ChemComm
FEATURE ARTICLE

# Chiral bicyclic lactams: useful precursors and templates for asymmetric syntheses[1]

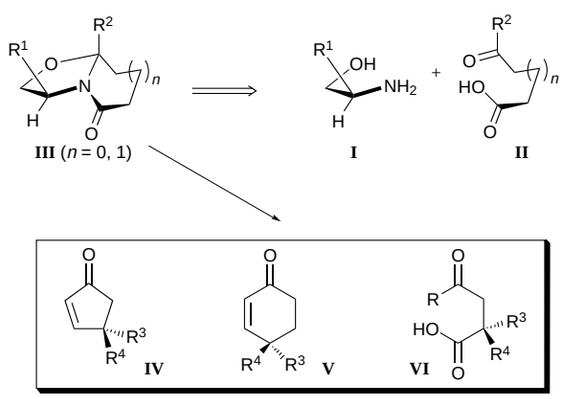
**A. I. Meyers and Gregory P. Brengel**

*Department of Chemistry, Colorado State University, Fort Collins, Colorado 80523, USA*

**A survey of the utilitarian bicyclic lactams is presented. These chiral templates have provided, and continue to provide, access to a plethora of natural and unnatural carbocyclic products in high enantiomeric purity. Their synthetic versatility has recently grown with the development of new methods for the construction of heterocycles. In addition to the cyclopentenone, cyclohexenone and hexahydroindenone systems, products derived from bicyclic lactams now include optically active piperidines, pyrrolidines, pyrrolidinones and tetrahydroisoquinolines. These favourable properties make the bicyclic lactams highly adaptable tools for asymmetric synthesis.**

Some recent progress achieved through the use of chiral, nonracemic bicyclic lactams **III** ($n$ = 0,1) has demonstrated that they are extremely useful and versatile building blocks for the preparation of a host of enantiomerically enriched, natural and unnatural products.[2] The preparation of these templates from their corresponding enantiomerically pure amino alcohols **III**, and their earlier utility in the synthesis of compounds containing quaternary stereocentres such as cyclopentenones **IV**, cyclohexenones **V** and carboxylic acids **VI**, has been previously reviewed (Scheme 1).[2a,d]

The synthesis of enantiopure carbocycles, which until recently was the major focus of our program, continues to serve as a vital goal for the development of new synthetic methods *via* bicyclic lactams. Examples of these included in the present discussion will describe enantiopure hexahydroindenones, benzindenones and cyclohexenones containing contiguous stereogenic centres (Scheme 2). The discovery that nitrogen-containing heterocycles could also be efficiently generated from these chiral lactams stimulated recent studies directed toward the syntheses of optically active pyrrolidine and piperidine derivatives. Thus, the reader will find that a large portion of this brief outline has been dedicated to the development and application of methods for the syntheses of enantiopure heterocyclic compounds from 5,5- and 5,6-bicyclic lactams (*vide infra*).



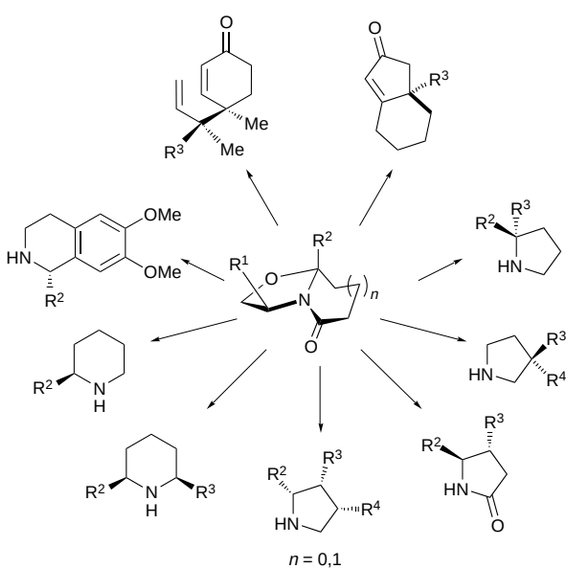

**Scheme 1**

## Recent syntheses of chiral non-racemic carbocycles

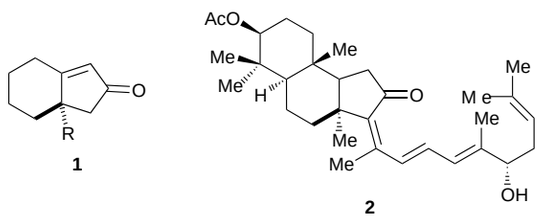
### *Hexahydroinden-2-ones and benz[e]inden-2-ones*

The hexahydroindenone ring system **1**, present in a number of naturally occurring compounds (*e.g.* Stelliferin A **2**[3]) was identified as a viable target for the bicyclic lactams. Since the preparation of enantiopure 3,3-disubstituted cyclopentenones *via* the bicyclic lactam had already been accomplished,[2a,c,h] modifications to access this ring system were investigated (Scheme 3).[4] The requisite bicyclic lactam **3**, which could undergo intramolecular cyclization affording the intermediate alcohol **4**, would serve as a key precursor. After hydrolysis and condensation to **5**, this should provide the desired tetrahydroindenone **1**.

The bromo lactam **8** was prepared *via* a two step process shown in Scheme 4. Thus, alkylation of bicyclic lactam **6** with butenyl bromide, followed by a second *endo* alkylation with an appropriate electrophile, afforded good yields of dialkylated product **7**.[2a,4] The latter was converted to the bromide **8** *via* hydroboration–oxidation followed by bromination in good overall yields. Metal–halogen exchange yielded the alcohol **4** *via* the organolithium **3** (Scheme 3). Hydrolysis to the diketone **5**, followed by base-catalysed condensation, produced optically




**Scheme 2**



pure hexahydroindenones **1** in modest overall yields. Similarly, alkylation of **6** with the appropriate aryl bromides furnished lactams **9**, and the D ring of the Stelliferin class was accessed in a single step providing the benzindenones **10**. Because epimerization of the quaternary centres was not possible, diastereomerically pure lactams **8** and **9** provided enantiomerically pure products. Further elaboration of **10** should yield Stelliferin A **2**.

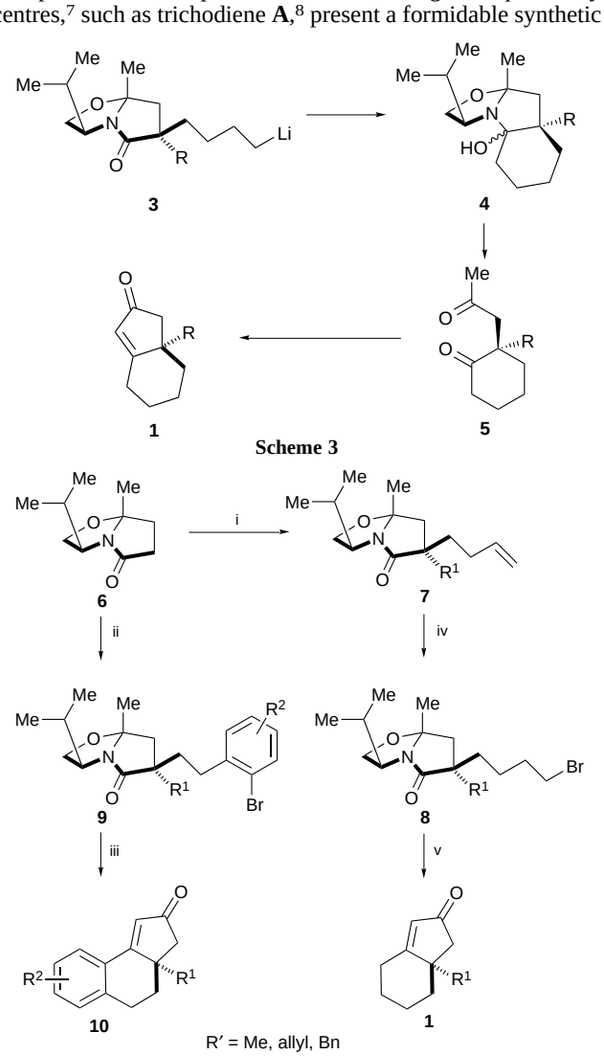
*Application of hexahydroindenones to the magellanine framework*

The above sequence leading to the hexahydroindenones has recently been applied to the construction of the Magellanine ring system **11** (Scheme 5).[5] The pivotal compound was the hexahydroindenone **1** (R = $CH_2Py$), which was obtained optically pure by hydrolysis–cyclization of diastereomerically pure lactam **7** (R = $CH_2Py$). Indenone **1** was cyclized *via* an intramolecular 1,4-addition of its enolate to the *N*-acylpyridinium salt and, after reoxidation, gave **12**. Successive stereoselective reductions provided the Magellanine framework **13**, whose structure was confirmed by single crystal X-ray analysis. The synthesis provided (−)-**13** in 13 steps from bicyclic lactam **6**, from which all of its six stereocentres had been derived.

*4,4-Disubstituted cyclohexenones with vicinal stereocentres*[6]

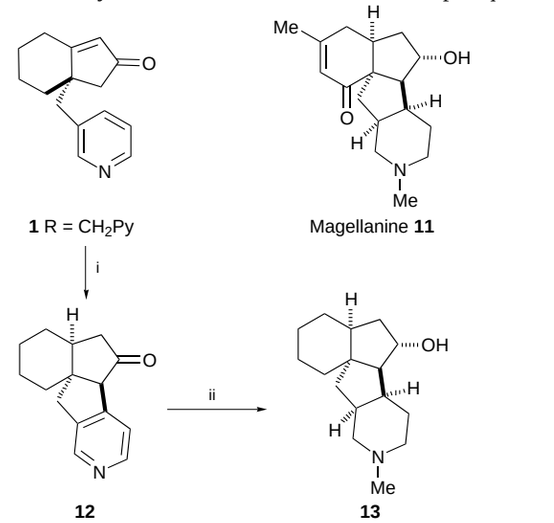
Compounds which possess vicinal stereogenic quaternary centres,[7] such as trichodiene **A**,[8] present a formidable synthetic challenge. Since one might imagine that this compound could be derived from the cyclohexenone **B**, it was envisioned that a bicyclic lactam might serve as a template for its synthesis (Scheme 6). Employment of the 5,6-bicyclic lactam, previously utilized in the synthesis of a number of optically active 4,4-disubstituted cyclohexenones,[2a,e] was feasible only if the properly substituted precursor **C** was available. Since the quaternary stereocentres could not be prepared through the usual dialkylation sequences, it was necessary to seek other means of installing these substituents with the correct stereochemistry. Undoubtedly, some form of the Claisen rearrangement (*e.g.* **D** → **C**) could produce the desired result. Unfortunately, lactam **14** could not, after numerous attempts, be directly *O*-alkylated to afford the Claisen precursor **16** (X = O) (Scheme 7). However, it was soon found that thiolactam **15**, obtained by treatment of **14** with Belleau's reagent,[9] underwent *S*-alkylation quite readily. Formation of the thioenolate with base, followed by addition of the appropriate allylic halides, produced the thioethers **16** (X = S) in good yields. The desired thio-Claisen rearrangement was smoothly implemented *via* thermal conditions to provide the rearranged thiolactams **17**.[10] The facial selectivity of the (3,3)-rearrangement was generally quite high, and the configuration of the new stereocentre was found to result from rearrangement on the *exo* face of the lactam. This is contrary to the *endo* selectivity normally observed during enolate alkylations of other 5,5- and 5,6-bicyclic lactams, however, this appears to be consistent with similar results obtained with these lactams of the type **14**.[2a,j] The subtle factors responsible for *exo* or *endo* selectivity with these lactams are still a matter of continuing investigation.†

The α,α-dialkylated thiolactams **17** were successfully transformed to the cyclohexenones **20** *via* the three step sequence

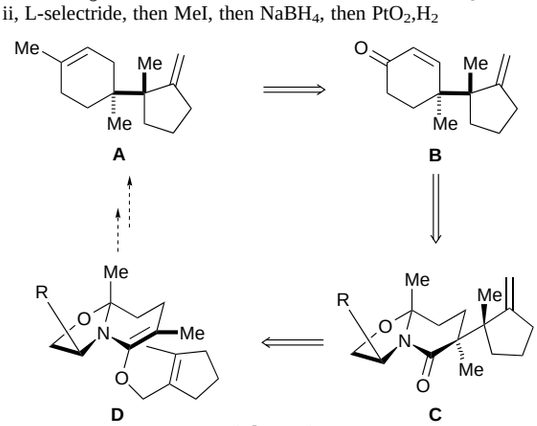



**Scheme 3**

**Scheme 4** *Reagents*: i, LDA, butenyl bromide, then LDA, $R^1X$; ii, LDA, $Ar(CH_2)_2Br$, then LDA, $R^1X$; iii, $Bu^tLi$, then $Bu_4NH_2PO_4$, then NaOEt; iv, $BH_3$, $H_2O_2$, then NBS, $PPh_3$; v, $Bu^tLi$,$Bu_4NH_2PO_4$, KOH




**Scheme 5** *Reagents*: i, PhOCOCl, $TiCl_4$, $Pr^i_2NEt$, then DDQ, then Pd–C, $H_2$; ii, L-selectride, then MeI, then $NaBH_4$, then $PtO_2$,$H_2$

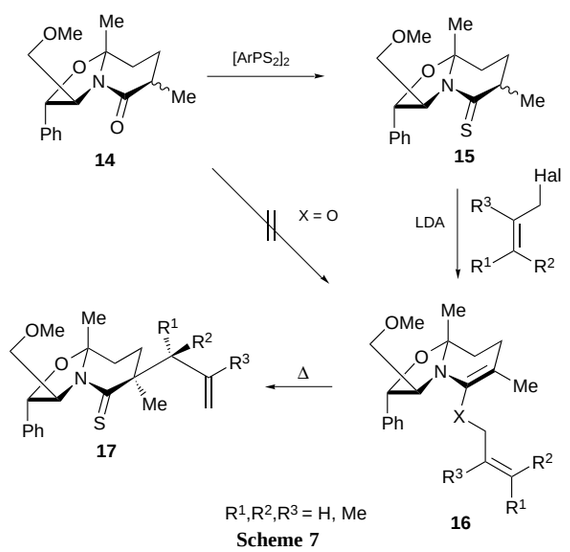



**Scheme 6**

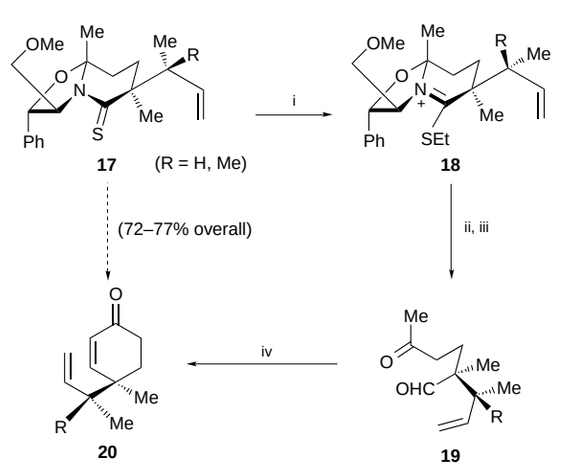
shown in Scheme 8. Generation of the thioiminium salts **18**, followed by reduction and hydrolysis, afforded the keto aldehydes **19** which were directly subjected to aldol cyclization to yield the optically pure ketone **20**, possessing vicinal quaternary centres in good overall yields.

### Syntheses of chiral non-racemic heterocycles

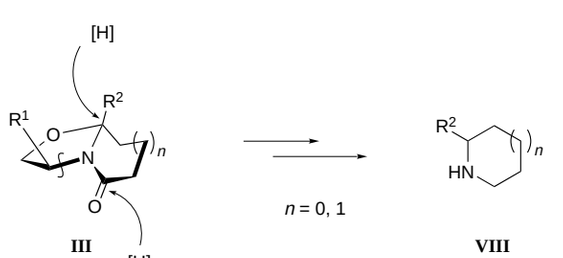
These highly useful[11a–c] substances should be readily obtained if the nitrogen atom present in the chiral auxiliary could be preserved in the final products **VIII** (Scheme 9). This was accomplished by simultaneous reduction of both the carbonyl and aminal centres in the lactams **III**, and was realized for both the 5,5- and 5,6-bicyclic systems. In this manner, enantiomerically pure pyrrolidines and piperidines **VIII** ($n$ = 0,1) were prepared (*vide infra*).




**Scheme 7**




**Scheme 8** *Reagents*: i, $Et_3OBF_4$; ii, Red-Al; iii, $H_3O^+$; iv, KOH, MeOH



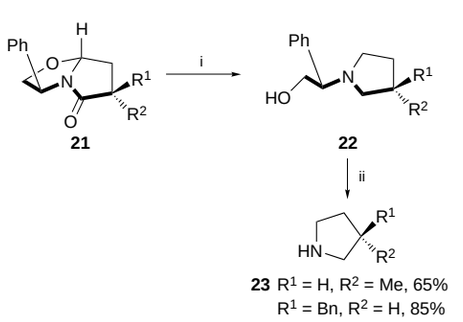

**Scheme 9**

### *Chiral pyrrolidines and pyrrolidinones*

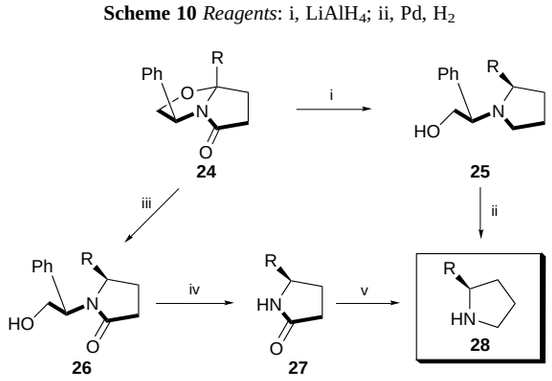
(i) *3-Substituted and 3,3-disubstituted pyrrolidines.* It was found that a number of angular hydrogen, dialkylated bicyclic lactams **21**,[2a] the utility of which had previously been demonstrated in the syntheses of chiral 5,5-disubstituted cyclopentenones,[2c] were simply and efficiently manipulated to provide enantiomerically pure 3,3-disubstituted pyrrolidines **23** (Scheme 10).[12] Specifically, the latter were obtained by reduction of lactams **21** with lithium aluminium hydride, followed by hydrogenolysis of the chiral auxiliary. It was noteworthy that monoalkylated lactams **21** ($R^1$ or $R^2$ = H) were also reduced, with no evidence of epimerization α to the lactam carbonyl group, to provide 3-substituted pyrrolidines **23** ($R^1$ or $R^2$ = H), in high optical purity.

(ii) *2-Substituted pyrrolidines and 5-substituted pyrrolidinones.* The angularly substituted, 5,5-bicyclic lactams **24** could be efficiently converted to 2-substituted pyrrolidines **28** and/or 5-substituted pyrrolidinones **27** by either of two short synthetic sequences (Scheme 11). Thus, treatment of lactam **24** directly with alane, or lithium aluminium hydride, reduced both the carbonyl and aminal centres to the pyrrolidines **25**, as single diastereomers. Hydrogenolysis of the nitrogen benzyl linkage then led to the free 2-substituted pyrrolidines **28** in good overall yields with greater than 98% enantiomeric purity.[11a] The utility of this sequence was recently demonstrated in the total asymmetric syntheses of the natural antibiotics (−)-irniine [R = $(CH_2)_9$Ph] and (−)-bgugaine [R = $(CH_2)_{13}$Me] by Jossang and co-workers.[13]

Alternatively, reduction of **24** by addition of triethylsilane and titanium tetrachloride to pyrrolidinone **26** (Scheme 11), followed by removal of the chiral auxiliary under dissolving metal conditions, provided the corresponding 5-substituted pyrrolidinones **27**, once again in high enantiomeric purity.[11a,14a,b] The pyrrolidinones, if desired, could be further reduced to the 2-substituted pyrrolidines **28**.[14c] Interestingly, both routes yielded pyrrolidines with the same absolute stereochemistry, namely, retention of configuration at the angular position in the lactams **21**.




**Scheme 10** *Reagents*: i, $LiAlH_4$; ii, Pd, $H_2$




**Scheme 11** *Reagents*: i, '$AlH_3$'; ii, Pd, $H_2$; iii, $Et_3SiH$, $TiCl_4$; iv, $Li^0$–$NH_3$; v, $LiAlH_4$

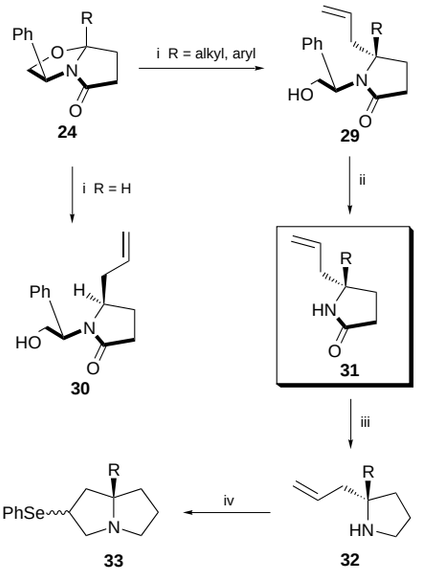
Although this stereochemical result was predictable for the alane reductions, having been previously observed in acetal cleavages,[15] it was surprising for the triethylsilane–titanium(IV) chloride system. Previous studies suggested that this reduction should have occurred in an $S_N2$ fashion to provide products with inversion of stereochemistry.[15] Fortunately, allylsilane additions to both angular hydrogen and angularly substituted bicyclic lactams **24** (Scheme 12) furnished some insight into the mechanism for these reductions (*vide infra*).

(iii) *2,2-Disubstituted pyrrolidines and 5,5-disubstituted pyrrolidinones.* In addition to hydride reductions, it was found that allylsilanes, under strong Lewis acidic conditions, could also be induced to add at the angular position of 5,5-bicyclic lactams **24** to furnish the disubstituted pyrrolidinones **29** and **30** (Scheme 12).[16] As seen for the hydride reductions, when R was either an alkyl or aryl substituent, the addition arose from *endo* entry to the lactam forming products with retention of configuration at the former angular position. Conversely, when the angular substituent was hydrogen, the observed stereochemistry was that from *exo* attack, or inversion of configuration. The chiral auxiliary in **29** may be cleaved under dissolving metal conditions to afford the 5,5-disubstituted pyrrolidinones **31** in good yield and with high enantiomeric excess. Again, if desired, pyrrolidinones **31** may be further reduced to pyrrolidines **32**. As an example of the utility of the newly installed allyl group, cyclization of pyrrolidines **32** was performed affording the backbone of the pyrrolizidine alkaloids **33**,[16b] an important class of natural products due to their potent biological activity.

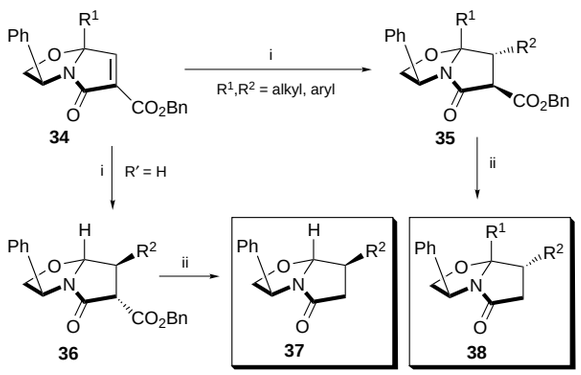
(iv) *Reactions with unsaturated 5,5-bicyclic lactams*. One of the most useful lactam substrates to date has been the unsaturated system **34** (Scheme 13)[2,17] The alkenic moiety has provided a functional handle on which a host of transformations have been carried out, including conjugate additions by various nucleophiles, pericyclic reactions,[2] and oxidations (*vide infra*). These transformations have proved invaluable in placing substituents in the 3- and 4-positions of both pyrrolidines and pyrrolidinones.

(v) *2,3*-trans-*Disubstituted pyrrolidines and 4-substituted and 4,5-disubstituted pyrrolidinones.* Lower order lithiocyanocuprates were found to efficiently add in a 1,4 fashion to activated unsaturated bicyclic lactams **34** producing **35** and **36** in good yields and high diastereoselectivities (Scheme 13).[18a,b] When the angular substituent in **34** was alkyl or aryl, addition proceeded mainly from the *endo* (α) face of the lactam, whereas the angular hydrogen lactams led to products resulting from *exo* (β) addition (**36**). This duality in the stereochemical outcome had been previously observed in cycloadditions to these unsaturated lactams,[2] and is believed to be primarily due to the steric effects created by the angular substituents. The benzyloxycarbonyl group ($R^2$ = $CO_2Bn$), which was found to be necessary for the cuprate additions, was efficiently removed *via* hydrogenolysis and decarboxylation. The resulting lactams **37** and **38** were subsequently converted to the corresponding pyrrolidines **39** and **41** respectively, or pyrrolidinones **40**, by one of the following sequences (Scheme 14).

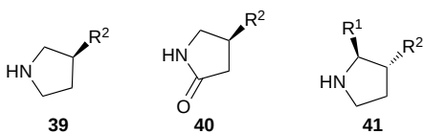
(vi) *2-Alkyl-3-amino- and 3,4-aziridino-pyrrolidines.* The 3-aminopyrrolidine **48** and 3,4-aziridinopyrrolidine **47** moieties are present in a diverse array of biologically active molecules,[19] and it was believed that these systems could be accessed *via* the unsaturated bicyclic lactam templates. It was observed that a series of primary and secondary amines efficiently added to the β-position of unsaturated lactams **42** to give the amino lactams **44** (Scheme 15).[19a] As previously seen with the cuprate additions, lactams bearing angular substituents (R = alkyl, aryl) led to products resulting from *endo* attack. The groups on the amine could be either chiral or achiral with no effect on the stereoselectivity. Surprisingly, the reaction was found to be irreversible. Thus, if the amino lactam adduct **44** was treated with base, generating the enolate, expulsion of the amine was



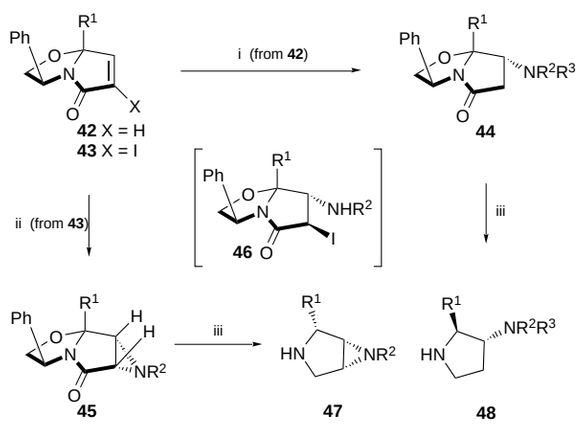

**Scheme 12** *Reagents*: i, (allyl)$SiMe_3$, $TiCl_4$; ii, $Li^0$–$NH_3$; iii, '$AlH_3$'; iv, PhSeSePh




**Scheme 13** *Reagents*: i, $R^2{}_2CuLiCN$; ii, Pd, $H_2$




**Scheme 14** *Reagents*: i, '$AlH_3$', then Pd, $H_2$; ii, $Et_3SiH$, $TiCl_4$, then $Li^0$–$NH_3$




**Scheme 15** *Reagents*: i, $R^2R^3NH$; ii, $R^2NH_2$; iii, '$AlH_3$', then Pd, $H_2$

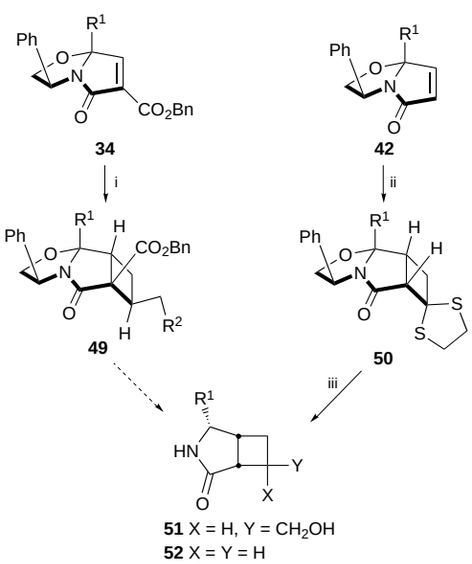
not observed, yet the enolate could be alkylated with an electrophile. This behaviour allowed for further elaboration of the pyrrolidine products (*vide infra*). However, by incorporating an α-halogeno substituent on the unsaturated lactam **43**,[17a] such as iodine, additions of primary amines efficiently led to aziridino products **45**, resulting from nucleophilic displacement of the halide *via* adduct **46**.[19b]

Both the amino and aziridino lactams were transformed to *trans*-2-alkyl-3-aminopyrrolidines **48** and *cis*-2-alkyl-3,4-aziridinopyrrolidines **47**, respectively, by the procedure identical to that used for the preparation of the other chiral pyrrolidine systems (*vide supra*).

(vii) *5-Alkyl-3,4-cyclobutanopyrrolidinones.* Organocuprate reagents and amines were not the only nucleophiles found to efficiently add to the unsaturated bicyclic lactams in a Michael fashion. During continuing studies to develop a diverse array of optically active pyrrolidines, the annulations of 2-methylenedithiolanes and allylsilanes with chiral bicyclic lactams were also investigated (Scheme 16).[20]

2-Methylenedithiolane, in the presence of dimethylaluminium chloride, added to unsaturated lactams **42** affording cyclobutanes **50** in high yields and as single diastereomers after chromatography.[20a] Although the removal of the thioketal to give the cyclobutanone derivatives failed, the dithioacetal could be reduced to the cyclobutane fused lactam, which was readily converted to the pyrrolidinones **52** *via* standard auxiliary removal procedures (*vide supra*). This Lewis acid-mediated annulation is complementary to the earlier photochemical additions of ethylene,[2a] and furthermore, these chiral cyclobutanopyrrolidinones **52** are potentially useful constrained GABA analogues.

Additions of allylsilanes to the unsaturated ester lactams **34** unexpectedly led to cyclobutane adducts **49** (Scheme 16).[20b] This was surprising in view of earlier reports of allylsilane annulations leading only to cyclopentanes. In fact, the silacyclobutane fused lactams **49** were among the first confirmed examples of this reaction manifold, which until recently was seriously questioned.[21] Although the cyclobutanes derived from triisopropylallylsilane ($R^2$ = $Pr^i_3Si$) are resistant to further chemical manipulation, the trityldimethylsilacyclobutanes ($R^2$ = $Ph_3CMe_2Si$) should allow ready substitution of the silicon moiety by a hydroxy substituent[22] to access chiral hydroxycyclobutanes of type **51**. Studies are currently in progress to evaluate these systems.

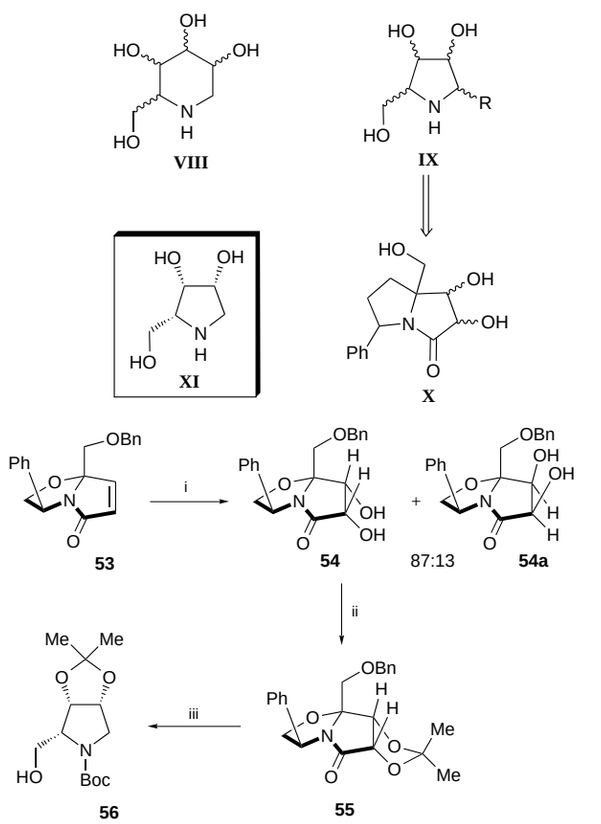



**Scheme 16** *Reagents*: i, (allyl)$R^2$ ($R^2$ = $SiPr^i_3$, $SiMe_2CPh_3$), $TiCl_4$; ii, 2-methylenedithiolane, $Me_2AlCl$, iii, Raney Ni, then $Et_3SiH$, $TiCl_4$, then $Li^0$–$NH_3$

(viii) *Chiral azasugars.* Azasugars **VIII** and **IX** are representative of a general class of compounds that have been reported to exhibit many biological properties including antitumour and anti-HIV activity. As a result, a great deal of interest has recently been generated in developing methods for their efficient syntheses.[23]

In view of this, 1,4-dideoxy-1,4-imino-D-lyxitol **XI** was selected as a target. In order to establish the correct absolute and relative stereochemistry of the hydroxymethyl and hydroxy substituents, the appropriate unsaturated lactam **53** was prepared (Scheme 17). The key step required installation of the *vic*-hydroxy groups in a *syn* fashion to the *endo* face of the lactam. This *cis* dihydroxylation was indeed accomplished, using *N*-methylmorpholine *N*-oxide (NMO) as an oxidant with a catalytic amount of osmium tetroxide, furnishing an 87 : 13 mixture of diastereomers **54** and **54a**. The major product **54**, predicted to be *endo* based on previous additions to unsaturated lactams, was readily separated from its *exo* epimer **54a** providing diastereomerically pure material. After protection of the diol as the acetonide **55**, the key reduction step was addressed. The reduction at the aminal centre required that inversion of configuration take place, in a stereoselective manner, to afford the correct stereochemistry of the hydroxymethyl substituent in **56**. Inversion at the angular position during reductions had been previously observed in the syntheses of cyclobutanes **51** and aziridines **47** (*vide supra*). It was anticipated that the cyclic acetonide **55** would serve as a blocking group and force reduction from the β-face. This was indeed the case, as reduction of **55** with 9-BBN produced, after hydrogenolysis of the auxiliary and protection of the nitrogen, the all-*cis* pyrrolidine **56** as a single diastereomer. Thus **56**, simply a protected version of **XI**, was prepared in a total of eight steps in 12% overall yield in high enantiomeric purity.

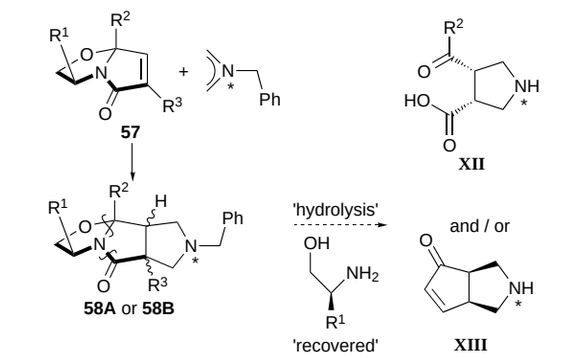
(ix) *3,4*-cis-*Disubstituted pyrrolidines.* It was anticipated that by fusing a pyrrolidine ring to the bicyclic lactam, *via* some type



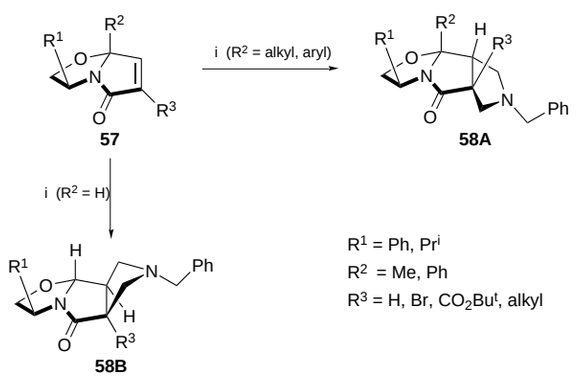

**Scheme 17** *Reagents*: i, $OsO_4$, NMO; ii, 2,2-dimethoxypropane, iii, 9-BBN, then Pd, $H_2$, $Boc_2O$

of [3 + 2] cycloaddition process, recovery of the amino alcohol auxiliary would be possible while still maintaining a nitrogen heteratom in the product. Thus, hydrolysis of the lactam adducts **58**, as previously demonstrated in earlier examples,[2a] would lead to the keto acids **XII** or cyclopentenones **XIII** (Scheme 18). In this manner, the requisite pyrrolidine ring would be in hand, and the amino alcohol auxiliary would not have to be sacrificed.

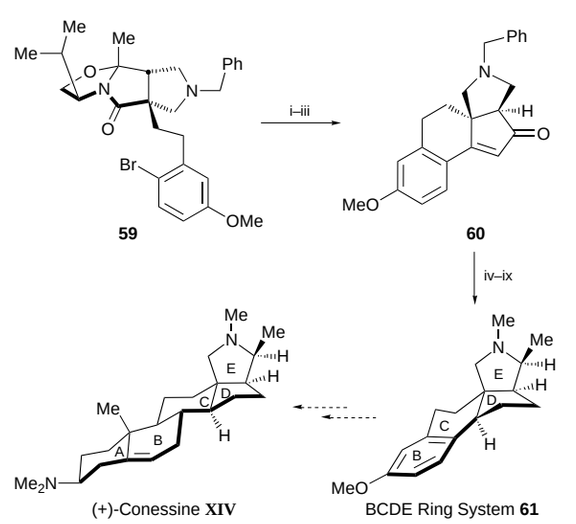
To this end, a study of the cycloaddition of azomethine ylides to chiral unsaturated bicyclic lactams was undertaken.[24] The ylides[25] led to high yields of cycloadducts **58A** and **58B** after addition to a variety of substituted bicyclic lactams **57** (Scheme 19). Once again, the angular substituent $R^2$ was the primary factor in determining *endo* or *exo* selectivity.




**Scheme 18**

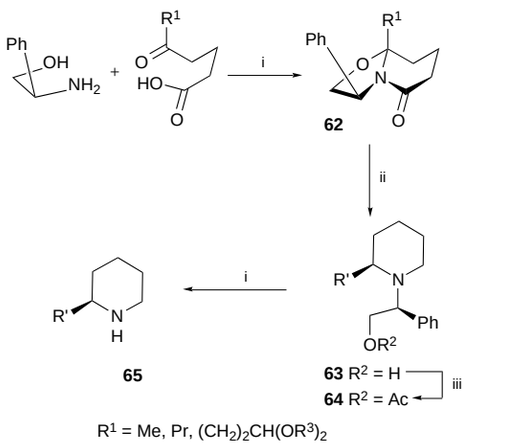



**Scheme 19** *Reagents*: i, $(Me_3SiCH_2)(MeOCH_2)(Bn)N$, TFA

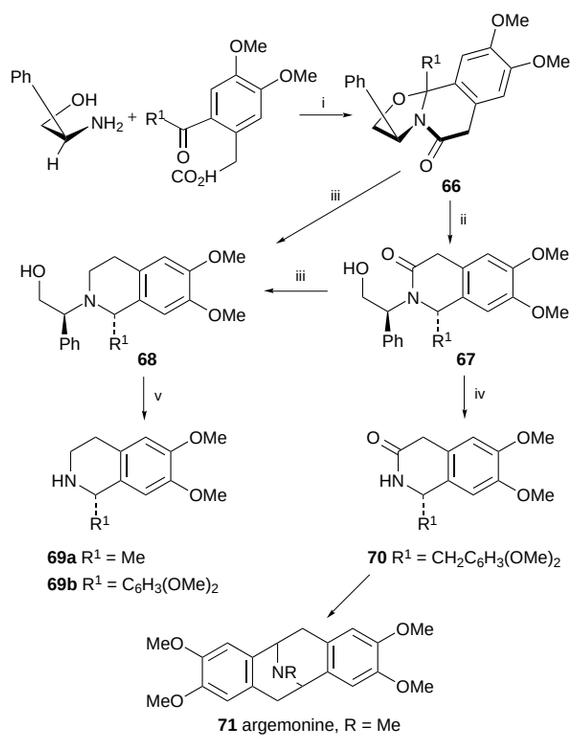



**Scheme 20** *Reagents*: i, $Bu^tLi$; ii, $Bu_4NH_2PO_4$; iii, NaOEt; iv, '$AlH_3$'; v, PhOCOCl; vi, $Bu^tOK$; vii, Pd, $H_2$; viii,$Bu^sLi$, MeI; ix, $LiAlH_4$

(x) *Asymmetric synthesis of conanine BCDE ring system.* (+)-Conessine **XIV**, a known amebicide, is just one in a family of alkaloids isolated from *Holarrhena antidysenterica*.[26] Common to each alkaloid in this family is the Conanine BCDE framework **61**, which contains a 3,4-disubstituted pyrrolidine subunit. A successful asymmetric synthesis of this structure would aptly demonstrate the versatility and utility of the chiral lactam template in pyrrolidine syntheses (Scheme 20).[27] The key step in implementing this sequence was the formation of cycloadduct **59**, containing the necessary bromoaryl side chain and the newly installed pyrrolidine E ring. The latter came directly from an azomethine cycloaddition to the appropriately functionalized unsaturated lactam **57** [$R^2 = (CH_2)_2Ar$].[18b] Other key steps in the synthesis involved construction of the BCD rings. This was accomplished *via* a method previously demonstrated for the preparation of the benz[*e*]inden-2-one ring system.[3] Metal–halogen exchange of aryl bromide **59**, followed by spontaneous cyclization, hydrolysis and aldol condensation, provided the requisite benzindenone **60** in high yield and in enantiomerically pure form. Reduction of the carbonyl group,




**Scheme 21** *Reagents*; i, heat; ii, Red-Al, heat; iii, $Ac_2O$; iv, $Pd(OH)_2$, $H_2$




**Scheme 22** *Reagents*: i, heat; ii, Red-Al; iii, $LiAlH_4$; iv, $Na^0$–$NH_3$; v, Pd, $H_2$

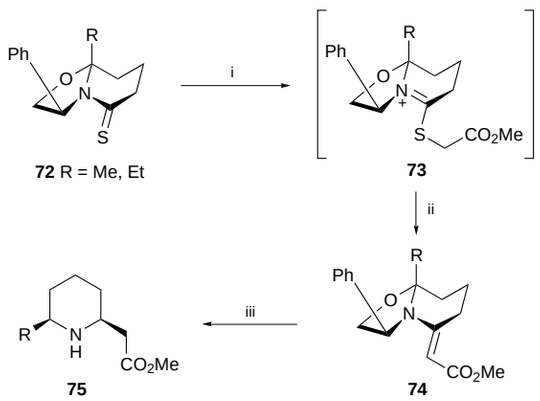
selective hydrogenation of the unsaturated C–D ring fusion and stereoselective alkylation of the pyrrolidine E ring resulted in the first asymmetric synthesis of the conanine BCDE framework **61**, in optically pure form and in 8% overall yield from **57**. Further elaboration of this framework to (±)–conessine **XIV** has previously been demonstrated.[26]

### *Piperidines and tetrahydroisoquinolines*

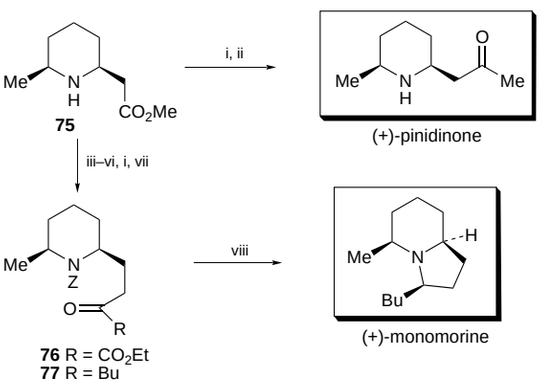
(i) *2-Substituted piperidines.* The presence of the piperidine ring system in a host of naturally occurring and biologically active alkaloids has generated considerable interest in the development of new methods for the preparation of these compounds in optically pure form.[11b,c,28a] Due to the success in the preparation of a number of enantiomerically pure pyrrolidines from 5,5-bicyclic lactams **III** ($n$ = 0), it was felt that similar techniques could be applied to the related 5,6-bicyclic lactam.

Red-Al reduction of a number of angular alkyl 5,6-bicyclic lactams **62**, derived from δ-keto acids as shown, furnished the piperidine derivatives **63** in good yields and with high diastereomeric excess (Scheme 21).[28b] Retention of configuration of the angular substituent in **62** was again maintained in the major piperidine products **63**. In all cases, the diastereomers, once converted to the acetates **64**, could be purified to provide, after hydrogenolysis of the chiral axuiliary, the enantiopure 2-substituted piperidines **65** in only two steps from the bicyclic lactam **62**. The efficient and versatile nature of this piperidine synthesis was featured in the total synthesis of natural (−)-pipecoline **65** ($R^1$ = Me), (+)-coniine **65** ($R^1$ = Pr), and the 1-azabicyclic system, (−)-coniceine.[28b,c]

(ii) *1-Substituted tetrahydroisoquinolines.* Owing to the successful preparation of 2-substituted piperidines from simple angular alkyl 5,6-bicyclic lactams **62**, it was proposed that 1-substituted tetrahydroisoquinolines **69** could also be obtained from an appropriately functionalized 5,6-bicyclic lactam




**Scheme 23** *Reagents*: i, $BrCH_2CO_2Me$; ii, $P(OMe)_3$, $Et_3N$, heat; iii, $Pd(OH)_2$, $H_2$




**Scheme 24** *Reagents*: i, MeNHOMe·HCl, $AlMe_3$; ii, MeMgBr; iii, 2Cl; iv, $OH^-$; v, $(COCl)_2$; vi, $CH_2N_2$, AgO; vii, BuMgBr; viii, Pd, $H_2$

(Scheme 22). Although there are a number of routes to the 1-alkylisoquinolines, there are relatively few which install 1-aryl substituents.

The requisite 5,6-bicyclic lactam **66** was simply prepared from the corresponding 2-acylphenylacetic acid and (*S*)-phenylglycinol, and the previously utilized reduction sequence for the piperidines was employed. Thus, reduction of **66** with $LiAlH_4$ to the tetrahydroisoquinoline derivatives **68** occurred with high diastereomeric excesses (Scheme 22). Again, the major products (>95% de) were those with retention of configuration at the angular position of **66**. After purification of the diastereomers by chromatography, hydrogenolysis of the chiral auxiliary provided the tetrahydroisoquinolines **69** in optically pure form.[29a,c] The efficiency of this process was aptly demonstrated in the syntheses of both 1-alkyl- and 1-aryl-tetrahydroisoquinolines, (−)-salsolidine **69a** and (+)-cryptostyline II **69b**, respectively.

Treatment of bicyclic lactam **66** [$R^1$ = $CH_2C_6H_3(OMe)_2$] with Red-Al reduced only the aminal carbon to produce lactam **67** (Scheme 22). Removal of the chiral auxiliary under dissolving metal conditions afforded the free lactam **70** which was further elaborated, *via* reduction and cyclization, to enantiomerically pure (−)-argemonine.[29b]

(iii) *2,6-Disubstituted piperidines.* The presence of biologically active piperidines **71**, containing substitution at both the 2- and 6-positions, has prompted a number of laboratories to pursue new and efficient methods to access these systems in enantiomerically pure form.[11b,c]

If the thiolactam **72** could be induced to undergo an Eschenmoser contraction,[30] a means of transforming the carbonyl group to a carbon–carbon linkage, a useful intermediate for further elaboration might be in hand. In this regard, addition of methyl α-bromoacetate to thiolactams **72**, prepared from oxolactam **62** *via* the Belleau reagent,[9] afforded the intermediate thioiminium salts **73** which, on treatment with triethylamine and trimethyl phosphite, gave the vinylogous urethanes **74** in high yield (Scheme 23). Hydrogenation of **74** with concomitant reduction of the aminal carbon, the C=C, and the benzylic carbon was achieved in a single step using palladium hydroxide to afford the *cis*-2,6-disubstituted piperidines **75** as single enantiomers. The reducible centres were attacked from the *endo* face of the lactam to provide only the *cis* isomers, with net retention of configuration at the former aminal centre. It was also shown that the unsaturated linkage is reduced prior to the aminal linkage.

The synthetic value of piperidines **75** (Scheme 24) was clearly demonstrated in the efficient syntheses of two alkaloids, (+)-pinidinone and the ant trail pheromone (+)-monomorine.[11c,31]

## Conclusions

Bicyclic lactams **III** ($n$ = 0,1) have, once again, proven themselves to be extremely versatile in preparing a host of optically active products (*vide supra*). Their utility is perhaps best exhibited by the shear diversity of compounds (*e.g.* Schemes 1 and 2) that may be accessed through this single set of chiral templates. The ready availability of these building blocks,‡ and their inherent ability to provide a variety of enantiomerically pure carbocycles and heterocycles, makes these bicyclic lactams both an important and general tool for asymmetric synthesis.

---

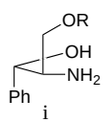
**Professor Meyers is a native of New York City and was educated at New York University where he received his Bachelors (1954) and PhD (1957) degrees. He was an NIH Special Fellow at Harvard University with Professor E. J. Corey and joined the faculty of Louisiana State University (New Orleans) where he rose to the rank of Boyd Professor. He was Professor of Chemistry at Wayne State University before joining Colorado State University in 1972. His research interests are new**

**synthetic methods, asymmetric synthesis, heterocycles and total synthesis of natural products. He has been the recipient of the ACS Award in Creativity in Organic Synthesis (1985), an Arthur C. Cope Scholar (1987), and elected to the National Academy of Sciences (1994). He has been Associate Editor of the *Journal of the American Chemical Society* and currently is a University Distinguished Professor and holder of the John K. Stille Chair in Chemistry.**

**Gregory Philip Brengel was born on Long Island, New York in 1968. He received a Bachelors of Science in Chemistry (with honours) from Indiana University in 1990, and carried out research with Professor Jeffrey M. Stryker. He then moved to Colorado State University where he began his doctoral studies with Professor Albert I. Meyers. His dissertation work has resulted in the stereoselective syntheses of cycloalkanols *via* allylsilane annulations to electron deficient alkenes and unsaturated bicyclic lactams. Gregory received his PhD in the autumn of 1996 and is currently employed with Union Carbide in New Jersey.**

## Footnotes

† It has been recently found that 5,5-bicyclic lactams **III**, derived from the Parke–Davis amino alcohol **i** (R = Me, $SiPh_2Bu^t$), undergo almost exclusive *exo* alkylation. The diastereoselectivities in these cases are extremely high and the results of the study will be reported in due course; A. I. Meyers and M. Seefeld, *J. Org. Chem.*, 1996, **61**, 5712. See also G. Roth *et al.*, *J. Org. Chem*., 1996, **61**, 5710. For *exo* selective alkylations of 5,6-bicyclic lactams, see ref. 2(*j*).



i

‡ A wide selection of saturated and unsaturated 5,5-bicyclic lactams **III** (*n* = 0) and **57**, respectively, are now commercially available from either Aldrich Chemical Co. or Salford Ultrafine Chemicals & Research Ltd., Research Park, Manchester (UK).

## References


1 For a recent authoratative review on asymmetric syntheses, see: *Houben-Weyl, Methods of Organic Chemistry, Vols. E21: Stereoselective Synthesis*, ed. G. Helmchen, R. W. Hoffman, J. Mulzer and E. Schaumann, Georg Thieme Verlag, 1995; *Asymmetric Synthesis*, ed. J. D. Morrison, Academic Press, Orlando, 1983–1985.

2 (*a*) D. Romo and A. I. Meyers, *Tetrahedron*, 1991, **47**, 9503; (*b*) D. Romo and A. I. Meyers, *J. Org. Chem.*, 1992, **57**, 6265; (*c*) A. I. Meyers and L. J. Westrum, *Tetrahedron Lett.*, 1993, **34**, 7701; (*d*) A. I. Meyers, in *Stereocontrolled Organic Synthesis*, ed. B. M. Trost, Blackwell Scientific Publications, 1994, pp. 145–161; (*e*) J. E. Resek and A. I. Meyers, *Synlett*, 1995, 145; (*f*) M. Es-Sayed, P. Devine, L. E. Burgess, A. de Meijere and A. I. Meyers, *J. Chem. Soc., Chem. Commun.*, 1995, 141; (*g*) C. J. Andres, N. Spetseris, J. R. Norton and A.I. Meyers, *Tetrahedron Lett.*, 1995, **36**, 1613; (*h*) J. B. Schwarz and A. I. Meyers, *J. Org. Chem.*, 1995, **60**, 6511; (*i*) for other reports on the use of these bicyclic lactams see, J. A. Ragan and M. C. Claffey, *Heterocycles*, 1995, **41**, 57; (*j*) T. Wunsch and A. I. Meyers, *J. Org. Chem.*, 1990, **55**, 4233.

3 M. Tsuda, M. Ishibashi, K. Agemi, T. Sasaki and J. Kobayashi, *Tetrahedron*, 1991, **47**, 2181; B. R. Gaikwad, T. Mayelvaganan, B. A. Vyas and S. V. Bhat, *Phytochemistry*, 1990, **29**, 3963.

4 A. I. Meyers and L. Snyder, *Synlett*, 1991, 863; L. Snyder and A. I. Meyers, *J. Org. Chem.*, 1993, **58**, 7507 and references cited therein.

5 D. A. Sandham and A. I. Meyers, *J. Chem. Soc., Chem. Commun.*, 1995, 2511 and references cited therein for previous syntheses of Magellanine.

6 P. N. Devine and A. I. Meyers, *J. Am. Chem. Soc.*, 1994, **116**, 2633.

7 For other routes to enantiomerically pure vicinal quaternary and tertiary stereocenters see: M. Yamaguchi, M. Hamada, H. Nakashima and T. Minami, *Tetrahedron Lett.*, 1987, **28**, 1785; H.-J. Knölker and R. Graf, *Tetrahedron Lett.*, 1993, **34**, 4765.

8 For a recent enantioselective (41% ee) synthesis of trichodiene, see J. C. Gilbert and R. D. Selliah, *J. Org. Chem.*, 1993, **58**, 6255.

9 G. Lajoie, F. Lepine, L. Maziak and B. Belleau, *Tetrahedron Lett.*, 1983, **24**, 3815.

10 For a review, see P. Metzner, *Synthesis*, 1992, 1185; Y. Tamaru, T. Harada and Z.-I. Yoshida, *J. Am. Chem. Soc.*, 1980, **102**, 2392 and references cited therein.

11 (*a*) L. E. Burgess and A. I. Meyers, *J. Org. Chem.*, 1992, **57**, 1656 and references cited therein; (*b*) A. D. Elbein and R. Molyneux, in *Alkaloids; Chemical and Biological Perspectives*, ed. S. W. Pelletier, 1987, vol. 57, p. 1; (*c*) M. J. Munchhof and A. I. Meyers, *J. Am. Chem. Soc.*, 1995, **117**, 5399 and references cited therein; (*d*) T. Mukaiyama and M. Asami, *Top. Curr. Chem.*, 1985, **127**, 133.

12 L. J. Westrum and A. I. Meyers, *Tetrahedron Lett.*, 1994, **35**, 973; for other syntheses of chiral 3-substituted pyrrolidines, see S. E. Denmark and L. R. Marcin, *J. Org. Chem.*, 1995, **60**, 3221.

13 A. Jossang, A. Melhaoui and B. Bodo, *Heterocycles*, 1996, **43**, 755.

14 (*a*) M. A. Tschantz, L. E. Burgess and A. I. Meyers, *Org. Synth.*, 1995, **73**, 221; (*b*) for other syntheses of 5-pyrrolidinones, see Z.-Y. Wei and E. E. Knaus, *Tetrahedron Lett.*, 1993, **34**, 4439; (*c*) for other syntheses of 2-pyrrolidines, see H. Suzuki, S. Aoyagi and C. Kibayashi, *Tetrahedron Lett.*, 1994, **35**, 6119.

15 K. Ishihara, A. Mori and H. Yamamoto, *Tetrahedron*, 1990, **46**, 4595; I. Mori, L. A. Flippin, K. Nozaki, H. Yamamoto, P. A. Bartlett and C. H. Heathcock, *J. Org. Chem.*, 1990, **55**, 6107; A. Alexakis and P. Mangeney, *Tetrahedron: Asymmetry*, 1990, **1**, 477.

16 (*a*) A. I. Meyers and L. E. Burgess, *J. Org. Chem.*, 1991, **56**, 2294; (*b*) L. E. Burgess and A. I. Meyers, *J. Am. Chem. Soc.*, 1991, **113**, 9858.

17 (*a*) B. J. Newhouse, A. I. Meyers,N. S. Sirisoma, M. P. Braun and C. R. Johnson, *Synlett*, 1993, 573; (*b*) J. E. Resek and A. I. Meyers, *Tetrahedron Lett.*, 1995, **36**, 7051.

18 (*a*) A. I. Meyers and L. Snyder, *J. Org. Chem.*, 1992, **57**, 3814; (*b*) A. I. Meyers and L. Snyder, *J. Org. Chem.*, 1993, **58**, 36; (*c*) for a recent synthesis of *cis*-2,3-disubstituted pyrrolidines, see T. Kercher and T. Livinghouse, *J. Am. Chem. Soc.*, 1996, **118**, 4200.

19 (*a*) C. J. Andres, P. H. Lee, T. H. Nguyen and A. I. Meyers, *J. Org. Chem.*, 1995, **60**, 3189 and references cited therein; (*b*) C. J. Andres and A. I. Meyers, *Tetrahedron Lett.*, 1995, **36**, 3491 and references cited therein; for recent syntheses of aminopyrrolidines see (*c*) G. M. Taylor, S. J. Baker, A. Gedney, D. J. Pearson and G. E. M. Sibley, *Tetrahedron Lett.*, 1996, **37**, 1297; (*d*) U. Chiacchio, F. Casuscelli, A. Corsaro, V. Librando, A. Rescifina, R. Romeo and G. Romeo, *Tetrahedron*, 1995, **51**, 5689.

20 (*a*) A. I. Meyers, M. A. Tschantz and G. P. Brengel, *J. Org. Chem.*, 1995, **60**, 4359; (*b*) G. P. Brengel, C. Rithner and A. I. Meyers, *J. Org. Chem.*, 1994, **59**, 5144.

21 H.-J. Knölker and R. Graf, *Tetrahedron Lett.*, 1993, **34**, 4765 and references cited therein.

22 G. P. Brengel and A.I. Meyers, *J. Org. Chem.*, 1996, **61**, 3230. see also I. Fleming, *Chemtracts: Org. Chem.*, 1996, **9**, 1.

23 (*a*) A. I. Meyers, C. J. Andres, J. E. Resek, M. A. McLaughlin, C. C. Woodall and P. H. Lee, *J. Org. Chem.*, 1996, **61**, 2586 and references cited therein; for other syntheses of hydroxypyrrolidines see (*b*) J. C. Carretero, R. G. Arrayás and I. S. de Gracia, *Tetrahedron Lett.*, 1996, **37**, 3379; (*c*) I. Burley and A. T. Hewson, *Tetrahedron Lett.*, 1994, **35**, 7099.

24 A. H. Fray and A. I. Meyers, *Tetrahedron Lett.*, 1992, **33**, 3575; A. H. Fray and A. I. Meyers, *J. Org. Chem.*, 1996, **61**, 3362.

25 A. Padwa and W. Dent, *J. Org. Chem.*, 1987, **52**, 235.

26 For the syntheses of (±)-conessine and the related (±)-conanine ring system, see G. Stork, S. D. Darling, I. T. Harrison and P. S. Wharton, *J. Am. Chem. Soc.*, 1962, **84**, 2018; M. Mukherjee and L. M. Mukherjee, *Indian J. Chem.*, 1981, **20B**, 1019 and references cited therein.

27 M. Kopach, A. H. Fray and A. I. Meyers, *J. Am. Chem. Soc.*, 1996, **118**, 9876.

28 (*a*) For a recent asymmetric synthesis of 2,3-disubstituted piperidines *via* chiral lactams, see L. Micouin, J.-C. Quirion and H.-P. Husson, *Tetrahedron Lett.*, 1996, **37**, 849; (*b*) M. J. Munchhof and A. I. Meyers, *J. Org. Chem.*, 1995, **60**, 7084; (*c*) for an asymmetric synthesis of (−)-coniine *via* chiral bicyclic lactam **62** ($R^1$ = H), see M. Amat, N. Llor and J. Bosch, *Tetrahedron Lett.*, 1994, **35**, 2223.

29 (*a*) M. J. Munchhof and A. I. Meyers, *J. Org. Chem.*, 1995, **60**, 7086 and references cited therein; (*b*) M. J. Munchhof and A. I. Meyers, *J. Org. Chem.*, 1996, **61**, in the press; (*c*) N. Uematsu, A. Fujii, S. Hashiguchi, T. Ikariya and R. Noyori, *J. Am. Chem. Soc.*, 1996, **118**, 4916.

30 A. Eschenmoser, *Pure Appl. Chem.*, 1973, **33**, 69.

31 For a recent asymmetric synthesis of (−)-dihydropinidine *via* angular hydrogen bicyclic lactam **62** ($R^1$ = H), see M. Amat, N. Llor, J. Hidalgo, A. Hernández and J. Bosch, *Tetrahedron: Asymmetry*, 1996, **7**, 977.

# Self-assembly of hyperbranched spheres; correlation between monomeric synthon and sphere size

**Wilhelm T. S. Huck,[a] Bianca H. M. Snellink-Ruël,[a] James W. Th. Lichtenbelt,[b] Frank C. J. M. van Veggel*[a] and David N. Reinhoudt*[a]**

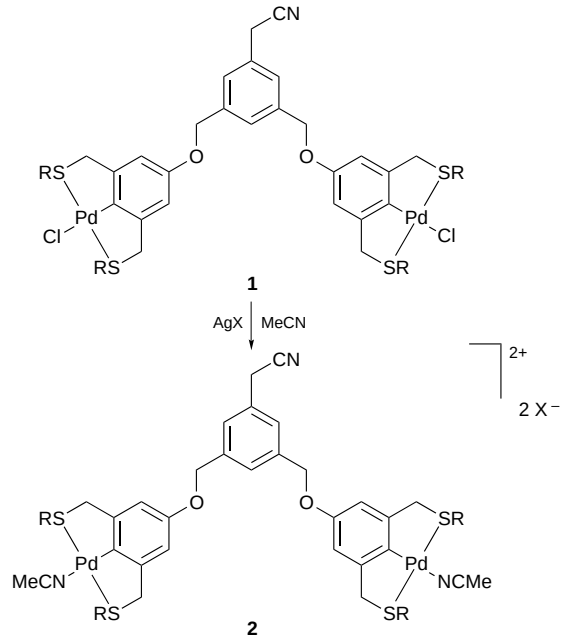
[a] *Laboratory of Organic Chemistry and Mesa Research Institute, University of Twente, PO Box 217, 7500 AE Enschede, The Netherlands*
[b] *AKZO NOBEL Research Laboratories, PO Box 9300, 6800 SB Arnhem, The Netherlands*

**Light-scattering experiments show that the size of self-assembled hyperbranched spheres can be varied from 100 to 400 nm, by variation of the building block structure and/or the counter anions.**

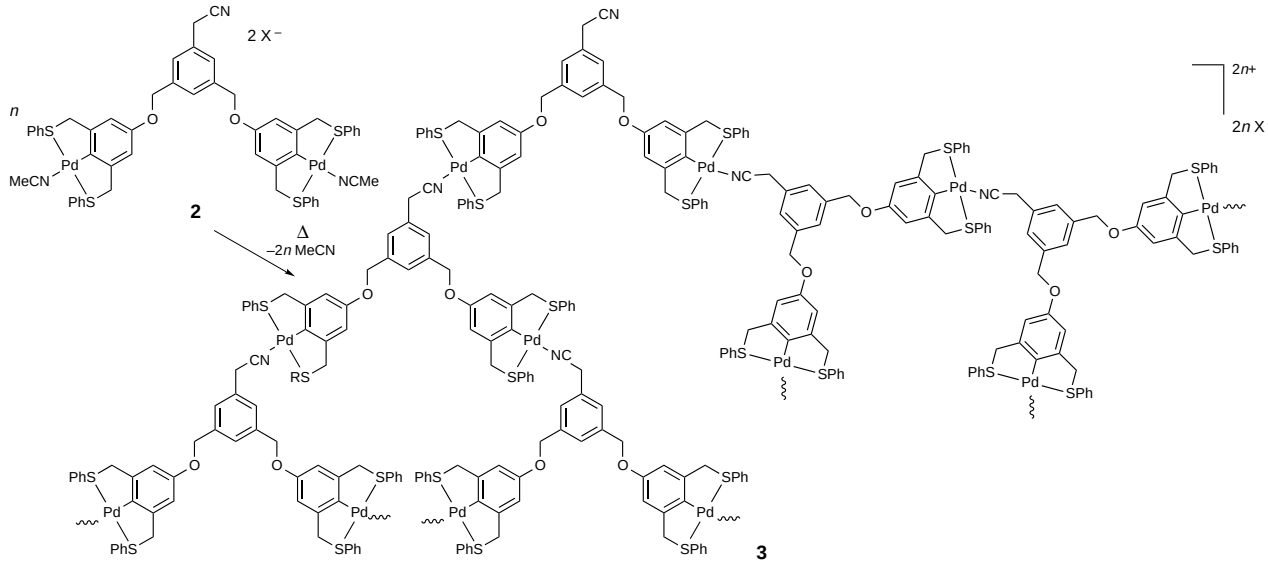
Recently, coordination chemistry has been exploited as a useful tool to form well-defined three-dimensional architectures *via* self-assembly. Transition metals can be used to control the geometry of architectures such as molecular squares,[1] helicates[2] and dendrimers.[3,4] Previously, we have reported the stepwise, non-covalent synthesis of dendrimers of nanosize dimensions *via* assembly of bis-Pd 'pincer' complexes **1** (R = Ph).[5]

The same building blocks can be used for the self-assembly of **2** (X = $BF_4^-$, R = Ph) into very large non-covalent structures. The size distribution of our self-assembled organo-palladium spheres was remarkably narrow (AFM: mean size 200 nm, σ *ca.* 30 nm).[6] These initial results prompted us to systematically study the influence of structural variations in the building block **1** and counter ions ($X^-$) on the size of the spheres, because the bulkiness of the non-coordinating anions and thioether moieties are likely to determine the assembly process.

The different anions were introduced by reacting the Pd–Cl complex **1** with the appropriate silver salt in MeCN (Scheme 1).† AgCl precipitated immediately giving the corresponding acetonitrile complex **2**. We have synthesized phenyl thioether building blocks with $BF_4^-$, $ClO_4^-$, $PF_6^-$, $CF_3SO_3^-$, *p*-$MeC_6H_4SO_3^-$ and $BPh_4^-$ counteranions. For **2b** (R = naphthyl) the $BF_4^-$, $PF_6^-$ and $CF_3SO_3^-$ systems were synthesized.




**Scheme 1** Structural variation in the building blocks




**Scheme 2** Schematic self-assembly of hyperbranched coordination polymers

Only the *p*-$MeC_6H_4SO_3^-$ could be isolated of the alkyl thioethers **2c**, **2d** because the Pd complexes were unstable with $BF_4^-$, $PF_6^-$ and $CF_3SO_3^-$ anions.

Removal of all acetonitrile by repeated evaporation and redissolving the residue in nitromethane results in the intermolecular coordination of the cyano groups of the building blocks to yield hyperbranched coordination polymers **3** (Scheme 2).‡

The size of the resulting assemblies was determined by quasi-elastic light-scattering (QELS). In general, we observed that larger anions or bulkier thioethers, gave smaller spheres (Fig. 1). The naphthyl thioether with $PF_6^-$ and $CF_3SO_3^-$ anions shows a similar decrease in size as the phenyl analogues.§ Comparing the entries for the $PF_6^-$, $CF_3SO_3^-$ and *p*-$MeC_6H_4SO_3^-$ anions it is evident from Fig. 1 that with increasing size of the thioether groups smaller particles are formed.

In addition, AFM and TEM were used to study the shape of some of the assemblies. Spherical assemblies are clearly observed.¶ From AFM data, sizes of 100 (±20) nm for **3b** ($X^-$ = $BF_4^-$) and of 110 (±20) nm for **3b** ($X^-$ = $CF_3SO_3^-$) were measured. This is in good agreement with the QELS data (140 and 104 nm, respectively). The TEM image shows assemblies of 225 nm for **3a** ($X^-$ = *p*-$MeC_6H_4SO_3^-$), in good agreement with QELS data (220 nm).

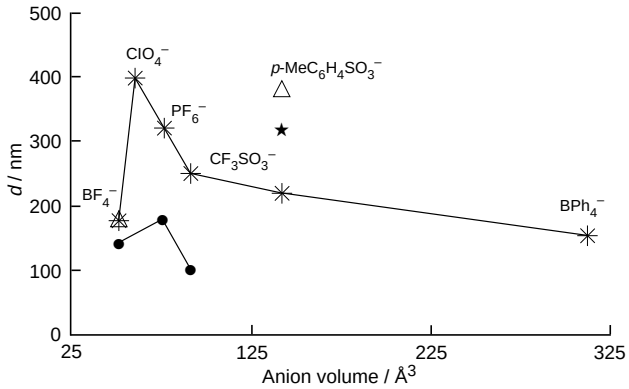



**Fig. 1** Sphere size *vs.* anions as measured by QELS in $MeNO_2$ at room temp. (△ = Et, * = Ph, ★ = Bu$^t$, ● = naphthyl)

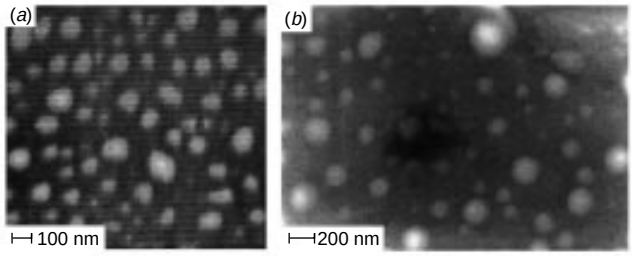



**Fig. 2** (*a*) AFM image of **3b** ($X^-$ = $CF_3SO_3^-$) and TEM image of **3a** ($X^-$ = *p*-$MeC_6H_4SO_3^-$)

The observed size dependency can be rationalized by combining the size of the anion and the distribution of charge in the polyelectrolyte assembly. The assembly process stops when the anions inside the sphere can no longer compensate for the accumulating charges and start to occupy the surface. Consequently, the different sizes of the spheres are determined both by the size and the charge density of the anion and the structure of bis-Pd complex.

The hyperbranched structure with a dense outer surface is supported by disassembly experiments that give information on kinetic stability. When *ca*. 20 equiv. of acetonitrile was added to a nitromethane solution of the spheres, these disassembled slowly in the course of 15–30 min. This slow disassembly indicates that acetonitrile can not easily penetrate the outer shell of building blocks. With a larger nitrile, like benzonitrile, the disassembly process is hardly evident, even after heating to 70 °C for 15 min. These data are indicative that a branching architecture leads to a closely packed surface, as has been observed in dendrimer chemistry.[7]

## Footnotes

† The Pd–Cl complexes were fully characterized by $^1$H and $^{13}$C NMR, FTIR, FAB–MS and elemental analysis. $^1$H NMR shows a characteristic shift at δ 4.5 (br) for the $CH_2S$ protons of the Pd-complex. Coordination of CN to the Pd-centres was evidenced by FTIR (2290 cm$^{-1}$).

‡ $^1$H NMR spectra in $CD_3NO_2$ of all assemblies show broad peaks, in agreement with large structures. Addition of $CD_3CN$ sharpened the spectra, which means that the self-assembly and disassembly processes are completely reversible. The original broad spectrum is restored when the solution is evaporated completely and redissolved in acetonitrile-free nitromethane.

§ The size of the anion was calculated using the option for Connolly Surfaces in CERIUS².[8] For unknown reasons the $BF_4^-$ anion behaves anomalously. The anion is, even inside the hyperbranched polymer, probably solvated and therefore appearing larger then the naked anion.

¶ The size distribution could not always be derived from these data because of (extensive) clustering. In the case of **3b** ($X^-$ = $PF_6^-$) only thin films were observed with AFM.

## References


1 P. J. Stang, D. H. Cao, S. Saito and A. M. Arif, *J. Am. Chem. Soc.*, 1995, **115**, 6273; P. J. Stang and B. Olenyuk, *Angew. Chem., Int. Ed. Engl.*, 1996, **35**, 732.

2 R. F. Carina, G. Bernardinelli and A. F. Williams, *Angew. Chem., Int. Ed. Engl.*, 1993, **32**, 1463; E. C. Constable, A. J. Edwards. P. R. Raithby and J. V. Walker, *Angew. Chem., Int. Ed. Engl.*, 1993, **32**, 1465; J.-M. Lehn, A. Rigault, J. Siegel, J. Harrowfield, B. Chevrier and D. Moras, *Proc. Natl. Acad. Sci. USA*, 1987, **84**, 2565.

3 S. Campagna, G. Denti, S. Serroni, A. Juris, M. Venturi, V. Ricevuto and V. Balzani, *Chem. Eur. J.*, 1995, **1**, 211.

4 S. Achar and R. J. Puddephatt, *Angew. Chem., Int. Ed. Engl.*, 1994, **33**, 847.

5 W. T. S. Huck, F. C. J. M. van Veggel and D. N. Reinhoudt, *Angew. Chem., Int. Ed. Engl.*, 1996, **35**, 1213.

6 W. T. S. Huck, F. C. J. M. van Veggel, B. L. Kropman, D. H. A. Blank, E. G. Keim, M. M. A. Smithers and D. N. Reinhoudt, *J. Am. Chem. Soc.*, 1995, **117**, 8293.

7 J. F. G. A. Jansen, E. M. M. de Brabander-van den Berg and E. W. Meijer, *Science*, 1994, **266**, 1226.

8 CERIUS2, Molecular Simulations Inc, Waltham, MA, USA.


*Received, 13th August 1996; Com. 6/05647D*

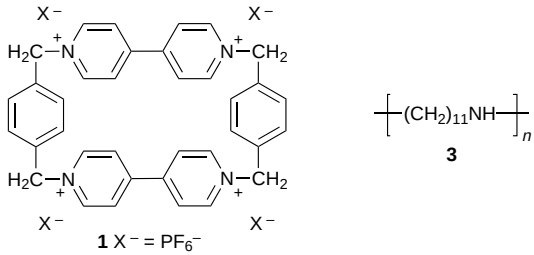
# Synthesis of some new polypseudorotaxanes

**Glynn J. Owen and Philip Hodge***

*University of Manchester, Department of Chemistry, Oxford Road, Manchester, UK M13 9PL*

**Linear polymers are synthesised which have hydroquinol ether units linked by several ethylene oxide units; in some cases the latter also contain ester groups and introduction of the tetracationic cyclophane cyclobis(paraquat-*p*-phenylene) 1 to solutions of the polymers in acetonitrile leads to the formation of polypseudorotaxanes; $^1$H NMR analysis of these solutions at −40 °C showed that in some cases up to 94% of the hydroquinol ether units were threaded through cyclophanes.**

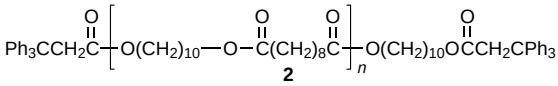
Interest in molecular assemblies of novel topology has increased enormously in recent years.[1–4] Numerous rotaxanes,† pseudorotaxanes† and catenanes have been synthesised.[3] Stoddart's group have exploited the favourable interactions between π-electron-rich moieties such as hydroquinol (HQ) ethers, where the ethers are formally derived from oligoethylene oxides (xEO), and π-electron-poor moieties such as those in the tetracationic cyclophane **1** for the self assembly of many rotaxanes and catananes.[3,5] The interest in molecular assemblies has extended to polymeric systems and various polyrotaxanes and polypseudorotaxanes have been prepared.[3] Polyrotaxanes have, for example, been prepared from polyester **2** and 30-crown-10,[6] and polypseudorotaxanes from polyacrylonitrile and 60-crown-20,[7] and from polymer **3** and β-cyclodextrin.[8] We wish to combine studies of polyrotaxanes and polypseudorotaxanes with our work on the synthesis of macrocycles[9,10] in order to build novel polymeric systems. As a first step we have synthesised polypseudorotaxanes based on polymers with dialkoxyaromatic units linked by several EO groups, plus in some cases ester groups, and Stoddart's cyclophane **1**, and we now report the results. Stoddart *et al.* have previously prepared two types of oligo- or poly-pseudorotaxanes.[11,12] One type was prepared, from compound **4**, which has five hydroquinol ether moieties, by 'threading' on one or two cyclophanes **1**.[11] The second type was prepared from the copolymer **5**, where the degree of polymerisation (DP) was approximately 9, and an excess of cyclophane **1** with respect to the repeat units.[12] With the former type detailed analysis of $^1$H NMR spectra provided proof of rotaxane formation;[11] with the latter type the main evidence of rotaxane formation was the expected colour change.[12] We have now assembled polypseudorotaxanes starting from polymers **6**–**10**, which have average DPs of up to 63, and have shown (i) that despite the relatively small number of end = groups present in most cases, polypseudorotaxanes can be rapidly obtained by 'threading' the polymers with cyclophane **1**, and (ii) that it is possible to obtain polypseudorotaxanes where a substantial fraction of the HQ ether units are present as rotaxane moieties and that this can be as high as 94% at −40 °C. Thus, it is possible for cyclophanes **1** to complex to HQ ether units which are adjacent in the polymer chain. This is the first occasion such 'close packing' of this charged cyclophane has been observed.



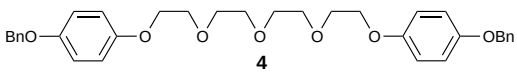
**1** $X^- = PF_6^-$



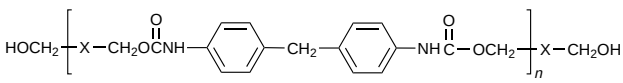
**3**

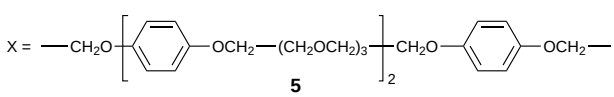


**2**

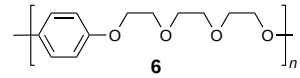


**4**

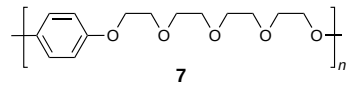




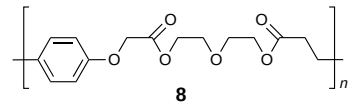
**5**



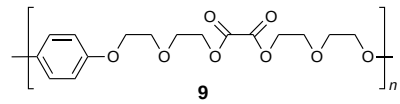
**6**



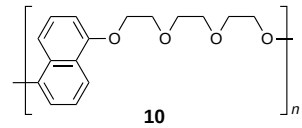
**7**



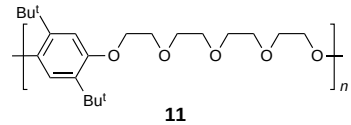
**8**



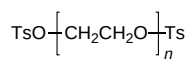
**9**



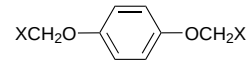
**10**



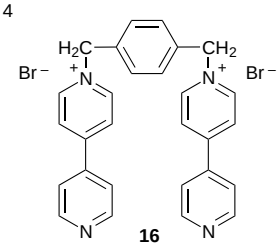
**11**



**12** *n* = 3
**13** *n* = 4



**14** X = $CO_2Et$
**15** X = $CH_2OCH_2CH_2OH$



**16**

Polymers **6**, **7**, **10** and **11** were prepared by reacting hydroquinol, 1,5-dihydroxynaphthalene (ND) or 2,5-di-*tert*-butylhydroquinol (DBHQ) with the ditosylate of either triethylene glycol (3EO) **12** or of tetraethylene glycol (4EO) **13** (Table 1). Diester **14** and diol **15** were prepared by reacting hydroquinol with ethyl chloroacetate or 2-(2-chloroethoxy)-ethanol respectively in the presence of potassium carbonate in ethanol. Reaction of diester **14** with diethylene glycol (2EO) in the presence of titanium tetraisopropoxide gave polyester **8**. Polyester **9** was similarly prepared from diol **15** and dimethyl oxalate (DMO). The molecular weights of the various polymers were estimated using gel permeation chromatography, Table 1. The $^1$H NMR spectra of the polymers were consistent with the assigned structures and $\overline{M}_n$ values; no phenolic end-groups were detected.

Attempts to prepare pseudopolyrotaxanes by reacting compound **16** and α,α′-dibromo-*p*-xylene **17** together in acetonitrile in the presence of polymer **6**, *i.e.* by 'clipping',[3] afforded complex mixtures that, by $^1$H NMR spectroscopy and UV spectroscopy, contained pseudopolyrotaxanes but the latter could not be isolated in a pure state.[13]

Polypseudorotaxanes were successfully prepared by 'threading', *i.e.* cyclophane **1** was prepared [from **16** and **17**][14] and purified, then it was added progressively to solutions of the polymers in acetonitrile at 20 °C. In each case the solution immediately became dark red, indicative of rotaxane formation, and as more cyclophane **1** was added the colour generally became more intense as monitored by UV spectroscopy. The solutions were analysed by $^1$H NMR spectroscopy at −40 °C.‡ At this temperature 'shuttling' of the threaded cyclophane was slow on the NMR timescale. In general the signals due to the starting polymer and the free cyclophane **1** were observed to decrease or disappear and signals characteristic of the rotaxane moiety, *i.e.* the HQ ether groups residing in the centre of the cyclophane plus the encircling cyclophane, appeared. The extents of 'threading' achieved with the various polymers are summarised in Fig. 1. It is evident in the cases of polymers **6**, **7** and **9** that up to the point when *ca*. 35% of cyclophane **1** has been added, essentially all the added cyclophane **1** becomes threaded. With polymer **6** the loading achieved, *i.e.* the percentage of HQ ether repeat units that are threaded, reaches a plateau at *ca*. 50% whilst with polymer **7** it reaches a plateau at *ca*. 70%. This latter percentage implies that a substantial fraction of the adjacent HQ ether units in the polymer chain are present as rotaxane moieties. Presumably with polymer **6**, which has only a 3EO spacer unit, such close proximity of the cyclophane rings is seriously inhibited because it results in electrostatic and/or steric interactions between the solvated cyclophanes. The presence of the ester linkage in polymer **8** clearly has an unfavourable effect on the 'threading' because the loading of this polymer, which formally has a 4EO spacer, reaches a plateau at *ca*. 55%, *i.e.* significantly lower than with polymer **7**. Polyester **9** on the other hand, which formally has a 5EO spacer, loads up to *ca*. 94%. Since this polymer has on average 21 HQ units in the chain, the result implies that on average each chain has 20 threaded rings. Similarly polyester **8** has on average, at maximum loading, 37 threaded rings per chain, *i.e.* is a [38]pseudopolyrotaxane. Polymer **10** also threads rapidly but the mixture obtained only dissolved in [$^2H_6$]DMF or [$^2H_6$]DMSO at *ca*. 100 °C. At this temperature the $^1$H NMR spectrum in [$^2H_6$]DMF was broad and whilst it was clear 'threading' occurred an accurate analysis was not possible. As expected on steric grounds, polymer **11** did not thread at all.

**Table 1** Synthesis and characterisation of polymers **6**–**11**

| Polymeric product | Starting compounds[a] | Yield (%) | Molecular weight[b] $\overline{M}_n$ | $\overline{M}_w$ | $\overline{DP}$[c] |
|---|---|---|---|---|---|
| **6** | HQ + **12** | 83 | 11 300 | 19 100 | 50 |
| **7** | HQ + **13** | 36 | 3500 | 4700 | 13 |
| **8** | **14** + 2EO | 89 | 18 600 | 23 400 | 63 |
| **9** | **15** + DMO | 47 | 7100 | 10 300 | 21 |
| **10** | ND + **12** | 77 | 7500 | 15 600 | 20 |
| **11** | DBHQ + **13** | 61 | 6600 | 13 200 | 17 |

[a] See text for abbreviations. [b] Determined by gel permeation chromatography. For polymers **6**, **7**, **10** and **11** polystyrene standards were used. For polymers **8** and **9** polyethylene glycol standards were used. [c] The average number of aromatic units per chain calculated from the $\overline{M}_n$ values, *i.e.* the values of *n* in formulae **6**–**11**. The actual average number of linkages formed during the syntheses are twice these values.

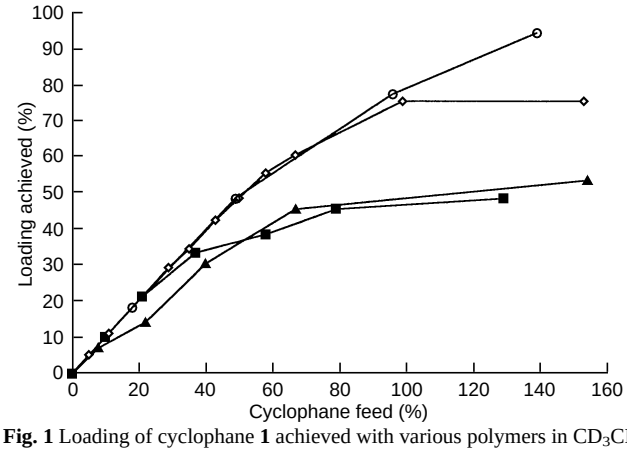



**Fig. 1** Loading of cyclophane **1** achieved with various polymers in $CD_3CN$ at −40 °C as a function of the cyclophane **1** feed. Polymer **6** —■—; **7** —◇—; **8** — ▲ —; **9** —○—. The cyclophane feed is the amount (mol%) of cyclophane added to the reaction mixture per polymer repeat unit.

We thank the EPSRC for a Research Studentship to G. J. O. and Dr F. Heatley for assistance with the NMR spectral analysis.

## Footnotes

† Rotaxanes have a rod or chain threaded through rings and end-groups that are sufficiently large to prevent the rings from slipping off. Pseudorotaxanes do not have the large end-groups and so can dissociate.

‡ The $^1$H NMR spectra shifts obtained agree closely with those reported by Stoddart's group for low-molecular-weight analogues,[11,16]

## References


1 J.-M. Lehn, *Supramolecular Chemistry*, VCH, Weinheim, 1995.
2 J.-M. Lehn, *Angew. Chem., Int. Ed. Engl.*, 1988, **27**, 89; 1990, **29**, 1304.
3 D.B. Amabilino and J. F. Stoddart, *Chem. Rev.*, 1995, **95**, 2725.
4 D. Philp and J. F. Stoddart, *Angew. Chem., Int. Ed. Engl.*, 1996, **35**, 1154.
5 See P. R. Ashton, S. Iqbal, J. F. Stoddart and N. D. Tinker, *Chem. Commun.*, 1996, 479 and references cited therein.
6 H. W. Gibson, S. Liu, P. Lecavalier, C. Wu and Y. X. Shen, *J. Am. Chem. Soc.*, 1995, **117**, 852.
7 H. W. Gibson and P. T. Engen, *New. J. Chem.*, 1993, **17**, 723.
8 G. Wenz and B. Keller, *Angew. Chem., Int. Ed. Engl.*, 1992, **31**, 197.
9 P. Hodge, M. P. Houghton and M. S. K. Lee, *J. Chem. Soc., Chem. Commun.*, 1993, 581.
10 P. Hodge, M. S. K. Lee, P. P. Peng, J. A. Semlyen and B. R. Wood, *Polym. Prepr.* (*Am. Chem. Soc. Div. Polym. Sci.*), 1994, **35**(**2**), 986.
11 P. R. Ashton, D. Philp, N. Spencer and J. F. Stoddart, *J. Chem. Soc., Chem. Commun.*, 1991, 1677.
12 X. Sun, D. B. Amabilino, I. W. Parsons and J. F. Stoddart, *Polym. Prepr.* (*Am. Chem. Soc. Div. Polymer Sci.*), 1993, **32**(**1**), 104.
13 M. Conroy, P. Hodge and G. J. Owen, unpublished work.
14 B. Odell, M. V. Reddington, A. M. Z. Slawin, N. Spencer, J. F. Stoddart and D. J. Williams, *Angew. Chem., Int. Ed. Engl.*, 1988, **11**, 1547.
15 G. J. Owen, P. Hodge and F. Heatley, unpublished results.
16 D. B. Amabilino, P.-L. Anelli, P. R. Ashton, G. R. Brown, E. Córdon, L. A. Godínez, W. Hayes, A. E. Kaifer, D. Philp, A. M. Z. Slawin, N. Spencer, J. F. Stoddart, M. S. Tolley and D. J. Williams, *J. Am. Chem. Soc.*, 1995, **117**, 11 142.


*Received, 8th October 1996; Com. 6/06895B*

# Stereochemistry of the oxidation of gibberellin 20-alcohols, $GA_{15}$ and $GA_{44}$, to 20-aldehydes by gibberellin 20-oxidases

**Jane L. Ward,[a] Graham J. Jackson,[a] Michael H. Beale,*[a] Paul Gaskin,[a] Peter Hedden,[a] Lewis N. Mander,[a] Andrew L. Phillips,[a] Hideharu Seto,[b] Manuel Talon,[c] Christine L. Willis,[d] Theresa M. Wilson[c] and Jan A. D. Zeevaart[c]**

[a] *IACR-Long Ashton Research Station, Department of Agricultural Sciences, University of Bristol, Long Ashton, Bristol, UK BS18 9AF*
[b] *Research School of Chemistry, Australian National University, Canberra ACT 0200, Australia*
[c] *MSU-DOE Plant Research Laboratory, Michigan State University, East Lansing, MI 48824, USA*
[d] *School of Chemistry, University of Bristol, Cantock's Close, Bristol, UK BS8 1TS*

**(20*R*)- and (20*S*)-[20-$^2H_1$]-gibberellins $A_{15}$ and $A_{44}$ have been used to determine the stereochemistry of the conversion to the 20-aldehyde catalysed by gibberellin 20-oxidases.**

The stepwise oxidation and subsequent removal of carbon-20 from $C_{20}$-precursors is one of the most important sequences of reactions in the biosynthesis of biologically active $C_{19}$ gibberellin (GA) plant hormones (Scheme 1). This conversion is unusual in that carbon-20 is lost at the aldehyde oxidation level in a reaction which also involves concerted formation of the 19,10-lactone function, a characteristic structural feature of the $C_{19}$-GAs, such as $GA_9$ and $GA_{20}$. The 20-carboxylic acid is also a biosynthetic product, but is not an intermediate in $C_{19}$-GA formation. Genes encoding GA 20-oxidases have been cloned from several plants.[1–5] These enzymes are 2-oxoglutarate-dependant dioxygenases, an important class of soluble, $Fe^{II}$-containing oxygenases .[6] Functional expression of GA 20-oxidase clones in *E. coli* has provided the means for a detailed study of the mechanism. Although studies in cell-free systems of spinach[7] indicated that more than one enzyme may be involved in the conversion of 20-methyl compounds *via* the 20-alcohol and 20-aldehyde to the $C_{19}$-lactone, all GA 20-oxidases so far cloned are able to convert substrates with 20-methyl functions through to $C_{19}$-lactones and/or 20-carboxylic acids.

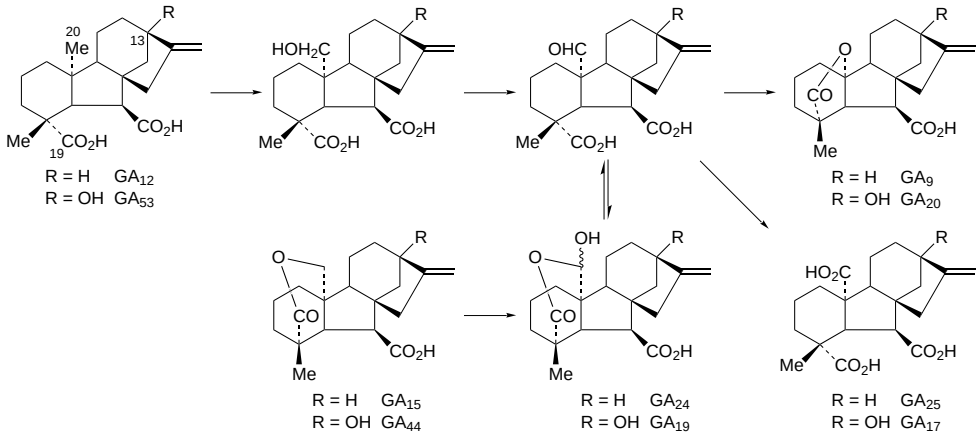
Here we report studies on the stereochemistry of the conversion of the 20-alcohol to the 20-aldehyde. Results are compared in cell-free systems from spinach with those obtained using recombinant enzyme from high-level expression of the *Arabidopsis thaliana* GA 20-oxidase clone At2353[2] in *E. coli* using the pET9d vector;† this enzyme converts $GA_{12}$ to $GA_9$ in high yield.

The syntheses of (20*R*)- and (20*S*)-[20-$^2$H]-$GA_{15}$ are summarised in Scheme 2. The route relies on the use of bulky *tert*-butyldiphenylsilyl (TBDPS) protecting groups to distinguish between the alcohol functions in the triol **1**, allowing manipulation of C-20, the most sterically hindered of the three hydroxymethyl groups. Triol **1** and its [$^2H_6$]-isotopomer **1a** were prepared by $LiAlH_4$ ($LiAlD_4$) reduction of $GA_{25}$ trimethyl ester, itself prepared by deoxygenation of $GA_{13}$ trimethyl ester.

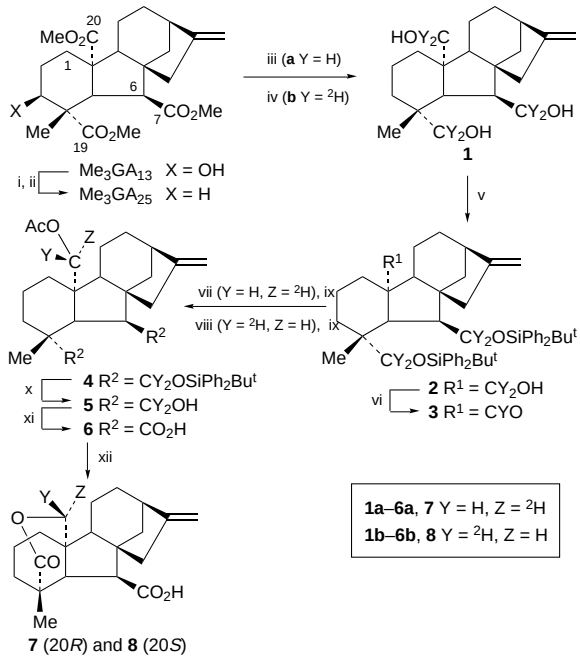
Treatment of **1** with TBDPSCl and imidazole gave the 7,19-*bis*-TBDPS derivative **2** in high yield. Swern oxidation of **2** gave the 20-aldehyde **3**. Reduction of the aldehyde with $NaBD_4$ was stereoselective (see later) and returned the [20-$^2H_1$]-alcohol **4**, which was protected as the acetate, before removal of the TBDPS groups with $Bu_4NF$ to give 7,19-diol **5**. Oxidation to the 7,19-dicarboxylic acid **6** followed by hydrolysis yielded (20*R*)-[20-$^2$H]$GA_{15}$ ($d_1$-65%, $d_0$-35%), in the lactone form **7**. The corresponding (20*S*) isomer **8** ($d_1$-99%, $d_0$-1%), was prepared in an analogous way from **1a,** reducing the 20-deuterio-aldehyde **3a** with $NaBH_4$ as shown in Scheme 2.

The configurations of **7** and **8** were assigned by $^1$H NMR spectroscopy. In fully protio species, the 20-hydrogens resonate at δ 4.12 (d, *J* 12.5 Hz) and 4.48 (dd, *J* 12.5 and 2.5 Hz). The downfield signal was assigned to the 20-*proR* proton by virtue of the long range W-coupling (2.5 Hz) to 1β-H, as confirmed by a difference NOE experiment, which revealed a clear NOE from 6-H to the signal at δ 4.48 and the absence of any enhancement of the upfield doublet at δ 4.12, assigned to the 20-*proS* hydrogen. Both **7** and **8** were labelled stereospecifically.

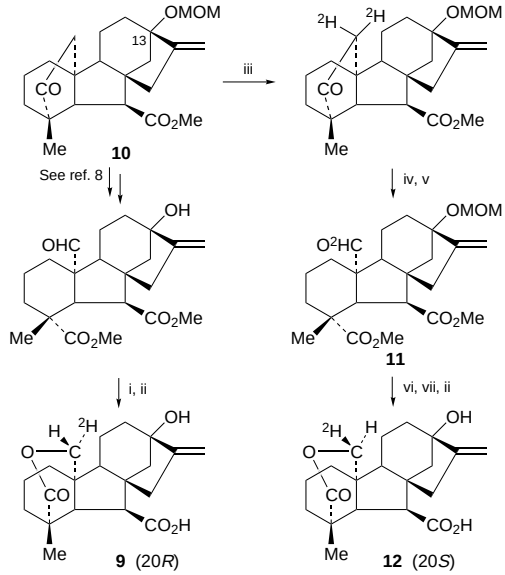
The corresponding [20-$^2H_1$] isotopomers of the 13-hydroxylated gibberellin, $GA_{44}$ **9** and **12**, were synthesised as shown in




**Scheme 1** Reactions catalysed by GA-20-oxidases




**Scheme 2** Synthesis of (20*R*)- and (20*S*)-[20-$^2H_1$]-$GA_{15}$. *Reagents*: i, KH, $CS_2$, MeI; ii, $Bu_3SnH$; iii, $LiAlH_4$; iv, $LiAl^2H_4$; v, $Bu^tPh_2SiCl$, imidazole; vi, $(COCl)_2$, $Me_2SO$, $Et_3N$; vii, $NaB^2H_4$; viii, $NaBH_4$; ix, $Ac_2O$, pyridine; x, $Bu_4N^+F^-$; xi, Jones oxidn; xii, NaOH, aq. MeOH.




**Scheme 3** Synthesis of (20*R*)- and (20*S*)-[20-$^2H_1$]-$GA_{44}$ *via* $GA_{19}$. *Reagents*: i, $NaB^2H_4$; ii, NaOH, aq. MeOH; iii, $^2H_2O$, $K_2CO_3$; iv, KH, DMF, THF, $O_2$; v, $CH_2N_2$; vi, Dowex 50W($H^+$); vii, $NaBH_4$.

Scheme 3. (20*R*)-[20-$^2H_1$]-$GA_{44}$ **9** ($d_1$-95%, $d_0$-5%) was produced by $NaBD_4$ reduction of $GA_{19}$ dimethyl ester followed by hydrolysis of the esters (2 mol $dm^{-3}$ aq. NaOH–MeOH, 1 : 1, reflux, 2 h). For the synthesis of (20*S*)-[20-$^2H_1$]-$GA_{44}$, the starting point was ketone **10**, an intermediate in the synthesis[8] of $GA_{19}$. Deuterium exchange at C-20, oxidative cleavage[8] and methylation gave [20-$^2H_1$]-$GA_{19}$ dimethyl ester, 13-methoxymethyl ether **11**. Deprotection at C-13 and then reduction of the aldehyde followed by demethylation gave the required (20*S*)-[20-$^2H_1$]-$GA_{44}$ **12** ($d_1$-61%, $d_0$-39%). The stereochemistry at C-20 was assigned by $^1H$ NMR spectroscopy as above.

Incubation of unlabelled $GA_{15}$, as the lactone or as the 20-hydroxy-19-carboxylic acid ('open lactone'),‡ with recombinant At2353 20-oxidase and analysis of the products by GC–MS revealed that only the open lactone was accepted as a substrate by the enzyme. A similar result has been obtained in cell-free systems from *C. maxima* endosperm[9] and pea cotyledons,[10] whereas homogenates of spinach leaves oxidise the closed-lactone form of $GA_{44}$.[7] Although the product of metabolism of $GA_{15}$ open lactone was mainly $GA_9$, under short incubation times§ the intermediate 20-aldehyde $GA_{24}$ was readily detectable by GC–MS.

Incubation§ of (20*R*)- and (20*S*)-[20-$^2H_1$]-$GA_{15}$ **7** and **8,** and $GA_{44}$ **9** and **12** in the open-lactone form‡ with recombinant enzyme and GC–MS analysis of the 20-aldehyde ($GA_{24}$ and $GA_{19}$, respectively) products, revealed that, for both $GA_{15}$ and $GA_{44}$ substrate, there is stereospecific loss of the 20-*proR* hydrogen (Table 1). In contrast, incubation of **9** and **12,** in the closed-lactone form, with the spinach cell-free system[7] and analysis of the 20-aldehyde ($GA_{19}$) produced showed that, in this case, the 20-*proS* hydrogen is lost (Table 1). Thus, this cell-free system contains an enzyme that is capable of oxidising C-20, presumably in the lactone form, and it does so with the opposite stereochemistry to that observed with the recombinant *A. thaliana* protein, which only accepts the open-lactone form. In the lactone form, the 20-*proR* hydrogen is fixed in a severely sterically hindered position under ring B and, thus, it is not surprising that the lactone 20-oxidase, present in spinach, removes the 20-*proS* hydrogen. However, in the enzymes that accept only the 'open-lactone' form, the substrate presumably is held such that the 20-*proR* hydrogen is more exposed.

**Table 1** Deuterium incorporations in enzymic products

| Substrate | $d_1 : d_0$(%) | Enzyme | Product | $d_1 : d_0$(%)[a] |
|---|---|---|---|---|
| **7** (20*R*) Open lactone | 65 : 35 | At2353 | $GA_{24}$ | 0 : 100 |
| **8** (20*S*) Open lactone | 99 : 1 | At2353 | $GA_{24}$ | 97 : 3 |
| **9** (20*R*) Open lactone | 95 : 5 | At2353 | $GA_{19}$ | 0 : 100 |
| **12** (20*S*) Open lactone | 61 : 39 | At2353 | $GA_{19}$ | 50 : 50 |
| **9** (20*R*) Lactone | 95 : 5 | Spinach | $GA_{19}$ | 85 : 15 |
| **12** (20*S*) Lactone | 61 : 39 | Spinach | $GA_{19}$ | 13 : 87 |

[a] $GA_{24}$ and $GA_{19}$ were identified by GC–MS comparison (KRI and spectra), as Me or Me, $Me_3Si$ derivatives, with authetic samples. Due to weak molecular ions isotope enrichments were calculated on $M^+ - 32$ (*m*/*z* 342) for $GA_{24}$ and $M^+ - 28$ (*m*/*z* 434) for $GA_{19}$.

## Footnotes

† Full details of the functional expression and characterisation of GA 20-oxidases will be reported elsewhere.

‡ The lactone-opened form of 20-hydroxymethyl GAs was produced by treatment with 2 mol $dm^{-3}$ NaOH.

§ Recombinant enzyme incubations were carried out in a total volume of 100 μl of TrisCl buffer (1 mol $dm^{-3}$, pH 7.5) containing 70 μl enzyme preparation [45% pure enzyme (estimated from SDS gel), 2.5 mg protein $ml^{-1}$]. GA substrate (5 μg), 2-oxoglutarate (8 mmol $dm^{-3}$), ascorbic acid (8 mmol $dm^{-3}$), dithiothreitol (8 mmol $dm^{-3}$), $FeSO_4$(1 mmol $dm^{-3}$), catalase (2 mg $ml^{-1}$) and bovine serum albumin (4 mg $ml^{-1}$).

## References


1 T. Lange, P. Hedden and J. E. Graebe, *Proc. Natl. Acad. Sci. USA*, 1994, **91**, 8552.
2 A. L. Phillips, D. A. Ward, S. Uknes, N. E. J. Appleford, T. Lange, A. K. Huttly, P. Gaskin, J. E.Graebe and P. Hedden, *Plant Physiol*., 1995, **108**, 1049.
3 Y-L. Xu, L. Li, K. Wu, A. J. M. Peeters, D. A. Gage and J. A. D. Zeevaart, *Proc. Natl. Acad. Sci. USA*, 1995, **92**, 6640.
4 K. Wu, D. A. Gage and J. A. D. Zeevaart, *Plant Physiol.* 1996, **110**, 547.
5 D. N. Martin, W. M. Proebsting, T. D. Parks, W. G. Dougherty, T. Lange, M. J. Lewis, P. Gaskin and P. Hedden, *Planta*, 1996, **200**, 159.
6 A. G. Prescott and P. John, *Ann. Rev. Plant Physiol. Plant Mol. Biol.*, 1996, **47**, 245.
7 S. J. Gilmour, J. A. D. Zeevaart, L. Schwenen and J. E. Graebe, *Plant Physiol*., 1986, **82**, 190.
8 R. D. Dawe, L. N. Mander and J. V. Turner, *Tetrahedron Lett.*, 1985, **26**, 363.
9 P. Hedden and J. E. Graebe, *J. Plant Growth Regul.*, 1982, **1**, 105.
10 Y. Kamiya, Y. Takahashi and J. E. Graebe, *Planta*, 1986, **169**, 524.


*Received, 6th September 1996; Com. 6/06158C*

# Continuous films of zeolite ZSM-5 on modified gold surfaces

**Svetlana Mintova,[a] Jonas Hedlund,[a] Brian Schoeman,[a] Valentin Valtchev[b] and Johan Sterte*[a]**

[a] *Department of Chemical Technology, Luleå University of Technology, S-97186, Luleå, Sweden*
[b] *Central Laboratory of Mineralogy and Crystallography, Bulgarian Academy of Sciences, 92 Rakovski St., 1000 Sofia, Bulgaria*

**Thin continuous films of zeolite ZSM-5 on gold surfaces are prepared by a novel method including silanization, charge modification and seeding of the surface prior to the hydrothermal crystallization of the zeolite.**

The preparation of continuous films of molecular sieves on various supports, including metallic and other inorganic as well as organic substrate surfaces, has recently attracted considerable attention.[1–5] The great interest in these materials is primarily motivated by their potential advantages in a number of applications such as membranes for separation and catalysis, chemical sensors, acoustic wave devices, and microelectronics.[6–10]

Several methods for the preparation of zeolite films on surfaces have been described.[11–14] Most of these methods involve the direct nucleation and crystallization of the desired zeolite on the substrate surface. A novel method for the preparation of thin zeolite films based upon a three-step procedure was recently presented.[15] In this method, the substrate surface is first treated with a cationic polymer in order to obtain a positive surface charge. Colloidal crystals of zeolite are then adsorbed as a monolayer on the surface by electrostatic attraction. Finally, the adsorbed crystals are induced to grow into a continuous film of intergrown crystals under hydrothermal conditions. Although very flexible and easy to control, this method has the disadvantage that it can only be applied on surfaces which have a substantial surface charge in aqueous solutions. This excludes surfaces of noble metals, a fact that significantly reduces the value of the method in several of the potential applications of zeolite films where films on gold or platinum surfaces would be desirable. Modification of this method to render it applicable for noble-metal substrate surfaces is therefore of great interest.

The purpose of this communication is to present a novel method for the controlled preparation of very thin continuous films of ZSM-5 on gold surfaces. Gold substrates consisting of a gold film with a thickness of approximately 50 nm on the surface of silver plates were prepared by sputtering. The surface of the silver plate was first cleaned for 10 min in acetone in an ultrasonic bath and then in a mixture of water, ammonium hydroxide and hydrogen peroxide (molar composition $280H_2O : 9H_2O_2 : 15NH_3$) for 10 min at room temp. The plates were then rinsed with distilled water and, subsequently, sonicated twice for 15 min in distilled water. Application of the gold film was achieved by sputtering in an MED 020 Coating System (BAL-TEC AG). The Au surfaces were silanized by treating the substrates for 3 h in a methanolic 20 mM γ-mercaptopropyltrimethoxysilane (MPT, OSi Specialties) solution and the silane was then hydrolysed in 0.10 M HCl for 15 h at room temp. The surface charge of the silanized gold surface was modified by treating the initially negative surface with a solution containing 1.0 mass% cationic polymer (Berocell 6100, Akzo Nobel) with the repeat unit $[CH_2CHOHCH_2NMe_2)]^+_n$ and an average molecular mass of 50 000 g $mol^{-1}$ for 1 h. Substrates were then rinsed twice with a 0.10 M ammonia solution to remove excess polymer. In order to adsorb a monolayer of ZSM-5 seed crystals onto the surface of the substrates, the substrates were treated with a purified colloidal suspension (4.5 mass%, pH = 10.5, average crystal size: $d_p$ = 90 nm) of discrete colloidal crystals of ZSM-5 for 1 h.[16] After this treatment, the substrates were rinsed 3 times with 0.10 M aq. $NH_3$, air dried and calcined for 1 h at 250 °C. Finally, the substrates were immersed in a synthesis solution with the molar composition $0.35Na_2O : 25SiO_2 : 0.5Al_2O_3 : 9TPAOH : 405H_2O$ for 40 h in order to induce continued growth (and intergrowth into a continuous film) of the crystals on the surface. The type of zeolite structure was confirmed by XRD with a Philips PW1710-00 powder diffractometer.

Particle size analysis and zeta potential measurements of the ZSM-5 seed sol were performed with a Brookhaven Instruments ZetaPlus. Adsorption of MPT was studied by reflection absorption Fourier transform IR spectroscopy (RAIRS, Perkin Elmer PE 2000 FTIR) and by VASE ellipsometry (J. A. Woolam Co). A Philips XL 30 scanning electron microscope (SEM) equipped with an LaB6 emission source was used for studies of surface morphology and to measure zeolite film thickness. Krypton adsorption was measured at liquid nitrogen temperature using a Micromeritics ASAP 2010 surface area and pore volume analyser.

In Fig. 1, a schematic illustration of the process is shown. The silanization of the gold surface by MPT was performed in solution resulting in a very thin silane layer (Fig. 1A). The RAIRS measurements of the silane layer were performed using an unsilanized substrate as the background and silanized samples as probes. The spectra were almost identical to that reported by Kurth and Bein[17] for adsorption of MPT on

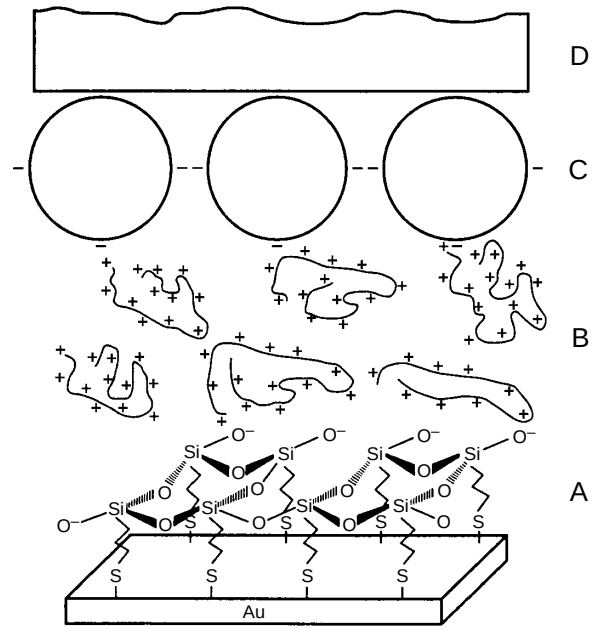



**Fig. 1** Schematic representation of the silanization of an Au surface with MPT (A), charge reversal of the negative siliceous interface to a positively charged interface by means of adsorption of a cationic polymer (B), electrostatic adsorption of negatively charged ZSM-5 crystals on silane-polymer modified Au (C) and the formation of a continuous zeolite film after hydrothermal treatment (D)

oxidized aluminium substrates. From their spectrum they concluded that MPT adsorbed on oxidized alumina is vertically oriented. The thickness of the MPT film was determined by ellipsometry to about 10 Å which is in good correspondence with a vertical orientation of MPT on the gold surface. Hydrolysis of the silane results in the formation of dissociated groups on the surface of the substrate resulting in a surface with a negative surface charge in neutral and alkaline aqueous solutions (Fig. 1A). This substrate surface readily adsorbed an excess of the cationic polymer, Fig. 1B, thus reversing the surface charge to a positive one and facilitating electrostatic adsorption of colloidal ZSM-5 crystals, Fig. 1C. The zeta potential of the colloidal ZSM-5 crystals in the purified sol (pH: 10.5) was determined to −54 mV. Fig. 2(*a*) shows an SEM micrograph of colloidal ZSM-5 crystals adsorbed on the gold substrate surface after modification of this surface by silanization, hydrolysis of the silane and charge reversal by treatment with the cationic polymer. The micrograph shows that the crystals are homogeneously adsorbed in a dense layer on the surface. After adsorption of the seed crystals, the sample was calcined in order to decompose the silane and the cationic polymer and to induce a stronger interaction between the adsorbed seed crystals and the substrate surface. Although the nature of the bonding of the seed crystals to the substrate surface is not entirely clear, the attachment of these crystals after the calcination process is strong enough to keep the zeolite firmly on the surface during the crystallization of the zeolite film. The formation of the zeolite film is achieved by contacting the substrate with adsorbed seed crystals with a synthesis solution with a composition suitable for the crystallization of zeolite ZSM-5 at hydrothermal conditions.[16] This treatment results in a continued growth of the seed crystals and eventually to the intergrowth of these crystals into a dense and continuous film, Fig. 1D. Fig. 2(*b*) and (*c*) show top and side views, respectively, of the final film obtained after 40 h of crystallization. From these and numerous other SEM micrographs it is clear that the ZSM-5 films produced are continuous, free from cracks and that they have an almost constant thickness. The film thickness estimated from the micrograph shown in Fig. 2(*c*) is 200–250 nm. The film thickness of this sample was also calculated from Kr adsorption data using the BET equation and the surface area (500 $m^2\ g^{-1}$) and density (1790 $kg\ m^{-3}$) of pure ZSM-5 as a reference. The value obtained in this manner is 230 nm which is in very good agreement with that measured from the SEM micrograph.

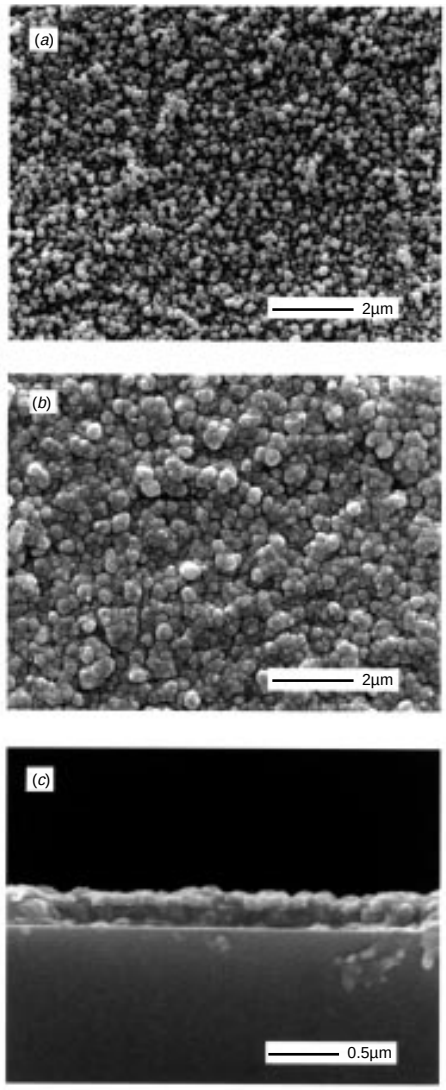



**Fig. 2** SEM micrographs showing the adsorbed 90 nm ZSM-5 seeds on the Au surface (*a*), the top view (*b*) and side view (*c*) of the continuous zeolite film after hydrothermal crystallization

The results presented in this communication show that continuous films of ZSM-5 on gold substrates can be prepared by a procedure involving four steps. The gold surface is first covered with a monomolecular layer of MPT which is hydrolysed under acidic conditions. The surface charge is then reversed by adsorption of a cationic polymer and a monolayer of colloidal seed crystals is adsorbed on the positively charged surface by electrostatic attraction. After decomposition of the silane and the cationic polymer by calcination, the seed crystals are grown into a continuous ZSM-5 film by further crystallization in a synthesis solution at hydrothermal conditions. The method is flexible and easy to control and allows for the preparation of films with a desired thickness of *ca*. 50 nm and upwards. Although only demonstrated in this communication for zeolite ZSM-5 on gold substrates, the method permits preparation of thin films of a number of zeolite types, *e.g*. zeolite-β, -A and -X, on various substrates. The flexible nature of the method employed gives new possibilities for the preparation of zeolite films with different physicochemical characteristics which may be of great interest in a number of applications.

The authors wish to thank the Swedish Research Council for Engineering Sciences (TFR) for financial support. S. M. is indebted to the Wenner-Gren Center Foundation for a scholarship.

## References

1 S. Feng and T. Bein, *Science*, 1994, **265**, 1839.
2 T. Sano, Y. Kiyozumi, K. Maeda, S. Niwa and F. Mizukami, *J. Mater. Chem*., 1992, **2**, 141.
3 V. Valtchev, B. J. Schoeman, J. Hedlund, J. Sterte and S. Mintova, *Microporous Mater*., 1996, in the press.
4 Y. Yan, S. Chaudhuri and A. Sarkar, *Chem. Mater*., 1996, **8**, 473.
5 J. Jansen, D. Kashchiev and A. Erdem-Senatalar, *Stud. Surf. Sci. Catal*., 1994, **85**, 215.
6 F. Bedioui and J. Devynck, *J. Phys. Chem*., 1996, **100**, 8607.
7 Z. Li and T. Mallouk, *J. Phys. Chem*., 1987, **91**, 643.
8 Z. Li, C. Lai and T. Mallouk, *Inorg. Chem*., 1989, **28**, 178.
9 Y. Yang and T. Bein, *J. Phys. Chem*., 1992, **96**, 9387.
10 D. Rolison, *Chem. Rev*., 1990, **90**, 867.
11 V. Valtchev and S. Mintova and L. Konstantinov, *Zeolites*, 1995, **15**, 679.
12 E. Geus, A. Mulder, D. Vischjager, J. Schoonman and H. van Bekkum, *Key Engineering Materials*, 1991, **61** & **62**, 57.
13 S. Feng and T. Bein, *Stud. Surf. Sci. Catal., 11th IZC*, Seoul, Korea, August 12–17, 1996, in the press.
14 E. Geus, H. van Bekkum, W. Bakker and J. Moulijn, *Microporous Mater*., 1993, **1**, 131.
15 J. Hedlund, B. J. Schoeman and J. Sterte, *Stud. Surf. Sci. Catal., 11th IZC*, Seoul, Korea, August 12–17, 1996, in the press.
16 A. Persson, B. J. Schoeman, J. Sterte and J.-E. Otterstedt, *Zeolites*, 1995, **15**, 611.
17 D. Kurth and T. Bein, *Langmuir*, 1993, **9**, 2965.

*Received, 8th October 1996; Com. 6/06906A*

# Ruthenium complexes of eilatin: face selectivity in octahedral geometry; synthesis of $[Ru(bpy)_2(eilatin)]^{2+}$ and $[Ru(phen)_2(eilatin)]^{2+}$

**Amira Rudi, Yoel Kashman,* Dalia Gut, Fabienne Lellouche and Moshe Kol***

*School of Chemistry, Raymond and Beverly Sackler Faculty of Exact Sciences, Tel-Aviv University, Tel-Aviv 69978, Israel*

**Eilatin, a marine alkaloid, is a potentially bifacial ligand that prefers to bind through its less hindered face in sterically demanding geometries as evident by the selective synthesis of two octahedral ruthenium complexes.**

A few years ago, several of us reported the isolation of eilatin **1a**, a marine alkaloid, from the tunicate *Eudistoma sp*.[1] This highly symmetric pyrido[2,3,4-*kl*]acridine was named after the location of its collection, the Gulf of Eilat. The bioactivity of eilatin[2] initiated a synthetic effort which yielded several syntheses,[3,4] the most efficient among them being biomimetic.[4] Herein we report a new aspect of eilatin character, namely its use as a face-selective ligand for transition metals.

The planar heptacyclic eilatin **1a** may be viewed as an all-conjugated 2,2′-bipyridine (bpy) and 2,2′-biquinoline (biq) fused rigidly back-to-back (**1b**). Both bpy and biq can serve as chelating ligands for various metals; however, their different steric bulk leads to different coordination behaviour. Thus, for instance, while both $[Ru(bpy)_3]^{2+}$ and $[Fe(bpy)_3]^{2+}$ are known compounds, the tris (biq) analogue is stable only for ruthenium,[5] while attempts to prepare the iron complex, $[Fe(biq)_3]^{2+}$, have been unsuccessful.[6] Accordingly, eilatin is expected to behave as a bidirectional ligand exhibiting face preference, depending on the steric crowding around the metal: in sterically demanding geometries such as octahedral or square-planar, eilatin is expected to bind to the metal through its 'head', while in loose geometries such as tetrahedral, both the 'head' and the 'tail' of eilatin are expected to be able to bind. Here, we describe the selective 'head' binding of eilatin to $Ru^{II}$ in octahedral environment.

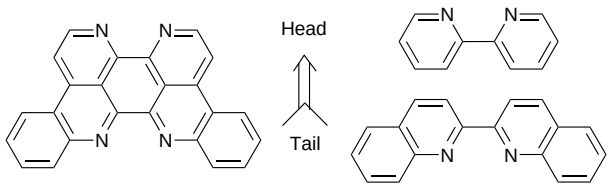
Octahedral complexes of the type $[RuL_nL'_{3-n}]^{2+}$ (L, L′ = bpy, phen, dppz,[7] HAT,[8] *etc*.) have attracted substantial scientific interest because of their remarkable MLCT properties,[9] directional electron and energy transfer,[10] DNA intercalation,[11,12] ability to serve as building blocks in supramolecular arrays,[13] and more. Reacting $[Ru(bpy)_2Cl_2]$ and eilatin in aqueous methanol and precipitating the product with ammonium hexafluorophosphate yielded $[Ru(bpy)_2(eilatin)][PF_6]_2$ **3a** as a dark green solid (Scheme 1).†

$^1$H NMR indicated the formation of a major product having $C_2$ symmetry in at least 90% selectivity, which was purified by crystallization.‡ Complete assignment of all the protons was possible using $^1$H COSY, NOESY and HMQC two-dimensional NMR techniques. Two pieces of evidence supported the assignment of the major product as the expected 'head' isomer: (*i*) NOE connectivity between the $H^a$ protons of eilatin and $H^6$ and $H^{6'}$ protons of the bipyridine units, indicating that the 'head' of eilatin is directed towards the metal, and (*ii*) ring-current effects on chemical shift: the $H^a$ protons of eilatin are strongly shifted to a higher field relative to free eilatin in $(CD_3)_2SO$, while the other protons are only slightly affected, indicating close proximity of these 'head' protons to the orthogonal bipyridine rings. FABMS was consistent with the proposed mononuclear structure, indicating that the 'tail' side is not coordinated to a second metal atom.

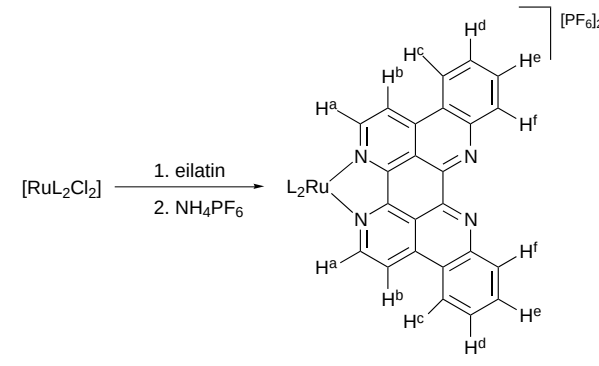
$[Ru(phen)_2Cl_2]$ reacted analogously yielding $[Ru(phen)_2(eilatin)][PF_6]_2$ **3b** as a dark green solid after work-up. The same high selectivity in formation of the major product was observed as for the bipyridine analogue. Using the same type of experiments and reasoning as for **3a** indicated that eilatin was bound 'head-on' in **3b** as well.‡

The $^1$H NMR spectra of **3a** and **3b** exhibit a strong dependence of chemical shift on temperature; this effect is more pronounced when $CD_3CN$ rather than $(CD_3)_2SO$ is used as solvent. Interestingly, different protons exhibit different temperature dependences: while the protons of the bpy or phen ligands in **3a** and **3b**, respectively, are almost unperturbed, the protons of the eilatin ligand (except for $H^a$) shift to lower field upon warming.§ Adding $C_6D_6$ to a $CD_3CN$ solution of the complexes at a constant temperature has the same effect on the chemical shifts as raising the temperature. A possible explanation for this behaviour is the formation of intermolecular π stacks between eilatin ligands in **3a** or **3b**, which are broken as the temperature is raised, or when a competing solvent is added. A similar effect has been reported for $[Ru(bpy)_2(tpphz)]^{2+}$.[14]

The dark green colour of the two eilatin complexes stands in sharp contrast to the orange–red colour of $[Ru(bpy)_3]^{2+}$ and $[Ru(phen)_3]^{2+}$ complexes. Table 1 lists the absorption maxima of free eilatin and its two ruthenium complexes. The two bands responsible for the green colour of **3a** and **3b** are the broad absorption centred at around 420 nm which is attributed to eilatin π–π* bands (perhaps overlapping Ru–bpy and Ru–phen MLCT bands in **3a** and **3b**, respectively), and the absorption at around 580 nm which is attributed to a Ru–eilatin MLCT band. This is one of the lowest energy MLCT bands reported for ruthenium polypyridyl complexes,[9] and is consistent with the




**1a** **1b**




**2a** L = bpy
**b** L = phen

**3a** L = bpy
**b** L = phen

**Scheme 1**

**Table 1** Optical absorption data for eilatin and its ruthenium complexes

| Compound | Absorption maxima[a] |
|---|---|
| **1a**[b] | 242 (4.8), 286 (3.7), 360 (1.1), 388 (2.1), 408 (3.0), 434 (2.7) |
| **3a**[c] | 241 (6.8), 286 (7.3), 341 (2.2), 405,[d] 424 (3.3), 460,[d] 583 (1.0) |
| **3b**[c] | 224 (5.4), 263 (6.3), 292 (2.9), 341 (1.2), 405,[d] 423 (2.3), 460,[d] 581 (0.7) |

[a] Absorption maxima are given in mm, and $10^{-4}$ ε (in parenthesis) in $M^{-1}$ $cm^{-1}$. [b] From ref. 1 in methanol. [c] In acetonitrile. [d] Shoulder.

low lying π* orbital of eilatin.¶ This directional electron transfer could be important in the design of molecular devices.

In summary, we have shown that the potentially bifacial ligand, eilatin, prefers to bind through its less hindered face in a sterically demanding octahedral environment. We are currently investigating the electronic properties of the mononuclear complexes as well as the preparation of eilatin-bridged heteropolynuclear complexes.

## Footnotes

† In a typical reaction 17 mg of $[Ru(bpy)_2Cl_2]\cdot 2H_2O$ and 1.5 equiv. of eilatin were heated to reflux in methanol–water for 5 h. Addition of water and evaporation of the methanol precipitated the excess eilatin, which was filtered off. Addition of $NH_4PF_6$ to the dark green aqueous solution precipitated **3a** as a $PF_6$ salt, which was purified by crystallization from an acetonitrile–ether mixture.

‡ *Spectroscopic data* for **1a**, **3a** and **3b**: **1a**, $^1$H NMR [500 MHz, $(CD_3)_2SO$, 298 K]: δ 9.18 ($H^a$), 8.84 ($H^b$), 8.41 ($H^c$), 8.02 ($H^d$), 7.90 ($H^e$), 8.95 ($H^f$). **3a**, $^1$H NMR [500 MHz, $(CD_3)_2SO$, 298 K]: δ 8.14 ($H^a$), 8.74 ($H^b$), 8.17 ($H^c$), 8.07 ($H^d$), 7.99 ($H^e$), 8.77 ($H^f$), 7.88 ($H^6$), 7.69 ($H^5$), 8.29 ($H^4$), 8.94 ($H^3$), 8.88 ($H^{3'}$), 8.17 ($H^{4'}$), 7.43 ($H^{5'}$), 7.98 ($H^{6'}$); FABMS, 771 $[M - 2PF_6 + H]^+$. **3b**, $^1$H NMR [500 MHz, $CD_3CN$–$(CD_3)_2SO$, 302 K]: δ 8.07 ($H^a$), 8.51 ($H^b$), 8.18 ($H^c$), 7.98 ($H^d$), 7.91 ($H^e$), 8.68 ($H^f$), 8.07 ($H^2$), 7.75 ($H^3$), 8.74 ($H^4$), 8.34 ($H^5$,H6), 8.70 ($H^7$), 7.75 ($H^8$), 8.42 ($H^9$); FABMS, 819 $[M - 2PF_6 + H]^+$, 963 $[M - PF_6 + H]^+$.

§ Compare, for example, the effect of temperature on the $^1$H NMR spectra of **3b** in $CD_3CN$. 298 K: δ 8.05 ($H^a$), 7.94 ($H^b$), 7.35 ($H^c$), 7.70 ($H^d$), 7.81 ($H^e$), 8.25 ($H^f$), 8.10 ($H^2$), 7.76 ($H^3$), 8.72 ($H^4$), 8.34 ($H^5$,$H^6$), 8.68 ($H^7$), 7.83 ($H^8$), 8.70 ($H^9$). 330 K: δ 8.07 ($H^a$), 8.23 ($H^b$), 7.89 ($H^c$), 7.89 ($H^d$), 7.89 ($H^e$), 8.48 ($H^f$), 8.12 ($H^2$), 7.76 ($H^3$), 8.70 ($H^4$), 8.33 ($H^5$,$H^6$), 8.67 ($H^7$), 7.80 ($H^8$), 8.55 ($H^9$).

¶ In contrast, the low-energy MLCT is absent from the spectra of pyridophenazine type complexes like $[Ru(bpy)_2(dppz)]^{2+}$[7] and $[Ru(bpy)_2(tpphz)]^{2+}$.[14]

## References


1 A. Rudi, Y. Benayahu, I. Goldberg and Y. Kashman, *Tetrahedron Lett.*, 1988, **29**, 6655.
2 N. R. Shochet, A. Rudi, Y. Kashman, Y. Hod, M. R. El-Maghrabi and I. R. Spector, *J. Cell. Phys.*, 1993, **157**, 481.
3 S. Nakahara, Y. Tanaka and A. Kubo, *Heterocycles*, 1993, **36**, 1139.
4 G. Gellerman, A. Rudi and Y. Kashman, *Tetrahedron*, 1994, **50**, 12 959.
5 D. M. Klassen, *Inorg. Chem.*, 1976, **15**, 3166.
6 C. M. Harris, S. Sokot, H. R. H. Patil, E. Sinn and H. Wong, *Aust. J. Chem.*, 1972, **25**, 1631.
7 E. Amouyal, A. Homsi, J. Chambron and J.-P. Sauvage, *J. Chem. Soc., Dalton Trans.*, 1990, 1841.
8 A. Kirsch-De Mesmaeker, L. Jacquet, A. Masschelein, F. Vanhecke and K. Heremans, *Inorg. Chem.*, 1989, **28**, 2465.
9 A. Juris, V. Balzani, F. Barigelletti, S. Campagna, P. Belser and A. Von Zelewsky, *Coord. Chem. Rev.*, 1988, **84**, 85.
10 T. J. Meyer, *Pure Appl. Chem.*, 1990, **62**, 1003.
11 N. J. Turro, J. K. Barton and D. A. Tomalia, *Acc. Chem. Res.*, 1991, **24**, 332.
12 D. S. Sigman, A. Mazumder and D. M. Perrin, *Chem. Rev.*, 1993, **93**, 2295.
13 S. Campagna, G. Denti, S. Serroni, A. Juris, M. Venturi, V. Ricevuto and V. Balzani, *Chem. Eur. J.*, 1995, **1**, 211.
14 J. Bolger, A. Gourdon, E. Ishow and J. Launay, *J. Chem. Soc., Chem. Commun.*, 1995, 1799.


*Received, 10th October 1996; Com. 6/06944D*

# Thermal isomerization process in benzene gels of L-glutamic acid-derived lipids with spiropyran head groups

**Hiroshi Hachisako,*[a] Hirotaka Ihara,[b] Teruo Kamiya,[a] Chuichi Hirayama[b] and Kimiho Yamada[a]**

[a] *Department of Industrial Chemistry, Kumamoto Institute of Technology, 4-22-1 Ikeda, Kumamoto 860, Japan*
[b] *Department of Applied Chemistry and Biochemistry, Faculty of Engineering, Kumamoto University, 2-39-1 Kurokami, Kumamoto 860, Japan*

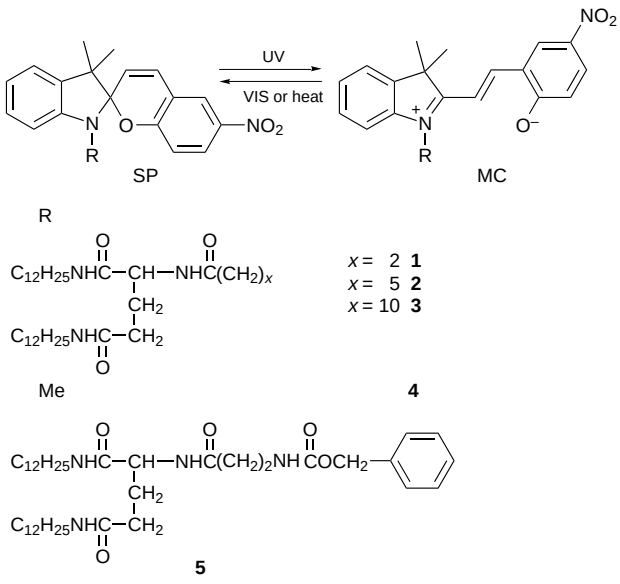
**First-order kinetic behaviour during the thermal isomerization process of lipids with photochromic spiropyran head groups in benzene strongly depends on the dispersion state of the lipids and this enables the determination of their critical aggregation concentrations.**

In recent years, organic gels arising from the formation of highly organized lipid assemblies in organic media have been attracting wide attention.[1–4] It is necessary to evaluate the critical gelling concentration (c.g.c.), at which the solution begins to form gels, as a measure of the stability of the aggregates of self-assembling lipids. In general, gelation has been considered successful if the cooled solution forms a nearly transparent mass that can be inverted without apparent flow.[4] However, this method is not applicable to fluid solutions containing fragmentary gels. On the other hand, the critical aggregation concentration (c.a.c.), at which lipids begin to aggregate, is believed to be almost identical to the c.g.c. However, this has not been verified because of the difficulty in direct evaluation of the c.a.c. in organic solutions (gels) by using conventional evaluation methods for aqueous solutions.† Therefore, an establishment of a direct evaluation method of c.a.c. in organic systems is very important.

On the other hand, it is well known that spiropyran (SP) shows reversible photochromism. Upon UV irradiation, a colourless and non-ionic SP is converted to a coloured and zwitterionic merocyanine (MC). This MC is reconverted to the SP thermally or upon exposure to visible light. We have previously reported that an L-glutamic acid-derived lipid **5** and related lipids with three amide bonds form organic gels through fibrous aggregates composed of a lipid membrane-like highly oriented structure.[1] Our present attention is focused on the application of photochromic behaviour of highly oriented aggregates of the SP-containing lipids **1**–**3** in organic media. Here, we propose an evaluation method for the c.a.c. of the L-glutamic acid-derived lipids with SP head groups, using MC–SP thermal isomerization (decolouration) behaviour in organic media.

SP-containing lipids **1**–**3** form transparent organic gels in benzene at concentrations of $2.0 \times 10^{-2}$ M. Differential scanning calorimetry (DSC) measurements of these gels (heating rate, 2 °C $min^{-1}$; temperature range, 5–100 °C) revealed that these lipids **1**–**3** showed sharp and single endothermic peaks‡ due to a gel-to-sol transition in the heating process in benzene, indicating that these SP-containing lipids self assemble into highly oriented structures in the gel state. Scanning electron micrographs of the cast film of **2** from a benzene solution revealed that the gel was composed of a network structure of fibrous aggregates with diameters of 300–2000 Å, close to those of aggregates of lipid **5** in benzene.[1]

SP-containing lipids **1**–**3** dissolved in benzene at 70 °C were gradually cooled to 20 °C to form gels. When the gels were exposed to UV light for 5 min at room temp. using a high-pressure mercury lamp in conjunction with a Toshiba UV-D35 colour filter ($330 < \lambda < 380$ nm), visible absorption spectral changes due to SP–MC conversion were observed. Fig. 1 shows a typical decolouration process of the UV-exposed lipid **2** in the benzene gel. Similar decolourations were observed in the gels of lipids **1** and **3**. The absorption maxima ($\lambda_{max}$ in benzene) of the



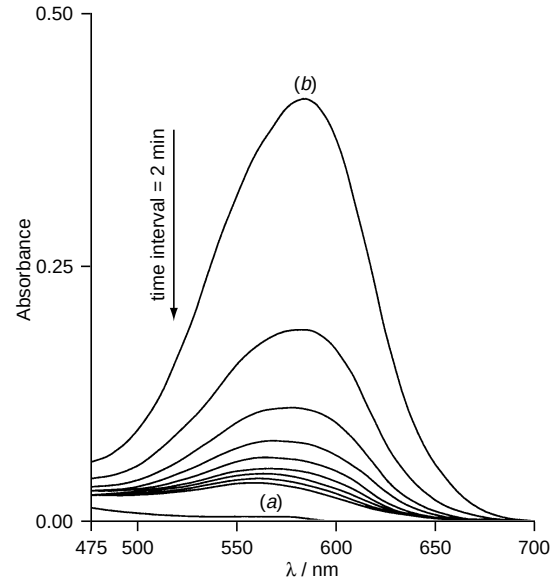




**Fig. 1** Visible absorption spectra of UV-irradiated **2** in benzene. [lipid] = $2 \times 10^{-2}$ M, 20 °C, path length of quartz cell 0.1 mm. (*a*) Before UV-irradiation; (*b*) measured immediately after UV irradiation for 5 min.

resulting MC species depended on the chemical structure of the *N*-substituents (R): 595, 585 and 571 nm for **1**, **2** and **3** respectively. The MC–SP thermal isomerizations were evaluated by first-order kinetic analyses. The plots of the MC–SP conversion process of lipids **1**– **3** in the gel states ($2.0 \times 10^{-2}$ M in benzene) did not obey simple first-order kinetics, whereas good linearities were obtained in the solution state ($1.0 \times 10^{-3}$ M in benzene). Similar deviations from linearity are, in general, observed in many other systems.[5] The first-order rate constants ($k_1$)§ for the MC–SP thermal isomerization for lipids **1**–**3** in benzene were calculated from the slope of these plots and are plotted against lipid concentrations as shown in Fig. 2. The $k_1$ values were remarkably dependent on the lipid concentrations. The critical concentrations shown by the dotted lines in Fig. 2 correspond closely to the critical gelling concentration (c.g.c.) determined by the inversion method.[4] Similar phenomena were observed in toluene. On the other hand, the thermal isomerization rate of the non-gelling SP **4** in benzene was slightly accelerated by increasing the concentration as shown in Fig. 2 and obeyed simple first-order kinetics. This difference can be explained by the fact that lipids **1**–**3** show lipid membrane-like highly oriented aggregation and SP **4** is in a molecularly dispersed state.¶ Fig. 1 shows the hypsochromic $\lambda_{max}$ shift from 585 to 560 nm at the later stage of the decolouration process. This species at 560 nm is ascribable to the H-like aggregates[7] of MC species with head-to-head stacking. These results indicate that the thermal MC–SP isomerization behaviour of the SP-containing lipids is sensitive to the aggregation of the lipid molecules. Therefore, it is concluded that the critical concentrations in Fig. 2 correspond to the c.a.c. of lipids **1**–**3**, respectively. This finding enabled us to detect the c.a.c. directly using first-order kinetics of thermal isomerization instead of *via* an indirect method through evaluation of the c.g.c. by conventional gelation tests, *e.g*. the inversion method.[4] Values of the c.a.c. determined from Fig. 2 were $3 \times 10^{-3}$, $2 \times 10^{-3}$ and $1 \times 10^{-2}$ M for **1**, **2** and **3** respectively. By comparison the corresponding c.g.c. values determined by the inversion method were $4 \times 10^{-3}$, $2 \times 10^{-3}$ and $1 \times 10^{-2}$ M.

In conclusion, we have established a direct method to determine the critical aggregation concentration of organic gels by using first-order kinetic analyses for the thermal MC–SP isomerization process of the component lipids with SP head groups. This finding will also help in clarification of the detailed aggregate structures of a series of organic gel-forming lipids.[1]

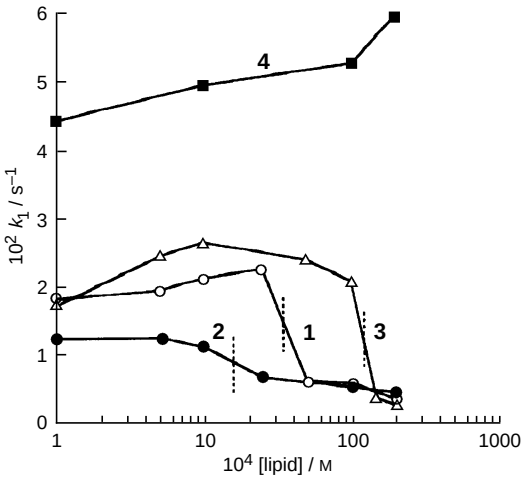



**Fig. 2** Concentration dependence of first-order rate constant ($k_1$) for MC–SP thermal isomerization of lipids **1**–**3** in benzene. 20 °C. Dotted lines indicate the c.a.c. values determined by this method. The error limits of $k_1$ values are within ±10%.‖

## Footnotes

† Surface tension, conductivity, fluorescence (using a fluorescent dye as a microenvironmental probe) and visible absorption spectral measurements (using a solvatochromic dye as a microenvironmental probe), *etc*. are used for the evaluation of c.a.c. in aqueous solution.

‡ Peak-top temperatures: 36 °C for **1**; 39 °C for **2**; 28 °C for **3** in benzene.

§ In the case of deviation from linearity, *e.g*. at $2 \times 10^{-2}$ M in benzene, $k_1$ values were calculated from the first two points and are plotted in Fig. 2.

¶ It has been reported that the thermal MC–SP isomerization is suppressed by aggregation of MC species.[6] Therefore, the retardation of the thermal isomerization rates of **1**–**3** and deviation of their first-order plots from linearity are ascribed to the existence of aggregated MC species.

‖ However, the error limits are much less than the change of $k_1$ values at the critical concentrations; therefore, the c.a.c. is not affected by the error of the of $k_1$ values and the method is safely applied to the determination of c.a.c. (c.g.c.) of the lipids.

## References


1 H. Ihara, H. Hachisako, C. Hirayama and K. Yamada, *J. Chem. Soc., Chem. Commun*., 1992, 1244; M. Takafuji, H. Ihara, C. Hirayama, H. Hachisako and K. Yamada, *Liq. Cryst*., 1995, **18**, 97; H. Ihara, K. Shudo, C. Hirayama, H. Hachisako and K. Yamada, *Liq. Cryst*., 1996, **20**, 807.

2 Y. Ishikawa, H. Kuwahara and T. Kunitake, *J. Am. Chem. Soc*., 1994, **116**, 5579.

3 K. Murata, M. Aoki, T. Nishi, A. Ikeda and S. Shinkai, *J. Chem. Soc., Chem. Commun*., 1991, 1715.

4 Y.-C. Lin, B. Kacher and R. G. Weiss, *J. Am. Chem. Soc*., 1989, **111**, 5542.

5 G. Smets, *Adv. Polym. Sci*., 1983, **50**, 17; T. Tsutsui, A. Hatakeyama and S. Saito, *Chem. Phys. Lett*., 1986, **132**, 563; E. Goldburt and V. Krongauz, *Macromolecules*, 1986, **19**, 247; H. Tomioka and T. Itoh, *Nippon Kagaku Kaishi*, 1988, 1031; K. Takagi, T. Kurematsu and Y. Sawaki, *J. Chem. Soc., Perkin Trans. 2*, 1995, 1667; T. Seki and K. Ichimura, *Macromolecules*, 1990, **23**, 31; M. Kikuchi, T. Kakurai and T. Noguchi, *Nippon Kagaku Kaishi*, 1972, 1323.

6 H. Tomioka and T. Itoh, *J. Chem. Soc., Chem. Commun*., 1991, 532.

7 A. H. Herz, *Adv. Colloid Interface Sci*., 1977, **8**, 237.



*Received, 17th September 1996; Com. 6/06386A*

# Singlet oxygen production from fullerene derivatives: effect of sequential functionalization of the fullerene core

**Takeshi Hamano,[a] Kensuke Okuda,[a] Tadahiko Mashino,[a] Masaaki Hirobe,[a] Kumi Arakane,[b] Akemi Ryu,[b] Shinrou Mashiko[c] and Tetsuo Nagano*[a]**

[a] *Faculty of Pharmaceutical Sciences, University of Tokyo, Hongo, Bunkyo-ku, Tokyo 113, Japan*
[b] *Research Laboratory, KOSÉ Corporation, Azusawa, Itabashi-ku, Tokyo 174, Japan*
[c] *Communication Research Laboratory, Iwaoka, Nishi-ku, Kobe 651-24, Japan*

**Singlet oxygen production efficiency of several laser-excited fullerene derivatives is compared by measuring the 1268 nm emissions; the efficiency was independent of the kind of addends, but it decreased with an increase in the number of addends, and addends at adjacent positions caused a greater decrease than remote addends.**

Fullerene and its derivatives produce singlet oxygen ($^1O_2$, $^1\triangle_g$) by energy transfer with high quantum yield;[1,2,3] [60]fullerene is a more efficient photosensitizer than rose bengal, methylene blue and eosin yellowish (tetrabromofluorescein sodium salt).[4] Singlet oxygen has been postulated to play important roles in many photochemical and photophysical processes in biological systems.[5] For example, it is thought to be responsible for phototoxicity in erythropoietic protoporphyria and for tetracyclin phototoxicity,[5] and it has also been applied for photodynamic therapy of cancer.[5] Thus, it is worthwhile to investigate in detail the photophysical or photochemical properties of fullerene and its derivatives from the standpoint of potential applications to biological systems. In particular, as fullerene derivatives have their UV–VIS absorption maxima at longer wavelengths, and have greater solubility in polar solvents, they may be preferable to the parent compound, [60]fullerene, for pharmaceutical application.[6]

We have already investigated the regiochemistry of several oxidation products of fullerene which were synthesized with the tetraphenylporphinatoruthenium(II) carbonyl–2,6-dichloropyridine-*N*-oxide–HBr system, and reported that [60]fullerene was multiply epoxidized (at least up to pentaepoxide, as determined by FAB mass spectroscopy), and that the second or the third oxygen was introduced at a position adjacent to the existing epoxide (confirmed by $^{13}C$ NMR spectroscopy employing $^{13}C$-enriched samples) (Fig. 1).[7] These epoxides might be good models to evaluate the effect of sequential functionalization on the photosensitizing activity of the fullerene structure. Anderson *et al*. have already reported on singlet oxygen production from dihydrofullerene, and discussed the effect of the functionalization.[2] However, they investigated only one derivative, and did not examine the effect of the number of addends, or the regiochemistry of bis or more highly functionalized fullerenes. We have also synthesized diethyl malonate-derivatized [60]fullerenes (see Fig. 1), which were previously reported by Hirsch *et al*.[8] As they have the addends at positions remote from each other (equatorial or *trans*-3),† they may have different photophysical properties from those of the corresponding epoxides.

In this work, we measured the near-infrared emission spectra corresponding to the $O_2(^1\triangle_g) \rightarrow O_2(^3\Sigma_g^-)$ transition at 1268 nm, which is highly specific to $^1O_2$, in solutions of fullerene derivatives under argon laser excitation (514.5 nm).[4] This is the most reliable method for $^1O_2$ detection developed so far. By this means, the amount of $^1O_2$ generated could be compared among the tested samples. We evaluated the efficiency of singlet oxygen production by calculating the value of emission intensity at 1268 nm/absorption coefficient at 514.5 nm ($I/\varepsilon$). As the absorption coefficient is a measure of the efficiency of a transition to an excited state ($S_1$ at a given wavelength, it can be thought that the $I/\varepsilon$ indicates the emission intensity from an unit of excited species ($S_1$) of sensitizer. That is, we evaluated the total efficiency of singlet oxygen production from the excited species by this value, and this value includes the efficiency of intersystem crossing and energy transfer from triplet state to molecular oxygen.

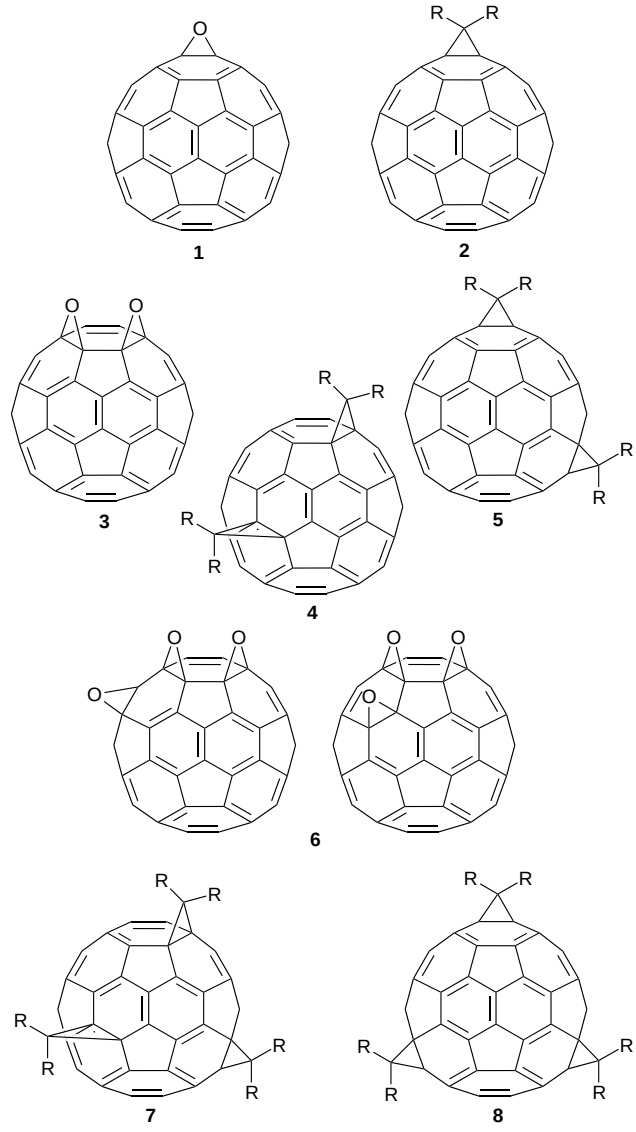



**Fig. 1**

Emission intensity increased in a concentration-dependent manner with all the compounds. The emission was diminished by the addition of excess β-carotene, a specific $^1O_2$ quencher, and was reduced by bubbling $N_2$ into the solution for a few minutes. These results confirm that all the compounds used in this study acted as photosensitizers, and that $^1O_2$ was responsible for the emission at 1268 nm.

First, we examined the effect of the number of addends on $^1O_2$-producing activity. As shown in Table 1, with both the epoxides and the diethyl malonate derivatives, $^1O_2$-producing ability decreased with an increase in the number of substituents. The size of the decrease was different between the two groups, and this will be discussed later. However, the order of diepoxide **3** and triepoxide **6** was exceptional, and the reason for this is still unknown.

Secondly we compared 1,2-epoxy[60]fullerene **1** and bis-(ethoxycarbonyl)[61]fullerene **2**. We did not observe any significant difference between **1** and **2** in $^1O_2$-producing ability. According to Anderson *et al*.,[2] dihydrofullerene had a reduced quantum yield of singlet oxygen production compared with [60]fullererne in $C_6D_6$. Our results are consistent with their report, even though a different laser wavelength was employed. It appears that functionalization of the fullerene core reduced the photodynamic activity, and the effect was not significantly dependent on the kind of addend, oxygen or diethyl malonate. However, it is noteworthy that the emission intensity itself was much greater with **2** than with **1** or [60]fullerene, because **2** has a greater value of ε at 514.5 nm (Table 1). This result suggests **2** would produce much more $^1O_2$ under given conditions, and could have significant implications for the pharmaceutical application of this class of compounds.

Next we compared 1,2;3,4-diepoxy[60]fullerene **3**, and tetra(ethoxycarbonyl)[62]fullerenes (equatorial) **4** and (*trans*-3) **5** in order to evaluate the effect of addend position on the fullerene structure. All three derivatives are bisadducts, but **3** has addends at adjacent positions, while **4** and **5** have them at remote positions. The emission intensity of **4** or **5** was stronger than that of [60]fullerene owing to the high ε value at 514.5 nm but, as expected the photodynamic efficiency was decreased after normalization, as described above. The results in Table 1 show that all of the derivatives have decreased $^1O_2$-producing ability ($I/\varepsilon$) compared with **1** or **2**, but the extent of the decrease was different between the two groups. That is, while **4** and **5** had 20–25% lower activity than **2**, **3** retained only 15% activity compared with that of **1**. This result suggests that a second addend introduced at an adjacent position to the existing one caused a greater perturbation of the electronic structure of the fullerene core than a second addend at a remote position. In the case of trisadducts **6**, **7** and **8**, the result was similar, that is to say, the photodynamic activity of **6** was greatly decreased compared with those of **7** and **8**, because of the proximity of the three addends on the fullerene core.

We also examined multihydroxylated fullerene (fullerenol) prepared by the literature method.[9] No peak was detected in $D_2O$ at concentrations up to about 10 mM (data not shown). This concentration is 10 000 times that of other fullerene derivatives used in this study. Thus, we concluded that extensive derivatization of the fullerene core results in loss of photodynamic activity. This is in accordance with the results reported by Cardullo *et al*. In the report, they showed that a fullerene hexaadduct had no photodynamic activity.[10]

As the results obtained in this study were relative efficiency of $^1O_2$ production of the fullerene derivatives, further investigation will be required for the clarification of their detailed photophysical properties, such as quantum yield of the energy transfer from triplet state to molecular oxygen, in the future.

**Table 1** Photodynamic efficiency of fullerene and its derivatives[a]

| Compound[b] | $I$[c] | $I/\varepsilon$[d] |
|---|---|---|
| $C_{60}$ | 1.0 | 1.0 |
| $C_{60}O$ **1** | 1.21 | 0.74 |
| $BECC_{61}$ **2** | 1.59 | 0.77 |
| $C_{60}O_2$ **3** | 0.29 | 0.11 |
| $TECC_{62}$ (equatorial) **4** | 2.09 | 0.59 |
| $TECC_{62}$ (*trans*-3) **5** | 2.15 | 0.53 |
| $C_{60}O_3$ **6** | 0.42 | 0.22 |
| $HECC_{63}$ (equatorial, equatorial) **7** | 1.71 | 0.42 |
| $HECC_{63}$ (*trans*-3, *trans*-3) **8** | 1.73 | 0.40 |
| $C_{60}O_4$ | 0.12 | 0.06 |
| $C_{60}O_5$ | 0.06 | 0.03 |

[a] The emission intensity at 1268 nm was measured in $CS_2$ solution for photosensitizers excited by Ar laser light at 514.5 nm with 25 mW output power. [b] Abbreviations: $BECC_{61}$ = bis(ethoxycarbonyl)$C_{61}$; $TECC_{62}$ = tetra(ethoxycarbonyl)$C_{62}$; $HECC_{63}$ = hexa(ethoxycarbonyl)$C_{63}$. The nomenclature follows the proposals of Hirsch *et al.* (ref. 8). [c] Emission intensity at 1268 nm. [d] Emission intensity at 1268 nm/absorption coefficient at 514.5 nm (relative value to that of [60]fullerene.

## Footnote

† The nomenclature follows the proposals of Hirsch *et al.* (ref. 8).

## References


1 J. W. Arbogast, A. P. Darmanyan, C. S. Foote, Y. Rubin, F. N. Diederich, M. M. Alvarez, S. J. Anz and R. L. Whetten, *J. Phys. Chem*., 1991, **95**, 11; J. W. Arbogast and C. S. Foote, *J. Am. Chem. Soc*., 1991, **113**, 8886.

2 J. L. Anderson, Yi-Zhong An, Y. Rubin and C. S. Foote, *J. Am. Chem. Soc*., 1994, **116**, 9763.

3 C. S. Foote, *ACS Symp. Ser*., 1995, **616**, 17 and references cited therein.

4 T. Nagano, K. Arakane, A. Ryu, T. Masunaga, K. Shinmoto, S. Mashiko and M. Hirobe, *Chem. Pharm. Bull*., 1994, **42**, 2291.

5 K. Arakane, A. Ryu, C. Hayashi, T. Masunaga, K. Shinmoto, S. Mashiko, T. Nagano and M. Hirobe, *Biochem. Biophys. Res. Commun*., 1996, **223**, 578; T. Hasan and A. U. Khan, *Proc. Natl. Acad. Sci. U.S.A.*, 1986, **83**, 4604; A. S. W. Li, C. F. Chignell and R. D. Hall, *Photochem. Photobiol*., 1987, **46**, 379; M. B. Poh-Fitzpatrick, *Semin. Liver Dis*., 1982, **2**, 164; K. R. Weishaupt, C. J. Gomer and T. J. Dougherty, *Cancer Res*., 1976, **36**, 2326; T. J. Dougherty, J. E. Kaufman, A. Goldfarb, K. R. Weishaupt, D. Boyle and A. Mittleman, *Cancer Res*., 1978, **38**, 2628; J. P. Keene, D. Kessel, E. J. Land, R. W. Redmond and T. G. Truscott, *Photochem. Photobiol*., 1986, **43**, 117; D. Brault, C. Vever-Bizet, M. Rougée and R. Bensasson, *Photochem. Photobiol*., 1988, **47**, 151.

6 A. S. Boutorine, H. Tokuyama, M. Takasugi, H. Isobe, E. Nakamura and C. Hélène, *Angew. Chem., Int. Ed. Engl*., 1994, **33**, 2462; Yi-Zhong An, Chi-Hong B. Chen, J. L. Anderson, D. S. Sigman, C. S. Foote and Y. Rubin, *Tetrahedron*, 1996, **52**, 5179.

7 T. Hamano, T. Mashino and M. Hirobe, *J. Chem. Soc., Chem. Commun*., 1995, 1537.

8 A. Hirsch, I. Lamparth and H. R. Karfunkel, *Angew. Chem., Int. Ed. Engl*., 1994, **33**, 437.

9 J. Li, A. Takeuchi, M. Ozawa, X. Li, K. Saigo and K. Kitazawa, *J. Chem. Soc., Chem. Commun*., 1993, 1784.

10 F. Cardullo, L. Isaacs, F. Diederich, J. P. Gisselbrecht, C. Boudon and M. Gross, *Chem. Commun*., 1996, 797.


*Received, 16th September 1996; Com. 6/06335G*

# Synthesis of 3-*O*-sialyl and 6-*O*-sulfo derivatives of dimeric *N*-acetyl lactosamine as specific acceptors for α-L-fucosyltransferases

**Rakesh K. Jain,† Bao-Guo Huang, E. V. Chandrasekaran and Khushi L. Matta***

*Department of Gynecologic Oncology, Rosewell Park Cancer Institute, Elm & Carlton Streets, Buffalo, NY 14263, USA*

**The stereoselective syntheses of 3-*O*-sialyl and 6-*O*-sulfo dimeric lactosamine derivatives 1–4 are accomplished through the use of key glycosyl donors 13 and 15.**

In continuation of our efforts towards the synthesis of biologically important oligosaccharides, we have developed an elegant synthesis of 3-*O*- and 6-*O*-substituted dimeric lactosamine derivatives. **1**–**4**[1] (Fig. 1), which were prepared from the key intermediates **5**–**13** (Fig. 2) by stereoselective transformation, as described in Schemes 1–3. Our approach is based upon the observation that an *O*-acetyl group can be selectively removed in the presence of a 6-*O*-pivaloyl substituent to give 6-*O*-pivaloyl β-D-galactopyranosyl linked compounds. Glycosylation of **5** with **9** under Mukaiyama's conditions ($SnCl_2$–AgOTf)[2] followed by acetylation with pyridine–acetic anhydride afforded the β(1→3) linked disaccharide **14** in 8% yield and the β(1→4) linked disaccharide **15** in 48% yield. The $^1$H NMR spectrum of **15** displayed characteristic signals for H-3, H-1 (δ 5.71–5.67), H-1′ (δ 4.50, d, $J$ = 8.0 Hz), 4 × OAc (δ 2.08, 2.04, 1.93 and 0.86) and 2 × $CMe_3$ (δ 1.25 and 1.17). Isopropylidenation of **11**, using Catelani's procedure,[3] followed by acetylation with pyridine–acetic anhydride and deacetonation provided the acceptor **16** in 66% yield. The $^1$H NMR spectrum gave characteristic signals at δ 5.70 (dd, H-3), 2.10 and 1.09 (2 × OAc) and 1.27 and 1.23 (2 × $CMe_3$). Condensation of the donor **15** with **16** under NIS–triflic acid conditions at −30 °C gave **17** in 76% yield. The $^1$H NMR spectrum of **17** displayed characteristic signals at δ 5.71–5.59 (2 × dd and d, H-3, H-3″ and H-4″), 5.46 (d, $J$ = 8.3 Hz, H-1″), 5.24 (d, $J$ = 8.5 Hz, H-1), 5.09 (dd, H-2‴), 4.97 (dd, H-2′), 4.53 (d, $J$ = 7.9 Hz, H-1‴), 4.43 (d, $J$ = 7.6 Hz, H-1′), 2.10–1.49 (cluster of singlets, 6 × OAc) and 1.25, 1.23 and 1.94 (4 × $CMe_3$) which confirmed a β(1→3) conformation of the newly incorporated glycosidic linkage. De-*O*-acetylation of **17** in MeOH–$CH_2Cl_2$ (1 : 1, *v*/*v*) with MeOH–MeONa (pH 10) at 0 °C provided the acceptor **18** in 95% yield. The $^1$H NMR spectrum gave characteristic signals at δ 5.58–5.69 (2 × dd, H-3″ and H-3), 5.34 (d, H-1″, $J$ = 8.2 Hz), 5.24 (d, H-1, $J$ = 8.4 Hz), 4.82 (dd, H-2′), 4.73 (d, $J$ = 7.8 Hz, H-1‴), 4.35 (d, $J$ = 7.7 Hz, H-1′), 1.84, 1.75 and 1.49 (each s, 3 × OAc) and 1.25, 1.23, 1.22 and 0.97 (each s, 4 × $CMe_3$) confirming the assigned structure.

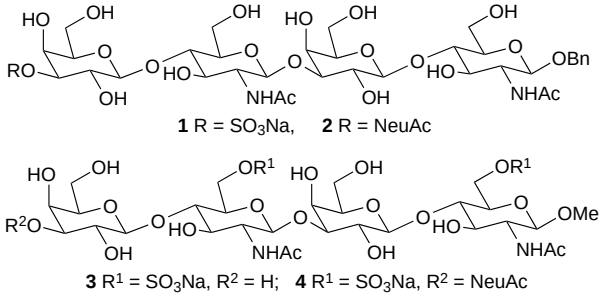



**Fig. 1** Target molecules sialyl and sulfated dimeric lactosamine **1**–**4**

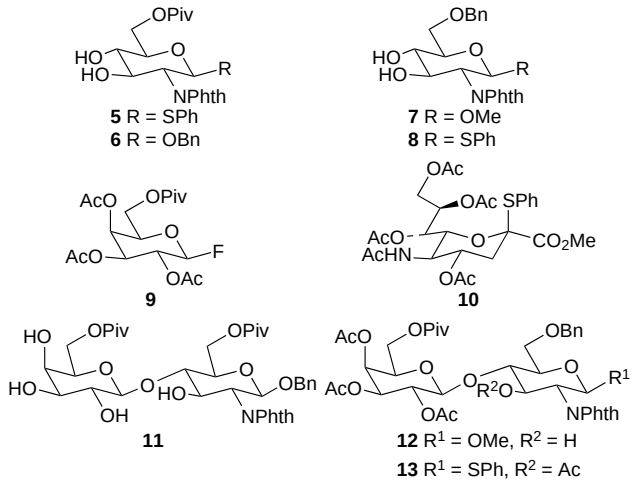
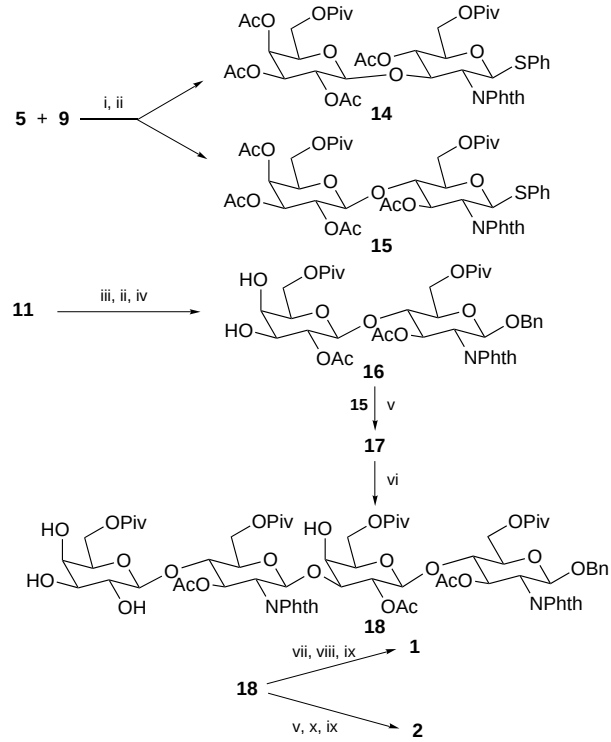
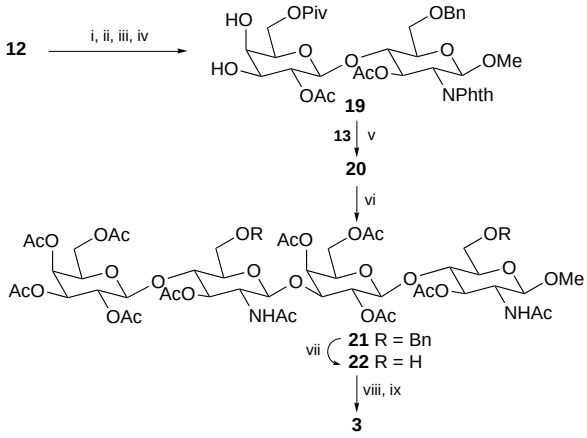



**Fig. 2** Key intermediates **5**–**13** involved in the synthesis of target molecules **1**–**4**




**Scheme 1** *Reactions and conditions*: i, **5** (1.0 equiv.), **9** (1.5 equiv.), AgOTf (1.20 equiv.), 4 Å molecular sieves, $CH_2Cl_2$–toluene (5 : 1, v/v), −15 °C to room temp., 5 h; ii, pyridine–$Ac_2O$ (2 : 1, v/v); iii, 0.15% CSA, DMP, 24 h, MeOH–$H_2O$ (10 : 1, v/v), 100 °C, 6 h; iv, 70% aq. AcOH, 70 °C, 2 h; v, **15** (1.05 equiv.), or **10** (3.0 equiv.), NIS (3.0 equiv.)–triflic acid, −30 °C, 2 h; vi, MeOH–$CH_2Cl_2$ (1 : 1, v/v), MeONa (pH 10), 2 h; vii, $SO_3$–pyridine complex in pyridine (6.0 equiv.), 5 °C, 16 h; viii, MeOH–hydrazine hydrate (4 : 1, v/v), 100 °C, 16 h, $Ac_2O$ (excess), MeOH–$CH_2Cl_2$ (1 : 1, v/v), 0 °C, 1 h; ix, MeOH–MeONa, 24 h; x, LiI (10 equiv.), pyridine, 120 °C, 3 h



**Scheme 2** *Reagents and conditions*: i, MeOH–$CH_2Cl_2$ (1 : 1, v/v), MeONa, 0 °C, 2 h, 85%; ii, DMP, PTS, room temp., 1.5 h, 89%; iii, pyridine–$Ac_2O$ (2 : 1, v/v), room temp., 12 h, 89%; iv, 70% aq. AcOH, 65 °C, 2.5 h, 66%; v, **13** (0.95 equiv.), NIS (3.0 equiv.)–triflic acid, −20 °C, 1 h, 54%; vi, EtOH–hydrazine hydrate (4 : 1, v/v), 100 °C, 16 h, pyridine–$Ac_2O$ (2 : 1, v/v), room temp., 12 h, 84%; vii, 10% Pd–C, $H_2$, MeOH, 16 h; 50%; viii, $SO_3$–pyridine complex in DMF (10 equiv.), 0 °C, 16 h; ix, MeOH–MeONa, 16 h; $Na^+$ resin, 35% from **22**

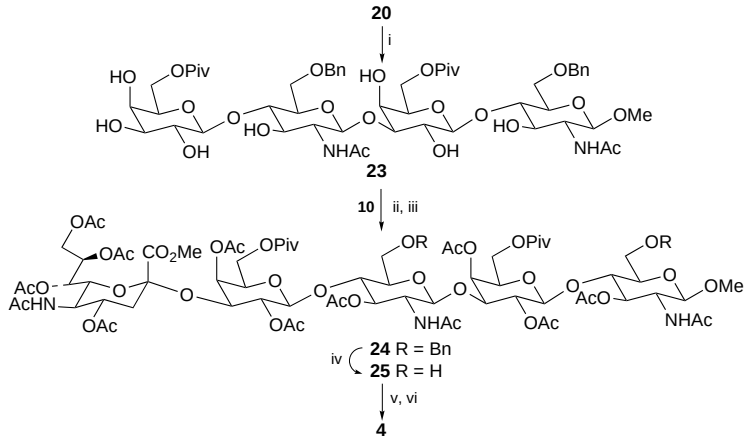
Removal of both the phthalimido and acetate groups from **20** was accomplished by treatment with hydrazine hydrate in ethanol (1 : 9, v/v) at 80 °C followed by N-acetylation to give **23** in 65% yield. Condensation of sialic acid donor **10** with **23** at −40 °C followed by *O*-acetylation gave **24** in 35% yield (based on **23** consumed). The synthesis of **4** from **24** was achieved by a sequence of reactions similar to those described for the preparation of **3** from **21**. The structures of **1**–**4** were confirmed by $^1H$ and $^{13}C$ NMR spectroscopy.†

Our preliminary examination of Galβ1,4(6-sulfo) GlcNAcβ1,3 Galβ1,4(6-sulfo) GlcNAcβ-O-Me (**3**) and Neu-Acα2,3Galβ1,4(6-sulfo)GlcNAcβ1,3Galβ1,4(6-sulfo) GlcNAcβ-O-Me (**4**) indicated that both of these compounds were equally active as acceptors for human colon tumour α1,3-L-fucosyltransferase.

These investigations were supported by Grant No. CA 63218 awarded by the National Cancer Institute.

## Footnote

† *Selected data* for **1**: $[\alpha]_D$ 7 (*c* 1.5, $H_2O$) [lit.,[12] −12.2 (*c* 0.5, $H_2O$)]; $^{13}C$ NMR ($D_2O$, 100.6 MHz): δ 101.86 (C-1‴), 101.72 (C-1′), 101.45 (C-1″), 98.81 (C-1), 81.04 (C-3′), 77.49 (C-3‴), 73.89 (C-4″), 73.85 (C-4), 59.90 (C-6‴ and C-6′), 59.09 (C-6″), 58.85 (C-6), 54.19 (C-2″), 53.99 (C-2). For **2**: $[\alpha]_D$ +186 (*c* 0.2, $H_2O$); $^1H$ NMR ($D_2O$, 400 MHz): δ 4.84 (d, *J* = 12 Hz,



**Scheme 3** *Reagents and conditions*: i, EtOH–hydrazine hydrate (9 : 1, v/v), 80 °C, 1 h, MeOH–$Et_3N$–$Ac_2O$ (4 : 2 : 1), room temp., 2 h, 65%; ii, **10** (2.50 equiv.), NIS (3.0 equiv.)–triflic acid, MeCN, −40 °C, 1 h; iii, pyridine–$Ac_2O$ (2 : 1, v/v), room temp., 12 h, 35% based on **23** consumed; iv, 10% Pd–C, $H_2$ MeOH, 24 h; v, $SO_3$–pyridine complex in DMF (10 equiv.), room temp., 2 h; vi, MeOH–MeONa, 48 h; $H_2O$, 4 h, $Na^+$ resin, 56% from **24**

Selective sulfation of **18** with $SO_3$–pyridine complex in pyridine at 5 °C provided the 3-*O*-sulfo compound which upon removal of its phthalimido group (MeOH–hydrazine hydrate, 100 °C) and *N*-acetylation followed by de-*O*-acetylation (MeOH–MeONa) gave the known compound **1** (55% from **18**).[4]

A similar NIS–triflic acid reaction of **18** with sialic acid donor **10** provided the crude pentasaccharide. The conversion of this intermediate into target compound **2** (23% from **18**) was then carried out in 4 steps: (i) LiI–pyridine (methyl ester to acid), (ii) MeOH–hydrazine hydrate (phthalimido group removal), (iii) $Ac_2O$–MeOH–$CH_2Cl_2$ (*N*-acetylation) and (iv) MeOH–MeONa (de-*O*-acetylation).

The synthesis of **3** and **4** (Schemes 2 and 3) involved the glycosylation of **8** with fluoride **9** under conditions similar to those described for the preparation of **15** (from **5**), followed by acetylation to give donor **13** along with some 1⟶3 linked disaccharide. Condensation of **13** with **19** under NIS–triflic acid conditions at −20 °C provided **20** in 54% yield. The formation of **21** from **20** was achieved by the treatment with hydrazine hydrate in ethanol (1 : 4, v/v) at 100 °C followed by acetylation with pyridine–acetic anhydride in 84% yield. The removal of *O*-benzyl (10% Pd–C) gave diol **22** which on sulfation with $SO_3$–pyridine complex in DMF and followed by de-*O*-acetylation gave compound **3** in 35% yield (from **22**).

H-1″), 4.69 (d, *J* = 11.0 Hz, H-1), 4.50 (d, *J* = 8.0 Hz, H-1‴), 4.41 (d, *J* = 8.0 Hz, H-1′), 2.71 (dd, J = 4.6 Hz, H-3‴e), 1.99 and 1.88 (each s, 3×NAc), 1.75 (t, *J* = 1.2 Hz, H-3‴a); $^{13}C$ NMR: δ 101.86 (C-1‴), 101.73 (C-1′), 101.55 (C-1″), 98.79 (C-1), 81.04 (C-3′), 77.49 (C-3‴), 74.49 (C-4″), 74.15 (C-4), 61.58 (C-9‴), 59.99 (C-6‴), 59.91 (C-6′), 59.09 (C-6″), 58.86 (C-6), 54.17 (C- 2″), 53.99 (C-2), 50.68 (C-5″), 38.63 (C-3‴); *m*/*z* 1128.5 $(M - Na)^-$. For **3**: $[\alpha]_D$ +21 (*c* 0.6, $H_2O$); $^{13}C$ NMR: δ 101.84 (C-1‴), 101.67 (C-1′), 101.56 (C-1″), 100.94 (C-1), 81.46 (C-3′), 76.88 (C-3‴), 74.33 (C-4″), 74.05 (C-4), 67.63 (C-6‴), 67.36 (C-6), 60.11 (C-6‴), 60.02 (C-6′), 56.19 (OMe), 54.15 (C-2″), 53.91 (C-2); *m*/*z* 942.9 $(M - Na)^-$. For **4**: $[\alpha]_D$ +24 (*c* 0.7, $H_2O$); $^{13}C$ NMR: δ 101.84 (C-1‴), 101.60 (C-1′), 101.15 (C-1″), 100.92 (C-1), 98.73 (C-2‴), 81.50 (C-3′), 76.79 (C-3‴), 74.29 (C-4″), 74.02 (C-4), 67.29 (C-6″), 67.08 (C-6), 61.52 (C-9‴), 60.01 (C-6′ and C-6‴), 56.17 (OMe), 54.09 (C-2″), 53.06 (C-2), 50.60 (C-5‴), 38.57 (C-3‴).

## References

1 R. K. Jain, R. Vig, R. D. Locke, A. Mohammad and K. L. Matta, *J. Chem. Soc., Chem. Commun.*, 1996, **65**.
2 T. Mukaiyama, Y. Murai and S. Shoda, *Chem. Lett.*, 1981, 431; T. Mukaiyama, Y. Hashimoto and S. Shoda, *Chem. Lett.*, 1983, 935.
3 G. Catelani, F. Colonna and A. Marra, *Carbohydr. Res.*, 1988, **182**, 297.
4 G. V. Reddy, R. K. Jain, R. D. Locke and K. L. Matta, *Carbohydr. Res.*, 1996, **280**, 261.

*Received, 5th August 1996; Com. 6/05439K*

# Proton migration on the [60]fullerene cage of 1-*tert*-butyl-1,4-dihydro[60]fullerene to yield the 1,2-isomer

**Fiachra Banim, David J. Cardin and Peter Heath**

*Department of Chemistry, University of Reading, Whiteknights, Reading Berkshire, UK RG6 6AD*

**Proton NMR data on the base catalysed rearrangement of 1-*tert*-butyl-1,4-dihydro[60]fullerene to the 1,2-isomer reveal a second order reaction and an activation energy of 56.1 kJ mol$^{-1}$.**

It has been reported that treatment of [60]fullerene with *tert*-butyllithium followed by acid quench gives both 1,2- and 1,4-isomers, and that the 1,4-compound rearranges to the more stable 1,2-isomer over a period of 12 h at 25 °C.[1] We now report that the pure 1,4-isomer is indefinitely stable in the solid form (no detectable rearrangement over eighteen months) while even in solution little conversion to the thermodynamic product occurs over two months in deuteriated chloroform. We also show that the rearrangement of the 1,4-isomer to the 1,2-isomer is base catalysed, and provide kinetic and thermodynamic data on this rearrangement.

1-*tert*-Butyl-1,2-dihydro[60]fullerene is the thermodynamically favoured adduct (by *ca.* 12 kJ mol$^{-1}$ from PM3 calculations[2]) not requiring (unlike the 1,4-adduct) the introduction of a double bond at the 6,5 ring junction (estimated from similar PM3 parameterisation of the MNDO Hamiltonian to add *ca*. 35 kJ mol$^{-1}$).[3] This unfavourable electronic effect is partly compensated by the absence of the eclipsing (steric) interaction that exists between addenda in the 1,2-position. This factor is clearly demonstrated by increasing the steric requirements of the adducts from Bu$^t$C$_{60}$H to a bulky 1-*tert*-butyl-1,4-dihydro-2-(3,6-dicyclopropylcyclohepta-2,4,6-trien-1-yl)[60]fullerene, when the 1,4-derivative becomes more favourable by a predicted 75 kJ mol$^{-1}$ (also from PM3 calculations).

Maximum yields of 1-*tert*-butyl-1-4-dihydro[60]fullerene were obtained if the reaction was acid quenched within 3 h, using toluene as solvent, and the lithium reagent was added in hexanes. After 24 h only the 1,2-isomer was obtainable. (Up to 85 : 15 1,4- : 1,2-adduct could be obtained). The ratio of the 1,4- : 1,2-adducts was not adversely affected when different protic species were introduced *e.g.* water, hydrogen chloride, water–hydrogen chloride, glacial acetic acid or trifluoroacetic acid. In an attempt to form the 1,4-adduct more selectively, the reaction was carried out at elevated temperature (60 °C), but this had little effect, and was not studied in more detail. The proton NMR spectrum of the reaction product shows two *tert*-butyl signals (at δ 2.08 and 1.88) and two 'cage' proton signals (at δ 6.67 and 6.32) in $CDCl_3$. A NOESY NMR experiment established that the lower field resonance at δ 6.67 and the *tert*-butyl resonance at δ 2.08 had a strong transient NOE. We conclude that these resonances represent the 1,2-isomer, which was verified by $^{13}$C NMR.† There was no transient NOE between the fullerenyl proton and the *tert*-butyl group for the second isomer, ruling out the unfavourable 1,6-adduct.[4]

In suitable environments, 1-*tert*-butyl-1,4-dihydro[60]fullerene is stable for prolonged periods of time, but can easily rearrange in the presence of trace impurities. Several acids were explored, but none gave any indication of isomerisation. Treatment of the isomeric mixture with various bases, by contrast, gave an immediate rearrangement reaction.‡ It is interesting to note that variation of the base showed that the p$K_a$ of the fullerenyl (cage) proton of the 1,4-isomer could be crudely estimated at 5.7 > p$K_a$ > 4.15 (these data were obtained in chloroform or deuteriochloroform solution), a range consistent with other estimates for a variety of such cage protons, and rather higher than that calculated recently (3.31) by quantum mechanical methods.[5]

Experiments were conducted using $^1$H NMR as a probe, and perdeuteriated pyridine as base catalyst, reactions being carried out in deuteriochloroform. When deuteriopyridine was added to solutions of the 1,4-isomer, the concentration of the latter was found to decrease, giving an increase in the 1,2-isomer concentration (Fig. 1),§ a *ca*. 96% conversion being generally observed. The 1,4-isomer concentration decayed exponentially with time, and an increase in the concentration of deuteriopyridine increased the rate of reaction.

A linear fit was obtained when the natural logarithm of the concentration of the 1,4-isomer was plotted against time, in agreement with a reaction first order with respect to the fullerene concentration (Fig. 2). A second order reaction was ruled out as a plot of the reciprocal of the substrate concentration with time gave a clearly non-linear relationship (Fig. 2).

A plot of ln $[A]_t$ against time allowed us to calculate $k'$ at different concentrations of deuteriopyridine (Fig. 3).¶ The results show that the reaction is second order overall and first order with respect to both the concentration of 1,4-Bu$^t$C$_{60}$H and deuteriopyridine. The exact value for the rate constant of the

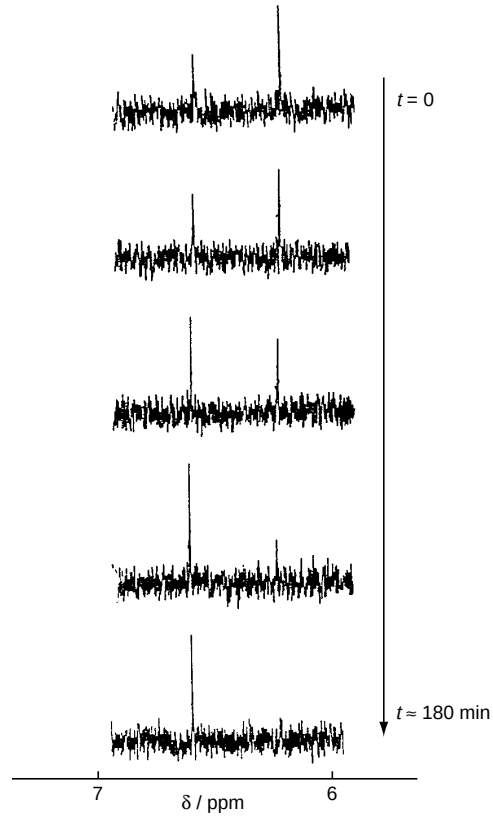



**Fig. 1** Variation of the $C_{60}H$ $^1$H NMR signals during isomerisation, recorded at 21 ± 1 °C in a 0.35 M solution of $C_5D_5N$ in $CDCl_3$

reaction $k_{expt}$ [2.1(1) × $10^{-3}$ $dm^3$ $mol^{-1}$ $s^{-1}$], was calculated from Fig. 3.¶

The rate of consumption of the reactant, 1-*tert*-butyl-1-4,-dihydro[60]fullerene, was determined at different temperatures in the range 20–50 °C for two concentrations. An Arrhenius plot gave an activation energy of 56.1 kJ $mol^{-1}$ (Fig. 4).

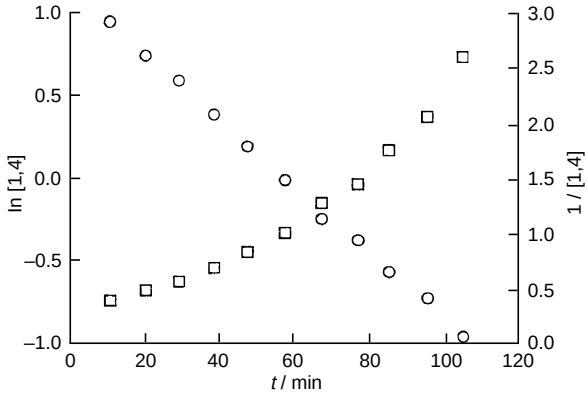



**Fig. 2** First- and second-order plots of the isomerisation reaction of the 1,4-isomer, recorded at 21 ± 1 °C. First order reaction (○) plotted *vs.* ln [1,4] (left axis) and second order reaction (□) plotted *vs.* 1/[1,4] (right axis). Recorded in 0.178.

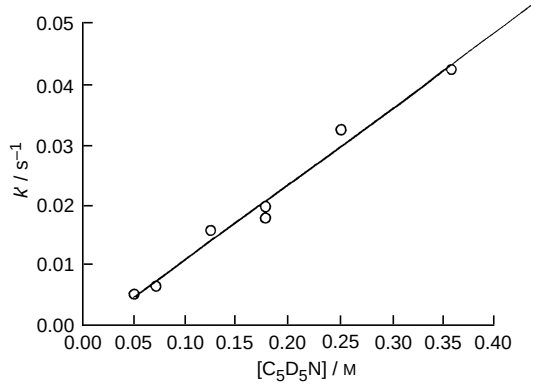



**Fig. 3** Plot of *k′ vs.* [$C_5D_5N$] at 21 ± 1 °C

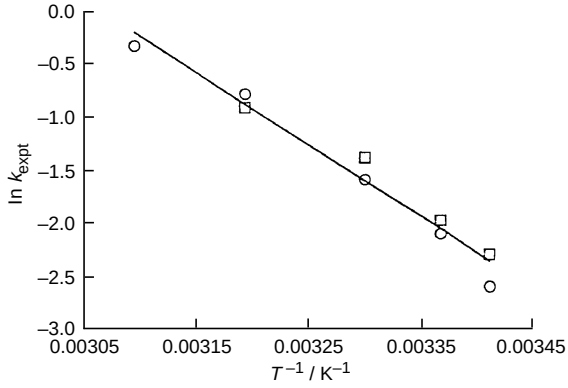



**Fig. 4** Arrhenius plot for the isomerisation reaction of the 1,4-isomer in 0.17 (□) and 0.07 M (○) $C_5D_5N$

In an attempt to elucidate the mechanism of the base catalysed reaction, the fullerenyl proton was substituted by a deuteron. Similar experiments to those employing 1,4-Bu$^t$$C_{60}$H were carried out on the 1,4-Bu$^t$$C_{60}$D derivative, again giving a reaction second order overall; first order with respect to 1,4-Bu$^t$$C_{60}$D and pyridine. The experimental value for the rate of reaction ($k_D$) was only marginally less than $k_{expt}$, yielding a value of *ca.* 1.2 for $k_{expt}/k_D$.

The mechanism of the hydrogen transfer step is currently under investigation. In initial experiments the 1,4-Bu$^t$$C_{60}$D reaction afforded substantially 1,2-Bu$^t$$C_{60}$H, the origin of the H atom (possibly adventitious water) and the details of the transfer are being studied.

We thank the authors of ref. 5 for providing details prior to publication.

## Footnotes

† The $^{13}$C NMR spectrum of pure 1-*tert*-butyl-1,2-dihydro[60]fullerene had 32 resonances indicative of the $C_s$ symmetry of a 1,2 adduct.

‡ Although the 1,4-isomer is stable as described above, on heating a mixture of the 1,2- and 1,4-isomers at 60 °C for 72 h, up to 25% of the 1,4-isomer rearranges. There may be a concerted, non-catalysed reaction also occurring, albeit at a substantially slower rate than the catalysed reaction. This route of rearrangement will be explored further.

§ Quantitative data were taken, however, from the *tert*-butyl signals, which had a substantially better signal-to-noise ratio.

¶ From the plots we can write eqn. (1) for the overall reaction,

$$[A] + [C_5D_5N] \rightarrow [B] + [C_5D_5N] \quad (1)$$

where A = 1,4-Bu$^t$$C_{60}$H and B = 1,2-Bu$^t$$C_{60}$H. This gives eqn. (2).

$$\text{rate of reaction} = k_{expt}\,[B][C_5D_5N] \quad (2)$$

If the concentration of deuteriopyridine is kept constant and the decrease in concentration of 1,4-Bu$^t$$C_{60}$H is monitored, this gives eqn. (3).

$$-d[A]/[A] = k'dt, \text{ where } k' = k_{expt}\,[C_5D_5N] \quad (3)$$

Integration of eqn. (3) gives eqn. (4).

$$\ln [A]_0 - \ln [A]_t = k't, \quad (4)$$

where $[A]_0$ is the concentration of [1,4-Bu$^t$$C_{60}$H] at $t = 0$ and $[A]_t$ is the concentration of [1,4-Bu$^t$$C_{60}$] at time $t$. Eqn. (4) then gives eqn. (5).

$$\ln [A]_t = -k't + \ln [A]_0 \quad (5)$$

## References

1 P. J. Fagan, P. J. Krusic, D. H. Evans, S. A. Lerke and E. Johnston, *J. Am. Chem. Soc.*, 1992, **114**, 9697.
2 T. Kitagawa, T. Tanaka, Y. Takata and K. Takeuchi, *J. Org. Chem.*, 1995, **60**, 1490.
3 N. Matsuzawa, D. A. Dixon and T. Fukunaga, *J. Phys. Chem.*, 1992, **96**, 7594.
4 A. Hirsch, A. Soi and H. R. Karfunkel, *Angew. Chem., Int. Ed. Engl.*, 1992, **31**, 766; *Angew. Chem.*, 1992, **104**, 808.
5 K. Choho, G. Van Lier, G. Lier, G. Van de Woude and P. Geerlings, unpublished results.

*Received, 23rd August 1996; Com. 6/05859K*

# Recognition of platinum(II) amine complexes by nucleotides: role of phosphate and carbonyl groups in ([$^{15}N_3$]diethylenetriamine)-(guanosine 5′-monophosphate)platinum(II)

**Zijian Guo, Peter J. Sadler*† and Erle Zang**

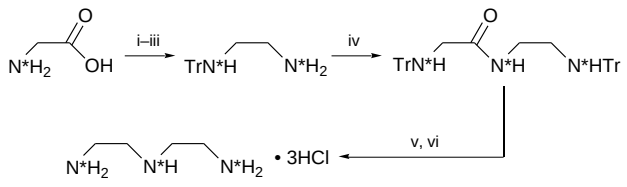
*Department of Chemistry, Birkbeck College, University of London, Gordon House, 29 Gordon Square, London, UK WC1H 0PP*

**Two-dimensional [$^1$H,$^{15}$N] NMR studies show that in the model monofunctional DNA adduct [Pt([$^{15}N_3$]dien)(5′-GMP-*N*7)]$^{2+}$ [5′-GMP = guanosine 5′-monophosphate, dien = 1,5-diamino-3-azapentane (prepared by a novel synthesis from glycine)], stereospecific hydrogen-bonding interactions involving Pt–NH protons are promoted by deprotonation of both the 5′-phosphate group and N$^1$H of coordinated 5′-GMP.**

A surprising recent finding is that monofunctional adducts of $[PtCl_2(NH_3)_2]$ (cisplatin) and $[Pt(NH_3)_2(H_2O)_2]^{2+}$ with one of the guanine bases in GG oligonucleotides can be very long lived.[1,2] It is therefore important to understand the factors which lead to stabilization of particular adducts between platinum am(m)ine complexes and DNA. Complexes of [Pt(dien)]$^{2+}$ with nucleotides have been widely studied since they represent stable monofunctional adducts, and the ability of [Pt(dien)]$^{2+}$ to introduce local denaturation of DNA has been demonstrated, for example by Brabec *et al*. using chemical probes.[3]

The NH groups on platinum am(m)ine ligands are thought to play a major role in determining the nature of the adducts *via* hydrogen-bonding interactions with DNA,[4] and we have shown previously that these can be investigated in solution using two-dimensional [$^1$H,$^{15}$N] NMR and $^{15}$N-labelled ligands.[5] Use of this method with dien complexes is complicated by the lack of an efficient synthesis of dien which can be adapted to $^{15}$N labelling. We report here briefly a novel efficient synthesis of [$^{15}N_3$]dien, and show that use of this allows an NMR study of hydrogen-bonding interactions in nucleotide complexes such as [Pt([$^{15}N_3$]dien)(5′-GMP-*N*7)]$^{2+}$. The NMR data implicate both the 5′-phosphate and C$^6$ carbonyl groups in pH-dependent stereospecific interactions with the Pt–$NH_2$ groups.

$^{15}$N-Labelled dien cannot readily be prepared by the Gabriel method[6] since [$^{15}$N]diethanolamine is required as a starting material. The preparation of this from ethylene oxide and excess $^{15}NH_3$ is uneconomic since the yield is low, the product cannot be readily separated from ethanolamine and triethanolamine, and the intermediate 2,2′-dichlorodiethylamine is unstable and difficult to handle. Therefore we have developed the new method shown in Scheme 1, which uses [$^{15}$N]glycine as starting material. The trityl group was used to protect the amino group throughout the synthesis. Amidation of [$^{15}$N]tritylglycine with $^{15}NH_3$ afforded [$^{15}N_2$]tritylglycinamide, which was then reduced to [$^{15}N_2$]monotritylethylenediamine by $LiAlH_4$. 1-([$^{15}$N]Tritylglycyl)-2-([$^{15}N_2$]trityl)ethylenediamine was obtained as a condensation product from [$^{15}N_2$]monotritylethylenediamine and [$^{15}$N]tritylglycine. After reduction and cleavage of the protecting group, the hydrochloride salt of [$^{15}N_3$]dien was obtained in 20% overall yield based on [$^{15}$N]glycine. Full details of the synthesis will be published elsewhere.




**Scheme 1** *Reagents and conditions*: i, TrCl, Tr = Trityl, Pr$^i$OH–$H_2O$, room temp.; ii, ethyl chloroformate, $^{15}NH_3$, $CHCl_3$, room temp.; iii, $LiAlH_4$, thf, room temp.; iv, ethyl chloroformate, $^{15}$N-tritylglycine, $CHCl_3$, room temp.; v, $LiAlH_4$, thf, 75 °C; vi, 4.8 M HCl, reflux

The platinum complex [Pt([$^{15}N_3$]dien)Cl]Cl was prepared according to the literature method for the unlabelled complex.[7] The two-dimensional [$^1$H,$^{15}$N] HSQC NMR spectrum of a fresh solution (*i.e*. prior to hydrolysis) of [Pt([$^{15}N_3$]dien)Cl]$^+$ **1** in $H_2O$–$D_2O$ (9 : 1) showed three sets of cross-peaks at δ 5.23/−33.9, 5.02/−33.9 and 6.65/8.13 (see Fig. 1). On the basis of their shifts,[8] the former two peaks can be assigned to non-equivalent protons on the two $NH_2$ groups, and the latter to the NH group.

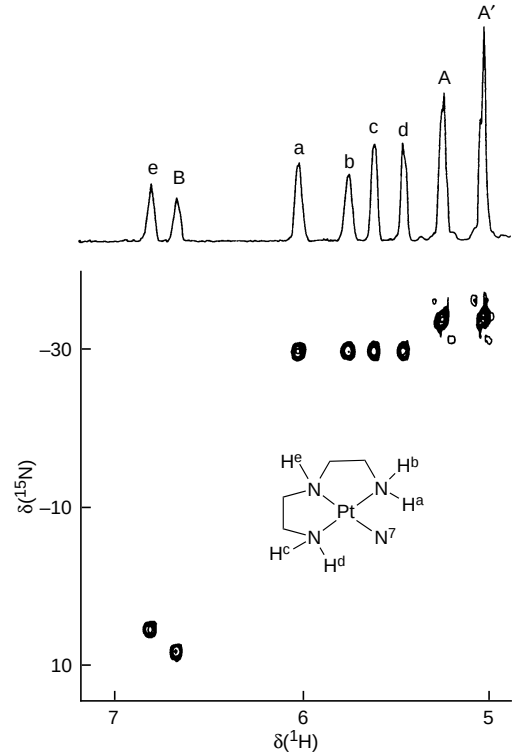


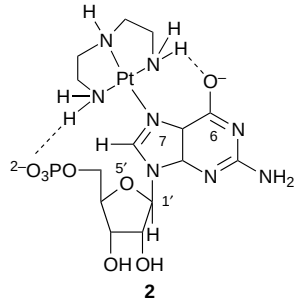

**Fig. 1** Reaction of [Pt([$^{15}N_3$]dien)Cl]$^+$ **1** with 5′-GMP. This two-dimensional [$^1$H,$^{15}$N] HSQC NMR spectrum was recorded 1.2 h after mixing and shows $NH_2$ and NH peaks for complex **1** labelled **A**, **A′** and **B**, respectively, and for the GMP adduct **2** labelled **a**–**e** (all five NH protons are non-equivalent). After 12 h the reaction was complete and only peaks for **2** were observable. The large downfield shift of peak **a** is notable. $^{195}$Pt satellites in both the $^1$H and $^{15}$N dimensions are evident for complex **1** but not for **2** (satellites broaden with increases in molecular size and chemical shift anisotropy). *Conditions*: mol ratio Pt : GMP 0.8 : 1 (5 mM), $H_2O$–$D_2O$ (9 : 1), pH 6.83, 298 K.

As an initial model for DNA binding, we studied the adduct formed from the reaction of 5′-GMP with **1** (5 mM, 1 : 1 mol ratio) at pH 6.8, 298 K. The two-dimensional spectrum after 1.2 h of reaction is shown in Fig. 1, where peaks assignable to the starting material **1** and to the product [Pt([$^{15}N_3$]dien)(GMP-*N*$^7$)]$^{2+}$ **2** are well resolved. Most notable is the presence of five cross-peaks for **2** showing that all the NH protons are magnetically non-equivalent. This might be expected in view of the chirality of the bound nucleotide. In order to understand the origin of the low-field shifts of the peaks for **2**, their pH dependence was studied over the range pH 3–11. There was little change in the $^1$H,$^{15}$N shift of peak **e** assigned to the central NH group over the range pH 3–9.5, but above this pH it broadened and disappeared, probably due to an increased exchange rate. The behaviour of the $NH_2$ peaks **a**, **b**, **c** and **d** is shown in Fig. 2. All four peaks show two-step titrations with p$K_a$ values of 5.58 and 8.54 (averages for peaks **a** and **c**). The shift changes for peaks **a** and **c** are much larger than those for peaks **b** and **d**.

The two p$K_a$ values can be associated with deprotonation of the 5′-phosphate (5.58) and the N$^1$H group (8.54) of coordinated 5′-GMP in **2**. For comparison, the phosphate p$K_a$ value for [Pt(en)(5′-GMP)$_2$]$^{2+}$ is 0.38 units lower than the value for free 5′-GMP (6.20) indicative of the presence of Pt–NH···ℑ-phosphate hydrogen bonding.[5] There are previous reports that the p$K_a$ of N$^1$H of guanine (*ca*. 9.5) is lowered by *ca*. 0.9–1.3 when guanine derivatives are coordinated to Pt$^{II}$ *via* N$^7$.[9] The large low-field PtNH$_2$ $^1$H NMR shifts observed for complex **2** (peaks **a** and **c**) on deprotonation of the N$^1$H group of bound GMP are intriguing since these PtNH$_2$ protons appear to be far away from N$^1$. This can be explained by an increase in the strength of hydrogen bonding between PtNH$_2$ and the C$^6$ carbonyl group due to an increase in electron density at C$^6$O on deprotonation of N$^1$. It is assumed that there is free rotation about Pt–N$^7$ and therefore both $NH_2$ groups are involved in hydrogen bonding. Keto–enol tautomerism could increase the negative charge on C$^6$O, as illustrated in the structure presented for complex **2**. Such hydrogen bonding involving C$^6$O has been found to play a role in determining the structure of Pt am(m)ine nucleotide complexes in the crystalline state, occurring for example in [Pt(dien){AGA-*N*$^7$(2)}],[10] but evidence for its presence in solution has previously proved difficult to obtain. The present data appear to provide evidence for such interactions at pH values close to those of biological relevance. Related NH···carbonyl interactions have been reported to play a major role in the stabilization of ternary complexes of zinc(II) cyclen complexes with thymine derivatives.[11]

The methods described here should also readily allow studies of chelate ring-opening reactions of [Pt([$^{15}N_3$]dien)]$^{2+}$ complexes. These have been the subject of much recent interest.[12] It is notable from our preliminary work that complex **2** showed no evidence for ring opening at pH 3.

We thank the Association for International Cancer Research, Biomolecular Sciences programme of the EPSRC and BBSRC, and EC HCM (ERBCHRXCT920016) and COST (D1-92/0002) programmes for their support for this work, and the MRC and ULIRS for the provision of NMR facilities.




**2**

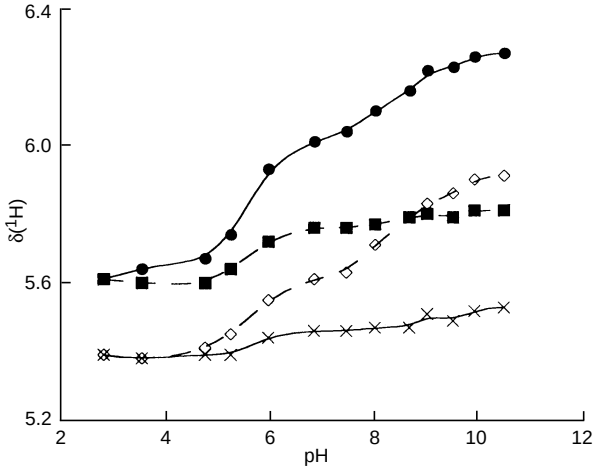



**Fig. 2** Dependence of the NH $^1$H NMR chemical shifts of complex **2** [Pt([$^{15}N_3$]dien)(5′-GMP-*N*$^7$)]$^{2+}$ on pH; peak **a** (●), **b** (■) **c** (◇), **d** (×). The large downfield shifts of two of the resonances between pH 5 and 7 can be associated with deprotonation of the 5′-phosphate group, and between 7 and 9 with deprotonation of N$^1$H of GMP. Little shift of peak **e** (Fig. 1) was observed over this pH range.

## Footnote

† Present address: Department of Chemistry, The University of Edinburgh, King's Buildings, West Mains Road, Edinburgh, UK EH9 3JJ.

## References

1 F. Gonnet, F. Reeder, J. Kozelka and J.-C. Chottard, *Inorg. Chem*., 1996, **35**, 1653; F. Gonnet, F. Reeder, J. Kozelka and J.-C. Chottard, *Chem. Eur. J*., 1996, **2**, 1068.
2 K. J. Barnham, S. J. Berners-Price, T. A. Frenkiel, U. Frey and P. J. Sadler, *Angew. Int., Ed. Ed. Engl*., 1995, **34**, 1874; S. J. Berners-Price, K. J. Barnham, U. Frey and P. J. Sadler, *Chem. Eur. J*., 1996, **2**, 1283.
3 V. Brabec, V. Boudny and Z. Balcarova, *Biochemistry*, 1994, **33**, 1316.
4 J. Reedijk, *Inorg. Chim. Acta*, 1992, **198–200**, 873.
5 S. J. Berners-Price, J. D. Ranford, U. Frey and P. J. Sadler, *J. Am. Chem. Soc*., 1993, **115**, 9285; S. J. Berners-Price, J. D. Ranford and P. J. Sadler, *Inorg. Chem*., 1994, **33**, 5842.
6 F. G. Mann, *J. Chem. Soc*., 1934, 461.
7 G. Annibale, M. Brandolisio and B. Pitteri, *Polyhedron*, 1995, **14**, 451.
8 S. J. Berners-Price and P. J. Sadler, *Coord. Chem. Rev*., 1996, **151**, 1.
9 K. Inagaki and Y. Kidani, *J. Inorg. Biochem*., 1979, **11**, 39; J.-C. Chottard, J.-P. Girault, G. Chottard, J.-Y. Lallemand and D. Mansuy, *J. Am. Chem. Soc*., 1980, **102**, 5565; J.-P. Girault, G. Chottard, J.-Y. Lallemand and J.-C. Chottard, *Biochemistry*, 1982, **21**, 1355; G. Schröder, B. Lippert, M. Sabat, C. J. L. Lock, R. Faggiani, B. Song and H. Sigel, *J. Chem. Soc., Dalton Trans*., 1995, 3767.
10 G. Admiraal, M. Alink, C. Altona, F. J. Dijt, C. J. van Garderen, R. A. G. de Graff and J. Reedijk, *J. Am. Chem. Soc*., 1992, **114**, 930.
11 M. Shionoya, E. Kimura and M. Shiro, *J. Am. Chem. Soc*., 1993, **115**, 6730; M. Shionoya, T. Ikeda, E. Kimura and M. Shiro, *J. Am. Chem. Soc*., 1994, **116**, 3848.
12 See for example, M. Mikola, J. Vihanto and J. Arpalahti, *J. Chem. Soc., Chem. Commun*., 1995, 1759.

*Received, 11th September 1996; Com. 6/06275J*

# Catalysis by calcium ion of the reoxidation of reduced PQQ by molecular oxygen

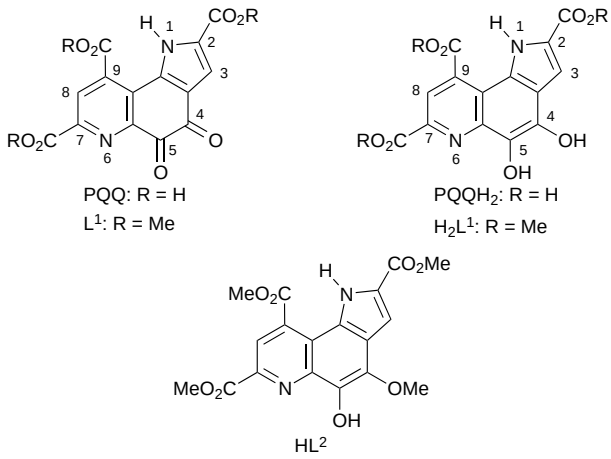
**Shinobu Itoh,* Hirokatsu Kawakami and Shunichi Fukuzumi***

*Department of Applied Chemistry, Faculty of Engineering, Osaka University, 2-1 Yamada-oka, Suita, Osaka 565, Japan*

**Reoxidation of reduced PQQ to the quinone by molecular oxygen is enhanced drastically by $Ca^{2+}$, the interaction of which has been recently demonstrated to exist in the enzyme active site by the X-ray crystallographic analysis of quinoprotein methanol dehydrogenase.**

PQQ (pyrroloquinolinequinone) is a novel coenzyme that was first isolated and identified from bacterial methanol dehydrogenases (MDH, E.C. 1.1.99.8) in 1979.[1] This coenzyme is the redox centre of MDH that catalyses the oxidation of methanol to formaldehyde and donates two electrons to a c-type cytochrome in biological systems.[2] Recently, the crystal structure of MDH from methylotrophic bacteria has been determined by two independent research groups to provide full particulars of the enzyme active centre. According to the reported X-ray structure, there is one calcium ion strongly bound to PQQ through its C-5 quinone carbonyl oxygen, N-6 pyridine nitrogen, and C-7 carboxylate group in the enzyme active site.[3,4]† In this context, we have recently demonstrated that the oxidation of methanol to formaldehyde by coenzyme PQQ is promoted significantly by $Ca^{2+}$, providing valuable insight into the role of $Ca^{2+}$ in the enzymatic alcohol-oxidation mechanism.[5] On the other hand, however, very little is known about the catalytic role of $Ca^{2+}$ in the reoxidation process of reduced PQQ. Here, we report that $Ca^{2+}$ also enhances the oxidation of reduced PQQ to the quinone by molecular oxygen, providing further information on the catalytic function of $Ca^{2+}$ in the enzymatic redox reactions.

The trimethyl ester of reduced PQQ in the quinol form ($H_2L^1$, $2.5 \times 10^{-5}$ mol dm$^{-3}$)[6] is oxidised by molecular oxygen very slowly in anhydrous acetonitrile (MeCN) as shown in Fig. 1 (line *a* in the inset). Addition of $Ca^{2+}$ ($8.2 \times 10^{-3}$ mol dm$^{-3}$) into the $O_2$-saturated MeCN solution of $H_2L^1$ results in significant acceleration of the oxidation rate (line *b* in the inset of Fig. 1). The absorbance at $\lambda_{max}$ = 326 nm due to $H_2L^1$ decreases accompanied by the increase in absorbance due to the quinone $L^1$ (Fig. 1). Quantitative formation of $H_2O_2$ in the final reaction mixture has been confirmed by iodometric titration using NaI. Rates of the reaction of $H_2L^1$ and $O_2$ in the presence of various concentrations of $Ca^{2+}$ in MeCN at 298 K were determined by monitoring the decrease in absorbance at $\lambda_{max}$ = 326 nm due to $H_2L^1$. The rates obeyed pseudo-first-order kinetics in the presence of a large excess of $O_2$ ($1.3 \times 10^{-2}$ mol dm$^{-3}$) and the observed pseudo-first-order rate constant ($k_{obs}$) increases with an increase in [$Ca^{2+}$] to exhibit first-order dependence on [$Ca^{2+}$] at low concentrations, changing to second-order dependence at high concentrations, as shown in Fig. 2.



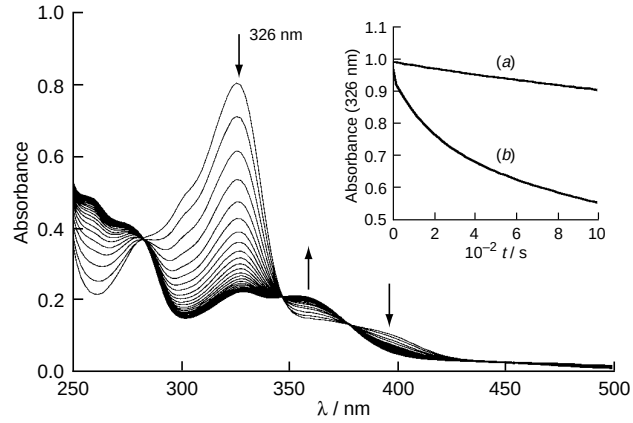




**Fig. 1** Spectral changes observed in the oxidation of $H_2L^1$ ($2.5 \times 10^{-5}$ mol dm$^{-3}$) by $O_2$ ($1.3 \times 10^{-2}$ mol dm$^{-3}$) in the presence of $Ca(ClO_4)_2$ ($8.2 \times 10^{-3}$ mol dm$^{-3}$) in $O_2$-saturated MeCN containing 0.8% $Me_2SO$ at 298 K. Inset: time course of the reaction followed at $\lambda$ = 326 nm under an $O_2$ atmosphere (*a*) in the absence and (*b*) in the presence of $Ca(ClO_4)_2$ ($1.0 \times 10^{-3}$ mol dm$^{-3}$) at 298 K.

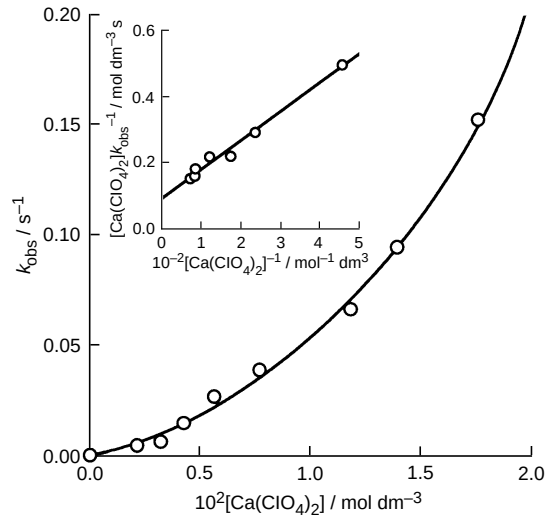
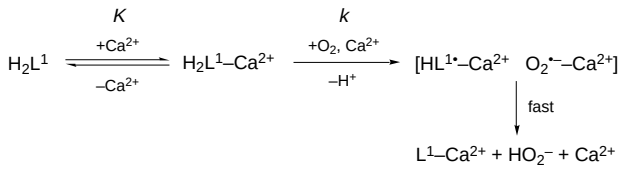



**Fig. 2** Plot of $k_{obs}$ *vs.* [$Ca(ClO_4)_2$] for the oxidation of $H_2L^1$ ($2.5 \times 10^{-5}$ mol dm$^{-3}$) by $O_2$ ($1.3 \times 10^{-2}$ mol dm$^{-3}$) in the presence of $Ca(ClO_4)_2$ in $O_2$-saturated MeCN containing 0.8% $Me_2SO$ at 298 K. Inset: plot of [$Ca^{2+}$]$k_{obs}^{-1}$ *vs.* [$Ca^{2+}$]$^{-1}$ for the reaction.

Addition of $Ca(ClO_4)_2$ to a deaerated MeCN solution of $H_2L^1$ results in a decrease in absorbance at $\lambda_{max}$ = 326 nm due to $H_2L^1$ accompanied by an increase in absorbance at $\lambda_{max}$ = 350 nm due to the $Ca^{2+}$ complex of a reduced species with a clear isosbestic point at 344 nm as the concentration of $Ca(ClO_4)_2$ is raised. From such a spectral change, one can obtain the 1 : 1 complex formation constant $K$ as $1.0 \times 10^2$ mol$^{-1}$ dm$^3$ using the relation $(A - A_0)/(A_\infty - A) = K[Ca^{2+}]$, where $A_0$ is the absorbance of $H_2L^1$ itself and $A_\infty$ is the absorbance of the $Ca^{2+}$ complex. Essentially the same spectral change was observed for 4-methoxy-substituted derivative $HL^2$ in the titration with $Ca(ClO_4)_2$ in deaerated MeCN, from which the $K$ value was determined as $1.1 \times 10^2$ dm$^3$ mol$^{-1}$.

Since the direct reaction with $O_2$ to give a covalent bond is spin forbidden, it has been proposed that the reaction of 1,5-dihydroflavin with $O_2$ occurs *via* an electron-transfer mechanism, resulting in a radical-ion pair, which collapses to form the covalent flavin-4*a*-hydroperoxide after spin conversion.[7,8] In this context, we have recently demonstrated that $Mg^{2+}$ catalyses the electron transfer step from 1,5-dihydroflavin anion to $O_2$ *via* the complex formation of $O_2^{\cdot-}$ and $Mg^{2+}$ to accelerate the overall two-electron oxidation of 1,5-dihydroflavin anion.[9] Thus, $Ca^{2+}$ may also catalyse the electron transfer step from $H_2L^1$ to $O_2$. The contribution of the second-order dependence of $k_{obs}$ on $[Ca^{2+}]$ in Fig. 2 indicates that the $H_2L^1$–$Ca^{2+}$ complex is a reactive electron donor rather than free $H_2L^1$ as shown in Scheme 1. The electron transfer from $H_2L^1$–$Ca^{2+}$ to $O_2$ is catalysed by $Ca^{2+}$ *via* the complex formation of $O_2^{\cdot-}$ and $Ca^{2+}$ as in the case of the $Mg^{2+}$-catalysed oxidation of 1,5-dihydroflavin anion.[9] The electron transfer may be accompanied with deprotonation and followed by fast hydrogen atom transfer to yield $H_2O_2$.

According to Scheme 1, the dependence of $k_{obs}$ on $[Ca^{2+}]$ is derived as $k_{obs} = kK[Ca^{2+}]^2[O_2]/(1 + K[Ca^{2+}])$, where $K$ is the complex formation constant of $H_2L^1$ with $Ca^{2+}$ and $k$ is the rate constant of the $Ca^{2+}$-catalysed oxidation of the reduced form by $O_2$ *via* formation of 1 : 1 complex between $O_2^{\cdot-}$ and $Ca^{2+}$. The kinetic equation can be rewritten as $[Ca^{2+}]k_{obs}^{-1} = (k[O_2])^{-1}[1 + (K[Ca^{2+}])^{-1}]$, where $[Ca^{2+}]k_{obs}^{-1}$ is linearly related to $[Ca^{2+}]^{-1}$. A linear plot of $[Ca^{2+}]k_{obs}^{-1}$ *vs.* $[Ca^{2+}]^{-1}$ is shown in the inset of Fig. 2. From the slope and intercept are obtained the rate constant $k = 8.6 \times 10^2$ dm$^3$ mol$^{-1}$ s$^{-1}$ and the complex formation constant $K = 1.0 \times 10^2$ dm$^3$ mol$^{-1}$. The $K$ value thus obtained agrees perfectly with the $K$ value ($1.0 \times 10^2$ dm$^3$ mol$^{-1}$) determined independently from the titration. Such an excellent agreement supports the validity of Scheme 1, where the $H_2L^1$–$Ca^{2+}$ complex is a reactive species for the oxidation by $O_2$. The spectral changes due to the formation of the $H_2L^1$–$Ca^{2+}$ and $HL^2$–$Ca^{2+}$ complexes are similar to that observed in the pH titration of $PQQH_2$ to $PQQH^-$.[6] Since the $K$ value of $H_2L^1$ is about the same as that of $HL^2$ (*vide supra*), the binding position of $Ca^{2+}$ with $H_2L^1$ and $HL^2$ may be the same. Thus, the coordination of $Ca^{2+}$ may occur to the hydroxy oxygen at the 5 position as well as the pyridine nitrogen at the 6 position, facilitating the deprotonation of C(5)–OH proton to produce a much stronger electron donor than free $H_2L^1$. This may be the reason why the $H_2L^1$–$Ca^{2+}$ complex acts as a reactive electron donor in the $Ca^{2+}$-catalysed electron transfer to $O_2$ (Scheme 1).




**Scheme 1**

The present study was financially supported in part by a Grant-in-Aid for Scientific Research on Priority Area (08249223) and a Grant-in-Aid for General Scientific Research (08458177) from the Ministry of Education, Science, Sports, and Culture of Japan. We also thank Takeda Science Foundation for financial support.

## Footnote

† The presence of $Ca^{2+}$ in the enzyme active site has been also suggested for other PQQ-dependent enzymes such as ethanol dehydrogenase from *Pseudomonas aeruginosa* and glucose dehydrogenase from *Acinetobacter calcoaceticus*, see ref. 10.

## References

1 S. A. Salisbury, H. S. Forrest, W. B. T. Cruse and O. Kennard, *Nature*, 1979, **280**, 843.
2 C. Anthony, M. Ghosh and C. C. F. Blake, *Biochem. J.*, 1994, **304**, 665 and references therein.
3 S. A. White, G. D. Boyd, F. S. Mathews, Z.-X. Xia, W.-W. Dai, Y.-F. Zhang and V. L. Davidson, *Biochemistry*, 1993, **32**, 12 955; Z.-X. Xia, W.-W. Dai, Y.-F. Zhang, S. A. White, G. D. Boyd and F. S. Mathews, *J. Mol. Biol.*, 1996, **259**, 480.
4 C. C. F. Blake, M. Ghosh, K. Harlos, A. Avezoux and C. Anthony, *Nature Struct. Biol.*, 1994, **1**, 102; M. Ghosh, C. Anthony, K. Harlos, M. G. Goodwin and C. Blake, *Structure*, 1995, **3**, 177.
5 S. Itoh, H. Kawakami and S. Fukuzumi, *J. Am. Chem. Soc.*, in contribution.
6 $PQQTMEH_2$ was synthesised according to the reported procedure: S. Itoh, Y. Ohshiro and T. Agawa, *Bull. Chem. Soc. Jpn*., 1986, **59**, 1911.
7 C. Kemal, T. W. Chan and T. C. Bruice, *J. Am. Chem. Soc*., 1977, **99**, 7272; E. J. Nanni Jr., D. T. Sawyer, S. S. Ball and T. C. Bruice, *J. Am. Chem. Soc*., 1981, **103**, 2797; G. Eberlein and T. C. Bruice, *J. Am. Chem. Soc*., 1982, **104**, 1449; 1983, **105**, 6685.
8 K. Maeda-Yorita and V. Massey, *J. Biol. Chem.*, 1993, **268**, 4134.
9 S. Fukuzumi and T. Okamoto, *J. Chem. Soc., Chem. Commun*., 1994, 521.
10 A. Mutzel and H. Görisch, *Agric. Biol. Chem.*, 1991, **55**, 1721; O. Geiger and H. Görisch, *Biochem. J*., 1989, **261**, 415.

*Received, 7th October 1996; Com. 6/06842A*

# An air-stable, primary alkylphosphine: $FcCH_2PH_2$ [Fc = $(\eta^5\text{-}C_5H_5)Fe(\eta^5\text{-}C_5H_4)$]

**Nicholas J. Goodwin, William Henderson*† and Brian K. Nicholson**

*Department of Chemistry, University of Waikato, Private Bag 3105, Hamilton, New Zealand*

**Sodium metabisulfite-mediated elimination of formaldehyde from the ferrocene-derived hydroxymethylphosphine $FcCH_2P(CH_2OH)_2$ yields the primary phosphine $FcCH_2PH_2$, which has been fully characterised, including an X-ray crystal structure; the phosphine is completely air-stable.**

Phosphine ligands containing ferrocene moieties are attracting interest for their coordination chemistry,[1] with significant recent emphasis on applications of metal complexes of chiral ferrocenylphosphines in asymmetric catalysis.[2] In a recent communication[3] we described the synthesis of the air-stable, crystalline hydroxymethylphosphine $FcCH_2P(CH_2OH)_2$ **1** from readily accessible $FcCH_2NMe_3^+I^-$ and $P(CH_2OH)_3$, and reasoned that this compound should be a versatile precursor for the synthesis of a wide range of other ferrocene-derived phosphines. Here we report that **1** can be used to synthesise the remarkably air-stable, crystalline primary alkylphosphine $FcCH_2PH_2$ **2**.

Reaction of **1** with 1 mol equiv. of aqueous sodium metabisulfite was carried out in a two-phase aqueous–light petroleum (bp 60–80 °C) mixture, at reflux. $FcCH_2PH_2$ **2** was isolated from the light petroleum layer in 60% yield. It is particularly noteworthy that this reaction may be carried out in air; indeed the use of an inert (dinitrogen) atmosphere provides no significant increase in yield or purity of the product. The synthesis of **2** demonstrates the use of $P(CH_2OH)_3$ as a masked, easily handled $PH_3$ equivalent. Orange crystals of **2**, of analytical purity,‡ and suitable for a single-crystal X-ray structure determination,§ were obtained by sublimation of the product *in vacuo*, onto a water-cooled coldfinger.

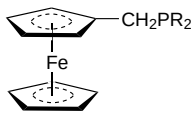
The molecular structure, shown in Fig. 1 together with selected bond distances and angles, unambiguously confirms **2** as the primary phosphine. Examination of the Cambridge Crystallographic Database[4] indicates that only two other X-ray structure determinations of free primary phosphines have been reported previously.[5] The P–C bond distance of **2**, 1.850(3) Å, is identical within experimental error to the P–C bond lengths calculated (1.8574 Å)[6] and measured by electron diffraction (1.858 ± 0.003 Å)[7] for $PH_2Me$.

The $^{31}P$ NMR spectrum ($CDCl_3$) of **2** shows a resonance at δ −129, showing a large $^1J$(PH) coupling of 194 Hz in the proton-coupled spectrum. This chemical shift is comparable with those of other primary phosphines, which give $^{31}P$ NMR resonances in the region δ −110 to −160.[8] The positive-ion electrospray mass spectrum (1 : 1 MeCN–$H_2O$) yielded the oxidised ion $\mathbf{2}^+$, as observed for other (low-basicity) ferrocene-derived species.[9]

Primary phosphines are typically highly air-sensitive; many derivatives, particularly those containing lower alkyl groups, are pyrophoric. Only a very small number of primary phosphines are known to us to have been reported as air-stable,[10] including other sterically unhindered primary phosphines of the type $[RR'_2N(CH_2)_nPH_2]I$.[11] Phosphine **2** appears to be completely air-stable both in the solid and solution states. The reasons for this are not immediately obvious, but the inclusion of the redox-active ferrocenyl group may be important in kinetically stabilising the phosphine towards oxidation. The structure of **2** shows that the $PH_2$ group is directed away from the Fe atom so there is no intramolecular interaction which would account for its lack of susceptibility to oxidation. After exposure of solid **2** to air at room temp. for 48 days no oxidation products could be detected by $^{31}P$ NMR.

In view of the air-stability of **2**, it was of interest to see whether it possessed typical ligand properties towards transition-metal centres. Preliminary studies suggest that the coordination chemistry of **2** is not significantly compromised by the factors that lead to its air-stability, since the *cis*-$[Mo(CO)_4(\mathbf{2})_2]$ complex **3** can be prepared by the thermal reaction of $Mo(CO)_6$ with **2** in decalin at 100 °C. Complex **3**, which is also air-stable, has been characterised by NMR spectroscopy ($^{31}P\{^1H\}$ NMR, $CDCl_3$, $\delta_P$ −63.2], electrospray mass spectrometry (negative-ion mode in MeOH with added NaOMe; $[M - H]^-$ at *m/z* 673), and by a single-crystal X-ray diffraction study, full details of which will be published separately.

The method of formaldehyde abstraction from **1** can also be extended to the synthesis of the secondary phosphine $FcCH_2PH(CH_2OH)$ **4**, when 0.5 mol equiv. of sodium metabisulfite is used. This phosphine is readily characterised by the doublet resonance [$^1J$(PH) 205 Hz] observed in the proton-coupled $^{31}P$ NMR spectrum at δ −50.7. In contrast to **2**, phosphine **4** cannot be readily sublimed under the same conditions, the lower volatility of **4** being presumably due to the presence of relatively strong hydrogen bonding involving the hydroxymethyl group. However, it is worth noting that the attempted conversion of **1** to **2** by pyrolysis (dynamic vacuum, 120 °C, < 0.05 mmHg) led to sublimation of mainly unreacted **1**, together with some **2** and **4**.




**1** R = $CH_2OH$
**2** R = H

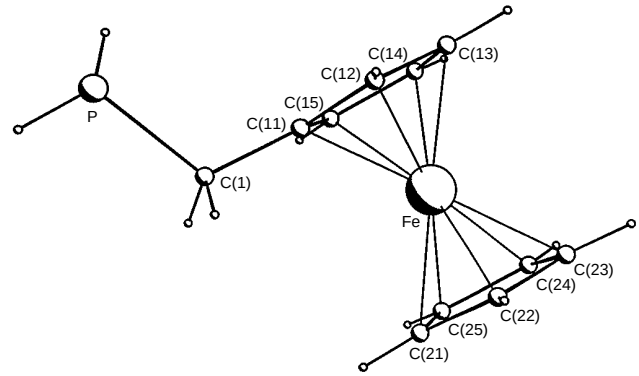



**Fig. 1** Molecular structure of $FcCH_2PH_2$ **2**, with atom numbering scheme. Selected bond lengths (Å) and angles (°): C(11)–C(1) 1.492(4), C(1)–P 1.850(3), Fe–C 2.022(3)–2.042(2), av. 2.035 Å; C(11)–C(1)–P 113.7(2).

In summary, the simplicity of synthesis and ease of handling of **2** make it ideal for studying the reactivity of a primary phosphine. The inclusion of the ferrocene centre will permit the ready development of organophosphine derivatives having excellent redox properties.

We thank the University of Waikato and the New Zealand Lottery Grants Board for financial support, Albright & Wilson Ltd., UK for a gift of $P(CH_2OH)_4Cl$, Professor Ward Robinson (Univerisity of Canterbury) for the X-ray data sets, and Professor Alistair Wilkins (University of Waikato) for GC–MS data. N. J. G. thanks the William Georgetti Trust for a scholarship.

## Footnotes

† E-mail: w.henderson@waikato.ac.nz

‡ Anal. (after sixty-one days storage of sample in air). Found: C, 57.07; H, 5.52. Calc. for $C_{11}H_{13}FeP$: C, 56.94; H, 5.65%. Mp. 44–46 °C.

§ *Crystal data* for **2**: $C_{11}H_{13}FeP$, $M_r$ = 232.04; monoclinic, space group $P2_1/c$, $a$ = 13.7111(9), $b$ = 7.5225(5), $c$ = 10.5662(7) Å, β = 107.448(5)° $U$ = 1039.7(1) Å$^3$, $D_c$ = 1.482 g cm$^{-3}$ for $Z$ = 4. $F$(000) = 480, μ(Mo-Kα) = 1.29 mm$^{-1}$, λ = 0.71073 Å, $T$ = −105 °C, crystal size = 0.52 × 0.44 × 0.24 mm. A total of 3190 reflections were collected using ω scans with 4 < 2θ < 60°. Of these 3032 were unique ($R_{merge}$ = 0.0279 after absorption correction applied, based on ψ scans, $T_{min,max}$ 0.403, 0.558). The structure was solved by direct methods and developed routinely. Full-matrix least-squares refinement was based on $F^2$, with all non-hydrogen atoms anisotropic and with hydrogen atoms (except for P–H hydrogens) included in calculated positions with isotropic temperature factors 1.2 times that of the $U_{iso}$ of the atom to which they are bonded. A penultimate electron density map showed two peaks which could be assigned to the H atoms on the P. These were included in fixed positions in the final refinement cycles. The refinement converged at $R_1$ = 0.0411 [for 2407 reflections with ($I$) > 2σ($I$)] and $wR_2$ = 0.1235 (all data) {$w$ = [σ$^2$($F_o^2$) + (0.0525$P$)$^2$ + 0.81$P$]$^{-1}$ where $P$ = [max($F_o^2$,0) + 2$F_c^2$/3]; final GOF = 1.032. The final difference map showed no peak greater than +0.639 e Å$^{-3}$ and no hole larger than −0.454 e Å$^{-3}$. Programs used were SHELXS-86[12] and SHELXL-93.[13] Atomic coordinates, bond lengths and angles, and thermal parameters have been deposited at the Cambridge Crystallographic Data Centre (CCDC). See Information for Authors, Issue No. 1. Any request to the CCDC for this material should quote the full literature citation and the reference number 182/302.

## References

1 For selected recent references, see: K.-S. Gan and T. S. A. Hor, *Ferrocenes*, ed. A. Togni and T. Hayashi, VCH, Weinheim, 1995, p. 1; I. R. Butler, M. Kalaji, L. Nehrlich, M. Hursthouse, A. I. Karaulov and K. M. A. Malik, *J. Chem. Soc., Chem. Commun*., 1995, 459.

2 A. Mernyi, C. Kratky, W. Weissensteiner and M. Widhalm, *J. Organomet. Chem*., 1996, **508**, 209; J. M. Brown, *Chem. Soc. Rev*., 1993, 25; O. Reiser, *Angew. Chem., Int. Ed. Engl*., 1993, **32**, 547; M. Sawamura and Y. Ito, *Chem. Rev*., 1992, **92**, 857; N. C. Zanetti, F. Spindler, J. Spencer, A. Togni and G. Rihs, *Organometallics*, 1996, **15**, 860; P. Barbaro and A. Togni, *Organometallics*, 1995, **14**, 3570; H. C. L. Abbenhuis, U. Burckhardt, V. Gramlich, C. Köllner, P. S. Pregosin, R. Salzmann and A. Togni, *Organometallics*, 1995, **14**, 759; M. Sawamura, H. Hamashima, M. Sugawara, R. Kuwano and Y. Ito, *Organometallics*, 1995, **14**, 4549.

3 N. J. Goodwin, W. Henderson and J. K. Sarfo, *Chem. Commun*., 1996, 1551.

4 April 1996 Release, F. H. Allen, J. E. Davies, J. J. Galloy, O. Johnson, O. Kennard, C. F. Macrae, E. M. Mitchell, G. F. Mitchell, J. M. Smith and D. G. Watson, *J. Chem. Inf. Comput. Sci*., 1991, **32**, 187.

5 R. A. Bartlett, M. M. Olmstead, P. P. Power and G. A. Sigel, *Inorg. Chem*., 1987, **26**, 1941; J. Wesemann, P. G. Jones, D. Shomburg, L. Heuer and R. Schmutzler, *Chem. Ber*., 1992, **125**, 2187.

6 P. C. Fox, J. P. Bowen and N. L. Allinger, *J. Am. Chem. Soc*., 1992, **114**, 8536.

7 L. S. Bartell, *J. Chem. Phys*., 1960, **32**, 832.

8 K. Dixon, in *Multinuclear NMR*, ed. J. Mason, Plenum Press, New York and London, 1987.

9 W. Henderson, A. G. Oliver and A. L. Downard, *Polyhedron*, 1996, **15**, 1165; X. Xu, S. P. Nolan and R. B. Cole, *Anal. Chem*., 1994, **66**, 119.

10 A. H. Cowley, J. E. Kilduff, T. H. Newman and M. Pakulski, *J. Am. Chem. Soc*., 1982, **104**, 5820; see also M. Yoshifuji, K. Shibayama, N. Inamoto, T. Matsushita and K. Nishimoto, *J. Am. Chem. Soc*., 1983, **105**, 2495.

11 D. J. Brauer, J. Fischer, S. Kucken, K. P. Langhans, O. Stelzer and N. Weferling, *Z. Naturforsch., Teil B*, 1994, **49**, 1511.

12 G. M. Sheldrick, SHELXS-86, Program for solving crystal structures, University of Göttingen, 1986.

13 G. M. Sheldrick, Program for refining crystal structures, University of Göttingen, 1993.

*Received, 25th September 1996; Com. 6/06580E*

# $NMe_4V_3O_7$: critical role of pH in hydrothermal synthesis of vanadium oxides

**Thomas G. Chirayil, Elizabeth A. Boylan, Marc Mamak, Peter Y. Zavalij and M. Stanley Whittingham*†**

*Chemistry Department and Materials Research Center, State University of New York at Binghamton, Binghamton, NY, 13902, USA*

**pH is critical in the formation of new mixed-valence vanadium oxides, $NMe_4V_3O_7$, $NMe_4V_4O_{10}$ and the dioxide $Li_xV_2O_4{\cdot}H_2O$, with $NMe_4^+$ cations or water molecules residing between vanadium oxide layers.**

In the last few years there has been much effort placed on the synthesis of new transition-metal oxides that might be active hosts for intercalation reactions. There is particular interest in oxides that react readily with lithium and might find application as cathodes in advanced lithium batteries.[1] Reis *et al*.[2] built on the pioneering work of Gunter *et al*.[3] and showed that two different tungsten oxides could be formed by hydrothermal reaction, and that pH controlled the phase formed. Subsequently, Guo *et al*.[4] expanded this work to molybdenum and discovered a new layered molybdenum oxide when tetramethylammonium ions were in the reaction medium. Most recently, several new vanadium oxide structures were formed also using the tetramethylammonium ion, including a new layered vanadium dioxide and $NMe_4V_4O_{10}$, both of which contain vanadium in square pyramids.[5] These two phases have now been completely characterized.[6–8]

In a systematic study of the impact of the pH of the reaction medium on the vanadium oxides formed, we have found that a whole range of new materials are formed. In this study the reactants $V_2O_5$, $NMe_4OH$, and LiOH in a molar ratio of 1 : 2 : 1 in water were acidified with acetic acid and heated at 185 °C in a Teflon-lined Parr reactor for 3 days; typically 20 g of reactants were reacted in 70 ml of water. X-Ray diffraction of the products formed showed that at least six different phases were formed depending on the initial pH. The pH range for the products is shown in Fig. 1. At the highest pH, 10, the known $Li_3VO_4$ is formed;[9] in this structure all the metal atoms are in tetrahedral sites. As the pH is lowered the new phase $NMe_4V_3O_7$ is formed whose structure is described below. This phase is also formed in the absence of lithium ions. At a pH of *ca*. 5 the new layered vanadium dioxide compound $Li_xV_{2-\delta}O_{4-\delta}{\cdot}H_2O$ is found, as reported earlier.[5–7] Lowering the pH further leads to the formation of another tetramethylammonium vanadate, $NMe_4V_4O_{10}$ whose structure we reported recently.[5,8] At the highest acidities two new compounds are formed, both of which contain tetramethylammonium ions; they appear to have layer structures with repeat distances of 11.5 Å and 19.1 Å at pH 3.3 and 2.6 respectively. We are presently trying to determine their structures from powder diffraction data.

Crystals of the trivanadate, $NMe_4V_3O_7$, have a lath-like appearance and their structure was determined by Rietveld analysis of powder diffraction data. It is related to that recently reported for $(DABCO)V_6O_{14}$,[10,11] (DABCO = 1,4-diazabicyclo[2.2.2]octane) but has some significant differences. The structure contains zigzag strings of edge-sharing $VO_5$ square pyramids; these strings are joined together by $VO_4$ tetrahedra, as indicated schematically in Fig. 2. The structure has lattice parameters of $a$ = 18.478, $b$ = 6.552, $c$ = 8.427 Å and $\beta$ = 91.1°, in space group $P2_1/n$; $b$ is the dimension along the chain, $c$ that perpendicular to the chain but in the plane of the vanadium oxide sheet, whereas $a$ is twice the distance between the sheets. The tetramethylammonium ions reside between the vanadium oxide layers, as indicated in Fig. 3. The sheets are almost planar in direct contrast to those of the DABCO hexavanadate $C_6H_{14}N_2V_6O_{14}{\cdot}H_2O$ which are highly puckered, leading to a longer $a$ and a shorter $c$ axis, $a$ = 19.20, $c$ = 7.547 Å and $\beta$ = 111.3°, whereas the dimension along the chain remains almost unchanged, $b$ = 6.625 Å.[10] This buckling is common for vanadium oxides, being also observed for the alkali-metal vanadium oxides.

The tetramethylammonium ions are lost on heating the trivanadate to 350 °C, with loss of the structure. However, at

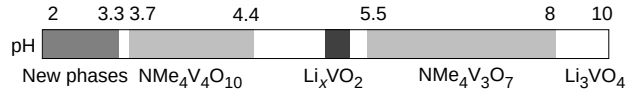



**Fig. 1** Structures formed as a function of the pH of the reaction medium

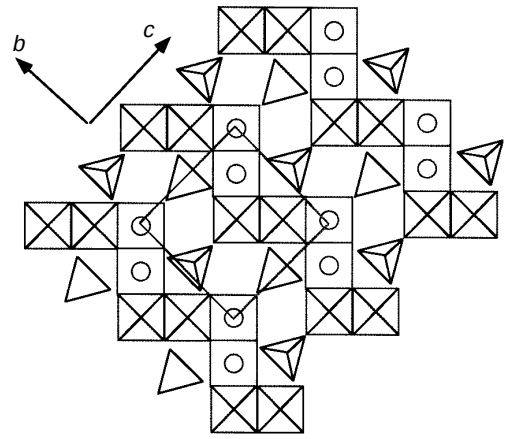



**Fig. 2** Schematic representation of the stucture of $NMe_4V_3O_7$, showing the zigzag chains of $VO_5$ square pyramids, joined together by $VO_4$ tetrahedra. The tetrahedra are shown separated from the chains for clarity. ☒ = $VO_5$ pyramid, apex up; ⊡ = $VO_5$ pyramid, apex down; ◬ = $VO_4$ tetrahedron, apex up; and △ = $VO_4$, apex down.

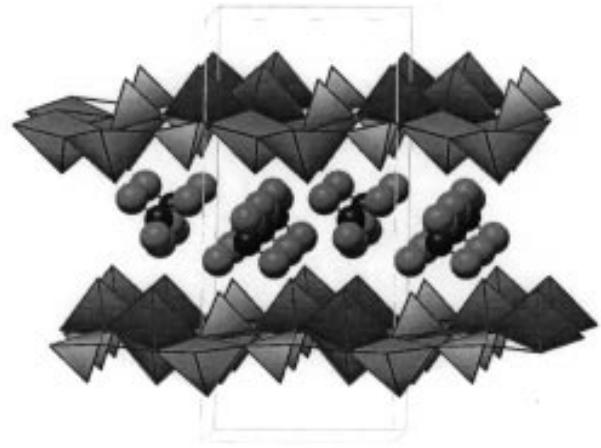


**Fig. 3** Side-view of $NMe_4V_3O_7$ looking down the $b$ axis

around 200 °C prior to the loss of the organic cations the structure takes up an additional oxygen atom to give the fully oxidized phase $NMe_4V_3O_8$. This appears to have a triclinic structure. Just like the tetravanadate, $NMe_4V_4O_{10}$, we have been unable so far to ion-exchange the tetramethyl ammonium ions out of the structure. In contrast the tetramethylammonium ions are expelled from the layered vanadium dioxide, $Li_xV_{2-\delta}O_{4-\delta}\cdot H_2O$, during synthesis; the structure is not formed in the absence of tetramethylammonium ions. This dioxide readily and reversibly undergoes dehydration and redox reactions with lithium[7] and organic molecules.

Some trends in the structures formed can be seen. $Li_3VO_4$ has all the vanadium in tetrahedral sites. As the pH is lowered the first phase formed, $NMe_4V_3O_7$, has vanadium in both tetrahedral and square-pyramidal sites. At still lower pH all the vanadium is found in square pyramids. Although the structures of the two phases formed under the most acidic conditions are not known it is probable by comparison with cluster complexes formed under similar acidic conditions that some of the vanadium will be found in octahedral sites. These cluster complexes often remain in solution during the hydrothermal reaction, and precipitate from the filtrate after standing under ambient conditions for several days; an example is $[NMe_4]_4$-$Li_2V_{10}O_{28}\cdot 12H_2O$, whose structure is also layered. It contains $V_{10}O_{28}$ clusters arranged in sheets together with $Li(H_2O)_4$ tetrahedra; the tetramethylammonium ions reside between these sheets.[12]

In conclusion, change of pH of the reaction medium in the hydrothermal synthesis of vanadium oxides results in a wide range of new structures, indicating the richness of the hydrothermal approach.[13] The first layered vanadium oxide[5] containing an organic species, $NMe_4V_4O_{10}$, has spawned a wide range of new compounds, including the dioxide $Li_xVO_2$ and $NMe_4V_3O_7$ whose structure is reported here. In addition, Nazar has recently found[14] an additional compound, $[NMe_4]_5V_{18}O_{46}$, which we have not yet seen in this investigation. Within the last year a number of other organic molecule–vanadium oxide complexes have been reported,[15] but so far only the tetramethylammonium ion has been found to form more than one structure type.

This work was supported by the National Science Foundation through grant DMR-9422667 and by the Department of Energy through Lawrence Berkeley Laboratory (Office of Transportation Technologies).

## Footnote

† E-mail: stanwhit@binghamton.edu

## References

1 *Solid State Ionics*, 1994, **69**.
2 K. P. Reis, A. Ramanan and M. S. Whittingham, *Chem. Mater.*, 1990, **2**, 219.
3 J. R. Günter, M. Amberg and H. Schmalle, *Mater. Res. Bull.*, 1989, **24**, 289.
4 J. Guo, P. Zavalij and M. S. Whittingham, *Chem. Mater.*, 1994, **6**, 357.
5 M. S. Whittingham, J. Guo, R. Chen, T. Chirayil, G. Janauer and P. Zavalij, *Solid State Ionics*, 1995, **75**, 257.
6 T. Chirayil, P. Zavalij and M. S. Whittingham, *Solid State Ionics*, 1996, **84**, 163.
7 T. Chirayil, P. Zavalij and M. S. Whittingham, *J. Electrochem. Soc.*, 1996, **143**, L193.
8 P. Zavalij, M. S. Whittingham, E. A. Boylan, V. K. Pecharsky and R. A. Jacobson, *Z. Krystallogr.*, 1996, **211**, 464.
9 R. D. Shannon and C. Calvo, *J. Solid State Chem.*, 1973, **6**, 538.
10 L. F. Nazar, B. E. Koene and J. F. Britten, *Chem. Mater.*, 1996, **8**, 327.
11 Y. Zhang, R. C. Haushalter and A. Clearfield, *Chem. Commun.*, 1996, 1055.
12 P. Zavalij, T. Chirayil, M. S. Whittingham, V. K. Pecharsky and R. A. Jacobson, *Acta Crystallogr.*, 1996, in the press.
13 M. S. Whittingham, *Curr. Op. Solid State Mater. Sci.*, 1996, **1**, 227.
14 L. F. Nazar, personal communication, 1996.
15 D. Riou and G. Férey, *J. Solid State Chem.*, 1995, **120**, 137; *Inorg. Chem.*, 1995, **34**, 6250; *J. Solid State Chem.*, 1996, **124**, 151; Y. Zhang, C. J. O'Connor, A. Clearfield and R. C. Haushalter, *Chem. Mater.*, 1996, **8**, 595.

*Received, 3rd October 1996; Com. 6/06772G*

# Changeover in a multimodal copper(II) catenate as monitored by EPR spectroscopy

**Frank Baumann,[a] Aude Livoreil,[b] Wolfgang Kaim*[a] and Jean-Pierre Sauvage*[b]**

[a] *Institut für Anorganische Chemie, Universität Stuttgart, Pfaffenwaldring 55, D-70550 Stuttgart, Germany*
[b] *Laboratoire de Chimie Organo-Minérale, URA 422 du CNRS, Institut le Bel, Université Louis Pasteur, 4, rue Blaise Pascal, 67070 Strasbourg, France*

**The electrochemically triggered rearrangement of a copper catenate is monitored by EPR spectroscopy; the initially generated tetrahedral copper(II) complex (with higher *g*-factor components and lower metal hyperfine splitting) is converted to a stable five-coordinate copper(II) species, within a few minutes at room temperature, in anhydrous MeCN.**

Molecular systems whose shape and internal motions can be controlled externally by applying a chemical or physical signal are fascinating.[1] They can be regarded as mimics of metalloproteins which may undergo drastic conformational changes (folding–unfolding), triggered by electron transfer from or onto an electrophore of the enzyme.[2]

Some of us have recently described a copper catenate which can experience a substantial yet controlled conformational change (gliding of one ring within the other), the process being induced electrochemically.[3] Indeed, transition-metal complexes are particularly suited for the design of such systems, since changes in the metal oxidation state can, at least in some cases, cause its coordination geometry to rearrange significantly.[4] The principle of the presently studied system is indicated in Fig. 1.

The square scheme of Fig. 1 contains alternating electrochemical steps and rearrangements, the latter steps leading to the most stable geometry of each oxidation state: four-coordinate for $Cu^{I}$ ($CuN_4^{+}$) and five-coordinate for $Cu^{II}$ ($CuN_5^{2+}$).

The isomerization of the compound from the $CuN_4^{2+}$ form to the $CuN_5^{2+}$ form involves an intramolecular change of the coordination number of the central metal ion from four to five. Such a change necessarily implies an altered coordination geometry and thus a modification of the d-orbital splitting pattern. For $Cu^{II}$ as the central ion, such a change may easily be monitored by EPR spectroscopy, considering the well established correlations[5] between crystallographically determined structures and the d-orbital situation as deduced from EPR data, in particular *g* factors and $^{63,65}Cu$ hyperfine coupling constants.

In the present EPR monitoring experiment (Fig. 2), the copper(I) form, $CuN_4^{+}$, with four-coordinate $d^{10}$ metal (distorted tetrahedral)[3] was oxidized to the paramagnetic copper(II) state $CuN_4^{2+}$ ($d^9$ configuration) in an electrolysis cell for EPR measurements (platinum anode in 2 mm capillary for EPR measurements; $CaH_2$-dried acetonitrile–0.1 M $NBu_4PF_6$). Following brief electrolysis at 293 K (5 min), the mixture was

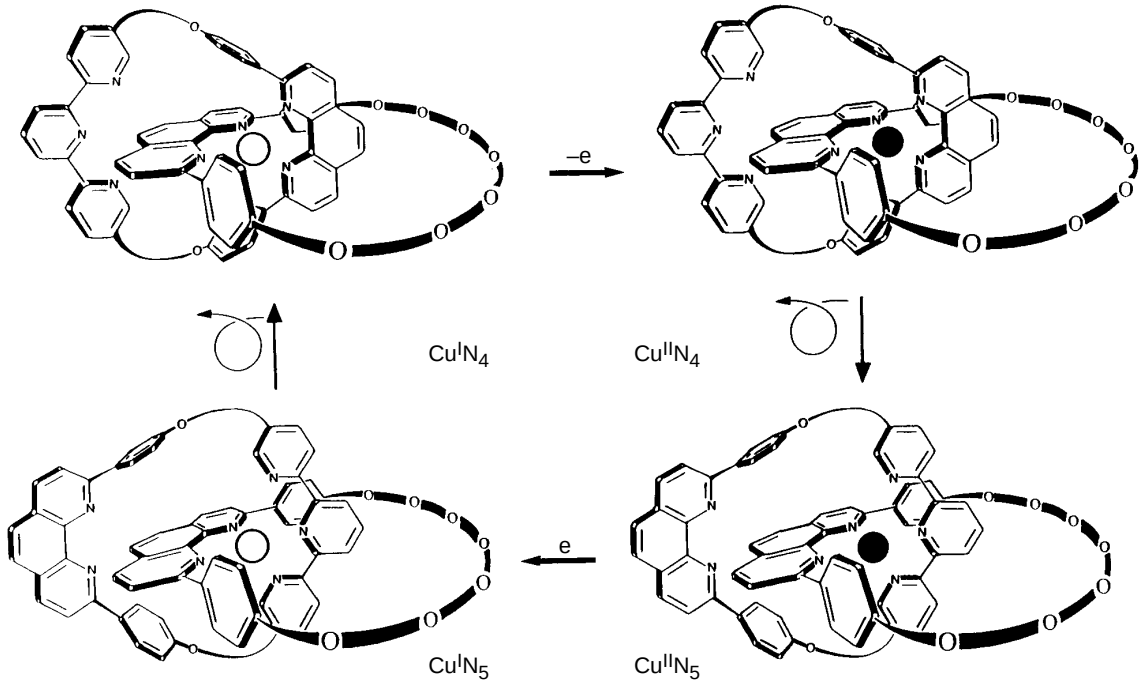



**Fig. 1** Electrochemically induced molecular rearrangements undergone by the copper catenate. The subscript 4 or 5 indicates the number of nitrogen atoms coordinated to the metal. White circles represents $Cu^{I}$ and black circles $Cu^{II}$. The organic backbone is a [2]catenate, consisting of two different interlocking rings. One ring incorporates a single chelate unit dpphen, whereas the other cycle contains two coordinating fragments (a dpphen unit and a terpy moiety; terpy = 2,2′:6′,2″-terpyridine).

immediately cooled to 110 K to form a glassy frozen solution. The initial anisotropic EPR spectrum is characterized by a relatively small $A_{\|}$ value of 12.1 mT and comparatively high $g$ components $g_{\|}$ = 2.276 and $g_{\perp}$ = 2.0735; $a_{\perp}$ and possible $^{14}N$ superhyperfine splitting could not be determined due to the linewidth. These values, corresponding to the 'metastable' form $CuN_4^{2+}$, are characteristic of four-coordinate $Cu^{II}$ in a distorted tetrahedral arrangement; similar numbers were measured for related complexes consisting of the same chelating units such as 2,9-diphenyl-1,10-phenanthroline (dpphen): the copper(II) state of catenate $[Cu(Cat_{30})]^{2+}$ ($g_{\|}$ = 2.282, $g_{\perp}$ = 2.075, $A_{\|}$ = 11.9 mT) and the non-catenate species $[Cu(dpphen)_2]^{2+}$ ($g_{\|}$ = 2.283, $g_{\perp}$ = 2.067, $A_{\|}$ = 12.2 mT).[6] In repeated cooling (110 K, EPR measurement) and warming cycles (308 K, 30 s, rearrangement reaction), there was a clear change in the EPR spectrum (Fig. 2), indicating the gradual formation of a new copper(II) species with quite different EPR characteristics. The hyperfine coupling component $A_{\|}$ = 16.6 mT is much larger than the value of 12.1 mT observed for the initial $CuN_4^{2+}$ form, whereas the $g$ components $g_{\|}$ = 2.233 and $g_{\perp}$ = 2.045 are smaller. These numbers are more in the typical range for geometrically relaxed copper(II) complexes,[5] which implies close to square-planar or, more likely, square-pyramidal geometry ($CuN_5^{2+}$). A structurally relevant five-coordinate complex, $[Cu(\eta^3\text{-L})(\eta^2\text{-L})][ClO_4]_2$, containing the potentially terdentate 2,6-bis(benzimidazol-2′-yl)pyridine ligand L and showing square-pyramidal configuration at the metal ion, has $g_{\|}$ = 2.23, $g_{\perp}$ = 2.03 and $A_{\|}$ = 16.7 mT.[7]

The EPR response illustrated in Fig. 2 thus supports the interpretation of a slow geometrical relaxation, $CuN_4^{2+} \rightarrow CuN_5^{2+}$, following the rapid heterogeneous oxidation of the copper(I) form (with preferred four-coordination), leading to the copper(II) state with its preferred five-coordinate geometry. The observed spectral differences are not only obvious (Fig. 2), they can also be rationalized straightforwardly, at least in a qualitative way. Both the $A_{\|}$ and $g$ value differences between the two copper(II) states support the above interpretation. According to eqn. (1) (where $j = x, y$ or $z$ coordinate, $\lambda$ is the spin–orbit coupling constant, $\Delta E_i$ is the energy separation between ground state $y_0$ and excited state $y_i$, and $L_j$ is a spin–orbit operator) and similar such approximations, high $g$ factors imply a small energy difference between the singly occupied molecular orbital (SOMO) and close-lying fully occupied MOs. Such a situation may be expected for a coordination geometry derived from the tetrahedron ($CuN_4^{2+}$) where the set of triply degenerate ($t_2$) or at least three close-lying uppermost d orbitals are occupied by five d electrons in a $d^9$ situation. On the other hand, the square or square-pyramidal geometry causes a large energy splitting between the SOMO ($d_{x^2-y^2}$) and the close-lying occupied d orbitals;[5] this splitting reduces the total energy of the system (Jahn–Teller effect) and leads to $g$ factors closer to the free electron value of $g_e$ = 2.0023, as observed here for the $CuN_5^{2+}$ state of the bimodal system.

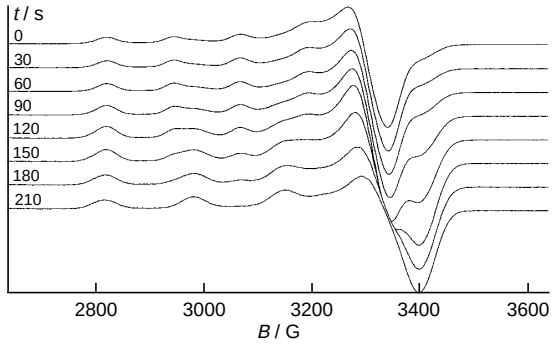



**Fig. 2** EPR spectra at 9.5938 GHz of the electrogenerated copper(II) state in acetonitrile–0.1 M $NBu_4PF_6$, following repeated cycling between cooling to 110 K (EPR measurements) and warming to 308 K (30 s, rearrangement reaction)

$$g = g_e + 2\lambda \sum_i \frac{\langle \psi_0 | L_j | \psi_i \rangle \langle \psi_i | L_j | \psi_0 \rangle}{\Delta E_i} \quad (1)$$

This work was supported by the CNRS (J. P. S.; A. L.), The Université Louis Pasteur (A. L.), the Deutsche Forschungsgemeinschaft and the Volkswagen Foundation (F. B.; W. K.).

## References

1 R. A. Bissell, E. Cordova, A. E. Kaifer and J. F. Stoddart, *Nature*, 1994, **369**, 133; Z. F. Liu, K. Hashimoto and A. Fujishima, *Nature*, 1990, **347**, 658; M. Harada, M. Sisido, J. Hirose and M. Nakanishi, *FEBS*, 1991, **286**, 6; F. Vögtle, W. M. Müller, U. Müller, M. Bauer and K. Rissanen, *Angew. Chem., Int. Ed. Engl.*, 1993, **32**, 1295; D. A. Parthenopoulos and P. M. Rentzepis, *Science*, 1989, **245**, 843; I. Willner, R. Blonder and A. Dagan, *J. Am. Chem. Soc.*, 1994, **116**, 3121; A. C. Benniston and A. Harriman, *Angew. Chem., Int. Ed. Engl.*, 1993, **32**, 1459; A. C. Benniston, A. Harriman and V. M. Lynch, *Tetrahedron Lett.*, 1994, **35**, 1473; M. Irie, O. Miyatake and K. Uchida, *J. Am. Chem. Soc.*, 1992, **114**, 8715; S. L. Gilat, S. H. Kawai and J. M. Lehn, *J. Chem. Soc., Chem. Commun.*, 1993, 1439.

2 J. Bixler, G. Bakker and G. McLendon, *J. Am. Chem. Soc.*, 1992, **114**, 6938; T. Pascher, J. P. Chesick, J. R. Winkler and H. Gray, *Science*, 1996, **271**, 1558.

3 A. Livoreil, C. Dietrich-Buchecker and J.-P. Sauvage, *J. Am. Chem. Soc.*, 1994, **116**, 9399.

4 S. Inomata, H. Tobita and H. Ogino, *Inorg. Chem.*, 1991, **30**, 3039; Y. Yao, M. W. Perkovic, D. P. Rillema and C. Woods, *Inorg. Chem.*, 1992, **31**, 3956; K. A. Gheysen, K. T. Potts, H. C. Hurrell and H. D. Abruna, *Inorg. Chem.*, 1990, **29**, 1589; W. E. Geiger, A. Salzer, J. Edwin, W. Von Philipsborn, U. Piantini and A. L. Rheingold, *J. Am. Chem. Soc.*, 1990, **112**, 7113; N. E. Katz and F. Fagalde, *Inorg. Chem.*, 1993, **32**, 5391; L. F. Joulie, E. Schatz, M. D. Ward, F. Weber and L. J. Yellowlees, *J. Chem. Soc., Dalton Trans.*, 1994, 799; A. Tomita and M. Sano, *Inorg. Chem.*, 1994, **33**, 5825 and references therein; A. M. Bond, T. W. Hambley, D. R. Mann and M. R. Snow, *Inorg. Chem.*, 1987, **26**, 2257; L. Zelikovich, J. Libman and A. Shanzer, *Nature*, 1995, **374**, 790.

5 See for example: B. A. Goodman and J. B. Raynor, *Adv. Inorg. Chem. Radiochem.*, 1970, **13**, 135; I. Bertini and A. Scozzafava, *Metal Ions in Biological Systems*, ed. H. Sigel, Marcel Dekker, New York, 1981, vol. 12, p. 31.

6 A. F. Stange, E.Waldhör, M. Moscherosch and W. Kaim, *Z. Naturforsch., Teil B*, 1995, **50**, 115; M. Geoffroy, M. Wermeille, C. O. Buchecker, J. P. Sauvage and G. Bernadinelli, *Inorg. Chim. Acta*, 1990, **167**, 157.

7 S. B. Sanni, H. J. Behm, P. T. Beurskens, G. A. Van Albada, J. Reedijk, A. T. H. Lenstra, A. W. Addison and M. Palaniandavar, *J. Chem. Soc., Dalton Trans.*, 1988, 1429.

8 W. Kaim, *Coord. Chem. Rev.*, 1987, **76**, 187.

*Received, 11th September 1996; Com. 6/06282B*

# Oxidation of NO to $NO_2$ on a Pt-MFI zeolite and subsequent reduction of $NO_x$ by $C_2H_4$ on an In-MFI zeolite: a novel de-$NO_x$ strategy in excess oxygen

**Masakazu Iwamoto,* Angel M. Hernandez and Tetsu Zengyo**

*Catalysis Research Center, Hokkaido University, Sapporo 060, Japan*

**Intermediate addition of reductant ($C_2H_4$) into an NO+$O_2$ stream between an oxidation catalyst for NO to $NO_2$ (Pt-MFI) and a reduction catalyst for $NO_x$ to $N_2$ (In-MFI), a so-called IAR method, is shown to be very effective in selectively reducing NO to $N_2$ in the presence of excess oxygen.**

The selective catalytic reduction of NO by hydrocarbons (SCR–HC) in the presence of excess oxygen is a potential method to remove $NO_x$ from various exhausts.[1] Although there have been many discussions on the reaction mechanism of the SCR–HC, the concept that NO is oxidized to $NO_2$ by oxygen and then the resulting $NO_2$ reacts with hydrocarbons to form an active intermediate is widely suggested on various catalysts.[2,3] Several efforts have been devoted to separate the functions of catalysts; for example, platinum and $Mn_2O_3$ are reported to be active for the oxidation of NO to $NO_2$ in the reaction system NO + $O_2$ + $CH_4$ on Pt/In/MFI[4] and NO + $O_2$ + $C_3H_6$ on $Mn_2O_3$ + Ce-MFI,[5] respectively. One of the most significant problems in these systems is that the oxidation catalyst for NO might be active for oxidation of the hydrocarbons, which would result in a decrease in the efficiency of the reductant. In the case of $CH_4$ as reductant, Pt can be used for NO oxidation because of the low oxidation activity of Pt towards $CH_4$.[4] With $C_3H_6$, $Mn_2O_3$ or $CeO_2$ should be employed because Pt or the other oxide catalysts are too active for $C_3H_6$ oxidation.[5]

It is well known that diesel exhausts contain very small amounts of unburned hydrocarbons. Thus addition of fuels or hydrocarbons into the diesel exhausts is required to reduce NO by the SCR–HC method. On the basis of the above reaction mechanism and the necessity of hydrocarbon addition, we propose here a novel strategy to reduce NO selectively, *viz*. the intermediate addition of a reductant into the NO-containing exhaust between an oxidation catalyst of NO and a reduction catalyst to $N_2$ (IAR method). In the present experiments Pt-MFI and In-MFI catalysts[6] have been employed as the model oxidation and reduction catalysts, respectively, in the reaction system NO + $O_2$ + $C_2H_4$.

Platinum and indium ion-exchanged MFI zeolites were prepared by a conventional method from aqueous tetraammineplatinum(II) nitrate and indium(III) nitrate solutions, respectively. The Si/Al molar ratio of the parent MFI zeolite was 11.7. The ion-exchange levels of Pt-MFI and In-MFI prepared were 101 and 83%, respectively. The zeolites were pressed, crushed and sieved to obtain particles of 250–425 μm. Catalytic reduction was carried out in a conventional flow system with twin quartz reactors and the flow diagram is shown in Fig. 1. The twin reactors were placed in a single furnace. The Pt-MFI catalyst was mounted in the first reactor and the In-MFI in the second. A mixture of NO, $O_2$ and He (balance) (total flow rate, 124 cm$^3$ min$^{-1}$) was introduced into the first reactor. The reductant, $C_2H_4$, diluted in He (26 cm$^3$ min$^{-1}$) was then added into the NO + $O_2$ mixture between the first and the second reactors. One can change the flow route of the NO + $O_2$ mixture to the bypass from the first reactor to evaluate the effect of the first catalyst bed. Before the catalytic reaction, the catalysts were pretreated *in situ* at 773 K for 3 h in a He flow. The reactants were 1000 ppm of NO, 857 ppm of $C_2H_4$, 2% of $O_2$ (helium balance) and the total flow rate of gases was 150 cm$^3$ min$^{-1}$. A gas chromatograph was employed to measure the respective concentrations of ethene, nitrogen, nitrous oxide, carbon dioxide and carbon monoxide. An $NO_x$ analyser was used to determine the degree of oxidation of NO to $NO_2$.

First, the effectiveness of Pt-MFI as the oxidation catalyst of NO was investigated and the results are plotted in Fig. 2. The conversion of NO to $NO_2$ on Pt-MFI was maximal at 523 K. Decrease in conversion at higher temperatures is due to the limitation of the equilibrium as clearly shown in Fig. 2. In the absence of the Pt-MFI catalyst, only a very small amount of $NO_2$ was produced under the present experimental conditions. One can therefore conclude that the Pt-MFI zeolite is a very active catalyst for the oxidation of NO to $NO_2$ and the catalytic activity is much higher than reported previously.[5,7] After the pretreatment, X-ray diffraction analysis of the Pt-MFI catalyst showed the formation of Pt particles on the MFI zeolite, which is in good agreement with a previous report.[8] The reproducibility of the results of Fig. 2 was very good within the temperature range 473–873 K and no deactivation of the Pt-MFI catalyst upon $NO_2$ formation was observed.

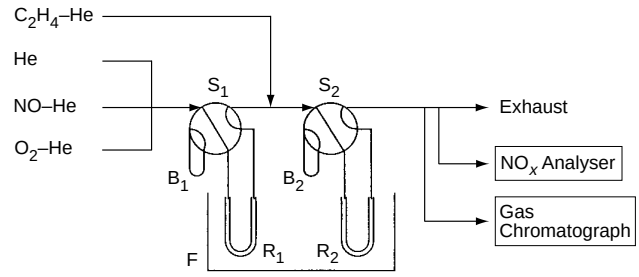



**Fig. 1** Flow system for SCR–HC by IAR method. B1 and B2, bypaths of the reactors; F, furnace; R1 and R2, reactors; S1 and S2, six-way valves.

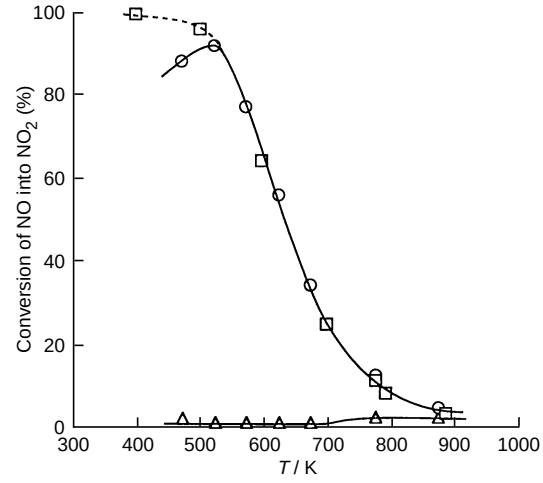



**Fig. 2** $NO_2$ formation in the NO + $O_2$ reaction on Pt-MFI (○). NO to $NO_2$ conversions without Pt-MFI (△) and under equilibrium (□) are also shown.

In Fig. 3, the activities of four kinds of catalytic systems are shown: (*i*) a series combination of the Pt-MFI catalyst (0.4 g) and the In-MFI catalyst (0.4 g) (Pt/In), (*ii*) the In-MFI catalyst alone (0.4 g) (In), (*iii*) physically mixed Pt-MFI (0.4 g) and In-MFI (0.4 g) catalysts (Pt + In) and (*iv*) a series combination of the Pt-MFI catalyst (0.4 g) and the parent Na-MFI catalyst (0.4 g) (Pt/Na). Fig. 3 clearly shows the great difference between the results of the Pt/In and the In systems. With Pt-MFI as the oxidation catalyst, the catalytic activity of In-MFI for NO reduction was greatly enhanced at 473–623 K. At the same time conversion levels of $C_2H_4$ also increased. It is evident that the increments of NO and $C_2H_4$ conversions are due to the formation of $NO_2$ on Pt-MFI. Fig. 3 also indicates formation of $N_2O$ at 473–623 K. This might suggest the easy formation of $N_2O$ in the presence of $NO_2$, although the reaction mechanism is, as yet, not clear.

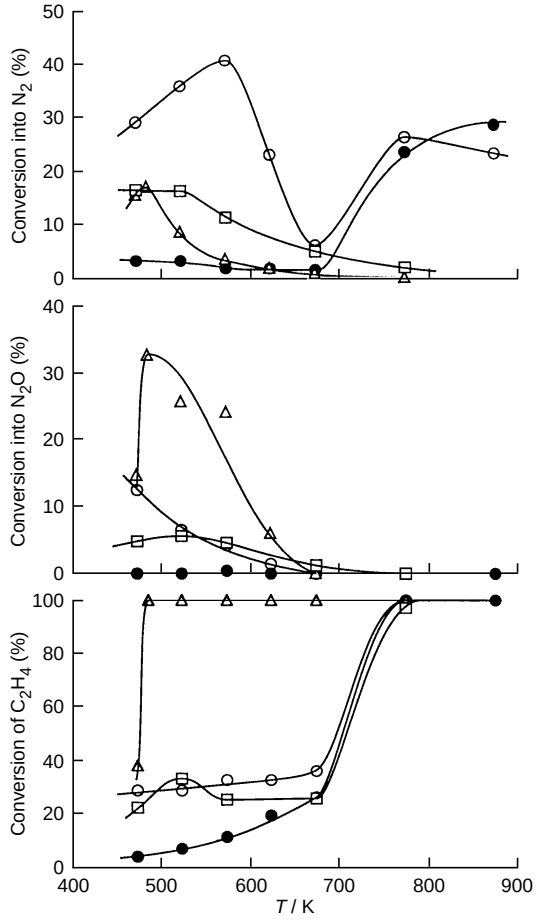



**Fig. 3** Reduction of NO by the IAR method on Pt/In (○), In (●), Pt + In (△) and Pt/Na (□) systems. The experimental conditions are described in the text.

The results on the Pt/In and In systems at 773–873 K were approximately the same. Taking the small amount of $NO_2$ formed at 773–873 K (Fig. 2) into consideration, the activity in this temperature region would result from the catalysis of In-MFI itself to the NO + $O_2$ + $C_2H_4$ mixture.

The results of the Pt/In system can be compared with those of the Pt + In system. The degree of conversion of NO to $N_2$ for the latter was much lower than that of the former as shown in Fig. 3, and almost the same as that of the Pt-MFI alone, as reported in a previous paper.[8] Therefore it follows that only Pt-MFI in the mixture of Pt-MFI and In-MFI is the active phase while In-MFI is essentially inactive. In addition, the results on the Pt/Na system reveal that indium ions are more effective than sodium ions in promotion of the catalytic reaction of $NO_2$ with hydrocarbons.

In conclusion, the results show the great effectiveness of the IAR method to reduce NO by hydrocarbons in the presence of an excess of oxygen. Although the effect of water addition to the system is yet to be investigated, it is clear that there is no longer a need to develop or search for catalysts which can oxidize NO to $NO_2$ but not oxidize the reductant, if we employ this method. There are many possible combinations of oxidation and reduction catalysts, depending on the condition of the exhausts and the nature of the reductants.

This work was supported by a grant-in-aid for Scientific Research from the Ministry of Education, Science, and Culture of Japan.

## References

1 M. Iwamoto and H. Yahiro, *Catal. Today*, 1994, **22**, 5.
2 H. Hamada, Y. Kintaichi, M. Sasaki, T. Ito and M. Tabata, *Appl. Catal.*, 1991, **70**, L15.
3 Y. Li and J. N. Armor, *J. Catal.*, 1994, **150**, 376; C. Yokoyama and M. Misono, *J. Catal*., 1994, **150**, 9; M. Shelef, C. M. Montreuil and H. W. Jen, *Catal. Lett*., 1994, **26**, 277; D. B. Lukyanov. G. Still, J. L. d'Itri and W. K. Hall, *J. Catal*., 1995, **153**, **265**; T. Beutel, B. J. Adelman, G.-D. Lei and W. M. H. Sachtler, *Catal. Lett.*, 1995, **32**, 83; K. A. Bethke, C. Li. M. C. Kung and H. H. Kung, *Catal. Lett.*, 1995, **31**, 287.
4 M. Ogura, S. Hiromoto and E. Kikuchi, *Chem. Lett*., 1995, 1135; E. Kikuchi, M. Ogura, N. Aratani, Y. Sugiura, S. Hiromoto and K. Yogo, *Catal. Lett.*, 1996, **27**, 35.
5 C. Yokoyama and M. Misono, *Catal. Lett.*, 1994, **29**, 1.
6 E. Kikuchi, M. Ogura, I. Terasaki and Y. Goto, *J. Catal.*, in the press.
7 A. Yu. Stakheev, C. W. Lee, S. J. Park and P. J. Chong, *Catal. Lett.*, 1996, **38**, 271.
8 H. K. Shin, H. Hirabayashi, H. Yahiro, M. Watanabe and M. Iwamoto, *Catal. Today*, 1995, **26**, 13.

*Received, 10th September 1996; Com. 6/06233D*

# Molybdenum and tungsten carbides as catalysts for the conversion of methane to synthesis gas using stoichiometric feedstocks

**Andrew P. E. York, John B. Claridge, Attila J. Brungs, Shik Chi Tsang† and Malcolm L. H. Green***

*The Catalysis Centre, Inorganic Chemistry Laboratory, University of Oxford, South Parks Road, Oxford, UK OX1 3QR*

**Molybdenum and tungsten carbides are extremely active and stable catalysts for the dry reforming, partial oxidation and steam reforming of methane to synthesis gas using stoichiometric feedstock; no bulk carbon deposition was observed.**

Recent estimates indicate that world reserves of natural gas will outlast those of oil by a considerable period.[1] Current industrial use of methane as a chemical feedstock proceeds by initial conversion to carbon monoxide and hydrogen (synthesis gas) by either steam reforming[2] [eqn. (1)] (a large scale process) or by dry reforming, [eqn (2)]; a further route is *via* partial oxidation [eqn. (3)].

$$CH_4 + H_2O = CO + 3\ H_2 \quad \Delta H^{\ominus}_{298} = +206\ \text{kJ mol}^{-1} \quad (1)$$

$$CH_4 + CO_2 = 2\ CO + 2\ H_2 \quad \Delta H^{\ominus}_{298} = +247\ \text{kJ mol}^{-1} \quad (2)$$

$$CH_4 + \tfrac{1}{2}O_2 = CO + 2\ H_2 \quad \Delta H^{\ominus}_{298} = -38\ \text{kJ mol}^{-1} \quad (3)$$

Nickel catalysts are used industrially for both the methane steam and dry reforming reactions because of their fast turnover rates, long term stability and low cost.[2] However, they have a major drawback since the nickel catalysts also catalyse carbon formation *via* methane decomposition and CO disproportionation, both of which lead to catalyst deactivation and the plugging of the reformer tubes by carbon deposits. Thus, in practice large excesses of oxidants are used in order to prevent carbon deposition. This results in synthesis gas with $H_2/CO$ and $CO_2/CO$ ratios which are not optimal for further conversion to major end products, such as methanol or gasoline. Considerable effort has been concentrated on exploring catalysts for eqns. (1)–(3) which are resistant to carbon formation at or near stoichiometric reactant ratios. Previously, sulfur passivated nickel catalysts[3] and noble metal catalysts[4–7] have been shown to exhibit kinetic resistance to carbon formation, but the low activities of sulfur passivated nickel and the high costs and limited availability of the noble metals have limited their application.

In the last 20 years, group VI transition metal carbides have been found to be active catalysts, comparable to platinum group metal catalysts for a number of reactions. Here we describe new catalysts, based on carbides of molybdenum and tungsten, for the reforming of methane using stoichiometric feedstocks at slightly elevated pressures. No carbon deposition is observed, and the consequential selectivities and conversions to carbon monoxide and hydrogen are those predicted by thermodynamic considerations.

The high surface area carbide catalysts were prepared by temperature programmed reduction of the oxides or supported oxides in a flow of methane or methane–hydrogen mixture, as previously described for β-$Mo_2C$,[8] WC[9] and $Mo_2C/Al_2O_3$.[10] Normally the catalysts were prepared *in situ* and tested immediately.

Table 1 shows the results obtained for the dry reforming of methane to synthesis gas with carbon dioxide, using β-$Mo_2C$ ($S_g$ = 91 $m^2\ g^{-1}$) and WC ($S_g$ = 39 $m^2\ g^{-1}$) as catalysts at both ambient and elevated pressure. The initial synthesis gas yields very closely approach those predicted from thermodynamic considerations, if carbon deposition is discounted.[7] At ambient pressure catalyst deactivation occurred, and this was clearly observable after 8 h [Fig. 1(*a*)]. Powder XRD (not given) showed that the initial β-$Mo_2C$ was converted to $MoO_2$, which has only very low activity for methane dry reforming. However, when the experiment was run at slightly elevated pressure

**Table 1** Catalytic performance of molybdenum and tungsten carbides for various methane reforming reactions

| Catalyst | $CH_4$: oxidant | Pressure/ bar | *T*/K | C[$CH_4$][a] (%) | Y[CO][b] (%) | $H_2/CO$[c] |
|---|---|---|---|---|---|---|
| β-$Mo_2C$ | 1 : 1[d] | 1.0 | 1120 | 92.4 | 92.5 | 0.93 |
| β-$Mo_2C$ | 1 : 1[d] | 8.3 | 1120 | 62.5 | 69.5 | 0.78 |
| WC | 1 : 1[d] | 8.3 | 1120 | 62.7 | 68.7 | 0.79 |
| 5% $Mo_2C/Al_2O_3$ | 1 : 1[d] | 8.3 | 1120 | 65.2 | 70.1 | 0.81 |
| β-$Mo_2C$ | 2 : 1[e] | 4.0 | 1170 | 94.7 | 89.6 | 2.01 |
| β-$Mo_2C$ | 2 : 1[e] | 8.7 | 1170 | 88.0 | 80.7 | 2.02 |
| WC | 2 : 1[e] | 8.7 | 1170 | 87.5 | 78.2 | 2.04 |
| 5% $Mo_2C/Al_2O_3$ | 2 : 1[e] | 8.7 | 1170 | 90.6 | 82.5 | 2.00 |
| β-$Mo_2C$ | 1 : 1[f] | 1.0 | 1220 | 91.5 | 90.1 | 3.08 |
| β-$Mo_2C$ | 1 : 1[f] | 8.3 | 1220 | 81.8 | 77.7 | 3.07 |
| WC | 1 : 1[f] | 8.3 | 1220 | 81.9 | 77.8 | 3.06 |
| 5% $Mo_2C/Al_2O_3$ | 1 : 1[f] | 8.3 | 1220 | 82.1 | 77.9 | 3.05 |

[a] C[$CH_4$] = (% conversion of $CH_4$ into all products). [b] Y[CO] = amount of CO in products)/(amount (C) in reagents.) [c] $H_2/CO$ = (amount of $H_2$ in products)/(amount of CO in products). [d] Dry reforming with carbon dioxide (inlet GHSV = 2.8 × $10^3\ h^{-1}$). [e] Partial oxidation with air (inlet GHSV = 5.2 × $10^3\ h^{-1}$). [f] Steam reforming with water (inlet GHSV = 2.8 × $10^3\ h^{-1}$).

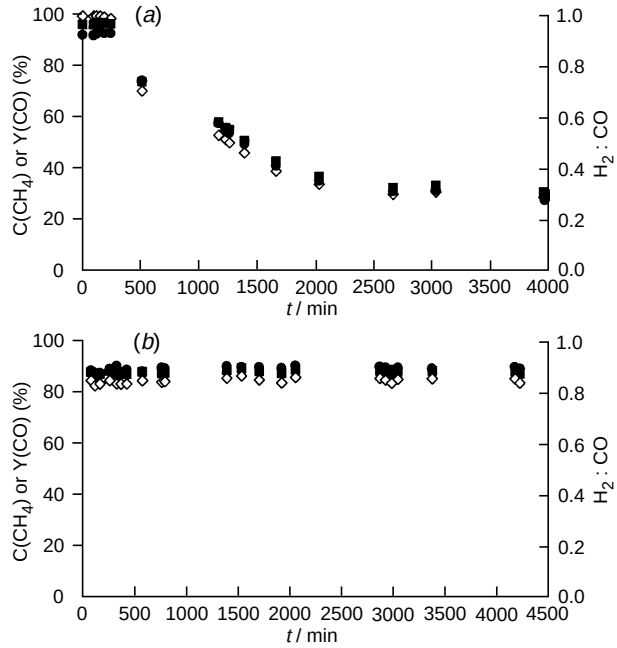



**Fig. 1** Catalyst stabilities for the dry reforming of methane ($T$ = 1220 K; $CH_4:CO_2$ = 1; GHSV = 2.8 × $10^3\ h^{-1}$); (*a*) pressure = 1 atm; (*b*) pressure = 8.3 atm; (■) Y[CO], (◇) C[$CH_4$], (●) $H_2:CO$

(about 8 bar), high activity was maintained for the duration of the experiments (typically 144 h), with no observable deterioration in the catalysts [Fig. 1(*b*)] providing, at least, an initial idea of the long term stability of the catalysts, although longer experiments need to be conducted. XRD studies of the quenched catalyst after use showed no trace of of $MoO_2$. Further, a high resolution transmission electron microscopy (HRTEM) study of the pre- and post-catalysis samples indicated that no bulk carbon deposition had occurred on the catalyst. In contrast, HRTEM examination of used nickel catalysts show the presence of large amounts of whisker carbon.[4] Activity studies of our carbide catalysts and of supported noble metal catalysts, for the dry reforming of methane under differential conditions (*i.e.* conversion kept < 10%), show that β-$Mo_2C$ has comparable activity on a gram basis to that of 5% Ir–$Al_2O_3$, which is well known as an active catalyst for steam and dry reforming.[5] Indeed, the relative activity of a number of the reforming catalysts has been established as: Ru > Rh > Ir ≈ $Mo_2C$ > WC > Pd > Pt.[5,11,12]

Table 1 also shows the results obtained for β-$Mo_2C$, WC and $Mo_2C$–$Al_2O_3$ as catalysts for the partial oxidation and steam reforming reactions, also at slightly elevated pressures. Again the reaction yields approach predicted thermodynamic equilibrium values, and have been carried out for 72 h or more without any evidence of macroscopic carbon deposition or catalyst deactivation. In the corresponding reactions at ambient pressure, catalyst deactivation was always observed due to the formation of inactive $MoO_2$.

The stabilisation of the active metal carbide phase under slightly elevated pressures is surprising since, although the carbides can be synthesised from the oxides by methane at high temperatures (> 1000 K), they are very reactive towards oxidation by oxygen, carbon dioxide and water.

We can offer no clear reasons to account for the high catalytic activity of the early transition metal carbides for the methane reforming reactions, nor for their resistance to macroscopic carbon formation. However, catalytic similarities between early transition metal carbides and the noble metals, which are active for steam reforming, have been noted before.[13–16]

## Footnote

† Present address: The Catalysis Research Centre, Department of Chemistry, University of Reading, Whiteknights, Reading, UK RG6 6AD.

## References


1 C. A. Jones and J. J. Leonard, *Energy Fuels*, 1981, **1**, 13.
2 J. R. Rostrup-Nielsen, in *Catalysis Science and Technology*, ed. J. R. Anderson and M. Boudart, Springer, Berlin, 1984, vol. 5, p. 1.
3 J. R. Rostrup-Nielsen, *J. Catal.*, 1984, **85**, 31.
4 J. B. Claridge, M. L. H. Green, S. C. Tsang, A. P. E. York, A. T. Ashcroft and P. D. Battle, *Catal. Lett.*, 1993, **22**, 299.
5 J. R. Rostrup-Nielsen and J. H. Bak Hansen, *J. Catal.*, 1993, **144**, 38.
6 A. T. Ashcroft, A. K. Cheetham, M. L. H. Green and P. D. F. Vernon, *Nature*, 1991, **352**, 225.
7 A. T. Ashcroft, A. K. Cheetham, J. S. Foord, M. L. H. Green, C. P. Grey, A. J. Murrell and P. D. F. Vernon, *Nature*, 1990, **344**, 319.
8 J. S. Lee, S. T. Oyama and M. Boudart, *J. Catal.*, 1987, **106**, 125.
9 F. H. Ribeiro, R. A. Dalla Betta, G. J. Guskey and M. Boudart, *Chem. Mater.*, 1991, **3**, 805.
10 J. S. Lee, K. H. Lee and J. Y. Lee, *J. Phys. Chem*., 1992, **96**, 362.
11 J. B. Claridge, M. L. H. Green and S. C. Tsang, *Catal. Today*, 1994, **21**, 455.
12 A. J. Brungs, J. B. Claridge, M. L. H. Green, S. C. Tsang and A. P. E. York, unpublished data.
13 R. B. Levy and M. Boudart, *Science*, 1973, **181**, 547.
14 L. Leclerq, in *Surface Properties and Catalysis by Non-Metals*, ed. J. P. Bonnelle, B. Delmon and E. Derouane, Riedel, Dordrecht, 1983, pp. 433.
15 S. T. Oyama and G. L. Haller, *Catalysis*, 1982, **3**, 333.
16 M. J. Ledoux, C. Pham-Huu, A. P. E. York, E. A. Blekkan, P. Delporte and P. Del Gallo, in *The Chemistry of Transition Metal Carbides and Nitrides*, ed. S. T. Oyama, Blackie Academic and Professional, Glasgow, 1966, p. 373.


*Received, 14th August 1996; Com. 6/05693H*

# Dynamics of adduct formation of hydroquinone under oxidative conditions observed by laser spectroscopy

**Victor Nadtochenko† and John Kiwi**

*Institute of Physical Chemistry II, Swiss Federal Institute of Technology, Lausanne 1015, Switzerland*

**Hydroxylated products of hydroquinone ($H_2Q$) are induced *via* $[Fe(ox)_3]^{3-}$–$H_2O_2$ under light and detected in the visible region by laser spectroscopy; reaction of hydroxyl radicals with ($H_2Q$) is observed leading to adduct formation.**

During the past few years the photochemistry of tris(oxaloferrate) has been studied.[1,2] Work has been reported recently[3,4] of the reactions of this complex with organic compounds using steady-state photolysis, flash photolysis and stopped-flow in the millisecond region and at longer times. Here, we report on the reactions of $[Fe(ox)_3]^{3-}$–$H_2O_2$ with hydroquinone ($H_2Q$) from the nanosecond timescale upwards. The findings reported here aim to further our understanding[4–7] about the mode of intervention of $[Fe(ox)_3]^{3-}$ during the degradation of $H_2Q$ in oxidative media.

$FeCl_3$, dihydrooxalic acid and hydroquinone were all Fluka p.a. and used as received. Laser photolysis was carried out using the second harmonic (λ = 347 nm) of a JK-2000 ruby laser operated in the Q-switched mode. The pulse width was *ca.* 10 ns and the energy *ca.* 10 mJ per pulse. The detection of the transient absorption changes was performed *via* an EGG photomultiplier with a rise time of *ca.* 5 ns. The basic system for kinetic spectroscopy detection has been described previously.[8]

Fig. 1(*a*) presents the transient species after the laser pulse for the traces (*i*) $H_2Q$ (40 mM) reacting with $H_2O_2$ (0.29 mM), (*ii*) $[Fe(ox)_3]^{3-}$ reacting with $H_2O_2$ (0.29 mM), (*iii*) the transient decay of $[Fe(ox)_3]^{3-}$ (0.6 mM) back to the ground state or to a metastable longer lived[6] intermediate $[(ox)_2Fe(ox^{\cdot-})]$ **I** (Scheme 1).

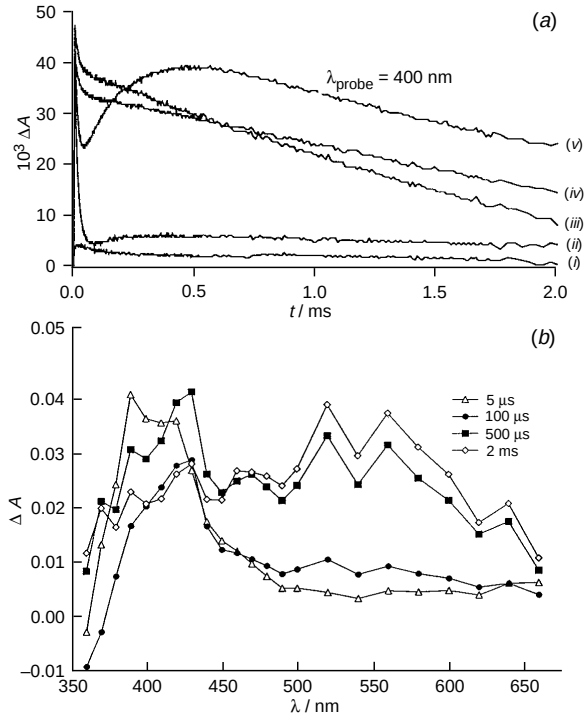



**Fig. 1** (*a*) Laser transients for different solutions of $[Fe(ox)_3]^{3-}$, $H_2O_2$ and hydroquinone ($H_2Q$). For other experimental details see text. (*b*) Transient decay spectra as a function of λ for the system $Fe(ox)_3^{3*-}$ [oxalate (0.6 mM)–$Fe^{3+}$ (18 mM), $H_2Q$ (40 mM) and $H_2O_2$ (0.29 M) at pH 6.5].

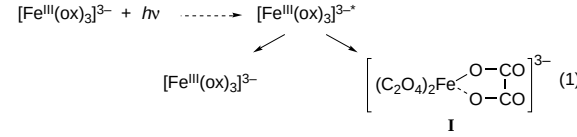
Trace (*iv*) in Fig. 1(*a*) shows $[Fe(ox)_3]^{3-}$ decay in the presence of $H_2Q$ (40 mM) where a quenching effect is noticeable. Finally, to this solution is added $H_2O_2$ (0.29 M) and the result is shown in Fig. 1(*a*) trace (*v*). The lifetimes (τ) of $[Fe^{III}(ox)_3]^{3-*}$ and **I** are *ca.* 5 μs and 2 ms, respectively, at neutral pH. The disappearance of the initial transient absorption is followed by the formation of a coloured species within *ca.* 600 μs. This is observed only in trace (*v*) for the complete chemical system $[Fe(ox)_3]^{3-}$–$H_2O_2$–$H_2Q$. It is not possible to rationalize this result in terms of formation of ·OH radicals by the usual Fenton mechanism [eqn. (2)][1,4] since (*a*) the

$$Fe^{2+} + H_2O_2 \rightarrow Fe^{3+} + OH^- + {}^{\cdot}OH; \quad k_2 = 41\text{–}75\ M^{-1}\ s^{-1} \qquad (2)$$

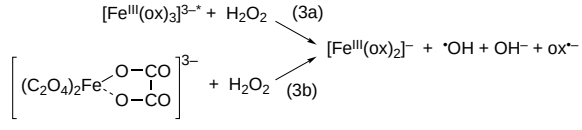
characteristic time for the reaction is about $10^3$ times longer[9] than the values observed in Fig. 1(*a*) when $[Fe(ox)_3]^{3-}$–$H_2O_2$ is photolysed in solution and (*b*) the observed rise time of the coloured product in Fig. 1(*a*) is seen to be close to the lifetime of the transient $[Fe(ox)_3]^{3-*} + H_2O_2$ as shown in Fig. 1(*a*) trace (*ii*). It is therefore impossible to assign the observed ·OH radical formation to the mechanism of eqn. (2) since only fast intermediates having lifetimes of microseconds would be able to hydroxylate $H_2Q$. Radical formation could be accounted for by reaction of $[Fe^{III}(ox)_3]^{3-*}$ or **I** with $H_2O_2$[6] (Scheme 2).

It has been previously reported[10] that $k_{OH + H_2Q} = 1.2 \times 10^{10}$ $M^{-1}\ s^{-1}$. Since $H_2Q$ (40 mM) was used in Fig. 1(*a*), trace (*i*), the characteristic time for ·OH radical attack would be *ca.* $2.1 \times 10^{-9}$ s. The second pathway of Scheme 2 [eqn. (3*b*)] therefore should be the limiting step for ·OH radical formation when $[Fe^{III}(ox)_3]^{3-*}$ reacts with $H_2O_2$ under light leading subsequently to adduct formation with $H_2Q$ as observed in trace (*v*) of Fig. 1(*a*). This conclusion is confirmed by the near independence observed for the formation of the coloured product of $H_2Q$ on the $H_2Q$ concentration in the range 2–40 mM at fixed $H_2O_2$ and $[Fe^{III}(ox)_3]^{3-}$ concentrations [as shown in Fig. 2(*b*)].

Fig. 1(*b*) shows the absorbances of the products formed after the laser pulse. Different transient lifetimes and absorbances (*A*) were observed as a function of λ due to the existence of different coloured intermediate transients between 350 and 550 nm. The




**Scheme 1**




**Scheme 2**

signals in Fig. 1(*b*) at λ = 450 nm and beyond would correspond to oxidized $H_2Q$–OH adducts in agreement with work by Adams and Michael[10] using pulse radiolysis. The spectrum at 5 μs after the pulse is mainly due to the initial quenching of the binary system $[Fe(ox)_3^{3-}]$–$H_2Q$ by $H_2O_2$. Kinetics of $H_2Q$ hydroxylation consistent with the observations can be rationalized by Schemes 1–3. The rate constants used have been previously reported.[11–13]

Under the experimental conditions used, $[H_2O_2] \gg [Fe^{2+}]$, $[H_2O_2] \gg [ox^{2-}]$ and $[H_2O_2] \gg [\cdot OH]$. The solution for this

$H_2Q + {}^{\bullet}OH \dashrightarrow H_2Q\text{–}OH(adduct)$ $k_4 = 1.2 \times 10^{10}\,M^{-1}s^{-1}$ (4)

$H_2O_2 + {}^{\bullet}OH \dashrightarrow HO_2^{\bullet} + H_2O$ $k_5 = 1.3 \times 10^{7}\,M^{-1}s^{-1}$ (5)

$ox^{2-} + {}^{\bullet}OH \dashrightarrow OH^- + ox^{\bullet-}$ $k_6 = 2 \times 10^{6}\,M^{-1}s^{-1}$ (6)

${}^{\bullet}OH + {}^{\bullet}OH \dashrightarrow H_2O_2$ $k_7 = 5.3 \times 10^{9}\,M^{-1}s^{-1}$ (7)

${}^{\bullet}OH + Fe^{2+} \dashrightarrow OH^- + Fe^{3+}$ $k_8 = 3 \times 10^{8}\,M^{-1}s^{-1}$ (8)

**Scheme 3**

$$[Fe(ox)_3^{3-*}] / dt = -k_q[Fe(ox)_3^{3-*}] - k_a[H_2O_2][Fe(ox)_3^{3-*}] \quad (9)$$

$$d[{}^{\bullet}OH] / dt = k_a[H_2O_2][Fe(ox)_3^{3-*}] - k_5[{}^{\bullet}OH][H_2O_2] - k_4[{}^{\bullet}OH][H_2Q] \quad (10)$$

$$d[adduct] / dt = k_4[{}^{\bullet}OH][H_2Q] \quad (11)$$

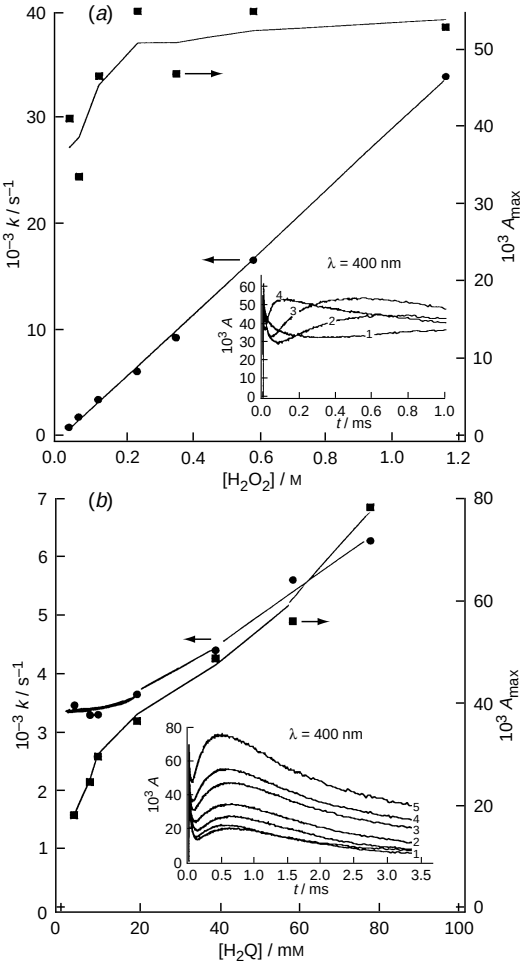



**Fig. 2** (*a*) Dependency of the reciprocal rise time of hydroquinone adducts (●) and absorbance $A_{max}$ (■) *vs.* $H_2O_2$ concentration. The same solution as in Fig. 1(*b*) was used. The insert shows the transient at λ = 400 nm when $H_2O_2$ is added at concentrations of (*i*) 0.029, (*ii*) 0.12, (*iii*) 0.58 and (*iv*) 1.16 M. (*b*) Dependency of the reciprocal rise time of hydroquinone ($H_2Q$) adducts (●) and absorbance $A_{max}$ (■) as a function of $H_2Q$ concentration. The insert shows the transient at λ = 400 nm when $H_2Q$ has been added in the following concentrations: (*i*) 10, (*ii*) 20, (*iii*) 39, (*iv*) 59 and (*v*) 79 mM.

system of differential equations can be stated in a simplified form

$$\Delta A(t) = A_{max} - (\text{cte}) \exp\{-(k_q + k_a[H_2O_2])t\} \quad (12)$$

where $A_{max} = k_4k_a[H_2O_2][H_2Q][Fe(ox)_3^{3*-}]_0/(k_q + k_a[H_2O_2])(k_5[H_2O_2] + k_4[H_2Q])$ and (cte) $= k_4k_a[H_2O_2][H_2Q][Fe(ox)_3^{3-*}]_0/\{[(k_5[H_2O_2] + k_4[H_2Ql]) - k_q + k_a[H_2O_2])](k_q + k_a[H_2O_2])\}$.

Fig. 2(*a*) and (*b*) show the dependency of the reciprocal rise time $k/s^{-1}$ and maximum amplitude for the coloured products ($A_{max}$) as a function of $H_2O_2$ and $H_2Q$ concentrations. Fig. 2(*a*) shows the dependency for $k/s^{-1}$ *vs.* [$H_2O_2$] for a solution oxalate 18 mM–$Fe^{3+}$ 0.6 mM at pH 6.5 and [$H_2Q$] = 59 mM. The insert in Fig. 2(*a*) shows the traces due to the coloured adduct formation (*A*) for different concentrations of added $H_2O_2$ in the millisecond range. The linear dependency of $k/s^{-1}$ *vs.* $H_2O_2$ in Fig. 2(*a*) with slope 2.9 ± 0.4 × $10^5$ $M^{-1}$ $s^{-1}$ is observed to be close to the value of the quenching reported[5] for $[Fe(ox)_3]^{3-*}$. This suggests the formation of ·OH radicals in reaction (3) as the limiting step for $H_2Q$ hydroxylation. This result is consistent with the relation $k/s^{-1} = k_q + k_a[H_2O_2]$. In the latter equation at high $H_2O_2$ concentrations $k_a[H_2O_2] > k_q$, the value of $A_{max}$ would be independent of the oxidant concentration. In effect Fig. 2(*a*) shows that the value of $A_{max}$ is almost independent of $H_2O_2$ concentration above *ca.* 0.25 M.

Fig. 2(*b*) shows the rate constant when experiments similar to those in Fig. 2(*a*) were carried out. The $H_2O_2$ concentration was kept constant at 0.145 M while the concentration of $H_2Q$ was varied in the range 2–78 mM. The growth of the transient at λ = 400 nm is shown in the insert. The value of $A_{max}$ near saturation at $H_2Q$ concentrations of 20–40 mM further increases at [$H_2Q$] > 40 mM. A kinetic model over the entire concentration range studied in Fig. 2 is not capable of accounting for all the features associated at higher $H_2Q$ concentrations.

This work has presented insight into adduct formation of $H_2Q$–OH. Fast hydroxylation of $H_2Q$ can only be explained by the presence of the ·OH radicals due to the fast reaction rate of ·OH with $H_2Q$.[10]

This work was supported by the grant N°EV5V-CT9-0249 from the Commission of European Communities (OFES Contract N°95 00 31, Bern) and through INTAS Cooperation Project Brussels N° 094-642.

## Footnote

† On leave of absence, Institute of Chemical Physics, Russian Academy of Sciences. Chernogolovka 142432, Moscow Region, Russia.

## References

1 V. Balzani and V. Carassiti, in *Photochemistry of Coordination Compounds*, Academic Press, London, 1970.
2 C. Hatchard and C. Parker, *Proc. R. Soc. London, Ser. A*, 1956, **235**, 518.
3 G. Cooper and B. DeGraff, *J. Phys. Chem*., 1971, **75**, 2897.
4 A. A. Safarzadeh-Amiri, J. Bolton and S. Carter, *J. Adv. Oxidation Technol.*, 1996, **1**, 18.
5 V. Nadtochenko and J. Kiwi, *Photochem. Photobiol. A*, 1996, **99**, 145.
6 Y. Zuo and J. Hoigné, *J. Environ. Sci. Technol.*, 1992, **26**, 1014.
7 D. Sawyer, K. Chang , A. Llobet, Ch. Redman and D. Barton, *J. Am. Chem. Soc*., 1993, **115**, 5817.
8 J. Kiwi and M. Grätzel, *J. Phys. Chem*., 1980, **84**, 1503.
9 C. Walling, *Acc. Chem. Res*., 1975, **8**, 125.
10 E. Adams and B. Michael, *Trans. Faraday. Soc*., 1967, **63**, 1171.
11 G. Buxton, W. Helman and A. Ross, *J. Phys. Chem. Ref. Data*, 1988, **17,** 513.
12 Y. Sun and J. Pignatello, *Environ. Sci. Technol*., 1993, **27**, 304.
13 D. Sedlak and J. Hoigné, *Atmos. Environ*., 1993, **27**, 2173.

*Received, 21st August 1996; Com. 6/05826D*

# Nanogram-scale derivatization of hydroxy groups for highly sensitive HPLC/MS/CD detection

**Ning Zhao,[a] Jin-Song Guo,[a] Lee-Chiang Lo,[a] Nina Berova,[a] Koji Nakanishi,*[a] Garner T. Haupert,[b] M. Warrack[c] and Adrienne A. Tymiak*[c]**

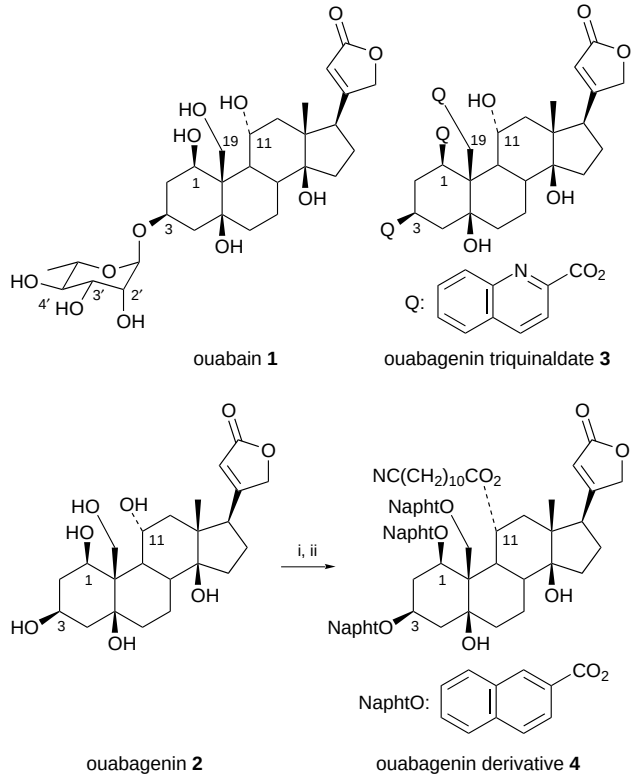
[a] *Department of Chemistry, Columbia University, New York, NY 10027, USA*
[b] *Renal Unit, Massachusetts General Hospital, Harvard Medical School, Charlestown, MA 02129, USA*
[c] *Bristol-Myers Squibb Pharmaceutical Research Institute, PO Box 4000, Princeton, NJ 08543-4000, USA*

**A strategy for performing submicrogram-scale structural studies of saponins and related compounds is worked out by: (*i*) naphthoylation to sensitize HPLC detection by fluorescence as well as configurational studies by exciton coupled CD; and (*ii*) ω-cyanoundecanoylation to increase LC/MS sensitivity (*ca*. 100-fold).**

The specific binding of plant-derived digitalis glycosides by mammalian Na,K-ATPase (sodium pump) raised the possibility that a mammalian analogue of digitalis might exist. Hamlyn *et al*. reported a molecule from human plasma which by mass spectrometry (MS), chromatographic behaviour, *etc*., was undistinguishable from the plant saponin ouabain **1** (ouabain-like compound or OLC).[1] We had also isolated from bovine hypothalamus an inhibitor of the Na,K-ATPase (hypothalamic inhibitory factor or HIF). Similar to ouabain, HIF had an L-rhamnoside moiety but sub-μg scale characterizations showed that it was some isomer of ouabain.[2] Since rhamnosidic saponins are unknown as natural products from mammalian sources, it became important to compare HIF, OLC and ouabain **1** directly. This was performed by converting 300–400 ng of each into their penta-2-naphthoates upon which it was found that the HPLC retention times of HIF and OLC pentanaphthoates were identical but differed from that of ouabain 2′,3′,4′,1,19-pentanaphthoate. Most uniquely, although ouabain **1** exhibited a typical positively split exciton couplet in its circular dichroic spectrum (CD) at 235 nm, *i.e.* 245 nm (Δε +209 $M^{-1}$ $cm^{-1}$)/229 nm (Δε −170), those of HIF and OLC were devoid of any clear Cotton effects (!), thus showing that the arrangements of the five naphthoates are such that the spatial interactions are intramolecularly cancelled.[3] In summary, HIF and OLC are in all likelihood identical but differ from ouabain **1**.

Subsequent rhamnosidation/naphthoylation studies of ouabagenin and CD measurements of the pentanaphthoates coupled with CD computations† suggest the possibility that the genins of HIF and ouabain **1** may indeed be different. Because of the extremely limited amount of the mammalian cardiotonic factor(s) available from natural sources (*e.g.* 5 kg of bovine hypothalamus yields 1 μg of HIF),[3] our strategy is to hydrolyse HIF with naringinase, determine the genin structure by highly sensitive methods, and eventually synthesize the genin and attach the rhamnose. The final structure will be compared with the natural sample by HPLC and CD of its pentanaphthoate and bioassay of the saponin.

In the following, we describe two-step derivatizations of hydroxy groups leading to facile HPLC collection, and increased LC/MS and CD sensitivities. The reaction conditions are chosen to perform partial derivatization with the fluorescent naphthoate chromophores, and this is followed by further acylation of the less reactive hydroxy group with an MS sensitivity-enhanced moiety. Since all properties of HIF are very similar to those of ouabain **1**, suggesting the close similarity (or identity?) of the two genins, ouabagenin is employed as a model. In our previous studies, the HIF hydroxy groups were converted into naphthoates because of many favourable attributes:[4] high derivatization yield (90–95%), fluorescence, intense UV absorption and hence favourable chromophore for exciton coupled CD,[5,6] *etc*. Because a positively charged nitrogen atom greatly enhances the sensitivity in ionspray MS, we first sought to employ 2-quinaldates, with UV properties similar to those of 2-naphthoates, thus simplifying the interpretation of exciton coupled CD, *i.e.* $\lambda_{max}$ of quinaldate in acetonitrile at 235 nm (ε 37 000 $M^{-1}$ $cm^{-1}$) *cf.* naphthoate at 234 nm (ε 58 000). Ouabagenin 1,3,19-triquinaldate **3**, which was prepared in a high-yield microscale reaction using conditions similar to those described for the naphthoate (see below), gave an intense split CD slightly weaker than that of the trinaphthoate: quinaldate **3**,‡ UV $\lambda_{max}$ in acetonitrile at 235 nm (ε 109 000 M $cm^{-1}$); CD 231 (Δε +125), 241 nm (−186), *A* (amplitude) −311, *cf.* trinaphthoate, $\lambda_{max}$ in acetonitrile at 231 nm (ε 147 000); CD 227 (+250), 240 nm (−292), *A* −542. Although the MS sensitivity of triquinaldate **3**




**Scheme 1** One-pot/two-step reaction (naphthoylation and 11-cyanoundecanoylation) of ouabagenin **2**. *Reagents*: i, 2-naphthoylimidazole, DBU, MeCN; ii, $[NC(CH_2)_{10}CO]_2O$, DBU, DMAP.

was enhanced, the quinaldate approach was abandoned because of the much weaker fluorescence.

Compound **4** was designed to overcome the disadvantages of **3**. In a one-pot/two-step reaction (Scheme 1), naphthoylation of ouabagenin was followed by 11-cyanoundecanoylation to give the strongly fluorescent **4**, 85% yield; 231 nm (ε 158 000 M cm$^{-1}$); CD 227 (+260), 240 (−317), $A$ −577; $\lambda_{ex}$ = 234 nm, $\lambda_{em}$ = 360 nm).§ A typical reaction is performed as follows. Ouabagenin (*ca.* 1 μg, dried in a silylated vial), was dissolved in 120 μl anhydrous acetonitrile, and treated with 2-naphthoylimidazole (3 mg) and DBU (0.4 μl). The reaction mixture was stirred for 1 h at room temperature followed by the addition of 11-cyanoundecanoic anhydride (5 mg),¶ and a catalytic amount of DMAP. After stirring for a further 8 h at room temperature, the reaction was quenched by adding 1 ml of 1 : 4 acetonitrile–water. After removal of acetonitrile, the mixture was applied to a Waters $C_{18}$ SepPak cartridge, and then washed sequentially with acetonitrile–water mixtures: 10 ml of 1 : 4, 10 ml of 2 : 3, 8 ml of 4 : 1 and 1 ml of 9 : 1. The final product was eluted with 4 ml acetonitrile, loaded onto a Vydac $C_{18}$ column (4.6 × 250 mm, 10 μm) and eluted isocratically with acetonitrile–water 82 : 18 at 1 ml min$^{-1}$. The products were detected by a fluorescence detector (Hewlett Packard 1046A fluorescence detector, $\lambda_{ex}$ = 234 nm, $\lambda_{em}$ = 360 nm). As depicted in Fig. 1(*a*), the HPLC peaks of ouabagenin trinaphthoate **3** overlap with the asterisked naphthoylation reaction byproducts, whereas the tetranaphthoate peak does not; introduction of the hydrophobic undecanoyl chain increases the retention time leading to no overlap [Fig. 1(*c*)]. Furthermore, **4** offered increased LC/MS detectability.‖ Whereas the limit of detection (LOD) for ouabagenin trinaphthoate was *ca.* 25 ng by single ion monitoring ionspray LC/MS, as little as 300 pg of acyl derivative **4** could be detected under the same conditions. Only part of the sensitivity enhancement observed with **4** is accounted for by increased hydrophobicity since LODs of 0.7 and 0.3 ng were measured for ouabagenin tetranaphthoate and 11-undecanoyl ouabagenin trinaphthoate, respectively.

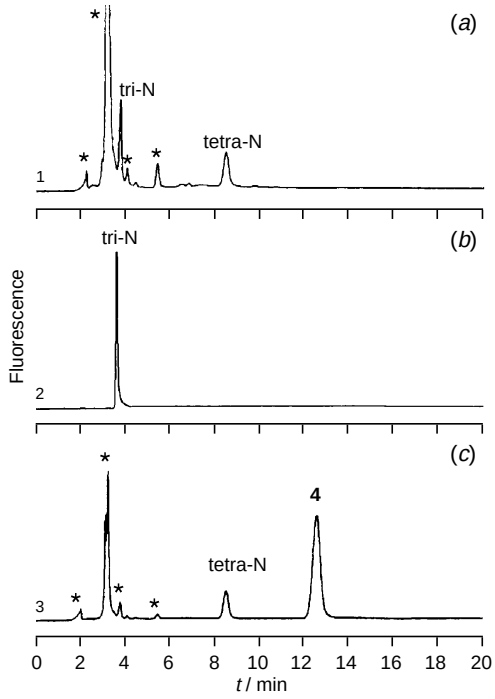



**Fig. 1** Fluorescence-detected HPLC profiles: (*a*) reaction mixture of naphthoylation of ouabagenin; (*b*) authentic ouabagenin trinaphthoate; (*c*) reaction mixture of one-pot/two-step derivatization. Asterisked peaks (*) are from reagents. tri-N = ouabagenin trinaphthoate; tetra-N = ouabagenin tetranaphthoate.

In summary, a general sub-μg derivatization/HPLC/MS/CD approach has been developed. The intense and fluorescent UV chromophore increases the sensitivity of fluorescence-detected HPLC and CD measurements, while the cyanoundecanoyl side chain increases the hydrophobicity to facilitate HPLC/MS analysis as well as increasing the MS sensitivity by *ca*. 100-fold as compared to a substrate without nitrogen. Application of this one-pot/two-step approach in HIF characterization is under way. It is clear that, with some modification, this approach is applicable to the identification, characterization, *etc.*, of other hydroxylated compounds.

The studies were supported by NIH grant GM 34509.

## Footnotes

† J. Dong, I. Akritopoulou-Zanze, J. Guo, N. Berova, K. Nakanishi and G. Haupert, in preparation.

‡ $^1$H NMR (400 MHz, $CDCl_3$) δ 8.22 (2 H, t, *J* 8.4 Hz), 6.97 (1 H, d, *J* 8.4 Hz), 5.89 (1 H, s, H-22), 5.87 (1 H, d, *J* 11.7 Hz, H-19), 5.71 (2 H, br s, H-1, H-3), 4.95 (1 H, d, *J* 18.2 Hz, H-21), 4.78 (1 H, d, *J* 11.7 Hz, H-19), 4.31 (1 H, m, H-11); FABMS 905 ($M^+$).

§ **4** exhibited the following characteristic peaks in $^1$H NMR (400 MHz, $CDCl_3$) δ 8.37 (1 H, s), 8.31 (1 H, s), 8.07 (1 H, s), 6.49 (1 H, s, H-1), 5.89 (1 H, s, H-22), 5.70 (1 H, br s, H-3), 5.33 (2 H, br s, 2 × H-19), 5.19 (1 H, m, H-11), 4.90 (1 H, d, *J* 17.8 Hz, H-21), 4.77 (1 H, d, *J* 17.8 Hz, H-21); FABMS 1093 ($M^+$).

¶ 11-Cyanoundecanoic anhydride was prepared from 11-cyanoundecanoic acid and DCC.

‖ Ionspray LC/MS was conducted on a Waters Nova-Pak C18 column (3.9 × 150 mm) with 1 ml min$^{-1}$ isocratic flow of 20% 2 mM $NH_4OAc$ in MeCN interfaced to a SCIEX API III mass spectrometer, using a 20 : 1 flow split and single-ion monitoring at the *m/z* of the $[M + NH_4]^+$ ion.

## References

1 J. M. Hamlyn, M. P. Balustein, S. Bova, D. W. DuCharme, D. W. Harris, F. Mandel, W. R. Mathews and J. H. Ludens, *Proc. Natl. Acad. Sci. USA*, 1991, **88**, 6259.
2 A. A. Tymiak, J. A. Norman, M. Bolgar, G. DiDonato, H. Lee, W. L. Parker, L.-C. Lo, N. Berova, K. Nakanishi, E. Haber and G. T. Haupert, *Proc. Natl. Acad. Sci. USA*, 1993, **90**, 8189.
3 N. Zhao, L.-C. Lo, N. Berova, K. Nakanishi, A. A. Tymiak, J. H. Ludens and G. T. Haupert, *Biochemistry*, 1995, **34**, 9893.
4 N. Ikemoto, L.-C. Lo and K. Nakanishi, *Angew. Chem., Int. Ed. Engl.*, 1992, **31**, 890.
5 N. Harada and K. Nakanishi, in *Circular Dichroic Spectroscopy—Exciton Coupling in Organic Stereochemistry*, University Science Books, Mill Valley, CA, 1983.
6 K. Nakanishi and N. Berova, in *Circular Dichroism, Principles and Applications*, ed. K. Nakanishi, N. Berova and R. E. Woody, VCH Publishers Inc., New York, 1994.

*Received, 20th August 1996; Com 6/05800K*

# NaY zeolite membrane for the pervaporation separation of methanol–methyl *tert*-butyl ether mixtures

**Hidetoshi Kita,*† Tsutomu Inoue, Hidetoshi Asamura, Kazuhiro Tanaka and Kenichi Okamoto**

*Department of Advanced Materials Science and Engineering, Faculty of Engineering, Yamaguchi University, Tokiwadai, Ube 755, Japan*

**NaY zeolite membrane grown hydrothermally on the surface of a porous alumina substrate shows a high alcohol selectivity in pervaporation, a membrane-based liquid separation process, of alcohol–benzene, cyclohexane or methyl *tert*-butyl ether.**

Pervaporation, a membrane process, has gained widespread acceptance in the chemical industry as an effective process for separation of azeotropic mixtures.[1] The process operates with a liquid feed, which contacts the upstream membrane face, and a vapour permeate under vacuum or a stream of inert gas and has been applied to the dehydration of organic liquids (ethanol, isopropyl alcohol, ethylene glycol, *etc*.) and many fundamental studies have been carried out.[2] Application of pervaporation to separate organic liquid mixtures such as aliphatic–aromatic hydrocarbons or alcohols–ethers, however, are still very limited because of the swelling of polymer membrane. On the other hand, membranes made from inorganic materials are generally superior to organopolymeric materials in thermal and mechanical stability, and chemical resistance. Among inorganic materials, zeolites are promising candidates as high-performance membranes because of the unique characteristics of zeolite crystals such as molecular sieving, ion exchange, selective adsorption and catalysis. Although there are many recent reports[3] on the preparation of zeolite membranes and gas permeation through them, only a limited number of publications[4–6] deal with pervaporation studies. Recently, we have reported a high pervaporation performance of NaA zeolite membrane for the separation of water–organic liquid mixtures.[6,7] Here, we report the synthesis of NaY zeolite membrane and its application to pervaporation.

NaY zeolite membrane was grown hydrothermally on the surface of a porous cylindrical alumina support (Nikkato Corp., 12 mm outer diameter, 1.5 mm thickness, 1.3 μm average pore size). The aluminosilicate gel used in the synthesis of NaY zeolite membrane was prepared by mixing a water-glass solution and alkaline aluminate solution as described in the literature.[8] After formation of the gel, the reaction mixture was stored at ambient temperature for 12 h. The molar composition of the resulting gel was $SiO_2/Al_2O_3$ = 10, $Na_2O/SiO_2$ = 1.4 and $H_2O/Na_2O$ = 60. The porous support was coated by a water slurry of seed crystals of NaY zeolite (HSZ-320NAA from Tosoh Co.) and then dried at 60 °C for 12 h. After ageing, the gel was poured into a polypropylene vessel and the support was placed in the gel. After hydrothermal treatment at 100 °C for 5 h, the support was taken out, washed with water and dried under reduced pressure.

The formulation of the NaY zeolite was verified by X-ray diffraction (XRD) with Cu-Kα radiation using a Shimadzu XD-D1 diffractometer. The XRD pattern of the NaY membrane grown on an alumina support consists of strong peaks corresponding to NaY zeolite and weak peaks of the alumina support. The surface of the membrane was examined by scanning electron microscopy (SEM) using a Hitachi S-2300 instrument. The surface of the alumina support was completely covered with randomly oriented, intergrown NaY zeolite crystals, 0.5–1 μm in size. The thickness of the membrane was about 20 μm judging from the cross-sectional view of the SEM image.

Pervaporation experiments were carried out using the apparatus described elsewhere.[6] The feed was introduced to the outer side of the zeolite membrane in a stainless-steel module that was placed in a thermostatted air-bath. Throughout the experiment the flow rate of the feed was held at 30–37 $cm^3$ $min^{-1}$. The effective membrane area was 47 $cm^2$ and the downstream pressure was maintained below 13.3 Pa. The membrane performance was evaluated by the permeation flux ($Q$/kg $m^{-2}$ $h^{-1}$) and the separation factor (α). The permeation flux was calculated by weighing the permeate collected by a liquid-nitrogen trap. The separation factor was determined as $\alpha_{A/B} = (Y_A/Y_B)/(X_A/X_B)$ where $X_A$, $X_B$, $Y_A$ and $Y_B$ denote the mass fraction of components A and B in the feed and the permeate, respectively, where A is the species which is preferentially pervaporated.

Table 1 shows the flux and the separation factor of pervaporation for liquid mixtures through NaY zeolite membrane together with previously reported pervaporation results for water–ethanol mixtures through NaA zeolite membranes.[6,7] The NaA zeolite membrane was highly selective for permeating water preferentially with high permeation flux because of the micropore filling of water in the zeolite pores or the intercrystalline pores between zeolite crystals to afford water-selective permeation through the membrane. NaY zeolite membrane also preferentially permeated water from water–alcohol mixtures. However, both the separation factor and the flux of the NaY zeolite membrane were lower than for the NaA zeolite membrane, probably due to the hydrophobic properties of NaY zeolite. On the other hand, NaY zeolite membrane showed a high alcohol selectivity for several feed mixtures with methanol or ethanol. Especially high separation factors were observed for methanol–methyl *tert*-butyl ether (MTBE) separation. In Fig. 1 pervaporation selectivity expressed as methanol mole fraction in the permeate is shown as a function of methanol mole fraction in the feed mixture. It can be observed that pervaporation through NaY zeolite membrane ensures MTBE enrichment in the feed phase by preferential methanol transfer. The corresponding vapour–liquid equilibrium (VLE) curve[9] is also shown and displays large deviation from ideality. This non-ideal behaviour results in the formation of a vapour–liquid azeotrope of composition 68.5 mol% MTBE at 51.27 °C and

**Table 1** Pervaporation performance of NaY zeolite membrane

| Zeolite | Feed solution (A/B) (mass% of A) | $T$/°C | α(A/B) | $Q$/kg $m^{-2}$ $h^{-1}$ |
|---|---|---|---|---|
| NaY | Water–Ethanol (10) | 75 | 125 | 1.59 |
| | Methanol–Benzene (14) | 50 | 1 400 | 0.62 |
| | Methanol–MTBE (10) | 50 | 7 600 | 0.32 |
| | | 40 | 6 500 | 0.21 |
| | Ethanol–Benzene (10) | 50 | 740 | 0.15 |
| | Ethanol–Cyclohexane (14) | 50 | 540 | 0.19 |
| NaA[a] | Water–Ethanol (10) | 75 | 10 000 | 2.15 |

[a] Ref. 6.

atmospheric pressure.[9] It is clear that pervaporation through NaY zeolite membrane can break up the azeotrope and is more selective than distillation (VLE).

Pervaporation flux and separation factors of NaY zeolite membrane for methanol–MTBE mixtures at 50 °C are plotted against the feed composition in Fig. 2. High separation factors were obtained over a wide range of feed compositions. The flux increased from 0.17 kg $m^{-2}$ $h^{-1}$ at 5.3 mol% methanol composition to 0.32 kg $m^{-2}$ $h^{-1}$ at 23 mol% composition while it was almost constant over the range 23–73 mol% composition. It is well known that the overall selectivity of a pervaporation process is determined by mobility selectivity and sorption selectivity. For methanol–MTBE mixtures, the kinetic diameters of these two molecules are approximately 0.38 and 0.62 nm, respectively, and are smaller than the intrinsic NaY zeolite pores of 0.74 nm.[8] Therefore, the sorption process presumably determines the pervaporation performance. Methanol sorption into the membrane increases with increasing methanol feed concentration and increasing sorption causes an increase in the pervaporation flux. When the methanol sorption approaches saturation, the flux becomes constant as shown in Fig. 2. Thus, the high selectivity of NaY zeolite membrane may be attributed to the selective sorption of methanol into the membrane.

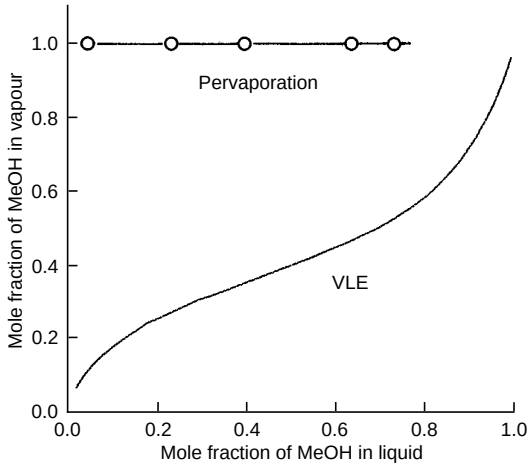



**Fig. 1** Pervaporation selectivity at 50 °C through NaY zeolite membrane and vapour–liquid equilibrium (VLE) at 101 kPa in the methanol–MTBE system

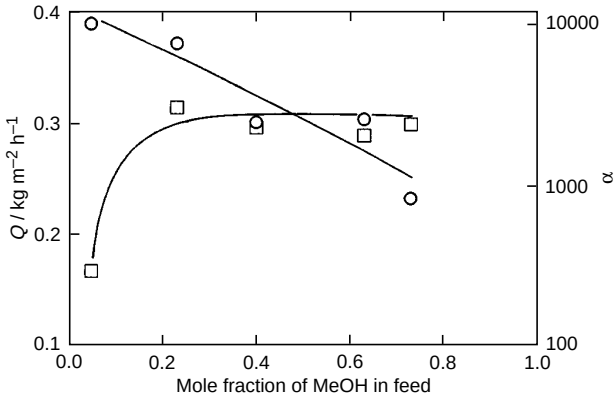



**Fig. 2** Flux $Q$ (□) and separation factor α (○) as a function of methanol feed concentration for pervaporation of methanol–MTBE mixtures through NaY zeolite membrane at 50 °C

## Footnote

† E-mail: kita@po.cc.yamaguchi-u.ac.jp

## References

1 H. L. Fleming, *Chem. Eng. Prog*., 1992, July, 46.
2 *Pervaporation Membrane Separation Processes*, ed. R. Y. M. Huang, Elsevier, Amsterdam, 1991; *Membrane Separations Technology Principles and Applications*, ed. R. D. Noble and S. A. Stern, Elsevier, Amsterdam, 1995.
3 E. R. Geus, M. J. den Exter and H. van Bekkum, *J. Chem. Soc., Faraday Trans*., 1992, **88**, 3101; Y. Y. Yan, M. E. Davis and G. R. Gavalas, *Ind. Eng. Chem. Res*., 1995, **34**, 1652; H. H. Funke, M. G. Kobalchick, J. L. Falconer and R. D. Noble, *Ind. Eng. Chem. Res*., 1996, **35**, 1575 and references therein.
4 P. Koelsch, D. Venzke, M. Noack, P. Toussaint and J. Caro, *J. Chem. Soc., Chem. Commun*., 1994, 2493.
5 T. Sano, H. Yanagishita, Y. Kiyozumi, F. Mizukami and K. Haraya, *J. Membr. Sci*., 1994, **95**, 221.
6 H. Kita, K. Horii, Y. Ohtoshi, K. Tanaka and K. Okamoto, *J. Mater. Sci. Lett*., 1995, **14**, 206; H. Kita, K. Horii, K. Tanaka, K. Okamoto, N. Miyake and M. Kondo, *Proceedings of 7th International Conference on Pervaporation Processes in the Chemical Industry*, ed. R. Bakish, Bakish Materials, Englewood, USA, 1995, p. 364.
7 H. Kita, *Maku* (*Membrane*), 1995, **20**, 169.
8 D. W. Breck, *Zeolite Molecular Sieves*, Wiley, New York, 1974, p. 245.
9 K. Alm and M. Ciprian, *J. Chem. Eng. Data*, 1980, **25**, 100.

*Received, 14th August 1996; Com. 6/05708J*

# Kinetics of nitric oxide scavenging by ruthenium(III) polyaminocarboxylates: novel therapeutic agents for septic shock

**Nathan A. Davies,[a] Mike T. Wilson,[a] Elizabeth Slade,*[b] Simon P. Fricker,[b] Barry A. Murrer,[b] Nigel A. Powell[b] and Graham R. Henderson[b]**

[a] *School of Biological and Chemical Sciences, Main Campus, University of Essex, Wivenhoe Park, Colchester, UK CO4 3SQ*
[b] *Johnson Matthey Technology Centre, Blount's Court, Sonning Common, Reading, Berks, UK RG9 4NH*

**The reaction of two representative ruthenium(III) polyaminocarboxylates with nitric oxide are rapid ($k$ > $10^7$ $M^{-1}$ $s^{-1}$ at pH 7.4 and 7.3 °C) forming tight ($K$ = $10^8$ $M^{-1}$) ruthenium(II) mononitrosyls.**

In the last decade nitric oxide (NO) has been found to be an essential component in many physiological processes and dysfunction in NO metabolism has been associated with a number of disease states such as epilepsy, arthritis, hypertension and septic shock.[1,2] In particular, overproduction of NO is implicated in the catastrophic drop in blood pressure associated with septic shock. This hypotension does not always respond well to conventional therapy such as intravenously administered adrenaline and dopamine.[3] Novel therapeutic approaches have largely concentrated on the development of inhibitors of the enzyme, inducible nitric oxide synthase (iNOS).[4] An alternative, however, is to remove NO by use of a specific, high affinity, non-toxic scavenger.

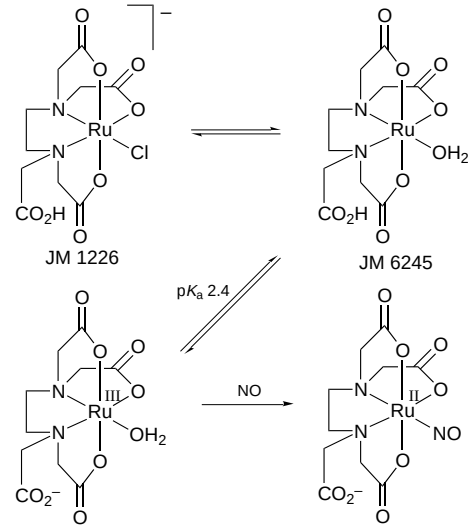
NO is a well characterised ligand for transition metals, having a high affinity for ferrous haem, indeed the biological effects of NO in regulation of blood pressure are brought about by the interaction of NO with the haem iron of the enzyme guanylate cyclase.[1] Ruthenium has a high affinity for NO and forms more nitrosyls than any other metal.[5] A strategy has been adopted in which ruthenium is chelated with suitable ligands which confer water solubility, allowing rapid *in vivo* clearance and unlike iron, low toxicity, whilst providing an available binding site for NO. The polyaminocarboxylates satisfy these requirements as ligands.

We have shown that the ruthenium(III) polyaminocarboxylates K[Ru(Hedta)Cl],[6] JM1226, and [Ru(Hedta)($H_2O$)],[6,7] JM6245 (Scheme 1) will reduce the level of nitrite in the cell culture medium of RAW264 macrophage cells stimulated to produce NO, and reverse lipopolysaccharide (LPS) induced hypotension in rats.[8,9]

Here, we report the NO binding properties of JM1226 and JM6245, JM1226 is water soluble at mM concentrations, forming a pale yellow solution in phosphate buffer over the pH range 6.5–8.0. Storage of JM1226 in phosphate buffer at pH 7.4 for more than 5 h at room temperature resulted in a change in the absorption spectrum due to formation of a dark green species. This green species is attributed to formation of a mixed valence $Ru^{III}Ru^{IV}$ μ-oxo dimer.[10] All experiments were therefore performed with freshly prepared solutions.

The absorption spectra of JM1226 at all pH values examined (6.5–8.0) are identical to the corresponding spectra for JM6245, indicating that the chloride is rapidly replaced in aqueous solution and that the mechanism of reaction of JM1226 with NO proceeds *via* the formation of the aqua species, JM6245, Scheme 1.

On addition of an aqueous NO solution to a solution of JM1226 a small change is observed in the near-UV region of the spectrum, leading to a loss of absorbance at 290 nm and an increase in absorbance below 270 nm, with an isosbestic point at 272 nm. We have utilized this absorbance change to determine the binding stoichiometry of NO to $Ru^{III}$ and to obtain an estimate of the binding affinity. Fig. 1 shows a titration of JM1226 (100 μM) with NO. The inset to Fig. 1 demonstrates that NO forms a 1:1 adduct with JM1226/




**Scheme 1** The proposed mechanism for the reaction of JM1226 with NO involves formation of the aqua complex, JM6245. Substitution at the aqua position is thought to proceed by associative ligand substitution[7] to give the ruthenium(II) mononitrosyl.

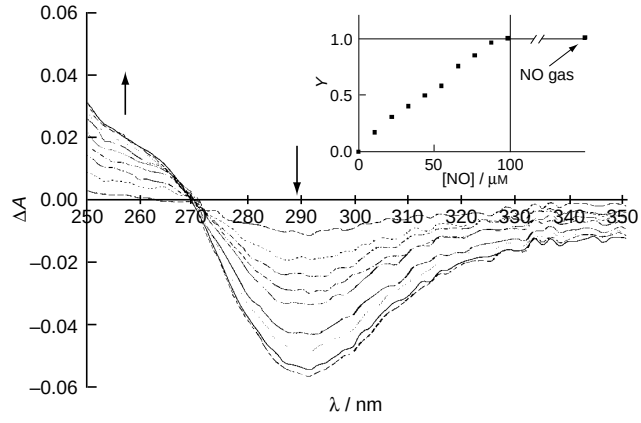



**Fig. 1** Difference spectrum of JM1226 in phosphate buffer (50 mM) at pH 7.4 titrated against an aqueous NO solution of known concentration calculated by titration of ferrous myoglobin with the NO solution.[11] Inset: the binding curve of JM1226 (100 μM) and NO is calculated for the absorbance change at 290 nm and indicates a 1:1 Ru–NO complex is formed. The fractional saturation, $Y$, is defined as $Y = (A - A_0)/(A_\infty - A_0)$, where $A_0$ and $A_\infty$ are absorbances in the absence and presence of saturating NO and $A$ is the absorbance after the addition of a sub-saturating concentration of NO.

JM6245. The affinity is high and cannot be determined from this figure directly, however the linearity of the binding curve approaching saturation indicates that the binding constant is $> 10^8$ M$^{-1}$. These findings are consistent with formation of a strong Ru–NO bond.[5]

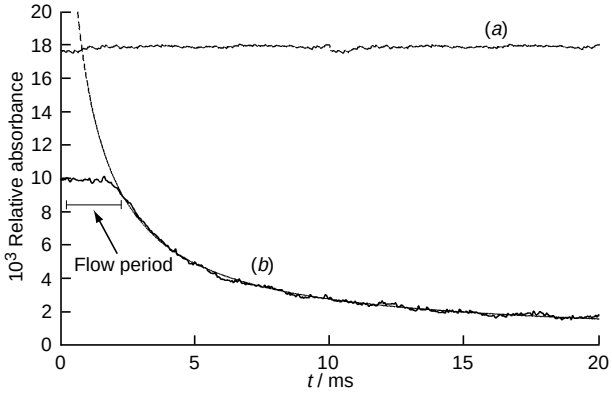



**Fig. 2** Change in absorbance of an anaerobic solution of JM1226 (25 μM) with time, in the absence (*a*) and presence (*b*) of NO (25 μM) in phosphate buffer (50 mM), pH 7.4 at 7.3 °C. The fit is to a second-order rate equation, traces are an average of six measurements. Spectra were recorded on an Applied Photophysics DX17 stopped-flow spectrometer with a measured deadtime of 1 ms.

**Table 1** Calculated second-order rate constants from stopped-flow experiments. All experiments were conducted in phosphate buffer (50 mM) at the pH and temperature stated. Errors represent standard deviation, $n = 6$, in each case

| Compound | pH | *T*/°C | $10^{-7}$ *k*/M$^{-1}$ s$^{-1}$ |
|---|---|---|---|
| JM1226 | 8 | 7.7 | 3.33 ± 0.17 |
| JM1226 | 7.4 | 7.3 | 2.24 ± 0.05 |
| JM1226 | 6.5 | 7.4 | 1.39 ± 0.01 |
| JM6245 | 8 | 7.2 | 3.29 ± 0.14 |
| JM6245 | 7.4 | 7.2 | 1.95 ± 0.06 |
| JM6245 | 6.5 | 7.5 | 2.18 ± 1.06 |

The binding of NO by JM1226/6245 is extremely rapid, Fig. 2, Table 1. As expected JM1226 and 6245 yield, within experimental error, the same rate constants and the reactions display little, if any, pH dependence. At room temperature most of the reaction occurs within the dead time of the apparatus (1 ms), hence the rate measurements were made at 7 °C. At this temperature we see a rapid NO concentration-dependent loss in absorbance, the amplitude of which is consistent with the spectral change on formation of the Ru–NO complex, Fig. 1. At wavelengths below the isobestic point (272 nm, Fig. 1) we observed an increase in absorbance (not shown) with the same course as that shown in Fig. 2 confirming that the process depicted in the figure is a result of the rapid binding of NO to the ruthenium complex. At pH 7.4 and 7.3 °C the rate constant is *ca*. $2 \times 10^7$ M$^{-1}$ s$^{-1}$, we therefore estimate that at physiological temperature the rate constant will exceed $10^8$ M$^{-1}$ s$^{-1}$.

We have shown that at physiological pH JM1226/JM6245 binds NO tightly and rapidly to form a stable 1 : 1 ruthenium(II) mononitrosyl. These properties confirm the pharmacological observations in a model of LPS induced endotoxic shock,[8] that ruthenium(III) polyaminocarboxylate complexes have potential as NO scavengers in NO mediated diseases.

## References


1 S. Moncada, R. M. J. Palmer and E. A. Higgs, *Pharmacol. Rev*., 1991, **43**, 109.
2 C. Nathan, *FASEB J*., 1993, **6**, 3051.
3 M. P. Glauser, G. Zanetti, J.-D. Baumgartner and J. Cohen, *Lancet*, 1991, **338**, 732.
4 J. F. Kerwin, Jr., J. R. Lancaster, Jr. and P. L. Feldman, *J. Med. Chem*., 1995, **38**, 4343.
5 F. Bottomley, *Coord. Chem. Rev*., 1978, **26**, 7.
6 A. A. Diamantis and J. V. Dubrawski, *Inorg. Chem*., 1981, **20**, 1142.
7 T. Matsubara and C. Creutz, *Inorg. Chem*., 1979, **18**, 1956.
8 S. P. Fricker, E. Slade, N. A. Powell, B. A. Murrer, I. L. Megson, G. D. Kennovin, S. T. Bisland, M. Loveland and F. W. Flitney, *The Biology of Nitric Oxide*, Portland Press, London, 1996, Part 5, p. 330.
9 S. P. Fricker, *Platinum Met. Rev*., 1995, **39**, 150.
10 J. Zhou, W. Xi and J. K. Hurst, *Inorg. Chem*., 1990, **29**, 160.
11 J. Torres and M. T. Wilson, *Methods Enzymol*., 1996, in the press.


*Received, 19th September 1996; Com. 6/06463I*

# Osmium(II) complexes of *N*-aryl-1,2-arylene diimines formed *via* *ortho*-dimerization of $ArNH_2$: synthesis, structure and redox properties

**Kedar Nath Mitra and Sreebrata Goswami*†**

*Department of Inorganic Chemistry, Indian Association for the Cultivation of Science, Calcutta 700 032, India*

**A family of *ortho*-arylene diimine chelates, $[OsBr_2L_2]$ (L = *N*-aryl-1,2-arylene diimine), which represent the first examples of osmium–quinonediimine complexes, are isolated from the reaction of $[NH_4]_2[OsBr_6]$ with aromatic amines, $ArNH_2$.**

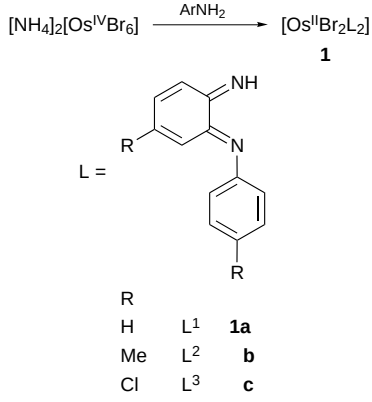
Here, we wish to introduce novel examples of bivalent osmium compounds of *N*-aryl-1,2-arylene diimines (L) which are formed *via* the template synthesis of L with osmium (Scheme 1). The compounds, $[OsBr_2L_2]$ **1**, represent the first examples[1] of osmium compounds of the *o*-arylene diimine family. This class of diimine[2] and dioxolene[3] complexes exhibits many interesting properties because of their redox propensities owing to the considerable mixing between metal and ligand orbitals. It may be noted[4] here that the above diimine ligands cannot be formed directly from the corresponding aminoarenes ($ArNH_2$).

In a typical experiment 0.25 g of $[NH_4]_2[OsBr_6]$ was mixed with a large excess of amine, $ArNH_2$ (*ca*. 0.5 g) and the resultant mixture was heated in an oil-bath at 130–135 °C in air for 1 h. After the removal of the excess of amine, the crude product was purified on a silica gel column eluting with chloroform–acetonitrile (9 : 1). Finally, the product was recrystallized from dichloromethane–hexane. Dark shiny crystals of $[OsBr_2L_2]$ **1** were obtained in *ca*. 50% yield.

The formation of **1** *via* the unusual oxidative *ortho*-dimerization reaction, $ArNH_2 \rightarrow L$, has been authenticated by the structure determination of a representative example, *viz*., $[OsBr_2L^1{}_2]$. A view of the molecule is shown in Fig. 1. The coordination sphere consists of $OsBr_2N_4$. Two bromides are *cis* to each other and the aryl-substituted imines are also in relative *cis* positions. The imine C–N bonds[5] [av. 1.323(19) Å] are shorter than the two C–N single bonds [C(19)–N(4), C(7)–N(2), av. 1.437(13) Å] present in the same molecule. Moreover, the average C–C lengths [1.349(26) Å] at positions that would have localized double bonds for the diimine form of the ligands are significantly shorter than the other C–C lengths [av. 1.418(20) Å] of the same ring. It is apparent from the structural data that there is very little delocalization in the coordinated diimine ligands with correspondingly no ambiguity in the bivalent oxidation state of osmium. The molecule approximates to overall $C_2$ symmetry. The twofold axis bisects the Br(1)–Os–Br(2) vector, as well as the N(2)–Os–N(4) vector.

All the osmium diimine compounds analysed satisfactorily. the $^1$H spectral features of the diamagnetic complexes consist of one relatively broad singlet resonance near δ 13.5, assignable[6] to NH (*e.g.* at δ 13.304 for **1b**), sharp methyl resonances (for **1b**) at δ 2.380 and 2.404 and resolved aromatic resonances in the range δ 6.5–8.0. Interestingly, each type of proton of L showed only one signal indicating magnetic equivalance of the two ligands in solution as found in the solid state. The electronic spectra of the complexes showed multiple charge-transfer transitions[7] occurring in the near-IR and visible regions [*e.g.* data for **1a** : λ/nm (ε/dm$^3$ mol$^{-1}$ cm$^{-1}$) 1150 (650), 900(780), 605(sh, 4310), 500(20050), 375(7290)].

Cyclic voltammetry of $[OsBr_2L_2]$ showed two oxidations and one reduction wave in the potential range 2.0 to −1.8 V *vs*. SCE. The two responses on the positive potentials are reversible ($\Delta E_p$ 60–65 mV, $i_{pa} = i_{pc}$) and assigned to successive one-electron transfers at the metal centre. The irreversible ligand reductions occur at negative potential. The potentials of the above couples shift anodically as the electron withdrawing ability of the substituent increases. For example, the potential of the $Os^{III}$–$Os^{II}$ couple shifts from 0.70 V for **1a** to 0.94 V for **1c**. This potential, 0.94 V for an $Os^{III}$–$Os^{II}$ couple, is one of the highest reported[8] in $[OsX_2\ L'_2]$ (X = Cl, Br; L′ = bidentate




**Scheme 1**

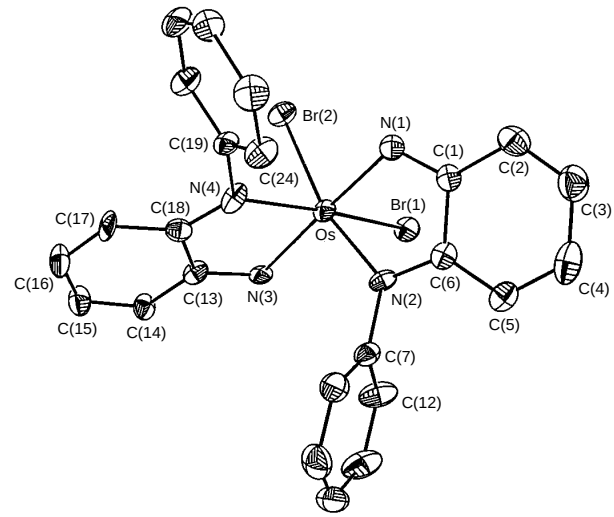



**Fig. 1** Molecular structure of $[OsBr_2L^1{}_2]$ showing the atom numbering scheme. Selected distances (Å) and angles (°): Os–Br(1) 2.519(2), Os–Br(2) 2.523(3), Os–N(1) 1.998(11), Os–N(2) 2.000(11), Os–N(3) 1.994(10), Os–N(4) 2.017(11), N(1)–C(1) 1.317(19), N(2)–C(6) 1.338(19), N(2)–C(7) 1.417(15), N(3)–C(13) 1.325(19), N(4)–C(18) 1.312(20), N(4)–C(19) 1.458(11); Os–N(1)–C(1) 116.7(7), Os–N(2)–C(6) 115.5(8), N(1)–C(1)–C(6) 113.6(12), N(2)–C(6)–C(1) 114.1(12), N(1)–Os–N(2) 77.9(4), N(3)–Os–N(4) 76.6(4), Os–N(3)–C(13), 118.2(6), Os–N(4)–C(18) 117.5(7), N(3)–C(13)–C(18) 112.8(12), N(4)–C(18)–C(13) 113.8(13).

ligand) systems. This may be attributed to the very strong π interactions between the metal and low-lying acceptor-ligand orbitals. This effect is also reflected in the short Os–N distance[7] (av. 2.002 Å) in $[OsBr_2L^1{}_2]$.

One-electron coulometric oxidation of **1a** at 0.9 V afforded a brown solution which can be quantitatively reduced to **1a** by electrolysis at 0.5 V. The brown solution of $\mathbf{1a}^+$ displayed a rhombic EPR spectrum with three distinct resonances at $g$ = 2.693, 2.401 and 1.638 indicating[9] the trivalent $d^5$ state of osmium in $\mathbf{1a}^+$.

The formation of L from $ArNH_2$ involves the transfer of four electrons and four protons. Therefore, a total of eight electrons and eight protons are released for the formation of two L in **1**. In contrast, the metal oxidation levels in $[NH_4]_2[OsBr_6]$ and **1** differ only by two units. The mechanism of the above reaction is, as yet, not established. However, we wish to note here that the above reaction does not proceed in an $N_2$ atmosphere in the absence of $O_2$. Presumably, *cis*-coordination of two aniline molecules followed by oxidative dimerization with the formation of a C–N bond in the presence of $O_2$ would be a plausible path for the formation of L in the above reaction. Osmium promoted oxidation of amine to imine by $O_2$ is known[10] in the literature. Interestingly, and as expected, 2,6-dimethylaniline did not react with $[OsBr_6]^{2-}$ under identical conditions.

Preliminary experiments indicate that compounds **1** serve as excellent starting materials for the syntheses of tris-chelates of osmium(II) diimines, the photochemistry and electrochemistry of which are of interest in contemporary research.[11] Detailed studies are in progress and will be reported elsewhere.

We are grateful to Professor A. Chakravorty and thank Dr P. Ghosh, IACS, Calcutta for their help in the X-ray analysis of **1a**. Financial support received from the UGC, New Delhi is acknowledged.

## Footnotes

† E-mail: icsg@iacs.ernet.in

‡ *X-Ray structure determination*: X-ray quality crystals (0.4 × 0.3 × 0.25 mm) of $[OsBr_2L^1{}_2]$ were obtained by slow diffusion of a dichloromethane solution of the complex into hexane. Cell parameters were obtained by least-square fits of 30 machine centred reflections. Data were collected ($3 \leqslant 2\theta \leqslant 43°$) on a Nicolet R3 m/V diffractometer (295 K) with graphite-monochromated Mo-Kα radiation (λ = 0.710 73 Å). Two check reflections were measured after 198 reflections did not show any significant change in intensity over 25 h exposure to X-rays. Data were corrected for Lorentz-polarization effect and absorption (azimuthal scan). Of the 2953 reflections collected 2858 were unique and 2386 reflections satisfying $I > 2\sigma(I)$ were used for structure solution by the Patterson heavy atom method using the SHELXTL-PLUS program[12] package on a MicroVax II computer. Refinement was done by the full-matrix least-squares method. All non-hydrogen atoms were made anisotropic. Hydrogen atoms were added at calculated positions and refined with fixed $U$ = 0.08 Å$^2$.

*Crystal data* for **2a**: $C_{24}H_{20}Br_2N_4Os$, $M$ = 712.2, triclinic, space group $P\bar{1}$, $a$ = 10.464(6), $b$ = 11.778(6), $c$ = 12.595(10) Å, α = 103.86(5), β = 112.72(6), γ = 107.79(4)°, $U$ = 1245.3(10) Å$^3$, $Z$ = 2, $D_c$ = 1.991 g cm$^{-3}$, $R$ = 0.046, $R'$ = 0.0521.

Atomic coordinates, bond lengths and angles, and thermal parameters have been deposited at the Cambridge Crystallographic Data Centre (CCDC). See Information for Authors, Issue No. 1. Any request to the CCDC for this material should quote the full literature citation and the reference number 182/298.

## References

1 A. A. Danopoulous, A. C. C. Wong, G. Wilkinson, M. B. Hursthouse and B. Hussain, *J. Chem. Soc., Dalton Trans.*, 1990, 315.
2 F. Hartl, T. L. Snoeck, D. J. Stufkens and A. B. P. Lever, *Inorg. Chem.*, 1995, **34**, 3887; H. Masui, A. B. P. Lever and E. S. Dodsworth, *Inorg. Chem.*, 1993, **32**, 258; A. Vogler and H. Kunkely, *Angew. Chem., Int. Ed. Engl.*, 1980, **19**, 221.
3 C. G. Pierpont and C. W. Lange, *Prog. Inorg. Chem.*, 1993, **41**, 381; A. S. Attia, S. Bhattacharya and C. G. Pierpont, *Inorg. Chem.*, 1995, **34**, 4427.
4 J. March, *Advanced Organic Chemistry*, 3rd edn., Wiley-Interscience, New York, 1985, p. 1034; R. L. Hand and R. F. Nelson, *J. Am. Chem. Soc.*, 1974, **96**, 850.
5 P. Belser, A. von Zelewsky and M. Zehnder, *Inorg. Chem.*, 1981, **20**, 3098; H. Y. Cheng and S.-M. Peng, *Inorg. Chim. Acta*, 1990, **169**, 23; A. M. Pyle, Y. M. Chiang and J. K. Barton, *Inorg. Chem.*, 1990, **29**, 4487.
6 L. F. Warren, *Inorg. Chem.*, 1977, **16**, 2814.
7 B. K. Ghosh, A. Mukhopadhyay, S. Goswami, S. Ray and A. Chakravorty, *Inorg. Chem.*, 1984, **23**, 4633.
8 B. K. Ghosh, S. Goswami and A. Chakravorty, *Inorg. Chem.*, 1983, **22**, 3358.
9 P. H. Rieger, *Coord. Chem. Rev.*, 1994, **135**/**136**, 203.
10 R. Tang, S. E. Diamond, N. Neary and F. Mares, *J. Chem. Soc., Chem. Commun.*, 1978, 562; S. E. Diamond, G. M. Tom and H. Taube, *J. Am. Chem. Soc.*, 1975, **97**, 2661; P. A. Lay, A. M. Sargeson, B. W. Skelton and A. H. White, *J. Am. Chem. Soc.*, 1982, **104**, 6161.
11 A. M. W. C. Thompson, *Coord. Chem. Rev.*, 1996, **152**, 157; J. R. Schoonover, P. Chen, W. D. Bates, R. B. Dyer and T. J. Meyer, *Inorg. Chem.*, 1994, **33**, 793.
12 G. M. Sheldrick, SHELXTL-PLUS 88, Structure Determination Software Programs, Nicolet Instrument Corp., Madison, WI, 1988.

*Received, 27th September 1996; Com. 6/06623B*

# Specific alkylidene coupling of the labile diruthenium bridging methylene complex $[(\eta\text{-}C_5H_5)_2Ru_2(\mu\text{-}CH_2)(CO)_2(MeCN)]$ with diazoalkanes ($N_2{=}CR_2$) giving alkenic products

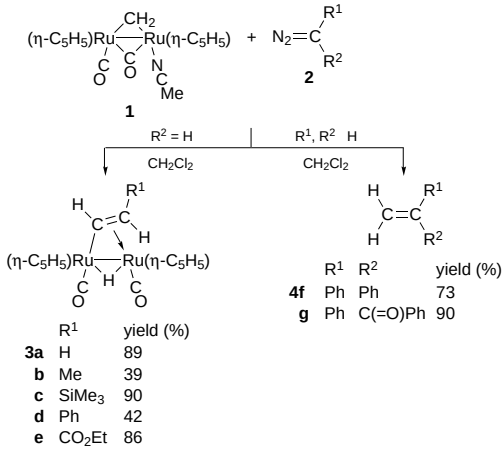
**Munetaka Akita,*[a] Ruimao Hua,[a] Selby A. R. Knox,*[b] Yoshihiko Moro-oka,*[a] Sadahiro Nakanishi[a] and Michael I. Yates[b]**

[a] *Research Laboratory of Resources Utilization, Tokyo Institute of Technology, 4259 Nagatsuta, Midori-ku, Yokohama 226, Japan*
[b] *School of Chemistry, University of Bristol, Bristol, UK BS8 1TS*

**Reaction of the labile diruthenium bridging methylene complex $[(\eta\text{-}C_5H_5)_2Ru_2(\mu\text{-}CH_2)(\mu\text{-}CO)(CO)(MeCN)]$ with diazoalkanes ($N_2{=}CR^1R^2$) results in specific C–C coupling to give alkenic products, *i.e.* the bridging alkenyl complex $[(\eta\text{-}C_5H_5)_2Ru_2(\mu\text{-}CH{=}CHR^1)(\mu\text{-}H)(CO)_2]$ ($R^2$ = H) or alkene $CH_2{=}CR^1R^2$ ($R^1$, $R^2 \neq$ H).**

C–C coupling mediated by transition-metal–alkylidene species is involved in many useful stoichiometric and catalytic organic transformations such as alkene cyclopropanation, metathesis and acetylene polymerization,[1] and most of the active species are mononuclear [$M{=}CR_2$] with an electrophilic vacant p orbital.[2a,b] In contrast, polynuclear bridging alkylidene species [$M_n(\mu\text{-}CR_2)$] appear to be sluggish with respect to C–C coupling, in particular, coupling with another $CR_2$ species, though they are recognized as better model compounds for surface-bound methylene species.[3] This is probably due to the σ character of the M–$CR_2$ bonds,[2c] and few successful examples of alkylidene coupling on a polynuclear system have been reported so far.[3] Herein we disclose the effective and specific C–C coupling of a labile diruthenium bridging methylene species $[(\eta\text{-}C_5H_5)_2Ru_2(\mu\text{-}CH_2)(\mu\text{-}CO)(CO)(MeCN)]$ **1**[4] with diazoalkanes ($N_2{=}CR^1R^2$ **2**), a reaction relevant to the carbon-chain propagation mechanism of catalytic CO hydrogenation.

When an ethereal solution of diazoalkane **2** was added to the labile bridging methylene species **1** at room temp. an instantaneous reaction took place with gas evolution (Scheme 1). In the case of the reaction with monosubstituted diazoalkane [$N_2{=}CR^1H$ (**2** $R^2$ = H); $R^1$ = H **a**, Me **b**, $SiMe_3$ **c**, Ph **d**, $CO_2Me$ **e**], the bridging alkenyl complexes $[(\eta\text{-}C_5H_5)_2Ru_2(\mu\text{-}CH{=}CHR^1)(\mu\text{-}H)(CO)_2]$ **3a**–**e**†,‡ were isolated in good yields after TLC separation. The products **3** were readily characterized on the basis of the NMR data† [(*i*) the separated $C_\alpha H_\alpha$ and $C_\beta H_\beta$ signals of the bridging alkenyl ligand ($\mu\text{-}C_\alpha H_\alpha{=}C_\beta H_\beta R^1$) and (*ii*) the hydride signal appearing around δ −15] and the absence




| | $R^1$ | yield (%) |
|---|---|---|
| **3a** | H | 89 |
| **b** | Me | 39 |
| **c** | $SiMe_3$ | 90 |
| **d** | Ph | 42 |
| **e** | $CO_2Et$ | 86 |

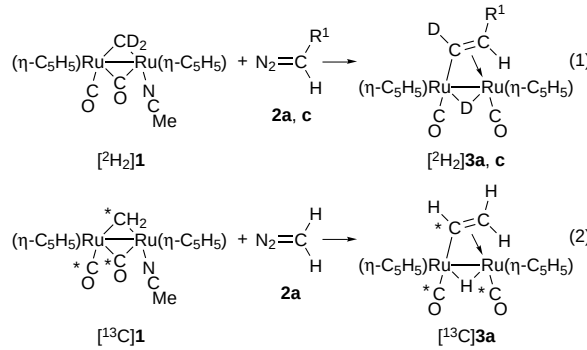
| | $R^1$ | $R^2$ | yield (%) |
|---|---|---|---|
| **4f** | Ph | Ph | 73 |
| **g** | Ph | C(=O)Ph | 90 |

**Scheme 1**

of a bridging CO stretching vibration. Derivatives of **3** including the structurally characterized **3b** have been previously obtained by a different route.[5] The reaction of **1** with disubstituted diazoalkane **2** [$R^1$ = $R^2$ = Ph **f**; $R^1$ = Ph, $R^2$ = C(=O)Ph **g**] afforded alkene $CH_2{=}CR^1$ $R^2$ **4f**,**g** and only a complicated mixture of organometallic products; the μ-H signal of **3** could not be detected.

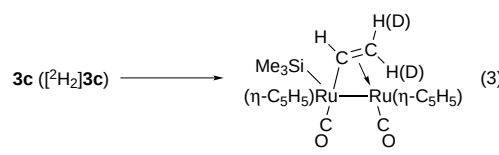
It is remarkable that the reaction conditions of the present C–C coupling are much milder than those of the thermal C–C coupling of the di(μ-alkylidene) complexes, $[(\eta\text{-}C_5H_5)_2Ru_2(\mu\text{-}CR_2)(\mu\text{-}CHR)(CO)_2]$ **5** (R = Me **a**,[6a] H **b**[6b]) (> 200 °C), and that the selectivity as well as the yield is superior to those of the latter systems.

In order to obtain an insight into the reaction mechanism, labelling experiments using $[^2H_2]$**1** (μ-$CD_2$) and $[^{13}C]$**1** (μ-$^{13}CH_2$) were carried out. Treatment of $[^2H_2]$**1** with **2a**,**c** produced $[^2H_2]$**3a**,**c** where the $H_\alpha$ and μ-H atoms were deuteriated completely [Scheme 2, eqn. (1)]. Similarly, the $^{13}C$-labelled methylene carbon atom in $[^{13}C]$**1** became the α carbon atom of the bridging alkenyl ligand in $[^{13}C]$**3a** [Scheme 2, eqn. (2)]. These labelling studies confirm that the C–C coupling is specific and that the α-CH and μ-H moieties in **3** come from the bridging $CH_2$ ligand in **1**.

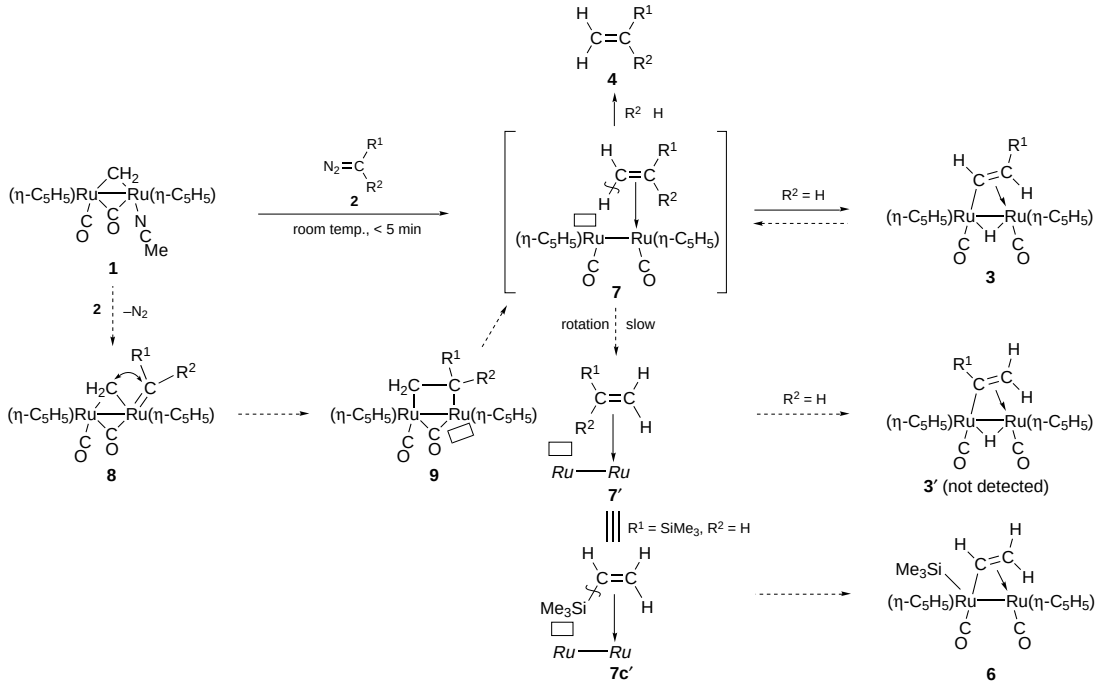



**Scheme 2** *C = $^{13}C$ enriched

It is also notable that thermolysis of the β-silylethenyl complex **3c** at 100 °C afforded the isomeric silyl–ethenyl complex **6** [eqn. (3)]. The rearrangement of $[^2H_2]$**3c** turned out to be specific as indicated by the formation of $[^2H_2]$**6** with the two β-methylene hydrogen atoms being deuteriated completely. Thus the β-$CH_2$ moiety in **6** originated from the μ-$CH_2$ ligand in **1**.




**6** ($[^2H_2]$**6**)



**Scheme 3** *Ru* = Ru(η-$C_5H_5$); □ = coordinatively unsaturated site

The specific alkylidene coupling and rearrangement can be interpreted in terms of the reaction mechanisms summarized in Scheme 3, involving the coordinatively unsaturated alkene species **7** as a key intermediate. Oxidative addition of a C–H bond in **7** would lead to the μ-alkenyl complex **3**, while in the case of the reaction with disubstituted diazoalkane (**2f**, **g**), the alkene **4** may be eliminated from the diruthenium centre due to the steric repulsion. The absence of the regioisomer **3′** and the results of the labelling experiments indicate that the C–H oxidative addition giving **3** must take place before the unsymmetrical structural information of **7** is lost (*e.g. via* rotation of the alkene ligand leading to **7′**). Because (*i*) the di(μ-alkylidene) complex **5** does not undergo C–C coupling under the present reaction conditions and (*ii*) the symmetrical structure of **5** cannot explain the results of the labelling experiments, the unsymmetrical η¹-alkylidene-μ-alkylidene species **8** and the dimetallacyclobutane **9** are plausible precursors of **7**. The different reactivities of complexes **8** and **5**, which have the same composition, may be attributed to the relative facility of migratory insertion *cf.* reductive elimination. Finally, thermolysis of the β-silylethenyl derivative **3c** is proposed to occur *via* reductive elimination to regenerate **7** with subsequent rotation of the alkene ligand (**7c′**) followed by oxidative addition of the Si–C bond giving rise to the silyl–ethenyl complex **6**.

The present study reveals that alkylidene units on a polynuclear system can be coupled with each other in a quite specific manner under very mild reaction conditions, if they are incorporated into the metal system in an appropriate way. In the present case, the C–C coupling is most probably realized *via* migratory insertion of the η¹-alkylidene-μ-alkylidene species **8**. A similar alkylidene coupling leading to an alkenic intermediate may occur on a heterogeneous catalyst surface, and, recently, a vinyl species has been proposed as an initiator of the carbon-chain propagation.[3e]

## Footnotes

† *Spectroscopic data*: **3a** (major isomer), $\delta_H$ (in $CDCl_3$) 8.48 (1 H, dd, *J* 7.8, 12.7 Hz, μ-C*H*=C$H_2$), 5.01, 4.84 (5 H × 2, s × 2, $C_5H_5$ × 2), 4.51 [1 H, d, *J* 7.8 Hz, μ-CH=C$H_2$ (*cis*)], 2.58 [1 H, d, *J* 12.7 Hz, μ-CH=C$H_2$ (*trans*)], −14.95 (1 H, s, μ-H); $\delta_C$ (in $C_6D_6$) 203.5, 202.4 (s × 2, CO), 144.4 (d, *J* 147 Hz, μ-*C*H=$CH_2$), 84.1 (d, *J* 176 Hz, $C_5H_5$), 83.5 (d, *J* 178 Hz, $C_5H_5$), 53.2 (t, *J* 156 Hz, μ-CH=*C*$H_2$); IR (in $CH_2Cl_2$) 1961, 1913 $cm^{-1}$. **3b** (major isomer), $\delta_H$ (in $C_6D_6$) 8.34 (1 H, d, *J* 11.7 Hz, μ-C*H*=CH), 4.76, 4.47 (5 H × 2, s × 2, $C_5H_5$), 3.54 (1 H, dq, *J* 5.9, 11.7 Hz, μ-CH=C*H*), 1.61 (3 H, d, *J* 5.9 Hz, $CH_3$), −14.44 (1 H, s, μ-H); IR (in $CH_2Cl_2$) 1954, 1911 $cm^{-1}$. **3c**, $\delta_H$ (in $CDCl_3$) 8.78 (1 H, d, *J* 13.9 Hz, μ-C*H* = CH), 5.06, 4.89 (5 H × 2, s × 2, $C_5H_5$ × 2), 2.55 (1 H, d, *J* 13.9 Hz, μ-CH=C*H*), −14.83 (1 H, s, μ-H); IR (in $CH_2Cl_2$) 1958, 1908 $cm^{-1}$. **3d** (major isomer), $\delta_H$ (in $C_6D_6$) 9.36 (1 H, d, *J* 12.5 Hz, μ-C*H*=CH), 7.2–7.0 (5 H, m, Ph), 4.80, 4.26 (5 H × 2, s × 2, $C_5H_5$ × 2), 4.64 (1 H, d, *J* 12.5 Hz, μ-CH=C*H*), −14.43 (1 H, s, μ-H); IR (in $CH_2Cl_2$) 1958, 1915 $cm^{-1}$. **3e** (major isomer), $\delta_H$ (in $CDCl_3$) 10.04 (1 H, d, *J* 11.7 Hz, μ-C*H*=CH), 5.20, 4.91 (5 H × 2, s × 2, $C_5H_5$ × 2), 4.18 (2 H, q, *J* 6.8 Hz, OC*H*$_2$CH$_3$), 3.55 (1 H, d, *J* 11.7 Hz, μ-CH=C*H*), 1.29 (3 H, t, *J* 6.8 Hz, OCH$_2$C*H*$_3$), −15.04 (1 H, s, μ-H); IR (in $CH_2Cl_2$) 1973, 1923, 1700 $cm^{-1}$..

‡ Complex **3** (except for **3c**) is composed of two isomers arising from the different configurations of the Ru auxiliaries ($C_5H_5$ and CO ligands) with respect to the $Ru_2$(μ-CH=CHR¹)(μ-H) core.[5]

## References


1 See, for example: J. P. Collman, L. S. Hegedus, J. R. Norton and Finke, *Principles and Applications of Organotransition Metal Chemistry*, University Science Books, Mill Valley, CA, 1987; G. W. Parshall and S. D. Ittel, *Homogeneous Catalysis*, 2nd edn., Wiley-Interscience, New York, 1992.

2 (*a*) H. Berke and R. Hoffmann, *J. Am. Chem. Soc*., 1978, **100**, 7224; (*b*) B. E. R. Schilling, R. Hoffmann and D. L. Lichtenberger, *J. Am. Chem. Soc*., 1979, **101**, 585; (*c*) N. M. Kostic and R. F. Fenske, *J. Am. Chem. Soc*., 1982, **104**, 3879.

3 W. A. Herrmann, (*a*) *Adv. Organomet. Chem*., 1982, **20**, 159; (*b*) *J. Organomet. Chem*., 1983, **250**, 319; (*c*) R. J. Puddephatt, *Polyhedron*, 1988, **7**, 767; (*d*) S. A. R. Knox, *J. Organomet. Chem*., 1990, **400**, 255; (*e*) P. M. Maitlis, H. C. Long, R. Quyoum, M. L. Turner and Z.-Q. Wang, *Chem. Commun*., 1996, 1. See also: (*f*) G. A. Somorjai, *Introduction to Surface Chemistry and Catalysis*, Wiley-Interscience, New York, 1994.

4 N. M. Doherty, J. A. Howard, S. A. R. Knox, N. J. Terril and M. I. Yates, *J. Chem. Soc., Chem. Commun*., 1989, 638.

5 R. E. Colborn, A. F. Dyke, S. A. R. Knox, K. Mead and P. Woodward, *J. Chem. Soc., Dalton Trans*., 1983, 2099.

6 (*a*) R. E. Colborn, D. L. Davis, A. F. Dyke, S. A. R. Knox, K. A. Mead and A. G. Orpen, *J. Chem. Soc., Dalton Trans*., 1989, 1799; (*b*) M. Akita, R. Hua, T. Oku and Y. Moro-oka, *Organometallics*, 1996, **15**, 2548.



*Received, 23rd September 1996; Com. 6/06525B*

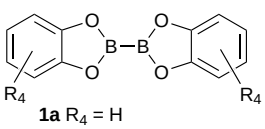
# Reaction between rhodium(III) bisboryls and diborane(4) compounds: evidence for a σ-bond metathesis process

**Todd B. Marder,*[a] Nicholas C. Norman,*[b] Craig R. Rice[b] and Edward G. Robins[b]**

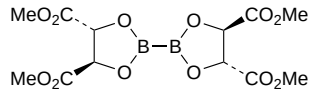
[a] *The University of Waterloo, Department of Chemistry, Waterloo, Ontario, Canada, N2L 3G1*
[b] *The University of Bristol, School of Chemistry, Bristol, UK BS8 1TS*

**The rhodium bis(boryl) complex [RhCl(PPh$_3$)$_2${B(cat)}$_2$] (cat = 1,2-O$_2$C$_6$H$_4$) reacts with the diborane(4) compounds B$_2$(O$_2$R)$_2$ {O$_2$R = 1,2-O$_2$C$_6$H$_3$Me-4, 1,2-O$_2$C$_6$H$_2$Bu$^t_2$-3,5 and dimethyl-L-tartrate [OCH(CO$_2$Me)CH(CO$_2$Me)O]} affording unsymmetrical metal bis(boryls) [RhCl(PPh$_3$)$_2${B(cat)}{B(O$_2$R)}] and diborane(4) compounds (cat)B–B(O$_2$R), one possible mechanism for which involves σ-bond metathesis.**

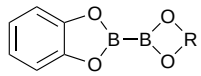
The oxidative addition of the B–B bond in certain diborane(4) compounds to low-valent transition-metal centres is now well established and results in metal bis(boryls) of the general formula [L$_n$M{BR$_2$}$_2$] some of which are active catalysts for the diboration of alkenes and alkynes.[1] During studies of the reactivity of metal boryls, we recently demonstrated that reversible oxidative addition–reductive elimination of B$_2$(cat)$_2$ **1a**[2] (cat = 1,2-O$_2$C$_6$H$_4$) occurs with the rhodium(III) tris(boryl) complex [Rh(PMe$_3$)$_3${B(cat)}$_3$],[3] and also that the platinum(II) bis(boryl) compound *cis*-[Pt(PPh$_3$)$_2${B(cat)}$_2$] reacts with the diborane(4) species B$_2$(1,2-O$_2$C$_6$H$_3$Bu$^t$-4)$_2$ **1b** to give the platinum bis(boryl) complex *cis*-[Pt(PPh$_3$)$_2${B(1,2-O$_2$C$_6$H$_3$-Bu$^t$-4)}$_2$] presumably *via* reductive elimination of **1a** followed by oxidative addition of **1b**.[1c] Reductive elimination of **1a** from the rhodium(III) bis(boryl) complex [RhCl(PPh$_3$)$_2${B(cat)}$_2$] **2a**[1a] in the presence of isocyanides has also been observed.[1f] In order to gain further insight into the factors which influence the oxidative addition–reductive elmination reaction of B–B bonds with transition-metal centres, we undertook a study of the reaction between complex **2a** and a series of diborane(4) compounds, preliminary results for which are described herein.



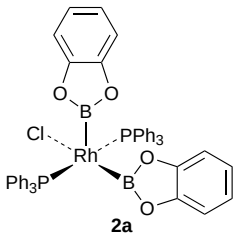
**1a** R$_4$ = H
**b** R$_4$ = 4-Bu$^t$-3,5,6-H$_3$
**c** R$_4$ = 4-Me-3,5,6-H$_3$
**d** R$_4$ = 3,5-Bu$^t_2$-4,6-H$_2$



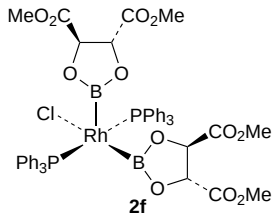
**1e**



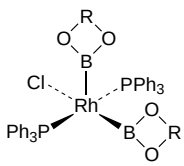
**1f** O$_2$R = 1,2-O$_2$C$_6$H$_3$Me-4
**g** O$_2$R = 1,2-O$_2$C$_6$H$_2$Bu$^t_2$-3,5
**h** O$_2$R = tartrate



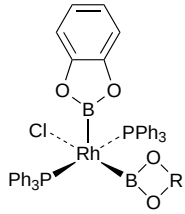
**2a**



**2f**



**2b** O$_2$R = 1,2-O$_2$C$_6$H$_3$Me-4
**d** O$_2$R = 1,2-O$_2$C$_6$H$_2$Bu$^t_2$-3,5



**2c** O$_2$R = 1,2-O$_2$C$_6$H$_3$Me-4
**e** O$_2$R = 1,2-O$_2$C$_6$H$_2$Bu$^t_2$-3,5
**g** O$_2$R = tartrate

The reaction between **2a** {generated *in situ* from the reaction between equimolar ratios of either [RhCl(PPh$_3$)$_3$] **3a** or [{RhCl(PPh$_3$)$_2$}$_2$] **3b** and **1a** in CH$_2$Cl$_2$ solution}[1a] and 1 equiv. of the diborane(4) compound B$_2$(1,2-O$_2$C$_6$H$_3$Me-4) **1c** was followed by $^{31}$P NMR spectroscopy which revealed the formation, after 2 h, of three products in a ratio of 1:2:1 (Fig. 1). One of these products was unreacted **2a** (δ 31.15, $J_{Rh–P}$ 112.9 Hz)[1a] and a second (δ 31.45, $J_{Rh–P}$ 114.8 Hz) was identified as the symmetrical bis(boryl) compound [RhCl(PPh$_3$)$_2${B(1,2-O$_2$C$_6$H$_3$Me-4)}$_2$] **2b**, prepared and identified independently from the reaction between **3b** and **1c**. The third, and major, product (δ 31.30, $J_{Rh–P}$ 114.8 Hz) we propose to be the mixed or unsymmetrical bis(boryl) complex [RhCl(PPh$_3$)$_2${B(cat)}{B(1,2-O$_2$C$_6$H$_3$Me-4)}] **2c** on the basis of the $^{31}$P NMR chemical shift, which is intermediate between those of the two symmetrical bis(boryls) **2a** and **2b**, and the value of $J_{Rh–P}$ which is almost identical to those of **2a** and **2b**. An identical $^{31}$P NMR spectrum to that shown in Fig. 1 was observed for the reaction between equimolar amounts of **2b** and **1a**.

Whilst the formation of the unsymmetrical bis(boryl) complex **3c** was unexpected, the generality of the reaction was

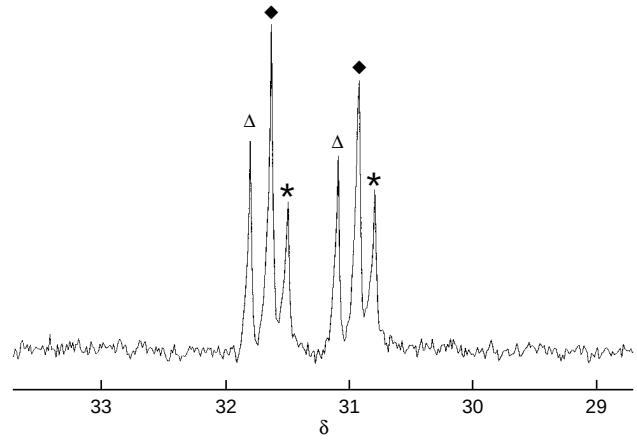
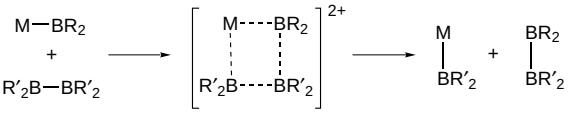



**Fig. 1** A $^{31}$P{$^1$H} NMR spectrum of the reaction between **2a** and **1c** in CH$_2$Cl$_2$ solution showing the presence of the compounds **2a** (*), **2b** (△) and **2c** (◆). Chemical shift and coupling constant data are given in the text. All spectra were recorded on a JEOL GX 400 spectrometer.

established with further examples. Thus the reaction between **2a** and $B_2(1,2\text{-}O_2C_6H_2Bu^t_2\text{-}3,5)_2$ **1d** afforded both the symmetrical species $[RhCl(PPh_3)_2\{B(1,2\text{-}O_2C_6H_2Bu^t_2 3,5)\}_2]$ **2d** (δ 31.85, $J_{Rh-P}$ 114.9 Hz)[1a] and the unsymmetrical compound $[RhCl(PPh_3)_2\{B(cat)\}\{B(1,2\text{-}O_2C_6H_2Bu^t_2\text{-}3,5)\}]$ **2e** (δ 31.70, $J_{Rh-P}$ 114.9 Hz) as well as unreacted **2a**, although in this case **2a** was present as the major species, the ratio of **2a** : **2e** : **2d** being *ca*. 7 : 1 : 1, and the reaction was observed to be considerably slower, taking about 24 h to reach completion.† Similarly, the reaction between **2a** and $B_2(tart)_2$‡ [tart = dimethyl L-tartrate, $OCH(CO_2Me)CH(CO_2Me)O$] **1e** afforded, in addition to unreacted **2a**, the symmetrical compound $[RhCl(PPh_3)_2\{B(tart)\}_2]$ **2f** (δ 32.05, $J_{Rh-P}$ 116.8 Hz) (prepared and identified independently from the reaction between **3b** and **1e**) and the unsymmetrical species $[RhCl(PPh_3)_2\{B(cat)\}\{B(tart)\}]$ **2g** (δ 31.55, $J_{Rh-P}$ 114.9 Hz), although the formation of **2f** was very slow and was only observed after about 9 days at which time the ratio of **2a** : **2g** : **2f** was 21 : 16 : 1.§ Interestingly, the reaction between **2f** and **1a** showed initial formation of **2a** and the unsymmetrical bis(boryl) **2g** was only observed after 6 days at which time the ratio of **2a** : **2g** : **2f** was 5 : 1 : 5.

All of these results imply that a scrambling of the diborane(4) compounds is occurring in solution in the presence of rhodium, further evidence for which was the observation and identification, by high-resolution mass spectrometry,¶ of the unsymmetrical diborane(4) compounds (cat)B–B(1,2-$O_2C_6H_3$Me-4) **1f**, (cat)B–B(1,2-$O_2C_6H_2Bu^t_2$-3,5) **1g** and (cat)B–B(tart) **1h** in their respective reaction solutions; no such compounds were observed in the absence of rhodium.

In terms of possible reaction mechanisms, we suspect that an oxidative addition–reductive elimination pathway, analogous to those described in the introductory paragraph, does occur since, in the reaction between **2f** and **1a**, the symmetrical bis(boryl) compound **2a** was observed prior to the appearance of the unsymmetrical species **2g**. The fact that unsymmetrical bis(boryls) and diborane(4) compounds are observed in all reactions, however, implies that an additional reaction mechanism must also be operating since simple oxidative addition–reductive elimination cannot afford such mixed products. Possible mechanisms which might account for the formation of the observed products include a double diborane(4) oxidative addition to give a rhodium(V) tetraboryl species such as $[RhCl(PPh_3)_n\{B(cat)\}_2\{B(O_2R)\}_2]$ ($O_2R$ = 1,2-$O_2C_6H_3$Me-4, 1,2-$O_2C_6H_2Bu^t_2$-3,5 and dimethyl-L-tartrate), or reductive elimination of ClB(cat) from a symmetrical bis(boryl) (for example, **2a**) followed by oxidative addition of diborane(4) to give a rhodium tris(boryl) complex $[Rh(PPh_3)_n\{B(cat)\}\{B(O_2R)\}_2]$, reductive elimination from either of which could afford the observed products. Whilst we cannot rule out either of these two possible mechanisms at this stage (particularly in view of the slowness of reactions involving **1d** and **1e** where the presence of trace amounts of undetected intermediates is a possibility), we note firstly the unlikelihood of the formation of a rhodium(V) complex in the former mechanism {although compounds which are formally rhodium(V) such as $[RhH_2(SiEt_3)_2(\eta\text{-}C_5Me_5)]$ have been described by Fernandez and Maitlis},[4] and, secondly, the lack of any evidence for oxidative addition of ClB(cat) to rhodium(I) triphenylphosphine centres (in this and other systems studied) which would subsequently be required in the latter mechanism in order to give the observed rhodium chloride bis(boryls). At this stage, the mechanism we prefer as the simplest explanation for these observations is one involving σ-bond metathesis, as shown in Scheme 1. Thus, whilst we have no direct evidence for this mechanism, we note that such mechanisms have been proposed by Smith[1d] to account for the reaction between **1a** and the platinum metallacyclopentane complex *cis*-$[Pt(PPh_3)_2\{(CH_2)_4\}]$ which affords *cis*-$[Pt(PPh_3)_2\{B(cat)\}_2]$ and (cat)$B(CH_2)_4$B(cat), and by Hartwig *et al.* in discussing the reaction between $[RuMe(PMe_3)_2(\eta\text{-}C_5H_5)]$ and HB(cat).[5] Furthermore, we note that complexes such as **2a** may be compared to the ruthenium(IV) alkylidene species of the form $[RuCl_2(=CR_2)(PR_3)_2]$ characterised by Grubbs and co-workers[6] which are known to be active alkene metathesis catalysts.




**Scheme 1**

Further studies relating to these observations are in progress, but the preliminary results described herein indicate the potential mechanistic complexity of systems involving metal boryls and diborane(4) compounds which will be an important consideration in any reactions in which metal boryls are employed as catalysts in diboration reactions.

T. B. M. thanks NSERC of Canada and N. C. N. thanks the EPSRC, Laporte plc and The Royal Society for research support, E. G. R. thanks EPSRC for a studentship and T. B. M. and N. C. N. thank NSERC and The Royal Society for supporting this collaboration *via* a series of Bilateral Exchange Awards. Johnson Matthey plc and E. I. Du Pont De Nemours and Co., Inc. are also thanked for generous supplies of rhodium salts.

## Footnotes

† We attribute the fact that the reaction between **2a** and **1d** is considerably slower than that between **2a** and **1c** to the fact that **1d** is much more sterically demanding than **1c**, consistent with which is the related observation that whilst **3a**,**b** react in minutes with **1a**, the corresponding reaction between **3a**,**b** and **1d** takes nearly 1 h to reach completion; steric congestion at the rhodium centre is also likely to favour a preponderance of the bis-B(cat) complex **2a** as observed.

‡ Compound **1e** was prepared from $B_2(NMe_2)_4$ and dimethyl-L-tartaric acid, $HOCH(CO_2Me)CH(CO_2Me)OH$, according to the general preparative routes described in ref. 2 and references therein; full details will be described in a future publication.

§ The slowness of this reaction is consistent with the observation that the reaction between **3a**,**b** and **1e** takes several days to go to completion.

¶ (cat)B–B(1,2-$O_2C_6H_3$Me-4) **1f** $C_{13}H_{10}B_2O_4$, ($M^+$) calc. *m/z* 252.076. Found *m/z* 252.076; (cat)B–B(1,2-$O_2C_6H_2Bu^t_2$-3,5) **1g** $C_{20}H_{24}B_2O_4$, ($M^+ - {}^{12}C^1H_3$) calc. *m/z* 335.163. Found *m/z* 335.163.

## References

1 (*a*) P. Nguyen, G. Lesley, N. J. Taylor, T. B. Marder, N. L. Pickett, W. Clegg, M. R. J. Elsegood and N. C. Norman, *Inorg. Chem.*, 1994, **33**, 4623; (*b*) R. T. Baker, P. Nguyen, T. B. Marder and S. A. Westcott, *Angew. Chem., Int. Ed. Engl.*, 1995, **34**, 1336; (*c*) G. Lesley, P. Nguyen, N. J. Taylor, T. B. Marder, A. J. Scott, W. Clegg and N. C. Norman, *Organometallics*, 1996, in the press; (*d*) C. N. Iverson and M. R. Smith, *J. Am. Chem. Soc.*, 1995, **117**, 4403; (*e*) T. Ishiyama, M. Matsuda, N. Miyaura and A. Suzuki, *J. Am. Chem. Soc.*, 1993, **115**, 11018; (*f*) R. T. Baker, J. C. Calabrese, S. A. Westcott, P. Nguyen and T. B. Marder, *J. Am. Chem. Soc.*, 1993, **115**, 4367.

2 F. J. Lawlor, N. C. Norman, N. L. Pickett, E. G. Robins, P. Nguyen, G. Lesley, T. B. Marder, J. A. Ashmore and J. C. Green, *Inorg. Chem.*, in the press.

3 C. Dai, G. Stringer, T. B. Marder, A. J. Scott, W. Clegg and N. C. Norman, *Inorg. Chem.*, in the press.

4 M. Fernandez and P. M. Maitlis, *J. Chem. Soc., Chem. Commun.*, 1982, 310.

5 J. F. Hartwig, S. Bhandari and P. R. Rablen, *J. Am. Chem. Soc.*, 1994, **116**, 1839.

6 P. Schwab, R. H. Grubbs and J. W. Ziller, *J. Am. Chem. Soc.*, 1996, **118**, 100 and references therein.

*Received, 14th October 1996; Com. 6/06993B*

# On the crystal structure of κ-alumina

**Hans-Leo Gross and Werner Mader***

*Institut für Anorganische Chemie der Universität Bonn, Römerstraße 164, 53117 Bonn, Germany*

**The idealized structure of κ-alumina is determined on the basis of lattice images by high-resolution electron microscopy and by applying crystallographic considerations and constraints of crystal chemistry.**

κ-Alumina was first observed in X-ray powder diffraction spectra of dehydration products of gibbsite by Stumpf *et al.*[1] in 1950. The unit-cell parameters as well as the space group of κ-alumina remained undetermined until 1991 when Liu and Skogsmo[2] performed electron diffraction on $Al_2O_3$ material generated by CVD. These authors determined the crystal system to be orthorhombic crystallising in the space group $Pna2_1$. The number of formula units is $Z = 8$ and a stacking sequence ABAC of closed-packed oxygen layers is the only possible one to be in accordance with that space group. Later, the lattice parameters were determined more precisely by means of X-ray powder diffraction to be $a = 0.4834$, $b = 0.8310$, $c = 0.8937$ nm by Halvarsson.[3] However, the crystal structure of κ-$Al_2O_3$, *i.e.* the cation distribution, was unknown up to now.

In the present study, κ-$Al_2O_3$ was produced by internal oxidation of a Nb–Al alloy with 5 atom% aluminium under the following conditions: $T = 1450$ °C, $p(O_2) = 10^{-4}$ mbar, $t = 30$ min. Using this method,[4] aluminium is internally oxidized to give $Al_2O_3$ precipitates within the metallic (Nb) matrix. Besides the modifications α-$Al_2O_3$ and θ-$Al_2O_3$, plate-like precipitates of κ-$Al_2O_3$ were observed using transmission electron microscopy (TEM). In the course of our TEM study we confirmed the results obtained by Liu and Skogsmo.[2] Furthermore, we were able to obtain high-resolution lattice images of κ-$Al_2O_3$ in different zone axes in order to obtain information on the (projected) cation distribution. The point-to-point resolution of 0.2 nm of the electron microscope (Philips CM30 SuperTwin, operated at 300 kV) does not allow the cations to be imaged separately. However, applying crystallographic considerations, the large amount of possible structural models can be reduced to only five structures, as outlined in the following.

Applying the ABAC stacking sequence and setting oxygen to (0,0,0), the positions of all the other oxygen ions in the idealized (undistorted) closed-packed anion sublattice are fixed. The *b* axis is parallel to a closed-packed direction in the oxygen layer and its length is three times the oxygen diameter. The *a* axis corresponds to the distance between two oxygen ions perpendicular to the closed-packed direction, while the *c* axis is parallel to the stacking direction of the layers (see Fig. 1). Since only one general position with multiplicity $M = 4$ exists in $Pna2_1$, four oxygen sites are symmetrically equivalent leaving six of the 24 anions in the unit cell symmetry-independent. This results in six independent octahedral sites and twelve tetrahedral sites, respectively. Owing to the stoichiometry, four of these independent interstitial sites have to be occupied resulting in 3060 principally possible structures calculcated by combination theory. (*i*) First we stipulate that the number of cations between the pairs of oxygen layers A–B, B–A, A–C, and C–A are identical. (*ii*) We can also exclude face-sharing and edge-sharing of $AlO_4$ tetrahedra with other tetrahedra as well as with $AlO_6$ octahedra, such elements do not exist in the structural chemistry of aluminium oxides. (*iii*) Since in aluminium oxides, aluminium preferentially occupies octahedral sites, a maximum value of 1 : 1 as the ratio of the occupied tetrahedral to octahedral sites is assumed. (*iv*) Cation layers showing exclusively tetrahedral occupation do not exist in the known aluminium oxides, and can be definitely excluded.

Following the boundary conditions (*i*)–(*iv*) for the cation occupation, five of the 3060 possible structures for κ-$Al_2O_3$ remain. Structures I–IV show only octahedrally coordinated aluminium, whereas structure V exhibits octahedral and tetrahedral coordination of aluminium with a ratio of 3 : 1. The latter structure is the structure we propose for κ-$Al_2O_3$. One indication of this structure is the spacing of 0.2234 nm of the closed-packed layers of κ-$Al_2O_3$, which corresponds better with the value of 0.2284 nm in the spinel aluminas relative to the value of 0.2165 nm in corundum. An even more substantial indication are the values of the Coulomb energies calculated for the five possible structure models and for corundum using the MAPLE program package.[5] The Coulomb energies are as follows. Structures I–IV: 3846–4024 kcal mol$^{-1}$. Structure V: 4232 kcal mol$^{-1}$. Corundum: 4354 kcal mol$^{-1}$ (cal = 4.184 J).

The proposed structure of κ-$Al_2O_3$ is shown in Fig. 1. From this it can be deduced that the most promising orientation for determining the cation positions is lattice imaging along [100] because the channels in the structure can be imaged best. A lattice image of κ-$Al_2O_3$ along [100] is shown in Fig. 2. The image simulation for a crystal thickness of 3.9 nm and focus setting of −78 nm shows very good matching with the observed image. Under these imaging conditions the brightest dots correspond to the channels between the octahedral double chains in the structure. The curved bright contrasts above represent the region of low atomic density, *i.e.* low scattering power along the chains of the $AlO_4$ tetrahedra. The dark contrast in the image corresponds to a region of high scattering power, produced in particular by the Al atoms, and forming intersecting dark lattice fringes of the planes (011) and ($0\bar{1}1$), respectively.

The crystal structure of κ-$Al_2O_3$ (Fig. 1) is isomorphous to that of $FeGaO_3$,[6] where aluminium occupies the iron and

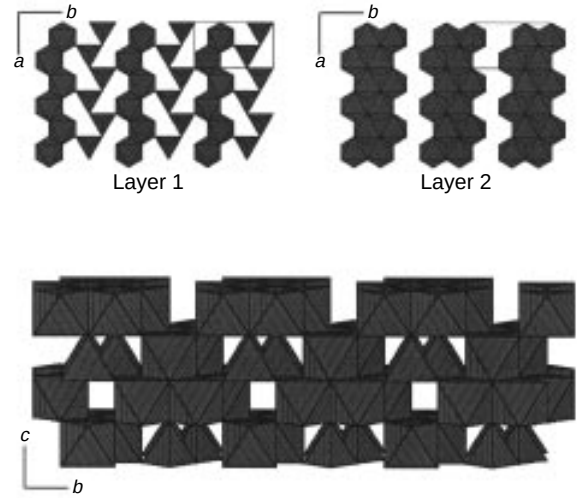



**Fig. 1** The idealized crystal structure of κ-$Al_2O_3$

gallium sites in the iron gallium oxide structure. The structure can be described as constituted by two different layers 1 and 2, which are stacked alternately along the direction of the *c* axis. Layer 1 consists of single chains of edge-sharing $AlO_6$ octahedra, which are connected *via* single chains of corner-sharing $AlO_4$ tetrahedra. Layer 2 is built up by edge-sharing $AlO_6$ octahedra, which are arranged as double chains parallel to the *a* axis, leaving channels of unoccupied octahedra in between. The repeat unit (length = *c* axis) contains four layers stacked as 121′2′, where the layers 1′ and 2′ are distinguished from the layers 1 and 2 by a rotation of 180° around the $2_1$-screw axis. In this structure the channels of unoccupied octahedra in layer 2 are bridged by the chains of tetrahedra of the adjacent layer 1.

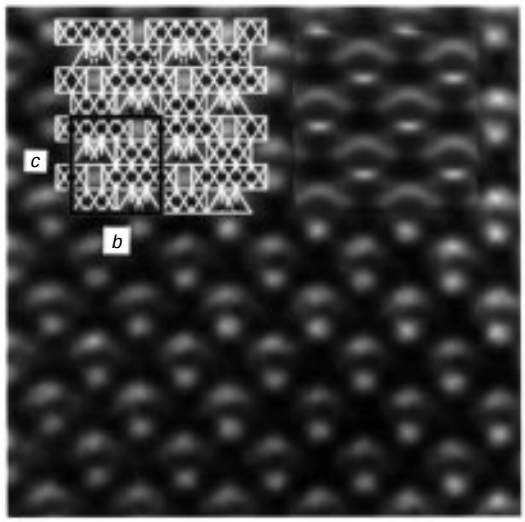



**Fig. 2** Lattice image of κ-$Al_2O_3$ along [100] with inserted image simulation, aluminium atoms and unit-cell dimensions

Further examinations using quantitative electron diffraction are currently being performed in order to evaluate the exact atomic coordinates of κ-$Al_2O_3$.

The help of Dr J. Mayer (MPI für Metallforschung, Stuttgart) in the electron microdiffraction is kindly acknowledged. We also thank Dr W. Assenmacher and Dr B. Freitag for experimental support and fruitful discussions. The financial support of the Ministerium für Wissenschaft und Forschung, NRW, Germany, under contract No. 10300892, is kindly acknowledged.

## References

1 H. C. Stumpf, A. S. Russell, J. W. Newsome and C. M. Tucker, *Ind. Eng. Chem.*, 1950, **42**, 1398.
2 P. Liu and J. Skogsmo, *Acta Crystallogr., Sect. B*, 1991, **47**, 425.
3 M. Halvarsson, PhD Thesis, Chalmers University of Technology, Göteborg, Sweden, 1994
4 W. Mader, *Z. Metallkd.*, 1989, **80**, 139.
5 R. Hoppe, *Angew. Chem*., 1970, **82**, 7.
6 S. C. Abrahams, J. M. Reddy and J. L. Bernstein, *J. Chem. Phys*., 1965, **42**, 3957

*Received, 30th September 1996; Com. 6/06661E*

# Direct transition from $S_A$ to antiferroelectric, ferroelectric or unknown phases of diastereomeric liquid-crystalline molecules with varying enantiomeric purities

**Koichi Mikami,*[a]† Tomoko Yajima,[a] Masahiro Terada,[a] Yoshiichi Suzuki[b] and Ichiro Kobayashi[b]**

[a] *Department of Chemical Technology, Tokyo Institute of Technology, Meguro-ku, Tokyo 152, Japan*
[b] *Central Research and Development Laboratory, Showa Shell Sekiyu K.K., 123-1 Shimokawairi, Atugi, Kanagawa 243-02, Japan*

**The phase sequences of diastereomeric α-trifluoromethyl-β-methyl-substituted liquid-crystalline molecules critically depend on the enantiomeric purities (% ee) not only for *ul*- but also for *lk*-diastereomers, to show eventually an unknown phase in the racemic region of either an *ul*- or an *lk*-diastereomer.**

New types of liquid-crystalline (LC) phases such as ferroelectric[1] (F) ($S_{C*}$), antiferroelectric[2] (AF) ($S_{C_A*}$), ferrielectric[3] ($S_{C_\alpha*}$ and $S_{C_\gamma*}$), and twist-grain boundary[4] (TGB) phases have recently been discovered in chiral LC molecules. Amongst these, the AF phase has been studied intensively both experimentally and theoretically, due to its potential applications in electro-optic devices.[5,6] However, only a limited number of AFLC molecules have been reported so far (Fig. 1) such as the methyl-substituted aryl ester (MHPOBC)[5a] and its trifluoromethyl analogue (TFMHPOBC),[5b] which bear a chiral alkyl terminus with a single stereogenic centre. In these, the direct phase transition from $S_A$ to $S_{C_A*}$ takes place in high enantiomeric excess (% ee) and the $S_{C*}$ phase occurs between the $S_A$ and $S_{C_A*}$ phases in the racemic region.[7] In order to investigate the relationship between molecular asymmetry and AFLC properties, we designed α-trifluoromethyl-β-methyl-substituted aryl esters which are diastereomers with double stereogenic centres. We report the intriguing feature that their phase sequence critically depends on the enantiomeric excesses (% ee) not only for *ul*- but also for *lk*-diastereomers.[8] Surprisingly, we also found a direct phase transition from $S_A$ to an unknown phase which shows an intriguing electro-optic response in the racemic composition for both diastereomers.

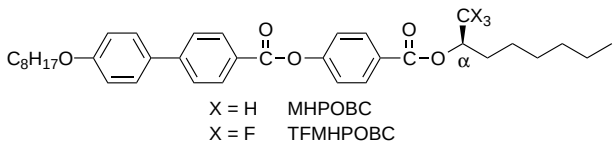
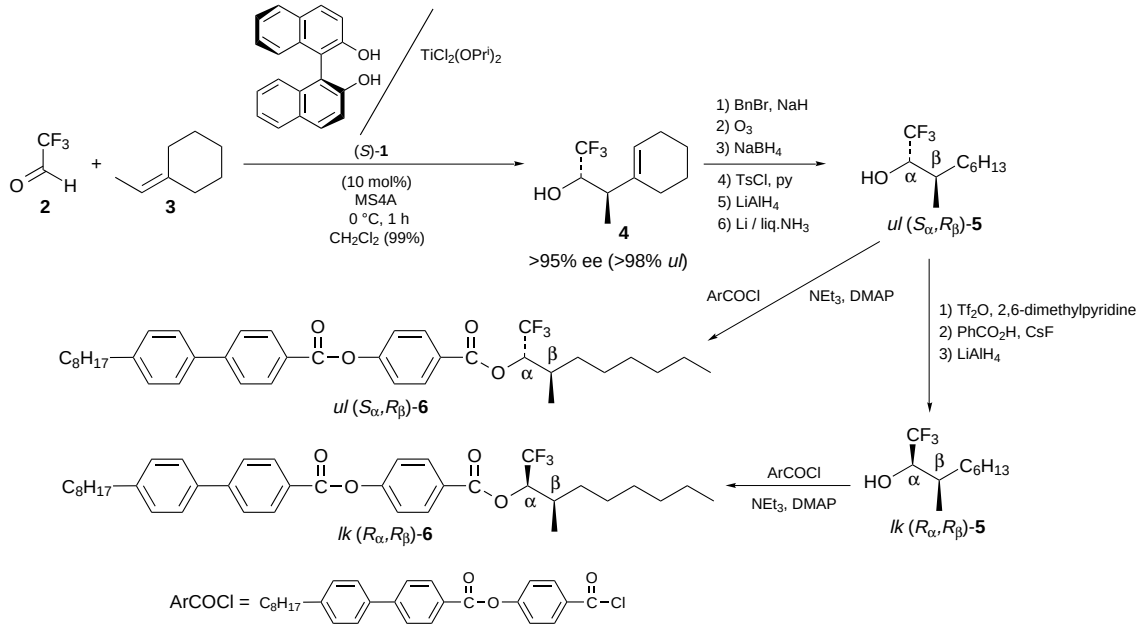



**Fig. 1**

Both enantiomers of diastereomeric LC molecules were synthesised through a chiral titanium complex-catalysed carbonyl–ene reaction[9] of fluoral **2** with ethylidenecyclohexane **3**,[10] using an (*S*)- or (*R*)-binaphthol-derived chiral titanium catalyst [(*S*)- or (*R*)-**1**][11] (Scheme 1). The *ul*($S_\alpha$,$R_\beta$)-alcohol **4** was thus obtained in an almost quantitative yield in more than 95% ee and 95% de, by the use of the (*S*)-binaphthol–titanium catalyst [(*S*)-**1**]. Protection of the alcohol, ozonolysis, reduction and deprotection led to the *ul*($S_\alpha$,$R_\beta$)-diastereomer **5** in an essentially stereopure form (> 95% ee, > 95% de). Inversion of the stereochemistry of a α-hydroxy group through the triflate derivative with benzoic acid by catalysis with caesium fluoride[12] produced an *lk*($R_\alpha$,$R_\beta$)-diastereomer **5** again in a stereochemically pure form (> 95% ee, > 95% de). Condensation of *ul*- and *lk*-**5** with 4-chlorocarbonylphenyl 4′-octyloxybiphenyl-4-carboxylate gave the diastereomeric LC molecules *ul*($S_\alpha$,$R_\beta$)- and *lk*($R_\alpha$,$R_\beta$)-**6**, respectively.

The phase sequences and transition temperatures for **6** were measured for varying enantiomeric excesses for the *ul*- and *lk*-




**Scheme 1**

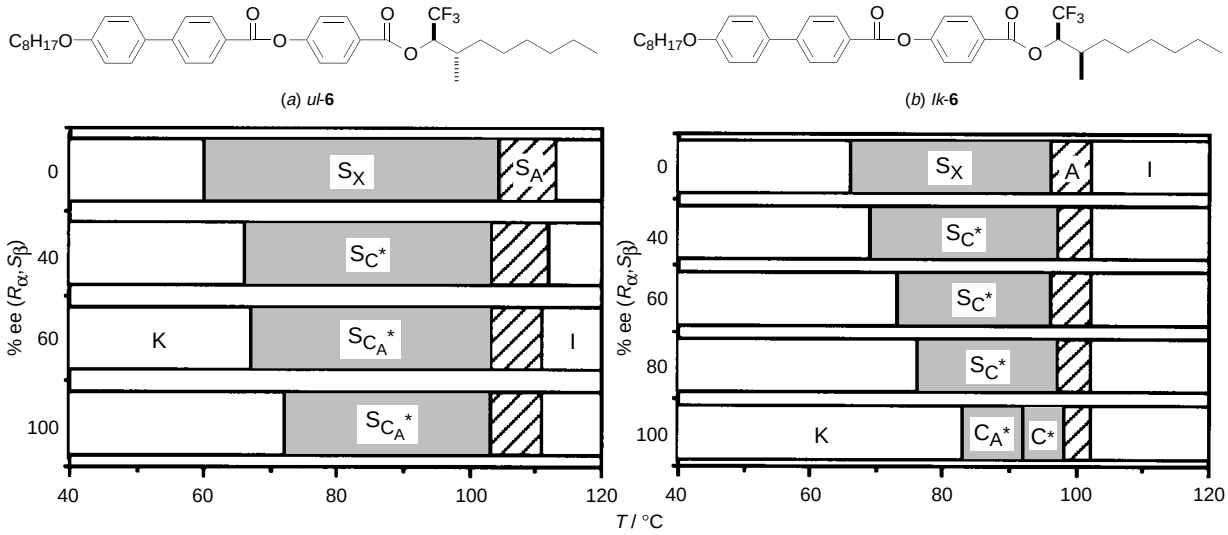



**Fig. 2**

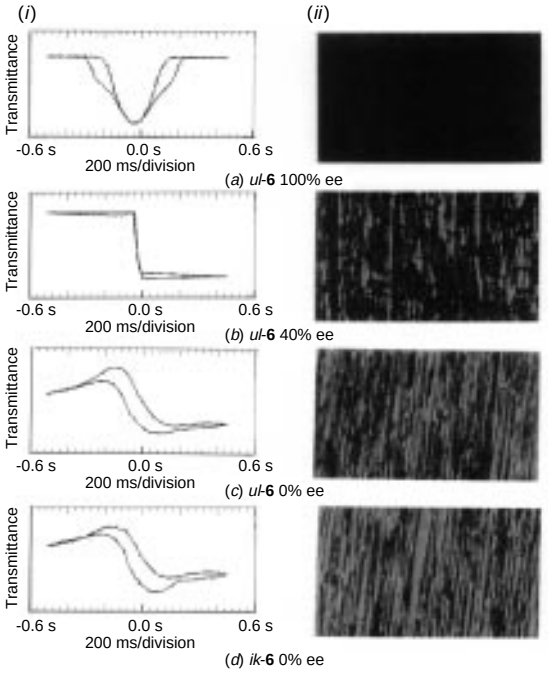



**Fig. 3** (*i*) Electro-optic switching characteristic at 90 °C and (*ii*) photomicrographs of the liquid-crystalline phases at 90 °C

diastereomers (Fig. 2). The phase transition from $S_A$ to $S_{C_A^*}$ takes place for medium-to-high enantiomeric excesses (60–100% ee) of the *ul*-diastereomer [Fig. 2(*a*)]. Interestingly, the transition from $S_A$ to $S_{C^*}$ takes place without any transition from $S_{C^*}$ to $S_{C_A^*}$ at low enantiomeric excess (40% ee). By contrast, the opposite *lk*-diastereomer shows the transition from $S_A$ to $S_{C^*}$ even in the enantiopure form (100% ee) [Fig. 2(*b*)]. Thus, the $S_{C_A^*}$ phase is likely to be stabilised in the *ul*-diastereomer. Surprisingly, an unknown phase appears in the racemic region of either the *ul*- or the *lk*-diastereomer. The phase in question is, therefore, referred to as $S_X$.

The *ul*-diastereomer **6** shows an AF double-loop hysteresis [Fig. 3(*i*)(*a*)] in the medium-to-high enantiomeric range (60–100% ee) and, by contrast, in the low enantiomeric purity (40% ee), a single-loop-hysteresis, characteristic of FLC [Fig. 3(*i*)(*b*)]. However, the electro-optic responses of $S_X$ phases of racemic LC diastereomers show an intriguing type of hysteresis for both *ul*- and *lk*-diastereomers [Fig. 3(*i*)(*c*) and (*d*)]. Furthermore, the kinds of texture in the $S_X$ phases [Fig. 3(*ii*)(*c*), (*d*)] are quite different from those in the $S_{C_A^*}$ [Fig. 3(*ii*)(*a*)] and $S_{C^*}$ [Fig. 3(*ii*)(*b*)] phases.

In summary, we have demonstrated the first proof that the appearances of antiferroelectric, ferroelectric and unknown phases are controlled by tuning the enantiomeric excesses in diastereomeric liquid-crystalline molecules.

## Footnote

† E-mail: kmikami@o.cc.titech.ac.jp

## References

1 N. A. Clark and S. T. Lagerwall, *Appl. Phys. Lett*., 1980, **36**, 899; R. B. Meyer, L. Liebert, L. Strzelecki and P. Keller, *J. Phys. Fr*., 1975, **36**, L69.
2 A. D. L. Chandani, T. Hagiwara, Y. Suzuki, Y. Ouchi, H. Takezoe and A. Fukuda, *Jpn. J. Appl. Phys*., 1988, **27**, L729; Y. Suzuki, T. Hagiwara, I. Kawamura, N. Okamura, T. Kitazume, M. Kakimoto, Y. Imai, Y. Ouchi, H. Takezoe and A. Fukuda, *Liq. Cryst*., 1989, **6**, 167.
3 A. D. L. Chandani, Y. Ouchi, H. Takezoe, A. Fukuda, K. Terashima, K. Furukawa and A. Kishi, *Jpn. J. Appl. Phys*., 1989, **28**, L1261; M. Fukui, H. Orihara, Y. Yamada, N. Yamamoto and Y. Ishibashi, *Jpn. J. Appl. Phys*., 1989, **28**, L849.
4 J. W. Goodby, M. A. Waugh, S. M. Stein, E. Chin, R. Pindak and J. S. Patel, *Nature*, 1989, **337**, 449.
5 (*a*) K. Furukawa, K. Terashima, M. Ichihashi, S. Saitoh, K. Miyazawa and T. Inukai, *Ferroelectrics*, 1988, **85**, 451; (*b*) Y. Suzuki, O. Nonaka, Y. Koide, N. Okabe, T. Hagiwara, I. Kawamura, N. Yamamoto, Y. Yamada and T. Kitazume, *Ferroelectrics*, 1993, **147**, 109.
6 Y. Takanishi, K. Hiraoka, V. K. Agrawal, H. Takezoe, A. Fukuda and M. Matsushita, *Jpn. J. Appl. Phys*., 1991, **30**, 2023; A. Fukuda, Y. Takanishi, T. Isozaki, K. Ishikawa and H. Takezoe, *J. Mater. Chem*., 1994, **4**, 997.
7 Y. Yamada, K. Mori, N. Yamamoto, H. Hayashi, K. Nakamura, M. Yamawaki, H. Orihara and Y. Ishibashi, *Jpn. J. Appl. Phys*., 1989, **28**, L1606.
8 For the definition of *ul* and *ik* nomenclature, see: D. Seebach and V. Prelog, *Angew. Chem., Int. Ed. Engl*., 1982, **21**, 654.
9 Reviews: K. Mikami, in *Advances in Asymmetric Synthesis*, ed. A. Hassner, JAI, London, 1995, vol. 1, pp. 1–44; K. Mikami and M. Shimizu, *Chem. Rev*., 1992, **92**, 1021.
10 K. Mikami, T. Yajima, M. Terada and T. Uchimaru, *Tetrahedron Lett*., 1993, **34**, 7591; K. Mikami, T. Yajima, M. Terada, E. Kato and M. Maruta, *Tetrahedron: Asymmetry*, 1994, **5**, 1087; K. Mikami, T. Yajima, T. Takasaki, S. Matsukawa, M. Terada, T. Uchimaru and M. Maruta, *Tetrahedron*, 1996, **52**, 85.
11 Reviews: K. Mikami, *Pure Appl. Chem*., 1996, **68**, 639; K. Mikami, M. Terada and T. Nakai, in *Advances in Catalytic Processes*, ed. M. P. Doyle, JAI, London, 1995, vol. 1, pp. 123–149; K. Mikami, M. Terada, S. Narisawa and T. Nakai, *Synlett*, 1992, 255.
12 T. Hagiwara, K. Tanaka and T. Fuchigami, *Abstr., 4H336 in the 70th Annual Meeting of the Chemical Society of Japan*, Tokyo, 1996.

*Received, 9th September 1996; Com. 6/06162A*

# Cycloaddition of nitrile oxides to [60]fullerene

**Tatiana Da Ros,[a] Maurizio Prato,*†[a] Fabiola Novello,[b] Michele Maggini,[b] Marco De Amici[c] and Carlo De Micheli[c]**

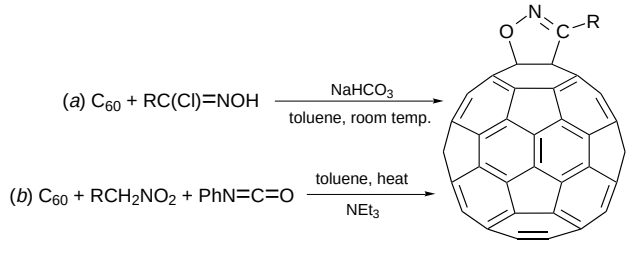
[a] *Dipartimento di Scienze Farmaceutiche, Università di Trieste, Piazzale Europa 1, 34127 Trieste, Italy*
[b] *Centro Meccanismi di Reazioni Organiche del CNR, Dipartimento di Chimica Organica, Università di Padova, Via Marzolo 1, 35131 Padova, Italy*
[c] *Istituto Chimico-Farmaceutico, Università di Milano, Viale Abruzzi 42, 20131 Milano, Italy*

**The addition of nitrile oxides to [60]fullerene is examined and it is found that the reaction products regenerate [60]fullerene under relatively mild conditions; the result is potentially useful for better control of fullerene functionalization.**

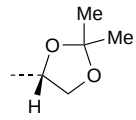
The use of fullerenes as frameworks for molecular assemblies is becoming increasingly popular.[1,2] The regiochemistry of multiple additions has been the subject of thorough investigations[3,4] and methodologies for the octahedral[4,5] or tetrahedral[6] functionalization of [60]fullerene have been successfully developed. However, complete control over the addition chemistry of fullerenes has yet to be reached, especially as new discoveries continue to emerge.[7,8] In connection with this, the reversibility of some reactions has been shown to be useful to reach challenging new targets.[6,9] Here we report that the products of the cycloaddition of nitrile oxides to [60]fullerene can regenerate quantitatively [60]fullerene under specific conditions and that this fact may be used to better control fullerene chemistry.

According to previous reports,[10,11] nitrile oxides, generated under different conditions, add readily to [60]fullerene giving rise to fullerene-fused isoxazolines (Scheme 1).‡

The most common way to generate nitrile oxides is the dehydrochlorination of hydroximoyl chlorides, which, in turn, can be prepared from the corresponding aldehydes (path *a*, Scheme 1, compounds **1a**–**e**, **h**, **i**). Alternatively, nitrile oxides can be efficiently prepared by dehydration of primary nitroalkanes (path *b*, Scheme 1, compounds **1f**, **g**). We have prepared, *via* path *a*, an optically active fullerene derivative, starting from the corresponding homochiral hydroximoyl chloride, readily available from D-mannitol[12] (**1i**, Scheme 1).




**a** R = $CH_2OCH_2CH_2OCH_2CH_2OMe$
**b** R = 9-anthryl
**c** R = COPh
**d** R = $CO_2Et$
**e** R = $C_6H_4$-4-OBn
**f** R = $CH_2CO_2Bu^t$
**g** R = $CH_2CH_2CO_2Me$
**h** R = $CH_2CH_2CH_2CH_2N(Boc)CH_2CO_2Bu^t$
**i** R =

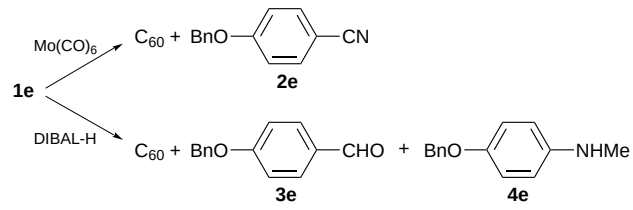


**Scheme 1**

Fullerene-fused isoxazolines (isoxazolinylfullerenes) are relatively stable and revert back to [60]fullerene only at very high temperatures (280–400 °C).[10] Compounds **1** are also stable to acids. Addition of 10 equiv. of trifluoroacetic acid to a solution of **1d** in chlorobenzene under reflux gave only traces of [60]fullerene after 10 d. Addition of *N*-phenylmaleimide as a retrocycloaddition trapping agent did not result in the formation of the corresponding adduct, even in chlorobenzene under reflux.

Conventional isoxazolines are versatile synthons in many transformations, as they are reduced under a variety of conditions to a range of functional groups (*e.g.* amino alcohols, amino carbonyls, nitrile alcohols, *etc.*).[13] On the contrary, isoxazolinylfullerenes appear to be resistant to further functionalization.[10] This could be due to two reasons. First of all, functionalities spatially close to the fullerene sphere have been found to be less reactive than usual.[14] Furthermore, if the N–O bond opens up, a hydroxy functionality directly attached to [60]fullerene would be generated. A single hydroxy group on a fullerene is presumed to be unstable, and is expected to eliminate.[7] Thus, it is not surprising that, when isoxazolines **1a**–**i** were treated with $Mo(CO)_6$ under conditions that usually favour N–O bond cleavage (anhydrous chlorobenzene under reflux for 24 h),[15] [60]fullerene was recovered quantitatively. The addition of protic solvents (either water or methanol, 0.025 M) accelerates the reaction.[15] Under these conditions, the reaction completed in 2 h. The reaction of **1e** with $Mo(CO)_6$ was investigated as a representative example (Scheme 2). Nitrile **2e** (identified by comparison to an authentic sample) was recovered quantitatively along with [60]fullerene. This result can be tentatively explained by initial N–O bond cleavage followed by expulsion of the fragments from [60]fullerene. More extended work will be necessary to clarify the detailed mechanism.

A similar result was obtained with the treatment of **1** with DIBAL-H (diisobutyl aluminium hydride, 10 equiv.) at room temperature in toluene. In this case, the reaction of **1e**, besides the quantitative production of [60]fullerene, yielded aldehyde **3e** and amine **4e** (identified by comparison with authentic samples) in 31 and 64% isolated yields respectively. Whereas aldehyde **3e** was probably formed by DIBAL-H reduction of

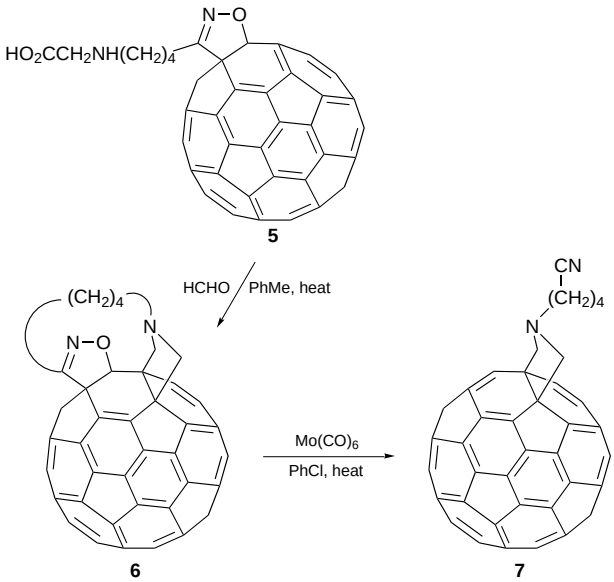



**Scheme 2**

nitrile **2e**, amine **4e** could have been formed from the rearrangement of nitrile oxide to the corresponding isocyanate[16] which was then reduced to **4e**. In any case, all attempts to trap the transient nitrile oxide under reductive conditions failed.

In light of the results reported here, several applications of the addition of nitrile oxides to fullerenes can be envisioned. The solubility of [60]fullerene, which is a real problem in a number of instances, can be improved by the temporary addition of a solubilizing appendage (see, for example, **1a**, Scheme 1). The examples reported here may be considered an attractive alternative to known methodologies.[17] In fact, the trioxanonane chain in **1a** can be easily attached *via* the corresponding nitrile oxide cycloaddition and then easily removed, in one single step, under two very different conditions, either of which are compatible with the reactivity of [60]fullerene and also with that of most functional groups. Furthermore, the use of a chiral chain (**1i**) can be used to chemically resolve racemic mixtures of chiral fullerenes or fullerene derivatives.[18]

As an example of the potential of the described methodology, isoxazoline **1h** was treted with trifluoroacetic acid to afford the corresponding glycine derivative **5** (as a trifluoroacetate salt) in quantitative yield (Scheme 3). When **5** was heated to reflux in toluene in the presence of 10 equiv. formaldehyde,[19] a single product was isolated by chromatography in 67% yield. Structure **6** is tentatively assigned to this product, based on analytical and spectroscopic data, with the help of AM1 optimization.§ Once treated with $Mo(CO)_6$, **6** led to **7** as the only isolated product. The structure of **7** was confirmed by the reaction of *N*-(4-cyanobutyl)glycine and formaldehyde with [60]fullerene.[19] Scheme 3 shows a specific site-directed functionalization of [60]fullerene using a temporary anchor point.




**Scheme 3**

Consiglio Nazionale delle Ricerche and MURST are gratefully acknowledged for financial support.

## Footnotes

† E-mail: prato@univ.trieste.it

‡ All new compounds exhibited satisfactory analytical and spectroscopic data.

§ Compound **6** is highly favoured over other possible positional isomers (MACSPARTAN program running on a Power Macintosh 9500).

## References

1 F. Diederich and C. Thilgen, *Science*, 1996, **271**, 317.
2 A. B. Smith, *Tetrahedron*, 1996, **52**, Tetrahedron Symposium in Print on Fullerene Chemistry.
3 A. Hirsch, I. Lamparth and H. R. Karfunkel, *Angew. Chem., Int. Ed. Engl.*, 1994, **33**, 437.
4 L. Isaacs, R. F. Haldimann and F. Diederich, *Angew. Chem., Int. Ed. Engl.*, 1994, **33**, 2339.
5 I. Lamparth, C. Maichle-Mössmer and A. Hirsch, *Angew. Chem., Int. Ed. Engl.*, 1995, **34**, 1607.
6 F. Cardullo, L. Isaacs, F. Diederich, J.-P. Gisselbrecht, C. Boudon and M. Gross, *Chem. Commun.*, 1996, 797.
7 P. R. Birkett, A. G. Avent, A. D. Darwish, H. W. Kroto, R. Taylor and D. R. M. Walton, *Chem. Commun.*, 1996, 1231.
8 T. Kusukawa and W. Ando, *Angew. Chem., Int. Ed. Engl.*, 1996, **35**, 1315.
9 B. Kräutler, T. Müller, J. Maynollo, K. Gruber, C. Kratky, P. Ochsenbein, D. Schwartzenbach and H.-B. Bürgi, *Angew. Chem., Int. Ed. Engl.*, 1966, **35**, 1204.
10 M. S. Meier and M. Poplawska, *Tetrahedron*, 1996, **52**, 5043.
11 H. Irngartinger, C. M. Köhler, U. Huber-Patz and W. Krätschmer, *Chem. Ber.*, 1994, **127**, 581.
12 K. E. Larsen and K. B. Torssell, *Tetrahedron*, 1984, **40**, 2985.
13 A. P. Kozikowski, *Acc. Chem. Res.*, 1984, **17**, 410.
14 W. W. Win, M. Kao, M. Eiermann, J. J. McNamara, F. Wudl, D. L. Pole, K. Kassam and J. Warkentin, *J. Org. Chem.*, 1994, **59**, 8571.
15 M. Nitta, A. Yi and T. Kobayashi, *Bull. Chem. Soc. Jpn.*, 1985, **58**, 991.
16 G. Bianchi, R. Gandolfi and P. Grünanger, *The Chemistry of Functional Groups, Supplement C*, Wiley, New York, N.Y., 1983, p. 748.
17 Y.-Z. An, G. A. Ellis, A. L. Viado and Y. Rubin, *J. Org. Chem.*, 1995, **60**, 6353.
18 J. M. Hawkins and A. Meyer, *Science*, 1993, **260**, 1918.
19 M. Maggini, G. Scorrano and M. Prato, *J. Am. Chem. Soc.*, 1993, **115**, 9798.

*Received, 20th September 1996; Com. 6/06503A*

# A new type of layered aluminium phosphate $[NH_4]_3[Co(NH_3)_6]_3[Al_2(PO_4)_4]_2$ assembled about a cobalt(III) hexammine complex

**Keith R. Morgan, Graeme J. Gainsford and Neil B. Milestone**

*Industrial Research Limited, PO Box 31-310, Lower Hutt, New Zealand*

**The formation of a novel layered aluminium phosphate containing a new type of layer stoichiometry is reported; the reaction is carried out under basic conditions using cobalt hexammine as a template.**

There have been a number of reports on the synthesis of microporous solids where metal complexes have been used as templating agents. Balkus *et al*.[1] synthesized a zeolite with the faujasite structure using metal phthalocyanine complexes as templating agents. Balkus and Shepelev[2] have used a bis(cyclopentadienyl)cobalt(III) complex to form a nonasil molecular sieve and more recently Freyhardt *et al*.[3] formed a novel large-pore high silica zeolite using bis(pentamethylcyclopentadienyl)cobalt(III) hydroxide. In order for a metal complex to be useful as a templating agent the metal complex must be stable under the reaction conditions. Cobalt(III) complexes are inert to substitution and remain stable at relatively high temperatures. We recently used this property to form a unique layered aluminium phosphate[4] about the chiral metal complex cobalt tris(ethylenediamine), $[Co(en)_3]^{3+}$. This was the first reported example where a metal complex was used as a template to form a layered structure. Bruce *et al*. have found that the cobalt tris(propylenediamine) complex[5] and the cobalt bis(diethylenetriamine) complex[6] can also act as a template to form a chiral layered material. We found that if either isomers of $[Co(en)_3]^{3+}$ was resolved and used as the template in the hydrothermal reaction then no crystalline material was formed. This suggests that there is no lattice compatible with the resolved complex, and that both isomers are required to obtain a stable structure.

The metal complex $[Co(en)_3]^{3+}$ is reasonably stable under the hydrothermal conditions used in these types of preparations. The cobalt hexammine complex, $[Co(NH_3)_6]^{3+}$, is not as stable and undergoes decomposition in boiling water with the loss of ammonium ion. The complex is, however, stable in concentrated ammonium ion solutions at temperatures up to 150 °C.

The reaction of aluminium oxyhydroxide, (0.5 g), $[Co(NH_3)_6]Cl_3$ (1 g) and 85% phosphoric acid (1.9 g) in concentrated ammonium hydroxide (10 ml) at 150 °C for 12 h resulted in the formation of long orange needles, up to 1 cm in length, large purple plates and a minor amount of unidentified small blue plates. The purple plates were identified by powder XRD as $NH_4CoPO_4$.[7] Since the colour of the orange needles suggested that the complex had acted as a template for formation of the structure and not undergone decomposition, this material was further characterised by single-crystal X-ray crystallography.†

The orange needles have a layered structure with the metal complex positioned between the layers. Water and ammonium ions fill the voids between the layer and the metal complex [Fig. 1(*a*)]. The composition of the layers is, however, different to those layered aluminium phosphates that have been reported to date, which have either the compositions $Al_3(PO_4)_4^{3-}$ (refs. 4–6, 8–11) or $Al_2(PO_4)_3^{3-}$ (ref. 12) and a range of unique layer topologies. The composition of this new layered phase is $Al_2(PO_4)_4^{6-}$. In most of the layered aluminium phosphates, the aluminium is tetrahedrally bonded through an oxygen to four phosphorus atoms. The structure described by Chippindale *et al*.[12] is unusual as it contains both tetrahedrally and trigonal-bipyramidal aluminium. In the $[Al_3(PO_4)_4^{3}]_n$[4–6,8–11] layered material the phosphorus is bonded through three oxygens to aluminium giving one non-coordinated P–O bond. In the $[Al_2(PO_4)_3^{3-}]_n$[12] layers there are two types of phosphorus. One type is bonded to four oxygens of which three are bonded to aluminium, the other is bonded to four oxygens but only two of these are bonded to aluminium.

For the structure reported here, $[Al_2(PO_4)_4^{6-}]_n$, there are two unique phosphorus atoms with each bonded to four oxygens. Only two of these oxygens are bonded to aluminium, the other two are nominally P–O double bonds. The solvent system of concentrated ammonium hydroxide used for forming the $Al_2(PO_4)_4^{6-}$ lattice is highly basic favouring P–O double bond formation. The $Al_2(PO_4)_4^{6-}$ lattice is the most basic type of the layered aluminium phosphates reported to date. There are three types of rings in the structure: two small four-membered rings and a large 20-membered ring [Fig. 1(*b*)]. The metal complexes reside within the larger ring. The density of the material is similar to that of the other layered aluminium phosphates.

There is an extensive hydrogen-bonding network involving the non-coordinated phosphoryl oxygens, the coordinated amines, the ammonium ions and the water molecules [O(phosphate)···N 2.71–2.96 Å], [O(4A)···O(water) 2.66 Å]. Six of the eight phosphoryl oxygens bind to more than one hydrogen. One

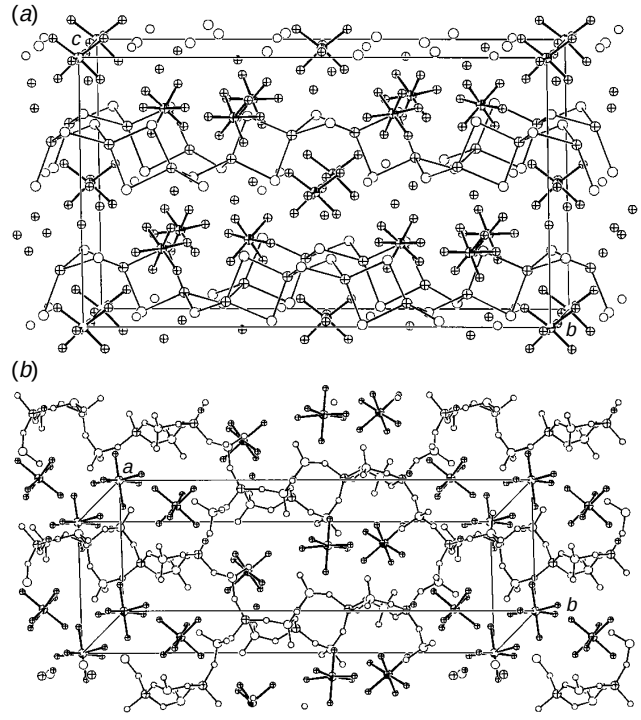



**Fig. 1** Views of structure: (⊕) N, (⊕) Al, (◯) P, (○) $H_2O$, (◒) Co. (*a*) View edge on to the $Al_2(PO_4)_2^{6-}$ layers; $PO_4$ and $AlO_4$ tetrahedron are shown linked as single atoms and hydrogens have been excluded. (*b*) View normal to the plane of just one layer at $z \approx 0.25$.

of the metal complexes is partially disordered and is bound weakly to one of the phosphoryl oxygens and the water molecule.

The layered phase $[NH_4]_3[Co(NH_3)_6]_3[Al_2(PO_4)_4]_2$ represents a new lattice type and layer topology. It is likely that a hydrothermal synthesis under similar basic conditions in the presence of suitable templates could yield other $Al_2(PO_4)_4^{6-}$ phases having different layer topologies.

## Footnote

† *Crystal data* for $[NH_4]_3[Co(NH_3)_6]_3[Al_2(PO_4)_4]_2 \cdot 2H_2O$: orthorhombic, *Aba2*, $a$ = 9.502(2), $b$ = 29.699(6), $c$ = 17.210(3) Å, $Z$ = 4, $D_c$ = 1.97 g cm$^{-3}$. 3845 reflections collected at 130(2) K on a Nicolet P4 diffractometer using Mo-K$\alpha$ radiation ($\lambda$ = 0.710 73 Å, graphite monochromator). The structure was solved by a direct method (SHELXS-90[13]) using empirical absorption-corrected data, and anisotropic temperature factors for the Co, P and Al atoms. During refinement a minor twinned component was detected; the twinned proportion parameter refined to 0.89(4).[14] Located ammine hydrogen atoms were refined[14] with isotropic temperature factors 1.2 times their parent nitrogen. The structure was refined on $F_0^2$ (358 parameters, 3324 independent reflections) to a conventional $R$ of 0.047 [$F_0 > 4\sigma(F_0)$]. Atomic coordinates, bond lengths and angles, and thermal parameters have been deposited at the Cambridge Crystallographic Data Centre (CCDC). See Information for Authors, Issue No. 1. Any request to the CCDC for this material should quote the full literature citation and the reference number 182/300.

## References


1 K. J. Balkus, C. D. Hargis and S. Kowalak, *ACS Symp. Ser*., 1992, **499**, 347.
2 K. J. Balkus and S. Shepelev, *Microporous Mater*., 1993, **1**, 383.
3 C. C. Freyhardt, M. Tsapatsis, R. F. Lobo, K. J. Balkus and M. E. Davies, *Nature*, 1996, **23**, 295.
4 K. Morgan, G. Gainsford and N. Milestone, *J. Chem. Soc., Chem. Commun*., 1995, 425.
5 D. A. Bruce, A. P. Wilkinson, M. G. White and J. A. Bertrand, *J. Chem. Soc., Chem. Commun*., 1995, 2059.
6 D. A. Bruce, A. P. Wilkinson, M. G. White and J. A. Bertrans, *J. Solid State Chem*., 1996, **125**, 228.
7 T. Duc, A. Durif, J.-C. Guitel and M.-T. Averbuch-Pouchot, *Bull. Soc. Chim. Fr*., 1968, 1760.
8 R. H. Jones, J. M. Thomas, R. Xu, Q. Huo, A. K. Cheetham and A. V. Powell, *J. Chem. Soc., Chem. Commun*., 1991, 126.
9 J. M. Thomas, R. H. Jones, R. Xu, J. Chen., A. M. Chippindale, S. Natarajan and A. K. Cheetham, *J. Chem. Soc., Chem. Commun*., 1992, 929.
10 R. H. Jones, A. M. Chippindale, S. Natarajan and J. M. Thomas, *J. Chem. Soc., Chem. Commun*., 1994, 565.
11 I. D. Williams, Q. Gao, J. Chen, L.-Y. Ngai, Z. Lin and R. Xu, *Chem. Commun*., 1996, 1781.
12 A. M. Chippindale, A. V. Powell, L. M. Bull, R. H. Jones, A. K. Cheetham, J. M. Thomas and R. Xu, *J. Solid State Chem*., 1992, **96**, 199.
13 G. M. Sheldrick, *Acta Crystallogr., Sect. A*, 1990, **46**, 467.
14 G. M. Sheldrick, SHELXL-93, University of Göttingen, 1993.


*Received, 30th August 1996; Com. 6/06006D*

# Surface adsorption in the gas–solid reaction between NO and $LaBaSrCu_2O_{6-\delta}$

**F. Munakata,*[a] Y. Akimune,[a] Y. Shichi,[b] M. Akutsu,[b] H. Yamaguchi[b] and Y. Inoue[b]**

[a] *Material Research Laboratory, Nissan Research Center, Nissan Motor Co. Ltd., 1 Natsushima-cho, Yokosuka 237, Japan*
[b] *Research Department, Nissan ARC Ltd., 1 Natsushima-cho, Yokosuka 237, Japan*

**The chemical state of NO over $LaBaSrCu_2O_{6-\delta}$ investigated by X-ray photoelectron spectroscopic analysis suggests the surface adsorption of $NO_2^-$ corresponds to NO trapped by oxygen vacancies.**

Since the discovery of high-$T_c$ superconducting cuprates,[1] a number of studies have been made on layered cuprates. The physical and chemical properties of layered cuprates have drawn attention in relation to their superconducting properties. Some of these oxides have been studied in the applications of $NO_x$ decomposition catalysis and gas sensors.[2–8] The catalytic applications of cuprates have been studied by Misono and coworkers[2–4] and by Shimada *et al*.[5] for direct decomposition or reduction of nitric oxides. These studies suggested that the redox properties of copper ions and the resultant oxygen vacancies may play an important role in the catalytic conversion of NO. Also, Machida *et al*.[9–11] have reported that rapid NO absorption by $BaCuO_{2+\delta}$ takes place through solid–gas reactions to produce barium nitrate and nitrite. By contrast, Misono and coworkers[12,13] suggested the possibility of NO uptake *via* direct incorporation into bulk $YBa_2Cu_3O_y$. They indicated that the NO–CO reaction took place through absorption owing to the defective structure of the layered cuprate. Recently, Machida *et al*.[14] reported the absorption–desorption properties of nitric oxide over the layered cuprate $La_{2-x}Ba_xSrCu_2O_6$ ($0 \leqslant x \leqslant 1.0$). These results suggest that the desorption process of NO contrasts to conventional NO absorption–desorption systems in the following ways: (*a*) NO absorption is not associated with the formation of nitrates or nitrites of barium and (*b*) the desorption temperature of $N_2$ is much higher than that of $O_2$. Therefore, it is worthwhile to study the adsorbed states of NO over $La_{2-x}Ba_xSrCu_2O_6$ in order to understand the absorption–desorption mechanism of NO over layered cuprates. Also, this mechanism indicates the existence of oxygen solubility in $La_{2-x}Ba_xSrCu_2O_6$. It is important to consider the oxygen non-stoichiometry effects for the adsorption–desorption properties of NO over $La_{2-x}Ba_xSrCu_2O_6$. However, the relation of the NO adsorption–desorption properties with the oxygen non-stoichiometry in $La_{2-x}Ba_xSrCu_2O_6$ has not been clearly defined.

In the present study, the surface adsorption of NO over $LaBaSrCu_2O_{6-\delta}$ was investigated by X-ray photoelectron spectroscopy (XPS) in order to understand the absorption–desorption process of NO over layered cuprate. We also discuss the chemical states of adsorbed nitric oxide near the surface of this compound and the effects of oxygen partial pressure on this surface reaction.

Powdered $LaBaSrCu_2O_{6-\delta}$ was prepared by coprecipitation of the citrates of the elements. After calcination at 1073 K for 5 h in air, the powder was ground and then heated at 1273 K for 10 h in air. The crystal phase of the powder was determined by powder X-ray diffraction (XRD) and the single-phase X-ray diffraction profiles are shown in ref. 14. The NO adsorbed samples were prepared by annealing at 627 K for 1 h upon introduction of 0.5 vol.% NO–5 vol.% $O_2$–94.5 vol.% $N_2$ or 0.5 vol.% NO–99.5 vol.% $N_2$. These powders were pressed into pellets, and analysed by X-ray photoelectron spectroscopy and powder X-ray diffraction. X-Ray photoelectron spectra (XPS) were measured using a commercial spectrometer (PHI ESCA-5600) with a base pressure in the chamber of *ca*. $10^{-12}$ atm. The X-ray source was monochromated Al-K$\alpha$ radiation (1486.6 eV) and the combined energy resolution was *ca*. 0.3 eV. Core-level binding energies were referenced to the C 1s peak at 284.5 eV to account for the surface charge-up, especially in the cases of samples that were poor electrical conductors.

The samples were prepared in a variety of process conditions as follows: (*a*) at 1273 K for 10 in air (sample A), (*b*) annealing sample A at 627 K for 1 h in the presence of 0.5 vol.% NO–99.5 vol.% $N_2$ (sample B), and (*c*) annealing sample A at 627 K for 1 h in the presence of 0.5 vol.% NO–5 vol.% $O_2$–94.5 vol.% $N_2$ (sample C). Fig. 1 shows N 1s XPS core-level spectra for these samples. The N 1s XPS peak was not detected for sample A. In Table 1, the binding energies of N 1s XPS core-level spectra are summarized for samples B and C, $NaNO_2$,[15] $Ba(NO_3)_2$[16] and $Sr(NO_3)_2$.[16] The data in Table 1 suggest that the N 1s XPS spectra of nitrates occur in the range $407 < E_b < 408$ eV, and those of nitrites at $E_b \approx 404$ eV. The N 1s XPS peak for sample B is observed at 403.1 eV, similar to that for $NaNO_2$ ($Na^+NO_2^-$).[15] It was considered that the N 1s XPS peak at *ca*. 404 eV indicated the surface adsorption of $NO_2^-$ corresponding

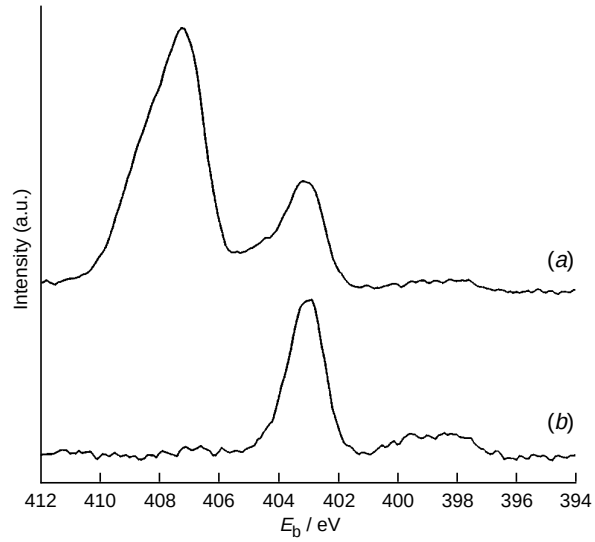



**Fig. 1** N 1s XPS core-level spectra for samples after NO absorption: (*a*) annealing at 627 K for 1 h after introducing 0.5 vol.% NO–5 vol.% $O_2$–94.5 vol.% $N_2$ and (*b*) annealing at 627 K for 1 h after introducing 0.5 vol.% NO–99.5 vol.% $N_2$

**Table 1** Binding energies of N 1s XPS core-level spectra

| | $E_b$/eV |
|---|---|
| Sample B | 403.1 |
| Sample C | 403.1, 407.3 |
| $NaNO_2$ | 403.9 |
| $NaNO_3$ | 407.4 |
| $Ba(NO_3)_2$ | 407.5 |
| $Sr(NO_3)_2$ | 408.1 |

to NO adsorption. Sample B showed an X-ray diffraction profile similar to $LaBaSrCu_2O_{6-\delta}$ and there were no additional reflections. The N 1s XPS peaks for sample C are observed at 407.3 and 403.1 eV, the former being similar to the N 1s XPS peak for $NaNO_3$ ($Na^+NO_3^-$).[15] On the other hand, the X-ray diffraction profile of sample C showed additional reflections due to the formation of barium and/or strontium nitrate, $(Ba_{0.5}Sr_{0.5})(NO_3)_2$.[17] The occurrence of the N 1s XPS peak at *ca*. 407.3 eV showed the formation of nitrates of $(Ba,Sr)(NO_3)_2$ in sample C. This process may be represented using Kröger–Vink notation [eqn. (1)]

$$4NO(g) + Ba_{Ba}^{x} + Sr_{Sr}^{x} + 2O_O^x + 3O_2(g) \rightarrow 2(Ba_{1/2}Sr_{1/2})(NO_3)_2 + V_{Ba}'' + V_{Sr}'' + 2V_O^{\cdot\cdot} \quad (1)$$

where V and g denote vacancy and gas, respectively. To simplify the discussion, the valences of Ba, Sr and O ions were assumed to be, respectively, +2, +2, and −2 on the lattice sites. The formation of nitrate is a consequence of the $NO–O_2$ atmosphere, according to eqn. (1). In the absence of $O_2$, the formation of nitrates and nitrites of Ba, Sr and Cu was not observed.

In Table 2, the binding energies of Cu $2p_{3/2}$ XPS core-level spectra are summarized for samples A, B and C, CuO[18] and $Cu(NO_3)_2$.[19] The XPS core-level spectra of samples A, B and C were similar to the spectrum of CuO in ref. 18. Also, the binding energy of the XPS core-level spectrum of Cu $2p_{3/2}$ in sample C is similar to that of $Cu(NO_3)_2$.[19] The binding energy of the Cu $2p_{3/2}$ XPS core-level spectrum of sample B was different from 933.7 eV (the binding energy of $Cu^{2+}$ ion in CuO) upon NO adsorption. As the formation of nitrates or nitrites was not observed in sample B, this result may reflect the intercalation of NO molecules into the layer structure.

Machida *et al.*[14] reported that NO absorption over $La_{2-x}Ba_xSrCu_2O_6$ was considered to proceed *via* intercalation of NO molecules into the layer structure. However, these compounds containing absorbed NO begin to desorb $NO–NO_2$ above 573 K.[14] It is considered that the present results shown in Fig. 1 and Table 2 reflect the adsorption–desorption reaction of NO near the surface. Therefore, the N 1s XPS peak at *ca*. 404 eV suggests surface adsorption of $NO_2^-$ resulting from NO absorption. Thus, this NO adsorption (or intercalation) near the surface induces a change of the chemical state of the Cu ions. On the other hand, layered cuprates have a large number of oxygen vacancies in the lattice as reflected in the chemical formula $LaBaSrCu_2O_{6-\delta}$.[14] Yasuda *et al*.[20] reported a mechanism in which the active sites for decomposition of NO over valency-controlled $La_2CuO_4$-based mixed oxides where coordinatively unsaturated $Cu^{2+}$ ions on the surface are easily oxidized to $Cu^{3+}$ upon NO adsorption. Misono and coworkers[2–4] and Shimada *et al*.[5] suggested that the redox characteristics of copper ions and the resultant oxygen vacancies should play an important role in the surface reaction of NO. Also, it is suggested that the chemical shift of Cu 2p XPS peak in Table 2 is related to the change of oxidation state of Cu ions which is caused by NO adsorption. Therefore, to explain the results of sample B, as shown in Fig. 1 and Table 2, we propose that NO gas is trapped by oxygen vacancies neighbouring the coordinatively unsaturated Cu ions on the surface of $LaBaSrCu_2O_{6-\delta}$.

**Table 2** Binding energies of Cu $2p_{3/2}$ XPS core-level spectra

| | $E_b$/eV |
|---|---|
| Sample A | 934.0 |
| Sample B | 933.1 |
| Sample C | 934.0 |
| $Cu(NO_3)_2$ | 935.5 |
| CuO | 933.0 |

In conclusion, the chemical state of NO over $LaBaSrCu_2O_{6-\delta}$ was investigated by X-ray photoelectron spectroscopy (XPS) and the results are interpreted as follows.

(*i*) The N 1s XPS peak was seen at a binding energy of *ca*. 404 eV for the sample annealed in 0.5 vol.% $NO–N_2$ and also seen at two binding energies of *ca*. 403.1 and 407.1 eV for the sample annealed in 0.5 vol.% NO–5 vol.% $O_2–N_2$.

(*ii*) From the X-ray-diffraction profile of the sample annealed in 0.5 vol.% NO–5 vol.% $O_2–N_2$, it is proposed that the N 1s XPS peak at 407.1 eV results from the formation of nitrates of Ba and/or Sr.

(*iii*) The N 1s XPS peak at *ca*. 403.1 eV suggests the surface adsorption of $NO_2^-$ group corresponding to NO trapped by oxygen vacancies.

## References


1 J. G. Bednorz and K. A. Muller, *Z. Phys. B*, 1986, **64**, 189.
2 N. Mizuno, M. Yamato, M. Tanaka and M. Misono, *Chem. Mater*., 1989, 1, 232.
3 N. Mizuno, Y. Fujisawa and M. Misono, *J. Chem. Soc., Chem. Commun*., 1989, 316.
4 H. Yasuda, N. Mizuno and M. Misono, *J. Chem. Soc., Chem. Commun*., 1990, 1094.
5 H. Shimada, S. Miyama and H. Kuroda, *Chem. Lett*., 1988, 1797.
6 H. Arai and M. Machida, *Catal. Today*, 1994, **22**, 97.
7 F. Munakata, K. Shinohara and M. Yamanaka, *MRS INT' 1 Mtg. Adv. Mater*., 1989, **6**, 15.
8 N. Koshizaki, K. Yasumoto and K. Suga, *Sens. Actuators B*, 1992, **9**, 17.
9 M. Machida, K. Yasuoka, K. Eguchi and H. Arai, *J. Chem. Soc., Chem. Commun*., 1990, 1165.
10 M. Machida, K. Yasuoka, K. Eguchi and H. Arai, *J. Solid State Chem*., 1991, **91**, 176.
11 M. Machida, S. Ogata, K. Yasuoka, K. Eguchi and H. Arai, *Proc. 10th Int. Congr. Catal*., ed. L. Guczi, F. Solymosi and P. Tetenyi, Elsevier, Amsterdam 1992, p. 2645.
12 K. Tabata, H. Fukui, S. Kohiki, N. Mizuno and M. Misono, *Chem. Lett.*, 1988, 799.
13 N. Mizuno, M. Yamato and M. Misono, *J. Chem. Soc., Chem. Commun*., 1988, 887.
14 M. Machida, H. Murakami and T. Kijima, *J. Mater. Chem*., 1994, **4**, 1621.
15 K. Burger, F. Tschismarov and H. Ebel, *J. Electron Spectrosc. Relat. Phenom*., 1977, **10**, 461.
16 A. B. Christie, J. Lee, I. Sutherland and J. M. Walls, *Appl. Surf. Sci*., 1983, **15**, 224.
17 MaMurdie *et al*., *Natl. Bur. Stand. U.S., Monogr*., 1975, **25**, 12.
18 N. S. McIntyre, S. Sunder, D. W. Shoesmith and F. W. Stanchell, *J. Vac. Sci. Technol*., 1981, **18**, 714.
19 V. I. Nefedov, A. K. Zhumadilov and T. Y. Konitova, *J. Struct. Chem., USSR*, 1977, **18**, 692.
20 H. Yasuda, T. Nitadori, N. Mizuno and M. Misono, *Bull. Chem. Soc. Jpn*., 1993, **66**, 3492.


*Received, 29th September 1996; Com. 6/05258D*

# Ruthenium porphyrin encapsulated in modified mesoporous molecular sieve MCM-41 for alkene oxidation

**Chun-Jing Liu,[a] Shou-Gui Li,[a] Wen-Qin Pang[b] and Chi-Ming Che*[a]**

[a] *Department of Chemistry, The University of Hong Kong, Pokfulam Road, Hong Kong*
[b] *Department of Chemistry, Jilin University, Changchun, China 130023*

**Ruthenium(II) *meso*-tetrakis(4-chlorophenyl)porphyrin encapsulated in MCM-41 modified with 3-aminopropyltriethoxysilane is a stable catalyst for alkene oxidation by *tert*-butyl hydroperoxide with high product turnovers.**

A useful means to improve the stability and selectivity of metalloporphyrin catalysts is by encapsulation in microporous materials such as zeolites.[1–5] However, the commonly employed zeolite Y has a small pore size and encapsulation of metalloporphyrins of second- and third-row transition metals is difficult. In this context, the large pore size of the MCM-41 mesoporous materials[6] is advantageous. Herein is described the encapsulation of a ruthenium porphyrin in modified MCM-41, and its catalytic properties.

MCM-41 was synthesized by a literature method[6] and was characterized by its XRD pattern, which shows a very strong peak at $d$ = 39.74 Å. [RuL(CO)(EtOH)] [$H_2$L = *meso*-tetrakis(4-chlorophenyl)porphyrin] was prepared according to the literature method.[7]

Direct encapsulation of [RuL(CO)(EtOH)] in MCM-41 was unsuccessful, presumably due to the interaction of the neutral ruthenium(II) porphyrin and the channel surface of MCM-41 being weak. To resolve this problem, the surface of MCM-41 was modified by using 3-aminopropyltriethoxysilane (APTES) as shown in Scheme 1. The modified MCM-41 characterized by IR (stretching and bending of the $NH_2$ group at 3470 and 1634 $cm^{-1}$), elemental analysis (found: C, 6.96; N, 2.49%) and XRD is designated as MCM-41(m).

In a typical experiment, MCM-41 (0.1 g) was mixed with a chloroform solution of APTES (10 ml, 0.1 M) and stirred at room temp. for 8–12 h. The MCM-41(m) was filtered and washed with chloroform and dichloromethane. As shown in Fig. 1, its XRD pattern is essentially the same as that of MCM-41.

MCM-41(m) exhibits a powerful encapsulation ability. Stirring a mixture of MCM-41(m) (0.1 g) and [RuL(CO)(EtOH)] (10 mg) in $CH_2Cl_2$ (10 ml) at room temp. for 1 h gave the encapsulated product containing 8.3 mass% of [RuL(CO)], designated 8.3 mass% Ru/M-41(m) (IR, $\nu_{C\equiv O}$ 1952.4 $cm^{-1}$; UV–VIS $\lambda_{max}$ 411, 528 nm). Products with different mass% [RuL(CO)] were obtained by varying the amount of [RuL(CO)(EtOH)] used in the reaction. The amount of [RuL(CO)] in Ru/M-41(m) was determined by dissolving the latter in an aqueous solution of HF (3 mass%) followed by extraction with dichloromethane. The UV–VIS absorption spectrum of the $CH_2Cl_2$ extract was essentially the same as that of [RuL(CO)(EtOH)] in $CH_2Cl_2$ ($\lambda_{max}$ 411.2, 528.8 nm). The solid diffuse-reflectance UV–VIS† and FT Raman spectra‡ of Ru/M-41(m) are very similar to those of [RuL(CO)], indicating that the molecule remains intact during the process of encapsulation.

As shown in Fig. 1, the XRD pattern of 8.3 mass% Ru/M-41(m) exhibits the characteristic peaks of MCM-41 but no peaks due to [RuL(CO)]. This indicates that the MCM-41 structure is retained and that the [RuL(CO)] molecules should be dispersed in the channels.

The immobilization of [RuL(CO)] onto the channel surface of MCM-41 is attributed to a ligand exchange reaction as shown in Scheme 2.

This suggestion is supported by the following experiments. First, [CuL] containing no axial ligands was found not to be encapsulated in MCM-41(m). Secondly, MCM-41 modified by trimethylsilation does not encapsulate [RuL(CO)(EtOH)], due to the conversion of surface –OH to –$SiMe_3$ groups which have little coordination ability.[6,8]

Ru/M-41(m) catalyses alkene oxidation by *tert*-butyl hydroperoxide (TBHP). In a typical experiment, a mixture of alkene (0.2 g), TBHP (0.1 g), Ru/M-41(m) (0.05 g, $5.84 \times 10^{-5}$ mmol) and dichloromethane (2 ml) in a sealed vial was stirred for 24 h under a nitrogen atmosphere at room temp. Products were analysed and quantified by gas–liquid chromatography and/or

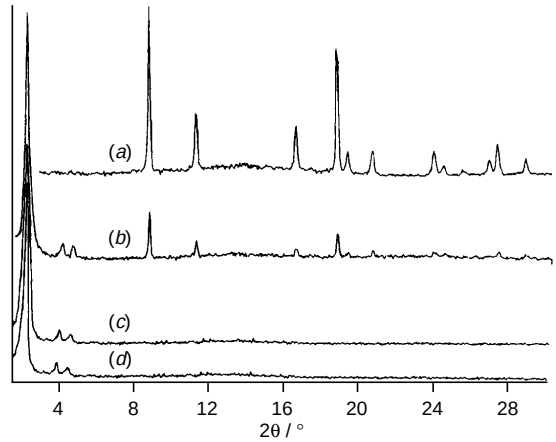
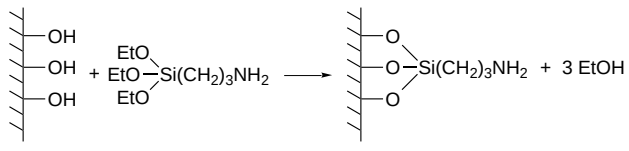
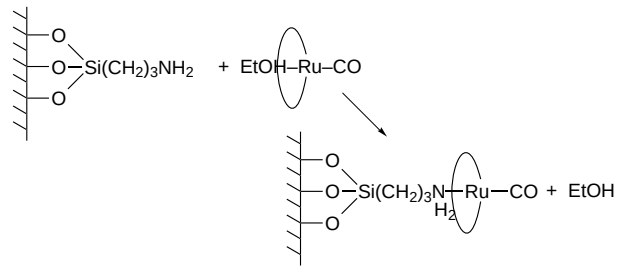



**Fig. 1** XRD patterns of (*a*) [RuL(CO)(EtOH)], (*b*) a physical mixture of [RuL(CO)(EtOH)] and MCM-41(m) in a mass ratio of 8 : 92, (*c*) 8.3 mass% Ru/M-41(m) and (*d*) MCM-41 and MCM-41(m)




**Scheme 1**




**Scheme 2**

**Table 1** Oxidation of alkenes by TBHP catalysed by [RuL(CO)(EtOH)] and 0.1 mass% Ru/M-41(m)

| | | 0.1 mass% Ru/M-41(m) | | [RuL(CO)(EtOH)] | |
|---|---|---|---|---|---|
| Substrate | Product | Turnover | % Yield[a] | Turnover | % Yield |
| Norbornene | *exo*-Norbornene oxide | 9003 | 52.6 | 230 | 53.8 |
| Cyclooctene | Cyclooctene oxide | 2044 | 11.9 | 69 | 11.9 |
| Styrene | Styrene oxide | 1878 | 11.0 | 52 | 12.2 |
| | Benzaldehyde | 4545 | 26.5 | 121 | 28.4 |
| Cyclohexene | Cyclohexene oxide | 377 | 2.2 | 20 | 4.6 |
| | Cyclohex-2-en-1-ol | 1219 | 7.1 | 26 | 6.1 |
| | Cyclohex-2-en-1-one | 2100 | 12.3 | 38 | 8.8 |
| *cis*-Stilbene[b] | *cis*-Stilbene oxide | 245 | 1.4 | 35 | 8.2 |
| | *trans*-Stilbene oxide | 1468 | 8.6 | 37 | 8.6 |
| | Benzaldehyde | 161 | 0.94 | 3 | 0.64 |
| *trans*-Stilbene[b] | *cis*-Stilbene oxide | 31 | 0.18 | 1 | 0.28 |
| | *trans*-Stilbene oxide | 1595 | 9.35 | 85 | 19.9 |
| | Benzaldehyde | 59 | 0.27 | Trace | — |

[a] Product yields were determined by GC and based on TBHP consumed. [b] The yield was determined by $^1$H NMR spectroscopy with 1,1-diphenylethylene as internal standard.

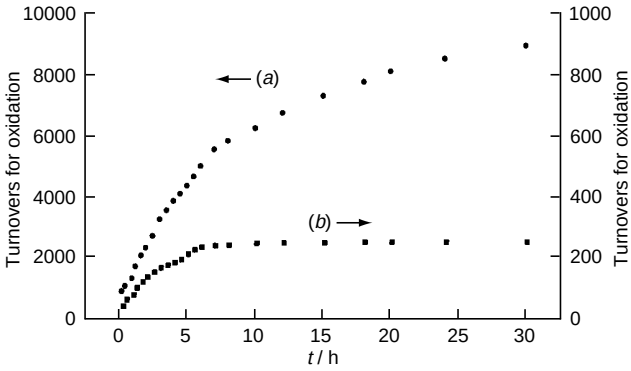



**Fig. 2** Time course of oxidation for norbornene by TBHP with (*a*) 0.1 mass% Ru/M-41(m) and (*b*) [RuL(CO)(EtOH)]

$^1$H NMR spectroscopy. Control experiments using [RuL(CO)(EtOH)] or MCM-41(m) as catalyst and under identical reaction conditions were also performed. TBHP in the absence of catalyst and/or MCM-41(m) showed very little catalytic activity compared with Ru/M-41(m).[9]

Ru/M-41(m) with a ruthenium content ranging from 0.1 to 8.3 mass% showed good catalytic activity. In norbornene oxidation, turnovers of *exo*-norbornene oxide with 0.1, 5 and 8.3 mass% Ru/M-41(m) as catalyst are 9003, 303 and 216, respectively, suggesting that the catalytic activity is high at low ruthenium content. Presumably this is due to efficient site isolation and diffusion pathways during the reaction. Owing to its better catalytic activity, the 0.1 mass% Ru/M-41(m) catalyst was used for further oxidation experiments. Table 1 compares the results obtained for the oxidation of norbornene (bicyclo-[2.2.1]hept-2-ene), cyclooctene, cyclohexene, styrene, *cis*- and *trans*-stilbenes catalysed by 0.1 mass% Ru/M-41(m) and free [RuL(CO)(EtOH)]. In general the product turnovers are 20–40 times higher with the former.

A typical time course for norbornene oxidation is shown in Fig. 2. With 0.1 mass% Ru/M-41(m), norbornene was oxidized to the *exo*-norbornene oxide at a rate of 300 turnovers $h^{-1}$ *cf.* 38 turnovers $h^{-1}$ with [RuL(CO)(EtOH)]. Also [RuL(CO)(EtOH)] was unstable and was completely deactivated after 6 h. By contrast, the 0.1 mass% Ru/M-41(m) catalyst appeared to be very stable and its catalytic activity did not change appreciably even after 48 h of reaction. Embedding of [RuL(CO)] molecules and their isolation from each other in the channels of MCM-41(m) precludes formation of stable inactive μ-oxo dimers. This may partly explain the stability of Ru/M-41(m) in the TBHP oxidation reaction. It is of note that the 0.1 mass% Ru/M-41(m) catalyst could be easily recovered by filtration and washing with $CH_2Cl_2$.

From Table 1, *trans*-stilbene oxide was the major product of *trans*-stilbene oxidation. However, oxidation of *cis*-stilbene catalysed by 0.1 mass% Ru/M-41(m) gave *trans*-stilbene oxide as the major product, in contrast to [RuL(CO)(EtOH)] for which an essentially 1 : 1 mixture of *cis*- and *trans*-stilbene oxides was obtained. This could be a consequence of the steric constraints imposed by the straight channels of MCM-41(m) which would favour the formation of linear *trans*-stilbene oxide.

We acknowledge supports from the Hong Kong Research Council and the University of Hong Kong.

## Footnotes

† Solid diffuse-reflectance UV–VIS spectrum of 0.1 mass% Ru/M-41(m) ($\lambda_{max}$/nm): 414, 535, 570.

‡ FT Raman spectrum of 8.3 mass% Ru/M-41(m) ($\tilde{\nu}$/cm$^{-1}$): 1591.7, 1545.0, 1488.3, 1462.9, 1363.9, 1235.4, 1206.5, 1088.5, 1036.4, 1012.9, 884.0, 848.3, 807.1, 708.7, 471.9, 397.3, 357.3, 337.9, 285.4, 159.7.

## References

1 M. Nakamura, T. Tatsumi and H. Tominaga, *Bull. Chem. Soc. Jpn.*, 1990, **63**, 3334.
2 F. Bedioui, *Coord. Chem. Rev.*, 1995, **144**, 39.
3 P. Battioni, R. Iwanejko, D. Mansuy, T. Mlodnicka, J. Poltowicz and F. Sanchez, *J. Mol. Catal.*, 1996, **109**, 91.
4 R. C. Sosa, R. F. Parton, P. E. Neys, O. Lardinois, P. A. Jacobs and P. G. Rouxhet, *J. Mol. Catal.*, 1996, **110**, 141.
5 B. Meunier, *Chem. Rev.*, 1992, **92**, 1441.
6 J. S. Beck, J. C. Vartuli, W. J. Roth, M. E. Leonowicz, C. T. Kresge, K. D. Schmitt, C. T.-W. Chu, D. H. Olson, E. W. Sheppard, S. B. McCullen, J. B. Higgins and J. L. Schlenker, *J. Am. Chem. Soc.*, 1992, **114**, 10 834.
7 D. P. Rillema, J. K. Nagle, L. F. Barringer Jr. and T. J. Meyer, *J. Am. Chem. Soc.*, 1981, **103**, 56.
8 G. A. Ozin and S. Özkar, *Chem. Mater.*, 1992, **4**, 511.
9 E. M. Gaigneaux, R. Maggi, P. Ruiz and B. Delmon, *J. Mol. Catal.*, 1996, **109**, 67.

*Received, 16th August 1996; Com. 6/05721G*

# $[Fe_3Cu(SPr^i)_6Cl_3]^{2-}$: a novel mixed-metal thiolate complex with a 'truncated' adamantane-like structure

**Hans-Oscar Stephan,[a,b] Gerald Henkel[b] and Mercouri G. Kanatzidis*[a]**

[a] *Department of Chemistry, Michigan State University, East Lansing, MI 48824, USA*
[b] *FB 6 - Fachgebiet Anorg. Chemie/Festkörperchemie, Gerhard-Mercator-Universität Duisburg, Lotharstr. 1, 47048 Duisburg, Germany*

**Reaction of $[Fe_2(SPr^i)_6]^{2-}$ with $FeCl_2$ and CuCl in a 1:1:1 molar ratio in hot tetrahydrofuran gives the complex anion $[Fe_3Cu(SPr^i)_6Cl_3]^{2-}$ which contains a $Fe_3Cu$ pyramidal core; the structure, magnetic properties and the solution $^1H$ NMR spectrum are reported.**

The chemistry of homometallic thiolate complexes has been developed to a remarkable extent in the last 20 years.[1,2] Nevertheless, there are amazingly few reports on analogous heterometallic clusters. The reason may be that these clusters are not as straightforward to stabilize as the homometallic ones because, in addition to the usual problems one has in isolating these labile complexes and crystallizing them, one is also faced with the problem of phase separation which leads to a mixture of homometallic complexes. To date, the most notable examples are $[Au_3Cu_3(SCH_2CH_2)_4]^{2-}$,[3] $[Au_2Cu_4(SCH_2CH_2)_4]^{2-}$,[3] $[Au_2Ag_4(SCH_2CH_2)_4]^{2-}$,[3] $[Cu_6In_3(SEt)_{16}]^{-}$,[4] $[Eu_2M_2(SPh)_8(py)_6]$ (M = Cd, Hg)[5] and $[Eu_2Zn_2(SPh)_8(thf)_6]$[5] as well as $[CuIn(ER)_4(PPh_3)_2]$[6] (E = S, Se). Focussing attention onto the chemistry of heterometallic thiolate complexes is now timely because, in addition to the novel properties and structures one might encounter, they could serve as molecular precursors to high-quality ternary heterometallic solids. This was shown earlier in the case of $[CuIn(ER)_4(PPh_3)_2]$ which leads cleanly to the photovoltaic material $CuInSe_2$.[6]

Our approach towards this class of complexes is to react well defined homometallic thiolate precursors with readily available sources of the heterometal such as metal halides.

Very recently, we found that the reaction of $[NMe_4]_2[Mn_2(SPr^i)_6]$[7] with CuCl gives the remarkable anion $[Mn_4Cu_4(SPr^i)_{12}(\mu_4\text{-}S)]^{2-}$.[8] The core of this cluster consists of a distorted $Mn_4Cu_4$ metal cube which is stabilized with an interstitial $\mu_4$-S ligand and edge-bridging thiolate ligands. Encouraged by this result, we started to explore the chemistry of the analogous $Fe^{2+}Cu^+$ system and discovered the novel mixed-metal cluster $[NMe_3(CH_2Ph)]_2[Fe_3Cu(SPr^i)_6Cl_3]$ **1**. Complex **1** is best accessible by a reaction of $[Fe_2(SPr^i)_6]^{2-}$ with solid $FeCl_2$ and CuCl (molar ratio 1:1:1) in hot tetrahydrofuran and can be isolated as orange–brown crystals upon addition of $[NMe_3(CH_2Ph)]Br$.†

The structure‡ of the tetranuclear cluster **1** is shown in Fig. 1. It contains a $Fe_3Cu$ trigonal pyramid with idealized $C_{3v}$ symmetry. The three Fe atoms define the vertices of the basal triangular plane with Fe···Fe separations of 3.852 Å. The apex of the pyramid is occupied by the Cu atom (Fe···Cu 3.205 Å). This metal core is held together by six thiolate groups. The observed Fe–S and Cu–S distances of 2.345 Å and 2.241 Å, respectively, are similar to the corresponding bond lengths in homoleptic homometallic Fe[9] and Cu[10] thiolate clusters. In contrast to the Fe atoms which each bind to terminal Cl ligands (Fe–Cl 2.313 Å) to adopt a tetrahedral coordination [S–Fe–S(Cl) 109.3°], the Cu atom resides inside the 'upper' $S_3$ face and thus has a trigonal planar environment (S–Cu–S 119.9°). This is the reason why the overall shape of **1** appears to be a truncated adamantane.

Complex **1** is a structural derivative of homometallic thiolate adamantanes of the formula $[M_4(SR)_6X_4]^{2-}$ (X = halogen).[7,11,12b] The central core of these complexes is an $M_4$ tetrahedron of tetrahedrally coordinated metal atoms. The formal replacement of one of these metal sites with a trigonal-planar M′ centre results in the loss of one terminal ligand. At the same time, the idealized symmetry of the $M_3M'$ core drops to $C_{3v}$ since M′ is shifted towards the centre of the cluster. However, the symmetry of the entire cluster is $C_3$ rather than $C_{3v}$, because of the orientation of the organic groups. The cluster shows the (3,−1,−1,−1) pattern§ with three axially oriented ligands within the basal $Fe_3S_3$ ring. The three $CuFe_2S_3$ rings have one axially disposed group each. This situation leads to a 'paddlewheel'-like arrangement of the thiolate ligands attached to Cu. The $C_3$ axis of the molecule thus runs through the Cu atom and the centre of the basal $Fe_3$ triangle.

Since **1** can be considered as an $[Fe_3(\mu\text{-}SR)_3(SR)_3Cl_3]^{3-}$ cluster which is stabilized by the incorporation of an additional $Cu^+$ ion, its structure is reminiscent of the trinuclear Fe clusters

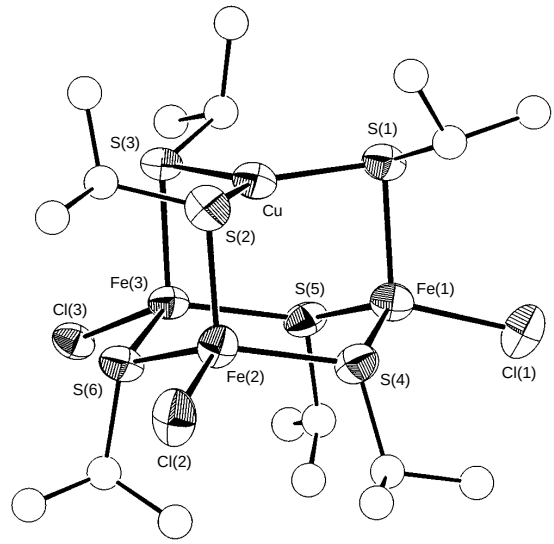



**Fig. 1** ORTEP plot of $[Fe_3Cu(SPr^i)_6Cl_3]^{2-}$ with labelling scheme. Selected bond distances (Å) and angles (°): Cu–Fe(1) 3.145(3), Fe(1)–Fe(2) 3.849(3), Cu–Fe(2) 3.234(3), Fe(1)–Fe(3) 3.851(3), Cu–Fe(3) 3.235(3), Fe(2)–Fe(3) 3.857(3), Cu–S(1) 2.228(4), Cu–S(2) 2.233(4), Cu–S(3) 2.261(4), Fe(1)–Cl(1) 2.307(5), Fe(1)–S(1) 2.334(5), Fe(1)–S(4) 2.356(5), Fe(1)–S(5) 2.347(4), Fe(2)–Cl(2) 2.313(4), Fe(2)–S(2) 2.345(5), Fe(2)–S(4) 2.334(4), Fe(2)–S(6) 2.355(4), Fe(3)–Cl(3) 2.321(4), Fe(3)–S(3) 2.350(4), Fe(3)–S(5) 2.343(4), Fe(3)–S(6) 2.344(4); S(1)–Cu–S(2) 127.6(2), S(1)–Cu–S(3) 114.4(2), S(2)–Cu–S(3) 117.9(2), S(1)–Fe(1)–S(4) 109.0(2), S(1)–Fe(1)–S(5) 99.9(2), S(4)–Fe(1)–S(5) 118.9(2), S(2)–Fe(2)–S(4) 103.1(2), S(2)–Fe(2)–S(6) 102.3(2), S(4)–Fe(2)–S(6) 119.7(2), S(3)–Fe(3)–S(5) 102.4(2), S(3)–Fe(3)–S(6) 104.2(2), S(5)–Fe(3)–S(6) 119.2(2), Cu–S(1)–Fe(1) 87.1(2), Cu–S(2)–Fe(2) 89.9(2), Cu–S(3)–Fe(3) 89.1(1), Fe(1)–S(4)–Fe(2) 110.3(2), Fe(1)–S(5)–Fe(3) 110.4(2), Fe(2)–S(6)–Fe(3) 110.4(2).

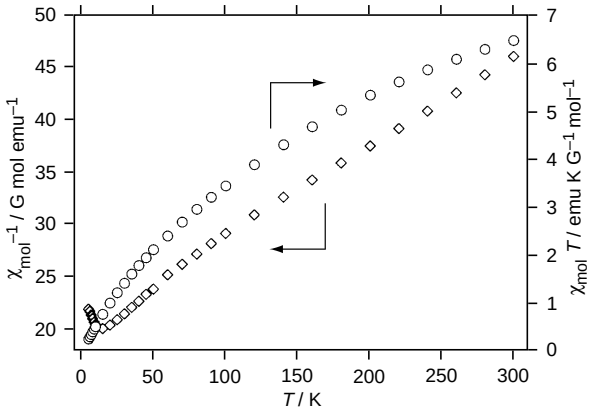



**Fig 2** Magnetic data for $[NMe_3(CH_2Ph)]_2[Fe_3Cu(SPr^i)_6Cl_3]$. The susceptibilitiy data were recorded on a powdered sample in the temperature range 5–300 K in a 2 kG applied magnetic field.

of composition $[Fe_3(\mu\text{-}SR)_3Cl_6]^{3-}$.[12] These clusters, however, exhibit strictly planar $Fe_3S_3$ rings with very large Fe–S–Fe bridging angles of *ca.* 140°. To examine if this major structural difference is reflected in the magnetic properties of **1**, we measured magnetic susceptibility data for $[NMe_3(CH_2Ph)]_2[Fe_3Cu(SPr^i)_6Cl_3]$ (Fig. 2). The data show antiferromagnetic exchange interactions with Curie–Weiss behaviour within the temperature range 120–300 K. The Weiss constant is calculated to be $\theta = -246$ K. The susceptibility data for $[Fe_3(\mu\text{-}SPh)_3Cl_6]^{3-}$,[12b] compare very well with the behaviour observed for **1**. Obviously, neither the presence of $Cu^+$ ions in **1** nor the fact that the Fe–S–Fe bridging angles in **1** are about 30° smaller than in $[Fe_3(\mu\text{-}SPh)_3Cl_6]^{3-}$, are followed by major changes in the magnetic behaviour.

The solution $^1$H NMR spectrum of $[NMe_3(CH_2Ph)]_2[Fe_3Cu(SPr^i)_6Cl_3]$ in $CD_3CN$ at room temperature was recorded. Since the isotropic shift of the SC*H*$Me_2$ signal is a function of the local magnetic moment of the iron atoms, we expected two signals, one in the neighbourhood of δ 163 in the downfield region of the spectrum. This value can be calculated from the known magnetic moments[12b] and paramagnetic shifts[9b] of the $CH_2$ groups of $[Fe(SEt)_4]^{2-}$ and $[Fe_4(SEt)_{10}]^{2-}$. In fact, we observed one resonance at δ 161 and an additional signal at δ 87. While the first peak most probably arises from SC*H*$Me_2$ ligands bridging two paramagnetic Fe atoms **1**, that at δ 87 could tentatively be assigned to SC*H*$Me_2$ ligands bridging one diamagnetic Cu and one paramagnetic Fe atoms.

In summary, we have presented the first mixed-metal FeCu thiolate complex, with a structure reminiscent of adamantane. This cluster might act as a useful starting material to novel mixed-metal thiolates or sulfido/thiolato compounds. In particular, the synthesis of mixed-metal cubanes of the formula $[Fe_3CuE_4(SR)_3]^{2-}$ (E = S, Se, Te), in which one iron atom of the $[Fe_4E_4]$ parent cluster core is replaced by a $Cu^+$ ion, might be accessible by reaction of **1** with elemental chalcogen.

H.-O. S. thanks the Deutsche Forschungsgemeinschaft for a postdoctoral fellowship. M.G.K. is a Camille and Henry Dreyfus Teacher–Scholar.

## Footnotes

† *Synthesis of* $[NMe_3(CH_2Ph)]_2[Fe_3Cu(SCPr^i)_6Cl_3]$. To a slurry of $NaSPr^i$ (0.59 g, 6 mmol) in 25 ml MeCN was added solid $FeCl_2$ (0.25 g, 2 mmol) and the mixture was stirred for 2 h. Then $[NMe(CH_2Ph)]Br$ (0.46 g, 2 mmol) was added and the stirring continued for 24 h. The solvent was evaporated and replaced by 25 ml of thf. Then, the mixture was filtered and the resulting solution of $[NMe_3(CH_2Ph)]_2[Fe_2(SPr^i)_6]$ was heated to its boiling point. Solid $FeCl_2$ (0.13 g, 1 mmol) and CuCl (0.10 g, 1 mmol) were added and the mixture was boiled for 20 min whereupon a small amount of a black precipitate was filtered off. The volume of the solution was reduced to *ca.* 15 ml. After stirring for 2 days at room temperature, the crude product precipitated. This material was recrystallized from MeCN–$Et_2O$ (1:5) to give 0.35 g (33%) of the desired compound. More material can be recovered from the mother-liquor to give an overall yield of 60%. The single crystal used for the X-ray structure determination was obtained from a solvothermal reaction of $[NMe_3(CH_2Ph)]_2[Fe_2(SPr^i)_6]$ with 2 equiv. of CuCl in thf at 80 °C.

‡ *Crystal data*: $[NMe_3(CH_3Ph)]_2[Fe_3Cu(SPr^i)_6Cl_3]$, monoclinic, space group $P2_1/n$ with $a$ = 10.846(4), $b$ = 12.018(5), $c$ = 41.23(1) Å, $\beta$ = 94.97(2)°, $U$ = 5354(3) Å$^3$, $Z$ = 4, $D_c$ = 1.351 g cm$^{-3}$ and $\mu$ = 15.9 cm$^{-1}$. Single-crystal X-ray diffraction data were collected (at −110 °C) on a Nicolet P3 four-circle diffractometer (Mo-K$\alpha$ radiation) with ω-scans, $4 < 2\theta < 45°$, and 3764 reflections with $F_o^2 > 3\sigma(F_o^2)$. An empirical absorption correction (DIFABS, N. Walker and D. Stuart, *Acta Crystallogr., Sect. A*, 1983, **39**, 158) was applied as recommended. The number of variables were 477, and final $R$, $R_w$ = 0.070, 0.045. The structure was solved with SHELXS86 and was refined with the TEXSAN Structure Analysis Package (Molecular Structure Corporation, 1985) of crystallographic programs. Sigma weights were used. The isopropyl group attached to S(5) is disordered over two positions. The structure of the $[NMe_3(CH_2Ph)]^+$ cations is normal and there are no bonding cation–anion contacts. Atomic coordinates, bond lengths and angles, and thermal parameters have been deposited at the Cambridge Crystallographic Data Centre (CCDC). See Information for Authors, Issue No. 1. Any request to the CCDC for this material should quote the full literature citation and the reference number 182/292.

§ An adamantane-like cluster of composition $[M_4(\mu\text{-}SR)_6X_4]^{2-}$ (X = Cl, Br, I, SR) is built up of four fused $M_3S_3$ rings in chair conformation in which the organic group bound to the μ-S atoms can either be axially or equatorially oriented. There are four independent conformers for $M_4(\mu\text{-}SR)_6$ cages which are symbolized by the following orientation patterns: (3,−2,−1,−0), (2,2,2,0), (3,−1,−1,−1) and (2,−2,−1,−1). The four numbers within the parentheses represent the number of axially oriented groups in each of the four $M_3(SR)_3$ six-membered rings. The most common one is (2,−2,−1,−1), while all other adamantane-like Fe thiolates known so far adopt the (3,−2,−1,−0) pattern.

## References

1 B. Krebs and G. Henkel, *Angew. Chem.*, 1991, **103**, 785; *Angew. Chem., Int. Ed. Engl.*, 1991, **30**, 769.
2 I. Dance and K. Fisher, *Prog. Inorg. Chem.*, 1994, **41**, 637.
3 G. Henkel, B. Krebs, P. Betz, H. Fietz and K. Saatkamp, *Angew. Chem.*, 1988, **100**, 1375; *Angew. Chem., Int. Ed. Engl.*, 1988, **27**, 1326.
4 W. Hirpo, S. Dhingra and M. G. Kanatzidis, *J. Chem. Soc., Chem. Commun.*, 1992, 557.
5 M. Brewer, J. Lee and J. G. Brennan, *Inorg. Chem.*, 1995, **34**, 5919.
6 W. Hirpo, S. Dhingra, A. C. Sutorik and M. G. Kanatzidis, *J. Am. Chem. Soc.*, 1993, **115**, 1597.
7 H.-O. Stephan and G. Henkel, *Polyhedron*, 1996, **15**, 501.
8 H.-O. Stephan, M. G. Kanatzidis and G. Henkel, *Angew. Chem., Int. Ed. Engl.*, 1996, **35**, 2135.
9 For example: (*a*) D. Swenson, N. C. Baenziger and D. Coucouvanis, *J. Am. Chem. Soc.*, 1978, **100**, 1932; (*b*) K. S. Hagen and R. H. Holm, *Inorg. Chem.*, 1984, **23**, 418; (*c*) G. Henkel and C. Chen, *Inorg. Chem.*, 1993, **32**, 1064.
10 See, for example: D. Coucouvanis, C. N. Murphy and S. K. Konodia, *Inorg. Chem.*, 1980, **19**, 2993; M. Baumgartner, H. Schmalle and E. Dubler, *Polyhedron*, 1990, **9**, 1155; I. G. Dance and J. C. Calabrese, *Inorg. Chim. Acta*, 1976, **19**, L41.
11 D. Coucouvanis, M. Kanatzidis, E. Simhon and N. C. Baenziger, *J. Am. Chem. Soc.*, 1984, **104**, 1874; D. Fenske, J. Meyer and K. Merzweiler, *Z. Naturforsch., Teil B*, 1987, **42**, 1207; P. A. W. Dean, J. Vittal and N. C. Payne, *Inorg. Chem.*, 1987, **26**, 1683; W. Tremel, B. Krebs, K. Greiwe, W. Simon, H.-O. Stephan and G. Henkel, *Z. Naturforsch., Teil B*, 1992, **47**, 1580; H.-O. Stephan, K. Griesar, W. Haase and G. Henkel, *Z. Naturforsch., Teil B*, 1994, **49**, 1620.
12 (*a*) K. S. Hagen and R. H. Holm, *J. Am. Chem. Soc.*, 1982, **104**, 5496; (*b*) M. A. Whitener, J. K. Bashkin, K. S. Hagen, J.-J. Girerd, E. Gamp and N. Edelstein, *J. Am. Chem. Soc.*, 1986, **108**, 5607; (*c*) R. H. Holm, K. S. Hagen and A. D. Watson, in *Chemistry for the Future*, ed. H. Grünewald, Pergamon, New York, 1984, pp. 115–124.

*Received, 10th October 1996; Com. 6/06962B*

# Cobalt tetraarylporphyrin-catalysed epoxidation of alkenes by dioxygen and 2-methylpropanal under fluorous biphasic conditions

**Gianluca Pozzi,*† Fernando Montanari and Silvio Quici**

*Centro CNR and Dipartimento di Chimica Organica e Industriale dell'Università, Via Golgi 19, I-20133 Milano, Italy*

**The aerobic epoxidation of alkenes with 2-methylpropanal can be carried out under fluorous biphasic conditions, in the presence of the perfluorocarbon soluble cobalt complex of tetraarylporphyrin 3 as catalyst.**

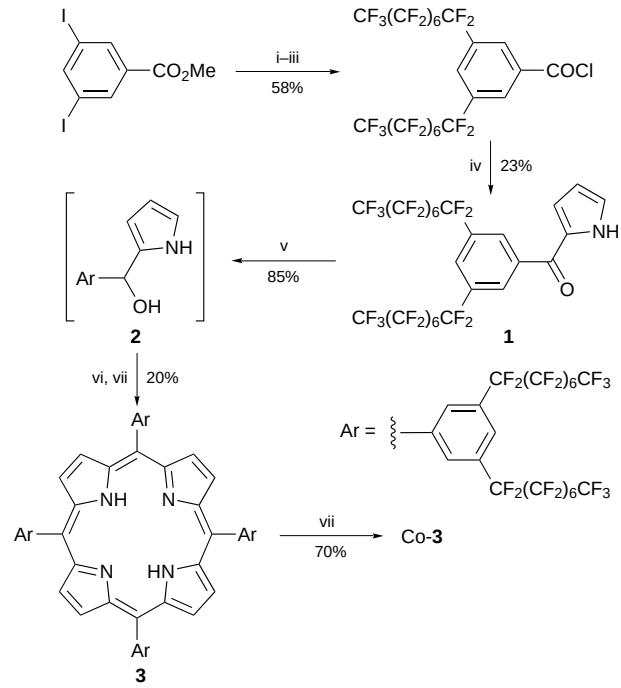
Catalysis under homogeneous two-phase conditions has been recognized as a viable alternative for many important chemical processes.[1] Several approaches to liquid–liquid biphasic catalytic reactions have been proposed, and among them the so-called 'fluorous biphase system' (FBS)[2] stands out for its peculiar characteristics. In this approach the low miscibilities of fluorocarbons with most organic solvents allows segregation of a catalyst soluble in the fluorocarbon phase from substrates and products dissolved in the organic phase. The FBS method shows appealing general features, such as the employment of nontoxic, reusable perfluorocarbons and the easy separation of catalyst from reactants and products.[3] Moreover, the inertness of perfluorocarbons and the high solubility of oxygen in these fluids would be particularly helpful in oxidation reactions.[4] In spite of this, the only examples of true FBS oxidation reported so far concern some simple reactions of phosphines and sulfides,[5] and the photooxidation of alkenes to hydroperoxides in the presence of a perfluorocarbon-soluble sensitizer.[6] The availability of efficient oxidation catalysts soluble in fluorocarbons is essential for applying the FBS concept to other synthetically useful reactions, such as the epoxidation of alkenes and hydroxylation of alkanes. These last reactions can be carried out under mild condition using a combination of molecular oxygen and reducing agent in the presence of transition metal complexes.[7] Here we report the synthesis of the perfluorocarbon-soluble tetraarylporphyrin **3**, bearing eight $C_8F_{17}$ chains, and the use of its cobalt complex Co-**3** as epoxidation catalyst under fluorous biphasic conditions.‡

All attempts to apply well-established synthetic procedures[8] to the preparation of **3** failed, as was found in the case of *meso*-perfluoroalkylporphyrins.[9] The synthesis of **3**, outlined in Scheme 1, was thus carried out by condensation of the pyrrole derivative **2**, according to a procedure originally devised by Kuroda and Ogoshi,[10] The presence of $Zn(OAc)_2$ as templating agent in the cyclisation step turned out to be essential for obtaining the porphyrin in reasonable yield. After removal of zinc, the free-base porphyrin **3** was metalated to form the cobalt complex Co-**3** according to a classical procedure.[11],§ Both **3** and Co-**3** were insoluble in common organic solvents, whereas they were easily dissolved in perfluorocarbons.¶

It is known that $Co^{II}$-tetraarylporphyrins are capable of binding dioxygen reversibly yielding oxygenated $Co^{III}$-complexes.[12] The UV-VIS spectra of Co-**3** in $CF_2ClCFCl_2$ and perfluorohexane both showed a broad Soret band with two maxima at 405 and 427 nm. The splitting of the Soret band as well as its breadth were consistent with the coexistence of $Co^{II}$ and $Co^{III}$ species in the aerated solutions.[13]

Co-**3** proved to be an efficient catalyst for the fluorous biphasic epoxidation of alkenes by molecular oxygen and 2-methylpropanal as reducing agent. Reaction conditions and results are detailed in Table 1.

Reactions were carried out at room temperature in flasks carefully shielded from direct sunlight. A solution of Co-**3** in




**Scheme 1** *Reagents and conditions*: i, $C_8F_{17}I$, Cu, DMF, 125 °C; ii, KOH, $H_2O$–MeOH, reflux; iii, $SOCl_2$, reflux; iv, pyrrole, EtMgBr, $Et_2O$, 0 °C; v, LAH, THF; vi, $Zn(OAc)_2.2H_2O$, propanoic acid, reflux, then 2,3-dichloro-5,6-dicyano-1,4-benzoquinone; vii, $CF_3CO_2H$, reflux, then aqueous $NaHCO_3$; viii, $Co(OAc)_2.4H_2O$, DMF, reflux

**Table 1** Epoxidation of alkenes under fluorous biphasic conditions catalysed by Co-**3**[a]

| Entry | Substrate | *t*/h | Conversion (%)[b] | Selectivity (%)[b,c] |
|---|---|---|---|---|
| 1 | *cis*-Cyclooctene[d] | 6 | — | — |
| 2 | *cis*-Cyclooctene | 3 | 100 | > 95 |
| 3 | *cis*-Cyclooctene[e] | 3 | 100 | > 95 |
| 4 | Norbornene | 5 | 95 | > 95 |
| 5 | 1-Methylcyclohexene | 3 | 100 | > 95 |
| 6 | 2-Methylundec-1-ene | 5 | 80 | 90 |
| 7 | Dodec-1-ene | 14 | 48 | 92 |
| 8 | Dodec-1-ene[f] | 14 | 60 | 87 |

[a] Conditions: [substrate] = 0.1 mol $dm^{-3}$ in MeCN; [2-methylpropanal] = 0.2 mol $dm^{-3}$ in MeCN; [Co-**3**] = 0.0001 mol $dm^{-3}$ in perfluorohexane; volume of MeCN = 1 ml; volume of perfluorohexane = 1 ml; stirring rate = 1300 rpm; $T$ = 25 °C. Reactions were carried out in the dark. [b] Determined by GC using the internal standard method. [c] Selectivity = (moles of epoxide)/(moles of substrate converted). Epoxides were identified by comparison with authentic samples or by GC–MS. [d] Reaction carried out in the absence of Co-**3**. [e] Using the perfluorohexane layer recovered from entry 2. [f] Using 3-methylbutanal instead of 2-methylpropanal.

perfluorohexane was added to a solution of alkene in MeCN containing a twofold excess of aldehyde with respect to the substrate. The resulting biphasic mixture was vigorously stirred under atmospheric pressure of dioxygen. Co-**3** was completely partitioned in the fluorous phase, as shown by the UV–VIS spectra of the two layers. At the end of the reaction, the two phases were easily separated and the MeCN layer was analysed by gas chromatography (GC). It is worthwhile noting that under these conditions, but in the absence of Co-**3**, alkenes did not react (Table 1, entry 1). In the presence of the perfluorocarbon soluble catalyst, high alkene conversions were generally obtained, epoxides being the major products.‖

As reported for reactions carried out under homogeneous conditions, the present procedure is less suited for unsubstituted terminal alkenes such as dodec-1-ene (entry 7) than for other substrates. Nevertheless, epoxide yields were still satisfactory, and could even be increased by raising the aldehyde–alkene ratio[7] or by choosing different aldehydes (entry 8).

Cobalt complexes of *meso*-tetraarylporphyrins have been recently used as homogeneous catalysts for the aerobic oxidation of organic substrates in the presence of 2-methylpropanal.[14] The positive effect of running the reaction under fluorous biphasic conditions can be appreciated by comparing the present results with those reported in the cited reference. We were able to use a much higher substrate–catalyst ratio (1000 : 1) than that previously reported (20 : 1). Moreover, after complete conversion of cyclooctene the perfluorocarbon layer, recovered by simple phase separation, could be used as such for a second run, without decreasing either the substrate conversion or the selectivity for cyclooctene oxide (entry 3).

Our current efforts are aimed at the synthesis of metal complexes of non-porphyrinic perfluorocarbon-soluble ligands, to be used as catalysts for hydrocarbon oxygenations in the presence of simple oxygen atom donors.

This work was supported by the European Community (Human Capital and Mobility Program-Contract No. ERBCHRXTC 94-0492). Fluorocarbon fluids were generously supplied by 3M Italia.

## Footnotes

† E-mail: research@iumchz.chimorg.unimi.it

‡ Introduction of one perfluoroalkyl tail on each *meso*-aryl group is not sufficient to impart solubility in perfluorocarbons (G. Pozzi and M. Miglioli, unpublished results).

§ *Selected data* for **1**: $^1$H NMR ($CDCl_3$): δ 9.64 (br s, 1 H), 8.30 (s, 2 H), 7.95 (s, 1 H), 7.22 (m, 1 H), 6.78 (m, 1 H), 6.39 (m, 1 H); $^{19}$F NMR ($CDCl_3$; $CFCl_3$): δ −81.3 (t, *J* 9 Hz, 3 F), −111.5 (t, *J* 13 Hz, 2 F), −121.6 (br s, 2 F), −122.3 (m, 6 F), −123.3 (br s, 2 F), −126.7 (br s, 2 F); $^{13}$C NMR ($CDCl_3$): δ 105–118 (m, $C_8F_{17}$), 112.0, 119.9, 126.6, 128.2, 130.2, 130.5, 130.8, 139.7, 181.2. For **3**: $^1$H NMR ($CF_2ClCFCl_2$, $C_6D_6$): δ 8.77 (s, 8 H), 8.72 (s, 8 H), 8.36 (s, 4 H), −2.85 (s, 2 H); $\lambda_{max}$ ($CF_2ClCFCl_2$) 413 nm (ε $7.2 \times 10^4$ dm$^3$ mol$^{-1}$ cm$^{-1}$). (Calc. for $C_{108}H_{22}F_{136}N_4$: C, 32.76; H, 0.56; N, 1.41; F, 65.27. Found: C, 32.72; H, 0.60; N, 1.34; F, 64.24%). For Co-**3**: $\lambda_{max}$ ($CF_2ClCFCl_2$) 405 nm (ε $1.6 \times 10^4$ dm$^3$ mol$^{-1}$ cm$^{-1}$), 427 (ε $1.6 \times 10^4$). The acid-sensitive alcohol **2** was not purified and it was used directly for the cyclisation step.

¶ The following perfluorocarbons, available from 3 M, were tested as solvents: FC-72 (mainly perfluorohexane, bp 56 °C), FC-75 (mainly perfluorobutyltetrahydrofuran, bp 102 °C), FC-43 (mainly perfluorotributylamine, bp 174 °C).

‖ Although the exact role of the metal complex in the epoxidation of alkenes by dioxygen with co-oxidation of aldehydes is still a matter of debate (see W. Nam, H. J. Kim, S. H. Kim, R. Y. N. Ho and J. S. Valentine, *Inorg. Chem*., 1996, **35**, 1045), consistent literature data demonstrate that its presence is crucial for ensuring conversion of linear alkenes and for obtaining high epoxide yields without using large amounts of aldehyde.

## References

1 B. Cornils, *Angew. Chem., Int. Ed. Engl*., 1995, **35**, 1575.
2 I. T. Horváth and J. Rábai, *Science*, 1994, **266**, 72.
3 Some examples of reactions carried out in fluorocarbons: D.-W. Zhu, *Synthesis*, 1993, 953; D. P. Curran and S. Hadida, *J. Am. Chem. Soc*., 1996, **118**, 2531; R. P. Hughes and H. A. Trujillo, *Organometallics*, 1996, **15**, 286; D. P. Curran, *Chemtracts. Org. Chem*., 1996, **9**, 75.
4 I. Klement and P. Knochel, *Synlett*, 1995, 113; R. D. Chambers, G. Sandford and A. Shah, *Synth. Commun*., 1996, **26**, 1861.
5 I. T. Horváth and J. Rábai, *U.S. Pat*. 5,463,082, 1995.
6 S. G. DiMagno, P. H. Dussault and J. A. Schultz, *J. Am. Chem. Soc*., 1996, **118**, 5312.
7 T. Mukaiyama and T. Yamada, *Bull. Chem. Soc. Jpn.*, 1995, **68**, 17 and references cited therein.
8 J. S. Lindsey, *Metalloporphyrins catalyzed oxidation*, ed. F. Montanari and L. Casella, Kluwer, Dordrecht, 1994, p. 49 and references cited therein.
9 S. G. DiMagno, R. A. Williams and M. J. Therien, *J. Org. Chem*., 1994, **59**, 6943.
10 Y. Kuroda, H. Murase, Y. Suzuki and H. Ogoshi, *Tetrahedron Lett*., 1989, **30**, 2411.
11 A. D. Adler, F. P. Longo, F. Kampas and J. Kim, *J. Inorg. Nucl. Chem*., 1970, **32**, 2443.
12 R. D. Jones, D. A. Summerville and F. Basolo, *Chem. Rev*., 1979, **79**, 139.
13 R. Iwanejko and T. Mlodnicka, *Bull. Pol. Acad. Sci., Chem*., 1987, **35**, 403.
14 A. K. Mandal, V. Khanna and J. Iqbal, *Tetrahedron Lett*., 1996, **37**, 3769.

*Received, 29th August 1996; Com. 6/05963E*

# Novel fluorescence sensor for 'small' saccharides

**Tony D. James,*[a] Hideyuki Shinmori[b] and Seiji Shinkai[b]**

[a] *The University of Birmingham, School of Chemistry, Edgbaston, Birmingham, UK B15 2TT*
[b] *Department of Chemical Science and Technology, Faculty of Engineering, Kyushu University, Fukuoka 812, Japan*

**The small binding pocket of compound 2 can exclude 'large' saccharides such as D-glucose, whereas 'small' saccharides such as D-sorbitol are strongly bound as 1 : 1 complexes; the binding events can be sensitively monitored by changes in the fluorescence intensity.**

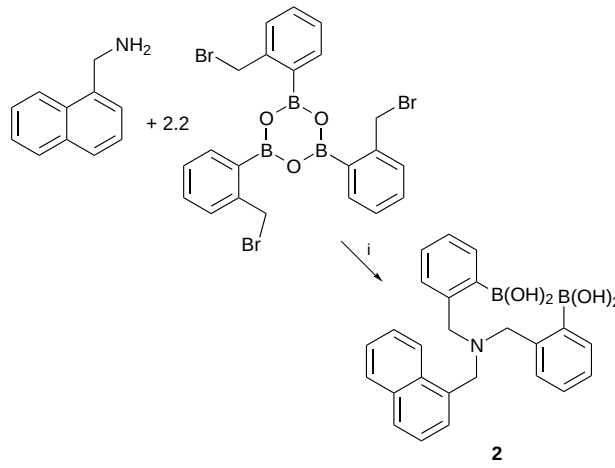
The development of boronic acid receptors for saccharides has recently gained much attention.[1] One problem with many of these systems is that they only function in basic aqueous media. Wulff was the first to report that a neighbouring nitrogen enhances the formation of boronate esters even under neutral pH conditions.[2] In a series of recent papers we employed the interaction between boronic acid and amine[3–7] to create photoinduced electron transfer (PET)[8,9] sensory systems for saccharides. When saccharides form cyclic boronate esters with boronic acids, the acidity of the boronic acid is enhanced[10] and therefore the Lewis acid–base interaction between the boronic acid and the tertiary amine is strengthened. The strength of this acid-base interaction modulates the PET from the amine (acting as a quencher) to anthracene (acting as a fluorophore). These compounds show increased fluorescence at pH 7.77 through suppression of the photoinduced electron transfer from nitrogen to anthracene on saccharide binding; a direct result of the stronger boron–nitrogen interaction.[3–7]

With diboronic acid **1** glucose selectivity was predicted from CPK models and then observed experimentally.[4] With other diboronic acids chiral discrimination[5] and metal ion allosterism[6] have been achieved. In these systems the formation of a 1 : 1 intramolecular complex which is classified as a saccharide-containing macrocycle was shown to be the important fluorescent species and the origin of the circular dichroism (CD) activity. With this work we have reduced the size of the cleft in order to modulate the selectivity of the boronic acid unit towards 'small' saccharides. From CPK models glucose cannot easily bind as a cyclic 1 : 1 complex with diboronic acid **2** and should be excluded from the binding pocket.

Compound **2** was synthesised from 1-aminomethylnaphthalene according to Scheme 1 and characterised using IR and $^1$H NMR spectral evidence and elemental analysis.

The absorption spectrum (25 °C, $H_2O$–MeOH, 300 : 1 v/v) and $\lambda_{max}$ were not affected over a large pH range (pH 1.7–11.8). The p$K_a$ values were determined using fluorescence spectroscopy (excitation 296 nm). The pH dependence of the relative fluorescence intensity ($I/I_0$; emission maximum 347 nm) is illustrated in Fig. 1. In the absence of saccharides, the $I/I_0$ is nearly constant from pH 1.5 to 8.0. Judging from the pH dependence of **1** a change from $\mathbf{2H}^+$ to **2** (*cf.* Scheme 2) should cause a large decrease in the fluorescence intensity. This means that deprotonation of $\mathbf{2H}^+$ occurs in a more acidic region. On the other hand, the $I/I_0$ gradually decreases above pH 8.0. This reflects the dissociation of boronic acid groups to $\mathbf{2}^-$ and $\mathbf{2}^{2-}$.

In the presence of saccharides, the $I/I_0$ increases from pH 4.0 and reaches a maximum at around pH 8.0. This change is ascribed to the intensified B–N interaction caused by the saccharide binding to the boronic acid group. Since the largest $I/I_0$ increase was observed at around pH 8.0, we determined the association constants ($K$) at pH 8.0 from plots of $I/I_0$ *vs.*




**2**

**Scheme 1** *Reagents*: i, $K_2CO_3$, MeCN, heat, 70%

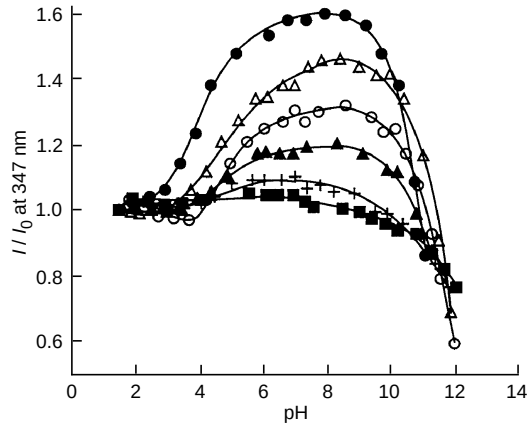
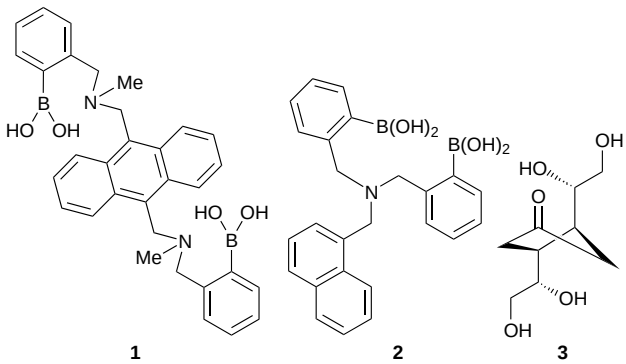
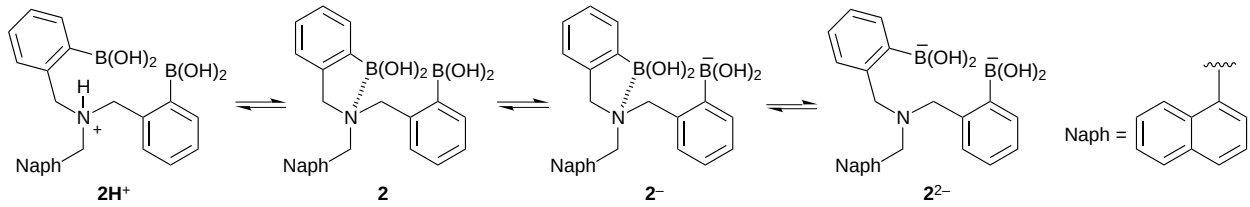



**Fig. 1** pH Dependence of the relative fluorescence intensity ($I/I_0$ at 347 nm) in the absence and presence of saccharides: [**2**] = $1.00 \times 10^{-5}$ mol dm$^{-3}$, [saccharide] = 0.10 mol dm$^{-3}$, 25 °C, $H_2O$–MeOH, 300 : 1 v/v buffered with HCl and NaOH, excitation 296 nm: (●) D-fructose, (△) pentaerythritol, (○) D-threitol, (▲) D-glucose, (+)-glycerine, (■) no saccharide




**1** **2** **3**




**Scheme 2**

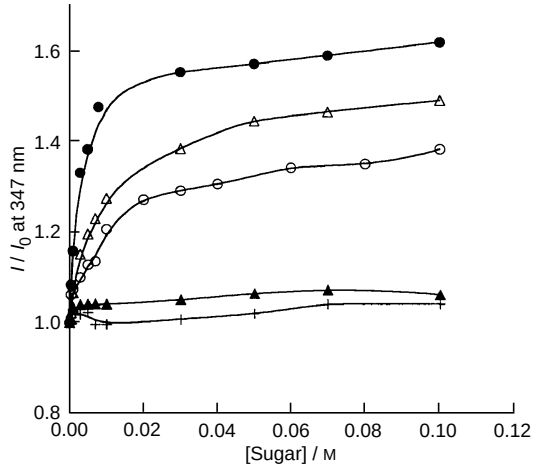



**Fig. 2** Plots of $I/I_0$ *vs.* [saccharide] for selected saccharides: (●) D-fructose, (△) pentaerythritol, (○) D-threitol, ( ▲ ) D-glucose, (+)-glycerine, (■) no saccharide

**Table 1** Association constants (*K*), number of binding sites and number of carbon separating two binding sites ($\Delta n$) at 25 °C and pH 8.0 in $H_2O$–MeOH, 300 : 1 *v/v*

| Sugar | log *K* | Binding site | $\Delta n$ |
|---|---|---|---|
| D-Sorbitol | 2.54 | 2 | 0–2 |
| D-Fructose | 2.52 | 2 | 0–1 |
| Dulcitol | 2.4 | 2 | 0–2 |
| Xylitol | 2.23 | 2 | 0–1 |
| D-Mannitol | 2.15 | 2 | 0–2 |
| Pentaerythritol | 2.11 | 2 | 0 |
| Ribitol | 1.97 | 2 | 0–1 |
| D-Threitol | 2.03 | 2 | 0 |
| D-Arabitol | 2.13 | 2 | 0–1 |
| D-Ribose | 1.91 | 2 | 0 |
| D-Fucose | 1.50 | 2 | 0 |
| Erythritol | 1.45 | 2 | 0 |
| D-Glucose | *a* | 2 | 1 |
| Glycerine | *a* | 1 | — |
| Propane-1,3-diol | *a* | 1 | — |
| **3**[b] | *a* | 2 | 2 |

[a] The *K* could not be determined because of the small fluorescence change. [b] $H_2O$–MeOH, 2 : 1 v/v (because of low solubility in water).

saccharide concentration (Fig. 2). The results are summarised in Table 1.

Examination of Table 1 reveals two important features of compound **2** as a PET sensor: that is, (i) **2** shows selectivity towards 'small' saccharides and (ii) only when they possess two binding sites (*i.e.* two diol units associative with a boronic acid) and they are not separated (*i.e.* the number of carbons separating the two diols, $\Delta n = 0$ in Table 1), do a large fluorescence increase and a large *K* value result. Glycerine and propane-1,3-diol, which have only one binding site, cannot enhance the fluorescence intensity. D-Glucose ($\Delta n = 1$) and mannitol derivative **3** ($\Delta n = 2$), in which two binding sites are separated by one or two carbons, cannot enhance the fluorescence either. Other compounds which can enhance the fluorescence intensity have two (or more than two) binding sites and $\Delta n = 0$ without exception. Even in those compounds with a choice of binding site, $\Delta n = 0$–2, the most stable complex should be the one with $\Delta n = 0$.

The formation of the cyclic structures is further supported by the fact that the complexes become CD active. For example, **2** ($1 \times 10^{-5}$ mol dm$^{-3}$) in the presence of sorbitol (0.10 mol dm$^{-3}$) gave $[\theta]_{max}$ $-2.16 \times 10^4$ deg cm$^2$ dmol$^{-1}$ for D-sorbitol and $2.16 \times 10^4$ deg cm$^2$ dmol$^{-1}$ for L-sorbitol at 228 nm (25 °C, pH 8.0 with 50 mmol dm$^{-3}$ phosphate buffer).

In conclusion we have clearly demonstrated that the selectivity of a diboronic acid cleft towards saccharides can be modified in a controlled manner by the correct spacing of two boronic acid units. This work illustrates the power of the synthetic saccharide sensor. Unlike enzymatic systems, selectivity can be designed for one particular saccharide. This offers the possibility of monitoring the concentrations of biologically important saccharides which are less abundant than D-glucose, in a variety of industrial and medicinal applications.

T. D. J. wishes to acknowledge the Royal Society for support through the award of a University Fellowship.

## References

1 G. Deng, T. D. James and S. Shinkai, *J. Am. Chem. Soc.*, 1994, **116**, 4567 and references cited therein; J. Yoon and A. W. Czarnik, *J. Am. Chem. Soc.*, 1992, **114**, 5874; G. T. Morin, M. P. Hughes, M.-F. Paugam and B. D. Smith, *J. Am. Chem. Soc.*, 1994, **116**, 8895 and references cited therein.
2 G. Wulff, *Pure Appl. Chem.*, 1982, **54**, 2093.
3 T. D. James, K. R. A. S. Sandanayake and S. Shinkai, *J. Chem. Soc., Chem. Commun.*, 1994, 477.
4 T. D. James, K. R. A. S. Sandanayake and S. Shinkai, *Angew. Chem., Int. Ed. Engl.*, 1994, **33**, 2207.
5 T. D. James, K. R. A. S. Sandanayake and S. Shinkai, *Nature*, 1995, **374**, 345.
6 T. D. James and S. Shinkai, *J. Chem. Soc., Chem. Commun.*, 1995, 1483.
7 T. D. James, P. Linnane and S. Shinkai, *Chem. Commun.*, 1996, 281; (b) T. D. James, K. R. A. S. Sandanayake and S. Shinkai, *Angew. Chem., Int. Ed. Engl.*, 1996, **108**, 2038.
8 R. A. Bissel, A. P. de Silva, H. Q. N. Gunaratna, P. L. M. Lynch, G. E. M. Maguire, C. P. McCoy and K. R. A. S. Sandanayake, *Top. Curr. Chem.*, 1993, **168**, 223.
9 A. W. Czarnik, *Fluorescent Chemosensors for Ion and Molecular Recognition*, ACS Books, Washington, 1993.
10 J. P. Lorand and J. D. Edwards, *J. Org. Chem.*, 1959, **24**, 769.

*Received, 24th September 1996; Com. 6/06552J*

# Synthesis of poly(anthracene-2,6-diyl) and a copolymer containing alternately anthracene-2,6-diyl and *p*-phenylene units

**Philip Hodge,* Gerald A. Power and M. A. Rabjohns**

*Department of Chemistry, University of Manchester, Oxford Road, Manchester, UK M13 9PL*

**The title polymers 1 and 2 are synthesised *via* precursor polymers assembled by organometallic couplings using a Diels–Alder adduct of 2,6-dibromoanthracene.**

Polymers with extended π-electron systems have long been of interest for theoretical reasons and also for possible applications in micro- and opto-electronics.[1] The synthesis of such polymers is, however, often complicated by their insolubility. In several such cases syntheses *via* precursor polymers have been successful.[2,3] In this type of approach a soluble readily characterised precursor polymer is synthesised which on heating, for example, is converted into the insoluble target polymer. A classical example is the Durham synthesis of polyacetylene.[2] Polymers with extended π-electron systems which electroluminesce are now also of interest as they may form the basis of electroluminescent display devices.[4] Examples of such polymers are various poly(phenylenevinylene)s.[5,6]

Many anthracene moieties are photoluminescent and polymers containing such units as part of a larger π-electron system are also likely to be electroluminescent. The only reported polymers where anthracene units are in the backbone and conjugated are some oligo(anthracene-9,10-diyl)s,[7] and some polyquinolines.[8] We now report syntheses, *via* precursor polymers **3** and **4** respectively, of poly(anthracene-2,6-diyl) **1** and a copolymer **2** containing alternately anthracene-2,6-diyl and *p*-phenylene units. The syntheses exploit the retro-Diels–Alder reaction. This has been exploited before, both in the synthesis of polymers with extended π-electron systems[2,8,9] and in the synthesis of polymers with nonconjugated anthracene moieties.[10,11]

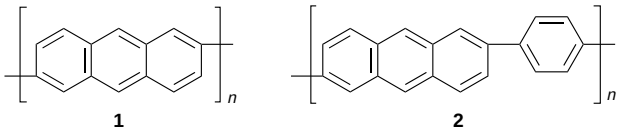
The synthesis of the Diels–Alder adduct **5** was conveniently achieved as outlined in Scheme 1. Thus, commercially available 2,6-diaminoanthraquinone **6** was converted into 2,6-dibromoanthraquinone **7** (60% yield) using a Sandmeyer reaction and the product **7** was reduced to 2,6-dibromoanthracene **8** (60% overall yield) by successive sodium borohydride reductions and acid catalysed dehydrations.[12] Treatment of compound **8** with an excess of maleic anhydride in xylene at reflux temperature gave the Diels–Alder adduct, which was then treated with methanol at reflux to give the half ester. The latter reacted smoothly with an $Et_2O$ solution of diazomethane to give the diester **5** (59% overall yield from compound **8**). This indirect route from compound **8** to diester **5** proved to be the most convenient route for obtaining a sufficient quantity of pure diester **5** for the subsequent synthetic work. Treatment of Diels–Alder adduct **5** in *N*,*N*-dimethylacetamide 80 °C with nickel(0)[13–15] gave precursor polymer **3** in 86% yield (Scheme 2). The infrared and $^1$H NMR spectra of the product were consistent with structure **3**. By gel permeation chromatography (GPC) the polymer had, relative to polystyrene standards, a number average molecular weight ($\overline{M}_n$) of 2700, a weight average molecular weight ($\overline{M}_w$) of 5400 and a peak molecular weight ($M_p$) of 5200. The $\overline{M}_w$ value corresponds to an average degree of polymerisation ($\overline{DP}$) of 17.

Copolymerisation of Diels–Alder adduct **5** and the 2,2-dimethylpropane-1,3-diol diester **9** of benzene-1,4-diboronic acid using a palladium(0) catalyst (Suzuki reaction)[16–18] gave precursor polymer **4** in 84% yield (Scheme 2). The infrared and $^1$H NMR spectra were consistent with structure **4**. By GPC the polymer had $\overline{M}_n$ 2300, $\overline{M}_w$ 5700 and $M_p$ 3000. The $\overline{M}_w$ value corresponds to a ($\overline{DP}$) of 28.

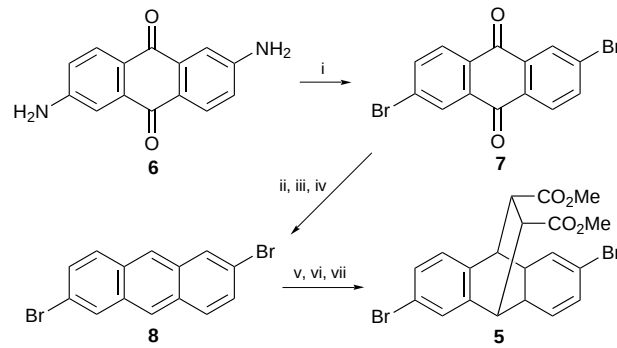
The precursor polymers **3** and **4** were soluble in many common solvents including THF and chloroform.

Conversions of the precursor polymers **3** and **4** into the target polymers **1** and **2** were achieved by thermal retro-Diels–Alder reactions which eliminated dimethyl maleate and produced the desired anthracene moieties. The reactions were monitored by thermogravimetric and spectroscopic methods. Thermogravimetric analysis showed that for both precursor polymers the onset on dimethyl maleate loss was at around 220 °C. Isothermal heating at atmospheric pressure showed that dimethyl maleate loss was significantly faster from polymer **4** than from polymer **3**. Heating polymer **3** at 260 °C for 3 h resulted in a weight loss corresponding to 73% of the theoretical maximum dimethyl maleate loss for this polymer. Similar treatment of polymer **4** at 240 °C for 1 h showed 95% of the theoretical maximum dimethyl maleate loss. It should be noted that these experiments were carried out at atmospheric pressure and that the observed weight losses would almost certainly be significantly greater for experiments carried out *in vacuo*. In all of these experiments both precursor polymers converted into the final polymers without melting.

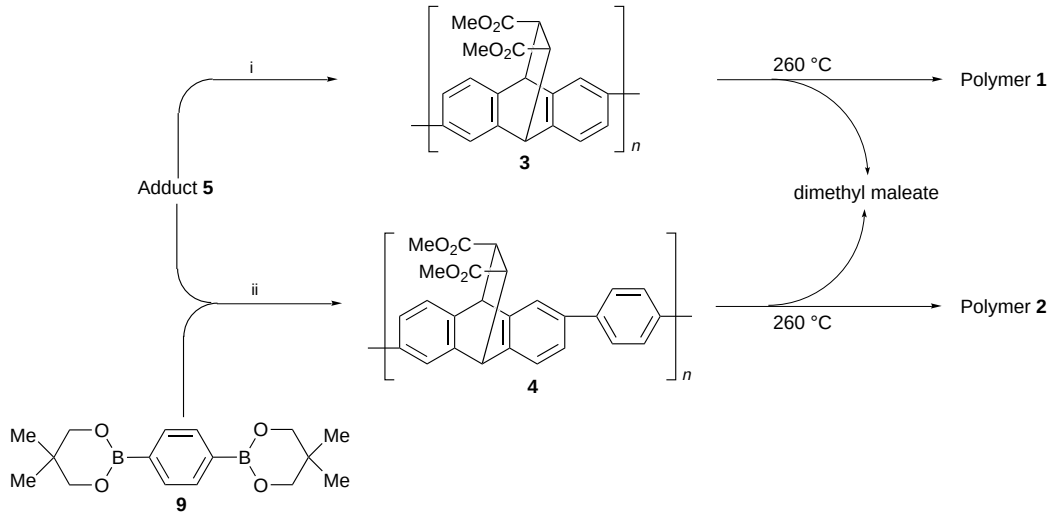
Having established the temperatures at which the retro-Diels–Alder reaction occurred, films of precursor polymers **3** and **4** were cast on sodium chloride discs and quartz discs in order to follow the reactions by FTIR and UV spectroscopy, respectively. On heating *in vacuo* for 12 h and 260 °C the clear polymer films were seen to change from colourless to an intense



**1** **2**




**Scheme 1** *Reagents and conditions*: i, *tert*-butyl nitrite, copper(II) bromide, MeCN, 80 °C; ii, $NaBH_4$, MeOH; iii, 5 M HCl, 90 °C, 6 h; iv, $NaBH_4$, $Pr^iOH$; v, maleic anhydride, *p*-xylene, 132 °C, 18 h; vi, MeOH, 56 °C, 16 h; vii, $CH_2N_2$, $Et_2O$, 20 °C




**Scheme 2** *Reagents and conditions*: i, $[Ni(PPh_3)_2Cl_2]$, $PPh_3$, Zn, 2,2′-bipyridyl, *N*,*N*-dimethylacetamide, 80 °C; ii, $[Pd(PPh_3)_4]$, toluene, aqueous potassium carbonate (2 M)

yellow. The final films were transparent and free from cracks. With both precursor polymers **3** and **4** the ester carbonyl stretch at 1747 $cm^{-1}$ was completely lost on heating and new bands due to anthracene moieties appeared respectively at 1623 $cm^{-1}$ and 1635 $cm^{-1}$. The UV spectrum of polymer **3** shifted from $\lambda_{max}$ 267 nm (absorbance arbitrarily assigned 1.00) to $\lambda_{max}$ 315 and 442 nm (relative absorbances 1.76 and 0.67). For polymer **4** there was a shift from $\lambda_{max}$ 294 nm (absorbance arbitrarily assigned 1.00) to $\lambda_{max}$ 322 and 427 nm (relative absorbances 1.48 and 0.62). This data is consistent with the formation of the desired final polymers **1** and **2**.

The electrical conductivities of polymers **1** and **2**, measured as thin films, were $<10^{-4}$ S $cm^{-1}$, but both showed significant conductivities after n- or p-type doping. Thus, after doping with potassium naphthalenide polymers, **1** and **2** had conductivities of $4.0 \times 10^{-2}$ and $1.4 \times 10^{-3}$ S $cm^{-1}$ respectively, and after doping with ferric chloride they had conductivities of $1.2 \times 10^{-1}$ and $5.5 \times 10^{-2}$ S $cm^{-1}$. It is evident that for a given dopant polymer **1** has the greater conductivity. When thin films were irradiated with UV light (366 nm), both polymers **1** and **2** gave a yellow–green luminescence.

We thank the EPSRC for financial support.

## References

1 W. J. Feast, J. Tsibouklis, K. L. Pouwer, L. Groenendaal and E. J. Meijer, *Polymer*, 1996, **37**, 5017.
2 J. H. Edwards, W. J. Feast and D. C. Bott, *Polymer*, 1984, **25**, 395; W. J. Feast and J. N. Winter, *J. Chem. Soc., Chem. Commun.*, 1985, 202.
3 R. A. Wessling and R. G. Zimmerman, *US Pat.* 3 401 152, 1968; 3 706 677, 1972; P. M. Lahti, D. A. Modarelli, F. R. Denton, R. W. Lenz and F. E. Karasz, *J. Am. Chem. Soc.*, 1988, **110**, 7258; W. B. Liang, M. A. Masse and F. E. Karasz, *Polymer*, 1992, **33**, 3101.
4 J. H. Burroughes, D. D. C. Bradley, A. R. Brown, R. N. Marks, K. Mackay, R. H. Friend, P. L. Burns and A. B. Holmes, *Nature*, 1990, **347**, 539.
5 N. C. Greenham, S. C. Moratti, D. D. C. Bradley, R. H. Friend and A. B. Holmes, *Nature*, 1993, **365**, 628.
6 D. H. Hwang, S. T. Kim, H. K. Shim, A. B. Holmes, S. C. Moratti and R. H. Friend, *Chem. Commun.*, 1996, 2241.
7 M. Baumgarten, U. Müller, A. Bohnen and K. Müllen, *Angew. Chem., Int. Edn. Engl.*, 1992, **31**, 448.
8 M. W. Pelter and J. K. Stille, *Macromolecules*, 1990, **23**, 2418.
9 G. A. Power, P. Hodge and N. B. McKeown, *Chem. Commun.*, 1996, 655.
10 R. Uddin, P. Hodge, M. S. Chisholm and P. Eustace, *J. Mater. Chem.*, 1996, **6**, 527.
11 M. A. Rabjohns, P. Hodge and P. A. Lovell, *Polymer*, 1997, **38**, in the press.
12 T. R. Criswell and B. H. Klanderman, *J. Org. Chem.*, 1974, **39**, 770.
13 I. Colon and G. T. Kwiatkowski, *J. Polym. Sci., Polym. Chem. Ed*, 1990, **28**, 367.
14 M. Ueda and F. Ichikawa, *Macromolecules*, 1990, **23**, 926.
15 V. Chaturvedi, S. Tanaka and K. Kaeriyama, *J. Chem. Soc., Chem. Commun.*, 1992, 1658; *Macromolecules*, 1993, **26**, 2607.
16 M. Rehahn, A. Schlüter, G. Wegner and W. J. Feast, *Polymer*, 1989, **30**, 1060.
17 U. Anton and K. Müllen, *Macromolecules*, 1993,**26**, 1248.
18 M. Rehahn, A. D. Schlüter and G. Wegner, *Makromol. Chem.*, 1990, **11**, 535.

*Received, 30th October 1996; Com. 6/07405G*

# 4-Substituted norsnoutanones: a new probe system for evaluating electronic effects in π-facial selectivity in nucleophilic additions

**Goverdhan Mehta,*[a] Chebolu Ravikrishna,[a] Bishwajit Ganguly[b] and Jayaraman Chandrasekhar*[b]**

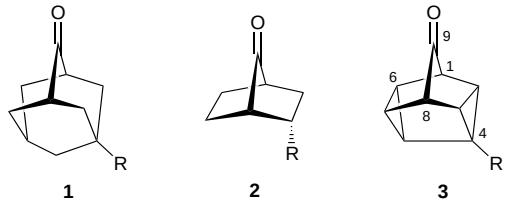
[a] *School of Chemistry, University of Hyderabad, Hyderabad 500 046, India*
[b] *Department of Organic Chemistry, Indian Institute of Science, Bangalore 560 012, India*

**Remotely substituted norsnoutanone derivatives show significant and consistent π-face selectivity in nucleophilic additions, revealing the interplay of orbital and electrostatic effects.**

Precise and predictable delineation of the various factors that can control π-face selectivities in additions to trigonal carbon centres has been a subject of intense scrutiny in recent years, as the desymmetrization of the two faces of the planar carbonyl/alkene group is a fundamental paradigm of stereoselective synthesis.[1] While the influence of steric factors in π-facial control is fairly well understood, the nature and role of the long range electronic effects (*e.g.* orbital *vs*. electrostatic) on face-selection is a matter of ongoing debate. In order to segregate the steric and electronic components, various research groups have devised substrates wherein the two π-faces are virtually isosteric with minimal conformational uncertainties and which can be electronically perturbed through distal modifications.[2–4] Among the systems that have been examined in detail, the sterically unbiased 5-substituted adamantan-2-ones **1**[4] and *endo*-substituted norbornan-7-ones **2**[3] have provided valuable insights into the factors governing the π-face selectivity during nucleophilic additions. Yet the relative importance and subtle interplay of various electronic factors in controlling face-selectivity remains controversial,[1] thus underscoring the need to examine newer systems.

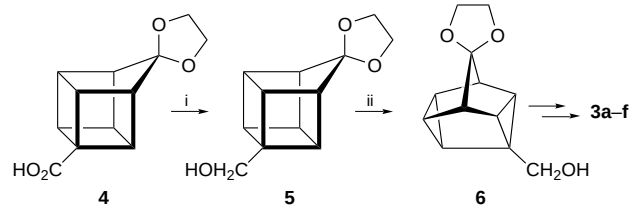
Herein we introduce 4-substituted norsnoutanone **3** (pentacyclo[4.3.0.0$^{2,4}$.0$^{3,8}$.0$^{5,7}$]nonan-9-one), a substrate with sterically unbiased π-faces and a distal substituent to desymmetrize and exert long range electronic perturbation, as a probe to study electronic control of face-selectivity. The pentacyclic system **3** has some interesting features and, in some ways, can be regarded as a hybrid of **1** and **2**. As the overlay diagram of the energy minimized **1**–**3** (R = CN) indicates, the substituent in **3** is farthest removed from the stereoinduction centre. Furthermore, the substituent at the 4-position in **3** is three bonds away (*cf*. three- and two-bond separation in **1** and **2**, respectively) from the C(9) carbonyl group, but it is linked through cyclopropane bonds which are expected to be better transmitters of electronic effects. Here we disclose our findings that in **3**, the C(4) substituent indeed exerts a dominant influence on the face-selectivity during nucleophilic additions. We also provide the results of calculated transition-state energetics for hydride addition to 4-substituted norsnoutanones that aid in the interpretation of the observed face-selectivities.

We have synthesized six derivatives **3a**–**f** for the present study from the homocubanone-4-carboxylic acid ketal **4**. LAH reduction to **5** and Ag$^{I}$ mediated rearrangement furnished the required framework **6**.[5] The hydroxymethyl functionality in **6** was elaborated through unexceptional but multi-step functional group modifications to furnish **3a**–**f** (Scheme 1).[6]

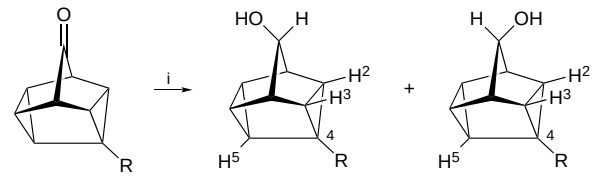



Pentacyclic ketones **3a**–**f** were subjected to hydride reduction with sodium borohydride to furnish (*E*)-**7a**–**f** and (*Z*)-**8a**–**f** alcohols in near quantitative yield; the diastereoselectivities are shown in Scheme 2.[6] The observed *E* : *Z* ratios were determined through $^1$H NMR analyses and remained insensitive to changes in the reaction solvent. The stereostructures of **7a**–**f** and **8a**–**f** have been unambiguously deduced on the basis of (i) the deshielding (*ca*. 0.3 ppm) of H(5) in *E*-alcohols compared to *Z*-alcohols, (ii) the relative deshielding of the H(2) and H(3) protons in *Z*-alcohols compared to *E*-alcohols, and (iii) the deshielding (7–8 ppm) of the quaternary C(4) carbon resonances in the *Z*-series compared to *E*-series. These observations were further fortified through selected shift reagent (LIS) studies.

The observed diastereoselectivities (Scheme 2) indicate a profound effect and consistent trend in the face-selectivity induced by the remote C(4) substituent. While strong electron-withdrawing groups (e.g. cyano, ester) exhibit marked preference for the *syn*-face approach of the hydride to furnish the (*E*)-alcohols, such preference is diminished in the moderately electron-withdrawing substituents present in **3c**–**e**. In the case of the alkyl-substituted derivative **3f** there is a marginal preference for *anti*-face addition. While these observations are generally similar to those reported for the adamantanone **1** and the norbornanone **2** derivatives, there are two notable features. There is a marked *increase* in the face-selectivity in **3** (*cf*. for




**Scheme 1** *Reagents and conditions*: i, $LiAlH_4$, THF, 82%; ii, Ag$^{I}$, MeOH, heat, 88%




| | | | |
|---|---|---|---|
| **3a** | R = $CO_2Me$ | (*E*)- **7a** 79% | (*Z*)- **8a** 21% |
| **b** | R = CN | **b** 84% | **b** 16% |
| **c** | R = C≡CH | **c** 76% | **c** 24% |
| **d** | R = CH=$CH_2$ | **d** 60% | **d** 40% |
| **e** | R = $CH_2OMe$ | **e** 56% | **e** 44% |
| **f** | R = Et | **f** 48% | **f** 52% |

**Scheme 2** *Reagents and conditions*: i, $NaBH_4$, MeOH, 0–5 °C

**Table 1** MNDO Heats of formation, *ab initio* total energies and relative energies of LiH addition transition states to the *syn*- and *anti*- faces

| | Heat of formation/kcal mol$^{-1}$ | *ab initio* Energy/$E_h$ | | |
|---|---|---|---|---|
| | MNDO //MNDO | HF/3-21G //HF/3-21G | HF/6-31G* //HF/3-21G | MP2/6-31G* //HF/3-21G |
| **3b** (*anti*) | 95.0 | 517.09150 | 519.98802 | 521.61734 |
| (*syn*) | 94.5 | 517.09315 | 519.98947 | 521.61899 |
| Relative energy[a]/kcal mol$^{-1}$ | 0.5 | 1.0 | 0.9 (0.4) | 1.0 (0.5) |
| **3d** (*anti*) | 80.3 | 502.32468 | 505.13354 | 506.74174 |
| (*syn*) | 80.2 | 502.32483 | 505.13358 | 506.74155 |
| Relative energy[a]/kcal mol$^{-1}$ | 0.1 | 0.1 | 0.0 (0.2) | −0.1 (0.1) |

[a] A positive value indicates *syn*-face addition transition state is more stable. Values in parentheses correspond to relative energies obtained by replacing LiH by a point charge at the location of the hydride.

**Table 2** MNDO Relative energies for *syn* and *anti* face addition calculated using the charge and hydride models as well as with LiH addition transition state geometries for substituted adamantanones, norbornanones and norsnoutanones[a]

| Substrate | Relative energy/kcal mol$^{-1}$ | | | Experimental *syn* : *anti* ratio[b] |
|---|---|---|---|---|
| | Charge | Hydride | Transition state | |
| **1** R = CN | 1.3 | 0.9 | 0.2 | 68 : 32 |
| **2** R = CN | 1.8 | 1.4 | 0.5 | 88 : 12 |
| **3** R = CN | 3.5 | 1.7 | 0.5 | 84 : 16 |
| **1** R = CH=$CH_2$ | −1.0 | 0.0 | 0.0 | — |
| **2** R = CH=$CH_2$ | −2.8 | −0.4 | −0.2 | 36 : 64[c] |
| **3** R = CH=$CH_2$ | 1.0 | 0.5 | 0.1 | 60 : 40 |

[a] A positive value indicates preference for *syn*-face addition. [b] For reduction with $NaBH_4$ or $LiAlH_4$. [c] For the divinyl derivative.

R = $CO_2$Me, *E* : *Z* ratios: 57 : 41 for **1**, 68 : 32 for **2** and 79 : 21 for **3**) despite the distal nature of the substituent. Another significant difference is that while the *endo*-vinyl and methoxymethyl substituents in the case of the norbornyl system **2** are, contrary to expectation based on Cieplak model, *anti*-directing, they are *syn*-directing in **3**, in keeping with the inductively withdrawing nature of these substituents.

To test some of the commonly used computational procedures for predicting face-selectivity and to interpret the observed results, transition-state energetics for LiH addition to two representative substrates **3b** and **3d** were calculated. Structures with vanishing gradients and a Hessian of 1 were optimized using MNDO[7] and *ab initio* (3-21G basis)[8] methods. Energies were also computed at HF and MP2 levels with the 6-31G* basis set.

At all levels of theory, the 4-cyano substituent in **3b** is correctly predicted to induce a clear *syn*-face selectivity for nucleophilic attack (Table 1). The energy differences are consistent with the observed product ratio. Much smaller relative energies (generally favouring *syn*-face addition) are computed for the vinyl derivative **3d**. The consistency of the MNDO procedure becomes evident when the results for **3d** are compared with those obtained for the *endo*-vinyl substituted norbornanone (Table 2). In the latter, *anti*-face addition is predicted to be favoured by 0.2 kcal mol$^{-1}$, as is indeed found experimentally.[3a]

Two procedures were used to examine the electrostatic effects in these systems. The LiH unit in the *ab initio* optimized transition state was replaced by a point negative charge (magnitude the same as the Mulliken charge) at the hydride location. The corresponding relative energies computed with the 6-31G* basis set reflect the differences in the electrostatic response between the nucleophile and the substrate at the transition state. These values for **3b** are smaller than the transition state energy differences but, significantly, are in the same direction (Table 1). Similar results were earlier obtained for the norbornanones.[9] An alternative approach[3b] to modelling electrostatic effects through a point negative charge and a hydride ion at an assumed distance from the ground state geometry of the substrate provides further insights. Due to the inherent assumptions in these models, unambiguous but exaggerated energy differences are obtained. In all the derivatives considered, the hydride model yields the same facial-selectivity as the transition state relative energies (Table 2), while the charge model reproduces the general trends.

The observed and calculated results can be understood by considering three factors. Cieplak-type hyperconjugative interactions[10] should favour *syn*-face addition in all the substrates with electron-withdrawing groups. Since these groups polarize the adjacent carbon atoms as well as the nearby *exo*-face hydrogen atoms, electrostatic interactions with the nucleophile would reinforce the *syn*-face preference. However, a direct through-space repulsive interactions between the nucleophile and the substituent is also possible, favouring *anti*-face approach. In the norbornanones, all three factors are important and their relative contributions determine the observed *syn*-face preference for the cyano and *anti*-face attack in the vinyl derivatives. All the interactions are reduced in the adamantanone series. Interestingly, the direct interaction between the nucleophile and the substituent is effectively eliminated in the norsnoutanones for geometric reasons. Hence, residual electrostatic and orbital effects favour *syn*-face approach in both **3b** and **3d**.

## References


1 Recent review: B. W. Gung, *Tetrahedron*, 1996, **52**, 5263.
2 P. Wipf and Y. Kim, *J. Am. Chem. Soc*., 1994, **116**, 11 678 and references cited therein; R. L. Halterman and M. A. McEroy, *J. Am. Chem. Soc*., 1990, **112**, 6690; H. Li, G. Mehta, S. Padma and W. J. le Noble, *J. Org. Chem*., 1991, **56**, 2006; G. Mehta, F. A. Khan, B. Ganguly and J. Chandrasekhar, *J. Chem. Soc., Chem. Commun*., 1992, 1711.
3 (*a*) G. Mehta and F. A. Khan, *J. Am. Chem. Soc*., 1990, **112**, 6140; (*b*) B. Ganguly, J. Chandrasekhar, F. A. Khan and G. Mehta, *J. Org. Chem*., 1993, **58**, 1734.
4 H. Li and W. J. le Noble, *Recl. Trav. Chim. Pays-Bas*, 1992, **111**, 199 and references cited therein.
5 G. Mehta, Ch. Ravikrishna and K. Ravikumar, *J. Chem. Soc., Chem. Commun*., 1994, 2321; L. A. Paquette, J. S. Ward, R. A. Boggs and W. B. Farnham, *J. Am. Chem. Soc*., 1975, **97**, 1101.
6 All new compounds reported here were fully characterized on the basis of spectral and analytical data. The details of the synthesis of compounds **3a**–**f** will be described in a full paper.
7 J. J. P. Stewart, *J. Comput. Aided Mol. Des.* 1990, **4**, 1.
8 W. J. Hehre, L. Radom, P. v. R. Schleyer and J. A. Pople, *Ab Initio Molecular Orbital Theory*, Wiley, New York, 1986.
9 M. N. Paddon-Row, Y.-D. Wu and K. N. Houk, *J. Am. Chem. Soc*., 1992, **114**, 10 638.
10 A. S. Cieplak, *J. Am. Chem. Soc*., 1981, **103**, 4540.



*Received, 29th July 1996; Revised M/S received 25th October 1996; Com. 6/07289E*

# Heterobimetallic early–late transition-metal tetrameric metallomacrocycles *via* self assembly

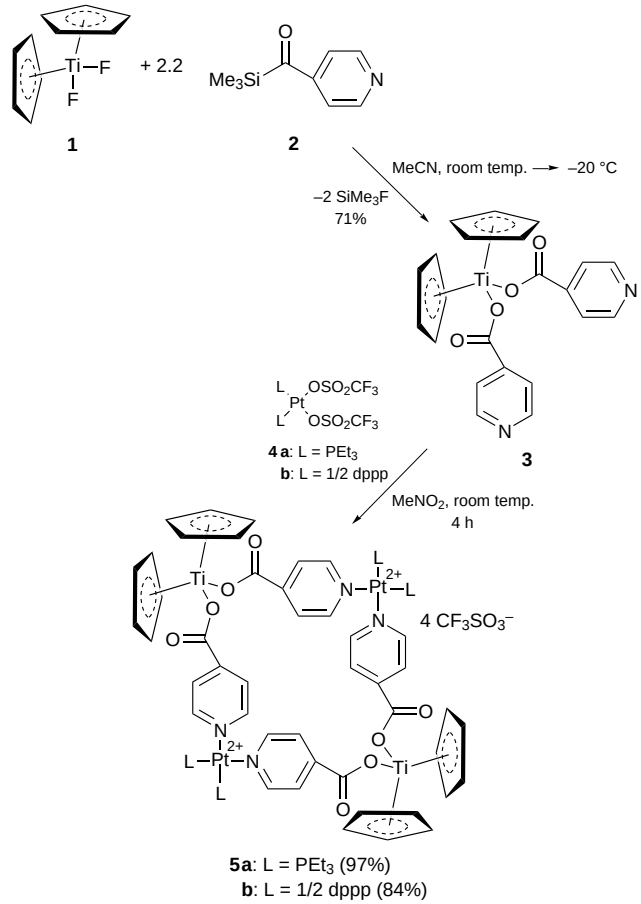
**Peter J. Stang*† and Neal E. Persky**

*Department of Chemistry, The University of Utah, Salt Lake City, Utah 84112, USA*

**Interaction of [Ti(η-$C_5H_5$)$_2$($O_2CC_5H_4N$)$_2$] with square-planar *cis*-[Pt($PR_3$)$_2$($OSO_2CF_3$)$_2$] in $MeNO_2$ gives mixed Ti–Pt tetrameric metallomacrocycles, *via* self assembly, in excellent yields.**

Dative metal–ligand coordination is becoming an increasingly important motif in the construction of discrete supramolecular species with well defined shapes and geometries.[1] The self assembly of diverse molecular squares with variable cavities using transition metals and the appropriate bidentate ligands as building blocks are elegant recent examples of the application of the above concept. To date all molecular squares have been constructed with the aid of either late-transition metals, like Pt and Pd,[2,3] Re,[4] or early-transition metals such as W and Cr,[5] or the main group element iodine[6,7] in its trivalent $I^{III}$ form.[8] Here, we report the formation *via* modular self assembly of the first examples of early–late transition-metal hybrid Ti–Pt hetero-bimetallic tetranuclear macrocycles.

Interaction of the known[9] Ti(η-$C_5H_5$)$_2$ complex **3** with the *cis*-square-planar platinum bistriflate complexes **4**[2] in $MeNO_2$ (0.12 M) at room temp. for 5 h afforded the desired novel macrocycles **5** in excellent isolated yields *via* self assembly, as shown in Scheme 1.‡ Work-up proceeded by simply reducing the solvent to *ca*. 2 ml under vacuum and subsequently precipitating and washing the macrocycles with diethyl ether. Macrocycles **5a**, **5b** are stable, orange, microcrystalline solids, characterized by spectroscopic means and, in the case of **5a**, by liquid secondary ion mass spectrometry (LSIMS). All spectral data are consistent with the proposed structures. Particularly characteristic of **5** are the respective single, sharp singlets (with appropriate Pt satellites) in the $^{31}$P NMR spectrum and the downfield shift of the pyridine hydrogens of **3** upon complexing to Pt in **5**, in particular the α-H shift of *ca*. 0.5 ppm and the β-H of *ca*. 0.3 ppm downfield in **5a** relative to precursor **3**. Most importantly the LSIMS of **5a** shows an $(M - 2\ OSO_2CF_3)^{2+}$ signal at *m/z* = 1002.6 whose experimental isotope pattern very closely matches the calculated value (Fig. 1), leaving little doubt about the tetranuclear nature and identity of this interesting metallomacrocycle. Fig. 2 displays an MM-2 minimized ball-and-stick (*a*) and space-filling model (*b*) of **5a**, illustrating the shape and cavity of this unique heterobimetallic metallomacrocycle with both square-planar Pt and distorted tetrahedral Ti as the shape-defining corner units.




**Scheme 1** Synthesis of macrocycle **5**; dppp = 1,3 bis(diphenylphosphino)propane

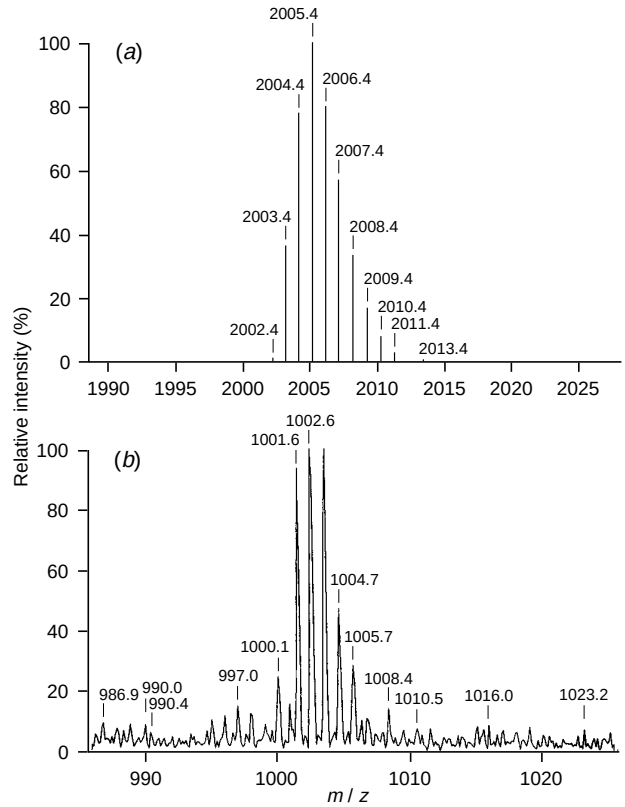



**Fig. 1** Selected region of the calculated (*a*) and experimental (*b*) LSIMS of macrocycle **5a** showing an $(M - 2\ OSO_2CF_3)^{2+}$ signal at *m/z* 1002.6

In summary, the first example of novel mixed Ti–Pt heterobimetallic tetranuclear metallomacrocycles are reported *via* self assembly from readily available precursors. LSIMS, along with spectral and physical data, are used to unambiguously characterize these new supramolecular species.

Financial support by the NSF (CHE-9529093) and the loan of $PtCl_2$ by Johnson-Matthey are gratefully acknowledged as is the A. von Humboldt Foundation and the hospitality of Professor M. Regitz during the summer of 1996.

(*a*)

(*b*)

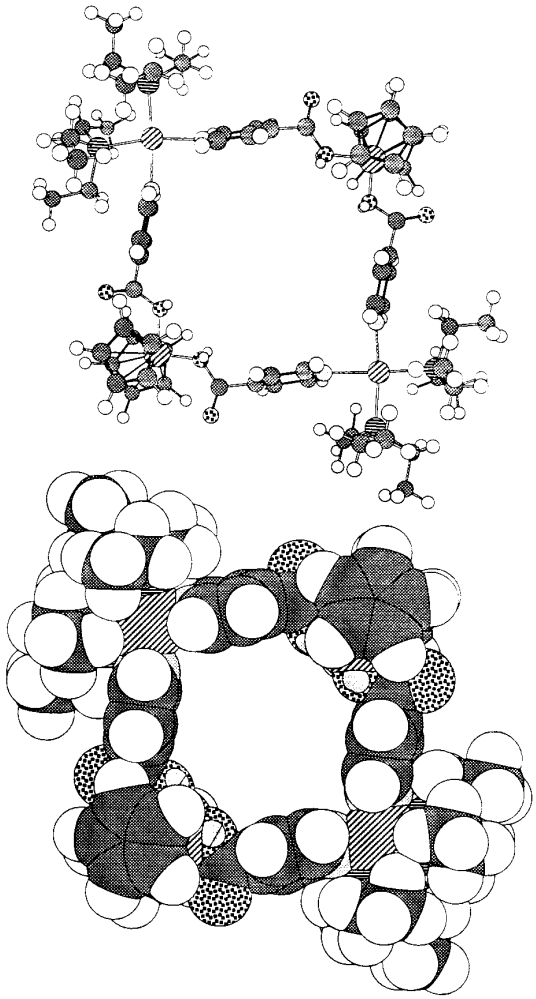


**Fig. 2** Chem-3D MM-2 minimized ball-and-stick (*a*) and space-filling model (*b*) of **5a**

## Footnotes

† E-mail: STANG@chemistry.utah.edu

‡For $^{31}P\{^1H\}$ spectra, 85% $H_3PO_4$ was used as an external reference at δ 0.00, and for $^{19}F\{^1H\}$ spectra $CFCl_3$ was used as an external reference at δ 0.00. *Selected spectroscopic data*: **3**, $^1H$ NMR ($CDCl_3$), δ 8.76 (d, 4 H, *J* 6.0 Hz), 7.80 (d, 4 H, *J* 6.0), 6.65 (s, 10H). $^{13}C\{^1H\}$ NMR ($CDCl_3$), δ 170.2 ($CO_2$), 150.6 ($C_\alpha$), 140.9 ($C_\gamma$), 123.4 ($C_\beta$), 119.2 ($C_5H_5$). **5a**, mp 198–200 °C (decomp.) (**5a**·$H_2O$ Found: C, 36.7; H, 4.4; N, 2.8; S, 5.7. Requires C, 37.0; H, 4.3; N, 2.4; S, 5.5%). IR ($CCl_4$) $\nu_{Ar}$ 3091w, $\nu_{CH_2}$ 2972w, $\nu_{CO_2}$ 1652s, 1540s, $\nu_{OTf}$ 1258s, 1221s, 1145s, 1028s $cm^{-1}$. $^1H$ NMR ($CD_3NO_2$), δ 9.30 (d, 8 H), 8.08 (d, 8 H), 6.68 (s, 20 H), 1.94 (t, 24 H), 1.37 (m, 36 H). $^{13}C\{^1H\}$ NMR ($CD_3NO_2$), δ 168.1 ($CO_2$), 152.6 ($C_\alpha$), 146.7 ($C_\gamma$), 128.7 ($C_\beta$), 121.6 ($C_5H_5$), 16.0 (m, $CH_2$), 8.3 ($CH_3$). $^{31}P\{^1H\}$ NMR ($CD_3NO_2$), δ 2.8 ($J_{PtP}$ 3060 Hz). $^{19}F\{^1H\}$ NMR ($CD_3NO_2$), δ −76. LSIMS, *m/z* 1002.6 (M −2 OTf)$^{2+}$. **5b**, mp 218–220 °C (decomp.). IR ($CCl_4$) $\nu_{Ar}$ 3106w, $\nu_{CH_2}$ 2920w, $\nu_{CO_2}$ 1655s, 1543s, $\nu_{OTf}$ 1253s, 1224s, 1150s, 1029s $cm^{-1}$. $^1H$ NMR ($CD_3NO_2$), δ 9.07 (8 H), 7.88–7.50 (m, 48 H), 6.59 (s, 20 H), 3.50–3.30 (m, 8 H), 2.65–2.35 (m, 4 H). $^{13}C\{^1H\}$ NMR ($CD_3NO_2$), δ 167.8 ($CO_2$), 152.3 ($C_\alpha$), 145.3 ($C_\gamma$), 134.5 (*o*-C), 134.0 (*p*-C), 130.9 (*m*-C), 127.6 ($C_\beta$), 125.9 (*ipso*-C), 122.7 (q, $J_{CF}$ 321 Hz, $OSO_2CF_3$), 121.3 ($C_5H_5$), 23.0 (m, $CH_2P$), 18.8 ($CH_2$). $^{31}P$ NMR ($CD_3NO_2$), δ −10.8 ($J_{PtP}$ 3009 Hz). $^{19}F\{^1H\}$ NMR ($CD_3NO_2$), δ −76.

## References

1 Reviews: D. Philip and J. F. Stoddart, *Angew. Chem*., 1996, **108**, 1242; D. S. Lawrence, T. Jiang and M. Levett, *Chem. Rev*., 1995, **95**, 2229; J. M. Lehn, *Supramolecular Chemistry: Concepts and Perspectives*, VCH, Weinheim, 1995; P. Ball, *Designing the Molecular World*, Princeton Univ. Press, 1994.

2 P. J. Stang and B. Olenyuk, *Angew. Chem., Int. Ed. Engl*., 1996, **35**, 732; P. J. Stang, B. Olenyuk, J. Fan and A. M. Arif, *Organometallics*, 1996, **15**, 904; P. J. Stang, D. H. Cao, S. Saito, and A. M. Arif, *J. Am. Chem. Soc*., 1995, **117**, 6273; P. J. Stang and D. H. Cao, *J. Am. Chem. Soc*., 1994, **116**, 4981; P. J. Stang and J. A. Whiteford, *Organometallics*, 1994, **13**, 3776.

3 M. Fujita, F. Ibukuro, K. Yamaguchi and K. Ogura, *J. Am. Chem. Soc*., 1995, **117**, 4175; M. Fujita, Y. J. Kwon, S. Washizu and K. Ogura, *J. Am. Chem. Soc*., 1994, **116**, 1151; M. Fujita, J. Yazaki and K. Ogura, *J. Am. Chem. Soc*., 1990, **112**, 5645.

4 R. V. Slone, D. I. Youn, R. M. Calhoun and J. T. Hupp, *J. Am. Chem. Soc*., 1995, **117**, 11 588.

5 P. M. Stricklen, E. J. Volcko and J. G. Verkade, *J. Am. Chem. Soc*., 1983, **105**, 2494.

6 P. J. Stang, K. Chen and A. M. Arif, *J. Am. Chem. Soc*., 1995, **117**, 8793; P. J. Stang and K. Chen, *J. Am. Chem. Soc*., 1995, **117**, 1667.

7 P. J. Stang and V. V. Zhdankin, *J. Am. Chem. Soc*., 1993, **115**, 9808.

8 Review: P. J. Stang and V. V. Zhdankin, *Chem. Rev*., 1996, **96**, 1123.

9 S. C. Dixit, R. Sharon and R. N. Kapour, *Inorg. Chem. Acta*, 1989, **158**, 109.

*Received, 9th July 1996; Com. 6/04842K*

# Phosphine-catalysed [3 + 2] cycloadditions of buta-2,3-dienoates with [60]fullerene

**Lian-He Shu,[a] Wei-Quan Sun,[a] Dan-Wei Zhang,[a] Shi-Hui Wu,*[a] Hou-Ming Wu,[b] Jing-Fei Xu[b] and Xia-Fei Lao[b]**

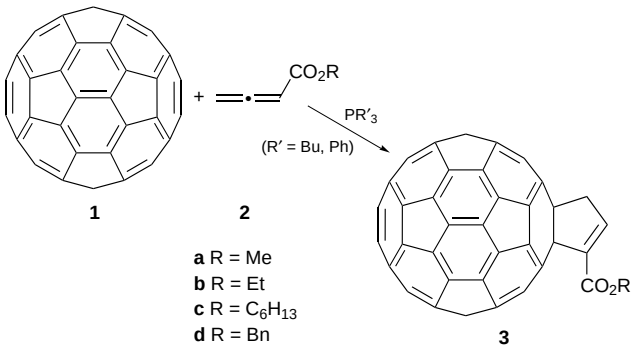
[a] *Department of Chemistry, Fudan University, Shanghai 200433, P.R. China*
[b] *State Key Laboratory of Bioorganic and Natural Products Chemistry, Shanghai Institute of Organic Chemistry, Shanghai 200032, P.R. China*

**[60]Fullerene reacts with buta-2,3-dienoates in the presence of phosphine to form alkyl 3′*H*-1,2-([1′,2′]cyclopenta)-[60]fullerene-5′-carboxylates.**

Cycloaddition reactions provide the most successful methodologies for the functionalization of fullerene.[1] A number of 1,3-dipoles, such as diazomethanes,[2] azides[3] and azomethine ylides[4] are known to react with [60]fullerene. Here we describe the phosphine-catalysed [3 + 2] cycloadditions of buta-2,3-dienoates with [60]fullerene. The [3 + 2] cycloadditions of buta-2,3-dienoates with electron-deficient alkenes have been reported by Zhang *et al*. recently.[5] This reaction provides a very efficient route to the synthesis of cyclopentene. Here [60]fullerene was used as the dipolarophile and the expected products were obtained with good yields (Scheme 1).

The reaction of [60]fullerene with **2a** and tributylphosphine was carried out at room temperature under nitrogen. Isolation on silica gel using toluene as eluent afforded **3a**† and unreacted [60]fullerene. The yield of **3a** was 42% (95% based on consumed [60]fullerene). For **2b**, **2c** and **2d**, the reactions were carried out at 80 °C and triphenylphosphine was used as catalyst. The yields (corrected for the recovered fullerene, shown in parentheses) for **3b**, **3c** and **3d** were 78 (81.6), 52 (89) and 88.5% (92%), respectively.

The FD-MS spectrum of **3a** gives the molecular ion peak at *m*/*z* 818 ($C_{65}H_6O_2$, 100%). In the FT-IR spectrum, the absorption bands for the alkenic and the carbonyl groups are located at 1638 and 1722 $cm^{-1}$, respectively. The $^1H$ NMR spectrum [600 MHz; $CS_2$–$(CD_3)_2CO$, 10 : 1] of **3a** shows three signals at δ 3.87 (3H, s, OMe), 4.61 (2H, d, *J* 2.64 Hz, $CH_2$) and 7.77 (1H, t, *J* 2.64 Hz, =CH). The $^{13}C$ NMR spectrum [150.9 MHz; $CS_2$–$(CD_3)_2CO$, 10 : 1] shows 35 signals in total, of which two signals are found to be overlapped. Peaks at δ 48.28, 52.09, 69.91, 72.08 and 163.13 are obviously due to the methylene group, the methoxy group, the two $sp^3$ carbons of the cage and the carbonyl group, respectively. The $^{13}C$ NMR spectrum is also consistent with the proposed structure, as $C_s$ symmetry requires 32 signals for the fullerene skeleton.



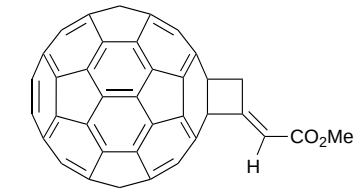

**Scheme 1**

Compound **3b** is almost insoluble in solvent, and only FT-IR and $^1H$ NMR spectra were obtained. For **3c** and **3d**,‡ all the spectra agree the proposed structure.

Recently, the phosphine-mediated reaction of but-2-ynoates with [60]fullerene was reported by Liou *et. al*.[6] The authors declared that [2 + 2] cycloaddition product **4** was formed from the reaction of [60]fullerene with methyl but-2-ynoate. The phosphine-catalysed [3 + 2] cycloadditions of but-2-ynoates and electron-deficient alkenes have been reported in literature.[5] Both the products and intermediates of this reaction have been proved to be the same as those of the reactions of buta-2,3-dienoates. This suggested to us that compound **4** was probably the same as **3a**. In fact, the FD-MS, FTIR, $^1H$ NMR and $^{13}C$ NMR spectra of **3a** are almost identical to those of **4**.

In order to prove our assumption, compound **4** was prepared from the reaction of methyl but-2-ynoates with [60]fullerene by the procedure described by Liou. It is reasonable to conclude that compound **4** is indeed identical to **3a**, for a mixture of **3a** and **4** showed only one peak by HPLC.§ This result encouraged us to check the structure of **3a** more carefully.

The cyclopentene structure of **3a** is further substantiated by the HMQC and HMBC NMR spectra. Assignable NMR spectral data are shown in Fig. 1. In the HMQC spectrum, the alkenic proton at δ 7.77 is found to be connected to the carbon atom at δ 144.05. In the HMBC spectrum, the alkenic proton (δ 7.77) shows correlations with both of the $sp^3$ carbons of the fullerene cage, which indicates that there are two or three bonds between this proton and the two carbon atoms. The structure with a four-membered ring **4** is ruled out, for the alkenic proton is either three or four bonds away from the addition site; this means that the HMBC spectrum for **4** would give only one correlation peak between the alkenic proton and the addition site carbons. The reasoning which led to the four-membered




**4**

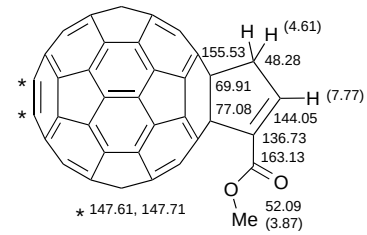
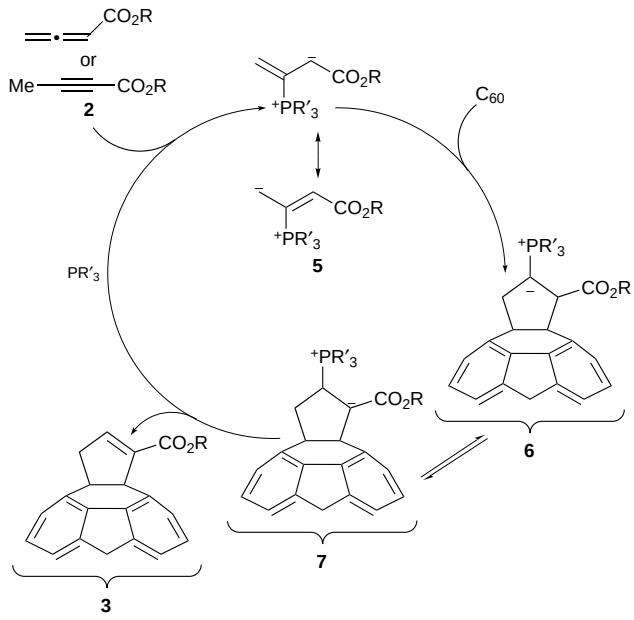



**Fig. 1** $^{13}C$ NMR and $^1H$ NMR (in parentheses) data for **3a**




**Scheme 2**

ring structure was that Liou assigned the small coupling constant observed to an allylic coupling. In fact, in the spectra of smaller rings, the coupling constant between aliphatic and alkenic protons (C$H_2$–C*H*=C) is quite small.[7] For example, the $J_{1,5}$ of cyclopentene is 2.1 Hz.[8]

A possible mechanism for the reaction is outlined in Scheme 2. As reported by Zhang *et. al*.,[5] phosphine first reacts with buta-2,3-dienoate or but-2-ynoate to form **5**, and then a [3 + 2] cycloaddition occurs. Product **3** is given with the regeneration of phosphine.

This work was supported by the National Science Foundation of China. We thank Professor Xiyan Lu of the Shanghai Institute of Organic Chemistry for kindly providing methyl but-2-ynoate and helpful discussions.

## Footnotes

† *Spectral data* for **3a**: FTIR ν(KBr)/cm$^{-1}$ 1722, 1638, 1428, 1328, 1240, 1188, 1116, 1090, 1000, 878, 766, 728, 575, 528; FD-MS *m*/*z* 818 ($C_{65}H_6O_2$, 100%), 720 ($C_{60}$, 5); $^{13}$C NMR [150.9 MHz; $CS_2$–$(CD_3)_2CO$, 10 : 1] $\delta_C$ (number of carbon atoms) 48.28 ($CH_2$), 52.09 ($OCH_3$), 69.91 and 77.08 ($sp^3$-C for $C_{60}$), 135.05 (2), 135.96 (2), 136.73 (quaternary alkenic C), 139.61 (2), 140.69 (2), 141.98 (2), 142.43 (4, overlapped), 142.54 (2), 142.59 (2), 142.86 (2), 143.10 (2), 143.13 (2), 143.52 (2), 144.05 (=CH), 144.85 (4, overlapped), 145.51 (2), 145.60 (2), 145.64 (2), 145.72 (2), 145.94 (2), 146.37 (2), 146.43 (2), 146.55 (2), 146.68 (2), 146.72 (2), 147.61 (1), 147.71 (1), 149.01 (2), 150.34 (2), 156.53 (2), 163.13 (C=O).

‡ *Selected data* for **3c**: FD-MS *m*/*z* 889 ($M^+$ + 1 for $C_{70}H_{16}O_2$, 100%); $^1$H NMR [600 MHz; $CS_2$–$(CD_3)_2CO$, 10 : 1] $\delta_H$ 0.91 (3H, t, Me), 1.33 (4H, m, $CH_2CH_2$), 1.40 (2H, m, $CH_2$), 2.00 (2H, m, $CH_2$), 4.24 (2H, t, $OCH_2$), 4.60 (2H, d, *J* 2.64 Hz, allyl–$CH_2$), 7.76 (1H, t, *J* 2.64 Hz); $^{13}$C NMR [150.9 MHz; $CS_2$–$(CD_3)_2CO$, 10 : 1] $\delta_C$ 15.00, 23.73, 26.76, 29.63, 32.43, 48.19, 65.64, 70.04, 77.05, 135.05, 135.97, 136.73 (quaternary alkenic C), 139.55, 140.74, 141.94, 142.43, 142.46, 142.54, 142.60, 142.86, 143.10, 143.13, 143.52, 143.84 (=CH), 144.86, 145.52, 145.59, 145.64, 145.72, 145.91, 146.37, 146.44, 146.55, 146.68, 146.72, 147.61, 147.70, 149.06, 150.45, 156.61, 162.78. For **3d**: FD-MS *m*/*z* 894 ($C_{71}H_{10}O_2$, 100%); $^1$H NMR [600 MHz; $CS_2$–$(CD_3)_2CO$, 10 : 1] $\delta_H$ 4.60 (2H, d, *J* 2.64 Hz, $CH_2$), 5.27 (2H, s, $OCH_2$), 7.23–7.28 (3H, m, arom.), 7.35 (2H, d, arom.), 7.81 (1H, t, *J* 2.64 Hz, =CH); $^{13}$C NMR [150.9 MHz; $CS_2$–$(CD_3)_2CO$, 10 : 1] $\delta_C$ 48.26, 67.28, 69.99, 77.06, 128.94, 129.13, 135.07, 135.99, 136.05, 136.64 (quaternary alkenic C), 139.57, 140.67, 141.95, 142.42, 142.52, 142.59, 142.85, 143.08, 143.12, 143.51, 144.58 (=CH), 144.85, 145.52, 145.59, 145.62, 145.71, 145.92, 146.36, 146.43, 146.54, 146.68, 146.71, 147.60, 147.70, 149.05, 150.28, 156.54, 162.60.

§ Experimental conditions: silica gel Si60 (5 μm), 240 × 5 mm; mixture of hexane and toluene (1 : 1, *v*/*v*) used as eluent; flow rate, 1.0 ml min$^{-1}$; detection, UV at 310 nm.

## References

1 R. Taylor and D. R. M. Walton, *Nature*, 1993, **363**, 685; A. Hirsch, *Angew Chem., Int. Ed. Engl*., 1993, **32**, 1138.
2 See, for example: J. C. Hummelen, B. W. Knight, F. LePeq, F. Wudl, J. Yao and C. L. Williams, *J. Org. Chem*., 1995, **60**, 532.
3 M. R. Banks, J. I. G. Cadogan, I. Gosney, P. K. G. Hodgson, P. R. R. Langridge-Smith, J. R. A. Millar and A. F. Taylor, *J. Chem. Soc., Chem. Commun*., 1995, 885 and references cited therein.
4 M. Maggini, G. Scorrano and M. Prato, *J. Am. Chem. Soc*., 1993, **115**, 9798.
5 C. Zhang and X. Lu, *J. Org. Chem*., 1995, **60**, 2906.
6 K.-F. Liou and C.-H. Cheng, *J. Chem. Soc., Chem. Commun*., 1995, 2473.
7 *The Sadtler Handbook of Proton NMR Spectra*, ed. W. W. Simons, Sadtler Research Laboratories, Inc., 1978, p. 51.
8 G. V. Smith and H. Kriloff, *J. Am. Chem. Soc*., 1963, **85**, 2016.

*Received, 28th August 1996; Com. 6/05923F*

# Phosphine-catalysed cycloaddition of buta-2,3-dienoates and but-2-ynoates to [60]fullerene

**Bryan F. O'Donovan, Peter B. Hitchcock, Mohamed F. Meidine, Harold W. Kroto, Roger Taylor and David R. M. Walton**

*School of Chemistry, Physics and Environmental Science, University of Sussex, Falmer, Brighton, East Sussex, UK BN1 9QJ*

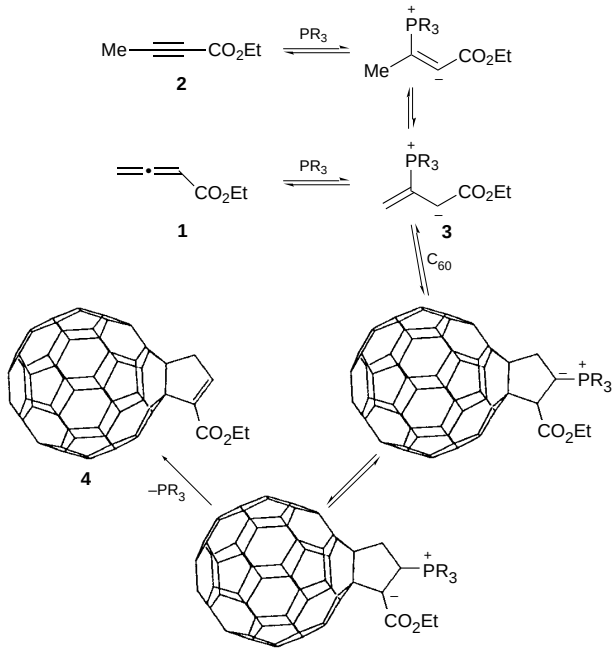
**In the presence of phosphine catalysts, ethyl buta-2,3-dienoate and ethyl but-2-ynoate undergo [3 + 2] as opposed to [2 + 2] dipolar cycloaddition to [60]fullerene.**

Cycloadditions have proved to be the most generally useful method yet devised for attaching organofunctional groups to fullerenes.[1] In these processes the cage often behaves as the electron deficient component, so that alkenes bearing electron-withdrawing groups serve as useful models for reactions. Recently Zhang and Lu[2] described a novel [3 + 2] annulation technique for preparing cyclopentenes, based on the phosphine-catalysed cycloadditions of buta-2,3-dienoates and but-2-ynoates to electron-deficient alkenes. We have successfully applied their methodology to [60]fullerene.

In a typical reaction, ethyl buta-2,3-dienoate **1** (21.26 mg, 0.19 mmol, 1.7 equiv.) and 5 mol% of tributylphosphine (1.92 mg, 9.5 μmol) were added successively to a solution of [60]fullerene (80.4 mg, 0.11 mmol) in toluene (200 $cm^3$), and the mixture was stirred at ambient temperature under nitrogen for 17 h. Thin layer chromatography (TLC) (silica) of a sample of the resulting red–brown solution revealed the presence of unreacted [60]fullerene and one major product **4**. Removal of the solvent *in vacuo* and flash chromatography (toluene–hexane, 7:3; silica gel) of the residue gave [60]fullerene, followed by **4** (43%, pure by TLC). Use of **1** in excess of 1.7 equiv. resulted in a lower yield of **4** due to a marked increase in the proportion of products arising from multiple cycloadditions to the cage.

When ethyl but-2-ynoate **2** was used instead of **1**, forcing conditions (refluxing benzene, 20 h) were required to produce **4**, albeit in lower yield (23%). At ambient temperature, all of the [60]fullerene was recovered together with unwanted byproducts due to slow decomposition of **2**.

Tricyclohexylphosphine ($PCy_3$) and $PBu_3$ showed comparable catalytic activity in the cycloaddition of **1** to [60]fullerene, whereas reaction was much slower with triphenylphosphine ($PPh_3$). The difference is greater with **2**; in this case $PPh_3$ appears not to catalyse the reaction. These observations are in line with the greater nucleophilicity of $PBu_3$ and $PCy_3$ relative to $PPh_3$ and are compatible with Scheme 1.




**Scheme 1**

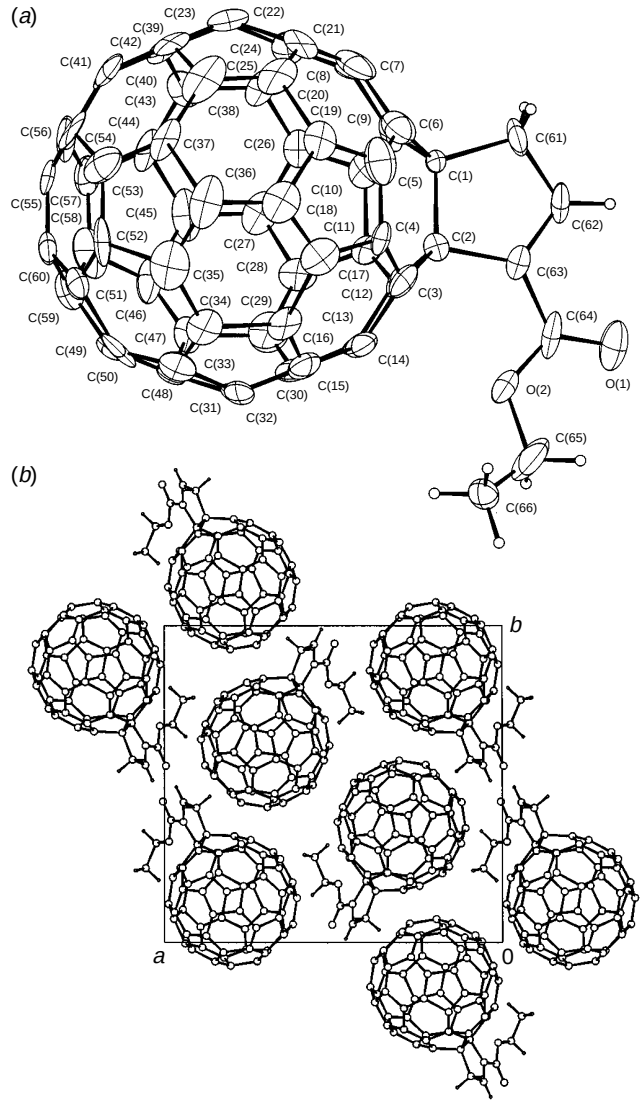



**Fig. 1** (*a*) X-Ray crystal structure of **4** and (*b*) representation of the crystal packing in the unit cell

The EI-MS of **4** displays the anticipated molecular ion peak at *m*/*z* 832, together with peaks at *m*/*z* 804 and 759 corresponding to loss of ethene and the ethyl carboxylate moiety, respectively.

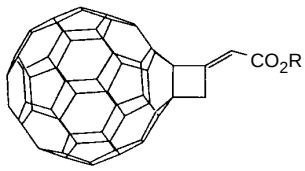
The FT-IR spectrum of **4** reveals a strong absorption at 1715 $cm^{-1}$ due to the ester carbonyl group. The 577 $cm^{-1}$ band, characteristic of the parent fullerene, is split into several weaker signals which, in conjuction with the strong 527 $cm^{-1}$ band, is commensurate with addition across the [6,6] double bond in [60]fullerene.

The $^1H$ NMR spectrum of **4** (300 MHz; $CS_2$–$CDCl_3$, 1 : 1) exhibits a triplet at δ 7.98 (*J* 2.6 Hz) due to the β vinyl proton, which is coupled to the adjacent methylene protons giving rise to a doublet at δ 4.77 (*J* 2.6 Hz).The ethyl group resonances are as expected: δ 4.53 (*J* 7.1 Hz, q) and δ 1.59 (7.1 Hz, t).

The high field $^{13}C$ NMR (125.76 MHz; $CS_2$–$CDCl_3$, 4 : 1) of **4** shows signals corresponding to the ethyl group (δ 14.49, 47.75), the methylene carbon (δ 61.29), and the fullerene cage $sp^3$ carbons (δ 69.54, 76.55). The $sp^2$ region exhibits 32 signals, one of which, the carbonyl carbon (δ 163.03), was assigned on the basis of its chemical shift. A further two signals (δ 128.34, 136.60) were assigned on the basis of $^{13}C\{^1H\}$ decoupling to the unsaturated carbons of the cyclopentene ring. The remaining 28 signals† correspond to the carbons of the fullerene core; two of single intensity, 24 of double intensity and two of quadruple intensity. Assuming that the latter are due to the incidental overlap of two sets of double intensity signals, and that the single intensity peaks correspond to the carbons which lie on the mirror plane, the number of resonances is consistent with the expected $C_s$ symmetry of the molecule.

Slow evaporation of a toluene–$CS_2$ solution of **4** yielded black needle-like crystals, suitable for X-ray analysis, on the basis of which the structure of **4** was conclusively assigned‡ (Fig. 1).

Recently Liou and Cheng[3] described the $PCy_3$-mediated reaction of alkyl 2-ynoates to [60]fullerene, and formulated the products as arising from a formal [2 + 2] cycloaddition generating **5**, as opposed to **4**. The authors based their structural conclusions exclusively on NMR evidence. We repeated this procedure with ethyl but-2-ynoate (reaction at ambient rather than the reflux temperature; 10-fold excess of ynoate) and found the NMR spectra of the product to be identical in all respects to **4**. We thus conclude that Liou and Cheng assigned the incorrect structure to the cycloadduct. It is noteworthy that Zhang and Lu[2] obtained only products arising from [3 + 2] as opposed to [2 + 2] cycloadditions of ynoates and butadienoates with electron-deficient alkenes




**5**

A viable mechanism for the reaction as originally proposed[2] is presented in Scheme 1. Nucleophilic attack of the tertiary phosphine on the β allenic or acetylenic carbon atom, followed by a prototropic shift (or series of shifts in the case of the ynoate substrate) generates the dipolar intermediate **3**, which undergoes a [3 + 2] cycloaddition to [60]fullerene. A further prototropic shift in the initial cycloadduct and subsequent β-elimination of the phosphine generates **4**.

B. F. O'D. thanks the Ivor Gray Nixon bursary fund for financial support.

## Footnotes

† *Selected spectroscopic data* for **4**; $^{13}C$ NMR: δ 156.00, 149.74, 148.33, 147.25, 147.15, 146.23, 146.20, 146.08, 145.95, 145.90, 145.46, 145.26, 145.17, 145.08, 144.95, 143.76, 144.37, 142.65, 142.61, 142.36, 142.11, 142.02, 141.94, 141.49, 140.21, 139.18, 135.52, 134.53.

‡ *Crystal structure data* for **4**: $C_{66}H_8O_2$, *M* = 832.7, orthorombic, space group $P_{na}2_1$ (no. 33), *a* = 18.531(3), *b* = 17.253(3), *c* = 10.022(5) Å, *U* = 3204(2) $Å^3$, *Z* = 4, $D_c$ = 1.73 g $cm^{-3}$, *F*(000) = 1680. Crystal size 0.2 × 0.2 × 0.02 mm, Mo-Kα radiation, λ = 0.71073 Å, μ = 0.1 $mm^{-1}$. Data collected on an Enraf-Nonius CAD4 diffractometer at 293 K. There were 2984 unique reflections measured for 2 < θ < 25°, with 1672 having $I > 2\sigma(I)$. Non-H atoms were located by direct methods (SHELXS-86) and refined on $F^2$ with all reflections (SHELXL-93). H-atoms were included in riding mode. The structure is disordered in the ratio 76 : 24, with the minor sites related to the major sites by reflection through a plane perpendicular to the *c* axis and passing through the centroid of the $C_{60}$ sphere. The coordinates for the minor occupancy molecule were generated from those of the major sites and then refined as a rigid body with isotropic thermal parameters. Final residuals were *R*1 = 0.062 [for $I > 2\sigma(I)$] and *wR*2 = 0.186 (for all data).

Atomic coordinates, bond lengths and angles, and thermal parameters have been deposited at the Cambridge Crystallographic Data Centre (CCDC). See Information for Authors, Issue No. 1. Any request to the CCDC for this material should quote the full literature citation and the reference number 182/304.

## References

1 S. Eguchi, M. Ohno, S. Kojima, N. Koide, A. Yashiro, Y. Shirakawa and H. Ishida, *Fullerene Sci. Technol.*, 1996, **4**, 303.
2 C. Zhang and X. Lu, *J. Org. Chem.*, 1995, **60**, 2906.
3 K. Liou and C. Cheng, *J. Chem. Soc., Chem. Commun.*, 1995, 2473.

*Received, 19th September 1996; Com. 6/06458B*

# Efficient and unique cooperation of three zinc(II) ions in the hydrolysis of diribonucleotides by a trinuclear zinc(II) complex

**Morio Yashiro,* Akira Ishikubo and Makoto Komiyama***

*Department of Chemistry and Biotechnology, Graduate School of Engineering, University of Tokyo, Hongo, Bunkyo-ku, Tokyo 113, Japan*

**A trinuclear $Zn^{2+}$ complex is prepared using a ligand having six pyridine moieties, *N*,*N*,*N*′,*N*′,*N*″,*N*″-hexakis(2-pyridylmethyl)[tris(2-aminoethyl)amine] ($L^3$), and efficiently hydrolyses diribonucleotides at pH 7 and 50 °C, showing much greater activity than a dinuclear $Zn_2L^2$ complex.**

A number of enzymes for phosphoester hydrolysis have two or three $Zn^{2+}$ ions in the catalytic centre.[1] Therefore, polynuclear metal complexes are expected to be useful as catalysts for the hydrolysis of nucleic acids. We have recently reported that a dinuclear zinc(II) complex with *N*,*N*,*N*′,*N*′-tetrakis(2-pyridylmethyl)-2-hydroxy-1,3-diaminopropane ($L^2$, Fig. 1) efficiently hydrolyses a diribonucleotide, the high activity arising from the cooperation of two $Zn^{2+}$ ions.[2]

It is important to elucidate the cooperation effect of three zinc(II) ions in phosphoester hydrolysis, since three $Zn^{2+}$ ions have been suggested to participate in enzymatic reactions.[1b] Thus, a new ligand $L^3$ was designed in this study.† $L^3$ is expected to bind three $Zn^{2+}$ ions, since each of the three dpa ($L^1$) units in $L^3$ should bind to $Zn^{2+}$ [dpa = bis(2-pyridylmethyl)amine].[3] Here, we report that the trinuclear complex $Zn_3L^3$ hydrolyses diribonucleotides much more efficiently than the dinuclear $Zn_2L^2$ complex.

The trinuclear zinc(II) complex was prepared in an aqueous solution by mixing $Zn(NO_3)_2$ and $L^3$ in a molar ratio of 3 : 1, and was characterized by $^1$H NMR spectroscopy. A mixture of $Zn(NO_3)_2$ (15 mM) and $L^3$ (5 mM) in $D_2O$ (pD 7) gave a very simple $^1$H NMR spectrum;‡ the six 2-pyridylmethyl moieties in $L^3$ were observed as one set of sharp signals, indicating the formation of a complex in which all the 2-pyridylmethyl moieties are equivalent. In contrast, when the concentration of $Zn(NO_3)_2$ was < 15 mM, the $^1$H NMR spectrum gave complicated signals, corresponding to the formation of several complex species having lower symmetries. These observations indicate the formation of a trinuclear complex having three-fold symmetry in a 3 : 1 $Zn(NO_3)_2$–$L^3$ mixture (Fig. 1).

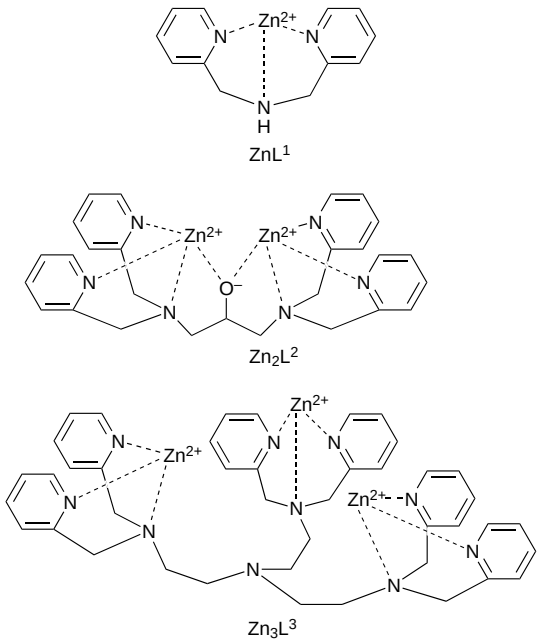



**Fig. 1** Structures of ligands. The proposed coordination modes of $Zn^{2+}$ are also shown. The drawn structures of the complexes are only partial, and additional molecules coordinating at the remaining sites of $Zn^{2+}$ are not specified.

Hydrolysis of ribonucleotide dimers, NpN′, by $Zn_3L^3$ was conducted at 50 °C and pH 6.9 (50 mM Hepes buffer).§ The reactions were followed by reversed-phase ODS HPLC. The products were nucleoside (N′), 3′- and 2′-monophosphates (3′-, 2′-NMP), and the 2′,3′-cyclic monophosphate (2′,3′-cNMP).¶ The reactions showed satisfactory pseudo-first-order kinetics.

The rate of NpN′ hydrolysis by the $Zn(NO_3)_2$–$L^3$ complex system is largely dependent on the metal ion-to-ligand ratio. Fig. 2 shows the rate constants for ApA hydrolysis at various concentrations of $L^3$ and a constant $Zn^{2+}$ concentration {[$Zn(NO_3)_2$] = 15 mM}. The maximal rate was observed at a ratio [$Zn(NO_3)_2$] : [$L^3$] = 3 : 1 indicating that the phosphoester hydrolysis is primarily promoted by the trinuclear $Zn_3L^3$ complex.

The results of hydrolyses of various diribonucleotides by the trinuclear complex are listed in Table 1 and for comparison, equivalent data for the dinuclear $Zn_2L^2$ complex are also listed. The trinuclear complex hydrolyses diribonucleotides efficiently, showing a considerable dependence on the structure of the substrate. For all the substrates examined, the activity of the trinuclear complex is much greater than that of the dinuclear complex. The half-life of CpA hydrolysis by the trinuclear $Zn_3L^3$ complex is 16 min (*cf.* 3 h for the dinuclear $Zn_2L^2$ complex).

Further, the trinuclear $Zn_3L^3$ complex-catalysed hydrolysis is unique in product formation with 3′-NMP preferentially formed

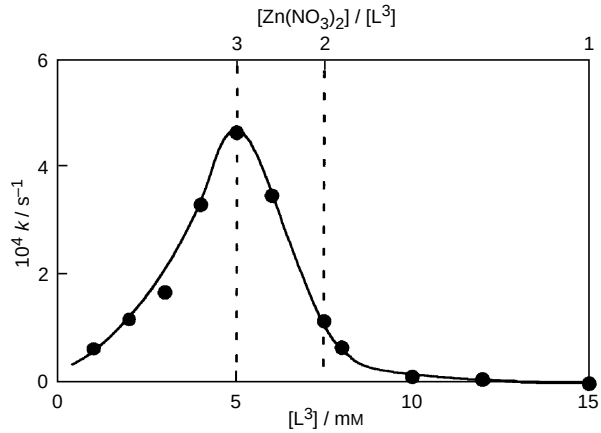



**Fig. 2** Rate constants for ApA hydrolysis with various concentrations of $L^3$ at a constant $Zn^{2+}$ concentration {[$Zn(NO_3)_2$] = 15 mM} at pH 6.9 and 50 °C

over 2′-NMP. In the hydrolysis of CpA, ApA, GpA and GpC, the formation ratio of 3′-NMP to 2′-NMP is > 90%. These results are significant, since 3′-NMP/2′-NMP selectivities are low in hydrolysis by $Zn_2L^2$.

Trinuclear metal centres have been found in crystals of P1 nuclease,[1a] phospholipase C,[1b] and alkaline phosphatase.[1c] On the basis of their crystal structures, participation of three $Zn^{2+}$ ions in the catalytic process has been proposed.[1b]‖ Although cooperative effects of two metal ions in phosphoester hydrolyses have been directly observed by using dinuclear complexes,[2,4] the cooperation of three metal ions in the catalytic process has not yet been clarified. The present results clearly show the efficiency of the trinuclear zinc(II) cluster in phosphoester hydrolysis.

In conclusion, a novel trinuclear zinc(II) complex is prepared using $L^3$. Because of the high efficiency and the selective formation of the 3′-monophosphate, the trinuclear zinc(II) complex is a unique catalyst for the hydrolysis of RNA.

This work was partially supported by Grants-in-Aid for Scientific Research on Priority Areas No. 08232219 and 08249206 from the Ministry of Education, Science and Culture.

**Table 1** Hydrolysis of diribonucleotides (NpN′) by polynuclear zinc(II) complexes at pH 6.9 and 50 °C[a]

| Substrate | $10^5$ $k$/s$^{-1}$ | $t_{1/2}$/s | 3′-NMP : 2′-NMP |
|---|---|---|---|
| $Zn_3L^3$ | | | |
| CpA | 72 | 960 | > 9 : 1 |
| ApA | 46 | 1400 | 9 : 1 |
| GpA | 26 | 2700 | 9 : 1 |
| UpA | 16 | 4500 | 7 : 3 |
| ApG | 17 | 4100 | 8 : 2 |
| GpC | 8 | 8500 | 9 : 1 |
| $Zn_2L^2$ | | | |
| CpA | 6 | 11 000 | 4 : 6 |
| ApA | 5 | 15 000 | 6 : 4 |
| GpA | 5 | 15 000 | 6 : 4 |
| UpA | 6 | 12 000 | 6 : 4 |
| $ZnL^1$ | | | |
| ApA | —[b] | —[b] | |

[a] $[Zn(NO_3)_2]$ = 15 mM, $[L^3]$ = 5 mM or $[L^2]$ = 7.5 mM, [NpN′] 0 = 0.1 mM. [b] No reaction after 24 h.

## Footnotes

† $L^3$ was prepared from tris(2-aminoethyl)amine and 2-picolylaldehyde in methanol, with subsequent reduction by $NaBH_3CN$ at room temp. and was isolated as a perchlorate salt.

**CAUTION**: although the perchlorate salt is moderately stable, it is a potential hazard and should therefore be handled with care and in small quantities. Anal. Calc. for $C_{42}H_{54}Cl_6N_{10}O_{24}$: C, 38.93; H, 4.20; N, 10.81. Found: C, 38.60; H, 4.37; N, 10.53%. $^1$H NMR (270 MHz, $D_2O$) δ 2.93 (6 H, t, *J* 6.5 Hz), 3.20 (6 H, t, 6.5), 3.79 (12 H, s), 7.30 (6 H, d, 7.8), 7.32 (6 H, t, 7.8), 7.77 (6 H, t, 7.8), 8.34 (6 H, d, 7.8).

‡ $^1$H NMR (270 MHz, $D_2O$, 50 °C) δ 2.91 (6 H, br), 2.94 (6 H, br), 4.17 (12 H, s), 7.57 (6 H, d, 7.8), 7.64 (6 H, t, 7.8), 8.15 (6 H, t, 7.8), 8.53 (6 H, d, 7.8).

§ Diribonucleotides, CpA, ApA, GpA, UpA, ApG and GpC, were purchased from Sigma.

¶ 2′,3′-cNMP is readily hydrolysed to 3′- and 2′-NMP, and is observed as an intermediate.

‖ Participation of three $Zn^{2+}$ in the phosphoester hydrolysis has been also suggested on the basis of the structure of a complex consisting of an inorganic phosphate and three mononuclear zinc(II) complexes (T. Koike, S. Kajitani, I. Nakamura, E. Kimura and M. Shiro, *J. Am. Chem. Soc.*, 1995, **117**, 1210).

## References

1 (*a*) E. Hough, L. K. Hansen, B. Birknes, K. Jynge, S. Hansen, A. Hordvik, C. Little, E. Dodson and Z. Derewenda, *Nature*, 1989, **338**, 357; (*b*) A. Volbeda, A. Lahm, F. Sakiyama and D. Suck, *EMBO J.*, 1991, **10**, 1607; (*c*) E. E. Kim and H. W. Wyckoff, *J. Mol. Biol.*, 1991, **218**, 449; (*d*) L. S. Beese and T. A. Steitz, *EMBO J.*, 1991, **10**, 25; (*e*) T. A. Steitz and J. A. Steitz, *Proc. Natl. Acad. Sci. USA*, 1993, **90**, 6498; (*f*) B. L. Vallee and D. S. Auld, *Biochemistry*, 1993, **32**, 6493; (*g*) J. B. Vincent, M. W. Crowder and B. A. Averill, *Trends Biochem. Sci.*, 1992, **17**, 105.

2 M. Yashiro, A.Ishikubo and M. Komiyama, *J. Chem. Soc., Chem. Commun.*, 1995, 1793.

3 D. W. Gruenwedel, *Inorg. Chem.*, 1968, **7**, 495; J. K. Romary, J. D. Barger and J. E. Bunds, *Inorg. Chem.*, 1968, **7**, 1142.

4 M. J. Young and J. Chin, *J. Am. Chem. Soc.*, 1995, **117**, 10 577; W. H. Chapman, Jr. and R. Breslow, *J. Am. Chem. Soc.*, 1995, **117**, 5462; R. Breslow, *Acc. Chem. Res.*, 1995, **28**, 146; M. W. Göbel, *Angew. Chem.*, 1994, **106**, 1201; M. Wall, R. C. Hynes and J. Chin, *Angew. Chem., Int. Ed. Engl.*, 1993, **32**, 1633; L. M. T. Schnaith, R. S. Hanson and L. Que, Jr., *Proc. Natl. Acad. Sci. USA*, 1994, **91**, 569; T. Koike, M. Inoue, E. Kimura and M. Shiro, *J. Am. Chem. Soc.*, 1996, **118**, 3091; D. Wahnon, A.-M. Lebuis and J. Chin, *Angew. Chem., Int. Ed. Engl.*, 1995, **34**, 2412; N. H. Williams and J. Chin, *Chem. Commun.*, 1996, 131.

*Received, 23rd September 1996; Com. 6/06505H*

# X-Ray crystallographic structure determination of some unique chiral sultam derivatives

**Hiroko Kakuda,*[a] Takanori Suzuki,[a] Yoshio Takeuchi[a] and Motoo Shiro*[b]**

[a] *Toyama Medical & Pharmaceutical University, Sugitani 2630, Toyama 930-01, Japan*
[b] *Rigaku Corporation, Matsubara 3-9-12, Akishima, Tokyo 196, Japan*

**X-Ray diffraction analyses of the novel structures of chiral sultams 1–3 reveal that the nitrogen atom in the *N*-sulfonamido sultam 1 is planar, whereas the N–H bond in the *N*-unsubstituted sultam 2 and the N–F bond in the *N*-fluoro sultam 3 are nonplanar on the side of the smaller alkyl substituent, contrary to expectation.**

In the course of developing new reagents for stereoselective fluorination,[1] we prepared several structurally interesting chiral sultam derivatives. Among those, we chose three representative sultams for X-ray analysis, *N*-sulfonamido sultam **1**, *N*-unsubstituted sultam **2** and its *N*-fluoro analogue **3**. Compounds **1** and **2** are synthetic intermediates for the potential fluorinating reagent **3**. In addition to the orientation of the N–F bond in **3**, the determination of the complete molecular structure is crucial for elucidation of the steric course of the asymmetric fluorination employing this reagent.

The molecular structures of compounds **1**, **2** and **3** are shown in Figs. 1, 2 and 3, respectively.† The sums of the bond angles around the nitrogen atom in these compounds are 359.4, 336.6 and 315.0°, respectively. Therefore, the configuration at the nitrogen atom in **1** is almost planar, while it is pyramidal in **2** and **3**.

The bond lengths N(2)–S(3) and N(2)–S(20) in **1** are 1,684(5) and 1.654(5) Å, respectively (Fig. 1). The latter is shorter than the former owing to the tendency of the nitrogen atom to donate its lone pair to the 3d orbital of S(20). Therefore, the presence of the exocyclic sulfonamido substituent contributes to the planarity of the nitrogen atom. Configurationally stable, pyramidal nitrogen atoms were observed when they are part of a three- to five-membered ring and when attached to electronegative substituents.[2] It is, however, not the case if the exocyclic

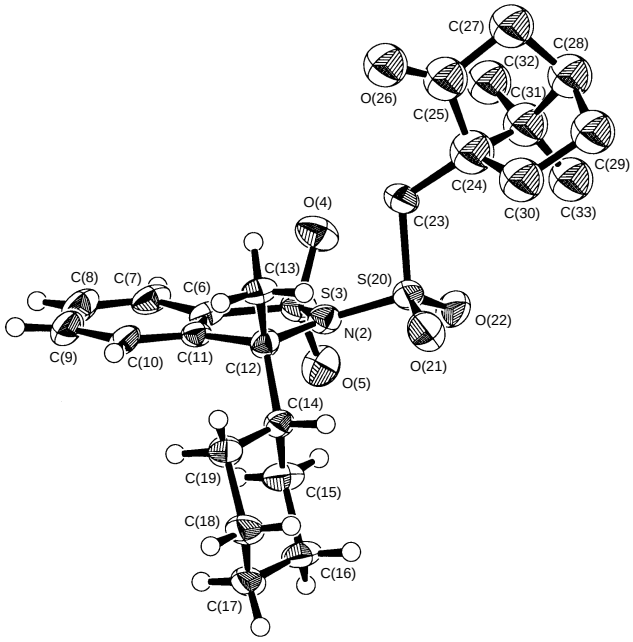



**Fig. 1** ORTEP diagram of **1** with 50% thermal ellipsoids. Two of minor disordered contributions of camphor moiety are omitted for clarity. Selected bond distances (Å) and angles (°): N(2)–S(3) 1.684(5), N(2)–S(20) 1.654(5), N(2)–C(12) 1.523(8); S(3)–N(2)–S(20) 117.6(3), S(3)–N(2)–C(12) 115.6(4), C(12)–N(2)–S(20) 126.2(4).

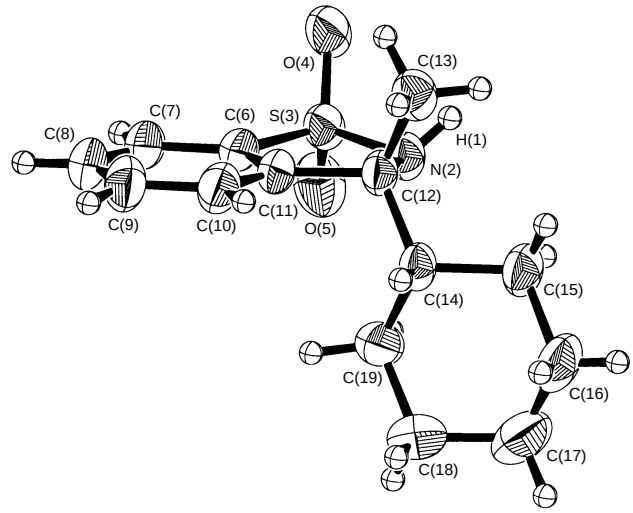



**Fig. 2** ORTEP diagram of **2** with 50% thermal ellipsoids. Selected bond distances (Å) and angles (°): N(2)–S(3) 1.620(2), N(2)–C(12) 1.487(4); S(3)–N(2)–C(12) 115.6(2), S(3)–N(2)–H(1) 108(2), C(12)–N(2)–H(1) 113(2).

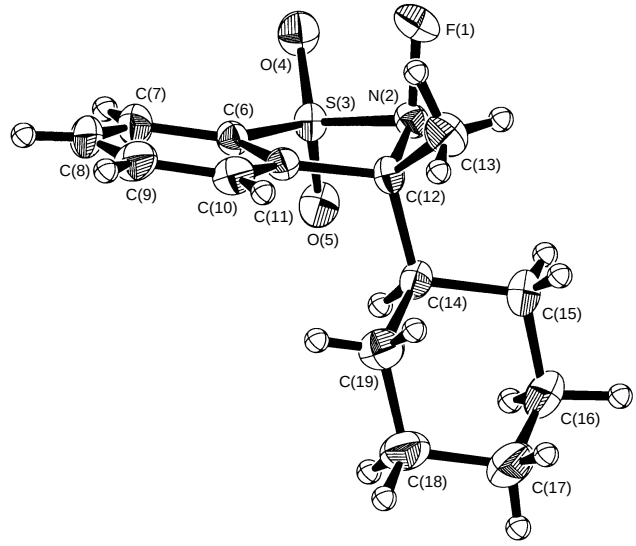
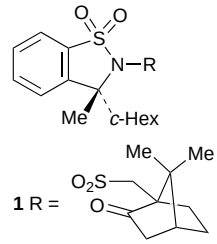



**Fig. 3** ORTEP diagram of **3** with 50% thermal ellipsoids. Selected bond distances (Å) and angles (°): N(2)–F(1) 1.435(3), N(2)–S(3) 1.738(2), N(2)–C(12) 1.523(4); F(1)–N(2)–S(3) 102.3(2), F(1)–N(2)–C(12) 105.7(2), S(3)–N(2)–C(12) 107.0(2).




substituent has an atom that interacts with the nitrogen lone pair, such as the sulfur atom of the sulfonyl in **1**.

The nitrogen atom in compound **2** (Fig. 2) apparently has $sp^3$ character based on the bond angles. The orientation of the amide proton is *syn* to the methyl group, namely, the lone pair of the nitrogen takes a position on the side of the larger alkyl substituent. Thus, the nitrogen pyramid is tilted in the opposite direction compared to a previous report,[2] although the reason is as yet unclear. The absence of the electronegative and rather bulky *N*-substituent such as a camphorsulfonyl group results in shortening the N(2)–S(3) distance [1.620(2) Å] and the N(2)–C(12) distance [1.487(4) Å] in **2**.

The structure of **3** was determined at 152 K (Fig. 3) since the thermal motion of the cyclohexyl group was high at room temperature. The nitrogen atom in **3** was found to be highly pyramidalized. The N(2)–S(3) bond [1.738(2) Å] is much longer than that in **1** and **2**, presumably owing to the highly electronegative character of the fluorine atom. The N(2)–F(1) bond [1.435(3) Å] is slightly elongated [*cf.*[3] 1.406(16) Å for F–$NR^1R^2$]. The dihedral angles F(1)–N(2)–C(12)–C(14) and F(1)–N(2)–C(12)–C(13) are −161.8(2) and −40.9(3)°, respectively. Therefore, the fluorine is antiperiplanar with the cyclohexyl group. The dihedral angles F(1)–N(2)–S(3)–O(4) and F(1)–N(2)–S(3)–O(5) are 30.5(2) and 159.4(2)°, respectively. Consequently, the nitrogen lone pair seems to bisect the O(4)–S(3)–O(5) angle, probably due to optimal orbital overlap with the d-orbital of the sulfur atom. The nitrogen atom is at a distance of 0.449 Å from the least-squares plane defined by S(3), C(6), C(11), C(12) and the five-membered ring has an envelope conformation. As a result, the N–F bond of **3** is nearly perpendicular to the least-squares plane (85.8°).

This work was partially supported by a Grant-in-Aid for Scientific Research (No. 07807193) from the Ministry of Education, Science and Culture, Japan.

## Footnotes

† *Crystal data* for **1**: $C_{24}H_{33}NO_5S_2$, $M$ = 479.65, orthorhombic, $a$ = 14.344(2), $b$ = 22.415(2), $c$ = 7.608(3) Å, $U$ = 2446(1) Å$^3$, $T$ = 163 K, space group $P2_12_12$ (no. 18), filtered Cu-Kα radiation, λ = 1.54178 Å, $Z$ = 4, $D_c$ = 1.302 Mg m$^{-3}$, $F$(000) = 1024, colourless prism, dimensions 0.35 × 0.20 × 0.10 mm, μ(Cu-Kα) = 2.259 mm$^{-1}$, Rigaku AFC7R diffractometer, ω–2θ scan, 4.0 < 2θ < 130.0°, 2420 reflections measured, 1960 reflections observed [$I > 3\sigma(I)$]. The structure was solved by direct methods (SIR92[4]) and expanded using Fourier techniques (DIRDIF94[5]). The camphor moiety [C(24)–C(33), O(26)] was disordered over three positions with a 43 : 29 : 28 distribution. All non-hydrogen atoms were refined anisotropically except those of the disordered group that were refined as a rigid group isotropically. For this reason, the $R$ value was slightly high. Hydrogen atoms were included but not refined, except those located with the disordered group and the C(23) atom attached to the disordered group, which were ignored. Isotropic temperature factors of the H atoms were set equal to $U_{eq}$ of the bonded C atom. The final cycle of full-matrix least-squares refinement (for 221 parameters) was converged with $R_w$ = 0.099, $R$ = 0.067 (gof = 1.32). For **2**: $C_{14}H_{19}NO_2S$, $M$ = 265.37, tetragonal, $a$ = 8.963(1), $c$ = 34.080(2) Å, $U$ = 2737.7(8) Å$^3$, $T$ = 296 K, space group $P4_32_12$ (no. 96), filtered Cu-Kα radiation, λ = 1.54178 Å, $Z$ = 8, $D_c$ = 1.288 mg m$^{-3}$, $F$(000) = 1136, colourless prism with dimensions 0.40 × 0.40 × 0.10 mm, μ(Cu-Kα) = 2.052 mm$^{-1}$, an empirical absorption correction based on azimuthal scans of several reflections, transmission factors 0.6093–0.9952; Rigaku AFC7R diffractometer, ω–2θ scan, 4.0 < 2θ < 120.0°, 1314 reflections measured, 1137 reflections observed [$I > 3\sigma(I)$]. The structure was solved by direct methods (SIR92) and expanded using Fourier techniques. The non-hydrogen atoms were refined anisotropically. Hydrogen atoms were refined isotropically. The final cycle of full-matrix least-squares refinement (for 240 parameters) was converged with $R$w = 0.051, $R$ = 0.040 (gof = 0.96). S(3)–O(4) distance [1.431(3) Å] is slightly longer than S(3)–O(5) [1.420(3) Å], which can be ascribed to the intermolecular hydrogen bonding between NH and O(4) [N(2)···O(4) 2.955(3) Å]. For **3**: $C_{14}H_{18}FNO_2S$, $M$ = 283.36, orthorhombic, $a$ = 12.704(3), $b$ = 13.518(4), $c$ = 8.263(4) Å, $U$ = 1419.0(6) Å$^3$, $T$ = 152 K, space group $P2_12_12_1$ (no. 19), graphite monochromated Mo-Kα radiation, λ = 0.71069 Å, $Z$ = 4, $D_c$ = 1.326 mg m$^{-3}$, $F$(000) = 600, colourless prism with dimensions 0.32 × 0.23 × 0.17 mm, μ(Mo-Kα) = 0.237 mm$^{-1}$, Rigaku AFC7R diffractometer, ω–2θ scan, 4.0 < 2θ < 55.0°, 1900 reflections measured, 1502 reflections observed [$I > 3\sigma(I)$]. The structure was solved by direct methods (SHELXS86[6]) and expanded using Fourier techniques. The non-hydrogen atoms were refined anisotropically. Hydrogen atoms were refined isotropically. The final cycle of full-matrix least-squares refinement (for 244 parameters) was converged with $R_w$ = 0.045, $R$ = 0.034 (gof = 1.12). Atomic coordinates, bond lengths and angles, and thermal parameters have been deposited at the Cambridge Crystallographic Data Centre (CCDC). See Information for Authors, Issue No. 1. Any request to the CCDC for this material should quote the full literature citation and the reference number 182/313.

## References

1 Y. Takeuchi, A. Satoh, T. Suzuki, A. Kameda, M. Dohrin, T. Satoh and K. L. Kirk, *Chem. Pharm. Bull*., submitted.
2 W. Oppolzer, M. Wills, C. Starkemann and G. Bernardinelli, *Tetrahedron Lett*., 1990, **31**, 4117.
3 F. H. Allen, O. Kennard, D. G. Watson, L. Brammer, A. G. Orpen and R. Taylor, in *International Tables for Crystallography*, ed. A. J. C. Wilson, Kluwer, Dordrecht, 1995, vol. C., pp. 685–706.
4 A. Altomare, M. C. Burla, M. Camalli, G. Cascarano, C. Giacovazzo, A. Guagliardi and G. Polidori, SIR92, *J. Appl. Crystallogr*., 1994, **27**, 435.
5 P. T. Beurskens, G. Admiraal, G. Beurskens, W. P. Bosman, R. de Gelder, R. Israel and J. M. M. Smits, DIRDIF94, The DIRDIF94 program system, Technical Report of the Crystallography Laboratory, University of Nijmegen, The Netherlands, 1994.
6 G. M. Sheldrick, SHELXS86, in *Crystallographic Computing 3*, ed. G. M. Sheldrick, C. Kruger and R. Goddard, Oxford University Press, 1986, pp. 175–189.

*Received, 28th October 1996; Com. 6/07312C*

# Synthesis of three novel supercharged β,γ-methylene analogues of adenosine triphosphate

**Xiaohai Liu, Xiu-Rong Zhang and G. Michael Blackburn***

*Krebs Institute, Department of Chemistry, University of Sheffield, Brook Hill, Sheffield, UK S3 7HF*

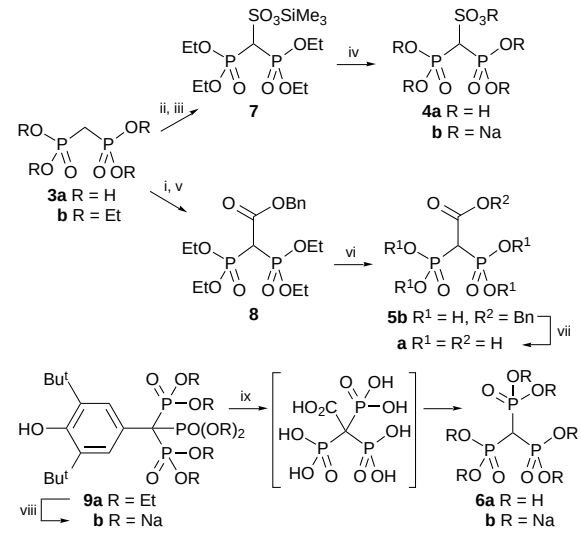
**Three derivatives of methylenebisphosphonic acid containing an additional ionisable acidic function are incorporated into β,γ-bridged derivatives of adenosine triphosphate to give the first examples of supercharged nucleotide analogues 2a–c.**

Adenosine triphosphate **1a** has multiple roles in cellular chemistry, among which its function as an energy source is predominant. However, a large variety of intra- and extracellular purinoceptors for adenine nucleotides is currently under intensive investigation and their affinities for nucleotides based on charge and metal ion-binding discrimination is likely to be of critical importance.[1] Also, the known higher affinity (*ca.* 1000-fold) of adenylate kinase for diadenosine 5′,5‴-pentaphosphate ($K_d$ 40 nM) over the corresponding tetraphosphate[2] ($K_d$ 20 μM) can be identified as arising from charge selectivity since the closed form of this enzyme has now been fully characterised in its stable ternary complex with AMP and β,γ-imino-ATP, which embraces six negative charges on phosphates in the reactive site without elongation of the polyphosphate structure.[3]

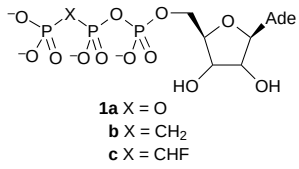
In previous studies, we have emphasised the significance of generating nucleotide analogues that are both isosteric and isopolar in character[4] with especial emphasis on the use of α-fluorophosphonates to ensure full ionisation of the phosphonate moiety.[5] We here describe supercharged analogues of nucleotides in which additional negative charge is provided without elongation of the polyphosphate chain. Such analogues **2** can be constructed by substituting the β,γ-methylene bridge of AMPPCP **1b** with an anionic function, *e.g.* $SO_3^-$, $CO_2^-$, or $PO_3H^-$. Such analogues will be especially important in the construction of bisubstrate analogues for kinases and related enzymes[2,6] where additional anionic charge cannot be accommodated within the phosphonate framework of simple isopolar nucleotide analogues.

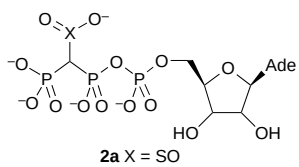
The preparation of such supercharged analogues of ATP and other nucleotides calls for convenient syntheses of derivatives of methylenebisphosphonic acid **3a** having an additional acidic OH function. We have identified 1,1-bis(phosphono)-methanesulfonic acid **4a**, 2,2-bis(phosphono)acetic acid **5a** and the known[7] methanetrisphosphonic acid **6a** as suitable polyanion equivalents to be incorporated into analogues of ATP and other nucleotides by standard methods. We here report syntheses of the first two of these bisphosphonates and an improved synthesis of **6a** along with their condensation with AMP to give three new supercharged analogues of ATP **2a-c**.

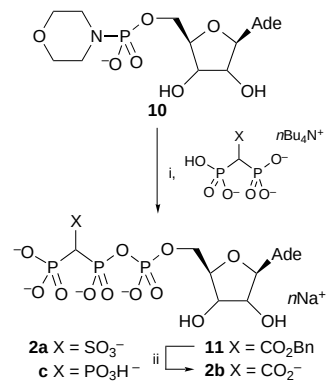
1,1-Bis(phosphono)methanesulfonic acid **4a** was prepared by trimethylsilylation[8] of tetraethyl methylenebisphosphonate **3b** and treatment of its anion with trimethylsilyl chlorosulfate in THF at room temperature. Without further purification, the product **7** was treated with an excess of bromotrimethylsilane in $CH_2Cl_2$ in the presence of triethylamine and solvolysed in MeOH to give the pentakis(triethylammonium) salt of 1,1-bis-(phosphono)methanesulfonic acid in 83% yield. This was converted into the free acid by ion exchange chromatography (Dowex-50, $H^+$) (Scheme 1).




**Scheme 1** *Reagents and conditions*: i, LiBu, THF, −78 °C, then $Me_3SiCl$, −78 to 0 °C; ii, LiBu, THF, −78 °C; $Me_3SiOSO_2CF_3$, −30 °C; iii, $Me_3SiOSO_2Cl$; iv, $Me_3SiBr$, $CH_2Cl_2$, $Et_3N$; v, BnOCOCl, THF; vi, $Me_3SiBr$, $CH_2Cl_2$; vii, Pd/C, $H_2$, MeOH; viii, $Me_3SiBr$, $CH_2Cl_2$, then $Na_2CO_3$ (aq); ix, $H_2O_2$, $F_3CCO_2H$




**Scheme 2** *Reagents and conditions*: i, pyridine, 20 °C, 12 h, camphorsulfonic acid; ii, Pd–$BaSO_4$, $H_2O$

**Table 1** NMR and mass spectral data for ATP and various β,γ-bridged nucleotide analogues

| Compound | $^{31}$P NMR data[a] | | | | | $^{1}$H NMR data ($P_2CHX$)[a] | | HRMS data[b] | |
|---|---|---|---|---|---|---|---|---|---|
| | $\delta_\alpha$ | $\delta_\beta$ | $\delta_\gamma$ | $^2J_{\alpha\beta}$ | $^2J_{\beta\gamma}$ | $\delta_H$ | $^2J_{PH}$ | Found $[M + 1]^+$ | Calc. |
| ATP[c] **1a** | −10.21 | −20.7 | −5.0 | 18.8 | 19.5 | — | — | — | — |
| AMPPCHFP[c] **1c** | −10.48 | +2.42 | +8.58 | 29.0 | 15.0 | 5.26 | 13.3 | — | — |
| AMPPC(S)P **2a** | −10.097 | +1.788 | +7.788 | 25.4 | 2.1 | 3.90 | 19.8, 21.6 | 695.8931 | 695.8908 |
| AMPPC(C)P **2b** | −10.217 | +4.589 | +11.160 | 27.3 | 9.4 | 3.49 | 20.0 | 659.9249 | 659.9238 |
| AMPPC(P)P **2c** | −9.415 | +7.848 | +13.225 | 26.3 | 8.8 | 2.85 | 21.3 | 695.9012 | 695.9003 |
| AMPPCP[c] **1b** | −10.35 | +14.36 | +12.14 | 26.8 | 7.9 | 2.38 | 19.4 | — | — |

[a] NMR at 161.97 MHz (phosphorus) and 400 MHz (proton) in $D_2O$ at pH 7.8. [b] Positive ion FAB-MS data for pentasodium salt $[M + 5Na - 4H]^+$. [c] Ref. 5.

Tetraethyl lithiotrimethylsilylmethylenebisphosphonate (*v.s.*) was reacted with benzyl chloroformate in anhydrous THF to give tetraethyl benzyloxycarbonylmethylenebisphosphonate **8** (43% yield). Treatment of ester **8** with bromotrimethylsilane[9] and methanolysis generated the free phosphonic acid **5b**, which was debenzylated by hydrogenolysis of its cyclohexylamine salt (Pd/C–$H_2$–MeOH) to give the tris(cyclohexyl)ammonium salt of **5a** (Scheme 1).

Hexaethyl (3,5-di-*tert*-butyl-4-hydroxyphenyl)methanetrisphosphonate[10] **9a** was transesterified with excess bromotrimethylsilane in $CH_2Cl_2$, the solvent evaporated and the residue treated with aqueous sodium carbonate, and the pH adjusted to 11 with sodium hydroxide. The sodium salt **9b** was precipitated by addition of MeOH and added to a mixture of hydrogen peroxide (8%, 30 volume strength) in trifluoroacetic acid and the reaction mixture quenched with EtOH and concentrated *in vacuo* to give the hexasodium salt of methanetrisphosphonic acid **6b**. This was converted into the free acid **6a** by ion exchange (Dowex-50, $H^+$) in 28% overall yield. It proved identical in spectroscopic properties to that described by Gross.[7] Evidently, the intermediate 2,2,2-trisphosphonoethanoic acid decarboxylates spontaneously.

The supercharged ATP analogues **2a**–**c** were prepared by condensation of the appropriate *n*-butylammonium salts of the free acids **4a**, **5b** and **6a** with adenosine 5′-phosphoromorpholidate[11] **10**. The free acids **4a**, **5b** and **6a** were treated with tetrabutylammonium hydroxide to pH 8.9, and the resulting tetrabutylammonium salts lyophilised repeatedly from anhydrous pyridine. The resulting dry salts were each reacted with **10** in anhydrous pyridine at room temperature to give the three nucleotide analogues as their tetrabutylammonium salts, purified by DEAE Sephadex chromatography (triethylammonium hydrogen carbonate gradient, pH 7.8). Promotion by 10-camphorsulfonic acid proved very effective for these condensations. The resulting triethylammonium salt products were dissolved in MeOH, from which their sodium salts were precipitated by addition of sodium iodide in propanone to give β,γ-sulfonatomethylene adenosine 5′-triphosphate **2a** (80% yield), β,γ-benzyloxycarbonylmethylene adenosine 5′-triphosphate **11** (75% yield) and β,γ-phosphonomethylene adenosine 5′-triphosphate **2c** (25% yield) as their sodium salts. Catalytic hydrogenolysis (Pd–$BaSO_4$–$H_2$) of **11** removed the benzyl ester function to give β,γ-carboxymethylene adenosine 5′-triphosphate **2b** as its pentasodium salt (61% yield) (Scheme 2).

All three ATP analogues **2a**–**c** were fully characterised by reverse phase high performance liquid chromatography (HPLC), high resolution MS, and $^1$H and $^{31}$P NMR (Table 1). Their phosphorus NMR spectra show AMX spectra for **2a** and **2b** and an $AMX_2$ spectrum for **2c.** The magnitude of the $^2J_{\alpha\beta}$ coupling constants is typical of ATP and its analogues while that for $^2J_{\beta\gamma}$ shows some variation, as is seen for other β,γ-bridged ATP species[5] (Table 1). The two supercharged analogues **2a**,**b** are necessarily mixtures of epimers with respect to the chiral centre in the β,γ-bridge though they are not resolved by HPLC (C-18 reverse phase MeCN–MeOH). The difference between the epimers is manifest most clearly in the $^{31}$P chemical shift for $P_\alpha$ for sulfonic acid **2a** where the signals for $P_\alpha$ in the two isomers are separated by 0.03 ppm. For all of the other phosphorus resonances, this diastereoisomeric separation appears to be not significantly greater than the phosphorus NMR line width (approx. 0.01 ppm). The proton NMR of the adenosine moieties of **2a**–**c** were unexceptional, while the chemical shifts of the methine proton in the β,γ-bridge lie between those for AMPPCP and AMPPCHFP, directly reflecting the increasing electronegativity of the functions: $PO_3H^- < CO_2^- < SO_3^-$ (Table 1). Accordingly, we see a clear need to generate supercharged nucleotides with this methine proton replaced by fluorine and such syntheses are in progress.

The positive ion FAB-MS spectra show a homologous series of peaks of mass increment 22 and having correct accurate masses for $[M + xH^+ + yNa^+]$ where $(x + y = 1)$. The sulfonic acid **2a** showed three to six sodium ions, the carboxylic acid **2b** zero to five sodium ions, and the trisphosphonate **2c** from three to six sodium ions. These data clearly reflect the strong cation binding potential of these nucleotide analogues and data on metal ion and proton affinities will be described elsewhere.

The spectroscopic properties of β,γ-sulfonatomethylene adenosine 5′-triphosphate **2a** most closely approximate to those of β,γ-fluoromethylene adenosine 5′-triphosphate, while it has the added feature of an extra negative charge on the molecule. Syntheses of the corresponding analogues of ADP are in progress and the affinities of various enzymes and receptors for analogues **2a**–**c** are being determined.

We thank the BBSRC for financial support (ROPA/MOLO4558) and Mr Peter Ashton (Birmingham University) for determination of high resolution mass spectra.

## References

1 G. Burnstock, in *CIBA Foundation Symposium*, 1996, vol. 198, pp. 1–305; N. J. Cusack and C. J. Pettey, *Drug Dev. Res.*, 1996, **37**, 212 and references cited therein.
2 R. Bone, Y. C. Cheng and R. Wolfenden, *J. Biol. Chem.*, 1986, **261**, 6410 and references cited therein.
3 M. B. Berry, B. Meador, T. Bilderback, P. Linag, M. Glaser and G. N. Phillips, *Proteins: Struct. Funct. Genet.*, 1994, **19**, 183.
4 G. M. Blackburn, *Chem. Ind. (London)*, 1981, 135.
5 G. M. Blackburn, D. E. Kent and F. Kolkmann, *J. Chem. Soc., Perkin Trans. 1*, 1984, 1119.
6 G. M. Blackburn, D. L. Jakeman, A. J. Ivory and M. P. Williamson, *Bioorg. Med. Chem. Lett.*, 1994, **4**, 2573.
7 H. Gross, B. Costisella, I. Keitel and S. Ozegowski, *Phosphorus Sulfur Silicon*, 1993, **83**, 203.
8 *cf.* Y. Zanella, S. Berté-Verrando, R. Dizière and P. Savignac, *J. Chem. Soc. Perkin Trans. 1*, 1995, 2835.
9 C. E. McKenna, M. R. Higa, N. H. Cheung and M.-C. McKenna, *Tetrahedron Lett.*, 1977, 155.
10 H. Gross, S. Ozegowski and B. Costisella, *Phosphorus Sulfur Silicon*, 1990, **47**, 7.
11 J. G. Moffatt and H. G. Khorana, *J. Am. Chem. Soc.*, 1961, **83**, 649.

*Received, 21st August 1996; Com. 6/05828K*

# Reversibility of *S*-nitrosothiol formation

**Pablo Herves Beloso† and D. Lyn H. Williams***

*Chemistry Department, University Science Laboratories, South Road, Durham, UK DH1 3LE*

**The nitrosation of thiols is sufficiently reversible to allow, in many cases, the low thiol concentration present at equilibrium to reduce $Cu^{2+}$ and bring about loss of nitric oxide from *S*-nitrosothiols.**

It is now clear that the decomposition of *S*-nitrosothiols in an aqueous buffer to give nitric oxide and the disulfide is brought about by $Cu^{+}$, which in turn is generated by reduction of $Cu^{2+}$ by thiolate ion,[1] or in principle by any other reducing agent. In many cases there is enough free $Cu^{2+}$ present in the aqueous buffer solution for this reaction to take place. Reduction of $Cu^{2+}$ sources where the copper is bound to peptides and proteins also occurs, thus allowing the possibility that these reactions could occur *in vivo*.[2] Currently there is considerable interest in the chemistry/biochemistry of nitrosothiols, since (*a*) they are being examined as possible drugs to effect vasodilation and to reduce platelet aggregation,[3] and (*b*) they are now believed to play an important part in some of the physiological processes involving nitric oxide.[4]

There is a question as to where the thiolate ion comes from, and it has been suggested that enough is present as an impurity, deriving from the nitrosothiol synthesis, whereas it has also been suggested that some partial hydrolysis of the nitrosothiol occurs.[1] We have eliminated the first possibility as a general explanation, by working with solutions of nitrosothiols generated *in situ*, using a very large excess of nitrous acid, when we find that reaction often still occurs.[5] We therefore looked at the possibility that the *S*-nitrosation is a reversible process.

Nitrosation of alcohols is a well-known reversible process in acid solution, [eqn. (1)],[6] and equilibrium constants have been

$$ROH + HNO_2 = RONO + H_2O \quad (1)$$

determined for many alcohols. Some typical values are 3.5 and 1.2 $dm^3\ mol^{-1}$ for methanol and ethanol respectively.[7] A kinetic method for demonstrating this reversibility is by the presence of a positive intercept at [ROH] = 0, when the first-order rate constant ($k_{obs}$) is plotted against [ROH], when reactions are carried out with [ROH] $\gg$ [$HNO_2$]. Equilibrium constants determined in this way[8] are in reasonable agreement with those obtained from direct measurements.[7] Such plots for the nitrosation of thiols showed no measurable intercepts;[9] it was generally assumed by us that the reactions are effectively (*i.e.* from a preparative point of view) irreversible, and this has been rationalised in terms of the difference in nucleophilicities (S > O), important for the forward reaction, and the difference in basicities (O > S), important in the reverse reaction, since *O*- or *S*-protonation occurs. We examined this more carefully in the case of the nitrosation of thiomalic acid. The results are shown in Fig. 1, for reaction at two different acidities. It is clear that there is no measurable intercept at [RSH] = 0. Nevertheless we have analysed solutions of nitrosothiols for thiol content, using Ellman's reagent.[10] Calibration experiments revealed that we were able to measure thiol concentrations in the range $8 \times 10^{-6}$ to $5 \times 10^{-5}$ mol $dm^{-3}$ very readily, from measurements at 412 nm of the absorbance due to the dianion of 2-nitro-5-thiobenzoic acid. All of our calibration measurements gave values for the extinction coefficient at this wavelength which were within 3% of the literature value[10] (14 150 $dm^3\ mol^{-1}\ cm^{-1}$).

Results were obtained for the product of nitrosation of penicillamine ($6.6 \times 10^{-4}$ mol $dm^{-3}$), using stoichiometric ratios of [RSH]:[$HNO_2$] ranging from 1:1 to 1:2. The nitrosation reactions were carried out under mildly acid conditions (*ca*. 0.05 mol $dm^3$ $H^+$), where it is known that reaction is very fast. Analysis for thiol content was carried out at pH 7.27 as described in the literature.[10] At this pH no reactions associated with eqn. (2) will occur. The results are

$$RSH + HNO_2 = RSNO + H_2O \quad (2)$$

presented in Table 1 in the form of the % [RSH] present at the equilibrium position. All of these *S*-nitrosations are very rapid processes. It is clear that thiol remains in all of these solutions, in a quite significant concentration for the 1:1 solution, dropping as expected as we move to the 1:2 mixture. These figures (ignoring the final value, where the concentration is very low and therefore subject to a large uncertainty), give an approximate equilibrium constant (*K*) for eqn. (2) of $3 \times 10^5$ $dm^3\ mol^{-1}$.

Values of *K* of this magnitude would not lead to a measureable intercept for plots such as that shown in Fig. 1, so this kinetic method is obviously not sufficiently sensitive to measure equilibrium constants of this magnitude. We have shown that this is the general situation for the nitrosation of thiols, by determining the equilibrium thiol concentration in a number of other cases. For *S*-nitrosocysteine generated *in situ*, we find 7.8% thiol remains at equilibrium from a 1:1 ratio of reactants (corresponding to an approximate *K* value of $6 \times 10^5$ $dm^3\ mol^{-1}$). The thiol content drops significantly on standing (to a fifth of its value in 1 h), no doubt because of aerial oxidation. Similarly, the nitrosation of thiomalic acid gives

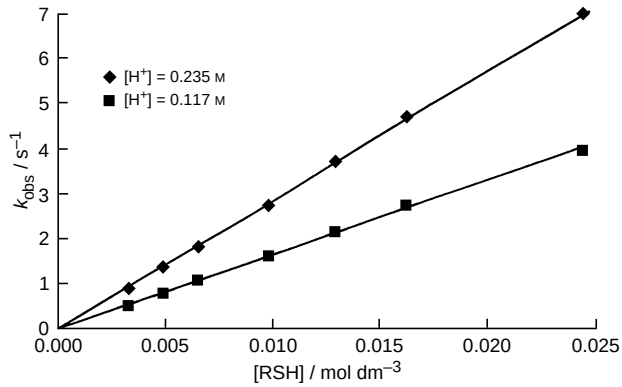



**Fig. 1** Plot of the first order rate constant ($k_{obs}$) *vs* [RSH] for the nitrosation of thiomalic acid by nitrous acid ($1 \times 10^{-4}$ mol $dm^{-3}$) at two different acidities

**Table 1** Percentage thiol remaining at equilibrium in the nitrosation of penicillamine ($6.7 \times 10^{-4}$ mol $dm^{-3}$)

| [RSH]:[$HNO_2$] | % RSH at equilibrium |
|---|---|
| 1:1 | 5.3 |
| 1:1.1 | 4.5 |
| 1:1.2 | 3.2 |
| 1:1.5 | 0.65 |
| 1:2 | 0.08 |

2.0% thiol at equilibrium from a 1 : 1 ratio of reactants, dropping to 0.11% for a 1 : 1.5 ratio, giving a $K$ value of *ca.* $3 \times 10^6$ $dm^3\ mol^{-1}$. Nitrosation of *N*-acetyl penicillamine gave 0.45% thiol from a 1 : 1 reactants ratio. It is not clear why this is so much smaller than that found for penicillamine. A fuller systematic study of the system is underway.

It follows that if *S*-nitrosation of thiols is significantly reversible in this way, then solutions of *S*-nitrosothiols, initially prepared in acid solution, will always contain a small thiol concentration. This will apply to solutions of nitrosothiols made up in any mildly acidic solution, but not presumably to solutions made up in basic solution. Solutions made up (directly in alkaline buffer) from two stable solid nitrosothiols, *S*-nitroso-*N*-acetyl penicillamine (SNAP) and *S*-nitrosoglutathione GSNO, analysed respectively for 0.78 and 0.80% thiol, probably derived from thiol impurity resulting from the incomplete *S*-nitrosation during synthesis. The difficulty in producing nitrosothiol samples totally free from thiol has been reported[11] in the case of GSNO.

Our results provide an explanation as to why reduction of $Cu^{2+}$ by thiolate (in solutions of *S*-nitrosothiols), eqn. (3),

$$2Cu^{2+} + 2RS^- = 2Cu^+ + RSSR \qquad (3)$$

occurs so readily in solutions where it would be expected that there would be no thiolate present. This applies whenever the *S*-nitrosothiol solution is prepared *in situ* from solutions of the thiol and nitrous acid, or in cases where mildly acidic solutions are first made up from solid samples.

We thank the Xunta de Galicia for a Research Training grant to P. H. B., and the EPSRC for a research grant for the purchase of a stopped flow spectrophotometer.

## References

1 A. P. Dicks, H. R. Swift, D. L. H. Williams, A. R. Butler, H. H. Al-Sadoni and B. G. Cox, *J. Chem. Soc., Perkin Trans. 2*, 1996, 481.
2 A. P. Dicks and D. L. H. Williams, *Chem. Biol.*, 1996, **3**, 655.
3 E. J. Langford, A. S. Brown, R. J. Wainwright, A. J. de Belder, M. R. Thomas, R. E. A. Smith, M. W. Radomski, J. F. Martin and S. Moncada, *Lancet*, 1994, **344**, 1458.
4 L. Jia, C. Bonaventura, J. Bonaventura and J. S. Stamler, *Nature*, 1996, **380**, 221.
5 P. Herves and D. L. H. Williams, to be published.
6 D. L. H. Williams, *Nitrosation*, 1988, Cambridge University Press, p. 150.
7 J. Casado, F. M. Lorenzo, M. Mosquera and M. F. R. Prieto, *Can. J. Chem.*, 1984, **62**, 136.
8 S. E. Aldred, D. L. H. Williams and M. Garley, *J. Chem. Soc., Perkin Trans. 2*, 1982, 777.
9 L. R. Dix and D. L. H. Williams, *J. Chem. Soc., Perkin Trans. 2*, 1984, 109.
10 P. W. Riddles, R. L. Blakeley and B. Zerner, *Anal. Biochem.*, 1979, **94**, 75.
11 A. C. F. Gorren, A. Schrammel, K. Schmidt and B. Mayer, *Arch. Biochem. Biophys.*, 1996, **330**, 219.

*Received, 23rd October 1996; Com. 6/07228C*

# Electronic origin of variable denitrosylation kinetics from isostructural {FeNO}$^7$ complexes: X-ray crystal structure of [Fe(oetap)(NO)]†

**D. Scott Bohle,*[a] Peter Debrunner,[b] Jeffrey P. Fitzgerald,[c] Bernhard Hansert,[a] Chen-Hsiung Hung[a] and Andrew J. Thomson[d]**

[a] *Department of Chemistry, University of Wyoming, Laramie, Wyoming 82071-3838, USA*
[b] *Department of Physics, University of Illinois Urbana-Champaign, Illinois 61801, USA*
[c] *Department of Chemistry, United States Naval Academy, Annapolis, Maryland 21402, USA*
[d] *School of Chemical Sciences, University of East Anglia, Norwich, UK NR4 7TJ*

**In contrast to the nitrosyl derivative of iron(II) octaethylporphyrin [Fe(oep)(NO)], the isostructural octaethyltetraazaporphyrin complex [Fe(oetap)(NO)] exhibits fast ligand-promoted nitric oxide dissociation in the presence of pyridine and *N*-methylimidazole.**

Iron(II) nitric oxide complexes of phthalocyanines have been known for over 30 years.[1–3] Although they are closely related to intensively studied porphyrin compounds,[4] they are in general not well characterized and very little is known about their solution reaction chemistry because of their poor solubility. We have begun to systematically explore the reactivity of iron(II) porphyrin nitrosyls and now extend our studies to include soluble iron(II) octaethyltetraazaporphyrins, [Fe(oetap)].[5,6] Herein we describe: (*i*) the synthesis of the nitrosyl derivative of iron(II) octaethyltetraazaporphyrin [Fe(oetap)(NO)] and its characterization by IR, EPR, Mössbauer spectroscopies, electrochemistry and elemental analysis; (*ii*) the structure of [Fe(oetap)(NO)] as determined by single-crystal X-ray diffraction; (*iii*) the comparison of the spectroscopic properties of [Fe(oetap)(NO)] and [Fe(oep)(NO)]; and (*iv*) the markedly different dissociation kinetics of nitric oxide from these two compounds promoted by pyridine and *N*-methylimidazole. Together these results illustrate the effect of the macrocyclic ligand on the properties and reactivities of ferrous nitrosyl complexes.

The iron(II) nitrosyl complexes [Fe(oep)(NO)] and [Fe(oetap)(NO)] are readily prepared under reductive nitrosylation conditions by treating [FeLCl] with nitric oxide in the presence of excess methanol and 2,6-dimethylpyridine.[7]‡ Their characterisation data, Table 1, are typical for paramagnetic five-coordinate iron(II) nitrosyl complexes in which the nitric oxide ligand adopts a bent geometry and the electronic structure is best described as a delocalized {FeNO}$^7$ configuration.[8] The most pronounced difference between [Fe(oep)(NO)] and [Fe(oetap)(NO)] is the potential of the first oxidation couple, {FeNO}$^6$–{FeNO}$^7$, which increases by 350 mV for [Fe(oetap)(NO)], indicating the more electron-withdrawing nature of the nitrogen atoms for the tetraaza derivative compared to the CH units in [Fe(oep)(NO)]. In addition, the larger quadrupolar splitting observed in the Mössbauer spectrum as well as the unusually clear anisotropy and hyperfine coupling observed near $g$ = 2.00 for the low-temperature EPR spectra of [Fe(oetap)(NO)], is indicative of there being a larger ligand field in the [Fe(oetap)(NO)] complex. In the case of the $^{14}$NO derivative two triplets are observed and assigned in the EPR spectrum as $g_z$ = 2.000 with $a_z$ = 17.77 G, and $g_y$ = 2.029, $a_y$ = 16.03 G. The third signal, $g_x$, is presumably part of the low-field shoulder of the overall manifold. The EPR spectra of [Fe(oep)(NO)] and other five-coordinate nitrosyl adducts of iron(II) porphyrins, in general do not exhibit such clear anisotropic signals with well resolved hyperfine coupling in their low-temperature spectra.[9] The decreased core size for the oetap ligand is the best explanation for these macrocyclic effects. In order to rule out aggregation as the origin of these spectroscopic features spectra with tenfold greater and smaller concentrations were measured under identical conditions; the resulting spectra retain all of these features.

Direct support for the interpretation of these spectroscopic results is found in the single-crystal X-ray diffraction structure of [Fe(oetap)(NO)].§ Unlike other related disordered structures, the bent nitrosyl ligand in this complex adopts a single geometry, Fig. 1, with the nitrosyl oriented away from the four ethyl groups on the same face of the macrocycle. In spite of the smaller core size of the tetraazaporphyrin, the {FeNO}$^7$ fragment in this complex adopts a very typical geometry in terms of the Fe–N–O bond angle [143.7(4)°], the iron displacement from the macrocycle [0.308(1) Å], and the dihedral angle N(3)–Fe–N(9)–O(1) [39.6(6)°].[10]

Considering the similarity in the structural and spectroscopic features of [Fe(oetap)(NO)] and [Fe(oep)(NO)], it is surprising to find that nitric oxide dissociation from the former is four orders of magnitude faster when they are treated with coordinating ligands such as pyridine and *N*-methylimidazole, *cf.* Table 1, eqn. (1).

$$[\text{Fe(oetap)(NO)}] + 2\text{L} \rightarrow [\text{Fe(oetap)L}_2] + \text{NO} \qquad (1)$$

The products from these reactions [Fe(oetap)L$_2$][5,6] form isosbestically with the same kinetics in both the presence and absence of dioxygen. However, as shown in Fig. 2, nitric oxide

**Table 1** Summary of physical and kinetic data for [Fe(oep)(NO)] and [Fe(oetap)(NO)]

| Compound | ν(NO)[a]/cm$^{-1}$ | $E_{\frac{1}{2}}$[b]/mV | $g_{iso}$ | $a$($^{14}$N)/G | Mössbauer data[d]/mm s$^{-1}$ Δ | δ | Added ligand L | [L]/M | $k_{obs}$[e]/s$^{-1}$ |
|---|---|---|---|---|---|---|---|---|---|
| [Fe(oep)(NO)] | 1672 | 390 | 2.05 | 18.0 | 1.258(1) | 0.348(1) | *N*-mim | 6.3 | 3.8(1) × 10$^{-5}$ |
| | | | | | | | py | 6.0 | 2.2(1) × 10$^{-5}$ |
| [Fe(oetap)(NO)] | 1666 | 733 | 1.99 | 17.0 | 1.951(1) | 0.209(1) | *N*-mim | 6.3 | 0.148(2) |
| | | | | | | | py | 6.0 | 0.072(1) |

[a] KBr pellet. [b] Potentials in mV *vs.* Ag$^+$/Ag in dichloromethane solution with 0.1 M $NBu_4PF_6$ as supporting electrolyte on a platinum-button working electrode. [c] Room-temp. EPR spectra measured in toluene solution. [d] At 100 K. [e] Pseudo-first-order rate constants for the rate of denitrosylation in 1 : 1 toluene–ligand solution at 25 °C.

dissociation from [Fe(oetap)(NO)] exhibits saturation behaviour and at high concentrations of *N*-mim reaches a limiting maximum rate of 0.148 $s^{-1}$. These observations suggest a mechanism which involves rapid equilibrium binding of axial ligand to [Fe(oetap)(NO)] followed by a rate-determining loss of nitric oxide from the six-coordinate intermediate. Thus the observed rates under saturation conditions correspond to nitric oxide dissociation rates as was found for [Fe(obtpp)(NO)].

Nitric oxide is now recognized as an ubiquitous intercellular messenger whose predominant and most well characterized signal transduction pathway involves the up-regulation of soluble guanylate cyclase (sGC) by binding to its iron(II) haem centre.[11] The denitrosylative down-regulation of this key enzyme remains poorly understood, with simple nitric oxide dissociation being frequently discounted due to the generally observed slow rate.[12] Several cases where facile ligand-promoted loss of nitric oxide are now known[10,13] and the factors which control these fundamental transformations are under investigation. The isostructural pair of complexes in this study are significant in that although they have almost identical steric constraints on axial ligand binding, they exhibit dramatic differences in reactivity. These results are clearly directly due to the marked differences in electronic structures of these compounds as shown in their Mössbauer and EPR spectra. Although an exact determination of the electronic structures of these species will require exacting levels of theory, it is clear that coordination of axial ligands populates orbitals with net Fe–NO antibonding character. The challenge is to determine which factors, under direct control of the polypeptide–haem–NO interaction, can also increase the lability of nitric oxide when bound to haem proteins such as sGC.

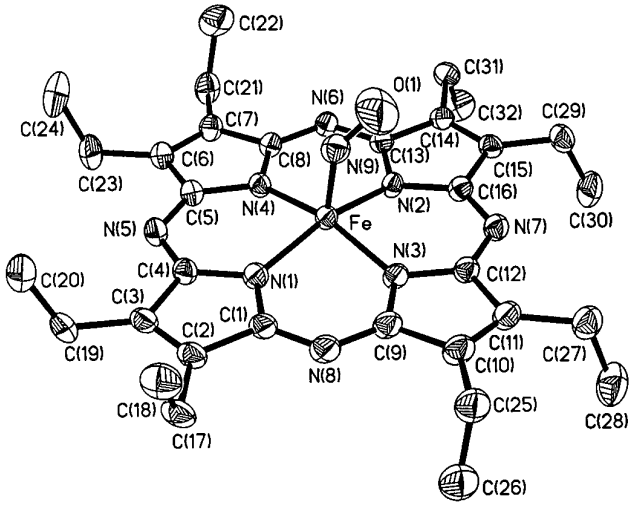



**Fig. 1** Molecular structure of [Fe(oetap)(NO)], with hydrogen atoms omitted for clarity. Important bond lengths (Å) and angles (°): Fe(1)–N(1–4) 1.922–1.941(3), Fe(1)–N(9) 1.721(4), N(9)–O(1) 1.155(5); Fe(1)–N(9)–O(1) 143.7(4).

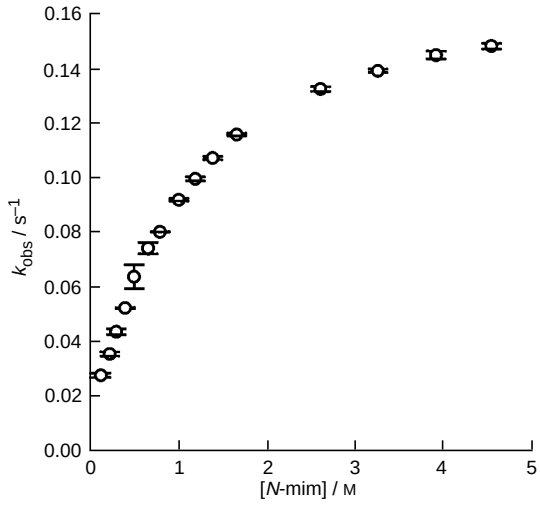



**Fig. 2** Observed rate of denitrosylation under pseudo-first-order conditions for [Fe(oetap)(NO)] as a function of *N*-methylimidazole concentration. *Conditions*: $[Fe(oetap)(NO)]_{initial}$ = 1.67 × $10^{-5}$ M, *T* = 25 °C, solvent mixture of *N*-methylimidazole with toluene and iodobenzene (19% volume).

We gratefully acknowledge support from the Department of Energy (DE-FCO2-91ER) Burroughs–Wellcome Foundation for a Hitchings–Elion Fellowship (D. S. B.), the Henry and Camille Dreyfus Foundation for a Teacher-Scholar award (D. S. B.) and the EPSRC and BBSRC for support for the Centre for Metalloprotein Spectroscopy and Biology at UEA (A. J. T.).

## Footnotes

† *Abbreviations*: oep = dianion of 2,3,7,8,12,13,17,18-octaethylporphine; oetap = dianion of 2,3,7,8,12,13,17,18-octaethyl-5,10,15,20-tetraazaporphine; obtpp = dianion of 2,3,7,8,12,13,17,18-octabromo-5,10,15,20-tetraphenylporphyrin, *N*-mim = *N*-methylimidazole.

‡ *Characterisation data* for [Fe(oetap)(NO)]: UV–VIS [$CHCl_3$, λ nm(log ε)] 316(4.57), 350(4.49), 590(4.49); IR(KBr, $cm^{-1}$) ν($^{15}$NO) = 1638.4 $cm^{-1}$; Anal: Calc. for $C_{32}H_{40}FeN_9O$, C, 61.73; H, 6.48; N, 20.25; Found: C, 61.71; H, 6.49; N, 20.14%.

§ *Crystal data*: [Fe(oetap)(NO)], $C_{32}H_{40}FeN_9O$, *M* = 622.6, triclinic, space group $P\bar{1}$ (no. 2), *a* = 10.378(2), *b* = 10.541(3), *c* = 14.290(3) Å, α = 79.36, β = 88.63(3), γ = 80.07(3)°, *U* = 1513.3(5) $Å^3$, *Z* = 2, $D_c$ = 1.366 Mg $m^{-3}$, λ = 0.71073 Å, μ = 0.541 $mm^{-1}$, *F*(000) = 658, *T* = 298 K. Data were collected on a Siemens P4 diffractometer for 2 < θ < 27.5°. The structure was solved by direct and Fourier methods and refined by least squares against $F^2$ to *R*1 = 0.0471 (*wR*2 = 0.0609) for 3870 unique intensity data with $I > 6\sigma(I)$. Atomic coordinates, bond lengths and angles, and thermal parameters have been deposited at the Cambridge Crystallographic Data Centre (CCDC). See Information for Authors, Issue No. 1. Any request to the CCDC for this material should quote the full literature citation and the reference number 182/307.

## References


1 G. Sartori and C. Ercolani, *Ricorca Sci*., 1963, **33**, 323.
2 C. Ercolani, A. M. Paoletti, G. Pennesi and G. Rossi, *J. Chem. Soc., Dalton Trans*., 1991, 1317.
3 C. Ercolani and C. Neri, *J. Chem. Soc. A*, 1967, 1715.
4 T. Yoshimura, *Bull Chem. Soc. Jpn*., 1991, **64**, 2819.
5 J. P. Fitzgerald, B. S. Haggerty, A. L. Rheingold, L. May and G. A. Brewer, *Inorg. Chem*., 1992, **31**, 2006.
6 J. P. Fitzgerald, G. Yap, A. L. Rheingold, C. T. Brewer, L. May and G. A. Brewer, *J. Chem. Soc., Dalton Trans*., 1996, 1249.
7 B. B. Wayland and L. W. Olson, *J. Am. Chem. Soc*., 1974, **96**, 6037.
8 R. D. Feltham and J. Enemark, *Coord. Chem. Rev*., 1974, **13**, 339.
9 T. Yoshimura, *J. Inorg. Biochem*., 1983, **18**, 263.
10 D. S. Bohle and C.-H. Hung, *J. Am. Chem. Soc*., 1995, **117**, 9584 and references therein.
11 L. J. Ignarro, *Biochem. Soc. Trans*., 1992, **20**, 465.
12 J. R. Stone and M. A. Marletta, *Biochemistry*, 1994, **33**, 5636.
13 J. M. C. Ribeiro, J. M. H. Hazzard, R. H. Nussenzveig, D. E. Champagne and F. A. Walker, *Science*, 1993, **260**, 539.


*Received, 8th October 1996; Com. 6/06880D*

# Alkene/alkane permselectivities of a carbon molecular sieve membrane

**Hiroyuki Suda* and Kenji Haraya**

*National Institute of Materials and Chemical Research, 1-1 Higashi, Tsukuba 305, Japan*

**A carbon molecular sieve membrane, whose pore dimension is slightly changed upon mild activation, exhibits excellent permselectivities for alkene/alkane gas pairs.**

Separation of light alkenes/alkanes has been recognized to be a key technology in the petrochemical industry. Propene/propane is a representative example, since propene is an important petrochemical feedstock and useful in the production of many chemicals. Several methods including distillation, adsorption, absorption and membrane separation have been employed for separation of propene from propane.[1] Among them, membrane separation is expected to be superior to other methods, since it is an energy saving process. Up to now, membrane separation of propene from propane has been investigated mainly by using polymeric membranes.[2–4] However, the drawbacks are the relatively lower permselectivity and lack of thermal and chemical stabilities of the polymeric membranes. These have led to further trials to develop thermally and chemically stable inorganic membranes which exhibit a better separation performance for propene/propane.[5,6] One of the candidates is a carbon molecular sieve (CMS) membrane obtained by pyrolysis of a polymeric precursor. The CMS membrane has been extensively studied and shown to have high gas permselectivities, *i.e.* a molecular sieving effect.[7–11] In our previous papers,[12,13] CMS membranes prepared by pyrolysis of both flat and capillary Kapton polyimides had been reported to exhibit the highest gas permselectivities for inorganic gas pairs. Here, we report the excellent propene/propane permselectivity of a CMS membrane whose pore dimension has been slightly expanded.

The original CMS membrane was fabricated by pyrolysis of a Kapton polyimide film (Toray - Du pont Inc.) between graphite blocks at 1273 K for 2 h at a heating rate of 10 K $min^{-1}$ at $10^{-5}$ Torr.[12] The membrane thus obtained was revealed by chemical analysis and IR spectroscopy to consist of almost only carbon. The membrane is essentially X-ray amorphous and was considered to have a turbostratic structure,[14] in which layer-planes of graphite-like structures are dispersed in a non-crystalline material. Because the original membrane has pores of only *ca.* 3.7 Å which are too small for permeation of hydrocarbons such as propene, the membrane was further calcined under mild activation in order to slightly enlarge the pore dimension. The original membrane was heated to 673 K at a heating rate of 10 K $min^{-1}$ under flowing Ar ( > 99.99%, 100 ml $min^{-1}$), and then He ( > 99.995%, 100 ml $min^{-1}$) containing water vapour (*ca*. 20 mmHg). After 10 min the He was replaced by Ar and the sample allowed to cool to room temperature.

Pore size distributions were obtained from analysis of adsorption isotherms at 298 K of probe gas molecules with different kinetic diameters σ[15] ($CO_2$, $C_2H_6$, n-$C_4H_{10}$, i-$C_4H_{10}$) by application of the Dubinin–Astakhov equation [eqn. (1)],[16]

$$W = W_0 \exp[-A/E)^n], A = RT \ln(P_s/P) \quad (1)$$

where $W$ is the pore volume, $A$ is the adsorption potential, $P_s$ is the saturated vapour pressure, $P$ is the equilibrium vapour pressure, $E$ is the characteristic energy of adsorption, and $W_0$ is the limiting micropore volume whose pore size is assumed to be larger than the kinetic diameter of each adsorbate. The samples were degassed at 573 K for 2 h under vacuum prior to each adsorption measurement. The adsorption isotherms obtained for both the CMS membranes before and after the mild activation step revealed that the former adsorbed only the smallest $CO_2$ molecule (σ = 3.3 Å), whereas the latter adsorbed even the larger $C_2H_6$ molecule (σ = 3.9 Å). The results suggest that the mild activation step is effective for the gradual increase of pore dimensions. It was clear from the obtained pore size distributions that the average pore size increased from *ca.* 3.7 to 3.9 Å due to the mild activation step. Fig. 1 demonstrates that larger pores of 4.0–4.3 Å which were not present in the original membrane appear to exist in the modified one.

Permeabilities of selected single gases were measured at 308–373 K with a high-vacuum time-lag method. The permeabilities of inorganic gases for the original CMS membrane were of the order of kinetic gas diameters[15] except for $H_2$ (Fig. 2). The permselectivities measured at 308 K for the

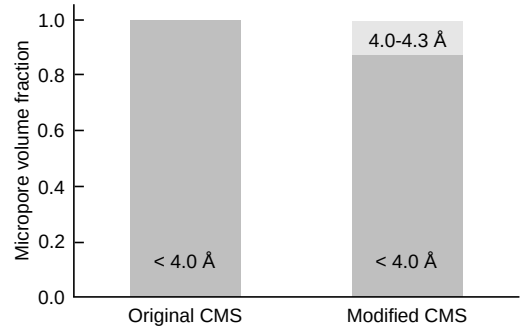



**Fig. 1** Change in micropore volume fraction of each pore size for the original and modified carbon molecular sieve (CMS) membranes

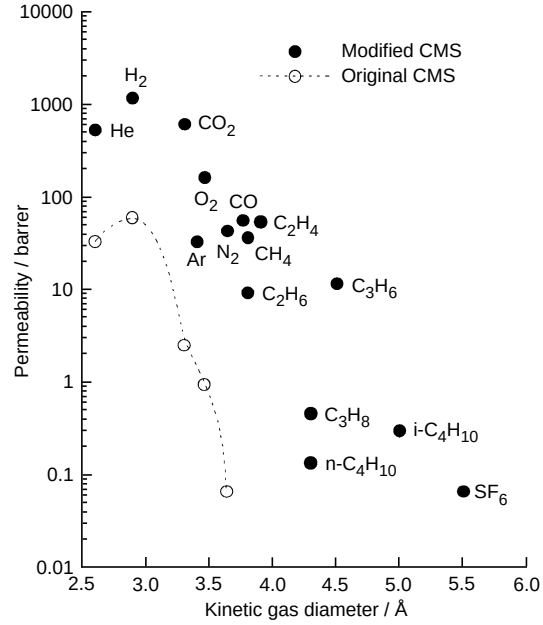



**Fig. 2** Permeabilities of selected gases for the original and modified CMS membranes measured at 373 K. Permeabilities are given in barrer, where 1 barrer = $1 \times 10^{-10}$ $cm^3$ (STP) cm $cm^{-2}$ $s^{-1}$ $(cmHg)^{-1}$.

membrane exceeded 1000 and 100 for $H_2$–$N_2$ and $CO_2$–$N_2$, respectively. These extremely high permselectivities, by which the membrane can discriminate between smaller and larger molecules, were a consequence of a pore dimension suitable for separation of such inorganic gas pairs.

The permeabilities for the modified CMS membrane were 10–700 times higher than those for the untreated membrane mainly due to the enlarged pore dimension. It was also shown from further permeation tests that there is an appreciable permeation of larger hydrocarbons. In particular, the permselectivities for light alkene/alkane gas pairs of the same carbon number were high. Permselectivities for propene/propane, for instance, were $>100$ at 308 K, much higher than previously reported values for polymeric membranes.[2–4] A rather high permselectivity of *ca.* 6 was also obtained at 308 K for ethene/ethane. These rather high permselectivities for the alkene/alkane gas pairs may arise from several factors including size effects, diffusivity and/or sorptivity, and the nature of surface functional groups that can be induced by the modification. A detailed study will now be undertaken on the permeation of hydrocarbons in modified CMS membranes to elucidate the factors leading to high permselectivities.

Considering the drawbacks of polymeric membranes (thermal and chemical instabilities *etc.*), the CMS membrane reported here activated under mild conditions is shown to be a promising candidate for alkene/alkane separation; other candidates for alkene/alkane separation are sol–gel derived inorganic membranes.[5,6] Silica membranes prepared by Asaeda *et al.*[5] exhibited permselectivities of 26 and 75 at 308 K for propene/propane single gas and gas mixtures, respectively, attributed to the selective adsorption of propene. However it appears to be difficult to prepare inorganic membranes which exhibit good propene/propane separation by the sol–gel method.[6]

## References


1 R. B. Eldridge, *Ind. Eng. Chem. Res.*, 1993, **32**, 2208.
2 O. M. Ilinitch, G. L. Semin, M. V. Chertova and K. I. Zamaraev, *J. Membr. Sci.*, 1992, **66**, 1.
3 A. Ito and S. T. Hwang, *J. Appl. Polym. Sci.*, 1989, **38**, 483.
4 K. R. Lee and S. T. Hwang, *J. Membr. Sci.*, 1992, **73**, 37.
5 M. Asaeda, A. Yamamichi, M. Satoh and M. Kamakura, *Proc. 2nd. Int. Conf. Inorg. Membr.*, 1993, p. 315.
6 B. N. Nair, K. Keizer, H. Verweij and A. J. Burggraf, *Sep. Sci. Tech.*, 1996, **31**, 1907.
7 J. E. Koresh and A. Soffer, *J. Chem. Soc., Faraday Trans. 1*, 1986, **82**, 2057.
8 H. Hatori, Y. Yamada, M. Shiraishi, H. Nakata and S. Yoshitomi, *Carbon*, 1992, **30**, 305.
9 M. B. Rao and S. Sircar, *J. Membr. Sci.*, 1993, **85**, 253.
10 C. W. Jones and W. J. Koros, *Carbon*, 1994, **32**, 1419.
11 J. Hayashi, M. Yamamoto, K. Kusakabe and S. Moorooka, *Ind. Eng. Chem. Res.*, 1995, **34**, 4364.
12 H. Suda and K. Haraya, *J. Chem. Soc., Chem. Commun.*, 1995, 1179.
13 K. Haraya, H. Suda, H. Yanagishita and M. Matsuda, *J. Chem. Soc., Chem. Commun.*, 1995, 1781.
14 R. E. Franklin, *Proc. R. Soc. London, Ser. A*, 1951, **209**, 196.
15 D. W. Breck, in *Zeolite Molecular Sieves—Structure, Chemistry, and Use*, Wiley, New York, 1974, p. 636.
16 V. A. Astakhov, M. M. Dubinin and P. G. Romankov, *Theor. Osn. Khim.*, 1969, **3**, 292.


*Received, 17th September 1996; Com. 6/06385C*

# $BiBr_3$-catalysed formation of cyclic carbonates from epoxides and DMF: a new oxidation reaction with molecular oxygen

**Véronique Le Boisselier, Michèle Postel and Elisabet Dunãch***

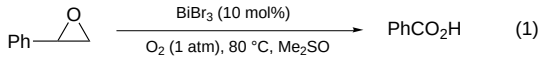
*Laboratoire de Chimie Moléculaire, U.R.A. 426 du C.N.R.S., Université de Nice-Sophia Antipolis, Parc Valrose, 06108 Nice Cedex 2, France*

**Cyclic carbonates are obtained in good yields from terminal epoxides and DMF in a $BiBr_3$-catalysed reaction with molecular oxygen as the oxidant.**

In the course of our ongoing research on the use of bismuth(III) derivatives as catalysts in oxidation reactions,[1] we have recently found a new $BiBr_3$-catalysed reaction which provides cyclic carbonates from terminal epoxides and DMF. Cyclic carbonates present interesting applications as polar aprotic solvents and as synthetic intermediates in organic synthesis,[2] and they are also important precursors to polycarbonates and other polymeric materials.[3]

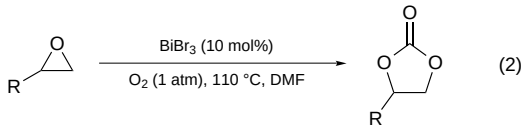
The synthesis of cyclic carbonates from epoxides is generally carried out with carbon dioxide, and various catalysts have been reported for this reaction.[4] To the best of our knowledge, no example in the literature reports the formation of carbonates from epoxides, DMF and $O_2$. Moreover, there has been no report of the use of $BiBr_3$ as the catalyst in oxidation reactions.

We have recently explored new possibilities for $Bi^{III}$ catalysis in the oxidation of epoxides[5] and α-ketols[6] to carboxylic acids by molecular oxygen. With $Bi^{III}$ mandelate[7] as the catalyst in $Me_2SO$, a C–C bond cleavage occurs on the oxirane ring or on the ketol, the carboxylic acids being obtained in 40–65% yield. When $BiBr_3$ was taken as the catalyst (10 mol%) for the oxidation of epoxides in $Me_2SO$ under $O_2$ (1 atm), the corresponding carboxylic acids were also formed. Thus, the reaction of styrene oxide led to benzoic acid in 46% yield [eqn. (1)].




(1)

Interestingly, when the same reaction was carried out in DMF, no oxidative C–C bond cleavage occurred and no carboxylic acid was obtained. The reaction selectively led to the formation of the cyclic carbonate 4-phenyl-1,3-dioxolan-2-one in 56% yield [eqn. (2)]. Thus, the nature of the solvent strongly




(2)

influences the reaction pathway, determining the nature of the reaction products.

The formation of cyclic carbonates from epoxides in DMF–$O_2$ catalysed by $BiBr_3$ appears to be specific to this catalytic system. Thus, when the experiment was carried out with 1,2-epoxydecane as the model epoxide, the corresponding cyclic carbonate was obtained in 70% yield. In the absence of the catalyst, no carbonate was formed. The replacement of $BiBr_3$ by $BiCl_3$ did not afford any carbonate, but led to the synthesis of 2-chloro alcohols (as a mixture of isomers) in 62% yield when 30 mol% $BiCl_3$ was used. It is worth noting that the corresponding bromo alcohols were not isolated in the analogous reaction with $BiBr_3$. Moreover, when $Bi^{III}$ mandelate was used as the catalyst in DMF, no reaction occurred, and the epoxide was quantitatively recovered. The reaction of the epoxide with $CO_2$ catalysed by $BiBr_3$ in refluxing THF did not give any carbonate.

When the reaction of 1,2-epoxydecane in DMF catalysed by $BiBr_3$ was carried out under an inert atmosphere ($N_2$), no carbonate was formed, although some polymerisation of the epoxide occurred. Thus, the presence of molecular oxygen is essential for carbonate formation. The consumption of $O_2$ during the reaction was measured, and reached 1.1 moles of $O_2$ per mole of epoxide at complete conversion (6 h reaction at 110 °C).

A series of epoxides were reacted in DMF under molecular oxygen (1 atm) at 110 °C, with a 10 mol% of $BiBr_3$ [eqn. (2)]. The results concerning the cyclic carbonate formation are presented in Table 1. The reactions were clean and selective, the only isolated products being the cyclic carbonates, the remaining by-products being attributed to epoxide polymerisation.

Aliphatic as well as aromatic terminal epoxides (entries 1–3) afforded the corresponding cyclic carbonates in good yields. An *o*-chlorine substituent on the aromatic ring (entry 4) was compatible with the reaction conditions, although it slowed the reaction rate, probably due to steric hindrance. Benzylic epoxides (entries 5, 6) and epibromohydrin (entry 7) led to the corresponding cyclic carbonates without elimination. No additional intramolecular cyclisation or double bond modification was observed in the reaction of 7,8-epoxyoct-1-ene (entry 8), indicating that carbonate formation does not involve radical intermediates. Several disubstituted epoxides were also tested

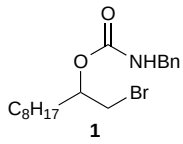
**Table 1** Oxidation of terminal epoxides to cyclic carbonates[a]

| Entry | R | Reaction time/h | Isolated yield of carbonate (%) |
|---|---|---|---|
| 1 | Ph | 7.5 | 56 |
| 2 | $C_8H_{17}$ | 6 | 70 |
| 3 | $C_6H_{13}$ | 8 | 64 |
| 4 | *o*-$ClC_6H_4$ | 31 | 68 (conversion 88%) |
| 5 | $PhOCH_2$ | 24 | 76 |
| 6 | *p*-$OMeC_6H_4OCH_2$ | 30 | 23 |
| 7 | $BrCH_2$ | 7 | 64 |
| 8 | $CH_2{=}CHC_4H_8$ | 31 | 32 (conversion 93%) |

[a] General reaction conditions: anhydrous DMF (5 ml) was stirred in the presence of $BiBr_3$ (134 mg, 0.3 mmol) at 110 °C for 30 min under molecular oxygen (1 atm), followed by the addition of the epoxide (3 mmol). The reaction was followed by GC until complete conversion of the substrate (unless stated). Acidic hydrolysis with aqueous 0.1 M HCl, diethyl ether extraction, drying of the organic layers with $MgSO_4$ and solvent evaporation led to the cyclic cabonates in the yields shown. The products were analysed by GC, $^1H$, $^{13}C$ NMR and mass spectroscopy, and their spectral data compared with those of authentic samples.

but did not afford cyclic carbonates under the same conditions. *trans*-5,6-Epoxydecane led to decane-5,6-dione in 56% yield.

The reaction presumably involves an epoxide ring opening with the incorporation and oxidation of the carbonyl moiety of DMF, the oxidant being $O_2$. 1,2-Diketones are not intermediates in this reaction; the reaction of hexane-3,4-dione did not afford any carbonate. In order to quench the amine residue eliminated from DMF, an equivalent amount of benzoyl chloride was added after the reaction with 1,2-epoxydecane. However, no *N*,*N*-dimethylbenzamide was isolated. In a different experiment, the reaction was carried out in *N*-benzylformamide. The epoxide consumption was slow (72 h) and no cyclic carbonate was formed. We could however isolate the carbamate **1**, arising from the oxidation of the benzylamine residue.†




**1**

Compound **1**, formed in 40% yield and purified by column chromatography, clearly establishes the epoxide–formamide coupling and the oxidation of the formamide group. The presence of a bromide on the less hindered side of the starting epoxide also shows the role of the catalyst in the initial oxirane ring opening. We can assume that an analogue of **1** is likely to be the intermediate in the carbonate formation in DMF. The reaction would be followed by oxygen transfer to the carbamate and ring closure with bromide elimination.

V. L. B. is grateful to the French MESR for a research grant.

## Footnote

† *Selected data* for compound **1**: $^1$H NMR ($CDCl_3$): δ 7.65–7.15 (5 H, m), 6.20 (NH, s), 4.50 (2 H, s), 3.85–3.60 (1 H, m), 3.12 (1 H, dd, *J* 15.0, 6.0 Hz), 3.08 (1 H, dd, *J* 15.0, 7.0 Hz), 1.40–0.78 (17 H, m). $^{13}$C NMR ($CDCl_3$): δ 164.1, 129.0–127.6, 71.2, 69.1, 53.1, 39.7–14.3; *m/z* (70 eV) 342 and 340 (1 : 1) ($M^+ - 29$, 5), 291(1), 262(3), 149(68), 91(100).

## References

1 M. Postel and E. Duñach, *Coord. Chem. Rev.*, 1996, in the press.
2 M. Brunner, L. Mussmann and D. Vogt, *Synlett*, 1993, 893.
3 S. Oi, K. Nemoto, S. Matsuno and Y. Inove, *Macromol. Rapid Commun.*, 1994, **15**, 133; *Organic and Bio-Organic Chemistry of Carbon Dioxide*, ed. S. Inoue and N. Yamazahi, Kodanska Ltd, Tokyo, 1982.
4 N. Kihara, N. Hara and T. Endon, *J. Org. Chem.*, 1984, **115**, 205; G. Rokicki, W. Kuran and B. P. Marcinick, *Monatsch. Chem.*, 1984, **115**, 205; T. Nishikubo, A. Kameyama, J. Yamashita and T. Tomoi, *J. Polym. Sci.*, 1993, **31**, 947; J. E. Bäckvall and O. Karlson, *Tetrahedron Lett.*, 1980, **21**, 4985; R. L. De Pasquale, *J. Chem. Soc., Chem. Commun.*, 1973, 157; M. Brunner, L. Mussmann and D. Vogt, *Synlett*, 1993, 893; P. Tascedda and E. Duñach, *J. Chem. Soc., Chem. Commun.*, 1995, 43.
5 T. Zevaco, E. Duñach and M. Postel, *Tetrahedron Lett.*, 1993, **34**, 2601; V. Le Boisselier, E. Duñach and M. Postel, *J. Organomet. Chem.*, 1994, **482**, 119.
6 V. Le Boisselier, C. Coin, M. Postel and E. Duñach, *Tetrahedron*, 1995, **51**, 4991.
7 T. Zevaco, M. Postel and N. Benali-Cherif, *Main Group Metal Chemistry*, 1992, **5**, 217.

*Received, 25th September 1996; Com. 6/06592I*

# Biosynthesis of macrophomic acid: plausible involvement of intermolecular Diels–Alder reaction

**Hideaki Oikawa,* Kenji Yagi, Kenji Watanabe, Mamoru Honma and Akitami Ichihara***

*Department of Bioscience and Chemistry, Faculty of Agriculture, Hokkaido University, Sapporo 060, Japan*

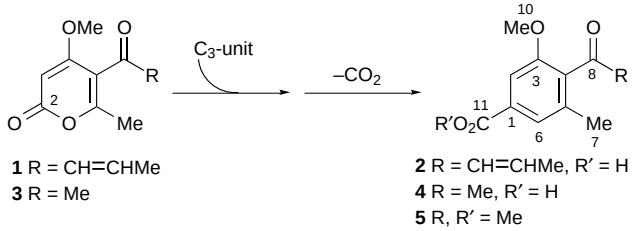
**The biosynthetic precursor of the fungal metabolite macrophomic acid 4 from *Macrophoma commelinae* has been studied by feeding experiments and enzymatic conversion from the pyrone 3 to 4 in a cell-free system. Based on the experimental data, a biosynthetic pathway for 4 involving an unprecedented intermolecular Diels–Alder reaction is proposed.**

In 1979 phytotoxin pyrenocine A **1**[1,2] was isolated from *Pyrenochaeta terrestris* by our group, and soon afterwards the structurally related pyrenochaetic acid A **2**[3] was also found from the same fungus. In spite of their striking structural similarity, we were unable to examine their biosynthetic origins due to their scarcity in the culture extracts. Later, Sakurai *et al*. reported that the fungus *Macrophoma commelinae* can convert pyrone **3** to macrophomic acid **4** (Scheme 1).[4,5] To our surprise, this fungus also converted **1** to **2** and its related analogues found in *P. terrestris*. Our continued interest in the biosyntheses of pyrenocines and pyrenochaetic acids prompted us to examine the unusual aromatic ring formation in *M. commelinae*.

Although Sakurai *et al*. established that the whole pyrone skeleton of **3** was directly transformed into benzoic acids with the loss of the C-2 carbon as $CO_2$, the origin of the $C_3$-unit of **4** remained to be established.[4,5] In order to answer this question, we employed several incorporation experiments. Administration of $^{13}C$- or $^{2}H$-labelled precursors to *M. commelinae*, followed by diazomethane treatment of the extracts, afforded methyl ester **5** which was examined by either $^{13}C$ or $^{2}H$ NMR analysis.

When [1-$^{13}$C]-L-serine was administered, an enhancement of the C-11 signal in the $^{13}C$ NMR spectrum of **5** formed in this experiment was observed. Normalization of the enhanced peak indicates an enrichment of 3.4 atom%. Similarly, after administration of [1-$^{13}$C]-L-alanine, high enrichment (6.3 atom%) at C-1 was observed. Since pyruvate is also incorporated without the loss of the C-1 carbon,[5] these data indicate that serine, alanine and pyruvate are converted to a common intermediate which is directly incorporated into **4**.

Next, a feeding experiment with [U-$^{13}$C]glycerol was conducted. In the $^{13}C$ NMR spectrum of the methyl ester **5** from the feeding experiment, two doublets at δ 166.5 (C-11, *J* 74.5 Hz) and 124.3 (C-6, *J* 60.3 Hz), and a doublet of doublets at δ 131.3 (C-1, *J* 74.5, 60.3 Hz) were observed. Both the splitting and the enrichment of the resonance show that incorporation of the labels, after the cycling of the $C_3$-unit through the tricarboxylic acid (TCA) and pentose-phosphate (PP) cycles, occurs at significant levels (Table 1). The observed coupling of the C-1 signal establishes the intact incorporation of glycerol.




**Scheme 1**

Administration of (1*RS*, 2*S*)- and (1*RS*, 2*R*)-[1-$^{2}$H]glycerols prepared from 1,2;5,6-di-*O*-isopropylidene-D-mannitol[6,7] to *M. commelinae* was then investigated. As expected, only one signal, assigned to 6-H, was observed at δ 7.36 in the spectra of **5** from both experiments. Enrichment of (2*R*)-[$^{2}$H]-glycerol was estimated to be 3.7%. On the other hand, negligible enrichment of $^{2}H$ (0.23%) was found in the case of (2*S*)-[$^{2}$H]glycerol. The results are explained by the intermediacy of the $C_3$-unit as a (2*R*)-3-phosphoglycerate (3-PG) derivative.

In order to obtain information on the origin of the hydrogen atom at C-6, feeding experiments with specifically $^{2}H$-labelled (1*R*, 2*R*)-[1-$^{2}$H]glycerol (58% ee) and (1*S*, 2*R*)-[1-$^{2}$H]glycerol (59% ee)† were conducted. Analysis of **5** formed in these experiments showed that the $^{2}H$-label at C-6 was retained at a 5.5 times higher level in the case of (1*R*, 2*R*)-glycerol compared with (1*S*, 2*R*)-glycerol. The observed selective labelling indicates that the C–C bond formation between the pyrone **3** and the $C_3$-unit is stereoselective, and that the pathway involves an intermediate which has diastereotopic methylene protons.

Intact incorporation of [U-$^{13}$C]glycerol and retention of the 1-$^{13}C$ label in the feeding experiments of L-serine and L-alanine exclude the possibility that TCA intermediates, *i.e.* oxaloacetate, directly convert into **4**. Among the other possible sources of the $C_3$-precursor, the observed results in the feeding experiment with specifically $^{2}H$-labelled glycerols exclude the possibility of the involvement of pyruvate and alanine as the $C_3$-unit. Experimental evidence in this study leaves the most obvious candidate, PEP, as an intact substrate in the novel aromatic ring formation. Since the previous study suggested that PEP was not incorporated into **4**,[5] we initiated a cell-free study. Using **3** and PEP as substrates, enzymatic formation of **4** in the cell-free system was found.‡§ This finding established that macrophomic acid **4** is formed from the pyrone **3** and PEP by the specific enzyme(s).

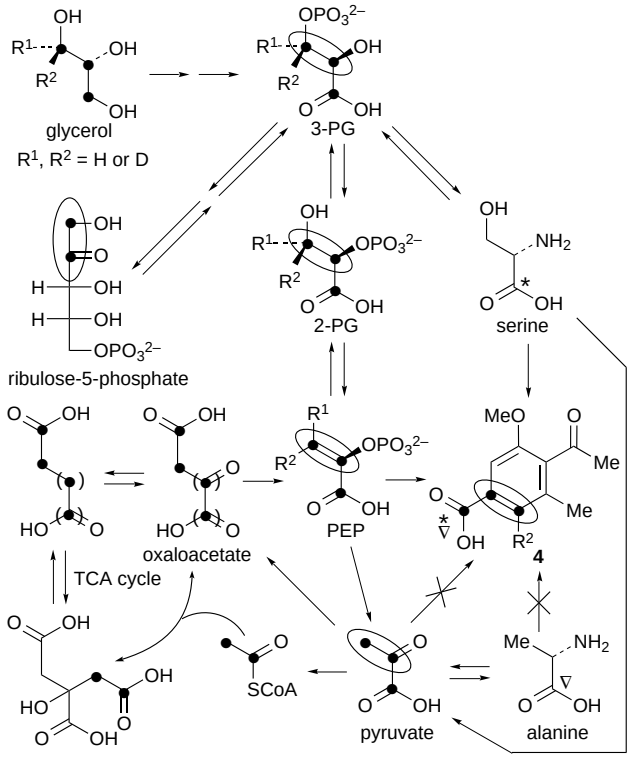
For the biosynthesis of macrophomic acid, Sakurai *et al*. proposed an anion-based condensation of **3** and PEP.[5] On the basis of our experimental data, we propose an alternative pathway for the conversion of **3** to **4**, as shown in Scheme 3. In this pathway, an intermolecular inverse-electron-demand Diels–Alder reaction of the pyrone **3** and the dienophile

**Table 1** Incorporation of $^{13}C$- or $^{2}H$-labelled precursors into **5** in *M. commelinae* in the presence of the pyrone **3**

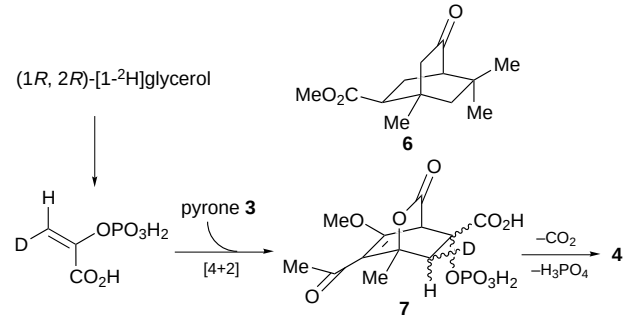
| | | Enrichment | | |
|---|---|---|---|---|
| Entry | Precursor | C-6 | C-1 | C-11 |
| 1 | [1-$^{13}$C]-L-alanine | | | 3.4 |
| 2 | [1-$^{13}$C]-L-serine | | | 6.3 |
| 3 | [U-$^{13}$C]glycerol | 1.9 | 1.6[a] (1.0, 1.9)[b] | 2.9 |
| 4 | (1*RS*, 2*R*)-[1-$^{2}$H]glycerol | 3.7 | | |
| 5 | (1*RS*, 2*S*)-[1-$^{2}$H]glycerol | 0.23 | | |
| 6 | (1*R*, 2*R*)-[1-$^{2}$H]glycerol | 34 | | |
| 7 | (1*S*, 2*R*)-[1-$^{2}$H]glycerol | 7.1 | | |

[a] Enrichment for doublet of doublets. [b] Enrichments for two doublets.

intermediate PEP affords a plausible adduct **7** which is transformed into **4** by successive retro-Diels–Alder reaction and *syn*-elimination of phosphoric acid. Compared with the hypothesis of Sakurai *et al*., our pathway significantly simplifies this unusual conversion. The results in the feeding experiments with (1*R*, 2*R*)- and (1*S*, 2*R*)-[1-$^2$H]glycerols are consistent with the selective retention of $^2$H at C-6 in **5** *via* [3-$^2$H]-PEP. Interestingly, pyrenochaetic acid A **2** was chemically synthesized from pyrenocine A **1** *via* the plausible biomimetic route.[8]




**Scheme 2**




**Scheme 3**

To test this mechanism, the bicyclic compound **6**[9] which mimicked the plausible intermediate **7**, was synthesized. As expected, the intermediate analogue **6** inhibited the enzymatic conversion of **3** (10 μM) and PEP (100 μM) to **4**. The $IC_{50}$ of **6** was determined to be 200 μM. This observation lends further support to our hypothesis, although the anion-based condensation is not rigorously excluded.

Currently, we are working on purifying the enzyme responsible for this unusual biological transformation.

We are grateful to Mr Watanabe and Mrs Fukushi in our department for the acquisition of mass spectra. This work was supported by a Grant-in-Aid from the Ministry of Education, Science, and Culture of Japan.

## Footnotes

† The stereospecifically labelled glycerols were synthesized by Sharpless asymmetric dihydroxylation of deuterium-labelled allyl benzyl ethers. Details will be reported elsewhere.

‡ The crude enzyme was prepared as follows. The mycelium of *M. commelinae* IFO 9570 was cultured under shaking as described by Sakurai *et al*. During preincubation for induction of the desired enzyme, mycelia were collected by filtration and suspended in 50 mM potassium phosphate (0.45% NaCl, pH 7.2) containing a 100 mM DMF solution of pyrone **3** (final concentration 1 mM). This was further incubated under shaking for 3 h. The mycelia were collected by filtration and suspended in the same buffer. The mixture was homogenized with a mortar and pestle. Cell debris was removed by centrifugation (1.207 g, 15 min) and the supernatant was used as a crude enzyme.

§ Reactions were carried out at 30 °C for 4 h in mixtures containing the crude enzyme (1 ml), the pyrone **3** in DMF (10 μl, final concentration 100 μM) and phosphoenolpyruvate in $H_2O$ (10 μl, final concentration 100 μM) in a total volume of 1.02 ml. Denatured enzyme (100 °C, 10 min) was used as a control. HPLC analysis of reaction products was performed with an ODS column (Wakosil-II 5C18, MeCN–$H_2O$, 3 : 2, 1 ml min$^{-1}$, UV 250 nm). Product formation was quantified *via* calibration with a standard. After 4 h, **3** and PEP were completely converted into **4**.

## References

1 H. Sato, K. Konoma and S. Sakamura, *Agric. Biol. Chem.*, 1979, **43**, 2409.
2 H. Sato, K. Konoma, S. Sakamura, A. Furusaki, T. Matsumoto and T. Matsuzaki, *Agric. Biol. Chem.*, 1981, **45**, 795.
3 H. Sato, K. Konoma and S. Sakamura, *Agric. Biol. Chem.*, 1981, **45**, 1675.
4 I. Sakurai, H. Suzuki, S. Shimizu and Y. Yamamoto, *Chem. Pharm. Bull.*, 1985, **33**, 5141.
5 I. Sakurai, H. Miyajima, K. Akiyama, S. Shimizu and Y. Yamamoto, *Chem. Pharm. Bull.*, 1988, **36**, 2003.
6 S. Takano, E. Goto, M. Hirama and K. Ogasawara, *Heterocycles*, 1981, **16**, 381.
7 S. Takano, K. Seya, E. Goto, M. Hirama and K. Ogasawara, *Synthesis*, 1983, 116.
8 A. Ichihara, K. Murakami and S. Sakamura, *Tetrahedron*, 1987, **43**, 5245.
9 R. A. Lee, *Tetrahedron Lett.*, 1973, 3333.

*Received, 10th June 1996; revised manuscript received 31st October 1996; Com. 6/07412J*

# Novel anion binding selectivity trends exhibited by new dinuclear rhenium(I), ruthenium(II) and osmium(II) bipyridyl cleft-type receptors

**Paul D. Beer,*[a]† Simon W. Dent,[a] Gerald S. Hobbs[a] and Trevor J. Wear[b]**

[a] *Inorganic Chemistry Laboratory, South Parks Road, Oxford, UK OX1 3QR*
[b] *Kodak Ltd, Headstone Drive, Harrow, Middlesex, UK HA1 4TY*

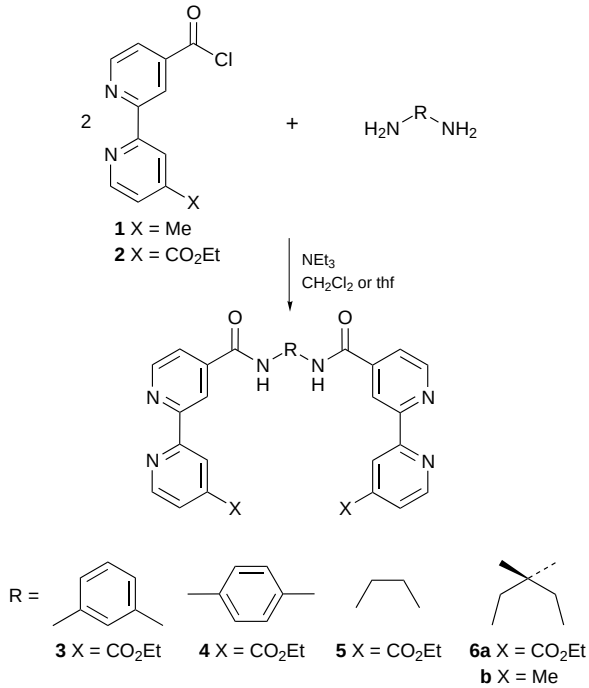
**Novel dinuclear rhenium(I), ruthenium(II) and osmium(II) bipyridyl cleft-type receptor systems exhibit remarkable selectivity for dihydrogenphosphate over halide anions dictated by the nature of the bridging linkage and the transition-metal Lewis-acidic centre.**

Anions are of crucial importance in many essential chemical and biochemical processes and therefore their binding and recognition is presently the subject of intensive research.[1] To date, a number of research groups have designed and synthesised anion binding reagents that use either favourable hydrogen-bonding interactions alone,[2,3] or hydrogen-bonding interactions in conjunction with electrostatic forces[4–6] to coordinate and, in some instances, sense anions. Examples of the latter which have been particularly successful in this respect are amide containing cobaltocenium[7,8] and ruthenium(II) polypyridyl molecules.[9–11] In an effort to enhance selective anion recognition through the design of new cooperative polymetallic Lewis-acidic systems, we report here the synthesis of novel dinuclear transition-metal bipyridyl, cleft-type receptors whose remarkable selectivity for the dihydrogenphosphate anion over halide anions is profoundly influenced by the nature of the bridging linkage, and the electronic character of the transition-metal Lewis-acidic centre.

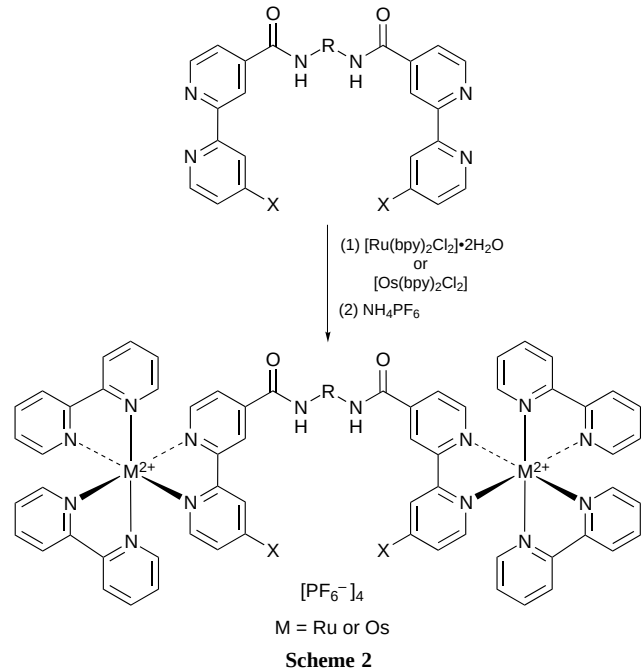
The reaction of 4-carboxy-4′-methyl-2,2′-bipyridine[12] or 4-carbonyl-4′-ethoxycarbonyl-2,2′-bipyridine[13] with thionyl chloride afforded the acid chlorides **1** and **2** respectively in quantitative yields. The condensation of 2 equiv. of **1** or **2** with 1 equiv. of diamine in dichloromethane solution afforded the new 'cleft'-type bipyridyl (bpy) ligands **3**–**6** in excellent yields (Scheme 1). The free ligands were chelated to the positively charged $[M(bpy)_2]^{2+}$ fragment (M = Ru, Os) unit by reaction with either 2 equiv. of *cis*-$[Ru(bpy)_2Cl_2]\cdot 2H_2O$[14] or *cis*-$[Os(bpy)_2Cl_2]$[15] in ethanol–water–acetic acid. The mixed ruthenium–osmium receptor, Ru–**6b**–Os, was prepared by reaction of ligand **6b** with 1 equiv. of *cis*-$[Ru(bpy)_2Cl_2]\cdot 2H_2O$, followed by 1 equiv. of *cis*-$[Os(bpy)_2Cl_2]$. The crude products were purified by column chromatography on Sephadex LH-20 and converted to the hexafluorophosphate salts with an excess of aqueous $NH_4PF_6$ (Scheme 2). The rhenium(I) receptor, Re–**6b**–Re, was prepared by reaction of the free ligand **6b** with 2 equiv. of $[Re(CO)_5Br]$ in thf and purified by recrystallisation from acetone–diethyl ether (Scheme 3).‡

Proton NMR titration experiments with $Cl^-$ and $H_2PO_4^-$ anions were carried out in $(CD_3)_2SO$ solution and revealed significant downfield shifts in the receptors' amide and 3,3′-bpy protons. For example, the amide protons of Ru–**6b**–Ru were perturbed by 0.93 ppm and the 3,3′-bpy protons by 0.84 ppm after the addition of an excess of tetrabutylammonium dihydrogenphosphate. In all cases the resulting titration curves (for example, Fig. 1) suggest complexes with a 1 : 1 receptor : anion stoichiometry are formed in solution. Stability constants were calculated from the titration data using the EQNMR computer program[16] and the values are presented in Table 1.§

Clearly the nature of the bridging linkage has a dramatic influence on the anion binding strength and selectivity these dinuclear cleft-type receptors display. Of particular note is the

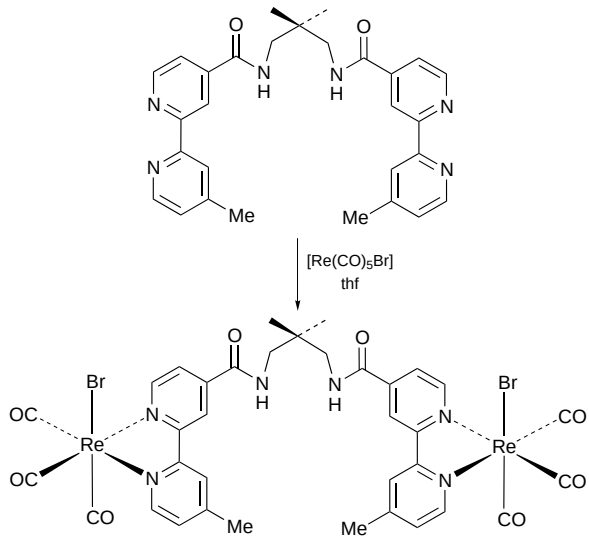



**Scheme 1**




**Scheme 2**

remarkable increase in the magnitude of stability constant of $H_2PO_4^-$ that results from simply altering the linkage from *m*-phenylene Ru–**3**–Ru ($K$ = 55 M$^{-1}$) to *p*-phenylene Ru–**4**–Ru ($K$ = 4320 M$^{-1}$), with the halide stability constant values remaining virtually unchanged. In addition, whereas the ethyl-bridged receptor Ru–**5**–Ru forms an extremely weak complex with $H_2PO_4^-$ and is $Cl^-$ selective, the 2,2′-dimethyl-1,3-propane-bridged analogue, Ru–**6a**–Ru forms an extremely strong and selective complex with $H_2PO_4^-$. Comparing Ru–**6a**–Ru and Ru–**6b**–Ru, it is also of interest to note there is a significant 4′-bipyridyl substituent effect, with $H_2PO_4^-$ anions favouring the ester containing receptor and chloride the methyl containing one.




**Scheme 3**

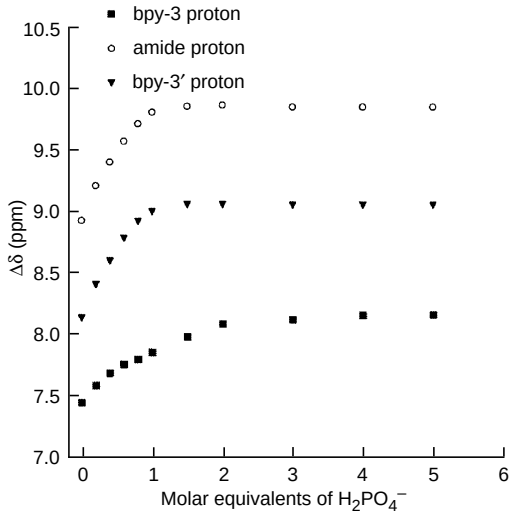



**Fig. 1** $^1$H NMR titration curve of Ru–**6b**–Ru with $NBu_4H_2PO_4$ in $(CD_3)_2SO$

**Table 1** Stability constant data for dinuclear cleft-anion receptors in $(CD_3)_2SO$

| Receptor | $K$ ($Cl^-$)[a,b]/ M$^{-1}$ | $K$ ($Br^-$)[a,b]/ M$^{-1}$ | $K$ ($H_2PO_4^-$)[a,b]/ M$^{-1}$ |
|---|---|---|---|
| Ru–**3**–Ru | 25 | 45 | 55 |
| Ru–**4**–Ru | 55 | 40 | 4320 |
| Ru–**5**–Ru | 70 | 60 | 10 |
| Ru–**6a**–Ru | 245 | 170 | 19700 |
| Re–**6b**–Re | 120 | —[c] | 1820 |
| Ru–**6b**–Ru | 310 | 220 | 15480 |
| Ru–**6b**–Os | 440 | —[c] | 22150 |
| Os–**6b**–Os | 825 | —[c] | > 30000 |

[a] Average for amide and bpy protons. [b] Errors estimated to be < 10%. [c] Not calculated.

Table 1 also demonstrates that the nature of the bipyridyl-coordinated transition-metal centre strikingly dictates the strength and degree of anion recognition selectivity. With both $H_2PO_4^-$ and $Cl^-$ anionic guest species the stability constants increase in magnitude in the order Re–**6b**–Re < Ru–**6b**–Ru < Ru–**6b**–Os < Os–**6b**–Os. From electrostatic considerations it is perhaps not surprising the neutral bis-rhenium(I) receptor forms the relatively weaker anion complexes. However, what is unexpected is the dramatic increase in magnitude of stability constant for the osmium-containing receptors, especially in respect to $H_2PO_4^-$ complexation. This observation suggests the $(bpy)_2Os^{2+}$ moiety is a particularly efficient Lewis-acidic centre to incorporate into this new cleft-type class of transition-metal bipyridyl amide anion receptor.

We thank Kodak Ltd for a studentship (S. W. D.) and Johnson Matthey for the generous loan of ruthenium and osmium salts.

## Footnotes

† E-mail: beer%server.icl.@ox.ac.uk
http://www.ncl.ox.ac.uk/icl/beer.html

‡ All new compounds were fully characterised by elemental analysis, $^1$H and $^{13}$C NMR and FABMS.

¶ The addition of chloride or dihydrogenphosphate anions to $(CD_3)_2SO$ solutions of $[M(bpy)_3)][PF_6]_2$ (M = Ru, Os) had no effect on the $^1$H NMR spectrum. The metal-free bipyridyl ligands exhibited extremely weak and insignificant interactions with both chloride and dihydrogenphosphate anions in $(CD_3)_2SO$.

## References

1 B. Dietrich, *Pure Appl. Chem.*, 1993, **65**, 1457.
2 A. M. Kelly-Rowley, V. M. Lynch and E. V. Ansyln, *J. Am. Chem. Soc.*, 1995, **117**, 3438.
3 P. A. Gale, J. L. Sessler, V. Král and V. Lynch, *J. Am. Chem. Soc.*, 1996, **118**, 5140.
4 P. D. Beer, C. A. Dickson, N. C. Fletcher, A. J. Goulden, A. Grieve, J. Hodacova and T. J. Wear, *J. Chem. Soc., Chem. Commun.*, 1993, 828.
5 V. Král, A. Andrievsky and J. L. Sessler, *J. Am. Chem. Soc.*, 1995, **117**, 2953.
6 N. Ohata, H. Masuda and O. Yamauchi, *Angew. Chem., Int. Ed. Engl.*, 1996, **35**, 531.
7 P. D. Beer, C. Hazelwood, D. Hesek, J. Hodacova and S. E. Stokes, *J. Chem. Soc., Dalton Trans.*, 1993, 1327.
8 P. D. Beer, M. G. B. Drew, A. R. Graydon, D. K. Smith and S. E. Stokes, *J. Chem. Soc., Dalton Trans.*, 1995, 403.
9 P. D. Beer, S. W. Dent and T. J. Wear, *J. Chem. Soc., Dalton Trans.*, 1996, 2341.
10 F. Szemes, D. Hesek, Z. Chen, S. W. Dent, M. G. B. Drew, A. J. Goulden, A. R. Graydon, A. Grieve, R. J. Mortimer, J. S. Weightman and P. D. Beer, *Inorg. Chem.*, 1996, **35**, 5868.
11 M. S. Goodman, V. Jubian and A. D. Hamilton, *Tetrahedron Lett.*, 1995, **36**, 2551.
12 D. G. McCafferty, B. M. Bishop, C. G. Wall, S. G. Hughes, S. L. Mecklenberg, T. J. Meyer and B. W. Erickson, *Tetrahedron*, 1995, **51**, 1093.
13 G. Vériot, J.-P. Dutasta, G. Matouzenko and A. Collet, *Tetrahedron*, 1995, **51**, 389.
14 B. P. Sullivan, D. J. Salmon and T. J. Meyer, *Inorg. Chem.*, 1978, **17**, 3334.
15 P. A. Lay, A. M. Sargeson and H. Taube, *Inorg. Synth.*, 1986, **24**, 291.
16 M. J. Hynes, *J. Chem. Soc., Dalton Trans.*, 1993, 311.

*Received, 17th October 1996; Com. 6/07086H*

# Design of an SHG-active crystal, 4-iodo-4′-nitrobiphenyl: the role of supramolecular synthons

**Jagarlapudi A. R. P. Sarma,*[a] Frank H. Allen,[b] Vanessa J. Hoy,[c] Judith A. K. Howard,[c] Ram Thaimattam,[d] Kumar Biradha[d] and Gautam R. Desiraju*[d]**

[a] *Physical and Inorganic Chemistry Division, Indian Institute of Chemical Technology, Hyderabad, 500 007, India*
[b] *Cambridge Crystallographic Data Centre, 12 Union Road, Cambridge, UK CB2 1EZ*
[c] *Department of Chemistry, University of Durham, South Road, Durham, UK DH1 3LE*
[d] *School of Chemistry, University of Hyderabad, Hyderabad 500 046, India*

**The crystal structure of 4-iodo-4′-nitrobiphenyl has been determined with packing calculations and the presence of polar and parallel iodo···nitro supramolecular synthons leads to non-centrosymmetry and measurable SHG activity**

We have, in previous publications, described the identification of the I···O mediated, iodo···nitro supramolecular synthon **1** and its use in retrosynthetically guided supramolecular synthesis.[1–3] We conclude from this earlier work that: (*i*) synthon **1** is a polarisation-based structural unit; (*ii*) **1** is reasonably robust and as such it can be employed reliably in the design of new crystal structures. Here, we show that these ideas can be further extended to the design of an organic crystal with the property of second harmonic generation (SHG).

Synthon **1** can be used as a linear extender and so the ribbon structures of 4-iodonitrobenzene **2** and the 1 : 1 complex **3** of 1,4-diiodobenzene and 1,4-dinitrobenzene are not hard to anticipate.[1,2] However, these structures are centrosymmetric and therefore not viable for SHG applications. In **3**, the constituent molecules are themselves centrosymmetric, while in **2** the polar ribbon pattern is stacked in an antiparallel fashion leading to centrosymmetry. This is a general problem and our inability to control tertiary structural features, such as parallel *vs.* antiparallel stacking of polar structural units, is a major challenge in the practice of crystal engineering.

In order to design a non-centrosymmetric crystal, we decided to introduce the iodo and nitro substituents on a biphenyl framework and 4-iodo-4′-nitrobiphenyl **4** was prepared according to literature procedures.[4] While we were reasonably sure that **4** would yield a ribbon structure like **2** and **3**, a twisted and therefore chiral molecular conformation was further anticipated in view of the known structural chemistry of the biphenyls.[5] Finally, it was hoped that the (microscopic) molecular chirality of the twisted biphenyls units would lead to (macroscopic) crystal chirality.[6,7] There is some precedent for this, for in many classes of molecules, chiral sub-structural units (say helices) of the same handedness pack better than those of opposite handedness.[8] In any case, our optimism was furthered when we noted that crystals of **4** were obtained in the *F*-centred orthorhombic system, because the most common space group here, *Fdd*2 is non-centrosymmetric. Crystals of **4** seemingly suitable for X-ray diffraction analysis were obtained by recrystallisation. In fact crystals of two different morphologies were obtained; long needles from benzene and prisms from nitromethane. However, both forms have the same cell parameters and space groups and single-crystal data were collected.†

At this stage, a problem arose. The structure failed to solve despite all reasonable attempts and it was decided to attempt structure solution with packing energy calculations. The Cerius[2] program from molecular simulations was used.[9] The starting points were the experimental unit cell ($a$ = 8.06, $b$ = 18.812, $c$ = 14.364 Å) and the measured crystal density of 1.98 g cm$^{-3}$ which together indicate that $Z$ = 8. Accordingly, the more likely space group is *Fdd*2 with the molecules bisected by [001], the twofold direction. Molecular optimisation with MOPAC[10] (AM1 Hamiltonian) gave a non-planar conformation which was used in the crystal optimisation with the crystal packer module of the Cerius[2] program. The structure rapidly moved into an energy minimum. The molecule was free to rotate about [001] during the minimisation and no effort was made to refine the unit cell. The final structure of **4** is shown in Fig. 1 and the final simulated X-ray powder pattern agrees very well with the experimentally recorded pattern (Fig. 2). In retrospect, it appears that all the crystals chosen for single-crystal data collection were flawed. Even when the coordinates obtained by

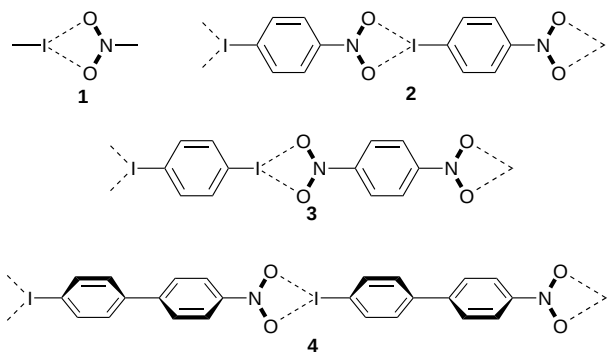


**Fig. 1** Stereoview of a molecular layer of 4-iodo-4′-nitrobiphenyl **4** as obtained by its crystal structure simulation. Notice the parallel arrangement of polar iodo···nitro synthons.

simulation were used in least-squares refinement, such refinements were unsatisfactory. The *R* values routinely fell to below 0.05, but the atomic displacement parameters were generally unacceptable. Alternative disordered or twinned structures in both *Fdd*2 and the alternative *Fddd* were considered but showed no improvement in the fit of the model to the data.

The appearance of the simulated diffraction pattern was found to depend on the assumed particle size along the three crystallographic directions and the value chosen were 300, 600 and 50 Å. These numbers were not picked at random but were obtained from an inspection of Fig. 1. The more numerous herringbone interactions along [100] and [010] were expected to lead to larger values of the particle size in these directions. Yet, the efficacy of the interactions (in effect, the growth rates) appear to be the same along either [100] or [010]. Therefore, noting the relative values of the *a* and *b* parameters, the particle size along [100] was taken, somewhat subjectively, to be half that along [010]. These considerations are important because it was found that the appearance of the spectrum is quite sensitive to the particle size chosen, though naturally the peak positions themselves do not change during these operations.

It may be noted from Fig. 1 that all the iodo···nitro synthons **1** in the structure of **4** are parallel, leading to macroscopic crystal polarity. Preliminary SHG measurements ($Nd^{3+}$/YAG laser, 1064 nm) indicate that crystalline **4** is SHG active. A higher initial activity falls rapidly because of material decomposition in the laser beam and the final activity is in the region of six times that of urea. More interestingly, the calculated molecular hyperpolarisability β is only $4.3 \times 10^{-36}$ esu. This observation hints that the crystal SHG has contributions also from the polarisation-based synthons, **1**. It is important to note that supramolecular synthons as defined previously,[3] not only have structural connotations but also are relevant to crystal properties. Many useful crystal properties are a consequence of molecular and supramolecular structure. It is therefore not surprising that supramolecular hyperpolarisability as manifested in synthons such as **1** is important and should be considered in studies of SHG materials.

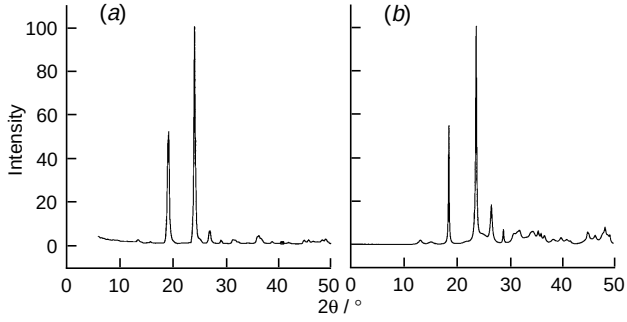



**Fig. 2** Experimental (*a*) and simulated (*b*) X-ray powder spectra of biphenyl **4**. These plots were obtained with the Cerius² program.

This study shows that: (*i*) the principles of supramolecular retrosynthesis may be combined with molecular engineering techniques to obtain non-centrosymmetric crystal structures; (*ii*) supramolecular synthons such as **1** are structural units that are also of relevance in determining the magnitude of SHG activity because they can contribute to supramolecular hyperpolarisability; (*iii*) the use of simulation software is a valuable alternative method of crystal structure determination when single-crystal X-ray diffraction methods prove problematic, and if partial crystallographic information, such as cell parameters and space group, is available.

We thank Molecular Simulations (Cambridge) for their support, Dr D. Narayana Rao and Dr A. Nangia for useful discussions and Mr. Y. Chandrasekhar for carrying out the SHG measurements. R. T. thanks UGC for financial assistance.

## Footnote

† Atomic coordinates have been deposited at the Cambridge Crystallographic Data Centre (CCDC). See Information for Authors, Issue No. 1. Any request to the CCDC for this material should quote the full literature citation and the reference number 182/309.

## References

1 F. H. Allen, B. S. Goud, V. J. Hoy, J. A. K. Howard and G. R. Desiraju, *J. Chem. Soc., Chem. Commun.*, 1994, 2729.
2 V. R. Thalladi, B. S. Goud, V. J. Hoy, F. H. Allen, J. A. K. Howard and G. R. Desiraju, *Chem. Commun.*, 1996, 401.
3 G. R. Desiraju, *Angew. Chem., Int. Ed. Engl.*, 1995, **34**, 2311.
4 J. Harley-Mason and F. G. Mann, *J. Chem. Soc.*, 1940, 1379.
5 C. P. Brock and G. L. Morelan, *J. Phys. Chem.*, 1986, **90**, 5631.
6 J. A. R. P. Sarma, M. S. K. Dhurjati, K. Ravikumar and K. Bhanuprakash, *J. Chem. Soc., Chem. Commun*., 1993, 440.
7 G. R. Desiraju and T. S. R. Krishna, *J. Chem. Soc., Chem. Commun.*, 1988, 192.
8 C. P. Brock, W. B. Schweizer and J. D. Dunitz, *J. Am. Chem. Soc.*, 1991, **113**, 9811.
9 Cerius² Program, BIOSYM/Molecular Simulations, 9685 Scranton Road, San Diego, CA 92121-3752, USA, and 240/250 The Quorum, Barnwell Road, Cambridge, UK CB5 8RE.
10 M. J. S. Dewar, E. G. Zoebisch, E. F. Healy and J. J. P. Stewart, *J. Am. Chem. Soc.*, 1985, **107**, 3902.

*Received, 12th July 1996; Com. 6/05044A*

# A styrylpyridinium salt in aqueous solution: unusual solution behaviour

**N. J. Crowther and D. Eagland***

*School of Pharmacy–Pharmaceutical Chemistry, University of Bradford, Bradford, UK BD7 1DP*

**The results of a series of physico-chemical experiments are presented which show that 4-(4-formylphenylethenyl)-1-methylpyridinium methanesulfonate, one example of a styrylpyridinium salt, undergoes a micellar type aggregation as a function of concentration in aqueous solution.**

The photosensitivity of the styrylpyridinium group was first reported by Williams and coworkers,[1,2] subsequently photoreactive styrylpyridinium salts have achieved widespread use in the production of photoresists for screen printing, since their use in this role was first patented by Ichimura and coworkers in 1988.[3,4] The reported mode of action of such salts is by an acid-catalysed aldol condensation reaction with the polymer poly(vinyl alcohol), and subsequently a photoinduced dimerisation, using UV light, of the attached pendant styrylpyridinium groups on adjacent polymer molecules.

Several papers have since been published[5–7] on various aspects of the fundamental photodimerisation reaction of styrylpyridinium, and related compounds, in solution and in the crystal form,[8,9] and of photodimerisation following the solubilisation of these compounds into micellar materials such as aerosol OT[10] but, as far as we are aware, nothing has been reported on the physico-chemical behaviour of such compounds in aqueous solution.

The structure of a molecule of the styrylpyridinium type is such that we considered that unusual aqueous solution behaviour might be expected, thus we report here a series of physico-chemical studies of one such compound, 4-(4-formylphenylethenyl)-1-methylpyridinium methylsulfonate, SbQ, in aqueous solution.

The sample of SbQ was kindly supplied by Sericol plc, purified by a recrystallisation procedure, with a quoted purity of better than 99.5% m/m, which was confirmed by the lack of a minimum in the observed surface tension data. Density measurements were made using previously reported techniques[11] and had a precision of $1 \times 10^{-4}$ kg m$^{-3}$; the microcalorimetric measurements, also using previously reported procedures,[12] had a precision of $1 \times 10^{-7}$ J. Surface tension measurements were undertaken using a drop profile measurement procedure, developed in this laboratory, with a precision of ±0.05 mN m$^{-1}$. Light-scattering measurements were made using a Sofica photogoniometer, model 42 000, modified to use a Uniphase 1 mW He–Ne laser, operating at 543 nm. Vapour-pressure measurements were made with a Knauer vapour-pressure osmometer, standardised against Analar NaCl solutions. Heats of dilution measurements were carried out using an LKB flow microcalorimeter, model 2107-121/127.

The vapour-pressure measurements, obtained at 37 °C, are presented in Fig. 1, where the ratio $\Delta t/c$ represents the difference in temperature between the solvent reference probe and the solution probe at a concentration $c$ in g kg$^{-1}$. The plot shows two linear regions, both with good correlation coefficients of 0.996 and 0.998, intersecting at a concentration value of 1.25% m/m. The intercept of the low range of solution concentrations was utilised in the usual manner to determine a value for the number average molar mass for SbQ of 341, close to the expected value of 335. The difference of slope at the higher concentrations suggests that, above the concentration of 1.25% m/m, some form of aggregation has occurred.

An analysis of the energy of the structure of the SbQ molecule, minimised in water, was performed, using a Hyperchem molecular modelling package, based on MM+ force-field calculations,[13] which produced a very planar structure. Such a structure for the molecule easily allows for the possibility of stacking of the molecules with the hydrophobic regions one above the other, with the aldehyde and NMe groups alternating, to produce an aggregate, shown energy minimised in water for four space-filled SbQ molecules in Fig. 2.

Taking the difference between the intercepts in Fig. 1 for the two concentration regions as being due to the aggregate, this yields a molar mass for the SbQ aggregate of about 2800, suggesting that the aggregate stack consists of about eight monomer units, with a critical concentration for the change of 1.25% m/m, close to 0.04 M

Surface tension measurements, as a function of concentration, for a series of solutions of SbQ, at 25 °C, are shown in Fig. 3; the pattern seen is the classic one for micellisation of a surfactant with the break occurring at about 0.06 M. This evidence therefore suggests that the SbQ aggregate is in fact a stacked rod-like micelle, with a c.m.c. value of 0.04 to 0.06 M, depending on the experimental measurement. The somewhat

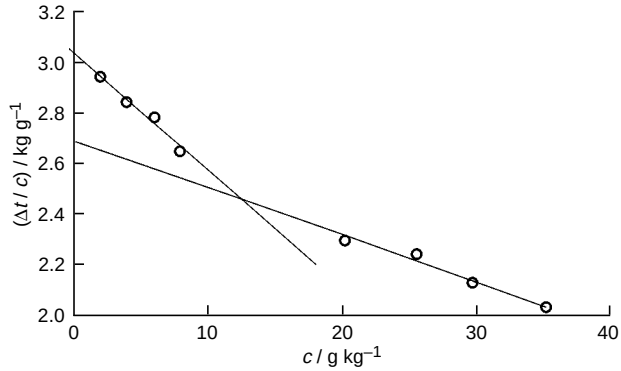



**Fig. 1** Vapour-pressure measurements on solutions of SbQ, at 37 °C, as a function of concentration

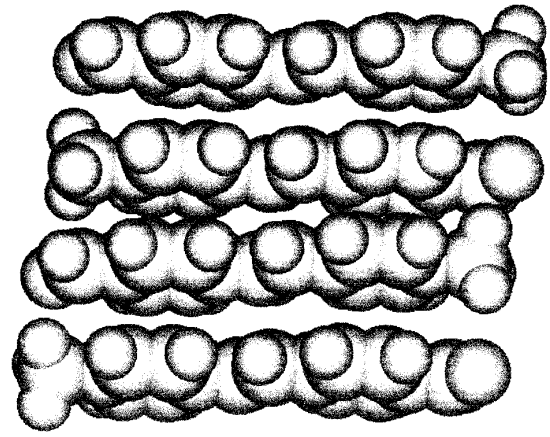


**Fig. 2** Energy-minimised structure of an SbQ aggregate in water

high equilibrium value of the surface tension, at 51 mN $m^{-1}$, is possibly due to the strongly hydrophilic groups present at each end of the molecule.[14]

Values of the apparent molar volume of the SbQ molecule, obtained from the density measurements at 25 °C, are also shown in Fig. 3; the sharp change of slope seen at 0.04 M means that the SbQ molecule adopts a more compact form above this concentration, exactly what might be expected to happen when aggregating to form a micelle. Such a change of slope at the c.m.c. of a surfactant has been reported by Perron *et al.*[15]

Values for the Rayleigh scattering at an angle of 90°, measured at a temperature of 25 °C, as function of concentration, are shown in Fig. 3; the sharp increase in scattering which occurs at concentrations approaching 0.04 M indicates the appearance of larger particles, the micelles in fact.

Heats of dilution measurements, at 25 °C, as a function of the initial concentration of the solution, Fig. 3, also show a sharp change of slope, in this case at 0.035 M, yet again indicating a major change in the solution state of the solute, from monomer to micelle[15] has occurred.

In conclusion, the close correlation between the concentration dependence behaviour of all the experimental measurements is good confirmation of the existence of a monomer–micelle equilibrium in the aqueous solutions of SbQ.

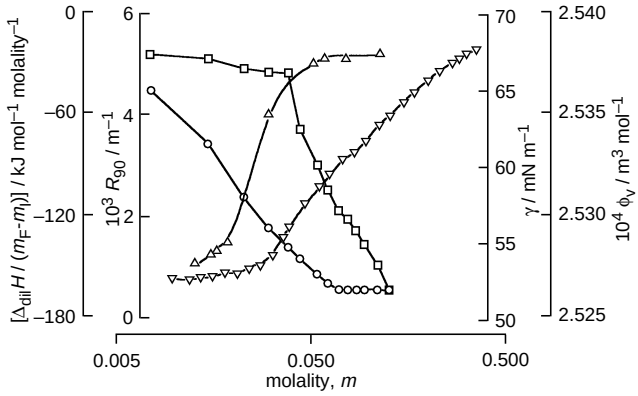



**Fig. 3** Surface tension measurements (○), apparent molar volume values (□), Raleigh scattering values at 90° (△) and heats of dilution (▽) of SbQ solutions at 25 °C, as a function of concentration

The SbQ molecule is one example of quite a large group of styrylpyridinium and styrylquinolinium compounds, all of similar structure; it is therefore very likely that, in general, compounds of this type will exhibit similar micellar behaviour. With regard to the broader implications of this behaviour, we are grateful to one of the referees for drawing our attention to the work of Tiddy *et al.*[16,17] who have reported what may be similar stacked aggregates in dilute aqueous solutions of azo and cyan dyes.

## References


1 D. G. Borden and J. L. R. Williams, *Makromol. Chem.*, 1964, **73**, 203.
2 J. L. R. Williams and D. G. Borden, *Makromol. Chem.*, 1977, **178**, 3053.
3 K. Ichimura, *UK Pat.* GB 2 030 575 B, 1978.
4 K. Ichimura, M.Ito, M. Yamana and H. Ito, *US Pat.* 4 777 114, 1988.
5 K. Ichimura, *Makromol. Chem*., 1987, **188**, 2973.
6 K. Ichimura and N. Oohara, *J. Polym. Sci.: Part A, Polym. Chem*., 1987, **25**, 3064.
7 M. Y. Li, E. M. Pearce, A. Reiser and S. Narang, *J. Polym. Sci.: Part A, Polym. Chem.*, 1988, **26**, 2517.
8 M. Hasegawa, K. Saigo, T. Mori, H. Uno, M. Nohara and H. Nakanishi, *J. Am. Chem. Soc.*, 1985, **107**, 2788.
9 M. Hasegawa, H. Arioka, H. Harashina, M. Nohara, M. Kubo and T. Nishikubo, *Isr. J. Chem.*, 1985, **25**, 302.
10 K. Takagi, B. R. Suddaby, S. L. Vadas, C. A. Backer and D. G. Whitten, *J. Am. Chem. Soc.*, 1986, **108**, 7865.
11 F. F. Vercauteren, W. A. B. Donners, N. J. Crowther and D. Eagland, *Eur. Polym. J.*, 1987, **23**, 711.
12 D. Eagland, N. J. Crowther and C. J. Butler, *Polymer*, 1993, **34**, 2804.
13 U. Burkert and N. L. Allinger, *Mol. Mech., ACS Monogr*., 1982, **177**.
14 A. R. Pitt, S. D. Morley, N. J. Burbridge and E. L. Quickenden, *Colloids Surf. A: Physicochem. Eng. Aspects*, 1996, **114**, 321.
15 G. Perron, F. Yamashita, P. Martin and J. E. Desnoyers, *J. Colloid Interface Sci.*, 1991, **144**, 222.
16 G. J. T. Tiddy, D. L. Mateer, A. P. Ormerod, W. J. Harrison and D. J. Edwards, *Langmuir*, 1995, **11**, 390.
17 W. J. Harrison, D. L. Mateer and G. J. T. Tiddy, *J. Phys. Chem.*, 1996, **100**, 2310.


*Received, 27th September 1996; Com. 6/06605D*

# Remarkable oxygen promotion of the selective reduction of nitric oxide by hydrogen over Au/NaY and Au/ZSM-5 zeolite catalysts

**Tarek M. Salama,† Ryuichiro Ohnishi and Masaru Ichikawa***

*Catalysis Research Center, Hokkaido University, Sapporo 060, Japan*

**A significant enhancement of the selective reduction of nitrogen oxide by $H_2$ is produced in the presence of oxygen over Au/NaY and Au/ZSM-5 catalysts by forming $NO_2$ and $N_2O_4$ intermediates, which are eventually reduced to $N_2$.**

More efficient engine performance would be desirable by using higher air–fuel ratios than those permitted by the 'window' required for conventional three-way catalysts.[1] Thus, there is much interest in the $O_2$-assisted reduction of nitric oxide by hydrocarbons such as methane and propane on Cu/ZSM-5[2] and Pt, Co, Ni and Fe exchanged ZSM-5;[3] however, synergism effected by added oxygen in NO decomposition and reduction with hydrocarbons has not been observed. Although gold has been recognized to be poorly active as a catalyst, Haruta *et al.*[4] have recently found that highly dispersed Au particles on $\alpha$-$Fe_2O_3$ and $Co_3O_4$ exhibit high activity for CO and $H_2$ oxidation at low temperatures. Recently, we reported the catalytic reduction of NO by CO[5] and $H_2$[6] over Au/NaY. Interestingly, the NO + CO reaction did proceed marginally at lower temperatures, *e.g.* 473–623 K, while adding $H_2$ significantly promoted the reaction on Au/NaY, where it assisted N–O dissociation with the formation of the intermediate NCO (with characteristic IR bands at 2280–2240 $cm^{-1}$).[5] The intermediate was converted into $N_2$ and $CO_2$ by interactions with NO in the gas phase. Here, we describe for the first time the remarkable enhancement of the selective reduction of NO by $H_2$ in the presence of oxygen over Au/NaY and Au/ZSM-5. The possible mechanism of $O_2$-assisted NO reduction by $H_2$ was also studied by means of *in situ* FTIR in order to identify the intermediates formed.

Au/NaY (Si/Al = 5.6; Linde, LZY-52, surface area 900 $m^2\ g^{-1}$) and Au/ZSM-5 (Si/Al = 23.8; Tosoh Co. Ltd, surface area 1000 $m^2\ g^{-1}$) samples were prepared by vaporization of $AuCl_3$ (Strem Chemical, 99% purity) into each zeolite, according to the monolayer dispersion technique.[7] The resulting $AuCl_3$ encapsulated in NaY or ZSM-5 was evidently reduced to AuCl by the extraframework hydroxy groups in the zeolites upon thermal treatment in vacuum at 338 K for 24 h. The catalysts contained 5% *m*/*m* Au, according to ICP analysis, and were characterized by EXAFS, XPS and XRD techniques.[7,8]

The catalytic performances in the reduction of nitric oxide by hydrogen in the presence and absence of oxygen were studied at atmospheric pressure in the steady-state flow mode. Four streams of NO–He, $H_2$, $O_2$ and He were supplied by mixing in a chamber using mass flow controller units to obtain a feed-gas mixture of 1375 ppm NO, 1.5% $H_2$ and 0.09–0.7% $O_2$ balanced with He at a total flow rate of 28 ml $min^{-1}$. Each catalyst (100 mg) was charged in a Pyrex glass tubular reactor. The stoichiometry of the feed stream was defined by $S$ = ([NO] +2[$O_2$])/[$H_2$] at zero time. The reactor effluent gas was sampled and analysed by on-line gas chromatography equipped with a thermal conductivity detector, using molecular sieve 5A and porapak-Q columns. Prior to the NO– $H_2$–$O_2$ reaction, the catalyst was reduced in a flowing gas mixture of 10% $H_2$ in He at 623 K. The catalytic activity was expressed in terms of percentage conversion of NO to $N_2$ as a function of the reaction time and $S$.

The selective reduction of NO by $H_2$ into $N_2$ proceeded in the temperature range 373–673 K over Au/NaY and Au/ZSM- 5. As shown in Fig. 1, the NO conversion to $N_2$ was markedly enhanced by 5–10 times by the addition of oxygen (0.2 % *v*/*v*) in the feed stream. Therefore, oxygen in the reaction gas stream plays a synergetic role in the NO–$H_2$ reaction. All the runs showed almost analogous trends of promotion by adding oxygen. The effect is greater on Au/NaY (*a*) than for Au/ZSM-5 (*b*) at the same oxygen level. The data militate against the claim that Cu/ZSM-5 is better than Cu/NaY for the oxygen promotion in NO reduction by hydrocarbons.[9] Control transient response experiments with pulse addition of $O_2$ into an NO–$H_2$ stream revealed that the differences in NO conversions obtained are related to competing reactions of NO and $H_2$ with $O_2$ over the gold catalysts. The oxygen promotion was linearly proportional to the oxygen concentration (0.09–0.21 %). After 2 h reaction time, the oxygen supply was turned off which resulted in a dramatic loss of the NO conversion (Fig. 1).

In the presence of $O_2$, NO reduction by hydrogen selectively goes to $N_2$ formation and neither $NH_3$ nor $N_2O$ were detected over Au/NaY and Au/ZSM-5 catalysts in the effluent stream at the outlet. By contrast, Hastvan *et al.*,[10] have reported for the same reaction over Pd-$MoO_3$/$\gamma$-$Al_2O_3$ catalysts that $NH_3$ and $N_2O$ are the major products. It has also been observed[11] that a better $N_2$ selectivity in the NO reduction by hydrogen is achieved by combining precious metals (Pt, Pd and Rh) and transition-metal oxides on $Al_2O_3$.

To gain insight into the mechanism of oxygen promotion in the selective NO redution by hydrogen, *in situ* FTIR studies were performed over Au/NaY and Au/ZSM-5 samples. *In situ* IR absorption spectra were recorded over the temperature range 474–573 K. A self-supporting wafer was placed in an IR cell

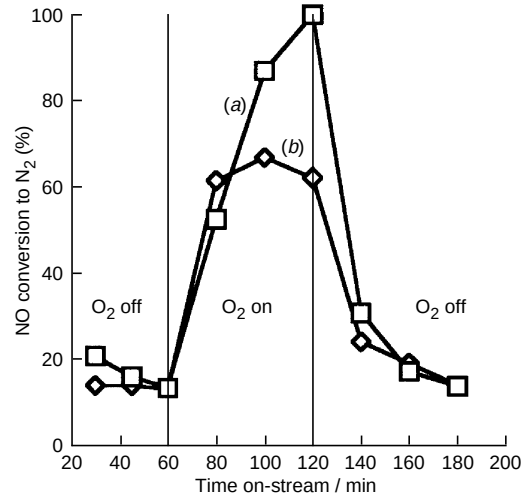



**Fig. 1** NO conversion (mol%) to $N_2$ as a function of time and $O_2$ (0.2% *v*/*v*) switch on–off in the NO (0.14% *v*/*v*)–$H_2$(1.5% *v*/*v*) flow mode reaction (flow rate = 28 ml $min^{-1}$) over Au/NaY (5% mass Au loading) (*a*) and Au/ZSM-5 (5% mass Au loading) (*b*) at 523 K, respectively

equipped with NaCl windows. The sample was reduced in circulating hydrogen (50 Torr) at 473 K before conducting the $NO–H_2–O_2$ reaction at the desired temperature. IR spectra were recorded with a Shimadzu 4100 FT IR double- beam spectrometer with a resolution of 2 $cm^{-1}$.

$^{15}NO_2$ and $^{15}N_2O_4$ were produced by the addition of $O_2$ to $^{15}NO$ (1 : 1 *v*/*v*) at 474 K on Au/ZSM-5. As shown in Fig. 2, after the $NO–O_2$ system reached a steady state [Fig. 2(*a*)], a pair of bands with an intensity ratio of *ca.* 1 : 1 developed at 1780 and 1760 $cm^{-1}$ arising from the stretching mode of monomeric $^{15}N–O$ on $Au^I$ and $Au^IO$, respectively. These bands were similarly assigned by Valyon and Hall[9] in NO chemisorption on Cu/ZSM-5. We did not observe such terminal NO species in the absence of oxygen on the Au/NaY and Au/ZSM-5 samples at identical NO chemisorption conditions. This implies that oxygen acts as a promoter for NO chemisorption on Au. The respective shift to lower wavenumbers (*ca.* 30 $cm^{-1}$) compared to those for $^{14}NO$ at 1811 and 1792 $cm^{-1}$ indicates that they are mononitrosyl species.

After heating the samples to 573 K, the ill resolved doublet bonds assigned to $^{15}N_2O_4$ completely vanished and were replaced by species at 1780 and 1760 $cm^{-1}$ [Fig. 2(*b*)]. The $^{15}NO_2$ bands were also decreased in intensity but to a lesser extent. This leads us to conclude that $^{15}N_2O_4$ together with $^{15}NO_2$ species dissociated back to monomeric NO and NO(O) at higher temperatures. It was previously reported that $NO_2$ dissociates on Au to form coadsorbed $NO_{(a)}$ and $O_{(a)}$ with a kinetic-energy barrier of $E_d \geqslant 17$ kcal mol[12] (1 cal = 4.184 J). The assignments of the observed IR bands associated with nitrogen oxides are summarized in Table 1.

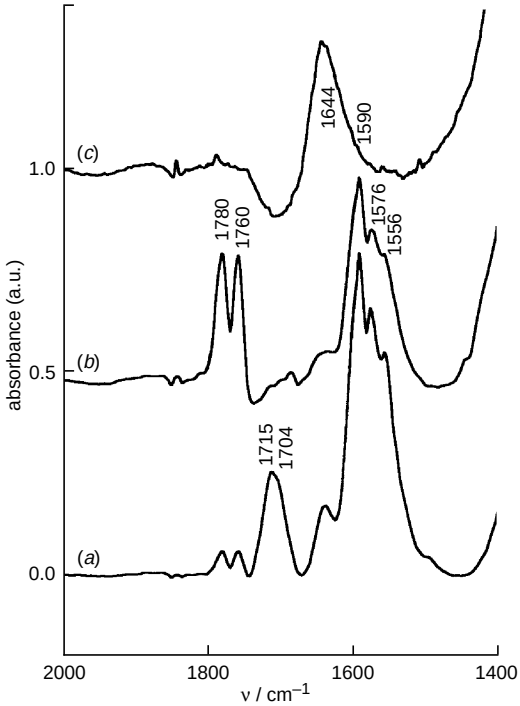



**Fig. 2** *In situ* IR spectra obtained on Au/ZSM-5 (5% Au loading) from (*a*) $^{15}NO$ (40 Torr)–$O_2$ (40 Torr) reaction at 474 K, (*b*) obtained upon increasing the reaction temperature to 573 K for 10 min, and (*c*) after admission of $H_2$ (100 Torr) at 573 K for 20 min

**Table 1** IR bands from the $NO–H_2–O_2$ reaction on Au/ZSM-5 and their assignment

| ν/$cm^{-1}$ | | | | |
|---|---|---|---|---|
| $^{14}NO^a$ | $^{15}NO^a$ | Calc.$^b$ | Assignment | Ref. |
| 1811 | 1780 | 1781 | NO accessible to $Au^I$ | This work |
| 1792 | 1760 | 1762 | NO on $Au^I$ carrying extralattice oxygen | This work |
| 1755 | 1715 | 1714 | Solid-state $N_2O_4$ | 13 |
| 1744 | 1704 | 1702 | Gas-phase $N_2O_4$ | 13 |
| 1630 | 1590 | 1591 | ⎫ | 14 |
| 1612 | 1576 | 1574 | ⎬ $NO_2$ and $NO_2^-$ | 14 |
| 1597 | 1556 | 1557 | ⎭ | 14 |

$^a$ NO stretching vibration. $^b$ Calculated using $\nu_{15} = \nu_{14}(\mu_{14}/\mu_{15})$ where $\mu_{14}$ is the reduced mass for $^{14}NO$ and $^{16}O$ and $\mu_{15}$ the reduced mass for $^{15}NO$ and $^{16}O$.

Subsequently, $H_2$ (100 Torr) was admitted to the reacting system [Fig. 2(*c*)], resulting in the complete disappearance of $NO_2$ and $N_2O_4$ species on Au/ZSM-5 with substantial formation of $N_2$ (*m*/*z* 28) and $H_2O$ (band at 1644 $cm^{-1}$). Oxygen promotion in the selective reduction of NO by $H_2$ on Au/NaY and Au/ZSM-5 is proposed to proceed as follows:

$$2NO + 2O_{ads} \xrightarrow[O_2]{\text{very fast}} [2NO_2 \rightleftharpoons N_2O_4]_{ads}$$

$$N_2O_4(NO_2) + 2H_2 \rightarrow N_2 + 2H_2O$$

$$2NO + 2H_2 \rightarrow N_2 + 2H_2O$$

Bands assignable to $N_2O$ and $NH_3$ were not detected by an *in situ* IR experiment in the presence of oxygen even when the reaction took place over a wide range of temperature. Nevertheless, we have previously reported that $N_2O$ and adsorbed $NH_4^+$ were partially detected as by-products due to NO dissociation in the $NO–H_2$ reaction over Au/NaY.[5] Accordingly, the results suggest that oxygen surpresses the dissociation of NO on Au/NaY, while promoting the formation of oxygenated intermediates such as $NO_2$ and $N_2O_4$, which are readily reduced by hydrogen selectively to $N_2$. Moreover, it is noteworthy that the synergism effected in the presence of excess oxygen is produced by inhibiting the sintering of Au due to a facile redox process between $Au^I$ and $Au^0$ in NaY and ZSM-5 even under the reductive $NO–H_2$ atmosphere.

## Footnote

† On leave from the Chemistry Department, Faculty of Science, Al-Azhar University, Cairo, Egypt.

## References


1 T. J. Truex, R. A. Searle and D. C. Sun, *Platinum Met. Rev.*, 1992, **36**, 1.
2 J. O. Petunchi, G. Still and H. K. Hall, *Appl. Catal. B: Environ.*, 1993, **2**, 303.
3 T. Li and J. N. Armer, *US Pat.* 5 149 512,1992, to Air Products and Chemicals, Inc.
4 M. Haruta, N. Yamada, T. Kobayashi and S. Iijima, *J. Catal.*, 1989, **115**, 301.
5 T. M. Salama, Y. Ohnishi and M. Ichikawa, *J. Chem. Soc., Faraday Trans,*. 1996, **92**, 301.
6 T. M. Salama, Y. Ohnishi, T. Shido and M. Ichikawa, *J. Catal.*, 1996, **162**, 169.
7 T. M. Salama, T. Shido, H. Minagawa and M. Ichikawa, *J. Catal.*, 1995, **152**, 322; S. L. Qiu, R. Ohnishi and M. Ichikawa, *J. Chem. Soc., Chem. Commun.*, 1992, 1425.
8 T. M. Salama, T. Shido, Y. Ohnishi and M. Ichikawa, *J. Phys. Chem.*, 1996, **100**, 3688.
9 J. Valyon and W. K. Hall, *J. Phys. Chem.*, 1993, **97**, 1204.
10 I. Halasz, A. Brenner and M. Shelef, *Catal. Lett.*, 1993, **18**, 289.
11 Y. J. Mergler, A. van Aals and B. E. Nieuwenhuys, *207th National Meeting*, American Chemical Society, 1994, vol. 39, p. 161.
12 D. T. Wickham, B. A. Banse and B. E. Koel, *Catal. Lett.*, 1996, **6**, 163.
13 U. Schwalke, J. E. Parmeter and W. H. Weinberg, *J. Chem. Phys.*, 1986, **84**, 4036.
14 J. W. London and A. T. Bell, *J. Catal.*,1973, **31**, 32.
15 K. Nakamoto, *Infrared and Raman Spectra of Inorganic and Coordination Compounds*, Wiley, New York, 1978, 3rd edn., p 9.


*Received, 2nd October 1996; Com. 6/06761A*

# A new carboxylate anion selective cobaltocenium calix[4]arene receptor

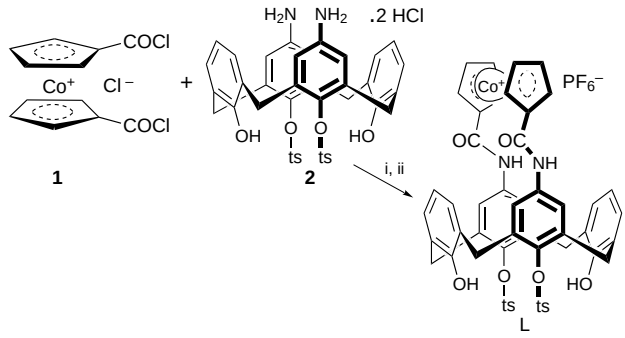
**Paul D. Beer,*[a] Michael G. B. Drew,[b] Dusan Hesek[a] and Kye Chun Nam[a]†**

[a] *Inorganic Chemistry Laboratory, University of Oxford, South Parks Road, Oxford, UK OX1 3QR*
[b] *Department of Chemistry, University of Reading, Whiteknights, PO Box 224, Reading, UK RG6 2AD*

**A new upper-rim cobaltocenium bridged calix[4]arene receptor L is synthesised and by virtue of its unique topology exhibits remarkable carboxylate anion selectivity.**

The synthesis of positively charged or neutral electron-deficient abiotic receptor molecules designed to non-covalently bind[1] and sense[2] anions of biochemical, medical and environmental importance is an area of intense current research activity. As a consequence of their inimitable upper- and lower-rim topologies the calixarenes[3] are attractive host molecules to modify and so create unique cavities for the recognition of target guest species. Although this has been exploited for the recognition of metal cations,[4] in contrast calixarene anion receptors are still relatively rare.[5] We report here the synthesis of a new upper-rim cobaltocenium-bridged calix[4]arene receptor L which by virtue of its topology exhibits remarkable carboxylate anion selectivity.

The condensation of 1,1′-bis(chlorocarbonyl)cobaltocenium chloride **1**[6] with the upper-rim bis-amine-substituted calix[4]-arene derivative **2**[7] in dry acetonitrile in the presence of triethylamine initially gave a crude product which after silica column chromatography and addition of ammonium hexafluorophosphate afforded L as a yellow powder in 38% yield (Scheme 1).



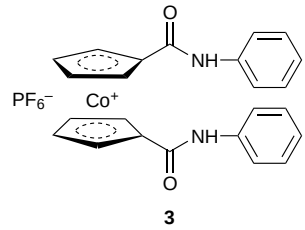

**Scheme 1** *Reagents*: i, MeCN–thf–py; ii, $NH_4PF_6$; ts = $O_2SC_6H_4Me$-*p*

**Table 1** Stability constant data in $(CD_3)_2SO$

| Anion | K[a]/dm³ mol⁻¹ L | **3** |
|---|---|---|
| $Cl^-$ | 70 | 35 |
| $Br^-$ | —[b] | — |
| $NO_3^-$ | 125 | — |
| $HSO_4^-$ | 40 | — |
| $H_2PO_4^-$ | 6 380 | 320 |
| $MeCO_2^-$ | 41 520 | 1560 |
| $PhCO_2^-$ | 38 400 | — |
| $PhCH_2CO_2^-$ | 22 270 | — |
| $C_{10}H_{17}CO_2^-$ | 19 750 | — |

[a] Errors estimated to be ≤10%. [b] Very weak binding, a stability constant value could not be calculated in this solvent.

The anion coordination properties of L were investigated by $^1H$ NMR anion titration experiments in $(CD_3)_2SO$ solution with various tetrabutylammonium halide, nitrate, dihydrogen phos-



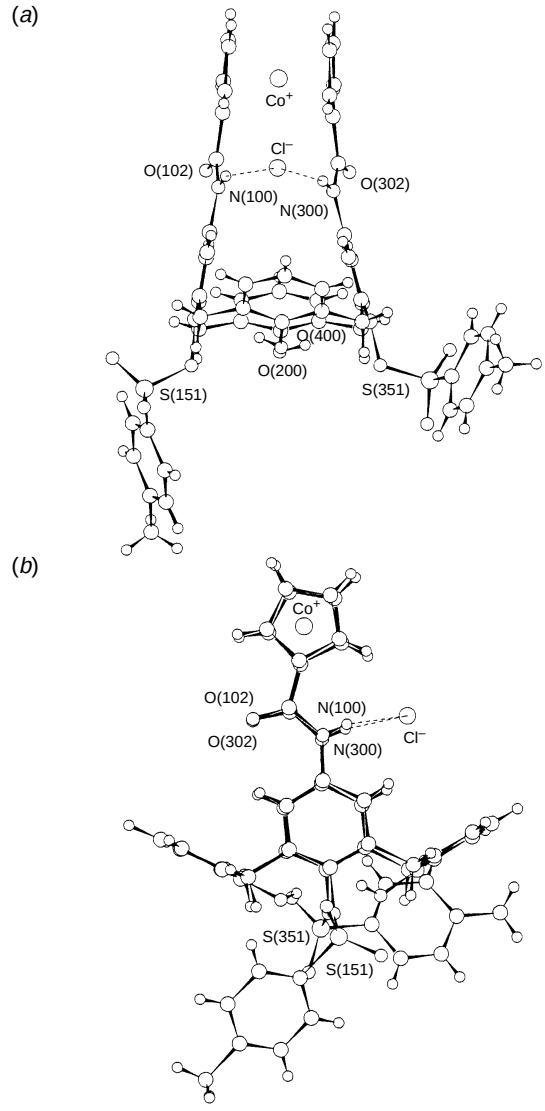




**Fig. 1** Structure of the chloride complex of L

phate, hydrogen sulfate and carboxylate salts. Substantial downfield perturbations of the receptor's amide and cyclopentadienyl protons were observed especially with carboxylate anionic guests, suggesting anion binding is taking place at the upper-rim vicinity of the receptor. It is noteworthy that with benzoate and β-naphthylcarboxylate anions large upfield perturbations of the receptor's aryl calix[4]arene protons of 0.6 ppm were also seen. Stability constants were calculated from the resulting titration curves using EQNMR[8] and these values are presented in Table 1 which includes stability constant data for acyclic receptor **3**. The receptor L exhibits remarkable thermodynamic stability and selectivity preferences for carboxylate anions, in particular for acetate over $H_2PO_4^- \gg NO_3^- > Cl^- > HSO_4^- > Br^-$. In comparison **3** forms a much weaker complex with the acetate anion (Table 1). These novel anion coordination properties may be attributable to the upper-rim rigidly held cobaltocenium bridging unit of L creating a unique and ideal bidentate amide (CO–NH) hydrogen-bond donor environment of complementary topology for recognising bidentate anions such as carboxylates. The X-ray crystal structure of the chloride complex of L corroborates this postulation‡ [Fig. 1(*a*), (*b*)]. As is clearly shown particularly in Fig. 1(*a*) the calix[4]arene has the typical flattened cone conformation with $C_2$ distortion. The angles made by the four phenyl rings and the plane of the four methylene carbon atoms are 106.8, 28.4, 98.9 and 29.8°. The two angles > 90° illustrate that the tops of the two phenyl rings of the calixarene are pulled together so that the cobaltocenium bridge can be formed [Fig. 1(*b*)]. However, despite being attached to the upper rim of the calixarene, the two cyclopentadiene rings are almost coplanar intersecting at an angle of 7.6°. The Co–C distances are in the range 2.04(1)–2.10(1) Å. In addition to the cobaltocenium linkage as shown in the Figure, the two N–H groups form hydrogen bonds to the chloride anion Cl(1)···N(100) 3.287, N(300) 3.298 Å.

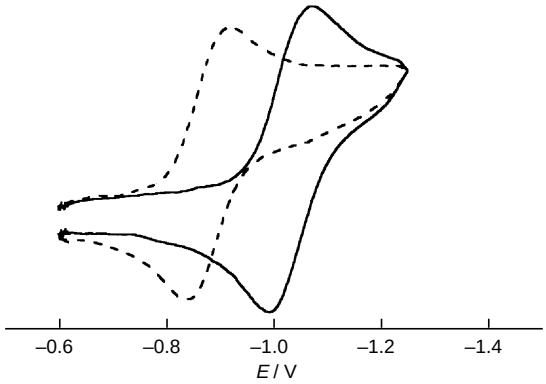



**Fig. 2** Cyclic voltammograms of L in MeCN in the absence (– – – –) and presence (——) of 3 equiv. $NBu_4O_2CMe$

**Table 2** Electrochemical data for L[a]

| Anion | $\Delta E$[b]/mV |
|---|---|
| $Cl^-$ | 60 |
| $NO_3^-$ | 20 |
| $HSO_4^-$ | 10 |
| $H_2PO_4^-$ | 130 |
| $MeCO_2^-$ | 155 |
| $PhCO_2^-$ | 140 |
| $PhCH_2CO_2^-$ | 150 |
| $C_{10}H_{17}CO_2^-$ | 135 |

[a] Obtained in acetonitrile solution containing 0.1 mol $dm^{-3}$ $NBu_4PF_6$ as supporting electrolyte. [b] Cathodic shift perturbations of cobaltocenium/cobaltocene redox couple of L produced by presence of anions (up to 5 equiv.) added as their tetrabutylammonium salts.

Electrochemical anion recognition studies in acetonitrile solutions reveal L to electrochemically sense carboxylate anions through substantial cathodic shift perturbations of up to $\Delta E$ = 155 mV of the reversible cobaltocenium–cobaltocene redox couple (Fig. 2, Table 2) at 0.85 V. Thus L is a first-generation prototype amperometric selective sensing reagent for carboxylate anionic guest species.

We thank the EPSRC for a postdoctoral fellowship to D. H. and for use of the mass spectrometry service at University College, Swansea. The University of Reading and the EPSRC are gratefully acknowledged for funding towards the crystallographic image-plate system.

## Footnotes

† Visiting scholar from Chonnam National University, Republic of Korea.

‡ *Crystal data* for LCl·MeCN, $C_{56}H_{47}ClCoN_3O_{10}S_4$, $M$ = 1080.5, orthorhombic, space group *Pbca*, $a$ = 15.401(12), $b$ = 17.418(13), $c$ = 31.43(4) Å, $U$ = 10 578 Å$^3$, $Z$ = 8, $D_m$ = 1.362 Mg $m^{-3}$, 15 659 reflections measured ($R_{int}$ = 0.065), 6660 independent reflections refined on $F^2$ to $R$ of 0.0871. Atomic coordinates, bond lengths and angles, and thermal parameters have been deposited at the Cambridge Crystallographic Data Centre (CCDC). See Information for Authors, Issue No. 1. Any request to the CCDC for this material should quote the full literature citation and the reference number 182/322.

## References

1 F. P. Schmidtchen, *Nachr. Chem. Tech. Lab*., 1988, **36**, 8; H. E. Katz, in *Inclusion Compounds*, ed. J. L. Atwood, J. E. D. Davies and D. D. MacNicol, Oxford University Press, New York, 1991, vol. 4, p. 391; B. Dietrich, *Pure Appl. Chem*., 1993, **65**, 1457.
2 P. D. Beer, *Chem. Commun*., 1996, 689 and references therein.
3 C. D. Gutsche, in *Calixarenes*, ed. J. F. Stoddart, Monographs in Supramolecular Chemistry, The Royal Society of Chemistry, Cambridge, 1989, vol. 1.
4 R. Ungaro and A. Pochini, in *Calixarenes, a Versatile Class of Macrocyclic Compounds*, ed. J. Vicens and V. Böhmer, Kluwer, Dordrecht, 1990, p. 133; F. Arnaud-Neu, G. Barrett, S. J. Harris, M. Owens, M. A. McKervey, M. J. Schwing-Weill and P. Schwinte, *Inorg. Chem*., 1993, **32**, 2644 and references therein.
5 P. D. Beer, M. G. B. Drew, C. Hazlewood, D. Hesek, J. Hodacova and S. E. Stokes, *J. Chem. Soc., Chem. Commun*., 1993, 229; Y. Morzheim, D. M. Rudkevich, W. Verboom and D. N. Reinhoudt, *J. Org. Chem*., 1993, **58**, 7602; J. W. Steed, R. K. Junega and J. L. Atwood, *Angew. Chem., Int. Ed. Engl*., 1994, **33**, 2456; P. D. Beer, Z. Chen, A. J. Goulden, A. Grieve, D. Hesek, F. Szemes and T. Wear, *J. Chem. Soc., Chem. Commun*., 1994, 1269.
6 J. E. Sheats and M. D. Rausch, *J. Org. Chem*., 1970, **35**, 3245.
7 P. D. Beer, M. G. B. Drew, D. Hesek, M. Shade and F. Szemes, *Chem. Commun*., 1996, 2161.
8 M. J. Hynes, *J. Chem. Soc., Dalton Trans*., 1993, 311.

*Received, 6th November 1996; Com. 6/07569J*

# Solvent directed aggregation of a metallocene; structures of $\{[Pb(\eta\text{-}C_5H_5)_2]_3\cdot C_6H_5Me\}_\infty$ and $[Pb(\eta\text{-}C_5H_5)_2]_6$

**Michael A. Beswick, Catherine Lopez-Casideo, Michael A. Paver,* Paul R. Raithby, Christopher A. Russell, Alexander Steiner and Dominic S. Wright***

*Department of Chemistry, University of Cambridge, Lensfield Road, Cambridge, UK CB2 1EW*

**The classic zigzagged chain structure of orthorhombic plumbocene, $[Pb(\eta\text{-}C_5H_5)_2]_\infty$, is obtained by crystal growth from the vapour phase; however, crystallisation from toluene results in modification of the conformation of the polymer chain, as observed in the solvate $[Pb(\eta\text{-}C_5H_5)\cdot C_6H_5Me]_\infty$ 1, and cyclisation into hexamers, as seen in the new hexagonal phase $[Pb(\eta\text{-}C_5H_5)_2]_6$ 2.**

We have recently observed that nucleophilic addition of the cyclopentadienide anion ($C_5H_5$) to plumbocene {$[Pb(\eta\text{-}C_5H_5)_2]$} produces a variety of complexes containing mononuclear and linear extended anions of general formulae $[Pb_n(\eta\text{-}C_5H_5)_{2n+1}]^-$.[1] The chain length of the homologue formed depends on the size and nature of the counter cations, and therefore on the lattice energy involved. Accordingly, the reaction of $[Pb(\eta\text{-}C_5H_5)_2]$ with $[Mg(\eta\text{-}C_5H_5)_2]$ in thf produces $[Mg(thf)_6]^{2+}\{[Pb(\eta\text{-}C_5H_5)_3]^-\}_2$ [1c] whereas the same reaction in the presence of 12-crown-4 gives the mixed anion complex $\{[Li(12\text{-crown-}4)_2]^+\}_2[Pb_2(\eta\text{-}C_5H_5)_5]^-[Pb_9(\eta\text{-}C_5H_5)_9]^-$.[1a] The formation of these anions points to the underlying structural flexibility of plumbocene itself. In this respect, two phases of plumbocene have been identified (triclinic and orthorhombic). However, only the orthorhombic polymeric phase $\{[Pb(\eta\text{-}C_5H_5)_2]_\infty\}$, grown from the vapour phase, has been structurally characterised.[2]

With the previous background in mind we have recently embarked on an investigation of the influence of solvation on the structure of plumbocene.[3] We report here that simple crystallisation of orthorhombic plumbocene from toluene solution results in major structural modification of the polymer chain. From such solutions two new complexes, the polymeric toluene solvate $\{[Pb(\eta\text{-}C_5H_5)_2]_3\cdot C_6H_5Me\}_\infty$ **1** and the cyclic molecular phase $[Pb(\eta\text{-}C_5H_5)_2]_6$ **2**, have been characterised.†

Complex **1** has an infinite polymer structure which is qualitatively similar to the orthorhombic form of plumbocene [Fig. 1(*a*)].‡ In both cases the association of the $[Pb(\eta\text{-}C_5H_5)_2]$ monomer units by bridging $\mu\text{-}C_5H_5$ ligands results in trigonal-planar metal environments {av. Cp–Pb–Cp 120.8° in **1**; *cf.* av. 120.0° in orthorhombic $[Pb(\eta\text{-}C_5H_5)_2]$;[2] Cp = centroid of cyclopentadienyl ring}. The pattern of $C_5H_5$–Pb bond lengths in **1** is also similar to that found in orthorhombic $[Pb(\eta\text{-}C_5H_5)_2]$, with a shorter interaction being made to the terminal $C_5H_5$ ligand (av. Pb–Cp 2.50 Å) and two longer interactions being made with the bridging ligands [av. Pb–($\mu$-Cp) 2.75 Å]. However, the presence of toluene solvation within the lattice has a marked effect on the conformation of the polymer chain of **1**. Rather than consisting of a simple two-dimensional zigzagged structure, as is observed in orthorhombic plumbocene, polymer strands of **1** adopt a sinusoidal pattern in order to avoid the interstitial toluene molecules [Fig. 1(*b*)].

Molecules of **2** are composed of six identical $[Pb(\eta\text{-}C_5H_5)_2]$ units which are linked together into a cyclic arrangement (Fig. 2).§ The mode of association of these units and the resulting environments of the metal centres are similar to those found in orthorhombic $[Pb(\eta\text{-}C_5H_5)_2]$ and **1**.[2] However, the monomers of **2** are less affected by their association than in either of the latter. The $[Pb(\eta\text{-}C_5H_5)_2]$ units resemble those found for monomeric plumbocene in the gas phase (Cp–Pb ≈ 2.50 Å and Cp–Pb–Cp 138°),[4] with the Pb centre of each monomer being bonded more closely to two of the $C_5H_5$ ligands [Cp(A)–Pb(1) 2.44 Å, Cp(B)–Pb(1) 2.53 Å and Cp(A)–Pb–Cp(B) 135.3°] than to the $C_5H_5$ ligand of the next monomer unit [Cp(B)···Pb(1b) 3.33 Å]. This pattern of $C_5H_5$–Pb interactions implies that the association of the monomers is extremely loose. The stacking of the $[Pb(\eta\text{-}C_5H_5)_2]_6$ rings results in infinite cylindrical channels through the crystal lattice.

The influence of substituents on the structures of p-block metallocenes is now well established. Increased substitution of the $C_5H_5$ rings with sterically demanding groups generally leads to the formation of oligomeric rather than polymeric species. For example, whereas $[E(\eta\text{-}C_5H_5)]_\infty$ (E = In, Tl)[5] have polymeric structures in the solid state, $[E\{C_5(CH_2Ph)_5\}]$[6] are essentially monomeric. The structural flexibility and subtle influence of the substituents are seen particularly in $[In(\eta\text{-}C_5Me_5)]_6$, which forms loosely associated In···In bonded octahedra in the solid state,[7] and $[Tl\{\eta\text{-}C_5H_3(SiMe_3)_2\text{-}1,3\}]_6$, containing Tl–{$\mu$-$\eta$-$C_5H_3(SiMe_3)_2$-1,3}–Tl linked cyclic molecules related to **2**.[8] Despite its similarity with the structure of the latter, the oligomeric structure of **2** is unique for any unfunctionalised main group metallocene.

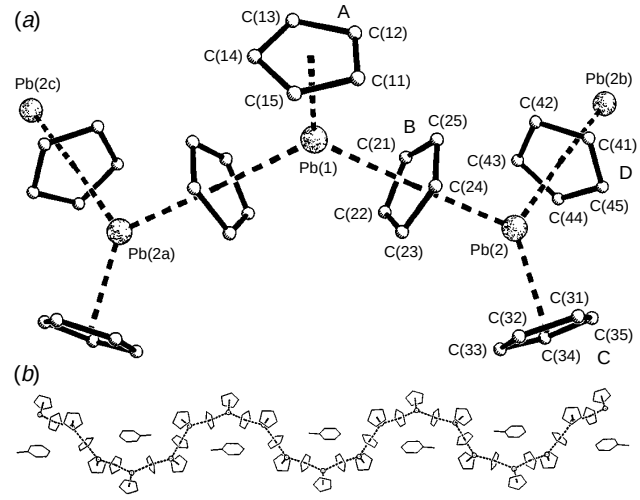



**Fig. 1** (*a*) Asymmetric unit of **1**. Hydrogen atoms have been omitted for clarity. Key bond lengths (Å) and angles (°): Pb(1)–C(11) 2.74(7), Pb(1)–C(12) 2.73(7), Pb(1)–C(13) 2.76(6), Pb(1)–C(14) 2.79(7), Pb(1)–C(15) 2.79(5), Cp(A)–Pb(1) 2.48, Pb(1)–C(21) 3.03(7), Pb(1)–C(22) 3.05(7), Pb(1)–C(23) 2.96(7), Pb(1)–C(24) 2.93(7), Pb(1)–C(25) 2.98(7), Cp(B)–Pb(1) 2.73, Pb(2)–C(21) 3.08(7), Pb(2)–C(22) 3.11(7), Pb(2)–C(23) 3.03(7), Pb(2)–C(24) 2.95(7), Pb(2)–C(25) 2.98(7), Cp(B)–Pb(2) 2.78, Pb(2)–C(31) 2.74(3), Pb(2)–C(32) 2.79(3), Pb(2)–C(33) 2.85(3), Pb(2)–C(34) 2.84(3), Pb(2)–C(35) 2.77(3), Cp(C)–Pb(2) 2.53, Pb(2)–C(41) 3.00(7), Pb(2)–C(42) 3.02(7), Pb(2)–C(43) 3.01(7), Pb(2)–C(44) 2.97(7), Pb(2)–C(45) 2.97(7); Cp(D)–Pb(2) 2.74, av. Cp–Pb–Cp 120.8°, av. Pb–Cp–Pb 175.1, Cp(C)–Pb···Pb–Cp(A) (dihedral) 74.3; Cp represents centroid of $\eta$-$C_5H_5$ ring. (*b*) Polymer structure of **1**.

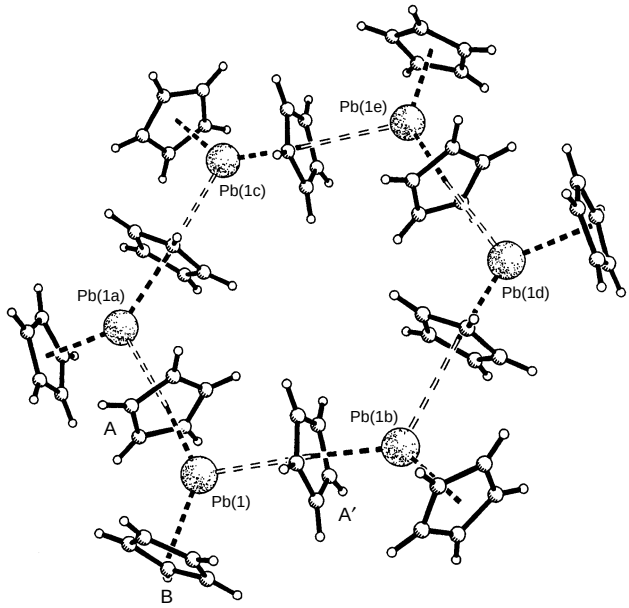



**Fig. 2** Molecular structure of **2** in the solid state. Hydrogen atoms have been omitted for clarity. Key bond lengths (Å) and angles (°): Pb(1)–C(1) 2.76(1), Pb(1)–C(2) 2.86(1), Pb(1)–C(3) 2.88(1), Pb(1)–C(4) 2.79(1), Pb(1)–C(5) 2.71(1), Cp(A)–Pb(1) 2.53, Pb(1)–C(6) 2.79(1), Pb(1)–C(7) 2.78(1), Pb(1)–C(8) 2.69(1), Pb(1)–C(9) 2.64(1), Pb(1)–C(10) 2.71(1), Cp(B)–Pb(1) 2.44, Pb(1)–C(1a,2a,3a,4a,5a) 3.53(2), Cp(A)–Pb(1b) 3.33, Cp(A)–Pb(1)–Cp(B) 135.3, Cp(B)–Pb(1)–Cp(A′) 116.2, Cp(A)–Pb(1)–Cp(A′) 108.5, Pb(1)···Cp(A)–Pb(1b) 179.2, Pb···Pb 5.56, Pb···Pb···Pb 120.0.

The characterisation of **1** and **2** illustrates, for the first time, that non-coordinating solvent interactions can have profound consequences on the conformation and overall structure adopted by a main group metallocene. Similar observations may well be expected for group 13 metallocenes {[E(η-$C_5H_5$)]; E = In, Tl}, for which polymeric structures have been determined for crystals grown from the vapour phase.[5]

## Footnotes

† Orthorhombic [Pb(η-$C_5H_5$)$_2$]$_\infty$ was prepared in the manner described in the literature and purified by sublimation (140 °C, 0.1 atm). Crystallisation from toluene at 5 °C gives a mixture of **1** and **2**. Owing to the composition of this mixture, elemental analysis (C, H) and $^1$H NMR spectroscopy indicate that there is *ca*. toluene molecule to each [Pb(η-$C_5H_5$)$_2$] monomer unit (*i.e.* consistent with largely **1**).

‡ *Crystal data*: **1**, $C_{37}H_{38}Pb_3$, $M$ = 1104.24, orthorhombic space group *Pnma*, $a$ = 16.421(3), $b$ = 24.375(5), $c$ = 8.234(2) Å, $U$ = 3296(1) Å$^3$, $Z$ = 4, λ = 0.710 73 Å, $T$ = 153(2) K, $D_c$ = 2.225 Mg m$^{-3}$, μ(Mo-Kα) = 15.311 mm$^{-1}$. Data were collected on a Siemens-Stoe AED diffractometer using an oil-coated crystal[9] of dimensions 0.3 × 0.2 × 0.2 mm using the θ–ω method (8.32 ⩽ 2θ ⩽ 45.06°). Of a total of 2284 reflections collected 2199 were independent. A semi-empirical absorption correction based on ψ-scans was applied (max., min. transmission = 0.981, 0.149). The structure was solved by direct methods and refined by full-matrix least squares on $F^2$ to final values of $R_1$ = 0.102 (for 2195 data with $F > 4\sigma F$) and $wR_2$ = 0.231 (all data) [$R_1 = \Sigma|F_o - F_c|/\Sigma|F_o|$, $wR_2 = \{[\Sigma w(F_o^2 - F_c^2)^2]/\Sigma wF_o^4\}^{0.5}$, $w = 1/[\sigma^2(F_o^2) + (xP)^2 + yP]$, $P = (F_o^2/3)$].[10] Largest peak and hole in the final difference map = 2.968 and −2.958 e Å$^{-3}$. The C atoms were refined isotropically. The $C_5H_5$ rings and toluene molecules were refined as rigid groups. $C_5H_5$(A) is disordered on an inversion centre and $C_5H_5$(D) is disordered on a mirror plane. Hydrogen atoms were set geometrically.

**2**, $C_{60}H_{60}Pb_6$, $M$ = 2024.22, hexagonal, space group $P6cc$, $a$ = 18.058(2), $c$ = 10.219(2) Å, $U$ = 2885.9(7) Å$^3$, $Z$ = 2, λ = 0.710 73 Å, $T$ = 153(2) K, $D_c$ = 2.329 Mg m$^{-3}$, μ(Mo-Kα) = 17.473 mm$^{-1}$. Data were collected on a Siemens-Stoe AED diffractometer using an oil-coated crystal[9] of dimensions 0.15 × 0.24 × 0.24 mm using the θ–ω method (8.40 ⩽ 2θ ⩽ 44.98°). Of a total of 4906 reflections collected 1268 were independent. A semiempirical absorption correction based on ψ-scans was applied (max., min. transmission = 0.953, 0.476). The structure was solved as for **1** to final values of $R_1$ = 0.041 (for 1261 data with $F > 4\sigma F$) and $wR_2$ = 0.124 (all data). Largest peak and hole in the final difference map = 3.118 and −0.749 e Å$^{-3}$. C atoms were refined isotropically and the $C_5H_5$ rings as rigid groups. Hydrogen atoms were set geometrically.

Atomic coordinates, bond lengths and angles, and thermal parameters have been deposited at the Cambridge Crystallographic Data Centre (CCDC). See Information for Authors, Issue No. 1. Any request to the CCDC for this material should quote the full literature citation and the reference number 182/319.

## References


1 (*a*) M. J. Duer, N. C. Page, M. A. Paver, P. R. Raithby, M.-A. Rennie, C. A. Russell, A. Steiner and D. S. Wright, *J. Chem. Soc., Chem. Commun.*, 1995, 1141; (*b*) M. A. Paver, C. A. Russell and D. S. Wright, *Angew. Chem.*, 1995, **107**, 1677; *Angew. Chem., Int. Ed. Engl.*, 1995, **34**, 1545; (*c*) D. R. Armstrong, M. J. Duer, D. Moncrieff, M. A. Paver, C. Stourton, C. A. Russell, D. Stalke, A. Steiner and D. S. Wright, unpublished work.

2 C. Panattoni, G. Bombieri and U. Croatto, *Acta Crystallogr., Sect. A*, 1966, **21**, 823.

3 M. A. Beswick, N. L. Cromhout, C. N. Harmer, P. R. Raithby, C. A. Russell, J. B. Smith, A. Steiner and D. S. Wright, *Chem. Commun.*, 1996, 1978.

4 A. Almenningen, A. Haaland and T. Motzfeld, *J. Organomet. Chem.*, 1967, **7**, 97.

5 C. Panattoni, E. Frasson and F. Menegus, *Nature*, 1963, **199**, 823.

6 H. Schumann, C. Janiak, F. Gölitz, J. Loebel and A. Dietrich, *Organometallics*, 1989, **363**, 243; L. S. Bartell, *J. Chem. Phys.*, 1964, **41**, 717; H. Schumann, C. Janiak, M. A. Khan and J. J. Zuckerman, *J. Organomet. Chem.*, 1988, **354**, 7.

7 O. T. Beachley, Jr., M. R. Churchill, J. C. Fettinger, J. C. Pazik and L. Victoriano, *J. Am. Chem. Soc.*, 1986, **108**, 4666.

8 S. Harvey, C. L. Raston, B. W. Skelton, A. H. White, M. F. Lappert and G. Srivastava, *J. Organomet. Chem.*, 1987, **238**, C1.

9 D. Stalke and T. Kottke, *J. Appl. Crystallogr.*, 1993, **26**, 615.

10 G. M. Sheldrick, SHELXL93, Göttingen, 1993.


*Received, 6th November 1996; Com. 6/07561D*

# Chiral monolayer of self-assembled Δ-[Os(bpy)$_2$L(Cl)]$^+$ [bpy = 2,2′-bipyridyl, L = 1,2-bis(4-pyridyl)ethane] on a platinum electrode

**Yasuo Inose,[a] Shinobu Moniwa,[a] Akiko Aramata,*[a] Akihiko Yamagishi[b] and Kyaw-Naing[b]**

[a] *Catalysis Research Center, Hokkaido University, Sapporo 060, Japan*
[b] *Graduate School of Science, Hokkaido University, Sapporo 060, Japan*

**A chiral osmium complex, Δ-(2,2′-bipyridyl) [1,2-bis(4-pyridyl)ethane] chloroosmium Δ-[Os(bpy)$_2$L(Cl)]$^+$, is successfully self-assembled at a monolayer molecular level on a clean Pt electrode in non-aqueous solutions; the self-assembled Δ-[Os(bpy)$_2$LCl]$^+$ ions show a phenomenally repulsive interaction with each other on Pt in chiral-field formation and also in the Os$^{II}$–Os$^{III}$ redox reaction, while racemic complexes interact less repulsively with each other.**

Chiral monolayer creation at an electrode interface is a stimulating subject for atomic level surface design. Study of chiral electrode surfaces has been attempted with a cholesteric liquid crystal physically adsorbed on glassy carbon or Pt electrodes.[1] In other work, a chiral metal complex was inserted into a clay mineral by cation exchange leading to a chiral metal complex-modified clay electrode, where the chiral complex was Δ- or Λ-[Ru(phen)$_3$]$^{2+}$ (phen = phenanthroline). Oxidation of racemic [Co(phen)$_3$]$^{2+}$ to Λ-[Co(phen)$_3$]$^{3+}$ on a Δ-[Ru(phen)$_3$]$^{2+}$ modified clay electrode showed chiral performance in a 17% optical yield,[2] and the partial oxidation of phenylcyclohexylsulfide to chiral (*R*)-(+)-phenylcyclohexylsulfoxide on a Λ-[Ru(phen)$_3$]$^{2+}$-modified clay electrode gave a 20% optical yield.[2] The properties of a chiral complex-modified clay in a dispersed colloid form were experimentally and theoretically clarified by Yamagishi *et al.*,[3–5] but the electrochemical features of chiral [Ru(bpy)$_3$]$^{2+}$ in a clay-modified electrode were reported to be different from those in a dispersed form by Villemure and Bard,[6] showing that the electrochemical chirality determination of a metal complex-modified clay electrode is quite complicated and likely to arise from a small fraction of complex ions in defects of layer films of a laminal clay.

Metal electrode modification was carried out by application of a monolayer *via* a thiol RSH on Au in the form of RS–Au, where R contains an electroactive species.[7–9] Recently, an organic thiol with asymmetric carbon, adsorbed on Hg in a self-assembled manner, was reported to show an atomically two-dimensional chiral surface by Mandler and coworkers.[10] As another metal electrode modification, osmium complexes [Os(bpy)$_2$L(Cl)]$^+$ (L = 4,4′-bipyridine or derivatives) were self-assembled onto a Pt electrode through an N atom of bipyridine,[11] and the electrochemical behaviour was examined in aqueous and non-aqueous solutions.[11–15] The electron-transfer mechanism and the adsorption thermodynamics of the osmium complex self-assembled on Pt were discussed in detail since the electron-transfer reaction between the electrode and the complex bound to the electrode is a fairly straightforward system to be theoretically treated for elucidation of electron-transfer processes. An STM image of ordered self-assembled osmium complexes on Pt(111) was successfully observed by Hudson and Abruña,[16] indicating that the self-assembled osmium complexes form a two-dimensional ordered phase on Pt(111). In these reports, the above osmium complexes were synthesized as racemic mixtures of chiral Δ- and Λ-complexes [Fig. 1(*a*), (*b*)], depicted by molecular modelling, and used as a racemic mixture in the following. These lead us to the study of the creation of a chiral electrode interface by self-assembled Δ- or Λ-metal complexes in a monolayer form.

The separation of chiral Δ-(2,2′-bipyridyl) [1,2-bis(4-pyridyl)ethane] chloroosmium hexafluorophosphate [Os(bpy)$_2$L(Cl)]PF$_6$ [L = 1,2-bis(4-pyridyl)ethane] was carried out from racemic [Os(bpy)$_2$L(Cl)]PF$_6$, which was prepared according to ref. 11. The latter was first purified by elution on a 300 mesh alumina column with acetone, and then subjected to anion exchange to give the water-soluble [Os(bpy)$_2$L(Cl)]Cl. Chiral separation from racemic [Os(bpy)$_2$L(Cl)]Cl was conducted at least three times by column treatment on CM Sephadex (Pharmatia) with a potassium antimony (+)-tartrate saturated aqueous solution as the eluting agent to yield the Δ-osmium

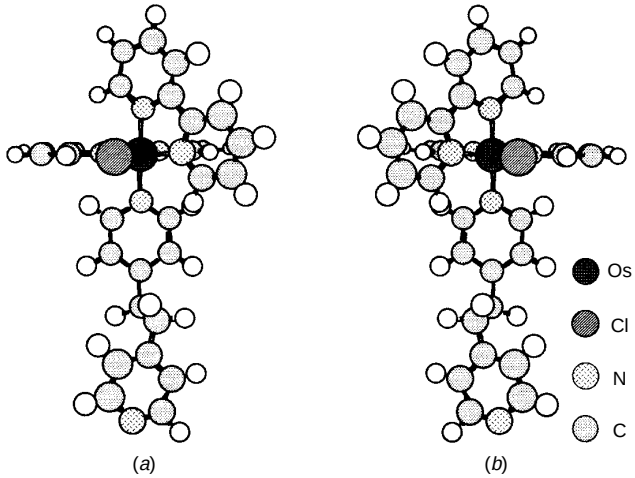



**Fig. 1** Structures of (*a*) Δ- and (*b*) Λ-[Os$^{II}$(bpy)$_2$L(Cl)]$^+$

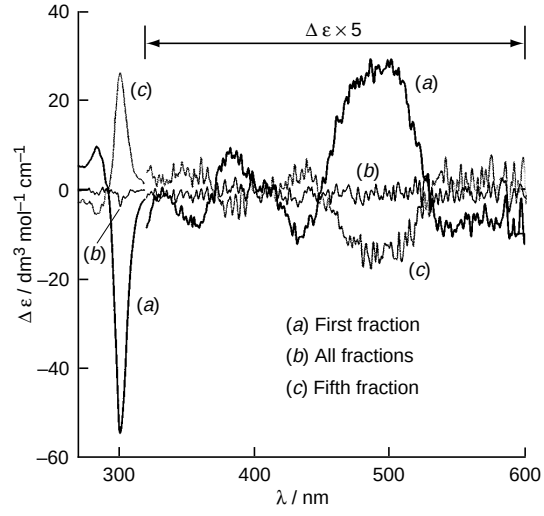



**Fig. 2** Circular dichromism spectra of [Os$^{II}$(bpy)$_2$L(Cl)]$^+$ after chiral separation. First fraction, fifth fraction and all fractions are assumed to be the Δ-, Λ-, and *rac*-species, respectively.

complex as the first of five fractions, since a clear column band separation was not observed. The last fraction containing the Λ-Os complex was also collected. This chiral column separation process also played the role of osmium complex purification. Thus, during the purification process of the racemic osmium complex, all fractions of the column band were collected. The circular dichromism spectra of Δ-, Λ-, and *rac*-complexes are shown in Fig. 2, where we find that the Δε of the first fraction is −55 $dm^3\ mol^{-1}\ cm^{-1}$ at 299 nm, while there is a report that Δε of Λ-$[Os(bpy)_3]^{2+}$ is 400 $dm^3\ mol^{-1}\ cm^{-1}$ at 300 nm.[17] The osmium complexes prepared were stored in a dark cold dry-box before use.

For the monolayer self-assembling procedure, a polycrystalline Pt electrode was inserted into 0.5 mM of Δ- or *rac*-$[Os(bpy)_2L(Cl)]Cl$ in $CH_2Cl_2$ solution for a given time, τ; before this the Pt had been electrochemically polished by cyclic voltammetry (CV) up to 1.2 V (SCE) in perchloric acid solution.

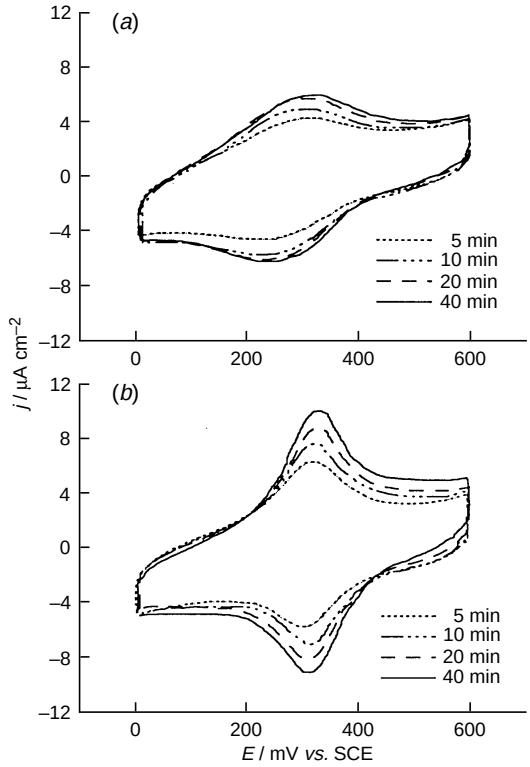



**Fig. 3** CVs of (*a*) Δ- and (*b*) *rac*-$[Os^{II}(bpy)_2L(Cl)]^+$ on a Pt electrode at 0.1 V $s^{-1}$ in 0.05 M TBAP–MeCN solution after Pt was inserted in 0.5 mM Δ- or *rac*-$[Os^{II}(bpy)_2L(Cl)]^+$ for different self-assembling times τ

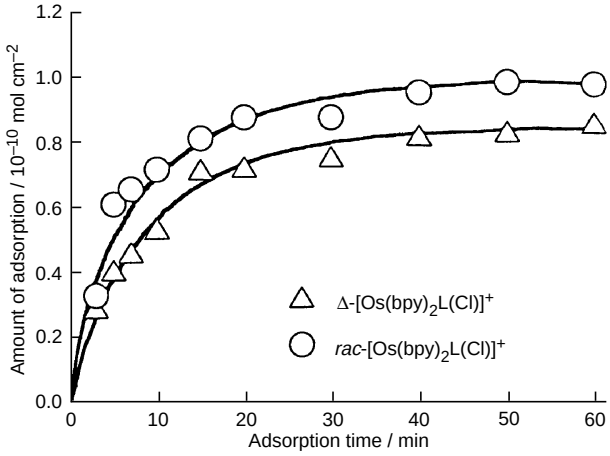



**Fig. 4** Amount of charge of CV peaks of Fig. 3 *vs.* self-assembling adsorption time τ. Ordinate of the amount of the charge densities is expressed in mol $cm^{-2}$.

At each τ, the Pt was subjected to CV measurement at a sweep rate ν of 0.1 V $s^{-1}$ in 0.05 M tetrabutylammonium perchlorate (TBAP) in $Me_2CN$, as shown in Fig. 3, for the electrode reaction of eqn. (1).

$$[Os^{II}(bpy)_2L(Cl)]^+ \rightleftharpoons [Os^{III}(bpy)_2L(Cl)]^{2+} + e \qquad (1)$$

Figs. 3(*a*) and (*b*) are for Δ- and *rac*-osmium complexes, respectively, with τ in the range 5–40 min. The sweep rate dependence of the CV current peak, $j_p$, showed a proportional relation *vs.* ν (at τ = 40 min) when $\nu \leqslant 200$ mV $s^{-1}$, irrespective of whether the electrode was modified by Δ- or *rac*-$[Os(bpy)_2L(Cl)]^+$, as found for a racemic osmium complex in ref. 11. As in that work, the effect of the electron-transfer reaction kinetics on the CV was observed at sweep rates > 100 V $s^{-1}$; the present data are indicative of a quasi-equilibrium state. Remarkable differences of CV characteristics, however, were observed between Δ- and *rac*-$[Os(bpy)_2L(Cl)]^+$ modified Pt electrodes (Fig. 3). Various parameters for the *rac*-Os complex are in good agreement with those of Acevedo and Abruña.[12] Potential differences ($\Delta E$) of anodic and cathodic current peaks are 70 and 30 mV for Δ- and *rac*-modified electrodes, respectively. The peak current height, $j_p$, of the Δ-osmium complex on Pt is roughly half that of the *rac*-osmium complex on Pt with half-height widths of 210 and 120 mV, respectively. The quantity of charge between anodic and cathodic reaction currents is plotted *vs.* τ in Fig. 4, where, at τ = 40 min, the amounts of charge Δ*Q* appear to be saturated at $0.85 \times 10^{-10}$ and $0.95 \times 10^{-10}$ mol $cm^{-2}$ for Δ- and *rac*-modified electrodes respectively, of which the latter amounts to a nearly complete monolayer assuming a cross-section of 1.54 $nm^2$ per molecule of the osmium complex.[11] These results show that a repulsive interaction energy is higher between chiral osmium complexes than between racemic osmium complexes or that a different ordered structure is suggested. The ordered STM structure has been observed for a self-assembled racemic osmium complex on Pt,[16] and the above values suggest that the self-assembled ordered structure should be different for chiral and racemic complexes if chiral complexes also form an ordered monolayer structure.† STM measurements upon the chiral complex self-assembled on Pt are now under way.

## Footnote

† The ordered molecule arrangement depicted in ref. 16 is for chiral complexes.

## References


1 R. D. Mariani and H. D. Abruña, *J. Electrochem. Soc.*, 1989, **136**, 113.
2 A. Yamagishi and A. Aramata, *J. Chem. Soc., Chem. Commun.*, 1984, 452; *J. Electroanal. Chem.*, 1985, **191**, 449.
3 A. Yamagishi and M. Soma, *J. Am. Chem. Soc.*, 1981, **103**, 4640.
4 A. Yamagishi, *J. Phys. Chem.*, 1982, **66**, 2472.
5 A. Sato and A. Yamagishi, *J. Am. Chem. Soc.*, 1994, **116**, 123.
6 G. Villemure and A. J. Bard, *J. Electroanal. Chem.*, 1990, **283**, 403.
7 C. E. D. Chidsey, C. R. Bertozzi, T. M. Putvinski and A. M. Mujace, *J. Am. Chem. Soc.*, 1990, **112**, 4301.
8 K. Uosaki, Y. Sato and H. Kita, *Langmuir*, 1991, **7**, 1510.
9 Y. Sato, S. Ye, T. Haba and K.Uosaki, *Langmuir*, 1996, **12**, 2726.
10 N. Muskal, I. Turyan, A. Shurky and D. Mandler, *J. Am. Chem. Soc.*, 1995, **117**, 1147.
11 D. Acevedo and H. D. Abruña, *J. Phys. Chem.*, 1991, **95**, 9590.
12 D. Acevedo, R. L. Bretz, J. D. Tirado and H. D. Abruña, *Langmuir*, 1994, **10**, 1300.
13 J. D. Tirado, D. Acevedo, R. L. Bretz and H. D. Abruña, *Langmuir*, 1994, **10**, 1971.
14 R. J. Forster and L. R. Faulkner, *J. Am. Chem. Soc.*, 1994, **116**, 5444; 5453.
15 R.J. Forster and J. P. O'Kelly, *J. Phys. Chem.*, 1996, **100**, 3695.
16 J. E. Hudson and H. D. Abruña, *J. Phys. Chem.*, 1996, **100**, 1036.
17 A. J. McCaffery, S. F. Mason and B. J. Norman, *J. Chem. Soc. A*, 1969, 1428.


*Received, 3rd October 1996; Com. 6/06791C*

# A tetraspiro nonacyclic compound by condensation of 1,1-bis(aminomethyl)cyclohexane with formaldehyde

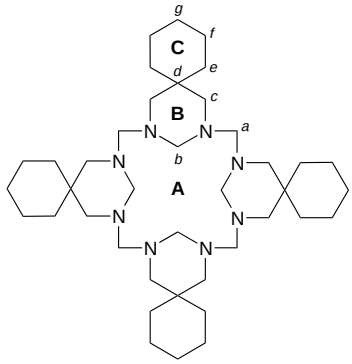
**M. Rachel Suissa,*[a,b] Christian Rømming[a] and Johannes Dale[a]**

[a] *Kjemisk Institutt, Universitetet i Oslo, 0315 Oslo, Norway*
[b] *Nesna College, 8700 Nesna, Norway*

**1,1-Bis(aminomethyl)cyclohexane condenses with formaldehyde to precipitate a polymer, which upon heating is readily isomerized to the nonacyclic compound tetraspiro[tetrakis(cyclohexane)-1,5‴′:1′,11‴′:1″, 17‴′:1‴,23‴′-[1,3,7,9,13,15,19,21]octaazapentacyclo[19.3.1.1$^{3,7}$.1$^{9,13}$.1$^{15,19}$]octacosane 1, whose structure has been determined by X-ray analysis and $^{13}$C NMR spectroscopy.**

The term 'strict covalent self assembly' has been defined as 'completely reversible reactions leading to products that are stable at thermodynamic equilibrium'.[1] Condensation of amines with formaldehyde to give multicyclic structures satisfies this criterion if all rings of the structure can obtain a geometry derivable from the diamond lattice. The earliest example is the formation from propane-1,3-diamine and formaldehyde of a pentacyclic octaaza compound, whose central ring is 16-membered.[2] In this laboratory it was shown that it can have two conformations, both of the diamond lattice type.[3] Subsequently, the corresponding product from 2,2-dimethylpropane-1,3-diamine and formaldehyde was also prepared and shown to exist only in the more symmetric ($D_{2d}$) of the two conformations.[4]

If each *gem*-dimethyl group is replaced by a spiro-linked pentamethylene chain, the resulting compound **1** would have four terminal cyclohexane rings (**C**) with high conformational mobility, while the central 16-ring (**A**) with its four laterally fused 6-rings (**B**) would remain rigid. A very special NMR spectroscopic situation can be predicted from the symmetry properties of the expected diamond lattice conformation of **1** as drawn in Fig. 1. The central part (**A** + 4**B**) has two 'vertical' planes of symmetry passing through atoms *b* and *d*, and two 'horizontal' two-fold axes passing through atoms *a*. At room temperature the terminal rings **C** will flip rapidly between the two chair forms to produce by averaging the NMR spectrum of the apparent 'planar' rings, and the molecular $D_{2d}$ symmetry is not destroyed. When the flipping becomes slow at low temperature, the $^{13}$C signal from carbons *c* will split into two, having very different shifts due to the upfield *gauche* interaction when carbons *f* are on the same side of the symmetry plane. The $^{13}$C signals of atoms *f* themselves will however remain unchanged since they will get the same interaction with carbons *c* on either side. Interestingly then, what is going on in ring **C** is not observed in its own spectrum but by 'remote sensing' in the spectrum of ring **B**.




**1**

A modest signal splitting should be expected also for the more distant 'corner' atoms *a* on the two-fold axes, each interacting weakly with two **C** rings. Assuming that the choice of frozen conformation is independent in each *C* ring, three situations are possible for each *a* carbon: the two neighbouring **C** chairs can either both be in the closest position, or one in the closest and one in the distant position (and *vice versa*), or both can be in their distant position. Statistically, this results in the splitting of the $^{13}$C NMR signal of carbon *a* into a triplet with 1 : 2 : 1 intensity.

An analysis in terms of possible species (conformers) can be carried out by looking down on a square projection of ring **A**. Each chair can be oriented clockwise (+) or counterclockwise (−), and if chirality is disregarded, four conformers are possible (Fig. 2). Of these, the conformer ++−−, drawn in full in Fig. 1, was chosen for clarity. The conformer found in the crystal structure is +++− (*vide infra*). The conclusion above that a 1 : 2 : 1 triplet should be expected statistically for carbon *a* in ring **A** is based on the assumption of equal populations of all four conformers.

Compound **1** was prepared as follows: malonodinitrile and 1,5-dibromopentane gave 1,1-dicyanocyclohexane (mp 63 °C, 65%), which by catalytic hydrogenation ($W_2$-Raney nickel, $NH_3$ saturated EtOH, 80 atm., 70 °C) yielded 1,1-bis(amino-

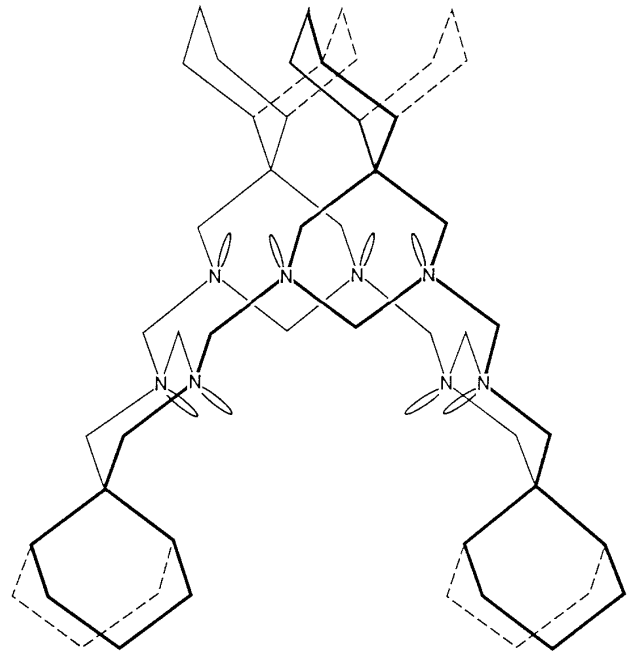



**Fig. 1** The postulated conformation of compound **1**. Both possible chair positions for each **C** ring are shown.

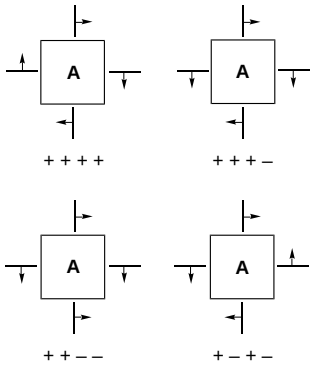



**Fig. 2** The four possible arrangements of rings **C**. The sign (+) represents a clockwise oriented **C** ring and (−) represents a counterclockwise oriented **C** ring.

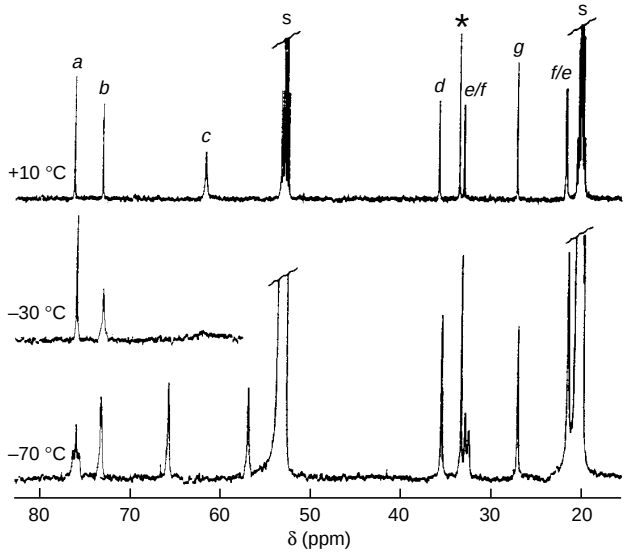



**Fig. 3** 125 MHz $^{13}C$ NMR spectra of **1** in [$^2H_8$]toluene–$CD_2Cl_2$ (1 : 1) at 10, −30 and −70 °C

methyl)cyclohexane as a viscous liquid (80%). Aqueous formaldehyde was dropped into a cooled aqueous solution (*ca.* 0 °C) of this diamine (ratio 2 : 1), causing immediate precipitation of a polymer. The polymer was heated for a few minutes in refluxing dioxane to give compound **1** (mp 215 °C, 100%). It is soluble in most organic solvents and crystallizes from dioxane, $CH_2Cl_2$ or toluene, giving extremely hard crystals; MS (EI, 70 eV) *m/z* 664 ($M^+$), 499 (3/4 M + 1), 333 (1/2 M + 1), 167 (1/4 M + 1), 137, 124, 95, 67, 42; $^{13}C$ NMR (125 MHz in $CD_2Cl_2$, 300 K): δ 76.7 ($C_a$), 73.5 ($C_b$), 62.1 ($C_c$), 36.2 ($C_d$), 33.6 ($C_{e/f}$), 27.6 ($C_g$), 22.2 ($C_{f/e}$).

The $^{13}C$ NMR signals at δ 33.6 and 22.2 (Fig. 3) represent two inner and two outer *e* and *f* carbons, but the splitting is barely visible. After lowering the temperature, the predicted broadening and splitting of the carbon *c* signal at δ 62.1 into a widely separated doublet takes place, while the carbon *a* signal at δ 76.7 splits into a narrow triplet.

The flipping process (or geminal $CH_2$ exchange) of ring **C** could in principle be determined directly by $^1H$ NMR spectroscopy, but this is prevented in practice by complex coupling. Full geminal site exchange of the remaining $CH_2$ groups in ring **A** and **B** would require the passage of much higher barriers, and while at 110 °C clear exchange broadening had started, $T_c$ could not be reached.

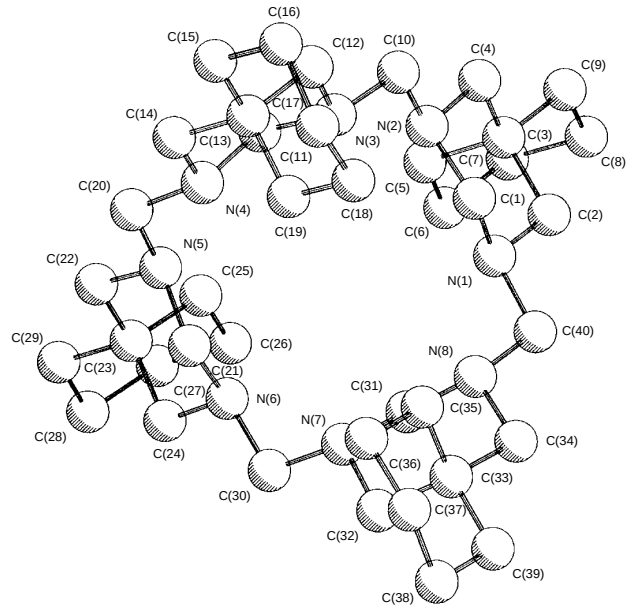



**Fig. 4** PLUTO plot of **1**

The X-ray analysis† of the crystal (Fig. 4) revealed that the unit cell contains four molecules all having the same +++− conformation, possibly chosen to obtain the efficient packing needed to explain the observed unusual hardness of the crystals. The molecules are arranged as two enantiomeric pairs; only one molecule of the pair is shown, the other having disorder in one of the **C** rings due to a 20% population of the +−+− conformer.

We thank NFR for financial support to C. R.

## Footnote

† *Crystal data* for **1**: $C_{40}N_8H_{72}$, colourless crystals, triclinic, space group $P\bar{1}$, $a$ = 15.309(3), $b$ = 16.244(3), $c$ = 19.699(3) Å, $\alpha$ = 69.57(1), $\beta$ = 84.63(2), $\gamma$ = 61.67(1)°, $V$ = 4025.5(1.3) Å$^3$, $Z$ = 4, $T$ = 138 K, spherical crystal, $\phi$ = 0.6 mm, 6614 reflections measured, range ($3 < 2\theta < 45°$), 4995 observed with $I > 3\sigma(I)$, $\mu$ = 1.2 cm$^{-1}$; final $R$ = 0.043 and $Rw$ = 0.042 [1283 parameters, $w = 1/\sigma^2(F_c^2)$; maximum shift/error = 0.27; $\rho_{max}$ = 0.22 e Å$^{-3}$, $\rho_{min}$ = −0.23 e Å$^{-3}$]; X-ray experimental procedures: Mo-K$\alpha$ radiation ($\lambda$ = 0.71069 Å), graphite crystal monochromator, NICOLET P 3F diffractometer ($\omega$ scan technique). The structure was determined by direct methods (MITHRIL) and anisotropically refined (NRCVAX), drawing made using PLUTO.

Atomic coordinates, bond lengths and angles, and thermal parameters have been deposited at the Cambridge Crystallographic Data Centre (CCDC). See Information for Authors, Issue No. 1. Any request to the CCDC for this material should quote the full literature citation and the reference number 182/306.

## References

1 D. Philip and J. F. Stoddart, *Angew. Chem., Int. Ed. Engl.*, 1996, **35**, 1154.
2 H. Krässig, *Makromol. Chem.*, 1955, **17**, 77.
3 J. Dale, C. Rømming and T. Sigvartsen, *Acta Chem. Scand.*, 1991, **45**, 1071.
4 J. Dale, F. Rise, C. Rømming and T. Sigvartsen, *Acta Chem. Scand.*, 1992, **46**, 1200.

*Received, 2nd September 1996; Com. 6/06014E*

# Selective stabilization of a bulged duplex of d(GCGAAACGC) oligonucleotide by thymine base-substituted naphthalene diimide

**Shigeori Takenaka,*[a] Makoto Yokoyama[b] and Hiroki Kondo[b]**

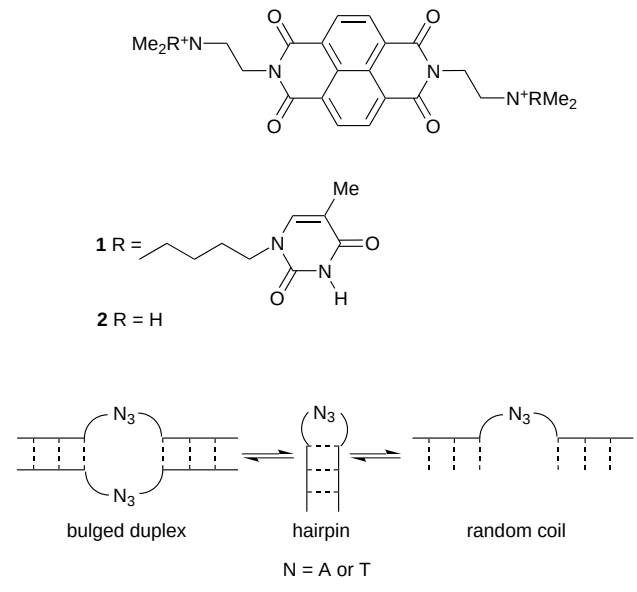
[a] *Department of Chemical Science and Technology, Kyushu University, Fukuoka 812-81, Japan*
[b] *Department of Biochemical Engineering and Science, Kyushu Institute of Technology, Iizuka 820, Japan*

**A naphthalene diimide carrying thymine moieties at the termini of its substituentsstabilized specifically the bulged duplex of d(GCGAAACGC), which is rarely found under ordinary conditions.**

Nucleic acids have a variety of higher-order structures, such as base bulge and hairpin, which are associated with many biological functions.[1] Compounds recognizing these structures are important for studying nucleic acid structure and can serve as new DNA-targeting agents. Many molecules have been synthesized to exhibit this.[2–10] For example, a macrocyclic bisacridine developed by Lehn and co-workers showed a selective binding to the DNA hairpin of d(GCGAAACGC), named $sA_3$.[10] We have shown that thymine base-substituted naphthalene diimide **1** has a high affinity for polyA.[11] It occurred to us that compound **1** might bind to the hairpin region of $sA_3$ specifically as well, since this oligonucleotide consists of single stranded adenines. Contrary to this expectation, however, **1** produced a bulged duplex rather than a hairpin structure on $sA_3$, as shown in Scheme 1.

In $sA_3$, the bulged structure is in equilibrium with a hairpin. The latter is the predominant species in solution under ordinary conditions, as exemplified by a melting profile in which two transition temperatures were observed.[10] The higher melting temperature ($T_{mH}$) is attributed to intramolecular transition from a hairpin to random coil. The lower melting temperature ($T_{mL}$), which is rarely found and $sA_3$ concentration-dependent, is attributed to intermolecular transition from a bulged duplex to a hairpin.

Fig. 1(*a*) shows the melting curve of $sA_3$ with a major transition temperature at 54 °C due to the collapse of the hairpin structure as described previously.[10] Two transition temperatures appeared at about 18 and 60 °C in the presence of **1**, and the lower temperature transition was raised with an increase in the amount of **1**. Since the absorbance of **1** alone was independent of temperature over the 15–90 °C range, the lower transition temperature was attributed to $T_{mL}$. These data indicated that **1** can stabilize the bulged structure of $sA_3$ specifically, although it stabilized the hairpin structure as well, albeit to a smaller extent [*ca*. 6 °C, compare curves (i) and (ii) in Fig. 1(*a*)]. On the other hand, naphthalene diimide **2**, without thymine moieties, showed a transition curve featuring mainly a rise in the $T_{mH}$ to 80 °C. This behaviour of **2** was largely unaffected by the presence of thymine. Ordinary intercalators insert themselves between adjacent base pairs in double stranded nucleic acids, thus effecting stabilization.[12] This is the case with **2**, where the $T_{mH}$ was raised by 26 °C when compared with the $T_{mH}$ of $sA_3$ alone. In summary, **1** stabilizes the bulged duplex of $sA_3$ much more than its hairpin structure, whereas **2** stabilizes mainly the hairpin structure, as do other ordinary intercalators. This difference arises presumably because **1** can bridge the two DNA strands through hydrogen bonding of its thymines moieties with the adenine moieties of $sA_3$. We estimate that 50 and 10% of $sA_3$ assumes the bulged structure in




**Scheme 1**

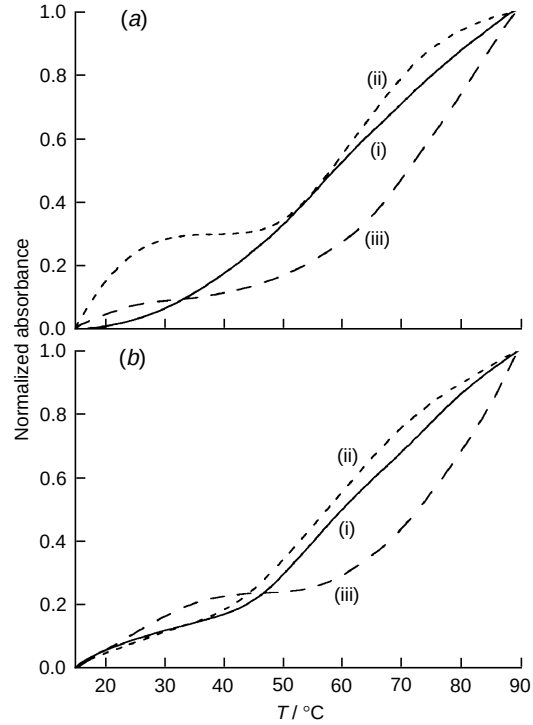



**Fig. 1** Melting profiles for (*a*) $sA_3$ and (*b*) $sT_3$: (i) no additive; (ii) in the presence of **1**; (iii) in the presence of **2**. Carried out in 10 mM MES (2-morpholinoethanesulfonic acid) and 1 mM EDTA (ethylenediaminetetraacetic acid) buffer (pH 6.25); oligonucleotide (in the double strand form) and additive concentration = 5.8 μM.

the presence of an equimolar amount of **1** and **2**, respectively, at 20 °C.

To investigate whether **1** can stabilize the bulged adenines specifically, the melting curve of d(GCGTTTCGC) ($sT_3$) was measured in the absence and presence of **1** or **2** under the same conditions [Fig. 1(*b*)]. This oligonucleotide showed two transition temperatures at *ca*. 15 and 60 °C, which can be attributed to the transition from a bulged duplex to hairpin and from a hairpin to random coil, respectively [(i) in Fig. 1(*b*)]. Neither the bulged duplex nor the hairpin was stabilized by **1**, whereas **2** stabilized the hairpin structure exclusively [(ii) and (iii) in Fig. 1(*b*)]. This result proves that **1** stabilizes the bulged adenines specifically.

The competitive binding to $sA_3$ of **1** and **2** with ethidium bromide was performed by monitoring ethidium fluorescence.

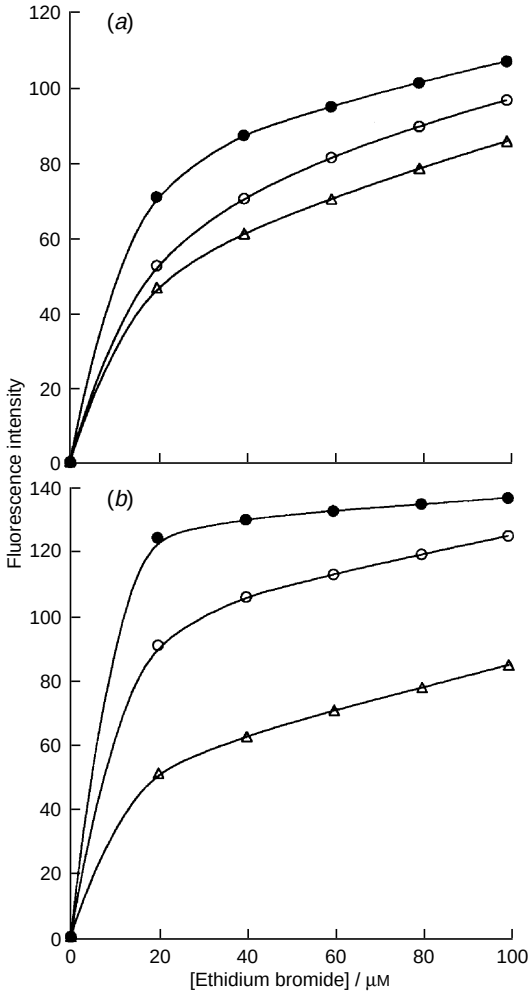



**Fig. 2** Changes in the fluorescence intensity upon addition of ethidium bromide to (*a*) $sA_3$ and (*b*) $sT_3$: (●) no additive; (△) in the presence of **2**; (○) in the presence of **1**. Carried out in 10 mM MES buffer (pH 6.25) containing 0.3% $Me_2SO$ at 20 °C; oligonucleotide (in the double strand form) and additive concentration = 5.8 μM.

Addition of ethidium bromide to $sA_3$ increased the fluorescence intensity at 595 nm ($\lambda_{ex}$ = 546 nm) at 20 °C as a result of binding to DNA as shown in Fig. 2(*a*). The fluorescence of ethidium bromide was suppressed with a mixture of $sA_3$ and **1** or **2**, and the quenching was more pronounced with **2** than with **1** [Fig. 2(*a*)]. On the other hand, **1** was not as effective as **2** in the quenching of the fluorescence of $sT_3$-bound ethidium bromide [Fig. 2(*b*)], demonstrating that the binding of **1** with $sT_3$ is weaker than with $sA_3$, whereas **2** can bind to both $sA_3$ and $sT_3$ equally well.

Since ethidium bromide binds to DNA by intercalation,[13] those intercalators which bind to the double stranded region of DNA compete with ethidium bromide to suppress its fluorescence. It follows therefore that **2** binds mainly to the double stranded region of $sA_3$, whereas **1** is away from such a region and binds mainly to the single stranded loop region. Both the bulge and hairpin structures of $sA_3$ have a loop, but the curvature of the loop is smaller for the bulge. Hence, the naphthalene diimide ring of **1** can stack more effectively with the adenine rings of the bulge. Moreover, since **1** possesses two thymine bases, it can hold together the two strands of $sA_3$ through complementary hydrogen bonding of the thymines with the adenines. We believe that this is the reason why **1** stabilizes the bulged structure of $sA_3$ specifically. Whatever the mechanism, this is the first example of the alteration of the secondary structure of an oligonucleotide using a small molecule.

This work was partially supported by a Grant-in-Aid for Scientific Research from the Ministry of Education, Science, Sports and Culture, Japan.

## References

1 M. Chastin and I. Tinoco, Jr., in *Progress in Nucleic Acids Research and Molecular Biology*, ed. W. E. Cohn and K. Moldave, Academic, New York, 1991, vol. 41, p. 131.
2 L. S. Ratmeyer, R. Vinayak, G. Zon and W. D. Wilson, *J. Med. Chem.*, 1992, **35**, 966.
3 J. L. Mergny, G. Duval-Valentin, C. H. Nguyen, L. Perrouault, B. Faucon, M. Rougee, T. B. Montenay-Garestier, E. Isagni and C. Hélène, *Science*, 1992, **256**, 1681.
4 W. D. Wilson, F. A. Tanious, S. Mizan, S. Yao, A. S. Kiselyov, G. Zon and L. Strekowski, *Biochemistry*, 1993, **32**, 10 614.
5 J. S. Lee, L. J. P. Latimer and K. J. Hampel, *Biochemistry*, 1993, **32**, 5591.
6 D. S. Pilch and K. J. Breslauer, *Proc. Natl. Acad. Sci. USA*, 1994, **91**, 9332.
7 K. R. Fox, P. Polucci, T. C. Jenkins and S. Neidle, *Proc. Natl. Acad. Sci. USA*, 1995, **92**, 7887.
8 S. C. Zimmerman, C. R. Lamberson, M. Cory and T. A. Fairley, *J. Am. Chem. Soc*., 1989, **111**, 6805.
9 J. M. Veal, Y. Li, S. C. Zimmerman, C. R. Lamberson, M. Cory, G. Zon and W. D. Wilson, *Biochemistry*, 1990, **29**, 10 918.
10 A. Slama-Schwok, M.-P. Teulade-Fichou, J.-P. Vigneron, E. Taillandier and J.-M. Lehn, *J. Am. Chem. Soc*., 1995, **117**, 6822.
11 S. Takenaka, M. Manabe, M. Yokoyama, M. Nishi, J. Tanaka and H. Kondo, *Chem. Commun*., 1996, 379.
12 M. Cory, D. D. McKee, J. Kagan, D. W. Henry and J. Miller, *J. Am. Chem. Soc*., 1985, **107**, 2528.
13 B. F. Cain, B. C. Baguley and W. A. Danny, *J. Med. Chem*., 1978, **21**, 658.

*Received, 28th October 1996; Com. 6/07303D*

# Molecular recognition induced aggregation and fusion between vesicles containing lipids bearing complementary hydrogen bonding head-groups

**Valérie Marchi-Artzner,[a] Ludovic Jullien,[a]† Thaddée Gulik-Krzywicki[b] and Jean-Marie Lehn*[a]**

[a] *Laboratoire de Chimie des Interactions Moléculaires, UPR285, Collège de France, 11, Place Marcelin Berthelot, F-75005 Paris, France*

[b] *Centre de Génétique Moléculaire, CNRS, 91190 Gif-sur-Yvette, France*

**Equimolar mixtures of large unilamellar vesicles, obtained from mixtures of egg lecithin and lipids containing complementary hydrogen bonding head-groups (barbituric acid and triaminopyrimidine), aggregate and fuse generating much larger vesicles.**

Molecular recognition research has focussed especially on the selective formation of discrete supermolecules from complementary receptor–substrate pairs.[1] Extension to polymolecular assemblies should allow the recognition-directed generation of well-defined, extended supramolecular entities *via* the introduction of suitable recognition features into the molecular components.

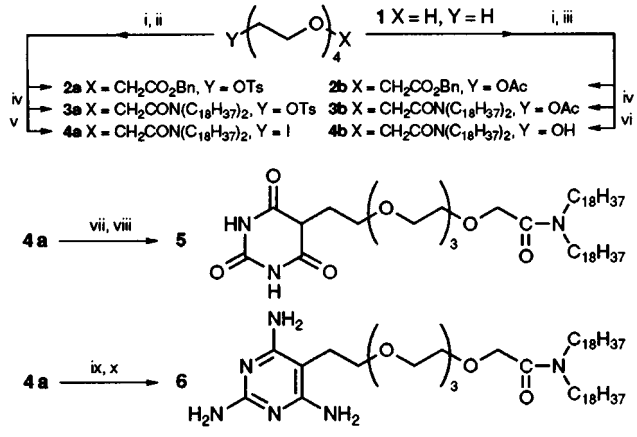
Thus, in previous work from our group, the self-assembly of units bearing complementary hydrogen bonding patterns has been used for generating liquid crystalline phases[2,3] and supramolecular polymers.[3,4] On the other hand, selective interactions take place at molecular layers into which recognition groups have been introduced.[5–7] Further on, molecular recognition may direct processes occuring between discrete polymolecular bodies such as liposomes. Indeed, surface recognition is a basic process controlling the interactions between biological cells.[8] Endowing artificial vesicles with recognition features may provide a means of provoking their interaction and for inducing processes such as aggregation and fusion. In the longer term it should permit the generation of polyvesicular architectures in a controlled fashion, a prerequisite for constructing organized assemblies of vesicles, of interest both as artificial functional nanoarchitectures and as models of biological tissue.

We report here some of our first results on the study of vesicles containing complementary lipids bearing as head groups the barbituric acid (BAR) and triaminopyrimidine (TAP) units which not only interact through three hydrogen bonds, but also, due to their double-faced nature, form self-assembled, extended ribbons.[9] the polymeric character of which is expected to enhance the global adhesion between complementary surfaces. We have previously studied the behavior of electrostatically complementary vesicles bearing opposite charges,[10] and recently the interaction between vesicles containing a biotinylated lipid and streptavidin in solution has been investigated.[11] For this work, we selected the complementary amphiphiles **5** and **6**; they were synthesized according to Scheme 1.‡ In view of the supramolecular organization imposed by hydrogen bonding interaction, a polyoxyethylenic spacer has been introduced in order to provide sufficient orientational freedom to the recognition sites.

Electron microscopy showed that **4b** and 1 : 9 mixtures of **5** or **6** with **4b** form lamellar phases in water under all conditions of vesicle preparation that have been investigated in the present study (detergent removal, sonication or lipid swelling in presence of an alternative electrical field). Large unilamellar vesicles were prepared from 1 : 9 mixtures of **5**, **6** or **4b** and egg lecithin (EPC) either by detergent dialysis[15] or extrusion[16] methods. As indicated by freeze-fracture electron microscopy [Fig. 1(*a*)] and by quasistatic and dynamic light scattering experiments, the size polydispersity of vesicles prepared by extrusion through Nucleopore filters was low, making them suitable to analyse the evolution of the vesicle solution by these techniques. Whereas aqueous suspensions of pure **5**, **6** and **4b** exhibited a sharp signal at 41 ± 1 °C by differential scanning calorimetry (DSC), the 1 : 9 mixtures with EPC did not display any transition, thus suggesting the absence of an extensive lipid segregation within the bilayer.

When identical amounts of weakly light scattering vesicular preparations of **5**-EPC 1 : 9 and **6**-EPC 1 : 9 were mixed, the solution became turbid after a few minutes whereas the appearance of individual preparations remained stable for a week. This observation was quantified by dynamic light scattering measurements (Table 1). The diameters of the starting vesicular suspensions were in the 150 nm range whereas the multimodal mathematical treatment of the data from the final state of the mixture provided an apparent diameter equal to 2000 nm. Considering the relation of size to scattered light intensity, this value can be reasonably assumed to represent the diameter of the largest objects.

In order to define more precisely the nature of the events taking place in these solutions, electron microscopy pictures were recorded at different times after mixing complementary vesicles. First, a rapid aggregation leading to the formation of large clusters of vesicles was observed [Fig. 1(B)]. After 15 min, two different populations of vesicles were visible [Fig. 1(C)]. A few very large vesicles (micrometer range) were surrounded by many smaller ones exhibiting size and morphology close to that of starting preparations. Support for the identification of vesicle fusion as the phenomenon triggering vesicle growth was provided by the observation of singular




**Scheme 1** *Reagents and conditions*: i, $N_2CHCO_2Bn$, $BF_3(OEt_2)$, $CH_2Cl_2$, room temp., 60%; ii, TsCl, pyridine, 0 °C, 69%; iii, $Ac_2O$, pyridine, room temp., 80%; iv, (*a*): $H_2$, Pd/C, $CH_2Cl_2$, (*b*) *N*-hydroxysuccinimide, DCC, DMAP, (*c*) $HN(C_{18}H_{37})_2$, 30 °C; v, NaI, butanone reflux, 93%; vi, NaOH, EtOH, 96%; vii, $CH_2(CO_2Me)_2$, NaOMe MeOH, reflux, 85%; viii, $OC(NH_2)_2$, NaOMe, MeOH, reflux, 72%; ix, $CH_2(CN)_2$, NaH, $Me_2SO$, 60%; x, $HNC(NH_2)_2$, NaOMe, MeOH, reflux, 70%

events such as the formation of necks between adhering vesicles and budding on large vesicles [Fig. 1(D)].

In the present system, different interactions may contribute to the observed coalescence phenomena. In view of the acidobasic properties of the BAR and TAP lipids leading to the formation of species of opposite charge, an attractive electrostatic interaction may also play a role as observed previously.[10] Furthermore, ion-pairing reinforced hydrogen bonding between BAR and TAP units has been observed.[17] Since polyoxyethyleneglycol is known to promote vesicle fusion, we established that the spacer itself did not do so, since vesicles prepared from 1 : 9 **4b**-EPC mixtures were stable at least for several days. The present experiments consequently suggest that surface recognition *via* complementary hydrogen bonding patterns plays an important role in the events observed. Studies in progress should provide more information about the nature of the interaction between complementary vesicles and about its role in the vesicle fusion event. The intervesicular processes described here represent a first step towards the controlled, recognition-directed construction of organized, functionally integrated assemblies of vesicles leading towards 'tissue-like' artificial entities.

We thank L'OREAL for a graduate fellowship to V. M. A.

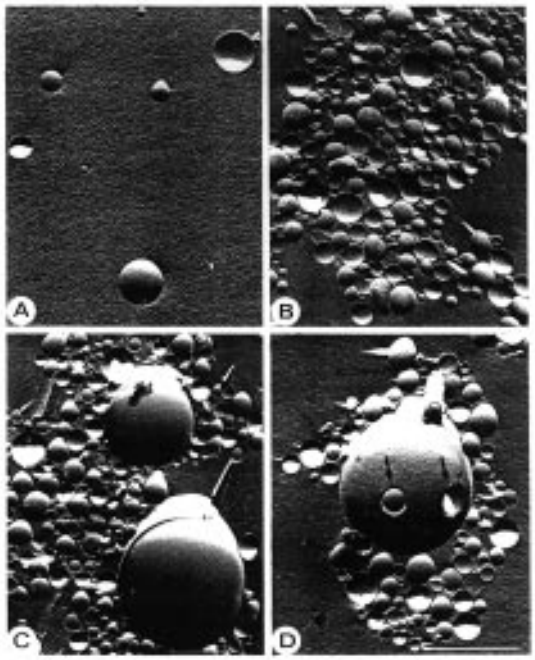



**Fig. 1** Freeze-fracture electron micrographs of the vesicles prepared from 9 : 1 mixtures of egg lecithin and lipids **5** or **6** containing either barbituric acid (BAR) or triaminopyrimidine (TAP) head-groups. (A) Typical image of vesicle preparations containing either BAR or TAP lipids. (B) Equimolar mixture of BAR and TAP vesicles immediately after mixing. (C), (D): the same as (B) but after more than 15 min incubation. Notice the aggregation of vesicles after mixing and the appearance of much larger vesicles after incubation, some of which show vesicle fusion [arrows in (D)]. All photographs are at the same scale; the bar on (D) represents 500 nm.

**Table 1** Diameters (in nm) of large unilamellar vesicles determined by dynamic light scattering (± 10nm)[a]

| Angle(°) | **6**-EPC vesicles | **5**-EPC vesicles | 1 : 1 Vesicle mixture |
|---|---|---|---|
| 90 | 137 | 135 | — |
| 70 | 144 | 153 | — |
| 50 | 155 | 156 | 2000 |

[a] Vesicles prepared by extrusion from 1 : 9 mixtures of **5** or **6** and EPC at 35 °C in 20 mM glucose; vesicle concentration: 0.5 mg $dm^{-3}$

## Footnotes

† Present address: Laboratoire de Chimie URA 1679, Ecole Normale Supérieure, 24, rue Lhomond, F. 75231 Paris Cedex 05, France

‡ The reaction of an excess of tetraethyleneglycol with benzyldiazoacetate.[12] followed by tosylation of the remaining alcohol group yielded compound **2a** which, *via* hydrogenolysis over Pd/C in $CH_2Cl_2$ followed by coupling with dioctadecylamine gave the amide **3a** which was converted to **4a**. This led to the barbituric acid derivative **5** by monoalkylation of dimethyl malonate followed by condensation with urea.[13] The substituted triaminopyrimidine **6** was obtained in a similar way *via* monoalkylation of malonodinitrile by **4a** and then condensation with guanidine.[14] The alcohol **4b** was synthesized by a modification of the pathway *via* **2b** and **3b**.

## References

1 J.-M. Lehn, *Supramolecular Chemistry*, VCH, Weinheim, 1995; *Comprehensive Supramolecular Chemistry*, ed. J. L. Atwood, J. E. D. Davies, D. D. MacNicol and F. Vogtle, Pergamon, Oxford, 1996, vol. 1–3.
2 J. Brienne, J. Gabard, J.-M. Lehn and I. Stibor, *J. Chem. Soc., Chem. Commun*., 1989, 1868.
3 C. Fouquey, J.-M. Lehn and A.-M. Levelut, *Adv. Mater*., 1990, **2**, 254; T. Gulik-Krzywicki, C. Fouquet and J.-M. Lehn, *Proc. Nat. Acad. Sci. USA*, 1993, **90**, 163.
4 Ref. 1, Ch. 9; J.-M. Lehn, *Makromol. Chem. Makromol. Symp*., 1993, **1**, 69; see also C. M. Paleos and D. Tsioulvas, *Angew. Chem., Int. Ed. Engl*., 1995, **34**, 1696; D. S. Lawrence, T. Jiang and M. Levett, *Chem. Rev*., 1995, **95**, 2229.
5 R. Ahuja, P. Lorenzo Casuro, D. Möbius, W. Paulus, H. Ringsdorf and G. Wildburg, *Angew. Chem., Int. Ed. Engl*., 1993, **105**, 1082.
6 N. Kimizuka, T. Kawasaki and T. Kunitake, *J. Am. Chem. Soc*., 1993, **115**, 4387; T. Kunitake, *Makromol. Chem. Makromol. Symp*., 1995, **98**, 45.
7 F. Pincet, E. Perez, G. Bryant, L. Lebeau and C. Mioskowski, *Phys. Rev. Lett*., 1994, **73**, 2780.
8 B. Albert, D. Bray, J. Lewis, M. Raff, K. Roberts and J. D. Watson, *Molecular Biology of the Cell*, 3rd edn, Garland, New York, 1994.
9 J.-M. Lehn, M. Mascal, A. Decian and J. Fischer, *J. Chem. Soc., Chem. Commun*., 1990, 479.
10 V. Marchi-Artzner, L. Jullien, L. Belloni, D. Raison, L. Lacombe and J.-M. Lehn, *J. Phys. Chem*., 1996, **100**, 13 844.
11 S. Chiruvolu, S. Walker, J. Israelachvili, F. J. Schmitt, D. Leckband and J. A. Zasadzinski, *Science*, 1994, **264**, 1753.
12 *Org. Synth*., 1973, **5**, 179.
13 A. C. Cope, H. L. Holmes and H. O. House, *Org. React.*, IX, ch. 4, 107.
14 P. B. Russel and G. H. Hitching, *J. Am. Chem. Soc*., 1952, **74**, 3443.
15 *Liposomes. A Practical Approach*, ed. R. R. C. New, Oxford University Press, New York, 1990; L. T. Mimms, G. Zampighi, Y. Nozaki, C. Tanford and J. A. Reynolds, *Biochemistry*, 1981, **20**, 833.
16 F. Szoka, Jr. and D Papahadjopoulos, *Proc. Natl. Acad. Sci. USA*, 1978, **75**, 4194.
17 M. Mascal, P. S. Fallon, A. S. Batsanov, B. R. Heywood, S. Champ and M. Coclough, *J. Chem. Soc., Chem. Commun*., 1995, 805.

*Received, 16th September 1996; Com. 6/06340C*

# Molecular recognition involving multiple cation–π interactions: the inclusion of the acetylcholine trimethylammonium moiety in resorcin[4]arene

**Kazutaka Murayama and Katsuyuki Aoki***

*Department of Materials Science, Toyohashi University of Technology, Tempaku-cho, Toyohashi 441, Japan*

**X-Ray analysis of the molecular complex formed between the neurotransmitter acetylcholine (ACh) and resorcin[4]-arene, ACh$^+$.resorcinarene.Cl$^-$.$H_2O$ shows that the ACh molecule is captured by the macrocyclic resorcinol tetramer through multiple cation–π interactions between the quaternary trimethylammonium group of ACh and the four π-rings of the cavitand.**

The cation–π interaction has attracted much attention because of its chemical,[1–3] biological[1] and theoretical[4] applications. It has been well documented that synthetic macrocyclic compounds comprised of aromatic rings exhibit a strong affinity for quaternary ammonium compounds including the neurotransmitter acetylcholine (ACh).[1a] Particular interest focuses on the origin of the strong molecular association: it has been proposed[1a] that the cationic ammonium group could bind to the π-faces of aromatic rings of its receptor through a cation–π interaction. Although a recent statistical analysis,[5] based on crystal structures from the Cambridge Structural Database, of the interactions between R–N$^+$Me$_3$ cations and phenyl rings demonstrates their preferable occurrence, X-ray evidence for such a cation–π interaction is still lacking† for artificial macrocyclic receptor systems,[1–3,6] involving synthetic ACh receptors.[1a,7] As the continuation of our X-ray investigations on the cation–π interaction,[8] we report here the crystal structure of the molecular complex formed between macrocyclic resorcin[4]arene **1**‡ and ACh, where the quaternary trimethylammonium group of ACh makes close contacts with the four π-rings of **1**. $^1$H NMR spectroscopy confirms that the cation–π interaction also occurs in solution. The biological relevance of the multiple cation–π interactions for the interaction between ACh and acetylcholine esterase (AChE) is suggested.

The ACh–resorcin[4]arene molecular complex was prepared from ACh$^+$.Cl$^-$ (2 mmol) and **1**§ (0.2 mmol) dissolved in ethanol (5 ml)–water (3 ml). The mixture (pH 6) was allowed to stand at room temperature for three weeks after which colourless crystals (plates) formed.¶ 3,3-Dimethylbutyl acetate **2** was synthesized in 83% yield from acetyl chloride (50 mmol) and 3,3-dimethylbutan-1-ol (6 ml, 50 mmol).

Fig. 1 shows the molecular structure of the complex, ACh$^+$.**1**.Cl$^-$.$H_2O$, where **1** is neutral. The most interesting structural feature is the host–guest complexation between **1** and ACh through cation–π interactions, that is, between the quaternary trimethylammonium group of ACh and the multiple π-rings system of the macrocyclic resorcinol tetramer. The choline group makes close contacts through its two methyl groups with the four rings of the bowl-shaped cavitand. To our knowledge, this is the first crystal structure in which ACh shows the cation–π interaction between the trimethylammonium group and the π-electrons of the aromatic ring. The ACh molecule adopts a *gauche* conformation about the choline group due to an N$^+$···O electrostatic interaction [the torsion angle O(10)–C(39)–C(40)–N(1) = −77(5)°], usually observed[9] for the O–C–C–N$^+$ system, and *trans* about the C(38)–O(10) bond [C(37)–C(38)–O(10)–C(39) = −173(2)°]. Furthermore, in the crystal lattice this ACh is capped on its acetyl terminal group by the adjacent resorcinarene molecule (at 3/2 − *x*, 1/2 + *y*, 1/2 − *z*), as shown in Fig. 2. Thus an ACh molecule is captured by two resorcinarene molecules in a head-to-tail arrangement. Interestingly, the polar carboxy oxygen O(9), rather than the apolar methyl group C(37), contacts with the aliphatic ethyl groups tethered to the tail of the cavitand [3.83(3) Å to C(29), 3.80(3) Å to C(31), 3.78(3) Å to C(33) and 3.68(3) Å to C(35)]. The chloride anion forms four hydrogen bonds with the hydroxy oxygen atoms O(1) [Cl···O(1) 3.04(1) Å], O(2) [3.12(1) Å] and O(7) [2.99(2) Å], each oxygen belonging to a different molecule, and a water oxygen atom O(11) [3.24(2) Å], but it does not contact with the cationic choline group of ACh.

The $^1$H NMR spectrum (270 MHz, $CD_3OD$) of the ACh–resorcinarene **1** complex (30 mmol dm$^{-3}$) shows a singlet at δ 2.107 for the *N*-methyl protons of ACh, while the corresponding signal of ACh alone appears at δ 3.215. This upfield shift of 1.108 ppm for the complex is probably due to the aromatic ring-current effect, indicating that the quaternary trimethylammonium group associates preferentially with the π-rings of resorcinarene in solution, where the resorcinarene molecule

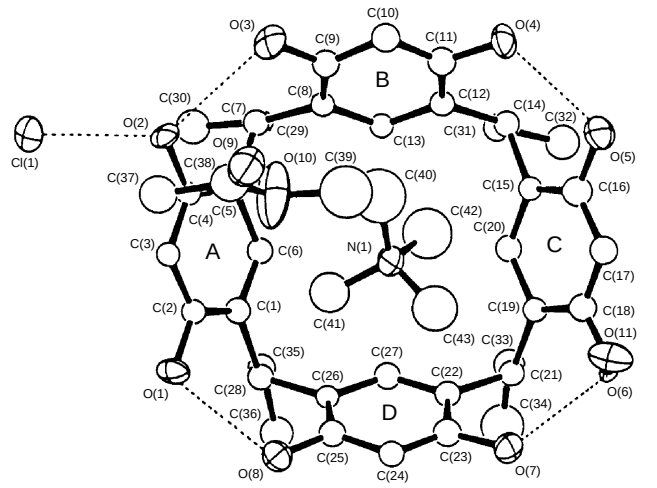
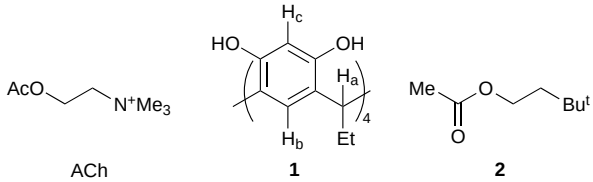



**Fig. 1** Top view of the molecular structure of ACh$^+$.**1**.Cl$^-$.$H_2O$, showing the host–guest complexation between a cyclic resorcinol tetramer and an ACh molecule through cation–π multiple interactions; close contacts (< 3.6 Å): C(41)···C(2) [3.51(4)], C(41)···C(25) [3.56(4)], C(42)···C(12) [3.57(5)], C(42)···C(15) [3.43(5)], C(42)···C(16) [3.54(5)] and C(42)···C(20) [3.48(5) Å]; relevant methyl C···π-centroid distances: C(41)···ring A [3.60], C(41)···ring D [3.87], C(42)···ring B [3.64] and C(42)···ring C [3.36 Å]; relevant methyl C···ring–plane perpendicular distances: C(41)···ring A [3.48], C(41)···ring D [3.59], C(42)···ring B [3.52] and C(42)···ring C [3.31 Å]. Broken lines denote hydrogen bonds.



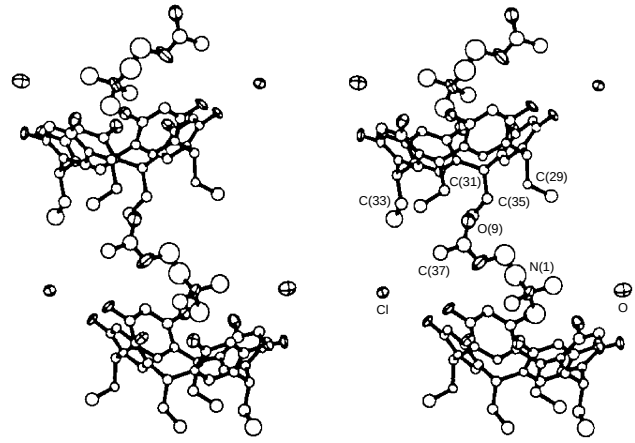



**Fig. 2** Stereoview of a segment of the crystal structure of $ACh^+$.**1**.$Cl^-$.$H_2O$, showing the encapsulation of an ACh molecule between two resorcinarene molecules and close C–H···O contacts between the carboxyl oxygen of ACh and four $CH_2$ moieties tethered to the lower rim of the cavitand

retains the bowl-shaped conformation.‖ In addition, the $^1H$ NMR spectrum (270 MHz, $CD_3OD$) of the solution containing ACh (30 mmol $dm^{-3}$) and resorcinol monomer as noncyclic reference compound in a 1 : 4 molar ratio does not show an appreciable upfield shift of the *N*-methyl protons (δ 3.195) of ACh, showing the importance of the defined structure of **1** in its effective association with ACh, where the preorganized cavity of **1** makes cation–π multiple interactions possible and stabilizes them.

In order to examine more closely the significance of the quaternary trimethylammonium group in the cation–π interaction, a comparative study was undertaken using 3,3-dimethylbutyl acetate **2**, an uncharged compound isosteric to ACh, where the trimethylammonium nitrogen of ACh is replaced with a carbon atom. The $^1H$ NMR spectrum (270 MHz, $CD_3OD$) of the solution containing acetate **2** and resorcinarene **1** (30 mmol $dm^{-3}$; equimolar ratio) and that of **2** alone show only a small upfield shift of 0.052 ppm for the *tert*-butyl protons of **2** in the mixture (δ 0.895 and 0.947, respectively). This indicates that the intensity of interaction between the terminal *tert*-butyl group of **2** and the π-rings of **1** may be minor. Thus it appears again[1a,8] that the cationic nature of the quaternary choline group could be responsible for its preferable association with the π-ring, that is, through cation–π interaction.

In summary, (i) the ACh molecule contacts simultaneously with more than one aromatic ring through multiple cation–π interactions, thus mimicking the ACh binding to AChE. A recent X-ray study[10] has revealed that a total of 14 aromatic residues line the 'active site gorge' of AChE. A biological role of the multiple cation–π interactions might be that simultaneous contacts could promote the gain of total energy for molecular associations which are needed for rapid transport of ACh through the gorge ('aromatic guidance'[10]) and also for the ACh-fixing at the bottom of the gorge. In this regard, the trimethylammonium moiety of ACh, where one positive formal-charge is smeared out over the three methyl groups,[1a] seems to be an excellent device to achieve cation–π multiple interactions. (ii) This study clearly demonstrates that the aromatic system interacts strongly with the cationic choline moiety in preference to the neutral *tert*-butyl group. In order to provide further insights into the significance of the trimethylammonium group of ACh in the cation–π interaction, X-ray and solution studies, by exchanging the $N^+Me_3$ group with $N^+H_nMe_{3-n}$ ($n$ = 1–3), are under way.

## Footnotes

† There have been reported, to our knowledge, two crystal structures[3,11] of host–guest complexes between synthetic macrocycles of aromatic rings and quaternary ammonium compounds: however, in $4Na^+$.(trimethylanilinium$^+$).(*p*-sulfonatocalix[4]arene$^{4-}$).$Cl^-$;[3] the trimethylammonium group is located out of the cavity of the host, and in $(Et_3HN^+)_2$.(tetramethylresorcin[4]arene).$SO_4^{2-}$.4EtOH,[11] no mention is made on the cation–π interaction.

‡ 2,8,14,20-Tetraethyl-4,6,10,12,16,18,22,24-octahydroxycalix[4]arene.

§ Compound **1** was synthesized according to a literature procedure.[12]

¶ *Crystal data* for: $ACh^+$.**1**.$Cl^-$.$H_2O$.$C_{43}H_{58}ClNO_{11}$. $M$ = 800.38, colourless plates, monoclinic, space group $P2_1/n$, $a$ = 12.450(9), $b$ = 21.598(7), $c$ = 15.717(7) Å, β = 95.15(5)°, $U$ = 4209(3) Å$^3$, $Z$ = 4, $D_m$ = 1.265 (measured by flotation in hexane–carbon tetrachloride), $D_c$ = 1.263 g $cm^{-3}$, μ(Mo-Kα) = 1.50 $cm^{-1}$, $T$ = 293 K, $F$(000) = 1712. A Rigaku AFC7R diffractometer with graphite-monochromated Mo-Kα (λ = 0.71069 Å) was used to collect 5847 unique data in the range $4 < 2\theta < 50°$, 1728 data with $I > 3\sigma(I)$ were used in the refinement. The diffraction pattern was in general quite weak and did not extend much beyond 2θ = 40°, mostly due to the small crystal size (0.08 × 0.30 × 0.30 mm) and some disorder of ACh molecules (as noted below). Residuals of $R$ = 0.110 and $R_w$ = 0.117 were obtained after 295 parameters had refined to convergence (TEXSAN), where only Cl, O and N atoms were treated anisotropically while all C atoms isotropically because of limited number of reflection data. The quality-of-fit index is 1.53, and the largest shift/esd = 0.18. High vibrational amplitudes [10–16 Å$^2$] for C(34), O(10), C(37), C(40), C(42) and C(43) of ACh might be due to disorder, that is, these atoms most likely occupy slightly different positions from molecule to molecule (attempts to find alternative chain conformations failed), causing the rather high $R$ values. No attempt to locate the H atoms was made. Atomic coordinates, bond lengths and angles, and thermal parameters have been deposited at the Cambridge Crystallographic Data Centre (CCDC). See Information for Authors, Issue No. 1. Any request to the CCDC for this material should quote the full literature citation and the reference number 182/317.

‖ In solution, resorcin[4]arene exists as mixtures of bowl-shaped (crown), saddle, boat and chair conformers.[13] In the ACh-1 system, the equivalency in the NMR spectra of four Ha protons (t, $\delta_H$ 4.175–4.233), four Hb (s, $\delta_H$ 6.248), and four Hc (s, $\delta_H$ 7.262) of **1** indicates that **1** has a symmetric macrocyclic skelton, suggesting **1** to have a bowl-shaped conformation.

## References


1 (*a*) D. A. Dougherty and D. A. Stauffer, *Science*, 1990, **250**, 1558 and references cited therein; (*b*) D. A. Dougherty, *Science*, 1996, **271**, 163.
2 H.-J. Schneider, *Angew. Chem., Int. Ed. Engl.*, 1991, **30**, 1417 and references cited therein.
3 S. Shinkai, K. Araki, T. Matsuda, N. Nishiyama, H. Ikeda, I. Takasu and M. Iwamoto, *J. Am. Chem. Soc.*, 1990, **112**, 9058, and references cited therein.
4 S. Mecozzi, A. P. West Jr. and D. A. Dougherty, *J. Am. Chem. Soc.*, 1996, **118**, 2307 and references cited therein; C. Chipot, B. Maigret, D. A. Pearlman and P. A. Kollman, *J. Am. Chem. Soc.*, 1996, **118**, 2998.
5 M. L. Verdonk, G. J. Boks, H. Kooijman, J. A. Kantors and J. J. Kroon, *J. Comput.-Aided Mol. Des.*, 1993, **7**, 173.
6 T. Merz, H. Wirtz and F. Vögtle, *Angew. Chem., Int. Ed. Engl.*, 1986, **25**, 567; A. Casnati, P. Jacopozzi, A. Pochini, F. Uggozoli, R. Cacciapaglia, L. Mandolini and R. Ungaro, *Tetrahedron*, 1995, **51**, 591.
7 M. Dhaenens, L. Lacombe, J.-M. Lehn and J.-P. Vigneron, *J. Chem. Soc., Chem. Commun.*, 1984, 1097; L. Garel, B. Lozach, J.-P. Dutasta and A. Collet, *J. Am. Chem. Soc.*, 1993, **115**, 11 652; R. Mélic, J.-M. Lehn and J.-P. Vigneron, *Bull. Soc. Chim. Fr.*, 1994, **131**, 579; M. Inouye, K. Hashimoto and K. Isagawa, *J. Am. Chem. Soc.*, 1994, **116**, 5517; K. N. Koh, K. Araki, A. Ikeda, H. Otsuka and S. Shinkai, *J. Am. Chem. Soc.*, 1996, **118**, 755.
8 K. Aoki, K. Murayama and H. Nishiyama, *J. Chem. Soc., Chem. Commun.*, 1995, 2221.
9 M. Sundaralingam, *Nature*, 1968, **217**, 35.
10 J. L. Sussman, M. Harel, F. Frolow, C. Oefner, A. Goldman, L. Toker and I. Silman, *Science*, 1991, **253**, 872.
11 T. Lippmann, H. Wilde, M. Pink, A. Schäfer, M. Hesse and G. Mann, *Angew. Chem., Int. Ed. Engl.*, 1993, **32**, 1195.
12 Y. Aoyama, Y. Tanaka and S. Sugahara, *J. Am. Chem. Soc.*, 1989, **111**, 5397.
13 A. G. S. Högberg, *J. Am. Chem. Soc.*, 1980, **102**, 6046.


*Received, 21st October 1996; Com. 6/07131G*

# Enhanced binding of a hexacyclic amidine analogue of Hoechst 33258 to the minor groove of DNA: $^1$H NMR and UV melting studies with the decamer duplex d(GGTAATTACC)$_2$

**Clare E. Bostock-Smith,[a] Kevin J. Embrey[b] and Mark S. Searle*[a]**

[a] *Department of Chemistry, University of Nottingham, University Park, Nottingham, UK NG7 2RD*
[b] *Queensland Pharmaceutical Research Institute, Griffith University, Nathan, Brisbane 4111, Australia*

**NMR and UV melting studies with the decamer duplex d(GGTAATTACC)$_2$ show that replacing the *N*-methylpiperazine ring of the DNA minor groove binding agent Hoechst 33258 with a hexacyclic amidine leads to both an increase in duplex stability ($\Delta T_m \approx 7$ °C) and enhanced A–T specific recognition; the amidine NH exchanges slowly with the solvent and has a small temperature coefficient ( < 3 ppb/°C) supporting its involvement in intermolecular hydrogen bonding, however, the data suggest that the ring is flipping rapidly even at 278 K even though the interaction appears to contribute significantly to complex stability.**

The bis-benzimidazole Hoechst 33258 [Fig. 1(*a*), **1**] binds to the minor groove of A–T rich DNA sequences.[1] Specific hydrogen bonding interactions between the benzimidazole NHs and adenine N3/thymine O2 of the DNA bases on the floor of the groove provide key components for binding and recognition; the complex has been studied extensively by NMR[2–6] and X-ray analysis.[7–12] In contrast, the role of the *N*-methylpiperazine ring in the recognition process is less well defined. Its cationic charge clearly contributes to complex stability, while van der Waals contacts are also observed with the floor of the minor groove.[10] However, both the conformation and orientation of the piperazine ring appear to be variable including, in some cases, the observation of preferential binding to G–C regions at the end of A–T tracts of DNA where the wider groove has been proposed to more readily accommodate this bulky substituent.[7,9,11]

One rational approach to the design of new Hoechst analogues with enhanced functional properties is to replace the *N*-methylpiperazine component with one capable of specific hydrogen bond-mediated recognition of the minor groove. Here we describe such an analogue containing a hexacyclic amidine group, Hoechst 43254 **2**. A recent X-ray structure[13] has shown that a Hoechst analogue with a five-membered amidine ring does not have the correct geometry to allow the amidine NH to hydrogen bond to the floor of the minor groove.

Energy minimisation of Hoechst 43254 using MACROMODEL[14] suggests that a twist of *ca*. 20° away from coplanarity is necessary to relieve steric repulsions between amidine NHs and phenyl hydrogens on the adjacent benzimidazole ring. Energy minimisation and molecular dynamics calculations on the DNA complex of **2** (modelled from the X-ray coordinates of the DNA complex of **1** described by Quintana *et al.*[10]) suggest that the ligand should bind with enhanced specificity to the 5′-AATT sequence through the interaction of an amidine NH with the N3 of the second adenine base [see Fig. 1(*b*) *vs*. 1(*c*)]. The twisted conformation of the six-membered amidine ring (*cf*. the five-membered ring) appears to optimise the geometry for such an interaction.

In Fig. 2, UV 'melting' curves for d(GGTAATTACC)$_2$ are shown plotted as absorbance at 260 nm *vs*. temperature at a duplex concentration of 3.2 μM (buffered with 0.01 M sodium phosphate and 0.11 M sodium chloride, pH 7.0). The duplex alone gives a broad melting curve with a $T_m$ of 27 °C. Hoechst 33258 **1** increases the $T_m$ significantly to 45 °C with the melting transition becoming appreciably more cooperative. However, with Hoechst 43254 **2** bound the stabilisation effect is even more pronounced with the $T_m$ rising further to 52 °C ($\Delta T_m \approx$ 7 °C), in good agreement with previous studies with related ligands and other A–T tract duplexes.[15]

In Fig. 3 we show by $^1$H NMR that **2** binds tightly to d(GGTAATTACC)$_2$ and is in slow exchange on the chemical shift time-scale. Binding of the asymmetric ligand lifts the dyad symmetry of the duplex such that the two strands of DNA are non-equivalent in the complex. The high field methyl region (δ 1–1.8) and low field imino proton region of the spectrum (δ 9.0–14.5) of the ligand-free and ligand-bound duplex are illustrated. The number of thymine methyl [(*a*) *vs.* (*b*)] and imino proton resonances from the A–T base pairs [(*c*) *vs.* (*d*)] doubles on ligand binding indicating that the drug is located at a single high affinity site. Generally, the pattern of ligand-induced perturbations to base H6/H8 (major groove) and deoxyribose H1′ resonances (minor groove) are suggestive of a very similar binding location for both **1** and **2** that spans the central AATT site of the decamer duplex (data not shown). Many intermolecular NOEs have so far been identified that support this model.

The $^1$H NMR spectrum of the complex shown in Fig. 3(*d*) also provides evidence for hydrogen bonding interactions between the ligand and minor groove. Downfield shifted resonances are observed for the benzimidazole NHs, one of which is resolved at δ 11.65, the other overlapped at δ 12.74.

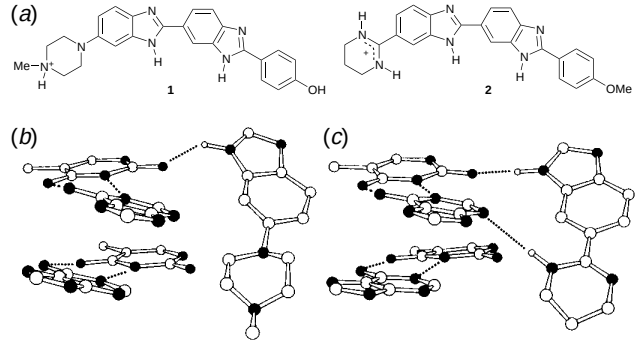



**Fig. 1** (*a*) Structure of Hoechst 33258 **1** and Hoechst 43254 **2**. (*b*) Portion of the X-ray structure of Hoechst 33258 (described by Quintana *et al.*[10]) illustrating the position and orientation of the *N*-methylpiperazine ring in the minor groove. (*c*) Hoechst 43254 complex modelled using the same X-ray coordinates and MACROMODEL software.[14] The ligand structure was energy minimised separately to determine the preferred conformation and orientation of the amidine ring. This conformation was adopted in initial modelling studies of the complex of **2**, keeping all other dihedral angles and ligand–DNA interactions the same as in the X-ray structure. The complex was subsequently energy minimised and subjected to 100 ps of unrestrained room temperature molecular dynamics. The resultant amidine NH → adenine N3 hydrogen bonding distance, which was not added as a constraint, was found to be 2.3 Å.

Both are shifted appreciably further downfield than the corresponding resonances in the complex of Hoechst 33258 with the same DNA sequence (δ 11.02 and 12.03, respectively).[5] Given that both ligands appear to bind similarly to the central AATT binding sequence, we interpret these larger binding shifts for **2** as consistent with stronger electrostatic interactions[16,17] and with overall tighter binding within the minor groove. Thus, introducing a more favourable interaction at the amidine end of the ligand appears to cooperatively enhance other intermolecular interactions at the ligand–DNA interface. Further, the well-resolved resonance at δ 9.39 is assigned to the amidine NH of the bound ligand on the basis of cross-peaks in 2D NOESY spectra to adjacent methylene protons (δ 3.82) on the ring. Identification of this resonance has enabled us to probe the role of the hexacyclic amidine ring in intermolecular interactions. The amidine NH has a small temperature coefficient (< 3 ppb/°C), a very slow rate of exchange (as judged by variable temperature and saturation transfer experiments), and gives a number of intermolecular NOEs that support both its close proximity to the floor of the minor groove, and possible involvement in specific hydrogen bonding with it. It is notable that the amidine NH signal has an integrated intensity equivalent to two protons, indicating that the solvent-exposed and solvent-buried ring NH are equivalent even at 278 K. Averaging of the signals from the C3 and C5 methylene protons adds further weight to the conclusion that in the bound state the ring is undergoing 180° flips (or free rotation) such as to rapidly interchange the environments on either side of the ring. Thus, a proposed hydrogen bond that appears to contribute significantly to complex stability also appears to be a dynamic interaction.

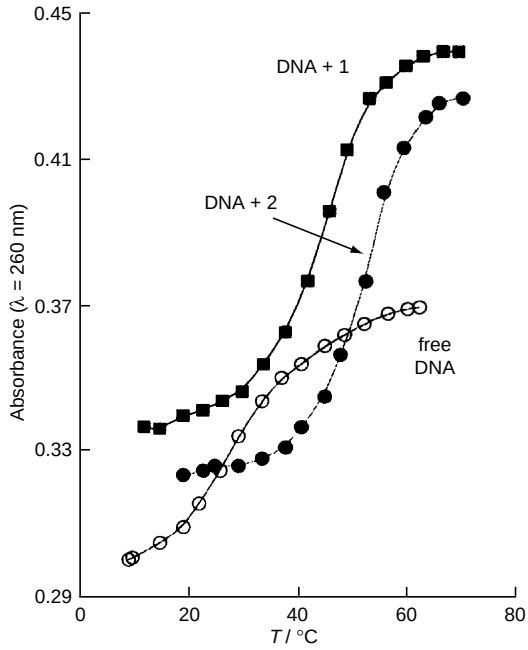



**Fig. 2** UV melting curves for the decamer duplex d(GGTAATTACC)$_2$ with and without bound ligands (**1** and **2**). Errors in $T_m$s were estimated to be less than ±2 °C. Sample concentrations and buffers are indicated in the text. The sample of Hoechst 33258 was purchased from Aldrich, while Hoechst 43254 was kindly provided by Hoechst, Frankfurt, Germany. Both samples were checked by $^1$H NMR and used without further purification. The oligonucleotide duplex was synthesised trityl-on using solid-phase phosphoramidite chemistry and purified by reverse-phase HPLC using 0.1 M triethylammonium acetate (TEAA) buffer and an acetonitrile gradient. The trityl group was removed by treatment with 50% aqueous acetic acid for 1 h at 35 °C and the oligonucleotide finally dialysed to remove TEAA and introduce $Na^+$ as the counter-ion.

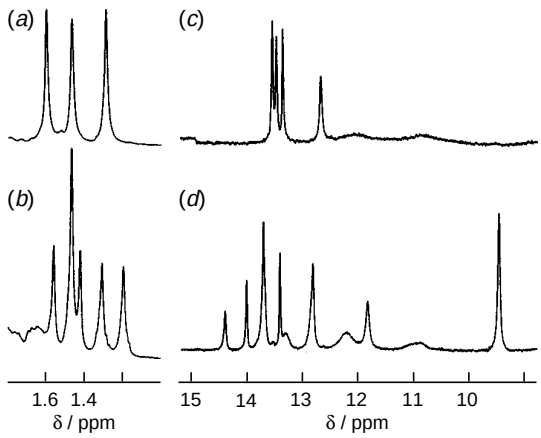



**Fig. 3** $^1$H NMR spectra (500 MHz) of ligand-free DNA (*a*) and (*c*), and of the complex with Hoechst 43254 (*b*) and (*d*), recorded in 90% $H_2O$ solution at 298 K using a 1-1 jump-return pulse sequence to suppress the solvent peak. A spectral width of 24 ppm was employed with a delay of 70 μs to optimise excitation at the position of the imino proton resonances (~ 13 ppm).

We thank the EPSRC for a research studentship to C. E. B. S. K. J. E. was the recipient of an Australian Postgraduate Research Award held at the Victorian College of Pharmacy, Parkville, Victoria, Australia. The Department of Chemistry at the University of Nottingham, the Nuffield Foundation and the Royal Society are gratefully acknowledged for financial support. We thank John Keyte for oligonucleotide synthesis.

## References

1 J. Portugal and M. J. Waring, *Biochim. Biophys. Acta*, 1988, **949**, 158.
2 M. S. Searle and K. J. Embrey, *Nucl. Acids Res.*, 1990, **18**, 3753.
3 J. A. Parkinson, J. Barber, K. T. Douglas, J. Rosamond and D. Sharples, *Biochemistry*, 1990, **29**, 10 181.
4 A. Fede, A. Labhardt, W. Bannwarth and W. Leupin, *Biochemistry*, 1991, **30**, 11377.
5 K. J. Embrey, M. S. Searle and D. J. Craik, *Eur. J. Biochem.*, 1993, **211**, 437.
6 A. Fede, M. Billeter, W. Leupin and K. Wuthrich, *Structure*, 1993, **1**, 177.
7 P. E. Pjura, K. Grzeskowiak and R. E. Dickerson, *J. Mol. Biol.*, 1987, **197**, 257.
8 M.-K. Teng, N. Usman, C. A. Frederick and A. H. J. Wang, *Nucl. Acids. Res.*, 1988, **16**, 2671.
9 M. A. A. F. deC. T. Carrondo, M. Coll, J. Aymami, A. H. J. Wang, G. A. van der Marel, J. H. van Boom and A. Rich, *Biochemistry*, 1989, **28**, 7849.
10 J. R. Quintana, A. A. Lipanov and R. E. Dickerson, *Biochemistry*, 1991, **30**, 10 294.
11 N. Spink, D. G. Brown, J. V. Skelly and S. Neidle, *Nucl. Acids Res.*, 1994, **22**, 1607.
12 M. C. Vega, I. Garcia Saez, J. Aymami, R. Eritja, G. A. van der Marel, J. H. van Boom, A. Rich and M. Coll, *Eur. J. Biochem.*, 1994, **222**, 721.
13 A. A. Wood, C. M. Nunn, A. Czarny, D. W. Boykin and S. Neidle, *Nucl. Acids. Res.*, 1995, **23**, 3678.
14 F. Mohamadi, N. G. J. Richards, W. C. Guida, R. Liskamp, M. Lipton, C. Caufield, G. Chang, T. Hendrickson and W. C. Still, *J. Comput. Chem.*, 1990, **11**, 440.
15 A. Czarny, D. W. Boykin, A. A. Wood, C. M. Nunn, S. Neidle, M. Zhao and W. D. Wilson, *J. Am. Chem. Soc.*, 1995, **117**, 4716.
16 M. S. Searle, M. S. Westwell and D. H. Williams, *J. Chem. Soc., Perkin Trans. 2*, 1995, 141.
17 G. J. Sharman, M. S. Searle, B. Benhamu, P. Groves and D. H. Williams, *Angew. Chem., Int. Ed. Engl.*, 1995, **34**, 1483.

*Received, 7th October 1996; Com. 6/06847B*

# Efficient polymer-supported Sharpless alkene epoxidation catalyst

**Laetitia Canali,[a] Jaana K. Karjalainen,[a] David C. Sherrington[a] and Osmo Hormi[b]**

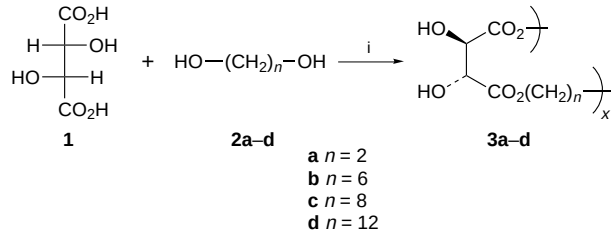
[a] *Department of Pure and Applied Chemistry, University of Strathclyde, 295 Cathedral Street, Glasgow, UK G1 1XL*
[b] *Department of Chemistry, University of Oulu, Oulu, Finland*

**Linear poly(tartrate ester) ligands provide high chemical yields and enantiomeric excesses in the epoxidation of *trans*-hex-2-en-1-ol using Ti(OPr$^i$)$_4$–*tert*-butyl hydroperoxide.**

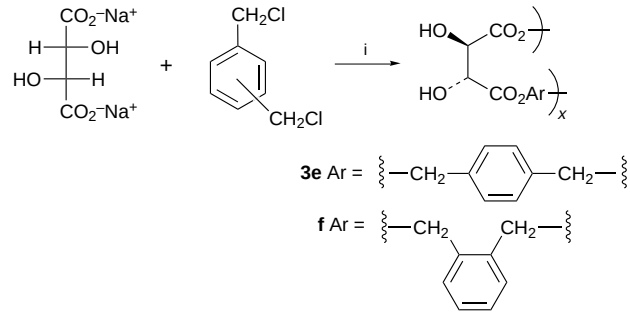
The advantages of polymer-supported reactive species are now widely recognised by organic chemists, and increasing exploitation of these systems is occurring both in academic and industrial laboratories.[1] The effective immobilisation of asymmetric catalysts, reagents and auxiliaries is a particularly important methodological target, especially for metal complex-based catalysts. Progress in the area has been reviewed by Hodge[2] and Sherrington.[1] Unfortunately, more often that not the supported systems display levels of induction below those of the corresponding low molecular weight species. However, a notable exception is the Zn-catalysed asymmetric alkylation of aldehydes using $ZnEt_2$ with chiral amino alcohols, where polymer-supported analogues yield very high levels of enantiomeric excess (ee).[3,4] Recently attention has focussed on a number of asymmetric alkene oxidation catalysts. Attempts to immobilise Jacobsen's asymmetric Mn$^{III}$-based alkene epoxidation catalyst[5] have led to polymeric species which offer only relatively low ees in typical reactions.[6,7] However, the results reported by Song *et al.*[8] on the Sharpless asymmetric dihydroxylation of alkenes[9] using catalytic levels of $OsO_4$ with $K_3Fe(CN)_6$–$K_2CO_3$ as secondary oxidant and polymeric alkaloids as the chiral ligand are remarkable, with essentially quantitative asymmetric induction coupled with high chemical yields.

Interestingly, there are no reports of the successful immobilisation of the Sharpless Ti–tartrate ester-based asymmetric alkene epoxidation catalyst, despite this being a relatively long-standing and well used methodology.[10] An early attempt to develop a polymer-supported system by Farrell *et al.*[11] employed a single tartrate ester unit bound to a polystyrene resin. However, the induction achieved (*ca.* 50–60% ee) was only modest. We now report on the synthesis of a group of poly(tartrate ester)s and their use with titanium tetraisopropoxide [Ti(OPr$^i$)$_4$] and *tert*-butyl hydroperoxide (tBHP) as the oxidant in epoxidising *trans*-hex-2-en-1-ol **4** in high chemical yield and good ee.

Poly(tartrate ester)s **3a**–**d** were synthesised from L-(+)-tartaric acid **1** and diols **2** using a standard polycondensation procedure[12] (Scheme 1). Water and unreacted diol were removed by distillation under high vacuum at the end of the reaction. The polymers were extracted with acetone in a Soxhlet apparatus and dried in a vacuum oven (50 °C) for *ca.* 15 h. Poly(tartrate ester)s **3e,f** were synthesised from L-(+)-tartartic acid disodium salt dihydrate dissolved in water and α,α′-dichloroxylene dissolved in $CHCl_3$ by a phase transfer catalysed procedure[13] using tetrabutylammonium bromide hydrate (TBAB) as the catalyst (Scheme 2). The results of polymerisations are shown in Table 1. All the polymers were soluble in $Me_2SO$ and so crosslinking side-reactions involving the secondary OH group on the tartrate residue appear to be absent. The polymers also display a positive optical rotation, and while it is not possible to say that no racemisation of the tartrate residues occurs during polymerisation, the values of the observed




**Scheme 1** *Reagents and conditions*: i, toluene-*p*-sulfonic acid (3 mass%), *ca.* 120 °C, 3 d




**Scheme 2** *Reagents and conditions*: i, $Bu_4NBr$ (20 mol%), $H_2O$, $CHCl_3$, reflux, 7 d

**Table 1** Synthesis of polyesters **3** derived from L-(+)-tartaric acid and diols

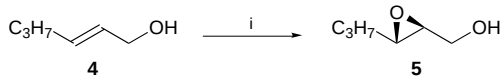
| Polyester | Conversion (%) | $[\alpha]_D^{25}$ [a] | $\nu_{max}$/cm$^{-1}$ (C=O, OH) | Elemental microanalysis (%) Calculated | Found |
|---|---|---|---|---|---|
| **3a** | 73 | +13[b] | 1755, 3479 | C, 40.92; H, 4.58 | C, 39.2; H, 4.6 |
| **3b** | 68 | +25 | 1755, 3479 | C, 51.72; H, 6.94 | C, 51.5; H, 6.5 |
| **3c**[c] | 95 | +17 | 1747, 3469 | C, 55.37; H, 7.74 | C, 56.4; H, 7.8 |
| **3d**[d] | 55 | +4[e] | 1755, 3470 | C, 60.74; H, 8.92 | C, 61.0; H, 9.2 |
| **3e** | 45 | +18 | 1748, 3430 | C, 57.14; H, 4.80 | C, 52.3; H, 5.1 |
| **3f** | 48 | +15 | 1747, 3420 | C, 57.14; H, 4.80 | C, 56.3; H, 5.1 |

[a] Concentrations: 0.2 g per 100 ml $Me_2SO$, Perkin-Elmer WM250. [b] Concentration: 0.4 g per 100 ml MeOH. [c] Washed with hexane. [d] $\overline{M}_w$ = *ca.* 4,200, $\overline{M}_W/\overline{M}_N$ = *ca.* 1.7, determined by GPC with polystyrene standards in THF. [e] Concentration: 0.8 g per 100 ml in $CHCl_3$.

**Table 2** Epoxidation of *trans*-hex-2-en-1-ol with tBHP catalysed by L-(+)-polyester **3** and $Ti(OPr^i)_4$

| Ligand | Molar ratio **4**; Ti : tartrate | *T*/°C | Reaction time/h[a] | Epoxide yield (%)[b] | Isolated yield (%)[c] | Work-up[d] | Ee[e] (%) |
|---|---|---|---|---|---|---|---|
| DMT | 100 : 5 : 6 | −30 | 3 | 91[g] | 44 | A | ⩾98[g] |
| **3a** | 100 : 17 : 20 | −20 | 3 | 51 | 50 | B | 8 |
| **3b** | 100 : 17 : 20 | −20 | 3 | 63 | 63 | B | 55 |
| **3c** | 100 : 5 : 10 | −20 | 3 | 22 | 59 | B | 79 |
| **3c** | 100 : 17 : 20 | −20 | 7 | 92 | 58 | B | 79 |
| **3d** | 100 : 12 : 12 | −20 | 3 | 65 | 60 | B | 41 |
| **3d** | 100 : 5 : 10 | −20 | 3 | 21 | 46 | B | 52 |
| **3d** | 100 : 10 : 30 | −20 | 3 | 80 | 61 | B | 77 |
| **3d** | 100 : 17 : 20 | −20 | 3 | 75 | 61 | B | 64 |
| **3e** | 100 : 17 : 20 | −20 | 3 | 73 | 42 | B | 47 |
| **3f** | 100 : 17 : 20 | −20 | 3 | 74 | 80 | B | 68 |

[a] From addition of **4**. [b] From GC analysis after 3 h. [c] After additional 12 h in freezer, work-up and Kugelrohr distillation. [d] A = ferrous sulfate, tartaric acid (ref. 15); B = non-acidic aqueous workshop (ref. 15). [e] (2*S*,3*S*)-(−)-Propyloxiranemethanol determined *via* chiral HPLC (Chiralcel OB, hexane–$Pr^iOH$. [f] DMT = L-(+)-dimethyl tartrate. [g] Chemical yield = 85%, ee = 94%; Sharpless using L-(+)-diethyltartrate (ref. 15).




**4** **5**

**Scheme 3** *Reagents and conditions*: i, poly(tartrate ester) (10–30 mol%), $Ti(OPr^i)_4$ (5–17 mol%), $Bu^tOOH$ (2 equiv.), 4 Å molecular sieves, $CH_2Cl_2$, −20 °C, 3 h

rotations are comparable with those reported[14] for dimethyl L-(+)-tartrate {$[\alpha]_D^{22}$ + 21 (*c* 2.5, $H_2O$)} and for diethyl L-(+)-tartrate {$[\alpha]_D^{20}$ + 8.5 (neat)}.

Polyesters **3a**–**f** were used as ligands in the epoxidation of **4** with $Ti(OPr^i)_4$–tBHP as shown in Scheme 3. Powdered activated 4 Å molecular sieves, polymeric ligand and $Ti(OPr^i)_4$ were first mixed in $CH_2Cl_2$ at −20 °C for 1 h, the tBHP was added and the mixture stirred for a further 1 h at −20 °C before **4** in $CH_2Cl_2$ was added. The reaction was then left to proceed for 3 h at *ca.* −20 °C, when the GC yield was determined. Each reaction mixture was then stored overnight in a freezer before work-up and isolation of pure **5** *via* Kugelrohr distillation. Enantiomeric excess was determined by chiral HPLC using a Chiralcel OB column and hexane–isopropyl alcohol (97.5 : 2.5) as eluent. The results are summarised in Table 2. Generally reactions are fast even at −20 °C with GC yields (3 h) in the range 20–90% depending upon the polymer ligand **3** used. In some instances isolated yields are higher than GC yields because the reactions continue in the freezer overnight. Isolated yields, however, are by no means optimised; pure **5** was isolated simply for optical rotation measurements and considerable scope remains for optimisation. Enantiomeric excesses generally fall in the range 40–80% with a significant dependence on the poly(tartrate ester) employed. Polymer (**3a**) is very poor, and polymer (**3c**) the most effective. The origin of the 'polymer effect' is not clear and may well involve a contribution from solubility and molecular weight variation, and from conformational factors. Polymers **3a** and **3b** are rather insoluble in $CH_2Cl_2$, as is **3c**. However, the latter does form a $CH_2Cl_2$ soluble complex with $Ti(OPr^i)_4$. This led us to prepare **3d** which is itself soluble in $CH_2Cl_2$; however, **3d** gave poorer levels of induction than **3c** under comparable conditions so that solubility alone is not the only factor. Solubility limitations have made molecular weight determination difficult, but two different batches of **3d** yielded $\overline{M}_w$ = 4150 and 4210, with $\overline{M}_w/\overline{M}_N$ = 1.7 (gel permeation chromatography; polystyrene standards in THF). Compound **3d** is therefore oligomeric rather than polymeric, and further work is underway to investigate this parameter. It seems most likely that the active species with simple dialkyl tartrate–$Ti(OPr^i)_4$ are rather complicated, possibly 2 : 2 complexes.[16] The effectiveness of poly(tartrate ester)s may well therefore depend also on the ability of these backbones to assume a conformation which allows maximum opportunity for the formation of such complexes. In this respect, in due course, investigation of poly(tartrate ester)s may well provide useful structural information on the active species themselves.

At the moment we are further optimising these reactions and pursuing the above structural aspects. We are also making crosslinked poly(tartrate ester) gels and immobilising linear poly(tartrate ester)s on supports such as poly(styrenedivinylbenzene) in an attempt to produce highly practical re-usable heterogeneous Sharpless epoxidation catalysts.

We acknowledge funding from the Neste Oy Foundation and the Finnish cultural Foundation. We also appreciate the molecular weight determinations carried out by RAPRA.

## References

1 D. C. Sherrington, 'Polymer-supported Synthesis', in *Chemistry of Waste Minimisation*, ed. J.H. Clark, Blackie, 1995, ch. 6, p. 141.
2 P. Hodge, 'Polymer-supported asymmetric organic synthesis', in *Innovation and Perspectives in Solid Phase Synthesis*, ed. R. Epton, SPCC UK, 1990, p. 273.
3 S. Itsuno, Y. Sakurai, K. Ito, T. Maruyama and J. M. M. Frechet, *J. Org. Chem*., 1990, **55**, 304.
4 P. Hodge, paper presented at SCI Meeting on Ion Exchange Resins as Catalysts, London, June 1994; also in *Macromolecules 1991*, ed. J. Kahovec, VSP, Utrecht, 1993, p. 441.
5 E. N. Jacobsen, W. Zhang, A. R. Muci, J. R. Echer and Li Deng, *J. Am. Chem. Soc*., 1991, **113**, 7063.
6 B. B. De, B. B. Lohray, S. Sivaram and P. K. Dhal, *Tetrahedron: Asymmetry*, 1995, **6**, 2105.
7 F. Minutolo, D. Pini and P. Salvadori, *Tetrahedron Lett*.,1996, **37**, 335.
8 C. E. Song, J. W. Yang, H. J. Ha and S.-G. Lee, *Tetrahedron: Asymmetry*, 1996, **7**, 645.
9 R. A. Johnson and K. B. Sharpless, 'Catalytic Asymmetric Dihydroxylation', in *Catalytic Asymmetric Synthesis*, ed. I. Ojima, VCH, New York, 1993, p. 227.
10 T. Katsuki and K. B. Sharpless, *J. Am. Chem Soc*., 1980, **102**, 5974.
11 M. J. Farrall, M. Alexis and M. Trecarten, *Nouv. J. Chim*., 1983, **7**, 449.
12 D. Seebach, H.-O. Kalinowski, W. Langer, G. Grass and E. M. Wilka, *Org. Synth*., 1983, **61**, 24.
13 J. March, *Advanced Organic Chemistry*, Wiley, New York, 3rd edn., 1985, p. 353.
14 *Aldrich Handbook of Fine Chemicals*, 1994–1995.
15 Y. Gao, R. M. Hanson, J. M, Klunder, S. Y. Ko, H. Masumune and K. B. Sharpless, *J. Am. Chem. Soc*., 1987, **109**, 5765.
16 M. G. Finn and K. B. Sharpless, *J. Am. Chem. Soc*., 1991, **113**, 113.

*Received, 10th October 1996; Com. 6/06954A*

# Polymer supported alkali metal naphthalenides: application in the generation of lithium and sodium reagents

**Tania R. van den Ancker,[a] Graeme R. Hanson,[b] Fu-Chin Lee[a] and Colin L. Raston[c]**

[a] *Faculty of Science and Technology, Griffith University, Nathan, Queensland 4111, Australia*
[b] *Centre for Magnetic Resonance, University of Queensland, St Lucia, Queensland 4072, Australia*
[c] *Department of Chemistry, Monash University, Clayton, Melbourne, Victoria 3168, Australia*

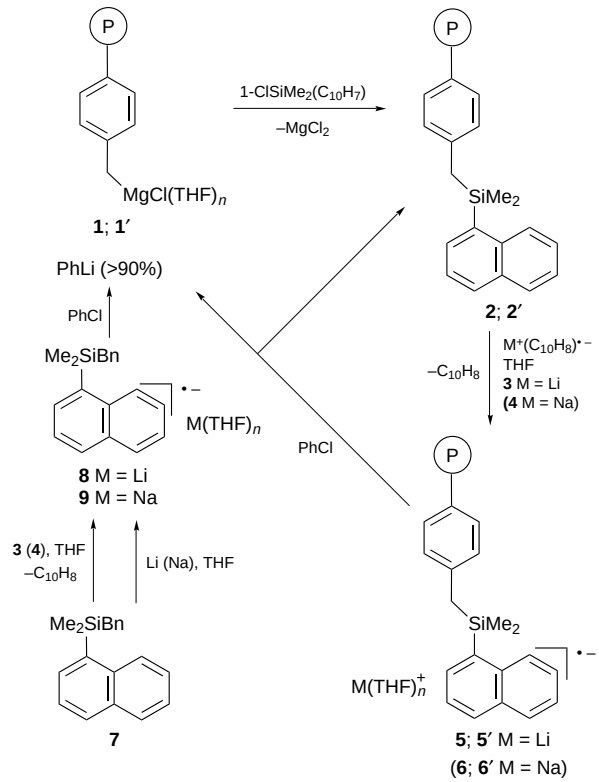
**Polymer supported lithium and sodium naphthalenide complexes are prepared from the reaction of THF solutions of lithium and sodium biphenylide with polystyrene bearing -$CH_2SiMe_2(1\text{-}C_{10}H_7)$ groups, generating highly coloured paramagnetic material, which afford lithium and sodium reagents in high yield when treated with organic halides, nitriles and phosphates.**

Lithium arene radical anion complexes afford organic lithium complexes in high yield;[1] the solutions of these reagents, however, are loaded with the arene by-product. Yus *et al*.[2] have developed a method for the preparation of lithium reagents by the reaction of lithium powder with catalytic amounts of arene (1–2%), resulting in a reduced amount of the by-product. A strategy that completely avoids generating solutions containing the arene is the use of supported lithium reagents. This is developed herein for polymer supported lithium reagents, along with analogous supported sodium reagents, due to their utility in generating lithium and sodium reagents which can be separated from the spent polymer by simple filtration. This work follows from our success in developing synthetically useful polymer[3,4] and silica[5] supported magnesium anthracene. These act as a source of magnesium in the generation of anthracene-free benzylic Grignard reagents.

The naphthalene functionalised polymer **2**; **2′** (Scheme 1) was prepared by the treatment of a THF slurry of the Grignard reagent of chloromethylated polystyrene[3,6] (microporous BIO-RAD S-X1, 1.34 mmol $g^{-1}$ **1** and 4.11 mmol $g^{-1}$ **1′**, 1.0% crosslinked) with an excess of 1-(chlorodimethylsilyl)naphthalene† at 0 °C, in greater than 95% yield based on weight increase (assuming two THF molecules attached to the metal centre), IR studies and analysis for residual chlorine content of $< 0.3$ mmol $g^{-1}$. Solutions of lithium biphenylide **3** in THF (or DME) were added to THF (or DME) slurries of polymers **2**; **2′** resulting in the formation of a red–brown paramagnetic material ($g_{av}$ = 2.0034, 2.0035/THF; $g_{av}$ = 2.0029, 2.0026/DME) of polymer supported lithium naphthalenide **5**; **5′**. Similarly addition of a THF (or DME) solution of sodium biphenylide **4** to THF (or DME) slurries of polymers **2**; **2′** resulted in the formation of a red–brown paramagnetic material ($g_{av}$ = 2.0034, 2.0035/THF; $g_{av}$ = 2.0029, 2.0100/DME) of polymer supported sodium naphthalenide **6**; **6′**. Lithium and sodium biphenylide were chosen as the electron transfer reagents because of the lower reduction potential of biphenyl (−2.70 V *vs*. SCE) relative to that of naphthalene (−2.50 V *vs*. SCE), thus favouring transfer from the biphenyl to naphthalene;[7] the presence of the silyl group on naphthalene in the polymer would further favour electron transfer since silicon stabilises charge by polarisation.[9] No reaction was evident between **2**; **2′** and activated lithium powders.

In an attempt to model the reaction of the functionalised polymers, 1-(benzyldimethylsilyl)naphthalene‡ **7** was prepared. Reaction with lithium or sodium metal yielded a deep green paramagnetic solution of lithium[1-(benzyldimethylsilyl)naphthalene](THF)$_n$ **8**, ($g_{av}$ = 2.0028) and sodium[1-(benzyldimethylsilyl)naphthalene](THF)$_n$ **9**, ($g_{av}$ = 2.0028) respectively (Scheme 1). Complexes **8** and **9** were also prepared by the reaction of **7** with THF solutions of **3** and **4** respectively.

EPR spectra of the polymer supported alkali naphthalenides **5** and **6** were obtained at room temperature in THF. The EPR spectrum of **5** is shown in Fig. 1(*a*), the simulated spectra in Fig. 1(*b*). The spectrum appears as a multiplet ($g_{av}$ = 2.00275) with hyperfine coupling. Extensive simulation using SOPHE[10] indicated the multiplet arises from the coupling of two equivalent lithium atoms [$A(^7\text{Li}) = 2.327(4) \times 10^{-4}$ cm$^{-1}$], four equivalent protons [$A(^1\text{H}) = 1.310(4) \times 10^{-4}$ cm$^{-1}$] and two other equivalent protons [$A(^1\text{H}) = 2.424(4) \times 10^{-4}$ cm$^{-1}$] to a single unpaired electron. Consequently, the EPR spectrum arises from an unpaired electron delocalised over two lithium centres rather than a contact ion pair involving a lithium and a radical anion. Polymer supported magnesium anthracene has radical anion sites with the divalent magnesium accounting for a pair of radicals.[3,4] The EPR spectrum of polymer supported sodium naphthalenide also gave a multiplet with hyperfine coupling, in this case there is a broadening of the signals, resulting in difficulty in the simulation. The broadening may arise from dipole–dipole interaction of the sodium atoms a phenomenon seen in sodium zeolite systems.[11]




**Scheme 1**

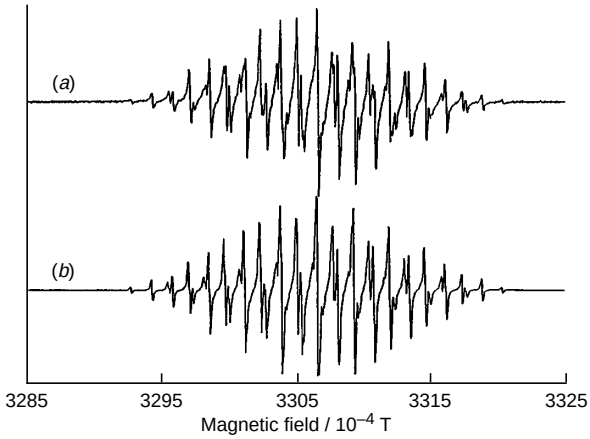



**Fig. 1** EPR spectra of polymer supported lithium naphthalenide **5**: (*a*) experimental (ν = 9.2776 GHz) and (*b*) simulated spectra

Polymer **5**; **5′** affords lithium reagents with a range of organic halides [*e.g.* chlorobenzene, 9-chloroanthracene, 2-(3′-chloropropyl)-2-methyl-1,3-dioxalane, 3-chloro-1-phenylpropan-1-ol], organo nitriles (acetonitrile, benzonitrile) and triorganophosphates [O=P(OR)$_3$, R = Et, Ph] in > 75% yield at *ca.* 0.1 M. These reactions are based on two different methods. The first involves the formation of the organoalkali, which is then quenched to give the desired complex.§ The second reaction involves the quenching of the organoalkali complex *in situ*, in a Barbier-type¶ reaction. Reaction of **8** and **9** with 0.5 equiv. of chlorobenzene or 9-chloroanthracene both gave the corresponding lithium or sodium complexes, respectively.

The spent polymers **2**; **2′** were tested for recycling potential and overall the uptake of lithium from **3** and the yield of lithium reagents obtained differ only slightly over successive cycles. As an example, for three such cycles for **5** the uptake of lithium from **3** was successively 110, 100 and 100% with the corresponding yields of lithiobenzene at 93, 91 and 89% (based on titrations). Each cycle involved quenching **5** with chlorobenzene, separating the polymer and washing it with THF followed by treatment with **3** to regenerate a deep red polymer. Investigations into the use of the sodium naphthalene polymer to generate the sodium reagent of chlorobenzene were also undertaken, with yields of > 80%. This work has also been extended to the use of metal oxide supported complexes.[12]

The main advantages in using polymers **5**; **5′** and **6**; **6′** in generating lithium and sodium reagents, which is possible for a variety of substrates, are that the reactions are high yielding, and the reaction mixtures are free of arene by-products. The ability to recycle the polymers is also noteworthy, as is the fact that the supported polymers offer a means of delivering a small amount of the equivalent of a Group 1 metal.

We thank the Australian Research Council for support of this work.

## Footnotes

† 1-(Chlorodimethylsilyl)naphthalene was prepared by quenching 1-lithionaphthalene with excess dichlorodimethylsilane.[8]

‡ 1-(benzyldimethylsilyl)naphthalene **8** was prepared by the treatment of benzylmagnesium chloride with **2**, in $Et_2O$ in 66% yield (bp 137 °C, 0.5 mmHg, satisfactory spectroscopic and analytical data obtained).

§ In a typical experiment the organic halide in THF was slowly added over 20 min to a THF slurry of the polymer supported lithium naphthalenide at −78 °C. This resulted in the dissipation of the red colour of the polymer supported lithium naphthalenide and the formation of an orange solution. The solution was stirred for a further 1–3 h then filtered to give the arene free organoalkali. In all cases target concentrations of the resulting lithium reagent were close to 0.1 M. For example the lithium reagent of chlorobenzene was generated in > 95% yield (by titration) with quenching by chlorotrimethylsilane affording trimethylsilylbenzene in 90% yield as the exclusive product.

¶ A mixture of the organic halide and electrophile in THF was slowly added over 45 min to a THF slurry of the polymer supported lithium naphthalenide at −30 or 0 °C. This resulted in the dissipation of the red colour and the formation of a pale yellow solution. The resulting solution was then stirred for 15 min, filtered, and the solution hydrolysed and the product extracted into $Et_2O$ and purified by distillation. As an example, benzonitrile gave trimethylsilylbenzene in 75% yield as the only product.

## References

1 J. L. Wardell, *Alkali Metals*, in *Comprehensive Organometallic Chemistry*, ed. G. Wilkinson, F. G. A. Stone and E. W. Abel, Pergamon Press, Oxford, 1982, vol. 8, ch. 24; J. L. Wardell, *Preparation and Use in Organic Synthesis of Organolithium and Group 1A Organometallics*, in *The Chemistry of Metal–Carbon Bond*, ed. F. R. Hartley, Wiley, Chichester, 1987.
2 M. Yus and D. J. Ramon, *J. Chem Soc., Chem. Commun.*, 1991, 398; D. J. Ramon and M. Yus, *Tetrahedron Lett.*, 1990, **31**, 3763; A. Guijarro, D. J. Ramon and M. Yus, *Tetrahedron*, 1993, **49**, 469; A. Guijarro and M. Yus, *Tetrahedron*, 1995, **51**, 231; A. Guijarro and M. Yus, *Tetrahedron Lett.*, 1993, **34**, 3487; D. Guijarro, B. Mancheno and M. Yus, *Tetrahedron*, 1994, **50**, 8551; D. Guijarro and M. Yus, *Tetrahedron*, 1994, **50**, 3447; D. Guijarro and M. Yus, *Tetrahedron Lett.*, 1994, **35**, 2965; D. Guijarro, G. Guillena, B. Mancheno and M. Yus, *Tetrahedron*, 1994, **50**, 3427; D. J. Ramon and M. Yus, *Tetrahedron Lett.*, 1990, **31**, 3767; J. F. Gil, D. J. Ramon and M. Yus, *Tetrahedron*, 1993, **49**, 4923.
3 S. Harvey and C. L. Raston, *J. Chem. Soc., Chem. Commun.*, 1988, 652.
4 T. R. van den Ancker, S. Harvey and C. L. Raston, *J. Organomet. Chem.*, 1995, **502**, 35.
5 T. R. van den Ancker and C. L. Raston, *Organometallics*, 1995, 584.
6 S. Itsuno, G. D. Darling, H. D. Stover and J. M. J. Frechet, *J. Org. Chem.*, 1987, **52**, 4644.
7 A. Streitwieser, *Molecular Orbital Theory for Organic Chemists*, Wiley, New York, 1961.
8 D. F. Fritz, A. Sahil, H. P. Keller and E. Kovals, *Anal. Chem.*, 1976, **98**, 5706.
9 P. v. R. Schleyer, T. Clark, A. J. Kos, G. W. Spitznagel, C. Rhode, D. Arad, K. N. Houk and N. G. Rhodan, *J. Am. Chem. Soc.*, 1984, **106**, 6467.
10 D. M. Wang, G. R. Hanson, *J. Magn. Reson.*, 1995, **117**, 1; D. Wang and G. R. Hanson, *Appl. Magn. Reson.*, 1996, **11**, 401.
11 P. A. Anderson and P. P. Edwards, *J. Chem. Soc., Chem. Commun.*, 1991, 915; P. P. Edwards, J. L. Woodall, P. A. Anderson, A. R. Armstrong and M. Slaski, *Chem. Soc. Rev.*, 1993, 305.
12 T. R. van den Ancker and C. L. Raston, unpublished results.

*Received, 9th September 1996; Com. 6/06181H*

# Zeolite as a reagent and as a catalyst: reduction and isomerization of alkenes by Ca Y

**K. Pitchumani, Abraham Joy, Nicolette Prevost and V. Ramamurthy***

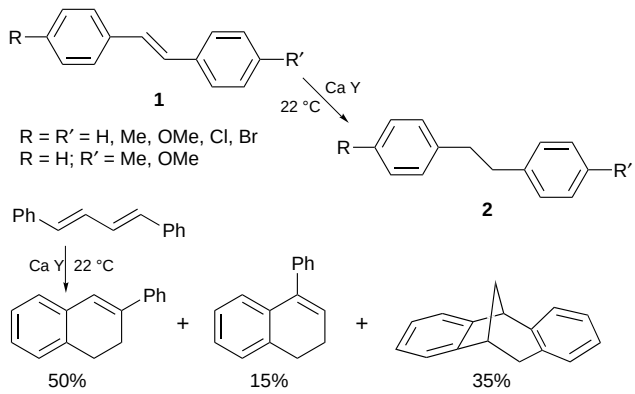
*Department of Chemistry, Tulane University, New Orleans, LA 70118, USA*

**Depending on the number of Brønsted acid sites present, Ca Y can act either as a reagent and reduce stilbenes to 1,2-diarylethanes or act as a catalyst and isomerize *cis*-stilbenes to the more stable *trans* form; Lewis acid sites generated by the activation process yield radical cations from stilbenes but these do not yield any stable products.**

In spite of its success as an industrial catalyst, the main use of zeolite in the laboratory is still only as a drying agent.[1] Here we show that zeolite can be used to carry out some routine organic transformations. Examples presented illustrate that the characteristics of the zeolite are essentially controlled by its activation procedure.

In this study Ca Y was used.† Since the exact nature of activation determines the behaviour of Ca Y, the activation method is described in detail. In method A, a known amount of the zeolite was placed inside a preheated (*ca*. 500 °C) oven under aerated conditions and activated for *ca*. 10 h. The zeolite was taken out of the oven at that temperature, cooled for *ca*. 2–3 min in the laboratory atmosphere and dropped into a hexane solution of stilbenes **1** (10 mg) after which the resultant slurry was stirred for 1 h. Extraction of the hexane–zeolite slurry with methylene chloride gave the corresponding 1,2-diarylethanes **2** in high yield ( > 90%) (Scheme 1). It is important to note that the reduction is fairly facile, nearly quantitative and is devoid of side reactions.

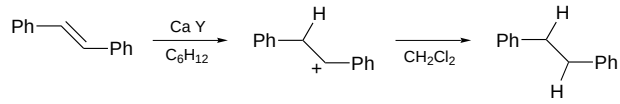
Reduction by Ca Y of a double bond activated by method A was found to be general. For example, 1,1-diphenylethylenes, *p*-methoxystyrene, β-methyl-*p*-methoxystyrene, 1-phenylcyclopentene and 1-phenycyclohexene were reduced to the corresponding hydrocarbons by Ca Y.[2] However, when this reaction was extended to 1,4-diphenylbutadiene, a surprising rearrangement occurred. Addition of Ca Y, activated by method A, to a hexane solution of 1,4-diphenylbutadiene (10 mg), resulted in quantitative conversion to the products shown in Scheme 1. This reaction was exceptionally rapid; the reaction was complete within 5 min of addition. While we are sure that a carbocation is involved in these rearrangements, we are not certain of the details of the mechanism. Work is underway to establish the mechanism.



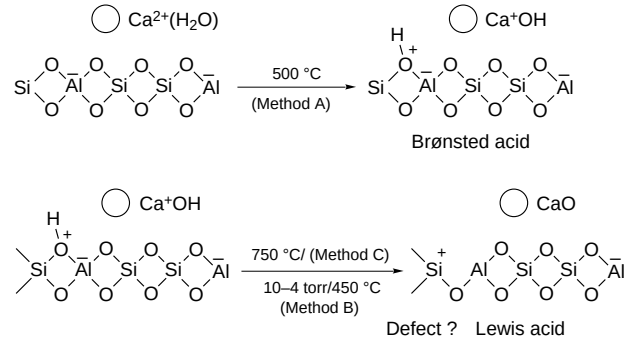

**Scheme 1**

The proposed mechanism for the reduction of stilbenes is shown in Scheme 2. It is known that activation of Ca Y at 500 °C under aerated conditions generates a large number of Brønsted acid sites within the supercages of the Y zeolite.[1] Formation of $H^+$ has been established to result from the dissociation of water by the strongly polarizing divalent cation $Ca^{2+}$ (Scheme 3). By the use of a combination of Ca Y ($H_2O$), Ca Y ($D_2O$) and deuteriated solvents ($C_6D_{12}$ and $CD_2Cl_2$), we showed that one of the hydrogen atoms comes from a water molecule present within the zeolite before activation and the other from the solvent. The carbocation derived from *p,p*′-dimethoxystilbene was found to be unusually stable. The diffuse reflectance spectrum of Ca Y included with *p,p*′-dimethoxystilbene showed transitions corresponding to the carbocation in the region *ca*. 300–370 nm.[3]

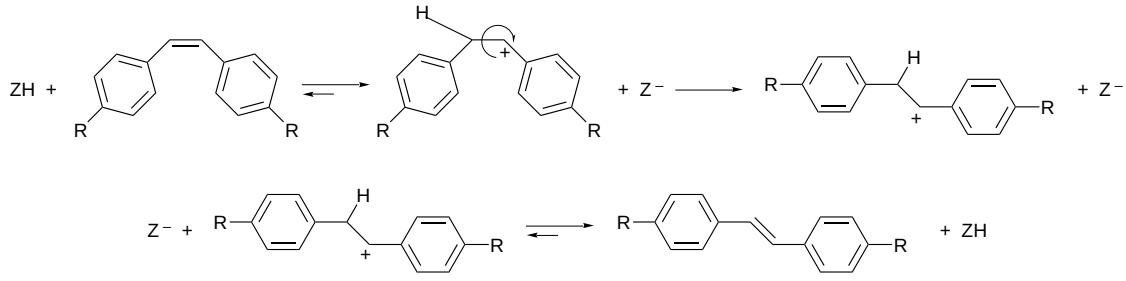
In the second method (method B), the zeolite was activated on a vacuum line at 450 °C. The procedure involved the following steps: a known amount of Ca Y taken in a quartz tube was degassed on a vacuum line at $5 \times 10^{-4}$ Torr for about 2 h. While maintaining the vacuum, the sample was heated to 450 °C at a rate of 20 °C $min^{-1}$ and maintained at 450 °C for *ca*. 10 h. The zeolite was cooled to room temperature and added to a hexane solution of *cis*-**1** and stirred for 3 h. Extraction of the solution gave *trans*-**1** in quantitative yield. Previous studies of alkaline earth cation exchanged zeolites have shown that the condition of activation dictates the generation of Brønsted and Lewis acid sites (Scheme 3).[1] It has been established that activation at higher temperatures ( > 750 °C) or at moderate temperatures ( > 400 °C) under vacuum results mostly in Lewis acid sites; only very few Brønsted acid sites are generated under such conditions. When we used the zeolite activated at 750 °C (method C) only isomerization was observed. Such zeolites failed to reduce the *trans*-**1**. In conclusion, the behaviour of Ca




**Scheme 2**




**Scheme 3**



**Scheme 4**

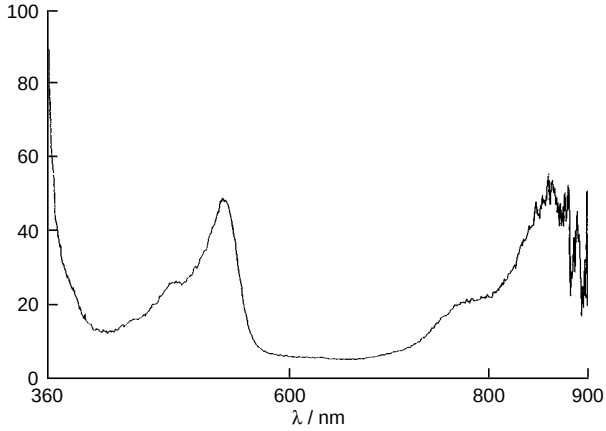



**Fig. 1** Diffuse reflectance spectrum of *p,p′*-dimethoxystilbene included within Ca Y activated at 450 °C under vacuum ($10^{-4}$ Torr)

Y activated by method A was different from the ones activated by methods B and C.

The proposed mechanism for the geometric isomerization of **1** is shown in Scheme 4. The acid–base equilibria represented in Schemes 2 and 4, we propose, are controlled by the number of Brønsted acid sites present in Ca Y. When the number of Brønsted acid sites is disproportionately large when compared to the number of alkene molecules present in a zeolite, the acid–base equilibrium favours the permanent formation of carbocations. These carbocations have a long lifetime and abstract a hydride ion from the solvent to yield **2**. When the number of Brønsted acid sites is relatively small, not enough carbocations are generated to yield significant amounts of **2**. However, when the *cis* isomer is the guest, the protonation results in the conversion of the *cis* isomer to the thermodynamically more stable *trans* form. From the above studies it has become evident that the key to effecting selective *cis* to *trans* isomerization (without reduction) is to control the number of Brønsted acid sites within a zeolite.

In addition to the carbocation, cation radicals were also formed when stilbenes **1** were added to activated Ca Y. The extent of cation radical formation dependent on the method of activaton of Ca Y. While methods B and C gave relatively large amount of radical cations, the method A gave only minor amounts. The diffuse reflectance spectrum displayed in Fig. 1 for *p,p′*-dimethoxystilbene can clearly be identified with the radical cation of the alkene.[4] Consistent with this assignment, EPR signals were observed with the sample. The EPR spectra in all cases were broad and structureless. The radical cations generated spontaneously within Ca Y were stable for several days. Although we rule out Brønsted acid sites as possible electron acceptor sites, we have no knowledge of the nature of the electron acceptor at this time.[5]

We have shown that both carbocations and cation radicals from alkenes can be generated within Ca Y. Further, we have established that by carefully controlling the conditions of activation, one can selectively generate long-lived organic carbocations and cation radicals within such zeolites. We are in the process of identifying the electron acceptor sites within zeolites and the source of hydride ion during the reduction process.

The authors thank the Division of Chemical Sciences, Office of Basic Energy Sciences, Office of Energy Research, U.S. Department of Energy and NSF-EPSCOR-LBR Center for Photoinduced Processes, Tulane University for support of this program.

## Footnote

† Ca Y was prepared by exchanging Na Y with calcium nitrate for 12 h at 100 °C. The exchange was repeated four times, the solid filtrate was washed thoroughly with water and dried at 90 °C for *ca.* 16 h. ICP analysis indicated the exchanged zeolite to have a composition of $Si_{138.7}Al_{53.3}Na_{7.5}$-$Ca_{23.3}O_{884}$.

## References

1 J. W. Ward, in *Zeolite Chemistry and Catalysis*, ed. J. A. Rabo, American Chemical Society, Washington, DC, 1976, p. 118; M. L. Poutsma, in *Zeolite Chemistry and Catalysis*, ed. J. A. Rabo, American Chemical Society, Washington DC, 1976, p. 437.
2 N. Prevost, P. H. Lakshminarasimhan, V. J. Rao and K. Pitchumani, unpublished results.
3 R. A. McClelland, C. Chan, F. Cozens, A. Modro and S. Steenken, *Angew. Chem., Int. Ed. Engl.*, 1991, **30**, 1337.
4 V. Ramamurthy, J. V. Caspar and D. R. Corbin, *J. Am. Chem. Soc.*, 1991, **113**, 594.
5 D. N. Stamires and J. Turkevich, *J. Am. Chem. Soc.*, 1964, **86**, 749; F. R. Chen and J. J. Fripiat, *J. Phys. Chem.*, 1992, **96**, 819; X. Liu, K. K. Iu, J. K. Thomas, H. He and J. Klinowski, *J. Am. Chem. Soc.*, 1994, **116**, 11 811; A. Corma, V. Fornes, H. Garcia, V. Marti and M. A. Miranda, *Chem. Mater.*, 1995, **7**, 2136.

*Received, 23rd September 1996; Paper 6/06578C*

# Catalytic activity of FSM-16 for photometathesis of propene

**Hisao Yoshida,* Koichi Kimura, Yoshitaka Inaki and Tadashi Hattori**

*Department of Applied Chemistry, Graduate School of Engineering, Nagoya University, Nagoya 464-01, Japan*

**Mesoporous silica (FSM-16) catalyses metathesis of propene under photoirradiation at a higher activity than amorphous silica whereas microporous silica crystals (silicalite-1) do not catalyse the reaction.**

Mesoporous silica materials such as MCM-41[1,2] and FSM-16[3,4] attract a great deal of attention as new materials and many applications are expected. Although the application of these materials for catalysis has been widely studied, attention has also been paid to the generation of catalytic activity through the introduction of other metal ions into the silica lattice, but not to the catalytic activity of unmodified mesoporous silica.

Here, we show that unmodified mesoporous silica (FSM-16) has a higher catalytic activity in the photometathesis of propene than does amorphous silica which was recently found to be catalytically active in this reaction.[5] To elucidate structural factors of mesoporous silica in this reaction, we compare the catalytic activities of other forms of $SiO_2$; amorphous silica, microporous crystalline silica (silicalite-1)[6] and high-silica zeolite (dealuminated mordenite).

Amorphous silica (AMS) was prepared by the sol–gel method[7] by hydrolysis of tetraethylorthosilicate (TEOS) followed by calcination at 773 K for 5 h. FSM-16 was prepared essentially in the same manner as described by Inagaki *et al.*[3,4] except that hexadecyltrimethylammonium bromide was used as a template and the resulting material was calcined at 873 K in an $N_2$ atmosphere for 1 h and subsequently in air for 5 h. Silicalite-1 was synthesized from TEOS and tetrapropylammonium bromide (TPABr) by hydrothermal synthesis (433 K, 24 h) followed by washing, drying and calcination at 823 K. Dealuminated mordenite (DM, $SiO_2/Al_2O_3$ = 328) was obtained by extraction (12×) of aluminium using 8 M HCl at 333 K for 24 h[8] from JRC-Z-HM15 (a reference catalyst,[9,10] Catalysis Society of Japan). The structures of the samples were confirmed by XRD and $N_2$ adsorption–desorption isotherms.

Photocatalytic conversion of propene was carried out under irradiation for 1 h using a 250 W Hg lamp in a closed static system (120 ml; propene 100 μmol) at room temperature. The powdered catalyst (200 mg) was spread on the flat bottom (12 $cm^2$) of a quartz reactor irradiated from beneath. Pretreatment of catalyst was performed at 873 K (or 1073 K) in air for 2 h and in the presence of 100 Torr oxygen for 1 h, followed by evacuation at the same temperature. After 1 h reaction, products and unreacted propene were collected with a liquid-$N_2$ trap when the catalyst was under irradiation, and were analysed by GC.

The XRD patterns of the samples pretreated at 873 K and that of silicalite-1 pretreated at 1073 K are shown in Fig. 1. AMS (*a*) showed a very broad diffraction peak at 2θ *ca.* 22°, indicating its amorphous nature. The FSM-16 sample (*b*) exhibited low-angle diffraction peaks at 2θ 2.36, 4.06 and 4.68° and a very broad diffraction peak at 2θ *ca.* 23° as reported,[3,4] indicating that this material has ordered hexagonal mesopores with XRD amorphous walls. Silicalite-1 (*c*) and DM (*d*) were clearly assigned by comparison with their published structures.[6,11] The structures of AMS, FSM-16 and DM were essentially unchanged upon calcination at 1073 K, while silicalite-1 calcined at 1073 K (*e*) gave an XRD pattern resembling that of amorphous silica.

The $N_2$ adsorption isotherms of AMS and FSM-16 were of type IV indicating the presence of mesopores; isotherms of silicalite-1 and DM were of type I, also suggesting microporous structures.

Table 1 shows the catalytic activities of the samples evacuated at 873 K for propene metathesis under photoirradiation. AMS catalysed the metathesis reaction quite slowly, the activity roughly corresponding to that reported previously.[5] By contrast, FSM-16 showed a much higher metathesis activity than AMS. It should be noted that FSM-16 seemed to exhibit a higher specific activity than AMS. This is because the ratio of catalytic activity of FSM-16 to that of AMS is larger than the ratio of BET surface areas (1170 and 580 $m^2\ g^{-1}$ for FSM-16 and AMS, respectively). The $C_2/C_4$ ratio on FSM-16 was close to unity, indicating the metathesis reaction proceeded selectively. In contrast, silicalite-1 showed no activity, indicating its microporous structure is of no advantage under the reaction conditions. DM also give no gaseous products and judging from

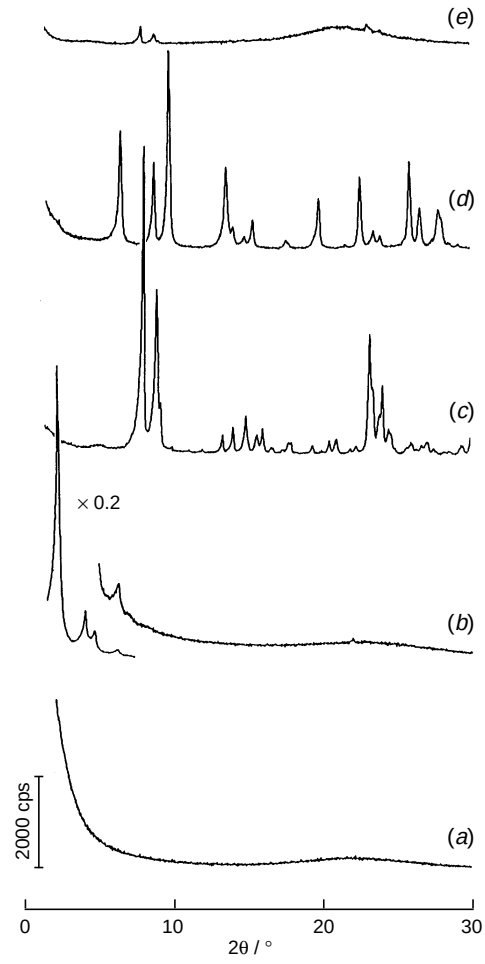



**Fig. 1** XRD patterns of porous silica materials: (*a*) amorphous silica (AMS), (*b*) FSM-16, (*c*) and (*e*) silicalite-1 and (*d*) dealuminated mordenite (DM). Samples (*a*)–(*d*) were calcined at 873 K and (*e*) at 1073 K. The intensity of the low-angle region of (*b*) is reduced to 1/5.

**Table 1** Results of tests for propene photometathesis on silica materials

| Pretreatment temperature/K | Sample | Yield (%) | | | | | Conv. (%) to metathesis | $C_2/C_4$ ratio |
|---|---|---|---|---|---|---|---|---|
| | | $C_2$[a] | *trans*-$C_4$ | *cis*-$C_4$ | 1-$C_4$ | Adsorbed | | |
| 873 | AMS | 1.4 | 1.0 | 0.7 | 0.0 | 1.0 | 3.1 | 0.82 |
| | FSM-16 | 8.2 | 5.7 | 2.8 | 0.3 | 5.8 | 16.9 | 0.94 |
| | Silicalite-1 | 0.0 | 0.0 | 0.0 | 0.0 | 2.3 | 0.0 | — |
| | DM | 0.0 | 0.0 | 0.0 | 0.0 | 100.0 | 0.0 | — |
| 1073 | AMS | 16.8 | 11.8 | 4.4 | 0.0 | 2.0 | 33.0[b] | 1.04 |
| | FSM-16 | 16.2 | 12.0 | 4.7 | 0.4 | 5.6 | 33.3[b] | 0.95 |
| | Silicalite-1 | 0.0 | 0.0 | 0.0 | 0.0 | 1.3 | 0.0 | — |
| | DM | 0.0 | 0.0 | 0.0 | 0.0 | 98.7 | 0.0 | — |

[a] $C_2$ = ethene, $C_4$ = butene. [b] Conversions on amorphous silica and FSM-16 reached equilibrium under the reaction conditions.[5]

the colour of DM after reaction, propene appears to have been adsorbed and polymerized on acid sites of DM.

Upon evacuation at higher temperature (1073 K), the activities of AMS and FSM-16 greatly increased, while DM produced no gaseous products, as shown in Table 1. Activation of amorphous silica upon evacuation at high temperature is in agreement with a previous report.[5]

Upon evacuation at 1073 K the zeolite structure of silicalite-1 was destroyed and became XRD amorphous (BET surface area 7.5 $m^2\ g^{-1}$). This amorphous sample gave no metathesis products even after 30 h reaction.

It is suggested from the results on the catalyst samples evacuated at 873 K that an amorphous phase of silica might be necessary for photometathesis on silica since reaction did not proceed on microporous crystalline silica, but only on amorphous silica (AMS) and on FSM-16 whose walls are amorphous.[2,12] The results on the catalysts evacuated at 1073 K, however, indicated that catalytic activity is governed by the other factors, since amorphous samples produced by evacuation of silicalite-1 showed no activity.

Another distinguishable factor between these samples is the concentration of surface hydroxy groups: microporous crystals have few hydroxy groups, while amorphous silica surfaces such as AMS and FSM-16 would possess a large amount of hydroxy groups, The increase of activity of AMS and FSM-16 evacuated at higher temperature indicates that this process produces active sites on the samples. Therefore it is suggested that sites produced by desorption of hydroxy groups would regulate the activity. For silicalite-1, there are only a small number of hydroxy groups prior to evacuation. Therefore, silicalite-1 evacuated at high temperature possesses few active sites, despite its amorphous surface.

There are two possibilities why FSM-16 exhibits higher activity than AMS. One is that FSM-16 has a larger number of surface hydroxy groups than AMS. The second is that the nature of the active sites differs from that of AMS as a consequence of the characteristic walls of FSM-16 which consist of double $SiO_4$ tetrahedral layers.[13]

In conclusion, the catalytic activity of unmodified mesoporous silica (FSM-16) has been investigated. FSM-16 exhibits higher photocatalytic activity for propene metathesis than amorphous silica. The key point is that FSM-16 has many hydroxy groups on the amorphous walls which constitute the hexagonal mesopore structure. The active sites are proposed to be produced by desorption by hydroxy groups from the amorphous surface of silica.

We thank Mr T. Abe, K. Nishi, T. Ishikura (Nagoya Univ.), S. Inagaki and Dr Y. Fukushima (Toyota Central R & D Labs., Inc.) for their help in the preparation of samples.

## References

1 C. T. Kresge, M. E. Leonowicz, W. J. Roth, J. C. Vartuli and J. S. Beck, *Nature*, 1992, **359**, 710.
2 J. S. Beck, J. C. Vartuli, W. J. Roth, M. E. Leonowicz, C. T. Kresge, K. D. Schmitt, C. T.-W. Chu, D. H. Olson, E. W. Sheppard, S. B. McCullen, J. B. Higgins and J. L. Schlenker, *J. Am. Chem. Soc.*, 1992, **114**, 10834.
3 S. Inagaki, Y. Fukushima and K. Kuroda, *J. Chem. Soc., Chem. Commun.*, 1993, 680.
4 S. Inagaki, A. Koiwai, N. Suzuki, Y. Fukushima and K. Kuroda, *Bull. Chem. Soc. Jpn.*, 1996, **69**, 1449.
5 H. Yoshida, T. Tanaka, S. Matsuo, T. Funabiki and S. Yoshia, *J. Chem. Soc., Chem. Commun.*, 1995, 761.
6 E. M. Flanigen, J. M. Bennett, R. W. Grose, J. P. Cohen, R. L. Patton, R. M. Kirchner and J. V. Smith, *Nature*, 1978, **271**, 512.
7 S. Yoshida, T. Matsuzaki, T. Kashiwazaki, K. Mori and K. Tarama, *Bull. Chem. Soc. Jpn.*, 1974, **47**, 1564.
8 A. Satsuma, T. Ishikura, T. Shimizu, M. Niwa, T. Hattori and Y. Murakami, *Kagaku Kogaku Ronbunshu*, 1995, **21**, 1120.
9 T. Hattori, H. Matsumoto and Y. Murakami, *Stud. Surf. Sci. Catal.*, 1987, **31**, 815.
10 T. Uchijima, in *Catalytic Science and Technology*, ed. S. Yoshida, N. Takezawa and T. Ono, Kodansha, VCH, Tokyo, 1991, vol. 1, p. 393.
11 M. M. J. Treacy, J. B. Higgins and R. von Ballmoos, *Zeolites*, 1996, **16**, 323.
12 C.-Y. Chen, H.-X. Li and M. E. Davic, *Microporous Mater.*, 1993, **2**, 17.
13 S. Inagaki, Y. Sakamoto, Y. Fukushima and O. Terasaki, *Chem. Mater.*, 1996, **8**, 2089.

*Received, 30th October 1996; Com. 6/07406E*

# Comparing the acidities of zeolites and SAPOs from first principles

**Rajiv Shah,[a] Julian D. Gale*[b] and Michael C. Payne[a]**

[a] *Cavendish Laboratory (TCM), University of Cambridge, Madingley Road, Cambridge, UK CB3 0HE*
[b] *Department of Chemistry, Imperial College, South Kensington, UK SW7 2AY*

**First-principles density functional calculations using periodic boundary conditions are used to demonstrate that SAPO-34 is less acidic than its aluminosilicate equivalent chabazite, based on the properties of the Brønsted-acid sites and their interaction with basic molecules.**

There is much interest in understanding the nature of microporous solid acid catalysts, which have many important applications in commercial processes. Two of the most commonly studied types of materials in this category are zeolites (aluminosilicates) and silicoaluminophosphates (SAPOs), which result from the substitution of aluminium for silicon and silicon for phosphorus, respectively, within the tetrahedral framework. Such negatively charged defect sites can be counterbalanced by the presence of a proton leading to the formation of Brønsted-acid sites which are believed to be the active sites for catalysis. If we are to gain any insight into the chemistry which occurs within the confines of microporous materials we need to understand the factors which can affect their acidity. In this study the relative acidity of a zeolite and SAPO with the same framework structure is considered, in order to examine the differences made by framework composition.

The question of Brønsted acidity in zeolites has been studied both experimentally,[1,2] and theoretically.[3] However the majority of the theoretical work has used small gas-phase clusters, often without reference to specific materials. More recent work has used periodic boundary conditions to study zeolites.[4] In a previous study[5] we have shown that inclusion of the full zeolite structure is essential if a proper characterisation of the energy surface around the acid site is to be achieved.

The current work uses the same methods to study a SAPO catalyst, allowing a comparison of the properties of these materials with zeolites. Gradient-corrected density functional theory (DFT) is used to calculate the electronic ground-state of the system, expanding the valence electronic wavefunctions in plane-waves upto a 650 eV cut-off and representing the nuclei and core electrons by norm-conserving pseudopotentials.† The framework structure was represented by a single unit cell of the material and periodic boundary conditions. All atoms were allowed to relax freely, except for the constraint of fixed cell shape. The material studied was SAPO-34, structurally analogous to the zeolite chabazite, used for our previous work. SAPO-34 has been observed to be an active catalyst for methanol conversion to hydrocarbons,[8] and so constitutes a realistic model. The structure has twelve tetrahedral sites in the unit cell. For simplicity the case of one Si substitution per unit cell has been considered.

The accuracy of gradient-corrected DFT to represent bonding and structure has been demonstrated by calculations of the lattice parameter of α-quartz and equilibrium bond lengths for a methanol molecule which are within ±1% of experimental values. The gas-phase proton affinity of a methanol molecule has also been reproduced within 1%.[5] The ability of these methods to represent hydrogen bonded systems was shown by Greatbanks *et al.*[9]

Initially we studied just the isolated framework Brønsted acid site. This is confirmed to consist of the proton forming a covalent bond with one of the oxygens around the Si site. A local minimum is found for the proton on any of the four symmetry inequivalent oxygens around the site. The relative energies and some other characteristics of these proton sites are listed in Table 1. The most stable site is O(1), but the difference in energy for O(3) is less than $kT$ at room temperature. The IR frequencies seen for these two sites may correspond to the distinct 3600 and 3625 $cm^{-1}$ O–H bands observed in dehydrated SAPO-34.[2] The range of energies of the sites is less than the 9 kJ $mol^{-1}$ spread seen for the four proton sites in the aluminosilicate chabazite, but it is O(1) which is most stable in both cases.[5] The O–H frequencies are higher and the O–H bond lengths slightly shorter than in the zeolite case. This would be consistent with the SAPO having a higher proton affinity due to a stronger O–H bond. The two bonds formed by the hydroxy group to the rest of the framework are more equal in length than seen in the aluminosilicate, where the bond to the Al is longer than that to Si.

Population analysis techniques[10] have been used to examine the bonding around such an acid site. This shows increasing ionic character around the substituted Si site. The Mulliken charge on the Si (+2.31) is not much higher than that found on substituted Al in zeolites (+2.14). The charges on the surrounding oxygens and hydroxy group are very similar, although the charge on the proton is slightly higher in the zeolite (+0.55) than in the SAPO (+0.53). Hence one would expect the leading term in a multipole expansion of the electrostatic potential to be similar for the zeolite and SAPO. However, the bond populations seen are quite different between the two systems, so higher terms in the expansion would differ. The overlap populations of the two bonds made by the hydroxy group to the framework are more equal in the SAPO (0.29 and 0.24) than in the zeolite (0.16 and 0.38), consistent with the more equal bond lengths.

Although the properties of the isolated Brønsted-acid sites give an indication of the relative O–H bond strengths between the different materials the real test of acidity comes from the interaction between the hydroxy group and a basic adsorbate. This depends not only on the proton affinity but also on the local electrostatic potential which is crucial in stabilising chemisorbed species. Experimentally, weak bases such as CO and $N_2$ are often used to probe acidity by measurement of the shift in

**Table 1** Energies, stretching frequencies and geometry around the O–H group for the four proton sites in SAPO-34. Energies relative to O(1). Values for the most stable site in the zeolite chabazite are also given for comparison. $\nu_{OH}^{harm}$ is the harmonic frequency, and $\nu_{OH}$ the anharmonicity corrected value (using a Morse potential[5])

| | O(1) | O(2) | O(3) | O(4) | Zeolite |
|---|---|---|---|---|---|
| $E$/kJ $mol^{-1}$ | 0 | 5 | 2 | 4 | — |
| $\nu_{OH}^{harm}$/$cm^{-1}$ | 3870 | 3860 | 3860 | 3865 | 3845 |
| $\nu_{OH}$/$cm^{-1}$ | 3610 | 3600 | 3600 | 3605 | 3590 |
| O–H/Å | 0.970 | 0.970 | 0.971 | 0.970 | 0.972 |
| Si–O/Å | 1.762 | 1.741 | 1.747 | 1.777 | 1.697 |
| Al–O/Å | 1.763 | 1.756 | 1.762 | 1.779 | 1.857 |
| Si–O–H/° | 110.6 | 109.0 | 109.3 | 111.0 | 113.5 |
| Al–O–H/° | 116.6 | 116.4 | 115.1 | 117.0 | 111.5 |
| Al–O–Si/° | 132.6 | 133.7 | 134.4 | 131.9 | 134.4 |

their stretching frequency. However, we have chosen to use methanol as a probe molecule because of the interest in the methanol to gasoline conversion process.[11] The adsorption of methanol in zeolites has been previously studied by us,[5] and here we extend this to consider the stable forms for methanol bound to a SAPO acid site. The case of one molecule per acid site was considered. From a number of different starting points the forces on the atoms were used to relax the atoms to the nearest local minimum by a BFGS technique. In the zeolite the geometry shown in Fig. 1 was found, with the proton transferred from the framework to the methanol. For the SAPO case a number of different geometries were found, but in none of these was proton transfer found to be stable. However, the framework O–H bond was lengthened by about 8%, and this hydrogen atom generally formed quite a short hydrogen bond (1.4–1.5 Å) to the methanol oxygen. The most stable geometry, with a binding energy of −77.9 kJ mol$^{-1}$, is illustrated in Fig. 2. Interestingly, although the molecule bridges across the Si site in the same way as it does across Al in zeolites, here the methanol hydrogen forms longer hydrogen bonds to two framework oxygens, rather than just one shorter bond to a single oxygen. Six-ring type geometries of the type found in zeolites were seen, but with the methanol hydrogen forming a single hydrogen bond, about 1.9 Å long, to one of the oxygens adjacent to Si. Such geometries were about 10 kJ mol$^{-1}$ higher in energy.

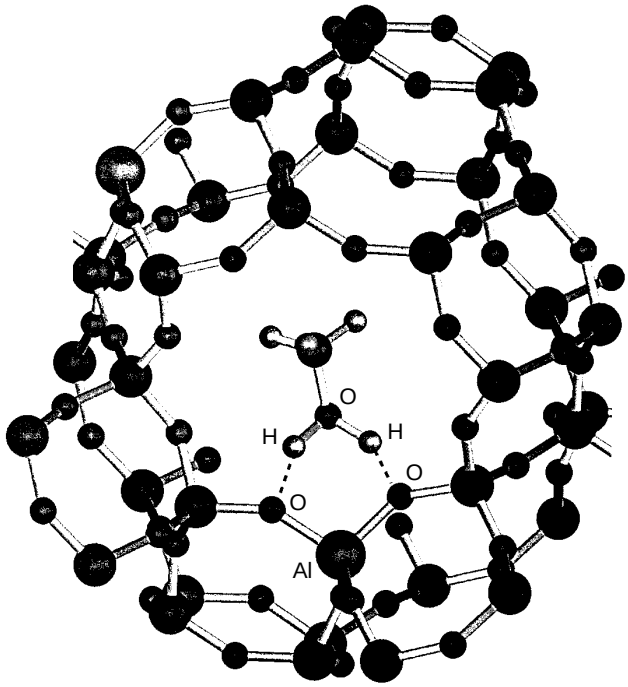



**Fig. 1** Six-ring geometry seen for protonated methanol in chabazite

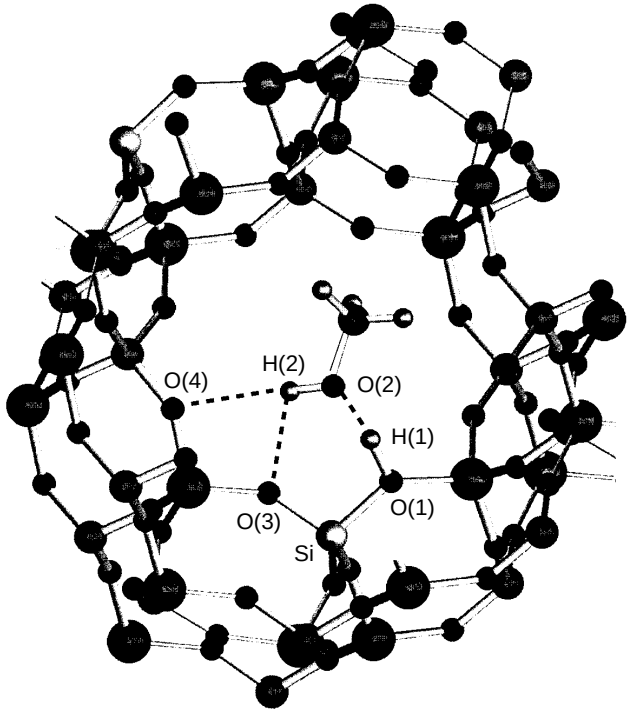



**Fig. 2** The most stable geometry found for methanol bound to acid site of SAPO-34. Selected distances (Å) are O(1)–H(1) 1.06, O(2)–H(1) 1.46, O(2)–H(2) 0.97, O(3)–H(2) 2.36, O(4)–H(2) 2.48.

Our results show that SAPO-34 appears unable to protonate methanol, whereas a zeolite of the same framework topology can. This suggests that, at least for this topology, SAPOs are less acidic than zeolites. This conclusion is different from that of Limtrakul,[12] who suggested SAPOs were more acidic. The differences are probably explained by the very small clusters used in his work, in particular for the SAPO only including one of the oxygens around the Si site while replacing the other oxygens by hydrogen atoms to saturate the edge of the cluster. This meant the only methanol geometry considered was for the molecule to bridge across Al rather Si, which we found to be about 20 kJ mol$^{-1}$ higher in energy. Our finding that at low loading methanol is not protonated in SAPOs, but can be protonated in zeolites, is consistent with the results recently reported by Thursfield and Anderson.[13] The results here have given useful insights into the nature of solid acid catalysts and further work will allow an examination of the IR spectra of adsorbed methanol, and a comparison with the adsorption of other basic molecules such as water, whose structure in SAPO-34 has recently been determined by X-ray crystallography.[2]

Computational work was performed on the Edinburgh Cray T3D, as part of the Materials Chemistry and UKCP consortia. The work of R. S. was supported by EPSRC, and that of J. D. G. by the Royal Society.

## Footnote

† The CETEP code[6] was used, based on the methods described in ref. 7.

## References

1 G. Mirth, J. A. Lercher, M. W. Anderson and J. Klinowski, *J. Chem. Soc., Faraday Trans.*, 1990, **86**, 3039.
2 L. Smith, A. K. Cheetham, R. E. Morris, L. Marchese, J. M. Thomas, P. A. Wright and J. Chen, *Science*, 1996, **271**, 799.
3 J. D. Gale, C. R. A. Catlow and J. R. Carruthers, *Chem. Phys. Lett.*, 1993, **216**, 155.
4 L. Campana, A. Selloni, J. Weber, A. Pasquarello, I. Papai and A. Goursot, *Chem. Phys. Lett.*, 1994, **226**, 245.
5 R. Shah, J. D. Gale and M. C. Payne, *J. Phys. Chem.*, 1996, **100**, 11 688.
6 L. J. Clarke, I. Stich and M. C. Payne, *Comput. Phys. Commun.*, 1992, **72**, 14.
7 M. C. Payne, M. P. Teter, D. C. Allan, T. A. Arias and J. D. Joannopoulos, *Rev. Mod. Phys.*, 1992, **64**, 1045.
8 Y. Xu, C. P. Grey, J. M. Thomas and A. K. Cheetham, *Catal. Lett.*, 1990, **4**, 251.
9 S. P. Greatbanks, I. H. Hillier, N. A. Burton and P. Sherwood, *J. Chem. Phys.*, 1996, **105**, 3770.
10 M. D. Segall, C. J. Pickard, R. Shah and M. C. Payne, *Mol. Phys.*, 1996, in the press.
11 S. L. Meisel, J. P. McCullogh, C. H. Lechthaler and P. B. Weisz, *Chemtech*, 1976, **6**, 86.
12 J. Limtrakul, *Chem. Phys.*, 1995, **193**, 79.
13 A. Thursfield and M. W. Anderson, *J. Phys. Chem.*, 1996, **100**, 6698.

*Received, 25th July 1996; Com. 6/05200B*

# A reductive rearrangement of iron acetylide hydride complexes

**Leslie D. Field,* Adrian V. George,* Elizabeth Y. Malouf, Trevor W. Hambley and Peter Turner**

*School of Chemistry, University of Sydney, NSW 2006, Australia*

**Iron acetylide hydride complexes of the type [Fe(H)(C≡CR)(dmpe)$_2$] [dmpe = 1,2-bis(dimethylphosphino)ethane] react with anions in a methanol solution to form substituted alkenyl complexes; the crystal structure of *trans*-FeN$_3$(CH=CHPh)(dmpe)$_2$] is presented.**

There is current interest in metal acetylide complexes as materials which may be used as components in non-linear optical materials,[1,2] the construction of organometallic polymers[2–4] and as new liquid crystals.[5] Metal σ-acetylide complexes have been prepared by a number of routes including ligand exchange reactions,[4,6] oxidative addition reactions[7,8] and by deprotonation of metal vinylidene complexes.[9]

Acetylide hydride complexes of iron [FeH(C≡CR)L$_4$] have been formed by reaction of a terminal acetylene with a coordinatively unsaturated iron complex [FeL$_4$] (L is usually a phosphine).[8,10] The acetylide hydride complexes of [Fe(PP)$_2$] [PP = 1,2-bis(dimethylphosphino)ethane (dmpe) or 1,2-bis-(diethylphosphino)ethane] are typically reactive, air-sensitive materials but they can be handled and stored as solids under an inert atmosphere.[11] They can be converted to the more stable acetylide chloride derivatives [FeCl(C≡CR)(PP)$_2$] by treatment with dichloromethane or other alkyl halides.‡

Treatment of the iron acetylide hydride complexes with a chloride, azide or thiocyanate salt in methanol solution, resulted effectively in substitution of the hydride by Cl$^-$, N$_3^-$ or SCN$^-$ with partial reduction of the bound acetylene. Treatment of *trans*-[FeH(C≡CPh)(dmpe)$_2$] **1** with a methanol solution of sodium azide resulted in formation of *trans*-[FeN$_3$(CH=CHPh)(dmpe)$_2$] **2** (Scheme 1).

The conversion of **1** to **2** was clean and quantitative and the $^{31}$P NMR spectrum indicated the reaction was complete within 30 min. Removal of the solvent and washing the residue with methanol produced *trans*-[FeN$_3$(CH=CHPh)(dmpe)$_2$] **2** as an orange solid. The $^1$H NMR spectrum exhibited two alkenyl protons (at δ 7.05 and 5.73) with a coupling ($^3J_{HH}$ 16.7 Hz) and this is consistent with a *trans* stereochemistry for the alkene. The vinyl resonance at δ 7.05 also showed coupling to the four equivalent phosphorus ligands ($^3J_{PH}$ 6.9 Hz). An analogous reaction between **1** and chloride or thiocyanate in methanol solvent quantitatively gave *trans*-[FeCl(CH=CHPh)(dmpe)$_2$] **3** and *trans*-[FeSCN-(CH=CHPh)(dmpe)$_2$] **4** respectively.

The crystal structure of **2** (Fig. 1)† confirms that the azide and alkenyl ligands adopt a *trans* configuration about the metal centre and the stereochemistry of the double bond is (*Z*). The three nitrogen atoms of the azide group are approximately collinear (176°) and form an approximate angle of 146° with the equatorial plane containing the metal and the four phosphorus donors.

A likely reaction course for the reduction of the acetylide complexes reported here, involves initial protonation of the σ-bound acetylide ligand at the carbon β to the metal centre to form a vinylidene complex. Metal-to-carbon hydride migration in the vinylidene complex with attack by the anion (Cl$^-$, N$_3^-$ or SCN$^-$) leads to the neutral complexes (Scheme 2).

Protonation (or the addition of other electrophiles) at the β carbon of metal acetylide complexes is well known[12] and the intramolecular hydride migration from the metal to the α carbon

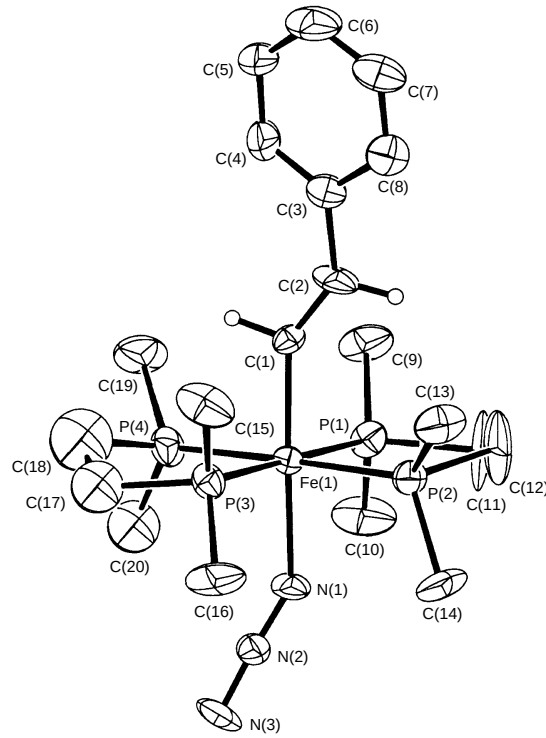
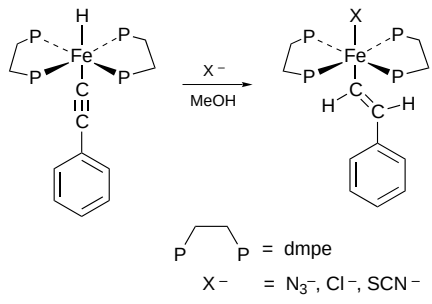
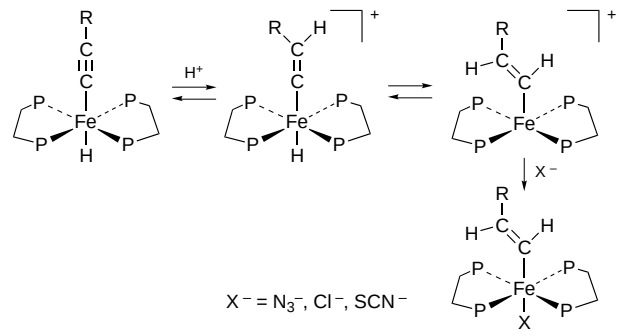



**Fig. 1** ORTEP[20] plot of *trans*-[FeN$_3$(CH=CHPh)(dmpe)$_2$] **2**




**Scheme 1**




**Scheme 2**

of the vinylidene complex is analogous to the mechanism proposed for formation of $\eta^3$-butenyne complexes from metal bis(acetylide)s.[13] The complex *trans*-[FeH(C≡C$C_6H_4$C≡CH)$(dmpe)_2$] **5** which has both metal- and non-metal-bound acetylides reacts with a methanol solution of sodium azide, to give *trans*-[$FeN_3$(CH=C$HC_6H_4$C≡CH)$(dmpe)_2$] **6** as the sole product. Exclusive formation of the vinyl metal product **6** from **5** supports the proposal that an intramolecular metal-to-carbon hydride migration is a key step in the mechanism.

Treatment of analogous ruthenium acetylide hydride complexes with a methanol solution of azide or chloride produces ruthenium alkenyl complexes, presumably by a similar mechanism.[14]

The partial hydrogenation of an acetylene by metal hydride complexes has previously been reported.[15] Reaction of excess phenylacetylene with [$FeH_2(dmpe)_2$] in methanol solution forms a bis(acetylide) complex (*via* an acetylide hydride complex) and 2 equiv. of styrene are produced in the reaction.[16] A reasonable intermediate in the conversion of the acetylide hydride complex to the bis(acetylide) is an acetylide styryl iron complex, [Fe(C≡CPh)(CH=CHPh)$(dmpe)_2$], which would undergo substitution of the styryl group in the presence of excess phenylacetylene to form the bis(acetylide) and free styrene.

The metal-to-carbon hydride migration reported here provides a novel method of reducing metal acetylides to vinyl metal complexes in protic solvents. The reduction is stereospecific and provides an alternative approach for the introduction of the vinyl group into metal complexes.

We gratefully acknowledge financial support from the Australian Research Council.

## Footnote

† *Crystal data* for *trans*-[$FeN_3$(CH=CHPh)$(dmpe)_2$] **2**: $C_{20}H_{39}N_3FeP_4$, $M$ = 501.29, monoclinic, space group $P2_1/c$, $a$ = 23.888(3), $b$ = 9.112(2), $c$ = 35.680(3) Å, β = 95.568(8)°, $Z$ = 12 (three independent complexes), $R$ = 0.055 [3624 $F$, $I > 1.50\sigma(I)$]. Orange acicular crystals of *trans*-[$FeN_3$(CH=CHPh)$(dmpe)_2$] **2** suitable for X-ray diffraction studies were grown by the slow evaporation of a methanol–tetrahydrofuran solution of the complex. A crystal was mounted in a glass capillary, on a Rigaku AFC7R diffractometer equipped with a graphite monochromator. All calculations were performed using the teXsan crystallographic software package of Molecular Structure Corporation.[17] Data were reduced and Lorentz, polarisation and absorption corrections (psi scan) were applied. The structure was solved by direct methods[18] and expanded using Fourier techniques.[19]

Atomic coordinates, bond lengths and angles, and thermal parameters have been deposited at the Cambridge Crystallographic Data Centre (CCDC). See Information for Authors, Issue No. 1. Any request to the CCDC for this material should quote the full literature citation and the reference number 182/303.

## References


1 *Materials for Nonlinear Optics*, ed. S. R. Marder, J. E. Sohn and G. D. Stucky, *ACS Symp. Ser.* 455, American Chemical Society, Washington, DC, 1991, pp. 605 and references therein; J. C. Calabrese, L.-T. Cheng, J. C. Green, S. R. Marder and W. J. Tam, *J. Am. Chem. Soc.*, 1991, **113**, 7227; P. N. Prasad and D. J. Williams, *Nonlinear Optical Effects in Molecules and Polymers*, Wiley, New York, 1991; D. R. Ulrich, *Mol. Cryst. Liq. Cryst.*, 1990, **189**, 3; E. Abraham, C. T. Seaton and S. D. Smith, *Sci. Am.*, 1983, **284**, no. 2, 85; W. A. G. Graham, *J. Organomet. Chem.*, 1986, **300**, 81.

2 S. Takahashi, H. Morimoto, E. Murata, S. Kataoka, K. Sonogashira and N. Hagihara, *J. Polym. Sci. Polym. Chem. Ed.*, 1982, **20**, 565; N. Hagihara, K. Sonogashira and S. Takahashi, *Adv. Polym. Sci.*, 1980, **41**, 149.

3 K. Onitsuka, T. Joh and S. Takahashi, *Bull. Chem. Soc. Jpn.*, 1992, **65**, 1179; S. Takahashi, E. Murata, K. Sonogashira and N. Hagihara, *J. Polym. Sci. Polym. Chem. Ed.*, 1980, **18**, 661; H. B. Fyfe, M. Mlekuz, D. Zargarian, N. J. Taylor and T. B. Marder, *J. Chem. Soc., Chem. Commun.*, 1991, 188; G. Jia, R. Puddephatt, J. J. Vittal and N. C. Payne, *Organometallics*, 1993, **12**, 263; G. Jia, N. C. Payne, J. J. Vittal and R. J. Puddephatt, *Organometallics*, 1993, **12**, 4771; S. Kotani, K. Shiina and K. Sonogashira, *Appl. Organomet. Chem.*, 1991, **5**, 417; H. S. Nalwa, *Appl. Organomet. Chem.*, 1991, **5**, 377.

4 M. S. Khan, A. K. Kakkar, S. L. Ingham, P. R. Raithby, J. Lewis, B. Spencer, F. Wittmann and R. H. Friend, *J. Organomet. Chem.*, 1994, **472**, 247; C. W. Faulkner, S. L. Ingham, M. S. Khan, J. Lewis, N. J. Long and P. R. Raithby, *J. Organomet. Chem.*, 1994, **482**, 139.

5 A. Abe, N. Kimura and S. Tabata, *Macromolecules*, 1991, **24**, 6238; T. Kaharu, H. Matsubara and S. Takahashi, *J. Mater. Sci*., 1991, **32**, 732; S. Takahashi, Y. Takai, H. Morimoto and K. Sonogashira, *J. Chem. Soc., Chem. Commun.*, 1984, 3.

6 See for example: L. D. Field, A. V. George, T. W. Hambley and E. Y. Malouf, *Organometallics*, 1991, **10**, 3842; L. D. Field, A. V. George, S. R. Pike, I. E. Buys and T. W. Hambley, *Polyhedron*, 1995, **14**, 3133; L. D. Field, A. V. George, D. C. R. Hockless, G. R. Purches and A. White, *J. Chem. Soc., Dalton Trans.*, 1996, 2011; M. P. Gamasa, J. Gimeno, E. Lastra, M. Lanfranchi and A. Tiripicchio, *J. Organomet. Chem.*, 1991, **405**, 333; D. Touchard, C. Morice, V. Cadierno, P. Haquette, L. Toupet and P. H. Dixneuf, *J. Chem. Soc., Chem. Commun.*, 1994, 859.

7 See for example: S. D. Ittel, C. A. Tolman, P. J. Krusic, A. D. English and J. P. Jesson, *Inorg. Chem.*, 1978, **17**, 3432; C. Bianchini, P. Barbaro, A. Meli, M. Peruzzini, A. Vacca and F. Vizza, *Organometallics*, 1993, **12**, 2505; P. J. Stang and R. Tykwinski, *J. Am. Chem. Soc.*, 1992, **114**, 4411; H. B. Fyfe, M. Mlekuz, G. Stringer, N. J. Taylor and T. B. Marder, B. *NATO ASI Ser.*, 1992, **206** (*Inorg. Organomet. Polym. Spec. Prop.*), Ser.E, 331; H. B. Fyfe, M. Mlekuz, D. Zargarian, N. J. Taylor and T. B. Marder, *J. Chem. Soc., Chem. Commun.*, 1991, 188.

8 S. D. Ittel, C. A. Tolman, A. D. English and J. P. Jesson, *J. Am. Chem. Soc.*, 1978, **100**, 7577.

9 See for example: A. Davison and J. P. Selegue, *J. Am. Chem. Soc.*, 1978, **100**, 7763; D. Touchard, C. Morice, V. Cadierno, P. Haquette, L. Toupet and P. H. Dixneuf, *J. Chem. Soc., Chem. Commun.*, 1994, 859; D. L. Hughes, M. Jimenez-Tenorio, G. J. Leigh and A. T. Rowley, *J. Chem. Soc., Dalton Trans.*, 1993, 3151; D. R. Senn, A. Wong, A. T. Patton, M. Marsi, C. E. Strouse and J. A. Gladysz, *J. Am. Chem. Soc.*, 1988, **110**, 6096; M. I. Bruce, A. G. Swincer and R. C. Wallis, *J. Organomet. Chem.*, 1979, **171**, C5; A. J. Hodge, S. L. Ingham, A. K. Kakkar, M. S. Khan, J. Lewis, N. J. Long, D. G. Parker and P. R. Raithby, *J. Organomet. Chem.*, 1995, **488**, 205.

10 M. V. Baker and L. D. Field, *J. Am. Chem. Soc.*, 1987, **109,** 2825; *J. Am. Chem. Soc.*, 1986, **108,** 7433; *Organometallics*, 1986, **5,** 821.

11 L. D. Field and A. V. George, *J. Organomet. Chem.*, 1993, **454**, 217.

12 M. I. Bruce and A. G. Swincer, *Adv. Organomet. Chem.*, 1983, **22**, 59; M. I. Bruce and R. C. Wallice, *J. Organomet. Chem.*, 1978, **161**, C1; B. E. Bolanad-Lussier and R. P. Hughes, *Organometallics*, 1982, **1**, 635.

13 L. D. Field, A. V. George, G. R. Purches and I. H. M. Slip, *Organometallics*, 1992, **11**, 3019.

14 L. D. Field, A. V. George and G. R. Purches, unpublished work.

15 J. López, A. Romero, A. Santos, A. Vegas, A. M. Echavarren and P. Noheda, *J. Organomet. Chem.*, 1989, **373**, 249; C. Bianchini, A. Meli, M, Peruzzini, F. Vizza and A. Albinati, *Organometallics*, 1990, **9**, 2283; J. M. Bray and R. J. Mawby, *J. Chem. Soc., Dalton Trans.*, 1989, 589; B. H. Lipshutz and E. L. Ellsworth, *J. Am. Chem. Soc.*, 1990, **112**, 7440; A. Andriollo, M. A. Esteruelas, U. Meyer, L. A. Oro, R. A. Sánchez-Delgado, E. Sola, C. Valero and H. Werner, *J. Am. Chem. Soc.*, 1989, **111**, 7431.

16 L. D. Field, A. V. George, T. W. Hambley, E. Y. Malouf and D. J. Young, *J. Chem. Soc., Chem. Commun.*, 1990, 931.

17 teXsan, Crystal Structure Analysis Package, Molecular Structure Corporation, The Woodlands, TX, 1984 and 1992.

18 A. Altomare, M. C. Burla, M. Camalli, M. Cascarano, C. Giacovazzo, A. Guagliardi and G. Polidori, SIR92, *J. Appl. Crystallogr.*, 1993, **26**, 343.

19 P. T. Beurskens, G. Admiraal, G. Beurskens. W. P. Bosman, R. de Gelder, R. Israel and J. M. M. Smits, DIRDIF94, Technical Report of the Crystallography Laboratory, University of Nijmegen, The Netherlands, 1994.

20 C. K. Johnson, ORTEP, A Thermal Ellipsoid Plotting Program, Oak Ridge National Laboratory, Oak Ridge, Tennessee, 1965.


*Received, 22nd August 1996; Com. 6/05846I*

# Dramatic solvent effect on the luminescence of a dinuclear gold(I) complex of quinoline-8-thiolate

**Biing-Chiau Tzeng,[a] Chi-Keung Chan,[a] Kung-Kai Cheung,[a] Chi-Ming Che*[a] and Shie-Ming Peng[b]**

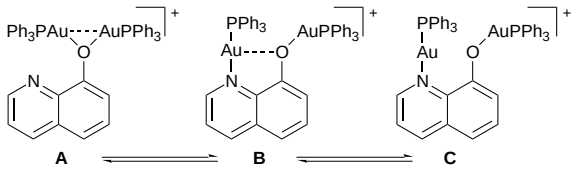
[a] *Department of Chemistry, The University of Hong Kong, Pokfulam Road, Hong Kong*
[b] *Department of Chemistry, National Taiwan University, Taipei, Taiwan*

**The complex $[\{Au(PPh_3)\}_2(8\text{-qnS})]BF_4$ (8-qnS = quinoline-8-thiolate) with intramolecular gold(I)···gold(I) distances of 2.991(2) and 3.081(2) Å in two independent asymmetric units, shows a long-lived emission at 640 nm which is quenched by polar solvents such as acetonitrile and alcohol.**

Study on the solvent and/or medium effect on the occurrence of gold(I)···gold(I) interactions could shed new insight into the molecular self-assembly of gold(I) atoms, which was found to give polynuclear gold(I) compounds with novel structural and electro-optical properties.[1] This is particularly important in understanding the chemistry of gold(I) drugs,[2] where such interaction might occur under biological conditions. Schmidbaur and co-workers had reported an interesting study indicating scrambling of the $[Au(PPh_3)]^+$ units in a solution of the complex (8-quinolinyl)bis[(triphenylphosphine)gold(I)]-oxonium tetrafluoroborate[3] (Scheme 1). Spectroscopic evidence in support of the equilibrium reactions depicted in Scheme 1 only came from $^{31}P$ NMR spectral data of **B**, which revealed two $^{31}P$ signals at low temperature. Herein is described the molecular structures and photophysical properties of $[Au(PPh_3)(8\text{-qnS})]$ (8-qnS = quinoline-8-thiolate) and $[\{Au(PPh_3)\}_2(8\text{-qnS})]BF_4$ indicating an interesting case, whereby a solvent effect on the association of the $[Au(PPh_3)]^+$ units through a bridging sulfur atom could be reflected by a distinct change in emissive properties.

Complexes **1** and **2**$BF_4$† were prepared by modified literature procedures[3,4] and perspective views of their structures‡ are shown in Figs. 1 and 2, respectively. In **1**, the Au(1) atom is two-coordinate, but the measured P(1)–Au(1)–S(1) angle of 163.7(3)° and Au(1)–N(1) distance of 2.627(9) Å suggest a weak Au(1)···N(1) interaction. This is different from the related $[Au(PPh_3)(2\text{-pyS})]$ (2-pyS = pyridine-2-thiolate) complex,[4] where an approximate linear geometry about the Au atom has been found [P–Au–S 177.9(1)°]. In **2**, there are two independent asymmetric units, and the 8-qnS is bonded to 2 nearly equivalent $[Au(PPh_3)]^+$ units through the sulfur atom. The intramolecular gold(I)···gold(I) contacts of 2.991(2) and 3.081(2) Å are longer than those in $[\{Au(PPh_3)\}_4S]^{2+}$ [Au···Au$_{av}$ 2.910(2) Å],[5] but shorter than those values of 3.110(3) Å in $[\{Au(PPh_3)\}_2SR]^+$[6] and 3.299(3) Å in $[\{Au(PPh_3)\}_3S]^+$.[7] It is noted that the mean Au–S–Au angle of 80.6(1)° lies in the range of values found in related complexes[6] which show intramolecular gold(I)···gold(I) interactions.

The absorption spectra of **1** and **2**$BF_4$ measured in dichloromethane and in acetonitrile are shown in Fig. 3. Irrespective of the solvents, complex **1** shows an intense absorption at 386 nm,




**Scheme 1**

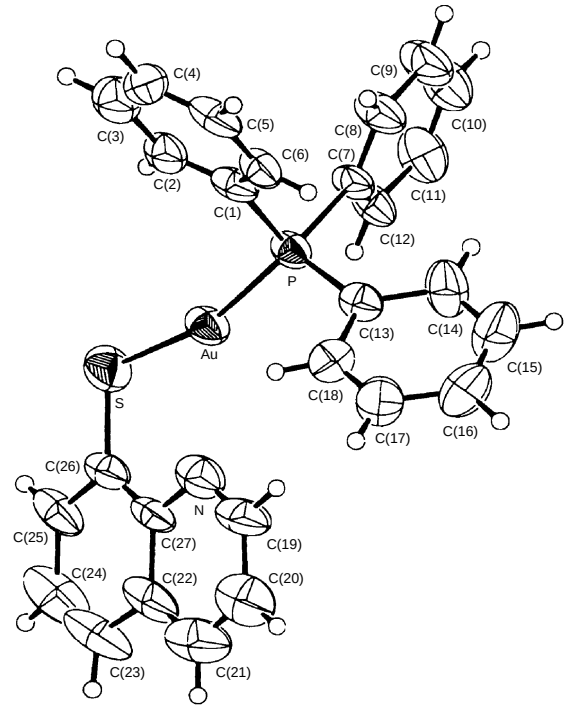



**Fig. 1** A perspective view of $[Au(PPh_3)(8\text{-qnS})]$ (bond lengths in Å, angles in °): Au(1)–S(1) 2.296(8), Au(1)–P(1) 2.248(7); S(1)–Au(1)–P(1) 163.7(3)

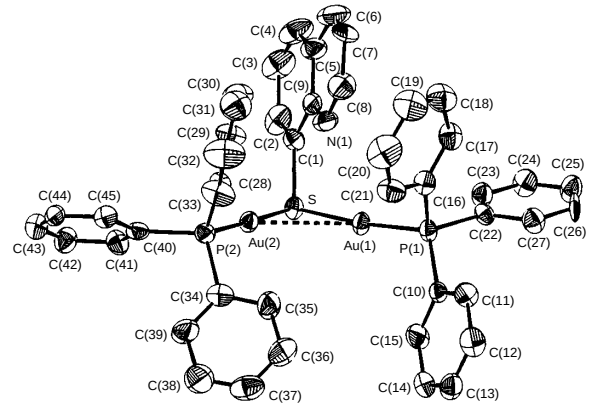



**Fig. 2** A perspective view of $[\{Au(PPh_3)\}_2(8\text{-qnS})]^+$ (bond lengths in Å, angles in °): Au(1A)···Au(2A) 3.081(2), Au(1B)···Au(2B) 2.991(2), Au(1A)–S(1A) 2.343(3), Au(2A)–S(1A) 2.342(3), Au(1A)–P(1A) 2.256(3), Au(2A)–P(2A) 2.268(3), Au(1B)–S(1B) 2.357(3), Au(2B)–S(1B) 2.351(3), Au(1B)–P(1B) 2.253(3), Au(2B)–P(2B) 2.254(3); S(1A)–Au(1A)–P(1A) 174.6(1), S(1A)–Au(2A)–P(2A) 178.6(1), S(1B)–Au(1B)–P(1B) 172.6(1), S(1B)–Au(2B)–P(2B) 169.6(1) (A and B represent two independent asymmetric units)

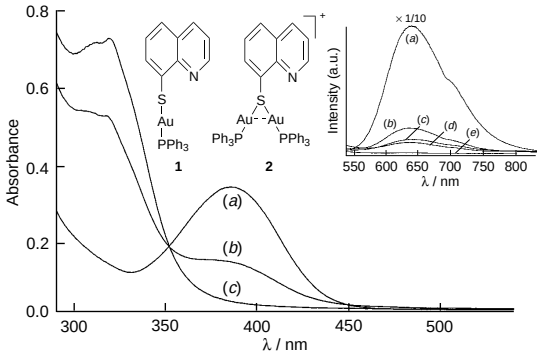
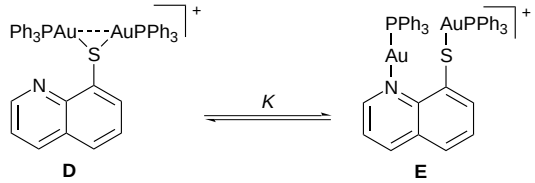



**Fig. 3** The absorption spectra of **1** in $CH_2Cl_2$ (*a*), **2**$BF_4$ in MeCN (*b*) and **2**$BF_4$ in $CH_2Cl_2$ (*c*); complex concentration = $9 \times 10^{-5}$ M. [Insert is the emission spectra of **2**$BF_4$ ($1 \times 10^{-4}$ M) in (*a*) $CH_2Cl_2$, (*b*) thf, (*c*) EtOH, (*d*) MeOH and (*e*) MeCN; excitation at 320 nm].

which is assigned to $S \rightarrow Au^I$ charge transfer (LMCT) transition. For **2**$BF_4$ there is a distinct difference in the spectra measured in dichloromethane and in acetonitrile. In dichloromethane, the complex shows an intense absorption band at *ca*. 320 nm, which is assigned to the $5d(d_{\sigma^*}) \rightarrow 6p(p_\sigma)$ transition modified by gold(I)···gold(I) interation. We suggest that coordinating the electrophilic $[Au(PPh_3)]^+$ unit on the sulfur atom of the [Au(8-qnS)] moiety would blue shift the $S \rightarrow Au^I$ transition and hence explain the apparent blue shift of the spectrum of **2**$BF_4$ from that of **1**. Notably, addition of acetonitrile to a dichloromethane solution of **2**$BF_4$ increases the absorption at *ca*. 386 nm with a concomitant decrease in the absorption at *ca*. 320 nm; the spectral changes with an isosbestic point at 352 nm. Other solvents such as MeOH and EtOH also give similar spectral changes. We rationalize this finding by the following equilibrium reaction (Scheme 2).




**Scheme 2**

Form **E** would be isostructural to form **B** in Scheme 1 and would show no intramolecular gold(I)···gold(I) interaction. Its absorption spectrum, therefore, is anticipated to be similar to that of **1**. Thus the spectral changes shown in Fig. 3 could be rationalized by a decrease in the equilibrium constant *K* (*K* = [**E**]/[**D**]) from acetonitrile to dichloromethane. The scrambling of the $[Au(PPh_3)]^+$ units is very fast on the NMR timescale, since the $^{31}P$ NMR spectrum of an acetonitrile solution of **2**$BF_4$ shows only a single peak (δ 34.12) at room temperature and even at −35 °C (δ 32.97).

The reaction in Scheme 2 could also be shown by emission spectroscopy. In solution, complex **1** shows a very weak emission at 477 nm. Excitation of a dichloromethane solution of **2**$BF_4$ gives a very weak emission at 460 nm and an intense low-energy one with a lifetime of 26 μs at 640 nm (Fig. 3, insert). The low energy emission is absent in **1** and a gold(I)···gold(I) interaction is most probably responsible for it. The excitation spectrum of the 640 nm emission matches with the absorption spectra. The excited state is tentatively assigned to come from the metal-centred $5d(d_{\sigma^*}) \rightarrow 6p(p_\sigma)$ excitation, although mixing with some $S \rightarrow Au$ charge-transfer character in the excited state could not be precluded. Notably, the emission depends on solvent polarity. Polar solvents such as MeCN, MeOH, EtOH and thf were found to quench it with quenching rate constants in the order MeCN > MeOH > EtOH > thf ($k_q = 1.25 \times 10^5$, $0.50 \times 10^5$, $0.32 \times 10^5$ and $0.24 \times 10^5$ $M^{-1}$ $s^{-1}$ respectively). In acetonitrile, the 640 nm emission virtually disappears, whereas it has the highest quantum yield and longest lifetime in dichloromethane. Importantly, addition of dichloromethane to a methanol solution revives the emission. Thus, the decrease in the 640 nm emission in polar solvents is consistent with the UV–VIS absorption data. Because the low-energy emission at 640 nm is associated with a gold(I)···gold(I) interaction, the reaction of Scheme 2 may well explain the apparent solvent-induced quenching of the emission of **2**$BF_4$.

We acknowledge support from the University of Hong Kong, the Hong Kong Research Grants Council, and the Croucher Foundation.

## Footnotes

† *Syntheses*: [Au(PPh$_3$)(8-qnS)] **1**: $NEt_3$ was added dropwise to a methanol solution (15 ml) of quinoline-8-thiol (8-HqnS, 99 mg). A dichloromethane solution of [AuCl(PPh$_3$)] (250 mg) was then added and stirred for 30 min. Then $Ag(CF_3SO_3)$ (130 mg) was added and the insoluble AgCl was filtered. The pale yellow filtrate was reduced to *ca*. 2 ml to give the product (yield = 50%).

[$Au_2$(8-qnS)(PPh$_3$)$_2$] **2**$BF_4$: A solution of Na(8-qnS) was prepared by adding 8-HqnS (99 mg) and NaOMe (30 mg) in $CH_2Cl_2$–MeOH (1 : 1, 25 ml). [AuCl(PPh$_3$)] (500 mg, 25 ml in dichloromethane) was added to the solution, which was stirred for 4 h at room temp. After addition of $NaBF_4$ (60 mg) the pale yellow solution was evaporated to dryness. The resulting solid was extracted with thf (yield = 45%).

‡ *Crystal data*: [Au(PPh$_3$(8-qnS)] **1**: $C_{27}H_{21}AuNPS$, $M$ = 619.47, monoclinic, space group $P2_1/n$, $a$ = 14.632(3), $b$ = 10.424(1), $c$ = 16.360(3) Å, β = 110.08(1)°, $U$ = 2344(1) Å$^3$, $Z$ = 4, $D_c$ = 1.756 g cm$^{-3}$, crystal dimensions 0.2 × 0.15 × 0.25 mm, μ(Mo-Kα) = 64.24 cm$^{-1}$, $F$(000) = 1200. Intensity data were collected on Rigaku AFC7R diffractometer with graphite-monochromated Mo-Kα radiation (λ = 0.7107 Å) using ω–2θ scan mode with $2\theta_{max}$ = 45°. 3489 unique reflections were measured and 1965 reflections with $I > 3\sigma(I)$ were used in the refinement. Refinement of positional and anisotropic thermal parameters for all non-hydrogen atoms (281 variables) converged to $R$ = 0.074 and $R_w$ = 0.090. The final Fourier difference map showed residual extrema in the range of 1.89 to −2.54 e Å$^{-3}$.

[{Au(PPh$_3$)}$_2$(8-qnS)]$BF_4$·0.5thf **2**$BF_4$·0.5thf: $C_{47}H_{40}Au_2BF_4NP_2SO_{0.5}$, $M$ = 1201.58, triclinic, space group $P\bar{1}$, $a$ = 14.049(5), $b$ = 17.319(6), $c$ = 19.623(8) Å, α = 90.09(3), β = 108.72(3), γ = 101.20(3)°, $U$ = 4425(3) Å$^3$, $Z$ = 4, $D_c$ = 1.805 g cm$^{-3}$, crystal dimensions 0.20 × 0.30 × 0.50 mm, μ(Mo-Kα) = 67.28 cm$^{-1}$, $F$(000) = 2300. Intensity data were collected on Enraf-Nonius CAD4 diffractometer with graphite-monochromated Mo-Kα radiation (λ = 0.7107 Å), 11585 unique reflection (2θ < 45°) were measured and 7758 with $I > 2\sigma(I)$ were used in the refinement. Refinement of positional and anisotropic thermal parameters for all non-hydrogen atoms (1046 variables) converged to $R$ = 0.035 and $R_w$ = 0.037. The final Fourier difference map showed residual extrema in the range of 1.34 to −2.34 e Å$^{-3}$.

Atomic coordinates, bond lengths and angles, and thermal parameters have been deposited at the Cambridge Crystallographic Data Centre (CCDC). See Information for Authors, Issue No. 1. Any request to the CCDC for this material should quote the full literature citation and the reference number 182/310.

## References

1 B.-C. Tzeng, W.-C. Lo, C.-M. Che and S.-M. Peng, *Chem. Commun.*, 1996, 181; B.-C. Tzeng, K.-K. Cheung, C.-M. Che and S.-M. Peng, *Chem. Commun.*, 1996, 1681; R.-H. Uang, C.-K. Chan, S.-M. Peng and C.-M. Che, *J. Chem. Soc., Chem. Commun.*, 1994, 2561; S.-J. Shieh, H. Xiao, S.-M. Peng and C.-M. Che, *J. Chem. Soc., Dalton Trans.*, 1994, 3067; D. M. P. Mingos, J. Yau, S. Menzer and D. J. Williams, *Angew. Chem., Int. Ed. Engl.*, 1995, **34**, 1894.

2 C. F. Shaw, III, M. T. Coffer, J. Klingbeil and C. K. Mirabelli, *J. Am. Chem. Soc.*, 1988, **110**, 729; M. T. Coffer, C. F. Shaw, III, M. K. Eidsness, J. W. Watkins, II and R. C. Elder, *Inorg. Chem.*, 1986, **25**, 333; A. A. Isab and P. J. Sadler, *J. Chem. Soc., Dalton Trans.*, 1982, 135.

3 A. Kolb, P. Bissinger and H. Schmidbaur, *Inorg. Chem.*, 1993, **32**, 5132.

4 P. D. Cookson and E. R. T. Tiekink, *J. Chem. Soc., Dalton Trans.*, 1993, 259.

5 F. Canales, M. C. Gimeno, P. G. Jones and A. Laguna, *Angew. Chem., Int. Ed. Engl.*, 1994, **33**, 769.

6 A. Sladek and H. Schmidbaur, *Chem. Ber.*, 1995, **128**, 907.

7 P. G. Jones, G. M. Sheldrick and E. Hädicke, *Acta Crystallogr., Sect. B*, 1980, **36**, 2777.

*Received, 20th September 1996; Com. 6/06494I*

# Solvent-free oxidation reactions with Ti-MCM-41 and TS-1 catalysts occluded in polydimethylsiloxane (PDMS) membranes

**Ivo Vankelecom,*† Karen Vercruysse, Nancy Moens, Rudy Parton, Jale Sudhakar Reddy and Pierre Jacobs**

*Centre for Surface Chemistry and Catalysis, Faculty of Agricultural and Applied Biological Sciences, Katholieke Universiteit Leuven, Kardinaal Mercierlaan 92, 3001 Leuven, Belgium*

**The incorporation of TS-1 and Ti-MCM-41 catalysts in PDMS is proven to enable the oxidation of hexane and epoxidation of *cis*-cyclooctene, respectively, with high conversions under solvent-free reaction conditions.**

In 1994,[1] we reported a new type of catalytically active membrane, consisting of a FePcY zeolite (ironphthalocyanine occluded in zeolite Y) that was dispersed in a polymeric phase (PDMS). This catalytic system enabled the oxidation of cyclohexane under solvent-free conditions in a counter-current membrane configuration. Furthermore, the new hydrophobic environment of the catalyst created by this PDMS membrane acted as a 'solvent phase' and led to strongly increased conversions.[1–3] Here, we describe two new examples of successful incorporation of oxidation catalysts in PDMS: mesoporous Ti-MCM-41[4] and microporous TS-1,[5] both Ti-containing structures. They are used in the epoxidation of *cis*-cyclooctene and in the oxidation of hexane respectively. A set of reactions have been carried out to demonstrate the influence of the hydrophobic PDMS membrane on the activity of these catalysts with or without any solvent.

Ti-MCM-41 and TS-1 were synthesised following known procedures.[4,6] In the synthesis of Ti-MCM-41 (Ti/Si = 52), 18.8 g Ludox AS-40 (40 mass% colloidal silica in water, Dupont) were mixed with 19.4 g tetraethylammonium hydroxide (TMAOH, 20 mass% in water, Fluka) and 16.1 g cetyltrimetylammonium chloride (CTMACl, 25 mass% in water, Aldrich). After stirring for 15 min, a second portion (32.2 g) of CTMACl was added followed by 3.64 g $Ti(OBu^n)_4$ (99%, Alfa) dissolved in 3.60 g of isopropyl alcohol (99.5%, Aldrich). The complete synthesis was performed in ice-cooled glass containers. After homogenization, the synthesis gel was poured into stainless-steel autoclaves which were placed in a rotating oven at 383 K for 24 h. After synthesis, the autoclaves were cooled and the catalyst was filtered, washed several times, and dried at 333 K over 10 h.

TS-1 (Ti/Si = 50) was prepared by stirring 1.94 g $Si(OEt)_4$ (98%, Aldrich), 0.20 g $Ti(OEt)_4$ (99%, Aldrich) and 20.3 g tetrapropylammonium hydroxide (40 mass% aqueous solution, Fluka) at 330 K under a nitrogen atmosphere over 3 h. The resulting clear solution was poured into a Teflon-lined stainless-steel autoclave which was placed in an oven at 450 K for 24 h. The catalyst was separated by centrifugation and washed several times with deionised water before it was dried at 333 K over 10 h. Both TS-1 and Ti-MCM-41 were calcined at 820 K over 12 h, using a heating rate of 1 K $min^{-1}$.

Before using the TS-1 and Ti-MCM-41 catalysts, they were thoroughly characterised by chemical analysis, XRD, IR and UV–VIS DRS. These characterization techniques indicated that these materials possessed properties similar to those reported in the literature. In the case of Ti-MCM-41, the peaks on the XRD pattern could be indexed on a hexagonal lattice with a pore diameter of 38 Å. Raman and UV–VIS revealed the absence of anatase impurities.

The earlier described method[7] to prepare zeolite-filled membranes could no longer be applied here as the PDMS prepolymer would completely obstruct the mesopores of Ti-MCM-41 during the membrane synthesis. Therefore, a new preparation method, developed by Vankelecom *et al.*,[8] was used in which a partially polymerised network is formed before the catalyst is added. PDMS-prepolymer and crosslinker (General Electric, RTV-615A and B respectively) were mixed in a 10 : 1 ratio. For Ti-MCM-41 containing membranes, a 20 mass% mixture of PDMS in 4-methylpentan-2-one (99.5%, Acros Chimica) was prepolymerised over 1 h at 343 K. When incorporating TS-1, a 15 mass% mixture of PDMS in 4-methylpentan-2-one was stirred at 328 K for 1.5 h. The catalyst was added in a 13 mass% (relative to PDMS) loading in the case of Ti-MCM-41 and in a 17 mass% loading for TS-1. After thorough mixing at room temperature, the suspension was poured into a Petri dish and the solvent was allowed to evaporate overnight. The final curing of the polymer took place in a vacuum oven at 423 K over 1 h. TS-1 and Ti-MCM-41 catalysts embedded in PDMS are denoted as TS-1/PDMS and Ti-MCM-41/PDMS, respectively. *n*-Hexane (10 g) was oxidised in a 100 ml capacity Parr reactor at 373 K using 25 g of a 35 mass% hydrogen peroxide (Acros Chimica) solution in water with 0.25 g TS-1. If a solvent was used in the reaction, 38 g was added to 5 g of hexane, 12 g of hydrogen peroxide and 0.25 g of TS-1. Heptane was used as external standard in the GC analysis of these reactions.

The epoxidation of *cis*-cyclooctene (95%, Aldrich) over Ti-MCM-41 was performed at 330 K in a round-bottomed flask with condensor. 8 g of substrate were reacted with 8.4 g of *tert*-butyl hydroperoxide (70 mass% aqueous solution, Acros Chimica) over 0.2 g of dry Ti-MCM-41. Chlorobenzene (99%, Acros Chimica) was used as external standard for quantitative GC analysis.

The results obtained in the oxidation of *n*-hexane are summarised in Table 1. Under solvent-free reaction conditions,

**Table 1** Oxidation of *n*-hexane with hydrogen peroxide over TS-1 at 373 K

| | No solvent[a] | | Methanol[b] | |
|---|---|---|---|---|
| | TS-1 | TS-1/PDMS | TS-1 | TS-1/PDMS |
| TON[c] | 280 | 870 | 520 | 440 |
| Product distribution (%) | | | | |
| Alcohols | 5 | 9 | 22 | 30 |
| Ketones | 50 | 51 | 70 | 62 |
| Acids | 38 | 38 | 4 | 6 |
| Other[d] | 7 | 3 | 4 | 3 |
| Peroxide efficiency (%)[e] | 26 | 80 | 65 | 59 |
| Peroxide conversion (%)[f] | 99 | 99 | 99 | 92 |

[a] *Reaction conditions*: TS-1 = 0.25 g; substrate = 10 g; $H_2O_2$ (35 mass% in water) = 25 g. [b] *Reaction conditions*: TS-1 = 0.25 g; substrate = 5 g; $H_2O_2$ (35 mass% in water) = 12 g; methanol = 36 g. [c] TON (turnover numbers) after 5 h reaction. [d] Mainly methyl ethers (when using methanol as solvent) and polyfunctional compounds. [e] Peroxide efficiency = 100 × (mmol peroxide utilized in product formation/mmol peroxide consumed). [f] Peroxide conversion = 100 × (mmol peroxide consumed/mmol peroxide at the end of the reaction). The remaining $H_2O_2$ was estimated by titration using a 0.1 M $Ce(SO_4)_2$ solution.

the positive role of the membrane is obvious: the TON (turnover number) is only 280 over TS-1 as compared to 870 over the TS-1/PDMS catalyst. The major products are hexan-2-ol, hexan-3-ol, hexan-2-one and hexan-3-one. By-products, mainly acids, are formed by consecutive oxidation reactions. The very high activity obtained over the membrane-occluded catalyst can be ascribed to the combination of two beneficial effects: (*i*) the hydrophobic nature of the PDMS membrane concentrates the non-polar *n*-hexane around the catalyst particle and (*ii*) the density of the composite membrane makes the incorporated catalyst reside at the interface of both reagent faces, whereas the non-embedded catalyst mainly resides in the aqueous phase at the bottom of the reactor. The conversion of hydrogen peroxide is almost complete in all cases.

When methanol is added as a solvent under comparable conditions, the catalyst powder performs better than the TS-1/PDMS. However, the TON is about halved as compared with TS-1/PDMS under solvent-free conditions. Clearly, the solvent causes a dilution of the reagents. On the other hand, the presence of methanol molecules in the zeolite pores reduces the secondary oxidation reactions by enhancing the removal of the reaction products out of the zeolite pores. Under solvent-free reaction conditions, the residence time of the primary oxidation products in the zeolite pores is higher.

The advantage of a PDMS membrane is further evidenced in the epoxidation of *cis*-cyclooctene with Ti-MCM-41. After only 7 h, 50% of the theoretical maximum conversion is reached, whereas only 8% is converted with the non-membrane resident catalyst a value which hardly exceeds the conversion in a blank reaction.

**Table 2** Epoxidation of *cis* cyclooctene with *tert*-butyl hydroperoxide over Ti-MCM-41 at 330 K[a]

| | Theoretical conversion (%)[b] | | Epoxide selectivity (%)[c] | | Peroxide efficiency (%)[d] | |
|---|---|---|---|---|---|---|
| *t*/h | 7 | 24 | 7 | 24 | 7 | 24 |
| No catalyst | —[e] | 10 | —[e] | 81 | —[e] | 90 |
| Ti-MCM-41 | 8 | 14 | 82 | 81 | 95 | 95 |
| Ti-MCM-41/PDMS | 50 | 72 | 70 | 75 | 97 | 95 |

[a] *Reaction conditions*: Ti-MCM-41 = 0.2 g; substrate = 8.4 g; *tert*-BHP (70 mass% in water) = 4 g. [b] Conversion (%) = 100 × (mmol products formed/mmol *tert*-BHP initially present). [c] Epoxide selectivity (%) = 100 × (mmol epoxide/mmol total products). [d] Per- oxide efficiency (%) = 100 × (mmol *tert*-BHP used in product formation/mmol *tert*-BHP consumed). [e] Not determined.

With these two examples, we have proved the versatility of our earlier reported membrane-occluded catalyst system (FePcY–PDMS). The results confirm that a membrane resident catalyst is able to create an excellent activity under biphasic reaction conditions. However, consecutive oxidation reactions might assume significance as a possible drawback in the absence of a solvent. The application of catalytic membranes in a counter-current membrane reactor might not only reduce this problem, but will most probably further improve the performance of membrane-resident catalysts.

We are grateful to the Belgian Government for the support in the frame of a IUAP-PAI grant on supramolecular Catalysis. R. P. and I. V. thank the Belgian National Fund of Scientific Research (N. F. W. O.) for grants as Post-Doctoral Researchers.

## Footnote

† E.mail: ivo.vankelecom@agr.kuleuven.ac.be

## References

1 R. F. Parton, I. F. J. Vankelecom, M. J. A. Casselman, C. P. Bezoukhanova, J.-B. Uytterhoeven and P. A. Jacobs, *Nature*, 1994, **370**, 541.
2 I. F. J. Vankelecom, R. F. Parton, M. J. A. Casselman, J. B. Uytterhoeven and P. A. Jacobs, *J. Catal.*, 1996, **163**, 457.
3 R. F. Parton, I. F. J. Vankelecom, D. Tas, K. Janssen, P.-P. Knops-Gerrits and P. A. Jacobs, *J. Mol. Catal.*, in the press.
4 A. Corma, M. T. Navarro and J. Perez-Pariente, *J. Chem. Soc., Chem. Commun.*, 1994, 147.
5 M. Taramasso, G., Perego and B. Notari, *US Pat.* 4,410,501, 1983.
6 E. Astorino, J. B. Peri, R. J. Willey and G. Busea, *J. Catal.*, 1995, **157**, 482.
7 I. F. J. Vankelecom, E. Scheppers, R. Heus and J.-B. Uytterhoeven, *J. Phys. Chem.*, 1994, **98**, 12 390.
8 I. F. J. Vankelecom, P. A. Jacobs and J.-B. Uytterhoeven, *Eur. Pat. Appl.*, 1996.

*Received, 8th October 1996; Com. 6/06907J*

# Perfluorovinyl–metal derivatives: a new one-pot synthesis

**Kulbinder K. Banger, Alan K. Brisdon* and Arti Gupta**

*Department of Chemistry, University of Manchester Institute of Science and Technology, PO Box 88, Manchester, UK M60 1QD*

**The one-pot reaction of the CFC replacement 1,1,1,2-tetrafluoroethane ($CF_3CFH_2$, HFC-134a) with 2 equiv. of butyllithium in diethyl ether at −78 °C followed by the addition of main-group or transition-metal halides results in good yields of the corresponding metal–perfluorovinyl compounds of high purity.**

Although fluorine is capable of replacing hydrogen in many organic systems usually without major structural changes the number of examples of organometallic complexes containing perfluorinated ligands is very much more limited than for the comparable perprotio analogues.[1] Of the examples that do exist in the literature many of the smaller fluorine-containing organic fragments are derived from bromofluorocarbons (BFCs) or chlorofluorocarbons (CFCs). However starting materials like these are currently being phased out under international and national agreements, such as the Montreal Protocol, due to their deleterious effect on the ozone layer. A case in point is the synthesis of perfluorovinyl ($CF_2$=CF–) derivatives which have previously used bromotrifluoroethene as the starting material. This pyrophoric compound is no longer commercially produced which will ultimately result in it being unavailable for pure research applications and thus this route will become obsolete. Very recent work[2] has focused on the use of one of the hydrofluorocarbon replacements for CFCs, 1,1,1,2-tetrafluoroethane ($CF_3CFH_2$, HFC-134a) as an alternative perfluorovinyl source for organic synthesis.

In view of the recent resurgence in interest in the chemistry of organofluorine compounds and in particular their coordination to metal centres to induce C–F bond activation[3] we report the 'one-pot' synthesis of metal perfluorovinyl compounds using HFC-134a as a perfluorovinyl source. The addition of 2 equiv. of *n*-butyllithium to a diethyl ether solution of HFC-134a at −78 °C results in the double deprotonation and elimination of 1 equiv. of lithium fluoride from HFC-134a to generate the $CF_2$=$CF^-Li^+$ reagent **1** in good yields. Compound **1** generated in this way is stable in solution for up to 24 h at this temperature but decomposes rapidly as the temperature is increased above −45 °C. The formation of metal perfluorovinyl complexes is readily achieved by adding concentrated cold diethyl ether or thf solutions of metal halides to the lithium reagent. This immediately results in reaction and the formation of an off-white precipitate of the lithium halide. Multinuclear NMR studies were found to be a convenient method to monitor the progress of these reactions and to determine the degree of perfluorovinyl substitution, prior to work-up procedures. Samples withdrawn from the organic phase of the reaction of $CF_2$=$CF^-Li^+$ and $HgCl_2$ in a 2 : 1 ratio were transferred to NMR tubes and allowed to warm to room temperature. $^{19}$F NMR spectra show replacement of the complex multiplet signals due to HFC-134a at δ −64.9 and −226.5 by three sets of doublets of doublets typical of the AMX pattern previously observed for perfluorovinyl metal complexes[4] each with associated mercury satellite structure. The extent of substitution of the product may also be conveniently determined by NMR, in this case from the $^{199}$Hg NMR spectra which exhibit a triplet of triplets of triplets so confirming unequivocally the product as $[Hg(CF{=}CF_2)_2]_2$ **2**. This compound was isolated as a clear liquid after allowing the reaction mixture to slowly warm to room temperature before being worked up using existing routes.[5] Extraction of the organic phases followed by drying and evaporation of the organic solvents results in the generation of the perfluorovinyl metal compound in good yield (typically > 90%, based on the metal complex).

An analogous reaction using a 1 : 1 ratio of mercury(II) chloride to perfluorovinyllithium reagent generates the mono-substituted complex. NMR studies suggest that a very small amount of bis(perfluorovinyl)mercury is also present (typically < 5%) in the crude product. The relatively high volatility of fluorine-containing compounds coupled with their thermally robust nature means that further purification of the products, if necessary, may often be achieved by distillation or sublimation. For example sublimation of the crude product from the 1 : 1 reaction at 100 °C (20 mmHg) results in an air-stable, white solid which is analytically pure $ClHg(CF{=}CF_2)$ **3**.

Having confirmed that this route may be used successfully to synthesise known perfluorovinyl complexes in high yield the extent of its utility as a general method of introducing the –CF=$CF_2$ moiety into a wide range of substrates was investigated by reaction with a variety of early- and late-transition metal coordination complexes and organometallic compounds. All reactions were carried out in a similar manner to that described above. Confirmation of the identity of the materials synthesised as perfluorovinyl metal complexes was obtained by elemental analysis and spectroscopic measurements.† In all cases $^{19}$F NMR spectra clearly demonstrated three sets of doublets of doublets with the anticipated satellite structure due to coupling with spin-active metal nuclei being evident where appropriate. A summary of these reactions is presented in Fig. 1.

The stability of these complexes is variable, with the majority of these complexes being thermally stable, although decomposition does occur in the presence of water or on extended contact with glassware, however the pentacarbonyl manganese perfluorovinyl complex decomposes rapidly under aqueous conditions.

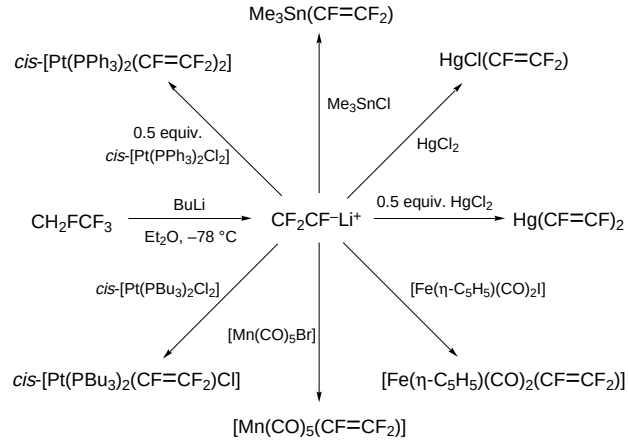



**Fig. 1** Reactions of perfluorovinyllithium, derived from $CF_3CH_2F$, with a variety of metal halides

We acknowledge ICI Klea for the donation of chemicals and R. L. Powell for useful discussions.

## Footnote

† *Selected spectroscopic data*: **2**, $Hg(CF{=}CF_2)_2$. IR ν/cm$^{-1}$ (neat) 1750, 1275, 1150, 1050. NMR: $^{19}$F (188.3 MHz, solvent $Et_2O$, standard $CFCl_3$) δ −90.1 [1 F, dd, *J*(FF) 37, 75 Hz, CF=CF*F*], −124.5 [1 F, dd, *J*(FF) 75, 109 Hz, CF=C*F*F], −185.4 [1 F, dd, *J*(FF) 37, 109 Hz, C*F*=$CF_2$]; $^{13}$C (75.49 MHz, neat, standard $SiMe_4$) δ 165.0 (1 C, m, CF=*C*$F_2$), 161.7 (1 C, m, *C*F=$CF_2$); $^{199}$Hg (35.8 MHz, neat, standard $HgMe_2$) δ 957 [ttt, *J*(HgF) 816, 224, 32 Hz].

**3**, $ClHg(CF{=}CF_2)$. Anal. Found: F, 17.6; Hg, 63.5. Calc. for $C_2ClF_3Hg$: F, 17.97; Hg, 63.27%; IR ν/cm$^{-1}$ (Nujol) 1750, 1277, 1160, 1011. NMR: $^{19}$F (188.3 MHz, solvent $Et_2O$, standard $CFCl_3$) δ −92.3 [1 F, dd, *J*(FF) 42, 69, *J*(HgF) 374 Hz, CF=CF*F*], −124.0 [1 F, dd, *J*(FF) 69, 111, *J*(HgF) 13 Hz, CF=C*F*F], −180.5 [1 F, dd, *J*(FF) 42, 111, *J*(HgF) 1169 Hz, C*F*=$CF_2$]; $^{199}$Hg (35.8 MHz, solvent $Et_2O$, standard $HgMe_2$) δ 876 (ddd).

$Me_3Sn(CF{=}CF_2)$. IR ν/cm$^{-1}$ (Nujol) 1646, 1219, 1146, 1036. NMR: $^{19}$F (solvent $Et_2O$) δ −88.6 [1 F, dd, *J*(FF) 33, 79 Hz, CF=CF*F*], −123.5 [1 F, dd, *J*(FF) 79, 113 Hz, CF=C*F*F], −194.6 [1 F, dd, *J*(FF) 33, 113 Hz, C*F*=$CF_2$].

*cis*-$[Pt(PEt_3)_2(CF{=}CF_2)_2]$. NMR: $^{19}$F (solvent $Et_2O$) δ −98.3 (1 F, m, CF=CF*F*), −129.7 [1 F, dd, *J*(FF) 100.7, 101.0, *J*(PF) 1.5, *J*(PtF) 41.5 Hz, CF=C*F*F], −160.8 [1 F, dd, *J*(FF) 101.0, 32.1, *J*(PF) 32, *J*(PtF) 389.1 Hz, C*F*=$CF_2$]; $^{31}$P (81.05 MHz, $CDCl_3$ solution, standard aq. $H_3PO_4$) δ 5.5 [m, *J*(PtP) 2111 Hz].

*cis*-$[Pt(PBu_3)_2(CF{=}CF_2)Cl]$. NMR: $^{19}$F (solvent $Et_2O$) δ −94.5 [1 F, m, *J*(FF) 38, 81 Hz, CF=CF*F*], −126.0 [1 F, m, *J*(FF) 81, 109 Hz, CF=C*F*F], −183.3 [1 F, m, *J*(FF) 38, 109 Hz, C*F*=$CF_2$].

$[Mn(CO)_5(CF{=}CF_2)]$. NMR: $^{19}$F δ −98.2 [1 F, dd, *J*(FF) 25, 55 Hz, CF=CF*F*], −109.0 [1 F, dd, *J*(FF) 55, 124 Hz, CF=C*F*F], −149.0 [1 F, dd, *J*(FF) 25, 124 Hz, C*F*=$CF_2$].

$[Fe(\eta\text{-}C_5H_5)(CO)_2(CF{=}CF_2)]$. NMR: $^{19}$F (solvent $Et_2O$) δ −85.0 [1 F, dd, *J*(FF) 42, 101 Hz, CF=CF*F*], −131.5 [1 F, dd, *J*(FF) 101, 115 Hz, CF=C*F*F), −183.0 [1 F, dd, *J*(FF) 42, 115 Hz, C*F*=$CF_2$].

## References

1 R. P. Hughes, *Adv. Organomet. Chem.*, 1990, **31**, 183.
2 J. Burdon, P. L. Coe, I. B. Haslock and R. L. Powell, *Chem. Commun.*, 1996, 46.
3 J. L. Kiplinger, T. R. Richmond and C. E. Osterberg, *Chem. Rev.*, 1994, **94**, 373.
4 R. B. Johannessen and R. W. Duerst, *J. Magn. Reson.*, 1971, **5**, 355.
5 P. Tarrant, P. Johncock and J. Savory, *J. Org. Chem.*, 1963, **28**, 839.

*Received, 16th August 1996; Com. 6/05732B*



Typeset and printed by Black Bear Press Limited, Cambridge, England

ChemComm
FEATURE ARTICLE

# Selective complexation and sensitive analysis of charge diffuse cationic species using lipophilic cyclodextrins

**David Parker and Ritu Kataky**

*Department of Chemistry, University of Durham, South Road, Durham, UK DH1 3LE*

**Lipophilic peralkylated cyclodextrins are useful ionophores for the selective binding of a variety of size-matched charge-diffuse cationic species. Chiral potentiometric sensors may be devised using plasticised membrane electrodes, while voltammetric sensors may be fabricated that allow sub-nanomolar levels of detection of electron-rich aromatic cations. The observation of the binding of size-matched tetraalkylammonium ions has led to the development of sensitive methods of detection for species such as acetylcholine. When lipophilic cyclodextrins are coupled to enzymes in a disposable biosensor, a highly specific method of analysis is achieved giving sub-picomolar levels of detection.**

## Introduction

Classical coordination chemistry focuses on the binding of metal ions by ligands and is an area of research activity that is relatively mature.[1] For example, the principles that govern how a ligand binds to a given ion are well established and selectivity in complexation may be quite accurately predicted from an appreciation of the preference of the ion for a particular type of donor atom, coordination number and geometry. Metal ions are usually charge dense species with large metal–ligand free energies of complexation. On the other hand, many organic cations—such as 'onium ions (of O, P, S and N)—are best considered to be charge diffuse species whose interaction with a ligand or receptor relies upon multiple, weaker binding forces. In the case of ammonium ions for example, the positive charge is usually delocalised over the adjacent carbon and hydrogen atoms. Complexation of such charge diffuse species usually requires both size and shape complementarity between the receptor and the ion and the presence of stabilising hydrogen-bonding interactions. Size and shape complementarity is often associated with a favourable solvophobic interaction, while directed hydrogen-bonding involves the cationic 'onium ion acting as a hydrogen-bond donor to proximate electron-rich acceptors. An early example of such an interaction with a synthetic neutral ionophore involves the complexation of a primary ammonium ion, $R\overset{+}{N}H_3$ with the lone-pairs of $C_3$-related ether oxygen atoms in an 18-crown-6 derivative.[2] Receptors that are rich in π-electron density may also serve as the hydrogen-bond acceptor:[3] in the enzyme acetylcholine esterase the interactions between the cationic $NMe_3$ head group of acetylcholine and the hydrophobic π-electrons of Trp-84 are believed to contribute over 20 kJ $mol^{-1}$ to the overall free energy of binding.[4]

Whilst cation-π interactions are undoubtedly an important binding interaction in supramolecular chemistry, for an $\overset{+}{N}$–CH group as a hydrogen bond donor the interaction with ether oxygens is more energetically favourable. The gas-phase dissociation enthalpies for $\overset{+}{N}Me_4$ with various n and π donors have been measured.[5] The interaction with $H_2O$, MeOH and benzene was considerably weaker than that found for the more polarisable dialkyl ethers, and polyethers gave the highest measured values consistent with multiple additive $\overset{+}{N}$C–H···O interactions. Ionic C–H···O hydrogen bonds are well-documented structurally in the solid-state, and 9 out of 10 of the shortest C–H···O contacts involve $[NCH]^{\delta+}$ as the hydrogen bond donor.[6] Multiple weak C–H···O interactions between alkylammonium ions and size-matched receptors may therefore make a very significant contribution to the overall free-energy of binding of 'onium ions.

## Chiral sensors

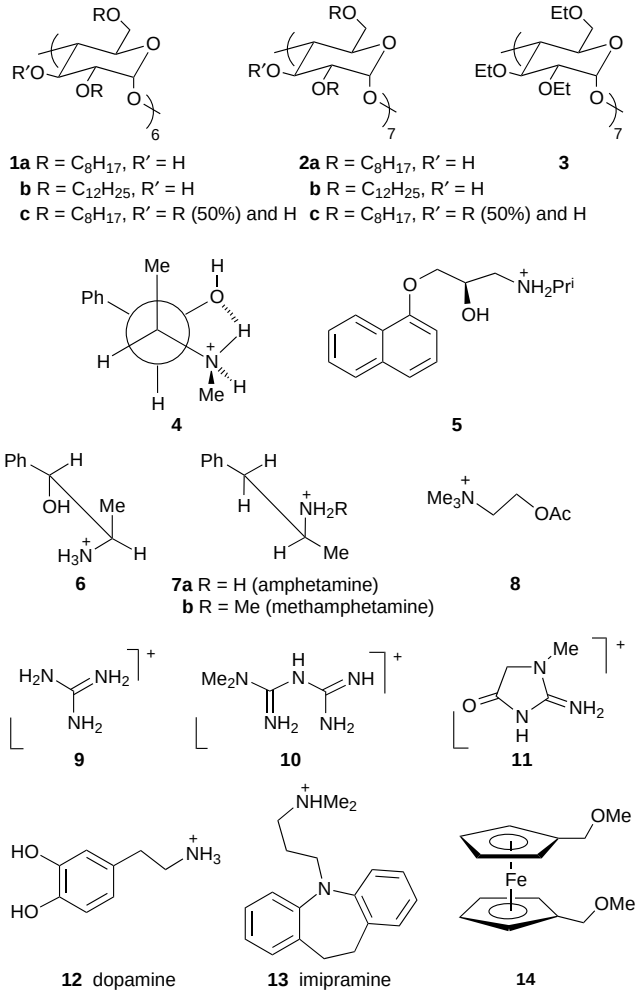
Our interest in the binding of charge diffuse organic species was sparked by the challenge of devising an enantioselective ion-selective electrode that exhibited reasonable chemoselectivity for the target ion. If analysis is to be carried out with a membrane-based potentiometric sensor, then a neutral ionophore is required that can reversibly bind the target ion, with fast exchange kinetics, *i.e.* a free energy of activation for exchange between free and bound forms of the analyte of less than, say, 65 kJ $mol^{-1}$. Chemoselectivity in binding the target analyte is important—rejecting competing charge-dense ions for example—and stereoselectivity is also required so that the potential difference that builds up at the aqueous-membrane interface is proportional to the activity of the ion and its enantiomeric purity. Earlier work on chiral sensors had examined certain lipophilic chiral crown ethers as ionophores[2] and although enantioselective sensors for chiral primary amines were defined, chemoselectivity was very modest (severe $Na^+/K^+$ interference) and *N*-alkyl substitution compromised the N–H···O binding interaction.

Given the developing role of alkylated cyclodextrins in GC[7] and HPLC[8] analysis, we were attracted by the possibility of devising lipophilic ionophores by modifying the 2, 3 and 6-OH groups of these chiral host molecules. Initial work therefore focused on the synthesis and characterisation of the lipophilic ionophores[9] and the evaluation of their use as chiral ionophores for size-matched arylammonium ions.[10] A series of alkylated cyclodextrins was prepared, **1**, **2** and **3**, systematically varying the size of the cyclodextrin cavity and the nature of the alkyl chain. α-Cyclodextrin derviatives, comprising six glucose sub-units, define a toroidal cavity that is sufficiently large to include monosubstituted benzene derivatives. The free energy of binding may be attributed to a favourable solvophobic interaction, with inclusion leading to the displacement of relatively 'high-energy' solvent molecules, and to attractive van der Waals' and dispersion forces in the complex. The β- and γ-cyclodextrin analogues containing seven and eight glucose units respectively define a larger cavity suitable for inclusion of larger substrates such as naphthyl derivatives in the former case and tricyclic molecules or ions in the latter.

Stepwise alkylation procedures were devised that allowed preferential 2,6-dialkylation, and the more hindered 3-OH group could be alkylated under more forcing conditions (*e.g.* NaH–THF–18-crown-6–RX). The precise degree of alkylation was assessed by a combination of NMR, reductive depolymerisation–GCMS and direct electrospray mass spectrometric methods[9] and the three independent methods of analysis showed excellent agreement. The per-*O*-ethyl β-cyclodextrin

**3**[11] is perhaps the simplest lipophilic cyclodextrin and is very soluble in non-polar organic solvents and almost completely insoluble in water.

Poly-*O*-octyl-α-cyclodextrin (containing an average of 15.4 octyl groups per cyclodextrin), when incorporated into a plasticised PVC membrane, gave an ion-selective electrode that showed a different response (in slope and in $E°$ values) to the (−)-(1*R*, 2*S*)-ephedrinium ion **4**, compared to its enantiomer and its diastereoisomers, the (+)- or (−)-pseudoephedrinium cations. The electrode could be calibrated to measure the enantiomeric purity of samples of ephedrinium salts (Fig. 1) even in the presence of the pseudo-ephedrinium diastereoisomers.[10] In order to measure the total ephedrinium concentration parallel measurements are needed using an achiral or non-selective ionophore: per-*O*-octyl maltose serves as a suitable ionophore for the latter purpose. Moreover, the electrode response was not significantly impaired by the presence of a simulated clinical electrolyte containing $Na^+$ (150 mM), $K^+$ (4.3 mM), $Ca^{2+}$ (1.26 mM) and $Mg^{2+}$ (0.9 mM), and an overall selectivity coefficient $-\log K^{pot}_{clin}$ of 3.7 was determined. The difference in the free energy of complexation for binding of the ephedrinium enantiomers was only 2.5 kJ $mol^{-1}$ with **1b** and **1c**, but this corresponds to a 26 mV differential response that is sufficient to be measured quite accurately. Using the size-matched β-cyclodextrins **2b** or **2d** as the ionophore, similar experiments were conducted with propranolol **5**, as the analyte. The observed enantiodifferentiation was also about 25 mV or 2.4 kJ $mol^{-1}$, but was sufficient to allow enantiomeric purity determinations to be effected using a calibrated electrode.




## Probing complexation

Complex formation was monitored by NMR methods and by electrospray mass spectrometry, and was probed further by variation of the host and guest structures. Confirmation of the formation of a 1 : 1 complex with ephedrinium or propranolol cations was provided by positive-ion ESMS spectra (Fig. 2), and measurements using pulsed-gradient spin echo $^1H$ NMR methods of the diffusion coefficient of the (+)-ephedrinium ion in the presence and absence of **1b** in $CDCl_3$ were consistent with 1 : 1 complex formation with an equilibrium constant of 137 (288 K).[12] The (−)-enantiomer was bound more weakly and when all of the OH groups in the 3-position were capped with methyl groups both enantiomers bound with the same affinity. Capping of the residual OH groups in the α-cyclodextrin hosts also markedly reduced the enantioselective response of the electrode and its sensitivity to the ephedrinium analyte, highlighting the importance of these groups *either* in rigidifying the CD structure through intramolecular hydrogen bonding *or* in acting as an orienting hydrogen-bond donor to the cationic guest. Variation of the structure of the β-arylammonium ion was also examined: the norephedrinium ion **6** behaved in a parallel manner to ephedrinium, while species lacking the α-hydroxy group—such as the amphetamines **7**—also gave an enantioselective response, suggesting that the configuration of the chiral centre β to the aryl ring was most important in defining enantioselectivity.[10]

Further details of the solution complexation process were provided by measurements of the $^1H$ NMR relaxation rates of the cyclodextrin and of the included ion. Changes in relaxation rate dependent upon which enantiomer was bound by **1c** were observed for both the cyclodextrin and the β-arylammonium ion. The rate of relaxation of the cyclodextrin $H^3$ proton, for example, increased differentially by 1.45 $s^{-1}$ on complexation

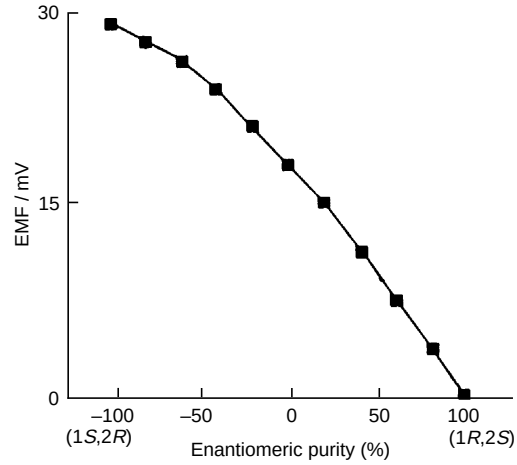



**Fig. 1** Calibrated electrode response for an ISE based on poly-*O*-octyl-α-cyclodextrin with the enantiomeric purity of the ephedrinium analyte (310 K, $I$ = 0.1)

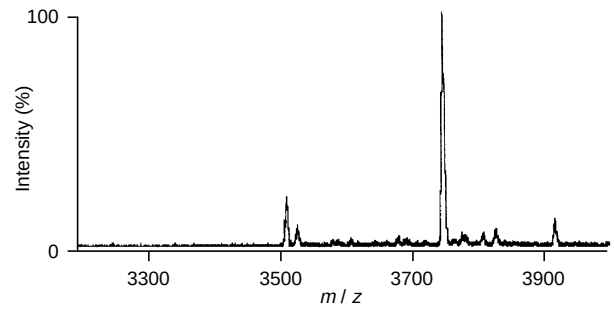



**Fig. 2** Electrospray mass spectrum of the complex formed between 2,6-didodecyl-β-cyclodextrin and (*R*)-propanolol

of (+)-ephedrinium compared to (−)-ephedrinium. It is well known that this proton is oriented towards the centre of the cyclodextrin cavity, and similar (albeit smaller) changes in rate have been observed following inclusion of (+)-Trp by α-cyclodextrin.[13] More marked enantiodependent changes in relaxation rate were measured for the diastereotopic $NH_2$ protons of the guest ephedrinium ion. A model has been proposed that accounts for the observed changes.[10] In the complex of the more strongly bound (+)-ephedrinium ion, the *C*-methyl (in the 2-position) group is oriented away from the H-3 and H-5 protons of the cyclodextrin. With the (−)-enantiomer, in order to avoid an unfavourable steric interaction the complex adopts an alternative structure lacking a stabilising N–H···O hydrogen-bond. Small differences in hydrogen-bonding (*i.e.* one H-bond mismatch) have recently been invoked to explain free-energy differences of the order of 2.5 kJ $mol^{-1}$ in DNA binding to intercalating molecules.[14]

## Binding and detection of 'onium ions

During the course of electrode-response experiments aimed at examining the effect of ionic strength on complexation, we quickly became aware of an *unusual* response in the presence of tetramethylammonium ions, when using poly-*O*-octyl-β- or tri-*O*-octyl-β-cyclodextrin as the membrane ionophore. The *absence* of any response was traced to competitive binding by the alkylammonium ion,[11,15] and 1:1 cyclodextrin: $NR_4^+$ complexes were observed by ESMS (Fig. 3) and were further characterised by $^{14}N$, $^2H$ and $^1H$ NMR measurements.[16] Both $NMe_4^+$ and $NEt_4^+$ have ionic diameters that are matched quite closely in size to a peralkylated cyclodextrin,[17] and complex formation is expected to be driven by a favourable solvophobic interaction and may be aided by multiple, weak $\overset{\delta+}{N}CH\cdots O$ interations.[5,6] This binding interaction allows the lipophilic cyclodextrins to be used as ionophores for the potentiometric detection of a variety of substituted alkylammonium ions (Table 1). Long-chain trimethylammonium ions may be detected sensitively at sub-micellar concentrations, and selectivity over $Na^+/K^+$ was found to reach a maximum at chain lengths that matched those of the alkyl groups in the cyclodextrin receptor.[11] Favourable hydrophobic interactions between alkyl chains may afford an extra stabilising interaction. Indeed, the lipophilic cyclodextrins **1a**, **1b**, **2a** and **2b** themselves form well-defined bilayers at an air–water interface.[18] Calculations of the surface area per molecule in these assemblies suggest that not only are the 'primary' alkyl chains (those bound to the 6-position) directed away from the aqueous phase but also that the chains linked to the 2-position are folded back tightly along the sides of the cyclodextrin. At a clean silicon or gold surface, atomic force microscopic measurements provided clear evidence for aggregation of the lipophilic cyclodextrins and aggregates varying in diameter from 2 to 0.1 μm were observed.[18]

Various other types of charge diffuse cations have been examined as analytes. For example, the strongly basic guanidinium ions such as **9** and **10** may be sensitively detected by potentiometric methods,[19] and the related metabolite creatinine **11** ($pK_a$ = 4.75) may also be assayed, provided that the electrode response is corrected to allow for dissociation of this weak acid.[11] With these hydrogen-bond donating cations, the independence of the observed electrode response to the structure of the sensing cyclodextrin (3-OH *vs.* 3-OR groups, α *vs.* β derivatives) indicated that the primary binding interaction involves $\overset{+}{N}–H\cdots O$ hydrogen-bonding.

Voltammetric methods of analysis, such as differential pulse voltammetry, allow lower concentrations of analytes to be measured, provided that the analyte possesses an accessible redox couple. The catecholamine oxidation of dopamine **12** occurs at +200 mV (*vs.* Ag/AgCl) on a screen-printed carbon electrode that has been coated with 2,3,6-tri-*O*-ethyl-β-cyclodextrin **3**.[20] Dopamine concentrations as low as $10^{-11}$ mol $dm^{-3}$ may be detected in this way, comparing favourably to the levels found in samples of cerebrospinal fluid ($10^{-8}$ mol $dm^{-3}$). The more sterically bulky cation, imipramine—an anti-depressive drug with a toxic level in blood of 5 μg per ml—is more effectively analysed using a sensor incorporating a poly-*O*-octyl-γ-cyclodextrin ionophore. In this case oxidation of the electron-rich aromatic moiety may be monitored by differential pulse voltammetry, and a linear current response was observed in the range $10^{-4}$ to $10^{-9}$ mol $dm^{-3}$ (Fig. 4).

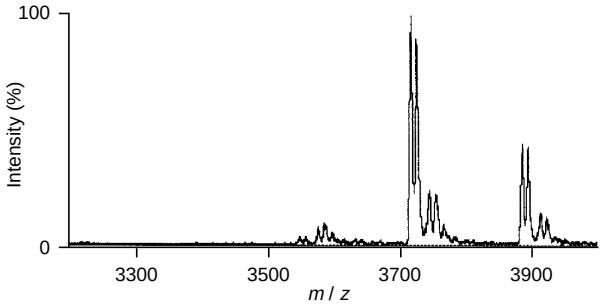



**Fig. 3** Electrospray mass spectrum of the 1:1 complexes between equimolar amounts of $C_{12}H_{25}N(CD_3)_3^+/C_{12}H_{25}NMe_3^+$ and 2,6-didodecyl-β-cyclodextrin ($Pr^iOH$; cone-voltage 30 V)

**Table 1** Response of ISEs to alkylammonium cations in the absence and presence of interferent ions using plasticised PVC-based membrane electrodes[a] (310 K)

| Analyte | Ionophore | Slope | Detection limit −log[c]/mol $dm^{-3}$ | $pK_{pot}^{clin}$ |
|---|---|---|---|---|
| $NMe_4^+$ | **1b** | 58.8 | 6.0 | 4.3 |
| $C_{12}H_{25}NMe_3^+$ | **2d** | 61.5 | 6.6 | 5.2 |
| acetylcholine **8**[b] | **1c** | 61.4 | 6.5 | 4.2 |
| choline **9** | **1c** | 61.4 | 6.4 | 3.4 |
| methacholine **10** | **1c** | 60.3 | 6.6 | 4.4 |

[a] $pK^{pot}$ values were determined in a simulated clinical electrolyte (refs. 11,16). [b] Protein interference (*e.g.* 40 g $dm^{-3}$ serum albumin) did not perturb the slope but raised the limit of detection to $10^{-5.1}$ mol $dm^{-3}$.

Whilst lipophilic cyclodextrins are very attractive ionophores for the sensitive detection of a broad spectrum of charge diffuse and size-matched cationic species, their relative lack of specificity needs to be addressed if practicable sensors are to be devised for environmental or clinical applications. For example,

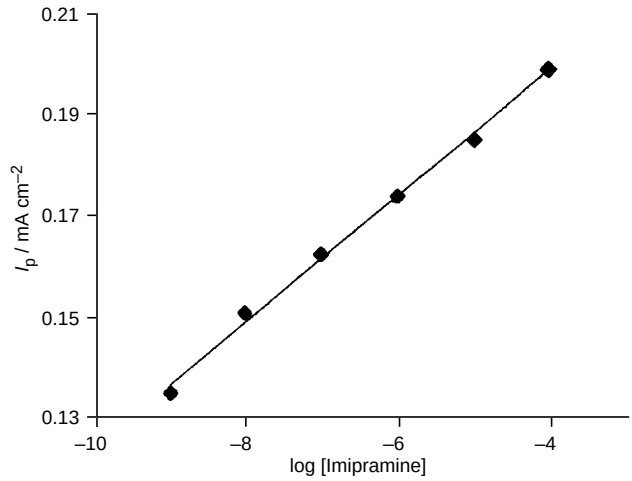
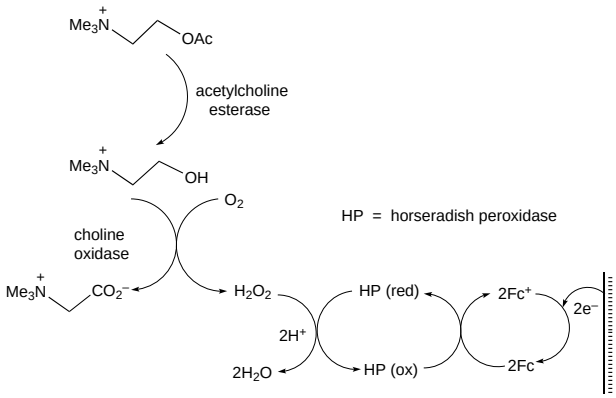



**Fig. 4** Variation of current response, measured by differential pulse voltammetry, with concentration of the tricyclic anti-depressant drug imipramine **13**

while choline and acetyl choline are bound selectively by **1c** or **3**, compared to sodium, potassium, calcium or magnesium, various other cationic aryl species may compete in binding to the cyclodextrin host. By coupling the analysis into an enzymic relay, excellent *specificities* may be achieved with very low limits of detection. Typically biosensors based on this approach have allowed sub-micromolar levels of analytes to be measured, but lower limits of detection have only been achieved if 'preconcentration' techniques are used, *e.g.* microdialysis[21] or HPLC[22] separation. Generally these biosensors are not particularly robust devices that have a limited lifetime.

We have studied recently a biosensor based on the well-established[23] horseradish peroxidase–choline oxidase–acetylcholine esterase relay system (Scheme 1), which is known to allow sub-micromolar levels of acetylcholine to be assayed *via* the relayed amperometric detection of hydrogen peroxide. Using a screen-printed disposable electrode, successive layers were deposited, first the charge shuttle of 1,1′-bis(methoxymethyl)ferrocene **14** then the three enzymes in phosphate buffer and finally a thin encapsulating film of plasticised polyurethane containing 5% by weight of tri-*O*-ethyl-β-cyclodextrin and a lipophilic counterion. The resultant 'dip-type' sensor, after conditioning in aqueous buffer, allows *sub-picomolar* levels of acetylcholine to be measured with negligible interference from compounds such as ascorbic acid, dopamine and atropine (Fig. 5). The electrode was stable to dry storage in air for a period of at least four months and was active in solution for several weeks. Following continuous contact with a $10^{-10}$ mol dm$^{-3}$ solution of acetylcholine, the measured current response had diminished only by 20%. Control experiments




**Scheme 1**

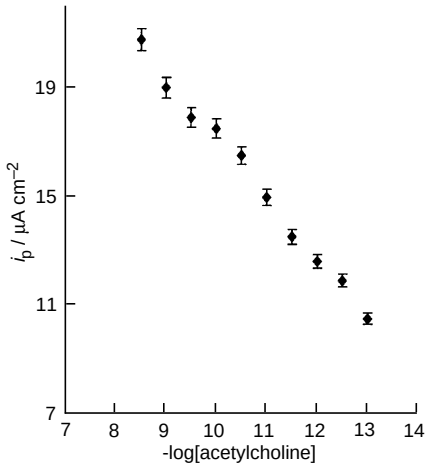



**Fig. 5** Calibration curve for an amperometric enzyme electrode for acetylcholine based on a coated screen printed carbon electrode using the enzyme system, acetylcholine esterase–choline oxidase–horseradish peroxidase encapsulated with a plasticised polyurethane thin film containing 2,3,6-tri-*O*-ethyl-β-cyclodextrin (see Scheme 1)

using an electrode that did not contain, in turn, either the encapsulating thin film or the cyclodextrin derivative have been undertaken. An acetylcholine sensor without the lipophilic anion and the plasticised thin film responded to acetylcholine only at micromolar concentration levels and with nanoamp current levels. The sensor with the cyclodextrin included showed a much improved current response and could be accurately calibrated over a much wider range of substrate concentrations.

The β-cyclodextrin derivative may serve a dual function: not only does it mediate transport of the acetylcholine through the thin polymeric film, but it can also reversibly bind the ferrocene derivative[24] (especially in the ferricenium state) promoting the relay of charge to the electrode. Given that many compounds with widely different uses target the acetylcholine esterase enzyme, *e.g.* organophosphorus pesticides or various chemical warfare agents, then such species may also be detected readily and at low concentration using such a biosensor.[25] More generally, lipophilic cyclodextrins that are designed to bind with some selectivity to other important charge diffuse cations, *e.g.* dopamine, may be coupled into a variety of relayed biosensors and may give excellent specificity and sensitivity in detection.


## Acknowledgements

It is a pleasure to thank the EPSRC for an Advanced Fellowship (R. K.), and the BBSRC for their support of this work.



**David Parker was born in Consett, County Durham. He gained a first class honours degree in Chemistry from Oxford University in 1978 and a DPhil in 1980, working on asymmetric catalysis, under the supervision of Dr John M. Brown in the Dyson Perrins Laboratory. He was a NATO Fellow in 1980/81 working with Professor Jean-Marie Lehn at the Université Louis Pasteur, Strasbourg and was appointed to a Lectureship at Durham University in 1982. He was subsequently promoted to a Senior Lectureship in 1989 and to a Chair in Chemistry in 1992. At present he is the Chairman of the Department of Chemistry at Durham. He was awarded the Hickinbottom Fellowship by the Royal Society of Chemistry in 1988, the Corday Morgan Medal and Prize of the RSC for 1987 and the ICI Research Prize in Organic Chemistry in 1991. In 1996, he gained the Interdisciplinary Award of the RSC and his research interests embrace many aspects of complexation phenomena in solution.**

**Ritu Kataky was born in Shillong, Assam, India and took her degree at the Indian Institute of Technology, New Delhi, India. After lecturing at St. Mary's College, Shillong, she took a PhD under the supervision of Professor Arthur Covington working on ion-selective electrodes in clinical analysis. In 1988 she began a post-doctoral fellowship at Durham University and in 1992 was awarded an EPSRC Advanced Fellowship. Her research interests are in physical aspects of analytical chemistry, focusing on electroanalysis of clinically important species.**


## References


1 *Perspectives in Coordination Chemistry*, ed. A. F. Williams, C. Floriani and A. E. Merbach, VCH, Basel, 1992.

2 S. C. Peacock and D. J. Cram, *J. Chem. Soc., Chem. Commun.*, 1976, 282; W. Bussmann, J.-M. Lehn, U. Oesch, P. Plumère and W. Simon, *Helv. Chim. Acta.*, 1981, **64**, 557.

3 D. A. Dougherty, P. C. Kearney, L. S. Mizoire, R. A. Kumpf, J. E. Forman and A. McCurdy, in *Computational Approaches in Supramolecular Chemistry*, ed. G. Wipff, NATO ASI Series C, vol. 426, Kluwer, London, 1994, pp. 301–309; P. C. Kearney, L. S. Mizoire, R. A. Kumpf, J. E. Forman, A. McCurdy and D. A. Dougherty, *J. Am. Chem. Soc.*, 1993, **115**, 9907.

4 M. Harel, D. M. Quinn, H. K. Nair, I. Silman and J. L. Sussman, *J. Am. Chem. Soc.*, 1996, **118**, 2340; J. L. Sussman, M. Harel, F. Frolow,

C. Oefner, A. Goldman, L. Tolker and I. Silman, *Science*, 1991, **253**, 872.
5 C. A. Deakyne and M. Meot-Ner, *J. Am. Chem. Soc.*, 1985, **107**, 474; M. Meot-Ner and C. A. Deakyne, *J. Am. Chem. Soc.*, 1985, **107**, 469.
6 O. Kennard, *Supramol. Chem.*, 1993, **1**, 277; T. Steiner and W. Saenger, *J. Am. Chem. Soc.*, 1992, **114**, 10 146.
7 W. A. Konig, R. Krebber and G. Wenz, *J. High Resolut. Chromatogr.*, 1989, **12**, 641.
8 S. Li and W. C. Purdy, *Chem. Rev.*, 1992, **92**, 1457.
9 P. S. Bates, R. Kataky and D. Parker, *J. Chem. Soc., Chem. Commun.*, 1992, 153; P. S. Bates, B. N. Green and D. Parker, *J. Chem. Soc., Chem. Commun.*, 1993, 693; P. S. Bates, D. Parker and A. F. Patti, *J. Chem. Soc., Perkin Trans. 2*, 1994, 657.
10 P. S. Bates, R. Kataky and D. Parker, *Analyst* (*London*), 1992, **117**, 1313; P. S. Bates, R. Kataky and D. Parker, *J. Chem. Soc., Perkin Trans. 2*, 1994, 669; R. Kataky, D. Parker and P. M. Kelly, *Scand. J. Clin. Lab. Invest.*, 1995, **55**, 409.
11 P. M. Kelly, R. Kataky, D. Parker and A. F. Patti, *J. Chem. Soc., Perkin Trans. 2*, 1995, 1955.
12 Y. Cohen, S. Palmer and D. Parker, unpublished results: for PGSE NMR methods in assessing complexation, see O. Mayzel and Y. Cohen, *J. Chem. Soc., Chem. Commun.*, 1994, 901; O. Mayzel, O. Aleksiuk, F. Grynszpan, S. Biali and Y. Cohen, *J. Chem. Soc., Chem. Commun.*, 1995, 1183.
13 K. B. Lipkowitz, S. Raghothama and D. Young, *J. Am. Chem. Soc.*, 1992, **114**, 1554.
14 G. C. Best and P. B. Dervan, *J. Am. Chem. Soc.*, 1995, **117**, 1187.
15 P. S. Bates, R. Kataky and D. Parker, *J. Chem. Soc., Chem. Commun.*, 1993, 691.
16 P. S. Bates, R. Kataky and D. Parker, *Analyst* (*London*), 1994, **117**, 181; increases in the rate of relaxation of the $^2$H nucleus in $C_{12}N(CD_3)_3^+$ were observed following addition of **1b** or **2b**; P. M. Kelly and D. Parker, unpublished observations.
17 F. Cramer, W. Saenger and H.-C. Spatz, *J. Am. Chem. Soc.*, 1967, **89**, 14.
18 M. H. Greenhall, P. Lukes, R. Kataky, N. E. Agbor, J. P. S. Badyal, J. Yarwood, D. Parker and M. C. Petty, *Langmuir*, 1995, **11**, 3997.
19 R. Kataky, P. M. Kelly, D. Parker and A. F. Patti, *J. Chem. Soc., Perkin Trans. 2*, 1994, 2381.
20 D. Parker, R. Kataky, P. M. Kelly and S. Palmer, *Pure Appl. Chem.*, 1996, **68**, 1219.
21 W. J. Albery, M. G. Boutelle, S. L. T. Durrant, M. Fillenz, A. R. Hopkins and B. P. Mangold *Phil. Trans. R. Soc. London A*, 1990, **333**, 49.
22 L. E. Webb and R. C. Johnston, *Clin. Biochem.*, 1986, **19**, 212.
23 A. Guerrieri, G. E. De Benedetto, F. Palmisano and P. G. Zambonin, *Analyst* (*London*), 1995, **120**, 2731.
24 A. Harada and S. Takahaslin, *J. Chem. Soc., Chem. Commun.*, 1984, 645.
25 R. Kataky and D. Parker, *Br. Pat. Appl.*, 9611499.6; R. Kataky and D. Parker, *Analyst* (*London*), 1996, 1829.

*6/03564G*

# Self-assembly of tetraalkylammonium salt-stabilized giant palladium clusters on surfaces

**Manfred T. Reetz,* Martin Winter and Bernd Tesche**

*Max-Planck-Institut für Kohlenforschung, Kaiser-Wilhelm-Platz 1, D-45470 Mülheim/Ruhr, Germany*

**Nanostructured palladium clusters, stabilized by a monomolecular coat of sufactants $N(C_8H_{17})_4Br$ or $N(C_{18}H_{37})_4Br$, self-assemble on carbon surfaces in an ordered manner with the formation of hexagonal close packed structures.**

Self-assembly of preformed nanostructured transition-metal clusters on solid surfaces in ordered structures constitutes a formidable preparative challenge.[1] Investigations in this field of material science is driven by the prospect of fabricating structurally uniform materials having unique electronic and/or magnetic properties. For example, placing finite-sized clusters onto surfaces in geometrically well defined arrays may open the way to single-electron tunnel devices. Recently we have shown that a variety of nanostructured metal clusters and bimetallic clusters stabilized by tetraalkylammonium salts can be prepared electrochemically in a size-selective manner by correct adjustment of the current density and proper choice of solvent.[2] A combined STM–TEM study revealed that each individual cluster is surrounded by a monomolecular layer of the $NR_4X$ salt.[3] Whereas many TEM studies of $NR_4X$- stabilized metal clusters have been carried out previously in order to determine the average size of the metal core,[2–4] unusual phenomena relating to self-assembly on the surface have not been observed to date. In this paper we describe ordering phenomena involving high purity monodisperse $NR_4X$-stabilized palladium clusters on carbon supports, as observed by transmission electron microscopy.

In all experiments the surfaces upon which the clusters were deposited consisted of carbon support films, produced by means of an impact evaporator, and placed on copper grids (400 mesh $in^{-1}$).[5] Simple dip-coating using solutions of $N(C_4H_9)_4Br$-, $N(C_8H_{17})_4Br$- or $N(C_{18}H_{37})_4Br$-stabilized palladium clusters[2] having average inner core sizes of 2.5, 5.9 and 5.9 nm, respectively, was performed,† followed by TEM analysis. In the case of the $N(C_4H_9)_4Br$-stabilized palladium clusters, the TEM micrographs failed to show any signs of order, irrespective of the conditions used in the dip-coating process. Completely random distributions of clusters on the surface were observed. Similar observations were made upon employing larger sized palladium clusters stabilized by $N(C_4H_9)_4Br$. In complete contrast, the samples stabilized by $N(C_8H_{17})_4Br$ led to high degrees of ordering. The respective clusters self-organize in a hexagonal close packing structure. Interestingly, the system self-assembles in ordered stacks of such layers, these being arranged in almost perfect steps and terraces. High-resolution TEM clearly reveals the first few individual layers (Fig. 1).

Besides the stacks of layers, clear domains of monolayers were obtained, as shown by typical TEM images (Fig. 2). Again hexagonal close packing occurs. The corresponding two-dimensional Fourier-transformed image is shown in Fig. 3. Close inspection of individual clusters at atomic resolution reveals lattice fringes characteristic of face centred cubic (fcc) crystallinity.

Careful analysis of the geometric features of the surface structure reveals some interesting features. We have previously shown by STM measurements that the thickness of the $N(C_8H_{17})_4Br$ protective coat surrounding palladium clusters having different core sizes amounts to 1.2 nm, which is in line with simple force-field calculations (1.1 nm).[3] In the present case assumption of a bilayer between the ordered clusters leads to the prediction that the distance between the centres of the metal cores should amount to 8.3 nm. The observed value of 8.2 nm is in excellent agreement with this expectation, which means

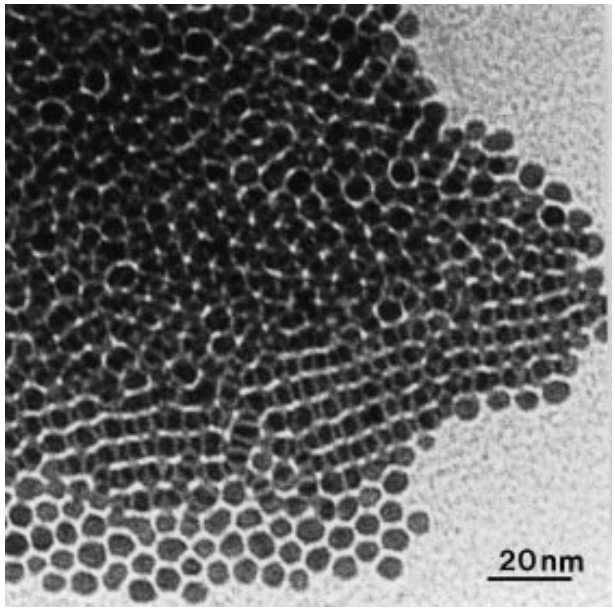



**Fig. 1** Electron micrograph of palladium colloid of the first, second and third monolayer, which are stepwise ordered in a three- dimensional structure after deposition on carbon support films

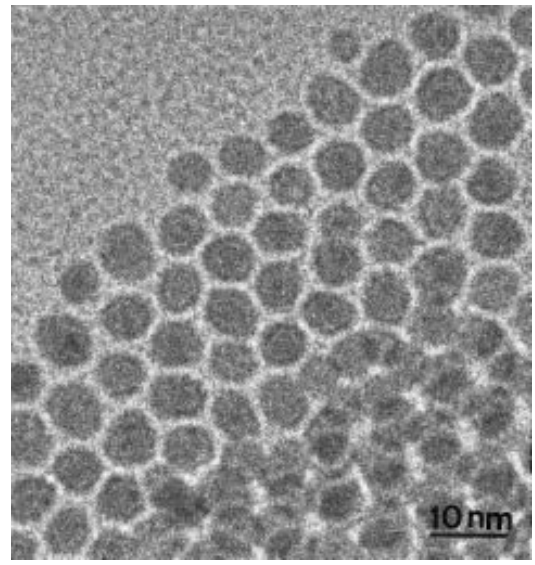



**Fig. 2** Electron micrograph of palladium colloid hexagonal close packed arranged in the first monolayer

that the protective mantles on the surface touch each other without damage or interpenetration. This means that nano-engineering on surfaces should be possible simply by varying the length of the alkyl groups of the ammonium stabilizer. For example, upon using $N(C_{18}H_{37})_4Br$-stabilized palladium clusters having an inner metal core size of 5.9 nm, it is predicted that the average distance between the centres of the clusters should be 10.3 nm. Indeed, upon employing the 5.9 nm sized $N(C_{18}H_{37})_4Br$-stabilized palladium clusters, hexagonal close packing was again observed, the distance between the centres of the clusters this time amounting to 10.2 nm.

An unusual effect was observed in the case of the $N(C_8H_{17})_4Br$-stabilized palladium clusters. A few highly ordered domains were discerned in which hexagonal close packing clearly does not occur (Fig. 4). Although cursory inspection suggests cubic close packing (coordination number four in the two-dimensional layer; twelve in the three-dimensional arrangement), careful analysis reveals that the material is in fact non-close packed. The distance between the centres of the clusters amounts to 6.3 nm. The reason for the formation of such unusual ordered domains is presently unclear. It appears that this molecular structure begins to have the characteristics of a three-dimensional crystalline superlattice (Fig. 4), in which the particles are ordered.

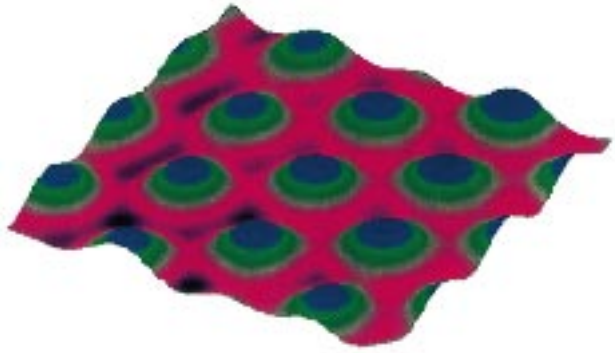


**Fig. 3** Individual hexagonal close packed palladium colloid after digital image processing

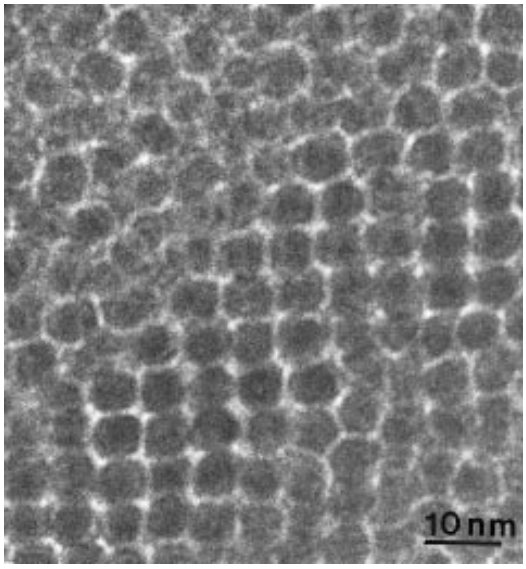



**Fig. 4** Electron micrograph of palladium colloid ordered in a non-closed packed cubic-like arrangement

In summary, we have demonstrated for the first time that certain $NR_4X$-stabilized metal clusters self-organize on supports, forming two-dimensional films and three-dimensional superlattices. By varying the length of the alkyl chains of the ammonium ions, predictable structural ordering is possible. Preliminary experiments show that variation of the palladium cluster core size is another useful parameter which also allows for nanoscale engineering. Extension to other metal clusters and bimetallic analogues as well as the corresponding nanostructured $NR_4X$-stabilized metal oxide clusters[6] should be straightforward.

## Footnote

† A TEM grid (400 mesh $in^{-1}$)[5] was dipped into a $10^{-3}$ M solution of a $NR_4Br$-stabilized palladium cluster[2] in thf for 2–3 s. Following removal from the solution, the grid was dried in air at room temp. for 2–3 h.

## References


1 M. Brust, D. Bethell, D. J. Schiffrin and C. J. Kiely, *Adv. Mater.*, 1995, **7**, 795; R. L. Whetten, J. T. Khoury, M. M. Alvarez, S. Murthy, I. Vezmar, Z. L. Wang, P. W. Stephens, C. L. Cleveland, W. D. Luedtke and U. Landman, *Adv. Mater.*, 1996, **8**, 428; R. H. Terrill, T. A. Postlethwaite, C. Chen, C.-D. Poon, A. Terzis, A. Chen, J. E. Hutchison, M. R. Clark, G. Wignall, J. D. Londono, R. Superfine, M. Falvo, C. S. Johnson, Jr., E. T. Samulski and R. W. Murray, *J. Am. Chem. Soc.*, 1995, **117**, 12537; P. C. Ohara, D. V. Leff, J. R. Heath and W. M. Gelbart, *Phys. Rev. Lett.*, 1995, **75**, 3466; M. Dorogi, J. Gomez, R. Osifchin, R. P. Andres and R. Reifenberger, *Phys. Rev. B: Condens. Matter*, 1995, **52**, 9071; W. D. Luedtke and U. Landman, *J. Phys. Chem.*, 1996, **100**, 13323; G. Schmid, A. Lehnert, U. Kreibig, Z. Adamczyk and P. Belouschek, *Z. Naturforsch., B: Chem. Sci.*, 1990, **45**, 989; C. A. Mirkin, R. L. Letsinger, R. C. Mucic and J. J. Storhoff, *Nature*, 1996, **382**, 607; A. P. Alivisatos, K. P. Johnsson, X. Peng, T. E. Wilson, C. J. Loweth, M. P. Bruchez Jr., and P. G. Schultz, *Nature*, 1996, **382**, 609; P. C. Hidber, W. Helbig, E. Kim and G. M. Whitesides, *Langmuir*, 1996, **12**, 1375; R. P. Andres, J. D. Bielefeld, J. I. Henderson, D. B. Janes, V. R. Kolagunta, C. P. Kubiak, W. J. Mahoney and R. G. Osifchin, *Science*, 1996, **273**, 1690.

2 M. T. Reetz and W. Helbig, *J. Am. Chem. Soc.*, 1994, **116**, 7401; M. T. Reetz, W. Helbig and S. A. Quaiser, *Chem. Mater.*, 1995, **7**, 2227; M. T. Reetz and S. A. Quaiser, *Angew. Chem.*, 1995, **107**, 2461; *Angew. Chem., Int. Ed. Engl.*, 1995, **34**, 2240.

3 M. T. Reetz, W. Helbig, S. A. Quaiser, U. Stimming, N. Breuer and R. Vogel, *Science*, 1995, **267**, 367.

4 N. Toshima, T. Takahashi and H. Hirai, *Chem. Lett.*, **1985**, 1245; M. Boutonnet, J. Kizling, R. Touroude, G. Maire and P. Stenius, *Appl. Catal.*, 1986, **20**, 163; K. Meguro, M. Torizuka and K. Esumi, *Bull. Chem. Soc. Jpn.*, 1988, **61**, 341; J. Wiesner, A. Wokaun and H. Hoffmann, *Prog. Colloid Polym. Sci.*, 1988, **76**, 271; N. Satoh and K. Kimura, *Bull. Chem. Soc. Jpn.*, 1989, **62**, 1758; H. Bönnemann, W. Brijoux, R. Brinkmann, R. Fretzen, T. Joussen, R. Köppler, B. Korall, P. Neiteler and J. Richter, *J. Mol. Catal.*, 1994, **86**, 129.

5 B. Tesche, *Vak.-Tech.*, 1975, **24**, 104; B. Tesche, T. Schilling, M. Wesemann and R. Schlögl, in *Electron Microscopy*, EUREM 92, Granada, Spain, 1992, vol. 2, 673.

6 M. T. Reetz, S. A. Quaiser, M. Winter, J. A. Becker, R. Schäfer, U. Stimming, A. Marmann, R. Vogel and T. Konno, *Angew. Chem.*, 1996, **108**, 2228; *Angew. Chem., Int. Ed. Engl.*, 1996, **35**, 2092.


*Received, 20th September 1996; Com. 6/06490F*

# High-intensity, laser-jet photochemistry: photodecarboxylation of 3,3-diphenyl-1*H*,3*H*-naphtho[*cd*][2]pyran-1-one

**R. Marshall Wilson,*[a] K. A. Schnapp,*[b] Martin Glos,[a] Cornelia Bohne*[c] and Andrew C. Dixon[c]**

[a] *Department of Chemistry, University of Cincinnati, Cincinnati, OH 45221-0172, USA*
[b] *Department of Chemistry, Northern Kentucky University, Highland Heights, KY 41099-1905, USA*
[c] *Department of Chemistry, PO Box 3065, University of Victoria, Victoria, BC, CA 3W8 3V6, Canada*

**The novel photodecarboxylation of an aryl δ-lactone from an upper triplet state is described.**

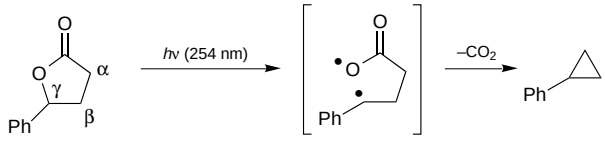
Although the photodecarboxylation of esters is a widely known process, loss of carbon dioxide from lactones is ordinarily a minor pathway in solution phase photochemistry.[1] The majority of cases reported indicate efficient photodecarboxylation requires that an excited aromatic chromophore cleave a benzyl ester bond to form a carboxy radical (Scheme 1).[2] Herein we report the novel high-intensity laser-jet photodecarboxylation of 3,3-diphenyl-1*H*,3*H*-naphtho[*cd*][2]pyran-1-one **1**.

The preparation of **1** in nearly quantitative yield involves the reaction of the ketone **2** with DBAHA [tris(2,4-dibromophenyl)ammonium hexachloroantimonate; Scheme 2] in an unprecedented SET Baeyer–Villiger lactonization.†

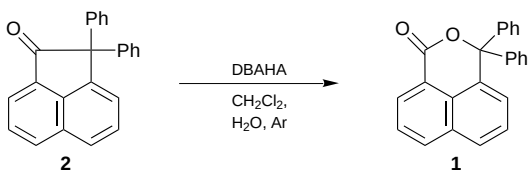
When **1** was irradiated under low-intensity conditions (356 nm, Rayonet Photochemical Reactor, $C_6H_6$, Ar, 7 days), no products were observed. However, under high-intensity, laser-jet conditions,[3] two new products were isolated: the carboxylic acid **3**, and the cycloheptatriene **4** (Scheme 3).‡

The mechanism for the formation of photoproducts **3** and **4** might be accounted for by either of two possible pathways [(*a*) and (*b*) in Scheme 3]. Pathway (*a*) involves absorption of a photon by **1** to form $^3$**1**, which upon absorption of a second photon could result in homolytic C–O bond scission to produce **5**, which in turn might lose $CO_2$ thermally to form the novel triarylmethyl biradical **6**. Alternatively, **5** may undergo a most unusual addition to benzene to produce **3**. A second possible pathway (*b*) requires that absorption of the first photon by **1** results in homolytic bond scission to form biradical **5**, which upon the absorption of a second photon produces a biradical excited state that might either react with solvent to form **3** or undergo decarboxylation to produce **6**. In either case, the triarylmethyl biradical **6** apparently cyclizes at the *ipso* position of a phenyl group to form the norcaradiene **7**. The thermally labile **7** undergoes ring opening followed by a photochemically allowed 1,7-phenyl migration to produce the observed cycloheptatriene **4**.[4] Related 1,7-phenyl shifts have been found to be so facile that only the phenyl-shifted final product could be isolated under some conditions.[4b]

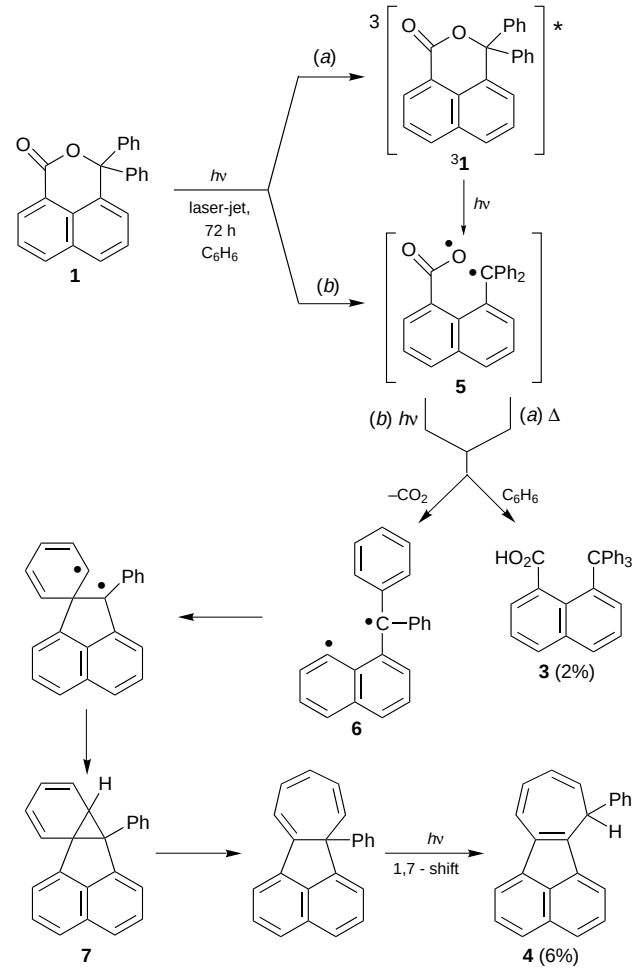
The transient absorption spectroscopy of pyranone **1** was examined in order to gain further insight into the mechanism of decarboxylation. Excitation of **1** produced a transient signal ($\lambda_{max}$ = 460 nm, $\tau \geqslant 10$ μs)§ which was independent of solvent (benzene, acetonitrile or cyclohexane). The transient spectrum for **1** was similar to the spectrum determined independently for triplet 1-acetonaphthone, which is expected to be the chromophore with lowest energy in **1**. The transient for **1** was quenched with similar efficiency by $O_2$ and cyclohexa-1,3-diene ($1–3 \times 10^9$ dm$^3$ mol$^{-1}$ s$^{-1}$). These results are consistent with an assignment of the transient of **1** to its triplet state. The biradicals can be ruled out as the transient, since these species would be expected to have shortened lifetimes in cyclohexane due to




**Scheme 1**




**Scheme 2**




**Scheme 3**

hydrogen abstraction from the solvent and probably would not be effciently quenched by cyclohexa-1,3-diene.

Two-laser experiments were performed in order to address the question of whether C–O bond scission occurs from an upper triplet state of **1**.[5]¶ Reactive upper triplet states have been observed for benzil[6] and 1,3-bis(1-naphthyl)propan-2-one.[7] In both of these instances, the first excited triplet state was unreactive, and 'reluctant' reactivity was observed only from upper triplet states. When the triplet of **1** in benzene was further excited at 355 nm, a small but detectable, amount of bleaching was observed within 10 ns following the YAG laser pulse (Fig. 1). The actual amount of bleaching is somewhat larger than shown in Fig. 1, since some triplet was formed by the irradiation of **1** with the 355 nm laser only. The same transient spectra were recorded before and after the irradiation of the triplet by the second laser pulse. This bleaching indicates that **1**[3] is photoreactive and this observation is consistent with pathway (*a*). It is worth noting that the energy of the photolysis (second) laser pulse corresponds to the energy employed in the high-intensity argon laser-jet experiments. When this energy was decreased by irradiating the triplet at 532 nm no bleaching was observed, suggesting that the bleaching quantum yield is dependent on the energy of excitation of the triplet.

Thus, the formation of the high intensity photoproducts **3** and **4** is probably initiated *via* pathway (*a*) (Scheme 3) involving a β-scission[3] in which an excited aromatic ring cleaves the benzyl C–O bond. In previous work,[2a,b] this type of bond was β to an excited phenyl group rather than to an excited naphthyl group. Apparently the higher energy triplet state of a phenyl group (82.5 kcal mol$^{-1}$ for toluene; 1 cal = 4.184 J)[8] leads to direct cleavage of the benzyl C–O bond, while the much lower energy naphthyl triplet state (59.6 kcal mol$^{-1}$ for 1-methyl naphthalene)[8] requires an additional photon to promote it to a higher energy triplet state, from which the benzyl C–O cleavage becomes energetically favourable. Once the decarboxylation has occurred, formation of the cycloheptatriene *via* collapse of **6** to the norcaradiene **7** has precedent in several reactions studied earlier.[4] Finally, it is interesting to note that while high intensity irradiation of the parent ketone **2** might also be expected to form the biradical **6** *via* photodecarbonylation, **2** was found to be photochemically unreactive.

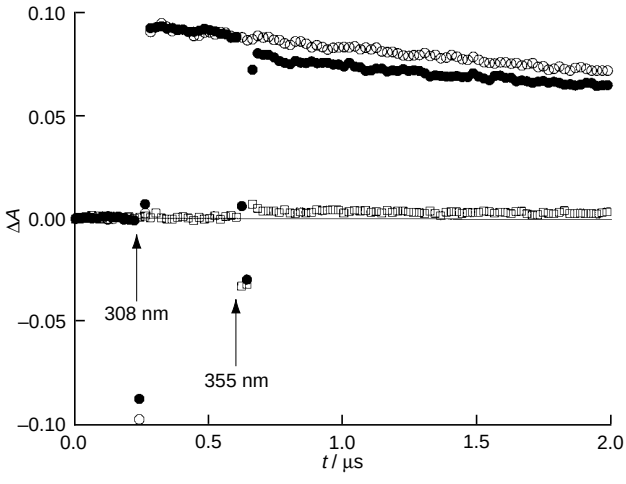



**Fig. 1** Transient signals at 460 nm for the excitation of **1** at (○) 308 nm only, (□) 355 nm only and (●) 308 nm followed by 355 nm

R. M. W. thanks the NSF (CHE-9122141), K. A. S. thanks the Research Corporation (C-3466) and the NSF EPSCoR (REG 1994), M. G. thanks the DAAD and C. B. thanks the Natural Sciences and Engineering Research Council of Canada for financial support. The authors thank Professor Waldemar Adam on the occasion of his 60th birthday for many useful discussions on laser photochemistry.

## Footnotes

† The details and further examples of this type of reaction will be reported shortly.

‡ *Selected data* for **1**: mp 208–209 °C (lit.,[9] 204 °C); $^1$H NMR (250 MHz; $CDCl_3$) δ 8.39 (d, *J* 7.2 Hz, 1 H), 8.15 (d, *J* 8.2 Hz, 1 H), 7.92 (d, *J* 8.3 Hz, 1 H), 7.63 (t, *J* 7.7 Hz, 1 H), 7.52 (t, *J* 7.5 Hz, 1 H), 7.31–7.18 (m, 10 H), 7.11 (d, *J* 7.2 Hz, 1 H); $\nu_{max}$ ($CH_2Cl_2$)/cm$^{-1}$ 3067, 3038, 1723 (vs), 1623, 1586, 1493, 1402, 1353; HRMS (EI) calc. for $C_{24}H_{16}O_2$ ($M^+$), 336.1172. Observed, 336.1175. For **3**: $^1$H NMR (250 MHz; $CDCl_3$) δ 9.05 (d, *J* 8.0 Hz, 1 H), 8.79 (d, *J* 8.3 Hz, 1 H), 8.71 (d, *J* 7.5 Hz, 1 H), 7.94 (dd, *J* 8.0, 8.0 Hz, 1 H), 7.76 (dd, *J* 6.7, 6.7 Hz, 1 H), 7.63–7.51 (m, 9H), 7.41 (brs, 3 H), 7.30–7.07 (m, 3 H), 6.64 (d, *J* 10.0 Hz, 1 H); $\nu_{max}$($CH_2Cl_2$)/cm$^{-1}$ 3400 (br), 1720, 1595; GC–MS *m/z* 414.45. For **4**: $^1$H NMR (250 MHz; $CDCl_3$) δ 7.79–7.71 (m, 3 H), 7.56 (d, *J* 7.1 Hz, 1 H), 7.50 (d, *J* 4.3 Hz, 2 H), 7.32 (d, *J* 7.0 Hz, 2 H), 7.23–7.12 (m, 4 H), 6.52 (dd, *J* 11.0, 6.2 Hz, 1 H), 6.40 (dd, *J* 10.3, 6.6 Hz, 1 H), 6.10 (dd, *J* 9.2, 9.2 Hz, 1 H), 5.10 (d, *J* 8.3 Hz, 1 H); $\nu_{max}$ ($CH_2Cl_2$)/cm$^{-1}$ 3066, 3027, 1599, 1482; HRMS (EI) calc. for $C_{23}H_{16}$ ($M^+$), 292.1252. Observed 292.1239.

§ The basic laser flash photolysis system is described in Y. Liao and C. Bohne, *J. Phys. Chem*., 1996, **100**, 734. Since some destruction of **1** was observed, most experiments were performed with a flow cell or the sample was subjected to less than 50 laser shots. The transient lifetime is limited by residual oxygen in the flow cell.

¶ The triplet state was formed by the excitation of **1** with an excimer laser (Lumonics EX-510) at 308 nm. The triplet was monitored at 460 nm, and was irradiated after a suitable delay (Stanford Research Delay Generator, model DG535) by a YAG laser (Spectra Physics GCR-12) at 355 or 532 nm. The excimer laser irradiated the sample at 90° to the monitoring beam, whereas the Yag laser beam irradiated the sample from the front at a small angle with respect to the monitoring beam. The negative Δ*A* values in Fig. 1 correspond to fluorescence of **1** and scattered light.

## References

1 R. Simonaitis and J. N. Pitts Jr., *J. Am. Chem. Soc.*, 1969, **91**, 108; J. S. Bradshaw, E. L. Loveridge and L. White, *J. Org. Chem.*, 1968, **33**, 4127.
2 (*a*) R. S. Givens and W. F. Oettle, *J. Am. Chem. Soc*., 1971, **93**, 3301; (*b*) R. S. Givens and W. F. Oettle, *J. Org. Chem.*, 1972, **37**, 4325; (*c*) G. W. Perold and G. Ourisson, *Tetrahedron Lett.*, 1969, 3871; (*d*) I. S. Krull and D. R. Arnold, *Tetrahedron Lett.*, 1969, 1247.
3 R. M. Wilson and K. A. Schnapp, *Chem. Rev*., 1993, **93**, 223.
4 (*a*) R. M. Wilson, T. N. Romanova, A. Azadnia, J. A. Krause Bauer and R. P. Johnson, *Tetrahedron Lett*., 1994, **35**, 5401; (*b*) K. A. Schnapp, P. L. Motz, S. M. Stoeckel, R. M. Wilson, J. A. Krause Bauer and C. Bohne, *Tetrahedron Lett.*, 1996, **37**, 2317.
5 L. J. Johnston, *Chem. Rev*., 1993, **93**, 251; J. C. Scaiano and L. J. Johnston, *Organic Photochemistry*, ed. A. Padwa, Marcel Dekker, New York, 1989, vol. 10, p. 309.
6 W. G. McGimpsey and J. C. Scaiano, *J. Am. Chem Soc.*, 1987, **109**, 2179.
7 L. J. Johnston and J. C. Scaiano, *J. Am. Chem. Soc.*, 1987, **109**, 5487.
8 S. L. Murov, *Handbook of Photochemistry*, Marcel Dekker, New York, 1973.
9 M. Zsuffa, *Ber*., 1910, **43**, 2915.

*Received, 3rd September 1996; Com. 6/06069B*

# *ortho*-Hydroxylation of 4-*tert*-butylphenol by nonheme iron(III) complexes as a functional model reaction for tyrosine hydroxylase

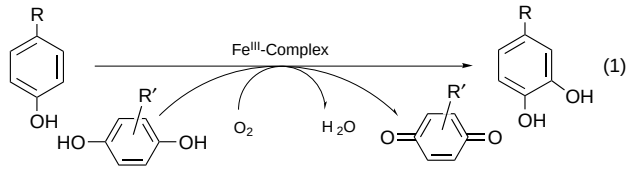
**Takuzo Funabiki,* Tomomasa Yokomizo, Shinko Suzuki and Satohiro Yoshida**

*Department of Molecular Engineering, Graduated School of Engineering, Kyoto University, Kyoto 606-01, Japan*

**Hydroxylation of 4-*tert*-butylphenol to 4-*tert*-butylcatechol is performed by a catecholatoiron(III) complex–hydroquinone–$O_2$ system which mimicks the roles of $Fe^{2+}$ and $Fe^{3+}$ in tyrosine hydroxylase; the *ortho*-hydroxylation of phenols by iron–oxygen active species is suggested.**

Tyrosine hydroxylase (TH) is one of the pteridine-dependent nonheme iron monooxygenases and converts tyrosine to DOPA by hydroxylation with molecular oxygen. Very little is known about not only the active site environment of the enzyme, but also the role of iron in oxygen activation. TH is isolated mostly in the form of $Fe^{3+}$ [TH($Fe^{3+}$), coordinated by DOPA],[1–4] but $Fe^{2+}$ [TH($Fe^{2+}$)] is suggested to be an active species.[1,5–7] Scheme 1[1,3] shows that $Fe^{3+}$ is reduced to an active TH($Fe^{2+}$) by tetrahydropterine ($BPH_4$)[1] and coordinated by catecholamine to give an inert species.[3,4,8,9] The active species has been proposed to be a peroxytetrahydropterin [($BPH_4$)–OOH] rather than an iron–oxygen species.[5,10,11]

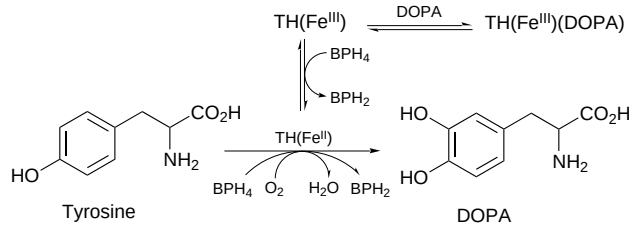
In model studies, on the other hand, results suggest that the hydroxylation proceeds *via* an iron—oxygen species in the enzymatic system. Inner-sphere transfer of a peroxo oxygen in $HOC_6H_4O$–$Fe^{III}$–OOR[12] or of the OH ligand in $HOC_6H_4O$–$Fe^{IV}$–OH[13] to the phenolate ligands has been proposed. In the latter case, $Fe^{II}$ complexes such as bis(2,6-dicarboxypyridine)iron(II) and reductants such as PhNHNHPh have been used.[13] Considering that cytochrome P450-type monooxygenations are catalysed by $Fe^{III}$ species, with donation of two electrons and two protons in a catalytic cycle, it is probable that the tyrosine hydroxylase-type *ortho*-hydroxylations are catalysed by $Fe^{III}$ species in the presence of electron and proton donors. In mimicking the processes of reduction of $Fe^{3+}$ to $Fe^{2+}$ by $BPH_4$ and inhibition by coordination of catechol, and in excluding the formation of the ($BPH_4$)–OOH type active species, we have performed hydroxylation of phenol with $O_2$ by iron(III) complexes in the presence of hydroquinones as proton and electron donors [eqn. (1)].




Catecholatoiron complexes formed *in situ*†[14,15] were used as the ferric complex, and 4-*tert*-butylphenol ($Bu^tC_6H_4OH$ **1**) was used as substrate.‡ The effect of four different hydroquinones was studied here: 2,6-di-*tert*-butylhydroquinone (DTBHQ), *tert*-butylhydroquinone (TBHQ), hydroquinone (HQ) and 1,4-dihydroxynaphthalene (DNH). Hydroxylation was performed at 25 °C with $O_2$ (1 atm). In a typical case, the reaction of **1** was started by addition of a MeCN solution (7.5 $cm^3$) of $FeCl_3$ (0.125 mmol) and pyridine (0.25 mmol) to **1** (25 mmol), catechol (0.125–1.25 mmol) and hydroquinone (5.0 mmol).

4-*tert*-Butylcatechol **2** was formed as the sole detectable product from **1**.§ The yield of **2** was greatly dependent on the substituents on catechol: hydroxylation was promoted by electron-withdrawing substituents. Thus, the yield of **2** per mol% Fe decreased in the order: 3,4,5,6-$Cl_4$ (560) > 4-$NO_2$ (410) > 4-Cl (230) > H (120) > 3,5-$Bu^t_2$ (80) > none (*i.e.* without catechol, 52), with [Fe] = [catechol] = 0.125 mmol and [DTBHQ] = 5 mmol. The reverse order was found for the relative rate of consumption of hydroquinones: 3,4,5,6-$Cl_4$ (0.08) < 4-$NO_2$ (0.24) < 4-Cl (0.65) < 3,5-$Bu^t_2$ (0.91) < none (2.18), indicating that electron-withdrawing substituents on catechols, which stabilize the catecholatoiron(III) complexes, are efficient for the *ortho*-hydroxylation of phenols.

It was noticed that after consumption of hydroquinone, **2** was converted to an unidentified polymeric product. As shown in Fig. 1(*a*), this consecutive reaction of **2** was prevented by addition of excess catechol which also, brought about an increase in the yield of **2**. This is probably because the excess catechol effectively controls the competitive coordination of **2**




**Scheme 1**

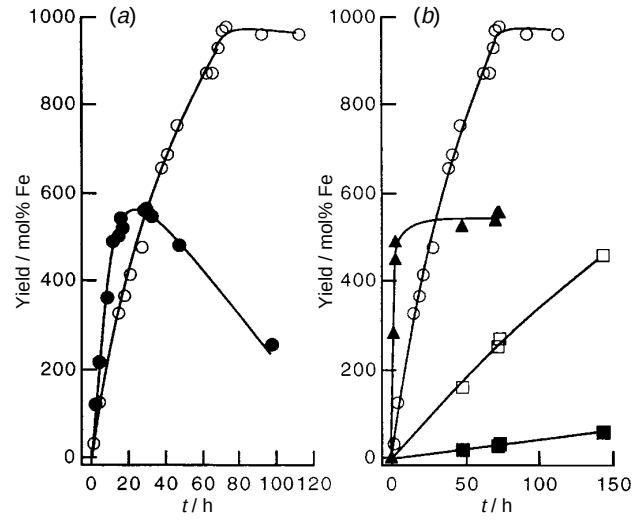



**Fig. 1** Formation of 4-*tert*-butylcatechol from 4-*tert*-butylphenol catalysed by a tetrachlorocatecholatoiron(III) complex under $O_2$ (1 atm). (*a*) Effect of tetrachlorocatechol concentration: [tetrachlorocatechol]:[Fe] = (●) 1 : 1 and (○) 10 : 1, $FeCl_3$ = 0.125 mmol, pyridine = 0.25 mmol, DTBHQ = 5.0 mmol, $Bu^tC_6H_4OH$ = 25 mmol in MeCN (7.5 $cm^3$). (*b*) Effect of different hydroquinones: (○) DTBHQ, (▲) DHN, (□) TBHQ and (■) HQ = 5.0 mmol, tetrachlorocatechol = 1.25 mmol, $FeCl_3$ = 0.125 mmol, pyridine = 0.25 mmol, $Bu^tC_6H_4OH$ = 25 mmol in MeCN (7.5 $cm^3$).

and hydroquinone to $Fe^{III}$. The end of hydroxylation does not mean the deactivation of the active species. The reaction is repeatedly performed by addition of hydroquinone, indicating that the active species is maintained in the form of a catecholatoiron(III) complex.

Hydroxylation is greatly influenced by the hydroquinones. As shown in Fig. 1(*b*), the initial rate of hydroxylation is correlated with the electron-transfer affinity of the hydroquinone (DHN > DTBHQ > TBHQ > HQ), as shown by the decrease in the intensity of the characteristic band of the catecholatoiron(III) complexes [Fig. 2(*a*)]. The rapid quenching of the reaction in spite of the initial rapid formation of **2** is caused by the oxidation of DHN to the corresponding ineffective quinone. Reduction of $Fe^{III}$ to $Fe^{II}$ by hydroquinones was also shown by the formation of a characteristic phenanthrolineiron(II) complex. In the presence of phenanthroline, the hydroxylation does not proceed, indicating that the active iron(II) species is trapped by phenanthroline. The effect of the catecholate ligand on the electron transfer shown in Fig. 2(*a*) indicates that tetrachlorocatecholatoiron(III) is less susceptible to the electron transfer from DTBHQ than the 4-chlorocatecholatoiron(III) complex.

Regardless of the importance of the iron(II) species for hydroxylation, the rapid formation and high yield of **2** was not observed when $FeCl_2$ was used in place of $FeCl_3$ in the tetrachlorocatechol–DTBHQ system. Since $Fe^{2+}$ can be oxidized to an $Fe^{3+}$ species under oxygen, it is difficult to perform the reaction only in the presence of $Fe^{II}$ species, but the result indicates that the $FeCl_3$ system is much better at hydroxylation than the $FeCl_2$ system.

The above results indicate not only that electron transfer to $Fe^{III}$ is essential for hydroxylation, but also that the presence of $Fe^{III}$ species in equilibrium with $Fe^{II}$ is important for the catalytic hydroxylation. This is similar to the participation of both $Fe^{3+}$ and $Fe^{2+}$ in the activity of tyrosine hydroxylase. The most favourable combination of conditions studied here is the use of the tetrachlorocatecholatoiron(III) complex and DTBHQ, which combine to form the most efficient active iron(II) species.

The importance of the presence of $Fe^{III}$ in equilibrium with $Fe^{II}$ suggests the mechanism shown in Scheme 2 for the hydroxylation of phenols. Unlike reactions catalysed by $Fe^{II}$ complexes,[13] the present results suggest that the $Fe^{III}$ species [$(L)Fe^{3+}$] is involved in the catalytic cycle. Support for formation of a free radical intermediate was not found, but addition of triphenylmethane did not affect the reaction. Observation of characteristic LMCT bands at around 600 nm indicated that phenols, including hydroquinones, coordinate to $Fe^{3+}$. Fig. 2(*b*) shows the coordination of phenol to $Fe^{III}$, either together with or replacing a catecholate ligand. The electron-withdrawing substituents on catechol might be effective in making the ferrous as well as ferric centre a better Lewis acid towards the phenolic substrate. It is very likely that the *ortho*-hydroxylation proceeds inside the coordination sphere, but whether the oxygen transfer to phenol proceeds directly *via* a hydroperoxoiron(III) or oxoiron(V) species is a problem to be solved in future.

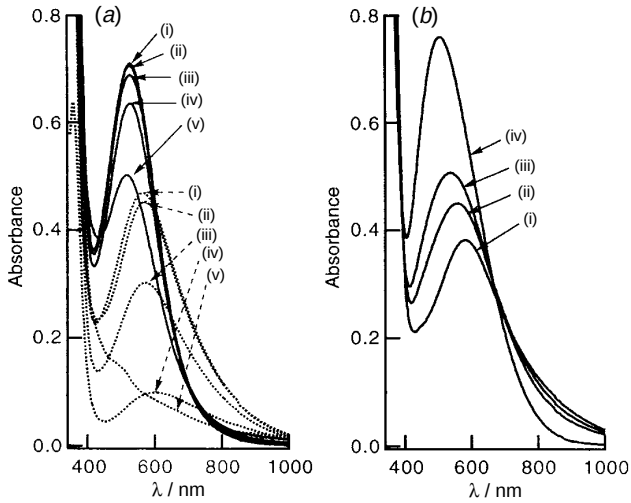
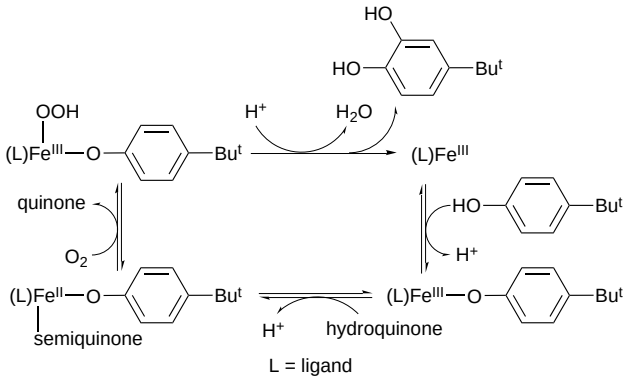



**Fig. 2**(*a*) Visible spectral changes caused by addition of hydroquinones to (- - - - -) tetrachloro- and (——) 4-chloro-catecholatoiron (III) complexes under argon: (i) none, (ii) HQ, (iii) TBHQ, (iv) DTBHQ and (v) DHN. $FeCl_3$ = catechol = 0.025 mmol, hydroquinone = 1.0 mmol, pyridine = 0.05 mmol in MeCN (7.5 $cm^3$). (*b*) Visible changes caused by addition of *tert*-butylphenol to a catecholatoiron (III) complex under argon: (i) $[Bu^tC_6H_4OH]:[catechol]$ = 0 : 1, (ii) 100 : 1, (iii) 250 : 1 (iv) 250 : 0. $FeCl_3$ = catechol = 0.025 mmol, pyridine = 0.05 mmol in MeCN (75 $cm^3$).




**Scheme 2**

## Footnotes

† Formation of three types of catecholatoiron complexes in solution, depending on the catechols used, has been reported:[13,14] $[FeCl(Cat)py_2]$ ($CatH_2$ = 3,5-di-*tert*-butylcatechol), $[FeCl_2(Cat)py]$ ($CatH_2$ = pyrocatechol, 4-methylcatechol, 4-chlorocatechol), $[FeCl_2(Cat)py_2]$ ($CatH_2$ = tetrachlorocatechol).

‡Although chlorophenol is reported to be more reactive than **1**, (ref. 12) we could not detect chlorocatechol in our conditions.

§ No product other than **1** has been detected, indicating that **2** and *tert*-butyl-1,2-benzoquinone **3** are converted to polymeric products.

## References


1 J. Haavik, K. K. Andersson, L. Petersson and T. Flatmark, *Biochim. Biophys. Acta*, 1988, **953**, 142.
2 I. Michaud-Soret, K. K. Andersson and L. Que Jr., *Biochemistry*, 1995, **34**, 5504.
3 K. K. Andersson, D. D. Cox, L. Que Jr., T. Flatmark and J. Haavik, *J. Biol. Chem*., 1988, **263**, 18621.
4 K. K. Andersson, C. Vassort, B. A. Brennan, L. Que Jr., J. Haavik, T. Flatmark, F. Gros and J. Thibault, *Biochem. J*., 1992, **284**, 687.
5 T. A. Dix, D. M. Kuhn and S. J. Benkovic, *Biochemistry*, 1987, **26**, 3354.
6 J. Haavik, B. Le Bourdelles, A. Martinez, T. Flatmark and J. Mallet, *Eur. J. Biochem*., 1991, **199**, 371.
7 P. F. Fitzpatrick, *Biochem. Biophys. Res. Commun*., 1989, **161**, 211.
8 K. K. Andersson, J. Haavik, A. Martinez, T. Flatmark and L. Petersson, *FEBS Lett*., 1989, **258**, 9.
9 J. Haavik, A. Martínez and T. Flatmark, *FEBS Lett*., 1990, **262**, 363.
10 P. F. Fitzpatrick, *Biochemistry*, 1991, **30**, 6386.
11 P. F. Fitzpatrick, *Biochemistry*, 1991, **30**, 3658.
12 N. Kitajima, M. Ito, H. Fukui and Y. Moro-oka, *J. Am. Chem. Soc*., 1993, **115**, 9335.
13 J. P. Hage and D. T. Sawyer, *J. Am. Chem. Soc*., 1995, **117**, 5617.
14 T. Funabiki, H. Kojima, M. Kaneko, T. Inoue, T. Yoshioka, T. Tanaka and S. Yoshida, *Chem. Lett*., 1991, 2143.
15 T. Funabiki, M. Ishikawa, Y. Nagai, J. Yorita and S. Yoshida, *J. Chem. Soc., Chem. Commun*., 1994, 1951.


*Received, 8th October 1996; Com. 6/06878B*

# Biosynthesis of ω-cyclohexyl fatty acids in *Alicyclobacillus acidocaldarius*: the stereochemistry of the initial 1,4-conjugate elimination

**Sandeep Handa and Heinz G. Floss***

*Department of Chemistry, Box 351700, University of Washington, Seattle, Washington 98195-1700, USA*

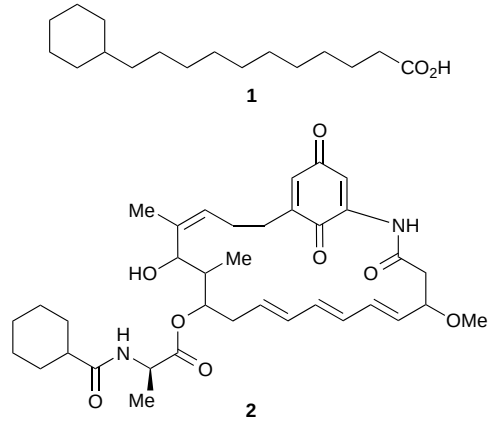
**The 1,4-conjugate elimination of $H_2O$ from shikimic acid 3, the initial step in the biosynthesis of ω-cyclohexyl fatty acids by the bacterium *Alicyclobacillus acidocaldarius*, has been shown to occur with an overall *anti* stereochemistry *via* loss of the *pro*-6*R* hydrogen of 3.**

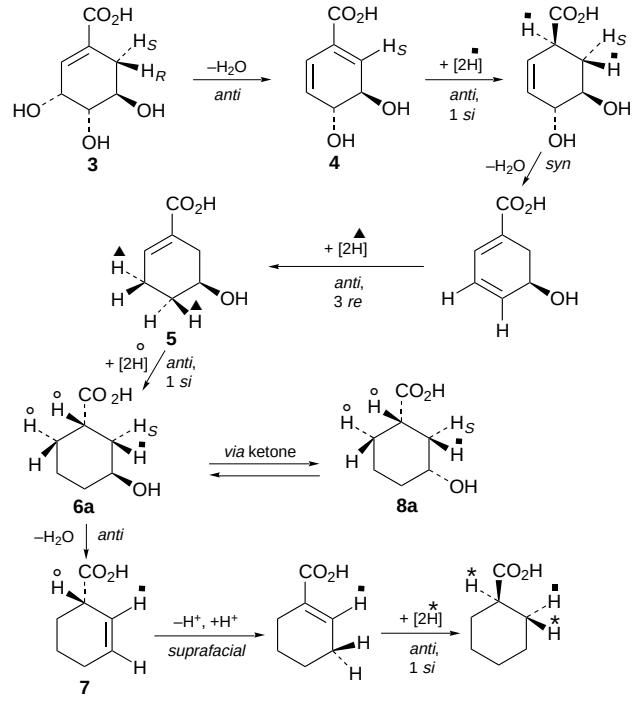
The thermoacidophilic bacterium *Alicyclobacillus acidocaldarius* (formerly *Bacillus acidocaldarius*) produces a series of ω-cyclohexyl fatty acids of which ω-cyclohexylundecanoic acid **1** is the most abundant.[1] It has been suggested that these unusual fatty acids have special physiological importance for the cells at the high temperatures and low pH at which they grow.[2] ω-Cyclohexyl fatty acids have also been isolated from the thermoacidophilic *A. acidoterrestis*[3] and the mesophilic *Curtobacterium pusillum*[4] and in all cases they are believed to arise *via* fatty acid biosynthesis from a cyclohexanecarboxylic acid starter unit (presumably as its coenzyme A thioester). This fully reduced cyclohexanecarboxylate moiety is relatively rare in nature although it is found attached, *via* a D-alanine unit, to the macrocycle of the ansamycin antibiotic ansatrienin A **2** produced by *Streptomyces collinus*.[5]

The biosynthesis of the cyclohexanecarboxylic acid moiety has been studied in *A. acidocaldarius*[6] and *S. collinus*[7] and it has been shown to arise from shikimic acid **3** *via* a series of dehydrations and double bond reductions such that no intermediate is ever aromatic. Previous studies have allowed us to delineate all the steps in the biosynthetic conversion and to establish the stereochemical course for all but one of the metabolic transformations. The biosynthetic pathway, which is common to both organisms, is shown in Scheme 1.

To date, however, the stereochemistry of the initial 1,4-conjugate elimination, resulting in the conversion of shikimic acid **3** to (3*R*,4*R*)-3,4-dihydroxycyclohexa-1,5-dienecarboxylic acid **4** by loss of an unactivated C-6 proton and the C-3 hydroxy group of **3**, has remained elusive. This is primarily due to the fact that both the C-6 protons of **3** are lost in the overall conversion to cyclohexanecarboxylic acid, thus obscuring the stereochemistry of the initial proton loss. This problem was overcome by the isolation of a blocked mutant of *A. acidocaldarius*[8] (designated as mutant 2) which is unable to convert the *trans*-3-hydroxycyclohexanecarboxylic acid intermediate **6a** to cyclohex-2-enecarboxylic acid **7**. This results in the accumulation of **6a**, isolated from the culture medium as its methyl ester **6b**,[6] and lower levels of its C-3 epimer *cis*-3-hydroxycyclohexanecarboxylic acid **8a** (again isolated as the corresponding methyl ester **8b**), postulated to arise from **6a** by a side reaction involving oxidation to the ketone and reduction with opposite stereochemistry.[6] Since both **6a** and **8a** contain the shikimate C-6 proton retained in the initial 1,4-conjugate elimination step, the *A. acidocaldarius* mutant 2 provided a system in which to investigate the stereochemistry of this elimination.

In order to synthesize the stereospecifically deuteriated (6*R*)-(−)-[6-$^2H_1$]shikimic acid **3a** required for these investigations, we decided to employ the route of Fleet,[9] as previously adapted by Zamir *et al.*[10] (Scheme 2). This adaptation allows for the stereospecific labelling to be introduced *via* enzymic reduction of the intermediate aldehyde **9a** (prepared from D-mannose) using horse liver alcohol dehydrogenase coupled to an $NAD^+$ recycling system employing [$^2H_6$]ethanol to supply the deuteride reducing equivalents. The intermediate alcohol **10a** thus produced was then taken through to **3a** as previously described.[9] We were also able use this strategy to synthesise (6*S*)-(−)-[6-$^2H_1$]shikimic acid **3b** *via* the corresponding enzymic reduction of the deuteriated aldehyde **9b** (prepared from **9a** by

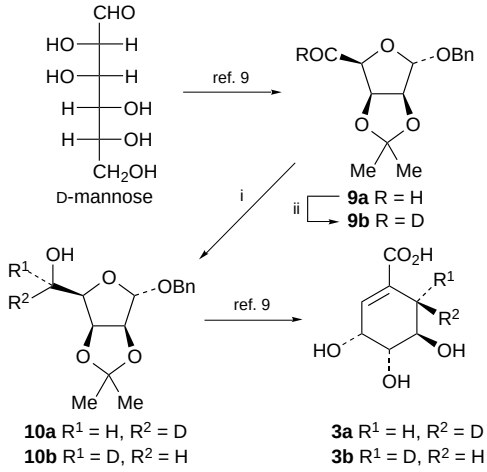



**Scheme 1**

an oxidation–reduction sequence) using unlabelled ethanol to supply the reducing equivalents.

With both specifically deuteriated shikimates **3a** and **3b** in hand feeding experiments were carried out with cultures of *A. acidocaldarius* mutant 2. The two accumulated intermediates **6a** and **8a** were isolated as their methyl esters **6b** and **8b**, employing similar conditions and experimental protocols to those previously described.[6] The isolated compounds were subsequently analysed by $^2$H NMR and two of the resulting spectra are shown in Fig. 1.




**Scheme 2** *Reagents*: i, Horse liver alcohol dehydrogenase, $NAD^+$, $C_2D_5OD$ (for **9a**), $C_2H_5OH$ (for **9b**); ii, $NaO_2Cl$, 2-methylbut-2-ene, $Bu^tOH$, $H_2O$, then $CH_2N_2$, $Et_2O$, then $LiAlD_4$, THF, then $Me_2SO$, $(COCl)_2$, $Pr^i_2EtN$, $CH_2Cl_2$

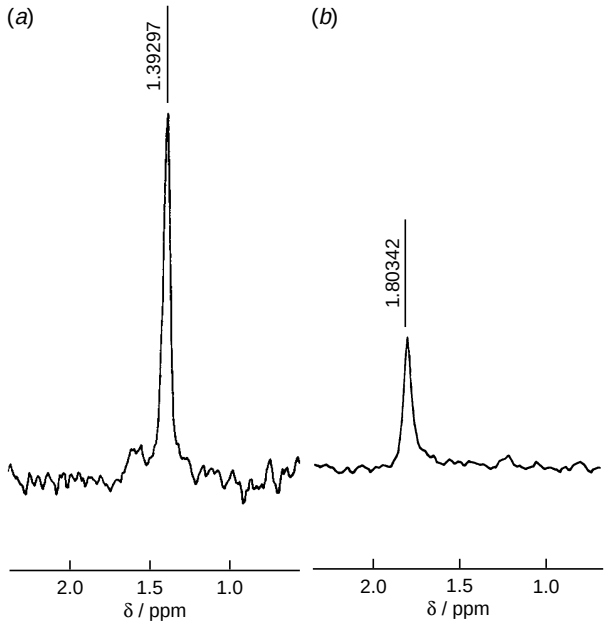



**Fig. 1** Partial 46.07 MHz $^2$H NMR spectra of (*a*) **8b** and (*b*) **6b** from the incorporation of (6*S*)-(−)-[6-$^2H_1$]shikimic acid **3b**. The spectra of **6b** and **8b** obtained from (6*R*)-(−)-[6-$^2H_1$]shikimic acid **3a** showed no signals in this region.

Previous studies[6] had already established that the proton retained in the initial 1,4-conjugate elimination from **3** occupies the *pro*-2*S* position in the acids **6a** and **8a** accumulated by the mutant organism. Furthermore, $^1$H NMR spectra of the corresponding methyl esters **6b** and **8b**, while not allowing definite identification of the signal attributable to this proton, had shown it to lie within a complex set of signals between δ 1.45–1.85 for the *trans*-isomer **6b** and between δ 1.15–1.45 or 1.78–1.96 for the *cis*-isomer **8b**.

Inspection of the $^2$H NMR spectra of **6b** and **8b** isolated from the feeding experiment with (6*S*)-(−)-[6-$^2H_1$]shikimic acid **3b** (Fig. 1) clearly shows that the deuterium label has been retained, giving rise to signals at δ 1.80 and 1.39 for **6b** and **8b**, respectively. The $^2$H NMR spectra of **6b** and **8b** isolated from the experiment with (6*R*)-(−)-[6-$^2H_1$]shikimic acid **3a** showed no discernible signals even after prolonged data accumulation.

Thus the results clearly indicate that it is the *pro*-6*R* hydrogen of shikimate that is lost in the initial 1,4-elimination step in the biosynthesis of cyclohexanecarboxylic acid by *A. acidocaldarius*. The elimination therefore occurs by an overall *anti* mechanism and as such mirrors exactly the analogous 1,4-elimination found in the 'normal' shikimate pathway involving the formation of chorismate from 5-enolpyruvylshikimate 3-phosphate.[11] While previous experiments[12] with *A. acidocaldarius* have shown that chorismate is not an intermediate on the biosynthetic pathway to cyclohexanecarboxylic acid, confirming divergence from the standard shikimate pathway prior to this stage, this new finding suggests that there may be a strong evolutionary relationship between the two metabolic processes, which share the feature of abstraction of an unactivated hydrogen. Additionally it removes the final stereochemical ambiguity of the biosynthetic pathway.

Further work will explore mechanistic aspects of this elimination (*e.g.* whether the hydroxy group is activated by phosphorylation prior to elimination, as is the case in the formation of chorismate) and will examine the stereochemistry of similar reactions in analogous biosynthetic pathways.

This work was supported by the U.S. National Institutes of Health through grant AI20264. We thank Mr Stefan Gröger for recording the NMR spectra.

## References

1 G. Darland and T. D. Brock, *J. Gen. Microbiol.*, 1971, **67**, 9.
2 M. DeRosa, A. Gambacorta, L. Minale and L. D. Bu'Lock, *J. Chem. Soc., Chem. Commun.*, 1971, 1334.
3 G. Deinhard, P. Blanz, K. Poralla and E. Altan, *Syst. Appl. Microbiol.*, 1987, **10**, 47.
4 K. Suzuki, K. Saito, A. Kawaguchi, S. Okuda and K. Komagata, *J. Gen. Appl. Microbiol.*, 1981, **27**, 261.
5 M. Damberg, P. Russ and A. Zeeck, *Tetrahedron Lett.*, 1982, **23**, 59.
6 B. S. Moore, K. Poralla and H. G. Floss, *J. Am. Chem. Soc.*, 1993, **115**, 5267.
7 B. S. Moore, H. Cho, R. Casati, E. Kennedy, K. A. Reynolds, U. Mocek, J. M. Beale and H. G. Floss, *J. Am. Chem. Soc.*, 1993, **115**, 5254.
8 W. Krischke and K. Poralla, *Arch. Microbiol.*, 1990, **153**, 463.
9 G. W. Fleet and T. K. M. Shing, *J. Chem. Soc., Chem. Commun.*, 1983, 849.
10 L. O. Zamir, C-D. Nguyen, S. W. Li, A. Nikolakakis and F. Sauriol, *J. Labelled Compd. Radiopharm.*, 1992, **31**, 875.
11 R. K. Hill and G. R. Newkome, *J. Am. Chem. Soc.*, 1969, **91**, 5893; D. K. Onderka and H. G. Floss, *J. Am. Chem. Soc.*, 1969, **91**, 5894.
12 B. S. Moore and H. G. Floss, *J. Nat. Prod.*, 1994, **57**, 382.

*Received, 18th October 1996; Com. 6/07122H*

# Highly functionalised monocyclic and bicyclic β-lactams *via* alkene metathesis

**Anthony G. M. Barrett,*[a] Simon P. D. Baugh,[a] Vernon C. Gibson,*[a] Matthew R. Giles,[a] Edward L. Marshall[a] and Panayiotis A. Procopiou[b]**

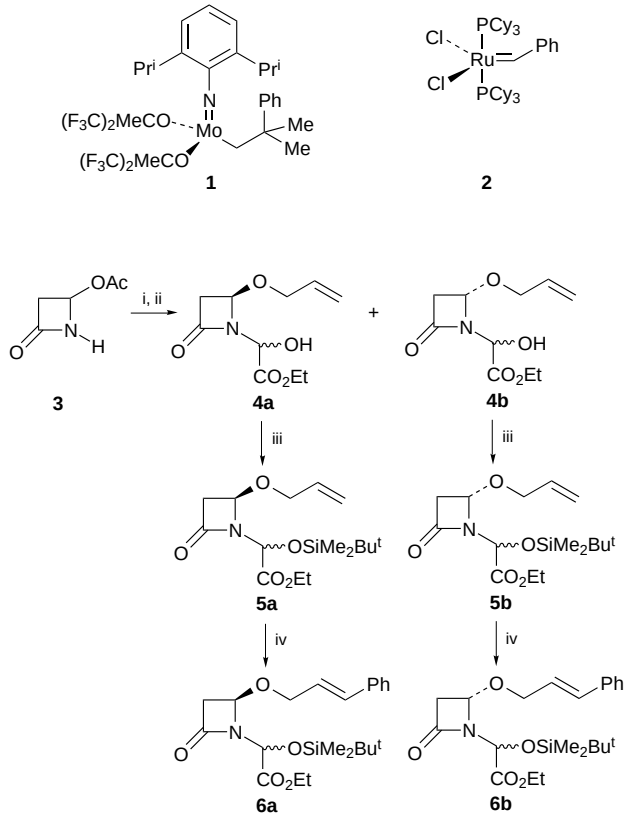
[a] *Department of Chemistry, Imperial College of Science, Technology and Medicine, London, UK SW7 2AY*
[b] *Department of Medicinal Chemistry, Glaxo Wellcome Research and Development Ltd, Gunnels Wood Road, Stevenage, Hertfordshire, UK SG1 2NY*

**Both monocyclic and bicyclic β-lactam systems are prepared *via* alkene metathesis reactions using Mo(=CHCPhMe$_2$)(=NC$_6$H$_3$Pr$^i_2$)[(OCMe(CF$_3$)$_2$]$_2$ or Ru(=CHPh)Cl$_2$(PCy$_3$)$_2$.**

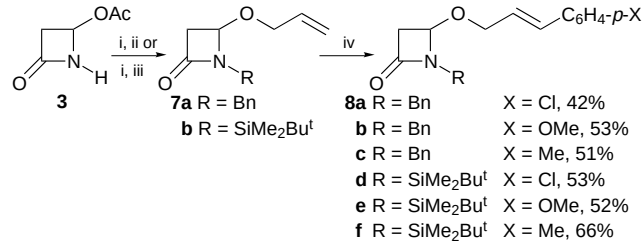
The elaboration of carbon skeletons *via* the construction of carbon–carbon bonds represents one of the most important endeavours in synthetic organic chemistry. Transition metal catalysed processes are especially valuable, particularly for the selective transformation of polyfunctional precursors into products of enhanced complexity. The pioneering work of Grubbs has shown that a wide variety of compounds may be synthesised *via* ring-closing metathesis (RCM) procedures[1] using molybdenum **1**[2] and ruthenium **2**[3] based catalysts. Other workers have extended this methodology which is now finding increasing use in synthesis.[4–8] Our group has recently shown that a number of previously unexplored systems are amenable to alkene metathesis.[9,10] In particular we have shown that β-lactams are well tolerated under metathesis conditions furnishing both mono- and bi-cyclic systems alike in good to excellent yields. Herein we report the extension of this work to the synthesis of more highly functionalised β-lactams.

Sequential reaction of the commercially available 4-acetoxyazetidin-2-one **3** with allyl alcohol and ethyl glyoxylate produced the diastereomeric alkenes **4a,b** (Scheme 1) which were separable by chromatography. Protection of **4a** and **4b** with *tert*-butyldimethylchlorosilane gave the metathesis substrates **5a,b**† in quantitative yield. In a similar manner treatment of 4-acetoxyazetidin-2-one **3** with allyl alcohol followed by benzyl bromide or *tert*-butyldimethylchlorosilane gave alkenes **7a** (69%) and **7b** (76%) respectively. Reaction of **5a** with excess styrene (4 equiv.) and a catalytic amount of carbene **1** (1 mol%) in dichloromethane at room temperature for 2 h produced the desired alkene **6a** (79%) (Scheme 1). Similarly epimer **5b** gave **6b** under the same conditions in comparable yield (67%). In all the cross metathesis processes reported herein only the *trans* double bond isomers were observed. We then explored a series of electronically diverse styrenes (*p*-Cl, *p*-OMe, *p*-Me) as the cross metathetic partners of protected β-lactams **7a** and **7b**. The reactions proceeded smoothly in the presence of **1** (1 mol%) to furnish *trans* alkenes **8a**–**f** (42–66%) (Scheme 2).

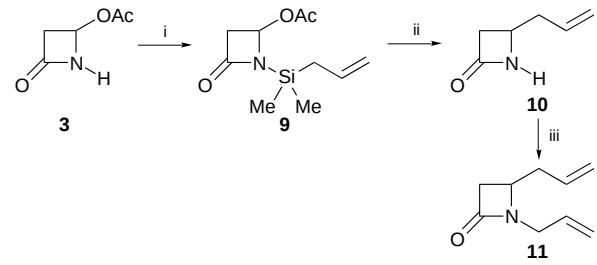
The synthesis of novel heteroatom-containing β-lactam substrates suitable for RCM were examined next. Following the procedure of Uyeo[11] a modified Sakurai-type reaction was utilised to synthesise 4-allylazetidin-2-one **10** (Scheme 3). Treatment of 4-acetoxyazetidin-2-one **3** with allylchlorodimethylsilane in the presence of an amine base followed by




**Scheme 1** *Reagents and conditions*: i, $HOCH_2CH{=}CH_2$, $Zn(OAc)_2$, PhH, heat, 4 h, 83%; ii, $H(O)CCO_2Et$, PhMe, heat 15 h, 79%; iii, Bu$^t$Me$_2$SiCl, DMAP, $CH_2Cl_2$, 25 °C, 2 d, 100%; iv, **1** (1 mol%), $PhCH{=}CH_2$, $CH_2Cl_2$, 25 °C

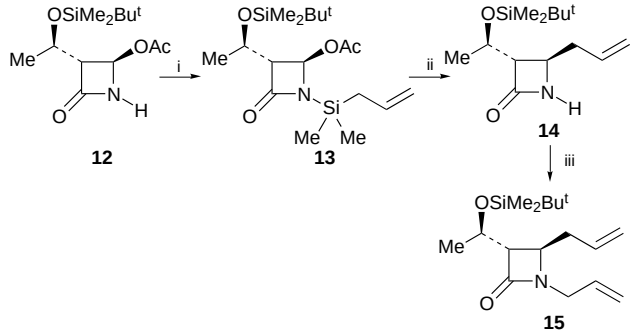



**Scheme 2** *Reagents and conditions*: i, $HOCH_2CH{=}CH_2$, $Zn(OAc)_2$, PhH, heat, 4 h, 83%; ii, $BrCH_2Ph$, NaH, DMF, 0 °C, 83%; iii, Bu$^t$Me$_2$SiCl, $NEt_3$, $CH_2Cl_2$, 0 °C, 92%; iv, **1** (1 mol%), *p*-X-$C_6H_4CH{=}CH_2$, $CH_2Cl_2$, 25 °C

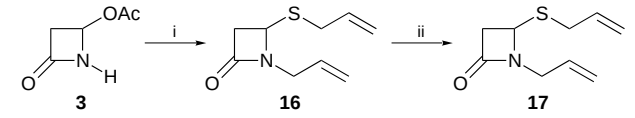



**Scheme 3** *Reagents and conditions*: i, $ClSiMe_2CH_2CH{=}CH_2$, $NEt_3$, $CH_2Cl_2$, 25 °C, 15 h, 85%; ii, $Me_3SiOTf$, $CH_2Cl_2$, 0 °C, 2 h, 71%; iii, $BrCH_2CH{=}CH_2$, KOH, 18-crown-6, PhH, 25 °C, 2 h, 77%

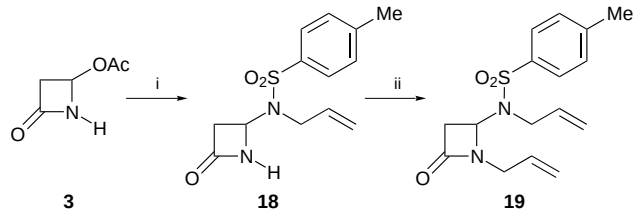
reaction with a catalytic quantity of trimethylsilyl trifluoromethanesulfonate ($Me_3SiOTf$) gave 4-allylazetidin-2-one **10** (59% over 2 steps). This proved to be rather unstable and was treated immediately with allyl bromide and potassium hydroxide to give the diene **11** (77%). In an analogous manner substrate **15** was synthesised, starting from commercially available (3*R*,4*R*)-3-[(*R*)-*tert*-butyldimethylsilyloxyethyl]azetidin-2-one **12** (Scheme 4, 46% over 3 steps). In this reaction sequence the $Me_3SiOTf$ mediated allyl transfer to produce **14** from **13** was a stereoselective process furnishing a single



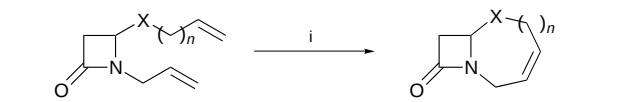

**Scheme 4** *Reagents and conditions*: i, $ClSiMe_2CH_2CH{=}CH_2$, $NEt_3$, $CH_2Cl_2$, 25 °C, 15 h, quant.; ii, $Me_3SiOTf$, $CH_2Cl_2$, 0 °C, 2 h, 91%; iii, $BrCH_2CH{=}CH_2$, KOH, 18-crown-6, PhH, 25 °C, 2 h, 92%




**Scheme 5** *Reagents and conditions*: i, $HSCH_2CH{=}CH_2$, NaOMe, MeOH, 25 °C, 90 min, 69%; ii, $BrCH_2CH{=}CH_2$, NaH, DMF, 0 °C, 1 h, 81%



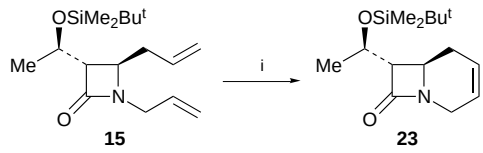

**Scheme 6** *Reagents and conditions*: i, *p*-$MeC_6H_4SO_2NHCH_2CH{=}CH_2$, KOBu$^t$, 18-crown-6, MeCN, 25 °C, 30 min, 67%; ii, $BrCH_2CH{=}CH_2$, NaH, DMF, 0 °C, 1 h, 89%




**11** X = $CH_2$, *n* = 0
**17** X = S, *n* = 1
**19** X = *p*-$MeC_6H_4SO_2N$, *n* = 1

**20** X = $CH_2$, *n* = 0
**21** X = S, *n* = 1
**22** X = *p*-$MeC_6H_4SO_2N$, *n* = 1

**Scheme 7** *Reagents and conditions*: i, X = $CH_2$, *n* = 0, **2** (5 mol%), $CH_2Cl_2$, 25 °C, 6 h, 81%; i, X = S, *n* = 1, **1** (5 mol%), $CH_2Cl_2$, 25 °C, 2 h, 78%: i, X = *p*-$MeC_6H_4SO_2N$, *n* = 1, **1** (5 mol%), $CH_2Cl_2$, 25 °C, 2 h, 91%




**Scheme 8** *Reagents and conditions*: i, **2** (5 mol%), $CH_2Cl_2$, 25 °C, 6 h, 78%

diastereomer. The novel diene **17** was obtained by sequential treatment of 4-acetoxyazetidin-2-one **3** with prop-2-enethiol and allyl bromide (Scheme 5, 56% over 2 steps). Alkene **19** was synthesised by reaction of 4-acetoxyazetidin-2-one **3** with *N*-tosylallylamine (67%) according to the procedure of Campbell and Connarty[12] followed by *N*-allylation of the resulting β-lactam **18** with allyl bromide (89%).

With the RCM substrates in hand, diene **11** was exposed to a catalytic quantity of ruthenium carbene **2** (5 mol%) in dichloromethane at room temperature. Diene **11** was rapidly converted into the bicyclic [2.4.0]carbacephem **20** in excellent yield (81%) (Scheme 7). In this and the other RCM processes (*vide infra*), only a single product component was evident by TLC analysis. In a similar manner diene **15** was converted into carbacephem **23** in high yield (Scheme 8, 78%). RCM of dienes **17** and **19** proceeded only slowly with ruthenium catalyst **2** (5 mol%) giving bicyclic lactams **21** and **22** in low isolated yield (22 and 36% respectively). However, replacement of the ruthenium catalyst **2** with the molybdenum catalyst **1** (5 mol%) resulted in rapid reactions leading to the isolation of homocephem **21** (78%) and homo-azacephem **22** in excellent yield (91%) (Scheme 7).

In conclusion we have shown that alkene metathesis is an extremely useful synthetic tool for the synthesis of highly functionalised monocyclic β-lactams and a variety of bicyclic β-lactams. The range of heteroatoms tolerated in the ring-closing metathesis reaction (C, O, N and S) suggests that this methodology should be of enormous use for the synthesis of a great range of antibiotics and their derivatives. The azacephem system is of particular interest as this is a relatively unexplored area. Recent work on azapenems has been published by Hegedus[13,14] and our work provides an alternative metal-mediated route to such systems.

We thank Glaxo Wellcome Research Ltd. for the most generous endowment (to A. G. M. B.) and for a CASE grant (to S. P. D. B.), the Wolfson Foundation for establishing the Wolfson Centre for Organic Chemistry in Medical Science at Imperial College, and the Engineering and Physical Science Research Council for a CASE grant (to S. P. D. B.).

## Footnote

† All new compounds were fully characterised spectroscopically and further by microanalysis and/or HRMS.

## References

1 G. C. Fu and R. H. Grubbs, *J. Am. Chem. Soc.*, 1992, **114**, 5426; O. Fujimura and R. H. Grubbs, *J. Am. Chem. Soc.*, 1996, **118**, 2499; Zuercher, M. Hashimoto and R. H. Grubbs, *J. Am. Chem. Soc.*, 1996, **118**, 6634.
2 R. H. Schrock, J. S. Murdzek, G. C. Bazan, J. Robbins, M. DiMare and M. O'Regan, *J. Am. Chem. Soc.*, 1990, **112**, 3875.
3 P. Schwab, M. B. France, J. W. Ziller and R. H. Grubbs, *Angew. Chem., Int. Ed. Engl.*, 1995, **34**, 2039.
4 W. E. Crowe and D. R. Goldberg, *J. Am. Chem. Soc.*, 1995, **117**, 5162.
5 S. F. Martin, H. J. Chen, A. K. Courtney, Y. Liao, M. Pätzel, M. N. Ramser and A. S. Wagman, *Tetrahedron Lett.*, 1996, **52**, 7251.
6 B. C. Borer, S. Deerenberg, H. Bieräugel and U. K. Pandit, *Tetrahedron Lett.*, 1994, **35**, 3191.
7 M. T. Crimmins and B. W. King, *J. Org. Chem.*, 1996, **61**, 4192.
8 M. Schuster, J. Permerstorfer and S. Blechert, *Angew. Chem., Int. Ed. Engl.*, 1996, **35**, 1979.
9 A. G. M. Barrett, J. C. Beall, V. C. Gibson, M. R. Giles and G. L. P. Walker, *Chem. Commun.*, 1996, 2229.
10 A. G. M. Barrett, S. P. D. Baugh, V. C. Gibson, M. R. Giles, E. L. Marhsall and P. A. Procopiou, *Chem. Commun.*, 1996, 2231.
11 S. Uyeo and H. Itani, *Tetrahedron Lett.*, 1991, **23**, 2143.
12 M. M. Campbell and B. P. Connarty, *Heterocycles*, 1982, **19**, 1853.
13 C. Betschart and L. S. Hegedus, *J. Am. Chem. Soc.*, 1992, **114**, 5010.
14 B. Ronan and L. S. Hegedus, *Tetrahedron*, 1994, **49**, 5549.

*Received, 28th October 1996; Com. 6/07308E*

# Structure of an amorphous polymer electrolyte, poly(ethylene oxide)$_3$ : LiCF$_3$SO$_3$

**Roger Frech,[a] Sangamithra Chintapalli,[a] Peter G. Bruce[b] and Colin A. Vincent[b]**

[a] *Department of Chemistry and Biochemistry, University of Oklahoma, Norman, Oklahoma 73019, USA*
[b] *School of Chemistry, University of St Andrews, St. Andrews, Fife, UK KY16 9ST*

**The amorphous phase formed on melting the crystalline polymer electrolyte PEO$_3$ : LiCF$_3$SO$_3$ has a short-range structure in which all of the lithium ions are located within the poly(ethylene oxide) helix.**

Polymer electrolytes are compounds formed by the dissolution of salts in polar high molar mass macromolecules which form strong interactions with cations. They form the basis of a new electrochemical technology which includes thin film all-solid-state lithium batteries. Electrolytes based on poly(ethylene oxide), PEO, may form crystalline or amorphous phases. A major advance has recently been made in establishing the structures of crystalline polymer electrolytes, but it is the amorphous materials which exhibit high ionic conductivity and it is therefore their structures which are of particular interest. By combining high-resolution IR spectroscopic studies of both crystalline and amorphous phases with the results of an X-ray diffraction analysis of the crystalline phase, we have established the structure of an amorphous polymer electrolyte consisting of a lithium salt, LiCF$_3$SO$_3$, dissolved in the high molecular mass PEO, such that there are three host oxygen atoms for each Li$^+$ ion present.

The structure of crystalline PEO$_3$ : LiCF$_3$SO$_3$ consists of a parallel array of separate PEO chains each associated with its own set of ions, in which each chain adopts a helical conformation.[1] A single lithium ion is located within each turn of the helix which is coordinated directly by three ether oxygens. The coordination environment around the Li$^+$ ion is completed by two further oxygens, one from each of two CF$_3$SO$_3^-$ anions thus forming a five-coordinate arrangement in an approximate trigonal-bipyramidal geometry. The CF$_3$SO$_3^-$ anions bridge neighbouring lithium ions by donating one of their oxygens to each of two lithiums, while the remaining oxygen of each CF$_3$SO$_3^-$ group is uncoordinated. The CF$_3$ groups sit outside the dimensions of the helix. The crystal structure does not change from −173 °C until the melting point at 179 °C.

In the molten phase there is no long-range order, as is evident from the absence of Bragg peaks.[2] It is clear from a study of vibrational spectra, however, that similar short-range order to that in the crystalline phase persists. Fig. 1 shows the symmetric stretching mode $\nu_s(SO_3)$ as a function of temperature. This mode is known to be affected by both changes in the ionic environment of CF$_3$SO$_3^-$ (*i.e.* by any alteration in neighbouring cation numbers or positions) and by variation in the way 'solvent' is coordinated to neighbouring cations.[3]

Distinct bands which appear in the IR spectra of low molar mass liquid PEO oligomer–LiCF$_3$SO$_3$ solutions in this region have been previously assigned as 'free' ions (1032 cm$^{-1}$), simple ion pairs (1041 cm$^{-1}$) and a more highly associated ionic species described as an ionic aggregate (1050 cm$^{-1}$), following the Raman spectra-based assignments of ref. 3. In the room-temperature IR spectrum of high molecular mass PEO$_3$ : LiCF$_3$SO$_3$ there is only a single band at 1046 cm$^{-1}$. It is seen that apart from the expected increase in bandwidth as the temperature is raised, the frequency shift of the band on melting is $< 1$ cm$^{-1}$.

IR spectra of PEO$_3$ : LiCF$_3$SO$_3$ are shown in Fig. 2 for the CF$_3$ symmetric deformation mode, $\delta_s(CF_3)$, over the temperature range 25–190 °C. This mode is particularly sensitive to variation in the ion association due to a shifting of the electron density between the CF$_3$ and the SO$_3$ ends of the anion as a result of association with a cation.[4] In this spectral region IR bands of oligomer–LiCF$_3$SO$_3$ solutions are assigned as 'free' ions (752 cm$^{-1}$), simple ion pairs (757 cm$^{-1}$), and an aggregate species (763 cm$^{-1}$). We will focus our attention on the $\delta_s(CF_3)$ region because of the more distinct frequency separation of the various triflate ion species in the PEO$_3$ : LiCF$_3$SO$_3$ compounds.

As in the case of $\nu_s(SO_3)$ there is only a single band in Fig. 2, at 760 cm$^{-1}$, which is assigned to the aggregate species. The lowering of this frequency from the value of 763 cm$^{-1}$ which is observed in liquid oligomer–LiCF$_3$SO$_3$ solutions is possibly due to packing effects in the crystalline state, *e.g.* from a decrease in the rotational or reorientational motion of the CF$_3$ groups. Knowledge of the crystal structure permits an unambiguous assignment of the $\nu_s(SO_3)$ mode and the $\delta_s(CF_3)$ mode shown in Figs. 1 and 2, respectively. These vibrational states arise from a CF$_3$SO$_3^-$ ion, two oxygen atoms of which bridge in a monodentate arrangement two Li$^+$ ions that lie adjacent to

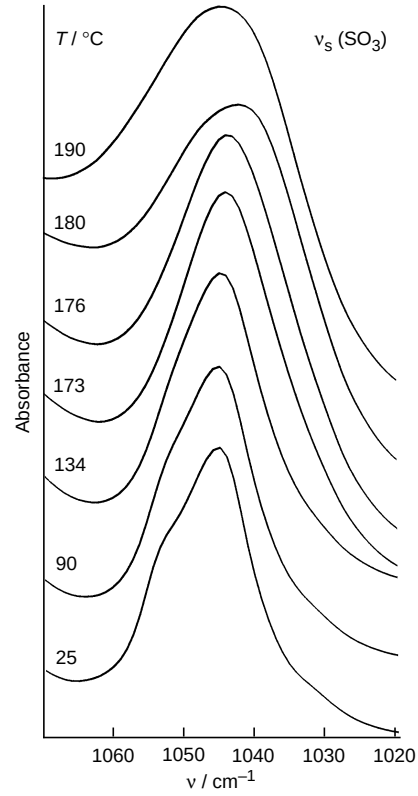



**Fig. 1** Symmetric stretching mode, $\nu_s(SO_3)$, as a function of temperature for poly(ethylene oxide)$_3$ : LiCF$_3$SO$_3$

each other within the polymer helix. Each anion is essentially a $[Li_2CF_3SO_3]^+$ species in terms of the vibrational modes of the $CF_3SO_3^-$ ion. This assignment is consistent with a study of $LiCF_3SO_3$ in acetone and poly(propylene oxide)[5] in which the highest frequency component in the $\nu_s(SO_3)$ spectral region was assigned to the isolated triple ion $[Li_2CF_3SO_3]^+$.

The frequency of the $\delta_s(CF_3)$ band does not change as the temperature is increased up to the onset of melting although thermal broadening of the band is apparent. Above the melting point there is a broad feature centred at 763 $cm^{-1}$, which is the frequency expected for a $[Li_2CF_3SO_3]^+$ species. The question arises: what is the nature of the $[Li_2CF_3SO_3]^+$ species? They cannot be individual, isolated $[Li_2CF_3SO_3]^+$ triple ions as have been previously observed in the oligomer–$LiCF_3SO_3$ solutions with somewhat lower salt concentrations,[6] since the presence of such moieties would necessarily require the presence of 'free' $CF_3SO_3^-$ ions on charge balance considerations. These would in turn give rise to a band at 752–753 $cm^{-1}$, and no absorption can be observed in this region. In principle, the charge balance might also be satisfied by a $[Li(CF_3SO_3)_2]^-$ species, which would be observed spectroscopically at *ca.* 757 $cm^{-1}$. There is indeed a shoulder at 180 °C (but not, apparently, at higher temperatures) which might correspond to such a species, but its intensity is very weak in comparison with the $[Li_2CF_3SO_3]^+$ band and hence is considered to be of minor importance.

Vibrational bands in the 800–1000 $cm^{-1}$ region are due to a mixture of $CH_2$ rocking and C–O stretching and are very sensitive to the local conformation of the polyether backbone.[7] We observe no major shift in the frequency of these modes between the spectrum of the highest temperature crystalline phase and the amorphous phase, suggesting that the basic lithium–polyether backbone interaction does not alter when the crystals melt.

We therefore conclude that the majority species is $[Li_2CF_3SO_3]^+$ and that in the absence of significant quantity of $CF_3SO_3^-$ or $[Li(CF_3SO_3)_2]^-$, this must be present in the amorphous phase largely as part of an extended ionic chain as in the crystal.

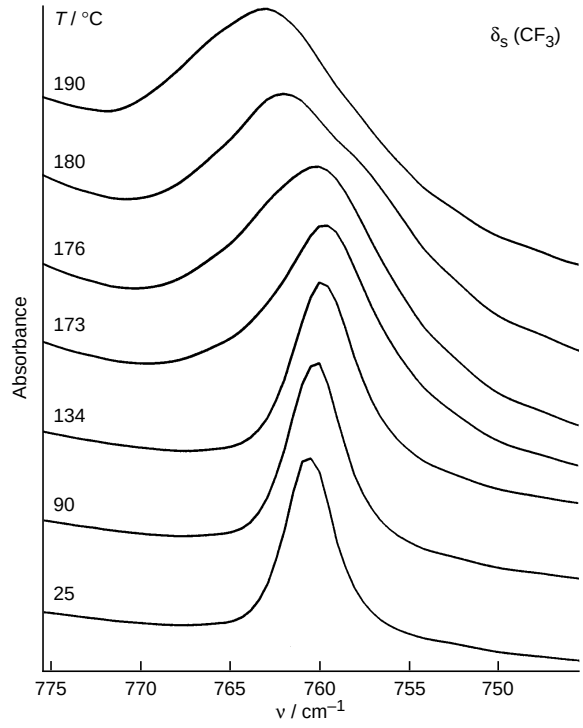



**Fig. 2** Symmetric deformation mode, $\delta_s(CF_3)$, as a function of temperature for poly(ethylene oxide)$_3$ : $LiCF_3SO_3$

It is evident that the structure of the amorphous phase is very similar to that of the crystalline state, with only a loss of long-range order arising from a loss of register between adjacent PEO chains and some disordering in the helical torsion angles. In particular each chain remains intact with its associated ions: *i.e.* every chain is associated with a dedicated set of cations and anions which do not bond to any of the other chains. In this sense each chain forms an isolated, infinitely long, coordination complex. Interchain interactions are only of the dipole–dipole or van der Waals type and are thus of second-order compared with the intrachain interactions. There is no evidence of cation or anion cross-linking between chains.

It seems unlikely, given the absence of interchain ionic cross-links at the high concentration of 3 : 1, that these would be present to any significant extent in amorphous phases with lower salt content. Beginning at a low salt concentration and then increasing the salt content will load each chain with ions and increase the intrachain cross-link density thus reducing segmental motion, raising $T_g$ and suppressing the ionic conductivity, as has been suggested in a recent study based on a detailed analysis of the polymer dynamics by NMR.[8] The consequences of the assertion that interchain cross-links are of minor significance in amorphous polymer electrolytes at higher oxygen/salt ratios (*i.e.* in phases which may be useful in an electrochemical device) will be considered elsewhere.[9]

It is tempting to speculate that the $Li^+$ ions may be transported along the chains while remaining within the helix, as suggested by Armand *et al.*[10] nearly twenty years ago. It is known that the polymer chain dynamics are intimately linked to the ionic motion, and it is therefore likely that the $Li^+$ ions would be 'handed-on' from coil to coil by an appropriate dynamic mode of the polymer, *e.g.* a concertina motion along the axis of the helix. A perfect 3 : 1 structure would have a lithium ion in every coil and conductivity would, as a result, not be possible. However, some defects ($Li^+$ vacancies) are likely which, although below the level that may be detected by the spectroscopic methods, are sufficient to endow the polymer with some conductivity. At lower salt concentrations (*i.e.* higher PEO : salt ratios) there will, of course, be a substantial proportion of $Li^+$ ion vacancies in the PEO coils. It is important to note also that for long-range ion transport (*e.g.* d.c. conductivity) it will be necessary to include interchain lithium ion transfer in the overall mechanism, since as we have argued, there is no significant centre-of-gravity motion of the polymer chains for host molecules above the entanglement limit.

## References


1 P. Lightfoot, M. A. Mehta and P. G. Bruce, *Science*, 1993, **262**, 883.
2 J. B. Thomson, Ph.D. Thesis, University of St Andrews, 1996.
3 G. Petersen, P. Jacobsson and L. M. Torell, *Electrochim. Acta*, 1992, **37**, 1495.
4 W. Huang, R. Frech and R. A. Wheeler, *J. Phys. Chem*., 1994, **98**, 100.
5 J. R. Stevens and P. Jacobsen, *Can. J. Chem*., 1991, **69**, 1980.
6 W. Huang and R. Frech, *Polymer*, 1994, **35**, 235.
7 H. Matsuura and K. Fukuhara, *J. Polym. Sci. B*, 1986, **24**, 1383.
8 M. E. Ries, M. G. Breeton, J. M. Cruickshank, P. G. Klein and I. M. Ward, *Macromolecules*, 1995, **28**, 3282.
9 R. Frech, S. Chintapalli, P. G. Bruce and C. A. Vincent, to be published.
10 M. B. Armand, J. M. Chabagno and M. Duclot, *Second International Meeting on Solid Electrolytes*, St. Andrews, Scotland, 1978, extended abstracts 6.5.


*Received, 10th September 1996; Com. 6/06264D*

# Highly defined pore size distribution in sol–gel silicate glasses induced by incorporation of an oligomeric siloxane

**Nico A. J. M. Sommerdijk, Ernst R. H. van Eck and John D. Wright***

*Centre for Materials Research, University of Kent, Canterbury, Kent, UK CT2 7NH*

**Doping of sol–gel derived tetramethoxysilane (TMOS) glasses with small amounts of octaphenylcyclotetrasiloxane (OPCTS) induces a remarkably narrow pore size distribution.**

The use of sol–gel techniques for the preparation of silicates employing surfactant aggregates as templates has opened the way to a range of possible applications of these well defined mesoporous materials.[1,2] Using surfactant aggregates displaying hexagonal,[1] cubic,[2] and lamellar[3] phases, highly ordered silicate materials with predefined pores could be obtained. Organically modified alkoxysilane precursors (ormosils) can also be used to modify the pores in sol–gel derived silica materials, but this does not lead to a better definition of the shape and size of the pores.[4,5] However, by the incorporation of non-crosslinking oligosiloxane units of defined size into the inorganic polymer network, better definition of the pore size may be achieved without the use of relatively large quantities of organic materials, and without the need for their removal.

The hydrolytic ring-opening of octaphenylcyclotetrasiloxane (OPCTS) **1** provides well defined ormosil units which may be incorporated into a silicate network. The resulting octaphenyltetrasiloxanediol (OPTSD) units would then provide segments of defined length which could be used to tailor the pore size in these mesoporous materials.

The ring-opening hydrolysis reaction of OPCTS should be carried out preferably in the presence of an excess of prehydrolysed TMOS in order to ensure reaction of the terminal OH groups of OPTSD with the sol–gel network and prevent polysiloxane formation. However, it was not possible to perform this reaction under standard hydrolysis conditions due to precipitation of the apolar OPCTS in aqueous media. This problem was circumvented by adding a 1 : 1 (*v*/*v*) mixture of thf and concentrated hydrochloric acid to a stirred thf solution of TMOS and OPCTS at 50 °C.† Nevertheless, no more than 10 mol% (based on silicon) could be added to the mixture without immediate precipitation. Gelation of the mixture occurred within 2 h and the gel was kept at 50 °C in a sealed vessel for 16 h. After ageing for two weeks at room temperature, small needle-shaped crystals had formed inside the transparent material. The crystalline material was removed by dissolution in thf followed by recrystallisation. Powder diffraction experiments demonstrated that they consisted of OPTSD. The glassy gels were washed with ethanol to remove remaining acid and aged for two more weeks. The diffraction patterns of the powdered ormosil revealed that washing had removed all the crystalline material and that the resulting glass was completely amorphous.

The glasses were transparent. However, drying in air or exposure to water turned them into opaque materials. Glasses prepared without the addition of OPCTS remained transparent upon exposure both to air and water.

The incorporation of ring-opened OPCTS units into the sol–gel network was examined using FTIR and solid-state $^{29}$Si NMR spectroscopy.‡ Comparison of both the FTIR and NMR spectra obtained for the ormosil with those obtained from a reference material prepared without OPCTS revealed that diphenylsiloxane units were incorporated into the new material. Both spectroscopic techniques showed furthermore that the presence of diphenylsiloxane units in the ormosil did not merely arise from entrapped OPTSD, but that it was chemically incorporated in the silica network.

Comparison of the FTIR spectra of the ormosil with those obtained from OPTSD revealed shifts to higher wavenumbers for two of the Si–Ph vibrations, from 741.7 to 744.5 and from 718.2 to 719.3 cm$^{-1}$, respectively,§ indicating restricted conformational motions of the OPTSD units due to incorporation in the silicate network. More concrete evidence was obtained from the solid-state NMR experiments which revealed that condensation with the silicate network must have been complete since the resonance at $\delta$ −39.6, assigned to the terminal $D_1$ unit[6] of OPTSD, was no longer present in the $^{29}$Si NMR spectrum of the ormosil (Fig. 1).¶

The pore size distribution of the ormosil was determined using thermoporometry[7,8] and compared to the pore size distribution found in the reference material. The results presented in Fig. 2 show that the addition of a small amount of OPCTS has a dramatic effect on the porosity of the material. The ormosil has small pores with diameters distributed over a range of 4–10 nm (*i.e.* a distinctly wider range than in the

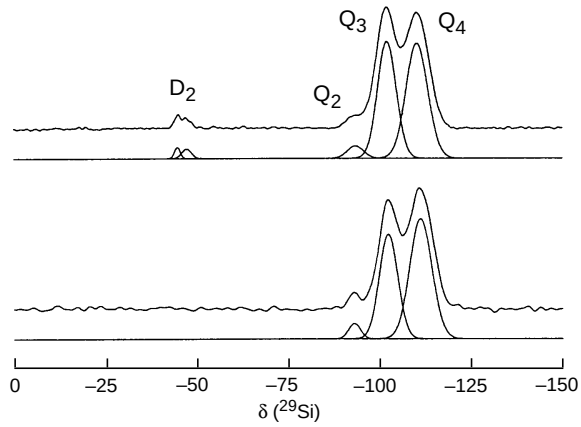
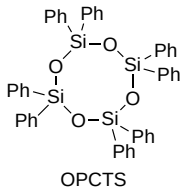
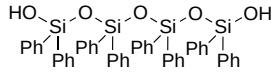



**Fig. 1** $^{29}$Si solid-state NMR spectra of sol–gel glasses prepared from 100% TMOS (lower trace) and from a 96 : 4 mixture (based on Si) of TMOS and OPCTS (upper trace). Gaussian fits are shown below each trace. The spectra were obtained at 59.665 MHz with single-pulse excitation at a MAS frequency of 5.0 kHz using high-power proton decoupling and a relaxation delay of 300 s.




OPCTS




OPTSD

reference compound) and also another type of pores with diameters of approximately 4.5 nm and a very narrow size distribution range. This result shows that incorporation of OPCTS modifies the overall network structure in the host material as well as generating new, sharply defined pore structures.

Remarkably, the $^{29}$Si NMR spectra (Fig. 1) reveal that only 1 mol% of OPTSD is incorporated into the sol–gel network. It is also clear from Fig. 1 that incorporation of OPTSD units causes only a small decrease in the functionality of the Q atoms (the average number of Si–O–Si bonds per Q atom) from 3.503 ± 0.008 to 3.470 ± 0.007. This change is due to an increase in the relative amount of $Q_3$ atoms (from 40 to 45%) and a decrease in $Q_4$ atoms (from 55 to 51%). The number of Si–O–Si links between OPTSD and the silicate network is not sufficient to explain this change in functionality or the dramatic changes in pore size distribution. However, the OPTSD modifies the overall network in other ways (*e.g. via* steric effects) as well as by changes in the type of linkages. Full understanding of these effects requires further experiments using similar modifiers with different substituents, which are in progress.

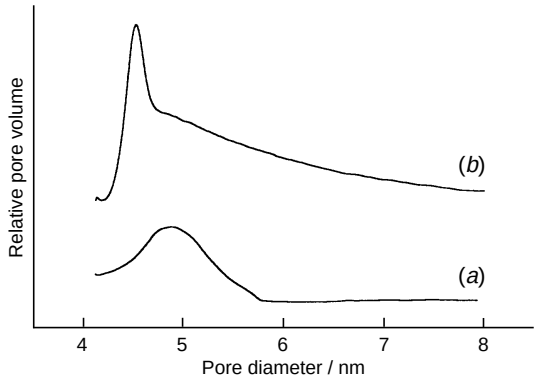



**Fig. 2** Pore size distributions of sol–gel glasses prepared from 100% TMOS (*a*) and from a mixture of TMOS and OPCTS (4% based on Si) (*b*) determined from thermoporometry experiments[7,8]

We would like to thank Drs R. H. Cragg and M. E. Smith for helpful discussions, and gratefully acknowledge the University of Kent for its strong support of NMR facilities.

## Footnotes

† Comparison of powder diffraction patterns of OPCTS before and after hydrolysis indicated that ring opening was complete when the described procedure was applied.

‡ Solid-state $^{29}$Si NMR experiments were performed using a Chemagnetics CMX 300 Infinity spectrometer, using magic angle spinning and proton decoupling.

§ Similar but reversed spectral changes are observed upon ring opening of OPCTS which leads to a shift of the same Si–Ph vibrations from 742.5 to 741.7 and from 720.3 to 718.2 $cm^{-1}$, respectively. These shifts to lower wavenumbers were interpreted as an increase in conformational motion due to a released ring strain.

¶ The notations $D_n$ and $Q_n$ are used to describe the chemical environment of silicon atoms which could form two and four possible Si–O–Si bonds, respectively. The number of bonds actually present is represented by *n*.

## References

1 C. T. Kresge, M. E. Leonowicz, W. J. Roth, J. C. Vartuli and J. S. Beck, *Nature*, 1992, **359**, 710.
2 J. S. Beck, J. C. Vartuli, W. J. Roth, M. E. Leonowicz, C. T. Kresge, K. G. Schmitt, C. T.-W. Chu, D. H. Holson, E. W. Sheppard, S. B. McCullen, J. B. Higgins and J. L. Schlenker, *J. Am. Chem. Soc.*, 1992, **114**, 10834.
3 P. T. Tanev and J. T. Pinnavaia, *Science*, 1996, **271**, 1267.
4 B. Lintner, N. Arfsten, H. Dislich, H. Schmidt, G. Philipp and B. Seiferling, *J. Non-Cryst. Solids*, 1988, **100**, 378.
5 J. D. MacKenzie and Y. Hu, *J. Mater. Sci.*, 1992, **27**, 4415.
6 D. Hoebbel, T. Reinert and H. Schmidt, *J. Sol–Gel Sci. Technol.*, 1996, **6**, 139.
7 M. Brun, A. Lallemand, J. F. Quinson and C. Eyraud, *Thermochim. Acta*, 1977, **21**, 59.
8 K. Ishikiriyama, M. Todoki and K. Motomoru, *J. Colloid Interface Sci.*, 1995, **171**, 92.

*Received, 5th November 1996; Com. 6/07518E*

# Amphoteric surfactant templating route for mesoporous zirconia

**Anthony Kim,* Paul Bruinsma, Yuan Chen, Li-Qiong Wang and Jun Liu**

*Pacific Northwest National Laboratory, Richland, Washington, 99352, USA*

**An amphoteric surfactant templating route permits the synthesis of hexagonal mesophases of zirconium compounds by self-assembly of the surfactant and soluble zirconium species in aqueous solution.**

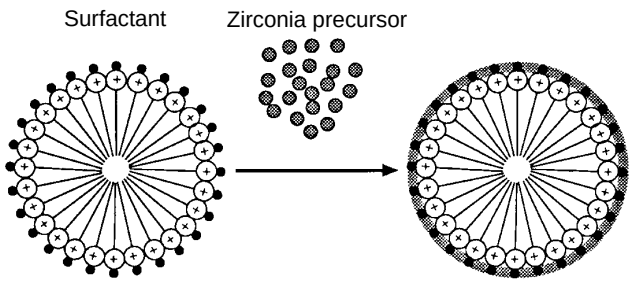
The invention of mesoporous silica molecular sieves[1,2] has generated wide interest in the synthesis of mesoporous materials based on self-assembly of ordered, surfactant/inorganic structures. Routes based on ionic,[1–4] hydrogen,[5,6] and covalent bonding[7–9] between the surfactant and the inorganic have been developed for the synthesis of mesoporous silica and other metal oxides. Previously, mesoporous zirconia has been produced; however, these methods involve expensive alkoxides,[10] rely on sulfate ion to link the surfactant and zirconium,[11,12] or do not involve self-assembly.[13,14] Here, we report a new synthesis route based on self-assembly of a soluble zirconia precursor and an amphoteric surfactant template. The amphoteric surfactant, cocamidopropyl betaine (CAPB), has quaternary ammonium and carboxylate functionalities for the head group and can therefore bond with both negatively and positively charged inorganic species. In contrast to quaternary ammonium surfactant routes,[11,12] CAPB does not require a bridging anion for the formation of the surfactant–Zr complex. CAPB also has the advantage of high solubility over wide ranges of pH and ionic strength[15] and may therefore find use in a variety of syntheses.

The proposed amphoteric surfactant templating route is shown in Scheme 1. Under the low pH conditions of the reaction, the quaternary ammonium group of CAPB is positively charged, and the carboxylate group is initially protonated.[16] Positively charged inorganic species attach to the surfactant by reaction with the carboxyl group. Concurrent surfactant bonding with the inorganic and aggregation of the micellar structures leads to formation of the hexagonal mesophase. The quaternary ammonium group serves two purposes: (*i*) it imparts high solubility for the otherwise insoluble carboxylic acid and (*ii*) it helps to ensure a large head-group area necessary for the formation of the rod-shaped micellar subunits of the hexagonal phase.[17]

The hexagonal mesophase was prepared from zirconyl chloride octahydrate (Aldrich Chemical), cocamidopropyl betaine (Amphosol CG, 30 mass%, Stepan Co.) and water, as follows. CAPB was purified of NaCl by ion exchange to pH = 2.6. Aqueous 0.25 M $ZrOCl_2$ was combined with CAPB until the Zr/CAPB mole ratio was 0.8. After reaction at 70 °C for four days the product was recovered by filtration.

Powder X-ray diffraction (XRD, Cu-K$\alpha$ radiation) of the as-synthesized mesophase (Fig. 1) revealed a primary (100) reflection corresponding to 41 Å and a secondary (110) reflection of the hexagonal phase. Higher order peaks of the hexagonal mesophase were unresolved, in part because of a broad peak centred at 2$\theta$ *ca*. 5.2°. This broad peak suggests that the walls of the mesostructure are made up of amorphous zirconium hydrate, since the peak approximately corresponds to a *d*-spacing of 17 Å, the average distance between zirconium centres in crystalline hydrates.[18] Other evidence for tetrameric species is given by three more broad peaks centred at 2$\theta$ *ca*. 27, 42 and 58° (XRD not shown) which correspond to zirconium tetramers in solution.[19] Transmission electron microscopy (TEM) of as-synthesized mesophase (Fig. 2) confirmed the formation of the hexagonally packed mesostructure. The 42 Å repeat distance from TEM agrees well with $d_{100}$ = 41 Å from XRD.

Bonding between the surfactant and zirconium precursor was probed by solution $^{13}C$ NMR spectroscopy. Betaine [(carboxymethyl)trimethylammonium hydroxide, Aldrich Chemical] was used to model the interactions of the surfactant head-group with zirconium species during the early stages of mesophase formation. The use of betaine in place of CAPB prevented precipitation, allowing the collection of simplified high-resolution solution NMR spectra (Fig. 3). Chemical shifts were referenced to dioxane ($\delta$ 67.4). Betaine on its own [pH adjusted to 1.3 with HCl, Fig. 3(*a*)] showed three distinct peaks: one at $\delta$ 54.00 corresponding to the methyl carbons, one at $\delta$ 63.63 corresponding to the methylene carbon and one at $\delta$ 167.03 corresponding to the carbon of the carboxyl group. Addition of zirconyl chloride [Zr/betaine molar ratio = 1, pH = 1.3, Fig. 3(*b*)] caused peak shifts for the carboxyl carbon ($\delta$ 2.04) and methylene carbon ($\delta$ 1.45). A previous study has shown that the carboxyl carbon peak shifts to lower field upon deprotonation (increasing pH).[20] Since the pH values were the same for the zirconium–betaine and betaine solutions, the significant peak shift is mainly caused by the interaction of the carboxylate




**Scheme 1** Proposed amphoteric surfactant templating route for hexagonal mesophase formation where the carboxylate group provides for the bonding of the surfactant with the inorganic species and the quaternary ammonium group maintains a large head-group area for hexagonal mesophase formation

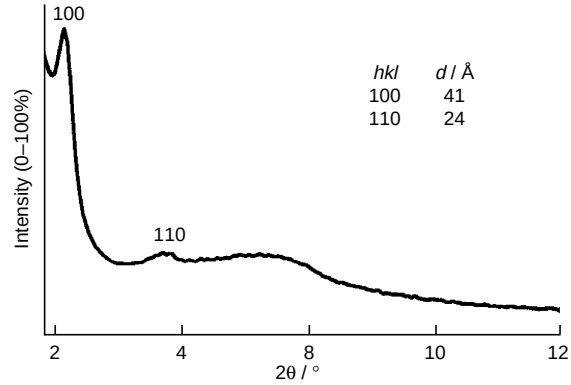



**Fig. 1** Powder X-ray diffraction pattern of the zirconyl chloride hexagonal mesophase showing the 100 and 110 reflections of a hexagonal lattice

group with the zirconium species. Furthermore, bonding between the carboxylate group and zirconium species is supported by a decrease in mobility, as indicated by the broadening of the carboxylate and methylene peaks. Multiple carboxylate peaks suggest a variety of bonding conformations in the betaine–zirconium complex. Peak shifting and broadening of the methyl carbon peak by zirconyl chloride were insignificant, indicating that the quaternary ammonium group does not bond with the zirconium species.

As-synthesized hexagonal mesophases prepared by the amphoteric surfactant templating route showed poor thermal stability. Calcination caused the (100) reflection of the hexagonal mesophase prepared from zirconium sulfate to shift to higher angle, indicating shrinkage of the mesostructure. Concurrently, higher order reflections of the hexagonal mesophase disappeared. Such loss of long-range order occurred as structural water, counter ions, and surfactant were removed simultaneously during calcination. These problems might be solved by innovative methods for removing the surfactant template and condensing the oxide precursors.[8,9] For example, controlled base treatment with NaOH proved to be efficient at removing the counter ions without destroying the mesostructure. Base-treated zirconium sulfate mesophase had surface areas of 130 $m^2\ g^{-1}$ after calcination at 350 °C and 40 $m^2\ g^{-1}$ after calcination at 450 °C, as compared to $< 5\ m^2\ g^{-1}$ for calcined, as-synthesized material.

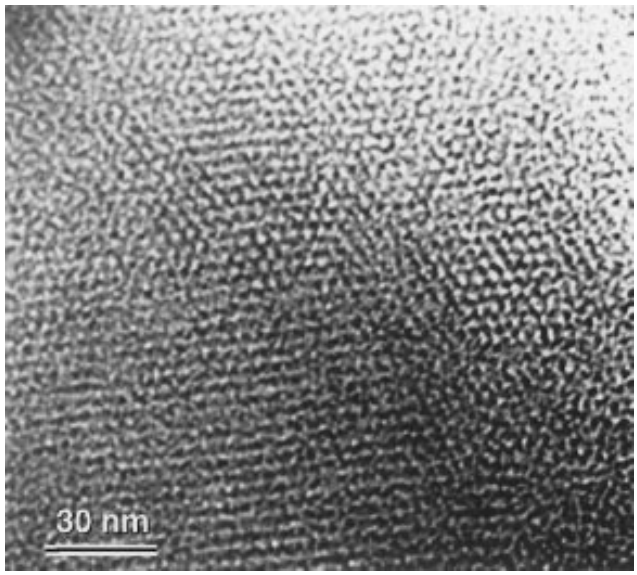



**Fig. 2** Transmission electron micrograph of the zirconyl chloride hexagonal mesophase produced by the amphoteric surfactant templating route showing the 42 Å repeat distance

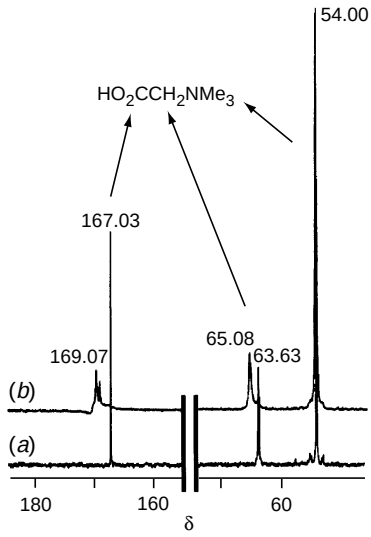



**Fig 3** Solution $^{13}C$ NMR spectra of betaine, pH adjusted to 1.3 (*a*) and of the betaine–zirconyl chloride complex; (*b*) Zr–betaine mole ratio = 1, pH = 1.3

In summary, an amphoteric surfactant templating method has been developed for the self-assembly of hexagonal mesophase zirconium compounds. Cocamidopropyl betaine provides the appropriate head-group area, solubility and chemical bonding to produce a hexagonal mesophase from aqueous solution. The quaternary ammonium group ensures large head-group area and high solubility, while the carboxylate group chemically attaches the precursor to the surfactant. Bifunctional surfactants, such as CAPB, offer new possibilities in mesoporous syntheses, particularly those involving cationic inorganic species.

This work was performed at Pacific Northwest National Laboratory, a multiprogram national laboratory operated by Battelle Memorial Institute for the US Department of Energy under contract DE-AC06-76RLO 1830. The authors greatly appreciate the X-ray diffraction work performed by D. E. McCready.

## References

1 C. T. Kresge, M. E. Leonowicz, W. J. Roth, J. C. Vartuli and J. S. Beck, *Nature*, 1992, **359**, 710.
2 J. S. Beck, J. C. Vartuli, W. J. Roth, M. E. Leonowicz, C. T. Kresge, K. D. Schmitt, C. T.-W. Chu, D. H. Olson, E. W. Sheppard, S. B. McCullen, J. B. Higgins and J. L. Schlenker, *J. Am. Chem. Soc.*, 1992, **114**, 10834.
3 Q. Huo, D. I. Margolese, U. Ciesla, D. G. Demuth, P. Feng, T. E. Gier, P. Sieger, A. Firouzi, B. F. Chmelka, F. Schüth and G. D. Stucky, *Chem. Mater.*, 1994, **6**, 1176.
4 Q. Huo, D. I. Margolese, U. Ciesla, P. Feng, T. E. Gier, P. Sieger, R. Leon, P. M. Petroff, F. Schüth and G. D. Stucky, *Nature*, 1994, **368**, 317.
5 P. T. Tanev and T. J. Pinnavaia, *Science*, 1995, **267**, 865.
6 S. A. Bagshaw, E.Prouzet and T. J. Pinnavaia, *Science*, 1995, **269**, 1242.
7 D. M. Antonelli and J. Y. Ying, *Angew. Chem., Int. Ed. Engl.*, 1995, **34**, 2014.
8 D. M. Antonelli and J. Y. Ying, *Chem. Mater.*, 1996, **8**, 874.
9 D. M. Antonelli and J. Y. Ying, *Angew. Chem., Int. Ed. Engl.*, 1996, **35**, 426.
10 M. S. Wong, D. M. Antonelli and J. Y. Ying, *Proc. Fifth World Cong. Chem. Eng.*, 1996, 549.
11 J. S. Reddy and A. Sayari, *Catal. Lett.*, 1996, **38**, 219.
12 F. Schüth, *Ber. Bunsen-Ges. Phys. Chem.*, 1995, **99**, 1306.
13 J. A. Knowles and M. J. Hudson, *J. Chem. Soc., Chem. Commun.*, 1995, 2083.
14 M. J. Hudson and J. A. Knowles, *J. Mater. Chem.*, 1996, **6**, 89.
15 E. G. Lomax, in *Amphoteric Surfactants*, ed. E. G. Lomax, Marcel Dekker, New York, 1996, ch. 1.
16 X. Domingo, in *Amphoteric Surfactants*, ed. E. G. Lomax, Marcel Dekker, New York, 1996, ch. 3.
17 J. N. Israelachvili, *Intermolecular and Surface Forces*, Academic Press, San Diego, 1992, pp. 380–382.
18 A. Clearfield and P. A. Vaughan, *Acta Crystallogr.*, 1956, **9**, 555.
19 G. M. Muha and P. A. Vaughan, *J. Chem. Phys.*, 1960, **33**, 194.
20 *Tables of Spectral Data for Structure Determination of Organic Compounds*, ed. E. Pretsch, T. Clerc, J. Seibl and W. Simon, Springer-Verlag, New York, 1989, C205.

*Received, 2nd July 1996; Com. 6/04578B*

# Synthetic ribofuranose-containing polymers show catalytic activity in the hydrolysis of phosphodiesters

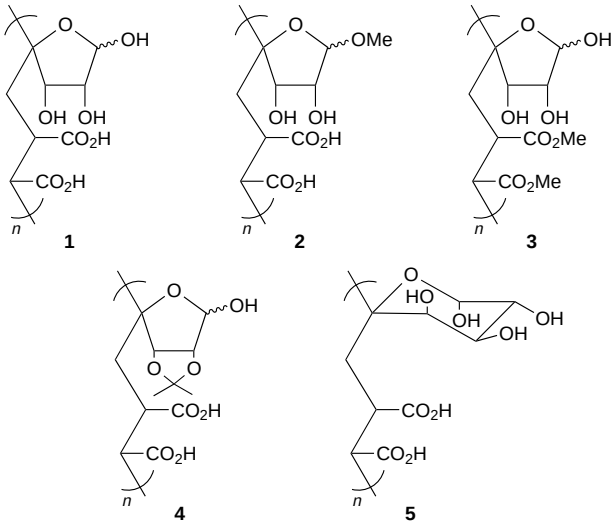
**Man Jung Han,*[a] Kyung Soo Yoo,[a] Tae Joon Cho,[a] Ji Young Chang,[a] Yu Jin Cha[b] and Seok Hyun Nam[b]**

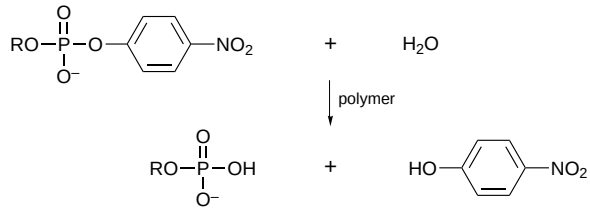
[a] *Department of Applied Chemistry, Ajou University, Suwon 442-749, Republic of Korea*
[b] *Department of Biological Science, Ajou University, Suwon 442-749, Republic of Korea*

**Synthetic polymers containing ribofuranose rings as pendent groups catalyse the cleavage of DNA and the hydrolysis of phosphodiesters with a rate acceleration of $10^3$ compared with that of the uncatalysed reactions.**

In the past three decades there has been great interest in the synthesis of enzyme-like polymers.[1,2] A few synthetic polymers have been found to show catalytic activity; for example, imidazole-containing polymers are reported to catalyse the hydrolysis of phenyl esters.[3,4] While investigating polynucleotide analogues,[5–8] we have found that synthetic ribofuranose-containing polymers show catalytic activity for the hydrolysis of phosphodiesters and the cleavage of oligodeoxyribonucleotides. This is the first example of synthetic polymer catalysis of phosphodiester hydrolysis.

The catalytic activity seemed to be caused by the hydroxy groups on the furanose rings of the polymers. In order to elucidate the structural requirements for the catalytic activity, five polymers were synthesized.† Polymers **1**–**4** contained ribofuranose derivatives, while polymer **5** had pyranose rings in their polymer chains. The number-average molecular weights of polymers **1**–**5** were measured to be 8.4, 13.0, 9.3, 9.5 and 17.0 $\times$ $10^3$ by gel permeation chromatography, respectively. The *vic*-OH groups at C-2′ and C-3′ on the furanose rings of **1**–**3** were in the *cis*-configuration, while the OH groups at C-1′, C-2′, C-3′ and C-4′ on the pyranose ring of **5** were in either the *aeea* or *eaae* conformations. Approximately 30% of the 1′-OH groups of **1** and **3** were in the *cis*-configuration with respect to 2′-OH on the same furanose rings.‡




Hydrolysis rates of ethyl *p*-nitrophenyl phosphate (substrate) were measured in Tris buffers (pH = 7.4, ionic strength = 0.02, KCl) *via* the UV absorption (400 nm) of the *p*-nitrophenol evolved. To check whether any side reaction other than the hydrolysis of the substrate occurred (Scheme 1), the reaction mixtures in the presence of **1** or **3** ([substrate] = $4.67 \times 10^{-4}$ M, [**1**] = [**3**] = $1.62 \times 10^{-5}$ M, pH = 7.4 at 50 °C, 24 h) were examined by $^{31}$P NMR. In both cases only two peaks, at $\delta$ 2.69 for ethyl phosphate and $\delta$ −5.97 for the substrate (relative to phosphoric acid at $\delta$ 0), were observed. The same result was also obtained by liquid chromatography analysis, indicating that the hydrolysis occurred exclusively.

By measuring the hydrolysis rates in the buffer solution alone and in the presence of the monomers (succinic acid and ribofuranose) and the polymers **1**–**5** at 50 °C, it was found that polymers **4** and **5** and the monomers showed no acceleration of the hydrolysis, while **1**, **2** and **3** with *vic*-*cis*-diols on the furanose rings exhibited catalytic activity. These results suggested that the *vic*-*cis*-diols of furanose rings were responsible for the catalytic activity. The *vic*-dicarboxyl groups of the polymers were of little importance for the catalytic activity, as seen in the results of the reactions of **3**, **4** and **5**.

In the hydrolysis, the measured rate ($v_m$) is the sum of the rate of the catalysed reaction ($v_c$) and the uncatalysed reaction ($v_b$) [eqn. (1)]. The value of $v_c$ was therefore obtained from eqn. (2).

$$v_m = v_c + v_b \quad (1)$$

$$v_c = v_m - v_b \quad (2)$$

The initial $v_c$ values were obtained at constant concentrations of **1**, **2** and **3** by changing the substrate concentrations. Michaelis–Menten kinetics for **1**, **2** and **3** were confirmed by performing the double reciprocal plot of Lineweaver and Burk $[v]^{-1}$ (*vs.* $[\text{substrate}]^{-1}$) (Fig. 1), which gave $K_m$ and $V_{max}$. The $k_{cat}$ was obtained from eqn. (3). We assumed that each polymer

$$k_{cat} = V_{max}/[E]_o \quad (3)$$

chain formed one active site, since no significant catalytic activity for the polymers with *M*n's lower than 4000 (PD = 4) was observed. The $k_{cat}$ values were found to be $4.22 \times 10^{-1}$ h$^{-1}$ for polymer **1**, $1.65 \times 10^{-1}$ h$^{-1}$ for **2**, and $9.04 \times 10^{-1}$ h$^{-1}$ for **3**. The $k_{cat}$ of **3** was about $10^3$ higher than that of the uncatalysed reaction ($9.12 \times 10^{-4}$ h$^{-1}$). Polymers **1** and **3** showed higher catalytic activities than **2**, probably because the former polymers contained *ca*. 30% more *vic*-*cis*-diol groups than the latter.

Noncompetitive inhibition was observed by addition of phenylboronic acid ($K_I = 3.33 \times 10^{-4}$ M) and $K_2HPO_4$ ($K_I = 2.38 \times 10^{-4}$ M). Competitive inhibition was found in the presence of acetate ions ($K_I = 6.02 \times 10^{-4}$ M). Both forms of inhibition seemed to occur because the *vic*-*cis*-diols were blocked by formation of hydrogen bonds with the inhibitors.

ssDNA of 30 bases was incubated in a buffer solution in the presence of the polymers, and developed on acrylamide gel

(Fig. 2). The extent of ssDNA cleavage was observed in the order of polymer **3** > polymer **1** > polymer **2**, which was coincident with the $k_{cat}$ of the polymers. Polymers **1**, **2** and **3** containing *vic*-*cis*-diol groups of the furanose ring showed clear DNase activity, while no cleavage was observed in the buffer solution or in the presence of **4** or **5**.

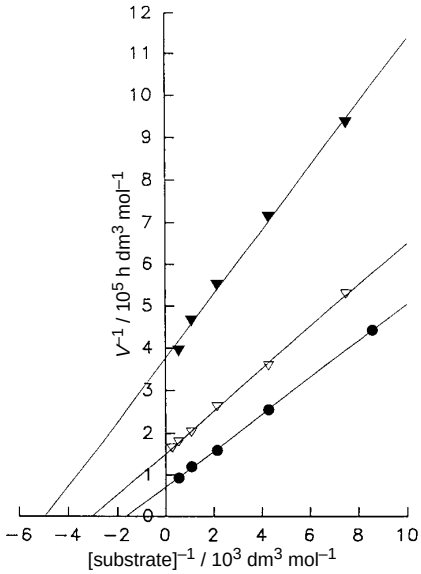



**Fig. 1** The reciprocals of the initial rates as a function of the reciprocals of the substrate concentrations for polymers (▽) **1**, (▼) **2** and (●) **3**: [polymer] = $1.62 \times 10^{-5}$ M in Tris buffer at pH = 7.4, 50 °C, ionic strength = 0.02 (KCl)

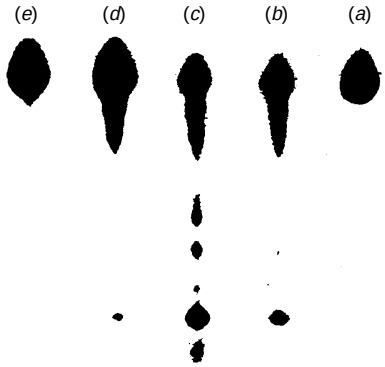



**Fig. 2** Autoradiogram of 7 M urea–8% acrylamide gel electrophoretic analysis of the reaction mixtures. $^{32}$P-Labelled ssDNA of 30 bases, d(CATGGCAAAGCCAGTATACAAATTGTAATA), corresponding to the human foamy virus proviral DNA in position nt. 3634-3611 (ref. 9), was incubated at 37 °C, ionic strength = 0.02 (KCl) and pH = 7.4 (Tris buffer), for 12 h (*a*) with no additive, in the presence of (*b*) polymer **1**, (*c*) polymer **3**, (*d*) polymer **2** and (*e*) polymer **4**. [DNA] = $7.5 \times 10^{-4}$ M, [polymer] = $7.3 \times 10^{-5}$ M. No DNA cleavage was observed in the buffer or in the presence of polymer **4**, while polymers **1**, **2** and **3** catalysed hydrolysis of DNA.

Since no activity was found for the monomer pair, the polymers are likely to form the active sites with a specific conformation. It seems possible that the furanose rings having *vic*-*cis*-diol groups were located inside the active sites, where the phosphodiester substrates were also accommodated. The *vic*-*cis*-diol groups seem to form hydrogen bonds with the two oxygen atoms of the phosphate so as to activate the phosphorus atoms attacked by nucleophiles ($H_2O$). Further investigation of the mechanism is in progress.

This work was supported by the Korea Science and Engineering Foundation and Korean Ministry of Education.

## Footnotes

† Copolymerization of 1-*O*-acetyl-5-deoxy-2,3-isopropylidene-D-*erythro*-pent-4-enofuranose with maleic anhydride (molar ratio 1 : 2) in bulk at 90 °C for 13 h in the presence of AIBN (2 mol%) resulted in the alternating copolymer, which was hydrolysed to give **1** using aqueous HCl–dioxane at 97 °C for 24 h and to give **4** using 0.1 M NaOH at room temperature for 24 h. Polymer **1** was esterified with $CH_2N_2$ to give **3**. Polymer **2** was obtained by copolymerization of 1-*O*-methyl-5-deoxy-2,3,-*O*-isopropylidene-D-*erythro*-pent-4-enofuranose with maleic anhydride under the same condition as described above and subsequent hydrolysis of the polymer using formic acid at 107 °C for 13 h. Polymer **5** was synthesized by copolymerization of 6-deoxy-1,2 : 3,4-di-*O*-isopropylidene-α-D-*galacto*-hex-5-enopyranose with maleic anhydride under the same conditions described above and subsequent hydrolysis in 68% formic acid at 100 °C for 13 h.

‡ To determine the configuration of the C-1 atoms of the monomers, 1,2,3-tri-*O*-acetyl-5-*O*-trityl-D-ribofuranose was prepared by tritylation and subsequent acetylation of D-ribose, from which the monomers were also prepared. The configuration of the C-1 atom remained intact during polymerization, and the protection and deprotection reactions of the C-1 hydroxy group. In the α form, the C-1 proton is *cis* with respect to the C-2 proton, while in the β form, the C-1 proton is *trans* with respect to the C-2 proton. In the $^1$H NMR spectrum of 1,2,3-tri-*O*-acetyl-5-*O*-trityl-D-ribofuranose in $CDCl_3$, two peaks appeared at δ 6.54 (d, $J$ = 4 Hz) and 6.22 (s) from the C-1 protons of the α and β forms. The singlet peak at δ 6.22 and the doublet peak at δ 6.54 were assigned to the proton of β form and the proton of α form, respectively, since the angle between the C-1 proton of the α form and the C-2 proton was nearly zero and thus a larger coupling constant was expected. The ratio of the α and β forms was calculated from the peak area ratio.

## References

1 T. Kunitake and Y. Okahata, *Adv. Polym. Sci.*, 1976, **20**, 159.
2 T. Kunitake, *Polymer-supported Reactions in Organic Synthesis*, ed. P. Hodge and D. C. Sherrington, Wiley, New York, 1980, p. 195.
3 C. G. Overberger, T. T. Pierre, N. Vorchheimer and S. Yaroslavsky, *J. Am. Chem. Soc.*, 1963, **85**, 3513.
4 C. G. Overberger and T. W. Smith, *Macromolecules*, 1975, **8**, 416.
5 M. J. Han, C. H. Lee, K. H. Kim and S. H. Lee, *Macromolecules*, 1992, **25**, 3528.
6 M. J. Han, S. M. Park, J. Y. Park and S. H. Yoon, *Macromolecules*, 1992, **25**, 3534.
7 M. J. Han, Y. S. Chang, J. Y. Park and K. H. Kim, *Macromolecules*, 1992, **25**, 6574.
8 M. J. Han, K. S. Kim, T. J. Cho, K. H. Kim and J. Y. Chang, *Macromolecules*, 1994, **27**, 2896.
9 B. Maruer, H. Barnnert, G. Darai and R. M. Flügel, *J. Virol.*, 1988, **62**, 1590.

*Received, 5th November 1996; Com. 6/07522C*

# Calculated details of a mechanism for conversion of $N_2$ to $NH_3$ at the FeMo cluster of nitrogenase

**Ian Dance**

*School of Chemistry, University of New South Wales, Sydney 2052, Australia*

**Density functional calculations mapping the geometry/energy hypersurface of the $Fe_7MoS_9$(*S*-cysteine)-(homocitrate)(histidine) cluster in nitrogenase and its binding of $N_2$, $H^+$, $e^-$ and N–H intermediates reveal mechanistic details for the formation of $NH_3$.**

The enzyme nitrogenase reduces $N_2$ to $NH_3$ at an $Fe_7MoS_9$(*S*-cysteine)(homocitrate)(histidine) cluster. While the structure of this active site is known in atomic detail, the mechanism for binding, activation, electronation and protonation of $N_2$ is still tantalisingly obscure.[1] In addition to numerous reports of model systems, and commentaries on chemical expectations about mechanism,[2] there are theoretical contributions to investigation of the mechanism which include calculations of $N_2$ binding geometries and electronic structure,[3] and a mechanism supported by density functional calculations has been outlined.[4]

Here I communicate new density functional calculations† mapping the geometry/energy hypersurface of the full cluster, as it binds the reactants $N_2$, $H^+$ (and $e^-$), rearranges the intermediate N–H species, and facilitates the sequential release of $2NH_3$.

Fig. 1 defines the 40 atoms included in the model of the active site. The redox level adopted as the reference state in the following corresponds to a core $[Fe_7Mo]^{22+}$, equivalent to $(Fe^{+2.57})_7Mo^{4+}$. As previously described[4] the protein surrounds favour one undercoordinated $(Fe^3)_4(S^3)_2(S^2)_2$ face‡ ($Fe^{3A}$, $Fe^{3B}$, $Fe^{3C}$, $Fe^{3D}$ in Fig. 1) as the reactive site. Fig. 2 shows three configurations for $N_2$ bound to this site: the lowest energy configuration has the least symmetrical geometry, and is dubbed the oblique arrow configuration. This optimised binding geometry differentiates the proximal N atom ($N^p$) bound to four Fe atoms, and the distal N atom ($N^d$) bound to two Fe atoms.

A characteristic of the oblique arrow configuration is that the distal N atom ($N^d$) is positioned between three of the

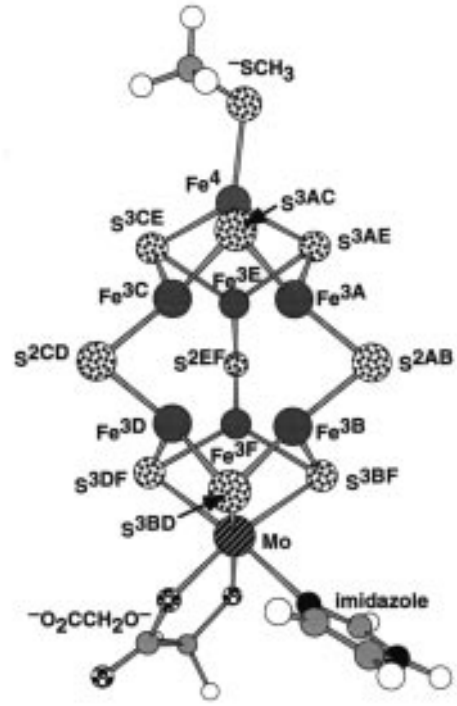



**Fig. 1** The $[Fe_7MoS_9(SCH_3)(imidazole)(O_2CCH_2O)]$ model calculated as the active site of nitrogenase. Numerical superscripts in atom identifiers are coordination numbers: N, black; C, small grey; H, open.

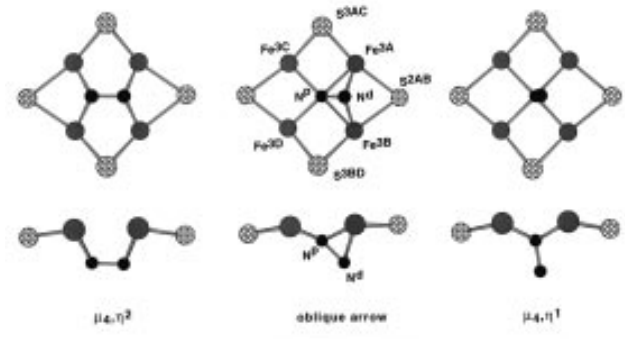



**Fig 2** The $\mu_4,\eta^2$, oblique arrow and $\mu_4,\eta^1$ geometries for $N_2$ bound to the $Fe^{3A}$ $Fe^{3B}$ $Fe^{3C}$ $Fe^{3D}$ face, with relative energies +83, 0, +37 kJ $mol^{-1}$. Other atoms (Fig. 1) included in the energy minimisations are omitted for clarity. In the lowest energy geometry, $N^p$, $N^d$ are proximal and distal to the $Fe_4$ face respectively: $N^p$–$Fe^3$ 1.93–1.98 Å; $N^d$–$Fe^{3A}$,$Fe^{3B}$ 2.07, 2.03 Å; $Fe^{3A}$–$Fe^{3C}$ 2.66, $Fe^{3B}$–$Fe^{3D}$ 2.64 Å, $Fe^{3A}$–$Fe^{3B}$ 2.65 Å, $Fe^{3C}$–$Fe^{3D}$ 2.56 Å.

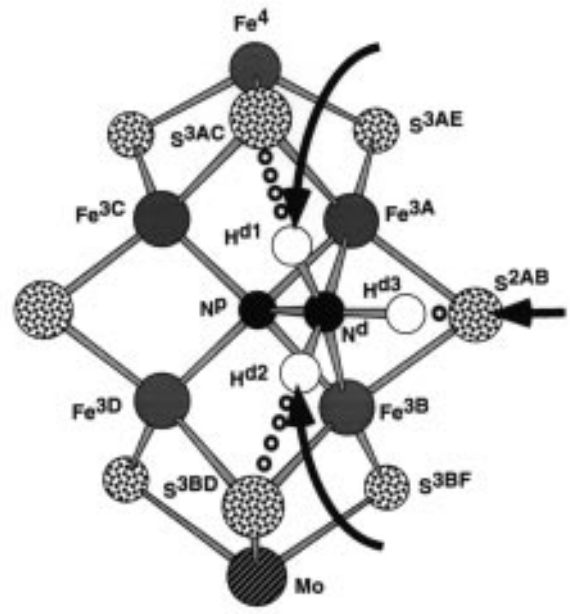



**Fig 3** Location of hydrogen atoms ($H^{d1}$, $H^{d2}$, $H^{d3}$) on $N^d$ prior to dissociation of $N^dH_3$. The rear $Fe^3$ and $S^2$ atoms and the complete coordination of $Fe^4$ and Mo are not shown for reasons of clarity. Open heavy circles show the hydrogen bonds from H to $S^3$ and $S^2$. Heavy arrows show probable trajectories for the three approaching hydrogen atoms (see text).

surrounding S atoms, $S^{2AB}$, $S^{3AC}$, $S^{3BD}$, such that protons on these S atoms are well positioned for transfer to $N^d$. Further, addition of two electrons to the cluster at this stage most affects the electron population at these S atoms: the changes in Mulliken partial charges are *ca.* −0.19 at $S^2$, *ca.* −0.11 at $S^3$, −0.04 at Mo, and *ca.* 0.00 at Fe. Therefore the possibility of reduction and protonation of the distal N atom was investigated by energy minimisation of a structure containing three H atoms between $N^d$ and S, hydrogen bonded to S, as detailed in Fig. 3. The electronic population at this stage was equivalent to addition of $N_2$, $4e^-$ and $3H^+$ relative to the reference state. Energy minimisation caused scission of the N–N bond and dissociation of the distal N atom as $NH_3$: Fig. 4 shows several stages in this dissociation. Because the calculation did not include the surrounding protein and its hydrogen bond acceptor sites, the dissociating $NH_3$ retains its hydrogen bonds to the three S atoms, and inverts during the dissociation; Fig. 4(*d*) also shows a later stage of dissociation after the hydrogen bonds have been broken.

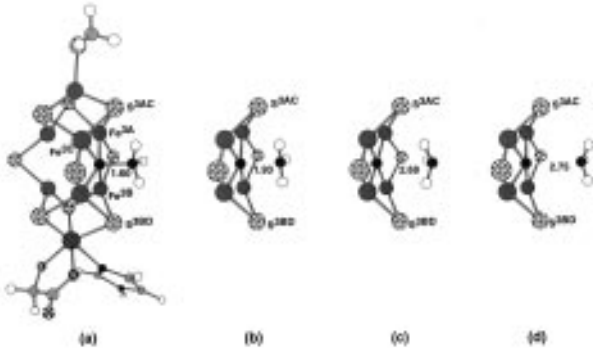


**Fig 4** Side views of four stages in the dissociation of $N^dH_3$, shown fully for stage (*a*) and as the dissociation face only for (*b*)–(*d*). $N^p\cdots N^l$ distances (Å) are marked (the N–N bond length at the beginning of this reaction was 1.28 Å). Relative energies for these intermediates are (*a*) 0, (*b*) −188, (*c*) –368, (*d*) –414 kJ $mol^{-1}$. Stages (*b*) and (*c*) demonstrate the inversion of $NH_3$ due to the strength of the S···H hydrogen bonds, which are broken in stage (*d*).

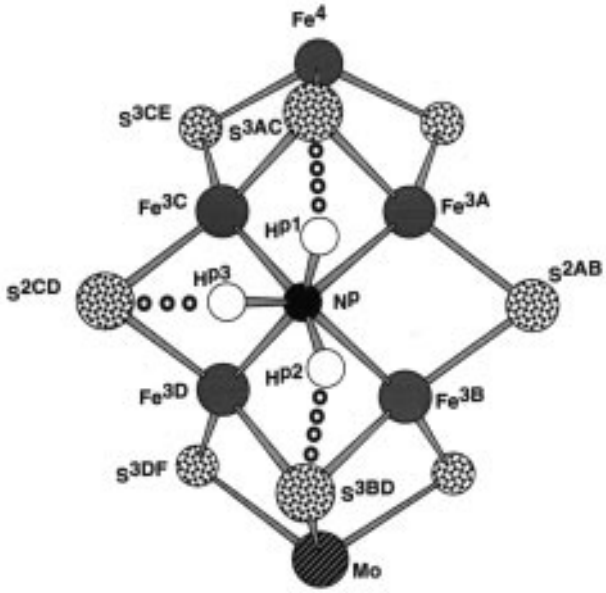



**Fig. 5** Location of hydrogen atoms ($H^{p1}$, $H^{p2}$, $H^{p3}$) on $N^p$ prior to dissociation of $N^pH_3$. The rear $Fe^3$ and $S^2$ atoms and the complete coordination of $Fe^4$ and Mo are not shown for reasons of clarity. Open heavy circles show the hydrogen bonds from H to $S^3$ and $S^2$.

After dissociation of $N^dH_3$ the proximal N atom is left bound to the $Fe_4$ face; the second stage of electronation and protonation of this N atom can also involve the surrounding S atoms, but the geometry is different because $N^p$ is close to the $Fe_4$ face. Fig. 5 shows an intermediate geometry containing three new H atoms associated with $N^p$ and hydrogen bonded to $S^2$ and $S^3$. On energy minimisation with an atom/electron population now corresponding to the reference state + $N_2$ + $6e^-$ + $6H^+$ − $NH_3$, $N^dH_3$ dissociates by sliding around one of the $Fe^3$ atoms.

These results provide the rudiments of a mechanism for binding of $N_2$, proton approach, introduction of electrons, and sequential dissociation of $NH_3$. They reinforce the chemical expectation that undercoordinated $Fe^3$ and $S^2$ atoms play key roles. During the processes described the Fe–Fe, Fe–S and S–Mo distances change as expected according to increases and decreases in coordination. Additional calculations reveal that H atoms can also bridge $Fe^3$–$S^3$ bonds, and that $Fe^3$ atoms as well as the $Fe^3$–$S^3$ bonds can mediate the passage of H atoms from protein to both the distal and proximal N atoms: likely trajectories for H approach to $N^d$ are shown in Fig. 3. Other mechanistic aspects currently being refined involve protonation and/or electronation of $N_2$ *en route* to the oblique arrow configuration, protonation/electronation of $N^p$ while $N^dH_3$ is dissociating, and the coupled formation of $H_2$. Further development will include relevant surrounding protein, which is essential for the ingress of protons and the egress of $NH_3$.

The support of this research by the Australian Research Council is gratefully acknowledged.

## Footnotes

† Calculations used non-local blyp functionals and double numerical basis sets, as implemented in the program DMol (MSI). The accuracy of these methods has been demonstrated by replication of the experimental geometries of related clusters such as $VFe_4S_6(SR)(PR_3)_4$.[5] All models have $C_1$ symmetry.

‡ Numerical superscripts signify coordination numbers.

## References

1 M. K. Chan, J. Kim and D. C. Rees, *Science*, 1993, **260**, 792; J. T. Bolin, A. E. Ronco, T. V. Morgan, L. E. Mortenson and N. H. Xuong, *Proc. Natl. Acad. Sci. USA*, 1993, **90**, 1078; D. C. Rees, M. K. Chan and J. Kim, *Adv. Inorg. Chem.*, 1993, **40**, 89; J. Kim and D. C. Rees, *Biochemistry*, 1994, **33**, 389; J. B. Howard and D. C. Rees, *Annu. Rev. Biochem.*, 1994, **63**, 235.

2 R. R. Eady and G. J. Leigh, *J. Chem. Soc., Dalton Trans.*, 1994, 2739; G. J. Leigh, *New J. Chem.*, 1994, **18**, 157; *Science*, 1995, **268**, 827; T. A. Bazhenova and A. E. Shilov, *Coord. Chem. Rev.*, 1995, **144**, 69; C. E. Laplaza and C. C. Cummins, *Science*, 1995, **268**, 861; C. E. Laplaza, A. R. Johnson and C. C. Cummins, *J. Am. Chem. Soc.*, 1996, **118**, 709; R. L. Richards, *Pure Appl. Chem.*, 1996, **68**, 1521; D. Coucouvanis, *J. Biol. Inorg. Chem.*, 1996, in the press; C. J. Pickett, *J. Biol. Inorg. Chem.*, 1996, in the press; D. Sellmann and J. Sutter, *J. Biol. Inorg. Chem.*, 1996, in the press; R. N. F. Thorneley and D. J. Lowe, *J. Biol. Inorg. Chem.*, 1996, in the press.

3 H. Deng and R. Hoffmann, *Angew. Chem., Int. Ed. Engl.*, 1993, **32**, 1062; W. Plass, *J. Mol. Struct.*, 1994, **315**, 53; R. J. Deeth and C. N. Field, *J. Chem. Soc., Dalton Trans.*, 1994, 1943; R. J. Deeth and S. A. Langford, *J. Chem. Soc., Dalton Trans.*, 1995, 1; K. K. Stavrev and M. C. Zerner, *Chem. Eur. J.*, 1996, **2**, 83; Q. Cui, D. G. Musaev, M. Svensson, S. Sieber and K. Morokuma, *J. Am. Chem. Soc.*, 1995, **117**, 12366.

4 I. G. Dance, *Aust. J. Chem.*, 1994, **47**, 979.

5 I. G. Dance, *ACS Symp. Ser.*, ed. E. I. Steifel and K. Matsumoto, American Chemical Society, Washington DC, 1996, in the press.

*Received, 21st October 1996; Com. 6/07136H*

# Site specific photo-crosslinking of single stranded oligonucleotides by a complementary sequence equipped with an internal photoactive probe

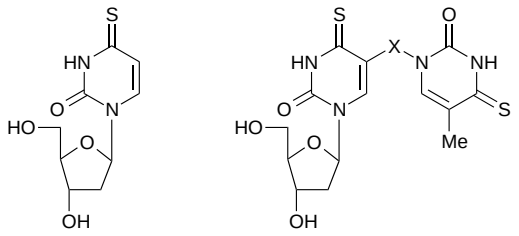
**Carole Saintomé,[a,b] Pascale Clivio,[a] Alain Favre,[b] Jean-Louis Fourrey*[a] and Philippe Laugâa[b]**

[a] *Institut de Chimie des Substances Naturelles, CNRS 91198, Gif-sur-Yvette Cedex, France*
[b] *Institut Jacques Monod, CNRS-Université Paris VII, 2 Place Jussieu, 75251 Paris Cedex 05, France*

**The photo-crosslinking behaviour of oligonucleotide constructs, incorporating photoactive residues 1–5 at a defined position, has been examined in the presence of their DNA (14-mer) and RNA (15-mer) complementary targets using a two-fold excess; it revealed a moderate but promising irreversible binding efficiency, the results of which could be anticipated by molecular mechanics in the case of 4.**

There are many instances in which oligodeoxynucleotides (ODN) or nuclease resistant oligonucleotide analogues, conjugated with chemical or photochemical reagents, are utilized as biochemical tools.[1,2] In nucleic acid studies, although simple oligonucleotide binding may not be sufficient to disrupt nucleic acid functions, inactivation will certainly occur if, after specific recognition, a modified oligonucleotide probe has the capacity to undergo irreversible covalent photo-crosslinking to its target.[3] In such probes, a photoactive label is usually introduced at their 5′-terminus, excepted for some examples with psoralens whose applications are specific of AT sites.[4]

Herein, we have examined the photochemical behaviour towards their DNA and RNA targets of strictly complementary constructs having a photoactive nucleoside residue which can be easily placed at a defined position within the sequence. Namely, we have compared the light-induced reactivity of a series of oligonucleotides, containing 4-thiodeoxyuridine ($s^4$dU) **1** with that of their analogues containing the recently synthesized nucleosides **2**–**5** (Fig. 1).[5] The latter have a chain of variable length at the C-5 position of 2′-deoxyuridine which permits the attachment at its other extremity of $N^1$-carboxymethyl-4-thiothymine. It is known that, upon light excitation (UVA, $\lambda_{max} \simeq 330$ nm), such sulfur-substituted pyrimidines (4-thiouracil and 4-thiothymine) undergo covalent bond formation with all the current nucleic bases with a higher preference for thymine.[6,7] In this study, nucleoside **1** and the modified analogues **2**–**5** were incorporated at position 1 (for nucleosides **1** and **4**) or position 7 according to a known synthetic and purification procedure[8] by means of their corresponding phosphoramidites,[5] of 14-mer oligonucleotides designated **Oi**-1 and **Oi**-7 (**i** corresponding to nucleosides **1**–**5** (Fig. 1). Oligonucleotides **Oi**-1 and **Oi**-7 were irradiated in two-fold excess in the presence of their RNA or DNA complements, designated **OR** or **OD** respectively, which had been $^{32}$P-labelled at their 5′-end (Table 1). Denaturing polyacrylamide gel electrophoresis (PAGE) showed formation of interstrand photoproducts manifested by the appearance of slow moving species on the gels, the yields of which were quantified using a phosphorimager. In contrast, there were no such reactions in the dark or with an oligonucleotide sequence unable to anneal to **Oi**-1 and **Oi**-7.




**i** = **1** ($s^4$dU)

**i** = **2**, **X** = $(CH_2)_2CONH(CH_2)_2NHCOCH_2$
**i** = **3**, **X** = $(CH_2)_2CONH(CH_2)_4NHCOCH_2$
**i** = **4**, **X** = $NH(CH_2)_2NHCOCH_2$
**i** = **5**, **X** = $C{\equiv}CCH_2NHCOCH_2$

**Oi**-1 5′d($N_i$ G C C C G T C T G T T G T)3′ with **i** = **1** ($s^4$dU) or **4**

**Oi**-7 5′d(T G C C C G $N_i$ C T G T T G T)3′ with **i** = **1** ($s^4$dU), **2**, **3**, **4** or **5**

**OR** 3′A C G G G C A G A C A A C A G5′

**OD** 3′d(A C G G G C A G A C A A C A )5′

**Fig. 1** Modified nucleosides **i** (i = **1**–**5**) and oligonucleotides **Oi**-1 and **Oi**-7 incorporating **i** at either position 1 or 7 ($N_i$ corresponds to nucleoside **i**). **OR** and **OD** designate the nucleotide sequences of their RNA (15-mer) and DNA (14-mer) complement, respectively. **OR** was obtained by transcription, and contains an extra G in 5′ which gives efficient initiation.

Oligonucleotide **O1**-1 having **1**, the $s^4$dU photoreactive label, placed at its 5′-extremity, exhibited a high photo-crosslinking capacity with both its DNA or RNA target, albeit with a lower efficiency in the latter case (55 *vs*. 33%). However, its analogue **O1**-7 having $s^4$dU at position 7 within the sequence yielded weak (0.5% with DNA) or no detectable (RNA) crosslinks. This indicates that, for a crosslinking reaction to occur, the photoreactive $s^4$dU should be placed at the 5′-dangling end of the duplex and it suggests that the conformational flexibility at this extremity might be higher for a type B DNA helix than for a type A RNA–DNA helix.

When the extended analogue **4** was placed at the 5′-end of the probe, to give **O4**-1, an efficient cross-linking reaction with the complementary target was observed as in the case of **1**. Again, compared to its RNA analogue, the DNA target proved to be more reactive (21 *vs*. 28%). In the **OR** case, the reaction was very selective and covalent bond formation took place with its complementary residue A15, exclusively (for mapping see below).

**Table 1** Crosslinking efficiency, relative yield and position of crosslinks for **Oi**-1 and **Oi**-7

| | Total cross-linking efficiency (%) | | Relative yields (%) and positions of crosslinks with **OR** | | | | |
|---|---|---|---|---|---|---|---|
| Probe | **OD** | **OR** | C3 | C6 | C10 | G11 | A15 |
| **O1**-1 | 53 | 33 | | | | | 100 |
| **O4**-1 | 28 | 21 | | | | | 100 |
| **O1**-7 | 0.5 | 0 | | | | | |
| **O2**-7 | 20 | 8 | | 85 | 6 | 7 | |
| **O3**-7 | 15 | 6 | | 88 | | 12 | |
| **O4**-7 | 10 | 3.5 | | 74[a] | | | |
| **O5**-7 | 22 | 18 | 40 | 60 | | | |

[a] Other crosslinks were not characterized due to their instability.

However, in sharp contrast with **1** at position 7 (Fig. 2), when the extended 2′-deoxyuridine residues **2**–**5** were placed within the sequence at this position, covalent crosslinking occurred with both their complementary **OD** and **OR** (Table 1). As for labels **1** and **4** at position 1, the crosslinking yields are better in the DNA series, varying from 10 to 22%. These moderate yields are not unexpected since the complementary sequences **OD** (DNA) and **OR** (RNA), containing the less reactive A, C and G residues compared to T or U, were chosen intentionally to be in the less favourable conditions for crosslinking.[6] On the other hand, protrusion of the label in the major groove of the double helix, which has the possibility to undergo covalent bonding with proximate intra- or inter-strand residues, could also account for these moderate yields. To examine the relative efficiency of the latter process, 5′ $^{32}$P-labelled **O5**-7 was first irradiated alone. Denaturating PAGE revealed the formation of intrastrand crosslinked species (60% yield) migrating faster than **O5**-7. When a similar experiment was performed with 5′ $^{32}$P-labelled **O5**-7 hybridized to **OR** (two fold excess), it showed a considerable decrease of the fast migrating species (30% yield) together with the appearance of a retarded crosslinked species corresponding to interstrand bridges (22% yield) as revealed by their limited digestion by RNase T1.[9] Interestingly, experiments with **OD** exhibited the same pattern of inter- and intra-strand bridges. Mapping of the exact sites for crosslink formation was carried out using limited alkaline hydrolysis[7c] of the complexes obtained with 5′-end labelled RNA (Fig. 2). The results, given in Table 1, show a preference (74 to 100%) for the residues on the 5′-side of the **OR** target with C6 being preferred (60 to 88%).

Finally, these experimental observations were compared with those predicted by molecular mechanics. A study was undertaken in the case of the **O4**-7–**OR** hybrid in order to determine which residues might participate in inter- and intra-strand photoproduct formation. Model building and computations were performed on a Silicon Graphics Iris 4D/35 equipped with an Evans and Sutherland PS390 graphic device using the SYBYL programme package (Tripos Associates, Saint Louis, Mo). The **O4**-7–**OR** hybrid was built according to the NMR data of Salazar *et al*.,[10] *i.e*. with a C(3′)-*endo* RNA strand and a O(4′)-*endo* DNA strand. The conformational space accessible to the s$^4$T moiety of **4** was explored *via* a systematic search performed along the torsional angles of the linker X (Fig. 1). Residues potentially available for photoaddition were determined through selection of the conformations satisfying both following criteria: (i) a distance of less than 6 Å between the midpoint of the C=S bond of the 4-thiothymine moiety and that of the C(6)=C(5) bond[7g] of the proximal pyrimidines or the midpoint of the C(8)=N(7) bond[11] of the proximal purines, and (ii) an angle between these bonds in the 0 ± 30° (parallel) or 180 ± 30° (antiparallel) ranges. It was found that about 30% of the selected conformations would yield intrastrand crosslinks, while 70% of the selected conformations would yield interstrand crosslinks with residues A5, C6, A7 and G8. When the selection criteria for bond distances and angles were narrowed to 0–4 Å and 0–20° ranges, respectively, the most properly oriented residues appeared to be C6 (50%) and to a lesser extent A7 (21%) and G8 (29%). It is noteworthy that in the case of C6, the plane of the s$^4$T ring is parallel to that of C6, whereas in the case of A7 and G8 it is perpendicular to those of A7 and G8. This might account for the fact that interstrand crosslinking has been detected with a higher preference for C6.

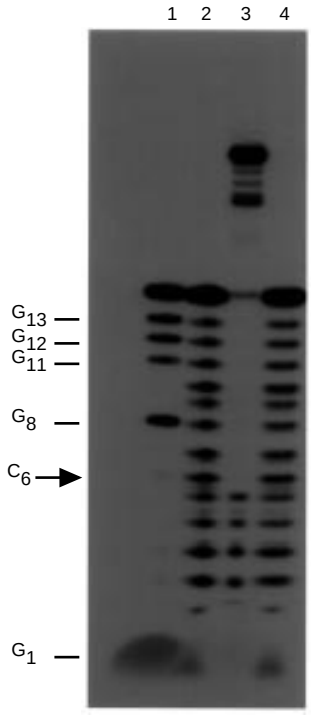



**Fig. 2** Identification of RNA residues involved in crosslinking. Sequencing gel of free and crosslinked **OR**. Lane 1: partial digestion of free **OR** with RNase T1; lanes 2 and 4: limited alkaline hydrolysis of **OR**; lane 3: limited alkaline hydrolysis of the major **OR**–**O4**-7 photoadduct. The spots corresponding to G positions are marked. The arrow points to nucleotide C6 involved in the crosslink.

We thank ACC-SV (MST) for financial support.

## References


1 U. Englisch and D. H. Gauss, *Angew. Chem., Int. Ed. Engl*., 1991, **30**, 613.
2 C. Hélène, T. Le Doan and N. T. Thuong, in *Photochemical Probes in Biochemistry*, ed. P. E. Nielsen, Kluwer, Dordrecht, 1989, p. 219.
3 D. G. Knorre and V. V. Vlassov, *Genetica*, 1991, **85**, 53.
4 For porphyrin labelling in 5′, see L. Mastruzzo, A. Woisard, M. D. F. Ma, E. Rizzarelli, A. Favre and T. Le Doan, *Photochem. Photobiol*., 1994, **60**, 316; D. Magda, M. Wright, R. A. Miller, J. L. Sessler and P. I. Sansom, *J. Am. Chem. Soc*., 1995, **117**, 3729. For psoralen labelling in 5′ or 3′, see J. M. Kean, A. Murakami, K. R. Blake, C. D. Cushman and P. S. Miller, *Biochemistry*, 1988, **27**, 9113; U. Pieles and U. Englisch, *Nucleic Acids Res*., 1989, **17**, 285; E. H. Chang, P. S. Miller, C. Cushman, K. Devadas, K. F. Pirollo and P. O. Ts'o, *Biochemistry*, 1991, **30**, 8283; J. Woo and P. B. Hopkins, *J. Am. Chem. Soc*., 1991, **113**, 5457; H. E. Johansson, G. J. Belshman, B. S. Sproat and M. W. Hentze, *Nucleic Acids Res*., 1994, **22**, 4591; G. Godard, J.-C. François, I. Duroux, U. Asseline, N. Thuong, C. Hélène, C. and T. Saison-Behmoaras, *Nucleic Acids Res*., 1994, **22**, 4789. For internal labelling with psoralens, see H. B. Gamper, G. D. Cimino and E. Hearst, *J. Mol. Biol*., 1987, **197**, 349; U. Pieles, B. S. Sproat, P. Neuner and F. Cramer, *Nucleic Acids Res*., 1989, **17**, 8967; M. A. Reynolds, T. A. Beck, R. I. Hogrefe, A. McCaffrey, L. J. Arnold and M. M. Vaghefi, *Bioconjugate Chem*., 1992, **3**, 366.
5 C. Saintomé, P. Clivio, J.-L. Fourrey, A. Woisard and A. Favre, *Tetrahedron Lett*., 1994, **35**, 873. Full characterization of these photoactive nucleosides will be described in a forthcoming article.
6 A. Favre, Y. Lemaigre Dubreuil and J.-L. Fourrey, *New J. Chem*., 1991, **15**, 593.
7 (*a*) P. Wollenzien, A. Expert-Bezançon and A. Favre, *Biochemistry*, 1991, **30**, 1785; (*b*) E. J. Sontheimer and J. A. Steitz, *Science*, 1993, **262**, 1989; (*c*) V. D. Dos Santos, A.-L. Vianna, J.-L. Fourrey and A. Favre, *Nucleic Acids Res*., 1993, **21**, 201; (*d*) D. Dos Santos, J.-L. Fourrey and A. Favre, *Biochem. Biophys. Res. Commun*., 1993, **190**, 377; (*e*) A. Woisard, J.-L. Fourrey and A. Favre, *J. Mol. Biol*., 1994, **239**, 366; (*f*) M. Tanaka, J.-L. Fourrey and A. Favre, *New J. Chem*., 1995, **19**, 469; (*g*) A. Favre and J.-L. Fourrey, *Acc. Chem. Res*., 1995, **28**, 375; (*h*) Z. Wang and T. M. Rana, *Biochemistry*, 1996, **35**, 6491.
8 P. Clivio, J.-L. Fourrey, J. Gasche, A. Audic, a. Favre, C. Perrin and A. Woisard, *Tetrahedron Lett*., 1992, **33**, 65.
9 J. M. D'Alessio, in *Gel Electrophoresis of Nucleic Acids*, ed. D. Richmond and B. D. Hames, 1991, p. 173.
10 M. Salazar, O. Y. Fedorov, J. M. Miller, N. S. Ribeiro and B. R. Reid, *Biochemistry*, 1993, **32**, 4207.
11 C. Saintomé, P. Clivio, A. Favre, J.-L. Fourrey and C. Riche, *J. Am. Chem. Soc*., 1996, **118**, 8142.


*Received, 13th September 1996; Com. 6/06330F*

# Glycosidase-catalysed synthesis of oligosaccharides: a one step synthesis of lactosamine and of the linear B type 2 trisaccharide α-D-Gal-(1 → 3)-β-D-Gal-(1 → 4)-β-D-GlcNAcSEt involved in the hyperacute rejection response in xenotransplantation from pigs to man and as the specific receptor for toxin A from *Clostridium difficile*

**Gabin Vic,† Chuong Hao Tran, Michaela Scigelova and David H. G. Crout***

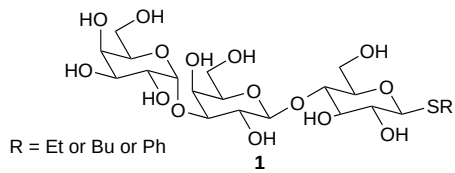
*Department of Chemistry, University of Warwick, Coventry, UK CV4 7AL*

**Sequential use of the β-galactosidase from *Bacillus circulans* and an α-galactosidase from *Aspergillus oryzae* give the linear B trisaccharide 2, identified as the epitope that binds anti-Gal antibodies during pig-to-man xenotransplantation and as the receptor for toxin A from *Clostridium difficile*.**

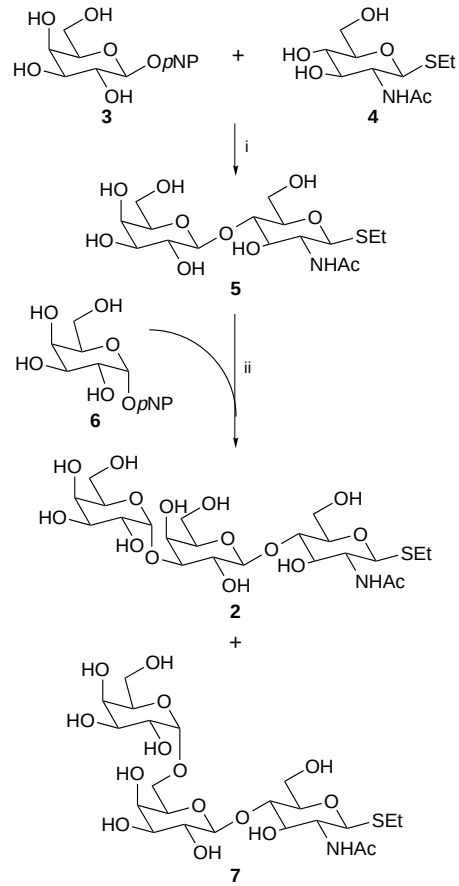
There is at present a worldwide shortage of organs available for human transplantation. The use of pigs' organs would be a solution to this problem if the hyperacute rejection that occurs after such transplantation could be prevented.[1] Two trisaccharides **1** and **2** bearing the α-D-Gal-(1 → 3)-β-D-Gal terminus have been identified to play a fundamental role in the process of hyperacute xenograft rejection in xenotransplantation from pigs to man.[2] Both of these trisaccharides are specific antigens for the binding of xenoreactive antibodies of the recipient on endothelial cells in the graft which inevitably destroy it within a few hours. Moreover trisaccharide **2** is also known as the receptor for toxin A from *Clostridium difficile* which is the major cause of antibiotic-associated diarrhoea and the causative agent of pseudomembranous colitis (PMC) particularly in elderly patients.[3] The significance of these findings prompted the development of an enzymatic synthesis of these trisaccharides because the application of glycosidases in oligosaccharide synthesis avoids the need for protection-deprotection steps required in non-enzymatic syntheses.

In a previous communication[4] the enzymatic synthesis was described of several derivatives of the linear B type 6 trisaccharide **1** starting from alkyl 1-thio-β-D-lactopyranoside as acceptor and *p*-nitrophenyl α-D-galactopyranoside as donor using the newly discovered α-galactosidase II from *Aspergillus oryzae*.‡ Here we report the synthesis of the linear B type 2 trisaccharide **2** in two enzymatic steps (Scheme 1). The synthesis required first the synthesis of a glycoside **5** of *N*-acetyllactosamine. *N*-Acetylglucosamine has been synthesised using glycosyltransferases. The routes of Wong *et al.*[5] and of Thiem and Wiemann[6] both required the use of six enzymes because, in addition to the galactosyl transferase, an enzyme system for the regeneration of the galactosyl donor, UDP-Gal, was included. In a recent improvement of this procedure, Zervosen and Elling have reduced the number of enzymatic steps required to three by using sucrose synthetase to regenerate UDP-Glc.[7] However, reduction to practice of this scheme required the use of two further enzymes: dTDP-glucose 4,6-dehydratase to synthesise dTDP-6-deoxy-D-*xylo*-4-hexulose required for reactivation of UDP-Glc 4′-epimerase and invertase to hydrolyse the excess of sucrose remaining at the end of the reaction.

The method reported here is based on the use of the β-galactosidase from *Bacillus circulans* which was used by Sakai *et al.* to synthesise *N*-acetyllactosamine from lactose and *N*-acetylglucosamine.[8] Some 1,6-isomer was simultaneously formed and isolation of the product required extensive chromatographic purification. This method has been refined by using the thioethyl glycoside of *N*-acetylglucosamine as acceptor and *p*-nitrophenyl β-D-galactoside as donor. With these substrates the glycosylation was found to proceed with complete regiocontrol for formation of the β 1 → 4 isomer and isolation of the product was also greatly simplified.




**1**




**3** **4** **5** **6** **2** **7**

**Scheme 1** *Reagents*: i, β-galactosidase from *Bacillus circulans*; ii, α-galactosidase II from *Aspergillus oryzae*

Ethyl 1-sulfanyl-(β-D-galactopyranosyl)-(1 → 4)-(2-acetamido-2-deoxy)-*O*-β-D-glucopyranoside **5** was obtained by incubation of *p*-nitrophenyl β-D-galactopyranoside **3** as galactosyl donor and ethyl 1-sulfanyl-(2-acetamido-2-deoxy)-*O*-β-D-glucopyranoside **4**[9] as acceptor using a crude β-galactosidase from *Bacillus circulans*.§ A simple procedure was followed: the donor **3** (0.55 g, 1.82 mmol) and the acceptor **4** (2.96 g, 11.15 mmol) in acetate buffer (pH 5.0, 50 mmol $dm^3$, 37 $cm^3$) were incubated with the crude β-galactosidase (3.8 mg, 7.4 U) at 22 °C for 7 h. After all of the donor has been consumed the reaction was stopped by heating at 100 °C for 5 min. *p*-Nitrophenol was extracted with diethyl ether (4 × 50 $cm^3$) and the aqueous layer was concentrated to a total volume of 12 cm.[3] This was applied in 4 $cm^3$ batches to a Biogel P2 column (120 × 2 cm) which was eluted with $H_2O$ (flow rate 0.6 $cm^3$ $min^{-1}$, fraction 6 $cm^3$) to give the disaccharide **5** in 50% yield (0.39 g). The structure of the product was confirmed by $^1H$ and $^{13}C$ NMR spectroscopy and mass spectrometry.[10]

Synthesis of the trisaccharide glycoside **2** was completed by transfer of the α-D-galactosyl residue (1 → 3) on to the disaccharide **5** using a partially purified α-galactosidase II from *Aspergillus oryzae*. This enzyme accepted *p*-nitrophenyl α-D-galactopyranoside **6** as an α-D-galactosyl donor giving a 1 : 0.9 mixture of the α 1 → 3 and α 1 → 6 linked trisaccharides **2** and **7**. These two trisaccharides were further purified to homogeneity by a combination of Biogel P2 and carbon–Celite column chromatography, and selective enzymatic hydrolysis. Thus donor **6** (79 mg, 0.26 mmol) and the acceptor **5** (0.40 g, 0.93 mmol) in citrate–phosphate buffer (pH 5.0, 50 mmol $dm^3$, 3.12 $cm^3$) were incubated with the partially purified α-galactosidase II (4 U) at 22 °C for 20 h. The reaction was stopped by heating at 100 °C for 5 min, the mixture was diluted with $H_2O$ (15 $cm^3$) and filtered. *p*-Nitrophenol was extracted with diethyl ether (4 × 10 $cm^3$). The aqueous layer was concentrated to 4 $cm^3$ and applied to a Biogel P2 column (120 × 2 cm) which was eluted with $H_2O$ (flow rate 0.6 $cm^3$ $min^{-1}$). The mixture of trisaccharides obtained in 32% overall yield (49 mg) was applied to a carbon–Celite column which was eluted with water–ethanol (75 : 25). The α 1 → 6 linked trisaccharide was eluted in the first fractions and a mixture of α 1 → 3 and a minor β linked trisaccharide were eluted in the following fractions. The presence of this β linked trisaccharide was due to the remaining β-galactosidase activity in the enzymatic preparation. The α 1 → 3 trisaccharide **2** was further purified to homogeneity by selective hydrolysis of the β linked trisaccharide using the β-galactosidase from *Bacillus circulans*¶ to give finally trisaccharide **2** (20 mg). The structure of **2** was confirmed by $^1H$ and $^{13}C$ NMR spectroscopy and mass spectrometry (Table 1). The method described here provides an easy access to this important trisaccharide but was not optimised. This may be realised by using the α-galactosidase II from *Aspergillus oryzae* free from β-galactosidase activity.

We thank the EPSRC and the BBSRC for financial support, Mr I. Katyal for mass spectra and Mrs S. Vic for useful discussions.

**Table 1** Selected $^1H$ NMR data for trisaccharides **2** and **7**[a,b]

| Trisaccharide | 1-H | 1′-H | 1″-H |
|---|---|---|---|
| **2** | 4.61 (d, 10.28) | 4.50 (d, 7.62) | 5.10 (d, 3.65) |
| **7** | 4.65 (d, 10.62) | 4.43 (d, 7.63) | 4.97 (d, 2.98) |

[a] $^1H$ NMR was carried out at 400 MHz using a Bruker AC 400 spectrometer in $D_2O$. [b] [Multiplicity, coupling constant (Hz)].

## Footnotes

† Present address: Unilever Research, Biorecognition Department, Colworth House, Sharnbrook, Bedford, UK MK44 1LQ.
‡ Isolated from the partially purified β-galactosidase of *A. oryzae*, a gift from the Sigma Chemical Company Ltd.
§ A gift from Daiwa Kasei Co., Japan.
¶ The mixture of trisaccharide **2** and β linked trisaccharide (25 mg, 0.042 mmol) in acetate buffer (pH 5.0, 50 mmol $dm^3$, 2 $cm^3$) was incubated with the β-galactosidase from *Bacillus circulans* (8.0 mg, 15.5 U) at 22 °C for 1 h and purified using a Biogel P2 column.

## References

1 W. Parker, S. Saadi, S. S. Lin, Z. E. Holzknecht, M. Bustos and J. L. Platt, *Immunology Today*, 1996, **17**, 373.
2 D. K. C. Cooper, E. Koren and R. Oriol, *Immunological Rev.*, 1994, **141**, 31.
3 G. F. Clark, H. C. Krivan, T. D. Wilkins and D. F. Smith, *Arch. Biochem. Biophys.*, 1987, **257**, 217.
4 G. Vic, M. Scigelova, J. J. Hastings, O. W. Howarth and D. H. G. Crout, *Chem. Commun.*, 1996, 1473.
5 C.-H. Wong, S. L. Haynie and G. M. Whitesides, *J. Org. Chem.*, 1982, **47**, 5416; C.-H. Wong, R. Wang and Y. Ichikawa, *J. Org. Chem.*, 1992, **57**, 4343.
6 J. Thiem and T. Wiemann, *Synthesis*, 1992, 141.
7 A. Zervosen and L. Elling, *J. Am. Chem. Soc.*, 1996, **118**, 1836.
8 K. Sakai, R. Katsumi, H. Ohi, T. Usui and Y. Ishido, *J. Carbohydr. Chem.*, 1992, **11**, 553.
9 T. Buska, P. J. Garreg, P. Kondarsson and J. L. Maloisel, *Tetrahedron: Asymmetry*, 1994, **5**, 2187.
10 G. Vic, J. J. Hastings, O. W. Howarth and D. H. G. Crout, *Tetrahedron: Asymmetry*, 1996, **7**, 709.

*Received, 24th October 1996; Com. 6/07255K*

# Synthesis of *p*-tolylsulfonyl-substituted dienes *via* radical cyclization of diynes

**Stephen Caddick,*[a] Craig L. Shering[a] and Sjöerd N. Wadman[b]**

[a] *The Chemistry Laboratory, University of Sussex, Falmer, Brighton, UK BN1 9QJ*
[b] *GlaxoWellcome, Medicines Research Centre, Gunnels Wood Road, Stevenage, Herts, UK SG1 2NY*

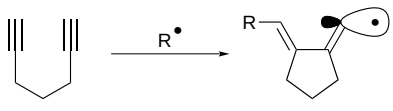
**A novel radical cyclization of hepta-1,6-diynes with toluene-*p*-sulfonyl bromide leads to two new classes of electron deficient sulfonyl dienes.**

The use of radical cyclizations for the synthesis of five-membered rings has become widespread in organic chemistry and radicals are now regarded as useful intermediates in synthesis.[1] The majority of commonly employed methods use tributyltin hydride (TBTH) to induce homolysis of an organic halide or alcohol derivative to generate the reactive carbon-centred radical species. An attractive alternative is to use the addition of a free-radical to a carbon–carbon π bond in order to generate the radical species; this has the advantage of incorporating some additional functional groups into the product. The synthetic utility of this type of approach using enyne and diene systems has been shown. Seminal work by Stork *et al.* has illustrated the synthetic advantages of using alkynes in radical based transformations.[2] Cyclization of diynes has attracted little attention, which is surprising considering the synthetic potential of the resultant diene.[3] Here we present our preliminary investigations relating to this novel type of radical cyclization (Scheme 1).

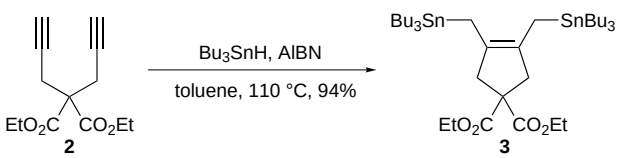
Our initial work illustrated the nature of the problem associated with the radical cyclization of diynes. Treatment of diyne **2** with TBTH under standard free-radical conditions led to the isolation of the bis(stannane) **3** in good yield[4] (Scheme 2).

This type of symmetrical allylic stannane may well be synthetically useful. However, we were never able to isolate a tin-substituted diene, although we note that, with substrate modification, this may be possible.[5] This reductive process is most likely a reflection of the relative rates of addition of the stannyl radical to an intermediate conjugated diene compared to that to acetylenes.† To address this problem we were attracted to the use of sulfonyl radicals which have, surprisingly, gained little use in synthesis.[6] In a diyne to diene transformation, we postulated that initial addition–cyclization would lead to an electronically deficient π-system; further addition would be disfavoured due to the inherent electrophilic nature of sulfonyl radicals.[7]

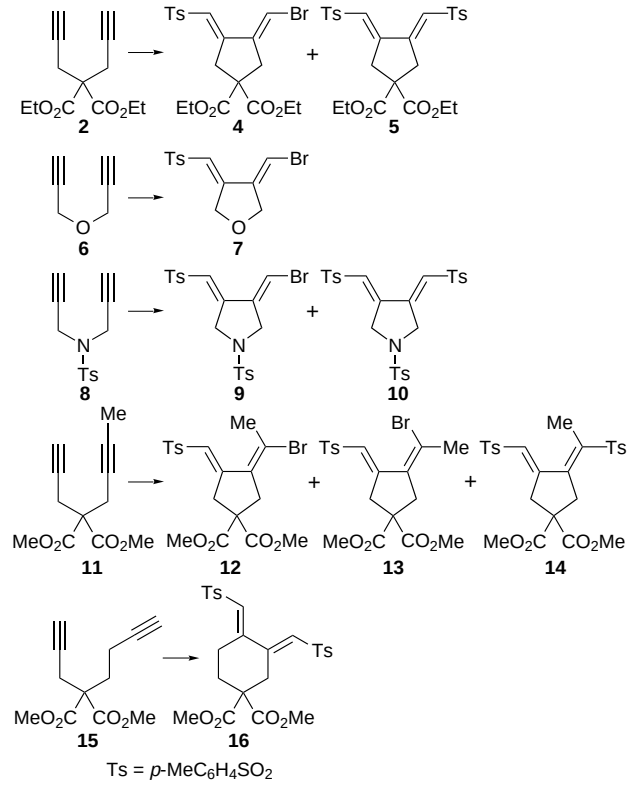
We elected to study the reaction of several readily available diynes with toluene-*p*-sulfonyl bromide (TsBr) under standard free-radical conditions (Scheme 3). Table 1 presents the detailed results of these experiments and several features are worthy of note. Entry 2 shows the optimised transformation of **2** to **4**. When the reaction was carried out under reflux the reaction proceeded with diminished yield and selectivity (entry




**Scheme 1**




**Scheme 2**




**Scheme 3**

**Table 1** Reaction of diynes with toluene-*p*-sulfonyl bromide

| Entry | Precursor | Products (yield, %) |
|---|---|---|
| 1[a] | **2** | **4** (46) **5** (18) |
| 2[b] | **2** | **4** (63) **5** (17) |
| 3[c] | **6** | **7** (72) |
| 4[b] | **8** | **9** (34) **10** (22) |
| 5[b] | **11** | **12** (40) **13** (17.5) **14** (13.5) |
| 6[d] | **2** | **5** (91) |
| 7[d] | **8** | **10** (87) |
| 8[d] | **15** | **16** (51) |

[a] A stirred benzene solution of diyne (*ca.* 0.04 M), TsBr (1 equiv.), AIBN (0.25 equiv.) under reflux over 24 hr. [b] A stirred benzene solution of diyne (*ca.* 0.04 M), TsBr (1 equiv.), AIBN (0.25 equiv.) (external temp. 63–65 °C) over 72 h. [c] A stirred benzene solution of excess diyne (*ca.* 0.04 M), TsBr (1 equiv.), AIBN (0.25 equiv.) in a sealed tube (external temp. 63–65 °C) with AIBN added portionwise (0.25 equiv.) every 24 h until reaction complete. [d] A stirred benzene solution of diyne (*ca.* 0.12 M), TsBr (3 equiv.), AIBN (0.4 equiv.) in a sealed tube (external temp. 98–100 °C) with AIBN added portionwise (0.4 equiv.) every 24 h until reaction complete.

1). Substrate **6** was the only precursor from which we isolated the bromo sulfone; we suspect that this is a result of the relatively insoluble nature of the bromide **7** (entry 3). In the synthesis of heterocycles there is no evidence of products derived from β-scission or double bond migration to yield the aromatic furan or pyrrole (entries 3 and 4).[8]

Entry 5 is particularly informative; it demonstrates the regio- and stereo-control which can be associated with reactions of this type.‡ The products appear to be uniquely derived from addition of the *p*-tolylsulfonyl radical to the least hindered end of the alkyne; we attribute this to a reversible addition of sulfonyl radicals to acetylenes. The stereochemical outcome of these reactions may be a consequence of the rapid rate of inversion of vinyl radicals.[9] If so, it is likely that the stereochemical course of a particular reaction could be predicted by comparison of the relative sizes of the bromine atom with other proximal substituents.§

Initially our efforts were directed at maximising the yield of bromo sulfone products and we were surprised by the isolation of the bis(sulfones). We assume that these products result from the further addition of toluene-*p*-sulfonyl bromide to the bromo sulfones followed by loss of bromine under radical or electrocyclic conditions. The bis(sulfones) have some obvious synthetic utility[10] and we decided to examine the prospect of transforming the diynes directly into the bis(sulfones) as the sole product. We found that this was possible with representative diynes **2** and **8** by treatment with excess toluene-*p*-sulfonyl bromide (entries 6 and 7). Using these conditions we were also able to prepare the cyclohexane derivative **16** from **15** in reasonable yield (entry 8).¶

We believe that cyclizations of this type can form the basis for a general synthetic methodology, however, if the bromo sulfones are required it is likely that any given example will require a particular set of reaction conditions. The shelf stable bis(sulfones) are likely to find some utility in synthesis as they are now readily available in good yield from the diyne precursor. The work presented here illustrates for the first time that diynes can be transformed into stable cyclic dienes[11] under radical conditions using toluene-*p*-sulfonyl bromide. The isolation of the bromo sulfone as the major product under appropriate conditions may support the original hypothesis that the electron deficient sulfonyl diene is relatively unreactive toward the electrophilic sulfonyl radical. The incorporation of two useful functional groups in the products derived from this and other toluene-*p*-sulfonyl radical mediated cyclizations is a clear advantage over related tin based transformations. Investigations of the synthetic utility of the two new classes of diene presented here are ongoing.

We gratefully acknowledge financial support from the EPSRC and GlaxoWellcome for a CASE award (C. L. S.). We also gratefully acknowledge support from Zeneca, Rhone-Poulenc Rorer and the BBSRC for financial support of our programme. We thank Dr A. G. Avent, Dr P. B. Hitchcock, Dr A. K. Abdul-Sada, C. Dadswell and the EPSRC Mass Spectrometry Service at Swansea.

## Footnotes

† The analogous silyl derivative of the intermediate conjugate diene has been successfully synthesised by the use of cuprate methodology, albeit in poor yield: I. Fleming and E. M. deMarigorta, *Tetrahedron Lett.*, 1993, **34**, 1201.

‡ All compounds exhibited data consistent with their formulae (IR, $^1$H and $^{13}$C NMR, MS, HRMS). *Selected data* for **4**: $\nu_{max}/cm^{-1}$ 1733, 1673, 1327, 1148; $\delta_H(CDCl_3$; 250 MHz) 1.23 (t, *J* 7.1, 6 H), 2.41 (s, 3 H), 3.04 (d, *J* 2.7, 2 H), 3.66 (d, *J* 2.4, 2 H), 4.17 (q, *J* 7.1, 4 H), 6.39 (t, *J* 2.4, 1 H), 6.78 (t, *J* 2.7, 1 H), 7.32 and 7.8 (AA′BB′, 4 H); $\delta_C(CDCl_3$; 75.5 MHz) 14.37, 22.04, 39.78, 40.26, 57.56, 62.54, 108.53, 121.17, 127.72, 130.35, 138.84, 142.82, 144.97, 150.32, 170.59 [HRMS: (M + H$^+$) $C_{20}H_{24}{}^{81}BrO_6S$ requires 473.0457. Found, 471.0448]. For **5**: $\nu_{max}/cm^{-1}$ 1732, 1597, 1332, 1149; $\delta_H(CDCl_3$; 250 MHz) 1.22 (t, *J* 7.1, 6 H), 2.41 (s, 6 H), 3.55 (d, *J* 2.3, 4 H), 4.16 (q, *J* 7.1, 4 H), 6.52 (t, *J* 2.3, 2 H), 7.32 and 7.76 (AA′BB′, 8 H); $\delta_C(CDCl_3$; 75.5 MHz) 14.66, 22.38, 38.05, 58.75, 62.96, 125.87, 128.16, 130.77, 138.24, 154.89, 160.80, 170.71 [HRMS: (M + H$^+$) $C_{27}H_{31}O_8S_2$ requires 547.140. Found, 547.1447].

§ The stereochemistry was determined by NMR experiments (NOE studies) and X-ray crystallography.

¶ We have been unable to isolate and characterise the expected bromo sulfone from the complex mixture which results from treatment of **15** with TsBr (1 equiv.).

## References

1 B. Giese, *Radicals in Organic Synthesis: Formation of Carbon Carbon Bonds*, Pergamon, Oxford, 1986; D. P. Curran, *Synthesis*, 1988, 414 and 489; C. P. Jasperse, D. P. Curran, T. Fervig, *Chem. Rev.*, 1991, 1237; D. P. Curran, in *Comprehensive Organic Synthesis*, ed. B. M. Trost and I. Fleming, Pergamon, 1990, vol. 4, p. 715; W. B. Motherwell and D. Crich, *Free Radical Chain Reactions in Organic Synthesis*, Academic Press, 1991.

2 G. Stork and R. Mook, *J. Am Chem. Soc.*, 1987, **109**, 2829; G. Stork and R. Mook, *J. Am. Chem. Soc.*, 1983, **105**, 3721.

3 A. Padwa, H. Nimmesgern and G. S. K. Wong, *J. Org. Chem.*, 1985, **50**, 5620.

4 M. Ramaiah, *Tetrahedron*, 1987, **43**, 3541.

5 D. Crich and S. M. Fortt, *Tetrahedron Lett.*, 1987, **28**, 2895.

6 For reviews of the area, see C. Chatgilialoglu, *The Chemistry of Sulfones and Sulfoxides: Sulfonyl Radicals*, 1988, Wiley, New York; M.-P. Bertrand, *Org. Prep. Proceed. Int.*, 1994, **26**, 257; see also, T. A. K. Smith and G. H. Whitham, *J. Chem. Soc., Perkin Trans 1*, 1989, 31; A. C. Serra, C. M. M. Correa da Silva and M. L. C. Do Vale, *Tetrahedron*, 1991, **47**, 9463; T. G. Back and K. R. Muralidharan, *J. Org. Chem.*, 1989, **54**, 121; M. C. D. Aldoim, A. D. Morris, W. B. Motherwell and D. M. O'Shea, *Tetrahedron Lett.*, 1988, **29**, 4173 and references cited therein.

7 A. S. Gozdz and P. Maslak, *J. Org. Chem.*, 1991, **56**, 2179 and references cited therein.

8 J. E. Brumwell, N. S. Simpkins and N. K. Terrett, *Tetrahedron Lett.*, 1993, **34**, 1215.

9 R. W. Fessenden and R. H. Schuler, *J. Chem. Phys.*, 1963, **39**, 2147.

10 N. S. Simpkins, *Sulfones in Organic Synthesis*, Pergamon Press, Oxford, 1993.

11 For interesting related work, see T. J. Woltering and H. M. R. Hoffman, *Tetrahedron*, 1995, **51**, 7389; M. Journet and M. Malacria, *J. Org. Chem.*, 1994, **59**, 718; P. J. Parsons, P. A. Willis and S. C. Eyley, *Tetrahedron*, 1992, **48**, 9461.

*Received, 21st October 1996; Com. 6/07127I*

# Catalytic asymmetric hydroboration–amination

**Elena Fernandez, Mark W. Hooper, Frances I. Knight and John M. Brown***

*Dyson Perrins Laboratory, South Parks Road, Oxford, UK OX1 3QY*

**A one-pot asymmetric synthesis of primary amines from vinylarenes *via* catalytic hydroboration is described.**

Despite considerable efforts to find alternatives, catecholborane is the most useful borane and rhodium complexes are the most useful catalysts in catalytic hydroboration.[1] Synthetic application of the resulting catecholborane adducts is however limited to oxidation with basic $H_2O_2$, and hence the asymmetric version[2] is in turn limited to the synthesis of secondary alcohols, for which many excellent alternative routes are already available.[3] Given the wealth of functional group transformations that can be performed with alkylboranes,[4] there is an incentive for developing further synthetic outlets for the catalysed case. Our initial efforts were directed to the reaction of isolated 1-phenylethylcatecholboronates† with electrophilic aminating agents such as $ClMgN(Me)OSiMe_3$, and although some success was achieved in controlling enantioselectivity, the chemoselectivity for secondary amine formation over alcohol was moderate.[5]

In considering a direct route from alkylcatecholboronates to amines, we were guided by prior results from Brown's research in which alkylboronates, which do not react directly with the standard aminating agent $H_2NOSO_3H$,[6] were converted by a practical, albeit multistep, route into amines *via* the more reactive dialkylborinate esters. In contrast, excess $R_2Zn$ is reported to effect clean transmetallation of a range of dialkylvinylboranes,[7a] trialkylboranes,[7b] alkylboronates and alkyldithioboronates,[7c] thus providing a route to less accessible alkenyl and alkylzinc compounds. Reaction intermediates have not been reported, although it is likely that the trialkylborane is an intermediate in boronate ester transmetallations (*vide infra*).

Our own initial experiments were conducted in toluene solution by reacting an isolated sample of catecholboronate ester **1** with 1 equiv. of $Et_2Zn$; we were delighted to observe that a clean and quantitative displacement took place, resulting in the transfer of two ethyl groups to boron to form **2** and removal of the Zn from the reaction medium as an insoluble catecholate.[8] The resulting borane was characterized by $^1H$ NMR [$\delta_H(C_7D_8)$ 1.20 (q), 0.95(t)] and MS (*m/z* 205). Oxidation of the borane **2** under standard conditions ($H_2O_2$, NaOH) demonstrated that the configurational integrity of the stereogenic centre had been maintained. At this point we became aware of an early report that primary alkylcatecholboronates react with 2 equiv. of RMgBr by complete displacement of the catechol residue giving the mixed trialkylborane.[9] In accord with this, complete displacement of catecholate without precipitation was observed when the reaction between MeMgCl and borane **1** was carried

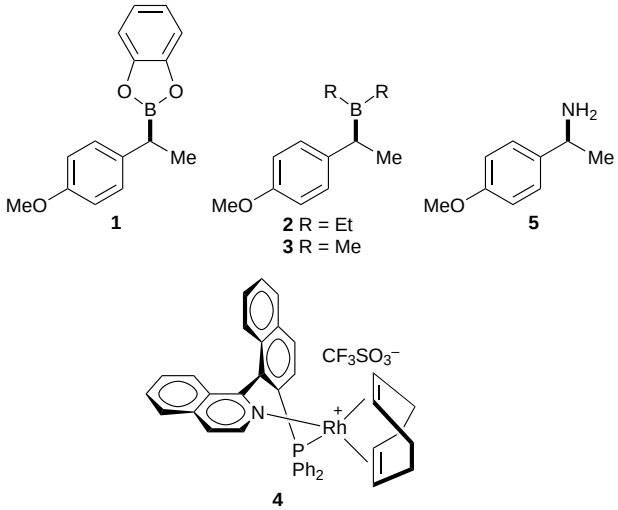
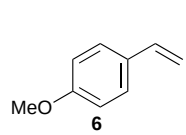
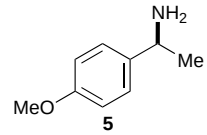
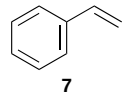
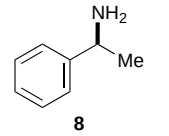
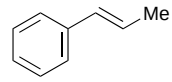
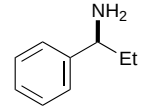
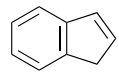
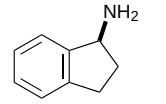
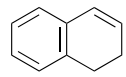
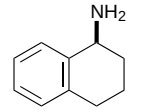
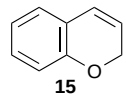
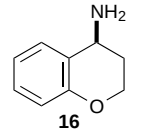
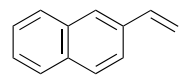
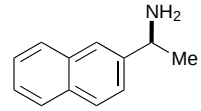



**Table 1** Hydroboration–amination of vinylarenes[a]

| Reactant | Product | Regioselectivity (%)[b] | Isolated yield (%) | Ee (%)[c] |
|---|---|---|---|---|
|  **6** |  **5** | > 98 | 56 | 98 |
|  **7** |  **8** | > 98 | 54 | 87 |
|  **9** |  **10** | > 98 | 50 | 90 |
|  **11** |  **12** | > 98[d] | 61 | 77 |
|  **13** |  **14** | 96 | 51 | 97 |
|  **15** |  **16** | 98[e] | 64 | 89 |
|  **17** |  **18** | 92[f] | 62 | 90 |

[a] Hydroboration–amination experiments as per typical protocol (see footnote ‡). [b] Minor component is regioisomeric primary amine. [c] Ees of amines or their acetamides were analysed by GC using a 25 m CHIRALDEX bonded silica column at 140–150 °C, achieving baseline separation in all cases. [d] From isolated organoborane. [e] Not previously obtained in enantiomerically enriched form, $[\alpha]_D^{23}$ −55.21 (*c* 0.36, $CHCl_3$) for acetylamino derivative; configuration assigned by comparison with (*S*)-chroman-4-ol (ref. 16) formed by hydroboration–oxidation. [f] Analysis by $^1H$ NMR using $Eu(tfc)_3$.

out in thf solution, the only product being **3** [$\delta_C$ 13.0 ($J_{BC}$ 82 Hz)].[10] These displacement reactions were also shown to be occur with other arylalkylboronates prepared by catalytic hydroboration of vinylarenes with catecholborane.

With a clean route to enantiomerically enriched trialkylboranes in hand, attention was then turned to developing a synthetically useful amination procedure. It is known that in aminations with $H_2NOSO_3H$, methyl is a poor migrating group,[11] and a protocol was developed accordingly. It was established in an initial experiment that successive addition of 2 equiv. of MeMgCl and 3 equiv. of $H_2NOSO_3H$ to an isolated sample of borane **1** (86% ee) in thf gave amine **5** in 83% ee and 65% yield. Catalytic hydroboration was then carried out for several vinylarenes in thf solution at ambient temperature, employing the rhodium complex of (*S*)-quinap (**4**) in the manner previously described.[12] On completion of the hydroboration reaction, 2 equiv. of MeMgCl (3 M solution in thf) were added followed after 30 min by 3 equiv. of $H_2NOSO_3H$. After stirring for 12 h the amine was isolated either directly, or as its acetamide (MeCOCl) and the ee analysed as described in Table 1. As far as can be determined, the ee values reflect the enantioselectivity of the catalytic hydroboration step, since $H_2O_2$–$OH^-$ oxidation at the trialkylborane stage provides a secondary alcohol whose enantiomeric purity is the same or slightly lower than that of the primary amine (within experimental error). For the acyclic side-chain amines derived from alkenes **6**, **7**, **9** and **17**, the results follow quite closely those observed previously in hydroboration–oxidation, but superior results have been obtained for the slower-reacting dihydronaphthalene **13** and 4-chromene **15** by very careful attention to catalyst purity and freshness, although indene **11** was somewhat inferior. A one-stage asymmetric synthesis of 1-aminotetralin **14** in 97% ee is of potential practical significance.

In summary, we have developed a method for the catalytic asymmetric synthesis of primary amines from alkenes that complements existing methods, which are most commonly based on imine[13] or enamide reduction,[14] or allylic alkylation procedures.[15] The activation of catecholborane adducts offers the possibility of further extending the range of catalytic hydroboration (*e.g.* to Suzuki couplings and other C–C bond forming reactions) and provides an incentive for us to improve the scope and selectivity of the catalytic reaction itself.

We thank the University of Tarragona for leave (to E. F.) and Johnson-Matthey for the loan of rhodium salts. F. I. K. was supported through a Studentship from LINK Asymmetric Synthesis, and we warmly thank Dr A. J. Blacker (Zeneca) for his help and interest. Dr H. Doucet made helpful contributions.

## Footnote

† IUPAC name: *ortho*-phenylene 1-phenylethylboronate.

‡ Freshly prepared complex **4** (4.0 mg, 0.005 mmol, 1.0 mol%) and thf (0.5 ml) were placed in a vial under argon with the alkene (0.5 mmol). Freshly distilled catecholborane (53.3 μl, 59.5 mg, 0.5 mmol) was added with stirring, then left for 1 h. MeMgCl (3 M in thf, 333 μl, 1.0 mmol) was added and the solution stirred for 30 min. The reactant solution was added to predried $H_2NOSO_3H$ (169 mg, 1.5 mmol), with 0.7 ml of thf or diglyme, and stirred under argon for *ca.* 15 h. HCl (1 M, 2 ml) was added, and the mixture poured into $H_2O$ (4 ml). The aqueous layer was extracted with $Et_2O$ (3 × 20 ml) and then was made strongly alkaline with NaOH (1 M, 3 ml). The mixture was then extracted with $Et_2O$ (3 × 20 ml). The $Et_2O$ extracts were combined and dried with magnesium sulfate, and the solvent removed *in vacuo*.

## References

1 S. Pereira and M. Srebnik, *Organometallics*, 1995, **14**, 3127; E. A. Bijpost, R. Duchateau and J. H. Teuben, *J. Mol. Catal.*, 1995, **95**, 121; X. M. He and J. F. Hartwig, *J. Am. Chem. Soc.*, 1996, **118**, 1696.
2 K. Burgess and M. J. Ohlmeyer, *Chem. Rev.*, 1991, **91**, 1089; J. M. Valk, G. A. Whitlock, T. P. Layzell and J. M. Brown, *Tetrahedron: Asymmetry*, 1995, **6**, 2593.
3 *E.g.* B. Weber and D. Seebach, *Tetrahedron*, 1994, **50**, 6117; A. Fujii, S. Hashiguchi, N. Uematsu, T. Ikariya and R. Noyori, *J. Am. Chem. Soc.*, 1996, **118**, 2521; A. W. Douglas, D. M. Tschaen, R. A. Reamer and Y. J. Shi, *Tetrahedron: Asymmetry*, 1996, **7**, 1303.
4 A. Pelter, K. Smith and H. C. Brown, *Borane Reagents*, Academic Press, New York, 1988.
5 F. I. Knight, A. J. Blacker, J. M. Brown, D. Lazzari and A. Ricci, unpublished results.
6 H. C. Brown, K. W. Kim, T. E. Cole and B. Singaram, *J. Am. Chem. Soc.*, 1986, **108**, 6761; H. C. Brown, M. V. Rangaishenvi and B. Singaram, *J. Org. Chem.*, 1991, **56**, 3286.
7 (*a*) W. Oppolzer and R. N. Radinov, *Helv. Chim. Acta*, 1992, **75**, 170; M. Srebnik, *Tetrahedron Lett.*, 1991, **32**, 2449; (*b*) F. Langer, A. Devasagayaraj, P. Y. Chavant and P. Knochel, *Synlett*, 1994, 410; H. Eick and P. Knochel, *Angew. Chem., Int. Ed. Engl.*, 1996, **35**, 218; (*c*) F. Langer, J. Waas and P. Knochel, *Tetrahedron Lett.*, 1993, **34**, 5261.
8 For the X-ray structure of a Zn catecholate, see H. E. Mabrouk, D. G. Tuck and M. A. Khan, *Inorg. Chim. Acta*, 1987, **129**, 75.
9 S. Cabiddu, A. Maccioni and M. Secci, *Gazz. Chim. Ital.*, 1972, **102**, 555; this work has occasionally been cited, but never been extended despite its obvious usefulness.
10 Dr K. K. Hii, personal communication.
11 B. Carboni and M. Vaultier, *Bull. Soc. Chim. Fr.*, 1995, **132**, 1003.
12 J. M. Brown, D. I. Hulmes and T. P. Layzell, *J. Chem. Soc., Chem. Commun.*, 1993, 1673.
13 N. Uematsu, A. Fujii, S. Hashiguchi, T. Ikariya and R. Noyori, *J. Am. Chem. Soc.*, 1996, **118**, 4916; C. A. Willoughby and S. L. Buchwald, *J. Am. Chem. Soc.*, 1994, **116**, 8952.
14 M. J. Burk, Y. M. Wang and J. R. Lee, *J. Am. Chem. Soc.*, 1996, **118**, 5142.
15 P. Von Matt, O. Loiseleur, G. Koch, A. Pfaltz, C. Lefeber, T. Feucht and G. Helmchen, *Tetrahedron: Asymmetry*, 1994, **5**, 573; A. Togni, U. Burckhardt, V. Gramlich, P. S. Pregosin and R. Salzmann, *J. Am. Chem. Soc.*, 1996, **118**, 1031; H. Kubota and K. Koga, *Heterocycles*, 1996, **42**, 543.
16 H. L. Holland, T. S. Manoharan and F. Schweizer, *Tetrahedron: Asymmetry*, 1991, **2**, 335.

*Received, 9th October 1996; Com. 6/06918E*

# Copper(II)-templated assembly of tetranuclear grid-like complexes from simple pyridine–pyrazole ligands

**John C. Jeffery, Peter L. Jones, Karen L. V. Mann, Elefteria Psillakis, Jon A. McCleverty,* Michael D. Ward* and Claire M. White**

*School of Chemistry, University of Bristol, Cantock's Close, Bristol, UK BS8 1TS*

**Reaction of $Cu(O_2CMe)_2·H_2O$ with $HL^1$ [3-(2-pyridyl)pyrazole] or $HL^2$ [6-(3-pyrazolyl)-2,2′-bipyridine] and $NH_4PF_6$ followed by crystallisation of the crude products from dmf–ether affords $[Cu_4L^1{}_6(dmf)_2][PF_6]_2$ 1 and $[Cu_4L^2{}_4(dmf)_4][PF_6]_4$ 2 respectively, in which the deprotonated pyrazolyl groups act as bridging ligands and the 2 × 2 grid–like architectures are a result of the preference of the $Cu^{II}$ ions for elongated square-pyramidal coordination geometries.**

Recent developments in the specific, efficient syntheses by self-assembly processes of coordination complexes have afforded a variety of unusual topologies such as molecular helicates, grids, ladders, rings, and boxes.[1–6] Such complexes are of interest not only for their unusual structures and the simple synthetic methods used to prepare them, but also because they allow the preparation of high-nuclearity complexes in which several potentially interacting metal centres are linked in a well defined spatial array.

We describe here the syntheses and structures of the copper(II) complexes of $HL^1$ [3-(2-pyridyl)pyrazole] and $HL^2$ [6-(3-pyrazolyl)-2,2′-bipyridine] in which the above principles have been used to prepare tetranuclear grid-like complexes. These complexes are of particular interest as they show (*i*) how the unusual stereoelectronic preferences of $Cu^{II}$ can be harnessed to assemble complex high-nuclearity structures that are not accessible with other metal ions, and (*ii*) how simple polydentate ligands containing terminal pyrazolyl fragments are appealing components for use in supramolecular chemistry.

$HL^1$ (a known ligand)[7,8] forms simple mononuclear octahedral tris-chelate complexes with $Ni^{II}$ and $Zn^{II}$.[9] We reasoned that this was unlikely with $Cu^{II}$. Reaction of $HL^1$ with $Cu(O_2CMe)_2·2H_2O$ (3 : 2) in methanol at room temperature afforded a clear deep green solution from which a blue–green solid precipitated on addition of $NH_4PF_6$. This was recrystallised from dmf–ether to give crystals of **1**·2 dmf in *ca.* 90% yield. FAB mass spectrometry showed the presence of numerous peaks corresponding to polynuclear species [up to $Cu_4L^1{}_6$] and the elemental analysis was consistent with the empirical formula $[Cu_2L^1{}_3(dmf)][PF_6]$.The crystal structure of **1** (Fig. 1) shows that **1** is in fact $[Cu_4L^1{}_6(dmf)_2][PF_6]_2$.† There are two approximately planar $Cu_2(\mu\text{-}L^1)_2$ units, related by an inversion centre, in which each $[L^1]^-$ acts as a terdentate bridge linking the two metal centres; these units are stacked parallel and face-to-face (mean plane separation 3.2–3.5 Å), with additional

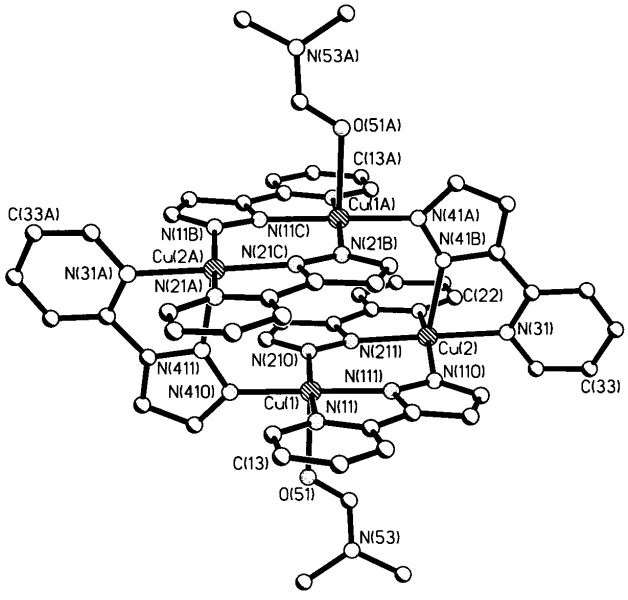



**Fig. 1** Structure of the complex cation of **1**. Selected bond lengths (Å) and angles (°): Cu(1)–N(410) 1.977(2), Cu(1)–N(210) 1.980(2), Cu(1)–N(111) 1.982(2), Cu(1)–N(11) 2.064(2), Cu(1)–O(51) 2.339(2), Cu(2)–N(211( 1.968(2), Cu(2)–N(110) 1.996(2), Cu(2)–N(31) 2.047(2), Cu(2)–N(21) 2.073(2), Cu(2)–N(411A) 2.198(2); N(11)–Cu(1)–N(111) 80.57(9), N(410)–Cu(1)–N(210) 91.57(9), N(210)–Cu(1)–N(111) 96.64(9), N(410)–Cu(1)–N(11) 90.51(9), N(410)–Cu(1)–N(111) 170.61(9), N(21)–Cu(1)–N(11) 168.85(9), N(211)–Cu(2)–N(110) 96.60(9), N(110)–Cu(2)–N(31) 90.31(9), N(211)–Cu(2)–N(21) 80.72(9), N(21)–Cu(2)–N(31) 91.31(9), N(211)–Cu(2)–N(31) 171.35(9), N(110)–Cu(2)–N(21) 165.66(9), N(31)–Cu(2)–N(411A) 78.44(9).

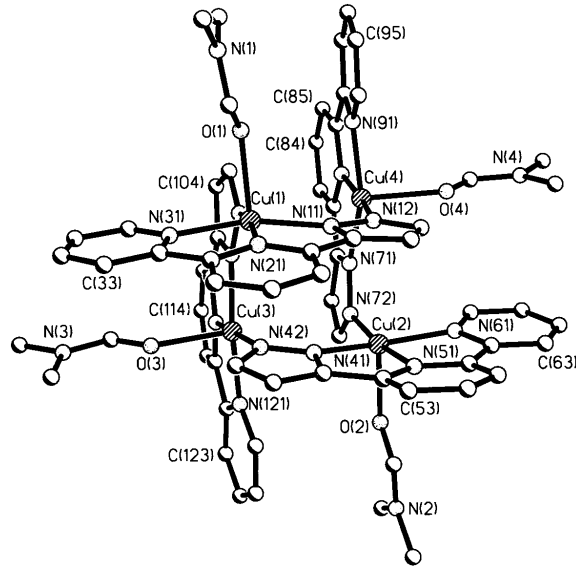



**Fig. 2** Structure of the complex cation of **2**. Selected bond lengths (Å) and angles (°): Cu(1)–N(102) 1.949(5), Cu(1)–N(21) 1.957(5), Cu(1)–N(11) 2.001(5), Cu(1)–N(31) 2.050(5), Cu(1)–O(1) 2.243(4), Cu(2)–N(72) 1.951(5), Cu(2)–N(51) 1.954(5), Cu(2)–N(41) 2.012(5), Cu(2)–N(61) 2.049(5), Cu(2)–O(2) 2.271(4), Cu(3)–N(42) 1.952(5), Cu(3)–N(111) 1.956(5), Cu(3)–N(101) 2.010(5), Cu(3)–N(121) 2.056(5), Cu(3)–O(3) 2.229(4), Cu(4)–N(12) 1.949(5), Cu(4)–N(81) 1.961(5), Cu(4)–N(71) 2.012(4), Cu(4)–N(91) 2.041(5), Cu(4)–O(4) 2.227(4); N(102)–Cu(1)–N(21) 168.4, N(11)–Cu(1)–N(31) 157.6(2), N(51)–Cu(2)–N(72) 171.5(2), N(41)–Cu(2)–N(61) 156.8(2), N(42)–Cu(3)–N(111) 170.2(2), N(101)–Cu(3)–N(121) 156.4, N(12)–Cu(4)–N(81) 171.9(2), N(71)–Cu(4)–N(91) 156.1(2).

deprotonated ligands $[L^1]^-$ perpendicular to the two $Cu_2(\mu\text{-}L^1)_2$ planes forming linking 'cross-pieces'. Two of the metals [Cu(1) and Cu(1A)] have additional dmf ligands attached, and therefore have a square-pyramidal $N_4O$ environment in which the O ligands (dmf) are axial; Cu(2) and Cu(2A) have square-pyramidal $N_5$ environments in which one of the pyrazole donor atoms is in the axial position. In every case the axial ligand is significantly further from the metal [Cu(I)–O(51) 2.339(2) Å, Cu(2)–N(411A) 2.198(2) Å] than the four equatorial ligands (lengths in the range 1.97–2.07 Å), in keeping with the requirements of the Jahn–Teller effect.

$HL^2$ was prepared in exactly the same way as $HL^1$,[8] but starting from 6-acetyl-2,2′-bipyridine. $HL^2$ forms simple mononuclear octahedral complexes with many first-row metal ions.[9] Reaction of $HL^2$ with $Cu(O_2CMe)_2\cdot 2H_2O$ (1 : 1) in methanol at room temperature followed by addition of aqueous $NH_4PF_6$ resulted in precipitation of a blue–green solid which was recrystallised from dmf–ether to give crystals of **2**·6dmf in *ca.* 80% yield. Electrospray mass spectrometry indicated the formation of a tetranuclear complex in solution, and the elemental analysis indicated the empirical formula $[Cu(L^2)][PF_6]$, *i.e.* a 1 : 1 metal : ligand ratio. The crystal structure of **2** is in Fig. 2,† and shows that **2** is the tetramer $[Cu_4L^2_4(dmf)_4][PF_6]_4$ and has many structural similarities to **1**. The overall structure is that of a 2 × 2 grid, with two pairs of parallel, stacked $[L^2]^-$ ligands mutually perpendicular to each other. The stacking distances again are in the range 3.2–3.5 Å. Each metal ion is coordinated by the terdentate pocket of one deprotonated ligand $[L^2]^-$, one pyrazole donor atom which is acting as a bridge to a ligand attached to another metal ion, and a dmf ligand. The result is an elongated $N_4O$ square-pyramidal geometry with the dmf ligand in the axial position; the axial bond lengths lie in the range 2.23–2.27 Å, in contrast to the equatorial ones which lie in the range 1.95–2.06 Å. The four metal ions are crystallographically independent but chemically very similar, and the complex has approximate $S_4$ symmetry (*cf.* the $S_2$ axis of **1** implied by its inversion centre).

The grid-like architecture of both complexes is emphasised in Fig. 3. Comparison with the simple mononuclear octahedral complexes that these ligands can also form[9] shows that assembly of these structures is directed principally by the stereoelectronic preference of the $Cu^{II}$ ions for elongated tetragonal geometry: to satisfy this requirement necessitates deprotonation of the pyrazole rings and bridging behaviour of the ligand. These structures are in interesting contrast to other grid- and ladder-like structures in which the necessary mutually perpendicular orientation of ligand strands is achieved by using ligands with bidentate compartments assembling around (pseudo-tetrahedral) $Cu^I$ or $Ag^I$ templates.[3,5,6]

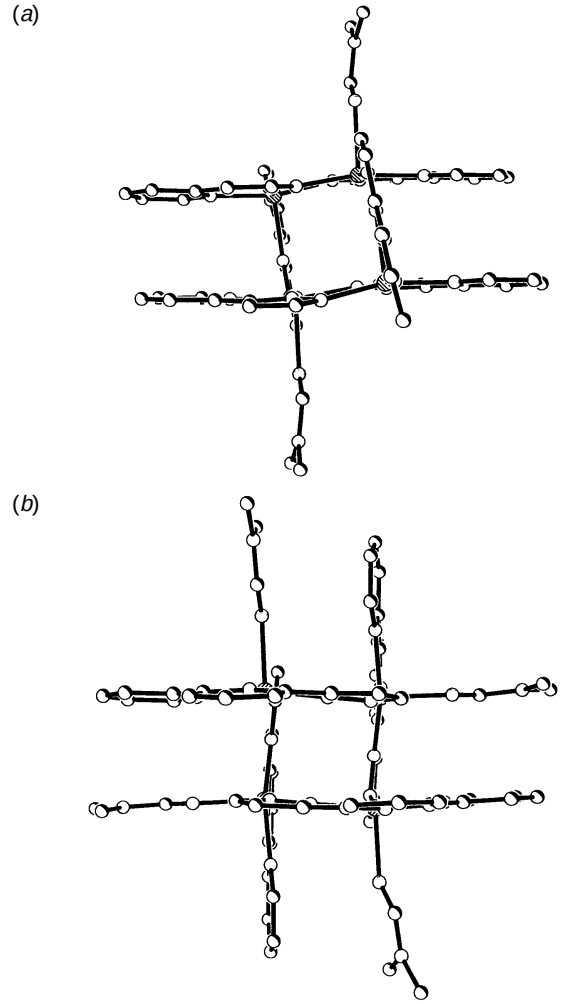



**Fig. 3** Alternative views of the complex cations of **1** (*a*) and **2** (*b*) emphasising the grid-like structure and the aromatic stacking

## Footnote

† *Crystallography*. Suitable crystals were mounted on a Siemens SMART diffractometer (graphite-monochromatised Mo-Kα X-radiation).

**1**·2dmf: $C_{60}H_{64}Cu_4F_{12}N_{22}O_4P_2$, $M$ = 1701.4, green plates, crystal size 0.5 × 0.4 × 0.1 mm; triclinic, space group $P\bar{1}$; $a$ = 10.410(2), $b$ = 13.282(3), $c$ = 14.170(2) Å, α = 85.254(10), β = 70.087(12), γ = 68.15(2)°; $U$ = 1707.5(6) Å$^3$; $Z$ = 1; $D_c$ = 1.655 g cm$^{-3}$; $F(000)$ = 864; μ(Mo-Kα) = 1.373 mm$^{-1}$. 8183 data were collected with $2\theta_{max}$ = 50° at −100 °C, and merged to give 5820 unique data ($R_{int}$ = 0.023).

**2**·6dmf: $C_{82}H_{106}Cu_4F_{24}N_{26}O_{10}P_4$, $M$ = 2450.0, green needles, crystal size 0.7 × 0.15 × 0.1 mm$^3$; monoclinic, space group $P2_1/n$; $a$ = 19.567(2), $b$ = 26.313(3), $c$ = 20.033(2) Å; β = 91.44(1)°; $U$ = 10311(3) Å$^3$; $Z$ = 4; $D_c$ = 1.578 g cm$^{-3}$; $F(000)$ = 5008; μ(Mo-Kα) = 0.987 mm$^{-1}$. 63 226 data were collected with $2\theta_{max}$ = 55° at −100 °C, and merged to give 23 223 unique data ($R_{int}$ = 0.079).

Both structures were solved by direct methods, and refined on all $F^2$ data using the SHELX suite of programs. All non-hydrogen atoms were refined with anisotropic thermal parameters; hydrogen atoms were included in calculated positions with fixed isotropic thermal parameters. For **1**·2dmf, $R_1$ = 0.036, $wR_2$ = 0.106. The complex is centrosymmetric so each asymmetric unit contains one half of the complex and one unique dmf molecule. For **2**·6dmf, $R_1$ = 0.079, $wR_2$ = 0.200. Each asymmetric unit contains one complete tetranuclear complex and six independent molecules of dmf. Atomic coordinates, bond lengths and angles, and thermal parameters have been deposited at the Cambridge Crystallographic Data Centre (CCDC). See Information for Authors, Issue No. 1. Any request to the CCDC for this material should quote the full literature citation and the reference number 182/323.

## References


1 D. Philp and J. F. Stoddart, *Angew. Chem., Int. Ed. Engl.*, 1996, **35**, 1155 and references therein.
2 B. Hasenknopf, J.-M. Lehn, B. O. Kneisel, G. Baum and D. Fenske, *Angew. Chem., Int. Ed. Engl.*, 1996, **35**, 1838 and references therein.
3 P. N. W. Baxter, G. S. Hanan and J.-M. Lehn, *Chem. Commun.*, 1996, 2019 and references therein.
4 E. C. Constable, *Prog. Inorg. Chem.*, 1994, **42**, 67.
5 M.-T. Youinou, N. Rahmouni, J. Fischer and J. A. Osborn, *Angew. Chem., Int. Ed. Engl.*, 1992, **31**, 733.
6 P. N. W. Baxter, J.-M. Lehn, J. Fischer and M.-T. Youinou, *Angew. Chem., Int. Ed. Engl.*, 1994, **33**, 2284.
7 P. L. Jones, J. C. Jeffery, J. A. McCleverty and M. D. Ward, *Polyhedron*, in the press.
8 A. J. Amoroso, A. M. W. Cargill Thompson, J. C. Jeffery, P. L. Jones, J. A. McCleverty and M. D. Ward, *J. Chem. Soc., Chem. Commun.*, 1994, 2751; H. Brunner and T. Scheck, *Chem. Ber.*, 1992, **125**, 701.
9 K. L. V. Mann, E. Psillakis, J. A. McCleverty and M. D. Ward, unpublished work.


*Received, 7th October 1996; Com. 6/06827H*

# Rings and linear polymers formed by addition of silver perchlorate to *trans*-[Pt(C≡CR)$_2$(PMe$_2$Ph)$_2$] (R = Bu$^t$, H)

**Shinsaku Yamazaki,*[a] Antony J. Deeming,*[b] Despo M. Speel,[b] David E. Hibbs,[c] Michael B. Hursthouse[c] and K. M. Abdul Malik[c]**

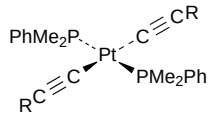
[a] *Chemistry Laboratory, Kochi Gakuen College, 292 Asahi Tenjin-Cho, Kochi 780, Japan*
[b] *Department of Chemistry, University College London, 20 Gordon Street, London, UK WC1H 0AJ*
[c] *School of Chemistry and Applied Chemistry, University of Wales, PO Box 912, Cardiff, UK CF1 3TB*

**Addition of AgClO$_4$ to *trans*-[Pt(C≡CR)$_2$(PMe$_2$Ph)$_2$] (R = Bu$^t$, H) gives 1 : 1 adducts of the general formula *trans*-[PtAg(ClO$_4$)(μ-C≡CR)$_2$(PMe$_2$Ph)$_2$] which are cyclic dimers when R = Bu$^t$ (ClO$_4^-$ not coordinated) or linear polymers when R = H (ClO$_4^-$ coordinated to silver).**

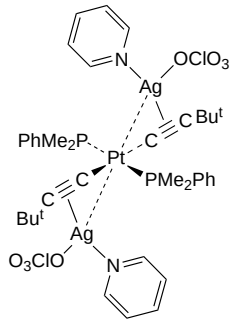
*cis*-Dialkynyl complexes of platinum behave as chelating bidentate ligands at copper(I) and silver(I). *cis*-[Pt(CuCl)(C≡CBu$^t$)$_2$(PMe$_2$Ph)$_2$] **1** contains Cu coordinated to two alkynes and a chloride ligand and the complexes [Pt$_2$M(C≡CPh)$_4$(dppe)$_2$][BF$_4$] (M = Cu[1], Ag[2]) and *cis*-[Pt$_2$Ag(C≡CPh)$_4$(PPh$_3$)$_4$][ClO$_4$][3] contain Ag or Cu atoms coordinated tetrahedrally to four alkyne groups. Some recent examples of coordination of Pt alkynyl complexes to silver(I)[1–4] and a review by Forniés and Lalinde have appeared.[5]

Attempting to form linear polymers containing M(μ-C≡CR)M′ components, we coupled CuCl with *trans*-[Pt(C≡CBu$^t$)$_2$(PMe$_2$Ph)$_2$]. Since the alkynyl ligands are *trans* at platinum, chelation is not possible and the linear polymer [{PtCu$_2$Cl$_2$(C≡CBu$^t$)$_2$(PMe$_2$Ph)$_2$}$_n$] with the polymer backbone ···Pt[(μ-C≡CR)CuCl$_2$Cu(μ-RC≡C)Pt]$_n$(μ-C≡CR)··· was obtained.[6] This paper describes our preparation of halide-free polymers with the backbone ···Pt(μ-C≡CR)[Ag(μ-RC≡C)Pt(μ-C≡CR)]$_n$Ag··· composed only of metal and bridging alkynyl ligands.

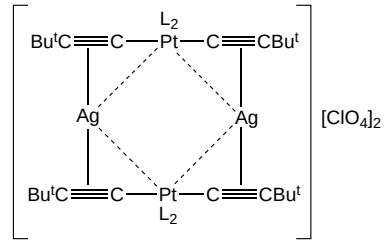
The complex *trans*-[Pt(C≡CBu$^t$)$_2$(PMe$_2$Ph)$_2$] **1a** reacts with AgClO$_4$ (2 mol/mol Pt) in acetonitrile to give *trans*-[PtAg$_2$(MeCN)$_x$(μ-C≡CBu$^t$)$_2$(PMe$_2$Ph)$_2$][ClO$_4$]$_2$ **2** (*x* is probably 4) and we have determined the X-ray structure of the corresponding copper complex with *x* = 4.[2] Treatment of **2** with pyridine gave the neutral derivative *trans*-[PtAg$_2$(ClO$_4$)$_2$(py)$_2$(μ-C≡CBu$^t$)$_2$(PMe$_2$Ph)$_2$] **3** which was characterised by single-crystal X-ray diffraction.[2] In **3** one silver ion coordinates to each of the two alkynyl ligands and polymerisation is prevented. However, with restricted addition of AgClO$_4$ (1 mol/mol Pt complex) to *trans*-[Pt(C≡CBu$^t$)$_2$(PMe$_2$Ph)$_2$] **1a**, a complex is formed which crystallised from benzene as *trans*-[Pt$_2$Ag$_2$(μ-C≡CBu$^t$)$_4$(PMe$_2$Ph)$_4$][ClO$_4$]$_2$·2C$_6$H$_6$ **4**·2C$_6$H$_6$.† The stoichiometry fits a linear polymer but in this case an alternative cyclic dimer is formed. The X-ray structure was determined at 150(2) K because of crystal degradation at 293 K (see Fig. 1).‡ In contrast to compound **3**, the silver atoms in **4** coordinate on the same face of the Pt coordination plane allowing two square-planar Pt complexes to be glued parallel to each other by two




**1a** R = Bu$^t$
**b** R = H




**3**




**4** (L = PMe$_2$Ph)

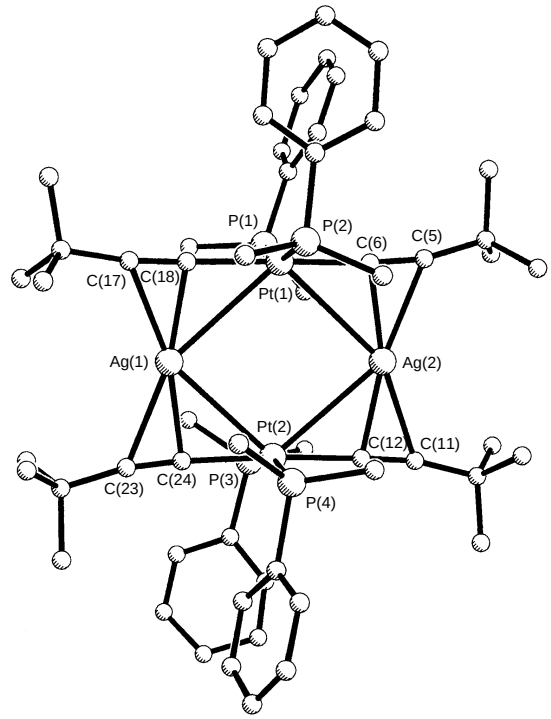



**Fig. 1** Structure of the square dicationic complex in *trans*-[Pt$_2$Ag$_2$(μ-C≡CBu$^t$)$_4$(PMe$_2$Ph)$_4$][ClO$_4$]$_2$·2C$_6$H$_6$ **4**·2C$_6$H$_6$. The non-coordinated perchlorate ions and the benzene molecule are not shown.

$Ag^+$ ions. The perchlorate ions are not coordinated. The $Pt_2Ag_2$ set of atoms is closely planar and approximately square [Pt–Ag distances 3.1960(10), 3.2161(9), 3.2080(9), 3.2683(10) Å; Pt–Ag–Pt angles 86.51(2), 85.44(2)°; Ag–Pt–Ag angles 93.26(2), 94.79(2)°; Pt···Pt 4.3938(9) Å and Ag···Ag 4.7138(9) Å]. The Ag atoms appear to be pulled in towards the centre of the square resulting in shorter contacts with the α than the β alkynyl carbon atoms [av. Ag–$C^{\alpha}$ 2.236 Å, av. Ag–$C^{\beta}$ 2.448 Å] (Fig. 2). Pt···Ag distances up to 2.95 Å have been considered to indicate donor interactions from Pt to Ag but in this case the average Pt···Ag distance of 3.22 Å shows that such interactions must be extremely weak.[7]

The $Bu^t$ groups in **4** are bent away from each other [av. $C^{\alpha}C^{\beta}C(Bu^t)$ 169.1°], as are the tertiary phosphines [P–Pt–P 160.06(8), 163.95(8)°], suggesting that replacement of the $Bu^t$ groups by smaller substituents would allow the cyclic molecules to relax into a tighter configuration. However, addition of $AgClO_4$ (1 mol/mol Pt) to *trans*-[$Pt(C{\equiv}CH)_2(PMe_2Ph)_2$] gives crystals of *trans*-[$PtAg(ClO_4)(\mu\text{-}C{\equiv}CH)_2(PMe_2Ph)_2$] **5**† which, rather than forming a cyclic dimer, gives a linear polymer (X-ray structure, Fig. 3).‡ Relaxation of crowding around Ag has allowed the perchlorate to coordinate to it and the *trans* $PMe_2Ph$ ligands to become closely linear [P–Pt–P 177.2(1)°]. The $Ag^+$ ions still coordinate on the same face of each Pt coordination plane (as in **4** but not **3**) forming a zigzag chain with a perchlorate ion in each cavity along the chain. In addition to the short coordinated Ag–O distance [Ag(1)–O(1) 2.65(1) Å], there are number of $ClO_4^-$-to-chain contacts which might help to stabilize this arrangement. The shortest C≡CH···O contact is too long to be considered a hydrogen bond. [$C^{\beta}$···O 3.56 Å]. Fig. 2 shows the differences in the geometries of $Ag^+$ coordination in compounds **4** and **5**. The $Ag^+$ ion is more closely coordinated to $C^{\alpha}$ than $C^{\beta}$ in **5**, the reverse of the situation in **4**, and Pt···Ag distance are much longer in **5** than in **4**.

We have tried to synthesise analogues of **5** with other counter ions such as $BPh_4^-$ which are too big to fit the cavities or unlikely to coordinate but no crystalline products could be obtained. We have still to assess properly the factors that control the mode of aggregation of [$PtAg(ClO_4)(C{\equiv}CR)_2(PMe_2Ph)_2$] units in complexes of this type.

We thank the Royal Society and the Japan Promotion of Sciences (S. Y.) for support for this collaboration.

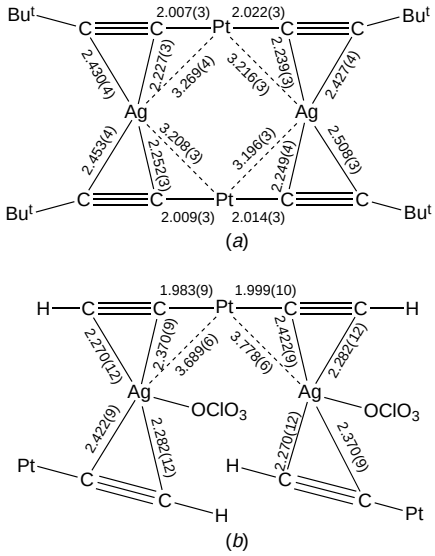
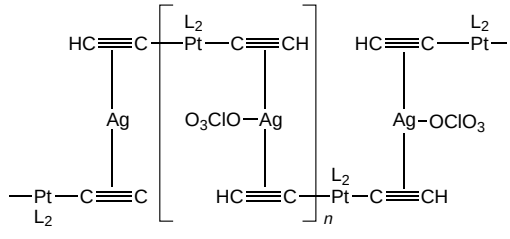



**Fig. 2** Details of the Ag/Pt/alkynyl ligand geometries in **4**·$2C_6H_6$ (*a*) and in **5** (*b*); distances in Å




**5** (L = $PMe_2Ph$)

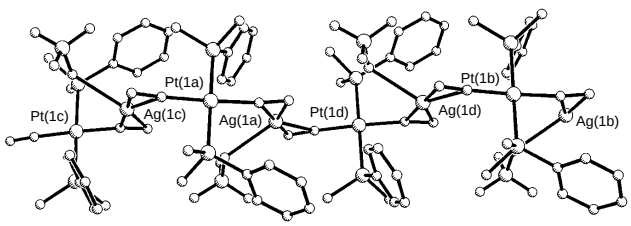



**Fig. 3** Structure of the linear polymer [{$PtAg(ClO_4)(C{\equiv}CH)_2(PMe_2Ph)_2$}$_n$] **5**; in this case the coordinated perchlorate ions are shown

## Footnotes

† *Synthesis and spectra* of Ag–Pt complexes. Compound **4**: a solution of **1a** (0.223 g) in acetonitrile was treated with $AgClO_4$ (0.081 g). Addition of benzene and slow evaporation at room temp. gave pale yellow crystals of **4**·$2C_6H_6$ (0.240 g, 98%); ν(C≡C) (Nujol), 2031w $cm^{-1}$; $^1H$ NMR ($CD_3CN$): δ 1.17 (s, $Bu^t$), 2.02 [t, *J*(PH) 7.4, *J*(PtH) 30.8 Hz, $PMe_2Ph$], 7.37 (s, $C_6H_6$), 7.4–8.0 ($PMe_2Ph$); $^{13}C\{^1H\}$ NMR ($CDCl_3$) δ 15.08 [t, *J*(PC) 39.1 Hz, $PMe_2Ph$], 30.82 ($CMe_3$), 32.55 ($CMe_3$); $^{31}P\{^1H\}$ NMR ($CDCl_3$) δ −14.79 [*J*(PtP) 2109 Hz].

Compound **5**: a solution of **1b** {prepared from *cis*-[$PtCl_2(PMe_2Ph)_2$] and $NaC_2H$ in liquid $NH_3$} (0.20 g) in acetonitrile was treated with $AgClO_4$ (0.088 g). Addition of benzene led to the gradual crystallization of pale yellow crystals (0.11 g, 40%), ν(C≡C) (Nujol), 1914 $cm^{-1}$; $^1H$ NMR spectra ($CD_3CN$) show a mixture, FABMS (NOBA matrix) showed $[Pt_2Ag(C_2H)_4(PMe_2Ph)_4]^+$ and $[PtAg(C_2H)_2(PMe_2Ph)_2]^+$ as the highest mass ions.

‡ *Crystal data*. Compound **4**·$2C_6H_6$: $C_{68}H_{92}Ag_2Cl_2O_8P_4Pt_2$, pale yellow crystals from benzene, 0.40 × 0.20 × 0.15 mm, $M$ = 1838.12, triclinic, space group $P\bar{1}$, $a$ = 14.608(2), $b$ = 16.338(2), $c$ = 16.356(3) Å, α = 87.28(1), β = 75.02(1), γ = 76.43(1)°, $U$ = 3665.3(13) Å$^3$, $Z$ = 2, $D_c$ = 1.66 g $cm^{-3}$, 9854 unique data, 9854 used, 723 parameters, $R_1$ = 0.0522, $wR_2$ = 0.0916. Compound **5**: $C_{20}H_{24}AgClO_4P_2Pt$, pale yellow crystals from acetonitrile–benzene, 0.09 × 0.22 × 0.40 mm, $M$ = 728.29, monoclinic, space group $P2_1/c$, $a$ = 10.481(2), $b$ = 12.236(2), $c$ = 18.868(3) Å, β = 101.53(1)°, $U$ = 2371.3(6) Å$^3$, $Z$ = 4, $D_c$ = 2.04 g $cm^{-3}$, 4173 unique data, 3163 used [$I_o > 3\sigma(I_o)$], 262 parameters, $R$ = 0.0387, $R_w$ = 0.0428.

Atomic coordinates, bond lengths and angles, and thermal parameters have been deposited at the Cambridge Crystallographic Data Centre (CCDC). See Information for Authors, Issue No. 1. Any request to the CCDC for this material should quote the full literature citation and the reference number 182/324.

## References

1 S. Yamazaki and A. J. Deeming, *J. Chem. Soc., Dalton Trans.*, 1993, 3051.
2 S. Yamazaki and A. J. Deeming, unpublished work.
3 I. Ara, J. R. Berenguer, J. Forniés, E. Lalinde and M. T. Moreno, *J. Organomet. Chem.*, 1996, **510**, 63.
4 P. Espinet, J. Forniés, F. Martínez, M. Tomás, E. Lalinde, M. T. Moreno, A. Ruiz and A. J. Welch, *J. Chem. Soc., Dalton Trans.*, 1990, 791; J. Forniés, M. A. Gómez-Saso, F. Martínez, E. Lalinde, M. T. Moreno and A. J. Welch, *New J. Chem.*, 1992, **16**, 483; J. Forniés, E. Lalinde, F. Martínez, M. T. Moreno and A. J. Welch, *J. Organomet. Chem.*, 1993, **455**, 271; I. Ara, J. Forniés, E. Lalinde, M. T. Moreno and M. Tómas, *J. Chem. Soc., Dalton Trans.*, 1994, 2735; J. Forniés, E. Lalinde, A. Martín and M. T. Moreno, *J. Organomet. Chem.*, 1995, **490**, 179; I. Ara, J. Forniés, E. Lalinde, M. T. Moreno and M. Tómas, *J. Chem. Soc., Dalton Trans.*, 1995, 2397.
5 J. Forniés and E. Lalinde, *J. Chem. Soc., Dalton Trans.*, 1996, 2587.
6 S. Yamazaki, A. J. Deeming, M. B. Hursthouse and K. M. A. Malik, *Inorg. Chim. Acta*, 1995, **236**, 147.
7 A. Erxleben and B. Lippert, *J. Chem. Soc., Dalton Trans.*, 1996, 2329.

*Received, 29th October 1996; Com. 6/07358A*

# Novel syntheses of heterodinuclear phosphaalkenyl complexes: X-ray structure of $[Ru\{P(AuPPh_3)=CHBu^t\}Cl_2(CO)(PPh_3)_2]$

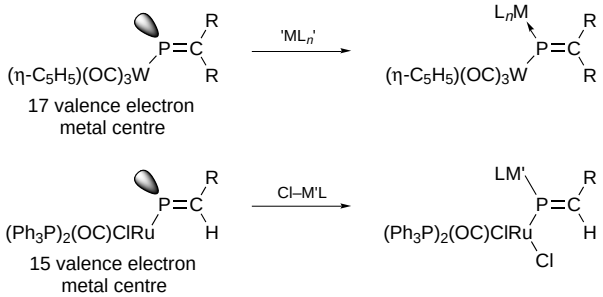
**Robin B. Bedford,[a] Anthony F. Hill,*†[a] Cameron Jones,*‡[b] Andrew J. P. White,[c] David J. Williams[c] and James D. E. T. Wilton-Ely[a]**

[a] *Department of Chemistry, Imperial College of Science, Technology and Medicine, South Kensington, London, UK SW7 2AY*
[b] *Department of Chemistry, University of Wales, Swansea Singleton Park, Swansea, UK SA2 8PP*
[c] *Chemical Crystallography Laboratory, Department of Chemistry, Imperial College of Science, Technology and Medicine, South Kensington, London, UK SW7 2AY*

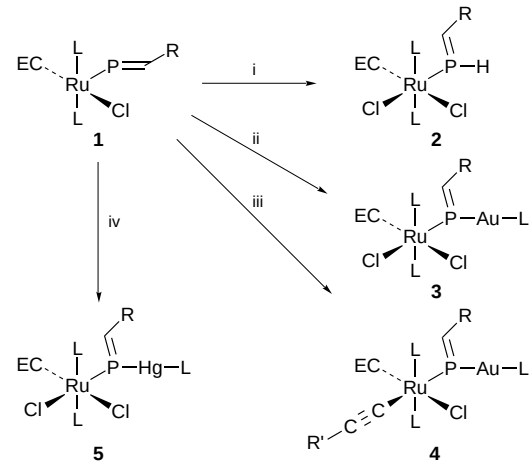
**The reaction of $[Ru(P{=}CHBu^t)Cl(CE)(PPh_3)_2]$ (E = O, S) with $[AuX(PPh_3)]$ (X = Cl, $C{\equiv}CC_6H_4Me$-4), $HgCl_2$ or $Hg_2Cl_2$ leads *via* addition of the Au–X or Hg–Cl bonds across the Ru–P linkage to the heterodinuclear phosphaalkene complexes $[Ru\{P(AuPPh_3){=}CHBu^t\}ClX(CE)(PPh_3)_2]$ and $[Ru\{P(HgCl){=}CHBu^t\}Cl_2(CE)(PPh_3)_2]$.**

Mononuclear phosphaalkenyl complexes remain rare.[1] Nevertheless, our recent observation[2] that hydroruthenation of phosphaalkynes provides an exceptionally facile entry into such compounds should presage a substantial broadening of the field. Polynuclear phosphaalkenyl complexes remain unknown, and only one example of a dinuclear complex has been structurally characterised, resulting from the reaction of the kinetically stabilised phosphaalkene $ClP{=}C(SiMe_3)_2$ with Collman's reagent.[3] The remaining examples involve the reactions of $[W\{P{=}C(R)SiMe_3\}(CO)_3(\eta\text{-}C_5H_5)]$ (R = Ph, $SiMe_3$) with $[Fe_2(CO)_9]$, $[Ni(CO)_4]$ or $[AuCl(PPh_3)]$.[4] In these reactions the lone pair of the phosphaalkenyl ligand coordinates to $Fe(CO)_4$, $Ni(CO)_3$ or AuCl fragments *via* a simple dative two-electron interaction. It is this aspect of phosphaalkenyl coordination chemistry with which this report is concerned, in illustrating for the first time the 1,2-addition of metal–halide and metal–carbon bonds across the P–C multiple bond of a phosphaalkenyl complex. This approach converts the three-electron phosphaalkenyl ligand into a formally neutral metallated phosphaalkene (Scheme 1). This has allowed the first structural characterisation of a heterobimetallic phosphaalkenyl complex.

The nucleophilicity of the phosphaalkenyl ligand in the complex $[Ru(P{=}CHBu^t)Cl(CO)(PPh_3)_2]$ **1a** has been recently demonstrated in its reactivity with HCl to provide the phosphaalkene complex $[Ru(HP{=}CHBu^t)Cl_2(CO)(PPh_3)_2]$ **2**.[2] Over the last decade, guided by isolobal considerations the fragment $AuPPh_3^+$ has come to be viewed as the cluster chemist's proton. Within this context, it is therefore noteworthy that the reaction of **1a** with $[AuCl(PPh_3)]$ leads to the smooth and high yield conversion of **1a** to a complex formulated as $[Ru\{P(AuPPh_3){=}CHBu^t\}Cl_2(CO)(PPh_3)_2]$ **3a** on the basis of spectroscopic§ and crystallographic¶ data (Scheme 2, Fig. 1). Most informative amongst the spectroscopic data is the upfield shift of the $^{31}P$ NMR signal associated with the phosphaalkenyl ligand from δ 450.4 in **1a** to δ 319.4 in **3a**. This resonance appears as a double triplet as a result of coupling to the phosphine phosphorus nuclei bound to gold [$J$(PP) 268.5 Hz] and ruthenium [$J$(PP′) 29.6 Hz]. The former suggests an essentially *trans* P–Au–P linkage, whilst the latter is con-




**Scheme 1** Phosphaalkenyl complexes as ligands; $ML_n$ = $Fe(CO)_4$, $Ni(CO)_3$, AuCl; M′L = HgCl, $AuPPh_3$




**Scheme 2** (L = $PPh_3$, R = $CMe_3$, R′ = $C_6H_4Me$-4, E = O, S). *Reagents and conditions*: i, HCl; ii, [AuCl(L)]; iii, [Au(C≡CR′)L]; iv, $Hg_2Cl_2$ or $HgCl_2$.

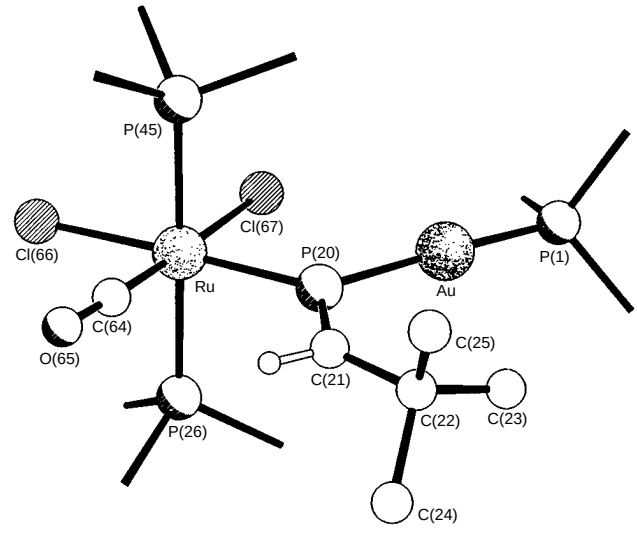



**Fig. 1** Molecular geometry for $[Ru\{P(AuPPh_3){=}CHBu^t\}Cl_2(CO)(PPh_3)_2]$ **3a**; phenyl groups omitted

siderably larger than that found in the precursor **1a** (10.0 Hz). The resonances due to the phosphine ligands both show coupling to the phosphaalkenyl phosphorus, however there is no resolvable coupling between the phosphine resonances consistent with the absence of an Ru–Au bond.

The formulation was confirmed by a single-crystal X-ray diffraction analysis,¶ the results of which are summarised in Fig. 1. The geometry at ruthenium is essentially octahedral with *cis*-interligand angles in the range 87.2(3)–93.0(1)°, whilst the geometry at gold is close to linear [P(1)–Au–P(20) 177.6(1)°]. The two ruthenium chloride distances are 2.481(2) and 2.464(2) Å indicating that the *trans* influence of the phosphaalkenyl ligand is only marginally greater than that of the carbonyl ligand. Interest focusses on the phosphaalkenyl bridge although the novelty of **3a** leaves us with little precedent for comparison. It is noteworthy that the coordination at phosphorus is trigonal [intersubstituent angles in the range 119.7(3)–120.2(3)°], indeed this planarity extends to include Au, P(1), C(22) and the equatorial ruthenium coordination plane [maximum deviation from planarity of 0.085 Å by Cl(66)]. The P(20)–C(21) bond length of 1.664(9) Å is clearly multiple in nature, and comparable to that observed [1.640(4) Å] in [Fe{μ-P=C(SiMe$_3$)$_2$}$_2$(CO)$_6$].[3] The two Au–P distances differ only marginally, with that to the phosphaalkenyl ligand [2.320(2) Å] being the longer of the two. The Ru–P(20) separation of 2.296(2) Å is however *ca*. 0.1 Å shorter than those to the phosphines [P(45) 2.397(2), P(26) 2.413(2) Å], indicating a π-acid role for the phosphaalkenyl ligand when bound to a retrodative metal centre. Finally the *trans* disposition of the ruthenium and the butyl group about the P=C double bond confirms our earlier suggestion that hydroruthenation of P≡CBu$^t$ to provide **1a** occurs in a regiospecifically *trans* manner.

The facility of the addition of [AuCl(PPh$_3$)] to **1a** bodes well for the future elaboration of heterobimetallic phosphaalkenyl complexes by the bridge-assisted methodology. Preliminary results indicate that the gold acetylide [Au(C≡CC$_6$H$_4$Me-4)(PPh$_3$)] also adds across the Ru–P bond to provide the ruthenium acetylide complex [Ru{P(AuPPh$_3$)=CHBu$^t$}(C≡CC$_6$H$_4$Me-4)Cl(CO)(PPh$_3$)$_3$] **4a**§ (Scheme 2). In a similar manner both mercury-(I) and -(II) chloride react with **1** to provide [Ru{P(HgCl)=PHBu$^t$}Cl$_2$(CO)(PPh$_3$)$_2$] **5a**, the former reaction being accompanied by deposition of elemental mercury. Bis(alkynyl)mercurials [Hg(C≡CR)$_2$], however, fail to react with **1a** in contrast to [Au(C≡CC$_6$H$_4$Me-4)(PPh$_3$)]. Similar reactions, and the products [Ru{P(AuPPh$_3$)=CHBu$^t$}XCl(CS)(PPh$_3$)$_2$] [X = Cl **3b**, C≡CC$_6$H$_4$Me-4 **4b**] and [Ru{P(HgCl)=PHBu$^t$}Cl$_2$(CS)(PPh$_3$)$_2$] **5b** are also observed between these reagents and the thiocarbonyl complex [Ru(P=CHBu$^t$)Cl(CS)(PPh$_3$)$_2$] **1b**, obtained from the reaction of [RuHCl(CS)(PPh$_3$)$_3$] and P≡CBu$^t$.

The chemistry described for the complexes **1** illustrates their unusual nature which makes them distinct from other phosphaalkenyl complexes for which the effective atomic number rule holds domain. For such complexes, the linear three-electron (electrophilic at P) or bent one-electron (nucleophilic at P) role of the phosphaalkenyl ligand is distinctly dichotomous. We have previously suggested[2] that the complexes **1** represent a special case: linearisation of the M = P=C linkage, and the attendant reduction of the nucleophilicity of the phosphorus is not apparently favoured by the 15-electron 'RuCl(CE)(PPh$_3$)$_2$' fragment. Such behaviour is typical of formally isoelectronic nitrosyl complexes of the late-transition metals. This leads in the unique case of **1** to the juxtaposition of a nucleophilic phosphaalkenyl phosphorus adjacent to a coordinatively unsaturated ruthenium centre, *i.e.* a 1,2-dipole predisposed to the 1,2-addition of dipolar reagents.

We gratefully acknowledge the generous loan of ruthenium salts by Johnson Matthey Chemicals and the Nuffield Foundation and the Engineering and Physical Sciences Research Council (UK) for financial support and the provision of a diffractometer.

## Footnotes

† E-mail: a.hill@ic.ac.uk
‡ E-mail: c.a.jones@swansea.ac.uk

§ *Spectral data*: for **3a**, IR/cm$^{-1}$ (Nujol) 1950 [ν(CO)]; (CH$_2$Cl$_2$) 1960 [ν(CO)]. NMR (CD$_2$Cl$_2$, 298 K) $^1$H: δ 0.95 (s, 9 H, Me), 7.22, 7.53, 7.99 (m × 3, 46 H, Ph + P=CH). $^{13}$C{$^1$H}: δ 199.4 [d, CO, *J*(PC) 10.7 Hz], 182.9 [d, P=C, *J*(PC) 19.6 Hz], 136–127 (Ph), 39.8 [d, CMe$_3$, *J*(PC) 9.0 Hz], 32.3 [d, CH$_3$, *J*(PC) 10.7 Hz]. $^{31}$P{$^1$H}: δ 319.4 [dt(br), P=C, *J*(PP) 268.5, *J*(PP′) *ca*. 30 Hz], 37.8 [d, AuPPh$_3$, *J*(PP) 265.8 Hz], 18.7 (d, RuPPh$_3$, *J* 29.6 Hz). FABMS: *m/z* (%) [assignment]; 1379(11) [Ru$_2$Cl$_2$(CO)$_2$(PPh$_3$)$_4$]$^+$, 1248(17) [M − HCl]$^+$, 1148(0.5) [M − HP=CClCMe$_3$], 1188(6) [H$_2$-Ru$_2$Cl$_2$(CO)$_2$(PPh$_3$)$_3$]$^+$, 987(11) [M − HCl − PPh$_3$]$^+$, 887(1) [M − HP=CClCMe$_3$ − PPh$_3$]$^+$, 689(4) [RuCl(CO)(PPh$_3$)$_2$]$^+$, 654(11) [Ru(CO)(PPh$_3$)$_2$]$^+$, 626 [HRu(PPh$_3$)$_2$]$^+$, 459(20) [AuPPh$_3$]$^+$, 363(8) [RuPPh$_3$]$^+$, 263(18) [HPPh$_3$]$^+$.

**4a**, IR/cm$^{-1}$ (Nujol) 2094 [ν(C≡C)], 1953 [ν(CO)], 817 [δ(C$_6$H$_4$)]; (CH$_2$Cl$_2$) 2095 [ν(C≡C)], 1954 [ν(CO)]. NMR (CD$_2$Cl$_2$, 298 K) $^1$H: δ 0.98 [s, 9 H, C(C*H*$_3$)$_3$], 2.25 [s, 3 H, C$_6$H$_4$C*H*$_3$], 6.79, 6.88 [(A B)$_2$, 4 H, C$_6$H$_4$, *J*(AB) 7.9 Hz], 7.55, 8.15 (m × 2, 45 H, Ph), 7.64 [d, 1 H, P=CH, *J*(PH) 23.1 Hz]. $^{13}$C{$^1$H}: δ 200.4 [d, CO, *J*(PC) 10.7 Hz], 186.3 [s(br), P=C], 135.6–126.8 (Ph and RuC≡*C*), 117.5 [d, RuC≡C, *J*(PC) 19.4 Hz], 39.5 [d, *C*Me$_3$, *J*(PC) 14.3 Hz], 32.3 [d, C(*C*H$_3$)$_3$, *J*(PC) 11.1 Hz], 20.9 (C$_6$H$_4$*C*H$_3$). $^{31}$P{$^1$H}: δ 312.8 [dt, P=C, *J*(PP) 227.5, *J*(PP′) 27.7 Hz], 40.0 [d, AuPPh$_3$, *J*(PP) 227.5 Hz], 26.4 (d, RuPPh$_3$, 27.7 Hz). FABMS: *m/z* (%) [assignment]; 1499(2) [M + nba − H$_2$O]$^+$, 1470(2) [M + nba − CO − H]$^+$, 1364(0.3) [M]$^+$, 1329(2) [M − Cl]$^+$, 1248(4) [M − HCCC$_7$H$_7$]$^+$, 1118(24) [M − HCCC$_7$H$_7$ − HPCHBu$^t$ − CO]$^+$. **5a**, IR/cm$^{-1}$ (Nujol) 1981(sh), 1967 [ν(CO)], 1260m, 1027m, 803m; (CH$_2$Cl$_2$) 1980 [ν(CO)]. NMR (CD$_2$Cl$_2$, 298 K) $^1$H: δ 0.85 [d, 9 H, CH$_3$, *J*(PH) 2.2 Hz], 7.40–7.97 (m × 4, 31 H, P=CH and Ph). $^{13}$C{$^1$H}: δ 197.3 (m, CO), 178.2 [d, P=C, *J*(PC) 26.7 Hz], 127.2–134.8 (Ph), 40.6 [d, CMe$_3$, *J*(PC) 14.3 Hz], 30.4 [d, CH$_3$, *J*(PC) 14.2 Hz]. $^{31}$P{$^1$H}: 257.9 [t, P=C, *J*(PP) 33.3, *J*(HgP) 7757 Hz], 18.2 (d, PPh$_3$, 27.7 Hz). FABMS: *m/z* (%) [assignment]; 1025(1) [M − Cl]$^+$, 689(14) [RuCl(CO)(PPh$_3$)$_2$]$^+$, 654(7) [Ru(CO)(PPh$_3$)$_2$]$^+$, 625(7) [Ru(PPh$_3$)$_2$]$^+$, 363(19) [RuPPh$_3$]$^+$.

¶ *Crystal data* for **3a**: C$_{60}$H$_{55}$AuCl$_2$OP$_4$Ru·2CH$_2$Cl$_2$, *M* = 1454.7, monoclinic, space group *P*2$_1$/*n*, *a* = 10.276(3), *b* = 29.300(7), *c* = 20.772(6) Å, β = 101.50(2)°, *U* = 6129(3) Å$^3$, *Z* = 4, *D*$_c$ = 1.577 g cm$^{-3}$, μ(Mo-Kα) = 30.4 cm$^{-1}$, λ = 0.710 73 Å, *F*(000) = 2896. A yellow prism of dimensions 0.83 × 0.67 × 0.27 mm was used. Data were measured on a Siemens P4/PC diffractometer with graphite monochromated Mo-Kα radiation (ω-scans). 7949 Independent reflections were measured (2θ ⩽ 45°) of which 5644 had $|F_o| > 4\sigma(|F_o|)$ and were considered to be observed. The structure was solved by direct methods and the non-hydrogen atoms were refined anisotropically by full-matrix least squares based on $F^2$ using absorption-corrected data to give $R_1$ = 0.047, $wR_2$ = 0.098 for the observed data and 578 parameters. Atomic coordinates, bond lengths and angles, and thermal parameters have been deposited at the Cambridge Crystallographic Data Centre (CCDC). See Information for Authors, Issue No. 1. Any request to the CCDC for this material should quote the full literature citation and the reference number 182/308.

## References

1 L. Weber, *Angew. Chem., Int. Ed. Engl.*, 1996, **35**, 271 and references therein.
2 R. B. Bedford, A. F. Hill and C. Jones, *Angew. Chem., Int. Ed. Engl.*, 1996, **35**, 547.
3 A. M. Arif, A. H. Cowley and S. Quashie, *J. Chem. Soc., Chem. Commun.*, 1985, 428.
4 E. Niecke, H.-J. Metternich, M. Nieger, D. Gudat, P. Wenderoth, W. Malisch, C. Hahner and W. Reich, *Chem. Ber.*, 1993, **126**, 1299.

*Received, 14th October 1996; Com. 6/06987H*

# Generation, entrapment and reactivity of long-lived organic carbocations and radical cations within a supramolecular assembly: Ca Y zeolite

**K. Pitchumani,[a] P. H. Lakshminarasimhan,[a] Nicolette Prevost,[a] D. R. Corbin[b] and V. Ramamurthy*[b]**

[a] *Department of Chemistry, Tulane University, New Orleans, LA 70118, USA*
[b] *Central Research and Development, The Du Pont Company, Wilmington, DE 19880, USA*

**Diarylethenes spontaneously form the corresponding radical cations and carbocations upon inclusion within activated Ca Y zeolite; oxygen plays an important role in the generation of the radical cations.**

By virtue of their ability to generate carbocations and radical cations, zeolites have been used in a number of catalytic processes.[1] Although the mechanism of carbocation formation is fairly well understood, the potential of such intermediates in routine organic transformations has not been fully realized. On the other hand, no agreement on the mechanism of cation radical generation within zeolites has been reached.[2] This communication addresses these concerns.

When Ca Y (300 mg) activated at 500 °C under aerated conditions for about 12 h, and cooled to room temperature, was dropped into a cyclohexane solution of 1,1-diphenylethene **1a**, (20 mg 3 ml) a bright green colour developed which, in the slurry, persisted for several weeks.† Extraction of the cyclohexane–zeolite slurry with dichloromethane gave 1,1-diphenylethane **2a** as the single product (Scheme 1). The zeolite residue after extraction was still coloured and remained so for at least 12 h under aerated conditions. When the zeolite turned colourless, it was extracted for a second time with dichloromethane to yield benzophenone. The overall yield of the two products was 90% diphenylethane and 10% benzophenone.

The diffuse reflectance spectra of the zeolite–**1a** complex as formed in cyclohexane, showed two strong absorptions with $\lambda_{max}$ at 432 and 615 nm (Fig. 1). The zeolite residue after the first extraction with dichloromethane showed only a peak at 615 nm. On the basis of literature reports, we assign the 432 nm peak to the $Ph_2C^+Me$ carbocation and the one at 615 nm to the radical cation of **1a**[3,4] The presence of a radical cation in the Ca Y sample is also indicated by EPR spectroscopy.[5] A strong EPR signal with a *g*-value of 2.00235 was obtained.

Ca Y activated in the temperature range 300–600 °C under aerated conditions was found to be ideal for carbocation generation. It has been established in the literature that such conditions of activation lead to the generation of Brønsted acid sites.[6] Through extensive deuteriation experiments, we have established that one of the hydrogens in diphenylethane **2a** (Scheme 1) comes from the water present within the zeolite and the other from dichloromethane which is used to extract the product from the zeolite. Results of the deuteriation experiments are summarized in Scheme 2.

Of the various activation conditions we attempted, Ca Y activated > 400 °C on a vacuum line under reduced pressure ($< 10^{-3}$ Torr) was found to be ideal for the generation of radical cations with minimum interference from carbocations. Two remarkable observations made by us in the case of 1,1-diarylethenes lead us to conclude that oxygen plays an important role in the generation of the radical cation within Ca Y. Inclusion of diphenylethene **1a** into Ca Y activated at 450 °C on a vacuum line and handled under nitrogen atmosphere generated only a very light green colour.‡ However, when oxygen was bubbled into such a solution, a dark green colour resulted and the benzophenone yield was enhanced from 1 to 10%. Enhancement of the yield of the radical cation was also confirmed by the diffuse reflectance spectral data. This observation suggested to us that oxygen is essential for radical cation generation. The following observation made with 4,4′-dimethylaminodiphenylethene **1c** further strengthened our view that oxygen plays a

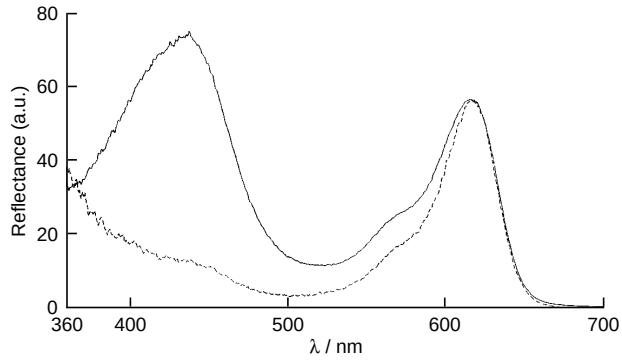
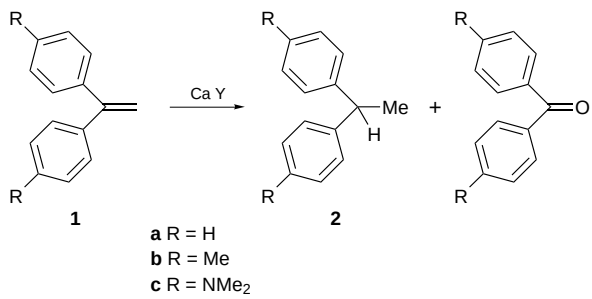
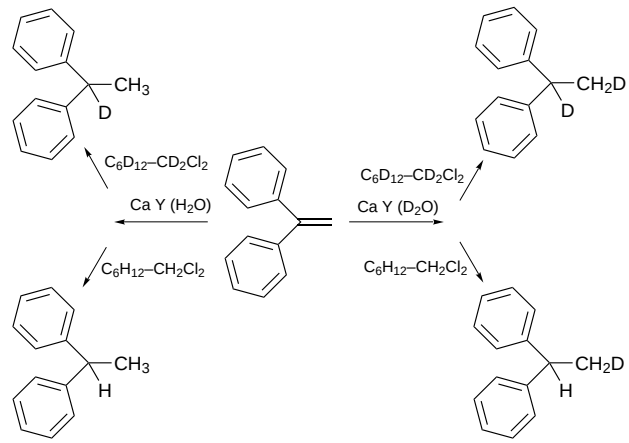



**Fig. 1** Diffuse reflectance spectra of diphenylethene included within activated (500 °C aerated) Ca Y. (—) Soon after the addition of Ca Y to a cyclohexane solution of diphenylethene and (---) after extracting the above solution with $CH_2Cl_2$.




**Scheme 1**




**Scheme 2**

crucial role in the generation of radical cations within zeolites. When 4,4′-dimethylaminodiphenylethene was included within activated Ca Y the corresponding radical cation was generated. The diffuse reflectance spectrum of **1c** within Ca Y is shown in Fig. 2. The blue coloured solid, when degassed on a vacuum line ($< 10^{-3}$ Torr) turned colourless and the diffuse reflectance spectrum no longer contained the peak due to the radical cation at 620 nm. Introduction of air into this sample, most surprisingly, regenerated the blue colour and the peak at 620 nm reappeared in the diffuse reflectance spectrum. This process was reversible for at least six cycles. This remarkable observation lead us to suggest that oxygen is most likely the electron acceptor at least in the case of 4,4′-dimethylaminodiphenylethene. The alkene **1c** was unique in its behaviour in several ways: (*a*) no other alkenes including **1a** and **1b** above showed the reversible behaviour exhibited by **1c**; (*b*) the radical cation from **1c** was generated even in monovalent cation-exchanged (Li, Na, K, Rb and Cs) Y zeolite. All other alkenes gave radical cations only in divalent cation-exchanged Y and in ZSM-5 zeolites.

Recently, Frei and coworkers have exploited the unique feature of divalent cation-exchanged zeolites to stabilize charge-transfer complexes between hydrocarbons and oxygen.[7] In the case of the alkenes used by Frei and coworkers, the permanent charge separation occurs only upon activation by light. However, the alkenes we have investigated, all possessing much lower oxidation potentials[8] than those studied by Frei and coworkers, are oxidized even in the absence of light. Most surprisingly, 4,4'-dimethylaminodiphenylethene, possessing a very low oxidation potential (0.66 V), establishes a reversible oxidation process with oxygen as the acceptor.[9] Absence of such a process with either diphenylethene (1.88 V) or 4,4′-dimethoxydiphenylethene (1.32 V) suggests to us that the acceptor for these alkenes may not be the free oxygen. Further work, in progress, with a series of alkenes with oxidation potential varying between 0.6 and 2.0 V is expected to clarify this aspect of the oxidation of alkenes within Ca Y.

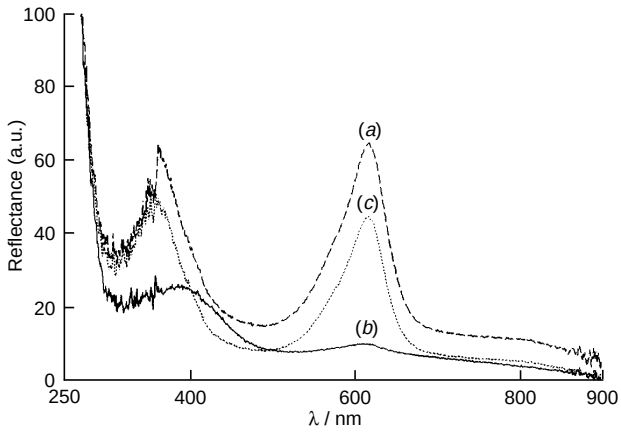



**Fig. 2** Diffuse reflectance spectra of 4,4′-dimethylaminodiphenylethene **1c** included in Ca Y. (*a*) (---) Sample after extraction with dichloromethane under aerated conditions. (*b*) (—) The above sample degassed on a vacuum line and under reduced pressure ($10^{-3}$ Torr). (*c*) (···) Sample (*b*) exposed to air.

The conditions under which radical cations and carbocations can be generated, independent of each other, within Ca Y zeolite have been established. Using this technique we have been able to generate long-lived radical cations and carbocations from a number of alkenes. We are in the process of characterizing the persistent carbocations and radical cations by CP MAS NMR and by EPR respectively. The mechanism of radical cation formation within activated zeolites is also being pursued.

We thank the Division of Chemical Sciences, Office of Basic Energy Sciences, Office of Energy Research, US Department of Energy and NSF-EPSCOR-LBR Center for Photoinduced Processes, Tulane University for support of this program.

## Footnotes

† ICP analysis indicated the zeolite used had the composition $Si_{138.7}Al_{53.3}Na_{7.5}Ca_{23.3}O_{384}$.

‡ Ca Y was placed in a quartz tube and heated at 450 °C under reduced pressure ($5 \times 10^{-4}$ Torr). Nitrogen was adsorbed onto this sample at room temp. and degassed. This process was repeated four times and finally the sample was left under nitrogen overnight. Further handling was done under nitrogen atmosphere. Very light colour formation is consistent with a report [ref. 2(*b*)] that it is difficult to remove strongly adsorbed oxygen from Ca Y.

## References

1 H. van Bekkum, E. M. Flanigen and J. C. Jansen, *Introduction to Zeolite Science and Practice*, Elsevier, Amsterdam, 1991.
2 (*a*) D. N. Stamires and J. Turkevich, *J. Am. Chem. Soc*., 1964, **86**, 749; (*b*) F. R. Chen and J. J. Fripiat, *J. Phys. Chem*., 1992, **96**, 819; (*c*) X. Liu, K. K. Iu, J. K. Thomas, H. He and J. Klinowski, *J. Am. Chem. Soc*., 1994, **116**, 11811; (*d*) A. Corma, V. Fornes, H. Garcia, V. Marti and M. A. Miranda, *Chem. Mater*., 1995, **7**, 2136.
3 R. A. McClelland, V. M. Kanagasabapathy and S. Steenken, *J. Am. Chem. Soc.*, 1988, **110**, 6913.
4 H. P. Leftin and W. K. Hall, *J. Phys. Chem*., 1960, **64**, 382; H. P. Leftin and W. K. Hall, *J. Phys. Chem*., 1962, **66**, 1457.
5 G. Turner, M. G. Bakker and V. Ramamurthy, unpublished work.
6 J. W. Ward, in *Zeolite Chemistry and Catalysis*, ed. J. A. Rabo, American Chemical Society, Washington, DC, 1976, p. 118; M. L. Poutsma, in *Zeolite Chemistry and Catalysis*, ed. J. A. Rabo, American Chemical Society, Washington, DC, 1976, p. 437; P. E. Eberly, *J. Phys. Chem*., 1968, **72**, 1042; H. Hattori and T. Shiba, *J. Catal*, 1968, **12**, 111; J. W. Ward, *J. Phys. Chem*., 1968, **72**, 4211; *J. Catal*, 1968, **10**, 34; J. B. Uytterhoeven, R. Schoonheydt, B. V. Liengme and W. K. Hall, *J. Catal.*, 1969, **13**, 425; J. W. Ward, *J. Catal.*, 1969, **14**, 365; M. L. Costenoble, W. J. Mortier and J. B. Uytterhoeven, *J. Chem. Soc., Faraday Trans., 1*, 1977, **73**, 466; 477.
7 For a recent publication, see: H. Sun, F. Blatter and H. Frei, *J. Am. Chem. Soc*., 1996, **118**, 6873.
8 K. Gollnick, A. Schnatterer and G. Utschick, *J. Org. Chem.*, 1993, **58**, 6049.
9 K. B. Yoon and J. K. Kochi, *J. Am. Chem. Soc*., 1988, **110**, 6586.
10 S. L. Mattes and S. Farid, *J. Am. Chem. Soc*., 1986, **108**, 7356; R. A. Neunteufel and D. R. Arnold, *J. Am. Chem. Soc*., 1973, **95**, 4080.

*Received, 18th October 1996; Com. 6/07124D*

# Shaping the cavity of calix[4]arene using transition metals and binding alkali-metal cations inside the cavity: the relevance of the alkali-metal cation–arene interaction

**Antonio Zanotti-Gerosa,[a] Euro Solari,[a] Luca Giannini,[a] Carlo Floriani,*[a]† Angiola Chiesi-Villa[b] and Corrado Rizzoli[b]**

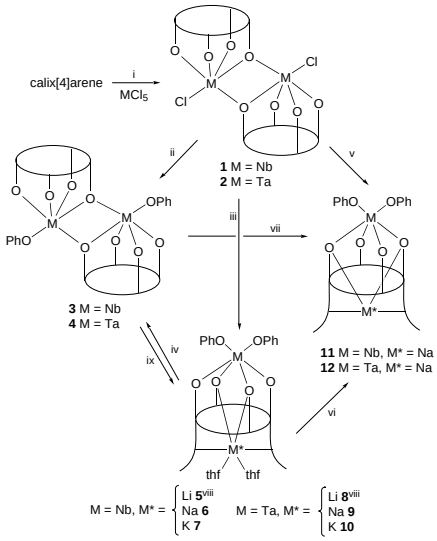
[a] *Institut de Chimie Minérale et Analytique, BCH, Université de Lausanne, CH-1015 Lausanne, Switzerland*
[b] *Dipartimento di Chimica, Università di Parma, I-43100 Parma, Italy*

**Transition metals can be used for shaping and electronically enriching the calix[4]arene cavity; in this approach, the π-basic cavities can be adapted to alkali-metal cation complexation in a very hydrophobic environment and these cations can even be transferred into aliphatic hydrocarbons; the η⁶-arene–alkali-metal cation interaction is structurally elucidated.**

Complexation by transition metals[1,2] can be used as a methodology for shaping[2c] and tuning the binding properties of the calix[4]arene cavity.[3] The present report deals with a simple and general strategy for binding alkali-metal cations inside the calix[4]arene cavity. Solvation of the alkali-metal cations by a π-cavity is a quite remarkable phenomenon, in the context of the role played by the cation–π interactions in chemistry and biology.[4] Typically, complexation of alkali-metal cations is achieved using the chemically modified lower rim of calix[4]arenes, thus rendering complexation outside the cavity, using a set of conventional donor atoms.[3c,5–7]

The metallation of calix[4]arene has been achieved using $NbCl_5$ and $TaCl_5$ and the functionalizable dimers **1**‡ and **2** were obtained as analytically pure crystalline solids.

The reaction of **1** and **2** with alkali-metal phenoxides under the conditions briefly specified in Scheme 1 gave complexes **5**–**12**,‡ which can be considered as alkali-metal cation carriers in hydrophobic environments since they are very soluble in aliphatic hydrocarbons. The formation of **5**–**12** proceeds *via* the intermediacy of the monophenoxo derivatives **3** and **4**, as shown in Scheme 1. Attainment of the thf solvated (**5**–**10**) or unsolvated (**11**, **12**) forms of the alkali-metal cation depends on the reaction solvent. Unexpectedly, the desolvation of **6** and **9** to **11** and **12** was quite easy, thus confirming that the major binding effect of the alkali-metal cation is provided by the calix[4]arene oxygens and the arene rings. X-Ray structural information is available for **1**, **3**, **5**, **6**, **9**, **10** and **11**.§ In particular, we found that complexes **6**, **9** and **10** are isostructural. Structural details are reported only for **9** (see Fig. 1).




**Scheme 1** *Reagents and conditions*: i, toluene, reflux; ii, 1 equiv. NaOPh, thf, room temp.; iii, excess of M*OPh, thf; iv, 1 equiv. of **1** in thf or 1 equiv. of **2** in $C_6H_6$; v, 2 equiv. NaOPh, $C_6H_6$, reflux; vi, azeotropic distillation, $C_6H_{14}$; vii, excess of NaOPh, $C_6H_6$; viii, a single thf is bonded to $Li^+$; ix, NaOPh, thf, room temp.

The two independent molecules A and B have an imposed crystallographic *m* symmetry so in the asymmetric unit of each complex there are two halves of crystallographically independent molecules. The mirror plane runs through the metal atoms and the oxygen atoms O(1) and O(3) bisecting the C(1)–C(4) and C(13)–C(16) rings. An alkali-metal cation is accommodated inside the cavity of the complex interacting with two oxygen atoms of the calixarene [O(2), O(2*)]. Two oxygen atoms from thf complete a planar (for symmetry requirements) coordination around the alkali metal.

As a consequence of the six-coordination of the metal, the calixarene ligand assumes a flattened cone conformation with the opposite C(5)···C(11) and C(3′)···C(11′) rings pushed outward and the opposite C(1)···C(4) and C(13)···C(16) rings inward relative to the cavity of the macrocycle. In both molecules A and B the sodium atom was found to be disordered over two positions (Na and Na′) which lie at a mean distance of 2.102(12) and 2.149(14) Å for molecules A and B respectively, from the reference plane. In both molecules, Na can be considered as η⁶-bonded to the C(1)···C(4) ring [Na···C 3.005(17)–3.415(16) Å, $Na^+$···η⁶-arene(centroid), 2.465(17) Å (molecule A) and 2.924(16)–3.231(16) Å (molecule B)]; $Na^+$ can be considered as η³-bonded to atoms C(13), C(16) and C(13*) of the opposite ring [Na′···C 3.001(16)–3.125(14) Å (molecule A) and 3.168(16)–3.289(15) Å (molecule B)]. The

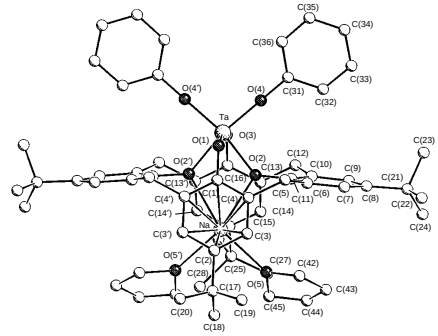


**Fig. 1** A SCHAKAL drawing of complex **6**. Selected interatomic distances (Å) and angles (°): Nb–O(1) 2.015(2), Nb–O(2) 1.969(2), Nb–O(3) 2.016(2), Nb–O(4) 1.975(2), Nb–O(5) 1.901(2), Nb–O(6) 1.896(3), Na–O(1) 2.296(3), Na–O(3) 2.309(3), Na–C(22) 2.975(4), Na–C(23) 3.034(4), Na–C(24) 3.072(4), Na–C(25) 3.047(4), Na–C(26) 2.992(4), Na–C(27) 2.937(4), Na–arene(centroid) 2.666(4); O(5)–Nb–O(6) 98.8(1), O(4)–Nb–O(5) 97.8(1), O(3)–Nb–O(5) 168.2(1), O(3)–Nb–O(4) 83.4(1), O(2)–Nb–O(5) 93.6(1), O(2)–Nb–O(4) 162.7(1), O(2)–Nb–O(3) 82.8(1), O(1)–Nb–O(6) 168.6(1), O(1)–Na–O(3) 65.3(1).

directions of the η bonds are nearly perpendicular to the O(2)O(5)O(2*)O(5*) coordination plane, the dihedral angles between the Na–centroid directions and the normal to the plane are in the range 16.3(2)–17.0(3)°. The sodium atoms are displaced from the coordination plane by 0.440(12) and −0.360(12) Å for Na and Na′ respectively (molecule A) and 0.416(10) and 0.199(14) Å for Na and Na′, respectively (molecule B).

The complexation of alkali-metal cations was achieved by forcing open the calix[4]arene cavity using an appropriate coordination number of the metal.[2c] In the case of **5**–**11**, the negative charge is certainly a determining factor for the binding ability of the cavity. The complexation of the alkali metals by the cavity takes advantage of the cation–π interactions. This has been conveniently revealed by Shinkai *et al.* using mass spectrometry in the case of the alkali-metal cation–calixarene interactions.[8] The structural support for this kind of cation–π interaction comes from the X-ray analyses performed on **5**, **6**, **9**, **10** and **11**. The X-ray analysis revealed, at least in the solid state, how this kind of alkali-metal cation–arene interaction depends on the presence of thf and on the size of the alkali-metal cation. The interaction varies from bis-$\eta^6$-coordination for potassium [$K^+$–$\eta^6$-arene(centroid) 2.742(10), 2.819(10) Å in **10**] to a single $\eta^6$-coordination for sodium [$Na^+$–$\eta^6$-arene(centroid) 2.606(8) Å in **6** and 2.666(4) Å in **11**], to $\eta^3$-coordination for lithium [$Li^+$–$\eta^3$-arene(centroid) 1.98(4) Å in **5**], for the solvated forms of **5**, **6**, **9** and **10**. We should emphasize that, for **11** and **12**, the solvation of the alkali-metal cation is provided mainly by the arene rings. For a comparison of the structural parameters related to alkali-metal cations interacting with aromatic rings we refer to the excellent review by Weiss.[9]

Work is in progress (*i*) to elaborate the strategy for shaping the cavity of calix[4]arene in order to bind organic and inorganic cations inside; (*ii*) to study alkali-metal cation exchange processes; the reaction of **6** with LiCl in thf led, in fact, to the easy displacement of $Na^+$ by $Li^+$ in the cavity; (*iii*) to use these compounds as alkali-metal cation carriers in hydrocarbon media, the calix[4]arene cavity being a very hydrophobic environment.

We thank the Fonds National Suisse de la Recherche Scientifique (Grant No. 20-40268.94) and Ciba-Geigy SA (Basel, Switzerland) for financial support.

## Footnotes

† E-mail: carlo.floriani@icma.unil.ch

‡ *Syntheses*: **1**: $NbCl_5$ (11.065 g, 41.0 mmol) was added to a suspension of calix[4]arene ($H_4L$) (26.58 g, 41.0 mmol) in toluene (200 $cm^3$) and the reaction mixture was refluxed for 14 h. The solvent was removed *in vacuo*, the red residue washed with toluene (150 $cm^3$), and collected (93%). Crystals suitable for X-ray analysis were grown from a saturated thf solution.

**9**: NaOPh (1.22 g, 10.5 mmol) was added to a suspension of $[TaL(Cl)]_2{\cdot}2CH_2Cl_2$ (4.66 g, 2.4 mmol) in thf (100 $cm^3$). The reaction mixture was stirred at room temp. for 12 h, then refluxed for 6 h to give a white suspension. The solid was collected and extracted with the mother-liquors for 30 h. Volatiles were removed *in vacuo* and the solid residue was washed with *n*-hexane (100 $cm^3$), collected and dried *in vacuo* (88%).

**11**: NaOPh (0.91 g, 7.84 mmol) was added to a suspension of **1** (3.32 g, 3.81 mmol) in benzene (150 $cm^3$). The reaction mixture was refluxed for 12 h and the red suspension became a yellow solution. The solvent was removed *in vacuo* and fresh benzene (200 $cm^3$) was added. The mixture was filtered twice, the solvent was concentrated to 10 $cm^3$, and *n*-hexane (200 $cm^3$) was added. Upon concentration of this solution, a yellow solid precipitated and was collected and dried *in vacuo* (77%). Crystal suitable for X-ray analysis were grown by slowly cooling a saturated toluene–hexane solution to 9 °C.

§ *Crystal data*: **3**: $C_{108}H_{130}Nb_2O_{17}{\cdot}5C_4H_8O$, $M$ = 2166.6, monoclinic, space group $P2_1/n$, $a$ = 19.617(3), $b$ = 13.256(2), $c$ = 22.489(5) Å, β = 100.52(2)°, $U$ = 5749.8(18) $Å^3$, $Z$ = 2, $D_c$ = 1.251 g $cm^{-3}$, $F(000)$ = 2312, Cu-Kα radiation (λ = 1.541 78 Å), μ(Cu-Kα) = 21.49 $cm^{-1}$; crystal dimensions 0.18 × 0.32 × 0.62 mm.

**5**: $C_{62}H_{68}LiNbO_7{\cdot}C_{60}H_{70}LiNbO_7{\cdot}0.5C_4H_8O{\cdot}0.25C_6H_{14}$, $M$ = 2085.7, triclinic, space group $P\bar{1}$, $a$ = 12.467(6), $b$ = 20.181(6), $c$ = 24.954(2) Å, α = 93.69(4), β = 90.85(5), γ = 99.31(3)°, $U$ = 6181(7) $Å^3$, $Z$ = 2, $D_c$ = 1.121 g $cm^{-3}$, $F(000)$ = 2205, Mo-Kα radiation (λ = 0.710 69 Å), μ(Mo-Kα) = 2.30 $cm^{-1}$; crystal dimensions 0.26 × 0.30 × 0.48 mm.

**9**: $C_{64}H_{76}NaO_8Ta{\cdot}0.5C_6H_{14}$, $M$ = 1220.3, monoclinic, space group $P2_1/m$, $a$ = 12.545(2), $b$ = 24.795(5), $c$ = 20.031(3) Å, β = 99.38(1)°, $U$ = 6147(2) $Å^3$, $Z$ = 4, $D_c$ = 1.319 g $cm^{-3}$, $F(000)$ = 2532, Mo-Kα radiation (λ = 0.710 69 Å), μ(Mo-Kα) = 4.02 $cm^{-1}$; crystal dimensions 0.10 × 0.32 × 0.68 mm. For 4538 unique observed reflections [$I > 2\sigma(I)$] collected at $T$ = 295 K on a Enraf-Nonius CAD4 diffractometer (6 < 2θ < 50°) and corrected for absorption the conventional $R$ is 0.036 ($wR_2$ = 0.075).

**11**: $C_{56}H_{62}NaNbO_6{\cdot}2C_7H_8{\cdot}0.3C_6H_{14}$, $M$ = 1157.1, monoclinic, space group $P2_1/n$, $a$ = 12.090(2), $b$ = 20.380(4), $c$ = 25.079(5) Å, β = 91.36(2)°, $U$ = 6178(2) $Å^3$, $Z$ = 4, $D_c$ = 1.244 g $cm^{-3}$, $F(000)$ = 2452, Mo-Kα radiation (λ = 0.710 69 Å, μ(Mo-Kα) = 4.02 $cm^{-1}$, crystal dimensions 0.13 × 0.16 × 0.32 mm.

Atomic coordinates, bond lengths and angles, and thermal parameters have been deposited at the Cambridge Crystallographic Data Centre (CCDC). See Information for Authors, Issue No. 1. Any request to the CCDC for this material should quote the full literature citation and the reference number 182/316.

## References

1 S. G. Bott, A. W. Coleman and J. L. Atwood, *J. Chem. Soc., Chem. Commun.*, 1986, 610; M. M. Olmstead, G. Sigel, H. Hope, X. Xu and P. P. Power, *J. Am. Chem. Soc.*, 1985, **107**, 8087; G. E. Hofmeister, F. E. Kahn and S. F. Pedersen, *J. Am. Chem. Soc.*, 1989, **111**, 2318; G. E. Hofmeister, E. Alvarado, J. A. Leary, D. I. Yoon and S. F. Pedersen, *J. Am. Chem. Soc.*, 1990, **112**, 8843; B. M. Furphy, J. M. Harrowfield, D. L. Kepert, B. W. Skelton, A. H. White and F. R. Wilner, *Inorg. Chem.*, 1987, **26**, 4231.

2 (*a*) F. Corazza, C. Floriani, A. Chiesi-Villa and C. Guastini, *J. Chem. Soc., Chem. Commun.*, 1990, 640; (*b*) 1083; (*c*) F. Corazza, C. Floriani, A. Chiesi-Villa and C. Rizzoli, *Inorg. Chem.*, 1991, **30**, 4465; (*d*) J. A. Acho, L. H. Doerrer and S. J. Lippard, *Inorg. Chem.*, 1995, **34**, 2542; (*e*) J. A. Acho, T. Ren, J. W. Yun and S. J. Lippard, *Inorg. Chem.*, 1995, **34**, 5226.

3 (*a*) C. D. Gutsche, *Calixarenes*, The Royal Society of Chemistry, Cambridge, UK, 1989; (*b*) *Calixarenes, A Versatile Class of Macrocyclic Compounds*, ed. J. Vicens and V. Böhmer, Kluwer, Dordrecht, Netherlands, 1991; (*c*) V. Böhmer, *Angew. Chem., Int. Ed. Engl.*, 1995, **34**, 713 and references therein.

4 D. A. Dougherty, *Science*, 1996, **271**, 163.

5 F. Arnaud-Neu, G. Barrett, S. J. Harris, M. Owens, M. A. McKervey, M.-J. Schwing-Weill and P. Schwinté, *Inorg. Chem.*, 1995, **32**, 2644; F. Arnaud-Neu, E. M. Collins, M. Deasy, G. Ferguson, S. J. Harris, B. Kaitner, A. J. Lough, M. A. McKervey, E. Marques, B. L. Ruhl, M.-J. Schwing-Weill and E. M. Seward, *J. Am. Chem. Soc.*, 1989, **111**, 8681; P. J. Dijkstra, J. A. J. Brunink, K.-E. Bugge, D. N. Reinhoudt, S. Harkema, R. Ungaro, F. Ugozzoli and E. Ghidini, *J. Am. Chem. Soc.*, 1989, **111**, 7567; P. D. Beef, M. G. B. Drew, P. A. Gale, P. B. Leeson and M. I. Ogden, *J. Chem. Soc., Dalton Trans.*, 1994, 3479; F. Arnaud-Neu, S. Fanni, L. Guerra, W. McGregor, K. Ziat, M.-J. Schwing-Weill, G. Barrett, M. A. McKervey, D. Marrs and E. M. Seward, *J. Chem. Soc., Perkin Trans. 2*, 1995, 113; J. L. M. Gordon, V. Böhmer and W. Vogt, *Tetrahedron Lett.*, 1995, **36**, 2445.

6 S. K. Chang and I. Cho, *J. Chem. Soc., Perkin Trans. 2*, 1986, 211; A. Arduini, A. Pochini, S. Reverberi, R. Ungaro, G. D. Andreetti and F. Ugozzoli, *Tetrahedron*, 1986, **42**, 2089; F. Arnaud-Neu, M. J. Schwing, K. Ziat, S. Cremin, S. J. Harris and M. A. McKervey, *New J. Chem.*, 1991, **15**, 33; A. Arduini, E. Ghidini, A. Pochini, R. Ungaro, G. D. Andreetti, G. Calestani and F. Ugozzoli, *J. Inclusion Phenom.*, 1988, **6**, 119; S. K. Chang, S. K. Kwon and I. Cho, *Chem. Lett.*, 1987, 947; F. Arnaud-Neu, S. Cremin, D. Cunningham, S. J. Harris, P. McArdle, M. A. McKervey, M. A. McManus, M. J. Schwing and K. Ziat, *J. Inclusion Phenom.*, 1991, **10**, 329; M. J. Schwing-Weill, F. Arnaud-Neu and M. A. McKervey, *J. Phys. Chem.*, 1992, **5**, 496.

7 A very particular, non-extendible, single case of $Cs^+$ inclusion by an upper-rim bridged monoanionic calix[4]arene has been reported: R. Assmus, V. Böhmer, J. M. Harrowfield, M. I. Ogden, W. R. Richmond, B. W. Skelton and A. H. White, *J. Chem. Soc., Dalton Trans.*, 1993, 2427.

8 F. Inokuchi, Y. Miyahara, T. Inazu and S. Shinkai, *Angew. Chem., Int. Ed. Engl.*, 1995, **34**, 1364.

9 E. Weiss, *Angew. Chem., Int. Ed. Engl.*, 1993, **32**, 1501.

*Received, 7th October 1996, Com. 6/06826J*

# Activity of carbonaceous deposits in the selective reduction of nitrogen oxides

**Jan Connerton, Richard W. Joyner* and Michael Stockenhuber**

*The Catalysis Research Laboratory, The Nottingham Trent University, Clifton Lane, Nottingham, UK NG11 8NS*

**Carbonaceous deposits, formed on the catalyst Cu/ZSM-5 by interaction at low temperature with propene, NO and oxygen, are characterised spectroscopically and shown to be able to carry out the selective catalytic reduction of NO; rates of reaction, which follow simple kinetics, are lower than in the absence of pre-deposited coke, and the results suggest an inverse correlation between catalyst Brønsted acidity and activity in $NO_x$ reduction.**

The selective reduction of nitrogen oxides by hydrocarbons in the presence of oxygen, using for example Cu/ZSM-5 catalysts, continues to attract attention.[1–5] Much interest now centres on the nature of the nitrogen-containing functionality in the reaction, with spectroscopic support emerging both for oxidised nitrogenous species such as nitro groups,[6,7] and also for reduced species, particularly cyanides.[7–12] Less attention has been paid to the characterisation of the hydrocarbon moieties which must be involved, although it is recognised that long-lived carbonaceous species can be formed within the pores of the zeolite, with possible mechanistic importance, as discussed by ourselves and others.[7,13] Here, we report on the nature and reactivity of hydrocarbon species deliberately deposited on Cu/ZSM-5 catalysts with different metal contents. We have previously shown that nitrogen is released from these deposits by reaction with oxygen[7] and now show that the deposits are also able to activate $NO_x$ directly. The reactivity of the coke towards $NO_x$ is also compared to the steady-state performance of these catalysts.

Catalysts have been prepared from H-ZSM-5 (Si/Al ratio 25) as described previously,[3] using conventional ion-exchange techniques. A range of catalysts from 50 to 130% nominal degree of exchange has been examined. Catalyst performance has been tested in a simple flow-through microreactor, equipped with a chemiluminescent analyser for nitrogen oxides (NOx Box, Signal Instruments Model 4000), and a gas chromatograph. Steady-state reaction conditions comprised 2% oxygen, 1200 ppm propene, 2000 ppm NO, balance helium and GHSV = 30 000 $h^{-1}$; the catalysts were initially activated by heating at 773 K for 1 h in 2% oxygen in helium. IR spectroscopy measurements were carried out in transmission mode using a specially constructed *in situ* vacuum cell which can be heated to > 800 K, and an ATI RS1 Fourier transform spectrometer.

Before studying the behaviour of deposited coke, the steady-state performance of the catalysts was measured, starting at 773 K and gradually reducing the temperature. As in our earlier study,[7] coke was then deposited by exposing the catalyst of interest to the reaction mixture at 473 or 573 K. The IR spectrum of the deposit on a 54% copper exchanged catalyst is shown in Fig. 1. The bands at 2879, 2937 and 2971 $cm^{-1}$ are typical of hydrocarbons adsorbed on acidic zeolites such as H-ZSM-5 and are due to C–H stretching vibrations. It is important to note that the band characteristic of the zeolite's Brønsted acidity (normally observed at *ca*. 3607 $cm^{-1}$) has been suppressed, indicating that these sites have played their expected role in hydrocarbon activation. The intense band at *ca*. 1600 $cm^{-1}$ is assigned to C=C stretching vibrations in adsorbed aromatic molecules, and is characteristic of hydrocarbon deposits on zeolites.[9] It is superimposed on an overtone band associated with the zeolite lattice vibrations. The other important features of the spectrum are the band at 2250 $cm^{-1}$, which it is now accepted is due to cyanide species,[10–12] and bands at 3300 and 3375 $cm^{-1}$. These are nitrogen–hydrogen stretches which probably reflect the presence both of =NH and $–NH_2$ groups, which have not been reported before in this system. Their observation provides important evidence that the organic nitro groups, which are formed first in the sequence of reactions leading to release of nitrogen,[5] can undergo sequential reduction to cyanide [eqn. (1)].

$$–NO_2 \rightarrow –NH–OH \rightarrow –NH_2 \rightarrow =NH \rightarrow \equiv N \qquad (1)$$

The zeolite is unable to activate oxygen at the relatively low temperatures where the hydrocarbon deposit is formed. Coupled with the presence of readily activated propene, the result is an atmosphere which is more strongly reducing than is the case where steady-state reactivity is high, and where the reduction sequence may not progress as far as cyanide.[5]

The reactivity of the carbonaceous deposit in NO reduction in the absence of other hydrocarbons has been studied by exposing it to the same NO–oxygen concentration as was used for steady-state reaction, and heating from 473 to *ca*. 920 K at 10 K $min^{-1}$. The results of experiments with two different catalysts are shown in Fig. 2, which show the instantaneous concentration of $NO_x$ ($NO + NO_2/N_2O_4$) at the reactor exit. In each case the deposit on the catalyst shows significant activity in $NO_x$ reduction, but the maximum of activity for the catalyst with 100% copper exchange occurs at *ca*. 100 K lower temperature than for the catalyst with only 54% exchange. The amount of $NO_x$ converted in each case is, however, rather similar, corresponding to *ca*. 25 mg NO (g catalyst)$^{-1}$. This is the same order of magnitude as that measured for deposited coke in our earlier study,[7] where 30 mg $g^{-1}$ of coke was formed on an overexchanged catalyst tested at 10 000 $h^{-1}$ GHSV. The kinetics of reaction between $NO_x$, oxygen and the carbonaceous deposits can be simply described. Fig. 2 also shows rates of reaction calculated by assuming first-order behaviour in both NO and hydrocarbon concentration, and zero order of reaction in oxygen (which is present in substantial excess throughout). There is very good agreement with experiment for such a simple model, particularly when it is realised that $NO_2$ is a reaction

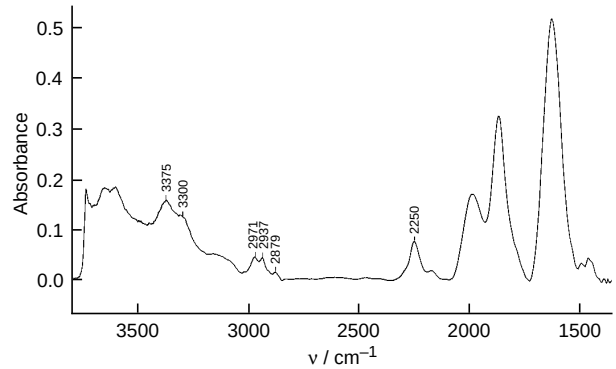



**Fig. 1** IR spectrum of the carbonaceous deposit on a 54% Cu-exchanged catalyst; frequencies of bands discussed in the text are marked

intermediate.[5] In line with the changes in activity, the apparent activation energy of the reaction decreases from *ca*. 92 to 82 kJ mol$^{-1}$ as the copper content of the zeolite is increased.

These results suggest that the presence of too many Brønsted zeolite acid sites inhibits the $NO_x$ reduction reaction. It is known that relatively few Brønsted sites remain in the so-called 'overexchanged' catalysts which are the most active for $NO_x$ reduction.[14] The present study shows that when the catalyst is pre-treated at low temperature in a way that allows the acid sites to have maximum influence in hydrocarbon activation, the result is to produce a hydrocarbonaceous deposit which is of lower activity in $NO_x$ reduction at low temperature than that formed at steady state. Comparison of Fig. 1 with our earlier steady-state results (ref. 3, Fig. 1) shows that the steady-state process occurs more quickly at temperatures up to *ca*. 720 K. Equally, the deposit produced on the catalyst with lower copper content, and therefore higher residual Brønsted acidity, is even less active in NO reduction. There is thus an inverse correlation between Brønsted acidity and catalyst performance. It is still not clear whether the small amount of residual Brønsted acidity which remains in the most active Cu/ZSM-5 catalysts is necessary for the reaction to occur, since it is possible that the Lewis acidity associated with the $Cu^{I}$ sites[14] is sufficient to activate the hydrocarbon species.

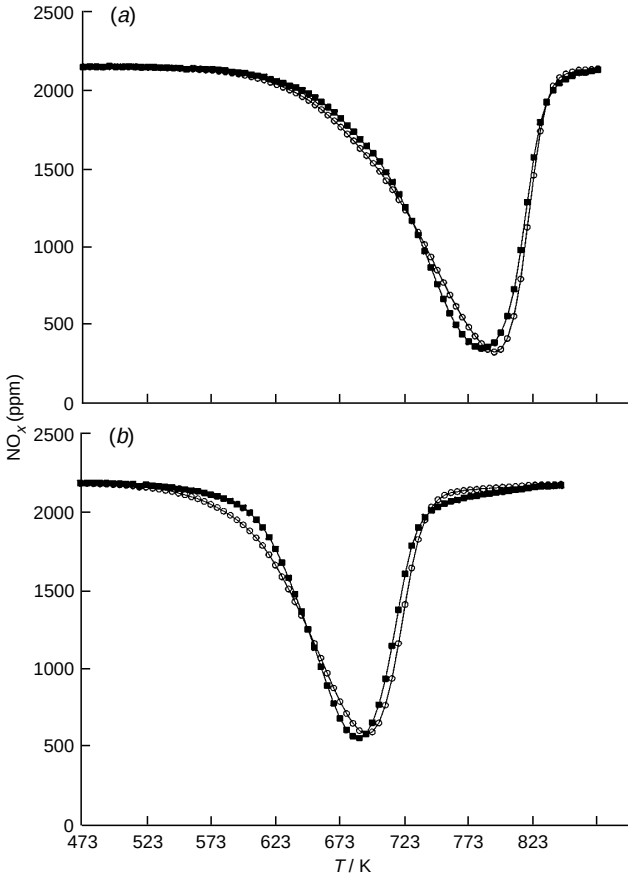



**Fig. 2** (*a*) Observed and calculated $NO_x$ concentration observed during heating at 10 K min$^{-1}$ in NO–oxygen, after the formation of hydrocarbon deposits at 473 K on a 54% Cu-exchanged catalyst as described in the text. (■) Experimental, (○) calculated using the simple model described in the text. (*b*) As (*a*), but for a 100% Cu-exchanged catalyst.

We have had many useful discussions related to this with work with Dr Olga Tkachenko and the late Professor Efim Shpiro, of the Zelinsky Institute of Organic Chemistry, Moscow, and with Drs J. C. Frost, A. Diwell, A. P. Walker and colleagues, of Johnson Matthey Technology Centre. We thank Professor J. A. Lercher for the design of the *in situ* cell for IR spectroscopy developed in his research group. We are grateful to Johnson Matthey PLC for financial support and some analytical assistance, and to EPSRC for financial support.

## References

1 M. Iwamoto, *Stud. Surf. Sci. Catal.*, 1990, **54**, 121.
2 J. O. Petunchi and W. K. Hall, *Appl. Catal.*, 1993, **2**, 303.
3 W. Grünert, N. W. Hayes, R. W. Joyner, E. S. Shpiro, M. R. H. Siddiqui and G. N. Baeva, *J. Phys. Chem.*, 1994, **98**, 10 832.
4 T. Beutel, B. Adelman and W. M. H. Sachtler, *Catal. Lett.*, 1996, **37**, 125.
5 N. W. Hayes, R. W. Joyner and E. S. Shpiro, *Appl. Catal. B*, 1996, **8**, 343.
6 T. Tanaka, T. Okuhara and M. Misono, *Appl. Catal. B*, 1994, **4**, L1.
7 N. W.Hayes, W. Grünert, G. J. Hutchings, R. W. Joyner and E. S. Shpiro, *J. Chem. Soc., Chem. Commun.*, 1994, 531.
8 F. Radtke, R. A. Koeppel and A. Baiker, *J. Chem. Soc., Chem. Commun.*, 1995, 427.
9 D. G. Blackmond, J. G. Goodwin and J. E. Lester, *J. Catal.*, 1982, **78**, 34.
10 C. Li, K. A. Bethke, H. H. Kung and M. Kung, *J. Chem. Soc., Chem. Commun.*, 1995, 813.
11 D. B. Lukyanov, J. L. d'Itri, G. Sill and W. K. Hall, *Stud. Surf. Sci. Catal.*, 1996, **101**, 651.
12 A. W. Aylor, L. J. Lobree, J. A. Reimer and A. T. Bell, *Stud. Surf. Sci. Catal.*, 1996, **101**, 661.
13 G. P. Ansell, A. F. Diwell, S. E. Golunski, J. W. Hayes, R. R. Rajaram, T. J. Truex and A. P. Walker, *Appl. Catal. B*, 1993, **2**, 81.
14 J. Connerton, M. B. Padley and R. W. Joyner, *J. Chem. Soc., Faraday Trans.*, 1995, **91**, 1841.

*Received, 27th September 1996; Com. 6/06618F*

# Synthesis, molecular structure and NMR spectroscopy of a transition-metal bifluoride complex: formation *via* C–F activation or reaction with $Et_3N{\cdot}3HF$

**Michael K. Whittlesey, Robin N. Perutz,* Bryan Greener and Madeleine H. Moore**

*Department of Chemistry, University of York, York, UK YO1 5DD*

**The bifluoride complex, *trans*-[Ru(dmpe)$_2$(H)(HF$_2$)] (dmpe = Me$_2$PCH$_2$CH$_2$PMe$_2$), is generated by reaction of *cis*-[Ru(dmpe)$_2$H$_2$] either with fluoroarenes (C$_6$F$_6$, C$_6$F$_5$H and others) or by reaction with Et$_3$N·3HF; its solid-state structure, established crystallographically, reveals a Ru(η$^1$-FHF) moiety with a long Ru–F bond and an F···F distance close to that in bifluoride salts, while the presence of the same complex in solution is shown by low-temperature NMR spectra.**

The C–F activation of hexafluorobenzene with transition-metal complexes may take two forms. Simple oxidative addition yields a metal pentafluorophenyl fluoride.[1,2] In a more puzzling process, several metal hydride complexes yield pentafluorophenyl hydride complexes.[2,3] A strong thermodynamic drive for this reaction is provided by the release of hydrogen fluoride, although its fate has not been determined.[4] We show here that the HF can be trapped as a complex of bifluoride, HF$_2$, which can also be accessed by reaction with a mild source of HF, Et$_3$N·3HF.[5] We have been prompted to publish at this stage by the recent report of [Mo(PMe$_3$)$_4$(H)$_2$F(HF$_2$)].[6]

We demonstrated earlier that the reaction of *cis*-[Ru(dmpe)$_2$-H$_2$] **1** (dmpe = Me$_2$PCH$_2$CH$_2$PMe$_2$) with C$_6$F$_6$ at −78 °C generates *trans*-[Ru(dmpe)$_2$(C$_6$F$_5$)H]. Reactions with partially fluorinated arenes yield analogues also arising from C–F activation.[3] In all these reactions, we noted the formation of a second hydride containing species, **2**, which is the subject of this paper. The $^1$H NMR spectrum (293 K) of **2** formed in the reaction of **1** with a twofold excess of C$_6$F$_n$H$_{6-n}$ (*n* = 6, 5, 4, 3) includes two broad singlet resonances at δ 13.8 and −25.8 in [$^2$H$_8$]thf. It is present in a ratio of *ca.*, 1:2 relative to the fluoroaryl hydrides. The $^{31}$P{$^1$H} spectrum shows a broad singlet; there are no resonances in the $^{19}$F NMR spectrum. Although the spectra of **2** were unaffected by running the reaction in an FEP-lined NMR tube, the formation of **2** was completely suppressed by triethylamine (fivefold excess). These observations suggested that **2** is *trans*-[Ru(dmpe)$_2$-(H)(HF$_2$)] formed from the HF released in the C–F activation reactions. A higher yield route to **2** was provided by the reaction of **1** with triethylamine trihydrofluoride.[7] Amine·HF adducts, R$_3$N·*x*HF, represent mild sources of HF which can be handled in solution without special precautions, and which have been employed to synthesise fluoride complexes.[8]

On addition of Et$_3$N·3HF to **1** (< 1 mol Et$_3$N·3HF per mol of **1**, both reagents dissolved in thf) at room temperature, **2** is formed. Although NMR spectra recorded at 293 K suggest that **2** is the single ruthenium-containing product, low-temperature spectra of recrystallised **2** resolve into two sets of resonances. The major species is indeed identified as *trans*-[Ru-(dmpe)$_2$(H)(HF$_2$)] from the full coupling pattern of $^1$H, $^{31}$P and $^{19}$F spectra (Fig. 1, 2).† The NMR spectra are unaffected by heating to 330 K and recooling to *ca.* 200 K. The IR spectrum of **2** (Nujol mull) shows a broad band for the bifluoride ligand at 1690 cm$^{-1}$, in the range reported for bifluoride ion salts.[9]

A suitable single crystal of **2** was obtained by slow evaporation of a thf solution. The structure determined by X-ray crystallography (Fig. 3)‡ showed a bifluoride group, F–H–F, coordinated to ruthenium and lying *trans* to the hydride ligand. The bifluoride bisects the two chelating dmpe groups and is tilted to give a Ru–F···F bond angle of 129.9(3)°. The F···F distance of 2.276(8) Å is very close to that found in bifluoride salts, MHF$_2$ (M = Na, K, NH$_4^+$),[9] or in pyridine·*n*HF,[10] and is significantly shorter (9 e.s.d.s) than the F···F separation of 2.351(8) Å found in [Mo(PMe$_3$)$_4$(H)$_2$F(HF$_2$)].[6] The Ru–F bond length [2.284(5) Å] is longer than in any conventional ruthenium–fluoride complexes (2.01–2.04 Å).[11] Indeed, **2** is a rare example of a complex containing M–H and M–F bonds, and is unique in the octahedral stereochemistry of hydride *trans* to fluorine.[12] Formation of platinum bifluoride complexes in solution has been suggested from $^1$H NMR data.[13] A crystal structure of a niobium dimer with two η$^2$-HF$_2$ groups has been reported but without evidence for this species in solution.[14] The molybdenum bifluoride complex[6] dissociates completely into [Mo(PMe$_3$)$_4$(H)$_2$F$_2$] and HF in solution.

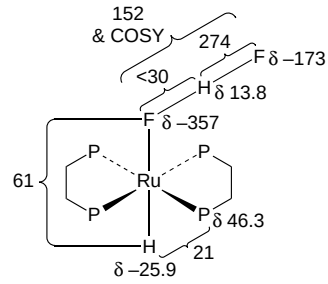



**Fig. 1** Coupling pattern (Hz) and chemical shifts in the low-temperature NMR spectra of *trans*-[Ru(dmpe)$_2$(H)(HF$_2$)] **2**

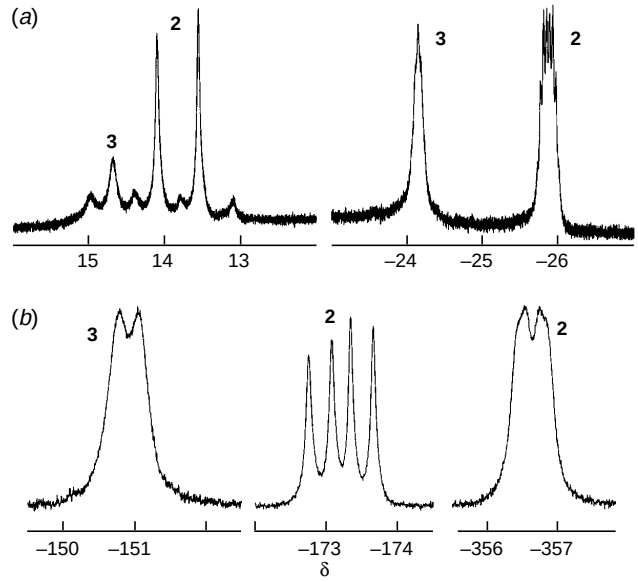



**Fig. 2** (*a*) $^1$H NMR spectrum (500 MHz) of bifluoride and hydride regions of recrystallised **2** in [$^2$H$_8$]thf at 188 K showing the presence of **2** and **3**. (*b*) $^{19}$F NMR spectrum (470 MHz) showing the bifluoride and metal–fluoride regions. The spectra in (*a*) and (*b*) are shown on a common scale in Hz cm$^{-1}$.

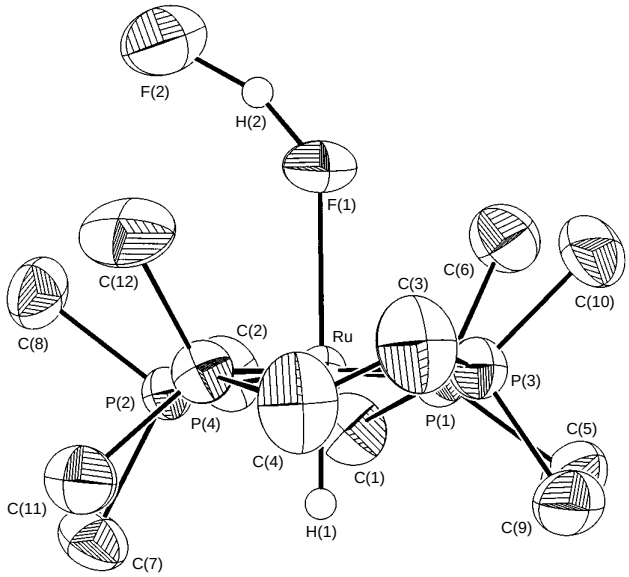



**Fig. 3** ORTEP diagram of the molecular structure of **2** (ellipsoids at 50% level). Principal bond lengths (Å), angles and torsional angles (°): Ru–F(1) 2.284(5), F(1)–F(2) 2.276(8), F(2)–F(1)–Ru 129.9(3), F(2)– F(1)–Ru–P(1) 114.9(4), F(2)–F(1)–Ru–P(2) 31.0(4).

The second species, **3**, observed at 188 K, shows a triplet resonance at δ 14.8 (*J* 145 Hz) in the $^1$H NMR spectrum [Fig. 2(*a*)] and a broad doublet resonance at δ −150.9 [Fig. 2(*b*)] in the $^{19}$F NMR spectrum consistent with the $HF_2^-$ anion.[15] It is identified provisionally as [Ru(dmpe)$_2$-H$^+$][$HF_2^-$].[16]§

A sequence for the formation of the bifluoride hydride that involves an intermediate dihydrogen hydride complex is shown in eqns. (1) and (2) {[Ru] = Ru(dmpe)$_2$}:

$$[Ru]H_2 + HF \longrightarrow [Ru](\eta^2\text{-}H_2)H^+F^- \quad (1)$$

$$[Ru](\eta^2\text{-}H_2)H^+F^- + HF \longrightarrow [Ru](H)(HF_2) + H_2 \quad (2)$$

The HF originates either in $Et_3N{\cdot}3HF$ or in reaction of **1** with fluoroarenes. These experiments show that the bifluoride group, $HF_2$, can be generated in an aprotic organic solvent under mild conditions. The fate of expelled HF in our C–F activation reactions is explained. Taken together with the molybdenum results[6] we may anticipate further bifluoride complexes with the hydrogen atom occupying a range of positions between the two fluorine atoms,¶ which may be probed *via* the values of $J_{HF}$. Our synthetic methods offer new routes to combination of hard and soft ligands as exemplified by *trans*-[Ru(dmpe)$_2$(OH)H], a complex closely related to **2**.[17] The exchange processes in **2** involving coordinated and free bifluoride are under investigation.

We acknowledge financial support from EPSRC and the loan of ruthenium from Johnson Matthey. We wish to thank Drs S. B. Duckett, O. Eisenstein, E. G. Hope and M. G. Partridge and Miss C. L. Higgitt for help and advice.

## Footnotes

† *Spectroscopic data* for *trans*-[Ru(dmpe)$_2$(H)(HF$_2$)], **2**: NMR {500 MHz, [$^2$H$_8$]thf, 188 K}: $^1$H δ −25.86 (dqnt, $^2J_{PH}$ 20.5, $^2J_{FH}$ 61.3 Hz, 1 H, Ru–H), 1.50 (s, 12 H, 4 × CH$_3$), 1.53 (s, 12 H, 4 × CH$_3$), 1.70 (br s, 4 H, 4 × PCH*H*), 1.92 (br s, 4 H, 4 × PC*H*H), 13.83 (d, $^1J_{HF}$ 273.9 Hz, 1 H, HF$_2$). $^{31}$P{$^1$H} δ 46.3(s). $^{19}$F δ −173.1 (dd, $^1J_{HF}$ 273.9, $^2J_{FF}$ 151.5 Hz, 1 F, Ru–F–H–*F*), −356.8 (br d, $^2J_{FF}$ 151.5 Hz, 1 F, Ru–*F*). IR (Nujol): 1690 cm$^{-1}$ ν(HF$_2$). FABMS, *m/z* 403 [Ru(dmpe)$_2$H]$^+$. The C, H analysis fitted [Ru(dmpe)$_2$(H)(F)], probably because of HF loss in the furnace.

‡ *Crystal data* for *trans*-[Ru(dmpe)$_2$(H)(HF$_2$)] **2**: 0.7 × 0.6 × 0.3 mm, $C_{12}H_{34}F_2P_4Ru$, *M* = 441.34, monoclinic, space group $P2_1$, *a* = 9.269(7), *b* = 11.848(8), *c* = 10.126(7) Å, β = 114.40(6)°, *U* = 1012.7(12) Å$^3$, *F*(000) = 456, $D_c$ = 1.447 Mg m$^{-3}$, *Z* = 2, λ(Mo-Kα) = 0.710 69 Å, μ = 1.095 mm$^{-1}$, $R_1[I > 2\sigma(I)]$ = 0.0305, $wR_2$ = 0.0831, GOF = 0.761, *T* = 293 K, 1873 unique reflections out of 1996 reflections measured. Diffractometer: Rigaku AFC6S, 2θ range 5–50°. After initial solution with the TEXSAN software package[18] by direct methods, SHELXL-93[19] was employed for full-matrix least-squares refinement. The hydride hydrogen atom and the bifluoride hydrogen atom were located from the difference map and refined isotropically. While the location of the hydride was unambiguous, that of the bifluoride hydrogen atom was not. All other hydrogen atoms were refined with a 'riding' model. Atomic coordinates, bond lengths and angles, and thermal parameters have been deposited at the Cambridge Crystallographic Data Centre (CCDC). See Information for Authors, Issue No. 1. Any request to CCDC for this material should quote the full literature citation and reference number 183/328.

§ *NMR data* for [Ru(dmpe)$_2$H]$^+$ **3**: NMR {500 MHz, [$^2$H$_8$]thf, 188 K}: $^1$H δ −24.14 (br qnt $^2J_{PH}$ 20.4 Hz, 1 H, Ru–H), (1.00 br s, (4 H, 4 × PCH*H*), 1.46 (s 12 H, 4 × CH$_3$), 1.57 (s 12 H, 4 × CH$_3$), 2.07 (br s, 4 H, 4 × PC*H*H). $^{31}$P{$^1$H} δ 44.5(s). The spectrum in toluene shows very similar chemical shifts and intensity ratio for **2** and **3**, indicating that **3** is not a solvent adduct.

¶ Preliminary effective core potential *ab initio* calculations by F. Maseras and O. Eisenstein confirm the stability of HF bound to *trans*-[Ru(PH$_3$)$_4$(H)F]. They reproduce the F···F and Ru–F distances satisfactorily and place the bifluoride hydrogen 0.25 Å closer to F(2) than F(1) in agreement with the NMR data.

## References

1 P. Hofmann and G. Unfried, *Chem. Ber.*, 1992, **125**, 659; J. L. Kiplinger, T. G. Richmond and C. E. Osterberg, *Chem. Rev.*, 1994, **94**, 373.
2 S. T. Belt, M. Helliwell, W. D. Jones, M. G. Partridge and R. N. Perutz, *J. Am. Chem. Soc.*, 1993, **115**, 1429.
3 M. K. Whittlesey, R. N. Perutz and M. H. Moore, *Chem. Commun.*, 1996, 787.
4 Catalytic hydrogenolysis of hexafluorobenzene has been reported with a rhodium hydride complex. The HF released in this reaction is trapped by added base. M. Aizenberg and D. Milstein, *J. Am. Chem. Soc.*, 1995, **117**, 8674.
5 The principal features of this work were submitted in January 1996 as a conference abstract: M. K. Whittlesey and R. N. Perutz. *Abstracts of 6th Int. Conf. on The Chemistry of the Platinum Group Metals*, York, UK, July 21–26, 1996; poster 80.
6 V. J. Murphy, T. Hascall, J. Y. Chen and G. Parkin, *J. Am. Chem. Soc.*, 1996, **118**, 7428.
7 R. Franz, *J. Fluorine Chem.*, 1980, **15**, 423; M. A. McClinton, *Aldrichchim. Acta*, 1995, **28**, 31.
8 A. Herzog, H. W. Roesky, F. Jäger and A. Steiner, *Chem. Commun.*, 1996, 29.
9 J. Emsley, *Chem. Soc. Rev.*, 1980, **9**, 91; B. S. Ault, *Acc. Chem. Res.*, 1982, **15**, 103.
10 D. Boenigk and D. Mootz, *J. Am. Chem. Soc.*, 1988, **110**, 2135.
11 C. J. Marshall, R. D. Peacock, D. R. Russell and I. L. Wilson, *Chem. Commun.*, 1970, 1643; S. A. Brewer, K. S. Coleman, J. Fawcett, J. H. Holloway, E. G. Hope, D. A. Russell and P. G. Watson, *J. Chem. Soc., Dalton Trans.*, 1995, 1073.
12 J. T. Poulton, M. P. Sigalas, K. Folting, W. E. Streib, O. Eisenstein and K. G. Caulton, *Inorg. Chem.*, 1994, **33**, 1476; N. M. Doherty and N. W. Hoffman, *Chem. Rev.*, 1991, **91**, 553.
13 D. R. Coulson, *J. Am. Chem. Soc.*, 1976, **98**, 3111; S. Hintermann, P. S. Pregosin, H. Rüegger and H. C. Clark, *J. Organomet. Chem.*, 1992, **435**, 225.
14 H. W. Roesky, M. Sotoodeh, Y. M. Xu, F. Schrumpf and M. Noltemeyer, *Z. Anorg. Allg. Chem.*, 1990, **580**, 131.
15 L. Gouin, J. Cousseau and J. A. S. Smith, *J. Chem. Soc., Faraday Trans. 2*, 1977, 1878; K. O. Christe and W. W. Wilson, *J. Fluorine Chem.*, 1990, **46**, 339; 1990, **47**, 117; B. K. Bennett, R. G. Harrison and T. G. Richmond, *J. Am. Chem. Soc.*, 1994, **116**, 11165.
16 Examples of similar five-coordinate cations. L. D. Field, T. W. Hambley and B. C. K. Yau, *Inorg. Chem.*, 1994, **33**, 2009; A. Mezzetti, A. Del Zotto, P. Rigo and E. Farnetti, *J. Chem. Soc., Dalton Trans.*, 1991, 1525; M. Ogasawara, K. Aoyagi and M. Saburi, *Organometallics*, 1993, **12**, 3393; M. Jiménez-Tenorio, M. C. Puerta and P. Valerga, *J. Am. Chem. Soc.*, 1993, **115**, 9794.
17 M. J. Burn, M. G. Fickes, J. F. Hartwig, F. J. Hollander and R. G. Bergman, *J. Am. Chem. Soc.*, 1993, **115**, 5875.
18 TEXSAN-TEXSRAY Structure Analysis Package, Molecular Structure Corporation, Houston, TX, 1985.
19 G. M. Sheldrick, SHELXL-93, University of Göttingen, Germany, 1993.

*Received, 25th September 1996; Com. 6/06598H*

# Asymmetric aromatic vicarious nucleophilic substitution of hydrogen

**Mark D. Drew,[a] David A. Jackson,[b] Nicholas J. Lawrence,*[a] John Liddle[a] and Robin G. Pritchard[a]**

[a] *Chemistry Department, University of Manchester Institute of Science and Technology, Manchester, UK M60 1QD*
[b] *ZENECA Process Technology Department, Huddersfield Works, PO Box A38, Leeds Road, Huddersfield, UK HD2 1FF*

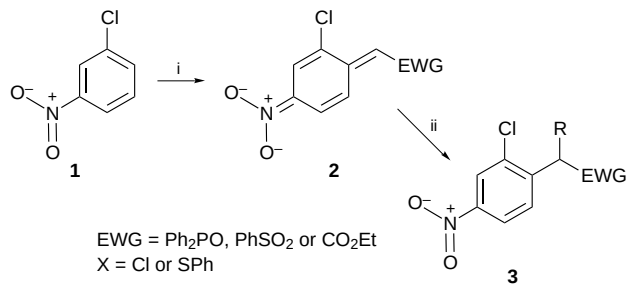
**A series of novel one-pot aromatic vicarious nucleophilic substitution of hydrogen/asymmetric alkylation reactions are described; the enolates of several chiral cyclohexyl phenylsulfanylacetates react readily with 3-chloronitrobenzene followed by subsequent stereoselective alkylation.**

The aromatic vicarious nucleophilic substitution[1,2] (VNS) of hydrogen provides a useful route to substituted arenes not readily prepared by electrophilic substitution. We recently reported[3,4] that the anion **2**, the initial product of the reaction between a nitrobenzene and a vicarious nucleophile, can be quenched with a variety of electrophiles (**1** → **3**, Scheme 1). It was clear to us that the relative and absolute stereochemical configuration of the newly created stereogenic centre might be controlled by an appropriate auxiliary incorporated into the nucleophile. Here we report an unprecedented asymmetric variant of this type of one-pot VNS–alkylation reaction which enables the stereocontrolled synthesis of a stereocentre adjacent to an electron deficient aryl group.

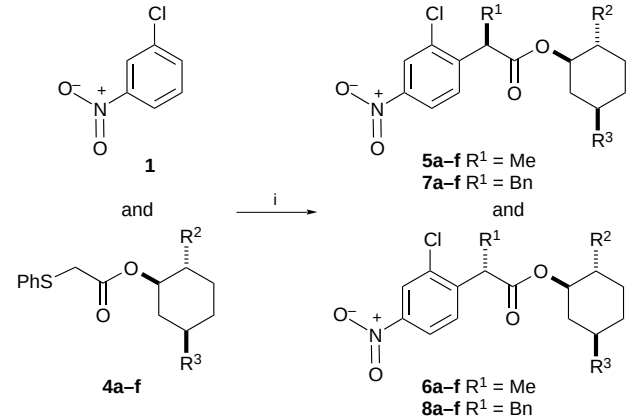
We chose to study the VNS reactions of a series of chiral esters **4a**–**f**. Menthol proved to be a poor auxiliary; reaction of the phenylsulfanylacetate **4a** with **1** followed by benzylation gave a 1 : 1 mixture of diastereoisomers in 60% yield. However the VNS–alkylation reaction of phenylsulfanylacetate **4b** derived from (−)-8-phenylmenthol[5] was much more successful. The enolate of **4b** reacted cleanly with 3-chloronitrobenzene **1** in DMF, with substitution taking place solely in the *para* position. Quenching the reaction mixture at −65 °C with a series of alkylating reagents gave moderate to good stereoselectivity.†,‡ Quenching with methyl iodide generated the corresponding diastereoisomeric esters **5b** and **6b** in a ratio of 3 : 1, in good yield. Benzylation proved to be the most diastereoselective reaction, giving the two α-benzylated diastereoisomers **7b** and **8b** in a ratio of 8 : 1 (Scheme 2, Table 1).

*trans*-2-Phenylcyclohexan-1-ol[6] has been extensively used in a wide variety of asymmetric reactions and is often used in place of (−)-8-phenylmenthol, since both enantiomeric forms are available by a variety of methods, most notably *via* asymmetric hydroboration[7] or dihydroxylation–reduction[8] of 1-phenylcylohexene. We therefore decided to apply this auxiliary to our VNS–asymmetric alkylation reaction. The enolate of (−)-*trans*-2-phenylcyclohexyl phenylsulfanylacetate **4c** reacted cleanly with 3-chloronitrobenzene, however no stereoselectivity was obtained upon methylation, while only a poor 2 : 1 diastereoselectivity was observed upon benzylation. We next tested the sterically more demanding esters phenylsulfanylacetates **4d**–**f** prepared from (±)-*trans*-2-biphenyl-, (±)-*trans*-2-(1′-naphthyl)- and (±)-*trans*-2-(2′-naphthyl)cyclohexan-1-ol, which are available *via* cuprate ring-opening of cyclohexene oxide.[9] The alcohols were converted to the phenylsulfanylacetates, reacted with 3-chloronitrobenzene under typical VNS conditions, and quenched with methyl iodide and benzyl bromide at −65 °C.§ The *trans*-2-(2′-naphthyl)cyclohex-1-yl group proved to be the most effective auxiliary, giving a 3 : 1 mixture of diastereoisomers **5f** and **6f** upon methylation and a 4 : 1 mixture of **7f** and **8f** upon benzylation.

Fortunately both products of the VNS reaction of (±)-*trans*-2-(2′-naphthyl)cyclohexyl phenylsulfanylacetate **4f** were crystalline; X-ray crystallography showed the major isomer **7f** to be the (1*RS*,2*SR*,α*RS*) diastereoisomer (Fig. 1).¶,‖ Since both




**Scheme 1** *Reagents and conditions*: i, NaH (2 equiv.), EWG–$CH_2X$ (1 equiv), room temp., DMF. ii, RX′ (1 equiv.), room temp.




**Scheme 2** *Reagents and conditions*: i, NaH (2 equiv.), 0 °C, DMF; ii, $R^1X$ (MeI or BnBr) (1 equiv.), −65 °C

**Table 1** Diastereoselectivity[a] of VNS–asymmetric alkylation reaction **1** + **4** → **5** + **6** or **7** + **8**

| Auxiliary | **4** | **5** : **6**[c] $R^1$ = Me | **7** : **8**[c] $R^1$ = Bn |
|---|---|---|---|
| (−)-Menthol | **a** | — | 1 : 1 (60) |
| (−)-8-Phenylmenthol | **b** | 3 : 1 (67) | 8 : 1 (70) |
| (−)-*trans*-2-Phenylcyclohexan-1-ol | **c** | 1 : 1 (55) | 2 : 1 (62) |
| (±)-*trans*-2-(4-Biphenyl)cyclohexan-1-ol | **d** | 1 : 1 (64) | 4 : 3 (64) |
| (±)-*trans*-2-(1′-Naphthyl)cyclohexan-1-ol | **e** | 3 : 2 (64) | 4 : 1 (57) |
| (±)-*trans*-2-(2′-Naphthyl)cyclohexan-1-ol | **f** | 3 : 1 (60) | 4 : 1[b] (62) |

[a] Measured by $^1H$ NMR (300 MHz) analysis of the crude reaction mixture. [b] Similar selectivity was obtained when (−)-**4f** was used. [c] Yields shown in parentheses. The relative stereochemistry of the major diastereoisomer is assigned by analogy to **7b** and **7f**.

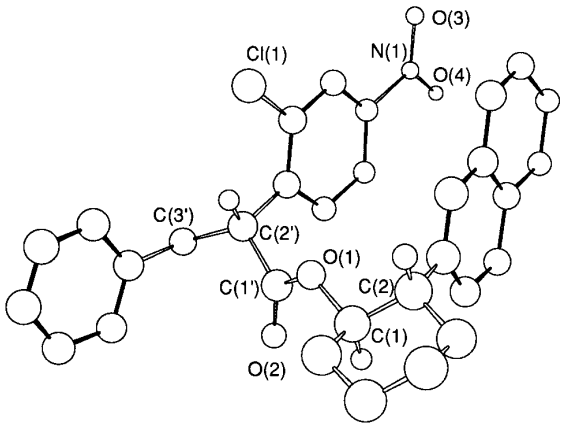
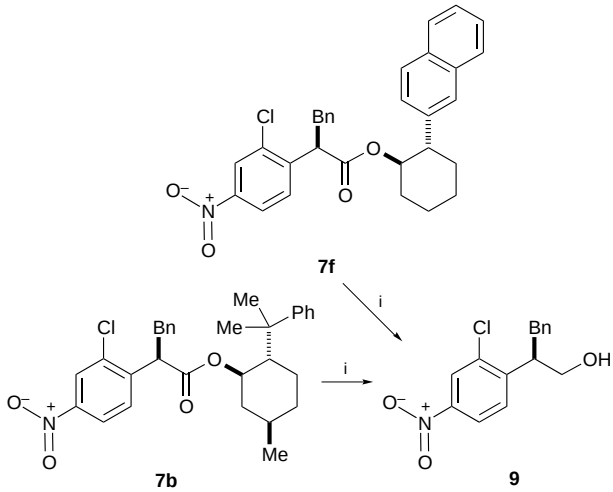



**Fig. 1** X-Ray crystal structure of the diastereoisomer **7f**




**Scheme 3** *Reagents and conditions*: i, DIBALH (2.1 equiv.), THF, room temp.

products **7b** and **8b** from the (−)-8-phenylmenthol derived VNS nucleophile **4b** were oils the alcohol **9**, obtained from DIBALH reduction of **5b**, was compared with that similarly obtained from (−)-*trans*-2-(2′-naphthyl)cyclohexyl phenylsulfanylacetate **4f** (Scheme 3). Enantiomerically pure (−)-*trans*-2-(2′-naphthyl)cyclohexan-1-ol was prepared from 1-(2′-naphthyl)cyclohexene using Sharpless's procedure.[10] The alcohols **9** derived from the two auxiliaries had the same sign of rotation, $[\alpha]_D$ − 36.4 (from **7f**) and $[\alpha]_D$ − 38.2 (from **7b**),** confirming that configuration of the newly created chiral centre in **7b** was also (*R*). It is interesting to note that the sense of stereochemical induction is the same as that reported for the alkylation of the enolate of 8-phenylmenthyl phenylacetate generated by deprotonation with butyllithium.[11]

We thank the EPSRC (CASE award to J. L.) and ZENECA for financial support.

## Footnotes

† Diastereoselectivity was determined by $^1$H NMR spectroscopy (300 MHz). All compounds were fully characterised and gave the expected spectral and analytical data.

‡ *Typical procedure*: To a nitrogen flushed slurry of sodium hydride (2.0 mmol) in dry DMF (3 cm$^3$) at 0 °C was added dropwise a mixture of phenylsulfanylacetate **4** (1 mmol) and 3-chloronitrobenzene (1.1 mmol) in dry DMF (3 cm$^3$). The mixture was allowed to reach room temperature over 2 h then cooled to −65 °C. The alkyl halide (1.0 mmol) was added and the reaction left to reach room temperature. The mixture was poured into dilute hydrochloric acid (20 ml) and extracted with chloroform (3 × 20 cm$^3$). The combined extracts were washed with distilled water, dried (magnesium sulfate) and concentrated *in vacuo*. The diastereoisomeric mixture of esters was separated by chromatography (silica, 1 : 1 chloroform–hexane, v/v).

§ *Selected data* for **7f**: $[\alpha]_D$ −71 (*c* 0.5, $CHCl_3$); $R_f$ 0.45 (silica, 1 : 1, chloroform–hexane, *v/v*); mp 89–91 °C. (Found: C, 72.3; H, 5.5; N, 2.8; Cl, 7.1; $C_{31}H_{28}ClNO_4$ requires C, 72.4; H, 5.5; N, 2.7; Cl, 6.9%); $\nu_{max}$(liquid film on CsI plates)/cm$^{-1}$ 2940 (m), 2860 (w), 1735 (s), 1530 (s), 1350 (s), 1170 (m), 1020 (w), 820 (w), 750 (m); $\delta_H$(300 MHz; $CDCl_3$) 1.26–1.65 (4 H, m, cyclohexyl), 1.76–1.90 (3 H, m, cyclohexyl), 2.02 (1 H, m, cyclohexyl), 2.65 (1 H, dt, *J* 4, 12 Hz, C*H*CHO), 2.66 (1 H, dd, *J* 7, 14 Hz, PhC$H_aH_b$), 3.14 (1 H, dd, *J* 9, 14 Hz, PhC$H_aH_b$), 4.23 (1 H, dd, *J* 7, 9 Hz, CHC=O) 5.09 (1 H, dt, *J* 4, 11 Hz, CHO), 6.73 (1 H, d, *J* 9 Hz, aromatic), 6.98–7.62 (14 H, cm, aromatic); $\delta_C$(75 MHz; $CDCl_3$) 24.71 ($CH_2$), 25.62 ($CH_2$), 32.20 ($CH_2$), 33.59 ($CH_2$), 38.54 ($CH_2$), 48.86 (CH), 50.14 (CH), 77.00 (CH), 121.07 (CH), 123.86 (CH), 125.15 (CH), 125.71 (CH), 125.93 (CH), 126.06 (CH), 126.57 (CH), 127.13 (CH), 127.53 (CH), 127.93 (CH), 128.30 (CH), 128.70 (CH), 132.08 (C), 132.79 (C), 133.73 (C), 137.77 (C), 139.76 (C), 142.69 (C), 146.03 (C), 171.00 (C=O); *m/z* (FAB) 552 [(M + K)$^+$, 45%], 513 [(M + H)$^+$, 50], 419 (40), 391 (40), 208 (60), 141 (100).

¶ *Crystal data* for **7f**. $C_{31}H_{28}ClNO_4$: *M* = 514.0 monoclinic, space group $P2_1/c$, *a* = 14.357(2), *b* = 20.227(3), *c* = 18.643(3) Å, β = 91.56(3)°, *V* = 5411.9(14) Å$^3$, *Z* = 8, $D_c$ = 1.262 g cm$^{-3}$, *T* = 293 K, colourless plates, μ = 1.78 cm$^{-1}$. *Data collection and processing*: A crystal of **7f** having approximate dimensions of 0.40 × 0.30 × 0.3 mm was mounted on a glass fibre. All measurements were made on a Siemens R3m/n diffractometer with graphite-monchromated Mo-Kα X-radiation. The data were collected at a temperature of 20 ± 1 °C using the ω–2θ scanning technique to a maximum of 2θ value of 50.0°. The structure was solved by direct methods using SHELXS-86.[12]

Full-matrix least-squares refinement using SHELXL93[13] yielded final residuals, based on $F^2$, of $wR^2$ = 0.207 and $R_1$ = 0.099 for 5025 observed [$I > 2\sigma(I)$] reflections with $w = 1/[\sigma^2(F_o) + (0.0766p)^2 + 3.2581p]$ where $p = (F_o^2 + 2F_c^2)/3$. In this room temperature study the atoms are undergoing substantial vibration leading to relatively high *R*-factors. Atomic coordinates, bond lengths and angles, and thermal parameters have been deposited at the Cambridge Crystallographic Data Centre (CCDC). See Information for Authors, Issue No. 1. Any request to the CCDC for this material should quote the full literature citation and the reference number 182/326.

‖ The asymmetric unit consists of two chemically identical and similarly configured molecules. For clarity, only one is shown in the Fig. 1.

** Both samples of **9**, derived from diastereoisomerically pure **7b** and **7f** were shown to be enantiomerically pure by $^1$H and $^{19}$F NMR analysis of their α-methoxy-α-(trifluoromethyl)phenylacetates.

## References

1 M. Makosza, *Chimia*, 1994, **48**, 499.
2 For reviews of aromatic vicarious nucleophilic substitution, see M. Makosza and J. Winiarski, *Acc. Chem. Res.*, 1987, **20**, 282; M. Makosza, *Synthesis*, 1991, 103; M. Makosza, J. Golinski and J. Barran, *J. Org. Chem.*, 1984, **49**, 1488; M. Makosza and S. Ludwiczak, *Synthesis*, 1986, 50; M. Makosza, *Russ. Chem. Rev.*, 1989, **58**, 747.
3 N. J. Lawrence, J. Liddle and D. A. Jackson, *Tetrahedron Lett.*, 1995, **36**, 8477.
4 N. J. Lawrence, J. Liddle and D. A. Jackson, *Synlett*, 1996, 55.
5 O. Ort, *Org. Synth.*, 1987, **65**, 203.
6 J. K. Whitesell, H. H. Chen and R. M. Lawrence, *J. Org. Chem.*, 1985, **50**, 4663.
7 H. C. Brown, J. V. N. Vara Prasad, A. K. Gupta and R. K. Bakashi, *J. Org. Chem.*, 1987, **52**, 310.
8 S. B. King and K. B. Sharpless, *Tetrahedron Lett.*, 1994, **35**, 5611.
9 D. Basavaiah and P. D. Rao, *Tetrahedron: Asymmetry*, 1994, **5**, 223.
10 D. A. Jackson, N. J. Lawrence and J. Liddle, unpublished results.
11 A. Solladie-Cavallo, A. G. Csaky, I. Gantz and J. Suffert, *J. Org. Chem.*, 1994, **59**, 5343.
12 G. M. Sheldrick, in *Crystallographic Computing 3*, ed. G. M. Sheldrick, C. Kruger and R. Goddard, OUP, 1985, pp. 175–189.
13 G. M. Sheldrick, SHELXL93, Program for the Refinement of Crystal Structures, University of Göttingen, Germany.

*Received, 9th October 1996; Com. 6/06921E*

# Spectroscopic evidence for cooperativity effects involving C–H···O hydrogen bonds: crystalline mestranol

**Thomas Steiner,*[a] Bert Lutz,[b] John van der Maas,[b] Nora Veldman,[c] Antoine M. M. Schreurs,[c] Jan Kroon[c] and Jan A. Kanters[c]**

[a] *Institut für Kristallographie, Freie Universität Berlin, Takustrasse 6, D-14195 Berlin, Germany*
[b] *Department of Analytical Molecular Spectrometry, Faculty of Chemistry, Utrecht University, PO Box 80083, 3508 TB Utrecht, The Netherlands*
[c] *Bijvoet Center for Biomolecular Research, Department of Crystal and Structural Chemistry, Utrecht University, Padualaan 8, 3584 CH Utrecht, The Netherlands*

**Combined crystallographic and IR spectroscopic study of the hydrogen bond network in the synthetic sex steroid mestranol indicates that a C≡C–H···O hydrogen bond can be considerably enhanced if the C≡C–H donor simultaneously accepts an O–H···C≡C interaction.**

It is well known that in arrays of conventional hydrogen bonds such as O–H···O and N–H···O, the strengths of the individual constituents are enhanced by cooperativity effects. Best known is σ-bond cooperativity in chains such as $O^{\delta-}$–$H^{\delta+}\cdots O^{\delta-}$–$H^{\delta+}\cdots O^{\delta-}$–H, where the individual hydrogen bonds enhance each other's strengths by mutual polarisation of the O–H groups.[1] A current topic of hydrogen bond research is directional interactions of the types C–H···Y[2] and X–H··π.[3] In crystal structures, these types of weak hydrogen bonds are often found interconnected with 'normal' or other weak hydrogen bonds, forming motifs that are topologically analogous with conventional hydrogen bond patterns. Several authors have taken this as a manifestation of cooperativity phenomena,[4] although structural analogy alone does not prove such an effect. There are conflicting views that suggest that weak hydrogen bonds are additive in nature, similar to van der Waals contacts.

Here we present a combined structural and spectroscopic study of the crystalline synthetic sex steroid mestranol **1**, which contains a remarkable system of interconnected conventional and non-conventional hydrogen bonds.

The crystal structure† of **1** contains two symmetry-independent molecules of virtually identical conformation‡ (Fig. 1), but which have different intermolecular contacts. A section of the crystal packing is shown in Fig. 2. Symmetry-independent molecules A and B are arranged in a head-to-head fashion, with their hydroxy and ethynyl groups forming a two-dimensional hydrogen bond network. This system of intermolecular interactons is shown in detail in Fig. 3 [only the HC≡C–C(17)–OH moieties are drawn]; geometric data is given in Table 1. The two symmetry-independent ethynyl groups donate antiparallel C≡C–H···O hydrogen bonds of very similar geometries, with C···O separations differing by only 0.035 Å (Table 1). However, these two C≡C–H···O hydrogen bonds have completely different functions in the hydrogen bond array: C≡C(A)–H simultaneously accepts an O–H···π hydrogen bond, and is thereby part of an infinite chain O(B)–H···C≡C(A)–H···O(A′)–H···O(B′)–H *etc.*, for which cooperativity enhancement might be suggested for all participating hydrogen bonds. The other ethynyl residue forms only the isolated hydrogen bond C≡C(B)–H···O(B)–H.

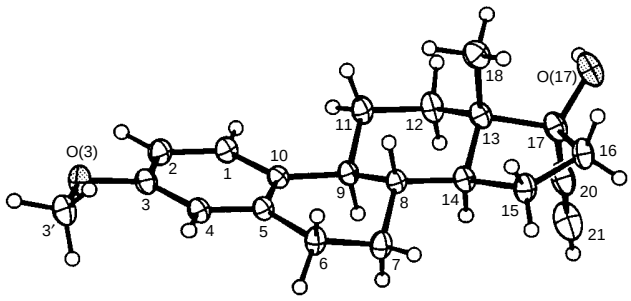



**Fig. 1** Molecular structure and atomic numbering scheme of **1**, molecule A. Oxygen atoms are shaded. Displacement ellipsoids are drawn at the 30% probability level.

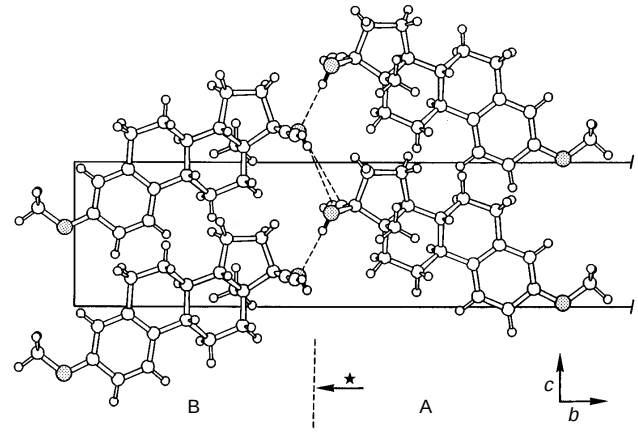



**Fig. 2** Section around $y/b = 1/4$ of the crystal packing. Oxygen atoms are shaded. The arrow marked by a star indicates the projection of Fig. 3.

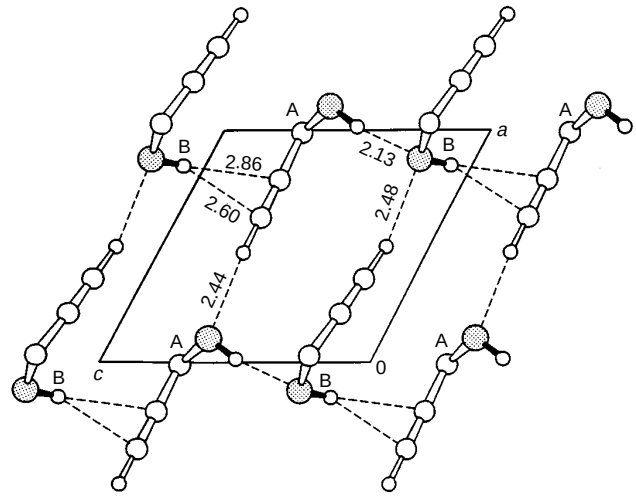



**Fig. 3** Hydrogen bond pattern in a projection perpendicular to Fig. 2. Oxygen atoms are shaded. Normalised H-positions are shown.

The infrared spectra were recorded§ for crystals and a dilute solution of **1** in $CCl_4$ (Table 2 and Fig. 4). As is to be expected, the spectrum shows two distinct O–H and two ≡C–H absorption bands present in the crystal phase, corresponding to the two symmetry-independent molecules. Of the two O–H bands, one is quite narrow and red-shifted by $-90.7$ cm$^{-1}$ compared to the 'free' O–H group in $CCl_4$ solution. This is typical for O–H···π hydrogen bonding, and the band is assigned to O(B)–H. The other O–H absorption band is significantly broader and more intense, and is therefore assigned to the conventionally hydrogen bonding O(A)–H. The two ≡C–H bands are shifted by $-21.3$ and $-59.8$ cm$^{-1}$ compared to free ethynyl groups, both values being indicative of C–H···O hydrogen bonding. Since these two red shifts differ by almost a factor of three, the two C≡C–H···O hydrogen bonds in the crystal must be markedly different despite their similar donor–acceptor separations.

The two C≡C–H···O interactions are formed by chemically identical groups; therefore, the large difference in the corresponding $\nu_{\equiv C-H}$ shifts can only be due to differences in the intermolecular environment. It is straightforward to suggest that the C–H···O interaction in the infinite chain is the stronger one, because it is donated by an ethynyl group which simultaneously accepts an O–H···π interaction. Therefore, the strongly shifted band is assigned to residue A, and the weakly shifted band to residue **B**; the difference is interpreted as a direct consequence of the cooperative effect.¶ This is compatible with spectroscopic investigations on 2-ethynyladamantan-2-ol,[5] where an unusually large $\nu_{\equiv C-H}$ red shift was found for a O–H···C≡C–H···O coupled system; that system, however, contains no non-cooperative C–H···O bonds for comparison.[4c]

These observations show conclusively that C–H···O interactions can be strongly influenced by their environment. The structural and spectral data for **1** are incompatible with the view that C–H···O and X–H·π interactions are too subtle to experience or to generate significant non-additivity effects. This is not relevant only to ethynyl groups. For all other residues that can simultaneously act as C–H donors and π acceptors, similar effects must be expected. A most important example is the phenyl group.

**Table 1** The hydrogen bonds of **1**; M = centroid of C(20)≡C(21) (for normalized H positions with C–H = 1.09 and O–H = 0.98 Å)

| | H···A/Å | D···A/Å | D–H···A (°) |
|---|---|---|---|
| O(17A)–H···O(17B) | 2.13 | 3.098(7) | 170 |
| O(17B)–H···C(20B) | 2.86 | 3.835(6) | 175 |
| O(17B)–H···M(B) | 2.67 | 3.636(7) | 170 |
| O(17B)–H···C(21B) | 2.60 | 3.524(8) | 158 |
| C(21A)–H···O(17A) | 2.44 | 3.443(5) | 153 |
| C(21B)–H···O(17B) | 2.48 | 3.478(5) | 151 |

**Table 2** Stretching frequencies

| Sampling | $\nu_{O-H}$/cm$^{-1}$ | $\nu_{\equiv C-H}$/cm$^{-1}$ |
|---|---|---|
| Dilute solution in $CCl_4$ at r.t. | 3614.0 | 3308.6 |
| Crystal (KBr) at r.t. | 3523.3, 3481.4 | 3287.3, 3248.8 |
| Crystal (KBr) at 92 K[a] | 3505.1, 3471.3 | 3278.9, 3233.8 |
| Shift $\Delta\nu_{cryst-soln}$ at r.t. | −90.7, −132.6 | −21.3, −59.8 |

[a] The low temperature data are not discussed in the text, because no corresponding X-ray crystal structure is available. The increase of the red shifts indicates further strengthening of all hydrogen bonds upon cooling. r.t. = room temperature.

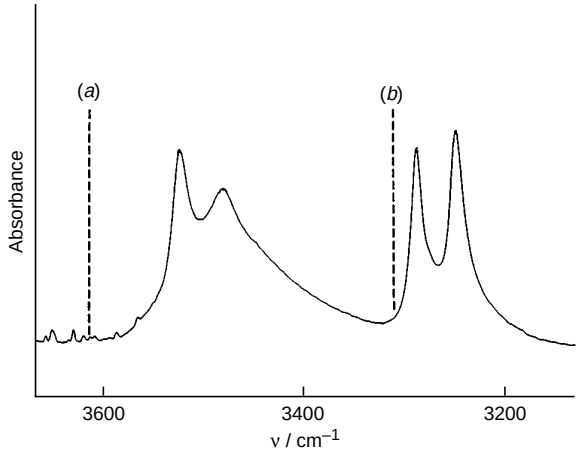



**Fig. 4** Section of the IR absorption spectrum of crystalline **1** at room temp. (KBr); numerical values are listed in Table 2: (*a*) $\nu_{OH}$ in $CCl_4$, (*b*) $\nu_{\equiv C-H}$ in $CCl_4$. The two left bands represent hydrogen bonding O–H, and the two right bands hydrogen bonding C≡CH groups.

## Footnotes

† Mestranol: 17α-ethynyl-3-methoxestra-1,3,5[10]-trien-17β-ol $C_{21}H_{26}O_2$, $M$ = 310.4 (commercially available from Sigma). Solvent-free crystals were obtained by slow evaporation of solutions in EtOH. Monoclinic, space group $P2_1$, $a$ = 6.8622(8), $b$ = 39.71(3), $c$ = 6.997(5) Å, β = 117.6(2)°, $V$ = 1690(2) Å$^3$, $Z$ = 4, $D_c$ = 1.22 g cm$^{-3}$. Enraf-Nonius FAST area-detector, Mo-Kα (λ = 0.71073 Å), graphite monochromator, 0.5 × 0.2 × 0.2 mm$^3$ crystal, room temperature, 14262 measured reflections, 8704 unique reflections ($R_{int}$ = 0.064), 6670 with $F^2 > 2\sigma(F^2)$, no absorption correction. Structure solution and refinement with standard methods (SHELXS-86, SHELXL-93). H-atoms refined isotropically. Final $R$ = 0.070 (for observed reflections), $wR(F^2)$ = 0.164 (for all reflections). Atomic coordinates, bond lengths and angles, and thermal parameters have been deposited at the Cambridge Crystallographic Data Centre (CCDC). See Informations for Authors, Issue No. 1. Any request to the CCDC for this material should quote the full literature citation and the reference number 182/305.

‡ The steroid skeleton does not significantly differ from 17α-ethynylestradiol as observed in the hemihydrate crystal structure; V. J. van Geerestein, *Acta Crystallogr., Sect. C*, 1987, **43**, 1206.

§ IR spectroscopy: Mattson Research Series spectrophotometer equipped with a DTGS detector. Cryostate Specac P/N 21.000 variable temperature cell. Scanning parameters: region 4000–500 cm$^{-1}$, resolution 2 cm$^{-1}$, 64 scans and triangular apodization.

¶ There is a further difference in the surroundings of the two ethynyl groups: as a consequence of the double-acceptor function of O17(B), there might be electrostatic repulsion between C(21B)–H and O(17A)–H donating hydrogen bonds to O(17B). This could destabilize the C(21B)–H···O interaction, and be responsible for a reduced red shift of $\nu_{C(21B)-H}$. Since the H[C(21B)]···H [O(17A)] distance is rather long (2.80 Å), it is assumed that this interaction is of only secondary importance compared to the O–H··π interaction accepted by the residue A. C(21A)–H does not form such a, possibly unfavourable, contact.

## References


1 G. A. Jeffrey and W. Saenger, *Hydrogen Bonding in Biological Structures*, Springer, Berlin, 1991.

2 G. R. Desiraju, *Acc. Chem. Res.*, 1991, **24**, 290; T. Steiner, *Cryst. Rev.*, 1996, **6**, 1.

3 (*a*) M. A. Viswamitra, R. Radhakrishnan, J.Bandekar and G. R. Desiraju, *J. Am. Chem. Soc.*, 1993, **115**, 4868; (*b*) H. S. Rzepa, M. H. Smith and M. L. Webb, *J. Chem. Soc., Perkin Trans. 2*, 1994, 703; (*c*) T. Steiner, E. B. Starikov, A. M. Amado and J. J. C. Teixeira-Dias, *J. Chem. Soc., Perkin Trans. 2*, 1995, 1321.

4 (*a*) S. Lakshmi, K. Subramanian, K. Rajagopalan, G. Koellner and T. Steiner, *Acta Crystallogr., Sect. C*, 1995, **51**, 2327; (*b*) T. Steiner, M. Tamm, B. Lutz and J. van der Maas, *Chem. Commun.*, 1996, 1127; (*c*) F. H. Allen, J. A. K. Howard, V. J. Hoy, G. R. Desiraju, D. S. Reddy and C. C. Wilson, *J. Am. Chem. Soc.*, 1996, **118**, 4081.

5 E. Steinwender, E. T. G. Lutz, J. van der Maas and J. A. Kanters, *Vib. Spectrosc.*, 1993, **4**, 217.


*Received, 2nd October 1996; Com. 6/06758A*

# Dioxygen and carbon monoxide binding in dendritic iron(II)porphyrins

**James P. Collman,*[a] Lei Fu,[a] Adrien Zingg[b] and François Diederich*[b]**

[a] *Department of Chemistry, Stanford University, Stanford, CA 94305, USA*
[b] *Laboratorium für Organische Chemie, ETH-Zentrum, Universitätstrasse 16, CH-8092 Zürich, Switzerland*

**Equilibrium $O_2$ and CO binding behaviour of two dendritic iron(II) porphyrin systems is reported.**

Tetrameric haemoglobin (Hb) and monomeric myoglobin (Mb) are haem proteins responsible for dioxygen storage and transport in biological systems. In the deoxy forms of both Hb and Mb the haem iron is bound to a single, 'proximal', axial imidazole resulting in a five-coordinate high-spin ($S$ = 2) $Fe^{II}$; upon oxygenation at the opposite 'distal' face, a diamagnetic $Fe^{III}O_2^-$ complex forms reversibly. The protein superstructure is responsible for the kinetic stabilization of the oxygenated form; amino acid residues on the 'distal' porphyrin face appear to destabilize a competing complex derived from the endogenous toxic CO. Thus the '*M*' value (*i.e.* the ratio of the two equilibrium binding constants $K_{CO}/K_{O_2}$) for Hb and Mb is about 100, small enough that the body can tolerate low, endogenous levels of CO. The 'picket fence' iron(II) model† complex also binds $O_2$ reversibly, exhibiting an $O_2$ affinity about the same as that of Mb; the polar $O_2$ binding cavity kinetically stabilizes the intrinsically bent $O_2$ adduct. In contrast, the linear CO ligand binds very strongly to the 'picket fence' porphyrin; *M* for the T (tense)-state model is 4280.[1] Several subsequent model systems such as 'pocket',[2] 'hybrid',[3] and 'capped'[4] porphyrins effect some distortion of the CO ligand and, as a consequence, *M* is lowered to *ca.* 150; with more hindered cavities, *M* can fall below 1.[5] The detailed interaction between structural distortion and equilibrium affinities of CO remains controversial.[6]

Stabilization of bound $O_2$ is also poorly understood. A distal histidine residue in Hb and Mb forms a weak [stability *ca.* 2 kcal $mol^{-1}$ (1 cal = 4.184 J)] hydrogen bond to the terminal oxygen in the $Fe^{III}O_2^-$ adduct. There have been some attempts to imitate such a hydrogen bond with model iron(II) porphyrins.[7] Some haem proteins have an unusually high $O_2$ affinity; for example in the blood worm *Ascaris*,[8] the $O_2$ affinity is $10^4$-fold higher compared with Hb. One can speculate that a strong hydrogen bond is responsible for this high $O_2$ affinity.

With the recent surge in dendrimer technology,[9] dendritic porphyrins were prepared as synthetic models of globular haem proteins.[10,11] It was shown for aqueous solutions that, in analogy to the protein surroundings in electron transfer proteins, a densely packed dendritic shell around a deeply buried iron haem profoundly influences the redox potential of the biologically relevant $Fe^{III}$–$Fe^{II}$ couple.[10*b*] Recently, Jiang and Aida[11*b*] reported a dendritic iron(II) porphyrin with aryl ether branches which exhibits reversible dioxygen binding. However, in their study, a 1-methylimidazole was used. This ligand is known to form a six-coordinate, low-spin iron(II) complex. This factor complicates any measure of $O_2$ affinity.

Herein we report a gas equilibrium binding study with two dendritic iron(II) porphyrins of first (G1-$Fe^{II}$, $M_r$ = 3956) and second (G2-$Fe^{II}$, $M_r$ = 11296) dendritic generation (Fig. 1). These were prepared from the corresponding free-base dendritic porphyrins[10*b*] *via* metallation with $FeBr_2$ in THF in an inert atmosphere box and subsequently purified chromatographically ($SiO_2$, MeOH–$CH_2Cl_2$).‡ The dendritic iron(II) porphyrins were each dissolved in toluene, 1000 mol equiv. of 1,2-dimethylimidazole (dmim) were added to form the five-coordinate, high-spin iron(II) complex, and the solution was loaded into a tonometer for gas binding studies. The dmim ligand forms only a 1 : 1 high-spin iron(II) adduct obviating the problem of controlling the number of axial ligands. Furthermore, the resulting iron(II) porphyrin is a good model for the lower affinity T-state of Hb.[12]

Gas flow: $O_2$, then $N_2$, then $O_2$ UV–VIS experiments showed reversible $O_2$ binding in toluene solution at 25 °C. Using a tonometer, we measured the $O_2$ and CO equilibrium binding constants ($K_{O_2}$ and $K_{CO}$)[13] for both dendrimers G1-$Fe^{II}$ and G2-$Fe^{II}$. These $P_{1/2}(O_2)$ ( = $1/K_{O_2}$) and $P_{1/2}(CO)$ ( = $1/K_{CO}$) values are displayed in Table 1 compared with those of T-state Hb, the corresponding T-state 'picket fence' model, and of the blood worm *Ascaris.*

It is remarkable that the $O_2$ affinities [$K_{O_2}$ = $1/P_{1/2}(O_2)$] of the dendritic porphyrins are about 1500 times greater than those of T-state Hb; these values approach the high affinity of *Ascaris* (Table 1). The CO affinities of the dendritic porphyrins are lower than those of the 'picket fence' model but are close to the value of Hb in the T-state. The combination of high $O_2$ and low

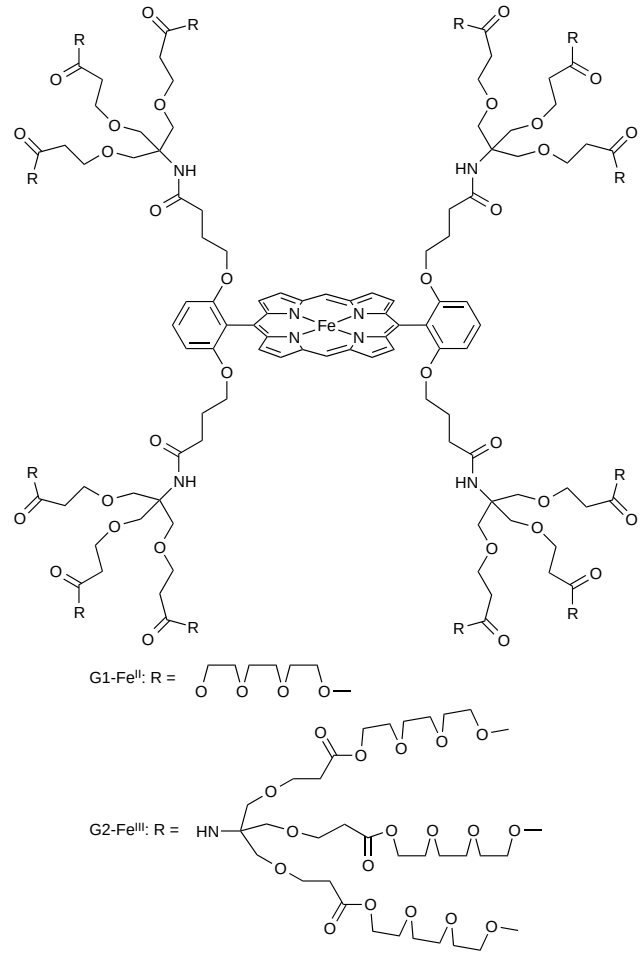



**Fig. 1** Dendritic porphyrins G1-$Fe^{II}$ and G2-$Fe^{II}$

**Table 1** Oxygen and carbon monoxide binding data

| | $P_{1/2}$/Torr | | $M$ $P_{1/2}(O_2)/P_{1/2}(CO)$ |
|---|---|---|---|
| | $O_2$ | CO | |
| Hb (T-state)[a] | 40 | 0.30 | 135[14] |
| Fe (picket fence)/dmim[b] | 38 | 0.0089 | 4280[2b] |
| *Ascaris*[c] | 0.002 | 0.1 | 0.02[8b] |
| G1-$Fe^{II}$/dmim[b] | 0.035 | 0.35 | 0.10 |
| G2-$Fe^{II}$/dmim[b] | 0.016 | 0.19 | 0.08 |

*Conditions*: [a] $H_2O$, pH 7, 25 °C. [b] Toluene, 25 °C. [c] $H_2O$, pH 7, 20 °C. Changing solvent polarity may slightly affect the affinities.[15]

CO affinities yields very low values for *M*. The dendritic *M* values show a trend similar to *Ascaris*.

Why are the $O_2$ affinities so great? These may result from a hydrogen bond to the amide N–H group. Molecular models suggest that the terminal O of bound $O_2$ can form such a hydrogen bond with the NH of the amide group linking together the porphyrin core and the first-generation dendritic branches, but more evidence is needed; studies are in progress. The lower CO affinities may be caused by a congested pocket over the CO binding site much like the sterically distorted model complexes mentioned above.

In conclusion, we have studied two dendrimer-based myoglobin T-state models. Each exhibits reversible $O_2$ and CO binding activities. The measured $O_2$ affinities are about 1500 times higher than those of a haemoglobin and 'picket fence' porphyrin, implying a possible hydrogen bonding between the terminal O of bound $O_2$ and an amide N–H group. In terms of CO affinity, the dendritic model systems are more like Hb than uncapped haem (*e.g.* 'picket fence' porphyrin) suggesting that, as with Hb, bound CO experiences a steric interaction that distorts binding from a favourable linear conformation.

## Footnotes

† 'Picket fence' porphyrin: *meso*-tetra(α,α,α-*o*-pivalamidophenyl)-porphyrin. For a general reference, see also: L. Stryer, *Biochemistry*, 4th edn., W. H. Freeman and Co., New York, 1955, pp. 152.

‡ UV–VIS spectra in toluene of G1-$Fe^{II}$: $\lambda_{max}$ (ε) = 428 nm ($4.1 \times 10^5$ $M^{-1}$ $cm^{-1}$); and G2-$Fe^{II}$: $\lambda_{max}$ (ε) = 408 nm ($2.2 \times 10^{-5}$ $M^{-1}$ $cm^{-1}$).

## References


1 J. P. Collman, J. I. Brauman, T. R. Halbert and K. S. Suslick, *Proc. Natl. Acad. Sci. USA*, 1976, **73**, 3333; J. P. Collman, R. R. Gagne, T. R. Halbert, J.-C. Marchon and C. A. Reed, *J. Am. Chem. Soc.*, 1973, **95**, 7868; J. P. Collman, R. R. Gagne, C. A. Reed, T. R. Halbert, G. Lang and W. T. Robinson, *J. Am. Chem. Soc.*, 1975, **97**, 1427.

2 K. Kim, J. Fettinger, J. L. Sessler, M. Cyr, J. Hugdahl, J. P. Collman and J. A. Ibers, *J. Am. Chem. Soc.*, 1989, **111**, 403; J. P. Collman, J. I. Brauman, B. L. Iverson, J. L. Sessler, R. M. Morris and Q. H. Gibson, *J. Am. Chem. Soc.*, 1983, **105**, 3052.

3 C. Tetreau, D. Lavalette, M. Momenteau, J. Fischer and R. Weiss, *J. Am. Chem. Soc.*, 1994, **116**, 11840.

4 C. Slebodnick, M. L. Duval and J. A. Ibers, *Inorg. Chem.*, 1996, **35**, 3607.

5 J. P. Collman, P. C. Herrmann, B. Boitrel, X. Zhang, T. A. Eberspacher and L. Fu, *J. Am. Chem. Soc.*, 1994, **116**, 9783; J. P. Collman, P. C. Herrmann, L. Fu, T. A. Eberspacher, M. Eubanks, B. Boitrel, P. Hayoz, X. Zhang, J. I. Brauman and V. Day, *J. Am. Chem. Soc.*, submitted for publication.

6 T. G. Spiro, *Science*, 1995, **270**, 221; G. B. Ray, X.-Y. Li, J. A. Ibers, J. L. Sessler and T. G. Spiro, *J. Am. Chem. Soc.*, 1994, **116**, 162; M. Lim, T. A. Jackson and P. A. Anfinrud, *Science*, 1995, **269**, 962; T. G. Traylor, N. Koga and L. A. Deardurff, *J. Am. Chem. Soc.*, 1985, **107**, 6504; T. G. Traylor, *Acc. Chem. Res.*, 1981, **14**, 102; B. A. Springer, S. G. Sligar, J. S. Olson and G. N. Phillips Jr., *Chem. Rev.*, 1994, **94**, 699.

7 G. E. Wuenschell, C. Tetreau, D. Lavalette and C. A. Reed, *J. Am. Chem. Soc.*, 1992, **114**, 3346.

8 Q. H. Gibson and M. H. Smith, *Proc. R. Soc. London, Ser. B*, 1965, **163**, 206; T. Okazaki and J. B. Wittenberg, *Biochim. Biophys. Acta*, 1965, **111**, 503; A. P. Kloek, J. Yang, F. S. Mathews and D. E. Goldberg, *J. Biol. Chem.*, 1993, **268**, 17669.

9 G. R. Newkome, C. N. Moorefield and F. Vögtle, *Dendritic Molecules, Concept–Synthesis–Perspectives*, VCH, Weinheim, 1996.

10 (*a*) P. J. Dandliker, F. Diederich, M. Gross, C. B. Knobler, A. Louati and E. M. Sanford, *Angew. Chem., Int. Ed. Engl.*, 1994, **33**, 1739; (*b*) P. J. Dandliker, F. Diederich, J.-P. Gisselbrecht, A. Louati and M. Gross, *Angew. Chem., Int. Ed. Engl.*, 1995, **34**, 2725.

11 (*a*) R.-H. Jin, T. Aida and S. Inoue, *J. Chem. Soc., Chem. Commun.*, 1993, 1260; (*b*) D. L. Jiang and T. Aida, *Chem. Commun.*, 1996, 1523; (*c*) R. Sadamoto, N. Tomioka and T. Aida, *J. Am. Chem. Soc.*, 1996, **118**, 3978; (*d*) Y. Tomoyose, D.-L. Jiang, R.-H. Jin, T. Aida, T. Yamashita, K. Horie, E. Yashima and Y. Okamoto, *Macromolecules*, 1996, **29**, 5236; (*e*) P. Bhyrappa, J. K. Young, J. S. Moore and K. S. Suslick, *J. Am. Chem. Soc.*, 1996, **118**, 5708; (*f*) K. W. Pollak, J. W. Leon and J. M. J. Fréchet, *Polym. Mater. Sci. Eng.*, 1995, **73**, 333.

12 J. P. Collman and C. A. Reed, *J. Am. Chem. Soc.*, 1973, **95**, 2048; M. Momenteau and C. A. Reed, *Chem. Rev.*, 1994, **94**, 659.

13 N. J. Rose and R. S. Drago, *J. Am. Chem. Soc.*, 1959, **81**, 6138; T. J. Beugelsdijk and R. S. Drago, *J. Am. Chem. Soc.*, 1975, **97**, 6466; J. P. Collman, J. I. Brauman and K. S. Suslick, *J. Am. Chem. Soc.*, 1975, **97**, 7185.

14 V. S. Sharma, M. R. Schmidt and H. M. Ranney, *J. Biol. Chem.*, 1976, **251**, 4267; R. C. Steinmeier and L. J. Parkhurst, *Biochemistry*, 1975, **14**, 1564.

15 K. S. Suslick and M. M. Fox, *J. Am. Chem. Soc.*, 1983, **105**, 3507; T. Hashimoto, R. L. Dyer, M. L. Crossley, J. E. Baldwin and F. Basolo, *J. Am. Chem. Soc.*, 1982, **104**, 2101.


*Received, 31st October 1996; Com. 6/07413H*

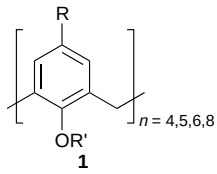
# Qualitative test for supramolecular complexation of $C_{60}$ using a mesoporous silica

**Alexander Drljaca, Christopher Kepert, Leone Spiccia, Colin L. Raston,* Christian A. Sandoval and Thomas D. Smith***

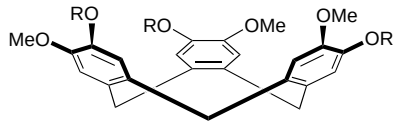
*Department of Chemistry, Monash University, Clayton, Victoria 3168, Australia*

**A new form of mesoporous silica with a surface area of 600 $m^2\ g^{-1}$, mean pore radius of 5.4 nm and total pore volume of 1.9 ml $g^{-1}$ uptakes $C_{60}$ in toluene; on removal of toluene or the addition of fullerene complexing agents the $C_{60}$ undergoes aggregation within the silica, identified by an inter-fullerene resonant transition at *ca*. 450 nm.**

Complexation of $C_{60}$ has been established for a variety of molecules including some hydrophobic calixarenes **1**[1–3] and cyclotriveratrylenes **2**[4,5] and is determined by the dimensions and shape of the cavity of the complexing agent, the nature of the interactions involving the spherical and otherwise non-polarised fullerene within the supermolecule, solvation effects, and fullerene–fullerene interactions.[5] The primary process in complexation of $C_{60}$ is most likely the formation of host–guest species with the resulting polarised fullerene aggregating as part of micelle-like species with a core of fullerenes surrounded by a sheath of host molecules.[5] The host–guest interactions are inherently weak and may not be evident in solution studies using UV–VIS spectroscopy, and where a discrete complex is not isolable, intimate contact between the two species in solution cannot be ruled out.




**1**




**2**

In addressing the difficulties in identifying and encouraging host–guest interactions, we have developed a new amorphous mesoporous silica ($MPSiO_2$) with sufficient pore size to allow mobilisation of $C_{60}$, and large enough to accommodate aggregates of fullerenes and associated host molecules, at least for small aggregates where conventional particle size analysis would be difficult. We show that when this material is loaded with $C_{60}$ it offers a qualitative test for supramolecular complexation of the fullerene, and that devoid of $C_{60}$ is a material for uptake of preformed micelles $\leqslant$5.4 nm in diameter. Other noteworthy features of the new mesoporous silica include: (*i*) the material has a narrow range of mesopores, (*ii*) it is prepared using inexpensive template materials; and (*iii*) its ability to allow solid-state diffusion or diffusion from organic solutions for a range of different classes of compounds including iodine at 293 K, ferrocene, nickelocene, and titanocene dichloride at 400 K, and 2-(2,4-dinitrobenzyl)pyridine at 383 K.[6] Mesoporous silicate (and aluminosilicate) materials containing pores in the range 1.6 to 10.0 nm are prepared by taking advantage of the self-assembling properties of liquid-crystal surfactant molecules,[7] and find application in catalysis. MCM-41 for example is effective for the epoxidation of bulky alkenes,[8,9] although the well defined structural arrangement of its mesopores requires relatively large amounts of liquid-crystal template material, which compromises any catalytic conversion of practical value. A zeolite-related microporous aluminophosphate with one-dimensional pores of diameter 12.5 Å can accommodate $C_{60}$.[10]

$MPSiO_2$ was prepared from sodium silicate, tetraethylammonium bromide, triethanolamine in a mixture of water, dmf and phosphoric acid, with the final product obtained after heating the isolated solid at 823 K:† particle fraction 60–80 mesh, surface area 600 $m^2\ g^{-1}$ with a mean pore radius window limit of 5.4 nm with no evidence of microporosity and a total pore volume of 1.9 ml $g^{-1}$. A sharp IR band at 3740 $cm^{-1}$ shows the presence of silanol groups, which decreased substantially after the adsorption studies. Contact of the magenta toluene solution of $C_{60}$ with $MPSiO_2$ results in magenta colouration of the silica which is retained after air drying, Fig. 1(*a*), but on heating at 320 K to remove the toluene the material changed to yellow, Fig. 1(*b*). This colour change and the associated appearance of a broad new band at 450 nm in the reflectance spectrum, which is ascribed to inter-fullerene resonant transitions, is consistent with disruption of toluene-solvated $C_{60}$ molecules,[11] affording aggregates of $C_{60}$ within the pores of $MPSiO_2$. The band is similar to that found in thin films and aggregates of colloidal $C_{60}$,[11,12] and that for the 1 : 1 complex of $C_{60}$ with **1** (R = Bu$^t$, R′ = H, *n* = 8), which has three fullerenes in the core of the micelle.[13] Contact of the yellow material with toluene restored the magenta colour of toluene-solvated $C_{60}$ in the pores.

Addition of toluene solutions of **1** or **2** to the magenta $MPSiO_2$ solid yields brown–yellow material, with representative reflectance spectra shown in Fig. 2. Except for spectrum

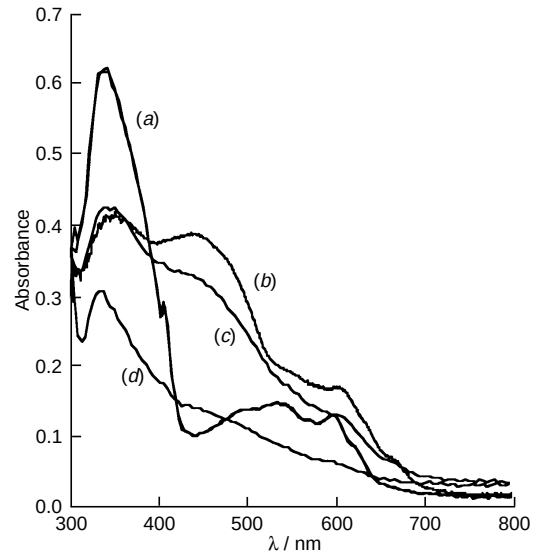



**Fig. 1** UV–VIS reflectance spectra of $MPSiO_2$ after (*a*) uptake of $C_{60}$ in toluene, (*b*) removal of toluene from the solid in (*a*), (*c*) treatment with a 1 : 1 mixture of $C_{60}$ : **2** (R = Me) in toluene and (*d*) treatment with a 1 : 10 mixture of $C_{60}$ : **2** (R = Me) in toluene

(*d*), Fig. 2 (see below), they show a similarly broad new band at *ca*. 450 nm, and is likewise consistent with the formation of aggregates of $C_{60}$, most likely as part of micelle-like structures with the fullerene cores surrounded by host molecules in the pores of $MPSiO_2$. In forming a host–guest interaction the host ligand, L, polarises the fullerene thereby encouraging the formation of aggregates, eqn. (1).[5] The new band is indicative of

$$C_{60} + L \overset{\text{toluene}}{\rightleftharpoons} (C_{60})_n L_x \qquad (1)$$

supramolecular complexation of the fullerene in the pores of the silica and is a qualitative test for host–guest interaction. In addition, we note that some molecules of type **1** and **2** failed to yield isolable host–guest complexes, and failed to show any host–guest interaction in solution, unlike in the pores of $MPSiO_2$, *e.g.* **1** (R = Bu$^t$, R′ = H, *n* = 4), **1** (R = *p*-$C_6H_4OPh$, R′ = Me, *n* = 4), **1** (R = Ph, R′ = Me, *n* = 4) and **2** (R = allyl). However, host–guest interaction is implied by the distinctly different crystal morphology of pure solid $C_{60}$ obtained on evaporation of toluene solutions of the fullerene and host, *e.g.* for **2** (R = allyl) (see below).[5] A toluene solution of $C_{70}$ (red–brown) in contact with $MPSiO_2$ coloured the silica particles red–brown, but in this case there was no marked change in the reflectance spectra on removal of the toluene, or on the addition of host molecules.

Addition of mixtures of $C_{60}$ with a selection of host molecules to $MPSiO_2$ also yielded brown material to varying degrees. A 1 : 1 mixture of $C_{60}$ : **2** (R = Me) gave a similar colour change and spectrum to that of adding the same host to $C_{60}$ already in the pores. However, for a 1 : 10 ratio there was little uptake of fullerene, Fig. 1(*d*), which is consistent with our earlier studies that micelle-like species are being formed under such conditions.[5] The bulk of these must be stable micelles > 5.4 nm in diameter. For **2** (R = allyl) the difference between the 1 : 1 and 1 : 10 mixtures added to the silica is reversed. The 1 : 1 mixture results in little uptake of the fullerene in the pores and thus most of the micelle-like structures are > *ca*. 5.4 nm whereas for the 1 : 10 mixture incorporation of smaller micelles prevails. Electronic spectra of the 1 : 10 solution itself suggests the presence of solvated host–guest species;[5] their intimate contact with the silica in the pores must then encourage fullerene–fullerene interactions.

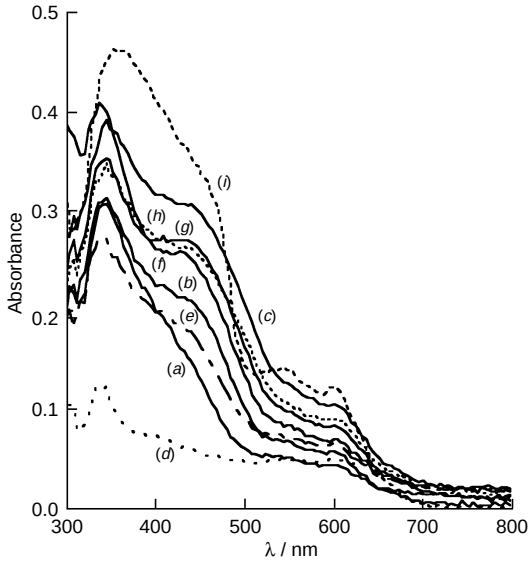



**Fig. 2** UV–VIS reflectance spectra of the solid from Fig. 1(*a*), after treatment with a toluene solution of **1**: (*a*) R = Bu$^t$, R′ = H, *n* = 4; (*b*) R = *p*-$C_6H_4OPh$, R′ = Me, *n* = 4; (*c*) R = Bu$^t$, R′ = H, *n* = 6; (*d*) R = H, R′ = H, *n* = 6; (*e*) R = CPh, R′ = Me, *n* = 4; (*f*) R = Bu$^t$, R′ = H, *n* = 5; (*g*) R = $CH_2Ph$, R′ = H, *n* = 5, (*h*) R = $CH_2Ph$, R′ = Me, *n* = 5, (*i*) R = Bu$^t$, R′ = H, *n* = 8

Unlike other calixarenes, addition of calix[6]arene to the magenta silica results in leaching of the fullerene from the silica, Fig. 2(*d*). However, addition of a mixture of the same calixarene and $C_{60}$ to $MPSiO_2$ gives the inter-fullerene resonant transition. It appears that an excess of the fullerene is required to encourage host–guest interactions/aggregation in the pores and in this context we note that the complex prepared from the calixarene and $C_{60}$ is rich in fullerene, analysing as the 2 : 1 complex.[1] The leaching of the $C_{60}$ by a solution of calix[6]arene may be due to encapsulation of each fullerene by two calixarenes as a toluene-soluble species, and/or the calixarene–fullerene association is more labile than for other calixarenes.

We thank the Australian Research Council for support of this work, and the CSIRO Division of Materials Science and Technology for the measurements of surface area, mean pore radius and pore volume.

## Footnote

† *Synthesis* of $MPSiO_2$: two solutions were prepared: solution A, which contained 30 ml of a stock solution of sodium silicate (density 1.36 g ml$^{-1}$; assay $Na_2O$ 8.55% m/m and $SiO_2$ 27.45% m/m) diluted to 100 ml with water containing 2.0 g of tetraethylammonium bromide, and solution B which consisted of 4 ml of triethanolamine in 10 ml of water to which was added 15 ml of dmf and 6 ml of phosphoric acid (85% m/m). Solution B was added to solution A with rapid stirring which was continued through the formation of a gel which formed within minutes and was allowed to stand overnight. Most of the water content was removed by heating the gel at 383 K for 12 h with stirring of the solid material at hourly intervals. The powdered product was washed successively with portions of hot water (5 × 200 ml) and after drying at 393 K was heated at 823 K in a muffle furnace for 48 h. The organic material was removed within a relatively short time with the longer heating period being required to remove coke which finally gives the white powdered product. After grinding, the particle fraction (60–80 mesh) was isolated and used for uptake of the various compounds.

## References

1 J. L. Atwood, G. A. Koutsantonis and C. L. Raston, *Nature*, 1994, **368**, 229.
2 K. Araki, K. Akao, A. Ikeda, T. Suzuki and S. Shinkai, *Tetrahedron Lett.*, 1996, **37**, 73 and references therein.
3 R. M. Williams, J. M. Zwier, G. H. Nachtegaal and A. P. M. Kentgens, *J. Am. Chem. Soc.*, 1994, **116**, 6965.
4 J. L. Atwood, M. J. Barnes, R. S. Burkhalter, P. C. Junk, J. W. Steed and C. L. Raston, *J. Am. Chem. Soc.*, 1994, **116**, 10346.
5 J. L. Atwood, M. J. Barnes, M. G. Gardiner and C. L. Raston, *Chem. Commun.*, 1996, 1449.
6 C. Kepert, L. Spiccia and T. D. Smith, unpublished work.
7 J. S. Beck, J. C. Vartuli, W. J. Roth, M. Leonowicz, C. T. Kresge, K. D. Schmitt, C. T.-W. Chu, D. H. Olsen, E. W. Sheppard, S. B. McCullen, J. B. Higgins and J. L. Schenker, *J. Am. Chem. Soc.*, 1992, **114**, 10834.
8 T. Maschmeyer, F. Rey, G. Sanker and J. M. Thomas, *Nature*, 1995, **378**, 159.
9 E. Klemn, D. Klemn and T. Kleinschmidt, *Chem. Phys. Lett.*, 1978, **55**, 113.
10 M. W. Anderson, J. Shi, D. A. Leight, A. E. Moody, F. A. Wade, B. Hamilton and S. W. Carr, *J. Chem. Soc., Chem. Commun.*, 1993, 533.
11 A. Beeby, J. Eastoe and R. K. Heenan, *J. Chem. Soc., Chem. Commun.*, 1994, 173.
12 F. Diederich, J. Effing, U. Jonas, L. Jullien, T. Plesnivy, H. Ringsdorf, C. Thilgen and D. Weinstien, *Angew. Chem., Int. Ed. Engl.*, 1992, **31**, 1599.
13 C. L. Raston, J. L. Atwood, P. J. Nichols and I. B. N. Sudria, *Chem. Commun.*, 1996, 2615.

*Received, 9th July 1996; Com. 6/04839K*

# Different donor binding modes of the pincer ligand 2,6-bis[(diethylamino)-methyl]phenyl: intermolecularly chelating in Li[2,6-$(NEt_2CH_2)_2C_6H_3$] and both mono- and bi-dentate in $BCl_2$\{2-[$BCl_3(NEt_2CH_2)$]-6-$(NEt_2CH_2)C_6H_3$\}

**Robert Schlengermann, Joachim Sieler, Svea Jelonek and Evamarie Hey-Hawkins***

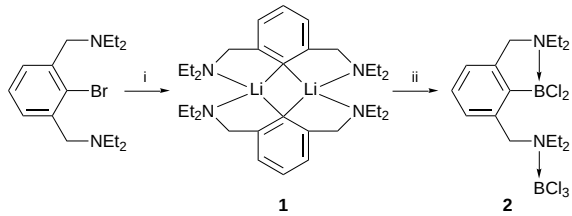
*Institut für Anorganische Chemie der Universität Leipzig, Talstrasse 35, D-04103 Leipzig, Germany*

**The reaction of dimeric Li[2,6-$(NEt_2CH_2)_2C_6H_3$] 1 with $BCl_3$ yields $BCl_2$\{2-[$BCl_3(NEt_2CH_2)$]-6-$(NEt_2CH_2)C_6H_3$\} 2, independent of the stoichiometric ratio (1:1 or 1:2) or reaction conditions (0 °C or boiling hexane).**

The lithium derivatives of monoanionic terdentate ligands 2,6-$(NR_2CH_2)_2C_6H_3$ (R = Me, Et) are valuable starting materials for the preparation of transition-metal or main-group element derivatives.[1] A variety of binding modes to late transition metals, *i.e.* as two-, four- and six-electron donor, have been observed.[2] Intramolecular coordination of the amino group strongly stabilises these compounds.[2] Thus, the intramolecularly stabilised five-coordinate 2,6-[bis(dialkylamino)-methyl]phenyl derivatives $AlX_2$[2,6-$(NMe_2CH_2)_2C_6H_3$] (X = Cl, H),[3] $GaMe_2$[2,6-$(NMe_2CH_2)_2C_6H_3$],[4] $InCl_2$[2,6-$(NEt_2CH_2)_2C_6H_3$],[5] InMe(Cl)[2,6-$(NEt_2CH_2)_2C_6H_3$],[5] $InEt_2$-[2,6-$(NEt_2CH_2)_2C_6H_3$][4] and $InR_2$[2,6-$(NMe_2CH_2)_2C_6H_3$] (R = Me, Et, Pr),[4] are liquids or low-melting solids and far less air-sensitive than trimethyl compounds; they are therefore suitable replacements for MOVPE.[4,5] Of the boron analogues, only the boronic acid derivative $B(OH)_2$[2,6-$(NMe_2CH_2)_2C_6H_3$][6] and the boronates $B(OCH_2CR_2O)$[2,6-$(NMe_2CH_2)_2C_6H_3$] (R = H, Ph),[7] $B(OCH_2CMe_2CH_2O)$[2,6-$(NMe_2CH_2)_2C_6H_3$][8] and $B(OCH_2CHMeO)$[2,6-$(NMe_2CH_2)_2$-$C_6H_3$],[8] which were synthesised from boronic acid and diols, have been reported in the literature. Since base-stabilised arylboron dichloride derivatives would appear to be useful starting materials for the preparation of transition-metal boranediyl complexes,[9] we attempted the preparation of these compounds.

The synthesis and *in situ* reactions of Li[2,6-$(NEt_2CH_2)_2C_6H_3$] **1** have been reported.† **1** (2.0 g, 7.8 mmol) reacts with $BCl_3(OEt_2)$ (15.6 mmol) in hexane (25 ml) at 0 °C to give $BCl_2$\{2-[$BCl_3(NEt_2CH_2)$]-6-$(NEt_2CH_2)C_6H_3$\} **2** in almost quantitative yield, independent of the stoichiometric ratio or reaction conditions (Scheme 1); formation of a $BCl_3$-free product was not observed. This suggests that **2** is the thermodynamically favoured product. In the comparable reaction of **1** with $InCl_3$, $InCl_2$[2,6-$(NEt_2CH_2)_2C_6H_3$] is obtained, in which both amino groups are coordinated to the In atom.[5]

In addition to being indispensable reagents for preparative organometallic and organic chemistry, lithium compounds often exhibit fascinating structures in the solid state.[10] In the compounds studied up to now, the Li atom exhibits a pronounced tendency to interact with electron-rich ligands or donor molecules, or aggregation through electron-deficient Li–C bonds is observed, leading to a large variety of structures.[10] A general principle for the dimerisation of lithium reagents has been described in the literature.[11]




**Scheme 1** *Reagents and conditions*: i, $Bu^nLi$, hexane, 0 °C, 12 h at room temp., 72%; ii, $BCl_3$, hexane, 0 °C, 99%

In the solid state Li[2,6-$(NEt_2CH_2)_2C_6H_3$] **1** consists of dimeric units in which the Li atoms are bonded to the two *ipso*-C atoms of the aryl rings by three-centre–two-electron bonds; the molecule has $C_2$ symmetry (Fig. 1).‡ The tetrahedral coordination of Li is completed by intra- and inter-molecular interactions with one amino group of each aryl ligand. The *ipso*-C atoms, C(1) and C(10), have tetrahedral rather than planar geometry. The structural parameters of **1** are in agreement with those of other structurally characterised dimeric lithium aryls.[12] § The structural data [Li–C, Li···Li, Li–N, bite angle N(2)–Li(1)–C(10) and N(1)–Li(1)–C(1)] as well as the overall structure ($C_2$ symmetry) and geometry of **1** [angle between planes C(1)–C(2a)/$C_2Li_2$ 56.8(1)°, C(10)–C(14a)/$C_2Li_2$ 56.9(2)°, C(1)–C(2a)/C(10)-C(14a) 66.20(8)°] are nearly identical to those of dimeric {2,3,5,6-tetrakis-[(dimethylamino)methyl]phenyl}lithium.[13] Other related lithium derivatives with two intra- and inter-molecularly chelating *ortho* substituents are tetrameric Li[2-$(NMe_2CH_2)C_6H_4$][14] and Li[2,6-$(NMe_2CH_2)_2C_6H_3$],[6,14] which is dimeric according to a molecular mass determination.

Like {Li[2,6-$(NMe_2CH_2)_2C_6H_3$]}$_2$,[14] dimeric **1** has $C_2$ symmetry. Therefore the C–C$H_2$-N and C$H_2$CH$_3$ groups are

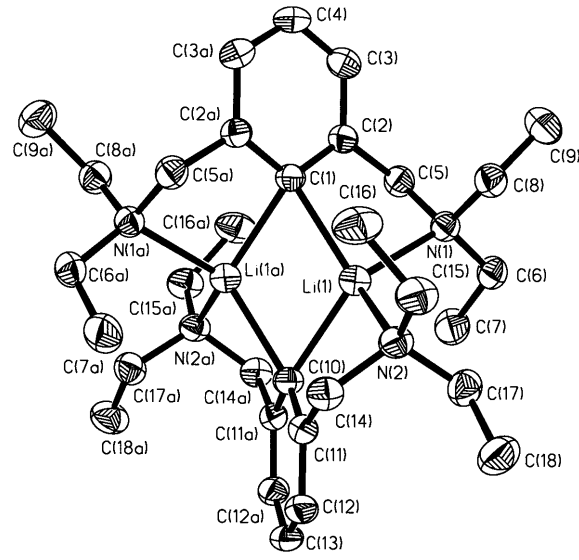



**Fig. 1** Molecular structure of dimeric Li[2,6-$(NEt_2CH_2)_2C_6H_3$] **1** showing the atom numbering scheme employed (ORTEP plot, 50% probability, SHELXTL PLUS; XP).[18] Selected bond lengths (Å) and angles (°): Li(1)–N(1) 2.178(3), Li(1)–N(2) 2.164(3), Li(1)–C(1) 2.228(3), Li(1)–C(10) 2.231(3), Li(1)···Li(1a) 2.483(5); N(2)–Li(1)–N(1) 111.01(12), N(2)–Li(1)–C(1) 134.67(13), N(1)–Li(1)-C(1) 86.07(10), N(2)–Li(1)–C(10) 85.92(10), N(1)–Li(1)–C(10) 134.27(13), C(1)–Li(1)–C(10) 112.32(12), Li(1)–C(1)–Li(1a) 67.73(14), Li(1)–C(10)–Li(1a) 67.62(14), C(2)–C(1)–C(2a) 114.9(2), C(11)–C(10)–C(11a) 114.4(2).

diastereotopic (below 16 °C); above 16 °C they become homotopic as the molecule becomes fluctional ($\Delta G^{\ddagger}$ = 54.6 ± 0.2 kJ mol$^{-1}$).[15]¶

Crystals of **2** were obtained from dichloromethane at −25 °C. The molecular structure of **2** is shown in Fig. 2.‡ In **2**, an arylboron dichloride is intramolecularly stabilised by interaction with one amino group, giving a five-membered B–C–C–C–N ring ($BC_3$ coplanar, N lies 0.5 Å below this plane). This leads to a distorted tetrahedral environment at B(1) [small C(1)–B(1)–N(2) bite angle and large C(1)–B(1)–Cl(1) bond angle]. The structural data of the C–C–C–N–B five-membered ring in **2** are similar to those of B(OCH$_2$CPh$_2$O)[2,6-(NMe$_2$CH$_2$)$_2$C$_6$H$_3$].[7] Due to the coordination number of five in InMe(Cl)[2,6-(NEt$_2$CH$_2$)$_2$C$_6$H$_3$], the C–In–N bite angles are even smaller [72.7(1), 72.3(1)°][5] than in **2** and the boronate. It is well known that $BCl_3$ forms stable adducts with ethers and amines, and the geometry of the $BCl_3$ group which is coordinated by the second amino group in **2** is comparable to that of undistorted tetrahedral $BCl_3$(NMe$_3$).[16] To our knowledge, **2** is the first example where the pincer ligand 2,6-(NEt$_2$CH$_2$)$_2$C$_6$H$_3$ acts as a monodentate ligand towards one molecule and as a bidentate ligand towards another. The only remotely related example is [WL(CO)$_3$(NCMe)] [L = 2-Ph$_3$SnC$_6$H$_4$CH$_2$N(Me)CH$_2$CH$_2$NMe$_2$], in which L exhibits $\eta^2$-N,N′ coordination to W and $\eta^1$-C coordination to Sn.[17]

While the related boronates B(OCH$_2$CR$_2$O)[2,6-(NMe$_2$CH$_2$)$_2$C$_6$H$_3$] (R = H, Ph) are dynamic in solution due to facile exchange of amine ligands,[7] in **2** this process is not possible due to the coordination of one amino group to the (aryl)$BCl_2$ fragment, while the other is coordinated to a $BCl_3$ molecule. Thus, in the proton NMR spectrum of **2** (in [$^2$H$_8$]thf),¶ the non-equivalence of the CC*HH*N (AB system) and NC*HH*CH$_3$ protons (one q for each H of both methylene groups) indicates that the five-membered chelate ring C–C–C–N–B is rigid in solution. For the C-C*H*$_2$N($BCl_3$)(C*H*$_2$CH$_3$)$_2$ group, these are equivalent (one s, one q). The chemical shifts and coupling patterns are solvent dependent.¶

The results presented here show that Li[2,6-(NEt$_2$CH$_2$)$_2$C$_6$H$_3$] **1** is dimeric in the solid state with $C_2$ symmetry. The reaction of **1** with $BCl_3$ yields the novel donor-stabilised arylboron dichloride, $BCl_2${2-[$BCl_3$(NEt$_2$CH$_2$)]-6-(NEt$_2$CH$_2$)C$_6$H$_3$} **2**; a $BCl_3$-free compound was not obtained. We are presently investigating the chemistry of **2** and its use in the preparation of transition-metal boranyl or boranediyl complexes.

We gratefully acknowledge financial support from the Deutsche Forschungsgemeinschaft (R. S.) and the Fonds der Chemischen Industrie; the company Chemetall GmbH has provided a generous donation of lithium alkyls, and Hoechst AG a generous donation of chemicals.

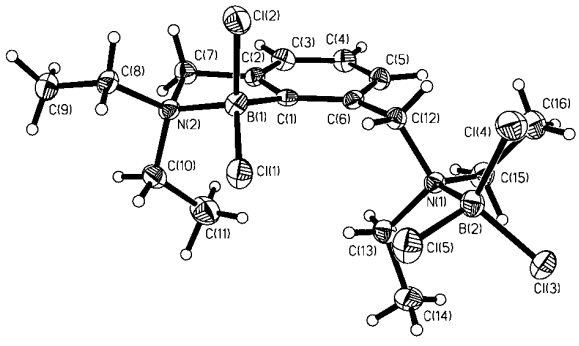



**Fig. 2** Molecular structure of $BCl_2${2-[$BCl_3$(NEt$_2$CH$_2$)]-6-(NEt$_2$CH$_2$)C$_6$H$_3$} **2** showing the atom numbering scheme employed (ORTEP plot, 50% probability, SHELXTL PLUS; XP).[18] Selected bond lengths (Å) and angles (°): B(1)–Cl(1) 1.842(4), B(1)–Cl(2) 1.882(5), B(2)–Cl(3) 1.855(5), B(2)–Cl(4) 1.852(5), B(2)–Cl(5) 1.841(5), B(1)–N(2) 1.649(5), B(2)–N(1) 1.639(5), B(1)–C(1) 1.598(5); C(7)–N(2)–B(1) 103.3(3), C(1)–B(1)–N(2) 100.5(3), C(2)–C(1)–C(6) 119.1(3), C(2)–C(1)–B(1) 107.7(3), C(6)–C(1)–B(1) 132.1(3).

## Footnotes

† Li[2,6-(NEt$_2$CH$_2$)$_2$C$_6$H$_3$] **1** was prepared according to the literature procedure.[4,5] Recrystallisation from hexane gave colourless crystals (72%).

‡ *Crystal data*: for **1**: $C_{32}H_{54}Li_2N_4$, $M$ = 508.68, white crystals, 0.5 × 0.5 × 0.5 mm, orthorhombic, space group *Pbcn* (no. 60), $T$ = 200(2) K, $a$ = 13.4959(9), $b$ = 16.9164(11), $c$ = 14.1022(9) Å, $U$ = 3219.6(4) Å$^3$, $Z$ = 4, $D_c$ = 1.049 g cm$^{-3}$, $F$(000) = 1120, μ(Mo-Kα) = 0.060 mm$^{-1}$, 13028 reflections collected with 2 < θ < 26°; of these 2956 were independent; 283 parameters, refinements converge to $R_1$ = 0.0477, $wR_2$ = 0.1004 [for reflections with $I > 2\sigma(I)$], $R_1$ = 0.0656, $wR_2$ = 0.1123 (all data). **2**: $C_{16}H_{27}B_2Cl_5N_2$, $M$ = 446.27, white crystals, 0.15 × 0.10 × 0.10 mm, triclinic, space group $P\bar{1}$ (no. 2), $T$ = 260(2) K, $a$ = 7.069(2), $b$ = 10.837(5), $c$ = 14.090(5) Å, α = 90.09(2), β = 104.16(2), γ = 97.35(2)°, $U$ = 1037.3(7) Å$^3$, $Z$ = 2, $D_c$ = 1.429 g cm$^{-3}$, $F$(000) = 464, μ(Mo-Kα) = 0.702 mm$^{-1}$, 4656 reflections collected with 1.5 < θ < 26°; of these 3409 were independent; 334 parameters, refinements converge to $R_1$ = 0.0460, $wR_2$ = 0.0889 [for reflections with $I > 2\sigma(I)$], $R_1$ = 0.0752, $wR_2$ = 0.1082 (all data).[18] Atomic coordinates, bond lengths and angles, and thermal parameters have been deposited at the Cambridge Crystallographic Data Centre (CCDC). See Information for Authors, Issue No. 1. Any request to the CCDC for this material should quote the full literature citation and the reference number 182/315.

§ In a structurally characterised dimeric aryllithium, Li–C ranges from 2.19 to 2.28 Å, Li···Li from 2.37 to 2.66 Å, and Li–C–Li from 64.2 to 67.4![14]

¶ Full spectroscopic discussion will be given in the full paper.

## References

1 A. A. H. van der Zeijden and G. van Koten, *Inorg. Chem.*, 1986, **25**, 4723; A. L. Wayda and R. D. Rogers, *Organometallics*, 1985, **4**, 1440; F. A. Cotton and G. N. Mott, *Organometallics*, 1982, **1**, 38; L. E. Manzer, *J. Am. Chem. Soc.*, 1978, **100**, 8068; and references therein.

2 G. van Koten, *Pure Appl. Chem.*, 1989, **61**, 1681; 1990, **62**, 1155; J. T. B. H. Jastrzebski and G. van Koten, *Adv. Organomet. Chem.*, 1993, **35**, 241.

3 L. Contreras, A. H. Cowley, F. P. Gabbai, R. A. Jones, C. J. Carrano and M. R. Bond, *J. Organomet. Chem.*, 1995, **489**, C1.

4 H. Schumann, U. Hartmann and W. Wassermann, *Chem. Ber.*, 1991, **124**, 1567.

5 H. Schumann, W. Wassermann and A. Dietrich, *J. Organomet. Chem.*, 1989, **365**, 11.

6 M. Lauer and G. Wulff, *J. Organomet. Chem.*, 1983, **256**, 1.

7 S. Toyota, T. Futawaka, H. Ikeda and M. Oki, *J. Chem. Soc., Chem. Commun.*, 1995, 2499.

8 M. Lauer, H. Böhnke, R. Grotstollen, M. Salehnia and G. Wulff, *Chem. Ber.*, 1985, **118**, 246.

9 The only known examples of transition-metal boranediyl complexes are [(CO)$_4$FeB(NMe$_2$)] (G. Schmid, W. Petz and H. Nöth, *Inorg. Chim. Acta*, 1970, **4**, 423) and [{(C$_5$H$_4$R)(CO)$_2$Mn}$_2$(μ-BX)], with X = NMe$_2$, R = H, Me; X = Bu$^t$, R = Me (H. Braunschweiger and T. Wagner, *Angew. Chem.*, 1995, **107**, 904).

10 W. N. Setzer and P. v. Rague-Schleyer, *Adv. Organomet. Chem.*, 1985, **24**, 353 and references therein.

11 P. v. Rague-Schleyer, R. Hacker, H. Dietrich and W. Mahdi, *J. Chem. Soc., Chem. Commun.*, 1985, 662.

12 S. Harder, J. Boersma, L. Brandsma, J. A. Kanters, W. Bauer and P. v. Rague-Schleyer, *Organometallics*, 1989, **8**, 1696; D. Thoennes and E. Weiss, *Chem. Ber.*, 1978, **111**, 3157; J. T. B. H. Jastrzebski, G. van Koten, K. Goubitz, C. Arlen and M. Pfeffer, *J. Organomet. Chem.*, 1983, **246**, C75; M. A. Beno, H. Hope, M. M. Olmstead and P. P. Power, *Organometallics*, 1985, **4**, 2117.

13 A. A. H. van der Zeijden and G. van Koten, *Recl. Trav. Chim. Pays-Bas*, 1988, **107**, 431.

14 J. T. B. H. Jastrzebski, G. van Koten, M. Konijn and C. H. Stam, *J. Am. Chem. Soc.*, 1982, **104**, 5490.

15 M. Hesse, H. Meier and B. Zeeh, *Spektroskopische Methoden in der Organischen Chemie*, Georg-Thieme-Verlag, Stuttgart–New York, 4th edn., 1991.

16 H. Hess, *Acta Crystallogr., Sect. B*, 1969, **25**, 2338.

17 B. P. Buffin, M. J. Poss, A. M. Arif and T. G. Richmond, *Inorg. Chem.*, 1993, **32**, 3805.

18 SHELXTL PLUS, Siemens Analytical X-ray Instruments Inc., 1990, XS: Program for Crystal Structure Solution, XL: Program for Crystal Structure Determination, XP: Interactive Molecular Graphics.

*Received, 30th September 1996; Com. 6/06670D*

# Spectroscopy with the polarizable solvent diiodomethane

**Fredric M. Menger* and Ana M. Sanchez**

*Department of Chemistry, Emory University, Atlanta, Georgia 30322, USA*

**The polarizable solvent $CH_2I_2$ causes $^1H$ NMR upfield chemical shifts of 1.5 ppm as well as bathochromic shifts of a dye greater than those caused by polar solvents such as methanol.**

Diiodomethane has a density of 3.3, a boiling point of 180 °C and a relative permittivity of 5.3. Its outstanding physical property is, however, a refractive index of 1.748. This compares with 1.333 for water and 1.560 for bromobenzene. Even carbon disulfide (with the highest refractive index among the common solvents) has a value of only 1.628. Refractive indices arise from a light wave's oscillating electric field being countered by a corresponding oscillating field from a molecule's electrons. The velocity of the propagating wave is thereby reduced. Thus, the refractive index of 1.748 for diiodomethane reflects a particularly high electron mobility around the two iodine atoms. More specifically, the longitudinal polarizability for C–I bonds is as much as 9 times greater than for the C–C bond.[1]

Compared to hydrogen-bonding, ion-pairing, charge-transfer and π-stacking, intermolecular polarizability effects on organic compounds are rather poorly understood. The question here, therefore, is how systems are perturbed when embedded in a sea of polarizable electrons as provided by diiodomethane. Judging from its relative permittivity of 5.3, the solvent appears to be apolar in nature. This may be misleading because the dielectric constant, derived from a 'bulk' measurement, fails to depict specific interactions occurring at the molecular level.

One indication that diiodomethane does in fact influence spectral properties comes from an NMR study of $^{129}Xe$ in 46 solvents.[2] Among these solvents, diiodomethane induces by far the largest chemical shift of δ 335. This may be compared to δ 225 for carbon disulfide, δ 248 for iodomethane and δ 196 for water. It was also shown that proton gas-to-liquid NMR shifts for $CH_4$, being a complex function of the refractive indices, is greatest for diiodomethane among several poly-brominated and chlorinated solvents.[3] Diiodomethane has also been used as one of 37 solvents for a study of the visible molecular absorption spectrum of cyanine dyes.[4] A modest red shift of *ca*. 25 nm was observed in switching from methanol to diiodomethane. Molecular absorption bands correlate with $(n^2 - 1)/(2n^2 + 1)$ where $n$ is the refractive index of the solvent.

Before carrying out any spectroscopy, we felt it desirable to obtain a sense of the solubilizing power of diiodomethane. The following compounds are miscible with diiodomethane: acetonitrile, benzene, chloroform, cyclohexene, dioxane, ethanol, ethyl acetate, ethyl ether and tetrahydrofuran. The following are immiscible: bromine, hexane, hexan-1-ol, ethyl vinyl ether and water. Acrylic acid and cyclohexane show modest solubility. In general, aromatic groups seem to help solubilize compounds in diiodomethane.

NMR spectra were obtained with a 500 MHz spectrometer on samples in 5 mm tubes containing 0.14 M solute in $CD_2I_2$. $SiMe_4$ in $CDCl_3$ was used as an external reference. Since no differences were observed between $CD_2I_2$ (Aldrich), (stabilized with copper) and $CD_2I_2$ purified by vacuum distillation, all experiments used the former.

A total of 17 diverse solutes in $CD_2I_2$ were examined by $^1H$ NMR. The vast majority of signals shifted upfield relative to those in $CDCl_3$, by 1.5 ± 0.1 ppm. For example, uncorrected[5] cyclohexene signals shifted from δ 5.58, 1.90 and 1.52 in $CDCl_3$ to δ 4.09, 0.43 and 0.03, respectively, in $CD_2I_2$. Other representative examples from the group of 17 (including an alkene, carboxylic acid, nitrile, ketone *etc*.) are given in Table 1. Since the shifts were more or less uniform regardless of the proton type, there was little simplification of the spectra except in four cases (anisole, phenetole, butyl phenyl ether and thioanisole). These simplifications arose from one proton of a multi-proton multiplet fortuitously shifting slightly differently (*ca*. 0.1 ppm) than the other components. Fig. 1 shows the improved peak resolution of the thioanisole spectrum in $CD_2I_2$ relative to $CDCl_3$. Note that since spectra in $CDCl_3$ and $CCl_4$ are very similar, the observed differences between $CD_2I_2$ and $CDCl_3$ cannot be ascribed to hydrogen-bonding to the latter solvent. A change from $CDCl_3$ to $CD_2I_2$ caused upfield shifts in the $^{13}C$ NMR spectra of less than 1 ppm.

No variation in chemical shift was observed with thioanisole in diiodomethane as the temperature was varied from 10 to 30 °C (6 °C being the freezing point of the solvent). The chemical shifts of the toluene signals in various mixtures of $CD_2I_2$ and $CDCl_3$ were found to be linearly related to the percentage of $CD_2I_2$ in the solvent. All these results point to a nonspecific solvent effect arising from solvent in the aggregate as opposed to definable molecular complexes. Accordingly, it appears that solutes are immersed in a continuum where their spontaneous electric moments create a reaction field in the solvent which, in turn, affects the magnetic shielding at the solute nuclei. Diiodomethane with its high refractive index would be expected to excel in this regard.[6]

Visible spectrophotometry gave more detailed information on the solvation properties of diiodomethane at the molecular level. The experiments used *N*,*N*-dimethindoaniline (phenol blue) dissolved at a concentration of $2 \times 10^{-5}$ M in several solvents including diiodomethane. Phenol blue has a solvent-

**Table 1** $^1H$ NMR chemical shifts in $CDCl_3$ and $CD_2I_2$

| Solute | δ ($CDCl_3$) | δ ($CD_2I_2$) | Δδ/ppm |
|---|---|---|---|
| Naphthalene | 7.789 | 6.309 | 1.480 |
| | 7.422 | 5.957 | 1.465 |
| *o*-Phenetidine | 6.675 | 5.125 | 1.550 |
| | 6.617 | 5.060 | 1.557 |
| | 3.953 | 2.471 | 1.482 |
| | 3.690 | 2.054 | 1.636 |
| | 1.327 | −0.124 | 1.451 |
| Acetophenone | 7.866 | 6.344 | 1.522 |
| | 7.475 | 6.071 | 1.404 |
| | 7.374 | 5.958 | 1.416 |
| | 2.519 | 1.088 | 1.431 |
| Ethyl benzoate | 7.947 | 6.369 | 1.578 |
| | 7.447 | 6.038 | 1.409 |
| | 7.333 | 5.910 | 1.423 |
| | 4.279 | 2.763 | 1.516 |
| | 1.294 | −0.153 | 1.457 |
| Toluene | 7.167 | 5.764 | 1.390 |
| | 7.055 | 5.674 | 1.402 |
| | 2.277 | 0.911 | 1.366 |
| Iodobenzene | 7.650 | 6.105 | 1.454 |
| | 7.277 | 5.811 | 1.466 |
| | 7.053 | 5.599 | 1.545 |

sensitive $\lambda_{max}$, and for this reason it has been widely exploited as a polarity probe.[7] Table 2 lists the absorbance maxima in select solvents ranging in polarity from hexane to water. It is seen that there is a red shift as the solvent becomes more polar. For example, $\lambda_{max}$ shifts from 545 nm in hexane to 654 nm in water. This is traditionally explained by the polar solvents stabilizing the transition dipole which resembles, as a crude model, the dipolar resonance contributor of the dye. The resulting spectral shift, of the dipole-induced dipole type, depends upon both the change in dipole moment of the solute and the refractive index of the solvent. A dispersive interaction is also possible in which a rapidly fluctuating transition moment creates an induced dipole in solvent molecules; this effect likewise depends upon the solvent polarizability and, hence, the refractive index.

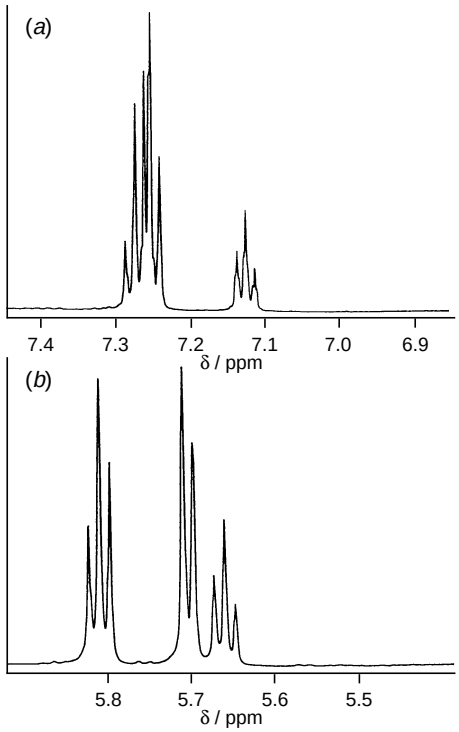
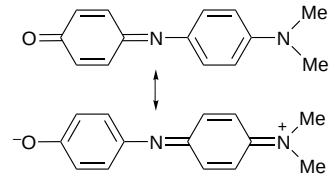



**Fig. 1** $^1$H NMR spectra of the aromatic portion of thioanisole in (*a*) $CDCl_2$ and (*b*) $CD_2I_2$. The simplification in $CD_2I_2$ results from the *ortho*-protons being shifted upfield 0.1 ppm more than the *meta*- and *para*-protons.

**Table 2** Absorbance maxima for phenol blue in several solvents

| Solvent | $\lambda_{max}$/nm |
|---|---|
| Hexane | 545 |
| Benzene | 573 |
| Dimethylformamide | 593.5 |
| Chloroform | 595 |
| Propan-2-ol | 603 |
| Ethanol | 605 |
| Methanol | 607.5 |
| Diiodomethane | 617 |
| Water | 654 |




Diiodomethane adopts a remarkable position in the list of solvents in Table 2. According to our particular reporter dye, only water exceeds diiodomethane in apparent 'polarity'. Even methanol is not quite as polar as diiodomethane. We know of no similar case in which there is such a large disparity between a 'bulk' polarity (as manifested by a relative permittivity of 5.3) and the corresponding 'spectrophotometrically-based' polarity (as manifested by the $\lambda_{max}$ of phenol blue). The shifts with phenol blue are, we presume, so much greater than with cyanine dyes because phenol blue extensively charge-separates in the excited state whereas cyanine dyes merely distribute a cationic charge. Diiodomethane clearly stabilizes transient ionic charge far beyond what is normally expected from an aprotic, and seemingly apolar, solvent.

Diiodomethane would be an interesting solvent with which to carry out kinetic studies, but experimental difficulties have thus far prevented us from doing so. Three problems were encountered: (*a*) insolubility of either the reactant or product in the solvent; (*b*) strong absorbance of the solvent below 400 nm; and (*c*) reactivity of the solvent under the reaction conditions. Information on the ability of polarizable systems to stabilize polar transition states would be particularly useful to those involved in enzyme mechanisms. Methionine, with its polarizable sulfur, frequently resides near active sites with no apparent function.

We thank the National Science Foundation for support of this work.

## References

1 N. S. Isaacs, *Physical Organic Chemistry*, Longman, Essex, 1987.
2 E. M. Arnett and P. C. Wernett, *J. Am. Chem. Soc.*, 1993, **115**, 12 187.
3 F. H. A. Rummens, *Chem. Phys. Lett.*, 1975, **31**, 596.
4 W. West and A. L. Geddes, *J. Phys. Chem.*, 1964, **68**, 837.
5 A. D. Buckingham, T. Schaefer, and W. G. Schneider, *J. Chem. Phys.*, 1960, **32**, 1227.
6 T. R. Stengle, N. V. Reo, and K. L. Williamson, *J. Phys. Chem.*, 1981, **85**, 3772.
7 L. G. S. Brooker and R. H. Sprague, *J. Am. Chem. Soc*, 1941, **63**, 3214.

*Received, 12th September 1996; Com. 6/06486H*

# Nickel(0)-catalysed diyne–maleimide double-cycloaddition copolymerisation to form poly(bicyclo[2.2.2]oct-7-ene)s

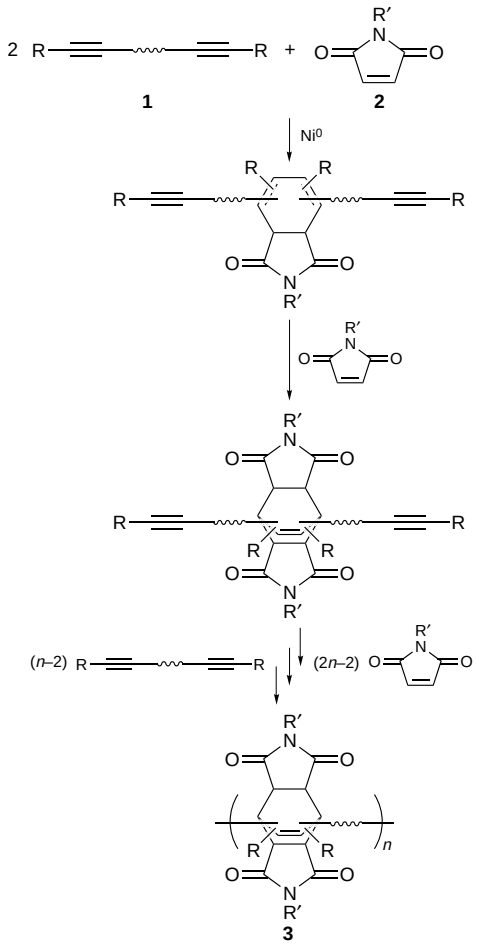
**Tetsuo Tsuda,*[a] Akihiko Tobisawa,[b] Haruna Mizuno[b] and Atsushi Takeda[b]**

[a] *Department of Polymer Chemistry, Graduate School of Engineering, Kyoto University, Yoshida, Kyoto 606-01, Japan*
[b] *Department of Synthetic Chemistry, Faculty of Engineering, Kyoto University, Yoshida, Kyoto 606-01, Japan*

**A nickel(0) catalyst effects the double-cycloaddition copolymerisation of diynes with *N*-substituted maleimides to form poly(bicyclo[2.2.2]oct-7-ene)s.**

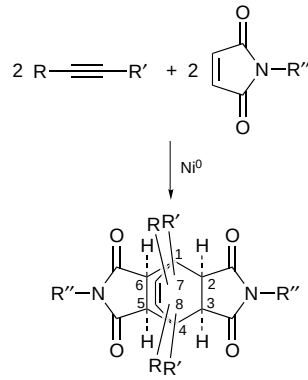
Recently we developed a transition metal-catalysed diyne cycloaddition copolymerisation[1] as a useful method of polymer synthesis, in which one molecule of a cycloaddition component such as carbon dioxide, an isocyanate, a nitrile or elemental sulfur reacts with two diyne molecules to afford a cycloaddition copolymer containing a heterocycle in its repeat unit.[2]

Here we report a new type of transition metal-catalysed diyne cycloaddition copolymerisation with an alkene to afford a cycloaddition copolymer containing a carbocycle in its repeat unit, *i.e.* a nickel(0)-catalysed diyne **1**–*N*-substituted maleimide **2** double-cycloaddition copolymerisation to form a poly(bicyclo[2.2.2]oct-7-ene) **3** having a wholly carbon backbone with an imide functionality (Scheme 1). This diyne–maleimide copolymerisation is characterised by a unique process in which two maleimide molecules connect two diyne molecules by double-cycloaddition to generate a copolymer repeat unit containing a bicyclo[2.2.2]oct-7-ene ring *via* nickel(0)-catalysed formation of a cyclohexadiene intermediate. Cycloaddition of two diyne molecules to one maleimide molecule is followed by Diels–Alder cycloaddition with the second maleimide molecule. This diyne–maleimide copolymerisation is based on our recent study of an efficient and chemoselective nickel(0)-catalysed 2 : 2 monoyne–maleimide double-cycloaddition to afford an *exo*,*exo*-bicyclo[2.2.2]oct-7-ene derivative stereoselectively (Scheme 2).[3]




**Scheme 1**

The results of the copolymerisation of 1,4-diethynylbenzene **1ad** with *N*-octylmaleimide **2g** are summarised in Table 1. The reaction was carried out in a 50 ml stainless steel autoclave under nitrogen. When a mixture of **1ad** (0.25 mmol) and **2g** (0.5 mmol) in THF (5 ml) was heated at 90 °C for 20 h in the presence of a $Ni(CO)_2(PPh_3)_2$ catalyst (Ni : **1ad** = 0.1), poly(bicyclo[2.2.2]oct-7-ene) **3adg** with $M_n$ = 27200 and




**Scheme 2**

**Table 1** Nickel(0)-catalysed double-cycloaddition copolymerisation of 1,4-diethynylbenzene **1ad** with *N*-octylmaleimide **2g** to form poly(bicyclo[2.2.2]oct-7-ene)s **3adg**[a]

| | | | | **3adg** | | |
|---|---|---|---|---|---|---|
| Catalyst | Ni : **1ad**[b] | **2g** : **1ad**[b] | *T*/°C | Yield (%)[c] | $M_n$[d] | $M_w/M_n$[d] |
| $Ni(CO)_2(PPh_3)_2$ | 0.1 | 4 | 90 | 50 | 19800 | 1.9 |
| $Ni(CO)_2(PPh_3)_2$ | 0.1 | 2 | 90 | 51 | 27200 | 2.1 |
| $Ni(CO)_2(PPh_3)_2$ | 0.05 | 2 | 90 | 50 | 26800 | 3.5 |
| $Ni(CO)_2(PPh_3)_2$ | 0.1 | 2 | 110 | 60 | 34600 | 1.9 |
| $Ni(CO)_2(PPh_3)_2$ | 0.1 | 2 | 130 | 36 | 27100 | 2.6 |
| $Ni(cod)_2$-$2PPh_3$ | 0.1 | 2 | 90 | 50 | 16000 | 2.4 |
| $Ni(cod)_2$ | 0.1 | 2 | 90 | 91[e] | | |

[a] Conditions: **1ad** (0.25 mmol), THF (5 ml), 20 h, isolation of **3adg** using $CH_2Cl_2$–AcOEt. [b] Molar ratio. [c] Based on 100% conversion of **1ad** to **3adg**. [d] Determined by GPC with polystyrene standards in $CHCl_3$. [e] A $CH_2Cl_2$-insoluble copolymer.

$M_w/M_n$ = 2.1 was obtained in 51% yield by concentration of the resulting reaction mixture under vacuum and by precipitation with $CH_2Cl_2$–AcOEt. Raising the reaction temperature to 110 °C increased the copolymer molecular weight to 34600. A nickel(0) catalyst generated from $Ni(cod)_2$ and 2 equiv. of $PPh_3$ was also effective, but $Ni(cod)_2$ alone gave an insoluble copolymer, probably due to copolymer branching and/or cross-linking[2c] originating from formation of diyne trimer in the copolymer. Compound **3adg** was formed as a pale yellow powder, which was soluble in THF, $CH_2Cl_2$ and $CHCl_3$ but insoluble in AcOEt and diethyl ether. The thermal stability of **3adg** was examined by thermogravimetric analysis (TGA) in air, and $T_{10}$ (the temperature causing a 10% weight loss) was 322 °C.

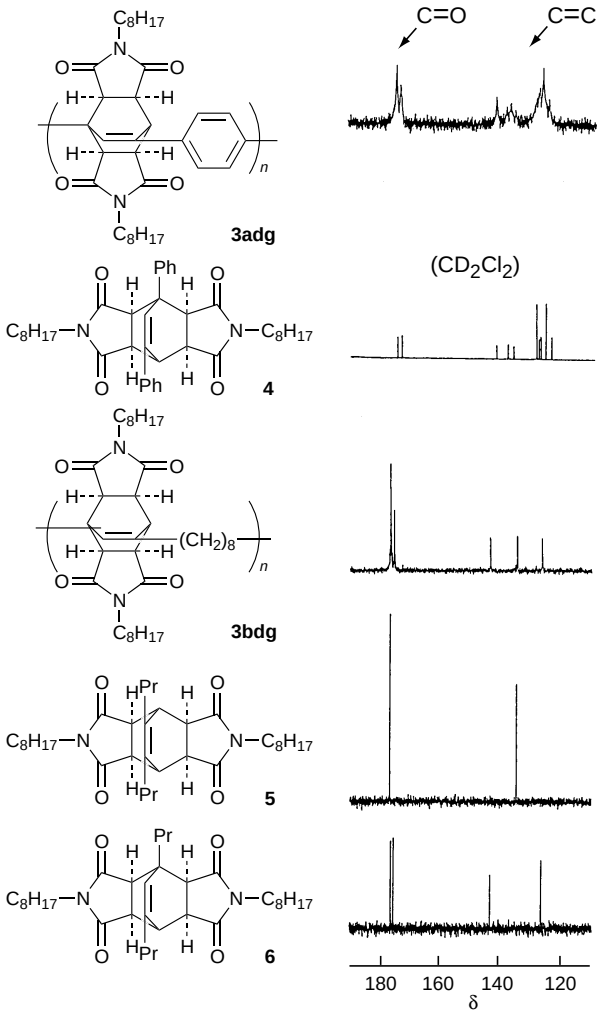



**Fig. 1** $^{13}C$ NMR C=O and C≡C signals of poly(bicyclo[2.2.2]oct-7-ene)s **3adg** and **3bdg** together with model compounds **4**–**6** ($CDCl_3$)

**Table 2** Nickel(0)-catalysed double-cycloaddition copolymerisation of diynes **1** with maleimides **2** to form poly(bicyclo[2.2.2]oct-7-ene)s **3**[a]

| | | | | **3** | | | |
|---|---|---|---|---|---|---|---|
| **1** | **2** | **2**:**1**[b] | *T*/°C | | Yield (%)[c] | $M_n$[d] | $M_w/M_n$[d] |
| **bd** | **f** | 4 | 110 | **bdf**[e] | 70 | 15900 | 1.3 |
| | | 2 | 110 | | 75 | 12400 | 2.3 |
| **bd** | **g** | 4 | 90 | **bdg** | 96 | 9300 | 1.8 |
| | | 2 | 90 | | 70 | 12400 | 2.4 |
| **bd** | **h** | 4 | 110 | **bdh**[e] | 78 | 5000 | 1.6 |
| **ce** | **f** | 4 | 110 | **cef** | 75 | 6300 | 2.8 |

[a] Conditions: **1** (0.25 mmol), $Ni(CO)_2(PPh_3)_2$: **1** = 0.1, THF (2 ml), 20 h, isolation of **3** using $CH_2Cl_2$–hexane. [b] Molar ratio. [c] Based on 100% conversion of **1** to **3**. [d] Determined by GPC with polystyrene standards in $CHCl_3$. [e] Isolation from $CH_2Cl_2$–$Et_2O$.

Copolymerisations of **1ad** with *N*-phenyl- and *N*-ethyl-maleimides **2f** and **2h** gave insoluble copolymers **3adf** and **3adh**. Thus introduction of a longer *N*-alkyl substituent, such as an octyl group, into the maleimide was necessary for the preparation of a soluble poly(bicyclo[2.2.2]oct-7-ene) from **1ad**.

Poly(bicyclo[2.2.2]oct-7-ene) **3adg** was identified by IR, $^1H$ and $^{13}C$ NMR spectroscopy. Comparison of $^{13}C$ NMR C=O and C=C signals of **3adg** and a model compound of the copolymer repeat unit was most informative. The $^{13}C$ NMR C=O and C=C signals of **3adg** were similar to those of model compound **4**,[3] obtained regio- and stereo-selectively by the nickel(0)-catalysed cycloaddition reaction of phenylacetylene with **2g** (Fig. 1). This result confirms that the structure of **3adg** contains an *exo*,*exo*-fused 1,8-phenylene-substituted bicyclo[2.2.2]oct-7-ene ring.

In contrast with the formation of insoluble copolymer **3adf**, dodeca-1,11-diyne **1bd** copolymerised with **2f** to afford soluble copolymer **3bdf**, the difference in solubility being due to the presence of the long alkylene chains (Table 2). Diyne **1bd** copolymerised with **2g** to afford **3bdg** as a colourless resinous solid. The $^{13}C$ NMR C=O and C=C signals of **3bdg** were a superposition of those of two model compounds **5** and **6**,[3] which were obtained stereo- but nonregio-selectively by nickel(0)-catalysed cycloaddition reaction of pent-1-yne with **2g** (Fig. 1). This fact demonstrates the copolymer structure and indicates that **3bdg** has two kinds of repeat units corresponding to **5** and **6**.

Use of a two-fold excess of the maleimide (maleimide : diyne = 4 : 1) did not influence significantly the copolymer yield and molecular weight when compared with the stoichiometric copolymerisation (maleimide : diyne = 2 : 1) (Tables 1 and 2). An internal diyne, tetradeca-3,11-diyne **1ce**, copolymerised with **2f** at 110 °C to afford **3cef**.

Poly(bicyclo[2.2.2]oct-7-ene)s **3adg** and **3bdg** containing two octyl groups per repeat unit have unique rigid and flexible fence-like structures, respectively, and are potentially interesting, as structurally related comb-like polymers are well known and attract considerable attention on account of their specific properties.[4]

This work was partly supported by a Grant-in-Aid for Scientific Research on Priority Areas (Nos. 06227235 and 07216237) from the Ministry of Education, Science, Sports and Culture, Japan.

## References

1 T. Tsuda, *Gazz. Chim. Ital.*, 1995, **125**, 101; T. Tsuda, in *The Polymeric Materials Encyclopedia*, ed. J. C. Salamone, CRC, Boca Raton, 1996, vol. 3, p. 1905; vol. 5, p. 3525.

2 For the diyne–carbon dioxide cycloaddition copolymerisation to form a poly(2-pyrone), see: (*a*) T. Tsuda, H. Yasukawa, H. Hokazono and Y. Kitaike, *Macromolecules*, 1995, **28**, 1312. For the diyne–carbon dioxide cycloaddition copolymerisation to form a poly(4-pyrone), see: (*b*) T. Tsuda, H. Hokazono and K. Toyota, *J. Chem. Soc., Chem. Commun.*, 1995, 2417. For the diyne–isocyanate cycloaddition copolymerisation to form a poly(2-pyridone), see: (*c*) T. Tsuda and A. Tobisawa, *Macromolecules*, 1995, **28**, 1360. For the diyne–nitrile cycloaddition copolymerisation to form a poly(pyridine), see: (*d*) T. Tsuda and H. Maehara, *Macromolecules*, 1996, **29**, 4544. For the diyne–elemental sulfur cycloaddition copolymerisation to form a poly(thiophene), see: (*e*) T. Tsuda and A. Takeda, *Chem. Commun.*, 1996, 1317. For the diyne–diene–carbon monoxide cycloaddition terpolymerisation to form a poly(enone), see: (*f*) T. Tsuda and F. Tsugawa, *Chem. Commun.*, 1996, 907. For the related monoyne–dimaleimide double-cycloaddition copolymerisation to form a poly(imide), see: (*g*) T. Tsuda, M. Shimada and H. Mizuno, *Chem. Commun.*, 1996, 2371.

3 T. Tsuda and H. Mizuno, The 69th Annual Meeting of The Chemical Society of Japan, Kyoto, 1995, 2H435.

4 For examples: N. A. Plate and V. P. Shibaev, *J. Polym. Sci., Macromol. Rev.*, 1974, **8**, 117; Y. Yuki, H. Kunisada and Y. Miyake, *Polym. J.*, 1991, **23**, 939.

*Received, 24th September 1996; Com. 6/06563E*

# The synthesis and structure of $[Zr(\eta\text{-}C_5H_5)_2(\eta^2\text{-}C_5H_3Bu^t_2)X]$

**Marco M. Corradi, David J. Duncalf, Gerard A. Lawless* and Martin P. Waugh**

*The Chemistry Laboratory, School of Chemistry, Physics and Environmental Science, University of Sussex, Brighton, UK BN1 9QJ*

**Reaction of 1 equiv. of $KC_5H_3Bu^t_2$ with $[Zr(\eta\text{-}C_5H_5)_2X_2]$ affords $[Zr(\eta\text{-}C_5H_5)_2(\eta^2\text{-}C_5H_3Bu^t_2)X]$ (X = Cl 1, Br 2); the molecular structure, and solid- and solution-state $^{13}C$ NMR data are presented.**

There is considerable interest in the catalysis of alkene polymerisation by Zr-based metallocenes. Overwhelming evidence exists supporting the proposal that cationic 14 electron metallocene alkyls $[Zr(\eta\text{-}C_5H_5)_2R]^+$ are the active species.[1–3] Two steps which are crucial to the proposed mechanism are (*i*) the binding of the alkene to the Zr centre and (*ii*) its subsequent insertion into the Zr–R bond. Given that for ethene the entire insertion process may be as fast as 70–170 fs,[4] it is hardly surprising that no examples of a π complex of an alkene and $[Zr(\eta\text{-}C_5H_5)_2R]^+$ have been structurally characterised, despite the synthesis of an ever increasing number of such cations. We now report that this $\eta^2$ coordination mode is observable when an alkene may act as a three-electron donor. We present as evidence the structure and $^{13}C$ NMR spectroscopic data for **2**.

The reaction of $KC_5H_3Bu^t_2$ with $[Zr(\eta\text{-}C_5H_5)_2X_2]$ in toluene or thf yields **1** and **2** respectively.† The molecular structure of **2** was determined‡ (Fig. 1). The $\eta^2$ coordination mode of the $^-C_5H_3Bu^t_2$ is evident from a comparison of the Zr–C(4) and Zr–C(5) bond lengths [2.490(3), 2.539(3) Å, respectively] with those for Zr–C(1), Zr–C(2) and Zr–C(3) [3.462(4), 3.834(5), 3.368(5) Å, respectively]. Zr, Br, C(4) and C(5) are coplanar to within 0.0165 Å. The M(1)–Zr–C(4) and M(1)–Zr–C(5) angles are 118(3) and 107.7(3)° respectively while the corresponding M(2)–Zr–C(4) and M(2)–Zr–C(5) angles are 108.2(3) and 98.6(3)° respectively. The M(1)–Zr–M(2) angle is unexceptional at 128.6(4). The size and asymmetry of the Zr–C(4) and Zr–C(5) interactions are in good agreement with those calculated for the ethene complex $\{Zr(\eta\text{-}C_5H_5)_2(\eta^2\text{-}C_2H_4)Me\}$ (2.50, 2.72 Å).[5] **2** may be formulated as a cyclopentadienyl adduct of a 14-electron Zr cation such as $[Zr(\eta\text{-}C_5H_4Bu^t)_2\{CH_2C(Me)C(Me)C(Me)CH_2\}]$[6] or $[Zr(\eta\text{-}C_5H_4Bu^t)_2\{OCMe_2CH_2CH_2CHCH_2\}]$,[7] [for which the $\eta^2$ Zr–C bond lengths are 2.602(7)–2.759(7) and 2.68(2), 2.89(2) Å respectively]. In this model the resulting anionic charge is delocalised on C(1), C(2) and C(3) (Scheme 1, **a**). The combination of such anionic and cationic centres within a neutral molecule has been recently demonstrated.[8] The high-frequency shifts exhibited in the $^{13}C$ NMR spectra of the β, C(1) and C(3) resonances and the corresponding low-frequency shift for C(2) (δ 170.6 and 87.6 respectively, for **2**) indicate, however, that a cationic formulation for C(1) and C(3) is more appropriate (Scheme 1, **b**–**d**). Thus the $^-C_5H_3Bu^t_2$ groups of **1** and **2** act as three-electron donors to 15-electron Zr centres resulting in 18-electron complexes. A similar bonding model has been previously proposed to account for the $\eta^2$-bonding in $[Ti(\eta\text{-}C_5H_5)_2(\eta^2\text{-}C_5H_5)]$.[9] The stability of this coordination mode requires both the availability of a third electron and the concomitant formation of a stable β cationic carbon centre. The Zr–C(4) and Zr–C(5) bond lengths compare well with those reported for the $\eta^2$ coordinated butadiene of $[Zr(\eta\text{-}C_5H_5)_2\{\mu\text{-}(1,2\text{-}\eta^2\text{-}Zr):(4\text{-}\eta^1\text{-}Al)\text{-}C_4H_6\}(\mu\text{-}Cl)AlCl_2]$[10] [2.348(2), 2.510(2) Å] and indenyl groups of the *ansa*-bridged systems $[Zr\{Me_2C(\eta\text{-}C_5H_4)(\eta^2\text{-}C_9H_6)\}(\eta\text{-}C_5H_5)Cl]$ [2.587(8), 2.497(8) Å] and $[Zr\{(CH_2)_5C(\eta\text{-}C_5H_4)(\eta^2\text{-}C_9H_6)\}(\eta\text{-}C_5H_5)Cl]$[11] [2.508(5), 2.564(4) Å]. The latter is characterised by a low-frequency $^{13}C$ NMR shift.§ For $[Zr\{(CH_2)_5C(\eta\text{-}C_5H_5)(\eta^2\text{-}C_9H_6)\}(\eta\text{-}C_5H_5)Cl]$, $[Zr\{Me_2C(\eta\text{-}C_5H_4)(\eta^2\text{-}C_9H_6)\}(\eta\text{-}C_5H_5)Cl]$ and $[Zr(\eta\text{-}C_5H_5)_2\{\mu\text{-}(1,2\text{-}\eta^2\text{-}Zr):(4\text{-}\eta^1\text{-}Al)\text{-}C_4H_6\}(\mu\text{-}Cl)AlCl_2]$ similar shifts have been noted. The long Zr–Br(1), 2.672(1) Å, is also consistent with an 18-electron configuration. A solid-state $^{13}C$ NMR study of **2** confirmed that the $\eta^2$-coordination

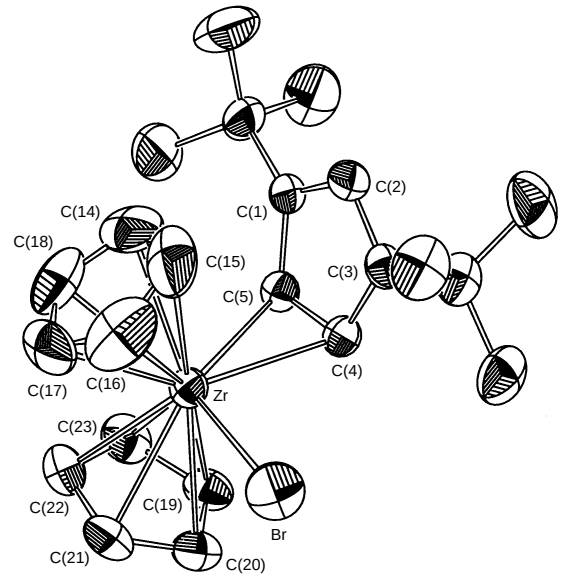
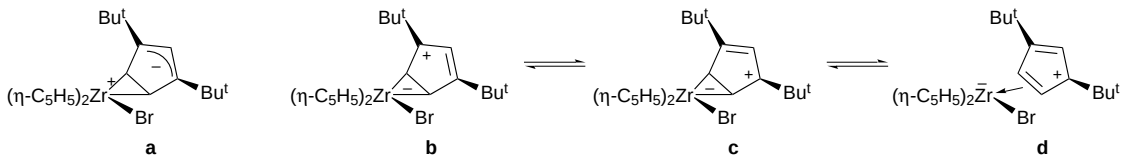



**Fig. 1** The molecular structure of $[Zr(\eta\text{-}C_5H_5)_2(\eta^2\text{-}C_5H_3Bu^t_2)Br]$ **2** and atom numbering scheme with selected bond lengths (Å) and angles (°): Zr–C(1) 3.462(4), Zr–C(2) 3.834(5), Zr–C(3) 3.368(5), Zr–C(4) 2.490(5), Zr–C(5) 2.539(3), Zr–Br 2.672(1), Zr–M(1) 2.21(1), Zr–M(2) 2.24(1), M(1)–Zr–C(4) 118.0(3), M(1)–Zr–C(5) 107.7(3), M(2)–Zr–C(4) 108.2(3), M(2)–Zr–C(5) 98.6(3), M(1)–Zr–M(2) 128.6(4), M(1) denotes the centroid of the ring C(14)–C(18), M(2) denotes the centroid of the ring C(19)–C(23)




**Scheme 1** Resonance structures for **2**

mode of the $^{-}C_5H_3Bu^t_2$ group is retained in toluene solution at 243 K, as all $^{13}C$ resonances, C(1)–C(5) are inequivalent. Upon warming to 297 K, however, C(4) and C(5) mutually exchange as do C(1) and C(3). The exchange mechanism may involve either $\eta^2$ to $\eta^1$ or $\eta^2$ to $\eta^5$ rearrangements.¶ We favour the latter for **2**, as the former would be extremely unfavourable sterically due to the β-Bu$^t$ substituents, and the twenty electron count associated with such an $\eta^5$ rearrangement has precedence in $[Zr(\eta\text{-}C_5H_5)_3(\eta^1\text{-}C_5H_5)]$.[12] For non-cyclopentadienyl based $\eta^2$ systems, clearly the former will be of greater importance. A comparison of the $^{13}C$ NMR data for **1** and **2** corroborates the presence of an $\eta^2$ bonding mode for the $^{-}C_5H_3Bu^t_2$ ligand of **1**, also. Initial studies indicate that both **1** and **2** are inactive as ethene polymerisation catalysts although the addition of MAO does produce an active system. Finally, a similar three electron interaction between say, ethene or propene, and a 14-electron Zr centre would sufficiently destabilize the corresponding metallocycle permitting facile insertion into a neighbouring Zr–C bond. Furthermore the tacticity of the resulting polymer would be dependent on the rate of insertion in comparison to the rate of $\eta^2$ to $\eta^1$ exchange.

We thank EPSRC (M. M. C., D. J. D., M. P. W.) for financial support.

## Footnotes

† *Syntheses*: $[Zr(\eta\text{-}C_5H_5)_2(\eta^2\text{-}C_5H_3Bu^t_2)Cl]$. To a Schlenk tube containing $[Zr(\eta\text{-}C_5H_5)_2Cl_2]$ (2.84 g, 9.72 mmol) and $KC_5H_3Bu^t_2$ (2.1 g, 9.72 mmol) was added 200 ml of dry, degassed toluene. The reaction mixture was stirred for 72 h during which time a gradual colour change from yellow to dark red was observed. After this time the toluene solution was filtered from the off-white precipitate and the toluene removed *in vacuo* to yield **1** as an orange powder, 85.5% (3.6 g, 8.31 mmol). Recrystallisation of **1** from toluene afforded dark orange platelets unsuitable for single-crystal diffraction. Mp (decomp.) 167–169 °C. $^1H$ NMR ($CDCl_3$, 400.13 MHz) δ 6.05 (s, 10 H) 5.96 [t, 1 H, $^4J(^1H–^1H)$ 1.75 Hz], 5.50 [d, 2 H, $^4J(^1H–^1H)$ 1.75 Hz], 1.28 (s, 18 H); $^{13}C\{^1H\}$ NMR ($CDCl_3$, 100.61 MHz) δ 170.2, 115.9 [$^1J(^{13}C–^1H)$ 158 Hz], 113.5 [$^1J(^{13}C–^1H)$ 174 Hz], 88.0 [$^1J(^{13}C–^1H)$ 158 Hz], 34.3, 31.9 [$^1J(^{13}C–^1H)$ 126 Hz].

$[Zr(\eta\text{-}C_5H_5)_2(\eta^2\text{-}C_5H_3Bu^t_2)Br]$. To a Schlenk tube containing $[Zr(\eta\text{-}C_5H_5)_2Br_2]$ (0.92 g, 2.41 mmol) in thf (40 ml) was added $KC_5H_3Bu^t_2$ (0.71 g, 3.29 mmol) slurried in thf (50 ml). An immediate colour change from pale yellow to orange was observed. After stirring for a further 12 h the thf was removed *in vacuo* and the resulting orange powder extracted into hexane. The solvent was removed *in vacuo* to yield **2** as an orange powder, 78%, (0.9 g, 1.88 mmol). Recrystallisation of **2** from toluene afforded dark orange platelets suitable for single-crystal diffraction. Mp (decomp) 139.8 °C. $^1H$ NMR ($C_7D_8$, 400.13 MHz) δ 5.96 [t, 1 H, $^4J(^1H–^1H)$ 1.75 Hz], 5.69 (s, 10 H), 5.38 [d, 2 H, $^4J(^1H–^1H)$ 1.75 Hz], 1.33 (s, 18 H); $^{13}C\{^1H\}$ NMR ($C_7D_8$, 100.61 MHz) δ 170.6, 115.9, 112.8, 87.6, 34.4, 31.6; $^{13}C\{^1H\}$ NMR ($C_7D_8$, 100.61 MHz, 243 K) δ 172.6, 169.9, 115.4, 112.8, 93.8, 80.9, 35.2, 34.1, 31.7; $^{13}C\{^1H\}$ CP MAS NMR (100.61 MHz) δ 178, 174, 122, 117, 98, 85, 44, 38, 36.

‡ *Crystal data* $[Zr(\eta\text{-}C_5H_5)_2(\eta^2\text{-}C_5H_3Bu^t_2)Br]$, $C_{30}H_{39}BrZr$. Crystallographic measurements were made on a Siemens three-circle diffractometer equipped with a SMART CCD area detector, using Mo-Kα radiation, λ = 0.71073 Å, 2θ < 57.18°, μ = 2.103 mm$^{-1}$. The heavy atoms were located by the Patterson interpretation of SHELXTL and refined on $F^2$ by a full-matrix least-squares procedure. Anisotropic thermal parameters were used for all non-H atoms. H atoms were given fixed isotropic temperature factors with the positions constrained by the heavy-atom geometry in the refinement. A molecule of toluene is present within the asymmetric unit. $T$ = 220(2) K. Specimen 0.40 × 0.35 × 0.20 mm, $M$ = 570.74, monoclinic, space group $P2_1/n$, $a$ = 11.082(2), $b$ = 10.224(2), $c$ = 21.675(4) Å, β = 96.02(3)°, $U$ = 2442.3(8) Å$^3$, $D_c$ = 1.554 g cm$^{-3}$, μ(Mo-Kα) = 2.103 mm$^{-1}$, $Z$ = 4. For reflections with 1.89 < θ < 28.59°, $R(F)$ = 0.0544 for 4570 observed reflections [$I > 2\sigma(I)$] and $wR(F^2)$ = 0.1162 for all 5724 reflections. Atomic coordinates, bond lengths and angles, and thermal parameters have been deposited at the Cambridge Crystallographic Data Centre (CCDC). See Information for Authors, Issue No. 1. Any request to the CCDC for this material should quote the full literature citation and the reference number 182/331.

§ The paramagnetic shift associated with these cations compared with those associated with classical trialkyl carbonium species is diminished due to the resonance stabilisation of the positive charge.

¶ Initial analysis of this lineshape at 298, 273, 253, 243, 233 K yields $\Delta H^‡$ = 66 kJ mol$^{-1}$, $\Delta S^‡$ = 68 J K$^{-1}$ mol$^{-1}$. At 298 K $\Delta G^‡$ = 46 kJ mol$^{-1}$.

## References

1 R. F. Jordan, *Adv. Organomet. Chem.*, 1991, **32**, 325.
2 A. S. Guram and R. F. Jordan, in *Comprehensive Organometallic Chemistry*, ed. E. W. Abel, F. G. A. Stone and G. Wilkinson, Pergamon, Oxford, 1995, vol. 4, p. 589.
3 M. Bochmann, *J. Chem. Soc., Dalton Trans.*, 1996, 255.
4 R. J. Meier, G. H. J. van Doremaele, S. Larlori and F. Buda, *J. Am. Chem. Soc.*, 1994, **116**, 7274.
5 T. K. Woo, L. Fan and T. Ziegler, *Organometallics*, 1994, **13**, 432.
6 A. D. Horton and A. G. Orpen, *Organometallics*, 1992, **11**, 8.
7 Z. Wu, R. F. Jordan and J. L. Petersen, *J. Am. Chem. Soc.*, 1995, **117**, 5867.
8 B. Temme, G. Erker, J. Karl, H. Luftmann, R. Frohlich and S. Kotila, *Angew. Chem., Int. Ed. Engl.*, 1995, **34**, 1755.
9 C. R. Lucas, M. L. H. Green, R. Forder and K. Prout, *J. Chem. Soc., Chem. Commun.*, 1973, 97.
10 G. Erker, R. Noe, C. Kruger and S. Werner, *Organometallics*, 1992, **11**, 4174.
11 G. M. Diamond, M. L. H. Green, P. Mountford, N. A. Popham and A. Chernega, *J. Chem. Soc., Dalton Trans.*, 1996, 921.
12 R. D. Rodgers, R. Vann Bynum and J. L. Atwood, *J. Am. Chem. Soc.*, 1978, **100**, 3238.

*Received, 27th September 1996; Com. 6/06638K*

# Quinoxalino-fused sultines and their application in Diels–Alder reactions

**Wen-Sheng Chung* and Jing-Horng Liu**

*Department of Applied Chemistry, National Chiao Tung University, Hsinchu, Taiwan 30050, R.O.C.*

**The synthesis of 7,8-disubstituted quinoxalino[2,3-*d*]-[1,2λ⁴]oxathiine 2-oxides 7a–c, precursors for quinoxalino-*o*-quinodimethanes 3a–c, and their application in the Diels–Alder reactions are reported.**

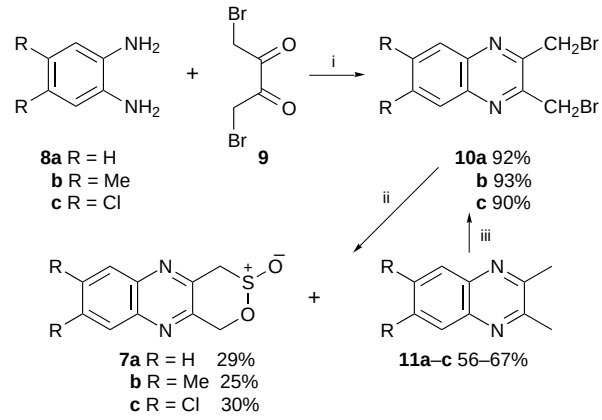
The chemistry of heterocyclic *o*-quinodimethanes **1** has attracted a great deal of attention recently.[1] Various methods for generating these highly reactive dienes have been developed.[2] Among them, cheletropic elimination of $SO_2$ from heteroaromatic-fused 3-sulfolenes **2** has drawn the most attention.[1–3] Quinoxalines are important naturally occurring heterocycles and are usually found to have biological and pharmaceutical activity.[4] Finding an easy, high-yield method for generating quinoxalino-*o*-quinodimethanes **3** is thus of particular interest.

Although Chou *et al*. reported[5] generating quinoxalino-*o*-quinodimethanes **3a** using $SO_2$ extrusion of the quinoxalino-fused sulfolene **4**, all their attempts to isolate the Diels–Alder adducts failed. Recently we described[6] the generation of nonclassical heteroaromatic *o*-quinodimethanes **5** by thermal extrusion of $SO_2$ from corresponding sultines **6**. A significant advantage of using sultines is that their thermolysis occurs at a much lower temperature than that of corresponding sulfolenes.[6–8] We report here our work on the synthesis of quinoxalino-fused sultines **7a**–**c** and their applications in Diels–Alder reactions with alkenes and alkynes.

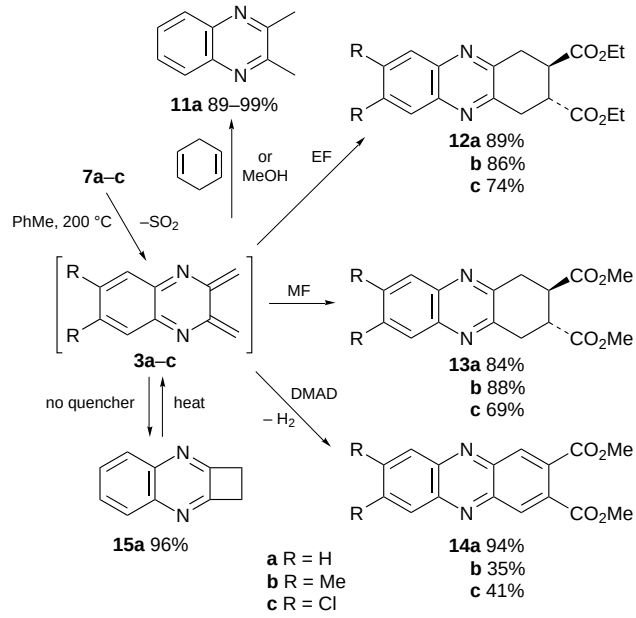
Previously unknown sultines **7a**–**c** were synthesized in two steps with good yields as shown in Scheme 1. Reaction of the appropriate *o*-diamino-substituted benzene **8** with 1,4-dibromobutane-2,3-dione **9** gave the known 2,3-bis(bromomethyl)quinoxaline **10a**,[9a] 6,7-dimethylquinoxaline **10b**,[4,9b] and 6,7-dichloroquinoxaline **10c**.[4] The desired quinoxalino-fused sultines **7a**–**c**† and by-products **11** were obtained by the use of Rongalite[8] (sodium formaldehyde sulfoxylate) with the corresponding dibromides **10a**–**c**. Although the yields of sultines **7a**–**c** were only *ca*. 30%, fortunately the by-product **11** can be converted back to dibromide **10** *via* *N*-bromosuccinimide bromination,[4b] which makes the syntheses of the sultines more efficient.

The Diels–Alder reactions of quinoxalino-fused sultines **7a**–**c** with several dienophiles are presented in Scheme 2. When heated in toluene (200 °C, sealed tube) in the presence of 3 equiv. of diethyl fumarate (EF) or dimethyl fumarate (MF), the sultines **7a**–**c** all underwent extrusion of $SO_2$ and the resulting quinoxalino-*o*-quinodimethanes **3a**–**c** were intercepted as the 1 : 1 adducts (**12** and **13**) in 69–89% yield. The reactions with dimethyl acetylenedicarboxylate (DMAD) went similarly to 1 : 1 adducts and after loss of $H_2$ gave **14a**–**c** in 35–94% yield.

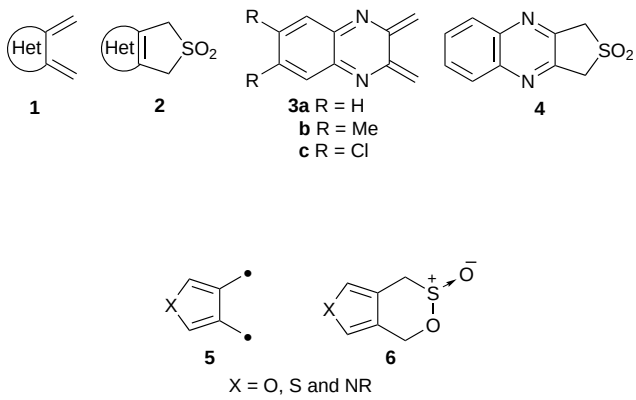
In the absence of a dienophile, sultine **7a** underwent thermal extrusion of $SO_2$ and formed the cyclobuta[1,2-*b*]quinoxaline **15a** almost quantitatively. In contrast, **15a** was reported[5] to be isolated only in low yield (10%) when the corresponding sulfolene **4** was flash pyrolysed at 500 °C followed by addition of excess *N*-phenylmaleimide (NPM). Thermolysis of **7a** in the presence of methanol or cyclohexa-1,4-diene, on the other hand, gave 2,3-dimethylquinoxaline **11a** in 89–99% yield. Inter-




**Scheme 1** *Reagents and conditions*: i, benzene, reflux, 1 h; ii, Rongalite, DMF, 0 °C, 7 h; iii, NBS




**Scheme 2**

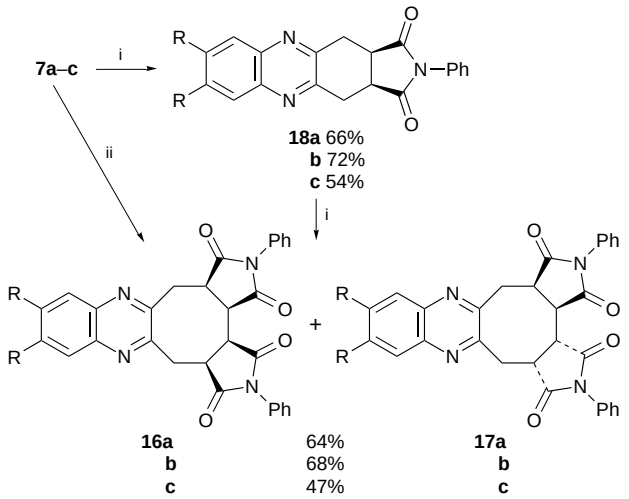


estingly, Diels–Alder adducts (such as **12**–**14a**) were also formed in excellent yield when the cyclobutene **15a** was heated in the presence of dienophiles at 200 °C, indicating that cyclobutene **15a** is also a good precursor of *o*-quinodimethane **3a**.

The reaction of **7a**–**c** with excess NPM at 200 °C gave a pair of new adducts **16** and **17** in 47–68% yields (Scheme 3). These 2 : 1 adducts showed similar spectral characteristics, consistent with the *cis* and *trans* cyclooctaquinoxalines **16** and **17**.‡ When only 1 equiv. of NPM was used, the yield of 1 : 1 adduct **18b** was optimized to 72% and the 2 : 1 adducts (**16** and **17**) were present in only trace amounts. Similar observation of these 2 : 1 adducts in the trapping of pyrimidine *o*-quinodimethanes by NPM has been reported recently by Tomé *et al.*[3a,c] We were, however, surprised to see that different adducts were reported[10] when **10a** was heated with sodium iodide in the presence of NPM, even though this method is generally assumed to give a synthetic equivalent of *o*-quinodimethane **3a**. The real reason for this difference may be just as the authors described:[10] the reaction of **10a** and sodium iodide probably did not involve dehalogenation to give a true *o*-quinodimethane **3a**, but rather the adducts might have been formed by a mechanism involving displacement of a halogen atom by the dienophile.

Thus our results, obtained by pyrolysing 7,8-disubstituted quinoxalino-fused sultines **7a**–**c**, strongly support the formation of quinoxalino-*o*-quinodimethanes **3a**–**c**, which differ from the products formed when sulfolene **4** is pyrolysed, or when **10a** and sodium iodide react.[10] The easily synthesized sultines **7a**–**c** reacted under milder conditions (200 °C) than the corresponding sulfolene **4** (⩾290 °C is required) and their reaction products were different in many cases. When generated in the presence of a dienophile, sultines **7a**–**c** provided elegant synthons for the formation of [4 + 2] cycloadducts. If no trapping agents were used, the sultines gave cyclobuta[1,2-*b*]quinoxaline **15** almost quantitatively, which again is a good precursor of *o*-quinodimethanes **3**. Further work to study the mechanism by laser flash photolysis is in progress.

We thank the National Science Council of the Republic of China for its financial support (Grant No. NSC 85-2113-M-009-002).




**Scheme 3** *Reagents and conditions*: i, NPM (1 equiv.), toluene, 200 °C; ii, NPM (3 equiv.), toluene, 200 °C

## Footnotes

† Cyclobuta[1,2-*b*]quinoxaline **15** has been reported in the literature (ref. 5) and our samples correspond in all aspects with the reported properties. Satisfactory spectral data were obtained for all products. *Selected data* for **7a**: white solid, mp 137–138 °C; $^1$H NMR (300 MHz, $CDCl_3$) δ 8.08–8.03 (2 H, m), 7.82–7.77 (2 H, m), 5.63 (1 H, AB, *J* 16.1 Hz), 5.32 (1 H, AB, *J* 15.6 Hz), 4.59 (1 H, A′B′, *J* 16.1 Hz) and 4.14 (1 H, A′B′, *J* 16.1 Hz); $^{13}$C NMR (75.4 MHz, $CDCl_3$), δ 147.11 ($C_q$), 142.51 ($C_q$), 142.10 ($C_q$), 141.45 ($C_q$), 130.68 (CH), 130.39 (CH), 128.82 (CH), 128.77 (CH), 62.56 ($CH_2$) and 57.92 ($CH_2$); *m/z* 220 ($M^+$, 23%), 156 ($M^+ - SO_2$, 100), 129 (16), 102 (15). For **7b**: white solid, mp 158–159 °C; $^1$H NMR δ 7.79 (2 H, s), 5.61 (1 H, AB, *J* 15.6 Hz), 5.28 (1 H, AB, *J* 15.6 Hz), 4.57 (1 H, A′B′, *J* 16.6 Hz), 4.08 (1 H, A′B′, *J* 16.6 Hz) and 2.50 (6 H, s); $^{13}$C NMR, 145.98 ($C_q$), 141.55 ($C_q$), 141.43 ($C_q$), 141.12 ($C_q$), 140.83 ($C_q$), 140.43 ($C_q$), 127.68 (CH), 127.65 (CH), 62.64 ($CH_2$), 57.93 ($CH_2$), 20.39 (Me) and 20.36 (Me); *m/z* 248 ($M^+$, 21), 184 ($M^+ - SO_2$, 100), 169 (38), 103 (9). For **7c**: orange solid, mp 205–206 °C, $^1$H NMR δ 8.17 (2 H, s), 5.59 (1 H, AB, *J* 16.1 Hz), 5.30 (1 H, AB, *J* 16.1 Hz), 4.54 (1 H, A′B′, *J* 16.5 Hz) and 4.13 (1 H, A′B′, *J* 16.4 Hz); $^{13}$C NMR, 148.40 ($C_q$), 143.53 ($C_q$), 141.15 ($C_q$), 140.16 ($C_q$), 135.46 ($C_q$), 135.20 ($C_q$), 129.48 (CH), 129.43 (CH), 62.32 ($CH_2$) and 57.76 ($CH_2$); *m/z* 288 ($M^+$, 8), 224 (100), 226 (63), 189 (40), 154 (2).

‡ *Selected data* for a 1 : 1 mixture of **16a** and **17a**: $^{13}$C NMR δ 178.93 ($C_q$), 177.22 ($C_q$), 176.13 ($C_q$), 175.90 ($C_q$), 151.80 ($C_q$), 151.12 ($C_q$), 141.51 ($C_q$), 140.69 ($C_q$), 132.23 ($C_q$), 131.35 ($C_q$), 130.26 (CH), 130.06 (CH), 129.17 (CH), 129.80 (CH), 128.96 (CH), 128.89 (CH), 128.82 (CH), 128.39 (CH), 126.47 (CH), 126.37 (CH), 42.42 (CH), 41.19 (CH), 39.64 (CH), 38.08 (CH), 34.27 ($CH_2$), 32.48 ($CH_2$); *m/z* 502 ($M^+$, 36), 381 (54), 329 ($M^+$ − NPM, 52), 181 (100) (Found: $M^+$, 502.1652. $C_{30}H_{22}N_4O_4$ requires *M*, 502.1641). Currently, stereochemistry cannot be assigned unambiguously.

## References

1 For recent review, see R. A. Aitken, I. Gosney and J. I. G. Cadogan, *Prog. Heterocycl. Chem*., 1992, **4**, 1; 1993, **5**, 1; T.-S. Chou, *Rev. Heteroatom Chem*., 1993, **8**, 65; K. Ando and H. Takayama, *Heterocycles*, 1994, **37**, 1417; K. Ando, M. Kankake, T. Suzuki and H. Takayama, *Tetrahedron*, 1995, **51**, 129.

2 J. L. Charlton and M. M. Alauddin, *Tetrahedron*, 1987, **43**, 2873; R. L. Funk and K. P. C. Vollhardt, *Chem. Soc. Rev*., 1980, **9**, 41; W. Oppolzer, *Synthesis*, 1978, 793; K. C. Nicolaou, W. E. Barnette and P. Ma, *J. Org. Chem*., 1980, **45**, 1463.

3 (*a*) A. C. Tomé, J. A. S. Cavaleiro and R. C. Storr, *Tetrahedron*, 1996, **52**, 1735; 1723; (*b*) L. A. White, P. M. O'Neill, B. K. Park and R. C. Storr, *Tetrahedron Lett*., 1995, **36**, 5983; (*c*) A. C. Tomé, J. A. S. Cavaleiro and R. C. Storr, *Tetrahedron Lett*., 1993, **34**, 6639; (*d*) P. M. S. Chauhan, A. P. A. Crew, G. Jenkins, R. C. Storr, S. M. Walker and M. Yelland, *Tetrahedron Lett*., 1990, **31**, 1487; 1491.

4 (*a*) D. Villemin and B. Martin, *Synth. Commun*., 1995, **25**, 2319; (*b*) R. B. Baudy, L. P. Greenblatt, I. L. Jirkovsky, M. Conklin, R. J. Russo, D. H. Bramlett, T. A. Emrey, J. T. Simmonds, D. M. Kowal, R. P. Stein and R. P. Tasse, *J. Med. Chem*., 1993, **36**, 331.

5 T.-S. Chou and C.-W. Ko, *Tetrahedron*, 1994, **50**, 10 721.

6 W.-S. Chung, W.-J. Lin, W.-D. Liu and L. G. Chen, *J. Chem. Soc., Chem. Commun*., 1995, 2537.

7 For a review of sultines, see D. C. Dittmer and M. D. Hoey, *The Chemistry of Sulphinic Acids, Esters and Their Derivatives*, Wiley, Chichester, 1990, pp. 239–273.

8 M. D. Hoey, D. C. Dittmer, *J. Org. Chem*., 1991, **56**, 1947; W. F. Jarvis, M. D. Hoey, A. L. Finocchio and D. C. Dittmer, *J. Org. Chem*., 1988, **53**, 5750; G. Attardo, W. Wang, J.-L. Kraus and B. Belleau, *Tetrahedron Lett*., 1994, **35**, 4743.

9 (*a*) M. M. Roland and R. C. Anderson, *J. Heterocycl. Chem*., 1977, **14**, 541; (*b*) J. Pohmer, M. V. Lakshimikantham and M. P. Cava, *J. Org. Chem*., 1995, **60**, 8283.

10 N. E. Alexandrou, G. E. Mertzanos, J. Stephanidou-Stephanatou, C. A. Tsoleridis and P. Zachariou, *Tetrahedron Lett*., 1995, **36**, 6777.

*Received, 2nd October 1996; Com. 6/06764F*

# Convergent syntheses of the pyrrolic marine natural products lamellarin-O, lamellarin-Q, lukianol-A and some more highly oxygenated congeners

**Martin G. Banwell,*[a] Bernard L. Flynn,[a] Ernest Hamel[b] and David C. R. Hockless[a]**

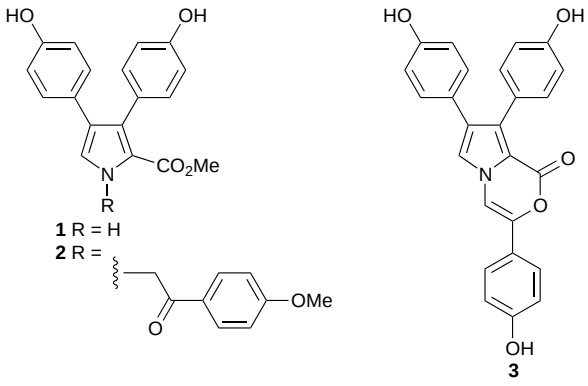
[a] *Research School of Chemistry, Institute of Advanced Studies, The Australian National University, Canberra, ACT 0200, Australia*

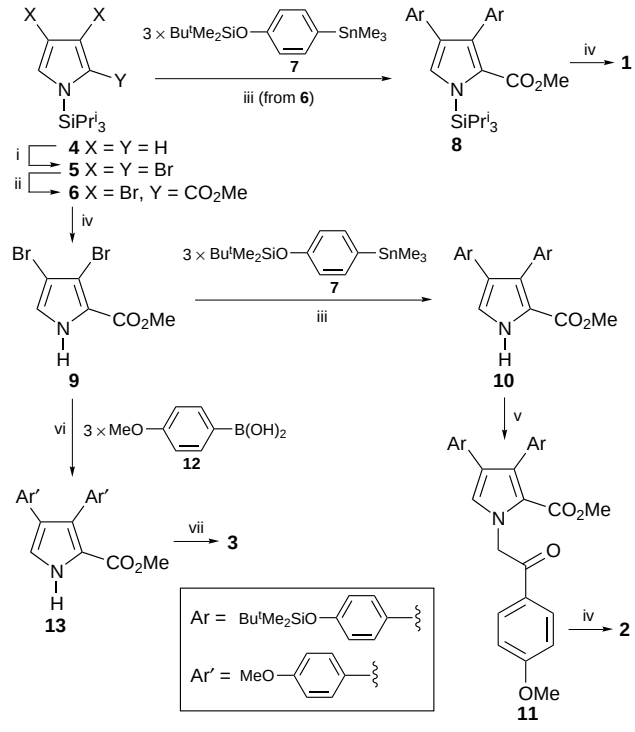
[b] *Laboratory of Molecular Pharmacology, DBS, National Cancer Institute, National Institutes of Health, Bethesda, Maryland 20892, USA*

**The marine alkaloids lamellarin-Q 1, lamellarin-O 2 and lukianol-A 3 as well as their more highly oxygenated congeners 22 and 23 are synthesised using Stille, Suzuki or Negishi cross-coupling reactions as the key step.**

Lamellarins A–R,[1–5] lukianols A–B,[6] storniamides A–D,[7] polycitrins A–B[8] and polycitone A[8] are marine natural products that possess a 3,4-diarylated pyrrole 2-carboxylic acid ester or amide moiety as the common structural subunit. These materials have been isolated from widely varying locations and organisms (molluscs, tunicates, sponges) and a number have been shown to possess interesting biological properties. For example, lukianol-A exhibits some activity against a cell line derived from human epidermaoid carcinoma[6] while the penta-*O*-methyl derivative of polycitone A was found to inhibit the growth of SV 40 transformed fibroblast cells at concentrations of 10 μg ml$^{-1}$.[8] Our own interest in such alkaloids stems from the notion that they are configurationally stable structural hybrids of the powerful anti-mitotic agents combretastatin A-4[9] and colchicine[10] and, as such, may represent new classes of compounds that are capable of inhibiting cell division.[11] Despite the foregoing, remarkably little attention has been given to the total synthesis of any of the above-mentioned marine natural products.[12] Consequently, we now report convergent syntheses of the title compounds **1**–**3** as well as two more highly oxygenated and differentially di-arylated congeners. In each case, the key synthetic step involves Stille[13] or Suzuki[14] or Negishi[15] cross-coupling of readily available pyrrole 2-carboxylic acid derivatives with the appropriate aryl stannane, boronic acid or iodide. These steps represent rare examples of the use of palladium-catalysed cross-coupling chemistry for the introduction of carbon-based substituents onto the pyrrole nucleus.[16]

The pivotal dibromopyrrole **6** (Scheme 1) required for all the syntheses was readily prepared from pyrrole itself using procedures developed by Muchowski and co-workers.[17] Thus, the triisopropylsilyl derivative, **4**,[17] of pyrrole was subjected to reaction with 3 molar equiv. of *N*-bromosuccinimide (NBS) in THF at −78 °C. In this manner the tribromo-derivative, **5** (91%, mp 44–46 °C; lit.,[17] mp 46 °C) was obtained. Subjection of this latter compound to reaction with PhLi followed by $ClCO_2Me$ afforded the previously unreported compound **6** (99%). Stille cross-coupling of pyrrole **6** with 2 equiv. of the $Bu^tMe_2Si$ protected stannane **7** using $Pd(PPh_3)_2Cl_2$ as catalyst gave the expected product **8** (66%). Three-fold deprotection of the tris-*O*-silylether **8** using $Bu_4NF$ then afforded lamellarin-Q **1** (98%, mp 227–228 °C) which was spectroscopically identical with the natural product. The synthesis of lamellarin-O followed very similar lines. Thus, compound **6** was desilylated and the resulting pyrrole **9** (99% mp 147–148 °C) coupled with arylstannane **7**. In this manner the two-fold coupling product **10** (66%) was obtained. Reaction of this latter compound with commercially available 2-bromo-4′-methoxyacetophenone in the presence of base then gave the *N*-substituted pyrrole **11** (84%) which was deprotected with $Bu_4NF$ to provide the natural



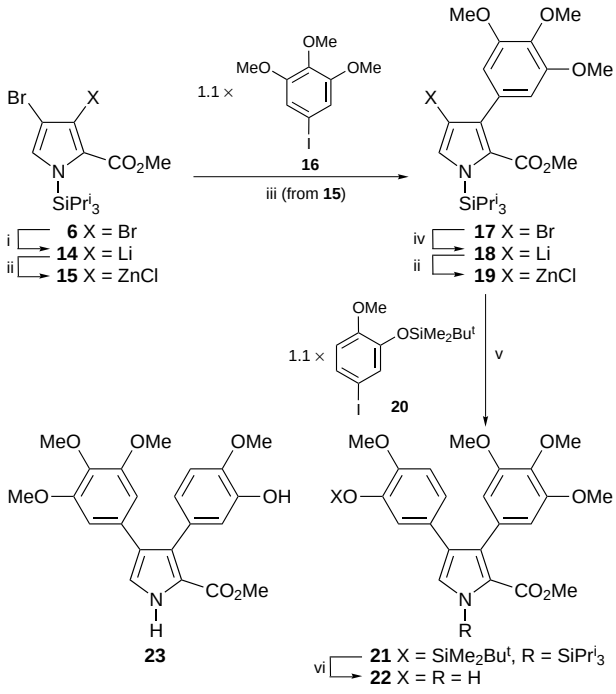




**Scheme 1** *Reagents and conditions*: i, NBS (3 equiv.), THF, −78 °C, 1 h then 20 °C for 4 h; ii, PhLi (1 equiv.), −78 °C, 0.16 h then $ClCO_2Me$ (1.05 equiv.), −78 to 20 °C, 1 h; iii, $Pd(PPh_3)_2Cl_2$ (10 mol%), 1,4-dioxane, 101 °C, 14 h; iv, $Bu_4NF$ (10 mol% excess), THF, 20 °C, 1 h then 0.5 M aq. HCl; v, *p*-$MeOC_6H_4COCH_2Br$ (3 equiv.), $K_2CO_3$ (5 equiv.), $Bu_4NCl$ (20 mol%), THF, 66 °C, 8 h; vi, $Pd(PPh_3)_4$ (5 mol%), sat. aq. $Na_2CO_3$ (6 equiv.), DMF, 153 °C, 23 h; vii, see ref. 12

product **2** (99%, mp 259–260 °C), the structure of which was confirmed by single-crystal X-ray analysis.†

Two-fold cross-coupling of pyrrole **9** with *p*-$MeOC_6H_4$-$B(OH)_2$ **12**[18] under standard Suzuki conditions afforded compound **13** (78% mp 170–171 °C; lit.,[12] mp 169–171 °C) which has previously been converted, over three steps and in 53% yield, into lukianol A **3** by Fürstner and co-workers.[12] The present work represents a superior synthesis of this natural product since the pivotal intermediate **13** is available in five steps and 69% overall yield from pyrrole by the methods just described while Fürstner's route provides the same material in six steps and *ca*. 15% overall yield.

In carrying out the Stille and Suzuki cross-coupling reactions described above we failed to observe any significant quantities of mono-arylated pyrroles even when shorter reaction times and 1 : 1 stoichiometries were employed. As a consequence, these types of coupling reactions would not seem useful in providing access to differentially di-arylated pyrroles–systems that would be required for the synthesis of the more complex lamellarins and in the preparation of various combretastatin A-4/colchicine hybrids. Such limitations were overcome by regioselective lithiation of compound **6** followed by transmetallation and Negishi cross-coupling reactions as outlined in Scheme 2 for the preparation of differentially diarylated and highly oxygenated pyrroles **22** and **23** (these compounds were chosen as targets because of their structural resemblance to combretastatin A-4). Thus, reaction of compound **6** at −78 °C with PhLi afforded the mono-lithio-derivative **14** which was transmetallated with $ZnCl_2$ to give the organozinc **15**. This last species was, in turn, cross-coupled with the aryl iodide **16**[19] to give the mono-arylated pyrrole **17** (69% from **6**, mp 154–155 °C). Compound **17** was subjected to a further lithiation–transmetallation sequence and intermediate **19** then cross-coupled with aryl iodide **20** (mp 36–38 °C) to give compound **21** (75%, mp 154–156 °C). This latter material was desilylated using $Bu_4NF$ thereby affording the target pyrrole **22** (91%, mp 158–159 °C).




**Scheme 2** *Reagents and conditions*: i, PhLi (1.0 equiv.), THF, −78 °C, 0.25 h; ii, $ZnCl_2$ (1.1 equiv.), THF, −78 to *ca*. 20 °C, 0.25 h; iii, Compound **16** (1.1 equiv.), $Pd(PPh_3)_4$ (5 mol%), THF, 20 °C, 8 h; iv, BuLi (equiv.), THF, −78 °C, 0.02 h; v, Compound **20** (1.1 equiv.), $Pd(PPh_3)_4$ (5 mol%), THF, 20 °C, 8 h; vi, $Bu_4NF$ (2.2 equiv.), THF, 20 °C, 1 h then 0.5 M aq. HCl

An exactly analogous reaction sequence where compound **15** was coupled with aryl iodide **20** and the resulting mono-arylated pyrrole (62%) subjected to metallation and coupling with aryl iodide **16** afforded, after deprotection, the isomeric system **23** (42% from **6**, mp 172–173 °C) the structure of which was confirmed by single-crystal X-ray analysis.†

We thank the Institute of Advanced Studies for financial support including the provision of a post-Doctoral Research Fellowship to B. L. F. Associate Professor R. J. Capon (University of Melbourne) is thanked for providing spectroscopic data on lamellarin-O and -Q.

## Footnote

† *Crystal data* for **2**: $C_{30}H_{30}NO_6$, $M$ = 500.57, $T$ = 193(1) K, $P\bar{1}$, $a$ = 10.260(3), $b$ = 11.127(4), $c$ = 12.125(2) Å, $\alpha$ = 108.39, $\beta$ = 99.97(2), $\gamma$ = 95.98(2)°, ($Z$ = 2. Atomic coordinates, bond lengths and angles, and thermal parameters have been deposited at the Cambridge Crystallograpic Data Centre (CCDC). See Information for Authors, Issue No. 1. Any request to the CCDC for this material should quote the full literature citation and the reference number 182/295.

## References

1 R. J. Andersen, D. J. Faulkner, H. Cun-heng, G. D. van Duyne and J. Clardy, *J. Am. Chem. Soc.*, 1985, **107**, 5492.
2 N. Lindquist, W. Fenical, G. D. van Duyne and J. Clardy, *J. Org. Chem.*, 1988, **53**, 4570.
3 A. R. Carroll, B. F. Bowden and J. C. Coll, *Aust. J. Chem.*, 1993, **46**, 489.
4 S. Urban, M. S. Butler and R. J. Capon, *Aust. J. Chem.*, 1994, **47**, 1919.
5 S. Urban, L. Hobbs, J. N. A. Hooper and R. J. Capon, *Aust. J. Chem.*, 1995, **48**, 1491.
6 W. Y. Yoshida, K. K. Lee, A. R. Carroll and P. J. Scheuer, *Helv. Chim. Acta*, 1992, **75**, 1721.
7 J. A. Palermo, M. Florencia Rodriguez Brasco and A. M. Seldes, *Tetrahedron*, 1996, **52**, 2727.
8 A. Rudi, I. Goldberg, Z. Stein, F. Frolow, Y. Benayahu, M. Schleyer and Y. Kashman, *J. Org. Chem.*, 1994, **59** 999.
9 R. T. Brown, B. W. Fox, J. A. Hadfield, A. T. McGown, S. P. Mayalarp, G. R. Pettit and J. A. Woods, *J. Chem. Soc., Perkin Trans. 1*, 1995, 577 and references cited therein.
10 M. G. Banwell, *Pure Appl. Chem.*, 1996, **68**, 539 and references cited therein.
11 For an example of the successful hybridisation of the combretastatin and colchicine structures see C. J. Andres, J. E. Bernardo, Q. Yan, S. B. Hastie and T. L. Macdonald, *Bioorg. Med. Chem. Lett.*, 1993, **3**, 565.
12 During the course of the work described here a very different approach to lukianol A and the dimethyl ether of lamellarin O was reported (A. Fürstner, H. Weintritt and A. Hupperts, *J. Org. Chem.*, 1995, **60**, 6637). Steglich *et al*. have reported a biomimetic synthesis of polycitrin A (A. Terpin, K. Polborn and W. Steglich, *Tetrahedron*, 1995, **51**, 9941).
13 (*a*) J. K. Stille, *Angew. Chem., Int. Ed. Engl.*, 1986, **25**, 508; (*b*) T. N. Mitchell, *Synthesis*, 1992, 803.
14 A. Suzuki, *Pure Appl. Chem.*, 1994, **66**, 213 and references cited therein.
15 (*a*) E. Negisihi, T. Takahashi and A. O. King, *Org. Synth.*, 1987, **66**, 67; (*b*) P. Knochel and R. D. Singer, *Chem. Rev.*, 1993, **93**, 2117.
16 For discussions of this matter see (*a*) A. Minato, K. Tamao, T. Hayashi, K. Suzuki and M. Kumada, *Tetrahedron Lett.*, 1981, **22**, 5319; (*b*) J. Wang and A. I. Scott, *Tetrahedron Lett.*, 1995, **36**, 7043; (*c*) C. K. Chang and N. Bag, *J. Org. Chem.*, 1995, **60**, 7030 and references cited therein. Also see K. Takahashi, A. Gunji, K. Yanagi and M. Miki, *J. Org. Chem.*, 1996, **61**, 4784.
17 B. L. Bray, P. H. Mathies, R. Naef, D. R. Solas, T. T. Tidwell, D. R. Artis and J. M. Muchowski, *J. Org. Chem.*, 1990, **55**, 6317.
18 K. S. Chan, X. Zhou, M. T. Au and C. Y. Tam, *Tetrahedron*, 1995, **51**, 3129.
19 B. F. Bowden, R. W. Read and W. C. Taylor, *Aust. J. Chem.*, 1981, **34**, 799.

*Received, 3rd October 1996; Com. 6/06793J*

# $C_{120}O_2$: The first [60]fullerene dimer with cages bis-linked by furanoid bridges

**Andrei Gromov,[a] Sergei Lebedkin,[c] Stephan Ballenweg,[a] Anthony G. Avent,[b] Roger Taylor[b] and Wolfgang Krätschmer*[a]**

[a] *Max-Planck-Institut für Kernphysik, Postfach 103980, D-69029 Heidelberg, Germany*
[b] *The Chemistry Laboratory, University of Sussex, Brighton, UK BNI 9QJ*
[c] *Forschungszentrum Karlsruhe, Institut für Nukleare Festkörperphysik, Postfach 3640, D-76021 Karlsruhe, Germany*

**$C_{120}O_2$ has been prepared, characterised by MALDI–TOF MS, UV–VIS, FTIR, and shown by $^{13}C$ NMR spectroscopy to have $C_{2v}$ symmetry, the [60]fullerene cages being linked by adjacent furanoid rings; thus the structure has a connecting bridge containing a four-membered ring, reminiscent of that conjectured for the [2 + 2] fullerene cycloadduct.**

Recently, we described the preparation and characterisation of $C_{120}O$, the first dimeric fullerene derivative.[1] The structure was subsequently confirmed.[2] As part of our ongoing interest in fullerene oxides, and the search for $C_{119}$ precursors,[3] we prepared and isolated $C_{120}O_2$ by thermolysis of $C_{120}O$.[4] Solid $C_{120}O$ was heated to 400 °C for 1 h at normal pressure in an Ar atmosphere. Under these conditions we observed (i) decay of $C_{120}O$ into $C_{60}$ (up to 60% with respect to the initial $C_{120}O$), (ii) the formation of $C_{120}O_2$ (*ca*. 15%) together with oligomeric oxides $(C_{60})_nO_m$ ($n$ = 3–5; $m$ = 3–9), and (iii) an insoluble uncharacterised residue (*ca*. 10%).[4] $C_{120}O_2$, isolated from the obtained mixture by a two-stage HPLC separation,† is a brown solid, stable under ambient conditions and in solution (HPLC analysis).

The mass spectrum of $C_{120}O_2$ [matrix-assisted laser desorption/ionisation time-of-flight (MALDI–TOF) MS, negative mode of ionisation, matrix 9-nitroanthracene] shows (Fig. 1) the intense molecular ion peak at 1473.3 amu (calculated for $C_{120}O_2$, 1473.32 amu). Weak peaks at 720.2 and 736.6 amu indicate minor fragmentation of $C_{120}O_2$ into $C_{60}$ and $C_{60}O$; a similarly weak peak at 1489.8 amu ($C_{120}O_3$) may indicate oxidation by the matrix under MALDI conditions.

Our initial attempts to obtain a $^{13}C$ NMR spectrum failed due to the low solubility of the substance in $CS_2$. To overcome this problem we produced enriched material with *ca*. 7% $^{13}C$.‡ The $^{13}C$ NMR spectrum is shown in Fig. 2 and consists of two lines in the $sp^3$ region and 27 in the $sp^2$ region (with three coincident peaks).§ The number of lines, and their intensity distribution is consistent with a molecule of $C_{2v}$ symmetry. The two groups of four equivalent $sp^3$-hybridised carbon atoms indicate that each [60]fullerene cage is bis-linked by adjacent furanoid rings.

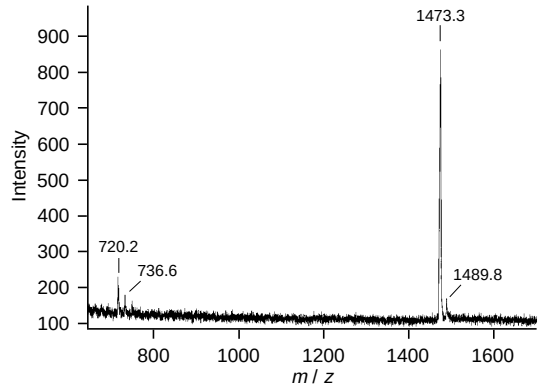



**Fig. 1** MALDI–TOF mass spectrum of $C_{120}O_2$

Thus, the connecting bridge contains a four-membered ring. The four half-intensity $sp^2$ peaks are due to the carbons on one of the $\sigma_v$ planes.

The $^{13}C$ NMR data suggest two most likely structures, in both of which a four-membered ring is part of the linkage between the cages: in one, the two furanoid rings link the cages *via* 6,6 junctions as in the case of $C_{120}O$[1] **1**, whereas the other structure involves 6,5 junctions for this purpose **2** (Fig. 3). Whilst structure **2** has a four-membered ring exactly analogous to that conjectured for photopolymerised fullerenes,[5] **2** may be disputed on two grounds: (i) it contains unfavourable double bonds in pentagons[6] (calculated to destabilise by *ca*. 8.5 kcal $mol^{-1}$ per double bond);[7] (ii) the structure is inappropriate to explain the position in the spectrum of the signals for the on-plane carbons. For structure **2** each on-plane pair is roughly equidistant from the addend, so that four lines in a similar region of the spectrum could be expected. By contrast, in structure **1** one of the pairs is adjacent to the addend site, and is *exo* to a pentagon containing two $sp^3$-hybridised carbons. These latter are less electron-withdrawing than $sp^2$-hybridised carbons and

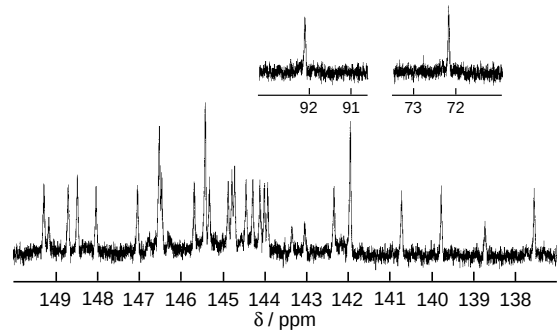



**Fig. 2** $^{13}C$ NMR spectrum of $C_{120}O_2$

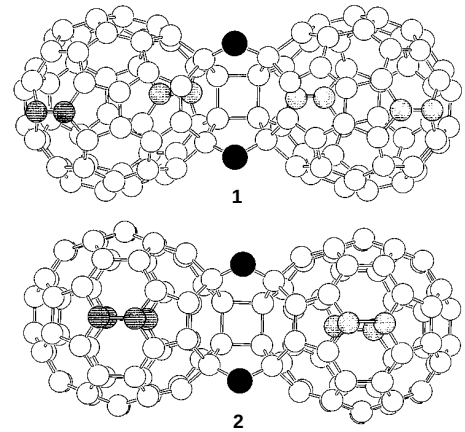



**Fig. 3** Possible structures of $C_{120}O_2$ with $C_{2v}$ symmetry: furan-ring linkage *via* 6,6 junctions **1** or *via* 6,5 junctions **2**. The oxygens are black, and the on-plane carbon pairs are hatched for clarity.

this will therefore induce a dipole in the adjacent double bond, resulting in one carbon (in the pentagon) appearing well upfield, the other carbon correspondingly downfield, as observed. The other on-plane pair is remote from the addend and so should appear at a similar position in the spectrum, also as observed. Lastly, in assigning the structure, we discounted the possibility (i) that all $sp^3$-hybridised carbons are located in one pentagon, implying a substantially larger number of double bonds in pentagons than in **2**; the structure should also have strong repulsive p-orbital interactions from the adjacent oxygens, and (ii) of the locations of the C–C and the C–O–C connections being reversed; this would produce severe strain because the cages would come into almost direct contact.

The UV–VIS spectrum (cyclohexane) resembles that for $C_{120}O$, showing peaks at 224, 256 and 318 nm, and a rather weak band at 422 nm. The FT–IR spectra [KBr for middle IR (MIR), Fig. 4(*a*); polyethylene for far IR (FIR), Fig. 4(*b*)] of $C_{120}O_2$ are compared to that of $C_{120}O$. The $^{13}C$ NMR data suggest that the furanoid bridges in $C_{120}O_2$ and $C_{120}O$ are rather similar and this similarity is also reflected in the IR spectra of both compounds. In the MIR, where the intra-cage vibrations occur, these similarities are especially striking [Fig. 4(*a*)]. However, the inter-cage vibrations of both dimers observable in the FIR show characteristic shifts. $C_{120}O$ exhibits one strong absorption band at 207 $cm^{-1}$ and a weak band at 124 $cm^{-1}$ (very close to 118 $cm^{-1}$ Raman band of photopolymerized [60]fullerene),[5] both of which are probably responsible for the inter-cage stretching modes. The corresponding FIR features of $C_{120}O_2$ occur at *ca*. 260 (line pair) and 161 $cm^{-1}$, and thus are shifted (approximately by a factor of 1.28) in frequency compared to $C_{120}O$. Such a shift indicates the more rigid bridge construction in $C_{120}O_2$, thus confirming the NMR data.

In conclusion, we note that $C_{120}O_2$ is the first characterised compound having a four-membered ring as part of the linkage between the two fullerene cages.

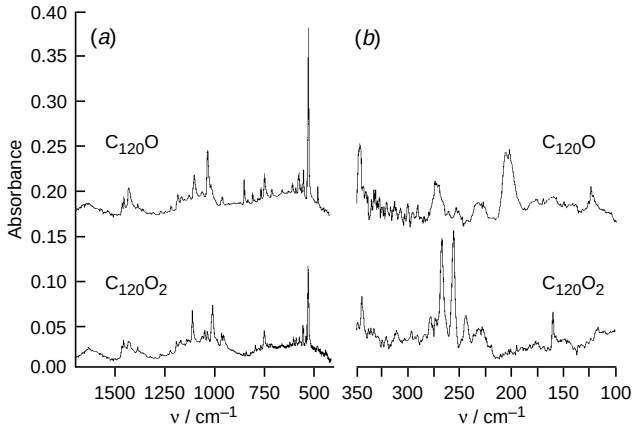



**Fig. 4** (*a*) MIR (KBr, 1 mg of sample) and (*b*) FIR (polyethylene, 20 mg of sample) spectra of $C_{120}O_2$ compared to that of $C_{120}O$. The spectra of $C_{120}O$ are shifted for clarity.

The authors appreciate the support of the Human Capital and Mobility Programme of the EU. A. G., S. B. and W. K. wish to thank the Deutsche Forschungsgemeinschaft and S. L. is grateful to the Bundesministerium für Bildung, Wissenschaft, Forschung und Technologie for financial support. The help of Dr G. Monninger and H. Stopka-Ebeler (Max-Planck-Institut für Kernphysik, Heidelberg) in measuring IR spectra, and the skillful assistance of Dr J. Gross (Organisch-Chemisches Institut, Universität Heidelberg) in acquiring mass spectra is greatly acknowledged.

## Footnotes

† $C_{120}O_2$ was first separated from $C_{60}$ and higher mass species using a 250 × 4.6 mm Cosmosil 5PBB column, *o*-dichlorobenzene eluent, flow rate 1.0 ml $min^{-1}$, 150 bar, detection at 340 nm. Final purification was carried out with a 250 × 4.6 mm Cosmosil Buckyprep column, toluene eluent, flow rate 1.0 ml $min^{-1}$, 60 bar, detection at 340 nm. Under these conditions, $C_{120}O_2$ eluted at 18.1 min (*cf.* 7.8 min for $C_{60}$ and 15.8 min for $C_{120}O$).

‡ $^{13}C$-enriched $C_{60}$ was obtained by the standard procedure[8] using graphite rods hollowed out and packed with a mixture of $^{13}C$ enriched powder and regular graphite; the enriched $C_{60}$ was used as starting material for $C_{120}O$ preparation (ref. 1).

§ The $^{13}C$ NMR spectrum [125.76 MHz, $CS_2$–$CDCl_3$ 98 : 2, *ca*. 35 mmol $dm^{-1}$ $Cr(acac)_3$, 60 h, 36 000 scans] exhibits peaks at δ 149.28 (4 C), 149.16 (2 C), 148.70 (4 C), 148.48 (4 C), 148.03 (4 C), 147.04 (4 C), 146.53 (8 C), 146.47 (4 C), 145.69 (4 C), 145.43 (8 C), 145.33 (4 C), 144.88 (4 C), 144.79 (4 C), 144.73 (4 C), 144.46 (4 C), 144.29 (4 C), 144.13 (4 C), 144.02 (4 C), 143.94 (4 C), 143.36 (2 C), 143.06 (2 C), 142.35 (4 C), 141.96 (8 C), 140.73 (4 C), 139.79 (4 C), 138.74 (2 C), 137.58 (4 C), 92.11 (4 C), 72.19 (4 C).

## References

1 S. Lebedkin, S. Ballenweg, J. Gross, R. Taylor and W. Krätschmer, *Tetrahedron Lett.*, 1995, **36**, 4971.
2 A. R. Smith, H. Tokuyama, M. Strongin, G. T. Furst and W. J. Romanov, *J. Am. Chem. Soc.*, 1995, **117**, 9359.
3 R. S. W. McElvany, J. H. Callagan, M. M. Ross, L. D. Lamb and D. R. Huffman, *Science*, 1993, **260**, 1632; R. Taylor, *J. Chem. Soc., Chem. Commun.*, 1994, 1629; G. B. Adams, J. B. Page, M. O'Keefe and O. F. Sankey, *Chem. Phys. Lett.*, 1994, **228**, 485; R. D. Beck, G. Bräuchle, C. Stoermer and M. Kappes, *J. Chem. Phys.*, 1995, **102**, 540; E. Albertazzi and F. Zerbetto, *J. Am. Chem. Soc.*, 1996, **118**, 2734.
4 A. Gromov, S. Lebedkin, S. Ballenweg and W. Krätschmer, in *Fullerenes and Fullerene Nanostructures*, Proceedings of the International Winterschool in the Electronic Properties of Novel Materials, World Scientific, Singapore, 1996, ed. H. Kuzmany, J. Fink, M. Mehring and S. Roth, p. 460.
5 A. M. Rao, P. Zhou, K.-A. Wang, G. T. Hager, I. M. Holden, Y. Wang, W.-T. Lee, X.-X. Bi, P. C. Eklund, D. S. Cornett, M. A. Duncan and J. J. Amster, *Science*, 1993, **259**, 955; P. Zhou, Z.-H. Dong, A. M. Rao and P. C. Eklund, *Chem. Phys. Lett.*, 1993, **211**, 337.
6 R. Taylor, *Tetrahedron Lett.*, 1991, **32**, 3731.
7 N. Matsuzawa, D. A. Dixon and T. Fukunaga, *J. Phys. Chem.*, 1992, **96**, 7594.
8 W. Krätschmer, L. D. Lamb, K. Fostiropoulos and D. R. Huffman, *Nature*, 1990, **347**, 354.

*Received, 3rd October 1996; Com. 6/06794H*

# Comparative evaluation of enantiocontrol for intramolecular cyclopropanation of diazoacetates with chiral Cu$^{I}$, Rh$^{II}$ and Ru$^{II}$ catalysts

**Michael P. Doyle,*[a] Chad S. Peterson,[a] Qi-Lin Zhou[b] and Hisao Nishiyama*[c]**

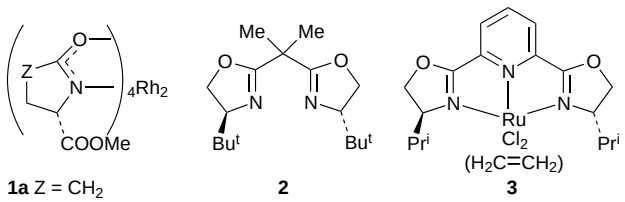
[a] *Department of Chemistry, Trinity University, San Antonio, Texas 78212, USA*
[b] *Institute of Fine Chemicals, East China University of Science and Technology, 130 Meilong Lu, Shanghai 200237, Peoples Republic of China*
[c] *School of Materials Science, Toyohashi University of Technology, Tempaku-cho, Toyohashi 441, Japan*

**Enantioselectivity for intramolecular cyclopropanation of allylic diazoacetates shows complementarity in comparisons of chiral Cu$^{I}$, Rh$^{II}$ and Ru$^{II}$ catalysts.**

A broad selection of chiral catalysts for enantioselective cyclopropanation with diazoacetates has been described.[1] The vast majority fall into two structural classes: (i) those, including the appropriately substituted semicorrin[2] and bis-oxazoline[3] complexes of copper(I) and (pybox)$RuCl_2$(ethene),[4] whose chiral ligands are $C_2$-symmetric and (ii) chiral dirhodium(II) carboxamidates whose ligand arrange- ment in these octahedral complexes places two distinguishing ester attachments *cis* to each other.[5] The success of chiral dirhodium(II) carboxamidates, especially dirhodium(II) tetrakis[methyl 2-oxopyrrolidine-5(*R* or *S*)-carboxylates], $Rh_2$(5*R*-MEPY)$_4$ and $Rh_2$(5*S*-MEPY)$_4$ **1a**,[6] for highly enantio-selective intramolecular cyclopropanation of allylic diazoacetates has been described but, surprisingly, these same synthetically useful transformations have not been examined using copper(I) with $C_2$-symmetric ligands nor comprehensively with chiral (pybox)Ru$Cl_2$(ethene). We now present our preliminary results which demonstrate complementarity in enantiocontrol between these diverse catalysts.

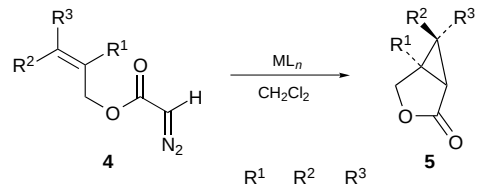
Treatment of a selection of allylic diazoacetates (Scheme 1) with 1.0 mol% Cu(OTf)/**2**[7] in $CH_2Cl_2$ resulted in the expected cyclopropanation products **5** in moderate to relatively low isolated yields and with often variable enantiomeric excesses (ee). Dramatic improvements in isolated yields without a corresponding change in enantioselectivity were achieved with the use of Cu(MeCN)$_4$PF$_6$/**2** (Table 1). The air stability and handling ease of Cu(MeCN)$_4$PF$_6$[8] render this copper(I) reagent superior to the universally employed[9] Cu(OTf) for catalytic cyclopropanation reactions. Comparative yields and enantiomeric excesses for $Rh_2$(5*S*-MEPY)$_4$ catalysed reactions (0.1–1.0 mol% **1a**)[5] and for **3** (3–5 mol%) are also given in Table 1. Surprisingly, the absolute configurations of cyclopropane products **5c** and **5d** from catalysis by CuPF$_6$/**2** are opposite to those formed with **3**.

Enantioselectivity in copper(I)/**2** catalysed reactions is higher with allylic diazoacetates that have 2-alkyl (**4e,f**)[10] substituents, and these are the substituents that give the lowest enantioselectivities in $Rh_2$(5*S*-MEPY)$_4$-catalysed reactions. With the (pybox)$RuCl_2$(ethene) catalyst **3**, these diazo substrates did not undergo intramolecular cyclopropanation under a variety of reaction conditions; carbene dimers were the only isolated products. However, use of $Rh_2$(4*S*-MPPIM)$_4$ **1b** instead of $Rh_2$(5*S*-MEPY)$_4$ causes an enormous enhancement in enantiocontrol for **5e** and **5f** as well as for intramolecular cyclopropanation of *trans*-2-hexen-1-yl diazoacetate (**4c**).[11] The preference for higher enantiocontrol with *trans*- disubstituted alkenes **4c** for **3** relative to *cis*-disubstituted systems **4d** with **1a** contrasts with the low % ee values observed for catalysis by CuPF$_6$/**2** of




**1a** Z = $CH_2$
**b** Z = $NCOCH_2CH_2Ph$

**2** **3**




**4** **5**

| | $R^1$ | $R^2$ | $R^3$ |
|---|---|---|---|
| **a** | H | H | H |
| **b** | H | Me | Me |
| **c** | H | H | Pr |
| **d** | H | Pr | H |
| **e** | Me | H | H |
| **f** | Bu | H | H |

**Scheme 1**

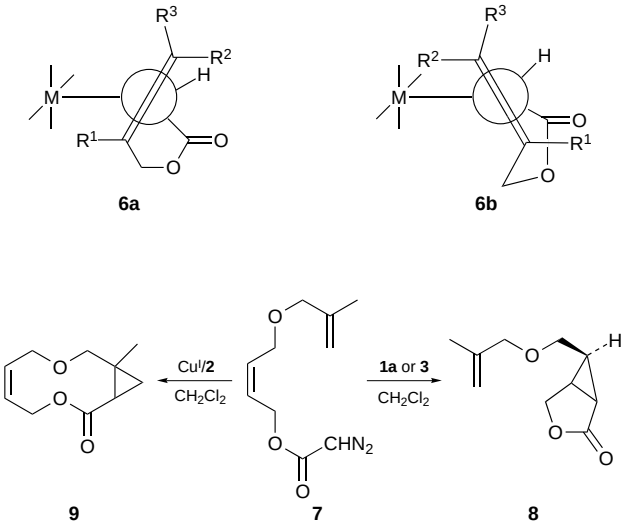
**Table 1** Comparative yields and enantioselectivities of Cu$^{I}$, Rh$^{II}$ and Ru$^{II}$ catalysed intramolecular cyclopropanation reactions of **4a–f**

| Cyclo-propane **5** | Cu(MeCN)$_4$PF$_6$/**2** | | $Rh_2$(5*S*-MEPY)$_4$ **1a** | | $Rh_2$(4*S*-MPPIM)$_4$ **1b** | | (pybox)$RuCl_2$(ethene) **3** | |
|---|---|---|---|---|---|---|---|---|
| | Yield (%) | ee (%)[a] | Yield (%) | ee (%)[a] | Yield (%) | ee (%)[a] | Yield (%) | ee (%)[a] |
| **a** | 61 | 20 (1*R*,5*S*) | 75 | 95 (1*R*,5*S*) | — | — | — | — |
| **b** | 80 | 13 (1*R*,5*S*) | 89 | 95 (1*S*,5*R*) | — | — | 91 | 76 (1*R*,5*S*) |
| **c** | 74 | 29 (1*S*,5*R*) | 93 | 95 (1*R*,5*S*) | 83 | 95 (1*R*,5*S*) | 68 | 78 (1*R*,5*S*) |
| **d** | 82 | 37 (1*S*,5*S*) | 88 | 94 (1*R*,5*S*) | — | — | 54 | 21 (1*R*,5*S*) |
| **e**[b] | 58 | 87 (1*S*,5*R*) | 72 | 7 (1*R*,5*S*) | 75 | 89 (1*S*,5*R*) | 0 | — |
| **f**[c] | 73 | 82 (1*S*,5*R*) | 72 | 35 (1*S*,5*R*) | 82 | 93 (1*S*,5*R*) | 0 | — |

[a] Configurational assignment in parentheses (ref. 5). [b] Absolute configuration determined from the X-ray structure of 1-(1-naphthyl)-ethylamide derivative (L. E. Overman, private communication). [c] Configuration assigned by analogy with **5e** and order of elution on a 30 m Chiraldex G-TA column.

either **4c** or **4d**. Thus each of these catalytic systems has unique capabilities for enantio- selection, independent of whether their ligands are $C_2$-symmetric (**2** and **3**) or if they have a *cis*-array of chiral attachments (**1**). However, as is evident from these data, chiral dirhodium(II) carboxamidates are the catalysts of choice for these intramolecular cyclopropanation reactions.

The selectivities for allylic cyclopropanation observed with catalysts **1**–**3** are consistent with the alkene approach trajectories that are depicted by the Newman projections of **6a,b**. In these representations the ligated metal (M) orients the carbon–carbon double bond to a frontside approach to the carbene centre; the backside approach produces the enantiomeric forms. For **6a**, which models selectivity with $Rh_2(MEPY)_4$ catalysts, interaction of $R^1$ with the catalyst face is most pronounced and, appropriate to the high enantiocontrol observed with *cis*-disubstituted allylic diazoacetates, $R^2$ is oriented away from the catalyst (**6b**). High enantiocontrol observed in cyclopropanation reactions of allylic diazoacetates having $R^3$ or $R^1$ groups (*e.g.* with $Cu^I$/**2** or **3**) is consistent with **6b**. However, the absence of cyclopropane products from **4e,f** with **3** suggests that conformation **6a** is required for these substrates, whereas **6b** is operative for **4b–d**. That catalysis by **3** and $CuPF_6$/**2** forms **5c** and **5d** which have opposite configura- tions demands a more subtle explanation than has heretofore been accorded these reactions.




**Scheme 2**

Another comparative measure of selectivity in intramolecular cyclopropanation reactions is regioselection, particularly with **7** which is designed to undergo either γ-lactone formation or macrocyclization (Scheme 2). With $CuPF_6$/**2** macrocycle formation was the predominant intramolecular process (**9**: 87% ee, 43% yield; **8**: 41% ee, 19% yield),[12] whereas only **8** was produced by catalysis with either **1a** (96% ee, 84% yield) or **3** (17% ee, 45% yield). The formation of **8** catalysed by **1a**, $CuPF_6$/**2** and **3** occurred with % ee values and enantiomer configurations that are similar to and predictable from results for **5d** in Table 1.

Support from the National Institutes of Health (GM 46503) and the Robert A. Welch Foundation to M. P. D. is greatly appreciated. We are grateful to L. E. Overman for the information that he provided.

## References

1 M. P. Doyle, in *Comprehensive Organometallic Chemistry II*, ed. L. S. Hegedus, Pergamon Press, New York, 1995, vol. 12, ch. 5; M. P. Doyle, in *Catalytic Asymmetric Synthesis*, ed. I. Ojima, VCH Publishers, New York, 1993, ch. 3.
2 A. Pfaltz, *Acc. Chem. Res.*, 1993, **26**, 39.
3 R. E. Lowenthal and S. Masamune, *Tetrahedron Lett.*, 1991, **32**, 7373; D. A. Evans, K. A. Woerpel and M. J. Scott, *Angew. Chem., Int. Ed. Engl.*, 1992, **31**, 430; D. Müller, G. Umbricht, D. Weber and A. Pfaltz, *Helv. Chim. Acta*, 1991, **74**, 232.
4 H. Nishiyama, Y. Itoh, Y. Sugaware, H. Matsumoto, K. Aoki and K. Itoh, *Bull. Chem. Soc. Jpn.*, 1995, **68**, 1247; S.-B. Park, K. Murata, H. Matsumoto and H. Nishiyama, *Tetrahedron: Asymmetry*, 1995, **6**, 2487.
5 M. P. Doyle, R. E. Austin, A. S. Bailey, M. P. Dwyer, A. B. Dyatkin, A. V. Kalinin, M. M. Y. Kwan, S. Liras, C. J. Oalmann, R. J. Pieters, M. N. Protopopova, C. E. Raab, G. H. P. Roos, Q.-L. Zhou and S. F. Martin, *J. Am. Chem. Soc.*, 1995, **117**, 5763.
6 M. P. Doyle, W. R. Winchester, J. A. A. Hoorn, V. Lynch, S. H. Simonsen and R. Ghosh, *J. Am. Chem. Soc.*, 1993, **115**, 9968.
7 D. A. Evans, K. A. Woerpel, M. M. Hinman and M. M. Faul, *J. Am. Chem. Soc.*, 1991, **113**, 726.
8 G. J. Kubas, *Inorg. Synth.*, 1979, **19**, 90.
9 T. G. Grant, M. C. Noe and E. J. Corey, *Tetrahedron Lett.*, 1995, **36**, 8745.
10 L. E. Overman was the first to report that high enantiocontrol was achieved in Cu(OTf)/**2** catalysed reactions of **4e**: 209th National Meeting of the American Chemical Society, Anaheim, California, April 2–6, 1995; ORGN-172.
11 M. P. Doyle, Q.-L. Zhou, A. B. Dyatkin and D. A. Ruppar, *Tetrahedron Lett.*, 1995, **36**, 7579.
12 M. P. Doyle, C. S. Peterson and D. L. Parker, Jr., *Angew. Chem., Int. Ed. Engl.*, 1996, **35**, 1334.

*Received, 7th October 1996; Com. 6/06893F*

# Non-biomimetic oxidation of 1,4-dihydropyridines†

**Rodolfo Lavilla,* Francisco Gullón, Xavier Barón and Joan Bosch***

*Laboratory of Organic Chemistry, Faculty of Pharmacy, University of Barcelona, 08028 Barcelona, Spain*

**The reaction between *N*-alkyl-1,4-dihydropyridines and dimethyldioxirane leads to dimeric tetrahydropyridines having oxygen atoms at the 2- and 3-positions in good yields and with good stereocontrol; these compounds are useful iminium ion precursors, and are satisfactorily transformed into 2-substituted 3-hydroxy-1,2,3,4-tetrahydropyridines.**

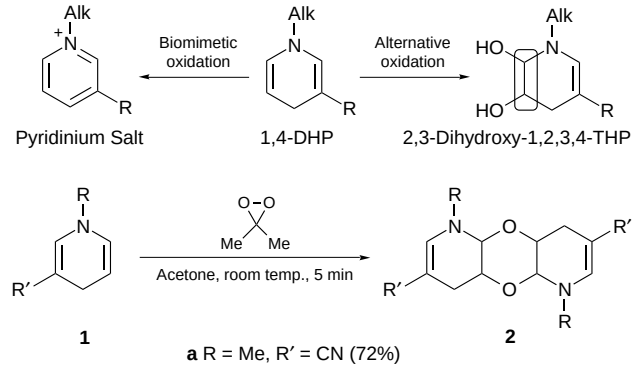
1,4-Dihydropyridines are interesting compounds and play an important role in synthetic, therapeutic and bioorganic chemistry.[1] New methods for their preparation[2] and transformations have been the subject of research in our laboratory: selective reductions,[3] electrophilic additions[4] and total syntheses of alkaloids[5] have been developed.

Here we report an efficient, mild and selective non-biomimetic oxidation of *N*-alkyl-1,4-dihydropyridines.‡ Although the conversion of these compounds to the corresponding pyridinium salts is a well-established process that has relevant significance in cell metabolism [NAD(P)H is commonly oxidized to $NAD(P)^+$ in many enzyme-assisted reductions], very little is known about 'alternative' dihydropyridine oxidations (*i.e.* epoxidations or dihydroxylations).[6,7] To our knowledge, no synthetically useful reports dealing with this subject have been published. After several unsuccessful attempts to oxidize *N*-alkyl-1,4-dihydropyridines with MCPBA or $OsO_4$, we turned our attention to the use of dimethyldioxirane (DMD), a reagent used in a wide range of functional group transformations,[8] including the oxidation of enamines.[9] It should be mentioned that a chemically related dioxetane was involved in the 'normal' oxidation of a NADH analogue.[10]

The required *N*-methyl-1,4-dihydropyridines **1** were prepared by sodium dithionite reduction of the corresponding pyridinium salts, following published procedures.[11] When dihydropyridines **1** were treated at room temperature with DMD for 5 min, the tricyclic dioxanes **2** were obtained in good yields.§¶ This process can be rationalized by considering the initial epoxidation of the enamine double bond with subsequent ring opening of the oxirane ring to give an iminium ion that undergoes dimerization.

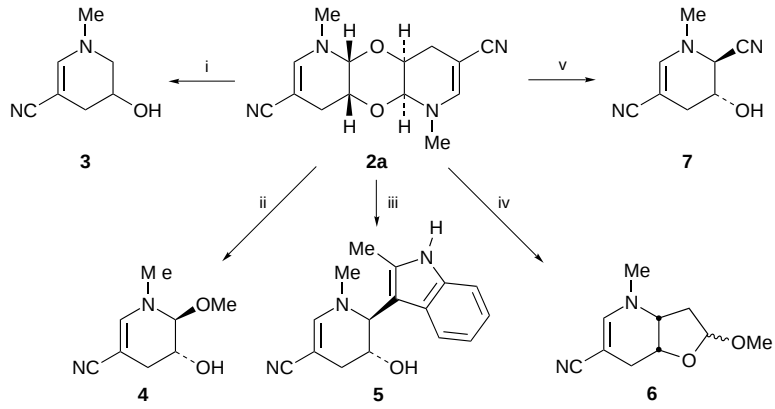
This transformation constitutes the first general, non-biomimetic oxidation of 1,4-dihydropyridines, avoiding the natural oxidation pathway to pyridinium salts. In contrast, the use of dioxiranes generated *in situ* from 2-chlorocyclohexanone or 1,1,1-trifluoroacetone in the presence of stochiometric amounts of Oxone®[12] was not satisfactory, showing the incompatibility of dihydropyridines with strong oxidants like peroxyacids. The major stereoisomers **2** have a centre of symmetry,[13] showing a *cis* stereochemistry for the oxygens at $C_2$–$C_3$ and a *anti* relationship between the two tetrahydropyridine moieties; minor amounts of other isomers were isolated, probably having a *syn* stereochemistry. The stereochemical assignments were based on the coupling constants in the $^1H$ NMR spectra and on $^1H$-$^1H$ COSY, HMQC and NOESY experiments. Dioxanes **2** were stable enough to be chromatographed, spectroscopically characterized and stored indefinitely in the freezer under an inert atmosphere. An additional interest of dimers **2** lies in the fact that they are highly functionalized iminium ion precursors.

A preliminary study of this type of reactivity was undertaken, including the generation of iminium ions under different conditions and their subsequent interaction with nucleophiles. Thus, reduction of **2a** with triethylsilane in the presence of




**a** R = Me, R′ = CN (72%)
**b** R = Me, R′ = $CO_2Me$ (76%)
**c** R = Bn, R′ = CN (69%)
**d** R = Bn, R′ = $CO_2Me$ (60%)

**Scheme 1**




**Scheme 2** *Reagents and conditions*: i, $Et_3SiH$, $TiCl_4$, THF, −60 °C, 5 min (95%); ii, MeOH, TFA, 0 °C, 5 min (72%; *cis* isomer 24%); iii, 2-methylindole, TFA, 20 °C, 5 min (60%; *cis* isomer 24%); iv, 1-methoxyethene, $BF_3{\cdot}Et_2O$, THF–$CH_2Cl_2$, −60 °C, 5 min (60%, mixture of isomers at the acetalic carbon); v, $Me_3SiCN$, $TiCl_4$, $CH_2Cl_2$, 0 °C, 5 min (40%; *cis* isomer 27%)

titanium tetrachloride afforded tetrahydropyridinol **3**, whereas TFA-induced addition of methanol gave the 'protected' α-alcoxy tetrahydropyridine **4**. On the other hand, addition of 2-methylindole was achieved under acid catalysis, affording adduct **5** with moderate stereoselectivity. In the latter two reactions, minor amounts of the *cis* isomers were isolated. Addition of methoxyethylene was achieved in the presence of boron trifluoride. In this case, the intramolecular trapping of the resulting carbonium ion by the hydroxy group allowed the formation of the partially reduced furopyridine **6** (ring fusion *cis*) in a one-pot transformation. Finally, $Me_3SiCN$ was added to give α-amino nitrile **7** (epimeric mixture at C-2) in good yield.‖

In conclusion, a useful, mild and selective method for the formal epoxidation of 1,4-dihydropyridines has been developed, and some relevant reactions of the resulting compounds, which act as iminium ion precursors, are reported. These results present interesting possibilities in the study of the chemical reactivity of dihydropyridines, a class of compounds with a significant role in biochemistry and in natural product synthesis (*e.g.* alkaloids and azasugars).

This work was supported by the Dirección General de Investigación Científica y Técnica, Spain, (PB94-0214) and by the Comissionat per Universitats i Recerca (Generalitat de Catalunya, Grant SGR95-00428).

## Footnotes

† Presented in part at the Eigth FECHEM Conference on Heterocycles in Bio-Organic Chemistry, September 1–4, 1996, Villa Olmo, Italy.

‡ The term non-biomimetic is used in a broad sense, meaning that the process involves an oxygen transfer rather than the usual two-electron oxidation observed in nature.

§ All new compounds were characterized by $^1$H and $^{13}$C NMR, IR, UV, MS and HRMS.

¶ *Typical procedure*: A 1.1 fold excess of DMD (0.07 M) in acetone[14] was added to a solution of the dihydropyridine **1a** (1 mmol) in acetone (20 ml) at 0 °C. The progress of the reaction was monitored by TLC. When all the starting material had been consumed (*ca.* 5 min), the solvent was removed under reduced pressure and the residue was chromatographed through neutral alumina ($CH_2Cl_2$–MeOH) to give the corresponding dioxane **2a** (72%). $^1$H NMR (300 MHz, $CD_3OD$) 2.16 (ddd, 1 H, *J* 16.3, 2.7 and 1.5 Hz, H-4), 2.53 (ddd, 1 H, *J* 16.3, 3.7 and 1.9 Hz, H-4), 3.15 (s, 3 H, $CH_3$), 3.83 (m, 1 H, H-3), 4.41 (dd, 1 H, *J* 2.6 and 1.5 Hz, H-2), 6.74 (d, 1 H, *J* 1.9 Hz, H-6); $^{13}$C NMR (75.4 MHz, $CD_3OD$) 24.4 (C-4), 39.3 ($CH_3$), 63.9 (C-3), 70.3 (C-5), 80.4 (C-2), 122.7 (CN), 146.0 (C-6). HRMS (e.i.) *m/z*: calc. 272.1273, found 272.1272.

‖ *Selected spectral data* for **3**: $^1$H NMR (300 MHz, $CDCl_3$) 2.20 (br s, 2 H, H-4 and OH), 2.49 (br d, 1 H, *J* 15.8 Hz, H-4), 2.95 (s, 3 H, $CH_3$), 3.01 (m, 1 H, *J* 12.6, 5.6, 2.5 and 0.9 Hz, H-2), 3.17 (ddd, 1 H, *J* 12.6, 2.6 and 1.1 Hz, H-2), 4.19 (br s, 1 H, H-3), 6.79 (d, 1 H, *J* 0.9 Hz, H-6); $^{13}$C NMR (75.4 MHz, $CDCl_3$): 30.0 (C-4), 42.9 ($CH_3$), 52.9 (C-2), 61.9 (C-3), 69.5 (C-5), 123.0 (CN), 147.5 (C-6). For **4** (major stereoisomer, *trans*): $^1$H NMR (300 MHz, $CDCl_3$) 2.12 (ddd, 1 H, *J* 16.6, 2.2 and 1.3 Hz, H-4), 2.40 (ddd, 1 H, *J* 16.6, 3.8 and 1.9 Hz, H-4), 3.09 (s, 3 H, $NCH_3$), 3.38 (s, 3 H, $OCH_3$), 3.93 (m, 1 H, H-3), 4.07 (dd, 1 H, *J* 3.2 and 1.2 Hz, H-2), 6.77 (dd, 1 H, *J* 2.0 and 1.0 Hz, H-6); $^{13}$C NMR (75.4 MHz, $CDCl_3$): 25.6 (C-4), 42.6 ($NCH_3$), 56.4 ($OCH_3$), 61.8 (C-3), 73.1 (C-5), 89.4 (C-2), 122.1 (CN), 145.2 (C-6). HRMS (e.i.) *m/z*: calc. 168.0899, found 168.0902. For **5** (major stereoisomer, *trans*): $^1$H NMR (300 MHz, $CDCl_3$) 2.33 (dd, 1 H, *J* 15.6 and 6.7 Hz, H-4), 2.43 (s, 3 H, $CH_3$), 2.50 (dd, 1 H, *J* 15.6 and 4.0 Hz, H-4), 2.81 (s, 3 H, $NCH_3$), 4.20 (ddd, 1 H, *J* 6.7, 5.4 and 4.0 Hz, H-3), 4.30 (d, 1 H, *J* 5.4 Hz, H-2), 7.02 (s, 1 H, H-6), 7.07–7.20 (m, 2 H, H-5 and H-6 indole), 7.33 (d, 1 H, *J* 8.0 Hz, H-7 indole), 7.47 (d, 1 H, *J* 7.7 Hz, H-4 indole), 8.10 (br s, 1 H, NH); $^{13}$C NMR (75.4 MHz, $CDCl_3$) 11.8 ($CH_3$), 28.3 (C-4), 40.9 ($NCH_3$), 60.6 (C-2), 66.4 (C-3), 69.2 (C-5), 108.0 (C-3 indole), 110.6 (C-7 indole), 117.8 (C-4 indole), 119.8 (C-6 indole), 120.0 (CN), 121.6 (C-5 indole), 122.2 (C-3a indole), 134.5 (C-2 indole), 136.1 (C-7a indole), 148.5 (C-6). HRMS (e.i.) *m/z*: calc. 267.1372, found 267.1381. For **6** (major stereoisomer): $^1$H NMR (300 MHz, $CDCl_3$): 1.97 (ddd, 1 H, *J* 13.7, 7.5 and 2.9 Hz, H-3), 2.40 (m, 1 H, H-3), 2.47 (m, 2 H, H-7), 2.92 (s, 3 H, $NCH_3$), 3.35 (s, 3 H, $OCH_3$), 3.55 (m, 1 H, H-3a), 4.25 (m, 1 H, H-7a), 5.02 (dd, 1 H, *J* 5.9 and 2.9 Hz, H-2), 6.72 (s, 1 H, H-5); $^{13}$C NMR (75.4 MHz, $CDCl_3$) 25.5 (C-7), 36.6 (C-3), 40.8 ($NCH_3$), 55.4 ($OCH_3$), 57.1 (C-3a), 73.5 (C-7a), 79.9 (C-6), 104.0 (C-2), 123.1 (CN), 147.1 (C-5). HRMS (e.i.) *m/z*: calc. 194.1055, found 194.1060. For **7** (major stereoisomer, *trans*): $^1$H NMR (300 MHz, $CDCl_3$) 2.30 (ddd, 1 H, *J* 16.8, 2.6 and 2.3 Hz, H-4), 2.75 (ddd, 1 H, *J* 16.8, 3.6 and 2.0 Hz, H-4), 3.08 (s, 3 H, $NCH_3$), 3.98 (dd, 1 H, *J* 2.6 and 2.3 Hz, H-2), 4.39 (m, 1 H, H-3), 6.77 (d, 1 H, *J* 2.0 Hz, H-6); $^{13}$C NMR (75.4 MHz, $CDCl_3$) 27.2 (C-4), 41.3 ($NCH_3$), 52.7 (C-2), 63.2 (C-3), 76.3 (C-5), 115.4 (CN), 120.7 (CN), 145.9 (C-6). HRMS (e.i.) *m/z*: calc. 163.0746, found 163.0746.

## References

1 For reviews on the chemistry of dihydropyridines, see: U. Eisner and J. Kuthan, *Chem. Rev.*, 1972, **72**, 1; D. M. Stout and A. I. Meyers, *Chem. Rev.*, 1982, **82**, 223.

2 R. Lavilla, T. Gotsens, M. Guerrero and J. Bosch, *Synthesis*, 1995, 382 and references cited therein.

3 R. Lavilla, T. Gotsens, F. Gullón and J. Bosch, *Tetrahedron*, 1994, **50**, 5233; M.-L. Bennasar, B. Vidal, A. Lázaro, R. Kumar and J. Bosch, *Tetrahedron Lett.*, 1996, **37**, 3541.

4 M.-L. Bennasar, B. Vidal and J. Bosch, *J. Chem. Soc., Chem. Commun.*, 1995, 125; M.-L. Bennasar, B. Vidal and J. Bosch, *J. Org. Chem.*, 1995, **60**, 4280.

5 M.-L. Bennasar, B. Vidal and J. Bosch, *J. Am. Chem. Soc.*, 1993, **115**, 5340; M.-L. Bennasar, B. Vidal and J. Bosch, *J. Org. Chem.*, 1996, **61**, 1916.

6 L. A. Negievich, O. M. Grishin and A. A. Yasnikov, *Ukr. Khim. Zh.*, 1968, **34**, 684 (*Chem. Abstr.*, 1969, **70**, 11513); L. A. Negievich, O. M. Grishin and A. A. Yasnikov, *Ukr. Khim. Zh.* 1968, **34**, 802 (*Chem. Abstr.*, 1969, **70**, 28776).

7 For a 4 + 2 cycloaddition involving *N*-acyl-1,2-dihydropyridines and singlet oxygen, see: M. Natsume, Y. Sekine, M. Ogawa, H. Soyagimi and Y. Kitagawa, *Tetrahedron Lett.*, 1979, 3476; for the osmylation of *N*-acyl-1,2-dihydropyridines, see: T. Tschamber, F. Backenstrass, M. Neuburger, M. Zehnder and J. Streith, *Tetrahedron*, 1994, **50**, 1135.

8 J. K. Crandall, in *Encyclopedia of Reagents for Organic Synthesis*, ed. L. A. Paquette, Wiley, Chichester, 1995, vol. 3, p. 2061; W. Adam, R. Curci and J. O. Edwards, *Acc. Chem. Res.*, 1989, **22**, 205; R. W. Murray, *Chem. Rev.*, 1989, **89**, 1187.

9 W. Adam, E.-M. Peters, K. Peters, H.-G. von Schnering and V. Voerckel, *Chem. Ber.*, 1992, **125**, 1263; W. Adam, M. Ahrweiler, K. Paulini, H.-U. Reissig and V. Voerckel, *Chem. Ber.*, 1992, **125**, 2719; L. E. Burgess, E. K. M. Gross and J. Jurka, *Tetrahedron Lett.*, 1996, **37**, 3255.

10 W. Adam, M. Heil and R. Hutterer, *J. Org. Chem.*, 1992, **57**, 4491.

11 M. E. Brewster, A. Simay, K. Czako, D. Winwood, H. Farag and N. Bodor, *J. Org. Chem.*, 1989, **54**, 3721.

12 D. Yang, M.-K. Wong and Y.-C. Yip, *J. Org. Chem.*, 1995, **60**, 3887.

13 For related structures, see: B. Koppenhoefer, W. Winter and E. Bayer, *Liebigs Ann. Chem.*, 1983, 1986; W. Adam, K. Peters and M. Sauter, *Synthesis*, 1994, 111; C. Agami, F. Couty, L. Hamon, B. Prince and C. Puchot, *Tetrahedron*, 1990, **46**, 7003; W. Adam, D. Reinhardt, H.-U. Reissig and K. Paulini, *Tetrahedron*, 1995, **51**, 12257.

14 DMD solutions were prepared according to W. Adam, J. Bialas and L. Hadjiarapoglou, *Chem. Ber.*, 1991, **124**, 2377, and the dioxirane content (*ca.* 0.07 M) was determined by iodometric titration.

*Received, 9th October 1996; Com. 6/06919C*

# Stabilization of neutral oxophlorin π-radicals by bulky meso-alkyl groups

**Richard G. Khoury,[a] Laurent Jaquinod,[a] Amy M. Shachter,[b] Nora Y. Nelson[a] and Kevin M. Smith*[a]†**

[a] *Department of Chemistry, University of California, Davis, CA 95616, USA*
[b] *Department of Chemistry, Santa Clara University, Santa Clara, CA 95053, USA*

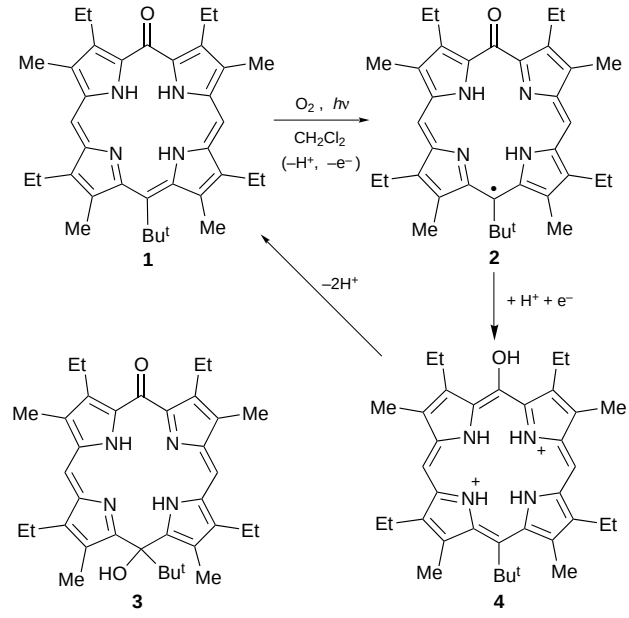
**The 15-*tert*-butyl-5-oxophlorin 1 forms a stable, neutral π-radical species 2, in high yield; the 13,17-bis-unsubstituted 5-oxophlorin analogue 5, under similar conditions, affords the 15-iso-5-oxophlorin 6 and 15-hydroxy compound 7 (both characterized by X-ray crystallography), the latter demonstrating the trapping of the π-radical by dioxygen.**

The syntheses and chemistry of tetrapyrrole π-free-radicals is one of the few fields of porphyrin chemistry which remains relatively undeveloped. It is also a fact that the preparation of other stable and useful π-radicals are found only infrequently in the literature. Published work on π-radicals has focused on the study of their electronic structure,[1] their use to create charge transfer species in molecular conductors,[2] their use in synthesis[3] and their involvement in biological systems.[4] Compounds such as quinones and related compounds play important roles as mediators in some electron-transfer processes which occur in mitochondria and in chloroplasts. Radicals also react with transition metal ions that have appropriate reduction potentials.[4] In biological systems, haemes in haemoglobin and myoglobin are degraded to bile pigments *via* a key intermediate, suspected to be a meso-oxyporphyrin π-neutral radical or an oxophlorin radical species reacting quickly with $O_2$.[4,5] In 1975, studies by Fuhrhop and co-workers showed that oxophlorins and their metal complexes are oxidized at low potentials yielding fairly unstable neutral π-radicals which underwent a variety of secondary reactions to generate, for instance, 5,15-dioxoporpho-10,20-dimethenes.[6] Examples of radical dimerizations of oxophlorins at the 15-positions[6] led us to believe that the meso-15-position has unique chemical reactivity.[5] We showed that electronic and steric features at the 15-position enable one to exert control over the oxidation potential of the oxophlorin, and direct a novel dimerization process to the 10-position, a phenomenon which has been used for the reversible self-assembly of a cyclic tetra-oxophlorin.[7] In order to further investigate the chemical properties associated with 15-meso-substituents, we targeted 15-*tert*-butyl-5-oxophlorins in the hope that radical formation and stabilization would take place at the 15-position.

MacDonald-type (*i.e.* 2 + 2) condensation of 1,9-diformyl-5-oxodihydrodipyrrin[8] with 5-*tert*-butyl-2,8-diethyl-3,7-dimethyldihydrodipyrrin-1,9-dicarboxylic acid‡ followed by basic treatment resulted in formation of the 15-*tert*-butyl-5-oxophlorin **1** in 43% yield. Exposure of compound **1** to air in $CH_2Cl_2$ and daylight (which accelerated the transformation) afforded the neutral π-radical **2** of 15-*tert*-butyl-5-oxophlorin§ in 90% yield. This compound possesses a Soret band at 410 nm and a typical organic π-radical EPR signal at 3000 G. The magnetic susceptibility of **2**, measured by the NMR Evans method[9] is $\mu_{eff}$ = 2.5 $\mu_B$ at 297 K, indicating that the compound exists entirely in the form of the neutral π-radical.[4]¶ This oxophlorin radical is stable to air for long periods of time in the solid form. It was found to be fairly stable in solution, showing only about 30% decomposition over two weeks in the presence of oxygen (to form 15-*tert*-butyl-15-hydroxy-5-oxophlorin **3**). Addition of acid to a $CH_2Cl$ solution of **2** generated, *via* the readily reduced π-cation porphyrin radical,[10] the diprotonated hydroxyporphyrin **4** (Scheme 1). This reduction–protonation process could be followed by spectrophotometry, which showed clean isobestic points (at $\lambda_{max}$ = 438 and 540 nm), furthermore demonstrating the quantitative radical character of **2**.

Fuhrhop had earlier demonstrated that the spin density distribution in 5-oxophlorin radicals lies predominately on the carbon atom at the 15-position.[6] By analogy, the free radical in **2** is also believed to be localized preferentially at the 15-position where it can be stabilized by hyperconjugation through the *tert*-butyl substituent.

In order to establish the effect of steric congestion upon the radical formation resulting from the interaction of the 15-substituent with abutting groups in the 13- and 17- positions, synthesis of 12,13,17,18-unsubstituted-15-*tert*-butyl-5-oxophlorin **5** was attempted using the same pathway as described for **1**.‖ This synthesis, however, yielded two products neither of which was a π-radical. The first product was characterized as 15-*tert*-butyl-15-iso-5-oxophlorin **6**** and the second was shown to be the 15-*tert*-butyl-15-hydroxy derivative **7**.†† Structure **7** presents evidence for the trapping of the π-radical at the 15-position (presumably by dioxygen) and further indicates the preferential localization of the radical at this position. A 15-peroxo bis(5-oxophlorin) derivative has been proposed earlier by Fuhrhop *et al.*[6a] The molecular structures of **6**‡‡ and **7**‡‡ were confirmed by X-ray crystallography (Fig. 1). Both macrocycles exhibit a slightly ruffled conformation with a mean deviation from there least-squares plane for the 24 core atoms of 0.263 Å for compound **6** and of 0.257 Å for compound **7**. The C=O bond length for structures **6** and **7** are 1.239 and 1.242 Å, respectively, in good agreement with expected C=O bonds lengths. For compound **7** the C–O bond length in the 15-position is 1.455 Å which is also in agreement with expected normal C–O bond lengths.




**Scheme 1**

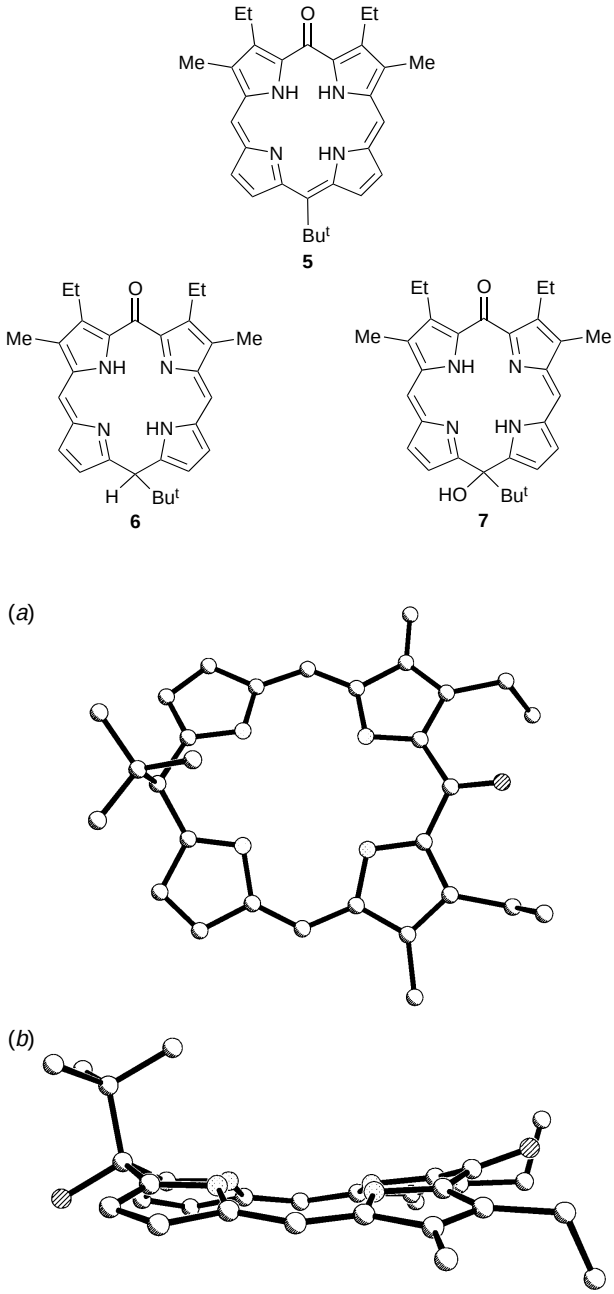



**Fig. 1** Molecular structure of (*a*) 15-*tert*-butyl-15-iso-5-oxophlorin **6** and (*b*) 15-*tert*-butyl-15-hydroxy derivative **7**

This work was supported by a grant from the National Science Foundation (CHE-96-23117). Mass spectrometric analyses were performed by the University of California, San Francisco, Mass Spectrometry Facility (A. L. Burlingame, Director) supported by the Biomedical Research Technology Program of the National Center of Research Resources, NIH NCRR BRTP 01614.

## Footnotes

† E-mail: smith@chem.ucdavis.edu

‡ Prepared by acidic condensation of trimethylacetaldehyde (TMA) with 2 equiv. of the corresponding α-free-pyrrole benzyl ester (K-10 clay catalyst, $CH_2Cl_2$–TFA (5 : 1), room temp., 4 d, chromatographed on silica gel eluted with $CH_2Cl_2$, deprotection with Pd-C/$H_2$, overall yield 35%).

§ Mp 180–182 °C. UV–VIS $\lambda_{max}(CH_2Cl_2)$/nm 410 (ε 66 700), 628 (11 700), 664 (11 000). $^1$H NMR (300 MHz, $CDCl_3$–[$^2$H]TFA) δ 1.48 (s, 9 H, Bu$^t$), 1.56 (t, 6 H, $CH_2CH_3$), 1.69 (t, 6 H, $CH_2CH_3$), 3.26 (s, 6 H, $CH_3$), 3.43 (s, 6 H, $CH_3$), 3.89 (m, 8 H, $CH_2CH_3$), 10.06 (s, 2 H, meso-H). MS: *m/z* 550.

¶ The magnetic susceptibility of the free radical was determined using Evans method.[9] Paramagnetic shifts of tetramethylsilane were determined for 2-4 × $10^{-3}$ M free radical solutions in chloroform and were obtained on a JEOL GSX 400 MHz ($^1$H NMR) spectrometer. At 24 °C, the molar magnetic susceptibility was 2.6 × $10^{-3}$ $cm^{-3}$ $mol^{-1}$ and the calculated magnetic moment was 2.5 $\mu_B$. Diamagnetic corrections were estimated from Pascal's constants.

‖ The 5-*tert*-butyl-3,7-di-unsubstituted half was prepared by condensation of TMA with 40 equiv. of pyrrole catalysed by TFA.[11]

** Mp 280–285 °C. UV–VIS $\lambda_{max}(CH_2Cl_2)$/nm 420 (ε 86 000), 644 (14 000). $^1$H NMR (300 MHz, $CDCl_3$) δ 0.83 (m, 6 H, $CH_2CH_3$), 1.25 (s, 9 H, Bu$^t$), 2.17 (s, 6 H, $CH_3$), 2.76 (m, 4 H, $CH_2CH_3$), 3.92 (s, 1 H, 15-meso H), 6.39 (s, 2 H, β-H), 6.81 (s, 2 H, β-H), 6.94 (s, 2 H, meso-H), 12.89 (br s, 2 H, NH). MS: *m/z* 467.

†† Mp 244–246 °C. UV–VIS $\lambda_{max}(CH_2Cl_2)$/nm 448 (ε 66 000), 510 (11 500). $^1$H NMR (300 MHz, $CDCl_3$) δ 1.04 (m, 6 H, $CH_2CH_3$), 1.53 (s, 9 H, Bu$^t$), 2.15 (s, 6 H, $CH_3$), 2.78 (m, 4 H, $CH_2CH_3$), 6.65 (s, 2 H, β-H), 6.84 (s, 2 H, β-H), 6.97 (s, 2 H, meso-H), 12.95 (br s, 2 H, NH). MS: *m/z* 483.

‡‡ *Crystal Data* for **6**: single crystals (purple) crystallized from MeOH–THF–$H_2O$, triclinic space group *P*$\bar{1}$, cell dimensions: *a* = 9.765(2), *b* = 11.719(2), *c* = 12.013(2) Å, α = 83.70(3), β = 68.72(3), γ = 81.20(3)°, *V* = 1263.8(4) Å$^3$, *Z* = 2. X-Ray diffraction data were collected at 130(2) K, λ(Cu-Kα) = 1.54178 Å, θ/2θ scan mode to $2\theta_{max}$ = 114°. Of 4882 reflections measured (±*h*,±*k*,+*l*), 3404 were unqiue and 2425 had $I > 2\sigma$. The structure was solved by direct methods and refined on $F^2$ using all data by full-matrix least-squares methods (SHELXL-94). Final *R* factors for observed data are *R* = 0.0569 and w*R*2 (all data) = 0.1472. For **7**: single crystals (green) crystallized from MeOH–THF–$H_2O$, triclinic space group *P*$\bar{1}$, cell dimensions: *a* = 10.154(2), *b* = 11.344(2), *c* = 12.285(2) Å, α = 82.63(3), β = 66.93(3), γ = 78.37(3)°, *V* = 1273.3(4) Å$^3$ and *Z* = 2. X-Ray diffraction data were collected at 130(2) K, λ(Cu-Kα) = 1.54178 Å, θ/2θ scan mode to $2\theta_{max}$ = 114°. Of 3707 reflections measured (±*h*,±*k*,+*l*), 2365 were unique and 1833 had $I > 2\sigma$. The structure was solved by direct methods and refined (based on $F^2$ using all data) by full-matrix least-squares methods (SHELXL-94). Final *R* factors for observed data are *R* = 0.0615 and w*R*2 (all data) = 0.1662. Atomic coordinates, bond lengths and angles, and thermal parameters have been deposited at the Cambridge Crystallographic Data Centre (CCDC). See Information for Authors, Issue No. 1. Any request to the CCDC for this material should quote the full literature citation and the reference number 182/332.

## References

1 C. Adamo, V. Barone and A. Fortunelli, *J. Chem. Phys*., 1995, **102**, 384; A. Hudson, D. Waterman and A. Alberti, *J. Chem. Soc., Perkin Trans. 2*, 1995, 2091.
2 C. D. Bryan, A. W. Cordes, R. M. Fleming, N. A. George, S. H. Glarum, R. C. Haddon, R. T. Oakly, T. T. M. Palstra, A. S. Perel, L. F. Schneemeyer and J. V. Waszczak, *Nature*, 1993, **365**, 821; D. Luneau, J. Laugier, P. Rey, G. Ulrich, R. Ziessel, P. Legoll and M. Drillon, *J. Chem. Soc., Chem. Commun*., 1994, 741; A. W. Cordes, R. C. Haddon and R. T. Oakley, *Adv. Mater*., 1994, **6**, 798.
3 A. F. Fontan, R. J. Kolt, Y. Q. Huang and D. D. M. Wayner, *J. Org. Chem*., 1994, **59**, 4671.
4 E. I. Ochiai, *J. Chem. Educ*., 1993, **70**, 128; I. Morishima, H. Fujii and Y. Shiro, *Inorg. Chem*., 1995, **34**, 1528.
5 A. H. Jackson, G. W. Kenner and K. M. Smith, *J. Chem. Soc. (C)*, 1968, 302; R. G. Khoury, L. Jaquinod, D. J. Nurco and K. M. Smith, *Chem. Commun*., 1996, 1143.
6 J.-H. Fuhrhop, S. Besecke, J. Subramanian, C. Mengersen, D. Riesner and D. Mauzerall, *J. Am. Chem. Soc*., 1975, **97**, 7141; A. L. Balch, B. C. Noll, S. L. Phillips, S. M. Reid and E. P. Zovinka, *Inorg. Chem*., 1993, **32**, 4730.
7 R. G. Khoury, L. Jaquinod, D. J. Nurco, R. K. Pandey, M. O. Senge and K. M. Smith, *Angew. Chem*., 1996, **108**, 2657.
8 P. S. Clezy, A. J. Liepa and G. A. Smythe, *Aust. J. Chem*., 1970, **23**, 589, 603.
9 D. F. Evans, *J. Chem. Soc*., 1959, 2003.
10 D. C. Borg, J. Fajer, R. H. Felton and D. Dolphin, *Proc. Natl. Acad. Sci. USA*, 1970, **67**, 813.
11 C. H. Lee and J. S. Lindsey, *Tetrahedron*, 1994, **39**, 11427.

*Received, 17th October 1996; Com. 6/07076K*

# Macropolyhedral boron-containing cluster chemistry: isolation and characterization of twenty-one-vertex $[(PMe_2Ph)_3HReB_{20}H_{15}Ph(PHMe_2)]$

**Pervinder Kaur,[a] Sarath D. Perera,[a]† Tomáš Jelínek,[a,b] Bohumil Stíbr,[b] John D. Kennedy,[a] William Clegg[c] and Mark Thornton-Pett[a]**

[a] *School of Chemistry of the University of Leeds, Leeds, UK LS2 9JT*
[b] *Institute of Inorganic Chemistry of the Czech Academy of Sciences, 25068 Rez, The Czech Republic*
[c] *Department of Chemistry of the University of Newcastle, Newcastle-upon-Tyne, UK NE1 7RU*

**Reaction of $B_{20}H_{16}$ with $[ReH_5(PMe_2Ph)_3]$ yields the twenty-one-vertex metallaborane $[(PMe_2Ph)_3HReB_{20}H_{15}Ph(PHMe_2)]$ which consists of a *closo* twelve-vertex $\{B_{12}\}$ unit and a *nido* eleven-vertex $\{B_{11}\}$ unit fused with a common triangular face, with the $\{(PMe_2Ph)_3HRe\}$ moiety capping *exo* to the *nido* $\{B_{11}\}$ unit with three Re–H–B bonds; an unusual reductive P-phenyl cleavage of a $PMe_2Ph$ moiety to give B-pendant *exo* $PHMe_2$ and *exo* Ph moieties on the open face of the eleven-vertex subcluster is also apparent.**

The extension of the contiguous cluster chemistry of polyhedral boron-containing compounds beyond about fourteen vertices into the so-called 'macropolyhedral' area requires either fusion chemistry of smaller clusters[1] or Aufbau chemistry on pre-formed macropolyhedral species. Aufbau reactions to incorporate metal centres into the two accessible isomers of $B_{18}H_{22}$ yield nineteen- and twenty-vertex metallaboranes,[2,3] but to use this approach for even bigger clusters requires bigger contiguous starting substrates. The next highest known contiguous binary borane, $B_{20}H_{16}$,[4] is very difficult to come by. Its bis(ligand) adduct formation was investigaterd some 30 years ago,[5,6] as well as some related hydrolysis and alcoholysis behaviour,[6] but any further chemistry is unexamined since then. We have now isolated small quantities of $B_{20}H_{16}$ from crude $B_{10}H_{14}$,[7] and here report preliminary results from its reaction with $[ReH_5(PMe_2Ph)_3]$ to generate the large, twenty-one-vertex, contiguous metallaborane $[(PMe_2Ph)_3HReB_{20}H_{15}Ph(PHMe_2)]$.

Reaction of $[ReH_5(PMe_2Ph)_3]$ (83 mg; 138 μmol) and $B_{20}H_{16}$ (32 mg; 138 μmol) in solution in $C_6H_6$ (7 $cm^3$) at reflux for 60 min, followed by chromatographic separation, revealed several coloured reaction products. Of these, two are identifiable as rhenaborane products in yields that are viable for further examination on this reaction scale. Repeated thin-layer chromatography [silica gel G (Fluka $GF_{254}$), $CH_2Cl_2$–$C_6H_{14}$ mixtures] and repeated recrystallization has now ultimately given one of these, $[(PMe_2Ph)_3HReB_{20}H_{15}Ph(PHMe_2)]$, as a pure, yellow, crystalline solid [4 mg; 5.5 μmol; 4% ($R_f$ 0.46, $CH_2Cl_2$–$C_6H_{14}$ 80 : 20)]. Crystals suitable for single-crystal X-ray work have been exceedingly difficult to grow. Ultimately (eleven months) one was obtained of suitable size for CCD work (Fig. 1 and schematic cluster structure **I**).‡ The results from the X-ray structural analysis are consistent with the results from NMR spectroscopy of the bulk material.§ The basic cluster structure is based on a *nido* eleven-vertex subcluster and a *closo* twelve-vertex subcluster fused with a common triangular three-boron face (schematics **I** and **II**). This twenty-vertex geometry is similar to those (*a*) of the bis(ligand) adducts of $B_{20}H_{16}$ such as $[B_{20}H_{16}(MeCN)_2]$[5] and (*b*) of $[(PMe_2Ph)_4Pt_2B_{18}H_{16}]$[2] formed *via* oxidative Aufbau from $B_{18}H_{22}$. These three incidences may suggest a particular stability of this twelve-vertex: eleven-vertex *closo* : *nido* structural format. In $[(PMe_2Ph)_3HReB_{20}H_{15}Ph(PHMe_2)]$ the twenty-first vertex is provided by the capping of a closed triangular three-boron face of the *nido*

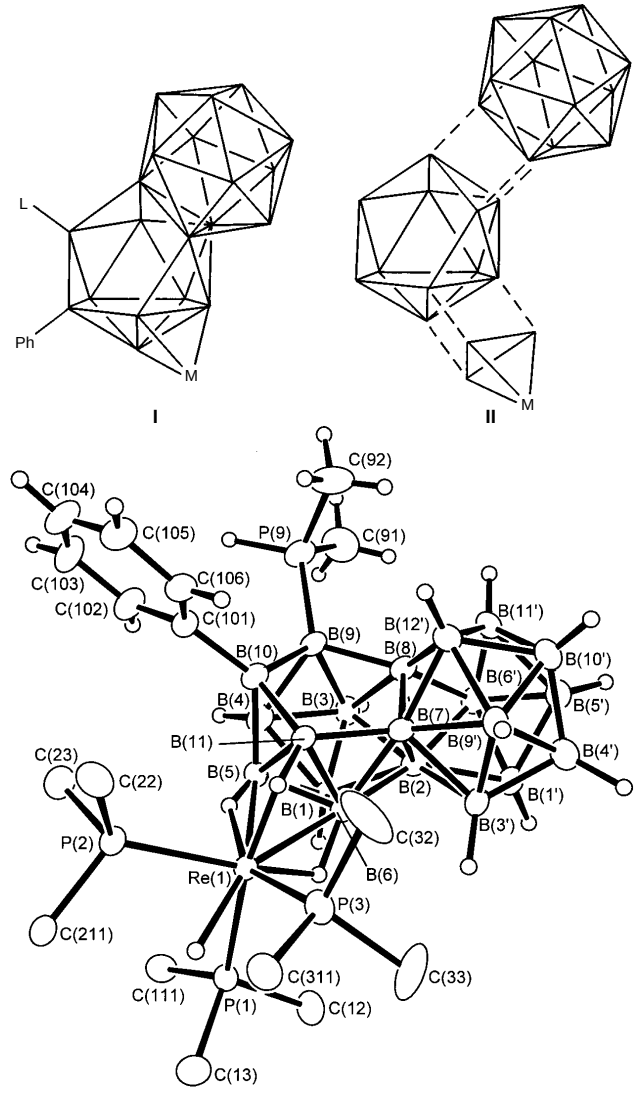



**Fig. 1** ORTEP-type diagram of the molecular structure of $[(PMe_2Ph)_3HReB_{20}H_{15}Ph(PHMe_2)]$. Selected distances (in Å) are as follows: from Re(1) to P(1) 2.3533(14), to P(2) 2.351(2), to P(3) 2.374(2), to B(5) 2.376(6), to B(6) 2.3561(7) and to B(11) 2.447(6); interboron B(2)–B(7) 1.800(9), B(2)–B(8) 1.772(9), B(7)–B(8) 1.841(10), B(8)–B(9) 1.756(9), B(9)–B(10) 1.736(9), B(10)–B(11) 1.748(9), B(7)–B(11) 1.755(9); B(2)–B(3) is long at 1.991(9), with the other interboron distances in the range 1.712(9)–1.914(9) for the *nido* subcluster and 1.729(11)–1.819(10) for the *closo* subcluster; shorter intercluster distances are B(3)–B(6′) 2.409(10) and B(3′)–B(6) 2.367(9); B(9)–P(9) is 1.888(7) and B(10)–C(101) 1.589(8). Selected angles (in °) at Re(1) are P(1)–P(2) 100.90(5), P(2)–P(3) 104.14(6), P(1)–P(3) 108.52(6), P(1)–H(12) 68.17(4), P(2)–H(12) 64.09(4) and P(3)–H(12) 65.61(4).

eleven-vertex subcluster by a $\{(PMe_2Ph)_3HRe\}$ centre *via* three B–H(*exo*)–Re linkages. This latter type of linkage has predecent in $[(PPh_3)_2ClRuB_{12}H_{11}(NEt_3)]$,[8] and, in Group VII chemistry, $[(CO)_3MnB_8H_{14}]$ and $[(CO)_3MnB_3H_8]$.[9] In sum, the twenty-one-vertex contiguous cluster structure is based upon a triple-cluster unit consisting of a central eleven-vertex $\{B_{11}\}$ *nido* subcluster conjoined by a common three-boron triangular face to a *closo* twelve-vertex $\{B_{12}\}$ subcluster and by a second common three-boron triangular face to a *nido*-type four-vertex $\{ReB_3\}$ subcluster (schematic **II**).

The compound has several other interesting features: (*a*) at twenty-one vertices it is the largest molecular contiguous boron-containing cluster yet characterized; (*b*) the twelve-vertex-*closo* : eleven-vertex-*nido* double-subcluster format with three-atoms-in-common appears to be a stable one; (*c*) the rhenium centre bonds *exo–nido*, rather than *endo* to form a *closo* cluster (there is contemporary interest[10] in this type of boron-to-metal bonding and the factors that may influence it); (*d*) the reductive P–phenyl cleavage of a $PMe_2Ph$ moiety and (*e*) the concomitant phenyl transfer to boron are both very unusual, and the compound may therefore model intermediates for the formation of $[(PH_3)_2(Ph_2PC_6H_4)IrB_9H_7(PPh_3)]$ *via* a so-far unique complete reductive $PAr_3 \rightarrow PH_3$ cleavage,[11] and for the formation of $[(CO)(PPh_3)(PPh_2)Os(PPh_3)PtB_5H_7Ph]$ *via* a phosphorus-to-boron phenyl-group transfer.[12] There is clearly much interesting chemistry to be revealed by the further examination of this and other related twenty-boron systems, and we currently attempt to do this.

Contribution no 57 from the Rez–Leeds Anglo–Czech Polyhedral Collaboration (ACPC). We thank the EPSRC (UK), the Czech Grant Agency, the Academy of Sciences of the Czech Republic, and the Royal Society for support, and Simon Barrett and Jonathan Vessey for assistance with NMR spectroscopy.

## Footnotes

† Present address: Department of Chemistry, The Open University of Sri Lanka, Nawala, Nugegoda, Sri Lanka.

‡ *Crystal data* for $[(PMe_2Ph)_3HReB_{20}H_{15}Ph(PHMe_2)]\cdot CHCl_3$: $C_{33}H_{62}B_{20}Cl_3P_4Re$, $M$ = 1091.58 (includes solvent), triclinic, space group $P\bar{1}$, $a$ = 12.8286(9), $b$ = 14.2985(10), $c$ = 15.4090(10) Å, $\alpha$ = 113.369(2)°, $\beta$ = 99.955(2)° $\gamma$ = 93.486(2)°, $U$ = 2529.2(3) Å$^3$, $Z$ = 2, $D_c$ = 1.43 Mg m$^{-3}$, $F(000)$ = 1092, $\mu$ = 2.577 mm$^{-1}$, $T$ = 160 K; crystal size 0.40 × 0.10 × 0.10 mm. 15960 reflections were measured on a Siemens SMART CCD area detector using graphite-monochromated Mo-K$\alpha$ radiation and narrow $\omega$-rotation frames. Data were corrected for absorption empirically using redundant and symmetry equivalent data. The structure was solved by heavy-atom methods[13] and was refined by full-matrix least-squares analysis on $F^2$ using all 11092 unique reflections ($R_{int}$ = 0.0421).[14] $wR = \{\Sigma[w(F_o^2 - F_c^2)^2]/\Sigma[w(F_o^2)^2]\}^{\frac{1}{2}}$ = 0.1001 for all data, conventional $R$ [on $F$ values of 9360 reflections with $F_o^2 > 2\sigma(F_o^2)$] = 0.0485, goodness of fit $S$ = 1.134 on all $F^2$ for 610 parameters. All non-hydrogen atoms were refined with anisotropic displacement parameters. Methyl, phenyl and methine hydrogen atoms were constrained to idealised positions with fixed isotropic displacement parameters of $nU_{eq}$ of the parent carbon atom (where $n$ = 1.5 for methyl and 1.2 for phenyl and methine). All other hydrogen atoms were located on Fourier difference syntheses and were freely refined apart from those hydrogen atoms bonded to rhenium which were not refined. Atomic coordinates, bond lengths and angles, and thermal parameters have been deposited at the Cambridge Crystallographic Data Centre (CCDC). See Information for Authors, Issue No. 1. Any request to the CCDC for this material should quote the full literature citation and the reference number 182/312.

§ Measured NMR data ($CDCl_3$) as follows (294–297 K) {ordered as $\delta(^{11}B)$ (in ppm rel. $F_3BOEt_3$) [$\delta(^1H)$ (in ppm rel. $SiMe_4$) of directly bound *exo* hydrogen atoms in square brackets]: +23.6 [no *exo*-H], +7.1 [+3.43], *ca.* +0.5 [+2.37], *ca.* +0.5 [+4.08], −1.5 [+2.50], −4.2 [+2.79], −4.7 [−6.53, ReHB bridge], −6.3 [+2.13], −8.0 [+1.96], −11.2 [no *exo*-H], −14.2 [+1.38], −15.0 [+1.54], −17.6 [+2.08], *ca.* −18.0 [no *exo*-H], *ca.* −18.5 [+1.55], *ca.* −18.6 [no *exo*-H], −19.2 [−8.30, ReHB bridge], −28.4 [no *exo*-H], −33.3 [+1.02], −36.2 [−5.66, ReHB bridge]; additionally $\delta(^1H)$(ReH) −6.27 [1 : 2 : 1 t, $^2J(^{31}P–^1H)$(mean) 60 Hz of 1 : 1 d, $^2J(^{31}P–^1H)$ 46 Hz], $\delta(^1H)$(PH) + 4.94 [d, $^1J(^{31}P–^1H)$ 394 Hz of m, $^3J(^1H–C–P–^1H)$(mean) 6 Hz], $\delta(^1H)$(PMe)($PHMe_2$) + 1.23 and +1.38 [for both, $^2J(^{31}P–^1H)$ *ca.* 13 Hz, $^3J(^1H–P–C–^1H)$ *ca.* 6 Hz], $\delta(^1H)$(PMe)($PMe_2Ph$) + 2.07, +1.91, +1.90, +1.77, +1.76 and +1.72 [one tentative, all $^2J(^{31}P–^1H)$ *ca.* 9–10 Hz], $\delta(^{31}P)$ (in ppm rel. 85% $H_3PO_4$) (223 K) −18.3 (sharp), −20.0 (sharp), −20.3 (sharp) and −30.9 (br, $PHMe_2$ group).

## References

1 For recent references see: T. Jelínek, J. D. Kennedy and B. Štíbr, *J. Chem. Soc., Chem. Commun*., 1994, 1415; P. Kaur, J. Holub, N. P. Rath, J. Bould, L. Barton, B. Štíbr and J. D. Kennedy, *Chem. Commun*., 1996, 273; L. Barton, J. Bould, J. D. Kennedy and N. P. Rath, *J. Chem. Soc., Dalton. Trans*., 1996, 3145.

2 Y. M. Cheek, N. N. Greenwood, J. D. Kennedy and W. S. McDonald, *J. Chem. Soc., Chem. Commun*., 1982, 80.

3 X. L. R. Fontaine, N. N. Greenwood, J. D. Kennedy, P. MacKinnon and M. Thornton-Pett, *J. Chem. Soc., Chem. Commun*., 1986, 1111.

4 L. B. Friedman, R. D. Dobrott and W. N. Lipscomb, *J. Am. Chem. Soc*., 1963, **85**, 3505; N. E. Miller and E. L. Muetterties, *J. Am. Chem. Soc*., 1963, **85**, 3506; R. D. Dobrott, L. B. Friedman and W. N. Lipscomb, *J. Chem. Phys*., 1964, **40**, 866.

5 J. Enemark, L. B. Friedman, J. A. Hartsuck and W. N. Lipscomb, *J. Am. Chem. Soc*., 1966, **88**, 3659.

6 N. E. Miller, J. A. Forstner and E. L. Muetterties, *Inorg. Chem*., 1964, **3**, 1690.

7 S. A. Barrett, P. N. Condick, X. L. R. Fontaine, M. A. Fox, R. Greatrex, T. Jelínek, P. Kaur, J. D. Kennedy, P. MacKinnon and B. Štíbr, *J. Chem. Soc., Dalton Trans*., submitted.

8 M. Elrington, N. N. Greenwood, J. D. Kennedy and M. Thornton-Pett, *J. Chem. Soc., Dalton Trans*., 1987, 415.

9 J. C. Calabrese, M. Fischer, D. F. Gaines and J. W. Lott, *J. Am. Chem. Soc*., 1974, **96**, 6318; S. J. Hildebrandt, D. F. Gaines and J. Calabrese, *Inorg. Chem*., 1978, **17**, 790; see also D. F. Gaines, M. Fischer, S. J. Hildebrandt, J. Calabrese and J. W. Lott, in *Inorganic Compunds with Unusual Properties*, Advances in Chemistry Series, 150, ed. R. B. King, American Chemical Society, Washington, DC, 1976, ch. 26, pp. 311–317.

10 See, for example, together with references therein: F. Teixidor, J. A. Ayllón, C. Viñas, R. Kivekäs, R. Sillanpää and J. Casabó, *Organometallics*, 1994, **13**, 2751; C. Viñas, R. Nuñek, M. A. Flores, F. Teixidor, R. Kivekäs and R. Sillanpää, *Organometallics*, 1995, **14**, 3952; I. Chisevsky, P. V. Petrovsky, P. V. Sorokin, V. I. Bregadze, F. M. Dolgushin, A. I. Yanovsky, Y. T. Struchkov, A. Demonceau and A. F. Noels, *Organometallics*, 1996, **15**, 2619; N. S. Hosmane, Y. Wang, A. R. Oki, H. Zhang and J. A. Maguire, *Organometallics*, 1996, **15**, 626. See also: F. Teixidor, J. A. Ayllón, C. Viñas, R. Kivekäs, T. Sillanpää and J. Casabó, *J. Chem. Soc., Chem. Commun*., 1992, 1281; J. D. Kennedy, *J. Chem. Soc., Dalton Trans*., 1993, 2545.

11 J. Bould, P. Brint, X. L. R. Fontaine, J. D. Kennedy and M. Thornton-Pett, *J. Chem. Soc., Chem. Commun*., 1989, 1763; J. Bould, P. Brint, J. D. Kennedy and M. Thornton-Pett, *J. Chem. Soc., Dalton Trans*., 1993, 2335.

12 J. Bould, J. E. Crook, N. N. Greenwood and J. D. Kennedy, *J. Chem. Soc., Dalton Trans*., 1991, 185.

13 G. M. Sheldrick, *Acta Crystallogr., Sect. A*, 1990, **46**, 467.

14 G. M. Sheldrick, SHELXL93, Program for refinement of crystal structures, University of Göttingen, 1993.

*Paper 6/07112K; Received, 18th October 1996*

# Trigold triacetylides: polymerization through gold···gold bonding or bridging ligands

**Michael J. Irwin,[a] Ljubica Manojlović-Muir,[b] Kenneth W. Muir,*[b] Richard J. Puddephatt*[a] and Dmitrii S. Yufit[b]**

[a] *Department of Chemistry, University of Western Ontario, London, Canada N6A 5B7*
[b] *Department of Chemistry, University of Glasgow, Glasgow, UK G12 8QQ*

**The new trigold(I) triacetylide $[C_6H_3(C{\equiv}CAu)_3$-1,3,5] reacts with monodentate ligands, L = isocyanide, phosphite or phosphine, to give $[C_6H_3(C{\equiv}CAuL)_3$-1,3,5] complexes which form polymeric solids with intermolecular Au···Au bonding; it also reacts with bidentate ligands to give covalently linked network polymers of the formula $[\{C_6H_3(C{\equiv}CAu)_3$-1,3,5$\}_2(\mu$-L–L$)_3]$, L–L = diisocyanide or diphosphine.**

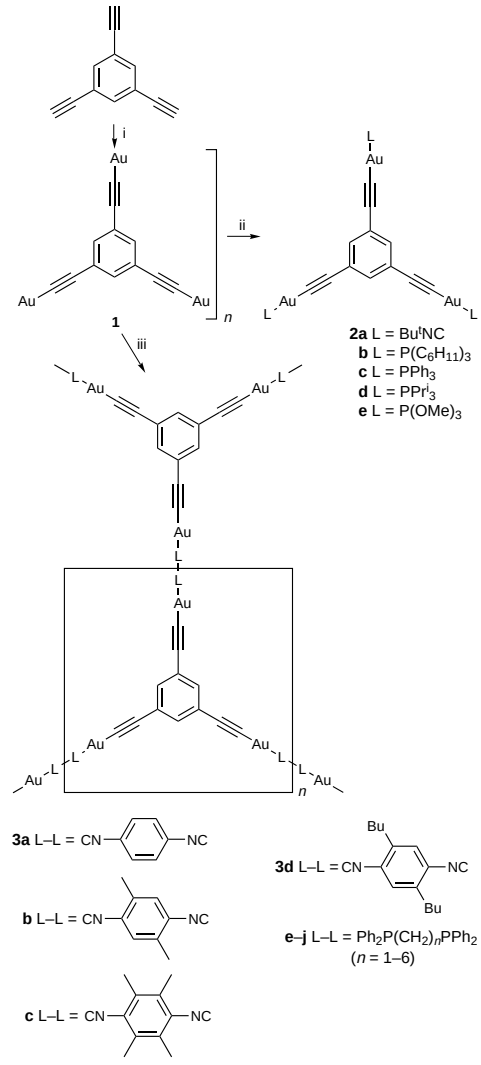
Linear digold(I) complexes have the interesting tendency to polymerize, either through weak intermolecular gold···gold binding, as in compounds with the chain structure derived from PhC≡C–Au–LL–Au–C≡CPh,[1,2] or through covalent binding of bridging bidentate ligands, as in the linear rigid-rod polymers $(–LL–Au–C{\equiv}C–Ar–C{\equiv}C–Au–)_n$, where L–L = diphosphine or diisocyanide and Ar = 1,4-$C_6H_4$ or a similar spacer group.[2] The former compounds are unique to gold chemistry, while the latter find an analogy in the well known polymers *trans*-$[M(PBu_3)_2(–C{\equiv}C–Ar–C{\equiv}C–)]_n$ (M = Ni, Pd, Pt) and in related complexes[3] whose conjugated structures might lead to materials applications.[4] There is currently much interest in extending this chemistry beyond the one-dimensional polymers, by using trifunctional core molecules, and the triacetylene 1,3,5-triethynylbenzene appears particularly well suited for this purpose.[5,6] In this article we report trigold(I) complexes of the type $[C_6H_3(C{\equiv}C–Au–L)_3]$, which can form loose polymers by intermolecular gold···gold association, as well as covalently linked polymers of the stoichiometry $[\{C_6H_3(C{\equiv}C–Au)_3\}_2(L–L)_3]$.

Reaction of $[AuCl(SMe_2)]$ in tetrahydrofuran–methanol with 1,3,5-triethynylbenzene and sodium acetate as base gave in high yield the insoluble, bright yellow solid $[C_6H_3(C{\equiv}CAu)_3]$ **1** (Scheme 1) which is expected to have a polymeric structure with bridging alkynyl groups.[7] (**CAUTION:** the pure complex **1** detonates easily and should be handled with extreme care and in small quantities only.) Reaction of 3 equiv. of ligand L (L = isocyanide, phosphite or phosphine) with a suspension of **1** in dichloromethane at room temperature yields the soluble complexes $[C_6H_3(C{\equiv}C–Au–L)_3]$ **2** in good yield. Complexes **2** are white or pale yellow, air-stable, analytically pure solids which are soluble in organic solvents. All have been characterized spectroscopically and those with L = $Bu^tN{\equiv}C$ **2a** and $P(OMe)_3$ **2e** by X-ray diffraction as well.† The last two appear to be the first complexes of the $C_6H_3(C{\equiv}C^-)_3$ ligand with any metal, as well as the first trigold triacetylides, to be characterised crystallographically.

The molecular structures of **2a** and **2e**, shown in Fig. 1, are closely similar. Each contains a planar $C_6H_3(C{\equiv}CAuX)_3$ nucleus (X = C or P) which displays approximate $D_{3h}$ symmetry. C–Au–X angles deviate from linearity by 8°.

In the solids of both compounds molecules related by lattice translations are interlinked through weakly attractive Au···Au interactions [3.234(1) Å in **2a**, 3.316(1) Å in **2e**] to form crinkled tapes which extend throughout the crystals (Fig. 1). The gold atoms involved in these interactions [Au(1) and Au(2) in **2a**, Au(1) and Au(3) in **2e**] thereby attain the T-shaped coordination geometry, with Au···Au–X (X = C, P) angles ranging from 73 to 103°.

In **2a** the shortest Au···Au separations between molecular tapes are 3.723(1) Å for Au(1) atoms related by inversion centres and 3.950(1) Å for Au(2) and Au(3) atoms in molecules related by translation along the *a*-axis; in **2e** the two-fold screw axes give rise to intermolecular Au(1)···Au(2) contacts of 3.973(1) Å. Although these inter-tape separations are larger than both the van der Waals diameter of gold (3.60 Å)[8,9] and the range of distances generally regarded as typical of normal $Au^I···Au^I$ attractive interactions (2.90–3.50 Å),[2,8,9] they provide geometrically similar environments for the gold atoms, in which




**Scheme 1** *Reagents*: i, $[AuCl(SMe_2)]$, NaOAc; ii, 3 equiv. L; iii, 1.5 equiv. L–L

the Au···Au–X (X = C, P) angles are 62–120° and the Au···Au···Au angles 135–151°. This directionality of the mutual approach of the gold atoms could be taken as evidence for intertape attractions yielding three-dimensional solids stabilized by cross-linking of ···Au–R–Au···Au–R–Au··· chains [R = $C_6H_3(C{\equiv}C)_3$]. It also appears that weak intermolecular Au···Au interactions leading to the T-shaped geometry, which is considered highly specific for gold(I) complexes,[8] may be a significant factor in driving molecular self-assembly in their solids. It is therefore conceivable that the synthon **A** may prove useful in the design of supramolecular solids with desirable chemical and physical properties.

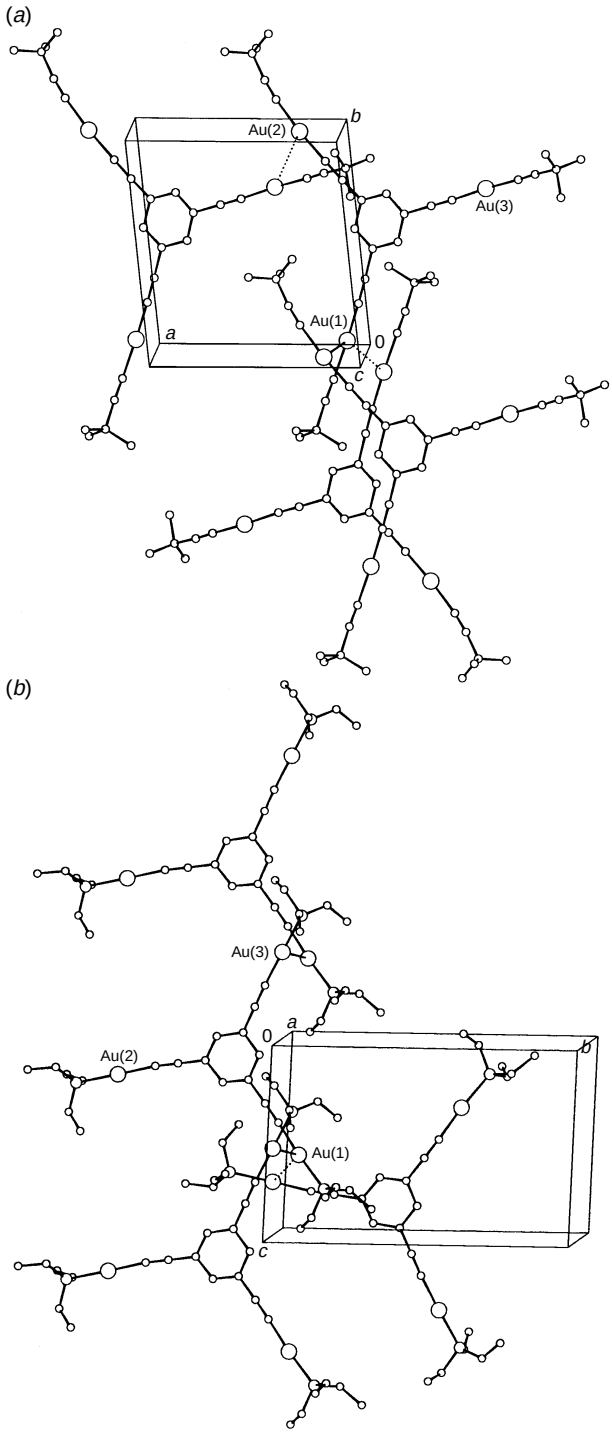



**Fig. 1** (*a*) The crystal structure of 1,3,5-$(Bu^tNCAuC{\equiv}C)_3C_6H_3{\cdot}C_2H_4Cl_2$ **2a**·$C_2H_4Cl_2$, with the solvent molecules omitted for clarity. Labels are shown for the gold atoms in the reference molecule only, the Au···Au interactions within the molecular tapes are shown by full lines, and those involving the gold atoms in different tapes, by dashed lines. Selected interatomic distances (Å) and angles (°): Au(1)–Au(1$^{i}$) 3.723(1), Au(1)–Au(2$^{ii}$) 3.234(1), Au(2)–Au(3$^{iii}$) 3.950(1). The symmetry transformations applied are: i $-x, -y, 1-z$; ii $x, y-1, z$; iii $1+x, y, z$; iv $x, 1+y, z$; (v) $x-1$, y, *z*. (*b*) The crystal structure of 1,3,5-$[(MeO)_3PAuC{\equiv}C]_3C_6H_3$ **2e**. Selected interatomic distances (Å) and angles (°): Au(1)–Au(2$^{i}$) 3.973(1), Au(1)–Au(3$^{ii}$) 3.316(1). The symmetry transformations applied are: i $2-x$, $1/2+y, 1-z$; ii $x, y, 1+x$; (iii) $2-x, -1/2+y, 1-z$; iv $x, y, z-1$. Disorder involving phosphite methoxy groups is not shown for clarity.

Covalently bridged polymers were readily prepared by reaction of **1** (addition) or **2a** (displacement of the $Bu^tN{\equiv}C$ ligands) with bidentate ligands [L–L = diisocyanide CN–Ar–CN, Ar = $C_6H_4$, $C_6H_2Me_2$, $C_6Me_4$, $C_6H_2Bu^t_2$, or diphosphine $Ph_2P(CH_2)_nPPh_2$, $n$ = 1–6] in acetone at room temperature. They precipitated as pale yellow solids which were insoluble in common organic solvents, and analysed as $[\{C_6H_3(C{\equiv}C{-}Au)_3\}_2(L{-}L)_3]_n$ **3**. Their proposed structures (Scheme 1) are supported by comparison of their IR and XPS data with those of the corresponding model compounds **2**.

In summary, the first trigold triacetylide complexes have been prepared and shown to have elegant planar molecular structures with approximate $D_{3h}$ symmetry. They can act as a core of loosely linked polymers formed by weak intermolecular gold···gold binding, or they can react with bidentate ligands to form covalently-linked network polymers.

We thank the NSERC (Canada) and EPSRC (UK) for financial support.

## Footnote

† *Crystallographic data*: **2a**·$C_2H_4Cl_2$: $C_{27}H_{30}Au_3N_3{\cdot}C_2H_4Cl_2$, $M$ = 1086.39, space group $P\bar{1}$, $a$ = 10.340(1), $b$ = 11.539(1), $c$ = 16.444(1) Å, $\alpha$ = 75.01(1), $\beta$ = 80.11(1), $\gamma$ = 81.33(1)°, $U$ = 1855.5(2) Å$^3$, $Z$ = 2.

Intensities were measured at 20 °C with Mo-K$\alpha$ radiation, $\lambda$ = 0.710 73 Å. The mean intensity of three standard reflections decreased by 27% during the experiment. The data were corrected for crystal decomposition and for absorption. Refinement on $F^2$ of 287 parameters, using 5082 observations, converged at $R_1$ = 0.054, $wR_2$ = 0.140 for 2825 reflections with $I > 2\sigma(I)$, $|\Delta\rho| < 1.31$ e Å$^{-3}$. The unit cell contains two molecules of the gold complex, one ordered and one disordered $C_2H_4Cl_2$ solvate molecules.

For **2e**: $C_{21}H_{30}Au_3O_9P_3$, $M$ = 1110.26, monoclinic, space group $P2_1$, $a$ = 0.979(2), $b$ = 15.630(2), $c$ = 10.453(2) Å, $\beta$ = 111.57(2)°, $U$ = 1516.2(5) Å$^3$, $Z$ = 2.

The data were corrected for absorption. Refinement of $F^2$ of 320 parameters using 5242 observations converged at $R_1$ = 0.043, $wR_2$ = 0.080 for 2613 reflections with $I > 2\sigma(I)$, $|\Delta\rho| < 1.43$ e Å$^{-3}$. The Flack absolute structure parameter $\chi$ = −0.015(13). Two oxygen and two carbon atoms of $P(OMe)_3$ ligands are disordered.

Atomic coordinates, bond lengths and angles, and thermal parameters have been deposited at the Cambridge Crystallographic Data Centre (CCDC). See Information for Authors, Issue No. 1. Any request to the CCDC for this material should quote the full literature citation and the reference number 182/321.

## References

1 S.-J. Shieh, X. Hong, S.-M. Peng and C.-M. Che, *J. Chem. Soc., Dalton Trans.*, 1994, 3067.
2 M. J. Irwin, G. Jia, N. C. Payne and R. J. Puddephatt, *Organometallics*, 1996, **15**, 51.
3 N. Hagihara, K. Sonogashira and S. Takahashi, *Adv. Polym. Sci*., 1980, **41**, 149.
4 A. Hirsch and M. Hanack, *Conjugated Polymeric Materials: Opportunities in Electronics, Optoelectronics and Molecular Electronics*, ed. J. L. Bredas and R. R. Chance, Kluwer Academic, New York, 1990, p. 163.
5 D. E. Ames, D. Bull and C. Takundwa, *Synthesis*, 1981, 364.
6 D. Tzalis and Y. Tor, *Chem. Commun*., 1996, 1043. G. B. Gardner, Y.-H. Kiang, S. Lee, A. Asgaonkar and D. Venkataram, *J. Am. Chem. Soc*., 1996, **118**, 6946.
7 D. M. P. Mingos, J. Yau, S. Menzer and D. J. Williams, *Angew. Chem., Int. Ed. Engl*., 1995, **34**, 1894.
8 S. S. Pathaneni and G. R. Desiraju, *J. Chem. Soc., Dalton Trans*., 1993, 319.
9 D. M. P. Mingos, *J. Chem. Soc., Dalton Trans*., 1996, 561.

*Received, 22nd October 1996; Com. 6/07214C*

# Excellent effect of lithium-doped sulfated zirconia catalysts for oxidative coupling of methane to give ethene and ethane

**Kazuhisa Murata,* Takashi Hayakawa and Ken-ichi Fujita**

*National Institute of Materials and Chemical Research, Tsukuba, Ibaraki 305, Japan*

**Li-doped sulfated zirconia catalysts are found to be effective for oxidative coupling of methane; *ca.* 80% $C_2$ selectivity is attained at 1073 K with 43% $CH_4$ conversion.**

In this decade, much attention has been paid to the conversion of methane into more valuable products under oxidative[1] or non-oxidative[2] conditions. Of many routes, oxidative coupling of methane (OCM) to give $C_2$ hydrocarbons is still one of the most promising choices for direct methane conversion. Generally, research efforts have been directed towards a search for new efficient catalysts and basic metal oxides such as MgO, CaO and $La_2O_3$ are mostly used as catalysts or supports. However, it seems likely that the strong basicities of the catalysts used are not always required.[3]

Here, fairly super-acidic metal oxides were examined as catalyst supports for the OCM reaction and lithium-doped sulfated zirconia systems were found to be excellent candidates for $C_2$ formation.

The catalysts were prepared as follows. Sulfated zirconia was prepared by the conventional two-step method,[4] in which amorphous zirconia was first synthesized by hydrolysing an aqueous $ZrO(NO_3)_2$ solution with ammonia, followed by calcination for 3 h at 573 K. Then, the resulting zirconia (BET surface area = 266 $m^2\ g^{-1}$) was added to $(NH_4)_2SO_4$ solution and evaporated to dryness, accompanied by calcination in air for 3 h at 973 K. The resultant sulfated zirconia (72.8 $m^2\ g^{-1}$) was impregnated with an aqueous solution of alkali- or alkaline earth-metal compounds such as $Li_2CO_3$ in which the alkali-metal content was 5 mass% (the mass percentage is defined as the ratio of Li to $ZrO_2$). This was then evaporated to dryness, drying overnight at 373 K with calcination in air at 873 K for 3 h (the surface area of the resulting catalyst = 7.3 $m^2\ g^{-1}$). The catalytic runs were carried out under atmospheric pressure and in a fixed-bed vertical-flow reactor constructed from a high-purity alumina tube (id = 6 mm) packed with 0.5 g of catalyst and mounted inside a tube furnace. The catalyst was pretreated in nitrogen at 1073 K for 1 h. Then, the reactant gas mixture (15% $CH_4$, 5% $O_2$ and 80% $N_2$, 50 ml $min^{-1}$) was introduced at $W/F$ = 4.1 g cat h $mol^{-1}$. The products were analysed on-line by gas chromatography (GC) equipped with a Syncarbon-S (FID) column for $C_2H_6$, $C_2H_4$, $C_2H_2$, $C_3H_6$ and $C_3H_8$, Porapack Q (2 m) and molecular sieve 5A (2 m) (TCD) columns for $CH_4$, $CO_2$, $H_2O$, $H_2$, $O_2$ and CO and another Porapack Q (1 m) (FID) column for small amounts of higher hydrocarbons such as $C_4H_8$ and benzene.

The major products of the oxidative coupling of methane are ethene, ethane, carbon monoxide and carbon dioxide with only trace amounts of acetylene, but-1-ene and benzene. The results obtained in the various $ZrO_2$ catalysts at 1073 K are presented in Table 1, where data were taken after 30 min of reaction. In the $ZrO_2$ and sulfated $ZrO_2$ catalysts, some reaction took place, carbon oxides being, however, the dominant products and $C_2$ compounds were obtained in only 3% yield. For the Li-doped $ZrO_2$ catalyst without sulfate, the $CH_4$ conversion was almost unaltered, but $C_2$ selectivity (*ca.* 50%) improved slightly. It was found that 80.2% $C_2$ selectivity was achieved at 32.1% $CH_4$ conversion over the Li-doped sulfated $ZrO_2$ catalyst at a $CH_4/O_2$ ratio of 3. This is the first example of the use of solid super-acid-based catalysts for the oxidative coupling of $CH_4$. The $C_2$ yield (34.5%) was improved by the use of a $CH_4/O_2$ ratio of 2,† although the $C_2$ selectivity was slightly decreased. The $C_2$ yield obtained here is found to be considerably better than results reported in the catalysts systems based on basic metal oxides such as MgO.[1] Moreover, at a $CH_4/O_2$ ratio of 9 without diluent, the $C_2$ selectivity was further increased; as high as 85.1% $C_2$ selectivity was attained at 30.7% $CH_4$ conversion,‡ which is desirable from the practical viewpoint. Fig. 1 shows the effects of reaction temperature on the $CH_4$ conversion and the

**Table 1** Catalytic performances for oxidative coupling of methane over Li-promoted sulfated zirconia catalysts[a]

| Catalyst[b] | Conversion (%) | Selectivity[c](%) | | | | | $C_2$ Yield[d](%) |
|---|---|---|---|---|---|---|---|
| | | $C_2H_2$ | $C_2H_4$ | $C_2H_6$ | CO | $CO_2$ | |
| $ZrO_2$ | 16.0 | 0.19 | 11.3 | 6.75 | 64.6 | 16.9 | 2.92 |
| $6\%SO_4^{2-}/ZrO_2$ | 16.8 | 0.27 | 11.7 | 6.29 | 66.2 | 15.3 | 3.06 |
| $5\%Li/ZiO_2$ | 17.2 | 0.62 | 27.2 | 22.9 | 16.4 | 31.9 | 8.74 |
| $5\%Li/6\%SO_4^{2-}/ZrO_2$ | 32.1 | 1.21 | 58.3 | 20.7 | 9.69 | 5.70 | 25.8 |
| $5\%Li/6\%SO_2^{2-}/ZrO_2$[e] | 35.5 | 1.72 | 58.9 | 9.99 | 21.2 | 4.79 | 25.1 |
| $5\%Li/6\%SO_4^{2-}/ZrO_2$[f] | 43.3 | 0.67 | 58.3 | 20.7 | 11.7 | 6.10 | 34.5 |
| $5\%Li/6\%SO_4^{2-}/ZrO_2$[g] | 30.7[h] | 0.62 | 56.8 | 27.7 | 5.36 | 4.27 | 25.7 |

[a] *Reaction conditions*: $T$ = 1073 K, $P$ = 0.1 MPa, total flow = 50 ml $min^{-1}$, reactant gas [$CH_4$ (15%)–$O_2$ (5%)–$N_2$ (80%)]. Results are after 30 min of reaction. [b] The sulfated zirconia was prepared using $(NH_4)_2SO_4$. [c] Conversion and selectivity are based on the amount of methane reacted. [d] $C_2$ yield is obtained from the product of conversion and $C_2$ selectivity, where $C_2$ selectivity is the sum of $C_2H_2$, $C_2H_4$ and $C_2H_6$. [e] The sulfated zirconia was prepared using 0.5 M $H_2SO_4$. [f] Reactant gas [$CH_4$ (10%)–$O_2$ (5%)–$N_2$ (85%)]. [g] Reactant gas [$CH_4$ (90%)–$O_2$ (10%)]. [h] In this run, carbon and hydrogen mass balances were 94 and 92%, respectively: C mass balance = $(2 \times C_2H_6 + 2 \times C_2H_4 + 2 \times C_2H_2 + 3 \times C_3H_6 + 3 \times C_3H_8 + 4 \times C_4H_8 + 5 \times C_5H_{10} + 6 \times$ benzene + $7 \times$ toluene + CO + $CO_2) \times 100/CH_4$ converted. H mass balance = $(3 \times C_2H_6 + 2 \times C_2H_4 + C_2H_2 + 3 \times C_3H_6 + 4 \times C_3H_8 + 4 \times C_4H_8 + 5 \times C_5H_{10}$ + $3 \times$ benzene + $4 \times$ toluene + $H_2$ + $H_2O) \times 100/CH_4$ converted. In other runs the C and H mass balances were also between 90 and 95%. In any run, the remainder of gaseous products must be a very small amount of oxygenates such as methanol. Also, the formation of bulk lithium carbonate during the reaction[9] was not detected by powder X-ray diffraction, the patterns of which remained unchanged before and after reaction. Further study is under way to improve the C and H mass balances.

selectivities under no-diluent conditions. The $CH_4$ conversion and $C_2$ selectivity increased with increasing reaction temperature up to 1073 K, whereas $CO_x$ selectivity decreased. These findings could be explained, at least partly, by a difference in the activation energy between $C_2$ and $CO_x$ formation.[5]

The effect of catalyst components were examined using other acid sources and other alkali metals. In the Li-doped acid-promoted $ZrO_2$ catalysts, the effect of acid precursors other than $(NH_4)_2SO_4$ was in the order: $(NH_4)_2SO_4$ (25.8) > 0.5 M $H_2SO_4$ (25.1) > $NH_4Cl$ (22.9) > trimethyleneborate (22.3) > $(NH_4)_3PO_4$ (19.3) > $NH_4NO_3$ (16.5) > none (8.7). (The values in parentheses represent the $C_2$ yield at 1073 K.) For the Na- and K-doped sulfated $ZrO_2$ catalysts, the $CH_4$ conversion was almost the same as for the Li-doped catalysts, but $C_2$ selectivity decreased to *ca.* 50%, nearly 30% lower than that for the Li-doped catalyst. Over catalysts promoted with 10 mass% of Li, both $CH_4$ conversion and $C_2$ selectivity were slightly reduced and, as a result, the $C_2$ yield decreased to *ca.* 19%.

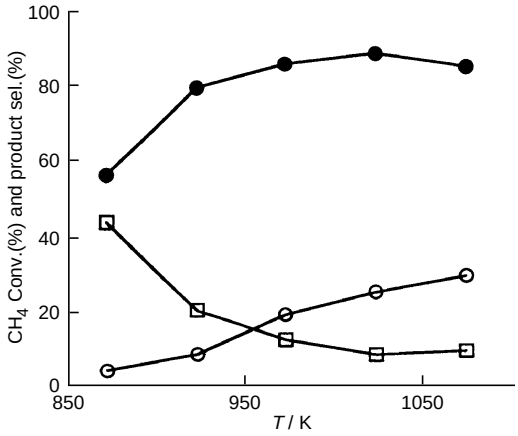



**Fig. 1** Effect of the reaction temperature on the oxidative coupling of methane over 5% Li-doped 6 mass% $SO_4^{2-}/ZrO_2$ catalysts without diluent. *Conditions*: $CH_4$ (90%)–$O_2$ (10%), feed 50 ml $min^{-1}$, catalyst 0.5 g. $CH_4$ conversion (○); selectivities: $C_2$ (●), $CO_x$ (□).

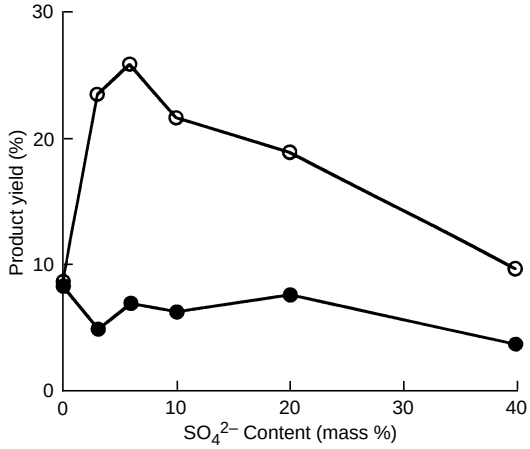



**Fig 2** Effect of sulfate content on the product yields. *Conditions*: $CH_4$ (15%)–$O_2$ (5%)–$N_2$ (80%), feed 50 ml $min^{-1}$, 1073 K. The mass% of sulfate content is defined as the ratio of $SO_4^{2-}$ to $ZrO_2$. Selectivities: $C_2$ (○), $CO_x$ (●).

The effectiveness of the Li-doped sulfated $ZrO_2$ catalysts on the oxidative coupling of $CH_4$ is still not clear. Since the effect of Li doping on MgO support has been already reported,[6] it seems likely that the preparation of sulfated $ZrO_2$ surface is a key step in our catalyst system. In fact, the catalyst performances depend on the sulfate content (Fig. 2) and calcination temperature: a maximum $C_2$ yield is attained over the catalysts which contain 6 mass% sulfate and are calcined at 923–973 K, being closely related to the preparation conditions of sulfated $ZrO_2$ as solid superacids.[7] If so, sulfated metal oxides other than $ZrO_2$[8] might be also effective as supports. We found that, for an Li-doped sulfated $SnO_2$ catalyst,§ 82.4% $C_2$ selectivity at 1073 K is achieved at 30.5% $CH_4$ conversion. Also, a $ZrO_2$ catalyst, impregnated with an aqueous solution containing both $(NH_4)_2SO_4$ and $Li_2CO_3$, followed by calcination in air at 873 K for 3 h, showed much lower reactivity than that prepared by the two-step method. By investigating all these findings, it is concluded that Li doping over a super-acid surface is required for the generation of high catalytic performances for the $ZrO_2$-based OCM reaction reported here.

Further work is in progress not only to carry out reaction on larger experimental scales, but also to elucidate the nature of the Li-doped solid super-acid catalysts.

## Footnotes

† In this run, after reaction for 5 h at 1073 K, methane conversion was decreased (43.3 to 39%), whereas $C_2$ selectivity was slightly increased (79.7 to 82.1%).

‡ In this run, the amount of oxygen required to reach 30.7% $CH_4$ conversion could approximately correspond to that contained in the feedstock, if we assume the following reaction steps including thermal cracking of ethane or ethene to form ethene or acetylene, although further investigation will be required for the reaction scheme. (1) $2CH_4 + 1/2O_2 \rightarrow C_2H_6 + H_2O$, (2) $C_2H_6 \rightarrow C_2H_4 + H_2$, (3) $C_2H_4 \rightarrow C_2H_2 + H_2$, (4) $CH_4 + 3/2O_2 \rightarrow CO + 2H_2O$, (5) $CO + 1/2O_2 \rightarrow CO_2$, (6) $CH_4 + H_2O \rightarrow CO + 3H_2$. In fact, in this run, the expected amount of hydrogen was observed by GC analysis. Also, in a separate experiment using the same catalyst, we confirmed that efficient $C_2H_4$ formation from $C_2H_6$ was observed even at 1023 K in the absence of $O_2$, consistent with a thermodynamical calculation.

§ $SnO_2$ impregnated with 6 mass% $(NH_4)_2SO_4$ was calcined at 873 K for 3 h.

## References


1 J. H. Lunsford, *Angew. Chem., Int. Ed. Engl.*, 1995, **34**, 970.
2 K. Murata and H. Ushijima, *J. Chem. Soc., Chem. Commun.*, 1994, 1157.
3 Z.-C. Jiang, C.-J. Yu, X.-P. Fang, S.-B. Li and H.-L. Wang, *J. Phys. Chem.*, 1993, **97**, 12 870.
4 X. Song and A. Sayari, *Catal. Rev. Sci. Eng.*, 1996, **38**, 329.
5 Y. Amenomiya, V. I. Birss, M. Goledzinowski, J. Galuszka and A. R. Sanger, *Catal. Rev. Sci. Eng.*, 1990, **32**, 163.
6 T. Ito and J. H. Lunsford, *Nature*, 1985, **314**, 721.
7 M. Hino and K. Arata, *J. Chem. Soc., Chem. Commun.*, 1979, 1148.
8 H. Matsuhashi, M. Hino and K. Arata, *Chem. Lett.*, 1988, 1027.
9 D. M. Ginter, E. Magni, G. A. Somorjai and H. Heinemann, *Catal. Lett.*, 1992, **16**, 197.


*Received, 27th September 1996; Com. 6/06624K*

# Hydration structure of $Eu^{III}$ on aqueous ion-exchange resins using laser-induced fluorescence spectroscopy

**Yoshio Takahashi,*[a]†‡ Takaumi Kimura,[b] Yoshiharu Kato,[b] Yoshitaka Minai[a] and Takeshi Tominaga[a]**

[a] *Department of Chemistry, School of Science, University of Tokyo, Hongo, Tokyo 113, Japan*
[b] *Japan Atomic Energy Research Institute (JAERI), Tokai, Ibaraki 310-09, Japan*

***Ca.* 2 and > 5 molecules of hydrated water are removed from the inner sphere of $Eu^{III}$ on strongly and weakly acidic ion-exchange resins, respectively, showing the different mechanisms between ion-exchange reactions occurring on these two types of resins.**

Recently, the hydration structure of metal ions on strongly acidic cation-exchange resins (denoted as SCR) has been investigated by neutron diffraction.[1] However, descriptions on the structures of the exchanged ion have not been fully clarified, despite the wide applications of cation-exchange resins in chemistry and biology.[2] This is perhaps due to difficulties encountered in analysing the adsorbed metal species at a solid–water interface. The present study provides direct information on the hydration structures of $Eu^{III}$ exchanged on SCR and weakly acidic cation-exchange resins (denoted as WCR) obtained through laser-induced fluorescence spectroscopy. This method has the advantages of having high sensitivity and good selectivity for $Eu^{III}$, and can be applied to the current resin system in the presence of an aqueous phase. Moreover, the method is able quantitatively to count the number of hydrated water molecules attached to $Eu^{III}$, unlike neutron diffraction.

The fluorescence lifetime of $Eu^{III}$ ($^5D_0 \rightarrow {}^7F$ manifold) is related to $N_{H_2O}$ (the number of $H_2O$ molecules in the primary coordination sphere of the $Eu^{III}$ ion) due to the energy transfer from the excited state of $Eu^{III}$ to OH vibrations of the hydrated $H_2O$.[3] The method was therefore applied to measure $N_{H_2O}$ values of $Eu^{III}$ in both aqueous and solid phases.[3] In the present study, the method is, for the first time, applied to the study of the hydration structure of $Eu^{III}$ at the solid–water interface.

AG 50WX8 (functional group: $-SO_3^-$; matrix: styrene divinylbenzonate; proton exchange capacity: 2.1 mequiv. $g^{-1}$) and Bio-Rex 70 (functional group: $-CO_2$; matrix: acrylate; proton exchange capacity: 3.5 mequiv. $g^{-1}$) purchased from Bio-Rad Lab., Inc. were used as the SCR and WCR samples, respectively. Linear poly(4-styrenesulfonic) acid (PSS) and linear polyacrylic acid (PAA) purchased from Aldrich were also employed. The concentrations of polyelectrolytes (SCR, WCR, PSS and PAA) and $Eu^{III}$ are listed in Fig. 1. The pH and supporting electrolyte concentration ($C_s$) were adjusted by addition of small amounts of NaOH or $HClO_4$ and $NaClO_4$ respectively. An aqueous solution of $Eu^{III}$ with no polyelectrolyte was also prepared (WP system). These solutions (or suspensions in the resin systems) were aged overnight prior to the subsequent procedures. The distribution of $Eu^{III}$ between the aqueous and solid phases was measured using a $^{152}Eu$ tracer after centrifugation at 3000 rpm for 1 min. The solution or suspension contained in a quartz cell and magnetically stirred was exposed to light (395 nm) from a dye laser giving rise to the excitation of $Eu^{III}$ ($^7F_0 \rightarrow {}^5L_6$). The decay curve for the emission at 615 nm was measured by a photomultiplier and recorded with a digital oscilloscope coupled with a personal computer.

The relation of $N_{H_2O}$ with the lifetimes $\tau_{H_2O}$ and $\tau_{D_2O}$ measured in the $H_2O$ and $D_2O$ systems, respectively, is as follows:[3]

$$N_{H_2O} = 1.05\,(1/\tau_{H_2O} - 1/\tau_{D_2O})/ms^{-1} \quad (1)$$

For SCR, WCR, PSS and PAA systems, $\tau_{D_2O}$ values were 1.10, 1.98, 3.00 and 3.05 ms, respectively. These $\tau_{D_2O}$ values allow us to evaluate $N_{H_2O}$ from the luminescence lifetime measurement data [eqn. (1)] and results are shown in Fig. 1 It is seen that $N_{H_2O}$ of the europium(III) aqua complex is 9.[3]

In the WP system, the $N_{H_2O}$ decreases from the $N_{H_2O}$ of $Eu^{III}$ (aq) which indicates the formation of inorganic complexes of $Eu^{III}$ such as $Eu(CO_3)^+$, $Eu(OH)^{2+}$ or $Eu(OH)_2^+$ between pH 6 and 7.5.[4] When pH > 7.5, the $^{152}Eu$ experiments shows that $Eu^{III}$ formed inorganic colloids or precipitates.[4] Formation of such inorganic colloids or precipitates of $Eu^{III}$ made its lifetime very short due to the non-radiative energy transfer among the neighbouring $Eu^{III}$ in the colloids or precipitates.[5] In this pH region therefore, $N_{H_2O}$ of $Eu^{III}$ in the WP system apparently becomes much greater than 9. Such short lifetime values were not observed in the polyelectrolyte systems; therefore inorganic colloidal species were not formed, and all the $Eu^{III}$ is completely complexed with the polyelectrolytes.

In the WCR system, $Eu^{III}$ was shown from $^{152}Eu$ experiments to be adsorbed at pH > 4. $N_{H_2O}$ decreased abruptly at pH *ca.* 3.5 due to the initiation of ion exchange. The $N_{H_2O}$ value in the WCR system decreased gradually from 3.5 to 2.5 between pH 4 and 9, in a manner similar to the PAA system. This decrease suggests that more carboxylates are bound to $Eu^{III}$ with increasing pH accompanied with an increasing degree of ionization of WCR or PAA.[6]

In the SCR system, $Eu^{III}$ was adsorbed at pH > 0.5 at which $N_{H_2O}$ of the adsorbed $Eu^{III}$ on SCR was *ca.* 7.5. The exchanged $Eu^{III}$ ion on WCR releases five to seven molecules of hydrated

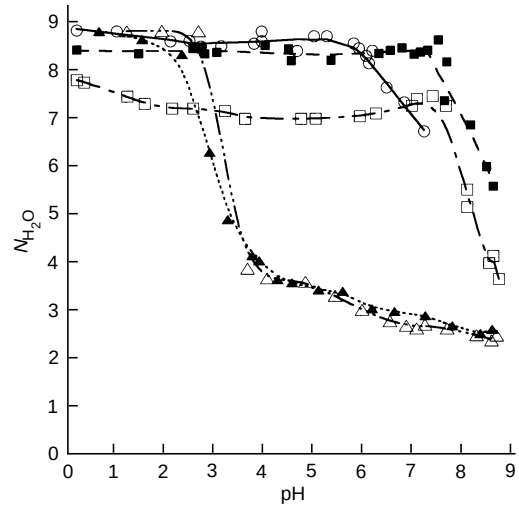



**Fig. 1** pH dependence of $N_{H_2O}$ in the SCR (□), WCR (△), PSS (■), PAA (▲) and WP (○) systems. Total concentration of $Eu^{III}$ is $2 \times 10^{-4}$ M. SCR and WCR systems: 4.0 g of AG 50WX8 and 10 g of Bio-Rex 70 suspended in 1 $dm^3$ water, respectively; PSS and PAA systems: aqueous solutions of polystyrenesulfonic acid (8.3 g $dm^{-3}$) and polyacrylic acid (3.0 g $dm^{-3}$), respectively; WP system: $Eu^{III}$ in water without added polyelectrolyte.

water, while only one or two water molecules are released when adsorbed on SCR. This indicates that the hydration structure of $Eu^{III}$ ion is much more affected by WCR than SCR. The present result suggests different mechanisms between the ion-exchange reactions in the SCR and WCR systems: the hydrated $Eu^{III}$ ion interacts with SCR, whereas the dehydrated $Eu^{III}$ ion interacts with WCR. Reports on the selectivities in the ion exchange of alkali, alkaline earth, and lanthanoid elements concludes that a metal ion with a larger ionic radius is more readily exchanged on SCR for metal ions having the same charge showing that hydrated ions interacts with SCR.[2] By contrast, WCR adsorbs a smaller ion more effectively, showing that the metal ion forms an inner-sphere complex with WCR.[2] The present results on the hydration structure of $Eu^{III}$ have provided spectroscopic evidence for the different mechanisms of ion-exchange reactions on SCR and WCR, as has been suggested by thermodynamic data.[2]

In the PSS and SCR systems at higher pH region, $N_{H_2O}$ begins to decrease at pH *ca.* 7.5. In contrast, in the absence of the polyelectrolytes (WP system), the decrease of $N_{H_2O}$ was observed at pH > 6 due to the formation of inorganic complexes, as described earlier. This shows that the $Eu^{III}$ ion was exchanged on PSS or SCR as a free hydrated ion accompanied by removal of the hydroxide or carbonate ligand at pH between 6 and 7.5. When pH > 7.5, the $N_{H_2O}$ values in the PSS and SCR systems decreased with an increase in pH. This indicates that the complex ion of europium(III) hydroxide or carbonate [*e.g.*, $Eu(CO_3)^+$, $Eu(OH)^{2+}$ or $Eu(OH)_2^+$] is directly adsorbed on PSS and SCR at these pH values.

Although it is suggested that the hydrated ion interacts with SCR, the $N_{H_2O}$ value of the adsorbed $Eu^{III}$ on SCR was less than that of $Eu^{3+}$ (aq). This shows that the SCR affects the hydration structure of $Eu^{III}$ to some extent. On the other hand, the $N_{H_2O}$ value of $Eu^{III}$ complexed with PSS (linear polyelectrolyte analogue of SCR) was similar to that of the aqua complex. On comparing the $N_{H_2O}$ values in the SCR and PSS systems, it is thought that the cross-linked structure of SCR may be responsible for its influence on the hydration structure of $Eu^{III}$. This is compatible with the result of neutron diffraction study[1] on the hydration structure of ion-exchanged $Ni^{2+}$ and $Li^+$, showing that a sulfonate group penetrates into the primary hydration sphere of these ions.

As $C_s$ (concentration of supporting electrolyte, $NaClO_4$) increases up to 1.0 M, $N_{H_2O}$ values in the WCR and SCR systems remained almost constant (Fig. 2). This was also found to be the case for the WP system in the $C_s$ region.[7] However, $N_{H_2O}$ values in the PAA (linear polyelectrolyte of acrylate) system decreased. This is perhaps due to change in conformation, since the shape of PAA was folded as a result of shielding the repulsive forces between the dissociated carboxylate groups with the supporting cations.[8] This suggests that network structures of WCR and SCR resins are more rigid than the linear structure of PAA.

This work was supported by a Grant-in-Aid for Scientific Research on Priority Areas 'New Development of Rare Earth Complexes' No. 08220212 from the Ministry of Education, Science, Sports, and Culture.

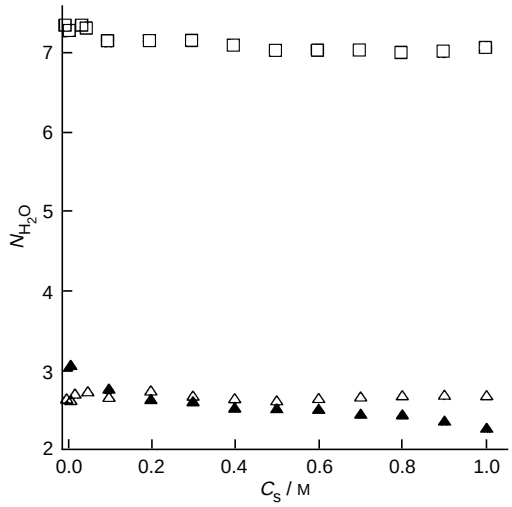



**Fig. 2** Dependence of $N_{H_2O}$ upon $C_s$ in the SCR (□), WCR (△) and PAA (▲) systems. Experimental conditions were similar to those for Fig. 1.

## Footnotes

† Research Fellow of the Japan Society for the Promotion of Science.

‡ E-mail: ytakaha@chem.s.u-tokyo.ac.jp

## References

1 R. H. Tromp and G. W. Neilson, *J. Phys. Chem.*, 1996, **100**, 7380.
2 M. Marhol, *Ion Exchangers in Analytical Chemistry. Their Properties and Use in Inorganic Chemistry*, Elsevier, Prague, 1982; J. Korkisch, *Handbook of Ion Exchanger*, CRC Press, Boca Raton, FL, 1989.
3 W. DeW. Horrocks, Jr. and D. R. Sundnick, *J. Am. Chem. Soc.*, 1979, **101**, 334; T. Kimura and G. R. Choppin, *J. Alloys Comp.*, 1994, **213**/**214**, 313; T. Kimura, G. R. Choppin, Y. Kato and Z. Yoshida, *Radiochim. Acta*, 1996, **72**, 61.
4 W. Runde, G. Meinrath and J. I. Kim, *Radiochim. Acta*, 1992, **58**/**59**, 93; A. J. Fairhurst, P. Wareick and S. Richardson, *Colloids Surf. A*, 1995, **99**, 187.
5 Y. Okamoto, Y. Ueba, N. F. Dzhanibekov and E. Banks, *Macromolecules*, 1981, **14**, 17; R. Resifeld, E. Greenberg and R. Velapoldi, *J. Chem. Phys.*, 1972, **56**, 1698.
6 T. H. Yoon, H. Moon, Y. J. Park and K. K. Park, *Environ. Sci. Technol.*, 1994, **28**, 2139.
7 F. Tanaka and S. Yamashita, *Inorg. Chem.*, 1984, **23**, 2044.
8 Y. Takahashi, T. Kimura, Y. Kato, Y. Minai and T. Tominaga, *J. Radioanal. Nucl. Chem., Lett.*, 1996, **212**, 11.

*Received, 14th October 1996; Com. 6/06996G*

# The fate of [2,3,3-$^2H_3$, 1,2-$^{13}C_2$]-D,L-glycerate in clavulanic acid biosynthesis

**Janos Pitlik and Craig A. Townsend***

*Department of Chemistry, The Johns Hopkins University, Baltimore, Maryland 21218, USA*

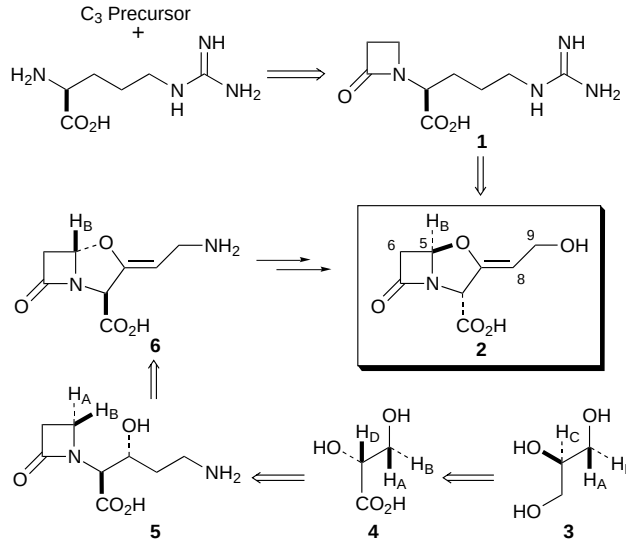
**The hydrogen at C-2 of glycerate is lost in the biosynthesis of clavulanic acid.**

Elusive to experiment and mechanistic understanding has been the biosynthesis of the 4-membered ring of deoxyguanidinoproclavaminic acid **1**, the first β-lactam-containing intermediate in the anabolic pathway to clavulanic acid **2**.[1] These three carbons are known to be derived efficiently from glycerol **3**, accompanied by the loss of $H_C$.[2,3] Subsequent radiochemical experiments with samples of this $C_3$-carbohydrate bearing tritium stereospecifically at the *pro*-(*R*) hydroxymethylene established that chiral information was delivered through the entire biosynthetic pathway to clavulanic acid **2** such that the (1*R*,2*S*)-hydrogen ($H_A$) of **3** is lost while $H_B$ is incorporated in **2** at C-5.[4] Similarly, in the clavaminate synthase-catalysed cyclization/dehydration of proclavaminic acid **5** to clavaminic acid **6** it was determined that formation of the oxazolidine ring involved specific replacement of the 4′*S*-label ($H_A$) with substrate oxygen (retention of configuration).[5] Finally, the demonstration that both $H_A$ and $H_B$ are retained from glycerol **3** to proclavaminic acid **5** allowed important deductions to be made about the cryptic formation of the β-lactam ring. Generation of the azetidinone N–C-4′ bond takes place with (*a*) loss of the glycerol oxygen, (*b*) no net change in oxidation state at this methylene carbon and, (*c*) overall retention of configuration,[6] unlike monocyclic β-lactam formation in nocardicin[7] and, presumably, the monobactams. Lastly, the stereochemical inversion that takes place between clavaminic acid **6** and clavulanic acid **2** must occur with retention of $H_B$.

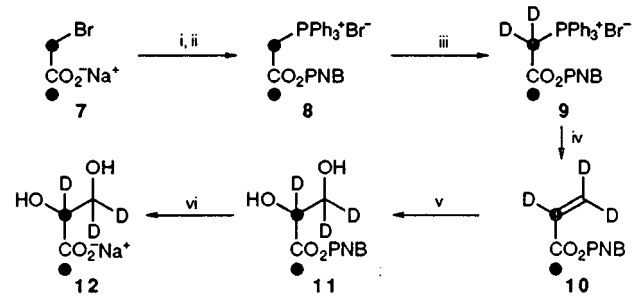
The complete loss of $H_C$ from glycerol **3**, but the retention of both $H_A$ and $H_B$ into proclavaminic acid **5** followed by their stereospecific loss and retention, respectively, into clavulanic acid **2** point to the intervention of conventional glycolytic metabolism, *e.g.* to glycerate **4**, prior to uptake into the β-lactam biosynthetic pathway. Earlier whole-cell studies revealed that [2-$^3$H, 1-$^{14}$C]-D-glycerate gave efficient incorporation of carbon label into the β-lactam ring (95–100%) of clavulanic acid, but only 4–11% of the tritium could be accounted for in the molecule by chemical degradation, principally at C-6 and C-8.[3] Given the inherent inaccuracies of low radioactivity in this technically difficult double label experiment, we have re-examined the fate of the glycerate C-2 hydrogen by a methodologically distinct means.

The experiment to test the retention or loss of H-2 was designed to use two $^{13}$C-labels as internal measures of intact and absolute carbon utilization and then multiple deuterium labels to monitor changes at H-2 knowing that one of the glycerate H-3 hydrogens would be cleanly retained in clavulanic acid **2**. Thus, (±)-[2,3,3-$^2H_3$, 1,2-$^{13}C_2$]glycerate **12** (Scheme 2) was prepared as follows. [1,2-$^{13}C_2$]Bromoacetate **7** was converted to its crystalline *p*-nitrobenzyl (PNB) ester and treated with $PPh_3$ to form the phosphonium salt **8**. Facile ylide formation in $D_2O$ allowed rapid exchange at the C-2 methylene followed by Wittig reaction with deuterioformaldehyde in $D_2O$[8,9] in the presence of anhydrous $K_2CO_3$ yielded *p*-nitrobenzyl [2,3,3-$^2H_3$, 1,2-$^{13}C_2$]acrylate **10** in excellent yield. Sharpless dihydroxylation[10,11] gave PNB glycerate **11**. Hydrogenolysis in the presence of $NaHCO_3$ and reverse-phase HPLC purification (Partisil 10 ODS 3, 25 × 250 mm, $H_2O$ elution) provided the desired quintuply labelled sodium glycerate **12** in nearly 60% overall yield. $^{13}C\{^1H\}$ NMR analysis of the product [Fig. 1(*a*)] displayed the expected carboxyl resonance as a clean doublet ($^1J_{CC}$ = 54.2 Hz) while the corresponding doublet for C-2 was further split into a pair of 1 : 1 : 1 triplets owing to the directly bound deuterium ($^1J_{CD}$ = 22.1 Hz) and broadened slightly by the adjacent C-3 deuteria.

Cultures (2.0 l) of *Streptomyces clavuligerus* (ATCC 27064) were grown as previously described (500 ml/4 l flask).[12] After 48 h, **12** (2.0 mmol/l) was administered in equal portions to the fermentations under sterile conditions. After an additional 96 h, the clavulanic acid produced was isolated by adsorption onto carbon, conversion to its *p*-bromobenzyl ester and purification by silica gel chromatography (40 mg).[2,13] Careful $^{13}C\{^1H\}$ NMR analysis of this product showed the natural abundance singlet for the β-lactam carbonyl, C-7, flanked by a doublet ($^1J_{CC}$ = 38.9 Hz) indicating 0.80–0.85% intact incorporation of the multiply labeled glycerate carbon skeleton [Fig. 1(*b*)].




**Scheme 1**




**Scheme 2** *Reagents and conditions*: i, PNB–OH, EDC, DMAP, $CH_2Cl_2$, room temp., 3 h, 95%; ii, $PPh_3$, THF–$CH_2Cl_2$, room temp., 24 h; iii, $D_2O$, room temp., 24 h; iv, $D_2CO$ in $D_2O$, $K_2CO_3$, 24 h, 80% for 3 steps; v, Bu$^t$OOH, cat. $OsO_4$, $Et_4NOAc$, acetone, 0 °C to room temp., 6 h, 85%; vi, $H_2$, 10% Pd–C, $NaHCO_3$, $H_2O$–THF, room temp., 24 h, then RP–HPLC, 92%

Centred upfield at δ 46.39, the natural abundance peak for C-6 could be found flanked by upfield α- and α/β-shifted doublets.[14] That marked by (▲) corresponds to $^{13}C$ at C-6 paired to $^{13}C$ at C-7 and $^{2}H$-label at C-5 (α- and β-heavy isotopes; $\Delta\delta$ = 0.144 ppm). This species represents 80% fully intact incorporation of **12**. The second, smaller doublet (●) is due to doubly $^{13}C$-labelled molecules, but having $^{1}H$ at C-5 (α-heavy isotope; $\Delta\delta$ = 0.019 ppm). While this 20% of incorporated precursor seems high, it is an artifact[4] of cummulative isotope effects[15] that discriminate against $^{2}H$-labelled molecules, but let the very small proportion of [$^{1}H$,$^{13}C$]-labelled precursor and intermediate molecules pass more swiftly along the pathway. These observations notwithstanding, notably absent is a 1 : 1 : 1 triplet corresponding to deuterium directly bound to C-6 and a concommitant β-isotope shift detectable in the doublet for C-7. In an attempt to establish an upper bound for incorporation of deuterium at C-6, a $^{2}H\{^{1}H\}$ NMR spectrum was recorded (data not shown). Deuterium label at C-5 was easily observed and, while some minor secondary incorporation at C-9 could be detected, none was seen at C-6. Within the limits of the NMR methods used, we place the possible level of deuterium incorporation at C-6 from each of these NMR experiments at < 0.05%.

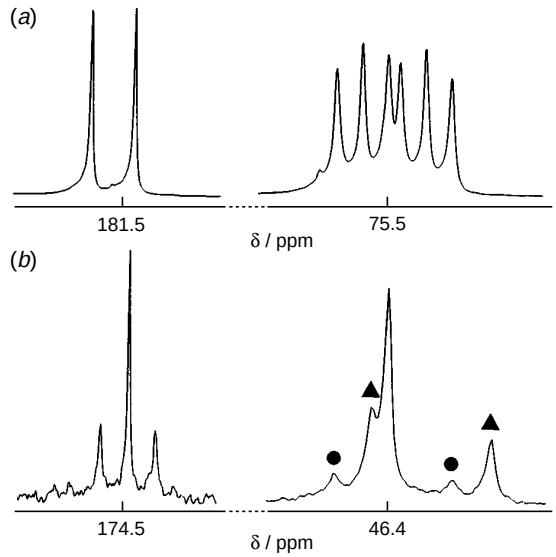



**Fig. 1** Partial $^{13}C\{^{1}H\}$ NMR spectra at 100 MHz of (*a*) [2,3,3-$^{2}H_3$, 1,2-$^{13}C_2$]-D,L-glycerate **12** in $D_2O$, referenced to DSS; (*b*) biosynthetically enriched *p*-bromobenzyl clavulanate in $CDCl_3$, referenced to $SiMe_4$, 21 000 transients

We are led to conclude from these data that $^{2}H$-2 is lost from **12** upon incorporation into clavulanic acid. There is a caveat, however remote, that H-2, unlike H-3, is labile among the intermediates of glycolysis despite the use of a triglyceride-based medium to favour gluconeogenesis.[3,12] The possibility exists that the metabolic flux among these intermediates is so great relative to the rate of entry into the biosynthetic pathway that the C-2 deuterium has exchanged for hydrogen before detectable incorporation at C-6 can occur. This proviso aside, the loss of H-2 from glycerate imposes new limitations on the mechanism of β-lactam formation in clavulanic acid biosynthesis, a process whose full understanding has thus far resisted experimental enquiry.

## References


1 S. W. Elson, K. H. Baggaley, M. Davidson, M. Fulston, N. H. Nicholson, G. D. Risbridger and J. W. Tyler, *J. Chem. Soc., Chem. Commun.*, 1993, 1212.
2 I. Stirling and S. W. Elson, *J. Antibiot.*, 1979, **32**, 1125.
3 C. A. Townsend and M.-F. Ho, *J. Am. Chem. Soc.*, 1985, **107**, 1066.
4 C. A. Townsend and S.-S. Mao, *J. Chem. Soc., Chem. Commun.*, 1987, 86.
5 A. Basak, S. P. Salowe and C. A. Townsend, *J. Am. Chem. Soc.*, 1990, **112**, 1654.
6 D. B. McIlwaine and C. A. Townsend, *J. Chem. Soc., Chem. Commun.*, 1993, 1346.
7 C. A. Townsend, A. M. Brown and L. T. Nguyen, *J. Am. Chem. Soc.*, 1983, **105**, 919.
8 M. Grayson and P. T. Keough, *J. Am. Chem. Soc.*, 1960, **82**, 3919.
9 C. A. Townsend, T. Scholl and D. Arigoni, *J. Chem. Soc., Chem. Commun.*, 1975, 921.
10 K. Akashi, R. E. Palermo and K. B. Sharpless, *J. Org. Chem.*, 1978, **43**, 2063.
11 H. C. Kolb, M. S. VanNieuwenhze and K. B. Sharpless, *Chem. Rev.*, 1994, **94**, 2483.
12 S. W. Elson and R. S. Oliver, *J. Antibiot.*, 1978, **31**, 586.
13 C. A. Townsend and M.-F. Ho, *J. Am. Chem. Soc.*, 1985, **107**, 1065.
14 J. C. Vederas, *Nat. Prod. Rep.*, 1987, 277.
15 S. P. Salowe, W. J. Krol, D. Iwata-Reuyl and C. A. Townsend, *Biochemistry*, 1991, **30**, 2281.


*Received, 17th October 1996; Com. 6/07078G*

# Hydrogen generation using water-insoluble polymer-bound ruthenium(II) complexes

**Masahiro Suzuki, Satoshi Kobayashi, Mutsumi Kimura, Kenji Hanabusa and Hirofusa Shirai***

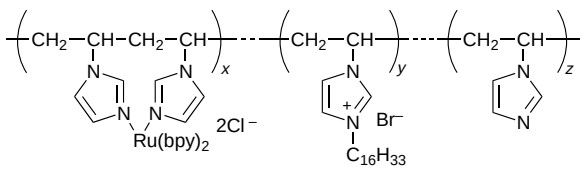
*Department of Functional Polymer Science, Faculty of Textile Science and Technology, Shinshu University, Ueda, Nagano 386, Japan*

**Water-insoluble free-standing films of partially quaternized poly(1-vinylimidazole)-bound ruthenium(II) complexes are prepared, and photoinduced hydrogen generation is observed with light irradiation (λ > 440 nm) of aqueous solutions containing the polymer-bound ruthenium(II) complex film, methyl viologen, triethanolamine and bis(2,2′-bipyridine)platinum(II).**

Tris(2,2′-diimine)ruthenium(II) complexes have attracted much attention as photosensitizers for application to solar-energy conversion.[1–3] In particular, tris(2,2′-bipyridine)ruthenium(II), $[Ru(bpy)_3]^{2+}$, has been widely employed as a photocatalyst for water cleavage and used as a photosensitizer in many hydrogen generation systems.[4–7] Metallopolymers, in which ruthenium(II) complexes are coordinated to poly(4-vinylpyridine) and poly(1-vinylimidazole), have been investigated, and applications to polymer catalysts, photosensitizers, and molecular diodes have been proposed.[8–10] However, there are no reports on the application of these photosensitizers to photoinduced hydrogen generation.

Recently, we have reported the preparation of partially quaternized poly(1-vinylimidazole)-bound ruthenium(II) complexes [Ru(QPIm)] and their films, and luminescence quenching and photosensitized charge separation using Ru(QPIm)s as photosensitizers.[11–13] These results indicated that Ru(QPIm)s and their films are sufficiently capable of utilization as photosensitizers. In this work, hydrogen generation using Ru(QPIm)s as photosensitizers was investigated in methanol–water and water.

The polymer photosensitizers were prepared according to the literature[11] and the structures were confirmed by $^1$H NMR and absorption spectroscopies (Fig. 1). The polymer films were prepared by casting from methanol solution, and the measured thicknesses were 0.182 mm for $C_{16}$RuQPIm-25 and 0.184 mm for $C_{16}$RuQPIm-44. 1,1′-Dimethyl-4,4′-bipyridinium ($MV^{2+}$) and 1,1′-dioctyl-4,4′-bipyridinium ($C_8V^{2+}$) were used as acceptors. Triethanolamine (TEA) was used as a sacrificial donor and bis(2,2′-bipyridine)platinum(II) $[Pt(bpy)_2]^{2+}$ was used as the catalyst for hydrogen evolution, respectively. Hydrogen generation was performed at 25 °C with light irradiation by a 300 W slide projector under an argon atmosphere. Light with λ < 440 nm was cut off by a Toshiba Y-44 filter.




| Polymers | *x* | *y* | *z* |
|---|---|---|---|
| $C_{16}$RuQPIm-25 | 0.0033 | 0.2531 | 0.7436 |
| $C_{16}$RuQPIm-44 | 0.0033 | 0.4404 | 0.5563 |

**Fig. 1** Chemical structure of Ru(QPIm)

Fig. 2 shows the relationship between hydrogen generation and irradiation time for Ru(QPIm)s in methanol–water (9 : 1 *v*/*v*) and RuQPIm films in aqueous solution.

The amount of generated hydrogen for $C_{16}$RuQPIm-25 was larger than that for $C_{16}$RuQPIm-44. This is attributed to electrostatic repulsion between viologen species and quaternized imidazolium residues and steric hindrance of alkyl side-chains.

Compared with $MV^{2+}$ systems, hydrogen generation for $C_8V^{2+}$ systems was lower. We have already reported that viologens with long alkyl groups show van der Waals interactions with alkyl side-chains on the polymer backbone.[11,12] After electron transfer from the photoexcited ruthenium(II) complex to $MV^{2+}$ in the polymer domain, the $MV^{\cdot+}$ species formed quickly diffuse into the bulk solution and readily react with the Pt catalyst. However, the $C_8V^{\cdot+}$ species barely diffuse into the bulk solution due to interaction with the polymer, leading to the inhibition of reaction with the positively charged Pt catalyst; consequently, hydrogen generation decreases.

In Ru(QPIm) film systems, 0.46 and 0.36 ml of hydrogen was evolved for $C_{16}$RuQPIm-25/$MV^{2+}$ and $C_{16}$RuQPIm-44/$MV^{2+}$, respectively, while hydrogen evolution was scarcely observed in the $C_8V^{2+}$ systems. During light irradiation, the colour of reaction solution and polymer film do not change, indicating that the $MV^{\cdot+}$ species formed react rapidly with the platinum catalyst. For $C_8V^{2+}$ systems, however, the colour of the polymer film changes from orange to deep blue (but the solution is

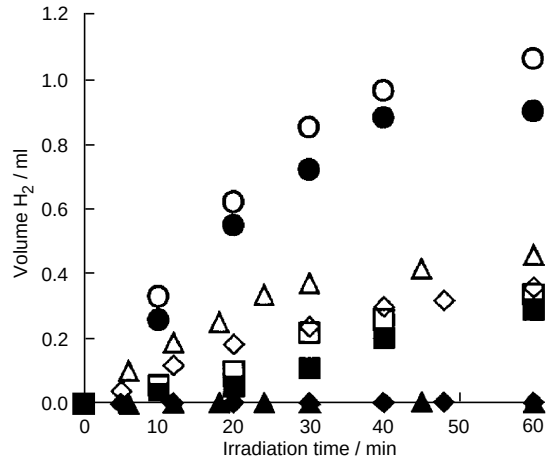



**Fig. 2** Hydrogen generation upon light irradiation of methanol–water (9 : 1 *v*/*v*) containing $5.0 \times 10^{-5}$ mol dm$^{-3}$ Ru(QPIm), $5.0 \times 10^{-3}$ mol dm$^{-3}$ viologen, 0.1 mol dm$^{-3}$ TEOA, and $3.0 \times 10^{-3}$ mol dm$^{-3}$ platinum catalyst for $C_{16}$RuQPIm-25/$MV^{2+}$ (○), $C_{18}$RuQPIm-44/$MV^{2+}$ (□), $C_{16}$RuQPIm-25/$C_8V^{2+}$ (●), $C_{16}$RuQPIm-44/$C_8V^{2+}$ (■), $C_{16}$RuQPIm-25film/$MV^{2+}$ (△), $C_{16}$RuQPIm-44film/$MV^{2+}$ (◇), $C_{16}$RuQPIm-25film/$C_8V^{2+}$ (▲) and $C_{16}$RuQPIm-44film/$C_8V^{2+}$ (◆)

unchanged), which indicates that a charge separation reaction occurs and the $C_8V^{\cdot+}$ species scarcely react with the platinum catalyst. In a previous paper,[13] we reported that $C_8V^{2+}$ species are adsorbed on the surface of the polymer film and only adsorbed $C_8V^{2+}$ species react with photoexcited ruthenium(II) complexes. Considering this fact, the present results can be explained as follows. After electron transfer from the photoexcited ruthenium(II) complex to the $MV^{2+}$ species on the surface of the polymer, the $MV^{\cdot+}$ species formed diffuse into the bulk solution and react with the platinum catalyst, leading to hydrogen generation. On the other hand, $C_8V^{2+}$ species are adsorbed on the surface of the polymer film and the charge separation takes place only on the film surface. Therefore, no evolution of hydrogen is observed since the adsorbed $C_8V^{\cdot+}$ species do not react with the positively charged platinum catalyst. Quantum yields for $H_2$ formation are summarized in Table 1.

**Table 1** Maximum amount of generated hydrogen and quantum yields for hydrogen generation for solution and film systems

| | $H_2$[a]/ml | $\phi(H_2)$ |
|---|---|---|
| In MeOH–$H_2O$ | | |
| $C_{16}$RuQPIm-25/$MV^{2+}$ | 1.01 | 0.026 |
| $C_{16}$RuQPIm-25/$C_8V^{2+}$ | 0.34 | 0.025 |
| $C_{16}$RuQPIm-44/$MV^{2+}$ | 0.91 | 0.022 |
| $C_{16}$RuQPIm-44/$C_8V^{2+}$ | 0.29 | 0.018 |
| In aqueous solution (film) | | |
| $C_{16}$RuQPIm-25/$MV^{2+}$ | 0.46 | 0.015 |
| $C_{16}$RuQPIm-25/$C_8V^{2+}$ | 0.36 | 0.014 |
| $C_{16}$RuQPIm-44/$MV^{2+}$ | < 0.01 | < 0.001 |
| $C_{16}$RuQPIm-44/$C_8V^{2+}$ | < 0.01 | < 0.001 |

[a] Irradiation for 1 h.

The present results demonstrate that partially quaternized poly(1-vinylimidazole)-bound ruthenium(II) complex films can be used for a photoinduced hydrogen generation reaction as new polymer-solid photosensitizers. Furthermore, it is found that the high efficiency of charge separation does not necessarily bring about high efficiency of hydrogen generation in the present systems. A detailed investigation on the hydrogen generation is now in progress in our laboratory.

## References


1 A. Juris, V. Balzani, F. Barigelletti, S. Campagna, P. Belser and A. von Zelewsky, *Coord. Chem. Rev.*, 1988, **84**, 85.
2 T. J. Meyer, *Pure Appl. Chem.*, 1986, **58**, 1193.
3 J. S. Connolly, *Photochemical Conversion and Storage of Solar Energy*, Academic Press, New York, 1981.
4 K. Kalyanasundarama, *Photochemistry of Polypyridine and Porphyrin Complexes*, Academic Press, London, 1981.
5 C. Creutz and N. Sutin, *Proc. Natl. Acad. Sci. USA*, 1975, **72**, 2858.
6 J. R. Norris and D. Meisel, *Photochemical Energy Conversion*, Elsevier, Amsterdam, 1988.
7 E. Pellizzetti and M. Schivavello, *Chemical Conversion Storage of Solar Energy*, Kluwer Academic, Dordrecht, 1990.
8 O. Haas, H. R. Zumbrunnen and J. G. Vos, *Electrochim. Acta*, 1985, **30**, 1551.
9 S. M. Geraty and J. G. Vos, *J. Chem. Soc., Dalton Trans.*, 1987, 3073.
10 R. J. Forster and J. G. Vos, *Macromolecules*, 1990, **23**, 4372.
11 M. Suzuki, Y. Mori, M. Kimura, K. Hanabusa and H. Shirai, *J. Chem. Soc., Faraday Trans.* 1996, in the press.
12 M. Suzuki, Y. Mori, N. Yokoyama, M. Kimura, K. Hanabusa and H. Shirai, *Macromol. Chem. Phys.*, 1996 in the press.
13 M. Suzuki, M. Kimura, K. Hanabusa and H. Shirai, *J. Phys. Soc.*, submitted.



*Received, 21st October 1996; Com. 6/07161I*

# A novel diaminoborate ligand system derived from 1,8-diaminonaphthalene and 9-BBN: preparation of titanium and zirconium complexes and crystal structure of the titanium complex

**Galia Bar-Haim, Romem Shach and Moshe Kol*†**

*School of Chemistry, Raymond and Beverly Sackler Faculty of Exact Sciences, Tel-Aviv University, Tel-Aviv 69978, Israel*

**1,8-Diaminonaphthalene reacts selectively with 1 equiv. of 9-BBN to form a bridging amine–aminoborane, and with 2 equiv. of 9-BBN to form a non-bridging bis(aminoborane); these aminoboranes give rise to a novel diaminoborate (4e,1−) ligand system by reactions with dimethylamides of titanium and zirconium.**

The search for new ligand systems, and especially ones that could replace the (6e,1−) cyclopentadienyl type ligands, is a major area of research in current inorganic and organometallic chemistry. Most progress has been achieved with ligands based on nitrogen donors like trispyrazolylborate,[1] benzamidinate,[2] silyl amide,[3] boryl amide[4] and others.[5] A major aspect in designing of such ligands, other than their electronic character, is their steric effects on the metal environment. In this report we describe a novel boron nitrogen ligand derived *via* two routes from 1,8-diaminonaphthalene and 9-BBN, and its complexes with titanium and zirconium.

Aniline was reported to react with 9-borabicyclo[3.3.1]-nonane (9-BBN) to form the corresponding *B*-phenylamino-9-BBN with evolution of hydrogen gas.[6] We found that 1,8-diaminonaphthalene can react with 9-BBN, with evolution of hydrogen gas, to form two isolable products, depending on the molar ratio of the reactants: addition of exactly 1 equiv. of 9-BBN to 1,8-diaminonaphthalene results in highly selective formation of an amine–aminoborane, $HL^1$, whereas addition of 2 equiv. of 9-BBN to 1,8-diaminonaphthalene yields a bis-(aminoborane), $L^2$, quantitatively. Adding 1 equiv. of 9-BBN to isolated $HL^1$ produces $L^2$ in high yield as well (Scheme 1). When stored and handled under dry nitrogen at room temperature, $HL^1$ and $L^2$ are stable for months.

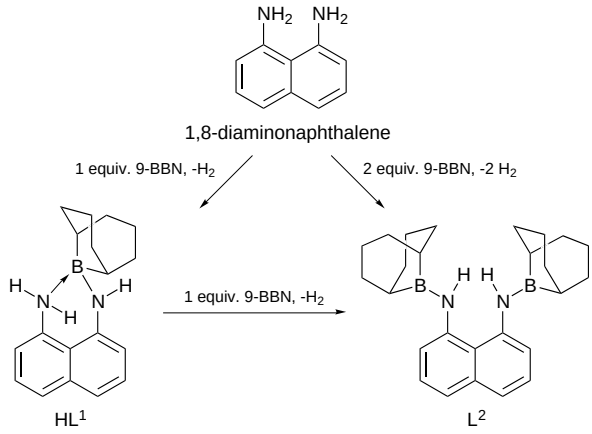
$^1$H, $^{13}$C and $^{11}$B NMR indicate that $HL^1$ is *pseudo*-$C_{2v}$-symmetrical on the NMR timescale, with the boron atom bridging between the two nitrogen atoms.‡ The three N–H protons appear as a sharp singlet in the $^1$H NMR spectrum even at −50 °C. These data are consistent with a fast dynamic process in which the bridging 9-BBN unit is rocking between the two faces of the naphthalene ring, while the three N–H protons rapidly equilibrate between the two nitrogen atoms.

On the other hand, the two boron atoms in $L^2$ are three-coordinate according to $^{11}$B NMR spectroscopy, *i.e.* they are not bridging between the two nitrogen atoms. Three peaks for six aromatic protons indicate a symmetrical naphthalene system. Two peaks for four bridgehead carbons of the two 9-BBN units indicate a high barrier to rotation of the 9-BBN groups around the B–N bonds attributed to $p_\pi$–$p_\pi$ interactions.§

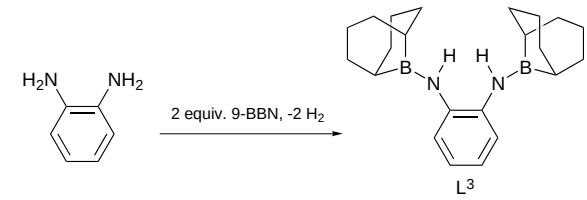
Interestingly, related aromatic diamines do not exhibit the same high selectivity in formation of an amine–aminoborane. Thus, reaction between 1,2-phenylenediamine and 2 equiv. of 9-BBN gave a bis(aminoborane), $L^3$, quantitatively, whose spectral properties are analogous to those of $L^2$ (Scheme 2).¶ However, reaction between 1,2-phenylenediamine and 1 equiv. of 9-BBN gave an inseparable mixture of products.

$HL^1$ reacted cleanly with tetrakis(dimethylamino)titanium in an amine elimination reaction giving $[TiL^1(NMe_2)_3]$ **1** and dimethylamine. **1** was isolated in high yield as an orange crystalline solid upon evaporation of the solvent and recrystallisation from diethyl ether–pentane at −35 °C. Tetrakis-(dimethylamino)zirconium reacted similarly yielding $[ZrL^1(NMe_2)_3]$ **2** as a white crystalline solid after a similar work-up (Scheme 3, route a). **1** and **2** exhibit almost identical NMR spectra that indicate that, in solution, $L^1$ is a (4e,1−) symmetrical chelating diaminoborate-type ligand.‖

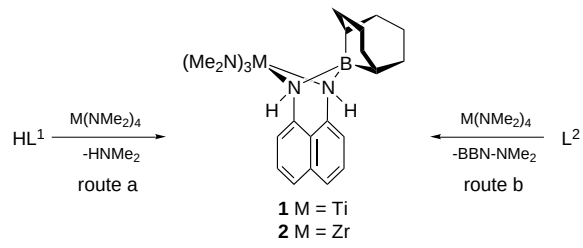
The X-ray crystal structure of the titanium complex **1** showed that the chelating diaminoborate ligand effectively blocks one face of the metal (Fig. 1).** The main structural feature is an almost perfectly symmetrical Ti–N–B–N four-membered ring, having B–N and Ti–N bond lengths of 1.60 and 2.29 Å, respectively, and N–B–N and N–Ti–N bond angles of 94.4 and 61.4°, respectively.




**Scheme 1**




**Scheme 2**




**Scheme 3**

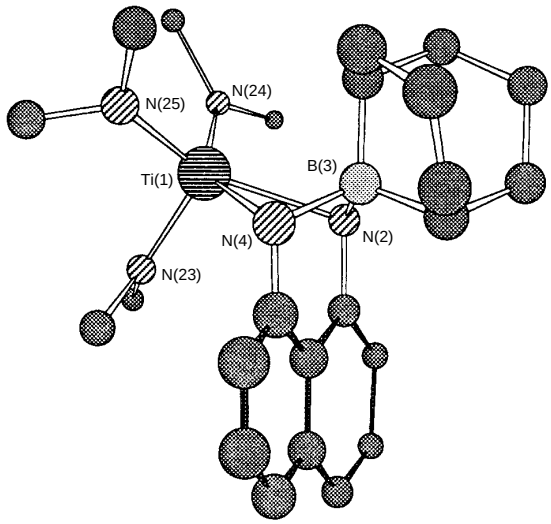



**Fig. 1** Molecular structure of [TiL$^1$(NMe$_2$)$_3$] **1**. Hydrogen atoms omitted for clarity. Selected distances (Å) and angles (°): Ti(1)–N(2) 2.302(3), Ti(1)–N(4) 2.282(4), Ti(1)–N(23) 1.874(3), Ti(1)–N(24) 1.927(5), Ti(1)–N(25) 1.912(3), B(3)–N(2) 1.586(7), B(3)–N(4) 1.604(5); N(2)–Ti(1)–N(4) 61.4(1), N(2)–B(3)–N(4) 94.4(4), Ti(1)–N(2)–B(3) 88.0(2), Ti(1)–N(4)–B(3) 88.3(3).

Several reports describing systems that include M–N–B–N four-membered rings have appeared (M = Ge, Sn, Ti, Zr, Cr).[7] However, in those cases the N–B–N unit either forms a (4e,2−) ligand, or it is a part of a larger heterocyclic system. The system we describe herein is the first case of a (4e,1−) diaminoborate ligand system, to the best of our knowledge. Unlike other (4e,1−) ligands, such as benzamidinate or acetylacetonate, the diaminoborate ligand consists of tetrahedral atoms rather than trigonal-planar atoms close to the metal centre. Since tetrahedral atoms are inherently more sterically demanding than trigonal-planar atoms, close control of the metal environment can be achieved by proper substitutions in this ligand system.

The *N,N′*-bis(trimethylsilyl) derivative of 1,8-diaminonaphthalene acts as a (4e,2−) ligand.[8] Considering the B–Si diagonal relationship one may expect that L$^2$ would act as a chelating (4e,2−) bis(borylamide) ligand[4] by double deprotonation. However, this was not the case. Instead, L$^2$ reacted cleanly with tetrakis(dimethylamino)-titanium and -zirconium to yield the diaminoborate complexes **1** and **2**, respectively, accompanied by 9-BBN–NMe$_2$ as a by-product[9] (Scheme 3, route b). The driving force for this unprecedented transformation is, apparently, the stability of the boron-bridged structure, in the 1,8-diaminonaphthalene skeleton.

Proximity effects have a strong effect on chemical reactivity in 1,8-disubstituted naphthalenes.[10] We think that the selective formation of HL$^1$ and of the (4e,1−) metal complexes of L$^1$ (**1** and **2**) are a result of such effects. We are currently investigating these effects as well as the reactivity of the novel diaminoborate complexes.

We thank the Israel Science Foundation administered by the Israel Academy of Sciences and Humanities for financial support.

## Footnotes

† E-mail: moshekol@ccsg.tau.ac.il

‡ HL$^1$ was prepared on a 20 mmol scale by adding 1 equiv. of 9-BBN in hexanes to a solution of 1,8-diaminonaphthalene in ether under nitrogen, and stirring at room temp. until hydrogen evolution ceased (*ca*. 30 min). The light yellow solid that precipitated was washed with ether and dried to give pure HL$^1$ in *ca*. 95% yield: $^1$H NMR ($C_6D_6$, 200 MHz) δ 0.58 (br s, 2 H, CH), 1.60–2.20 (m, 12 H, 6 $CH_2$), 4.06 (s, 3 H, NH), 6.12 (d, 2 H, *J* 8 Hz), 7.08 (t, 2 H, *J* 8 Hz), 7.24 (d, 2 H, *J* 8 Hz). $^{13}$C{$^1$H} NMR ([$^2H_8$]thf, 50.4 MHz) δ 24.4 (CH), 27.3 ($CH_2$), 33.2 ($CH_2$), 113.4 (CH), 120.6 (CH), 128.3 (CH). $^{11}$B NMR ($C_6D_6$, 115.5 MHz) δ −1.7.

§ L$^2$ was prepared on a 10 mmol scale, by adding 2 equiv. of 9-BBN in hexanes to a solution of 1,8-diaminonaphthalene in ether under nitrogen, and stirring at room temp. until hydrogen evolution ceased (*ca*. 30 min). Removing the solvents under vacuum yielded white crystalline L$^2$ quantitatively: $^1$H NMR ($C_6D_6$, 200 MHz) δ 1.29–1.95 (m, 14 H), 6.92 (s, 2 H, NH), 7.04 (d, 2 H, *J* 8 Hz), 7.15 (t, 2 H, *J* 8 Hz), 7.44 (d, 2 H, *J* 8 Hz). $^{13}$C{$^1$H} NMR ($C_6D_6$ 50.4 MHz) δ 22.9 (CH), 28.1 (CH), 24.4 ($CH_2$), 33.8 ($CH_2$), 34.4 ($CH_2$), 126.2 (CH), 123.6 (CH), 126.3 (CH). $^{11}$B NMR ($C_6D_6$, 115.5 MHz) δ 49.9.

¶ L$^3$: $^1$H NMR ($C_6D_6$, 200 MHz) δ 1.30–2.04 (m, 14 H), 5.67 (s, 2 H, NH), 7.02 (m, 2 H), 7.23 (m, 2 H); $^{13}$C{$^1$H} NMR ($C_6D_6$, 50.4 MHz) δ 23.2, 28.0 (CH), 24.5, 34.0, 34.8 ($CH_2$), 125.3, 125.9 (CH); $^{11}$B NMR ($C_6D_6$, 115.5 MHz) δ 51.6.

‖ [TiL$^1$(NMe$_2$)$_3$] **1**: $^1$H NMR ($C_6D_6$, 200 MHz) δ 0.63 (br s, 1 H, CH), 0.67 (br s, 1 H, CH), 1.75–2.20 (m, 12 H, 6 $CH_2$), 2.84 (s, 18 H), 4.11 (s, 2 H, NH), 6.39 (d, 2 H, *J* 7 Hz), 7.13 (t, 2 H, *J* 7 Hz), 7.20 (d, 2 H, *J* 7 Hz). $^{11}$B NMR ($C_6D_6$, 115.5 MHz) δ −2.8. [ZrL$^1$(NMe$_2$)$_3$] **2**: $^1$H NMR ($C_6D_6$, 200 MHz) δ 0.69 (br s, 2 H, CH), 1.68–2.11 (m, 12 H, 6 $CH_2$), 2.69 (s, 18 H) 3.99 (s, 2 H, NH), 6.37 (d, 2 H, *J* 7 Hz), 7.08 (t, 2 H, *J* 7 Hz), 7.22 (d, 2 H, *J* 7 Hz). $^{11}$B NMR ($C_6D_6$, 115.5 MHz) δ −4.4.

** *Crystal data* for $C_{24}H_{40}BN_5Ti$, *M* = 457.32, monoclinic, space group $P2_1/a$, *a* = 15.649(4), *b* = 18.949(2), *c* = 18.404(3) Å, β = 111.72(2)°, *U* = 5070(2) Å$^3$, *Z* = 8, $D_c$ = 1.198 g cm$^{-3}$, λ(Mo-Kα) 0.71073 Å, $2\theta_{max}$ = 45.96°. Data were collected on an Enraf-Nonius CAD4 diffractometer using an orange crystal mounted in a sealed glass capillary at room temperature. Of a total of 6245 collected reflections, 6027 were unique ($R_{int}$ = 0.0387). The structure was solved by direct methods. The final cycle of full-matrix least-squares refinement was based on 6027 observed reflections ($I > 0$) and 571 variable parameters and converged with unweighted and weighted agreement factors of $R$ = 0.0995, $R_w$ = 0.1391 for the entire data. GOF = 1.010. Residual electron densities: +0.20, −0.29 e Å$^{-3}$.

Atomic coordinates, bond lengths and angles, and thermal parameters have been deposited at the Cambridge Crystallographic Data Centre (CCDC). See Information for Authors, Issue No. 1. Any request to the CCDC for this material should quote the full literature citation and the reference number 182/314.

## References

1 S. Trofimenko, *Chem. Rev.*, 1993, **93**, 943.
2 R. Gomez, R. Duchatteau, A. N. Chernega, J. H. Teuben, F. T. Edelman and M. L. H. Green, *J. Organomet. Chem.*, 1995, **491**, 153; D. Herskovics-Korine and M. S. Eisen, *J. Organomet. Chem.*, 1995, **503**, 307.
3 A. D. Horton, J. de With, A. J. van der Linden and H. van de Weg, *Organometallics*, 1996, **15**, 2672.
4 T. H. Warren, R. R. Schrock and W. M. Davis, *Organometallics*, 1996, **15**, 562.
5 R. Kempe, S. Brenner and P. Arndt, *Organometallics*, 1996, **15**, 1071.
6 B. Singaram, *Heteroatom Chem.*, 1992, **3**, 245.
7 D. Fest, C. D. Habben, A. Meller, G. M. Sheldrick, D. Stalke and F. Pauer, *Chem. Ber.*, 1990, **123**, 703; H. Fußstetter and H. Nöth, *Chem. Ber.*, 1979, **112**, 3672; N. Kuhn, A. Kuhn, R. Boese and N. Augart, *J. Chem. Soc., Chem. Commun.*, 1989, 975; G. Schmid, D. Kampmann, W. Meyer, R. Boese, P. Paetzold and K. Delpy, *Chem. Ber.*, 1985, **118**, 2418.
8 J. C. D. Schaeffer and J. J. Zuckerman, *J. Am. Chem. Soc.*, 1974, **96**, 7160; Z. Ziniuk and M. Kol, unpublished work.
9 S. F. Nelsen, C. R. Kessel, D. J. Brien and F. Weinhold, *J. Org. Chem.*, 1980, **45**, 2116.
10 H. A. Staab and T. Saupe, *Angew. Chem., Int. Ed. Engl.*, 1988, **27**, 865.

*Received, 22nd October 1996; Com. 6/07194E*

# Structure determination from sparse data: geometries of the monohalogenophosphines

**Bruce A Smart and David W. H. Rankin***

*Department of Chemistry, University of Edinburgh, West Mains Road, Edinburgh, UK EH9 3JJ*

**Use of restraints calculated *ab initio* allows the refinement of the structures of the halogenophosphines, $PH_2X$ (X = F, Cl, Br, I), from published rotation constants.**

It is well known that combining experimental information obtained from methods such as gas-phase electron diffraction, rotational spectroscopy and liquid-crystal NMR spectroscopy in least-squares refinements yields more accurate structures than can be obtained using any one method alone.[1] The development of very fast and inexpensive computers has also made it practicable to utilise information calculated *ab initio* to improve the quality of molecular structures. Until recently, where experimental information was insufficient to determine the values of some parameters, normal practice was to fix them at values calculated *ab initio*.[2] This procedure is less than ideal, first because a fixed parameter is tacitly assumed to be absolutely correct and so its effect on other refining parameters cannot be gauged and, secondly, because unrealistically low standard deviations for correlated parameters can result.

We have recently described a method for assigning uncertainties to *ab initio* data, allowing theoretical information to be entered into structure refinements as predicate observations or flexible restraints (the SARACEN method).[3] A sensible choice of uncertainties can be obtained either by performing a graded series of calculations in which the basis set and level of correlation is systematically varied, or by consideration of the known accuracy of calculations at the highest level. The original aim of the SARACEN method was to enhance electron diffraction studies, giving complete molecular structures which were previously inaccessible. The method can also be used with rotation constants, providing a quick and relatively inexpensive way of extracting structural information from small sets of data. It is thus related to the 'diagnostic least-squares' method,[4] with the very important distinction that the restraints are now based on high-level calculations, instead of being more or less inspired guesses.

Recent reports of the rotation constants of the unstable monohalogenophosphines, $PH_2F$,[4,5] $PH_2Cl$,[5,6] $PH_2Br$[6,7] and $PH_2I$,[6,8] have provided an ideal opportunity to demonstrate the utility of this technique, leading to structures of these important molecules.

A graded series of *ab initio* molecular orbital calculations was undertaken to provide values and uncertainties used in structural refinements and to obtain vibrational corrections for conversion from the $B_0$ to $B_z$ structural type.† Calculated molecular geometries for the monohalogenophosphines are reported in Table 1.

Most parameters were insensitive to the adopted theoretical method, a notable exception being the phosphorus–halogen distances, which require the use of large polarisation sets. For

**Table 1** The molecular structure of $PH_2X$ (X = F, Cl, Br, I) compounds from theory and experiment[a]

| X | Method | $r$(P–X) | $r$(P–H) | θ(XPH) | θ(HPH) | X | $r$(P–X) | $r$(P–H) | θ(XPH) | θ(HPH) |
|---|---|---|---|---|---|---|---|---|---|---|
| F | 6-31G**/SCF | 159.95 | 140.57 | 98.64 | 93.70 | Br | 223.54 | 140.11 | 97.20 | 94.44 |
| | 6-31G**/MP2 | 162.72 | 141.04 | 98.89 | 92.21 | | 224.38 | 140.61 | 96.78 | 93.48 |
| | 6-311G**/SCF | 160.11 | 140.75 | 98.27 | 93.78 | | 225.17 | 140.37 | 96.91 | 94.60 |
| | 6-311G**/MP2 | 162.43 | 141.23 | 98.40 | 92.15 | | 225.06 | 140.88 | 96.65 | 93.06 |
| | 6-311G**MP3 | 161.81 | 141.29 | 98.05 | 92.21 | | 225.95 | 140.94 | 96.46 | 93.00 |
| | 6-311G**/MP4SDQ | 162.46 | 141.52 | 98.15 | 92.11 | | 226.26 | 141.12 | 96.45 | 92.98 |
| | 6-311G**/QCISD | 162.49 | 141.64 | 98.08 | 92.14 | | 226.47 | 141.26 | 96.40 | 92.96 |
| | 6-311+G**/MP2 | 163.97 | 141.16 | 97.38 | 92.94 | | 225.09 | 140.84 | 96.69 | 93.20 |
| | 6-311G(2df,2pd)/MP2 | 160.33 | 141.25 | 98.53 | 91.80 | | 223.74 | 140.79 | 96.16 | 92.58 |
| | QZ3P(f,d)/MP2 | 161.57 | 141.12 | 97.88 | 92.25 | | 222.26 | 140.82 | 96.48 | 92.63 |
| | SARACEN ($r_z$) | 160.4(1) | 142.3(4) | 98.1(5) | 92.1(3) | | 223.1(1) | 141.9(2) | 96.5(5) | 92.5(2) |
| | SARACEN ($r_e$) | 159.9(2) | 140.8(4) | 98.1(5) | 92.1(3) | | 222.6(2) | 140.4(2) | 96.5(5) | 92.5(2) |
| | Exptl. ($r_z$)[b] | 160.7(1) | 142.9(1) | 97.8(1) | 92.0(1) | | | | | |
| | Exptl. ($r_e$)[b] | 160.2(2) | 141.5(3) | 97.8(2) | 92.0(2) | | | | | |
| Cl | 6-31G**/SCF | 207.29 | 140.18 | 97.46 | 94.55 | I | 247.96 | 140.12 | 96.61 | 94.62 |
| | 6-31G**/MP2 | 207.27 | 140.67 | 97.53 | 93.41 | | 247.33 | 140.16 | 96.52 | 93.51 |
| | 6-311G**/SCF | 208.40 | 140.33 | 97.24 | 94.53 | | 248.95 | 140.37 | 96.33 | 94.71 |
| | 6-311G**/MP2 | 208.11 | 140.80 | 97.20 | 92.96 | | 248.98 | 140.88 | 95.48 | 93.21 |
| | 6-311G**/MP3 | 208.65 | 140.89 | 97.02 | 92.90 | | | | | |
| | 6-311G**/MP4SDQ[c] | — | — | — | — | | | | | |
| | 6-311G**/QCISD | 209.20 | 141.20 | 96.93 | 92.87 | | | | | |
| | 6-311+G**/MP2 | 208.06 | 140.82 | 97.22 | 93.05 | | 249.02 | 140.87 | 95.56 | 93.33 |
| | 6-311G(2df,2dp)/MP2 | 207.00 | 140.81 | 96.82 | 92.53 | | 244.39 | 140.80 | 95.65 | 92.71 |
| | QZ3P(f,d)/MP2 | 206.09 | 140.85 | 97.02 | 92.65 | | 244.32 | 140.82 | 95.82 | 92.67 |
| | SARACEN ($r_z$) | 206.4(1) | 141.8(3) | 97.2(7) | 92.6(2) | | 245.3(1) | 141.4(2) | 96.1(5) | 92.7(2) |
| | SARACEN ($r_e$) | 205.9(2) | 140.3(3) | 97.2(7) | 92.6(2) | | 244.8(2) | 139.9(2) | 96.1(5) | 92.7(2) |
| | Exptl. ($r_z$)[b] | 206.8(1) | 142.3(1) | 96.4(1) | 92.8(1) | | | | | |
| | Exptl. ($r_e$)[b] | 206.3(2) | 141.1(3) | 96.4(2) | 92.8(2) | | | | | |

[a] Distances in pm, angles in degrees. [b] Experimental geometry from ref. 20. [c] Molecular geometry not calculated at this level.

example, when the basis set is improved from 6-311G** to 6-311G(2df,2p) at the MP2 level of theory the P–F bond in $PH_2F$ is shortened by more than 2 pm. An analogous effect is found for the heavier $PH_2X$ compounds and has previously been observed for $PF_3$.[19] In all four compounds predictions of the P–H bond lengths proved to be far less sensitive to changes in the adopted theoretical method, with improvements beyond 6-31G**/MP2 having little effect on the value of this parameter. The H–P–X and H–P–H angles were found to be sensitive only to the inclusion of diffuse functions and a large polarisation set, although these effects are small and act in opposing directions.

Values chosen for use in SARACEN refinements were those calculated at the QZ3P(f,d)/MP2 level, corrected to allow for small differences between $r_e$ and $r_z$ structural types. Conservative estimates of uncertainties of geometric parameters were made in accordance with the level of convergence achieved with respect to improvements in the theoretical treatment. Uncertainties of 2.0 and 1.0 pm were used for P–X and P–H bonds while the two angle parameters were assigned uncertainties of 1.0°. Corrections of 1.5(2) and 0.5(2) pm for $r_z$ minus $r_e$ were adopted for the P–H and P–X bond lengths while angle corrections were 0.0(2)°, based on comparisons of the two structural types previously reported for $PH_3$ and $PF_3$.[20,21]

All rotation constants were converted from $B_0$ to $B_z$ structural type using vibrational corrections obtained from scaled 6-31G**/MP2 force fields, before inclusion in least-squares refinements. Uncertainties of 10% were attached to all corrections. In all cases values of rotation constants for the refined structures fell within about one standard deviation of the corrected values.

Flexible restraints derived from *ab initio* calculations were used for all four parameters in refinements for each molecule. In each case molecular parameters ($r_e$) refined to values which fell within one standard deviation of the flexible restraint (see Table 1). The refined e.s.d.s for the P–X and P–H bond lengths were found to be much smaller than the uncertainties used for the predicate observations, suggesting that most of the information about these refined parameters is derived from experimental information. The e.s.d.s of angles were much closer to the uncertainties of the restraints, indicating that less information about these parameters is provided by the rotation constants. In particular, the standard deviation of the X–P–H angle is as high as 0.7° in the case of $PH_2Cl$, indicating that this parameter is poorly defined by experimental information.

The structure of the $–PH_2$ unit in the monohalogenophosphines was found to be surprisingly independent of the attached halogen. The P–H bond lengths in the four compounds fell across a range of just a few tenths of a pm, while the H–P–H bond angles were indistinguishable. Increasing the size of the halogen results in slight narrowing of the X–P–H angle. Our final structures for $PH_2X$ molecules (where X = F, Cl, Br) are in good agreement with recent results based on more extensive experimental data (see Table 1).[22,23] This method therefore provides acceptable structural parameters, making optimum use of a restricted data set to yield a full structure.

We thank the EPSRC for the provision of the Edinburgh *ab initio* facilities (grant GR/K/04194). We are grateful to Dr J. Demaison for very helpful discussions, and for his willingness to provide us with results prior to publication.

## Footnote

† All calculations were carried out on a DEC Alpha APX 1000 workstation using the Gaussian 94 program.[9] Geometry optimisations and vibrational frequencies were calculated from analytic first and second derivatives respectively, with bond lengths and angles converging to at least 0.01 pm or 0.01°. Geometries for all molecules were calculated using the standard 6-31G**[10–12] and 6-311G**[13–14] basis sets at the SCF and MP2 levels of theory. The iodine basis sets used in 6-31G** and 6-311G** calculations are due to Dunning and Sadlej, respectively.[15,16] To explore the effects of diffuse functions and a larger polarisation set on the molecular geometry additional calculations were carried out at the 6-311+G**/MP2 and 6-311G(2df,2pd)/MP2 levels. For the fluorine, chlorine and bromine compounds the effects of more complete correlation treatments were investigated at the MP3, MP4SDQ and QCISD levels. Final geometry optimisations for all $PH_2X$ molecules were performed at the MP2 level of theory using a QZ3P(f,d) basis set due to Huzinaga,[17,18] comprising 7s3p1d/4s3p1d (H), 15s10p3d1f/10s5p3d1f (F), 18s13p3d1f/13s8p3d1f (P, Cl), 20s14p11d1f/14s10p7d1f (Br) and 24s19p16d1f/18s14p12d1f (I) basis sets. Vibrational frequency calculations were performed at the 6-31G**/MP2 level to obtain harmonic force fields, which were scaled by 0.95 and 0.90 for bond stretches and angle bends respectively before being used to obtain predictions of vibrational corrections for rotational constants.

## References

1 *Molecular Structure by Diffraction Methods*, Specialist Periodical Reports, The Chemical Society, London, 1975, p. 72.
2 V. J. Klimkowski, J. D. Ewbank, C. v. Alsenoy, J. N. Scarsdale and L. Schäfer, *J. Am. Chem. Soc.*, 1982, **104**, 1476.
3 A. J. Blake, P. T. Brain, H. McNab, J. Miller, C. A. Morrison, S. Parsons, D. W. H. Rankin, H. E. Robertson and B. A. Smart, *J. Phys. Chem.*, 1996, **100**, 12 280; P. T. Brain, C. A. Morrison, S. Parsons and D. W. H. Rankin, *J. Chem. Soc., Dalton Trans.*, 1996, 4589.
4 R. F. Curl, *J. Comput. Phys.*, 1970, **6**, 367.
5 H. Beckers, H. Bürger and M. Paplewski, *J. Mol. Spectrosc.*, 1995, **171**, 546.
6 H. Beckers, H.Bürger, M. Paplewski and W. Thiel, *J. Chem. Phys.*, 1994, **101**, 5585.
7 M. Paplewski, P. Drean, J. Demaison, H. Beckers and H. Bürger, *Chem. Commun.*, 1996, 2015.
8 H. Beckers, H. Bürger, J. Demaison, P. Drean, J.-M. Flaud and M. Paplewski, *J. Mol. Spectrosc.*, 1995, **172**, 78.
9 Gaussian 94 (Revision C.2), M. J. Frisch, G. W. Trucks, H. B. Schlegel, P. M. W. Gill, B. G. Johnson, M. A. Robb, J. R. Cheesman, T. A. Keith, G. A. Petersson, J. A. Montgomery, K. Raghavachari, M. A. Al-Laham, V. G. Zakrzewski, J. V. Ortiz, J. B. Foresman, J. Cioslowski, B. B. Stefanov, A. Nanayakkara, M. Challacombe, C. Y. Peng, P. Y. Ayala, W. Chen, M. W. Wong, J. L. Andres, E. S. Replogle, R. Gomperts, R. L. Martin, D. J. Fox, J. S. Binkley, D. J. Defrees, J. Baker, J. P. Stewart, M. Head-Gordon, C. Gonzalez and J. A. Pople, Gaussian Inc., Pittsburgh, PA, 1995.
10 W. J. Hehre, R. Ditchfield and J. A. Pople, *J. Chem. Phys.*, 1972, **56**, 2257.
11 P. C. Hariharan and J. A. Pople, *Theor. Chim. Acta*, 1973, **28**, 213.
12 M. S. Gordon, *Chem. Phys. Lett.*, 1980, **76**, 163.
13 R. Krishnan, J. S. Binkley, R. Seeger and J. A. Pople, *J. Chem. Phys.*, 1980, **72**, 650.
14 A. D. McLean and G. S. Chandler, *J. Chem. Phys.*, 1980, **72**, 5639.
15 T. H. Dunning, unpublished work.
16 A. J. Sadlej, *Theor. Chim. Acta*, 1992, **81**, 339.
17 S. Huzinaga and M. Klobukowski, *J. Mol. Struct.*, 1988, **167**, 1.
18 S. Huzinaga, *J. Chem. Phys.*, 1965, **42**, 1293.
19 M. Bühl, personal communication.
20 G. A. McRae, M. C. L. Gerry and E. A. Cohen, *J. Mol. Spectrosc.*, 1986, **116**, 58.
21 N. Ben Sari-Zizi, H. Bürger, M. Litz, H. Najib and J. Radtke, *J. Mol. Spectrosc.*, 1996, **177**, 46.
22 P. Drean, M. Paplewski, J. Demaison, J. Breidung, W. Thiel, H. Beckers and H. Bürger, *Inorg. Chem.*, in the press.
23 J. Demaison, personal communication.

*Received, 23rd October 1996; Com. 6/07243G*

# *N*-Methylidene[bis(trimethylsilyl)methyl]amine: the first isolable and stable monomeric methanimine allowing thermal [2 + 2] cycloadditions with ketenes

**Claudio Palomo,* Jesus M. Aizpurua, Marta Legido and Regina Galarza**

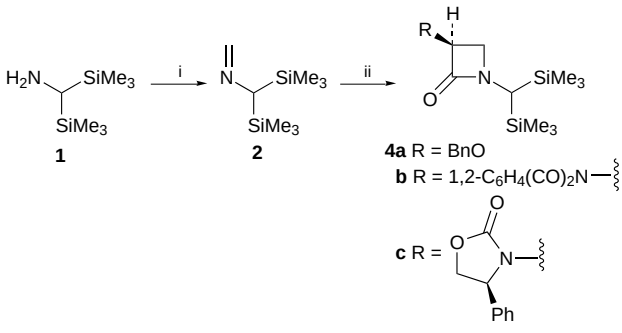
*Departamento de Química Orgánica, Facultad de Química, Universidad del Pais Vasco, Aptdo 1072, 20080 San Sebastián, Spain*

***N*-Methylidene[bis(trimethylsilyl)methyl]amine acts as a stable methanimine synthon [$CH_2$=NH] equivalent in [2 + 2] cycloadditions to ketenes, generated from acid chlorides and triethylamine, to provide 4-unsubstituted β-lactams in a single step.**

Although the chemistry of the C=N double bond has been extensively exploited over the years, reactions with formaldehyde imines have been virtually ignored.[1] Two main reasons have contributed to this fact: on the one hand the inaccessibility of monomeric methanimine in the condensed state[2] and, on the other hand, their great instability caused by spontaneous tri- or oligo-merization.[3] A very limited number of investigations have been conducted to address this problem. For example, Barluenga's group[4] has demonstrated that both *N*-methylenearyl- and *N*-methylenealkyl-amines are stable at −60 °C and can be generated *in situ* by the reaction of organometallic reagents with *N*-(alkoxymethyl)arylamines and *N*-alkyl-*N*-(alkylthiomethyl)ammonium chlorides, respectively. Independently to this group, Overman *et al.*[5] has also revealed that formaldehyde imines can be produced in solution, generally at −70 °C, from the reaction of *N*-(cyanomethyl)amines with strong bases. Although these authors also noticed the low temperature trapping of such methyleneamine species with carbon nucleophiles, no report on the reactivity of a methanimine species withstanding higher temperature reaction conditions has been published to date.

Here we report the chemical behaviour of some ketenes of interest in the context of β-lactam antibiotic chemistry,[6] (Scheme 1) towards the first isolable and stable methanimine,[7] easily prepared by the simple mixing of 33% formaldehyde aqueous solution and the readily available *C,C*-bis(trimethylsilyl)methylamine **1**.[8,†] To establish the correct reaction conditions for the expected [2 + 2] cycloaddition reaction, Table 1, we investigated the behaviour of imine **2** towards benzyloxyketene generated *in situ* from the carboxylic acid chloride **3a** and triethylamine. As entries 1 and 2 show, only poor yields of the expected β-lactam were obtained when the reactions were performed either at low temperature or under reflux of $CH_2Cl_2$ but, interestingly, the chromatographic analysis (GC–MS) of the reaction mixtures after 16 h revealed the presence of important quantities of unreacted imine **2** (typically 30–35%) surviving these reaction conditions. After several runs increasing the temperature by changing the solvent and using two- and four-fold excesses of the acid chloride **3a** (entries 3 and 4) a reasonable 62% yield of the isolated β-lactam **4a** was obtained after column chromatography. In view of this result, we next examined the suitability of this approach to the construction of the 3-amino 4-unsubstituted azetidin-2-one ring owing to its importance as a key structural element for the development of β-lactam antibiotics.[6] Actually, comparatively good yields of **4b** (65%, mp 207–209 °C) and **4c** {75%, mp 150–151 °C, $[\alpha]_D^{25}$ +89.6 (*c* 1.0, $Cl_2CH_2$)} could be reached, without the need for an excess acid chloride, by simply performing the reaction in refluxing benzene or chloroform as solvents (entries 5 and 6). This result contrasts with the fact that the cycloaddition between the Evans–Sjögren acid chloride **3c** and methanimine trimers, derived from benzylamine and trimethylsilylmethylamine, under the reported conditions[9] only affords traces of the expected β-lactams ( < 15%) together with major amounts of 3-[(4*S*)-2-oxo-4-phenyloxazolidin-3-yl]-acetic acid. In addition, the total asymmetric induction observed during the single step convergent formation of the β-lactam **4c**‡ was unaffected by the reaction temperature (entries 6 and 7), and it was particularly noteworthy when compared with the limited diastereomeric excesses achieved in comparable approaches reported to date.[10]

On the other hand, because the easy cleavage of the bis(trimethylsilyl)methyl moiety was fundamental in β-lactams **4** finding synthetic applications, we tried several deprotection methods using compound **5** {mp 124–126 °C, $[\alpha]_D^{25}$ +13.6 (*c* 1.0, $Cl_2CH_2$)} as a model, Scheme 2. This compound was easily obtained in 70% yield through the oxazolidinone moiety cleavage[11] and further *N*-Boc protection of the resulting free amino derivative. After screening our previously reported method[12] we found that exposure of **5** to the action of

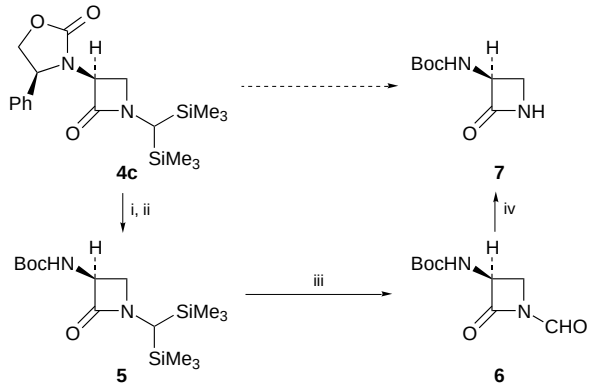



**Scheme 1** *Reagents and conditions*: i, 30% HCHO (1.2 equiv.), $H_2O$, room temp., 20 h, 75%; ii, $RCH_2COCl$ **3a**–**c**, $NEt_3$, for conditions, see Table 1

**Table 1** Cycloaddition reaction of methanimine **2** with alkoxy- and amidoketenes derived from acyl chlorides **3**

| Entry | Product **4** | Conditions[a] Solvent; *T*/°C; *t*/h | Yield (%)[b] |
|---|---|---|---|
| 1 | **a** | $CH_2Cl_2$; −78 → 20; 16 | 28 |
| 2 | **a** | $CH_2Cl_2$; 0 → 40; 16 | 30 |
| 3 | **a** | $CHCl_3$; 0 → 80[c]; 2 | 39 |
| 4 | **a** | $CHCl_3$; 80[d]; 1 | 62 |
| 5 | **b** | $C_6H_6$; 0 → 80; 16 | 65 |
| 6 | **c** | $C_6H_6$; 0 → 80; 16 | 75[e] |
| 7 | **c** | $CH_2Cl_2$; −78 → 20; 16 | 33[e] |

[a] Unless otherwise stated, the acid chloride (1.2 equiv.) was added to the imine **2** (1 equiv.) and triethylamine (2.4 equiv.) at the first temperature, and the reaction mixture was then stirred at the second temperature for the indicated time. [b] Yields of pure isolated products after column chromatography (silica gel, hexanes). [c] A twofold excess of the acid chloride and triethylamine was used. [d] The acid chloride (4.0 equiv.) was dropwise added to the imine **2** (1 equiv.) and triethylamine (8.0 equiv.) at reflux temperature. [e] Product obtained as single stereoisomer.




**Scheme 2** *Reagents and conditions*: i, Li (6 equiv.), THF, Bu$^t$OH, $NH_3$ (10 : 1 : 33), −78 °C, 10 min, then 1 M HCl, 5 min, 70%; ii, $(Boc)_2O$, room temp., 3 h; iii $(NH_4)_2Ce(NO_3)_6$, MeCN, $H_2O$, room temp., 3 h, 84%; iv, $NaHCO_3$, $Na_2CO_3$, $Me_2CO$, $H_2O$, room temp., 2 h, 78%

cerium(IV) ammonium nitrate in acetonitrile–water furnished the intermediate formyl derivative **6** [mp 134–136 °C, $[\alpha]_D^{25}$ −17.7 (*c* 1.0, $Cl_2CH_2$)] in a clean and high-yielding (90%) reaction. Further exposure of **6** to *N*-deformylation under usual conditions[12,13] afforded **7** [mp 172–174 °C, $[\alpha]_D$ −18.4 (*c* 1.0, MeOH), lit.,[14] mp 171–172 °C], which was identical in all respects to that previously described. Therefore, the bis-(trimethylsilyl)methyl group must be considered as a new protecting group for β-lactam synthesis.[15]

This work was supported by Basque Government (Project PI 95/93) and, in part, by Basque Country University (EHU/UPV : 170.215-EB147/94). A grant from Ministerio de Educacion y Ciencia (Spanish Government) to M. L. is gratefully acknowledged.

## Footnotes

† In sharp contrast to this result, analogous condensation of *C*-trimethylsilylmethylamine and formaldehyde afforded only the corresponding 1,3,5-tris(trimethylsilylmethyl)-1,3,5-triazine, see: T. Morimoto, Y. Nezu and K. Achiwa, *Chem. Pharm. Bull.*, 1985, **33**, 4596.

‡ For **4c** the 3*S* stereochemistry, relative to the known 4′*S* configuration of the oxazolidinone ring, was unambiguously established by X-ray analysis. *Crystal data* for **4c**. $C_{19}H_{30}N_2O_3Si_2$, $M$ = 390.63; crystal dimension 0.20 × 0.15 × 0.30 mm, orthorhombic, $P2_12_12_1$, $a$ = 6.444(1), $b$ = 22.025(2), $c$ = 32.083(3) Å, $V$ = 4553.5(3) Å$^3$, $T$ = 293 K, $Z$ = 8, $D_c$ = 1.140 g cm$^{-3}$, μ (Cu-Kα) = 1.527 mm$^{-1}$, λ = 1.54178 Å, 3608 total reflections, 1962 observed [$I > 2\sigma(I)$], 709 refined parameters, final conventinal $R$ = 0.047, $wR$ = 0.067, residual electron density 0.25 eÅ$^3$. The asymmetric unit was formed by two independent molecules with different conformation around the $(SiMe_3)_2CH$–N bond. Atomic coordinates, bond lengths and angles and thermal parameters have been deposited at the Cambridge Crystallographic Data Centre (CCDC). See Information for Authors, Issue No. 1. Any request to the CCDC for this material should quote the full literature citation and the reference number 182/329.

## References

1 *The Chemistry of the Carbon-Nitrogen Double Bond in The Chemistry of Functional Groups*, ed. S. Patai, Interscience Publishers, London, 1970.
2 B. Braillon, M. C. Lasne, J. L. Ripoll and J. M. Denis, *New J. Chem.*, 1982, **6**, 121; G. A. Harff, A. Sinnema and B. B. Wepster, *Recl. Trav. Chim. Pays-Bas*, 1979, **98**, 71; H. Möhrle, U. Scharf, E. Rühmann and R. Schmid, *Arch. Pharm.*, 1983, **316**, 222; M. D. Hurwitz, *US Pat.* 2 582 128 (*Chem. Abstr.*, 1952, **46**, 8146).
3 M. Dal Colle, G. Distefano, D. Jones, A. Guerrino, G. Seconi and A. Modelli, *J. Chem. Soc., Perkin Trans. 2*, 1994, 789.
4 J. Barluenga, A. M. Bayón and G. Asensio, *J. Chem. Soc., Chem. Commun.*, 1983, 1109; 1984, 427.
5 L. E. Overman and R. M. Burk, *Tetrahedron Lett.*, 1984, **25**, 1635.
6 *Chemistry and Biology of* β-*Lactam Antibiotics*, ed. R. B. Morin and M. Gorman, Academic, New York, 1982, vols. 1–3; *Recent Advances in the Chemistry of* β-*Lactam Antibiotics*, ed. A. G. Brown and S. M. Roberts, The Royal Society of Chemistry, London, 1984; W. Dürckheimer, J. Blumbach, R. Latrell and K. H. Sheunemann, *Angew. Chem., Int. Ed. Engl.*, 1985, **24**, 180.
7 A. Capperucci, A. Ricci, G. Seconi, J. Dunogues, S. Grelier, J. P. Picard, C. Palomo and J. M. Aizpurua, *J. Organomet. Chem.*, 1983, **458**, C1.
8 J. P. Picard, S. Grelier, T. Constantieux, J. Dunoguès, J. M. Aizpurua, C. Palomo, M. Petraud, B. Barbe, L. Lunnazi and J. M. Leger, *Organometallics*, 1993, **12**, 1378; C. Palomo, J. M. Aizpurua, J. M. Garcia and M. Legido, *J. Chem. Soc., Chem. Commun.*, 1991, 524.
9 O. Nakaguchi, T. Oku, H. Takeno, M. Hashimoto and T. Kamiya, *Chem. Pharm. Bull.*, 1987, **35**, 3985.
10 B. Alcaide, L. Casarrubios, G. Dominguez and M. A. Sierra, *J. Org. Chem.*, 1994, **59**, 7934; Y. Narukawa, K. N. Juneau, D. Snustad, D. B. Miller and L. S. Hegedus, *J. Org. Chem.*, 1992, **57**, 5453; C. Palomo, A. Arrieta, B. Lecea and F. P. Cossio, *J. Org. Chem.*, 1988, **53**, 3784; L. E. Overman and T. Osawa, *J. Am. Chem. Soc.*, 1985, **107**, 1698.
11 D. A. Evans and E. B. Sjögren, *Tetrahedron Lett.*, 1985, **26**, 3783; 3787.
12 J. Lasarte, C. Palomo, J. P. Picard, J. Dunogues and J. M. Aizpurua, *J. Chem. Soc., Chem. Commun.*, 1989, 72.
13 V. Farina, S. I. Hauck and D. Walker, *Synlett*, 1992, 761; G. I. Georg, P. He, J. Kant and Z. Wu, *J. Org. Chem.*, 1993, **58**, 5771.
14 P. G. Mattingly and M. J. Miller, *J. Org. Chem.*, 1980, **45**, 410.
15 C. Palomo, J. M. Aizpurua, M. Legido, R. Galarza, P. M. Deya, J. Dunogues, J. P. Picard, A. Ricci and G. Seconi, *Angew. Chem., Int. Ed. Engl.*, 1996, **35**, 1239; D. DiPietro, R. M. Borzilleri and S. M. Weinreb, *J. Org. Chem.*, 1994, **59**, 5856; G. H. Hakimelahi, M.-J. Shiao, J. R. Hwu and H. Davari, *Helv. Chim. Acta*, 1992, **75**, 1940; B. Alcaide, J. Perez Castells, B. Sanchez Vigo and M. A. Sierra, *J. Chem. Soc., Chem. Commun.*, 1994, 587.

*Received, 28th October 1996; Com. 6/07348D*

# Novel production of quinol-2(1*H*)-one derivatives from quinol-4(1*H*)-one derivatives

**Theodorus van Es[a] and Benjamin Staskun*[b]**

[a] *Department of Biochemistry and Microbiology, Cook College, Rutgers, The State University of New Jersey, 08903-0231, USA*
[b] *Department of Chemistry, University of the Witwatersrand, Johannesburg, South Africa*

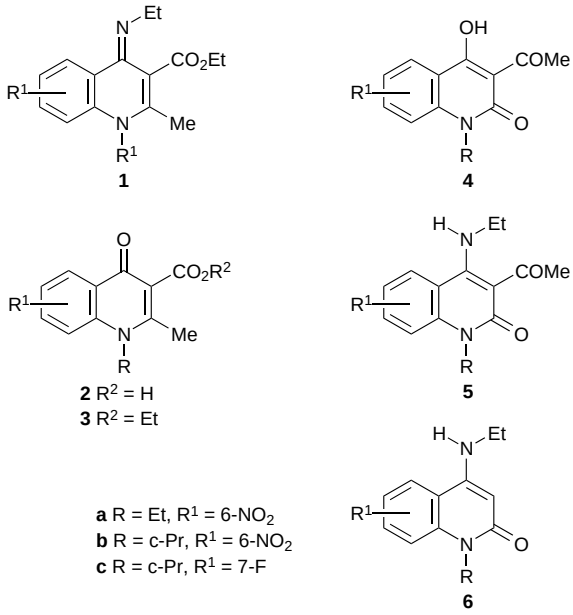
**Certain 1-alkyl-4-ethylimino-1,4-dihydro-2-methylquinoline-3-carboxylates transform in alkaline solution to give a variety of 1-alkylquinol-2(1*H*)-one derivatives by competitive C-2 attack by hydroxide followed by rearrangement.**

The venerable and extensive field of quinoline chemistry contains numerous and diverse molecular transformations.[1] Here we report the first examples, as far as we are aware, of a quinol-4(1*H*)-one derivative transforming to a quinol-2(1*H*)-one derivative. Alkaline hydrolysis of the recently available ethyl 1-ethyl- or 1-cyclopropyl-4-ethylimino-1,4-dihydro-2-methylquinoline-3-carboxylate **1** in most cases afforded the expected corresponding 4-oxoquinoline-3-carboxylic acid **2** *via* the intermediate ester **3**. However, the saponification of 1-ethyl-6-nitro substituted imine **1a**†‡ was accompanied by a rearrangement which yielded unexpected quinol-2(1*H*)-ones as major products. Thus with very dilute alkali the alkali-soluble 3-acetyl-1-ethyl-4-hydroxy-6-nitroquinol-2(1*H*)-one **4a**‡ (isomeric with the anticipated acid **2a**) and alkali-insoluble 3-acetyl-1-ethyl-4-ethylamino-6-nitroquinol-2(1*H*)-one **5a**‡ were obtained, while with a greater amount of NaOH **4a** and alkali-insoluble 1-ethyl-4-ethylamino-6-nitroquinol-2(1*H*)-one **6a**‡ were obtained (Table 1). The 1-cyclopropyl-6-nitro imine **1b** similarly gave the corresponding compounds **4b**, **5b** and **6b**, respectively. The relative proportions of the aforementioned products varied with the NaOH concentration and the reaction conditions (Table 1). An indication that the rearrangement is not restricted to imine **1** bearing a 6-$NO_2$ group was shown with the 1-cyclopropyl-7-fluoro substituted **1c** which in aqueous $(Me)_4NOH$–dioxane mixture (to minimise nucleophilic displacement of the fluorine) formed 3-acetyl-1-cyclopropyl-7-fluoro-4-hydroxyquinol-2(1*H*)-one **4c** and the expected quinoline-3-carboxylic acid **2c**.

Of mechanistic significance were the findings that on alkaline hydrolysis (i) even ethyl 1-ethyl-1,4-dihydro-2-methyl-6-nitro-4-oxoquinoline-3-carboxylate **3a** furnished 3-acetyl-4-hydroxyquinol-2(1*H*)-one **4a** (together with the expected 4-oxoquinoline-3-carboxylic acid **2a**) and (ii) 4-ethylaminoquinol-2(1*H*)-one **5a** converted to **4a**, the latter of which was not obtained from acid **2a**.

A tentative rationale based on the available evidence which accounts for the conversion **1** → **4**, **5** and **6** is outlined in Scheme 1 (with imine **1a**): Competitive attachment of $OH^-$ at C-2 of **1a** and at C-2 of 4-oxo ester **3a** (generated from **1a** by conventional hydrolysis of the imine function) gives rise to alcohol intermediates **A** and **B**, respectively. Ring-opening of **B** to a species such as **C** (depicted as a resonance contribution) followed on by an intramolecular *N*-acylation of the ester function in **C** results in **4a**. Similar events stemming from intermediate **A** result in enamine **5a**. The latter substance may subsequently undergo competitive hydrolysis of the 3-acetyl group to yield **6a**, and of the 4-ethylamino function to give **4a**.

It would appear from these preliminary results and the mechanistic analysis that electron-withdrawing group substituted substrates would be especially prone to this rearrange-

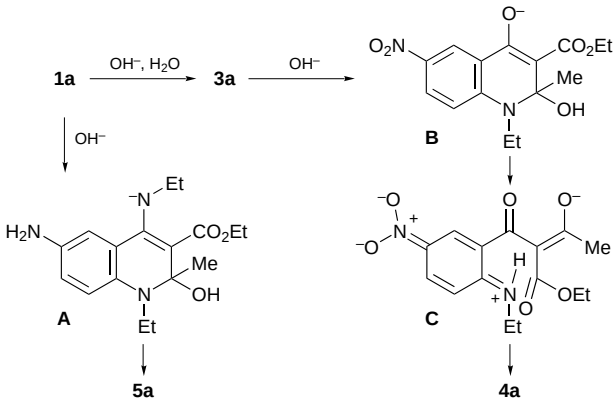



**a** R = Et, $R^1$ = 6-$NO_2$
**b** R = c-Pr, $R^1$ = 6-$NO_2$
**c** R = c-Pr, $R^1$ = 7-F

**Table 1** Production of quinol-2(1*H*)-one derivatives from quinol-4(1*H*)-one derivatives

| Substrate | R | $R^1$ | Amount/ mmol‡ | Method§ | Product(s)[a] (% yield)[b] |
|---|---|---|---|---|---|
| **1a** | Et | 6-$NO_2$ | 1 | A | **4a**(10), **5a**(63) |
| | | | 1 | B | **4a**(66), **5a**(15) |
| | | | 10 | C | **4a**(54), **6a**(35) |
| **1b** | cyclo-$C_3H_5$ | 6-$NO_2$ | 1 | A | **5b** (*ca.* 10)[c] |
| | | | 10 | C | **4b**(61), **6b**(35) |
| **1c** | cyclo-$C_3H_5$ | 7-F | 7.2 | D | **4c**( > 6%), **2c**(38%) |
| **3a** | Et | 6-$NO_2$ | 0.28 | E | **4a** (*ca.* 18%), **2a** (*ca.* 54%) |

[a] The products after purification [silica gel, benzene–acetone (4 : 1), followed by crystallisation] were fully characterised from their $^1$H NMR ($CDCl_3$) spectra (supplemented on occasion by NOE experiments) and accurate mass measurements (HRMS). [b] Crude. [c] Separated from alkali-insoluble co-product **6b** (silica gel, benzene–acetone, 4 : 1).




**Scheme 1**

ment, and that the reaction could be extrapolated to include the 2-demethylated analogues of **1** and **3**. Work is currently underway to optimise yields, identify other $R^1$ substituents in **1** and **3** which favour the rearrangement and to evaluate the synthetic utility of the finding.

In summary, we describe a novel 4-ethyliminoquinoline ⟶ quinol-2(1*H*)-one conversion reaction which leads to products of potential pharmacological interest,[2] and draw attention to the possibility, hitherto unforeseen, of rearrangements having occurred in certain cases during the numerous literature saponifications of 4-oxoquinoline-3-carboxylic esters.

We are grateful to Dr L. Carlton for conducting the NOE experiments and for helpful discussion, and to Mrs S. Heiss for the acquisition of NMR spectra. B. S. thanks the University of the Witwatersrand for financial support.

## Footnotes

† *Preparation of imine ester* **1a**. 2-chloro-*N*-ethyl-5-nitrobenzenecarboximidoyl chloride (10 mmol; from the corresponding amide and $SOCl_2$) and ethyl 3-ethylaminobut-2-enoate (11 mmol) were reacted in dry $CHCl_3$ (40 ml) at 0–5 °C for 4–5 d. The solvent was evaporated and the residual mixture of *C*-imidoylated crotonate and cyclised product **1a** was warmed to effect complete conversion to the title compound. Treatment with 2.0 mol $dm^{-3}$ NaOH liberated the acid-soluble substrate **1a** (crude yield, *ca.* 50%).

‡ *Selected spectroscopic data* for **1a**: yellow crystals, mp 111 °C (from EtOAc–hexane); $^1$H NMR ($CDCl_3$) 1.28–1.45 (m, 9 H), 2.44 (s, 3 H), 3.28 (q, *J* 7 Hz, 2 H), 4.06 (q, *J* 7 Hz, 2 H), 4.28 (q, *J* 7 Hz, 2 H), 7.23 (d, *J* 9.2 Hz, 1 H), 8.21 (dd, *J* 2.7, 9.2 Hz, 1 H), 9.10 (d, *J* 2.7 Hz, 1 H). For **4a**: yellow crystals, mp 172–173 °C (from MeOH); $^1$H NMR ($CDCl_3$) 1.37 (t, *J* 7.2 Hz, 3 H), 2.85 (s, 3 H), 4.34 (q, *J* 7.2 Hz, 2 H), 7.42 (d, *J* 9.4 Hz, 1 H), 8.50 (dd, *J* 2.7, 9.5 Hz, 1 H), 9.10 (d, *J* 2.7 Hz, 1 H), 17.03 (s, 1 H, removed by $D_2O$). For **5a**: yellow crystals, mp 160 °C (from MeOH); $^1$H NMR ($CDCl_3$) 1.35 (t, *J* 7.1 Hz, 3 H), 1.48 (t, *J* 7.1 Hz, 3 H), 2.73 (s, 3 H), 3.82–3.95 (8 line m, converted to quartet by $D_2O$, 2 H), 4.29 (q, *J* 7.1 Hz, 2 H), 7.37 (d, *J* 9.4 Hz, 1 H), 8.40 (dd, *J* 2.5, 9.4 Hz, 1 H), 9.0 (d, *J* 2.5 Hz, 1 H), 12.0 (br s, 1 H, removed by $D_2O$). For **6a**: yellow crystals, mp 266–268 °C (from MeOH); $^1$H NMR ($CDCl_3$) 1.34 (t, *J* 7.2 Hz, 3 H), 1.42 (t, *J* 7.2 Hz, 3 H), 3.25–3.38 (m, converted to quartet by $D_2O$, 2 H), 4.34 (q, *J* 7.1 Hz, 2 H), 4.92 (br s, 1 H, removed by $D_2O$), 5.79 (s, 1 H), 7.42 (d, *J* 9.4 Hz, 1 H), 8.38 (dd, *J* 2.4, 9.4 Hz, 1 H), 8.53 (d, *J* 2.4 Hz, 1 H).

§ *Method A*: EtOH (15 ml) containing aqueous 0.50 mol $dm^{-3}$ NaOH (0.50 ml), 55–60 °C, 22 h, evaporate, additional 0.50 mol $dm^{-3}$ NaOH, extract with $CHCl_3$, evaporate $CHCl_3$ phase ⟶ **5**, **6** [separate, silica gel (benzene–acetone, 4 : 1)], acidify (50% HOAc) aqueous phase ⟶ **4**, **2** (separate, *vide supra*), *Method B*: EtOH (15 ml) containing aqueous 0.50 mol $dm^{-3}$ NaOH (2.0 ml), then as in A. *Method C*: MeOH (50 ml) + aqueous 2.0 mol $dm^{-3}$ NaOH (20 ml), reflux, 1.5 h, then as in A (exclude alkali addition). *Method D*: $(Me)_4NOH$ (aqueous 25% solution, 10 ml)—dioxan (20 ml)—$H_2O$ (30 ml), reflux 3 h, evaporate dioxane and approx ½ volume $H_2O$, extract with $CHCl_3$ ⟶ 0.56 g (alkali-insoluble) complex mixture, acidify (50% HOAc) aqueous phase ⟶ 0.83 g (alkali-soluble) **4c** + **2c**, extract with boiling MeOH ⟶ 120 mg (MeOH-soluble) **4c** + 710 mg (MeOH-sparingly soluble) **2c**. *Method E*: MeOH (15 ml) + aqueous 2.0 mol $dm^{-3}$ NaOH (10 ml), reflux, 1.5 h, evaporate, acidify (50% HOAc), extract with $CHCl_3$ ⟶ **2a** + **4a** (total 56 mg) [molar ratio **2a** : **4a** ≈ 3 : 1, by $^1$H NMR ($CDCl_3$)].

## References

1 *Quinolines*, ed. G. Jones, Wiley, London, Part I, 1977; Part II, 1982.
2 A. Afonso, J. Weinstein, M. J. Gentles and S. B. Rosenblum, Schering Corp., US Pat. 1995, 5 378 694 (*Chem. Abstr.*, 1995, **122**, 213951k).

*Received, 30th October 1996; Com. 6/07385I*

# Reactions of $C_{2v}$-symmetrical $C_{60}$ pentakis-adducts with diazomethane: regioselective formation of hexakis- to octakis-adducts and mechanism of methanofullerene formation by addition of diazomethane followed by dinitrogen extrusion

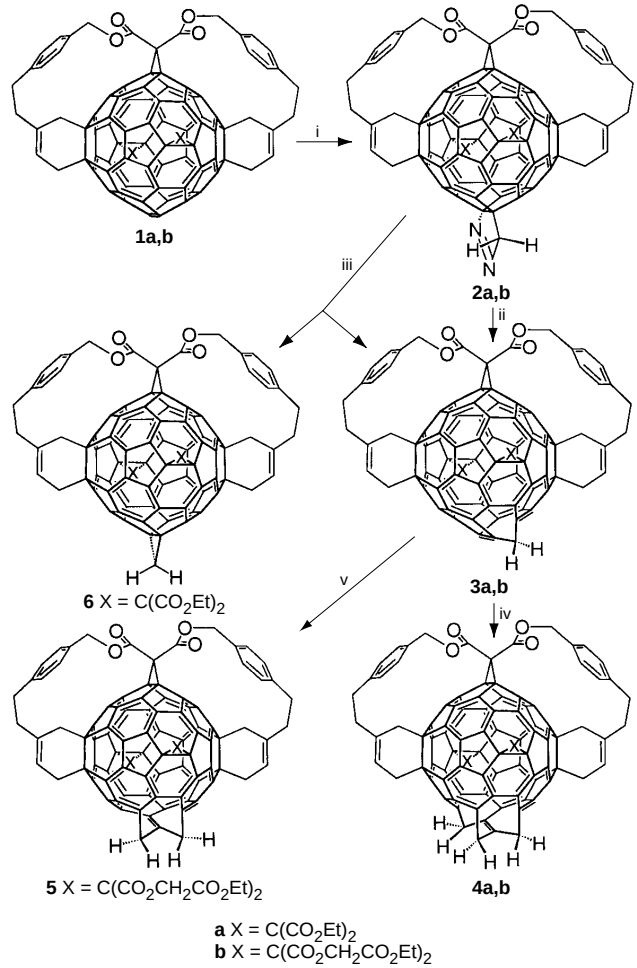
**Richard F. Haldimann,[a] Frank-Gerrit Klärner[b] and François Diederich*[a]**

[a] *Laboratorium für Organische Chemie, ETH-Zentrum, Universitätstrasse 16, CH-8092 Zürich, Switzerland*
[b] *Institut für Organische Chemie, Universität-GH Essen, Universitätstrasse 5, D-45141 Essen, Germany*

**Repeated treatment of the $C_{2v}$-symmetrical $C_{60}$ pentakis-adducts 1a,b with diazomethane provided with high regioselectively the novel heptakis- 5 and octakis-adducts 4a,b *via* hexakis-adducts 3a,b; an orbital symmetry-controlled reaction mechanism for the thermal dinitrogen extrusion from the pyrazoline intermediates in the addition of diazomethane to fullerenes is proposed.**

The 1,3-dipolar cycloaddition of diazomethane to $C_{60}$ or $C_{70}$ occurs at 6-6-bonds (bonds at the junction between two 6-membered rings) under formation of isolable pyrazoline derivatives.[1,2] Photolysis of these intermediates under $N_2$-extrusion provides an isomeric mixture of methanofullerenes, namely 6-6-closed ones, in which the 6-6-bond is bridged in a cyclopropane-type fashion, and 6-5-open ones, in which the methano group bridges the open junction between a 6- and 5-membered ring,[2] similar to the bonding in 1,6-methano-[10]annulene.[3] In contrast, thermolysis of the pyrazolines proceeds with high regioselectivity and yields 6-5-open adducts almost exclusively.[1,2a,c] As part of our research on higher adducts of $C_{60}$,[4] we became interested in exploring whether diazomethane would still add to highly functionalised carbon spheres of considerably reduced electrophilicity[4c] and dienophile character and whether the product distribution obtained by $N_2$-extrusion from the intermediate pyrazolines would be similar to that observed for the parent fullerenes. The $C_{2v}$-symmetrical pentakis-adducts **1a** and **1b**[4b] (Scheme 1) were chosen as starting materials in these investigations since their reactivity is limited to a single 6-6-bond in pseudo-octahedral position.[5] Addition to this bond is particularly favourable since it generates a residual fullerene π-chromophore consisting of eight stable benzenoid ring sub-structures.[6] Here, we report the stepwise addition of diazomethane to **1a**,**b** under formation of novel hexakis- to octakis-adducts of $C_{60}$ and propose a mechanism for the $N_2$-extrusion from the intermediate pyrazolines to give methanofullerenes.

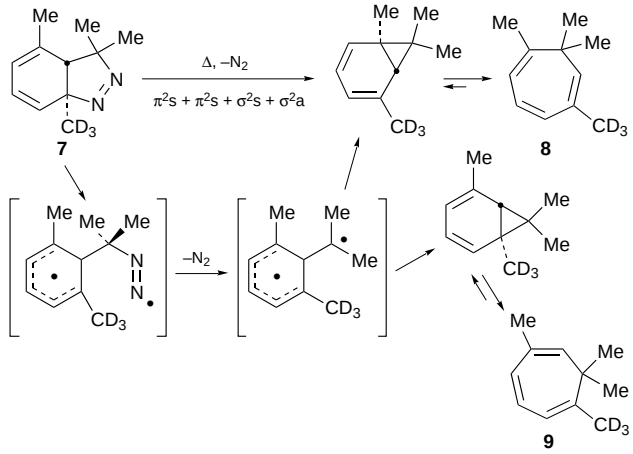
Reaction of **1a**,**b** with $CH_2N_2$ (*ca*. 60-fold excess) in $CHCl_3$ at 0 °C afforded the corresponding yellow, $C_s$-symmetrical pyrazolines **2a**,**b** in high yields (Scheme 1).† Upon heating to reflux in $CCl_4$, $N_2$-extrusion led to the orange-coloured, $C_1$-symmetrical 6-5-open methanofullerenes **3a**,**b** in nearly quantitative yield. Treatment of **3a**,**b** with $CH_2N_2$ (*ca*. 40-fold excess) in $CHCl_3$ at 0 °C gave within 15 min the yellow–orange, $C_1$-symmetrical octakis-adducts **4a**,**b** in an astonishing 90% yield. A further reaction of **4a**,**b** with additional diazomethane was not observed. When **3b** was reacted with $CH_2N_2$ (*ca*. 20-fold excess) for 10 min in $CH_2Cl_2$ at −80 to −60 °C, followed by quenching of the excess reagent with AcOH at −60 °C and workup at room temperature, heptakis-adduct **5** was directly obtained. Neither in the formation of **4a**,**b** nor in the preparation of **5** were pyrazoline intermediates observed. When pyrazoline **2a** was photolysed, the $C_{2v}$-symmetrical hexakis-adduct **6** and the $C_1$-symmetrical regioisomer **3a** were obtained in *ca*. 1 : 1 ratio and a combined yield of 15%. The isomeric mixture could not be separated by column chromatography. Therefore, **6** was purified by adding $CH_2N_2$ at 0 °C to the mixture in $CH_2Cl_2$ which transformed **3a** into octakis-adduct **4a** while leaving **6** unchanged. Chromatographic purification ($SiO_2$, $CH_2Cl_2$) was subsequently feasible, yielding **6** as a bright yellow solid. Thus, the reaction of diazomethane with pentakis-adducts **1a** ultimately yielded similar products to those observed in the addition to $C_{60}$: diazomethane added to the 6-6-bond and



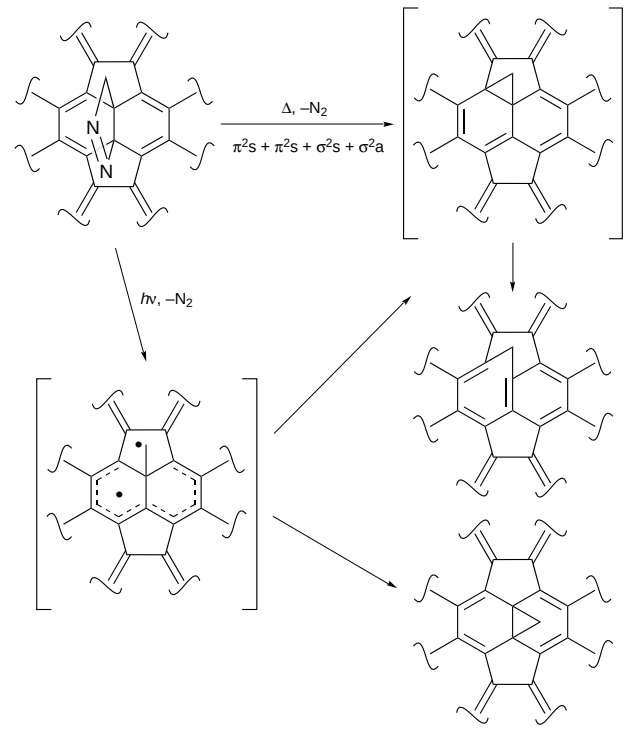

**Scheme 1** *Reagents and conditions*: i, $CH_2N_2$ (*ca*. 60 equiv.), $CHCl_3$, 0 °C, 1.5 h; 71% (**2a**), 93% (**2b**); ii, $CCl_4$, reflux, 15 min; 93% (**3a**, **b**); iii, *h*ν (Hg medium pressure lamp, 250 W), $C_6D_6$, $c$ = 9.6 mmol dm$^{-3}$, $T$ = 5–10 °C, 8 min, 15% (**6** and **5a** in *ca*. 1 : 1 ratio); iv, excess $CH_2N_2$ (*ca.* 40 equiv.), $CHCl_3$, 0 °C, 15 min; 90% (**4a, b**); v, $CH_2N_2$ (*ca*. 20 equiv.), $CH_2Cl_2$, −80 to −60 °C, 10 min, then excess HOAc, −60 °C, and workup at 20 °C; 79% (**3**)

photolysis of **2a** gave a mixture of 6-6-closed **6** and 6-5-open **3a** methanofullerenes, whereas thermolysis exclusively provided the 6-5-open derivative **3a**. None of the isomeric 6-6-closed methanofullerene **6** was detected in the $^1$H NMR spectrum of the crude thermolysis product.

According to semiempirical PM3 calculations,[4a,7] the 6-6-closed methanofullerene **6** is 2.1 kcal mol$^{-1}$ (1 cal = 4.184 J) more stable than the 6-5-open isomer **3a**. The preferred formation of the thermodynamically less stable product suggested that thermolysis proceeded under kinetic control, and one of us (F. G. K.) recognised the close analogy of the $N_2$-elimination of diazomethane–fullerene adducts to 6-5-open methanofullerenes to the previously reported $N_2$-elimination from diazoalkane–toluene adducts (Scheme 2).[8] Starting from **7**, thermolysis provides in an orbital symmetry controlled [$\pi^2$s + $\pi^2$s + $\sigma^2$s + $\sigma^2$a] rearrangement with high regioselectivity




**Scheme 2** Proposed mechanism for the thermal and photochemical $N_2$-extrusion from diazoalkane adducts of toluene




**Scheme 3** Proposed mechanism for the thermal and photochemical $N_2$-extrusion from diazalkane adducts of fullerenes (shown only in part)

cycloheptatriene **8**, resulting from ring-opening of the intermediate norcaradiene. In contrast, photolysis of **7** presumably proceeds *via* a diradical mechanism, leading to a mixture of **8** and isomeric **9**. We propose a similar mechanism (Scheme 3) to explain the product distribution obtained during thermolysis and photolysis of diazomethane–fullerene adducts. Even the surprising formation of **5** and **4a**,**b** can be rationalized by this mechanism. A 1,3-dipolar cycloaddition of diazomethane to **3a**,**b** or **5** is followed by rapid, regioselective, concerted $N_2$-elimination and valence bond isomerisation. It might also be responsible for the analogous preference of azide adducts of $C_{60}$ to thermally form 6-5-open azafullerenes.[9]

Support from the Swiss National Science Foundation is gratefully acknowledged.

## Footnote

† All compounds were fully characterised by $^1$H and $^{13}$C NMR ($CDCl_3$), IR, UV–VIS, and FABMS (3-nitrobenzyl alcohol). *Selected data* for **2a**: IR ($CHCl_3$): 1569 cm$^{-1}$ (N=N); $^1$H NMR: δ 5.73 (s, pyrazoline $CH_2$); $^{13}$C NMR: 23 of the 24 expected resonances expected for the fullerene sp$^2$-C-atoms; FABMS: *m/z* 1522.6 (22, M$^+$), 1492.5 (100 [M − $N_2$]$^+$). For **3a**: $^1$H NMR: δ 4.71 and 2.13 (2 × d, *J* 9.9 Hz, methano $CH_2$); $^{13}$C NMR: 44 of the 50 resonances expected for fullerene sp$^2$-C-atoms; FABMS: *m/z* 1493.7 (100, M$^+$). For **6**: $^1$H NMR: δ 2.57 (s, methano $CH_2$); $^{13}$C NMR: all 12 resonances expected for fullerene sp$^2$-C-atoms; FABMS: *m/z* 1493.7 (100, M$^+$). For **5**: $^1$H NMR: δ 4.48 (d, *J* 10.9, 2 H, methano CH), 2.75 (d, *J* 10.9, 2 H, methano CH); $^{13}$C NMR: all 26 resonances expected for fullerene sp$^2$-C-atoms; FABMS: *m/z* 1739.1 (M$^+$). For **4b**: $^1$H NMR: δ 4.53 (d, *J* 15.6, 1 H), 4.46 (d, *J* 15.2, 1 H), 4.10 (d, *J* 10.2, 1 H), 3.49 (d, *J* 15.6, 1 H), 3.38 (d, *J* 15.2, 1 H), 2.02 (d, *J* 10.2, 1 H) all methano CH; $^{13}$C NMR: 48 of the 50 resonances expected for the fullerene sp$^2$-C-atoms; FABMS: *m/z* 1753.3 (M$^+$, 100).

## References

1 T. Suzuki, Q. Li, K. C. Khemani and F. Wudl, *J. Am. Chem. Soc.*, 1992, **114**, 7301.
2 (*a*) A. B. Smith, III, R. M. Strongin, L. Brard, G. T. Furst, W. J. Romanow, K. G. Owens and R. C. King, *J. Am. Chem. Soc.*, 1993, **115**, 5829; (*b*) A. B. Smith, III, R. M. Strongin, L. Brard, G. T. Furst, W. J. Romanow, K. G. Owens and R. J. Goldschmidt, *J. Chem. Soc., Chem. Commun.*, 1994, 2187; (*c*) A. B. Smith, III, R. M. Strongin, L. Brard, G. T. Furst, W.J. Romanow, K. G. Owens, R. J. Goldschmidt and R. C. King, *J. Am. Chem. Soc.*, 1995, **117**, 5492.
3 E. Vogel, *Pure Appl. Chem.*, 1993, **65**, 143.
4 (*a*) L. Isaacs, R. F. Haldimann and F. Diederich, *Angew. Chem., Int. Ed. Engl.*, 1994, **33**, 2339; (*b*) L. Isaacs, P. Seiler and F. Diederich, *Angew. Chem., Int. Ed. Engl.*, 1995, **34**, 1466; F. Cardullo, L. Isaacs, F. Diederich, J.-P. Gisselbrecht, C. Boudon and M. Gross, *Chem. Commun.*, 1996, 797; (*c*) C. Boudon, J.-P. Gisselbrecht, M. Gross, L. Isaacs, H. L. Anderson, R. Faust and F. Diederich, *Helv. Chim. Acta*, 1995, **78**, 1334.
5 I. Lamparth, A. Herzog and A. Hirsch, *Tetrahedron*, 1996, **52**, 5065.
6 P. Seiler, L. Isaacs and F. Diederich, *Helv. Chim. Acta*, 1996, **79**, 1047; I. Lamparth, C. Maichle-Mössmer and A. Hirsch, *Angew. Chem., Int. Ed. Engl.*, 1995, **34**, 1607; B. Kräutler, T. Müller, J. Maynollo, K. Gruber, C. Kratky, P. Ochsenbein and D. Schwarzenbach, *Angew. Chem., Int. Ed. Engl.*, 1996, **35**, 1203; P. J. Fagan, J. C. Calabrese and B. Malone, *J. Am. Chem. Soc.*, 1991, **113**, 9408.
7 J. P. Stewart, *J. Comput. Chem.*, 1989, **10**, 209; F. Diederich, L. Isaacs and D. Philp, *J. Chem. Soc., Perkin Trans. 2*, 1994, 391.
8 F.-G. Klärner, V. Glock and J.-L. Hemmes, *Chem. Ber.*, 1990, **123**, 1869; F.-G. Klärner, R. Band, V. Glock and W. A. König, *Chem. Ber.*, 1992, **125**, 197.
9 M. Prato, Q. Chan Li, F. Wudl and V. Lucchini, *J. Am. Chem. Soc.*, 1993, **115**, 1148; A. B. Smith, III and H. Tokuyama, *Tetrahedron*, 1996, **52**, 5257; G. Schick, T. Grösser and A. Hirsch, *J. Chem. Soc., Chem. Commun.*, 1995, 2289; T. Grösser, M. Prato, V. Lucchini, A. Hirsch and F. Wudl, *Angew. Chem., Int. Ed. Engl.*, 1995, **34**, 1343.
10 A. Hirsch, *Tetrahedron*, 1996, **52**, 5065.

*Received, 4th November 1996; Com. 6/07483I*

# Radical cyclization reactions of 4-bromo vinylogous-esters, vinylogous-amides and enones

**Chin-Kang Sha,* Wei-Hong Tseng, Kuan-Tsau Huang, Kuan-Miao Liu, Herng-Yih Lin and San-Yan Chu***

*Department of Chemistry, National Tsing Hua University, Hsinchu 300, Taiwan, R.O.C.*

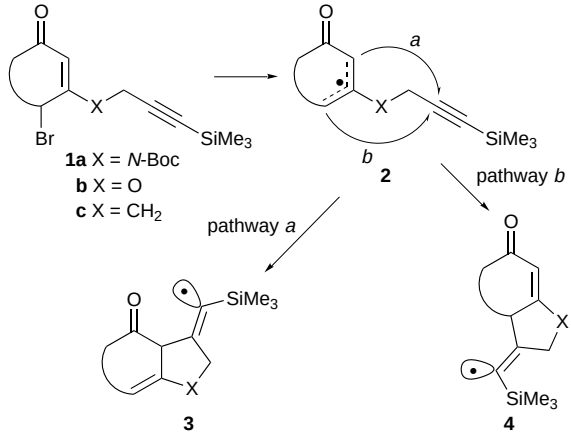
**Radicals generated from 4-bromo vinylogous-esters, vinylogous-amides and enones cyclize to a tethered acetylene side-chain preferentially at the γ-position; theoretical calculations of the spin density of the radicals and the relative stability of the radical intermediates are performed to rationalize the experimental observations.**

Radical reactions have emerged as one of the most useful synthetic methodologies in the formation of carbon–carbon bonds.[1] Previously we have described intramolecular cyclization reactions of α-ketone[2] and α-enone[3] radicals. As an extension to our work in this area, we investigated the intramolecular cyclization reactions of allylic enone radicals **2**, Scheme 1. Both from theoretical and experimental points of view, it is of special interest to discover whether radicals **2**, generated from 4-bromo cycloalkenones **1**, would cyclize at the α- or γ-position due to delocalization of the radical. Here we report the preliminary results of this investigation.

Vinylogous-esters **5** and **8** and vinylogous-amides **11**, **14** and **17** were prepared by literature methods.[4] Thus, 3-trimethylsilylprop-2-yn-1-ol[5] was condensed with cyclohexane-1,3-dione and cyclopentane-1,3-dione to afford vinylogous-esters **5** and **8**. Condensation of 3-trimethylsilylpropynylamine[6] with the corresponding cycloalkane-1,3-diones, followed by reaction with di-*tert*-butyl dicarbonate and 4-dimethylaminopyridine gave *tert*-butoxycarbonyl (Boc) protected vinylogous-amides **11**, **14** and **17**. Enones **21** and **24** were synthesized by treatment of the corresponding 3-ethoxycycloalkenones with 4-trimethylsilylbut-3-ynylmagnesium bromide followed by treatment with dilute HCl.[7] Bromination of **5**, **8**, **11**, **14**, **17**, **21** and **24** with *N*-bromosuccinimide (NBS) and AIBN in refluxing $CCl_4$ afforded the corresponding 4-bromo compounds **6**, **9**, **12**, **15**, **18**, **22** and **25**. Radical cyclizations were then carried out using tin hydride,[2] the results of which are summarized in Table 1. 4-Bromo vinylogous-esters and vinylogous-amides cyclized in acceptable yields. 4-Bromo enone **22** underwent radical cyclization with some difficulty to give both the cyclized product **23** and the reduction product **21** in equal amounts. 4-Bromo enone **25** did not cyclize to **26** but gave only the reduction product **24**. In general, radicals generated from 4-bromo cyclohexenones **6**, **12** and **22** were found to cyclize in better yields than the radicals generated from 4-bromo cyclopentenones **9**, **15** and **25**. However, it is interesting to note that most of radical cyclizations occurred at the γ-carbon. Only in entry 5, the radical generated from compound **18** with a highly hindered γ-position cyclized both at the γ- and α-positions to give **19** and **20** (1 : 2.5). Exocyclic double bonds formed after cyclization were isomerised into conjugated systems under the reaction condition (entries 1, 2 and 4, Table 1). In entry 6, the enone double bond was deconjugated after cyclization to give **23**.

To understand this unusual regioselectivity of radical cyclization at the γ-carbon, we performed PM3 calculations[8] on model radical systems **27** and **28**. Spin densities at the α- and γ-positions, expressed as the square of atomic orbital coefficients in SOMO, are 0.34 and 0.49 for **27**, and 0.33 and 0.53 for **28**. For the reaction under kinetic control, these coefficients are in accordance with the experimental observations. It is noteworthy that HOMO electron densities at the α- and γ-positions of the corresponding anionic species **29** are 0.47 and 0.32, which are opposite to the radical species. It is well known that reactions of anion **29** usually occur at the α-position.[9] We also calculated the relative stability of intermediates **30** and **31** which were formed *via* the α- or γ-cyclization (pathway *a* or *b* in Scheme 1). We found that **31** is 4.5 kcal $mol^{-1}$ (1 cal = 4.184 J) more stable than **30**. This probably reflects that cyclization at the γ-position, maintaining the conjugate enone π system in the transition state, is the pathway having the lower activation energy.

We gratefully acknowledge a grant (NSC 85-2113-M-007-016) from the National Science Council of the Republic of China.




Scheme 1

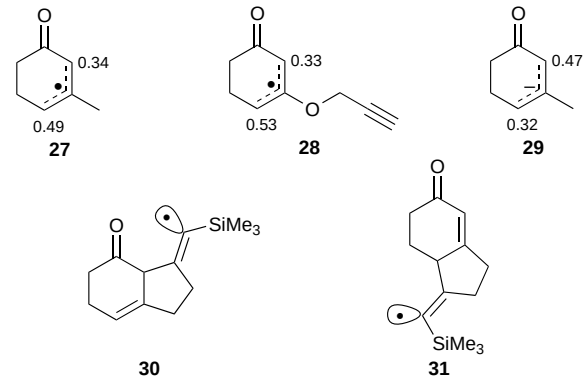
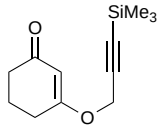
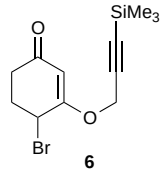
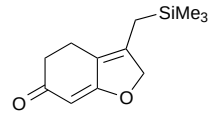
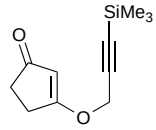
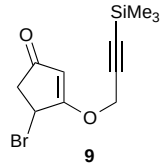
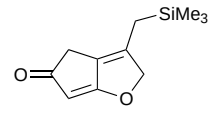
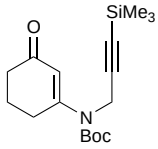
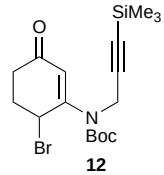
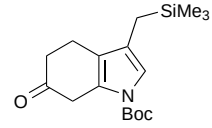
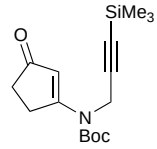
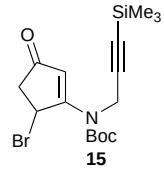
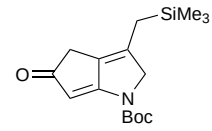
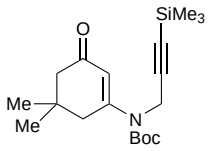
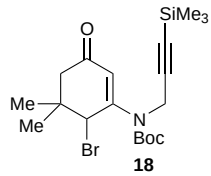
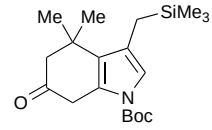
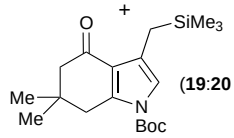
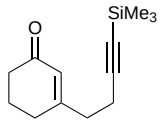
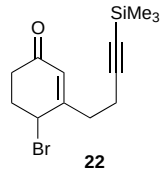
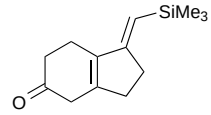
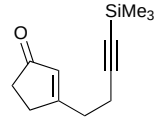
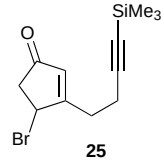
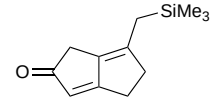


**Table 1** Radical cyclization of 4-bromo vinylogous-amides, vinylogous-esters and enones

| Entry | Starting material | 4-Bromo compound (%) | Cyclized product (%) | Reduction (%) |
|---|---|---|---|---|
| 1 |  **5** |  **6** 63[a] |  **7** 68[c] | — |
| 2 |  **8** |  **9** 27[b] |  **10** 42[c] | 52 |
| 3 |  **11** |  **12** 81 |  **13** 70[d] | — |
| 4 |  **14** |  **15** 60 |  **16** 51[e] | 23 |
| 5 |  **17** |  **18** 81 |  **19** +  **20** (**19**:**20** = 1:2.5) 50[d] | — |
| 6 |  **21** |  **22** 83 |  **23**[f] 31 | 31 |
| 7 |  **24** |  **25** 63 |  **26** 0 | 85 |

[a] Yield based on 67% conversion; 33% of **5** was recovered. [b] Yield based on 73% conversion; 27% of **8** was recovered. [c] The reaction was carried out in refluxing toluene. [d] The unstable crude cyclization product was treated with $I_2$ and DBU to give the pyrrolo compound which was isolated by flash column chromatography (florisil, 6 : 1 hexane–ethyl acetate). [e] The reaction was carried out in refluxing xylene. [f] The geometry of the vinylsilane group in **23** was tentatively assigned *E*.

## References


1 D. P. Curran, in *Comprehensive Organic Synthesis*, vol. 4, ed. B. M. Trost and I. Fleming, Pergamon Press, New York, 1991, p. 715–831.
2 C.-K. Sha, T.-S. Jean and D.-C. Wang, *Tetrahedron Lett.*, 1990, **31**, 3745.
3 C.-K. Sha, C.-Y. Shen, T.-S. Jean, R.-T. Chiu and W.-H. Tseng, *Tetrahedron Lett.*, 1993, **34**, 7641.
4 D. S. Middleton and N. S. Simpkins, *Tetrahedron Lett.*, 1988, **29**, 1315.
5 H. Westmijze and P. Vermeer, *Synthesis*, 1979, 392; R. L. Danhciser, D. J. Carini, D. M. Fink and A. Basak, *Tetrahedron Lett.*, 1983, **39**, 935.
6 L. F. Tietze, M. Bratz and M. Pretor, *Chem. Ber.*, 1989, **122**, 1955.
7 D. Becker, Z. Harel, M. Nagler and A. Gillon, *J. Org. Chem.*, 1982, **47**, 3297.
8 J. J. P. Stewart, MOPAC Version 6.0, J. Frank, Seiler Research Laboratory, United States Air Force Academy, CO 80840.
9 N. W. Atwater, *J. Am. Chem. Soc.*, 1960, **82**, 2847; J. M. Conia and A. S.-L. Craz, *Tetrahedron Lett.*, 1962, **12**, 505.



*Received, 4th November 1996; Com. 6/07487A*

# The first observation of 'NMR-invisible phosphorus' in cobalt-substituted aluminophosphate molecular sieves

**L. Canesson and A. Tuel***

*Institut de Recherches sur la Catalyse, C.N.R.S. 2 av. A. Einstein, 69626 Villeurbanne Cedex, France*

**A spin-echo mapping technique is used to record the total $^{31}$P NMR signal of CoAPO molecular sieves for which a large proportion of phosphorus nuclei are not accessible by conventional NMR techniques.**

Framework substitution of divalent cations for aluminium in aluminophosphate molecular sieves ($MeAPO_4$) has been a matter of interest over the last years as it provides AlPO materials with interesting properties in catalytic reactions.[1,2] Therefore, it is of prime importance to have an extensive characterisation of these catalysts, and to determine the nature and location of the metal ions within the channels and cavities of the structure. Among all the spectroscopic techniques that can be used, solid-state NMR is very attractive as both $^{31}$P and $^{27}$Al nuclei possess a natural abundance of 100%. It is expected that substitution of divalent cations for aluminium modifies the chemical shift of neighbouring $^{31}$P nuclei, as observed in $^{29}$Si NMR spectra of zeolites with aluminium incorporation. Up to now, the method has been successfully applied for the study of the environment of phosphorus nuclei in magnesium-substituted aluminophosphates MAPOs.[3–5] However, as far as paramagnetic transition-metal cations like $Co^{2+}$ are concerned, conventional NMR sequences cannot be applied. NMR signals are broadened and numerous spinning side-bands are observed, due to various interactions between cobalt and phosphorus nuclei.[6] The presence of these side-bands as well as the decrease in both the $T_1$ and $T_2$ relaxation times of $^{31}$P nuclei has sometimes been considered as a proof for the framework cobalt siting.[7] However, such modifications are also observed in Co-impregnated aluminophosphates, which makes the discrimination between framework and non-framework cobalt almost impossible with this technique. Peeters *et al.*[8] have shown that, when cobalt is incorporated into the AlPO framework, phosphorus nuclei in the first and third coordination spheres around the metal cannot be detected by NMR and become 'NMR-invisible'.

We report here for the first time a method that allowed us to observed these so-called 'NMR-invisible phosphorus' nuclei and to record the total $^{31}$P NMR spectrum of CoAPO materials. The method is based on a spin-echo mapping technique that has been successfully applied for the characterisation of paramagnetic VPO catalysts.[9,10] Schematically, the method consists of recording a series of spectra using a Hahn echo sequence at different irradiation frequencies. For each spectrum, the intensity is corrected taking into account the relaxation of the magnetisation before acquisition of the signal. The total NMR signal is then obtained by addition of all individual spectra. Tong[11] has recently shown that, under specific conditions, the spectrum obtained by spin-echo mapping could reproduce the real line shape. Therefore, it was possible to make quantitative measurements by comparing the NMR intensities with those of pure AlPO-5. All experiments were carried out on a Bruker DSX 400 spectrometer operating at 161.9 MHz. The 90° pulse was 3 μs and the defocalisation time between the 90 and 180° pulses in the echo sequence was 20 μs. All CoAPO molecular sieves were synthesised following literature procedures.

Fig. 1 compares the $^{31}$P NMR spectra of CoAPO-50 obtained under various conditions. Almost no signal is observed under MAS conditions, due to the high Co content in the sample (11 mass% Co). With a Hahn echo, a broad signal is observed at δ *ca.* −20 (ref. $H_3PO_4$), the intensity of which corresponds to < 10% of the total amount of phosphorus in the material. This shows that > 90% of $^{31}$P nuclei are not detected under these conditions. Using the spin-echo mapping technique, a very broad signal is observed between δ *ca.* 0 and 10 000. The integrated intensity of the obtained spectrum corresponds to 98% of the phosphorus atoms present in the sample, which shows that the total signal has been recorded. In fact, most of the signal (*ca.* 85%) is shifted towards low fields, which is the reason why it could not be observed using conventional echo sequences. The invisibility of $^{31}$P nuclei is thus not due to very fast relaxation processes but to the fact that the signal cannot be observed when the irradiation frequency is centred on δ 0. As for VPO catalysts, the shift probably results from an electron–nuclear dipolar-plus contact term between the electrons of $Co^{2+}$ and $^{31}$P nuclei. We have already reported that the frequency shift is proportional to a fractional contribution of the unpaired electron spin to the $^{31}$P nucleus.[10] In order to obtain more information about the nature and the assignments of the NMR

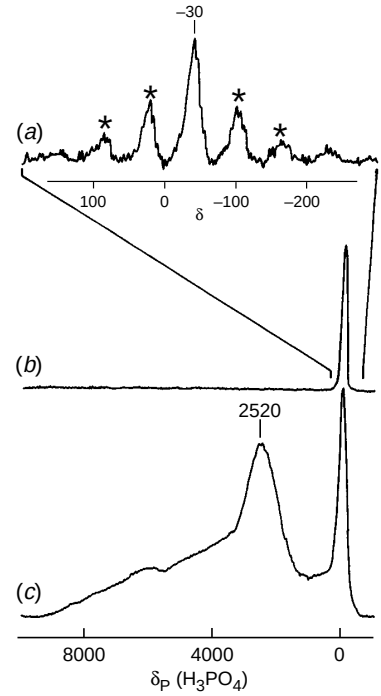



**Fig. 1** $^{31}$P NMR spectra of CoAPO-50. (*a*) $^{31}$P MAS spectrum. Pulse length: 2 μs, recycle delay: 20 s, spinning rate: 10 kHz. 1600 scans were accumulated (asterisks denote spinning side-bands). (*b*) Spectrum obtained with a Hahn echo sequence with the irradiation frequency at 0 Hz. (*c*) Spin-echo mapping spectrum obtained by addition of 22 spectra. For each individual spectrum, 1800 FIDs were accumulated.

signals, we have recorded the spectrum of DAF-2, a cobalt phosphate made of alternating $CoO_4$ and $PO_4$ tetrahedra.[12] The signal is composed of a broad peak at δ *ca*. 9500 and corresponds to P atoms surrounded exclusively by four Co atoms. As the shift is proportional to the electron density of $Co^{2+}$ on the $^{31}P$ nucleus, it is expected that it will depend on the number of Co atoms in the first coordination sphere around P. Therefore, we can suggest that the signal observed between δ *ca*. 500 and 10 000 corresponds to P atoms with at least one Co in the first coordination sphere, whilst the peak at δ *ca*. 0 corresponds to P(4A1) species. This was confirmed by studying a series of CoAPO molecular sieves with various Co contents. The relative intensity of the signal above δ 500 increases with the Co content but, in all cases, integration of the spectrum indicates that all phosphorus atoms were detected (Table 1). More details about the evolution of the line shape and intensity with the amount of Co incorporated will be given in a forthcoming paper.

CoAPO-50 clearly shows a distinct NMR peak at δ *ca*. 2500 which corresponds to approximately one quarter of the shift observed for DAF-2. We can thus assume that this line corresponds to P(1Co,3Al) units. Unfortunately, NMR lines are very broad and deconvolution of the signal into several lines corresponding to P(*n*Co, 4 − *n*Al) is not trivial. However, our assumption was supported by the study of samples containing low amounts of cobalt, like CoAPO-34 (2.95 mass% Co) or CoAPO-5 (3.05 mass% Co). For these samples, if we assume a random distribution of Co in the lattice, the relative contribution of P(2Co,2Al) species is expected to be negligible compared to that of P(1Co,3Al). Experimentally, spectra are essentially composed of two lines centred around δ 0 and 2500 without significant contribution above δ 5000. Moreover, we found that the relative intensity of the signal at δ 0 could be directly correlated with the Co content in the various samples, which makes the method very interesting not only for observing the total $^{31}P$ NMR signal but also to estimate the chemical composition. The line shape is slightly modified upon calcination of CoAPO materials in air (Fig. 2). As a general trend, we have noticed that the intensity in the range δ 500–1500 increases upon calcination whilst that above δ 2500 decreases, but the total intensity remained unchanged. As the observed shift strongly depends on the geometry and electronic density around P atoms, such modifications might be explained by changes in bond angles and lengths or by partial oxidation of $Co^{II}$ to $Co^{III}$ species upon calcination. Indeed, oxidation is expected to reduce the electronic density on the phosphorus nuclei and thus to decrease the observed NMR shift as already reported for VPO.[9]

Finally, we have studied a CoAPO-5 sample (10 mass% Co) obtained by impregnation of calcined AlPO-5 with cobalt(II) nitrate followed by calcination in air at 500 °C. As previously reported,[8] numerous spinning side bands are observed in the MAS NMR spectrum and $T_1$ and $T_2$ relaxation times considerably decrease with respect to pure AlPO-5. However, no signal is detected in the range δ 500–10 000 using the spin-echo mapping technique. This strongly suggests that the presence of an NMR signal in this region is characteristic of the incorporation of Co in the AlPO framework. The presence of Co–O–P bridges is probably necessary to delocalise the unpaired electrons of the metal on $^{31}P$ nuclei.

All these experiments show that the spin-echo mapping technique is a rapid and very powerful method to characterise CoAPO molecular sieves and to prove the incorporation of the metal in the framework. A detailed attribution of the different signals as well as the possibility of applying the method to the characterisation of other transition-metal substituted molecular sieves is in progress.

**Table 1** Percentage of phosphorus nuclei observed by $^{31}P$ NMR in various samples

| Sample | Co (mass%) | $I_E$ (%)[a] | $I_{SEM}$ (%)[b] |
|---|---|---|---|
| CoAPO-50 | 11.7 | 9.5 | 98 |
| CoAPO-46 | 7.9 | 17 | 103 |
| CoAPO-39 | 2.95 | 71 (65[c]) | 101 (97[c]) |
| CoAPO-5 | 3.05 | 67 (66[c]) | 99 (102[c]) |

[a] $I_E$ is the percentage of $^{31}P$ nuclei detected using a Hahn echo with irradiation frequency at 0 Hz. [b] $I_{SEM}$ is the percentage of $^{31}P$ nuclei detected with the spin-echo mapping technique. [c] Values obtained on calcined samples.

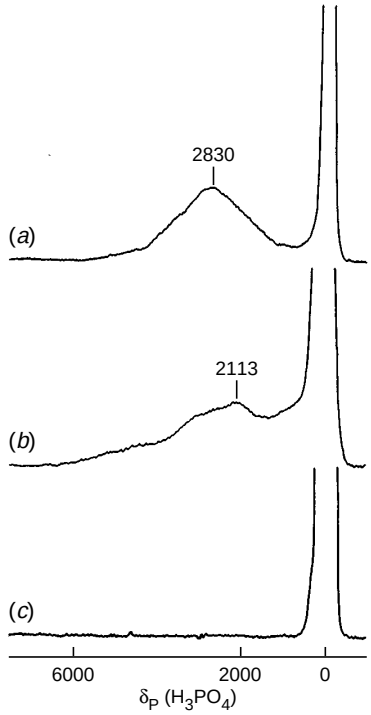



**Fig. 2** $^{31}P$ NMR spectra by spin-echo mapping of as-synthesised CoAPO-5 (*a*), calcined CoAPO-5 (*b*) and cobalt impregnated AlPO-5 (*c*)

## References


1 B. Akolekar, *J. Catal.*, 1993, **143**, 227.
2 J. Chen and J. M. Thomas, *J. Chem. Soc., Chem. Commun.*, 1994, 603.
3 F. Deng, Y. Yue, T. Xiao, Y. Du, C. Ye, L. An and H. Wang, *J. Phys. Chem.*, 1995, **99**, 6029.
4 J. P. Barrie and J. Klinowski, *J. Phys. Chem.*, 1989, **93**, 5972.
5 A. Tuel, I. Arcon, N. Novak Tušar, A. Meden and V. Kaucic, *Microporous Mater.*, 1996, **7**, 271.
6 C. Montes, M. E. Davis, B. Murray and N. Narayana, *J. Phys. Chem.*, 1990, **94**, 6431.
7 S. H. Chen, S. P. Sheu and K. J. Chao, *J. Chem. Soc., Chem. Commun.*, 1992, 1504.
8 M. P. J. Peeters, J. L.M. Van de Ven, J. W. de Haan and J. H. C. van Hooff, *Colloids Surf. A: Physicochem. Eng. Aspects*, 1993, **72**, 87.
9 M. T. Sananes, A. Tuel, G. J. Hutchings and J. C. Volta, *J. Catal.*, 1994, **148**, 395.
10 M. T. Sananes and A. Tuel, *Solid State Nucl. Magn. Reson.*, 1996, **6**, 157.
11 Y. Tong, *J. Magn. Reson.*, 1996, **119**, 22.
12 J. Chen, R. H. Jones, S. Natarajan, M. B. Hursthouse and J. M. Thomas, *Angew. Chem., Int. Ed. Engl.*, 1994, **33**, 639.


*Received, 8th November 1996; Com. 6/07603C*

# Synthesis of the first homo-3′,5′-cyclic nucleotide

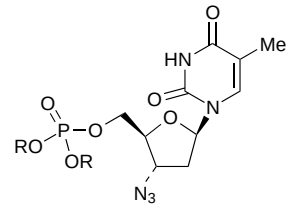
**Jayne H. M. Gould and John Mann***

*Department of Chemistry, Reading University, Whiteknights, Reading, UK RG6 6AD*

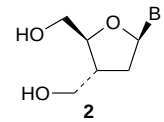
**Syntheses of 2′,3′-dideoxy-3′-hydroxymethylcytidine-6′-diphenylphosphate and the corresponding 5′,6′-cyclicphenylphosphate from 5(*S*)-*tert*-butyldimethylsilyloxymethylfuran-2(5*H*)-one are achieved.**

In the search for drugs with activity against HIV reverse transcriptase, novel analogues of the natural nucleosides have always been the most popular targets for synthesis. Recent discoveries include biologically potent L-series nucleosides[1] and variously protected phosphates like **1**, which are prodrugs of AZT.[2] Our synthesis of 2′,3′-dideoxy-3′-hydroxymethyl nucleosides of general structure **2** demonstrated that the cytidine derivative (B = cytosine) and 5-fluorocytidine derivative (B = 5-fluorocytosine) had particularly potent activity against a range of viruses,[3] and this encouraged us to try to prepare the monophosphate and cyclic phosphate derivatives for biological evaluation. Here we describe the successful attainment of these goals.

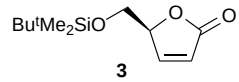
We have previously described the photoinduced addition of methanol to 5(*S*)-*tert*-butyldimethylsilyloxymethylfuran-2(5*H*)-one **3** to produce adduct **4**,[4] but for the present work this reaction was carried out on the 30 g scale with yields in the range 45–50%. Protection of the free hydroxy as its benzoate ester **5a** allowed selective reduction of the lactone (disiamyl borane in THF) and derivatisation of the resultant lactols to yield the anomeric acetates **6a** (overall yield 52%). These were reacted with bis-trimethysilylcytosine in the presence of tin(IV) chloride to yield the protected nucleoside analogue **7a** as a *ca.* 1 : 1 anomeric mixture, which could not be separated by flash chromatography. Selective removal of the benzoate was



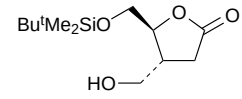
**1** R = subst. aryl or $RCOSCH_2CH_2$



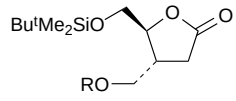
**2**



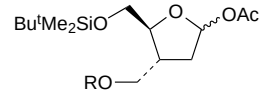
**3**



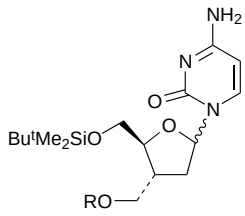
**4**



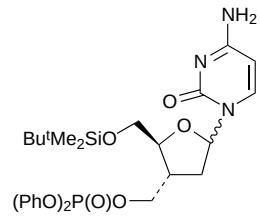
**5a** R = Bz
**b** R = $Bu^tMe_2Si$



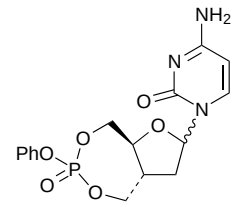
**6a** R = Bz
**b** R = $Bu^tMe_2Si$



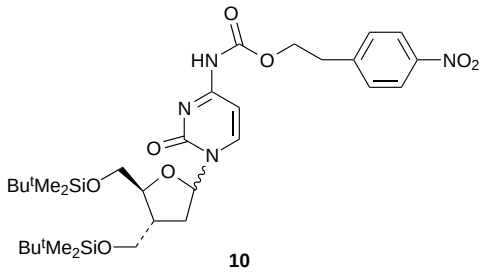
**7a**,**b**



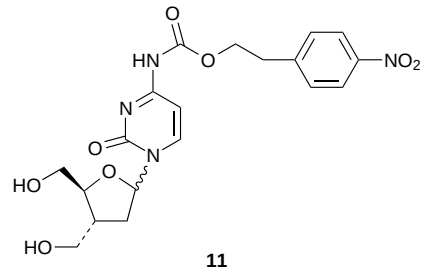
**8**



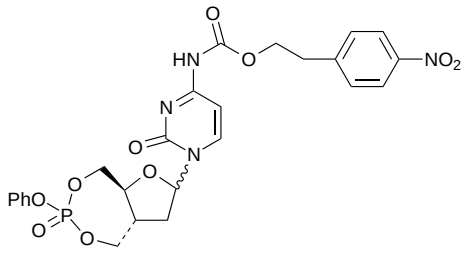
**9**



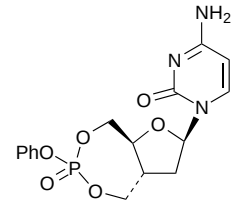
**10**



**11**



**12**



**13**

possible using base (1% NaOH in MeOH) and the free hydroxy was selectively phosphorylated using a modification of the method of Uchiyama *et al*.[5] This involved reaction of the nucleoside with 1 equiv. of *tert*-butylmagnesium chloride in the presence of diphenylphosphorochloridate to produce the desired 6′-diphenylphosphate **8** (63% yield). We had hoped to convert this compound into the cyclic phosphate **9**, but despite considerable efforts, this goal eluded us.

We thus turned our attention to the bis-silylated adduct **5b** which was reduced (DIBAL-H) and derivatised to provide lactol esters **6b** and thence the protected nucleoside anomers **7b** (52% overall). Protection of the free amino group of the cytosine as its 2-(*p*-nitrophenyl)ethyl carbamate[6] yielded the fully-protected nucleoside anomers **10**, and to our delight the anomers could now be separated (with relative ease) by flash chromatography. (Indeed we have used this protecting group to facilitate separation of anomeric mixtures of several substituted cytidines.) The silyl ether groups of these individual anomers were now removed (toluene-*p*-sulfonic acid in MeOH) and the resultant diols **11** were reacted in pyridine with bis(benzotriazolyl)phenyl phosphate[7] (from 2 equiv. of 1-hydroxybenzotriazole and phenylphosphodichloridate in the presence of triethylamine), to produce the desired cyclic phosphates **12** (35% α and 31% β after chromatography.† The α-anomer was more easily recrystallised than the β-anomer, and an X-ray crystallographic study confirmed the structure of this compound.‡ Finally, the carbamate group was removed from the β-anomer using triethylamine to yield the novel homo-cyclic nucleotide **13**,§ which was submitted for biological evaluation. We had hoped that the compound would act as a prodrug from compound **2** (B = cytosine), a compound with good activity against several viruses.[3] It did in fact show modest activity against HIV-1 ($EC_{50}$ 350 μmolar) and is presently being evaluated in other systems.

All of the reactions as far as compound **11** have been carried out routinely on the half-gram scale (though the cyclic phosphate formation has only been accomplished thus far on the 100 mg scale). One obvious extension of this work is to replace the phenyl group with other aryl groups or by *S*-acyl-2-thioethyl groups as in prodrugs like **1**, in an attempt to improve the bioavailability of the compounds. However, given the pivotal importance of cyclic-3′,5′-AMP and -GMP in biological processes, a more urgent task is to extend this methodology to the purine series in order to make homologues of these very important compounds.

J. G. thanks the MRC for a studentship under the AIDS Initiative Programme and we thank Dr Naheed Mahmood (MRC) for the (ongoing) biological evaluation. We are also very grateful for the advice given by Professor Colin Reese and for the numerous FAB mass spectra provided by the EPSRC Mass Spectrometry Centre at the University of Swansea.

## Footnotes

† *Selected spectroscopic data* for the α-anomer of **12**: $\delta_H$ (400 MHz, $CDCl_3$ and $CD_3OD$), integration values for the discrete diastereoisomers have not been given but were in the approximate ratio of 2 : 1 with respect to the signals for the discrete diastereoisomers, 1.75–1.84 (m, 2 × 2′-H), 2.45–2.51 (m, 2′-H), 2.80–2.87 (m, 2 × 3′-H), 2.93–2.99 (m, 2′-H), 3.14 (t, *J* 6.6 Hz, $CH_2$-npeoc), 3.51 (dd, $J_{gem}$ 11.0, $J_{6',3'}$ 6.6 Hz, 6′-H), 3.59 (dd, $J_{gem}$ 11.0, $J_{6',3'}$ 5.1 Hz, 6′-H), 3.76 (dd, $J_{gem}$ 11.0, $J_{6',3'}$ 4.4 Hz, 6′-H), 3.82 (dd, $J_{gem}$ 11.0, $J_{6',3'}$] 4.0 Hz, 6′-H), 4.12–4.25 (m, 5′-H, 2 × 4′-H), 4.40 (ddd, $J_{5',P}$ 24.9, $J_{gem}$ 11.7, $J_{5',3'}$ 3.7 Hz, 5′-H), 4.47 (t, *J* 6.6 Hz, 2 × $CH_2$-npeoc), 4.50–4.55 (m, 5′-H), 4.59 (ddd, $J_{5',P}$ 19.2, $J_{gem}$ 10.3, $J_{5',4'}$ 4.2 Hz, 5′-H), 6.02 (t, $J_{1',2'}$ 5.9 Hz, 1′-H), 6.09 (t, $J_{1',2'}$ 6.6 Hz, 1′-H), 7.20–7.27 (m, 2 × 5-H, 4 × Ar), 7.38 (t, *J* 7.7 Hz, 6 × Ar), 7.46 (d, *J* 8.8 Hz, 4 × Ar npeoc), 7.95 (d, $J_{6,5}$ 7.7 Hz, 6-H), 7.99 (d, $J_{6,5}$ 7.3 Hz, 6-H) and 8.19 (d, *J* 8.8 Hz, 4 × Ar npeoc); $\delta_C$ (100.4 MHz, $CDCl_3$ and $CD_3OD$) 34.8 ($CH_2$-npeoc), 35.7 (C-2′), 36.6 (C-2′), 42.7 (C-3′), 42.8 (C-3′), 62.4 (C-6′), 65.0 (C-6′), 65.4 ($CH_2$-npeoc), 67.2 (C-5′), 68.4 (C-5′), 81.5 (C-4′), 84.4 (C-4′), 88.3 (C-1′), 88.7 (C-1′), 119.7 (2 × C-5), 123.6 (Ar), 123.8 (Ar), 125.7 (Ar), 129.8 (Ar), 142.8 (Ar), 142.9 (Ar), 143.3 (C-6), 143.4 (C-6), 145.2 (C–$NO_2$), 146.9 (C-quart), 150.0 (C-quart), 152.8 (2 × C-4), 155.6 (2 × C=O, npeoc) and 163.2 (2 × C-2).

For the β-anomer of **12**: $\delta_H$ (400 MHz, $CDCl_3$), integration values for the discrete diastereoisomers have not been given but were in the approximate ratio of 5 : 1 with respect to the signals for the discrete diastereoisomers, 2.29–2.43 (m, 4 × 2-H′), 2.56–2.64 (m, 2 × 3-H′), 3.11 (t, *J* 6.6 Hz, 2 × $CH_2$-npeoc), 4.09 (dd, $J_{gem}$ 12.8, $J_{6',3'}$ 10.3 Hz, 6′-H), 4.14–4.24 (m, 3 × 6′-H), 4.32 (dd, $J_{gem}$ 11.7, $J_{5',4'}$ 3.7 Hz, 5′-H), 4.34–4.42 (m, 2 × 4′-H, 5′-H), 4.45 (t, *J* 6.6 Hz, 2 × $CH_2$-npeoc), 4.49–4.58 (m, 5′-H), 4.67 (ddd, $J_{5',P}$ 18.3, $J_{gem}$ 10.6, $J_{5',4'}$ 4.4 Hz, 5′-H), 6.05 (dd, $J_{1',2'}$ 6.8, $J_{1',2'}$ 1.6 Hz, 1′-H), 6.12 (d, $J_{1',2'}$ 7.0 Hz, 1′-H), 7.22 (d, *J* 7.7 Hz, 4 × Ar), 7.32–7.38 (m, 2 × 5-H, 6 × Ar), 7.41 (d, *J* 8.4 Hz, 4 × Ar npeoc), 7.76 (d, $J_{6,5}$ 7.3 Hz, 6-H), 7.89 (d, $J_{6,5}$ 6.6 Hz, 6-H) and 8.17 (d, *J* 8.4 Hz, 4 × Ar npeoc); $\delta_P$ (81 MHz, $CDCl_3$) −5.2 and −5.7; *m/z* 572.1294 ($M^+$) ($C_{25}H_{25}N_4O_{10}P$ requires 572.1308).

‡ We thank A. Jahans and Dr M. G. B. Drew for the X-ray structure determination, which will be described in detail elsewhere. Suffice to say, the compound crystallised in an extended conformation.

§ *Selected spectroscopic data* for **13**: $\delta_H$ (400 MHz, $CD_3OD$), integration values for the discrete diastereoisomers have not been given but were in the approximate ratio of 2 : 1 with respect to the signals for the discrete diastereoisomers, 2.16–2.21 (m, 4 × 2-H′), 2.71–2.78 (m, 2 × 3-H′), 4.0 (dd, $J_{5',P}$ 20.9, $J_{gem}$ 11.0 Hz, 5′-H), 4.05–4.17 (m, 2 × 4′-H, 2 × 5′-H), 4.23 (ddd, $J_{6',P}$ 22.3, $J_{gem}$ 10.3, $J_{6',3'}$ 8.2 Hz, 6′-H), 4.32–4.44 (m, 3 × 6′-H), 4.49 (ddd, $J_{5',P}$ 20.0, $J_{gem}$ 10.3, $J_{5',4'}$ 3.9 Hz, 5′-H), 5.81 (d, $J_{5,6}$ 7.7 Hz, 5-H), 5.83 (d, $J_{5,6}$ 7.7 Hz, 5-H), 5.99 (dd, $J_{1',2'}$ 6.6, $J_{1',2'}$ 3.7 Hz, 1′-H), 6.03 (dd, $J_{1',2'}$ 6.9, $J_{1',2'}$ 2.9 Hz, 1′-H), 7.15 (t, *J* 7.9 Hz, 6 × Ar), 7.30 (t, *J* 7.9 Hz, 4 × Ar), 7.57 (d, *J* 7.7 Hz, 6-H) and 7.59 (d, *J* 7.7 Hz, 6-H); *m/z* 380.1011 [$(M + H)^+$] ($C_{16}H_{19}N_3O_6P$ requires 380.1011).

## References

1 J. W. Beach, L. S. Jeong, A. J. Alves, D. Pohl, H. O. Kim, C.-N. Chang, S.-L. Doong, R. F. Schirazi, Y.-C. Cheng and C. K. Chu, *J. Org. Chem.*, 1992, **57**, 2217; T.-S. Lin, M.-Z. Luo, M.-C. Liu, Y.-L. Zhu, E. Gullen, G. E. Dutschman and Y.-C. Cheng, *J. Med. Chem.*, 1996, **39**, 1757; T.-S. Lin, M.-Z. Luo and M.-C. Liu, *Tetrahedron*, 1995, **51**, 1055; T.-S. Lin, M.-Z. Luo, M.-C. Liu, S. B. Pai, G. E. Dutschman and Y.-C. Cheng, *J. Med. Chem.*, 1994, **37**, 798.

2 X. Pannecouke, G. Parmentier, G. Schmitt, F. Dolle and B. Luu, *Tetrahedron*, 1994, **50** 1173; I. Lefebre, C. Perigaud, A. Pompon, A.-M. Aubertin, J.-L. Girardet, A. Kirn, G. Gosselin and J.-L. Imbach, *J. Med. Chem.*, 1995, **38**, 3941; C. McGuigan, R. N. Pathirana, J. Balzarini and E. De Clerq, *J. Med. Chem.*, 1993, **36**, 1048; C. McGuigan, R. N. Pathirana, M. P. H. Davies, J. Balzarini and E. De Clerq, *Bioorg. Med. Chem. Lett.*, 1994, **4**, 427.

3 J. Mann and A. C. Weymouth-Wilson, *J. Chem. Soc., Perkin Trans. 1*, 1994, 3141.

4 J. Mann and A. C. Weymouth-Wilson, *Synlett*, 1992, 67.

5 M. Uchiyama, Y. Aso, R. Noyori and Y. Hayakawa, *J. Org. Chem.*, 1993, **58**, 373.

6 F. Himmelsbach, B. S. Schulz, T. Trichtinger, R. Charubala and W. Pfleiderer, *Tetrahedron*, 1984, **40**, 59.

7 G. van der Marel, C. A. A. van Boeckel, G. Wille and J. H. van Boom, *Tetrahedron Lett.*, 1981, **22**, 3887.

*Received, 12th November 1996; Com. 6/07699H*

# Self-assembling polymeric mixed donor (O/N) *N*-ethylmorpholine adducts of alane ($AlH_3$)

**Philip C. Andrews,[a] Colin L. Raston,*[a] Brian W. Skelton[b] and Allan H. White[b]**

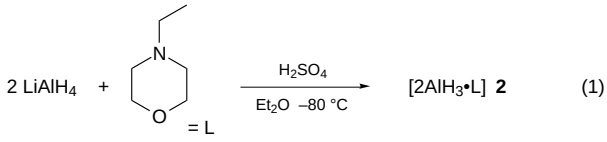
[a] *Department of Chemistry, Monash University, Clayton, Victoria 3168, Australia*
[b] *Department of Chemistry, The University of Western Australia, Nedlands, W. A., Australia 6907*

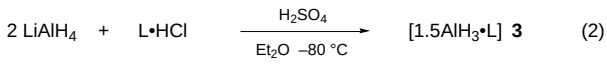
**The 2:3 and 1:2 stoichiometric reactions of *N*-ethyl morpholine with the $Et_2O$ adduct of $AlH_3$, prepared from $LiAlH_4$ and $H_2SO_4$ in $Et_2O$ at −80 °C, afford alane-rich hydride-bridged polymers exhibiting a range of bonding modes of Lewis bases to $AlH_3$ including unprecedented mono Al···H hydride bridging.**

Lewis-base adducts of alane ($AlH_3$) are important precursors in CVD production of thin films.[1] The stability of such compounds and hence ease of decomposition is often determined by the nature of the Lewis bases present. Attempts at rationalising the stability of such complexes has led to a great deal of solid-state structural information on N-amine and P-phosphine stabilised adducts, for example $AlH_3{\cdot}2$quinuclidine, $AlH_3{\cdot}2NMe_3$ and $AlH_3{\cdot}PBu^t_3$ which are monomeric five- or four-coordinate species, dimeric $[AlH_3{\cdot}NMe_2(CH_2Ph)]_2$ with weak hydride bridging and thus five-coordinate metal centres, and polymeric $[AlH_3{\cdot}tmen]_\infty$ and $[AlH_3{\cdot}Pr^i_2PCH_2CH_2PPr^i_2]_\infty$ which have polydentate ligands associated with five-coordinate metal centres.[2] In contrast the only structurally authenticated alane derivatives involving Lewis bases donating through an O atom are $AlH_3{\cdot}2$thf, $[AlH_2(\mu\text{-}H{\cdot}thf)]_2$[3] and the mixed-donor complex $[AlH_3{\cdot}$*N*-methylmorpholine$]_\infty$ **1**.[4] Such complexes are important since they give insight into the possible decomposition processes for alane and gallane ($GaH_3$), Lewis-base adducts in the presence of air and/or moisture where simple O-complexation at the metal centre is likely to be the primary process for decomposition, as well as how such adducts bind to oxidised silica surfaces.[5]

Herein, we report the synthesis and crystal structures of two alane adducts of *N*-ethylmorpholine (L): namely $[2AlH_3{\cdot}L]_\infty$ **2** and $[1.5AlH_3{\cdot}L]_\infty$ **3**. The compounds spontaneously self-assemble into one- or two-dimensional polymeric structures with head-to-head hydride bridging and/or two O-donating groups to the same metal centre. This has implications for building even more complex systems for polydentate donor ligands in general. In addition, a new structural type for alane has been established, and overall both structures taken together summarise the structural variety found for all other characterised Lewis base adducts of alane and gallane.

Complexes **2** and **3** were prepared as shown in reactions (1) and (2).† In reaction (1) the *N*-ethylmorpholine is




added immediately on cooling to −80 °C an $Et_2O$ solution of alane preformed from sulfuric acid (98%) and an $Et_2O$ solution of $LiAlH_4$. In reaction (2) the hydrochloride salt of the morpholine is present together with the $LiAlH_4$ in $Et_2O$ prior to the addition of the sulfuric acid. The use of the hydrochloride salt in reaction (2) is important in finely controlling the stoichiometry of the reaction. Therefore an $L : AlH_3{\cdot}xEt_2O$ ratio of 1:2 for **2** and 1:1.5 for **3** is ensured. Colourless crystals of both **2** and **3** are obtained at −30 °C from an $Et_2O$ solution, although the colourless rhomboidal crystals of **3** were also obtained from *in vacuo* sublimation. Both sets of crystals are stable at room temperature with **2** melting with gas evolution *in vacuo* at 66–67 °C and finally decomposing to metal at *ca*. 137 °C, and **3** decomposing > 150 °C.

Due to the quadrupolar $^{27}Al$ nucleus the only meaningful information from the NMR studies was the relative chemical shifts of the $AlH_3$ protons, giving a relatively broad singlet, and the protons and $^{13}C$ in the complexed *N*-ethylmorpholine.

The solid-state structures of **2** and **3** are shown in Figs. 1 and 2 respectively.‡ Both structures are polymeric crystallising in the space group $P\bar{1}$, albeit showing significant differences: **2** forms a polymeric chain due to the linking of discrete N and O bound $AlH_3$ units *via* hydride bridging, while this is also a feature of **3** there are several other important additional features which give rise to a two-dimensional net-like structure. The repeating unit in **3** consists of four L moieties and two lots of three different types of $AlH_3$ units giving in total three different trigonal-bipyramidal Al environments. One Al centre behaves in a similar fashion to that as seen in **2**. However the two other

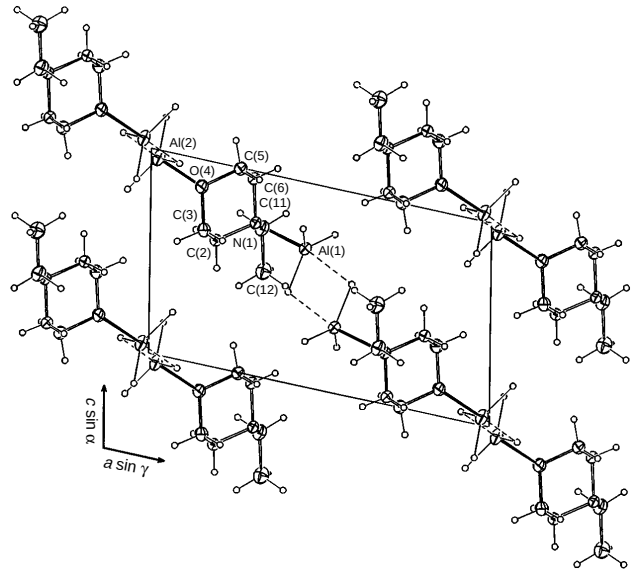



**Fig. 1** Crystal structure of **2** showing 20% ellipsoids; selected distances (Å) (bridging hydride distances in italics) and angles (°): Al(1)–N(1) 2.133(3), Al(2)–O(4) 1.993(3), 3[Al(1)–H] *1.56(3)*, 1.48(2), 1.47(2), 3[Al(2)–H] 1.54(3), 1.49(3), *1.56(3)*, Al(1)···H(01a) 2.11(3), Al(2)···H(02c) 1.93(3); N(1)–Al(1)–Al(1′) 138.95(8), O(4)–Al(2)–Al(2″) 136.46(9), Al(1)–N(1)–C(11) 107.4(2), Al(1)–N(1)–C(6) 110.3(2), 3[N(1)–Al(1)–H] 95(1), 94(1), 101(1); 3[H–Al(1)–H], 122(2), 113(1), 120(1). 3[O(4)–Al(2)–H], 94(1), 94(1), 94(1); 3[H–Al(2)–H] 128(2), 116(2), 114(2)

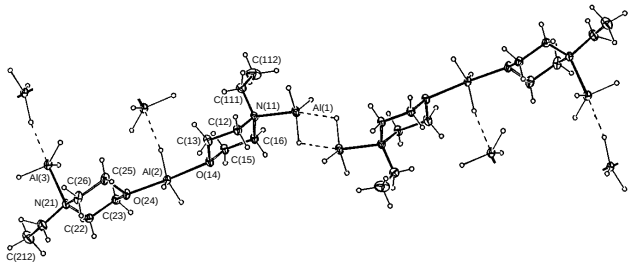



**Fig. 2** Crystal structure of **3** showing 20% ellipsoids; selected distances (Å) (bridging hydride distances in italics) and angles (°): Al(1)–N(11) 2.099(3), Al(2)–O(14), 2.172(3), Al(2)–O(24) 2.034(3), Al(3)–N(21) 2.182(3), 3[Al(1)–H] 1.49(5), *1.46(4)*, 1.46(3); 3[Al(2)–H] *1.43(4)*, 1.49(3), 1.55(4); 3[Al(3)–H] 1.32(5), 1.49(6), 1.58(6); Al(1)···H(01b) 2.13(3), Al(3)···H(02a) 2.29(4); Al(1)–N(11)–C(16) 109.0(2), Al(1)–N(11)–C(111) 111.6(3), O(14)–Al(2)–O(24) 174.7(1), Al(2)–O(14)–C(13) 110.7(2), Al(2)–O(24)–C(23) 120.8(2), Al(3)–N(21)–C(22) 114.8(2), Al(3)–N(21)–C(211) 108.3(3), 3[N–Al(1)–H] 95(2), 93(1), 102(1); 3[O(14)–Al(2)–H] 84(2), 88(1), 90(2); 3[O(24)–Al(2)–H] 94(2), 89(1), 95(2); 3[N(21)–Al(3)–H] 104(2), 99(2), 84(2)

Al centres which are both five-coordinate help form the two-dimensional structure through the formation of single Al–H hydride bridging, which is unprecedented for alane species. The Al which is bound by two O atoms contributes a $H^{\delta-}$ while it is the N-bound Al centre which provides the electropositive metal centre, thus achieving five-coordination. It is interesting that the polymer **1**, which is formed from the 1 : 1 reaction of $LiAlH_4$ with the hydrochloride salt of *N*-methylmorpholine (L′·HCl) gives a simpler asymmetric unit in compliance with the stoichiometry of the reaction; repeating $AlH_3$·L′ with each five-coordinate Al centre bound by both O and N from different morpholine moieties and with no intermolecular hydride bridging and with the donor ligands arranged head-to-tail rather than head-to-head as seen in **2** and **3**. In complete contrast the 1 : 1 L′ adduct of trimethylaluminium shows no Al–O bonding although it is observed in the 2 : 1 adduct which forms a monomer.

The reaction of $AlH_3$ in $Et_2O$ with 4-(2-chloroethyl)morpholine hydrochloride affords the *N*-ethylmorpholine adduct, $[(AlH_3)(AlClH_2)\cdot L]_\infty$ **4**, which exhibits another variation in the polymeric framework, containing features of both **2** and **3**.†‡ Essentially it has the same hydrogen-bonded backbone as **2** but the cross-linking features of **3** with the close electrostatic interactions being between the bis O-bound Al (on which hydride/chloride exchange has occurred between the $AlH_3$ and $NCH_2CH_2Cl$ units) and Cl instead of Al···H.

The variety in structural motifs contained within **2** and **3** are clearly seen from an analysis of the bond lengths and angles. In **2** the Al–O bonds are relatively short, 1.993(3) Å, in comparison to the longer bonds of 2.172 and 2.034 Å in **3** and 2.19(2) Å in **1** reflecting the lower covalent interactions at the Al centre {*cf.* also the mono [1.967(2) Å] and bis [av. 2.066(3) Å] thf adducts of alane cited above}. In **3** the O–Al–O bond angle bisecting the trigonal-planar $AlH_3$ unit is almost linear at 174.7(1)°. The intermolecular $Al_2\cdots H_2$ distances of 2.11(3) and 1.93(3) Å in **2** and 2.13(3) Å in **3** are significantly longer than those within the $AlH_3$ units, 1.47(2)–1.58(6) Å. The N–Al···H–Al polymer linking bonds in **3** are longer again at 2.29(3) Å. All the Al–N distances are comparable with those found in related amine–alane adducts.

The use of ethereal solutions of alane by-passes the typical, and as yet unfavourable, ligand substitution reactions with $AlH_3\cdot NMe_3$ for forming exclusively O-donor ligand bound complexes. It also allows for the possibility of determining the relative stability of the Lewis-base O-donating species in comparison with their amine or phosphine stabilised analogues.

We thank the Australian Research Council for support of this work.

## Footnotes

† **2**. The $Et_2O$ complex of $AlH_3$ was generated *in situ* at −80 °C from the reaction of $LiAlH_4$ (0.46 g, 12 mmol) with $H_2SO_4$ (98%, 0.59 g, 6.12 mmol) in $Et_2O$ (30 ml). Almost immediately *N*-ethylmorpholine (0.69 g, 6 mmol) was added dropwise while the reaction mixture was stirred. This was then allowed to warm slowly to room temp. and stirred for a further 2 h. The white suspension was filtered leaving a clear $Et_2O$ solution from which rhomboidal colourless crystals were obtained at −30 °C (1.4 g, 73%). Alternatively a white powder can be formed on quick removal of $Et_2O$ from the clear solution and sublimed *in vacuo* to give the same rhomboidal crystals. Melting with gas evolution at 66–67 °C, further gas evolution from 94 °C until decomposition to metal at *ca*. 137 °C. $^1$H NMR (300 MHz, 25 °C, $C_6D_6$) δ 4.14 (s, AlH), 3.62 (m, $OCH_2$), 2.15 (m, $NCH_2$), 0.87 (t, $CH_3$), $^{13}$C NMR (75.5 MHz, 25 °C, $C_6D_6$) δ 63.16, 54.84, 52.87, 8.81. Anal. required (found) C, 41.14 (41.48); H, 10.93 (10.98); N, 8.00 (8.13)%.

**3**. $H_2SO_4$ (98%, 0.38 g, 3.90 mmol) was added dropwise to a stirred reaction mixture of *N*-ethylmorpholine hydrochloride (L·HCl) (0.61 g, 4 mmol) and $LiAlH_4$ (0.30 g, 8 mmol) in $Et_2O$ (25 ml) at −80 °C. This was allowed to stir and warm slowly to room temp. at which point it was stirred for a further 2 h. The white suspension was filtered and the clear $Et_2O$ solution cooled to −30 °C at which temperature fine colourless crystals of **3** were obtained (0.43 g, 62%); decomp. > 151 °C, $^1$H NMR (300 MHz, 25 °C, $C_6D_6$) δ 4.15 (s, AlH), 3.65 (m, $OCH_2$), 2.20 (m, $NCH_2$), 0.85 (t, $CH_3$), $^{13}$C NMR (75.5 MHz, 25 °C, $C_6D_6$) δ 63.25, 54.77, 52.91, 8.91. Anal: required (found) C 44.99 (41.88), H 11.01 (11.06), N 8.74 (8.51)%.

**4**. This was prepared from the reaction of 2 equiv. of $LiAlH_4$ and 1 equiv. of 4-(2-chloroethyl)morpholine hydrochloride in $Et_2O$ at −80 °C. Large colourless crystals were grown from the filtered clear ether solution at 4 °C, mp 123 °C.

‡ *Crystal structure determinations* (CAD4 diffractometer, crystals mounted in capillaries): **2**. $C_6H_{19}Al_2NO$, $M$ = 175.2, triclinic, space group $P\bar{1}$, $a$ = 11.941(6), $b$ = 7.021(3), $c$ = 6.963(3) Å, α = 101.68(3), β = 98.29(4), γ = 103.27(4)°, $U$ = 544.1 Å$^3$. $D_c$ ($Z$ = 2) = 1.069 g cm$^{-3}$, $F$(000) = 192. $\mu_{Mo}$ = 2.2 cm$^{-1}$, specimen: 0.27 × 0.18 × 0.15 mm, $A^*_{min,\ max}$ = 1.03, 1.04. $2\theta_{max}$ = 50°, final $R$, $R_w$ = 0.044, 0.042. $N_0$ = 1301 'observed' [$I > 3\sigma(I)$] reflections out of $N$ = 1905 unique.

**3**. $C_{12}H_{35}Al_3N_2O_2$, $M$ = 320.4. Triclinic, space group $P\bar{1}$, $a$ = 15.388(4), $b$ = 10.233(5), $c$ = 6.676(3) Å, α = 73.15(4), β = 77.95(4), γ = 81.62(4)°, $U$ = 980 Å$^3$, $D_c$ ($Z$ = 2) = 1.086 g cm$^{-3}$, $F$(000) = 352. $\mu_{Mo}$ = 1.9 cm$^{-1}$, specimen: 0.50 × 0.49 × 0.48 mm (no correction), $2\theta_{max}$ = 55°, final $R$, $R_w$ = 0.049, 0.051, $N$ = 2625, $N_0$ = 1868.

**4**. $C_{12}H_{34}Al_3ClO_2N_2$, $M$ = 354.8 triclinic, space group $P\bar{1}$, $a$ = 12.964(7), $b$ = 12.447(6), $c$ = 6.887(2) Å, α = 83.54(3), β = 77.30(4), γ = 71.06(4)°. $U$ = 1003 Å$^3$, $D_c$ ($Z$ = 2) = 1.18 g cm$^{-3}$, $F$(000) = 384. $\mu_{Mo}$ = 3.2 cm$^{-1}$, specimen: 0.55 × 0.50 × 0.40 mm (no correction), $2\theta_{max}$ = 50°, final $R$, $R_w$ = 0.055, 0.062. $N$ = 3512, $N_0$ = 2655. Refinement abnormalities, including a significant difference map residue, were modelled in terms of disorder of Cl(1) to either side of Al(3), populations of Cl(1,1′) being ($x$, 1 − $x$) $x$ = 0.840(3). Hydrogen atoms were refined in ($x$, $y$, $z$, $U_{iso}$)$_H$ leaving an effectively featureless final difference map (max. residue 0.45 e Å$^{-3}$). Atomic coordinates, bond lengths and angles, and thermal parameters have been deposited at the Cambridge Crystallographic Data Centre (CCDC). See Information for Authors, Issue No. 1. Any request to the CCDC for this material should quote the full literature citation and the reference number 182/327.

## References

1 W. L. Gladfelter, D. C. Boyd and K. F. Jensen, *Chem. Mater*., 1989, **1**, 339; T. H. Baum, C. E. Larson and R. L. Jackson, *Appl. Phys. Lett*., 1989, **55**, 1264; A. T. S. Wee, A. J. Murrell, N. K. Singh, D. O'Hare and J. S. Foord, *J. Chem. Soc., Chem. Commun*., 1990, 11; A. A. Melas, *US Pat*., 4740606, 1988; L. H. Dubois, B. R. Zegarski, M. E. Gross and R. G. Nuzzo, *Surf. Sci*., 1991, **244**, 89; P. Zannella, G. Rossetto, N. Brianese, F. Ossola and M. Prorchia, *Chem. Mater*., 1991, **3**, 225.

2 C. Jones, G. A. Koutsantonis and C. L. Raston, *Polyhedron*, 1993, **15**, 1829; C. L. Raston, *J. Organomet. Chem*., 1994, **475**, 15.

3 I. B. Gorrell, P. B. Hitchcock and J. D. Smith, *J. Chem. Soc., Chem. Commun*., 1993, 189.

4 J. L. Atwood, K. W. Butz, M. G. Gardiner, C. Jones, G. A. Koutsantonis, C. L. Raston and K. D. Robinson, *Inorg. Chem*., 1993, **32**, 3482.

5 F. M. Elms, R. N. Lamb, P. J. Pigram, M. G. Gardiner, B. J. Wood and C. L. Raston, *J. Chem. Soc., Chem. Commun*., 1992, 1423; K. W. Butz, F. M. Elms, C. L. Raston, R. N. Lamb and P. J. Pigram, *Inorg. Chem*., 1993, **32**, 3985.

*Received, 22nd November 1996; Com. 6/07916D*



Typeset and printed by Black Bear Press Limited, Cambridge, England

ChemComm
FEATURE ARTICLE

# Open chain compounds with preferred conformations[1]

**Richard Göttlich, B. Colin Kahrs, Joachim Krüger and Reinhard W. Hoffmann***

*Fachbereich Chemie der Philipps-Universität Marburg, Hans-Meerwein-Strasse, 35032 Marburg, Germany*

**The shape of a flexible molecule, *i.e.* the preferred conformation of a multi-substituted alkyl chain, may be controlled by the nature and location of the pendant substituents. Steric interactions between those substituents themselves as well as the main chain, or sterically demanding end-groups, can be used to realize conformation design of flexible molecules.**

## Introduction

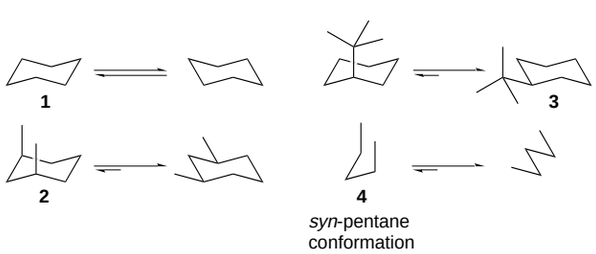
Compounds may be described in terms of a molecular backbone and of the functional groups attached to it. The distance and spatial arrangement of the functional groups frequently defines the activity of biologically active compounds. In cases of flexible, open chain compounds, it is the conformational space of the molecular backbone that limits and defines the possible distance between the functional groups attached. Definite arrangements may prevail, if the backbone of the molecule shows a marked conformational preference.

For instance, extended hydrogen bonding networks lead in polypeptides and proteins to the secondary and tertiary structure. Oligosaccharides composed of pyranoses have more defined spatial structures than saccharides composed of furanoses due to the conformational preferences of six membered rings. In polypropionate natural products steric interactions between the pendant methyl groups may restrict the conformational space and lead to oligo-conformational systems.[2] At the present time, when the design of peptidomimetics, artificial receptors and synthetic hosts is of interest, the properties of molecular backbones, especially their conformational properties, merit more detailed consideration. It is important to recognize the principles that render segments of a flexible molecular backbone mono-conformational, and to identify typical substructures of backbones, which populate to more than 90% a single conformation.

Well known examples are the 'conversion' of a bi-conformational cyclohexane nucleus **1** into a monoconformational situation by 1,3-*cis* disubstitution (*cf.* **2**) or by attachment of a conformational anchor, *e.g.* a *tert*-butyl group, *cf.* **3** (Scheme 1). One should keep in mind that the molecules **2** and **3** are still conformationally fully flexible. It is only that a single conformation predominates substantially.

Commonly, this effect is ascribed to the destabilization of one conformer by 1,3-diaxial interactions, which are a special case of the (destabilizing) *syn*-pentane interaction, *cf.* **4**. *syn*-Pentane interactions between two $CH_2$ groups result in a destabilization of *ca.* 3 kcal mol$^{-1}$ (1 cal = 4.184 J).[3,4,5] The avoidance of *syn*-pentane interactions is thus a powerful tool to reduce the number of low energy conformations of open chain compounds.[2,5] While pentane **5** is multiconformational, having five low energy conformations $E_r \leqslant 3.0$ kcal,[3] placement of substituents, *e.g.* methyl residues, in the 2,4 positions leads to 2,4-dimethylpentane **6**. The latter is 'bi-conformational' having only two low energy conformations **6a** and **6b** (Scheme 2). All other diamond lattice-type conformations are destabilized by *syn*-pentane interactions. Likewise, placement of substituents in the 2,4,6,8-positions of longer hydrocarbon chains will substantially reduce the number of low energy conformations available, creating bi-conformational situations in each dimethylpentane subsegment.

Placement of further substituents on the particular segment will not necessarily lead to a mono-conformational situation, since the additional *syn*-pentane interactions generated now affect all of the remaining low energy conformations. Different approaches towards reaching mono-conformational entities are the topic of this present account.




**Scheme 1**

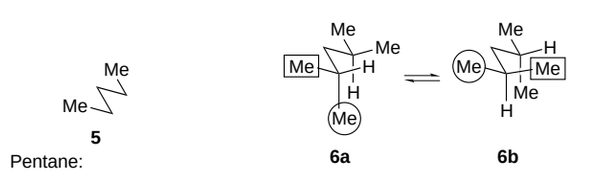
## Heteroatoms as pending substituents

In 2,4-dimethylpentane **6** the two methyl groups within each pair of end groups are identical. Hence, the conformers **6a** and **6b** are enantiomorphous, *i.e.* isoenergetic. The two conformers of **6** are formally interconverted by a +120° rotation about one skeletal bond and a −120° rotation about the other one. Considering an individual methyl group, *e.g.* the squared one, it has no *gauche* interactions in conformer **6a** and one gauche interaction in **6b**. If the end groups (squared or circled) in **6** were different, the energetic degeneracy would be lifted. On replacement of the squared methyl group by a group of smaller size, as measured *e.g.* by the *A*-value, the conformer equilibrium should be shifted towards **6b**.

The $^1$H–$^1$H vicinal coupling constants recorded for 2,4-dimethoxypentane[6] **7** or 2,4-dichloropentane[7] **8** document the expected shift in the conformer equilibrium; the conformer **b** (with the larger methyl group in the extended chain position) being preferred (Scheme 3).

The analysis of the conformer equilibria in such bi-conformational situations rests on the determination of vicinal coupling constants. The coupling constants between two individual hydrogens, *e.g.* $H_a$ and $H_b$ in **9** differ for the two conformers (Scheme 4).

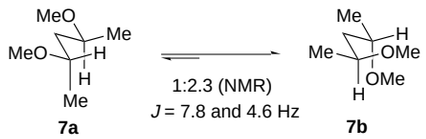
The measured coupling constant is the weighted time average over the conformer population. If, for example, **9a** and **9b** are present in a 1 : 1 ratio, an average coupling constant of about 6–7 Hz should be observed. Any bias of the equilibrium towards one side leads to a divergence of the coupling constants. By



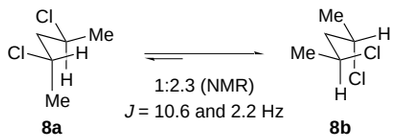

**Scheme 2**

comparison of the measured coupling constants with those calculated[8] for the individual conformers, the position of the equilibrium can be estimated.

At this point some general remarks are appropriate: We restrict our discussion to diamond lattice-type conformers. By this we imply backbone conformations with dihedral angles of 180 ± 15° or 60 ± 15°. If a conformation involving a *syn*-pentane interaction relaxes into the nearest energy minimum, this usually results in a skewed backbone conformation with dihedral angles of 90 ± 15°. These conformers are generally ⩾ 3 kcal higher in energy[9] than the lowest energy conformer. For this reason these skewed conformers contribute little to the overall conformer population and are not further considered here. Experimental information regarding the position of conformer equilibria derives from vicinal $^1H–^1H$ coupling constants between protons along the backbone of the molecule. The accuracy of these coupling constants obtained from first order multiplets in the $^1H$ NMR spectra is around ±0.1 Hz. If higher order multiplets have to be simulated, as is the case for all $C_2$-symmetrical structures such as **10** (Scheme 5), the coupling constants are accurate to about ±0.2 Hz. The experimental coupling constants are the weighted average of those of the populated conformers. In order to estimate the position of the conformer equilibrium for the bi-conformational backbone segments the coupling constants for the individual conformers have to be calculated. This is done by minimizing the individual conformer structures by the MM3* force field implemented in the MACROMODEL program.[8] This program also has a routine by which vicinal coupling constants are predicted for a given structure based on Karplus relationships. This routine makes provision for changes in the magnitude of coupling constants due to electronegative substituents on the backbone.[10] Clearly, coupling constants predicted this way will not be better than ±0.2 Hz. It is obvious that equating[11] experimental coupling constants with ±0.2 Hz accuracy with calculated coupling constants with ±0.2 Hz accuracy can give only a crude estimate of the conformer population. Nevertheless, the conformer population estimated this way agrees by and large with those calculated by MM3. Since it is not our aim to determine conformer populations accurately, but rather to identify substitution patterns that lead to a biased conformer equilibrium, the approach delineated above is sufficient for that purpose.




**7a** **7b**




**8a** **8b**

**Scheme 3**

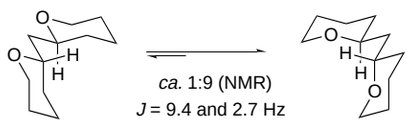



**9a** **9b**

$J_{a,b}$ = large
$J_{a,c}$ = small

$J_{a,b}$ = small
$J_{a,c}$ = large

**Scheme 4**




**10a** **10b**

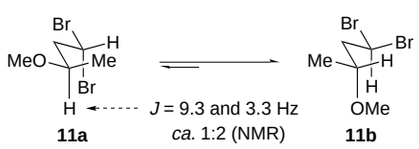
**Scheme 5**

The bias in the conformer equilibrium of the dimethoxy compound **7** can be attributed to a difference in effective size of a methoxy group *vs*. a methyl group—*cf* the *A*-values: Me = 1.74, MeO = 0.60. However, the conformer population depends not only on the differences in the van der Waals radii, but also on the restrictions in conformational space experienced by the methoxy group. This concerns both the energy and the number of the local C–C–O–$CH_3$ rotamers. The number of low energy rotamers for **7a** is 9 and for **7b** it is 4, giving more statistical weight to **7a**. The latter term affecting the conformer population of the backbone in **7** can be eliminated by tying the methoxy group into a ring. This is achieved by going from the dimethoxy compound **7** to the bis(tetrahydropyranyl)-methane **10**. In doing so, the methyl groups of **7** are also changed to $CH_2R$ groups. But the latter should have no effect on the conformer equilibrium, since the R residue, being held in a ring, does not lead to any additional gauche interactions in either conformer **10a** or **10b**. When comparing the conformer equilibria of **7** and **10**, it becomes apparent that the equilibrium of **10** lies considerably more on the **b** side, as judged by the $^1H$ NMR coupling constants.[1] The situation in **10** probably reflects the true difference in effective size between an ether oxygen and a methylene group.

Our goal was to convert a bi-conformational situation as found in **6** into a mono-conformational one, as approximated by **10**. The key was to replace one of the 'methyl groups' in **6**, *e.g.* the squared one by a group of different size than the remaining circled group. For a broader study on how the effective sizes of two groups effect the conformer population, we wanted to avoid $C_2$-symmetric systems, such as **7** or **10**, and turned to derivatives of 1,1-dibromobutane such as **11** (Scheme 6). In doing so we use a dibromomethyl group as a conformational lock to secure a bi-conformational situation and we determine than, to what extent the differences in effective size, *e.g.* of a methoxy and a methyl group, shift the conformer population toward a mono-conformational situation. In fact, the coupling constant of the hydrogen α to the oxygen substituent in **11** revealed a noticeable shift of the conformer equilibrium towards **11b**.

Increasing the size of the methyl group in **11**—the latter prefers to go into the sterically less encumbered chain end position—to an isopropyl group results in only a negligeable change in the conformer equilibrium, as seen from the coupling constants of **12** (Scheme 7). The small difference between a methyl and isopropyl group in such a system is also evident from the coupling constants recorded for **13**.[12] A sizeable effect is, however, attained when going to a *tert*-butyl group, as seen for **14**.

When changes are made at the oxygen substituent, the effect of tying the methoxy group into a ring can also be picked up within the dibromomethyl series, *cf*. the differences in coupling constants between **11** and **15** (Scheme 8). A change of the methoxy group in **12** to a trimethylsilyloxy group in **16** has, on the other hand, only a small effect. Thus, a trimethylsilyloxy group is hardly larger than a methoxy group as viewed from the dibromomethyl reporter unit.




**11a** **11b**

**Scheme 6**

## End-group control of conformation

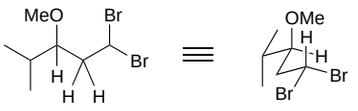
Coming back to the starting point **6**: when one replaces the squared methyl group in **6** by a really space-demanding substituent one should populate just the conformer **6a**. This is realized by going from **11** to **14**. The sizeable effect of the *tert*-butyl end group on the conformer population as seen for **14** has long been known as the *tert*-butyl effect,[13] according to which a *trans*-conformation is induced in structures such as **17** at the bond indicated (Scheme 9). Any other diamond lattice conformation around this bond would lead to *syn*-pentane interactions.

Hence, a combination of the structural elements **17** and **6**, as in compound **18**, should induce a t,g$^+$-conformation[14] as shown. In fact, a high tendency to adopt a single conformation has been reported for this compound by Luisi[15] based on measurements of the molecular rotation.

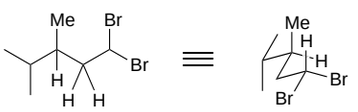
A more intricate situation of end-group control is seen in the examples **19** and **20** (Scheme 10). Obviously, steric bulk is not all that counts. In **19** and **20** an α-methoxyisobutyl residue is considered as the end group for the neighbouring bi-conformational segment. Since this segment is no longer symmetrically substituted, there are two sets of coupling constants, one large and one small in each. For the sake of simplicity we quote in Scheme 10 only the average value of the large coupling constants on the one side and of the small ones on the other side.

To evaluate the effect of the α-methoxyisobutyl group on the conformation of the C3–C4 bond (which in turn controls the conformation of the C4–C5 bond) in **19** and **20** we may consider just the number of low energy conformations which are free of *syn*-pentane interactions: For **19** there are three such conformations: (2,3g$^+$ 3,4t); (2,3t, 3,4t); and (2,3t 3,4g$^-$). Thus, in the bi-conformational segment C3 to C5, the 3,4t conformers are favoured by 2 : 1 over the 3,4g conformers according to this simplified analysis. The $^1$H NMR coupling constants indicate a 1.5 : 1 preference for the t conformation in this segment.

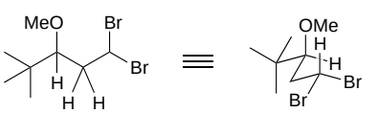
When going to **20** the situation is markedly different: there is only one conformer, the (2,3t 3,4t) conformer, which is free of *syn*-pentane interactions. Hence, compound **20** should have only one low energy conformation, the one shown, a fact that is reflected in the strong difference of the coupling constants recorded for **20**.[16] This effect can be used to selectively exert local conformation control in more extended molecular backbones such as **21** (Scheme 11).[17]




**12** major conformer
*J* = 9.4 and 3.1 Hz by *ca.* 3:1 (NMR)

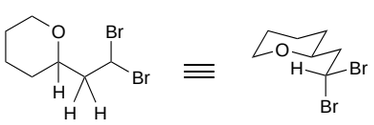



**13** major conformer
*J* = 8.7 and 4.5 Hz by *ca.* 1.5:1 (NMR)

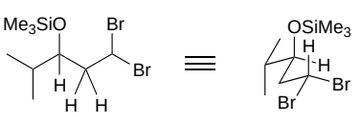



**14** major conformer
*J* = 10.8 and 2.7 Hz by > 10:1 (NMR)

**Scheme 7**

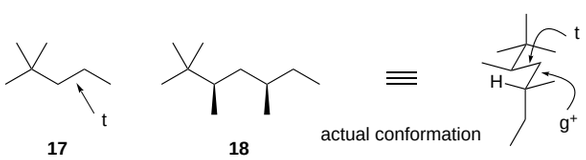



**15** major conformer
*J* = 9.7 and 2.7 Hz by > 9:1 (NMR)




**16** major conformer
*J* = 9.2 and 3.0 Hz by *ca.* 2:1 (NMR)

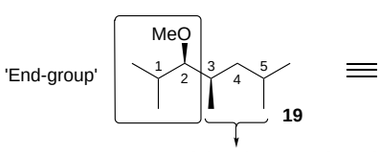
**Scheme 8**




**17** **18** actual conformation

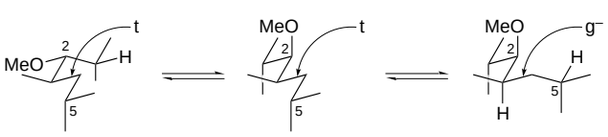
t = *trans*
g = *gauche*

**Scheme 9**

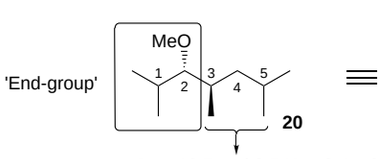



**19**

$J_{av}$ = 8.6 and 5.7 Hz 3,4t : 3,4g = *ca.* 1.5 : 1 (NMR)

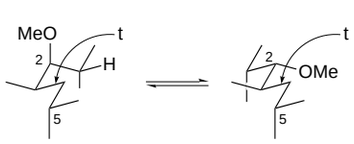



2,3g$^+$3,4t **19a** 2,3t 3,4t **19b** 2,3t 3,4g$^-$ **19c**



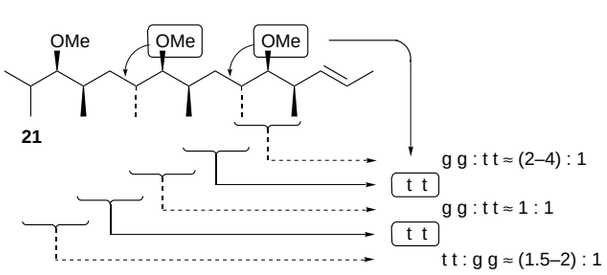

**20**

$J_{av}$ = 10.7 and 3.5 Hz 3,4t : 3,4 others = *ca.* 15 : 1 (NMR)




2,3g$^+$3,4t **20a** 2,3t 3,4t **20b**

**Scheme 10**




**Scheme 11**

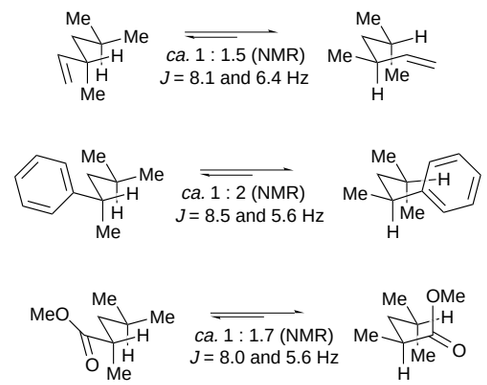
### sp²-Hybridized substituents

sp²-Hybridized end groups, such as vinyl, phenyl and methoxycarbonyl are, on the other hand, slimmer than a $CH_2R$ group. Therefore, in bi-conformational situations the former groups should be preferentially found in those positions, which are subject to the higher number of gauche interactions. This has been tested with a number of model compounds (Scheme 12).[16]

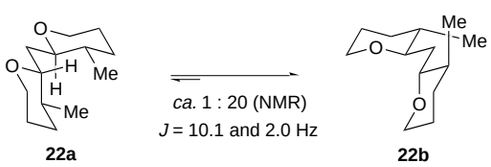
As can be seen from the coupling constants, the effects caused by a single sp²-hybridized substituent are rather small; $\Delta G$ values which affect the conformer equilibrium, do not exceed *ca*. 0.5 kcal mol$^{-1}$.

### Conformation design

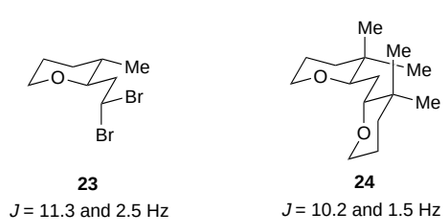
Many of the effects described above, which bias a bi-conformatonal towards a mono-conformational situation, are small or not far-reaching. For this reason effective conformation design to attain mono-conformational situations in larger molecular backbones would have to rely on the combination of several control elements. The introduction of polar repulsions, of hydrogen bonding networks, or of situations that profit from the attractive gauche effect,[18] would obviously offer additional strategies. At the present stage of the development of the field, we were interested to see how far one could go simply by using the effects discussed in the previous sections.



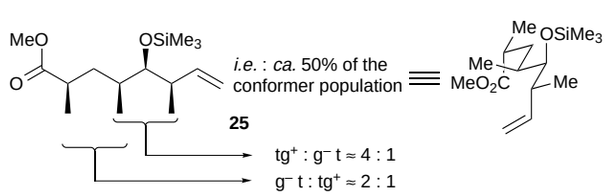

**Scheme 12**




**Scheme 13**




**Scheme 14**




**Scheme 15**

For example, in the case of **10**, introduction of two methyl groups to give **22** should reinforce the conformational preference. The two methyl groups in **22** have been strategically placed in the equatorial position to selectively destabilize the conformer **22a** by *syn*-pentane interactions between the methyl group and the backbone each relative to the conformer **22b** (Scheme 13).[1]

The same effect is seen[19] on comparison of the conformational preference of compound **23** with that of **15**. Since an essentially mono-conformational situation is already reached in compounds **22** and **23** by these tools, introduction of further methyl groups as in **24** has only a minor effect (Scheme 14).[1]

The effects that may be attained by multiple substitution of a chain with sp²-hybridized substituents are less striking. Nevertheless, the coupling constants recorded for **25**[16] indicate that about 50% of the total conformer population has a central g$^-$ttg$^+$ conformation (Scheme 15).

The various principles mentioned above are clearly manifest in nature's conformation design as illustrated by zincophorin **26**,[20] a natural ligand conformationally preorganized to complex $Zn^{2+}$. Inspection of part of its crystal structure lets one read nature's conformations design (Fig. 1).

The awareness of these and other factors, which render backbones of flexible molecules oligo- or mono-conforma-

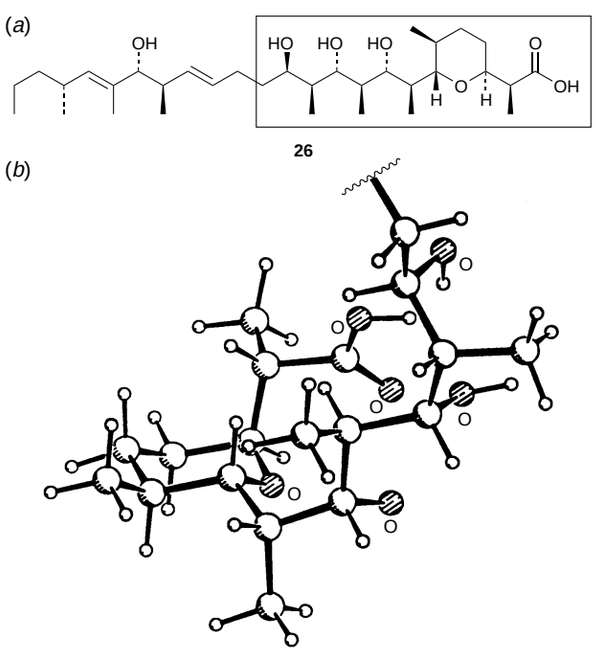
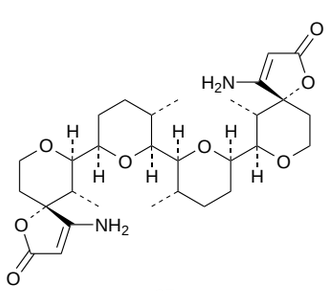



**Fig. 1** (*a*) Structure of zincophorin with fragment highlighted, and (*b*) partial crystal structure of highlighted fragment



tional, is obviously important for contemporary drug design and the design of tailor-made host molecules. This has recently been demonstrated by W. C. Still[21] with the synthesis of artificial ligands such as **27**.


## Acknowledgements

C. K. gratefully acknowledges a fellowship from the Graduierten-Kolleg 'Metallorganische Chemie' at the Philipps-Universität Marburg and R. G. acknowledges one from the Fonds der Chemischen Industrie. Additional support came from the Volkswagenstiftung and the European Community, grant HMC-ERB-CHRXCT 930141.



**Reinhard W. Hoffmann (born 1933) studied chemistry at the University of Bonn, where he received his PhD under the supervision of Professor B. Helferich. Two years as a postdoctoral associate in the group of Professor G. W. Brindley at the Pennsylvania State University were followed by another postdoctoral year in the group of Professor G. Wittig at the University of Heidelberg. Professor Hoffmann gained his habilitation from the University of Heidelberg in 1964. In 1967 he moved to the Technical University of Darmstadt and in 1970 he was appointed to a chair of organic chemistry at the University of Marburg.**

**Professor Hoffmann was a visiting Professor at the University of Wisconsin (1968), the University of Bern (1978) and the University of Berkeley (1981). In 1993 he was awarded the Liebig-Denkmünze from the Gesellschaft Deutscher Chemiker.**

**Björn Colin Kahrs (born (1968) studied chemistry at the University of Göttingen, where he graduated in 1993. He earned his PhD under the supervision of Professor R. W. Hoffmann from the University of Marburg and in 1996 he took a position at Merck AG, Darmstadt.**

**Richard Göttlich (born 1969) studied chemistry in Marburg and received his PhD under the supervision of Professor R. W. Hoffmann in 1996. Currently he is a postdoctoral associate with Professor M. Shibasaki at the University of Tokyo.**

**Jochen Krüger (born 1969) studied chemistry at the Technical University of Munich and at the University of Marburg where he graduated in 1994. Presently he is working as a PhD student in the group of Professor R. W. Hoffmann.**


## References


1 Flexible Molecules with Defined Shape, Part IV; for Part III see: R. W. Hoffmann, B. C. Kahrs, J. Schiffer and J. Fleischhauer, *J. Chem. Soc., Perkin Trans. 2*, 1996, 2407.
2 R. W. Hoffmann, *Angew. Chem.*, 1992, **104**, 1147; *Angew. Chem., Int. Ed. Engl.*, 1992, **31**, 1124.
3 K. B. Wiberg and M. A. Murcko, *J. Am. Chem. Soc.*, 1988, **110**, 8029.
4 R. A. Scott and H. A. Scheraga, *J. Chem. Phys.*, 1966, **44**, 3054; A. Abe, R. L. Jernigan and P. J. Flory, *J. Am. Chem. Soc.*, 1966, **88**, 631; S. Sykora, *Collect. Czech. Chem. Commun.*, 1968, **33**, 3514.
5 P. W. Smith and W. C. Still, *J. Am. Chem. Soc.*, 1988, **110**, 7917.
6 K. Matsuzaki, K. Sakota and M. Okada, *J. Polym. Sci., Part A*, 1969, **7**, 1444.
7 B. Schneider, J. Stokr, D. Doskocilova, S. Sykora, J. Jakes and M. Kolinsky, *J. Polym. Sci., Ser. C.*, 1969, 1073; T. Moritani and Y. Fujiwara, *J. Chem. Phys.*, 1973, **59**, 1175.
8 F. Mohamadi, N. G. J. Richards, W. C. Guida, R. Liskamp, M. Lipton, C. Caufield, G. Chang, T. Hendrickson and W. C. Still, *J. Comput. Chem.*, 1990, **11**, 440.
9 S. Tsuzuki, L. Schäfer, H. Goto, E. D. Jemmis, H. Hosoya, K. Siam, K. Tanabe and E. Osawa, *J. Am. Chem. Soc.*, 1991, **113**, 4665.
10 C. A. G. Haasnoot, F. A. A. M. de Leeuw and C. Altona, *Tetrahedron*, 1980, **36**, 2783; C. A. G. Haasnoot, F. A. A. M. de Leeuw, H. P. M. de Leeuw and C. Altona, *Org. Magn. Reson.*, 1981, **15**, 43.
11 For example see: C. A. G. Haasnoot, *J. Am. Chem. Soc.*, 1993, **115**, 1460.
12 K. Brumm, *Dissertation*, University of Marburg, 1993.
13 S. Cauwberghs and P. J. De Clercq, *Tetrahedron Lett.*, 1988, **29**, 2493; R. W. Alder, C. M. Maunder and A. G. Orpen, *Tetrahedron Lett.*, 1990, **31**, 6717.
14 For the t,g nomenclature see for example ref. 2.
15 S. Pucci, M. Aglietto and P. L. Luisi, *J. Am. Chem. Soc.*, 1967, **89**, 2787.
16 R. Göttlich, *Dissertation*, University of Marburg, 1996.
17 R. Göttlich, T. Fäcke, U. Rolle and R. W. Hoffmann, *J. Chem. Soc., Perkin Trans. 2*, 1996, 2059.
18 S. Wolfe, *Acc. Chem. Res.*, 1972, **5**, 102; E. Juaristi, *J. Chem. Edu.*, 1979, **56**, 438.
19 R. W. Hoffmann, H.-C. Stiasny and J. Krüger, *Tetrahedron*, 1996, **52**, 7421.
20 H. A. Brooks, D. Gardner, J. P. Poyser and T. J. King, *J. Antibiot.*, 1984, **37**, 1501; S. J. Danishefsky, H. G. Selnick, R. E. Zelle and M. P. DeNinno, *J. Am. Chem. Soc.*, 1988, **110**, 4368.
21 M. T. Burger, A. Armstrong, F. Guarnieri, D. Q. McDonald and W. C. Still, *J. Am. Chem. Soc.*, 1994, **116**, 3593; G. Li and W. C. Still, *J. Am. Chem. Soc.*, 1993, **115**, 3804.



*6/03040H*

# Cyano adduct-anions of [60]fullerene observed by electrospray mass spectrometry

**George Khairallah and J. Barrie Peel***

*School of Chemistry, La Trobe University, Bundoora, Victoria 3083, Australia*

**Negative-ion electrospray mass spectrometry of $C_{60}$–$CN^-$ solutions are used to study the cyano adduct-anions of [60]fullerene, revealing three abundant species, namely $C_{60}(CN)_n^-$, $n$ = 1, 3, 5, with $C_{60}(CN)^-$ as the dominant anion.**

The nucleophilic addition reactions of [60]fullerene demonstrate its behaviour as an electron deficient polyalkene.[1] Thus $C_{60}$ undergoes amination reactions such as with triethylamine,[2] where the intermediate radical anion, $C_{60}^{\cdot -}$, is thought to be involved. The $C_{60}$ reaction with cyanide anion[3] forms the mono-adduct anion, $C_{60}(CN)^-$, as a soluble salt. Electrospray mass spectrometry (ESMS) examining both positive and negative ions has been demonstrated as a powerful technique in the study of fullerenes and their adducts. The study of $C_{60}$ and $C_{70}$ anions by negative-ion ESMS,[4] led to observation of higher fullerene anions.[5] Tagged fullerenes[6] and polyamine adducts of $C_{60}$[7] have been studied by positive-ion ESMS, and the methoxylated anions of $C_{60}$ and $C_{70}$ by negative-ion ESMS.[5,8]

It has been noted that electrospray response varies according to source design as well as instrument conditions,[8] which offers an explanation for the different spectra observed for the methoxylated anions of $C_{60}$ by Wilson and Wu[8] and by Hiraoka and coworkers.[5] The former observed only the even-electron species, $C_{60}(OMe)_n^-$, $n$ = 1, 3, 5, which are the more likely long-lived anions in solution, as confirmed by semi-empirical theoretical studies.[9] By contrast the latter workers observed one odd-electron species, $C_{60}(OMe)_2^{\cdot -}$, as well.[5] It is possible that this ion results from collision-induced dissociation of the stable higher ions within the electrospray source. However an electrospray source can also behave as an electrochemical cell,[10,11] and $C_{60}^{\cdot -}$ is observed in the ESMS of $C_{60}$ solutions.[11] Hence the odd-electron species $C_{60}(OMe)_2^{\cdot -}$ is possibly resulting from electron attachment (reduction) of neutral $C_{60}(OMe)_2$.

We have used the reaction of $C_{60}$ (MER Corporation) in dry 1,2-dichlorobenzene with NaCN in dry DMF to provide various solutions for examination by ESMS. Mass spectra were obtained with a VG BioQ triple-quadrupole system (VG Biotech, Altrincham, UK). The freshly prepared mixtures, which contained $C_{60}$ total concentrations of *ca*. 0.5 mmol dm$^{-3}$ and NaCN of *ca*. 5–100 mmol dm$^{-3}$, were injected directly into the spectrometer using a Rheodyne injector incorporating a 50 mm$^3$ loop. The mobile phase used was 1 : 1 propan-2-ol–water as recommended for its proven negative-ion sensitivity.[12] A flow rate of 5 mm$^3$ min$^{-1}$ was used and spectra were acquired in the negative-ion mode with the nozzle/skimmer (cone) voltage of 40 V. Scanning was from *m/z* 700–900, with 25 scans being signal-averaged over a 120 s period to produce each mass spectrum.

Visual observation of typical $C_{60}$–$CN^-$ solutions showed an initial olive green colour which changed progressively over a period of around an hour through dirty brown shades to a brown–yellow colour. The ESMS data presented here were obtained for solutions up to 1 h following mixing.

Typical spectra measured for various $CN^-$ concentrations and at various times, Fig. 1, exhibit strong peaks in the 740–800 *m/z* range. The three peaks located at *m/z* values of 746, 798 and 850 indicate the presence of the even-electron cyano adduct-anions $C_{60}(CN)_n^-$ $n$ = 1, 3, 5. At higher resolution each peak clearly demonstrates the appropriate isotope ratios based on natural $^{12}C/^{13}C$ as illustrated for the 746 peak in Fig. 2. The four discernible isotopes of $C_{60}(CN)^-$, of *m/z* 746, 747, 748 and 749, have theoretical relative abundances of 100 : 68 : 23 : 5. However the peak at 772, of *m/z* corresponding to the odd-electron $C_{60}(CN)_2^{\cdot -}$ species, as also shown in Fig. 2, exhibits an isotope distribution revealing 0.5 amu spacings, contrary to this formula. This pattern is suggestive of a doubly-charged ion containing two $C_{60}$ units, and our conjecture is that it is an ion–molecule complex, namely $C_{60}(CN)_4^{2-}.C_{60}$. This is supported by our observation that $C_{60}(CN)_4^{2-}$ at *m/z* 412 is also present in some $C_{60}$–$CN^-$ solutions.[13] Likewise the 824 peak is probably due to the analogous $C_{60}(CN)_8^{2-}.C_{60}$ species.

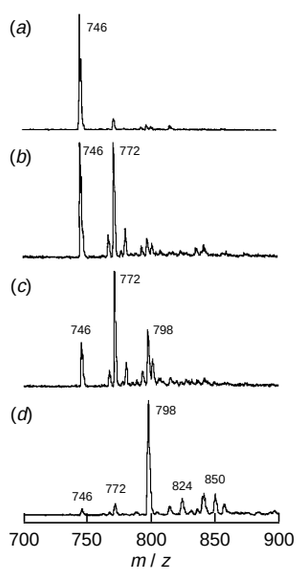



**Fig. 1** Negative-ion electrospray mass spectra for *m/z* = 700–900 of $C_{60}$–$CN^-$ solutions (*a*) [$CN^-$] = *ca*. 5 mmol dm$^{-3}$, (*b*) [$CN^-$] = *ca*. 50 mmol dm$^{-3}$ at 25 min, (*c*) [$CN^-$] = *ca*. 50 mmol dm$^{-3}$ at 50 min, and (*d*) [$CN^-$] = *ca*. 100 mmol dm$^{-3}$

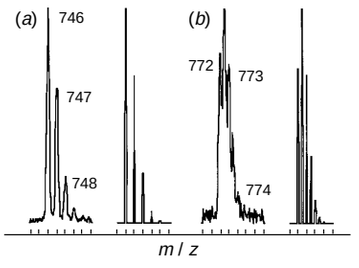



**Fig. 2** Comparison of experimental and theoretical $^{12}C/^{13}C$ isotope distributions for the negative-ion mass spectra of (*a*) $C_{60}(CN)^-$ and (*b*) $C_{60}(CN)_4^{2-}.C_{60}$

The spectra of fresher and lower concentration solutions are dominated by $C_{60}(CN)^-$ in agreement with the observation of this species as the intermediate in the reactions described by Majid *et al.*[3] For older and more concentrated solutions the relative abundance of $C_{60}(CN)_3^-$ increases and then $C_{60}(CN)_5^-$ likewise, with all three ($n$ = 1, 3, 5) present in some cases in comparable amounts. There are various other weak peaks in this mass region, and these can be assigned to species containing oxygen indicative of some degree of oxidation.

A comparison with the ESMS data reported[5,8] for $C_{60}(OMe)_n^-$ shows that the same even-electron species ($n$ = 1, 3, 5) are dominant. However the $C_{60}^{\cdot -}$ observed in the $C_{60}$–$OMe^-$ mixtures is not observed here with the $C_{60}(CN)_n^-$ species.

The results of semi-empirical molecular orbital calculations obtained using the AM1 approximation with the MOPAC program[14] are presented in Table 1. On the basis of earlier calculations[9] on the $OMe^-$ adducts the likely isomers for the $C_{60}(CN)_n^-$ ($n \geqslant 2$) species are relatively few in number. An analysis of the charge distribution for $C_{60}(CN)^-$ shows that the negative charge is located mostly on and near the CN group, analogous to the case of $C_{60}OMe^-$.[9] So for the higher isomers the structures with reasonably localized CN groups should adequately support the excess negative charge in their vicinity.

The calculated ionization energies and heats of formation, and the derived mean binding energies per CN of the chosen isomeric structures for each $C_{60}(CN)_n^-$ for $n$ = 1, 3, 5 are given in Table 1. The latter parameters offer a simple quantitative comparison of the relative stabilities of the respective anion species.

**Table 1** MOPAC/AM1 results for selected isomers of $C_{60}(CN)_n^-$, $n$ = 1, 3, 5; calculated ionization energies, IE (in eV) and heats of formation, $\Delta H_f$ with mean binding energies per CN, $\Delta H_b$ (kJ mol$^{-1}$)

| Molecule | Structure[a] | IE | $\Delta H_f$ | $\Delta H_b$[b] |
|---|---|---|---|---|
| $C_{60}$ | | 9.64 | 4072 | |
| $C_{60}^{\cdot -}$ | | 3.31 | 3771 | |
| $CN^-$ | | 3.13 | 184 | |
| $C_{60}(CN)^-$ | | 4.99 | 3817 | 439 |
| $C_{60}(CN)_3^-$ | 1,4,11- | 5.37 | 3950 | 197 |
| | 1,4,55- | 5.13 | 3994 | 182 |
| | 1,4,15- | 5.19 | 4016 | 175 |
| $C_{60}(CN)_5^-$ | 1,4,11,15,30- | 6.09 | 4042 | 157 |
| | 1,2,39,57,60- | 5.31 | 4169 | 131 |
| | 1,4,39,53,57- | 5.31 | 4176 | 130 |

[a] The numbering system used is that given in ref. 15. [b] $\Delta H_b$ is given by $\Delta H/n$ for the reaction $C_{60} + n\ CN^- \rightarrow C_{60}(CN)_n^-$.

Since the ionization energies (IEs) of the anions are significantly positive and increasing with increasing $n$, it is not surprising that the strong ionic environment is able to support the negative charge state of these species. So $C_{60}^{\cdot -}$, with its much lower calculated IE of 3.31 eV, is not supported in this environment, while $C_{60}(CN)^-$ with its higher IE of 4.99 eV is present at moderate $CN^-$ concentration. Hence the favoured isomers of $C_{60}(CN)_3^-$ and $C_{60}(CN)_5^-$ with their higher IEs of 5.37 and 6.09 eV, respectively, are formed at higher $CN^-$ concentration and over time. However the $CN^-$ concentration may not be high enough to produce the $C_{60}(CN)_7^-$ species, possibly because of an unfavourable equilibrium with $C_{60}(CN)_6$, which, with a structure likely to be the same as $C_{60}Cl_6$,[15] is expected to be the most stable of the neutral species considered. Overall these results show good correspondence with the ESMS observation of the dominance of $C_{60}(CN)^-$ represented in the spectra of Fig. 1.

We thank J. C. Traeger and I. M. thomas for assistance with the ESMS measurements, and the Australian Research Council for financial support.

## References

1 F. Wudl, A. Hirsch, K. C. Khemani, T. Suzuki, P.-M. Allemand, A. Koch, H. Eckert, G. Srdanov and H. M. Webb, in *Fullerenes: Synthesis, Properties and Chemistry of Large Carbon Clusters*, ed. G. S. Hammond and V. J. Kuck, ACS Symposium Series 481, American Chemical Society, Washington, DC, 1992.
2 J. Pola, A. D. Darwich, R. A. Jackson, H. W. Kroto, A. K. Abdulsada, R. Taylor and D. R. M. Walton, *Fullerene Sci. Tech.*, 1995, **3**, 299.
3 K.-K. Majid, B. Knight, G. Srdanov and F. Wudl, *J. Am. Chem. Soc.*, 1995, **117**, 11 371.
4 K. Hiraoka, I. Kudaka, S. Fujimaki and H. Shinohara, *Rapid. Commun. Mass Spectrom.*, 1991, **6**, 254.
5 S. Fujimaki, I. Kudaka, T. Sato, K. Hiraoka, H. Shinohara, Y. Saito and K. Nojima, *Rapid. Commun. Mass Spectrom.*, 1993, **7**, 1077.
6 S. R. Wilson and Y. Wu, *J. Am. Soc. Mass Spectrom.*, 1993, **4**, 596.
7 S. R. Wilson and Y. Wu, *Org. Mass Spectrom.*, 1994, **29**, 1864.
8 S. R. Wilson and Y. Wu, *J. Am. Chem. Soc.*, 1993, **115**, 10 334.
9 J. B. Peel, *Aust. J. Phys.*, 1996, **49**, 435.
10 A. T. Blades, M. G. Ikonomou and P. Kebarle, *Anal. Chem.*, 1991, **63**, 2109.
11 A. Dupont, J. P. Gisselbrecht, E. Leize, L. Wagner and A. Van Dorsselaer, *Tetrahedron Lett.*, 1994, **35**, 6083.
12 R. F. Straub and R. D. Voyksner, *J. Am. Soc. Mass Spectrom.*, 1993, **4**, 578.
13 G. Khairallah and J. B. Peel, unpublished results.
14 M. B. Coolidge and J. J. P. Stewart, Frank J. Seiler Research Laboratory, United States Air Force Academy, Colorado 80840 USA, 1990.
15 P. R. Birkett, A. G. Avent, A. D. Darwish, H. W. Kroto, R. Taylor and D. R. M. Walton, *J. Chem. Soc., Chem. Commun.*, 1993, **15**, 1230.

*Received, 23rd October 1996; Com. 6/07229A*

# Aqueous-phase p$K_a$ of the methyl group in acetic acid

**Joseph J. Grabowski**

*Department of Chemistry, University of Pittsburgh, Pittsburgh, PA, 15260, USA*

**The gas-phase acidity of the α-hydrogens of acetic acid and the aqueous-phase p$K_a$ of ethyl acetate are combined with other literature values in a thermodynamic cycle to provide the aqueous-phase p$K_a$ of the methyl group of acetic acid as 22.7 ± 1.0 and the p$K_a$ of the enol of acetic acid as 3.3 ± 1.0.**

Enolate anions of carboxylic acids are postulated as intermediates in a number of biologically important reactions that include addition,[1] racemization[2] and elimination processes.[3] Despite their importance and the attempts to understand how such energetic species could be stabilized,[4] little is known about α-C–H acidities in carboxylic acids including the prototypical acetic acid itself. Arguable exceptions are limited to compounds with special structural features that provide kinetic or thermodynamic stabilization[5,6] or those that can be generated as products from the decay of reactive intermediates produced by laser flash photolysis.[7]

An alternative strategy for determining an aqueous phase p$K_a$ is to translate a gas-phase acidity into its condensed-phase counterpart by using an appropriate thermochemical cycle such as that for acetic acid shown in Scheme 1.[8] Knowing any four of the five parameters in Scheme 1 allows one to obtain the missing thermochemical value. This approach has been used to determine hydration enthalpies of alkyl ammonium[9] and aliphatic carboxylate ions,[8,10] and takes advantage of recently determined, accurate gas-phase basicities[11,12] or acidities.[13]

Several distinct advantages over conventional approaches are realized for p$K_a$ determinations *via* Scheme 1. First, gas-phase acidities can be accurately determined across the full range of acidities, and in a well-defined common environment (*i.e.* the gas-phase), while condensed-phase values are easily and accurately determined only in water. Second, all gas-phase acidities, by their very nature, are for the direct ionization process depicted in the top equation of Scheme 1 and do not require any consideration for ion-pairing or other aggregation effects. Third, the control accessible to modern gas-phase ion chemistry techniques allows nearly equal ability to measure absolute acidities of two or more different types of protons in the same molecule, a process more difficult to address in the condensed-phase.

Recent determinations of the gas-phase acidity of the α-C–H of acetic acid[14,15] and the p$K_a$ of ethyl acetate as a carbon acid in aqueous solution[16] can now be combined with other calorimetric data from the literature, as described below, to provide a direct evaluation of the aqueous phase p$K_a$ of the less acidic proton in acetic acid. Inspection of Scheme 1 provides the necessary equation with which to evaluate the aqueous-phase ionization energy of acetic acid as a carbon acid, $\Delta G^{aq}_{acid}\{CH_3CO_2H\}$ [eqn. (1)]. (All thermochemical values are summarized in Table 1.)

$$\Delta G^{aq}_{acid}\{CH_3CO_2H\} = \Delta G^{g}_{acid}\{CH_3CO_2H\} - \Delta G^{g\rightarrow aq}_{solv}\{CH_3CO_2H\} + \Delta G^{g\rightarrow aq}_{solv}\{H^+\} + \Delta G^{g\rightarrow aq}_{solv}\{H_2C{=}C(O^-)OH\} \quad (1)$$

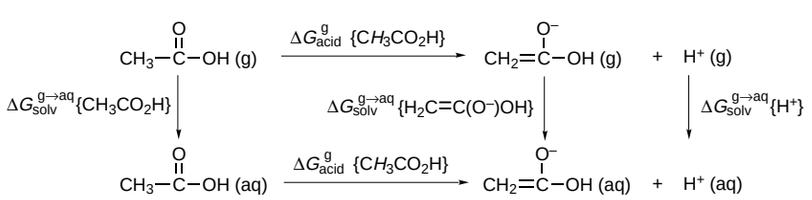
Several years ago we discovered that gas-phase deprotonation of acetic acid by hydroxide and other bases led to competitive proton abstraction from the O and C sites;[14] bracketing studies in both directions led to the determination that $\Delta G^{g}_{acid}\{CH_3CO_2H\}$ = 361.2 kcal mol$^{-1}$ (1 cal = 4.184 J). Additional proton abstraction studies of the monoenolate anion of acetic acid prepared by a fluorodesilylation reaction are entirely consistent with this value.[15]

Free energies of hydration of many neutrals are available in the literature[17–19] and simple unknown values can be estimated to within an accuracy of better than 0.25 kcal mol$^{-1}$.[19] For acetic acid, $\Delta G^{g\rightarrow aq}_{solv}\{CH_3CO_2H\}$ is −6.70 kcal mol$^{-1}$, an experimental value reproduced to within 0.1 kcal mol$^{-1}$ by group contributions.[19]

Prior uses of the thermochemical cycle in Scheme 1 have variously considered the free energy of hydration of the proton[20,21] to be well established,[22] at −259.5 kcal mol$^{-1}$, as well as the 'object of much dispute',[8] at −262.4 kcal mol$^{-1}$. While this value is critical for determining absolute energies of solvation for anions, as previously demonstrated, it is completely unimportant herein because the value appears in eqn. (1) and in estimating $\Delta G^{g\rightarrow aq}_{solv}\{H_2C{=}C(O^-)OH\}$ and therefore cancels. Thus, while the value used by Wilson and co-workers[8] is adopted for Table 1, it is important to recognize that changing this solvation energy will have no effect on the p$K_a$ that is derived.

To date, the major hindrance in using Scheme 1 to estimate p$K_a$ values has been the lack of reliable anion hydration energies; this is the situation for the monoenolate anion of acetic acid. Scheme 1, therefore, is most commonly used when both gas and aqueous-phase acidities are known, to derive ion energies of hydration.[8,10,22] By using Scheme 1 to determine the free energy of hydration of the enolate anion for methyl acetate, and using this value to estimate the energy of hydration of the monoenolate anion of acetic acid, one can overcome two problems at once: namely, the uncertainty in the absolute hydration energy of the proton and the unknown hydration energy of the monoenolate anion of acetic acid.

Rearranging eqn. (1) for methyl acetate and to determine an anion hydration energy, requires: p$K_a\{CH_3CO_2CH_3\}$ = 25.6 (assumed to be identical to ethyl acetate[16]) or $\Delta G^{aq}_{acid}\{CH_3CO_2CH_3\}$ = 34.9 kcal mol$^{-1}$;




**Scheme 1**

$\Delta G^{g}_{acid}\{CH_3CO_2CH_3\}$ = 365.1 kcal mol$^{-1}$ and[13] $\Delta G^{g\rightarrow aq}_{solv}\{CH_3CO_2CH_3\}$ = −3.32 kcal mol$^{-1}$.[19] Combining these values with the hydration energy of the proton provides $\Delta G^{g\rightarrow aq}_{solv}\{H_2C{=}C(O^-)OCH_3\}$ = −71.1 kcal mol$^{-1}$. If we assume the hydration energy of the monoenolate anion of acetic acid is equal to that of the enolate anion of methyl acetate plus a correction term for the mutation of a methyl group into a hydrogen, then the hydration energy of the proton drops out of consideration for the p$K_a\{CH_3CO_2H\}$ determination.

The remaining question concerns the correction term. Inspection of Table 1 reveals that $CH_3CO_2H$ has a more negative solvation free energy than $CH_3CO_2CH_3$ by 3.4 kcal mol$^{-1}$. Likewise, literature data[19] for propanoic acid *vs.* methyl propanoate, butanoic acid *vs.* methyl butanoate and methanol *vs.* dimethyl ether shows that mutating a methyl into a hydrogen enhances solvation free energy in each case by 3.42 ± 0.15 kcal mol$^{-1}$. Using this value as the correction term therefore allows us to predict $\Delta G^{g\rightarrow aq}_{solv}\{H_2C{=}C(O^-)OH\}$ = −74.54 kcal mol$^{-1}$. Using this latter value, the aqueous C–H acidity of acetic acid thus derived (Scheme 1, Table 1) is p$K_a\{CH_3CO_2H\}$ = 22.7. More complex corrections might have been required if the monoenolate anion of acetic acid possessed an internal hydrogen bond in the gas-phase. However, high level *ab initio* calculations clearly demonstrate the lack of such an interaction.[15,23]

A consideration of the approach used to derive the p$K_a$ shows that the error in the derived value is determined by the error in four terms. Relative gas-phase acidities are good to better[24] than 1.0 kcal mol$^{-1}$ while relative solvation energies have an estimated error of 0.1 kcal mol$^{-1}$. The stated error for the p$K_a$ of ethyl acetate is 0.5 p$K_a$ units (± 0.7 kcal mol$^{-1}$) and little extra error will result from the assumption of equivalent p$K_a$ values for methyl and ethyl acetates. The standard deviation for the four sets of literature examples used to derive an average $\delta\Delta G^{g\rightarrow aq}_{solv}$ for mutation of a methyl group into a hydrogen is 0.15 kcal mol$^{-1}$. Thus the best estimate is p$K_a\{CH_3CO_2H\}$ = 22.7 ± 1.0.

The p$K_a$ value derived here is entirely consistent with the oft-cited value of 24 that is obtained from an extrapolation of a correlation of ionization rate to p$K_a$s[25] and may be compared to the p$K_a\{CH_3COCH_3\}$[26] = 19.27, p$K_a${α-hydroxy-α-phenylacetic acid}[7] = 22 and p$K_a\{CH_3COSCH_2CH_3\}$[27] = 21.0. Combination of p$K_a\{CH_3CO_2H\}$ = 22.7 with p$K_E$ = 19.4 (where $K_E$ is the equilibrium constant for formation of the enol from the keto tautomer)[28–30] leads to the prediction that p$K_a\{H_2C = C(OH)_2\}$ = 3.3 (±1.0).[16]

In summary, an approach has been outlined that allows one to determine p$K_a$ values in aqueous solution by hydrating the reaction for the corresponding gas-phase value. This approach is limited by the availability and accuracy of the necessary thermochemical values. Even the simplest 'thermochemical literature history' reveals a constant refinement and improvement in accuracy as time and experimental methodologies progress. All values used in this work are, therefore, summarized in Table 1. In the event that one of the values used to derive this p$K_a$ is refined in the future, one simply needs to replace that value in Table 1 and thereby derive the new and presumably more accurate p$K_a$. For comparison, the hydration energy of acetate ion and acetone enolate are also included in Table 1; these values were obtained using a method analogous to that in Scheme 1.

Acknowledgment is made to the National Science Foundation for financial support for this work and to Professors Chris Cramer and Chris Maricondi for valuable discussion.

**Table 1** Free energies and p$K_a$s (at 298 K) used and derived in this work[a]

| | $CH_3CO_2CH_3$ | $CH_3CO_2H$ | $CH_3COCH_3$ | $CH_3CO_2H$ |
|---|---|---|---|---|
| Gas-phase acid data[b] | 365.1 | 361.2[c] | 361.9 | 341.5 |
| Neutral solvation data[d] | −3.32 | −6.70 | −3.85 | −6.70 |
| $H^+$ Solvation data[e] | −262.4 | −262.4 | −262.4 | −262.4 |
| Aqueous acidity data | | | | |
| p$K_a$ | 25.6[f] | 22.7[g] | 19.27[i] | 4.76 |
| $\Delta G^{aq}_{acid}$ | 34.91[g] | 31.0[b] | 26.28[g] | 6.49[g] |
| Anion solvation data | −71.12[h] | −74.52[i] | −77.09[h] | −79.3[h] |

[a] All values except p$K_a$'s are in kcal mol$^{-1}$. [b] All gas-phase acidities are obtained from ref. 13 unless noted. [c] Ref. 14. [d] All neutral free energies of hydration are obtained from ref. 19. [e] Derived from the $\Delta H$ and $\Delta S$ values cited in ref. 8. Note that while this value is crucial for deriving absolute solvation energies using gas- and aqueous-phase acidities, the p$K_a$ derived for the methyl position of acetic acid is insensitive to this value as discussed in the text. [f] Assumed to the same as ethyl acetate and obtained from ref. 16. [g] Derived from $\Delta G = -RT\ln K_a$. [h] Derived from the other values in this Table and a consideration of Scheme 1. [i] Ref. 24. [j] See text.

## References


1 P. Dowd, R. Hersline, S. W. Ham and S. Naganathan, *Science*, 1995, **269**, 1684.
2 G. L. Kenyon, J. A. Gerlt, G. A. Petsko and J. W. Kozarich, *Acc. Chem. Res.*, 1995, **28**, 178.
3 J. P. Richards, in *The Chemistry of Enols*, ed. Z. Rappoport, Wiley, New York, 1990, pp. 651–689.
4 Y. Apeloig, in *The Chemistry of Enols*, ed. Z. Rappoport, Wiley, New York, 1990, pp. 1–74.
5 A. F. Hegarty and P. O'Neil, in *The Chemistry of Enols*, ed. Z. Rappoport, Wiley, New York, 1990, pp. 639–650.
6 B. M. Allen, A. F. Hegarty, P. O'Neil and M. T. Nguyen, *J. Chem. Soc., Perkin Trans. 2*, 1992, 927.
7 Y. Chiang, A. J. Kresge, P. Pruszynski, N. P. Schepp and J. Wirz, *Angew. Chem., Int. Ed. Engl.*, 1990, **29**, 792.
8 B. Wilson, R. Georgiadis and J. E. Bartmess, *J. Am. Chem. Soc.*, 1991, **113**, 1762.
9 D. H. Aue, H. M. Webb and M. T. Bowers, *J. Am. Chem. Soc.*, 1976, **98**, 318.
10 P. Haberfield and A. K. Rahshit, *J. Am. Chem. Soc.*, 1976, **98**, 4393.
11 S. G. Lias, J. E. Bartmess, J. F. Liebman, J. L. Holmes, R. D. Levin and W. G. Mallard, *J. Phys. Chem. Ref. Data*, 1988, **17**, suppl. No. 1.
12 S. G. Lias, J. F. Liebman, R. D. Levin and S. A. Kafafi, *Positive Ion Energetics: NIST Standard Reference Database 19A*, 2nd edn., 1993.
13 J. E. Bartmess, *NIST Negative Ion Energetics Database, Version 3.0, Standard Reference Database 19B*, National Institute of Standards and Technology, 3rd edn., 1993.
14 J. J. Grabowski and X. Cheng, *J. Am. Chem. Soc.*, 1989, **111**, 3106.
15 R. A. J. O'Hair, S. Gronert, C. H. DePuy and J. H. Bowie, *J. Am. Chem. Soc.*, 1989, **111**, 3105.
16 T. L. Amyes and J. P. Richard, *J. Am. Chem. Soc.*, 1996, **118**, 3129.
17 D. D. Wagman, W. H. Evans, V. B. Parker, R. H. Schumm, I. Halow, S. M. Bailey, K. L. Churney and R. L. Nuttall, *J. Phys. Chem. Ref. Data*, 1982, **11**, suppl. No. 2.
18 J. Hine and P. K. Mookerjee, *J. Org. Chem.*, 1975, **40**, 292.
19 S. Cabani, P. Gianni, V. Mollica and L. Lepori, *J. Sol. Chem.*, 1981, **10**, 563.
20 H. F. Halliwell and S. C. Nyburgh, *Trans. Faraday Soc.*, 1963, **59**, 1126.
21 C. E. Klots, *J. Phys. Chem.*, 1981, **85**, 3585.
22 R. G. Pearson, *J. Am. Chem. Soc.* 1986, **108**, 6109.
23 M. S. Gordon, D. R. Gano and E. Curtiss, *J. Am. Chem. Soc.*, 1996, in the press.
24 J. E. Bartmess and R. T. McIver, in *Gas-Phase Ion Chemistry*, ed. M. T. Bowers, Academic Press: New York, 1979, vol. 2, pp. 87–121.
25 R. G. Pearson and R. L. Dillon, *J. Am. Chem. Soc.*, 1953, **75**, 2439.
26 A. J. Kresge, *Acc. Chem. Res.*, 1990, **23**, 43.
27 T. L. Amyes and J. P. Richard, *J. Am. Chem. Soc.*, 1992, **114**, 10 297.
28 N. Heinrich, W. Koch, G. Frenking and H. Schwarz, *J. Am. Chem. Soc.*, 1986, **108**, 593.
29 J. P. Guthrie and Z. Liu, *Can. J. Chem.*, 1995, **73**, 1395.
30 J. P. Guthrie, *Can. J. Chem.*, 1993, **71**, 2123.


*Received, 4th June 1996; Revised manuscript received, 28th October 1996; Com. 6/07539H*

# Isolation and characterization of a unique heterocyclic ring system from nickel-ion catalysed polymerization of phenylisocyanide

**William B. Euler,* Jiun-Tang Huang, Misoo Kim, Lynne Spencer and William Rosen***

*Department of Chemistry, 51 Lower College Road, University of Rhode Island, Kingston, RI 02881, USA*

**Nickel-ion catalysed polymerization of phenylisocyanide (PhNC) produces the expected major product, poly(*N*-phenyliminomethylene), and a minor product of low molecular mass with a structure that gives insight into the mechanism of polymerization.**

The nickel(II) catalysed polymerization of isocyanide derivatives has been formulated as producing helical structures by a process described as a 'merry-go-round mechanism'.[1] Intermediates that seem to confirm this proposed mechanism[2] have been isolated and the structures of these characterized nickel(II) complexes have been established.[3] Recently, Deming and Novak[4] have challenged the assumption that $Ni^{II}$ is the active catalytic centre; their data implicating $Ni^{I}$ as the centre around which the helical polymers are constructed.

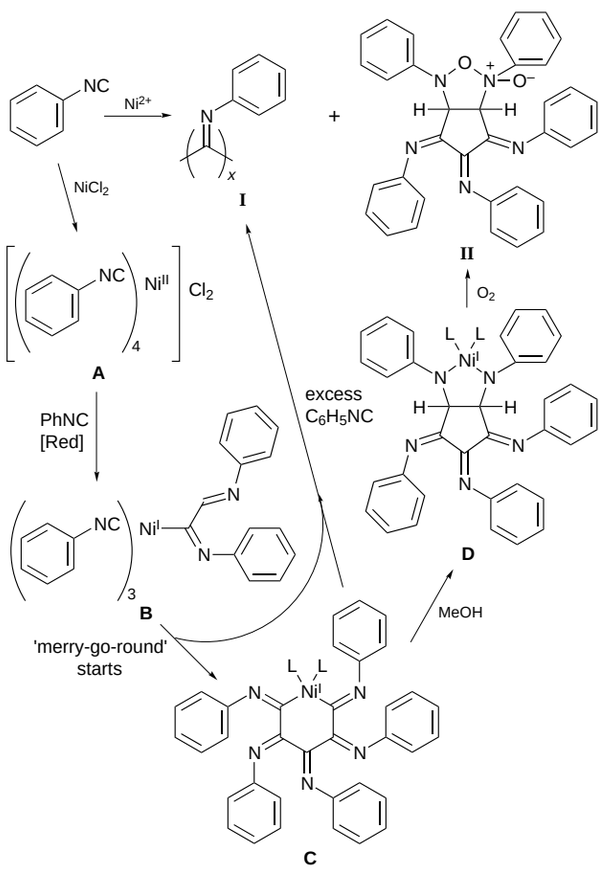
In the hopes of taking advantage of the interesting helical polymers that can be produced when isocyanide derivatives are catalytically polymerized, we embarked upon a study of the polymerization process as applied to phenylisocyanide (PhNC). As part of these studies we reported that the 'as-prepared' poly(*N*-phenyliminomethylene) **I**[5] is indeed substantially helical when first formed mechanistically but that dissolution of **I** in a non-polar solvent leads to an unravelling of the helical conformation. Our conclusion from this study, along with speculation in the literature,[6] is that the 'merry-go-round mechanism' is applicable initially but subsequent processing of the resultant helical polymers is liable to lead to non-helical structures if the side-chain group is not sterically demanding.[7]

As part of our initial investigation we reported[5] that polymer **I** is always accompanied by a low molecular mass component which is produced in very low yield when the polymerization is carried out in methanol as described.† We have now characterized the low molecular mass component from the polymerization of PhNC, structure **II** in Scheme 1, and this leads to some interesting conclusions concerning the polymerization mechanism. Structure **II** is unique[8] in the chemical literature‡ and allows us to speculate on the 'merry-go-round mechanism'[1] and its application when $Ni^{I}$ is the active catalytic centre.[4]

Preparation of the 'as-prepared' polymer **I** and GPC analysis of this polymer has been described elsewhere.[5] The bulk of the soluble product consisted of a polymer with $M_n \approx 2000$ and broad polydispersity but GPC always showed a low molecular mass band whose intensity was dependent upon the method of polymerization; those preparations done under a blanket of $N_2$ had a much more pronounced low molecular mass peak than those done under ambient air. Isolation of this low molecular mass fraction from the GPC column led to a colourless, crystalline solid with mp 263.5–264 °C. From preparations that yielded 2 g of the 'as-prepared' polymer **I** we were able to isolate about 20 mg of **II** when a blanket of $N_2$ was employed during the reaction.

The isolated crystalline solid **II** was structurally characterized by high-resolution mass spectrometry and $^1H$ and $^{13}C$ NMR and IR spectra. The high-resolution mass spectrum, using $NH_4^+$ in the LSIMS mode, yielded an $(M+H)^+$ molecular ion with $m/z$ = 550.22353 which most closely fits the molecular formula $C_{35}H_{27}N_5O_2$.§ The $^1H$ NMR spectrum displays 27 protons of which 23 resonate as a complex multiplet centred at δ 7.25 while the remainder resonate as doublets at δ 5.89 (1H, $J$ = 2 Hz), 6.03 (2H, $J$ = 7 Hz) and 6.52 (1H, $J$ = 2 Hz). The $^{13}C$ NMR spectrum exhibits 35 signals with peaks at δ 166.0, 151.5 and 150.5 assigned to imine carbons, those at δ 146.2, 144.2, 140.8, 138.1 and 135.0 are assigned to *ipso* carbons on the phenyl rings, 25 peaks between δ 130.2 and 119.2 are associated with *o*-, *m*- and *p*-carbons on the phenyl rings, and two at δ 74.6 and 67.0 which are assigned to saturated bridgehead carbons.¶ The $^1H$–$^{13}C$ HETCOR spectrum connects the δ 5.89 proton to the δ 74.6 carbon and the δ 6.52 proton to the δ 67.0 carbon.‖ The $^1H$–$^{13}C$ COLOC (long-range HETCOR) correlates the δ 5.89 proton with both the δ 151.5 and 166.0 carbons and the δ 6.52 proton with both the δ 150.5 and 151.5 carbons. Finally, the IR spectrum shows a strong absorption at 1668 $cm^{-1}$ assigned to an imine stretching mode. The spectral information is compatible with structure **II**.

The mechanism that is implied by the isolation of **II** accommodates both the 'merry-go-round'[1] concept and the idea that $Ni^{I}$ is the active catalytic centre,[4] as indicated in Scheme 1. Initiation of the process begins with the formation of **A**[3] and if an amine nucleophile is present, and a sterically hindered




**Scheme 1**

isocyanide derivative is being polymerized, then a nickel(II)–carbene intermediate can be isolated.[9] However, in the absence of a good nucleophile (such as an amine), attack by the reducing isocyanide (in excess) should lead to the intermediate **B** which contains a nickel(I) carboiminoyl diradical moiety rather than a nickel(II) carbene moiety.[9] The intermediate **B** can initiate the 'merry-go-round' for which the activation barrier is very low and the polymerization proceeds until either $O_2$ terminates the reaction or isocyanide is depleted. Under anaerobic conditions the chain-growth process is slowed[4] because of an increased activation barrier that leads through **C** to products (again, the presence or absence of an excess of isocyanide determines the ultimate course of reaction). The enhanced stability of **C** may be due to the fact that the pentamer corresponds to the first turn of a $4_1$ helix and this puts the fifth monomer in a geometry to readily coordinate to the metal. From **C**, when either depletion of isocyanide or anaerobic conditions dictate the course, the solvent (MeOH) acts as a reducing agent which leads to an intermediate such as **D**, which should be isolable. Once $O_2$ is introduced into the system, intermediate **D** is quickly oxidized to **II** and the $Ni^{II}$ regenerated.**

We thank the US Army Research Office for financial support for this work under grant number DAAL03-92-G-0391.

## Footnotes

† *Polymer preparation*: PhNC was added to a stirred solution of anhydrous $NiCl_2$ in MeOH, either under a blanket of $N_2$ or in contact with air, and the mixture was stirred for one week. A solid precipitate began to form after a short time and polymerization was virtually complete within one or two days but the odour of PhNC was still present so that stirring was always continued for one week. The solid precipitate was removed by filtration, washed thoroughly with MeOH, dried, and analysed by GPC.[5]

‡ An unstable intermediate (2,3,5-triphenyltetrahydro-1,2,5-oxadiazole-*N*-oxide) having a similar structure to **II** has been isolated[8] but little spectral information is available for it. Compound **II** shows some decomposition after several months but is much more stable than intermediates reported in the literature.[8]

§ The observed *m*/*z* value of 550.22353 for $(M + H)^+$ deviates from the calculated value for $C_{35}H_{28}N_5O_2^+$ of 550.22370 by $< 0.73$ ppm. Anal. Calc. for $C_{35}H_{27}N_5O_2$ C, 76.48; H, 4.95; N, 12.74. Found, C, 76.08; H, 5.14; N, 12.37%.

¶ A DEPT spectrum confirmed the assignment of the quaternary carbons.

‖ Based on the size of the coupling constant, the ring fusion seems to be in the *cis* conformation. MM2 calculations show that the *cis* isomer is of lower energy than the *trans* isomer, supporting this conclusion.

** We have noted that the amount of **II** produced is approximately the same as the molar amount of $NiCl_2$ used to initiate the catalysis, but how intermediate **C** evolves into intermediate **D** is still unclear. We have been unable to isolate either **C** or **D** and we have been unable to characterize the oxidation product derived from the presumed reducing agent, methanol.

## References

1 R. J. M. Nolte, *Chem. Soc. Rev.*, 1994, **23**, 11.
2 W. Drenth and R. J. M. Nolte, *Acc. Chem. Res.*, 1979, **12**, 30.
3 P. C. J. Kamer, R. J. M. Nolte, W. Drenth, H. L. L. M. Nijs and J. A. Kanters, *J. Mol. Catal.*, 1988, **49**, 21.
4 T. J. Deming and B. M. Novak, *J. Am. Chem. Soc.*, 1993, **115**, 9101.
5 J.-T. Huang, J. Sun, W. B. Euler and W. Rosen, *J. Polym. Sci., Part A, Polym. Chem.*, 1996, in the press.
6 B. Hong and M. A. Fox, *Macromolecules*, 1994, **27**, 5311.
7 C. Kollmar and R. Hoffmann, *J. Am. Chem. Soc.*, 1990, **112**, 8230.
8 N. F. Hepfinger and C. E. Griffin, *Tetrahedron Lett.*, 1963, 1361.
9 P. C. J. Kamer, R. J. M. Nolte and W. Drenth, *Recl. Trav. Chim. Pays-Bas*, 1988, **107**, 175.

*Received, 13th August 1996; Com. 6/05684I*

# A β-amino-cyclodextrin monolayer-modified Au electrode: a command surface for the amperometric and microgravimetric transduction of optical signals recorded by a photoisomerizable bipyridinium–azobenzene diad

**Michal Lahav, Koodali T. Ranjit, Eugenii Katz and Itamar Willner***

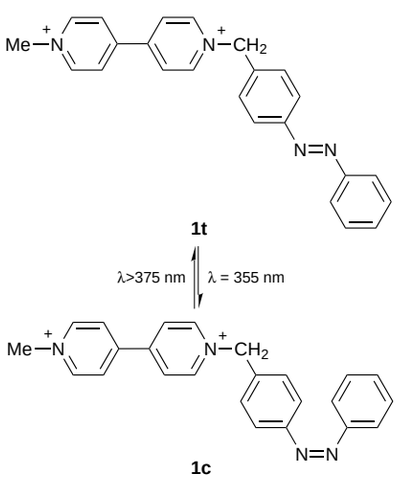
*Institute of Chemistry and the Farkas Center for Light-Induced Processes, The Hebrew University of Jerusalem, Jerusalem 91904, Israel*

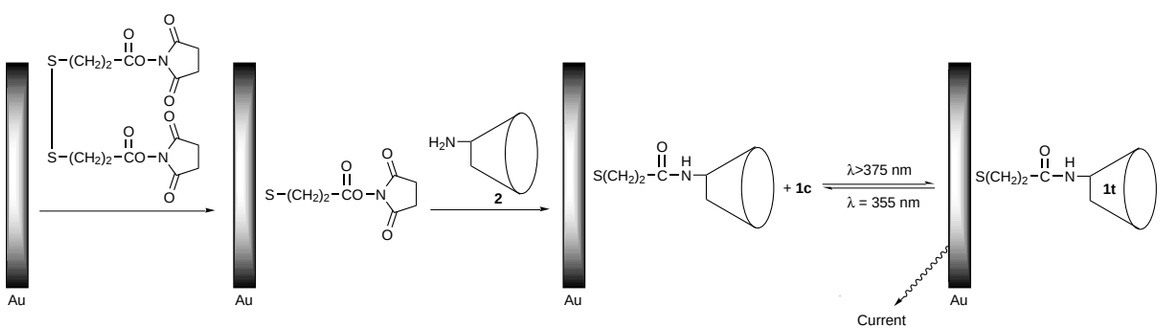
**A β-amino-cyclodextrin monolayer assembled onto Au electrodes acts as an active interface for the electrochemical and microgravimetric transduction of optical signals recorded by a bipyridinium–azobenzene diad.**

Molecular electronic and optoelectronic devices are the subject of recent extensive research efforts.[1,2] Electrical triggering of molecular functions and physical transduction of the activated chemical functionality provide the grounds for molecular electronic systems.[3,4] Photonic or optical triggering of molecular functions and transduction of the light-activated chemical functionality represent the basic features of molecular optoelectronics.[5,6] Photochemical activation of the formation or dissociation of donor–acceptor complexes in the presence of photoisomerizable electron acceptors[7] or light-induced molecular isomerization into a redox-active photoisomer state[5] allows the spectroscopic or electrical transduction of the recorded optical signals. To design molecular electronic or optoelectronic devices integration of the molecular assembly with a transducing element (surface) is essential. Functionalized monolayers assembled onto electrode surfaces were applied as active interfaces for sensing,[8] concentration of redox-active compounds[9] and discrimination of molecular redox activities at electrode surfaces.[10] Recently, the assembly of functionalized photoisomerizable monolayers onto electrode surfaces enabled the amperometric and piezoelectric transduction of optical signals recorded by the monolayer.[11–13] Here, we report on the use of a β-amino-cyclodextrin monolayer-modified Au electrode as a command surface for electrochemical transduction of optical signals, recorded by *N*-methyl-*N*′-[1-phenylazobenzyl]-4,4′-bipyridinium **1**.

*N*-Methyl-*N*′-[1-phenylazobenzyl]-4,4′-bipyridinium exhibits reversible photoisomerizable properties. Irradiation of *trans*-*N*-methyl-*N*′-[1-phenylazobenzyl]-4,4′-bipyridinium **1t**, λ = 355 nm, yields the *cis* isomer **1c**† and further irradiation of **1c**, λ > 375 nm, regenerates the **1t** state. The two photoisomers reveal different association features to **2**. The association constants of **1t** and **1c** to **2** were determined spectroscopically by following the absorbance changes at λ = 420 nm, and correspond to $K_a$ = 1700 and 180 M$^{-1}$, respectively.

A primary monolayer of thiopropionic acid-active ester was assembled onto the electrode followed by coupling β-amino-cyclodextrin[14] **2** to the functionalized surface (Scheme 1).[15] The **2**-functionalized monolayer electrode acts as a command interface for the amperometric or microgravimetric quartz crystal microbalance (QCM) transduction of optical signals recorded by the photoisomerizable diad **1**.‡ Fig. 1 shows the cyclic voltammograms of **1t** and **1c** in the presence of the **2**-modified electrode. A high amperometric response corresponding to the one-electron reduction of the bipyridinium redox-active unit is observed for **1t** while the redox wave for **1c** is substantially lower.§ The peak currents of the redox waves of **1t** and **1c** show a linear relation with the scan rates ($i \propto \nu$ for $\nu \leqslant 3$ V s$^{-1}$) implying that the redox waves originate from surface-confined redox-active species. Control experiments at a bare Au electrode reveal that **1t** and **1c** yield under the same conditions identical, very weak, redox waves. The enhanced electrical responses of the photoisomerizable diad in the presence of the **2**-monolayer-modified electrode are attributed to its concentration at the electrode interface by association to



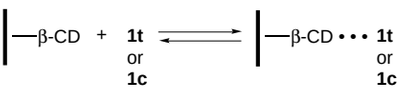




**Scheme 1** Assembly of the **2** monolayer onto Au surfaces

the cyclodextrin cavity. The photoisomer **1t** exhibits high affinity for **2** and yields a high amperometric response. The photoisomer **1c** exhibits a low association constant to the receptor sites and results in a low redox signal. Coulometric analysis of the redox waves of **1t** and **1c** implies surface coverages of the functionalized cyclodextrin by **1t** and **1c** that correspond to $2.7 \times 10^{-11}$ and $1.5 \times 10^{-11}$ mol cm$^{-2}$, respectively. These values are consistent with the surface coverages evaluated by the microgravimetric experiments. By reversible photoisomerization of the diad between the states **1t** and **1c**, cyclic high and low amperometric signals are transduced from the system (inset, Fig. 1).

Microgravimetric analysis of the association of **1t** to the **2** interface and the dissociation of **1c** from the functionalized monolayer using a quartz crystal microbalance provides a further means for the electronic transduction of the recorded optical signals.[16] The Au electrodes associated with a quartz crystal (9 MHz) were modified by the **2** monolayer as described in Scheme 1. Fig. 2 shows the crystal frequency changes upon its interaction with **1c** and **1t** [curves (*a*) and (*b*), respectively]. A high frequency change of $\Delta f = -11 \pm 1$ Hz is observed for **1t**, while a substantially lower frequency change, $\Delta f = -5 \pm 0.5$, is detected for **1c**. These results clearly demonstrate that **1t** associates to the **2** receptor interface while **1c** reveals a substantially lower affinity for the monolayer electrode. From the frequency changes observed upon interaction of photoisomers **1t** and **1c** with the **2**-monolayer electrode, and by the application of the Sauerbrey equation [eqn. (1), where $\Delta f$ is the crystal frequency change upon changing the crystal mass by $\Delta m$, and $A$ is the surface area], the surface densities of **1t** and **1c** on the monolayer electrode are estimated to be $2.8 \times 10^{-11}$ and $1.3 \times 10^{-11}$ mol cm$^{-2}$, respectively.¶ By cyclic photoisomerization of the diad between the states **1t** and **1c**, reversible high- and low-frequency changes of the modified quartz crystal are observed [Fig. 2 (inset)].

$$\Delta f = (-2.3 \times 10^{-6}) f_0^2 (\Delta m/A) \quad (1)$$




(2)

In conclusion, we have demonstrated that the β-amino-cyclodextrin-modified Au electrodes or piezoelectric crystals provide active interfaces for electronic transduction of optical signals recorded by the photoisomerizable electroactive bipyridinium–azobenzene diad **1**.

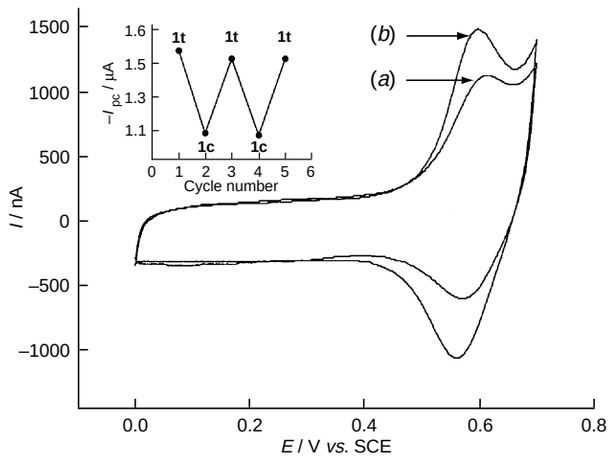



**Fig. 1** Cyclic voltammograms of (*a*) [**1c**] = $1 \times 10^{-6}$ M and (*b*) [**1t**] = $1 \times 10^{-6}$ M in 0.01 M phosphate buffer, pH = 10.8, scan rate 100 mV s$^{-1}$, $T$ = 25 °C. Inset: Cyclic cathodic responses of the **2**-monolayer electrode measured at 0.6 V upon reversible photoisomerization of the diad between **1t** and **1c**, respectively.

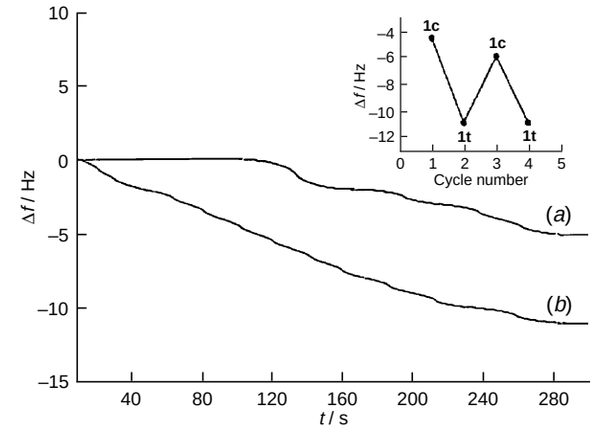



**Fig. 2** Frequency changes of the **2**-modified quartz crystal upon interaction with: (*a*) [**1c**] = $3 \times 10^{-6}$ M; (*b*) [**1t**] = $3 \times 10^{-6}$ M. Inset: cyclic frequency changes of the crystal upon reversible photoisomerization of the diad between state **1c** and **1t**, respectively. Frequencies are measured after 300 s of interaction of the crystal with the respective isomer. Experiments were performed in an aqueous environment.

## Footnotes

† A photostationary state corresponding to 92% of **1c** is formed.
‡ Microgravimetric QCM analysis of the modified monolayer indicates a surface coverage of $(4.7 \pm 0.1) \times 10^{-10}$ mol cm$^{-2}$ of β-amino-CD.
§ As the **1c** state represents a photostationary state where *ca*. 8% of **1t** is present (*ca*. 90 nA) of the total current response of **1c** (1.12 μA) is attributed to residual **1t** in the system.
¶ By following the frequency changes of the β-amino-CD modified crystal at different bulk concentrations of **1t** and **1c**, the association constants of the two photoisomers to the monolayer receptor sites, [eqn. (2)] were estimated to be $K_a$(**1t**) = 7000 M$^{-1}$ and $K_a$(**1c**) = 3000 M$^{-1}$.

## References


1 *Nanosystems: Molecular Machinery, Manufacturing and Computation*, ed. E. Drexler, Wiley, New York, 1992.
2 P. Ball, *Nature*, 1993, **362**, 123; F. L. Carter, A. Schultz and D. Duckworth, *Molecular Electronic Devices*, ed. F. L. Carter, Marcel Dekker, New York, 1987, p. 183.
3 R. A. Bissel, E. Cordova, A. E. Kaifer and J. F. Stoddart, *Nature*, 1994, **363**, 133.
4 M. T. Rojas and A. E. Kaifer, *J. Am. Chem. Soc*., 1995, **117**, 5883.
5 J. Daub, C. Fischer, J. Salbeck and K. Ulrich, *Adv. Mater*., 1990, **3**, 366; S. L. Gilat, S. H. Kawai and J.-M. Lehn, *Chem. Eur. J*., 1995, **1**, 275; S. H. Kawai, S. L. Gilat, R. Ponsinet and J.-M. Lehn, *Chem. Eur. J*., 1995, **1**, 285; S. L. Gilat, S. H. Kawai and J.-M. Lehn, *J. Chem. Soc., Chem. Commun*., 1993, 1439.
6 J. Daub, J. Salbeck, T. Knochel, C. Fischer, H. Kunkely and K. M. Rapp, *Angew. Chem., Int. Ed. Engl*., 1989, **28**, 1494; B. L. Feringa, W. F. Jager and B. de Lange, *J. Am. Chem. Soc*., 1991, **113**, 5468; J. Achatz, C. Fischer, J. Salbeck and J. Daub, *J. Chem. Soc., Chem. Commun*., 1991, 504.
7 I. Willner, S. Marx and Y. Eichen, *Angew. Chem., Int. Ed. Engl*., 1992, **31**, 1243.
8 K. D. Schierbaum, T. Weiss, E. U. T. van Velzen, J. F. J. Engbersen, D. N. Reinhoudt and W. Göpel, *Science*, 1995, **265**, 1413.
9 M. T. Rojas, R. Koniger, J. F. Stoddart and A. E. Kaifer, *J. Am. Chem. Soc*., 1995, **117**, 336.
10 F. Malem and D. Mandler, *Anal. Chem*., 1993, **65**, 37; E. Katz, M. Lion-Dagan and I. Willner, *J. Electroanal. Chem*., 1995, **382**, 25.
11 Z. F. Liu, K. Hashimoto and A. Fujishima, *Nature*, 1990, **347**, 658.
12 A. Doron, E. Katz, M. Portnoy and I. Willner, *Angew. Chem., Int. Ed. Engl*., 1996, **35**, 1535.
13 S. Marx-Tibbon, I. Ben-Dov and I. Willner, *J. Am. Chem. Soc*., 1996, **118**, 4717.
14 H. Parrot-Lopez, Ch. Ling, P. Zhang, A. Baszkin, G. Albrecht, C. Rango and A. W. Coleman, *J. Am. Chem. Soc*., 1992, **114**, 5479.
15 E. Katz, *J. Electroanal. Chem*., 1990, **291**, 257.
16 D. A. Buttry, *Electroanalytical Chemistry*, ed. A. J. Bard, Marcel Dekker, New York, 1991, vol. 17, p. 1.


*Received, 9th September 1996; Com. 6/06189C*

# 1,3-Dipolar cycloadditions to methylenespiro[2.2]pentane: a complementary access to spiro cyclopropanated azaheterocycles

**Beatrice Anichini,[a] Andrea Goti,[b] Alberto Brandi,*[a] Sergei I. Kozhushkov[c] and Armin de Meijere*[c]**

[a] *Dipartimento di Chimica Organica 'U. Schiff', Università di Firenze, Via G. Capponi 9, I-50121 Firenze, Italy*
[b] *Centro di Studio C.N.R. sui Composti Eterociclici, Università di Firenze, Via G. Capponi 9, I-50121 Firenze, Italy*
[c] *Institut für Organische Chemie der Georg-August-Universität Göttingen, Tammannstrasse 2, D-37077 Göttingen, Germany*

**The domino cycloaddition–thermal rearrangement of nitrile oxides and methylenespiro[2.2]pentane gives 5-azaspiro-[2.5]oct-6-en-8-one derivatives; with a nitrone the process complements the one using bi(cyclopropylidene) for the synthesis of α-spiro cyclopropanated heterocyclic ketones.**

We have recently reported on the 'domino' cycloaddition–rearrangement process involving 1,3-dipoles such as nitrones **1** or nitrile oxides and bi(cyclopropylidene) **2**.[1] The process, essentially 'one pot', led to new 5-azaspiro[2.5]octan-8-ones **4** with high selectivities and in good yields (Scheme 1). Some of these spirocyclopropanated heterocycles also showed interesting biological activity, as they were found to cleave a DNA plasmid.[2]

However, isoxazolines **5**, derived by addition of **2** to nitrile oxides under the rearrangement conditions did not give the analogous derivatives **6**, instead affording exclusively the 2-substituted dihydrofuro[2,3-*c*]pyridine derivatives **7**[1] due to a non-selective rearrangement of both cyclopropane units in **5** under the required thermolytic conditions (Scheme 2).

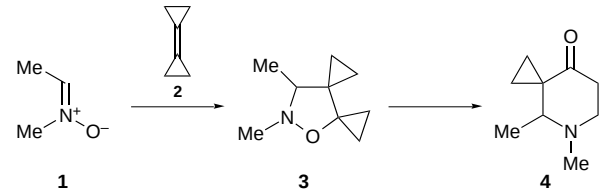
We now report the synthesis of 6-substituted 5-azaspiro-[2.5]oct-6-en-8-ones **11** by a different approach, utilising methylenespiro[2.2]pentane **8** as the dipolarophile (Scheme 3).

Methylenespiro[2.2]pentane **8**,[3,4] easily available from methylenecyclopropane[4a] or by thermal isomerization of bi(cyclopropylidene),[4b] has already been used in [2+1] addition processes for the synthesis of triangulanes.[5] The cycloaddition of benzonitrile oxide **9a**, generated slowly *in situ* at room temperature from the corresponding hydroximoyl chloride, to **8** afforded the isoxazoline **10a** in 64% yield with high regioselectivity, while the stable 2,4,6-trimethylbenzonitrile oxide **9b** gave the corresponding adduct **10b** quantitatively. Compared to bi(cyclopropylidene) **2**,[1] methylenespiro-[2.2]pentane **8** showed higher reactivity towards nitrile oxides, as demonstrated by the milder conditions required for the reaction with the stable nitrile oxide **9b** and the considerable decrease in formation of the undesired side-product generated by dimerization of the unstable nitrile oxide **9a**.

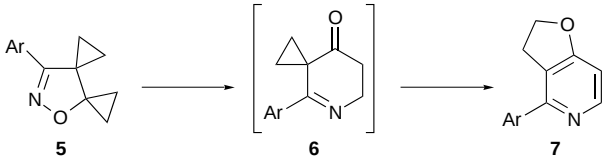
Isoxazolines **10** underwent thermal rearrangement more easily than their counterparts (**5**) from bi(cyclopropylidene)[1] and provided the ketones **11**, which contained a spiro-cyclopropane ring on the pyridone structure (Scheme 3). The structural assignment was based on the observation of characteristic signals in the NMR spectra for the C=C–C=O system, the olefinic proton and the methylene group adjacent to nitrogen. The higher lability of compounds **6** (Scheme 2), where the cyclopropane ring did not survive the rearrangement conditions, can be ascribed to the double spiro-conjugated cyclopropane ring.[6]

The highly regioselective opening of the spiro cyclopropane ring in **10** is noteworthy. This selectivity is opposite to that obtained when the process was applied to alkyl or aryl-substituted methylenecyclopropanes.[7] If a homolytic N–O bond cleavage is involved, as indicated by previous observations,[7a] this selectivity can be explained by the higher preference for the route (*a*) (Scheme 4) with ring opening to the diradical intermediate **A**, where the disubstituted cyclopropane carbon maintains the $sp^3$-like hybridization lost in intermediate **C** (Scheme 4).

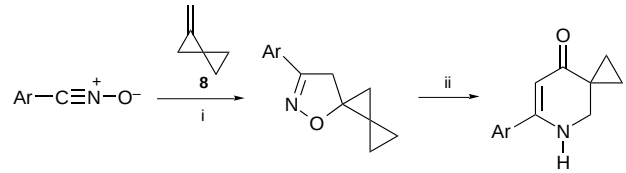
However, cyclopropyl methyl radicals **A** are known to rearrange readily to homoallylic radicals **E**,[8] which would eventually lead to products not observed in our process. This high regio- and chemo-selectivity, therefore, cannot rule out the



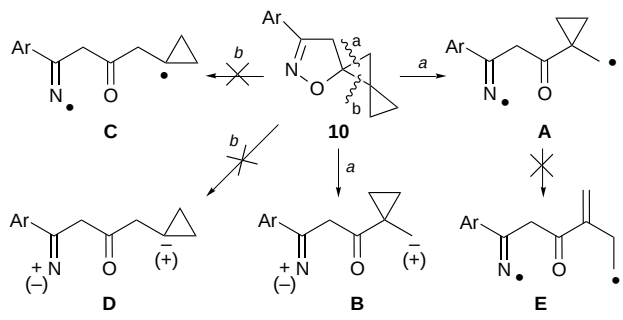

**Scheme 1**




**Scheme 2**




**Scheme 3** *Reagents and conditions* for **9a**: i, $C_6H_6$, room temp. 16 h, 64%; ii, *o*-dichlorobenzene, 160 °C, 14 h, 70%; for **9b**: i, $C_6H_6$, 60 °C, 4 h, 95%; ii, mesitylene, 163 °C, 4 h, 92%

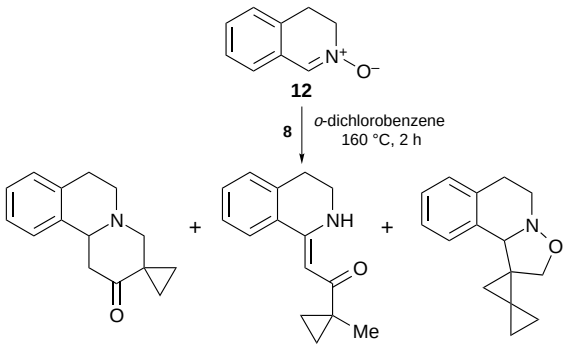



**Scheme 4**

presence of zwitterionic intermediates such as **B** in the rearrangement of isoxazolines **10**, although a solvent effect on the process could not be observed. Further investigations are required to assess the origin of the high regio- and chemoselectivity observed.

With nitrones the process suffers from low selectivity. For example, heating a solution of nitrone **12** and **8** in *o*-dichlorobenzene at 160 °C for 2 h in a 'one pot' process gives the ketone **13** (30%) as well as the enaminone **14** and the regioisomeric cycloadduct **15** (Scheme 5).[1,5*a*,7] The regioselectivity of the cyclopropane opening was confirmed, but, as expected, besides the product of diradical coupling (**13**), a 1,5-hydrogen shift in the intermediate diradical led to the open-chain isomer **14**, as the major product.[7]

The authors are indebted to CRUI-Italy (Conferenza dei Rettori delle Università Italiane) and the German Academic Exchange Service (DAAD) for partial financial support of this project within the Vigoni Program. This work was also supported by the Fonds der Chemischen Industrie as well as by BASF, Bayer and Degussa AG (gifts of chemicals).




**Scheme 5**

## References

1 A. Brandi, A. Goti, S. Kozhushkov and A. de Meijere, *J. Chem. Soc., Chem. Commun.*, 1994, 2185; A. Goti, B. Anichini, A. Brandi, S. Kozhushkov, C. Gratkowski and A. de Meijere, *J. Org. Chem.*, 1996, **61**, 1665.

2 A. Goti, B. Anichini, A. Brandi, A. de Meijere, L. Citti and S. Nevischi, *Tetrahedron Lett.*, 1995, **36**, 5811.

3 W. R. Dolbier, Jr., K. Akiba, J. M. Riemann, C. A. Harmon, M. Bertrand, A. Bezaguet and M. Santelli, *J. Am. Chem. Soc.*, 1971, **93**, 3933.

4 (*a*) S. Arora and P. Binger, *Synthesis*, 1974, 801; (*b*) A. de Meijere and S. I. Kozhushkov, in *Carbocyclic Three-Membered Ring Compounds*, ed. A. de Meijere, Thieme, Stuttgart, 1996, vol. E17, in the press.

5 (*a*) A. Goti, F. M. Cordero and A. Brandi, *Top. Curr. Chem.*, 1996, **178**, 1; (*b*) N. S. Zefirov, S. I. Kozhushkov, B. I. Ugrak, K. A. Lukin, O. V. Kokoreva, D. S. Yufit, Y. T. Struchkov, S. Zoellner, R. Boese and A. de Meijere, *J. Org. Chem.*, 1992, **57**, 701.

6 S. Danishefsky, *Acc. Chem. Res.*, 1979, **12**, 66 and references cited therein.

7 (*a*) A. Brandi, F. M. Cordero, F. De Sarlo, A. Goti and A. Guarna, *Synlett*, 1993, 1; (*b*) F. M. Cordero, A. Brandi, C. Querci, A. Goti, F. De Sarlo and A. Guarna, *J. Org. Chem.*, 1990, **55**, 1762; (*c*) A. Brandi, S. Garro, A. Guarna, A. Goti, F. M. Cordero and F. De Sarlo, *J. Org. Chem.*, 1988, **53**, 2430.

8 D. C. Nonhebel, *Chem. Soc. Rev.*, 1993, 347; J. Walton, in *Carbocyclic Three-Membered Ring Compounds*, ed. A. de Meijere, Thieme, Stuttgart, 1996, vol. E17, in the press; S.-Y. Choi and M. Newcomb, *Tetrahedron*, 1995, **51**, 654; H. Venkatesan and M. M. Greenberg, *J. Org. Chem.*, 1995, **60**, 1053; D. J. Hastings and A. C. Weedon, *J. Org. Chem.*, 1991, **56**, 6326; D. Becker, N. Haddad and Y. Sahali, *Tetrahedron Lett.*, 1989, **30**, 2661.

*Received, 18th September 1996; Com. 6/06434E*

# *p*-Fluoroacetophenone molecule as a probe to study zeolite acidity by $^{19}F$ solid-state NMR spectroscopy

**A. Simon,*[a] L. Delmotte,[a] J.-M. Chezeau[a] and L. Huve[b]**

[a] *Laboratoire de Matériaux Minéraux, URA CNRS 428, Ecole Nationale Superieure de Chimie, 3 rue Alfred Werner, 68093 Mulhouse Cedex, France*

[b] *Shell Recherche, Centre de Recherche de Grand-Couronne, 76530 Grand-Couronne, France*

**$^{19}F$ chemical shift variations of *p*-fluoroacetophenone adsorbed on a MFI zeolite show that this compound is a promising probe for measurements of zeolite acidity strength.**

Zeolites are used as acid catalysts in important industrial processes such as the cracking of hydrocarbons in refineries. 'Direct' methods (IR spectroscopy and $^{1}H$ NMR of OH groups)[1–3] and methods using probe molecules (titration, calorimetric measurements, NMR of adsorbed bases, *etc.*)[4–6] have been employed to study zeolite acidity properties. However, the evaluation of the acidity strength of these materials still represents a real difficulty. In this work, the use of $^{19}F$ MAS NMR using a new probe molecule is presented.

The $^{19}F$ nucleus is very interesting for NMR studies with a nuclear spin $I$ of 1/2, a natural abundance of 100%, a high detection sensitivity (83% relative to H), and a large chemical shift range. The principle of the method we propose is to relate the chemical shift of the $^{19}F$ nucleus in the adsorbed probe molecule to the strength of the acid sites in the zeolite. This paper presents preliminary results on the adsorption of *p*-fluoroacetophenone on MFI. This organic compound is a good indicator of zeolite acidity strength because it contains a functionality whose $pK_{BH^+}$ value (−6.2)[7] falls in the acidity strength range of zeolites.[9] $^{19}F$ chemical shift variation as a function of acidity strength has been determined for *p*-fluoroacetophenone by Taft and Levins[7] and found to vary from δ −107.0 (Hammett acidity function: $H_0$ = 0) to δ −79.4 ($H_0$ = −11) with a shift of 4.9 ppm per $H_0$ unit near its $pK_{BH^+}$.

Prior research shows that $^{19}F$ NMR of alkaline probe molecules has made pH measurements in biological systems[9] possible. Nicholas *et al.*[10] studied adsorption of *p*-fluoroaniline and *p*-fluoronitrobenzene in zeolites. However, they could only determine the boundaries of the acidity strength for the MFI and FAU zeolites under study.

MFI zeolites were prepared in fluoride media in our laboratory.[11] Acid zeolites with Si/Al ratios of 35.5 and 55 [HZSM-5(35.5), HZSM-5(55)] and a non-acid purely siliceous MFI zeolite [HZSM-5(∞)] were calcined up to 823 K for 6 h under ambient atmosphere. Under these calcination conditions no residual $F^-$ (δ *ca.* −64) is observed in the $^{19}F$ MAS NMR spectra. After hydration, the zeolite samples were mounted in glass tubes with a bed depth of 5 mm and heated to 673 K at a heating rate of 15 K $h^{-1}$ *in vacuo*. At this temperature, samples were evacuated for 20 h at a pressure of $10^{-1}$ Pa. After cooling, samples were exposed to a saturated vapour of dehydrated *p*-fluoroacetophenone. After adsorption, samples were transferred into the NMR rotor in an argon atmosphere. $^{19}F$ MAS NMR spectra (reference $CFCl_3$) were recorded at 282.4 MHz on a Bruker MSL-300 with a 4 mm Doty probe (pulse length of 4 μs for the π/2 pulse, recycle delay of 6 or 10 s, spinning rate of 7–8 kHz).

Fig. 1 shows the spectra thus obtained for two days adsorption realized at room temperature. The amount of adsorbed *p*-fluoroacetophenone was determined by comparison of $^{19}F$ MAS NMR spectra with that of a known amount of an as-synthesized uncalcined MFI zeolite with no aluminium prepared in fluoride medium[11] which contains $4F^-$ ions per unit cell (Table 1). The maximum loading of the probe molecule in the zeolite structure based on geometric constraints alone is eight species per unit cell.

The narrow peak ($\Delta\nu_{1/2}$ = 375 Hz) which appears at δ −106.6 for HZSM-5(∞) [Fig. 1(*a*)] has a chemical shift

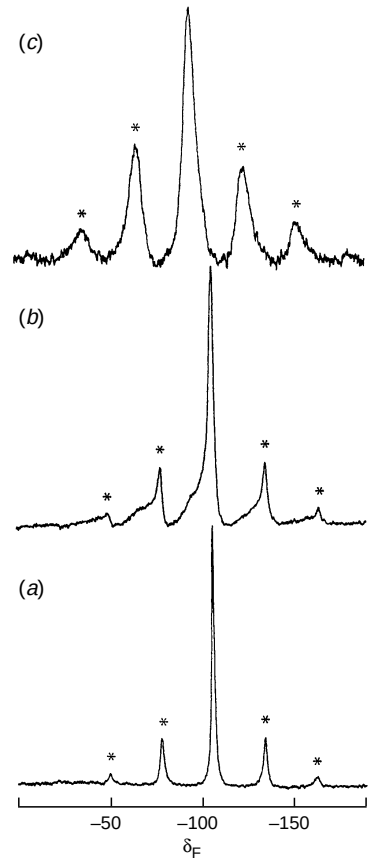



**Fig. 1** $^{19}F$ MAS NMR spectra of (*a*) HZSM-5(∞), (*b*) HZSM-5(55) and (*c*) dehydrated HZSM-5(35.5) treated with *p*-fluoroacetophenone for 2 days at room temperature; * MAS side-bands

**Table 1** Concentration of bridging OH (framework aluminium as determined by $^{27}Al$ MAS NMR) and *p*-fluoroacetophenone (as determined by $^{19}F$ MAS NMR)

| | Concentration in species per unit cell | |
|---|---|---|
| Sample | Bridging OH (framework aluminium) | *p*-Fluoroacetophenone |
| HZSM-5(35.5) | 2.3 | 1.6 |
| HZSM-5(55) | 1.7 | 4.0 |
| HZSM-5(∞) | — | 1.5 |

which is practically identical to that of *p*-fluoroacetophenone molecules in the liquid state (δ −107.0). Furthermore, the symmetrical shape of the signal indicates that fluorinated molecules have no preferential orientation and the small linewidth suggests a high mobility. We assign the peak at δ −106.6 to *p*-fluoroacetophenone molecules involved in weak interactions with this non-acidic zeolite framework.

When the Si/Al ratio decreases to 55, we distinguish different fluorinated molecules populations [Fig. 1(*b*)]. The first corresponds to a relatively narrow ($\Delta\nu_{1/2}$ = 845 Hz) peak situated at δ −106.6. By analogy with the HZSM-5(∞) [Fig. 1(*a*)] this is attributed to molecules which are in weak, interaction with the zeolite framework. The two other populations correspond to broader peaks ($\Delta\nu_{1/2}$ = 1740 and 1630 Hz) situated at lower fields (δ −95.3 and −100.5 respectively). The relative areas of various fluorinated species [δ −95.3 (23.3%), δ −100.5 (16.9%), *ca*. −106.6 (59.3%)] show that for four adsorbed fluorinated molecules per unit cell, the amount of *p*-fluoroacetophenone associated with the peaks situated at δ −95.3 and −100.5 represents 1.6 molecules per unit cell. This value corresponds approximately to the number of zeolite acid sites (Table 1). From the chemical shift values determined by Taft and Levins,[7] it can be deduced that these molecule populations are in interaction with acid sites which have a strength $H_0$ of −6.4 (δ −95.3) and $H_0$ −5.4 (δ −100.5). The increase in linewidths could be related to a decrease of the mobility of fluorinated molecules which reveals a stronger interaction with the zeolite framework. However, many interactions, such as homonuclear dipolar interactions (F–F), heteronuclear dipolar interactions (F–H, F–Al), chemical shift anisotropy, magnetic susceptibility and/or chemical exchange could contribute to the increase in linewidth. A more detailed study will be published elsewhere. Furthermore, measurement of areas corresponding to *p*-fluoroacetophenone molecules in strong interaction with acid sites and *p*-fluoroacetophenone in weak interaction with zeolite framework [Fig. 1(*b*)] shows that this method is quantitative.

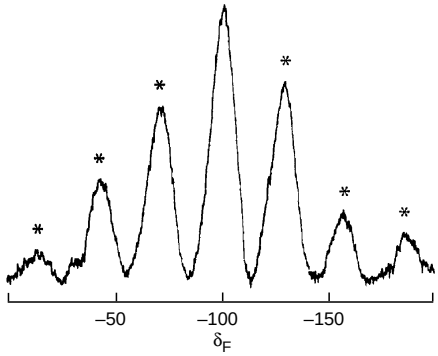



**Fig. 2** $^{19}$F MAS NMR spectrum of hydrated HZSM-5(35.5) treated with *p*-fluoroacetophenone for 15 days at room temperature; * MAS side-bands

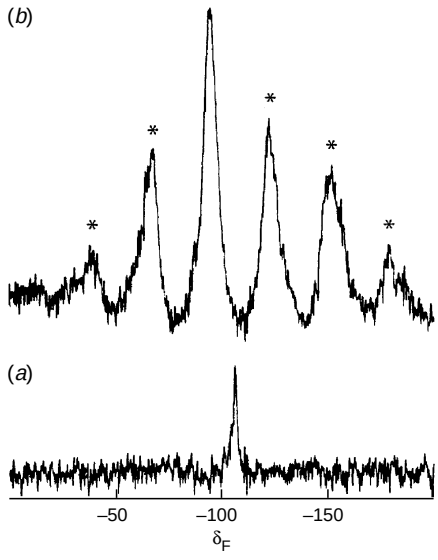



**Fig. 3** $^{19}$F MAS NMR spectra of (*a*) dehydrated HZSM-5(∞) and (*b*) HZSM-5(35.5) treated with *p*-fluoroacetophenone for 70 h at 423 K; * MAS side-bands

In the HZSM-5(35.5) sample, the $^{19}$F MAS NMR spectrum reveals only one broad peak ($\Delta\nu_{1/2}$ = 1830 Hz) situated at δ −95.6 [Fig. 1(*c*)]. Analysises (Table 1) show that there are fewer adsorbed fluorinated molecules than zeolite acid sites. At such an Si/Al ratio, most acid sites in the MFI zeolite structure should be accessible. The main reason for this low adsorption rate may be the blocking up of the channels by molecules in interaction with acid sites because channels are not blocked prior to adsorption of *p*-fluoroacetophenone (*n*-hexane adsorption rate at 298 K is 11.6%).

On partially hydrated HZSM-5(35.5) (3–8%) loaded with *p*-fluoroacetophenone, we observed only one broad peak ($\Delta\nu_{1/2}$ = 3340 Hz) situated at δ −100.2 ($H_0$ −5.4) (Fig. 2). This is indicative of a decrease of acidity induced by water molecules which react with zeolite acid sites[12] and level their acidity. Chemical shift exchange between water and *p*-fluoroacetophenone molecules, and important dipolar interactions between F and H of $H_2O$ and $H_3O^+$ chemical species may induce the increase in linewidth.

When adsorption on dehydrated zeolites is realized at 423 K (Fig. 3) only a few *p*-fluoroacetophenone molecules are trapped inside HZSM-5(∞) unlike HZSM-5(35.5). In the latter, strong zeolite acid sites related to aluminium interact with *p*-fluoroacetophenone and the thermal energy is not high enough at 423 K to break these interactions.

In conclusion, this work shows that *p*-fluoroacetophenone acts as a quantitative acidity strength indicator *via* $^{19}$F MAS NMR. The $^{19}$F chemical shift value allows the acidity strength to be determined, whereas the area of the signal can be related to the number of acid sites. However, we can foresee several limitations to this method. In aluminium-rich zeolites, the adsorption of a probe molecule might prevent another molecule to reach an acid site close to the first one. In some structures, small cavities could be inaccessible to the *p*-fluoroacetophenone molecules, whereas in structures with only one-dimensional channels, the adsorption of such a molecule could prevent others to progress inside the channels. All these limits are also encountered by reacting molecules when zeolites are used as catalysts.

We thank Professor J. L. Guth for valuable discussions.

## References

1 W. E. Farneth and R. J. Gorte, *Chem. Rev.*, 1995, **95**, 615.
2 H. Pfeifer, D. Freude and J. Kärger, *Catalysis and Adsorption by Zeolites*, ed. G. Ohlmann *et al.*, Elsevier, Amsterdam, 1991.
3 P. Batamack, C. Dorémieux-Morin and J. Fraissard, *J. Chim. Phys.*, 1992, **89**, 423.
4 L. Moscou and R. Moné, *J. Catal.*, 1973, **30**, 417.
5 H. Van Bekkum, E. M. Flanigen and J. C. Jansen, *Introduction to Zeolite Science and Practice*, Elsevier, Amsterdam, 1991, **58**, 270.
6 E. Brunner, *J. Mol. Struct.*, 1995, **355**, 61.
7 R. W. Taft and P. L. Levins, *Anal. Chem.*, 1962, **34**, 436.
8 L. W. Beck and J. F. Haw, *J. Phys. Chem.*, 1995, **99**, 1076.
9 C. J. Deutsch and J. S. Taylor, *Annu. NY Acad. Sci.*, 1987, **508**, 33.
10 J. B. Nicholas, J. F. Haw, L. W. Beck, T. R. Krawietz and D. B. Ferguson, *J. Am. Chem. Soc.*, 1995, **117**, 12 350.
11 J. L. Guth, H. Kessler, J. M. Higel, J. M. Lamblin, J. Patarin, A. Seive, J. M. Chézeau and R. Wey, *Zeolite Synthesis*, ed. M. L. Ocelli and H. E. Robson, ACS Symp. Ser., 1989, **398**, 176.
12 F. Deng, Y. Du, C. Ye, J. Wang, T. Ding and H. Li, *J. Phys. Chem.*, 1995, **99**, 15 208.

*Received, 23rd September 1996; Com. 6/06648H*

# Photochemical C–C coupling reaction of an iron acetylide complex $[Fe(\eta^5\text{-}C_5Me_5)(CO)_2(C{\equiv}CPh)]$ with alk-1-ynes (RC≡CH) leading to cyclic compounds including paramagnetic iron(I) cyclopentadienone complexes $[Fe(\eta^5\text{-}C_5Me_5)(\eta^4\text{-}2\text{-}Ph\text{-}5\text{-}R\text{-}C_5H_2O)]$

**Munetaka Akita,* Masako Terada and Yoshihiko Moro-oka***

*Research Laboratory of Resources Utilization, Tokyo Institute of Technology, 4259 Nagatsuta, Midori-ku, Yokohama 226, Japan*

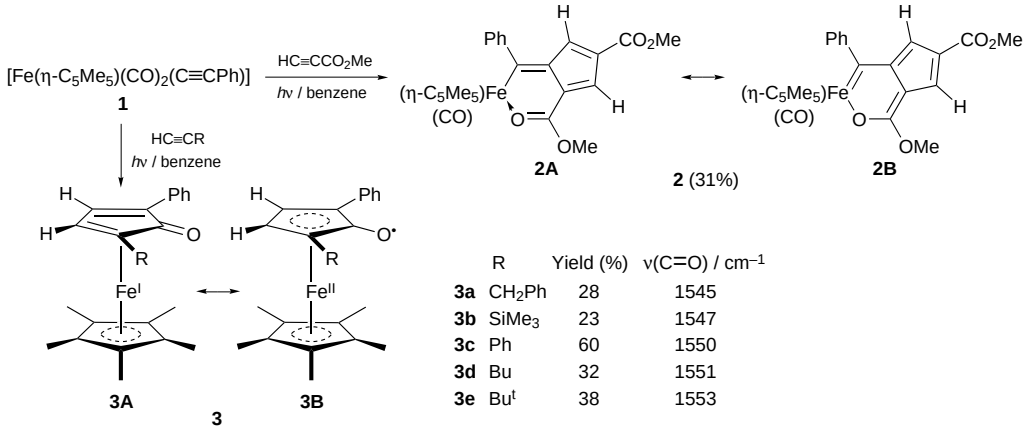
**Photolysis of $[Fe(\eta^5\text{-}C_5Me_5)(CO)_2(C{\equiv}CPh)]$ with methyl propynoate which bears a coordinating substituent ($CO_2Me$) affords a metallabicyclic compound incorporating two molecules of the alkyne, whereas the reaction with alk-1-ynes (RC≡CH) bearing a non-coordinating substituent (R = alkyl, Ph, $SiMe_3$) produces paramagnetic 17e iron(I)-cyclopentadienone complexes $[Fe(\eta^5\text{-}C_5Me_5)(\eta^4\text{-}2\text{-}Ph\text{-}5\text{-}R\text{-}C_5H_2O)]$.**

C–C coupling reactions of alkynes have been realized by the action of a transition-metal species.[1] One versatile transformation is insertion into an M–C bond leading to oligomeric or polymeric conjugated systems.[2] In a previous paper, we reported the photochemical dimerization of iron acetylides $[Fe(\eta\text{-}C_5Me_5)(CO)_2(C{\equiv}CR)]$ (R = H, Ph), giving dinuclear complexes with an enyne ligand.[3] The study reveals that, when a C≡C group is introduced into the coordination sphere of the acetylide complex, insertion takes place quite readily. Herein we disclose photochemical reactions of the phenylacetylide complex with alk-1-ynes leading to cyclic products including iron(I) cyclopentadienone complexes.[4]

Irradiation of a benzene solution of $[Fe(\eta\text{-}C_5Me_5)(CO)_2(C{\equiv}CPh)]$ **1**[5] with a high-pressure mercury lamp in the presence of methyl propynoate (5 equiv.) afforded a red–brown complex **2** in 31% yield (Scheme 1). The NMR spectrum of the mononuclear complex **2**† showed two MeO signals [$\delta_H(CDCl_3)$ 3.74, 3.80] and revealed the incorporation of two molecules of the alkyne. The bicyclic structure of **2** has been determined by X-ray crystallography (Fig. 1)‡ and the contribution of a carbene structure **2B** in addition to the dominant resonance structure **2A** is evident as indicated by the structural parameters as well as the spectroscopic data {$\delta_C$(C2) 280.7 (s), $\nu$[C(23)=O(3)] 1600 $cm^{-1}$}.

In contrast to the reaction with alk-1-yne bearing a coordinating substituent ($CO_2R$) mentioned above, the photochemical reaction with alk-1-ynes (RC≡CH) bearing a non-coordinating substituent (R) afforded air-stable orange products **3** (R = $CH_2Ph$ **a**, $SiMe_3$ **b**, Ph **c**, Bu **d**, $Bu^t$ **e**) after separation by alumina column chromatography. The striking features of **3** are (*i*) paramagnetism, (*ii*) loss of the $\nu$(C≡O) absorption, and (*iii*) the appearance of an IR absorption around 1550 $cm^{-1}$ (KBr) which is assignable to a $\nu$(C=O) vibration. Complex **3** has been characterized as a 17e iron(I) cyclopentadienone complex, $[Fe(\eta\text{-}C_5Me_5)(\eta^4\text{-}2\text{-}Ph\text{-}5\text{-}R\text{-}C_5H_2O)$, on the basis of the results of X-ray crystallography of the $SiMe_3$ and Ph derivatives **3b**,**c**.§ A view of **3c** is shown in Fig. 2. The Fe–C(1) distance [2.22(1) Å] is substantially longer than the Fe–C(2)–(5) distances [2.090(9), 2.029(9), 2.028(9), 2.075(9) Å; suggesting that the cyclopentadienone ring C(1)–(5) is coordinated to the Fe centre essentially in an $\eta^4$-mode (**3A**) [C(1)–C(2) 1.43(1), C(1)–C(5) 1.48(1), C(2)–C(3) 1.42(1), C(3)–C(4) 1.50(1), C(4)–C(5) 1.42(1) Å], like an $\eta^4$-diene ligand. However, the considerably elongated C(1)–O bond [1.26(1) Å] and the lowered wavenumber of the $\nu$(C=O) vibration (Scheme 1) are indicative of a minor contribution of the iron(II) $\eta^5$-cyclopentadienoxyl structure (**3B**), where the unpaired electron is localized on the oxygen atom and the Fe centre attains an 18e configuration. The cyclopentadienone ring is located virtually parallel to the $C_5Me_5$ ring [Fe–C($C_5Me_5$) 2.06–2.10(1) Å], and the two Ph groups at the 2 and 5 positions are arranged almost coplanar with the central five-membered ring to extend the conjugated $\pi$ system.

A possible formation mechanism of **2** and **3** is summarized in Scheme 2. Initial photodecarbonylation followed by coordination of the alk-1-yne gives an $\eta^2$-alkyne intermediate **4**. Subsequent insertion of the C≡C moiety into the Fe–C≡ bond with the orientation of the substituent directing toward the metal centre gives an ynenyl species **5**. In the case of the reaction with methyl propynoate, a sequence of (*i*) further insertion of the acetylene substrate **6**, (*ii*) insertion of the terminal PhC≡C part into the Fe–C($sp^2$) bond, and (*iii*) coordination of the ester C=O moiety would give **2**. On the other hand, the reaction of




| | R | Yield (%) | ν(C=O) / $cm^{-1}$ |
|---|---|---|---|
| **3a** | $CH_2Ph$ | 28 | 1545 |
| **3b** | $SiMe_3$ | 23 | 1547 |
| **3c** | Ph | 60 | 1550 |
| **3d** | Bu | 32 | 1551 |
| **3e** | $Bu^t$ | 38 | 1553 |

**Scheme 1**

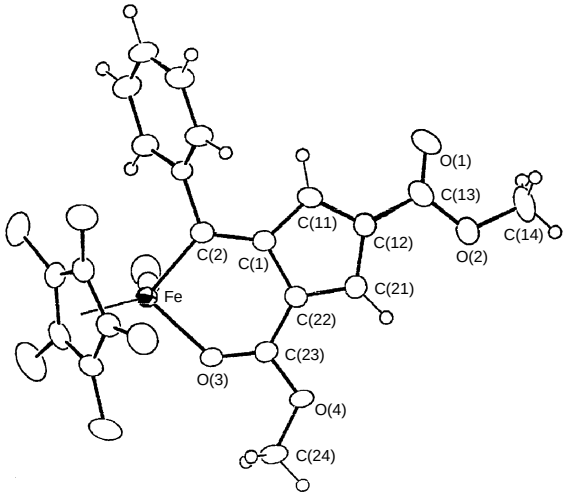



**Fig. 1** Molecular structure of **2** with thermal ellipsoids drawn at the 30% probability level. Selected bond distances (Å): Fe–C(2) 1.922(4), Fe–O(3) 1.995(3), C(2)–C(1) 1.406(6), C(1)–C(11) 1.435(6), C(1)–C(22) 1.451(6), C(11)–C(12) 1.379(6), C(12)–C(21) 1.428(6), C(21)–C(22) 1.365(6), C(22)–C(23) 1.427(6), C(23)–O(3) 1.234(5), C(13)–O(1) 1.197(6).

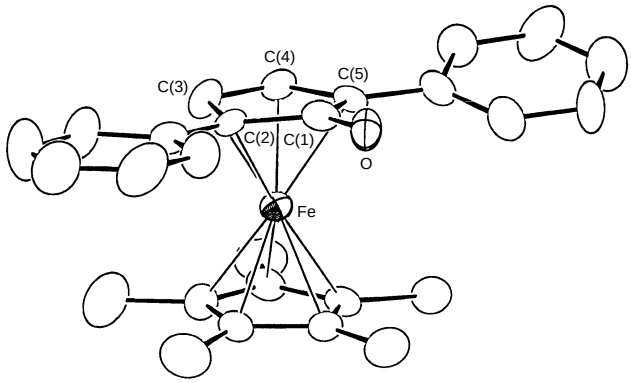
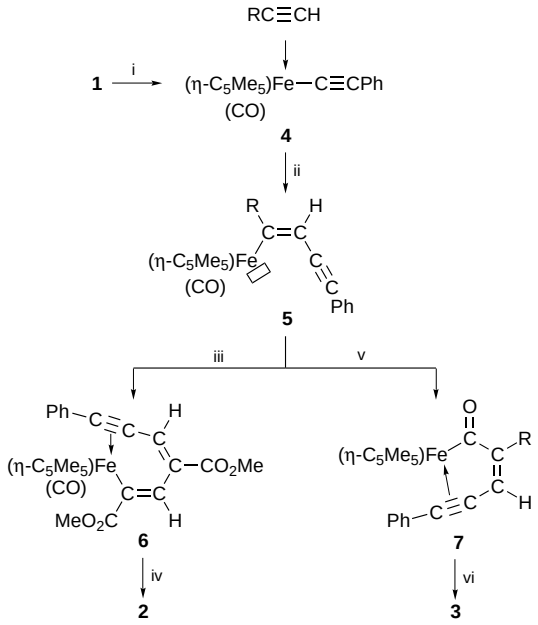



**Fig. 2** An overview of **3c** with thermal ellipsoids drawn at the 30% probability level




**Scheme 2** i, Photodecarbonylation and coordination of RC≡CH; ii, insertion of alk-1-yne; iii, insertion of a second molecule of alk-1-yne; iv, insertion of the PhC≡C part and coordination of the ester C=O group; v, CO insertion; vi, PhC≡C insertion and H abstraction

alk-1-yne with a non-coordinating substituent follows CO insertion of the ynenyl moiety to form the acyl intermediate **7**. Successive ring closure *via* C≡C insertion and H abstraction from the reaction medium gives the cyclopentadienone complex **3**. The reaction pathways may depend on the nucleophilicity of the α-carbon atom of the ynenyl group in **5** as well as the coordinating ability of the alk-1-yne substituent (R).

In summary, a C≡C functional group incorporated in a metal coordination sphere readily inserts into the M–C≡ bond to form a conjugated system *via* C–C coupling. The obtained 17e species **3**, which can be viewed as a dehydrogenated form of the classical hydroxyferrocene or a paramagnetic counterpart of well known cyclopentadienone complexes,[4] belongs to a rare class of iron(I) compounds.[6] Despite the paramagnetic character, **3** is air stable and passes through an alumina column. A study on the physical properties and reactivity of **3** is now under way.

## Footnotes

† *Selected spectroscopic data* for **2**: NMR data for the ring: $\delta_H(CDCl_3)$ 6.62, 7.64 [d × 2, *J* 2 Hz, C(11 H) and C(21 H)]. $\delta_C(CDCl_3)$ 280.7 [s, C(2)], 174.1 [s, C(23)], 166.6 [s, C(13)], 155.7 [t, *J* 7 Hz, C(12)], 148.9 [q, *J* 4 Hz, C(1)], 131.4, 118.3 [d × 2, *J* 164 Hz, C(11) and C(21)], 116.4 [d, *J* 9 Hz, C(22)]. IR (KBr) ν(C≡O) 1927, ν(C=O) 1703, 1600 $cm^{-1}$.

‡ *Crystallographic data*: **2**: $C_{27}H_{28}FeO_5$, *M* = 488.4, triclinic, space group $P\bar{1}$, *a* = 11.190(2), *b* = 12.181(3), *c* = 8.812(2) Å, α = 97.60(2), β = 96.42(2), γ = 90.21(2)°, *U* = 1182.9(5) $Å^3$, *Z* = 2, $D_c$ = 1.37 g $cm^{-3}$, $R(R_w)$ = 0.046 (0.049) for 2474 unique data with $I > 3\sigma(I)$ and 298 variables.

**3c**: $C_{26}H_{27}FeO$, *M* = 423.4, monoclinic, space group $P2_1/n$, *a* = 11.901(5), *b* = 9.235(6), *c* = 19.77(1) Å, β = 94.94(4)°, *U* = 2165(2) $Å^3$, *Z* = 4, $D_c$ = 1.30 g $cm^{-3}$ $R(R_w)$ = 0.064 (0.065) for 1711 unique data with $I > 3\sigma(I)$ and 262 variables.

**3b**: $C_{24}H_{31}OSiFe$, *M* = 419.4, monoclinic, space group $P2_1/n$, *a* = 12.003(3), *b* = 12.186(3), *c* = 16.258(3) Å, β = 104.90(3)°, *U* = 2298(2) $Å^3$, *Z* = 4, $D_c$ = 1.21 g $cm^{-3}$, $R(R_w)$ = 0.078 (0.081) for 1994 unique data with $I > 3\sigma(I)$ and 186 variables. Atomic coordinates, bond lengths and angles, and thermal parameters have been deposited at the Cambridge Crystallographic Data Centre (CCDC). See Information for Authors, Issue No. 1. Any request to the CCDC for this material should quote the full literature citation and the reference number 182/320.

§ Slippage of the cyclopentadienone ring is more evident for the $SiMe_3$ derivative **3b** [Fe–C(1) 2.29(1), Fe–C(2) 2.09(1), Fe–C(3) 2.014(9), Fe–C(4) 1.996(9), Fe–C(5) 2.10(1) Å]; however, the relative arrangement of the ring with respect to the $C_5Me_5$ ligand can not be determined satisfactorily because of the severe disorder of the $C_5Me_5$ ligand, which was refined by using rigid models.

## References

1 For leading references, see: *Comprehensive Organometallic Chemistry II*, ed. E. W. Abel, F. G. A. Stone and G. Wilkinson, Pergamon, Oxford, 1995, vol. 12, ch. 7; J. P. Collman, L. S. Hegedus, J. R. Norton and R. G. Finke, *Principles and Applications of Organotransition Metal Chemistry*, 2nd edn., University Science Book, California, 1987; G. W. Parshall and S. D. Ittel, *Homogeneous Catalysis*, 2nd edn., Wiley-International, New York, 1992.

2 For polymerization, see C. I. Simionescu and V. Percec, *Prog. Polym. Sci*., 1982, **8**, 133; T. Masuda and T. Higashimura, *Adv. Polym. Sci*., 1986, **81**, 121.

3 M. Akita, S. Sugimoto, M. Terada and Y. Moro-oka, *J. Organomet. Chem*., 1993, **447**, 103.

4 For related hydroxyferrocenes and diamagnetic cyclopentadienone complexes, see: D. P. Dawson, W. Yongskulrote, J. M. Bramlett, J. B. Wirht, B. Durham and N. T. Allison, *Organometallics*, 1994, **13**, 3873; C. Slugovc, K. Mauthner, K. Mereiter, R. Schmid and K. Kirchner, *Organometallics*, 1996, **15**, 2954; K. Mauthner, K. Mereiter, R. Schmid and K. Kirchner, *Organometallics*, 1994, **13**, 5054 and references therein.

5 M. Akita, M. Terada, S. Oyama and Y. Moro-oka, *Organometallics*, 1990, **9**, 816. See also: M. Akita and Y. Moro-oka, *Bull. Chem. Soc. Jpn*., 1995, **68**, 420.

6 For 19e iron(I) species, see: D. Astruc, *Chem. Rev*., 1988, **88**, 1189. For organometallic 17e species, see: M. C. Baird, *Chem. Rev*., 1988, **88**, 1217.

*Received, 7th October 1996; Com. 6/06836G*

# A versatile route to $[Ru_3(CO)_{11}(alkyne)]$ complexes

**Silvio Aime,*† Walter Dastrù, Roberto Gobetto, Luciano Milone and Alessandra Viale**

*Dipartimento di Chimica Inorganica, Chimica Fisica e Chimica dei Materiali, V. Pietro Giuria 7, 10125 Torino, Italy*

**Alkynes react at low temperature with $[Ru_3H(\mu\text{-}H)(CO)_{11}]$ to afford the novel $[Ru_3(CO)_{11}(alkyne)]$ complexes, which correspond to the first stage of the coordination of alkynes to metal clusters and are the precursors of the previously reported $[Ru_3(CO)_9(\mu\text{-}CO)(\mu_3\text{-}\eta^2\text{-}alkyne)]$ derivatives.**

Although the reactions between alkynes and trimetallic carbonyl clusters $[M_3(CO)_{12}]$ (M = Fe, Ru, Os) have been under intense scrutiny in the last two to three decades and a large number of derivatives have been characterized,[1] no report has yet appeared on derivatives corresponding to the first step of alkyne coordination, *i.e.* to $[M_3(CO)_{11}(alkyne)]$ species containing an alkyne ligand coordinated in a $\eta^2$-mode to a single metallic centre. It is reasonable to think that the lack of observation of these compounds is an indication of their instability and their prompt transformation to $[M_3(CO)_x(alkyne)]$ derivatives:[2,3] [eqn. (1); M = Fe, $x$ = 9; M = Ru, Os, $x$ = 10].

$$[M_3(CO)_{12}] + \text{alkyne} \xrightarrow{-CO} [M_3(CO)_{11}(\text{alkyne})] \xrightarrow{-CO} [M_3(CO)_x(\text{alkyne})] \quad (1)$$

Thus the thermally activated dissociation of CO ligands from $[M_3(CO)_{12}]$ occurs at temperatures which appear to be too high to allow the observation of detectable amounts of $[M_3(CO)_{11}(alkyne)]$ derivatives.

A way to overcome this problem lies in the possibility of forming the coordinatively unsaturated '$Ru_3(CO)_{11}$' species at low temperature and then to allow its reaction *in situ* with the alkyne ligand.

Some years ago, Keister and coworkers[4] reported that $[Ru_3H(\mu\text{-}H)(CO)_{11}]$, in the presence of carbon monoxide, decomposes cleanly to $[Ru_3(CO)_{12}]$ (97% isolated yield). They also showed that the kinetics of this conversion are first order in $[Ru_3H(\mu\text{-}H)(CO)_{11}]$ and independent of CO concentration. The proposed mechanism consists of the reductive elimination of $H_2$ (through a three-centre transition state) leading to the formation of the coordinatively unsaturated '$Ru_3(CO)_{11}$' intermediate.

On the basis of this background information, we thought that $[Ru_3H(\mu\text{-}H)(CO)_{11}]$ may represent an interesting 'lightly stabilized' derivative[5] for carrying out substitution reactions at low temperature.

The reaction between $[Ru_3H(\mu\text{-}H)(CO)_{11}]$ and acetylene was carried out directly in the NMR tube, in $CD_2Cl_2$ at 183 K. After few minutes the $^1H$ NMR spectrum of the reaction mixture shows two doublets at $\delta$ 8.45 and 5.97 ($^3J_{HH}$ 8.6 Hz) assigned to $[Ru_3(CO)_{11}(\eta^2\text{-}C_2H_2)]$, and two singlets at $\delta$ 5.42 and 1.80 assigned to free $C_2H_4$‡ and $C_2H_2$ respectively. The $^{13}C$ NMR spectrum at 183 K of the reaction mixture obtained by using a $^{13}CO$-enriched sample of $[Ru_3H(\mu\text{-}H)(CO)_{11}]$ is shown in Fig. 1. In the spectrum there are eleven carbonyl resonances of equal intensity at $\delta$ 215.0, 196.1, 194.9, 193.8, 193.1, 191.1, 190.1, 189.0, 188.4, 187.8 and 185.9.

As we approach ambient temperature, we observe that the transformation of $[Ru_3(CO)_{11}(\eta^2\text{-}C_2H_2)]$ to $[Ru_3(CO)_9(\mu\text{-}CO)(\mu_3\text{-}\eta^2\text{-}C_2H_2)]$ takes place as clearly assessed from both $^1H$ and $^{13}C$ NMR spectroscopy.[3] The observation of distinct $^1H$ and $^{13}C$ resonances for all the ligands present in $[Ru_3(CO)_{11}(\eta^2\text{-}C_2H_2)]$ is indicative of a 'frozen' asymmetric structure in which the acetylene occupies an axial coordination site. The observation of a carbonyl resonance significantly downfield shifted ($\delta$ 215.0) is reminiscent of a semi-bridging ligand which 'disperses' excess of charge to a neighbouring metallic centre. This may be an indication of the occurrence of some interaction of the acetylene ligand with a second ruthenium centre as shown in Fig. 2. The source of molecular asymmetry would then arise from a partial alignment of the alkyne ligand along one of the metal–metal bonds and this arrangement anticipates to some extent the coordination geometry found in $[Ru_3(CO)_9(\mu\text{-}CO)(\mu_3\text{-}\eta^2\text{-}alkyne)]$.[3]

An estimation of the distance between the two hydrogens in the alkyne moiety was obtained by measuring the $^1H$ NMR relaxation times at 213 K. Both hydrogens show the same $T_1$ value of 1.6 s. On the assumption that the relaxation pathway is largely dominated by the dipolar contribution, the $r_{HH}$ distance can be determined by eqn. (2):[6]

$$\frac{1}{T_1} = \frac{3}{2}\left(\frac{\mu_0}{4\pi}\right)^2 \frac{\gamma_H^4 \hbar^2 \tau_c}{r^6} \quad (2)$$

where $\mu_0$ is the magnetic susceptibility in a vacuum, $\gamma_H$ is the gyromagnetic value for a proton and $\tau_c$ is the molecular reorientational time of the complex. Since $[Ru_3(CO)_{11}(\eta^2\text{-}C_2H_2)]$ and $[Ru_3(CO)_{12}]$ have very similar molecular sizes, we used a value of 172 ps for $\tau_c$ at 213 K as evaluated from a recent NMR relaxation study of $[Ru_3(CO)_{12}]$.[7] The obtained $r_{HH}$ distance is 2.48 Å. On the basis of a carbon–carbon distance of

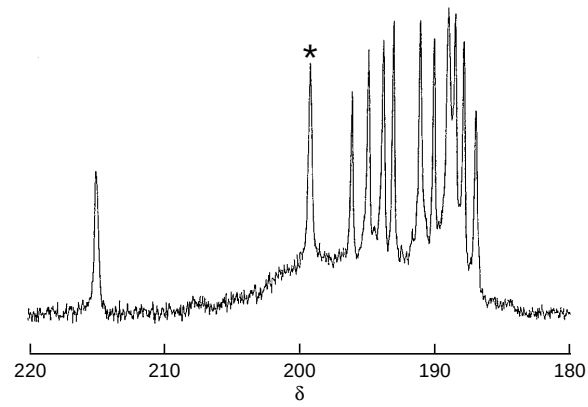



**Fig. 1** $^{13}C\{^1H\}$ NMR spectrum of a $^{13}CO$ enriched sample of $[Ru_3(CO)_{11}(\eta^2\text{-}C_2H_2)]\{CD_2Cl_2$, 183 K; * is assigned to $[Ru_3(CO)_{12}]\}$

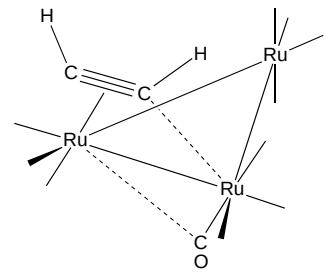



**Fig. 2** Proposed structure for $[Ru_3(CO)_{11}(\eta^2\text{-}C_2H_2)]$

1.27 Å (as found for mononuclear systems containing an $\eta^2$-bonded acetylene molecule[8]) and a carbon–hydrogen distance of 1.1 Å an average value of 123.5° for the H–C–C angle was obtained.

Analogous results were obtained when $[Ru_3H(\mu\text{-}H)(CO)_{11}]$ was reacted with substituted acetylenes. In the case of phenylacetylene only one of the two possible isomers of $[Ru_3(CO)_{11}(\eta^2\text{-}HC_2Ph)]$ was detected as clearly established by the single resonance for the acetylenic proton observed at $\delta$ 6.18 in the NMR spectrum.

In summary the results herein reported show that $[Ru_3H(\mu\text{-}H)(CO)_{11}]$ may represent a useful starting material for the synthesis of $[Ru_3(CO)_{11}L]$ derivatives where L may be an alkyne as well as a number of other two-electron donor ligands. This novel synthetic route to $[Ru_3(CO)_{11}L]$ species may also provide useful insights into the further development of the cluster–surface analogy,[9] since the first stages of the chemisorption processes are probably represented by the interaction of Lewis-base substrates at single metallic centres followed by the eventual set-up of multicentre bonding schemes.

We thank Ministero dell' Università e della Ricerca Scientifica e Tecnologica (MURST) and the Consiglio Nazionale delle Ricerche (Comitato 03) for financial support.

## Footnotes

† E-mail: aime@ch.unito.it

‡ The detection of $C_2H_4$ seems to imply that the reactivity of $[Ru_3H(\mu\text{-}H)(CO)_{11}]$ could not be limited to the loss of $H_2$ to give '$Ru_3(CO)_{11}$'. Another mechanism involving intermediates like $[Ru_3H_2(C_2H_2)(CO)_{11}]$ and $[Ru_3H(CHCH_2)(CO)_{11}]$ which react with $C_2H_2$ to yield $[Ru_3(CO)_{11}(\eta^2\text{-}C_2H_2)]$ and $C_2H_4$ may occur. However, it has been observed that $[Ru_3(CO)_{11}(\eta^2\text{-}C_2H_2)]$ is also formed in the reaction between $[Ru_3(CO)_{11}(NCMe)]$ and $C_2H_2$ at room temperature {even if it can be detected only in small amounts as it rapidly transforms to $[Ru_3(CO)_9(\mu\text{-}CO)(\mu_3\text{-}\eta^2\text{-}C_2H_2)]$}.[10] As MeCN is known to be a good leaving group, this observation supports the view that $[Ru_3(CO)_{11}(\eta^2\text{-}C_2H_2)]$ may be formed *via* the intermediate '$Ru_3(CO)_{11}$' species.

## References

1 E. Sappa, *J. Cluster Sci.*, 1994, **5**, 211; A. J. Deeming, *Adv. Organomet. Chem.*, 1986, **26**, 1; A. J. Deeming, S. H. Hasso and M. Underhill, *J. Chem. Soc., Dalton Trans.*, 1975, 1614; B. F. G. Johnson, J. Lewis, B. E. Reicherd, K. T. Schropp and G. M. Sheldrick, *J. Chem. Soc., Dalton Trans.*, 1977, 1417; B. F. G. Johnson, R. Khattar, J. Lewis and P. R. Raithby, *J. Organomet. Chem.*, 1987, **335**, C17; C. G. Pierpont, *Inorg. Chem.*, 1977, **16**, 636.
2 J. F. Blount, L. F. Dahl, C. Hoogzand and W. Hübel, *J. Am. Chem. Soc.*, 1966, **88**, 292.
3 S. Aime, R. Gobetto, L. Milone, D. Osella, L. Violano, A. J. Arce and Y. De Sanctis, *Organometallics*, 1991, **10**, 2854; S. Rivomanana, G. Lavigne, N. Lugan and J. J. Bonnet, *Organometallics*, 1991, **10**, 2285.
4 L. R. Nevinger, J. B. Keister and J. Maher, *Organometallics*, 1990, **9**, 1900.
5 A. D. Adams and J. P. Selegue, in *Comprehensive Organometallic Chemistry*, Pergamon, Oxford, 1982, p. 1025; B. F. G. Johnson, J. Lewis and D. A. Pippard, *J. Chem. Soc., Dalton Trans.*, 1989, 407; M. Tachikawa and J. R. Shapley, *J. Organomet. Chem.*, 1977, **124**, C19.
6 R. K. Harris, *Nuclear Magnetic Resonance Spectroscopy*, Pitman, London, 1983.
7 S. Aime, W. Dastrù, R. Gobetto, J. Krause and L. Milone, *Organometallics*, 1995, **14**, 4435.
8 G. R. Davies, W. Hewertson, R. H. B. Mais, P. G. Owston and C. G. Patel, *J. Chem. Soc. A*, 1970, 1873.
9 R. Ugo, *Catal. Rev.*, 1975, **11**, 225; E. L. Mutterties, T. N. Rhoding, E. Band, C. F. Brucker and W. R. Pretzer, *Chem. Rev.*, 1979, **79**, 91.
10 S. Aime *et al.*, to be published.

*Received, 14th October 1996; Com. 6/06984C*

# Novel vanadium(III/IV) compounds with the diamidate ligand 1,2-bis(2-pyridinecarboxamide)benzene ($H_2$bpb)

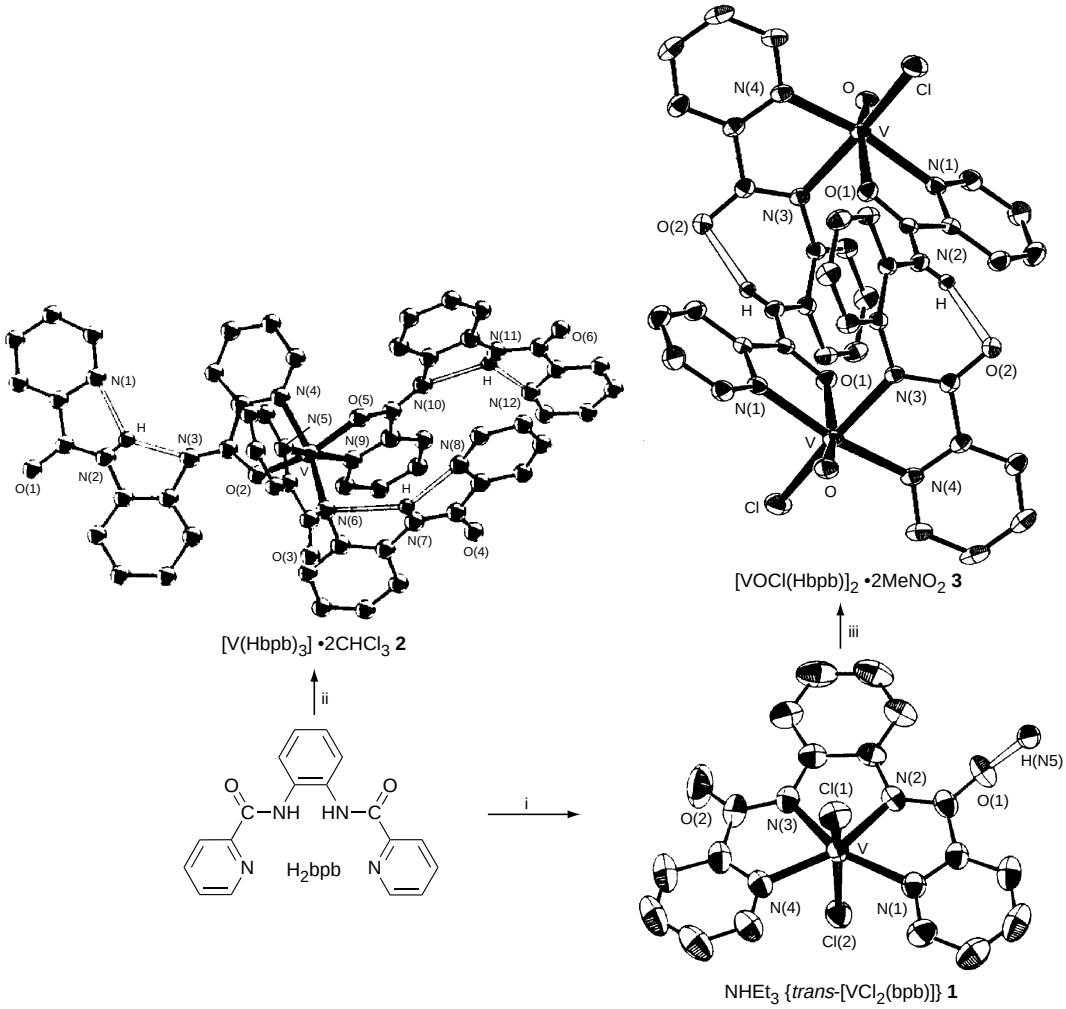
**Antonis T. Vlahos,[a] Themistoklis A. Kabanos,*[a] Catherine P. Raptopoulou[b] and Aris Terzis[b]**

[a] *Department of Chemistry, Section of Inorganic and Analytical Chemistry, University of Ioannina, 45 110 Ioannina, Greece*
[b] *NRPCS Demokritos, Institute of Materials Science, 15 310 Agia Paraskevi Attikis, Greece*

**Reaction of the diamidate ligand $H_2$bpb with $VCl_3$ depending on the base affords either the compound $NHEt_3${*trans*-$[V^{III}Cl_2(bpb)]$} 1 or $[V^{III}(Hbpb)_3]\cdot 2CHCl_3$ 2; aerial oxidation–hydrolysis of 1 gives the dimeric species $[VOCl(Hbpb)]_2\cdot 2MeNO_2$ 3; the X-ray crystal structures of 1, 2 and 3 are reported.**

Vanadium is a bioessential element,[1] but its role in biological systems is not yet well understood. The synthesis as well as the structural and spectroscopic characterization of low molecular mass model complexes of the biologically important oxidation states (+II to +V) of vanadium will help in making further progress in the elucidation of the biological role of vanadium.

Currently our group[2a] in parallel with others[2b] have embarked on a study of the interaction of vanadium with the amide(peptide) functionality, –NHCO–, which is a potential metal-ion binding site in biomolecules. Herein we wish to report the synthesis and structural characterization of vanadium(III) and oxovanadium(IV) compounds, $NHEt_3${*trans*-$[V^{III}Cl_2(bpb)]$} **1**, $[V^{III}(Hbpb)_3]\cdot 2CHCl_3$ **2** and $[V^{IV}OCl(Hbpb)]_2\cdot 2MeNO_2$ **3** (Scheme 1). The structure of **1** is the first example of a vanadium(III) centre that is bound by two deprotonated amidate nitrogens, while the structures of **2** and **3** are the first examples of vanadium(III/IV) centres with simultaneous ligation of a deprotonated amide nitrogen and of an amide oxygen from two different amide functionalities.




**Scheme 1** Synthesis and X-ray crystal structures of complexes **1**, **2** and **3**. *Conditions*: i, $VCl_3$, $NEt_3$, toluene; ii, $VCl_3$, $NH_3$, toluene; iii, $CH_3NO_2$, air. Selected interatomic distances (Å): for **1**, V–N(3) 1.996(2), V–N(2) 2.016(2), V–N(4) 2.136(2), V–N(1) 2.141(2), V–Cl(1) 2.350(1), V–Cl(2) 2.357(1). For **2**, V–O(5) 1.936(3), V–O(2) 1.974(3), V–N(6) 2.011(4), V–N(9) 2.114(4), V–N(5) 2.118(4), V–N(4) 2.186(4). For **3**, V–Cl 2.355(1), V–O 1.587(2), V–N(3) 2.086(2), V–N(4) 2.115(2), V–N(1) 2.145(2), V–O(1) 2.217(2).

Refluxing a mixture of vanadium(III) chloride (1.30 mmol), $H_2$bpb (1.30 mmol) and triethylamine (6.50 mmol) in dry toluene under argon for 14 h yielded the mononuclear brick red complex **1** and $NHEt_3Cl$ [eqn. (1)].

$$VCl_3 + H_2bpb + 2NEt_3 \rightarrow NHEt_3\{trans[VCl_2(bpb)]\} + NHEt_3Cl \quad (1)$$

**1**

By layering diethyl ether into a chloroform solution of **1** and $NHEt_3Cl$ brick-red crystals of complex **1** (yield 20%) suitable for X-ray structure analysis† were obtained. Because the solubilities of complex **1** and $NHEt_3Cl$ were almost identical in various organic solvents **1** could not be separated from $NHEt_3Cl$ and so gaseous ammonia (bubbling) was substituted for triethylamine whereupon crystals of **2** were obtained in a very low yield (5%) (this is under further investigation). When a nitromethane solution of **1** was exposed to the atmosphere the dimeric species **3** is formed as green crystals (yield 80%).

As shown in Scheme 1, the structure of complex **1** exhibits distorted octahedral coordination at the vanadium centre. The two chlorine atoms are *trans* and the angle Cl(1)–V–Cl(2) is bisected by the plane defined by the four nitrogen atoms of the ligand $bpb^{2-}$. The mean $V–N_{amide}$ bond length [2.006(2) Å] is slightly longer (0.024 Å) than the only other known vanadium(III)–amidate distance[2a] and this might be due to the stronger, dianionic ligand set in complex **1**, which results in a lower effective charge on the vanadium(III) centre and therefore longer V–N distances. The bond lengths to N(1) [2.141(2) Å] and N(4) [2.136(2) Å] the pyridine nitrogens lie at the lower limit of $V–N_{py}$ distances seen in the literature.[2a,3] The V–Cl bond lengths [V–Cl(1) 2.350(1), V–Cl(2) 2.357(1) Å] are in the range expected for vanadium(III) complexes.[2a,4] Comparison of the structure of complex **1** described herein with its iron analogue,[5] *i.e.* $NHEt_3\{trans$-$[FeCl_2(bpb)]\}\cdot MeCN$, reveals a close similarity, except that there is a small reduction in the average V–N bond length (*ca.* 0.04 Å) [V–N (av.) 2.07(8), Fe–N (av.) 2.11(1) Å] that results in a slight increase of the *cis*-bite angles of the vanadium complex.

The structure of complex **3** (Scheme 1) consists of discrete dimers. The vanadium(IV) centres are related by a centre of symmetry. In this dimeric species, each vanadium has a distorted octahedral environment and is bonded to two pyridine nitrogens, one amidic oxygen, one amidic nitrogen (from two bridging $\mu_2$-$\eta^4$-$Hbpb^-$ ligands), to a chlorine atom and to an oxo group. The ligated pyridine nitrogens are *trans* to each other and the amidic oxygen is *trans* to the oxo ligand. The V=O and the V–Cl (the chlorine atom is *cis* to the oxo group) bond lengths of 1.587(2) A and 2.355(1) Å, respectively, are in good agreement with those reported in the literature for octahedral oxovanadium(IV) compounds.[6,7] The $V–O_{amide}$ bond distance [2.217(2) Å] is almost identical with the only other known vanadium(IV)–amidate O distance[6] [2.206(1) Å], while the $V–N_{amide}$ bond [2.086(2) Å] is substantially longer (*ca.* 0.09 Å) than the mean $V–N_{amide}$ distance [2.00(1) Å] for various oxovanadium(IV)–amidate compounds,[2] and this might be due to the substantial deviation from planarity of the bridging ligand $Hbpb^-$. Compound **3**, unlike the double-helical complexes of Constable *et al.*,[8] resembles instead the non-helical dimer of Williams and coworkers.[9]

While the formation of **1** is straightforward, the reasons for the preferential formation of **2** when ammonia is substituted for triethylamine are not at all clear. The vanadium atom in **2** is coordinated to three singly deprotonated chelated rings ($\eta^2$-$Hbpb^-$) in a distorted octahedral coordination, environment with two different modes of coordination, *i.e.* $N_{py},O_{am}$ (two chelate rings) and $N_{py},N_{am}$ (one chelate ring). One might expect a tris-chelate vanadium(III) complex through pyridine and deprotonated amide nitrogen atoms, since the deprotonated amides normally coordinate *via* N.[10] To this general trend there are only two other exceptions.[11,12] Steric hindrance, or strong preference of the vanadium(III) centre for oxygen ligation might be an explanation for amidate-O ligation and not deprotonated amidate-N ligation in two chelate rings of **2** (theoretical calculations are under way).

We gratefully acknowledge support of this research by the Greek General Secretariat of Research and Technology (Grant No. 1807/95) and Mrs F. Masala for typing the manuscript of this paper.

## Footnotes

† *Crystal data*: for **1**, $C_{24}H_{28}Cl_2N_5O_2V$, $M$ = 540.37, monoclinic, space group $P2_1/n$, $a$ = 10.501(1), $b$ = 20.958(3), $c$ = 11.781(2) Å, β = 90.340(4)°, $U$ = 2592.7(6) Å$^3$, $Z$ = 4, $D_c(D_m)$ = 1.384(1.36) g cm$^{-3}$, $T$ = 298 K, no. of unique reflections = 5086, no. of parameters 372, $R1$ = 0.0359, $wR2$ = 0.0935 with $I > 2\sigma(I)$.

For **2**, $C_{56}H_{41}Cl_6N_{12}O_6V$, $M$ = 1241.65, monoclinic, space group $P2_1/c$, $a$ = 16.380(2), $b$ = 26.182(3), $c$ = 14.573(1) Å, β = 113.568(3)°, $U$ = 5728.6(10) Å$^3$, $Z$ = 4, $D_c(D_m)$ = 1.440(1.42) g cm$^{-3}$, $T$ = 293 K, no. of unique reflections = 7313, no. of parameters = 840, $R1$ = 0.0461, $wR2$ = 0.1076 with $I > 2\sigma(I)$.

For **3**, $C_{38}H_{32}Cl_2N_{10}V_2$, $M$ = 961.63, triclinic, space group $P\bar{1}$, $a$ = 12.672(3), $b$ = 10.961(2), $c$ = 8.950(2) Å, α = 112.069(6), β = 99.993(8), γ = 109.705(8)°, $U$ = 1018.35 Å$^3$, $Z$ = 1, $D_c(D_m)$ = 1.567(1.55) g cm$^{-3}$, $T$ = 296 K, no. of unique reflections = 3890, no. of parameters = 333, $R(R_w)$ = 0.0362(0.0377) with $F > 6\sigma(F)$.

Atomic coordinates, bond lengths and angles, and thermal parameters have been deposited at the Cambridge Crystallographic Data Centre (CCDC). See Information for Authors, Issue No. 1. Any request to the CCDC for this material should quote the full literature citation and the reference number 182/341.

## References

1 *Metal Ions in Biological Systems*, ed. H. Sigel and A. Sigel, Marcel Dekker, New York, 1995, vol. 31.
2 (*a*) A. D. Keramidas, A. B. Papaioannou, A. Vlahos, T. A. Kabanos, G. Bonas, A. Makriyannis, C. P. Raptopoulou and A. Terzis, *Inorg. Chem.*, 1996, **35**, 357; A. J. Tasiopoulos, A. T. Vlahos, A. D. Keramidas, T. A. Kabanos, Y. G. Deligiannakis, C. P. Raptopoulou and A. Terzis, *Angew. Chem., Int. Ed. Engl.*, 1996, **35**, 2531; (*b*) A. S. Borovik, T. M. Dewey and K. N. Raymond, *Inorg. Chem.*, 1993, **32**, 413; C. R. Comman, E. P. Zovinka, Y. D. Boyajian, K. M. Geiser-Bush, P. O. Boyle and P. Singh, *Inorg. Chem.*, 1995, **34**, 4213; D. C. Crans, H. Holst, A. D. Keramidas and D. Rehder, *Inorg. Chem.*, 1995, **34**, 2524; F. W. B. Einstein, R. J. Batchelor, S. J. Angus-Dunne and A. S. Tracey, *Inorg. Chem.*, 1996, **35**, 1680.
3 J. G. Reynolds, S. C. Sendlinger, A. M. Murray, J. C. Huffman and G. Christou, *Inorg. Chem.*, 1995, **34**, 5745.
4 M. Marranti, S. Gambarotta, C. Floriani, A. Chiesi-Villa and C. Guastini, *Inorg. Chem.*, 1986, **25**, 2308.
5 Y. Yang, F. Diederich and J. S. Valentine, *J. Am. Chem. Soc.*, 1991, **113**, 7195.
6 T. A. Kabanos, A. D. Keramidas, A. Papaioannou and A. Terzis, *Inorg. Chem.*, 1994, **33**, 845.
7 I. Cavaco, J. C. Pessoa, D. Costa, M. T. Duarte, R. D. Gillard and P. Matias, *J. Chem. Soc., Dalton Trans.*, 1994, 149; M. Mohan, M. R. Bond, T. O. Tieno and C. J. Carrano, *Inorg. Chem.*, 1995, **34**, 1233.
8 E. C. Constable, M. D. Ward and D. A. Tocher, *J. Chem. Soc., Dalton Trans.*, 1991, 1675.
9 S. Rüttimann, C. Riguet, G. Bernardinelli, B. Bocquet and A. F. Williams, *J. Am. Chem. Soc.*, 1992, **114**, 4230.
10 H. Sigel and R. B. Martin, *Chem. Rev.*, 1982, **82**, 385.
11 V. Scheller-Krattiger, K. H. Scheller, E. Sinn and R. B. Martin, *Inorg. Chim. Acta*, 1982, **60**, 45.
12 W. Leung, T. S. M. Hun, K. Hui, I. D. Williams and D. Vanderveer, *Polyhedron*, 1996, **15**, 421.

*Received, 11th October 1996; Com. 6/06980K*

# Low-temperature water–gas shift reaction over gold deposited on $TiO_2$

**Hiroaki Sakurai,*† Atsushi Ueda, Tetsuhiko Kobayashi and Masatake Haruta**

*Osaka National Research Institute, AIST, Midorigaoka 1, Ikeda, Osaka 563, Japan*

**Gold exhibits very high catalytic activities, comparable with that of a conventional $Cu/ZnO/Al_2O_3$ catalyst, for forward and reverse water–gas shift reactions when supported on titanium oxide by the deposition–precipitation method.**

The water–gas shift reaction is used as one of the important industrial processes to adjust the $CO/H_2$ ratio for methanol synthesis and to produce $H_2$ for ammonia synthesis. For this reaction, two kinds of catalysts are commercially used.[1] One is a high-temperature shift catalyst, which is based on iron oxide structurally promoted with chromium oxide and is used in the temperature range 583–723 K and at 2.5–3.5 MPa. Another is a low-temperature shift catalyst composed of copper, zinc oxide and alumina, and is used between 483 and 513 K. Recently, Andreeva *et al*. reported that Au deposition enhances the catalytic activity of iron oxide for the water–gas shift reaction.[2,3] The activity is comparable with that of a conventional copper catalyst. Here, we report a novel and more active catalyst, Au deposited on $TiO_2$, which contains neither copper nor iron oxide, but exhibits low-temperature activities both for the forward and reverse water–gas shift reactions.

The catalysts were prepared by deposition–precipitation (DP) of gold hydroxide from $HAuCl_4$ on titanium dioxide powder (P25, Japan Aerosil Co.).[4] To obtain fine gold particles, magnesium citrate solution was added during preparation.[5,6] The catalyst was finally calcined in air at 673 K. Gold loading in the starting solutions is expressed as atom% [100Au/(Au+M) for $Au/M_xO_y$]. For comparison, other gold and copper catalysts were prepared by coprecipitation (Cop) and impregnation (Imp) methods.

Table 1 shows the catalyst parameters and some kinetic data under forward water–gas shift conditions. Other than Au catalysts, a commercial $Cu/ZnO/Al_2O_3$ catalyst (Catalysts and Chemicals Inc., Far East) was examined for comparison. The reactant gas containing CO (1%), $H_2O$ (2%) and He (balance) was fed at a space velocity of 12 600 $h^{-1}$ ml (g cat)$^{-1}$ and under a pressure of 0.1 MPa, and the introduction of $H_2O$ was carried out using a micro-feeder or by bubbling. At 373 K, CO conversion was < 20% and much lower than the equilibrium conversion (99.97%), therefore, the reaction rate, TOF, and activation energy were calculated around this temperature. The catalysts tested were stable during catalytic activity measurements and the change of CO conversion during 2.5 h was less than < 0.5%. In the calculation of TOF for supported metal catalysts, generally, the number of exposed metal atoms is determined by titration using CO and $H_2$. In the case of supported gold, the titration method is not applicable because of the lack of irreversible stoichiometric adsorption of these molecules on the surface of gold. The number of gold atoms exposed to the surface was thus simply calculated from the mean diameter of the gold particle. The shape of the gold particles deposited on the $TiO_2$ surface was well defined and hemispherical by TEM observation.[4]

**Table 1** Catalytic activity of supported gold catalysts for the water–gas shift reaction[a]

| Catalyst[b] | $D_{metal}$[c] /nm | Rate at 373 K/mol $s^{-1}$ (g cat)$^{-1}$ | TOF at 373 K/$s^{-1}$ | $E_a$/kJ $mol^{-1}$ |
|---|---|---|---|---|
| $Au/TiO_2$(DP, 3.4%)[d] | 4.4 | $1.0 \times 10^{-7}$ | $7.9 \times 10^{-4}$ | 46 |
| $Au/TiO_2$(DP, 5%)[d] | — | $1.4 \times 10^{-7}$ | — | 45 |
| $Au/TiO_2$(DP, 10%)[d] | 4.4 | $3.0 \times 10^{-7}$ | $9.2 \times 10^{-4}$ | 31 |
| $Au/TiO_2$(Cop, 33%)[d] | 2.8 | $6.4 \times 10^{-8}$ | $5.6 \times 10^{-5}$ | 47 |
| $Au/Fe_2O_3$(Cop, 5%) | 3.3 | $2.2 \times 10^{-8}$ | $9.1 \times 10^{-5}$ | 52 |
| $Au/Al_2O_3$(Cop, 5%) | 3.7 | $3.4 \times 10^{-8}$ | $1.1 \times 10^{-4}$ | 24 |
| Au/ZnO(Cop, 5%) | 4.9 | $9.0 \times 10^{-9}$ | $5.7 \times 10^{-5}$ | 34 |
| $Cu/ZnO/Al_2O_3$[e] | 13.4 | $1.2 \times 10^{-7}$ | $2.0 \times 10^{-4}$ | 53 |

[a] Reactant gas CO(1%)–$H_2O$(2%)–He(balance); SV = 12 600 $h^{-1}$ ml (g cat)$^{-1}$; pressure 0.1 MPa. [b] DP, deposition–precipitation; Cop, coprecipitation, Au loading in atom%. [c] Calculated from XRD by using Scherrer's equation. [d] Addition of magnesium citrate during preparation. [e] Commercial catalyst, with Cu content of 42 atom% by XRF analysis.

Particle sizes of Au and Cu given in Table 1 were calculated from the XRD data. The titania powder P25 is composed of both anatase and rutile. Because the broad diffraction peaks for gold overlapped with these diffraction lines, the diffraction profile of $TiO_2$ itself was mathematically subtracted from the profile of $Au/TiO_2$, and then the Au particle size was calculated by using Scherrer's equation. It was found that Au was deposited on the oxide surface with diameters < 5 nm.

Among gold catalysts (Table 1), $Au/TiO_2$ showed the highest reaction rates. While the reaction rate at 373 K increased with increasing Au loading for a series of $Au/TiO_2$ catalysts prepared by the deposition–precipitation method, $Au/TiO_2$ prepared by coprecipitation showed a lower rate despite the higher metal loading and the smallest gold particle sizes. This may be attributed to differences in exposure of gold particles on the surface and the crystalline nature of $TiO_2$ depending on the preparation method. The activation energies listed in Table 1, except for $Au/Al_2O_3$ and Au/ZnO, are close to the reported values for $Cu/Al_2O_3$ (55.6 kJ $mol^{-1}$) and $Au/Al_2O_3$ (48.8 kJ $mol^{-1}$), both prepared by incipient wetness impregnation.[7] However, the reaction rate and turnover frequency were very different depending on the preparation method. The TOF reported for $Au/Al_2O_3$(Imp) was only 1/342 that of the value for $Cu/Al_2O_3$(Imp).[7] On the other hand, $Au/Al_2O_3$(Cop) was more active and had half of the TOF of the $Cu/ZnO/Al_2O_3$ catalyst. The activities of $Au/TiO_2$ (DP) were much more striking. The rates of reaction at 373 K were comparable and the TOF was more than 4 times higher than that of $Cu/ZnO/Al_2O_3$. Although this comparison is not made under industrial reaction conditions and the lifetime (the commercial Cu catalyst has a lifetime of *ca*. 2–4 years by adding the alumina component[1]) has not yet been examined, the results clearly show that gold is potentially as active as copper, when highly dispersed on suitable support oxide.

Fig. 1 shows the activities of gold catalysts under the reverse water–gas shift conditions. The reactant gas mixture $CO_2$(23%)– $H_2$(67%)–Ar(balance) was passed through the catalyst bed at a space velocity of 3000 $h^{-1}$ ml (g cat)$^{-1}$ and under a pressure of 0.1 or 5 MPa. Catalytic activities are expressed by $k$ defined as $[CO][H_2O]/[CO_2][H_2]$. The concentration of each component was calculated from analytical data and the material balance equations.[8] Au on $TiO_2$ and $Al_2O_3$ showed higher activities than $Au/Fe_2O_3$, and the most active $Au/TiO_2$ reached thermodynamic equilibrium at a temperature as low as 423 K at 5 MPa. However, $Au/TiO_2$ and $Cu/TiO_2$

prepared by impregnation methods were only poorly active, and did not reach equilibrium even at 673 K.

As reported previously, these gold catalysts produce methanol, methane and other hydrocarbons under such high- pressure conditions, and the product selectivity greatly differs depending on the nature of the oxide supports.[8–10] When the total pressure was decreased from 5 to 0.1 MPa, the activity decreased as shown in Fig. 1, however, CO selectivities were very much improved. For example, $Au/TiO_2$ produced methanol, methane and CO with selectivities of 4, 10 and 86%, respectively, at 523 K and 5 MPa, CO selectivity reached values > 99% at 0.1 MPa.

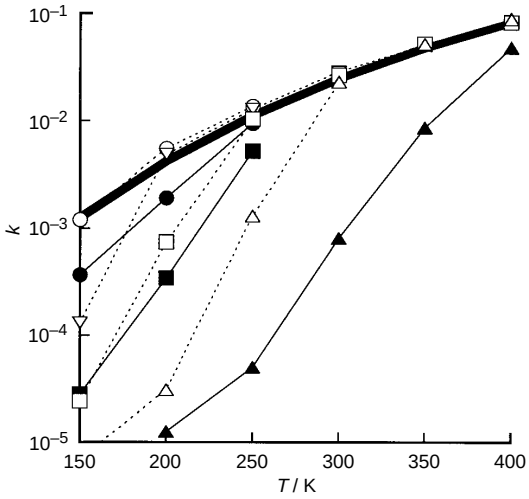



**Fig. 1** Catalytic activities of supported gold catalysts for the reverse water–gas shift reaction. Reactant gas mixture $CO_2$(23%)–$H_2$(67%)–Ar(balance); SV = 3000 $h^{-1}$ ml (g cat).$^{-1}$ Activities are expressed in terms of $k$ at a total pressure of 5 MPa over (○) $Au/TiO_2$ (DP, 2 atom%), (▽) $Au/Al_2O_3$ (Cop, 5 atom%), (□) $Au/Fe_2O_3$ (Cop, 5 atom%), (△) Au/ZnO (Cop, 5 atom%) and 0.1 MPa over (●) $Au/TiO_2$ (DP, 2 atom%), (■) $Au/Fe_2O_3$ (Cop, 5 atom%), (▲) Au/ZnO (Cop, 5%). The thick continuous line shows the thermodynamic equilibrium limit.

Gold deposited on $TiO_2$ is known to exhibit very high activity for CO oxidation to $CO_2$ even below 273 K.[4,5] $CO_2$ formation is further enhanced when moisture is added to the reactant mixture of CO and air.[11] This enhancement is not due to the shift reaction of CO and water because the shift activity is almost zero at 273 K under the conditions used here.

## Footnote

† E-mail: sakurai@onri.go.jp

## References

1 C. Rhodes, G. J. Huchings and A. M. Ward, *Catal. Today*, 1995, **23**, 43.
2 D. Andreeva, V. Idakiev, T.Tabakova and A. Andreev, *J. Catal.*, 1996, **158**, 354.
3 D. Andreeva, V. Idakiev, T. Tabakova, A. Andreev and R. Giovanoli, *Appl. Catal.*, 1996, **134**, 275.
4 S. Tsubota, D. A. H. Cunningham, Y. Bando and M. Haruta, *Preparation of Catalysts VI*, ed. G. Poncelet *et al*., Elsevier, Amsterdam, 1995, p. 227.
5 S. Tsubota, M. Haruta, T. Kobayashi, A. Ueda and Y. Nakahara, *Preparation of Catalysts*, ed. V. G. Poncelet *et al.*, Elsevier, Amsterdam, 1991, p. 695.
6 H. Sakurai and M. Haruta, *Catal. Today*, 1996, **29**, 361.
7 D. C. Grenoble, M. M. Estadt and D. F. Ollis, *J. Catal.*, 1981, **67**, 90.
8 H. Sakurai and M. Haruta, *Appl. Catal. A*, 1995, **127**, 93.
9 H. Sakurai, S. Tsubota and M. Haruta, *Appl. Catal. A*, 1993, **102**, 125.
10 H. Sakurai, S. Tsubota and M. Haruta, *Science and Technology in Catalysis*, ed. Y. Izumi *et al*., Kodansha, Tokyo, 1995, p. 111.
11 S. Tsubota, A. Ueda, H. Sakurai, T. Kobayashi, and M. Haruta, *Environmental Catalysis*, ed. J. N. Armor, American Chemical Society, Washington DC, 1994, p. 420.

*Received, 9th September 1996; Com. 6/06192C*

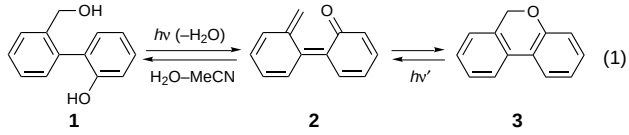
# Photocyclization of a 1,1′-bisnaphthalene: planarization of a highly twisted biaryl system after excited state ArOH dissociation

**Yijian Shi and Peter Wan***

*Department of Chemistry, Box 3065, University of Victoria, Victoria, British Columbia, Canada V8W 3V6*

**Photolysis of the highly twisted 1,1′-bisnaphthalene 6 gives the much more planar dinaphthopyran 10 with high quantum yield (Φ = 0.17) in aqueous MeCN, demonstrating that the expected enhanced electronic communication between the connected aromatic rings of biaryls in $S_1$ is sufficient to drive thermally unfavourable reactions requiring initial planarization of these biaryl systems.**

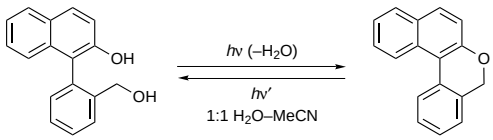
Twisted ground state structures of biphenyls and biaryls in general become much more planar when electronically excited.[1] However, this phenomenon has been utilized only on a limited basis to design or induce new photochemistry.[2] We demonstrated several years ago that photolysis of twisted (dihedral angle of 72°) 2-(2′-hydroxyphenyl)benzyl alcohol **1** in aqueous solution or in 100% MeCN gave the essentially planar 5*H*-dibenzo[*b*,*d*]pyran **3** *via* the proposed *o*,*o*′-biphenyl quinone methide **2** with high quantum efficiency (Φ up to 0.5) [eqn. (1)].[2c,d] We wondered whether the reaction could be




**1** **2** **3** (1)

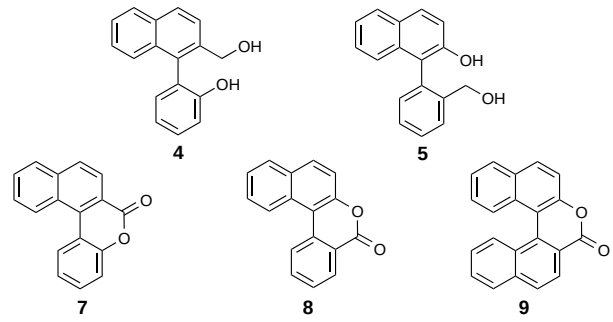
extended to binaphthyls and related compounds since large biaryls are of interest in a variety of areas including supramolecular chemistry where photoflexible systems are useful as photoswitches,[3] and as ligands in catalysis design.[4] Since 1,1′-binaphthyls are more twisted than biphenyls in general due to the additional steric interactions from introduction of two additional benzene rings, the notion that electronically excited binaphthyls can undergo extensive twisting to a more planar form even under these additional constraints would be relevant chemical information for use in supramolecular chemistry where large torsional motions are of intrinsic value in molecular switching.

Biarylmethyl alcohols **4**–**6** were made *via* LAH reduction of the corresponding lactones **7**–**9**, which were synthesized according to method of Bringmann *et al*.[5] All of **4**–**6** were smoothly converted to their corresponding pyrans on photolysis in MeCN or aqueous MeCN at 254 nm [*e.g.* eqn. (2)].† Shown




**6** **10** (2)

in Fig. 1 is the UV–VIS spectra for conversion of **6** to pyran **10** in 1 : 1 $H_2O$–MeCN at 254 nm showing the clean conversion to almost 100% **7**, with Φ = 0.17. Photolysis of the pyran **10** at > 350 nm resulted in > 50% conversion back to **6** illustrating the reversibility of the photoreaction. Although reaction of **5** was clean and reversible, the quantum yield for cyclization (Φ ≈ 0.04) was substantially lower than observed for **4** and **6** (*vide infra*). Molecular mechanics calculations of **5** and **6** and an X-ray crystal structure‡ of **4** showed that these biaryls are highly twisted with dihedral angles approaching 90°. However, the corresponding pyran products are much more planar. For example, the dihedral angle for **10** (the most non-planar of the pyrans products) is 37° from X-ray crystallography.‡ Thus, these photocyclizations involve a very substantial twisting motion to planarity on the excited state surface. Moreover, the photoreversibility of the reaction shows that there is an equally substantial twisting motion out of planarity in the ring opening reaction, which formally requires conrotatory motion of the orbitals involved (a photochemically induced electrocyclic ring opening). Indeed, the degree of twisting motion displayed in these systems on photolysis approach those observed for *cis*–*trans* photoisomerization of alkenes.




**4** **5** **7** **8** **9**

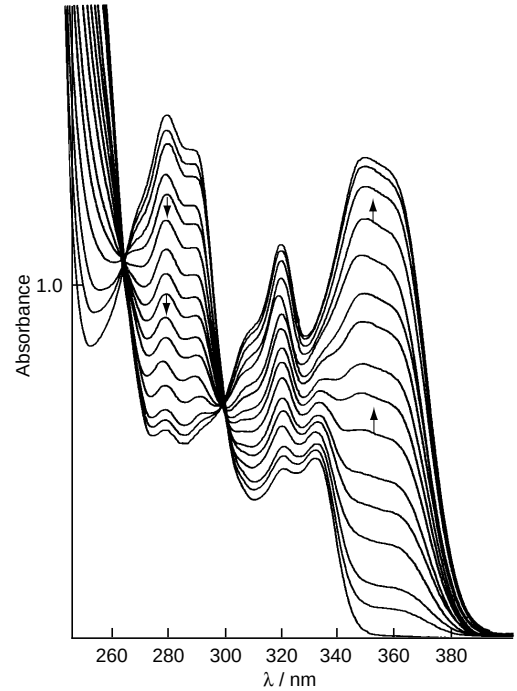
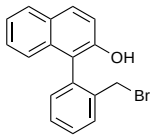



**Fig. 1** UV–VIS traces of conversion of **6** to **10** on photolysis of at 254 nm in 1 : 1 $H_2O$–MeCN. Each trace taken after about 5–20 s irradiation in a UV cuvette.

Bromide derivative **11** was photolyzed in 1 : 1 $H_2O$–MeCN and gave **10** in > 90% yield ($\Phi \approx 0.35$) along with a dramatic decrease in the pH of the aqueous solution (from pH 7 to 2.6) indicating that these binaphthyl systems can also photo release strong acid concurrent with geometric change [eqn. (3)]. The



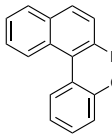

**11**

$$\xrightarrow[\text{1:1 } H_2O\text{–MeCN}]{h\nu} \mathbf{10} + \text{HBr} \qquad (3)$$

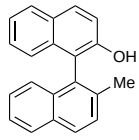
additional fact that **11** was found to be thermally stable to 125 °C makes these systems potentially useful for the photodeprotection of esters and related functional groups by making the required naphthylmethyl derivatives from bromide **11**.

The twisting motion of biaryls towards planarity on the excited state surface has been generally rationalized[2a,6] by noting that the coefficients of the two carbons joining the two aryl rings in the LUMO have the same sign whereas they have opposite sign in the HOMO. Thus population of the LUMO on electronic excitation causes an increase in the π-bond strength joining the two aryl groups; hence a twisting motion to a more planar structure.

However, simple twisting of the two aryl rings to a more planar geometry on electronic excitation does not completely explain why these compounds cyclize and lose water. Additional chemical steps are required, *viz.* dissociation of the hydroxynaphthalene (or phenol) proton and loss of hydroxide ion from the arylmethyl (benzylic) position to form the corresponding biaryl naphthoquinone methide. In our first report of this type of reaction[2c] [eqn. (1)], we were not able to address whether twisting took place before proton dissociation from the phenol or *vice versa*, or that they took place together, although it was clear that the phenolate ion in the excited state was the reactive species. We now report that a better understanding is available for **4**–**6**. We have studied the fluorescence behaviour of model compounds **12** and **13** (for **4** and **6**, whose fluorescence were too weak for proper study due to their high photoreactivity for cyclization) and **5** (which is sufficiently fluorescent), and found that there is a correlation




**12**




**13**

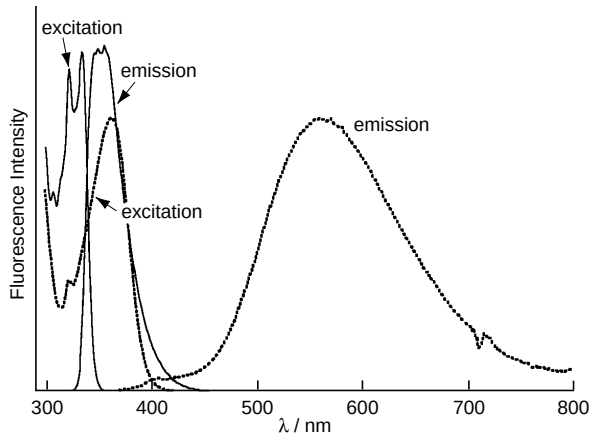



**Fig. 2** Fluorescence excitation and corrected emission spectra of **13** in 100% MeCN (solid lines) and in 1 : 1 MeCN–0.01 mol $dm^{-3}$ NaOH (dashed lines). The measured Stokes shifts are 1700 and 7500 $cm^{-1}$ for the protonated (ArOH) and naphthoate ($ArO^-$) forms of **13**, respectively.

between the amount of observed Stokes shift (a useful measure of the degree of change in geometry between the Franck–Condon and the fluorescent states)[1] and the quantum efficiency of cyclization.

All of **5**, **12** and **13** display only a modest Stokes shift in 100% MeCN (*ca.* 1700 $cm^{-1}$, Fig. 2) where the fluorescence is from the protonated form. This implies that the degree of twisting of the excited protonated phenol or naphthol is insignificant. However, when their fluorescence spectra were taken in pH 12 (excitation of the phenolate or naphthoate forms), the Stokes shifts of the emission from the deprotonated forms were substantial for **12** and **13** (*ca.* 7500–8000 $cm^{-1}$) (Fig. 2) but much less for **5** (*ca.* 3000 $cm^{-1}$). We can conclude that these systems twist to become more planar only after (adiabatic) excited state deprotonation. That is, the mechanism for cyclization must involve initial adiabatic deprotonation from the twisted (Franck–Condon) structure followed by twisting to a more planar form, which then loses hydroxide ion from the arylmethyl position to generate the required (naphtho)quinone methide intermediate. The much lower quantum yield of cyclization observed for **5** is most likely due to the lesser degree in which this system is capable of twisting (to the more planar form) after deprotonation although the exact reasons for this is unknown at this time. A possible explanation we are currently investigating is that there is a dependence of the degree of twisting and the amount of available electron density to the $ArCH_2OH$ moiety from the electronically excited $ArO^-$ ring. We believe the above new results and improved understanding of the reaction mechanism will help us design supramolecular systems which can incorporate these chromophores for use as photoactivatable systems.

We acknowledge support of this research by the Natural Sciences and Engineering Research Council (NSERC) of Canada.

## Footnotes

† Oxygen had no measurable effect on these photocyclizations. The fluorescence results reported here and previously[2c,d] indicate that these are most likely reactions from the singlet excited state. Although we have not been able to directly observe the proposed *o,o′*-biaryl quinone methides by nanosecond laser flash photolysis (presumably due to their very short lifetimes), we have observed[2d] similar quinone methides when they cannot cyclize to the corresponding pyrans. This argues in favour of a photocyclization mechanism *via* such intermediates rather than, for example, simple displacement of the hydroxide of the methylene carbon by the phenol oxygen.

‡ Details of the X-ray crystal structure analyses will be published in due course.

## References

1 T. C. Werner, in *Modern Fluorescence Spectroscopy*, vol. 2, ed. E. Wehry, Plenum, New York, 1976; I. B. Berlman, *J. Chem. Phys.*, 1970, **74**, 3085, I. B. Berlman, *Handbook of Fluorescence Spectra of Aromatic Molecules*, 2nd ed, Academic, New York, 1971.

2 (*a*) H. E. Zimmerman and D. S. Crumrine, *J. Am. Chem. Soc.*, 1972, **94**, 498; (*b*) K. Mislow and A. J. Gordon, *J. Am. Chem. Soc.*, 1963, **85**, 3521; (*c*) C.-G. Huang, K. A. Beveridge and P. Wan, *J. Am. Chem. Soc.*, 1991, **113**, 7676; (*d*) Y. Shi and P. Wan, *J. Chem. Soc., Chem. Commun.*, 1995, 1217.

3 V. Balzani and F. Scandola, *Supramolecular Photochemistry*, Ellis Horwood, New York, 1991, ch. 7.

4 G. Bringmann, R. Walter and R. Weirich, *Angew. Chem., Int. Ed. Engl.*, 1990, **29**, 977.

5 G. Bringmann, T. Hartung, L. Göbel, O. Schupp, C. L. J. Ewers, B. Schöner, R. Zagst, K. Peters, H. G. von Schnering and C. Burschka, *Liebigs Ann. Chem.*, 1992, 2245; G. Bringmann, B. Schöner, O. Schupp, K. Peters, E.-M. Peters and H. G. von Schnering, *Liebigs Ann. Chem.*, 1994, 91.

6 A. Imamura and R. Hoffmann, *J. Am. Chem. Soc.*, 1968, **90**, 5379.

*Received, 10th September 1996; Com. 6/06487F*

# Magnetic properties of charge-transfer complexes based on TEMPO radicals

**Shin'ichi Nakatsuji,[a] Atsushi Takai,[a] Kazuyoshi Nishikawa,[b] Yukio Morimoto,[b] Noritake Yasuoka,[b] Kazuya Suzuki,[c] Toshiaki Enoki[d] and Hiroyuki Anzai[a]**

[a] *Department of Material Science, Faculty of Science, Himeji Institute of Technology, Kanaji 1479-1, Kamigori, Hyogo 678-12, Japan*
[b] *Department of Life Science, Faculty of Science, Himeji Institute of Technology, Kanaji 1479-1, Kamigori, Hyogo 678-12, Japan*
[c] *Department of Chemistry, Faculty of Engineering, Yokohama National University, 156 Tokiwadai, Hodogaya-ku, Yokohama 240, Japan*
[d] *Department of Chemistry, Faculty of Science, Tokyo Institute of Technology, Meguro-ku, Tokyo 152, Japan*

**TEMPO (2,2,6,6-tetramethylpiperidinyloxy) radical 1 and its derivatives 2–5 are found to form charge-transfer complexes with some acceptors such as $TCNQF_4$ (2,3,5,6-tetrafluoro-7,7,8,8-tetracyanoquinodimethane) or DDQ (2,3-dichloro-5,6-dicyano-1,4-benzoquinone) being isolated as solid substances.**

The development of new molecular magnetic materials, especially organomagnetic materials is current interest and a number of compounds carrying stable radicals as the key building blocks have been prepared and their magnetic behaviour has been elucidated in recent years.[1] In the course of our study for the development of new organomagnetic compounds, we have been interested in preparing some donor or acceptor molecules carrying stable radicals, especially TEMPO radicals, and the charge-transfer (CT) complexes derived therefrom to build up and to arrange the spins in the solid state/crystal structures.[2] Here we report that some TEMPO radicals themselves are able to form CT complexes with appropriate acceptors, that is to say, TEMPO radicals can act as donors to form CT complexes which can be isolated as solids.

When TEMPO radical **1** was treated with an equimolecular amount of $TCNQF_4$ in acetonitrile, the resulting deep-blue solid was confirmed by elemental analysis to be the 1 : 1 complex **6**. Moreover, bands corresponding to the $TCNQF_4$ radical anion, at 856 and 753 nm in acetonitrile were clearly observed in the visible absorption spectrum of **6** and the lower wavenumber of νCN (νCN 2190 $cm^{-1}$) observed in its IR spectrum compared with the neutral acceptor ($TCNQF_4$: νCN 2237 $cm^{-1}$) was also consistent with the formation of the CT complex **6** (Table 1).† To our knowledge, this is a rare example of a isolated charge-transfer complex in which a radical acts as a donor (Scheme 1).[3,4]‡

**Table 1** Summary of magnetic data of **1**–**5** as well as complexes **6**–**15**

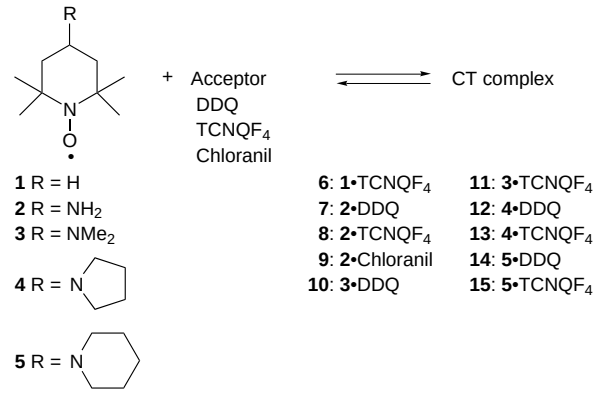
| Compound | Magnetic interaction | $\theta^a$/K |
|---|---|---|
| **1** | antiferromagnetic[b] | −3.0[b] |
| **2** | antiferromagnetic | −0.2 |
| **3** | antiferromagnetic | −7.5[c] |
| **4** | antiferromagnetic | −6.3[c] |
| **5** | ferromagnetic | 0.5 |
| **6** | weak susceptibility | — |
| **7** | ferromagnetic | 0.1 |
| **8** | antiferromagnetic | −0.1 |
| **9** | ferromagnetic | 0.1 |
| **10** | antiferromagnetic | −0.4 |
| **11** | antiferromagnetic | −1.8 |
| **12** | antiferromagnetic | −1.1 |
| **13** | antiferromagnetic | −0.3 |
| **14** | antiferromagnetic | −6.2[c] |
| **15** | antiferromagnetic | −0.9 |

[a] Fitting for Curie–Weiss rule. [b] *Cf.* ref. 5 in text. [c] Short-range order is suggested from the susceptibility data in this case.

A magnetic susceptibility measurement on **6** was carried out on a polycrystalline sample using a SQUID susceptometer in the temperature range 2–300 K. It was found from the data that while TEMPO **1** itself shows antiferromagnetic interactions with a Weiss constant θ of −3.0 K,[5] a drastic decrease of magnetic susceptibility was observed in complex **6** suggesting a strong tendency for singlet formation between the radical centres.§

An X-ray analysis of single crystals of **6** grown by recrystallization from acetone gave confirmative structural elucidation of the complex as shown in Fig. 1.¶ Relatively small bond alternation in each $TCNQF_4$ molecule of the complex **6** suggests the delocalization of π electrons on the whole molecule upon formation of the radical anion (Fig. 1, upper).[6] It is apparent from Fig. 1 that both donors and acceptors form segregated column structures along the *a*-axis with a zigzag structure in the latter. The following features are also disclosed from the analysis. (*i*) The nearest O···O distance found is that between donor molecules in the column which amounts to 6.99 Å. (*ii*) The interplanar stacking distance between $TCNQF_4$ molecules is *ca*. 6.99 Å. Partial insertion with some slipping of another $TCNQF_4$ molecule results in the zigzag column structure. (*iii*) The nearest distance between oxygen of a donor molecule and a $TCNQF_4$ molecule is that of O(1)···F(2) of 2.78 Å (Fig. 1, upper), somewhat shorter than the sum of the van der Waals radii of each atom. The magnetic behaviour of the complex would then be interpreted as follows: the charge accepted by the $TCNQF_4$ species is from TEMPO radicals which leads to the formation of oxoammonium ions, *i.e.* TEMPO is converted into $TEMPO^+$ resulting a singlet while the loss of the spins of $TCNQF_4$ radical anions is supposed to be derived from their columnar structure as described above.

Following the results obtained above, we then prepared a series of similar CT complexes derived from 4-amino-TEMPO




**Scheme 1**

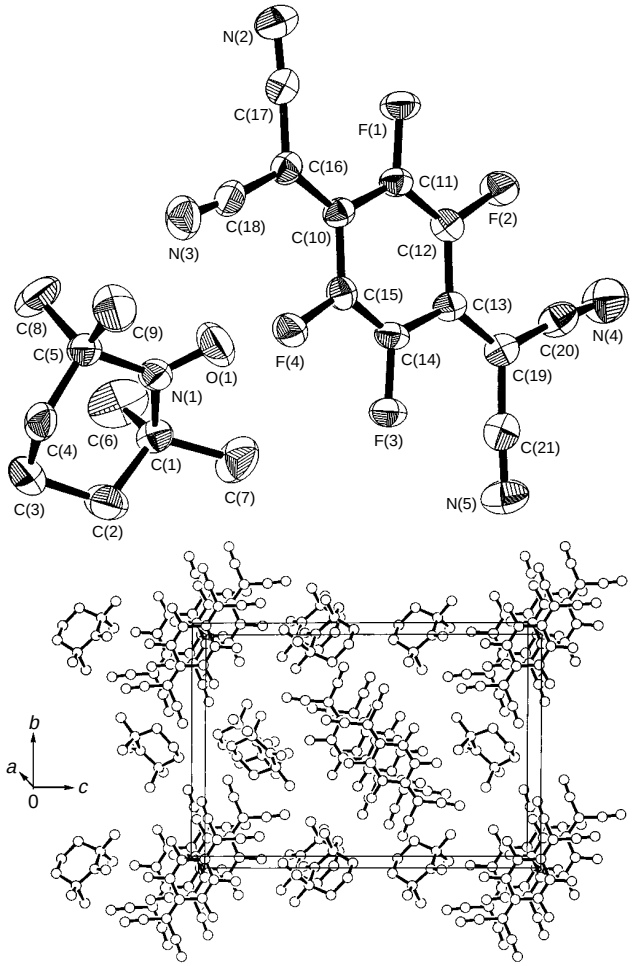



**Fig. 1** Upper: structure of **6**. Lower: crystal structure of **6** viewed almost along the *a* axis. Selected interatomic distances (Å) and angles (°): O(1)–N(1) 1.195(5), N(1)–C(1) 1.526(6), N(1)–C(5) 1.531(6), O(1)–N(1)–C(1) 117.6(5), O(1)–N(1)–C(5) 117.2(5), C(1)–N(1)–C(5) 125.2(5), C(10)–C(11) 1.423(6), C(11)–C(12) 1.350(7), C(12)–C(13) 1.418(7), C(13)–C(14) 1.416(7), C(14)–C(15) 1.340(7), C(10)–C(15) 1.414(7), C(10)–C(16) 1.407(7), C(13)–C(19) 1.398(7).

**2** and its alkylated derivatives **3**–**5** (Scheme 1) having stronger electron-donating ability than **1**.[4]‖ The latter radicals (**3**–**5**) were prepared by the reductive amination of 4-oxo-TEMPO with alkyl amines using sodium cyanoborohydride as a reducing reagent and those radicals **2**–**5** gave complexes with weaker acceptors than $TCNQF_4$, *e.g.* DDQ or chloranil. As summarized in Table 1, acceptor-dependent antiferromagnetic or ferromagnetic interactions were suggested in each complex on the basis of their Weiss constants, *e.g.* for the complexes prepared from 4-amino-TEMPO **2**, weak ferromagnetic interactions were suggested in the DDQ complex **7** or chloranil complex **9** ($\theta$ = 0.1 K for both) while antiferromagnetic interactions were suggested in the $TCNQF_4$ complex ($\theta$ = −1.0 K). Among other complexes prepared from 4-alkylated amino-TEMPO derivatives **3**–**5**, short-range antiferromagnetic spin order in the very low-temperature region was suggested for the complex **14** as depicted in Fig. 2.

In summary, we have prepared a series of CT complexes **6**–**15** based on TEMPO radicals having variable and acceptor-dependent magnetic behaviour. The TEMPO–$TCNQF_4$ complex **6** was structurally elucidated by X-ray analysis to rationalize its low magnetic susceptibility.

Because the CT complexes could be easily prepared from simple nitroxyl radicals and acceptors and because the finding described above may be possibly applied to a variety of hitherto known nitroxyls, it would be expected to enrich sources of novel

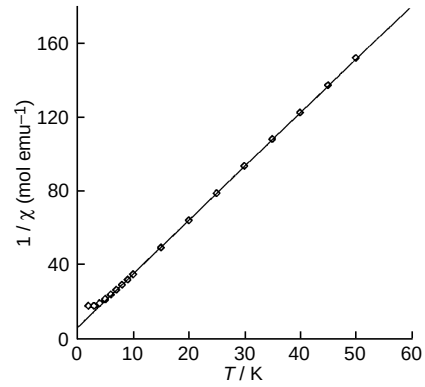



**Fig. 2** Temperature dependence of 1/χ below 50 K for complex **14**. The straight line was drawn to show deviation from Curie–Weiss behaviour in the lower temperature region.

organomagnetic materials and further studies to prepare related complexes and their single crystals are now under way.

This research was supported by a Grant-in-Aid for Scientific Research on Priority Area 'Molecular Magnetism' (No. 228/04242104) from the Ministry of Education, Science and Culture, Japan and a Scientific Research Grant from The Foundation of Himeji Institute of Technology, which are gratefully acknowledged.

## Footnotes

† In the EPR spectrum of **6**, triplet absorptions due to the nitroxy radical were observed in acetone solution, suggesting partial dissociation of the complex in the solution.

‡ Independently and almost at the same time, Sugawara and coworkers have prepared and isolated a charge-transfer complex based on *p*-dimethylamino-nitronyl nitroxide and chloranil.

§ The Curie constant *C* for **6** was very low with a value of $1.57 \times 10^{-3}$ emu K $mol^{-1}$.

¶ *Crystal data* for **6**: $C_{21}H_{18}F_4N_5O$, $M$ = 432.40, monoclinic, space group $P2_1/n$ (no. 14), $a$ = 6.985(2), $b$ = 14.407(4), $c$ = 20.427(3) Å, β = 93.70(2)° ($T$ = 23.0 °C), $U$ = 2051.4(7) Å$^3$, $Z$ = 4, $D_c$ = 1.400 g $cm^{-3}$, $F(000)$ = 892.00. 3482 measured reflections, 3188 unique reflections, collected on a Rigaku AFC5R four-circle diffractometer with monochromated Cu-Kα radiation (1.541 78 Å). Final conventional $R$ factor = 0.059 for 1762 independent reflections with $F_o > 3\sigma(F_o)$ and 280 parameters. Atomic coordinates, bond lengths and angles, and thermal parameters have been deposited at the Cambridge Crystallograpic Data Centre (CCDC). See Information for Authors, Issue No. 1. Any request to the CCDC for this material should quote the full literature citation and the reference number 182/235.

‖ The first oxidation potentials of radicals **1**–**5** measured by cyclic voltammetry are ($E$/V *vs.* SCE in acetonitrile, 0.1 mol $dm^{-3}$ TBAP as supporting electrolyte, scan rate = 50 mV): **1**, 0.70; **2**, 0.68; **3**, 0.61; **4**, 0.56; **5**, 0.65.

## References

1 *Cf.* H. Iwamura, *Adv. Phys. Org. Chem.*, 1990, **26**, 179; O. Kahn, *Molecular Magnetism*, VCH, Weinheim, 1993; J. S. Miller and A. J. Epstein, *Angew. Chem., Int. Ed. Engl.*, 1994, **33**, 385.

2 For donors: S. Nakatsuji, S. Satoki, K. Suzuki, T. Enoki, N. Kinoshita and H. Anzai, *Synth. Met.*, 1995, **71**, 1819; S. Nakatsuji, N. Akashi, K. Suzuki, t. Enoki, N. Kinoshita and H. Anzai, *Mol. Cryst. Liq. Cryst.*, 1995, **268**, 153; for acceptors: S. Nakatsuji, N. Akashi, Y. Komori, K. Suzuki, T. Enoki and H. Anzai, *Mol. Cryst. Liq. Cryst.*, 1996, **279**, 73; S. Nakatsuji, N. Akashi, K. Suzuki, T. Enoki and H. Anzai, *J. Chem. Soc., Perkin Trans. 2*, 1996, 2555.

3 *Cf.* Y. Murata and N. Mataga, *Bull. Chem. Soc. Jpn.*, 1971, **44**, 354.

4 H. Sakurai, R. Kumai, A. Izuoka and T. Sugawara, presented at *The Vth International Conference on Molecular-based Magnets* (*ICMM 96*), Osaka, July, 1996, Abstract, p. 172, to be published.

5 C. Veyret and A. Balise, *Mol. Phys.*, 1973, **25**, 873.

6 T. Sugimoto, K. Ueda, M. Tsujii, H. Fujita, N. Hosoito, N. Kanehisa, Y. Shibamoto and Y. Kai, *Chem. Phys. Lett.*, 1996, **249**, 304.

*Received, 12th September 1996; Com. 6/06293H*

# Hydrothermal synthesis of an iron silicate with layered structure

**Ramesh B. Borade and Abraham Clearfield**

*Department of Chemistry, Texas A&M University, College Station, TX 77840, USA*

**A method is provided for the synthesis of a crystalline layered iron silicate using a particular reaction gel composition containing an organic directing agent and possessing significant quantities of iron (Si/Fe = 38.6) in trivalent oxidation state; the present layered iron silicate has a structure related to kenyaite and/or silica-X.**

Kenyaite is a hydrous sodium silicate mineral first found in the lake beds of Lake Magadi in Kenya.[1] Synthetic forms of similar silicates using potassium instead of sodium ions, with layered structures, were subsequently prepared.[2–5] Synthetic kenyaite has the chemical formula $K_2Si_{20}O_{41}{\cdot}xH_2O$. The intercalation behaviour of this material was used to establish its layered structure. The crystal structure of kenyaite remains unknown at present. The layered silicate, identified as silica-X, was first reported by Heidemann.[6] Silica-X was synthesized hydrothermally using silicic acid and KOH solution at 175 °C for 3–10 days,[6,7] Attempts made by Greenwood,[8] to synthesize silica-X using silicic acid and $Na^+$, $Mg^{2+}$ and $NH_4^+$ cations instead of $K^+$, were unsuccessful. However, the synthesis of silica-X using diaquat-4 halide[9] and of kenyaite using poly-(diethyldiallylammonium chloride)[5] as a structure-directing template is reported in the literature. Incorporation of Al in kenyaite or silica-X by synthetic routes was also achieved.[5,9] Comparison of X-ray powder diffraction patterns of silica-X with kenyaite suggests that these materials are closely related to each other. Here, we report the synthesis of an iron silicate with a kenyaite/silica-X type structure using hexamethyleneimine (HMI) as template.

A typical procedure to synthesize the iron containing layered silicate is as follows. Solution A was obtained by adding appropriate quantities of water and the nitrogen-containing template to a sodium silicate solution (27% $SiO_2$, 14% NaOH and 69% water, Aldrich). Solution B was prepared by dissolving iron(III) sulfate [$Fe_2(SO_4)_3{\cdot}5H_2O$, Fluka] in water. Then, solution B was added (dropwise addition) to A. The addition of the $Fe_2(SO_4)_3{\cdot}5H_2O$ solution is a crucial step. Slow addition produces a lemon-coloured solution and fast addition produced a red–brown mixture. When addition was complete, the mixture was stirred for another 20 min. Finally, conc. $H_2SO_4$ (98%, EM Science) was added to adjust the final pH of the mixture. The final mixture was a lemon-coloured turbid solution with the chemical formula: 20–40 $SiO_2$ : 1 $Fe_2O_3$ : 9.8 $Na_2O$ : 13.7 HMI : 1360 $H_2O$ : 9.8 $H_2SO_4$. This solution was then transferred into stainless-steel autoclaves of 300 ml capacity, which were heated at 150 °C for 15 days without stirring. The resultant solid product was recovered by filtration and washed with demineralized hot water. This product is denoted as as-made kenyaite. The Na-form of the sample was prepared by air calcination of the as-made sample at 540 °C for 4 h. This material was repeatedly ion-exchanged with 5 M ammonium chloride solution at 80 °C to obtain the $NH_4$-form of kenyaite. The H-form was obtained by calcination of the $NH_4$-form in air at 400 °C for 2 h. Using this procedure, highly crystalline iron silicate samples with input $SiO_2/Fe_2O_3$ ratios of 20–40 were obtained.

The X-ray powder diffraction pattern was obtained on a Rigaku Ru200 automated powder diffractometer using Cu-Kα radiation (λ = 1.5418 Å). The XRD pattern, presented in Fig. 1, is similar to kenyaite and or silica-X type materials. Scanning electron micrographs of the iron silicate (Fig. 2) show spherical

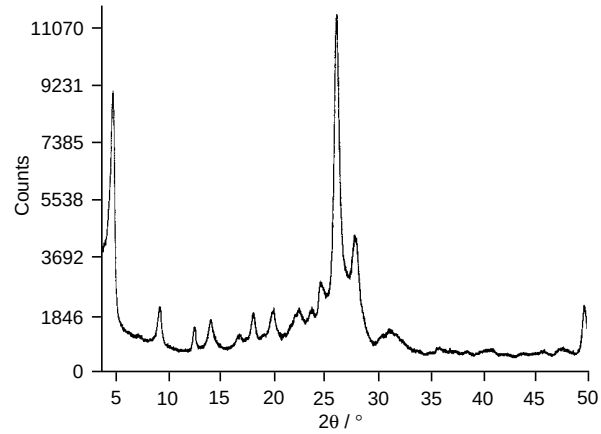



**Fig. 1** X-Ray powder diffraction pattern of iron-containing kenyaite (as-made)

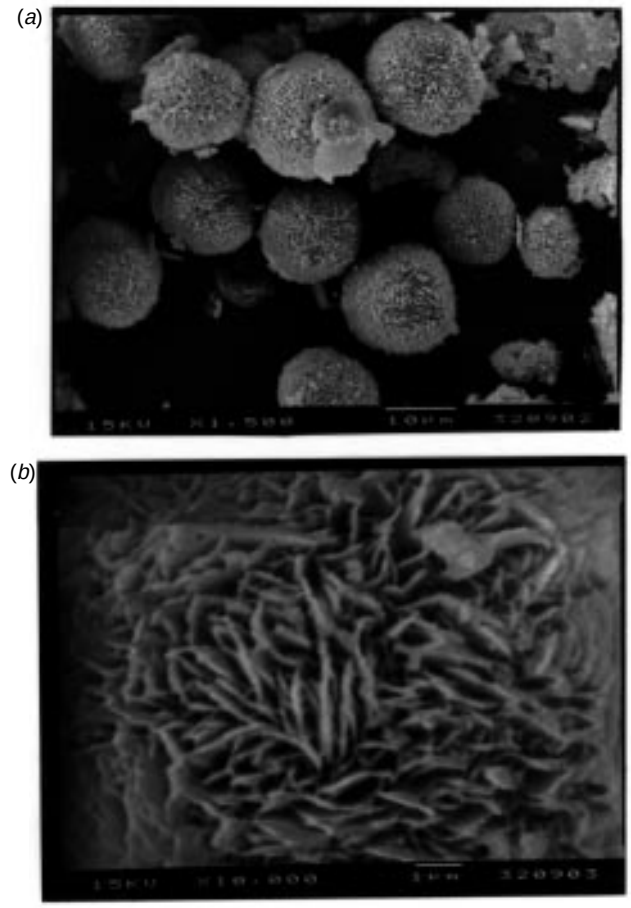



**Fig. 2** Scanning electron micrographs of iron-containing kenyaite at different magnifications

particles 5–15 μm in diameter. The spherical aggregates are made up of a variety of thin stacked crystals in rosette form. This platelet morphology is very similar to those of kenyaite[5] and ferrierite type materials.[10,11] After calcination at 540 °C for 4 h, the peak at 3.25 Å disappeared completely and all peaks were shifted towards lower *d* values. The relative shift in *d* values was significant for the first two peaks. For kenyaite, Eugster[1] indexed these two peaks as 001 and 002 reflections, assuming tetragonal symmetry. In as-synthesized iron silicate these 00*l* reflections appear at 20.2 and 10.1 Å and in the calcined sample at 17.6 and 8.8 Å. Similar observations have been made by Schwieger *et al.*[5] for kenyaite. TGA experiments were carried out using a DuPont (Model 951) thermal analyser. About 20 mg of the sample was placed in a quartz bucket and heated in a nitrogen–oxygen atmosphere at a heating rate of 10 °C $min^{-1}$. The TGA curve clearly showed three mass losses. The first step (25–200 °C) is due the desorption of water and the second (200–600 °C) and third steps (600–950 °C) are due to desorption/decomposition of the organic template and dehydroxylation of iron silicate, respectively. The (Na + organic)/(Si + Fe) ratio in as-made kenyaite is 0.073/1. The mass loss associated with each step was 4.7, 6.6 and 4.0%, respectively. That the third step is indeed due to dehydroxylation and not due to the residual carbon was confirmed by carrying out additional TGA experiments with $Na^+$ and $H^+$ forms of kenyaite containing no template. The chemical composition and sorption capacity of iron silicate are reported in Table 1. The constancy in the Si/Fe ratio before and after ion exchange indicates that Fe is not present in occluded form or in ion-exchangeable sites. Sorption data presented in Table 1 suggest that the iron silicate of the present study sorbs water as well as *n*-hexane in amounts 3–4 times greater than silica-X.[9] The measured $N_2$ BET surface area of the iron silicate was 170 $m^2$ $g^{-1}$.

The presence of most of the Fe in the trivalent oxidation state and indeed situated in the layered silicate framework position is confirmed by studying the O 1s XPS and EPR spectra of iron silicate. The surface Si/Fe ratio determined by XPS was 32.8 and by bulk chemical analysis 38.9 for the Na-form of the iron silicate indicating a somewhat inhomogeneous Fe distribution and/or the presence of a small amount of extraframework iron oxidic species on the surface of the sample. In addition, the O 1s XPS spectra (not shown) gave a main peak at 532.4 eV and a shoulder at 530.7 eV corresponding to oxygen species associated with the silicate framework and extraframework iron oxidic species, respectively. The relative area contribution due to the shoulder peak to the main O 1s peak was *ca*. 13%. When the Na-form of the iron silicate was exchanged with $NH_4Cl$ the relative contribution of the O 1s shoulder peak to the main peak reduced to 7%, indicating that there are some iron oxidic species that can be washed away by $NH_4^+$ treatment. Since the Na/Fe ratio was close to 1 in the Na-form of the material, the possibility of the presence of Fe in an ion-exchangeable site is less likely. It is obvious that these excess Fe species must be occluded iron oxidic/hydroxidic species. The formation of such small amounts of extraframework iron oxidic species during the synthesis of iron-containing zeolites was previously observed.[12–14] X-Band EPR spectra were obtained at room temperature using a Bruker ER-200 D spectrometer. The spectrum shown in Fig. 3 shows four signals at $g = 2.0$, *ca*. 2.9, 4.3 and 9.6. The signal at $g = 4.3$ in conjunction with the signal at $g = 9.6$ is commonly assigned to incorporation of $Fe^{3+}$ on a strongly distorted rhombic site.[15–18] The signal at $g = 2.8$ has been assigned to Fe as iron oxidic or hydroxidic phases. This is consistent with the O 1s XPS results. The signal at $g = 2.0$ may be due to framework or non-framework $Fe^{3+}$ species.[15] These two species can be distinguished by EPR by conducting dehydration–rehydration studies with the same sample. Thus, an EPR study in combination with XPS clearly shows the presence of most of the $Fe^{3+}$ in framework positions. The FTIR spectra of chemisobed $NH_3$ revealed the formation of $NH_4^+$ ions (*ca*. 1460 $cm^{-1}$) with Brønsted-acid sites indirectly suggesting that Fe is present in the framework position.[19]

To summarize, synthesis of an iron silicate with a kenyaite and/or silica-X type material using a hexamethyleneimine template is reported.

The authors acknowledge with thanks the R. A. Welch Foundation for partial support of this study under grant No. A673.

**Table 1** Chemical composition and sorption capacity of iron silicate in various forms

| Sample | Template (mass%) | Mass% Na | Si | Fe | Mole ratio Na/Fe | Si/Fe | Mass% Water | *n*-Hexane |
|---|---|---|---|---|---|---|---|---|
| As-made | 6.6 | 0.72 | 36.88 | 1.77 | 0.99 | 38.6 | — | — |
| Na Form | — | 0.80 | 37.20 | 1.91 | 0.98 | 38.9 | 5.86 | 3.90 |
| H Form | — | 0.05 | 37.10 | 1.85 | 0.06 | 40.1 | 5.67 | 4.00 |

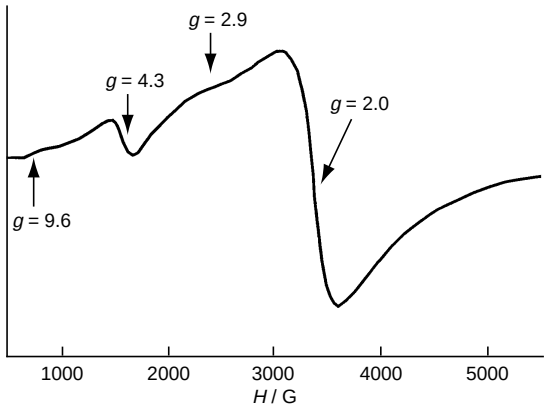



**Fig. 3** Room-temperature EPR spectrum of as-made iron-containing kenyaite

## References

1 H. Eugster, *Science*, 1967, **157**, 1177.
2 G. Lagaly and K. Beneke, *Am. Mineral.*, 1975, **60**, 642.
3 R. K. Iler, *J. Colloid Sci.*, 1964, **19**, 648.
4 W. Schwieger, D. Heidemann and K. H. Bergk, *Rev. Chim. Mineral.*, 1985, **22**, 639.
5 W. Schwieger, D. Freude, P. Werner and D. Heidemann, *Synthesis of Microporous Materials*, ed. M. L. Occelli and H. Robson, Van Nostrand Reinhold, New York, vol. 2, ch. 11, p. 229.
6 A. Heidemann, *Beit. Mineral. Petrogr.*, 1964, **10**, 242.
7 C. Frondel, *Am. Mineral.*, 1979, **64**, 799.
8 R. Greenwood, *Am. Mineral.*, 1967, **52**, 1662.
9 E. W. Valyocsik, *US Pat.*, 4 632 815, 1986.
10 R. B. Borade and A. Clearfield, *Zeolites*, 1994, **14**, 458.
11 L. Schreyeck, P. Caullet, J.-C. Mougenel, J.-L. Guth and B. Marler, *J. Chem. Soc., Chem. Commun.*, 1995, 2187.
12 R. B. Borade and A. Clearfield, *Chem. Commun.*, 1996, 2267.
13 R. B. Borade, *Zeolites*, 1987, **7**, 398.
14 R. B. Borade, A. Adnot and S. Kaliaguine, *Zeolites*, 1991, **11**, 710.
15 D. Goldfarb, M. Bernardo, K. G. Strohmaier, D. E. W. Vaughan and H. Thomann, *J. Am. Chem. Soc.*, 1994, **116**, 6344.
16 B. D. McNicol and G. T. Pott, *J. Catal.*, 1972, **25**, 223.
17 E. G. Derouane, M. Mestagh and L. Vieloye, *J. Catal.*, 1972, **33**, 69.
18 A. Bruckner, R. Luck, W. Weiker, B. Fahlke and H. Mehner, *Zeolites*, 1992, **12**, 380.
19 R. B. Borade and A. Clearfield, unpublished work.

*Received, 16th September 1996; Com. 6/06343H*

# Stereoselective synthesis of 2-phosphino-1-zirconaindenes and related 2-phosphinophospholes and stiboles

**Y. Miquel,[a] A. Igau,[a] B. Donnadieu,[a] J.-P. Majoral,*[a] L. Dupuis,[b] N. Pirio[b] and P. Meunier*[b]**

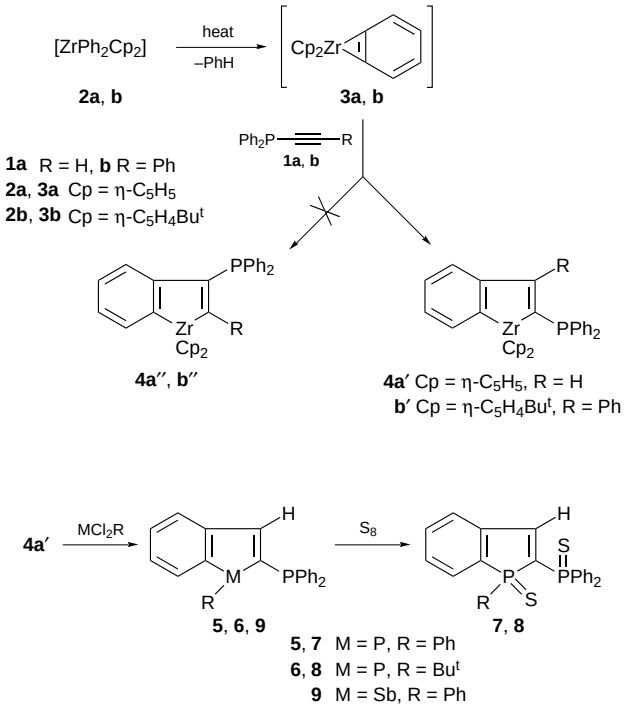
[a] *Laboratoire de Chimie de Coordination du CNRS, 205 route de Narbonne, 31077 Toulouse Cedex, France*
[b] *Laboratoire de Synthèse et d'Electrosynthèse Organométalliques associé au CNRS (UMR 5632), Université de Bourgogne, Faculté des Sciences Gabriel, 6 boulevard Gabriel, 21000 Dijon, France*

**2-Phosphinophospholes and stiboles are prepared from the reaction of benzynezirconocene with alkynylphosphines followed by addition either of dichlorophosphines or a dichlorostibene.**

The development of new and practical methods of stereoselective synthesis of main-group element derivatives is currently among the major objectives of a number of research groups throughout the world. Our ongoing investigations concern the study of interactions between group IV element and main-group element species[1] and are focused on the discovery of new methodologies of ring formation, opening or expansion but also on the preparation of ligands which have been regarded as laborious to prepare by conventional means.

The present report deals with an efficient synthesis of substituted zirconaindene compounds and their use as starting reagents for the formation of a variety of 2-phosphinophospholes and of a 2-phosphinostibole. Indeed phospholes[2] continue to attract considerable attention because of their use in different fields (*e.g.* catalysis, coordination chemistry) and therefore there is a need to diversify ways of preparation of these useful phosphorus heterocycles as well as the nature of these derivatives. To the best of our knowledge only one report described the preparation of a 2-thiophosphinophosphole which was obtained *via* a sequence of reactions involving metallation of the 1-phenyl-3,4-dimethyl-2-thiophosphole followed by addition of diphenylchlorophosphane.[3]

Treatment of the alkynylphosphine **1a** with [$ZrPh_2(\eta\text{-}C_5H_5)_2$] **2a** in benzene at 80 °C for 6 h leads to the formation of a phosphinozirconaindene **4a** arising from insertion of the carbon–carbon triple bond of **1a** into a zirconium–carbon bond of the transient benzyne zirconocene **3a**. The reaction gave rise to only one phosphorus species as indicated by $^{31}P$ NMR spectroscopy (**4a**, δ 6.9) (Scheme 1). **4a** was further characterized by $^{1}H$ and $^{13}C$ NMR† but the spectroscopic data did not distinguish between the two possible structures for **4a**: the 2-phosphinozirconaindene form **4a′** or the 3-phosphinozirconaindene form **4a″**. In order to have a better knowledge of the structure of **4a**, exchange reactions with phenyl or *tert*-butyl dichlorophosphanes were attempted. Addition of these dichlorophosphanes $RPCl_2$ to a solution of **4a** in thf afforded the phosphinophosphol derivatives **5** (R = Ph) or **6** (R = $Bu^t$) (Scheme 1). $^{31}P$ NMR spectra exhibit as expected two doublets [**5**, δ −14 ($PPh_2$), 10.6 (PPh); **6**, δ −12 ($PPh_2$), 3.7 ($PBu^t$)] with a large $^{2}J_{PP}$ of 50 Hz for **5** and 52 Hz for **6**. Compounds **5** and **6** were fully characterized as their disulfide adducts **7** and **8** {**7**, δ($^{31}P$) 39.2 [$P(S)Ph_2$], 51.4 [P(S)Ph], $^{2}J_{PP}$ 24.7 Hz; **8**, δ ($^{31}P$) 38.9 [$P(S)Ph_2$],† 78.6 [$P(S)Bu^t$], $^{2}J_{PP}$ 24.9 Hz}. Confirmation of the identity of **8** was achieved by a single-crystal X-ray study‡ which shows that the 2- and not the 3-substituted thiophosphole




**Scheme 1**

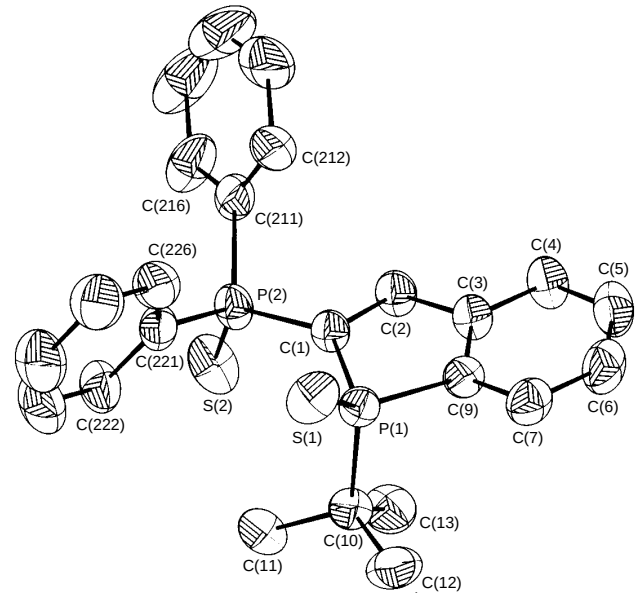



**Fig. 1** Molecular structure of **8** with crystallographic numbering scheme. Selected bond lengths (Å) and angles (°): P(1)–C(1) 1.831(3), P(1)–C(9) 1.814(3), C(1)–C(2) 1.340(4), C(2)–C(3) 1.468(4), C(3)–C(9) 1.391(4), P(2)–C(1) 1.804(3); C(1)–P(1)–C(9) 91.4(1), P(1)–C(1)–C(2) 109.2(2), P(1)–C(1)–P(2) 130.7(2).

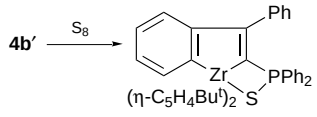
was formed. A molecule of **8** is shown in Fig. 1 and important bond lengths and angles are summarized.

Therefore these results clearly demonstrate that the 2-phosphinozirconaindene form **4a′** is selectively prepared when the acetylenic phosphane **1a** is treated with the benzynezirconocene **3a**.

A similar exchange reaction involving **4a′** and phenyldichlorostibene led to the formation of the corresponding 2-phosphinostibole **9** [δ ($^{31}$P) −2] (Scheme 1).

Remarkably such a stereoselective synthesis of 2-phosphinophospholes was also observed with more hindered acetylenic phosphanes such as **1b** and more hindered diphenylzirconocenes such as [$ZrPh_2(\eta\text{-}C_5H_4Bu^t)_2$] **2b**.

Indeed treatment of **1b** with **2b** affords exclusively the complex **4b′** [δ ($^{31}$P) −27.1]. Addition of $S_8$ to **4b′** led to the corresponding sulfide **10** [δ ($^{31}$P) 34.3]† (Scheme 2). Successful X-ray diffraction analysis of a single crystal of **10**‡ shows several interesting features (Fig. 2). First, it corroborates that, here also, the insertion reaction of the benzynezirconocene **3b** into the carbon–carbon triple bond of **1b** is stereoselective and leads to an α-substituted zirconaindene. Secondly the structure reveals an interaction between zirconium and sulfur. The Zr–S distance is 2.797(1) Å, and compares well, for example, with the Zr–S bond lengths found in compounds with a chelating dithiocarbamate ligand such as [$ZrCl(S_2CNEt_2)(\eta\text{-}C_5H_5)_2$] [Zr–S 2.635(2), 2.723(2) Å].[4,5]




**10**

**Scheme 2**

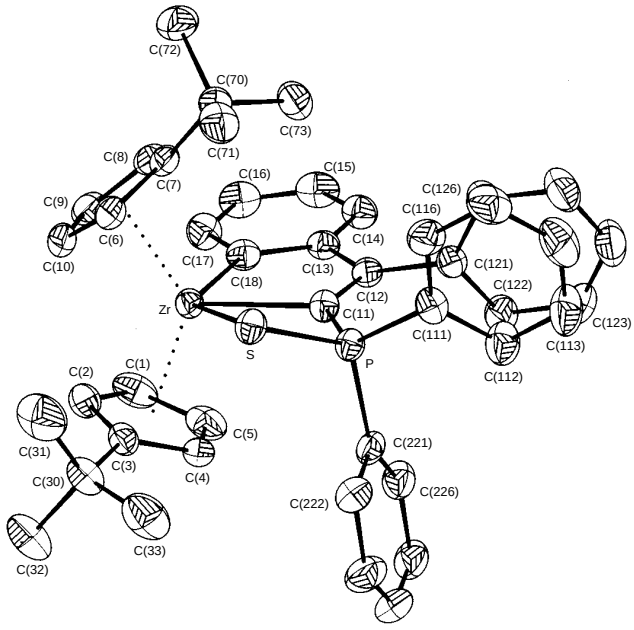



**Fig. 2** Molecular structure of **10** with crystallographic numbering scheme. Selected bond lengths (Å) and angles (°): P–S 2.005(1), P–C(1) 1.749(3), S–Zr 2.797(1), Zr–C(1) 2.490(4), Zr–C(8) 2.580(3), C(8)–C(3) 1.391(4), C(3)–C(2) 1.406(5), C(1)–C(2) 1.389(6), Zr–C(1)–P 106.4(2), Zr–S–P 85.4(4).

As a consequence the P–S bond length is found to be slightly larger [2.005(1) Å] than those generally observed for thiophosphoryl groups (1.93–1.95 Å). Indeed, the P–S bond length lies in between those of a single and a double P–S bond.

In conclusion, we have discovered a new and easy approach to the synthesis of 2-phosphinophospholes and a related 2-phosphinostibole. The remarkable stereoselectivity in these reactions arises from the strong interaction between the phosphorus lone pair in **1a** or **1b** and zirconium in **3a** or **3b**. Such an interaction has been already demonstrated to be the driving force in many reactions involving phosphorus and zirconium.[6]

## Footnotes

† Satisfactory analytical and/or spectral data were obtained for all new compounds. *Selected spectroscopic data* for compounds **8** and **10**. For **8**: DCIMS, *m/z* 439 ([M + 1]$^+$, 100%). NMR: $\delta_H$ ($C_6D_6$) 1.06 [d, $^3J$(HP) 18.2 Hz, 9 H, $CH_3$], 6.80–7.14 (m, 8 H, $CH_{Ph}$), 7.45 (m, 1 H, $CH_{Ph}$), 7.80 [dd, $^2J$(HP) 35.5, $^3J$(HP) 17.6 Hz, 1 H, CH], 8.18, 8.24, 8.50, 8.58 (m, 1 H, $CH_{Ph}$); $\delta_C$ 136.1 [dd, $^1J$(CP) 27.5, $^1J$(CP) 66.3 Hz, PCP], 138.1 [dd, $^1J$(CP) 78.9, $^3J$(CP) 3.2 Hz, CPBu$^t$], 140.9 [dd, $J$(CP) 17.2, $J$(CP) 22.0 Hz, CCPBu$^t$], 157.1 [dd, $^2J$(CP) 10.2, $^2J$(CP) 6.2 Hz, CH].

For **10**: DCIMS, *m/z* 727 ([M + 1]$^+$, 100%). NMR: $\delta_H$ ($C_6D_6$) 1.14 (s, 18 H, $C_5H_4Bu^t$), 5.75 (m, 4 H, $C_5H_4Bu^t$), 5.87, 6.16 (2 pseudo q, 4 H, $C_5H_4Bu^t$), 6.68 (m, 1 H, $CH_{Ar}$), 6.86–6.90 (m, 3 H, $CH_{Ar}$), 6.96–6.99 (m, 1 H, $CH_{Ar}$), 7.04–7.07 (m, 2 H, $CH_{Ar}$), 7.13–7.16 (m, 1 H, $CH_{Ar}$), 7.26–7.30 (m, 4 H, $CH_{Ar}$), 7.36–7.41 (m, 6 H, $CH_{Ar}$), 7.45–7.46 (m, 1 H, $CH_{Ar}$); $\delta_C$ 154.7 [d, $^2J$(CP) 6.3 Hz, ZrC=*C*Ph], 154.8 [d, $^1J$(CP) 33.3 Hz, ZrCP], 170.5 [d, $^3J$(CP) 5.5 Hz, ZrC=*C*], 194.2 [d, $^3J$(CP) 6.5 Hz, ZrC].

‡ Crystal data recorded on an IPDS STOE diffractometer using a φ rotation scan, Mo-Kα radiation was used (λ = 0.710 73 Å). For **8**: $C_{24}H_{24}P_2S_2{\cdot}0.5C_6H_6$, crystal dimensions 0.50 × 0.37 × 0.25 mm, monoclinic, space group *I*2/*a*, *a* = 19.156(4), *b* = 10.131(2), *c* = 28.391(6) Å, β = 109.50(2)°, *U* = 5193.8 Å$^3$; $D_c$ = 1.22 g cm$^{-3}$, μ = 3.29 cm$^{-1}$, number of reflections collected 16191, number of independent reflections 4100 ($R_m$ = 0.049), *R* = 0.0429, $R_w$ = 0.0445, GOF = 1.04.

For **10**: $C_{44}H_{35}PSZr$, crystal dimensions 0.60 × 0.50 × 0.50 mm, monoclinic, space group $P2_1/c$, *a* = 12.247(2), *b* = 19.746(4), *c* = 15.970(1) Å, β = 106.41(1)°, *U* = 3704.8 Å$^3$; $D_c$ = 1.31 g cm$^{-3}$, μ = 4.16 cm$^{-1}$, number of reflections collected 23721, number of independent reflections 4163 ($R_m$ = 0.047), *R* = 0.0314, $R_w$ = 0.0364, GOF = 0.8.

Atomic coordinates, bond lengths and angles, and thermal parameters have been deposited at the Cambridge Crystallographic Data Centre (CCDC). See Information for Authors, Issue No. 1. Any request to the CCDC for this material should quote the full literature citation and the reference number 182/340.

## References


1 See for example: J.-P. Majoral, M. Zablocka and A. Igau, *Chem. Ber.*, 1996, **129**, 879 and references therein; A. Mahieu, A. Igau, J. Jaud and J.-P. Majoral, *Organometallics*, 1995, **14**, 944.

2 For a review see: F. Mathey, *Chem. Rev.*, 1988, **88**, 429; A. N. Hughes, *Handbook of Organophosphorus Chemistry*, Marcel Dekker, New York, 1992, p. 483.

3 B. Deschamps and F. Mathey, *Organometallics*, 1992, **11**, 1411.

4 S. L. Buchwald, R. B. Nielsen and J. C. Dervan, *J. Am. Chem. Soc.*, 1987, **109**, 1590.

5 The covalent Zr–S bond length was found to be 2.514(2) Å in a germazirconaheterocycle: J. Bodiguel, P. Meunier, M. M. Kubicki, P. Richard and B. Gautheron, *Organometallics*, 1992, **11**, 1423.

6 M. Zablocka, A. Igau, N. Cénac, B. Donnadieu, F. Dahan, J.-P. Majoral and K. M. Pietrusiewicz, *J. Am. Chem. Soc.*, 1995, **117**, 8083; N. Cénac, M. Zablocka, A. Igau, J.-P. Majoral and A. Skowronska, *Organometallics*, 1996, **15**, 1208; N. Cénac, M. Zablocka, A. Igau, J.-P. Majoral and A. Skowronska, *J. Org. Chem.*, 1996, **61**, 796.



*Received, 30th September 1996; Com. 6/06672K*

# Anomalous role of molecular sieves 4A in the preparation of a binaphthol-derived active $\mu_3$-oxo titanium catalyst

**Masahiro Terada,[a] Yousuke Matsumoto,[a] Yoshiyuki Nakamura[b] and Koichi Mikami*[a]**

[a] *Department of Chemical Technology, Tokyo Institute of Technology, Meguro-ku, Tokyo 152, Japan*
[b] *Research Laboratory of Resources Utilization, Tokyo Institute of Technology, Midori-ku, Yokohama 27, Japan*

**The active species of binaphthol-derived titanium catalyst 1, which is used as an efficient catalyst for glyoxylate–ene reactions, is primarily composed of a $\mu_3$-oxo ($Ti_3O$) species, for which the molecular sieves 4A employed in the catalyst preparation act as a $H_2O$ donor.**

Recently, much attention has been focused on the development of chiral Lewis-acid catalysts for a variety of carbon–carbon bond forming reactions.[1] We have already reported the asymmetric glyoxylate–ene reaction catalysed by the chiral titanium complex **1** prepared from optically pure binaphthol (BINOL) and $[TiCl_2(OPr^i)_2]$ in the presence of molecular sieves (MS) 4A [Scheme 1, eqn. (1)].[2] The MS 4A employed in the catalyst preparation has been proven to serve as a catalyst for the ligand-exchange reaction.[2a] Thus, the structure of the active titanium catalyst is assumed to be the BINOL-derived titanium dichloride **2**. Herein we report that, by elucidating the significant role of MS 4A,[3,4] the active species of the chiral titanium catalyst **1** is not the dichlorotitanium complex **2** but a $\mu_3$-oxo species ($Ti_3O$) on the basis of $^{17}O$ NMR and elemental analyses (Scheme 1).

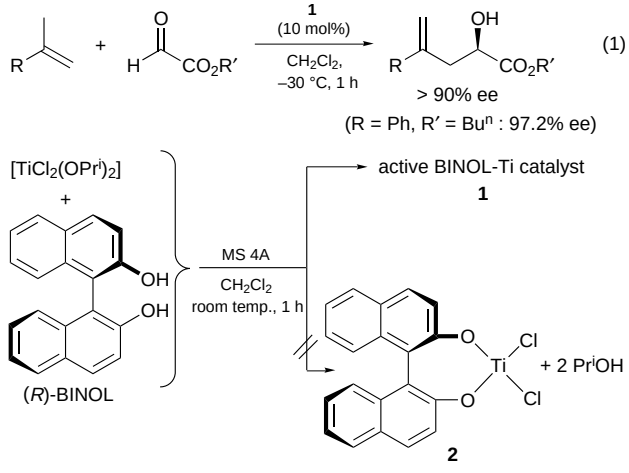
As shown in Scheme 2, it can be confirmed that the dichlorotitanium complex **2**, prepared from $TiCl_4$ and BINOL dilithium salt in dichloromethane according to the preparative procedure of dichlorotitanium 3,3′-dimethylbinaphthoxide,[5] is probably not the active species in the glyoxylate–ene reaction; the dichlorotitanium complex **2** only gives the ene product in low yield along with a low % ee.† By contrast, treatment of **2** with commercially available MS 4A‡ without activation significantly increases the chemical yield along with a higher level of % ee. These results reveal that the MS 4A converts the pre-catalyst **2** into the active BINOL–Ti catalyst **1**.

In order to elucidate the role of MS 4A to give the active catalyst **1**, the chiral titanium catalyst was prepared from BINOL and $[TiCl_2(OPr^i)_2]$ in the presence of highly activated (320 °C, < 0.05 mmHg, 12 h) and, hence, dehydrated MS 4A (< 0.2% m/m $H_2O$).[7] Inspection of the data in Scheme 3 reveals, in turn, a significant role of an 'unactivated' MS 4A; a quite low chemical yield is observed by using activated MS 4A. In contrast, titanium complex prepared in the presence of commercially available and unactivated MS 4A following our original procedure[2a,c] gives the ene product in high chemical yield with a high level of enantioselectivity. From gravimetric analysis of the $H_2O$ content in the unactivated MS 4A, the commercially available MS 4A employed in the catalyst preparation[2] is found to contain 5.3% m/m $H_2O$.§ These results, coupled with the catalytic activity, imply that $H_2O$ thus contained in MS 4A is important in giving the active BINOL–Ti catalyst **1**.¶

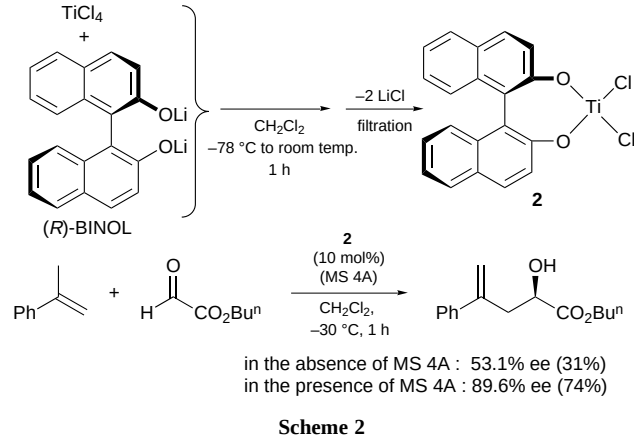
In order to obtain evidence for the involvement of $H_2O$ in the active catalyst **1**, we next turned our attention to the $^{17}O$ NMR analysis of the active BINOL–Ti catalyst **1**. An analytical sample of **1** was prepared from BINOL and $[TiCl_2(OPr^i)_2]$ in the presence of MS 4A doped with $H_2{}^{17}O$ [5.3% m/m $H_2{}^{17}O$ (10 atom% enriched)]. The $^{17}O$ NMR spectrum of the active BINOL–Ti catalyst **1** in $[^2H_8]$toluene reveals peaks only in the $\mu_3$-oxo ($Ti_3O$) region (δ 520–590).‖

Furthermore, elemental analysis of **1** reveals only a low amount of Cl (Found: Ti, 11.4; Cl, 0.6%; Cl/Ti = 0.07. Calc. for **2**: Ti, 11.9; Cl; 17.6%). These results strongly suggest that the MS 4A not only serves as an $H_2O$ donor to hydrolyse the titanium pre-catalyst but also as a base to trap HCl.

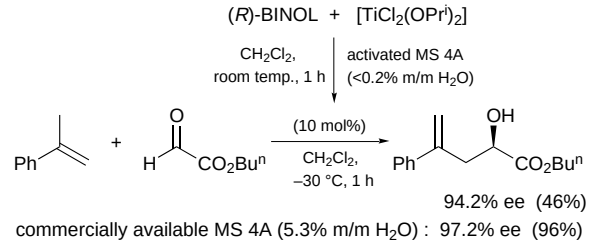
In summary, we have uncovered that the MS 4A, despite being a desiccant, serves anomalously as a $H_2O$ donor towards




**Scheme 1**




**Scheme 2**




**Scheme 3**

a titanium pre-catalyst and also acts as a base to trap HCl to give the active BINOL–Ti catalyst **1**. We have further disclosed by $^{17}O$ NMR spectroscopy that the active BINOL–Ti catalyst **1** is composed of $\mu_3$-oxo species.

## Footnotes

† In our previous report,[2] the dichlorotitanium complex **2** prepared in ether according to Reetz's procedure[6] exhibits high levels of enantioselectivity (93% ee). However, in our hands, the reproducibility of the enantioselectivity is poor ranging from 37 to 93% ee.

‡ Molecular sieve 4A, powder (catalogue no. 23,366-8) was purchased from Aldrich.

§ Quite recently,[8] the amount of $H_2O$ content externally introduced in MS 4A was reported to affect the % ee in an asymmetric Diels–Alder reaction catalysed by the BINOL-derived chiral titanium complex **1** prepared according to our modified procedure.[2d]

¶ Binaphthoxytitanium diisopropoxide **3**, which was prepared from $[Ti(OPr^i)_4]$ and BINOL with azeotropic removal of isopropyl alcohol and recrystallization, exhibited only low catalytic activity (12% yield), but after treatment with unactivated MS 4A, gives high chemical yield (98%) and enantioselectivity (97.3% ee) to suggest that MS 4A also acts as a $H_2O$ donor for **3**.

‖ The oxygen chemical shifts of titanium(IV) polyoxo–alkoxides have been reported to be strongly dependent on the titanium bridging mode; $\mu_3$-oxo ($Ti_3O$) and $\mu$-oxo ($Ti_2O$) oxygens have chemical shifts at $\delta$ 450–650 and 650–850, respectively.[9]

## References


1 *Advances in Catalytic Processes: Asymmetric Chemical Transformations*, ed. M. P. Doyle, JAI Press, Greenwich, Connecticut, 1995, vol. 1; R. Noyori, *Asymmetric Catalysis in Organic Synthesis*, Wiley, New York, 1994; *Catalytic Asymmetric Synthesis*, ed. I. Ojima, VCH, New York, 1993; *Asymmetric Catalysis*, ed. B. Bosnich, Martinus Nijhoff, Dordrecht, 1986; H. B. Kagan, *Comprehensive Organometallic Chemistry*, Pergamon, Oxford, 1982, vol. 8.

2 (*a*) K. Mikami, M. Terada and T. Nakai, *J. Am. Chem. Soc*., 1990, **112**, 3949; (*b*) 1989, **111**, 1940; (*c*) K. Mikami, M. Terada, S. Narisawa and T. Nakai, *Org. Synth*., 1993, **71**, 14; (*d*) K. Mikami, Y. Motoyama and M. Terada, *J. Am. Chem. Soc*., 1994, **116**, 2812.

3 D. W. Breck, *Zeolite Molecular Sieves*, Wiley, New York, 1974; J. M. Thomas and C. R. Theocaris, *Modern Synthetic Methods*, Springer, Berlin, 1989, T. Onaka and Y. Izumi, *J. Synth. Org. Chem. Jpn*., 1989, **47**, 233; A. Dyer, *An Introduction to Zeolite Molecular Sieves*, Wiley, Chichester, 1988; M. E. Davis, *Acc. Chem. Res*., 1993, **26**, 111.

4 M. G. Finn and K. B. Sharpless, *Asymmetric Synthesis*, Academic Press, New York, 1985, vol. 5, p. 249; R. M. Hanson and K. B. Sharpless, *J. Org. Chem*., 1986, **51**, 1922; Y. Gao, R. M. Hanson, J. M. Klunder, S.-Y. Ko, H. Masamune and K. B. Sharpless, *J. Am. Chem. Soc*., 1987, **109**, 5765. Also see: K. Narasaka, N. Iwasawa, M. Inoue, T. Yamada, M. Nakashima and J. Sugimori, *J. Am. Chem. Soc*., 1989, **111**, 5340.

5 T. J. Boyle, N. W. Eilerts, J. A. Heppert and F. Takusagawa, *Organometallics*, 1994, **13**, 2218.

6 M. T. Reetz, S.-H. Kyung, C. Bolm and T. Zierke, *Chem. Ind*., 1986, 824.

7 D. R. Burfield, G.-H. Gan and R. H. Smithers, *J. Appl. Chem. Biotechnol*., 1978, **28**, 23.

8 G. H. Posner, H. Dai, D. S. Bull, J.-K. Lee, F. Eydoux, Y. Ishihara, W. Welsh, N. Pryor and S. Petr Jr., *J. Org. Chem*., 1996, **61**, 671.

9 V. W. Day, T. A. Eberspacher, W. G. Klemperer, C. W. Park and F. S. Rosenberg, *J. Am. Chem. Soc*., 1991, **113**, 8190; V. W. Day, T. A. Eberspacher, Y. Chen, J. Hao and W. G. Klemperer, *Inorg. Chim. Acta*, 1995, **229**, 391; J. Blanchard, S. Barboux-Doeuff, J. Maquet and C. Sanchez, *New J. Chem*., 1995, **19**, 929.



*Received, 15th October 1996; Com. 6/07036A*

# β-*trans*-$[N_4\{P(Ph)(C_6H_{11}N)\}_4]^{4-}$; a tetraanionic ligand system exhibiting two separated tetradentate coordination sites of concave-shaped cavities

**Alexander Steiner* and Dominic S. Wright**

*Department of Chemistry, University of Cambridge, Lensfield Road, Cambridge, UK CB2 1EW*

**β-*trans*-$[N_4\{P(Ph)(C_6H_{11}NH)\}_4]$ can be deprotonated at all four N–H functions with BuLi in toluene yielding $Li_4\{$β-*trans*-$[N_4\{P(Ph)(C_6H_{11}NH)\}_4]\}$, using an excess of BuLi in the presence of thf, the lithium enolate co-complex $Li_6\{$β-*trans*-$[N_4\{P(Ph)(C_6H_{11}N)\}_4](CH_2{=}CHO)_2\}\cdot 4$thf is formed, in which the tetraanionic ligand β-*trans*-$[N_4\{P(Ph)(C_6H_{11}N)\}_4]^{4-}$ exhibits two separated coordination sites; both act in a tetradentate way and form concave-shaped cavities.**

Multianionic ligand systems have scarcely been investigated in metallo-organic coordination chemistry.[1] Their high reactivity and low solubility, due to their exceptional high polarity, limit their synthetic applications in aprotic solvents. Recently we discovered, that highly charged ligand systems can be stabilized by introducing cyclophosphazene backbones into the ligand cores as shown in the hexaanionic $[N_3P_3(C_6H_{11}N)_6]^{6-}$ **A** ($C_6H_{11}$ = cyclohexyl).[2] Its structural and spectroscopic features suggest, that the negative charge is stabilised by delocalisation from the terminal amido onto the central ring-nitrogen functions. The dimeric lithium complex $Li_{12}[N_3P_3(CyN)_6]_2\cdot 4$thf **1** (Cy = $C_6H_{11}$) is soluble in aprotic solvents and therefore a potential transfer reagent for introducing this ligand system into a wide range of diverse metal complexes. In systems such as **A**, where there is an extensive surface of donating N-centres, a variety of metal coordination modes is expected. This paper is concerned with manipulating the ligand sphere of these systems by partial substitution of donating centres with organic substituents. The introduction of non-coordinating substituents should provide steric control and therefore a specific design of the ligand surface. Consequently the overall equatorial arrangement of the phosphorus-bonded phenyl substituents in the novel tetraanionic ligand system β-*trans*-$[N_4\{P(Ph)(C_6H_{11}N)\}_4]^{4-}$ **B**, presented here, should provide a sterically controlled separation of coordination sites within this ligand system.

The β-*trans* isomer of 2,4,6,8-tetraphenyl-2,4,6,8-tetrakis(cyclohexylamino)cyclotetraphosphazene **1** can be obtained with retention of configuration by the aminolysis reaction of the corresponding nongeminal tetrachlorotetraphenylcyclotetraphosphazene[3] with cyclohexylamine in the presence of triethylamine in diethyl ether in 50% yield. Further reaction with 4 equiv. of BuLi in toluene gives almost quantitatively the tetrametallated derivative $Li_4\{$β-*trans*-$[N_4\{P(Ph)(CyN)\}_4]\}$ **2**. Carrying out the reaction in thf by using an excess of BuLi yielded a colourless crystalline material, which was suitable for X-ray structure analysis‡ and could be identified as $Li_6\{$β-*trans*-$[N_4\{P(Ph)(C_6H_{11}N)\}_4](CH_2{=}CHO)_2\}\cdot 4$thf **3**. The presence of two equivalents of lithium enolate in **3** is derived from the reaction of excess BuLi with thf. However, this is a common decomposition pathway of thf in the presence of strong bases and inclusion of $CH_2{=}CHOLi$, caused by fragmentation of thf, has been reported recently.[4]

The molecular structure of **3** exhibits $C_i$ symmetry and is composed of the centrally arranged tetraanionic ligand encapsulated by two triangular $Li_3$ faces, each capped by an O-donor function of the monoanionic enolate moieties (Fig. 1). The equatorial configuration of all four phenyl substituents and the overall axial arrangement of the cyclohexylamido substituents at the puckered chair-shaped $P_4N_4$ ring separate the donating ligand surface into two coordination spheres. Both form concave-shaped cavities, due to the shielding arrangement of the surrounding organic substituents, and act in a tetradentate way *via* two terminal and two ring-nitrogen centres. Fig. 2 illustrates the central core of **3**, which approximately can be described as three interlocked distorted hexagonal prisms, in which the central one is surrounded by the $P_4N_4$ ring. Each N(r)-function (r = ring) coordinates one and each N(t)-function (t = terminal) coordinates two Li centres, resulting in three different coordination patterns towards the three crystallo-

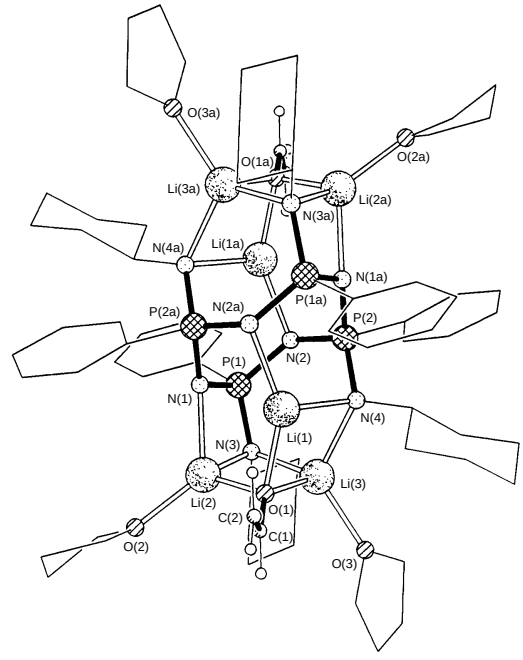
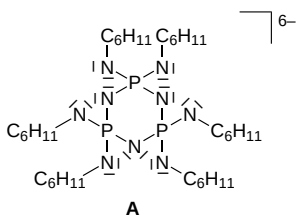
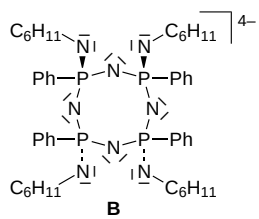



**Fig. 1** Molecular structure of **3**. Selected bond lengths (Å) and angles (°): P(1)–N(1) 1.626(6), P(1)–N(2) 1.635(6), P(1)–N(3) 1.624(6), P(2)–N(2) 1.603(6), P(2)–N(4) 1.622(6), P(2)–N(1a) 1.660(6), Li(1)–N(2a) 2.07(1), Li(1)–N(4) 2.10(1), Li(1)–O(1) 1.94(1), Li(2)–N(1) 2.08(1), Li(2)–N(3) 2.06(1), Li(2)–O(1) 1.91(1), Li(2)–O(2) 1.96(1), Li(3)–N(3) 2.09(1), Li(3)–N(4) 2.08(1), Li(3)–O(1) 2.02(1), Li(3)–O(3) 2.06(1), O(1)–C(1) 1.339(9), C(1)–C(2) 1.28(1); N(1)–P(1)–N(2) 112.9(3), N(1)–P(1)–N(3) 103.0(3), N(2)–P(1)–N(3) 119.5(3), N(2)–P(2)–N(1a) 110.0(3), N(2)–P(2)–N(4) 111.5(3), N(4)–P(2)–N(1a) 115.9(3), P(1)–N(1)–P(2a) 124.0(3) P(1)–N(2)–P(2) 127.6(4), O(1)–C(1)–C(2) 128.9(9). Atoms labelled a are generated by a centre of inversion.



graphically independent Li centres; while Li(1) and Li(3) can be seen as parts of two different six-membered heterocycles [Li(1)–N(r)–P–N(r)–P–N(t) and Li(3)–N(t)–P–N(r)–P–N(t)], Li(2) is chelated by a N(r)–P–N(t) unit. Four- and six-membered heterocyclic P–N ring-systems containing s-block metals were observed also in the presence of monoanionic linear phosphazene ligands.[5] All Li centres in **3** are further saturated by an enolate O-function, in addition Li(2) and Li(3) are coordinated by thf donor molecules, resulting in trigonal-planar [Li(1)] and tetrahedral [Li(2) and Li(3)] metal environments.

Structural parameters of the central $P_4N_8$ unit are comparable with those of the $P_3N_9$ unit in **1** and suggest an equal distribution of the negative charge onto all eight N-functions. As observed in **1** there is no significant difference in bond lengths from the phosphorus atoms toward the ring [av. P–N(4) 1.63 Å] and those toward the terminally located nitrogen centres [av. P–N(t) 1.62 Å]. On the other hand, neutral amino-substituted cyclophosphazenes exhibit significantly shorter P–N-ring bond distances compared to their terminal located counterparts, as illustrated in the structurally related β-*trans*-$[N_4\{P(Ph)(MeNH)\}_4]$ [P–N(r) 1.60 Å, P–N(t) 1.68 Å (av.)].[3b]

Ligand systems such as **A** and **B** show that there is a vast potential in multianionic ligand systems. Coordination mode and charge can be varied by formal successive substitution of donating centres with steric organic groups, thus introducing a specific design of the ligand surface. It would be interesting to investigate the nature of delocalisation of the negative charge throughout the P–N cores and its influence on coordination behaviour. There is also the possibility that anion **B** could accommodate two mixed-valent metal centres in its separate cavities, interacting electronically *via* the P–N core.[6]

We thank Dr J. M. Rawson for providing a sample of $[N_4\{P(Ph)Cl\}_4]$. A. S. gratefully acknowledges the EU Human Capital and Mobility Program for a research fellowship.

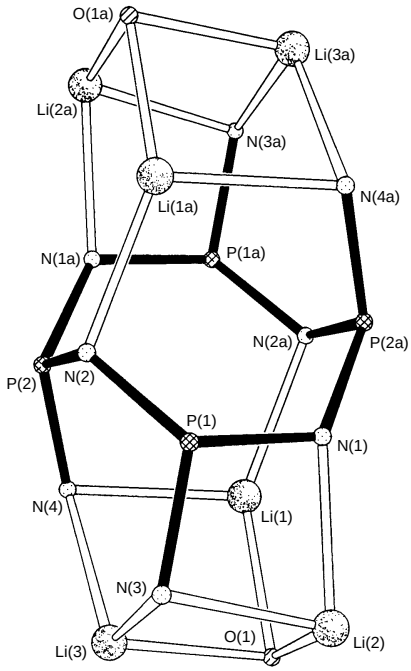



**Fig. 2** Core structure of **3**

## Footnotes

† *Selected NMR data* (25 °C): **1**: $^1$H NMR ($C_6D_6$) δ 0.8–1.6 (m, $CH_2$, $C_6H_{11}$, 40 H), 2.6 (m, CH, $C_6H_{11}$, 4 H), 7.0–7.4 (m, Ph, 12 H), 8.3 (m, Ph, 8 H); $^{31}$P NMR ($C_6D_6$, relative to $H_3PO_4$) δ 3.2. **2**: $^1$H NMR ($C_6D_6$) δ 1.0–2.0 (m, $CH_2$, $C_6H_{11}$, 40 H), 2.8 (m, CH, $C_6H_{11}$, 4 H), 7.1–7.5 (m, Ph, 12 H), 8.6 (m, Ph, 8 H); $^{31}$P NMR ($C_6D_6$, relative to $H_3PO_4$ δ 24.6. **3**: $^1$H NMR ($C_6D_6$) δ 0.8–1.8 (m, $CH_2$, $C_6H_{11}$, 40 H), 1.5 (m, thf, 16 H), 2.4 (m, CH, $C_6H_{11}$, 4 H), 3.6 (t, thf, 16 H), 3.7–4.0 (m, $CH_2$, OCH=$CH_2$, 4 H), 7.0 (dd, CH, OCH=$CH_2$, 2 H), 7.2–7.5 (m, Ph, 12 H), 8.6 (m, Ph, 8 H); $^{31}$P NMR ($C_6D_6$, relative to $H_3PO_4$) δ 24.3.

‡ *Crystal data* for **3**: $C_{68}H_{102}Li_6N_8O_6P_4$, $M_w$ = 1293.10, triclinic, space group $P\bar{1}$, $a$ = 10.969(2), $b$ = 13.022(3), $c$ = 14.760(3) Å, α = 64.12(3), β = 69.62(3), γ = 86.52(3)°, $U$ = 1767.7(6) Å$^3$, $Z$ = 1, λ = 0.71073 Å, $T$ = 153(2) K, $D_c$ = 1.215 Mg m$^{-3}$, μ(Mo-Kα) = 0.161 mm$^{-1}$. Data were collected on a Siemens-Stoe AED diffractometer (θ–$\bar{\omega}$ method, 8 ⩽ 2θ ⩽ 45°) using an oil-coated rapidly cooled crystal[7] of dimensions 0.4 × 0.5 × 0.5 mm. Of a total of 5662 reflections, 4574 were independent ($R_{int}$ = 0.14). The structure was solved by direct methods[8] and refined by full-matrix least squares on $F^2$ using all data to final values of $R1$ = 0.084 [$F > 4\sigma F$ (3471 reflections)], $wR2$ = 0.300 (all data). [$R1 = \Sigma||F_o| - |F_c||/\Sigma F_o$ and $wR2 = \{\Sigma w(F_o^2 - F_c^2)/\Sigma w(F_o^2)^2\}^{0.5}$].[9] Largest features in the final difference map, 0.491 and −0.754 e Å$^{-3}$. Atomic coordinates, bond lengths and angles, and thermal parameters have been deposited at the Cambridge Crystallographic Data Centre (CCDC). See Information for Authors, Issue No. 1. Any request to the CCDC for this material should quote the full literature citation and the reference number 182/335.

## References

1 *Comprehensive Coordination Chemistry*, ed. G. Wilkinson, R. D. Gillard and J. A. McCleverty, Pergamon, Oxford, 1987, vol. 2.
2 A. Steiner and D. S. Wright, *Angew. Chem.*, 1996, **108**, 712; *Angew. Chem., Int. Ed. Engl.*, 1996, **35**, 636.
3 (*a*) B. Grushkin, A. Berlin, J. McClanahan and R. G. Rice, *Inorg. Chem.*, 1966, **5**, 172; (*b*) G. J. Bullen and P. R. Mallinson, *Chem. Commun.*, 1969, 691.
4 S. De Angelis, E. Solari, C. Floriani, A. Chiesi-Villa and C. Rizzoli, *J. Chem. Soc., Dalton Trans.*, 1994, 2467.
5 M. Witt and H. W. Roesky, *Chem. Rev.*, 1994, **94**, 1163; A. Steiner and D. Stalke, *Inorg. Chem.*, 1993, **32**, 1977; R. Hasselbring, S. K. Pandey, H. W. Roesky, D. Stalke and A. Steiner, *J. Chem. Soc., Dalton Trans.*, 1994, 3447; S. K. Pandey, A. Steiner, H. W. Roesky and D. Stalke, *Angew. Chem.*, 1993, **105**, 625; *Angew. Chem. Int. Ed. Engl.*, 1993, **32**, 596; J. F. van der Maelen Uria, S. K. Pandey, H. W. Roesky and G. M. Sheldrick, *Acta Crystallogr., Sect. C*, 1994, **50**, 671.
6 C. Creutz and H. Taube, *J. Am. Chem. Soc.*, 1973, **95**, 1086.
7 T. Kottke and D. Stalke, *J. Appl. Crystallogr.*, 1993, **26**, 615.
8 G. M. Sheldrick, SHELXS-86, crystal structure solution program, Göttingen, 1986.
9 G. M. Sheldrick, SHELXL-93, crystal structure refinement program, Göttingen, 1993.

*Received, 16th October 1996; Com. 6/07055H*

# A cluster model for the catalytic hydrogenation of CFCs and the synthesis and structural characterisation (when X = Br) of $[Pd_4(\mu_3\text{-}CF)(\mu\text{-}X)_3(PBu^t_3)_4]$ (X = Cl, Br)

**Ramón Vilar, Simon E. Lawrence, D. Michael P. Mingos* and David J. Williams**

*Department of Chemistry, Imperial College of Science, Technology and Medicine, South Kensington, London, UK SW7 2AY*

**The syntheses, characterisation and crystal structure (when X = Br) of $[Pd_4(\mu_3\text{-}CF)(\mu\text{-}X)_3(PBu^t_3)_4]$ (X = Cl, Br) are reported; the $\mu_3$-CF moiety is hydrogenated to $CFH_3$ under mild conditions and serves as a model for the heterogeneous hydrogenation of CFCs to HCFCs.**

The cluster–surface analogy has a long history which can be traced back to Muetterties pioneering work.[1] Molecular clusters with coordinated organic fragments have proved to be invaluable for providing definitive spectroscopic data which have been used to identify analogous species on metal surfaces.[2] The study of such systems on clean and well defined metal surfaces has implications for understanding the heterogeneous catalysed transformations of organic feedstocks. The lack of reactivity of molecular clusters, specifically catalytic reactivity, has, however, limited the development of the cluster–surface analogy.

Alkylidyne ligands have been extensively studied when coordinated to group 8 and 9 metals.[3,4] However, fluoromethylidyne cluster compounds have been structurally characterised only for iron[5–7] and molybdenum.[8] Recently, $[Pd_4(\mu_3\text{-}CH)(\mu\text{-}Cl)_3(PBu^t_3)_4]$, the first example of a palladium methylidyne cluster, has been described and structurally characterised.[9] Herein we report the syntheses of $[Pd_4(\mu_3\text{-}CF)(\mu\text{-}X)_3(PBu^t_3)_4]$ (X = Cl **1**, Br **2**) and the first structural characterisation of a palladium $\mu_3$-CF cluster. Interestingly the CF group of $[Pd_4(\mu_3\text{-}CF)(\mu\text{-}Cl)_3(PBu^t_3)_4]$ is readily cleaved when the cluster is reacted with $H_2$ under mild conditions.

When 1 mol equiv. of $[Pd_2(dba)_3]\cdot C_6H_6$, 2 mol equiv. of $PBu^t_3$ and 0.5 mol equiv. of $CFCl_3$ were reacted in toluene for 6 h the reaction mixture turned dark brown. The solvent was removed under reduced pressure and the crude product was recrystallised from toluene–acetone at 4 °C to give $[Pd_4(\mu_3\text{-}CF)(\mu\text{-}Cl)_3(PBu^t_3)_4]$ **1** as dark green crystals. The formulation of this product was confirmed on the basis of IR, $^{31}P\{^1H\}$ NMR, $^{19}F$ NMR, FABMS and elemental analyses.†

A solution of $[Pd_4(\mu_3\text{-}CF)(\mu\text{-}Cl)_3(PBu^t_3)_4]$ in toluene was treated with 3 mol equiv. of LiBr in acetone for 4 h and $[Pd_4(\mu_3\text{-}CF)(\mu\text{-}Br)_3(PBu^t_3)_4]$ **2** was obtained. After removing the solvents under reduced pressure the remaining dark green solid was extracted with benzene and crystals of $[Pd_4(\mu_3\text{-}CF)(\mu\text{-}Br)_3(PBu^t_3)_4]$ were obtained from benzene–acetone after cooling to 4 °C overnight. The formulation was confirmed by the IR, $^{31}P\{^1H\}$ NMR, $^{19}F$ NMR, FABMS and analytical data.‡ A single-crystal X-ray analysis§ of compound **2** has confirmed that the cluster has a structure similar to that previously reported for $[Pd_4(\mu_3\text{-}CH)(\mu\text{-}Cl)_3(PBu^t_3)_4]$.[9] It consists of a tetrahedral cluster with a face-capping fluoromethylidyne ligand. The molecular structure (Fig. 1) demonstrates that the chlorine atoms of the starting material have been substituted by three bromine atoms, whilst retaining the effective $C_{3v}$ symmetry of the metal cluster skeleton. The Pd–Pd bonds in the cluster are in the range 2.727(2)–3.123(2) Å compared with 2.668(1)–3.143(1) Å in the analogous $[Pd_4(\mu_3\text{-}CH)(\mu\text{-}Cl)_3(PBu^t_3)_4]$ cluster compound.

The presence of the $\mu_3$-CF capping ligand in these clusters is interesting in terms of the cluster–surface analogy. It is known that palladium black and palladium supported in alumina may be used as heterogeneous catalysts for the hydrogenation of chloroflurocarbons (CFCs) to hydrochlorofluorocarbons (HCFCs) and hydrofluorocarbons (HFCs).[11] Recently these reactions have taken on considerable industrial importance because of the need for HFCs as possible substitutes for the ozone-damaging CFCs. However, to our knowledge only heterogeneous catalytic processes for converting CFCs to HCFCs have been reported.[12] $[Pd_4(\mu_3\text{-}CF)(\mu\text{-}Cl)_3(PBu^t_3)_4]$ derived from $CFCl_3$ may be converted to $CFH_3$ homogeneously under mild conditions and therefore provides an effective model for such a process.

A solution of $[Pd_4(\mu_3\text{-}CF)(\mu\text{-}Cl)_3(PBu^t_3)_4]$ in toluene was reacted with $H_2$–$NEt_3$ and 4 mol equiv. of $PBu^t_3$ under mild conditions (at STP). The products formed in this reaction were $[Pd(PBu^t_3)_2]$, $[HNEt_3]Cl$ and $CFH_3$ (in > 50% yield after 2 h as detected by gas chromatography).¶ No other volatile fluorocarbon compounds were detected by gas chromatography. $[Pd(PBu^t_3)_2]$ was detected using $^{31}P\{^1H\}$ NMR, by its characteristic resonance at δ 85.5[13] and monitoring its signal indicated that the reaction was complete after 4 h. This confirms that a $\mu_3$-CF moiety, derived by an oxidative-addition process from $CFCl_3$, may be hydrogenated to $CFH_3$ under mild conditions.

When the hydrogenation reaction was repeated using the mononuclear compound $[Pd(PBu^t_3)_2]$, generated *in situ* from $[Pd_2(dba)_3]$ and $PBu^t_3$, with an excess of $CFCl_3$ {50 : 1 relative

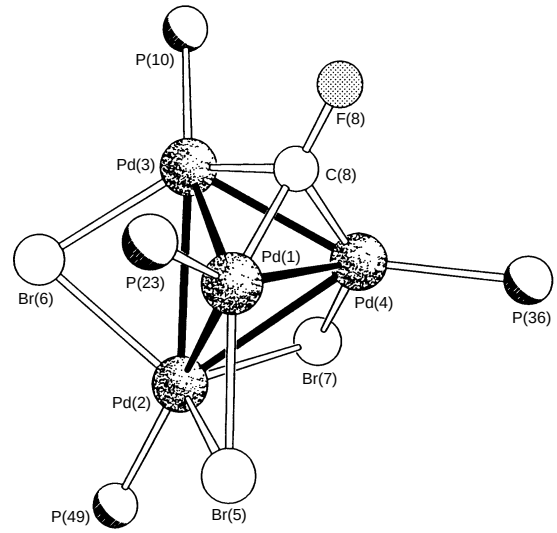


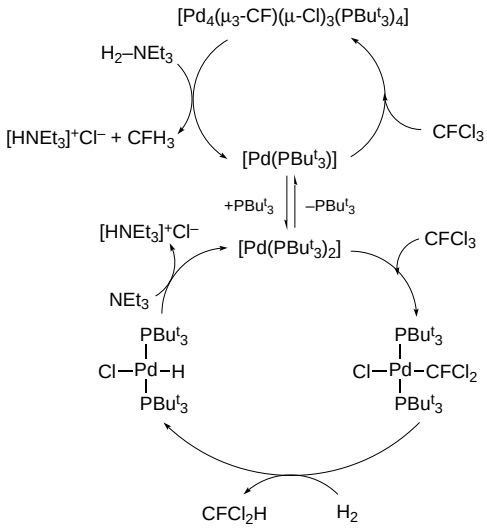

**Fig. 1** The molecular structure of the cluster $[Pd_4(\mu_3\text{-}CF)(\mu\text{-}Br)_3(PBu^t_3)_4]$ showing the numbering used (the phosphine substituents are omitted for clarity). Important bond lengths (Å): Pd(1)–C(8) 1.94(2), Pd(3)–C(8) 1.96(2), Pd(4)–C(8) 1.96(2), Pd(1)–Br(5) 2.524(3), Pd(2)–Br(5) 2.668(3), Pd(2)–Br(6) 2.666(3), Pd(2)–Br(7) 2.639(3), Pd(3)–Br(6) 2.531(3), Pd(4)–Br(7) 2.529(2), Pd(1)–P(23) 2.397(5), Pd(2)–P(49) 2.361(5), Pd(3)–P(10) 2.403(6), Pd(4)–P(36) 2.392(5), Pd(1)–Pd(2) 3.112(2), Pd(1)–Pd(3) 2.727(2), Pd(1)–Pd(4) 2.729(2), Pd(2)–Pd(3) 3.097(2), Pd(2)–Pd(4) 3.123(2), Pd(3)–Pd(4) 2.731(2), C(8)–F(8) 1.36(2).

to $[Pd_2(dba)_3]$}, the only hydrogenation product observed was $CFCl_2H$. Complete conversion of the $CFCl_3$ to $CFCl_2H$ required 24 h. No traces of $CFH_3$ or any other gas were detected, suggesting that the cluster $[Pd_4(\mu_3\text{-}CF)(\mu\text{-}Cl)_3(PBu^t_3)_4]$ plays an essential role in the hydrogenation of $CFCl_3$ to $CFH_3$.

Although the formation of $[Pd_4(\mu_3\text{-}CF)(\mu\text{-}Cl)_3(PBu^t_3)_4]$ from $CFCl_3$ and its subsequent hydrogenation provides an illustration of how $CFCl_3$ may be hydrogenated to $CFH_3$ on a metal surface, the cluster compound itself is not an effective homogeneous catalyst. When $H_2$ was bubbled through a solution of $[Pd_4(\mu_3\text{-}CF)(\mu\text{-}Cl)_3(PBu^t_3)_4]$ in toluene in the presence of $NEt_3$ and with a 50-fold excess of $CFCl_3$, the gases produced were identified as $CFH_3$ and $CFCl_2H$ with a ratio of $CFCl_3H/CFH_3$ of *ca*. 2.3. $^{31}P\{^1H\}$ NMR data confirmed that the cluster had fragmented during this reaction.

Scheme 1 summarises plausible mechanistic cycles involving the reactions for the mono- and tetra-nuclear palladium compounds. Although in the absence of hydrogen the formation of the tetranuclear cluster with the $\mu_3$-CF group proceeds at a sufficient rate to compete with the formation of the simple oxidative-addition products, the hydrogenation step proceeds more quickly for the mononuclear product than for the tetranuclear compound leading to the formation of $CFCl_2H$ in addition to $CFH_3$. Attempts are currently being made to use variations in the ligands to change the relative rates of the competing cycles and thereby improve the selectivity of the catalytic hydrogenation process.

We thank CONACYT and ORS for scholarships to R. V., EPSRC for financial support to S. E. L., BP plc for endowing D. M. P. M.'s chair and ICI for providing reference samples of $CFCl_2H$ and $CFH_3$.




**Scheme 1** Reactions involved in the palladium-assisted hydrogenation of $CFCl_3$

## Footnotes

† *Selected data* for **1**: yield 18%. (Found C, 42.4; H, 7.4. $C_{49}H_{108}Cl_3FP_4Pd_4$ requires C, 42.9; H, 7.9%). $^{31}P\{^1H\}$ NMR ([$^2H_6$]benzene) δ 103.4 (q), 68.6 (dd); $^{19}F$ NMR ([$^2H_6$]benzene) δ 111.0 [dq, $^3J$(PP) 132.2, $^3J$(PF) 39.7, $^4J$(PF) 8.5 Hz]. IR ν(C–F) 1052 $cm^{-1}$.

‡ *Selected data* for **2**: yield 61%. (Found C, 40.9; H, 6.8 $C_{49}H_{108}Br_3FP_4Pd_4\cdot0.75C_6H_6\cdot0.75Me_2CO$ requires C, 41.0; H, 7.1%). $^{31}P\{^1H\}$ NMR ([$^2H_6$]benzene) δ 117.0 (q), 70.5 (dd); $^{19}F$ NMR ([$^2H_6$]benzene) δ 116.0 [dq, $^3J$(PP) 173.0, $^3J$(PF) 40.1, $^4J$(PF) 11.0 Hz]. The metathesis reaction of **1** to **2** was monitored at different reaction times by $^{31}P\{^1H\}$ and $^{19}F$ NMR spectroscopy. The asymmetric mixed-halogen clusters $[Pd_4(\mu_3\text{-}CF)(\mu\text{-}Br)(\mu\text{-}Cl)_2(PBu^t_3)_4]$ **3** and $[Pd_4(\mu_3\text{-}CF)(\mu\text{-}Br)_2(\mu\text{-}Cl)(PBu^t_3)_4]$ **4** were identified as intermediates, suggesting that the substitution reaction takes place sequentially.

§ *Crystal data* for **1**: $C_{49}H_{108}Br_3FP_4Pd_4\cdot0.75Me_2CO\cdot0.75C_6H_6$, $M$ = 1607.7, monoclinic, space group $C2/c$; $a$ = 25.989(4), $b$ = 25.529(4), $c$ = 24.216(4) Å, β = 118.77(1)°; $U$ = 14083(4) Å$^3$, $Z$ = 8, $D_c$ = 1.517 g $cm^{-3}$; μ(Mo-Kα) = 2.833 $mm^{-1}$; $F(000)$ = 6524. Data were measured on a Siemens P4/PC diffractometer with graphite-monochromated Mo-Kα radiation using ω scans. The structure was solved by direct methods and the non-hydrogen atoms of the cluster refined anisotropically by full-matrix least-squares based on $F^2$ to give $R_1$ = 0.0783, $wR_2$ = 0.1446 (SHELXTL)[10] for 3824 unique observed reflections ($|F| > 4\sigma|F_o|$, $2\theta \leqslant 50°$) and 609 parameters. Atomic coordinates, bond lengths and angles, and thermal parameters have been deposited at the Cambridge Crystallographic Data Centre (CCDC). See Information for Authors, Issue No. 1. Any request to the CCDC for this material should quote the full literature citation and the reference number 182/330.

¶ *Selected data for chromatographic studies*: the chromatographic studies were performed in a Perkin Elmer 8500-GC with an FID detector and a Carbopack B/5% Fluorocol column special to detect fluorinated compounds. The oven temperature was set to 60 °C, the detector to 250 °C and the injection temperature to 200 °C. The carrier gas ($N_2$) flow rate was adjusted to 25 ml $min^{-1}$. Samples: 200 μl of sample (gases produced in the reaction) was injected using a gas-tide syringe. The assignment of the peaks was made by comparison with standards of $CFH_3$, $CFCl_2H$ and $CFCl_3$ at the same temperature and flow rate conditions.

## References

1 E. L. Muetterties, *J. Organomet. Chem.*, 1980, **200**, 177.
2 *Metal–Metal Bonds and Clusters in Chemistry and Catalysis*, ed. J. P. Fackler, Texas A&M University Press, USA, 1990.
3 J. B. Keistler, *Polyhedron*, 1988, **7**, 847; D. Seyferth, J. E. Hallgreen and P. L. K. Hung, *J. Organomet. Chem.*, 1973, **50**, 265.
4 B. R. Penfold and B. H. Robinson, *Acc. Chem. Res.*, 1973, **6**, 73.
5 D. Lentz and H. Michael-Shulz, *Inorg. Chem.*, 1990, **29**, 4396.
6 D. Lentz and H. Michael, *Inorg. Chem.*, 1989, **28**, 3396.
7 D. Lentz, *Coord. Chem. Rev.*, 1995, **143**, 383.
8 W. Schulze, H. Hartl and K. Seppelt, *J. Organomet. Chem.*, 1987, **319**, 77.
9 A. D. Burrows, D. M. P. Mingos, S. Menzer, R. Vilar and D. J. Williams, *J. Chem. Soc., Dalton Trans.*, 1995, 2107.
10 G. M. Sheldrick, SHELXTL, Siemens Analytical Instruments, Madison, WI, 1990; SHELXL 93, University of Göttingen, 1993.
11 B. Coq, J. M. Cognion, F. Figuéras and D. Tournigant, *J. Catal.*, 1993, **141**, 21.
12 B. Dhandapani and S. T. Oyama, *Catal. Lett.*, 1995, **35**, 353.
13 R. Vilar and D. M. P. Mingos, *J. Cluster Sci.*, in the press.

*Received, 16th October 1996; Com. 6/07048E*

# Optical control over $Pb^{2+}$ binding to a crown ether-containing chromene

**Mark T. Stauffer, David B. Knowles, Carrie Brennan, Lance Funderburk, Fu-Tyan Lin and Stephen G. Weber***

*Department of Chemistry, University of Pittsburgh, Pittsburgh, PA 15260 USA*

**Naphthochromene 1 binds $Pb^{2+}$ in the dark, and the complex is photodissociated by a novel mechanism.**

Metal-ion chelation by crown ethers has been the subject of intense investigation by researchers[1] for over thirty years. Functionalization of crown ethers[2] leads to pH, redox, and photochemical control over metal-ion binding. Several reports of metal-ion chelation by crown ether groups coupled to photochromic azobenzenes,[2] spiropyrans,[3] and spirooxazines[4] have appeared in the literature. Binding strategies described include the 'butterfly'[2] configuration (*i.e.* a crown ether attached to each end of azobenzene) and use of ionic 'caps'.[2–4] We present here a crown ether-containing chromene that binds $Pb^{2+}$ in the dark, with dissociation of $Pb^{2+}$ upon irradiation with near-UV light. The process is photoreversible. We monitor $Pb^{2+}$ binding by observing the changes in the cathodic reduction of $Pb^{2+}$. To our knowledge, there are no published accounts of metal-ion binding using photochromic chromenes. In metal-binding azobenzenes,[2] spiropyrans,[3] and spirooxazines,[4] the binding affinity is controlled by light through its influence on the chelator's geometry and/or the large increase in donor strength of the pyran oxygen following cleavage of the spiro carbon–oxygen bond. In contrast, compound **1** functions by taking advantage of the decrease in electron donor strength on ligating heteroatoms that can also stabilize, by electron donation, the positive charge created following photolysis.

Compound **1** was synthesized from 1-phenyl-1-(3,4-benzo-1,4,7,10,13-pentaoxacyclopentadeca-3-ene)prop-2-yn-1-ol and β-naphthol under acidic conditions, and purified by re-crystallization (mp 83 °C). Perchlorate salts, benzo-15-crown-5, and methanol (MeOH) were used as received. Simultaneous photochemistry and square-wave voltammetry of solutions of $Pb^{2+}$ and **1** [MeOH–$H_2O$ (9 : 1)–$5.0 \times 10^{-2}$ mol $dm^{-3}$ $LiClO_4$] were carried out at amalgamated Au in a 1 mm quartz cuvette. Square-wave voltammetry of solutions of $Pb^{2+}$ and benzo-15-crown-5 was performed at amalgamated Au in a conventional three-electrode electrochemical cell, in the same medium used for the photoelectrochemistry.

We used the model compound benzo-15-crown-5 to study the effect of $Pb^{2+}$ binding by a crown ether upon the voltammetry of $Pb^{2+}$ (Fig. 1). In the absence of benzo-15-crown-5, we observed reduction of free $Pb^{2+}$ (−346 mV *vs.* Ag/AgCl). Increasing the concentration of benzo-15-crown-5 in solution caused the $Pb^{2+}$ reduction peak to shift and decrease in intensity, indicative of binding of $Pb^{2+}$ by benzo- 15-crown-5. We carried out competitive binding between $Pb^{2+}$ and $Na^+$, in the presence of an excess of $Na^+$, to confirm that the decrease in the $Pb^{2+}$ reduction wave upon addition of benzo-15-crown-5 was due to binding of $Pb^{2+}$ by the crown ether. Addition of $7.0 \times 10^{-2}$ mol $dm^{-3}$ $NaClO_4$ to a solution containing $1.83 \times 10^{-5}$ mol $dm^{-3}$ $Pb^{2+}$ and $1.0 \times 10^{-2}$ mol $dm^{-3}$ benzo-15-crown-5 yielded the reduction wave (*ca.* −420 mV, *vs.* Ag/AgCl) for free $Pb^{2+}$ during voltammetry of this solution. Thus, the change in the voltammetry of $Pb^{2+}$ observed in Fig. 1 was due to binding by the crown ether.

Compound **1** ($\lambda_{max}$ = 284, 302, 346, 358 nm) yields a visible band ($\lambda_{max}$ = 476 nm) during irradiation with 300–400 nm light. Photoswitching of **1** in the presence of $Pb^{2+}$ (Fig. 2) reveals that **1** is fairly photostable. Voltammetry of **1** in the dark

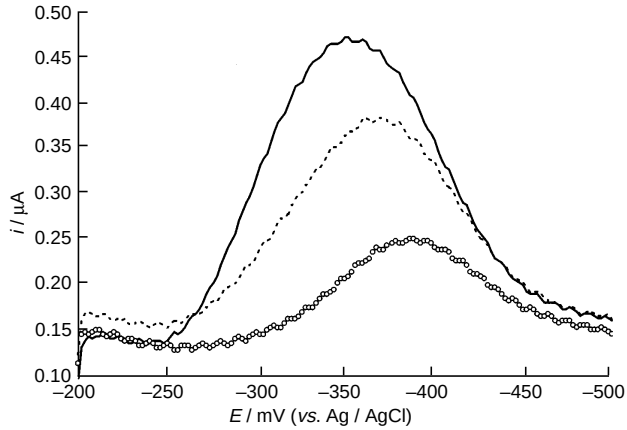



**Fig. 1** Cathodic reduction of $4.0 \times 10^{-5}$ mol $dm^{-3}$ $Pb^{2+}$ in MeOH–$H_2O$ (9 : 1) containing 0.1 mol $dm^{-3}$ $LiClO_4$ in the absence and presence of excess benzo-15-crown-5. (——) $4.0 \times 10^{-5}$ mol $dm^{-3}$ $Pb^{2+}$; (---) $9.6 \times 10^{-3}$ mol $dm^{-3}$ benzo-15-crown-5 added; (ooo) $3.3 \times 10^{-2}$ mol $dm^{-3}$ benzo-15-crown-5 added.

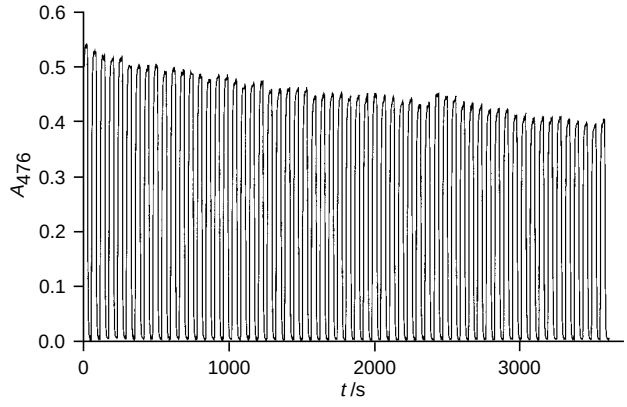
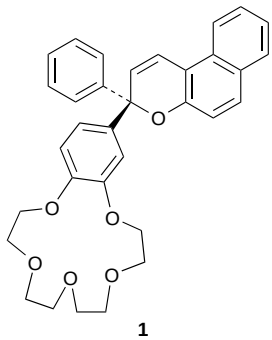
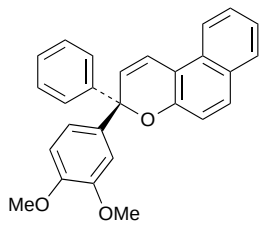



**Fig. 2** Photoswitching of $4.93 \times 10^{-4}$ mol $dm^{-3}$ **1** in the presence of $5.39 \times 10^{-3}$ mol $dm^{-3}$ $Pb^{2+}$, in MeOH–$H_2O$ (9 : 1) containing $5 \times 10^{-2}$ mol $dm^{-3}$ $LiClO_4$. Each cycle consists of 30 s irradiation with 300–400 nm light, followed by 30 s irradiation with > 420 nm light.




**1**




**2**

or during illumination yields no waves in the −300 to −1000 mV region. Fig. 3 illustrates the results of our photoelectrochemical studies of $Pb^{2+}$ in the presence of **1**. In the dark, we do not see the wave at *ca.* −400 mV (*vs.* Ag) corresponding to reduction of free $Pb^{2+}$. Instead, we observe a very broad wave at *ca.* −600 mV, indicating that the $Pb^{2+}$ binds to the crown ether. Upon irradiation with 300–400 nm light, we obtain the wave (*ca.* −420 mV, *vs.* Ag) for reduction of free $Pb^{2+}$, showing that the $Pb^{2+}$–crown complex has dissociated due to photoisomerization of **1** (Scheme 1). Irradiation with > 420 nm light yields the same result observed in the dark, indicating the $Pb^{2+}$ binds again to **1**. $^1$H and $^{13}$C NMR spectroscopies† of **1** upon addition of $Pb^{2+}$ (2 : 1 $Pb^{2+}$: **1** in $CD_3CN$) in the dark give further

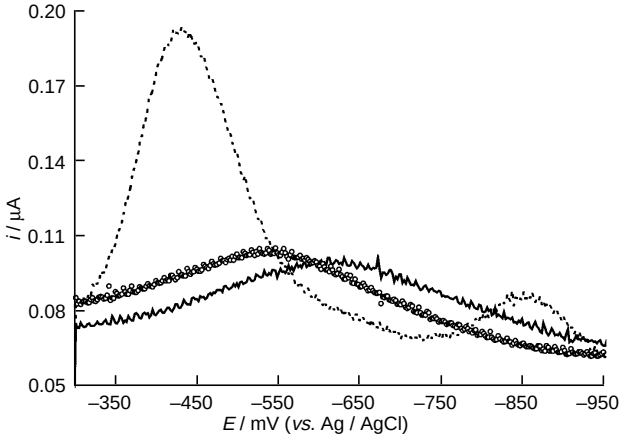
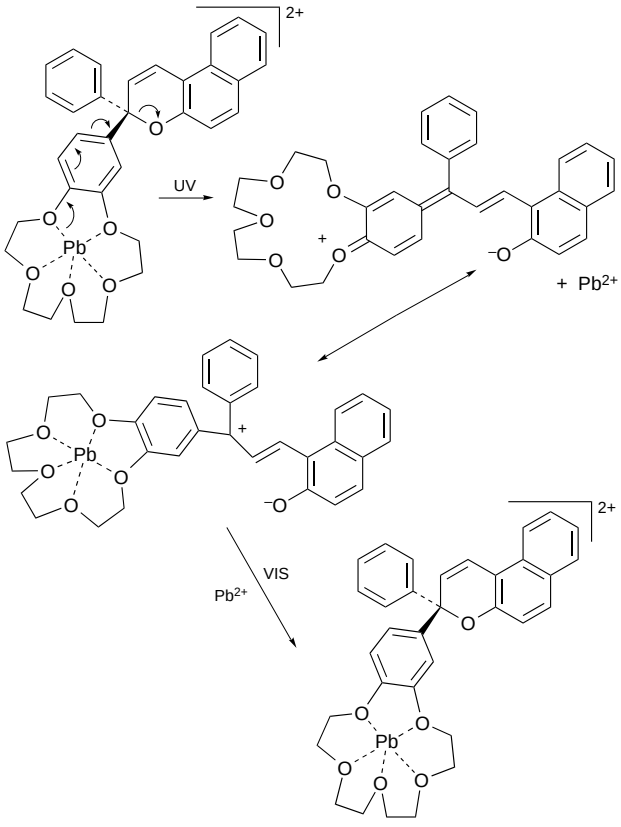



**Fig. 3** Photoelectrochemistry of $5.8 \times 10^{-5}$ mol dm$^{-3}$ $Pb^{2+}$ + $2 \times 10^{-3}$ mol dm$^{-3}$ **1** in MeOH–$H_2O$ (9 : 1) containing $5 \times 10^{-2}$ mol dm$^{-3}$ $LiClO_4$. (——) dark; (---) UV photolysis; (ooo) visible photolysis.




**Scheme 1**

evidence of binding by $Pb^{2+}$. For $^1$H NMR, the crown ether methylene proton resonances are in the region δ 3.73–4.33 with $Pb^{2+}$ *cf.* δ 3.56–4.00 in the absence of $Pb^{2+}$. Resonance shifting and line broadening occur in both $^1$H and $^{13}$C NMR spectra of **1** in the presence of $Pb^{2+}$.

Further evidence suggests that the $Pb^{2+}$ binds to the crown ether moiety. In the dark, we observe the same trend for cathodic reduction of $Pb^{2+}$ in the presence of a large excess of **1** (Fig. 3) as that in excess benzo-15-crown-5 (Fig. 1). In each case, the reduction potential of $Pb^{2+}$ becomes more negative upon addition of the crown ethers. Control experiments involving the dimethoxylated analogue of **1** (*i.e.*, **2**) show no indication of $Pb^{2+}$ binding. We observe no shift in the $Pb^{2+}$ reduction peak potential upon addition of **2** in the dark. Also, $^1$H and $^{13}$C NMR spectroscopies† reveal no changes in the chemical shifts and shapes of the resonances of **2** upon addition of $Pb^{2+}$ in the dark, indicating that $Pb^{2+}$ does not bind to **2**.

Unlike previously designed crowned photochromics,[2–4] in which UV photolysis enhances the cation-binding abilities of the ligands through the creation of additional binding sites or geometry changes, UV-induced photoisomerization of **1** causes open **1** to lose its cation-binding ability due to withdrawal of electron density from the crown ether moiety (Scheme 1). Kimura *et al.*[5] observe a similar occurrence for $Na^+$ bound to a crowned malachite green leuconitrile. The difference between **1** and Kimura's[5] leuconitrile is that the coordination by **1** is photoreversible. There is a significant technical advantage to exerting optical control over metal-ion binding in this manner. The system using the photochromic chelator (*e.g.* sensor or extractor) functions in the dark, and only needs to be exposed to light, with consequent photodegradation, for brief periods of forced dissociation.

We gratefully acknowledge the financial support of the Office of Naval Research.

## Footnote

† **1** $^1$H NMR (500 MHz, $CD_3CN$, 298 K) δ 3.58 (t, 8 H, $OCH_2$), 3.71 (t, 4 H, $OCH_2$), 3.98 (t, 4 H, OMe), 6.42–8.00 (naphthopyran and phenyl, 16 H). $^{13}$C NMR (125 MHz, $CD_3CN$, 298 K) δ 69.5, 69.7, 69.9, 70.9, 71.4 ($OCH_2$), 83.0 ($CPh_2$), 113.7–151.3 (naphthopyran and phenyl).

**2** $^1$H NMR (500 MHz, $CD_3CN$, 298 K) δ 3.70 (s, 3 H, OMe), 3.72 (s, 3 H, OMe), remaining δ values same as those of **1** for naphthopyran and phenyl moieties. $^{13}$C NMR (125 MHz, $CD_3CN$, 298 K) δ 56.2 (OMe), 83.0 ($CPh_2$), 111.5–151.3 (naphthopyran and phenyl).

## References

1 C. J. Pedersen, *J. Am. Chem. Soc.*, 1967, **89**, 2495, 7017; *Angew. Chem., Int. Ed. Engl.*, 1988, **27**, 1021; R. M. Izatt, R. E. Terry, D. P. Nelson, Y. Chan, D. J. Eatough, J. S. Bradshaw, L. D. Hansen and J. J. Christensen, *J. Am. Chem. Soc.*, 1976, **98**, 7626; J. D. Lamb, R. M. Izatt, J. J. Christensen and D. J. Eatough, *Thermodynamics and Kinetics of Cation-Macrocycle Interaction*, in *Coordination Chemistry of Macrocyclic Compounds*, ed. G. A. Melson, Plenum, NY, 1979, pp. 145–217.

2 S. Shinkai, *Dynamic Control of Cation Binding*, in *Cation Binding by Macrocycles*, ed. Y. Inoue and G. W. Gokel, Marcel Dekker, NY, 1990, pp. 397–428 and references therein; F. C. J. M. van Veggel, W. Verboom and D. N. Reinhoudt, *Chem. Rev.*, 1994, **94**, 279 and references therein; S. Shinkai, T. Nakaji, Y. Nishida, T. Ogawa and O. Manabe, *J. Am. Chem. Soc.*, 1980, **102**, 5860.

3 M. Inouye, Y. Noguchi and K. Isagawa, *Angew. Chem., Int. Ed. Engl.*, 1994, **33**, 1163; K. Kimura, T. Yamashita and M. Yokoyama, *J. Chem. Soc., Perkin Trans. 2*, 1992, 613; H. Sasaki, A. Ueno, J.-I. Anzai and T. Osa, *J. Am. Chem. Soc.* 1986, **59**, 1953.

4 K. Kimura, T. Yamashita, M. Kaneshige and M. Yokoyama, *J. Chem. Soc., Chem. Commun.*, 1992, 969.

5 K. Kimura, M. Kaneshige and M. Yokoyama, *J. Chem. Soc., Chem. Commun.*, 1994, 1103.

*Received, 21st October 1996; Com. 6/07141D*

# Novel calamitic side-chain metallomesogenic polymers with ferrocene in the backbone: synthesis and properties of thermotropic liquid-crystalline poly(ferrocenylsilanes)

**Xiao-Hua Liu,[a] Duncan W. Bruce*[b] and Ian Manners*[a]**

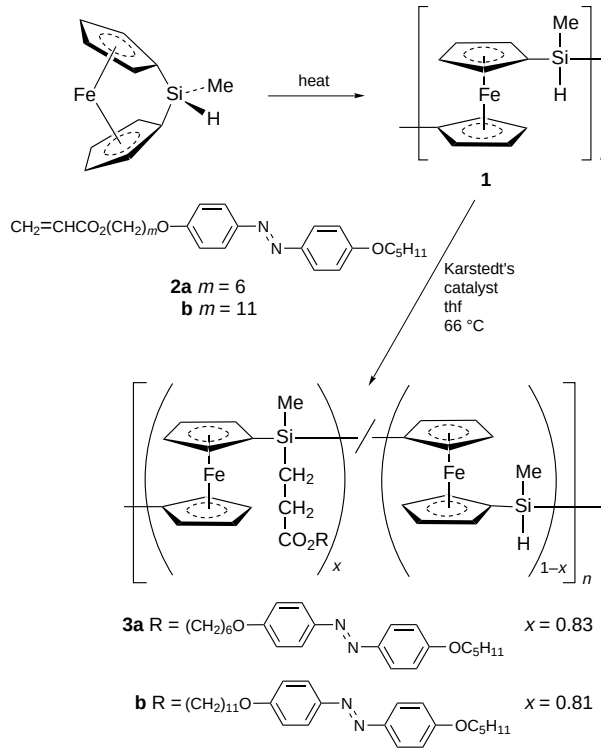
[a] *Department of Chemistry, University of Toronto, 80 St. George Street, Toronto M5S 3H6, Ontario, Canada*
[b] *Department of Chemistry, University of Exeter, Stocker Road, Exeter, UK EX4 4QD*

**Novel thermotropic, metallomesogenic polymers with a poly(ferrocenylsilane) main chain and 4-pentoxy-4′-hydroxyhexanoxyazobenzene or 4-pentoxy-4′-hydroxy-undecyloxyazobenzene acrylate side chains have been prepared; each material displays a nematic mesophase.**

The study of the incorporation of metals into the structures of low molar mass liquid crystals with the aim of accessing novel physical properties is now a well established area of materials chemistry.[1,2] Metallomesogenic polymers are particularly attractive as they have the potential to combine the advantageous properties of polymers (*e.g.* excellent mechanical properties, low thermal expansion, and excellent processability) with those of transition-metal complexes (*e.g.* colour, polarizability, magnetic characteristics).[3,4] Ferrocene units are of considerable interest as components of liquid-crystalline (LC) materials due to their high thermal stability, tunable redox characteristics and their structural variability which might lead to intriguing effects on mesophase morphology.[5] A range of low molecular mass calamitic (rod-like) systems can be prepared by monosubstitution or by 1,2-, 1,3- or 1,1′-disubstitution of the ferrocene nucleus.[6] Several examples of calamitic side-chain metallomesogenic polymers with ferrocene in the side-group structure are known.[7] For example, thermotropic ferrocene-containing side-chain LC polymers have been prepared from ferrocene-containing monomers.[7a,b] Ferrocene-containing side chain LC polymers where the liquid crystallinity is derived from the organic mesomorphic monomers have also been reported.[7c] Although main-chain, LC polymers with ferrocene in the backbone are more common (*e.g.* main-chain polyester incorporating ferrocene units substituted at 1,1′-positions[8]) these are limited to materials in which the ferrocene units are a significant distance apart, making the exploitation of cooperative interactions between the iron atoms difficult. Here, we report on the synthesis and thermal properties of the first side-chain metallomesogenic polymers with ferrocene units in the main chain. These materials were prepared by the functionalization of poly(ferrocenylmethylhydrosilane) and represent the first well characterized, liquid-crystalline poly(ferrocenylsilanes).

Recent work has shown that high molar mass poly(ferrocenylsilanes) are accessible *via* the ring-opening polymerization of silicon-bridged [1]ferrocenophane precursors.[9] To prepare side-chain LC poly(ferrocenylsilanes) a hydrosilylation strategy was used. First, poly(ferrocenylmethylsilane) **1** was synthesized by thermal ring-opening polymerization of the appropriate [1]ferrocenophane precursor.[10] Secondly, azobenzene-based mesogens, **2a** and **2b**,† were then attached to the backbone of polymer **1** *via* a platinum-catalysed hydrosilylation reaction (Scheme 1). Analysis of the orange polymers **3a** and **3b** by $^1$H NMR gave a hydrosilylation yield of $>80\%$ for both polymers, although a significant amount of unreacted Si–H bonds was present in the resulting polymers, as indicated by IR and by $^{29}$Si and $^1$H NMR spectroscopy.‡

The mesomorphic behaviour of the azobenzene derivatives and the polymers was investigated by a combination of differential scanning calorimetry (DSC) and polarized optical microscopy. Thus, on heating, polymer **3b** underwent a glass transition at 35 °C followed by melting at 53 °C; polymer **3a** underwent a coincident glass transition and melting event at 36 °C (Fig. 1). Following melting, a birefringent phase was found which was readily identified as corresponding to a




**Scheme 1**

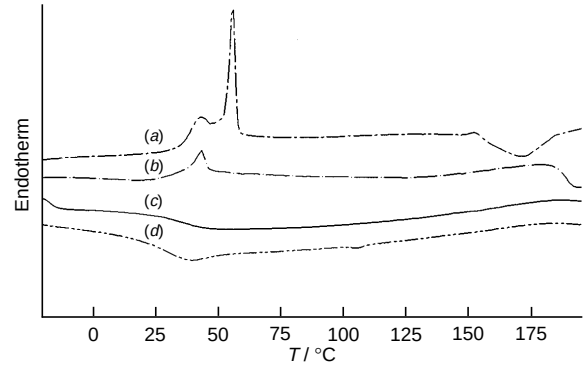



**Fig. 1** Differential scanning calorimetry thermograms of polymers **3a** and **3b** (10 °C min$^{-1}$); (*a*) the first heating of **3b**, (*b*) the first heating of **3a**, (*c*) the first cooling of **3a**, (*d*) the first cooling of **3b**

nematic phase on account of the characteristic 'flashing' seen when the sample was subject to mechanical stress (although the 'flashing' was, of course, much slower than that normally observed in low molar mass systems on account of the much higher viscosity of the polymer). Thus, the polymers melted at much lower temperature than the free azobenzene groups and by comparing the transition temperature of the two liquid-crystal polymers **3a** and **3b**, it is apparent that as the number of carbon atoms in the flexible spacer is increased, the melting point increases. On further heating, the nematic phase was found to persist above 250 °C, by which time decomposition of the sample was becoming rapid. By DSC, **3a** and **3b** showed broad exothermic transitions at 185 and 153 °C, which did not correspond to any event observable by microscopy, and which we therefore suppose represented the onset of decomposition. The nature of the decomposition is, however, unclear at present, as neither the parent, unfunctionalized polymer, nor the free azobenzene fragments decomposed below 300 °C. On cooling, **3a** and **3b** did not recrystallize. Table 1 shows the transition types, temperatures, molecular mass data and $^{29}$Si NMR chemical shifts.

In conclusion, we have reported the synthesis and mesogenic properties of two novel calamitic thermotropic side-chain LC polymers containing ferrocene in the backbone. The optical microscopy showed a well defined texture for the nematic phase. These functionalized poly(ferrocenylmethylsilanes) represent the first examples of calamitic thermotropic side-chain LC polymers with ferrocene units in the backbone, and in particular, it is interesting to note that whereas the precursor mesogen **2a** is not liquid-crystalline, mesophase stabilization is apparent in polymer **3a**. This synthetic route offers ample opportunities for structural variations and we are exploring these and the properties of the materials in detail. Of particular interest[11] is the study of the liquid-crystal properties in the three oxidation states accessible for these materials (neutral, oxidised at alternate iron sites, and fully oxidised).[9]

We thank the University of Sheffield for the award of a Postgraduate Scholarship to Xiao-Hua Liu, and Ron Rulkens for assistance in synthesis of the starting polymer **1**. I. M. thanks the Natural Science and Engineering Research Council of Canada (NSERC) for funding and the Alfred P. Sloan Foundation for a Research Fellowship (1994–1998), and D. W. B. thanks the University of Exeter for support.

**Table 1** Molecular masses, $^{29}$Si NMR, thermal transition temperatures and assignments for **1**, **2a**, **2b** and the metallomesogenic polymers **3a** and **3b**

| Compound | $M_w$[a] | $M_n$[a] | PDI[a] | δ($^{29}$Si)[b] | Transition[c] | $T$/°C |
|---|---|---|---|---|---|---|
| **1** | $2.1 \times 10^5$ | $9.6 \times 10^4$ | 2.2 | −20.3 | $T_g$ | 9 |
| **2a** | | | | | K–I | 89 |
| **2b** | | | | | K–I | 96 |
| | | | | | (I–N) | (84) |
| | | | | | $(N–S)_A$ | (82) |
| **3a** | $3.8 \times 10^4$ | $1.4 \times 10^4$ | 2.7 | −20.3 | $T_g$ | *ca.* 30 |
| | | | | −4.5 | K–N | *ca.* 36 |
| | | | | | N–d | > 250[d] |
| **3b** | $4.2 \times 10^4$ | $1.7 \times 10^4$ | 2.5 | −20.3 | $T_g$ | 35 |
| | | | | −4.5 | K–N | 53 |
| | | | | | N–d | > 250[d] |

[a] Estimated by gel permeation chromatography (GPC) in thf using polystyrene standards, PDI = $M_w/M_n$. [b] $^{29}$Si NMR spectra were recorded in $CDCl_3$. [c] The transition temperatures were measured by DSC at 10 °C min$^{-1}$. Notation: crystal (K), glass transition ($T_g$), smectic A ($S_A$), nematic (N), and isotropic (I) phases, and decomposition temperature (d). [d] DSC suggests that decomposition begins around 185 °C for **3a** and around 153 °C for **3b**, although 250 °C represents a temperature at which it becomes rapid.

## Footnotes

† The synthesis of **2a** and **2b** was achieved in five steps from *p*-acetamidophenol. The steps involved reaction with i, *n*-$C_5H_{11}Br$; ii, $H^+$–$H_2O$; iii, phenol, HCl and $NaNO_2$; iv, $HO(CH_2)_mBr$ and v, $CH_2CHCOCl$. Both compounds gave satisfactory IR, $^1$H and $^{13}$C NMR and mass spectra.

‡ **3a**: The catalyst [$Pt_2\{(\eta\text{-}CH_2{=}CHSiMe_2)O\}_3$] (4 mg) in xylenes (20 μl) was added to a mixture of polymer **1** (0.3 g, 1.32 mmol) and compound **2a** (0.58 g, 1.32 mmol) in dry thf (100 ml). The reaction mixture was heated to reflux and $^1$H NMR was used to follow the hydrosilylation reaction. After three days $^1$H NMR showed that a small amount of unreacted Si–H bonds still existed. The product was purified by precipitation into hexanes twice. An orange coloured polymer was obtained. Yield 0.55 g (63%). $^1$H NMR (200 MHz, $CDCl_3$): δ 0.4–0.65 (br m, 6 H, C*H*$_3$SiCH$_2$ and C*H*$_3$SiH), 0.85–1.1 (m, 5 H, C*H*$_3$CH$_2$ and SiCH$_2$), 1.25 −1.95 [br m, 14 H, $(CH_2)_7$], 2.34 (br s, 2 H, $CH_2CO_2$), 4.0–4.2 (br m, 22 H, $C_5H_4$, C*H*$_2$OPh and $CO_2CH_2$), 4.9 (br s, 1 H, SiH), 6.95–7.1 (d, 4 H, Ph), 7.85–8.0 (d, 4 H, Ph). $^{13}$C NMR (50 MHz, $CDCl_3$): δ −3.9, −2.7, 11.4, 14.1, 22.5, 25.6, 26.0, 28.2, 28.7, 28.9, 29.1, 29.3, 29.4, 29.5, 31.5, 64.6, 67.9, 68.3, 71.5, 72.9, 73.0, 114.6, 124.2, 146.9, 161.0, 174.8. $^{29}$Si NMR (79 MHz, $CDCl_3$) δ 4.5 ($SiCH_2$), −20.3 (SiH, $^1J_{SiH}$ 51 Hz). The hydrosilylation yield was confirmed by $^1$H NMR.

**3b** was synthesised by using the same method as **3a**. Similar analytical data were obtained.

## References

1 D. W. Bruce, in *Inorganic Materials*, 2nd edn., ed. D. W. Bruce and D. O'Hare, Wiley, Chichester, 1966; *J. Chem. Soc., Dalton Trans.*, 1993, 2983; P. M. Maitlis and A.-M. Giroud-Godquin, *Angew. Chem., Int. Ed. Engl.*, 1991, **30**, 402; S. A. Hudson and P. M. Maitlis, *Chem. Rev.*, 1993, **93**, 861; P. Espinet, J. L. Serrano, L. A. Oro and M. A. Esteruelas, *Coord. Chem. Rev.*, 1992, **30**, 402.

2 D. W. Bruce and X.-H. Liu, *J. Chem. Soc., Chem. Commun.*, 1994, 729; *Liq. Cryst.*, 1995, **18**, 165.

3 L. Oriol and J. L. Serrano, *Adv. Mater.*, 1995, **7**, 348.

4 M. Altmann and U. H. F. Bunz, *Angew. Chem., Int. Ed. Engl.*, 1995, **34**, 569; R. Deschenaux, I. Kosztics, J. L. Marendaz and H. Stoeckli-Evans, *Chimia*, 1993, **47**, 206; M. Altmann, V. Enkelmann, G. Lieser and U. H. F. Bunz, *Adv. Mater.*, 1995, **7**, 726; A. A. Dembek, R. R. Burch and A. E. Feiring, *J. Am. Chem. Soc.*, 1993, **115**, 2087.

5 R. Deschenaux and J. W. Goodby, in *Ferrocenes*, ed. A. Togni and T. Hayashi, VCH, Weinheim, 1995, ch. 9.

6 R. Deschenaux, J. L. Marendaz and J. Santiago, *Helv. Chim. Acta*, 1993, **76**, 865; R. Deschenaux and J. L. Marendaz, *J. Chem. Soc., Chem. Commun.*, 1991, 909.

7 (*a*) R. Deschenaux, V. Izvolenski, F. Turpin, D. Guillon and B. Heinrich, *Chem. Commun.*, 1996, 439; (*b*) R. Deschenaux, I. Kosztics, U. Scholten, D. Guillon and M. Ibn-Elhaj, *J. Mater. Chem.*, 1994, **4**, 1351; (*c*) A. Wiesemann and R. Zentel, *Liq. Cryst.*, 1994, **16**, 349.

8 P. Singh, M. D. Rausch and R. W. Lenz, *Polym. Bull.*, 1989, **22**, 247.

9 D. A. Foucher, B-Z. Tang and I. Manners, *J. Am. Chem. Soc.*, 1992, **114**, 6246; I. Manners, *Adv. Organomet. Chem.*, 1995, **37**, 131; Y.-Z. Ni, R. Rulkens and I. Manners, *J. Am. Chem. Soc.*, 1996, **118**, 4102.

10 D. Foucher, R. Ziembinski, R. Peterson, J. Pudelski, M. Edwards, Y.-Z. Ni, J. Massey, C. R. Jaeger, G. J. Vancso and I. Manners, *Macromolecules*, 1994, **27**, 3992.

11 R. Deschenaux, M. Schweissguth and A-M. Levelut, *Chem. Commun.*, 1996, 1275.

*Received, 10th October 1966; Com. 6/07238K*

# Selective two-electron reduction of $C_{60}$ by 10-methyl-9,10-dihydroacridine *via* photoinduced electron transfer

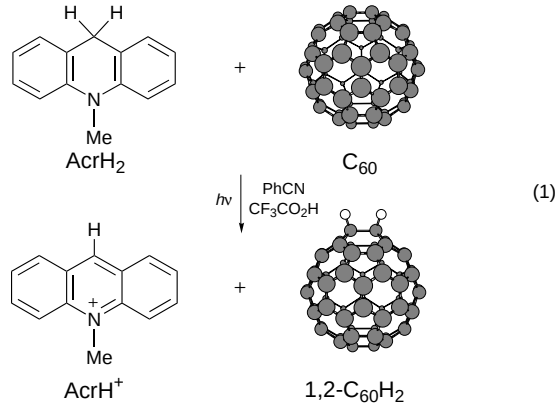
**Shunichi Fukuzumi,*[a] Tomoyoshi Suenobu,[a] Shuichiro Kawamura,[a] Akito Ishida[a] and Koichi Mikami*[b]**

[a] *Department of Applied Chemistry, Faculty of Engineering, The Institute of Scientific and Industrial Research, Osaka University, Suita, Osaka 565, Japan*

[b] *Department of Chemical Technology, Tokyo Institute of Technology, Meguro-ku, Tokyo 152, Japan*

**The selective two-electron reduction of $C_{60}$ to 1,2-dihydro[60]fullerene is attained *via* photoinduced electron transfer from 10-methyl-9,10-dihydroacridine to the triplet excited state of $C_{60}$ in the presence of trifluoroacetic acid in benzonitrile under irradiation of visible light.**

The preparation of dihydro[60]fullerene ($C_{60}H_2$) has recently attracted considerable interest, since it is the simplest $C_{60}$ hydrocarbon derivative.[1,2] The reduction of $C_{60}$ has so far been achieved by the use of strong reductants such as $BH_3$, which yield not only $C_{60}H_2$ but also polyhydride mixtures ($C_{60}H_{2n}$, $n$ = 2 and 3).[1,2] Thus, the use of relatively mild reductants to achieve the selective reduction of $C_{60}$ to $C_{60}H_2$ is desirable. However, $C_{60}$ in the ground state has proved extremely difficult to reduce with mild reductants. We report herein the selective two-electron reduction of $C_{60}$ by a mild hydride donor, 10-methyl-9,10-dihydroacridine ($AcrH_2$), *via* photoinduced electron transfer from $AcrH_2$ to the triplet excited state of $C_{60}$ ($^3C_{60}{}^*$) in the presence of trifluoroacetic acid in benzonitrile (PhCN) to yield 1,2-$C_{60}H_2$ selectively [eqn. (1)].




The hydride donor $AcrH_2$ and its deuteriated analogue 10-methyl[9,9-$^2H_2$]acridine ($AcrD_2$) were prepared as previously described.[3] To a solution of $C_{60}$ (10.1 mg, 0.014 mmol) in deaerated PhCN (50 ml) was added $AcrH_2$ (2.7 mg, 0.014 mmol) and $CF_3CO_2H$ (0.014 mmol), and the solution was irradiated with a Xe lamp equipped with a UV-cut filter ($\lambda$ < 540 nm) for 30 min. After evaporation of PhCN under reduced pressure, the residue was separated by washing with MeCN and centrifuged to give 1,2-$C_{60}H_2$ exclusively in 70% yield.† In the dark, however, no reaction occurred even at high temperatures (*e.g.* 373 K). No appreciable amount of polyadducts was obtained even after a prolonged irradiation time under the present experimental conditions. The $^1$H NMR signal at $\delta$ 5.91 (s, 2H) of 1,2-$C_{60}H_2$ (400 MHz, in $C_6D_6$) agrees well with that reported previously.[1] The visible spectrum exhibits an absorption maximum at $\lambda_{max}$ = 434 nm, which is known to be characteristic of a 1,2-monoadduct resulting from 1,2-addition to a 6–6 bond.[2] Theoretical investigation also indicates that 1,2-$C_{60}H_2$ is the most stable form among 23 different regioisomers.[4]

When the photoreduction of $C_{60}$ by $AcrH_2$ is carried out in the presence of NaI, the reaction is strongly inhibited. Since NaI is a well-known triplet quencher,[5] the photoreduction of $C_{60}$ probably proceeds *via* $^3C_{60}{}^*$, which is quenched by NaI to retard the photoreduction. In fact, the lifetime of the transient $^3C_{60}{}^*$ triplet–triplet (T–T) absorption at $\lambda_{max}$ = 740 nm is significantly reduced by the presence of $AcrH_2$. The bimolecular quenching rate constant ($k_q$) of $^3C_{60}$* by $AcrH_2$ was determined to be 4.3 × $10^9$ dm$^3$ mol$^{-1}$ s$^{-1}$ from the decay kinetics of transient T–T absorption at 740 nm following excitation at 355 nm. The quantum yields ($\Phi$) were also determined from an increase in absorbance due to 1,2-$C_{60}H_2$ by using a ferrioxalate actinometer[6] under irradiation of monochromatized light of $\lambda$ = 546 nm. The $\Phi$ value for the photoreduction of $C_{60}$ by $AcrH_2$ in PhCN increases with an increase in the concentration of $AcrH_2$ to reach a limiting value ($\Phi_\infty$) as shown in Fig. 1. From the dependence of $\Phi$ on [$AcrH_2$] is obtained the quenching constant $K_{obs}$ ( = $k_{obs}\tau_T$), which is converted to the rate constant ($k_{obs}$) for the reaction of $^3C_{60}$* with $AcrH_2$ (5.0 × $10^9$ dm$^3$ mol$^{-1}$ s$^{-1}$) by using $\tau_T$ for $^3C_{60}$* (32 μs) in PhCN.[7] The $k_{obs}$ value agrees with a $k_q$ value (4.3 × $10^9$ dm$^3$ mol$^{-1}$ s$^{-1}$) determined independently (*vide supra*). Such an agreement confirms that the photoreduction of $C_{60}$ proceeds *via* the triplet excited state.

The free energy change of the photoinduced electron transfer from $AcrH_2$ to $^3C_{60}$* is negative ($\Delta G^0_{et}$ = −32 kJ mol$^{-1}$) judging from the fact that the one-electron oxidation potential of $AcrH_2$ ($E^0_{ox}$ *vs.* SCE = 0.81 V)[8] is lower than the one-electron reduction potential of $^3C_{60}$* ($E^0_{red}$ *vs.* SCE = 1.14 V).[9] In such

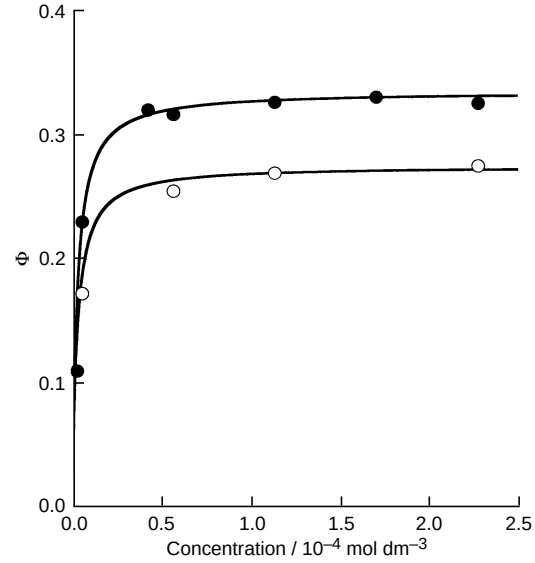
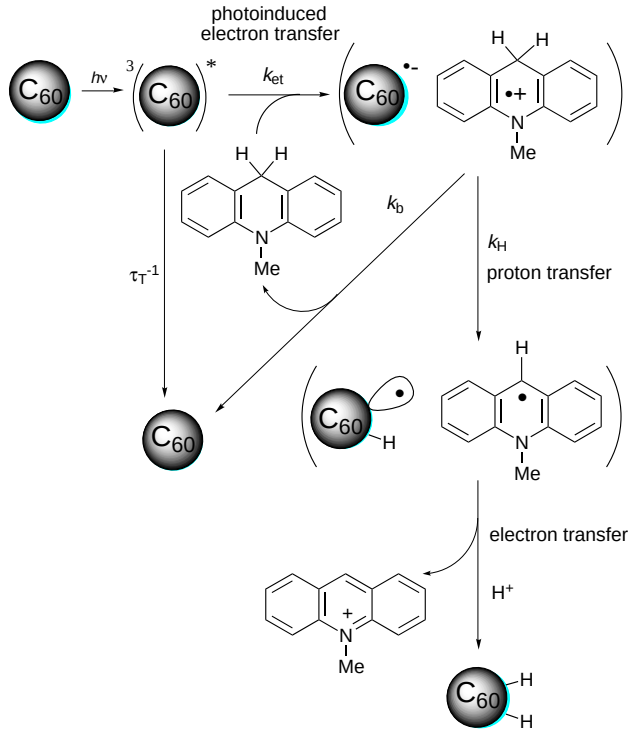



**Fig. 1** Dependence of the quantum yield on the concentration of $AcrH_2$ and $AcrD_2$ for the photoreduction of $C_{60}$ (2.8 × $10^{-4}$ mol dm$^{-3}$) by ● $AcrH_2$ and ○ $AcrD_2$ in the presence of $CF_3CO_2H$ (5.6 × $10^{-4}$ mol dm$^{-3}$) in PhCN at 298K.

a case the electron transfer rate constant ($k_{et}$) may reach the diffusion-limited value in PhCN ($5.6 \times 10^9$ dm$^3$ mol$^{-1}$ s$^{-1}$),[9] which agrees with both the $k_{obs}$ and $k_q$ values (*vide supra*). Thus, the photoreduction of $C_{60}$ by $AcrH_2$ may proceed *via* photoinduced electron transfer from $AcrH_2$ to $^3C_{60}$* ($k_{et}$) as shown in Scheme 1. The photoinduced electron transfer gives the radical ion pair in competition with the decay to the ground state ($k_T = \tau_T^{-1}$). Since $AcrH_2^{\cdot+}$ is known to be a very strong acid,[8] proton transfer from $AcrH_2^{\cdot+}$ to $C_{60}^{\cdot-}$ ($k_H$) may occur in the radical ion pair in competition with the back electron transfer to the reactant pair ($k_b$), to give $C_{60}H^{\cdot}$, which is converted to 1,2-$C_{60}H_2$ by fast electron transfer from $AcrH^{\cdot}$ in the presence of $CF_3CO_2H$. By applying the steady-state approximation to the reactive species, $^3C_{60}$* and the radical ion pair in Scheme 1, the dependence of $\Phi$ on [$AcrH_2$] can be derived as given by eqn. (2), which agrees with the observed dependence of $\Phi$ on

$$\Phi = (k_H/(k_H + k_b))k_{et}\tau_T[AcrH_2]/(1 + k_{et}\tau_T[AcrH_2]) \quad (1)$$




**Scheme 1**

[$AcrH_2$] in Fig. 1. The limiting quantum yield $\Phi_\infty$ corresponds to $k_H/(k_H + k_b)$. Thus, the $\Phi_\infty$ value being smaller than unity (0.33) may be ascribed to the competition of the proton transfer process ($k_H$) with the back electron transfer process ($k_b$). The existence of a protonation step following the photoinduced electron transfer is confirmed by the observed deuterium isotope effect in the limiting quantum yield ($\Phi^\infty_H/\Phi^\infty_D = 1.2$ in Fig. 1) when $AcrH_2$ is replaced by the deuteriated compound ($AcrD_2$). In contrast, no kinetic isotope effect was observed for the rate constant of electron transfer.

Alternatively, $C_{60}^{\cdot-}$ produced in the initial photoinduced electron transfer from $AcrH_2$ to $C_{60}$ could be protonated by the acid, and hydrogen transfer from $AcrH_2^{\cdot+}$ to $C_{60}H^{\cdot}$ gives the final products. However, no increase in the quantum yield was observed with an increase in the amount of $CF_3CO_2H$. In addition, the reduction potential of $C_{60}$ was not affected by the presence of $CF_3CO_2H$ in PhCN, as previously observed.[10] Thus, the protonation of $C_{60}^{\cdot+}$ probably occurs *via* $AcrH_2^{\cdot+}$ in the radical ion pair rather than *via* $CF_3CO_2H$ (Scheme 1).

## Footnote

† The yield was determined by HPLC equipped with an analytical 'Buckyclutcher I' column (Regis, Morton Grove, IL). A hexane– toluene mixture was used as eluent with a flow rate of 2 ml min$^{-1}$. The product was monitored at 434 nm with a UV-VIS detector.

## References


1 C. C. Henderson and P. A. Cahill, *Science*, 1993, **259**, 1885; S. Ballenweg, R. Gleiter and W. Krätschmer, *Tetrahedron Lett*., 1993, **34**, 3737; L. Becker, T. P. Evans and J. L. Bada, *J. Org. Chem*., 1993, **58**, 7630; T. F. Guarr, M. S. Meier, V. K. Vance and M. Clayton, *J. Am. Chem. Soc*., 1993, **115**, 9862.

2 A. Hirsch, *The Chemistry of the Fullerenes*, Georg Thieme Verlag, New York, 1994, p. 115.

3 S. Fukuzumi, S. Koumitsu, K. Hironaka and T. Tanaka, *J. Am. Chem. Soc*., 1987, **109**, 305.

4 N. Matsuzawa, D. A. Dixon and T. Fukunaga, *J. Phys. Chem*., 1992, **96**, 7594.

5 S. Fukuzumi, S. Kuroda and T. Tanaka, *J. Am. Chem. Soc*., 1985, **107**, 3020.

6 C. G. Hatchard and C. A. Parker, *Proc. R. Soc. London, Ser. A*, 1956, **235**, 518.

7 K. Mikami, S. Matsumoto, A. Ishida, S. Takamuku, T. Suenobu and S. Fukuzumi, *J. Am. Chem. Soc*., 1995, **117**, 11134.

8 S. Fukuzumi, Y. Tokuda, T. Kitano, T. Okamoto and J. Otera, *J. Am. Chem. Soc*., 1993, **115**, 8960.

9 J. W. Arbogast, C. S. Foote and M. Kao, *J. Am. Chem. Soc*., 1992, **114**, 2277.

10 D. E. Cliffel and A. J. Bard, *J. Phys. Chem*., 1994, **98**, 8140.


*Received, 31st October 1996; Com. 6/07417K*

# Synthesis, crystal structure and rearrangement of a methylene(ylene)-phosphorane containing a $CH_2$-moiety at an $sp^2$-hybridized phosphorus(v) centre

**Bernd Schinkels, Alexander Ruban, Martin Nieger and Edgar Niecke***

*Anorganisch-Chemisches-Institut der Universität Bonn, Gerhard Domagk Str.1, D-53121 Bonn, Germany*

**The reaction of the iminophosphane, $(Me_3Si)_3C–P=N–Mes^*$, with $Me_2S=CH_2$ affords the first methylenephosphorane containing a $CH_2$ moiety at an $sp^2$-hybridized phosphorus(v) centre; the crystal structure as well the rearrangement of which is reported.**

Methylenephosphoranes **I**, which may be formally regarded as a phosphane stabilized methylene ($CH_2$), are well established[1] and their chemistry with respect to organic and organometallic syntheses has long been known.[2]

In contrast, only one kinetically stable derivative of a methylenephosphane,[3] **II**, is known so far in which the $CH_2$ moiety is linked to a phosphinidene unit. Methylene(ylene)-phosphoranes **III**, which also contain an $sp^2$-hybridized phosphorus centre as in **II** but with phosphorus(v) are known so far only as transient species, and their existence has only been inferred from trapping experiments.[4] Here we report the synthesis and X-ray structure of the first example of a stable derivative of a methylenephosphorane of the type **III** (Fig. 1).

In a typical experiment, a THF solution of the iminophosphane, $(Me_3Si)_3CP=NMes^*$, **1** [obtained by the treatment of $ClP=NMes^*$[5] with an equimolar quantity of $LiC(SiMe_3)_3$ in THF at −78 °C†] was added under stirring to an equimolar quantity of $Me_2S=CH_2$ in THF at −40 °C.

The solvent was removed under vacuum and the residue was taken up in 40 ml of hexane. The LiI present was removed by filtration and the filtrate concentrated and the resulting residue recrystallized from hexane to give **2** as pale colourless crystals (82.6% yield).

Compound **2** was shown to be a monomer from the observation of the molecular ion in the high-resolution mass spectrum at *m/z* 534 (6%). The formation of an imino(methylene)phosphorane and not of the valence isomeric azaphosphirane[6] is readily demonstrated by the low field $^{31}P$ NMR chemical shift (δ 157.8), while the lowest field signal in the $^{13}C$ NMR spectrum (δ 64.2, $^1J_{CP}$ 108.2 Hz) manifests the existence of a methylene carbon atom attached to a phosphorus(v) centre. The direct proximity of two chemical inequivalent hydrogens attached to this atom (d δ 3.07; dd 3.38, $^2J_{PH}$ 14.1, $^2J_{HH}$ 7.7 Hz) unambiguously proves the presence of a $>P=CH_2$ moiety (Scheme 1).

The new methylenephosphorane **2** was conclusively characterized by X-ray crystallography‡ for which suitable crystals were obtained from hexane at room temperature (Fig. 2). As in all structurally investigated bis(ylene)phosphoranes,[7] the central phosporus atom exhibits a trigonal planar environment (sum of the angles at P = 360°). The methylene carbon atom, both the hydrogen atoms bonded to it, and the atoms P(1)–N(1)–C(12) are almost planar (mean deviation from plane = 0.005 Å). The aryl substituent at N(1) is approximately orthogonal to the central π-bond system (the angle between the plane P(1)–N(1)–C(1)–C(2) and the aryl plane is 89°) and in an *E*-configuration relative to the $(Me_3Si)_3C$ substituent at P(1), as is found in the iminophosphane **1** (Scheme 1). As compared to known imino(methylene)phosphoranes,[8] the P(1)–N(1)-bond length [1.556(2) Å] in **2** is elongated which may be interpretated in terms of the small P(1)–N(1)–C(12) angle [121.2(2)°], whereas the P(1)–C(1) distance [1.612(3) Å] is significantly shorter. Other bond lengths and angles do not show any peculiarities.

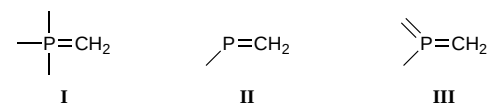
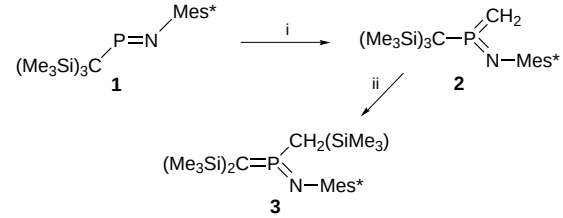



**Fig. 1**

While compound **2** is stable at ambient temperatures it easily isomerizes by heating a toluene solution of **2** at about 100 °C to give the corresponding imino(methylene)phosphorane **3**, which was isolated by recrystallization from non-polar solvents as a colourless powder (84.7% yield). The isomerization **2** → **3** by [1,3] silyl migration in the C–P=C triad results in chemical equivalence and the shielding of the two hydrogens atoms, as shown by $^1H$ NMR, (δ 2.0, $^2J_{PH}$ 16.1 Hz), which reflects the change in hybridization from $sp^2$ to $sp^3$. Furthermore the three equivalent silyl groups in **2** split into a set of three resonances in **3**. The tricoordinated phosphorus(v) centre maintains the characteristic low field shift in the $^{31}P$ NMR spectrum (δ 129.5), whereby the chemical shift of the methylene carbon in the $^{13}C$ NMR spectrum (δ 68.3, $^1J_{PC}$ 43.1 Hz) falls in the same spectral




**Scheme 1** *Reagents and conditions*: i, $Me_2SCH_2$, THF, −40 °C, 82.6%; ii, toluene, 1 h, reflux, 84.7%

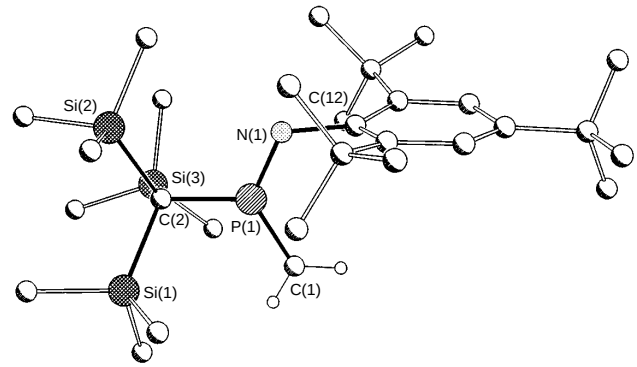



**Fig. 2** Molecular structure of **2**. Disordered parts and methyl and aromatic hydrogen atoms were omitted for clarity. Selected bond lengths (Å) and angles (°): P(1)–C(1) 1.612(3), P(1)–N(1) 1.556(2), P(1)–C(2) 1.803(2); C(1)–P(1)–N(1) 124.8(1), C(1)–P(1)–C(2) 118.6(1), N(1)–P(1)–C(2) 116.7(1), P(1)–N(1)–C(12) 121.2(2), C(1)–P(1)–N(1)–C(12) 2.6(3), C(2)–P(1)–N(1)–C(12) −178.5(2).

region as in **2**. The composition of **3** was further deduced from the high-resolution mass spectrum.

We thank the Deutsche Forschungsgemeinschaft, the Fonds der Chemischen Industrie for generous financial support and the Graduierten Kolleg for a grant (A. R.).

## Footnotes

† *Spectroscopic data* for **1**: Yield 76.1% mp 78–81 °C. $^{31}$P NMR ($C_6D_6$): δ 500.4; $^{1}$H NMR ($C_6D_6$): δ 0.53 (s, 27 H, $SiMe_3$), 1.50 (s, 9 H, *p*-Bu$^t$), 1.68 (s, 18 H, *o*-Bu$^t$), 7.67 (s, 2 H, $C_6H_2$); $^{13}$C NMR ($C_6D_6$): δ 5.4 (d, $^{3}J_{PC}$ 4.4 Hz, $SiMe_3$), 32.2 (s, *o*-C*C*H$_3$), 34.6 (d, $J_{PC}$ 2.6 Hz, *p*-C*C*H$_3$), 34.9 (s, *p*-*C*CH$_3$), 37.2 (s, *o*-*C*CH$_3$), 47.9 (d, $^{1}J_{PC}$ 100.3 Hz, *p*-*C*Si$_3$), 122.7 (s, *m*-Ar), 137.2 (d, $^{3}J_{PC}$ 11.7 Hz, *o*-Ar), 143.0 (s, *p*-Ar), 150.7 (d, $^{2}J_{PC}$ 15.7 Hz, *ipso*-Ar). MS (20 eV, EI) *m/z* (%) 521 (7%) [M$^+$], 290 (100) [PNMes*$^+$]. For **2**: Yield 82.6%, mp 86–90 °C. $^{31}$P NMR ($C_6D_6$): δ 157.8; $^{1}$H NMR ($C_6D_6$): δ 0.56 (s, 27 H, $SiMe_3$), 1.51 (s, 9 H, *p*-Bu$^t$), 1.84 (s, 18 H, *o*-Bu$^t$), 3.10 (d, $^{2}J_{HH}$ 7.7 Hz, $^{2}J_{PH}$ < 1.0 Hz, 1 H, P=C$H_2$), 3.38 (dd, $^{2}J_{HH}$ 7.7, $^{2}J_{PH}$ 14.1 Hz, 1 H, P=C$H_2$), 7.65 (d, $^{6}J_{PH}$ 2.2 Hz, 2 H, $C_6H_2$); $^{13}$C NMR ($C_6D_6$): δ 6.0 (d, $^{3}J_{PC}$ 3.1 Hz, $SiMe_3$), 17.2 (d, $^{1}J_{PC}$ 28.5 Hz, P-*C*Si$_3$), 32.3 (d, $^{7}J_{PC}$ 1.7 Hz, *p*-*C*CH$_3$), 33.2 (d, $^{5}J_{PC}$ 1.4 Hz, *o*-*C*CH$_3$), 35.0 (d, $^{6}J_{PH}$ 1.9 Hz, *p*-*C*CH$_3$), 37.5 (d, $^{4}J_{PH}$ 2.3 Hz, *o*-*C*CH$_3$), 64.2 (d, $^{1}J_{PC}$ 108.2 Hz, P=C$H_2$), 123.0 (d, $^{4}J_{PH}$ 5.7 Hz, *m*-Ar), 141.5 (d, $^{3}J_{PC}$ 11.8 Hz, *o*-Ar), 142.2 (d, $^{5}J_{PH}$ 6.5 Hz, *p*-Ar), 146.2 (d, $^{2}J_{PC}$ 13.4 Hz, *ipso*-Ar). The $CH_2$ group is confirmed by a DEPT 135 experiment. MS (20 eV, EI) *m/z* (%) 535 (4) [M$^+$], 73 (100) [$(CH_3)_3Si^+$] (Found: M$^+$, 535.3614. $C_{29}H_{58}N_1{:}Si_3P_1$ requires 535.3620). For **3**: Yield 84.7%, mp 82–84 °C. $^{31}$P NMR ($C_6D_6$): δ 129.5; $^{1}$H NMR ($C_6D_6$): δ 0.29 (s, 9 H, $SiMe_3$), 0.31 (s, 9 H, $SiMe_3$), 0.39 (s, 9 H, $SiMe_3$), 1.51 (s, 9 H, *p*-Bu$^t$), 1.74 (s, 18 H, *o*-Bu$^t$), 2.0 (d, $^{2}J_{PH}$ 16.1 Hz, 2 H, $SiMe_3CH_2$), 7.55 (d, $^{6}J_{PH}$ 2.2 Hz, 2 H, $C_6H_2$); $^{13}$C NMR ($C_6D_6$): δ 1.14 (d, $^{3}J_{PC}$ 3.4 Hz, P=CSi*Me*$_3$), 4.37 (d, $^{3}J_{PC}$ 4.9 Hz, P=CSi*Me*$_3$), 5.6 (d, $^{3}J_{PC}$ 5.0 Hz, Si*Me*$_3$CH$_2$), 21.7 (d, $^{1}J_{PC}$ 62.3 Hz, P–*C*(SiMe$_3$)H$_2$), 32.1 (d, $^{7}J_{PC}$ 1.2 Hz, *p*-C*C*H$_3$), 32.3 (d, $^{5}J_{PC}$ 1.7 Hz, *o*-C*C*H$_3$), 35.0 (d, $^{6}J_{PH}$ 1.5 Hz, *p*-*C*CH$_3$), 37.0 (d, $^{4}J_{PH}$ 1.9 Hz, *o*-*C*CH$_3$), 68.3 [d, $^{1}J_{PC}$ 43.1 Hz, P=C(SiMe$_3$)$_2$], 122.5 (d, $^{4}J_{PH}$ 4.2 Hz, *m*-Ar), 140.0 (d, $^{3}J_{PC}$ 10.3 Hz, *o*-Ar), 142.2 (d, $^{5}J_{PH}$ 5.0 Hz, *p*-Ar), 144.7 (d, $^{2}J_{PC}$ 10.3 Hz, *ipso*-Ar). MS (20 eV, EI) *m/z* (%) 535(3) [M$^+$], 73 (100) [$(CH_3)_3Si^+$].

‡ *Crystal data* for **1**: $C_{28}H_{56}NPSi_3$, $M$ = 522.0, triclinic space group $P\bar{1}$ (no. 2), red crystals, dimensions 0.10 × 0.20 × 0.38 mm$^3$, $a$ = 9.814(3), $b$ = 13.580(5), $c$ = 14.113(4) Å, α = 64.38(3), β = 82.94(2), γ = 79.20(3)°, $U$ = 1664(1) Å$^3$, $D_c$ = 1.04 mg m$^{-3}$, $Z$ = 2, μ(CuKα) = 1.87 mm$^{-1}$, $T$ = 200(2) K, $F$(000) = 576.5647 symmetry independent reflections were used for the structure solution (direct methods) and refinement (full-matrix least-squares on $F^2$, 316 parameters). Non-hydrogen atoms were refined anisotropically, H atoms localized by difference electron density and refined using a 'riding' model. *wR*2 = 0.136 {$R_1$ = 0.049 [$I > 2\sigma(I)$]}. An empirical absorption correction on the basis of Ψ-scans was applied. Selected bond lengths (Å) and angles (°): P(1)–N(1) 1.566(3), P(1)–C(19) 1.837(3), N(1)–C(1) 1.429(4); P(1)–N(1)–C(1) 120.2(2), C(19)–P(1)–N(1) 110.4(2), C(1)–N(1)–P(1)–C(19)–178.7(2). For **2**: $C_{29}H_{58}NPSi_3$, $M$ = 536.0, triclinic, space group $P\bar{1}$ (no. 2), yellow crystals, dimensions 0.60 × 0.70 × 0.80 mm$^3$, $a$ = 9.182(3), $b$ = 13.539(5), $c$ = 15.247(5) Å, α = 65.59(3), β = 84.94(3), γ = 82.42(3)°, $U$ = 1710(1) Å$^3$, $D_c$ = 1.04 mg m$^{-3}$, $Z$ = 2, μ(MoKα) = 0.20 mm$^{-1}$, $T$ = 293(2) K, $F$(000) = 592.6025 symmetry independent reflections were used for the structure solution (direct methods) and refinement (full-matrix least-squares on $F^2$, 444 parameters, 540 restraints). Non-hydrogen atoms were refined anisotropically, H atoms localized by difference electron density and refined using a 'riding' model, *wR*2 = 0.184 {$R_1$ = 0.062 [$I > 2\sigma(I)$]}. The *p*-Bu$^t$ and the C(SiMe$_3$)$_3$ group were disordered. Atomic coordinates, bond lengths and angles, and thermal parameters have been deposited at the Cambridge Crystallographic Data Centre (CCDC). See Information for Authors, Issue No. 1. Any request to the CCDC for this material should quote the full literature citation and the reference number 182/318.

## References

1 A. W. Johnson, in *Ylids and Imines of Phosphorus*, Wiley, New York, 1993.
2 B. E. Maryanoff and A. B. Reitz, *Chem. Rev.*, 1989, **89**, 863; H. Schmidbaur, *Angew. Chem., Int. Ed. Engl.*, 1983, **22**, 907.
3 R. Appel, C. Casser, M. Immenkeppel and F. Knoch, *Angew. Chem., Int. Ed. Engl.*, 1984, **23**, 895; *J. Organomet. Chem.*, 1985, **293**, 213; K. Issleib, H. Schmidt and C. Wirkner, *Z. Anorg. Allg. Chem.*, 1982, **488**, 75.
4 E. Niecke and D.-A. Wildbredt, *Chem. Ber.*, 1980, **113**, 1549.
5 E. Niecke, M. Nieger and F. Reichert, *Angew. Chem.*, 1988, **100**, 1781; *Angew. Chem., Int. Ed. Engl.*, 1988, **27**, 1715.
6 E. Niecke, A. Seyer and D.-A. Wildbredt, *Angew. Chem.*, 1981, **93**, 687; *Angew. Chem., Int. Ed. Engl.*, 1981, **20**, 675.
7 M. Regitz and O. J. Scherer, *Multiple Bonds and Low Coordination in Phosphorus Chemistry*, Thieme Verlag, New York, 1989.
8 W. Schilbach, V. von der Gönna, D. Gudat, M. Nieger and E. Niecke, *Angew. Chem.*, 1994, **106**, 1037; *Angew. Chem., Int. Ed. Engl.*, 1994, **33**, 982.

*Received, 30th October 1996; Com. 6/07402B*

# Formation of a novel $Re_3$(μ-ethyne) cluster and the possible involvement of Re=Re electrons in the bonding

**Wei-Wei Zhuang and David M. Hoffman***

*Department of Chemistry, University of Houston, Houston, TX 77204, USA*

**The homoleptic neopentoxide cluster $[Re_3(\mu\text{-}OCH_2Bu^t)_3(OCH_2Bu^t)_6]$ reacts with ethyne to give a novel adduct having ethyne bridged perpendicular to one edge of a $Re_3$ triangle and with substituted alkynes to yield alkenyl clusters and pivaldehyde.**

The chemistry of $[Re_3(\mu\text{-}X)_3X_6]$ clusters, which have a robust triangular $Re_3$ core with three Re–Re double bonds, is characterized primarily by reactions involving X substitution or transformation, ligand adduct formation and, in a few cases, cluster breakdown.[1] Herein we report the formation of a novel ethyne adduct derived from a $[Re_3(\mu\text{-}X)_3X_6]$ cluster, $[Re_3(\mu\text{-}OCH_2Bu^t)_2(OCH_2Bu^t)_7(\mu\text{-}HCCH)]$, which may be best described as a dimetallatetrahedrane.

The homoleptic neopentoxide cluster $[Re_3(\mu\text{-}OCH_2Bu^t)_3(OCH_2Bu^t)_6]$, synthesized by the same method used to prepare $[Re_3(\mu\text{-}OPr^i)_3(OPr^i)_6]$,[2] reacts in hot hexane with 10 equiv. of ethyne (closed flask heating at 50 °C for 12 h) to give $[Re_3(OCH_2Bu^t)_9(HCCH)]$. The product was isolated in 61% yield as green crystals from a cold saturated hexane solution. A single-crystal X-ray crystallographic analysis shows that ethyne bridges perpendicularly to one edge of a $Re_3$ triangle (Fig. 1).† The ethyne-bridged Re–Re bond is slightly longer (0.021 Å) than the neopentoxide-bridged bond, and both distances are significantly longer than the Re–Re distances in $[Re_3(\mu\text{-}OCH_2Bu^t)_3(OCH_2Bu^t)_6]$ [av. 2.368 (1) Å][3] and other $Re_3$ alkoxide clusters.[2,4,5] The C–C bond distance [1.414(33) Å] is between those of a single and double bond but the large e.s.d. indicates the distance should be interpreted with caution. The Re–C distances are close to those found, for example, in $[Re_3Me_9(PPhEt_2)_2]$,[6] and the Re–$O_t$ distances are normal. The bridging neopentoxide is 0.2 Å closer to Re(1) than Re(2).

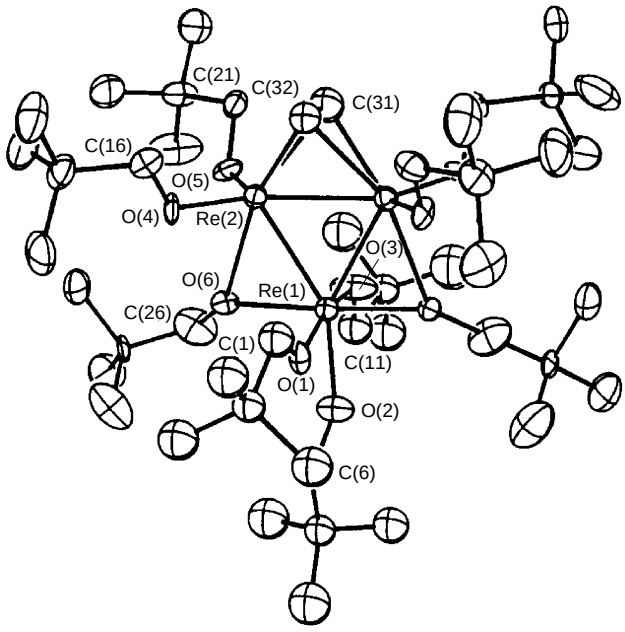



**Fig. 1** View of the $[Re_3(\mu\text{-}OCH_2Bu^t)_2(OCH_2Bu^t)_7(\mu\text{-}HCCH)]$ molecule showing the atom numbering scheme. Only one orientation of each disordered group is shown. Bond lengths (Å) and angles (°): Re(1)–Re(2) 2.496(1), Re(1)–O(1) 1.895(13), Re(1)–O(2) 2.025(16), Re(1)–O(3) 1.912(14), Re(1)–O(6) 1.990(11), Re(2)–Re(2′) 2.517(2), Re(2)–O(4) 1.910(10), Re(2)–O(5) 1.902(10), Re(2)–O(6) 2.203(10), Re(2)–C(31) 2.143(22), Re(2)–C(32) 2.155(18), C(31)–C(32) 1.414(33); O(1)–Re–O(2) 84.1(6), O(1)–Re–O(3) 165.6(6), O(6)–Re–O(6′) 175.1(6), O(4)–Re(2)–O(5) 111.6(5), O(6)–Re(2)–O(4) 82.5(4), O(6)–Re(2)–O(5) 83.7(4).

The room-temperature $^1H$ NMR spectrum of $[Re_3(OCH_2Bu^t)_9(HCCH)]$ is fully consistent with the solid-state structure. The coupling constants associated with the ethyne ligand were obtained for $[Re_3(OCH_2Bu^t)_9(H^{13}C^{13}CH)]$ from proton and carbon-13 spectra, which each consisted of one-half of an expected AA′XX′ pattern in the ethyne region. Two of the four constants, $^1J_{CH}$ = 210 Hz and $^2J_{CH}$ = 4.5 Hz, were determined analytically from the spectrum,[7] and the other two, $^1J_{CC}$ = 23–26 Hz and $^3J_{HH}$ = 0–3 Hz, were obtained by a combination of analytical methods and spectrum simulations. The small one-bond $^{13}C$–$^{13}C$ coupling constant (*cf.* $^1J_{CC}$ = 172 Hz for ethyne)[8] suggests there is substantial electron transfer from the Re=Re bonds to the coordinated ethyne. The observed $^1J_{CC}$ is comparable, in fact, to those for $[M_2(OR)_6(py)_n(\mu\text{-}C_2H_2)]$ complexes (M = Mo, 23–28 Hz; M = W, 10–19 Hz), which have been described as closely approaching the dimetallatetrahedrane description on the basis of structural, theoretical, spectroscopic and reactivity studies.[9] The lengthening of the Re–Re bonds in the adduct compared to the parent cluster is also consistent with the dimetallatetrahedrane model.

Steric factors are important in the formation of the ethyne adduct. The reactions of $[Re_3(OCH_2Bu^t)_9]$ with MeCCMe, $Me_3CCH$ and PhCCPh, for example, all give alkenyl products and pivaldehyde [eqn. (1)]. Analogous products were observed previously in reactions between $[Re_3(\mu\text{-}OPr^i)_3(OPr^i)_6]$ and alkynes, including ethyne.[4] The proposed mechanism for formation of the alkenyl products in these systems is alkoxide β-hydrogen elimination from $[Re_3(\mu\text{-}OR)_3(OR)_6]$ to give the terminal hydride cluster $[Re_3H(\mu\text{-}OR)_3(OR)_5]$, and subsequent trapping of the hydride by alkyne.

$$[Re_3(\mu\text{-}OCH_2Bu^t)_3(OCH_2Bu^t)_6] + RCCR' \xrightarrow[50\ °C]{C_6D_6} [Re_3(\mu\text{-}OCH_2Bu^t)_3\{\eta^1\text{-}CR{=}C(H)R'\}(OCH_2Bu^t)_5] + Bu^tC(O)H \quad (1)$$

(R = R′ = Me, Et or Ph; R = H, R′ = $Bu^t$)

To summarize, $[Re_3(\mu\text{-}OCH_2Bu^t)_3(OCH_2Bu^t)_6]$ and ethyne react to give $[Re_3(\mu\text{-}OCH_2Bu^t)_2(OCH_2Bu^t)_7(\mu\text{-}HCCH)]$, a triangular cluster in which ethyne bridges perpendicularly to a Re–Re edge. There are a few low-valent transition-metal alkyne clusters having cores resembling that in $[Re_3(\mu\text{-}OCH_2Bu^t)_2(OCH_2Bu^t)_7(\mu\text{-}HCCH)]$,[10,11] but there appear to be no other mid- or high-valent examples. The ethyne in $[Re_3(\mu\text{-}OCH_2Bu^t)_2(OCH_2Bu^t)_7(\mu\text{-}HCCH)]$ is substantially reduced as judged by the long C–C bond and small $^{13}C$–$^{13}C$ coupling constant, suggesting there is electron transfer from the Re=Re bonds to the ethyne. Although this appears to be the first example of this type of internal electron-transfer behaviour in the $[Re_3(\mu\text{-}X)_3X_6]$ system, it is a common feature in the chemistry of mid-

valent early transition-metal multiply bonded compounds. Two prototypical examples are the reactions of triply bonded $[M_2(OR)_6]$ (M = Mo, W) compounds with CO and alkynes to form, respectively, alkylidene- and dimetallatetrahedrane-like $[M_2(OR_6)(\mu\text{-CO})]$ and $[M_2(OR)_6(\mu\text{-alkyne})]$ complexes. In contrast to the reaction between ethyne and $[Re_3(\mu\text{-}OCH_2Bu^t)_3(OCH_2Bu^t)_6]$, reactions involving substituted alkynes give pivaldehyde and alkenyl clusters *via* a proposed hydride intermediate.

We thank the Robert A. Welch Foundation for financial support and Dr J. Korp for his technical assistance with the X-ray crystallographic analysis of $[Re_3(OCH_2Bu^t)_9(HCCH)]$.

## Footnote

† *Crystal data* for $[Re_3(\mu\text{-}OCH_2Bu^t)_2(OCH_2Bu^t)_7(\mu\text{-HCCH})]$ at −50 °C, $C_{47}H_{101}O_9Re_3\cdot 2CH_2Cl_2$, dark olive green plate, 0.12 × 0.40 × 0.45 mm, $M$ = 1538.94, monoclinic, space group $P2_1/m$, $a$ = 11.879(2), $b$ = 22.847(5), $c$ = 12.004(2) Å, β = 95.46(1)°, $U$ = 3243 Å$^3$, $Z$ = 2, $D_c$ = 1.58 g cm$^{-3}$, μ(Mo-Kα) = 58.7 cm$^{-1}$. Data were collected on a Nicolet R3m/V diffractometer with graphite-monochromated Mo-Kα radiation (λ = 0.710 73 Å) in the ω scan mode. Lorentz and polarization corrections as well as an empirical absorption correction based on ten reflections having χ values between 70 and 90° were applied to the data. A total of 5023 reflections were collected in the range $4 < 2\theta < 48°$; 3452 unique reflections with $I > 3\sigma(I)$ were used in the structure solution. Three of the neopentoxide groups [C(1), C(6), C(11)] were treated as independently rotating rigid bodies because of disorder. Two significant areas of residual electron density were noted on the mirror plane which were indicative of a severe positional disorder of the entire molecule, and these were refined as partial Re atoms having a total of 3% occupancy. $R(F)$ = 0.061; $R_w(F)$ = 0.054 where $w = [\sigma(F)]^{-2}$.

Atomic coordinates, bond lengths and angles, and thermal parameters have been deposited at the Cambridge Crystallographic Data Centre (CCDC). See Information for Authors, Issue No. 1. Any request to the CCDC for this material should quote the full literature citation and the reference number 182/338.

## References

1 F. A. Cotton and R. A. Walton, *Multiple Bonds Between Metal Atoms*, Clarendon Press, Oxford, 1993.
2 D. M. Hoffman, D. Lappas and D. A. Wierda, *J. Am. Chem. Soc.*, 1993, **115**, 10 538.
3 W. W. Zhuang and D. M. Hoffman, submitted for publication.
4 D. M. Hoffman, D. Lappas and D. A. Wierda, *Organometallics*, in the press.
5 A. C. C. Wong and G. Wilkinson, *Polyhedron*, 1988, **7**, 1363.
6 P. Edwards, K. Mertis, G. Wilkinson, M. B. Hursthouse and K. M. A. Malik, *J. Chem. Soc., Dalton Trans.*, 1980, 334.
7 H. Günther, *Angew. Chem., Int. Ed. Engl.*, 1972, **11**, 861; *Angew. Chem.*, 1972, **84**, 907.
8 K. Kamien'ska-Trela, *Ann. Rep. NMR Spectrosc.*, 1995, **30**, 131.
9 M. H. Chisholm, B. K. Conroy, D. L. Clark and J. C. Huffman, *Polyhedron*, 1988, **7**, 903.
10 M. Green, J. A. K. Howard, A. P. James, C. M. Nunn and F. G. A. Stone, *J. Chem. Soc., Dalton Trans.*, 1986, 187.
11 L. E. Bogan, Jr., G. R. Clark and T. B. Rauchfuss, *Inorg. Chem.*, 1986, **25**, 4050.
12 M. H. Chisholm, D. M. Hoffman and J. C. Huffman, *Chem. Soc. Rev.*, 1985, 69.

*Received, 1st November 1996; Com. 6/07432D*

# Chromogenic reagent for mercury based on Kemp's acid imide

**Zhen-He Wang,[a] Takuji Hirose,*[a] Bruce W. Baldwin[a] and Yanyan Yang[b]**

[a] *National Institute of Materials and Chemical Research, 1-1 Higashi, Tsukuba, Ibaraki 305, Japan*
[b] *Department of Chemistry, University of Tsukuba, Tsukuba, Ibaraki 305, Japan*

**Kemp's acid imide type chromogenic reagent showed a significant colour change with excellent selectivity for $Hg^{II}$ over other transition- and heavy-metal ions.**

Recently, we reported that Kemp's acid imides were useful carriers for the transport of various metal ions.[1,2] Amongst these carriers, the aromatic Kemp's acid imide **2** had an especially high transport ability and efficiency for $Hg^{II}$. By substituting a chromogenic moiety in place of the *n*-butyl group of **2**, a molecular sensor for mercury was constructed. Here, we present an excellent chromogenic reagent **1**, which is different from the usual reagents having either sulfur atoms or a macrocyclic structure,[3–5] for $Hg^{II}$ with high selectivity over other transition- and heavy-metal ions.

Chromophore **1** was synthesized in 59% yield in the same manner as **2** by the reaction of Kemp's triacid anhydride acid chloride and *N*,*N*-dimethyl-4,4′-azodianiline **3**.[6] Characterization of **1** was accomplished using $^1H$ and $^{13}C$ NMR spectroscopy, high-resolution mass spectrometry, and elemental analysis. UV–VIS spectra were measured on a Jasco V-550 spectrophotometer in acetonitrile containing 0.01 mol $dm^{-3}$ $LiClO_4$ as electrolyte; a large excess of $LiClO_4$ did not affect the spectra of **1** under these conditions. A 1.00 cm optical pathlength quartz cell, stirred magnetically, and thermostatted at 25.0 ± 0.2 °C, was used in the spectral measurements.

The titration experiments were carried out using $3.00 \times 10^{-5}$ mol $dm^{-3}$ of chromophore **1**, with the addition of 0.0–10.0 mol equiv. of $Hg(ClO_4)_2$. After the addition of an acetonitrile solution of $Hg(ClO_4)_2$, the yellow chromophoric solution ($\lambda_{max}$ = 418 nm) dramatically changed colour to red with the appearance of a new peak ($\lambda_{max}$ = 519 nm), as shown in Fig. 1. As clearly seen upon the addition of $Hg^{II}$ from 0.0 to 10.0 mol equiv. the original absorption band ($\lambda_{max}$ = 418 nm) intensity decreased, while the new absorption band ($\lambda_{max}$ = 519 nm) intensity increased. The two absorption bands, with an isosbestic point at 462 nm, indicated an equilibrium between at least two species. The simplest case would involve two species present in solution, assumed to be the chromophore itself ($\lambda_{max}$ = 418 nm), and the complex ($\lambda_{max}$ = 519 nm) in a 1 : 1 (and/or 2 : 2) chromophore : metal ratio. The 1 : 1 (and/or 2 : 2) complex was also proposed by $^{13}C$ NMR titration of **2**.[1] Moreover, **1** showed a significant response to $Hg^{II}$ cation at concentrations as low as $4.0 \times 10^{-6}$ mol $dm^{-3}$. Assuming 1 : 1 complexation of $Hg^{II}$, the stability constant derived from the absorption spectral data was $8.0 \times 10^4$ $dm^3$ $mol^{-1}$.

The same experiments were also carried out using different metals, and the results summarized in Table 1. Clearly, **1** is the most sensitive to $Hg^{II}$ among the transition- and heavy-metal ions studied. The sensitivities of $Zn^{II}$ and $Cd^{II}$ with respect to $Hg^{II}$ are 1/75 and < 1/7500, respectively. It is very interesting that **1** has high selectivity towards highly toxic mercury over the biologically important zinc cation.[7] Although the detectable concentration limit of **1** was not as low as dithizone,[4] which is the usual chromogenic reagent for mercury, its selectivity for mercury was very high, even though it contains no sulfur atom unlike most other mercury selective chromophores.[3,4] The high selectivities (sensitivities) shown in Table 1 show that no preorganization of a suitable cavity seems to be necessary for ideal complexation as discussed by Lerchi *et al*.[3] The selectivity is similar to that previously reported in the transport results of imide **2**.[1] The only unusual phenomenon was observed in the

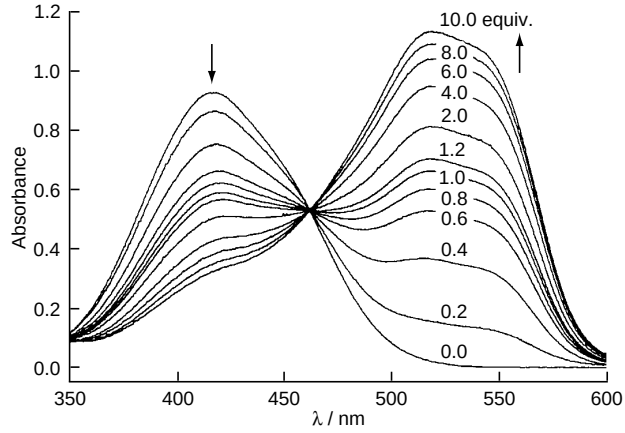



**Fig. 1** UV–VIS spectra of **1** ($3.00 \times 10^{-5}$ mol $dm^{-3}$) and upon incremental addition of $Hg(ClO_4)_2$ in MeCN containing 0.01 mol $dm^{-3}$ $LiClO_4$ as electrolyte

**Table 1** Detection limits (mol $dm^{-3}$) of **1**[a]

| Metal ion[b] | $10^4c$/mol $dm^{-3}$ | Selectivity ([M]/[Hg]) |
|---|---|---|
| $Hg^{II}$ | 0.040 | 1.0 |
| $Cd^{II}$ | > 300 | > 7500 |
| $Zn^{II}$ | 3.0 | 75 |
| $Co^{II}$ | 9.0 | 230 |
| $Ni^{II}$ | 30 | 750 |
| $Cu^{II}$ | 0.15 | 3.8 |
| $Pb^{II}$ | 0.12 | 3.0 |
| $Ag^{I}$ | 16 | 400 |

[a] $3.00 \times 10^{-5}$ mol $dm^{-3}$ in MeCN containing 0.01 mol $dm^{-3}$ $LiClO_4$ as electrolyte at 25.0 ± 0.2 °C. [b] The counter anion was $ClO_4^-$ except for $Cd(NO_3)_2$.

**2** **3** **1** R = $NMe_2$ **4** R = $NO_2$

UV–VIS spectra in titration with $Cu^{II}$. In this case, in addition to the new absorption band ($\lambda_{max}$ = 519 nm), another ($\lambda_{max}$ = 610 nm) also appeared (not shown). The maximum absorbance at 519 nm was reached upon the addition of 1 mol equiv. of $Cu^{II}$. However, further addition of $Cu^{II}$ decreased the 519 nm absorption and increased the new absorption at 610 nm until 2.0 mol equiv. of $Cu^{II}$ was added. We propose that this new absorption band arises from the interaction between excess $Cu^{II}$ and the dimethylamino group of chromophore **1**, as a consequence of the higher affinity of $Cu^{II}$ for nitrogen compared to other metal cations investigated.

The time-dependent spectra of **1** and **3** in the presence of 1 mol equiv. $Hg^{II}$ were taken over a period of 5–60 min to elucidate the spectroscopic features of chromophore **1**. These spectra showed that although **3** showed large absorbance changes with time, no spectral change was observed for **1** under the same conditions. In other words, there was no time dependence for the interaction of $Hg^{II}$ cation and chromophore **1**.

In order to investigate the mechanism of colour change, hydrochloric acid and sodium hydroxide solution were used in place of $Hg^{II}$, the complexation of Kemp′s acid imide **2** with $Na^{I}$ is very weak[2] while the spectrum of the 1 : 1 chromophore–HCl solution was exactly the same as that of the 1 : 1 chromophore–$Hg^{II}$ solution. This meant **1** was also a good molecular sensor for acid. On the other hand, when an NaOH solution was put into the above solution, the absorption at 519 nm decreased, and disappeared upon addition of 1 equiv. of NaOH. This suggested that protonation played a very important role in changing the colour. A plausible mechanism for the colour change is that when transition- or heavy-metal ions are added to the chromophoric solution, the carboxylic acid proton is removed during complex formation, and that this proton binds to the azo group, changing the conjugate feature of **1**, while the dimethylamino group acts as an electron donating group aiding protonation. This mechanism of the colour change is different from other ionizable cyclic or bicyclic molecular sensors.[5] To obtain further evidence, the nitro-substituted derivative **4** was also prepared. Since the nitro group acts as an electron attracting group which decreases the electronic density at the azo group, the released proton cannot interact with the azo group to change the conjugate feature of **4**, such that, as predicted, no colour change occurred even in the presence of excess metal ion.

In summary, a novel Kemp's acid imide **1** was prepared as a chromogenic reagent for $Hg^{II}$. The selectivity of **1** for $Hg^{II}$ was very high over that of other transition- and heavy-metal ions such as $Co^{II}$, $Ni^{II}$, $Cu^{II}$, $Zn^{II}$, $Cd^{II}$, $Pb^{II}$ and $Ag^{I}$. The mechanism of the colour change was demonstrated as being due to the formation of a complex in 1 : 1 (and/or 2 : 2) chromophore : metal ratio after the addition of the transition- or heavy-metal ion to the chromophoric solution. The complexation causes proton transfer from the carboxyl group to the azo group, changing the colour of the original chromophore **1**.

## References


1 T. Hirose, B. W. Baldwin, Z.-H. Wang, K. Kasuga, T. Uchimaru and A. Yliniemelä, *Chem. Commun.*, 1996, 391.

2 T. Hirose, B. W. Baldwin, T. Uchimaru, S. Tsuzuki, M. Uebayashi and K. Taira, *Chem. Lett.*, 1995, 231.

3 M. Lerchi, E. Reitter, W. Simon and E. Pretsch, *Anal. Chem*., 1994, **66**, 1713.

4 F. D. Snell, *Photometric and Fluorometric Methods of Analysis*, Wiley, New York, 1978, Part 1.

5 For example, see: T. Kaneda, S. Umeda, H. Tanigawa, S. Misumi, Y. Kai, H. Morii, K. Miki and N. Kasai, *J. Am. Chem. Soc*., 1985, **107**, 4802; R. C. Helgeson, B. P. Czech, E. Chapoteau, C. R. Gebauer, A. Kumar and D. J. Cram, *J. Am. Chem. Soc*., 1989, **111**, 6339; K. Nakashima, Y. Yamawaki, S. Nakatsuji, S. Akiyama, T. Kaneda and S. Misumi, *Chem. Lett.*, 1983, 1415; A. Mason, A. Sheridan, I. O. Sutherland and A. Vincent, *J. Chem. Soc., Chem. Commun.*, 1994, 2627; H.-G. Löhr and F. Vögtle, *Acc. Chem. Res*., 1985, **18**, 65.

6 J. Rebek, Jr., L. Marshall, R. Wolak, K. Parris, M. Killoran, B. Askew, D. Nemeth and N. Islam, *J. Am. Chem. Soc.*, 1985, **107**, 7476; D. S. Kemp and K. S. Petrakis, *J. Org. Chem*., 1981, **46**, 5140; F. M. Menger and M. Ladika, *J. Am. Chem. Soc*., 1988, **110**, 6794; Y. Ikeura, Y. Honda, K. Kurihara and T. Kunitake, *Chem. Lett*., 1990, 169.

7 J.-M. Lehn and F. Montavon, *Helv. Chim. Acta*, 1978, **61**, 67 and references therein.



*Received, 4th November 1996; Com. 6/07470G*

# Non-linear optical properties of the inorganic cluster $[(\eta\text{-}C_5H_5)CoFe_2SSe(CO)_6]$

**Sudeep Banerjee,[a] G. Ravindra Kumar,*[a]† Pradeep Mathur*[b]‡ and P. Sekar[b]**

[a] *Tata Institute of Fundamental Research, Homi Bhabha Road, Mumbai 400 005, India*
[b] *Department of Chemistry, Indian Institute of Technology, Powai, Mumbai 400 076, India*

**Non-linear refraction and absorption have been studied in a mixed-metal, mixed chalcogenide cluster. The cluster displays optical limiting significantly superior to that displayed by $C_{60}$.**

The relentless search for materials with good non-linear optical response has led to impressive strides in understanding existing materials as well as the design and synthesis of new types of molecules.[1] In particular, there has been great interest in finding better non-linear media for the process of optical limiting.[2] Organic systems like dyes, porphyrins and fullerenes have been explored in considerable detail.[2–4] Some transition-metal cluster compounds have also been investigated for their potential for response comparable to or exceeding that of $C_{60}$.[5–8]

Cluster compounds which contain one or more bridging chalcogen ligands have recently been attracting considerable attention.[9] It is possible to design the construction of certain classes of mixed-metal clusters in which different combinations of chalcogen ligands can be incorporated.[10] Recently we have synthesised and structurally characterised the first example of a mixed-metal cluster containing both S and Se ligands $[(\eta\text{-}C_5H_5)CoFe_2(CO)_6(\mu_3\text{-}S)(\mu_3\text{-}Se)]$.[11] Here, we report on its optical limiting characteristics. Among the key requirements for a good optical limiter are (*a*) large transmission at low intensities followed by low transmission at high intensities and (*b*) a low threshold for the onset of non-linear attenuation of the input beam.[2] We show that, on both these counts, the present cluster displays superior performance compared to other materials.

The linear absorption spectrum of a solution of $[(\eta\text{-}C_5H_5)CoFe_2SSe(CO)_6]$ in *n*-hexane is shown in Fig. 1. There is weak absorption in the visible and near-IR regions. Commonly used laser wavelengths (Nd-YAG, dye and diode) exist in these regions and hence limiting applications are important here. The non-linear optical properties of the solution were measured by the *Z*-scan technique[12] at 1064 and 532 nm using an Nd-YAG laser emitting 35 ps pulses at a 10 Hz repetition rate. Typical *Z*-scans are shown in Fig. 2. The large peak to valley difference (nearly 40%) in the closed aperture case [Fig. 2(*a*)] indicates considerable non-linear refraction and the occurrence of the peak at positive *z* indicates positive non-linearity or self-focussing. The non-linear refraction coefficient $\gamma$ can be extracted from the difference in transmission between the peak and the valley.[12] Table 1, which summarises the experimental parameters and the extracted non-linear coefficients, indicates that our $\gamma$ value at 532 nm is two orders of magnitude larger than the values reported by Shi and coworkers for other inorganic clusters at the same wavelength.[13] The $\gamma$ at 1064 nm for our

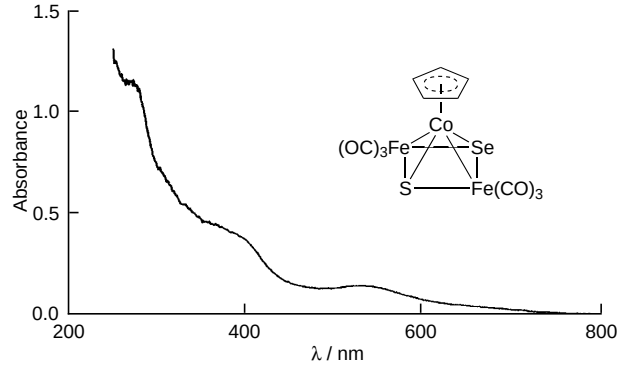



**Fig. 1** Linear absorption spectrum of $[(\eta\text{-}C_5H_5)CoFe_2SSe(CO)_6]$ in *n*-hexane. The inset shows the structure of this cluster.

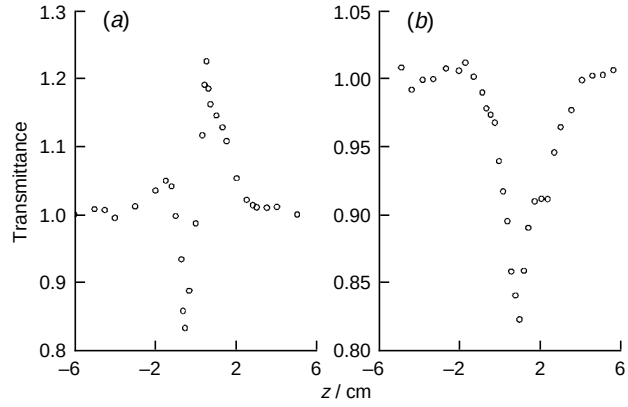



**Fig. 2** Results of a *Z*-scan at 532 nm. A lens with 50 cm focal length was used, giving a focussed spot radius of about 25 μm. The sign convention for *z* is as defined in ref. 12. $z = 0$ is the focus. The fluence at focus is 0.80 J cm$^{-2}$. (*a*) Non-linear refraction, (*b*) non-linear absorption.

**Table 1** Experimentally determined values for $[(\eta\text{-}C_5H_5)CoFe_2SSe(CO)_6]$ and those reported for other materials. The maximum (at focus) intensity in our *Z*-scan experiment was 23 GW cm$^{-2}$, corresponding to a maximum fluence of 0.8 J cm$^{-2}$. The sample concentration was 50 μmol ml$^{-1}$; $\gamma$ is the non-linear refractive index coefficient (see ref. 12). $F_t$ is the limiting threshold fluence at 532 nm

| Material | $\gamma$ (532 nm)/ m$^2$ W$^{-1}$ | $\gamma$ (1064 nm)/ m$^2$ W$^{-1}$ | $F_t$ (with ap.)/ J cm$^{-2}$ | $F_t$ (no. ap.)/ J cm$^{-2}$ | Ref. |
|---|---|---|---|---|---|
| $[(\eta\text{-}C_5H_5)CoFe_2SSe(CO)_6]$ | $2.7 \times 10^{-14}$ | $-5.8 \times 10^{-18}$ | $2.1 \times 10^{-3}$ | $11.0 \times 10^{-3}$ | This work |
| $C_{60}$ | $-9 \times 10^{-17}$ | — | — | $175 \times 10^{-3}$ | 14, 15 |
| $[MoOS_3(CuNCS)_3]^{2-}$ | $-2.3 \times 10^{-16}$ | — | — | 7.0 | 13, 16 |
| $[Mo_8O_8Cu_{12}S_{24}]^{4-}$ | $-3.5 \times 10^{-16}$ | — | — | — | 13 |
| $[Cu_4(SPh)_6]^{2-}$ | $5.0 \times 10^{-17}$ | — | — | — | 13 |

cluster is also of a significant magnitude (no other data exist for a comparison to be made at this wavelength). Note that the sign of the non-linearity changes at 1064 nm, where the non-linear refraction is found to be due to self-defocussing. Moving on to the open aperture data [Fig. 2(*b*)], it is evident that there is non-linear absorption, indicated by the dip in the transmission as the sample is moved towards the focus. The non-linear absorption of about 16% at the maximum fluence of 0.80 J $cm^{-2}$, is significant considering the low fluence levels we have used. The solvent *n*-hexane did not give any signals. It is also clear from Table 1 that the $\gamma$ is considerably superior to that measured for $C_{60}$.[14]

The significant non-linear refraction as well as non-linear absorption displayed by this cluster have been used to design optical limiters with and without apertures. Fig. 3 shows the measurements of transmission at 532 nm as a function of input energy density (fluence) with an aperture of 1 mm in the output beam. The input pulse was focussed by a lens with a focal length of 50 cm. The concentration of the sample was adjusted such that the transmission of the limiter at low fluences is quite large (80%). The transmission starts decreasing as the input increases to a fluence of 1.0 mJ $cm^{-2}$ (28 MW $cm^{-2}$) and comes down to 30% at 3.5 mJ $cm^{-2}$. The onset of non-linear transmission in other inorganic clusters has been found to occur at values that are two orders of magnitude larger than that for the present cluster.[7] The benchmark limiting material, $C_{60}$, also shows onset of non-linear transmission at 80 mJ $cm^{-2}$.[15] The threshold for limiting,[2] defined as the fluence at which the transmission decreases to half of the value at low input fluences, is found to be 2.1 mJ $cm^{-2}$ for our cluster. This value is about 250 times smaller than the smallest value obtained for other inorganic clusters studied recently.[16] Even without an aperture (the open aperture case), our limiting threshold is 11 mJ $cm^{-2}$, which is a factor of over 45 times smaller compared to the other clusters[16] and about 15 times smaller than that for $C_{60}$. An additional advantage of our cluster is that it has a large transmission at low input intensities, a characteristic required for an ideal optical limiter.

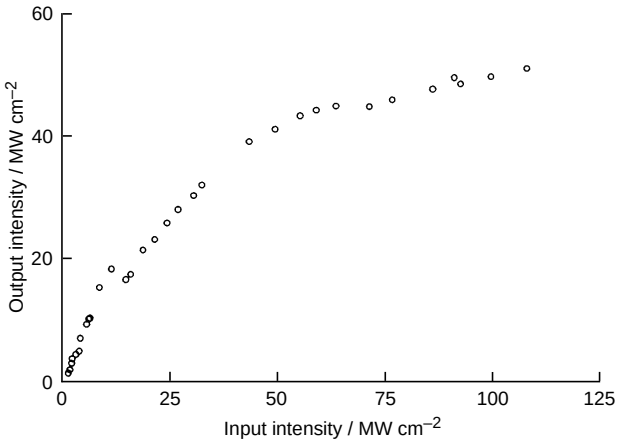



**Fig. 3** Output–input characteristics of a solution of the cluster in *n*-hexane at 532 nm with an aperture of 1 mm in the transmitted beam. Linear (low intensity) transmission of the limiter was 80%. The sample was contained in a 1 mm path length quartz curvette.

In conclusion, we have shown that the mixed-metal, mixed chalcogenide cluster [($\eta$-$C_5H_5$)$CoFe_2SSe(CO)_6$] displays large optical non-linearity. We have demonstrated that it has optical limiting characteristics which are considerably superior to $C_{60}$ and other recently investigated inorganic clusters.

## Footnotes

† E-mail: grk@tifrvax.tifr.res.in
‡ E-mail: mathur@ether.chem.iitb.ernet.in

## References

1 *Materials for Nonlinear Optics—Chemical Perspectives*, ed. S. R. Marder, J. E. Sohn and G. D. Stucky, *ACS Symp. Ser.*, American Chemical Society, Washington, DC, 1991, 455; J.-L. Bredas, C. Adant, P. Tackx, A. Persoons and B. M. Pierce, *Chem. Rev.*, 1994, **94**, 243.
2 L. W. Tutt and T. F. Boggess, *Prog. Quant. Electron.*, 1993, **17**, 299.
3 M. Ravikanth and G. R. Kumar, *Curr. Sci.*, 1995, **68**, 1010.
4 G. R. Kumar and F. A. Rajgara, *Appl. Phys. Lett.*, 1995, **67**, 3871; A. Sevian, M. Ravikanth and G. R. Kumar, *Chem. Phys. Lett.*, in the press.
5 L. W. Tutt and S. W. McCahon, *Opt. Lett.*, 1990, **15**, 700.
6 S. Shi, W. Ji, S. H. Tang, J. P. Lang and X. Q. Xin, *J. Am. Chem. Soc.*, 1994, **116**, 3615; S. Shi, W. Ji, J. P. Lang and X. Q. Xin, *J. Phys. Chem.*, 1994, **98**, 3750.
7 W. Ji, S. Shi, H. J. Du, P. Ge, S. H. Tang and X. Q. Xin, *J. Phys. Chem.*, 1995, **99**, 17 297.
8 W. Ji, H. J. Du, S. H. Tang and S. Shi, *J. Opt. Soc. Am. B*, 1995, **12**, 876.
9 L. C. Roof and J. W. Kolis, *Chem. Rev.*, 1993, **93**, 1037; K. H. Whitmire, *Coord. Chem.*, 1988, **17**, 95; M. A. Ansari and F. A. Ivers, *Coord. Chem. Rev.*, 1990, **100**, 223; P. Mathur, D. Chakravarty and I. J. Mavunkul, *J. Cluster. Sci.*, 1993, **4**, 351.
10 P. Mathur, M. M. Hossain, S. B. Umbarkar, C. V.V. Satyanarayana, A. L. Rheingold, L. M. Liable-Sands and G. P. A. Yap, *Organometallics*, 1996, **15**, 1898; P. Mathur and P. Sekar, *Chem. Commun.*, 1996, 727.
11 P. Mathur, P. Sekar, C. V. V. Satyanarayana and M. F. Mahon, *Organometallics*, 1995, **14**, 2115.
12 M. Sheik-Bahae, A. A. Said, T.-H. Wei, D. J. Hagan and E. W. Van Stryland, *IEEE J. Quant. Elec.*, 1990, **26**, 760.
13 S. Shi, X. Zhang and X. F. Shi, *J. Phys. Chem.*, 1995, **99**, 14 911.
14 S. Couris, E. Koudoumas, A. A. Ruth and S. Leach, *J. Phys. B*, 1995, **28**, 4537.
15 C. Li, R. Wang, Y. Song and Y. Wang, *J. Opt. Soc. Am. B*, 1994, **11**, 1356.
16 D. Long, S. Shi, X. Xin, B. Luo, L. Chen, X. Huang and B. Kang, *J. Chem. Soc., Dalton Trans.*, 1996, 2617.

*Received, 4th November 1996; Com. 6/07485E*

# Extensively π-conjugated soluble oligothienylenevinylenes

**El Hadj Elandaloussi, Pierre Frère* and Jean Roncali***

*Ingénierie Moléculaire et Matériaux Organiques, CNRS UMR 6501, Université d'Angers, 2 Bd Lavoisier, F-49045 Angers, France*

**Soluble oligothienylenevinylenes are synthesized; the longest oligomers exhibit small bandgaps and can be oxidized to the dication by a two-electron transfer.**

Conjugated oligomers are subject to considerable current interest related to their potential applications in diodes,[1] field-effect transistors,[2] light-emitting diodes,[3] or molecules for non-linear optics (NLO).[4] From a fundamental viewpoint, π-conjugated oligomers are widely investigated as models for the electronic and electrochemical properties of the parent polymers.[5] While these two fields of research have been extensively developed for thiophene oligomers (nTs),[1–5] oligothienylenevinylenes (nTVs) have attracted less attention. Due to the presence of ethylene linkages, nTVs are expected to exhibit less rotational disorder and lower aromatic character than nTs and hence enhanced electron delocalization. Although advantage has been taken of these efficient electron-transmission properties for the design of NLO molecules,[6] attempts to prepare nTVs of well defined structure have remained scarce.[7] Thus, Nakayama and Fujimori synthesized nTVs containing up to seven thiophene rings,[7b] but their electrochemical properties were not analysed.

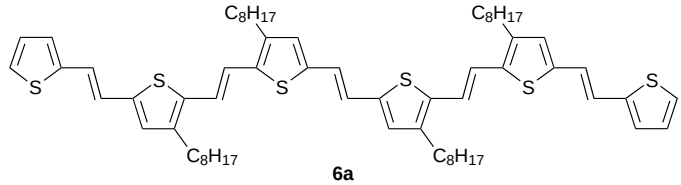
Here, we report preliminary results on the synthesis of the first examples of alkyl substituted nTVs, that are also the longest ever reported. The solubility of these nTVs allowed the analysis of their electrochemical properties providing a first evidence for direct two-electron generation of a dication on a conjugated oligomer.

Oligomers containing two (**2a**,**b**), four (**4a**,**b**) and eight thiophene rings (**8a**,**b**) have been synthesized from 3-octylthiophene and 3,4-dibutylthiophene using an iterative strategy involving formylation of a nTV of degree *n* followed by McMurry dimerization. Compounds **6a** and **10b** were prepared by double Wittig–Horner alkenation of the appropriate dialdehyde and with thienylmethylphosphonate (TP), while **6b** was prepared from 3,4-dibutyl-2,5-thiophenedicarbaldehyde by

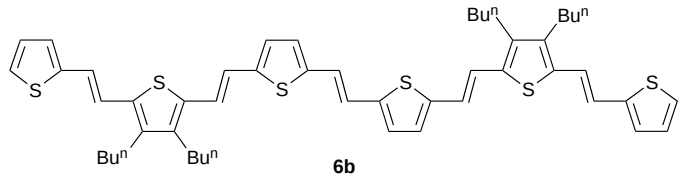
**Table 1** Electrochemical[a] and optical[b] data for nTVs

| Compound | $E_{pa_1}$ | $E_{pa_2}$ | $E_{pa_2} - E_{pa_1}$ | $\lambda_{max}$/nm | $\Delta E^c$/eV |
|---|---|---|---|---|---|
| **2a** | 1.06 | 1.39 | 0.33 | 354 | 2.94 |
| **4a** | 0.70 | 0.88 | 0.18 | 473 | 2.09 |
| **6a** | 0.60 | 0.70 | 0.10 | 526 | 1.93 |
| **8a** | 0.56 | | 0.00 | 552 | 1.84, 1.70[d] |
| **2b** | 0.97 | 1.32 | 0.35 | 360 | 2.94 |
| **4b** | 0.60 | 0.78 | 0.18 | 488 | 2.13 |
| **6b** | 0.57 | 0.69 | 0.12 | 522 | 1.99 |
| **8b** | 0.45 | | 0.00 | 572 | 1.78 |
| **10b** | 0.43 | | 0.00 | 586 | 1.72 |

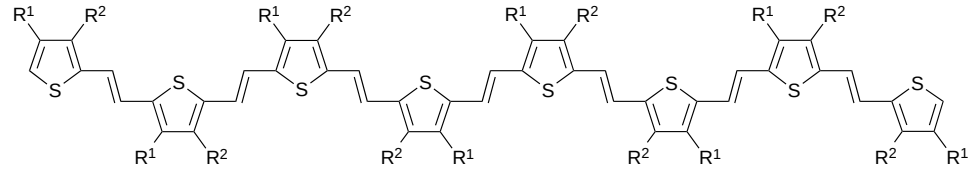
[a] $10^{-4}$ M in 0.1 M $NBu_4PF_6$–$CH_2Cl_2$, scan rate 100 mV $s^{-1}$, reference SCE (*E* in V). [b] In $CH_2Cl_2$. [c] Estimated from the absorption edge. [d] On film.



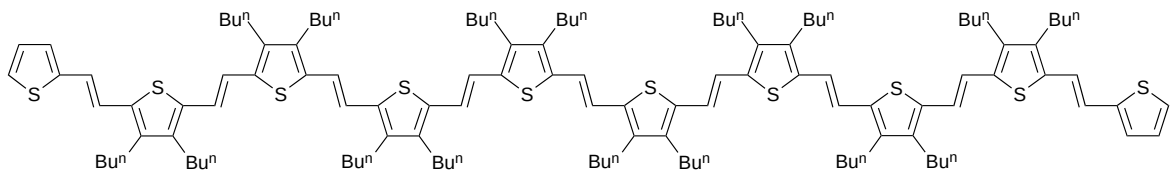
**6a**



**6b**



**8a** $R^1$ = H, $R^2$ = $C_8H_{17}$
**b** $R^1$ = $R^2$ = $Bu^n$



**10b**

double Wittig–Horner alkenation with TP followed by monoformylation and McMurry coupling.

Table 1 lists the main electrochemical and optical data of the new nTVs. Due to the +I effect of the two butyl chain, nTVs **b** show lower oxidation potentials and absorb at longer wavelengths than nTVs **a**. The CV of **2a** and **2b** shows two irreversible oxidation waves with peak potentials $E_{pa1}$ and $E_{pa2}$ around 1.00 and 1.30–1.40 V corresponding to the successive generation of the radical cation and dication. Extension of the conjugation length in **4a**,**b** and **6a**,**b** leads to a negative shift of the peak potentials and to a decrease of their difference $E_{pa2} - E_{pa1}$ indicative of a weaker coulombic repulsion between positive charges in the dication. In parallel, both oxidation waves become reversible. For **8a**,**b**, the dication is formed directly through a single-step two-electron transfer. Furthermore, two additional reversible one-electron waves occur around 0.80 and 1.00 V showing that the system can be charged up to the tetracationic state (Fig. 1). Further chain extension to **10b** produces a further decrease of $E_{pa1}$ to 0.43 V. However, the combined effects of chain extension and of the absence of alkyl chains on the terminal thiophenes produce a dramatic decrease of the solubility.

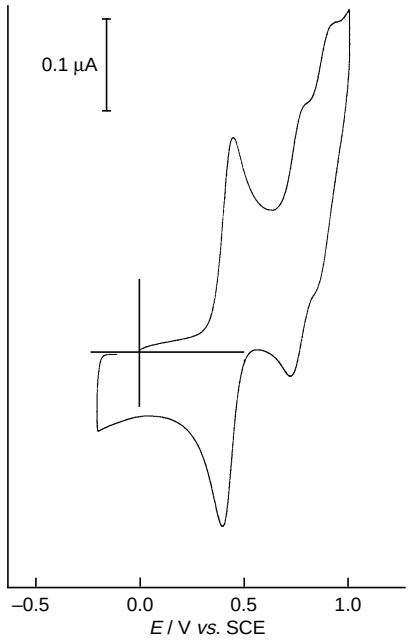



**Fig. 1** Cyclic voltammogram of **8b**, $10^{-4}$ M in 0.1 M $NBu_4PF_6$–$CH_2Cl_2$, scan rate 100 mV $s^{-1}$, reference SCE

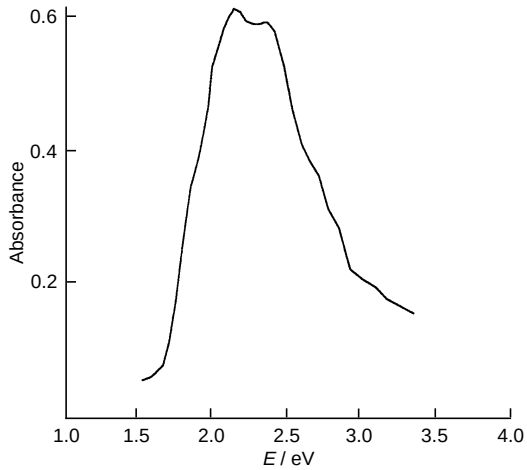



**Fig. 2** Optical spectrum of a film of **8a** cast from a $CH_2Cl_2$ solution

Although two-electron oxidations have already been reported,[8] it is to our knowledge the first time that such a process is observed for oligomers based on the repetition of a single basic unit. This result suggests that soluble nTVs could be of great interest for modelling bipolarons in conjugated polymers.

The solution optical spectra of all nTVs exhibit a well defined vibronic fine structure consistent with an all *trans* rigid geometry. Optical data (Table 1) show that chain extension leads to the expected red shift of $\lambda_{max}$ which reaches 586 nm for **10b** while the HOMO–LUMO gap ($\Delta E$) decreases to 1.72 eV. The optical spectrum of a solution-processed film of **8a** (Fig. 2) reveals the persistence of the vibronic fine structure and a bandgap of *ca.* 1.70 eV. This value, slightly smaller than that of the parent poly(thienylenevinylene) (PTV),[9] suggests that for PTV prepared by thermal elimination the mean conjugation length is limited to *ca.* 8 TV units. On the other hand, the steady decrease of $\Delta E$ with chain extension and the absence of saturation observed for both series of nTVs strongly suggest that longer nTVs could exhibit even lower gaps. Further support to this conclusion is provided by the extrapolation of the plot of $\Delta E$ *vs.* the reciprocal number of conjugated carbons for nTVs **b** which leads to a predicted bandgap of 1.45 eV for PTV.

## References


1 D. Fichou, Y. Nishikitani, G. Horowitz, J. Roncali and F. Garnier, *Synth. Met.*, 1989, **28**, C729.
2 F. Garnier, R. Haijalaoui, A. Yassar and P. Srivastava, *Science*, 1994, **265**, 1684.
3 F. Geiger, M. Stoldt, R. Schweizer, P. Bäuerle and E. Umbach, *Adv. Mater.*, 1993, **5**, 922.
4 H. Thienpont, G. L. J. A. Rikken, E. W. Meijer, W. ten Hoeve and H. Wynberg, *Phys. Rev. Lett.*, 1990, **65**, 2141; F. Würthner, F. Effenberger, R. Wortmann and P. Krämer, *Chem. Phys.*, 1993, **173**, 305.
5 D. Jones, M. Guerra, L. Favaretto, A. Modelli, M. Fabrizio and G. Distefano, *J. Phys. Chem.*, 1990, **94**, 5761; J. V. Caspar, V. Ramamurthy and D. R. Corbin, *J. Am. Chem. Soc.*, 1991, **113**, 600; P. Bäuerle, *Adv. Mater.*, 1992, **4**, 102; J. Guay, P. Kasai, A. Diaz, R. Wu, J. M. Tour and L. H. Dao, *Chem. Mater.*, 1992, **4**, 1097.
6 V. P. Rao, Y. M. Cai and A. K.-Y. Jen, *J. Chem. Soc., Chem. Commun.*, 1994, 1689.
7 (*a*) G. Kossmehl, M. Hätel and G. Manecke, *Makromol. Chem.*, 1970, **131**, 15; (*b*) J. Nakayama and T. Fujimori, *Heterocycles*, 1991, **32**, 991.
8 J. P. Parakka, A. S. Jeevarajan, L. D. Jeevarajan, L. D. Kispert and M. P. Cava, *Adv. Mater.*, 1996, **8**, 54; E. Elandaloussi, P. Frère and J. Roncali, *Tetrahedron Lett.*, 1996, **37**, 6121.
9 S. Yamada, S. Tokito, T. Tsuisui and S. Saito, *J. Chem. Soc., Chem. Commun.*, 1987, 1448.


*Received, 7th November 1996; Com. 6/07574F*

# A conjugated polymer/redox polymer hybrid with electronic communication between metal centres

**Colin G. Cameron and Peter G. Pickup***

*Department of Chemistry, Memorial University of Newfoundland, St. John's, Newfoundland, Canada A1B 3X7*

**Enhanced electrochemical charge transport rates in a conjugated metallopolymer formed by complexation of $[Ru(2,2'\text{-bpy})_2]^{2+}$ moieties to donor N-atoms in the backbone of a benzimidazole-based polymer provide strong evidence for electronic communication between metal centres.**

In the study of electrodes coated with electroactive polymers,[1,2] a clear distinction has been made between 'conducting polymers' whose redox sites are delocalised over a conjugated π system, and 'redox polymers' which have localised redox sites. Although redox polymers based on transition-metal complexes have many potential advantages in applications such as electrocatalysis and electronic devices, the development of commercial applications has been much more successful for conducting polymers.[3,4] There could therefore be significant opportunities for the exploitation of transition-metal centres in conducting polymers. Indeed, there has been much work in this area,[5] but in most cases the complex has been electronically isolated from the conjugated polymer backbone by saturated linkages. The few examples which involve direct electronic interaction between the conjugated polymer and the complex have demonstrated novel electronic, electrochemical and catalytic properties.[6–10]

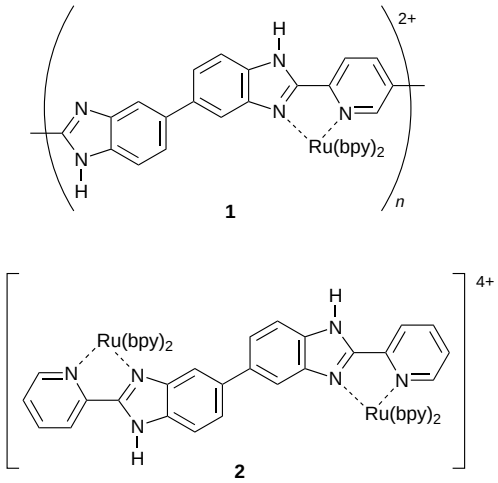
We report here a benzimidazole-based conjugated polymer with coordinated $Ru(bpy)_2^{2+}$ moieties (**1**, bpy = 2,2′-bipyridine). The Ru redox centres are coordinated to nitrogen atoms in the conjugated backbone of the polymer, providing direct electronic communication between the complex and the polymer. Work on an analogous binuclear complex (**2**) has indicated that there is a weak electronic interaction between adjacent Ru centres, which can be increased by removal of the imidazole proton.[11] These interactions are manifested most strikingly in polymer **1** by a high, pH-dependent electron transport rate.

Polymer **1** was prepared following standard literature procedures for the preparation of polybenzimidazoles[12] and $[Ru(bpy)_2L]^{2+}$ complexes[13] (glycerol was used as the solvent for complexation). Gel permeation chromatography indicated that the molar mass of the ruthenium-complexed polymer was $> 50\,000$ g mol$^{-1}$. Elemental analysis indicated that *ca*. 60% of the bidentate pyridine–benzimidazole sites were occupied. Polymer films were deposited on Pt disc electrodes by evaporation of acetonitrile–water (12 : 1).

Fig. 1 shows cyclic voltammograms of a film of **1** in acetonitrile containing acid or base. The formal potentials are close to values reported for the dimer complex **2**. The shift in potential with increasing pH is due to deprotonation of the imidazole ring.

Fig. 2 shows complex impedance plots for similar films in basic (*a*) and acidic (*b*) electrolyte solutions. In each case the impedance was measured at the formal potential. These impedance data are typical for a redox polymer film on an electrode and the electron diffusion coefficient ($D_e$) can be obtained from the difference between the high-frequency intercept ($R_{high}$) and the low-frequency limiting real impedance ($R_{low}$): $D_e = d^2/[3(R_{low} - R_{high})C_{lf}]$, where $d$ is the film thickness and $C_{lf}$ is the low-frequency capacitance.[14] Values of $d$ were obtained from the surface coverage, determined from a slow voltammogram, using a ruthenium site concentration of 1.6 M based on the dry density of similar materials.[15] Although this concentration is an estimate, it does not compromise the validity of our conclusions because (*a*) it is the same value used to obtain $D_e$ values for the comparison material, poly-$[Ru(bpy)_2(vpy)_2]^{2+}$ (vpy = 4-vinylpyridine),[16] and (*b*) it is unlikely to be significantly overestimated, since the Ru site concentration in a $[Ru(bpy)_3][PF_6]_2$ crystal is only 1.75 M.[17] $D_e$ values obtained from impedance measurements on **1** in acidic and basic acetonitrile were $6 \times 10^{-9}$ and $1 \times 10^{-8}$ cm$^2$ s$^{-1}$, respectively. For comparison, $D_e$ for poly-$[Ru(bpy)_2(vpy)_2]^{3+/2+}$ in acetonitrile is *ca*. $7 \times 10^{-10}$ cm$^2$ s$^{-1}$.[16]

In both acidic and basic media, electron transport is significantly faster in **1** than in poly-$[Ru(bpy)_2(vpy)_2]^{3+/2+}$, suggesting enhanced electronic communication between Ru centres. $D_e$ is higher in the basic solution than in the acidic solution, consistent with the known increase in electron



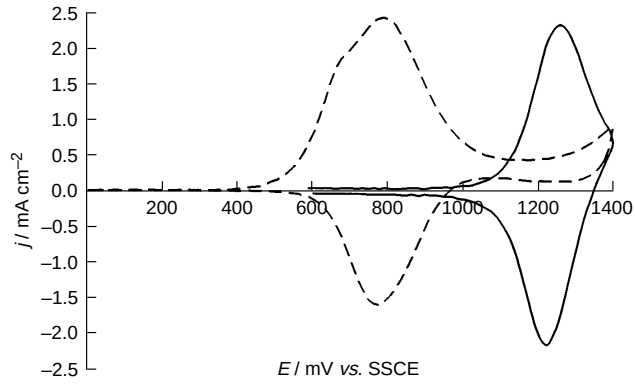




**Fig. 1** Cyclic voltammograms (100 mV s$^{-1}$) of a Pt electrode (0.0052 cm$^2$) coated with a thin ($\Gamma_{Ru} = 3.6 \times 10^{-8}$ mol cm$^{-2}$) film of **1** in 0.1 M $NEt_4ClO_4$–MeCN containing *ca*. 5 mM $NBu_4OH$ (---) or *ca*. 50 mM $HClO_4$ (—)

delocalization between Ru centres connected by a benzimidazole bridge.[11] Furthermore, $D_e$ values for **1** were found to decrease with time spent at high potentials in the basic electrolyte (*i.e.* during impedance measurements or cyclic voltammetry), consistent with the expected deactivation (over-oxidation) of the conjugated polymer backbone.[18] As far as we know, the $D_e$ value obtained for **1** in basic acetonitrile is the highest value yet reported for a Ru–bpy based redox polymer.[19]

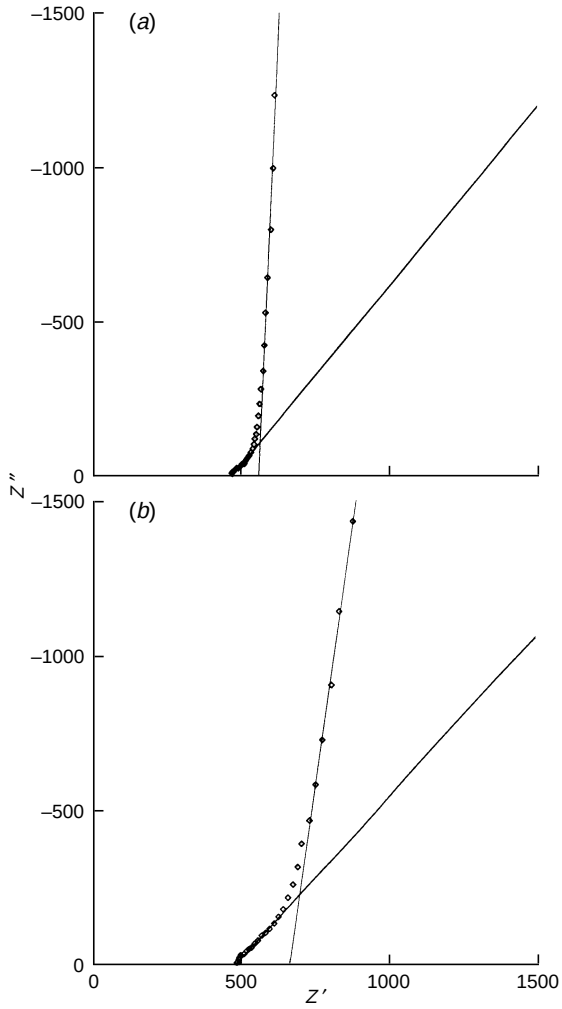



**Fig. 2** Complex plane impedance plots for Pt electrodes (0.0052 $cm^2$) coated with thin films of **1** in 0.1 M $NEt_4ClO_4$–MeCN containing (*a*) *ca.* 5 mM $NBu_4OH$ ($\Gamma_{Ru} = 1.5 \times 10^{-8}$ mol $cm^{-2}$) or (*b*) *ca.* 50 mM $HClO_4$ ($\Gamma_{ru} = 1.4 \times 10^{-8}$ mol $cm^{-2}$). Lines show extrapolations to the real axis intercepts, $R_{high}$ and $R_{low}$.

These results provide conclusive evidence that the conjugated polybenzimidazole backbone of **1** is involved in electron transfer between Ru sites. Since the Ru-free polymer does not exhibit electrochemical activity in the potential region of the Ru formal potential in either medium studied, electron transport is presumably facilitated by an electronic interaction between metal centres through the polymer backbone, rather than by hopping *via* the polymer backbone. This type of long-range, multi-metal centre interaction could provide the basis for useful electrocatalytic and electronic materials.

This work was supported by the Natural Sciences and Engineering Research Council of Canada and Memorial University.

## References

1 M. E. G. Lyons, in *Electroactive Polymer Electrochemistry, Part 1: Fundamentals*, ed. M. E. G. Lyons, Plenum Press, New York, 1994, pp. 1–235.
2 G. Inzelt, *Electroanal. Chem*., 1994, **18**, 89.
3 J. S. Miller, *Adv. Mater*., 1993, **5**, 587.
4 J. S. Miller, *Adv. Mater*., 1993, **5**, 671.
5 A. Deronzier and J.-C. Moutet, *Coord. Chem. Rev*., 1996, **147**, 339.
6 H. Nishihara, T. Shimura, A. Ohkubo, N. Matsuda and K. Aramaki, *Adv. Mater*., 1993, **5**, 752.
7 M. O. Wolf and M. S. Wrighton, *Chem. Mater*., 1994, **6**, 1526.
8 T. Yamamoto, T. Maruyama, Z.-H. Zhou, T. Ito, T. Fukuda, Y. Yoneda, F. Begum, T. Ikeda, S. Sasaki, H. Takezoe, A. Fukuda and K. Kubota, *J. Am. Chem. Soc*., 1994, **16**, 4832.
9 T. Maruyama and T. Yamamoto, *Inorg. Chim. Acta*, 1995, **238**, 9.
10 S. S. Zhu and T. M. Swager, *Adv. Mater*., 1996, **8**, 497.
11 M. Haga, T. Ano, K. Kano and S. Yamabe, *Inorg. Chem*., 1991, **30**, 3843.
12 J. A. Osaheni and S. A. Jenekhe, *Macromolecules*, 1995, **28**, 1172.
13 E. A. Seddon and K. R. Seddon, *The Chemistry of Ruthenium*, Elsevier, Amsterdam, New York, 1984.
14 M. F. Mathias and O. Haas, *J. Phys. Chem*., 1992, **96**, 3174.
15 P. Denisevich, H. D. Abruna, C. R. Leidner, T. J. Meyer and R. W. Murray, *Inorg. Chem*., 1982, **21**, 2153.
16 P. G. Pickup, W. Kutner, C. R. Leidner and R. W. Murray, *J. Am. Chem. Soc*., 1984, **106**, 1991.
17 D. P. Rillema, D. S. Jones and H. A. Levy, *J. Chem. Soc., Chem. Commun*., 1979, 849.
18 A. A. Pud, *Synth. Met*., 1994, **66**, 1.
19 N. Oyama and T. Ohsaka, in *Molecular Design of Electrode Surfaces*, ed. R. W. Murray, Wiley, New York, 1992, pp. 333–402.

*Received, 12th November 1996; Com. 6/07671H*

# Synthesis, crystal and molecular structure of a novel organoantimony cage compound, $C_4Bu^t_4P_4Sb_2$

**Steven J. Black, Matthew D. Francis and Cameron Jones*†**

*Department of Chemistry, University of Wales, Swansea, Singleton Park, Swansea, UK SA2 8PP*

**The reaction of the hetero-ring anion $[P_2SbC_2Bu^t_2]^-$ with $FeCl_3$ affords the organoantimony cage compound, $C_4Bu^t_4P_4Sb_2$, *via* a proposed oxidative coupling reaction; the X-ray crystal structure of the cage displays weak intermolecular interactions.**

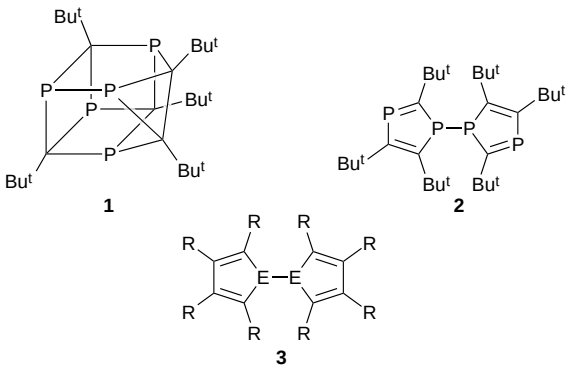
The chemistry of organophosphorus cage compounds is a rapidly expanding area that derives its current importance from the remarkable similarities such compounds show to their hydrocarbon cage counterparts.[1] Several synthetic routes to these compounds have been developed but the oxidative coupling of polyphospholyl ions is the route most relevant to the work described here.[2] For example, Nixon and coworkers have reported that the treatment of a 1:1 mixture of the ions $[1,2,4\text{-}P_3C_2Bu^t_2]^-$–$[1,3\text{-}P_2C_3Bu^t_3]^-$ with $FeCl_3$ leads to low yields of the cage, $P_5C_5Bu^t_5$ **1**, *via* an unknown mechanism.[3] The formation of organophosphorus cage compounds *via* oxidative coupling reactions can be blocked if the reacting polyphospholyl ion is sufficiently sterically protected, as is the case in the reaction of $[1,3\text{-}P_2C_3Bu^t_3]^-$ with $[RuCl_2(\eta^4\text{-}C_8H_{12})]_n$ which yields **2** among other products.[4] Moreover, the absence of any known uncoordinated poly-arsolyl, -stibolyl or -bismolyl anions precludes the existence of heavier group 15 element organometallic cages derived from oxidative coupling reactions. However, coupling of their monosubstituted counterparts is known to yield compounds of the type **3**, which can possess solid-state intermolecular interactions (E = Sb, Bi) that impart thermochromic properties to these species.[5]

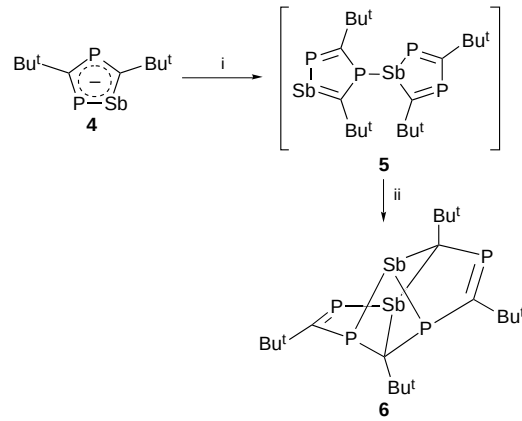
We have recently developed a high-yielding synthetic route to the diphosphastibolyl ring anion $[P_2SbC_2Bu^t_2]^-$ **4**,[6] which we have incorporated into a range of organometallic complexes, *viz*. $[Ru(\eta^5\text{-}C_5R_5)(\eta^5\text{-}P_2SbC_2Bu^t_2)]$ (R = H, Me),[7] $[M(\eta^5\text{-}P_2SbC_2Bu^t_2)(\eta^4\text{-}C_8H_{12})]$ (M = Rh, Ir) and $[Co(\eta^5\text{-}P_2SbC_2Bu^t_2)(\eta^4\text{-}P_2SbC_2HBu^t_2)]$.[8] Our interests have now extended to an examination of the formation of organometallic cages *via* oxidative coupling reactions of **4**. The results of these investigations are reported herein.

Treatment of a dme solution of $FeCl_3$ with 1 equiv. of $[Li(tmeda)_2]$ **4** (Scheme 1) leads to the formation of the air- and moisture-stable cage compound, $C_4Bu^t_4P_4Sb_2$ **6** (mp 82 °C decomp.), in good yield (61%) after chromatographic work-up (Kieselgel, hexane). Compound **6** can also be prepared in lower yields by the reactions of $[Li(tmeda)_2]$ **4** with either $InCl_3$, $PbCl_2$ or $SbF_3$. It seems likely that the reaction mechanism involves an initial coupling to give the intermediate, **5**, which then undergoes a [4 + 2] cycloaddition reaction to give the final product, **6**. If this is so, it is surprising that the coupling occurs through the most sterically hindered heterocentre on one of the rings, *i.e.* the P centre adjacent to two *tert*-butyl substituted C centres. It is also surprising that only one set of enantiomers is formed despite the numerous isomers that are possible if the coupling reaction were to occur through any of the heterocentres on each ring and if there was no specificity to the possible subsequent cycloaddition reactions.

The spectroscopic data‡ for **6** support its proposed structure. Its $^{31}P\{^1H\}$ NMR spectrum is pseudo-first order and has been successfully simulated as an AMNX spin system with four inequivalent phosphorus resonances; two at low field ($P_A$, $P_X$) in the region consistent with phosphaalkenes, and two in the higher field saturated phosphorus region ($P_M$, $P_N$). The lowest field signal (δ 363.4) shows considerable broadening which suggests it arises from the low-coordinate phosphorus centre, P(1), adjacent to the quadrupolar antimony centre, Sb(1). This would necessitate the highest field signal (δ −18.6) to originate from P(2) due to its two-bond coupling (28 Hz) to P(1). The assignment of the remaining signals, P(4) (δ 356.5) and P(3) (δ 32.5) logically follows. Interestingly, there is a very large two-bond coupling (137 Hz) between P(2) and P(3). This is perhaps best explained as a through space coupling which results from the very short intramolecular P(2)–P(3) distance (*vide infra*). Both the $^1H$ and $^{13}C$ NMR spectra of **6** are as expected and highlight four inequivalent *tert*-butyl groups. The mass spectrum of **6** exhibits a molecular-ion peak with the correct isotopic distribution.

The molecular structure of **6**§ is depicted in Fig. 1. All bond lengths within the structure are normal for single bonded interactions except those for P(1)–C(2) [1.681(4) Å] and P(4)–C(12) [1.689(4) Å] which are consistent with localised




**Scheme 1** *Reagents and conditions*: i, $FeCl_3$, dme, 18 h, 25 °C; ii, [4 + 2] cycloaddition

P–C double bonds. Compound **6** contains the first example of a structurally characterised diphosphastibacyclobutane fragment [Sb(2)–P(3)–C(1)–P(2)] which has very short cross-ring P···P (2.822 Å) and Sb···C (3.024 Å) distances which are well within the sum of the van der Waals radii (3.8 and 4.04 Å respectively[9]) for these atom combinations. There are also two polyhetero six-membered rings within the structure [P(1)=C(2)–P(2)–Sb(2)–C(11)–Sb(1) and P(4)=C(12)–P(3)–C(1)–Sb(1)–C(11)] which are also the first examples of such heterocyclic fragments. Another feature of the structure of **6** became evident from an examination of its cell packing diagram (Fig. 2) which shows the molecules to be linked in infinite one-dimensional arrays through weak intermolecular interactions [Sb(2)···P(1) 3.621(6) Å, P(2)···P(1) 3.652(5) Å] which are less than the sum of the van der Waals radii of the atoms involved [Sb–P (4.1 Å), P–P (3.8 Å)].

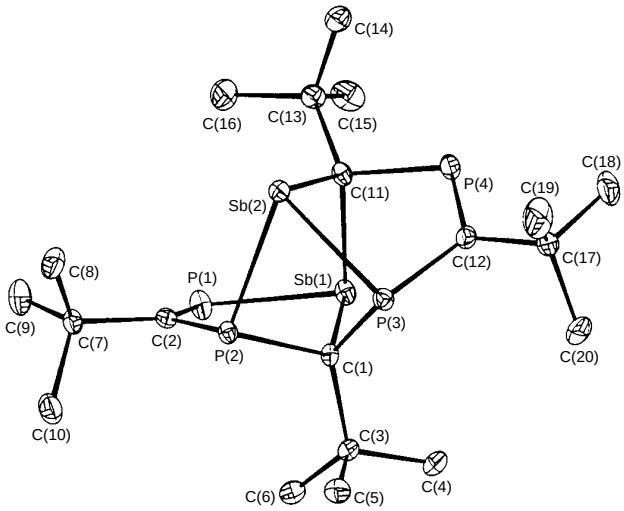



**Fig. 1** Molecular structure of $C_4Bu^t_4P_4Sb_2$ **6**. Selected bond lengths (Å) and angles (°): Sb(1)–C(1) 2.200(4), Sb(1)–C(11) 2.223(4), Sb(1)–P(1) 2.531(1), Sb(2)–C(11) 2.221(4), Sb(2)–P(3) 2.516(1), Sb(2)–P(2) 2.529(1), P(1)–C(2) 1.681(4), P(2)–C(2) 1.827(4), P(2)–C(1) 1.874(4), P(3)–C(12) 1.852(4), P(3)–C(1) 1.925(4) P(4)–C(12) 1.689(4), P(4)–C(11) 1.844(4), C(1)–Sb(1)–C(11) 88.7(1), C(1)–Sb(1)–P(1) 91.6(1), C(11)–Sb(1)–P(1) 98.5(1); C(11)–Sb(2)–P(3) 82.6(1), C(11)–Sb(2)–P(2) 96.2(1), P(3)–Sb(2)–P(2) 68.0(4), C(2)–P(1)–Sb(1) 98.8(1), C(2)–P(2)–C(1) 107.6(2), C(2)–P(2)–Sb(2) 104.1(1), C(1)–P(2)–Sb(2) 85.6(1), C(12)–P(3)–C(1) 109.2(2), C(12)–P(3)–Sb(2) 94.7(1), C(1)–P(3)–Sb(2) 84.9(1), P(2)–C(1)–P(3) 95.9(2), P(2)–C(1)–Sb(1) 107.0(2), P(3)–C(1)–Sb(1) 111.8(2), P(1)–C(2)–P(2) 124.9(2), P(4)–C(11)–Sb(2) 107.9(2), P(4)–C(11)–Sb(1) 97.1(2), Sb(2)–C(11)–Sb(1) 109.2(2), P(4)–C(12)–P(3) 121.8(2).

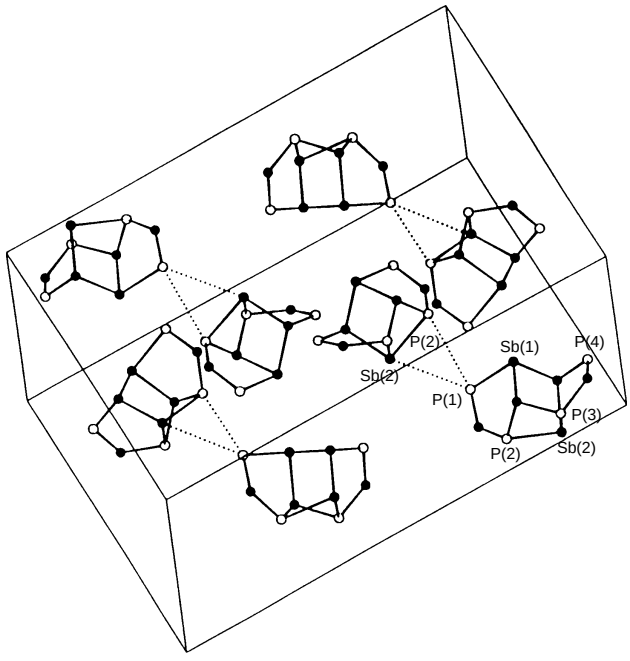



**Fig. 2** Unit-cell diagram for $C_4Bu^t_4P_4Sb_2$ **6** showing intermolecular interactions. *tert*-Butyl groups omitted for sake of clarity

We have recently discovered that the highly strained cage compound **6** undergoes facile intramolecular rearrangement reactions, either in solution (even at −30 °C) or when treated with transition-metal fragments, *e.g.* $[W(CO)_5]$. The results of these investigations will be presented in a later publication.

We gratefully acknowledge financial support from The Leverhulme Trust (S. J. B.) and The Nuffield Foundation. We also thank Professor M. B. Hursthouse and Mr D. E. Hibbs (EPSRC Crystallography Service, Cardiff) for the X-ray data collection and many helpful discussions.

## Footnotes

† E-mail: c.a.jones@swansea.ac.uk

‡ *Spectroscopic data* for **6**: $^1$H NMR (250 MHz, $C_6D_6$, $SiMe_4$) δ 1.16 (s, 9 H, Bu$^t$), 1.28 (s, 9 H, Bu$^t$), 1.48 (s, 9 H, Bu$^t$), 1.62 (s, 9 H, Bu$^t$); $^{13}$C NMR (100.6 MHz, $C_6D_6$) δ 30.7 (dd, C*C*H$_3$, $^3J_{PC}$ 7.5, 7.8 Hz), 31.8 (dd, C*C*H$_3$, $^3J_{PC}$ 11.4, 10.0 Hz), 32.7 (dd, C*C*H$_3$, $^3J_{PC}$ 6.0, 9.1 Hz), 36.3 (d, C*C*H$_3$, $^3J_{PC}$ 10.4 Hz), 38.6 (d, *C*CH$_3$, $^2J_{PC}$ 16.2 Hz), 42.1 (dd, *C*CH$_3$, $^2J_{PC}$ 22.0, 21.0 Hz), 46.2 (dd, *C*CH$_3$, $^2J_{PC}$ 14.9, 12.6 Hz), 47.7 (dd, *C*CH$_3$, $^2J_{PC}$ 12.1, 14.2 Hz), 79.0 (ddd, PCP, $^1J_{PC}$ 50, 51, $^3J_{PC}$ 8 Hz), 90.5 (d, SbCP, $^1J_{PC}$ 65 Hz), 212.0 (ddd, PCP, $^1J_{PC}$ 77, 74, $^3J_{PC}$ 10.1 Hz), 240.2 (ddd, PCP, $^1J_{PC}$ 89, 87, $^3J_{PC}$ 9.6 Hz); $^{31}$P{$^1$H} NMR (101.4 MHz, $C_6D_6$) δ −18.6 (dd, P$^2$, $^2J_{P2,3}$ 137, $^2J_{P1,2}$ 28 Hz), 32.5 (dd, P$^3$, $^2J_{P2,3}$ 137, $^2J_{P3,4}$ 31 Hz), 356.5 (d, P$^4$, $^2J_{P3,4}$ 31 Hz), 363.4 (d, P$^1$, $^2J_{P1,2}$ 28 Hz); CIMS (70 kV) 645 (MH$^+$, 8%), 523 (MH$^+$ − Sb, 10%), 169 (Bu$^t$CPCBu$^{t+}$, 15%), 57 (Bu$^{t+}$, 100%). Suitable analytical data were obtained.

‡ *Crystal data* for **6**: $C_{20}H_{36}P_4Sb_2$, $M$ = 643.87, orthorhombic, space group *Pbca*, $a$ = 12.9730(5), $b$ = 19.0530(7), $c$ = 21.052(2) Å, $U$ = 5203.5(6) Å$^3$, $Z$ = 8, $D_c$ = 1.644 g cm$^{-3}$, $F(000)$ = 2544, μ = 23.26 cm$^{-1}$, crystal 0.23 × 0.31 × 0.18 mm, radiation Mo-Kα (λ = 0.710 69 Å), 150(2) K.

All crystallographic measurements were made using a FAST area detector diffractometer. The structure was solved by direct methods and difference synthesis and refined on $F^2$ by full-matrix least squares using all unique data. All non-hydrogen atoms are anisotropic with H atoms included in calculated positions (riding model). Final $wR$ (on $F^2$) and $R$ (on $F$) were 0.0647 and 0.0446 for all data. Atomic coordinates, bond lengths and angles, and thermal parameters have been deposited at the Cambridge Crystallographic Data Centre (CCDC). See Information for Authors, Issue No. 1. Any request to the CCDC for this material should quote the full literature citation and the reference number 182/336.

## References

1 R. Streubel, *Angew. Chem., Int. Ed. Engl.*, 1995, **34**, 436 and references therein.
2 F. Mathey, *Coord. Chem. Rev.*, 1994, **137**, 1 and references therein.
3 R. Bartsch, P. B. Hitchcock and J. F. Nixon, *J. Organomet. Chem.*, 1989, **375**, C31.
4 S. S. Al-Juaid, P. B. Hitchcock, R. M. Matos and J. F. Nixon, *J. Chem. Soc., Chem. Commun.*, 1993, 267.
5 A. J. Ashe, W. Butler and T. R. Diephouse, *J. Am. Chem. Soc.*, 1981, **103**, 207; *Organometallics*, 1983, **2**, 1005; A. J. Ashe and F. J. Drone, *Organometallics*, 1984, **3**, 495.
6 M. D. Francis, D. E. Hibbs, M. B. Hursthouse, C. Jones and K. M. A. Malik, *J. Organomet. Chem.*, in the press.
7 M. D. Francis, D. E. Hibbs, M. B. Hursthouse, C. Jones and K. M. A. Malik, *Chem. Commun.*, 1996, 1591.
8 S. J. Black and C. Jones, *J. Organomet. Chem.*, in the press.
9 J. Emsley, *The Elements*, 2nd edn., Oxford University Press, 1991.

*Received, 12th November 1996; Com. 6/07672F*

# Self-assembly of supramolecular boxes

**Michael J. Hannon,* Claire L. Painting and William Errington**

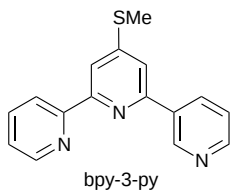
*Department of Chemistry, University of Warwick, Gibbet Hill Road, Coventry, UK CV4 7AL*

**Supramolecular boxes are prepared from a dinucleating ligand and redox-active metal centres incorporated into the cavity framework without the need for ancillary ligands to block coordination sites on the metal; crystal structures of copper(I) and cadmium(II) cage structures of 4-thiomethyl-6-(3-pyridyl)-2,2′-bipyridine are reported.**

There is much interest in the use of the supramolecular synthetic approach to assemble large molecular aggregates.[1] The metallosupramolecular approach has enjoyed particular success and nanoscale arrays containing up to 15 components have been assembled.[2] Following the elegant work of Fujita *et al*.[3] and others[4] we were drawn to the assembly of supramolecular species containing cavities as they represent readily prepared analogues of organic macrocycles. As described by Fujita *et al*., a square-shaped cyclophane analogue results from mixing the pre-prepared complex $[Pd(en)(NO_3)_2]$ with the bis-monodentate ligand 4,4′-bipyridine.[3] In this reaction the ethylenediamine ligand acts as a blocking ligand sealing up two coordination sites on the palladium centre. In the absence of blocking ligands polymeric arrays result.[8]

We reasoned that, with judicious design, it should be possible to assemble boxes from ligands incorporating chelating units. The incorporation of chelating units into the framework is desirable as it should (*a*) remove the need for ancillary blocking ligands and (*b*) permit the incorporation of a more varied selection of metal ions into the cage arrays. Using our design, cage structures might be assembled in a single self-assembly process involving simple mixing of metals and ligands rather than the stepwise approach, involving pre-preparation of the blocked metal complex, inherent in the previous work.[3,4] Such a design requires the preparation of ligands which contain two coordination sites, linked in such a fashion that they cannot both coordinate to the same metal ion. Moreover the position of the link must lead logically to the formation of a defined closed structure when metal ions coordinate to the ligand, and the closed structure that results must contain an aryl-linked cavity. The coordination sites used might be either two polydentate sites or one polydentate and one monodentate site. We have chosen to initiate our studies with the latter and wish to report our preliminary results in this area.

Following our design, we have prepared the substituted terpyridine ligand 4-thiomethyl-6-(3″-pyridyl)-2,2′-bipyridine (bpy-3-py). This ligand is constrained by its connectivity to act as a dinucleating ligand, presenting a didentate binding site to one metal ion and a monodentate to the other. The ligand was prepared in good yield (64%) in a one-pot Potts[5] reaction of 3,3-bis(methylthio)-1-(2′-pyridinyl)prop-2-en-1-one with the potassium enolate of 3-acetylpyridine, followed by ring closure with ammonium acetate.



bpy-3-py

Warming methanolic or acetonitrilic solutions of the ligand with 1 equiv. of copper(I) salts $[Cu(MeCN)_4]X$ (X = $PF_6$, $BF_4$) leads to the rapid formation of red solutions from which red–brown salts of formula $[Cu_2(bpy\text{-}3\text{-}py)_2(MeCN)_2]X_2$ are isolated on cooling. Mass spectrometric analysis (FAB) shows the presence of dinuclear $M_2L_2$ and $M_2L_2X$ peaks consistent with this formulation. Cyclic voltammetric analysis of acetonitrilic solutions of the complexes shows a single reversible oxidation at +0.13 V (*vs*. $Fc–Fc^+$) consistent with copper(I) in an $N_4$ coordination environment.[6] More importantly this implies that there are not two different types of copper(I) centre present in the molecule. The absorption spectra of acetonitrilic solutions of the complexes show charge-transfer bands centred at 537 ($\varepsilon$ = 1300) and 426 nm (2300 $M^{-1}$ $cm^{-1}$), which are also consistent with an $N_4$ coordination set containing polypyridyl units.[6] The $^1H$ NMR spectra of $CD_3CN$ solutions of the salts show the expected number of resonances in the aromatic region and the presence of a single thiomethyl resonance. The spectra are slightly broadened at room temperature, most probably as a result of 'ring-wobbling' processes similar to those that we have previously observed[6,7] in other oligopyridine assemblies.

Recrystallisation of the hexafluorophosphate salt from acetonitrile solution by the slow diffusion of diethyl ether afforded deep red crystals, the structure of which has been determined† and which is shown in Fig. 1. As anticipated the bpy-3-py ligand bridges between two metal centres. Each copper(I) centre is bound to a bipyridyl unit from one ligand and a pyridyl from the other, resulting in the formation of a dimeric $M_2L_2$ species. The pseudo-tetrahedral coordination sphere of the metal centre is completed by an acetonitrile solvent molecule. The metal–ligand bond lengths and angles are unremarkable and the intermetallic Cu···Cu distance is 5.178(1) Å. The pyridyl and bipyridyl binding domains are twisted with respect to each other [dihedral angle 50.26(13)°] and a cavity between the pyridyl units of the two ligands results. This twisting is anticipated; indeed we have previously used it to generate double-helical complexes.[6] In this case the twisting results in the aromatic rings defining the desired aryl-lined cavity.

The cage structure furnishes each metal ion with only three donor atoms (one from the pyridyl unit of one ligand and two from the bipyridyl of the ligand). The box structure is

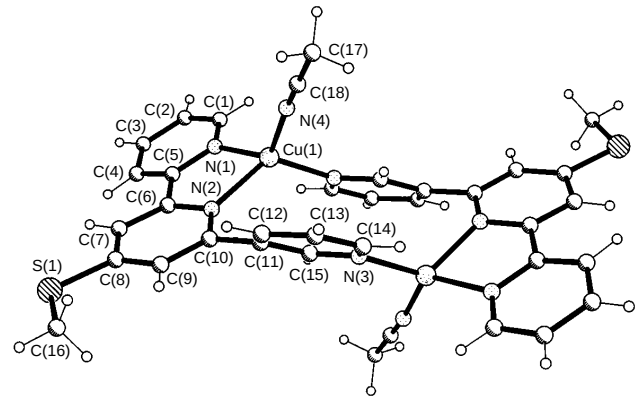



**Fig. 1** Crystal and molecular structure of the cation $[Cu_2(bpy\text{-}3\text{-}py)_2(MeCN)_2]^{2+}$

nevertheless formed with the tetrahedral copper(I) ion. We have therefore investigated whether the structure might also be supported by metal ions with a higher coordination number requirement.

Reaction of a methanolic solution of the ligand with cadmium(II) acetate gives a pale green solution from which beautiful green blocks crystallise on the addition of methanolic ammonium hexafluorophosphate. On isolation the crystals rapidly lose solvent to give an apple-green solid. An X-ray crystallographic study has been undertaken on the crystalline material† and the structure is shown in Fig. 2. Once again a dimeric $M_2L_2$ cage structure is formed with the ligand bridging between the two metal centres and each cadmium(II) ion bound to a pyridyl group from one ligand and a bipyridyl unit from the other ligand. The twisting about the aryl–aryl bonds between the pyridyl and bipyridyl units [dihedral angle 55.40(13)°] again results in the desired aryl-lined cavity. In contrast to the pseudo-tetrahedral copper(I) cations the cadmium(II) dications occupy a pseudo-octahedral environment. The remaining coordination sites are completed by a didentate acetate ligand and a methanol solvent molecule. The two cadmium centres are separated by 5.6788(8) Å.

The structure may be contrasted with the polymeric species obtained from mixing cadmium(II) salts with 4,4′-bipyridine.[8] While the reaction of $[Pd(en)(NO_3)_2]$ with 4,4′-bipyridine gives rise to a molecular square, the reaction of the cadmium(II) metal salt, which does not contain a blocking ethylenediamine ligand, gives rise to a polymeric array of squares. As anticipated, the introduction of the chelating unit within our system does lead to the formation of the box structure, rather than a polymeric array.

We have thus established a novel ligand which allows us to form metallosupramolecular cage species with a variety of metal ions without the need for ancillary ligands which deliberately block coordination sites. We are also applying the principles learnt in this study to the development of polymeric arrays ('crystal engineering') and will address our studies in that area in a subsequent paper.

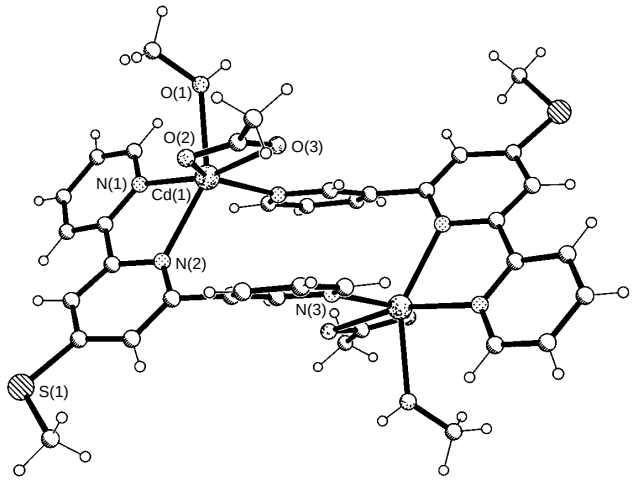



**Fig. 2** Crystal and molecular structure of the cation $[Cd_2(bpy\text{-}3\text{-}py)_2(O_2CMe)_2(MeOH)_2]^{2+}$

We are grateful to the Royal Society for a grant enabling the purchase of an electrochemical workstation (M. J. H.), the EPSRC for a studentship (C. L. P.) and the EPSRC and Siemens for grants enabling the purchase of the diffractometer.

## Footnote

† *Crystal data*: $[Cu_2(bpy\text{-}3\text{-}py)_2(MeCN)_2][PF_6]_2\cdot 2MeCN$; $C_{40}H_{38}Cu_2F_{12}N_{10}P_2S_2$, $M$ = 1139.94, monoclinic, space group $P2_1/n$, $a$ = 7.4991(4), $b$ = 20.3814(4), $c$ = 15.6175(3) Å, β = 101.837(3)°, $U$ = 2336.25(14) Å$^3$, 200 K; final $R1$, $wR2$ and $S$ are 0.046, 0.118 and 1.13 for 310 parameters.

$[Cd_2(bpy\text{-}3\text{-}py)_2(MeOH)_2(O_2CMe)_2][PF_6]_2\cdot 2MeOH$; $C_{40}H_{48}Cd_2F_{12}N_6O_8P_2S_2$, $M$ = 1319.70, triclinic, space group $P\bar{1}$, $a$ = 7.99110(10), $b$ = 12.9262(3), $c$ = 13.5037(4) Å, α = 107.7130(10), β = 95.8010(10), γ = 107.1700(10)°, $U$ = 1241.28(5) Å$^3$, 180 K; final $R1$, $wR2$ and $S$ are 0.049, 0.110 and 0.968 for 358 parameters.

Data were collected using a Siemens SMART CCD area-detector diffractometer. Refinement was by full-matrix least squares on $F^2$ for all data using SHELXL-96.[9] Atomic coordinates, bond lengths and angles, and thermal parameters have been deposited at the Cambridge Crystallographic Data Centre (CCDC). See Information for Authors, Issue No. 1. Any request to the CCDC for this material should quote the full literature citation and the reference number 182/342.

## References

1 J.-M. Lehn, *Supramolecular Chemistry—Concepts and Perspectives*, VCH, Weinheim, 1995; D. Philp and J. F. Stoddart, *Angew. Chem., Int. Ed. Engl.*, 1996, **35**, 1155; E. C. Constable, *Prog. Inorg. Chem.*, 1994, **42**, 67.
2 P. N. W. Baxter, J.-M. Lehn, J. Fischer and M.-T. Youinou, *Angew. Chem., Int. Ed. Engl.*, 1994, **33**, 2284.
3 M. Fujita, J. Yazaki and K. Ogura, *J. Am. Chem. Soc.*, 1990, **112**, 5645; M. Fujita, S. Nagao and K. Ogura, *J. Am. Chem. Soc.*, 1995, **117**, 1649; M. Fujita and K. Ogura, *Bull. Chem. Soc. Jpn.*, 1995, **69**, 1471 and references therein.
4 P. J. Stang and K. Chen, *J. Am. Chem. Soc.*, 1995, **117**, 1667 and references therein; H. Rauter, E. C. Hillergis, A. Erxleben and B. Lippert, *J. Am. Chem. Soc.*, 1994, **116**, 616; F. S. McQuillan, C. J. Jones and J. A. McCleverty, *Polyhedron*, 1995, **14**, 3157; R. V. Slone, D. I. Yoon, R. M. Calhoun and J. T. Hupp, *J. Am. Chem. Soc.*, 1995, **117**, 11 813; A. Bilyk, M. M. Harding, P. Turner and T. W. Hambley, *J. Chem. Soc., Dalton Trans.*, 1994, 2783.
5 K. T. Potts, M. J. Cipullo, P. Ralli and G. Theodoridis, *J. Org. Chem.*, 1982, **47**, 3027.
6 E. C. Constable, M. J. Hannon, A. J. Edwards and P. R. Raithby, *J. Chem. Soc., Dalton Trans.*, 1994, 2669.
7 R. C. Chotalia, E. C. Constable, M. J. Hannon and D. A. Tocher, *J. Chem. Soc., Dalton Trans.*, 1995, 3571.
8 M. Fujita, Y. J. Kwon, S. Washizu and K. Ogura, *J. Am. Chem. Soc.*, 1994, **116**, 1151.
9 G. M. Sheldrick, SHELXL-96, Program for Crystal Structure Refinement, University of Göttingen, Germany, 1996.

*Received, 18th November 1996; Com. 6/07826E*

# Oxidative desulfurization–fluorination of alkanol xanthates. Control of the reaction pathway to fluorination or trifluoromethoxylation

**Kiyoshi Kanie, Yoichiro Tanaka, Masaki Shimizu, Manabu Kuroboshi† and Tamejiro Hiyama***

*Research Laboratory of Resources Utilization, Tokyo Institute of Technology, 4259 Nagatsuta, Midori-ku, Yokohama, Kanagawa 226, Japan*

**The reagent consisting of 70% HF–py (py = pyridine) and a halonium oxidant converts R–$OCS_2Me$ into either R–$OCF_3$ (R = primary) or R–F (R = secondary, tertiary or benzylic) whereas the 50% HF–py system converts R–$OCS_2Me$ (R = secondary) into R–$OCF_3$.**

Exploitation of novel and efficient fluorination reactions has been the subject of extensive research,[1] because organofluorine compounds very often play key roles in material and pharmaceutical science. The oxidative desulfurization–fluorination reaction[2] recently disclosed by us transforms the xanthates derived from phenols and primary alkanols to the corresponding trifluoromethyl ethers.[3] To achieve this transformation, a readily available reagent system consisting of hydrogen fluoride and 30% pyridine (70% HF–py)[4] and a halonium oxidant is extremely effective.

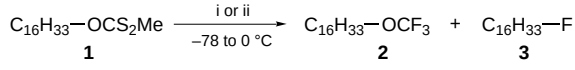
Very recently, Motherwell and his co-workers reported that the xanthates of primary and secondary alkanols were converted into the corresponding fluorides by means of 4-methyl(difluoroiodo)benzene ($TolIF_2$).[5] This paper, indicating that the xanthates of primary alkanols gave different products, prompted us to study in more detail the oxidative desulfurization–fluorination of the xanthates of various secondary and tertiary alkanols. Herein we report that R–$OCS_2Me$ (R = primary) could be converted into R–$OCF_3$, whereas R–$OCS_2Me$ (R = secondary, tertiary or benzylic) was fluorinated to give R–F. Furthermore, we also found that 50% HF–py could convert R–$OCS_2Me$ (R = secondary) into the corresponding R–$OCF_3$ with R–F being undetected. According to the presented method, secondary alkyl trifluoromethyl ethers are prepared for the first time from the corresponding alcohols.

To compare the selectivity of the reagent 70% HF–py–$X^+$ with $TolIF_2$, we first chose *O*-hexadecyl *S*-methyl dithiocarbonate **1** for the model substrate. Upon treatment with $TolIF_2$, **1** was reportedly converted into 1-fluorohexadecane **3** in 48% yield.[5] When **1** was treated with 1,3-dibromo-5,5-dimethylhydantoin (DBH, 3.0 mol) and 70% HF–py (80 mol) in dichloromethane at −78 to 0 °C for 1 h, 1-trifluoromethoxyhexadecane **2** was isolated in 95% yield, and no trace of **3** could be detected. To confirm the difference between the two reagents, we used bis(trifluoroacetoxy)iodobenzene (3.0 mmol) in place of DBH; trifluoromethyl ether **2** was obtained again as the sole product in 67% yield (Scheme 1) Thus, the reagent system consisting of 70% HF–py and an oxidant exhibits unique reactivity, contrasting sharply to $TolIF_2$, and the reaction pathway appears to be governed by a fluorinating agent rather than by an oxidant.

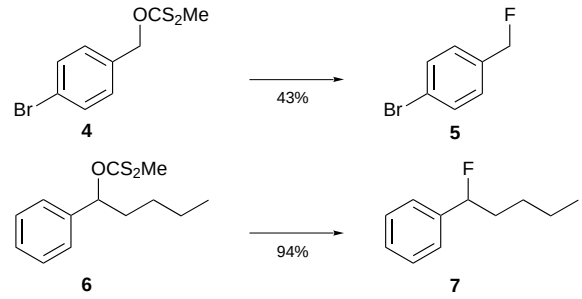
In contrast to the xanthates of primary alcohols, those of benzylic, secondary or tertiary alcohols underwent the fluorination reaction under the standard oxidative desulfurization–fluorination conditions. Examples are the reactions of the benzylic xanthates **4**‡ and **6**; both gave fluorination products **5** and **7**, respectively (Scheme 2).

Xanthate **8** also was successfully fluorinated to give **9** in 70% yield using *N*-iodosuccinimide (NIS) as the oxidant (Scheme 3). With DBH, bromination of the phenyl ring accompanied the fluorination reaction.§

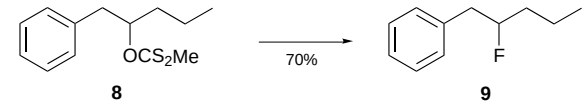
The fluorination conditions were applied to the xanthates derived from secondary or tertiary alcohols. The isolated yield is shown below the formula of each product (Scheme 4). As readily seen, both secondary and tertiary alkyl fluorides could be prepared in good yields.¶ The xanthate of menthol gave **11c** as an isolable single product. Although the reaction appears to have proceeded with retention of configuration, we consider **11c** was produced through a carbocationic intermediate. Similar stereochemical results are reported with other fluorination reagents.[5,6]



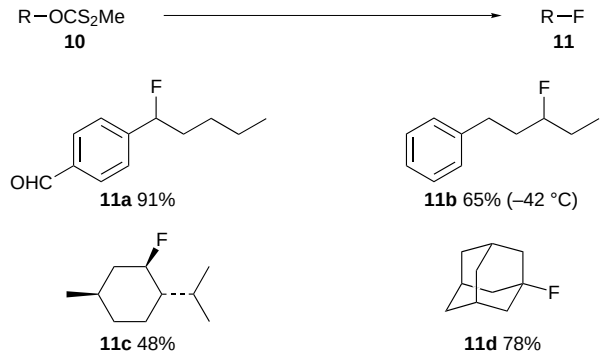

**Scheme 1** *Reagents and conditions*: i, 70% HF–py, DBH, **2** 95%; ii, 70% HF–py, $PhI(OCOCF_3)_2$, **2** 67%




**Scheme 2** *Reagents and conditions*: 70% HF–py (40 mol), DBH (3.0 mol), $CH_2Cl_2$, −78 to 0 °C, 1 h




**Scheme 3** *Reagents and conditions*: 70% HF–py (20 mol), NIS (3.0 mol), $CH_2Cl_2$, −42 °C, 1 h

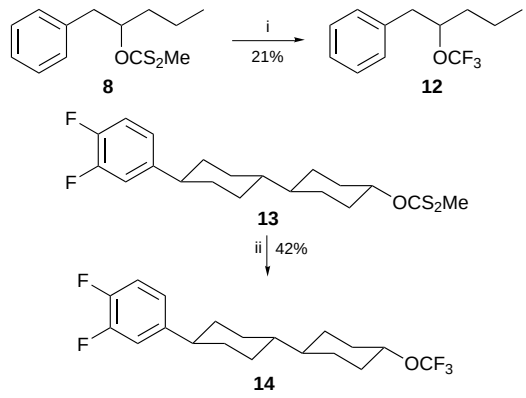



**Scheme 4** *Reagents and conditions*: 70% HF–py (40 mol), NIS (3.0 mol), $CH_2Cl_2$, −78 to 0 °C, 0.5–1 h

The fluorination reaction may be attributed to an easy elimination of the $–OCS_2Me$ group from secondary and tertiary aliphatic xanthates under the acidic conditions, followed by the subsequent fluoride attack at the resulting electrophilic carbon to complete the fluorination. Hence we envisaged that, if the acidity of the reaction conditions was controlled by proper choice of the reagent system, we could switch the reaction pathway to the trifluoromethyl ether formation. Thus, we used 50% HF–py as the fluorinating reagent that was prepared by dilution of 70% HF–py with pyridine. Indeed, xanthate **8** afforded the corresponding trifluoromethyl ether **12** in 21% yield by treatment with 50% HF–py (40 mol) and *N*-bromosuccinimide (NBS, 5.0 mol) at −78 to 0 °C for 30 min (Scheme 5).‖ Herein no trace of alkyl fluoride **9** could be detected. Furthermore, xanthate **13** was also converted into the corresponding trifluoromethyl ether **14** in 42% yield.

In conclusion, the reagent system consisting of 70% HF–py and a halonium ion oxidant is extremely effective for the conversion of $R–OCS_2Me$ (R = alkyl) into either $R–OCF_3$ (R = primary) or R–F (R = benzylic, secondary or tertiary), depending on the structure of the substrate. In particular, the xanthates of primary alcohols give trifluoromethyl ethers in striking contrast to the reaction with $TolIF_2$. The difference may be attributed to the difference between the reactive species involved.[5,6] Furthermore, the synthesis[7] of secondary alkyl trifluoromethyl ethers is achieved with a readily adjustable reagent system consisting of 50% HF–Py and NBS. Thus, the reaction pathway to secondary alkyl fluoride or to trifluoromethyl ether is controlled simply by an appropriate choice of the fluorination reagent starting with the same substrate.

The present work is partially supported financially by a grant from the Asahi Glass Foundation and by a Grant-in-Aid (No. 07405042) for Scientific Research (A) from the Ministry of Education, Science, Sports and Culture.




**Scheme 5** *Reagents and conditions*: i, 50% HF–py (40 mol), NBS (5.0 mol), $CH_2Cl_2$, −78 to 0 °C, 0.5 h; ii, 50% HF–py (40 mol), NBS (5.0 mol), $CH_2Cl_2$, 0 °C, 1 h

## Footnotes

† Present address: Department of Applied Chemistry, Faculty of Engineering, Okayama University, Tsushima-naka, Okayama 700, Japan.

‡ To obtain the product in high yield, 40 mol of 70% HF–py was enough. When 80 mol of 70% HF–py was used, halogenation of the aromatic moiety simultaneously took place, and a mixture of monobromo, dibromo and tribromo derivatives resulted.

§ When 40 mol of 70% HF–py was used, iodination of the phenyl group occurred to some extent.

¶ A procedure for the synthesis of 4-(1-fluoropentyl)benzaldehyde **11a** is representative. To a suspension of NIS (1.5 mmol) in dichloromethane (2.5 ml) were added 70% HF–py[4] (0.5 ml, 2.2 mmol, 20 mmol of $F^-$) and *O*-{1-(4-formylphenyl)pentyl} *S*-methyl dithiocarbonate (0.5 mmol) at −78 °C. The mixture was stirred at 0 °C for 1 h, poured into a pH = 10 buffer solution ($NaHCO_3$, $NaHSO_3$ and NaOH) and extracted with diethyl ether three times. The combined ethereal layers were dried over $MgSO_4$, filtered and concentrated under reduced pressure. Flash column chromatography on silica gel (hexane–$Et_2O$, 20 : 1) afforded **11a** in 91% yield.

‖ A procedure for the preparation of trifluoromethyl ether **12** is as follows. To a suspension of NBS (5.0 mmol) in dichloromethane (2.5 ml) was added pyridine (0.46 ml); subsequently 70% HF–py (1.0 ml, 4.4 mmol, 40 mmol of $F^-$) was slowly added dropwise at −78 °C, and the resulting mixture was stirred at room temp. for 5 min and then recooled to −78 °C. A dichloromethane (2.5 ml) solution of xanthate **8** (1.0 mmol) was added dropwise to the suspension at −78 °C. The resulting mixture was stirred at 0 °C for 30 min, poured into a pH = 10 buffer solution ($NaHCO_3$, $NaHSO_3$ and NaOH) and extracted with diethyl ether three times. The combined ethereal layers were dried over $MgSO_4$, filtered and concentrated under reduced pressure. Flash column chromatography on silica gel (cyclohexane) afforded 1-phenylpent-2-yl trifluoromethyl ether **12** in 21% yield.

** Under the similar conditions, trifluoromethyl ethers of β-cholestanol and 1-phenylpentan-3-ol were prepared in 24 and 16% yield, respectively.

## References

1 J. T. Welch, *Tetrahedron*, 1987, **43**, 3123; H. Nohira, *Yuki Gosei Kagaku Kyokai Shi*, 1991, **49**, 467; N. Yoneda, *Tetrahedron*, 1991, **47**, 5329; J. A. Wilkinson, *Chem. Rev*., 1992, **92**, 505; M. Hudlicky and A. E. Pavlath, *Chemistry of Organic Fluorine Compounds II. A Critical Review*, ACS Monograph 187, Washington, DC, 1995 and references cited therein.

2 M. Kuroboshi and T. Hiyama, *Yuki Gosei Kagaku Kyokai Shi*, 1993, **51**, 1124; M. Kuroboshi and T. Hiyama, *Tetrahedron Lett.*, 1992, **33**, 4177; M. Kuroboshi and T. Hiyama, *Synlett*, 1991, 909; M. Kuroboshi and T. Hiyama, *Chem. Lett.*, 1992, 827.

3 M. Kuroboshi, K. Suzuki and T. Hiyama, *Tetrahedron Lett.*, 1992, **33**, 4173.

4 G. A. Olah, J. T. Welch, Y. D. Vankar, M. Nojima, I. Kerekes and J. A. Olah, *J. Org. Chem.*, 1979, **44**, 3872.

5 M. J. Koen, F. L. Guyader and W. B. Motherwell, *J. Chem. Soc., Chem. Commun.*, 1995, 1241.

6 C. M. Sharts and W. A. Sheppard, *Org. React.*, 1974, **21**, 125.

7 β-Fluoroalkyl trifluoromethyl ethers are prepared alternatively by treatment of alkenes with $CF_3OF$, albeit in low yields. See: D. H. R. Barton, L. J. Dankas, A. K. Ganguly, R. H. Hesse, G. Tarzia and M. M. Pechet, *J. Chem. Soc., Chem. Commun.*, 1969, 227; S. Rozen, *Chem. Rev.*, 1996, **96**, 1717; C. Corvaja, F. Cremonese, W. Navarrini, C. Tonelli and V. Tortelli, *Tetrahedron Lett.*, 1995, **36**, 3543.

*Received, 21st November 1996; Com. 6/07897D*

# Directional photochemical processes with an amphiphilic anthraceno–ruthenium complex in dihexadecyl phosphate vesicles

**Joe Otsuki,*[a] Naotoshi Okuda,[b] Takeyuki Amamiya,[b] Koji Araki[a] and Manabu Seno[b]**

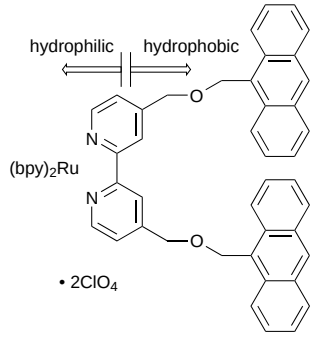
[a] *Institute of Industrial Science, University of Tokyo, 7-22-1 Roppongi, Minato-ku, Tokyo 106, Japan*
[b] *College of Science and Technology, Nihon University, 1-8-14 Kanda Surugadai, Chiyoda-ku, Tokyo 101, Japan*

**Excitation of an amphiphilic anthraceno–ruthenium complex, which serves as an antenna-sensitizer complex, leads to two kinds of anthracene triplet states, one of which is bleached by a hydrophilic acceptor and the other by a hydrophobic acceptor in dihexadecyl phosphate vesicles; the latter process is directional from the surface to the interior of the bilayer membrane.**

Numerous model studies have appeared on photo-induced electron-transfer systems across vesicle membranes, since vesicles have been considered to be useful in providing desirable microheterogeneous environments for the charge separation processes required in photosynthesis.[1] However, nearly all studies involve diffusional processes of redox-active components and the organization of components is thus limited. O'Brien and coworkers recently addressed this problem and reported some systems in which components are partitioned selectively in various parts of the membrane.[2] Another approach would be to connect the components covalently and incorporate them into vesicles with a defined direction by rational design of the hydrophobic–hydrophilic balance. There are only a few reports on covalently linked chromophores in vesicles[3] in spite of the fact that the covalent approach has been met with great success in elucidating factors determining the rate of electron transfer in homogeneous solutions.[4,5] Here we report on vectorial processes effected by a covalently linked anthraceno–ruthenium complex **1** in dihexadecyl phosphate (DHP) vesicles.

The $[Ru(bpy)_3]^{2+}$–anthracene system was chosen as the covalently linked photoactive centre because the intramolecular triplet energy transfer process of a related compound from the ruthenium centre to the anthracene unit is well documented and its excited-state lifetime is longer than that of $[Ru(bpy)_3]^{2+}$ itself.[6] The antenna-sensitizer complex **1**, which has two anthracenes on one of the bipyridine ligands, is designed so that half of the molecule (Ru centre) is hydrophilic, whereas the other half including anthracene is hydrophobic.

The bis-anthracene ligand was prepared from 9-anthracenemethanol and 4,4′-bis(bromomethyl)-2,2′-bipyridine[7] with KOH in $Me_2SO$ (64%, mp 184–185 °C). The complexation of this ligand with *cis*-$[Ru(bpy)_2Cl_2]\cdot 2H_2O$[8] followed by the addition of $NaClO_4$ provided **1** (80%, mp 175–179 °C). *N*,*N*′-Didodecylpyromellitimide **2** was prepared from pyromellitic anhydride and 1-aminododecane in refluxing dmf (82%, mp 156.5–158.5 °C).†




**1**

The absorption spectrum of **1** is nearly the superposition of $[Ru(bpy)_3]^{2+}$ and 9-anthracenemethanol, thus the intramolecular electronic interaction in the ground state is negligible. On the other hand, emission properties of **1** are totally different from the model compounds as shown in Table 1.‡ Upon excitation of **1** at 455 or 470 nm, the emission intensity from the metal-to-ligand charge transfer (MLCT) state is diminished by a factor of 20 from that of $[Ru(bpy)_3]^{2+}$. It was established by Meyer and coworkers[8] that the quenching is caused by the intramolecular triplet energy transfer to anthracene (An). Although anthracenemethanol also quenches the emission from $[Ru(bpy)_3]^{2+}$ in DHP vesicles, the intramolecular quenching in **1** is more efficient. The fluorescence from $^1$An is diminished by a factor of 100 in the vesicular solution. The loss of emission may be caused by an enhanced rate for $^1$An to $^3$An intersystem crossing facilitated by the spin–orbit coupling due to the heavy-atom effect of ruthenium.[8] Indeed, the transient absorption spectrum§ after excitation at 337 nm coincides with that of $^3$An (data not shown). According to these observations, it is concluded that excitation, either to MLCT or to $^1$An, leads to $^3$An.

The triplet anthracene in **1** in vesicular solution decays by two exponential processes of comparative amplitudes with lifetimes of 3 and 13 μs [Fig. 1(*a*)], whereas the decay in MeCN is single exponential ($\tau$ = 150 μs). In the presence of 0.2 mM of methyl viologen ($MV^{2+}$), which is known to adsorb on the surface of DHP vesicles,[10] only the longer lifetime component is bleached, while the shorter one is unaffected, as shown in Fig. 1(*b*).

An acceptor with alkyl chains, **2**, was prepared aiming at being incorporated in bilayer membranes, which was indeed confirmed by gel permeation chromatography. Electron-transfer quenching of the MLCT state by the imide should be possible on the basis of redox potentials {−0.84 V for $[*Ru(bpy)_3]^{2+/3+}$[11] and −0.71 V for the diimide[1−/0][12] *vs.* SCE}. However, the emission intensity of $[Ru(bpy)_3]^{2+}$ adsorbed on the vesicle surface is unaltered by up to *ca.* 50 μM of **2**. Hence, **2** must be separated from the ruthenium complex on the membrane surface and so located in the hydrophobic part of the bilayer membrane. In sharp contrast to the case with $MV^{2+}$,

**Table 1** Relative emission intensities[a]

| | MeCN | | DHP vesicles | |
|---|---|---|---|---|
| $\lambda_{ex}$/nm | 455 | 364 | 470 | 366 |
| $\lambda_{em}$/nm | 610 | 410 | 630 | 415 |
| **1** | 0.05 | 0.09 | 0.06 | 0.01 |
| $[Ru(bpy)_3]^{2+}$, AnMeOH | 1.07 | 0.96 | 0.16 | 0.32 |
| $[Ru(bpy)_3]^{2+}$ | 1 | — | 1 | — |
| AnMeOH | — | 1 | — | 1 |

[a] The concentrations of Ru units were 3 and 30 μM, while those of An units were 6 and 60 μM in MeCN and in vesicle dispersions, respectively. AnMeOH = 9-anthracenemethanol.

transient absorption of **1** with **2** (10 μM) in DHP vesicles shows that the shorter-lifetime component is completely bleached [Fig. 1(*c*)], suggesting electron transfer from $^3$An to **2**,¶ whereas the longer-lifetime component is not affected at all.

To summarize, there are two types of $^3$An in DHP vesicles with different lifetimes, the longer-lifetime component being located near the surface of the membrane and bleached by $MV^{2+}$, while the shorter-lifetime component is located deeper in the membrane and bleached by the diimide (Fig. 2).‖ In the latter process, the photochemical events proceed directionally from the initial excitation of the ruthenium centre on the membrane surface to the final bleaching by the imide in the hydrophobic region in the membrane. Thus it is demonstrated that the covalent approach is useful to effect directional processes across the interface.

This work was partly supported by a Grant-in-Aid for Scientific Research from the Ministry of Education, Science and Culture. The authors acknowledge Professor K. Horie and Dr T. Yamashita of the University of Tokyo for help in establishing the photolysis system. Part of the photolysis equipment was made by S. Furuya and T. Shinohara of the Central Workshop of our Institute.

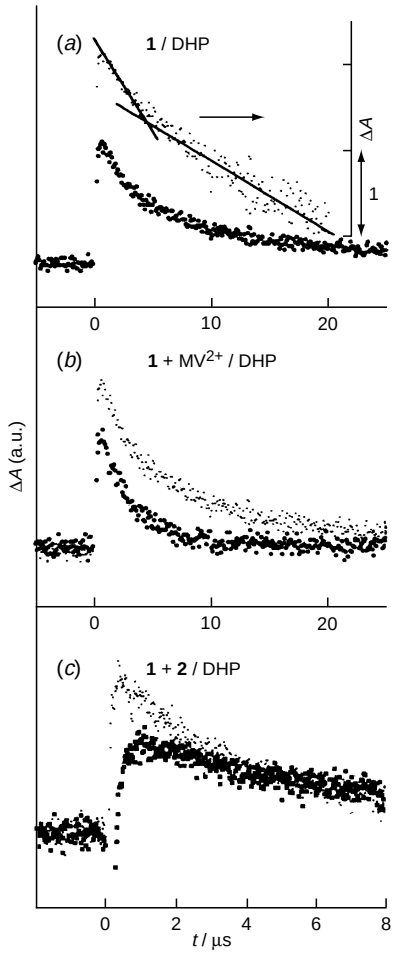



**Fig. 1** (*a*) Transient absorption decay of **1** incorporated in DHP vesicles at 418 nm following excitation at 337 nm. The logarithm plot is also shown. (*b*) The transient absorption in the presence of $MV^{2+}$. (*c*) The transient absorption in the presence of **2**. In (*b*) and (*c*), the decay curve without an acceptor is also shown for comparison by small dots. The experimental conditions are the same as in Table 1.

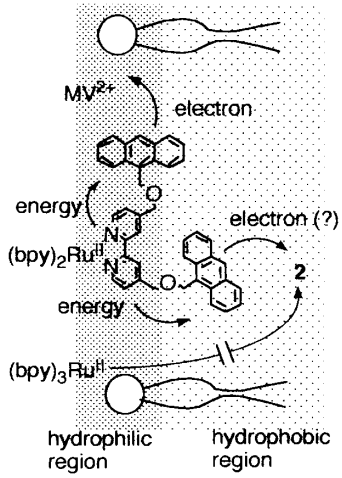



**Fig. 2** Schematic representation of the processes taking place in DHP vesicles involving **1** and acceptors

## Footnotes

*Selected data for* **1**: $^1$H NMR [$(CD_3)_2SO$] δ 4.90 (s, 4 H), 5.68 (s, 4 H), 7.36 (d, 2 H, *J* 6 Hz), 7.48–7.57 (16 H), 7.64 (d, 2 H, *J* 6 Hz), 7.67 (d, 2 H, *J* 6 Hz), 8.07 (d, 4 H, *J* 8 Hz), 8.13 (t, 2 H, *J* 8 Hz) , 8.15 (t, 2 H, *J* 8 Hz), 8.44 (d, 4 H, *J* 8 Hz), 8.58 (s, 2 H),8.75 (d, 2 H, *J* 8 Hz), 8.76 (d, 2 H, *J* 8 Hz); IR (KBr, $cm^{-1}$) 1622, 1464, 1446, 1121, 1094, 765, 624; Anal. Calc. for $C_{62}H_{48}Cl_2N_6O_{10}Ru{\cdot}2.5H_2O$: C, 59.38; H, 4.26; N, 6.70. Found: C, 58.96; H, 3.61; N, 7.40%. For **2**: $^1$H NMR ($CDCl_3$) δ 0.87 (t, 6 H), 1.2–1.4 (36 H), 1.69 (m, 4 H), 3.73 (t, 4 H), 8.26 (s, 2 H); IR (KBr, $cm^{-1}$) 2917, 2848, 1720, 1694, 1408, 1061, 723; HRMS Calc. for $C_{34}H_{52}N_2O_4$: *m/z* 552.4106; found *m/z* 552.3907; Anal Calc. C, 73.87; H, 9.48; N, 5.08. Found C, 73.84; H, 9.33; N, 5.26%.

‡ DHP vesicles were prepared according to a reported procedure.[9] Incorporation of the respective components was confirmed by passing the vesicle solution through Sephadex G50 and observing the coelution of vesicles and the components. Samples were substituted by Ar prior to measurements.

§ Laser flash photolysis experiments were conducted using a home- made system including an $N_2$ laser as the excitation source and a Xe lamp as the monitor light.

¶ We were unable to detect any direct evidence of $\mathbf{2}^-$ probably due to its small concentration and fast (< 0.2 μs with our instrumentation) back electron transfer. Bleaching by energy transfer is unlikely, since the triplet energy of the diimide (2.54 eV for *N*,*N*′-dimethylpyromellitimide[13]) is much larger than that of anthracene (1.85 eV).[8]

‖ It is not clear whether the two $^3$An species belong to the same molecule (as implied in Fig. 2) or to different molecules.

## References

1 J. N. Robinson and D. J. C. Hamilton, *Chem. Soc. Rev.*, 1991, **20**, 49.
2 P. J. Clapp, B. Armitage, P. Roosa and D. F. O'Brien, *J. Am. Chem. Soc.*, 1994, **116**, 9166 and references therein.
3 H. Nakamura, A. Motonaga, T. Ogata, S. Nakao, T. Nagamura and T. Matsuo, *Chem. Lett.*, 1986, 1615.
4 M. R. Wasielewski, *Chem. Rev.*, 1992, **92**, 435.
5 D. Gust, T. A. Moore and A. L. Moore, *Acc. Chem. Res.*, 1993, **26**, 198.
6 S. Boyde, G. F. Strouse, W. E. Jones, Jr. and T. J. Meyer, *J. Am. Chem. Soc.*, 1989, **111**, 7448.
7 S. Gould, G. F. Strouse, T. J. Meyer and B. P. Sullivan, *Inorg. Chem.*, 1991, **30**, 2942.
8 B. P. Sullivan, D. J. Salmon and T. J. Meyer, *Inorg. Chem.*, 1978, **17**, 3334.
9 Y.-M. Tricot, D. N. Furlong and W. H. F. Sasse, *Aust. J. Chem.*, 1984, **37**, 1147.
10 D. N. Furlong, Y.-M. Tricot, J. D. Swift and W. H. F. Sasse, *Aust. J. Chem.*, 1984, **37**, 703.
11 A. Juris, V. Balzani, F. Barigelletti, S. Campagna, P. Belser and A. V. Zelewsky, *Coord. Chem. Rev.*, 1988, **84**, 85.
12 A. Viehbeck, M. J. Goldberg and C. A. Kovac, *J. Electrochem. Soc.*, 1990, **137**, 1460.
13 R. N. Nurmukhametov, L. I. Semenova, N. V. Korol'kova, G. A. Val'kova and I. I.Ponomarev, *Russ. J. Chem.*, 1990, **64**, 1604.
14 Y.-M. Tricot, D. N. Furlong, W. H. F. Sasse, P. Davis, I. Snook and W. V. Megen, *J.Colloid Interf. Sci.*, 1984, **97**, 380.

*Received, 2nd December 1996; Com. 6/08105C*

# Iodine intercalation in the oxide-ion conductor $BaBi_8O_{13}$

**Darren P. Scarfe, Sai Bhavaraju and Allan J. Jacobson***

*Department of Chemistry and Texas Center for Superconductivity, University of Houston, Houston, TX 77204-5641, USA*

**The intercalation compound $I_3BaBi_8O_{13}$ forms on reaction of iodine with the layered oxide-ion conductor $BaBi_8O_{13}$; the location of iodine within the structure and the ac conductivity of the iodine intercalated phase are described.**

Intercalation reactions of neutral molecules with neutral layered host lattices are restricted to a few guest–host combinations.[1] In insulating host lattices, host–guest interactions include hydrogen bonding, for example in formamide–kaolinite intercalation compounds,[2] and coordination of a base to a metal centre in pyridine–$VOPO_4$.[3] In conducting host lattices, intercalation of neutral molecules is usually accompanied by oxidation of the host lattice and reduction of the guest species. The formation of graphite intercalation compounds with bromine and arsenic pentafluoride are among the most studied examples of neutral molecule intercalation reactions that proceed by this mechanism.[4] A closely related recent example was provided by the observation of iodine intercalation in bismuth cuprate high $T_c$ superconductors, for example, $Bi_2Sr_2CaCu_2O_8$.[5] Iodine is intercalated by direct reaction with the oxide to form a stage 1 structure with iodine located between the double Bi–O sheets and the composition $IBi_2Sr_2CaCu_2O_8$. The nature of the intercalated iodine species remains controversial though the preponderance of the evidence from Raman, XPS, and XAS measurements suggests that the intercalated species is $I_3^-$ charge balanced by the formation of holes in the $CuO_2$ planes.[6–12] Here, we describe a new example of the intercalation of iodine into the layered bismuth oxide host lattice, $BaBi_8O_{13}$. In this case, the host lattice is a good oxide ion conductor but is electronically insulating.

The composition $BaBi_8O_{13}$ is part of the solid solution series observed in the $Bi_2O_3$–BaO phase diagram between *ca*. 20 to 25 mole% BaO that is characterized by a rhombohedral layer structure.[13] The same layered structure type is also observed in the $Bi_2O_3$–MO (M = Ca, Sr) systems.[14] Each macrolayer is composed of a slab built of octahedrally coordinated (Ba,Bi)–O units sandwiched between two planar hexagonal Bi–O sheets. The structure of each complex layer can be related to that of fluorite and is distinctly different from the structure of the square-planar BiO layers in $Bi_2Sr_2CaCu_2O_8$. In each rhombohedral unit cell of $BaBi_8O_{13}$ (space group $R\bar{3}m$) three interlayer spaces are located between the hexagonal Bi–O sheets (a significant fraction of the oxygen atoms in the Bi–O layers are missing). The macrolayers are held together by van der Waals forces and there are no interlayer ions in the pristine host lattice. The rhombohedral phase has been studied in detail because of its very high oxide ion conductivity.[13–19] Two previous structural studies have investigated possible oxygen transport pathways and have suggested that migration *via* the empty interlayer sites is important in the anionic conduction mechanism.[16,19] In this study, we have synthesized the new intercalation compound $I_3BaBi_8O_{13}$ and measured its ac conductivity. The conductivity difference between the host and the intercalated lattice gives further insight into the conductivity mechanism.

The host material was prepared by reaction of a stoichiometric mixture of $Bi_2O_3$ and $Ba(NO_3)_2$ with repeated grinding and annealing at 710 °C in air. The lattice parameters of the single-phase product ($BaBi_8O_{13}$) were determined from the powder X-ray diffraction (XRD) pattern shown in Fig. 1(*a*) [*a* = 3.984(1), *c* = 28.491(2) Å]. Iodine intercalation was carried out by reaction of single-phase $BaBi_8O_{13}$ with $I_2$ (4–5 molar excess) in a sealed evacuated (*ca*. 50 mTorr) Pyrex tube for 1–5 d. The optimum conditions for intercalation were investigated by varying reaction temperatures from 50 to 350 °C and analysing the reaction products by XRD. The yellow colour of the starting material changes to brown on intercalation. For temperatures ≤150 °C, the XRD patterns showed no reaction between the host material and excess iodine. Reactions at temperatures ≥300 °C resulted in a decomposition of the starting materials to $BiI_3$ and other unidentified impurity phases. XRD patterns of samples reacted at 150–275 °C showed the formation of a single-phase layered iodine intercalated compound [Fig. 1(*b*)]. Electron microprobe analysis (EMPA‡) was used to determine the stoichiometry of the reaction product. Analyses of elemental composition and the backscattered electron images indicated the formation of a single-phase product with an average composition $I_{3.10}Ba_{0.98}Bi_{8.06}O_{13.42}$.‡ The stability of the iodine intercalated phase was studied by thermogravimetric analysis (TGA) under flowing $N_2$ saturated with water at 298 K using a TA 2950 Instrument. TGA and XRD showed that the iodine intercalated structure is stable up to temperatures of *ca*. 450 °C, although this is accompanied by the evolution of 1.3 moles of iodine. Above 650 °C the host material is the majority phase observed together with small

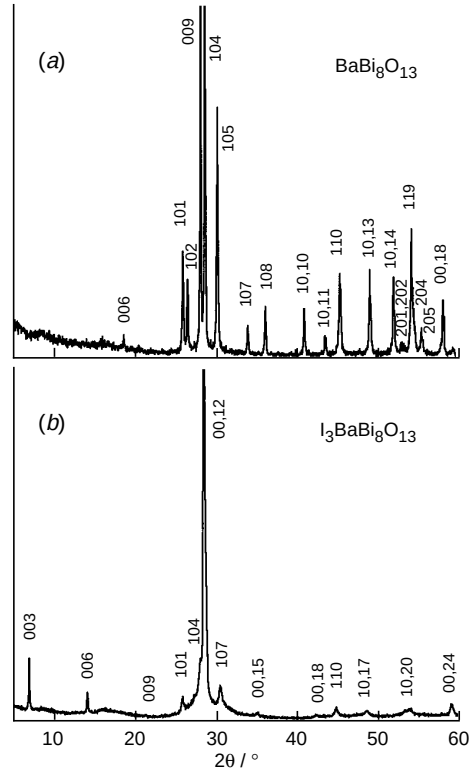



**Fig. 1** Powder X-ray diffraction patterns for (*a*) the host compound $BaBi_8O_{13}$ and (*b*) the iodine intercalated phase $I_3BaBi_8O_{13}$

amounts of unidentified impurity phases. Single-phase host material is obtained only after heating at 700 °C for 10 h. In agreement with the EMPA data, the weight loss given by TGA indicates an iodine content of 3.15(2).

The X-ray diffraction data for the iodine intercalation compound [Fig. 1(*b*)] show several (*h*0*l*) and a well defined series of (00*l*) reflections. The mixed reflections are weak relative to the (00*l*) series most probably due to a combination of preferred orientation effects and some stacking disorder. We note that the observed (*h*0*l*) reflections obey rhombohedral absences suggesting that the layer stacking sequence is preserved. The *a* axis expands from 3.984(1) to 4.01(1) Å on intercalation. The X-ray data show no evidence of any superstructure.

The positions of the (00*l*) reflections were used to determine the *c* axis of the intercalation compound. A value of $c$ = 38.46(5) Å was obtained corresponding to an increase of 9.97 Å per unit cell assuming that the rhombohedral symmetry is preserved. Each unit cell contains three layers and therefore each iodine layer expands the *c* axis by *ca*. 3.32 Å. Refinement of the intensities of the observed (00*l*) reflections was used to confirm a structural model in which the intercalated iodine species form a stage 1 compound with a monolayer of iodine located in the van der Waals gap mid-way between the Bi–O layers. In the refinement, the Ba, Bi and O atom positions were fixed at positions corresponding to the host structure. A scale factor, iodine atom *z* coordinate, occupancy and thermal parameters were refined. The best fit to the data gave an iodine stoichiometry of 3.12(4) corresponding to approximately one iodine atom intercalated into each interlayer space within the unit cell of the host material. Because only a limited number of mixed reflections are observed, the nature and the arrangement of iodine species within the *ab* plane is not yet known. Further studies on single crystal samples are in progress.

Conductivity measurements were made using a two-probe ac impedance technique in the temperature range 260–440 °C. The conductivities of the pristine host material and the iodine intercalated phase are shown in Fig. 2 in the form of an Arrhenius plot. The conductivity of the intercalated phase is approximately 1.5–2 orders of magnitude lower than the host material. The lower conductivity supports previous suggestions that oxide-ion conductivity involves the participation of interlayer sites. At higher temperatures, the difference between the conductivities of the two materials decreases possibly due to the increase in the number of vacant interlayer sites available to oxide ions as iodine is removed from the structure. A larger value of the activation energy due to the migration of oxide ions *via* intralayer sites is a further possibility.

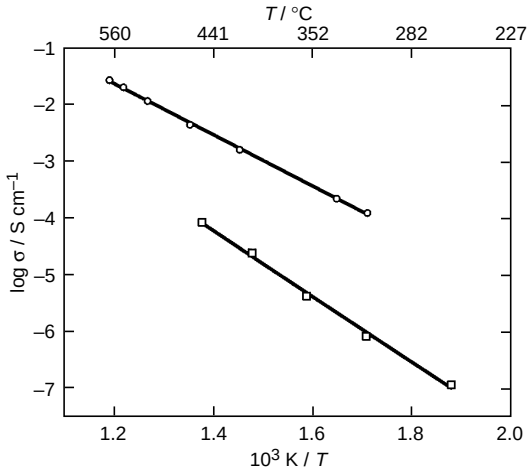



**Fig. 2** Ac conductivity *vs.* $10^3/T$ for $BaBi_8O_{13}$ (○) and $I_3BaBi_8O_{13}$ (□)

At present, the nature of the intercalated iodine species (*e.g.* $I_3^-$, $I^-$, $I_2$), and its structural arrangement within the *ab* plane are not known. Further studies are required in order to determine the nature of the host–guest interactions and the extent of charge transfer in this new example of an intercalation compound formed by reaction of a neutral guest species with a neutral insulating host lattice. Iodine intercalation experiments in compounds with different Bi : Ba ratios and in the related rhombohedral phases in which Ba is substituted with Sr, Ca or La are in progress.

We thank the Robert A. Welch Foundation and the Texas Center for Superconductivity for support of this work.

## Footnotes

† E-mail: ajjacob@uh.edu

‡ Electron microprobe analysis (EMPA) was carried out with a JEOL JXA-8600 instrument operated at 15 keV with a 10 μm beam diameter and a beam current of 30 nA. Counting times in the range of 40–100 s were used for both peaks and background. The uncertainties in the data are approximately ±1% (relative) for the cations and ±10% (relative) for oxygen.

## References

1 R. Schöllhorn, in *Inclusion Compounds*, ed. J. L. Atwood, J. E. D. Davies and D. D. MacNicol, Academic Press, New York, 1984, vol. 1, ch. 7, p. 249.
2 J. M. Adams and D. A. Jefferson, *Acta Crystallogr., Sect. B*, 1976, **32**, 1180.
3 J. W. Johnson, A. J. Jacobson, J. F. Brody and S. M. Rich, *Inorg. Chem.*, 1982, **21**, 3820.
4 *Graphite Intercalation Compounds*, Springer Series in Materials Science 18, ed. H. Zabel and S. Solin, Springer–Verlag, Berin, 1992.
5 X-D. Xiang, S. McKernan, W. A. Vareka, A. Zettl, J. L. Corkill, T. W. Barbee III and M. L. Cohen, *Nature*, 1990, **348**, 145.
6 X-D. Xiang, A. Zettl, W. A. Vareka, J. L. Corkill, T. W. Barbee III and M. L. Cohen, *Phys. Rev. B*, 1991, **43**, 11 496.
7 E. Faulques and R. E. Russo, *Solid State Commun.*, 1992, **82**, 531.
8 D. Pooke, K. Kishio, T. Koga, Y. Fukuda, N. Sanada, M. Nagoshi, K. Kitazawa and K. Yamafuji, *Physica C*, 1992, **198**, 349.
9 H. J. Trodahl, D. Pooke, G. J. Gainsford and K. Kishio, *Physica C*, 1993, **213**, 427.
10 P. V. Huong and A. L. Verma, *Phys. Rev. B*, 1993, **48**, 9869.
11 G. Liang, A. Sahiner, M. Croft, W. Xu, X.-D. Xiang, D. Badresingh, W. Li, J. Chen, J. J. Peng, A. Zettl and F. Lu, *Phys. Rev. B*, 1993, **47**, 1029.
12 T. Soto, D. Pooke and K. Kishio, *Phys. Rev. B*, 1995, **51**, 16 220.
13 T. Takahashi, T. Esaka and H. Iwahara, *J. Solid State Chem.*, 1976, **16**, 317.
14 T. Takahashi, H. Iwahara and K. Nagai, *J. Appl. Electrochem.*, 1972, **2**, 97.
15 P. Conflant, J. C. Boivin and D. Thomas, *J. Solid State Chem.*, 1980, **35**, 192.
16 J. C. Boivin and D. Thomas, *Solid State Ionics*, 1981, **5**, 523.
17 R. J. D. Tilley, *J. Solid State Chem.*, 1982, **41**, 233.
18 H. D. Baek and A. V. Virkar, *J. Electrochem. Soc.*, 1992, **11**, 139.
19 D. Mercurio, J. C. Champarnaud-Mesjard, B. Frit, P. Conflant, J. C. Boivin and T. Vogt, *J. Solid State Chem.*, 1994, **112**, 1.

*Received, 10th September 1996; Com. 6/06263F*

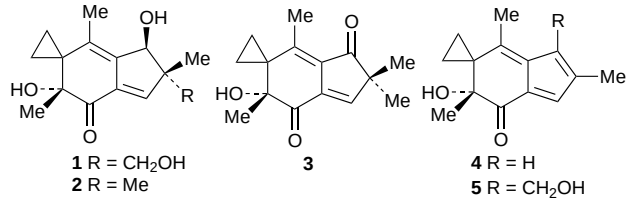
# Total synthesis of hydroxymethylacylfulvene, an antitumour derivative of illudin S

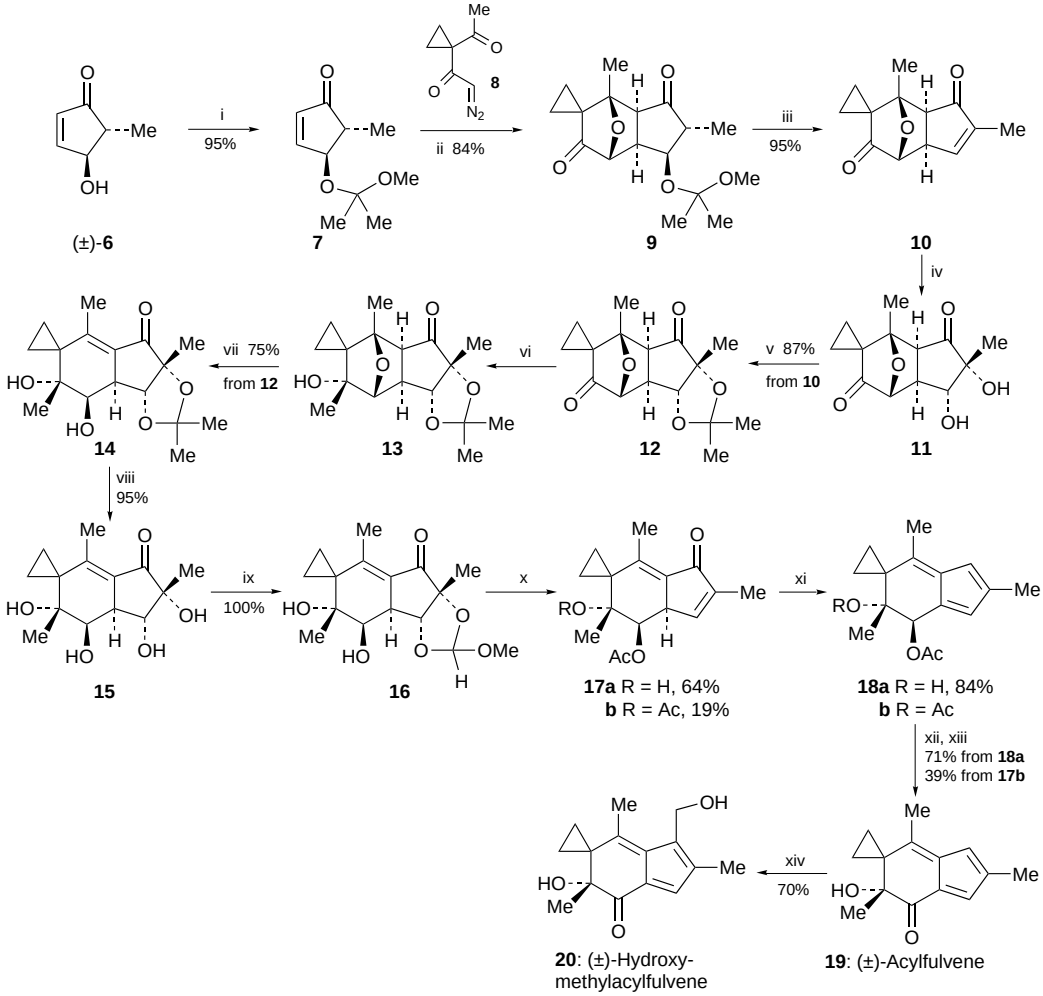
**Trevor C. McMorris,*[a] Yi Hu,[a] Jian Yu[a] and Michael J. Kelner[b]**

[a] *Department of Chemistry and Biochemistry, University of California, San Diego, La Jolla, CA 92093, USA*
[b] *Department of Pathology, University of California, San Diego, La Jolla, CA 92093, USA*

**(±)-Hydroxymethylacylfulvene is synthesized in 14 steps from 4-hydroxy-5-methyl-2-cyclopenten-1-one and 1-acetyl-1-(diazoacetyl)cyclopropane in 15% overall yield.**

Acylfulvenes are a new class of potent antitumour compounds derived from the toxic sesquiterpene illudin S **1**.[1,2] The latter and illudin M **2** are produced in cultures of the basidiomycete *Omphalotus illudens*.[3] These two compounds also possess antitumour activity but were found to have poor therapeutic indices when tested *in vivo*, particularly in solid tumour systems. Studies on the mechanism of toxicity of illudins have led to the preparation of illudin derivatives with greatly improved therapeutic indices compared to the parent compounds. Thus first generation analogue dehydroilludin M **3**[4] showed better efficacy against metastatic MV 522 lung carcinoma xenografts (established in 4-week old athymic




**Scheme 1** *Reagents and conditions*: i, 2-Methoxypropene, $POCl_3$, room temp., 12 h; ii, $Rh_2(OAc)_4$, $CH_2Cl_2$, DMF, reflux, 1.5 h; iii, KOH–MeOH, room temp., 1 h; iv, $OsO_4$, NMO, THF, $H_2O$, room temp., 24 h; v, dimethoxypropane, *p*-TsOH, MeCN, room temp., 10 h; vi, MeMgCl, THF, −78 °C, 2.5 h; vii, KOH–MeOH, 80 °C, 2 h; viii, Dowex resin, $H^+$ form, MeOH, room temp., 12 h; ix, $HC(OMe)_3$, *p*-TsOH, room temp., 2 h; x, $Ac_2O$, reflux, 1.5 h; xi, $CeCl_3·7H_2O$, $NaBH_4$, MeOH–THF (1 : 3), 0 °C to room temp., 5% HCl; xii, $LiAlH_4$, diethyl ether; xiii, Dess–Martin reagent, $CH_2Cl_2$, room temp., 1 h; xiv, $(CH_2O)_n$, $H_2SO_4$, $H_2O$–acetone, room temp., 20 h

Balb/c nu/nu mice) than nine known anticancer agents including cisplatin, cytoxan and paclitaxel. Its efficacy was comparable to that of mitomycin C.[5] The efficacy of second generation analogue acylfulvene **4** exceeded that of dehydroilludin M and mitomycin C.[6] Although these compounds prolonged lifespan in the MV 522 model, they did not induce regression of the primary tumour implants. However, a third generation analogue hydroxymethylacylfulvene (HMAF) **5** caused complete tumour regression in all animals at the maximum tolerated dose of 10 mg $Kg^{-1}$ (iv or ip) three times per week for three weeks. This resulted in an increase in life span of more than 150%.[7] HMAF has also been found to exhibit outstanding activity against breast, colon and skin cancer cell lines derived from human tumours. This compound is now undergoing clinical trials.[8]

HMAF can be prepared readily from acylfulvene **4**, with paraformaldehyde in dilute $H_2SO_4$ solution in 73% yield, or directly from illudin S. However, the total synthesis of acylfulvenes remains a very desirable objective, because it will make available a variety of analogues for structure–activity investigations. The synthesis of (±)-hydroxymethylacylfulvene has been accomplished as follows.

(±)-4-Hydroxy-5-methylcyclopent-2-enone (±)-**6**†[9] was converted to the acetal **7** (2-methoxypropene, $POCl_3$). The latter and rhodium acetate were added to dichloromethane containing dimethylformamide. A solution of diazoketone **8**[10] in dichloromethane was added slowly to the refluxing solution.[10,11] The intermediate carbonyl ylide underwent a 1,3-dipolar cycloaddition reaction with the cyclopentenone to form the adduct **9** in 84% yield, isolated as one enantiomeric pair. Compound **9** was sensitive to base and was converted in high yield (95%) to cyclopentenone **10** with methanolic KOH at room temperature. Further base treatment of **10**, in an attempt to cleave the oxygen bridge, led to extensive decomposition. Because of the electrophilicity of the cyclopropyl ring and reactivity of the unsaturated ketone, many other efforts also failed to give the desired oxygen bridge-opened compound. The double bond was therefore masked by forming diol **11** with $OsO_4$, NMO in THF at room temperature. Diol **11** was converted to the acetonide **12** with dimethoxypropane and *p*-TsOH (87% for two steps). Regioselective reaction of **12** with methylmagnesium chloride (THF, −78 °C) afforded the Grignard product **13**. Treatment of **13** with 10% KOH–MeOH at 80 °C for 2 h cleaved the oxygen bridge giving the diol **14** (75% for the two steps). The acetonide was next hydrolysed (Dowex resin, $H^+$ form, MeOH, 12 h) giving the tetraol **15** (95%).[12] Compound **15** was converted to the orthoester **16** (trimethyl orthoformate, *p*-TsOH, room temp.) and the latter was heated in acetic anhydride (reflux, 1.5 h).[13] A mixture of mono- and di-acetate (**17a** 64%, **17b** 19%) was obtained. Reduction of **17a** with $NaBH_4$, $CeCl_3 \cdot 7H_2O$ in THF and methanol gave an unstable product and the hydroxy group was eliminated on work up yielding the fulvene **18a** (84%). Reduction of the acetate **18a** ($LiAlH_4$, diethyl ether, room temp., 10 min) followed by oxidation of the resulting alcohol with Dess–Martin reagent[14a,b] yielded (±)-acylfulvene **19** (71%) as a yellow gum. Diacetate **17b** could also be converted similarly to **19** (40%). Finally, (±)-hydroxymethylacylfulvene **20** was obtained from **19** following the known procedure.[2]

The spectral properties of (±)-hydroxymethylacylfulvene **20** and (±)-acylfulvene **19** were identical to those of the hydroxymethylacylfulvene and acylfulvene derived from illudin S.

This investigation was supported by MGI Pharma Inc., Minnetonka, Minnesota, USA.

## Footnote

† The new compounds **6**–**20** were fully characterised by spectroscopic data including HRMS.

## References

1 T. C. McMorris, M. J. Kelner, W. Wang, M. A. Diaz, L. A. Estes and R. Taetle, *Experientia*, 1996, **52**, 75.
2 T. C. McMorris, M. J. Kelner, W. Wang, J. Yu, L. A. Estes and R. Taetle, *J. Nat. Prod.*, 1996, **59**, 896.
3 T. C. McMorris and M. Anchel, *J. Am. Chem. Soc.*, 1965, **87**, 1594.
4 T. C. McMorris, M. J. Kelner, W. Wang, L. A. Estes, M. A. Montoya and R. Taetle, *J. Org. Chem.*, 1992, **57**, 6876.
5 M. J. Kelner, T. C. McMorris and R. Taetle, *Anticancer Res.*, 1995, **15**, 873.
6 M. J. Kelner, T. C. McMorris, L. A. Estes, M. A. Montoya, R. Starr, K. Samson and R. Taetle, *Cancer Res.*, 1995, **55**, 4936.
7 M. J. Kelner, T. C. McMorris, L. A. Estes, W. Wang, K. M. Samson and R. Taetle, *Investigational New Drugs*, 1996, **14**, 161.
8 Unpublished data provided by MGI Pharma Inc., Minneapolis. This company has been licensed by the University of California to develop illudin analogues for treating tumours. U.S. Patents 5,439,936, 5,439,942, 5,523,490 and 5,563,176 on these compounds have been issued to the University of California, and several more are pending.
9 G. Piancatelli, A. Scettri and S. Barbadoro, *Tetrahedron Lett.*, 1976, **39**, 3555.
10 A. Padwa, E. A. Curtis and V. P. Sandanayaka, *J. Org. Chem.*, 1996, **61**, 73.
11 F. R. Kinder and K. W. Bair, *J. Org. Chem.*, 1994, **59**, 6965.
12 M. Kitamura, M. Isobe, Y. Ichikawa and T. Goto, *J. Am. Chem. Soc.*, 1984, **106**, 3252.
13 P. Camps, J. Cardellach, J. Font, R. M. Ortuno and O. Ponsati, *Tetrahedron*, 1982, **38**, 2395.
14 D. B. Dess and J. C. Martin, *J. Am. Chem. Soc.*, 1991, **113**, 7277; R. E. Ireland and L. Liu, *J. Org. Chem.*, 1993, **58**, 2899.

*Received, 17th October 1996; Com. 6/07077I*

# Photochemistry of acetone in the presence of exocyclic olefins: an unexpected competition between the photo-Conia and Paternò–Büchi reactions

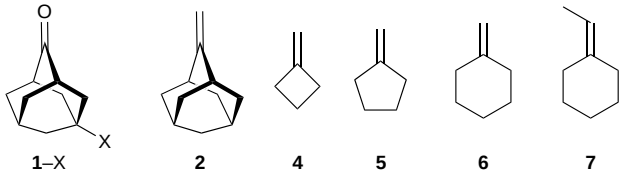
**Wen-Sheng Chung* and Chia-Chin Ho**

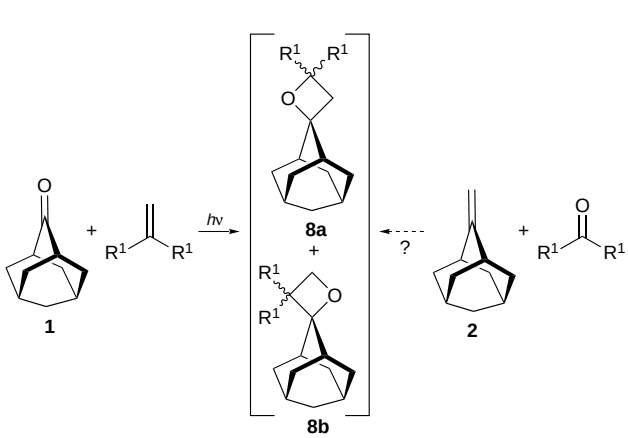
*Department of Applied Chemistry, National Chiao Tung University, Hsinchu, Taiwan 30050, ROC*

**When irradiated in the presence of several exocyclic olefins, acetone undergoes homoalkylation with the olefins to form a series of 4-cycloalkylbutan-2-ones (with quantum yields of 0.14 ± 0.01) rather than exhibiting the expected Paternò–Büchi reaction; in contrast, the photolysis of perdeuteriated acetone gave both types of products.**

Carbonyl group photochemistry has been covered in many excellent reviews and books over the last four decades.[1] It has long been known that when irradiated in the presence of olefins, aliphatic ketones undergo the Paternò–Büchi reaction,[2] Norrish type I or Type II reactions,[2,3] the former of which gives oxetane products, and the latter, pinacols, alcohols and hydrocarbon dimers. In some rare cases they may also lead to ene-reaction products.[4] Results other than those described above have been reported[5] but the reports have long been ignored.[1] For example, the photochemistry of acetone with norbornene was reported[5a] to proceed by chain addition of acetonyl radicals to norbornene, a process analogous to the addition of cyclohexanone to oct-1-ene[5b] and to cyclohexene.[5c] The same outcome, when obtained thermochemically, is known as the Conia reaction.[6] Thus, we shall call the latter reactions photo-Conia reactions.

In the course of studying face selectivity in the photocycloaddition reaction of 5-substituted adamantan-2-ones **1**–Xs, we have used many different olefins with nitrile or alkoxy substituents and have found that they all give oxetane products in excellent yields.[7] It is of interest to know whether the photocycloaddition occurs when **1**–X is replaced with methyleneadamantane **2** and the olefin is replaced with a ketone (Scheme 1). It is also surprising to note that the photochemistry of ketones in the presence of exocyclic olefins has not been systematically studied.[1] We report here the photochemistry of acetone **3a** with methyleneadamantane **2** and a series of exocyclic alkenes, *e.g.* methylenecyclobutane **4**, methylenecyclopentane **5**, methylenecyclohexane **6** and ethylidenecyclohexane **7**.



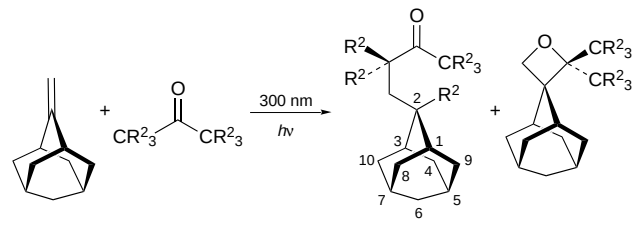




**Scheme 1**

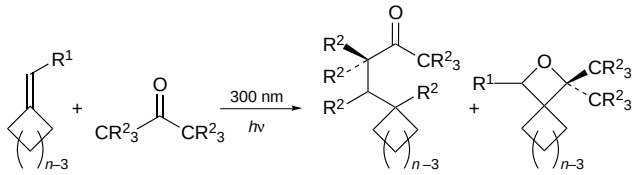
Irradiation at 300 nm of a degassed solution of 0.1 g of **2** in 20 ml spectrograde acetone **3a** at room temp. for 12 h leads to the formation of a novel photo-Conia[6] adduct **9** as a major product† (52% isolated yield), some oxetane **10** (5%), and many other minor reaction products (each less than 5% as determined by GC) (Scheme 2). The major product was first identified as a 1 : 1 adduct by GC–MS which indicated a molecular ion peak at *m/z* 206. If oxetane **10** were the major product, ring metathesis fragments[3b,7] would have been observed in the mass spectrum, *e.g. m/z* at 176 ($M^+ - HCOH$) and 148 (**2**), however, the major peaks were observed at *m/z* 191 ($M^+ - Me$), 188 ($M^+ - H_2O$) and 163 ($M^+ - COMe$). This observation along with information from $^1H$ and $^{13}C$ NMR spectra (*vide infra*) confirmed structure **9** as the major product.

It has been reported[7,8] that hydrogen on the carbon α to the oxygen of an oxetane ring has a chemical shift of δ 4–5, whereas hydrogen on the β-carbon atom has a chemical shift of δ 2.5–3.6. The $^1H$ NMR spectrum of **9** had a triplet at δ 2.38 for hydrogens α to carbonyl and a singlet at δ 2.12 for Me, which is incompatible with an oxetane structure. One expects to see only singlet oxetane ring protons no matter whether the oxetane is **8a** or **10**. The $^{13}C$ NMR and DEPT signals of the major product included 7 lines for adamantane and one methyl at δ 29.80, two methylene carbons at δ 26.57 and 42.04 due to the 3,4-carbons of adamant-4-ylbutan-2-one, and a quaternary carbon at δ 209.63 due to carbonyl carbon, which provide further evidence for the photo-Conia product **9**.

In order to determine the proton source on C-2 of product **9**, we also irradiated **2** in deuteriated [$^2$H]acetone **3b** for comparison. The ratio of photo-Conia product to oxetane **9**/**10** was about 11 in acetone, but about 2 (**11** : **12**) in [$^2H_6$]acetone. Comparing the $^1H$ NMR spectra of **11** with **9**, three dramatic changes are observed: (i) the triplet at δ 2.38 for hydrogens α-to carbonyl, (ii) the singlet at δ 2.12 for Me, and (iii) the multiplet at δ 1.55 for proton at C-2 had all disappeared. These deuteriated acetone **3b** results indicate that the proton at C-2 was abstracted from acetone. Note that oxetane **12** has now been isolated in good yield, but was only trace when acetone **3a** was used. The large deuterium isotope effect observed implies that




**Scheme 2**




| | | | |
|---|---|---|---|
| **4** $n$ = 4, $R^1$ = H | **3a** $R^2$ = H | **13** (14%) | trace |
| **5** $n$ = 5, $R^1$ = H | **3a** $R^2$ = H | **14** (12%) | trace |
| **6** $n$ = 6, $R^1$ = H | **3a** $R^2$ = H | **15** (60%) | trace |
| **7** $n$ = 6, $R^1$ = Me | **3a** $R^2$ = H | **16** (17%) | **17** (17%) |
| **7** $n$ = 6, $R^1$ = Me | **3b** $R^2$ = D | **18** (5%) | **19** (32%) |

**Scheme 3**

a C–H bond cleavage was involved in the transition state of this novel photo-Conia reaction.

Note that the photo-Conia reaction of **2** occurs only in neat acetone and deuteriated acetone, but not in other organic solvents such as acetonitrile, benzene and cyclohexane. Compound **2** would also neither react photochemically in dilute acetone solutions (≤1 mol $dm^{-3}$ in organic solvents), nor would it react with acetone in the dark. In order to explore the scope of this photo-Conia reaction, we also photolysed **2** in acetophenone, benzophenone and butan-2-one for 24 h. No reaction was found in the aryl ketones. Although the photo reaction in butan-2-one revealed evidence of formation of some Conia-type products under GC–MS analysis, they were too complex to be isolated.

We then turned our attention to the variation of **2** into a series of exocyclic olefins **4**–**7**. The photolysis of methylenecyclobutane **4**, methylenecyclopentane **5** and methylenecyclohexane **6** in acetone gives photo-Conia products **13**–**15** as the only isolable products (Scheme 3).† Due to many possible secondary photochemical reactions, the yields from methylenecyclobutane **4** and methylenecyclopentane **5** are poor. Nevertheless, methylenecyclohexane **6** gave the homo-alkylation product **15** as the major product in 60% yield. The expected oxetane product from the Paternò–Büchi reaction was detected in trace by GC–MS but was not isolated. On the other hand, when a trisubstituted olefin such as **7** was photolysed in acetone, adducts **16** and **17** were obtained as a 1 : 1 mixture. The Paternò–Büchi reaction product **19** became dominant when **7** was photolysed in deuteriated acetone **3b**. The quantum yields for the photo-Conia reaction products of **2** and **6** in acetone (*i.e.* Φ for **9** and **15**) were determined‡ to be 0.15 and 0.13, respectively.

Kharasch[5b,9] suggested that in the reaction of aldehydes with terminal olefins to form ketones, it is the acyl radical [R(O=)C·] that attacks the olefin. Acetone[5a] or cyclohexanone[5b,c] undergoing Type I cleavage would not, however, explain the observed photo-Conia products. Our results may be explained as follows: the rate-determining step involves an α-hydrogen abstraction of acetone by another excited acetone to give an α-keto radical,[5c] which is then added further to a molecule of exocyclic olefin. In deuteriated acetone **3b**, the C–D bond cleavage step is hampered with respect to that of a C–H bond, thus the Paternò–Büchi reaction is comparable. Although the mechanism of this photo-Conia reaction is still unclear at present, it provides a novel and good-yield method for homoalkylation,[11] which has long been neglected in carbonyl photochemistry.

We thank the National Science Council of the Republic of China for its financial support (Grant No. NSC 84-2113-M-009-002).

## Footnotes

† Satisfactory spectral data were obtained for all products. *Selected data* for **9**: colourless oil; $^1$H NMR (300 MHz, $CDCl_3$), δ 2.38 (2 H, t, *J* 8.7 Hz), 2.12 (3 H, s) and 1.85–1.44 (17 H, m); $^{13}$C NMR (75.4 MHz, $CDCl_3$), δ 209.63 (C=O), 43.96 (CH), 42.04 ($CH_2$), 39.06 ($CH_2$), 38.25 ($CH_2$), 31.66 (CH), 31.43 ($CH_2$), 29.80 (Me), 28.17 (CH), 27.93 (CH) and 26.57 ($CH_2$); *m/z* 206 ($M^+$, 2), 191 (5), 188 (24), 163 (20), 148 (100%), 106 (36) and 92 (52); (Found: $M^+$ 206.1674. $C_{14}H_{22}O$ requires 206.1671). For **11**: colourless oil; $^1$H NMR, δ 1.88–1.81 (6 H, m), 1.72–1.65 (8 H, m) and 1.52–1.48 (2 H, m); $^{13}$C NMR, δ 210.04 (C=O), 43.95 (CD), 38.98 ($CH_2$), 38.27 ($CH_2$), 31.60 (CH), 31.45 ($CH_2$), 31.33 ($CH_2$), 28.18 (CH), 27.97 (CH) and 26.48 ($CH_2$); *m/z* 212 ($M^+$, 3), 194 (22), 192 (5), 166 (10), 148 (100%), 92 (48) and 80 (40); (Found: $M^+$ 212.2054. $C_{14}H_{16}OD_6$ requires 212.2047). For **12**: colourless oil, $^1$H NMR, δ 4.19 (2 H, s), 2.30 (2 H, br s) and 1.82–1.60 (12 H, m); $^{13}$C NMR, δ 87.87 ($C_q$), 75.59 ($CH_2$), 49.52 ($C_q$), 37.07 ($CH_2$), 34.65 ($CH_2$), 34.35 ($CH_2$), 32.07 (CH), 26.79 (CH) and 26.55 (CH); *m/z* 212 ($M^+$, 31), 194 (100%), 182 (95), 148 (7), 135 (28) and 65 (36). For **15**: colourless oil; $^1$H NMR, δ 2.44 (2 H, t, *J* 7.8 Hz), 2.14 (3 H, s), 1.71–1.63 (5 H, m), 1.50–1.43 (2 H, m), 1.26–1.15 (4 H, m) and 0.93–0.86 (2 H, m); $^{13}$C NMR, δ 209.58 (C=O), 41.26 ($CH_2$), 37.12 (CH), 32.99 ($CH_2$), 31.10 ($CH_2$), 29.73 (Me), 26.42 ($CH_2$) and 26.13 ($CH_2$); *m/z* 154 ($M^+$, 15), 136 (11), 96 (77), 81 (65) and 55 (100%); (Found: $M^+$ 154.1361. $C_{10}H_{18}O$ requires 154.1358).

‡ We used *trans*-stilbene as an actinometer when taking the quantum yield for its *trans* to *cis* isomerization as 0.32 at 300 nm light and measured the quantum yield for **9** and **15**. For the use of this actinometer see ref. 10.

## References

1 For reviews on the Paternò–Büchi reaction see: D. R. Arnold, *Adv. Photochem.*, 1968, **6**, 301; J. C. Dalton and N. J. Turro, *Ann. Rev. Phys. Chem.*, 1970, **21**, 499; N. J. Turro, J. C. Dalton, K. Dawes, G. Farrington, R. Hautala, D. Morton, M. Niemczyk and N. Schore, *Acc. Chem. Res.*, 1972, **5**, 92; N. J. Turro, *Modern Molecular Photochemistry*, Benjamin, Menlo Park, 1978, ch. 10 and 11; G. Jones, II, in *Organic Photochemistry*, ed. A. Padwa, Wiley, New York, 1981, vol. 5. pp. 1–122; S. W. Schreiber, *Science*, 1985, **227**, 858; H. A. J. Carless, in *Synthetic Organic Photochemistry*, ed. W. M. Horspool, Plenum, New York, 1984, pp. 425–487; M. Demuth and G. Mikhail, *Synthesis*, 1989, 145; A. G. Griesbeck, in *Organic Photochemistry and Photobiology*, ed. W. M. Horspool and P.-S. Song, CRC, New York, 1994, p. 522; p. 550.

2 L. Paternò and G. Chieffi, *Gazz. Chim. Ital.*, 1909, **39**, 341; G. Büchi, C. G. Inman and E. S. Lipinsky, *J. Am. Chem. Soc.*, 1954, **76**, 4327.

3 (*a*) R. G. W. Norrish and C. H. Bamford, *Nature*, 1936, **138**, 1016; (*b*) J. S. Bradshaw, *J. Org. Chem.*, 1966, **31**, 237; (*c*) W. M. Nau, F. L. Cozens and J. C. Scaiano, *J. Am. Chem. Soc.*, 1996, **118**, 2275.

4 E. H. Gold and D. Ginsburg, *Angew. Chem., Int. Ed. Eng.*, 1966, **5**, 246; To compare a thermal ene reaction see: F.-G. Klärner, B. M. J. Dogan, O. Ermer, W. v. E. Doering and M. P. Cohen, *Angew. Chem., Int. Ed. Eng.*, 1986, **25**, 108.

5 (*a*) W. Reusch, *J. Org. Chem.*, 1962, **27**, 1882; (*b*) M. S. Kharasch, J. Kuderna and W. Nudenberg, *J. Org. Chem.*, 1953, **18**, 1225; (*c*) P. de Mayo, J. B. Stothers and W. Templeton, *Can. J. Chem.*, 1961, **39**, 488.

6 For reviews on Conia reactions and ene reactions see: J. M. Conia and P. le Perchec, *Synthesis*, 1975, 1; W. Oppolzer and V. Snieckus, *Angew. Chem., Int. Ed. Eng.*, 1978, **17**, 476; B. B. Snider, *Acc. Chem. Res.*, 1980, **13**, 426.

7 W.-S. Chung, N. J. Turro, S. Srivastava, H. Li and W. J. le Noble, *J. Am. Chem. Soc.*, 1988, **110**, 7882; W.-S. Chung, N. J. Turro, S. Srivastava and W. J. le Noble, *J. Org. Chem.*, 1991, **56**, 5020; W.-S. Chung, N.-J. Wang, Y.-D. Liu, Y.-J. Leu and M. Y. Chiang, *J. Chem. Soc., Perkin Trans. 2*, 1995, 307; W.-S. Chung, Y.-D. Liu and N. J. Wang, *J. Chem. Soc. Perkin Trans. 2*, 1995, 581.

8 D. R. Arnold, R. L. Hinman and A. H. Glick, *Tetrahedron Lett.*, 1964, 1425.

9 M. S. Kharasch, W. H. Urry and B. M. Kuderna, *J. Org. Chem.*, 1949, **14**, 248.

10 T.-I. Ho, T.-M. Su and T.-C. Hwang, *J. Photochem. Photobiol. A. Chem.*, 1988, **41**, 293.

11 For other homoalkylation methods by metal oxides or organic peroxides see: Von A. Rieche, E. Schmitz and E. Gründemann, *Z. Chem.*, 1964, **4**, 177; E. I. Heiba and R. M. Dessau, *J. Am. Chem. Soc.*, 1971, **93**, 524; A. Citterio, F. Ferrario and S. Bernardinis, *J. Chem. Res.* (*S*), 1983, 310, see ref. 6.

*Received, 31st October 1996; Com. 6/07415D*

# Unexpected structure of 1,3-diphenyl-2-azaallylpotassium–*N*,*N*,*N*′,*N*″,*N*″-pentamethyldiethylenetriamine: infinite, zigzag chains of alternating cations and two distinct types of anion, one azaallyl bonded, the other allyl bonded

**Philip C. Andrews,[a] David R. Armstrong,[a] William Clegg,[b] Fiona J. Craig,[a] Lorraine Dunbar[a] and Robert E. Mulvey*[a]**

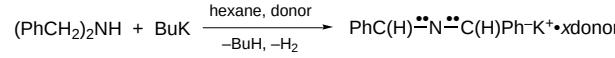
[a] *Department of Pure and Applied Chemistry, University of Strathclyde, Glasgow, UK G1 1XL*
[b] *Department of Chemistry, University of Newcastle, Newcastle-upon-Tyne, UK NE1 7RU*

**[{[PhC(H)⋯N⋯C(H)Ph]$^-$K$^+$·pmdeta}$_\infty$] adopts a novel crystal structure exhibiting separate η$^3$-C⋯N⋯C and η$^3$-C⋯C⋯C ligating modes, surprisingly leaving one electronegative N centre not bonded to K$^+$; reaction of the azaallyl K with its parent imine PhC(H)=NCH$_2$Ph in toluene affords the interesting, metal-free, chiral product PhC(H)=NCH(Ph)CH(Ph)N(H)CH$_2$Ph.**

With numerous studies devoted to the structural chemistry of synthetically important lithium organic derivatives having taken place since the early sixties,[1] attention is now turning to their more reactive, and less easily handled, heavier congeners.[2] One recent report[3] focused on the structure of the 1,3-diphenyl-2-azaallyl anion–potassium ion pair [{PhC(H)⋯N⋯C(H)Ph}$^-$K$^+$] in the presence of 18-crown-6: a simple discrete monomer with the anion η$^2$-C,N-bonded to the cation. Previously we had described the structure of the pmdeta-ligated sodium analogue [{PhC(H)⋯N⋯C(H)Ph}$^-$Na$^+$],[4]† which is also monomeric, though its anion is only N-bonded to the smaller Na$^+$ cation. Given this background, the crystal structure of the potassium analogue, [{[PhC(H)⋯N⋯C(H)Ph]$^-$K$^+$·pmdeta}$_\infty$] **1**, revealed herein, is novel on three counts: first, it is a polymer as opposed to a monomer; second, the anion engages in unique η$^3$–C⋯N⋯C interactions with K$^+$; third, and most significantly, a second type of anion–cation coordination is present, remarkable for not involving the central highly electronegative N atom, but the adjacent *o*-C⋯*ipso*-C⋯α-C units. The existence of the previously reported bis-solvated variant [{PhC(H)⋯N⋯C(H)Ph}$^-$K$^+$·2pmdeta}] **2**,[5] a suspected monomer,‡ makes these findings all the more intriguing. We also demonstrate the synthetic value of the azaallyl potassium system in reporting an addition reaction which produces the interesting chiral compound PhC(H)=NCH(Ph)CH(Ph)N(H)CH$_2$Ph **3**.

The aforementioned crown complex was prepared by deprotonating the imine PhC(H)=NCH$_2$Ph with KH in a 12 h long reflux procedure.[3] However, our alternative method for generating the azaallyl potassium ion pair starting from dibenzylamine can be accomplished in minutes (Scheme 1). As discussed in depth elsewhere,[5] mechanistically this process appears to involve also the imine and KH, but as short-lived intermediates, of enhanced reactivity. Originally we thought that only bis-adduct **2** was affordable by this method, as 2 equiv. of pmdeta were necessary to achieve complete dissolution of the initially formed dibenzylamidopotassium. But it transpires that hot toluene mixtures containing 1 equiv. of pmdeta, when filtered through Celite to remove fine solids, afford solutions that on cooling deposit some crystalline **1** mixed with **2**.§

The crystal structure of **1**¶ consists of infinite chains of contacted ions, the salient feature of which is the two distinct types of bridging-anion (Fig. 1). These lie approximately perpendicular to each other (87.7°). Predictably, type 1 ligates through the central azaallyl C(1)⋯N(1)⋯C(1A) unit. More surprisingly, type 2 ligates through the off-centre allyl C(8)–C(9)–C(9A) unit, leaving N(2) not bonded to K(1); this N atom lies 3.648 Å from two adjacent K$^+$ ions. Both types use their delocalised π systems to bridge to pairs of K$^+$ cations, disposed on either side of the planar PhC(H)NC(H)Ph frameworks. Chelating tridentate triamine ligands complete the coordination of the cations. Two-fold disorder of each type of anion limits the precision of the structure. Nevertheless, it is still discernible that the metal–anion contacts are decidedly shorter for type 1 than for type 2 (by about 0.35 Å on average), and




**Scheme 1**

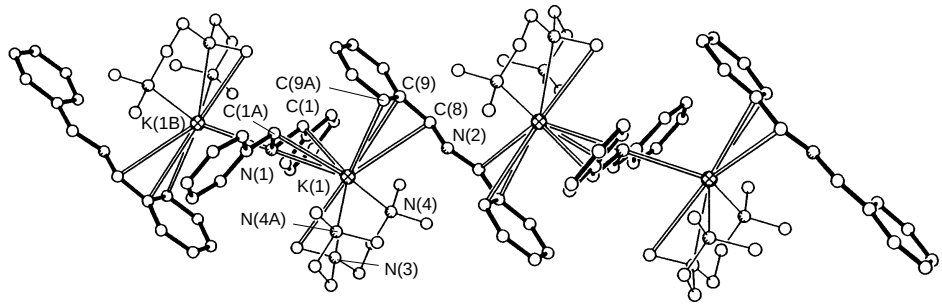
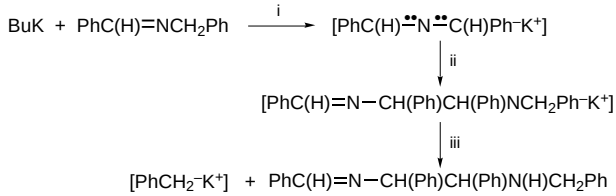



**Fig. 1** Section of the infinite chain structure of **1** with labelling of selected atoms. Hydrogen atoms are omitted for clarity and only one disorder component of each anion is shown. Key dimensions (Å): K(1)–N(1) 2.996(2), K(1)–C(1) and K(1)–C(1A) 2.930(6), K(1)–C(8) 3.366(7), K(1)–C(9) and K(1)–C(9A) 3.268(5), K(1)–N(3) 2.868(5), K(1)–N(4) and K(1)–N(4A) 2.889(4), N(1)–C(1) 1.513(6), N(2)–C(8) 1.347(10), K(1)···N(2) 3.648(3). Symmetry operators: A *x*, 1 − *y*, *z*; B 1 − *x*, 1 − *y*, 1 − *z*.

linked to this, that the C⋯N bonds in the former have substantially less double bond character than those in the latter. This implies that the structure is primarily dictated by strong metal-to-azaallyl anion (electrostatic) bonding, the steric characteristics of which permit the loose attachment of the allyl fragment of another anion [the 'loose' K–C bonds are slightly longer than those producing the polymeric arrangement in the benzyl structure mentioned below, which lie in the range 3.150–3.265 Å; while the strong cation–anion interaction is considerably shorter, and is more representative of that in the monomeric crown analogue described above (3.044 Å)]. The observation that a second pmdeta molecule can readily displace one of the two anions from the coordination sphere of the cation (*i.e.* as in **2**), supports this interpretation. In a search for comparable structures to **1**, [{$PhCH_2K$·pmdeta·0.5toluene}$_\infty$][6] stands out in view of its zigzag polymeric set-up and two distinct multihapto anion–$K^+$ coordinations; however, the similarity is only superficial as it contains a single type of anion, and one devoid of a heteroatom (*i.e.* incapable of offering a seat of high electron density). Pyridyl-substituted [$K(2\text{-}C_5H_4N)CHPPh_2CHPPh_2$·2thf][7] is also noteworthy in exhibiting a 1-azaallyl (N⋯C⋯C) unit (**1** displays a 2-azaallyl alternative).

Preliminary studies probing the chemistry of the azaallyl–K ion pair have uncovered the interesting reaction sequence shown in Scheme 2. A second equivalent of imine gives the addition product which appears to metallate toluene. Chiral product **3** with no K present, crystallises from solution, its identity being unambiguously established by a $^1$H NMR spectrum.‖ The yield of **3** still needs to be optimised, but it is significant that it is also found in reactions containing a 1 : 1, BuK : imine stoichiometry. Earlier it was reported that the reaction between the azaallyl and [$ZrCl_2(\eta\text{-}C_5H_5)_2$] yielded [$Zr(\eta^2\text{-PhCH-N-CH(Ph)CH(Ph)-N=CPh-}\eta^1)(\eta\text{-}C_5H_5)_2$][3] the coupling of the azaallyl moieties was ascribed to an oxidative addition process in which $Zr^{IV}$ is reduced to $Zr^{II}$ then oxidised back to $Zr^{IV}$. The implication of our new finding is that similar coupling processes can occur even without the mediation of a transition-metal redox centre.

We thank the EPSRC for its continuing financial support (studentship to F. J. C. and research equipment to W. C.) and Dr Daniel R. Baker (Solvay Interox) for many helpful discussions.




**Scheme 2** *Reagents*: i, hexane; ii, PhC(H)=$NCH_2$Ph; iii, *N*,*N*,*N*′,*N*′-tetramethylethylenediamine (3 mol equiv.), toluene

## Footnotes

† pmdeta = *N*,*N*,*N*′,*N*″,*N*″-pentamethyldiethylenetriamine.

‡ An attempted crystal structure determination confirmed the monomeric nature and bis-pmdeta solvation; however, the quality of the data was poor and not of a publishable standard.

§ The relative amounts of **1** and **2** appear variable and inconsistent, though **2** generally predominates. As our efforts to separate this mixture have so far failed, we are unable to give an absolute yield of **1**. However, the possibility that **1** is a rogue crystal can be ruled out as the unit-cell parameters of a number of crystals (from repeated syntheses of **1**), have been checked and found to conform to those reported here.

¶ *Crystal data* for **1**: $C_{23}H_{35}KN_4$, $M$ = 406.65, monoclinic, space group $C2/m$, $a$ = 11.1901(8), $b$ = 17.6135(13), $c$ = 12.6609(10) Å, β = 107.272(2)°, $U$ = 2382.9(3) Å$^3$, $Z$ = 4, $D_c$ = 1.134 g cm$^{-3}$, μ = 0.24 mm$^{-1}$ (Mo-Kα, λ = 0.710 73 Å), $T$ = 160 K. 6177 Reflections were measured on a Siemens SMART CCD area detector diffractometer, yielding 2165 unique reflections ($2\theta_{max}$ = 50° , $R_{int}$ = 0.0207). The structure was solved by direct methods and refined on $F^2$ values with anisotropic atomic displacement parameters, constrained hydrogen atoms, and twofold disorder across 2/*m* ($C_{2h}$) positions for both independent anions. Final $R^1$ = $\Sigma[w(F_o^2 - F_c^2)^2]/\Sigma[w(F_o^2)^2]^{\frac{1}{2}}$ = 0.1938 for all data, conventional $R$ = 0.0861 for $F$ values of 1846 reflections with $F_o^2 > 2\sigma(F_o^2)$, goodness of fit = 1.103 for all $F^2$ values and 173 refined parameters; extremes of difference map +0.29 and −0.85 e Å$^{-3}$. Atomic coordinates, bond lengths and angles, and thermal parameters have been deposited at the Cambridge Crystallographic Data Centre (CCDC). See Information for Authors, Issue No. 1. Any request to the CCDC for this material should quote the full literature citation and the reference number 182/343.

‖ $^1$H NMR (400 MHz, $C_7D_8$, 298 K): δ 1.91 (m, 1 H, NH), 3.38 (m, 1 H, PhC*H*$^1$H$^2$), 3.65 m, 1 H, PhCH$^1$*H*$^2$), 4.16 (m, 1 H, NHC*H*Ph), 4.37 (d, 1 H, C*H*Ph), 7.70 (s, 1 H, PhC*H*=N).

## References

1 Review: E. Weiss, *Angew. Chem.*, 1993, **105**, 1565; *Angew. Chem., Int. Ed. Engl.*, 1993, **32**, 1501.
2 Review: C. Schade and P. v. R. Schleyer, *Adv. Organomet. Chem.*, 1987, **27**, 169.
3 P. Veya, C. Floriani, A. Chiesi-Villa and C. Guastini, *J. Chem. Soc., Chem. Commun.*, 1991, 991.
4 P. C. Andrews, R. E. Mulvey, W. Clegg and D. Reed, *J. Organomet. Chem.*, 1990, **386**, 287.
5 P. C. Andrews, D. R. Armstrong, D. R. Baker, R. E. Mulvey, W. Clegg, L. Horsburgh, P. A. O'Neil and D. Reed, *Organometallics*, 1995, **14**, 427.
6 D. Hoffman, W. Bauer, F. Hampel, N. J. R. v. Eikema Hommes, P. v. R. Schleyer, P. Otto, U. Pieper, D. Stalke, D. S. Wright and R. Snaith, *J. Am. Chem. Soc.*, 1994, **116**, 528.
7 H. Schmidbaur, U. Deschler and B. Milewski-Mahrla, *Chem. Ber.*, 1982, **115**, 3290.

*Received, 8th November 1996; Com. 6/07601G*

# Crystal engineering of inorganic/organic composite solids: the structure-directing role of aromatic ammonium cations in the synthesis of the 'step'-layered molybdenum oxide phase [4,4′-$H_2$bpy][$Mo_7O_{22}$]·$H_2O$

**Pamela J. Zapf,[a] Robert C. Haushalter*[b] and Jon Zubieta*[a]**

[a] *Department of Chemistry, Syracuse University, Syracuse, NY 13244, USA*
[b] *NEC Research Institute, 4 Independence Way, Princeton, NJ 08540, USA*

**The hydrothermal reaction of $MoO_3$, Mo metal, $NiCl_2$ and 4,4′-bipyridine yields a step-layered molybdenum oxide [4,4′-$H_2$bpy)][$Mo_7O_{22}$]·$H_2O$, a material structurally related to layered $MoO_3$.**

Among the inorganic materials enjoying widespread contemporary interest, the metal oxide-based solid phases occupy a prominent position by virtue of their applications to catalysis, sorption, molecular electronics, energy storage, optical materials and ceramics.[1,2] The evolution of metal oxide chemistry is critically dependent on the synthesis of new solids possessing unique structures and properties.[3] While the synthesis of solid-state materials remains a challenge,[4,5] the techniques of hydrothermal synthesis, in combination with the structure-directing properties of organic components, may be exploited in the isolation of metastable inorganic/organic composites which retain the structural elements of the synthetic precursors.[6,7] The cooperative assembly of metal oxide/organic phases has been demonstrated by the recent reports of novel one-dimensional molybdenum oxide polymers, incorporating organoammonium cations.[8,9] More significantly, we have demonstrated that incorporation of organoammonium or amine-ligated transition- or post-transition-metal cations situated between mixed-valence vanadium oxide layers yields materials structurally related to $V_2O_5$, with the degree of reduction and condensation within the layers reflected in the charge per volume ratio of the interlamellar cation. In addition to functioning as structure-directing cations or as components of complex cations, organoamines may serve as multifunctional ligands, forming an integral part of the covalent skeleton of the solid. While crystal 'engineering' based on transition-metal coordination to appropriate ligands has evolved dramatically since the seminal work of Robson and Hoskins,[10,11] applications to metal oxides have remained largely unexplored. We have shown recently that 4,4′-bipyridine may be incorporated into metal oxide phases as a ligand serving to buttress the inorganic layers, as illustrated by [$MoO_3$(4,4′-bpy)$_{0.5}$].[12] It was anticipated that under more acidic reaction conditions, protonation of the aromatic amine would provide an aromatic ammonium cation which would serve as a structure-directing template by virtue of the interplay of hydrophobic/hydrophilic interactions[13] and of multipoint hydrogen bonding between the cation and the metal oxide scaffolding of the composite.

The title compound [4,4′-$H_2$bpy][$Mo_7O_{22}$]·$H_2O$ (**1**·$H_2O$) was prepared as colourless rhombs in 10–15% yield in the hydrothermal reaction of $MoO_3$, Mo (250 mesh), 4,4′-bipyridine, $NiCl_2$ and $H_2O$ in the mole ratio 5 : 1 : 2 : 2 : 300 at 200 °C for 93 h in a Parr acid-digestion bomb.

Under the acidic conditions of the reaction, the pyridyl nitrogen atoms are protonated, precluding coordination to the oxide skeleton and resulting in incorporation of the organic component as the bipyridinium dication.

As shown in Fig. 1, the structure of **1**·$H_2O$† consists of the molybdenum oxide layers, separated by an interlamellar region populated by [4,4′-$H_2$bpy]$^{2+}$ cations and $H_2O$ molecules of crystallization. The inorganic subunit of **1**·$H_2O$ is both structurally and compositionally related to the layered oxide $MoO_3$. In a formal sense, **1**·$H_2O$ may be considered to derive from $MoO_3$ through intercalation of [4,4′-$H_2$bpy]$^{2+}$ cations and water, requiring the addition of an oxide anion to the inorganic framework to achieve charge compensation. Since charge/volume considerations result in one bipyridinium cation for seven molybdenum oxide sites, compound **1**·$H_2O$ may be reformulated as [4,4′-$H_2$bpy][$(MoO_3)_7O$]·$H_2O$ to reflect its relationship to the $MoO_3$ parent.

However, while the $[Mo_7O_{22}]_n^{2n-}$ layers are constructed from edge- and corner-sharing {$MoO_6$} octahedra as observed for $MoO_3$,[14] the consequences of adding one $O^{2-}$ group every seven molybdenum sites are manifested in a layer structure significantly different from that adopted by $MoO_3$. The $MoO_3$ layer is constructed from linear ribbons, two polyhedra thick, of edge-sharing {$MoO_6$} octahedra; adjacent ribbons are linked through corner-sharing to produce the layer structure. Consequently, each Mo site in $MoO_3$ displays three triply bridging, two doubly bridging, and one terminal oxo group.

In contrast to the planar layers adopted by $MoO_3$, the oxide layers of **1**·$H_2O$ are distinctly stepped. Examinations of the detailed structure of the layers of **1**·$H_2O$ reveals a motif again based on ribbons of edge-sharing {$MoO_6$} octahedra. However, as shown in Fig. 2, the ribbon executes a 90° turn and shifts one polyhedral length along the *b*-direction at the 'step' juncture at every seventh Mo site. Adjacent ribbons are again linked through corner-sharing interactions, but in such a fashion as to produce three distinct {$MoO_6$} sites. The molybdenum centres Mo(2) and Mo(3) exhibit bonding patterns essentially identical to that observed for $MoO_3$: each projects a single terminal oxo

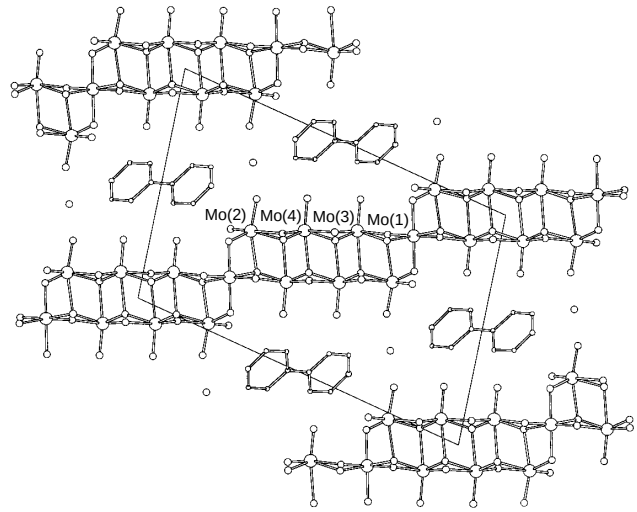



**Fig. 1** A view of the structure of **1**·$H_2O$, showing the $[Mo_7O_{22}]_n^{2n-}$ inorganic layers and the $H_2O$ molecules and $[C_{10}H_{80}N_2]^{2+}$ cations occupying the interlamellar regions

group to either surface of the metal oxide layers and participates in three triply bonding oxo interactions within the ribbon and two doubly bonding oxo linkages to adjacent ribbons. On the other hand, the Mo(4) site is constrained by the folding of the ribbon to provide a second terminal oxo unit, which projects into the 'step' domain of the metal oxide network and adopts the conventional *cis* configuration with respect to the terminal oxo group directed toward the interlamellar region. The most unusual coordination site is occupied by Mo(1) which exhibits only doubly and triply bridging oxo groups and provides the locus of the dislocation of the layer structure of **1**·$H_2O$ with respect to the parent $MoO_3$ structure.

There is an extensive hydrogen-bonding network formed among the $-NH^+$ groups of the bipyridinium cations, the waters of crystallization, and the *cis* terminal oxo groups of Mo(4). This extensive hydrogen-bonding motif causes water and the organic component to be released only at elevated temperatures. Thermogravimetric analysis of **1**·$H_2O$ at a heating rate of 10 °C $min^{-1}$ under $N_2$ revealed no mass loss until 170 °C when release of water commences. The organic component is not removed until *ca*. 250–300 °C.

There has been considerable interest in $MoO_3$ for its catalytic properties in the oxidation of methanol to formaldehyde[15] and for its intercalation properties,[16] for example, intercalation of hydrogen from oxide bronzes of the $H_xMoO_3$ family with applications to electrochromic displays and proton mobility in solids.[17] Oxide **1**·$H_2O$ represents a new class of organically based molybdenum oxides which are different from those obtained from intercalation reactions.[18] The structural modifications of composite metal oxide/organic solids may be realized by introducing organic components as ligands, tethers or structure-directing cations, roles which reflect hydrophobic–hydrophilic interactions and/or multipoint directional hydrogen bonding. Thermal removal of the organic templates from these materials may lead to new metal oxides, with different physical properties and selectivities with respect to interactions with organic substrates. The characterization of the thermal decomposition products of **1**·$H_2O$ is in progress, and their structures and physical properties will be presented in future publications.

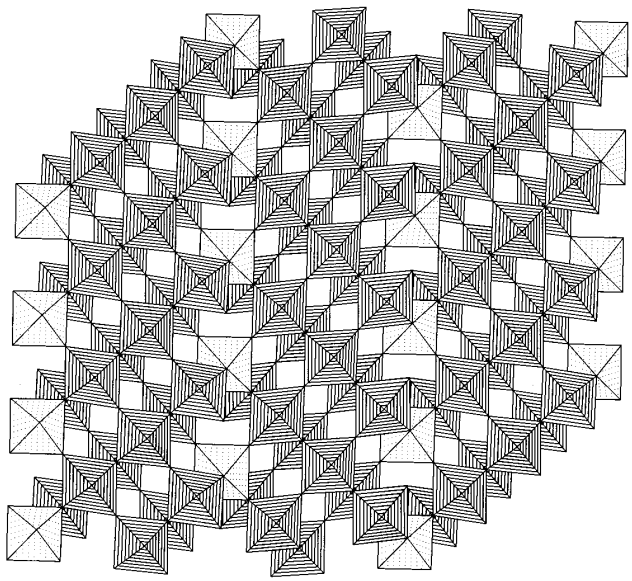


**Fig. 2** A polyhedral representation of the $[Mo_7O_{22}]_n^{2n-}$ layer. The stippled polyhedra represent the Mo(1) sites which provide the location of the dislocations in the **1**·$H_2O$ structure with respect to the parent $MoO_3$ structure.

The work at Syracuse University was funded by NSF grant CHE9318824.

## Footnote

† *Crystal data* for **1**·$H_2O$, $C_{10}H_{12}Mo_7N_2O_{23}$: monoclinic, space group *P*2/*n*, *a* = 12.219(2), *b* = 5.532(1), *c* = 18.322(4) Å, β = 103.28(3)°, *U* = 1205.4(7) Å$^3$, *Z* = 2; *R* = 0.032 for 2107 reflections with $I_0 \geqslant 3.0\sigma(I_0)$ (Mo-Kα radiation, μ = 36.35 $cm^{-1}$). Atomic coordinates, bond lengths and angles, and thermal parameters have been deposited at the Cambridge Crystallographic Data Centre (CCDC). See Information for Authors, Issue No. 1. Any request to the CCDC for this material should quote the full literature citation and the reference number 182/347.

## References

1 A. J. Cheetham, *Science*, 1994, **264**, 794 and references therein.
2 P. A. Cox, *Transition Metal Oxides*, Clarendon Press, Oxford, England, 1995.
3 N. S. P. Bhuvanesh, B. Prasad, R. C. K. Subramanian and J. Gopalakrishnan, *Chem. Commun*., 1996, 289.
4 A. Stein, S. Keller and T. E. Mallouk, *Science*, 1993, **259**, 1558.
5 F. J. DiSalvo, *Science*, 1990, **247**, 649.
6 J. Gopalakrishnan, *Chem. Mater*., 1995, **7**, 1265.
7 Q. S. Huo, D. I. Margolese, U. Clesla, P. Y. Feng, T. E. Gier, P. Sieger, R. Leon, P. M. Petroff, F. Schüth and G. D. Stucky, *Nature*, 1994, **368**, 317.
8 M. I. Khan, Q. Chen and J. Zubieta, *Inorg. Chim. Acta*, 1993, **213**, 328.
9 Y. Xu, L.-H. An and L.-L. Koh, *Chem. Mater*., 1996, **8**, 814.
10 R. Robson, D. P. Abraham, S. R. Batten, R. W. Gable, B. F. Hoskins and J. Liu, in *Supramolecular Architecture*, ed. T. Bein, *ACS Symp. Ser.*, 1992, **499**, 256.
11 D. P. Abraham, B. F. Hoskins and R. Robson, *J. Am. Chem. Soc*., 1991, **113**, 3603.
12 P. J. Zapf, R. L. LaDuca, R. C. Haushalter and J. Zubieta, *Chem. Commun*., submitted for publication.
13 R. C. Haushalter and L. A. Mundi, *Chem. Mater*., 1992, **4**, 31.
14 L. Kihlborg, *Ark. Kemi*, 1963, **21**, 357.
15 E. McCarron, III and A. W. Sleight, *Polyhedron*, 1986, **5**, 129.
16 D. O'Hare, in *Inorganic materials*, ed. D. W. Bruce and D. O'Hare, Wiley, New York, 1992.
17 R. C. T. Slade, T. K. Halstead and P. G. Dickens, *J. Solid State Chem*., 1980, **34**, 183.
18 J. W. Johnson, A. J. Jacobson, S. M. Rich and J. F. Brody, *J. Am. Chem. Soc*., 1981, **103**, 8246.

*Received, 15th October 1996; Com. 6/07022A*

# Highly efficient and flexible total synthesis of coelenterazine

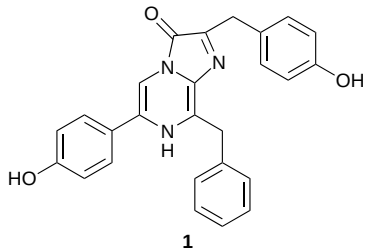
**Martine Keenan, Keith Jones* and Frank Hibbert**

*Department of Chemistry, King's College London, Strand, London, UK WC2R 2LS*

**A new total synthesis of the bioluminescent chromophore coelenterazine 1 is described.**

Coelenterazine **1** found in the jellyfish *Aequorea victoria* was the second imidazopyrazine-based chromophore to be isolated from luminescent marine organisms.[1] Its structure was determined in 1974[2] and it has been synthesised using an approach developed by Kishi[3] in which the fully-substituted pyrazine ring is synthesised by a condensation reaction between an α-amino nitrile and an α-nitroso ketone. In the jellyfish, coelenterazine is bound covalently to a protein which is activated to bioluminescence by reaction with calcium ions. The fact that the protein has been cloned and over-expressed means that a very sensitive system for the detection of calcium ions within cells is available.[4] In addition, the gene for this protein has recently been suggested to be an ideal reporter of gene expression.[5] Both these techniques require the addition of coelenterazine itself to the system in order to observe the desired luminescence. In addition coelenterazine on its own undergoes chemiluminescence with superoxide anion and this has been used as an assay of respiratory burst in neutrophils.[6] These wide-ranging analytical uses make coelenterazine a sought-after molecule for both medical and molecular biological use. Our interest in this area arose from a desire to couple the useful luminescent properties of coelenterazine, with a metal-binding site in the same molecule to explore the possibility of luminescent detection of specific metals. To achieve this goal, we needed a flexible, high-yielding synthesis of coelenterazine which could be adapted to incorporate suitable metal-binding sites. We chose to adopt a different strategy to the Kishi synthesis and start with the pyrazine ring intact to allow late introduction of the substituents.

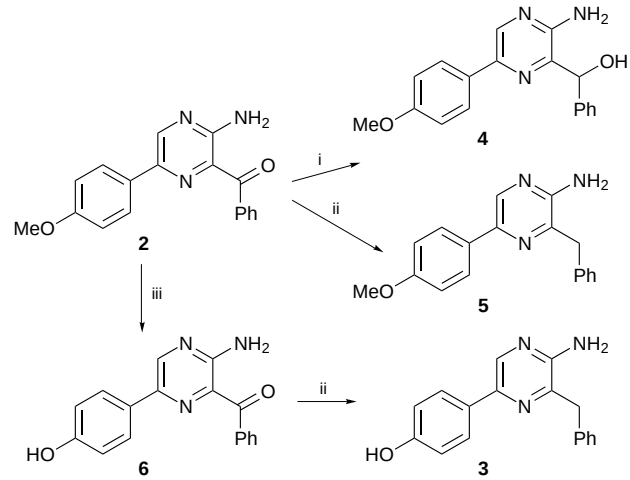
We recently reported the synthesis of the aminopyrazine **2** involving as a key step the formation of the aryl–heteroaryl bond by a high yielding Suzuki coupling reaction between a bromopyrazine and 4-methoxyphenylboronic acid.[7] We further demonstrated that this coupling could give a range of aryl-substituted pyrazines in excellent yield by varying the boronic acid. In order to convert this compound into the desired aminopyrazine **3** representing the southern hemisphere of coelenterazine, two transformations were required, namely reduction of the ketone to a methylene unit and deprotection of the methyl ether (Scheme 1). A two-step procedure was explored involving reduction of the ketone to the alcohol **4** in 60% yield using $NaBH_4$ in MeOH for 15 min.[8] However, reduction of the alcohol **4** with a variety of reagents ($Et_3SiH$ and $CF_3CO_2H$,[9] $ZnBr_2$ and $NaBH_3CN$[10] and radical-based deoxygenation[11]) failed to give any trace of **3**. Reduction of the ketone *via* the alcohol was abandoned and direct reduction to the alkane was investigated. After the failure of a number of methods, a Wolff–Kishner reduction of **2** was explored. Reaction of **2** with hydrazine hydrate and KOH in ethylene glycol at 240 °C for 3 h[12] gave an extremely insoluble red compound, the mass spectrum of which indicated reduction had occurred to give some **5**. However, the insolubility of this material led us to believe that **5** was a minor component and that extensive decomposition had occurred. Consequently, we decided to deprotect the methyl ether prior to reduction of the ketone moiety. Cleavage of methyl aryl ethers has been reported under a variety of conditions but the only successful deprotection of **2** was achieved using ethanethiolate in DMF at 100 °C for 10 h.[13] This gave phenol **6** as a brown solid (mp 176–177 °C) in 81% yield. Finally we were gratified to find that exposure of **6** to the Wolff–Kishner conditions as described above gave the aminopyrazine **3** as a powdery yellow solid (mp 220–222 °C) in 84% yield. This compound was readily purified by chromatography and was fully characterised.



**1**

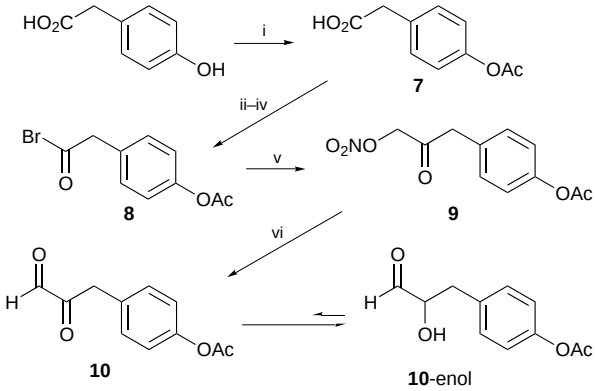
In order to complete the synthesis of coelenterazine, a suitable α-keto aldehyde representing the northern hemisphere was required. After exploring a variety of dithiane-based routes to this compound, we settled on the route shown in Scheme 2.[14] Acetylation of the phenol group in 4-hydroxyphenylacetic acid was carried out in 84% yield using NaOAc in $Ac_2O$. Formation of the acid chloride ($SOCl_2$) and reaction with $CH_2N_2$ gave the α-diazo ketone in high yield. This was not isolated but was reacted with dry HBr to give the bromomethyl ketone **8** in 89% overall yield from **7**. Reaction of the rather sensitive **8** with $AgNO_3$ in MeCN overnight gave the nitrate ester **9** as a colourless solid (mp 65–70 °C) in 98% yield. Finally, reaction of **9** with NaOAc in $Me_2SO$ at room temperature for 25 min gave the α-keto aldehyde **10** in 88% yield as a colourless solid (mp 134–136 °C). Interestingly, NMR studies on **10** indicated that it exists entirely in the enol form in a range of solvents.

The stage was now set for the condensation of **3** and **10** which should lead directly to coelenterazine.[14,15] Model condensations

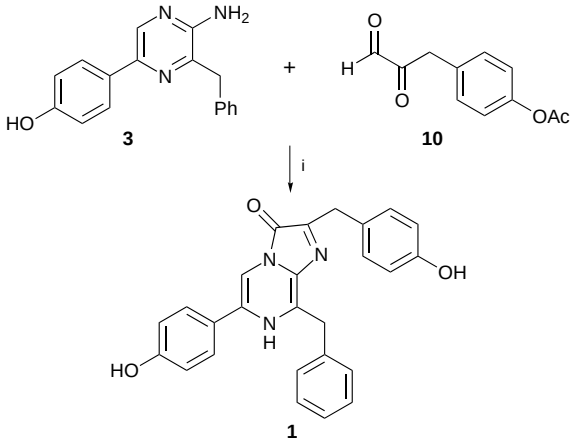


**Scheme 1** *Reagents and conditions*: i, $NaBH_4$, MeOH, 0 °C, 15 min; ii, hydrazine hydrate, KOH, ethanediol, 240 °C 3 h; iii, EtSH, NaH, DMF, 100 °C, 10 h

using the methoxy analogue of the acetoxy α-keto aldehyde **10** had proceeded in poor yield and subsequent cleavage of the methyl ether had proven impossible. The choice of the acetate group for protection of the phenol in the α-keto aldehyde unit was in order to allow deprotection to the phenol to occur under the acidic conditions of the coupling reaction. Reaction of **3** and **10** in EtOH containing conc. HCl and water for 4.5 h at 80 °C in the dark gave coelenterazine **1** as a methanol-soluble orange–brown solid (mp 177 °C, lit.,[14] 175–178 °C) in 62% yield after chromatography. This material forms brilliant yellow-coloured solutions which are both light- and air-sensitive but is relatively stable as a solid. The spectral properties of **1** agreed with those reported in the literature.[3,14] This new, highly convergent synthesis of coelenterazine involves 14 steps in total, although there are only 8 linear steps, and proceeds in 25% overall yield from commercially available 2-chloropyrazine. We are now in a position to prepare a wide range of analogues and explore their chemical and luminescent properties.




**Scheme 2** *Reagents and conditions*: i, NaOAc, $Ac_2O$, reflux, 2 h; ii, $SOCl_2$ (excess), room temp., 12 h; iii, $CH_2N_2$, $Et_2O$, 0 °C, 90 min; iv, dry HBr, 0 °C, 30 min; v, $AgNO_3$, MeCN, room temp., 12 h; vi, NaOAc·3 $H_2O$, $Me_2SO$, room temp., 25 min




**Scheme 3** *Reagents and conditions*: i, EtOH, conc. HCl, 80 °C, 4.5 h with light and air excluded

We thank the BBSRC for a studentship (M. K.) and Professor F. McCapra for useful discussions.

## References


1 O. Shimomura, F. H. Johnson and Y. Saiga, *J. Cell. Comp. Physiol*., 1962, **59**, 223; O. Shimomura and F. H. Johnson, *Tetrahedron Lett*., 1973, **14**, 2963.
2 O. Shimomura, F. H. Johnson and H. Morise, *Biochemistry*, 1974, **13**, 3278.
3 O. Shimomura, B. Musicki and Y. Kishi, *Biochem. J*., 1989, **261**, 913.
4 C. C. Ashley and E. B. Ridgway, *Nature (London)*, 1968, **219**, 1168; M. R. Knight, A. K. Campbell, S. M. Smith and A. J. Trewavas, *Nature (London)*, 1991, **352**, 524.
5 M. N. Badminton, G. B. Sala-Newby, J. M. Kendall and A. K. Campbell, *Biochem. Biophys. Res. Commun*., 1995, **217**, 950.
6 M. Lucas and F. Solano, *Anal. Biochem*., 1992, **206**, 273.
7 K. Jones, M. Keenan and F. Hibbert, *Synlett*, 1996, 509.
8 K. Teranishi and T. Goto, *Bull. Chem. Soc. Jpn*., 1990, **63**, 3132.
9 D. N. Kursanov, Z. N. Parnes and N. M. Loim, *Synthesis*, 1974, 633.
10 C. K. Lau, C. Dufresne, P. C. Bélanger, S. Piétré and J. Scheigetz, *J. Org. Chem*., 1986, **51**, 3038.
11 W. B. Motherwell and D. Crich, in *Free Radical Chain Reactions in Organic Synthesis*, Academic Press, London, 1992, pp. 37–52.
12 W. Schwaiger and J. P. Ward, *Recl. Trav. Chim. Pays-Bas*, 1972, **91**, 1175.
13 G. I. Feutrill and R. N. Mirrington, *Aust. J. Chem*., 1972, **25**, 1719.
14 S. Inoue, S. Sugiura, H. Kakoi and K. Hasizume, *Chem. Lett*., 1975, 141.
15 S. Inoue, S. Sugiura, H. Kakoi and T. Goto, *Tetrahedron Lett*., 1969, **10**, 1609.


*Received, 4th November 1996; Com. 6/07460J*

# Reaction of 1,8-diazabicyclo[5.4.0]undec-8-ene with methyl 3,5-dinitrobenzoate and 1,3,5-trinitrobenzene

**James K. Sutherland**

*Chemistry Department, University of Manchester, UK M13 9PL*

**1,8-Diazabicyclo[5.4.0]undec-8-ene (DBU) undergoes a double addition reaction with the title compounds forming crimson 2-aminoindole derivatives.**

In the course of examining the complexation of 3,5-dinitrobenzoates of cholic acids with a variety of compounds it was observed that with DBU a red colour rapidly developed in $CHCl_3$ and that, after some time, stable red compounds were formed. In order to determine whether these reactions were solely a function of the complexing ability of the cholic esters or due to the dinitrobenzoate function, methyl 3,5-dinitrobenzoate was treated in $CHCl_3$ or EtOAc with DBU whereupon deep red solutions were formed with the colour intensity increasing for up to 2 d. Chromatography yielded starting material and two orange compounds. The less polar orange compound (19%) was shown by spectroscopy† to have structure **1**. The structure of the more polar product was assigned by spectroscopy.‡ Assuming that DBU is also acting as a C-nucleophile in forming this product, structure **3** was assigned.

DBU reacts in a similar manner with 1,3,5-trinitrobenzene to give **2** (11%).§

A scheme to account for the formation of **1** and **3** is the initial reaction giving the Meisenheimer complexes **4** and **5** (the original red colour formed on mixing) from the ester and DBU acting as a C-nucleophile,¶ followed by oxidation of the adducts to form the aryl compounds **6** and **7**; *ipso* displacement of the nitro group of **6** would then give the indole **1** whilst **7** cyclises to form the isoquinolone **3** (Scheme 1). There are a number of examples of DBU reacting as a C- and N-nucleophile,[1] but the order in which reaction occurs is not clear; in the current example DBU appears to be acting initially as a C-nucleophile.

1,3-Dimethylpiperidino-2-indole is reported[2] to absorb at $\lambda_{max}$/nm 230 (ε 25 400), 290 (9300) and 296 (8950) thus the introduction of the electron accepting $NO_2$ and $CO_2Me$ groups effects a large bathochromic shift of *ca*. 180 nm, presumably due to the donating power of both nitrogens of the enediamine system.

I thank Dr G. A. Morris for valuable discussions.

## Footnotes

† $C_{17}H_{19}N_3O_4$, $\lambda_{max}$/nm 332 (ε 13 100) and 475 (5500); $\nu_{max}$/cm$^{-1}$ 1706; $\delta_H$ 8.41 (1 H, d, *J* 1.9), 7.81 (1 H, d, *J* 1.9), 3.85 (3 H, s) and 7 × (2 H, m) with the connectivities $\delta_H$ 4.08–2.10–3.38 and 3.48–1.95–1.91–2.78 (2D-COSY); in addition the signal at $\delta_H$ 4.08 showed an NOE to that at 7.81 (37%) and the 3.85 signal was enhanced by irradiation of these at 8.41 (15%) and 7.81 (9%). $\delta_C$ 166.95, 152.10, 135.33, 125.18, 119.85, 115.90, 111.16, 95.68, 54.01, 51.88, 48.99, 39.96, 28.42, 25.26, 24.51 and 21.80.

‡ $C_{16}H_{16}N_4O_4$; $\lambda_{max}$/nm 462 (11 000); $\nu_{max}$/cm$^{-1}$ 1661; $\delta_H$ 9.17 (1 H, d, *J* 2.6), 8.65 (1 H, d *J* 2.6), and 7 × (2 H, m) with the connectivities δ 4.16—2.10–3.38 and 3.62–1.94–1.75–2.28 (2D-COSY).

§ $C_{15}H_{16}N_4O_4$, $\lambda_{max}$/nm 340 (6000) and 470 (25 000); $\delta_H$ 8.62 (1 H, d, *J* 1.9), 7.92 (1 H, d, *J* 1.9) and 7 × (2 H, m) with the connectivities $\delta_H$ 4.10–2.36–3.44 and 3.59–2.04–1.95–2.78 (2D-COSY); irradiation of the signal at $\delta_H$ 4.10 generated an NOE at 7.92 (22%).

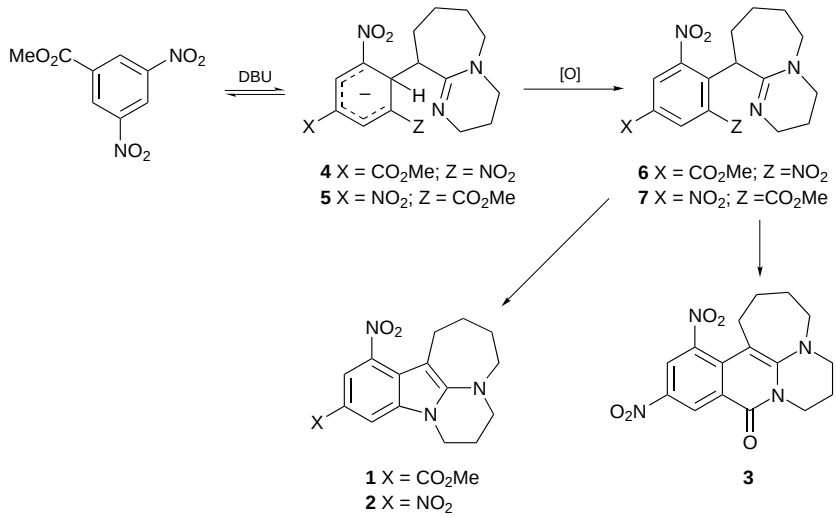
¶ The exact nature of the nucleophile is not known and there are a number of possible formulations.

## References

1 L. L. McCoy and D. Mal, *J. Org. Chem.*, 1981, **46**, 1016; M. Perbost, M. Lucas, C. Chavis and J.-L. Imbach, *J. Heterocycl. Chem.*, 1993, **30**, 627; R. D. Chambers, A. J. Roche, A. S. Batsanov and J. A. K. Howard, *J. Chem. Soc., Chem. Commun.*, 1994, 2055; L. Ma and D. Dolphin, *J. Chem. Soc., Chem. Commun.*, 1995, 2251.

2 T. Hino, M. Makagawa, T. Hashisumi, N. Yamagi, Y. Miwa, K. Tsuneaka and S. Akabashi, *Tetrahedron*, 1971, **27**, 775.

*Received, 13th November 1996; Com. 6/07723D*




**Scheme 1**

# A trisbipyridine tripodal ligand as toluene gelator. Phase transition-triggered binding of iron(II)

**Jean-Ernest Sohna Sohna and Frédéric Fages***

*Photophysique et Photochimie Moléculaire (URA 348 CNRS), Université de Bordeaux I, 351 Cours de La Libération, 33405 Talence Cedex, France*

**The formation of a physical gel with toluene is reported for a trisbipyridine ligand which exhibits iron(II) binding properties triggered by the gel-to-liquid phase transition.**

During the course of investigations on the synthesis of new molecular receptors for transition-metal ions,[1] we discovered that the trisbipyridine ligand $L^1$ exhibited unanticipated solvent gelation properties.†

At room temperature, a solution of ligand $L^1$ in toluene is entirely transformed into a highly viscous thermoreversible gel. In a typical gelation experiment, a 1 mg sample of $L^1$ ($M_W$ = 838) was added to 1 $cm^3$ of toluene in a test tube, and the mixture was either heated or sonicated at room temperature until total dissolution. The resulting solution was allowed to stand undisturbed for *ca*. 2 h at room temperature. The obtained transparent gel mass could be inverted without any flow, and remained stable for several months in a stoppered tube. Using 2 mg of $L^1$, the gelation of the same volume of toluene was effected in only a few minutes. One molecule of the gel-forming tripodal molecule can therefore bind up to 8000 molecules of toluene. We determined $T_{gel}$ of $L^1$ by the spectroscopic turbidity method. We measured the absorbance at 600 nm of a gel {[$L^1$] = 1.15 mg $g^{-1}$} prepared in a 10 mm optical cell. A value of 72 ± 1 °C was obtained by raising the temperature of the sample at a rate of 1 °C $min^{-1}$.

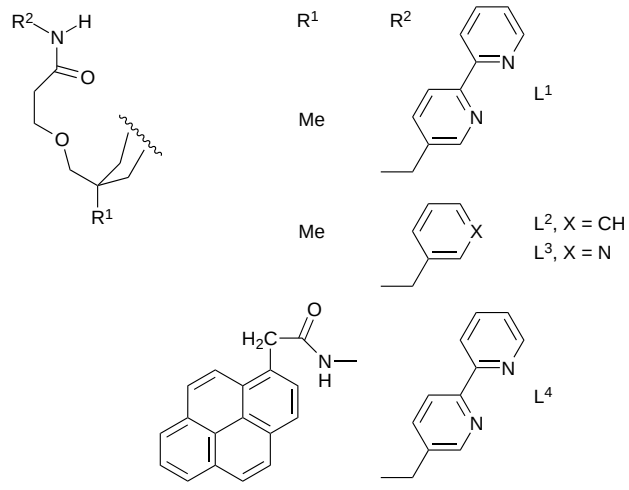
It was also found that 1 : 4 (molar ratio) $CH_2Cl_2$–diethyl ether and 2 : 3 $CH_2Cl_2$–*tert*-butyl methyl ether solvent mixtures could be gelated quite effectively {[$L^1$] = 1.2 mg $g^{-1}$}. $L^1$ did not form gels with cyclohexane, pentane, methanol, $Me_2SO$, dichloromethane, chloroform, nitrobenzene, or *o*-xylene. The structurally related compounds $L^2$–$L^4$ did not gelate toluene.‡

Over the last few years, the ability of several classes of low molecular-mass organic molecules to promote physical gelation of organic solvents has been reported.[2] This phenomenon has been explained on the basis of gelator molecules self-aggregation, which produces a three-dimensional network encaging solvent molecules.[2,3] van der Waals interactions and/or hydrogen bonding were invoked to account for supramolecular network formation. The FTIR spectrum (KBr) of a xerogel, obtained by the slow evaporation of toluene from a gel sample, was compared to that of $L^1$ crystallized from methanol. Bands at 3281 (NH), 1636 (amide I), and 1548 $cm^{-1}$ (amide II) $cm^{-1}$ were observed in the spectrum of the xerogel, whereas the corresponding bands in the spectrum of $L^1$ obtained from methanol were found at 3424, 3284, 1649 and 1556 $cm^{-1}$. This data are indicative of an enhanced manifestation of hydrogen-bonding interactions in the former sample relative to the latter. While intramolecular hydrogen bonds were shown to prevail in solution for a series of related tripod-like molecules incorporating amido linkages in each of the tripod chains,[4] it is very likely that gelation of the apolar toluene solvent by $L^1$ could rather result from molecular self-aggregation through extensive intermolecular hydrogen bonding. The bipyridine subunits might play a specific role in the assembling process leading to gelation, although, as yet, this remains undemonstrated.§

A great variety of complexing agents containing three 2,2′-bipyridine chelating units have been synthesized previously and were shown to exhibit a strong affinity towards first-row transition-metal cations ($M^{2+}$).[5] Especially, some receptors bearing pendent 2,2′-bipyridyl-5-ylmethyl arms were found to form extremely stable $[M(bipy)_3]^{2+}$ complexes in solution.[6] Consistently, $[FeL^1]^{2+}$, prepared by reaction of $L^1$ with 1 mol equiv. of $FeCl_2{\cdot}4H_2O$, was observed to be quite stable in aqueous media, and could be isolated by addition of an excess of potassium hexafluorophosphate. Its VIS spectrum in acetone ($\lambda_{max}$ = 520 nm, $\varepsilon_{max}$ = 7220 $dm^3\ mol^{-1}\ cm^{-1}$) was very close to that of $[Fe(bipy)_3]^{2+}$ and of iron(II) complexes[6] of related ligands. The formation of the 1 : 1 complex in methanol ([$L^1$] < $10^{-5}$ mol $dm^{-3}$) was confirmed spectrophotometrically by the method of continuous variations (Job plot).

Shinkai's group reported previously the case of a cholesterol-based gelator bearing a crown ether moiety. The gelation ability of this system was shown to respond to alkali-metal cations.[7] To our knowledge, $L^1$ is the first example of a molecular receptor for transition-metal ions endowed with solvent gelation properties. A gelled toluene solution of ligand $L^1$ showed drastically reduced complexation ability towards iron(II) salts.

When 0.5 $cm^3$ of water was carefully deposited at the top of a toluene gel sample prepared in a 10 mm diameter test-tube from 0.5 $cm^3$ of toluene {[$L^1$] = 1.2 mg $g^{-1}$), we observed that (*i*) the aqueous phase, despite being denser, occupied the upper layer and (*ii*) the biphasic system remained stable indefinitely. When the same experiment was carried out with water containing an excess of $Fe(SO_4){\cdot}7H_2O$, the gel mass was similarly unaltered after 24 h. As compared to the blank experiment, only a slight modification of the shape of the interface layer between gelled toluene and isotropic water was noticed. Furthermore, the latter phase slowly turned pink, probably due to the extraction of some ligand molecules from the gel into the isotropic water phase driven by complexation equilibria. When the system was heated above $T_{gel}$, the gel collapsed, which led to mixing and the inversion of toluene and water, with, simultaneously, a deep red colouring of the aqueous



solution. VIS absorption spectroscopy indicated that the total amount of ligand $L^1$ initially dissolved in toluene was then transferred to water as the iron(II) chelate. In the blank experiment, $L^1$ was not extracted into water.

Polymer gels that can take up or release molecules upon phase transition are of considerable interest for a wide range of applications.[8] The properties of the new gelator $L^1$ could lead to the development of supramolecular devices for applications.

We are grateful to the CNRS, the Université de Bordeaux I and La Région Aquitaine for financial support.

## Footnotes

† Compound $L^1$ was prepared by a simple two-step procedure. 1,1,1-Tris-(carboxyethoxymethyl)ethane was activated *via* DCC-mediated condensation with *N*-hydroxysuccinimide to give the corresponding active triester. The latter was reacted in dmf with 3.3 mol equiv. of 5-aminomethyl-2,2′-bipyridine to afford $L^1$ (white solid) in 80% yield. Mp 91 °C, $^1$H NMR ($CD_3OD$): δ 0.80 (s, 3 H), 2.45 (t, 6 H), 3.25 (s, 6 H), 3.65 (t, 6 H), 4.45 (s, 6 H), 7.4 (m, 3 H), 7.8 (m, 6 H), 8.25 (m, 6 H), 8.60 (m, 6 H). Satisfactory elemental analyses and mass spectrometry data were obtained.

‡ $L^2$–$L^4$ were characterized by proton NMR spectroscopy and mass spectrometry. The synthesis of $L^4$, together with its metal cation binding and photophysical studies, will be published elsewhere.

§ $L^2$ and $L^3$ do not gelate. Furthermore, we also noticed the conspicuous propensity of a series of related molecular systems symmetrically substituted with two or three 5-amidomethyl-2,2′-bipyridine moieties to aggregate strongly even in polar solvents.

## References

1 F. Fages, B. Bodenant and T. Weil, *J. Org. Chem.*, 1996, **61**, 3956.
2 T. Brotin, R. Utermöhlen, F. Fages, H. Bouas-Laurent and J.-P. Desvergne, *J. Chem. Soc., Chem. Commun.*, 1991, 416; H. T. Stock, N. J. Turner and M. McCague, *J. Chem. Soc., Chem. Commun.*, 1995, 2063 and references therein.
3 P. Terech, I. Furman, R. G. Weiss, H. Bouas-Laurent, J.-P. Desvergne and R. Ramasseul, *Faraday Discuss.*, 1995, **102**, 345.
4 I. Dayan, J. Libman, A. Shanzer, C. E. Felder and S. Lifson, *J. Am. Chem. Soc.*, 1991, **113**, 3431.
5 R. Ziessel and J.-M. Lehn, *Helv. Chim. Acta*, 1990, **73**, 1149 and references therein; P. Belser, A. von Zelewsky, M. Franck, C. Seel, F. Vögtle, L. De Cola, F. Barigelletti and V. Balzani, *J. Am. Chem. Soc.*, 1993, **115**, 4076.
6 P. Sheldon, W. Errington, P. Moore, S. C. Rawle and S. M. Smith, *J. Chem. Soc., Chem. Commun.*, 1994, 2489; R. F. Beeston, S. L. Larson and M. C. Fitzgerald, *Inorg. Chem.*, 1989, **28**, 4187.
7 K. Murata, M. Aoki, T. Nishi, A. Ikeda and S. Shinkai, *J. Chem. Soc., Chem. Commun.*, 1991, 1715.
8 T. Tanaka, C. Wang, V. Pande, A. Y. Grosberg, A. English, S. Masamune, H. Gold, R. Levy and K. King, *Faraday Discuss.*, 1995, **102**, 201.

*Received, 28th October 1996; Com. 6/07346H*

# Water-soluble poly(4,7,10,13-tetraoxatetradecylmethylsilane): enhanced yield and improved purity *via* polymerization using graphite-potassium ($C_8K$) as reducing agent

**Thomas J. Cleij, Stellar K. Y. Tsang and Leonardus W. Jenneskens*†**

*Debye Institute, Department of Physical Organic Chemistry, Utrecht University, Padualaan 8, 3584 CH Utrecht, The Netherlands*

**Application of graphite-potassium ($C_8K$, THF, 0 °C), instead of convential Wurtz-type coupling conditions (Na, toluene, 110 °C), as reducing agent for the preparation of non-ionic, watersoluble poly(4,7,10,13-tetraoxatetradecylmethylsilane) 1 gives a markedly enhanced yield as well as a high molecular weight polymer of high purity.**

Polysilanes, *viz*. polysilylenes, exhibit (photo)physical and electronic properties of interest for application in materials science.[1] Although with the conventional Wurtz-type coupling conditions (Na, toluene, 110 °C) a number of polysilanes with alkyl and/or aryl substituents have been prepared, a drawback is that the severe polymerization conditions impair the use of monomers with functionalized side chains.[2] Hence, introduction of, for example, ionic groups has to be achieved by side chain functionalization after polymerization.[2–4] Notwithstanding using the conventional Wurtz-type coupling procedure, polysilanes containing ether linkages in their side chains[5] and, more recently, the first non-ionic water-soluble polysilanes possessing oligo(oxyethylene) side chains have become available,[6,7] albeit in low yields. Moreover, especially in the case of the non-ionic water-soluble polysilanes, their remarkable solubility in common organic solvents as well as water hampered their purification by simple (repeated) precipitation. High molecular weight material had to be separated from low molecular weight impurities (*vide infra*) by laborious preparative size exclusion chromatography (SEC). Hence as shown for poly(4,7,10,13-tetraoxatetradecylmethylsilane) **1**,[6,7] isolated yields varied considerably (**1**; $\ll$ 1.0[7] up to 11%[6]). This is unfortunate, since polar polysilanes in general attract attention due to their propensity to Langmuir film formation at the air–water interface[2,3] and their potential application in (self)-assembly.[8]

Here we report that with graphite-potassium ($C_8K$),[9] instead of Na, as reducing agent, non-ionic, water-soluble **1** is accessible in a markedly enhanced yield. Furthermore, the high molecular weight fraction isolated by preparative SEC is shown to possess considerably improved purity (Scheme 1). The choice of $C_8K$ was based on reported results for poly(methylphenylsilane)[10] and poly(phenylsilyne).[11] $C_8K$ was shown to be applicable at subambient temperature and to be compatible with a wide range of solvents.‡ Hence in contrast to the conventional Wurtz-type coupling procedure (Na, toluene, 110 °C), polymerization *via* the $C_8K$ route requires considerably less severe conditions.

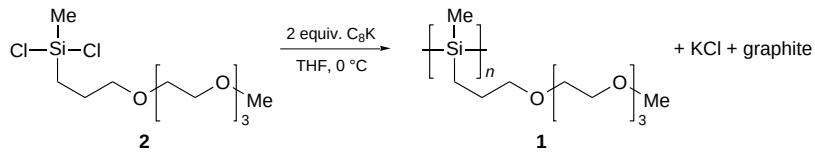
To establish the suitability of $C_8K$ for the preparation of **1**, the monomer 4,7,10,13-tetraoxatetradecylmethyldichlorosilane **2**[6] was polymerized under various conditions.§ Initial experiments revealed that both the formation of **1** as well as its final yield are strongly dependent on the ratio $C_8K$ : **2**, reaction temperature and duration of polymerization, respectively. In THF, the high molecular weight polymer **1** was only obtained with a ratio $C_8K$ : **2** of 2 and a reaction temperature of 0 °C. No **1** could be identified if either excess $C_8K$ (ratio $C_8K$ : **2** > 2) was used or in polymerizations executed with *ca*. 2 equiv. $C_8K$ at $T > 0$ °C. To determine optimal polymerization conditions the effect of reaction time was studied in more detail (Table 1). The data show that for optimal formation of **1** a reaction time of 2–2.5 h is required (Table 1, entry 3). Longer reaction times lead to degradation of **1** (Table 1, entries 4 and 5, SEC). Under optimized conditions similar molecular weight distributions were found as those reported previously for **1** (Wurtz-type coupling reaction; Table 1, entry 6; $M_w$ *ca*. 1.5 × 10[4]).[6] In contrast to results reported for poly(methylphenylsilane) prepared *via* the $C_8K$ route,[10] no polymer **1** could be extracted from the graphite phase after filtration.

After preparative SEC, polymer **1** was isolated in yields ranging from 20 to 35%. This is a considerable enhancement with respect to the yields obtained using conventional Wurtz-type coupling conditions (**1**; $\ll$ 1.0[7] up to 11%[6]). $^{29}$Si NMR analysis only gave the characteristic silicon backbone resonance at δ −31.4 (Table 1, entry 3 and Fig. 1). The absence of resonances attributable to end-groups and/or siloxane moieties indicates that **1** prepared using $C_8K$ after purification by preparative SEC is completely free from low-molecular weight material (*vide infra*). This is supported by $^1$H and $^{13}$C NMR

**Table 1** Salient features of **1** obtained *via* the $C_8K$ route ($C_8K$ : **2** = 2.0, THF, 0 °C) with different reaction times after purification by preparative SEC.§¶

| Entry | *t*/h | Yield (%) | $M_w$ × 10$^{-3}$ [a] | $M_w$/$M_n$ [b] | $\lambda_{max}$/nm [c] | ε(Si–Si)/10$^3$ dm$^3$ mol$^{-1}$ cm$^{-1}$ [c] |
|---|---|---|---|---|---|---|
| 1 | 1.0 | 30 | 6.9 | 1.3 | 300 | 1.6 |
| 2 | 1.5 | 34 | 10.7 | 1.5 | 301 | 2.1 |
| 3 | 2.0 | 22 | 14.0 | 1.9 | 304 | 4.8 |
| 4 | 2.5 | 33 | 14.4 | 2.0 | 304 | 2.4 |
| 5 | 3.0 | 18 | 8.8 | 1.6 | 301 | 3.2 |
| 6 [d] | 2.0 | 11 | 15.1 | 1.4 | 299 | 1.8 |

[a] Molecular weight distributions determined with analytical SEC (UV detection λ 300 nm, polystyrene standards). [b] Polydispersity [see footnote (*a*)]. [c] Solvent MeCN. [d] Prepared using conventional Wurtz-type coupling conditions.[6]




**2** **1**

**Scheme 1**

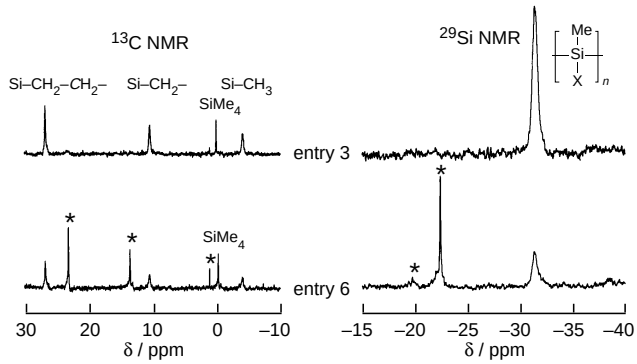



**Fig. 1** $^{13}C$ and $^{29}Si$ NMR spectra of **1** prepared using either $C_8K$ [THF, 0 °C (entry 3)] or conventional Wurtz-type coupling conditions [Na, toluene, 110 °C (entry 6)]. Peaks marked with * are due to impurities such as cyclosiloxanes‖ and low molecular weight oligomers (for X see Scheme 1).

spectroscopy (Fig. 1, $^{13}C$ NMR).¶ While for **1** prepared *via* the conventional Wurtz-type coupling reaction broad and split $^1H$ NMR signals were observed for the $SiCH_3$, $SiCH_2$ and $SiCH_2CH_2$ moieties,[6] discrete resonances, similar to those reported for poly(γ-methoxypropylmethylsilane),[5] were found for **1** prepared using $C_8K$.¶

Additional evidence for the improved purity of **1** prepared *via* the $C_8K$ method was obtained from its UV spectrum. The $\lambda_{max}$ value at *ca*. 300 nm ($\sigma \rightarrow \sigma^*$ transition) in combination with the increase of the extinction coefficient ε are in agreement with the presence of only a high molecular weight polymer (Table 1; entries 2–5 *vs*. entry 6).[1,6]

$^{29}Si$ NMR and FAB-MS of the low molecular weight fractions indicate that they mainly consist of cyclosiloxanes [$D_n$ with $n$ = 3, 4 and 5], which apparently are formed during work-up.‖ This result differs from that found for the low molecular weight fractions for **1** prepared using conventional Wurtz-type coupling conditions. In that case the low molecular weight fraction primarily consists of cyclosilanes (five- and six-membered) and cyclosiloxanes [$D_n$ with $n$ = 4 and 5].[6]‖

## Footnotes

† E-mail: jennesk@chem.ruu.nl

‡ It is noteworthy that it was recently reported that the yield of poly(methylphenylsilane) prepared using $C_8K$ (THF, −78 to 25 °C) appears to be sensitive to the addition of a co-solvent such as 1,2-dimethoxyethane.[13]

§ All polymerizations were carried out in dried glassware under an Ar atmosphere. In a typical experiment, 4,7,10,13-tetraoxatetradecylmethyldichlorosilane (**2**, 1.66 g, 5.2 mmol) was slowly added *via* a syringe to a suspension of THF (10 ml) and $C_8K$ [prepared by stirring graphite (1.00 g, 83.2 mmol) and potassium (0.41 g, 10.4 mmol) for 1 h at 150 °C][9] cooled at 0 °C. After the appropriate reaction time (see Table 1) the reaction mixture was quenched by adding MeOH (2 ml) followed by filtering off the graphite and precipitated KCl. To the filtrate a solution of $KHCO_3$ (0.5 g) in water (30 ml) was added to neutralize dissolved HCl and to prevent polymer degradation. After removal of solvents *in vacuo* the oily residue was redissolved in $CH_2Cl_2$ (30 ml) and the precipitated $KHCO_3$ as well as additional KCl were removed by filtration. The filtrate was concentrated *in vacuo* and the high molecular weight polymer fraction was subsequently isolated by preparative SEC (Biobeads SX-1, eluent $CH_2Cl_2$). Polysilane **1** was characterized with analytical SEC, DSC, TGA, UV, $^1H$, $^{13}C$ and $^{29}Si$ NMR spectroscopy.¶

¶ Polysilane **1** prepared using $C_8K$ possesses improved purity compared to **1** obtained with the conventional Wurtz-type coupling procedure (Fig. 1).[6] $^1H$ NMR (300.13 MHz, $CDCl_3$) $\delta_H$ 0.26 (br, 3 H), 0.77 (br, 2 H), 1.60 (br, 2 H) and 3.38–3.66 (br, 17 H); $^{13}C$ NMR (75.47 MHz, $CDCl_3$) $\delta_C$ −4.1, 10.4, 26.8, 59.0, 70.1, 70.5, 70.6, 72.0 and 74.4; $^{29}Si$ NMR (59.63 MHz, $CDCl_3$) $\delta_{Si}$ −31.4.

‖ Cyclosiloxanes $D_n$ {$\overline{[–Si(R^1R^2)–O–]_n}$ with $R^1$=$R^2$=Me} possess $^{29}Si$ NMR chemical shifts at δ −8.93, −20.00 and −22.62 for $n$ = 3, 4 and 5, respectively. For the low molecular weight fractions isolated from the crude reaction mixture $^{29}Si$ NMR chemical shifts at δ −11.94 and −12.32, −21.06 and −22.0 assigned to $D_3$, $D_4$ and $D_5$ species, respectively, were found.[12] This assignment is corroborated by FAB-MS.

## References


1 For a review: R. D. Miller and J. Michl, *Chem. Rev.*, 1989, **89**, 1359.
2 For a review: S. Hayase, CHEMTECH, 1994, October 19 and references cited therein.
3 T. Seki, A. Tohnai, T. Tamaki and K. Ueno, *J. Chem. Soc., Chem. Commun.*, 1993, 1876; T. Seki, N. Tanigaki, K. Yase, A. Kaito, T. Tamaki, K. Ueno and Y. Tanaka, *Macromolecules*, 1995, **28**, 5609.
4 J. S. Hrkach and K. Matyjaszewski, *Macromolecules*, 1990, **23**, 4042; K. Matyjaszewski, J. S. Hrkach, H.-K. Kim and K. Ruehl, in *Silicon Based Polymer Science: A Comprehensive Resource*, ed. J. M. Ziegler and F. W. Gordon Fearon, Advances in Chemistry Series 224, ACS, Washington DC, 1990.
5 C. H. Yuan and R. West, *Macromolecules*, 1993, **26**, 2645; H. Frey, G. J. J. Out, M. Möller, D. Greszta and K. Matyjaszewski, *Macromolecules*, 1993, **26**, 6231; J. S. Hrkach and K. Matyjaszewski, *J. Polym. Sci. Part A: Polym. Chem.*, 1994, **32**, 1949.
6 C. A. van Walree, T. J. Cleij, J. W. Zwikker and L. W. Jenneskens, *Macromolecules*, 1995, **28**, 8696.
7 K. Oka, N. Fujiue, S. Nakanishi, T. Takata, T. Dohmaru, C.-H. Yuan and R. West, *Chem. Lett.*, 1995, 875.
8 T. Seki, A. Tohnai, T. Tamaki and A. Kaito, *Macromolecules*, 1996, **29**, 4813; T. Seki, A. Tohnai, T. Tamaki and A. Kaito, *Chem. Lett.*, 1996, 361; M. Yoshida, T. Seki, F. Nakanishi, K. Sakamoto and H. Sakurai, *Chem. Commun.*, 1996, 1381.
9 A. Fürstner and H. Weidman, *J. Organomet. Chem.*, 1988, **354**, 15; R. Csuk, B. I. Glänzer and A. Fürstner, *Adv. Organomet. Chem.*, 1988, **28**, 85; A. Fürstner, *Angew. Chem., Int. Ed. Engl.*, 1993, **32**, 164.
10 B. Lacave-Goffin, L. Hevesi and J. Devaux, *J. Chem. Soc., Chem. Commun.*, 1995, 769; R. G. Jones, R. E. Benfield, P. J. Evans and A. C. Swain, *J. Chem. Soc., Chem. Commun.*, 1995, 1465.
11 W. Uhlig, *Z. Naturforsch.*, 1995, **50b**, 1674 and references cited therein.
12 E. A. Williams and J. D. Cargioli, in *Annual Reports on NMR Spectroscopy*, ed. G. A. Webb, Academic Press, 1979, vol. 9, p. 221.
13 B. Lacave-Goffin, J. Devaux and L. Hevesi, *XIth International Symposium on Organosilicon Chemistry*, Montpellier, France, Sept. 1–6, 1996; abstract OC16.


*Received, 18th November 1996; Com. 6/07786B*

# Modelling the active sites of heterogeneous titanium epoxidation catalysts using titanium silasequioxanes: insight into specific factors that determine leaching in liquid-phase processes

**Hendrikus C. L. Abbenhuis,* Simon Krijnen and Rutger A. van Santen**

*Schuit Institute of Catalysis, Eindhoven University of Technology, PO Box 513, 5600 MB Eindhoven, The Netherlands*

**Active catalysts for the epoxidation of alkenes by *tert*-butyl hydroperoxide are provided by silasesquioxane titanium(IV) derivatives; a non-leaching catalyst, not prone to irreversible protic cleavage of its siloxy functions by the oxidizing agent, contains a terdentate silasesquioxane ligand.**

In the current search for non-leaching heterogeneous liquid-phase oxidation catalysts detailed studies of how the catalytically active metal species are bonded to the support are rare. Often, more attention is paid to the performance of the catalyst, rather than to the fundamental question whether the catalyst is truly heterogeneous or not. In order to approach this problem at a molecular level, we report here on epoxidations catalysed by titanium silasesquioxanes. In these silasesquioxanes, the titanium is incorporated *via* spatially oriented siloxy bonds (Ti–O–Si) which structurally resemble surface sites that have been purportedly identified on silica surfaces.

Heterogeneous titanium catalysts are very important in oxidation processes but at the same time have been reported to undergo some leaching in liquid-phase applications. For instance, the highly active Shell titanium/silica epoxidation catalyst[1,2] becomes only truly heterogeneous after a certain time on stream.[3] Similar materials, that are currently being reported as the result of grafting silica[4] or MCM-41 mesoporous silica[5] with titanium derivatives, or even novel titanosilicates,[6] might therefore be only partially heterogeneous when applied in liquid-phase oxidation reactions.

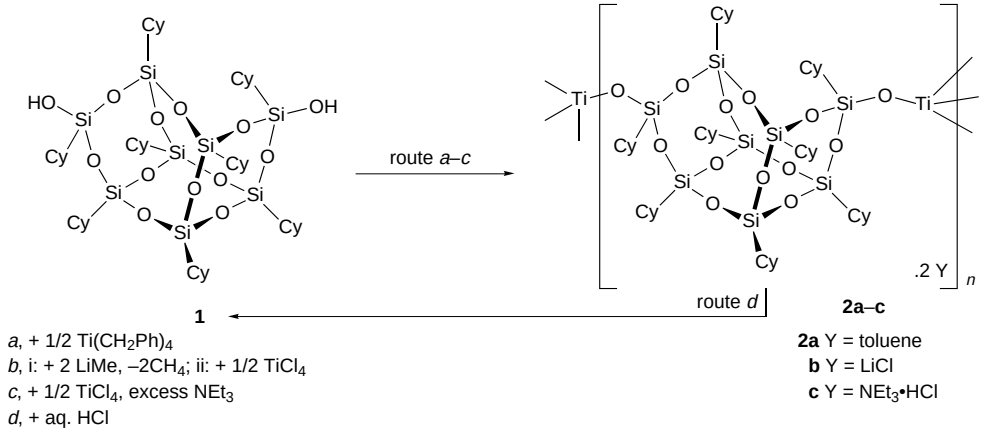
The silasesquioxane **1** (Scheme 1) possesses a well defined structure which includes two reactive, isolated hydroxy groups that occupy '*exo*' positions above nearby $Si_4O_4$ rings, that are part of an interdigitated $Si_8O_{11}$ skeleton. Several functionalizations of **1** have already been achieved *via* clean silanol centred reactions and were in most cases reported to leave the silasesquioxane skeleton intact.[7–9] Recently, we reported on the construction of a very active, truly heterogeneous catalyst from **1** for Diels–Alder reactions of enones.[10]

We found that, in toluene, the silanol groups present in **1** easily react with tetrabenzyltitanium (Scheme 1, route *a*), resulting in concomitant formation of toluene and a pale yellow titaniumsilasesquioxane gel **2a** that occludes the entire volume of the solvent used. When subjected to prolonged centrifugation (20 min at 900 g), the gel releases toluene until a toluene/silasesquioxane mass ratio of *ca.* 18 is reached. Upon drying *in vacuo*, the gel collapses into a powder, yielding **2a** free of solvent in 90% yield. The swelling capacity of the dried titaniumsilasesquioxane gel **2a** for toluene is reduced to approximately 0.5 ml $g^{-1}$.

Related titaniumsilasesquioxane gels were also prepared from the building block **1** involving reactions with titanium tetrachloride and a base (Scheme 1, routes *b* and *c*). As a result of these synthetic methods, the gels obtained contain enclosed lithium chloride or $[NHEt_3]Cl$.

The silanol-mediated functionalizations that lead to the formation of the silasesquioxane gels **2** are straightforward and find precedent in the well exploited silanol-centred reactivity of the related silasesquioxane $(C_6H_{11})_7Si_7O_9(OH)_3$.[11] Powder reflection UV–VIS measurements on **2a–c** show the onset of significant UV absorption only below 350 nm, with a maximum at 220–240 nm. This indicates that in **2a–c** the titanium centres exist as four-coordinate titanium(IV) siloxy units.

Analysis of the titaniumsilasesquioxane gels **2** by single-pulse 79.5 MHz $^{29}Si$ MAS NMR provides a method to establish the degree of silanol functionalization during their formation. Upon substitution, the originally lower field resonance of the silanol silicon atoms at δ −58.9 shifts towards the higher field part of the spectrum where the other silasesquioxane silicon resonances are already found (δ −65 to −75). Comparison of the integrals over the two distinct parts of the spectra indicates that the fraction of remaining silanol units in the titanium gels **2a–c** is, typically, 0.05 (*cf.* 0.25 in the silasesquioxane **1**), *i.e. ca.* 80% of the silanol units of the starting material **1** have been functionalized in the gel-forming process.




**Scheme 1** Synthetic routes to the titaniumsilasesquioxane gels **2a–c** (Cy = cyclohexyl)

Interestingly, when any of the gels **2** are subjected to acid hydrolysis followed by organic work-up, the silasesquioxane **1** can be recovered in near to quantitative yield (Scheme 1, route *d*). From this observation, it can be concluded that the silanol deprotonations involved in the formation of the gels **2** do not induce any change in the silasesquioxane framework.

The titanium silasesquioxane gels **2** efficiently catalyse the epoxidation of alkenes under mild conditions (see Table 1). In a typical reaction equimolar amounts of alkene and *tert*-butyl hydroperoxide (TBHP) were reacted over the catalyst (*ca.* 1 mol% Ti with respect to the substrates) in hexane at 50 °C. Though for the reactions studied, the silasesquioxane gels **2** were reasonable to good catalysts, attempts to filter the catalyst off during epoxidation, and thus to stop the reaction, met with complications which were indicative of severe leaching of catalytically active species from the titanium gels. Interestingly, NMR studies showed that during epoxidation, rapid hydrolysis of the gel by TBHP occurs resulting in the quantitative reformation of the silasesquioxane **1** and concomitant formation of non-siloxy titanium species that are catalytically active.

An essential feature of several of the proposed mechanisms of alkene epoxidation by titanium silicalites involves hydrolysis of a titanium siloxy function in a four-coordinate active site.[12–15] For the titanium gel **2**, such a hydrolysis step would lead to rapid degeneration of the material since the titanium siloxy units (Ti–O–Si) result here from functionalization of isolated silanol groups, the silasesquioxane being a bifunctional monodentate ligand (Scheme 2, route i). This would therefore imply that silasesquioxane titanium species where the silasesquioxane can bind to titanium as a multidentate ligand are more robust epoxidation catalysts.

In order to verify this hypothesis, we have tested the activity of the known silasesquioxane complex **3**, that has a terdentate silasesquioxane ligand,[8,16] for similar alkene epoxidations (Table 1). Interestingly, complex **3** turned out to be an epoxidation catalyst that is effective at low concentration and which selectively produces alkene oxides in high yield with good peroxide economy. Especially the somewhat difficult epoxidation of oct-1-ene is catalysed more effectively by **3**. The same catalytic performance was found for **3** that was repeatedly recrystallized from toluene–acetonitrile, which seems to exclude the possibility that undetected trace impurities in **3** are responsible for the observed catalytic activity. It is likely that due to multidentate silasesquioxane coordination, **3** does not hydrolyse irreversibly during epoxidation reactions (Scheme 2, route ii); in fact, the complex is even stable in 1 M aq. HCl! Under catalytic conditions, complex **3** can be easily monitored by $^{1}H$ and $^{13}C$ NMR, it's cyclopentadienyl unit providing a convenient and sensitive NMR probe. From these NMR experiments it could be concluded that after *ca.* 100 turnovers, complex **3** is still the only observable silasesquioxane species present and that it does not lose the cyclopentadienyl ligand during epoxidation catalysis. These findings are consistent with a mechanism for alkene epoxidation in which reversible hydrolysis of a titanium siloxy function occurs. In our opinion, these observations support the mechanism of heterogeneous alkene epoxidation by titanium silicalites proposed by Clerici, Ingallina, Sheldon and Van Doorn.[12–15]

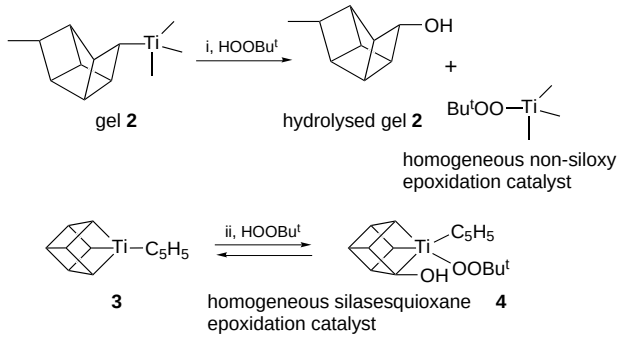
In conclusion, we have shown that new titanium-containing silasesquioxane gels effectively catalyse the epoxidation of alkenes by TBHP under mild conditions. The active catalyst, however, is a soluble, non-siloxy titanium species. Alternatively, the titanium complex **3**, that contains a terdentate silasesquioxane ligand, has excellent performance in the same epoxidations. In this case, the catalysis occurs exclusively through titanium siloxy complexes. As such, liquid-phase, silica-supported titanium epoxidation catalysts are predicted to be accessible and active in many cases but will be truly heterogeneous only when stringent conditions are met. More work on the structural characterization of the titanasilasesquioxane gels as well on their use in catalysis is currently in progress together with experimental work on the heterogenization of complex **3**.

The research of H. C. L. A. has been made possible by a fellowship of the Royal Netherlands Academy of Arts and Sciences (KNAW). S. K. thanks the Netherlands Institute for Catalysis Research (NIOK) for financial support.

**Table 1** Epoxidation of alkenes with TBHP catalysed titanasilasesquioxanes[a]

| Catalyst | Alkene | *t*/h | Conv. (%) | Selectivity in alkene (%) |
|---|---|---|---|---|
| **2a** | Oct-1-ene | 24 | 15 | 60 |
| **2b** | Oct-1-ene | 24 | 25 | 60 |
| **3** | Oct-1-ene | 24 | 80 | 80 |
| **2a** | Cyclooctene | 4 | 50 | > 95 |
| **2b** | Cyclooctene | 4 | 90 | > 95 |
| **3** | Cyclooctene | 3 | 90 | > 95 |
| **2a** | Norbornylene | 4 | 60 | > 95 |
| **2b** | Norbornylene | 3.5 | 90 | > 95 |
| **3** | Norbornylene | 3 | 90 | > 95 |

[a] All reactions were performed using equimolar amounts (1.6 mmol) of alkene and dried *tert*-butyl hydrogen peroxide (1.6 mmol) in hexane (1.0 ml). Reactions were performed at 50 °C in sealed vials that were magnetically stirred using 25 mg of catalyst. Conversions and yields were determined by $^{1}H$ NMR spectroscopy.




**Scheme 2** Schematic representation of the reaction of silasesquioxane titanium species with TBHP rendering species capable of alkene epoxidation: i, the irreversible hydrolysis of the silasesquioxane gels **2** and ii, the reversible hydrolysis of a silasesquioxane complex (the lines in the cube-type ligands represent Si–O–Si, with cyclohexyl units at the corners)

## References

1 H. P. Wulff, *US Pat.*, 3 923 843, 1975 [*Chem. Abstr.*, 84 : 89977d].
2 H. P. Wulff and F. Wattimena, *US Pat.*, 4 021 454, 1977 [*Chem. Abstr.*, 87 : 22393d].
3 R. A. Sheldon, *J. Mol. Catal.*, 1980, **7**, 107 and unpublished work from Schram and Van Broekhoven cited therein.
4 R. Hutter, D. C. M. Dutoit, T. Mallat, M. Schneider and A. Baiker, *J. Chem. Soc., Chem. Commun.*, 1995, 163.
5 T. Maschmeyer, F. Rey, G. Sankar and J. M. Thomas, *Nature*, 1995, **378**, 159.
6 M. A. Roberts, G. Sankar, J. M. Thomas, R. H. Jones, H. Du, J. Chen, W. Pang and R. Xu, *Nature*, 1996, **381**, 401.
7 J. F. Walzer, D. A. Newman and F. J. Feher, *J. Am. Chem. Soc.*, 1989, **111**, 1741.
8 F. J. Feher, T. A. Budzichowski, K. Rahimian and J. W. Ziller, *J. Am. Chem. Soc.*, 1992, **114**, 3859.
9 T. S. Haddad and J. D. Lichtenhan, *J. Inorg. Organomet. Polymers*, 1995, **5**, 237.
10 H. C. L. Abbenhuis, H. W. G. Van Herwijnen and R. A. Van Santen, *Chem. Commun.*, 1996, 1941.
11 F. J. Feher, and T. A. Budzichowski, *Polyhedron*, 1995, **14**, 3239.
12 M. G. Clerici and P. Ingallina, *J. Catal.*, 1993, **140**, 71.
13 M. G. Clerici, *Appl. Catal.*, 1991, **68**, 249.
14 R. A. Sheldon and J. A. Van Doorn, *J. Catal.*, 1973, **31**, 427.
15 R. A. Sheldon, *J. Mol. Catal.*, 1980, **7**, 107.
16 I. E. Buys, T. W. Hambley, D. J. Houlton, T. Maschmeyer, A. F. Masters and A. K. Smith, *J. Mol. Catal.*, 1994, **86**, 309.

*Received, 22nd November 1996; Com. 6/07935K*



Typeset and printed by Black Bear Press Limited, Cambridge, England

ChemComm
FEATURE ARTICLE

# Vectorial transfer of electronic energy in rod-like ruthenium–osmium dinuclear complexes

**Francesco Barigelletti,[a] Lucia Flamigni,[a] Jean-Paul Collin[b] and Jean-Pierre Sauvage[b]**

[a] *Istituto FRAE-CNR, Via P. Gobetti 101, 40129 Bologna, Italy*
[b] *Laboratoire de Chimie Organo-Minerale, Université Louis Pasteur, Faculté de Chimie, 1 rue Blaise Pascal, F-67008, Strasbourg, France*

**Dinuclear complexes containing ruthenium and osmium-based bis-terpyridyl chromophoric termini are prepared and their luminescence properties investigated. The two chromophoric units are connected by 1,4-phenylenes only, or phenylene and bicyclooctane spacers. In this way complete control of the geometry of the dinuclear complexes is achieved and these rigid species resemble molecular rods or girders featuring intermetal distances in the range 11–24 Å. The Ru → Os transfer of electronic excitation is energetically allowed and we have studied the effect on this process both of the intermetal separation and the electronic properties of the spacers. The main conclusions are that the phenylene spacers are very efficient in transmitting the intermetal electronic communication but an important role is also played by the spatial localization of the metal-to-ligand charge-transfer excited states involved in the excitation-transfer process.**

## Introduction

The study of vectorial photoinduced processes is of great importance in large-size molecular assemblies that combine light-sensitive components and molecular functionalities for carrying out useful functions (artificial photochemical molecular devices, PMD[1]). Basically, these molecular assemblies can be obtained either by action of weak intermolecular forces[2] or by covalently linking molecular subunits.[3] The latter approach may lead to the building up of very large species where the spatial organization of the active components is provided by suitable bridging ligands, BLs. Thus, in the presence of properly arranged energy gradients for intercomponent energy- or electron-transfer steps, light absorption may drive the intercomponent processes sought for. For instance, bearing in mind the mimicry of natural systems, investigated systems include high-nuclearity light-harvesting assemblies[4] and di-, tri- or multi-partite systems for performing charge separation.[5] In all cases, the BL is expected not only to provide the spatial organization of the active components but also to be responsible for a certain amount of electronic interaction between them. Clearly, it is of importance to achieve control of the electronic factor in order to tune the various kinetic steps and ensure an efficient energy cascade.

Systems convenient for study are those in which the BLs contain a variable number of identical molecular subunits. This allows the construction of series of compounds in which (*i*) the distance between the active components is gradually varied and, as a consequence, (*ii*) the electronic interaction between them is modulated. We survey here results for relatively simple but geometrically well defined dinuclear species (Figs. 1 and 2).† These contain ruthenium- and osmium-based centres (the photochemically active units[6]), connected by bischelating BLs. In the cases illustrated here, the bridges contain (*i*) terpyridyl-[7,8] or bipyridylbenzene-like[9] chelating sites; the external ligand being 4′-*p*-tolylterpyridine in each case, and (*ii*) a spacer S that includes phenylene and bicyclooctane units. The employed BLs allow a high degree of geometric control of the dinuclear species because the metal centres are kept at fixed distances and are linearly aligned with BL.

We will only be concerned with intramolecular (intercomponent) processes because in dilute solutions (concentration *ca.* $10^{-5}$ mol $dm^{-3}$) intermolecular processes do not take place within the considered timescales. Recent reports deal with the behaviour of BLs which include spacers like cyanide,[10] ethenyl,[11] ethenylbenzene,[12] ethenylbicyclooctane,[13] ethynylbenzene,[14] ethynylbicyclooctane[15] and polyenes.[16] These BLs are capable of providing a high degree of rigidity to the dinuclear species. We will not concern ourselves with a close comparison between our and other results;[17–19] instead we will only briefly comment on problems arising with dinuclear complexes where the ruthenium- and osmium-based photoactive units employ a tris-bipyridine instead of the bis-terpyridine-type coordination discussed here.

## Synthetic strategies

The strategy employed for the synthesis of Ru–BL–Os dinuclear complexes starts with the synthesis of the symmetrical BLs (terpyridyl- or dipyridylbenzene-type ligand). Two successive steps with the suitable precursor (Ru or Os) afford the heterodinuclear complexes. In fact, the key step is the preparation of the mononuclear ruthenium complex bearing a free coordination site. The yield for this reaction can be optimized by using an excess of bridging ligand *vs.* the labile solvated ruthenium precursor, $[Ru(ttp)(Me_2CO)_3]^{2+}$. All the compounds reported here were isolated as $PF_6^-$ salts and characterized by $^1H$ NMR and FABMS.

The terpyridyl-type BLs were prepared by homocoupling of the appropriate terpyridine units either following the method reported by Constable and Ward,[20] or by the method of Kröhnke[21] in the case of the series with the tpy–$ph_n$–tpy BLs. Suzuki's cross-coupling procedure[22] was used for the bis-terpyridine BL incorporating the bicyclo[2.2.2]octane spacer, tpy–ph–bco–ph–tpy.

The bis-cyclometallating dipyridylbenzene BLs were also prepared by reductive coupling or Suzuki's cross-coupling reaction utilizing 1-bromo-3,5-dipyridylbenzene as the building block.[23] This latter compound was prepared by a palladium-catalysed C–C coupling procedure based on aromatic stannanes.[24]

## The experimental approach

In our systems, the lowest-lying excited energy levels centred on the ruthenium- and osmium-based active components are triplet states of metal-to-ligand charge-transfer (MLCT) nature.[6] These excited levels can be populated by absorption of visible light. In order to observe the Ru → Os electronic energy transfer we have performed both steady-state and time-resolved measurements.[7–9] Unfortunately, selective excitation of the donor is not possible and in the former case we have excited the Ru–BL–Os dinuclear species corresponding to an isosbestic point for the absorption of the ruthenium- and osmium-based

reference complexes. In this way 50% of the excited dinuclear species will have excitation centred on the ruthenium-based chromophore and 50% will have excitation centred on osmium-based chromophores [eqn. (1)].

$$2\ \text{Ru–BL–Os} + h\nu \rightarrow \text{*Ru–BL–Os} + \text{Ru–BL–*Os} \quad (1)$$

The ruthenium- and osmium-based luminescence spectra fall in different wavelength regions and with steady-state luminescence spectroscopy it has been possible to monitor the quenching of the ruthenium-based luminescence and sensitization of the osmium-based luminescence, owing to the Ru → Os transfer of the excitation energy [eqn. (2)].

$$\text{*Ru–BL–Os} \rightarrow \text{Ru–BL–*Os} \quad (2)$$

The same information has been obtained by employing time-resolved spectroscopic methods. In this case we have monitored the lifetime of the excited ruthenium-based unit (the energy donor), $\tau$, in the dinuclear complex, with respect to the lifetime of the excited reference compound, $\tau_o$, and derived the energy transfer rate, $k$ [eqn. (3)].

$$k = \frac{1}{\tau} - \frac{1}{\tau_0} \quad (3)$$

In some cases it has also been possible to observe time-resolved sensitization of the osmium-based component, followed by its decay.[8]

## Transfer of electronic excitation energy

From the spectroscopic properties of the ruthenium- and osmium-based components,[6–9] it is possible to see that the Ru → Os transfer of electronic excitation energy [eqn. (2)] is exoergonic. This transfer takes place according to the exchange (Dexter)[25] mechanism, whereas the Coulombic (Förster)[26] mechanism has been found to be negligible.[7,9]

The exchange mechanism may be conveniently visualized as a simultaneous double electron exchange between the donor and the acceptor partners.[27] On this basis, it is possible to follow a classical approach that parallels that for non-adiabatic electron transfer.[28] Thus, in the weak interaction limit between involved centres, the Dexter energy transfer can be cast in terms of thermodynamic quantities [eqn. (4)].

$$k = \nu \exp(-\Delta G^{\ddagger}/RT) \quad (4a)$$

$$\nu = \frac{2H^2}{h}\left(\frac{\pi^3}{\lambda RT}\right)^{1/2} \quad (4b)$$

$$\Delta G^{\ddagger} = \frac{\lambda}{4}\left(1 + \frac{\Delta G^0}{\lambda}\right)^2 \quad (4c)$$

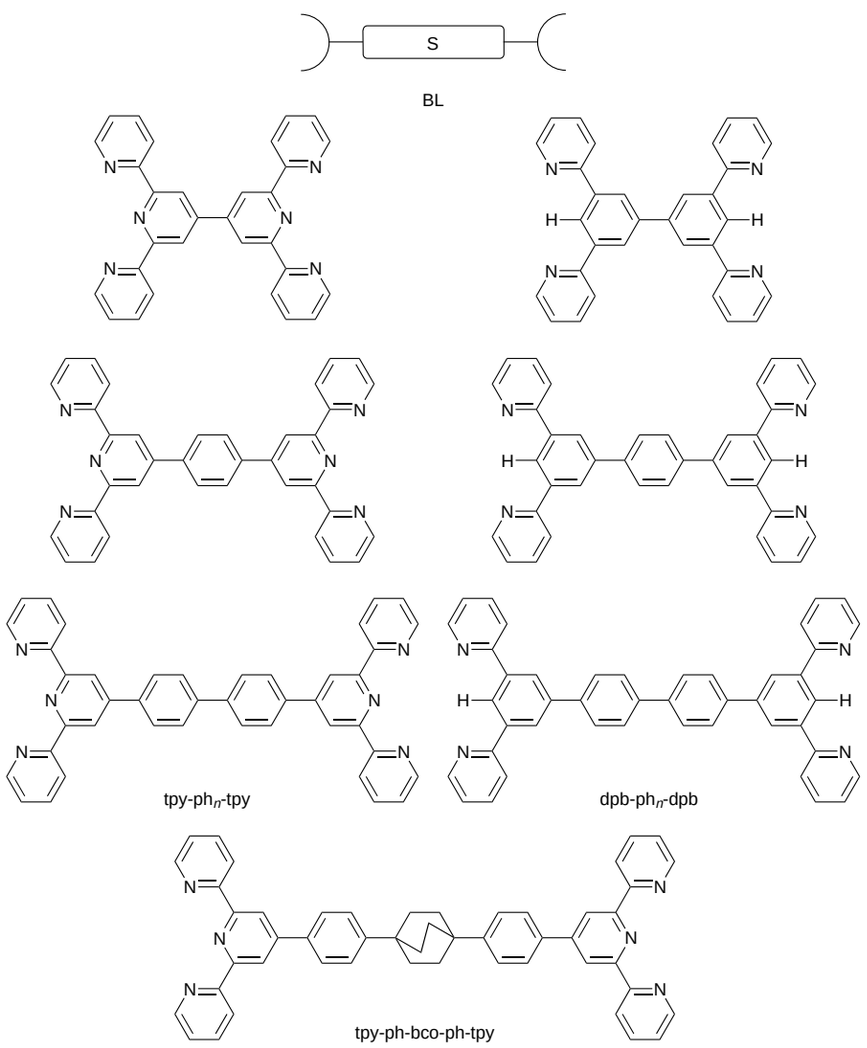



**Fig. 1** The employed bridging ligands, BLs: tpy–ph$_n$–tpy is a series of bis-tpy BLs containing phenylene spacers, $n$ = 0–2; dpb–ph$_n$–dpb is a series of bis-dipyridylbenzene BLs containing phenylene spacers, $n$ = 0–2 (in the Ru–BL–Os complexes, these latter BLs are dianions); and tpy–ph–bco–ph–tpy is a BL where a bicyclooctane unit has been interposed between two phenylene groups

In these equations ν is a frequency factor, λ is the reorganization energy, $H$ is the intercomponent electronic interaction energy and $\Delta G^{\ddagger}$ and $\Delta G^0$ are the activation energy and the free energy change, respectively, for the transfer of excitation energy. The free energy change is evaluated from the maxima of the emission bands of the donor and acceptor reference compounds, as measured at 77 K.[6–9] For the osmium-based complexes, the reorganization energy, $\lambda^{Os}$, may be estimated from the Stokes shift of absorption and emission spectra, $2\lambda^{Os}$ = SS.[29] For structurally similar ruthenium- and osmium-based complexes, it is usually assumed that $\lambda^{Ru} = \lambda^{Os}$.[9,13] Table 1 collects estimates for $\Delta G^0$ and λ values concerned with some structurally similar ruthenium- and osmium-based couples of reference complexes.

From Table 1, it can be seen that electronic excitation transfer between the selected donor and acceptor couples occurs under nearly activationless conditions since $\Delta G^0 \approx -\lambda$ [eqn. (4a–c)]. Thus the double electron exchange is expected to be governed by electronic factors. Under these conditions, the distance dependence of the interaction energy, $H$, can be described by eqn. (5).

$$H = H_0 \exp(-\beta d_{MM}) \quad (5)$$

where $d_{MM}$ indicates the distance between the metal centres, β is an attenuation factor and $H_0$ is the interaction energy at intercomponent orbital contact.

### Energy transfer in the series of complexes containing the tpy–ph$_n$–tpy BLs

Pertinent photophysical data for the [(ttp)Ru(tpy–ph$_n$–tpy)Os(tpy)]$^{4+}$ series of complexes are collected in Table 2. For these complexes, the $d_{MM}$ intermetal distance changes from 11 to 20 Å, depending on $n$. The excited Ru(ttp)$_2^{2+}$ chromophore exhibits a room-temperature lifetime $\tau$ = 0.95 ns in acetonitrile. Thus, because of the competition with intrinsic deactivation of the ruthenium-based component, only Ru → Os processess occurring with rates $k > 10^9$ s$^{-1}$ are expected to take place. Actually, the transfer of energy was found to occur with $k > 10^{10}$ s$^{-1}$ even for $n$ = 2 and one concludes that the polyphenylene bridge behaves as an extremely good energy transducer over the remarkable intermetal separation of 20 Å.[7] Interposition of a bicyclooctane (bco) unit in [(ttp)Ru(tpy–ph–bco–ph–tpy)Os(tpy)]$^{4+}$ leads to an intermetal separation of 24 Å, and results in a dramatic decrease of the energy transfer rate, $k = 4.4 \times 10^6$ s$^{-1}$ as measured at 77 K,[8] Table 2. To some extent, this effect is due to the increased intermetal distance, however a major role must be ascribed to the electronically insulating properties of the bco saturated group. This group breaks the ππ* frame of molecular orbitals centred on the phenylene units and only provides less efficient σσ* orbitals for the transmission of the intermetal interaction.

### Energy transfer in the series of complexes containing the dpb–ph$_n$–dpb biscyclometallating BLs

The dinuclear complexes that contain these dianionic BLs exhibit the same geometrical properties as the previous series, with distances between the metal centres ranging from 11 to 20 Å, depending on the size of the phenylene spacer.[9] For the cyclometallated series, the rate of Ru → Os energy transfer proved to be much lower than for the structurally identical series seen in the previous section. Thus, at room temperature no energy transfer was observed, despite the fact that the excited [Ru(ttp)(dpb)]$^+$ chromophore exhibits a lifetime $\tau_o$ = 4.5 ns in

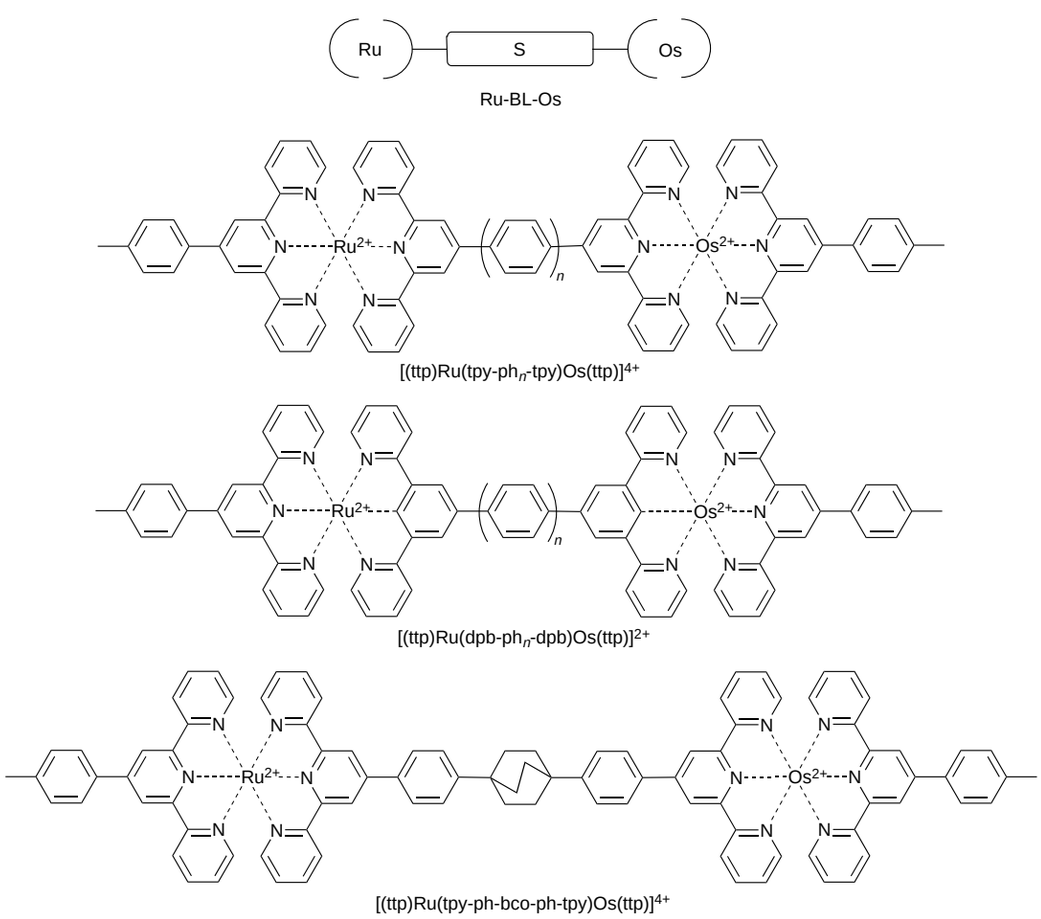



**Fig. 2** The Ru–BL–Os dinuclear complexes

acetonitrile, *i.e.* significantly longer than that of its $[Ru(ttp)_2]^{2+}$ homologue ($\tau_o$ = 0.95 ns). As a consequence, it was necessary to monitor the process at 77 K, where the intrinsic deactivation of the excited $[Ru(ttp)(dpb)]^+$ species is sufficiently slow, $\tau_o$ = 496 ns, Table 2. The Ru → Os energy- transfer rates for the $[(ttp)Ru(dpb–ph_n–dpb)Os(ttp)]^{2+}$ series were obtained both according to the steady-state approach outlined above (in this case we used 550 or 514 nm light excitation so as to excite 40 and 60% of the ruthenium- and osmium-based chromophores, respectively), and by time-resolved experiments [eqn. (3)]. As one can see from Table 2, the energy-transfer rate is affected to a large degree by the presence of the phenylene spacers and it was possible to draw a sizeable attenuation factor $\beta$ = 0.33 Å$^{-1}$ [eqn. (5)] for the phenylene units.[9]

**Table 1** Parameters for Ru → Os electronic energy transfer[a]

| Reference donor | Reference acceptor | $\Delta G^{0\,b}$/eV | $\lambda^c$/eV | Ref. |
|---|---|---|---|---|
| $[(ttp)Ru(ttp)]^{2+}$ | $[(ttp)Os(ttp)]^{2+}$ | −0.25 | 0.15 | 7 |
| $[(ttp)Ru(dpb)]^+$ | $[(ttp)Os(dpb)]^+$ | −0.18 | 0.15 | 9 |
| $[(bpy)_2Ru(bpy)]^{2+}$ | $[(bpy)_2Os(bpy)]^{2+}$ | −0.38 | 0.40 | 13 |

[a] See eqn. (4a–c), solvent is acetonitrile, butyronitrile or dmf–$CH_2Cl_2$ (9 : 1). [b] Estimated from luminescence band maxima of the reference donor and acceptor complexes at 77 K. [c] Estimated from Stokes shifts for the acceptor complex.

### Electronic properties of the chromophores in the $[(ttp)Ru(tpy–ph_n–tpy)Os(ttp)]^{4+}$ and $[(ttp)Ru(dpb–ph_n–dpb)Os(ttp)]^{2+}$ series

For the two series of complexes, which are geometrically identical (see Fig. 2), there is a difference of orders of magnitude in the Ru → Os energy-transfer rate, Table 2. As the energy-transfer step is nearly activationless in both cases, a minor rôle is played by nuclear (reorganization) factors [eqn. (4a–c)] whereas a possible explanation relies on a different role of the electronic factor.

A pictorial description of the energy-transfer process for the two smallest members of the two series is provided in Fig. 3. Here we emphasize the spatial properties of the ruthenium- and osmium-centred MLCT states involved in the excitation transfer. In particular (*a*) for the case of the tpy–tpy BL the MLCT excited states are described with the promoted electron residing on the tpy fragment of BL, and (*b*) for the dpb–$dpb^{2-}$ BL the promoted electron is placed on the external ttp ligand. Actually, in the former case the tpy–tpy bridging ligand is a better electron acceptor with respect to the ttp terminal ligand because of electronic delocalization[7] and in the latter case the ttp terminal ligand is a better electron acceptor than the dianionic dpb–$dpb^{2-}$ BL.[9]

Fig. 3 describes the Ru → Os simultaneous double electron exchange in terms of a metal–metal hole transfer (HT) and a ligand–ligand electron transfer (ET).[30] Clearly, HT occurs over identical distances in the two series (for the same *n*, $d_{HT} = d_{MM}$)

**Table 2** Photophysical results and Ru → Os energy-transfer rates[a]

| | | 293 K | | | 77 K | | | |
|---|---|---|---|---|---|---|---|---|
| | $d_{MM}$/Å | $\tau_0{}^b$/ns | $\tau^b$/ns | $k^c$/s$^{-1}$ | $\tau_o{}^b$/ns | $\tau^b$/ns | $k^c$/s$^{-1}$ | Ref. |
| $[(ttp)Ru(ttp)]^{2+}$ | | 0.95 | | | 9100 | | | 7 |
| $[(ttp)Ru(tpy–tpy)Os(ttp)]^{4+}$ | 11 | | < 0.03 | > $10^{10}$ | | < 0.03 | > $10^{10}$ | 7 |
| $[(ttp)Ru(tpy–ph–tpy)Os(ttp)]^{4+}$ | 15.5 | | < 0.03 | > $10^{10}$ | | < 0.03 | > $10^{10}$ | 7 |
| $[(ttp)Ru(tpy–ph–ph–tpy)Os(ttp)]^{4+}$ | 20 | | < 0.03 | > $10^{10}$ | | < 0.03 | > $10^{10}$ | 7 |
| $[(ttp)Ru(tpy–ph–bco–ph–tpy)Os(ttp)]^{4+}$ | 24 | | 0.95 | —[d] | | 220 | $4.4 \times 10^6$ | 8 |
| $[(ttp)Ru(dpb)]^+$ | | 4.5 | | | 496 | | | |
| $[(ttp)Ru(dpb–dpb)Os(ttp)]^{2+}$ | 11 | | 0.35 | $2.6 \times 10^9$ | | 0.72 | $1.4 \times 10^9$ | 9 |
| $[(ttp)Ru(dpb–ph–dpb)Os(ttp)]^{2+}$ | 15.5 | | 3.5 | $6.3 \times 10^7$ | | 42 | $2.2 \times 10^7$ | 9 |
| $[(ttp)Ru(dpb–ph–ph–dpb)Os(ttp)]^{2+}$ | 20 | | 4.9 | $< 2.2 \times 10^7$ | | 178 | $3.6 \times 10^6$ | 9 |

[a] Solvent is acetonitrile, butyronitrile or dmf–$CH_2Cl_2$ (9 : 1). [b] Lifetimes of the ruthenium-based chromophore. [c] $k = (1/\tau) - (1/\tau_o)$. [d] No energy transfer takes place at room temperature.

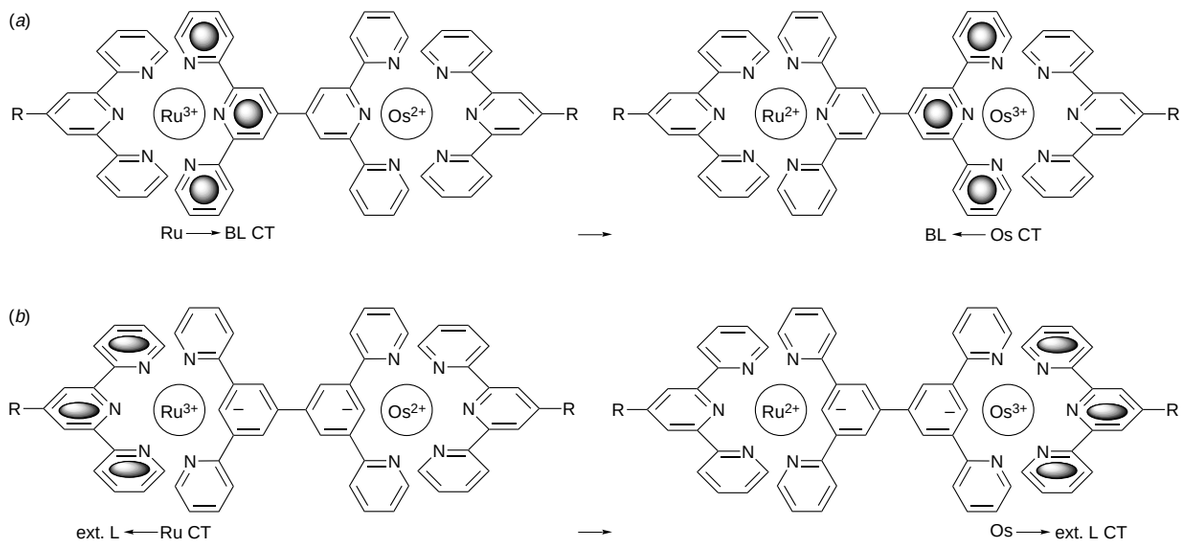



**Fig. 3** Spatial properties of the MLCT excited states involved in the Ru → Os excitation-transfer step for $[(ttp)Ru(tpy–tpy)Os(ttp)]^{4+}$ (*a*) and $[(ttp)Ru(dpb–dpb)Os(ttp)]^{2+}$ (*b*); R = 4′-*p*-tolyl. The shaded areas indicate localization regions for the promoted electron of the MLCT excited state: M → BL (*a*) and M → external L (*b*).

and is thought to involve the available highest- occupied molecular orbitals (HOMOs) of the bridge.[31] In contrast, ET involves the chelating sites of BL for case (*a*), $d_{ET} < d_{MM}$, and the external ligands for case (*b*), $d_{ET} > d_{MM}$. Thus ET occurs in remarkably different conditions in the two series, both in terms of intercentre spatial separation and of electronic coupling. The latter point may be appreciated by noting that around each metal centre the external ligand system is arranged perpendicularly with respect to the chelating site belonging to the bridge (Fig. 3). Given that ET occurs by involving the available lowest $\pi^*$ unoccupied molecular orbitals (LUMOs, which are ligand-centred), the electron travelling from one external ligand to the opposite external ligand will cross at least two regions where the $\pi$ orbital systems are perpendicularly arranged. In this case therefore, one expects a low electronic coupling for the ligand–ligand ET. In conclusion, it seems possible that the difference in energy-transfer rates between the two series is mainly ascribable to a different rôle of the electronic factor for the two cases.

## Future developments

One limitation in the development of larger species for the study of long-range vectorial energy transfer is related to the lifetime of the excited donor, the ruthenium-based chromophore. This happens because the energy-transfer process, which becomes slower and slower with increasing size of the bridge, is in direct competition with intrinsic deactivation of the excited donor. Actually, long-lived ruthenium-based chromophores with the tris-bpy coordination ($\tau \approx$ hundreds of ns)[6] are employed in building dinuclear and higher nuclearity complexes.[30,32] Unfortunately, this latter type of coordination results in some geometric disadvantages with respect to that based on the bis-tpy coordination. For the purpose of illustration, Fig. 4 depicts some geometrical properties of such a complex, $[(bpy)_2Ru(bpy–S–bpy)Os(bpy)_2]^{4+}$, where S includes double bonds and a bicyclooctane unit.[13] Because of the properties of the tris-bpy coordination, the bpy–S–bpy BL is not linearly aligned with the metal centres (and with the peripheral ligands). In addition, because of rotations around single bonds, the intermetal separation is 17 Å as an average, with an uncertainty estimated at ±1 Å.

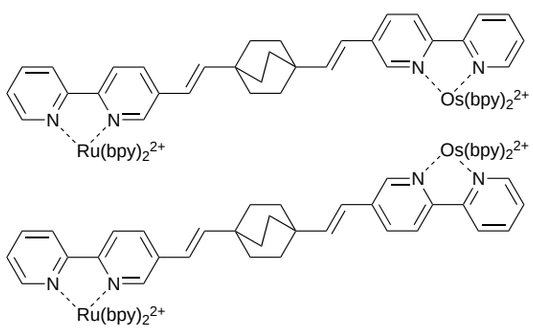



**Fig. 4** Two possible nuclear configurations resulting from the use of the tris-bpy coordination in a $[(bpy)_2Ru(bpy–S–bpy)Os(bpy)_2]^{4+}$ dinuclear complex: there is no linear alignment along the M–BL–M axis and the intermetal distance is subject to some uncertainty

For the building up of new dinuclear complexes there may be different strategies. One useful approach is to combine the electronic properties of the tris-bpy arrangement and the geometrical properties of a perfectly aligned, more symmetric bridge. An example of such type of approach is illustrated in Fig. 5. In this species, the $Ru(bpy)_2(phen)^{2+}$ chromophore exhibits a long-lived excitation, $\tau$ = 145 ns, and the phen–adamantane–phen BL ensures the sought-for alignment of the various components, with a fixed intermetal separation of 21 Å.[33]

Another useful approach may be based on the improvement of the spectroscopic properties of Ru–tpy type fragments by appending suitable groups at the 4′ position of the external tpy ligand. Actually, by using both electron-withdrawing and attracting appended groups[34] or groups that affect electronic delocalization over the tpy fragment[14] it has been possible to obtain long-lived Ru–tpy type units. Also, the use of protonable appended sites to the Ru–tpy chromophore may be of interest.[35] Literature examples of these possible approaches are illustrated in Fig. 6.

## Conclusions

In order to develop molecular assemblies it is of obvious importance to gain control of the energetic and geometric factors. Our studies show that, for assemblies incorporating ruthenium– and osmium–terpyridine type and related cyclometallated analogues, the additional possibility exists of a fine

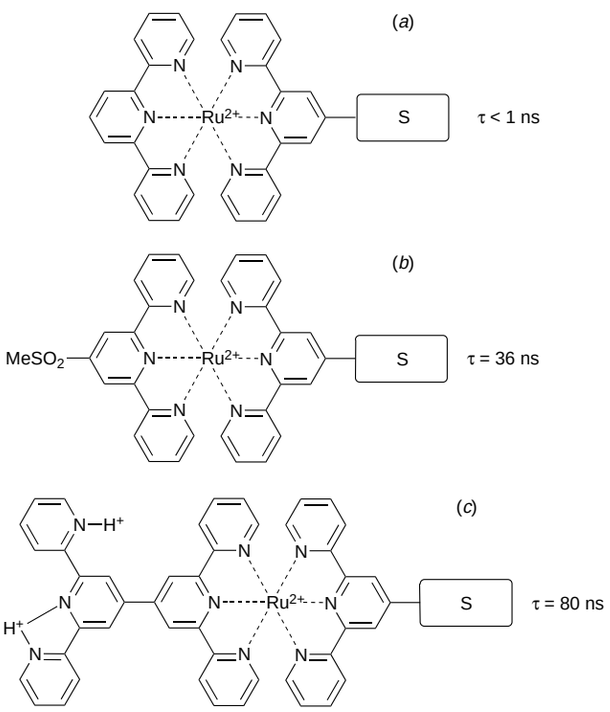



**Fig. 6** Perturbation of the basic $Ru(tpy)_2^{2+}$ chromophore (*a*),[7] may result in long-lived excited states centred on the ruthenium-based unit: (*b*) ref. 34 and (*c*) ref. 35. The diagrams show various Ru–tpy chromophores linked to a spacer for incorporation in dinuclear complexes.

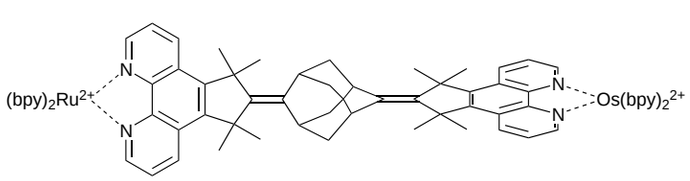



**Fig. 5** A linear alignment of the metals and the BL results from the use of the phen–adamantane–phen BL;[33] the metal centres are at a fixed separation of 21 Å

modulation of photoinduced intermetal processes which is based on control of the spatial distribution of the metal-to-ligand charge-transfer excited states involved in the processes. We have performed our studies by employing cyclometallating analogues of the terpyridine ligand but a similar approach is likely to work with other types of ligand fragments. In principle, our results indicate ways for substantial manipulation of rates of energy transduction along molecular rods.


### Acknowledgements

This work was supported by the Progetto Strategico Tecnologie Innovative of CNR. A NATO grant (No. 920446, Supramolecular Chemistry) is acknowledged. Thanks are also due to A. Sour, S. Chodorowski-Kimmes and M. Beley.



**Francesco Barigelletti was born in 1944. He obtained his 'Laurea' in Chemistry in 1970 at the Faculty of Science, University of Bologna. After a postdoctoral fellowship spent in the Photochemical and Radiation Chemistry Laboratory (later, FRAE Institute) that was established a few years before and leave for a draft in the Army, he joined the National Research Council of Italy in 1973. His current interests include the photochemistry and photophysics of molecular and supramolecular systems for light-energy conversion and storage.**

**Lucia Flamigni obtained her 'Laurea' in Chemistry in 1973 at the University of Bologna. She had postdoctoral experience at the Chemistry Department of the University of Manchester and at the Center for Fast Kinetic Research, University of Texas at Austin. She has been researcher at the FRAE Institute since 1982. Her current interests include photoreactivity of dyes in organized media and photoinduced energy and electron transfer in molecular assemblies containing ruthenium and osmium centres.**

**Jean-Paul Collin was born in 1945 in Metz. After his PhD in electrochemistry with Professor J. P. Schwing at the Louis Pasteur University, Strasbourg, he did postdoctoral work with Professor Jean-Marie Lehn on water photolysis. He is now a CNRS research director. He joined Dr Jean-Pierre Sauvage's group in 1983 and his present research field concerns photoinduced charge separation in multicomponent molecular systems.**

**Jean-Pierre Sauvage was born in 1944 in Paris. After studying at Strasbourg University, he did his PhD with J.-M. Lehn on cryptates and spent some time as a post-doc with M. L. H. Green at Oxford, UK. He is now a research director (CNRS) at the Faculty of Chemistry. His main scientific interests range from chemical topology (catenanes and knots) to models of the photosynthetic reaction centres and one-dimensional multicomponent transition complexes.**


### Footnote

† Abbreviations used: tpy = 2,2′:6′,2″-terpyridine, Hdpb = di-2-pyridyl-1,3-benzene, bpy = 2,2′-bipyridine, phen = 1,10-phenanthroline, ph = phenylene unit, bco = bicyclo[2.2.2]octane unit, BL = bridging ligand, ttp = 4′-*p*-tolyl-2,2′:6′,2″-terpyridine, S = spacer, *i.e.* unit(s) included in a BL, ext. L = external or peripheral or terminal ligand, Ru–BL–Os = dinuclear complex.

### References


1 V. Balzani and F. Scandola, *Supramolecular Photochemistry*, Horwood, Chichester, UK, 1991, ch. 12.
2 J.-M. Lehn, *Supramolecular Chemistry*, VCH, Weinheim, 1995.
3 A representative, but not exhaustive, collection of contributing lines of work can be found in *Supramolecular Chemistry*, ed. V. Balzani and L. De Cola, Kluwer, Dordrecht, 1992.
4 F. Denti, S. Campagna and V. Balzani, in *Mesomolecules. From molecules to materials*, ed. G. D. Mendenhall, A. Greenberg and J. F. Liebaman, Chapman and Hall, New York, 1995, ch. 3.
5 Comprehensive reviews in this field can be found in special issues of *Tetrahedron*, 1989, **45**; and *Top. Curr. Chem.*, 1990, **156**; 1990, **158**; 1991, **159**; no attempt has been made here to cover more recent literature.
6 T. J. Meyer, *Pure Appl. Chem.*, 1986, **58**, 1193; A. Juris, V. Balzani, F. Barigelletti, S. Campagna, P. Belser and A. von Zelewsky, *Coord. Chem. Rev.*, 1988, **84**, 85; J.-P. Sauvage, J.-P. Collin, J.-C. Chambron, S. Guillerez, C. Coudret, V. Balzani, F. Barigelletti, L. De Cola and L. Flamigni, *Chem. Rev.*, 1994, **94**, 993.
7 F. Barigelletti, L. Flamigni, V. Balzani, J.-P. Collin, J.-P. Sauvage, A. Sour, E. D. Constable and A. M. W. Cargill Thompson, *J. Am. Chem. Soc.*, 1994, **116**, 7692.
8 F. Barigelletti, L. Flamigni, V. Balzani, J.-P. Collin, J.-P. Sauvage and A. Sour, *New J. Chem.*, 1995, **19**, 793.
9 F. Barigelletti, L. Flamigni, M. Guardigli, A. Juris, M. Beley, S. Chodorowski-Kimmes, J.-P. Collin and J.-P. Sauvage, *Inorg. Chem.*, 1996, **35**, 136; M. Beley, S. Chodorowski-Kimmes, J.-P. Collin, J.-P. Sauvage, L. Flamigni and F. Barigelletti, *Inorg. Chem.*, 1994, **33**, 2543.
10 F. Scandola, R. Argazzi, C. A. Bignozzi and M. T. Indelli, *Photochem. Photobiol. A: Chem.*, 1994, **82**, 191.
11 S. Boyde, G. F. Strouse, W. E. Jones Jr. and T. J. Meyer, *J. Am. Chem. Soc.*, 1990, **112**, 7395.
12 J. R. Show, R. T. Webb and R. H. Schmehl, *J. Am. Chem. Soc.*, 1990, **112**, 11 117.
13 L. De Cola, V. Balzani, F. Barigelletti, L. Flamigni, P. Belser, A. von Zelewsky, M. Franck and F. Vögtle, *Inorg. Chem.*, 1993, **32**, 5228.
14 A. C. Benniston, V. Groosshenny, A. Harriman and R. Ziessel, *Angew. Chem., Int. Ed. Engl.*, 1994, **33**, 1884.
15 F. Vögtle, M. Franck, M. Nieger, P. Belser, A. von Zelewsky, V. Balzani, F. Barigelletti, L. De Cola and L. Flamigni, *Angew. Chem., Int. Ed. Engl.*, 1993, **32**, 1643.
16 A. C. Benniston, V. Goulle, A. Hariman, J.-M. Lehn and B. Marczinke, *J. Phys. Chem.*, 1994, **98**, 7798.
17 For the development of large-size molecular wires based on ethynyl-containing bridges, see V. Groosshenny, A. Harriman and R. Ziessel, *Angew. Chem., Int. Ed. Engl.*, 1995, **34**, 1100; 2705; V. Groosshenny, A. Harriman, M. Hissler and R. Ziessel, *Platinum Met. Rev.*, 1996, **40**, 26.
18 A rich metallosupramolecular chemistry arises from the use of various oligopyridines, see E. C. Constable and A. M. W. Cargill Thompson, *J. Chem. Soc., Dalton Trans.*, 1992, 3467; E. C. Constable, *Prog. Inorg. Chem.*, 1994, **42**, 67; E. C. Constable and A. M. W. Cargill Thompson, *New J. Chem.*, 1996, **20**, 65.
19 Linear polynuclear complexes can also contain cyano-bridged *trans*-tetrakis-pyridine metal units, B. J. Coe, T. J. Meyer and P. S. White, *Inorg. Chem.*, 1995, **34**, 3600.
20 E. C. Constable and M. D. Ward, *J. Chem. Soc., Dalton Trans.*, 1990, 1405.
21 F. Krönke, *Synthesis*, 1975, 1.
22 N. Miyama, T. Yanagi and A Suzuki, *Synth. Commun.*, 1981, **11**, 513.
23 M. Beley, S. Chodorowsky, J.-P. Collin and J.-P. Sauvage, *Tetrahedron Lett.*, 1993, **34**, 2933.
24 J. K. Stille, *Angew. Chem., Int. Ed. Engl.*, 1986, **25**, 508.
25 D. L. Dexter, *J. Chem. Phys.*, 1993, **21**, 836.
26 Th. H. Förster, *Discuss. Faraday Soc.*, 1959, **27**, 7.
27 P. Closs and J. R. Miller, *Science*, 1989, **244**, 35.
28 V. Balzani, F. Bolletta and F. Scandola, *J. Am. Chem. Soc.*, 1980, **102**, 2552; F. Scandola and V. Balzani, *J. Chem. Educ.*, 1983, **60**, 814.
29 N. Sutin, *Acc. Chem. Res.*, 1982, **15**, 275.
30 F. Scandola, M. T. Indelli, C. Chiorboli and C. A. Bignozzi, *Top. Curr. Chem.*, 1990, **158**, 73.
31 From intervalence studies of homometallic dinuclear complexes it has been found that there is a strong intermetal electronic communication when the coordination environment includes cyclometallating positions, see M. Beley, J.-P. Collin and J.-P. Sauvage, *Inorg. Chem.*, 1993, 32, 4539; E. C. Constable, A. M. W. Cargill Thompson and S. Greulich, *J. Chem. Soc., Chem. Commun.*, 1993, 1444.
32 V. Balzani, A. Juris, M. Venturi, S. Campagna and S. Serroni, *Chem. Rev.*, 1996, **96**, 759.
33 V. Balzani, F. Barigelletti, P. Belser, S. Bernhard, L. De Cola and L. Flamigni, *J. Phys. Chem.*, 1996, **100**, 16 786.
34 M. Maestri, N. Armaroli, V. Balzani, E. C. Constable and A. M. W. Cargill Thompson, *Inorg. Chem.*, 1995, **34**, 2759.
35 F. Barigelletti, L. Flamigni, M. Guardigli, J.-P. Sauvage, J.-P. Collin and A. Sour, *Chem. Commun.*, 1996, 1329.



*6/03623F*

# Diversity of linking modes by *N*,*N*′-*p*-phenylenedimethylenebis(pyridin-4-one) [*p*-XBP4] in the novel 'linked lantern' framework complex $\{[Nd_2(p\text{-XBP4})_6(H_2O)_4](p\text{-XBP4})(H_2O)_3(ClO_4)_6\}_n$

**David M. L. Goodgame, Stephan Menzer, Amanda M. Smith and David J. Williams**

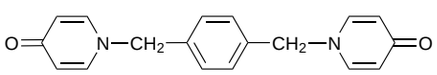
*Department of Chemistry, Imperial College of Science, Technology and Medicine, London, UK SW7 2AY*

**The title compound has a complex framework structure in which pairs of Nd atoms are linked by four *p*-XBP4 ligands to form 'lanterns' which are further connected by interwoven Nd–(*p*-XBP4)–Nd bridges, and yet again by non-coordinated *p*-XBP4 molecules hydrogen bonded to aqua ligands on the Nd centres.**

The field of supramolecular chemistry has undergone a veritable explosion of activity opening up a wide diversity of themes and applications.[1] A particularly interesting topic within this field is the use of the 'self-assembly' process for the formation of, for example, macrocycles, catenanes and cages and the range of approaches for achieving these objectives has very recently been reviewed.[2] We have shown that a particularly versatile ligand for forming such materials is *N*,*N*′-*p*-phenylenedimethylenebis(pyridin-4-one) (**I**, *p*-XBP4). It has the ability to form interwoven metallomacrocyclic networks[3,4] and also to bring pairs of metal ions into close proximity within these arrays by forming μ-O atom bridges.[3] Further studies with **I** have produced an extensive range of lanthanide (Ln) compounds with unusual stoichiometries;[5] examples include $Ln_4(p\text{-XBP4})_7(NO_3)_{12}\cdot 4H_2O$ (Ln = La–Eu), $Ln_2(p\text{-XBP4})_3(NO_3)_6\cdot 2H_2O$ (Ln = Gd–Yb) and $Ln_2(p\text{-XBP4})_7(ClO_4)_6\cdot 7H_2O$ (Ln = La, Nd, Sm, Gd). In view of our previous observations of the propensity for **I** to generate novel structures with transition-metal ions, the non-integral stoichiometries of the lanthanide compounds pointed to the formation of yet further types of framework arrays. Full X-ray characterisation of most of these compounds has been hindered by their formation only as poorly crystalline powders. However X-ray quality crystals have been obtained for $Nd_2(p\text{-XBP4})_7(ClO_4)_6\cdot 7H_2O$ **1**,† and the structural study‡ of this reveals not only a particularly novel framework array but also a new type of networking role for **I**.

This analysis reveals that each neodymium atom is eight coordinate (Fig. 1) being bound to one oxygen atom from each of six different *p*-XBP4 ligands [Nd–O in the range 2.373(4)–2.433(4) Å] and to two aqua ligands with Nd–O(aqua) distances of 2.551(4) and 2.639(4) Å. The coordination geometry around each neodymium atom is essentially bicapped trigonal prismatic with O(21) and O(91) as the capping atoms. There are four different *p*-XBP4 ligand geometries (A, B, C and D)§ in the structure, and, although all the *p*-XBP4 ligands act as bridges, they do so in three quite different ways.

Pairs of adjacent neodymium centres are directly bridged by four *p*-XBP4 ligands, two each of types A and B (shown in red in Fig. 2), forming a 'pumpkin'- or 'lantern'-like oblate spheroidal 'box', with a Nd···Nd separation of 11.9 Å and with distances between the centroids of the opposite pairs of *p*-$C_6H_4$ rings of *ca*. 14 Å, thereby producing an effective cage volume




**I** (*p*-XBP4)

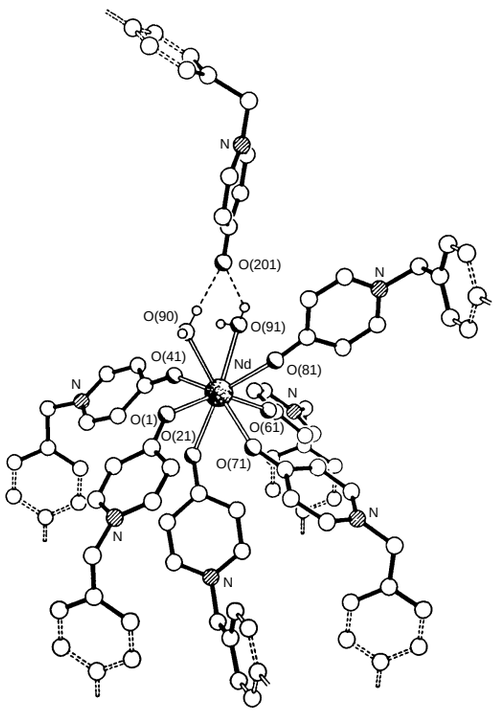



**Fig. 1** The neodymium coordination environment in **1** showing also the hydrogen bonding of part of a D-type *p*-XBP4 molecule to the aqua ligands

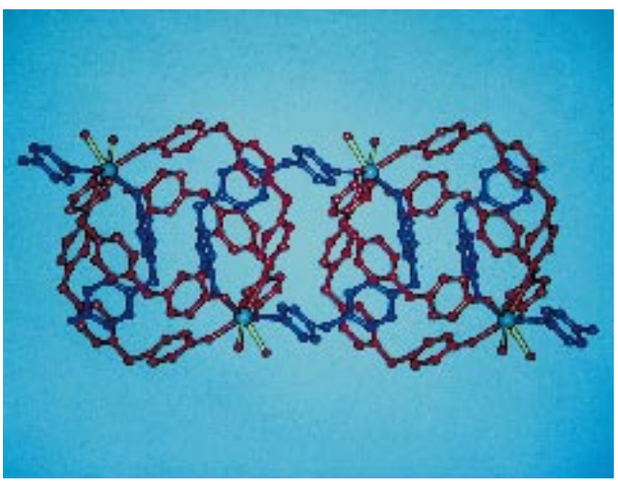


**Fig. 2** Part of one of the covalently linked chains of 'lanterns' formed by **1** in the solid state. Ligands of types A and B are shown in red and the interpenetrating C-type linkages are shown in blue.

of *ca*. 1260 Å$^3$. The 'surfaces' of these globular lanterns comprise sets of 34-membered metallocycles which are sufficiently large to permit the interweaving capability of **I** to operate. Pairs of type C ligands (shown in blue in Fig. 2) are initially directed into the central cavity but then fold and pass through the centres of the rings that form the opposite lantern faces and, by interpenetrating adjacent lanterns, form a further set of 34-membered macrocycles and link them into chains.

Pyridinone rings from the type C ligands form π–π stacked pairs within the central cavity of each lantern (Fig. 2) (mean interplanar separation of 3.37 Å and centroid–centroid distance of 3.66 Å). There is a further strong π–π interaction between pairs of pyridinone rings of type B ligands of adjacent lanterns (mean interplanar separation of 3.34 Å and centroid–centroid distance of 3.73 Å).

The solid-state structure of **1** also reveals a further type of bridging role for the *p*-XBP4 molecule not seen hitherto. The chains of lanterns are connected into sheets by cross-struts comprising non-coordinated *p*-XBP4 molecules of type D *via* strong hydrogen bonds between each of the carbonyl oxygen atoms and the pairs of aqua ligands bonded to each neodymium centre (Fig. 3).¶ The resulting voids within each sheet, *i.e.* between the D-type molecules, are occupied by the perchlorate ions, water molecules of solvation and the lantern-like spheroids of offset adjacent sheets.

The 'superstructure' described above demonstrates the ability of the *p*-XBP4 molecule to act, not only as a unit for the self-assembly of complex networks by virtue of its versatile ligand coordination behaviour, but also as an efficient hydrogen-bonding acceptor, thereby extending its crystal engineering potential.

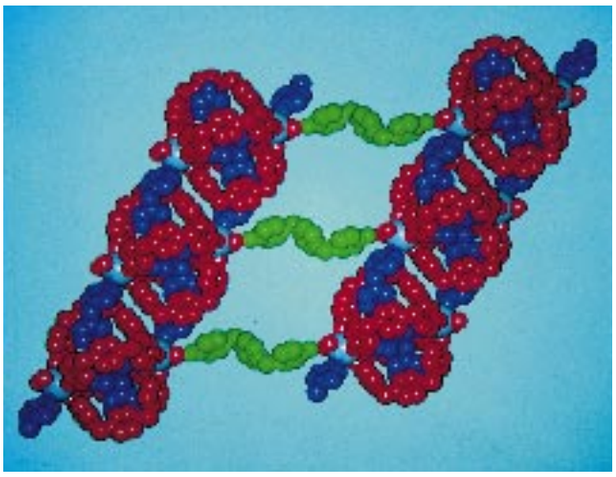


**Fig. 3** The linking of adjacent chains *via* hydrogen bonds from the aqua ligands to D-type *p*-XBP4 molecules (shown in green)

We thank the EPSRC for a Research Studentship (to A. M. S.), the BBSRC for a postdoctoral fellowship (to S. M.) and the Wolfson Foundation for equipment.

## Footnotes

† Pale mauve crystals of **1** were obtained in 43% yield by slow (2 weeks) evaporation of a solution of $Nd(ClO_4)_3{\cdot}6H_2O$ (0.04 mmol) and **I**·$4H_2O$ (0.2 mmol) in a mixture of methanol (6 cm$^3$), acetonitrile (4 cm$^3$) and water (1 cm$^3$). Satisfactory analyses were obtained.

‡ *Crystal data*: $C_{63}H_{63}Cl_3N_7NdO_{22.5}$ **1**, crystal dimensions 0.10 × 0.16 × 0.17 mm, triclinic, space group $P\bar{1}$, $a$ = 14.083(2), $b$ = 15.754(2), $c$ = 17.519(2) Å, α = 67.01(1), β = 73.51(1), γ = 69.08(1)°, $U$ = 3294.8(6) Å$^3$, $Z$ = 2, $M$ = 1528.8, $D_c$ = 1.541 g cm$^{-3}$, λ = 0.710 73 Å, μ(Mo-Kα) = 0.993 mm$^{-1}$, $T$ = 293 K, Siemens P4/PC diffractometer, graphite-monochromated Mo-Kα radiation, ω scans. The structure was solved by the heavy-atom method and was refined anisotropically, on $F^2$ data, using the SHELXTL program package (version 5.03)[6] to $R_1$ = 0.0454, $wR_2$ = 0.1168 for 7016 independent observed reflections [$|F_o| > 4\sigma(|F_o|)$, 2θ = 3.5–45.0°]. Atomic coordinates, bond lengths and angles, and thermal parameters have been deposited at the Cambridge Crystallographic Data Centre (CCDC). See Information for Authors, Issue No. 1. Any request to the CCDC for this material should quote the full literature citation and the reference number 182/351.

§ In type A ligands, the pyridinone rings have a skewed open-book conformation with respect to the central *p*-$C_6H_4$ rings, whereas in type B the geometry is closer to orthogonal. The type C ligands have their pyridinone rings oriented so that one is essentially orthogonal to the central *p*-$C_6H_4$ ring whilst the other is in an open-book conformation. Type D molecules have their pyridinone rings in an *anti* open-book arrangement.

¶ The O(aqua)···O(*p*-XBP4) distances are 2.65 and 2.70 Å and the O···O(*p*-XBP4)···O angle [O(90)···O(201)···O(91)] is 67.6°, with associated H···O and O–H···O distances and angles of 1.76 Å, 174° and 1.92 Å, 144° respectively.

## References

1 An extensive and thorough overview is provided by: *Comprehensive Supramolecular Chemistry*, ed. J. L. Atwood, J. E. D. Davies, D. D. MacNicol and F. Vögtle, Elsevier Science, 1996.
2 See *e.g.*: M. Fujita, ch. 7 of vol. 9 of ref. 1.
3 D. M. L. Goodgame, S. Menzer, A. M. Smith and D. J. Williams, *J. Chem. Soc., Chem. Commun*., 1995, 1975 and references therein.
4 D. M. L. Goodgame, S. Menzer, A. M. Smith and D. J. Williams, *Angew. Chem*., 1995, **107**, 605; *Angew. Chem., Int. Ed. Engl*., 1995, **34**, 574.
5 A. M. Smith, PhD Thesis, London University, 1995.
6 G. M. Sheldrick, SHELXTL version 5.03, University of Göttingen, 1995.

*Received, 15th November 1996; Com. 6/07764A*

# A tetranuclear neodymium cage which tightly binds sodium carbonate molecules

**Glen B. Deacon,*[a] Tiecheng Feng,[a] David C. R. Hockless,[b] Peter C. Junk,[a] Brian W. Skelton[b] and Allan H. White[b]**

[a] *Chemistry Department, Monash University, Clayton, Victoria 3168, Australia*
[b] *Department of Chemistry, University of Western Australia, Nedlands, WA 6907, Australia*

**The complexes $[Na_2Nd_4L_4(CO_3)L'_4]$ [$H_3L$ = (*o*-$HOC_6H_4CH{=}NCH_2)_2CHOH$, L′ = tetrahydrofuran or $L'_2$ = 1,2-dimethoxyethane] have novel cage structures in which $Nd_4O_{12}N_8$ bowl-shaped frameworks of $Nd_4L_4$ molecules entrap solvated $Na_2CO_3$ molecules within the cavity of the bowl.**

Lanthanoid alkoxide cage complexes are of great interest,[1] but aryloxide analogues are much less common. Some rare examples are based on the 4-methylphenoxide ion and include $[Na_3La_2(\mu_4\text{-}OAr)_3(\mu\text{-}OAr)_6(thf)_5]$, (thf = tetrahydrofuran, Ar = 4-$MeC_6H_4$).[2] Cage complexes have the capacity to act as hosts for a variety of guest species,[3] and there is a current focus on incorporation of anionic species, *e.g.* environmentally important contaminants such as phosphate.[4] The Schiff-base ligand (*o*-$HOC_6H_4CH{=}NCH_2)_2CHOH$ ($H_3L$), which is known to give bimetallics for d-block metals,[5] has the potential, on deprotonation to $L^{3-}$, to form mixed aryloxo–alkoxo cages with lanthanoid metals. We now report the synthesis and structure of a tetranuclear neodymium cage based on this ligand. This host tightly encapsulates solvated sodium carbonate within the cavity of the cluster, and a novel binding mode of $CO_3^{2-}$ is observed.

Reaction of anhydrous $NdCl_3$, $H_3L$, sodium amide and sodium carbonate in thf at room temperature (Scheme 1) resulted in triple deprotonation of the ligand and gave a blue solution from which was isolated air- and moisture-sensitive pink $[Na_2Nd_4L_4(CO_3)(thf)_4]$ **1**, in good yield.† Recrystallisation of **1** from 1,2-dimethoxyethane (dme) yielded the air- and moisture-sensitive pink complex $[Na_2Nd_4L_4(CO_3)(dme)_2]\cdot 1.5$ dme, **2**·1.5 dme.†

A synthesis in the absence of sodium carbonate gave a product with analytical composition $NdL(thf)_2$ which could not be crystallized in a form suitable for X-ray studies nor were the solubility properties suitable for characterization in solution.

The molecular structures of both **1** and **2** (Fig. 1), established by X-ray crystallography,‡ feature a tetranuclear, bowl-shaped, cage $[Nd_4L_4]$ with quasi-twofold symmetry. Within the cavity of the cage resides a multiply anchored, solvated sodium carbonate molecule, $Na_2CO_3L'_4$ (L′ = thf or $L'_2$ = dme). One carbonate oxygen bridges two sodium atoms, whilst each of the others bridges one sodium and two neodymium atoms. The carbonate coordination appears unique in combining $\mu_6$-bridging with chelation to two of the bridged atoms (**I**). This contrasts the known simple $\mu_6$-bridging[6] for the unique $CO_3^{2-}$ in the centre of $[(VO)_6(\mu_6\text{-}CO_3)(\mu\text{-}CO_3)_3(OH)_9]^{5-}$, and the recently observed $\mu_9$-bridging in a lithium siloxane complex.[7] Each sodium is five-coordinate, being bound not only by the chelating carbonate and thf or dme, but also by a bridging aryloxide oxygen of the cage (see below). Thus, sodium carbonate is securely bonded to the cage.

The $Nd_4L_4$ cage contains square-antiprismatic eight-coordinate neodymium atoms with Nd(1) and Nd(1a) of **2** different from Nd(1′) and Nd(1a′) (Fig. 1). The former are coordinated by two imide nitrogens, one $\eta^1$- and two $\mu$-aryloxide (NdONd and NdONa) oxygens, one $\mu_3$- and one $\mu$-alkoxide oxygen, and a $\mu_3$-carbonate oxygen ($ONd_2Na$). By contrast, the latter pair are

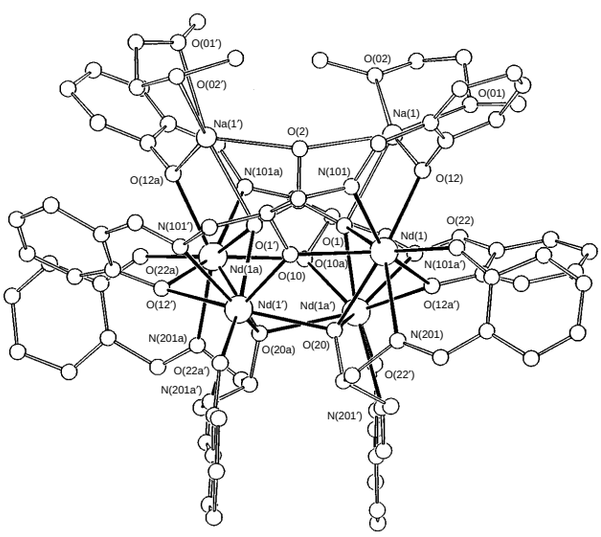
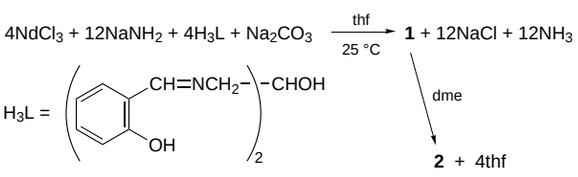
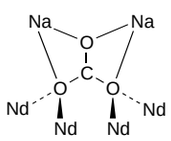



**Fig. 1** Molecular projection of $[Na_2Nd_4L_4(CO_3)(dme)_2]$ **2** normal to the quasi-twofold axis; hydrogen atoms have been omitted for clarity. Selected bond distances (Å): Nd–($\eta^1$-OAr), Nd(1)–O(22) 2.24(3), Nd(1a)–O(22a) 2.32(3), Nd(1′)–O(22a′) 2.35(2), Nd(1a′)–O(22′) 2.22(2); M–($\mu$-OAr), Nd(1)–O(12) 2.26(1), Nd(1)–O(12a′) 2.57(2), Nd(1a)–O(12a) 2.34(1), Nd(1a)–O(12′) 2.61(2), Nd(1′)–O(12′) 2.42(2), Nd(1a′)–O(12a′) 2.39(2), Na(1)–O(12) 2.34(3), Na(1′)–O(12a) 2.25(3); M–($\mu$-OCH), Nd(1)–O(10) 2.40(1), Nd(1a)–O(10a) 2.34(2), Nd(1′)–O(10) 2.36(2), Nd(1a′)–O(10a) 2.43(2); M–($\mu_3$-OCH), Nd(1)–O(20) 2.54(2), Nd(1a)–O(20a) 2.57(1), Nd(1′)–O(20) 2.47(1), Nd(1′)–O(20a) 2.46(2), Nd(1a′)–O(20) 2.49(2), Nd(1a′)–O(20a) 2.48(1); Na–($\mu$-$OCO_2$), Na(1)–O(2) 2.37(2), Na(1′)–O(2) 2.35(2); M–($\mu_3$-$OCO_2$), Nd(1)–O(1) 2.51(2), Nd(1a)–O(1′) 2.48(2), Nd(1′)–O(1′) 2.56(1), Nd(1a′)–O(1) 2.51(1), Na(1)–O(1) 2.56(1), Na(1′)–O(1′) 2.50(1); Nd–N, 2.51(2)–2.63(2); Na–O(dme), 2.48(2)–2.60(2). Selected bond angles (°) O(1)–C(1)–O(1′) 123(1), O(1)–C(1)–O(2) 117(2), O(1′)–C(1)–O(2) 120(2).




**Scheme 1**




**I**

coordinated by two nitrogens, one $\eta^1$- and one $\mu$-(NdONd)-aryloxide oxygen, one $\mu$- and two $\mu_3$-alkoxide oxygens and a $\mu_3$-carbonate oxygen.

The deprotonated ligands are bridging pentadentate and bind to each of two Nd atoms with three donor atoms, and to a further Nd by one donor atom. However, two ligands have $\mu_3$-alkoxo donors [O(20) or O(20a)] and two $\eta^1$-aryloxide oxygens whereas the other two contain $\mu$-alkoxo donors [O(10) or O(10a)], and two $\mu$-aryloxide oxygens.

The Nd–OAr distances (Fig. 1) feature short bonds to the $\eta^1$-bonded oxygens and the $\mu$-oxygens bridging to sodium, whilst the Nd–O(Ar)–Nd bonds are significantly longer for Nd(1,1a) but only marginally longer for Nd(1′,1a′). The Nd–($\eta^1$-O) bond lengths are comparable with those of La–($\eta^1$-OAr) of seven-coordinate lanthanum in the rare aryloxo cluster $NMe_4[Na_2La_2(\mu_4\text{-OAr})(\mu_3\text{-OAr})_2(\mu\text{-OAr})_4(\eta^1\text{-OAr})_2(thf)_5]$, (Ar = 4-$MeC_6H_4$).[2] (The effect of the higher coordination number of **2** offsets that of the smaller lanthanoid radius.) For Nd(1, 1a), Nd–($\mu$-OCH) distances are markedly shorter than Nd–($\mu_3$-OCH), whereas these distances differ less for Nd(1′, 1a′) (Fig. 1). However, the range is similar to that for previously reported Nd–($\mu$ or $\mu_3$-OR) bonds (*e.g.* R = $CH_2Bu^t$, $CHPr^i_2$).[1,8] Average Na–($\mu$-OAr) distances are somewhat longer than those of four-coordinate $[Na\{OC_6H_2(CF_3)_3\text{-}2,4,6\}(thf)_2]_2$[9] as is reasonable for the coordination number difference. Nd–O–$CO_2$ distances are comparable with those in the eight-coordinate Nd cage, $[Nd_8(thd)_8(H_2O)_2(\mu\text{-}Bu^tCO_2)_6(\mu_3\text{-}OH)_6(\mu_6\text{-}CO_3)_2]$, (thd = 2,2,6,6-tetramethylheptane-3,5-dionate).[10] Although there is considerable variation in the Na–$OCO_2$ distances (Fig. 1), this can be attributed to the expected difference between bonding to $\mu$- and $\mu_3$-bridged oxygens. Moreover, a similar range has been observed for 'strongly bonded' Na–($\mu$-O) in $[Na_3\{Ru_2(CO_3)_4\}\cdot 6H_2O]_n$.[11] The Nd···Nd separations [3.803(3)–3.844(4) Å] are not much larger than the sum (3.63 Å)[12] of the six-coordinate metal radii encouraging our planned investigation of the magnetic properties to explore possible Nd···Nd interactions.

We have also recently prepared and crystallographically characterized other complexes which incorporate the $Nd_4L_4$ stoichiometry. These include $[Na_5Nd_4L_4(OH)(OMe)_4(HOMe)(dme)_3]$, which contains the $Nd_4L_4$ cage in a different arrangement and encapsulates NaOH and NaOMe molecules.[13] This indicates the cage can be prepared independently of $Na_2CO_3$ and will accommodate other species.

We are grateful to the Australian Research Council for support of this work.

## Footnotes

† All operations were carried out under an atmosphere of purified $N_2$ or Ar because of the extreme sensitivity of the compounds to air and moisture. **1**: a mixture of $NdCl_3$ (0.50 g, 2.0 mmol), $H_3L$ (0.59 g, 2.0 mmol), $NaNH_2$ (0.40 g, 8.0 mmol) and $Na_2CO_3$ (0.20 g, 1.7 mmol) in thf (50 ml), was rapidly stirred at ambient temperature for 48 h, whereupon a light blue solution and a white precipitate was produced. After filtration, concentration and addition of a small amount of pentane (*ca*. 5 ml), dichroic light pink crystals of **1** deposited on prolonged standing (yield 66%) (Found: C, 47.4, H, 4.5, N, 5.5, Nd, 28.2, Na, 1.9%. $C_{85}H_{92}N_8Na_2Nd_4O_{19}$ requires C, 47.4, H, 4.3, N, 5.2, Nd, 26.8, Na, 2.1%). IR (Nujol): 1629vs, 1596s, 1550m, 1538s, 1347s, 1323s, 1302s, 1245w, 1218m, 1193m, 1145s, 1124m, 1107w, 1063m, 1040s, 1026s, 965w, 896m, 865m, 848w, 791w, 756s, 738s, 702m, 646w, 592m $cm^{-1}$. $\lambda_{max}$ (thf)/nm ($\varepsilon$/$dm^3$ $mol^{-1}$ $cm^{-1}$): 575 (213), 582 (209), 737 (130).

**2**: complex **1** was recrystallised from dme, and dichroic light pink crystals of **2** were obtained on prolonged standing (Found: C, 46.4, H, 4.8, N, 5.4%. $C_{83}H_{95}N_8Na_2Nd_4O_{22}$ requires C, 45.7, H, 4.4, N, 5.1%). IR (Nujol): 1627vs, 1596s, 1540m, 1341m, 1322m, 1290m, 1193w, 1146w, 1125w, 1057w, 1028m, 974w, 896w, 865w, 851w, 789w, 758s, 738m, 728m, 694w, 624w, 588w $cm^{-1}$. $\lambda_{max}$ (thf)/nm ($\varepsilon$/$dm^3$ $mol^{-1}$ $cm^{-1}$): 528 (78), 577 (100), 583 (115), 737 (93), 756 (89).

‡ *Crystallographic data*: **2**: air-sensitive pink crystals, $C_{83}H_{95}N_8Na_2Nd_4O_{22}$, $M$ = 2179.8, monoclinic, space group $P2_1/c$, $a$ = 25.90(1), $b$ = 22.88(2), $c$ = 15.331(6) Å, $\beta$ = 90.89(4)°; $2\theta_{max}$ = 45°. $N$ (unique) = 10733; $N_0$ [$I > 3\sigma(I)$; absorption corrected] = 4197. $R$, $R_w$ = 0.066, 0.052. Anisotropic thermal parameter refinement for Nd, Na, O, N; $(x, y, z, U_{iso})_H$ included at constrained estimates. Abnormal features: high thermal motion on the ether ligands.

**1** (a less satisfactory result): $C_{85}H_{92}N_8Na_2Nd_4O_{19}$, $M$ = 2152.7, modelled as orthorhombic; space group *Pnca*, $a$ = 25.30(3), $b$ = 23.67(1), $c$ = 15.077(5) Å; $2\theta_{max}$ = 40°. $N$, $N_o$ = 4868, 2773. $R$, $R_w$ = 0.092, 0.097. (Nd, Na anisotropic) with similar connectivity to **2** which it predates. The result of **2** raises the possibility that **1** is actually isomorphous, pseudo-orthorhombic, with monoclinic $\beta$ = 90°; no further adequately crystalline material has been forthcoming to pursue the point further.

Atomic coordinates, bond lengths and angles, and thermal parameters have been deposited at the Cambridge Crystallographic Data Centre (CCDC). See Information for Authors, Issue No. 1. Any request to the CCDC for this material should quote the full literature citation and the reference number 182/345.

## References

1 D. C. Bradley, *Chem. Rev.*, 1989, **89**, 13; K. G. Caulton and L. G. Hubert-Pfalzgraf, *Chem. Rev.*, 1990, **90**, 969; R. C. Mehrotra, A. Singh and U. M. Tripathi, *Chem. Rev.*, 1991, **91**, 1287; L. G. Hubert-Pfalzgraf, *New J. Chem.*, 1995, **19**, 727.
2 W. J. Evans, R. E. Golden and J. W. Ziller, *Inorg. Chem.*, 1993, **32**, 3041.
3 J. L. Atwood, G. W. Orr and K. D. Robinson, *Supramol. Chem.*, 1994, **3**, 89; J. W. Steed, C. P. Johnson, C. L. Barnes, R. K. Juneja, J. L. Atwood, S. Reilly, R. L. Hollis, P. H. Smith and D. L. Clark, *J. Am. Chem. Soc.*, 1995, **117**, 11426.
4 P. D. Beer, Z. Chen, A. J. Goulden, A. Graydon, S. E. Stokes and T. Wear, *J. Chem. Soc., Chem. Commun.*, 1993, 1834; D. M. Rudkevich, Z. Brzozka, M. Palys, H. C. Visser, W. Verboom and D. N. Reinhoudt, *Angew. Chem.*, 1994, **106**, 480; *Angew. Chem., Int. Ed. Engl.*, 1994, **33**, 467.
5 G. D. Fallon, A. Markiewicz, K. S. Murray and T. Quach, *J. Chem. Soc., Chem. Commun.*, 1991, 198; K. Bertoncello, G. D. Fallon, K. S. Murray and E. R. T. Tiekink, *Inorg. Chem.*, 1991, **30**, 3562.
6 T. C. W. Mak, P.-J. Li, C.-M. Zheng and K.-Y. Huang, *J. Chem. Soc., Chem. Commun.*, 1986, 1597.
7 K. Hyvarinen, M. Klinga and M. Leskela, *Polyhedron*, 1996, **15**, 2171.
8 D. M. Barnhart, D. L. Clark, J. C. Gordon, J. C. Huffman, J. G. Watkin and B. D. Zwick, *J. Am. Chem. Soc.*, 1993, **115**, 8461; D. M. Barnhart, D. L. Clark, J. C. Huffman, R. L. Vincent and J. G. Watkin, *Inorg. Chem.*, 1993, **32**, 4077.
9 S. Brooker, F. T. Edelmann, T. Kottke, H. W. Roesky, G. M. Sheldrick, D. Stalke and K. H. Whitmire, *J. Chem. Soc., Chem. Commun.*, 1991, 144.
10 N. P. Kuz'mina, Z. An'Tu, A. P. Pisarevskii, L. I. Martynenko and Yu. T. Struchkov, *Koord Khim.*, 1994, **20**, 712.
11 A. J. Lindsay, G. Wilkinson, M. Moteralli and M. B. Hursthouse, *J. Chem. Soc., Dalton Trans.*, 1987, 2723.
12 N. N. Greenwood and A. Earnshaw, *Chemistry of the Elements*, Pergamon Press, Oxford, 1984, p. 1430.
13 G. B. Deacon, T. Feng, D. C. R. Hockless, P. C. Junk, B. W. Skelton and A. H. White, unpublished work.

*Received, 2nd October 1996; Com. 6/06743H*

# Photoreduction of carbon dioxide by metal phthalocyanine adsorbed Nafion membrane

**J. Rajan Premkumar and Ramasamy Ramaraj***

*School of Chemistry, Madurai Kamaraj University, Madurai-625 021, India*

**Formic acid is photosynthesised from carbon dioxide upon reduction by metal phthalocyanines adsorbed onto a Nafion membrane (photocatalyst) in acidic aqueous solution containing triethanolamine as a hole scavenger.**

The rise of carbon dioxide ($CO_2$) concentration in the atmosphere because of the 'greenhouse effect' has now become a global environmental issue. In this context, the reduction of $CO_2$ into other useful chemicals has attracted much attention.[1,2] Electrochemical reduction of $CO_2$ has been reported using modified electrodes[2–4] while its photochemical reduction has been reported using semiconductor colloids[5] and metal complexes[6] in homogeneous solution. The development of more efficient photocatalysts in the solid phase is desirable for the efficient multielectron photoreduction of $CO_2$. Catalysts immobilized in Nafion membranes are particularly advantageous due to their spatial separation from the solution phase which normally contains very many species. In the present investigation, we have used metal phthalocyanines (MPCs) adsorbed into a Nafion membrane for the photocatalytic reduction of $CO_2$. The MPC film behaves as p-type material.[7] The dopant/electron acceptor, $CO_2$, diffuses into the phthalocyanine matrix which is adsorbed in the Nafion membrane. The presence of such defect sites is a fundamental prerequisite for a good performance of the MPC film in photovoltaic/photoelectrochemical cells and for their electrical conductivity as well as photoconductivity.[7,8]

MPCs [cobalt(II) phthalocyanine (CoPC), zinc(II) phthalocyanine (ZnPC)] and Nafion membrane (type 115, 1100 equiv. wt., thickness 0.13 mm) were purchased from Aldrich. The Nafion membrane (1 $cm^2$) was pretreated by boiling in concentrated $HNO_3$ followed by washing with distilled water.[9] The MPC-adsorbed Nafion membrane was prepared by immersing the membrane in a solution containing a known concentration of CoPC or ZnPC in dmf. Then the MPC-adsorbed Nafion membrane (represented as Nf/CoPC or Nf/ZnPC) was washed and dipped in distilled water. The CoPC and ZnPC were adsorbed irreversibly and the amounts of CoPC and ZnPC adsorbed into the Nafion membrane were determined by measuring the changes in absorbance of CoPC and ZnPC in solution before and after dipping the Nafion membrane.[10] The Nf/MPC membrane was characterized by absorption and emission spectra. Fig. 1 shows the surface morphology of the

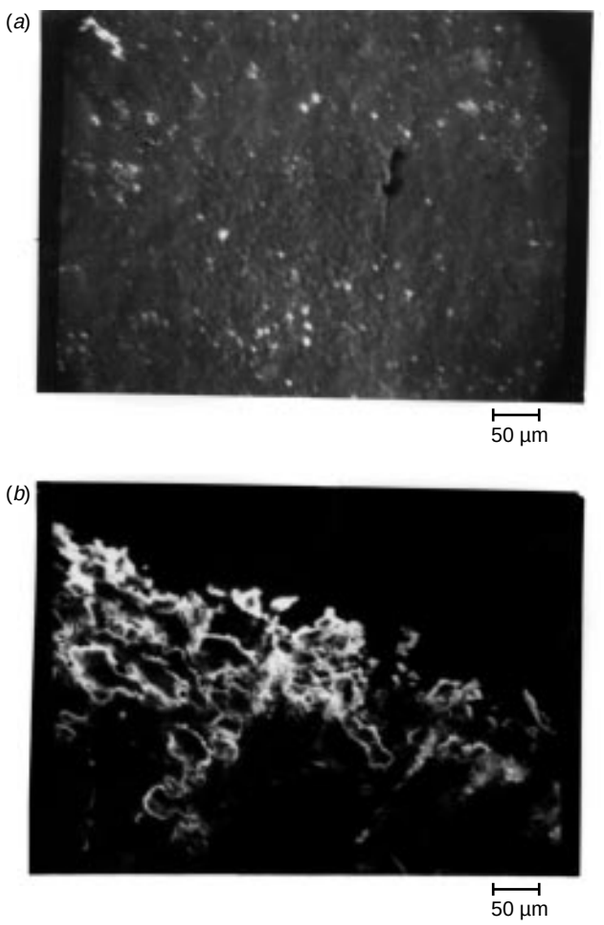



**Fig. 1** SEM photographs of (*a*) Nafion and (*b*) Nf/CoPC membranes

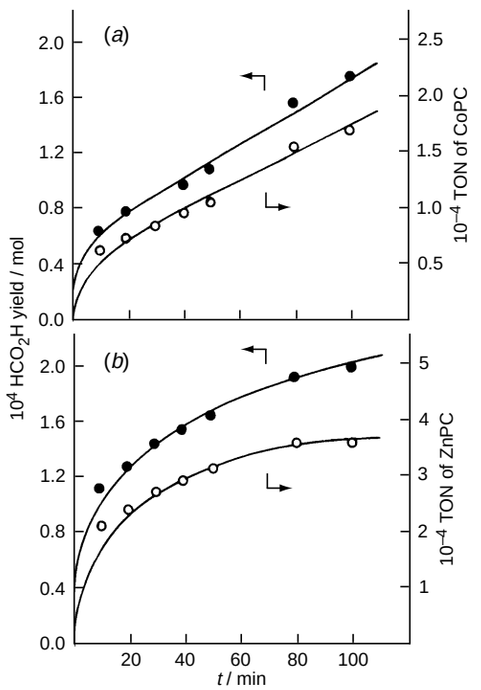



**Fig. 2** Yield of formic acid and turnover number (TON) of (*a*) Nf/CoPC and (*b*) Nf/ZnPC (1 $cm^2$ area Nafion membrane) at different light irradiation times (*t*). Adsorbed amounts: (*a*) $2.046 \times 10^{-8}$ mol CoPC and (*b*) $1.057 \times 10^{-8}$ mol ZnPC.

Nafion and Nf/CoPC membranes recorded using a scanning electron microscope (SEM) (Hitachi S-450). Adsorption of CoPC into the Nafion membrane [Fig. 1(*b*)] is evident when compared to the SEM of a blank Nafion membrane [Fig. 1(*a*)]. The adsorbed CoPC then agglomerates into larger deposits.

The prepared Nf/MPC was used for photocatalytic reduction of $CO_2$. The Nf/CoPC and Nf/ZnPC were dipped into a photolysis cell containing a $CO_2$-saturated aqueous solution of triethanolamine (TEA) (0.1 mol $dm^{-3}$) and $HClO_4$ (0.1 mol $dm^{-3}$) and then irradiated with visible light. A 500 W tungsten–halogen lamp was used as the light source with a water filter cell (6 cm pathlength with Pyrex glass windows) and a Pyrex-glass filter to cut off IR and UV radiation. The distance between the light source and the Nafion membrane was 40 cm. After 10–100 min of irradiation the cell solution was tested for formic acid, formaldehyde and oxalic acid using HPLC (Shimadzu, LC-8A modular HPLC system, reverse-phase column (ODS), 70% methanol mobile phase) and spectrophotometric methods.[4,11] Formic acid alone was detected as the $CO_2$ reduction product. The yields of formic acid formed at different light irradiation times at Nf/CoPC and Nf/ZnPC were determined and the corresponding turnover numbers (TONs) of CoPC and ZnPC are shown in Fig. 2. The TONs of MPCs were obtained using the relation 2 × (mol of formic acid produced/mol of MPC in Nafion membrane). The TON of ZnPC was higher than that of CoPC (Fig. 2). This may be due to the greater interaction of ZnPC with $CO_2$ than that of CoPC with $CO_2$. The axial coordinating ability of other central metals is relatively lower when compared to ZnPC.[7,12] The experiments were repeated several times and reproducible results were obtained. The Nf/MPC membrane was found to be very stable for weeks and was reused in the experiments.

In the absence of any one of the reaction components (visible light, MPC, TEA, $H^+$ and $CO_2$) formic acid was not observed. The p-type semiconductor nature of MPC film has already beenreported[7,8] and the probable photocatalytic reactions are given below [eqns. (1)–(3)]:

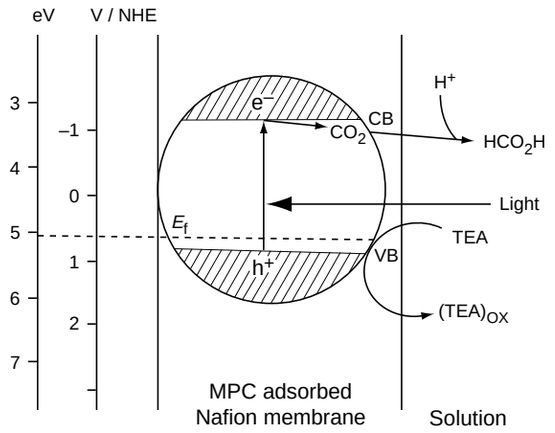
$$\text{MPC} + h\nu \longrightarrow \text{MPC*}\ (e^-_{CB} + h^+_{VB}) \quad (1)$$

$$2\ \text{TEA} + 2\ h^+_{VB} \longrightarrow 2\ (\text{TEA})_{ox} \quad (2)$$

$$CO_2 + 2\ e^-_{CB} + 2\ H^+ \longrightarrow HCO_2H \quad (3)$$

where $e^-_{CB}$ and $h^+_{VB}$ denote an electron in the conduction band and a positive hole in the valence band of the Nf/MPC system, respectively.

In the bulk of the Nf/MPC film, $CO_2$ plays an active role as a dopant of the p-type phthalocyanine. For MPCs, in the intrinsic case, the width of the bandgap in a slip-stack orientation of adjacent molecules is *ca*. 2.0 eV.[8] Light irradiation results in an $S_0 \rightarrow S_1$ transition, *i.e.* the formation of MPC* located about 0.2 eV below the conduction band edge. The ionized intermediates $MPC^{\cdot+}$ and $CO_2^{\cdot-}$ are formed by electron transfer. It is assumed that in a semiconductor catalyst, the photoexcited electrons in the more negative conduction band have the greater ability to reduce $CO_2$ in solution (Scheme 1). It is also reasonable to assume that the field in the microenvironmental sites as well as the highly acidic nature of the Nafion membrane[13,14] accelerate further the $CO_2$ reduction process. Investigations on the role of the MPC catalyst in the Nafion membrane in the selective production of formic acid by $CO_2$ reduction are under way.




**Scheme 1** Schematic illustration of the photocatalytic reduction of carbon dioxide at MPC adsorbed in a Nafion membrane. The circle describes the semiconducting nature of the adsorbed MPC Nafion membrane. MPC = CoPC or ZnPC, TEA = triethanolamine, CB = conduction band, VB = valence band and $E_F$ = Fermi level.

Generous financial support from the Department of Science and Technology (DST) and the Council of Scientific and Industrial Research (CSIR) is gratefully acknowledged. J. P. acknowledges the CSIR for a Senior Research Fellowship. We thank Professor G. Kulandaivelu for his help in recording SEM images.

## References

1 P. Braunstein, D. Matt and D. Nobel, *Chem. Rev.*, 1988, **88**, 747.
2 T. Yoshida, K. Kamato, M. Tsukamoto, T. Iida, D. Schlettwein, D. Wohrle and M. Kaneko, *J. Electroanal. Chem.*, 1995, **385**, 209 and references therein.
3 M. N. Mahmood, D. Masheder and C. J. Harty, *J. Appl. Electrochem.*, 1987, **17**, 1159.
4 J. R. Pugh, M. R. M. Bruce, B. P. Sullivan and T. J. Meyer, *Inorg. Chem.*, 1991, **30**, 86.
5 S. Kuwabata, H. Uchida, A. Ogawa, S.Hirao and H. Yoneyama, *J. Chem. Soc., Chem. Commun.*, 1995, 829 and references therein.
6 H. Hori, F. P. A. Johnson, K. Koike, O. Ishitani and T. Ibusuki, *J. Photochem. Photobiol. A: Chem.*, 1996, **96**, 171 and references therein.
7 J. J. Simon and J. J. Andre, *Molecular Semiconductors*, Springer-Verlag, Berlin, 1985.
8 D. Schlettwein, M. Kaneko, A. Yamada, D. Wohrle and N. I. Jeager, *J. Phys. Chem.*, 1991, **95**, 1748.
9 F. R. Fan, H. Y. Liu and A. J. Bard, *J. Phys. Chem.*, 1985, **89**, 4418.
10 B. D. Berezin and V. G. Vopion, *Coordination Compounds of Porphyrins and Phthalocyanines*, Wiley, New York, 1981.
11 T.Yoshida, K. Tsutsumida, S. Teratani, K. Yasufuku and M. Kaneko, *J. Chem. Soc., Chem. Commun.*, 1993, 631.
12 P. Day and R. J. P. Williams, *J. Chem. Phys.*, 1962, **37**, 567.
13 *Perfluorinated Ionomer Membranes*, ed. A. Eisenberg and H. L. Yeager, ACS Symposium Series 180, American Chemical Society, Washington, 1982.
14 G. A. Olah, G. K. Prakash and J. Sommer, *Super Acids*, Wiley-Interscience, New York, 1985.

*Received, 16th October 1996; Com. 6/07069H*

# Solubilization of a self-assembled metallocryptand by addition of $K^+$

**Markus Albrecht* and Oliver Blau**

*Institut für Organische Chemie, Universität Karlsruhe, Richard-Willstätter-Allee, D-76131 Karlsruhe, Germany*

**The insoluble self-assembled neutral coordination compound $Ga_2L^1_3$ can be solubilized by binding of $K^+$ if the ligand $H_2L^1$ with internal oxygen atoms is used.**

Helicates are formed in spontaneous self-assembly processes from linear oligo-donor ligands and appropriate metal ions. If nitrogen donors are used, cationic[1] or neutral[2] complexes are obtained, while oxygen donor ligands lead to anionic supramolecular species.[3,4] In recent studies we could show that anionic helicates, which are formed from alkyl-bridged dicatecholate ligands and titanium(IV) ions, are able to bind alkali-metal counter ions in a cryptate-type fashion.[4]

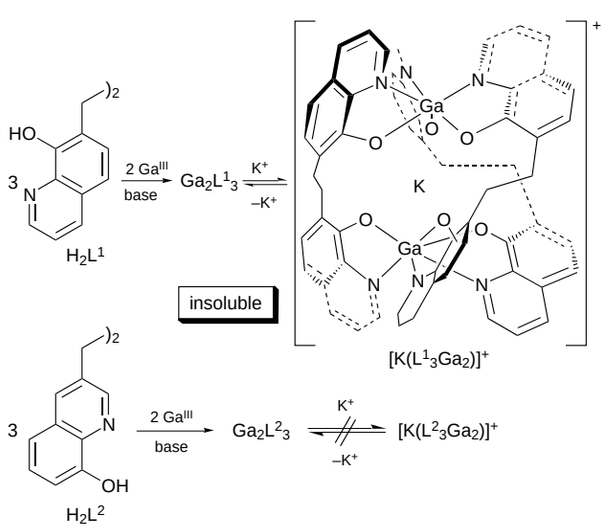
To investigate the cation binding ability of neutral self-assembled metallo-supramolecular hosts[5] we synthesized the ethylene-bridged di(8-hydroxyquinoline) ligands $H_2L^1$ and $H_2L^2$.[6] Upon formation of dinuclear triple-stranded complexes with metal ions $M^{3+}$ either a cryptand-type compound $M_2L^1_3$ with internal oxygen atoms or a cage molecule $M_2L^2_3$ without internal donor atoms should be obtained. The latter is not able to bind alkali-metal cations in its interior.[7]

To prove this hypothesis we performed the reaction of $H_2L^1$ or $H_2L^2$ (3 equiv.) with $Ga(NO_3)_3{\cdot}H_2O$ (2 equiv.) in the presence of sodium carbonate (3 equiv.) as base in methanol (Scheme 1). Heating overnight afforded yellow solids in quantitative yields. The compounds were insoluble in common solvents but elemental analysis shows the composition $Ga_2L_3{\cdot}xH_2O$ ($L^1$, $x$ = 8; $L^2$, $x$ = 7).†

If $Ga_2L^1_3$ is suspended in $(CD_3)_2SO$ and a large excess of potassium chloride or potassium chlorate is added and the sample is heated to 160 °C, the solution starts to turn yellow. The $^1H$ NMR spectrum (500 MHz, 296 K, Fig. 1) reveals the signals of the ligating moieties of $L^1$ at δ 8.67 (dd, *J* 1.0, 8.4 Hz), 7.94 (dd, *J* 1.0, 4.8 Hz), 7.76 (d, *J* 8.4 Hz), 7.62 (dd, *J* 4.8, 8.4 Hz), and 7.31 (d, *J* 8.4 Hz). Resonances of diastereotopic protons of the alkyl spacer at δ 3.08 (m) and 2.69 (m) show the presence of chiral metal complex units. Corresponding $^{13}C$ NMR signals (125 MHz, 296 K) are observed at δ 153.5 (C), 144.8 (CH), 141.2 (CH), 136.1 (C), 132.0 (CH), 128.2 (C), 125.7 (C), 121.7 (CH), 112.5 (CH) and 31.0 ($CH_2$). In accordance with our earlier work on related dinuclear catecholate–titanium systems the compound should adopt the chiral helicate[4] and not the achiral *meso*-helicate[8] structure.

Preparation of $Ga_2L^1_3$ in the presence of a large amount of potassium chloride (70 equiv.) leads to a yellow precipitate from methanol which is soluble in $(CD_3)_2SO$ and gives rise to an NMR spectrum as discussed above. FAB(+) mass spectrometry [Fig. 2, 3-nitrobenzyl alcohol (3-NBA) matrix] confirms that a cationic species $[K(L^1_3Ga_2)]^+$ is obtained. At high molar masses exclusively the peak of $[K(L^1_3Ga_2)]^+$ can be observed (*m/z* 1121, correct isotopic pattern). An analytically pure sample of $[K(L^1_3Ga_2)]Cl{\cdot}8H_2O$† was obtained by washing the solid material with a small amount of water. Extracting $[K(L^1_3Ga_2)]Cl$ with a large amount of water leads to the removal of KCl to give the insoluble neutral complex $Ga_2L^1_3$. Upon heating of $[K(L^1_3Ga_2)]Cl$ in $(CD_3)_2SO$ no dynamic behaviour can be observed by NMR spectroscopy up to 430 K indicating a remarkable configurational stability of the complex.[3,8]

$[K(L^1_3Ga_2)]Cl$ can be crystallized from dmf–diethyl ether. Preliminary results of an X-ray structure analysis[9] unambiguously show that the complex in the solid state adopts a helical structure and that the $K^+$ ion is located in the interior of the dinuclear gallium cryptand.




**Scheme 1** Preparation of $Ga_2L^1_3$, $[K\subset(L^1_3Ga_2)]Cl$ and $Ga_2L^2_3$

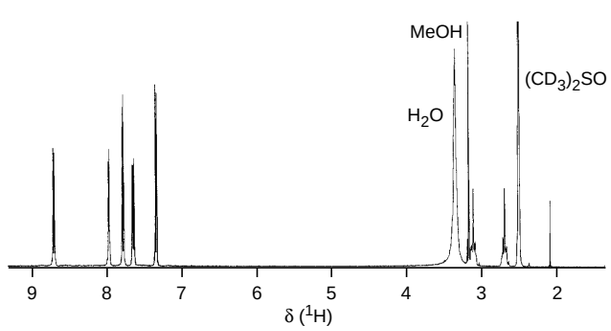



**Fig. 1** $^1H$ NMR spectrum of $[K\subset(L^1_3Ga_2)]Cl$ in $(CD_3)_2SO$

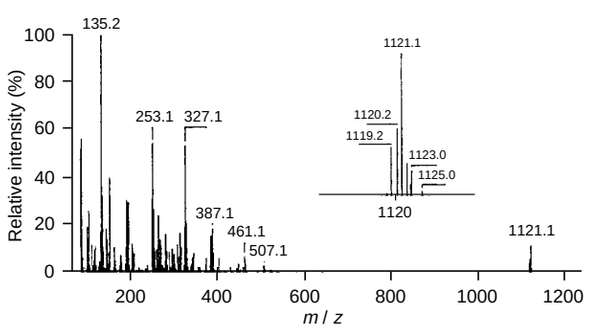



**Fig. 2** Positive FAB mass spectrum of $[K\subset(L^1Ga_2)]Cl$ (3-NBA matrix)

Due to the lack of internal oxygen donors, $Ga_2L^2_3$ is not solubilised by addition of potassium cations and heating to 160 °C. No endohedral complex with the alkaline-metal cation is formed in this case.

To summarise, we introduced a new ligand $H_2L^1$ for metallo-supramolecular chemistry which upon coordination to $Ga^{III}$ forms the neutral insoluble complex $Ga_2L^1_3$. Addition of potassium salts leads to the soluble inclusion compound $[K\subset(L^1_3Ga_2)]Cl$. By contrast, no soluble material can be obtained by addition of $K^+$ to the ligand $H_2L^2$, which does not possess internal oxygen atoms. Future work will focus on the nature of the insoluble coordination compound $Ga_2L^1_3$ and on its behaviour in the presence of different metal cations.

This work was supported by the Deutsche Forschungsgemeinschaft.

## Footnote

† Anal. Calc. for $C_{60}H_{42}Ga_2N_6O_6\cdot8H_2O$ ($Ga_2L^1_3\cdot8H_2O$): C, 58.75; H, 4.77; N, 6.85. Found: C, 58.62; H, 4.38; N, 6.89. Calc. for $C_{60}H_{42}ClGa_2KN_6O_6\cdot8H_2O$ {$[K(L^1_3Ga_2)]Cl\cdot8H_2O$}: C, 55.39; H, 4.49; N, 6.46. Found: C, 55.11; H, 4.40; N, 6.23. Calc. for $C_{60}H_{42}Ga_2N_6O_6\cdot7H_2O$ ($Ga_2L^2_3\cdot7H_2O$): C, 59.63; H, 4.67; N, 6.95. Found: C, 59.80; H, 4.46; N, 6.81%.

## References

1 Review: E. C. Constable, *Prog. Inorg. Chem.*, 1994, **42**, 67.
2 G. Stuckmeier, U. Thewalt and J.-H. Furhop, *J. Am. Chem. Soc.*, 1976, **98**, 278; W. S. Sheldrick and J. Engel, *J. Chem. Soc., Chem. Commun.*, 1980, 5; see also: R. C. Scarrow, D. L. White and K. N. Raymond, *J. Am. Chem. Soc.*, 1985, **107**, 6540.
3 B. Kersting, M. Meyer, R. E. Powers and K. N. Raymond, *J. Am. Chem. Soc.*, 1996, **118**, 7221; E. J. Enemark and T. D. P. Stack, *Angew. Chem., Int. Ed. Engl.*, 1995, **34**, 996.
4 M. Albrecht and S. Kotila, *Angew. Chem., Int. Ed. Engl.*, 1996, **35**, 1208; M. Albrecht, H. Röttele and P. Burger, *Chem. Eur. J.*, 1996, **2**, 1264.
5 For comparison see *e.g.*: A. Schepartz and J. P. McDevitt, *J. Am. Chem. Soc.*, 1989, **111**, 5976.
6 M. Albrecht and O. Blau, *Synthesis*, in the press.
7 For other self-assembled cryptands and crown ethers see *e.g.*: R. W. Saalfrank, R. Burak, A. Breit, D. Stalke, R. Herbst-Irmer, J. Daub, M. Porsch, E. Bill, M. Müther and A. X. Trautwein, *Angew. Chem., Int. Ed. Engl.*, 1994, **33**, 1621; R. W. Saalfrank, N. Löw, F. Hampel and H.-D. Stachel, *Angew. Chem., Int. Ed. Engl.*, 1996, **35**, 2209.
8 M. Albrecht and S. Kotila, *Angew. Chem., Int. Ed. Engl.*, 1995, **34**, 2134; M. Albrecht and C. Riether, *Chem. Ber.*, 1996, **129**, 829.
9 M. Albrecht, O. Blau and R. Fröhlich, unpublished work.

*Received, 21st October 1996; Com. 6/07185F*

# *N*,*N*-Dialkylcarbodiimide synthesis by palladium-catalysed coupling of amines with isonitriles

**Ilan Pri-Bar[a] and Jeffrey Schwartz*[b]**

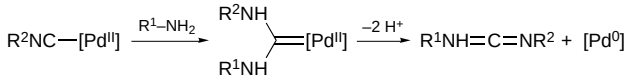
[a] *Radiochemistry Department, Rotem Industries Ltd., Beer-Sheva, 84190, Israel*
[b] *Department of Chemistry, Princeton University, Princeton, New Jersey, 08544-1009, USA*

**Catalytic condensation of amines and isonitriles can be accomplished efficiently at 100 °C using a palladium complex catalyst, oxygen, and iodine to give *N*,*N*-dialkylcarbodiimides.**

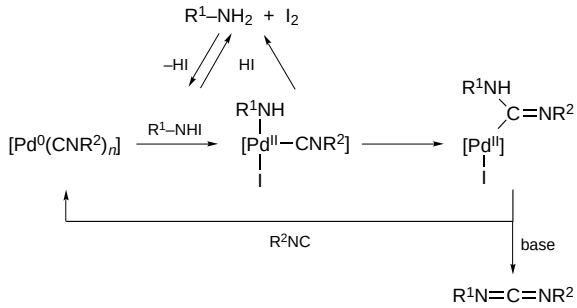
We recently reported[1] that $I_2$ can promote the homogeneous carbonylation of amines to urethanes using a palladium complex catalyst in an alcohol,† and we suggested that an *N*-iodoamine intermediate was involved. Isonitriles are isoelectronic with carbon monoxide, and we now wish to report that amines will condense with isonitriles, under conditions similar to those noted for amine carbonylation, to give good yields of *N*,*N*-dialkylcarbodiimides. This $I_2$-promoted reaction provides an alternative to conventional syntheses of carbodiimides which are accomplished *via* phosgenation of thiourea,[2] thermal coupling of isocyanates (for which synthesis also entails phosgene),[3] or catalytic dehydration of ureas.[4] Furthermore, this new route, which uses $O_2$, seems advantageous compared with another palladium complex catalysed procedure that uses silver oxide as a stoichiometric oxidant.[5]

$$R^1NH_2 + R^2NC \xrightarrow[I_2,\ O_2]{\text{Pd cat.}} R^1N{=}C{=}NR^2 + H_2O$$

**Scheme 1**



**Scheme 2**



**Scheme 3**

In a typical procedure (Scheme 1), palladium acetate (22 mg, 0.1 mmol), iodine (50 mg, 0.2 mmol), and anhydrous sodium carbonate (320 mg, 3.0 mmol) were placed in a pressure vessel. Cyclohexylamine (0.11 ml, 1.0 mmol) and cyclohexyl isocyanide (0.1 ml, 0.8 mmol) were dissolved in acetonitrile (10 ml) and added to the reaction mixture which was then pressurized with $O_2$ (40 psi) and heated to 100 °C for 3 h. The initially deep-red reaction mixture turned yellow–orange; no Pd black precipitation was observed. (There was no obvious reaction rate dependence on $O_2$ pressure.) The mixture was cooled to ambient temperature, depressurized, filtered, and analysed by GC. Carbodiimide isolation was accomplished by evaporative removal of solvent and residual amine, followed by vacuum distillation. Representative results are given in Table 1.

As shown in Table 1, aliphatic amines give some carbodiimide when $O_2$ is used as the sole oxidizing reagent (entries 2, 7). This may derive from a process (Scheme 2) which is similar to that reported[5] for a palladium complex-catalysed carbodiimide synthesis *via* a palladium(II) carbene complex; here, $O_2$ replaces $Ag_2O$ as the oxidant. Indeed, the initial rate of carbodiimide synthesis increases with increasing $O_2$ pressure. However, in the absence of iodine, the carbodiimide product undergoes subsequent hydrolysis to the urea.

We have proposed[1] that oxidative addition of an *in situ* generated *N*-iodoamine intermediate to a low-valent palladium species occurs in the context of carbamate synthesis.‡ Donor substituents could contribute to the stability of such oxidized amine intermediates and, by concentration enhancement, favour overall reaction with $Pd^0$. Relative rates for amine carbonylation were: *p*-$Me_2NC_6H_4NH_2$ > *p*-$MeOC_6H_4NH_2$ ≫ $PhNH_2$ > *p*-$ClC_6H_4NH_2$ > *p*-$MeO_2CC_6H_4NH_2$; aliphatic amines were

**Table 1** Oxidative coupling of amines with isonitriles

| Entry | Amine/mmol | Isonitrile/mmol | $I_2$/mmol | Yield[a] |
|---|---|---|---|---|
| 1 | $C_6H_{11}NH_2$ (1.4) | $C_6H_{11}NC$ (0.8) | (0.2) | 67[b] |
| 2 | $C_6H_{11}NH_2$ (1.4) | $C_6H_{11}NC$ (0.8) | — | 35[c] |
| 3 | $C_6H_{11}NH_2$ (1.4) | $Me_3CNC$ (0.9) | (0.2) | 41[5] |
| 4 | $Me_3CNH_2$ (1.4) | $C_6H_{11}NC$ (0.9) | (0.2) | 46[5] |
| 5 | $Me_3CNH_2$ (19) | $C_6H_{11}NC$ (1.2) | (0.2) | 76[5] |
| 6 | $Me_3CNH_2$[d] (38) | $Me_3CNC$ (0.9) | (0.2) | 86, 70[e] |
| 7 | $Me_3CNH_2$[d] (10) | $Me_3CNC$ (0.9) | — | 31[f] |
| 8 | *p*-$MeOC_6H_4NH_2$ (1.4) | $C_6H_{11}NC$ (0.9) | (0.2) | 67[6] |
| 9 | $Me_3CNH_2$ (1.4) | $Me_3CNC$ (0.9) | (0.2) | 4 (sym)[g] |
| | *n*-$C_4H_9NH_2$ (1.4) | | | 63 (asym)[g,5] |

[a] Carbodiimide yield determined by GC; yield based on added isonitrile. [b] An unknown byproduct was also formed; no urea was produced. [c] Dicyclohexyl urea was also formed (10%) in the absence of $I_2$. [d] Reaction performed in neat amine. [e] No $Na_2CO_3$ added. [f] Di-*tert*-butyl urea was also formed (30%) in the absence of $I_2$. [g] Sym = *N*,*N*-di-*tert*-butylcarbodiimide; asym = *N*-*tert*-butyl-*N*-*n*-butylcarbodiimide.

the most reactive. Carbodiimide synthesis was slower than carbonylation for each amine investigated, and only aliphatic amines and *p*-methoxyaniline were especially reactive.§ Highest yields of carbodiimide were realized when excess amine was employed (Table 1, entries 4, 5, 6). A mechanistic alternative for the $I_2$-enhanced pathway involves oxidative addition of the *N*-iodoamine to a palladium(0) isonitrile complex,¶ which may be rate determining, or reversible. In this latter proposal (Scheme 3), migratory 'insertion' of the amido ligand‖ could be rate determining, and relative rates for insertion** *vs*. reversion to the starting amine would contribute to the overall success of the synthetic procedure, as would the presence of base, such as carbonate or excess amine. The preferred formation of the asymmetrical carbodiimide from a mixture of *tert*-butylamine and *n*-butylamine and *tert*-butyl isocyanide (Table 1, entry 9) is likely sterically controlled.

## Footnotes

† For example, palladium acetate (22 mg, 0.1 mmol), iodine (254 mg, 1.0 mmol), $Na_2CO_3$ (276 mg, 2.0 mmol), aniline (92 mg, 1.0 mmol), methanol (10 ml) 50 psi CO; 100 °C; 30 min yields methyl phenylcarbamate (74%).

‡ Aniline treated with $I_2$ under carbonylation reaction conditions (ref. 1), but in the absence of Pd or $O_2$, gave azobenzene (15%), consistent with the intermediate formation of *N*-iodoaniline.

§ A small amount of carbodiimide was produced, as determined by GC–MS, by reaction between *p*-$ClC_6H_4NH_2$ and $C_6H_{11}NC$.

¶ For oxidative addition to $(RNC)_2Pd^0$, see L. Malatesta, *J. Chem. Soc*., 1955, 3924. Relative rate trends for oxidative addition of a series of *N*-iodoamines to either $(RNC)_2Pd^0$ or $Pd^0(CO)_n$ species could be similar.

‖ Deprotonation of a palladium(II)-coordinated amine to give an amido complex has been reported using strong bases such as disilylamide (J. Louie, F. Paul and J. F. Hartwig, *Organometallics*, 1996, **15**, 2794) or *tert*-butoxide (see, for example, R. A. Widenhoefer and S. L. Buchwald, *Organometallics*, 1996, **15**, 3534). No similarly strong base is present in the system described herein.

** The rate of alkyl group 'insertion' in a $Pd^{II}(RNC)$ complex increases with increasing nucleophilicity of the migrating carbon. See S. Otsuka and K. Ataka, *J. Chem. Soc., Dalton Trans*., 1976, 327. Relative rates for amido group insertion might also follow this trend.

## References


1 I. Pri-Bar and J. Schwartz, *J. Org. Chem*., 1995, **60**, 8124.
2 M. Mikolajczyk, *Tetrahedron*, 1981, **37**, 233; H. Ulrich and A. A. R. Sayigh, *Angew. Chem., Int. Ed. Engl*., 1966, **5**, 704.
3 For a general review see F. Kurzer and K. Douraghi-Zadeh, *Chem. Rev*., 1967, **67**, 107; isonitriles may be prepared in good yield by the phosgene-free Hofmann carbamine synthesis. See: W. P. Weber and G. W. Gokel, *Tetrahedron Lett*., 1972, **17**, 1637.
4 C. L. Stevens, G. A. Singhal and A. B. Ash, *J. Org. Chem*., 1967, **32**, 2895.
5 Y. Ito, T. Hirao and T. Saegusa, *J. Org. Chem*., 1975, **40**, 2981.
6 K. Taniguchi, S. Shigenaga, T. Ogahara, T. Fujitsu and M. Matsuo, *Chem. Pharm. Bull*., 1993, **41**, 301.



*Received, 2nd September 1996; Com. 6/06012I*

# Photochemical host–guest interaction in $Tb^{3+}$ and $Eu^{3+}$ ion-exchanged $K_{2-x}H_xTi_2O_5$ layered oxides

**Akihiko Kudo* and Eichi Kaneko**

*Department of Applied Chemistry, Faculty of Science, Science University of Tokyo, 1-3 Kagurazaka, Shinjuku-ku, Tokyo 162, Japan*

**Luminescence of $Eu^{3+}$ and $Tb^{3+}$ intercalated in $K_{2-x}H_xTi_2O_5$ layered oxides is observed by exciting the layered titanate host indicating that the energy transfer *via* electron–hole trapping from the layered host to the guest in the interlayers occurred.**

Energy- and electron-transfer processes have been studied using various types of organic and inorganic host–guest materials. This phenomenon is especially important for rare-earth phosphors doped in inorganic bulk materials.[1] Ion-exchangeable layered oxides with structural regularity are one of the interesting host materials. Applications of the layered oxides to photochemistry, materials chemistry *etc.* have been extensively investigated.[2] The photochemical interaction in energy- and electron-transfer processes between oxide layers (hosts) and substances in interlayers (guests) is of particular interest from the viewpoint of the development of new host–guest systems. Recently, the host–guest interaction in the luminescent properties of $[Ru(bpy)_3]^{2+}$ intercalated in layered titanates and niobates has been reported.[3] Here, the photochemical host–guest interaction induced by the excitation of layered oxide hosts is revealed by the photoluminescence properties of $K_{2-x}H_xTi_2O_5$ layered oxides exchanged with rare-earth metal ions.

$K_2Ti_2O_5$ was synthesized by melting a mixture of $TiO_2$ (Kanto Chemicals, 99.0%) and $K_2CO_3$ (Kanto Chemicals) at 1270 K for 1 h in air using a platinum crucible.[4,5] $H^+$- and $Ln^{3+}$-exchanged derivatives were prepared in aqueous $LnCl_3$ (0.02 M, 40 ml) containing 1 g of $K_2Ti_2O_5$ powder. About 50% of $K^+$ in $K_2Ti_2O_5$ can easily be exchanged with $H^+$ even in distilled water.[5] Therefore, the $H^+$-exchange should partly take place during the ion-exchange reactions in aqueous $LnCl_3$ solutions; the trivalent rare-earth metal ion-exchanged derivatives are denoted $K_{2-x-3y}H_xLn_yTi_2O_5$. The compositions of the ion-exchanged derivatives were determined by EDX (Kevex, DeltaPlus). Photoluminescence was measured for powdered samples at room- and liquid-nitrogen-temperatures using a quartz cell and a fluorometer (Spex, Fluoromax™).

Fig. 1 shows the emission spectra of $H^+$-, $Eu^{3+}$- and $Tb^{3+}$-exchanged $K_{2-x}H_xTi_2O_5$ obtained by excitation at 320 nm at 77 K. The compositions of obtained materials were $K_{0.7}H_{1.3}Ti_2O_5$, $K_{0.60}H_{1.2}Eu_{0.04}Ti_2O_5$ and $K_{0.85}H_{1.0}Tb_{0.05}Ti_2O_5$, respectively. A broad emission band was observed at 520 nm for $K_{0.7}H_{1.3}Ti_2O_5$ although an emission band was observed at 420 nm by excitation at 270 nm for $K_2Ti_2O_5$.[6] Such a shift by $H^+$-exchange in emission spectra has also been observed for layered potassium niobates.[7] It is noteworthy that the emission comes from the host of two-dimensional titanate sheets. For $K_{0.60}H_{1.2}Eu_{0.04}Ti_2O_5$ and $K_{0.85}H_{1.0}Tb_{0.05}Ti_2O_5$, the host emission was partly quenched and emission of the rare-earth metal ions was observed ($Eu^{3+}$, $^5D_0 \rightarrow {}^7F_{1,2}$; $Tb^{3+}$, $^5D_4 \rightarrow {}^7F_{4,5,6}$). Moreover, the ratios of luminescence intensities of $Eu^{3+}$ and $Tb^{3+}$ to those of the hosts were increased by increasing the degree of ion exchange.

Fig. 2 shows the excitation spectra of the ion-exchanged derivatives at 77 K. A broad excitation band with an onset at 350 nm was observed for $K_{0.7}H_{1.3}Ti_2O_5$. For $K_{0.60}H_{1.2}Eu_{0.04}Ti_2O_5$ and $K_{0.85}H_{1.0}Tb_{0.05}Ti_2O_5$, broad excitation bands with onsets at 350 nm were observed in addition to the peaks due to direct excitation of the rare-earth metal ions (360, 376 and 393 nm for $Eu^{3+}$, 367 and 377 nm for $Tb^{3+}$). Especially for $K_{0.85}H_{1.0}Tb_{0.05}Ti_2O_5$, the intensity of the broad band was larger than that of the direct excitation of $Tb^{3+}$. These broad bands were similar to that for $K_{0.7}H_{1.3}Ti_2O_5$. Luminescence of $K_{0.7}H_{1.3}Ti_2O_5$ was not observed at 300 K because non-radiative transitions in titanate layers and/or electron transfer quenching by $H^+$ in interlayers occurred. At 300 K, only the peaks due to the direct excitation of $Eu^{3+}$ and $Tb^{3+}$ were observed for the $K_{0.60}H_{1.2}Eu_{0.04}Ti_2O_5$ and $K_{0.85}H_{1.0}Tb_{0.05}Ti_2O_5$ powder but broad bands were not obtained. Moreover, such a band was not obtained in the excitation spectrum of an aqueous $Tb^{3+}$ solution. From these results, it was concluded that the broad band was due to the excitation of titanate layers. Accordingly, the

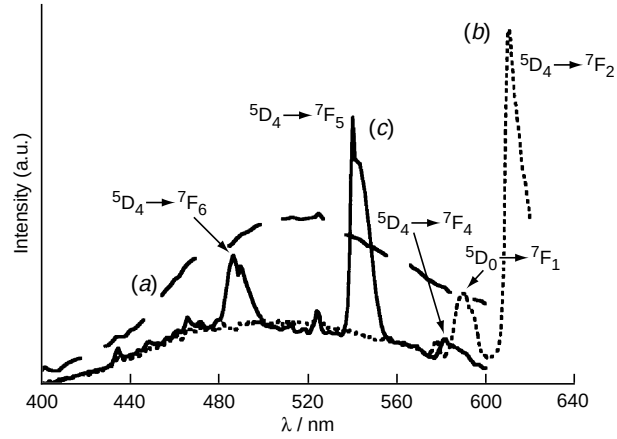



**Fig. 1** Emission spectra of (*a*) $K_{0.7}H_{1.3}Ti_2O_5$, (*b*) $K_{0.60}H_{1.2}Eu_{0.04}Ti_2O_5$ and (*c*) $K_{0.85}H_{1.0}Tb_{0.05}Ti_2O_5$ at 77 K obtained by excitation at 320 nm

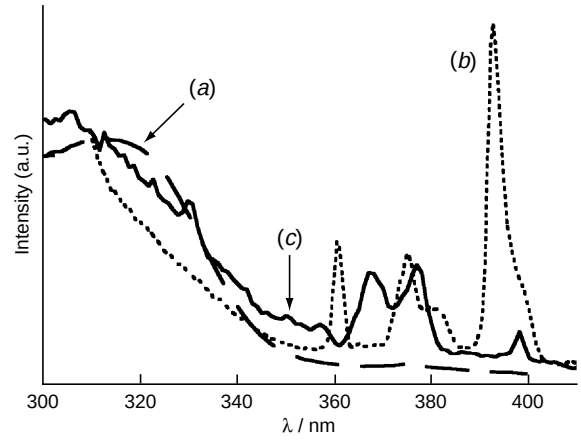



**Fig. 2** Excitation spectra of (*a*) $K_{0.7}H_{1.3}Ti_2O_5$ (monitored at 520 nm), (*b*) $K_{0.60}H_{1.2}Eu_{0.04}Ti_2O_5$ (monitored at 591.5 nm) and (*c*) $K_{0.85}H_{1.0}Tb_{0.05}Ti_2O_5$ (monitored at 541.5 nm) at 77 K

emission spectra in Fig. 1 which had been obtained by excitation at 320 nm were due to the host excitation.

The absorption spectra of $Pr^{3+}$, $Sm^{3+}$, $Eu^{3+}$, $Tb^{3+}$, $Dy^{3+}$ and $Er^{3+}$ ions more or less overlap with the host emission spectra.[8] Therefore, the resonant energy transfer would have been possible energetically for all the rare-earth metal ion-exchanged derivatives. Unexpectedly, however, only $Eu^{3+}$ and $Tb^{3+}$ showed luminescence by the host excitation even though the amounts of rare-earth metal ions exchanged were similar in all samples ($K_{0.60}H_{1.2}Eu_{0.04}Ti_2O_5$, $K_{0.58}H_{1.4}Pr_{0.02}Ti_2O_5$, $K_{0.85}H_{1.0}Tb_{0.05}Ti_2O_5$, $K_{1.2}H_{0.68}Sm_{0.04}Ti_2O_5$, $K_{0.57}H_{1.4}Dy_{0.02}Ti_2O_5$ and $K_{0.64}H_{1.3}Er_{0.03}Ti_2O_5$). Only the host emission was observed for the $K_{0.58}H_{1.4}Pr_{0.02}Ti_2O_5$, $K_{1.2}H_{0.68}Sm_{0.04}Ti_2O_5$, $K_{0.57}H_{1.4}Dy_{0.02}Ti_2O_5$ and $K_{0.64}H_{1.3}Er_{0.03}Ti_2O_5$ powders indicating the lack of the energy transfer from the host layer to the guest ion. $Eu^{3+}$ and $Tb^{3+}$ can easily assume other oxidation numbers such as $Eu^{2+}$ and $Tb^{4+}$. Therefore, the present result can be explained as follows; electrons and holes produced by host excitation in titanate layers can be trapped by $Eu^{3+}$ and $Tb^{3+}$ located in interlayers, respectively, and holes and electrons successively can recombine at their ions resulting in the luminescence, *i.e.* electrons and holes act as carriers of the excitation energy. Photocatalytic reactions proceed at interlayers of $K_{2-x}H_xTi_2O_5$[9] indicating that the electrons and holes can actually be transferred to substances in the interlayers. The energy levels of the conduction and valence bands of the titanate layers would satisfy the redox reactions of $Eu^{3+}$ and $Tb^{3+}$ judging from the band structures of various titanates.[10,11]

In conclusion, in the $K_{2-x-3y}H_xLn_yTi_2O_5$ layered oxide system, $Eu^{3+}$ and $Tb^{3+}$ in interlayers showed luminescence upon excitation of the titanate layers. This observation indicates energy-transfer processes *via* electron–hole trapping from layered titanate hosts to guests in interlayers. The present study demonstrates the energy transfer in two-dimensional systems by probing luminescence of guests of rare-earth metal ions. This will be of particular interest as the novel photochemical host–guest system in which the direct excitation of stable layered oxide hosts plays an important role.

Support by the Tokuyama Science Foundation is gratefully acknowledged.

## References

1 R. C. Powell and G. Blasse, *Struct. Bonding* (*Berlin*), 1980, **42**, 43 and references therein.
2 M. Ogawa and K. Kuroda, *Chem. Rev.*, 1995, **95**, 399 and references therein.
3 T. Nakato, K. Kusunoki, K. Yoshizawa, K. Kuroda and M. Kaneko, *J. Phys. Chem.*, 1995, **99**, 17896.
4 S. Anderson and A. D. Wadsley, *Nature* (*London*), 1960, **187**, 499; S. Anderson and A. D. Wadsley, *Acta Chem. Scand.*, 1961, **15**, 663.
5 Y. Fujiki and T. Ohsaka, *Yogyo Kyokai-shi* (*Ceramics*), 1982, **90**, 19.
6 A. Kudo and T. Sakata, *J. Mater. Chem.*, 1993, **3**, 1081.
7 A. Kudo and T. Sakata, *Chem. Lett.*, 1994, 2179; *J. Phys. Chem.*, 1996, **100**, 17323.
8 H. L. Smith and A. J. Cohen, *Phys. Chem. Glasses*, 1963, **4**, 173.
9 M. Shibata, A. Kudo, A. Tanaka, K. Domen, K. Maruya and T. Onishi, *Chem. Lett.*, 1987, 1017.
10 D. E. Scaife, *Sol. Energy*, 1980, **25**, 41.
11 A. Kudo and T. Sakata, *J. Phys. Chem.*, 1995, **99**, 15963.

*Received, 16th September 1996; Com. 6/06338A*

# Scandium(III) or lanthanide(III) triflates as recyclable catalysts for the direct acetylation of alcohols with acetic acid

**Anthony G. M. Barrett* and D. Christopher Braddock**

*Department of Chemistry, Imperial College of Science, Technology and Medicine, South Kensington, London UK SW7 2AY*

**Scandium(III) or lanthanide(III) triflates are found to efficiently catalyse the direct acetylation of primary, secondary or tertiary alcohols with acetic acid; the catalyst can be recovered quantitatively and re-used with no loss of activity.**

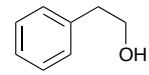
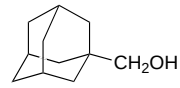
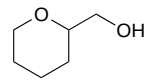
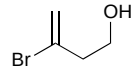
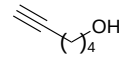
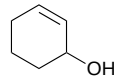
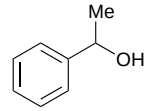
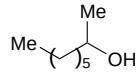
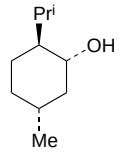
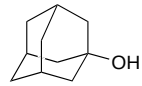
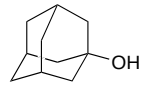
Esterification of carboxylic acids and the acylation of alcohols are fundamental processes in organic chemistry.[1,2] The direct acylation of alcohols with carboxylic acids, the Fischer esterification, can be brought about with mineral acids or sulfonic acids where the only by-product is water, *i.e.* formally an atom economic process.[3] However, the reaction is reversible and typically large excesses of either the alcohol or acid are required. Alternatively, Fischer esterifications can be driven to completion by azeotropic removal of water. However the use of strong mineral acids leads to highly acidic waste streams posing an environmental problem for industrial processes.

In order to circumvent the problem of equilibria, typically acylation of alcohols is performed with activated acyl groupings such as (mixed) acid anhydrides or acid chlorides with a stoichiometric quantity of amine base in the presence of basic catalysts such as 4-dimethylaminopyridine or 4-pyrrolidinopyridine.[2,4] These acylations work extremely well, but from an atom economic standpoint are found wanting when compared to the Fischer esterification. Acylation of alcohols can also be brought about by the action of Lewis acidic reagents in conjunction with carboxylic acids, but the Lewis acid is destroyed in the work-up procedure.[5] Similarly, Lewis acids are known to activate acid anhydrides for the acylation of alcohols,[6] but the conversion is inherently wasteful since half of every acid anhydride molecule is lost as a carboxylic acid. Furthermore, from an industrial point of view, and tonne for tonne, anhydrides are significantly more expensive than the corresponding carboxylic acid.

Lanthanides have found increasing use as mild and selective reagents in organic synthesis.[7] In particular, scandium(III) or lanthanide(III) trifluoromethanesulfonates (triflates)[8] have been used to good effect as Lewis acids in Diels–Alder,[9] allylation,[10] Friedel–Crafts[11] and Mukaiyama aldol[12,13] reactions. Many of these publications stress the ability of the catalyst to function effectively in protic media.[13,14] Indeed, for the Mukaiyama reaction the optimum solvent system was found to be aqueous THF, the catalyst recycled *via* aqueous work up and used repeatedly with little detriment to rate or yield.[13] Recently the catalytic use of scandium(III) triflate has been described for the acylation of alcohols with acid anhydrides, or with carboxylic acids in the presence of 1.5 equiv. of *p*-nitrobenzoic anhydride.[15,16] In a similar vein, the methanolysis of methoxyacetates with ytterbium(III) triflate has also been reported.[17] The compatibility of lanthanide(III) triflate salts with water and other protic solvents and yet their apparent ability to function as strong Lewis acids is somewhat paradoxical. We sought to harness this water tolerant Lewis acidity and have instigated a program in the area of clean technology using lanthanide(III) triflates for atom economic transformations.† In the course of our investigations we found that these lanthanide salts were active acylation catalysts. Herein we report the direct acylation of primary, secondary and tertiary alcohols using acetic acid in the presence of a catalytic quantity of scandium(III) or lanthanide(III) triflates. The use of acetic acid rather than acetic anhydride or acetyl chloride is both economically and environmentally advantageous. Furthermore, the catalysts are readily recyclable *via* a simple aqueous work-up.

**Table 1** Direct acetylation of alcohols with acetic acid catalysed by scandium(III) triflate




| Entry | Alcohol[a] | $Sc(OTf)_3$ (mol%) | *t*/h | *T*/°C | Conv. (%)[b] | Yield (%) |
|---|---|---|---|---|---|---|
| 1 |  | 5 | 24 | room temp. | > 99 | 99 |
| | | — | 48 | room temp. | 10 | — |
| | | 5 | 0.5 | reflux | > 99 | 98 |
| | | — | 0.5 | reflux | 37 | — |
| 2 |  | 5 | 24 | room temp. | > 99 | 92 |
| | | — | 48 | room temp. | 11 | — |
| 3 |  | 5 | 24 | room temp. | > 99 | 96 |
| | | — | 48 | room temp. | trace | — |
| 4 |  | 5 | 24 | room temp. | > 99 | 88 |
| | | — | 48 | room temp. | 36 | — |
| 5 |  | 5 | 24 | room temp. | > 99 | 95 |
| | | — | 48 | room temp. | 10 | — |
| 6 |  | 5 | 1 | room temp. | > 99 | 97 |
| | | — | 24 | room temp. | trace | — |
| 7 |  | 5 | 2 | 65 | > 99 | 98 |
| | | | 18 | 65 | 17 | — |
| 8 |  | 5 | 6 | 65 | > 99 | 98 |
| | | — | 18 | 65 | 23 | — |
| 9 |  | 5 | 24 | 65 | > 99 | 95 |
| | | — | 18 | 65 | 16 | — |
| 10 |  | 5 | 0.5 | reflux | 71 | — |
| | | — | 0.5 | reflux | trace | — |
| | | 5 | 3 | reflux | 71 | — |
| | | — | 0.5 | reflux | trace | — |
| 11 |  | 5 | 0.5 | reflux | 88 | — |
| | | — | 0.5 | reflux | trace | — |
| | | 5 | 18 | reflux | 88 | 81[c] |
| | | — | 18 | reflux | 23 | — |

[a] 1 mmol of alcohol in 2 ml HOAc, except entry 10 (1 mmol in 5 ml HOAc) and entry 11 (1 mmol in 25 ml HOAc). [b] GC–MS determination. [c] After flash chromatography on silica gel.

The experimental procedure for these acetylations is remarkably simple, requiring neither dry glassware nor inert atmospheres: a catalytic quantity of lanthanide(III) salt (5–10 mol%) was added to a stirred solution of the alcohol (1 mmol) in acetic acid (2 ml). In the case of primary alcohols the reactions can be run at room temperature: quantitative acetylation occurs over 24 h and a range of functional groups can be tolerated (Table 1, entries 1–5). In the control experiments with no lanthanide(III) salts only small quantities of the alcohols were converted to their acetates over the same reaction time. Alternatively, the reaction can be carried out at higher temperature and acetylation is essentially complete in the time taken to bring the reaction mixture to reflux. For simple secondary alcohols somewhat elevated temperatures are required for acceptable reaction times, and again quantitative acetylation occurred (Table 1, entries 6–9). It is of interest to note that no elimination adducts were observed. Cyclohex-2-enol, an allylic alcohol, was acetylated remarkably quickly, the reaction being complete within 1 h at room temperature, while in the corresponding control experiment only traces of the acetate were detected after 24 h (Table 1, entry 5). Acetylation of adamantan-1-ol, an extremely bulky tertiary alcohol, was somewhat less successful (Table 1, entries 10 and 11). However a remarkable rate acceleration was observed and the equilibrium position was obtained in less than 0.5 h in refluxing acetic acid in the presence of a catalytic quantity of scandium(III) triflate.

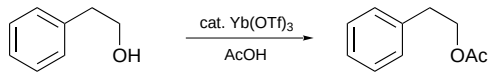
Partition work-up with $CH_2Cl_2$ and water leads to the isolation of the acetylated alcohols which are essentially single components by standard analytical techniques ($^1H$ and $^{13}C$ NMR) and require no further purification (primary and secondary alcohols). The aqueous phase containing both the catalyst and acetic acid can be evaporated under reduced pressure to furnish the lanthanide(III) salt as a white solid which can be recycled and used repeatedly without loss of activity (Table 2).‡

Of the metal triflates examined in this study, scandium(III) triflate was found to be the most effective. The lanthanide(III) triflates were less active but ytterbium(III) triflate was appreciably more effective than lanthanum, praeseodymium or europium triflates (Table 3).

In conclusion, we have demonstrated the use of scandium(III) or lanthanide(III) triflates for the acetylation of alcohols using acetic acid only as the acetyl source and where the catalyst is readily recovered and re-used. This underscores the use of lanthanide salts as environmentally acceptable catalysts for atom economic transformations.

The Imperial College group thank Air Products and Chemicals, Inc. for support of our research under the auspices of the Joint Strategic Alliance, Glaxo Group Research Ltd. for the most generous endowment (to A. G. M. B), the EPSRC and the Wolfson Foundation for establishing the Wolfson Centre for Organic Chemistry in Medical Science at Imperial College.

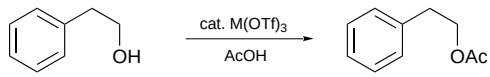
**Table 2** Recycling ytterbium(III) triflate for the acetylation of phenethyl alcohol with acetic acid




| Run[a] | Isolated yield (%) | Recovery $Yb(OTf)_3$ (%) |
|---|---|---|
| 1 | 95 | 98 |
| 2 | 99 | > 99 |
| 3 | 97 | > 99 |
| 4 | 98 | > 99 |

[a] Phenethyl alcohol (3 mmol) in refluxing acetic acid (5 ml) for 0.5 h with ytterbium(III) triflate (10 mol% for run 1).

**Table 3** The effect of various lanthanide(III) triflates for the acetylation of phenethyl alcohol with acetic acid[a]




| | Conversion (%)[c] | |
|---|---|---|
| $M(OTf)_3$[b] | After 3 h | After 21 h |
| Sc | 79 | 100 |
| La | 22 | 63 |
| Pr | 28 | 77 |
| Eu | 23 | 70 |
| Yb | 41 | 92 |

[a] All reactions run with alcohol (1 mmol) in acetic acid (2 ml) at room temp. [b] 10 mol%. [c] GC–MS determination.

## Footnotes

† Scandium(III) and lanthanide(III) triflates are commercially available from the Aldrich chemical company as their hydrated forms.
‡ The FT-IR spectrum of the recovered material was identical to that of the commercially available salt.

## References

1 M. A. Ogliaruso and J. F. Wolfe, in *The Chemistry of Functional Groups*, ed. S. Patai, Wiley, Chichester, suppl. B, part 1, p. 411; H. Pielartzik, B. Irmisch-Pielartzik and T. Eicher, in *Methoden Org. Chem. (Houben-Weyl)*, 1985, **5**, (E), 659; I. O. Sutherland, in *Comprehensive Organic Chemistry*, ed. D. H. R. Barton and W. D. Ollis, Pergamon Press, Oxford, 1979, vol. 2, p. 869.
2 J. Mulzer, in *Comprehensive Organic Synthesis*, ed. B. M. Trost and I. Fleming, Pergamon Press, Oxford, 1991, vol. 6, p. 323.
3 B. M. Trost, *Angew. Chem., Int. Ed. Engl.*, 1995, **34**, 259.
4 G. Höfle, W. Steglich and H. Vorbrüggen, *Angew. Chem., Int. Ed. Engl.*, 1978, **17**, 569. For the use of tributylphosphine as an acylation catalyst, see E. Vedejs and S. T. Diver, *J. Am. Chem. Soc.*, 1993, **115**, 3358; E. Vedejs, N. S. Bennet, L. M. Conn, S. T. Diver, M. Gingrass, S. Lin, P. A. Oliver and M. J. Peterson, *J. Org. Chem.*, 1993, **58**, 7286.
5 J. Izumi, I. Shiina and T. Mukaiyama, *Chem. Lett.*, 1995, 141; I. Shiina and T. Mukaiyama, *Chem. Lett.*, 1994, 677; A. K. Kumar and T. K. Chattopadhyay, *Tetrahedron Lett.*, 1987, **28**, 3713.
6 R. H. Baker and F. G. Bordwell, *Org. Synth.*, 1955, Coll. Vol III, 141; E. Vedejs and O. Daugulis, *J. Org. Chem.*, 1996, **61**, 5702.
7 T. Imamaoto, in *Lanthanides in Organic Synthesis*, Academic Press, London, 1994.
8 R. W. Marshmann, *Aldrichim. Acta*, 1995, **28**, 77.
9 S. Kobayshi, H. Ishitani, I. Hachiya and M. Araki, *Tetrahedron*, 1994, **50**, 11623; S. Kobayshi, M. Araki and I. Hachiya, *J. Org. Chem*., 1994, **59**, 3758; L. B. Yu, D. P. Chen and P. G. Wang, *Tetrahedron Lett.*, 1996, **37**, 2169.
10 V. K. Aggarwal and G. P. Vennall, *Tetrahedron Lett.*, 1996, **37**, 3745; C. Belluci, P. G. Cozzi and A. Umanironchi, *Tetrahedron Lett.*, 1995, **36**, 7289; H. C. Aspinall, A. F. Browning, N. Greeves and P. Ravenscroft, *Tetrahedron Lett.*, 1994, **35**, 4639; I. Hachiya and S. Kobayshi, *J. Org. Chem.*, 1993, **58**, 6958.
11 T. Tsuchimoto, K. Tobita, T. Hiyama and S. I. Fukuzawa, *Synlett*, 1996, 557; I. Hachiya, M. Moriwaki and S. Kobayashi, *Bull. Chem. Soc. Jpn*., 1995, **68**, 2053; A. Kawada, S. Mitamura and S. Kobayashi, *Chem. Commun.*, 1996, 183.
12 S. Kobayashi, I. Hachiya and M. Yasuda, *Tetrahedron Lett.*, 1996, **37**, 5569.
13 S. Kobayashi and I. Hachiya, *J. Org. Chem.*, 1994, **59**, 3590 and references cited therein.
14 D. P. Chen, L. B. Wu and P. G. Wang, *Tetrahedron Lett.*, 1996, **37**, 4467; S. Kobayashi and I. Hachiya, *J. Synth. Org. Chem. Jpn*., 1995, 53, 370; S. Kobayashi, *Synlett*, 1994, 689 and references cited therein.
15 K. Ishihara, M. Kubota, H. Kurihara and H. Yamamoto, *J. Org. Chem.*, 1996, **61**, 4560; K. Ishihara, M. Kubota, H. Kurihara and H. Yamamoto, *J. Am. Chem. Soc.*, 1995, **117**, 4413, 6639 (corrections).
16 For an active scandium acylation catalyst derived from trifluoromethanesulfonimide see: K. Ishihara, M. Kubota and H. Yamamoto, *Synlett*, 1996, 265.
17 T. Hanamoto, Y. Sugimoto, Y. Yokoyama and J. Inanaga, *J. Org. Chem.*, 1996, **61**, 4491.

*Received, 20th September 1996; Com. 6/06484A*

# New reductive deiodination reaction by hydrogen atom transfer from cyclohexane

**Jean Boivin,[a] Béatrice Quiclet-Sire,[b] Laure Ramos[a] and Samir Z. Zard*[a,b]**

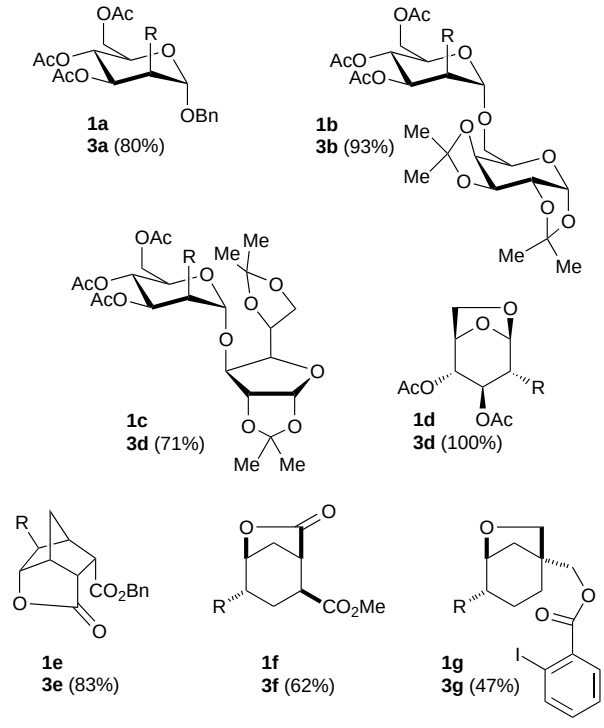
[a] *Laboratoire de Synthèse Organique associé au CNRS, Ecole Polytechnique, 91128 Palaiseau, France*
[b] *Institut de Chimie des Substances Naturelles, CNRS, 91198 Gif-Sur-Yvette, France*

**Secondary iodides flanked by one or more inductive electron-withdrawing groups can be reduced *via* a radical chain reaction involving a hydrogen atom transfer from cyclohexane, the process being triggered by a small amount of an initiator such as dilauroyl peroxide.**

Although organoiodine compounds are seldom found in nature and are therefore rarely synthetic targets themselves, they are nevertheless very useful intermediates in organic synthesis in general.[1] Iodides are not only starting materials in a wide variety of organometallic transformations: the introduction of an iodine atom is often an integral part of the creation of another bond, as in the iodo-lactonisation reaction and other related processes.[2] When introduced in this way, and after its task has been accomplished, the iodine atom must then often be reductively removed. The most generally employed reagent for this purpose is tributylstannane, used either in stoichiometric amounts or, when possible, regenerated *in situ* by an auxiliary reducing agent such as sodium borohydride or cyanoborohydride.[3,4] Other procedures include catalytic hydrogenation, reduction with dissolving metals or low valent metal salts and, in some cases, with complex hydrides.[4] Apart perhaps from catalytic hydrogenation, most of these methods are not generally applicable to iodides derived from iodo-lactonisation since they usually cause either reductive opening of the lactone ring or reduce the lactone itself. We now report a new radical chain process where reduction is achieved by an unusual hydrogen atom transfer from cyclohexane.

The reaction of iodides with radicals is a fast and reversible process, the equilibrium lying normally to the side of the most stable radical. This important property is the basis of the Kharasch-type atom transfer reactions, which have been elegantly exploited in organic synthesis in recent years.[5] It seemed that if an *unstabilised* secondary radical generated from the corresponding iodide and rendered electrophilic by one or more inductively electron-withdrawing groups (represented by a β-acetoxy group in **1**) present in the vicinity, then it should be possible to establish the chain process outlined in Scheme 1. The key, and rate determining, step is the hydrogen abstraction from cyclohexane.[6] This process is not normally efficient with ordinary aliphatic radicals, allowing cyclohexane to be used for example as solvent in replacement of the more toxic benzene.[6] However, when the radical has electrophilic character then the hydrogen abstraction rate is promoted by favourable polar factors.[7] The requirement for secondary radicals that are not stabilised by resonance comes from a need to make the process nearly thermoneutral (and preferably slightly exothermic) rather than strongly endothermic. With primary iodides, the hydrogen abstraction step (step B) would be even more favoured, but the subsequent iodine transfer equilibrium (step A) would shift to the wrong side.

This conjecture was reduced to practice as shown by the examples (and yields) compiled in Fig. 1. The reaction is performed in the following way: a solution of the iodide in cyclohexane (0.1 M) is heated to reflux under an inert atmosphere for 20–30 min and dilauroyl peroxide (typically 17 mol% with respect to the iodide, but this amount can be decreased or increased depending on the scale and purity of the iodide) is added in one portion to the deoxygenated reaction mixture. After heating for 2–3 h (TLC monitoring), the solution is concentrated under partial vacuum and the residue purified by column chromatography. The concomitant formation of cyclohexyl iodide was confirmed by GC–MS analysis of the reaction mixture. Carbohydrate-derived iodides are ideal substrates since the presence of several carbon–oxygen bonds around the radical centre make them especially electrophilic. It is worth




**Scheme 1**

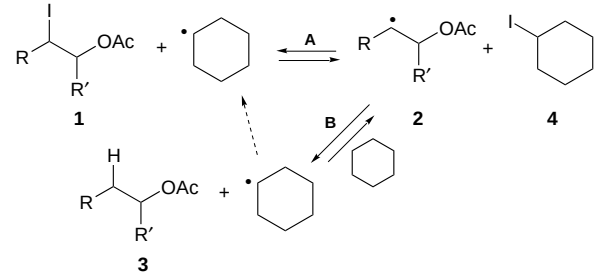



**Fig. 1** Reduction of iodides **1a–g** (R = I) into **3a–g** (R = H)

pointing out that all the substrates were constructed using either an iodo-etherification or an iodo-lactonisation reaction,[2,8] both powerful processes that introduce at the same time the iodide and an electron-withdrawing group. For example, **1b** and **1c** were made by reacting tri-*O*-acetyl-D-glucal with a 1,2:3,4-di-*O*-isopropylidene-D-galactopyranose or diacetone-D-glucose in the presence of iodosuccinimide.[8]

The importance of the electron-withdrawing group is shown by the behaviour of iodo lactones **1e** and **1f** and iodo ether **1g**. These compounds contain only one electron-attracting group next to the incipient radical centre, in contrast to the carbohydrate examples; consequently, the reaction required more dilauroyl peroxide (up to 37%). In the case of the cyclic iodo ether **1g** the yield was modest, reflecting the poorer electron-withdrawing ability of the ether linkage. Moreover, when a *mixture* of both **1f** and **1g** was subjected to the reaction conditions, lactone **1f** reacted much faster (about 5 times), as ascertained by GC–MS monitoring of the reaction. It is interesting to note that the aromatic iodide in **1g** remains largely unaffected. In fact, this competition experiment reveals aspects of selectivity that could be exploited in synthesis, and work aimed at exploring such possibilities is under way.

The present process represents a convenient and inexpensive method for reducing an important class of iodides. A number of useful and commonly encountered functional groups are tolerated. From a more fundamental point of view, it strengthens the notion that it is polar[7] and not steric effects[9] that play a predominant role in the so-called β-C–O bond effect discovered Barton and his collaborators[10] several years ago. It was noted at the time that xanthates derived from carbohydrates underwent deoxygenation more smoothly and sometimes at a lower temperature than simpler derivatives when exposed to tributyltin hydride.

## References


1 R. D. Chambers and S. R. James, in *Comprehensive Organic Chemistry*, ed. D. H. R. Barton and W. D. Ollis, Pergamon Press, Oxford, 1979, vol. 1, pp. 493–575.
2 S. Knapp, in *Advances in Heterocyclic Natural Product Synthesis*, ed. W. H. Pearson, JAI Press, Connecticut, 1996, pp. 57–98; K. E. Harding and T. H. Tiner, in *Comprehensive Organic Synthesis*, ed. B. M. Trost, I. Fleming and M. F. Semmelhack, Pergamon Press, Oxford, 1991, vol. 4, ch. 1.9, pp. 363–421; G. Cardillo and M. Orena, *Tetrahedron*, 1990, **46**, 3321; M. D. Dowle and D. I. Davies, *Chem. Soc. Rev*., 1979, 171.
3 M. Pereyre, J.-P. Quintard and A. Rahm, *Tin in Organic Synthesis*, Butterworths, London, 1987; W. P. Neumann, *Synthesis*, 1987, 665.
4 T. Imamoto, in *Comprehensive Organic Synthesis*, ed. B. M. Trost and I. Fleming, Pergamon Press, Oxford, 1991, vol. 8, pp. 793–809.
5 D. P. Curran, in *Comprehensive Organic Synthesis*, ed. B. M. Trost and I. Fleming, Pergamon Press, Oxford, 1991; vol. 4, pp. 715–831. D. P. Curran, *Synthesis*, 1988, 417, 489.
6 B. Quiclet-Sire and S. Z. Zard, *J. Am. Chem. Soc*., 1996, **118**, 9190.
7 I. D. Jenkins, *J. Chem. Soc., Chem. Commun*., 1994, 1227; W. K. Busfield, I. D. Grice, I. D. Jenkins and M. J. Monteiro, *J. Chem. Soc., Perkin Trans. 2*, 1994, 1071; W. K. Busfield, I. D. Grice and I. D. Jenkins, *J. Chem. Soc., Perkin Trans. 2*, 1994, 1079; B. P. Roberts and A. J. Steel, *J. Chem. Soc., Perkin Trans. 2*, 1994, 2411; P. Kaushal, L. H. Mock and B. P. Roberts, *J. Chem. Soc., Perkin Trans. 2*, 1990, 1663 and references cited therein. For reviews on the polar effects in radical reactions, see J. M. Tedder, *Angew. Chem., Int. Ed. Engl*., 1982, **21**, 401; *Tetrahedron*, 1982, **38**, 313; G. A. Russell, in *Free Radicals*, ed. J. K. Kochi, Wiley, New York, 1973, vol. 1, ch. 7.
8 J. Thieme, H. Karl and J. Schwentener, *Synthesis*, 1978, 696.
9 D. Crich, A. L. J. Beckwith, C. Chen, Q. Yao, I. G. E. Davison, C. Anaya de Parrodi, L. Quintero-Cortes and J. Sandoval-Ramirez, *J. Am. Chem. Soc*., 1995, **117**, 8575.
10 D. H. R. Barton, W. Hartwig and W. B. Motherwell, *J. Chem. Soc., Chem. Commun*., 1982, 447.


*Received, 4th November 1996; Com. 6/07459F*

# Practical heterogenisation of an active manganese triazacyclononane epoxidation catalyst *via* surface glycidylation

**Y. V. Subba Rao,[a] Dirk E. De Vos,[a] T. Bein[b] and Pierre A. Jacobs*[a]**

[a] *Center for Surface Science and Catalysis, K.U. Leuven, Kardinaal Mercierlaan 92, 3001 Leuven, Belgium*
[b] *Chemistry Department, Purdue University, IN 47907 West Lafayette, USA*

**A convenient immobilisation of triazacyclononane ligands on a glycidylated surface leads to a new group of active, heterogeneous manganese epoxidation catalysts.**

The catalytic activity of complexes of Mn and 1,4,7-triazacyclononane (tacn) type ligands in oxidation catalysis has only recently been unveiled.[1] Working in the right solvent and temperature conditions can greatly improve epoxidation activity and selectivity, although both catalytic parameters are also largely influenced by the nature of the substituents on the nitrogen atoms.[2] We now exploit this knowledge in devising an easy procedure for covalently anchoring Mn–tacn complexes on a mesoporous MCM-41 support material. Considerable research has been devoted to the covalent anchoring of first-row transition-metal catalysts, but most of this work concentrated on porphyrins. These are heterogenised on inorganic carriers *via* substitution at the periphery of the macrocycle, or *via* a coordinative bond with a covalently attached axial ligand.[3] While some non-haem transition-metal complexes have been covalently attached to the MCM-41 surface,[4] there seem to be few reports on the catalytic activity of these systems. We now report that our anchoring of tacn on a glycidylated support provides a heterogeneous catalyst in which the catalytic activity of the Mn–tacn core is well preserved.

The mesoporous, siliceous MCM-41 material was synthesised by a slightly modified literature procedure.[5] Its quality was established by XRD and by sorption measurements. In the surface modification, the dried surface of MCM-41 was first reacted with (3-glycidyloxypropyl)trimethoxysilane in dry toluene.† IR spectroscopy shows that the reaction of the silanol groups ($\nu_{OH}$ *ca.* 3745 $cm^{-1}$) is almost complete. Next tacn is added and reacts selectively with the glycidyloxypropyl (GP) residue, producing a 3-propoxy-2-hydroxypropyl substituent on the tacn macrocycle. This type of oxirane opening is well known from the preparation of 2-hydroxyalkyl-substituted tacn ligands.[6] In a third step, the remaining secondary amine groups of the anchored tacn are further functionalised, for instance through reaction with propylene oxide (Scheme 1). Careful Soxhlet extractions after the surface modification ensure that only covalently attached ligands reside on the host material. The different steps in the build-up at the surface were followed by $^{13}C$ MAS NMR, and by thermal analysis. For instance, after reaction with the glycidylating agent, the MAS NMR spectrum shows peaks at δ 73.4, 50, 44, 23 and 9, which is in close agreement with the peaks of the glycidyloxypropyltrimethoxysilane precursor. Only the $CH_2Si$ resonance is slightly shifted downfield (from δ 5.26 to 9) as a result of the surface bonding. Loadings with tacn were determined with thermogravimetric analysis; a typical loading is 0.4 mmol tacn per gram of modified MCM-41. Porosity measurements indicate that the pore volume with a radius under 20 Å substantially decreases after anchoring of the tacn (from 1.62 to 0.98 ml $g^{-1}$). For the sake of comparison, tacn was also anchored on a silica, glycidylated *via* the same method (Sil-GP–tacn); a commercial chloropropyl functionalised silica was also reacted with tacn (Sil-P–tacn).

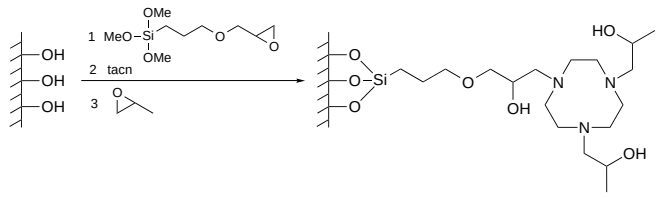
The metal-binding properties of the functionalised surfaces were thoroughly characterized by EPR spectroscopy. Therefore the materials were doped with a small amount of $Mn^{2+}$ or $Cu^{2+}$ probe ions, corresponding to 10% of the estimated metal binding capacity.‡ The EPR parameters of $Cu^{2+}$ are highly sensitive to the composition of the primary coordination sphere, and can be used to distinguish between mono- and bis-chelated complexes [Table 1 and Fig. 1(*a*)–(*c*)].[7] In a $Cu^{2+}$ doped MCM-GP–tacn, $Cu^{2+}$ binds selectively on the bound ligand, and not on the siliceous surface. At low $Cu^{2+}$ concentrations, bis-complexes are formed. This shows that the mobility of the bound ligands and the surface coverage are sufficiently high to allow an interaction between neighbouring attached ligands. At contrast, not only bis- but also mono-complexes are observed with the $Cu^{2+}$ doped Sil-P–tacn sample. This proves that the metal binding sites are more isolated in this material. In the case of $Mn^{2+}$–MCM-GP–tacn, the selective metal binding to the ligand is evidenced by the appearance of 'non-central' lines in the X-band EPR spectrum [Fig. 1(*d*)].[8,9]

Most importantly, the catalytic activity of Mn–tacn is preserved intact after this mild anchoring procedure. Before reaction, a solution of $MnSO_4$ (8 μmol) was reacted for 1 h with the heterogenised ligand (20 mg) under an $N_2$ atmosphere. Subsequently the alkene (1 mmol) and $H_2O_2$ (2 mmol, diluted in the organic solvent in a 1 : 1 mass ratio) were added, bringing the oxidant : alkene : Mn ratio to 250 : 125 : 1. Results are given in Table 2. Especially encouraging are the high epoxide selectivities (up to 90%) obtained for styrene and cyclohexene

**Table 1** EPR parameters of crystalline and supported Cu–tacn complexes

| Complex | $g_{\parallel}$ | $\lvert A_{\parallel}\rvert$ [a] | $g_{\perp}$ |
|---|---|---|---|
| $Cu^{2+}$ on MCM-41 | 2.409 | 131 | 2.08 |
| $Cu^{2+}$ on Sil-P–tacn | 2.289 | 159 | 2.05–2.06 |
| | 2.223 | 181 | 2.05–2.06 |
| $Cu^{2+}$ on MCM-GP–tacn | 2.229 | 176 | 2.05 |
| $[Cu(tacn)Br_2]$[b] | 2.278 | 158 | 2.050 |
| $[Cu(tacn)_2]$ $[Cu(CN)_3]$[b] | 2.229 | 177 | 2.055 |

[a] $10^{-4}$ $cm^{-1}$. [b] See ref. 7.




**Scheme 1**

with an Mn–MCM-GP–tacn modified with propylene oxide. This means that radical reactions are unimportant in product formation. In the particular case of styrene oxidation in methanol, the epoxide is further converted *via* acid catalysis into phenylacetaldehyde and phenylethanediol. As the siliceous MCM-41 is not acidic, the low pH of aqueous $H_2O_2$ may well be at the basis of these reactions. A typical turnover number for reactions in methanol is 50. Somewhat lower turnover numbers were obtained with other solvents such as acetone and acetonitrile, but epoxide selectivities were higher. The glycidylation approach is not limited to the MCM support. Thus a considerable activity was obtained with tacn, anchored on a glycidylated silica surface. The catalytic data prove that for tacn anchoring, the newly proposed glycidylation approach is clearly more successful than the more traditional approach *via* substitution of a silica-bound chloropropyl chain.

Summarizing, our work presents to our knowledge the first example of a catalytically active, non-aromatic Mn complex which is covalently heterogenised on an inorganic support. The reaction of the glycidyl residue with tacn is not only a very facile anchoring step; the opening of the oxirane ring by tacn also creates a hydroxy group which can assist in the metal binding.

We thank the Belgian Government for supporting this work in the framework of an I.U.A.P. project. Y. V. S. R. and D. D. V. thank K.U. Leuven and FWO (Belgium) for post-doctoral fellowships. T. B. acknowledges funding from the US Department of Energy.

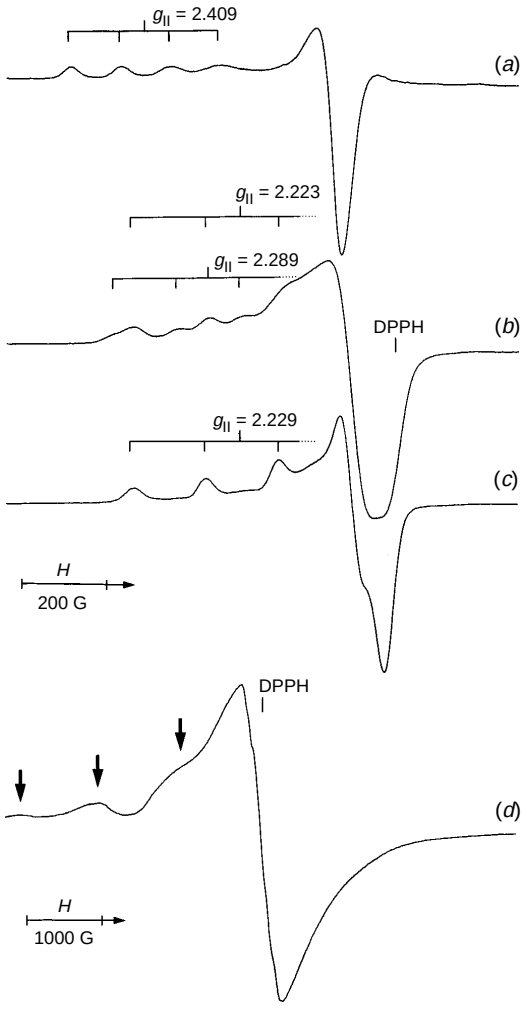



**Fig. 1** X-Band EPR spectra (130 K) of $Cu^{2+}$, adsorbed on (*a*) siliceous MCM-41, (*b*) Sil-P–tacn, (*c*) MCM-GP-tacn; (*d*) is the spectrum, recorded at 293 K under $N_2$, of $Mn^{2+}$ on MCM-GP–tacn. The clear non-central transitions (indicated by arrows) prove a strong distortion of the $Mn^{2+}$ coordination symmetry from spherical and thus coordination of $Mn^{2+}$ by a surface-bound tacn macrocycle.

**Table 2** Catalytic activity of complexes of Mn and tacn, covalently anchored on silica carriers[a]

| Substrate | Catalyst | Solvent | T.O.[b] | Selectivity[c] |
|---|---|---|---|---|
| Styrene | MCM-GP–tacn | Acetone | 4.1 | 87 (88) |
| | MCM-GP–tacn[d] | Acetone | 16 | 87 (90) |
| | MCM-GP–tacn[d] | Methanol | 52 | 24 (76) |
| | MCM-GP–tacn[d] | Acetonitrile | 15 | 62 (88) |
| | Sil-P–tacn | Acetone | 2.6 | 79 (82) |
| | Sil-P–tacn[d] | Acetone | 3.0 | 67 (82) |
| | Sil-GP–tacn | Acetone | 6.1 | 72 (81) |
| | Sil-GP–tacn[d] | Acetone | 18 | 83 (89) |
| Cyclohexene | MCM-GP–tacn[d] | Methanol | 16 | 86 |

[a] *Reaction conditions*: 1 mmol of substrate, 2 mmol of aqueous 35% $H_2O_2$, 20 mg of support with the covalently attached ligand, 8 μmol of $MnSO_4$, 1 g of solvent, 1 h, 273 K. [b] T.O. = turnover number, *i.e.* moles of epoxide and epoxide-derived products $h^{-1}$ (mole Mn)$^{-1}$. [c] Epoxide selectivity. Numbers within parentheses includes products directly derived from the epoxide, *e.g.* phenylacetaldehyde and phenylethanediol in the case of styrene. [d] Modified with propylene oxide.

## Footnotes

† 1.0 ml (4.5 mmol) of 3-glycidyloxypropyltrimethoxysilane (Fluka) was added to 3.0 g of a freshly calcined MCM-41 in 25 ml of dry toluene and refluxed for 24 h in an $N_2$ atmosphere. After reaction the resulting solid was filtered, washed thoroughly with toluene and methanol and subjected to toluene Soxhlet extraction. The oxirane ring on the glycidylated support (1 g) was opened with tacn (80 mg) in toluene (50 ml, 50 °C, 24 h). 2-Hydroxypropyl substituents were introduced by adding an excess of propylene oxide in ethanol (293 K, 10 h). For anchoring on silica supports, analogous procedures were adopted. Silica was from Fluka (70–230 mesh) and 3-chloropropyl silica was from Aldrich (230–400 mesh).

‡ For the EPR measurements, 0.1 g of the functionalised support was stirred for 2 h in 4 ml of a 1 mM $MnSO_4{\cdot}H_2O$ or $CuSO_4{\cdot}5H_2O$ solution in methanol–water (9 : 1), and collected by filtration. For Mn, an inert atmosphere was used. The metal concentration was limited to avoid dipolar line broadening.

## References

1 R. Hage, J. Iburg, J. Kerschner, J. Koek, E. Lempers, R. Martens, U. S. Racherla, S. W. Russell, T. Swarthoff, M. Van Vliet, J. Warnaar, L. van der Wolf and B. Krijnen, *Nature*, 1994, **369**, 637.
2 D. E. De Vos and T. Bein, *Chem. Commun.*, 1996, 921; *J. Organomet. Chem.*, 1996, **520**, 195; D. E. De Vos, J. Heinershagen and T. Bein, *Angew. Chem., Int. Ed. Engl.*, 1996, **35**, 2211.
3 A. W. van der Made, J. W. H. Smeets, R. J. M. Nolte and W. Drenth, *J. Chem. Soc., Chem. Commun.*, 1983, 1204; P. Battioni, E. Cardin, M. Louloudi, B. Schöllhorn, G. A. Spyroulias, D. Mansuy and T. G. Traylor, *Chem. Commun.*, 1996, 2037; K. Miki and Y. Sato, *Bull. Chem. Soc. Jpn.*, 1993, **66**, 2385; G. Labat and B. Meunier, *J. Chem. Soc., Chem. Commun.*, 1990, 1414; P. R. Cooke and J. R. Lindsay Smith, *J. Chem. Soc., Perkin Trans. 1*, 1994, 1913.
4 P. Sutra and D. Brunel, *Chem. Commun.*, 1996, 2485.
5 J. S. Beck, J. C. Vartuli, W. Roth, M. Leonowicz, C. T. Kresge, K. D. Schmitt, C. Chu, D. H. Olson, E. W. Sheppard, S. McCullen, J. B. Higgins and J. L. Schlenker, *J. Am. Chem. Soc.*, 1992, **114**, 10 834.
6 A. A. Belal, P. Chaudhuri, I. Fallis, L. J. Farrugia, R. Hartung, N. M. McDonald, B. Nuber, R. D. Peacock, J. Weiss and K. Wieghardt, *Inorg. Chem.*, 1991, **30**, 4397.
7 R. D. Bereman, M. R. Churchill, P. M. Schraber and M. E. Winkler, *Inorg. Chem.*, 1979, **18**, 3122; P. Chaudhuri, K. Oder, K. Wieghardt, J. Weiss, J. Reedijk, W. Hinrichs, J. Wood, A. Ozarowski, H. Stratemaier and D. Reinen, *Inorg. Chem.*, 1986, **25**, 2951.
8 G. M. Woltermann and J. R. Wasson, *Inorg. Chem.*, 1973, **12**, 2366; H. W. De Wijn and R. F. van Balderen, *J. Chem. Phys.*, 1967, **46**, 1381; D. E. De Vos, B. M. Weckhuysen and T. Bein, *J. Am. Chem. Soc.*, 1996, **118**, 9615.
9 D. Zhao and D. Goldfarb, *J. Chem. Soc., Chem. Commun.*, 1995, 875.

*Received, 27th November 1996; Com. 6/08016B*

# X-Ray structure of the 1 : 1 complex of a tripodal receptor and *cis*-cyclohexane-1,3,5-tricarboxylic acid

**Pablo Ballester,[a] Antoni Costa,[a] Pere M. Deyà,[a] Ghislain Deslongchamps,[b] Daniel Mink,[b] Andreas Decken,[b] Rafael Prohens,[a] Salvador Tomàs[a] and Manuel Vega[a]**

[a] *Departament de Química, Universitat de les Illes Balears, 07071 Palma de Mallorca, Spain*
[b] *Department of Chemistry, University of New Brunswick, Fredericton, N.B., E3B 6E2, Canada*

**The X-ray crystal structure of the 1 : 1 complex of a tripodal abiotic receptor and *cis*-cyclohexane-1,3,5-tricarboxylic acid is reported; the 1 : 1 complex is devoid of $C_3$-symmetry and packs into a multi-columnar self-assembly.**

Two years ago, some of us reported[1] the synthesis and binding properties of the tripodal receptor **1**, designed to bind tricarboxylic acids.[2] The receptor **1** shows high selectivity[3] for binding *cis*-cyclohexane-1,3,5-tricarboxylic acid **2** (Fig. 1) and forms a very stable complex with it in chloroform solution. Molecular modeling studies[4] suggested that two different $C_3$-symmetric geometries, **3a** and **3b**, were possible for the binding of triacid **2** by receptor **1**. In both cases, six intermolecular hydrogen bonds could form between the three carboxylic acids of the guest and the three amidopyridine 'arms' of the receptor.

ROESY[5] $^1$H NMR studies of the complex in $CHCl_3$ revealed intermolecular contacts that agreed with a predominance in solution of the '*endo*'† supramolecular complex **3a**. Slow diffusion of cyclohexane into a 1 : 1 solution of **1** and **2** in $CH_2Cl_2$ produced colourless plates that were relatively unstable when removed from the mother liquor. After numerous attempts to obtain a suitable dataset, the X-ray crystal structure was solved,‡ revealing that **2** is docked into the receptor *via* six intermolecular hydrogen bonds (Fig. 2). This structure shows a complex geometry which is in general agreement with the solution structure **3a** proposed previously based on NMR data. However, the triacid complex does not possess the anticipated $C_3$-symmetry axis. The O···N distances for all six hydrogen-bonded interactions are different, ranging from 2.612 (0.010) to 2.739 (0.010) Å (N···HO) and from 2.854 (0.010) to 2.910 (0.010) Å (O···HN). The dihedral angles about the carboxy–cyclohexyl single bonds vary by as much as 94°. The asymmetry is also evident in the three propyl chains, where two are in different *anti* conformations while the third chain is *gauche*. Deviation from $C_3$-symmetry undoubtedly arises from the presence of disordered cyclohexane, which was found to be present at an occupancy less than 1 in the difference map.

Further inspection of the crystal packing reveals a columnar motif. The 1 : 1 complexes stack on top of each other in an alternating top-to-top and bottom-to-bottom fashion and form columnar supramolecular arrangements (Fig. 3). The bottom-to-bottom interaction involves π–π interaction[6] between the two central benzene rings of the receptor in a perfect face-to-face geometry separated by *ca*. 3.9 Å. The absolute stereochemistry of the complexes alternates within a single column. Thus, any two adjacent complexes within a column (whether top-to-top or bottom-to-bottom) form a perfectly centrosymmetric dimer, a direct consequence of the $C_2/c$ space group in which the complex crystallizes.

The columnar structures pack in parallel fashion to form palisade-like sheets, which are stabilized by antiparallel π–π

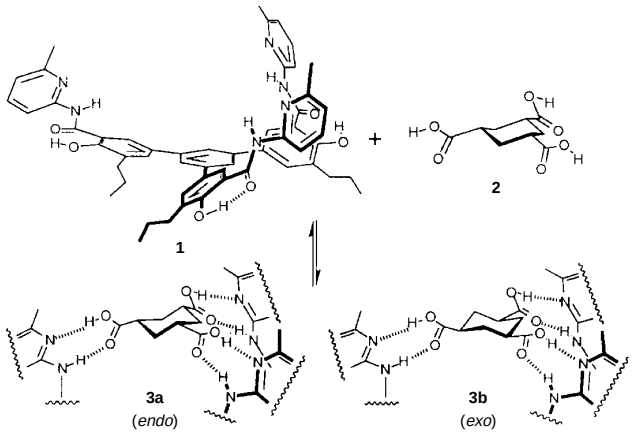



**Fig. 1** Possible binding geometries for the 1 : 1 complex of **1** and **2**

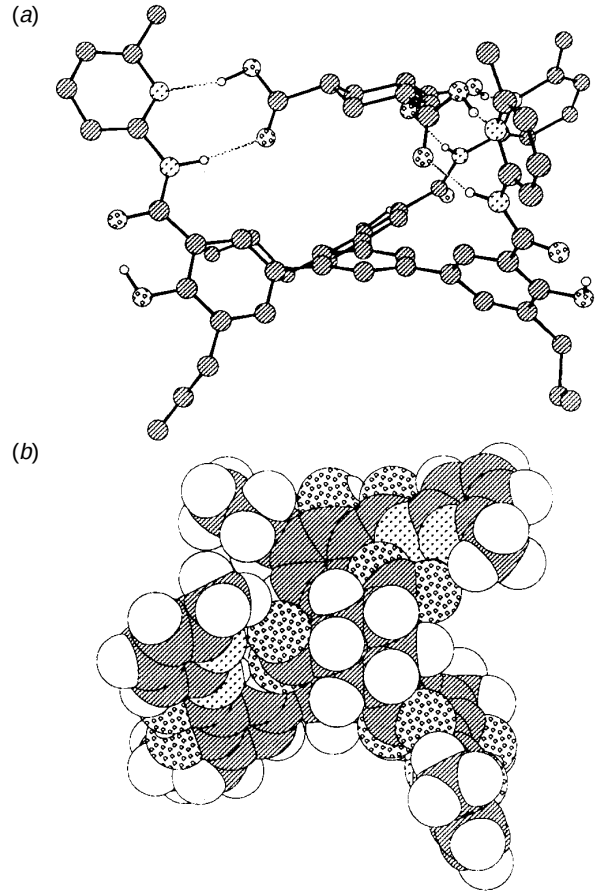



**Fig. 2** X-Ray structure of 1 : 1 complex between **1** and **2**: (*a*) side view (only polar hydrogens in calculated positions are shown, dotted lines indicate intermolecular hydrogen bonds) and (*b*) top view of a CPK representation

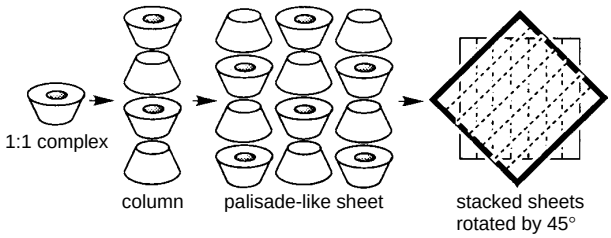



**Fig. 3** Schematic crystal packing of the 1 : 1 complex

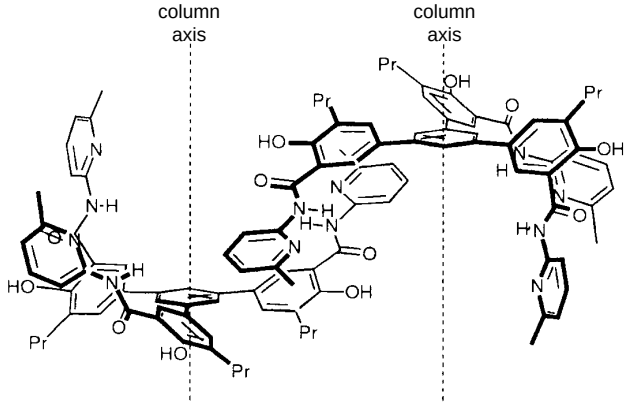



**Fig. 4** Antiparallel π-stacking between arylamidopyridine arms

stacking between arylamidopyridine 'arms' from adjacent columns (Fig. 4). The sheets stack on top of each other to complete the packing and are rotated with respect to each other by about 45°. Attempts at the X-ray characterization of other supramolecular complexes of triacids are under way, including *trans*-cyclohexane-1,3,5-tricarboxylic acid, and we will report on these findings in due course.

We thank the DGICYT (Project PB92-0251), NSERC and NATO (SRG 930949) for financial support. We are most grateful to Dr T. Stanley Cameron (Dalhousie University, Halifax, Canada) for acquisition of the X-ray data.

## Footnotes

† The terms '*endo*' and '*exo*' refer to the orientation of the three equatorial carboxy groups of **2** with respect to the receptor cavity.

‡ *Crystal data* for $C_{54}N_6O_6H_{54}\cdot C_9O_6H_{12}\cdot 0.5\ C_6H_{12}$: $M$ = 1141.30, crystallizes from dichloromethane–cyclohexane as colourless plates; crystal dimensions 0.25 × 0.25 × 0.08 mm, monoclinic, $a$ = 32.562(6), $b$ = 14.825(8), $c$ = 27.201(4) Å, β = 105.93(1)°, $U$ = 12626(8) Å$^3$, $Z$ = 8, $D_c$ = 1.201 g cm$^{-3}$, space group $C2/c$, $F(000)$ = 4848. Three-dimensional, room-temperature X-ray data were collected in the range 33 to 60° in 2θ on a Rigaku AR5F diffractometer by the θ–2θ scan method using Cu-Kα radiation; 9388 independent reflections ($R_{int}$ = 0.054 on $F^2$) were collected. The structure was solved by direct methods and refined by full-matrix least-squares methods on $F^2$. Hydrogen atoms were included in calculated positions and refined using a riding model. Refinement converged at a final $R1$ = 0.0741 ($wR2$ = 0.2098 for all 9326 data, 747 parameters, mean and maximum δ/σ 0.003, 0.043), with allowance for the thermal anisotropy of all non-hydrogen atoms. Minimum and maximum final electron density −0.307 and 0.549 e Å$^{-3}$. A weighting scheme $w = 1/[\sigma^2(F_0^2) + (0.030P)^2 + (0.00P)]$ where $P = [\max(F_0^2, 0) + 2F_c^2]/3$ was used in the latter stages of the refinement. Complex scattering factors were taken from the software package.[7]

Atomic coordinates, bond lengths and angles, and thermal parameters have been deposited at the Cambridge Crystallographic Data Centre (CCDC). See Information for Authors, Issue No. 1. Any request to the CCDC for this material should quote the full literature citation and the reference number 182/344.

## References

1 P. Ballester, A. Costa, P. M. Deyà, J. F. González, M. C. Rotger and G. Deslongchamps, *Tetrahedron Lett*., 1994, **35**, 3813.
2 For references related to the binding of carboxylic acids and carboxylates, see for example: E. Kimura, A. Sakonaka, T. Yatsunami and M. Kodama, *J. Am. Chem. Soc*., 1981, **103**, 3041; M. W. Hosseini and J. M. Lehn, *J. Am. Chem. Soc*., 1982, **104**, 3525; J. Rebek, Jr., D. Nemeth, P. Ballester and F.-T. Lin, *J. Am. Chem. Soc*., 1987, **109**, 3474; Y. Tanaka, Y. Kato and Y. Aoyama, *J. Am. Chem. Soc*., 1990, **112**, 2807; J. M. Lehn, R. Méric, J. P. Vigneron, I. Bkouche-Waksman and C. Pascard, *J. Chem. Soc., Chem. Commun*., 1991, 62; V. Alcazar and F. Diederich, *Angew Chem., Int. Ed. Engl*., 1992, **31**, 1521; M. Crego, C. Raposo, M. Caballero, E. García, J. G. Saez and J. R. Morán, *Tetrahedron Lett*., 1992, **33**, 7437; A. Galán, D. Andreu, A. M. Echavarren, P. Prados and J. de Mendoza, *J. Am. Chem. Soc*., 1992, **114**, 1511; E. Fang, S. A. V. Arman, S. Kincaid and A. D. Hamilton, *J. Am. Chem. Soc*., 1993, **115**, 369; B. C. Hamann, N. R. Branda and J. Rebek, Jr., *Tetrahedron Lett*., 1993, **34**, 6837; L. Owens, C. Thilgen, F. Diederich and C. B. Knobler, *Helv. Chim. Acta*, 1993, **76**, 2757; P. Schiessl and F. P. Schmidtchen, *Tetrahedron Lett*., 1993, **34**, 2449.
3 P. Ballester, unpublished results.
4 F. Mohamadi, N. G. Richards, W. C. Guida, R. Liscamp, M. Lipton, C. Gaulfield, G. Chang, T. Hendrickson and W. C. Still, MACROMODEL, ver.4.5, *J. Comput. Chem*., 1990, **11**, 440.
5 A. A. Bothner-By, R. L. Stephens and J. Lee, *J. Am. Chem. Soc*., 1984, **106**, 811.
6 C. A. Hunter, *Chem. Soc. Rev*., 1994, **23**, 101; C. A. Hunter and J. K. M. Sanders, *J. Am. Chem. Soc*., 1990, **112**, 5525.
7 G. M. Sheldrick, SHELXTL PLUS, ver. 4.21, Siemens Analytical X-ray Instruments, Inc., 1990; G. M. Sheldrick, SHELXL93, University of Göttingen, 1993.

*Received, 4th November 1996; Com. 6/07461H*

# Convenient preparation of trifluoroacetyl Meldrum's acid and its use as a building block for trifluoromethyl-containing compounds

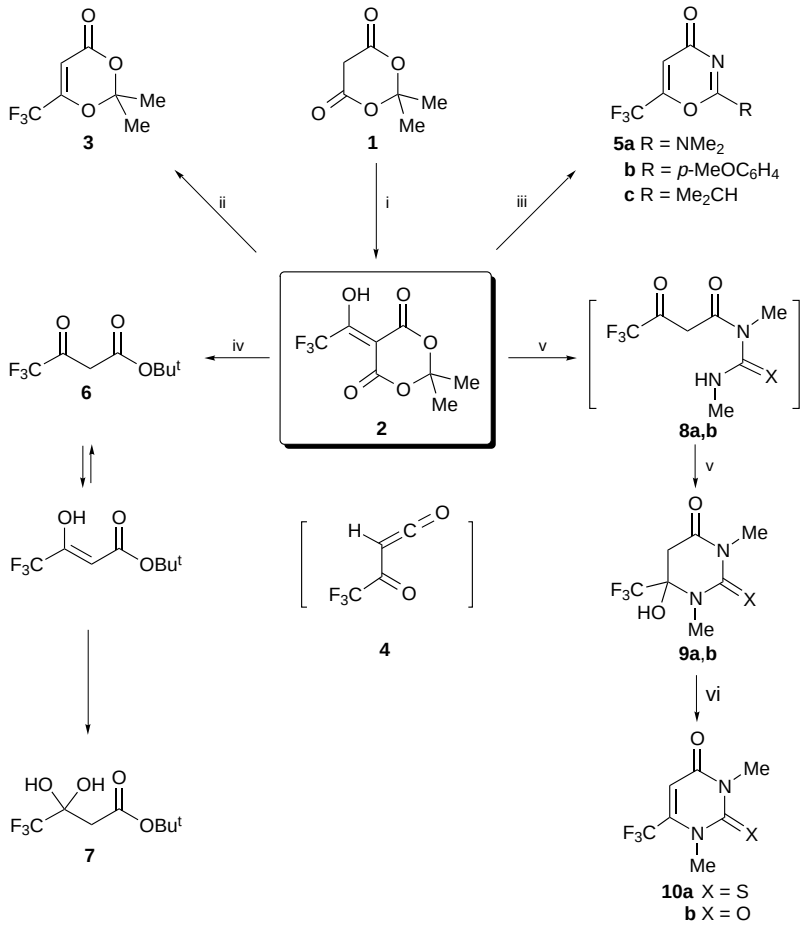
**Yasuo Morita, Rika Kamakura, Masaki Takeda and Yutaka Yamamoto***

*Tohoku College of Pharmacy, 4-4-1 Komatsushima, Aoba-ku, Sendai 981, Japan*

**Trifluoroacetyl Meldrum's acid is conveniently prepared and applied to the synthesis of trifluoromethyl-containing compounds.**

Building block approaches are currently of major interest for the construction of biologically significant trifluoromethyl-containing organic compounds.[1] Additionally, acylketenes are reactive intermediates that have been widely used in organic synthesis.[2] In this context, trifluoroacetylketene will serve as one of the most useful building blocks. However, only a few publications have appeared concerning trifluoromethyl-containing acyl ketenes, which are generated *in situ* by the thermolysis of 4*H*-1,3-dioxin-4-one[3] or by the trifluoroacetylation of ketene.[4] Acyl Meldrum's acids[5] (5-acyl-2,2-dimethyl-1,3-dioxane-4,6-dione) also behave as a precursor of acylketene. Here we describe our preliminary findings on the simple preparation of trifluoroacetyl Meldrum′s acid and its successful application to the preparation of trifluoromethyl-containing compounds such as 6-trifluoromethyl-2*H*,4*H*-1,3-dioxin-4-one, *tert*-butyl trifluoroacetoacetate, 6-trifluoromethyl-4*H*-1,3-oxazin-4-ones and 6-trifluoromethyl (thio)uracil derivatives.†

Existing methods for the preparation of acyl Meldrum's acid include the reaction of Meldrum's acid **1** with acyl chloride[6] in the presence of a tertiary amine, the reaction of **1** with a carboxylic acid[7] in the presence of a dehydrating agent and the reaction with an *in situ* generated acyl imidazolide.[8] It may be possible to carry out the acylation reaction with commercially available trifluoroacetyl chloride. However, this reagent is rather expensive and somewhat difficult to handle (bp −27 °C). Thus, we employed the imidazolide method for the preparation of trifluoroacetyl Meldrum's acid **2**. The reaction of isolated *N*-trifluoroacetylimidazole[9] with **1** in the presence of imidazole at room temperature afforded **2** in 71% yield.‡ Attempts to generate the acyl imidazolide *in situ*, however, were un-




**Scheme 1** *Reagents and conditions*: i, *N*-trifluoroacetylimidazole (1.1 equiv.), imidazole (1 equiv.); ii, acetone; iii, nitrile–solvent (benzene or toluene) or neat; iv, Bu$^t$OH (1.1 equiv.); v, *N*,*N*′- dimethyl(thio)urea; vi, cat. *p*-TsOH

successful. Treatment of trifluoroacetic acid with carbonyldiimidazole, followed by the reaction with **1**, gave none of the desired compound and recovery of a small amount of **1**.

Compound **2** was found to be labile even at room temperature. Thus, upon standing in chloroform at room temperature for 2 days or refluxing in $CH_2Cl_2$ for 1.5 h in the presence of acetone, 6-trifluoromethyl-2,2-dimethyl-2*H*,4*H*-1,3-dioxin-4-one **3**,[4]§ was obtained in moderate yield. The conversion of **2** to **3** is rationalized in terms of generation of trifluoroacetylketene **4** followed by cycloaddition across the carbon–oxygen double bond of acetone.[10]

The hetero-Diels–Alder reaction of acylketene with a variety of dienophiles is one of the most useful methods for the synthesis of heterocyclic compounds.[2b] Treatment of **2** with dimethylcyanamide in benzene under reflux (1 h) gave 2-dimethylamino-6-trifluoromethyl-4*H*-1,3-oxazin-4-one **5a** in 46% yield. Similarly, **5b** was obtained by the reaction of **2** with anisonitrile (toluene, reflux, 1 h, 60%). Treatment of **2** with a large excess of isobutyronitrile (40 equiv.) under reflux (1 h) gave **5c** in 71% yield. However, the cycloaddition reaction of acylketene with carbon–nitrogen triple bonds is limited to substituted acylketenes. Thus, the reaction of an unsubstituted acylketene such as benzoylketene with an aromatic nitrile gives only dimerized or polymerized products of acylketene and none of the cycloaddition product with nitrile was obtained.[11] The first example of a cycloaddition reaction of an unsubstituted acylketene with a simple nitrile was achieved with the trifluoroacetylketene **4**. These 1,3-oxazin-4-ones would also be useful building blocks for the synthesis of trifluoromethyl-containing nitrogen heterocycles *via* ring transformations.[12]

Reactions of **2** with nucleophiles such as *tert*-butyl alcohol, dimethylthiourea and dimethylurea were examined. Treatment of **2** with 1.1 equiv. of *tert*-butyl alcohol in chloroform at room temperature for 3 days, followed by vacuum distillation, afforded the previously unknown *tert*-butyl trifluoroacetoacetate **6** (80%). When **6** was left without protection from atmospheric moisture, solid **7** was formed. On the basis of the spectral and analytical characteristics, **7** was assigned the structure of the hydrated product of **6**. The hydration of compounds containing the trifluoromethylcarbonyl moiety is a well known phenomenon.[13] However, to the best of our knowledge, this is the first example of the isolation of the hydrated form of a trifluoromethylated β-keto ester.

The reaction with 1,3-dimethylthiourea (THF, room temperature, 24 h) gave the dihydrouracil derivative **9a** (90%) *via* trifluoroacetoacetyl derivative **8a**. Subsequent dehydration of **9a** in toluene under reflux with a catalytic amount of toluene-*p*-sulfonic acid afforded 6-trifluoromethyluracil **10a** (80%). Similarly, 2-oxo analogue **9b** (THF, room temperature, 24 h, 45%) and **10b** (91%) were obtained.

Further investigation of the application of **2** as a convenient method for the synthesis of biologically important heterocycles is in progress.

## Footnotes

† All new compounds gave satisfactory analytical and spectral data.

‡ The procedure for the preparation of **2** is as follows: to a solution of **1** (10 mmol) and imidazole (10 mmol) in 20 ml of $CHCl_3$ was added a solution of *N*-trifluroacetylimidazole (11 mmol) in 20 ml of $CHCl_3$ over a period of 30 min at room temperature. After stirring for an additional 5 min the solution was washed with 10% HCl (10 ml × 3), dried ($MgSO_4$) and the solvent evaporated while maintaining the temperature below 20 °C. Washing the resulting colourless solid with small amount of cold diethyl ether gave analytically pure **2**.

§ Preparation of compound **3** by trifluoroacetylation of *in situ* generated ketene with trifluoroacetic anhydride is reported by Boivin *et al.*,[4] but the reported yield is 8%. Iwaoka *et al.*[3] reported the preparation of 6-trifluoromethyl-4-oxo-4*H*-1,3-dioxine-2-spirocyclohexane from 4,4,4-trifluoro-3-oxobutanoic acid, cyclohexanone and acetic anhydride in the presence of a catalytic amount of sulfuric acid.

## References


1 J. T. Welch and S. Eswarakrishnan, *Fluorine in Bioorganic Chemistry*, Wiley, New York, 1991; M. Hudlicky and A. E. Pavlath, *Chemistry of Organic Fluorine Compounds II*, American Chemical Society, Washington DC, 1995.

2 (*a*) T. T. Tidwell, *Ketenes*, Wiley, New York, 1995; (*b*) C. Wentrup, W. Heilmayer and G. Kollents, *Synthesis*, 1994, 1219; (*c*) C. Kaneko, M. Sato, J. Sakaki and Y. Abe, *J. Heterocycl. Chem.*, 1990, **27**, 25.

3 T. Iwaoka, T. Murohashi, M. Sato and C. Kaneko, *Synthesis*, 1992, 977.

4 J. Boivin, L. E. Kaim and S. Z. Zard, *Tetrahedron*, 1995, **51**, 2585.

5 B. C. Chen, *Heterocycles*, 1991, **32**, 529.

6 Y. Oikawa, K. Sugano and O. Yonemitsu, *J. Org. Chem.*, 1978, **43**, 2087; I. Shinkai, T. Liu, R. A. Reamer and M. Sletzinger, *Tetrahedron Lett.*, 1982, **23**, 4899; J. Obaza and F. X. Smith, *Synth. Commun.*, 1982, **12**, 19.

7 Y. Hamada, Y. Kondo, M. Shibata and T. Shioiri, *J. Am. Chem. Soc.*, 1989, **111**, 669; J. Maibaum and D. H. Rich, *J. Med. Chem.*, 1989, **32**, 1571; W. R. Ewing and M. M. Joullie, *Heterocycles*, 1988, **27**, 2843.

8 R. F. Chapman, N. I. J. Phillips and R. S. Ward, *Tetrahedron*, 1985, **41**, 5229; D. Alker, S. F. Campbell, P. E. Cross, R. A. Burges, A. J. Carter and D. G. Gurdiner, *J. Med. Chem.*, 1989, **32**, 2381; L. Lermere, E. G. Neeland, J. P. Ounsworth, R. J. Sim, S. A. Tishler and L. Weiler, *Can. J. Chem.*, 1992, **70**, 1427.

9 H. A. Stabb and G. Walther, *Chem. Ber.*, 1962, **95**, 2070.

10 M. Sato, H. Ogasawara, K. Oi and T. Kato, *Chem. Pharm. Bull.*, 1983, **31**, 1896.

11 M. Sato, N. Kanuma and T. Kato, *Chem. Pharm. Bull.*, 1984, **32**, 106.

12 See as reviews T. Kato, N. Katagiri and Y. Yamamoto, *Heterocycles*, 1980, **14**, 1333; Y. Yamamoto and Y. Morita, *J. Synth. Org. Chem. Japan*, 1992, **50**, 887.

13 A. N. Fomin, V. I. Saloutin, K. I. Pashkevich, D. V. Bazhenov, Y. K. Grishin and Y. A. Ustynyuk, *Izv. Akad. Nauk SSSR, Ser. Khim.*, 1983, 2626; M. Tordeux and C. Wakselman, *Synth. Commun.*, 1991, **21**, 1243; J. P. Begue, D. B. Delpon and A. Dogbeavou, *Synth. Commun.*, 1992, **22**, 573; J. P. Bouillon, Z. Janousek and H. V. Viehe, *Pol. J. Chem.* 1994, **68**, 2315.


*Received, 2nd December 1996; Com. 6/08104E*

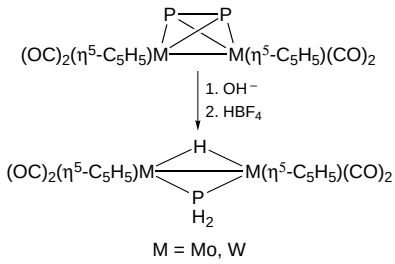
# Synthesis and characterisation of $[M_2(\eta^5\text{-}C_5H_5)_2(CO)_4(\mu\text{-}PH_2)(\mu\text{-}H)]$ (M = Mo, W); a new route to $\mu\text{-}PH_2$ complexes involving novel activation of a bridging diphosphorus ligand

**John E. Davies, Martin J. Mays,* Paul R. Raithby, Gregory P. Shields and Peter K. Tompkin**

*Department of Chemistry, Lensfield Road, Cambridge, UK CB2 1EW*

**Reaction of the known diphosphorus complexes $[M_2(\eta^5\text{-}C_5H_5)_2(CO)_4(\mu,\eta^2\text{-}P_2)]$ (M = Mo 1a, W 1b) with M′OH (M′ = Na, K) in thf–water followed by addition of $HBF_4$ affords the new phosphido complexes $[M_2(\eta^5C_5H_5)_2(CO)_4(\mu\text{-}PH_2)(\mu\text{-}H)]$ (M = Mo 3a, W 3b) in good yield; 3a is the subject of a single-crystal X-ray diffraction study.**

The preparation and characterisation of complexes containing naked group 15 ligands has been an active area of research for some years now,[1] although the subsequent reactivity of these complexes has been relatively poorly investigated, being in the main restricted to the coordination of 16-electron fragments to lone pairs present on the main-group fragment.[2] We recently showed with the formation of $[Mo_2(\eta^5\text{-}C_5H_5)_2(CO)_3\{\mu,\eta^3\text{-}PPh_2C(H)SP_2S\}]$ from $[Mo_2(\eta^5\text{-}C_5H_5)_2(CO)_4(\mu,\eta^2\text{-}P^2)]$ **1a** the hitherto unsuspected potential of naked $P_n$ ligands as precursors to otherwise inaccessible ligands.[3] We now report that the reaction of $[M_2(\eta^5\text{-}C_5H_5)_2(CO)_4(\mu,\eta^2\text{-}P_2)]$ (M = Mo **1a**, W **1b**) with M′OH (M′ = Na, K) in thf–$H_2O$ gives the dimetallic anions $[M_2(\eta^5\text{-}C_5H_5)_2(CO)_4(\mu\text{-}PH_2)]^-$ (M = Mo **2a**, W **2b**).† Protonation of **2a**,**b** then affords the new phosphido complexes $[M_2(\eta^5\text{-}C_5H_5)_2(CO)_4(\mu\text{-}PH_2)(\mu\text{-}H)]$ (M = Mo **3a**, W **3b**) in typically 70–80% yield based on **1a**,**b** (Scheme 1). This new route to $\mu\text{-}PH_2$ complexes avoids the potentially hazardous use of $PH_3$ gas often used in previous syntheses,[4] and to our knowledge there are no previous examples of the preparation of $\mu\text{-}PH_2$ complexes from complexes containing naked phosphorus ligands.




**Scheme 1**

Reaction of a solution of **1a** (400 mg, 0.806 mmol), synthesised by the method of Scherer *et al.*,[5] in thf (80 ml)–water (0.2 ml) with a large excess of M′OH pellets at 80 °C affords an air-sensitive purple solution of $[M']^+[M_2(\eta^5\text{-}C_5H_5)_2(CO)_4(\mu\text{-}PH_2)]^-$ **2a**. Filtration through a glass sinter followed by addition of a slight excess of $HBF_4{\cdot}OEt_2$ and filtration through silica affords **3a** (289 mg, 0.617 mmol, 77%) as the only isolable product. Similar treatment of a solution of **1b** (400 mg, 0.604 mmol) affords **3b** (268 mg, 0.416 mmol, 69%).

The structure of **3a** has been determined by X-ray diffraction analysis.‡ The molecular structure is shown in Fig. 1, and includes selected bond parameters. The spectroscopic data† for **3a** are consistent with this structure. An 18-electron configuration is achieved at each Mo atom only if an Mo–Mo bond is proposed; the metal–metal distance is increased from 3.0406(8) Å in **1a**[5] to 3.2818(9) Å in **3a**, this being slightly longer than the 3.244(1) Å distance observed in the diphenylphosphido analogue $[Mo_2(\eta^5\text{-}C_5H_5)_2(CO)_4(\mu\text{-}PPh_2)(\mu\text{-}H)]$ **4**.[6] The MoHMoP core of the complex is essentially planar. The Mo–P bond distances [av. 2.402(1) Å] are slightly shorter than in **4**; this may reflect the reduced steric bulk of the $PH_2$ fragment as compared to the $PPh_2$ fragment.

Both the general applicability of this new, convenient high-yield synthesis of $\mu\text{-}PH_2$ complexes and a comparison of their chemistry to that of the well studied $\mu\text{-}PR_2$ complexes is in progress.

We thank the EPSRC for funding the X-ray diffractometer and for financial support to J. E. D., G. P. S. and P. K. T., and the Cambridge Crystallographic Data Centre for support to J. E. D. and G. P. S.

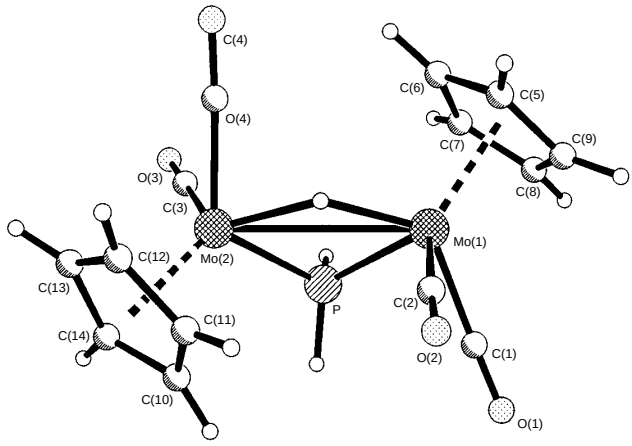



**Fig. 1** Molecular structure of **3a**. Selected bond lengths (Å) and angles (°): Mo(1)–Mo(2) 3.2818(9), Mo(1)–P 2.403(2), Mo(2)–P 2.401(2), Mo(1)–P–Mo(2) 86.19(5), P–Mo(1)–Mo(2) 46.88(4), P–Mo(2)–Mo(1) 46.93(4).

## Footnotes

† *Selected spectroscopic data*: [IR ($\nu_{CO}$/cm$^{-1}$) recorded in thf (**2a**, **2b**) or $CH_2Cl_2$ (**3a**, **3b**) solution; $^1$H, $^{13}$C and $^{31}$P NMR recorded in $CDCl_3$ solution; $^{31}$P NMR shifts recorded relative to $P(OMe)_3$ at δ 0.0 with upfield shifts negative; *J* in Hz]. For **2a**: $\nu_{CO}$ 1843vs, 1798s; $^1$H NMR 4.81 (s, 10 H, $C_5H_5$), 4.17 (d, 2 H, $^1J_{HP}$ 319, $PH_2$); $^{31}$P NMR −89.7 (s, $PH_2$). For **2b**: $\nu_{CO}$ 1835vs, 1789s; $^1$H NMR 4.90 (s, 10 H, $C_5H_5$), 4.56 (d, 2 H, $^1J_{HP}$ 336, $PH_2$); $^{31}$P NMR −89.7 (s, $PH_2$, $^1J_{PW}$ 728). For **3a**: $\nu_{CO}$ 1940vs, 1875s; $^1$H NMR 5.14 (s, 10 H, $C_5H_5$), 4.82 (d, 2 H, $^1J_{HP}$ 353, $PH_2$), −12.97 (d, 1 H, $^2J_{HP}$ 39, MoHMo); $^{13}$C NMR 90.1 ($C_5H_5$), 235.4 (s, CO), 240.6 (d, $^2J_{CP}$ 92, CO); $^{31}$P NMR −107.3 (s, $PH_2$); FABMS 468 ($M^+$); 440, 412, 384 ($M^+ - n$CO, *n* = 1–3); microanalysis (calculated values in parentheses) C, 35.79 (35.90); H, 2.71 (2.78); P, 6.33 (6.62). For **3b**: $\nu_{CO}$ 1929vs, 1861vs; $^1$H NMR 5.27 (s, 10 H, $C_5H_5$), 4.90 (d, 2 H, $^1J_{HP}$ 373, $PH_2$), −15.52 (d, 1 H, $^2J_{HP}$ 28, $^1J_{HW}$ 28.4, WHW); $^{31}$P NMR −180.7 (s, $^1J_{PW}$ 508); FABMS 644 ($M^+$); microanalysis (calculated values in parentheses) C, 25.57 (26.09); H, 2.17 (2.02); P, 4.40 (4.73).

‡ *Crystal data*: suitable crystals of **3a** were grown by diffusion of hexane into a concentrated dichloromethane solution at room temp. $C_{14}H_{13}Mo_2O_4P$, $M$ = 468.09, monoclinic, space group $P2_1/n$, $a$ = 9.071(2), $b$ = 15.667(3), $c$ = 11.010(2) Å, β = 97.32(2)°, $U$ = 1551.9(6) Å$^3$ (by least-squares refinement on diffractometer angles from 25 centred reflections 25 < 2θ < 30°), $T$ = 150 K, graphite-monochromated Mo-Kα radiation, λ = 0.710 73 Å, $Z$ = 4, $D_c$ = 2.003 Mg m$^{-3}$, $F$(000) = 912, orange block 0.20 × 0.18 × 0.17 mm, μ(Mo-Kα) = 1.729 mm$^{-1}$, semi-empirical absorption correction based on ψ-scans, relative transmission 0.940–0.997, Rigaku AFC7R diffractometer, ω–2θ scans, data collection range 5.20 < 2θ < 55.0°, +$h$, +$k$, ±$l$, three standard reflections measured at intervals of 200 reflections showed no significant variation in intensity. 3784 reflections measured, 3565 unique ($R_{int}$ = 0.037) used in all calculations. Solution by direct methods (SHELXTL-PLUS)[7] and subsequent Fourier-difference syntheses, anisotropic full-matrix least-squares refinement on $F^2$ (SHELXL 93).[8] Cyclopentadienyl hydrogen atoms placed in geometrically idealised positions and included using riding model. Phosphido hydrogen atoms located in final difference density map and coordinates were allowed to refine. The bridging hydride was located using the program HYDEX.[9] Final $wR(F^2)$ = 0.110 on all data, conventional $R(F)$ = 0.040 for 2903 observed reflections [$I$ > 2σ($I$)]; weighting scheme $w^{-1}$ = [σ$^2$($F_o^2$) + (0.0423$P$)$^2$ + 4.63$P$] where $P$ = ($F_o^2$ + 2$F_c^2$)/3, 196 parameters, GOF = 1.046, maximum Δ/σ = 0.002, max, min Δρ = 1.16, −1.03 e Å$^{-3}$.

Atomic coordinates, bond lengths and angles, and thermal parameters have been deposited at the Cambridge Crystallographic Data Centre (CCDC). See Information for Authors, Issue No. 1. Any request to the CCDC for this material should quote the full literature citation and the reference number 182/349.

## References


1 For a review of the field, see O. J. Scherer, *Angew. Chem., Int. Ed. Engl.*, 1990, **29**, 1104.
2 O. J. Scherer, H. Sitzmann and G. Wolmershäuser, *Angew. Chem., Int. Ed. Engl.*, 1984, **23**, 968; H. Lang, L. Znolsai and G. Huttner, *Angew. Chem. Suppl.*, 1983, 1464; H. Lang, L. Znolsai and G.Huttner, *Angew. Chem., Int. Ed. Engl.*, 1983, **22**, 976; A. Visi-Orosz, G. Pàlyi, L. Markò, R. Boese and G. Schmid, *J. Organomet. Chem.*, 1985, **288**, 179; L. Y. Goh, R. C. S. Wong and T. W. C. Mak, *J. Organomet. Chem.*, 1989, **373**, 71.
3 J. E. Davies, M. J. Mays, P. R. Raithby, G. P. Shields and P. K. Tompkin, *Chem. Commun.*, 1996, 2051.
4 B. F. G. Johnson, J. Lewis, E. Nordlander, S. M. Owen and P. R. Raithby, *J. Chem. Soc., Dalton Trans.*, 1996, 1567; A. Herrmann, B. Koumbouris, E. Herdtweck, M. L. Ziegler and P. Weber, *Chem. Ber.*, 1987, **120**, 931; E. A. V. Ebsworth, R. O. Gould, R. A. Mayo and M. Walkinshaw, *J. Chem. Soc., Dalton Trans.*, 1987, 2831.
5 O. J. Scherer, H. Sitzmann and G. Wolmershäuser, *J. Organomet. Chem.*, 1984, **268**, C9.
6 H. Hartung, B. Walther, U. Baumeister, H.-C. Böttcher, A. Krug, F. Rosche and P. G. Jones, *Polyhedron*, 1992, **11**, 1563.
7 G. M. Sheldrick, SHELXTL PLUS, Siemens Analytical Instruments, Madison, WI, 1990.
8 G. M. Sheldrick, SHELXL 93, University of Göttingen, 1993.
9 A. G. Orpen, *J. Chem. Soc., Dalton Trans.*, 1980, 2509.



*Received, 5th December 1996; Com. 6/08219J*

# A new route to the antitumour drug temozolomide, but not thiotemozolomide

**Yongfeng Wang,[a,b] Philip R. Lowe,[b] William T. Thomson,[c] Jonathan Clark[a] and Malcolm F. G. Stevens*[a]**

[a] *Cancer Research Laboratories, Department of Pharmaceutical Sciences, University of Nottingham, Nottingham, UK NG7 2RD*
[b] *Pharmaceutical Sciences Institute, Aston University, Birmingham, UK B4 7ET*
[c] *Aston Molecules Ltd., 10 Holt Court South, Aston Science Park, Birmingham, UK B7 4EJ*

**Interaction of 5-aminoimidazole-4-carboxamide with alkyl isocyanates yields *N*-substituted 1-carbamoylimidazoles which can be cyclised to imidazo[5,1-*d*][1,2,3,5]tetrazin-4(3*H*)-ones, including temozolomide 3a, on nitrosation; a similar reaction with methyl isothiocyanate, followed by nitrosation, affords the nitrosomethylamino derivative 11 of a new ring-system, imidazo[1,5-*b*][1,2,4]thiadiazole.**

The antitumour drug temozolomide **3a** has shown useful clinical activity against brain tumours[1] and metastatic melanoma,[2] two malignancies hitherto considered poorly treatable.

The original synthesis of temozolomide[3] started with 5-diazoimidazole-4-carboxamide **1** which was reacted with methyl isocyanate following a route to azolotetrazinones originally discovered by Ege.[4] The (presumed) dipolar intermediate **2a** cyclised spontaneously to temozolomide in high yield in a $Me_2SO$–ethyl acetate mixed solvent system at 25 °C (Scheme 1). Analogues of temozolomide **3b**–**d** can be prepared similarly. The diazoimidazole **1** does not react with methyl isothiocyanate in $Me_2SO$ at 40 °C nor in the same solvent containing the Lewis acids zinc iodide and boron trifluoride–diethyl ether or the base triethylamine, so 4-thiotemozolomide (**3a**; O = S) is not available by this route.

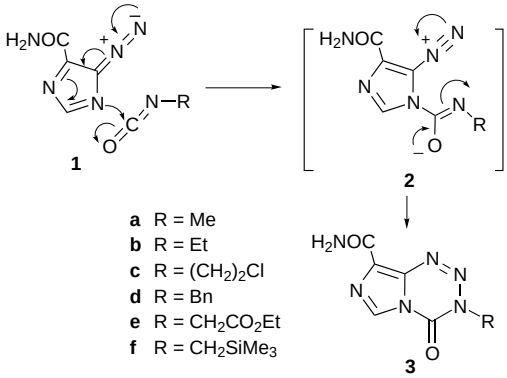
Our earlier work to develop alternative syntheses of temozolomide had exploited imidazotetrazinones *e.g.* **3e**,**f** prepared from less volatile 'masked' methyl isocyanates, which can be deprotected under conditions which retain the integrity of the base-fragile ring-system.[5] Here we report a new synthesis of temozolomide starting with 5-aminoimidazole-4-carboxamide hydrochloride **4**, which adapts another route developed by Ege[6] for the synthesis of pyrazolotetrazinones, so obviating the use of the potentially unstable diazoimidazole **1**. A parallel synthesis designed to furnish 4-thiotemozolomide surprisingly took an entirely different path and led to the construction of a new ring-system, imidazo[1,5-*b*][1,2,4]thiadiazole.

Interaction of the free base of **4** with methyl, ethyl, 2-chloroethyl and benzyl isocyanates in $Me_2SO$ or acetonitrile afforded the ureas **5a**–**d**†‡ regioselectively (75–95%) despite the availability of competing sites for carbamoylation. Nitrosative cyclisation of **5a** in 2 M hydrochloric acid in the temperature range 5–25 °C gave a red solution from which temozolomide **3a** precipitated in 30–35% yield. A by-product, 2-azahypoxanthine (15%), is probably formed by competing nitrosative cyclisation to the primary carboxamide group followed by loss of methyl isocyanate. Compared with the ease with which *N*-alkylanthranilamides cyclise to 3-alkyl-1,2,3-benzotriazin-4(3*H*)-ones[7] the yield of temozolomide is disappointing, but accountable for by the weakly acidic nature of the urea proton in the diazonium species **6a** which suppresses generation of the dipolar intermediate **2a**, the presumed precursor to temozolomide. Higher yields of the imidazotetrazinones **3b**–**d** were isolated (50–70%) by cyclisation of the corresponding ureas **5b**–**d**: also we have shown previously[5] that, in the case of the urea **5e** formed from ethyl isocyanatoacetate, cyclisation gave the imidazotetrazine **3e** (93%) consistent with the hypothesis that an electron-withdrawing group R facilitates ionisation of the urea proton, and hence cyclisation (Scheme 2).

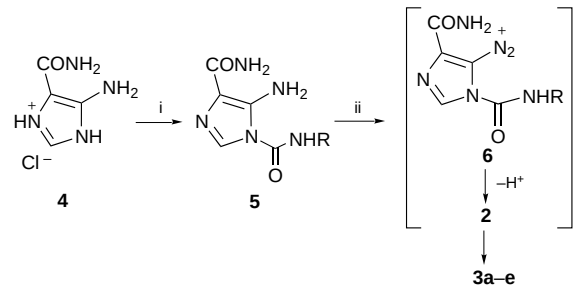
Interaction of the aminoimidazole carboxamide **4** with methyl isothiocyanate gave a thiourea (90%) which on nitrosation with excess nitrous acid at 25 °C gave a red product (85%), originally considered to be thiotemozolomide on the basis of its $^1H$ and $^{13}C$ NMR spectra which were comparable with that of temozolomide. However, elemental and mass spectral analysis confirmed a molecular formula $C_6H_6N_6O_2S$ (thiotemozolomide + 16 mass units). An X-ray structure determination (Fig. 1) revealed that the product was 2-nitrosomethylaminoimidazo[1,5-*b*][1,2,4]thiadiazole-4-carboxamide **11**.

A logical route to this unexpected compound is outlined in Scheme 3. Methylsulfanylcarbamoylation of the free base of amine **4** evidently affords the thiourea **7**†‡ substituted at the exocyclic amino group. Nitrosation of the thiol tautomer **7′** would generate an *S*-nitroso intermediate **8** which might cyclise to the imidazothiadiazole **10** directly (−HNO) or, probably, undergo further oxidation in the excess nitrous acid to the *S*-nitro intermediate **9** which would then cyclise ($-HNO_2$) to afford the bicycle **10**. Further nitrosation of the *sec*-amine group of **10** to afford the nitrosamine **11**‡§ is to be expected, although the exact timing of this step is not clear.

Of the five other imidazothiadiazole ring-systems reported in the literature only one, imidazo[1,2-*b*][1,2,4]thiadiazole,[8] contains an imidazole bridgehead nitrogen atom attached to sulfur.




**Scheme 1**




**Scheme 2** *Reagents and conditions*: i, RNCO, $Me_2SO$ or MeCN, 0–25 °C, $NEt_3$; ii, $NaNO_2$ in 2 M HCl, 0–25 °C

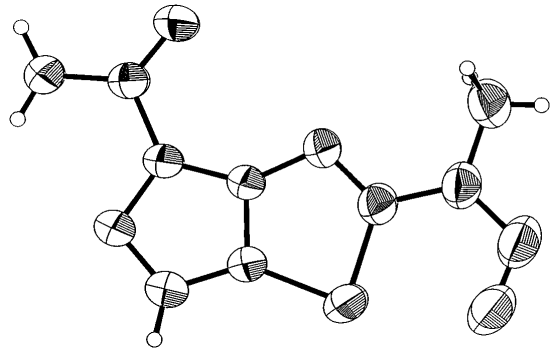
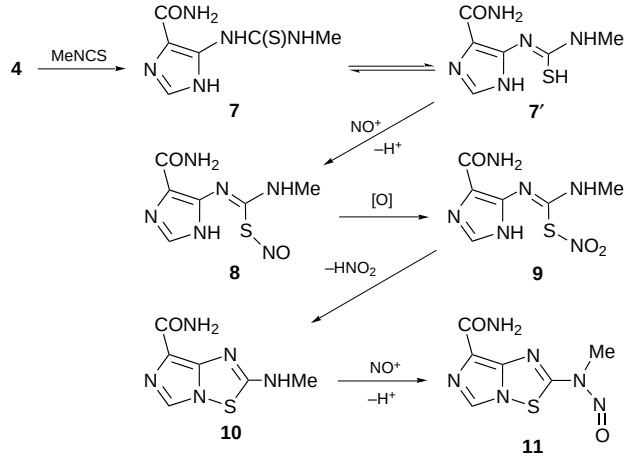


**Fig. 1** ORTEP view of the structure of 2-nitrosomethylaminoimidazo-[1,5-*b*][1,2,4]thiadiazole-4-carboxamide **11**. Displacement elipsoids are shown at the 50% probability level.




**Scheme 3**

This new synthesis of **11** in two steps from the aminoimidazole **4** is notable for the high yield and mild conditions and may be adapted for the synthesis of other examples of this intriguing new bicyclic system.

This work was supported by the Cancer Research Campaign, UK. We thank collaborators at Aston Molecules Ltd, Birmingham, UK and Schering-Plough Research Institute, Kenilworth, New Jersey, USA for helpful discussions.

## Footnotes

† *General experimental method* for ureas **5** and thiourea **7**. A solution or suspension of 5-aminoimidazole-4-carboxamide hydrochloride (0.5 g) and dry triethylamine (1 ml) in dry $Me_2SO$ or acetonitrile (10 ml) was treated dropwise (1 h) with the isocyanate or isothiocyanate (1.2 equiv.) at 10 °C (−10 °C in the case of acetonitrile). The mixture was stirred overnight at 25 °C, quenched with water (25 ml), and products collected and washed successively with water and ethyl acetate. Yields of ureas were **5a** (85%), **5b** (75%), **5c** (70%), **5d** (95%) and the thiourea **7** (85%). Satisfactory microanalytical data were obtained for new compounds.

‡ *Selected physical data* for ureas **5**, thiourea **7** and imidazothiadiazole **11**. 5-Amino-1-(*N*-methylcarbamoyl)imidazole-4-carboxamide **5a**: mp 170 °C (decomp.); $\nu_{max}$ (KBr) 3409, 1718, 1661, 1535, 1453, 1311, 1241, 947 cm$^{-1}$; $\delta_H$ [$(CD_3)_2SO$] 8.46 (q, 1 H, NH), 7.62 (s, 1 H, H-2), 6.93 (br s, 1 H, NH), 6.83 (br s, 1 H, NH), 6.39 (br s, 2 H, $NH_2$), 2.78 (d, 3 H, $CH_3$); $\delta_C$ [$(CD_3)_2SO$] 167.2, 151.6, 144.3, 127.0, 112.1, 27.5; *m/z* 184 ($M^+$ + 1); 5-Amino-1-(*N*-ethylcarbamoyl)imidazole-4-carboxamide **5b**: mp 150–152 °C (decomp.); $\nu_{max}$ (KBr) 3476, 3360, 3276, 1718, 1656, 1532, 1294, 847 cm$^{-1}$; $\delta_H$ [$(CD_3)_2SO$] 8.51 (m, 1 H, NH), 7.64 (s, 1 H, H-2), 6.92 (br s, 1 H, NH), 6.81 (br s, 1 H, NH), 6.37 (br s, 2 H, $NH_2$), 3.22 (m, 2 H, $CH_2$), 1.11 (t, 3 H, $CH_3$); $\delta_C$ [$(CD_3)_2SO$] 167.2, 150.2, 150.9, 144.4, 127.1, 112.1, 35.8, 15.3; *m/z* 198 ($M^+$ + 1); 5-Amino-1-[*N*-(2-chloroethyl)carbamoyl]imidazole-4-carboxamide **5c**: mp 102–105 °C (decomp.); $\nu_{max}$ (KBr) 3432, 3364, 3257, 1720, 1651, 1550, 1502, 1325 cm$^{-1}$; $\delta_H$ [$(CD_3)_2SO$] 8.79 (m, 1 H, NH), 7.68 (s, 1 H, H-2), 6.92 (br s, 1 H, NH), 6.84 (br s, 1 H, NH), 6.40 (br s, 2 H, $NH_2$), 3.78 (t, 2 H, $CH_2CH_2Cl$), 3.59 (q, 2 H, $CH_2CH_2Cl$);$\delta_C$ [$(CD_3)_2SO$] 170.3, 154.4, 147.6, 130.1, 115.3, 46.9, 45.9; *m/z* 231/233 ($M^+$); 5-Amino-1-(*N*-benzylcarbamoyl)imidazole-4-carboxamide **5d**: mp 163–168 °C (decomp.); $\nu_{max}$ (KBr) 3323, 3202, 1735, 1637, 1532, 1492, 1316, 1250 cm$^{-1}$; $\delta_H$ [$(CD_3)_2SO$] 9.09 (t, 1 H, NH), 7.74 (s, 1 H, H-2), 7.34 (m, 5 H, Ph), 6.92 (br s, 1 H, NH), 6.84 (br s, 1 H, NH), 6.42 (br s, 2 H, $NH_2$), 4.45 (d, 2 H, $CH_2$); $\delta_C$ [$(CD_3)_2SO$] 168.2, 152.3, 145.5, 140.2, 130.3, 129.2, 129.0, 128.0, 113.1, 45.2; *N*-(4-Carbamoylimidazol-5-yl)-*N*′-methylthiourea **7**; mp 200–205 °C (decomp.); $\nu_{max}$ (KBr) 3374, 3205, 2914, 1663, 1574, 1528, 1481, 1327 cm$^{-1}$; $\delta_H$ [$(CD_3)_2SO$] 12.63 (br s, 1 H, NH), 10.26 (br s, 1 H, NH), 9.89 (br s, 1 H, NH), 7.82 (s, 1 H, H-2), 7.43 (br s, 2 H, $NH_2$), 3.08 (d, 3 H, $CH_3$); $\delta_C$ [$(CD_3)_2SO$] 183.8, 167.6, 149.5, 139.1, 110.9, 37.2; *m/z* 199 ($M^+$); 2-Nitrosomethylaminoimidazo[1,5-*b*][1,2,4]thiadiazole-4-carboxamide **11**; mp 145–150 °C (decomp.); $\nu_{max}$ (KBr) 3481, 3423, 3365, 3139, 3126, 3039, 1675, 1625 1507, 1125 cm$^{-1}$; $\delta_H$ [$(CD_3)_2SO$] 8.08 (s, 1 H, H-6), 7.30 (br s, 1 H, NH), 7.16 (br s, 1 H, NH), 4.50 (s, 3 H, $CH_3$); $\delta_C$ [$(CD_3)_2SO$] 163.9, 154.8, 145.1, 126.4, 119.9, 31.6; *m/z* 227 ($M^+$ + 1).

§ *Crystal data* for **11**: $C_6H_6N_6O_2S$, $M$ = 226.23, monoclinic, space group $P2_1/n$, $a$ = 7.522(7), $b$ = 9.121(2), $c$ = 13.383(7) Å, $b$ = 97.73(6)°, $U$ = 910(1) Å$^3$, $Z$ = 4, $D_c$ = 1.65 g cm$^{-3}$, $F(000)$ = 464, (Cu-K$\alpha$) = 1.54180 Å, $\mu$ = 3.148 mm$^{-1}$, A lath 0.65 × 0.40 × 0.24 mm grown from $Me_2SO$–$Et_2O$ was mounted on an Enraf-Nonius CAD 4 diffractometer. 1734 unique reflections were collected by $\bar{\omega} - 2\theta$ for $2° \leqslant \theta \leqslant 75°$ and phased by direct methods.[8] Full-matrix least-squares refinement[10] on $F^2$ with anisotropic thermal parameters for non hydrogen atoms and all hydrogen atom positions determined from difference Fourier synthesis. At convergence, $R$ = 0.076, $R_w$ = 0.22 and GOF = 1.105 for 1479 observed reflections [$I > 2\,\delta I$]. Atomic coordinates, bond lengths and angles, and thermal parameters have been deposited in the Cambridge Crystallographic Data Centre (CDDC). See information for Authors, Issue No. 1. Any requests to the CDDC for this material should quote the full literature citation and the reference number 182/301.

## References

1 S. M. O'Reilly, E. S. Newlands, M. G. Glaser, M. Brampton, J. M. Rice-Edwards, R. D. Illingworth, P. G. Richards, C. Kennard, I. R. Colquhoun, P. Lewis and M. F. G. Stevens, *Eur. J. Cancer*, 1993, **29A**, 940.
2 N. M. Bleehen, E. S. Newlands, S. M. Lee, N. Thatcher, P. Selby, A. H. Calvert, G. J. S. Rustin, M. Brampton and M. F. G. Stevens, *J. Clin. Oncol.*, 1995, **13**, 910.
3 M. F. G. Stevens, J. A. Hickman, R. Stone, N. W. Gibson, G. U. Baig, E. Lunt and C. G. Newton, *J. Med. Chem.*, 1984, **27**, 196.
4 G. Ege and K. Gilbert, *Tetrahedron Lett.*, 1979, 4253.
5 Y. Wang, M. F. G. Stevens, W. T. Thomson and B. P. Schutts, *J. Chem. Soc., Perkin Trans. 1*, 1995, 2783.
6 G. Ege, K. Gilbert and K. Maurer, *Chem. Ber.*, 1987, **120**, 1375.
7 J. G. Erickson, in *The Chemistry of Heterocyclic Compounds*, ed. J. G. Erickson, P. F. Wiley and V. P. Wystrach, Interscience Publishers, Inc., New York, 1956, vol. 10, pp. 1–43; M. F. G. Stevens, *Progr. Med. Chem.*, 1976, **13**, 205.
8 C. C. Beard, USP 3 979 404/1976 (*Chem. Abstr.*, 1977, **86**, P29815).
9 G. M. Sheldrick, SHELX86, Program for Crystal Structure Solution, *Acta Crystallogr., Sect. A*, 1990, **46**, 467.
10 G. M. Sheldrick, SHELX93, University of Göttingen, Germany, 1993.

*Received, 6th September 1996; Com. 6/06159A*

# From monomeric iminosilane to a monomeric aminoalane: synthesis and crystal structures

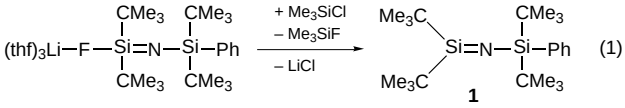
**Jörg Niesmann,[a] Uwe Klingebiel,*[a] Mathias Noltemeyer[a] and Roland Boese[b]**

[a] *Institut für Anorganische Chemie der Universität, Tammannstr. 4, D-37077 Göttingen, Germany*
[b] *Institut für Anorganische Chemie, Universität-GH Essen, Universitätsstr. 5-7, D-45117 Essen, Germany*

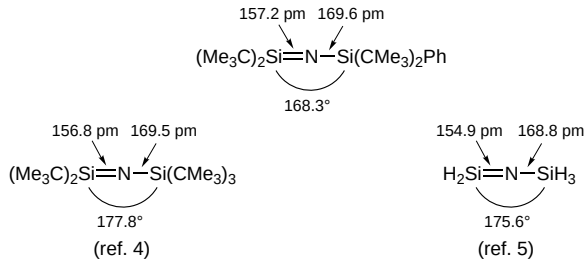
**The reaction between the iminosilane $R_2Si{=}NR'$ [R = $CMe_3$, R′ = $Si(CMe_3)_2Ph$] 1 and $AlMe_3$ in *n*-hexane at −78 °C affords the first monomeric aminodimethylalane $Me_2Al{=}N(R')R''$ [R″ = $Si(CMe_3)_2Me$] 2; the crystal structure of 2 is presented.**

Compounds of multiple bond systems involving heavier main group elements were long considered to be unstable and synthetically inaccessible.[1–3] The first silaethenes and disilenes were synthesised at the beginning of the 1980s, and the first iminosilanes were reported in the mid-1980s.[1–3]

The uncoordinated and thermally stable iminosilane $R_2Si{=}NR'$ [R = $CMe_3$, R′ = $Si(CMe_3)_2Ph$] **1** is formed in quantitative yield in the reaction between the lithiated fluorosilylamine compound and $SiClMe_3$.[1] It is based on a fluorine/chlorine exchange with subsequent thermal LiCl elimination [eqn. (1)].[1]




The crystal structure of **1** shows a trigonal arrangement of the $C_2Si{=}N$ unit around the silicon atom. In solid state the iminosilane is monomeric and the Si=N–Si skeleton is nearly linear (168.3°). The Si–N bond lengths are drastically different. The Si–N single bond is 169.6 pm, and the Si=N double bond is 157.2 pm. The results are consistent with Wiberg's experimental[4] and von Rague Schleyer's calculated[5] results.

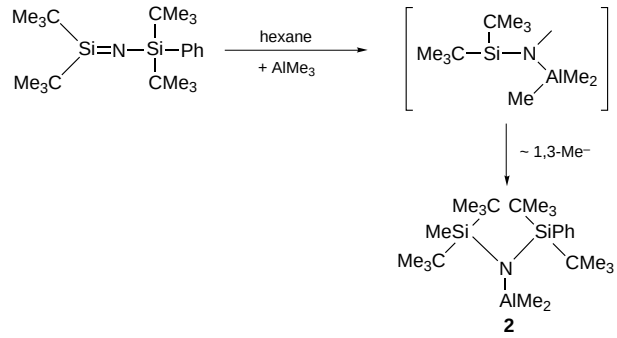



Iminosilanes react with Lewis bases, for example, with ethers or tertiary amines with formation of adducts. The adducts are often thermally stable and can be distilled without decomposition.[1,6] Reactions of iminosilanes with Lewis acids are not described so far. We found that di-*tert*-butyl(di-*tert*-butylphenylsilyl)iminosilane **1** reacts with trimethylalane, $AlMe_3$, to give the monomeric aminoalane, $Me_2AlN[Si(CMe_3)_2Me]Si(CMe_3)_2Ph$ **2** (Scheme 1).†‡

Unassociated compounds of the form $R_2M–NR'_2$ (M = B, Al, *e.g.* **2**) have the potential for π bonding between the main group 3 element (M) and nitrogen through overlap of the lone pair on nitrogen with the empty p orbital on boron or aluminium. Such π bonding is well established in molecules containing boron–nitrogen bonds.

The chemistry of the heavier group 3 elements, *e.g.* Al, is dominated by the tendency to form dimers or more highly associated structures. However, three-coordination is achieved by the use of bulky substituents.[7]

For the first time a monomeric aminodimethylalane is obtained by a nucleophilic methanide-ion migration from aluminium to silicon. The methanide-ion migration can be explained by the strong Lewis acidity of the three-coordinate silicon, which must be stronger than the Lewis acidity of the three-coordinate aluminium.




**Scheme 1**

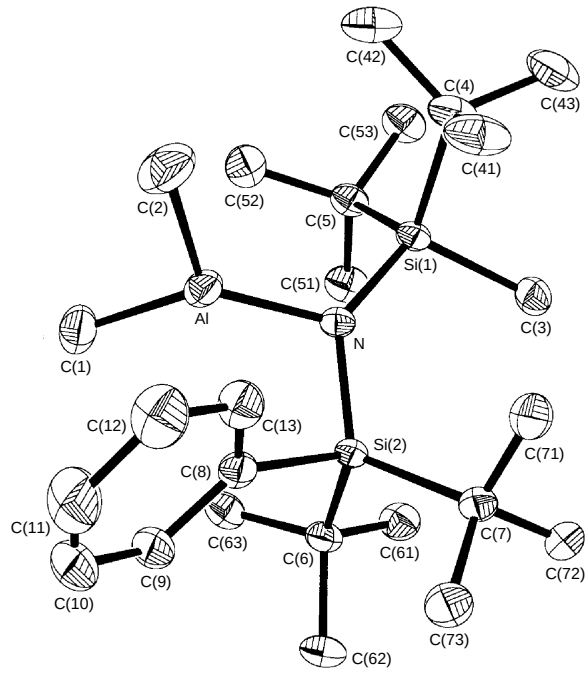



**Fig. 1** Molecular structure of **2** (ORTEP, thermal ellipsoids at the 50% probability level). Principal distances (pm) and angles (°): Al–N 186.9(2), Al–C(2) 195.4(2), Al–C(1) 196.4(2), Al–C(8) 256.4(3), Al–Si(2) 284.43(8), Si(1)–N 175.2(2), Si(2)–N 175.0(2); C(2)–Al–C(1) 108.03(11), C(1)–Al–N 125.66(9), C(2)–Al–N(1) 124.09(10), Σ < Al(1) = 357.8°, Si(2)–N–Si(1) 133.88(9), Al–N–Si(2) 103.56(7), Al–N–Si(1) 122.53(8), Σ < N(1) = 360.0°. Torsion angle C(1)–Al–N–Si(1) −57.5°.

The structure of **2**§ which is depicted in Fig. 1 consists of well separated $Me_2AlN(R')R$ monomers. The Al–N bond length is 186.9 pm. The geometry of the Al atom is nearly planar (sum of angles = 357.8°). The C–Al–C angle is 108.03°. The geometry of the nitrogen centre is also planar (sum of angles = 360.0°) with the widest angle, 133.9°, between the silyl groups. The torsion angle of the C(2)–Al–N–Si(1) axis is −57.5°. There is a weak intramolecular interaction of the electron deficient aluminium atom with the C(8) atom of the phenyl ring facing the metal, Al–C(8) 256.4 pm. This decreases the Al–N–Si(2) angle (103.6°) and brings the Al and Si(2) atoms into close proximity [Al–Si(2) 284.4 pm]. The Al–N bond length is short in comparison to the simple sum of the aluminium and nitrogen covalent radii, *i.e*. 200 pm, which suggests the presence of Al–N $p_\pi$–$p_\pi$ bonding. However, the dihedral angle C(1)–Al–N–Si(1) of −57.5° makes this very limited. Therefore most of the shortening of the Al–N bond should be attributed to the difference of the electronegativity. The Al–N bond length is comparable the Al–N distances of $Bu^t_2AlN$ compounds.[7]

This work was supported by the Deutsche Forschungsgemeinschaft and the Fonds der Chemischen Industrie.

## Footnotes

† *Preparative details*. Starting materials: **1**,[8] yellow oil, bp 108 °C (0.01 Torr), trimethylaluminium, 2.0 M solution in toluene. Reaction under dry argon. To 4.31 g (11.5 mmol) of di-*tert*-butyl(di-*tert*-butylphenylsilyl)iminosilane **1**,[8] which was freshly distilled into a Schlenk bulb, was added 60 ml of degassed dry hexane. Then 5.74 ml (11.5 mmol, 2.0 M solution in toluene) trimethylaluminium were added at −78 °C. The solution was stirred at −78 °C for 2 h and at 25 °C for 1 day. After removal of the solvent *in vacuo* ($10^{-2}$ Torr) and recrystallisation of the residue from toluene crystalline compound **2** was obtained in 74% yield; mp 121 °C; MS (EI): *m/z* (%) = 432(30) $[M - CH_3]^+$, 390(100) $[M - C_4H_9]^+$.

‡ *NMR data*: **2** ($C_6D_6$–toluene): $^1$H, δ −0.63 (s, 6H, $AlMe_2$), 0.40 (s, 3H, SiMe), 1.21 (s, 18H, $CMe_3$), 1.23 (s, 18H, $CMe_3$), 6.97– 8.06 (m, 5H, Ar-H); $^{13}$C, δ −0.13 (s, SiMe), 1.82 (br s, $AlMe_2$), 22.83/23.56 (s, $CMe_3$), 30.97/31.54 (s, $CMe_3$), 129.29 [s, Ph (C-3, C-5)], 132.56 [s, Ph (C-4)], 137.60 [s, Ph (C-2, C-6)], 137.65 [s, Ph (C-1)]; $^{29}$Si, δ -3.37 (s, SiPh), 7.13 (s, SiMe).

§ *Crystal data for* **2**: a crystal of size 0.4 × 0.6 × 0.8 $mm^3$ was measured on a STOE/Siemens AED2 four circle diffractometer with Mo-Kα radiation at 153 K. The space group is monoclinic, $P2_1/n$, with unit-cell dimensions $a$ = 11.1930(10), $b$ = 15.601(2), $c$ = 16.622(3) Å, β = 105.750(10)°, $U$ = 2793.6(7) $Å^3$, $Z$ = 4, refined from 30 reflections centred at positive and negative 2θ positions; μ = 0.170 $mm^{-1}$ and $F$(000) = 992. 3401 reflections up to 2θ = 45° were collected, of which 3396 were independent ($R_{int}$ = 0.014). The structure was solved using direct methods (SHELXS) and refined on $F^2$ (SHELX93) with no disorder indicated: $R_1[I > 2\sigma(I)]$ = 0.0347, $wR_2$ = 0.0852; for all 3391 data $R_1$ = 0.0391, $wR_2$ = 0.092, GOF = 1.071.

Atomic coordinates, bond lengths and angles, and thermal parameters have been deposited at the Cambridge Crystallographic Data Centre (CCDC). See Information for Authors, Issue No. 1. Any request to the CCDC for this material should quote the full literature citation and the reference number 182/311.

## References

1 I. Hemme and U. Klingebiel, *Adv. Organomet. Chem*., 1996, **39**, 159.
2 R. West, *Angew. Chem., Int. Ed. Engl*., 1987, **26**, 1201.
3 A. G. Brook and K. M. Baines, *Adv. Organomet. Chem.*, 1986, **25**, 1.
4 N. Wiberg, K. Schurz, G. Reber and G. Müller, *J. Chem. Soc., Chem. Commun*., 1986, 591.
5 P. von Ragué-Schleyer and P.O. Stout, *J. Chem. Soc., Chem. Commun.*, 1986, 1373.
6 S. Walter, U. Klingebiel and D. Schmidt-Bäse, *J. Organomet. Chem.*, 1991, **412**, 319.
7 P. J. Brothers and P. P. Power, *Adv. Organomet. Chem.*, 1996, **39**, 1.
8 D. Grosskopf, L. Marcus, U. Klingebiel and M. Noltemeyer, *Phosphorus Sulfur Silicon*, 1994, **97**, 113.

*Received, 22nd August 1996; Com. 6/05842F*

# Reaction of furans with trithiazyl trichloride: new synthesis of isothiazoles

**Xiao-Lan Duan, Charles W. Rees and Tai-Yuen Yue**

*Department of Chemistry, Imperial College of Science, Technology and Medicine, London, UK SW7 2AY*

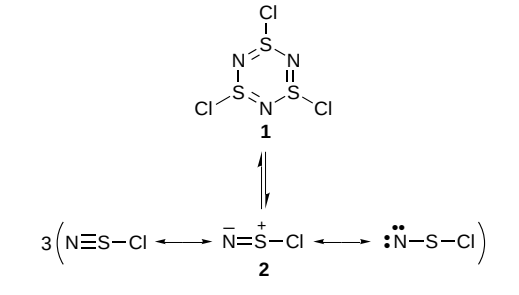
**Trithiazyl trichloride 1 converts 2,5-disubstituted furans into isothiazoles (*e.g.* 3, 6, 7) regiospecifically and in good yield, providing a new, one-step synthesis of isothiazoles, for which a novel mechanism involving formation and ring-opening of a β-thiazylfuran 4 is proposed.**

Trithiazyl trichloride **1**[1] is a stable but moisture-sensitive, yellow crystalline solid, prepared by heating ammonium chloride and sulfur with disulfur dichloride, and chlorination of the resulting salt, $S_3N_2Cl_2$.[2] The cyclic trimer **1** is in thermal equilibrium with the highly reactive monomer, thiazyl chloride **2** (Scheme 1). It is reactive towards many simple organic substrates and has considerable potential in the synthesis of sulfur-nitrogen compounds.[3]

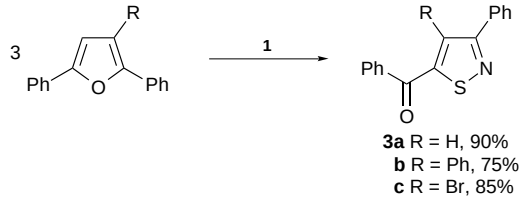
We thought that the monomer **2** might be selectively intercepted by furans in a Diels–Alder reaction.[4] Trithiazyl trichloride **1** reacted very cleanly with 2,5-diphenylfuran in boiling $CCl_4$, converting 3 equiv. into 5-benzoyl-3-phenylisothiazole **3a** in high yield (90%) (Scheme 2). 2,3,5-Triphenylfuran and 3-bromo-2,5-diphenylfuran reacted similarly to give the analogous isothiazoles **3b** (75%) and **3c** (85%). No isomers of the products were detected and so cleavage of the furan ring and incorporation of the S–N unit is apparently regiospecific. This represents a new opening of the furan ring and a new, mild, one-step synthesis of isothiazoles. Closely related, but fully substituted furans, such as 3,4-dibromo-2,5-diphenyl- and 3-bromo-2,4,5-triphenyl-furan did not react with the reagent **1**; clearly a ring hydrogen is required for the formation of HCl, which is evolved during the reactions. 2,5-Bis-(4-methylphenyl)-, 2,5-bis(4-methoxyphenyl)- and 2,5-di-*tert*-butylfuran all gave the analogous isothiazoles in boiling $CCl_4$ or toluene, although in somewhat lower yields (50–60%).

All of these products could have been formed by Diels–Alder reactions with thiazyl chloride **2**, followed by rearrangement of the adduct with loss of HCl,[3] but the above results led us to consider an alternative mechanism. This is based upon electrophilic substitution of the furan ring at an unsubstituted β-position to give a β-thiazyl derivative **4**, which could then rearrange to the isothiazole by a ring-opening, ring-closing mechanism (Scheme 3). We hoped to distinguish between these mechanisms by reacting the trimer **1** with polarised, unsymmetrical 2,5-disubstituted and 2,3,5-trisubstituted furans.

2-(4-Methoxyphenyl)-5-(4-nitrophenyl)furan **5a** in boiling THF gave 5-(4-methoxybenzoyl)-3-(4-nitrophenyl)isothiazole **6** (85%) very cleanly and regiospecifically (Scheme 4). This agreed well with the substitution mechanism (Scheme 3) since the aryl groups at C-2 and C-5 would strongly direct electrophilic attack to C-3, which leads to the observed isomer **6**. However, this result is harder to reconcile with the Diels–Alder mechanism since the expected orientation, based on the polarities of the furan **5a** and thiazyl chloride ($N^+{=}S^-{-}Cl$) would most reasonably lead to the undetected isothiazole isomer. The more nucleophilic furan ring position (C-3) of **5a** was then 'blocked' by bromination to give **5b**, which was treated with the trimer **1** under the same conditions. The reaction of **5b** was considerably slower than that of **5a**, but it too gave only one product, 4-bromo-2-(4-methoxyphenyl)-5-(4-nitrobenzoyl)isothiazole **7** (65%) with the *opposite* regiochemistry. This follows from the substitution mechanism, where the thiazyl substituent is introduced at the only available (deacti-

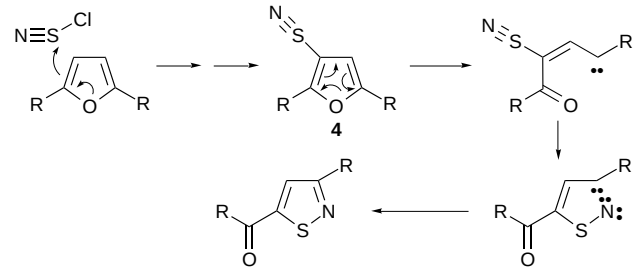


**Scheme 1**

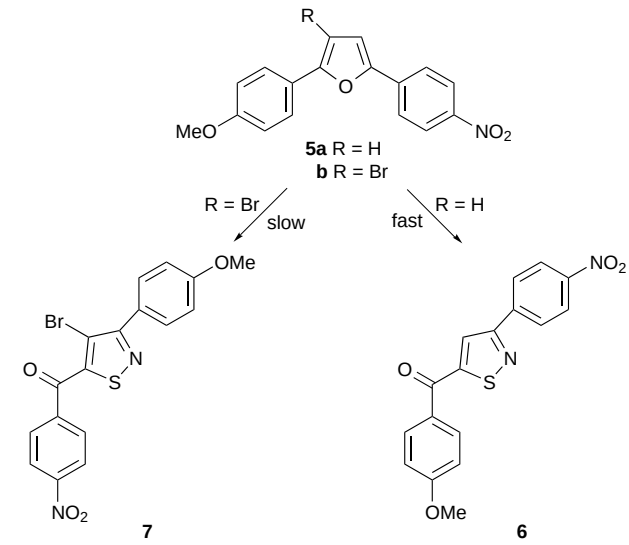


**3a** R = H, 90%
**b** R = Ph, 75%
**c** R = Br, 85%

**Scheme 2**



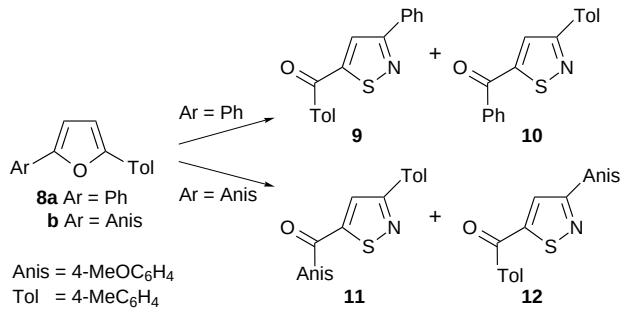
**Scheme 3**



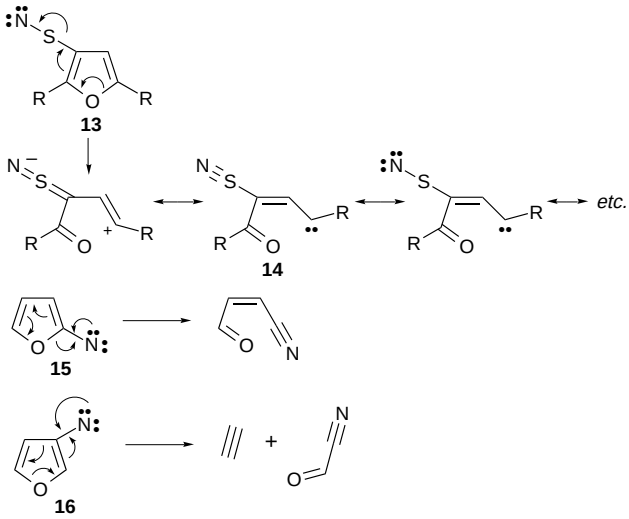
**Scheme 4**

vated) site, which leads to the observed isomer (Scheme 3). The Diels–Alder mechanism would require the complete reversal of orientation of cycloaddition, on passing from furan **5a** to **5b**, which seems unlikely.

Each of these highly polarised furans gave only one isothiazole; it seemed likely that if the degree of polarisation was reduced both possible isomeric isothiazoles might be formed, and this proved to be so. Thus 2-(4-methylphenyl)-5-phenylfuran **8a** and 2-(4-methoxyphenyl)-5-(4-methylphenyl) furan **8b** were treated with the trimer in boiling THF




**Scheme 5**




**Scheme 6**

(Scheme 5). Detailed analysis of the $^1$H NMR spectra showed that each gave mixtures of two isomeric isothiazoles which were inseparable by chromatography; these were **9** and **10** (3.3 : 1) (56%) and **11** and **12** (3.9 : 1) (65%) respectively. Thus in each case the more electron-releasing aryl group in the furan becomes part of the 5-aroyl group of the major isomer, in agreement with the reaction of the more highly polarised furan **5a**, where only the 'major' isomer was observed. On the mechanism of Scheme 3, substitution of SN should predominate at the ring position adjacent to the more electron-releasing group, which then transforms into the 5-aroyl group, as observed. The expected orientation in the Diels–Alder reaction would have led to the minor rather than the major isomer.

From all this evidence we favour the mechanism of Scheme 3. The initially puzzling step, ready opening of the β-thiazyl furan ring, is comprehensible when the nitrenoid character **13** of this intermediate is considered. The highly reactive thiazyl substituent could induce cleavage of the furan ring (arrows in **4** ≡ **13**) to give the delocalised intermediate **14** which then collapses to the isothiazole (Scheme 6). This unusual ring-opening is somewhat analogous to the well established cleavage reactions of nitrenes (and carbenes) directly attached to furan and other five-membered heterocyclic rings (*cf.* **15** and **16**).[5]

The structures of all the new compounds reported here are based on a detailed analysis and comparison of their spectra, particularly NMR and mass spectra, with model compounds. These data, and syntheses of the compounds, will be presented in a full paper.

We thank Zeneca Specialities, the Commonwealth Scholarship Commission and MDL Information Systems (UK) Ltd for financial support, and the Wolfson Foundation for establishing the Wolfson Centre for Organic Chemistry in Medical Science at Imperial College.

## References

1 *Gmelin Handbook of Inorganic Chemistry*, 8th edn., *Sulfur-Nitrogen Compounds*, Part 2, Springer-Verlag, Berlin, 1985, p. 92.
2 W. L. Jolly and K. D. Maguire, *Inorg. Synth.*, 1967, **9**, 107.
3 X.-G. Duan, X.-L. Duan, C. W. Rees and T.-Y. Yue, *J. Heterocycl. Chem.*, 1996, **33**, 1419.
4 *cf.* J. Passmore and M. J. Schriver, *Inorg. Chem.*, 1988, **27**, 2749; A. Haas and T. Mischo, *Can. J. Chem.*, 1989, **67**, 1902.
5 T. L. Gilchrist, *Adv. Heterocycl. Chem.*, 1987, **41**, 41.

*Received, 12th December 1996; Com. 6/08345E*

# Trimethylsilyl chloride-accelerated reduction and pinacol coupling of carbonyl compounds by means of samarium diiodide

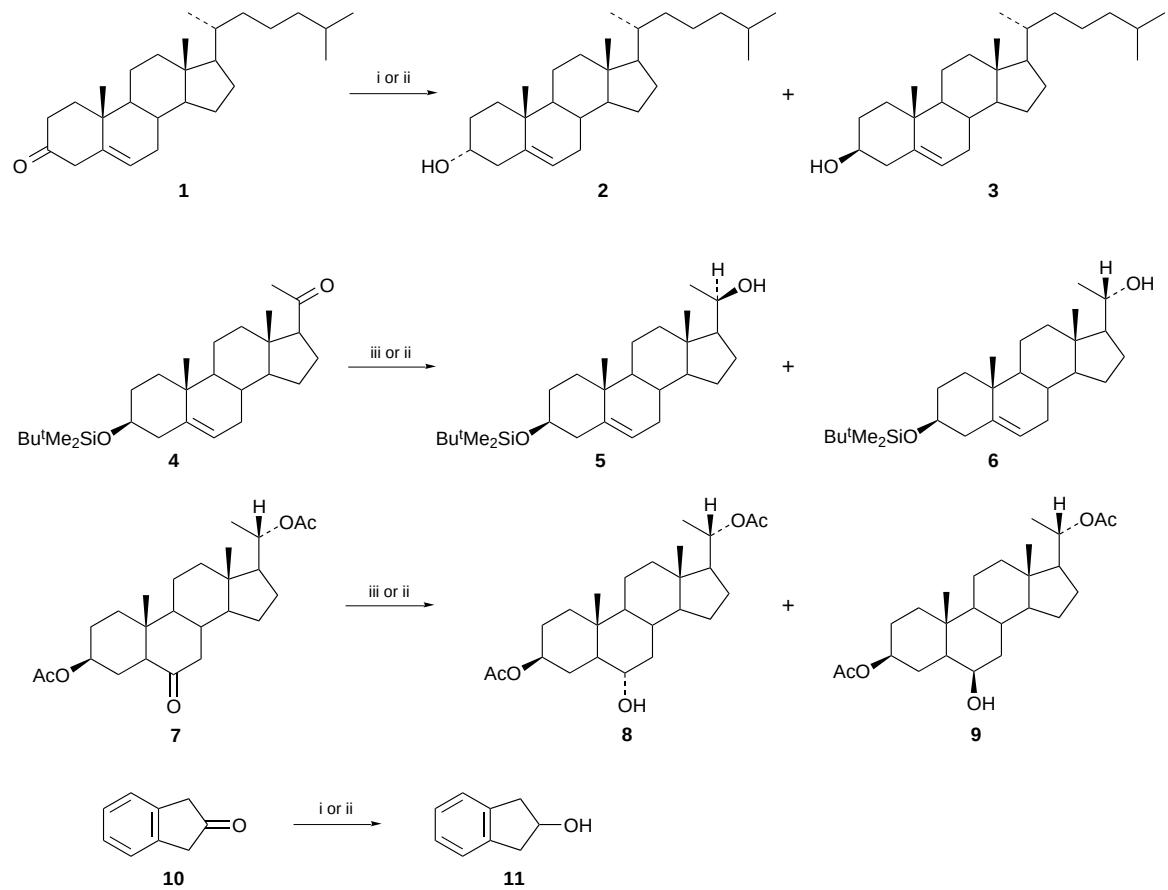
**Toshio Honda* and Miho Katoh**

*Institute of Medicinal Chemistry, Hoshi University, Ebara 2-4-41, Shinagawa-ku, Tokyo 142, Japan*

**The combination of samarium diiodide ($SmI_2$) and trimethylsilyl chloride ($Me_3SiCl$) in THF–HMPA is found to accelerate the reduction of sterically hindered and enolisable ketones, and also to accelerate pinacolisation of the carbonyl compounds depending on the reaction conditions.**

Samarium(II) diiodide, originally introduced by Kagan and co-workers[1] into organic synthesis, has been established as a useful synthetic reagent and a number of interesting reactions have been developed by application of this reagent.[2] $SmI_2$ is a powerful one-electron reducing agent and serves as an effective reductant of carbonyl compounds. $SmI_2$-promoted reduction of carbonyl compounds usually proceeds quickly and completes within a few minutes when the reaction is carried out in the presence of a proton donor such as an alcohol or water in tetrahydrofuran to prevent the formation of the pinacol coupling product.[1–3] During the course of our work on the synthesis of physiologically active compounds employing $SmI_2$, we observed that the reduction of ketones with $SmI_2$ in THF–HMPA was accelerated in the presence of $Me_3SiCl$ to give the corresponding alcohol(s) with Birch-type reduction stereochemistry in good yields.

Treatment of the 3-keto steroid **1** with 3 equiv. of $SmI_2$ in the presence of 3 equiv. of Bu$^t$OH as a proton donor in THF–HMPA at ambient temperature for 10 min afforded the corresponding alcohols [**2** (3α) : **3** (3β) = 28 : 57%].† When this reduction was carried out in the presence of 3 equiv. of $Me_3SiCl$ as an additive instead of Bu$^t$OH under the same reaction conditions, the yield improved to 90% [**2** (3α) : **3** (3β) = 30 : 60%].‡ Interestingly, reduction of the 20-keto steroid **4** with $SmI_2$ and Bu$^t$OH in THF–HMPA at room temperature required 6 h to afford the corresponding alcohols [**5** (20*S*) : **6** (20*R*) = 26 : 23%]. However, reduction of **4** under similar reaction conditions in the presence of $Me_3SiCl$ proceeded within 10 min to provide the alcohols (**5** and **6**)‡ in 93% yield, in a ratio of 1 : 1. The reaction became significantly faster in the presence of $Me_3SiCl$. A dramatic change was observed in the reduction of 6-keto steroid **7**, which on treatment with $SmI_2$ in THF–HMPA gave none of the desired alcohol, although HMPA was recognised to increase the rate of the reaction of $SmI_2$.[4]



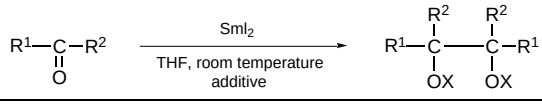

**Scheme 1** *Reagents and conditions*: i, $SmI_2$, Bu$^t$OH, THF–HMPA, room temp., 10 min; ii, $SmI_2$, $Me_3SiCl$, THF–HMPA, room temp., 1 min, then $Bu_4NF$, THF, room temp.; iii, $SmI_2$, Bu$^t$OH, THF–HMPA, room temp., 6 h

However, reduction of **7** was carried out with $SmI_2$ and $Bu^tOH$ for 6 h to afford the alcohols [**8** (6α) : **9** (6β) = 39 : 22%) in moderate yields. Moreover treatment for 10 min of **7** with $SmI_2$ in the presence of $Me_3SiCl$ afforded **8** as the sole product‡ in 91% yield. These varied reaction times and yields are reflected by the steric hindrance of the carbonyl groups (6-keto > 20-keto > 3-keto) and the above results clearly suggest that $Me_3SiCl$ accelerates the $SmI_2$-mediated reduction of sterically hindered ketones, although it is premature to present a detailed mechanistic rationale at the present time. This type of reduction was found to be effective to the enolisable ketones. Thus, the reduction of indan-2-one **10** with $SmI_2$ in THF–HMPA at ambient temperature in the presence of $Me_3SiCl$ proceeded within 1 min to give indan-2-ol **11** in 79% yield, whereas similar reduction with $SmI_2$ and $Bu^tOH$ after 10 min afforded **11** in 66% yield. The reduction was typically carried out as follows—to a stirred solution of $SmI_2$ in dry THF (7 $cm^3$), prepared from samarium metal (0.76 mmol) and diiodoethane (0.69 mmol), under argon at room temperature, was added HMPA (0.9 $cm^3$) and the resulting mixture was stirred for a further 15 min. After the successive addition of a solution of ketone (0.23 mmol) in THF (1 $cm^3$) and $Me_3SiCl$ (0.7 mmol), the mixture was stirred for the appropriate time and then treated with saturated aqueous sodium hydrogen carbonate. A stream of air was bubbled through the solution and an excess of Celite and $Et_2O$ were added. The solution was filtered and the filtrate was extracted with ethyl acetate. Evaporation of the solvent followed by treatment of the residue with $Bu_4NF$ (0.5 mmol) in THF (10 $cm^{-1}$) at room temperature afforded the desired alcohol.

The effectiveness of $Me_3SiCl$ for $SmI_2$-mediated pinacol coupling of the ketones in THF was also investigated. HMPA was used as co-solvent to reduce the formation of reduction products.[5] The results are summarised in Table 1 and indicate that the pinacol coupling of both aldehyde and ketone was also accelerated by the presence of $Me_3SiCl$. For example, it was reported that the pinacol coupling of hexyl methyl ketone with $SmI_2$ in THF–HMPA required 24 h to give the corresponding coupling product in 80% yield.[5] However, the same reaction in the presence of $Me_3SiCl$ proceeded within 3 min to give the coupling product in 77% yield (entry 2). Similar results were also obtained (see entires 5, 8 and 10), clearly indicating that $Me_3SiCl$ as an additive accelerated the pinacol coupling compared to the results previously reported.[5] A typical experimental procedure for the pinacol coupling is as follows—to a stirred solution of $SmI_2$ (5.1 mmol) in dry THF (50 $cm^3$), prepared from samarium metal and diiodoethane as above, were added a solution of ketone (1.55 mmol) in THF (2 $cm^3$) and $Me_3SiCl$ (4.7 mmol). The resulting solution was stirred for the appropriate time (see Table 1) under argon at room temperature. The mixture was worked-up as described above to give the coupling product.

In conclusion, we have found that $Me_3SiCl$ is an effective additive for the $SmI_2$-promoted reduction of ketones and also for pinacol coupling. Recently, Kagan and co-workers[6] reported the improved reactivity of $SmI_2$ by catalysis with transition metal salts, in which Barbier-type reactions were found to be accelerated in the presence of such metal salts. $Me_3SiCl$ in this work may play a similar role as the metal salts.

**Table 1** Pinacol coupling of the ketones




| Entry | Starting material R1 | Starting material R2 | Reaction conditions Additive | Reaction conditions Time | Product X | Yield (%)[c] |
|---|---|---|---|---|---|---|
| 1 | $C_6H_{13}$ | Me | — | 12 h | H | 75 |
| 2 | $C_6H_{13}$ | Me | $Me_3SiCl$[a] | 3 min | H | 77 |
| 3 | $C_6H_{13}$ | Me | — | 24 h | H | 80[d] |
| 4 | $C_7H_{15}$ | H | — | 45 min | H | 81 |
| 5 | $C_7H_{15}$ | H | $Me_3SiCl$[a] | 1 min | H[b] / $SiMe_3$ | 37 / 45 |
| 6 | $C_7H_{15}$ | H | — | 3 h | H | 85[d] |
| 7 | $PhCH_2CH_2$ | Me | — | 10 h | H | 78 |
| 8 | $PhCH_2CH_2$ | Me | $Me_3SiCl$[a] | 5 min | H | 78 |
| 9 | $PhCH_2CH_2$ | H | — | 1 h | H | 65 |
| 10 | $PhCH_2CH_2$ | H | $Me_3SiCl$[a] | 1 min | H[b] / $SiMe_3$ | 53 / 30 |

[a] 1.0 equiv. of starting material, 3.3 equiv. of $SmI_2$ and 3.0 equiv. of $Me_3SiCl$ were used. [b] A mixture of the alcohol and its trimethylsilyl ether was isolated. [c] Isolated yields. [d] This yield was based on the literature value (ref. 6).

## Footnotes

† The stereochemistry of the reduction products (**2, 3, 5, 6, 8** and **9**) were determined by comparison with authentic samples prepared according to literature procedures.

‡ The products from this reaction were trimethylsilyl ethers and the yields were obtained after their conversion into the corresponding alcohols by treatment with $Bu_4NF$ in THF.

## References


1 J. L. Namy, P. Girard and H. B. Kagan, *Nouv. J. Chim*., 1977, **1**, 5; P. Girard, J. L. Namy and H. B. Kagan, *J. Am. Chem. Soc*., 1980, **102**, 2693.

2 H. B. Kagan and J. L. Namy, *Tetrahedron*, 1986, **42**, 6573; J. Inanaga, *J. Synth. Org. Chem. Jpn*., 1989, **47**, 200; H. B. Kagan, *New J. Chem*., 1990, **14**, 453; J. A. Soderquist, *Aldrichimica Acta*, 1991, **24**, 15; G. A. Molander, *Chem. Rev*., 1992, **92**, 29; G. A. Molander and C. R. Harris, *Chem. Rev*., 1996, **96**, 307.

3 J. Souppe, J. L. Namy and H. B. Kagan, *Tetrahedron Lett*., 1982, 3497.

4 J. Inanaga, M. Ishikawa and M. Yamaguchi, *Chem. Lett*., 1987, 1485.

5 J. L. Namy, J. Souppe and H. B. Kagan, *Tetrahedron Lett*., 1983, **24**, 765.

6 F. Machrouhi, B. Hamann, J. L. Namy and H. B. Kagan, *Synlett*., 1996, 633.


*Received, 18th November 1996; Com. 6/07774I*

# Synthesis of potential inhibitors of GTP-cyclohydrolase I: an efficient synthesis of 8-substituted 7-deazaguanines

**Colin L. Gibson,† Klaus Paulini and Colin J. Suckling***

*Department of Pure & Applied Chemistry, University of Strathclyde, 295 Cathedral Street, Glasgow, UK G1 1XL*

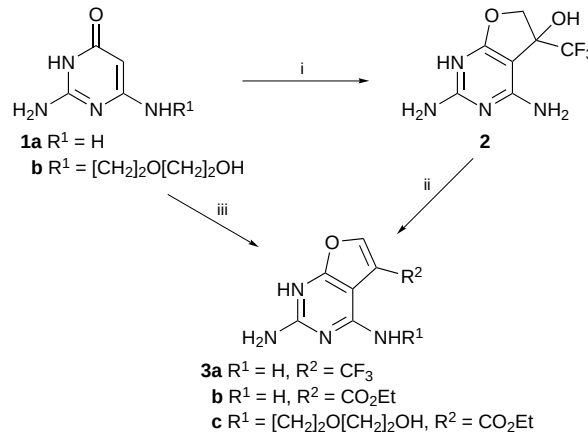
**A novel two step synthesis of 8-substituted 7-deazaguanines is developed and involves the regioselective alkylation of pyrimidinones 1a and 1b with nitrosoalkenes derived from α-halo oximes followed by transoximation to give the 7-deazaguanines 6a–d in 41–65% overall yield**

GTP-cyclohydrolase I catalyses the conversion of GTP into dihydroneopterin triphosphate and involves the opening of the imidazole and ribose rings with the loss of C-8 as formate, and Amadori rearrangement of the ribose portion.[1] Very little is known about the elementary steps of the process but the mechanism has been the subject of some discussion.[2–4] While there is consensus that the first step of the sequence involves attack of a nucleophile at C-8, the nature of the nucleophile ($H_2O$, $cys_{110}$-S-S-$cys_{181}$ or his) is still the subject of speculation. In order to address the issue of the nature of the nucleophile we wished to prepare potential inhibitors of GTP cyclohydrolase that had been designed to give stable tetrahedral nucleophilic C-8 addition intermediates. In this context, we proposed that 7-deazaguanines {pyrrolo[2,3-*d*]pyrimidin-4(3*H*)-ones} would not undergo subsequent imidazole ring opening and that by locating a strongly electron-withdrawing substituent at C-8, would afford stable tetrahedral intermediates.

Linear syntheses of 8-alkyl-7-deazaguanines have been reported involving the condensation of substituted ethyl cyanoacetate derivatives with guanidine hydrochloride.[5] This approach has been exploited by Seela and Chen for the synthesis of 8-methyl-7-deazaguanosine which was used in the synthesis of modified DNA oligionucleotides.[6] More direct convergent syntheses of 8-alkyl-7-deazaguanines have been carried out by the condensation of 2,6-diaminopyrimidin-4(3*H*)-ones with α-halo carbonyl compounds.[7] This latter approach suffers from problems of regiochemistry in that either 7-deazaguanines or furo[2,3-*d*]pyrimidines or mixtures of both are produced. In view of the fact that linear syntheses were unattractively long we carried out an initial study of the viability of the condensation routes involving α-halo ketones carrying α-electron-withdrawing groups. Thus, reaction of 2,6-diaminopyrimidin-4(3*H*)-one **1a** with 3-bromo-1,1,1-trifluoropropanone afforded, exclusively, the dihydrofuro[2,3-*d*]pyrimidine **2** in 67% yield (Scheme 1). The dihydrofuro[2,3-*d*]pyrimidine **2** could be dehydrated to the corresponding furo[2,3-*d*]pyrimidine **3a** (71% from **1a**) by treatment with concentrated sulfuric acid. Similarly, condensation of ethyl bromopyruvate with pyrimidinones **1a** or **1b** yielded the furo[2,3-*d*]pyrimidines **3b** and **3c**, directly, in 92 and 33% yields, respectively.

The failure of pyrimidinones **1a** and **1b** to yield 7-deazaguanines on reaction with α-halo ketones led to an evaluation of alternative novel routes to such species. In this context, nitrosoalkenes, generated *in situ* from α-halo oximes, are powerful electrophiles that have been shown to react with carbon nucleophiles at the β-carbon.[8] Given this reactivity pattern of nitrosoalkenes we anticipated that reaction with 2,6-diaminopyrimidin-4(3*H*)-one would provide short convergent syntheses of 8-substituted 7-deazaguanines. Accordingly, 3-bromo-1,1,1-trifluoropropanone oxime **4a** reacted with excess pyrimidinone **1a** in DMF to afford the C-5 alkylated pyrimidinone **5a** in 80% yield (entry 1, Table 1 and Scheme 2). Similarly, the oximes **4b**–**d** were treated with pyrimidinone **1a** in DMF in the presence of a base (excess **1a**, $Na_2CO_3$ or $Et_3N$) to give the C-5 alkylated pyrimidinones **5c** (57–79%, entries 5–7), **5e**‡ (38%, entry 10) and **5f** (47%, entry 11), respectively. The pyrimidinone **1b** carrying the 2-(2-aminoethoxy)ethanol side chain was also reacted with the oximes **4a** and **4b** in the presence of triethylamine or potassium carbonate to afford the C-5 alkylated pyrimidinones **5b** (43–58%, entries 3 and 4) and **5d** (47–61%, entries 8 and 9), respectively. In the syntheses of the pyrimidinones **5a**–**f** the only products were those derived from nucleophilic substitution of the C-5 position of pyrimidinones **1a** and **1b** at the α-carbon of the halo oximes **4a**–**d**, thus substantiating the potential of this method.

With an efficient method for the syntheses of pyrimidinones **5** with a C-5 alkyl oxime group we turned our attention to the cyclisation of these compounds to give 8-substituted 7-deaza-



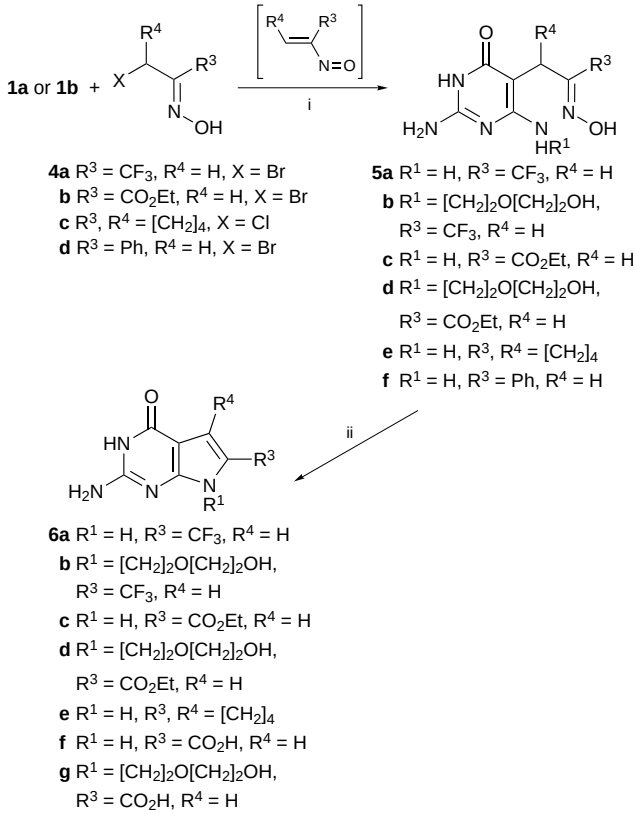

**Scheme 1** *Reagents and conditions*: i, 3-bromo-1,1,1-trifluoropropanone, DMF, 60 °C; ii, C $H_2SO_4$; iii, ethyl bromopyruvate, DMF, 60 °C

**Table 1** Synthesis of alkylated pyrimidinones **5** and cyclisation to 7-deazaguanines **6**

| Entry | Base | Product **5** | Yield of **5** (%) | Aldehyde | Product **6** | Yield of **6** (%) |
|---|---|---|---|---|---|---|
| 1 | **1a** | **a** | 80 | PhCHO | **a** | 81 |
| 2 | NaOAc[a] | **a** | 42 | [b] | **a** | 43 |
| 3 | $Et_3N$ | **b** | 58 | PhCHO | **b** | 71 |
| 4 | $Na_2CO_3$ | **b** | 43 | EtCHO | **b** | 52 |
| 5 | **1a** | **c** | 79 | PhCHO | **c** | 60 |
| 6 | $Na_2CO_3$ | **c** | 63 | MeCHO[c] | **c** | 30 |
| 7 | $Et_3N$ | **c** | 57 | — | — | — |
| 8 | $Et_3N$ | **d** | 61 | MeCHO[c] | **d** | 71 |
| 9 | $Na_2CO_3$ | **d** | 47 | PhCHO | **d** | 49 |
| 10 | $Na_2CO_3$[d] | **e** | 38[e] | — | — | — |
| 11 | $Et_3N$ | **f** | 47 | PhCHO or MeCHO[c] | decomp. | 0 |

[a] Reaction carried out in MeOH at 50–60 °C, 5 min. [b] Reaction carried out in DMF at 100–120 °C without aldehyde. [c] At room temperature. [d] At 60 °C for 96 h. [e] 64 : 36 Mixture of **5e** and **6e**.

guanines **6**. Thermal cyclisation of the trifluoro compound **5a** by heating in DMF at 100–120 °C gave the 8-trifluoromethyl-7-deazaguanine **6a** in 43% yield (Table 1, entry 2).[1] Unfortunately, this thermal procedure was not successful for the remaining oximes as slow decomposition was observed. An alternative method of transoximation involving heating the C-5 alkyl oximes **6a**–**d** with benzaldehyde in aqueous ethanol with a catalytic quantity of hydrochloric acid proved highly successful to afford the 8-substituted 7-deazaguanines **6a** (81%, entry 1), **6b** (71%, entry 3), **6c** (60%, entry 5) and **6d** (49%). The more reactive C-5 alkyl oximes **5b,c** and **d** could also be cyclised to the deazaguanines **6b** (52%, entry 4), **6c** (30%, entry 6) and **6d** (71%, entry 8) using the transoximation procedure with propanal or acetaldeyde. The phenyl substituted oxime **5f** failed to cyclise but underwent decomposition under a variety of conditions.




**Scheme 2** *Reagents and conditions*: i, DMF, base (see Table 1), room temp. 4–72 h; ii, EtOH–$H_2O$, benzaldehyde or acetaldehyde, cat. HCl, heat, 24–72 h

The 8-carboxy-7-deazaguanines **6f** (85%) and **6g** (83%) were also available by lithium hydroxide saponification of the respective esters **6c** and **6d**. Investigation of the 8-substituted 7-deazaguanines **6a**–**d** and **6f,g** and their triphosphorylated derivatives as inhibitors of GTP cyclohydrolase I is currently underway and these results will be reported in due course.

Grateful acknowledgement is made to the European Union for a Human Capital and Mobility Award (K. P.) (contract ERBCHRX CT93-0243).

## Footnotes

† E-mail: c.1.gibson@strath.ac.uk

‡ 64 : 36 mixture of oxime **5e** and 7-deazaguanine **6e**.

## References

1 G. M. Brown and J. M. Williamson, *Escherichia coli and Salmonella typhimurium*, Cellular and Molecular Biology, ed. F. C. Neidhardt, American Society of Microbiology, 1987, vol. 1, pp. 521–538.
2 W. Wolf and G. M. Brown, *Biochim. Biophys. Acta*, 1969, **192**, 468; J. J. Yim and G. M. Brown, *J. Biol. Chem*., 1976, **251**, 5087.
3 H. Nar, R. Huber, W. Meining, A. Bracher, M. Fischer, C. Hosl, H. Ritz, C. Schmid, S. Weinkauf and A. Bacher, *Biochem. Soc. Trans*., 1996, **24**, 375.
4 M. J. Dufton, C. L. Gibson, A. R. Pitt, S. Athmani and C. J. Suckling, unpublished results.
5 J. Davoll, *J. Chem. Soc*., 1960, 131; F. Seela and U. Lüpke, *Chem. Ber*., 1977, **110**, 1462; H. D. Winkeler and F. Seela, *J. Org. Chem*., 1983, **48**, 3119.
6 F. Seela and Y. Chen, *Chem. Commun*., 1996, 2263.
7 J. A. Secrist and P. S. Liu, *J. Org. Chem*., 1978, **43**, 3937.
8 T. L. Gilchrist and T. G. Roberts, *J. Chem. Soc*., *Perkin Trans. 1*, 1983, 1283 and references cited therein; H. C. Ottenheijm, R. Plate, J. H. Noordik and J. D. M. Herscheid, *J. Org. Chem*., 1982, **47**, 2147; R. Zimmer and H.-U. Reissig, *J. Org. Chem*., 1992, **57**, 339.

*Received, 10th December 1996; Com. 6/08297A*

# Diphosphines with large natural bite angles lead to the formation of non-classical *cis*-(diphosphine)$_2$Ru(H)(H$_2$)$^+$ complexes

**Mirko Kranenburg,[a] Paul C. J. Kamer,[a] Piet W. N. M. van Leeuwen*[a] and Bruno Chaudret*[b]**

[a] *J. H. van't Hoff Research Institute, Department of Inorganic Chemistry, University of Amsterdam, Nieuwe Achtergracht 166, 1018 WV Amsterdam, The Netherlands*

[b] *Laboratoire de Chimie de Coordination du CNRS, lié par conventions à l'Université Paul Sabatier, 205, Route de Narbonne, 31077 Toulouse Cédex, France*

**The application of diphosphine ligands with large natural bite angles leads to the formation of thermo-labile, non-classical *cis*-(diphosphine)$_2$Ru(H)(H$_2$)$^+$ complexes.**

The discovery of the first $\eta^2$-dihydrogen complex by Kubas *et al.*[1] has led to numerous studies on the factors determining the properties of such complexes. The bond between the transition metal and the $H_2$ ligand is a subtle balance between σ donation and π back-donation. Morris and coworkers have reported several studies on the effect of electronic modifications in diphosphine ligands on the stability of ruthenium dihydrogen complexes and on the acidity of the $H_2$ ligand.[2–9]

So far, few detailed studies have dealt with the effect of geometrical changes on the nature and reactivity of $\eta^2$-dihydrogen complexes.

Recently, Morokuma and coworkers reported that, with an increasing bite angle of the diphosphine, the nature of the (diphosphine)$_2$Ru('H$_3$')$^+$ complexes changes from *trans*-hydrido–dihydrogen to classical trihydride and to *cis*-hydrido–dihydrogen complexes.[10]

We recently developed[11] diphosphines based on xanthene-like backbones that allow the investigation of the effect of large bite angles on the properties of transition-metal complexes (Fig. 1). Here, we report that the geometrical constraints of these rigid bidentate phosphine ligands have a large effect on the structure and stability of ruthenium dihydrogen complexes.

*cis*-(Diphosphine)$_2$RuH$_2$ complexes **1** were prepared from Ru(cod)(cot) (cod = cycloocta-1,5-diene, cot = cycloocta-1,3,5-triene) and 2 equiv. of the diphosphine under 5 kPa $H_2$ (Fig. 2).†

Protonation of (thixantphos)$_2$RuH$_2$ **1a** at 176 K with HBF$_4$·OEt$_2$‡§ results in one product, which exhibits a broad symmetric signal in the $^1$H NMR spectrum at δ −6.7 and a double triplet in the $^{31}$P{$^1$H} NMR spectrum. Based on the $^{31}$P NMR spectrum and the $T_1$(min) for the hydride signal in the high-field region of the $^1$H NMR spectrum (17 ms at 240 K), we assign these signals to a *cis*-Ru(H$_2$)H species (**2a**). Upon raising the temperature slowly from 220 to 260 K, the signals from **2a** decrease and signals of a new species appear (Fig. 3). This new component gives rise to a sharp 14 line signal centred at δ −6.28 in the high-field region of the $^1$H NMR spectrum, and an ABMX splitting in the $^{31}$P{$^1$H} NMR spectrum. At 260 K this is the only species present. The nature of this new species was unambiguously determined by measurement of selective hydride-coupled $^{31}$P NMR as the cationic species (thixantphos)$_2$RuH$^+$ **3a**, resulting from the evolution of $H_2$ [$T_1$ (240 K) 242 ms]. The vacant site probably interacts with the counter ion or a solvent molecule (L).

Upon protonation of (sixantphos)$_2$RuH$_2$ **1b** at 176 K three products are formed as concluded from $^1$H and $^{31}$P NMR. In the high-field region of the $^1$H NMR spectrum one sharp 14 line multiplet centred at δ −5.6, similar to the signal observed for **3a**, and two broad signals located at δ −6.9 (major) and at δ −6.6 (minor) are present. Based on the $^{31}$P NMR spectrum and the $T_1$(min) value of the combined $^1$H signals at −6.9 to −6.6 (23 ms at 200 K), these signals are assigned to two *cis*-Ru(H$_2$)H isomers, **2b** and **2b′**. The ratio of these complexes is 1 (**2b′**) : 4 (**2b**) : 9 (**3b**). Increasing the temperature to 200 K results in a slight decrease of the amount of **2b**, **b′** and an increase of **3b** and at 210 K only the 14 line hydride signal of **3b** remains [$T_1$ (200 K) = 622 ms].

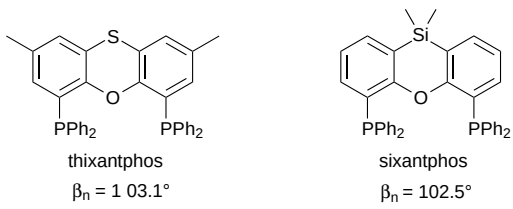



**Fig. 1** Structure and natural bite angles of the ligands. Bite angles calculated using molecular mechanics (CAChe WorkSystem),[12] with a P–Ru bond length of 2.424 Å[10] and a P–Ru–P angle bending force constant of 0 mdyn Å rad$^{-1}$ (1 dyn = 1 × 10$^{-5}$ N). The natural bite angle is defined as the preferred chelation angle determined only by ligand backbone constraints and not by metal valence angles.[13]

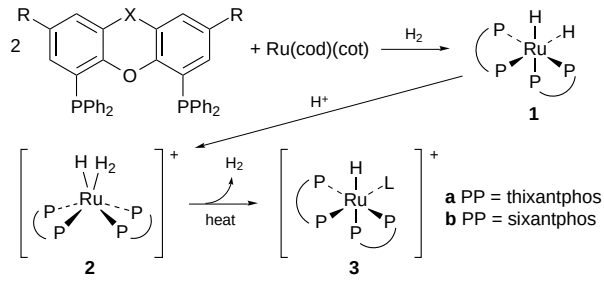



**Fig. 2** Reaction sequence leading to the products investigated

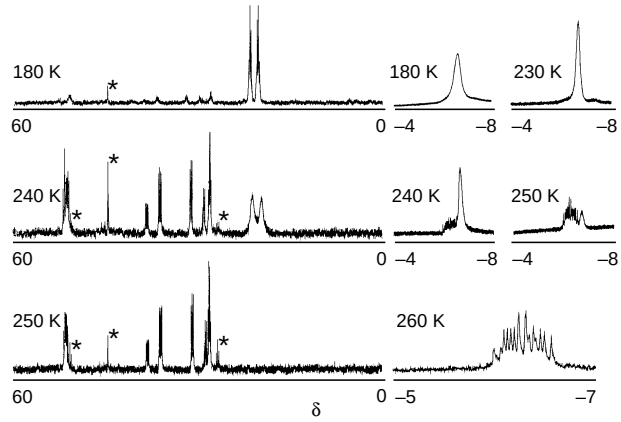



**Fig. 3** Change with temperature of the $^{31}$P{$^1$H} and high-field region of the $^1$H NMR spectra of the reaction mixture arising from protonation of **1a** with HBF$_4$·OEt$_2$; * denotes an impurity

The short $T_1$ values observed for **2** are indicative of the presence of short H–H distances (0.84 Å and 0.89 Å for **2a** and **2b** respectively as calculated from $T_1(H_2)$ and $T_1(H)$: see ef. 6.

Comparison of the $^{31}P\{^1H\}$ NMR spectra obtained for **2a** and **2b** reveals a notable difference in geometry for the complexes of these similar ligands. We used molecular modelling to investigate the possible geometries for these $(diphosphine)_2Ru(H)(H_2)^+$ complexes. The relative orientation of the backbones of the diphosphines when coordinated to the metal centre allows us to distinguish two types of complexes (Fig. 4). In complexes of type **A**, every P nucleus has a different environment, therefore all P nuclei are magnetically inequivalent and an ABMX splitting in the $^{31}P$ NMR spectrum is expected. In complexes of type **B**, we can distinguish two pairs of magnetically different P nuclei and an $A_2B_2$ splitting in the $^{31}P$ NMR spectrum is expected. In type **A** complexes the aromatic rings are more densely packed, compared to type **B** complexes, resulting in energetically favourable π-stacking interactions. This would be the favoured product (as seen in **2b**), but for thixantphos these stabilizing interactions are hampered by the methyl groups on the backbone, resulting in the formation of type **A** only.

The low thermal stability of **2a** and **2b** compared to other $(diphosphine)_2RuH_3^+$ complexes may be explained by the fact that the xantphos-type diphosphines enforce large bite angles, and therefore induce significant distortion of the octahedral ruthenium complex. INDO/1 calculations show that this distortion of the octahedral geometry induced by the xantphos-type diphosphines can lead to less optimal orbital overlap, resulting in decomplexation of $H_2$. Experimentally, for all three $(diphosphine)_2RuH_3^+$ complexes presented here, there is one signal corresponding to the '$H_3$' in the $^1H$ NMR spectra, indicating very rapid exchange as a result of the *cis* relative position of the hydride and dihydrogen ligands, unlike other $(diphosphine)_2MH_3^+$ complexes (M = Fe, Ru, Os), which only coalesce at higher temperatures.[2–7,9,14–17] Addition of $CF_3CO_2D$ to **1** leads for the product to the same $^1H$ and $^{31}P\{^1H\}$ NMR spectra as for protonation with $HBF_4{\cdot}OEt_2$. There is no resolvable H–D coupling, but in the $^{31}P\{^1H\}$ NMR spectrum all signals have small shoulders due to downfield isotopic shifts.

The application of diphosphines with large bite angles in the synthesis of $(diphosphine)_2Ru(H)(H_2)^+$ complexes emphasises the delicate nature of the bonding of $H_2$ to a transition metal. The distortion of the octahedral geometry of the complex favours the hydrogen atom exchange and destabilises the bond of $H_2$ to the metal centre by reducing the back-donation to the $H_2$ ligand. The results reported here provide experimental evidence for the predictions by Morokuma and coworkers[10] that an increase of the P–Ru–P bite angle might lead to a change from *trans*-hydride–dihydrogen complexes[14] to equilibria between *cis* and *trans* complexes,[15] and further to *cis* complexes. Furthermore these results show that tuning a steric parameter such as the natural bite angle of diphosphines dramatically influences the electronic properties of a transition-metal complex.

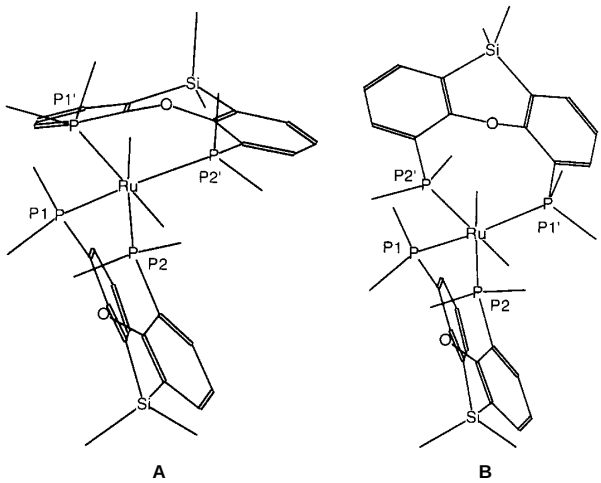



**Fig. 4** Two types of isomer for **2b**. Only $C_{ipso}$ atoms of phenyl groups are shown for clarity.

We thank F. Lacassin, G. Commenges (LCC du CNRS) and J. M. Ernsting (UoA) for assistance with NMR experiments, and the EU Human Capital and Mobility Program (MMCOS network) for financial support (in part) to M. K.

## Footnotes

† *Synthesis* of starting material: 0.120 g of Ru(cod)(cot) (0.381 mmol) and 2 equiv. of diphosphine were added to a Fisher–Porter bottle. The flask was flushed with argon, and 10 $cm^3$ of thf was added. Upon stirring a bright yellow solution formed, which was flushed with $H_2$, then pressurized to 5 kPa, and heated to 433 K for 20 h, during which time the reaction mixture turned dark brown. After cooling to room temp., the solvent was evaporated, and an extensive washing procedure yielded the pure product **1** (50–60%).

‡ *Protonation experiments*: a solution of **1** (*ca*. 0.01 g, *ca*. 7 μmol) in 0.5 $cm^3$ of $CD_2Cl_2$ was frozen in liquid $N_2$. $HBF_4{\cdot}Et_2O$ was added (3 $mm^3$, 35 μmol). The NMR tube was allowed to warm just to the melting point of the solution, shaken to dissolve the frozen $HBF_4{\cdot}Et_2O$, then immediately lowered into the NMR probe at 180 K. The first $^1H$ and $^{31}P\{^1H\}$ NMR spectra and the $T_1$ measurements were performed at this temperature. Subsequent measurements were performed at 10 K intervals up to 300 K.

§ *Selected NMR data*: $^1H$ and $^{31}P\{^1H\}$ NMR spectra measured in $CD_2Cl_2$ at 300 and 121.5 MHz respectively, except for **3a**, for which a separate experiment was performed in $(CD_3)_2CO$ with $^1H$ and $^{31}P\{^1H\}$ NMR spectra at 400 and 160 MHz, respectively. The $^1H$ data refers to the hydride region. **1a**; δ −8.32 (dt); $^{31}P\{^1H\}$, δ 36.3 (t), 33.5 (t). **2a**; $^1H$, δ −6.69 [br, $T_1$(min) 17 ms (240 K)]; $^{31}P\{^1H\}$, δ 21.7 (apparent t), 20.3 (apparent t). **3a**; $^1H$, δ −6.15 (m); $^{31}P\{^1H\}$, δ 33.5 (m), 35.0 (m), 42.5 (m), 57.2 (m).

## References

1 G. J. Kubas, R. R. Ryan, B. I. Swanson, P. J. Vergamini and H. J. Wasserman, *J. Am. Chem. Soc.*, 1984, **106**, 451.
2 R. H. Morris, F. F. Sawyer, M. Shiralian and J. Zubkowski, *J. Am. Chem. Soc.*, 1985, **107**, 5581.
3 M. Bautista, K. A. Earl, R. H. Morris and A. Sella, *J. Am. Chem. Soc.*, 1987, **109**, 3780.
4 M. Bautista, K. A. Earl, R. H. Morris and A. Sella, *J. Am. Chem. Soc.*, 1988, **110**, 7031.
5 E. P. Cappelani, P. A. Maltby, R. H. Morris, C. T. Schweitzer and M. R. Steele, *Inorg. Chem.*, 1989, **28**, 4437.
6 M. Bautista, E. P. Cappelani, S. D. Drouin, R. H. Morris, C. T. Schweitzer, A. Sella and J. Zubkowski, *J. Am. Chem. Soc.*, 1991, **113**, 4876.
7 K. L. Earl, G. Jia, P. A. Maltby and R. H. Morris, *J. Am. Chem. Soc.*, 1991, **113**, 3027.
8 B. Chin, A. J. Lough, R. H. Morris, C. T. Schweitzer and C. D'Agostino, *Inorg. Chem.*, 1994, **33**, 6278.
9 E. P. Cappelani, S. D. Drouin, G. Jia, P. A. Maltby, R. H. Morris and C. T. Schweitzer, *J. Am. Chem. Soc.*, 1994, **116**, 3375.
10 F. Maseras, N. Koga and K. Morokuma, *Organometallics*, 1994, **13**, 4008.
11 M. Kranenburg, Y. E. M. van der Burgt, P. C. J. Kamer, P. W. N. M. van Leeuwen, K. Goubitz and J. Fraanje, *Organometallics*, 1995, **14**, 3081.
12 CAChe WorkSystem, CAChe Scientific Inc., 18700 N.W. Walker Road, Building 92-01, Beaverton, OR 97006, USA.
13 C. P. Casey and G. T. Whiteker, *Isr. J. Chem.*, 1990, **30**, 299.
14 M. Saburi, K. Aoyagi, T. Takahashi and Y. Uchida, *Chem. Lett.*, 1990, 601.
15 M. Saburi, K. Aoyagi, H. Takeuchi, T. Takahashi and Y. Uchida, *Chem. Lett.*, 1990, 991.
16 M. Saburi, K. Aoyagi, T. Komada, T. Takahashi, Y. Uchida, K. Kozawa and T. Uchida, *Chem. Lett.*, 1990, 1909.
17 T. Tsukahara, H. Kawano, Y. Ishii, T. Takahashi, M. Saburi, Y. Uchida and S. Akutagawa, *Chem. Lett.*, 1988, 2055.

*Received, 12th August 1996; Com. 6/05635K*

# An elusive phase transition in $Na_2RbC_{60}$

**Luigi Cristofolini,[a] Konstantinos Kordatos,[a] Gerard A. Lawless,*[a] Kosmas Prassides,*[a] Katsumi Tanigaki*[b] and Martin P. Waugh[a]**

[a] *The Chemistry Laboratory, School of Chemistry, Physics and Environmental Science, University of Sussex, Brighton, UK BN1 9QJ*

[b] *NEC Fundamental Research Laboratories, Tsukuba 305, Japan*

**The ternary $Na_2RbC_{60}$ fulleride is studied by variable-temperature solid-state $^{13}C$ and $^{23}Na$ NMR spectroscopies; in addition to the well known orientational order/disorder transition, a phase transformation to a low-symmetry phase which likely contains bonded $C_{60}^{3-}$ moieties is identified at low temperature for the first time.**

Intercalation of solid $C_{60}$ with electron donors, like the alkali metals, results in a wealth of intercalated fulleride salts. All salts with stoichiometry $A_2A'C_{60}$ are metallic and display superconductivity (except $Li_2CsC_{60}$)[1] at critical temperatures as high as 33 K at ambient pressure,[2] surpassed only by the high $T_c$ superconducting oxides. All superconducting salts have been classified into two distinct, strictly cubic, families, distinguished through the orientational state adopted by the $C_{60}^{3-}$ ions in the crystal structure. For large alkali metals (A = K, Rb) occupying the tetrahedral interstices, a merohedrally disordered fcc structure in which the $C_{60}^{3-}$ ions are randomly distributed between two orientations related by 90° rotations about the cubic axes is adopted.[3] The second structural family is encountered when $Na^+$ resides in the tetrahedral interstices and both $Na_2RbC_{60}$[4] and $Na_2CsC_{60}$[5] have been shown to adopt a primitive cubic structure in which the majority of the $C_{60}^{3-}$ ions are rotated counterclockwise by *ca.* 98° about the appropriate [111] cube diagonal, with the remaining adopting minor orientations. Near room temperature, these salts also show a transition to an fcc structure, comprising orientationally disordered quasi-spherical $C_{60}^{3-}$ ions.[6] Here, we report the solid-state $^{13}C$ and $^{23}Na$ NMR spectra of $Na_2RbC_{60}$ in the temperature range 210–350 K. Our results reveal that in addition to the fcc → primitive cubic phase transition near room temperature, further cooling leads to a very slow phase transformation to a novel unsuspected low-symmetry structural form of $Na_2RbC_{60}$.

A high-resolution synchrotron X-ray diffraction profile of the $Na_2RbC_{60}$ sample† at 370 K reveals an fcc structure [$a$ = 14.1402(9) Å, space group $Fm\bar{3}m$] comprising quasi-spherical $C_{60}^{3-}$ ions, as expected. Fig. 1 shows the solid-state $^{13}C$ (MAS, spinning frequency = 6 and 8 kHz) and $^{23}Na$ (static) NMR spectra‡ of $Na_2RbC_{60}$ at 333, 253 and 213 K. The MAS $^{13}C$ NMR spectrum at 333 K [Fig. 1(*a*)] displays a single sharp peak at δ 189, consistent with fast rotational motion of the $C_{60}^{3-}$ ions in the fcc phase.[7] On cooling, a second peak appears gradually at δ 186 [Fig. 1(*a*) inset], with its intensity growing at the expense of the δ 189 resonance which becomes less intense until it completely disappears [Fig. 1(*b*)]. It can be assigned to the primitive cubic phase and remains sharp at 253 K, consistent with rapid large-amplitude librational motions of the $C_{60}^{3-}$ ions about their equilibrium orientations.[7] The temperature dependence of the static $^{23}Na$ NMR spectra mirrors that of $^{13}C$ NMR with the observation of both orientationally disordered (at 333 K) and ordered (at 253 K) phases, characterised by single resonances at δ 198 and 68 and linewidths at half height, $\nu_{\frac{1}{2}}$, of 1500 and 3300 Hz, respectively [Fig. 1(*d*) and (*e*)]. The increased linewidth in the orientationally ordered phase can arise from increased asymmetry due to two contributing factors: (*i*) the space group $Pa\bar{3}$ allows the displacement of the $Na^+$ ions (local symmetry $C_3$) from the ideal tetrahedral ($\frac{1}{4}$, $\frac{1}{4}$, $\frac{1}{4}$) positions along the [111] cube diagonals, and (*ii*) the coordination environment of the $Na^+$ ions is no longer symmetric, as they lie above the centre of a hexagonal face of one $C_{60}^{3-}$ ion and the midpoints of 6:6 bonds of three other neighbouring $C_{60}^{3-}$ ions.[5]

Further cooling to 213 K initially reveals little change in either $^{13}C$ or $^{23}Na$ NMR spectra. However, upon standing at 213 K, a continuous decrease in the intensity of the $^{13}C$ resonance (3 s repetition time, 8 kHz spinning frequency) is observed, until after *ca.* 4 h a plateau is reached at a value of *ca.* 50% of the original intensity. Prolonged time averaging (3700 repetitions)

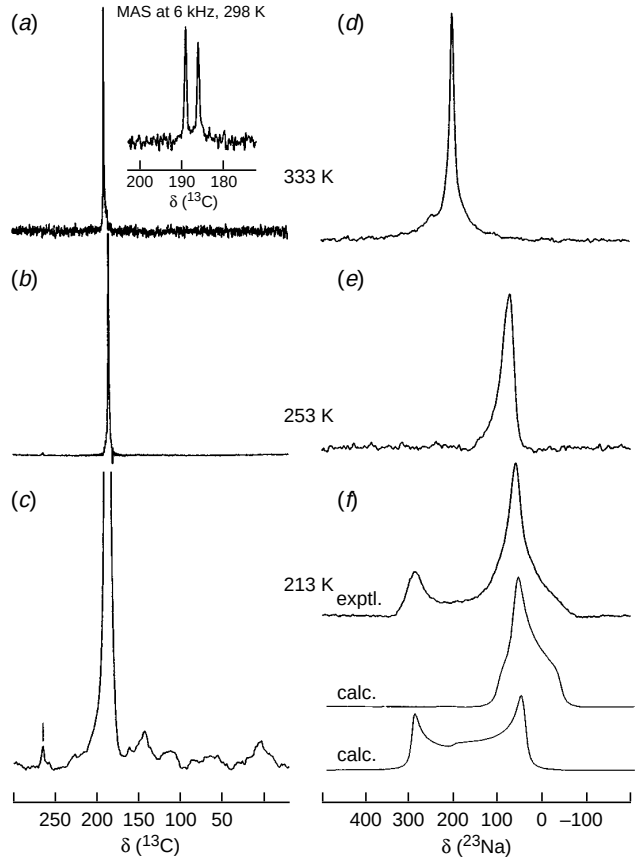



**Fig. 1** The solid-state $^{13}C$ (MAS) and $^{23}Na$ (static) NMR spectra of $Na_2RbC_{60}$: (*a*) $^{13}C$, fcc phase at $T$ = 333 K; the inset shows the spectrum at 298 K whence the two resonances signify coexistence of the fcc and primitive cubic phases. (*b*) $^{13}C$, primitive cubic phase at $T$ = 253 K. (*c*) expanded $^{13}C$, coexistence of primitive cubic and orthorhombic phases at 213 K; the vertical bar marks a spinning sideband. (*d*) $^{23}Na$, fcc phase at $T$ = 333 K. (*e*) $^{23}Na$, primitive cubic phase at $T$ = 253 K. (*f*) $^{23}Na$, coexistence of primitive cubic and orthorhombic phases at 213 K; the simulated spectra of the two resonances are also shown.

revealed numerous new features over the chemical shift range δ 0–250 [Fig. 1(*c*)], implying low crystalline symmetry and substantial distortion of the $C_{60}^{3-}$ ions. The shape of the static $^{23}$Na NMR spectrum also mirrors this change and evolves with time at 213 K; a new feature appears, saturating again after *ca.* 4 h [Fig. 1(*f*)]. Although the two $^{23}$Na resonances partially overlap, they can be separated by judicious choice of the relaxation delay in inversion recovery experiments, as they have very different longitudinal relaxation times, $T_1$ *ca.* 6 and 60 ms, respectively. Simulations of the complete spectrum are included in Fig. 1(*f*), using values of the NMR shift (arising from the combined effects of the chemical shift and the Knight shift), δ 60 and 208, of the quadrupole coupling constant, $(e^2qQ/h)$ = 2.51 and 4.63 MHz, and of the asymmetry parameter, η = 1.0 and 0.03 for the two resonances, respectively. The two phases exist in almost equal amounts.

The above NMR results are consistent with the presence of two phase transitions for $Na_2RbC_{60}$ in the temperature range 210–350 K. Firstly, the fcc → primitive cubic transformation is essentially complete, before a very slow transition, never going to completion, to a low-symmetry highly distorted structure occurs. Complementary high-resolution synchrotron and neutron diffraction experiments are in good agreement with this picture.[8] The low-symmetry phase at low temperature is identified as orthorhombic (space group *Immm*) with lattice constants at 180 K of *a* = 9.3819(8), *b* = 9.943(1) and *c* = 14.559(1) Å; it co-exists with the remaining fraction of the primitive cubic phase with *a* = 14.064(1) Å. The structural results for the orthorhombic phase are indicative of $C_{60}^{3+}$–$C_{60}^{3-}$ bonding in the low-temperature phase, as manifested by the existence of a very short temperature-independent interfullerene separation along *a* (9.38 Å), analogous to the situation encountered in the polymerised phases of $AC_{60}$ (A = K, Rb, Cs) salts[9] which show partial covalent bonding between strongly deformed $C_{60}^{-}$ ions. The broad $^{13}$C NMR spectra of the orthorhombic $Na_2RbC_{60}$ phase are also reminiscent of those measured for polymerised $AC_{60}$.[10] Work is in progress to search for the resonances associated with the bridging C atoms. An orthorhombic phase with comparable lattice dimensions had been observed at high pressures but it was thought that the application of pressure was essential for the phase transition and the resulting interfullerene bonding to occur.[11]

In conclusion, variable-temperature solid-state NMR measurements on $Na_2RbC_{60}$ establish the following sequence of phase transitions in the 210–350 K temperature range at ambient pressure: orthorhombic → primitive cubic → fcc. The NMR results are consistent with highly restricted $C_{60}^{3-}$ ions, most probably due to the formation of bonds between adjacent $C_{60}^{3-}$, as is found in the mono-alkali-metal fullerides. The hitherto unsuspected existence of the orthorhombic phase which completely eluded all earlier studies, presumably because of its slow kinetics, should aid rationalisation of many of the puzzling features of the physical properties of $Na_2RbC_{60}$.[12] In addition, its observation and the associated novel interfullerene bonding should not represent an isolated example, but rather a widespread phenomenon, begging a thorough reinvestigation of sodium (and lithium) fulleride chemistry.

We thank EPSRC for financial support [L. C., M. P. W. (ROPA)].

## Footnotes

† The $Na_2RbC_{60}$ sample used in the present work was prepared by reaction of stoichiometric quantities of $C_{60}$, Na and Rb contained in a sealed tantalum cell inside a sealed glass tube filled with He to 500 Torr at 480 K for 3 h, at 570 K for 12 h and at 620 K for 72 h; after an intermittent regrinding, the sample was annealed at 673 K for 25 days, employing the same experimental setup. Phase purity was confirmed by X-ray diffraction using a Siemens D5000 diffractometer.

‡ Solid-state $^{13}$C and $^{23}$Na NMR experiments with and without magic angle spinning (MAS) in an applied 9.395 T field were performed in the temperature range 210–350 K on a Bruker DMX-400 spectrometer (89 mm wide-bore magnet) with a 4 mm variable temperature double-bearing probe. The 50 mg sample was packed into a zirconia rotor with Kel-F end caps inside a glovebox and spun with $N_2$. A 30° excitation pulse was used for the $^{13}$C NMR experiments while the $^{23}$Na NMR spectra were acquired with a quad-echo pulse sequence.

## References

1 I. Hirosawa, K. Prassides, J. Mizuki, K. Tanigaki, M. Gevaert, A. Lappas and J. K. Cockcroft, *Science*, 1994, **264**, 1294.
2 A. F. Hebard, M. J. Rosseinsky, R. C. Haddon, D. W. Murphy, S. H. Glarum, T. T. M. Palstra, A. P. Ramirez and A. R. Kortan, *Nature*, 1991, **350**, 600; K. Tanigaki, T. W. Ebbesen, S. Saito, J. Mizuki, J. S. Tsai, Y. Kubo and S. Kuroshima, *Nature*, 1991, **352**, 222.
3 P. W. Stephens, L. Mihaly, P. L. Lee, R. L. Whetten, S. M. Huang, R. Kaner, F. Deiderich and K. Holczer, *Nature*, 1991, **351**, 632.
4 K. Kniaz, J. E. Fischer, Q. Zhu, M. J. Rosseinsky, O. Zhou and D. W. Murphy, *Solid State Commun.*, 1993, **88**, 47.
5 K. Prassides, C. Christides, I. M. Thomas, J. Mizuki, K. Tanigaki, I. Hirosawa and T. W. Ebbesen, *Science*, 1994, **263**, 950.
6 K. Tanigaki, I. Hirosawa, T. Manako, J. S. Tsai, J. Mizuki and T. W. Ebbesen, *Phys. Rev. B*, 1994, **49**, 12307.
7 C. Christides, K. Prassides, D. A. Neumann, J. R. D. Copley, J. Mizuki, K. Tanigaki, I. Hirosawa and T. W. Ebbesen, *Europhys. Lett.*, 1993, **24**, 755.
8 K. Prassides, K. Vavekis, K. Kordatos, K. Tanigaki, G. M. Bendele and P. W. Stephens, *J. Am. Chem. Soc.*, 1997, **119**, 834.
9 P. W. Stephens, G. Bortel, G. Faigel, M. Tegze, A. Janossy, S. Pekker, G. Oszlanyi and L. Forro, *Nature*, 1994, **370**, 636; S. Pekker, L. Forro, L. Mihaly and A. Janossy, *Solid State Commun.*, 1994, **90**, 349.
10 T. Kalber, G. Zimmer and M. Mehring, *Z. Phys. B*, 1995, **97**, 1; H. Alloul, V. Brouet, E. Lafontaine, L. Malier and L. Forro, *Phys. Rev. Lett.*, 1996, **76**, 2922.
11 Q. Zhu, *Phys. Rev. B*, 1995, **52**, R723.
12 K. Tanigaki and K. Prassides, *J. Mater. Chem.*, 1995, **5**, 1515; Y. Maniwa, T. Saito, K. Kume, K. Kikuchi, I. Ikemoto, S. Suzuki, Y. Achiba, I. Hirosawa, M. Kosaka and K. Tanigaki, *Phys. Rev. B*, 1995, **52**, R7054.

*Received, 2nd October 1996; Com. 6/06908H*

# Ruthenium maltolato complexes

**Michael D. Fryzuk,* Michael J. Jonker and Steven J. Rettig**

*Department of Chemistry, University of British Columbia, 2036 Main Mall, Vancouver, B.C., Canada V6T 1ZI*

**Two maltol molecules can be deprotonated and coordinated to Ru$^{II}$ to generate a series of octahedral complexes having the general formula Ru(ma)$_2$L$_2$ (ma = C$_6$H$_5$O$_3$; L = PPh$_3$, Me$_2$SO; L$_2$ = cycloocta-1,5-diene); when L = PPh$_3$, a precursor for the dimerization of phenylacetylene is obtained.**

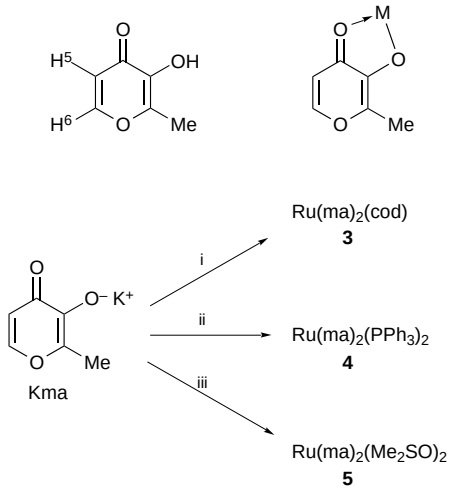
Maltol **1** is a naturally occurring, water-soluble, non-toxic food additive.[1] When deprotonated (p$K_a$ = 8.38),[2] it forms an anionic system capable of acting as a chelating, bidentate, O,O′ ligand of the type shown as **2**.

Because this ligand can confer water solubility on its metal complexes, even when the complexes are uncharged, there have been many reports on the use of this ligand in biological studies. For example, Al(ma)$_3$ has been used in studies related to Alzheimer's disease,[3] Fe(ma)$_3$ has been found to have potential as a treatment for iron-deficiency anaemia[4] and VO(ma)$_2$ has been tested as an insulin mimetic.[5–7] However, little work has been done on the use of this ligand in organometallic type complexes or in homogeneous catalysis.[8–10] Here we report the preparation and structure of a series of octahedral bis(maltolato) complexes of ruthenium[11] and show that one of these complexes shows activity for the dimerization of phenylacetylene.

The reaction of potassium maltolate, Kma (prepared by the addition of KOBu$^t$ to **1** in Et$_2$O), with a variety of ruthenium(II) complexes in organic solvents proved to be successful as a preparative route for the incorporation of the maltolato ligand. Thus, reaction of Kma with [Ru(cod)Cl$_2$]$_x$ in thf led to the formation of Ru(ma)$_2$(cod) **3** as orange–red crystals in 95% yield; similarly, addition of Kma to RuCl$_2$(PPh$_3$)$_3$ and RuCl$_2$(Me$_2$SO)$_4$ generated Ru(ma)$_2$(PPh$_3$)$_2$ **4** and Ru(ma)$_2$(Me$_2$SO)$_2$ **5**, respectively. These reactions are outlined in Scheme 1.

The solid-state structures of the cod complex **3** and the bis(dimethyl sulfoxide) derivative **5** were obtained and are shown in Figs. 1 and 2 respectively, along with selected bond lengths and angles.† Complex **3** is the first alkene complex of ruthenium(II) having only oxygen donors as ancillary ligands to be structurally characterized. Both structures display similar *cis* octahedral geometries; in fact upon close examination of the two structures in the solid state, the same $C_1$ molecular symmetry is found for each derivative. Because the maltolato ligand has two different oxygen donors, it can be considered as an anionic AB bidentate ligand; for an octahedral molecule having the general formula M(AB)$_2$L$_2$ (L = monodentate ligand), such a complex can exist in five stereoisomeric forms (*trans* and *cis* descriptors refer to disposition of L$_2$): two *trans* stereoisomers with $C_{2h}$ and $C_{2v}$ symmetry, respectively and three *cis* stereoisomers two of which have $C_2$ symmetry while the last is completely asymmetric ($C_1$). For the situation where L$_2$ is a symmetrical bidentate ligand, such as cod, only the three *cis* isomers are possible.

From the NMR spectroscopic data, the solid-state structure of **3** is maintained in solution such that only one species is observed and it displays peaks characteristic of a molecule with low symmetry. On the other hand, the bis(phosphine) complex **4** exists as a mixture of three of the possible five stereoisomers; one isomer shows two inequivalent phosphines by $^{31}$P{$^1$H}-NMR spectroscopy and resonances in the $^1$H NMR spectrum that compare to the asymmetric *cis* isomer found for **3** above. The remaining two stereoisomers of **4** have equivalent phosphines and equivalent maltolato ligands and thus could either




**Scheme 1** *Reagents and conditions*: i, [Ru(cod)Cl$_2$]$_x$, thf, 65 °C, 16 h; ii, RuCl$_2$(PPh$_3$)$_3$, thf, 22 °C, 16 h; iii, RuCl$_2$(Me$_2$SO)$_4$, toluene, 90 °C, 16 h

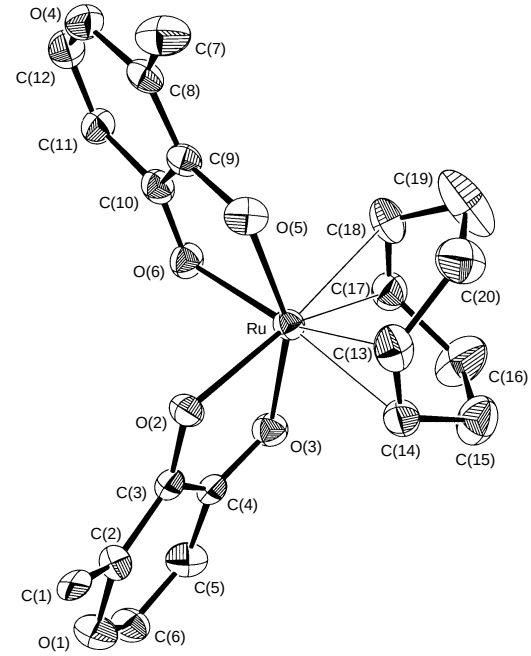



**Fig. 1** X-Ray crystal structure of Ru(ma)$_2$(cod) (**3**) (ellipsoids drawn at the 33% probability level). Selected interatomic distances (Å) and bond angles (°): Ru–O(2) 2.126(4), Ru–O(3) 2.098(5), Ru–O(5) 2.072(4), Ru–O(6) 2.114(4), Ru–C(13) 2.138(5), Ru–C(14) 2.157(7), Ru–C(17) 2.153(7), Ru–C(18) 2.161(6), O(2)–C(3) 1.306(7), O(3)–C(4) 1.288(7), C(3)–C(4) 1.43(1), O(5)–C(9) 1.335(7), O(6)–C(10) 1.262(9), C(9)–C(10) 1.45(1), C(13)–C(14) 1.34(2), C(17)–C(18) 1.46(1); O(2)–Ru– O(3) 79.5(2), O(5)–Ru–O(6) 79.5(2), O(3)–Ru–O(5) 156.0(2), O(2)–Ru–O(6) 92.7(2).

have *trans* or *cis* geometries. The situation for the $Me_2SO$ complex is more complex since isomers are also apparent in the crude reaction mixture but their $^1H$ NMR spectra overlap too much to be able to distinguish them.

While homoleptic maltolato complexes, $M(ma)_n$, are generally water soluble we found that only the bis(dimethyl sulfoxide) complex **5** exhibited any water solubility;[10] both the cod derivative **3** and the bis(phosphine) **4** were insoluble in $H_2O$. These complexes also displayed differences in their reactivity patterns. In this case, addition of phenylacetylene to either the cod complex **3** or the bis(dimethyl sulfoxide) **5** led to no reaction and recovery of starting materials. However, the bis(phosphine) derivative **4** was found to dimerize PhC≡CH to give the two possible linear isomers in a 1:1 ratio with turnover rates of *ca.* 20 $h^{-1}$ (Scheme 2).

Attempts to detect intermediates in this process by monitoring the reaction by $^{31}P\{^1H\}$ NMR spectroscopy were unsuccessful; however, when the dimerization was performed in the presence of excess $PPh_3$ the rate of the dimerization reaction was noticeably retarded. Thus, phosphine dissociation from **4** is required for activity, and this is reasonable given that this 18-electron complex contains two rather large, monodentate ligands. One can speculate further that the mechanism of alkyne dimerization involves a vinylidene intermediate[12,13] as required for the production of both *E* and *Z* isomeric forms of the eneyne product. Internal alkynes were generally found to be unreactive with all three of the bis(maltolato) complexes of Ru.

In this study we have demonstrated that organometallic type complexes and catalytic activity can be observed for Ru derivatives that are stabilized by the maltolato ancillary ligand. In addition, the cyclooctadiene complex **3** represents the first reported alkene-type complex of Ru stabilized by only oxygen donor ligands.

This work was supported by NSERC of Canada. We also acknowledge Johnson Matthey for the loan of Ru salts.

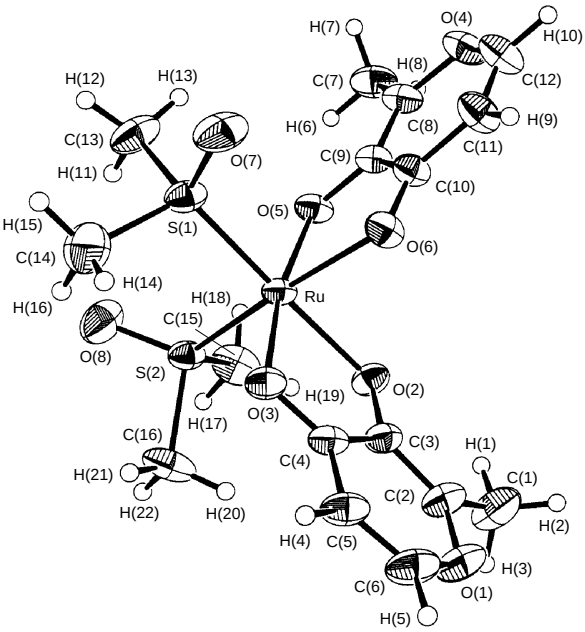
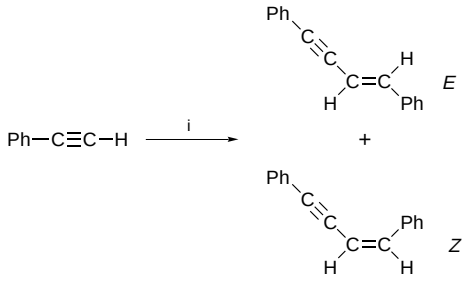



**Fig. 2** X-Ray crystal structure of $Ru(ma)_2(Me_2SO)_2$ **5** (ellipsoids drawn at the 33% probability level). Selected interatomic distances (Å) and bond angles (°): Ru–O(2) 2.106(2), Ru–O(3) 2.090(2), Ru–O(5) 2.078(2), Ru–O(6) 2.105(2), O(2)–C(3) 1.311(3), O(3)–C(4) 1.277(3), C(3)–C(4) 1.447(4), O(5)–C(9) 1.314(3), O(6)–C(10) 1.266(4), Ru–S(1) 2.2068(8), Ru–S(2) 2.1957(8), S(1)–O(7) 1.474(2), S(2)–O(8) 1.470(2); S(1)–Ru–S(2) 96.25(3), O(2)–Ru–O(3) 80.56(7), O(5)–Ru–O(6) 81.07(8), O(3)–Ru–O(5) 169.81(8), O(2)–Ru–O(6) 85.33(8).




**Scheme 2** *Reagents and conditions*: i, 1 mol% $Ru(ma)_2(PPh_3)_2$ **4**, 50 °C, toluene: *E*:*Z* ratio = 1:1

## Footnote

† *Crystal data*: **3**, $C_{20}H_{22}O_6Ru$, $M$ = 459.46, orthorhombic, space group $Pna2_1$ (no. 33), $a$ = 16.542(2), $b$ = 9.684(2), $c$ = 11.480(8) Å, $U$ = 1839.2(6) Å$^3$, $Z$ = 4, $D_c$ = 1.659 g cm$^{-3}$, μ(Mo-Kα) = 8.68 cm$^{-1}$, $F$(000) = 936. An orange–red prism of dimensions 0.10 × 0.10 × 0.15 mm was used. 3755 reflections were measured on a Rigaku AFC6S with Mo-Kα radiation using ω–2θ scans. The structure was solved by Patterson methods using full-matrix least-squares on $F$ for all non-hydrogen atoms using Lorentz polarization and absorption corrections to give $R$ = 0.034 and $R_w$ = 0.029 for 1775 independent observed reflections with $I > 3\sigma(I)$ and 244 variables for $2\theta_{max}$ = 65°.

**5**, $C_{16}H_{22}O_8RuS_2{\cdot}2.5C_6H_6$, $M$ = 702.82, triclinic, space group $P\bar{1}$ (no. 2), $a$ = 12.015(2), $b$ = 16.509(2), $c$ = 8.7933(8) Å, α = 99.853(9), β = 100.225(9), γ = 94.28(1)°, $U$ = 1681.2(4) Å$^3$, $Z$ = 2, $D_c$ = 1.388 g cm$^{-3}$, μ(Mo-Kα) = 6.19 cm$^{-1}$, $F$(000) = 726. An orange prism of dimensions 0.30 × 0.35 × 0.45 mm was used. 8104 relections were measured of which 7729 were unique using a Rigaku AFC6S with Mo-Kα radiation using ω–2θ scans. The structure was solved using direct methods using full-matrix least squares on $F$ for all non-hydrogen atoms using Lorentz polarization and absorption corrections to give $R$ = 0.038 and $R_w$ = 0.043 for 5946 independent observed reflections with $I > 3\sigma(I)$ and 379 variables for $2\theta_{max}$ = 55°. Atomic coordinates, bond lengths and angles, and thermal parameters have been deposited at the Cambridge Crystallographic Data Centre (CCDC). See Information for Authors, Issue No. 1. Any request to the CCDC for this material should quote the full literature citation and the reference number 182/293.

## References

1 L. F. Cavalieri, *Chem. Rev.*, 1947, **41**, 525.
2 T. Hedlund and L.-O. Öhman, *Acta Chem. Scand., Ser. A*, 1988, **42**, 702.
3 M. M. Finnegan, S. J. Rettig and C. Orvig, *J. Am. Chem. Soc.*, 1986, **108**, 5033.
4 M. T. Ahmet, C. S. Frampton and J. Silver, *J. Chem. Soc., Dalton Trans.*, 1988, 1159.
5 J. H. McNeill, V. G. Yuen, H. R. Hoveyda and C. Orvig, *J. Med. Chem.*, 1992, **35**, 1489.
6 P. Caravan, L. Gelmini, N. Glover, F. G. Herring, H. Li, J. H. McNeill, S. J. Rettig, I. A. Setyawati, E. Shuter, Y. Sun, A. S. Tracey, V. G. Yuen and C. Orvig, *J. Am. Chem. Soc.*, 1995, **117**, 12759.
7 K. Elvingson, A. G. Baro and L. Pettersson, *Inorg. Chem.*, 1996, **35**, 3388.
8 A. M. El-Hendawy and M. S. El-Shahawi, *Polyhedron*, 1989, **8**, 2813.
9 A. M. El-Hendawy, *Transition Met. Chem.*, 1992, **17**, 250.
10 L. Carter, D. L. Davies, J. Fawcett and D. R. Russell, *Polyhedron*, 1993, **12**, 1599.
11 S. J. Greaves and W. P. Griffith, *Polyhedron*, 1988, **7**, 1973.
12 C. Bianchini, P. Frediani, D. Masi, M. Peruzzini and F. Zanobini, *Organometallics*, 1994, **13**, 4616.
13 A. Dobson, D. S. Moore, S. D. Robinson, M. B. Hursthouse and L. New, *Polyhedron*, 1985, **4**, 1119.

*Received, 10th October 1996; Com. 6/06961D*

# Unprecedented dimethyl sulfoxide conformational equilibria and kinetics on $[Ir(Me_2SO)_3(\eta\text{-}C_5Me_5)][PF_6]_2$

**Antonio Cusanelli, Urban Frey and André E. Merbach***

*Institut de Chimie Minérale et Analytique, Université de Lausanne, CH-1015 Lausanne, Switzerland*

**Intermolecular dimethyl sulfoxide exchange on $[Ir(Me_2SO)_3(\eta\text{-}C_5Me_5)][PF_6]_2$ 1 proceeds *via* a dissociative mechanism, exclusively from a conformational isomer of 1 (1c) which is itself in equilibrium with a second more compact conformer (1a).**

The coordination chemistry of dimethyl sulfoxide was initially extended to the half-sandwich complexes $[M(Me_2SO)_3(\eta\text{-}C_5Me_5)][PF_6]_2$ (M = Rh, Ir) by Maitlis and coworkers.[1] These workers showed that these complexes were valuable intermediates for the synthesis of related compounds and that, more interestingly, these complexes were capable of rapidly exchanging bound $Me_2SO$ with free $Me_2SO$, although the kinetics of this exchange process were left unexplored. We now report the results of a dynamic $^1H$ NMR study on the iridium complex $[Ir(Me_2SO)_3(\eta\text{-}C_5Me_5)][PF_6]_2$ **1** which provides evidence in support of novel conformational equilibria and kinetics for the dimethyl sulfoxide exchange process.

In solution $Me_2SO$ coordinates to the relatively soft metal centre in **1** exclusively through the sulfur atom. This bonding assignment was initially confirmed by Maitlis and coworkers from IR investigations conducted on both $Me_2SO$ and $(CD_3)_2SO$ analogues of this complex[1] and this assignment is further corroborated by numerous X-ray crystal structures for similar iridium(III) complexes, which in all cases show the $Me_2SO$ ligand to be S bonded.[2] The spectroscopic results we have obtained for **1**† are in complete agreement with this assignment.

The low temperature $^1H$ NMR spectrum of **1**, acquired at 243.2 K in $CD_3NO_2$ containing excess free $Me_2SO$, did not show the expected two resonances corresponding to bound and free $Me_2SO$ respectively, but instead exhibited five resonances at δ 3.16, 3.15, 3.11, 2.99 and 2.56 (Fig. 1); the latter was unequivocally assigned to free solvent and the remaining signals were attributed to **1**.

Also present in this spectrum were two unequally populated resonances at δ 1.79 and 1.64 assigned to two unique $C_5Me_5$ groups. The three resonances at δ 3.16–3.13 integrated to six protons each with respect to the more populated of the $C_5Me_5$ signals whereas the remaining bound $Me_2SO$ resonance at δ 2.99 integrated to 18 protons with respect to the less populated $C_5Me_5$ moiety. Taken together, these results clearly suggest the presence of two stereoisomers of **1** (denoted as major and minor in Fig. 1), each composed of a $C_5Me_5$ group and three $Me_2SO$ ligands.

Considering first the major isomer of **1**, two conformers can account for the three resonance pattern observed for this species and these are depicted as structures **1a** and **1b** in Fig. 2; the symmetry of both structures is defined by a plane bisecting the $C_5Me_5$ centroid, Ir, and an S–O bond such that two $Me_2SO$ molecules and two Me groups are related by the mirror plane.

Upon closer inspection of the low-temperature limit NMR spectrum in Fig. 1, it is evident that the most deshielded resonance has a smaller linewidth at half-height ($\Delta\nu_{1/2}$ 1.7 Hz at 243.2 K) than the two adjacent resonances ($\Delta\nu_{1/2}$ 2.3, 2.2 Hz, respectively, at 243.2 K) which are broader but similar due, most likely, to a small unresolved $^4J_{HH}$ coupling ($^4J_{HH}$ couplings are *ca.* 0.1–0.4 Hz). Thus, one can assign the two broader resonances to the geminal methyl groups of the $Me_2SO$ molecules, labelled as A and B in Fig. 2, which are expected to be coupled. The most deshielded signal is then assigned to the remaining methyl groups, labelled as C in Fig. 2. These experimental results are thus consistent with conformer **1a**, rather than conformer **1b**, since the methyl groups (*i.e.* $Me_C$) in the former structure are expected to be more deshielded because of their close proximity to the ring current induced by the π electrons of the $C_5Me_5$ moiety. In addition, conformer **1a** is also the sterically preferred structure since it minimises the contacts between the bulky $C_5Me_5$ group and the $Me_2SO$ methyl groups.

With respect to the minor isomer of **1**, the single $^1H$ NMR resonance assigned to this conformer (Fig. 1) indicates that all three bound $Me_2SO$ groups in this species have the same

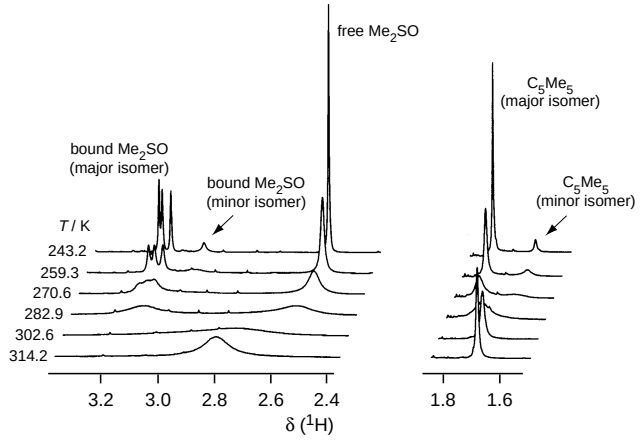



**Fig. 1** Experimental $^1H$ NMR (400 MHz) spectra of **1** (0.010 m) in $CD_3NO_2$ diluent ([free $Me_2SO$] = 0.028 m) at various temperatures

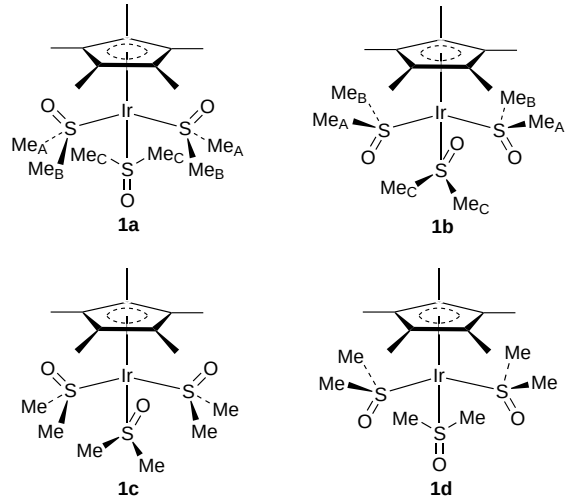



**Fig. 2** Structural representations of the plausible conformers of **1**

chemical environment. This can be accounted for by structures **1c** or **1d**. However, structure **1c** is obviously the less sterically demanding structure and thus we suggest that it is the most likely candidate for the minor isomer of **1**. Finally, and of utmost importance, the major:minor isomer ratio observed for complex **1** is seen to reflect the differing steric demands imposed by the bulky $C_5Me_5$ and $Me_2SO$ groups within the half-sandwich geometry and also supports assigning the major and minor isomers to **1a** and **1c** respectively.

As the temperature was raised to 314.2 K, all five resonances began to broaden, indicating that an intramolecular process and/or an intermolecular exchange(s) with free solvent was occurring over the same temperature interval (Fig. 1). Similar spectra were obtained when the variable-temperature study was repeated without excess $Me_2SO$, thus corroborating the interconversion between the two isomers of **1**. Notably, $^{13}C\{^1H\}$ NMR spectra of **1**, in the absence of free $Me_2SO$, acquired over a similar temperature interval also exhibited behaviour consistent with an interconversion process.

Having assigned the conformational identities of the two conformers of **1**, it is reasonable to conclude that their interconversion between structures **1a** and **1c** proceeds *via* a restricted rotation of the metal–sulfur bond. However, the question which remains unanswered is which of the conformers of **1** participates in the intermolecular exchange with free $Me_2SO$ or are both involved? A two-dimensional $^1H$ NMR EXCSY (exchange correlation spectroscopy) spectrum of **1** in $CD_3NO_2$ at 243.5 K with excess $Me_2SO$ provided the answer (Fig. 3).

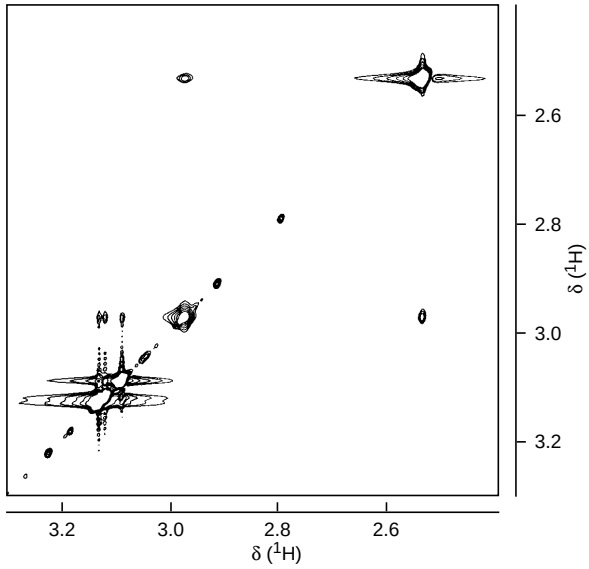



**Fig. 3** Two-dimensional $^1H$ NMR (400 MHz) EXCSY spectrum of **1** (0.010 m) in $CD_3NO_2$ diluent ([free $Me_2SO$] = 0.026 m) at 243.5 K (see Fig. 1)

Under these conditions, the most intense cross-peak relates the resonance of the minor conformer **1c** with that of free $Me_2SO$, confirming that this intermolecular exchange is the fastest process. The cross-peaks between conformers **1a** and **1c** were smaller, and most importantly, the cross-peaks diagnostic of an intermolecular exchange between the major isomer **1a** and free $Me_2SO$ were not observed, thus indicating that (*i*) the interconversion between **1a** and **1c** proceeds by an intramolecular pathway [eqn. (1)] and (*ii*) the exchange with free $Me_2SO$ proceeds solely from conformer **1c** [eqn. (2)].

$$\text{major-}[Ir(Me_2SO)_3(\eta\text{-}C_5Me_5)]^{2+} \underset{}{\overset{k_{intra}}{\rightleftharpoons}} \text{minor-}[Ir(Me_2SO)_3(\eta\text{-}C_5Me_5)]^{2+} \quad (1)$$

$$\text{minor-}[Ir(Me_2SO)_3(\eta\text{-}C_5Me_5)]^{2+} + 3{*}Me_2SO \overset{k_{inter}}{\rightleftharpoons} \text{minor-}[Ir(*Me_2SO)_3(\eta\text{-}C_5Me_5)]^{2+} + 3Me_2SO \quad (2)$$

A detailed kinetic study of complex **1** and other related half-sandwich solvento complexes is presently under way in our laboratory to gain more insight into the mechanistic details of solvent exchange on these complexes.

We thank the Swiss National Science Foundation for financial support.

## Footnote

† Complex **1** was prepared by modification to the literature method.[1] *Spectral data* for **1**: IR (acetone): 1126 $cm^{-1}$ ν(SO). $^1H$ NMR ($CD_3NO_2$, 400 MHz, 243.2 K): δ 1.64 (s, 15 H, $C_5Me_5$; **1c**), 1.79 (s, 15 H, $C_5Me_5$; **1a**), 2.99 (s, 18 H, $Me_2SO$; **1c**), 3.11 (s, 6 H, $Me_2SO$; **1a**), 3.15 (s, 6 H, $Me_2SO$; **1a**), 3.16 (s, 6 H, $Me_2SO$; **1a**). $^{13}C\{^1H\}$ NMR ($CD_3NO_2$, 100 MHz, 243.2 K): δ 8.92 (s, $C_5Me_5$; **1c**), 9.56 (s, $C_5Me_5$; **1a**), 39.33 (s, $Me_2SO$; **1c**), 39.55 (s, $Me_2SO$; **1a**), 40.36 (s, $Me_2SO$; **1a**), 41.59 (s, $Me_2SO$; **1a**), 85.40 (s, $C_5Me_5$; **1c**), 94.10 (s, $C_5Me_5$; **1a**). Elemental analysis: Calc.: C, 22.56; H, 3.91; F, 26.77; S, 11.29. Found: C, 22.70; H, 3.84; F, 26.51; S, 11.12%.

## References

1 C. White, S. J. Thompson and P. M. Maitlis, *J. Chem. Soc., Dalton Trans*., 1977, 1654.
2 J. M. Kisenyi, J. A. Cabeza, A. J. Smith, H. Adams, G. J. Sunley, N. J. S. Salt and P. M. Maitlis, *J. Chem. Soc., Chem. Commun*., 1985, 770; G. J. Sunley, P. Menanteau, H. Adams, N. A. Bailey and P. M. Maitlis, *J. Chem. Soc., Dalton Trans*., 1989, 2415. R. Krämer, K. Polborn and W. Beck, *J. Organomet. Chem*., 1991, **410**, 111.

*Received, 11th October 1986; Com. 6/06982G*

# A self-assembled macrocyclic tetranuclear molecular square $[Co(HL)]_4^{4+}$ [$H_2L$ = tetra(2-pyridyl)thiocarbazone]

**Chun-ying Duan,*[a] Ze-hua Liu,[a] Xiao-zeng You,[a] Feng Xue[b] and Thomas C. W. Mak*[b]**

[a] *Coordination Chemistry Institute and The State Key Laboratory of Coordination Chemistry, Nanjing University, Nanjing 210093, P.R. China*

[b] *Department of Chemistry, The Chinese University of Hong Kong, Shatin, New Territories, Hong Kong*

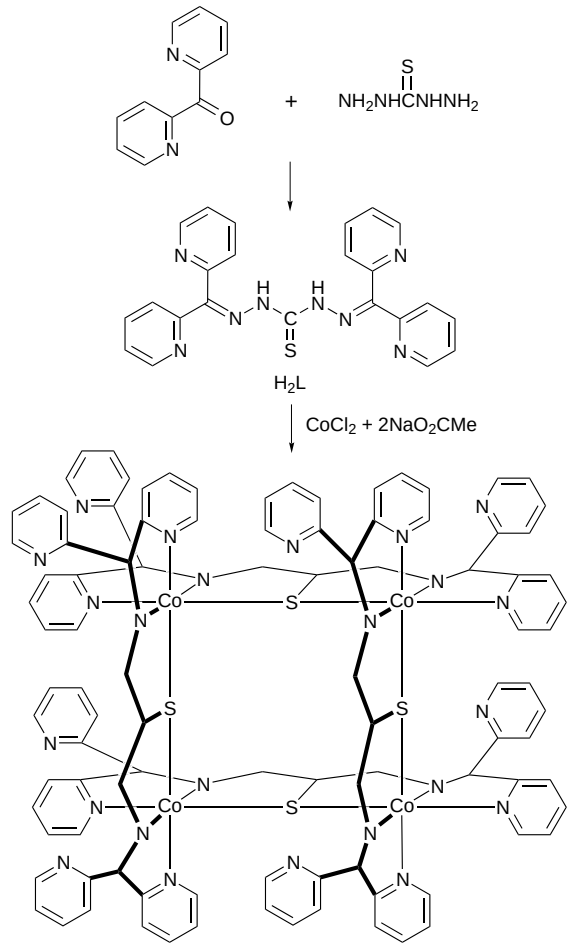
**A novel conformationally rigid, cobalt-based cationic molecular square achieved *via* self-assembly from tetra(2-pyridyl)thiocarbazone is synthesized and structurally characterized.**

Recently, conformationally rigid, tetranuclear macrocyclic ring systems with approximately 90° bond angles about each corner atom have been prepared in high yields *via* self-assembly from rigidly available precursors, thereby adding a new dimension to supramolecular as well as potentially biomimetic chemistry.[1–7] Hitherto only two related types of supramolecules have been reported. One is a square molecular box bridged by bifunctional nitrogen donors such as 4,4′-bipyridine,[1] 2,6-diazanthracene,[2] 2,6-diazanthracene-9,10-dione,[3] *cis*- or *trans-meso*-dipyridyl porphyrins[4] and the uracil monoanion,[5] where polyvalent iodine or heavy transition metals (Pd and Pt) occupy the corners. A second system is the $n \times n$ inorganic grid bridged by a linear polytopic ligand containing bidentate chelating sites for which the square-matrix arryas are occupied by tetrahedrally coordinating metal centres.[6,7]

In the present work, we report the synthesis and structural characterization of the first example of a cobalt-based cationic molecular square achieved *via* self-asembly with a novel rigid pentadentte ligand containing sulfur and nitrogen donor sites.

When di(pyridyl)ketone was treated with thiocarbazide in methanol at reflux, a yellow solid was readily formed. Elemental analysis supports the formation of the new pentadentate $N_4S$ ligand $(C_5H_4N)_2C{=}NN(H)C(S)N(H)N{=}C(C_5H_4N)_2$, tetra(2-pyridyl)thiocarbazone, $H_2L$. Interaction of $CoCl_2{\cdot}6H_2O$ with $H_2L$ and $NaO_2CMe$ in methanol at boiling temperature gave the tetranuclear complex $[Co(HL)]_4[O_2CMe]_4{\cdot}H_2O$ **1** *via* self-assembly, as shown in Scheme 1.† Macrocyclic complex **1** is a remarkably stable dark brown crystalline solid and is soluble in most organic solvents. An X-ray crystallographic study‡ has unequivocally confirmed the existence of a tetranuclear cationic molecular square in **1**.

In compound **1**, the sulfur atom of the $HL^-$ monocation exhibits twofold positional disorder, and its scattering power is represented by two 'half-atoms' S(1) and S(1′) separated by 0.93 Å. For the sake of clarity, only S(1) is shown in Fig. 1 and referred to in subsequent discussion. The tetranuclear $[Co(HL)]_4^{4+}$ cation is located at the $\bar{4}$ site with four cobalt(II) atoms at the corners of a square of edge length Co···Co of 4.43 Å, each metal centre being octahedrally coordinated by atoms S(1), N(2) and N(3) of one $HL^-$ ligand and S(1a), N(6a) and N(7a) from a second ligand (Fig. 1). These two $HL^-$ ligands bind to cobalt(II) in the *mer* configuration (with pairs of S atoms and pyridyl N atoms each bearing a *cis* relationship, whereas the thiocarbazone N atoms are *trans* to each other) as found in related octahedral cobalt thiocarbazone complexes.[8] The sulfur atoms lie alternately above and below the mid-points of the edges of the square, each being connected to two cobalt atoms with a bond angle Co–S–Co of 151°. The measured C–S bond distance of 1.814(4) Å is within the normal range of a C–S single bond,[9] indicating that the thiocarbazone moiety $HL^-$ adopts the thiol tautomeric form in acting as a mononegative ligand.[10] The C–N and N–N bond distances in $HL^-$ are intermediate between formal single and double bonds (see Fig. 1), pointing to extensive electron delocalization over the entire molecular skeleton. The imino H atom of the $HL^-$ monocation could not be located from the difference Fourier map, and is most likely disordered over both N(1) and N(5) sites. Except for the uncordinated pyridine rings and the disordered sulfur atom, the atoms in the monoanion are nearly coplanar, the mean deviation from the best plane being 0.080 Å. The dihedral angle between two $HL^-$ ligands coordinated to the same $Co^{II}$ atom is exactly 90° due to the symmetry of the $I4_1/a$ space group, the closest intermolecular distance between two $HL^-$ planes coordinated to different $Co^{II}$ centres is 4.43 Å, indicating weak π–π interaction. The crystal structure of **1** consists of a packing of tetranuclear $[Co(HL)]_4^{4+}$ cations




$[Co(HL)_4]^{4+}$ macrocyclic square in **1**

**Scheme 1**

imbedded in a matrix of highly disordered acetate ions and water molecules.

The UV–VIS spectra of **1** in methanol shows a strong broad absorption band at *ca.* 264 nm (log ε = 5.3) which is assigned to intraligand transitions and a quite broad band at *ca.* 490 nm (log ε = 4.2) which might be assigned to an MLCT transition. This result suggests that the square molecular box may be retained in solution. Solid-state spectra in the range 550–850 nm exhibit only a strong bond at *ca.* 600 nm, which can be assigned to d–d transitions of the central metal.

The components used in the construction of the cationic molecular square $[Co(HL)]_4^{4+}$ by self-assembly are novel in several respects. Previous studies generally made use of bidentate nitrogen donor ligands as the edges and iodonium or heavy transition-metal ions as the corners of the square unit. In our synthesis of this type of tetranuclear macrocycle we have introduced a newly designed, rigid pentadentate $N_4S$ ligand for binding to a first-row transition metal, thereby offering the potential of broadening the scope of further work in this area.

This work is supported by the National Nature Science Foundation of China and Hong Kong Research Grants Council Earmerked Grant CUHK 311/94p.

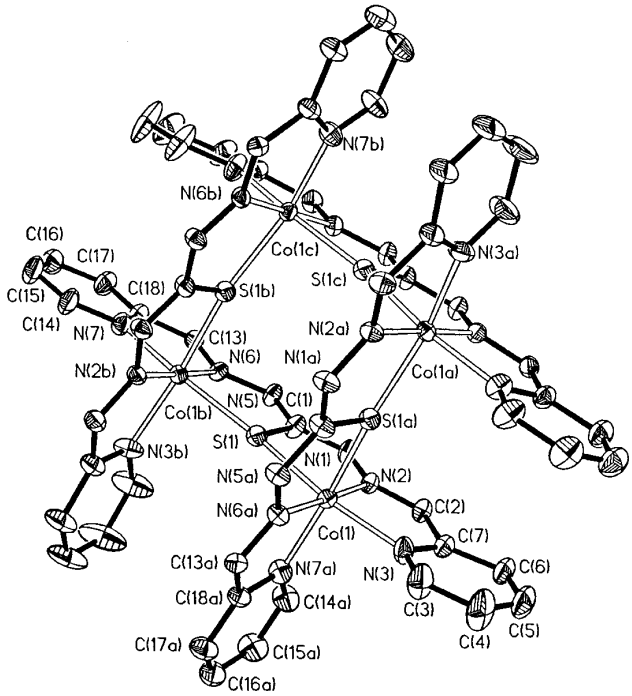



**Fig. 1** Perspective view of the molecular skeleton of the square macrocycle $[Co(HL)_4]^{4+}$ in **1**, showing the non-hydrogen atoms as 25% probability thermal ellipsoids. The uncoordinated pyridine rings and hydrogen atoms are omitted for clarity. The Co···Co separation is 4.43 Å. Selected bond lengths (Å) and angles (°): Co(1)–S(1) 2.268(3), Co(1)–N(2) 1.905(5), Co(1)–N(3) 1.983(5), Co(1)–S(1a) 2.300(3), Co(1)–M(6a) 1.915(5), Co(1)–N(7a) 1.971(5). S(1)–C(1) 1.813(6), C(1)–N(1) 1.318(7), C(1)–N(5) 1.321(6), N(2)–C(2) 1.314(7), N(6)–C(13) 1.317(6), N(1)–N(2) 1.353(6), N(5)–N(6) 1.356(6); S(1)–Co(1)–N(2) 84.7(1), S(1)–Co(1)–N(3) 162.4(2), S(1)–Co(1)–S(1a) 115.4(1), S(1)–Co(1)–N(6a) 93.5(1), S(1)–Co(1)–N(7a) 78.9(2), N(3)–Co(1)–N(2) 81.4(2), N(3)–Co(1)–S(1a) 77.2(2), N(3)–Co(1)–N(6a) 100.3(2), N(3)–Co(1)–N(7a) 92.2(2), Co(1)–S(1)–Co(1b), 151.3(1). Symmetry codes: a −0.25 + *y*, 1.25 − *x*, 0.25 − *z*; b 1.25 − *y*, 0.25 + *x*, 0.25 − *z*.

## Footnotes

† Complex **1** was synthesized by combining methanol solutions of $H_2L^1$ (0.44 g, 1 mmol), $CoCl_2·6H_2O$ (0.24 g, 1 mmol) and $NaO_2CMe$ (0.16 g, 2 mmol). The dark brown crystalline solid which formed after refluxing for 2 h was isolated and dried under vacuum to give **1** in 62% yield. Crystals suitable for an X-ray structure determination were obtained from slow evaporation of a DMF solution of **1** in air. Anal. Found: C, 54.1; H, 3.9; N, 19.5. Calc. for $C_{100}H_{80}Co_4N_{32}O_8S_4·H_2O$: C, 53.6; H, 3.7; N, 20.0%.

‡ *Crystal data* for **2**: tetragonal, space group $I4_1/a$ (no. 88); $a$ = 14.467(1), $c$ = 47.411(1) Å, $U$ = 9923(5) Å$^3$, $Z$ = 4, $F(000)$ = 4560, $\mu$ = 0.82 mm$^{-1}$; 5240 independent reflections measured, 2662 observed [$F > 6.0\sigma(F)$], number of parameters = 408; $R$ = 0.057, $R_w$ = 0.079. The intensities were collected at 294 K on a Rigaku Raxis IIC imaging-plate diffractometer using Mo-Kα radiation (λ = 0.710 73 Å) from a rotating-anode generator operating at 50 kV and 90 mA ($2\theta_{max}$ = 55.2°); 60 oscillation frames in the range 0–180°, exp osure time 8 min per frame. The crystal structure was solved by direct methods with distance restraints of C–C = 1.38 ± 0.01 Å and C–N = 1.34 ± 0.01 Å for uncoordinated pyridyl groups. The S atom [site occupancy factor (sof) for S(1) and S(1′) fixed at 0.5] and acetate ions [sof = 0.5 for O(1), O(2), C(24) and C(25) of one acetate group, sof = 1/4 for O(3), O(4) C(26), C(27) and O(5), O(6), C(28) and C(29) of the two other acetate groups with distance restraints of C–C = 1.520 ± 0.005 Å, C–O = 1.254 ± 0.005 Å, O···O = 2.16 ± 0.01 Å], as well as the water molecule (sof = 0.25) were found disordered. All non-hydrogen atoms were refined anisotropically by full-matrix least-squares. Hydrogen atoms were placed in their calculated positions with C–H = 0.96 Å, assigned fixed isotropic thermal parameters and allowed to ride on their respective parent atoms. The contributions of these hydrogen atoms were included in the structure-factor calculation. All computations were carried out on a PC-486 usig the SHELXTL-PLUS program package. Atomic coordinates, bond lengths and angles, and thermal parameters have been deposited at the Cambridge Crystallographic Data Centre (CCDC). See Information for Authors, Issue No. 1. Any request to the CCDC for this material should quote the full literature citation and the reference number 182/356.

## References

1 M. Fujita, Y. J. Kwon, S. Washizu and K. Ogura, *J. Am. Chem. Soc.*, 1994, **116**, 1151.
2 P. J. Stang and B. Olenyuk, *Angew. Chem., Int. Ed. Engl.*, 1995, **35**, 372.
3 C. M. Drain and J. M. Lehn, *J. Chem. Soc., Chem. Commun.*, 1994, 2313.
4 R. Holger, E. C. Hillgeris, A. Erxleben and B. Lippert, *J. Am. Chem. Soc.*, 1994, **116**, 616.
5 P. J. Stang and K. Chen, *J. Am. Chem. Soc.*, 1995, **117**, 1667.
6 M. T. Youinou, N. Rahmouni, J. Fischer and J. A. Osborn, *Angew. Chem., Int. Ed. Engl.*, 1992, **31**, 733.
7 P. N. W. Baxter, J. M. Lehn, J. Fischer and M. T. Youinou, *Angew. Chem., Int. Ed. Engl.*, 1994, **33**, 2284.
8 M. F. Nelicchi, G. F. Gasparri, G. Pelosi, M. C. Rodriguez-Arguelles and P. Tarasconi, *J. Chem. Soc., Dalton Trans.*, 1995, 3035.
9 A. G. Orpen, L. Brammer, F. H. Allen, O. Kennard, G. G. Watson and R. Taylor in, *Structure Correlation*, ed. H. B. Burgi and J. D. Dunitz, VCH, Weinheim, 1994, vol. 2, Appendix A, pp. 751–857.
10 S. Padhyé and G. B. Kauffman, *Coord. Chem. Rev.*, 1985, **63**, 127.

*Received, 12th November 1996; Com. 6/07689K*

# A new method for the quantitative determination of zeolitic Brønsted acidity

**Manfred Richter,* Barbara Parlitz, Reinhard Eckelt and Rolf Fricke**

*Institut für Angewandte Chemie, Rudower Chaussee 5, D-12484 Berlin, Germany*

**A new method for the quantitative determination of zeolitic Brønsted acidity is proposed utilizing the specific low-temperature reaction of $NH_4^+$ ions fixed to Brønsted sites with $NO–O_2$ thus preventing the loss of acid sites normally encountered for the conventional temperature-programmed mode of $NH_3$ thermodesorption.**

Acidity is one of the most prominent features established for microporous zeolite materials, besides the geometric diversities of crystal structures, pore sizes and pore arrangements. The term acidity mostly discriminates between sites of Brønsted character (protonic sites) and Lewis character (coordinatively unsaturated surface atoms or ions). For acidity characterization, among others, the temperature-programmed desorption of ammonia (TPDA) is routinely used today.[1,2] Interaction of Brønsted-acid sites with $NH_3$ converts the latter into $NH_4^+$ ions fixed to the zeolite framework, and the energy (equivalent to the temperature of desorption) required to release gaseous $NH_3$ is correspondingly high. Peak positions on the temperature axis during TPDA are indicative of the acid strength of sites whereas the peak areas contain information on the concentration of sites.

Mostly, the contributions of weak and strong acid sites overlap in the desorption profiles. Moreover, certain zeolite structures are thermally labile losing a part of the framework aluminium and thus acid sites. Thus it is reported[3] that calcination of zeolite mordenite at 770 K resulted in a degree of dealumination of about 70%. The thermal conversion of zeolite Y (Si/Al atomic ratio = 2.4) from its $NH_4^+$ form into the $H^+$ form is accompanied by a loss of *ca*. 44% of its framework aluminium.[4]

This obvious drawback can be avoided by utilization of the method proposed in the following. The method is based on the isothermal catalytic low-temperature conversion (CLTC) of zeolite-fixed $NH_4^+$ ions to $N_2$ by reaction with $NO–O_2$ at 373–393 K. Simultaneously, the $NH_4^+$ form of zeolite structures is transformed into the $H^+$ form. Three representative examples will be given (see Table 1) documenting the reliability of the new method.

**Table 1** Brønsted acidity of zeolite structures as determined by conventional TPD of ammonia in comparison with the catalytic low-temperature conversion of zeolitic $NH_4^+$ ions by $NO–O_2$

| Zeolite | Theoretical composition (Na form) | $V_p$[a]/ cm$^3$ g$^{-1}$ | Brønsted acidity/ mmol g$^{-1}$ | | |
|---|---|---|---|---|---|
| | | | TPD of $NH_4^+$ | TPD[b] of $NH_3$ | CLTC[c] of $NH_4^+$ |
| ZSM-5 | $Na_6[Al_6Si_{90}O_{192}]$ (Si/Al = 15.0) | 0.16 | 0.85 | 0.65 | 0.90 |
| Mordenite | $Na_8[Al_8Si_{40}O_{96}]$ (Si/Al = 5.0) | 0.18 | 2.51 | 1.40 | 2.40 |
| Y | $Na_{58}[Al_{58}Si_{134}O_{384}]$ (Si/Al = 2.3) | 0.32 | 3.75 | 1.65 | 3.82 |

[a] Micropore volume from nitrogen adsorption isotherms. [b] Adsorption of $NH_3$ after thermal decomposition of the $NH_4^+$ form and subsequent temperature-programmed desorption (TPD). [c] Catalytic low-temperature conversion of $NH_4^+$ by $NO–O_2$.

Zeolites ZSM-5, Y and mordenite whose ideal compositions and resulting Si/Al atomic framework ratios are given in Table 1, were obtained commercially in their ammonium form. The actual Si/Al framework ratios were determined to be 20.3 (ZSM-5), 2.6 (zeolite Y), and 5.6 (zeolite mordenite).

The CLTC of the $NH_4^+$ ions were performed in an integral flow reactor with a feed containing 0.5 vol.% NO, 10 vol.% $O_2$ and helium as diluent. The gas analysis was accomplished by on-line gas chromatography.

After admission of the $NO–O_2$–He mixture to the $NH_4^+$ form of the zeolite the NO is completely converted to $N_2$ with consumption of $NH_4^+$ ions. The reaction does not proceed in the absence of $O_2$. Obviously, NO has to be oxidized to $NO_2$, at least partially, to enable the subsequent reduction step [eqn. (1)],

$$2\ ZNH_4^+ + NO + NO_2 \rightarrow 2\ N_2 + 3\ H_2O + 2\ ZH^+ \quad (1)$$

where Z symbolizes the zeolite, $ZNH_4^+$ indicates the ammonium form of the zeolite and $ZH^+$ its protonic form. The formation of $NO_2 \cdot NO$ adducts, formally equivalent to $N_2O_3$, has been reported to occur on ZSM-5 either non-promoted or promoted following exposure to NO and $O_2$ at 295 K by Adelmann *et al*.[5]

Fig. 1 shows the result of characteristic experiments, where the $NH_4^+$ forms of three different zeolites representative of wide-pore (Y, MOR) and medium-pore (MFI) structures have been charged with an $NO–O_2$ gas mixture at 383 and 373 K, respectively. Prior to reaction the samples were flushed at 425

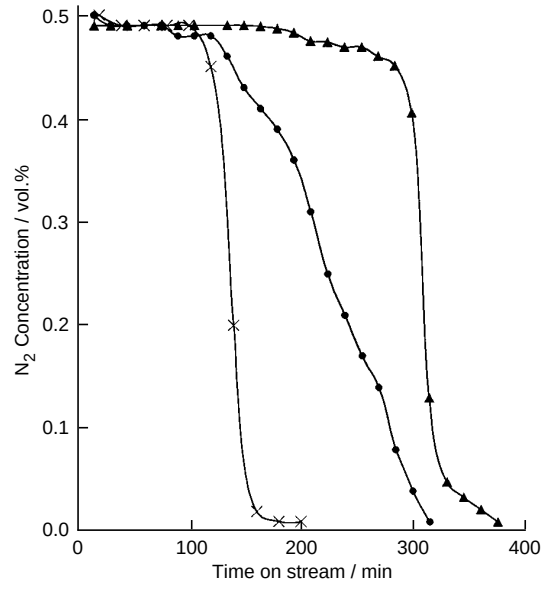



**Fig. 1** Quantitative determination of zeolitic Brønsted acidity by catalytic low-temperature conversion (CLTC) of $NH_4^+$ ions by $NO–O_2$ at low temperatures. Formation of $N_2$ *vs*. time on stream for (×) zeolite ZSM-5 (Si/Al ratio = 20.3), (●) zeolite mordenite (Si/Al ratio = 5.6) and (▲) zeolite Y (Si/Al ratio = 2.6). *Reaction conditions*: sample volume = 3.6 cm$^3$, feed = 0.5 vol.% NO, 10 vol.% $O_2$, carrier gas helium, flow rate = 1 cm$^3$ s$^{-1}$, reaction temperature = 373 K (ZSM-5) or 383 K (zeolite Y, mordenite).

K for 2 h with helium inside the reactor to remove physisorbed water.

All three investigated zeolite structures start with complete conversion of NO to $N_2$ during the first 120 min on stream. According to the concentration of $NH_4^+$ ions (equivalent to the concentration of Brønsted-acid sites) the $N_2$ formation ceases. Note that the reaction temperature in the cases of zeolite Y and zeolite mordenite was slightly higher, 383 K, in order to accelerate the process. Because only one N atom comes from the NO, and the other one from $NH_4^+$ surface ions, the volume concentration of $N_2$ is equal to that of NO, *viz*. 0.5 vol.%. The overall molar amount of $N_2$ formed was determined by numeric integration of the concentration–time curve and corresponds to the concentration of Brønsted-acid sites. The distinctly modified curve shape observed for the mordenite is tentatively attributed to the pore architecture where pores run only parallel to each other without crossings. Further experiments showed that the access of NO–$NO_2$ to the small side channels (2.6 × 3.7 Å) of the mordenite structure is hindered so that the CLTC of $NH_4^+$ ions is further slowed down.

Values given in Table 1 underline that the concentration of Brønsted-acid sites calculated from a thermal decomposition of the $NH_4^+$ form favourably coincides with that derived from the new method. A second run of temperature-programmed desorption following a reloading of the zeolite with gaseous $NH_3$ confirms that during the thermal decomposition of initial $NH_4^+$ ions a dealumination had taken place, most severe for zeolite Y and zeolite mordenite.

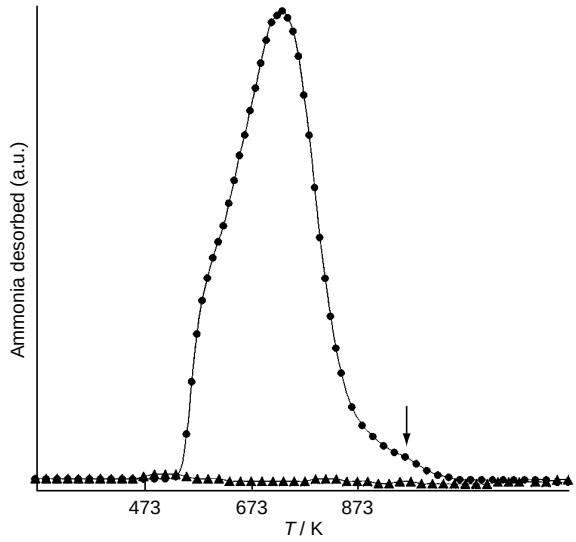



**Fig. 2** Temperature-programmed decomposition of $NH_4^+$ ions fixed to zeolite ZSM-5 before the CLTC (●) and after completion of the reaction (▲) according to curve (×) in Fig. 1. Sample mass = 0.2 g, heating rate = 10 K $min^{-1}$, carrier gas helium, flow rate = 0.5 $cm^3$ $s^{-1}$. The arrow indicates the end of the temperature increase. Decomposition is completed isothermally at 923 K.

The consumption of $NH_4^+$ ions according to eqn. (1) is confirmed for zeolite ZSM-5 by the results shown in Fig. 2. Following an exhaustive treatment of the sample with NO–$O_2$ at 373 K the sample was checked for the presence of residual $NH_4^+$ ions. As can be seen, no ammonia release is observed during temperature-programmed heating, *i.e*. no residual $NH_4^+$ ions remain.

The $NH_4^+$ form of the unused ZSM-5 is thermally decomposed with maximum release of ammonia at around 720 K. The Brønsted acidity calculated on the basis of this desorption profile amounts to 0.85 mmol $g^{-1}$ and is included in Table 1.

This result demonstrates that in turn the treatment by NO–$O_2$ might be utilized for the mild transformation of the zeolitic $NH_4^+$ form into the $H^+$ form which customarily requires temperatures higher than 770 K when performed thermally. The dealumination that accompanies this thermal treatment is demonstrated by the data given in the penultimate column of Table 1. Initial concentrations of Brønsted-acid sites cannot be reproducibly determined.

A further advantageous application of the described method is seen in the abatement of $NO_x$ from exhaust gases by an alternating process including a period of regeneration where the zeolite is reloaded with the required $NH_4^+$ ions.[6,7]

This work was supported by the Federal Ministry of Education, Science, Research and Technology of the FRG and the Berlin Senate, Department for Science, Research and Culture (Project No. 03C3005).

## References

1 R. J. Cvetanovic and Y. Amenomiya, *Adv. Catal*., 1967, **17**, 103.
2 N. Topsoe, K. Petersen and E. Derouane, *J. Catal*., 1981, **70**, 41.
3 H. Stach, J. Jänchen, H.-G. Jerschkewitz, U. Lohse, B. Parlitz, B. Zibrowius and M. Hunger, *J. Phys. Chem*., 1992, **96**, 8473.
4 U. Lohse, I. Pitsch, E. Schreier, B. Parlitz and K.-H. Schnabel, *Appl. Catal. A: General*, 1995, **129**, 189.
5 B. J. Adelman, G.-D. Lei and W. M. H. Sachtler, *Catal. Lett*., 1994, **28**, 119.
6 R. Eckelt, M. Richter and R. Fricke, *Ger. Pat. Appl*., 196 16 227, 0 1996.
7 M. Richter, R. Eckelt, B. Parlitz and R. Fricke, *Appl. Catal. B: Environ*., submitted for publication.

*Received, 29th November 1996; Com. 6/08077D*

# Unique binding site for bis-benzimidazoles on transfer RNA

**S. E. Sadat Ebrahimi, Amanda N. Wilton and Kenneth T. Douglas*†**

*School of Pharmacy and Pharmaceutical Science, University of Manchester, Manchester, UK M13 9PL*

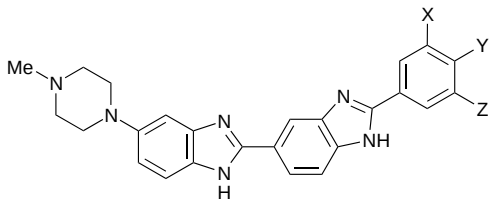
**Ligands based on bis-benzimidazole structures related to Hoechst 33258 bind to transfer RNA with 1 : 1 stoichiometry and dissociation constants in the micromolar range, their interaction appearing significantly different in nature from that with duplex DNA, based on the ribonucleic acid-induced quenching of their fluorescence.**

With ligand binding to RNA increasingly being recognised as a potential drug target, especially in the HIV field, an understanding of the molecular features which lead to strong, specific binding to RNA is a prerequisite to designing RNA-directed ligands as drug leads.[1,2] Use of *in vitro* selection of RNA sequences can determine preferred RNA sequences and structures (*e.g.* for tobramycin[3]), but this does not produce new RNA-binding structures. The complementary approach is to find novel RNA ligand structures and understand the basis of their binding interaction.[2]

Early studies indicated that netropsin and distamycin bind strongly to the minor groove of DNA but weakly to RNA (probably electrostatically to the phosphate ion sites on the backbone).[4] However, classical DNA-minor-groove ligands such as berenil[5] and benzimidazoles[6] have recently been reported to have strong interactions with RNA duplexes based on melting temperature determinations. However, these studies gave no indication of RNA-specifying interactions. The grooves of DNA and RNA differ in many respects. Thus, 4′,6-diamidino-2-phenylindole (DAPI) binds to AT stretches of B-DNA in the minor groove but intercalates into AU-RNA.[1] Strong evidence that DNA minor groove binders can bind in the tRNA groove is provided by an X-ray diffraction study with netropsin and distamycin, which shows specific hydrogen bonds to G51, U52 and G53 and electrostatic interactions with phosphates P61, P62 and P63 in this region,[7] but binding strengths were not measured. Porphyrins also bind brewer's yeast $tRNA^{Phe}$ in the TψC arm near the T54 and ψ55 residues.[8] Hoechst 33258 **1** binds strongly to B-DNA in AT-rich regions but except for specially designed synthetic oligonucleotides the absolute sequence specificity is low. Thus on calf thymus or plasmid DNA there are many sites for **1**. We now report a contrasting situation for RNA, namely specific binding to a unique site on tRNA of ligands based on **1**, *viz*. the 3,4-dimethoxy **2** and 3,4,5-trihydroxy **3** analogues.

Stock solutions of tRNA (from brewer's yeast, Boehringer Mannheim) were prepared in 0.1 M sodium phosphate buffer pH 7.80. Ligand stock solutions, initially in dimethyl sulfoxide (10 mM), were further diluted with phosphate buffer to the required concentration. Samples for fluorescence studies were filtered through a sterile Nalgene™ 0.2 μm syringe filter. Trihydroxy-Hoechst **3** was from a previous study[9] and 3,4-dimethoxy-Hoechst **2** was synthesised similarly by condensing ethyl 3,4-dimethoxybenzimidic hydrochloride (mp 143.5–145 °C, litr., 142–143 °C,[10] accurate mass, 210.1122. $C_{11}H_{16}NO_3$ requires 210.1130) with 2-(3,4-diaminophenyl)-6-(4-methylpiperazinyl)benzimidazole:[11] **2** was characterised by NMR and mass spectroscopy.‡ UV–VIS spectra were recorded at 25 °C using a Peltier-thermostatted cuvette holder in a Cary model 1E UV-Visible spectrophotometer using the Cary Base System Software and fluorescence emission spectra using a Hitachi F-2000 fluorescence spectrophotometer. The ligands were excited at wavelengths corresponding to their absorption maxima.

In the absorption spectra of a series of mixtures of tRNA (brewers' yeast) and **3** [Fig. 1(*a*)] the $\lambda_{max}$ value of **3** was found to shift from 326 nm to longer wavelength as the proportion of tRNA increased, becoming approximately 338 nm (broad) for a 1 : 1 molar mixture. These UV–VIS spectra were recorded for a series of tRNA : **3** mixtures (prepared from 50 μM stock solutions of **3** and tRNA) varying the molar ratio of the components but keeping a constant total concentration of the components. The absorbance at 360 nm for each ratio, corrected




**1** X = Z = H, Y = OH
**2** X = Y = OMe, Z = H
**3** X = Y = Z = OH

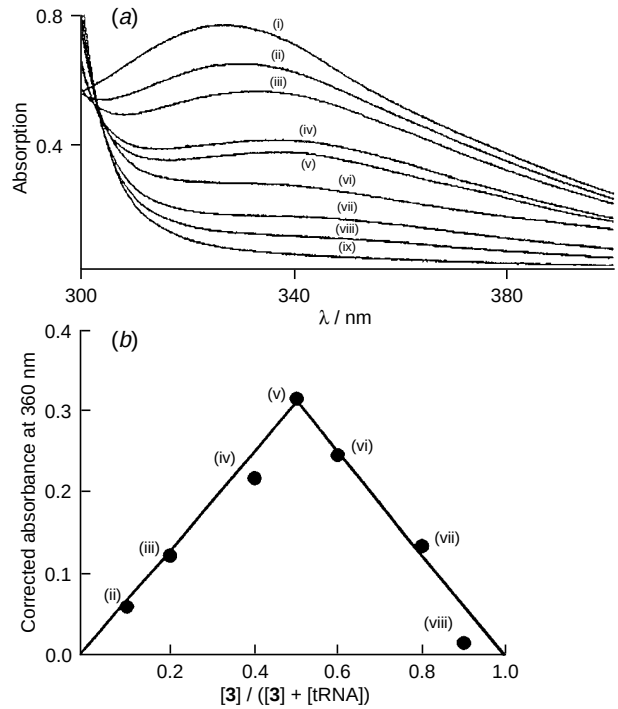



**Fig. 1** (*a*) UV–VIS absorption spectra of 3, 4, 5-trihydroxy-Hoechst **3** and brewer's yeast tRNA (combined concentration 50 μM) in 0.1 M sodium phosphate buffer pH 7.80. Mole fraction of **3**: (i) 1, (ii) 0.9, (iii) 0.8, (iv) 0.6, (v), 0.5, (vi) 0.4, (vii) 0.2, (viii) 0.1 and (ix) 0. (*b*) Job plot of the data from (*a*), corrected as described in the text.

for the contribution from unbound **3** or tRNA assuming 1 : 1 tight binding, plotted against the mole fraction of **3** to produce a Job plot [Fig. 1(*b*)] showed 1 : 1 complex formation and tight binding.

Addition of tRNA to a solution of **2**, **3** or related ligands leads to extensive fluorescence quenching, which is easier to study for some ligands than others depending on the initial fluorescence intensity of the free ligand. A sample of **2** (1 ml of a 10 μM solution in 0.1 M sodium phosphate buffer, pH 7.80) was excited at 338 nm and its fluorescence emission spectrum recorded between 300 and 600 nm after each addition of a series of aliquots of $tRNA^{Phe}$ (20 μl from 100 μM stock). A plot of the change in the fluorescence intensity, corrected for dilution *vs.* [$tRNA^{Phe}$] added was fitted by the equation for a single-site binding [eqn. (1)],

$$\text{Fluorescence } (F) = F_{max}[tRNA^{Phe}]/(K_{diss} + [tRNA^{Phe}]) \quad (1)$$

with a value for $K_{diss}$ of 14.8 + 0.9 μM. There is also evidence of a much weaker binding site(s). The binding site for ligands in this class remains to be identified but the binding is both specific, as shown by the Job analysis for **3**, and reasonably strong based on the dissociation constant determined for **2**. The environment of these bis-benzimidazole ligands on the RNA is clearly different in detail from that on DNA as the fluorescence of Hoechst 33258 is highly enhanced on binding to the minor groove of B-DNA[12,13] in contrast to the strong quenching seen here with tRNA. This may be an indirect effect, as seen for bromouridine quenching in DNA, or may indicate that the angles between the planes of the benzimidazole rings and the terminal aryl groups and their molecular environments differ substantially on DNA and RNA for such compounds. However, in spite of the detailed knowledge of binding interactions and such angles for Hoechst and its congeners in the DNA groove from NMR[12,14,15] and X-ray diffraction[16,17] studies, there is no information on the basis of RNA recognition by this family of structures. The molecular frameworks of **2** and **3** and their specific sequestration of tRNA (selectively occupying a unique run of 4–5 base-pairs out of approximately 75) provides a new lead for analogue design to increase the strength of binding to RNA-based grooves and to understand some aspects of ligand–RNA recognition at an atomic level.

## Footnotes

† E-mail: Ken.Douglas@man.ac.uk

‡ *Selected data* for **2**: $\delta_H$ [270 MHz, $(CD_3)_2SO$], 2.24 (s, 3 H, $NCH_3$), 3.12 [m, 4 H, $N(CH_2)_2$], 3.60 (m, 4 H, $N(CH_2)_2$], 3.84 (s, 3 H, $OCH_3$), 3.88 (s, 3 H, $OCH_3$), 6.93 (d, 1 H, Ar-H, *J* 8.6 Hz), 7.00 (s, 1 H, Ar-H), 7.13 (d, 1 H, Ar-H, *J* 8.6 Hz), 7.43 (d, 1 H, Ar-H, *J* 8.25 Hz), 7.65 (d, 1 H, Ar-H, *J* 8.25 Hz), 7.81 (d, 1 H, Ar-H, *J* 7.9 Hz), 7.82 (s, 1 H, Ar-H), 7.96 (d, 1 H, Ar-H, *J* 8.6 Hz), 8.27 (s, 1 H, Ar-H); FAB MS: Calc. for $C_{27}H_{29}N_6O_2$, 469.2352. Found, 469.2354. % (M + 1): Calc., 32.7; Found, 31.9%. % (M + 2): Calc., 4.91; Found, 4.83%.

## References

1 F. A. Tanious, J. M. Veal, H. Buczak, L. S. Ratmeyer and W. D. Wilson, *Biochemistry*, 1992, **31**, 3103.
2 M. J. Gait and J. Karn, *Trends Biotechnol*., 1995, **13**, 430.
3 Y. Wang and R. R. Rando, *Chem. Biol*., 1995, **2**, 281.
4 C. Zimmer, K. E. Reinert, G. Luck, U. Wahnert, G. Lober and H. Thrum, *J. Mol. Biol*., 1971, **58**, 329.
5 D. S. Pilch, M. A. Kirolos, X. Liu, E. Plum and K. J. Breslauer, *Biochemistry*, 1995, **34**, 9962.
6 W. D. Wilson, L. Ratmeyer, M. Zhao, L. Srekowski and D. Boykin, *Biochemistry*, 1993, **32**, 4098.
7 J. Rubin and M. Sundaralingam, *J. Biomol. Struct. Dyn*., 1984, **2**, 165.
8 W. J. Birdsall, Anderson, Jr. and N. Foster, *Biochim. Biophys. Acta*, 1989, **1007**, 176.
9 S. S. Ebrahimi, K. J. Embrey, K. T. Douglas, J. P. Parkinson, F. G. Loontiens and R. M. Clegg, *J. Biomol. Struct. Dyn*., 1995, **12**, a202.
10 A. P. T. Easson and F. L. Pyman, *J. Chem. Soc. (C)*, 1931, 2991.
11 S. E. S. Ebrahimi, M. C. Bibby, K. R. Fox and K. T. Douglas, *Anti-Cancer Drug Des*., 1995, **10**, 463.
12 J. A. Parkinson, J. Barber, K. T. Douglas, J. Rosamund and D. Sharples, *Biochemistry*, 1990, **29**, 10 181.
13 F. G. Loontiens, L. W. McLaughlin, S. Diekmann and R. M. Clegg, *Biochemistry*, 1991, **30**, 182.
14 M. S. Searle and K. J. Embrey, *Nucleic Acids Res*., 1990, **18**, 3753.
15 J. A. Parkinson, S. E. Ebrahimi, J. H. McKie and K. T. Douglas, *Biochemistry*, 1994, **33**, 8442.
16 M. Teng, N. Usman, C. A. Frederick and A. H. Wang, *Nucleic Acids Res*., 1988, **16**, 2671.
17 J. R. Quintana, A. A. Lipanov and R. E. Dickerson, *Biochemistry*, 1991, **30**, 10 294.

*Received, 2nd December 1996; Com. 6/08106A*

# Template synthesis of $[Cr(en)_3][Te_6]$: a novel polytelluride with a framework structure, whose cavities are filled with a $[Cr(en)_3]^{3+}$ template

**Christian Reisner and Wolfgang Tremel***

*Institut für Anorganische Chemie und Analytische Chemie der Johannes Gutenberg-Universität Mainz, Becherweg 24, D-55099 Mainz, Germany*

**$[Cr(en)_3][Te_6]$ (en = ethylenediamine) is obtained by a template synthesis under solvothermal conditions from $Cr(CO)_6$ and $BaTe_4$; its crystal structure contains a polymeric $Te_6^{3-}$ framework whose pores contain the $Cr(en)_3^{3+}$ template; $[Cr(en)_3][Te_6]$ is the first chalcogenide with a porous three-dimensional framework structure.**

Microporous materials with a three-dimensional framework of condensed $MO_4$ tetrahedra (M = *e.g.* Al, Si, P) have been known for a long time as zeolites. They have great technical importance as molecular sieves and catalysts.[1,2] Their sorptive properties are based on the regular arrangement of cavities with defined diameter and size, which can be varied by the use of templates.[3] On the other hand, the complexing properties of compounds with porous structures can be used for the stabilisation of various cluster species (*e.g.* $Cd_mS_n$ or $Si_8$).[4]

Recent examples of Si- or Al-free compounds with microporous structures based on tetrahedral building elements have been found in the gallophosphate cloverit, whose cavities are formed from twenty-membered rings,[5] in the nitridophosphate $Zn_7[P_{12}N_{24}]Cl_2$[6] and in several transition-metal phosphates.[7] The substitution of tetrahedral structure motifs in known aluminosilicates by octahedral or by square-pyramidal $MO_n$ building groups in early transition-metal phosphates opens the way to a new and versatile structural chemistry.[8] A nice example, the $[V_{10}O_{10}(H_2O)_2(OH)_4(PO_4)_7]^{6-}$ polyanion, which can be synthesized by self-assembly from simple reagents and whose structure can be viewed as an inorganic double helix built from vanadium phosphate units, has recently been reported by Haushalter *et al.*[9]

Except for a few examples, all compounds with porous structures are oxidic. This explains their thermal stability and insulating electrical properties. On the other hand, metal chalcogenides (*e.g.* $CuInS_2$, MnQ, CdQ; Q = S, Se, Te) are important materials for electronic devices because of their magnetic or semiconducting properties.[10] Sulfides possess enormous compositional and structural variety.[11,12] Therefore, in view of the utility of microporous oxides in chemical catalysis and the wide applicability of chalcogenides in electronic devices a new class of compounds with a combination of the properties of zeolitic and sulfidic materials should be an attractive synthetic target. Solvothermal methods or reactive flux methods are possible preparative routes to these new materials.† Sheldrick and Braunbeck have described the solvothermal synthesis of chalcogenostannates.[13] Dhingra and Kanatzidis obtained $[PPh_4][M(Se_6)_2]$, a compound with an open-layer structure by reacting gallium, indium and thallium with low-melting polychalcogenide fluxes.[14] Herein we report the synthesis and characterization of $[Cr(en)_3][Te_6]$ **1** whose structure is built up from a polytelluride framework with pores filled by templating $Cr(en)_3^{3+}$ ions.

The title compound was first obtained by the reaction of $Cr(CO)_6$ with an alloy of the nominal composition $BaAs_4Te_4$. Based on the assumption that reactions of polytellurides with hard 3d metal cations (*e.g.* $Cr^{3+}$ or $Mn^{2+}$) only lead to products with isolated oligotelluride anions $Te_n^{2-}$ ($n$ = 2, 3) and $[M(en)_3]^{m+}$ ($m$ = 2, 3), the initial target was the assembly of a framework structure with bridging $AsTe_n$ ($n$ = 3, 4) elements stabilized by templating $Cr(en)_3^{3+}$ cations which are formed by oxidative decarbonylation of $Cr(CO)_6$.[15] Further investigations and the results of the X-ray analysis revealed that **1** represents the crystalline part of the reaction products.‡ It can also be prepared by the reaction of $Cr(CO)_6$ with a melt of nominal composition $BaTe_4$ [eqn. (1)].§

$$Cr(CO)_6 + 2\ BaTe_4 \xrightarrow[\text{closed quartz tube}]{\text{en, 200 °C, 7 d}} [Cr(en)_3][Te_6] + 2\ BaTe + 6\ CO \qquad (1)$$

Whereas reaction of the educts in boiling en under normal pressure yields powder-like products, the combination of the reaction with $Te_x^{2-}$ polytellurides as mineralizers leads to well crystallized products. **1** was removed from the reaction mixture by crystallization and should be the kinetically stable reaction product. The homogeneity of the product was confirmed from Guinier powder data.

The structure of **1** contains a polymeric $[Te_6]^{3-}$ polyanion,[16] whose pores are filled by isolated octahedrally coordinated $Cr(en)_3^{3+}$ cations. The characteristic structural features of the $Te_6^{3-}$ polyanion are puckered sheets of Te atoms parallel to the *ab*-plane which are shown in Fig. 1(*a*) in a projection along [001]. Fig. 1(*b*) shows a view of the structure along [100]. Each of these sheets is made up from $Te_6$ fragments which are linked to each other by Te–Te single bonds [$d_{Te-Te}$ = 2.763(1) Å]. The $Te_6$ fragments contain a central $Te_3$ ring with one exocyclic Te atom bonded to each atom of the ring. The Te–Te distances of 3.138(1) Å within the ring are approximately 0.3 Å longer than a typical Te–Te single bond distance (2.84 Å in the structure of elemental tellurium[17]). A formal bond order of 0.32 can be calculated using Paulings's rule [$d(n) = d(1) - 0.61 \log(n)$, $d(1)$ = 2.796 Å].[18] The exocyclic Te–Te separations of 2.918(1) Å are approximately 0.2 Å longer than typical Te–Te bond distances in polytellurides (*e.g.* $d_{Te-Te}$ = 2.726 Å in $Te_4^{2-}$[19]), but they are comparable with the Te–Te distances in $Te_2$ units encountered in the structures of $K_4M_3Te_{17}$ (M = Zr, Hf).[20] The shortest Te–Te distances of 3.376(1) Å between the layers are much shorter than the sum of the van der Waals radii of 4.4 Å[19] and comparable with the Te–Te distances in the polytelluride cluster $[NbTe_{10}]^{3-}$.[21] According to the results of an MO study these values correspond to significant Te–Te bonding interaction.[22] The computed Pauling bond order is 0.11. Therefore, the Te sheets in the structure of **1** should not be viewed as isolated layers.

An alternative description may be given based on the hierarchy of the bonding. (*i*) Considering only distances in the range of 2.7 Å to 3.0 Å as bonding, the structure consists of isolated $Te_4^{2-}$ chains. This description is in accord with conventional bonding considerations in polychalcogenides. However, the presence of additional partially bonding Te–Te bonding interactions indicates that this description does not allow to fully understand the bonding situation in the $Te_6^{3-}$ polyanion. (*ii*) Alternatively, if we consider all Te–Te distances shorter than 3.15 Å as bonding, a puckered layer structure with $Te_6$ motifs linked by Te–Te single bonds ($d_{Te-Te}$ = 2.763 Å) is

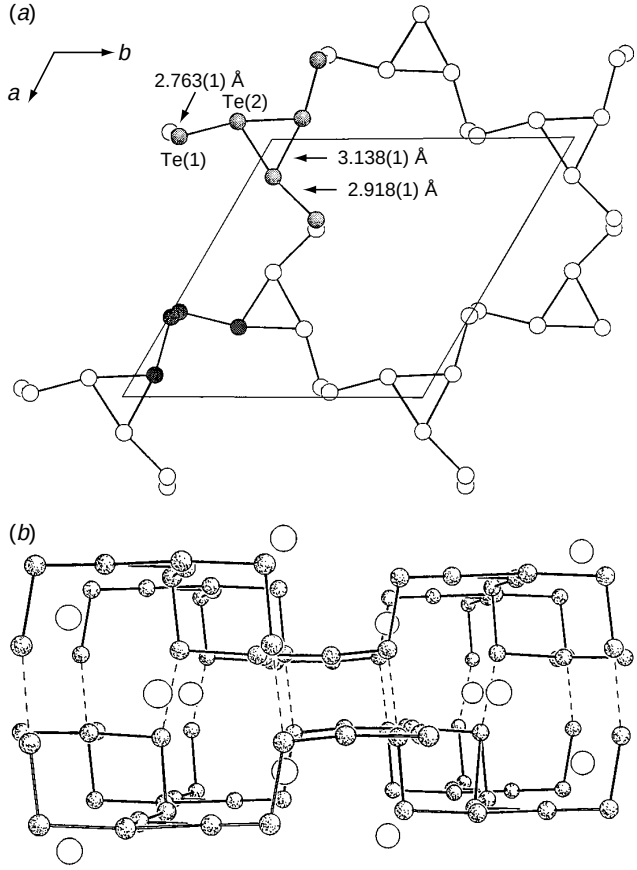



**Fig. 1** (*a*) Structure of the $Te_6^{3-}$ polyanion depicted in a view along [001]. (*b*) Two Te layers in a view along [100]. The positions of the $Cr(en)_3^{3+}$ cations are indicated by open spheres.

found [see Fig. 1(*a*)]. (*iii*) Counting all Te–Te distances shorter than 3.4 Å as bonding leads to a three-dimensional framework structure with pores containing solvated $Cr(en)_3^{3+}$ cations (Λ and Δ isomer, two crystallographically independent cations per unit cell. **1** is air-stable for several weeks. Thermal decomposition starts at 200 °C and is complete at 280 °C. Above 360 °C **1** transforms to other still uncharacterized products.

Although the electronic reasons for the stability of **1** can be rationalized by qualitative MO arguments, the mechanism of its formation is still unclear. The templating properties of the highly charged $Cr(en)_3^{3+}$ seems to be essential for the synthesis of **1**. Attempts to synthesize other related compounds with various $M(en)_3^{2+}$ cations (M = alkaline earth or 3d metal) only yield known chain-like polytellurides. The synthesis of further polytellurides with porous structures by means of coordinating ligands and highly charged cations is currently under investigation.

## Footnotes

† This corresponds to the formation conditions of naturally occurring sulfidic minerals.

‡ *Crystal data* for $[Cr(en)_3][Te_6]$: $C_6H_{12}CrN_6Te_6$, $M$ = 985.8, trigonal, space group $R32$ (no. 155), $Z$ = 6, $a$ = 14.292(2), $b$ = 14.292(2), $c$ = 18.076(3) Å, $U$ = 3197.56 Å$^3$, $D_c$ = 1.536 g cm$^{-3}$. Siemens P4, MoK$\alpha$, $\mu$ = 8.58 mm$^{-1}$, crystal size 0.15 × 0.15 × 0.15 mm, θ–2θ scan, $2\theta_{max}$ = 54°, 5446 reflections collected, 1564 independent reflections, 1485 reflections with $I > 2\sigma(I)$, $R(R_w)$ = 0.021(0.021). Atomic coordinates, bond lengths and angles, and thermal parameters have been deposited at the Cambridge Crystallographic Data Centre (CCDC). See Information for Authors, Issue No. 1. Any request to the CCDC for this material should quote the full literature citation and the reference number 182/337.

§ $[Cr(en)_3][Te_6]$: 44 mg of $Cr(CO)_6$ (0.2 mmol) and 259 mg of an alloy with the nominal composition $BaTe_4$ were loaded into a quartz tube (volume *ca.* 20 ml). After introducing 2 ml of en, the tube was sealed under vacuum (*ca.* $10^{-3}$ bar). After 7 days of heating at 200 °C, the tube was cooled at 1 °C min$^{-1}$ and opened. Black cubic crystals could be isolated from the colourless solution. The crystals were washed with tetrahydrofuran and dried *in vacuo*. Yield: 127 mg (63.3%), satisfactory elemental analysis, IR data: (KBr pellet) 3397m, 3480m, 3030s, 2912s, 2870s, 1547s, 1447s cm$^{-1}$.

## References


1 D. W. Breck, *Zeolite Molecular Sieves*, Krieger, Malabar, FL., 1984.
2 J. M. Thomas, *Angew. Chem.*, 1994, **106**, 963; *Angew. Chem., Int. Ed. Engl.*, 1994, **33**, 913.
3 G. D. Stucky, *Prog. Inorg. Chem.*, 1992, **40**, 99.
4 G. D. Stucky and J. E. MacDougall, *Science*, 1990, **247**, 669.
5 M. Estermann, L. B. McCusker, C. Baerlocher, A. Merrouche and H. Kessler, *Nature*, 1991, **352**, 320.
6 W. Schnick and J. Lücke, *Angew. Chem.*, 1992, **104**, 208; *Angew. Chem., Int. Ed. Engl.*, 1992, **31**, 213.
7 W. T. A. Harrison, T. E. Martin, T. E. Gier and G. D. Stucky, *J. Mater. Chem.*, 1992, **2**, 175.
8 R. C. Haushalter, K. G. Strohmaier and F. W. Lai, *Science*, 1989, **246**, 1289.
9 V. Soghomonian, Q. Chen, R. C. Haushalter, J. Zubieta and C. J. O'Connor, *Science*, 1993, **259**, 1596.
10 J. L. Shay and J. H. Wernick, *Ternary Chalcopyrite Semiconductors: Growth, Electronic Properties and Applications*, Pergamon, Elmsford, New York, 1975.
11 D. J. Vaughn and J. R. Craig, *Mineral Chemistry of Metal Sulfides*, Cambridge University Press, Cambridge, 1978.
12 B. Krebs, *Angew. Chem.*, 1983, **95**, 113; *Angew. Chem., Int. Ed. Engl.*, 1983, **22**, 113.
13 W. S. Sheldrick and H. G. Braunbeck, *Z. Anorg. Allg. Chem.*, 1993, **619**, 1300; *Z. Naturforsch., Teil B*, 1989, **44**, 1397; see also W. S. Sheldrick and M. Wachhold, *Angew. Chem.*, 1995, **107**, 490; *Angew. Chem., Int. Ed. Engl.*, 1995, **35**, 450; *Chem. Commun.*, 1996, 607; W. S. Sheldrick and B. Schaaf, *Z. Naturforsch., Teil B*, 1994, **49**, 993.
14 S. Dhingra and M. G. Kanatzidis, *Science*, 1992, **258**, 1769.
15 C. Reisner, Ph.D. Dissertation, University of Mainz, 1996.
16 P. Böttcher, *Angew. Chem.*, 1988, **100** 781; *Angew. Chem., Int. Ed. Engl.*, 1988, **27**, 758.
17 A. F. Wells, *Structural Inorganic Chemistry*, 5th edn., Clarendon Press, Oxford, 1984.
18 L. Pauling, *The Chemical Bond*, Cornell University Press, Ithaca, New York, 1976, p. 167.
19 J. C. Huffman and R. C. Haushalter, *Z. Anorg. Allg. Chem.*, 1984, **518**, 203.
20 P. M. Keane and J. A. Ibers, *Inorg. Chem.*, 1991, **30**, 1327.
21 W. A. Flomer and J. A. Kolis, *J. Am. Chem. Soc.*, 1988, **110**, 690.
22 W. Tremel, *Inorg. Chem.*, 1992, **31**, 1030.


*Received, 3rd December 1996; Com. 6/08173H*

# Novel molecular receptors capable of forming $Cu_2$–$O_2$ complexes. Effect of preorganization on $O_2$ binding

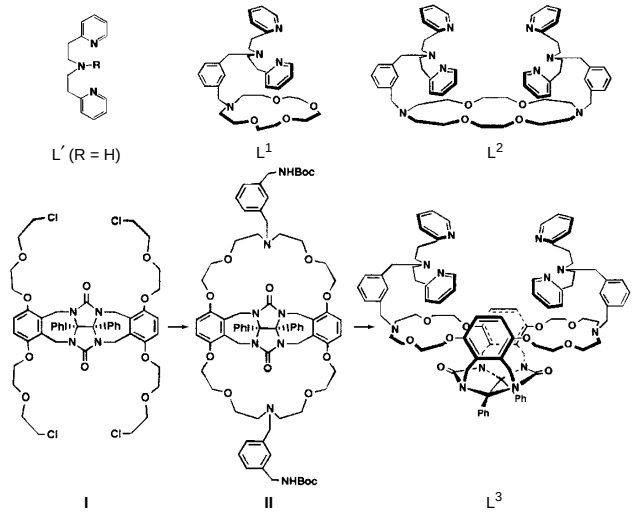
**Robertus J. M. Klein Gebbink,[a] Constantinus F. Martens,[a] Martinus C. Feiters,[a] Kenneth D. Karlin*[b] and Roeland J. M. Nolte*[a]**

[a] *Department of Organic Chemistry, NSR Centre, University of Nijmegen, Toernooiveld, 6525 ED, Nijmegen, The Netherlands*
[b] *Department of Chemistry, The Johns Hopkins University, Baltimore, Maryland 21218, USA*

**Novel biomimetic copper(I) receptors react with $O_2$ to form metastable $O_2$ complexes and the rate of these reactions depends on the preorganization of the ligands.**

The binding and activation of molecular oxygen by dinuclear copper enzymes has attracted much attention in recent years.[1,2] Using model studies it was proposed,[1d,3] and later confirmed,[4] that molecular oxygen is bound between the two copper centres in the active site of haemocyanin *via* an unusual $\mu$-$\eta^2$:$\eta^2$ binding mode.† Several groups have demonstrated that synthetically derived $Cu_2$–$O_2$ complexes can carry out oxygenation reactions,[5] in particular, upon the ligands of the complex. One aim of our research is to design systems which may be used in oxygenation reactions on exogeneous substrates. For this reason we have attached the previously studied ligand L′[5a–d] (Scheme 1) to particular crown ethers and to a known molecular receptor,‡ for the potential to bind substrates in close proximity of an $Cu_2O_2$ centre. Here, we describe initial studies with three new ligands $L^1$–$L^3$ (Scheme 1) and their copper(I) complexes **1**–**3**, and characterization of their molecular oxygen binding ability.

Ligands $L^1$ and $L^2$ were synthesized from the commercially available crown ethers aza-15-crown-5 and diaza-18-crown-6. The secondary nitrogen atoms of the latter compounds were alkylated with 3-cyanobenzyl bromide, and the cyano groups were reduced with $LiAlH_4$. The resulting primary amines were alkylated with vinylpyridine under high-pressure conditions (15 kbar)[6] using acetic acid as a catalyst, providing pure $L^1$ and $L^2$ in 27 and 58% overall yield, respectively. For the preparation of $L^3$ the tetrachloro compound **I**[7] was subjected to a double ring closure reaction with 2 equiv. of mono-Boc protected *m*-diaminoxylene to give **II**. After removal of the Boc groups with TFA and treatment of the resulting compound with vinylpyridine under high-pressure conditions compound $L^3$ was obtained in 80% overall yield.§




**Scheme 1**

Copper(I) complexes **1**–**3** were synthesized by adding the ligands $L^1$–$L^3$, dissolved in $CH_2Cl_2$, to the appropriate amount of $[Cu^I(MeCN)_4]ClO_4$ under strictly anaerobic conditions. After several precipitations with $Et_2O$ the complexes were isolated as yellow–brown powders. Elemental analysis and spectral data were in agreement with the structures $[Cu^IL^1]$-$ClO_4$ **1**, $[Cu^I_2L^2][ClO_4]_2$ **2** and $[Cu^I_2L^3][ClO_4]_2$ **3**.§

Complexes **1**–**3** all formed metastable $O_2$ adducts in $CH_2Cl_2$ at −85 °C (Scheme 2). The rates of formation of these adducts were quite different, whereas their UV–VIS spectra were very similar (Table 1). Complex **2**·$O_2$ was obtained within 1–2 min after bubbling pre-cooled $O_2$ through a $CH_2Cl_2$ solution of **2** at −85 °C. During the reaction the colour of the solution changed from yellow to purplish green. Under the same conditions the bright orange complex **3**·$O_2$ was formed in 10–20 min. In contrast, both the colour of a solution of **1** and the absorption spectrum of this solution remained initially unchanged. If, however, an $O_2$-saturated solution of this complex was allowed to stand for 3–5 h at −85 °C, an orange complex formulated as $\mathbf{1}_2$·$O_2$ was formed slowly; this diminished $O_2$-binding rate and stoichiometry is in keeping with that observed for other L′ (R = Me, $PhCH_2$, Ph) copper(I) mononuclear complexes.[5c] In view of the spectral and structural similarities with previously reported $Cu_2$–$O_2$ complexes[1c–e,3] we propose that complexes $\mathbf{1}_2$·$O_2$, **2**·$O_2$, and **3**·$O_2$ all contain a peroxo ligand in a (bent) $\mu$-$\eta^2$:$\eta^2$ binding mode; the distinctive absorption around 364 nm

$$2\ Cu^IL^1 + O_2 \xrightarrow{-85\ °C} (Cu^{II}L^1)_2O_2$$

$$Cu^I_2L^n + O_2 \xrightarrow[(n = 2,3)]{-85\ °C} Cu^{II}_2L^nO_2$$

$\lambda_{max}$ = 364 nm
orange-green

**Scheme 2**

**Table 1** UV–VIS characteristics [$\lambda$/nm ($\varepsilon$/dm$^3$ mol$^{-1}$ cm$^{-1}$)] of copper complexes **1**–**3** and haemocyanin

| Complex | $Cu^I$ | $Cu_2O_2$ | $Cu^{II}$ |
|---|---|---|---|
| **1** | 340 (2150) | 364 (4900)<br>428 (960)<br>656 (450) | 346 (3900)<br>616 (600) |
| **2** | 344 (5800) | 364 (12800)<br>526 (1000)<br>642 (800) | 344 (4000)<br>628 (300)<br>768 (100) |
| **3** | 340 (5000) | 364 (13100)<br>418 (2900)<br>524 (150)<br>650 (100) | 358 (3400)<br>630 (500) |
| Haemocyanin[a] | | 345 (20000)<br>570 (1000) | 700 (200) |

[a] Taken from ref. 9(*b*).

points to this type of binding.¶ The low absorption coefficients observed, particularly in $\mathbf{1}_2\cdot O_2$, are ascribed to lack of complete formation of $O_2$ adducts, and with concurrent temperature dependent decomposition (*vide infra*).

We found that the formation of complex $\mathbf{1}_2\cdot O_2$ can be accelerated if $KClO_4$ is added to the solution containing **1**, before $O_2$ is bubbled through it. In the presence of $KClO_4$ the $O_2$ complex reached its maximum concentration after 30–45 min, whereas without $KClO_4$ it took approximately 5 h for the complex to be formed completely. For 15-crown-5 and related compounds it is known that $K^+$ ions induce the formation of sandwich complexes, as these cations are too large to fit in the crown ether rings. Apparently, $K^+$ ions have the same effect on complex **1**: two mononuclear complexes are brought together and are pre-organized in order to bind one molecule of $O_2$. The proposed structure of such a sandwich complex, as shown in Fig. 1, may represent an intermediate state, more than it represents the final product. The enhanced oxygen affinity of complex **1** in the presence of $K^+$ cations mimics to some extent the allosteric effect of $Mg^{2+}$ ions on the oxygen binding by molluscan haemocyanin.[8] For the formation of $\mathbf{2}\cdot O_2$, and $\mathbf{3}\cdot O_2$ no acceleration effect of $K^+$ ions was observed.

Purging solutions $\mathbf{2}\cdot O_2$ with argon at −85 °C did not result in the decolourization of these solutions. When a solution of $\mathbf{2}\cdot O_2$ was rapidly heated under vacuum a green solution was obtained. These results indicate that the formation of the $O_2$ adducts is an irreversible process. As mentioned above the oxygen complexes are metastable; at −85 °C the loss in absorption intensity in the UV–VIS region was 5–10% after 1 h. Upon warming to room temperature the solutions of the complexes turned green within minutes. The resulting products could all be isolated as pale green powders in reasonable yields. IR and mass spectroscopy indicated that dinuclear copper(II) hydroxide complexes were formed. The starting ligands $L^1$–$L^3$ could be isolated from the corresponding copper(II) complexes after removal of the $Cu^{II}$ ions with aqueous ammonia. Yields were above 70% for $L^1$ and $L^3$, whereas $L^2$ was recovered in approximately 50% yield, indicating that some ligand degradation had occurred.

In summary, we have shown that the new complexes **1**–**3** all form stable $O_2$ complexes, which after warming yield copper(II) complexes in which the ligand remains intact to a major extent. This opens the possibility to use these complexes as oxygenation catalysts for exogeneous substrates, which is currently under study. The $O_2$ affinity and rate of formation of the copper(I) complexes is determined by the degree of pre-organization present in the starting complex.

The authors are grateful to NATO for a grant in their Supramolecular Chemistry Programme (CRG950904). R. K. G. and R. N. would like to thank SON–NWO for financial support and K. D. K. in addition acknowledges the National Institutes of Health.

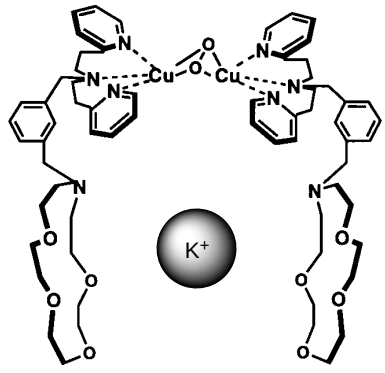



**Fig. 1** Proposed structure of $\mathbf{1}_2\cdot O_2$ formed in the presence of $K^+$ ions

## Footnotes

† Tolman and co-workers have recently demonstrated that interconversion of a $Cu_2(\mu\text{-}\eta^2:\eta^2\text{-}O_2)$ complex and a $Cu_2(\mu\text{-}O)_2$ complex is possible: J. A. Halfen, S. Mahaparta, E. C. Wilkinson, S. Kaderli, V. G. Young Jr., l. Que Jr., A. D. Zuberbühler and W. B. Tolman, *Science*, 1996, **271**, 1397.

‡ We have shown before that a similar complex with pyrazole instead of pyridine ligands, is capable of selectively oxidizing alcohols that are complexed in its cavity. C. F. Martens, R. J. M. Klein Gebbink, M. C. Feiters and R. J. M. Nolte, *J. Am. Chem. Soc*., 1994, **116**, 5667.

§ Compounds L′–$L^3$ and **1**–**3** were fully characterized by spectroscopic methods; data were made available for the reviewers.

¶ $Cu:O_2$ stoichiometries of the novel complexes are based on spectral similarities with structurally related systems [see refs. 1(*c*)–(*e*) and 3].

## References

1 For selected reviews see: (*a*) Z. Tyeklár and K. D. Karlin, *Acc. Chem. Res*., 1989, **22**, 241; (*b*) T. N. Sorrell, *Tetrahedron*, 1989, **45**, 3; (*c*) K. D. Karlin, Z. Tyeklár and A. D. Zuberbühler, in *Bioinorganic Catalysis*, ed. J. Reedijk, Marcel Dekker Inc., New York, 1993, pp. 261–315; (*d*) N. Kitajima and Y. Moro-oka, *Chem. Rev*., 1994, **94**, 737; (*e*) S. Fox and K. D. Karlin, *Dioxygen Reactivity in Copper Proteins and Complexes*, in *Reactive Oxygen in Biochemistry*, ed. J. S. Valentine, C. S. Foote, A. Greenberg and J. F. Liebman, Blackie Academic & Professional, Chapman & Hall, Glasgow, 1995, pp. 188–231.

2 *Bioinorganic Chemistry of Copper*, ed. K. D. Karlin and Z. Tyeklár, Chapman & Hall, New York, 1993.

3 N. J. Blackburn, R. W. Strange, A. Farooq, M. S. Haka and K. D. Karlin, *J. Am. Chem. Soc*., 1988, **110**, 4263; N. Kitajima, K. Fujisawa and Y. Moro-oka, *J. Am. Chem. Soc*., 1989, **111**, 8976; N. Kitajima, K. Fujisawa, C. Fujimoto, Y. Moro-oka, S. Hashimoto, T. Kitagawa, K. Toriumu, K. Tatsumi and A. Nakamura, *J. Am. Chem. Soc*., 1992, **114**, 1277; N. Kitajima and Y. Moro-oka, *J. Chem. Soc., Dalton Trans*., 1993, 2665.

4 K. A. Magnus, H. Ton-That and J. E. Carpenter, *Chem. Rev*., 1994, **94**, 727.

5 (*a*) K. D. Karlin, J. C. Hayes, Y. Gultneh, R. W. Cruse, J. W. McKown, J. P. Hutchinson and J. Zubieta, *J. Am. Chem. Soc*., 1984, **106**, 2121; (*b*) K. D. Karlin, B. I. Cohen, R. R. Jacobson and J. Zubieta, *J. Am. Chem. Soc*., 1987, **107**, 6194; (*c*) I. Sanyal, M. Mahroof-Tahir, M. S. Nasir, P. Ghosh, B. I. Cohen, Y. Gultneh, R. W. Cruse, A. Farooq, K. D. Karlin, S. Liu and J. Zubieta, *Inorg. Chem*., 1992, **31**, 4322; (*d*) M. S. Nasir, B. I. Cohen and K. D. Karlin, *J. Am. Chem. Soc*., 1992, **114**, 2482; (*e*) L. Casella, M. Gulloti, G. Pallanza and L. Rigoni, *J. Am. Chem. Soc*., 1988, **100**, 4221; (*f*) M. Réglier, C. Joraud and B. Waegell, *J. Chem. Soc., Chem. Commun*., 1990, 1752; (*g*) O. J. Gelling, A. Meetsma and B. L. Feringa, *Inorg. Chem*., 1990, **29**, 2816; (*h*) R. Menif, A. E. Martell, P. J. Squattrito and A. Clearfield, *Inorg. Chem*., 1990, **29**, 4723; (*i*) S. Mahaparta, J. A. Halfen, E. C. Wilkinson, L. Que Jr. and W. B. Tolman, *J. Am. Chem. Soc*., 1994, **116**, 9785.

6 C. F. Martens, R. J. M. Klein Gebbink, M. C. Feiters, H. Kooijman, W. J. J. Smeets, A. L. Spek and R. J. M. Nolte, *Inorg. Chem*., 1994, **33**, 5541.

7 J. W. H. Smeets, R. P. Sijbesma, L. van Dalen, A. L. Spek, W. J. J. Smeets and R. J. M. Nolte, *J. Org. Chem*., 1989, **54**, 3710.

8 K. I. Miller, E. Schabtach and K. E. van Holde, *Proc. Natl. Acad. Sci. USA*, 1990, **87**, 1496.

9 (*a*) E. I. Solomon, in *Copper Coordination Chemistry: Biochemical and Inorganic Perspectives*, ed. K. D. Karlin and J. Zubieta, Adenine Press, Guilderland, New York, 1983, pp. 1–22; (*b*) N. C. Eickman, R. S. Himmelwright and E. I. Solomon, *Proc. Natl. Acad. Sci. USA*, 1979, **76**, 2094.

*Received, 25th October 1996; Com. 6/07284D*

# Novel synthesis of two *tert*-butyl ketenyl phosphinidine ligands on a trinuclear ruthenium framework. X-Ray structure determination of $[Ru_3(\mu\text{-dppm})(CO)_7\{\mu_3\text{-PC(=C=O)Bu}^t\}_2]$

**Lindsay T. Byrne,[a] Julian A. Johnson,[b] George A. Koutsantonis,*[a] Brian W. Skelton[a] and Allan H. White[a]**

[a] *Department of Chemistry, University of Western Australia, Nedlands, Perth 6907, Australia*
[b] *CSIRO Division of Minerals, Port Melbourne, Victoria 3207, Australia*

**The reaction of an excess of $Bu^tC{\equiv}P$ with $[Ru_3(\mu\text{-dppm})(CO)_{10}]$ 1 in refluxing thf gives $[Ru_3(\mu\text{-dppm})(CO)_7\{\mu_3\text{-P(C=C=O)Bu}^t\}_2]$ 2 with two bridging phosphinidine ligands as the major product after chromatography.**

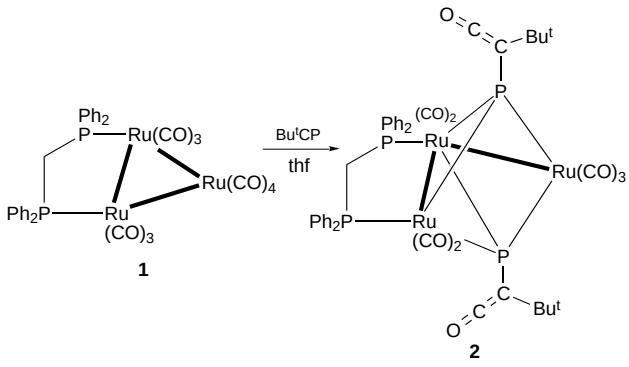
The considerable attention focussed on the chemistry of phosphaalkynes has been manifested in a sharp increase in numbers of papers dealing with the subject over the last ten years. This work is described in several excellent reviews which deal with both organometallic[1–3] and organic aspects.[4,5]

The chemistry of $[Ru_3(\mu\text{-dppm})(CO)_{10}]$ **1** [dppm = 1,2-bis(diphenylphosphino)methane], is characterised by its enhanced reactivity over that of the unsubstituted carbonyl $[Ru_3(CO)_{12}]$. Pyrolysis results in the elimination of benzene from dppm and metallation of one of the remaining phenyl groups.[6] Phosphines readily add to the unsubstituted Ru atom[7–9] and internal and terminal alkynes add readily to the ruthenium triangle.[10] As part of a continuing study of the reactivity of the activated cluster **1**, the reaction with 2-*tert*-butyl-1-phosphaalkyne was examined and the results are reported herein.

The reaction (Scheme 1)† in refluxing thf gave a mixture of products that are readily separated by thin layer chromatography, the major yellow band providing a moderate yield (*ca.* 27%) of $[Ru_3(\mu\text{-dppm})(CO)_7\{\mu_3\text{-PC(=C=O)Bu}^t\}_2]$ **2**, a 50-electron cluster. The compound remarkably contains two $\mu_3$-$Bu^t$ ketenyl phosphinidine ligands and is noteworthy for the lack of oligomerisation normally exhibited in the reactions of several equivalents of $Bu^tCP$ on transition-metal centres.

The FABMS of **2** showed a molecular ion $M^+$ at *m/z* 1141 that appeared to indicate the incorporation of two $Bu^tCP$ units and the sequential loss of nine CO groups. This latter fact is normally a reliable indication of the number of metal bound carbonyl groups and the fact that **1** readily adds substrates at the unsubstituted ruthenium[9] suggested a localised dimer at that atom occupying one coordination site. This formulation was at odds with the spectroscopic data which indicated the presence of four inequivalent phosphorus atoms. The fact that the phosphinidine ligands were found to be inequivalent was puzzling and seemingly at odds with the solid-state structure. The $^{31}P$ NMR spectrum of **2** contained four resonances that remained essentially unchanged within the temperature range 190 to 360 K indicating that the complex was rigid on the NMR timescale. The $^{31}P$ NMR spectrum was reproducible from a number of different samples and in different solvents. This suggests that the possibility of impurities or other structural isomers can be discounted.

The results of the room-temperature single-crystal X-ray structure study‡ are consistent with the stoichiometry and connectivity as expressed in **2** above and Fig. 1, a pair of substrate carbonyl ligands having been incorporated by the $Bu^tCP$ reactants to form a pair of $Bu^tC(CO)P$ phosphinidine entities. The phosphorus atoms of the latter approach the $Ru_3$ triangle from above and below the plane with approximately equivalent distances to the ruthenium atoms, much more precisely so about P(4). Notwithstanding, the phosphorus atoms are displaced from above the centroid of the triangle (and from




**Scheme 1**

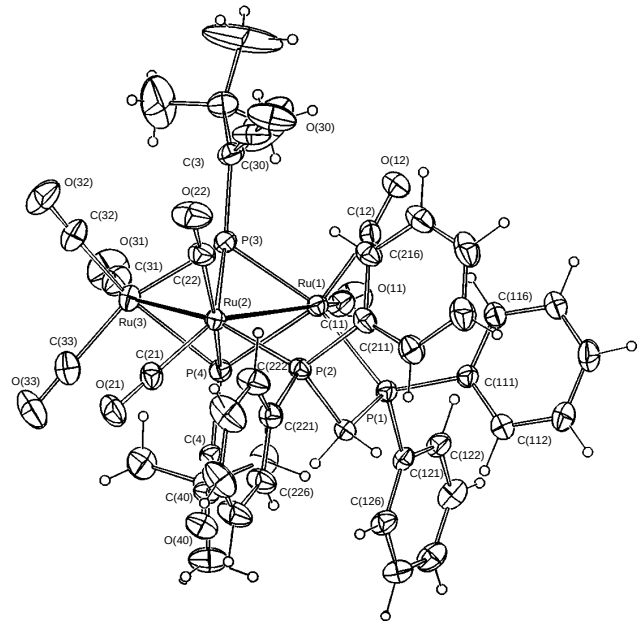
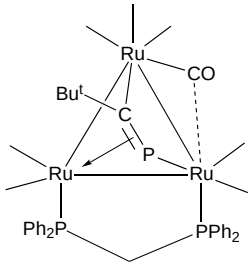
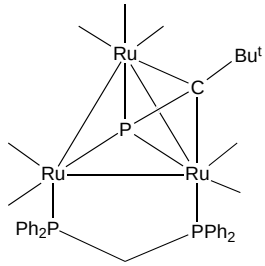



**Fig. 1** Projection of **2** approximately through the $Ru_3$ plane. 20% thermal ellipsoids are shown for non-hydrogen atoms; hydrogen atoms have arbitrary radii of 0.1 Å. Selected bond lengths (Å) and angles (°): Ru(1)–Ru(2) 2.916(1), Ru(2)–Ru(3) 2.831(1), P(3)–Ru(1–3), 2.296(2), 2.381(2), 2.330(2), P(4)–Ru(1–3) 2.380(2), 2.378(2), 2.377(2), Ru(1)–P(1) 2.386(2), Ru(2)–P(2) 2.306(2), P(3)–C(3) 1.807(7), C(3)–C(30) 1.27(1), C(30)–O(30) 1.19(1), P(4)–C(4) 1.809(7), C(4)–C(40) 1.293(9), C(40)–O(40) 1.176(8), Ru(3)–Ru(2)–Ru(1) 83.80(3), P(3)–C(3)–C(30) 114.7(6), P(4)–C(4)–C(40) 113.6(5), C(3)–C(30)–O(30) 179(1), C(4)–C(40)–O(40) 180(1), P(1)–C(0)–P(2) 110.4(3), C(3)–P(3)–Ru(1–3) 121.6(7), 126.9(2), 125.0(3), C(4)–P(4)–Ru(1–3) 129.6(3), 127.3(2), 121.4(3).




**3**




**4**

the dppm) so that they bridge one pair of ruthenium atoms, with the associated Ru···Ru distance lengthened to 3.839(1) Å, and with an unsymmetrical dppm disposition. The major difference observed lies in the Ru(1)–P(*n*)–Ru(3) angles [for $n$ = 3, 112.14(7)°; $n$ = 4, 107.59(6)°] and this possibly affects the observed $^{31}$P NMR resonances for these nuclei. It is of note that the $^{31}$P NMR shifts of μ-phosphido ligands in a series of structurally characterised compounds were greatly affected by small variations in Ru–P–Ru angle.[11] In the dppm ligand the two now inequivalent phosphorus atoms, bound to a pair of inequivalent ruthenium atoms, with inequivalent Ru–P [2.386(2), 2.306(2) Å], lie necessarily to one side of the $Ru_3$ plane so that the molecule's incipient *m* symmetry is lost. Despite this, the pair of phosphinidine ligands are almost eclipsed in projection, with the ketenyl moieties in surprisingly close proximity to other moieties in the coordination sphere [O(30)···O(22), H(216) 2.951(8), 2.69; O(40)···H(0a) 2.66 Å] and adjacent molecules [O(30)···H(0b) 2.50 Å]. The geometries of the Bu$^t$ ketenyl phosphinidine ligands are similar to those observed in $[Re_2Pt(CO)_8(dppe)\{\mu_3\text{-}PC(=C=O)(Bu^t)\}]$[12] and $[Fe_3(CO)_7(Se)(PBu^t)(Bu^tC_2H)\{\mu_3\text{-}PC(=C=O)Bu^t\}]$.[13]

In the absence of oligomerisation it is likely that the formation of **2** results from the stepwise addition of Bu$^t$CP (which can act as either a four- or six-electron donor) units with cleavage of a Ru–Ru bond. Further work is required to determine the mechanism operating in this reaction but a likely sequence of events would involve addition of Bu$^t$CP presumably through the labile equatorial site on the unsubstituted Ru atom, which adopts initially a $\mu_3$-$\eta^2$ (∥) **3** or (⊥) **4** ligating mode followed by addition of the liberated or metal-bound CO to the CP bond, the process being repeated to give the other ligand.

Work is in progress to identify the minor products from this reaction in the belief that they will shed further light on the course of this reaction.

We thank the ARC for financial support and the Department of Chemistry for a start up grant (G. A. K.).

## Footnotes

† *Synthesis of* **2**: an excess of Bu$^t$CP (0.05 ml) was added to a solution of $[Ru_3(CO)_{10}(\mu\text{-dppm})]$ (0.104 g, 0.107 mmol) in thf (20 ml) and heated to reflux for 40 min. After cooling the solvent was removed *in vacuo*, and the residue was dissolved in the minimum amount of $CH_2Cl_2$ and chromatographed (TLC, silica $GF_{254}$ 0.5 mm; 3 : 1 hexanes–$CH_2Cl_2$). Three bands were resolved but only the major yellow band ($R_f$ 0.6) was isolated, being crystallised from $CH_2Cl_2$–MeOH to give **2** (0.033 g, 27%). [Found: C, 46.44; H, 3.39; M(FAB MS) 1141 ($M^+$). $C_{44}H_{40}O_9P_4Ru_3$ requires C, 46.35; H, 3.54; M, 1141.] IR($C_6H_{12}$) ν(CO) 2092m, 2077m 2055s, 2002s, 1973w, 1949w cm$^{-1}$. $^{31}$P NMR ($C_6D_6$, 202.48 MHz) δ 14.8 (ddd, $Ph_2P^1CH_2$, $^2J_{P1P3}$ 163, $^2J_{P1P2}$ 73, $^2J_{P1P4}$ 18 Hz), 30.0 ($Ph_2P^2CH_2$, $^2J_{P2P3}$ 22, $^2J_{P2P4}$ 5 Hz), 111.2 [ddd, $P^3$(Bu$^t$)(CCO), $^2J_{P3P4}$ 172 Hz], 236.8 [ddd, $P^4$(Bu$^t$)(CCO)].

‡ *Crystal/refinement data* for **2**: $C_{44}H_{40}O_9P_4Ru_3$, $M$ = 1139.9, monoclinic, space group $P2_1/c$, $a$ = 15.001(5), $b$ = 17.930(4), $c$ = 20.131(6) Å, β = 116.43(3)°, $U$ = 4849 Å$^3$, $D_c$ ($Z$ = 4) 1.56 g cm$^{-3}$, 4727 independent, absorption corrected, 'observed' [$I > 3\sigma(I)$], diffractometer data being refined by full-matrix least squares to $R$ = 0.035, $R_w$ = 0.030 (statistical weights). Monochromatic Mo-Kα radiation, λ = 0.710 73 Å, $T$ = 295 K; anisotropic thermal parameter refinement for the non-hydrogen atoms, ($x$, $y$, $z$, $U_{iso}$)$_H$ included constrained. Atomic coordinates, bond lengths and angles, and thermal parameters have been deposited at the Cambridge Crystallographic Data Centre (CCDC). See Information for Authors, Issue No. 1. Any request to the CCDC for this material should quote the full literature citation and the reference number 182/333.

## References

1 J. F. Nixon, *Chem. Rev.*, 1988, **88**, 1327.
2 J. F. Nixon, *Chem. Ind.*, 1993, **7**, 404.
3 J. F. Nixon, *Chem. Soc. Rev.*, 1995, 319.
4 M. Regitz, *Chem. Rev.*, 1990, **90**, 191.
5 M. Regitz, *J. Heterocycl. Chem.*, 1994, **31**, 663.
6 N. Lugan, J.-J. Bonnet and J. A. Ibers, *J. Am. Chem. Soc.*, 1985, **4**, 484.
7 M. I. Bruce, J. R. Hinchliffe, R. Surynt, B. W. Skelton and A. H. White, *J. Organomet. Chem.*, 1994, **469**, 89.
8 M. I. Bruce, P. A. Humphrey, R. J. Surynt and E. Tiekink, *Aust. J. Chem.*, 1994, **47**, 477.
9 G. A. Koutsantonis, B. W. Skelton and A. H. White, in preparation.
10 M. I.Bruce, P. A. Humphrey, H. Miyamae, B. W. Skelton and A. H. White, *J. Organomet. Chem.*, 1992, **429**, 187.
11 A. J. Carty, in *Catalytic Aspects of Metal Phosphine Complexes, Adv. Chem. Ser.*, 1981, **196**, 163.
12 S. I. Alresayes and J. F. Nixon, *J. Chem. Soc., Chem. Commun.*, 1987, 928.
13 W. Imhof and W. Huttner, *J. Organomet. Chem.*, 1993, **447**, 1993.

*Received, 22nd December 1996; Com. 6/07943A*

# Destruction of cyanobacterial toxins by semiconductor photocatalysis

**Peter K. J. Robertson, Linda A. Lawton, Burkhard Münch and Julien Rouzade**

*School of Applied Science, The Robert Gordon University, St Andrew Street, Aberdeen, UK AB25 1HG*

**The rapid destruction of microcystin, a cyanobacterial toxin, using a titanium dioxide photocatalyst is observed; the process is extremely efficient with high concentrations of toxin completely undetectable within 10–40 min, depending on the initial concentration.**

Cyanobacterial (blue-green algal) toxins are extremely toxic naturally occurring substances which display hepato- and neuro-toxic behaviour.[1,2] Several genera of freshwater cyanobacteria including *Microcystis*, *Oscillatoria*, *Anabaena* and *Aphanizomenon* produce a range of potent natural toxins. These toxins can be classified in two general categories, neurotoxins [*e.g.* anatoxin-a, anatoxin-a(s) and saxitoxins] and hepatotoxins, namely microcystins which are the subject of this investigation. The heptapeptide microcystins are a family of *ca.* 50 congeners which exhibit potent inhibition of protein phosphatase 1 and 2A resulting in a range of clinical symptoms. Acute doses of microcystin, such as that recently experienced by patients undergoing dialysis, results in death due to hepatic failure.[3] Longer-term exposure to sub-lethal levels, however, is suspected of promoting primary liver cancer. The incidence of cyanobacterial blooms in freshwaters, including drinking water reservoirs, appears to have increased over the past few decades due to rising nutrient levels caused by intensive farming practices, sewage generation and detergent usage.[4] Microcystins are chemically very stable[5] and conventional water treatment processes fail to remove them, furthermore the use of more advanced methods such as granular carbon filtration and photochemical degradation have shown only limited efficacy.[6,7] The use of semiconductor photocatalysis for destruction of environmental pollutants is a well established technique with the mineralisation of a wide range of materials being reported.[8] When semiconductors are illuminated with light of an appropriate wavelength, electrons are promoted from the occupied valence band (producing oxidising sites) to the unoccupied conductance band (producing reducing sites). It is believed that hydroxyl radicals are generated at the valence band which promote the mineralisation of the pollutants.[9]

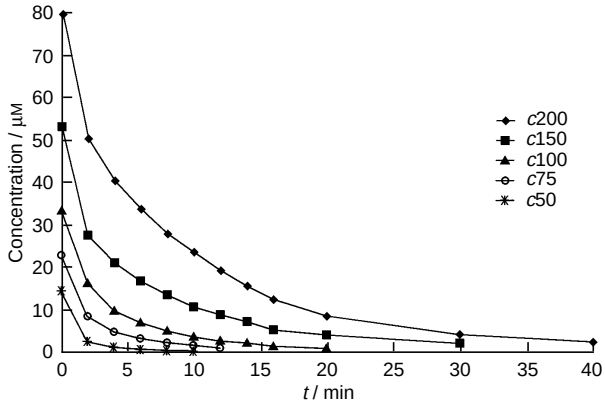



**Fig. 1** The destruction of a range of concentrations of microcystin-LR using a titanium dioxide photocatalyst. Samples were quantified by HPLC using the previously described method of Lawton *et al.* (ref. 11).

**Table 1** Rates of decomposition of microcystin-LR in the presence of $TiO_2$ photocatalyst

| Initial toxin concentration/μM | Initial rate/ μM $min^{-1}$ | Specific activity/ μM $min^{-1}$ $cm^{-2}$ ($\times 10^{-6}$)[a] | Specific rate/ μM $cm^{-2}$ $min^{-1}$ μM $photon^{-1}$ ($\times 10^{-3}$)[b] |
|---|---|---|---|
| 50 | 5.95 | 108.3 | 33.4 |
| 75 | 7.20 | 130.8 | 40.4 |
| 100 | 9.51 | 155.1 | 47.9 |
| 150 | 12.22 | 233.2 | 72.1 |
| 200 | 14.60 | 265.5 | 82.0 |

[a] The specific activity represents the rate of destruction per unit area of catalyst assuming a catalyst surface area of 50 $m^2$ $g^{-1}$. [b] The specific rate represents the rate of destruction per unit area of catalyst per photon absorbed assuming the number of photons absorbed by the reactor as $1 \times 10^{-4}$ photons $min^{-1}$ determined using potassium ferrioxalate actinometry (ref. 19).

We have discovered that this technique is extremely effective in the destruction of microcystin-LR (molecular weight 994)[2] one of the most commonly occurring cyanobacterial toxins. This toxin, a heptapeptide with the generic structure of a microcystin and leucine (L) and arginine (A) in the variable positions, was purified from a natural sample of *Microcystis aeruginosa*.[10] Aqueous solutions of microcystin-LR (pH 4, 306 K) were illuminated in the presence of air and a $TiO_2$ catalyst (1% m/v solution of $TiO_2$ Degussa P-25) using a xenon UV lamp (280 W UVASpot 400 Lamp, Uvalight Technology Ltd, spectral output 330–450 nm). The investigation was performed on a series of solutions containing varying concentration of microcystin-LR. The concentrations (μM) used to evaluate the photocatalytic destruction of microcystin-LR greatly exceeded that which occurs naturally (nM–pM). This, however, enabled us to directly quantify the toxin by HPLC (as described elsewhere[11]) without multi-step processing which is necessary to quantify the much lower levels found in the environment. Very rapid destruction of microcystin-LR was observed for all concentrations (Fig. 1) even at the highest level tested (200 μM) with the toxin virtually undetectable after 40 min. It was found that the initial rate of decomposition was influenced by the initial toxin concentration (Table 1). In fact, at concentrations below those shown the rate of destruction was so rapid that microcystin-LR was undetectable by the first sampling point (2 min). These data suggest that the much lower concentrations which can be present in drinking water will be rapidly removed by this technique. The samples that were illuminated without $TiO_2$ displayed no degradation. As was observed with the initial rates of destruction, the specific rates and specific activities for the process were also reduced with increasing toxin concentration.

The Langmuir–Hinshelwood kinetic rate model has been widely applied to the initial rate of the photocatalytic destruction of a wide series of compounds.[12] Eqn. (1) displays the Langmuir–Hinshelwood kinetic rate law where $r_0$ is the initial rate of disappearance of the substrate and $C_0$ is the initial

substrate concentration, $k$ is the rate constant of the reaction and $K$ is the Langmuir adsorption constant.

$$r_0 = \frac{kKC_0}{1 + kKC_0} \quad (1)$$

The constants $k$ and $K$ may be determined from a plot of $1/r_0$ *vs*. $1/C_0$. If the system obeys the Langmuir–Hinshelwood model this plot should be linear. The intercept of the line provides us with $1/k$ while the slope is equal to $1/kK$. We examined the suitability of applying this model to our system. The reciprocal of initial rate *vs*. initial concentration values for the microcystin decomposition reactions were plotted (Fig. 2) and a linear relationship was observed, confirming that our system does indeed follow the Langmuir–Hinshelwood model. From the graph we determined that $k$ and $K$ for the destruction of microcystin were 19.23 μM min$^{-1}$ and $2.9 \times 10^{-2}$ dm$^3$ μmol$^{-1}$ respectively. Rate and adsorption constants reported for the photocatalytic destruction for other organic compounds are comparable with those reported here.[8,13–15] Examples include 4-chlorophenol ($k$ = 79.3 μM min$^{-1}$, $K$ = $4.88 \times 10^{-3}$ dm$^3$ μmol$^{-1}$),[13] benzene ($k$ = 39 μM min$^{-1}$, $K$ = $1.8 \times 10^{-2}$ dm$^3$ μmol$^{-1}$)[14] perchloroethylene ($k$ = 34 μM min$^{-1}$, $K$ = $8.6 \times 10^{-3}$ dm$^3$ μmol$^{-1}$)[14] and phenol ($k$ = 12.9 μM min$^{-1}$, $K$ = $2.19 \times 10^{-2}$ dm$^3$ μmol$^{-1}$).[15]

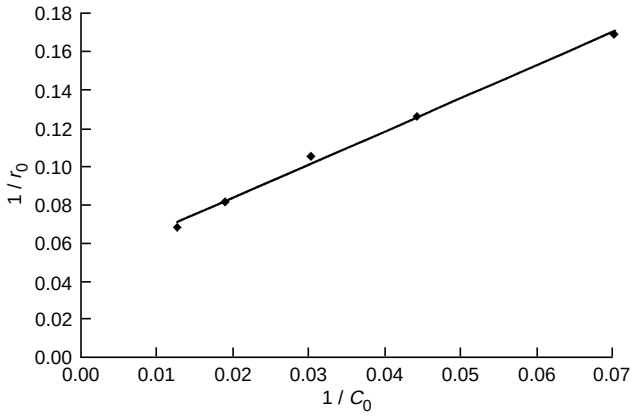



**Fig. 2** Plot of the reciprocal of the initial rate ($1/r_0$) *vs*. the reciprocal of the initial concentration ($1/C_0$)

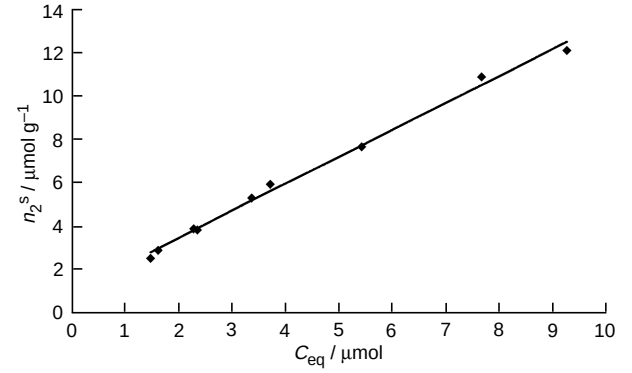



**Fig. 3** Dark adsorption isotherm of microcystin-LR on $TiO_2$. The number of moles of microcystin-LR attached per gram of $TiO_2$ is $n_2^S$ while $C_{eq}$ represents the equilibrium concentration of microcystin after 24 h.

Dark adsorption isotherms, for the adsorption of microcystin on $TiO_2$, were prepared in order to compare the value of the Langmuir adsorption constant determined by this method with that of the constant determined using the initial rates method for the photocatalytic model. Universal bottles containing the toxin solution plus $TiO_2$ were shaken at room temperature in the dark using a flask shaker for 24 h. The dissolved microcystin-LR was separated from the catalyst and quantified by HPLC. The dark adsorption isotherm for microcystin-LR was plotted (Fig. 3) and the $K$ value was found to be $2.9 \times 10^{-4}$ dm$^3$ μmol$^{-1}$. This is 100 times lower than the value obtained using the initial rates method. Similar differences have been observed by other workers.[16,17] It has been proposed that this may be due to photoadsorption reactions at the $TiO_2$ surface or that decomposition of the substrate may not occur exclusively at the catalyst surface but may be promoted by hydroxyl radicals released from the catalyst surface.[16,17]

Preliminary results from our laboratory have shown that this system can also be successfully applied to the destruction of other classes of cyanobacterial toxins.[18] The efficient removal of microcystins and the benefits of the reported removal of other organic contaminants, indicates that photocatalysis is an extremely attractive treatment method for potable water supplies.

We thank J. McElhiney and B. Cornish for assistance with HPLC analysis throughout the project, and S. M. Henderson and C. Edwards (Biotage UK, Hertford) for their collaboration in the purification of microcystin-LR.

## References

1 W. W. Carmichael, *Sci. Am*., 1994, **2**, 64.
2 L. A. Lawton, C. Edwards, K. A. Beattie, S. Pleasance, G. J. Dear and G. A. Codd, *Nat. Toxins*, 1995, **3**, 50.
3 J. Dunn, *Br. Med. J*., 1996, **312**, 1183.
4 C. S. Reynolds, in *Advances in Botanical Research*, ed. J. A. Callow, Academic Press, London, 1987, vol. 13, p. 63.
5 K. Tsuji, S. Nalto, F. Kondo, N. Ishikawa, M. F. Watanabe, M. Suzuki and K.-I. Harada, *Environ. Sci. Technol*., 1994, **28**, 173.
6 K. Tsuji, T. Watanuki, F. Kondo, M. Wanatabe, S. Suzuki, H. Nakazawa, M. Suzuki, H. Uchida and K. Harada, *Toxicon*, 1995, **33**, 1619.
7 K. Himberg, A.-M. Keijola, L. Husvirta, H. Pyysalo and K. Sivonen, *Water. Res*., 1989, **23**, 979.
8 M. R. Hoffmann, S. T. Martin, W. Choi and D. W. Bahnemann, *Chem. Rev*., 1995, **95**, 69.
9 A. Mills, R. H. Davies and D. Worsley, *Chem. Soc. Rev*., 1993, **93**, 417.
10 C. Edwards, L. A. Lawton, S. M. Coyle and P. Ross, 1996, **734**, 163.
11 L. A. Lawton, C. Edwards and G. A. Codd, *Analyst (London)*, 1994, **119**, 1525.
12 D. F. Ollis, E. Pelizzetti and N. Serpone, in *Photocatalysis, Fundamentals and Applications*, ed. N. Serpone and E. Pelizzetti, Wiley, New York, 1989, p. 603.
13 R. W. Matthews, *J. Catal*., 1988, **111**, 264.
14 C. S. Turchi and D. F. Ollis, *J. Catal*., 1989, **119**, 483.
15 R. W. Matthews and S. R. McEvoy, *J. Photochem. Photobiol. A: Chem*., 1992, **66**, 355.
16 J. Cunningham and G. Al-Sayyed, *J. Chem. Soc., Faraday Trans*., 1990, **86**, 3935.
17 A. Mills and S. Morris, *J. Photochem. Photobiol. A: Chem*, 1993, **71**, 75.
18 J. Rouzade, Internal Report, The Robert Gordon University, Aberdeen, Scotland, 1996.
19 C. G. Hatchard and C. A. Parker, *Proc. R. Soc. London, A, Math. Phys. Sci*., 1956, **235**, 518.

*Received, 25th November 1996; Com. 6/07965B*

# Photophysics of xanthione and 4*H*-1-benzopyran-4-thione in β-cyclodextrin complexes

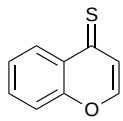
**Marek Sikorski,[a,b] Miquel Mir[a] and Francis Wilkinson[a]**

[a] *Department of Chemistry, Loughborough University, Loughborough, Leicestershire, UK LE11 3TU*
[b] *Faculty of Chemistry, University of A. Mickiewicz, 60 780 Poznan, Poland*

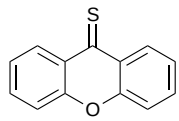
**The phosphorescence decays of β-cyclodextrin (β-CD) complexes of xanthione (XT) and 4*H*-1-benzopyran-4-thione (BPT) show that self-quenching and oxygen quenching are not important in such complexes, and that the existence of bimodal inclusion in solid complexes can be identified using the width of the distribution parameter of the Gaussian distribution of the logarithm of the observed rate constants for decay.**

Aromatic thioketones show interesting photochemical behaviour including fluorescence from the second excited singlet state, $S_2$, room temperature phosphorescence from the first excited triplet state, $T_1$, thermally activated delayed fluorescence from the first excited singlet state, $S_1$, and photochemistry arising from the $T_1$ state as well as from the $S_2$ state.[1] In addition, the $S_2$ and $T_1$ states of thiones are quenched at or near diffusion limited rates by a wide variety of substances including ground state thione (self-quenching) and oxygen. Moreover, studies of $S_2$ are complicated by the fact that thione non-radiative decay rates are extremely sensitive to the nature of the solvent since quenching by many common solvents occurs at diffusion-limited rates.[1] Attempts to overcome the self-quenching problem in solution have involved the incorporation of thiones in micelles.[2] In these organised media a decrease in the contribution of the self-quenching process to the decay of $T_1$ states of thioketones was achieved as a consequence of the compartmentalisation process.[2]

Recently, the formation of β-CD inclusion complexes of xanthione (XT) and 4*H*-1-benzopyran-4-thione (BPT) in aqueous solution have been reported.[3] Cyclodextrins (CDs) are cyclic oligosacharides of six to eight α-D-glucose units (α-CD, six; β-CD, seven; γ-CD, eight) that posses internal hydrophobic cavities able to include a great variety of guest molecules in aqueous solutions.[4] These complexes have been used for studying the photophysics and photochemistry of the guest molecules in an organised environment.[5] Here we report a preliminary account on the photophysics of XT and BPT β-CD complexes in water and in the solid state.†



BPT



XT

The absorption spectrum of BPT in water shows a maximum at 376 nm ($S_0 \rightarrow S_2$ band). Upon addition of 0.011 M β-CD, a small blue shift is observed ($\lambda_{max}$ = 373 nm). The absorption spectrum of XT in water could not be recorded by us in 1 cm pathlength cells due to the low solubility ($S = 2.5 \times 10^{-7}$ M, $\varepsilon = 1.5 \times 10^4$ dm$^3$ mol$^{-1}$ cm$^{-1}$).[2b] The solubility of XT increases upon addition of β-CD and the absorption spectrum was recorded ($S_0 \rightarrow S_2$ band, $\lambda_{max}$ = 406 nm).

Steady-state emission spectra of XT and BPT in air-equilibrated aqueous solution show dramatic changes in the emission intensity upon addition of β-CD to the solution. The positions of the wavelength maxima are collected in Table 1. These changes are depicted in Fig. 1(*a*) for XT. In the case of BPT there is a substantial increase in the $S_2 \rightarrow S_0$ fluorescence and in the $T_1 \rightarrow S_0$ phosphorescence, and a blue shift of the phosphorescence band (not shown). In the case of XT we were able to observe very little emission, if any, without β-CD. However, in the presence of β-CD, $S_2 \rightarrow S_0$ fluorescence and $T_1 \rightarrow S_0$ phosphorescence appear. These results confirm earlier reports[3] about the formation of β-CD inclusion complexes of XT and BPT in aqueous solution and show the protection offered by the β-CD cavity from oxygen quenching of thione molecules in such inclusion complexes. A similar conclusion was reached for other guest molecules in CD inclusion complexes in aqueous media[6] and also for solid state complexes.[7]

Ground state diffuse reflectance absorption spectra of XT–β-CD and BPT–β-CD solid complexes do not show noticeable changes in relation to the spectra observed in aqueous solution in the presence of β-CD (see Table 1). Steady-state emission spectra of XT–β-CD [Fig. 1(*b*)] and BPT–β-CD air-equilibrated solid complexes were recorded (see Table 1). In both cases, $S_2 \rightarrow S_0$ fluorescence and $T_1 \rightarrow S_0$ phosphorescence are observed. The relative intensity fluorescence/phosphorescence is very similar in both cases to that observed for the complexes in aqueous solution. For the sake of comparison fluorescence measurements were performed for XT and BPT on cellulose mechanical mixtures with similar concentrations to those employed for the β-CD solid complexes. Practically no phosphorescence was observed for these mechanical mixtures presumably because in these cases efficient oxygen quenching occurred. Moreover, no emission was observed from XT crystals.

Time resolved phosphorescence of XT–β-CD and BPT–β-CD solid complexes was studied using diffuse reflectance

**Table 1** Spectral properties of XT and BPT in different media

| | Absorption $\lambda_{max}(S_0 \rightarrow S_2)$/nm | Fluorescence $\lambda_{max}(S_0 \rightarrow S_2)$/nm | Phosphorescence $\lambda_{max}(S_0 \rightarrow S_2)$/nm |
|---|---|---|---|
| BPT in water | 376 | 425 | 644 |
| BPT in water + 0.011 M β-CD | 373 | 427 | 628 |
| BPT–β-CD solid complex | 370 | 439 | 618 |
| XT in water | —[a] | — | — |
| XT in water + 0.011 M β-CD | 406 | 430–490 | 667 |
| XT–β-CD solid complex | 408 | 457 | 661 |

[a] Solubility too low to be measured ($S = 2.5 \times 10^{-7}$ M, $\varepsilon = 1.5 \times 10^4$ dm$^3$ mol$^{-1}$ cm$^{-1}$) [ref. 2(*b*)].

laser flash photolysis equipment.‡,[8] The phosphorescence decays were fitted according to the Albery model[9] for dispersive kinetics§ [see Fig. 1(*b*) for XT as example]. The mean rate constants for triplet state decay obtained using the Albery model in the β-CD solid complexes [$k = (2.61 \pm 0.05) \times 10^5$ s$^{-1}$ for BPT and $k = (2.24 \pm 0.01) \times 10^5$ s$^{-1}$ for XT] are comparable to the values previously reported in solution at infinite dilution for BPT[10] and XT.[11] The mean decay constant of a XT–β-CD complex sample with eight times less XT loading was practically identical [$k = (2.04 \pm 0.02) \times 10^5$ s$^{-1}$] to the mean decay constant of the sample with higher loading. Practically identical phosphorescence decay of a XT–β-CD complex sample was observed when the sample was degassed prior to excitation, presumably due to the protection from oxygen quenching offered by the CD in the solid state.[7] These results suggest that self-quenching and oxygen quenching do not play an important role in the photophysics of thioketones in solid β-CD inclusion complexes.

It is interesting to note the difference in the width of the distribution parameter, γ, obtained from fitting to the Albery model the phosphorescence decay of the XT–β-CD and BPT–β-CD complexes ($\gamma = 1.11 \pm 0.02$ for BPT and $\gamma = 0.62 \pm 0.01$ for XT). The higher value for the BPT complex can be attributed to the existence of two non interconverting¶ major orientations of the BPT molecules within the β-CD cavity (see Fig. 2). By contrast, XT can only be fitted within the cavity in one major orientation due to its symmetry. The existence of multimodal inclusion of the guest molecules in the CD cavity has been studied in solution by different methods: electron paramagnetic resonance (EPR),[13] electron nuclear double-resonance (ENDOR),[14] fluorescence methods[15] and theoretical methods.[16]

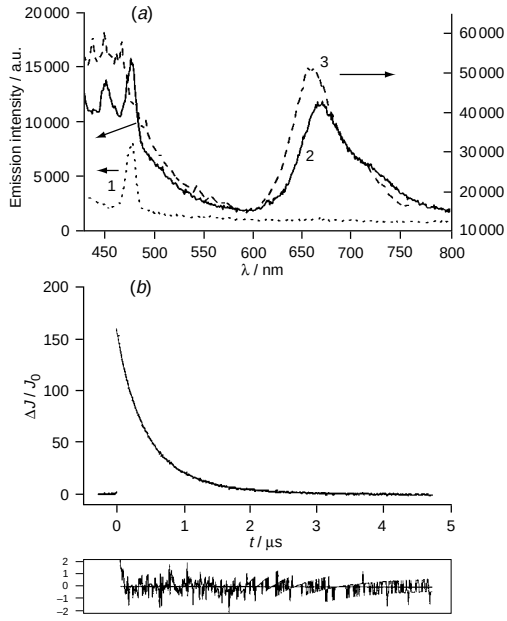



**Fig. 1** (*a*) Steady-state emission spectra of XT ($\lambda_{exc}$ = 410 nm, non deoxygenated samples at room temperature) in water (1), in water with β-CD 0.011 M (2) and in the β-CD complex in the solid state (3). (*b*) Phosphorescence decay trace of the XT–β-CD solid complex at 660 nm and fit according to the Albery model (ref. 9) with the plot of residuals.

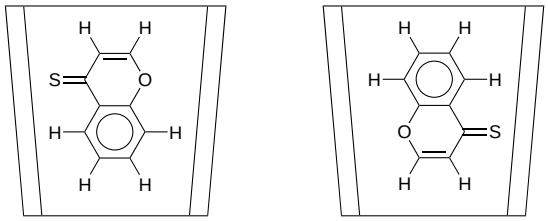


**Fig. 2** Major orientations of the BPT molecules within the β-CD cavity

In summary, the results presented here show that β-CD inclusion complexes in aqueous solution and in the solid state might be a particularly useful media for studying the intramolecular photophysics of aromatic thioketones due to the fact that self-quenching and quenching by oxygen are not important in such inclusion complexes. As far as we know, this is the first reported example of bimodal inclusion in solid state cyclodextrin complexes. The methodology applied in the present work (analysis of the phosphorescence decay according to the Albery model) is a new alternative to the fluorescence method and might be a powerful tool for investigating in the microsecond domain the existence of different inclusion orientations in solid cyclodextrin complexes.‖

We thank the Royal Society/Central and East European Postdoctoral Fellowship and The Foreign and Commonwealth Office for a postdoctoral grant (to M. S.) and DGICYT (Ministerio de Educación y Ciencia) of Spain for a postdoctoral grant (to M. M.).

## Footnotes

† CD solid complexes were prepared by dissolving a certain amount of the thione in 0.011 M β-CD aqueous solutions under magnetic stirring at 70 °C for 4 h. After evaporation of water *in vacuo* with a rotary evaporator, the solid obtained was dried under vacuum at 40 °C for 4 h. Sample loading were around 0.5–2 mg of the thione per gram of β-CD.

‡ A detailed description of the laser system can be found in ref. 8. The excitation wavelength was 355 nm.

§ Complex kinetics are normally observed in heterogeneous media (*i.e.* solid surfaces, polymer matrices, biological membranes) due to the variety of solute environments, every one with its own decay mode. The Albery model (ref. 9) describes the kinetics of heterogeneous systems by a Gaussian distribution of the logarithm of the observed rate constants with two parameters: the mean rate constant, *k*, and a distribution parameter, γ, that defines the spread of the Gaussian distribution (if $\gamma = 0$, the Albery model becomes a simple first-order exponential decay equation).

¶ The diameter of the β-CD cavity (ref. 4) is 6.0–6.4 Å and the largest diameter of the BPT molecule is *ca* 6.5 Å according to standard bond lengths (ref. 12). Therefore the molecule of BPT does not have inside the solid complex the possibility of interchanging the orientations depicted in Scheme 1.

‖ A lifetime distribution study of xanthone and benzophenone triplets in cyclodextrin complexes in the solid state using an exponential series method has been reported in the literature (ref. 7).

## References

1 A. Maciejewski and R. P. Steer, *Chem. Rev.*, 1993, **93**, 67 and references cited therein.
2 (*a*) V. Ramesh and V. Ramamurthy, *J. Photochem.*, 1982, **20**, 47; (*b*) A. Maciejewski, A. Jakubowska, E. Dutkiewicz and W. Augustyniak, *J. Colloid Interface Sci.*, 1996, **177**, 528.
3 M. Milewski, W. Augustyniak and A. Maciejewski, unpublished results.
4 M. L. Bender and M. Komiyama, *Cyclodextrin Chemistry*; Springer-Verlag, New York, 1977.
5 P. Bortolus and S. Monti, *Adv. Photochem.*, 1996, **21**, 1.
6 N. J. Turro, G. S. Cox and X. Li, *Photochem. Photobiol.*, 1983, **37**, 149.
7 M. Barra and J. C. Scaiano, *Photochem. Photobiol.*, 1995, **62**, 60.
8 F. Wilkinson and G. Kelly, *Handbook of Organic Photochemistry*, ed. J. C. Scaiano, CRC Press, Boca Raton, FL, 1989, vol. 1, pp. 293–314.
9 W. J. Albery, P. N. Bartlett, C. P. Wilde and J. R. Darwent, *J. Am. Chem. Soc.*, 1985, **107**, 1854.
10 M. Sikorski, W. Augustyniak, I. V. Khmelinski, V. V. Korolev and N. M. Bazhin, *Chem. Phys. Lett.*, 1993, **209**, 403.
11 U. Bruhlmann and J. R. Huber, *Chem. Phys. Lett.*, 1978, **54**, 606.
12 J. March, *Advanced Organic Chemistry*, Wiley, New York, 4th edn., 1992, p. 21.
13 Y. Kotate and E. G. Janzen, *J. Am. Chem. Soc.*, 1988, **110**, 3699.
14 Y. Kotate and E. G. Janzen, *J. Am. Chem. Soc.*, 1992, **114**, 2872.
15 (*a*) F. V. Bright, G. C. Catena and J. Huang, *J. Am. Chem. Soc.*, 1990, **112**, 1343; (*b*) A. Nakamura, K. Saitoh and F. Toda, *Chem. Phys. Lett.*, 1991, **187**, 110.
16 F. Pérez, C. Jaime and X. Sánchez-Ruiz, *J. Org. Chem.*, 1995, **60**, 3840.

*Received, 9th December 1996; Com. 6/08281E*

# Catalytic oxidation of methane to methyl hydroperoxide and other oxygenates under mild conditions

**Galina V. Nizova,[a] Georg Süss-Fink,*[b]† and Georgiy B. Shul'pin*[a]‡**

[a] *Semenov Institute of Chemical Physics, Russian Academy of Sciences, ul. Kosygina 4, Moscow 117977, Russia*
[b] *Institut de Chimie, Université de Neuchâtel, Avenue de Bellevaux 51, CH-2000, Neuchâtel, Switzerland*

**Methane is oxidized by air in acetonitrile solution to give methyl hydroperoxide (easily reduced to methanol), formaldehyde and formic acid in the presence of $[NBu_4]VO_3$–pyrazine-2-carboxylic acid as the catalyst and $H_2O_2$ as a promoter.**

The oxidation of saturated hydrocarbons with hydrogen peroxide and molecular oxygen catalysed by transition-metal complexes constitutes a convenient route for the direct transformation of these inert compounds to valuable products such as peroxides, ketones, alcohols and carboxylic acids.[1] Complexes of vanadium are known to catalyse the oxidation of various organic compounds by peroxides.[2,3]

We report here on the efficient oxidation of methane with air catalysed by the combination $[NBu_4]VO_3$–pyrazine-2-carboxylic acid (PCA) in the presence of hydrogen peroxide. The reactions of methane (and of cyclohexane as well) were carried out at various temperatures and pressures.§ The process was monitored by withdrawing aliquots at specific intervals and analysing each sample twice, *i.e.* before and after the addition of an excess of solid triphenylphosphine. This method described by us earlier[3,4] (and used then also by other workers[5]) allows one to detect alkyl hydroperoxides and to measure also the real concentrations of all three products (alkyl hydroperoxide, alcohol and aldehyde or ketone) present in the reaction solution, because usually alkyl hydroperoxides are decomposed in the gas chromatograph to produce the corresponding alcohol and ketone.¶

We have found that the combination of $[NBu_4]VO_3$ and PCA catalyses the oxidation of methane in acetonitrile solution in the presence of air and hydrogen peroxide to produce methyl hydroperoxide, formaldehyde and (after an induction period) formic acid (Table 1). Methyl hydroperoxide slowly decomposes to give methanol and formaldehyde. No methanol peak has been detected after opening the autoclave prior to the reduction with $PPh_3$. After the reduction with $PPh_3$ the MeOH peak appeared, while the concentration of HCHO in the solution dropped. The average rates of oxidation at 20, 40 and 75 °C are 7.5, 30 and 105 turnovers $h^{-1}$, respectively.

**Table 1** Oxidation of methane by air in the presence of $[NBu_4]VO_3$–PCA–$H_2O_2$[a]

| Pressure/bar | | | | Products (concentration/ $10^2$ mol $dm^{-3}$) | | | |
|---|---|---|---|---|---|---|---|
| Methane | Air | *T*/°C | *t*/h | MeOOH | HCHO | $HCO_2H$ | Total turnover[b] |
| 75 | 10 | 23 | 6 | 0.5 | 0.04 | 0 | 54 |
| | | | 16 | 1.3 | 0.13 | 0 | 143 |
| | | | 24 | 1.6 | 0.16 | 0 | 176 |
| 75 | 10 | 40 | 1 | 1.6 | 0.18 | 0 | 178 |
| | | | 4 | 1.0 | 0.32 | 0.5 | 182 |
| | | | 6 | 0.5 | 0.37 | 1.5 | 207 |
| | | | 17 | 0.1 | 0.03 | 5.0 | 513 |
| 40 | 10 | 75 | 4 | 0 | 0.20 | 4.0 | 420 |

[a] Conditions and concentrations of components, see Footnote §. Standard deviations of analytic methods ±20%; value 0 means below detection limit ($0.01 \times 10^{-2}$ for MeOH, MeOOH and HCHO; $0.1 \times 10^{-2}$ mol $dm^{-3}$ for $HCO_2H$). [b] Moles of all detected products per mole of vanadate ion.

The oxidation of methane, catalysed by $[NBu_4]VO_3$–PCA, requires the presence of air and hydrogen peroxide. We believe that hydrogen peroxide, although present in stoichiometric amounts, acts only as a promoter, while molecular oxygen is the oxidant. In order to prove the implication of $O_2$ from air in the oxidation process, we studied the analogous reaction with liquid cyclohexane in the place of methane. When the reaction was carried out in the presence of $H_2O_2$ but in the absence of air ($N_2$ atmosphere, 40 °C, 2 h) no formation of oxygenated products was observed. However, when the reaction vessel was opened to air, the reaction started immediately with the same rate as observed in the presence of air.

Finally, the cyclohexane oxidation under an $^{18}O_2$ atmosphere unambiguously showed a high degree of $^{18}O$ incorporation into the oxygenated products.‖ Thus, according to the GCMS analysis, the measured extent of $^{18}O$ incorporation into cyclohexanol after the reduction with triphenylphosphine is *ca.* 75%. Prior to the reduction with $PPh_3$, the $^{18}O$ labelling of cyclohexanol was noticeably lower (*ca.* 50%), and only *ca.* 5% of $^{18}O$ was found in cyclohexanone. The triphenylphosphine oxide formed from the reduction of the reaction mixture with $PPh_3$ also contained $^{18}O$. On the basis of these results one can assume that all oxygen present in the primary product of the oxidation (alkyl hydroperoxide, ROOH) stems from atmospheric dioxygen. Unlabelled oxygen (*ca.* 25%) detected in the cyclohexanol after the reduction with $PPh_3$ could originate from gaseous $^{16}O_2$, formed by catalytic decomposition of $H_2{}^{16}O_2$ in the reaction vessel. Such a decomposition proceeds rapidly in the injector of the chromatograph at high temperature. Cyclohexanone seems to be formed in the injector from cyclohexyl hydroperoxide completely *via* a mechanism involving the generation of alkyl radicals, R·, which react then with $^{16}O_2$.

We presume that in the presence of catalytic amounts of $[NBu_4]VO_3$–PCA, hydrogen peroxide is an efficient generator of hydroxyl radicals. The radicals HO· thus formed attack the alkane molecule, RH, abstracting a hydrogen atom. As a result, alkyl radicals, R·, are produced which rapidly react with molecules of oxygen to yield peroxyl radicals ROO· (see ref. 6). These latter species can then be transformed into ROOH. Stoichiometric quantities of $H_2O_2$ are presumably required in order to reactivate the catalyst system.

Thus it may be concluded that in the system described in the present work, hydrogen peroxide is only the promoter of the oxygenation, while molecular oxygen is the true oxidant. Such a scheme seems to be operative in many alkane oxidations with $H_2O_2$ in air (small amounts of molecular oxygen necessary for the addition to alkyl radicals can be formed by the decomposition of $H_2O_2$ even if the reaction is carried out in an inert atmosphere[6]). Indeed, previously we have found that alkyl hydroperoxides are formed as main products when higher alkanes are oxidized with $H_2O_2$ in air under the catalysis not only by the vanadium system studied in the present work,[3] but also by manganese porphyrinates, palladium complexes and iron salts,[4c] as well as by methyltrioxorhenium.[7] The reagent

described in this paper is one of the most efficient ones (in terms of catalytic turnovers) for methane oxidation[8] under mild conditions (temperatures below 100 °C).

We thank BASF, the International Science Foundation, INTAS, the Russian Basic Research Foundation and the Swiss National Science Foundation for support and Dr. Arthur Höhn (BASF, Ludwigshafen, Germany) for fruitful discussions.

## Footnotes

† E-mail: Suess-Fink@ich.unine.ch
‡ E-mail: gb@shulpin.msk.ru

§ The oxidations were carried out in glass-lined stainless-steel autoclaves with vigorous stirring (volume of the reaction solution = 10 ml, total volume of autoclave = 100 ml). Usually the following concentrations of the reagents were used: $[NBu_4]VO_3$, $1.0 \times 10^{-4}$ mol dm$^{-3}$; PCA, $4.0 \times 10^{-4}$ mol dm$^{-3}$; $H_2O_2$ (35% aq), 0.2 mol dm$^{-3}$. Before the oxidation the autoclave was charged with air and then with methane under appropriate pressures. (**CAUTION**: the combination of air and $H_2O_2$ with organic compounds at elevated pressures and temperatures may be explosive!) The reactions were stopped by cooling with ice and the reaction solution was analysed by GC (DANI-86.10; fused silica capillary column 60 m × 0.25 mm × 0.25 μm, SPB-1; integrator SP-4400). The concentration of formaldehyde was measured spectrophotometrically after its transformation into 2,6-dimethyl-3,5-diacetyl-1,4-dihydropyridine according to method described in ref. 9.

¶ If an excess of solid $PPh_3$ is added to the reaction solution 10–20 min before the GC analysis, the alkyl hydroperoxide present is completely reduced to the corresponding alcohol. As a result, the chromatogram differs completely from that of a sample not subjected to the reduction (the alcohol peak increases, while the intensity of the ketone peak decreases). If there is no difference between chromatograms of the same sample before and after reduction, this testifies to the absence of an alkyl hydroperoxide in the solution. If, by contrast, the chromatogram prior to the reduction exhibits the peaks for the ketone and the alcohol, whereas after the reduction with $PPh_3$ only a peak for the alcohol is observed, one may conclude that only the alkyl hydroperoxide was present in the solution. This method allows one to determine alkyl hydroperoxides in the presence of hydrogen peroxide.

‖ The reaction was carried out in a sealed ampoule (10 ml) at 20 °C under an atmospheric pressure of $^{18}O_2$ (content 98%, Cambridge Isotope Laboratories) over 3 days; concentrations: cyclohexane, 0.46 mol dm$^{-3}$; $H_2O_2$ (35% aq), 0.2 mol dm$^{-3}$; $[NBu_4]VO_3$, $1.0 \times 10^{-4}$ mol dm$^{-3}$, PCA, $4.0 \times 10^{-4}$ mol dm$^{-3}$. The resulting solution was analysed by GCMS (NERMAG R 30-10, capillary column 50 m × 0.25 mm × 0.25 μm, Carbowax 20M).

## References

1 *The Activation of Dioxygen and Homogeneous Catalytic Oxidation*, ed. D. H. R. Barton, A. E. Martell and D. T. Sawyer, Plenum, New York, 1993; R. H. Crabtree, *Chem. Rev.*, 1995, **95**, 987; A. E. Shilov and G. B. Shul'pin, *Activation and Catalytic Reactions of Hydrocarbons*, Nauka, Moscow, 1995.

2 A. Butler, M. J. Clague and G. E. Meister, *Chem. Rev.*, 1994, **94**, 625; M. Bonchio, V. Conte, F. Di Furia, G. Modena, S. Moro, T. Carofiglio, F. Magno and P. Pastore, *Inorg. Chem.*, 1993, **32**, 5797; R. Neumann, M. Chava and M. Levin, *J. Chem. Soc., Chem. Commun.*, 1993, 1685; M. Bonchio, V. Conte, F. Di Furia, G. Modena and S. Moro, *J. Org. Chem.*, 1994, **59**, 6262; A. E. Gekhman, N. I. Moiseeva and I. I. Moiseev, *Russ. Chem. Bull.*, 1995, **44**, 584; M. J. Clague and A. Butler, *J. Am. Chem. Soc.*, 1995, **117**, 3475; V. Conte, F. Di Furia and S. Moro, *J. Phys. Org. Chem.*, 1996, **9**, 329.

3 G. B. Shul'pin, D. Attanasio and L. Suber, *Russ. Chem. Bull.*, 1993, **42**, 55; G. B. Shul'pin, D. Attanasio and L. Suber, *J. Catal.*, 1993, **142**, 147; G. B. Shul'pin, A. N. Druzhinina and G. V. Nizova, *Russ. Chem. Bull.*, 1993, **42**, 1326; G. V. Nizova and G. B. Shul'pin, *Russ. Chem. Bull.*, 1994, **43**, 1146; G. B. Shul'pin and G. Süss-Fink, *J. Chem. Soc., Perkin Trans. 2*, 1995, 1459; G. B. Shul'pin, R. S. Drago and M. Gonzalez, *Russ. Chem. Bull.*, 1996, **45**, 2386; M. C. Guerreiro, U. Schuchardt and G. B. Shul'pin, *Russ. Chem. Bull.*, in the press; G. B. Shul'pin, M. C. Guerreiro and U. Schuchardt, *Tetrahedron*, 1996, **52**, 13 051.

4 (*a*) G. B. Shul'pin and A. N. Druzhinina, *Mendeleev Commun.*, 1992, 36; (*b*) *React. Kinet. Catal. Lett.*, 1992, **47**, 207; (*c*) G. B. Shul'pin and G. V. Nizova, *React. Kinet. Catal. Lett.*, 1992, **48**, 333; (*d*) G. B. Shul'pin, A. N. Druzhinina and L. S. Shul'pina, *Neftekhimiya*, 1993, **33**, 335; (*e*) G. B. Shul'pin, M. M. Bochkova and G. V. Nizova, *J. Chem. Soc., Perkin Trans. 2*, 1995, 1465.

5 D. L. Vanoppen, D. E. De Vos, M. J. Genet, P. G. Rouxhet and P. A. Jacobs, *Angew. Chem., Int. Ed. Engl.*, 1995, **34**, 560.

6 I. W. C. E. Arends, K. U. Ingold and D. D. M. Wayner, *J. Am. Chem. Soc.*, 1995, **117**, 4710; J. Kim, R. G. Harrison, C. Kim and L. Que, Jr., *J. Am. Chem. Soc.*, 1996, **118**, 4373; R. H. Fish, M. S. Konings, K. J. Oberhausen, R. H. Fong, W. M. Yu, G. Christou, J. B. Vincent, D. K. Coggin and R. M. Buchanan, *Inorg. Chem.*, 1991, **30**, 3002.

7 U. Schuchardt, D. Mandelli and G. B. Shul'pin, *Tetrahedron Lett.*, 1996, **37**, 6487.

8 P. E. Ellis, Jr. and J. E. Lyons, *Coord. Chem. Rev.*, 1990, **105**, 181; A. S. Goldstein and R. S. Drago, *J. Chem. Soc., Chem. Commun.*, 1991, 21; R. A. Periana, D. J. Taube, E. R. Evitt, D. G. Löffler, P. R. Wentrcek, G. Voss and T. Masuda, *Science*, 1993, **259**, 340; M. W. Grinstaff, M. G. Hill, J. A. Labinger and H. B. Gray, *Science*, 1994, **264**, 1311; A. Sen, M. A. Benvenuto, M. Lin, A. C. Hutson and N. Basickes, *J. Am. Chem. Soc.*, 1994, **116**, 998; K. Nakata, Y. Yamaoka, T. Miyata, Y. Taniguchi, K. Takaki and Y. Fujiwara, *J. Organomet. Chem.*, 1994, **473**, 329; A. S. Goldstein, R. H. Beer and R. S. Drago, *J. Am. Chem. Soc.*, 1994, **116**, 2424; M. Kurioka, K. Nakata, T. Jintoku, Y. Taniguchi, K. Takaki and Y. Fujiwara, *Chem. Lett.*, 1995, 244; Y. Taniguchi, S. Horie, K. Takaki and Y. Fujiwara, *J. Organomet. Chem.*, 1995, **504**, 137; M. Lin, T. E. Hogan and A. Sen, *J. Am. Chem. Soc.*, 1996, **118**, 4574.

9 T. Nash, *Biol. J.*, 1953, **55**, 416; S. E. Halliday and P. Skett, *Biochem. Pharmacol.*, 1990, **39**, 229.

*Received, 15th November 1996; Com. 6/7765J*

# The isolation and structure of bacillariolide III, an extracellular metabolite of the diatom, *Pseudo-nitzschia multiseries*

**Naiyu Zheng and Yuzuru Shimizu***

*Department of Biomedical Sciences, College of Pharmacy, University of Rhode Island, Kingston, RI 02881, USA*

**The marine diatom, *Pseudo-nitzschia multiseries* was found to excrete a metabolite formed by the cleavage of an eicosanoid, and its structure is determined.**

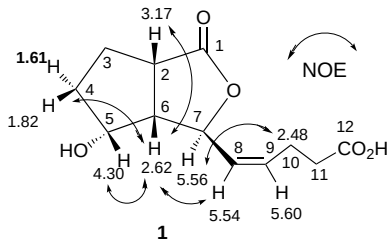
In the previous papers,[1,2] we reported the isolation and structure determination of two novel eicosanoids from the wild and cultured cells of the diatom, *Pseudo-nitzschia multiseries*,† a causative organism of so-called amnesic shellfish poisoning (ASP).[3] In the continuing study, we have noticed that the organism also produces extracellular metabolites. In this communication, we report the chemical characterization of one of the metabolites, bacillariolide III, **1** and its biosynthetic relationship with the previously reported compounds.

The clonal strain of *P. mutiseries* S2-184-1,‡ which had been isolated from Narragansett Bay in October, 1995 by N.Z., was cultured in F/2 + Si medium at 23 °C under fluorescent illumination (16 h/8 h L/D cycle) and sterile conditions. After centrifugation, the acidified culture medium (pH 3.0) was passed through silica gel C18. The C18 layer was washed with water and extracted with MeOH. The MeOH eluate was successively chromatographed on LH-20 (MeOH) and on silica gel C18 (10% MeCN + 0.5% acetic acid). The fraction which showed a single spot on TLC was passed through Chelex 100 $Na^+$ form to give the $Na^+$ salt of **1**. The free acid was obtained as an amorphous solid after acidification with 0.1 M HCl and extraction with $CHCl_3$. About 2 mg of pure bacillariolide III was obtained from a 20 l batch of culture.

**Table 1** $^1H$ and $^{13}C$ NMR data of Bacillariolide III, **1** ($^1H$: 400 MHz and $^{13}C$: 100 MHz in $CD_3OD$)

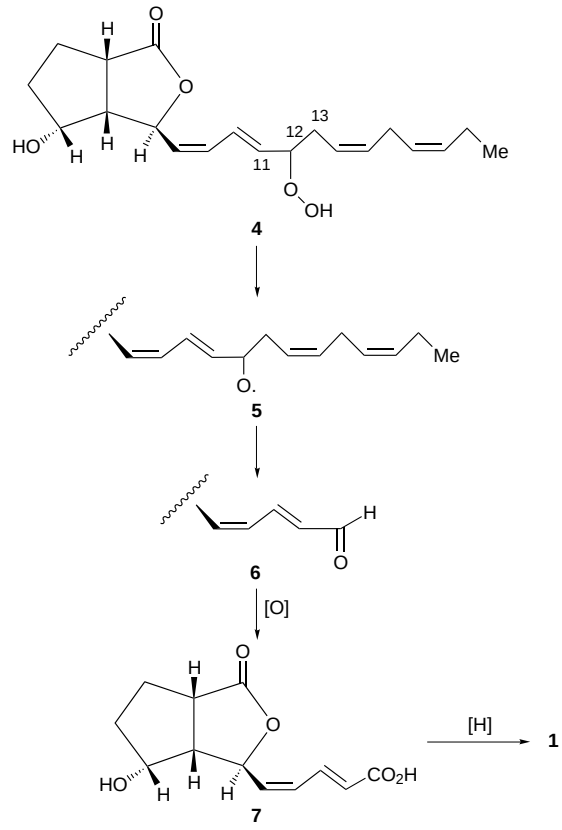
| Position | $\delta_C$ | $\delta_H$ | $^1H$–$^1H$ COSY cross peaks/δ |
|---|---|---|---|
| 1 | 183.6 | | |
| 2 | 44.8 | 3.17, dt (9.6, 6.6) | 1.98, 2.62 |
| 3 | 27.3 | 1.98, m | 3.17, 1.61, 1.82 |
| 4 | 34.7 | a. 1.61, m | 1.82, 1.98, 4.30 |
| | | b. 1.82, m | 1.61, 1.98, 4.30 |
| 5 | 74.7 | 4.30, ddd (1.5, 5.1, 6.3) | 1.61, 1.82, 2.62 |
| 6 | 52.1 | 2.62, ddd (10.0, 6.4, 1.8) | 3.17, 4.30 5.56 |
| 7 | 76.6 | 5.56,[b] dd (3.1, 12.0) | 2.62, 5.54 |
| 8 | 131.0 | 5.54[b], dd (6.4, 3.3) | 5.56, 5.60 |
| 9 | 133.5 | 5.60, dt (10.4, 6.0) | 5.54, 2.48 |
| 10 | 24.8[a] | 2.48, dt (6.5, 10.7) | 5.60, 2.41 |
| 11 | 36.0[a] | 2.41, t (6.5) | 2.48 |
| 12 | 183.3 | | |

[a] Assigned from the HMQC spectrum. [b] Overlapped signals.




**1**

**2**: 7α-H
**3**: 7β-H




**4** **5** **6** **7**

**Scheme 1** A possible biosynthetic pathway of bacillariolide III, **1**

Bacillariolide III, $[\alpha]_D^{24}$ −25.3 (*c* 0.28, MeOH), UV: end absorption, has the molecular formula of $C_{12}H_{16}O_5$ [*m*/*z* calc. 240.099774; found (EIMS) 240.099646]. The IR spectrum showed absorption bands, ν/cm$^{-1}$ ($CHCl_3$): 3500 (OH), 1770 (γ-lactone) and 1730 (γ-lactone). The $^1H$, $^{13}C$ and HMQC NMR spectra (Table 1) suggested the presence of two carbonyl groups, one disubstituted double bond, four methylene groups and four methine groups, of which two are bearing oxygen atoms. Thus the compound must be bicyclic. From the $^1H$–$^1H$ COSY and HMQC spectra, the entire spin system was easily established as shown in the structure **1**. The relative stereochemistry were established by NOE difference and NOESY experiments (shown on the structure). The geometry of the double bond was concluded as *Z* from the coupling constant of

the olefinic protons (6 Hz), which was also supported by the NOE data. The absolute configuration was assumed by the perceivable biosynthetic relationship of **1** with the co-occurring bacillariolide I, **2**, whose absolute configuration was unequivocally established by the X-ray crystallography of a derivative having a known chirality.[2]

The biosynthetic origin of **1** would never have been easily speculated, had it been a sole metabolite found with the diatom. However, the structures of the two previously isolated compounds, bacillariolide I, **2**, and II, **3**, suggest that **1** is a metabolite derived from bacillariolide I, **2** by the cleavage of the carbon chain at C-12 and C-13. It can be explained by the formation of 12-hydroperoxide **4** and alkoxyl radical **5**, followed by fragmentation to the aldehyde **6**, oxidation to carboxylic acid **7** and reduction to **1** (Scheme 1).§ Such cleavage of the polyene chain by 'homolytic-type' hydroperoxide lyases has been previously found in the algae.[4] Here, we can not rule out the possibility that these 12-hydroperoxide formation and chain cleavage may precede the bicyclic lactone ring formation. However, the large amount of **2** found in the cell, and late appearance of **1** in the medium seems to support the former case.

Interestingly, **1** is strictly an extracellular metabolite and not found in the cells. On the other hand bacillariolide I, **2** and II, **3** are found only in the cells and not in the culture medium, which indicates that **1** is discharged to the outside of the cells as soon as it is biosynthesized. Diatoms are the most abundant microalgae in the oceans in both quantity and number of species. However, in contrast to the case of some other microalgal families, only a very few secondary metabolites have been found in the cells of diatoms.[5,6] We have speculated that those organisms with solid siliceous skeletons tend not to store the metabolites but rather excrete them outside. The finding of a fairly large quantity of **1** and some other metabolites in the medium certainly supports this assumption.

The biological function of this extracellular metabolite is still under investigation, but its structural resemblance with the well-known plant growth regulators, jasmonates[7,8] and cucurbic acid[9] draws our attention. Bacillariolide I is known to possess significant inhibitory activity against phospholipase $A_2$.[6]

This work was supported by NIH grants GM 28754 and CA67775.

## Footnotes

† This organism was previously called *Nitzschia (Pseudo-nitzschia) pungens f. multiseries*, but its name has been recently changed to *Pseudo-nitzschia multiseries* (Hasle) Hasle by the original namer: G. R. Hasle, *J. Phycol.*, 1995, **31**, 428.

‡ The electron microscopic identification of this species was done by Professor Paul E. Hargraves, University of Rhode Island, who is gratefully acknowledged.

§ The proposed biosynthetic pathway was modified according to a suggestion by Professor William Gerwick, Oregon State University, who is thanked for his advice.

## References

1 R. Wang and Y. Shimizu, *J. Chem. Soc., Chem. Commun.*, 1990, 413.
2 R. Wang, Y. Shimizu, J. R. Steiner and J. Clardy, *J. Chem. Soc., Chem. Commun.*, 1993, 379.
3 Atlantic Research Laboratory Technical Report 56, NRCC 29083, Atlantic Research Laboratory, NRC, Halifax, Canada, 1988.
4 H. W. Gardner, *Biochim. Biophys. Acta*, 1991, **1084**, 221.
5 Y. Shimizu, *Chem. Rev.*, 1993, **93**, 1685.
6 Y. Shimizu, *Annu. Rev. Microbiol.*, 1996, **50**, 431.
7 J. R. Hanson, *J. Chem. Soc.*, 1965, 5036.
8 E. E. Farmer and C. A. Ryan, *Plant Cell*, 1992, **4**, 129.
9 H. Fukui, K. Koshimizu, S. Usuda and Y. Tamazaki, *Agric. Biol. Chem.*, 1977, **41**, 175.

*Received, 12th December 1996; Com. 6/08369B*

# $[M_4(Se_2)_2(PSe_4)_4]^{8-}$: a novel, tetranuclear, cluster anion with a stellane-like core

**Konstantinos Chondroudis and Mercouri G. Kanatzidis***

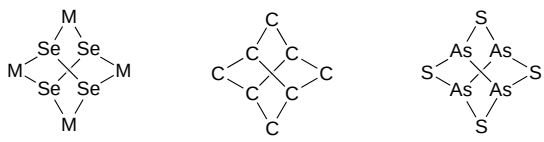
*Department of Chemistry, Michigan State University, East Lansing, Michigan 48824, USA*

**The molecular cluster compounds $[M_4(Se_2)_2(PSe_4)_4]^{8-}$ (M = Cd, Hg) form by the reaction of Cd and Hg with basic polychalcophosphate fluxes.**

The polychalcophosphate fluxes are a powerful tool for the synthesis of new ternary and quaternary chalcophosphate compounds.[1–12] In the presence of metal ions, these reactive fluxes give rise to highly anionic $[P_yQ_z]^{n-}$ (Q = S, Se) ligands which bind in an amazing number of ways to the metals, forming new materials.[1] The variation of the flux composition stabilizes different ligands such as $[PQ_4]^{3-}$, $[PSe_5]^{3-}$, $[P_2Q_6]^{4-}$, $[P_2Q_7]^{4-}$, $[P_2Se_9]^{4-}$, *etc*.[1–12] which become the building blocks of various polymeric solid-state structures. Lately, we demonstrated that the same fluxes can be used to provide access to molecular compounds if appropriate conditions are employed.[8] This includes modification (usually increase) of the flux Lewis basicity, which can be achieved by increasing the concentration of the $[P_yQ_z]^{n-}$ ligands in it. Application of this technique to group 12 yielded the tetranuclear, stellane-like $Rb_8[M_4(Se_2)_2(PSe_4)_4]$ (M = Cd, Hg) and herein, we report the synthesis,† structural characterization, optical and thermal properties of this novel complex.

$Rb_8[Cd_4(Se_2)_2(PSe_4)_4]$ and $Rb_8[Hg_4(Se_2)_2(PSe_4)_4]$‡ are isostructural. The single-crystal structure determination was performed on the mercury compound. The discrete $[Hg_4(Se_2)_2(PSe_4)_4]^{8-}$ anion is a tetranuclear complex, of approximate $D_{2d}$ symmetry, containing the relatively rare $[PSe_4]^{3-}$ ligand but also diselenide $Se_2^{2-}$ ligands in a novel cluster arrangement [Fig. 1(*a*)]. The most intriguing feature of the molecule is its stellane-like, $[Hg_4(Se_2)_2]^{4+}$ core, composed of four $Hg^{2+}$ ions and two $Se_2^{2-}$ ligands. In this arrangement every $Se_2^{2-}$ ligand coordinates to all four metals and the two diselenides are perpendicular to each other (Scheme 1, structure **A**). The four metal centres define a perfect 3.612(1)×3.612(1) Å square and the entire molecule resides on a $\bar{4}$ crystallographic site. A similar cage structure, has been observed in the organic molecule tricyclo[3.3.0.0$^{3,7}$]octane,[13,14] (Scheme 1, structure **B**). Its projection is reminiscent of a four-pointed star and because of that is also known as stellane. β-Tetraarsenic tetrasulfide is known to crystallize in discrete $As_4S_4$ molecules with a similar cage structure,[15] only in this molecule the sulfur atoms occupy the four corners of the 'star' (Scheme 1, structure **C**).

The stereoview in the Graphical Abstract can be useful in perceiving the cage core structure. This core acting as a gigantic metal centre is being coordinated by four $[PSe_4]^{3-}$ ligands. Each $[PSe_4]^{3-}$ employs two of its four available donor sites to bind to two neighboring metal atoms. In polyhedral terms, each $[PSe_4]^{3-}$ tetrahedron shares two corners with the four-pointed $[M_4(Se_2)_2]^{4+}$ star giving rise to the $[M_4(PSe_4)_4(Se_2)_2]^{8-}$ formula. Even though the $[PSe_4]^{3-}$ ligand is bidentate, its disposition is such that one of its non-coordinating Se atoms interacts with the diselenide ligand [Fig. 1(*b*)], as evidenced by the Se(3)–Se(5) distance of 3.327(3)Å (van der Waals radii sum is 3.8 Å).[16] In support of this observation the diselenide bond of 2.416(4) Å for Se(5)–Se(5″) is relatively long, for this coordination mode, compared, for example, to $[Hg_7Se_{10}]^{4-}$,[17] where a similarly bound $Se_2^{2-}$ ligand has a 2.349(6) Å bond length. This is consistent with partial electron transfer from the terminal Se(3) atoms to the σ* orbital of the Se(5)–Se(5″) ligand.




**A** $[M_4(Se_2)_2]^{4+}$ **B** Stellane **C** β-$As_4S_4$

**Scheme 1**

In $Rb_8[Hg_4(Se_2)_2(PSe_4)_4]$ the Hg–Se distances average at 2.68(5) Å which compare well with those of $[Hg_7Se_{10}]^{4-}$,[17] and $Hg_2P_2Se_6$.[18] Each cell contains two $[Hg_4(Se_2)_2(PSe_4)_4]^{8-}$ molecules which are separated by the nine-coordinate Rb(1) [range of Rb(1)–Se distances, 3.511(3)–3.800(3) Å; av. 3.661 Å], and by the six-coordinate Rb(2) cation [range of Rb(2)–Se distances, 3.478(3)–3.786(3) Å; av. 3.644 Å]. Selected bond distance and angles are given in the caption of Fig. 1.

$Rb_8[M_4(PSe_4)_4(Se_2)_2]$ (M = Cd, Hg) are insoluble in dmf and acetonitrile but soluble in a solution of crown ether,

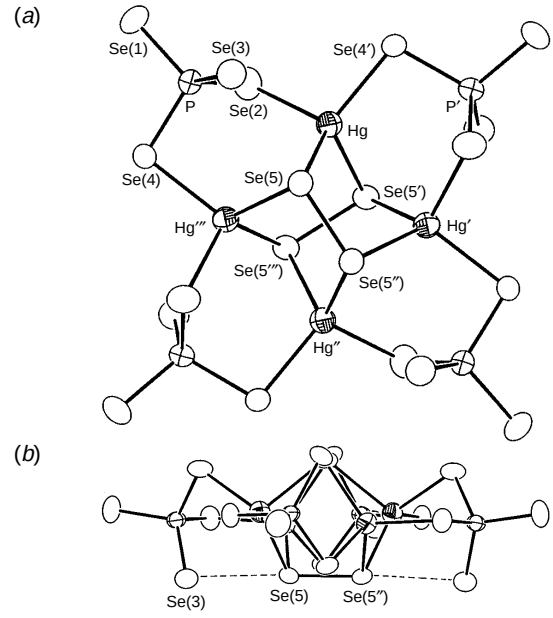



**Fig. 1** (*a*) ORTEP representation and labelling of a single $[Hg_4(Se_2)_2(PSe_4)_4]^{8-}$ anion. Selected bond distances (Å) and angles (°): Hg–Se(2) 2.713(2), Hg–Se(4) 2.623(2), Hg–Se(5) 2.669(2), Hg–Se(5′) 2.725(2), P–Se(1) 2.175(5), P–Se(2) 2.221(5), P–Se(3) 2.184(5), P–Se(4) 2.237(5), Se(5)–Se(5″) 2.416(4), Se(3)–Se(5) 3.327(3); Se(2)–Hg–Se(4) 101.44(7), Se(2)–Hg–Se(5) 114.33(6), Se(2)–Hg–Se(5′) 101.98(7), Se(4)–Hg–Se(5) 125.45(7), Se(4)–Hg–Se(5′) 110.70(6), Se(5)–Hg–Se(5′) 100.84(8), Hg–Se(2)–P 96.5(1), Hg–Se(4)–P′ 97.9(1), Hg–Se(5)–Hg‴ 84.07(6), Hg–Se(5′)–Se(5″) 109.43(7), Se(1)–P–Se(2) 108.7(2), Se(1)–P–Se(3) 111.6(2), Se(1)–P–Se(4) 107.9(2), Se(2)–P–Se(3) 110.9(2), Se(2)–P–Se(4) 107.0(2). (*b*) Perpendicular view of the same molecule. Dashed lines indicate Se– Se interactions.

18-crown-6, in dmf. The solution is green–brown and stable, according to UV– VIS, for up to 2–3 days. The dmf–complexant solution gives a different spectrum from the solid material with one medium absorption at *ca.* 585 nm (2.12 eV) and a shoulder at *ca.* 400 nm (3.10 eV), suggesting that the cluster undergoes rearrangement in solution. The solid-state UV–VIS diffuse reflectance spectrum shows sharp optical gaps consistent with semiconducting behaviour (for M = Cd, $E_g$ = 2.57 eV, whereas for M = Hg, $E_g$ = 2.32 eV). The solid-state IR spectrum shows peaks that are characteristic of both the nature and bonding mode of the $[PSe_4]^{3-}$ ligand.§ Differential thermal analysis (DTA), followed by XRD analysis of the residues, shows incongruent melting at 456 and 413° C for M = Cd and Hg, respectively. The decomposition product is a mixture of the starting compound and amorphous $Rb_xP_ySe_z$ flux. Some CdSe or HgSe should also be formed but they are either amorphous or in concentrations and particle sizes undetectable by XRD analysis.

The extremely high charge of this molecular unit would make its synthesis through conventional 'wet' chemistry very difficult, perhaps prohibitive. This accentuates the value of the flux technique in stabilizing highly charged molecular entities. The novelty of the compositional and structural features of the $[M_4(Se_2)_2(PSe_4)_4]^{8-}$ cluster, provides a stimulating example of the new chemistry that becomes accessible and suggests that the molten alkali-metal polychalcogenide approach has not yet been fully exploited.

Financial support from the National Science Foundation DMR-9527347 is gratefully acknowledged. This work made use of the SEM and TEM facilities of the Center for Electron Optics at Michigan State University.

## Footnotes

† *Syntheses:* $Rb_8[Cd_4(Se_2)_2(PSe_4)_4]$ was synthesized from a mixture of Cd (0.25 mmol), $P_2Se_5$ (0.50 mmol), $Rb_2Se$ (1.00 mmol) and Se (2.50 mmol) heated to 550 °C for 4 d followed by cooling to 150 °C at 2 °C $h^{-1}$. Most of the excess $Rb_xP_ySe_z$ flux was removed with degassed dmf. Following this, the product was washed with *ca.* 2 ml of tributyl phosphine to remove residual Se. Further washing with anhydrous diethyl ether revealed light yellow, needle-like crystals that are air-stable but sensitive in $H_2O$. (Yield *ca.* 66% based on Cd). Microprobe analysis gave an average composition of $Rb_{8.0}Cd_{4.0}P_{4.4}Se_{19.6}$. *Cell data* at 23 °C: $a = b = 17.564(3)$, $c = 7.275(2)$ Å, $U = 2244.3(8)$ Å$^3$.

$Rb_8[Hg_4(Se_2)_2(PSe_4)_4]$ was synthesized from a mixture of HgSe (0.50 mmol), $P_2Se_5$ (0.25 mmol), $Rb_2Se$ (1.00 mmol) and Se (2.50 mmol) heated to 500 °C for 4 d followed by cooling to 150 °C at 2 °C $h^{-1}$. Isolation as above revealed light yellow, needle-like crystals that are air-stable but sensitive in $H_2O$. (Yield *ca.* 78% based on Hg). Microprobe analysis gave an average composition of $Rb_{8.0}Hg_{4.4}P_{4.0}Se_{20.0}$.

‡ *Crystal data* at 23 °C: tetragonal, space group $P4_2/n$ (no. 86) $a = b = 17.654(2)$, $c = 7.226$ (2) Å, $U = 2253.6(9)$ Å$^3$, $Z = 2$, $D_c = 4.699$ g cm$^{-3}$, μ(Mo-Kα) = 380.81 cm$^{-1}$, $2\theta_{max} = 50°$, total data collected, 2162; unique data, 1838; data with $F_o^2 > 3\sigma(F_o^2)$, 1254. Number of variables: 82. An empirical absorption correction based on ψ scans was applied to the data during initial stages of refinement. DIFABS correction was applied after full isotropic refinement as recommended in N. Walker, *Acta Crystallogr., Sect. A*, 1983, **39**, 158. Final $R$, $R_w$ = 0.040, 0.049 (0.46, 0.56 before DIFABS).

Atomic coordinates, bond lengths and angles, and thermal parameters have been deposited at the Cambridge Crystallographic Data Centre (CCDC). See Information for Authors, Issue No. 1. Any request to the CCDC for this material should quote the full literature citation and the reference number 182/358.

§ The far-IR spectrum displays three strong absorptions at *ca.* 461, 434 and 417 cm$^{-1}$. These vibrations can be assigned to $PSe_4$ stretching modes and are of diagnostic value in distinguishing this selenophosphate ligand from others.[1,6] Weak absorptions below 200 cm$^{-1}$ can be assigned to M–Se vibrations.[1]

## References

1 T. J. McCarthy and M. G. Kanatzidis, *Inorg. Chem.*, 1995, **34**, 1257 and references therein.
2 T. J. McCarthy, T. Hogan, C. R. Kannewurf and M. G. Kanatzidis, *Chem. Mater.*, 1994, **6**, 1072.
3 T. J. McCarthy and M. G. Kanatzidis, *J. Alloys Compd.*, 1996, **236**, 70.
4 T. J. McCarthy and M. G. Kanatzidis, *J. Chem. Soc., Chem. Commun.*, 1994, 1089.
5 T. J. McCarthy and M. G. Kanatzidis, *Chem. Mater.*, 1993, **5**, 1061.
6 K. Chondroudis, T. J. McCarthy and M. G. Kanatzidis, *Inorg. Chem.*, 1996, **35**, 840.
7 K. Chondroudis and M. G. Kanatzidis, *Inorg. Chem.*, 1995, **34**, 5401.
8 K. Chondroudis and M. G. Kanatzidis, *Chem. Commun.*, 1996, 1371.
9 K. Chondroudis, T. J. McCarthy and M. G. Kanatzidis, *Inorg. Chem.*, 1996, **35**, 3451.
10 K. Chondroudis, A. J. Hanko and M. G. Kanatzidis, submitted for publication.
11 K. Chondroudis and M. G. Kanatzidis, *C. R. Acad. Sci. Paris, Ser. B*, 1996, **322**, 887.
12 J. H. Chen and P. K. Dorhout, *Inorg. Chem.*, 1995, **34**, 5705; J. H. Chen, P. K. Dorhout and J. E. Ostenson, *Inorg. Chem.*, 1996, **35**, 5627.
13 P. K. Freeman, V. N. M. Rao and G. E. Bigam, *Chem. Commun*. 1965, **21**, 511.
14 J. L. Adcock and H. Zhang, *J. Org. Chem*., 1996, **61**, 1975.
15 E. J. Porter and G. M. Sheldrick, *J. Chem. Soc., Dalton Trans*., 1972, 1347.
16 A. Bondi, *J. Phys. Chem*., 1964, **68**, 441.
17 K-W. Kim and M. G. Kanatzidis, *Inorg. Chem.*, 1991, **30**, 1966.
18 M. Z. Jandali, G. Eulenberger and H. Hahn, *Z. Anorg. Allg. Chem*., 1978, **447**, 105.

*Received, 5th November; Com. 6/07549E*

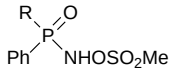
# Sulfonylation in the rearrangement of an *N*-phosphinoyl-*O*-sulfonylhydroxylamine: demonstration of a phosphonamidic-sulfonic anhydride intermediate and $^{18}O$-labelling evidence on how it may be formed

**Martin J. P. Harger**

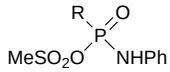
*Department of Chemistry, The University, Leicester, UK LE1 7RH*

**The rearrangement reaction of R(Ph)P(O)NHOSO$_2$Bn (R = PhMeCH) (57% enriched with one $^{18}O$ atom in the SO$_2$ group) with Bu$^t$NH$_2$ in CH$_2$Cl$_2$ gives the sulfonamide BnSO$_2$NHBu$^t$ (43.7% enriched with one $^{18}O$ atom) as one of the products; this indicates a phosphonamidic-sulfonic anhydride intermediate [R(BnSO$_2$O)P(O)NHPh], formed with partial equilibration of the sulfonate oxygen atoms and attacked (in part) at the sulfonyl group.**

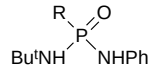
*N*-Phosphinoylhydroxylamines are the phosphorus analogues of hydroxamic acids, and their *O*-sulfonyl derivatives **1** (R = alkyl or phenyl) undergo rearrangement with base,[1] *e.g.* **1** gives **3** with Bu$^t$NH$_2$. The product-forming species may be a transient metaphosphonimidate [RP(O)=NPh], analogous to the isocyanate in a Lossen rearrangement,[2] although some evidence points instead to a phosphonamidic-sulfonic mixed anhydride **2**.[3,4] In principle this anhydride could react with a nucleophile at sulfur rather than phosphorus,[5] but in practice such products have not hitherto been seen. We now report the first direct chemical evidence for a mixed anhydride intermediate in the rearrangement, and $^{18}O$-labelling information on how it may be formed.



**1**

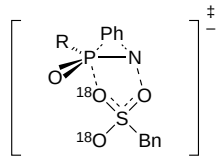


**2**

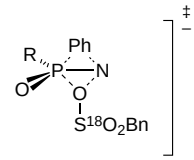


**3**

The benzylic sulfonyl derivative **4** was prepared by treating PhMeCH(Ph)P(O)NHOH (mixture of diastereoisomers)[3] with $^{18}O$-enriched BnSO$_2$Cl in pyridine (ice cooling). It was obtained as a mixture of diastereoisomers [$\delta_P$(CDCl$_3$) 42.6 and 41.0 (ratio 5:1); $\delta_H$(CDCl$_3$) 4.61 (major) and 4.19 (both AB; $\Delta\delta$ 0.12 or 0.14 ppm, $J_{AB}$ 14 Hz; SO$_2$C*H*$_2$Ph)] having 57% of the molecules enriched with one $^{18}O$ atom in the sulfonyl (SO$_2$) group [*m/z* (FAB) 416 and 418 (M + H)$^+$; negligible amount of double-labelled material]. With 2 mol dm$^{-3}$ Bu$^t$NH$_2$ (40 equiv.) in CH$_2$Cl$_2$ it gave mainly the 'normal' phosphonamide rearrangement product **7** [$\delta_P$(CDCl$_3$) 22.7 and 22.4 (diastereoisomers, ratio 3:1)] together with the sulfonate anion **6** [$\delta_H$(CDCl$_3$) 4.07 (s, PhC*H*$_2$SO$_3^-$)]. Significantly, however, it also gave a substantial amount (*ca.* 17%) of the sulfonamide product **8** [$\delta_H$(CDCl$_3$) 4.25 (s, PhC*H*$_2$SO$_2$) and 1.36 (s, NBu$^t$)] together with the phosphonamidate anion **9** [$\delta_P$(CDCl$_3$) 19.5].



**10**



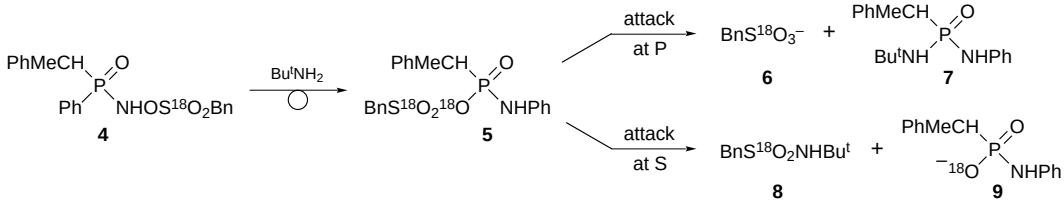
**11**

This behaviour is clearly indicative of a phosphonamidic-sulfonic anhydride intermediate **5** and competing attack at the P and S atoms by the Bu$^t$NH$_2$ nucleophile (Scheme 1).

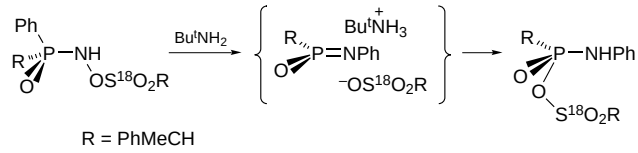
Mass spectrometric examination of the products, after esterification with diazaomethane in the case of the anions, indicated their isotopic enrichment (±0.5%):† **6** had 57.6% one $^{18}O$ atom [methyl ester, *m/z* (EI) 186 and 188 (M$^+$)], **7** had no enrichment [*m/z* (EI) 316 (M$^+$)], **8** had 43.7% one $^{18}O$ atom [*m/z* (CI) 245 and 247 (M + NH$_4$)$^+$] and **9** had 13.7% one $^{18}O$ atom [methyl ester, *m/z* (EI, GC–MS) 275 and 277 (M$^+$)].

For the products of attack at the phosphorus atom of the mixed anhydride, the results are as expected: all the label originally in the substrate **4** ends up in the sulfonate anion **6** and none in the phosphonamide rearrangement product **7**. Of more interest are the products of attack at sulfur, since it is from these that the distribution of the label in the mixed anhydride intermediate can be inferred. With 76% of the available $^{18}O$ label ending up in the sulfonamide product **8**, and only 24% in the phosphonamidate anion **9**, it would seem that, on rearrangement, the label in the sulfonyl group of the substrate **4** is transferred to the bridging and non-bridging positions of the mixed anhydride **5** in a ratio of 24:76.

Concerted rearrangement of the substrate, after removal of a proton (N*H*) by the amine, would most plausibly involve a transition state resembling **10**. This would give rise to a bridging:non-bridging $^{18}O$ ratio of 50:50 in the mixed anhydride. Subsequent scrambling of the label, after formation of the anhydride but before its conversion into product, might reduce the ratio, but not beyond the statistical value of 33:67; the experimentally observed value of 24:76 could never be attained. At the other extreme, if concerted rearrangement involved a transition state resembling **11**, the mixed anhydride would be formed with none of the label in the bridging position (ratio 0:100). In this case, however, subsequent scrambling could give rise to an (average) ratio of 24:76, so long as it occurred at approximately the same rate as the conversion of the




**Scheme 1**




**Scheme 2**

anhydride into product. Such scrambling is certainly not unreasonable; like a phosphonamidic chloride,[6] the phosphonamidic-sulfonic anhydride will tend to react with $Bu^tNH_2$ at phosphorus by a dissociative substitution mechanism (stepwise preassociative elimination-addition).[7] Nonetheless, the geometry of the transition state **11** makes this concerted pathway seem rather improbable.

The alternative to these is a non-concerted mechanism (Scheme 2), in which the sulfonate group becomes completely detached from the nitrogen atom before it begins to bond to phosphorus. At the limit this must result in a uniform (statistical) distribution of the label between the three sulfonate oxygen atoms of the mixed anhydride (ratio 33 : 67). Initially, however, the sulfonate oxygen atom (unlabelled) released from the N–O bond will not be equivalent to the other two, because of differences in solvation (by $CH_2Cl_2$ or $Bu^tNH_2$) and/or association (with $Bu^tNH_3^+$). If the new bond to phosphorus is formed before equilibration of the oxygen atoms is complete, and makes preferential use of this (unlabelled) oxygen atom, the mixed anhydride will be formed with less than a third of the available $^{18}O$ label located in the bridging position. The observed result (24% of the available $^{18}O$ in the bridging position) could then reflect a rather modest bias for incorporation of the unlabelled oxygen atom in the new P–O bond, or a strong bias with some subsequent scrambling. There is at least one precedent for a rearrangement involving migration of a sulfonate anion in which the oxygen atom released by bond breaking is preferentially employed in subsequent bond making;[8] in that case, however, it is a cation with which the sulfonate anion recombines, not an uncharged species.

Two conclusions can be drawn from the present study: a phosphonamidic-sulfoninc mixed anhydride **5** is involved in the rearrangement reactions of the hydroxylamine derivative **4**, even at a high amine concentration,‡ and the transformation of **4** into **5** is most probably non-concerted (Scheme 2). Some of the initial metaphosphonimidate intermediate may go directly to the phosphonamide product, by reaction with $Bu^tNH_2$, but some—perhaps most—rapidly recombines with the sulfonate anion to form the mixed anhydride.

I am grateful to Dr G. Eaton for recording mass spectra and Professor P. M. Cullis for advice and encouragement.

## Footnotes

† In all mass spectrometric measurements of $^{18}O$ enrichment, allowance was made for $^{34}S$ and natural abundance $^{18}O$ by comparing directly the spectrum of the enriched material with that of a natural abundance sample.

‡ A high concentration of $Bu^tNH_2$ was used for two reasons. First, it affords a rigorous test of the generality of mixed anhydride formation; at very low amine concentrations a metaphosphonimidate intermediate might have an atypically high disposition towards recombination with the sulfonate anion. Second, it limits the complications associated with the phosphonamidate anion **9** that is released when the amine attacks the mixed anhydride **5** at sulfur. This anion is a powerful nucleophile and competes with $Bu^tNH_2$ for another molecule of **5** (attack at the P atom of **5** produces a symmetrical phosphonamidic anhydride).

## References

1 M. J. P. Harger, *J. Chem. Soc., Perkin Trans. 1*, 1983, 2699; M. J. P. Harger and A. Smith, *J. Chem. Soc., Perkin Trans. 1*, 1987, 683.
2 E. S. Wallis and R. D. Dripps, *J. Am. Chem. Soc*., 1933, **55**, 1701; H. L. Yale, *Chem. Rev*., 1943, **33**, 209; L. Bauer and O. Exner, *Angew. Chem., Int. Ed. Engl*., 1974, **13**, 376.
3 M. J. P. Harger and R. Sreedharan-Menon, *J. Chem. Soc., Perkin Trans. 1*, 1994, 3261 and references cited therein.
4 M. J. P. Harger and R. Sreedharan-Menon, *Chem. Commun*., 1996, 867. (A very low concentration of $Bu^tNH_2$ had to be used in this study; the conclusions might not be valid under more normal conditions.)
5 J. Michalski, W. Dabkowski and J. Wasiak, *Pol. J. Chem*., 1992, **66**, 879 (review).
6 S. Freeman and M. J. P. Harger, *J. Chem. Soc., Perkin Trans. 2*, 1988, 81; *J. Chem. Soc., Perkin Trans. 1*, 1988, 2737.
7 W. P. Jencks, *Acc. Chem. Res*., 1980, **13**, 161; *Chem. Soc. Rev*., 1981, **10**, 345.
8 U. Gessner, A. Heesing, L. Keller and W. K. Homann, *Chem. Ber*., 1982, **115**, 2865 (see especially rearrangement in methanol).

*Received, 27th November 1996; Com. 6/08043J*

# Association of two incomplete cubane $WS_3Cu_3$ clusters in the crystal structures of $[PPh_4]_2[\{(C_5Me_5)WS_3\}_2Cu_6(NCS)_6]$ and $[PPh_4]_2[\{(C_5Me_5)WS_3\}_2Cu_6Br_6]$

**Jianping Lang, Hiroyuki Kawaguchi, Shiho Ohnishi and Kazuyuki Tatsumi***

*Department of Chemistry, Faculty of Science, Nagoya University, Furo-cho, Chikusa-ku, Nagoya 464-01, Japan*

**Two double cubane-like clusters, $[PPh_4]_2[\{(C_5Me_5)WS_3\}_2Cu_6(NCS)_6]$ 1 and $[PPh_4]_2[\{(C_5Me_5)WS_3\}_2Cu_6Br_6]$ 2, are self-assembled by the reactions of $[PPh_4][(C_5Me_5)WS_3]$ with CuNCS and CuBr in acetonitrile, respectively, the crystal structures of which consist of two $WS_3Cu_3$ incomplete cubes linked by NCS and Br bridges.**

The linkage of transition-metal clusters has been the subject of recent interest.[1–4] It has been shown that cubane clusters of homo- and hetero-metallic sulfides can be assembled in various ways. An example is the thiolate-bridged double-cubane cluster $[Mo_2Fe_6S_8(SPh)_9]^{3-}$, which was obtained from the reaction of $FeCl_3$ with $[NH_4]_2[MoS_4]$ and NaSPh.[5] The similar self-assembly of $FeCl_3$, $[NBu^n_4]_2[MoS_4]$ and NaSEt gave rise to $[Mo_2Fe_7S_8(SEt)_{12}]^{3-}$.[6] Two molecules of the cubane cluster $[Fe_4S_4Cl_4]^{2-}$ were linked upon treatment with $Li_2S$ to generate $[(Fe_4S_4Cl_3)_2S]^{4-}$,[7] while the incomplete cubane-like cluster $[Mo_3S_4(H_2O)_9]^{4+}$ also served as a starting material for the synthesis of double-cubane complexes such as $[(H_2O)_9Mo_3S_4CuCuS_4Mo_3(H_2O)_9]^{8-}$.[8] More recently, the preformed mixed-metal cubane clusters $[MoFe_3S_4Cl_3(Cl_4cat)(L)]^{2-}$ (cat = catechol; L = coordinating solvent molecule) have been assembled into various double-cubane clusters in the presence of the appropriate polycarboxylic acid.[9]

Recently we found a facile route to the organometallic trithiotungsten(VI) complex $[PPh_4][(C_5Me_5)WS_3]$ *via* C–S bond cleavage of ethanedithiolate.[10] The terminal sulfides in $[(C_5Me_5)WS_3]^-$ appear to be more reactive than those of $[PPh_4]_2[WS_4]$, and they react readily with alkyl halides and even with non-activated alkynes such as PhC≡CPh and PhC≡CH. Having noted that $[(C_5Me_5)WS_3]^-$ may be a potential building block for heterometallic sulfide clusters, we examined its reactions with CuNCS and CuBr. In this paper we report two double cubane-like clusters, $[PPh_4]_2[\{(C_5Me_5)WS_3\}_2Cu_6(NCS)_6]$ **1** and $[PPh_4]_2[\{(C_5Me_5)WS_3\}Cu_6Br_6]$ **2**, obtained from these reactions.

Compound **1** was prepared by the following procedure. CuNCS (0.05 g, 0.42 mmol) was added to $[PPh_4][(C_5Me_5)WS_3]$ (0.11 g, 0.14 mmol) in MeCN (20 ml) and the mixture was stirred for 24 h at room temperature. After filtering off insoluble materials, the resultant solution was concentrated to *ca*. 5 ml under reduced pressure, and $Et_2O$ (5 ml) was added. On standing for two days, dark red needles of **1**·MeCN were obtained in 75% yield. Compound **2** was prepared as dark red crystals in 84% yield by a procedure similar to that above, starting from CuBr. **1** and **2** are stable to oxygen and moisture and soluble in MeCN and $Me_2SO$.†

The X-ray analysis of **1**‡ revealed that the asymmetric unit consists of two crystallographically independent halves of $[\{(C_5Me_5)WS_3\}_2Cu_6(NCS)_6]^{2-}$ dianions, two $[PPh_4]^+$ cations, and one MeCN solvent molecule. The structure of one of the two cluster dianions of **1** is presented in Fig. 1, where an inversion centre resides at the centre of the molecule. The structure of the other cluster dianion is nearly the same as that shown in Fig. 1. Three CuNCS molecules are bound to a $(C_5Me_5)WS_3$ fragment, forming a $WS_3Cu_3$ incomplete cubane structure. Two such incomplete cubes are linked *via* interactions between the sulfur end of one NCS ligand in each cluster and three coppers of the other cluster. Thus the NCS sulfur fills a void of the $WS_3Cu_3$ incomplete cubane. The occurrence of triple bridging of the NCS sulfur is unprecedented, although double bridging was observed in the polymeric structures of $[Hpy][Cu_2(NCS)_3]$[11] and $[NEt_4]_3[WS_4Cu_4(NCS)_5]$.[12] The eight-membered Cu(1)N(1)C(11)S(4)Cu(1*)N(1*)C(11*)S(4*) ring is nearly planar. The $(C_5Me_5)WS_3$ unit has a slightly distorted three-legged piano-stool structure, and the $S_3$ plane is parallel (179°) to the $C_5Me_5$ ring. The W–S bond lengths of 2.267(3)–2.290(3) Å fall between the W–S (thiolate) single bonds and W=S double bonds in $[(C_5Me_5)W(S)_2(SCH_2Ph)]$ [2.328(4) *vs*. 2.149(3) Å] and $[(C_5Me_5)W(S)\{SC(Ph)=C(Ph)S\}]^-$ [2.326(2) Å *vs*. 2.186(2) Å].[10] The short W–Cu distances of 2.638(2)–2.682(2) Å suggest a dative interaction between $d^0$ $W^{VI}$ and $d^{10}$ $Cu^I$, which are comparable to those observed in $[NEt_4]_3[WS_4Cu_4(NCS)_5]$ [2.624(2)–2.708(2) Å][12] and $[NEt_4]_3[WOS_3(CuBr)_3(\mu\text{-Br})]$ [2.665(3)–2.681(2) Å].[13] The coordination geometry at each copper atom is approximately trigonal planar, to which an NCS sulfur is weakly bound from the direction perpendicular to the plane. Thus the Cu–S(NCS) bond lengths of 2.742(4)–3.060(3) Å are significantly longer than the Cu–S(sulfide) distances of 2.214(4)–2.249(4) Å in the trigonal plane, and the Cu–S(NCS)–

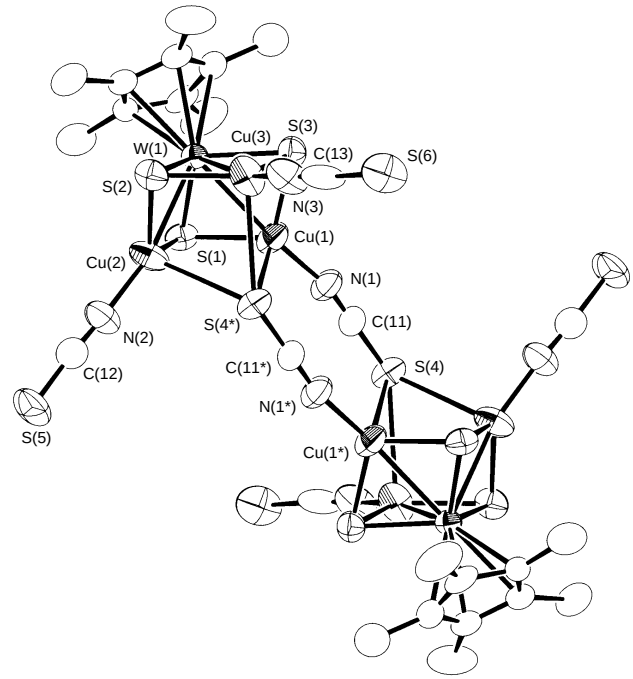



**Fig. 1** ORTEP drawing of one of the two cluster dianions of **1**, with labelling scheme and 50% thermal ellipsoids. Hydrogen atoms are omitted for clarity. Selected bond distances (Å) and angles (°): W–Cu(1) 2.644(2), W–Cu(2) 2.668(2), W–Cu(3) 2.644(2), W–S(av.) 2.281(2), Cu–S(av.) 2.230(2), Cu–S(4*)(av.) 2.952(4), Cu–N(av.) 1.88(3); S–W–S(av.) 105.8(1), S–Cu–S(av.) 109.3(1), S–Cu–S(4*)(av.) 97.4(1), W–S–Cu(av.) 72.0(1), Cu–S(4*)–Cu(av.) 65.7(1), S(4*)–Cu(1)–N(1) 98.4(3), Cu(1)–N(1)–C(11) 168(1), N(1)–C(11)–S(4) 179(1).

Cu angles [61.83(1)–70.34(8)°] are acute compared with the other Cu–S–Cu angles [88.0(1)–95.2(1)°].

The crystal of **2**‡ consists of one discrete $[\{(C_5Me_5)WS_3\}_2Cu_6Br_6]^{2-}$ dianions and two $[PPh_4]^+$ cations. The cluster dianion, shown in Fig. 2, is composed of two incomplete $WS_3Cu_3$ cubes of $[(C_5Me_5)WS_3Cu_3Br_3]^-$, which are interconnected by a four-membered $CuBr_2Cu$ ring. A crystallographic inversion centre is again located at the centre of the dianion. The main framework of the cluster dianion of **2** is similar to that of $[NEt_4]_4[(MoOS_3)_2Cu_6I_6]$.[14] In the $CuBr_2Cu$ ring, the Cu(1)–Br(1*) [or Cu(1*)–Br(1)] bond distance of 2.876(1) Å is 0.52 Å longer than that of Cu(1)–Br(1) [or Cu(1*)–Br(1*)]. Therefore, the interaction between the two incomplete cubes in **2** is weak, as in the case of **1**. A notable difference between the structures of **1** and **2** is that Br(1) [or Br(1*)] of **2** coordinates to one copper of the other incomplete cube while for **1** the terminal sulfur of NCS is bound to three coppers. As a consequence, there are two different types of copper geometries in the cluster dianion of **2**. Cu(2) and Cu(3) are trigonal planar, while Cu(1) adopts a distorted tetrahedral geometry. Owing to the different coordination environment, the W–Cu(1) distance of 2.676(8) Å is slightly longer than those of W–Cu(2) [2.657(8) Å] and W–Cu(3) [2.649(1) Å]. In each $(C_5Me_5)WS_3$ unit, the $S_3$ plane is parallel (178°) to the $C_5Me_5$ ring, and the three W–S distances of 2.280(2)–2.284(2) Å are very close to those of **1**.

The successful syntheses of **1** and **2** in high yields are interesting examples of how relatively complicated clusters can be formed by the self-assembly of two $[PPh_4][(C_5Me_5)WS_3]$ and six CuX (X = NCS, Br) components. As the linkage of two incomplete cubes is weak in either case, they may be cleaved easily in the presence of strong donor ligands such as $PPh_3$, dppm and bipyridine. In fact, **2** reacts readily with $PPh_3$ in acetonitrile to give $[(C_5Me_5)WS_3Cu_3Br_2(PPh_3)_2]$.[15] Details of their reactivity will be described elsewhere.

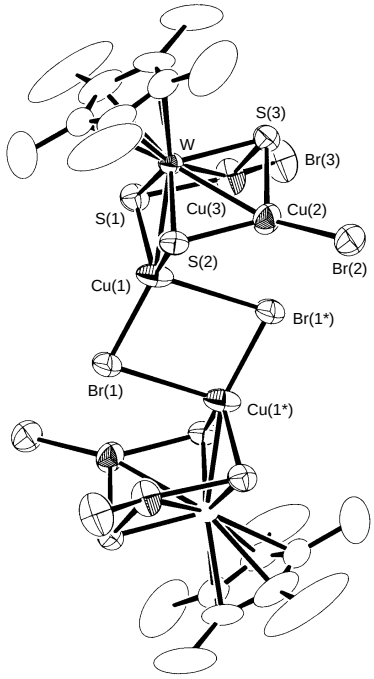



**Fig. 2** ORTEP drawing of the cluster dianion of **2**, with labelling scheme and 50% thermal ellipsoids. Hydrogen atoms are omitted for clarity. Selected bond distances (Å) and angles (°): W–Cu(1) 2.676(8), W–Cu(2) 2.657(1), W–Cu(3) 2.649(1), W–S(av.) 2.282(2), Cu–S(av.) 2.234(2), Cu–Br(av.) 2.308(1), Cu(1)–Br(1*) 2.876(1); S–W–S(av.) 105.8(1), S–Cu–S(av.) 109.2(2), W–S–Cu(av.) 71.2(2), Cu(1)–Br(1)–Cu(1*) 83.00(4), Br(1)–Cu(1)–Br(1*) 97.00(4).

J. P. Lang thanks the Japan Society for the Promotion of Science for a post-doctoral fellowship (1995–1997).

## Footnotes

† Synthetic manipulations were carried out under an argon atmosphere. *Spectroscopic data* for **1**: $^1$H NMR ($Me_2SO$, 500 MHz, 25 °C), δ 7.72–7.97 ($PPh_4^+$, m, 40 H), 2.14 ($C_5Me_5$, s, 30 H). Anal. Calc. for $C_{74}H_{70}Cu_6N_6P_2S_{12}W_2$: C, 39.69; H, 3.16; N, 3.75; S, 16.84. Found: C, 39.63; H, 3.11; N, 3.87; S, 16.51%. IR (Nujol mull, CsI): ν(W–$S_{br}$) 470w, 455m, 410m cm$^{-1}$. UV–VIS (MeCN) $\lambda_{max}$/nm ($10^{-3}$ $\varepsilon_{max}$/M$^{-1}$ cm$^{-1}$): 472 (0.297), 445 (0.334), 329 (0.891). For **2**: $^1$H NMR ($Me_2SO$, 500 MHz, 25 °C), δ 7.72–7.99 ($PPh_4^+$, m, 40 H), 2.10 ($C_5Me_5$, s, 30 H). Anal. Calc. for $C_{68}H_{70}Br_6Cu_6P_2S_6W_2$: C, 34.46; H, 2.98; S, 8.12. Found: C, 34.21; H, 2.95; S, 7.86%. IR (KBr pellet): ν(W–$S_{br}$) 453m, 409m cm$^{-1}$. UV–VIS (MeCN) $\lambda_{max}$/nm ($10^{-3}$ $\varepsilon_{max}$/M$^{-1}$ cm$^{-1}$): 486 (0.156), 445 (0.152), 329 (0.621).

‡ *Crystal data* for **1**·$CH_3CN$: $C_{76}H_{73}Cu_6N_7P_2S_{12}W_2$, $M$ = 2280.10, triclinic, space group $P\bar{1}$, $a$ = 17.059(5), $b$ = 26.508(7), $c$ = 9.515(4) Å, α = 90.36, β = 91.98(3), γ = 87.53(2)°, $U$ = 4295(2) Å$^3$, $Z$ = 2. Of 11384 reflections collected (Mo-Kα 2θ = 55.0°, 296 K) on a Rigaku AFC7R diffractometer; 11336 were unique and 6823 [$I > 3.00\sigma(I)$] were observed. The structure was solved by direct methods and expanded using Fourier techniques. All atoms except for the phenyl carbons and MeCN were refined anisotropically. H atoms were included but not refined. The final cycle of full-matrix least-squares refinement was converged with $R = \Sigma(|F_o| - |F_c|)/\Sigma|F_o| = 0.037$ and $R_w = [\Sigma w(|F_o| - |F_c|)^2/\Sigma w|F_o|^2]^{1/2} = 0.038$. For **2**: $C_{68}H_{70}Br_6Cu_6P_2S_6W_2$, $M$ = 2370.00, monoclinic, space group $P2_1/a$, $a$ = 9.871(1), $b$ = 27.789(5), $c$ = 14.496(3) Å, β = 100.53(1)°, $U$ = 3909(1) Å$^3$, $Z$ = 4. Of 9701 reflections collected (Mo-Kα 2θ = 55.0°, 296 K) on a Rigaku AFC7R diffractometer, 6134 [$I > 3.00\sigma(I)$] were observed. The structure was solved by direct methods and expanded using Fourier techniques. All the heavy atoms were refined anisotropically. H atoms were included but not refined. The final cycle of full-matrix least-squares refinement was converged with $R = \Sigma(|F_o| - |F_c|)/\Sigma|F_o| = 0.036$ and $R_w = [\Sigma w(|F_o| - |F_c|)^2/\Sigma w|F_o|^2]^{1/2} = 0.040$.

Atomic coordinates, bond lengths and angles, and thermal parameters have been deposited at the Cambridge Crystallographic Data Centre (CCDC). See Information for Authors, Issue No. 1. Any request to the CCDC for this material should quote the full literature citation and the reference number 182/349.

## References

1 F. A. Cotton, P. A. Kibala and W. J. Roth, *J. Am. Chem. Soc.*, 1988, **110**, 298.
2 J. M. Lehn, *Supramolecular Chemistry*, VCH, Weinheim, 1995.
3 A. Müller and C. Beugholt, *Nature*, 1996, **383**, 296.
4 V. A. Grillo, Z. Sun, K. Folting, D. N. Hendrickson and G. Christou, *Chem. Commun.*, 1996, 2233.
5 G. Christou, C. D. Garner, F. E. Mabbs and T. J. King, *J. Chem. Soc., Chem. Commun.*, 1978, 740.
6 T. E. Wolff, J. M. Berg, P. P. Power, K. O. Hodgson and R. H. Holm, *J. Am. Chem. Soc.*, 1979, **101**, 5454.
7 P. R. Challen, S. M. Koo, W. R. Dunham and D. Coucouvanis, *J. Am. Chem. Soc.*, 1990, **112**, 2455.
8 T. Shibahara, H. Akashi and H. Kuroya, *J. Am. Chem. Soc.*, 1988, **110**, 3313.
9 K. D. Demadis and D. Coucouvanis, *Inorg. Chem.*, 1995, **34**, 436.
10 H. Kawaguchi and K. Tatsumi, *J. Am. Chem. Soc.*, 1995, **117**, 3885.
11 C. L. Raston, B. Walter and A. H. White, *Aust. J. Chem.*, 1979, **32**, 2757.
12 J. M. Manoli, C. Potvin, F. Secheresse and S. Marzak, *Inorg. Chim. Acta*, 1988, **150**, 259.
13 Z. R. Chen, H. W. Hou, X. Q. Xin, K. B. Yu and S. Shi, *J. Phys. Chem.*, 1995, **99**, 8717.
14 H. W. Hou, D. L. Long, X. Q. Xin, X. X. Houng, B. S. Kang, P. Ge, W. Ji and S. Shi, *Inorg. Chem.*, 1996, **35**, 5363.
15 J. P. Lang and K. Tatsumi, to be published.

*Received, 2nd December 1996; Com. 6/08131B*

# 2′,3′-Anhydrouridine

**Anwar Miah, Colin B. Reese* and Quanlai Song**

*Department of Chemistry, King's College London, Strand, London, UK WC2R 2LS*

**The previously unreported title compound 4 is readily obtained by treating 2,2′-anhydro-1-β-D-arabinofuranosyluracil 1 with sodium hydride in dry dimethyl sulfoxide at room temperature.**

In the course of their early and pioneering studies on the chemistry of pyrimidine anhydronucleosides, Brown, Todd and co-workers reported[1] that when 2,2′-anhydro-1-β-D-arabinofuranosyluracil **1** washeated at 100 °C in *N*,*N*-dimethylformamide (DMF) solution with a very large excess of sodium ethanethiolate, the 3′-ethylsulfanyl derivative **2** was obtained and isolated as a colourless glass in *ca*. 55% yield. We subsequently showed that when the anhydronucleoside **1** was heated in DMF solution at 60 °C with an excess both of ethanethiol and $N^1$, $N^1$, $N^3$, $N^3$-tetramethylguanidine (TMG), 2′-deoxy-2′-(ethylsulfanyl)uridine **3** was obtained and isolated as a crystalline solid in 93% yield.

Brown *et al*.[1] rationalized their observations by suggesting that, under their reaction conditions, the 2,2′-anhydronucleoside **1** first isomerized to 2′,3′-anhydrouridine **4** which then underwent nucleophilic attack at C-3′ to give the observed product **2**. At the time of our earlier study,[2] we were unable to explain why the sodium and $N^1$, $N^1$, $N^3$, $N^3$-tetramethylguanidinium salts of ethanethiol should react in a different manner with the 2,2′-anhydronucleoside **1**, and previous attempts[3] to prepare 2′,3′-anhydrouridine **4** have been unsuccessful. We now report that when 2,2′-anhydro-1-β-D-arabinofuranosyluracil[4] **1** was treated with 1.5 equiv. of sodium hydride in dry dimethyl sulfoxide (DMSO) at room temperature for 20 min, it was virtually quantitatively converted into 2′,3′-anhydrouridine **4** which was isolated as a colourless crystalline solid† in 69% yield. The characterization of this epoxy compound **4** is based on microanalytical data (found: C, 47.63; H, 4.34; N, 12.36. $C_9H_{10}N_2O_5$ requires: C, 47.79; H, 4.46; N, 12.38%) and on $^1$H and $^{13}$C NMR spectroscopic evidence. It can be seen from Fig. 1 that the $^{13}$C NMR spectra [$(CD_3)_2SO$] of 2′,3′-anhydrouridine **4** [Fig. 1(*a*)] and the previously reported[5] and much more stable 2′,3′-anhydro-1-β-D-lyxofuranosyluracil **5** [Fig. 1(*b*)] are closely similar. The comparatively high field C-2′ and C-3′ resonance signals (δ 59.5 and 58.9 for the *ribo*-compound **4**; δ 55.9 and 55.6 for the *lyxo*-compound **5**) in the $^{13}$C NMR spectra of these compounds are particularly noteworthy.

When 2′,3′-anhydrouridine **4** was allowed to stand in triethylamine–methanol (1 : 9 v/v) solution at room temperature, it was quantitatively converted back into the 2,2′-anhydronucleoside **1** within 1 h. The interconversion of compounds **1** and **4** is reminiscent of the previously reported interconversion[6] of 2′,3′-anhydro-7,8-dihydro-8-oxoadenosine **6** and the isomeric 8,2′-anhydronucleoside **7**. Perhaps the reason why the preparation of 2′,3′-anhydrouridine **4** has eluded previous workers is that stringently anhydrous conditions are required if the irreversible conversion of **1** into 1-β-D-arabinofuranosyluracil **8** is to be avoided. It should be added that the preparation of 2′,3′-anhydro-3-*N*-methyluridine **9** has been reported.[7]

When 2,2′-anhydro-1-β-D-arabinofuranosyluracil **1** (1.0 mmol) was allowed to react with sodium ethanethiolate [prepared from ethanethiol (4.0 mmol) and sodium hydride (2.0 mmol)] in dry DMF (10 cm$^3$) solution at room temperature for

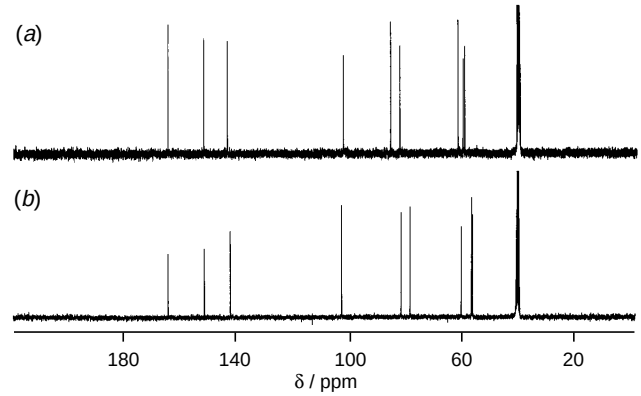
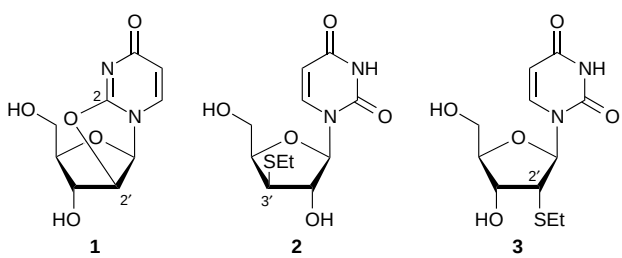
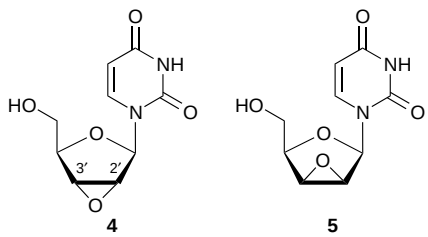
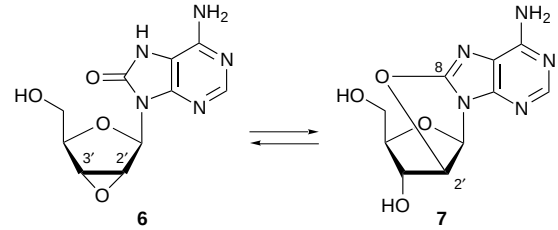
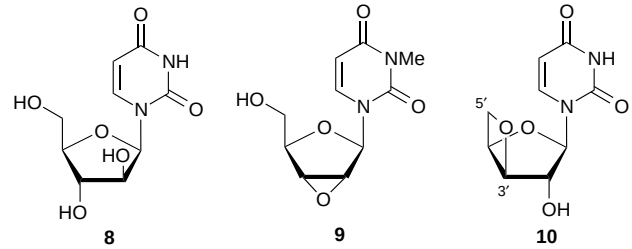



**Fig. 1** $^{13}$C NMR spectra in $(CD_3)_2SO$ of (*a*) 2′,3′-anhydrouridine **4** and (*b*) 2′,3′-anhydro-1-β-D-lyxofuranosyluracil **5**



18 h, 2′-deoxy-2′-(ethylsulfanyl)uridine **3** (mp 184–185 °C, lit.,[2] mp 183.5 °C) was obtained as the sole nucleoside product in 92% isolated yield. The course of this reaction corresponds with that of the previously reported[2] reaction between compound **1**, ethanethiol and TMG. However, when the 2,2′-anhydronucleoside **1** (1.0 mmol) was first treated with sodium hydride (4.0 mmol) in DMF (10 $cm^3$) for 2 h at room temperature and then, following the addition of ethanethiol (2.0 mmol), the reactants were stirred at room temperature for a further period of 18 h, the 3′-ethylsulfanyl derivative **2** (mp 130–132 °C)‡ was obtained in 90% isolated yield. It would therefore seem likely that the discrepancy between the results obtained by us in our previous study[2] and by Brown *et al*.[1] was due to the latter workers' sodium ethanethiolate being contaminated with a strong base (*e.g*. sodium methoxide). Finally, when the 2,2′-anhydronucleoside **1** was heated at 60 °C for 18 h with a five-fold excess of sodium hydride in dry *N*,*N*-dimethylacetamide in the absence of an additional nucleophile, 3′,5′-anhydro-1-β-D-xylofuranosyluracil **10** [mp 214–217 °C (decomp.), lit.,[8] mp 214–216 °C] was obtained and isolated in 62% yield. The fact that 2,2′-anhydro-1-β-D-arabinofuranosyluracil **1** can so easily be converted *in situ* into the isomeric 2′,3′-epoxide **4** makes it a particularly versatile synthetic intermediate.

## Footnotes

† It was not possible to determine the melting point of 2′,3′-anhydrouridine **4** as, on heating, it isomerized back to 2,2′-anhydro-1-β-D-arabinofuranosyluracil **1** before it melted. Compounds **1** and **4** have $R_f$ = 0.12 and 0.44, respectively, in chloroform–methanol (85 : 15 v/v).

‡ Found: C, 45.80; H, 5.58; N, 9.65. Calc. for $C_{11}H_{16}N_2O_5S$: C, 45.82; H, 5.59; N, 9.72%; $\delta_H$ [$(CD_3)_2SO$] 1.19 (3 H, t, *J* 7.4 Hz), 2.60 (2 H, quart, *J* 7.4 Hz), 3.36 (1 H, m), 3.64 (2 H, m), 4.11 (1 H, m), 4.29 (1 H, m), 5.06 (1 H, t, *J* 4.4 Hz), 5.69 (2 H, m), 5.82 (1 H, d, *J* 5.6 Hz), 7.93 (1 H, d, *J* 8.1 Hz), 11.34 (1 H, br s); $\delta_C$ [$(CD_3)_2SO$] 15.2, 26.1, 50.4, 61.4, 78.5, 80.3, 87.8, 101.9, 140.9, 150.9, 163.1; $R_f$ 0.50 in chloroform–methanol (85 : 15 v/v) (the $R_f$ of the 2′-ethylsulfanyl isomer **3** is 0.43 in the same solvent system).

## References


1 D. M. Brown, D. B. Parihar, A. Todd and S. Varadarajan, *J. Chem. Soc*., 1958, 3028.
2 K. J. Divakar and C. B. Reese, *J. Chem. Soc., Perkin Trans. 1*, 1982, 1625.
3 J. G. Buchanan and D. R. Clark, *Carbohydr. Res*., 1979, **68**, 331.
4 J. P. H. Verheyden, D. Wagner and J. G. Moffatt, *J. Org. Chem*., 1971, **36**, 250.
5 J. F. Codington, R. Fecher and J. J. Fox, *J. Org. Chem*., 1962, **27**, 163.
6 J. B. Chattopadhyaya and C. B. Reese, *J. Chem. Soc., Chem. Commun*., 1976, 860.
7 M. Màrton-Merész, J. Kuszmann, I. Pelczer, L. Pèrkànyi, T. Koritsànszky and A. Kàlmàn, *Tetrahedron*, 1983, **39**, 275.
8 I. L. Doerr, J. F. Codington and J. J. Fox, *J. Org. Chem*., 1965, **30**, 467.


*Received, 4th December 1996; Com. 6/08179G*

# Structure and physical properties of hexacyanomanganate(IV), $[Mn^{IV}(CN)_6]^{2-}$

**Wayne E. Buschmann,[a] Carlos Vazquez,[b] Michael D. Ward,[b]† Nancy C. Jones[b]‡ and Joel S. Miller*[a,b]**

[a] *Department of Chemistry, University of Utah, Salt Lake City, UT 84112, USA*
[b] *Science & Engineering Laboratories, DuPont, Experimental Station, Wilmington, DE 19880, USA*

**Hydrolytically unstable d³ $[Mn^{IV}(CN)_6]^{2-}$ as the $[N(PPh_3)_2]^+$ salt is crystallographically, spectroscopically, and magnetically characterized.**

The observation of magnetic ordering at relatively high temperature and including ambient temperature,[1] the photo-[2a] and electro-chemical[2b] switching between magnetic states as well as the reversible binding of oxygen[3] has led to a resurgence of interest in cyanometalates. The putative mechanism of spin coupling leading to ferromagnetic behaviour for some of these materials is that of spins on adjacent spin sites residing in orthogonal orbitals in the same spatial region.[4] An example is the ferromagnet $CsNi[Cr(CN)_6]\cdot 2H_2O$ ($T_c$ = 90 K) with the $e_g^2$ spins on each $Ni^{II}$ and orthogonal $t_{2g}^3$ spins on adjacent $Cr^{III}$ sites. Since $Mn^{IV}$ is isoelectronic to $Cr^{III}$, we targeted the preparation of $[Mn^{IV}(CN)_6]^{2-}$.

$K_2[Mn^{IV}(CN)_6]$ has been reported to be prepared from the oxidation of $K_3[Mn^{III}(CN)_6]$ with NOCl and exhibits $\nu_{CN}$ absorptions at 2240 vs and 2150 s $cm^{-1}$ and a room-temperature magnetic moment of 3.93 $\mu_B$.[5a] Although $[Mn^{IV}(CN)_6]^{2-}$ is hydrolytically unstable,[5b] several $[Mn^{IV}(CN)_6]^{2-}$ salts including $K_2[Mn^{IV}(CN)_6]$[5c,d] ($\nu_{CN}$ = 2151 $cm^{-1}$; $\mu_{RT}$ = 3.79 $\mu_B$) and $Mn^{II}[Mn^{IV}(CN)_6]\cdot 1.15H_2O$ have been prepared.[6] The latter is a ferrimagnet below an ordering temperature of 49 K.[5d] In order to develop non-aqueous routes to magnetic cyanometalates we prepared $[N(PPh_3)_2]_2[Mn^{IV}(CN)_6]$ the first structurally characterized simple salt which is stable in MeCN and $CH_2Cl_2$.§

The asymmetric unit of the unit cell‖ consists of a cation and half-anion, Fig. 1. The Mn–C and CN distances average 1.97 and 1.15 Å, respectively, and the *cis*-CNC and MnCN angles average 90.0 and 177.2°, respectively. The Mn–C and CN distances in this structure are comparable with the mean values reported for $Na_4[Mn^{II}(CN)_6]\cdot 10H_2O$ (1.95, 1.16 Å)[7] and $K_3[Mn^{III}(CN)_6]$ (1.98, 1.15 Å).[8] Within the accuracy of the crystal structure determination there is no evidence for a Jahn–Teller distortion as predicted for $^4A$ ground state. The cation is typical with an average PN distance of 1.579 Å and PNP angle of 139.6°. Each anion is surrounded by twelve cations in the solid state.

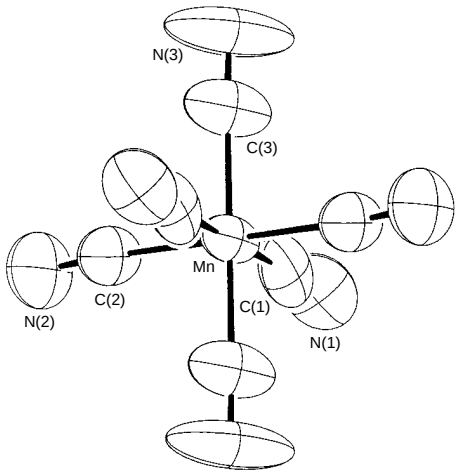



**Fig. 1** ORTEP drawing depicting atom labelling for $[Mn^{IV}(CN)_6]^{2-}$ in $[N(PPh_3)_2]_2[Mn^{IV}(CN)_6]$; atoms shown as 50% probability ellipsoids. Selected bond lengths (Å) Mn–C(1) 1.970(12), Mn–C(2) 1.965(8), Mn–C(3) 1.988(8), C(1)–N(1) 1.176(12), C(2)–N(3) 1.132(9), C(3)–N(3) 1.153(9).

The 2132 $cm^{-1}$ $\nu_{MnC\equiv N}$ absorption for $[Mn^{IV}(CN)_6]^{2-}$ is at higher energy than the 2092 and 2098 $cm^{-1}$ values for $[N(PPh_3)_2]_3[Mn^{III}(CN)_6]$. Coordination to $K^+$ leads to a significant increase in the energy of the $\nu_{C\equiv N}$ absorption, although an overall similar trend is observed for $\nu_{MnC\equiv NK}$: $K_2[Mn^{IV}(CN)_6]$ (2240, 2150 $cm^{-1}$)[5a] and $K_3[Mn^{III}(CN)_6]$ (2129, 2112 $cm^{-1}$).[9]

$[N(PPh_3)_2]_2[Mn^{IV}(CN)_6]$ exhibits a corrected room-temperature magnetic moment of 4.10 $\mu_B$ consistent with being a d³ octahedral complex with isolated anions. The expected six-line hyperfine for $^{55}Mn$ ($I$ = 5/2) is isotropic in the solution, frozen-solution, and even the solid-state spectra and is centred at $g$ = 1.996. This is strong evidence for a well behaved anion which exhibits very little or no distortion in its electronic configuration. At 78 K the electron paramagnetic resonance is 340 G wide with an average hyperfine coupling constant $|A|$ = 68 G, Fig. 2. The derivative peak to peak linewidths are essentially the same for the room-temperature and 78 K spectra with a slight variation from line to line. They proceed as 33, 30, 28, 31, 32, 27 (±1) G, from low to high field. This slight inhomogeneity is expected for manganese ions.[6]

The $Mn^{III/IV}$ couples of the octahedral cyanide anions are fully reversible one-electron events. $[Mn^{IV}(CN)_6]^{2-}$ {and $[Mn^{III}(CN)_6]^{3-}$} have a reversible $Mn^{III/IV}$ couple at $E_{1/2}$ = +0.14 V in MeCN *vs.* SCE, $\Delta E_{pp}$ = 0.09 V (10 mV $s^{-1}$ scan rate) using glassy carbon disk, Pt wire and $Ag/AgCF_3SO_3$ electrodes and ferrocene as an external standard. A reduction wave for the $Mn^{III/II}$ couple was not observed. The presence of any other metal cations affect the electrochemical response by precipitating out a cyanide complex onto the working electrode. By comparison, the $[Fe^{III/II}(CN)_6]^{3/4-}$ $E_{1/2}$ couple in MeCN is −0.42 V *vs.* SCE.[10]

The electronic spectrum of $[Mn^{IV}(CN)_6]^{2-}$ in MeCN, Fig. 3, unlike that of the isoelectronic $[Cr^{III}(CN)_6]^{3-}$,[11] possesses several charge-transfer bands. In contrast to $[Cr^{III}(CN)_6]^{3-}$ which has two d → d transitions at 26 500 ($\varepsilon$ = 90 $M^{-1}$ $cm^{-1}$)

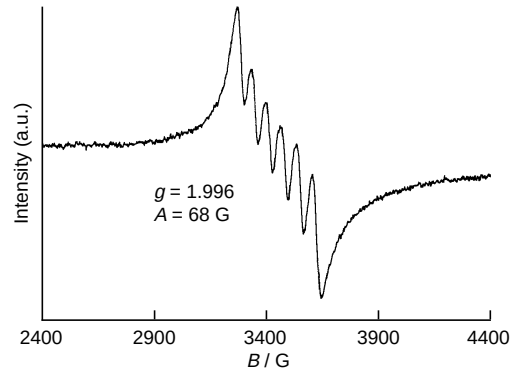



**Fig. 2** EPR spectrum of $[N(PPh_3)_2]_2[Mn^{IV}(CN)_6]$ at 78 K, 1.0 mM in $CH_2Cl_2$ at 9.6464 GHz

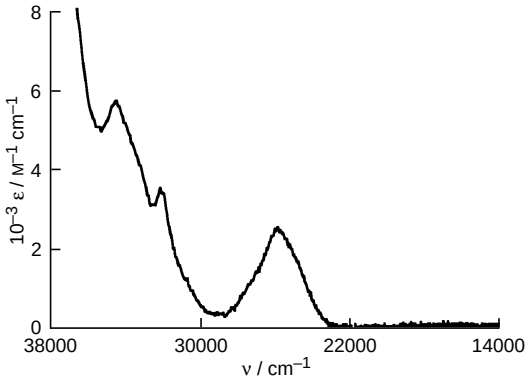



**Fig. 3** Electronic spectrum of $[N(PPh_3)_2]_2[Mn^{IV}(CN)_6]$ in MeCN

and 32 400 cm$^{-1}$ (ε = 65 M cm$^{-1}$) and one intense M → L charge-transfer absorption at 38 000 cm$^{-1}$ (ε = 6240 M$^{-1}$ cm$^{-1}$), $[Mn^{IV}(CN)_6]^{2-}$ possesses an intense band centred at 25 700 cm$^{-1}$ (ε = 2500 M$^{-1}$ cm$^{-1}$) which appears to be at least two overlapping bands. This band tails well into the visible region and is likely to be responsible for the extreme photosensitivity of this compound. There is a second band at 32 000 cm$^{-1}$ (ε = 3500 M$^{-1}$ cm$^{-1}$) and a third at 34 400 (ε = 5700 M$^{-1}$ cm$^{-1}$) on the tail of the aromatic π → π* transitions of the $[N(PPh_3)_2]^+$ cation which obscures the region above 36 000 cm$^{-1}$. This is the first electronic spectrum of a manganese cyanide taken without excess KCN[11] or perchloric acid[12] to prevent decomposition of the hydrolytically unstable anions. Reaction of $[Mn^{IV}(CN)_6]^{2-}$ to form molecule-based magnets is in progress.

W. E. B. and J. S. M. gratefully acknowledge the support from the US Department of Energy (Grant No. DE-FG03-93ER45504). We also thank C. M. Wynn (The Ohio State University) for measuring the magnetic susceptibility.

## Footnotes

† Present address: Department of Chemical Engineering & Materials Science, University of Minnesota, Minneapolis, MN 55455, USA.

‡ Present address: Department of Chemistry, La Salle University, Philadelphia, PA 19141, USA.

§ In a typical experiment a MeCN solution (20 ml) of $[Fe(\eta\text{-}C_5H_5)_2][BF_4]$ (2.42 mmol, 1.00 g) was added to a $CH_2Cl_2$ solution (50 ml of $[N(PPh_3)_2]_3[Mn^{III}(CN)_6]$¶ (2.42 mmol, 4.42 g). The green colour of the $[Fe(\eta\text{-}C_5H_5)_2]^+$ gradually changed over 1.5 h to give a dark orange solution. The product was precipitated with $Et_2O$, isolated and recrystallized from MeCN–$CH_2Cl_2$–$Et_2O$ to give small, yellow needles in 33% yield. IR: $\nu_{CN}$ (Nujol) = 2132 cm$^{-1}$. Raman: $\nu_{CN}$ = 2135 cm$^{-1}$, $\nu_{MC}$ = 365 cm$^{-1}$. mp 142 °C (decomp.). Anal. Calc. for $C_{78}H_{60}MnN_8P_4$: C, 72.73; H, 4.70; N, 8.40. Found: C, 72.49; H, 4.51; N, 8.58%.

¶ $K_3[Mn(CN)_6]$ (1.50 g, 4.57 mmol) was quickly added to a solution of $[N(PPh_3)_2]Cl$ (7.87 g, 13.7 mmol) disolved in 825 ml of water. The precipitated product was recovered by filtration and dried in *vacuo*. Recrystallization from a dry, oxygen-free MeCN solution layered with $Et_2O$ gave large orange–yellow prisms in 77% yield. IR: $\nu_{CN}$(Nujol) = 2092.2098 cm$^{-1}$. Raman: $\nu_{CN}$ = 2099, 2110 cm$^{-1}$, $\nu_{MC}$ = 359 cm$^{-1}$. mp 272 °C (decomp.). Anal. Calc. for $C_{114}H_{90}MnN_9P_6$: C, 74.95; H, 4.97; N, 6.90. Found: C, 74.90; H, 5.02; N, 6.96%.

‖ *Crystal data* for $C_{78}H_{60}MnN_8P_4$, $M$ = 1288.16, monoclinic, space group $P2_1/n$, $a$ = 10.707(2), $b$ = 13.402(2), $c$ = 23.662(4) Å, β = 100.41(1)°, $U$ = 3339.5 Å$^3$, $Z$ = 2, $D_c$ = 1.281 g cm$^{-3}$, λ = 0.710 73 Å, crystal size 0.52 × 0.42 × 0.50 mm, $T$ = −70 °C, $2\theta_{max}$ = 48°, $R_w$ (on $F$) [$R$ (on $F$)] = 0.069(0.065), for 2855 unique reflections with $I > 3\sigma(I)$. Data were collected on a Syntex $P\bar{1}$ diffractometer and the crystal structure solved using MOLEN software distributed by Enraf Nonius. Atomic coordinates, bond lengths and angles, and thermal parameters have been deposited at the Cambridge Crystallographic Data Centre (CCDC). See Information for Authors, Issue No. 1. Any request to the CCDC for this material should quote the full literature citation and the reference number 182/357.

## References

1 V. Gadet, T. Mallah, I. Castro and M. Verdaguer, *J. Am. Chem. Soc*., 1992, **114**, 9213; T. Mallah, S. Ferlay, C. Auberger, C. Helary, F. L.'Hermite, F. Ouahes, F. J. Vaissermann, M. Verdaguer and P. Veillet, *Mol. Cryst. Liq. Cryst*., 1995, **273**, 579; S. Ferlay, T. Mallah, R. Ouahes, P. Veillet and M. Verdaguer, *Nature*, 1995, **378**, 701; W. R. Entley and G. S. Girolami, *Science*, 1995, **268**, 297; *Inorg. Chem*., 1994, **33**, 5165.

2 (*a*) O. Sato, T. Iyoda, A. Fujishima and K. Hashimoto, *Science*, 1996, **272**, 704; (*b*) O. Sato, T. Iyoda, A, Fujishima and K. Hashimoto, *Science*, 1996, **271**, 49.

3 D. Ramprasad, G. P. Pez, B. H. Toby, T. J. Markley and R. M. Pearlstein, *J. Am. Chem. Soc*., 1995, **117**, 10 694.

4 O. Kahn, *Molecular Magnetism*, VCH, Weinheim, 1993; J. S. Miller and A. J. Epstein, *Angew. Chem., Int. Ed. Engl*., 1994, **33**, 385; *Angew. Chem*., 1994, **106**, 399; *Chem. Eng. News*, 1995, **73**, 30; O. Kahn, *Struct. Bonding (Berlin)*, 1987, **68**, 89.

5 (*a*) J. R. Fowler and J. Kleinberg, *Inorg. Chem*., 1970, **9**, 1005; G. Trageser and H. H. Eysel, *(b*) *Inorg. Chim. Acta*, 1978, **26**, L56; (*c*) *Z. Anorg. Allg. Chem*., 1976, **420**, 273; (*d*) R. Klenze, B. Kanellalopulos, B. G. Trageser and H. H. Eysel, *J. Chem. Phys*., 1980, **72**, 5819.

6 F. K. Hurd, M. Sachs and W. D. Hershberger, *Phys. Rev*., 1954, **93**, 373; R. G. Hayes and R. J. Myers, *J. Chem. Phys*., 1964, **40**, 877; R. B. Garrett and L. O. Moran, *J. Chem. Phys*., 1966, **44**, 890.

7 A. Tullberg and V. Nils-Gösta, *Acta Chem. Scand., Ser. A*, 1974, **28**, 551.

8 M. P. Gupta and H. J. Milledge, *Acta Crystallogr., Sect. B*, 1974, **30**, 656.

9 W. P. Griffith and G. T. Turner, *J. Chem. Soc. A*, 1970, 858.

10 G. Gritzner, K. Danksagmüller and V. Gutmann, *J. Electroanal. Chem*., 1976, **72**, 177.

11 J. J. Alexander and H. B. Gray, *J. Am. Chem. Soc*., 1968, **90**, 4260.

12 I. D. Chawla and M. J. Frank, *J. Inorg. Nucl. Chem*., 1970, **32**, 555.

*Received, 11th October 1996; Com. 6/06979G*



Typeset and printed by Black Bear Press Limited, Cambridge, England

ChemComm
FEATURE ARTICLE

# Control and applications of remote asymmetric induction using allylmetal reagents

**Eric J. Thomas**

*Department of Chemistry, University of Manchester, Manchester, UK M13 9PL*

**Treatment of hydroxy- and alkoxy-substituted allylstannanes with tin(IV) halides effects transmetallation and the stereoselective formation of allyltin trihalides. These react with aldehydes and imines derived from glyoxylates with useful levels of remote asymmetric induction. Aspects of this chemistry are discussed, together with the conversion of the products into tetrahydrofurans and dihydropyrans.**

During a study of the chemistry of (*S*)-4-benzyloxypent-2-enylstannane **1**,[1] it was found that stereo- and regio-selective reactions in favour of the 1-substituted *syn*-(*Z*)-5-benzyloxyhex-3-en-1-ols **2** were achieved if the allylstannane was treated with tin(IV) chloride for a few minutes at −78 °C followed by addition of an aldehyde (Scheme 1).[2] This reaction attracted our interest because of its high level of 1,5-asymmetric induction. This review discusses the scope of remote asymmetric induction using allyltin reagents.

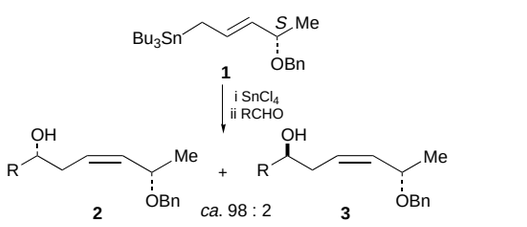
## Background

At the onset of our work, it was known that allylstannanes react with aldehydes on heating and in the presence of Lewis acids.[3,4] The thermal reactions proceed stereo- and regio-selectively and are believed to involve six-membered, cyclic, chair-like, transition structures. For example, the *anti* and *syn* products **6** (X = H) and **9** are obtained from the (*E*)- and (*Z*)-but-2-enylstannanes **4** (X = H) and **7**,[5] consistent with participation of the transition structures **5** and **8**.[5]

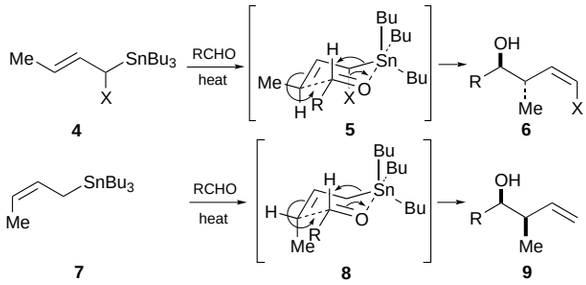
1-Substituted (*E*)-but-2-enylstannanes **4** (X = Me, OR) react with aldehydes on heating (Scheme 2) with excellent stereoselectivity in favour of the *anti*-(*Z*)-but-3-en-1-ols **6** (X = Me, OR).[6,7] The formation of *Z* double bonds in these reactions is consistent with participation of the transition structures **5** (X = Me, OR) in which the substituent next to tin is axial. This preference controls the facial selectivity of reactions of enantiomerically enriched 1-substituted but-2-enylstannanes with aldehydes.[8] Thus the (1*R*)- and (1*S*)-1-alkoxybut-2-enylstannanes **10** and **13** react with benzaldehyde to give the *anti* products **12** and **15** by selective attack on the *Si*- and *Re*-faces of the aldehyde, respectively (Scheme 3). Ozonolysis of these products gives rise to enantiomeric *anti*-aldol products, but the use of this reaction in synthesis is limited to aromatic and secondary aliphatic aldehydes because of the high temperatures required.[8]

Two processes are involved in the Lewis acid promoted reactions of allylstannanes and aldehydes. Boron trifluoride–diethyl ether promotes the reaction at −78 °C, and leads to the formation of the *syn* product **9** from both the (*E*)- and (*Z*)-but-2-enylstannanes **4** (X = H) and **7**,[9] albeit less selectively from the (*Z*)-allylstannanes.[10] This stereoconvergence has been explained in terms of open-chain transition structures, the antiperiplanar arrangement of aldehyde and stannane being proposed by Yamamoto (Scheme 4),[9] although the *gauche* arrangement was suggested by Denmark.[11] In these reactions, the boron trifluoride–diethyl ether is accelerating the reaction by coordinating to the aldehyde.

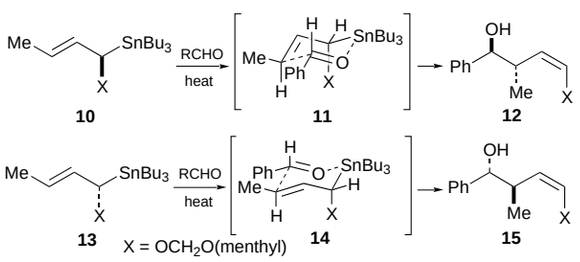
Other Lewis acids react with the allylstannane to generate more reactive allylmetal reagents which then react with the aldehyde.[4] The transmetallation reactions normally involve SE′ processes so terminal allylstannanes give 1-substituted allylmetal reagents. These react with aldehydes to give linear products, but can be unstable with respect to 1,3-rearrangement to give terminal allyl metal reagents which react with aldehydes to give branched products.[12] For example, the 1-phenylprop-2-enyltin dichloride **18** is generated from the 3-phenylpropenylstannane **17** and butyltin trichloride (Scheme 5), and reacts with aldehydes to give the linear products **20**. On standing it isomerises to the 3-phenyl isomer **19** which gives the *anti* products **21** with aldehydes. Transition structures analogous to **5** are believed to be involved.[13]



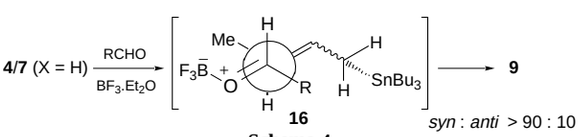

**Scheme 1**




**Scheme 2**




**Scheme 3**




**Scheme 4**

## Remote asymmetric induction in reactions of allylstannanes with aldehydes

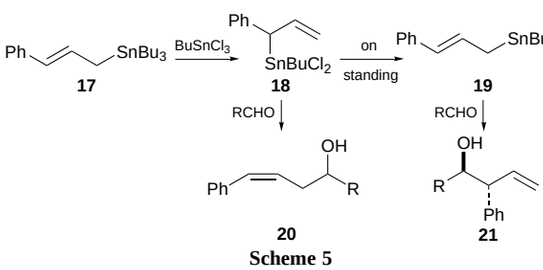
How can the regio- and stereo-selective formation of the 1,5-*syn* products **2** be explained? Since the tin(IV) halide is allowed to react with the stannane before the aldehyde is added, it is believed that transmetallation of the allylstannane is the first step.[14] This transmetallation is thought to involve delivery of the tin(IV) halide to the double bond of the allylstannane by the benzyloxy group to give the allyltin trichloride **22** which contains a four-membered oxastannane ring (Scheme 6). It is suggested that this transmetallation is stereoselective, with the isomer in which the vinyl and methyl groups are *trans*-disposed about the four-membered ring being preferred, perhaps due to kinetic control, although there may also be some equilibration of the *cis* and *trans* diastereoisomers under the reaction conditions. The allyltin trichloride **22** then reacts with the aldehyde *via* the transition structure **23** in which the group next to tin is axial, leading to the formation of the *cis* double bond in the product. Since the reaction between the tin(IV) chloride and an aldehyde is not reversible at −78 °C, this selectivity must be due to kinetic control. The initially formed product, before aqueous work-up, is the medium-ring dioxastannane **24**. Molecular modelling indicates that a *cis* double bond is more readily accommodated in the 8-membered ring of **24** than a *trans* double bond because of strain. If this strain is present in the transition structure **23**, it could account for the faster formation of the *cis* double bonded isomer **2**.[14]

The overall 1,5-asymmetric induction is therefore controlled by the stereoselectivity of the transmetallation step, and the preference of the group next to tin to be axial in the transition structure **23**. Coordination of the tin to the benzyloxy group is important in both of these steps. To investigate this coordination, the behaviour of the 4-*tert*-butyldimethylsilyloxypent-2-enylstannane **25** was investigated.[15]

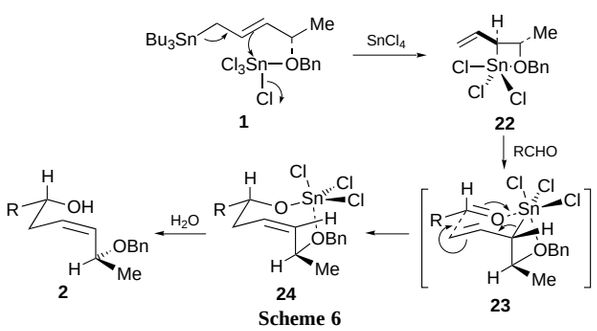
With benzaldehyde three products, the 1,5-*anti*-(*E*)-alkenol **26**, the 1,5-*syn*-(*Z*)-isomer **27** and a minor component which was not fully characterised (ratio 60 : 30 : 10, respectively) were formed (Scheme 7). The formation of the *anti*-(*E*)-alkenol **26** is consistent with participation of the allyltin trichloride **28**, which has the opposite configuration at the tin-bearing carbon to that of the allyltin trichloride **22**, and which reacts with the aldehyde *via* the transition structure **29**. It may be that, in this case, the transmetallation is taking place by intermolecular attack of the tin(IV) chloride on the allylstannane mainly in the conformation in which the allylic hydrogen is in the plane of the double bond. Approach of the tin(IV) chloride to the face away from the bulky silyloxy substituent,[16] would give the postulated intermediate **28**. The formation of the *trans* double bond in the products implies that the *tert*-butyldimethylsilyloxyethyl group adopts the equatorial position in the transition structure **29**. Perhaps, as no medium-ring strain is present, the bulky silyloxyethyl group is simply adopting the less hindered equatorial position.[15]

The scope of the tin(IV) halide-mediated reaction between alkoxy substituted allylstannanes and aldehydes has been widely investigated. The 4-(2-trimethylsilylethoxymethoxy)-, *p*-methoxybenzyloxy-, and hydroxy-pentenylstannanes **31** react with similar 1,5-induction to the 4-benzyloxypent-2-enylstannane **1**, although slightly reduced stereoselectivity is observed in reactions of the hydroxystannane **31** (R = H) with aliphatic aldehydes. Tin(IV) bromide leads to slightly better, and butyltin trichloride to similar, stereoselectivity, although the other Lewis acids investigated to date, $BF_3.Et_2O$, $TiCl_4$, $AlCl_3$, have proved less useful.

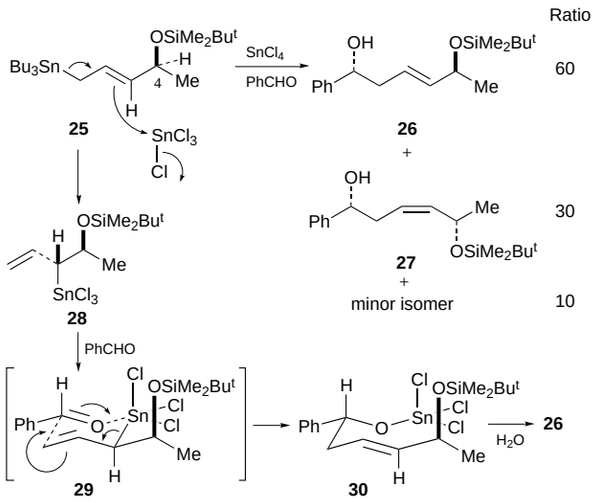
The 5-substituted pent-2-enylstannanes **32** ($R^1$ = Bn, PMB, SEM, H; $R^2$ = H) also react with aldehydes with useful levels of 1,5-induction after treatment with tin(IV) chloride or bromide (Scheme 8).[17,18] In this case the major product (*ca*. 95 : 5) is the



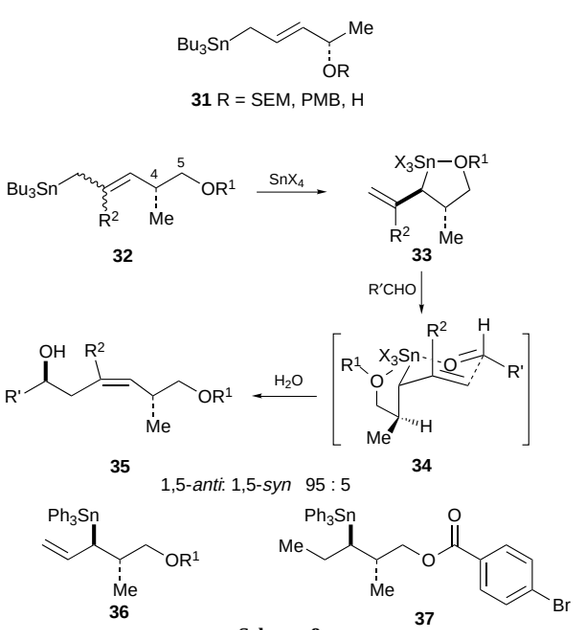

**Scheme 5**




**Scheme 6**




**Scheme 7**




**Scheme 8**

1,5-*anti*-(*Z*) stereoisomer **35** ($R^2$ = H). This is consistent with participation of the corresponding allyltin trihalide **33** ($R^2$ = H) which reacts with the aldehyde *via* the transition structure **34**. The formation of the *cis* double bond implies that the group next to tin is axial, so determining the facial selectivity of the reaction with the aldehyde and the configuration of the hydroxy bearing chiral centre in the product.

In the 5-substituted series, the *tert*-butyldimethylsilyl group has less effect on the overall selectivity, the stannane **32** ($R^1$ = $SiMe_2Bu^t$) giving the 1,5-*anti* product **35** ($R^1$ = $SiMe_2Bu^t$), albeit with reduced stereoselectivity (*ca.* 80 : 20).[15] An alkyl group at C(2) in the allylstannane, or the geometry of the double bond, have little effect. Thus both the (*E*)- and (*Z*)-2-methylpentenylstannanes **32** ($R^2$ = Me) give the 1,5-*anti*-(*Z*) products **35** ($R^2$ = Me) containing less than 2% of their *syn* diastereoisomers.[19]

In this series, the intermediate allyltin trichlorides **33** ($R^2$ = H; X = Cl) have been trapped by phenyllithium. Addition of phenyllithium to the allyltin trichloride from the benzyloxystannane **32** ($R^1$ = Bn; $R^2$ = H) gave the internal triphenylstannane **36** ($R^1$ = Bn) with excellent stereoselectivity (95 : 5) and similar stereoselectivity was observed for the hydroxy- and *tert*-butyldimethylsilyloxy-stannanes **32** ($R^1$ = H, $SiMe_2Bu^t$; $R^2$ = H). The structures of the major trapping products were established by X-ray diffraction of the *p*-bromobenzoate **37** which was prepared from the hydroxystannane **36** ($R^1$ = H) by reduction using diimide and esterification.[20]

This work is of interest since not only does it confirm the configurations originally assigned to the allyltin chlorides **33** on mechanistic grounds, but it also provides the regioisomeric triphenylallylstannanes **36** for transmetallation studies.

Transmetallation of allylstannanes with chiral centres at the 5- and 6-positions generates allyltin trihalides which react with aldehydes with 1,6- and 1,7-induction. In practice better stereoselectivities were observed with hydroxy substituted allylstannanes using tin(IV) bromide rather than tin(IV) chloride as the Lewis acid, although 1,6-induction was also observed for a 5-methoxyallylstannane. Thus the 5-hydroxy- and 5-methoxyhex-2-enyl and the 6-hydroxy-5-methylhex-2-enylstannanes **38** ($R^1$ = H, Me)[21] and **41**[22] were transmetallated with tin(IV) bromide to give allyltin tribromides, which reacted with aldehydes to give the 1,6-*syn* and the 1,6-*anti* products **40** ($R^1$ = H, Me) and **43**, respectively, with useful levels of 1,6-asymmetric induction (Scheme 9). Similarly the 6-hydroxyhept-2-enylstannane **44** gave the 1,7-*syn* products **46** with *ca.* 90 : 10 stereoselectivity.[23]

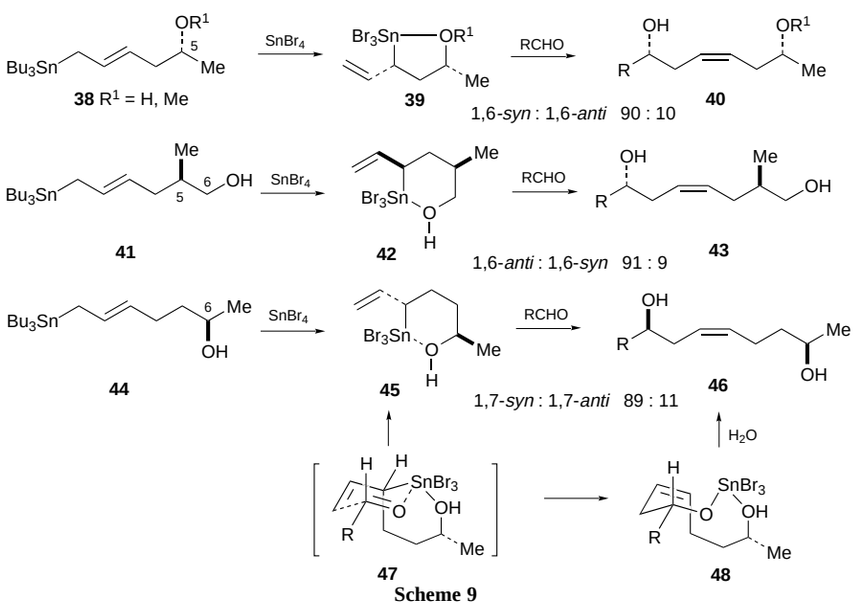
The stereoselectivities of these reactions are consistent with transmetallation giving the allyltin tribromides **39** ($R^1$ = H, Me), **42** and **45**, which react with aldehydes *via* six-membered, chair-like transition states in which the group next to tin is axial, *e.g.* **47** for the reaction of the allyltin tribromide **45**. The transmetallations are believed to generate allyltin tribromide in which the vinyl and methyl groups are both equatorial, as in the six-membered cyclic intermediates **42** and **45**, or pseudo-equatorial, as in the five-membered ring intermediate **39** (*cf.* also **33**), *i.e.* the more stable intermediates are believed to be involved, albeit formed kinetically.

The stereoselectivities of reactions with aldehydes of allylstannanes with nitrogen- and sulfur-containing functional groups have been investigated and found to parallel the reactions of their oxygen analogues. For example, treatment of the 4-aminopent-2-enylstannane **49** with tin(IV) bromide followed by the addition of an aldehyde gave the 1,5-*syn* products **51** with excellent stereoselectivity,[24] and the 5-benzylthiopent-2-enylstannane **52** similarly gave the 1,5-*anti* products **54**, with *ca.* 90 : 10 selectivity (Scheme 10).[25] The allyltin tribromides **50** and **53** are believed to be involved.

Rather different selectivity was observed for 5-acyloxyallylstannanes. The 5-acetoxypent-2-enylstannane **55** (R = Me) gave a mixture of products in which the *anti*-(*E*)-isomer **56** was the major component (Scheme 11).[26] The formation of this product is consistent with participation of the 7-membered ring containing allyltin trichloride **58** which reacts with the aldehyde *via* the transition structure **59**. Perhaps there is enough flexibility to accommodate an incipient *trans* double bond in this transitional structure so that the group next to tin can be equatorial. The use of different acyloxystannanes **55** (R = Ph, $Bu^t$, OMe, *etc*), failed to improve the selectivity to reliably useful levels.[26] The allylstannane **60** also gives rise to *E* double bonds in products from reactions with aldehydes, albeit with only low 1,8-*syn/anti* selectivity.[27]

## Remote asymmetric induction in reactions of allylstannanes and imines

Allylstannanes react with imines in the presence of strong Lewis acids,[28] but preliminary investigations showed that allyltin trichlorides did not react at −78 °C with *N*-alkyl and *N*-aryl imines prepared from benzaldehyde. However, the more



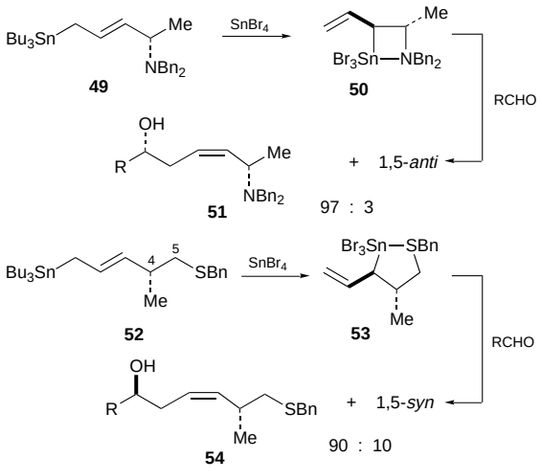

**Scheme 9**

electrophilic *N*-ethoxycarbonyl imine **61** and the chiral imine **63** prepared from butyl glyoxylate reacted efficiently with propenyltin trichloride to give the homoallylic amine derivatives **62** and **64**; (ratio 93 : 7, Scheme 12).[29] Of interest is the facial selectivity observed with the chiral imine **63** which is the opposite of that observed for an allylborane.[30]

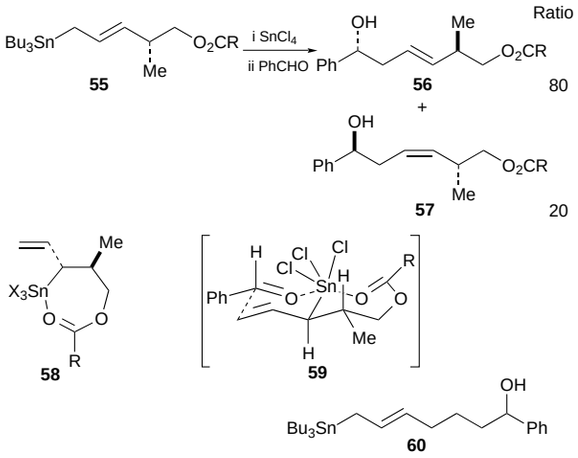
The imine **63** reacted with the allyltin trichloride **22** (Scheme 13) generated from the 4-benzyloxypent-2-enylstannane **1** with effective 1,5-induction in favour of the 1,5-*anti* isomer **66** (selectivity 90 : 10) even though this had involved attack of the allyltin trichloride on the less reactive face of the imine, *cf.* the facial stereoselectivity observed during the reaction of the imine **63** with propenyltin trichloride. With the enantiomeric imine *ent*-**63**, the formation of the 1,5-*anti* product was matched with the facial preference of the imine, and the major product was the 2*R* epimer **68**, selectivity 96 : 4. In both cases, all products isolated from the reactions between the imines **63** and *ent*-**63** were (*E*)-alkenes, in contrast to the selective formation of (*Z*)-alkenols in reactions with aldehydes.[29] The preference for formation of 1,5-*anti* products was maintained for the achiral *N*-arylthio, *N*-benzhydryl and *N*-dimethylbenzyl imines **70**–**72**, which gave the 1,5-*anti* products **73**–**75**, in *ca*. 90 : 10 stereoselectivity.[31]

The mechanisms of these reactions are not clear, although it is supposed that the allyltin trichloride **22** is involved since its formation takes place before addition of the electrophile. By analogy with the boron trifluoride–diethyl ether-promoted reactions of allylstannanes and aldehydes, which give (*E*)-alkenes,[32] perhaps the reaction between the allyltin trichloride **22** and imines involves an open-chain process. The transition structure **76** shows one possible orientation of the allyltin trichloride and the matched imine *ent*-**63** leading to the major product **68**. However, the cyclic transition structure **77** is also consistent with the observed stereoselectivity. In this case, the group on nitrogen, which must be axial if the nitrogen is to be coordinated to the tin, forces the group next to tin into the equatorial position to avoid severe 1,3-diaxial interactions, compare **23** and **77**.[29]

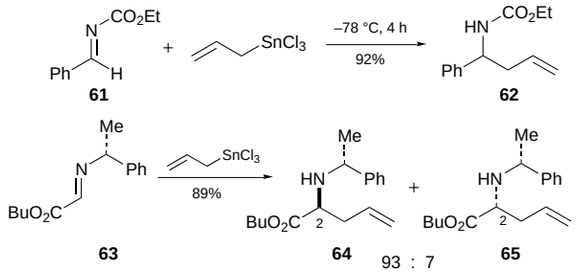
Of interest is the stereoselectivity of the reaction between the 4-*tert*-butyldimethylsilyloxypent-2-enylstannane **25** and imines. The achiral imines **70**–**72** react to give more of the 1,5-*syn* products **78**–**80** (Scheme 14), although the stereoselectivity, being *ca*. 75 : 25, is less than with the benzyloxystannane **1**.[15] The 1,5-*syn* products **81** and **82** are also preferred in reactions with the chiral imines **63** and *ent*-**63** (Scheme 15). This stereoselectivity is consistent with participation of the allyltin trichloride **28** which has the (*R*)-configuration at the tin bearing



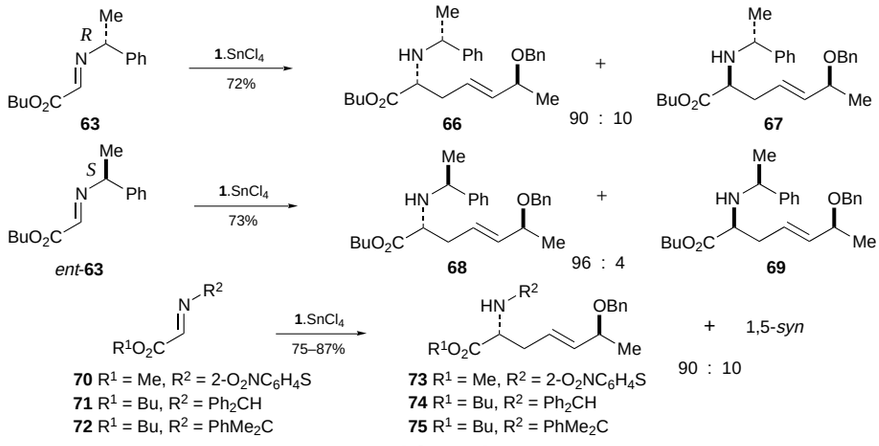

**Scheme 10**




**Scheme 11**




**Scheme 12**




**70** $R^1$ = Me, $R^2$ = 2-$O_2NC_6H_4S$
**71** $R^1$ = Bu, $R^2$ = $Ph_2CH$
**72** $R^1$ = Bu, $R^2$ = $PhMe_2C$

**73** $R^1$ = Me, $R^2$ = 2-$O_2NC_6H_4S$
**74** $R^1$ = Bu, $R^2$ = $Ph_2CH$
**75** $R^1$ = Bu, $R^2$ = $PhMe_2C$

**Scheme 13**

carbon. This prefers to approach the *Si* face of the imine, giving rise to the 1,5-*syn* product (see transition structure **83**).[15]

The allyltin trichloride generated from the 5-benzyloxypent-2-enylstannane **32** ($R^1$ = Bn; $R^2$ = H) reacts with the achiral imines **70** and **71** with useful 1,5-induction in favour of the 1,5-*syn* products **84** and **85** (Scheme 16).[31] With the matched (*R*)-imine **63** this selectivity is enhanced, but it is significantly reduced in reaction with the mismatched (*S*)-imine *ent*-**63**.[29] The formation of these 1,5-*syn* products is consistent with participation of the allyltin trichloride **33** ($R^1$ = Bn; $R^2$ = H; X = Cl) which reacts with the imine through either an open-chain or cyclic transition structure analogous to **76** or **77**.

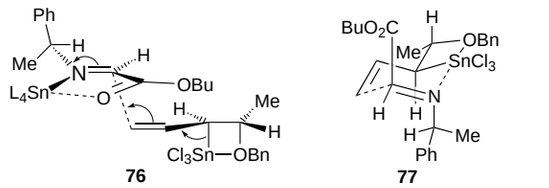
## Aspects of the chemistry of the products

The 4-benzyloxypent-2-enylstannane **1** reacts with chiral 3-alkoxy aldehydes with selectivity controlled by the stannane, not by the aldehyde, *e.g.* the 1,5-*syn* products **91** and **93** were the dominant products from the 3-alkoxybutanals **90** and **92** (Scheme 17), although some matching and mismatching was observed with 2-alkoxy aldehydes.[33] Since remote chiral centres in the aldehyde do not affect the 1,5-*syn*-stereoselectivity, it is possible to use repetitively the remote induction of alkoxystannanes to synthesize open-chain polyols.

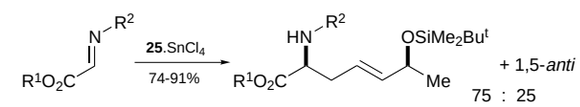
The 4-benzyloxyocta-2,7-dienylstannane **94** gave the 1,5-*syn* product **95** with 2-methylpropanal (*syn* : *anti* selectivity = 95 : 5) (Scheme 18). Protection and hydroboration–oxidation gave the aldehyde **96**, which reacted with the pent-2-enylstannane **1** to give the all-*syn* product **97**. Selective hydrogenation and hydrogenolysis gave the 15-methylhexadeca-2,6,10,14-tetraol **98** containing less than 5% of any other diastereoisomer. The aldehyde **96** was also treated with the stannane **94** to give the 1,5-*syn* product **99** which was protected and taken through to the corresponding aldehyde which gave the hexaol derivative **100** on treatment with the pent-2-enylstannane **1**.[34]

The 1,5-*syn*-alkenols **2** were converted stereoselectively into the all-*syn* epoxides **101** using $VO(acac)_2$ and *tert*-butyl hydroperoxide (Scheme 19).[35] The regioselectivity of hydride reduction of these epoxides was dependent upon the reducing agent. The 1,4- and 1,3-diols **102** and **103** were obtained as a mixture (33 : 67) using diisobutylaluminium hydride, but lithium aluminium hydride gave predominantly (99 : 1), and Red-Al† gave exclusively, the 1,4-diol **102**. Treatment of the 1,4-diol **102** (R = Ph) with lithium diisopropylamide and toluene-*p*-sulfonyl chloride gave the 2,5-*trans*-disubstituted tetrahydrofuran **104** by selective tosylation and displacement of the benzylic hydroxy group, but this sequence gave mixtures of products from other 1,4-diols **102** (R ≠ Ar).[36]

A synthesis of *cis*-2,5-disubstituted tetrahydrofurans, was developed from the alkenols **2**.[36] Treatment with toluene-*p*-sulfonyl chloride in pyridine gave the toluene-*p*-sulfonates **105**, which were oxidised stereoselectively using osmium tetraoxide (Scheme 20). The intermediate diols **106** were not isolated. Instead they cyclised *in situ* to give tetrahydrofurans,

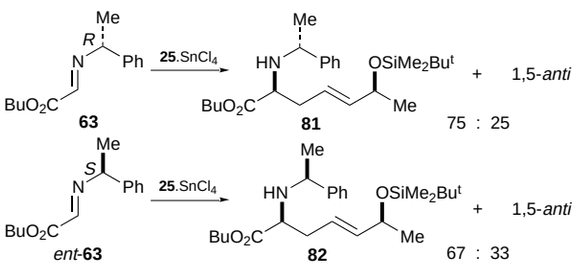


**76** **77**

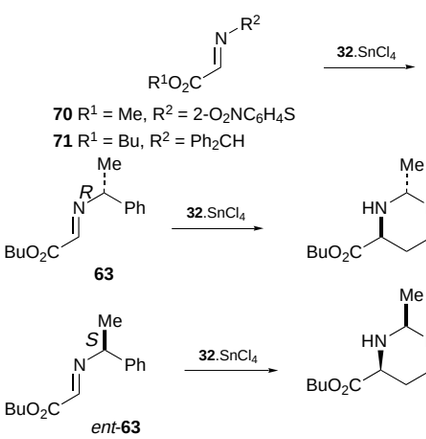


**70** $R^1$ = Me, $R^2$ = 2-$O_2NC_6H_4S$ **78** $R^1$ = Me, $R^2$ = 2-$O_2NC_6H_4S$
**71** $R^1$ = Bu, $R^2$ = $Ph_2CH$ **79** $R^1$ = Bu, $R^2$ = $Ph_2CH$
**72** $R^1$ = Bu, $R^2$ = $PhMe_2C$ **80** $R^1$ = Bu, $R^2$ = $PhMe_2C$

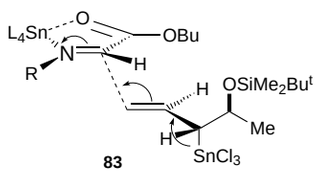
**Scheme 14**



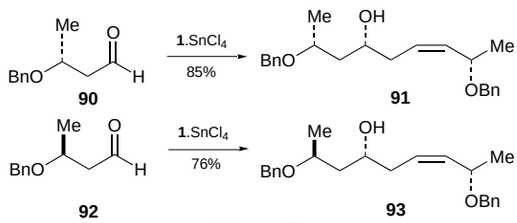
**Scheme 15**



**Scheme 16**



**83**



**Scheme 17**

*e.g.* **107** and **109** (ratio 85 : 15) and **108** and **110** (ratio 95 : 5). The stereoselectivity of formation of these tetrahydrofurans is consistent with the diastereofacial selectivity of oxidation of the alkenyl tosylates being controlled by the allylic benzyloxy group, and, for the 5-isopropyltetrahydrofuran **107**, was confirmed by NMR (NOE) studies on the ketone **111**.

This synthesis of tetrahydrofurans **107**–**110** involves three steps from the starting aldehyde, namely reaction with the allylstannane, tosylation and oxidation–cyclisation. This three step sequence was used to give polycyclic tetrahydrofurans. The major tetrahydrofuranyl-2-carboxylate **108** was taken through to the allylstannane **112**. Treatment with tin(IV) bromide and an aldehyde (Scheme 21) proceeded with useful levels (⩽ 90 : 10) of 1,5-induction to give the 1,5-*syn* products **113** (R = Ph, Pr$^i$, $CO_2$Bu), the allylic tetrahydrofuranyl chiral centre controlling the 1,5-induction. Tosylation and oxidation of the 2-hydroxyhexenyltetrahydrofuran **113** (R = Pr$^i$) then gave the bis(tetrahydrofuran) **114** (23%) together with a minor isomer, ratio 87 : 13.[36] As an alternative strategy, the tetrahydrofuranyl-2-carboxylate **108** was converted by protection and reduction into the aldehyde **115** (Scheme 22). This was treated under the usual conditions with stannane **1** and tin(IV) chloride to give the 1,5-*syn* product **116** (74%, no minor isomer being detected by HPLC). Tosylation and oxidation with osmium tetraoxide gave the diol **117** and a minor isomer (85 : 15). Treatment with sodium hydride instigated cyclisation to the bis(tetrahydrofuran) **118**.[36]

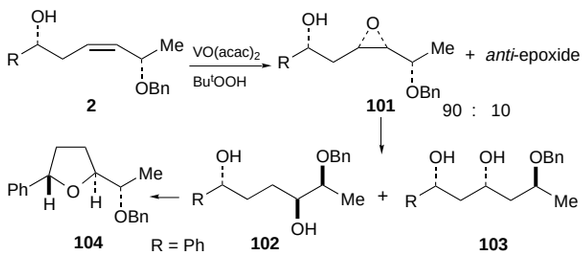
This synthesis of tetrahydrofurans is limited to products prepared from 4-alkoxyalkenylstannanes, since the alkoxy group is important in controlling the stereoselectivity of the oxidation using osmium tetraoxide as well as the reaction of the allylstannane with the aldehyde. However, another route to 2,5-*cis*-substituted tetrahydrofurans has been developed which is applicable to products prepared from 5-alkoxyalkenylstannanes. Epoxidation of the *anti*-alkenol **35** ($R^1$ = Bn, $R^2$ = H, R′ = Pr$^i$) using $VO(acac)_2$ and Bu$^t$OOH gave the *syn* epoxide **119** (Scheme 23). Treatment of this with diphenyldiselenide and sodium borohydride in ethanol gave a mixture of the dihydroxyselenides **120** and **121** corresponding to nonregioselective opening of the epoxide ring by sodium phenylselenide.[37] This mixture was not separated; rather it was treated with perchloric acid which gave the tetrahydrofuran **123** *via* the selenonium ion **122**. Reduction using tributyltin hydride gave the tetrahydrofuran **124**.[38]

Functionalised aldehydes were used in syntheses of dihydropyrans.[39,40] The tin(IV) chloride-promoted reaction of the 4-alkoxypent-2-enylstannane **31** (R = SEM) with toluene-*p*-sulfonyloxyacetaldehyde gave the 1,5-*syn* adduct **125** (Scheme 24). Treatment of this with anhydrous potassium carbonate gave the *syn* epoxide **126** which, on deprotection with trifluoroacetic acid, was converted into the 2,6-*cis*-disubstituted dihydropyran **127** containing *ca*. 20% of its 2,6-*trans* epimer. Conversely, the *anti* epoxide **129** was available *via* treatment of the 1,5-*syn* product **128**, prepared from stannane **31** (R = SEM) and benzoyloxyacetaldehyde, with mesyl chloride and triethylamine followed by saponification and cyclisation using potassium carbonate. Deprotection of this epoxide gave the 2,6-*trans*-disubstituted dihydropyran **130** containing *ca*. 20% of its 2,6-*cis* epimer.[39,40]

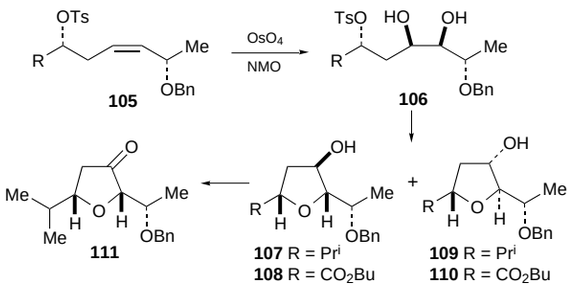
## Remote asymmetric induction using other allylmetal reagents

Although allylstannanes are useful in synthesis, there is often a problem in removing unwanted tin-containing residues from the products and so it was of interest to see whether the intermediate allyltin trihalides, important for remote induction, could be generated stereoselectively from starting materials other than allylstannanes.

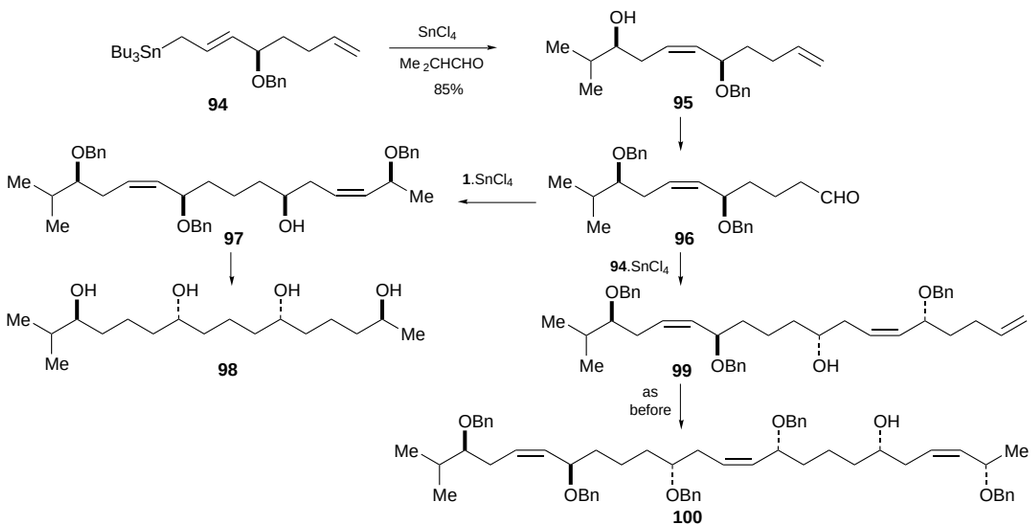
Stannous fluoride promotes reactions between 3-iodopropene and aldehydes, perhaps by formation of allyltin trihalides which




**Scheme 19**

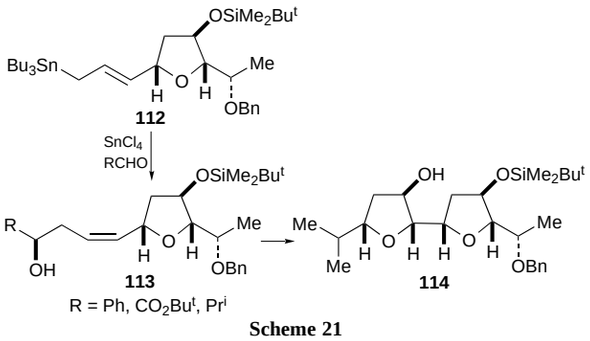



**Scheme 20**

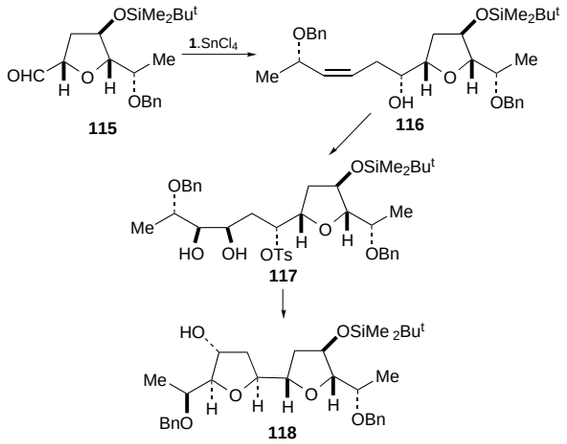



**Scheme 18**

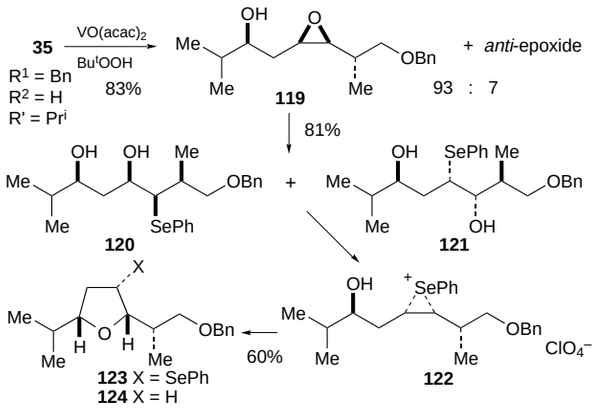
then react with the aldehyde.[41] However, treatment of either the allylic iodide or bromide **131** (X = I, Br) with stannous fluoride, chloride or triflate in the presence of benzaldehyde gave low yields of mixtures of products containing mainly the branched alkenols **132**.[42] The use of metallic tin with the iodide was similarly unsuccessful. However, some success was attained with allylsilanes. The (*Z*)- and (*E*)-pent-2-enylsilanes **134** and **135** were prepared from the aldehyde **133** (Scheme 25). Treatment of the (*Z*)-isomer **134** with tin(IV) chloride at −78 °C for 1–2 h generated an intermediate, perhaps the allyltin trihalide **33** (X = Cl, $R^1$ = Bn, $R^2$ = H), which reacted with benzaldehyde to give the 1,5-*anti* and 1,5- *syn* products **35** (R′ = Ph, $R^1$ = Bn, $R^2$ = H) and **136** (R′ = Ph), ratio 85 : 15. The (*E*)-allylsilane **135** similarly gave the 1,5-*anti* and 1,5-*syn* products **35** (R′ = Ph, $Pr^i$, Et, $R^1$ = Bn, $R^2$ = H) and **136** (R′ = Ph, $Pr^i$, Et), but with slightly reduced selectivity (1,5-*anti* : 1,5-*syn* = *ca*. 75 : 25).[43] Attempts to improve the 1,5-induction of allylsilanes to the levels observed with allylstannanes have not yet proved successful.



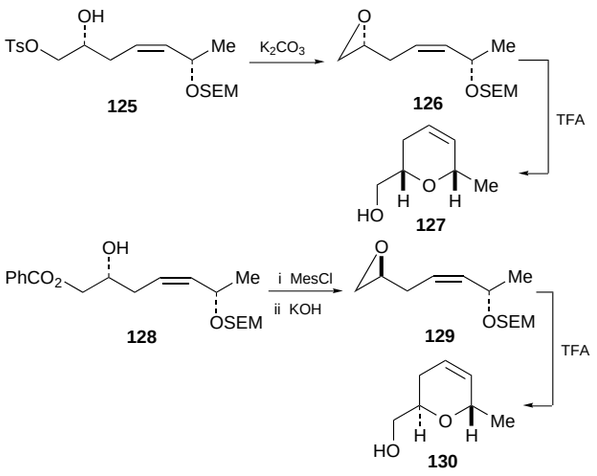

**Scheme 21**



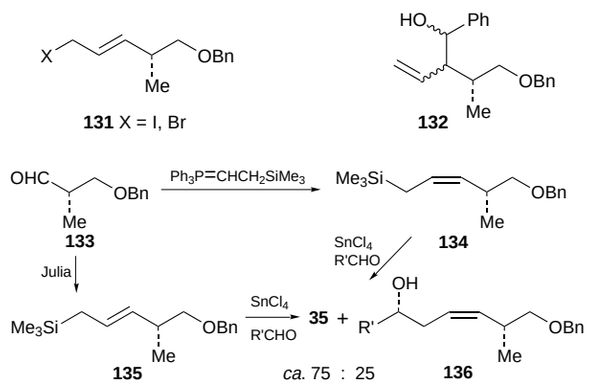

**Scheme 22**




**Scheme 23**




**Scheme 24**

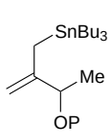



**Scheme 25**

## Summary and conclusions

The work outlined in this article shows that 4-, 5- and 6-substituted alkenylstannanes, after transmetallation with tin(IV) halides, react with aldehydes and imines with useful levels of 1,5-, 1,6- and 1,7-asymmetric induction.

Recently, a complementary approach to remote induction using allylstannanes has been introduced based on the chemistry of 2-(substituted-alkyl)propenylstannanes. For example, stereodivergent approaches to 1,4-asymmetric induction were developed based on the chemistry of 2-(1-substituted ethyl)propenylstannanes **137** (P = Me, Ac) and related compounds.[44–47] Advances in this area are expected.





## Acknowledgements

I should like to thank all my collaborators who have been involved in this work, including G. W. Bradley, C. T. Brain, J. S. Carey, T. S. Coulter, E. K. Dorling, M. Gruttadauria, D. J. Hallett, L. A. Hobson, V. J. Jephcote, R. Maguire, A. H. McNeill, S. V. Mortlock, A. J. Pratt, S. Stanway, A. Teerawutgulrag and A. I. Townsend. We acknowledge financial support from the EPSRC, the EPSRC-DTI LINK Asymmetric Synthesis Programme, the EU Human Capital and Mobility Programme, Rhone Poulenc Rorer, SmithKline Beecham, Glaxo-Wellcome and Zeneca.

## Footnote

† A 3.4 M solution of sodium bis(2-methoxyethoxy)aluminium hydride in toluene.

**E. J. Thomas studied at Cambridge University, carrying out research for his PhD under the supervision of Dr I. Fleming. He spent two years in the Dyson Perrins Laboratory, Oxford, as a post-doctoral research assistant working under the supervision of Dr G. H. Whitham, then moved to King's College, London as a University Lecturer in Organic Chemistry. After six years he returned to Oxford as a University Lecturer and Fellow of Exeter College. In 1988 he was appointed Professor of Organic Chemistry at the University of Manchester. His research interests are concerned with synthetic organic chemistry including both synthetic methodology and the synthesis of complex natural products. He was awarded a Hickinbottom Fellowship by the RSC in 1982, a Pfizer Academic Award in 1986 and was an RSC Tilden Lecturer in 1995/96.**

## References


1 S. V. Mortlock and E. J. Thomas, *Tetrahedron Lett*., 1988, **29**, 2479.
2 A. H. McNeil and E. J. Thomas, *Tetrahedron Lett*., 1990, **31**, 6239.
3 Y. Nishigaichi, A. Takuwa, Y. Naruta and K. Maruyama, *Tetrahedron*, 1993, **49**, 7395; Y. Yamamoto and N. Shida, *Adv. in Detailed Reaction Mechanisms*, 1994, **3**, 1.
4 E. J. Thomas, in *Houben Weyl*, *Methods of Organic Chemistry*, ed. G. Helmchen, R. W. Hoffmann, J. Mulzer and E. Schaumann, Thieme, 1995, vol. E21b, p. 1508.
5 C. Servens and M. Pereyre, *J. Organomet. Chem*., 1972, **35**, C20.
6 C. Hull, S. V. Mortlock and E. J. Thomas, *Tetrahedron Lett*., 1987, 5343; C. Hull, S. V. Mortlock and E. J. Thomas, *Tetrahedeon*, 1989, **45**, 1007.
7 A. J. Pratt and E. J. Thomas, *J. Chem. Soc. Chem. Commun*., 1982, 1115; A. J. Pratt and E. J. Thomas, *J. Chem. Soc., Perkin Trans 1*, 1989, 1521.
8 V. J. Jephcote, A. J. Pratt and E. J. Thomas, *J. Chem. Soc. Chem. Commun*., 1984, 800; V. J. Jephcote, A. J. Pratt and E. J. Thomas, *J. Chem. Soc., Perkin Trans 1*, 1989, 1529.
9 Y. Yamamoto, H. Yatagai, Y. Ishihara, N. Maeda and K. Maruyama, *Tetrahedron*, 1984, **40**, 2239.
10 G. E. Keck, S. M. Dougherty and K. A. Savin, *J. Am. Chem. Soc*., 1995, **117**, 6210.
11 S. E. Denmark and E. J. Weber, *J. Am. Chem. Soc*., 1984, **106**, 7970.
12 G. E. Keck, D. E. Abbott, E. P. Boden and E. J. Enholm, *Tetrahedron Lett*., 1984, **25**, 3927; S. E. Denmark, T. Wilson and T. M. Willson, *J. Am. Chem. Soc*., 1988, **110**, 984; S. E. Denmark, E. J. Weber, T. M. Wilson and T. M. Willson, *Tetrahedron*, 1989, **45**, 1053; G. E. Keck, M. B. Andrus and S. Castellino, *J. Am. Chem. Soc*., 1989, **111**, 8136; Y. Naruta, Y. Nishigaichi and K. Maruyama, *Tetrahedron*, 1989, **45**, 1067; A. Gambaro, A. Boaretto, D. Marton and G. Tagliavini, *J. Organomet. Chem*., 1984, **260**, 255; H. Miyake and K. Yamamura, *Chem. Lett*., 1992, 1369; A. Gambaro, P. Ganis, D. Marton, V. Peruzzo and G. Tagliavini, *J. Organomet. Chem*., 1982, **231**, 307; A. Boaretto, D. Marton, G. Tagliavini and P. Ganis, *J. Organomet. Chem*., 1987, **321**, 199; A. Boaretto, D. Marton, G. Tagliavini and A. Gambaro, *Inorg. Chim. Acta*, 1983, **77**, L196.
13 H. Miyake and K. Yamamura, *Chem. Lett*., 1993, 1473.
14 A. H. McNeill and E. J. Thomas, *Synthesis*, 1994, 322; E. J. Thomas, *Chemtracts: Org. Chem*., 1994, 207.
15 G. W. Bradley, D. J. Hallet and E. J. Thomas, *Tetrahedron: Asymmetry*, 1995, **6**, 2579.
16 K. Mikami and M. Shimizu, *Adv. Detailed Reaction Mechanisms*, 1994, **3**, 45.
17 J. S. Carey and E. J. Thomas, *Synlett*, 1992, 585.
18 J. S. Carey, T. S. Coulter and E. J. Thomas, *Tetrahedron Lett*., 1993, **34**, 3933.
19 A. Teerawutgulrag and E. J. Thomas, *J. Chem. Soc., Perkin Trans. 1*, 1993, 2863.
20 L. A. Hobson and E. J. Thomas, unpublished observations.
21 J. S. Carey and E. J. Thomas, *Tetrahedron Lett*., 1993, **34**, 3935.
22 S. J. Stanway and E. J. Thomas, *Tetrahedron Lett*., 1995, **36**, 3417.
23 J. S. Carey and E. J. Thomas, *J. Chem. Soc., Chem. Commun.*, 1994, 283.
24 S. J. Stanway and E. J. Thomas, *J. Chem. Soc., Chem. Commun*., 1994, 285.
25 S. J. Stanway and E. J. Thomas, *Synlett*., 1995, 214.
26 T. S. Coulter, A. Teerawutgulrag and E. J. Thomas, unpublished observations.
27 E. K. Dorling and E. J. Thomas, unpublished observations.
28 G. E. Keck and E. J. Enholm, *J. Org. Chem*., 1985, **50**, 146; Y. Yamamoto, T. Komatsu and K. Maruyama, *J. Org. Chem*., 1985, **50**, 3115.
29 D. J. Hallett and E. J. Thomas, *J. Chem. Soc., Chem. Commun*., 1995, 657.
30 Y. Yamamoto, S. Nishii, K. Maruyama, T. Komatsu and W. Ito, *J. Am. Chem. Soc*., 1986, **108**, 7778.
31 D. J. Hallett and E. J. Thomas, *Tetrahedron: Asymmetry*, 1995, **6**, 2575.
32 J. A. Marshall, *Chemtracts: Org. Chem*., 1992, **5**, 75; J. A. Marshall and W. Y. Gung, *Tetrahedron*, 1989, **45**, 1043; B. W. Gung, A. J. Peat, B. M. Snook and D. T. Smith, *Tetrahedron Lett*., 1991, **32**, 453; B. W. Gung, *Tetrahedron Lett*., 1991, **32**, 2867.
33 A. H. McNeill and E. J. Thomas, *Tetrahedron Lett*., 1992, **33**, 1369.
34 A. H. McNeill and E. J. Thomas, *Tetrahedron Lett*., 1993, **34**, 1669.
35 E. D. Mihelich, K. Daniels and D. J. Eickhoff, *J. Am. Chem. Soc*., 1981, **103**, 7690.
36 G. W. Bradley and E. J. Thomas, unpublished observations.
37 E. D. Mihelich, *J. Am. Chem. Soc*., 1990, **112**, 8995.
38 M. Gruttadauria and E. J. Thomas, unpublished observations.
39 R. J. Maguire and E. J. Thomas, *J. Chem. Soc., Perkin Trans. 1*, 1995, 2477.
40 R. J. Maguire and E. J. Thomas, *J. Chem. Soc., Perkin Trans. 1*, 1995, 2487.
41 T. Mukaiyama, T. Harada and S-i. Shoda, *Chem. Lett*., 1980, 1507; T. Mukaiyama and T. Harada, *Chem. Lett*., 1981, 1527; J. Nokami, J. Otera, T. Sudo and R. Okawara, *Organometallics*, 1983, **2**, 191.
42 T. S. Coulter and E. J. Thomas, unpublished observations.
43 C. T. Brain and E. J. Thomas, unpublished observations.
44 Y. Nishigaichi, H. Kuramoto and A. Takuwa, *Tetrahedron Lett*., 1995, **36**, 3353.
45 M. Gruttadauria and E. J. Thomas, *J. Chem. Soc., Perkin Trans. 1*, 1995, 1469.
46 Y. Nishigaichi and A. Kakuwa, presented at the VIIIth International Conference on the Organometallic Chemistry of Germanium, Tin, and Lead, Sendai, Japan, 17–21 September 1995.
47 R. J. Maguire, J. Mulzer and J. W. Bats, *J. Org. Chem.*, 1996, **61**, 6936.


*6/03881F*

# Selective catalytic oxidation of benzyl alcohols to benzaldehydes with a dinuclear manganese(IV) complex

**Charon Zondervan,[a] Ronald Hage[b] and Ben L. Feringa*[a]†**

[a] *Department of Organic and Molecular Inorganic Chemistry, Groningen Centre for Catalysis and Synthesis, University of Groningen, Nijenborgh 4, 9747 AG Groningen, The Netherlands*
[b] *Unilever Research Laboratory Vlaardingen, PO Box 114, 3130 AC Vlaardingen, The Netherlands*

**A dinuclear manganese(IV) catalyst is capable of oxidising benzylic alcohols to benzaldehydes with very high turnovers numbers (up to 1000) and high selectivities (above 99%).**

A key reaction in synthetic organic chemistry is the transformation of alcohols to aldehydes. Many procedures have been developed over the years, most notably the Oppenhauer and Swern oxidations and reactions utilising high valent metal compounds such as $MnO_2$, ammonium perruthenates and pyridinium chlorochromate.[1] However, almost all require stoichiometric amounts of metal compounds and sometimes co-oxidants, with concomitant environmental problems. Only a few examples are known in which metal complexes are used in a catalytic fashion. Benzaldehydes are obtained from benzyl alcohols with $RuCl_2(PPh_3)_3$[2] and $ZrO(OAc)_2$ using PhIO or *tert*-butyl hydroperoxide as oxidants,[3] and similar results were obtained with $SeO_2$–bis(4-anisyl) selenoxide.[4] A valuable alternative is the $[NBu_4][RuO_4]$–*N*-methylmorpholine oxide system.[5] These procedures typically require 1–10 mol% of catalyst and 100–300 mol% oxidant. Herein we report a novel method for the efficient and highly selective oxidation of benzylic alcohols to benzaldehydes using an active dinuclear manganese(IV) complex as catalyst and hydrogen peroxide or *tert*-butyl hydroperoxide as oxidant.

The excellent bleaching and epoxidation properties of **1** in water[6a] and acetone[6b,c] were recently reported. This complex consists of two manganese(IV) ions held together by three oxo ligands, with both metals bound to an *N*,*N*′,*N*″-trimethyl-1,4,7-triazacyclononane ligand.[7] The intriguing coordination chemistry of this ligand and its analogues has been reviewed.[8]

Initial results of the benzylic oxidation by using 0.6 μM **1**, 5 mM $H_2O_2$ and 0.6 mM benzyl alcohol in acetone in air were quite promising as highly selective aldehyde formation was observed, although the catalytic activity was modest (280 turnovers; entry 1, Table 1). Due to the efficient catalase activity of **1** under these conditions, we anticipated that excess of oxidant is required, but in attempting to increase the turnover number by using a very large excess hydrogen peroxide we only observed formation of benzoic acid (entry 2).‡ This could be overcome by adding 2000 equiv. of oxidant over a 10 h period, which cleanly gave 380 turnovers to benzaldehyde (entry 3). The mononuclear $Mn^{III}$ complex **2** gives a somewhat higher conversion with benzyl alcohol, but the bis(μ-acetato)(μ-oxo) complex **3** was virtually unreactive (entries 4 and 5). Complexes such as **3** are most probably dead ends in the catalytic cycle when, starting with **1** or **2**, traces of benzoic acid are formed during the oxidation reaction. Indeed, addition of a few equivalents of benzoic acid with respect to **1** completely inhibits any turnover on benzylic alcohols when the reaction is carried out under nitrogen atmosphere (entry 6). Exposure to air eventually leads to full conversion to benzoic acid. For practical synthetic applications further improvements with complete conversion to benzaldehydes were highly desirable.

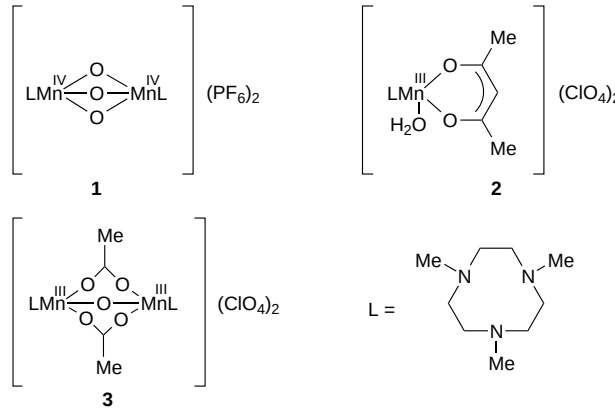



**Table 1** Effects of changing various parameters on the reactivity of benzyl alcohol

| Entry | Catalyst and oxidant[a] | Variation | Turnover[b] | *t*/min | Selectivity[c] |
|---|---|---|---|---|---|
| 1 | **1** + $H_2O_2$ | | 280 | 100 | > 99 |
| 2 | **1** + $H_2O_2$ (80 000 equiv.) | | 1000 | 60 | > 99[d] |
| 3 | **1** | [e] | 380 | 600 | > 99 |
| 4 | **2**[f] + $H_2O_2$ | | 660 | 100 | > 99 |
| 5 | **3**[g] + $H_2O_2$ | | 16 | 60 | > 99 |
| 6 | **1** + $H_2O_2$ | BnOH (2 equiv.) added | 0 | — | — |
| 7 | **1** + $Bu^tO_2H$ | | 0 | — | — |
| 8 | **1** + $Bu^tO_2H$ | Pretreatment with $H_2O_2$ | 480 | 150 | > 99 |
| 9 | **1** + $H_2O_2$ | Pretreatment with $H_2O_2$ | 360 | 150 | > 99 |
| 10 | $H_2O_2$ | No catalyst added | 0 | — | — |

[a] In all cases 1000 equiv. alcohol and 8000 equiv. oxidant were used in acetone in air; the reaction was followed by GC and terminated when conversion ceased to give benzaldehydes as product (the selectivity on aldehyde in all cases was above 99%). [b] Turnover number in mol aldehyde per mol **1**. [c] Selectivity in mol aldehyde per mol converted substrate. [d] Benzoic acid was the only product. [e] 2000 equiv. $H_2O_2$ in acetone were added over a 10 h period. [f] Ref. 9. [g] Ref. 7*b*.

**Table 2** Reactivity of substituted benzyl alcohols using two different procedures

| | | Method A | | Method B | |
|---|---|---|---|---|---|
| Entry | Substrate[a] | Turnover[b] | *t*/min | Turnover[b] | *t*/min |
| 1 | Benzyl alcohol | 360 | 60 | 480 | 150 |
| 2 | 4-Methoxybenzyl alcohol | 710 | 45 | 1000 | 45 |
| 3 | 3,4-Dimethoxybenzyl alcohol | 300 | 60 | 1000 | 20 |
| 4 | 4-(Dimethylamino)benzyl alcohol | — | | 1000 | 20 |
| 5 | 4-Chlorobenzyl alcohol | 700 | 45 | 1000 | 25 |
| 6 | 2-Chlorobenzyl alcohol | 490 | 45 | 1000 | 40 |
| 7 | 2,6-Dichlorobenzyl alcohol | 80 | 90 | — | |
| 8 | 4-Nitrobenzyl alcohol | 530 | 15 | 1000 | 45 |
| 9 | 3-Nitrobenzyl alcohol | 580 | 20 | 1000 | 25 |
| 10 | 2-Nitrobenzyl alcohol | 240 | 15 | 1000 | 35 |
| 11 | 4-Trifluoromethylbenzyl alcohol | 340 | 210 | 600 | 50 |
| 12 | Octan-2-ol | 360 | 100 | 360 | 90 |

[a] In all cases 1000 equiv. alcohol were used in acetone under inert atmosphere; the reaction was followed by GC and terminated when conversion ceased to give benzaldehydes as product (the selectivity on aldehyde in all cases was above 99%). [b] Turnover number in mol aldehyde per mol **1**.

To our surprise we found that the activity is significantly increased by employing a modified procedure. First the catalyst is mixed with 3000 equiv. of hydrogen peroxide in acetone for 30 min during which all hydrogen peroxide is decomposed (probably *via* catalase activity of **1**).§ Addition of an aliquot of substrate and hydrogen peroxide (1000 and 8000 equiv., respectively) to the thus pretreated catalyst leads to quantitative formation of benzoic acid, but under an inert atmosphere to selective formation of benzaldehyde (360 turnovers, entry 9). For substituted benzyl alcohols generally 400–700 turnovers to the corresponding benzaldehydes are found with over 99% selectivity with or without inert atmosphere conditions (Table 2, method A).

Although compound **1** with *tert*-butyl hydroperoxide (TBHP) is not active in the benzylic oxidation (Table 1, entry 7), the use of TBHP as oxidant in the second step, *i.e*. after pretreating **1** with hydrogen peroxide for 30 min, was found to have a highly beneficial influence on both turnover number and reaction rate (Table 1, entry 8). Nearly all substituted benzylic alcohols were fully converted to the corresponding benzaldehydes with excellent selectivities within an hour at room temperature using 0.1 mol% of catalyst **1** (Table 2, method B).¶

From the results with method A, we see a small but distinct steric effect as *ortho*-substituted substrates react more sluggishly than either *meta*- or *para*-substituted benzyl alcohols. In fact 2,6-disubstituted substrates are largely unreactive (entry 7). Substrates with electron-donating properties, *e.g*. (di)methoxy and dimethylamine benzyl alcohol (entries 2, 3 and 4), also appear to react faster under the conditions of method A than those with electron-withdrawing substituents such as nitro and trifluoromethyl groups (entries 8 and 11). The latter one even failed to give full conversion under the conditions of method B. As expected, secondary alcohols are selectively converted to ketones although the outcome is indifferent towards the procedure used. A typical example is given in entry 12.

In conclusion, we have demonstrated that manganese complex **1** is an excellent catalyst or catalyst precursor in novel procedures employing either $H_2O_2$ or TBHP as oxidant for the highly selective and very fast conversion of substituted benzyl alcohols to benzaldehydes. Further studies to elucidate the role of the pretreatment procedure and the exact nature of the catalytic species are in progress.

## Footnotes

† E-mail: feringa@chem.rug.nl

‡ A control experiment showed that **1** is capable of oxidising benzaldehyde to benzoic acid in air. In 90 min, 125 turnovers were found in acetone, whereas a blank reaction, *i.e*. without **1**, gave no reaction at all. 3-Nitrobenzaldehyde is not oxidised by **1** in air, or by **1** and $H_2O_2$ under turnover conditions.

§ From the 16 line spectrum obtained from EPR measurements at 77 K we inferred that **1** is reduced to a dinuclear $Mn^{III}$–$Mn^{IV}$ mixed valent species instantaneously when mixed with excess hydrogen peroxide in acetone, although we do not know if this reaction goes to full completion.[6a] Within 20 min the spectrum gradually changes to ultimately give a 6 line spectrum, indicative of $Mn^{II}$ species.

¶ A general experimental procedure is as follows: 1.0 ml of a 0.6 mM stock solution of crystallised **1** in acetone and 0.5 ml of hydrogen peroxide (30 wt%) are mixed for 30 min at room temperature under a nitrogen atmosphere. Simultaneously 0.6 mmol substrate and 0.5 ml hydrogen peroxide (30 wt%) (method A) or 0.6 mmol substrate and 0.5 ml of aqueous *tert*-butyl hydroperoxide (70 wt%) (method B) are added and the reaction is followed by GC until the maximum conversion is reached (usually within 1 h).

## References

1 *Organic Synthesis by Oxidation with Metal Compounds*, ed. W. J. Mijs and C. R. H. I. De Jonge, Plenum, New York, 1986; E. J. Corey and J. W. Suggs, *Tetrahedron Lett*., 1975, 2647; J. March, *Advanced Organic Chemistry*, Wiley, New York, 1992, 4th edn., p. 1167.
2 P. Müller and J. Godoy, *Tetrahedron Lett*., 1981, **22**, 2361; S. Kanemoto, K. Oshima, S. Matsubara, K. Takai and H. Nozaki, *Tetrahedron Lett*., 1983, **24**, 2185.
3 K. Kaneda, Y. Kawanishi and S. Teranishi, *Chem. Lett*., 1984, 1481.
4 F. Ogura, T. Otsubo, K. Ariyoshi and H. Yamagushi, *Chem. Lett*., 1983, 1833.
5 W. P. Griffith, S. V. Ley, G. P. Whitcombe and A. D. White, *J. Chem. Soc., Chem. Commun*., 1987, 1625.
6 (*a*) R. Hage, J. E. Iburg, J. Kerschner, J. H. Koek, E. L. M. Lempers, R. J. Martens, U. S. Racherla, S. W. Russell, T. Swarthoff, M. R. P. Van Vliet, J. B. Warnaar, L. Van der Wolf and B. Krijnen, *Nature*, 1994, **369**, 637; (*b*) D. De Vos and T. J. Bein, *Chem. Commun*., 1996, 917; (*c*) D. De Vos, J. L. Meinershagen and T. Bein, *Angew. Chem., Int. Ed. Engl*., 1996, **35**, 2211.
7 (*a*) K. Wieghardt, U. Bossek, B. Nuber, J. Weiss, J. Bonvoisin, M. Corbella, S. E. Vitols and J. J. Girerd, *J. Am. Chem. Soc*., 1988, **110**, 7398; (*b*) J. H. Koek, S. W. Russell, L. Van der Wolf, R. Hage, J. B. Warnaar, A. L. Spek, J. Kerschner and J. DelPizzo, *J. Chem. Soc., Dalton Trans*., 1996, 353.
8 P. Chauduri and K. Wieghardt, *Prog. Inorg. Chem*., 1987, **35**, 329.
9 K. Wieghardt, K. Pohl, U. Bossek, B. Nuber and J. Weiss, *Z. Naturforsch*., 1988, **43b**, 1184.

*Received, 18th November 1996; Com. 6/07779J*

# Efficient preparation of a linear, symmetrical, metal–metal bonded tricobalt compound; should we believe there is a bond stretch isomer?

**F. Albert Cotton, Lee M. Daniels and Glenn T. Jordan IV**

*Department of Chemistry and Laboratory for Molecular Structure and Bonding, Texas A&M University, College Station, TX 77843, USA*

**The synthesis in 42% yield of a linear, symmetrical, fully Co–Co bonded [2.3178(9) Å] trinuclear complex $[Co_3(dpa)_4Cl_2]$ [Hdpa = bis(2-pyridyl)amine] is reported, and its crystal structure presented.**

While the preparation, characterization and theoretical study of compounds containing strong, short metal–metal (M–M) bonds has become a major field of inorganic chemistry,[1] the study of compounds with linear chains of three or more bonded metal atoms is still in an embryonic state. The first such compound, which contained the $[Ru_3Cl_{12}]^{4-}$ ion, was first reported[2] in 1980 and the phosphine derivatives of this ion were extensively studied[3] in 1989–1991. Only very recently have other M–M bonded linear trinuclear species been reported.[4–7]

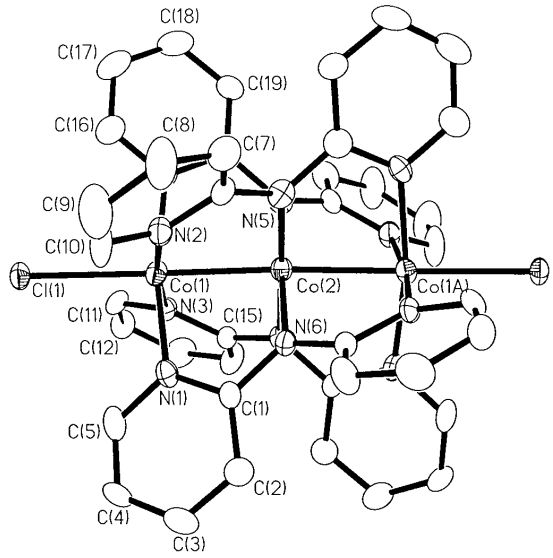



**Fig. 1** A side view of the $[Co_3(dpa)_4Cl_2]$ molecule. Selected bond lengths (Å) and angles (°): Co(1)–Co(2) 2.3178(9), Co(1)–Cl(1) 2.520(2), Co(1)–N(av) 1.991, Co(2)–N(av) 1.903; Co(1)–Co(2)–Co(1A) 177.0(1), Cl(1)–Co(1)–Co(2) 178.44(8).

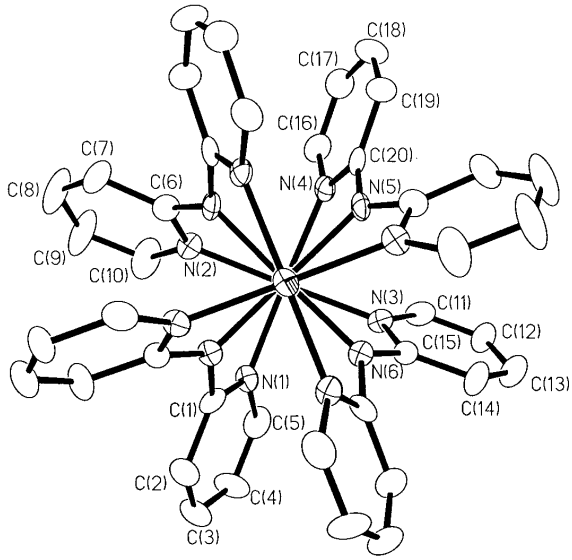



**Fig. 2** A view of the $Co_3(dpa)_4$ portion of the molecule looking down the $Co_3$ axis

One such compound[4] is $[Co_3(dpa)_4Cl_2]$ [Hdpa = bis(2-pyridyl)amine]. The yield quoted was only 2–5% and there were other features (*vide infra*) of the product that caused us concern. Therefore, we decided to look into this matter, beginning with the development of a synthetic method that gives a decent yield.

Our preparative procedure† which has been repeated many times, gives yields on the order of 40%. We have determined the crystal structure‡ of our product, which has the formula $[Co_3(dpa)_4Cl_2]\cdot CH_2Cl_2$, and find it to be significantly different from that previously reported[4] for $[Co_3(dpa)_4Cl_2]\cdot 2CH_2Cl_2\cdot H_2O$. Not only do we find a different space group (*Pnn*2), which is, however, the same space group in which Cu, Ru, and Rh analogues[5,6] crystallize, but we find a rigorously symmetrical molecule as was the case in all other $[M_3(dpa)_4Cl_2]$ compounds.[5–7] Our structure of $[Co_3(dpa)_4Cl_2]$ is shown in Figs. 1 and 2. The Co–Co distances are identical at 2.3178(9) Å as contrasted with values of 2.290(3) and 2.472(3) Å reported for the molecule described in ref. 4.

It is noteworthy that we find $[Co_3(dpa)_4Cl_2]\cdot CH_2Cl_2$ to be crystallographically isomorphous and molecularly isostructural with its symmetric rhodium analogue[5] for which Rh–Rh distances of 2.3920(5) Å were reported. The relationship between the M–M distances in these two isostructural compounds, 2.318 and 2.392 Å for the Co and Rh compounds, respectively, is very similar to that in the $[M_2\{PhNC(Ph)NPh\}_4]$ compounds,[8] where the Co–Co and Rh–Rh distances are, respectively, 2.302(1) and 2.389(1) Å.

One more important observation we made is that the UV–VIS and IR spectra of our compound are the same as those mentioned in ref. 4.

One way to resolve the discrepancy between our structure and that in ref. 4 is to postulate that they are 'bond stretch' isomers, which of course, become identical, one way or the other, in solution. Since all prior claims to this sort of isomerism have turned out to be erroneous (and the whole idea is not credible, anyway) we reject this possibility. There seems no other explanation except to propose that the previously reported structure is in error, although with reported residuals of $R = 0.049$ and $R_w = 0.039$, it is not, *prima facie*, obvious how. We look forward to a full report on the work described two and a half years ago in ref. 4.

## Footnotes

† Bis(2-pyridyl)amine (Hdpa, 0.480 g, 2.80 mmol) was placed in a 100 ml round-bottomed flask and dissolved in 16 ml of thf. The solution was cooled to −78 °C, and then 2.0 ml of 1.4 M LiMe was added. The solution immediately turned milky white, but quickly became a clear pale yellow solution upon warming. Anhydrous $CoCl_2$ (0.275 g, 2.12 mmol) was then

added to the reaction from a solid addition tube. The resulting brown solution was refluxed for 5.5 h, and then stirred overnight. After filtration of the mixture, a dark red powder was collected and washed several times with small portions of thf. The powder was dissolved in $CH_2Cl_2$ and layered with hexanes to yield a large crop of dark green crystals. Additional product was obtained from work-up of the filtrate. The solvent was removed from the filtrate under vacuum, leaving behind a dark residue. The residue was dissolved in 10 ml of $CH_2Cl_2$, filtered to remove LiCl, and layered with hexanes. Crystals from both solutions were collected, washed with hexanes, and dried under vacuum (0.300 g, 0.296 mmol, 42.3% yield). UV–VIS ($CH_2Cl_2$): 323, 390(sh), 568 nm.

‡ *Crystal data* for $[Co_3(dpa)_4Cl_2]\cdot CH_2Cl_2$ (−105 °C): orthorhombic, space group *Pnn*2, $a$ = 12.8145(9), $b$ = 13.955(1), $c$ = 11.1660(9) Å, $U$ = 1996.8(3) Å$^3$, $D_c$ = 1.685 g cm$^{-3}$, $Z$ = 2; CAD4 diffractometer with graphite-monochromated Mo-Kα radiation; ψ-scan absorption correction was made; 1449 unique reflections ($2\theta < 45°$) were measured. Full-matrix least-squares refinement on $F^2$ of positional and anisotropic thermal parameters for all non-hydrogen atoms (287 variables) converged to $R$ = 0.047 and $wR_2$ = 0.084 (all data) with the largest peak in difference map = 0.48(7) e Å$^{-3}$. The absolute configuration was confirmed by the Flack method.[9] Atomic coordinates, bond lengths and angles, and thermal parameters have been deposited at the Cambridge Crystallographic Data Centre (CCDC). See Information for Authors, Issue No. 1. Any request to the CCDC for this material should quote the full literature citation and the reference number 182/355.

## References


1 F. A. Cotton and R. A. Walton, *Multiple Bonds Between Metal Atoms*, 2nd edn., Oxford University Press, Oxford, 1993.
2 A. Bino and F. A. Cotton, *J. Am. Chem. Soc*., 1980, **102**, 608.
3 F. A. Cotton, M. Matusz and R. C. Torralba, *Inorg. Chem*., 1989, **28**, 1516; F. A. Cotton and R. C. Torralba, *Inorg. Chem*., 1991, **30**, 3293; 4386.
4 E. C. Yang, M. C. Cheng, M. S. Tsai and S. M. Peng, *J. Chem. Soc., Chem. Commun*., 1994, 2377.
5 J. T. Sheu, C. C. Liu, I. Chao, C. C. Wang and S. M. Peng, *Chem. Commun*., 1996, 315.
6 L. P. Wu, P. Field, T. Morrissey, C. Murphy. P. Nagle, B. Hathaway, C. Simmons and P. Thornton, *J. Chem. Soc., Dalton Trans*., 1990, 3835; G. J. Pyrka, M. El-Mekki and A. A. Pinkerton, *J. Chem. Soc., Chem. Commun*., 1991, 84.
4 S. Aduldecha and B. Hathaway, *J. Chem. Soc., Dalton Trans*. 1991, 993.
8 L. P. He, C. L. Yao, M. Naris, J. C. Lee, J. D. Korp and J. L. Bear, *Inorg. Chem*., 1992, **31**, 620.
9 H. D. Flack, *Acta Crystallogr., Sect. A*, 1983, **39**, 876; G. Bernardinelli and H. D. Flack, *Acta Crystallogr., Sect. A*, 1985, **41**, 500.



*Received, 18th December 1996; Com. 6/08482F*

# Energy *vs.* electron transfer processes involving a novel cobalt cage complex

**Christian Königstein,*[a,b,c]† Albert W. H. Mau,*[a]‡ Peter Osvath,*[a,b]§ and Alan M. Sargeson*[b]¶**

[a] *Division of Chemicals and Polymers, CSIRO, Clayton, Victoria 3169, Australia*
[b] *Research School of Chemistry, The Australian National University, Canberra ACT 0200, Australia*
[c] *Institute of Physical Chemistry, Vienna University of Technology, Getreidemarkt 9/156, A-1060 Wien, Austria*

**A novel cage complex, $[Co(Me_2\text{-}N_3S_3absar)]^{3+}$, able to undergo fast and efficient electron transfer reactions, is examined as an electron transfer agent in photocatalytic systems aimed at generating $H_2$; its electrochemical behaviour and excited state quenching properties are described.**

The ability to capture energy and transfer it *via* redox reactions is a key issue in the photochemical conversion of solar energy. Artificial systems have used the viologens,[1,2] polypyridinium complexes,[3] or cobalt cage complexes[4–6] as electron transfer agents. The high chemical stability of the cobalt cages allows the $Co^{II}$–$Co^{III}$ redox states to be cycled repeatedly without decomposition. Systems using $[Co(sep)]^{3+}$, $[Co(sar)]^{3+}$ (Fig. 1) and their derivatives as electron relay compounds gave comparable rates of $H_2$ formation[4–6] to those using methyl viologen ($MV^{2+}$). Although their overall efficiency of conversion of light to hydrogen ($\phi_{\pm}H_2$) was only *ca.* 10%, their turnover numbers were at least three orders of magnitude higher than those of the viologens, and there is potential for improvement.

The rate of photoinduced $H_2$ formation is controlled by the generation of an excited state S* of the sensitiser (1), and three distinct electron transfer processes [eqns. (2), (3), (3a)].

$$S + h\nu \rightarrow S^* \quad (1)$$

$$S^* + Co^{III} \rightarrow S^+ + Co^{II} \quad (2)$$

$$Co^{II} + H^+ \xrightarrow{Pt/pva} 1/2H_2 + Co^{III} \quad (3)$$

$$Co^{II} + S^+ \rightarrow S + Co^{III} \quad (3a)$$

Step (3) is essentially quantitative in the presence of the colloidal Pt/pva catalyst.[4] The rate constants of the electron transfer processes are governed by the respective reduction potentials and the electron self-exchange rate constants of the reaction partners. As the driving force for eqn. (2) is reduced (*i.e.* the reduction potential of the cobalt complex becomes more negative), energy transfer from the excited state competes with electron transfer. On the other hand, a more negative reduction potential is desirable for $H_2$ evolution [eqn. (3)]. These conflicting demands need to be optimised.

The electron transfer rates of the $CoN_6$ cages are lower than that of $MV^{2+}$, because of their lower self-exchange rates ($k_{11}$ *ca.* 1–5 $M^{-1}\ s^{-1}$),[7] and this is a limiting factor in their use. The $CoN_3S_3$ cages however, have much higher self-exchange rate constants ($k_{11}$ *ca.* $10^4\ M^{-1}\ s^{-1}$),[8,9] but their cobalt(II) complexes are weaker reductants than the $CoN_6$ cages (by *ca.* 350 mV) so $H_2$ production is modest at pH ⩽ 5.[4,10] Synthetic efforts were therefore directed to the preparation of $CoN_3S_3$ cages with contracted cavities,[10] as these should have a more negative reduction potential. Recent efforts to prepare $[Co(Me_2\text{-}N_3S_3sar)]^{3+}$ led to a novel and efficient method of synthesising the contracted cavity cage $[Co(Me_2\text{-}N_3S_3absar)]^{3+}$ ($[CoL]^{3+}$, Fig. 1), in which a methylene unit is missing from the cap.[11] The smaller cavity, and the inductive effect of the apical methyl group lowered the reduction potential by *ca.* 200 mV compared with other $CoN_3S_3$ cages[10] ($E$ = −0.20 V *vs.* NHE, reversible one-electron process).‖ The cobalt(II) complex should reduce protons in the presence of a colloidal platinum catalyst (at pH ⩽ 3), and together with the high electron self-exchange rate ($k_{11} = 1.3 \times 10^4\ M^{-1}\ s^{-1}$),[9] this made it a promising candidate for use as an electron transfer agent for light-induced $H_2$ formation.

Excited-state quenching reactions were studied with both $[Ru(bpy)_3]^{2+}$ and anthracene carboxylate ($AA^-$) as sensitisers. Earlier results with $MV^{2+}$ had shown that $AA^-$ had a much higher cage escape yield ($\phi_{ce}$ = 1) than $[Ru(bpy)_3]^{2+}$ ($\phi_{ce}$ = 0.25).[12] The rate constants for energy and electron transfer involving the excited singlet and triplet states of $AA^-$ with $[CoL]^{3+}$ are shown in Fig. 2. Both the excited $^1AA^-$ and $^3AA^-$ states were quenched by $[CoL]^{3+}$ at pH = 7, but linear Stern–Volmer plots (indicating dynamic quenching) were obtained only for the $^3AA^-$ quenching ($[CoL]^{3+} \leqslant 5 \times 10^{-3}$ M).** The non-linear Stern–Volmer plots obtained for $^1AA^-$ quenching imply some initial ground-state complex formation. This was also concluded from $k_q = 2 \times 10^{11}\ M^{-1}\ s^{-1}$ (obtained for low quencher concentrations where a degree of linearity was observed in the Stern–Volmer plots), which is higher than diffusion limited rate constants (*ca.* $10^{10}\ M^{-1}\ s^{-1}$). Both excited states are capable of reducing $[CoL]^{3+}$ [Fig. 2, $E°(^1AA^{\bullet}\text{–}AA^-)$ = −2.2 V *vs.* NHE, $E°(^3AA^{\bullet}\text{–}AA^-)$ = −0.88 V].[12] However, with an energy of 2.67 eV for the $^1A_1 \rightarrow {}^1T_1$ transition of $[CoL]^{3+}$, energy transfer from $^1AA^-$ to $Co^{III}$ is also possible.

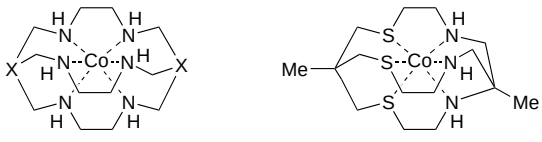



**Fig. 1** Cobalt cage complexes

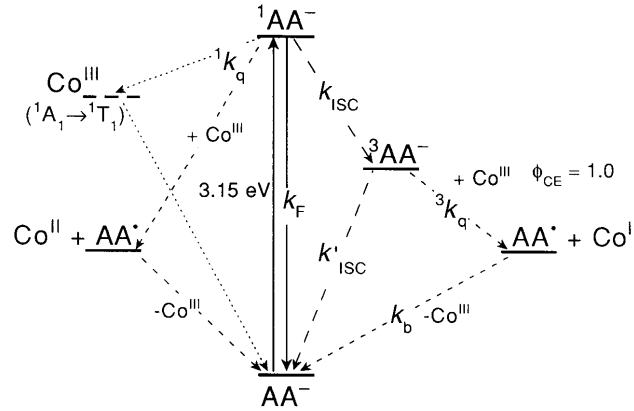



**Fig. 2** Energy and electron transfer processes between $AA^-$ and $[CoL]^{3+}$. Radiative transitions (———), non-radiative transitions (— — —), electron transfer processes (- - - - - -), energy transfer processes (·····). $^{III}Co$ = $[CoL]^{3+}$; $Co^{II}$ = $[CoL]^{2+}$.

$^3AA^-$ quenching to yield $[CoL]^{2+}$ occurs exclusively *via* excited-state electron transfer (efficiency *ca.* 100%, $k_q = 3 \times 10^9$ м$^{-1}$ s$^{-1}$). The very high cage escape yield and the enhanced intensity of the $^1A_1 \rightarrow {}^1T_1$ transition of $[CoL]^{3+}$ ($\lambda_{max}$ = 460 nm, $\varepsilon$ = 640 м$^{-1}$ cm$^{-1}$) allowed us to measure for the first time the bleaching†† of the ground-state absorption of a cobalt(III) cage complex due to electron transfer (Fig. 3). The cage escape yield was determined to be close to unity, and interestingly, the rate constant for the back electron transfer ($k_b = 7 \times 10^8$ м$^{-1}$ s$^{-1}$, Fig. 2) was smaller than that obtained with $MV^{2+}$ ($k_b = 2.7 \times 10^9$ м$^{-1}$ s$^{-1}$).[12] Thus, the overall quantum yield for the light-induced charge separation giving $[CoL]^{2+}$ and AA· is very high. Assuming a quencher concentration of $5 \times 10^{-4}$ м, 13% of the excited singlet state is deactivated *via* electron/energy transfer to $[CoL]^{3+}$, 6% is reemitted as fluorescence, and the yield of triplet formation is 81%. If only the triplet state participates effectively in the electron transfer to $[CoL]^{3+}$, 80% of the initially absorbed photons lead to the charge-separated state ($[CoL]^{2+}$ + AA·). Steady-state photolysis experiments with $H_4$edta as a sacrificial electron donor confirmed the quantum yield of $\eta$ = 0.8 for the formation of $[CoL]^{2+}$. The main contribution to the electron transfer and charge separation is from the $^3AA^-$ state, whereas energy transfer predominates over electron transfer from $^1AA^-$, which is also the case for $MV^{2+}$.[12] Comparing the excitation energy (3.15 eV) with the energy of the products (1.13 eV) after charge separation, 36% of the excitation energy is stored (Fig. 2).

$[CoL]^{3+}$ excited-state electron transfer with $[Ru(bpy)_3]^{2+}$ as photosensitiser ($k_q = 8.9 \times 10^8$ м$^{-1}$ s$^{-1}$) has a comparable quenching rate constant to $MV^{2+}$ ($k_q = 9.6 \times 10^8$ м$^{-1}$ s$^{-1}$),[4] but is higher than those for $Co^{III}N_6$ cages with similar reduction potentials ($[Co(Cl_2\text{-sar})]^{3+}$: $k_q = 2.2 \times 10^8$ м$^{-1}$ s$^{-1}$, $[Co(sep)]^{3+}$: $k_q = 1.4 \times 10^8$ м$^{-1}$ s$^{-1}$),[4] as expected on the basis of the higher self-exchange rates of the $CoN_3S_3$ cages.[8,9]

Unfortunately, the back-electron transfer rate constant and the yield of electron transfer and charge separation could not be measured because of the overlap of the $[CoL]^{3+}$ and $[Ru(bpy)_3]^{2+}$ absorptions at *ca.* 460 nm.

$[CoL]^{3+}$ was able to mediate the photoinduced $H_2$ formation at pH 5 (standard conditions with $MV^{2+}$) with $[Ru(bpy)_3]^{2+}$ as photosensitiser‡‡ ($\eta$ = 0.004) despite the relatively positive potential compared with that of $MV^{2+}$–$MV^{\cdot+}$ ($\eta$ = 0.1; $E°$ = −0.44 V). A similar complex with a potential of *ca.* −0.4 V should give very efficient conversion, and this is now being sought.

Although $AA^-$ does not possess an absorption band in the visible region of the spectrum, as long as energy transfer processes to the $^3AA^-$ state take place, its favourable high cage escape yield can be utilised. Energy transfer from the $^3$MLCT state of $[Ru(bpy)_3]^{2+}$ to $AA^-$ gives the $^3AA^-$ state in very high yield.[13] More efficient storage of solar energy could thus be achieved using a series of molecules designed with the appropriate properties to optimise the efficiency of each step in the system. Antenna molecules which absorb a large part of the solar spectrum[14] can be used to transfer light energy efficiently to anthracene. An assembly consisting of an antenna molecule, anthracene and a stable $CoN_3S_3$ cage of the type described here has the potential for efficient conversion of light energy to chemical energy.

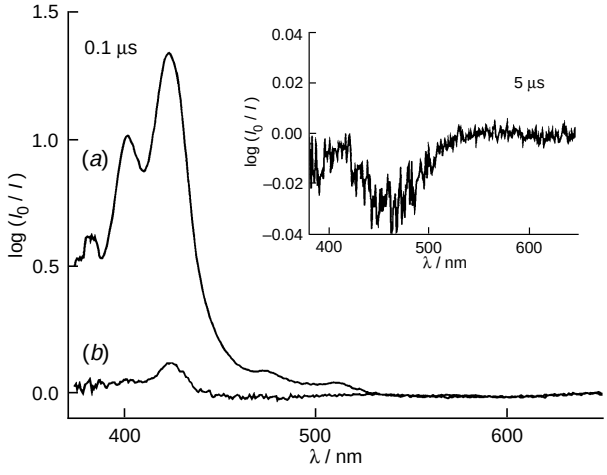



**Fig. 3** Transient absorption spectra. (*a*) $AA^-$ ($5 \times 10^{-4}$ м) in water; 100 ns after laser pulse ($XeF_2$ excimer, 50 mJ pulse$^{-1}$). (*b*) $AA^-$ ($5 \times 10^{-4}$ м) + $[CoL]^{2+}$ ($3.33 \times 10^{-3}$ м); 100 ns after laser pulse. Insert: as (*b*) but 5 μs after laser pulse.

C. K. thanks the 'Fonds zur Förderung der Wissenschaftlichen Forschung' (Project J0951-CHE) for financing his stay both at the ANU and at the CSIRO, Australia.

## Footnotes

† E-mail: ckoenigs@fbch.tuwien.ac.at
‡ E-mail: a.mau@chem.csiro.au
§ E-mail: p.osvath@chem.csiro.au
¶ E-mail: sargeson@rsc.anu.edu.au

‖ Cyclic voltammetry was performed in 1.0 м KCl (purged with $N_2$) using an EG & G Princeton Applied Research model 174 A polarographic analyser and a model 175 universal programmer, a platinum flag counter electrode, a Ag/AgCl reference electrode, and either a hanging mercury drop electrode (EG&G PAR model 303) or a F-doped $SnO_2$ covered glass sheet (TCO-glass, electrode area 1.5 cm$^2$) as working electrode. The concentration of $[CoL]^{3+}$ was $4 \times 10^{-3}$ м.

** Stern–Volmer plots of excited singlet state quenching were obtained using fluorescence emission, measured with a Perkin Elmer LS 50 luminescence spectrometer. The kinetics of quenching of $^3AA^-$ and $^3$MLCT of $[Ru(bpy)_3]^{2+}$ were investigated by measuring the lifetime of the triplet–triplet absorption of anthracene at 425 nm, using a 150 W xenon lamp (analysing light), a Bausch & Lomb high-intensity monochromator (1350 grooves mm$^{-1}$), and an AMI 9658b photomultiplier. Transient absorption spectra were obtained using an EG & G Princeton Applied Research Model 1460 optical multichannel analyser. As excitation light ($\lambda_{ex}$ = 351 nm), a Lambda Physik LPX 100 excimer laser was used ($XeF_2$).

†† $[CoL]^{2+}$ has a much weaker absorption at 465 nm ($\varepsilon$ = 100 м$^{-1}$ cm$^{-1}$) and a weak band at 550 nm ($\varepsilon$ = 80 м$^{-1}$ cm$^{-1}$).

‡‡ Buffered solutions (pH 5) containing $3.75 \times 10^{-4}$ м $[Ru(bpy)_3](ClO_4)_2$, $2 \times 10^{-3}$ м electron transfer agent ($MV^{2+}$ or $[CoL]^{3+}$), $5 \times 10^{-5}$ м colloidal platinum catalyst (stabilised by polyvinyl alcohol), and $2 \times 10^{-2}$ м $H_4$edta, were irradiated using a 150 W tungsten lamp. The amount of $H_2$ evolved was measured by GC as described in ref. 4.

## References

1 C. Königstein, *J. Photochem. Photobiol. A: Chem.*, 1995, **90**, 141.
2 S. Hühnig and H. Berneth, *Top. Curr. Chem.*, 1980, **92**, 1.
3 K. Kalyanasundaram, *Coord. Chem. Rev.*, 1982, **46**, 159.
4 I. I. Creaser, L. R. Gahan, R. J. Geue, A. Launikonis, P. A. Lay, J. D. Lydon, M. G. McCarthy, A. W. H. Mau, A. M. Sargeson and W. H. F. Sasse, *Inorg. Chem.*, 1985, **24**, 2671.
5 V. Houlding, T. Geiger, V. Kölle and M. Grätzel, *J. Chem. Soc., Chem. Commun.*, 1982, 681.
6 M. A. R. Scandola, F. Scandola, A. Indelli and V. Balzani, *Inorg. Chim. Acta*, 1983, **76**, L67.
7 I. I. Creaser, A. M. Sargeson and A. W. Zanella, *Inorg. Chem.*, 1983, **22**, 4022.
8 P. Osvath, A. M. Sargeson, B. W. Skelton and A. H. White, *J. Chem. Soc., Chem. Commun.*, 1991, 1036.
9 P. Osvath, A. M. Sargeson and A. W. Zanella, 1996, unpublished results.
10 P. A. Lay, J. Lydon, A. W.-H. Mau, P. Osvath, A. M. Sargeson and W. H. F. Sasse, *Aust. J. Chem.*, 1993, **46**, 641.
11 P. Osvath, A. M. Sargeson, A. MacAuley, R. E. Mendelez, S. Subramanian, M. J. Zaworotko and L. M. Broge, to be submitted.
12 O. Johansen, A. W. H. Mau and W. H. F. Sasse, *Chem. Phys. Lett.*, 1983, **94**, 107.
13 O. Johansen, A. W. H. Mau and W. H. F. Sasse, *Chem. Phys. Lett.*, 1983, **94**, 113.
14 A. W. H. Mau, O. Johansen and W. H. F. Sasse, *Photochem. Photobiol.*, 1985, **41**, 503.

*Received, 4th December 1996; Com. 6/08199A*

# Synthesis and catalytic properties of large-pore Sn-β and Al-free Sn-β molecular sieves

**N. K. Mal and A. V. Ramaswamy***

*National Chemical Laboratory, Pune-411 008, India*

**Sn-β and Al-free Sn-β (large pore, 12-membered ring channels) molecular sieves prepared by hydrothermal synthesis and characterised by XRD, FTIR and sorption techniques are distinguished by their acidic and oxidation properties, in the acetylation of 1,3,5-trimethylbenzene (1,3,5-TMB) with acetyl chloride and in the oxidation of *m*-cresol and 1,3,5-TMB with aqueous $H_2O_2$, respectively.**

Following the synthesis of medium-pore (10-membered ring) TS-1[1] and its use in shape-selective oxidation reactions on a commercial scale in the hydroxylation of phenol,[2] many attempts have been made to synthesize large pore (12 MR), three-dimensional Al-free Ti-β, without much success, unless trivalent metal ions of $Al^{3+}$ were present in the lattice.[3–6] Recently, Camblor *et al.*[7] reported the synthesis of Al-free Ti-β using seed crystals, and this material has been used effectively for the epoxidation of alkenes and for oxidation of relatively bulkier organic substrates.[8] We earlier reported the synthesis of medium-pore Sn-sil-1 (MFI structure), which was found to be less active than TS-1 in the hydroxylation of phenol[9] but more active than TS-1 in the oxidation of ethylbenzene[10] under similar conditions. In this report, for the first time, we describe the synthesis of large-pore, Sn-β and Al-free Sn-β molecular sieves, their characterization by XRD, FTIR and sorption techniques and catalytic activity in the hydroxylation of phenol, oxidation of *m*-cresol and 1,3,5-TMB in presence of aqueous $H_2O_2$ and acetylation of 1,3,5-TMB with acetyl chloride (AcCl).

The hydrothermal synthesis of Sn-β was carried out using gels with the following molar composition: 1.0 $SiO_2$ : 0.0–0.0125 $SnO_2$ : 0.0–0.03 $Al_2O_3$ : 0.52–0.70 TEAOH : 20 $H_2O$. In a typical preparation, 0.71 g of $SnCl_4 \cdot 5H_2O$ (98%, Loba Chem) in 10 g of $H_2O$ was added to 41.7 g of tetraethylorthosilicate (TEOS) (99.9%, Aldrich). After 15 min, 58.9 g of tetraethylammonium hydroxide (TEAOH) (35 mass% aqueous solution, Aldrich) was added under vigorous stirring for 1 h. To this reaction mixture 0.63 g of $Al_2(SO_4)_3 \cdot 16H_2O$ in 15 g $H_2O$ was added and stirred for another 1 h. 8.7 g of $H_2O$ was then added to the clear solution and stirred for 2 h. The resultant clear solution was charged into a stainless-steel autoclave and heated at 415 K under autogenous pressure and static conditions for 10 days to complete the crystallization. The resultant product was filtered, washed with deionized water, dried at 383 K and calcined at 823 K for 16 h. This sample is referred to as A. One more such Sn-β sample was prepared with different Al and Sn contents (Si/Al = 30.0 in gel and 14.7 in crystalline product and Si/Sn = 200 in gel and 150 in crystalline product). Dealuminated Sn-β (sample B) was prepared by refluxing 4 g of sample A with 60 ml of 5 M HCl for 3 h at 383 K. This treatment was repeated once more after filtration. This sample was filtered and washed thoroughly with distilled water until free of all acid and finally dried and calcined at 723 K for 12 h. Sample C was prepared following a similar procedure that was used for the synthesis of sample A, except that 0.5 g of B was added in place of 0.63 g of $Al_2(SO_4)_3 \cdot 16H_2O$. Two β zeolite samples (without Sn) were also prepared with different $SiO_2/Al_2O_3$ ratios (30.0 and 250). Al-free β (or silicalite) was prepared by the dealumination of zeolite-β of $SiO_2/Al_2O_3$ molar ratio of 250.

The XRD profiles of all as-synthesized and calcined samples match well with the BEA topology. No peaks due to $SnO_2$ or crystalline impurity phases are seen. The crystallinity of as-synthesized β is maximum, and this sample was considered to be the reference sample. Sn-β (A), Al-free Sn-β (C), dealuminated Sn-β (B) and dealuminated β (silicalite) are relatively less crystalline (approximately 96, 87, 67 and 55%, respectively) with respect to the reference sample. The SEM micrographs show that the particle size of all the samples is $< 0.3$ μm. The framework IR spectra of Sn samples (in Nujol mull) show a peak at *ca.* 957 $cm^{-1}$ (Fig. 1). This band which is intense in the case of Al-free Sn-β (C), is not observed in Sn-free β-zeolites. This band has been assigned to Si–O–M vibrations or Si–O(H) defect groups promoted by framework M from the possible substitution of heteroatom (M) in the Si–O–Si units.[9,10] $N_2$ adsorption isotherms at 77 K of Sn-β samples are characteristic of microporous materials. The surface areas are typically in the region of 650 $m^2\ g^{-1}$ for all the samples (Table 1). The mesopore (*t*-area) contribution is rather small in the case of Sn-β and Al-free Sn-β samples (35.6 and 57.0 $m^2\ g^{-1}$, respectively) but significant in the dealuminated β samples (120–160 $m^2\ g^{-1}$). The micropore volumes are in the range 0.20–0.25 ml $g^{-1}$ for all samples. The amounts of $H_2O$, *n*-hexane, cyclohexane and *m*-xylene adsorbed on these samples at 298 K and at $p/p_o$ of 0.5 (gravimetric, Cahn electrobalance) are included in Table 1. The comparable sorption capacity of Sn-containing and Sn-free β samples indicates that the micropore volumes are well maintained and that occluded $SnO_2$-type species may not be present in the Sn-containing samples.

The results on the catalytic activity of all the β samples are summarised in Table 2. The catalytic activity of the β, Sn-β and

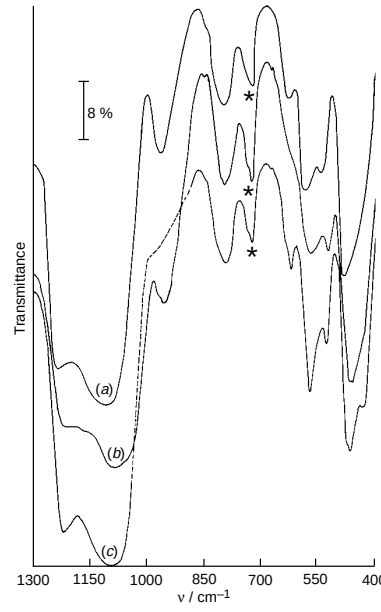



**Fig. 1** FTIR spectra of Al-free Sn-β sample (*a*), Sn-β sample with Si/Al = 28.5 and Si/Sn = 78.8 (*b*) and β sample with Si/Al = 50.3 (*c*). The absorption at 957 $cm^{-1}$ is similar to that observed for Ti-, V- and Sn-MFI and -MEL structures. * Nujol peak.

**Table 1** Physicochemical characteristics of Sn-β zeolites[a]

| Sample | In gel, molar ratio | | Products, molar ratio[a] | | Sorption capacity[b] (mass%) | | | | Surface area[c]/m$^2$ g$^{-1}$ | Micropore volume/ml g$^{-1}$ |
|---|---|---|---|---|---|---|---|---|---|---|
| | Si/Sn | Si/Al | Si/Sn | Si/Al | $H_2O$ | *n*-hexane | cyclohexane | *m*-xylene | | |
| Sn-β (A) | 100 | 100 | 78.8 | 28.5 | 26.7 | 19.3 | 21.2 | 25.0 | 670 | 0.25 |
| deAl-Sn-β (B) | — | — | 85.4 | > 3000 | 23.3 | 18.6 | 20.4 | 23.9 | 665 | 0.22 |
| Al-free Sn-β (C) | 100 | — | 54.5 | > 4000 | 25.6 | 19.4 | 21.3 | 25.4 | 677 | 0.25 |
| β | — | 125 | ∞ | 50.3 | 20.5 | 18.8 | 20.7 | 24.2 | 652 | 0.23 |
| deAl-β (silicalite) | — | — | — | > 3000 | 18.4 | 18.2 | 19.7 | 22.3 | 645 | 0.20 |

[a] Chemical analysis using EDX and ICP. [b] Gravimetric adsorption at $p/p_o$ = 0.5 and at 298 K (Cahn electrobalance). [c] $N_2$ adsorption isotherms (Coulter 100 CX analyser) at 77 K.

**Table 2** Reactions over Sn-containing β zeolites[a]

| Sample | Products, molar ratio | | Phenol hydroxylation[b] | | Oxidation of *m*-cresol[c] | | Oxidation of 1,3,5-TMB[d] | | | Acetylation of 1,3,5-TMB[e] | |
|---|---|---|---|---|---|---|---|---|---|---|---|
| | Si/Sn | Si/Al | TON | $H_2O_2$ efficiency | TON | $H_2O_2$ efficiency | TON | $H_2O_2$ efficiency | Selectivity[f] | AcCl conv.[g] | Selectivity[h] |
| Sn-β (A) | 78.8 | 28.5 | 30.3 | 33.0 | 6.6 | 20.3 | 1.0 | 4.2 | 50 | 32.5 | 96.5 |
| deAl-Sn-β (B) | 85.4 | > 4000 | 83.6 | 44.7 | 32.3 | 52.3 | 7.7 | 18.9 | 80 | — | — |
| Al-free Sn-β (C) | 54.5 | > 3000 | 80.1 | 65.0 | 30.6 | 75.4 | 6.6 | 24.5 | 77 | 6.4 | 99.1 |
| β | ∞ | 50.3 | 8.8 | 8.1 | 1.3 | 4.6 | 0.0 | 0.0 | 0.0 | 34.8 | 83.6 |
| Sn-β | 150 | 14.7 | — | — | — | — | — | — | — | 99.9 | 94.6 |
| β | ∞ | 13.9 | — | — | — | — | — | — | — | 99.9 | 82.0 |

[a] Catalyst/substrate = 10, 20, 20 mass% in the case of phenol, *m*-cresol and 1,3,5-TMB, respectively; substrate/$H_2O_2$ (mole) = 3.0; solvent/substrate (mole) = 20; reaction time = 15 h; TON is defined as the mole of substrate converted per mole of metal ion (Al + Sn). [b] Batch reactor; $T$ = 348 K; solvent = $H_2O$, $H_2O_2$ efficiency = mol% $H_2O_2$ consumed in the formation of parabenzoquinone, catechol and hydroquinone. [c] Parr autoclave; $T$ = 373 K; solvent = $H_2O$ : acetonitrile (2 : 1), $H_2O_2$ efficiency = mol% $H_2O_2$ consumed in the formation of 2,5-dihydroxytoluene, 3,4-dihydroxytoluene, 3-hydroxybenzyl alcohol and 3-hydroxybenzaldehyde. [d] Batch reactor; $T$ = 348 K; solvent = acetonitrile, $H_2O_2$ efficiency = mol% $H_2O_2$ consumed in the formation of 3,5-dimethylbenzyl alcohol, 3,5-dimethylbenzaldehyde and 2-hydroxy-1,3,5-TMB. [e] Down-flow, fixed-bed reactor; $T$ = 428 K; 1,3,5-TMB/acetyl chloride (AcCl) (mol) = 3.0, WHSV = 1.0 h$^{-1}$, analysis after 1 h run. [f] Product selectivity (mass%) for 3,5-dimethylbenzaldehyde. [g] Conversion (mass%) of acetyl chloride (AcCl). [h] Product selectivity for 2,4,6-trimethylacetophenone.

Al-free Sn-β samples can be rationalised in terms of activity due to acidic properties (depending on the Si/Al ratio) and oxidation properties (isolated $Sn^{4+}$ sites) or a combination of the two. All the Sn-containing samples are active in the hydroxylation of phenol, and oxidation of *m*-cresol and 1,3,5-TMB with aqueous $H_2O_2$ to different degrees. Both deAl-Sn-β (B) and Al-free Sn-β (C) samples show consistantly higher $H_2O_2$ efficiency in all the three test reactions, indicating the absence of acid sites (Si/Al > 3000). Al-free β (silicalite) shows negligible activity in the oxidation of *m*-cresol and 1,3,5-TMB (no active $Sn^{4+}$ ions) and in the acetylation of 1,3,5-TMB (no acidity). In the hydroxylation of phenol and oxidation of *m*-cresol and 1,3,5-TMB, the $H_2O_2$ efficiency over deAl-Sn-β (B) was lower than over Al-free Sn-β (C), while the TON is in the same order. The $H_2O_2$ efficiency in hydroxylation of phenol over Sn-containing β samples was less than that obtained with Sn-sil-1 (MFI structure).[9] This may be due to the more selective nature of the medium-pore Sn-sil-1 than the large pore Sn-containing β samples for relatively small molecules like phenol. In the oxidation of *m*-cresol, 75.4 mol% $H_2O_2$ efficiency could be achieved over Al-free Sn-β and 2-methylhydroquinone was detected as the major product. In the oxidation of *m*-cresol, both deAl-Sn-β (B) and Al-free Sn-β (C) show better $H_2O_2$ efficiency (18.9 and 24.5%, respectively) and TON (7.7 and 6.6, respectively) than Sn-β (A) ($H_2O_2$ efficiency = 4.2% and TON = 1.0). Sn-β (A) is not a good catalyst for the oxidation reaction. 3,5-Dimethylbenzaldehyde was detected as the major product in the oxidation of 1,3,5-TMB.

The β and Sn-β zeolites are active in the acetylation of 1,3,5-TMB with acetyl chloride. Under the conditions of the reaction, the conversion of acetyl chloride is related to the acidity (Si/Al ratio) of the sample. While both Sn-β (Si/Sn = 150 and Si/Al = 14.7) and β (Si/Al = 13.9) give a very high conversion (99.9%) of acetyl chloride, the selectivity for 2,4,5-trimethylacetophenone is higher on Sn-β (94.6%) than on β zeolite (82.0 mass%). The reason for the enhancement of selectivity over Sn-containing β zeolite is not clear at the moment. When the acetylation of 1,3,5-TMB was carried out in the absence of any catalyst (only porcelain beads were loaded in the reactor), the conversion of acetyl chloride was only 5.2%, which is slightly less than over Al-free Sn-β (C) sample (6.4%). This indicates that very weak acidity is associated with $Sn^{4+}$ ions in the zeolite structure.

In conclusion, a large-pore zeolite (BEA) with Sn in the framework has been synthesized for the first time, which is able to catalyse oxidation of bulkier organic substrates with aqueous $H_2O_2$ in the absence of acidity (Al-free state) and acetylation with acetyl chloride when acidic (low Si/Al ratio), with some selectivity advantages due to the presence of $Sn^{4+}$ ions.

Nawal Kishore is thankful to CSIR, New Delhi for a senior research fellowship.

## References

1 M. Taramasso, G. Perego and B. Notari, *US Pat.*, 4,410,501, 1983.
2 B. Notari, *Stud. Surf. Sci. Catal.*, 1987, **47**, 413.
3 R. B. Borade and A. Clearfield, *Microporous Mater.*, 1996, **5**, 289.
4 M. A. Camblor, M. Constantini, A. Corma, P. Esteve, L. Gilbert, A. Martinez and S. Valencia, *Appl. Catal. A: General*, 1995, **133**, L185.
5 M. A. Camblor, A. Corma, A. Martinez and J. Pèrez-Pariente, *Zeolites*, 1993, **13**, 82.
6 M. A. Camblor, A. Corma, A. Martinez and J. Pèrez-Pariente, *J. Chem. Soc., Chem. Commun.*, 1992, 589.
7 M. A. Camblor, M. Costantini, A. Corma, L. Gilbert, P. Esteve, A. Martinez and S. Valencia, *Chem. Commun.*, 1996, 1339.
8 A. Corma, M. A. Camblor, P. Esteve, A. Martinez and J. Pèrez-Pariente, *J. Catal.*, 1994, **145**, 151.
9 N. K. Mal, V. Ramaswamy, S. Ganapathy and A. V. Ramaswamy, *J. Chem. Soc., Chem. Commun.*, 1994, 1933.
10 N. K. Mal and A. V. Ramaswamy, *Appl. Catal. A: General*, 1996, **143**, 75.

*Received, 15th October 1996; Com. 6/07038H*

# Non-polymeric molybdenum(II) complexes of dicarboxylic acids: synthesis, structure and catalytic properties

**Elizabeth Whelan,[a] Michael Devereux,[a] Malachy McCann[b] and Vickie McKee[c]**

[a] *Dublin Institute of Technology, Cathal Brugha Street, Dublin, Ireland*
[b] *Chemistry Department, St. Patrick's College, Maynooth, Co. Kildare, Ireland*
[c] *School of Chemistry, Queen's University, Belfast, N. Ireland, UK BT9 5AG*

**$[Mo_2(MeCN)_8][BF_4]_4$ reacts with α,ω-dicarboxylic acids $[HO_2C(CH_2)_nCO_2H$, $n$ = 0–8] to form salts with empirical formula $[Mo_2\{O_2C(CH_2)_nCO_2\}(MeCN)_x][BF_4]_2$; the X-ray crystal structure of the butanedioic salt $[Mo_4\{\eta^2\text{-}\mu\text{-}O_2C(CH_2)_2CO_2\text{-}\mu\text{-}\eta^2\}_2(MeCN)_{12}][BF_4]_4\cdot 3MeCN$ is reported together with the use of the complexes as catalysts for the polymerization of norbornene.**

The $Mo^{II}Mo^{II}$ quadruply bonded neutral complex $[Mo_2(\mu\text{-}O_2CMe)_4]$ is known to react with dicarboxylic acids to give insoluble polymeric powders[1] which cannot be fully structurally characterized and which have limited subsequent chemical reactivity. Herein we detail the reactions of the tetracationic $Mo^{II}Mo^{II}$ salt $[Mo_2(MeCN)_8][BF_4]_4$[2] with α,ω-dicarboxylic acids $[HO_2C(CH_2)_nCO_2H$, $n$ = 0–8] to form red, soluble complex salts with empirical formula $[Mo_2\{O_2C(CH_2)_nCO_2\}(MeCN)_x][BF_4]_2$.‡ The tetranuclear butanedioic salt $[Mo_4\{\pi^2\text{-}\mu\text{-}O_2C(CH_2)_2CO_2\text{-}\mu\text{-}\eta^2\}_2(MeCN)_{12}][BF_4]_4\cdot 3MeCN$ **1** represents the first structurally characterized M–M quadruply bonded dicarboxylate complex (Fig. 1).§ The unit cell contains one centrosymmetric complex ion of formula $[Mo_4\{\eta^2\text{-}\mu\text{-}O_2C(CH_2)_2CO_2\text{-}\mu\text{-}\eta^2\}_2(MeCN)_{12}]^{4+}$ along with four $BF_4^-$ counter ions and three MeCN solvent molecules. The $Mo^{II}$ atoms are six-coordinate and their environments are very similar. They are linked by a short [2.1415(6) Å] quadruple bond and, *trans* to this, each has a long interaction with an axial MeCN molecule [Mo(1)–N(50) 2.712(5), Mo(2)–N(60) 2.674(5) Å]. The remaining donors, nitrogen atoms from two MeCN molecules (mean Mo–N 2.162 Å) and an oxygen atom from each of two carboxylate groups (mean Mo–O 2.084 Å) occupy a square plane with *cis* geometry. The two butanedioic dianions each have two bridging functions. First, each of the carboxylate groups bridges the Mo–Mo bond; secondly, each butanedioic ligand links the two halves of the tetranuclear complex together. The coordination environment about each of the quadruply bonded Mo–Mo cores is essentially identical to that of the structurally characterized, red dimolybdenum(II,II) monocarboxylate salt *cis*-$[Mo_2(\mu\text{-}O_2CMe)_2(MeCN)_6][BF_4]_2$.[3] The coordination of the dicarboxylate ligands in **1** is the same as in the tetranuclear ruthenium(I) pentanedioate complex $[Ru_4(CO)_8\{O_2C(CH_2)_3CO_2\}_2(PBu_3)_4]$[4] and the polymeric copper(II) butanedioate complex $\{[Cu_2\{O_2C(CH_2)_2CH_2)_2\}(H_2O)_2]\cdot 2H_2O\}_n$,[5] where again the individual bimetallic centres are spanned by two $^-O_2C(CH_2)_nCO_2^-$ ligands in a *cisoid* fashion.

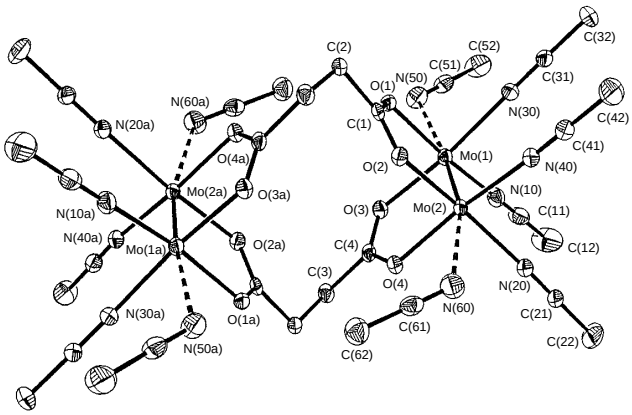



**Fig. 1** Crystal structure of **1**. Selected bond lengths (Å) and bond angles (°): Mo(1)–O(1) 2.091(3), Mo(1)–O(3) 2.088(3), Mo(2)–O(2) 2.080(3), Mo(2)–O(4) 2.077(3), Mo(1)–N(10) 2.162(4), Mo(1)–N(30) 2.172(4), Mo(1)–N(50) 2.712(5), Mo(2)–N(20) 2.163(4), Mo(2)–N(40) 2.152(4), Mo(2)–N(60) 2.674(5), Mo(1)—Mo(2) 2.145(6); O(3)–Mo(1)–O(1) 91.53(12), O(3)–Mo(1)–Mo(2) 91.21(9), O(1)–Mo(1)–Mo(2) 91.10(9), O(3)–Mo(1)–N(10) 88.66(14), O(1)–Mo(1)–N(10) 166.2(2), Mo(2)–Mo(1)–N(10) 102.72(13), O(3)–Mo(1)–N(30) 166.3(2), O(1)–Mo(1)–N(30) 89.18(14), Mo(2)–Mo(1)–N(30) 102.43(11), N(10)–Mo(1)–N(30) 87.4(2), O(3)–Mo(1)–N(50) 86.0(2), O(1)–Mo(1)–N(50) 84.01(13), Mo(2)–Mo(1)–N(50) 174.28(11), N(10)–Mo(1)–N(50) 82.2(2), N(30)–Mo(1)–N(50) 80.5(2), O(4)–Mo(2)–O(2) 90.64(12), O(4)–Mo(2)–Mo(1) 90.70(9), O(2)–Mo(2)–Mo(1) 90.80(9), O(4)–Mo(2)–N(40) 166.2, O(2)–Mo(2)–N(40) 86.00(14), Mo(1)–Mo(2)–N(40) 102.75(11), O(4)–Mo(2)–N(20) 90.11(14), O(2)–Mo(2)–N(20) 168.6(2), Mo(1)–Mo(2)–N(20) 100.52(12), N(40)–Mo(2)–N(20) 90.6(2), O(4)–Mo(2)–N(60) 76.1(2), O(2)–Mo(2)–N(60) 83.3(2), Mo(1)–Mo(2)–N(60) 165.43(11), N(40)–Mo(2)–N(60) 90.2(2), N(20)–Mo(2)–N(60) 85.9(2).

The IR spectrum of the solid (KBr matrix) contained prominent carboxylate $\nu_{asym}$(OCO) and $\nu_{sym}$(OCO) vibrations at 1536 and 1443 $cm^{-1}$, respectively, with the value of $\Delta\nu$(OCO) $\{\nu_{asym} - \nu_{sym} = 93\ cm^{-1}\}$ in keeping with that recorded for complexes in which the carboxylate ligand bridges short M–M bonds {*e.g.* $\Delta\nu$(OCO) = 85 $cm^{-1}$ for $[Mo_2(\mu\text{-}O_2CMe)_4]$}. The $[Mo_2\{O_2C(CH_2)_nCO_2\}(MeCN)_x][BF_4]_2$ complexes with $n$ = 3–8 had $\Delta\nu$(OCO) values in the region 74–99 $cm^{-1}$, suggesting that the dicarboxylate ligands in these species were also bridging bidentate. $\Delta\nu$(OCO) values for the ethanedioate ($n$ = 0) and propanedioate ($n$ = 1) complexes were significantly larger (251 and 155 $cm^{-1}$, respectively), implying a different coordination mode of the dicarboxylate OCO moieties. The shorter hydrocarbon chain linking the two carboxylate functions of the ethanedioate and propanedioate ligands probably imposes steric constraints which inhibit the formation of a discrete tetranuclear entity.

As with *cis*-$[Mo_2(\mu\text{-}O_2CMe)_2(MeCN)_6][BF_4]_2$ complex **1** is quite air-sensitive both in solution (acetonitrile) and in the solid state and therefore must be stored under $N_2$. However, the cyclic voltammogram of **1** in acetonitrile solution and under $N_2$ showed the complex to be electroinactive between the switching potentials of +2.0 to −2.0 V (*vs.* Ag/AgCl).¶

In the presence of $EtAlCl_2$ as a cocatalyst the molybdenum complexes ($n$ = 2–8) catalysed the room temperature ring-opening metathesis polymerization of norbornene (as a solution in chlorobenzene). The reactions were instantaneous, and GPC analysis of the products showed that they comprised mainly a mixture of high molecular mass polymer ($\bar{M}_w$ ranged from 125 000 to 691 000) and low molecular mass oligomers ($\bar{M}_w$ *ca.* 500). $^{13}C\{^1H\}$ NMR spectral analysis of the polymers[6] showed them to have a blocky distribution of *cis* and *trans* double bonds. The *cis* content ($\sigma_c$) of the polymers was in the narrow

range 0.34–0.44, indicating that the microstructure of the polynorbornene was essentially independent of the catalyst composition (*i.e.* the chain length of the dicarboxylate ligand).

E. W. thanks the Postgraduate Scholarship Fund (DIT) for financial assistance.

## Footnotes

† E-mail: MMCANN@MAY.IE

‡ Procedures conducted under $N_2$ using dry solvents. $[Mo_2(MeCN)_8][BF_4]_4$ (0.23 mmol), $HO_2C(CH_2)_nCO_2H$ (0.23 mmol) and MeCN (25 $cm^3$) gently heated for 1 h. The red solution was reduced *in vacuo* to low volume and small amounts of $CH_2Cl_2$ (or hexane) added periodically to slowly induce product precipitation.

§ *Crystal data* for **1**: $C_{38}H_{53}B_4F_{16}Mo_4N_{15}O_8$, red plate, crystal dimensions 0.68 × 0.30 × 0.18 mm, triclinic, space group $P\bar{1}$, $a$ = 9.842(1), $b$ = 10.744(1), $c$ = 16.792(2) Å, $\alpha$ = 92.35(1), $\beta$ = 92.77(1), $\gamma$ = 113.65(1)°, $U$ = 1621.1(3) $Å^3$, $\mu$ = 1.617 $mm^{-1}$, $Z$ = 1, $F(000)$ = 782. Data were collected at 153(2) K on a Siemens P4 four-circle diffractometer using graphite-monochromated Mo-K$\alpha$ radiation ($\lambda$ = 0.710 73 Å). Unit-cell parameters were determined by non-linear least-squares refinement of 37 accurately centred reflections ($10 < 2\theta < 25°$). Using 1.2° ω-scans at 6° $min^{-1}$, 6083 reflections were collected in the range $4 < 2\theta < 50°$, 5716 unique reflections ($R_{int}$ = 0.021) were used in the refinement. Crystal stability was monitored by recording three check reflections every 97 reflections and no significant variation was observed, although the crystal cracked towards the end of the data collection. The data were corrected for Lorentz and polarisation effects and a semi-empirical absorption correction was applied ($T_{max}$ = 1.000, $T_{min}$ = 0.838). The structure was solved by direct methods,[7] which revealed most of the structure and the remaining non-hydrogen atoms were located from difference Fourier maps. Hydrogen atoms were inserted at calculated positions (except for those on the partial occupancy acetonitrile) and assigned isotropic temperature factors tied to the equivalent isotropic $U$ of their carrier atoms. The non-hydrogen atoms were refined with anisotropic atomic displacement parameters. All the data were used for refinement on $F^2$ which converged with $wR2$ = 0.1319, GOF = 1.028 and the conventional $R$ = 0.0463 [$I > 2\sigma(I)$] for 404 parameters. 15 restraints were applied to the geometry and anisotropic displacement parameters of the partial occupancy solvent molecule. The final difference map showed no significant residual electron density, the largest peak (1.0 e $Å^{-3}$) being close to Mo(1). All programs used in the structure refinement are contained in the SHELXL-93 package.[8]

Atomic coordinates, bond lengths and angles, and thermal parameters have been deposited at the Cambridge Crystallographic Data Centre (CCDC). See Information for Authors, Issue No. 1. Any request to the CCDC for this material should quote the full literature citation and the reference nunmber 182/354.

¶ Cyclic voltammetry: glassy carbon disc and platinum wire as working and counter electrodes, respectively; Ag/AgCl as reference electrode; MeCN–$[NBu_4][ClO_4]$ as solvent–supporting electrolyte; $E_{\frac{1}{2}}$ = +0.49 V (*vs.* Ag/AgCl) for the ferrocene–ferrocenium couple.

## References

1 T. A. Stephenson, E. Bannister and G. Wilkinson, *J. Chem. Soc.*, 1964, 2538; R. J. Murenick, *J. Inorg. Nucl. Chem.*, 1976, **38**, 1275.
2 F. A. Cotton and K. J. Wiesinger, *Inorg. Chem.*, 1991, **30**, 871; *Inorg. Synth.*, 1992, **29**, 134.
3 F. A. Cotton, A. H. Reid, Jr. and W. Schwotzer, *Inorg. Chem.*, 1985, **24**, 3965; W. Clegg, G. Pimblett and C. D. Garner, *Polyhedron*, 1986, **5**, 31; G. Pimblett, C. D. Garner and W. Clegg, *J. Chem. Soc., Dalton Trans.*, 1986, 1257.
4 M. Bianchi, G. Menchi, F. Piacenti, A. Scrivanti and U. Matteoli, *J. Mol. Catal.*, 1989, **50**, 277.
5 B. H. O'Connor and E. N. Maslen, *Acta Crystallogr.*, 1966, **20**, 824.
6 K. J. Ivin, *Olefin Metathesis*, Academic Press, London, 1983, ch. 11.
7 G. M. Sheldrick, SHELXS-86, *Acta Crystallogr., Sect. A*, 1990, **46**, 467.
8 G. M. Sheldrick, SHELXL-93, University of Göttingen.

*Received, 6th November 1996; Com. 6/07560F*

# Hydride and proton transfer reactions in gaseous ion–molecule complexes [$PhCH_2^+$ $HOCH_2CH_2OH$]

**Henri E. Audier,*[a] Fadil Dahhani,[a] Arielle Milliet[a] and Dietmar Kuck*†[b]**

[a] *Département de Chimie, Laboratoire des Mécanismes Réactionnels, URA CNRS 1307, École Polytechnique, F-91128 Palaiseau, France*

[b] *Fakultät für Chemie, Universität Bielefeld, D-33501 Bielefeld, Germany and Fachbereich Chemie und Chemietechnik, Universität-GH Paderborn, D-33046 Paderborn, Germany*

**Benzyl cations and ethylene glycol react in the gas phase and form covalently bound adducts, as shown by slow and site-selective proton exchange, but also undergo irreversible hydride transfer giving two ion–neutral complexes, [$PhCH_3$ $HOCH_2CHOH^+$] and [$PhHCH_3^+$ $HOCH_2CHO$], which interconvert by a rapid and non-selective proton exchange.**

Ion–molecule reactions in the gas phase are often proceeded by hydride transfer from the neutral to the cationic partner of the encounter complex. For example, loss of methane and isobutane from protonated dimethyl ether[1] and protonated alkylbenzenes,[2–4] respectively, have been shown to occur by hydride abstraction within a complex between a cationic and a neutral fragment. In many cases, however, this process is inhibited by a variety of competing reactions; in particular, the cation may react as a proton donor (*i.e*. a Brønsted acid) rather than as a hydride acceptor (*i.e*. a Lewis acid).

A particularly interesting hydride-abstracting agent is the benzyl cation. In contrast to many alkyl cations, in particular *iso*-$C_3H_7^+$ and *tert*-$C_4H_9^+$, benzyl cations cannot react as a proton donor. Moreover, $PhCH_2^+$ is a 'soft' hydride abstractor owing to the relative weakness of the benzylic C–H bonds of toluene, and skeletal rearrangement would lead to an inert isomer, *viz*. the tropylium ion.

Here we present our preliminary results on the ion–molecule reactions between benzyl cations and ethylene glycol, a rare case in which the formation of isomeric covalent and complex-bound intermediates resulting from a hydride transfer reaction can be demonstrated. Benzyl cations were generated in the presence of ethylene glycol in the chemical ionization source of a double-focusing mass spectrometer using water as a reagent gas.‡ Adduct ions of elemental composition $C_9H_{13}O_2^+$ (charge-to-mass ratio *m/z* 153) were formed and then accelerated and separated from all other ions by a fixed, constant magnetic sector field. In general, ions thus selected have lifetimes of at least *ca*. 10–30 μs. A fraction of ions having internal energies slightly above the fragmentation threshold are 'metastable' and may decompose spontaneously within the field-free region following the magnetic sector. The fragmentation products of these metastable ions is determined by scanning the subsequent electrostatic sector field, and the MIKE spectrum[5]§ obtained provides information on the unimolecular reactions occurring during the lifetime of the (adduct) ions.

Metastable adduct ions (*m/z* 153) formed from $C_7H_7^+$ and ethylene glycol undergo essentially three competing reactions: (i) reformation of the reactants to give ions of *m/z* 91, (ii) hydride abstraction to give ions of *m/z* 61, and, as the major contribution, (iii) formation of ions of *m/z* 93, *i.e*. protonated toluene, by a formal double hydrogen transfer.[6,7]

Protonation of 2-benzyloxyethanol yields the same products with different relative contributions (given above in parentheses), an effect which is attributed to the differences in the internal energies of the adduct ions formed by the two alternative routes.[8] Water loss is only a minor process in both cases [9(2)%].

All of the three major reaction channels (i)–(iii) are subject to mass shifts if suitable deuterium labelled precursors are studied. The results of these experiments (Table 1) indicate that only the phenylic and hydroxy group hydrogen atoms undergo exchange whereas the benzylic methylene group participates neither in hydrogen exchange nor in hydrogen transfer steps (*cf*. entries 1 and 2). The metastable adduct ions $C_9H_{13}O_2^+$ form slowly interconverting covalently bound intermediates (**2** and **3**), and rapidly interconverting ion–molecule complexes (**4** and **5**), as illustrated in Scheme 1.

Only one adduct reaction (**1** → **4**) is irreversible. Introduction of methylene group labels in the glycol molecule (entry 3) leads to distinct mass shifts for channels (ii) and (iii) together with a decrease in their relative weight; at the same time, channel (i) does not undergo a mass shift but strongly gains importance. The data clearly show that the benzyl cation abstracts a hydride ion from one of the glycol methylene groups and that this is the rate-determining step of both channels (ii) and (iii). In agreement with this, labelling of the glycol hydroxy groups (entry 4) does not significantly affect the relative weights of the three channels; however, it reveals a proton exchange between the OH groups and the aromatic nucleus [*cf*. *m/z* 61–63 (ii), *m/z* 91–93 (i) and *m/z* 94–95 (iii)].

The existence of a rate-determining step allows us to distinguish two kinds of proton exchange processes. In particular, the formation of $C_7(H,D)_7^+$ is preceded by a slow exchange whereas the ions $C_2(H,D)_5O_2^+$ and $C_7(H,D)_9^+$ generated after hydride transfer are the subject of a relatively fast exchange. Moreover, the data from the (ring-[$^2H_3$])-labelled isotopomer (entry 5) demonstrates that the exchange preceding the re-formation of $C_7H_7^+$ involves only the hydroxy protons and those at the *ortho* positions of the benzene ring, as is evident from the exclusive formation of $C_7H_4D_3^+$ ions (*m/z* 94, instead of ions *m/z* 92–94). In contrast, the other two channels again show much more efficient H/D exchange, apparently involving all of the ring protons.¶ Finally, all the above-mentioned features, including the altered relative weights of the three reaction channels, are confirmed when perdeuteriated benzyl cations are used as precursors (entries 6 and 7); in particular, the slow $H^{OH}/H^{ortho}$ exchange occurring in channel (i) is corroborated by the formation of $C_7HD_6^+$ (*m/z* 97).

The site-specific proton exchange necessarily occurs *via* covalently bound species **2** and **3**.‖ The fact that neither the benzylic methylene nor the *meta* and *para* protons are involved

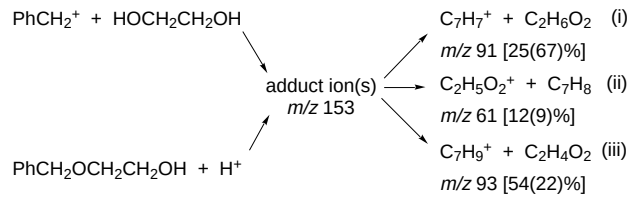
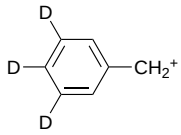
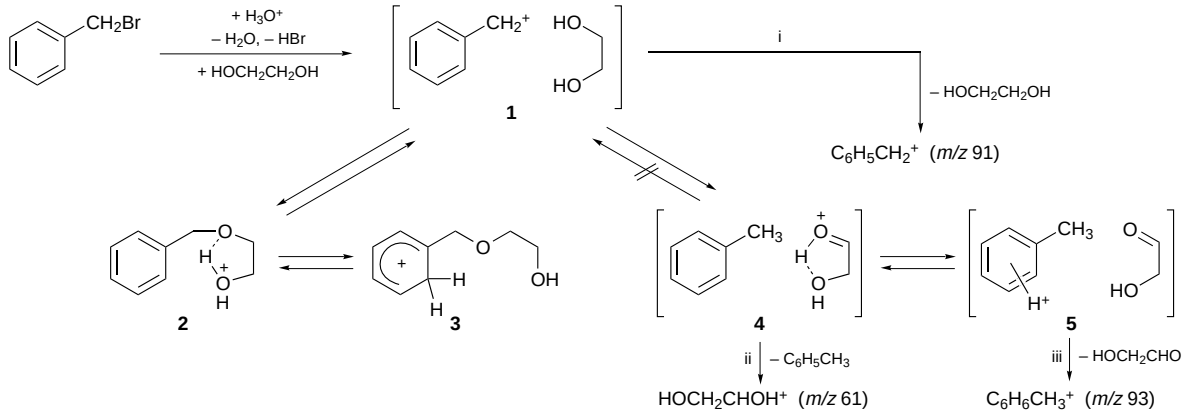


**Table 1** Partial MIKE spectroscopic data of deuterium labelled adduct ions of benzyl cations and ethylene glycol‡[a]

| | Precursors | | Product ions [glycol − H]$^+$ *m/z* | | | | | | Product ions [$C_7(H,D)_7^+$] and [$C_7(H,D)_9^+$] *m/z* | | | | | | | | | | |
|---|---|---|---|---|---|---|---|---|---|---|---|---|---|---|---|---|---|---|---|
| Entry | Benzyl cation | Glycol | 61 | 62 | 63 | 64 | 65 | 66 | 91 | 92 | 93 | 94 | 95 | 96 | 97 | 98 | 99 | 100 | 101 |
| 1 | $PhCH_2^+$ | $HOC_2H_4OH$ | 12 | | | | | | 25 | | 54 | | | | | | | | |
| 2 | $PhCD_2^+$ | $HOC_2H_4OH$ | 12 | | | | | | — | — | 22 | — | 54 | | | | | | |
| 3 | $PhCH_2^+$ | $HOC_2D_4OH$ | — | — | — | 8 | — | | 49 | — | — | 35 | — | — | — | | | | |
| 4 | $PhCH_2^+$ | $DOC_2H_4OD$ | 3 | 5 | 4 | | | | 18 | 4 | 3 | 24 | 30 | | | | | | |
| 5 |  | $HOC_2H_4OH$ | 7 | 5 | 1 | — | | | — | — | — | 29 | 15 | 42 | | | | | |
| 6 | $C_6D_5CD_2^+$ | $HOC_2H_4OH$ | 2.5 | 3.0 | 2.5 | — | — | — | | — | — | — | — | — | 3 | 38 | 25 | 19 | |
| 7 | $C_6D_5CD_2^+$ | $HOC_2D_4OH$ | | | | 1.5 | 2.0 | 1.5 | | | | | | — | 6 | 53 | — | 15 | 11 |

[a] Relative abundances given in % Σ.




**Scheme 1**

clearly excludes the intermediacy of the tropylium ion.[9,10] In agreement with this, a *meta*-methyl group strongly enhances the efficiency of the proton exchange owing to an increase of the local proton affinity of the ring positions *ortho* to the side chain.[11,12]

This work has been supported by the European Commission (HUCAMO Project No. CHRX-CT93 0291, 'Fundamental Studies in Gas-phase Ion Chemistry and Mass Spectrometry') and by the Fonds der Chemischen Industrie.

## Footnotes

† E-mail: kuck@chema.uni-bielefeld.de

‡ All experiments were performed using a ZAB-2F double focusing mass spectrometer (VG Micromass, Manchester) with reversed Nier-Johnson geometry. Ions were generated by a chemical ionization source at a nominal pressure of *ca.* $10^{-5}$ mbar and at *ca.* 150 °C after introduction of the corresponding benzyl bromide (10 μl), ethylene glycol (10 μl) and water (30 μl).

§ MIKES: Mass-analysed ion kinetic energy spectrometry.

¶ The proton exchange **4** ⇌ **5** is apparently statistical if the predominant interchange of the *ortho* and *para* protons of the aromatic ring and the two oxygen-bound protons of the glycol is assumed. This result is in agreement with the almost identical proton affinities of toluene [190 kcal mol$^{-1}$ [13] (for *para* protonation) and 188 kcal mol$^{-1}$ (for *ortho* protonation[11,12]] and that of hydroxyacetaldehyde [189 kcal mol$^{-1}$ (measured recently in our laboratories)] (1 cal = 4.184 J).

‖ Hydrogen atom transfer giving the complex [6-methylenecyclohexadiene$^{\cdot+}$ ·$OC_2H_4OH$] can be safely discarded as it requires *ca.* 250 kJ mol$^{-1}$ starting from **1**.

## References

1 H. E. Audier, G. K. Koyanagi, T. B. McMahon and D. Thölmann, *J. Phys. Chem*., 1996, **100**, 8220.
2 D. Berthomieu, V. Brenner, G. Ohanessian, J. P. Denhez, P. Millié and H. E. Audier, *J. Phys. Chem*., 1995, **99**, 712; see also H. E. Audier, C. Monteiro, P. Mourgues and D. Berthomieu, *Org. Mass Spectrom*., 1990, **25**, 245.
3 D. Kuck and C. Matthias, *J. Am. Chem. Soc*., 1992, **114**, 1901.
4 C. Matthias, K. Weniger and D. Kuck, *Eur. Mass Spectrom*., 1995, **1**, 445; see also D. Kuck, *Int. J. Mass Spectrom. Ion Process*, 1992, **117**, 441.
5 R. G. Cooks, J. H. Beynon, R. M. Caprioli and G. R. Lester, *Metastable Ions*, Elsevier, Amsterdam, 1973; J. R. Chapman, *Practical Organic Mass Spectrometry*, Wiley, Chichester, 2nd edn., 1993.
6 R. D. Bowen, *Acc. Chem. Res*., 1991, **24**, 364.
7 D. Kuck and U. Filges, *Org. Mass. Spectrom*., 1988, **23**, 643.
8 F. W. McLafferty and F. Tureček, *Interpretation of Mass Spectra*, University Science Books, Mill Valley, 4th edn., 1993, ch. 7.
9 D. Kuck, *Mass Spectrom. Rev*., 1990, **9**, 187 and references cited therein.
10 For a recent review on the chemistry of gaseous benzyl and tropylium ions, see C. Lifshitz, *Acc. Chem. Rec*., 1994, **27**, 138.
11 J. L. Devlin, J. F. Wolf, R. W. Taft and W. J. Hehre, *J. Am. Chem. Soc*., 1976, **98**, 1990.
12 D. Kuck, *Mass Spectrom. Rev*., 1990, **9**, 583 and references cited therein.
13 S. G. Lias, J. E. Bartmess, J. F. Liebman, J. L. Holmes, R. D. Levin and W. G. Mallard, *J. Phys. Chem. Ref. Data*, 1988, **17**, Suppl. No. 1.

*Received, 21st August 1996; Revised manuscript received, 14th November 1996; Com. 6/07744G*

# Surface characterisation of zirconium-doped mesoporous silica

**D. J. Jones,[a] J. Jiménez-Jiménez,[b] A. Jiménez-López,[b] P. Maireles-Torres,*[b] P. Olivera-Pastor,[b] E. Rodriguez-Castellón[b] and J. Rozière*[a]**

[a] *Laboratoire des Agrégats Moléculaires et Matériaux Inorganiques, ESA CNRS 5072, Université Montpellier 2, 34095 Montpellier cedex 5, France*
[b] *Departamento de Química Inorgánica, Cristalografía y Mineralogía, Universidad de Málaga, Campus de Teatinos, 29071 Málaga, Spain*

**Zirconium-doped mesoporous silicas of mole ratio Si/Zr from 50 to 5 are Lewis-acid catalysts, with a linear correlation between the zirconium content and total acidity.**

Much attention has been devoted to the synthesis of new mesoporous materials using surfactants as templates[1,2] since the first reports on MCM-41 type solids.[3] Mesoporous silica displays a hexagonal arrangement of cylindrical channels with diameters that vary between 16 and >100 Å, partially overcoming the small pore dimension limitations of zeolites. The low acidity of siliceous MCM-41 can be enhanced by isomorphous substitution of *e.g.* Al or $Ti^{IV}$ for Si[3–5] which specifically increases the number of Lewis-acid sites. The presence of $Zr^{IV}$ may also increase the acidity but, in addition, its invariable oxidation state may be an advantage compared with *e.g.* substitution with $Ti^{IV}$, in particular with regard to thermal stability.

The preparation of zirconium-containing mesoporous silica assisted by surfactant species (hexadecylamine) and its activity in redox catalysis has recently been described.[6] We report here a synthesis of Zr-doped mesoporous silica using hexadecyltrimethylammonium as template, and describe the total acidity and types of acid site, and structural information derived from X-ray photoelectron spectroscopy (XPS) coupled with depth profile analysis.

Si/Zr MCM-41 type compounds were prepared by adding tetraethoxysilane and zirconium tetrapropoxide to an ethanol–propanol solution at room temperature. Si/Zr ratios of 5, 25 and 50 gave samples SiZr5B, SiZr25B and SiZr50B. The solution was stirred for 15 min and then added to an aqueous solution of hexadecyltrimethylammonium bromide (25 mass%), previously stirred at 80 °C for 30 min. The surfactant/($SiO_2$ + $ZrO_2$) ratio was 0.5. For these samples, the pH was adjusted to 10.5 by addition of tetraethylammonium hydroxide. The resulting gels were stirred at 80 °C for 24 h and then at 25 °C for 48 h. The solids were recovered by filtration and washed with ethanol–propanol. A purely siliceous sample was prepared using the same experimental conditions (SiB). A further sample of Si/Zr ratio 50 was prepared, but the pH was adjusted to 2.8 by the addition of HCl (SiZr50A). All precursors were calcined in air at 540 °C, for 6 h. The ramp rate was 1 °C $min^{-1}$. Complete removal of surfactant was confirmed by elemental and thermogravimetric analyses.

Fig. 1 shows the powder X-ray diffraction patterns of the calcined Si/Zr materials. In all cases, a single diffraction peak was observed, consistent with short-range hexagonal order. Indeed, transmission electron microscopy allows a roughly hexagonal arrangement of pores to be observed. Owing to the breadth of the diffraction line, no correlation between its position and the Zr content was apparent. Neither XRD nor UV spectroscopy showed evidence for zirconium oxide.

Chemical analyses indicated that the Si/Zr ratio in the calcined phases is the same as that in the initial mixture. However, in each case, the ratio of Si/Zr at the surface, as determined from XPS, is higher than this bulk ratio. This is expected, given the greater rate of hydrolysis of Zr alkoxides relative to that of Si alkoxides. Depth profile analysis of sample SiZr25B was performed by etching with an $Ar^+$ gun, and observing the evolution of the Si/Zr ratio with time. After 5 min the surface ratio of 66 decreases to 23, and a constant value of 17 was reached after 15 min [Fig. 2(*a*)]. Single peaks were

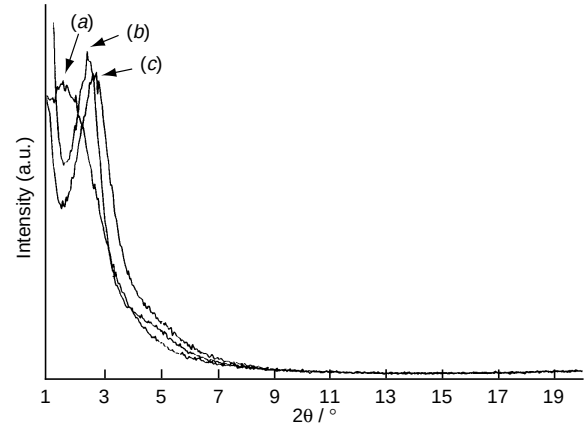



**Fig. 1** Powder X-ray diffraction patterns of (*a*) SiZr50A, (*b*) SiZr50B and (*c*) SiZr25B calcined at 540 °C

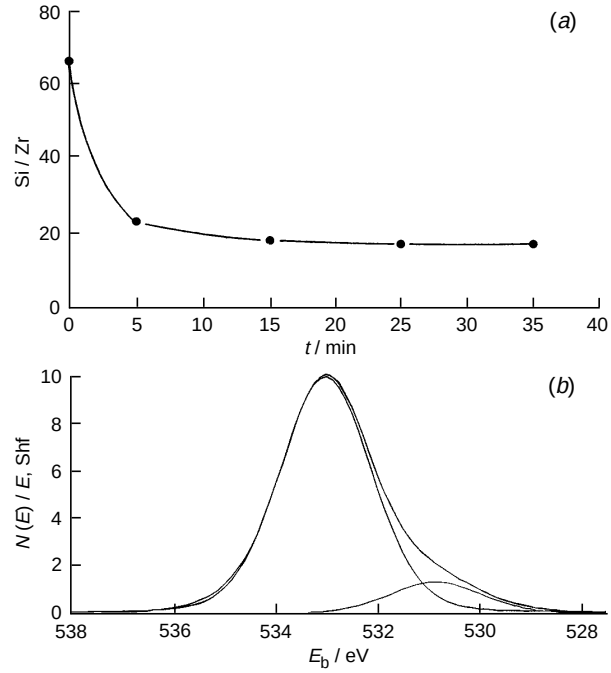



**Fig. 2** (*a*) Variation of the Si/Zr ratio in sample SiZr25B as determined by depth profile analysis using XPS as a function of time of etching; (*b*) O 1s XPS spectrum of SiZr5B

**Table 1** Textural parameters of prepared samples

| Sample | $S_{BET}$ (540 °C)/m² g⁻¹ | $\Sigma Vp^a$/ cm³ g⁻¹ | $S_{BET}$ (800 °C)/m² g⁻¹ | $d$p(av.)$^b$ (540 °C)/Å | $d$p(av.) (800 °C)/Å | % shrinkage$^c$ | $D^d$ (540 °C, air)/Å |
|---|---|---|---|---|---|---|---|
| SiZr50A | 1140 | 0.788 | — | 27.5 | — | — | 34.1 |
| SiB | 1157 | 1.000 | 985 | 30.2 | 22.5 | 5.2 | 9.9 |
| SiZr50B | 1302 | 0.923 | 1072 | 27.6 | 24.2 | 4.3 | 12.5 |
| SiZr25B | 1386 | 0.879 | 876 | 24.6 | 20.4 | 12.4 | 12.0 |
| SiZr5B | 973 | 0.687 | 700 | 27.5 | 23.8 | 5.2 | 16.3 |

[a] At $P/P_0 = 0.97$. [b] Calculated using the Cranston and Inkley method.[8] [c] Reduction in lattice parameter $a_0$ after calcination at 540 °C. [d] Pore wall thickness, $D$, after calcination at 540 °C; $D = a_0 - d_p$(av.), and $a_0 = 2d_{100}/\sqrt{3}$.

observed for both Si 2p and Zr $3d_{5/2}$ and the percentage of oxygen remained constant at 63% throughout the etching treatment. The O 1s peak becomes asymmetric as the amount of Zr in the samples increases. Thus for ZrSi5B, O 1s can be deconvoluted into two components, indicating two different environments for oxygen, *viz.* Si–O–Si (component at 533.0 eV) and Si–O–Zr (530.9 eV) [Fig. 2(*b*)]. The intensity ratio of these two peaks closely matches the surface Si/Zr ratio. In such heteroatom-substituted analogues of siliceous MCM-41 materials, the question arises as to the true incorporation of the heteroatom in the framework, as opposed to its presence as a segregated oxide phase. Here, the XPS signals of O 1s are at least 0.7 eV higher than that of $ZrO_2$ (530.2 eV), strong evidence in favour of the presence of framework zirconium. Further, the binding energies of Zr $3d_{5/2}$ (183.1–183.6 eV) are higher than that of $ZrO_2$ (182.2 eV) and are closer to that of $ZrSiO_4$ (183.3. eV). Preliminary results from extended X-ray absorption fine structure spectroscopy at the zirconium edge show the local structure to differ from that of $ZrO_2$, with evidence for silicon in the next nearest neighbour coordination shell.

The $^{29}$Si MAS NMR spectra of as-prepared SiZr25B shows resonances at δ−107.3, −98.6 and −89.4. After calcination, the increase in intensity of the two lower field resonances relative to that at δ−107.3 can be explained on the basis of the formation of Si–O–Zr bonds, as previously suggested for mixed $ZrO_2$–$SiO_2$ materials.[7]

All calcined compounds exhibited a reversible type IV nitrogen adsorption–desorption isotherm, with a sharp inflection at $P/P_o$ = 0.35–0.40, as is typical for MCM-type mesoporous materials. Table 1 gives the textural parameters derived from the isotherms. Surface areas lie between 973 and 1376 m² g⁻¹. The average pore size of the silica-only compound after calcination at 800 °C is lower by 25% that of its value after calcination at 540 °C. Zirconium-doped samples are more resistant, the average pore size being reduced by 12–17%. Even after calcination at 800 °C, all materials retain their mesoporous character and a high surface area. The wall thicknesses of all zirconium-containing phases are higher than that of the purely siliceous analogue, in agreement with the incorporation of zirconium into the framework. The particularly strong increase observed for the synthesis under acidic conditions may be a result of the synthetic mechanism which controls the precipitation of a solid phase from the gel mixture.

IR spectra of calcined samples after adsorption of pyridine show a virtual absence of Brønsted acid sites, and an increasing number of Lewis-acid sites with an increase in the amount of Zr present. The origin of the Lewis acidity may be attributed to the presence of $Zr^{IV}$ species with low coordination. Total acidity, determined by thermally programmed desorption of $NH_3$ follows the same trend, ranging between 0.17 and 0.77 mmol $NH_3$ g⁻¹. In particular, sample ZrSi5B is considerably more acidic than MCM-41 aluminosilicates.[5] Confirmation of the acidic character of the zirconium-doped samples is provided by their activity in the decomposition of isopropyl alcohol. Whilst purely siliceous MCM-41 (sample SiB) is not active in this reaction, calcined Si/Zr samples displayed, in contrast, a high catalytic activity (30 μmol g⁻¹ s⁻¹ at 200 °C for sample SiZr5B) and a selectivity of 99% towards production of propene, which was maintained after 20 h of reaction (Fig. 3). Inasmuch as both the location and number of active sites are key factors in the observed catalytic properties, knowledge of the ion distribution is essential. In this respect, this study has demonstrated the important contribution that XPS can make in the study of heteroatom-substituted mesoporous materials.

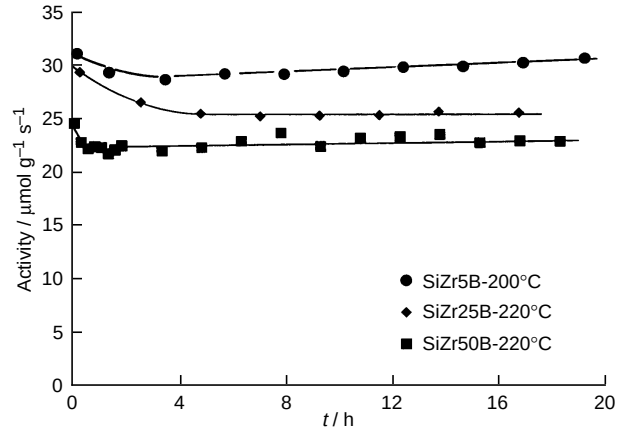



**Fig. 3** Catalytic activity of SiZr50B, SiZr25B and SiZr5B for *iso*- propyl alcohol decomposition as a function of time on stream

We thank the European Commission for support under Brite-EuRam contract BRE2-CT93-0450 and the CICYT (Spain), project MAT94-0678 for financial support.

## References

1 N. K. Raman, M. T. Anderson and J. Brinker, *Chem. Mater*., 1996, **8**, 1682.
2 A. Sayari, *Chem. Mater*., 1996, **8**, 1840.
3 C. T. Kresge, M. E. Leonowicz, W. J. Roth, J. C. Vartuli and J. S. Beck, *Nature*, 1992, **359**, 710.
4 J. S. Beck, J. C. Vartuli, W. J. Roth, M. E. Leonowicz, C. T. Kresge, K. D. Schmitt, C. T.-W. Chu, D. H. Olson, E. W. Sheppard, S. B. McCullen, J. B. Higgins and J. C. Schlenker, *J. Am. Chem. Soc*., 1992, **114**, 10 834.
5 A. Corma, V. Fornes, M. T. Navarro and J. Pérez-Pariente, *J. Catal*., 1994, **184**, 569.
6 A. Tuel, S. Gontier and T. Teissier, *Chem. Commun*., 1996, 651.
7 M. Andrianainarivelo, R. Corriu, D. Leclercq, P. H. Mutin and A. Vioux, *J. Mater. Chem*., 1996, **6**, 1665.
8 R. W. Cranston and F. A. Inkley, *Adv. Catal*., 1957, **9**, 143.

*Received, 3rd December 1996; Com. 6/08145B*

# Nucleophilic substitution of (alkoxymethylene)dimethylammonium chloride with potassium phthalimide; a convenient procedure for the synthesis of imides with inversion of configuration

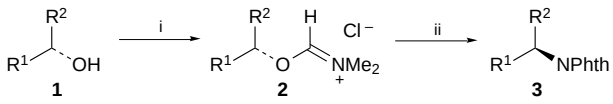
**Anthony G. M. Barrett,*[a] D. Christopher Braddock,[a] Rachel A. James[a] and Panayiotis A. Procopiou*[b]**

[a] *Department of Chemistry, Imperial College of Science, Technology and Medicine, London, UK SW7 2AY*
[b] *Department of Medicinal Chemistry, Glaxo Wellcome Research and Development Ltd, Gunnels Wood Road, Stevenage, Hertfordshire, UK SG1 2NY*

**Secondary alcohols are converted into their phthalimido derivatives with inversion of configuration *via* sequential reaction with (chloromethylene)dimethylammonium chloride and potassium phthalimide.**

The Mitsunobu reaction is the process *par excellence* for the conversion of secondary alcohols into esters with inversion of stereochemistry.[1] In this reaction an alcohol is treated with diethyl azodicarboxylate, triphenylphosphine and a carboxylic acid to provide the required ester. The reaction can be extended to a wide range of nucleophiles in addition to carboxylic acids to provide a variety of $S_N2$ substitution products. The stereoselective preparation of amines from the corresponding alcohol can be effected *via* formation of the phthalimido derivative.[2] There are however disadvantages associated with the Mitsunobu reaction. Diethyl azodicarboxylate is unstable and potentially explosive and the by-products, triphenylphosphine oxide and diethyl hydrazinedicarboxylate, are of considerable mass making the process non-ideal from the point of view of atom economy.[3] Recently, one of us reported the use of Vilsmeier chemistry to effect the stereospecific cyclisation of hydroxyphenols to provide benzodioxans, dihydrobenzopyrans and dihydrobenzofurans *via* (alkoxymethylene)dimethylammonium salts and intramolecular $S_N2$ displacement by phenoxide.[4] This Vilsmeier chemistry has also been extended to the conversion of alcohols into esters with inversion of stereochemistry.[5,6] Herein we report a further application of this methodology to form the phthalimide derivatives of secondary alcohols.

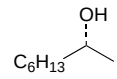
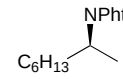
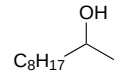
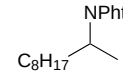
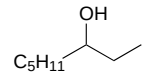
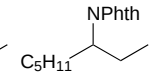
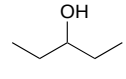
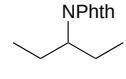
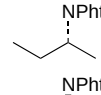
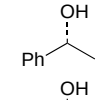
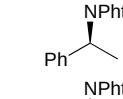
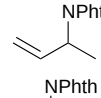
Treatment of a series of secondary alcohols **1** with (chloromethylene)dimethylammonium chloride, generated from oxalyl chloride and dimethylformamide,[7] provided the corresponding imidate salts **2**. These were then treated with potassium phthalimide at 60–70 °C to provide the phthalimide derivative **3** with inversion of stereochemistry (Scheme 1 and Table 1).† Enantiomeric purities (entries 1, 5, and 6) were established by HPLC. Clean inversion of stereochemistry was observed for entries 1 and 5 but substitution of (*R*)-1-phenylethanol proceeded with partial racemisation (entry 6, 72% ee). It is reasonable to speculate that this example either involved a mixed $S_N2/S_N1$ reaction or took place partially *via* the corresponding benzylic chloride. Several solvents were examined in these reactions of which acetonitrile was found to be superior. No reaction was observed in THF whereas reaction in DME or DMF gave the desired product in moderate yield. Furthermore the use of DMF as solvent led to partial racemisation in the preparation of (*S*)-*N*-2-octylphthalamide (58% ee). It is reasonable to assume that such partial racemisation was the result of partial substitution *via* 2-octyl chloride or *via* nucleophilic participation of the solvent (DMF) leading to inverted imidates. The imidate methodology in this paper should be of use as an alternative to the Mitsunobu reaction particularly for larger scale applications as the side products are innocuous (DMF and potassium chloride). The method is mechanistically similar to the synthesis of glycosides[8] and benzyl, allyl and *tert*-butyl ethers[9] *via* trichloroacetimidate activation.




**Scheme 1** *Reagents and conditions*: i, $CHCl{=}NMe_2^+Cl^-$, MeCN, 0 °C; ii, KPhth, 60–70 °C, 1–3 d

We thank Glaxo Group Research Ltd. for the most generous endowment (to A. G. M. B.) and for providing a CASE studentship (to R. A. J.); the Wolfson Foundation for establishing the Wolfson Centre for Organic Chemistry in Medical Science at Imperial College and the EPSRC for providing a CASE studentship (to R. A. J.).

**Table 1** Formation of phthalimido derivatives with inversion of stereochemistry[a]

| Entry | Substrate | Product[b] | Yield (%) | ee[c] (%) | Ref. |
|---|---|---|---|---|---|
| 1 |  |  | 95 | 96 [α]$_D$ +14.0 (*c* 1.1, $CHCl_3$) | 10[e] |
| 2 |  |  | 77 | —[d] | ‡ |
| 3 |  |  | 90 | —[d] | § |
| 4 |  |  | 91 | —[d] | 11[e] |
| 5 |  |  | 92 | 92 [α]$_D$ –12.8 (*c* 1.1, $CHCl_3$) | 12[e] |
| 6 |  |  | 73 | 72 [α]$_D$ –31.4 (*c* 0.5, $CHCl_3$) | 12[e] |
| 7 |  |  | 98 | —[d] | 13[e] |
| 8 |  |  | 34 | —[d] | 14[e] |

[a] All reactions performed with 7 equiv. of potassium phthalimide in acetonitrile for 1–3 d; [b] NPhth = phthalimido derivative; [c] Determined by HPLC on a chiral stationary phase; [d] Racemic substrate employed; [e] The spectroscopic data were identical to those reported in the literature.

## Footnotes

† In a typical procedure, oxalyl chloride (0.10 $cm^3$, 1.15 mmol) was added dropwise with stirring to a solution of DMF (0.09 $cm^3$, 1.17 mmol) in dry dichloromethane (1 $cm^3$) at 0 °C under nitrogen. After 5 min, the white solid was suspended in dry acetonitrile (30 $cm^3$) and (*R*)-octan-2-ol (0.16 $cm^3$, 1.0 mmol) and potassium phthalimide (1.3 g, 7 mmol) were added sequentially. The reaction mixture was heated to 65 °C for 16 h cooled and filtered. The residue, after rotary evaporation, was chromatographed on silica gel (5% ethyl acetate in hexanes) to provide (*S*)-*N*-2-octylphthalimide (0.25 g, 95%) as a colourless oil.

‡ *Selected data* for *N*-2-decylphthalimide: $R_f$ = 0.40 (light petroleum–ethylacetate, 10 : 1); $\delta_H$ (300 MHz; $CDCl_3$) 0.84 (3 H, t, *J* 6.7 Hz, $CH_3$), 1.24 (12 H, m, 6 × $CH_2$), 1.47 (3 H, d, *J* 6.9 Hz, $CH_3$), 1.74 (1 H, m, $CH_2$), 2.05 (1 H, m, $CH_2$), 4.34 (1 H, m, CH), 7.70 (2 H, m, PhH), 7.82 (2 H, m, PhH); $\delta_C$ (75 MHz; $CDCl_3$) 14.1, 18.7, 22.6, 26.8, 29.2, 29.2, 29.4, 31.8, 33.7, 47.5, 123.0, 132.1, 133.8, 168.6; $\upsilon_{max}$ (thin film)/$cm^{-1}$ 2927s, 2856m, 1774m, 1710s; *m/z* ($CI^+$; $NH_3$), 305 (*M* + $NH_4^+$, 100), 288 (*M* + $H^+$, 45%); HRMS: $C_{18}H_{25}NO_2$ requires: 287.1885. Found: 287.1873.

§ *Selected data* for *N*-3-octylphthalimide: $R_f$ = 0.23 (light petroleum–ethyl acetate 20 : 1); $\delta_H$ (300 MHz; $CDCl_3$) 0.86 (6 H, m, 2 × $CH_3$), 1.26 (6 H, m, 3 × $CH_2$), 1.82 (1 H, m, $CH_2$), 2.06 (1 H, m, $CH_2$), 4.12 (1 H, m, CH), 7.72 (2 H, m, PhH), 7.83 (2 H, m, PhH); $\delta_C$ (75 MHz; $CDCl_3$) 11.1, 14.0, 22.5, 25.6, 26.4, 31.5, 32.2, 54.0, 123.1, 131.9, 133.8, 168.9; $\upsilon_{max}$ (thin film)/$cm^{-1}$ 2960s, 2931s, 2860m, 1770s, 1711s; *m/z* ($CI^+$; $NH_3$), 277 (*M* + $NH_4^+$, 100), 260 (*M* + $H^+$, 69%); HRMS: $C_{16}H_{21}NO_2$ requires: 259.1572. Found: 259.1583.

## References


1 O. Mitsunobu, *Synthesis*, 1981, 1; D. L. Hughes, *Org. React*., 1992, **42**, 335; J. A. Dodge, J. I. Trujillo and M. Presnell, *J. Org. Chem*., 1994, **59**, 234.

2 O. Mitsunobu, M. Wada and T. Sano, *J. Am. Chem. Soc*., 1972, **94**, 680; J. Mulzer and G. Funk, *Synthesis*, 1995, 101; J. Mulzer and C. Brand, *Tetrahedron*, 1986, **42**, 5961; C. Simon, S. Hosztafi and S. Maklut, *Tetrahedron*, 1994, **50**, 9757; G. L. Grunewald, V. M. Paradklar, B. Pazhenchevsky, M. A. Pleiss, D. J. Sall, W. L. Seibel and T. J. Reitz, *J. Org Chem*., 1983, **48**, 2321.

3 B. M. Trost, *Angew. Chem., Int. Ed. Engl*., 1995, **34**, 259.

4 P. A. Procopiou, A. C. Brodie, M. J. Deal and D. F. Hayman, *Tetrahedron Lett*., 1993, **34**, 7483; P. A. Procopiou, A. C. Brodie, M. J. Deal and D. F. Hayman, *J. Chem. Soc., Perkin Trans. 1*, 1996, 2249.

5 A. G. M. Barrett, N. Koike and P. A. Procopiou, *J. Chem. Soc., Chem. Commun*., 1995, 1403.

6 H. Brechbuhler, H. Buchi, E. Hatz, J. Schreiber and A. Eschenmoser, *Helv. Chim. Acta*, 1965, **48**, 1747.

7 C. Reichardt and K. Schagerer, *Angew. Chem., Int. Ed. Engl*., 1973, **12**, 323.

8 R. R. Schmidt, *Synthesis of Glycosides in Comprehensive Organic Synthesis*, ed. B. M. Trost, I. Fleming and E. Winterfeldt, Pergamon, Oxford, 1991, vol. 6, pp. 49–54.

9 A. Armstrong, I. Brackenridge, R. F. W. Jackson and J. M. Kirk, *Tetrahedron Lett*., 1988, **29**, 2483; H.-P. Wessel, T. Iversen and D. R. Bundle, *J. Chem. Soc., Perkin Trans. 1*, 1985, 2247; T. Iversen and D. R. Bundle, *J. Chem. Soc., Chem. Commun*., 1981, 1240.

10 D. Landini and F. Rolla, *Synthesis*, 1976, 389; J. Castro and V. G. Matassa, *J. Org. Chem*., 1994, **59**, 2289.

11 Y. Shibata, M. Shickita, K. Sasaki, K. Nishimura, Y. Hashimoto and S. Iwasaki, *Chem. Pharm. Bull*., 1995, 177.

12 F. Toda, S. Soda and I. Goldberg, *J. Chem. Soc., Perkin Trans. 1*, 1993, 2357.

13 Y. Inoue, M. Taguchi, M. Toyofuku and H. Hashimoto, *Bull. Chem. Soc. Jpn*., 1984, **57**, 3021; O. Mumm and H. Richter, *Chem. Ber*., 1940, 843.

14 P. G. Sammes and D. Thetford, *J. Chem. Soc., Perkin Trans. 1*, 1989, 655.



*Received, 4th November 1996; Com. 6/07482K*

# A new monoclinic phase of superconducting $Tl_2Ba_2CuO_{6+\delta}$

**D. R. Pederzolli, G. M. Wltschek and J. P. Attfield**

[a] *Interdisciplinary Research Centre in Superconductivity, University of Cambridge, Madingley Road, Cambridge, UK CB3 0HE*
[b] *Department of Chemistry, University of Cambridge, Lensfield Road, Cambridge, UK CB2 1EW*

**High-resolution time-of-flight neutron and synchrotron X-ray powder diffraction studies of the 'orthorhombic' form of the high-$T_c$ superconductor $Tl_2Ba_2CuO_{6+\delta}$ evidence both the orthorhombic (*Fmmm*) phase and a new monoclinic (*F*112/*m*) form at high excess oxygen contents δ.**

$Tl_2Ba_2CuO_{6+\delta}$ (Tl-2201) is the first member of the $Tl_2Ba_2Ca_{n-1}Cu_nO_{4+2n}$ series of high critical temperature ($T_c$) copper oxide superconductors. Unlike the other homologues, which are all tetragonal, Tl-2201 exhibits both tetragonal and orthorhombic symmetries and the physical properties of both forms vary from non-superconducting to superconducting with $T_c$ values up to 90 K.[1] Physical measurements[2] and a resonant synchrotron X-ray diffraction study[3,4] have shown that the two forms have slightly different compositions $(Tl_{2-x}Cu_x)Ba_2CuO_{6+\delta}$. The orthorhombic form obtained at 800–850 °C is cation stoichiometric ($x = 0$) whereas tetragonal Tl-2201 formed above 850 °C has a significant degree of Cu substitution at the Tl site with $x = 0.1$. The synchrotron diffraction study also detected a possible phase separation in orthorhombic Tl-2201, evidenced by small splittings of certain diffraction peaks *e.g.* 040. Here we report further high-resolution synchrotron X-ray and time-of-flight (TOF) neutron powder diffraction studies of 'orthorhombic' Tl-2201. These have led to the discovery of a new monoclinic form of this important superconductor.

A 20 g batch of orthorhombic $Tl_2Ba_2CuO_{6+\delta}$ was synthesised at 820 °C under flowing $O_2$ and quenched to room temperature. Portions of this 'as-prepared' sample were annealed for 5 h under flowing Ar at temperatures between 200 and 700 °C to systematically decrease the excess oxygen content δ, and a further portion was treated under 600 atm $O_2$ pressure at 600 °C to increase δ. Synchrotron X-ray powder diffraction patterns were recorded on diffractometer 9.1 at the Synchrotron Radiation Source, Daresbury, UK and TOF neutron diffraction data were collected from instrument HRPD at the Rutherford Appleton Laboratory, UK. Rietveld refinements[5] were performed using the GSAS package.[6] Diffraction peaks from traces of $BaCO_3$ and $Tl_4O_3$[7] were also observed in some of the profiles and were fitted in the refinements. Magnetisations were measured on a Quantum Design SQUID magnetometer in a field of 500 G.

The neutron diffraction pattern of the as-prepared $Tl_2Ba_2CuO_{6+\delta}$ sample contained small splittings of many *hk*0 and *hkl* diffraction peaks *e.g.* 220 (Fig. 1) although the *h*00 and 0*k*0 diffraction peaks were unsplit. These splittings are inconsistent with orthorhombic symmetry and with the previously reported phase separation model,[4,5] and show that the crystal symmetry is monoclinic. Lowering the symmetry of the structural model from orthorhombic *Fmmm* to monoclinic *F*112/*m* (a non-standard setting of space group *C*2/*m* with the *c*-axis unique) gave a good fit to the profile ($R_{wp}$ = 8.8%). Monoclinic splittings were not observed for the 700 °C Ar-annealed sample (Fig. 1) and the data were fitted by the orthorhombic *Fmmm* model ($R_{wp}$ = 9.7%). Results are summarised in Tables 1 and 2.

The synchrotron X-ray diffraction profiles showed monoclinic splittings for the high pressure $O_2$-annealed, as-prepared, and 200 and 400 °C Ar-annealed Tl-2201 samples, but the 600 and 700 °C Ar-annealed samples were orthorhombic. Good fits to the data with $R_{wp}$ ranging from 5.4 to 9.7% were obtained using the monoclinic *F*112/*m* or orthorhombic *Fmmm* models as appropriate (Table 1).

The Tl-2201 superconductor is notable for having three different macroscopic symmetries due to small variations in chemical composition. The extent of the monoclinic distortion (Table 1) is dependent upon the oxygen content, as the largest

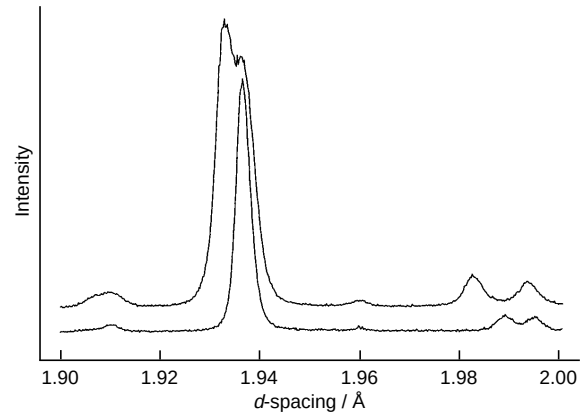



**Fig. 1** Part of the TOF neutron powder patterns of as-prepared (upper curve) and 700 °C Ar-annealed (lower curve) Tl-2201 samples. A monoclinic splitting of the 220 peak ($d$ = 1.935 Å) is seen for the as-prepared sample and the relative magnitudes of the orthorhombic distortions are apparent from the separation of the 208 and 028 reflections at 1.98–2.00 Å.

**Table 1** Cell data for monoclinic (γ > 90°) and orthorhombic (γ = 90°) $Tl_2Ba_2CuO_{6+\delta}$ samples from high-resolution synchrotron X-ray (X) (λ = 0.871 94 Å) and TOF neutron (N) refinements, with e.s.d.s in parentheses. Samples are listed in order of decreasing excess oxygen content δ

| Sample treatment | $a$/Å | $b$/Å | $c$/Å | γ/° | $10^3\ 2(b-a)/(b+a)$ |
|---|---|---|---|---|---|
| 600 atm $O_2$ X | 5.43846(7) | 5.50419(8) | 23.1563(3) | 90.189(1) | 12.01(2) |
| As-prepared X | 5.44667(8) | 5.50601(9) | 23.1556(3) | 90.120(1) | 10.84(2) |
| As-prepared N | 5.44760(6) | 5.50496(7) | 23.1560(3) | 90.114(1) | 10.47(2) |
| 200 °C, Ar X | 5.44527(11) | 5.50388(12) | 23.1494(4) | 90.119(2) | 10.71(2) |
| 400 °C, Ar X | 5.44989(10) | 5.50152(11) | 23.1638(4) | 90.124(2) | 9.43(2) |
| 600 °C, Ar X | 5.46383(8) | 5.49577(9) | 23.2168(4) | 90 | 5.83(2) |
| 700 °C, Ar X | 5.46622(7) | 5.49173(8) | 23.2223(3) | 90 | 4.66(2) |
| 700 °C, Ar N | 5.46576(7) | 5.49766(7) | 23.2265(3) | 90 | 5.82(2) |

**Table 2** Atomic parameters from neutron refinements of the as-prepared *F*112/*m* (normal type) and 700 °C Ar-annealed *Fmmm* (in italics where different) Tl-2201 samples, with e.s.d.s in parentheses

| Atom | Multiplicity | *x* | *y* | *z* | $U_{iso}$/Å$^2$ | Occupancy |
|---|---|---|---|---|---|---|
| Tl | 16 | −0.0049(6) | 0.0260(3) | 0.20253(3) | 0.0226(3) | 0.5 |
| | | *0* | *0.0175(8)* | *0.20271(5)* | *0.0210(4)* | |
| Ba | 8 | 0.5 | 0 | 0.08388(4) | 0.0196(3) | 1 |
| | | | | *0.08271(7)* | *0.0159(4)* | |
| Cu | 4 | 0 | 0 | 0 | 0.0184(2) | 1 |
| | | | | | *0.0132(4)* | |
| O(1a)[a] | 4 | 0.25 | 0.75 | 0 | 0.0207(2) | 1 |
| | | | | | *0.0152(3)* | |
| O(1b)[a] | 4 | 0.25 | 0.25 | 0 | 0.0207 | 1 |
| | | | | | *0.0152* | |
| O(2) | 8 | 0 | 0 | 0.11573(4) | 0.0207 | 1 |
| | | | | *0.11651(7)* | *0.0152* | |
| O(3) | 16 | −0.0203(6) | 0.0740(3) | 0.28895(8) | 0.0514(6) | 0.5 |
| | | *0* | *0.0587(5)* | *0.28838(11)* | *0.0471(8)* | |
| O(4) | 8 | 0.25 | 0.25 | 0.25 | 0.0207 | 0.096(2) |
| | | | | | *0.0152(3)* | *0.075(3)* |

[a] These sites are equivalent in orthorhombic *Fmmm* symmetry.

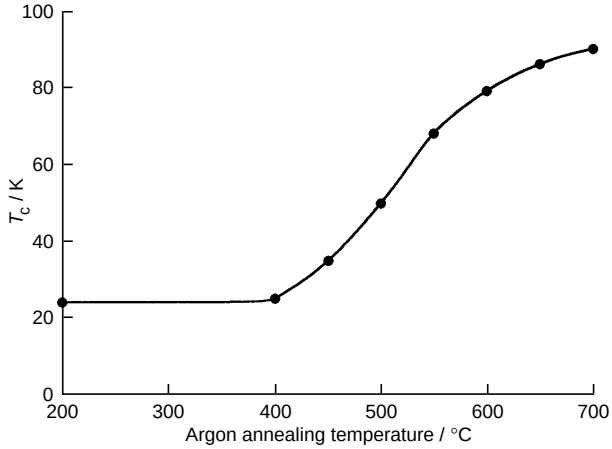



**Fig. 2** Variation of $T_c$ with Ar-annealing temperature in 'orthorhombic' Tl-2201

value of $\gamma = 90.2°$ is found in the sample treated under a high oxygen pressure, whereas the as-prepared material and samples annealed ⩽400 °C under Ar all have $\gamma \approx 90.1°$ and those annealed above 600 °C are orthorhombic. A similar reduction in the orthorhombic distortion, quantified by the orthorhombicity $2(b - a)/(b + a)$, is also observed with decreasing δ. The monoclinic to orthorhombic transition occurs between Ar-annealing temperatures of 400 and 600 °C and is accompanied by a sharp decrease in the orthorhombicity and an abrupt increase in *c* from 23.15–23.16 Å in monoclinic samples to 23.22–23.23 Å in the orthorhombic ones. The maximum slope in the variation of $T_c$ with Ar-annealing temperature (Fig. 2) also occurs within this region, showing that the structural or chemical changes at the monoclinic to orthorhombic transition enhance $T_c$.

Comparing the neutron-refined atomic parameters of the monoclinic as-prepared and orthorhombic 700 °C Ar-annealed $Tl_2Ba_2CuO_{6+\delta}$ samples (Table 2) enables small structural changes to be discerned. The reduction in excess oxygen content from $\delta = 0.192(4)$ to 0.150(6) is consistent with the change from overdoped non-superconducting behaviour to superconductivity with $T_c = 90$ K. This is accompanied by a significant increase in the distance from Cu to the apical oxygen atom O(2) from 2.676(1) Å in the non-superconducting monoclinic structure to 2.702(1) Å in the $T_c = 90$ K orthorhombic sample, whereas the Tl–O(2) distance decreases slightly from 2.012(1) to 2.001(2) Å. Hence, the observed expansion of 0.07 Å in *c* is due to the overall increase of 0.10 Å in the four Cu–O(2) contacts which is partly offset by a total decrease of 0.04 Å of the four Tl–O(2) bonds. This adds to the large amount of evidence for the crucial role of the apical Cu–O bond distance in determining the value of $T_c$ in these notable superconductors.[8,9]

In conclusion, small changes in the amount of excess oxygen in 'orthorhombic' $Tl_2Ba_2CuO_{6+\delta}$ play a critical role in determining the crystal symmetry and electronic properties. Oxygen-rich compositions with $T_c$ values up to *ca.* 50 K are monoclinic whereas less oxidised samples with $T_c$ values of 50–90 K are orthorhombic. The monoclinic to orthorhombic phase change occurs due to loss of interstitial oxygen, whereas the orthorhombic to tetragonal change at higher temperatures involves the loss of $Tl_2O_3$ from the structure accompanied by the substitution of 5% Cu at the Tl site.

## References


1 Y. Kubo, Y. Shimakawa, T. Manaho and H. Igarashi, *Phys. Rev. B*, 1991, **43**, 7875.
2 Y. Shimakawa, *Physica C*, 1993, **204**, 247.
3 M. A. G. Aranda, D. C. Sinclair, J. P. Attfield and A. P. Mackenzie, *Phys. Rev. B*, 1995, **51**, 12 747.
4 M. A. G. Aranda, D. C. Sinclair and J. P. Attfield, *Physica C*, 1994, **235**–**240**, 965.
5 H. M. Rietveld, *J. Appl. Crystallogr*., 1969, **2**, 65.
6 A. C. Larson and R. B. Von Dreele, Los Alamos National Laboratory Report No. LA-UR-86-748, 1987.
7 R. Marchand and M. Tournoux, *C. R. Hebd. Seances Acad. Sci., Ser. C, Sci. Chim*., 1973, **277**, 863.
8 Y. Ohta, T. Tohyama and S. Maekawa, *Phys. Rev. B*, 1991, **43**, 2968.
9 K. Eid, M. Matlak and J. Zielinski, *Physica C*, 1994, **220**, 61.



*Received, 27th November 1996; Com. 6/08024C*

# A facile dialkyl ether cleavage and rearrangement under mildly basic conditions during the Williamson synthesis with β-cyclodextrin

**Christopher T. Bibeau, Brian K. Hubbard and Christopher J. Abelt***

*Department of Chemistry, College of William and Mary, Williamsburg, VA 23187-8795, USA*

**Alkyl (9,10-dicyanoanthracenyl-2-methyl) ethers undergo facile transetherification with a variety of alkoxides.**

The ether bond is generally resistant to base cleavage.[1] Well-known exceptions occur when the alkoxide leaving group is stable, as with a phenoxide, and when cleavage relieves strain, as with an epoxide. Benzyl ethers are often used at protecting groups for alcohols.[2] These arylalkyl ethers are stable even with strong bases and are cleaved by catalytic hydrogenation or dissolving metal reduction. Thus, the ether bond should be an ideal linking group in the construction of supramolecular systems, especially when such systems will be used as reaction catalysts requiring their continued molecular integrity. In this paper we report a case involving construction of a cyclodextrin assembly wherein an arylalkyl alkyl ether bond undergoes facile cleavage under relatively mild conditions.

The Williamson ether synthesis can be applied to the regioselective alkylation of β-cyclodextrin (β-CD) at the glucose C2–OH. The regioselectivity arises from the greater acidity of the C2–OH relative to the C3 or C6–OH. The C2 alkoxide is stabilized by an intramolecular H-bond with the C3–OH of an adjacent glucose unit. D'Souza and Rong have shown that β-CD alkoxide will react by nucleophilic substitution with a variety of electrophiles to give C2 ethers.[3] We have applied this reaction to link together a 9,10-dicyanoanthracene (DCA) group with β-cyclodextrin *via* the 2-bromomethyl derivative **1**.[4] The reaction did not give rise to selective substitution at C2; in fact, a 3 : 1 ratio of C6 and C2-ethers was isolated (Scheme 1). In this communication we report the results of several experiments probing the origin of the observed regiochemistry.

In all of the following experiments the relative proportions of the DCA–β-CD ethers were determined through HPLC analysis of the reaction mixture.† The base used was β-CD alkoxide, and the base strength was controlled by the quantity of NaH used to deprotonate the β-cyclodextrin; for example, a 50% molar excess of NaH was used to generate a 1 : 1 mixture of β-CD C2-alkoxide and C2,C2′-dialkoxide. All reactions were conducted in DMF which was distilled from $CaH_2$ *in vacuo* before use.

The etherification reaction requires more than stoichiometric base to form ether products. The reaction with 50% excess base was monitored as a function of time. HPLC results reveal that **2** is formed initially, but disappears rapidly with concomitant formation of **3**. Ether formation is nearly complete within 30 min, but the fraction of **3** in the product mixture continues to increase well after this period. Two other unidentified species are revealed by the HPLC results.‡ These species form faster than **3**; then, like **2**, they disappear. We tentatively assign these as C3 ethers **4a,b** (*vide infra*), which are inside–outside (conformational) isomers. The faster eluting compound **4a** is assigned to the inside isomer since its hydrophobic interaction with the reverse-phase layer is less than that of the outside isomer.

Compound **2**, available from our previous work, is isomerized to **3** and **4a**,**b** by cyclodextrin alkoxide solutions. The final product distribution depends upon the initial alkoxide composition. When **2** is treated with β-CD alkoxide, the isomerization proceeds mainly to **4a**,**b**, whereas when a nearly equal mixture of β-CD alkoxide and β-CD dialkoxide is used, **3** becomes the ultimate product.

We set out to determine whether the isomerization was intra- or inter-molecular in nature. For this study we synthesized 6-*O*-per(*tert*-butyldimethylsilyl)-2-*O*-(9,10-dicyanoanthracenyl-2-methyl)-β-cyclodextrin **5**.§ The conditions for the isomerization of **2** were repeated: reaction with a stoichiometric amount of β-CD alkoxide and with 1 : 1 alkoxide/dialkoxide. The product composition at various times was probed by HPLC in two ways: (i) by direct injection of the reaction mixture and (ii) after removal of the silyl ethers with HF. Any product (**2**, **3** or **4a**,**b**) seen in the first set can arise only by an intermolecular process. The mixture from the second determination derives from a combination of both inter- and intra-molecular processes. Treatment of **5** with β-CD alkoxide gives rise to an intramolecular isomerization to the persilylated C3 ethers **6a** and **b**. However, treatment with a β-CD alkoxide/dialkoxide mixture produces **3** *via* an intermolecular process.

The assignment of **4a** and **b** as C3 ethers rests on their appearance in both the isomerization of **2** and especially of **5**. In

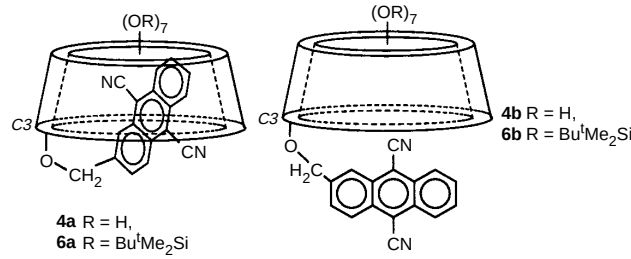
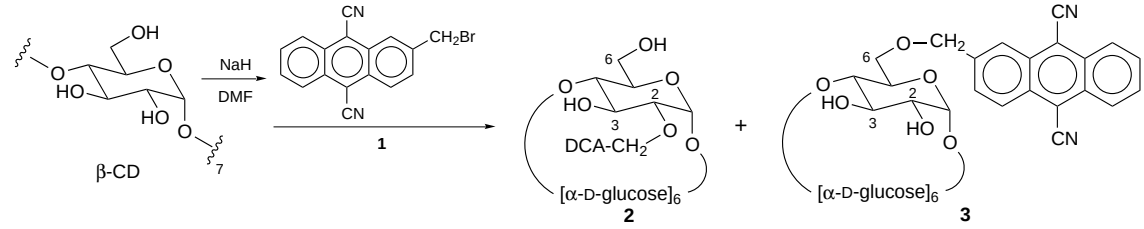


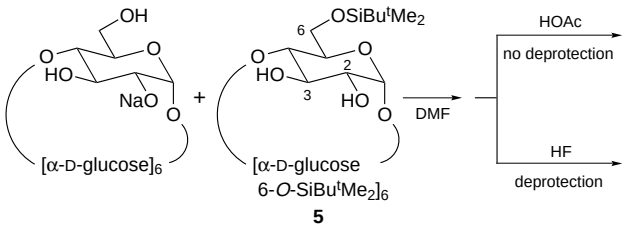

**Fig. 1** 9,10-dicyanoanthracenyl-2-methyl-C3-*O*-β-CD ethers **4a**,**b** and **6a**,**b**




**Scheme 1** Reaction of β-cyclodextrin alkoxide with 2-bromomethyl-9,10-dicyanoanthracene **1**

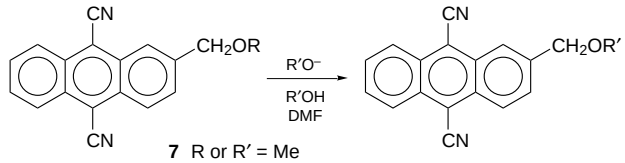
the latter result, the C3 position is the only one possible for a DCA ether product since the C6 hydroxy groups are blocked and the C2 isomer is the starting material. The faster elution of C3 ethers relative to C2 and C6 ethers in reverse-phase HPLC has been documented.[6] The kinetic stability of a self-included C3 ether has been reported recently for a C3 tethered 2-naphthylmethyl group.[7] The DCA group is longer than the naphthyl group, and the C3-inside ether should be even more kinetically stable than the reported naphthyl ether.

The scope of the transetherification was probed through attempted interconversions of compounds **7**–**9** (Scheme 3).¶ The reactions were conducted in DMF using 1.5 equiv. of alkoxide to mimic the above conditions and were monitored by HPLC.‖ Table 1 shows that ether exchange is a general reaction




**5**

**Scheme 2** Reaction of **5** with β-CD alkoxide and subsequent analysis




**7** R or R′ = Me
**8** R or R′ = Bn
**9** R or R′ = $HOCH_2CH_2$

**Scheme 3** Transetherification reactions of alkyl (9,10-dicyanoanthracenylmethyl) ethers

**Table 1** Transetherification yields[a]

| Ether (DCA–$CH_2$–OR) R= | Alkoxide (R′$O^-$) R′= | Yield (%)[b] (DCA–$CH_2$–OR′) | t/min |
|---|---|---|---|
| Me | β-CD[c] | 6 | 360 |
| Me | Bn | 30 | 23 |
| Me | $HOCH_2CH_2$ | 35 | 130 |
| Bn | β-CD[c] | 6 | 360 |
| Bn | Me | 27 | 105 |
| Bn | $HOCH_2CH_2$ | 32 | 1320 |
| $HOCH_2CH_2$ | Me | 58 | 105 |
| $HOCH_2CH_2$ | Bn | 52 | 23 |

[a] Reaction conditions: [DCA–$CH_2$–OR] = *ca*. 0.01 mol $dm^{-3}$, [R′$O^-$] *ca*. 0.015 mol $dm^{-3}$, [R′OH] = *ca*. 10% *v/v* in DMF, 23 °C. [b] Determined by HPLC results. [c] [R′$O^-$] + [R′OH] = *ca*. 0.01 mol $dm^{-3}$.

for DCA-2-methyl ethers. In fact, both **7** and **8** can be used to prepare the DCA- tethered β-CD **3**.

The electron-withdrawing nature of the DCA group as well as the presence of H-bonding[8] should be important factors in the ether exchange process. Other CD ether tethers without such an electron-withdrawing aryl groups do not undergo isomerization.[3] While substitution of electron-withdrawing groups onto benzyl ethers renders them more reactive than benzyl ethers, usually it is the functional group which is attacked, and ether cleavage still requires forcing conditions. The reactivity of **2** is unusual in that ether bond *migrates* instead of just cleaving. The ease with which the dicyanoanthracenylmethyl group is released may render it a useful protecting group for alcohols. We are pursuing independent syntheses of **4a** and **b**, as well as the mechanism of the transetherification reaction.

This work was supported by the National Science Foundation (CHE-9412515). We thank Cerestar for a gift of β-cyclodextrin.

## Footnotes

† Compounds **2**[4] and **3** elute at 21.8 and 22.9 min, respectively, from a 250 × 4.6 mm Whatman ODS-3 column using a linear gradient elution (80 : 20 to 50 : 50 $H_2O$–MeCN over 30 min) at 1.0 ml $min^{-1}$. The absorption at 254 nm was detected, and peak area percentages are reported as mole fractions.

‡ Compounds **4a** and **b** show retention times of 18.8 and 19.9 min, respectively.

§ Compound **5** was prepared from per-6-*O*-(*tert*-butyldimethylsilyl)-β-CD[5] by first forming the alkoxide with NaH in THF, then alkylating with **1**. It was purified by HPLC on silica gel, characterized by NMR, and gave satisfactory combustion analysis.

¶ Compounds **7**–**9** were prepared by $Ag_2O$-assisted alcoholysis reactions of **1**.

‖ Compounds **7** and **8** elute at 7.6 and 6.3 min, respectively, from a 250 × 4.6 mm Alltech Econosil column using an isocratic elution ($CHCl_3$) at 0.7 ml $min^{-1}$. Compound **9** elutes at 15.2 min using a linear gradient elution (0–20% MeOH in $CHCl_3$ over 20 min) at 1.0 ml $min^{-1}$. The absorption at 420 nm was detected, and an internal standard was used to determine the yields at 100% conversion.

## References

1 E. Staude and F. Patat, *The Chemistry of the Ether Linkage*, ed. S. Patai, Wiley, New York, 1967, pp. 22–81.
2 T. W. Greene, *Protective Groups in Organic Synthesis*, Wiley, New York, 1981, pp. 29–32.
3 D. Rong and V. T. D'Souza, *Tetrahedron Lett*., 1990, **30**, 4275.
4 B. K. Hubbard, L. A. Beilstein, C. E. Heath and C. J. Abelt, *J. Chem. Soc., Perkin Trans. 2*, 1996, 1005.
5 M. J. Pregel and E. Buncel, *Can. J. Chem*., 1991, **69**, 130.
6 S. H. Smith, S. M. Forrest, D. C. Williams Jr., M. F. Cabell, M. F. Acquavella and C. J. Abelt, *Carbohydr. Res*., 1992, **230**, 289.
7 S. R. McAlpine and M. Garcia-Garibay, *J. Am. Chem. Soc*., 1996, **118**, 2750.
8 D. H. Buchanan, N. Takemura and J. N. O. Sy, *J. Org. Chem*., 1986, **51**, 4291.

*Received, 18th November 1996; Com. 6/07829J*

# A new enzymatic enantioselective synthesis of dialkyl sulfoxides catalysed by monooxygenases

**Stefano Colonna,*[a] Nicoletta Gaggero,[a] Giacomo Carrea[b] and Piero Pasta[b]**

[a] *Istituto di Chimica Organica, Facolta'di Farmacia dell'Universita', Via Venezian 21, 20133 Milano, Italy*
[b] *Istituto di Chimica degli Ormoni, CNR, Via Mario Bianco, 9, 20131 Milano, Italy*

**Numerous dialkyl sulfides were enantioselectively oxidized to optically active sulfoxides catalysed by chloroperoxidase or cyclohexanone monooxygenase.**

The use of sulfoxides as chiral synthons in asymmetric synthesis is well documented and reliable.[1] Intensive research has demonstrated the efficiency of sulfoxides for controlling the stereoselectivity of a large number of reaction types: alkylation of carbanions, Michael addition, aldolisation reactions, cycloadditions, Pummerer rearrangement and so on. Several sulfoxides also have attractive pharmacological or biological activities.[2] There has been extensive research in recent years trying to develop new methods for the preparation of enantiomerically pure sulfoxides.

The wider application of methodologies based on the sulfinyl function is limited, however, by the relative paucity of general one-step procedures for obtaining enantiomerically pure sulfoxides, especially dialkyl sulfoxides.

Alkyl methyl sulfoxides of high enantiomeric purity have been prepared from cholesterol methyl sulfinates. This process requires a separation of diastereoisomers which are then treated with the relevant alkyl Grignard reagent to furnish the optically active sulfoxide.[3] Similarly, diacetone-D-glucose (DAG) has been used to induce chirality at sulfur.[4] Reaction of diastereoisomerically pure DAG-alkyl sulfinates with Grignard reagents gives optically active dialkyl sulfoxides with high ee (up to ⩾98%).[4]

Optical active cyclic sulfites derived from (*S*)-ethyl lactate have also found use in the preparation of optically active dialkyl sulfoxides.[5] In this case two consecutive displacements with Grignard reagents are required before the chiral transfer agent is released, but separation of intermediate sulfinate esters is still required. Optically active oxazolidinones derived from norephedrine and phenylalanine have also been used in a chiral auxiliary based route to dialkyl sulfoxides.[6]

A different approach to optically active sulfoxides involves an asymmetric oxidation of prochiral sulfides by the Sharpless procedure, modified independently by Kagan[7] and Modena;[8] in the case of dialkyl sulfoxides the ee values ranged between 50–71%. A new catalytic asymmetric oxidation by cumyl hydroperoxide using a chiral titanium complex as catalyst has been reported by Kagan recently (68% ee in the case of octyl methyl sulfoxide).[9] The asymmetric sulfoxidation with enantiomerically pure oxaziridines has been little used for the synthesis of optically active dialkyl sulfoxides.[10,11]

An alternative to asymmetric oxidation with chiral chemical oxidants is the enzymatic oxidation.[12] The only systematic study on an enzymatic asymmetric aliphatic sulfoxidation was carried out by May and co-workers.[13] *Pseudomonas oleovorans*, a non-haem monooxygenase, catalyses stereoselective sulfoxidation of methyl thioether substrates. The ee values of the prevailing sulfoxide are in the range 2–88%, depending upon the structure of the second alkyl chain. Apart from the necessity of a terminal methyl group, the biotransformation catalysed by *Pseudomonas oleovorans* suffers from a poor chemical yield.

Here we present a new enzymatic general approach to the synthesis of dialkyl sulfoxides with high ee. The enzymes used were chloroperoxidase from *Caldariomyces fumago* (CPO) and cyclohexanone monooxygenase (CMO) from *Acinetobacter* NCIB 9871, an iron-haem and a flavin-dependent oxidoreductase, respectively.

Previously, we have shown that these enzymes can catalyse the asymmetric sulfoxidation of numerous alkyl aryl sulfides with high enantioselectivity.[14] The versatility of CMO in promoting enantioselective sulfoxidations has been recently exploited also with 1,3-dithioacetals.[15]

Yields and enantiomeric excesses of the CPO and CMO catalysed oxidation of the dialkyl sulfides tested are reported in Tables 1 and 2. Cyclopentyl methyl sulfide **1**, allyl methyl sulfide **3**, isopropyl methyl sulfide **6** and bis(thiomethyl) methane **9** are excellent substrates for CPO in terms of chemical yield and ee. The increase in the size of the cycloalkane bound to the sulfur (cyclohexyl **2** instead of cyclopentyl **1**), leads to an appreciable decrease in chemical and optical yield. The importance of steric factors on chemical yield and ee is confirmed by the results obtained with methyl sulfides with different alkyl chains **4**, **5**. An increase in the branching of the alkyl chain causes similar effects **6**, **7**. These results can be rationalized by taking into account the higher contribution of the competitive spontaneous oxidation of the more hindered starting materials for which the enzymatic oxidation is slower. As already observed for alkyl aryl sulfides,[14] the oxidation of

**Table 1** CPO catalysed oxidation of sulfides to the corresponding sulfoxides [a]

| Sulfide | Conversion (%) | Ee (%) | Configuration |
|---|---|---|---|
| **1** Cyclopentyl methyl sulfide | ⩾98 | ⩾98 | *R*[b] |
| **2** Cyclohexyl methyl sulfide | 85 | 85 | *R* |
| **3** Allyl methyl sulfide | ⩾98 | ⩾98 | *R* |
| **4** Pentyl methyl sulfide | 75 | ⩾98 | *R* |
| **5** Octyl methyl sulfide | 40 | 54 | *R* |
| **6** Isopropyl methyl sulfide | ⩾98 | ⩾98 | *R* |
| **7** *tert*-Butyl methyl sulfide | 80 | 85 | *R* |
| **8** *tert*-Butyl ethyl sulfide | 30 | 35 | *R* |
| **9** Bis(thiomethyl)methane | 75 | ⩾98 | *R* |

[a] The sulfide (0.42 mmol) and CPO (Sigma) ($6.7 \times 10^{-6}$ mmol) were magnetically stirred in 40 ml of 0.05 mol $dm^{-3}$ citrate buffer, pH 5 at 25 °C for 5 min. $H_2O_2$ (0.42 mmol) in 480 μl of buffer, pH 5, was added in 18 aliquots at 3 min intervals. The reaction was quenched with sodium sulfite, extracted with diethyl ether and dried. The enantiomeric excesses of sulfoxides were determined by chiral HPLC on a Chiralcel OB column (Daicel), using the proper mixture of hexane and propan-2-ol as the mobile phase. The absolute configuration of sulfoxides was determined by comparison with authentic samples prepared by Sharpless oxidation and using chiral HPLC. [b] The absolute configuration of cyclopentyl methyl sulfoxide was determined by analysis of its $^1$H NMR spectrum in the presence of the chiral shift reagent (*S*)-(+)-α-methoxy-α-phenylacetic acid (ref. 17).

**Table 2** CMO catalysed oxidation of sulfides to the corresponding sulfoxides [a]

| Sulfide | Conversion (%) | Ee (%) | Configuration |
|---|---|---|---|
| **1** Cyclopentyl methyl sulfide | 80 | ⩾98 | *R*[b] |
| **2** Cyclohexyl methyl sulfide | 86 | ⩾98 | *R* |
| **3** Allyl methyl sulfide | 82 | ⩾98 | *R* |
| **4** Pentyl methyl sulfide | 58 | 60 | *S* |
| **5** Octyl methyl sulfide | 50 | 50 | *S* |
| **6** Isopropyl methyl sulfide | 75 | ⩾98 | *R* |
| **7** *tert*-Butyl methyl sulfide | 85 | ⩾98 | *R* |
| **8** *tert*-Butyl ethyl sulfide | 30 | 35 | *R* |
| **10** *tert*-Butyl vinyl sulfide | 78 | ⩾98 | *R* |
| **11** Cyclohexyl ethyl sulfide | 8 | 47 | *R* |
| **12** 4-Hydroxyethyl methyl sulfide | 80 | 33 | *R* |

[a] The sulfide (0.1 mmol) was magnetically stirred in 4 ml of 0.05 mol $dm^{-3}$ Tris–HCl buffer, pH 8.6, containing 2 μmol NADPH, 0.4 mmol glucose-6-phosphate, 5 units of CMO and 10 units of glucose-6-phosphate dehydrogenase. After overnight reaction, the solution was extracted with 4 portions (4 ml each) of diethyl ether and the organic extract was dried and evaporated. The enantiomeric excesses of sulfoxides were determined by chiral HPLC on a Chiralcel OB column (Daicel), using the proper mixture of hexane and propan-2-ol as the mobile phase. The absolute configuration of sulfoxides was determined by comparison with authentic samples prepared by Sharpless oxidation and using chiral HPLC. [b] The absolute configuration of cyclopentyl methyl sulfoxide was determined by analysis of its $^1$H NMR spectrum in the presence of the chiral shift reagent (*S*)-(+)-α-methoxy-α-phenylacetic acid.[17]

dialkyl sulfides affords predominantly or exclusively the corresponding (*R*)-sulfoxide.

For CMO promoted sulfoxidation, high enantioselectivity is observed for cycloalkyl methyl sulfoxides (**1**, **2**), and methyl sulfoxides with a linear or branched alkyl chain of up to four carbon atoms (**3**, **6**, **7**). In all these cases the absolute configuration of the prevailing enantiomer is *R*. A longer alkyl chain not only causes a drastic drop in the chemical and optical yield **4**, **5**, but also changes the stereochemical course of the sulfoxidation, since the resulting enantiomer now has the *S* absolute configuration.

The predictive active site model for the cyclohexanone monooxygenase catalysed oxidation of sulfides to sulfoxides, already proposed by us,[16] is compatible with these results but does not offer conclusive evidence due to the high conformational freedoms of dialkyl sulfides.

A comparison of the results obtained in the oxidation of dialkyl sulfides with CPO and CMO leads to the following conclusions: (i), both enzymes exibit high enantioselectivity in the oxidation of cycloalkyl methyl and alkyl methyl sulfides with limited steric requirements; (ii), the two enzymatic systems are enantiocomplementary for pentyl methyl sulfide and for octyl methyl sulfide, leading in all other cases to the (*R*)-sulfoxides; (iii) chloroperoxidase is more convenient than cyclohexanone monooxygenase since it is commercially available, uses hydrogen peroxide as oxidant and does not require the regeneration of the cofactor, as in the case with CMO.

This work was partially supported by EEC Human Capital and Mobility Programme and by COST Programme.

## References

1 G. Solladie', *Synthesis*, 1981, 185; J. Drabowicz and K. M. Mikolajczyk in, *The Chemistry of Sulfones and Sulfoxides*, ed. S. Patai , Z. Rappoport and C. J. M. Stirling, Wiley, 1988, pp. 233–278; K. K. Andersen, pp. 55–94, G. H. Posner, pp. 823–849.
2 M. C. Carreňo, *Chem. Rev*, 1995, **95**, 1717.
3 K. K. Andersen, B. Bujnicki, J. Drabowicz, M. Mikolajczyk and J. B. O'Brien, *J. Org. Chem.*, 1984, **49**, 4070.
4 I. Fernandez, N. Khiar, J. Llera and F. Alcudia, *J. Org. Chem*, 1992, **57**, 6789.
5 F. Rebiere, O. Samuel, L. Ricard and H. B. Kagan, *J. Org. Chem.*, 1991, **56**, 5991.
6 D. A. Evans, M. M. Faul, L. Colombo, J. J. Bisaha, J. Clardy and D. Cherry, *J. Am. Chem. Soc.*, 1992, **114**, 5977.
7 P. Pitchen, E. Duňach, M. N. Deshmukh and H. B. Kagan, *J. Am. Chem. Soc.*, 1984, **106**, 8188.
8 F. Di Furia, G. Modena and R. Seraglia, *Synthesis*, 1984, 325.
9 J. M. Brunel and H. B. Kagan, *Synlett.*, 1996, 404.
10 F. A. Davis, R. T. Reddy, W. Han and R. E. Reddy, *Pure Appl. Chem.*, 1993, **65**, 633 and references cited therein.
11 P. C. Bulman Page, J. P. Heer, D. Bethell, E. W. Collington and D. M. Andrews, *Tetrahedron: Asymmetry*, 1995, **6**, 2911.
12 H. L. Holland, *Chem. Rev.*, 1988, **88**, 473.
13 A. G. Katopodis, H. A. Smith, Jr and S. W. May, *J. Am. Chem. Soc.*, 1988, **110**, 897.
14 S. Colonna, N. Gaggero, L. Casella, G. Carrea and P. Pasta, *Tetrahedron: Asymmetry*, 1992, **3**, 95 and references cited therein; S. Colonna, N. Gaggero, P. Pasta and G. Ottolina, *Chem. Commun.*, 1996, 2303 and references cited therein.
15 S. Colonna, N. Gaggero, A. Bertinotti, G. Carrea and P. Pasta, *J. Chem. Soc., Chem. Commun.*, 1995, 1123; S. Colonna, N. Gaggero, G. Carrea, P. Pasta and A. Bernardi, *Tetrahedron: Asymmetry*, 1996, **7**, 565.
16 G. Ottolina, P. Pasta, G. Carrea, S. Colonna, S. Dallavalle and H. L. Holland, *Tetrahedron: Asymmetry*, 1995, **6**, 1375.
17 H. L. Holland, F. M. Brown and B. G. Larsen, *Bioorg. Medicinal Chem.*, 1994, **2**, 647.

*Received, 12th December 1996; Com. 6/08352H*

# An ω-functionalized perfluoroalkyl chain: synthesis and use in liquid crystal design

**Sandrine Pensec and François-Genès Tournilhac*†**

*ESPCI (CNRS URA429), Chimie et Electrochimie des Matériaux Moléculaires, 10 rue Vauquelin, 75231 Paris Cedex 05, France*

**A multiblock polyphilic compound incorporating a perfluoroalkyl spacer and associating groups at both extremities exhibits smectic A and smectic C mesophases.**

Perfluoroalkyl iodides permit the formation of stable C–C bonds by the Ullman reaction[1] or by free-radical addition to alkenes followed by dehalogenation.[2] They have been widely used in the design of highly fluorinated mesomorphic materials.[3,4] In the course of our research into polyphilic mesogens,[5] the need arose for new molecular architectures incorporating a central perfluoroalkyl bridge. Symmetric α,ω-diiodoperfluoroalkanes are available by several routes[6,7] but, to our knowledge, there is no efficient procedure for the synthesis of a perfluoroalkyl chain bearing two different reactive groups in the α and ω positions.

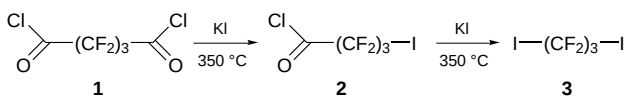
When reacting perfluoroglutaryl chloride with potassium iodide at 200–400 °C, McLoughlin noticed the formation of some 4-iodoperfluorobutyryl chloride,[7] which was isolated in the form of the free acid (Scheme 1).

In this original work,[7] relatively high yields (50–60%) of **3** were obtained when using high temperatures and long reaction times. In our experiments, all precautions were taken: (*i*) to stop the progression of the reaction at the optimum time; (*ii*) to avoid the hydrolysis of **2** into the corresponding acid; and (*iii*) to form a versatile derivative of **2** which may be easily purified and characterized.

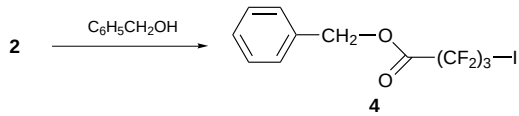
The starting material (hexafluoroglutaryl chloride), obtained from hexafluoroglutaric acid and oxalyl chloride, was vaporized at 220 °C with a nitrogen flow and passed at 350 °C through a glass tube packed with finely ground potassium iodide. The reaction time was determined by the flow of nitrogen. The products were trapped at −78 °C. The degree of conversion estimated by the relative intensities of the 1793 $cm^{-1}$ (C=O stretch) and 1128 $cm^{-1}$ (CF stretch) IR bands; was taken as a criterion for optimizing the reaction time. The products **1**, **2** and **3** were immediately treated with benzyl alcohol in toluene in the presence of pyridine and benzyl-4-iodoperfluorobutanoate **4** was isolated by liquid chromatography with an overall yield of 16% (Scheme 2).‡

Bifunctional spacer units are useful in the chemistry of covalently grafted surfaces, artificial membranes, liquid crystalline polymers, *etc.* Compound **4** allows the preparation of new mesomorphic materials as will be exemplified below.

Polyphilic compounds are made up of a sequence of molecular fragments differing in their chemical nature. In the mesomorphic state, unlike fragments have a tendency to segregate, hence leading to the formation of smectic layers.[4,5,8–10] Perfluoroalkyl chains have been widely used in the design of such materials, but always as end-groups. Starting from benzyl 4-iodoperfluorobutanoate, we have initiated the synthesis of new polyphilic compounds incorporating a perfluoroalkyl spacer in the central part of the molecule. Compound **7** was synthesized in three steps starting from **4** (Scheme 3).



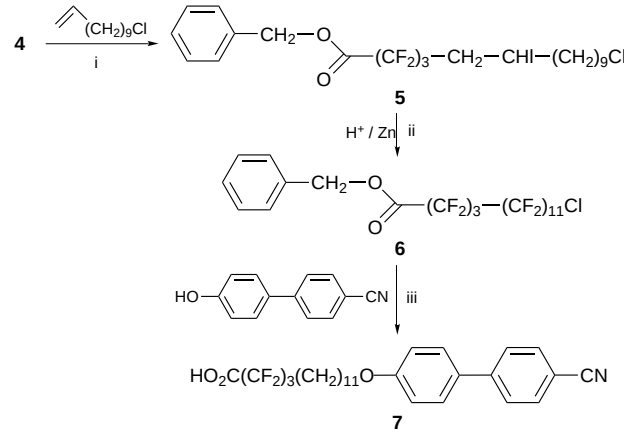

**Scheme 1**



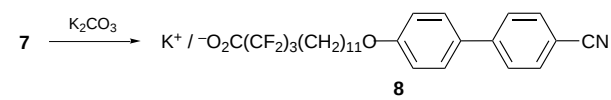

**Scheme 2**

Compound **4** was treated with 1-chloroundec-10-ene in the presence of azoisobutyronitrile (AIBN) to give benzyl 15-chloro-2,2,3,3,4,4-hexafluoro-6-iodopentadecanoate **5** which was in turn reduced to benzyl 15-chloro-2,2,3,3,4,4-hexafluoropentadecanoate **6** using Zn/HCl. Compound **6** was reacted with 4-cyano-4′-hydroxybiphenyl in the presence of $K_2CO_3$ in DMF to give the polyphilic compound **7**.† Compound **7** melts at 124.5 °C and is not mesomorphic. The p$K_a$ value of **7** is < 2. The potassium salt **8** was prepared by treatment with an aqueous solution of $K_2CO_3$ (Scheme 4).

The mesomorphic properties of **8** have been investigated by differential scanning calorimetry, optical microscopy and X-ray diffraction. On cooling from the isotropic phase, birefringence was detected at 186 °C by the growth of *bâtonnets*[11] which gradually merge to form the well known focal conic texture. This mesophase was identified as smectic A since homeotropic domains were also evident in the same temperature range. The focal conic texture is stable down to 135 °C, the temperature at which the focal domains become divided into subdomains showing different interference colours (broken fan texture[12,13]). At the same temperature, the *schlieren* texture appears in the previously homeotropic domains. These texture changes are




**Scheme 3** *Reagents and conditions*: i, AIBN, heptane, 90 °C, 4 h, 81%; ii, isooctane + acetic acid, 110 °C, 2 h, 72%; iii, $K_2CO_3$, DMF, 90 °C, 3 h, then HCl, 68%




**Scheme 4**

characteristic of the smectic A → smectic C transition.[13] This second fluid mesophase is monotropic, it may be observed for a few minutes in the 135–110°C range, whereupon crystallization rapidly occurs.

The DSC trace shows, on heating, two endotherms at 135 and 190 °C with enthalpies of 8.9 and 4.3 kJ mol$^{-1}$ respectively, corresponding to the K → $S_A$ and $S_A$ → I transitions. On cooling the reverse transitions take place at 186 and 123 °C.

Thus, whilst **7** is isotropic in the 135–190 °C range, the appearance of lamellar order in **8** may be related to the segregation of the ionic head from all other hydrophobic moieities.

X-Ray diffraction experiments were carried out on unoriented samples using Cu-Kα radiation. Attempts to investigate **8** in the smectic C phase failed due to its metastable character. The X-ray diffraction pattern recorded at 150 °C in the smectic A phase of **8** is presented in Fig. 1.

At large angles, a broad diffuse ring with a maximum at $2\pi/q = 4.9$ Å ($q = 4\pi \sin\theta/\lambda$) confirms the identification as smectic A and gives an estimate of the average intermolecular distance (*ca.* 5.7 Å). At narrow angles, the diagram shows three 00*l* reflections corresponding to an interlayer distance of 42.2 Å. The distance is intermediate between once and twice the molecular length (32 Å); a partially bilayered packing of the smectic $A_d$ type[14] may therefore be proposed. A similar observation was reported for other rodlike mesogens with ionic head-groups.[15] In $Na^+$ and $K^+$ long-chain carboxylates, a lipidic sublayer thickness 1.3 times greater than the alkyl chain length was interpreted by the formation of a double layer with strongly disordered alkyl chains.[16] In our case, the rigid cyanobiphenyl cores cannot be accommodated in any conformation, however, these fragments usually tend to optimize their packing by partial interdigitation. As already mentioned for polyphilic mesogens with cyanobiphenyl cores, the appearance of the smectic $A_d$ and C phases can be related to the close packing of lengthwise dimers associated through the cyano groups.[9]

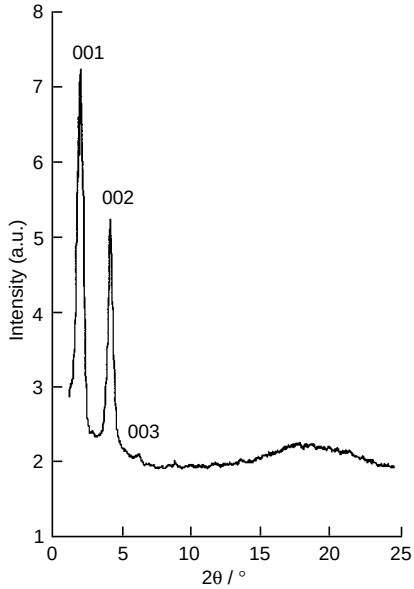



**Fig. 1** X-Ray (Debye–Scherrer) diffraction diagram of compound **8** recorded at 150 °C (densitometric profile of the photographic film)

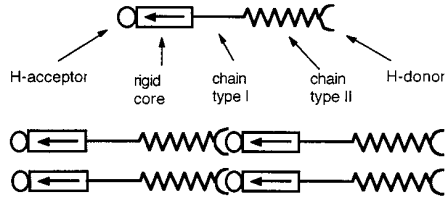



**Fig. 2** Polar rows of molecules expected from polyphilic compounds bearing hydrogen-bond donor and acceptor groups at the extremities

The potentialities of hydrogen-bond associated systems in the design of new mesomorphic architectures have been evidenced by several authors.[17] The synthetic scheme described in this paper permits the grafting of hydrogen-bond donor and acceptor groups at each molecular end of a polyphilic compound. It is noteworthy that polar rows of molecules may be formed in the liquid phases of such materials (Fig. 2).

J. Simon is thanked for helpful and stimulating discussions, D. Lelièvre for her help in X-ray measurements.

## Footnotes

† E-mail: fgt@cis.espci.fr

‡ *Selected analytical data*: **4**: MS (EI, *m/z*): 412 [M]$^+$, 277 [M − $CO_2CH_2C_6H_5$]$^+$, 227 [M − $CF_2CO_2CH_2C_6H_5$]$^+$, 177 [M − $(CF_2)_2CO_2CH_2C_6H_5$]$^+$, 127 [M − $(CF_2)_3CO_2CH_2C_6H_5$]$^+$, 91 [M − $I(CF_2)_3CO_2$]$^+$. IR (KBr, cm$^{-1}$) 1778.9 (C=O), 1190.1, 1145.0 (C–F), 770 (C–H arom., out of plane). $^1$H NMR ($CDCl_3$, $Me_4Si$, 300 MHz, δ) 7.43 (s, 5 H, $C_6H_5$), 5.4 (s, 2 H, $CH_2$). $^{13}$C NMR ($CDCl_3$, 75 MHz, δ) 158.45 (t, *J* 29.9 Hz, $CF_2$*C*OOR), 133.23 (s, arom.), 129.11 (s, arom.), 128.73 (s, arom.), 128.48 (s, arom.), 108.45 (m, *J* 265.5, 31.75 Hz, $CF_2$*C*$F_2CF_2$COOR), 106.94 (m, *J* 267.95, 33.6 Hz, $CF_2$*C*$F_2$COOR), 93.39 (m, *J* 319.8, 41.5 Hz, $ICF_2CF_2CF_2$), 69.75 (s, $COCH_2$). **7**: MS (CI, *m/z*): 561 [M + $NH_4$]$^+$, 543 [M]$^+$. Anal. Found: C, 61.29; H, 5.87; N, 2.61. Calc. C, 61.87; H, 5.74; N, 2.57. IR (KBr, cm$^{-1}$): 3649 (OH), 2921.5 (C–H asym.), 2850.3 (C–H sym.), 2246.1 (CN), 1781.8 (C=O), 1603.7 (C=C), 1178.1, 1142.5 (C–F), 827.0 (C–H, out of plane). $^1$H NMR ([$^2H_6$]acetone, 300 MHz, δ) 8.19 (s, 1 H, COOH), 7.79 (4 H, arom.), 7.67 (2 H, *J* 9.18 Hz, arom.), 7.05 (2 H, *J* 9.18 Hz, arom.), 4.03 (t, 2 H, *J* 6.6 Hz, $OCH_2$), 2.13 (m, 2 H, $CH_2CF_2$), 1.78 (qnt, 2 H, *J* 6.6 Hz, C*H*$_2$$CH_2CF_2$), 1.2 (m, alkyl). $^{13}$C NMR ([$^2H_6$]acetone, 75 MHz, δ) 160.86 (s, arom.), 160.75 (t, *J* 28.7 Hz, $CF_2$*C*OOH), 145.87 (s, arom.), 133.46 (s, arom.), 131.80 (s, arom.), 129.17 (s, arom.), 127.86 (s, arom.), 119.61 [m, *J* 251.4, 31 Hz, $(CH_2)_{11}$*C*$F_2CF_2CF_2$], 119.51 (s, CN), 115.94 (s, arom.), 112.06 (m, *J* 263 Hz, $CF_2$*C*$F_2CF_2$COOH), 110.84 (s, arom.), 109.57 (m, *J* 263, 32 Hz, $CF_2$*C*$F_2$COOH), 68.72 (s, $OCH_2$), 31.43 [t, *J* 22 Hz, *C*H$_2$$(CF_2)_3$], 29.8 ($CH_2$), 26.76 [s, $OCH_2CH_2$*C*H$_2$$(CH_2)_8$], 20.94 [s, $(CH_2)_9$*C*H$_2$$CH_2(CF_2)_3$].

## References


1 V. C. R. McLoughlin and J. Thrower, *Tetrahedron*, 1969, **25**, 5921.
2 R. N. Haszeldine, *J. Chem. Soc.*, 1962, 4491; N. O. Brace, *J. Org. Chem.*, 1962, **27**, 4491; 3033.
3 V. V. Titov, T. I. Zverkova, E. I. Kovshev, Yu. N. Fialkov, S. V. Shelazhenko and L. M. Yagupolski, *Mol. Cryst. Liq. Cryst.*, 1978, **47**, 1.
4 P. Kromm, M. Cotrait, J. C. Rouillon, P. Barois and H. T. Ngugen, *Liq. Cryst.*, 1996, **21**, 121 and references therein.
5 F. Tournilhac, L. Bosio, J. F. Nicoud and J. Simon, *Chem. Phys. Lett.*, 1988, **145**, 482.
6 R. N. Haszeldine, *Nature*, 1951, **167**, 139; V. Tortelli and C. Tonelli, *J. Fluorine Chem.*, 1990, **47**, 199 and references therein.
7 V. C. R. McLoughlin, *Tetrahedron Lett.*, 1968, **46**, 4761.
8 F. Tournilhac, L. Bosio, J. Simon, L. M. Blinov and S. V. Yablonsky, *Liq. Cryst.*, 1993, **14**, 405; E. Dietzmann, W. Weissflog, S. Markscheffel, A. Jákli, D. Lose and S. Diele, *Ferroelectrics*, 1996, **180**, 341; P. Kromm, M. Cotrait and H. T. Nguyen, *Liq. Cryst.*, 1996, **21**, 95.
9 B. I. Ostrovskii, F. G. Tournilhac, L. M. Blinov and W. Haase, *J. Phys. II (France)*, 1995, **5**, 979; M. Ibn-Elhaj, H. J. Coles, D. Guillon and A. Skoulios, *J. Phys. II (France)*, 1993, **3**, 1807.
10 J. G. Jegal and A. Blumstein, *J. Polym. Sci. A*, 1995, **33**, 2673; D. Markovitsi, A. Mathis, J. Simon, J.-C. Wittman and J. le Moigne, *Mol. Cryst. Liq. Cryst. Lett.*, 1980, **64**, 121.
11 G. Friedel, *Ann. Phys. (France)*, 1922, **18**, 273.
12 G. W. Gray and J. W. Goodby, *Smectic Liquid Crystals*, Leonard Hill, Glasgow, 1984.
13 D. Demus and H. Richter, *Textures of liquid crystals*, Verlag Chemie, Weinheim, 1978.
14 F. Hardouin, A. M. Levelut, M. F. Achard and G. Sigaud, *J. Chim. Phys.*, 1983, **80**, 53; D. Guillon and A. Skoulios, *J. Phys. (France)*, 1984, **45**, 607.
15 S. Ujiie and K. Iimura, *Macromolecules*, 1992, **25**, 3174.
16 A. Skoulios, *Adv. Colloid Interface Sci.*, 1967, **1**, 79.
17 T. Kato and J. M. J. Fréchet, *Macromolecules*, 1989, **22**, 3819; J. M. Lehn, *Angew. Chem., Int. Ed. Engl.*, 1990, **29**, 1304; C. Alexander, C. P. Jariwala, C. M. Lee and A. C. Griffin, *Polym. Prepr.*, 1993, **34**, 168.


*Received, 3rd January 1997; Com. 7/00085E*

# Energy filtered transmission electron microscopy (EFTEM) in the characterization of supported $TiO_2$ photocatalysts

**Alexander Starosud,[a] David P. Bazett-Jones[b] and Cooper H. Langford*[a]**

*Departments of [a]Chemistry and [b]Medical Biochemistry, The University of Calgary, A110-2500 University Dr. NW, Calgary, Alberta, Canada T2N 1N4*

**Energy filtered transmission electron microscopy demonstrates whether $TiO_2$ is on the surface or enters the pore channel system of zeolites.**

The widely studied photocatalyst, $TiO_2$, is often supported, either to simplify material handling or to modify the properties of the catalyst. Our group[1,2] and others[3] have exploited silica and zeolite supports. Our intention has been to modify the catalytic behaviour of the systems through convolution of the very general, non-selective, photocatalytic oxidation activity of $TiO_2$ with the absorption characteristics and specific oxidative catalysis available with high silica zeolites. In order to understand and manipulate such systems, it is necessary to develop tools for the detailed examination of the distribution of $TiO_2$ on and in the supports. In our earlier papers,[1,2] we described the information derivable from scanning electron microscopy, powder X-ray diffraction and vibrational spectroscopy. These indicated that $TiO_2$ thin films or microparticles on the zeolites were the most photoactive. In the case of large silica particles which could be examined in the cross-section, it was possible to gain insight into the behaviour of photocatalytic sites in the interior of the particles.[2] However, a severe limitation was the inability to image the distribution of $TiO_2$ in conventional small zeolite particles.

This communication describes a technique for imaging such a distribution. It exploits energy filtered transmission electron microscopy (EFTEM) (which has been used for mapping other elements[4–6]) to image cross-sections of micron-sized zeolite particles with varying sizes of mesopores which favour different distributions of $TiO_2$. The basis of the technique is that energy losses of electrons that pass through a sample are characteristic of the chemical elements present. Electrons are separated according to energy loss by a spectrometer which also acts as a lens.[7] The Ti-specific ionization edge L2,3 occurs at 456 eV. Consequently, a 430 eV image does not contain any Ti-specific information, whereas a 460 eV image is 'Ti-enhanced'. A net Ti distribution can be determined by subtracting the pre-edge reference image from the post-edge Ti-enhanced image. Samples were imbedded in QUETOL and thin-sectioned with an ultramicrotome to sections 30 nm thick. Energy loss micrographs were recorded with a Zeiss EM902 instrument equipped with an imaging spectrometer. A 500 μm condenser aperture, a 60 μm objective aperture and a 20 eV energy selecting slit aperture were used. Images were recorded at a magnification of 13 000 × on SO-163 electron image film (Kodak). The film was then digitized and analysed as described previously.[7]

We report here on the contrast of a demonstration sample pair that illustrates the power of the technique. Our preferred method[1] for $TiO_2$ loading of zeolites is to stir a colloid of $TiO_2$ with zeolite, remove the solvent and calcine at a moderate temperature (450 °C). Some experiments have suggested that the $TiO_2$ colloids may be labile so that smaller particles in equilibrium with the dominant ones might enter pores of the support which are smaller than the nominal particle size in the colloid, leading to distribution of $TiO_2$ into the particle interior. To test this, we have studied the loading of 'Q-sized' $TiO_2$ particles with diameters of 20–40 Å[8] into two compositionally similar zeolites of the mesoporous MCM-41 family,[9] one of which had an average pore diameter of 20 Å (MCM-20), the other with an average pore diameter of 60 Å (with pores up to 120 Å) (MCM-60). The pore size distributions of these two were measured by $N_2$ absorption in an ASDI RXM-100 catalyst characterization system. Penetration of Q-sized particles into the larger pore-sized MCM-41 should be facile. In contrast, penetration into the smaller pore size (20 Å) requires that the Q-sized colloid is in labile equilibrium with fragments smaller than the nominal particle size.

In Fig. 1, we show the net images (lower) resulting from the subtraction of the pre-edge reference image (upper) from the post-edge Ti-enhanced image (middle). The MCM-60 is shown in Fig. 1(*b*) and images of MCM-20 are shown in Fig. 1(*a*). These two images are representative of a number we recorded, and it must be understood that we do not control the orientation of the particles with respect to cutting direction of the ultramicrotome. A dark region across the centre of the particle shown in Fig. 1(*b*) (lower) indicates that $TiO_2$ particles did not fully penetrate the zeolite but the distribution of light dots clearly reveals deep penetration of $TiO_2$. In Fig. 1(*a*), we see that little penetration of $TiO_2$ into MCM-20 particles occurs.

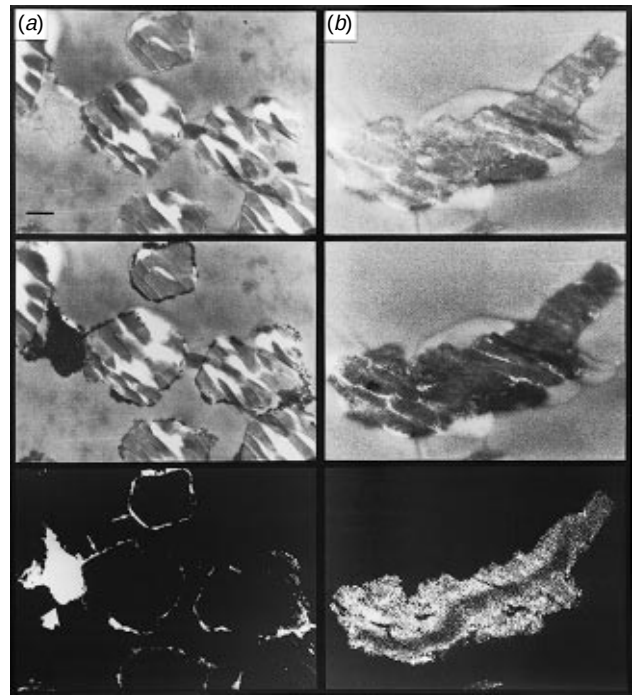



**Fig. 1** Energy filtered images of zeolites MCM-41 with average pore diameters of 20 Å (*a*) and 60 Å (*b*). Pre-edge images were recorded at 430 eV (upper panels), post Ti-edge images were recorded at 460 eV (middle panels). The lower panels show the net images after alignment, subtraction and inversion of contrast (Ti-rich regions shown as white on black background). Scale bar = 210 nm.

The hint that labile equilibration of the colloid particles with smaller $TiO_2$ polycations occurs is refuted. Where the colloid is prepared at particle sizes greater than the pore size, penetration is unimportant. Fig. 1(*a*) also shows that not all of the $TiO_2$ has been distributed in a uniform thin layer over the zeolite (small arrows, lower), but that aggregates of $TiO_2$ can form (large arrow, lower). The spatial detail in these images approaches the resolution limits of the electron microscope at 13 000 $\times$ magnification. Structure in the maps, therefore, is better resolved by about two orders of magnitude than can be obtained with X-ray microanalysis in the scanning electron microscope.

We thank the National Sciences and Engineering Research Council of Canada for support.

## References

1 Y. Xu and C. H. Langford, *J.Phys. Chem.*, 1995, **99**, 11501.
2 G. P. Lepore, L. Persaud and C. H. Langford, *J. Photochem. Photobiol*. A, 1996, 1.
3 S. Sampath, H. Uchida and H. Yoneyma, *J. Catal*., 1994, **149**, 189.
4 F. P. Ottensmeyer, *J. Ultrastruct. Res.*, 1984, **88**, 121.
5 D. E. Taylor, E. G. Walter, R. Sherburne and D. P. Bazett-Jones, *J. Ultrastruct. Res.*, 1988, **99**, 18.
6 P. A. Crozier and M. R. McCartney, *J. Catal*., 1996, **163**, 245.
7 M. J. Hendzel and D. P. Bazett-Jones, *J. Microsc.*, 1996, **182**, 1.
8 W. Choi, A. Termin and M. R. Hoffman, *J. Phys. Chem*., 1994, **98**, 13669.
9 J. S. Beck, *US Pat.* 5 057 296, 1991.

*Received, 8th August 1996; Com. 6/05530C*

# Rearrangement of *p*-methoxybenzyl-protected allylic alcohols to aldehydes

**Johan Wennerberg, Lars Eklund, Magnus Polla and Torbjörn Frejd***

*Organic Chemistry 1, Department of Chemistry, Lund University, S-22100, Lund, Sweden*

**Allyl *p*-methoxybenzyl ethers undergo an acid-catalysed 1,4-rearrangement to give *p*-methoxyphenylbutyraldehyde derivatives, which can be ring-closed to give substituted naphthalene derivatives.**

During our work with the Lewis acid-induced carbonyl-ene reaction,[1] a key step in our studies towards the synthesis of taxanes,[2,3] we recently discovered a new type of rearrangement (Scheme 1). When a mixture of **1c** and methyl or ethyl glyoxylate was treated with zeolite β or $BF_3{\cdot}Et_2O$, the ene reaction did not occur. Instead, **1c** rearranged to give aldehyde **2c** in good yield, which also occurred in the absence of the alkyl glyoxylate. Although allylic benzyl ethers are a well known class of compounds we were surprised to find that a literature search did not reveal any similar reactions under acidic conditions. One reason for this could be the fact that the reaction does not occur when an unsubstituted benzyl group is used instead of a *p*-methoxybenzyl (PMB) group. Thus, electron rich aromatic rings seems to be necessary. Another reason is that only zeolite β and $BF_3{\cdot}OEt_2$ among fifteen Lewis acids tested effected the rearrangement. The outcome of the reaction is similar to a 1,4-Wittig rearrangement,[4,5] although the reaction conditions and the mechanisms are quite different. While the 1,4-Wittig rearrangement needs strongly basic conditions and is usually a minor side reaction, the present rearrangement proceeds under acidic conditions (zeolite β is an acidic zeolite[6]) and gives moderate to good yields.

We propose the following mechanism; the initial step is the coordination of the Lewis acid (or protic acid) to the ether oxygen (**A**). This possibly leads to increased positive charge at the benzylic carbon, which explains why the *p*-methoxy group is necessary for the charge delocalization. Next, the π-electrons in the double bond attack the benzylic position to form cation **B**, which then undergoes a 1,2-hydride shift to give the aldehyde. The hydride shift was indicated by essentially complete statistical recovery of deuterium at the carbonyl α-position of **2c** after rearrangement of **1c**, which was 50% deuteriated at the allylic methylene group.

We have performed the reaction with four different PMB-protected allylic alcohols. The reaction is very simple to carry out, and easy access to allylic ethers together with the utility of aldehydes of type **2** should make this rearrangement quite useful in organic synthesis.† As a simple demonstration of this we cyclized one of the products, **2c**, using PPA(polyphosphoric acid)[7] to give the naphthalene derivative **3** in good yield. Aromatisation *via* elimination of water followed by oxidation (presumably due to dissolved air) took place directly in the PPA reaction mixture. The scope and limitations, together with various applications, of the described rearrangement will be reported shortly.

This work was financially supported by the Swedish Natural Science Research Council, The Knut and Alice Wallenberg Foundation and The Crafoord Foundation.

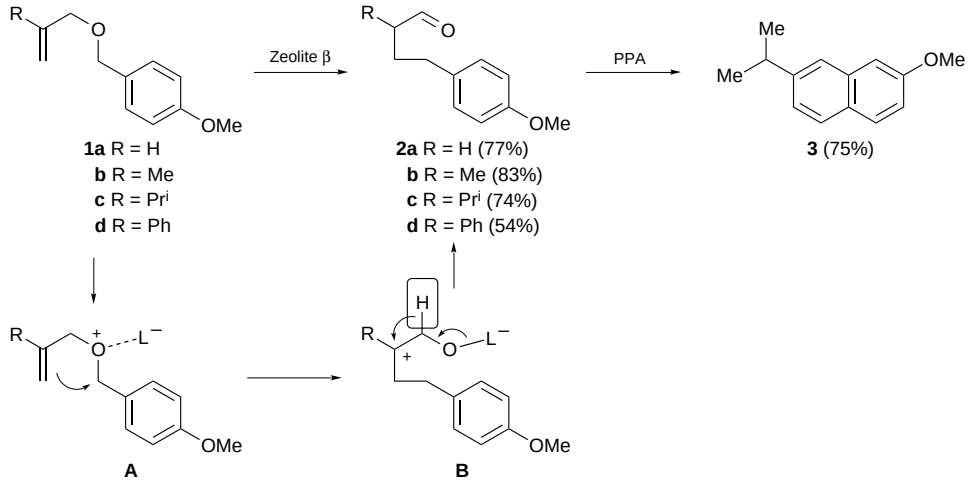
## Footnote

† *Typical procedure*: A solution of the PMB-protected allylic alcohol (1.0 mmol) in $CH_2Cl_2$ (2 ml) was stirred together with zeolite β (125 mg activated at 400 °C for 4 h) overnight at room temperature. The resulting orange–red mixture was then filtered through Celite. The Celite was washed with $CHCl_3$ (2 × 5 ml) and the combined organic extracts were concentrated at reduced pressure. The crude materials were purified by column chromatography ($SiO_2$, heptane–ethyl acetate, 95 : 5).

## References

1 K. Mikami and M. Shimizu, *Chem. Rev.*, 1992, **92**, 1021.
2 M. Polla and T. Frejd, *Tetrahedron*, 1993, **49**, 2701.
3 M. Polla, PhD Thesis, Lund University, 1993.
4 J. A. Marshall, in *Comprehensive Organic Synthesis*, ed. G. Pattenden, Pergamon Press, Oxford, 1991, vol. 3, p. 975.
5 T. Nakai and K. Maikami, in *Organic Reactions*, ed. R. M. Joyce, Wiley New York, 1994, vol. 46, p. 105.
6 M. Linsten, EKA Chemicals AB, personal communication.
7 T. S. Chen, P. Canonne and L. C. Leitch, *Synthesis*, 1973, 620.

*Received, 27th November 1996; Com. 6/08020K*




**Scheme 1**

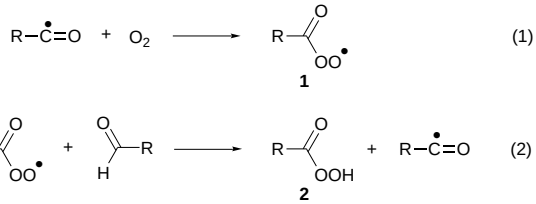
# Oxidation of organic substrates by molecular oxygen mediated by *N*-hydroxyphthalimide (NHPI) and acetaldehyde

**Cathy Einhorn,* Jacques Einhorn, Céline Marcadal and Jean-Louis Pierre**

*Laboratoire de Chimie Biomimétique, UMR CNRS 5616, Université J. Fourier, 38041 Grenoble, France*

**Various organic substrates, in particular hydrocarbons, are efficiently oxidized under mild conditions using molecular oxygen, *N*-hydroxyphthalimide and acetaldehyde, in the absence of metal catalysts.**

The use of molecular oxygen for the selective oxidation of organic substrates, especially hydrocarbons under mild conditions, is still a major challenge for organic chemistry.[1] It constitutes an environmentally safe alternative to more conventional oxidants used in stoichiometric amounts and is therefore of high economic value in industrial chemistry.[2] Catalysis by transition metal complexes is the main way of controlling the partial oxidation of alkanes, alkenes and aromatic hydrocarbons.[3] Although they have been known for a long time, autoxidations *without transition metal catalysis* are often of low efficiency and selectivity. They proceed *via* a free radical chain mechanism promoted by catalytic amounts of radical initiators.[4] Aldehydes are exceptions among organic compounds as their autoxidation rates are very high with long propagation chains [reactions (1) and (2)] even at room temperature and atmospheric pressure. This property has been used in the so-called 'cooxidation' processes, in which a mixture of an aldehyde and another organic substrate is submitted to molecular oxygen. The autoxidation of the aldehyde then promotes the oxidation of the less reactive partner. Aldehyde-mediated cooxidations have been used for the epoxidation of alkenes,[5] Bayer–Villiger oxidation of ketones[6] and oxidation of alcohols and of some hydrocarbons.[7] We describe herein the oxidation of organic substrates, in particular hydrocarbons, under aldehyde-promoted cooxidation conditions, in the presence of *N*-hydroxyphthalimide (NHPI). NHPI has been used previously as an electron carrier for electrochemical oxidations.[8] More recently various oxidations have been conducted using molecular oxygen and NHPI, generally combined with transition metal salts, under nonelectrochemical conditions.[9] Our new combination of $O_2$–aldehyde–NHPI reveals several interesting features. When a 0.2 M solution of ethylbenzene, acetaldehyde (1 equiv.) and NHPI (0.1 mol%) in MeCN was vigorously stirred at room temperature under an oxygen atmosphere for 48 h, a 26% yield of acetophenone and a 6% yield of 1-phenylethanol were formed, with no further reaction after a longer reaction time. No further oxidation was observed after the addition of a second equivalent of acetaldehyde and an additional 48 h stirring time. No NHPI was recovered at the end of this experiment but an almost quantitative amount of phthalimide was isolated. Surprisingly, the same experiment carried out in the *absence of stirring* led to substantially different results; after keeping the reaction medium under oxygen without any stirring for 48 h the yields of ketone and alcohol were 50 and 6%, respectively, while TLC analysis of the solution indicated only a partial degradation of NHPI. The addition of a second equivalent of acetaldehyde and another 48 h standing period led to increased yields of 67 and 9%, respectively. Obviously the rate of aldehyde autoxidation, controlled by oxygen diffusion in the solution, plays a decisive role in the outcome of the reaction. High aldehyde autoxidation rates lead to fast NHPI degradation, no more ethylbenzene being oxidized after its complete disappearance.




Passive diffusion of oxygen in bulk solutions is very sensitive to geometric characteristics of the reactor and therefore difficulties in the reproducibility and scaling up of such experiments may be anticipated. We found that an efficient and reproducible way to perform such oxidations is to add *slowly* the aldehyde to the vigorously stirred reaction medium; when 1 equiv. of acetaldehyde was added over 5 h to a solution of ethylbenzene and NHPI under oxygen, and fast stirring maintained for an additional 5 h period, a 66% yield of acetophenone and a 4% yield 1-phenylethanol were obtained.† Table 1 shows further examples of oxidations performed under the same conditions: 4-nitro-1-ethylbenzene is oxidized with lower efficiency than ethylbenzene itself (run 3) whereas 4-methoxy-1-ethylbenzene is oxidized almost quantitatively (runs 4, 5). 1-Phenylethanol is oxidized only slowly to acetophenone (runs 6, 7) indicating that a direct pathway leading from ethylbenzene to acetophenone is likely. In the case of cumene, demethylation giving acetophenone competes with hydroxylation (run 8). Indane and isochromane are oxidized almost quantitatively (runs 9, 10). Surprisingly diphenylmethane is oxidized with a lower conversion (49%) than ethylbenzene (70%), with a relatively high alcohol : ketone ratio (run 11). A high conversion (94%) is obtained on the other hand with xanthene (run 12). Inactivated hydrocarbons are oxidized at a slow but nevertheless significant rate: 8% conversion of cyclohexane is observed after a 72 h reaction time, with a 1 : 7 alcohol : ketone ratio (run 13). Adamantane is oxidized almost exclusively to adamantan-1-ol with only trace amounts of adamantan-2-one (runs 14, 15).

In order to obtain information about the reaction mechanism of this oxidation, several parameters have been investigated. No oxidation occurs in the presence of either hydroquinone or TEMPO (1 mol%), confirming the free radical pathway of the reaction. No oxidation is observed at room temperature with NHPI alone.‡ Cooxidation of ethylbenzene and acetaldehyde (1 equiv.) in the absence of NHPI furnishes, after 48 h, only 7% ketone and 2% alcohol, indicating a strong cooperative effect of both NHPI and aldehyde under cooxidation conditions. Virtually no oxidation is observed when acetaldehyde is replaced by peracetic acid, clearly indicating that the species involved in these oxidations is not the peracetic acid **2** (R = Me) formed *in situ*, but is probably the acetylperoxy radical **1**. This radical **1** may in turn oxidize NHPI to phthalimide *N*-oxyl **3** [reaction (3)], a fairly stable but highly reactive free radical, which has been proposed as a key intermediate in NHPI-mediated oxidations.[8d,8h,9c]

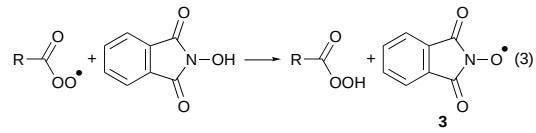
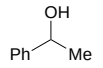
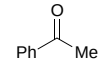
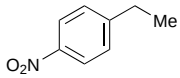
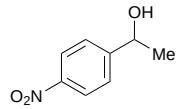
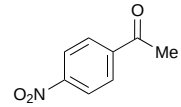
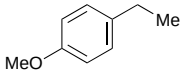
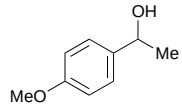
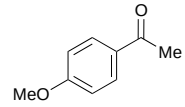
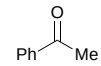
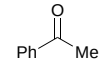
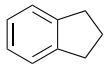
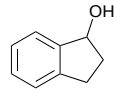
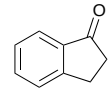
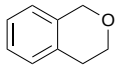
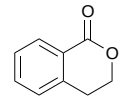
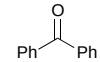
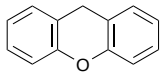
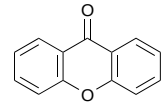
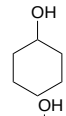
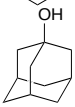
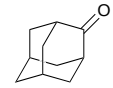


**Table 1** Molecular oxygen oxidation of various substrates mediated by NHPI and acetaldehyde[a]

| Run | Substrate | *t*/h[b] | Conversion (%)[c] | Products (yield, %)[d] | | | |
|---|---|---|---|---|---|---|---|
| 1 |  | 5 | 48 |  | (4) |  | (41) |
| 2 |  | 10 | 70 |  | (4) |  | (66) |
| 3 | | 10 | 24 | | (2) | | (22) |
| 4 |  | 5 | 75 |  | (7) |  | (68) |
| 5 |  | 21 | 97 | — | (7) |  | (90) |
| 6 |  | 5 | 3 |  | |  | (3) |
| 7 | | 72 | 37 | | | | (37) |
| 8 |  | 19 | 75 |  | (46) |  | (29) |
| 9 |  | 10 | 99 | — | (5) |  | (94) |
| 10 |  | 15 | 100 |  | |  | (99) |
| 11 | | 10 | 49 | | (10) | | (36) |
| 12 |  | 19 | 94 | — | |  | (70) |
| 13 |  | 72 | 8 |  | (1) |  | (7) |
| 14 | | 9 | 5 |  | (5) |  | (trace) |
| 15 |  | 24 | 10 | | (10) | | (trace) |

[a] Performed on a 1 mmol scale, in the presence of 0.1 mmol NHPI, in 3 ml MeCN. A solution of 1 mmol acetaldehyde in 3 ml MeCN was added over 5 h *via* a syringe pump. [b] Including the aldehyde addition period. [c] Determined by calibrated quantitative GLC analysis using an internal standard. [d] Absolute yield determined by GLC.

The new oxidation system developed here allows aerobic oxidation of organic substrates under very mild conditions without any metal catalyst, and will therefore find many applications in synthesis. Further studies on the reaction mechanisms involved here are currently under way.

## Footnotes

† Comparative experiments have been performed with benzaldehyde or isobutyraldehyde but with poorer results.

‡ Autoxidations of benzylic derivatives catalysed by NHPI alone have been described [see ref. 9(*a*)], but they occur at significant rates only at comparatively high temperature (100 °C) in benzonitrile as the solvent.

## References


1 C. L. Hill, *Activation and Functionalization of Alkanes*, Wiley, New York, 1989; D. H. R. Barton, A. E. Martell and D. T. Sawyer, *The Activation of Dioxygen and Homogeneous Catalytic Oxidation*, Plenum Press, New York, 1993; A. L. Feig and S. J. Lippard, *Chem. Rev.*, 1994, **94**, 759; B. A. Arndtsen, R. G. Bergman, T. A. Mobley and T. H. Peterson, *Acc. Chem. Res.*, 1995, **28**, 154.

2 U. Schuchardt, W. A. Carvalho and E. V. Spinacé, *Synlett*, 1993, 713.

3 R. A. Sheldon and J. K. Kochi, *Metal-Catalyzed Oxidations of Organic Compounds*, Academic Press, New York, 1981; L. Simandi, *Catalytic Activation of Dioxygen by Metal Complexes*, Kluwer, Boston, 1992.

4 C. L. Hill, *Activation and Functionalization of Alkanes*, Wiley, New York, 1989, p. 17.

5 F. Tsuchiya and T. Ikawa, *Can. J. Chem.*, 1969, **47**, 3191; A. D. Vreugdenhil and H. Reid, *Recl. Trav. Chim. Pays-Bas*, 1972, **91**, 237; K. Kaneda, S. Haruna, T. Imanaka, M. Hamamoto, Y. Nishiyama and Y. Ishii, *Tetrahedron Lett.*, 1992, **33**, 6827.

6 K. Kaneda, S. Ueno, T. Imanaka, E. Shimotsuma, Y. Nishiyama and Y. Ishii, *J. Org. Chem.*, 1994, **59**, 2915.

7 B. M. Choudary and Y. Sudha, *Syn. Commun.*, 1996, **26**, 1651; A. Bravo, F. Fontana, F. Minisci and A. Serri, *Chem. Commun.*, 1996, 1843.

8 (*a*) S. Ozaki and M. Masui, *Chem. Pharm. Bull.*, 1977, **25**, 1179; (*b*) M. Masui, T. Ueshima and S. Ozaki, *J. Chem. Soc., Chem. Commun.*, 1983, 479; (*c*) M. Masui, S. Hara, T. Ueshima, T. Kawaguchi and S. Ozaki, *Chem. Pharm. Bull.*, 1983, **31**, 4209; (*d*) M. Masui, K. Hosomi, K. Tsuchida and S. Ozaki, *Chem. Pharm. Bull.*, 1985, **33**, 4798; (*e*) M. Masui, T. Kawaguchi and S. Ozaki, *J. Chem. Soc., Chem. Commun.*, 1985, 1484; (*f*) M. Masui, S. Hara and S. Ozaki, *Chem. Pharm. Bull.*, 1986, **34**, 975; (*g*) M. Masui, T. Kawaguchi, S. Yoshida and S. Ozaki, *Chem. Pharm. Bull.*, 1986, **34**, 1837; (*h*) C. Ueda, M. Noyama, H. Ohmori and M. Masui, *Chem. Pharm. Bull.*, 1987, **35**, 1372; (*i*) For a review, see M. Masui, *Stud. Org. Chem.*, 1987, **30**, 137.

9 (*a*) Y. Ishii, K. Nakayama, M. Takeno, S. Sakaguchi, T. Iwahama and Y. Nishiyama, *J. Org. Chem.*, 1995, **60**, 3934; (*b*) T. Iwahama, S. Sakaguchi, Y. Nishiyama and Y. Ishii, *Tetrahedron Lett.*, 1995, **36**, 6923; (*c*) Y. Ishii, T. Iwahama, S. Sakaguchi, K. Nakayama and Y. Nishiyama, *J. Org. Chem.*, 1996, **61**, 4520; (*d*) Y. Ishii, S. Kato, T. Iwahama and S. Sakaguchi, *Tetrahedron Lett.*, 1996, **37**, 4993.



*Received, 4th November 1996; Com. 6/07463D*

# A disaccharide polyphosphate mimic of 1D-*myo*-inositol 1,4,5-trisphosphate

**David J. Jenkins, Rachel D. Marwood and Barry V. L. Potter*†**

*Department of Medicinal Chemistry, School of Pharmacy & Pharmacology, University of Bath, Claverton Down, Bath, UK BA2 7AY*

**A concise route from D-glucose and D-ribose to a potent sugar polyphosphate second messenger mimic related to adenophostin A is described; a role for the adenine base of the adenophostins is suggested.**

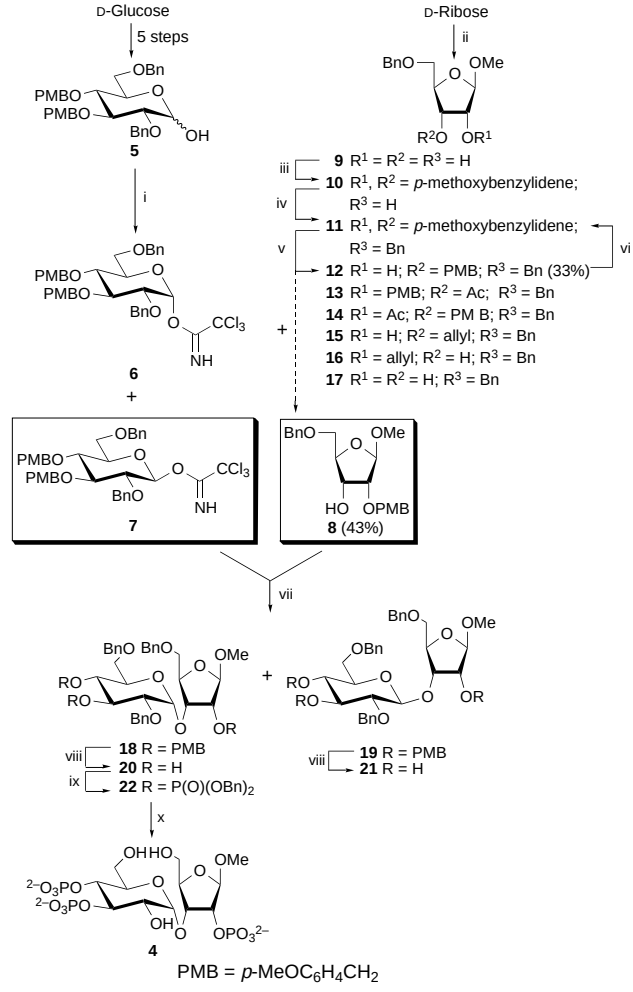
1D-*myo*-Inositol 1,4,5-trisphosphate [Ins(1,4,5)$P_3$, **1**] is a second messenger responsible for increasing the intracellular $Ca^{2+}$ concentration in stimulated cells.[1] Structure–activity studies now allow a good understanding of the relationship between **1** and its receptor.[2] A specific vicinal D-*threo* bisphosphate is essential for activity, while the third phosphate and 6-hydroxy group help to enhance binding affinity.

Most active inositol polyphosphates and related compounds tested at the Ins(1,4,5)$P_3$ receptor exhibit potencies comparable to or less than that of **1**.[2] However, in 1993 a Japanese group reported the isolation of two potently agonistic trisphosphate glyconucleotides from culture broths of *Penicillium brevicompactum*,[3] named adenophostins A and B and identified as **2a** and **2b**, respectively.[4] The structure of **2a** has now been confirmed by total synthesis.[5] Both adenophostins are effective at concentrations 10–100-fold lower than for **1**; these relative potencies are consistent with binding data.[6,7] Thus, **2a** and **2b** are by far the most potent agonists yet described at the Ins(1,4,5)$P_3$ receptor, despite their structural dissimilarity to **1**, and are attractive leads to carbohydrate-based Ins(1,4,5)$P_3$ mimics and receptor modulators.

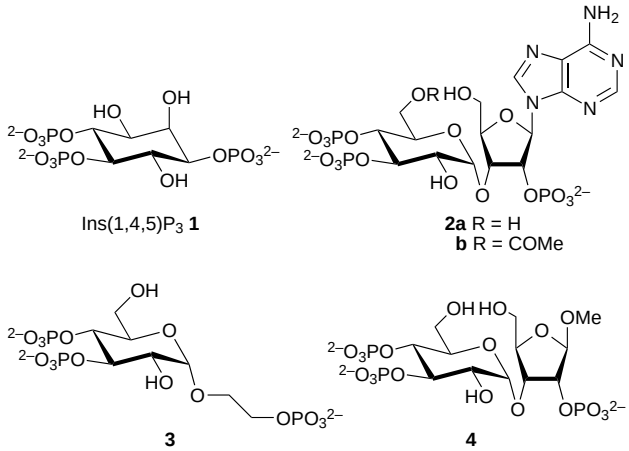
To elucidate the structural motifs of the adenophostins responsible for their activity we[8] and others[9] prepared the minimal structure **3**, which exhibited a potency 10-fold lower than **1**, demonstrating that while the glucose bisphosphate contained the pharmacophore responsible for $Ca^{2+}$ release, at least part of the adenosine moiety was responsible for the high activity of the adenophostins. Molecular modelling studies on **3** established[9] that the staggered conformation of its bimethylene chain did not allow the 2′-phosphate to mimic the corresponding phosphate of either **1** or **2a**. We report here the synthesis of methyl 3-*O*-(α-D-glucopyranosyl)-β-D-ribofuranoside 2,3′,4′-trisphosphate **4**, in which the adenine ring of **2a** has effectively been deleted, but the third phosphate is held similarly to **2a**, and which should clarify the relative importance of conformational restriction of this phosphate for the potency of **2a**.

2,6-Di-*O*-benzyl-3,4-di-*O*-(*p*-methoxybenzyl)-D-glucopyranose **5** was prepared in five steps from D-glucose.[8b] Reaction of **5** with $Cl_3CCN$ in the presence of $K_2CO_3$[10] gave the α-trichloroacetimidate **6** ($[\alpha]_D$ +13.6) and the crystalline β-anomer **7** (mp 80–81 °C; $[\alpha]_D$ +16.5), separated by flash chromatography, in the ratio of 1 : 2.5, based on isolated products.

With a suitable glycosyl donor in hand, we required **8** as an acceptor. D-Ribose was converted into known[11] **9**. Reaction of **9** with 1.05 equiv. of *p*-methoxybenzaldehyde dimethyl




**Scheme 1** *Reagents and conditions*: i, $Cl_3CCN$, $K_2CO_3$, $CH_2Cl_2$, $N_2$, room temp. 2 h, 65%; ii, MeOH, $H_2SO_4$, room temp., 20 h (β-anomer obtained by crystallisation); iii, *p*-$MeOC_6H_4CH(OMe)_2$, PTSA, DMF, 70 °C, −MeOH, 4 h, 93%; iv, NaH, BnBr, DMF, 3 h, 82%; v, DIBAL-H, $CH_2Cl_2$, room temp., 3 h, 76%; vi, DDQ, $CH_2Cl_2$, 3 Å sieves, room temp., 3 h, 71%; vii, $Me_3SiOSO_2CF_3$, $Et_2O$, 3 Å sieves, room temp., 10 min; viii, DDQ, $CH_2Cl_2$–$H_2O$ (10 : 1), room temp., 1 h, 56%; ix, $(BnO)_2PNPr^i_2$, 1*H*-tetrazole, room temp., 30 min, then MCPBA, −78 °C to room temp., 10 min, 82%; x, $H_2$, Pd–C, 40 psi, MeOH–$H_2O$ 4:1, room temp., 18 h, 70%



acetal,[12] with continuous removal of the liberated MeOH *via* an air condenser,[13] gave the 2,3-*O*-(*p*-methoxybenzylidene) derivative **10** ($[\alpha]_D$ −43.0) as a *ca.* 3 : 2 diastereoisomeric mixture, as judged by NMR. Benzylation of **10** gave **11** ($[\alpha]_D$ −27.2). Cleavage of the acetal with $LiAlH_4$–$AlCl_3$ in refluxing THF,[14] $NaCNBH_3$–$Me_3SiCl$ in MeCN[12] or DIBAL-H in $CH_2Cl_2$[15] all gave the required **8** (mp 42–43 °C; $[\alpha]_D$ +34.6), and the more polar **12** ($[\alpha]_D$ −28.8), in approximately equal proportions, the latter reagent giving by far the best yield. The structures of **8** and **12** were confirmed by preparation of acetates **13** ($[\alpha]_D$ +17.5) and **14** ($[\alpha]_D$ +21.5), the $^1$H NMR spectra of which respectively revealed a triplet at δ 5.13 (*J* 5.3 Hz) corresponding to H-3, and a doublet at δ 5.18 (*J* 4.4 Hz; H-1 presented as a singlet) corresponding to H-2. Although the regioselectivity of acetal cleavage was disappointing, isomer **12** was easily reoxidised to **11** (as a 92 : 8 diastereoisomeric mixture, $[\alpha]_D$ −26.4; diastereoisomers not assigned) using DDQ in dry $CH_2Cl_2$.[16]

A preparation of the related allyl-protected ribosides **15** and **16** by a different route has recently been reported.[17] Anomerisation of methyl 5-*O*-benzyl-2,3-*O*-isopropylidene-β-D-ribofuranoside on acidic hydrolysis, to give a *ca.* 1 : 4 α : β-anomeric mixture of products was described. We found that the more labile *p*-methoxybenzylidene acetal of **11** could be removed without anomerisation by treatment with 80% (*v*/*v*) aqueous acetic acid at 60 °C for 25 min, to give **17** ($[\alpha]_D$ −42.0; lit.[17] −47.7). Therefore, **10** may be a more suitable intermediate than methyl 2,3-*O*-isopropylidene-β-D-ribofuranoside to prepare derivatives of methyl β-D-ribofuranoside substituted at position 5.

Coupling of **7** and **8** was achieved using $Me_3SiOSO_2CF_3$ as promoter.[10] The $^1$H NMR spectrum indicated that although the α-glucopyranosyl compound **18** was the major product (H-1′, δ 5.09, *J* 3.4 Hz), the anomer **19** was present as a *ca.* 20% contaminant which could not be removed at this stage. However, on treatment with DDQ, the required triol **20**‡ (mp 103–105 °C; $[\alpha]_D$ +28.3) could be separated from **21** by column chromatography. Phosphitylation of **20** followed by oxidation gave the trisphosphate **22** ($[\alpha]_D$ +34.7). Compound **22** was hydrogenolysed to give the required trisphosphate **4**§ which was purified on Q Sepharose resin eluting with a 0–1 mol $dm^{-3}$ gradient of triethylammonium hydrogen carbonate, pH 7.5. The triethylammonium salt of **4** eluted at *ca.* 800–850 mmol $dm^{-3}$ buffer. As this form was surprisingly poorly soluble in water, it was converted to the freely soluble hexapotassium salt ($[\alpha]_D$ +67.3 calc. for free acid, $H_2O$, pH 8.5) before quantification by total phosphate assay[18] and biological evaluation.

Preliminary biological evaluation of 'ribophostin' **4** using permeabilised hepatocytes[19] revealed a $Ca^{2+}$-mobilising potency 10-fold better than **3** and very close to that of Ins(1,4,5)$P_3$. Full biological characterisation will be reported elsewhere. Noting that 2′-dephosphorylation of **2a** reduces its binding affinity 1000-fold,[4] this suggests that conformational restriction of the 2′-phosphate alone can engender Ins(1,4,5)$P_3$-like, but not adenophostin-like, potency. Therefore the adenine base of adenophostin plays an important, but as yet undefined, role in enhancing activity. We believe that it probably contributes to the positioning of the ribose phosphate such that it can mimic the 1-phosphate of Ins(1,4,5)$P_3$ in a unique way. Further clarification must now await the synthesis of suitably conformationally restricted compounds for accurate positioning of the 2′-phosphate group.

We thank Dr H. Dietrich for discussions, Dr C. Taylor for preliminary biological evaluations, the Wellcome Trust for a Prize Studentship (R.D.M.) and the BBSRC (Intracellular Signalling Programme) for financial support.

## Footnotes

† E-mail: B.V.L.Potter@bath.ac.uk

‡ *Spectroscopic data* for compound **20**: $\delta_H$ (400 MHz; $CDCl_3$; *J*/Hz) 1.69 (1 H, br s, exch. $D_2O$, OH), 2.74, 2.87 (2 H, 2 br s, exch. $D_2O$, 2 × OH), 3.32 (3 H, s, $OCH_3$), 3.38 (1 H, dd, *J* 3.4, 9.8, 2′-H), 3.45–3.57 (5 H, m, 4′-H, 5-Ha, 5-Hb, 6′-Ha, 6′-Hb), 3.74 (1 H, dt, *J* 3.9, 9.8, 5′-H), 3.92 (1 H, t, *J* 9.3, 3′-H), 4.01 (1 H, m, 3-H), 4.22 (2 H m, 2-H, 4-H), 4.44, 4.52 (2 H, AB, $J_{AB}$ 12.2, C$H_2$Ph), 4.51 (2 H, s, C$H_2$Ph), 4.69, 4.74 (2 H, AB, $J_{AB}$ 11.7, C$H_2$Ph), 4.69 (1 H, d, *J* 3.4, 1′-H), 4.88 (1 H, s, 1-H), 7.23–7.36 (15 H, m, 3 × Ph); $\delta_C$(100.4 MHz; $CDCl_3$) 55.03 (q, $OCH_3$), 69.00 (t, C-5 or C-6′), 70.74 (d, C-4′), 70.84 (d, C-5′), 71.69 (t, C-5 or C-6′), 73.24 (d, C-3′), 73.28 (d, C-3), 73.32, 73.55, 74.14 (3 t, C$H_2$Ph), 78.35 (d, C-2′), 79.11 (d, C-2 or C-4), 80.27 (d, C-2 or C-4), 97.79 (d, C-1′), 108.34 (d, C-1), 127.57, 127.63, 127.69, 127.74, 128.33, 128.42, 128.51, 128.75 (8 d, Ph), 137.18, 137.86, 138.06 (3 s, 3 × C-1 of phenyl ring); *m*/*z* ($FAB^+$) 597 [$(M + 1)^+$, 12%], 565 [$(M - OCH_3)^+$, 48], 343 [$(M - C_{13}H_{18}O_5)^+$, 3], 255 [$(M - C_{20}H_{24}O_5)^+$, 2]; *m*/*z* ($FAB^-$) 595 [$(M - 1)^-$, 28%], 505 [$(M - C_7H_7)^-$, 15], 253 [$(M - C_{20}H_{24}O_5)^-$, 25].

§ *Spectroscopic data* for compound **4** (triethylammonium salt): $\delta_H$(400 MHz; $CD_3OD$; *J*/Hz) 3.35 (3 H, s, $OCH_3$), 3.54 (1 H, ABX, $^2J_{AB}$ 11.9, $^3J$ 6.4, 5-Ha), 3.62 (1 H, dd, *J* 3.8, 9.6, 2′-H). 3.66 (1 H, br s, OH), 3.69–3.73 (3 H, m, 5-Hb, 5′-H, 6′-Ha), 3.93 (1 H, ABX, $^2J_{AB}$ 13.0, $^3J$ 3.5, 6′-Hb), 4.04–4.11 (2 H, m, 4-H, 4′-H), 4.44 (1 H, dd, *J* 4.3, 7.3, 3-H), 4.45 (1 H, q, $J_{3\text{-H, 2-H}} = J_{3\text{-H, 4-H}} = J_{HP}$ = 9, 3′-H), 4.58 (1 H, dd, *J* 4.3, $J_{HP}$ 9.5, 2-H), 4.94 (1 H, s, 1-H), 5.03 (2 H, br s, 2 × OH), 5.13 (1 H, d, *J* 3.7, 1′-H); $\delta_C$(100.4 MHz; $CD_3OD$) 55.18 (q, $OCH_3$), 61.98, 64.87 (2 t, C-5, C-6′), 73.32, 73.52, 73.78, 76.29, 76.46 (with C–P coupling), 78.83 (6 d, C-2, C-3, C-2′–C-5′), 82.71 (d, C-4), 98.93 (d, C-1′), 108.96 (dd, $^3J_{CP}$ 3.7, C-1); $\delta_P$(161.7 MHz; $CD_3OD$) −0.38, 1.05, 1.10 (3s); *m*/*z* ($FAB^-$) 565 [$M^-$, 100%] (Found: $M^-$, 565.012. $C_{12}H_{24}O_{19}P_3$ requires, 565.012).

## References

1 M. J. Berridge, *Nature (London)*, 1993, **361**, 315.
2 B. V. L. Potter and D. Lampe, *Angew. Chem., Int. Ed. Engl.*, 1995, **34**, 1933.
3 M. Takahashi, T. Kagasaki, T. Hosoya and S. Takahashi, *J. Antibiot.*, 1993, **46**, 1643.
4 S. Takahashi, T. Kinoshita and M. Takahashi, *J. Antibiot.*, 1994, **47**, 95.
5 H. Hotoda, M. Takahashi, K. Tanzawa, S. Takahashi and M. Kaneko, *Tetrahedron Lett.*, 1995, **36**, 5037; N. C. R. van Straten, G. A. van der Marel and J. H. van Boom, *Tetrahedron Lett.*, 1996, **37**, 3599.
6 M. Takahashi, K. Tanzawa and S. Takahashi, *J. Biol. Chem.*, 1994, **269**, 369.
7 J. Hirota, T. Michikawa, A. Miyawaki, M. Takahashi, K. Tanzawa, I. Okura, T. Furuichi and K. Mikoshiba, *FEBS Lett.*, 1995, **368**, 248.
8 (*a*) D. J. Jenkins and B. V. L. Potter, *J. Chem. Soc., Chem. Commun.*, 1995, 1169; (*b*) *Carbohydr. Res.*, 1996, **287**, 169.
9 R. A. Wilcox, C. Erneux, W. U. Primrose, R. Gigg and S. R. Nahorski, *Mol. Pharmacol.*, 1995, **47**, 1204.
10 R. R. Schmidt, J. Michel and M. Roos, *Liebigs Ann. Chem.*, 1984, 1343.
11 R. Barker and H. G. Fletcher, Jr., *J. Org. Chem.*, 1961, **26**, 4605.
12 R. Johansson and B. Samuelsson, *J. Chem. Soc., Perkin Trans. 1*, 1984, 2371.
13 D. Horton and W. Weckerle, *Carbohydr. Res.*, 1975, **44**, 227.
14 D. Joniak, B. Košíková and L. Kosáková, *Collect. Czech. Chem. Commun.*, 1978, **43**, 769.
15 D. A. Evans, S. W. Kaldor, T. K. Jones, J. Clardy and T. J. Stout, *J. Am. Chem. Soc.*, 1990, **112**, 7001.
16 A. F. Sviridov, M. S. Ermolenko, D. V. Yashunsky, V. S. Borodin and N. K. Kochetkov, *Tetrahedron Lett.*, 1987, **28**, 3835.
17 T. Desai, J. Gigg and R. Gigg, *Carbohydr. Res.*, 1996, **280**, 209.
18 D. A. Sawyer and B. V. L. Potter, *J. Chem. Soc., Perkin Trans. 1*, 1992, 923.
19 C. W. Taylor, M. J. Berridge, A. M. Cooke and B. V. L. Potter, *Biochem. J.*, 1989, **259**, 645.

*Received, 5th December 1996; Com. 6/08208D*

# Absolute stereochemistry of 1,2′-linked bi(naphthoquinone)s

**Robert W. Baker, Song Liu, Melvyn V. Sargent,* Brian W. Skelton and Allan H. White**

*Department of Chemistry, The University of Western Australia, Nedlands, Western Australia 6907, Australia*

**Asymmetric syntheses of the enantiomers of the naturally occurring atropisomerically chiral 1,2′-linked bi(naphthoquinone)s 8′-hydroxyisodiospyrin and isodiospyrin have allowed their absolute configurations to be assigned by X-ray and circular dichroism spectral studies of synthetic intermediates.**

There is a small number of naturally occurring bi(naphthoquinone)s which exhibit axial chirality.[1] Two of these compounds, (−)-8′-hydroxyisodiospyrin **1**[2,3] (which also occurs naturally in racemic form)[3] and (−)-isodiospyrin **2**,[1] are both 1,2′-linked and are of unknown but identical absolute configuration since isodiospyrin has been converted into 8′-hydroxyisodiospyrin in poor yield.[2]

We now report the synthesis of the enantiomers of both of these compounds which have been previously synthesised in racemic form.[4]

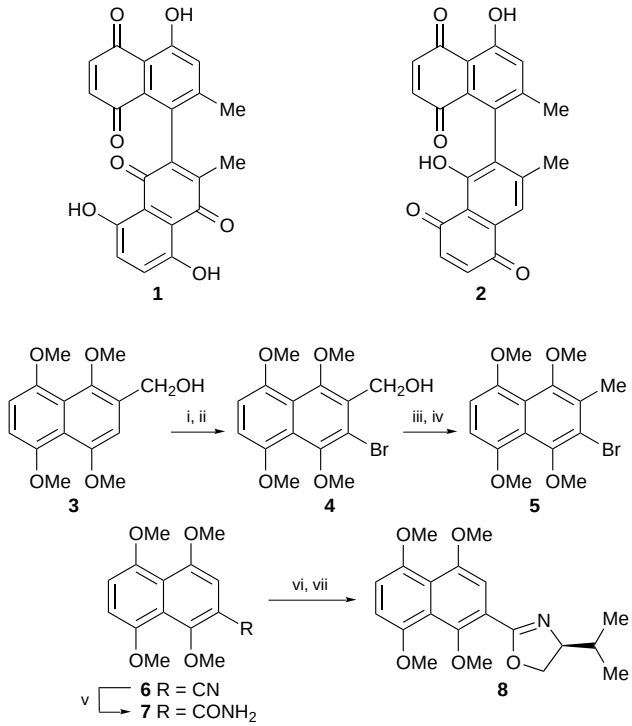
The known hydroxymethyl compound **2**,[5] on treatment with Schlosser's base[6] followed by 1,2-dibromo-1,1,2,2-tetrafluoroethane, afforded the bromo compound **4** (Scheme 1), and hence the bromo compound **5**. The known nitrile **6**[5] was converted into the amide **7** which under standard conditions[7] gave the dihydrooxazole **8**.

When the dihydrooxazole **8** was allowed to react with an excess of the Grignard reagent derived from the bromo compound **5** (Scheme 2), a 45% yield of the coupled product resulted which consisted of an inseparable mixture of two diastereoisomers, as shown by the $^1$H NMR spectrum, in the ratio 7 : 1. The major diastereoisomer was predicted to possess structure **9** (*i.e. R*) since the stereochemical outcome of the coupling is controlled by the chelating ability of the *ortho*-substituents (Fig. 1).[8] This stereochemistry was confirmed by an X-ray study† of a sample of the derived iodide **10** (Fig. 2) obtained by crystallisation of the diastereoisomeric mixture to constant specific rotation.

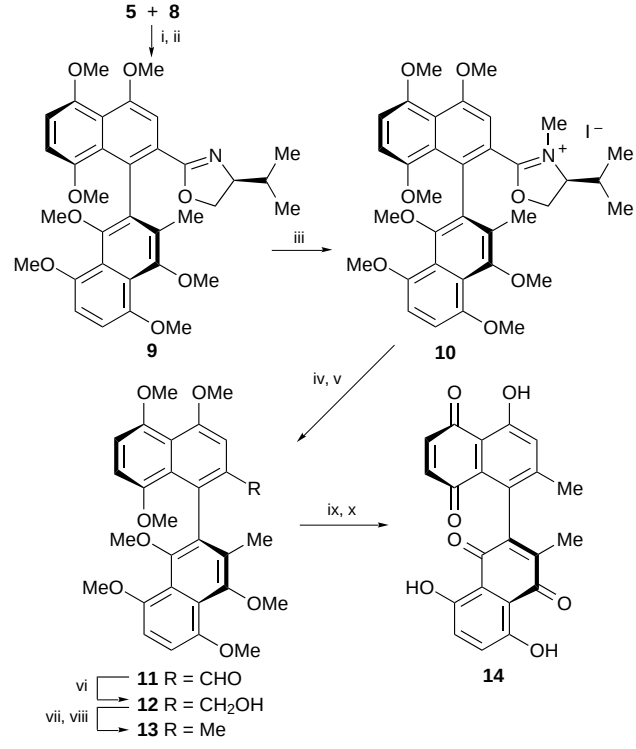
The iodide, enriched in the diastereoisomer **10**, was converted sequentially into the aldehyde **11**, the hydroxymethyl compound **12** and finally into the methyl compound **13**. The Mosher ester[9] of the hydroxymethyl compound indicated the presence of two diastereoisomers in the ratio 7 : 1, thus confirming that no racemisation has occurred during these transformations.

The circular dichroism (CD) spectrum[10] of the methyl compound **13** indicated the *S*-configuration in agreement with both mechanistic prediction and the X-ray study.

The methyl compound was oxidatively demethylated by treatment with ammonium cerium(IV) nitrate and the crude mixture of quinones so obtained was completely demethylated by exposure to aluminium chloride. Fractional crystallisation of the crude product allowed the separation of the (+)-(*S*)




**Scheme 1** *Reagents and conditions*: i, Bu$^t$OK, BuLi, THF, −78 °C, Ar, 5 h; ii, $BrCF_2CF_2Br$, −78 °C, Ar, 38%; iii, $MeSO_2Cl$, $NEt_3$, $CH_2Cl_2$, 25 °C, Ar, 3.5 h; iv, $NaBH_3CN$, $ZnCl_2$, $Et_2O$, 25 °C, Ar, 2 h, 67%; v, KOH, Bu$^t$OH, reflux, Ar, 2 h, 94%; vi, $Et_3OBF_4$, $(ClCH_2)_2$, 25 °C, Ar, 24 h; vii, (*S*)-valinol, reflux, Ar, 48 h, 45%




**Scheme 2** *Reagents and conditions*: i, 1.5 equiv. **5**, Mg, THF, reflux, Ar, 3 h; ii, **8**, THF, reflux, Ar, 5 h, 45%; iii, MeI, $MeNO_2$, 60 °C, Ar, 24 h, 100%; iv, $NaBH_4$, THF, MeOH, 0 °C, Ar, 1 h; v, $H^+$, 25 °C, Ar, 2 h, 67%; vi, $NaBH_4$, aq. NaOH, THF, 0 °C, Ar, 1 h, 100%; vii, $MeSO_2Cl$, $NEt_3$, $CH_2Cl_2$, 25 °C, Ar, 3.5 h; viii, $LiAlH_4$, THF, reflux, Ar, 3 h, 83%; ix, aq. CAN, MeCN, 0–25 °C, 30 min; x, $AlCl_3$, $CH_2Cl_2$, 0–25 °C, 1 h, 45%

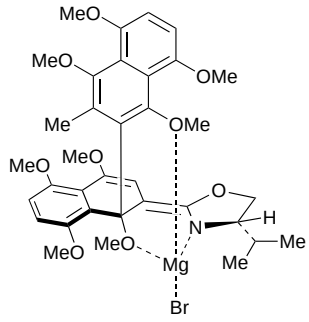
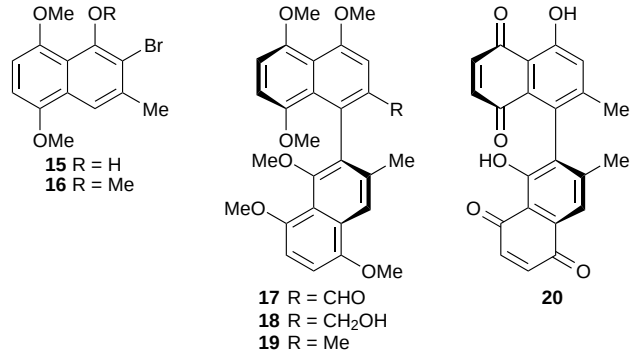



**Fig. 1** Preferred transition state for the coupling reaction leading to diastereoisomer **9**



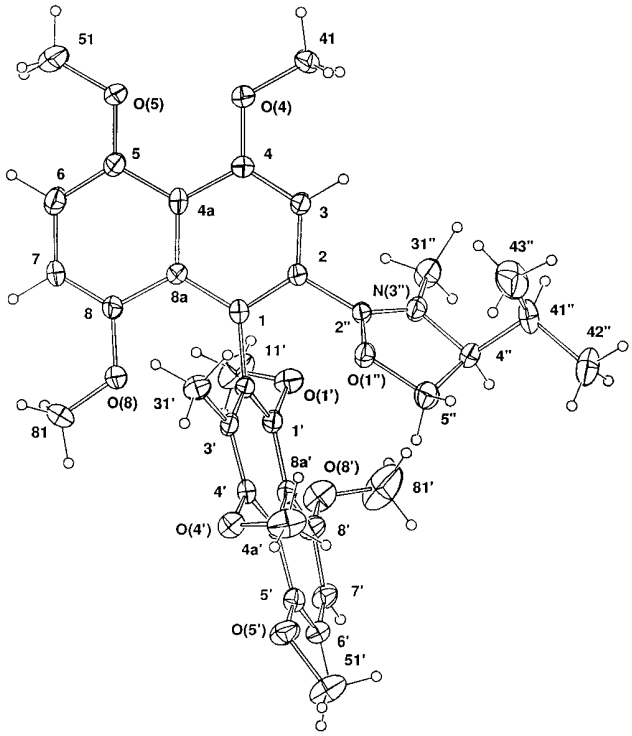




**Fig. 2** The cation of **10** as derived from the X-ray study; 20% thermal ellipsoids are shown for the non-hydrogen atoms, hydrogen atoms having arbitrary radii of 0.1 Å. Carbon atom labelling is shown by numbers only. Dihedral angles between central (unprimed) and pendant (fused) ring skeletal planes (prime and double prime): 81.2(2), 54.0(2)°.

enantiomer **14** of 8′-hydroxyisodiospyrin, mp 274 °C, from its less soluble racemate **1**. The spectroscopic properties of these compounds were identical with those of the natural materials.[2–4] Since the (+)-(*S*) enantiomer **14** absorbs strongly at the D-line it was not possible to obtain a precise value for the specific rotation; the CD spectrum (dioxane), however, exhibited maxima at λ 298, 354 and 480 nm (Δε 11.3, 6.9 and 2.4) and minima at λ 265 and 419 nm (Δε −22.8 and −1.4). The natural product thus possesses the *R* configuration.

The synthesis of isodiospyrin followed similar methodology. The required bromo compound **16**, obtained by methylation of the naphthol **15**,[11] was allowed to react as its Grignard reagent with the dihydrooxazole **8**. In this case the diastereoisomeric ratio of the coupled products was 10 : 1. At the stage of the aldehyde **17** in the synthetic sequence optical purification could readily be achieved by crystallisation, as shown by the $^1$H and $^{19}$F NMR spectra of the Mosher ester of the derived alcohol **18** when compared with those of the derivative of the racemic alcohol. These spectral data and those for the Mosher ester of the alcohol **12** allowed the configuration of the alcohol **18** to be assigned as *S*,[12] which was confirmed by the CD spectrum of the methyl compound **19**. Synthetic (+)-(*S*)-isodiospyrin **20**, mp 233 °C (lit.[13] for enantiomer, 233 °C), proved to be identical in physical properties, except rotation {$[\alpha]_D^{20}$ +138 (*c* 0.38, $CHCl_3$) [lit.[13] for enantiomer, −150 (*c* 0.27, $CHCl_3$)]}, with those of an authentic sample of the racemate.‡ The natural product thus possesses the *R* configuration.

## Footnotes

† *Crystal data* for **10**: $C_{35}H_{42}NO_8^+I^-\cdot H_2O$, $M$ = 749.6. Orthorhombic, $P2_12_12_1$, $a$ = 33.27(1), $b$ = 10.473(8), $c$ = 10.247(3) Å, $V$ = 3570 Å$^3$, $D_c$ ($Z$ = 4) = 1.39$_5$ g cm$^{-3}$. $N_0$ Independent 'observed' [$I > 3\sigma(I)$] out of $N$ measured absorption-corrected diffractometer reflections [$2\theta_{max}$ = 50°; 2θ–θ scan mode (extended counter arm); monochromatic Mo–*K*α radiation, λ = 0.7107$_3$ Å, $\mu_{Mo}$ = 9.5 cm$^{-1}$, specimen: 0.53 × 0.70 × 0.37 mm, $A^*_{min,\,max}$ = 1.39, 1.46] were refined by full-matrix least-squares to convergence [anisotropic thermal parameter forms for non-hydrogen atoms $(x,y,z,U_{iso})_H$ (cation) constrained at estimated values, difference map residue modelled as water molecule O ($H_O$ not observed)]. Conventional $R$,$R_w$ (statistical weights) on $|F|$: for *hkl* ($N$,$N_0$ = 3564, 2723) 0.050, 0.055 (alternative hand: 0.055, 0.061); for *hkl* ($N$,$N_0$ = 3563, 2730) 0.050, 0.055 (0.057, 0.062); for all data ($N$,$N_0$ = 6589, 5731) Flack '$x$' = −0.02(4). The assigned chirality is harmonious with that of the internal L-valine reference.

‡ We thank Professor H. Laatsch for this sample.

## References


1 R. H. Thomson, *Naturally Occurring Quinones III*, Chapman and Hall, London, 1987.
2 M. Tezuka, C. Takahashi, M. Kuroyanagi, M. Satake, K. Yoshihira and S. Natori, *Phytochem*., 1973, **12**, 175.
3 A. Coreia Alves, M. A. C. Costa and M. A. Ferreira, *An. Fac. Farm. Porto*., 1973, **33**, 5; M. A. Ferreira, M. A. C. Costa, A. Correia Alves and M. H. Lopes, *Phytochem*., 1974, **13**, 1587.
4 H. Laatsch, *Liebigs Ann. Chem*., 1984, 319; 1986, 1669.
5 Y. Tanoue, A. Terada, K. Torisu and H. Taniguchi, *Bull. Chem. Soc. Jpn*., 1989, **62**, 1211.
6 M. Schlosser, *Pure Appl. Chem*., 1988, **60**, 1627.
7 T. G. Grant and A. I. Meyers, *Tetrahedron*, 1994, **50**, 2297.
8 A. I. Meyers and H. Moorlag, *Tetrahedron Lett*., 1993, **34**, 6989; R. W. Gable, R. L. Martin and M. A. Rizzacasa, *Aust. J. Chem*., 1995, **48**, 2013.
9 J. A. Dale, D. L. Dull and H. S. Mosher, *J. Org. Chem*., 1969, **34**, 2543.
10 N. Harada and K. Nakanishi, *Circular Dichroic Spectroscopy: Exciton Coupling in Organic Spectrochemistry*, University Science Books, Mill Valley, 1983.
11 H. Laatsch, *Liebigs Ann. Chem*., 1985, 2420.
12 G. Billen, U. Karl, T. Scholl, K. D. Stroesch and W. Steglich, in *Natural Products Chemistry III*, ed. Atta-ur-Rahman and P. W. LeQuesne, Spinger, Berlin, 1988, 305.
13 K. Yoshihira, M. Tezuke and S. Natori, *Tetrahedron Lett*., 1970, 7.


*Received, 13th November 1996; Com. 6/07720J*

# Highly active ruthenium complexes with bidentate phosphine ligands for the solvent-free catalytic synthesis of *N*,*N*-dimethylformamide and methyl formate

**Oliver Kröcher, René A. Köppel and Alfons Baiker***

*Department of Chemical Engineering and Industrial Chemistry, Swiss Federal Institute of Technology, ETH-Zentrum, CH-8092 Zürich, Switzerland*

**Complexes of the type $[RuCl_2L_2]$ [L = $Ph_2P(CH_2)_nPPh_2$ ($n$ = 1–3), $Me_2P(CH_2)_2PMe_2$] are shown to be highly active and selective catalysts for the synthesis of formic acid derivatives from carbon dioxide, hydrogen and dimethylamine or methanol–triethylamine, respectively, without any additional solvent, affording at 373 K with $[RuCl_2(dppe)_2]$ an extremely high turnover frequency (TOF) of 360 000 $h^{-1}$ in *N*,*N*-dimethylformamide synthesis and a TOF of 830 $h^{-1}$ in methyl formate synthesis.**

Recently, carbon dioxide has gained renewed interest as an ideal source of carbon in synthetic chemistry because of its abundance, low cost and non-toxicity.[1,2] Among the possible valuable chemicals, special attention is given to formic acid and its derivatives like *N*,*N*-dimethylformamide [eqn. (1)] and methyl formate [eqn. (2)].[3,4]

$$CO_2 + H_2 + Me_2NH \rightarrow Me_2NC(O)H + H_2O \quad (1)$$

$$CO_2 + H_2 + MeOH \rightarrow HC(O)OMe + H_2O \quad (2)$$

The progress made up to 1995 in the homogeneously catalysed synthesis of *N*,*N*-dimethylformamide (dmf) and methyl formate from carbon dioxide has been reviewed recently.[3,4] Among various transition-metals investigated, ruthenium and rhodium complexes were found to exhibit high activity. Although remarkable efforts have been made to increase the activity of the catalytic complexes used, the turnover numbers (TON) and turnover frequencies (TOF) achieved remained realtively low.[3,4]

More recently, the use of $[RuCl_2(PMe_3)_4]$ as a catalyst for the synthesis of formic acid, dmf and methyl formate from carbon dioxide, hydrogen and dimethylamine or methanol, respectively, has been reported by Jessop *et al.*[3,5] The application of supercritical carbon dioxide (sc-$CO_2$) as a solvent for hydrogen and the catalyst enabled the authors to produce dmf with overall rates of up to 10000 $h^{-1}$ and methyl formate with overall rates of up to 55 $h^{-1}$. The use of sc-$CO_2$-soluble complexes was reported to be crucially important for achieving high activities. Although the process reported by Jessop *et al.* is far more efficient compared to the liquid-phase synthesis of dmf and methyl formate, overall reaction rates are still relatively low and the catalysts are sensitive to air, which impairs technical utilisation. The aim of our study was to find more active and stable catalysts for the synthesis of dmf and methyl formate, obviating these limitations.

Ruthenium complexes of the type $[RuCl_2L_2]$, with L representing the chelating ligands dppm = $Ph_2PCH_2PPh_2$, dppe = $Ph_2P(CH_2)_2PPh_2$ or dppp = $Ph_2P(CH_2)_3PPh_2$, were prepared,[6] which are easy to characterize, relatively cheap, and stable to water and air.

Table 1 lists the experimental conditions and the catalytic results obtained with the various ruthenium complexes for the synthesis of *N*,*N*-dimethylformamide and methyl formate, respectively. Note that catalytic results presented in Table 1 were confirmed by at least two repetitive experiments. Blank tests without catalyst performed repeatedly throughout the study revealed no catalytic activity.

The synthesis of dmf proceeded very rapidly at 373 K with up to 99% yield and always with 100% selectivity to dmf. Analysis of the gas phase by GC confirmed that no gaseous by-products (CO, $CH_4$) were formed. A TOF of 360 000 $h^{-1}$ could be reached with $[RuCl_2(dppe)_2]$, which is 36 times higher than that with $[RuCl_2(PMe_3)_4]$, the best catalyst reported so far.[3,5] In an experiment using 110 g dimethylamine a maximum TON of 740 000 was achieved, which indicates the upper limit of the catalyst's lifetime under the conditions applied. Calculated on the basis of 1 g of ruthenium, 530 kg dmf can be produced within 2 h. Further improvement in TOF may be possible by optimizing the reaction parameters. High TOFs could also be reached with $[RuCl_2(dppm)_2]$, whereas $[RuCl_2(dppp)_2]$ exhibited much lower activity (Table 1).

The extremely high catalytic activity achieved with such *trans*-$[RuCl_2L_2]$ complexes was not *a priori* expected, since the formation of a monohydride species was reported to be a prerequisite for catalytic activity for this type of hydrogenation

**Table 1** Catalytic properties of ruthenium complexes in the production of *N*,*N*-dimethylformamide and methyl formate from $CO_2$[a]

| Complex (μmol) | Reactant [additive] (mol) | *t*/h | Product | TON[b] | TOF[c]/$h^{-1}$ |
|---|---|---|---|---|---|
| $[RuCl_2(PMe_3)_4]$[d] (6.4) | Dimethylamine (3.80) | 70.0 | dmf | 420 000 | 6 000 |
| $[RuCl_2(dppe)_2]$ (0.58) | Dimethylamine (2.44) | 2.05 | dmf | 740 000 | **360 000** |
| $[RuCl_2(dppe)_2]$ (0.73) | Dimethylamine (0.78) | 0.75 | dmf | 200 000 | 265 000 |
| $[RuCl_2(dppm)_2]$ (1.0) | Dimethylamine (0.72) | 0.50 | dmf | 95 000 | 190 000 |
| $[RuCl_2(dppp)_2]$ (3.1) | Dimethylamine (0.72) | 4.05 | dmf | 10 700 | 2 650 |
| $[RuCl_2(dmpe)_2]$ (8.7) | Dimethylamine (0.72) | 15.0 | dmf | 30 000 | 2 000 |
| $[RuCl_2(PMe_3)_4]$[d,e] (2.9) | Methanol (0.08) [triethylamine] (0.030) | 64.0 | Methyl formate | 3 500 | 55 |
| $[RuCl_2(dppe)_2]$ (3.8) | Methanol (0.74) [triethylamine] (0.370) | 15.5 | Methyl formate | 12 900 | **830** |
| $[RuCl_2(dppe)_2]$[e] (2.3) | Methanol (0.74) [triethylamine] (0.074) | 15.5 | Methyl formate | 10 100 | 650 |

[a] *Reaction conditions*: 500 ml stainless-steel autoclave equipped with magnetically coupled stirrer. Analysis: GC equipped with Supelco SPB-1 fused silica capillary column. $p(H_2)$ = 8.5 MPa, $p(CO_2)$ = 13.0 MPa, $T$ = 373 K. [b] TON = mol product/mol complex. [c] TOF = TON $h^{-1}$. [d] Lit. data[3] for the hitherto best catalyst $[RuCl_2(PMe_3)_4]$. 300 ml autoclave. [e] $T$ = 353 K.

catalyst.[5,7] No conversion of *trans*-$[RuCl_2L_2]$ complexes to the corresponding monohydrides at normal pressure is described in the literature.[8,9] Despite this, $[RuHCl(dppe)_2]$, identified by NMR, could be found in the reactor after pretreatment of $[RuCl_2(dppe)_2]$ with 40 bar of hydrogen and dimethylamine, confirming monohydrides as key intermediates in the catalytic cycle. The monitored pressure in the reactor as well as the catalytic results indicated no further induction period after addition of carbon dioxide.

Jessop *et al.* investigated visually the phase behaviour in the reactor under comparable conditions for different reactants and additives. They found that a supercritical phase of carbon dioxide and hydrogen exists besides a liquid phase, highly swelled by dissolved gases.[5] Thus, high concentrations of carbon dioxide and possibly hydrogen could be assumed in the liquid-amine phase. Leitner *et al.* reported high concentrations of dissolved carbon dioxide in the liquid phase also under subcritical conditions.[10] Due to their insolubility in the sub- or super-critical carbon dioxide, the complexes *trans*-$[RuCl_2L_2]$ are expected to operate in the liquid phase, which is also supported by the fact that the catalysts could only be found in the liquid-product mixture after reaction. Moreover, cleaning of the lower part of the autoclave was sufficient to exclude any activity in subsequent blank tests. Variations of the carbon dioxide partial pressure from super- to sub-critical conditions, using $[RuCl_2(dppe)_2]$ as catalyst, resulted in a decrease of activity from 360 000 $h^{-1}$ (8.5 MPa $CO_2$) to 150 000 $h^{-1}$ (1.8 MPa $CO_2$), but no drastic activity drop was observed, indicating supercritical conditions not to be a necessary prerequisite for high catalytic activity.

Despite their similar solubility properties, the three related complexes $[RuCl_2(dppm)_2]$, $[RuCl_2(dppe)_2]$ and $[RuCl_2(dppp)_2]$ exhibited substantially different activities, with $[RuCl_2(dppp)_2]$ being far less active than $[RuCl_2(dppm)_2]$ and $[RuCl_2(dppe)_2]$ (Table 1). In order to compare the catalytic properties of these complexes, which are insoluble in sc-$CO_2$, with a complex soluble in the supercritical phase, $[RuCl_2(dmpe)_2]$ [dmpe = $Me_2P(CH_2)_2PMe_2$] was prepared,[11] using bidentate methyl phosphine ligands instead of phenyl phosphine ligands. Interestingly, $[RuCl_2(dmpe)_2]$ exhibited similar low activity to $[RuCl_2(dppp)_2]$, suggesting a more pronounced influence of the phosphine ligands than of the catalysts solubility properties.

$[RuCl_2(dppe)_2]$ was also tested for methyl formate synthesis at 353 K and exhibited a 12 times higher activity (TOF = 650 $h^{-1}$) than $[RuCl_2(PMe_3)_4]$ (TOF = 55 $h^{-1}$) under comparable conditions. Increasing the triethylamine concentration and the temperature resulted in an even higher TOF of 830 $h^{-1}$, which is 15 times higher than the best previous results.[5] Analysis of the reaction mixture by $^1H$ NMR spectroscopy revealed the formation of an adduct of formic acid and triethylamine beside methyl formate. Methyl formate synthesis with our complexes is favourable compared to that with $[RuCl_2(PMe_3)_4]$, because higher temperatures can be applied, which is crucial for an effective esterification of the initially formed formic acid.

In conclusion, we can state that ruthenium complexes with bidentate phosphine ligands exhibit much higher activity for the solvent-free synthesis of *N*,*N*-dimethylformamide (dmf) and methyl formate from carbon dioxide than hitherto reported catalytic systems.[3,5] The high concentrations of hydrogen and carbon dioxide in the liquid dimethylamine or methanol–triethylamine phase afford high concentrations of all reactants at the catalytic centres in an ideal reaction design. We have demonstrated that further improvements in the homogeneous hydrogenation of carbon dioxide are achievable not only by developing complexes soluble in the supercritical medium, but also by the utilisation of better suited ligands for this reaction in combination with a solvent-free reaction design.

## References


1 B. Cornils and W. A. Herrmann, in *Applied Homogeneous Catalysis with Organometallic Compounds*, VCH, Weinheim, 1996, pp. 1048–1072.
2 T. Clifford and K. Bartle, *Chem. Ind.*, 1996, 449.
3 P. G. Jessop, T. Ikariya and R. Noyori, *Chem. Rev.*, 1995, **95**, 259.
4 W. Leitner, *Angew. Chem., Int. Ed. Engl.*, 1996, **34**, 2207.
5 P. G. Jessop, Y. Hsiao, T. Ikariya and R. Noyori, *J. Am. Chem. Soc.*, 1996, **118**, 344.
6 R. Mason, D. W. Meek and G. R. Scollary, *Inorg. Chim. Acta*, 1976, **16**, L11.
7 E. A. Seddon and K. R. Seddon, *The Chemistry of Ruthenium*, ed. R. J. H. Clark, Elsevier, Amsterdam, 1984.
8 J. Chatt and R. G. Hayter, *J. Chem. Soc.*, 1961, 2605.
9 M. T. Bautista, E. P. Cappellani, S. D. Drouin, R. H. Morris, C. T. Schweitzer, A. Sella and J. Zubkowski, *J. Am. Chem. Soc.*, 1991, **113**, 4876.
10 W. Leitner, E. Dinjus and F. Gaßner, *J. Organomet. Chem.*, 1994, **475**, 257.
11 J. Chatt and R. G. Hayter, *J. Chem. Soc.*, 1961, 896.


*Received, 3rd December 1996; Com. 6/08150I*

# Boomerang shaped aggregates from a histidine surfactant

**Nico A. J. M. Sommerdijk, Mark H. L. Lambermon, Martinus C. Feiters, Roeland J. M. Nolte* and Binne Zwanenburg***

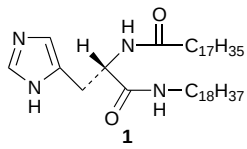
*Department of Organic Chemistry, NSR-Institute for Molecular Structure, Design and Synthesis, University of Nijmegen, Toernooiveld, 6525 ED Nijmegen, The Netherlands*

**Complexation of copper(II) ions to a long-chain histidine derivative leads to the formation of a new type of chiral architecture having the shape of a boomerang.**

Following the discovery that phospholipid molecules can form vesicular, rod-like, and even helical aggregates,[1] many researchers have shown that similar supramolecular structures can be obtained from synthetic surfactants.[2–5] Here, we report that the synthetic histidine derivative **1** in aqueous solution in the presence of copper(II) triflate forms boomerang-like scrolls. This novel architecture may be an intermediate state in the transformation of closed bilayers to helical structures.

Compound **1** was synthesized from Boc-protected L-histidine following a standard procedure;† **1** was not soluble in water at neutral pH, even at elevated temperatures. Protonation of **1** by dispersion in water adjusted to pH 2.5, led to the formation of very long thin fibres [Fig. 1(*a*)] which assembled side-by-side to yield bundles. Some of them showed a tendency to curl up into a right-handed, twisted structure [Fig. 1(*b*)].

Monolayer experiments indicated that **1** forms stable monolayers. The isotherm recorded at pH 6.5 displayed a sharp increase of the surface pressure at a molecular area of 60 Å$^2$ indicative of a non-compressible state (Fig. 2). When **1** was spread on a subphase adjusted to pH 2.5, the isotherm revealed an increase of the compressibility of the monolayer, as well as an increase in the area per molecule. The formation of a rigid monolayer at pH 6.5 is attributed to the presence of a high degree of preorganisation in the molecules, probably caused by strong intermolecular hydrogen bonds between the imidazole groups and by the formation of so-called amide polymers, *i.e.* linear arrays of hydrogen-bonded amide groups. Protonation of the imidazole groups at pH 2.5 apparently alters this hydrogen-bonding pattern, breaking up the preorganisation in the monolayer. It seems likely that the same strong intermolecular forces prevent the molecules of **1** from dissolving at neutral pH. Here also protonation is required to allow the head-groups of **1** to become hydrated and to form fibres.




**1**

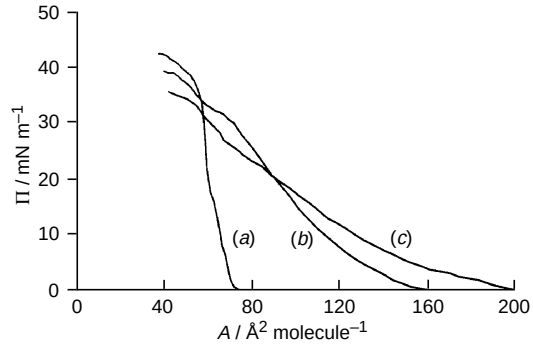



**Fig. 2** Monolayer isotherms of **1** recorded at 20 °C on subphases containing (*a*) water of pH 6.5, (*b*) water adjusted to pH 2.5, and (*c*) 10 mM aqueous copper(II) triflate

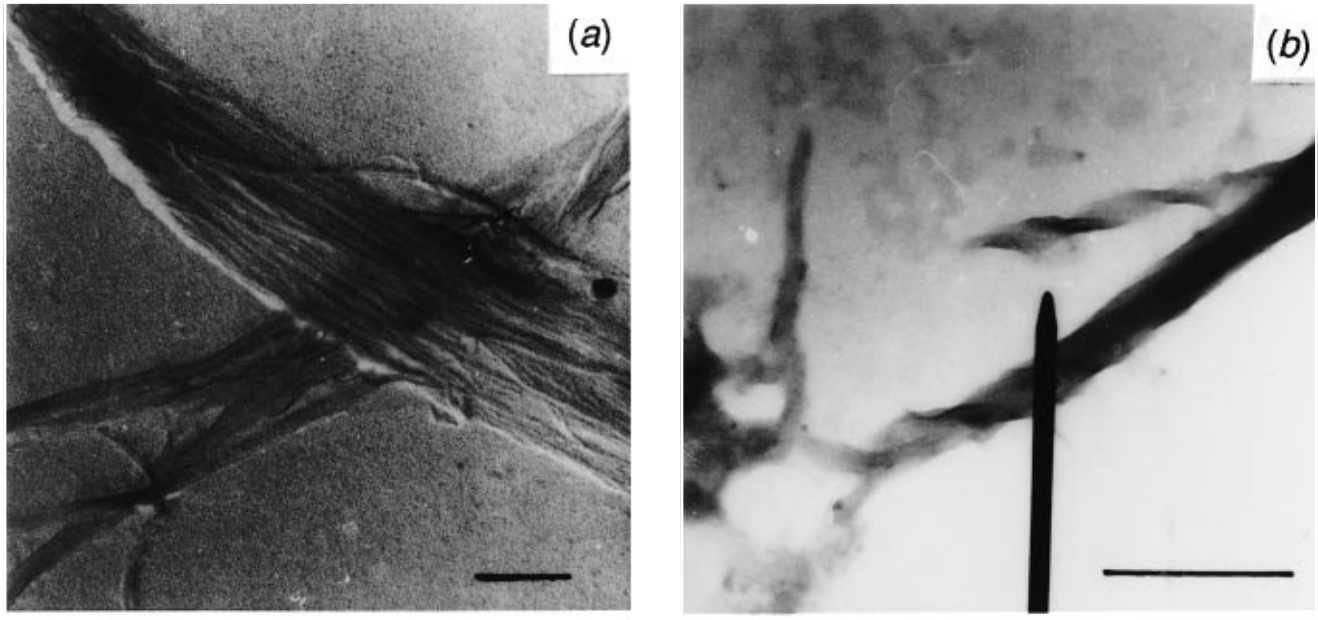



**Fig. 1** Electron micrographs of aqueous 0.1% (m/m) dispersion of **1** adjusted to pH 2.5; bars represent 250 nm

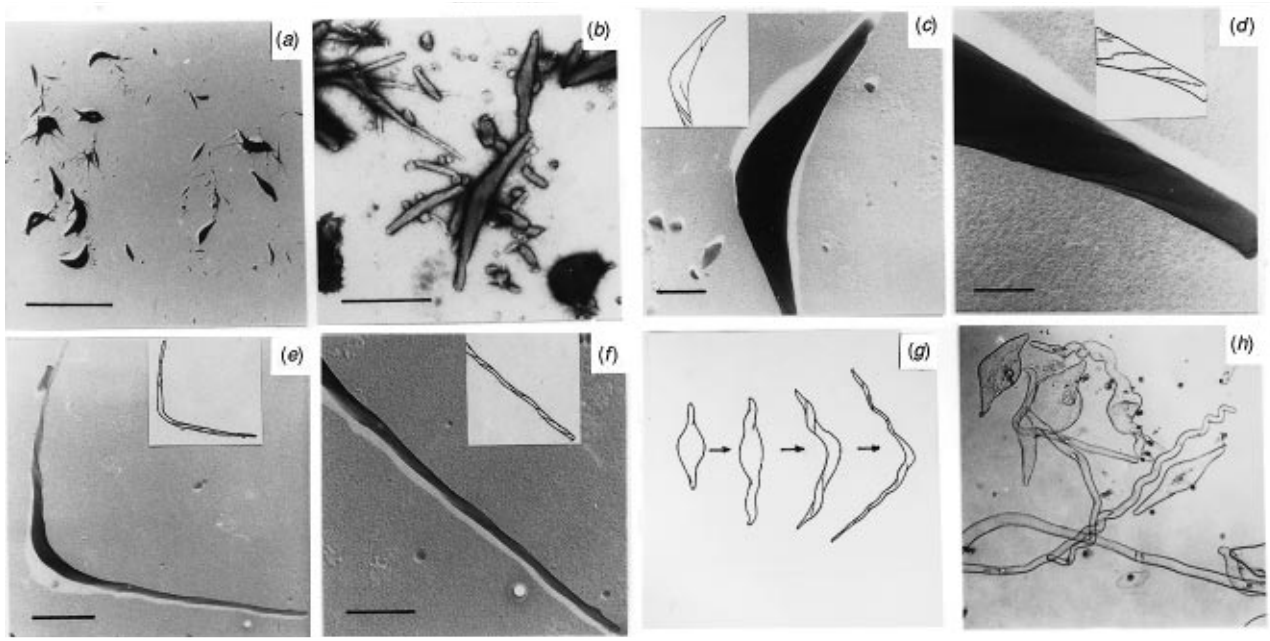



**Fig. 3** (*a*)–(*f*) Transmission electron micrographs of a 0.1% (m/m) dispersions of **1** containing 0.25 molar equivalents of copper(II) triflate. (*a*) Pt shadowing, bar 5 μm, (*b*) negative staining, bar 1 μm, (*c*) Pt shadowing, bar 250 nm, (*d*) Pt shadowing, bar 500 nm, (*e*) Pt shadowing, bar 500 nm, (*f*) Pt shadowing, bar 200 nm. Insets: graphic representations of the observed structures. (*g*) Schematic representation of the process of boomerang formation is deduced from the different observed structures, (*h*) optical micrograph of protoplasts at different stages of growth after addition of fusicoccin, kindly provided by Dr A. N. M. van Amstel.[6]

When copper triflate was added to **1** in a 1:4 ratio,‡ boomerang-like scrolls were generated [Fig. 3(*a*), (*b*)]. These had different thicknesses, but all showed a left-handed turn [Fig. 3(*d*), (*f*)]. Electron micrographs taken of samples stained with 2% uranyl acetate indicated that these scrolls were not massive, but contained an aqueous interior [Fig. 3(*b*)]. The different stages of scroll formation shown in Fig. 3 suggest that these boomerangs are formed by stretching and twisting of the vesicle membranes in a stereospecific manner. According to the overall shape of the scrolls, this twisting starts initially at opposite sides of the vesicle [Fig. 3(*g*)], resulting in a structure with a thickened centre and thin twisted ends [Fig. 3(*c*)], and eventually in thinner species which are also helical in the central part of the aggregate [Fig. 3(*e*)]. The aggregate structures in Fig. 3 show features that strongly resemble the spiral growth of protoplasts induced by the action of fusicoccin as reported by van Amstel [Fig. 3(*h*)].[6]

Remarkably, complexation of copper triflate leads to a monolayer which displays an even higher degree of compressibility, as compared to the monolayers formed on subphases of pure water adjusted to pH 6.5 and 2.5 (Fig. 2). This implies that addition of copper triflate leads to a lower degree of pre-organisation in the two-dimensional surfactant layer. This is most likely due to a preference of hydrogen-bond formation between molecules within the same complex, as opposed to the formation of long linear arrays of intermolecular hydrogen bonds. A similar situation may be present in the three-dimensional aggregates allowing the molecules to pack in such a way that their chirality is expressed at the supramolecular level. The boomerang shaped aggregates may be considered as being metastable states in the transformation of closed bilayer structures of helical ribbons. Further studies are in progress.

The authors thank H. P. M. Geurts for his assistance in performing electron microscopy experiments, W. Wong for providing artwork and Professor G. I. Tesser and P. J. H. M. Adams for the kind donation of Boc-protected L-histidine and helpful discussions.

## Footnotes

† Surfactant **1** was conveniently prepared from Boc-protected L-histidine. One alkyl chain was introduced by a DCC coupling with octadecylamine (yield 60%). Deprotection of this Boc–amide with trifluoroacetic acid and subsequent acylation with *N*-stearoyloxy–succinimide resulted in the introduction of the second alkyl chain (yield 75%). Anal. **1** Calc. C, 74.9; H, 12.0; N, 8.3. Found: C, 74.2; H, 11.5; N, 8.4%.

‡ Comparable ligand systems have been shown to form copper complexes of the type $[Cu(Him)_4]$ (Him = imidazole), see ref. 4*b*.

## References

1 A. D. Bangham and R. W. Horne, *J. Mol. Biol.*, 1964, **8**, 660; D. Papahadjopoulos, W. J. Vail, K. Jacobson and G. Poste, *Biochim. Biophys. Acta*, 1975, **394**, 483; K. Inoue, K. Suzuki and S. Nojima, *J. Biochem.*, 1977, **81**, 1097.

2 J. H. Fuhrhop and W. Helfrich, *Chem. Rev.*, 1993, **9**, 1565 and references therein.

3 J. M. Schnur, *Science*, 1993, **262**, 1669 and references therein.

4 N. A. J. M. Sommerdijk, P. J. J. A. Buynsters, A. M. A. Pistorius, M. Wang, M. C. Feiters, R. J. M. Nolte and B. Zwanenburg, *J. Chem. Soc., Chem. Commun.*, 1994, 1941; (*b*) R. J. H. Hafkamp, M. C. Feiters and R. J. M. Nolte, *Angew Chem.*, 1994, **106**, 1054.

5 J.-H. Fuhrhop and J. Mathieu, *Angew. Chem.*, 1984, **96**, 124; T. Kunitake and S. Shinkai, *Adv. Phys. Org. Chem.*, 1980, **17**, 435.

6 A. N. M. van Amstel, Ph.D. Thesis, University of Nijmegen, 1994.

*Received, 19th December 1996; Com. 6/08500H*

# Pinacol coupling of aromatic aldehydes catalysed by a titanocene complex: a transition metal catalysed radical reaction

**Andreas Gansäuer**

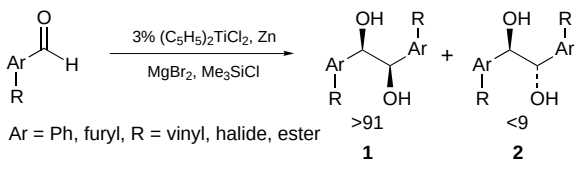
*Institut für Organische Chemie der Georg-August-Universität, Tammannstr. 2, D-37077 Göttingen, Germany*

**A trinuclear complex derived from titanocene chloride and magnesium bromide is an efficient catalyst for the pinacol coupling of aromatic aldehydes; the 1,2-diols are obtained with good diastereoselectivity and a wide variety of sensitive functional groups are tolerated.**

The reductive coupling of carbonyl compounds is the most direct way to 1,2-diols by forming a functionalized carbon–carbon bond.[1] Many stoichiometric reagents for this reaction have been developed[2] and the pinacol coupling has also been applied as a key step in the synthesis of several natural products.[3] To avoid the use of expensive and toxic reagents the development of an efficient transition metal catalysed pinacol coupling is desirable. Here the first titanocene dichloride catalysed pinacol coupling of aromatic aldehydes is described yielding the corresponding 1,2-diols at room temperature in good yields with good diastereoselectivities. Pinacol coupling is not only a shortcut of the otherwise existing two-step sequence, coupling of the aldehydes to an (*E*)-stilbene with stoichiometric amounts of titanium reagents as in McMurry coupling reactions, and a *syn,vic*-dihydroxylation of the central double bond. More importantly the pinacol route to 1,2-diols tolerates certain functional groups that are sensitive to the McMurry reagent and/or to the dihydroxylation reaction. The pinacol coupling used here catalytically uses cheap, readily available, non-toxic reagents.

The only reported catalytic pinacol couplings involve harsh reaction conditions, low selectivities and low functional group tolerance.[4] The catalysts, ruthenium complexes[4a] or samarium iodide,[4b] do not allow control of diastereoselectivity or enantioselectivity by ligand variations.

Based on the ability of cyclopentadienyl-bonded titanium(III) reagents[2a,c] to induce stoichiometric pinacol couplings it seemed possible to develop a catalytic cycle. For this purpose the formed diol has to be removed from titanium with concomitant regeneration of $(C_5H_5)_2TiCl_2$.[5] *In situ* reduction to the titanium(III) reagent then finishes the catalytic cycle.[6] Benzaldehyde coupling in the presence of Zn and $Me_2SiCl_2$ with 10% $(C_5H_5)_2TiCl_2$ gives complete conversion to pinacol after hydrolysis in less than 10 min. $Me_3SiCl$ as additive also gives clean product formation. Without the catalyst, conversion was not observed with $Me_2SiCl_2$ as additive. $Me_3SiCl$ and Zn react to give pinacol over 20 h albeit without diastereoselectivity.[7] Catalylic acceleration of the reaction was therefore significant as was the improvement in diastereoselectivity. Interestingly, however, lowering the temperature at which the catalytic coupling was performed leads to reduced selectivity and pronouncedly longer reaction times. One step in the catalytic cycle was slow and thus a competing, less selective pathway operated. It is known that titanium alkoxides are less selective stoichiometric reagents in pinacol couplings[8] and that both coupling and reduction of $(C_5H_5)_2TiCl_2$ are fast at and below room temperature.[2,6] Thus, silylation is the rate determining step in the catalytic cycle. To improve the diastereoselectivity a solution of benzaldehyde and $Me_3SiCl$ in THF was slowly added to a mixture of $(C_5H_5)_2TiCl_2$ and Zn in THF. The selectivity increased and the yield remained high. Selectivity is further improved by adding 1 equiv. of $MgBr_2$ to the benzaldehyde solution. This gave a tighter dimeric titanium catalyst by replacing Zn with Mg.




**Scheme 1** Titanocene catalysed pinacol coupling of aromatic aldehydes

Diethyl ether and dichloromethane gave inferior results. Other silylating reagents, *e.g.* $Me_2Bu^tSiCl$, did not give any reaction.

Under the optimised conditions a variety of symmetrical 1,2-diols were synthesised in good yields and selectivities and could be obtained diastereomerically pure after a single recrystallisation. Functional groups interfering with McMurry couplings or dihydroxylation reactions such as chlorides, double bonds, phenolate esters and α,β-unsaturated esters are readily tolerated. Although initial experiments were performed on a small scale, the reaction can be readily scaled up and gave the same results using 0.5, 5 or 50 mmol of substrate. In the latter case 320 mg of catalyst was used. This compared favourably with the use of 24.9 g of $(C_5H_5)_2TiCl_2$ in the stoichiometric reaction. In effect $(C_5H_5)_2TiCl_2$ is replaced by the cheaper $Me_3SiCl$. A stoichiometric reductant was needed in both cases. Other stoichiometric or catalytic reagents, *e.g.* $SmI_2$, are even more expensive and less selective. The cheapest source of inherently toxic osmium for a dihydroxylation reaction is about 40 times more expensive than the essentially non-toxic $(C_5H_5)_2TiCl_2$.

Mechanistically it seems reasonable to assume that the catalytically active species in the catalytic cycle is a dimeric

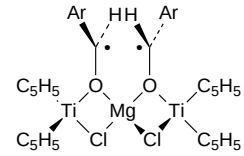



**Fig. 1** Likely catalytically active species for the dimerisation of ketyl radicals both bound to the dimeric titanium catalyst

**Table 1** Coupling of benzaldehyde at 0.1 M in the presence of $Me_2SiCl_2$ or $Me_3SiCl$

| Amount of catalyst (%) | *t*/h | *T*/°C | Yield (%) | **1**:**2** |
|---|---|---|---|---|
| 10 | 1.2 | 0 | 93 | 86:14 |
| 10 | 22 | −40 | 92 | 70:30 |
| 3 | 0.25 | 25 | 96 | 84:16[a] |
| 3 | 3 | 25 | 88 | 89:11[a,b] |
| 3 | 3 | 25 | 90 | 95:5[a,c] |

[a] 1.5 equiv. of $Me_3SiCl$. [b] Slow addition of PhCHO and $Me_3SiCl$. [c] Slow addition in the presence of $MgBr_2$

titanium complex binding both ketyl radicals. The observed *syn*-selectivity can then be readily explained by minimization of steric interference through *anti*-orientation of the R groups in the complex. This reaction is therefore an example of a transition metal catalysed radical reaction.

This work was generously supported by the Fonds der Chemischen Industrie. I thank Professor R. Brückner for his constant encouragement and generous support.

**Table 2** Pinacol coupling of substituted aldehydes under optimised conditions

| R-Ar | *t*/h | Yield (%) | **1**:**2** |
|---|---|---|---|
| 4-Methylphenyl | 2.5 | 82 | 92:8 |
| 4-Chlorophenyl | 3 | 78 | 93:7 |
| 3-Chlorophenyl | 3 | 87 | 93:7 |
| 4-Vinylphenyl | 2 | 91 | 92:8 |
| 4-Acetoxyphenyl | 3 | 83 | 92:8 |
| 4-Crotonyloxy-phenyl | 2 | 79 | 92:8 |
| 4-*tert*-Butylphenyl | 3 | 80 | 94:6 |
| 2-Furyl | 1.5 | 88 | 92:8 |

## References

1 G. M. Robertson, in *Comprehensive Organic Synthesis*, ed. B. M. Trost, I. Fleming and G. Pattenden, Pergamon Press, Oxford, 1991, vol. 3, p. 563; T. Wirth, *Angew. Chem*., 1996, **108**, 65; *Angew. Chem., Int. Ed. Engl*., 1996, **35**, 61.
2 (*a*) Y. Handa and J. Inanaga, *Tetrahedron Lett*., 1987, **28**, 5717; (*b*) A. W. Konradi, S. J. Kemp and S. F. Pedersen, *J. Am. Chem. Soc*., 1987, **109**, 6551; (*c*) M. C. Barden and J. Schwartz, *J. Am. Chem. Soc*., 1996, **118**, 5484.
3 K. C. Nicolaou, Z. Yang, J. J. Chin, H. Ueno, P. G. Nantermet, R. K. Guy, C. F. Clairborne, J. Renaud, E. A. Coulardos, K. Paulvannan and E. J. Sorensen, *Nature*, 1994, **367**, 630.
4 (*a*) H. Shinada, J.-P. Qü, H. Matsuzaka, Y. Ishii and Y. Hidai, *Chem. Lett*., 1995, 671; (*b*) R. Nomura, T. Matsuno and T. Endo, *J. Am. Chem. Soc*., 1996, **118**, 11 666.
5 A. Fürstner and A. Hupperts, *J. Am. Chem. Soc*., 1995, **117**, 4468; A. Fürstner and N. Shi, *J. Am. Chem. Soc*., 1996, **118**, 2533.
6 M. L. H. Green and C. R. Lucas, *J. Chem. Soc., Dalton Trans*., 1972, 1000; T. V. Rajan Babu and W. A. Nugent, *J. Am. Chem. Soc*., 1994, **116**, 986.
7 J.-H. So, M.-K. Park and P. Boudjouk, *J. Org. Chem*., 1988, **53**, 5871.
8 A. Clerici, L. Clerici and O. Porta, *Tetrahedron Lett*., 1996, **37**, 3035.
9 R. L. Halterman, *Chem. Rev*., 1992, **92**, 965.

*Received, 17th December 1996; Com. 6/08438I*

# First example of thiolate-bridged square-pyramidal and octahedral nickel(II) ions: $[Ni_2(L_{SO})(NCS)_2(dmf)]$

**Sally Brooker*† and Paul D. Croucher**

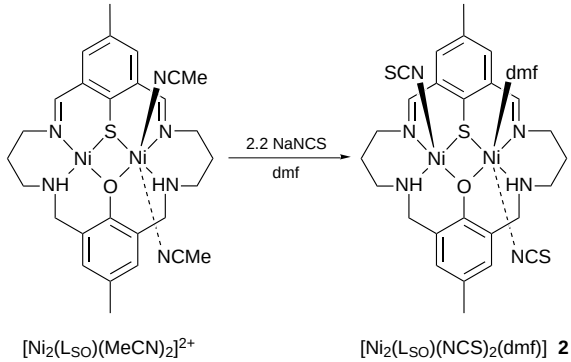
*Department of Chemistry, University of Otago, PO Box 56, Dunedin, New Zealand*

**A structure determination reveals that $[Ni_2(L_{SO})(NCS)_2(dmf)]$ 2 is one of the best structural models to date for the active site of [Ni,Fe] hydrogenases: it also contains the first example of a high-spin thiolate-bound square-pyramidal nickel(II) ion.**

There is currently intense interest in dinickel thiolate-bridged complexes as first-generation models for the active site in [Ni,Fe] hydrogenases,[1] yet only a handful of such complexes have been isolated and fully characterised.[2] The coordination environment of the dinuclear hydrogenase active site is thought to consist of a combination of five-coordinate nickel and six-coordinate iron ions bridged by two thiolate donors (one axial, one equatorial bridge) and one unknown, possibly oxygen-derived, equatorial bridge.[1] Unfortunately the vast majority of nickel mixed-donor thiolate complexes are poor structural models as they exhibit square-planar nickel ion geometries due to the strong ligand field imposed by the thiolate donors.[1–4] There are therefore relatively few examples of geometries other than square planar:[2,5–8] the coordination number five is especially rare, and, to our knowledge, the known examples of this coordination number are all low spin.[2,8] In Schiff-base macrocyclic complexes in which two bridging thiolates are provided this tendency is also observed, with the nickel(II) ions adopting square-planar $N_2S_2$ stereochemistry.[3,4] Clearly the synthesis of complexes which have coordination environments similar to those observed in the metalloprotein is highly desirable. Hence our research efforts are currently directed towards preparing mixed-donor dinickel thiolate-bridged complexes, in which a range of stereochemistries are observed at nickel(II), as first-generation structural models for hydrogenase.[4–7]

Recently we isolated a unique complex, $[Ni_2(L_{SO})(MeCN)_2][ClO_4]_2$ **1**, in which, despite the macrocycle $L_{SO}^{2-}$ providing potentially identical metal-binding environments, two differing geometries were observed for the nickel(II) ions, specifically $N_4SO$ octahedral and $N_2SO$ square planar (Scheme 1).[6] Given that this occurred in the presence of only rather weak ligand field ancilliary ligands (acetonitrile solvent molecules and perchlorate ions) it seemed likely that greater coordination numbers could be imposed on the nickel(II) ions. This paper concerns the intriguing result of adding thiocyanate ions to $[Ni_2(L_{SO})(MeCN)_2][ClO_4]_2$ **1**.

The addition of 2.2 equiv. sodium thiocyanate to an acetonitrile solution of complex **1**[6] causes precipitation of a solid which on recrystallisation from dmf by vapour diffusion of diethyl ether yields $[Ni_2(L_{SO})(NCS)_2(dmf)]$ **2** in which there has been a dramatic alteration in the nickel ion stereochemistries (Scheme 1). The X-ray structure determination reveals that each nickel ion in **2** is bound by an identical set of macrocycle donors (one amine nitrogen, one imine nitrogen, one bridging thiophenolate sulfur and one bridging phenolate oxygen), yet adopts differing stereochemistry (Fig. 1).‡ Ni(1) is octahedral binding one thiocyanate ion and a dmf solvent molecule to the remaining 'axial' sites, whilst Ni(2) is square-pyramidal binding one thiocyanate ion only. Comparison of the Ni–X bond lengths with related complexes[3–8] clearly indicates that Ni(2) is high spin [as is Ni(1)], as does the observation that Ni(2) is 0.26




**Scheme 1** Formation of $[Ni_2(L_{SO})(NCS)_2(dmf)]$ **2**

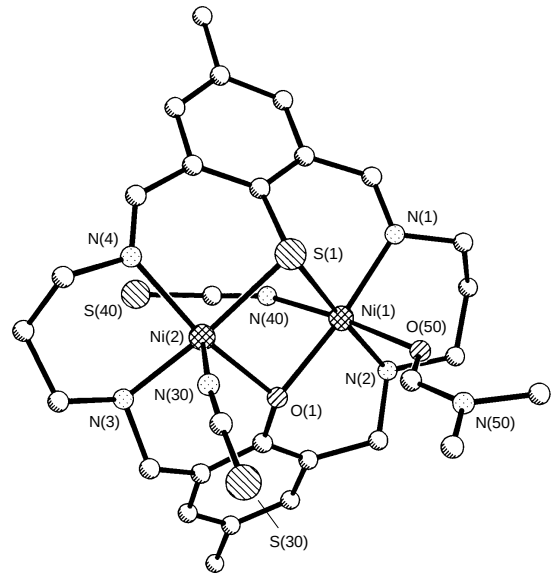



**Fig. 1** Perspective view of $[Ni_2(L_{SO})(NCS)_2(dmf)]$ **2**. Selected bond distances (Å) and angles (°): Ni(1)–N(40) 2.066(7), Ni(1)–N(2) 2.073(7), Ni(1)–N(1) 2.074(7), Ni(1)–O(50) 2.102(6), Ni(1)–O(1) 2.121(6), Ni(1)–S(1) 2.373(3), Ni(2)–N(30) 2.005(8), Ni(2)–N(3) 2.061(6), Ni(2)–N(4) 2.085(7), Ni(2)–O(1) 2.113(6), Ni(2)–S(1) 2.341(3), Ni(1)···Ni(2) 3.172(2), S(1)···O(1) 3.036(6); N(40)–Ni(1)–N(2) 91.7(3), N(40)–Ni(1) 94.8(3), N(2)–Ni(1)–N(1) 92.9(3), N(40)–Ni(1)–O(50) 175.5(3), N(2)–Ni(1)–O(50) 86.4(3), N(1)–Ni(1)–O(50) 89.4(3), N(40)–Ni(1)–O(1) 84.9(2), N(2)–Ni(1)–O(1) 95.9(3), N(1)–Ni(1)–O(1) 171.2(3), O(50)–Ni(1)–O(1) 91.2(2), N(40)–Ni(1)–S(1) 92.6(2), N(2)–Ni(1)–S(1) 175.7(2), N(1)–Ni(1)–S(1) 86.4(2), O(50)–Ni(1)–S(1) 89.3(2), O(1)–Ni(1)–S(1) 84.8(2), N(30)–Ni(2)–N(3) 94.3(3), N(30)–Ni(2)–N(4) 99.7(3), N(3)–Ni(2)–N(4) 91.1(3), N(30)–Ni(2)–O(1) 95.8(3), N(3)–Ni(2)–O(1) 93.2(2), N(4)–Ni(2)–O(1) 163.5(2), N(30)–Ni(2)–S(1) 98.4(2), N(3)–Ni(2)–S(1) 167.3(2), N(4)–Ni(2)–S(1) 86.6(2), O(1)–Ni(2)–S(1) 85.8(2), Ni(2)–S(1)–Ni(1) 84.59(9), Ni(2)–O(1)–Ni(1) 97.0(2).

Å out of the $N_2SO$ donor plane towards the bound thiocyanate ion.[9] The assignment of Ni(2) as high spin is also consistent with a preliminary magnetic measurement of 4.5 $\mu_B$ for **2** at room temperature.[7] This contrasts dramatically with the situation found in **1**: in both **1** and **2** one nickel(II) ion is octahedral, however the second nickel(II) ion is low-spin square planar in **1** whereas it is high-spin square pyramidal in **2**. To our knowledge this is the first example of a thiolate-bound high-spin square-pyramidal nickel(II) ion. Overall complex **2** is currently one of the best first-generation structural models available for the hydrogenase active site.

It is interesting that reaction of $[Ni_2(L_{SO})(MeCN)_2][ClO_4]_2$ with an excess of thiocyanate ions also yields **2**: further thiocyanate ions are not bound at the vacant axial site on the high-spin Ni(2) ion or as a replacement for the dmf molecule on Ni(1). This is presumably due to each nickel ion already satisfying the electroneutrality principle due to the coordination of anionic thiophenolate, phenolate and thiocyanate donors. This interpretation is consistent with the observation that one thiocyanate ion binds to each nickel ion in **2** in contrast with the situation in **1** where both neutral ancilliary ligands bind to just one of the two nickel ions. Once two thiocyanate ions are bound the complex is neutral so lack of solubility may also play an important role in the formation and isolation of **2**.

The macrocycle is very bent: the two phenyl ring planes intersect at 100.5° and the two macrocycle $N_2SO$ donor planes intersect at 143°. This is due in part to the differing geometries of the thiophenolate sulfur and phenolate oxygen atoms;[10,11] the former is tetrahedrally distorted [Ni–S(1)–X 84.6–103.3°] whilst the latter is closer to trigonal planar [Ni–O(1)–X 97.0–124.1°]. However, the Ni(1)–O(1)–Ni(2) angle of 97.0° is the smallest observed to date for a phenolate-bridged dinickel macrocyclic complex, and is far from trigonal.[11] The small Ni–X–Ni angles in **2** should have interesting consequences magnetically and this is under investigation.[7]

In summary, the ligand $L_{SO}^{2-}$ is of intermediate field strength, and the macrocyclic cavity quite flexible, so that it is able to accommodate a combination of either high-spin–high-spin or high-spin–low-spin nickel(II) ions as is demonstrated herein. This is a unique situation and augurs well for the ability of the $L_{SO}^{2-}$ macrocycle to yield further exciting first-generation models for the active site of the [Ni,Fe] hydrogenases. Hence further binding studies are under way, as are redox and XAS investigations.[7]

This work was supported by grants from the University of Otago. We thank Professor W. T. Robinson (University of Canterbury) for the X-ray data collection. S. B. thanks the University of Otago for the granting of study leave which has facilitated the writing of this paper, and gratefully acknowledges her host Professor K. Wieghardt and the financial support of the Alexander von Humboldt Stiftung.

## Footnotes

† E-mail: chemsab@otago.ac.nz

‡ *Crystal data* for **2**·$Et_2O$: $C_{33}H_{47}N_7Ni_2O_3S_3$, yellow oblong plate, 0.7 × 0.3 × 0.1 mm, triclinic, $P\bar{1}$, $a$ = 11.391(4), $b$ = 12.617(4), $c$ = 14.082(4) Å, $\alpha$ = 75.450(10), $\beta$ = 78.29(2), $\gamma$ = 85.78(2)°, $U$ = 1918(1) Å$^3$, $Z$ = 2, $\mu$ = 1.19 mm$^{-1}$, $D_c$ = 1.391 g cm$^{-3}$. Data were collected at 168 K on a Siemens P4 four-circle diffractometer using graphite-monochromated Mo-K$\alpha$ radiation. 5088 Reflections were collected, $4 < 2\theta < 45°$, and the 4992 independent reflections were used in the structural analysis after a semi-empirical absorption correction had been applied. The structure was solved by direct methods (SHELXS-86)[12] and refined against all $F^2$ data (SHELXL-93)[13] to $R_I$ = 0.062 [for 2662 $F > 4\sigma(F)$; w$R_2$ = 0.145 and goodness of fit = 0.85 for all 4992 $F^2$; 428 parameters; all non-hydrogen atoms except the disordered diethyl ether molecule of crystallisation anisotropic; max., min. residual electron density +0.62, −0.52 e Å$^{-3}$]. Atomic coordinates, bond lengths and angles, and thermal parameters have been deposited at the Cambridge Crystallographic Data Centre (CCDC). See Information for Authors, Issue No. 1. Any request to the CCDC for this material should quote the full literature citation and the reference number 182/366.

## References

1 A. Volbeda, M.-H. Charon, C. Piras, E. C. Hatchikian, M. Frey and J. C. Fontecilla-Camps, *Nature*, 1995, **373**, 580; J. C. Fontecilla-Camps, *J. Biol. Inorg. Chem.*, 1996, **1**, 91.
2 See for example: A. F. Kolodziej, *Prog. Inorg. Chem*., 1994, **41**, 493; M. A. Halcrow and G. Christou, *Chem. Rev*., 1994, **94**, 2421.
3 G. A. Lawrance, M. Maeda, T. M. Manning, M. A. O'Leary, B. W. Skelton and A. H. White, *J. Chem. Soc., Dalton Trans*., 1990, 2491; A. J. Atkins, A. J. Blake and M. Schröder, *J. Chem. Soc., Chem. Commun*., 1993, 1662.
4 S. Brooker, P. D. Croucher and F. M. Roxburgh, *J. Chem. Soc., Dalton Trans*., 1996, 3031 and references therein.
5 S. Brooker and P. D. Croucher, *J. Chem. Soc., Chem. Commun*., 1995, 1493.
6 S. Brooker and P. D. Croucher, *J. Chem. Soc., Chem. Commun*., 1995, 2075.
7 S. Brooker, P. D. Croucher, T. C. Davidson, G. S. Dunbar, S. P. Cramer, C. Y. Ralston, S. S. Iyer, A. McAuley and E. Bill, unpublished work.
8 See for example: J. J. Wilker, A. Gelasco, M. A. Pressler, R. O. Day and M. J. Maroney, *J. Am. Chem. Soc*., 1991, **113**, 6324; M. Cha, C. L. Gatlin, S. C. Critchlow and J. A. Kovacs, *Inorg. Chem*., 1993, **32**, 5868; D. C. Goodman, P. J. Farmer, M. Y. Darensbourg and J. H. Reibenspies, *Inorg. Chem*., 1996, **35**, 4989 and references therein.
9 P. L. Orioli, *Coord. Chem. Rev*., 1971, **6**, 285.
10 See for example: I. G. Dance, *Polyhedron*, 1986, **5**, 1037.
11 In the series of bis(phenolate-bridged) dinickel(II) complexes studied by Nag and coworkers these angles were in the range 99.2–105.7°: K. K. Nanda, L. K. Thompson, J. N. Bridson and K. Nag, *J. Chem. Soc., Chem. Commun*., 1994, 1337.
12 G. M. Sheldrick, *Acta Crystallogr., Sect. A*, 1990, **46**, 467.
13 G. M. Sheldrick, manuscript in preparation.

*Received, 19th November 1996; Com. 6/07833H*

# Catalytic dehydrogenation of ethylbenzene and tetrahydrofuran by a dihydrido iridium P–C–P pincer complex

**Mukta Gupta,†[a] William C. Kaska[b] and Craig M. Jensen*[a]**

[a] *Department of Chemistry, University of Hawaii, Honolulu, HI 96822, USA*
[b] *Department of Chemistry, University of California, Santa Barbara, CA 93106, USA*

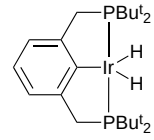
**The P–C–P pincer complex, $[IrH_2\{C_6H_3(CH_2PBu^t_2)$-2,6$\}]$ catalyses the transfer dehydrogenation of the donor-bearing substrates, ethylbenzene and tetrahydrofuran at temperatures as low as 150 °C.**

The catalytic dehydrogenation of aliphatic C–H bonds in the presence of functional groups is of major industrial importance. For example, the direct dehydrogenation of ethylbenzene accounts for 85% of the commercial production of styrene.[1] The reaction is carried out commercially at *ca*. 620 °C in the vapour phase over catalysts which primarily consist of iron oxide and potassium salt promoters.[1] Recently there has been considerable interest in the development of higher activity dehydrogenation catalysts which are also more selective for styrene over the degradation products, benzene and carbon.[1] Several soluble metal complexes have been found which catalyse the dehydrogenation of alkanes under moderate conditions.[2–4] However, none of these species have been reported to effect the catalytic dehydrogenation of aliphatic C–H bonds of functionalized substrates. This is apparently due to catalyst deactivation through strong coordinative interactions with donor groups. For example, $[IrH_2\{OC(O)CF_3\}(PPr^i_3)_2]$ effects the dehydrogenation of alkanes to arenes at 150 °C but fails to turnover catalytically since arenes are released from the metal centre only at temperatures at which complex decomposition occurs.[5]

We recently found that the iridium P–C–P pincer complex, $[IrH_2\{C_6H_3(CH_2PBu^t_2)_2$-2,6$\}]$ **1** is a highly active homogeneous catalyst for transfer dehydrogenation of cycloalkanes to alkenes and arenes.[4] In this system, the P–C–P framework of the catalyst is sufficiently robust that decomposition does not occur at temperatures required to achieve arene elimination. It was therefore of interest to explore whether alkylbenzenes and other weaker donor substrates such as cyclic ethers could be dehydrogenated by this catalytic system. We have found **1** will in fact catalyse the transfer dehydrogenation of ethylbenzene and tetrahydrofuran (thf).

Complex **1** was prepared as previously described.[4] The catalytic activity was investigated using solutions consisting of 4 ml of substrate (ethylbenzene, 32.6 mmol; thf, 49.3 mmol) *tert*-butylethene (tbe) (0.2 ml, 1.55 mmol) and **1** (3 mg, 0.005 mmol). The orange solutions were sealed in tubes under argon and fully immersed in an oil-bath for the prescribed reaction periods. The solutions became red upon heating and gradually change colour to yellow–orange during the reaction period. The reactivity was unaffected by the addition of metallic mercury to the solution indicating that metallic iridium is not involved in the hydrogen transfer.[6]

The results of the catalytic dehydrogenation experiments are summarized in Table 1. The products were identified by GCMS‡ analysis and quantified by gas chromatography.‡ Our product quantification balances the number of dehydrogenated C–C bonds within 5% to the amount of tbe hydrogenated to *tert*-butylethane (tba) in all experiments. No significant difference was found in either the amounts or distributions of products upon increasing the reaction time of the 200 °C experiments beyond 0.5 h. The amounts of products obtained in the 150 °C experiments increase over a longer period of time but are limited to lower levels than the 200 °C experiments. These results indicate that the amounts of products that are obtainable by these systems are restricted by thermodynamics. The direct dehydrogenation of ethylbenzene was explored at higher temperatures where a hydrogen acceptor such as tbe is not thermodynamically required. Unfortunately, **1** rapidly decom-




**1**

**Table 1** Catalytic dehydrogenations with **1**

| Substrate | *t*/h | *T*/°C | Products (mol/mol of **1**) | Dehydrogenated/ hydrogenated C–C bonds |
|---|---|---|---|---|
| thf | 1.0 | 150 | Dihydrofurans: 2,3 (46); 3,4 ( < 1) furan (31), tba (103) | 1.05 |
| thf | 3.0 | 150 | Dihydrofurans: 2,3 (41); 3,4 (5), furan (57), tba (154) | 1.04 |
| thf | 0.5 | 200 | Dihydrofurans: 2,3 (84); 3,4 (5), furan (54), tba (190) | 1.04 |
| thf | 1.0 | 200 | Dihydrofurans: 2,3 (86); 3,4 (6), furan (53), tba (192) | 1.03 |
| Ethylbenzene | 1.0 | 150 | Styrene (8), tba (8) | 1.00 |
| Ethylbenzene | 12.0 | 150 | Styrene (10), tba (10) | 1.00 |
| Ethylbenzene | 0.5 | 200 | Styrene (50), tba (51) | 0.98 |
| Ethylbenzene | 1.0 | 200 | Styrene (50), tba (52) | 0.96 |
| Ethylcyclohexane | 1.0 | 150 | Ethylcyclohexenes (3.5), ethylbenzene (8), styrene (7), tba (84) | 1.04 |
| Ethylcyclohexane | 12.0 | 150 | Ethylcyclohexenes (47), ethylbenzene (18), styrene (35), tba (274) | 1.05 |
| Ethylcyclohexane | 0.5 | 200 | Ethylcyclohexenes (58), ethylbenzene (35), styrene (34), tba (310) | 0.97 |
| Ethylcyclohexane[a] | 1.0 | 200 | Ethylcyclohexenes (13), ethylbenzene (43), styrene (76), tba (441) | 1.01 |

[a] An additional 0.2 ml (1.55 mmol) of tbe was added to the reaction mixture after 0.5 h.

poses at temperatures in excess of 200 °C and no dehydrogenation activity was observed.

The catalytic activity of **1** for the dehydrogenation of the functionalized substrates is significantly lower than previously found for cycloalkanes.[3,4] This suggests that arene and oxygen donor interactions with the metal centre inhibit the catalytic system. The findings of product inhibition and tbe concentration sensitivity in the transfer dehydrogenation of cyclooctane and cyclohexane also suggest that the catalytic activity of **1** is inhibited by species bearing donor groups.[3] In order to probe this possibility, the activity of **1** for the transfer dehydrogenation of ethylcyclohexane was investigated. As seen in Table 1, significantly higher styrene production was observed than in the case of ethylbenzene. This is apparently due to the reduced arene concentration in the ethylcyclohexane experiments. Nitrogen has been found to poison the transfer dehydrogenation of cyclooctane by **1**.[3] Similarly, no dehydrogenation of either ethylbenzene or thf was observed in experiments conducted under 1 atm of $N_2$ in place of argon at 150 °C. Thus the catalytic system is sensitive to even the weak donor, $N_2$.

Despite the limitations of this catalytic system, it represents a step forward in the development of improved catalysts for the production of styrene. It is also the first report of a homogeneous catalytic system for dehydrogenation of saturated C–H bonds in presence of functionalization. Modified catalysts of this type could provide an entrance into new chemical processes through previously inaccessible catalytic pathways.

The support of this research by the US Department of Energy Hydrogen Program is gratefully acknowledged.

## Footnotes

† 1995 J. J. Zuckermann fellow.

‡ GC analyses were performed on a temperature programmed (ethylbenzene, 70 °C isothermal for 1 min, 5 °C $min^{-1}$ to 130 °C; thf, 35 °C isothermal for 1 min; 1 °C $min^{-1}$ to 45 °C; ethylcyclohexane, 60 °C isothermal for 1 min, 5 °C $min^{-1}$ to 150 °C) Hewlett Packard 5890 gas chromatograph using a 250 μm × 25 m OV-1 capillary column. For GCMS analyses the column was coupled to a VG 70SE dual sector high-resolution mass spectrometer.

## References

1 D. H. James and W. M. Castor, in *Ullmann's Encyclopedia of Industrial Chemistry*, 5th edn., ed. B. Elvers, S. Hawkins and W. Russey, VCH Verlagsgesellschaft, Weinheim, 1994, p. 332.

2 D. Baudry, M. Ephritikhine and H. Felkin, *J. Chem. Soc., Chem. Commun*., 1983, 788; H. Felkin, T. Fillebeen-Khan, R. Holmes-Smith and J. Zakrzewski, *Tetrahedron Lett*., 1984, **25**, 1279; H. Felkin, T. Fillebeen-Khan, R. Holmes-Smith and Y. Lin, *Tetrahedron Lett*., 1985, **26**, 1999; M. W. Burk, R. H. Crabtree and D. V. McGrath, *J. Chem. Soc., Chem. Commun*., 1985, 1829; M. W. Burk and R. H. Crabtree, *J. Am. Chem. Soc*., 1987, **109**, 8025; K. Nomura and Y. Saito, *J. Chem. Soc., Chem. Commun*., 1988, 161; K. Nomura and Y. Saito, *J. Mol. Catal*., 1989, **54**, 57; T. Sakakura, T. Sodeyama and M. Tanaka, *New J. Chem*., 1989, **13**, 737; J. A. Maguire, W. T. Boese and A. S. Goldman, *J. Am. Chem. Soc*., 1989, **111**, 7088; T. Sakakura, T. Sodeyama, F. Abe and M. Tanaka, *Chem. Lett*., 1991, 297; J. A. Maguire and A. S. Goldman, *J. Am. Chem. Soc*., 1991, **113**, 6706; J. A. Maguire, A. Petrillo and A. S. Goldman, *J. Am. Chem. Soc*., 1992, **114**, 9492; T. Fujii and Y. Satio, *J. Chem. Soc., Chem. Commun*., 1990, 757; T. Fujii, Y. Higashino and Y. Satio, *J. Chem. Soc., Dalton Trans*., 1993, 517; T. Aoki and R. H. Crabtree, *Organometallics*, 1993, **12**, 294; J. A. Miller and L. K. Knox, *J. Chem. Soc., Chem. Commun*., 1994, 1449; J. Belli and C. M. Jensen, *Organometallics*, 1996, **15**, 1532.

3 M. Gupta, C. Hagen, W. C. Kaska, R. Flesher and C. M. Jensen, *Chem. Commun*., 1996, 2083.

4 M. Gupta, W. C. Kaska, R. Cramer and C. M. Jensen, *J. Am. Chem. Soc*., 1997, **119**, 840.

5 D. R. Anton and R. H. Crabtree, *Organometallics*, 1982, **2**, 855.

*Received, 29th October 1996; Com. 6/07381F*

# Effect of [60]fullerene on the radical polymerization of alkenes

**Sanjiv Mehrotra, Asutosh Nigam and Ripudaman Malhotra***

*Chemistry and Chemical Engineering Laboratory, SRI International, 333 Ravenswood Avenue, Menlo Park, CA 94025, USA*

**AIBN-initiated radical polymerization of 2-cyanoethyl acrylate and cyanovinyl acetate in the presence of [60]fullerene produces copolymers in good yields, whereas for most other vinyl monomers [60]fullerene almost completely inhibits the polymerization.**

The synthesis and isolation of macroscopic quantities of [60]fullerene has stimulated great interest in fullerene polymers. Along with the development of its chemistry, several different polymers incorporating [60]fullerene have been reported consisting of covalently linked fullerenes and copolymers in which fullerenes are a part of the polymer backbone.[1] In all previous reports on radical polymerization of vinyl monomers, conducted mostly with styrene or methyl methacrylate, the yields of polymers formed in solution were either very low or the reaction was completely inhibited.[2,3] It has been suggested that in the case of styrene, the free radicals are trapped by fullerene, and the resulting fullerene radicals do not propagate but instead can terminate. Recently, Camp *et al*. have reported the copolymerization of [60]fullerene and styrene in the presence of a large excess of the initiator AIBN.[4] According to the authors, the radicals from the initiator undergo multiple additions on [60]fullerene, ultimately changing its nature sufficiently such that it would not inhibit polymerization.

We report here findings of our study on AIBN-initiated radical polymerization of a range of vinyl monomers in the presence of [60]fullerene. The objective of this study was to determine how general is the inhibition of radical polymerization by [60]fullerene and to see if the fullerene radicals, which do not readily add to methyl methacrylate and styrene, would add to certain reactive monomers. The vinyl monomers studied were styrene, methyl acrylate, methyl methacrylate (MMA), acrylonitrile, vinyl acetate, 1-vinyl-2-pyrrolidone, 2-cyanoethyl acrylate (CEA) and 1-cyanovinyl acetate (CVA).

In a typical experiment, 60–100 equiv. of vinyl monomer was added to a suspension of [60]fullerene (50 mg, 0.07 mmol) in dry THF (2 ml) under argon atmosphere, followed by the addition of a catalytic amount of AIBN. The reaction mixture was heated under reflux (65 °C) for 22 h, the solvent was evaporated and the weight of the residue was taken as the first indication for the formation of a polymer. Control experiments with these monomers without [60]fullerene were also conducted under otherwise identical conditions. The results for the eight vinyl monomers studied are given in Table 1.

In the absence of [60]fullerene, polymer formation was observed in greater than 75% yield in all cases . However, in the presence of [60]fullerene, polymerization in six out of the eight monomers was substantially inhibited and yielded 15% or less of the polymeric products. For example, the reaction of methyl acrylate produced only 9% of the polymer. The presence of an α-methyl group on the vinyl moiety increases the polymer yield only marginally to 14%. Substitution with cyano, as in acrylonitrile, also did not lead to the production of substantial yields of the polymer in the presence of [60]fullerene. Surprisingly, we found that cyanovinyl acetate gave the polymer in about 50% yield. We wondered if the acetoxy group itself is responsible for this activity, but the polymerization of vinyl acetate was almost completely inhibited by [60]fullerene. Also noteworthy is the reactivity exhibited by 2-cyanoethyl acrylate (65% polymer yield), which is structurally very similar to methyl acrylate. The cyano group in this molecule is remote from the vinyl portion, and points to some cyclic intermediate in which the cyano group stabilizes the intermediate radical. It would be interesting to correlate the polymer formation with the partial reactivity factors of the various vinyl monomers. Unfortunately, we were unable to find literature reports on the partial reactivity factors for CEA and CVA, the two cases where we observed substantial copolymerization.

[60]Fullerene can inhibit the chain propagation by reacting with the initiator radical and/or by terminating the propagating chain. It has been reported that [60]fullerenes react effectively with isobutyronitrile radicals produced by the thermal decomposition of AIBN.[4] Therefore it is possible that [60]fullerene intercepts the initiating radicals in the polymerization reaction. To further understand the role of [60]fullerene as an inhibitor of propagating chains, we conducted the AIBN-initiated polymerization of MMA and quenched it with [60]fullerene at different time intervals. Polymerization of MMA was conducted for 1 or 2 h by heating 615 mg (6.14 mmol) of MMA in dry THF (2 ml) under reflux (65 °C) in the presence of 6 mg (0.036 mmol) of AIBN. Then 50 mg (0.07 mmol) of [60]fullerene was added to these reaction mixtures and heated overnight. The reaction mixture was evaporated to dryness, dissolved in MeCN, filtered to remove unconverted [60]fullerene and dried to recover the copolymers. In contrast to the complete inhibition of MMA polymerization when [60]fullerene was added at the start of the reaction, the yield of the copolymer increased to 264 mg (40%) when [60]fullerene was added following 1 h reaction, and 370 mg (56%) if the addition of [60]fullerene was delayed for 2 h. The number average molecular weights for [60]fullerene–PMMA polymers obtained in these cases were around 8,000 and 22,000 respectively. $^{13}C$ NMR spectra of the product do not show a peak at δ 143 corresponding to the starting [60]fullerene, which suggests complete reaction of fullerene with propagating radical chain. The low yields of polymerization in the above reactions and the difference in molecular weights further confirms that [60]fullerene quenches the propagating chains very effectively.

As mentioned above, the more reactive monomers, CVA and CEA, underwent facile copolymerization with [60]fullerene yielding 53 and 65% of the copolymers, respectively (Table 1).

**Table 1** Effect of [60]fullerene on the yield of polymers from AIBN-initiated polymerization of various vinyl monomers at 65 °C

| Monomer | Polymer yield (%) | |
|---|---|---|
| | With $C_{60}$ | Control |
| Methyl acrylate | 9 | 97 |
| Methyl methacrylate | 14 | 98 |
| Acrylonitrile | 11 | 76 |
| Cyanovinyl acetate | 53 | 92 |
| Vinyl acetate | 9 | 75 |
| 2-Cyanoethyl acrylate | 65 | 99 |
| Styrene | 15 | 85 |
| *N*-vinylpyrrolidone | 8 | 100 |

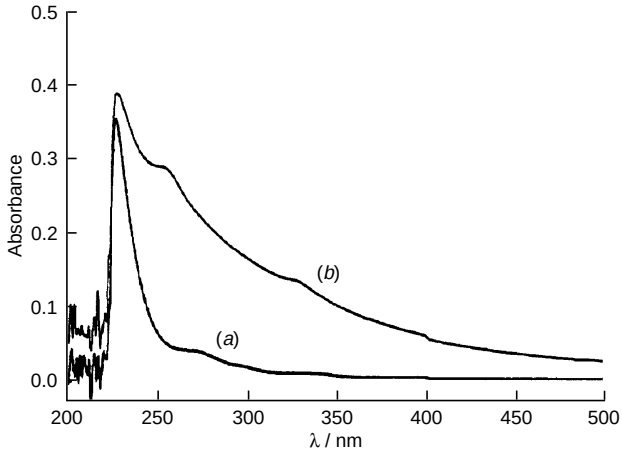



**Fig. 1** UV–VIS absorption spectra of (*a*) poly(2-cyanoethylacrylate) and (*b*) the copolymer formed with [60]fullerene

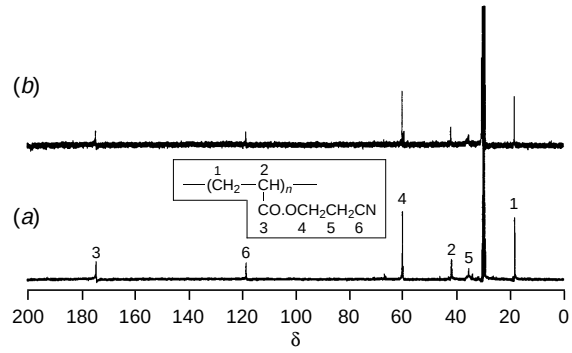



**Fig. 2** $^{13}C$ NMR spectra of (*a*) poly(2-cyanoethyl acrylate) and (*b*) the copolymer formed with [60]fullerene

It was also observed that the initially free flowing reaction mixture became viscous as the reaction proceeded. Evidently, these monomers are reactive enough that fullerene-based radical(s) formed by the addition of a growing polymer chain can add to them and continue the polymerization process. However, before we can make this conclusion, we have to eliminate the possibility of these monomers are undergoing polymerization by a different mechanism, *e.g.* polymerization promoted by traces of moisture. Thus, we attempted polymerization of CVA and CEA in the absence of AIBN and in the presence of traces of water. In none of these cases did we observe any polymerization. Therefore we conclude that the polymerization was indeed following a radical chain pathway.

The copolymer of [60]fullerene and CVA was completely soluble in MeCN. A small amount of material that did not dissolve in MeCN was identified as [60]fullerene. In contrast, only about half of the copolymer of [60]fullerene and CEA was soluble in MeCN. We believe that the insoluble portion has either a branched or a cross-linked structure which is obtained by the multiple addition of propagating chains to the fullerene surface. We also studied the effect of [60]fullerene on the propagating chains of CEA and CVA monomers. Two experiments were conducted for each of these monomers. Polymerization was initiated by heating the monomer in dry THF in the presence of a catalytic amount of AIBN, and [60]fullerene was added to the reaction mixture after 1 h. In one experiment the reaction was quenched immediately, and in the second, the heating was continued for another 22 h. For CVA, the yield of the polymer was only 18% when the reaction was quenched immediately after adding [60]fullerene, and 50% when the mixture was heated for the additional 22 h. These results further show that [60]fullerene does not completely inhibit the polymerization of reactive monomers. CEA, being an even more reactive substrate, yielded 83% of the polymer in the first hour and continued heating after the addition of [60]fullerene did not increase the yield any further. Analogous reactions with MMA yielded 24% of polymer after the first hour and 40% of the polymer if the mixture was heated overnight compared to 98% of the polymer after 22 h in the absence of [60]fullerene and 14% of polymer in the presence of [60]fullerene.

Structural characterization of the copolymers was performed using IR, NMR and UV spectroscopic techniques and thermogravimetric analysis (TGA). The presence of fullerene moieties is evident from the absorption spectra of the copolymers of [60]fullerene with CEA and CVA. Fig. 1 shows the absorption spectra for poly(CEA) and the copolymer formed with [60]fullerene. Whereas the absorption bands of the homopolymers cut off at much shorter wavelengths, the copolymers show broad overlapping bands extending from the UV region to almost 500 nm. Sun and coworkers[2] have also observed a similar broadening of the characteristic absorption bands of fullerenes when incorporated into a polymer matrix. Analogous data (not shown) were obtained for the CVA system. Fig. 2 shows the identical $^{13}C$ NMR spectra of the homopolymer and the copolymers for CEA. The spectrum for the copolymer does not show any signals due to the [60]fullerene moiety. The absence of any fullerene peaks may be due to the fact that the concentration of the fullerene units is very low, which is further exacerbated by the loss of the 60-fold degeneracy of the original [60]fullerene once it has undergone reaction to produce adducts. However, it is also significant that there is no peak at δ 143, corresponding to *free* [60]fullerene, in the case of the copolymer. Thus, the extended UV absorption must be due to the fullerene units that are now a part of the polymer. Again, similar data (not shown) were obtained for the CVA system. Thermal characterization of the polymers showed that the presence of the fullerene did not affect the onset of decomposition, although the char yield was higher with the fullerene copolymers when compared to the homopolymer.

We therefore conclude that [60]fullerene acts as an efficient inhibitor or a retarder in the radical polymerization of most vinyl monomers and results in the formation of [60]fullerene-terminated structures. However, with certain reactive vinyl monomers such as cyanoethyl acrylate and cyanovinyl acetate, it can form copolymers. Evidently, these monomers can add to the fullerene-based radical intermediate to propagate the polymerization. The role of reactivity ratios and general dependence on the structural and chemical nature of the vinyl monomers on polymerization reaction in the presence of [60]fullerene is currently under investigation in more detail in our laboratory.

This work was conducted under the program, 'Advanced Chemical Processing Technology', consigned to the Advanced Processing Technology Research Association from the New Energy and Industrial Technology Development Organization, which is carried out under the Industrial Science and Technology Frontier Program administered by the Agency of Industrial Science and Technology, the Ministry of International Trade and Industry, Japan.

## References

1 T. Cao and S. Webber, *Macromolecules*, 1995, **28**, 3741.
2 C. E. Bunker, G. E. Lawson and Y.-P. Sun, *Macromolecules*, 1995, **28**, 3744.
3 R. D. McClain, *Fullerenes: Recent Advances in the Chemistry and Physics of Fullerenes and Related Materials*, ed. R. S. Ruoff and K. M. Kadish, Electrochemical Society, Pennington, NJ, 1995, p. 71.
4 A. G. Camp, A. Lary and W. T. Ford, *Macromolecules*, 1995, **28**, 7959.

*Received, 8th August 1996; Com. 6/05555I*

# Dynamics of H/D and D/H exchanges in β-cyclodextrin dodecahydrate observed in real time: effects from zero-point vibrational energy

**Aida Moreira da Silva,[a] Thomas Steiner,[b] Wolfram Saenger,[b] José Empis,[c] and José J. C. Teixeira-Dias*[d]**

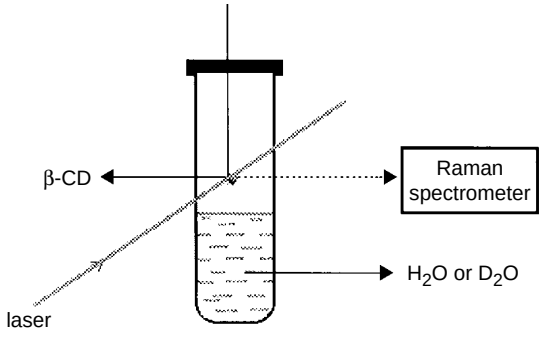
[a] *School of Agriculture, Polytechnical Institute of Coimbra, P-3000 Coimbra, Portugal*
[b] *Institut für Kristallographie, Freie Universität Berlin, D-14195 Berlin, Germany*
[c] *Laboratory of Biotechnology, Technical University, P-1000 Lisboa, Portugal*
[d] *Department of Chemistry, University of Aveiro, P-3810 Aveiro, Portugal*

**Cyclic H/D and D/H exchange processes in crystalline β-cyclodextrin dodecahydrate exposed to $D_2O$ (or $H_2O$) vapour, monitored in real time by the integrated intensity of the O–H Raman stretching band, exhibit different rate constants and activation energies ascribed to different zero-point vibrational energies of OH and OD.**

Crystalline hydrates of β-cyclodextrin (cyclomaltoheptaose, β-CD) are good models for the study of hydration processes in biomolecular structures.[1–8] The water molecules contained in the crystal[1,2] and most of the 21 β-CD hydroxy groups display appreciable positional and/or orientational disorder, with jump rates up to $10^{10}$–$10^{11}$ $s^{-1}$.[4,5] At atmospheres with humidities < 100%, the water content is reduced, and equilibration to changes of humidity takes place within minutes. This shows that, despite the absence of permanent channels, rapid water diffusion takes place in the crystal lattice.[2] If crystalline β-CD hydrate is exposed to an $H_2{}^{18}O$ atmosphere, all water molecules are replaced by the labelled species, showing that there are no 'fixed' water sites.[6] If a sample is exposed to a $D_2O$ atmosphere, complete H(O)/D(O) exchange takes place. Both exchange mechanisms occur on the same timescale, showing that long-range transport must be by diffusing intact water molecules, but since the H/D exchange also extends to β-CD hydroxy groups which are sterically inaccessible to diffusing water molecules, there must be local chains of proton transfer processes.[6] The previous studies were based on measurements on samples in equilibrium at room temperature. In the present work, we present, for the first time, real-time observations on the H/D exchange, and also report on temperature-dependent experiments.

In an H(O)/D(O) exchange experiment, the quantity of H(O) in the sample can be measured by the relative integrated intensity of the O–H Raman stretching band ($I_{OH}$).[7] Recently, we reported on a Raman spectroscopic real-time method to monitor $I_{OH}$,[7] which is here applied to the observation of the H/D exchange kinetics in β-CD dodecahydrate. The experimental setup is shown in Scheme 1.

Crystalline β-CD dodecahydrate† was placed in a closed cell over a reservoir of $D_2O$, and the Raman spectra of the region of O–H and O–D stretching vibrations were recorded at short time intervals (by use of a CCD detector, the 2100–3800 $cm^{-1}$ region could be recorded within *ca.* 1.5 min).‡ As $D_2O$ diffuses into, and $H_2O$ out of, the sample, and H/D exchange processes at the β-CD hydroxy groups take place, $I_{OH}$ continuously decreases, and, in parallel, $I_{OD}$ increases.§ A typical series of spectra is shown in Fig. 1; the invariant central peak represents a complex band of C–H stretching vibrations and is conveniently used as an internal reference intensity. During H(O)/D(O) exchange, the relevant kinetic variable is the fraction of remaining H(O) atoms, θ, which is experimentally measured by $I_{OH}/I_{OH}$(max.). As shown by the inset of Fig. 1, the relative H(O) concentration decreases according to approximate first-order kinetics (here with 50% exchange within 43 min). After equilibration, the $D_2O$ reservoir of the experimental cell was quickly replaced by an $H_2O$ reservoir,¶ so that the reverse exchange process [D(O)/H(O)] could be monitored on the same sample. After equilibration, another H(O)/D(O) exchange experiment could follow, and so on. The results obtained from a two-cycle sequence of experiments H/D → D/H → H/D → D/H are listed in Table 1.




**Scheme 1**

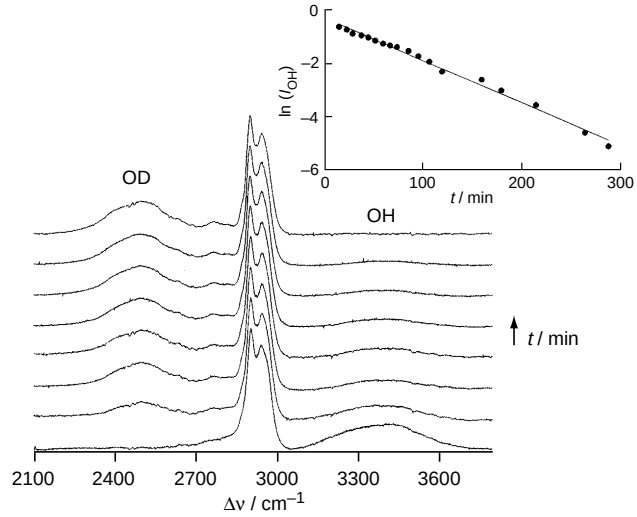



**Fig. 1** Examples of Raman spectra in the relevant spectral region 2100–3800 $cm^{-1}$, for on-line observation of H/D exchange

**Table 1** Results for a two-cycle exchange/back-exchange experiment: sample quantity *ca.* 20 mg, *n* is the number of spectra used, *k* the effective rate constant, and $t_{\frac{1}{2}}$ the time for 50% exchange[9¶]

| Experiment | *n* | $k$/$min^{-1}$ | $t_{\frac{1}{2}}$/min | $t_{\frac{1}{2}}$ (95% confidence) |
|---|---|---|---|---|
| First cycle, H → D | 18 | −0.0160 | 43 | 40–46 |
| First cycle, D → H | 15 | −0.0126 | 55 | 52–59 |
| Second cycle, H → D | 18 | −0.0175 | 40 | 37–43 |
| Second cycle, D → H | 13 | −0.0116 | 60 | 54–67 |

In all experiments, the exchange processes follow first-order kinetics. Although the determination of the $t_{\frac{1}{2}}$ values suffers some uncertainty, the data indicate different rate constants for the H/D and D/H exchange processes (the H/D and D/H values are each clearly outside the other 95% confidence interval), with the D/H process being the slower. Comparing the first and second cycles, the two H/D values are within each other's confidence intervals, as are the two D/H values, showing that the process as a whole can be reproduced cyclically.

As mentioned previously,[6] the macroscopic rate constant $k$ is sample dependent: owing to shorter diffusion paths, the exchange must be faster in samples with larger surface-to-mass ratios. Therefore, when repeating the above experiment with a different sample, the same general behaviour with somewhat different absolute $t_{\frac{1}{2}}$ values must be expected. This was in fact observed for another set of experiments, where again H/D exchange was observed to be faster than the D/H back-exchange.

These observations are in consonance with recent quantum mechanical calculations which indicate that OD hydrogen bonds are stronger owing to a lowering of the zero-point vibrational energy (ZPVE).[10] Therefore, OD hydrogen bonds should be more difficult to break, and D(O)/H(O) substitution should be slower than the reverse process. A consequence is that intact water molecules, which are the carriers of H or D through the lattice, diffuse more slowly when of the $D_2O$ type than of the $H_2O$ type (DHO should be in between these two extremes).

In order to assess the effect of temperature on the exchange rate constants, a different set of experiments was performed. At a number of defined temperatures, crystalline β-CD($H_2O$) dodecahydrate was exposed to the atmosphere over a reservoir of $D_2O$, for 30 min. Then, small samples were removed, sealed in capillary tubes and Raman spectra were recorded (batch method).‖ The fraction of remaining H(O) was determined from $I_{OH}$, allowing the calculation of $k$ and $t_{\frac{1}{2}}$ [from $I_{OH} = I_{OH}(\text{max.}) \exp(-kt)$ with $t$ = 30 min]. Analogous experiments were performed for β-CD($D_2O$) exposed to the atmosphere over $H_2O$. Numerical results are given in Table 2: as expected, the exchanges are appreciably faster at elevated temperatures. In a plot of $1n|1n\theta|$ *vs.* $1/T$, linear correlations are obtained for both processes (Fig. 2), suggesting Arrhenius type dependences of the rate constants. Linear regression calculation obtains activation energies, $E_a$, of 26 kJ mol$^{-1}$ for H/D exchange, and 33 kJ mol$^{-1}$ for D/H back-exchange. Again, this is in consonance with the theoretical calculations mentioned above,[10] which indicate that substitution of H(O) by D(O) lowers both the intramolecular and the intermolecular ZPVE.

**Table 2** Temperature-dependent H/D and D/H exchange experiments

| Experiment | $T$/K | $t_{\frac{1}{2}}$/min |
|---|---|---|
| H → D | 279 | 26 |
| | 291 | 16 |
| | 308 | 10 |
| | 343 | 3 |
| D → H | 280 | 47 |
| | 299 | 23 |
| | 315 | 13 |
| | 341 | 3 |

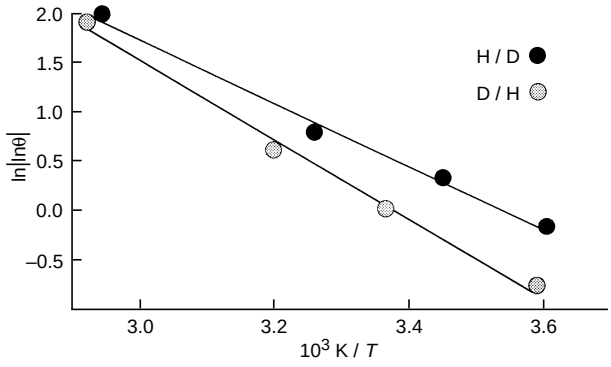



**Fig. 2** $1n|1n\theta|$ *vs.* $1/T$ for H/D [$\theta = I_{OH}/I_{OH}(\text{max.})$] and D/H [$\theta = I_{OD}/I_{OD}(\text{max.})$] exchange experiments

The experimental setup used (Scheme 1) allows the real-time observation of cyclic H/D and D/H exchange processes. Since the data are obtained from the same sample under the same conditions, the macroscopic rate constants for H/D and D/H exchange can be compared directly. The results indicate different rate constants for H/D and D/H exchanges in crystalline β-CD dodecahydrate. Presumably, the origin of this phenomenon is found in the different zero-point vibrational energies of OH and OD. It is of interest that this microscopic effect leads to noticeably different behaviour in the macroscopic diffusion properties.

This work was carried out in the Molecular Physical Chemistry Research Unit No. 70/94, University of Coimbra, financially supported by JNICT, Lisboa. The Berlin authors acknowledge support from Deutsche Forschungsgemeinschaft (Sa 196/26-1), Fonds der Chemischen Industrie and Deutscher Akademischer Austauschdienst (322-inida-dr).

## Footnotes

†β-CD, kindly donated by Wacker Chemie, München (Germany), was recrystallized by cooling concentrated aqueous solutions in a Dewar flask from *ca*. 80 °C to room temperature. Crystals were taken from the solvent and exposed to an atmosphere of moderate temperature and humidity (*ca*. 25 °C and 60% relative humidity). After equilibration with the atmosphere, crystals were ground, not sieved, to obtain a microcrystalline powder. Care was taken that all samples were prepared similarly.

‡ Jobin-Yvon T64000 Raman spectrometer, subtractive configuration, relevant slit widths set to 300 μm, intermediate slit between pre-monochromator and spectrograph wide open (14 mm), CCD detector, integration time 15 s. An Ar ion laser (Coherent-Innova 300-05 model with power track) provided *ca*. 100 mW at the sample position. Integrated intensities were determined using the machine software.

§ The sum $I_{OH}/I_{OH}(\text{max.}) + I_{OD}/I_{OD}(\text{max.})$ is *ca*. 1.0 at all times (deviations from unity were < 5%), *i.e*. the total number of OH/D oscillators was conserved during the exchange experiments. Separate normalization of each term is required because the OH and OD stretching vibrations have different Raman activities.

¶ Owing to the necessary manipulations at the start of the experiment and at the exchange of reservoirs, the zero point of the time scale is ill defined. Therefore, only data for $t \geqslant 15$ min are used for data analysis; this affects only the intercept, but not the kinetically relevant slope in Fig. 1.

‖ In this series of experiments, each measurement had necessarily to be performed on a different sample. Although all care was used to ensure that close to identical sample conditions were provided each time, the numerical reliability is reduced compared to the data in Table 1, which was obtained from only one sample.

## References

1 K. Lindner and W. Saenger, *Carbohydr. Res*., 1982, **99**, 103.
2 Th. Steiner and G. Koellner, *J. Am. Chem. Soc*., 1994, **116**, 5122.
3 Ch. Betzel, W. Saenger, B. E. Hingerty and G. M. Brown, *J. Am. Chem. Soc*., 1984, **106**, 7545.
4 Th. Steiner, W. Saenger and R. E. Lechner, *Mol. Phys*., 1991, **72**, 1211.
5 M. G. Usha and R. J. Wittebort, *J. Mol. Biol*., 1989, **208**, 669; *J. Am. Chem. Soc*., 1992, **114**, 1541.
6 Th. Steiner, A. M. Moreira da Silva, J. J. C. Teixeira-Dias, J. Müller and W. Saenger, *Angew. Chem., Int. Ed. Engl*., 1995, **34**, 1452.
7 A. M. Moreira da Silva, Th. Steiner, W. Saenger, J. Empis and J. J. C. Teixeira-Dias, *Chem. Commun*., 1996, 1871.
8 A. Marini, V. Berbenni, G. Bruni, V. Massarotti, P. Mustarelli and M. Villa, *J. Chem. Phys*., 1995, **103**, 7532.
9 E. Kreyszig, *Statistische Methoden und ihre Anwendungen*, Vandenhock & Ruprecht, Göttingen, 1991, 7th edn.
10 S. Scheiner and M. Cuma, *J. Am. Chem. Soc*., 1996, **118**, 1511.

*Received, 13th November 1996; Com. 6/07721H*

# Self-assembly directed by NH···O hydrogen bonding: a neutron study of a trilayered supramolecular array formed between 1,2-diaminoethane and benzoic acid

**Kenneth R. Adam,[a] Ian M. Atkinson,[a] R. Lindsay Davis,[b] Leonard F. Lindoy,[c] Myrna S. Mahinay,[a] Brian J. McCool,[a] Brian W. Skelton[d] and Allan H. White[d]**

[a] *School of Molecular Sciences, James Cook University, Qld., 4811, Australia*
[b] *Australian Nuclear Science and Technology Organisation, Menai, NSW, 2234, Australia*
[c] *School of Chemistry, University of Sydney, NSW, 1006, Australia*
[d] *Chemistry Department, University of Western Australia, Nedlands, Western Australia, 6009, Australia*

**The supramolecular array formed by co-crystallisation of 1,2-diaminoethane and benzoic acid is investigated by neutron diffraction; the system self-assembles into an unusual layered structure composed of two-dimensional hydrogen-bonded networks sandwiched between layers of edge-to-face stacked aromatic systems; the number of hydrogen-bond donors and acceptors is balanced in the structure.**

The self-assembly of two of more molecular components into well defined, solid-state supramolecular structures has been a topic of considerable recent interest.[1–3] Such 'crystal engineering' involves the attempted regulation of the subtle non-covalent interactions that dictate crystal packing in order to produce new materials showing unusual properties, including novel electrical and optical properties. Co-crystallisation of selected complementary molecules provides one means of generating new extended supramolecular frameworks of this type;[4] such an approach was employed in the study now reported.

Of the variety of intermolecular interactions commonly identified in solid-state supramolecular structures (hydrogen bonding, electrostatic, van der Waals, π–π stacking),[1,2,5–7] hydrogen bonds tend to have the highest strength and selectivity.[1,2]

Here, we report the single-crystal neutron structure of the 1 : 2 molecular assembly formed between 1,2-diaminoethane and benzoic acid.† Crystallisation of this adduct can be effected by slow evaporation of a stoichiometric mixture of the components dissolved in methanol. Large transparent crystals (*ca*. 0.4 × 0.8 × 0.8 cm, mp = 153.5 °C) grew rapidly overnight. The structure of the resulting supramolecular array (Fig. 1 and 2) is predominantly directed by π–π stacking and strong hydrogen-bond formation in which acid protons have transferred onto the amine nitrogens (analogous to 'intermolecular zwitterions') such that each amine in the structure is in its $-NH_3^+$ form. Polarised hydrogen-bond interactions of this type can be very strong[8] and, as often observed in related systems,[7,9,10] all the amine and acid protons within the structure take part in NH···O bonding. In the asymmetric unit as defined, the two independent benzoate moieties attached on opposite sides to a 1,2-diaminoethane moiety (*via* one strong hydrogen bond) lie approximately parallel [interplanar dihedral angle 3.1(2)°]. All hydrogen bonds in the array are very similar with N···O, N–H, H···O, N–H···O all very closely ranged [2.727(5)–2.764(6); 1.02(1)–1.09(1); 1.65(1)–1.78(1); 156(1)–172(1)°].

A two-dimensional planar layer is formed by parallel 'rows' of the acid/amine motifs being stacked side-by-side, each row being offset with respect to the next.

An edge-on projection of this layer is shown in Fig. 1; this illustrates that a pair of benzoate sheets effectively sandwich a sheet of 1,2-diaminoethane molecules parallel to the *ab* plane. The layer is 'stitched' together by hydrogen bonds between adjacent benzoic acids and 1,2-diaminoethanes of different motif units. Each benzoate participates in three strong hydrogen bonds, two to one oxygen in each case, with H···O···H 113.0(6), 112.6(6)°; C–O to that oxygen being slightly longer [1.264(5), 1.265(5) Å] than for those distances to the oxygens which have single hydrogen bonds [1.231(5), 1.241(5) Å]. It is noted that while each side adduct layer is very similar, they are not crystallographically equivalent, although the array has pseudo-symmetry.

Planar layers of acid/amine motifs are in turn stacked such that adjacent layers are bound together by edge-to-face (T-oriented) aromatic stacks in a herringbone arrangement (Fig. 1). The overall pattern of the layers can be expressed as . . .bab′bab′. . . where b and b′ are the non-identical benzoate layers and a is the amine layer. Owing to the proton transfer, a charge separation exists within the hydrogen-bonded layers, so that the amine layer is formally positively charged with the adjacent benzoate face being formally negatively charged.

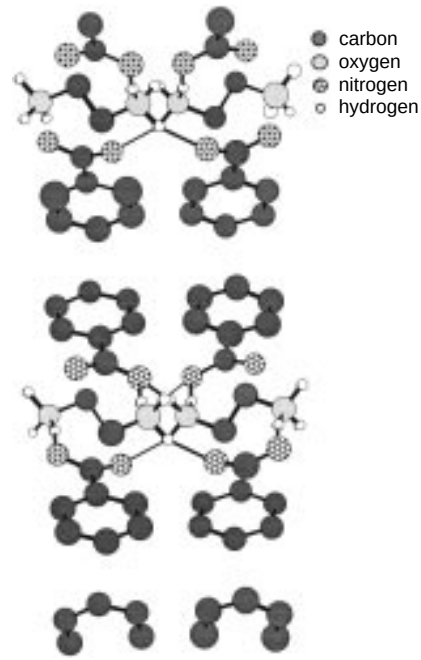



**Fig. 1** The structure of the 1 : 2 adduct between 1,2-diaminoethane and benzoic acid; projection down *a* (*c* horizontal). Only hydrogens participating in NH···O hydrogen bonds are illustrated.

In an attempt to gain further insight into the nature of the proton transfer, hydrogen-bond geometry optimisations were performed on isolated 1 : 2 adducts using density functional theory (DFT) involving the G94 package.[10] At the SVWN5/6-31G* or B3LYP/6-31G* levels of theory[12,13] it is predicted that the protons in the (observed) NH···O bonds are transferred from the amine to the acid moieties, so that the hydrogen bond becomes N···HO in character. Calculations in the presence of a solvent reaction field (either $H_2O$, $CHCl_3$ or methanol) all follow this pattern.‡ This suggests that the proton-transfer (ionic) hydrogen bonds within the solid-state structure are stabilised by the extensive hydrogen-bonding array within the solid-state lattice. Supporting this proposition are the results of similar DFT[14] and semi-empirical[9] calculations on our previously reported cyclam : 4-*tert*-butyl benzoic acid 1 : 2 adduct. In this system the network of NH···O hydrogen bonds is confined within a single adduct and proton transfer is predicted by DFT and semi-empirical calculations.

Finally, the B3LYP/6-31G* calculated dipole moment of a single 1,2-diaminoethane/benzoic acid motif is $6.41 \times 10^{-30}$ C m; this moment, coupled with the non-centrosymmetric nature of the crystalline structure suggests this material may have interesting SHG (second harmonic generation) properties.

In summary, we have demonstrated that benzoic acid and 1,2-diaminoethane self-assemble to discrete 2 : 1 aggregates held together by extensive hydrogen bonding and π-stacking interactions. This study acts as a prototype for the synthesis of a range of other closely related carboxylic acid/diamine arrays, a class of new (charged-separated) assemblies of potential interest as new opto-electronic materials.

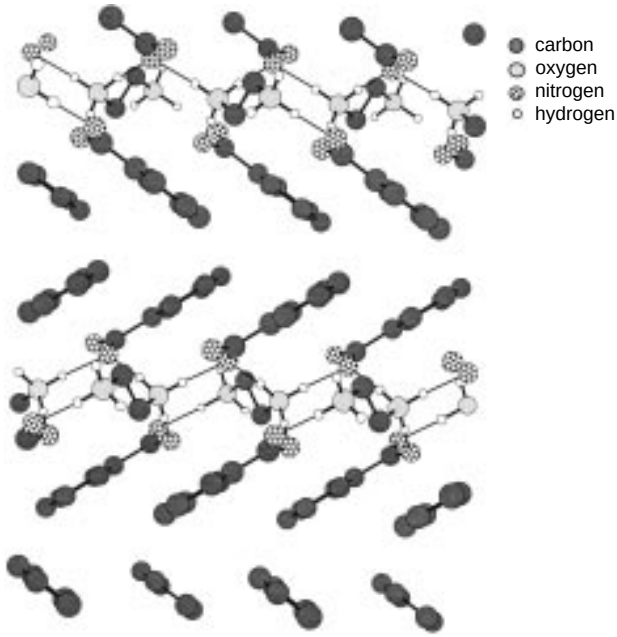



**Fig. 2** The structure of the 1 : 2 adduct between 1,2-diaminoethane and benzoic acid; projection down *b* (*c* horizontal). Only hydrogens participating in NH···O hydrogens bonds are illustrated.

We wish to thank the Australian Research Council and the Australian Nuclear Science and Technology Organisation for financial assistance.

## Footnotes

† *Crystallographic data*: $C_{16}H_{20}N_2O_4$, $M$ = 304.4, orthorhombic, space group $Pca2_1$, $a$ = 8.425(3), $b$ = 9.144(3), $c$ = 21.000(5) Å, $U$ = 1618 Å$^3$, $D_c$ ($Z$ = 4) = 2.14$_9$ g cm$^{-3}$.

*X-Ray study*: $N$ = 2942 unique diffractometer reflections [derived from a hemisphere to $2\theta_{max}$ = 65°; monochromatic Mo-K$\alpha$ radiation, $\lambda$ = 0.7107$_3$]; $R_{int}$ = 0.017, $N_0$ [$I \geqslant 3\sigma(I)$] = 1625 'observed' refining to conventional $R$ on $|F|$ = 0.041, $R_w$ (statistical weights) = 0.034. Anisotropic thermal parameter forms for C, O, ($x$, $y$, $z$, $U_{iso}$)$_H$ refined. ($x$, $y$, $z$) (C, O) resulting constrained in the refinement on neutron data. *T ca*. 295 K.

*Neutron study*: $N$ = 1679 reflections [HIFAR reactor, 2TANA diffractometer, Lucas Heights, Australia; $\lambda$ = 1.233(2) Å], $N_0$ = 981 refining to $R$ = 0.046, $R_w$ = 0.027. Anisotropic thermal parameter forms for C, O, ($x$, $y$, $z$, $U_{iso}$)$_H$ refined. Atomic coordinates, bond lengths and angles, and thermal parameters have been deposited at the Cambridge Crystallographic Data Centre (CCDC). See Information for Authors, Issue No. 1. Any request to the CCDC for this material should quote the full literature citation and the reference number 182/346.

‡ Similar results have been recorded in calculations on amino acid zwitterions where it has been found that proton transfers in such molecules are mediated by solvent molecules (J. H. Jensen and M. S. Gordon, *J. Am. Chem. Soc*., 1995, **117**, 8159).

## References

1 G. R. Desiraju, *Crystal Engineering: The Design of Organic Solids*, Elsevier, Amsterdam, 1989; C. B. Aakeröy and K. R. Seddon, *Chem. Soc. Rev*., 1993, **22**, 397.
2 S. Subramanian and M. J. Zaworotko, *Coord. Chem. Rev*., 1994, **137**, 401.
3 M. Mascal, P. S. Fallon, A. S. Batsonov, B. R. Heywood, S. Champ and M. Colclough, *J. Chem. Soc., Chem. Commun*., 1995, 805.
4 S. Hanessian, A. Gomtsyan, M. Simard and S. Rolens, *J. Am. Chem. Soc*., 1994, **116**, 4495.
5 Y.-L. Chang, M.-A. West, F. W. Fowler and J. W. Lauher, *J. Am. Chem. Soc*., 1993, **115**, 5991; C. B. Aakeröy and M. Nieuwenhuyzen, *J. Am. Chem. Soc*., 1994, **116**, 10983.
6 C. A. Hunter and J. K. Sanders, *J. Am. Chem. Soc*., 1990, **112**, 5525.
7 O. Ermer and A. Eling, *J. Chem. Soc., Perkin Trans. 2*, 1994, 925.
8 S. E. Scheiner, *Acc. Chem. Res*., 1994, **12**, 402.
9 K. R. Adam, M. Antolivich, B. J. McCool, R. Davis, C. H. L. Kennard, A. J. Leong, I. M. Atkinson, L. F. Lindoy and P. A. Tasker, *J. Chem. Soc., Chem. Commun*., 1994, 1539.
10 J. S. Nowick, M. A. Keith, K. A. Bellamo, J. A. Love, E. J. Martinez, G. Noronha, E. M. Smith and J. W. Ziller, *J. Am. Chem. Soc*., 1995, **117**, 89; D. E. Lynch, G. Smith, K. A. Byriel and C. H. L. Kennard, *Acta Crystallogr., Sect. C*, **50**, 1259; C. K. Fair and E. O. Schlemper, *Acta Crystallogr., Sect. B*, **33**, 1337.
11 Gaussian 94 (Revision B.3), M. J. Frisch, G. W. Trucks, H. B. Schlegel, P. M. W. Gill, B. G. Johnson, M. A. Robb, J. R. Cheeseman, T. Keith, G. A. Petersson, J. A. Montgomery, K. Raghavachari, M. A. Al-Laham, V. G. Zakrzewski, J. V. Ortiz, J. B. Foresman, C. Y. Peng, P. Y. Ayala, W. Chen, M. W. Wong, J. L. Andres, E. S. Replogle, R. Gomperts, R. L. Martin, D. J. Fox, J. S. Binkley, D. J. Defrees, J. Baker, J. P. Stewart, M. Head-Gordon, C. Gonzalez and J. A. Pople, Gaussian, Inc., Pittsburgh, PA, 1995.
12 S. H. Vosko, L. Wilk and M. Nusair, *Can. J. Phys*., 1980, **58**, 1200.
13 A. D. Becke, *J. Chem. Phys*., 1993, **98**, 5648.
14 K. R. Adam and I. M. Atkinson, unpublished work.

*Received, 19th August 1996; Com. 5/05748I*

# Construction of a self-assembling porphyrin trimer system

**Yasuhisa Kuroda,*[a] Yusuke Kato[b] and Hisanobu Ogoshi*[b]**

[a] *Department of Polymer Science, Kyoto Institute of Technology, Sakyo-ku, Matsugasaki, Kyoto 606, Japan*
[b] *Department of Synthetic Chemistry, Kyoto University, Sakyo-ku, Kyoto 606, Japan*

**A quaternary self-assembling system consisted of three porphyrin molecules and one linker molecule is constructed.**

The chemical construction of self-assembling systems is currently of interest to chemists because self-assembly is expected to be essential methodology to overcome the synthetic difficulties encounted in the preparation of highly complicated and ordered molecular systems.[1] Recently, we found a receptor based on a doubly bridged porphyrin molecule (trench porphyrin) which recognizes dialkyl tartrates selectively *via* four point hydrogen bonds.[2] The most important requirement for this system is the core conformations of the tartrate, *gauche* OH/OH and *anti* $CO_2R/CO_2R$, in which two carbonyl and two hydroxy oxygen atoms are practically planar. In contrast, the system is rather insensitive towards the properties of alkyl ester groups.[2] Thus, it is an interesting challenge to extend the system to a large scale assembly by modifying these alkyl moieties. We report here a self-assembling porphyrin trimer system consisting of two different types of porphyrin molecules and one tartrate derivative as a linker molecule.[3]

For this purpose, we designed a new tartrate linker molecule **1** which has two pyridine moieties arranged in a way so that the pyridine and tartrate moieties may act as independent recognition sites for the porphyrin molecules. Compound **1** was prepared by acid-catalysed reaction of L-tartaric acid with an excess of 3-(3′-pyridyl)propanol in toluene. The complex formation between **1** and *meso* trench porphyrin **2** was confirmed by UV–VIS spectroscopic titration showing a red shift of the Soret band of **2** (428 nm) with a clear isosbestic point, giving an association constant of 2300 ± 100 $dm^3\ mol^{-1}$ at 288 K. $^1H$ NMR data (Table 1) reveal further details of the present complex formation. Upon complexation with **2**, two hydroxy and $H_t$ protons (see Fig. 1) of **1** exhibit an unusual upfield shift as previously reported for simple alkyl tartrates.[2] The association constant is estimated to be $>1 \times 10^5$ $dm^3\ mol^{-1}$ at 223 K. In contrast, the proton signals of the pyridyl moiety are observed in the normal aromatic region and show only a 0.1–0.3 ppm upfield shift upon complexation. These observations indicate that **1** complexes with **2** at the tartrate site *via* four hydrogen bonds and the pyridyl moieties practically remain free. Another porphyrin component of the present assembly, octaethylporphyrin Rh complex **3**, also forms a complex with **1** giving a stable 2 : 1 complex which is isolable giving *m/z* of 1729.77 in a FABMS spectrum (calc. for $C_{92}H_{113}N_{10}O_6Rh_2Cl_2$, *m/z* 1729.63). As shown in Table 1, the pyridyl protons of this complex are shifted upfield by 2.0–8.5 ppm with respect to those of free **1**, while the $H_t$ protons show a relatively small upfield shift. The very large upfield shifts of $H_c$ and $H_d$ demonstrate the coordination of the pyridyl moieties of **1** on Rh atoms[4] and that the tartrate moiety does not directly participate in the complex formation. Thus, the tartrate and pyridyl moieties of **1** are confirmed to act as independent binding sites for porphyrins **2** and **3**. Based on these results, we attempted to construct a porphyrin trimer self-assembly. The $^1H$ NMR spectrum of the mixture of **1** (1.0 mM), **2** (1.0 mM) and **3** (2.0 mM) in $CDCl_3$ indicated that, at 223 K, no free pyridyl moieties of **1** were observed and new pyridyl signals (Table 1) appear in addition to those of the 2 : 1 complex of **3** and **1**. This behaviour is independent of the mixing sequences of the three components. It should be noted that both the tartrate and pyridyl moieties simultaneously show large upfield shifts which indicates the binding of the tartrate moiety on **2** and the pyridyl moiety on **3** respectively. Integration data for these protons gives the association constant between **2** and the 2 : 1 complex of **3** and **1** as 3000 ± 500 $dm^3\ mol^{-1}$ at 223 K which is much smaller than that for **2** and **1**, while the pyridyl moieties of **1**

**Table 1** $^1H$ NMR chemical shifts (δ) of **1** in $CDCl_3$ under various conditions[a]

| | Tatrate moiety | | Pyridyl moiety | | | |
|---|---|---|---|---|---|---|
| Host | $H_t$ | OH | $H_a$ | $H_b$ | $H_c$ | $H_d$ |
| none | 4.55 | —[b] | 7.51 | 7.22 | 8.44 | 8.45 |
| **2**[c] | 0.68 | −3.81 | 7.22 | 7.15 | 8.45 | 8.20 |
| | 0.56 | −4.13 | 7.24 | 7.08 | 8.38 | 7.89 |
| **3** | 2.70 | 4.00[d] | 5.52 | 4.65 | 0.20 | −0.06 |
| **2** + **3**[c,e] | 0.02 | −4.18 | 5.13 | 4.59 | −0.15[f] | −0.48 |
| | −0.18 | −4.43 | 5.00 | 4.54 | | −0.73 |

[a] The data are obtained at 223 K except those of **1** (288 K). [b] Unclear. [c] Two signals are observed due to the unsymmetrical structure of **2**. [d] Owing to heavy overlap with the ethyl signals of **3**, the position is assigned from COSY data. [e] [**1**] = [**2**] = $1 \times 10^{-3}$ M; [**3**] = $2 \times 10^{-3}$ M. Under these conditions, *ca*. 60% of **2** forms the assembly with a 1 : 2 complex of **1** and **3**. [f] No separation for $H_c$ was observed.

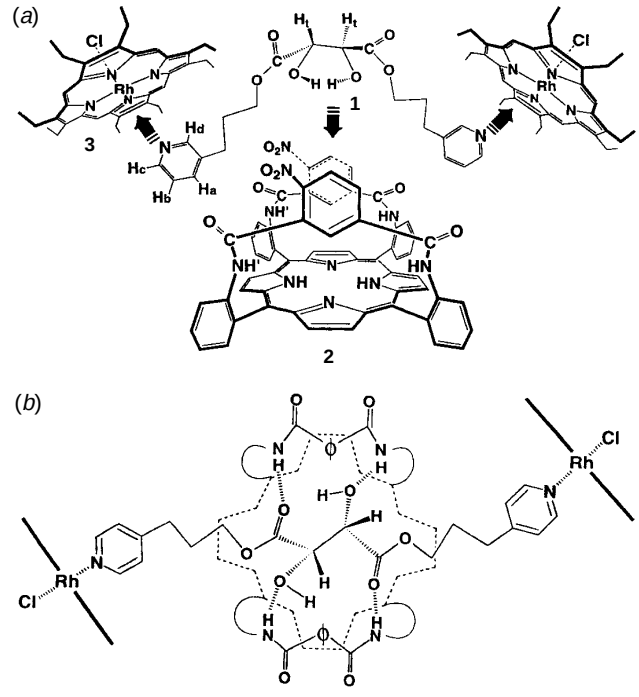



**Fig. 1** Self-assembling porphyrin trimer system. (*a*) Component structures. (*b*) Schematic assembly structure.

quantitatively form complexes with **3** even under the present conditions. Although the smaller association constant suggests the existence of significant steric hindrance between the core porphyrin **2** and the two terminal porphyrins **3** due to the short alkyl chains of **1**, the results clearly indicate that the present system affords the quaternary self-assembly shown in Fig. 1 without any confusion between the different types of binding sites.

## References


1 G. M. Whitesides, J. P. Mathias and C. T. Seto, *Science*, 1991, **254**, 1312; J. M. Lehn, *Science*, 1993, **260**, 1762; A. C. Bennist-on, A. Harriman and V. M. Lynch, *Tetrahedron Lett*., 1994, **35**, 1473; H. L. Anderson, S. Anderson and J. K. M. Sanders, *J. Chem. Soc., Perkin Trans. 1*, 1995, 2231; M. S. Goodman, V. Jubian, B. Linton and A. D. Hamilton, *J. Am. Chem. Soc*., 1995, **117**, 11 610; C. Valdes, U. P. Spitz, L. M. Toledo, S. W. Kubik and J. Rebek Jr., *J. Am. Chem. Soc.*, 1995, **117**, 12 733. J. P. Mathias, C. T. Seto, E. E. Simanek and G. M. Whitesides, *J. Am. Chem. Soc*., 1994, **116**, 1725; J. P. Collin, A. Harriman, V. Heitz, F. Odobel and J. P. Sauvage, *J. Am. Chem. Soc*., 1994, **116**, 5679; M. Fujita, S. Nagao and K. Ogura, *J. Am. Chem. Soc*., 1995, **117**, 1649; A. V. Chernook, A. M. Shulga, E. I. Zenkevich, U. Rempel and C. V. Borczyskowski, *J. Phys. Chem*., 1996, **100**, 1918.

2 Y. Kuroda, Y. Kato, M. Ito, J. Hasegawa and H. Ogoshi, *J. Am. Chem. Soc*., 1994, **116**, 10 338.

3 For porphyrin dimer system, see: C. M. Drain, R. Fischer, E. G. Nolen and J. M. Lehn, *J. Chem. Soc., Chem. Commun*., 1993, 243; Y. Kobuke and H. Miyaji, *J. Am. Chem. Soc*., 1994, **116**, 4111; J. L. Sessler, B. Wang and A. Harriman, *J. Am. Chem. Soc.*, 1995, **117**, 704; Y. Aoyama, T. Kamohara, A. Yamagishi, H. Toi and H. Ogoshi, *Tetrahedron Lett*., 1987, **28**, 2143; Y. Kuruoda, A. Kawashima, T. Urai and H. Ogoshi, *Tetrahedron Lett*., 1995, **46**, 8440.

4 H. Ogoshi, H. Hatakeyama, K. Yamamura and Y. Kuroda, *Chem. Lett*., 1990, 51.



*Received, 9th December 1996; Com. 6/08282C*

# Ti-beta-catalysed selective oxidation of sulfides to sulfoxides using urea–hydrogen peroxide adduct

**T. Indrasena Reddy and Rajender S. Varma***

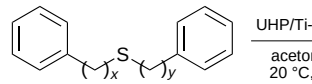
*Department of Chemistry and Texas Regional Institute for Environmental Studies (TRIES), Sam Houston State University, Huntsville, TX 77341-2117, USA*

**Ti-Beta zeolite catalyses the selective oxidation of organic sulfides to sulfoxides with urea–hydrogen peroxide adduct (UHP) as oxidant.**

Crystalline microporous titanium silicate 1 (TS-1)[1] has found applications in the catalytic oxidation of a variety of organic compounds[2] with aqueous hydrogen peroxide as an oxygen source. TS-1, the titanium analogue of the ZSM-5 zeolite, is reported to catalyse the oxidation of hydrocarbons,[1,3] arenes,[1,4] alkenes,[2a–d] amines[5] and sulfides.[6a] Apart from their unique catalytic properties, these thermally stable solid materials can be recycled many times without any loss of activity, thus emphasizing their environmentally benign character. However, one serious limitation of catalysis by zeolites is the steric hindrance that stops bulkier molecules from reaching the active sites, as has been highlighted in a recent report that states that thioanisole and ethyl phenyl sulfide can access the catalytic sites for oxidation to the corresponding sulfoxides and sulfones whereas diphenyl sulfide fails under the same conditions.†,‡ Herein we report a thorough study of the oxidation of sulfides that determines the limitations of various oxidative catalysts (TS-1, VS-1 and Ti–beta; Table 1) in terms of their comparative reactivity and selectivity. Benzyl phenyl sulfide, bearing a benzylic methylene group, is used as a substrate in these reactions as it is easy to monitor the relative formation of sulfoxide/sulfone by $^1$H NMR.

In the case of TS-1 and VS-1 (pore size 5.5 Å), no product could be detected, presumably on account of the inability of the substrate to enter the channel. At higher temperature, on the other hand, a poor yield of a mixture of products could be obtained. However, complete conversion to sulfoxides and sulfones occurs with a large pore (6.5 Å) zeolite, Ti-beta[7] (Table 1, entry 7), at room temperature using hydrogen peroxide.§,¶ Finally, selectivity is achieved‖ by replacing the potentially explosive hydrogen peroxide with the safer crystalline urea adduct of hydrogen peroxide (UHP), which compares favourably with existing protocols;[8] UHP adduct is known for the controlled release of the oxidant and is a well recognized source of oxygen.[2a,9]

Under these conditions, a facile and highly selective oxidation of bulkier organic sulfides [diphenyl sulfide, benzyl phenyl sulfide and dibenzyl sulfide, eqn. (1) and Table 2, entries




(1)

$x = y = 0$; $x = 0$, $y = 1$; $x = y = 1$
conversion, mass balance and yield = >90%

9–11] to the corresponding sulfoxides occurs with UHP in excellent yields.

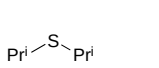
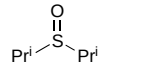
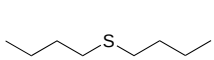
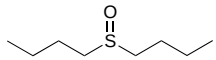
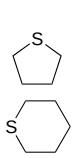
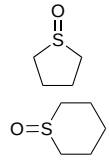
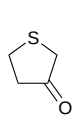
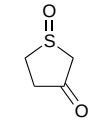
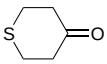
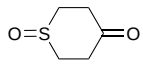
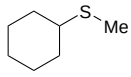
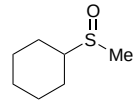
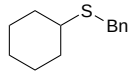
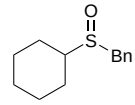
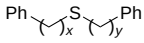
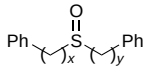
The scope of this protocol was further explored with a variety of sulfides (acyclic, cyclic and aromatic; Table 2) which were selectively oxidized to the corresponding sulfoxides in high yields with more than 95% mass balance. Acyclic and cyclic sulfides (Table 2, entries 1–4) were completely converted to the corresponding sulfoxides in 2 h at room temperature with 1.2 equiv. of UHP and 10 wt% of Ti-beta, whereas cyclic sulfides bearing a carbonyl functionality in their ring (Table 2, entries 5 and 6) required 3–4 h for complete conversion. All aromatic sulfides [as shown in eqn. (1)] produced clean sulfoxides with 100% selectively in 2 h.** Mechanistically, it is believed[2a] that the titanyl (Ti=O) function,[3a] the active site of the titanium silicates, binds with hydrogen peroxide to form a hydroxyhydroperoxo complex. This complex mimics *meta*-chloroperbenzoic acid and provides the required reactive oxygen (O*) species which oxidizes[2,3] sulfides to sulfoxides, generating water as a byproduct. Although it is not known whether the urea adduct (UHP) or free $H_2O_2$ enters the channels, it is known that the UHP complex is in equilibrium with free $H_2O_2$ and that the complex releases $H_2O_2$ at a rate which is, to some extent, solvent dependent.[9] In view of our own data and the background literature,[2a,3a] the use of the urea complex has two main advantages, namely the controlled release of $H_2O_2$ and the anhydrous nature of the oxidant. The sulfides and sulfoxides may enter or leave the zeolite channels at differing rates, but the oxidation undoubtedly occurs inside the zeolite catalyst.[2a,3a]

**Table 1** Oxidation of benzyl phenyl sulfide with 30% aqueous hydrogen peroxide catalysed by Ti- and V-silicates[a]

| Entry | Catalyst | Pore size/Å | *T*/°C | *t*/h | Conversion (%)[b] | Yield (%)[c] | Mass balance (%) |
|---|---|---|---|---|---|---|---|
| 1 | — | — | 60 | 12 | — | — | 87 |
| 2 | TS-1 | 5.5 | 20 | 12 | trace | trace | 83 |
| 3 | TS-1 | 5.5 | 60 | 12 | 24 | > 95 | 87 |
| 4 | VS-1 | 5.5 | 20 | 12 | trace | trace | 90 |
| 5 | VS-1 | 5.5 | 60 | 12 | 22 | 92 | 80 |
| 6 | VS-1 | 5.5 | 60 | 24 | 27 | 77 | 71 |
| 7 | Ti-beta | 6.5 | 20 | 02 | 95 | 95 | 95 |

[a] Reactions were carried out in $(CD_3)_2CO$ with sulfide (1 equiv.), oxidant (1.2 equiv.) and 10 wt% of catalyst. Variation in the amount of catalyst did not increase the conversion and at one stage ( > 50 wt%) it reduced the mass balance instead. [b] Conversions are based on $^1$H NMR spectroscopic analysis of the characteristic methylene signal in the crude reaction mixture (error ±5% of the stated values). [c] Yields refer to isolated products and are based on substrate consumption.

**Table 2** Selective oxidation of sulfides to sulfoxides with UHP catalysed by Ti-beta[a]

| Entry | Sulfide | Sulfoxide | Yield (%)[b] |
|---|---|---|---|
| 1 |  |  | 89 |
| 2 |  |  | 94[c] |
| 3 |  |  | 95 |
| 4 |  |  | 95 |
| 5 |  |  | 82 |
| 6 |  |  | 85 |
| 7 |  |  | 92 |
| 8 |  |  | 94 |
| 9 | | $x = y = 0$ | 92 |
| 10 | | $x = 0, y = 1$ | 95 |
| 11 | | $x = y = 1$ | 94 |

[a] The reactions were carried out in acetone at room temperature with sulfide (1 equiv.), UHP (1.2 equiv.) and 10 wt% of catalyst Ti-beta; all the sulfides reached complete conversion in 2 h except tetrahydrothiophen-3-one (entry 5) and tetrahydrothiopyran-4-one (entry 6), which required 3–4 h. [b] Yields refer to the pure isolated product. [c] Traces of sulfone were observed by $^1$H NMR spectroscopy.

Since a catalytic amount of the zeolite is used in this process and the reaction takes place at room temperature, we conclude that there are no restrictions placed on the sulfoxide as it leaves the channels. Apparently, the more reactive sulfide is oxidized more rapidly than the sulfoxide and the conversion of sulfoxide to sulfone is disfavoured due to the unavailability of a large excess of oxidant and possible steric crowding.

In conclusion, we have shown the versatility of the zeolite Ti-beta as a catalyst for selective oxidation of a variety of sulfides. The substrates which are not oxidized by TS-1 on account of their inaccessability are easily oxidized with this Ti-beta catalyst because of its larger pore size. The advantages of our environmentally benign approach over the conventional methods are the relative ease of separation of the catalyst and its recyclable nature.

We thank Dr M. Sasidharan, NCL, Pune, India for the supply of zeolite catalyst and the Texas Advanced Research Program (ARP) in Chemistry (Grant # 003606-023) and the Retina Research Foundation, Houston for generous support.

## Footnotes

† Thioanisole, under the reported conditions, produced the corresponding sulfoxide and sulfone in 3.55 : 1 ratio. However, diphenyl sulfide does not have access to the catalytic sites, the channel size of the zeolite TS-1 being only 5.5 Å [ref. 6(*a*)].

‡ While writing this manuscript, an article has appeared in which bulky substrates such as diphenyl sulfide and dibenzyl sulfide were oxidized to the corresponding sulfoxides with 30% $H_2O_2$ catalysed by CrS-2 [ref. 6(*b*)].

§ A peroxide test showed complete consumption of hydrogen peroxide.

¶ Various equivalents of hydrogen peroxide were used for the oxidation of benzyl phenyl sulfide. Experiments were carried out in deuteriated acetone and the ratios determined by $^1$H NMR analysis of characteristic signals in the crude reaction mixture (error ±5% of the stated values). Variation in the amount of catalyst used in the reaction did not produce any encouraging results in terms of selectivity.

| | | Yield (%) | |
|---|---|---|---|
| Equiv. $H_2O_2$ | Conversion (%) | Sulfoxide | Sulfone |
| 1.00 | 80 | 87 | 13 |
| 1.25 | 90 | 91 | 09 |
| 1.50 | 100 | 80 | 20 |

‖ Typical experimental procedure: Benzyl phenyl sulfide (100 mg, 0.64 mmol) in acetone (5 ml) was added to a well stirred mixture of UHP (72 mg, 0.77 mmol) and catalyst (10 mg, 10 wt% of sulfide) in the same solvent (10 ml) at 20 °C. This heterogenous mixture was then stirred for 2 h at the same temperature to complete the conversion of the sulfide to the corresponding sulfoxide. The reaction was monitored by TLC. The reaction mixture was then diluted with 10 ml of acetone and the catalyst filtered off and washed with acetone (2 × 5 ml). The combined solution was concentrated under reduced pressure to afford benzyl phenyl sulfoxide in 95% (105 mg, mp 118 °C).

** Other substrates investigated for their chemoselectivity include vinyl, allyl and prop-2-ynyl sulfides where alkenic moieties are preserved in the sulfoxide products. We have also performed the reactions with 1,4-thioxane, 5*H*-thiophen-2-one and thiomorpholine bearing a variety of substituents. The details of this work including stereoselectivity aspects will be published elsewhere.

## References

1 M. Taramasso, G. Perego and B. Notari, *U.S. Pat*., 1983, 4 410 501 (*Chem. Abstr*., 1982, **96**, 37802w); B. Notari, *Stud. Surf. Sci. Catal*., 1988, **37**, 413.

2 (*a*) W. Adam, R. Kumar, T. I. Reddy and M. Renz, *Angew. Chem., Int. Ed. Engl*., 1996, **35**, 880 and reference cited therein; (*b*) W. Adam, A. Corma, T. I. Reddy and M. Renz, unpublished results; (*c*) C. B. Khouw, C. B. Dartt, J. A. Labinger and M. E. Davis, *J. Catal*., 1994, **149**, 195; (*d*) C. B. Khouw and M. E. Davis, *J. Catal*., 1995, **151**, 77. For recent papers on the use of zeolites in oxidation reactions, see (*e*) K. Pitchumani, D. R. Corbin and V. Ramamurthy, *J. Am. Chem. Soc*., 1996, **118**, 8152; (*f*) K. Pitchumani and V. Ramamurthy, *Tetrahedron Lett*., 1996, **37**, 5297; (*g*) X. Li and V. Ramamurthy, *Tetrahedron Lett*., 1996, **37**, 5235; (*h*) For commentary on the proceedings of the 11th International Congress on Catalysis, see J. Haggin, *Chem. Eng. News*, August 5, 1996, 26.

3 (*a*) D. R. C. Huybrechts, L. DeBruycker and P. A. Jacobs, *Nature*, 1990, **345**, 240; (*b*) T. Tatsumi, M. Nakamura, S. Negishi and H. Tominaga, *J. Chem. Soc., Chem. Commun*., 1990, 476; (*c*) M. G. Clerici, *Appl. Catal*., 1991, **68**, 249.

4 A. V. Ramaswamy, S. Sivasanker and P. Ratnasamy, *Microporous Mater*., 1994, **2**, 451.

5 P. Roffia, M. Padovan, E. Moretti, G. De Alberti and Montedipe, *European Patent*, 1987, 208311 (*Chem. Abstr*., 1987, **106**, 155944s); T. Selvam and A. V. Ramaswamy, *Chem. Commun*., 1996, 1215.

6 (*a*) R. S. Reddy, J. S. Reddy, R. Kumar and P. Kumar, *J. Chem. Soc., Chem. Commun*., 1992, 84; (*b*) S. V. N. Raju, T. T. Upadhya, S. Ponratnam, T. Daniel and A. Sudalai, *Chem. Commun*., 1996, 1969.

7 M. A. Camblor, A. Corma and J. Perez-Pariente, *SP Pat*., 9101 798, 1991; M. A. Camblor, A. Corma, A. Martinez and J. Perez-Pariente, *J. Chem. Soc., Chem. Commun*., 1992, 589; T. Blasco, M. A. Camblor, A. Corma and J. Perez-Pariente, *J. Am. Chem. Soc*., 1993, **115**, 11806; M. A. Camblor, A. Corma and J. Perez-Pariente, *Zeolites*, 1993, **13**, 82; M. A. Camblor, A. Corma A. Martinez, J. Perez-Pariente and S. Valencia, in *New Developments in Selective Oxidation II*, ed. V. C. Corberan and S. Vic Bellon, Elsevier, New York, 1994.

8 For the oxidation of sulfides with other reagents, see G. W. Breton, J. D. Fields and P. J. Kropp, *Tetrahedron Lett*., 1995, **36**, 3825; W. Adam, C. M. Mitchell and C. R. Saha-Moller, *Tetrahedron*, 1994, **50**, 13121.

9 A. A. Oswald and D. L. Guerin, *J. Org. Chem*., 1963, **28**, 651; A. M. A. R. Gonsalves, R. A. W. Johnstone, M. M. Pereira and J. Shaw, *J. Chem. Res*. (S), 1991, 208.

*Received, 15th November 1996; Com. 6/07832J*

# Synthesis, reactivity, X-ray crystal and molecular structures of a novel dimeric tungsten(VI) polyoxoperoxo complex: $[PPh_4]_2[Ph_2SiO_2\{W_2O_2(\mu\text{-}O_2)_2(O_2)_2\}]$ and of a molybdenum(VI) analogue

**Jean-Yves Piquemal,[a] Claudette Bois[b] and Jean-Marie Brégeault*[a]†**

[a] *Catalyse Homogène et Chimie des Surfaces, Département de Chimie, Université Pierre et Marie Curie, URA 1428 du CNRS, Tour 54, Case 196; 4 place Jussieu, 75252 Paris Cedex 05, France*

[b] *Chimie des Métaux de Transition, Département de Chimie, Université Pierre et Marie Curie, URA 419 du CNRS; 4 place Jussieu, 75252 Paris Cedex 05, France*

**Tungsten and molybdenum complexes containing a diphenylsilanediolato ligand are structurally characterised; the overall structures of the anions are conserved in organic solvents.**

The chemistry of heteropolyoxoperoxometalates has received much attention in recent years.[1–8] In the course of systematic investigations of peroxidic $d^0$ transition-metal complexes involving different assembling ligands, model complexes with silicon-based anionic moieties were considered, in relation to attempts to prepare metal complexes supported on and/or inserted in silica. Monomeric silicic acid, $Si(OH)_4$, exists only in dilute aqueous solution; since this polymerizes,[9] $[SiO_4]^{4-}$ or hydrogenosilicates may be thought difficult to use as assembling ligands in the same way as $[HPO_4]^{2-}$,[6] $[HAsO_4]^{2-}$,[7] $[SO_4]^{2-}$,[8] *etc*. In some cases, $Si(OH)_4$ reacts directly and oligomeric species are known to depolymerize *e.g*. in the synthesis of $H_4[SiM_{12}O_{40}](aq)$ (M = Mo, W).[10] The corresponding silicopolyoxoperoxo-molybdates or -tungstates, $[SiO_4\{M_2O_2(\mu\text{-}O_2)_2(O_2)_2]^{4-}$, have been synthesized, but in our hands, are not easily purified. Organodisilanols can model geminal hydroxy groups which are much more reactive on silica surfaces than single silanols. Preliminary results obtained with diphenylsilanediol, $Ph_2Si(OH)_2$, are presented here. This compound is known as a chelating agent, either in mono- or in di- to tetra-meric forms.[11–14] The complexes $[PPh_4]_2[Ph_2SiO_2\text{-}\{M_2O_2(\mu\text{-}O_2)_2(O_2)_2\}]$ (M = W **1** or Mo **2**) can be isolated from water–ethanol mixtures.

'$WO_3{\cdot}H_2O$' (or '$MoO_3{\cdot}H_2O$') was first reacted with a 30% m/v solution of hydrogen peroxide and this solution was then added to ethanolic $Ph_2Si(OH)_2$. After 45 min, slow addition of ethanolic $PPh_4Cl$ precipitated **1** (or **2**) in good yield. The white (yellow) precipitate was filtered off, washed with water and diethyl ether and then air-dried (yields: 75–90%).‡ Crystals of **1** and **2** were grown by slow evaporation of acetonitrile solutions.

**1** and **2** are isomorphous compounds. A representation§ of the dinuclear anion, $[Ph_2SiO_2\{W_2O_2(\mu\text{-}O_2)_2(O_2)_2\}]^{2-}$, is shown in Fig. 1. It consists of an assembling anion, $[Ph_2SiO_2]^{2-}$, and of a dimeric moiety, $\{W_2O_{10}\}$, resulting from the association of two pentagonal bipyramids sharing one edge, O(6)···O(12), of the non-basal planes. Each of these atoms is on the girdle axis of a bipyramid with a typical lengthening of the M–O distances, the other axial positions being occupied by oxo ligands with normal bond lengths.[1–3,6–8] The W atoms are located outside the mean equatorial plane defined by the five O atoms corresponding to two peroxo groups and to the oxygen atom of the assembling ligand {0.375 [0.392] for W(1) [Mo(1)] and 0.366 [0.382] Å for W(2) [Mo(2)], respectively}. There is one non-bridging peroxo group with $\eta^2$ side-bound configuration and one bridging $\mu\text{-}\eta^2:\eta^1$ peroxo group. The Si–O and Si–C bond distances are similar to those found in cyclic siloxanes.

The IR spectra of complexes **1** and **2** show features comparable to those observed for other dinuclear species;[6–8] in addition a strong band at 1586 $cm^{-1}$ is assigned as ν(C–C, phenyl),[12,15] and a very sharp band at 1107 $cm^{-1}$ is due to an in-plane deformation of the phenyl ring with some ν(Si–C) character.[12,15] The phenyl vibrations occur in expected positions. Consistent with the structural data and the existence of two distinct M=O bonds, there are strong ν(M=O) bands at 978s and 964s for **1** and at 968s and 955s for **2**; Si–O stretches appear at *ca*. 926 $cm^{-1}$ as a very strong maximum for both compounds. Bands at 862s for **2** and 841s for **1** are assigned to ν(O–O) of the peroxo ligands and bands at *ca*. 580 and 530 $cm^{-1}$ are assigned to asymmetric and symmetric $[M(O_2)]$ stretches, respectively. For **1** and **2**, comparison of the ν(O–O) and ν(Si–O) vibrations (IR and Raman) in the solid state and MeCN solution suggests that the overall structures of the two anions are conserved in solution.

Epoxidation of cycloalkenes by **1** was markedly more successful than for linear analogues; the larger the cycloalkene ring, the greater the degree of conversion to epoxide. In all

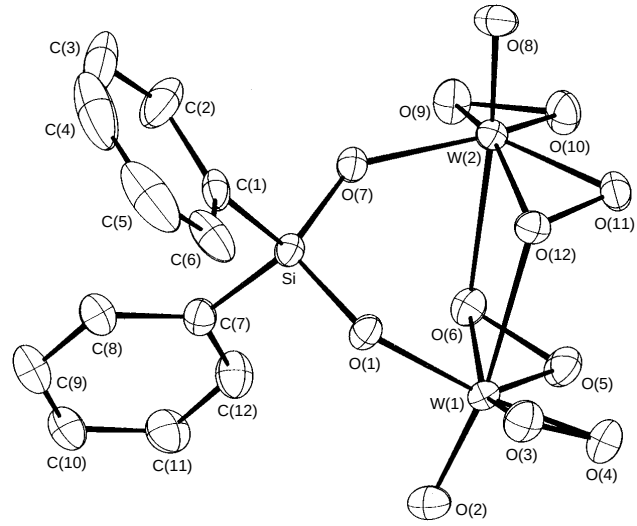



**Fig. 1** CAMERON representation of $[Ph_2SiO_2\{W_2O_2(\mu\text{-}O_2)_2(O_2)_2\}]^{2-}$ showing the atom labelling scheme. Selected bond lengths (Å) for **1** [**2**]: M(1)–O(1) 1.954(3) [1.964(2)], M(1)–O(2) 1.701(4) [1.681(2)], M(1)–O(3) 1.926(4) [1.928(2)], M(1)–O(4) 1.922(4) [1.931(2)], M(1)–O(5) 1.934(4) [1.927(2)], M(1)–O(6) 2.031(4) [2.006(2)], M(1)–O(12) 2.398(4) [2.444(2)], M(2)–O(6) 2.408(4) [2.459(2)], M(2)–O(7) 1.951(3) [1.959(2)], M(2)–O(8) 1.691(4) [1.672(2)], M(2)–O(9) 1.938(4) [1.937(2)], M(2)–O(10) 1.932(4) [1.929(2)], M(2)–O(11) 1.937(4) [1.927(2)], M(2)–O(12) 2.031(4) [2.014(2)], Si–O(1) 1.618(4) [1.619(2)], Si–O(7) 1.616(4) [1.620(2)], Si–C(1) 1.871(5) [1.874(3)], Si–C(7) 1.871(6) [1.884(3)], O(3)–O(4) 1.505(6) [1.481(4)], O(5)–O(6) 1.491(5) [1.470(3)], O(9)–O(10) 1.503(5) [1.473(3)], O(11)–O(12) 1.496(5) [1.468(3)].

cases, the order of increasing activity of PTC systems was $[Ph_2SiO_2(Mo_2O_{10})]^{2-} \ll [Ph_2SiO_2(W_2O_{10})]^{2-} < [HAsO_4(W_2O_{10})]^{2-}$, which confirms the assembling anion effect, but there is also a dramatic influence of the onium moiety.[16] Spectral data show that the diphenylsilanediolato compounds are recovered without any change if, at the end of the reaction, there is an excess of $H_2O_2$. Work is in progress to optimize conversions and selectivities.

Two novel anionic polyoxoperoxo species have been synthesized with $Ph_2Si(OH)_2$, $H_2O_2$–$H_2O$–EtOH and '$WO_3{\cdot}H_2O$' or '$MoO_3{\cdot}H_2O$'. They should be useful to model grafted polyoxoperoxo species which can be obtained on silica surfaces with geminal or single silanols or siloxane bridges and analogous complexes.[16,17]

## Footnotes

† E-mail: bregeaul@ccr.jussieu.fr

‡ All new complexes gave satisfactory elemental analyses (C, H, P, Si, Mo/W).

§ *Crystal data and collection parameters*: $C_{60}H_{50}O_{12}P_2SiW_2$ **1**, $M$ = 1420.78, monoclinic, space group $C2/c$ (no. 15), $a$ = 46.380(5), $b$ = 13.345(5), $c$ = 18.988(2) Å, β = 113.259(9)°, $U$ = 10797(7) Å$^3$ (by least-squares refinement on diffractometer angles from 25 centred reflections, 11.5 < 2θ < 12.5), $T$ = 290 K, graphite-monochromated Mo-Kα radiation, λ = 0.710 73 Å, $Z$ = 8, $D_c$ = 1.75 Mg m$^{-3}$, $F$(000) = 5564, yellow parallelepiped with dimensions 0.30 × 0.45 × 0.65 mm, μ(Mo-Kα) = 44.92 cm$^{-1}$, Nonius CAD4 four-circle diffractometer, ω–2θ scans, data collection range 1.0 < θ < 28.0°, three standard reflections showed no significant variation in intensity; 13 009 unique data collected of which 8923 with $(F_o)^2 > 3\sigma(F_o)^2$ were used in all calculations. Corrections were made for Lorentz and polarisation effects, extinction correction was also applied[18] and absorption correction based on DIFABS program[19] applied before anisotropic refinements (min. 0.81, max. 1.24).

$C_{60}H_{50}Mo_2O_{12}P_2Si$ **2**, $M$ = 1244.96, monoclinic, space group $C2/c$ (no. 15), $a$ = 46.331(5), $b$ = 13.343(3), $c$ = 19.027(4) Å, β = 113.35(1)°, $U$ = 10799(7) Å$^3$ (by least-squares refinement on diffractometer angles from 25 centred reflections, 11.5 < 2θ < 12.5), $T$ = 290 K, graphite-monochromated Mo-Kα radiation, $Z$ = 8, $D_c$ = 1.53 Mg m$^{-3}$, $F$(000) = 5045, colourless parallelepiped with dimensions 0.40 × 0.30 × 0.40 mm, μ(Mo-Kα) = 5.94 cm$^{-1}$, Nonius CAD4 four-circle diffractometer with ω–2θ scans, collection range 1.0 < θ < 28°, two standard reflections showed no significant variation in intensity; 13 005 unique reflections measured, 8945 with $(F_o)^2 > 3\sigma(F_o)^2$ were used in all calculations. Lorentz and polarisation effects with extinction correction as above for **1**; absorption correction based on DIFABS program[19] was applied before anisotropic refinements (min. 0.85, max. 1.12).

*Structure solution and refinement*: atomic form factors for neutral W (or Mo), Si, P, O, C and H were taken from ref. 20. Real and imaginary parts of anomalous dispersion were taken into account. The structures were solved by direct methods and subsequent Fourier difference techniques, and refined anisotropically. Refinements were carried out in four blocks by minimising the function $\Sigma w(|F_o| - |F_c|)^2$, where $F_o$ and $F_c$ are the observed and calculated structure factors (program CRYSTALS).[21] All hydrogen atoms were found on difference Fourier maps; their positions were not refined and they were considered with an overall isotropic thermal parameter $0.9_0$ < C–H < $1.0_5$ Å for both **1** and **2**, $U_{iso}$ = 0.074(3) for **1** and 0.075(2) for **2**. The final $R$ factors as defined in ref. 21 were $R$ = 0.034, $R_w$ = 0.037 for **1** and $R$ = 0.032, $R_w$ = 0.034 for **2** for 697 parameters, and unit weighting scheme, GOF = 2.21 for **1** and 2.04 for **2**, maximum Δρ = 0.77 and 0.40 e Å$^{-3}$ for **1** and **2** respectively. Atomic coordinates, bond lengths and angles, and thermal parameters have been deposited at the Cambridge Crystallographic Data Centre (CCDC). See Information for Authors, Issue No. 1. Any request to the CCDC for this material should quote the full literature citation and the reference number 182/352.

## References


1 C. Venturello, R. d'Aloisio, J. C. J. Bart and M. Ricci, *J. Mol. Catal*., 1985, **32**, 107.
2 N. M. Gresley, W. P. Griffith, B. C. Parkin, A. J. P. White and D. J. Williams, *J. Chem. Soc., Dalton Trans*., 1996, 2039.
3 W. P. Griffith, B. C. Parkin, A. J. P. White and D. J. Williams, *J. Chem. Soc., Chem. Commun*., 1995, 2183.
4 C. L. Hill and C. M. Prosser-McCartha, *Coord. Chem. Rev*., 1995, **143**, 407.
5 I. V. Kozhevnikov, *Catal. Rev. Sci. Eng*., 1995, **37**, 311.
6 L. Salles, C. Aubry, R. Thouvenot, F. Robert, C. Dorémieux-Morin, G. Chottard, H. Ledon, Y. Jeannin and J.-M. Brégeault, *Inorg. Chem*., 1994, **33**, 871.
7 J.-Y. Piquemal, L. Salles, C. Bois, F. Robert and J.-M. Brégeault, *C. R. Acad. Sci. Paris, Sér. II*, 1994, **319**, 1481.
8 L. Salles, F. Robert, V. Semmer, Y. Jeannin and J.-M. Brégeault, *Bull. Soc. Chim. Fr*., 1996, **133**, 319.
9 R. K. Iler, *The Chemistry of Silica*, Wiley, New York, 1979.
10 C. Rocchiccioli-Deltcheff, M. Fournier, R. Franck and R. Thouvenot, *Inorg. Chem*., 1983, **22**, 207.
11 V. A. Zeitler and C. A. Brown, *J. Am. Chem. Soc*., 1957, **79**, 4618.
12 N. M. Rutherford, Ph. D. Thesis, University of California, Berkeley, 1987.
13 M. Lazell, M. Motevalli, S. A. A. Shah, C. K. S. Simon and A. C. Sullivan, *J. Chem. Soc., Dalton Trans*., 1996, 1449 and references therein.
14 E. Samuel, J. F. Harrod, M. J. McGlinchey, C. Cabestaing and F. Robert, *Inorg. Chem*., 1994, **33**, 1292.
15 R. G. J. Miller and H. A. Willis, *Infrared Structural Correlation Tables*, Heyden and Son Ltd., London, 1969, Table 9.
16 J.-M. Brégeault, R. Thouvenot, S. Zoughebi, L. Salles, A. Atlamsani, E. Duprey, C. Aubry, F. Robert and G. Chottard, *Studies in Surface Science and Catalysis, New Developments in Selective Oxidation II*, ed. V. Cortés Corberán and S. Vic Bellón, Elsevier, 1994, **82**, 571.
17 R. Murugavel, A. Voigt, M. G. Walawalkar and H. W. Roesky, *Chem. Rev*., 1996, **96**, 2205.
18 A. C. Larson, *Crystallographic Computing*, ed. F. R. Ahmed, S. R. Hall and C. P. Huber, Munksgaard, Copenhagen, 1970, p. 291.
19 N. Walker and D. Stuart, *Acta Crystallogr., Sect. A*, 1983, **39**, 158.
20 D. T. Cromer and J. T. Waber, *International Tables for X-Ray Crystallography*, Kynoch Press, Birmingham, 1974, vol. IV, p. 99.
21 D. J. Watkin, J. R. Carruthers and P. W. Betteridge, CRYSTALS, An Advanced Crystallographic Program System, Chemical Crystallographic Laboratory, University of Oxford, 1989.


*Received, 14th October 1996; Com. 6/07014K*

# Copper dioxygen complexes stable at ambient temperature: optimization of ligand design and solvent

**Kenneth D. Karlin,*[a] Dong-Heon Lee,[a] Susan Kaderli[b] and Andreas D. Zuberbühler*[b]**

[a] *Department of Chemistry, The Johns Hopkins University, Baltimore, MD 21218, USA*
[b] *Institute of Inorganic Chemistry, University of Basel, CH-4056 Basel, Switzerland*

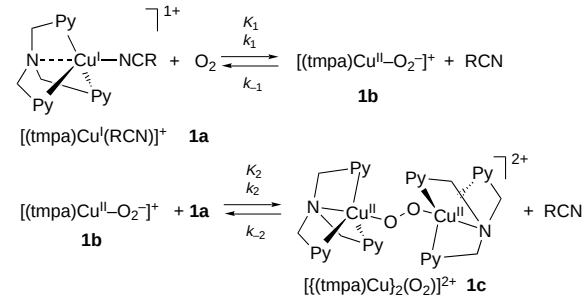
**Entropic destabilization of low-molecular mass μ-peroxo-dicopper(II) complexes are overcome using a new binucleating open-chain ligand by the combination of an optimized linking unit with a less competing solvent; complete formation and satisfactory stability at room temperature are thus obtained.**

As with efforts by synthetic chemists to design systems which mimic the $O_2$-binding of haemoglobin/myoglobin using modified iron porphyrinates, there has been considerable recent interest in studies of $O_2$-binding by copper complexes,[1,2] relevant to the arthropodal and molluscan haemolymph $O_2$-carrier haemocyanins.[3] In the deoxygenated state, these possess a dinuclear copper(I) centre; oxygenation proceeds *via* oxidative addition, producing a side-on bound μ-$\eta^2$:$\eta^2$-peroxo-dicopper(II) species (Cu···Cu 3.6 Å). Using tridentate nitrogen-containing ligands, synthetic models with this structure and accompanying spectroscopic properties have been generated and characterized at reduced temperatures (either in solution or as isolated solids).[1,2,4]

With tetradentate ligands such as tris(2-pyridylmethyl)amine (tmpa), divergent copper–dioxygen structure–spectroscopic types form. Kinetic/spectroscopic studies[5–7] reveal that copper(I) complexes with tmpa, its quinolyl substituted analogues, and binucleating version $L^2$, form sequentially both $Cu:O_2 = 1:1$ [superoxocopper(II)] and 2:1 [peroxodicopper(II)] products, stable only at reduced temperatures (*i.e.* −80 °C); X-ray structure analysis[8] establishes [{(tmpa)Cu}$_2$($O_2$)]$^{2+}$ **1c** (Scheme 1) to possess a *trans*-μ-1,2-peroxo ligation. The quinolyl[5] and dinucleating ligand[6] variations measurably affect $Cu^I_n/O_2$ stoichiometric preferences, reaction rates, and $Cu_n$–$O_2$ structural distortions or strain.[6,7] Here, however, we report dramatic effects upon reaction rates and copper–dioxygen complex stability, elicited by ligand synthetic modification or alteration of reaction solvent. In fact, the long sought goal of generating a fully formed and reasonably stable copper–dioxygen complex at room temperature in solution, has been achieved.

Kinetic–spectroscopic monitoring of [(tmpa)Cu$^I$(RCN)]$^+$ **1a** reacted with $O_2$ in EtCN at −90 °C typically reveals initial {*t ca*. 50 ms, [**1a**] = 0.4 mM; [$O_2$] = 4.5 mM} growth of the band at $\lambda_{max}$ = 410 nm, associated with a 1:1 intermediate adduct [(tmpa)Cu$^{II}$($O_2^-$)]$^+$ **1b** ($k_1 = 1.8 \times 10^4$ M$^{-1}$ s$^{-1}$). The final peroxo product [{(tmpa)Cu$^{II}$}$_2$($O_2^{2-}$)]$^{2+}$ **1c** ($\lambda_{max}$ = 525 nm) subsequently builds up at the expense of **1b** (and **1a**; Scheme 1) such that at *t ca*. 10 s at this temperature, **1b** mostly disappears and **1c** is nearly fully formed. The room-temperature stability of **1c** (and other copper–dioxygen complexes in general)[6,7] is precluded by a highly unfavoured reaction entropy ($\Delta S_{on}° = -220 \pm 11$ J K$^{-1}$ mol$^{-1}$),[6] and the 525 nm absorption essentially disappears, either in favour of Cu$^I$ (short times) or Cu$^{II}$ decomposition products.

These results stand in marked contrast to reactions now carried out in acetone as solvent. At −90 °C, [{(tmpa)Cu$^{II}$}-($O_2^-$)]$^+$ **1b** fully forms within the mixing time of the stopped-flow apparatus (< 2 ms), Fig. 1(*a*), providing a lower limit $k_1 \geqslant 10^6$ M$^{-1}$ s$^{-1}$. This $O_2$-binding to [{(tmpa)Cu$^I$}(Me$_2$CO?)]$^+$ **1a′** at −90 °C is at least comparable with the room-temperature reaction of $O_2$ with deoxyhaemocyanin ($k_{on}$ *ca*. $10^7$ M$^{-1}$ s$^{-1}$).[9] Thus, with the right ligand and medium, there is little, if any, restriction to $O_2$-binding to Cu$^I$, and these observations point to




**Scheme 1**

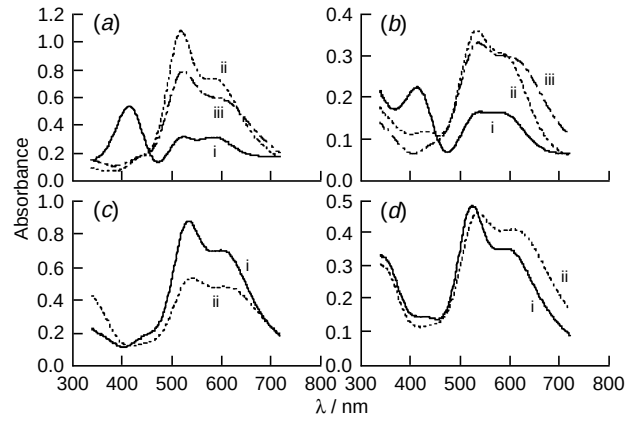
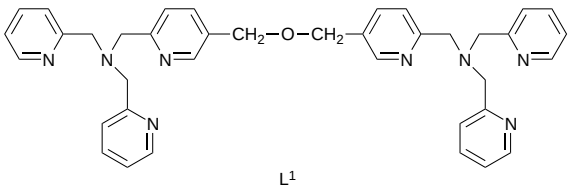
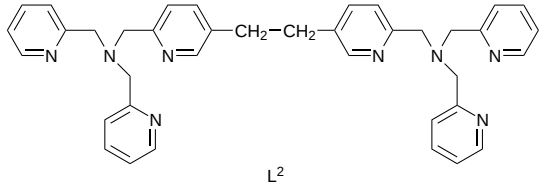



**Fig. 1** Stopped-flow spectral monitoring of the reaction in acetone of $O_2$ (5.1 mM) with (*a*) [(tmpa)Cu$^I$(RCN)]$^+$ (**1a**, 0.9 mM) and (*b*) [$L^2Cu_2$(EtCN)$_2$]$^{2+}$ (**2a**, 0.26 mM). Superoxo formation with some admixture of peroxo complex (2.6 ms after mixing) (i, superoxo −90 °C; ii, peroxo −90 °C; iii, peroxo +20 °C). Reaction of $O_2$ (5.1 mM) with [$L^1Cu_2$(EtCN)$_2$)]$^{2+}$ (**3a**, 0.55 mM) in (*c*) propionitrile or (*d*) acetone (0.28 mM) (i, peroxo −90 °C; ii, peroxo +20 °C).



nitrile coordination and rate-limiting dissociation being critical in the chemistry of tripod copper(I) complexes detailed for EtCN solutions.[5–7] The stability of $[\{(tmpa)Cu^{II}\}_2(O_2^{2-})]^{2+}$ **1c** [$\lambda_{max}$ = 525 nm, shoulders at *ca*. 430 and 600 nm; Fig. 1(*a*)][10]† is increased even more dramatically, with $\beta_2 = K_1K_2 \geqslant 5 \times 10^5$ M$^{-2}$ ($5 \times 10^2$ M$^{-2}$ in EtCN) at room temperature. Formation of 70% **1c** is obtained within the mixing time (EtCN: not observable, calculated formation 0.2%). At 20 °C, **1c** decomposes with $t_{1/2}$(decomp.) *ca*. 45 s.

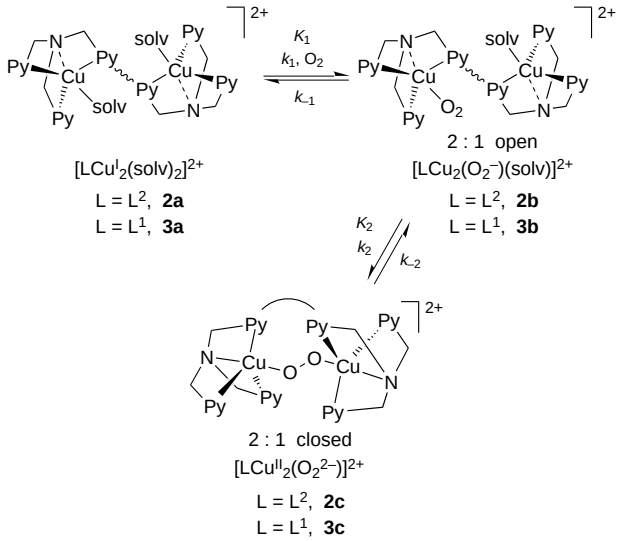
We previously showed that $[L^2Cu_2(EtCN)_2]^{2+}$ **2a** reacts with $O_2$ in EtCN giving both Cu : $O_2$ = 1 : 1 and 2 : 1 intermediates; $[L^2(Cu^ICu^{II})(O_2^-)(EtCN)]^{2+}$ **2b** reacts intramolecularly giving closed peroxo species $[L^2Cu_2(O_2)]^{2+}$ **2c** (Scheme 2).[6] The dinucleating nature of $L^2$ (compared to tmpa) results in considerable reduction of the entropic handicap found for formation of $[\{(tmpa)Cu\}_2(O_2)]^{2+}$ **1c**, by 130–140 J K$^{-1}$ mol$^{-1}$. However comparison of the $\Delta H_{on}°$ for **1c** *vs*. **2c** formation (−81 *vs*. −35 kJ mol$^{-1}$)[6] revealed the latter to be significantly strained, resulting in rearrangement to trimeric $[L^2Cu_2(O_2)]_3^{6+}$. In acetone, **2a** reaction with $O_2$ again results in enhanced stability of copper–dioxygen adducts. As with tmpa, 1 : 1 complex adduct formation occurs within the stopped-flow mixing time even at −90 °C, giving the characteristic $\lambda_{max}$ = 414 nm absorption [Fig. 1(*b*)], assigned to a bis-superoxocopper(II) species $[L^2Cu_2(O_2)_2]^{2+}$ **2b′**. Formation of peroxo complex $[L^2Cu_2(O_2)]^{2+}$ **2c** is essentially complete even at 20 °C [Fig. 1(*b*)], yielding $K_1K_2 > 4 \times 10^3$ M$^{-1}$ (27 M$^{-1}$ in EtCN),[6] but precluding calculation of thermodynamic parameters $\Delta H°$ and $\Delta S°$. Enhanced decomposition of **2c** [$t_{1/2}$(decomp.) *ca*. 4 s] *vs*. $t_{1/2}$(decomp.) *ca*. 40 s for **1c** may reflect the still considerably strained nature of adduct $[L^2Cu_2(O_2)]^{2+}$.

In combination, the new ligand $L^1$,‡ a modification designed to relieve the strain in **2c**, [11] is the most successful in giving a pseudoreversible $Cu_2$–$O_2$ complex stable at room temperature. Curiously, for both EtCN and acetone solvents, there is no spectral indication of any 1 : 1 adducts (*e.g*. **3b**, Scheme 2) upon reaction of dicopper(I) precursor $[L^1Cu_2(MeCN)_2]^{2+}$ **3a**‡ with $O_2$.§ Their formation appears to be inhibited and slow relative to the subsequent reactions leading to peroxo complex $[L^1Cu_2(O_2)]^{2+}$ **3c** ($\lambda_{max}$ = 535 nm). However, in EtCN, formation of **3c** is complete within the experimental mixing time even at −60 °C. Theoretical calculations[11] and preliminary analyses of the present kinetic data suggest that the longer linker arm in $L^1$ indeed relieves the strain observed for $[L^2Cu_2(O_2)]^{2+}$ **2c**, significantly enhancing adduct formation at room temperature to 60% [$K_1K_2$ = 300 M$^{-1}$ *vs*. 27 M$^{-1}$ for $L^2$, Fig. 1(*c*),† with $t_{1/2}$(decomp.) increased to 20 s]. $L^1$ seems to afford significant entropic advantage for formation of $[L^1Cu_2(O_2)]^{2+}$ **3c** compared to $[\{(tmpa)Cu\}_2(O_2)]^{2+}$ **1c**, with little enthalpic loss.

Acetone once more confers additional stability to **3c**. Peroxo formation is immediate and complete within experimental error at room temperature, thus precluding quantitative determination of $K_1K_2$, but we may safely assume that thermodynamic stability is still increased relative to $L^2$ in acetone. In line with this, enhanced persistence of the characteristic $[L^1Cu_2(O_2)]^{2+}$ **3c** spectrum [Fig. 1(*d*); $t_{1/2}$(decomp.) *ca*. 60 s] may be indicative of released strain and leads to the most stable of all copper–dioxygen complexes thus far studied by us.[7]¶

The results further demonstrate the importance in ligand design/modification, here shown to confer solution room-temperature stability to $Cu_2$–$O_2$ complexes. $L^1$ utilizes a dinucleating design which appears to be strain minimized. Acetone is shown to be a remarkable solvent for enhancing rates of formation and thermal stability of $Cu_n$–$O_2$ species, probably by virtue of its poor ability to ligate to $Cu^I$. Further analyses and investigations are aimed at further detailing of factors which can be controlled *via* ligand design (*i.e*. steric, electronic and medium effects), and which are critical to $Cu_n$–$O_2$ formation, structure, stability and reactivity.

We thank the National Institutes of Health (K. D. K.) and Swiss National Science Foundation (A. D. Z.) for financial support of this research.




**Scheme 2**

## Footnotes

† Solution spectral broadening and intensity diminution is expected with increase in temperature. See S. F. Rice, R. B. Wilson and E. I. Solomon, *Inorg. Chem*., 1980, **19**, 3425.

‡ Ether $L^1$ was synthesized by condensation of previously described hydroxymethyl and chloromethyl precursors.[6] Reaction of $L^1$ with 2 equiv. of $[Cu(MeCN)_4]ClO_4$ gave **3a**$(ClO_4)_2$, for which satisfactory C, H and N analyses were obtained.

§ We are investigating the hypothesis that **3a** in solution exists as a tight dinuclear complex (with pyridyl ligand stacking), altering the more typical and previously observed process of $Cu$–$O_2$ 1 : 1 complex formation. See L. F. Newcomb and S. H. Gellman, *J. Am. Chem. Soc*., 1994, **116**, 4993, for examples of solution stacking of aromatics connected with a propylene spacer.

¶ A recent report describes the use of a macrocycle dicopper complex which (irreversibly) binds dioxygen at room temp. See J. E. Bol, W. L. Driessen, R. Y. N. Ho, B. Moase, L. Que, Jr. and J. Reedyk, *Angew. Chem., Int. Ed. Engl*., in the press.

## References

1 N. Kitajima and Y. Moro-oka, *Chem. Rev*., 1994, **94**, 737.
2 S. Fox and K. D. Karlin, in *Dioxygen Reactivity in Copper Proteins and Complexes*, ed. J. S. Valentine, C. S. Foote, A. Greenberg and J. F. Liebman, Glasgow, 1995; K. D. Karlin and Z. Tyeklár, *Adv. Inorg. Biochem*., 1994, **9**, 123.
3 K. A. Magnus, H. Ton-That and J. E. Carpenter, *Chem. Rev*., 1994, **94**, 727; E. I. Solomon, U. M. Sundaram and T. E. Machonkin, *Chem. Rev*., 1996, **96**, 2536.
4 W. E. Lynch, D. M. Kurtz, Jr., S. Wang and R. A. Scott, *J. Am. Chem. Soc*., 1994, **116**, 11030; T. N. Sorrell, W. E. Allen and P. S. White, *Inorg. Chem*., 1995, **34**, 952; J. A. Halfen, S. Mahapatra, E. C. Wilkinson, S. Kaderli, V. G. Young, Jr., L. Que, Jr., A. D. Zuberbühler and W. B. Tolman, *Science*, 1996, **271**, 1397.
5 K. D. Karlin, N. Wei, B. Jung, S. Kaderli, P. Niklaus and A. D. Zuberbühler, *J. Am. Chem. Soc*., 1993, **115**, 9506.
6 D.-H. Lee, N. Wei, N. N. Murthy, Z. Tyeklár, K. D. Karlin, S. Kaderli, B. Jung and A. D. Zuberbühler, *J. Am. Chem. Soc*., 1995, **117**, 12498.
7 K. D. Karlin, S. Kaderli and A. D. Zuberbühler, *Acc. Chem. Res*., 1997, in the press.
8 Z. Tyeklár, R. R. Jacobson, N. Wei, N. N. Murthy, J. Zubieta and K. D. Karlin, *J. Am. Chem. Soc*., 1993, **115**, 2677.
9 C. R. Andrew, K. P. McKillop and A. G. Sykes, *Biochim. Biophys. Acta*, 1993, **1162**, 105.
10 M. J. Baldwin, P. K. Ross, J. E. Pate, Z. Tyeklár, K. D. Karlin and E. I. Solomon, *J. Am. Chem. Soc*., 1991, **113**, 8671.
11 P. Comba, P. Hilfenhaus and K. D. Karlin, *Inorg. Chem*., submitted for publication.

*Received, 20th November 1996; Com. 6/07862A*

# Structural consequences of competing noncovalent forces: the out–out conformation of the doubly protonated [2.2.2]cryptand

**Leonard R. MacGillivray and Jerry L. Atwood*†**

*Department of Chemistry, University of Missouri-Columbia, Columbia, Missouri 65211, USA*

**The reaction of [2.2.2]cryptand 1 with 2,6-dihydroxybenzoic acid (dhbH) in toluene affords the complex [1-2H]-[(2,6-dhb)$_2$]; its crystal structure exhibits the first solid state evidence of the out–out form of the doubly protonated macrobicycle and illustrates the role of C–H···O hydrogen bonds in providing additional stability to the cavity of the ligand.**

Although it is now generally accepted that noncovalent interactions (*e.g.* hydrogen bonds, π–π interactions, ion pairs) play an important role in determining the conformation and corresponding ionophoric properties of macro(poly)cyclic receptors (*e.g.* crown ethers, cryptands)[1] in solution,[2a] the gas phase,[2b] and the solid state,[2c] less is known about their structure determining roles in the presence of competing forces.[3] This is, perhaps, not surprising considering the difficulty in generating and analysing discrete, multi-component supramolecular assemblies and delineating the contributions of each interaction to the resulting structure.[4] Indeed, understanding the cooperativity[5] exhibited by noncovalent interactions, especially in the context of molecular recognition processes, promises to yield insight into areas of both chemical and biological relevance including the nucleation and crystallization of molecules[6] and the mechanisms by which the secondary structures of proteins (*e.g.* α-helices) are formed.[3]

Extensive work has demonstrated the self-assembly of proton cryptate complexes of the flexible macrobicyclic ionophore [2.2.2]cryptand **1** with inorganic anions isolated from liquid clathrate media.[7] In particular, we have illustrated the ability of two trifurcated intraionic $N^+$–H···O hydrogen bonds to slow down its rapid in–in, in–out, and out–out equilibrium[8] in solution and reorganize its structure to a chiral, in–in conformation with approximate $D_3$ symmetry in the solid state.[7a] In such a context, recent molecular dynamics simulations have shown the doubly protonated in–in form of **1** to be more stable than its corresponding out–out conformer by 21 kcal mol$^{-1}$.[9] This additional stability has been attributed, in part, to the intraionic $N^+$–H···O hydrogen bonds within the cavity.

As part of our ongoing studies of proton cryptates, we now report the synthesis and X-ray crystal structure of a complex, [**1**-2H][(2,6-dhb)$_2$] **2** (dhb = dihydroxybenzoate, dhbH = dihydroxybenzoic acid), which provides the first solid state evidence of the out–out form of the doubly protonated **1**. The complex exhibits two 2,6-dhb ions which interact with the outer surface of the cryptate *via* two interionic $N^+$–H···$O^-$ hydrogen bonds. As a consequence of these interactions, the ligand has undergone a structural reorganization from the in–in form, by breakage of its internal $N^+$–H···O hydrogen bonds, to the out–out conformation. Furthermore, in response to this reorganization, the ligand has formed four intraionic C–H···O interactions[10] inside its cavity. Such observations provide insight into molecular recognition processes involving hydrogen bond cooperativity where understanding the structural consequences of competing noncovalent forces is of much current interest.[5a,b]

Addition of **1** (0.040 g) to a hot toluene solution (40 ml) containing 2,6-dhbH (0.033 g) according to eqn. (1) immediately yielded a white precipitate **2**. Colourless crystals of **2** suitable for X-ray analysis were obtained by dissolving a portion of the precipitate in MeCN and allowing the solution to evaporate to dryness. The formulation of **2** was confirmed by single-crystal X-ray diffraction‡ and analytical data.§

$$\mathbf{1} + 2(2,6\text{-dhbH}) \rightarrow [\mathbf{1}\text{-2H}][(2,6\text{-dhb})_2]\ \mathbf{2} \qquad (1)$$

An ORTEP perspective of **2** is shown in Fig. 1. *Exo* protonation leads to the formation of two interionic $N^+$–H···$O^-$ hydrogen bonds between constituent ions, and hence, an out–out conformation is adopted by the cryptate. As a result, the cavity of the ligand is substantially distorted from approximate $D_3$ symmetry. This is illustrated by N(1)–CCO and N(2)–CCO torsion angles, which range from −65.6 to 171.1° and −60.0 to 174.4°, and the distances for the edges of each triangular face, which range from 4.228 to 4.931 Å and 4.070 to 4.867 Å, for atoms O(1), O(3), O(5) and O(2), O(4), O(6), respectively.¶ These values compare favourably to those of the *N*,*N*′-dimethyl-**1** diiodide salt[13] and the bisborohydride of **1**[14] which adopt similar *exo* conformations owing to the bulk of the substituents which precludes their entrance in the cavity. The corresponding torsion angles and O···O separations in [$H_3O$]$_2$[**1**-2H][4Cl]·4 $H_2O$ **5** range from −53.7(7) to −58.3(8)° and 3.69(2) to 3.79(2) Å, respectively.[7a] Furthermore, the nonbonding N···N separation (6.33 Å), which is shorter than that of the empty cryptand (6.87 Å),[14] is longer than in **5** (5.71 Å) but comparable to that of **3** (6.67 Å) and **4** (6.77 Å).

The geometry of the cavity of the cryptate in **2** may be attributed to the contributions of four C–H···O hydrogen bonds involving four α-hydrogen atoms, from two different methylene groups, and the four ethereal oxygen atoms which are directed inward toward the cavity. Indeed, Fig. 1 illustrates that *exo* protonation facilitates inversion at each bridgehead nitrogen

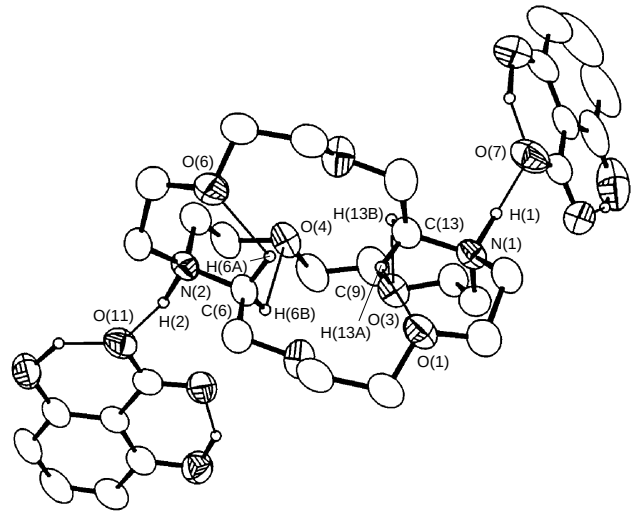



**Fig. 1** X-Ray crystal structure of **2**. Selected interatomic distances (Å) and angles (°): N(1)···O(7) 2.687(4), N(1)–H(1)–O(7) 177(2), N(2)···O(11) 2.689(4), N(2)–H(2)–O(11) 166(2), C(6)···O(4) 3.010(4), C(6)–H(6B)–O(4) 111, C(6)···O(6) 2.919(4), C(6)–H(6A)–O(6) 110, C(13)···O(3) 3.042(4), C(13)–H(13B)–O(3) 117, C(13)···O(1) 2.964(4), C(13)–H(13A)–O(1) 117.

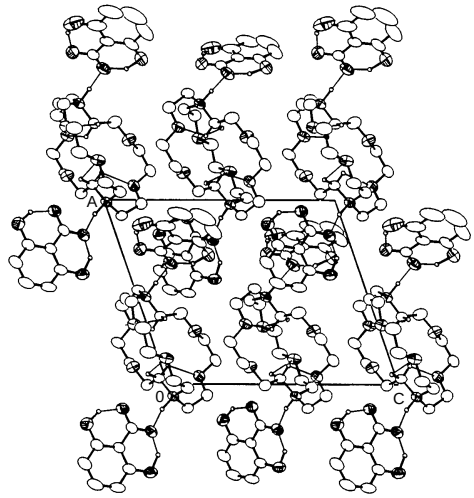



**Fig. 2** Crystal packing of **2** viewed along the crystallographic *b* axis

atom which subsequently enables one methylene group at each end of the cryptate to extend its hydrogen atoms inside the cavity and form the C–H···O interactions‖ The ability of C–H···O hydrogen bonds to provide structural stability to macrocyclic polyether components (*e.g.* cyclophanes) is known[15] and there is growing evidence that such interactions play a role in stabilizing the tertiary structures of biomolecules.[16] To our knowledge, this is the first case in which C–H···O hydrogen bonds have been recognized to impart conformational stability to the out–out topology of **1**.

A view along the crystallographic *b* axis depicting the crystal structure of **2** is shown in Fig. 2. The assembly process results in an alternating assembly of aliphatic and aromatic layers, involving cations and anions, respectively, within the *ac* plane. Interestingly, **5** exhibits a similar layered architecture despite the fact that its proton cryptate adopts the in–in topology.[7a]

The results reported herein lie at the heart of molecular recognition. By simply introducing an appropriate hydrogen bond acceptor along its outer surface, the [**1**-2H]$^{2+}$ ion has undergone a structural reorganization, *via* breakage of its internal N$^+$–H···O hydrogen bonds, to the out–out form which recognizes the anion *via* interionic N$^+$–H···O$^-$ interactions. In response, the cryptate has formed four C–H···O interactions inside its cavity. Such observations may provide insight into understanding those factors which influence the secondary structures of proteins since similar competing noncovalent forces are thought to play a role in contributing to their stability.[3a]

We are grateful for funding from the National Science Foundation, the Natural Sciences and Engineering Research Council of Canada (NSERC) for a research fellowship (L. R. M.) and the International Centre For Diffraction Data for a research scholarship (L. R. M.).

## Footnotes

† Email: chemja@mizzou1.missouri.edu

‡ *Crystal data* for [**1**-2H][(2,6-dhb)$_2$]; monoclinic, space group $P2_1/c$, $a$ = 12.346(1), $b$ = 20.519(1), $c$ = 14.626(1) Å, β = 109.27(4)°, $U$ = 3497(1) Å$^3$, $D_c$ = 1.30 g cm$^{-1}$, Cu-Kα radiation (λ = 1.54060 Å) for $Z$ = 4. Least-squares refinement based on 3206 reflections with $I_{net} > 2.0\sigma(I_{net})$ (out of 5176 unique reflections) collected on an Enraf Nonius CAD-4 diffractometer equipped on a rotating anode generator and 449 parameters on convergence gave a final value of $R$ = 0.063. Methylene, aromatic and hydroxy hydrogen atoms were placed by modelling the moieties as rigid groups with idealised geometry, maximising the sum of the electron density at the calculated hydrogen positions. Quaternary ammonium hydrogen atoms were loacted *via* inspection of a difference Fourier map and refined at a restrained distance of 1.10 Å from the N atoms to which they are bonded. Structure solution was accomplished with the aid of SHELXS-86[11] and refinement was conducted using SHELX93[12] locally implemented on a pentium-based IBM compatible computer. Atomic coordinates, bond lengths and angles, and thermal parameters have been deposited at the Cambridge Crystallographic Centre (CCDC). See Information for Authors, Issue No. 1. Any request to the CCDC for this material should quote the full literature citation and the reference number 182/361.

§ Anal. Calcd: C, 56.13; H, 7.07; N, 4.09. Found: C, 56.30; H, 7.00; N, 4.06.

¶ Two oxygen atoms from each triangular face [O(1), O(3) and O(4), O(6)] are directed inward toward the cavity.

‖ We have recently demonstrated the ability of the α-hydrogen atoms of the [**1**-2H]$^{2+}$ ion to contribute to the structural stability of the cavity of the ligand by participating in a cation–π interaction.[7c]

## References

1 G. Gokel, in *Crown Ethers Cryptands*, ed. J. F. Stoddart, The Royal Society of Chemistry, Cambridge, 1991.
2 Lead references: (*a*) L. Troxler and G. J. Wipff, *J. Am. Chem. Soc.*, 1994, **116**, 1468; (*b*) S. Lee, T. Wyttenbach, G. Von Helden and M. T. Bowers, *J. Am. Chem. Soc.*, 1995, **117**, 10 159; (*c*) G. Papoyan, K. Gu, J. Wiorkiewicz-Kuczera, K. Kuczera and K. Bowman-James, *J. Am. Chem. Soc.*, 1996, **118**, 1354.
3 (*a*) M. J. Bodkin and J. M. Goodfellow, *Protein Science*, 1995, **4**, 603; (*b*) K. A. Dill, K. M. Fiebig and H. S. Chan, *Prod. Natl. Acad. Sci. USA*, 1993, **90**, 1942.
4 I. J. Kurnig, M. M. Szczęśniak and S. Scheiner, *J. Am. Chem. Soc.*, 1986, **90**, 4253.
5 (*a*) H. Guo and M. Karplus, *J. Phys. Chem.*, 1994, **98**, 7104; (*b*) G. Maes and J. Smets, *J. Phys. Chem.*, 1993, **97**, 1818; (*c*) P. L. Huyskens, *J. Am. Chem. Soc.*, 1977, **99**, 2578.
6 L. Turi and J. J. Dannenberg, *J. Am. Chem. Soc.*, 1994, **116**, 8714.
7 (*a*) L. R. MacGillivray and J. L. Atwood, *J. Org. Chem.*, 1995, **60**, 4972; (*b*) L. R. MacGillivray and J. L. Atwood, *Chem. Commun.*, 1996, 735; (*c*) L. R. MacGillivray and J. L. Atwood, *Angew. Chem., Int. Ed. Engl.*, 1996, **35**, 1828.
8 R. W. Alder and S. P. East, *Chem. Rev.*, 1996, **96**, 2097.
9 P. Auffinger and G. J. Wipff, *J. Inclusion Phenom.*, 1991, **11**, 71.
10 G. R. Desiraju, *Acc. Chem. Res.*, 1996, **29**, 441.
11 G. M. Sheldrick, *Acta Crystallogr., Sect. A*, 1990, **46**, 467.
12 G. M. Sheldrick, SHELX-76, University of Cambridge, 1976.
13 N. Korber and M. Jansen, *Acta Crystallogr., Sect. C*, 1993, **49**, 1220.
14 B. Metz, D. Moras and R. Weiss, *J. Chem. Soc., Perkin Trans. 2*, 1976, 423.
15 D. B. Amabilino, P.-L. Anelli, P. R. Ashton, G. R. Brown, E. Córdova, L. A. Godínez, W. Hayes, A. E. Kaifer, D. Philip, A. M. Z. Slawin, N. Spencer, J. F. Stoddart, M. S. Tolley and D. J. Williams, *J. Am. Chem. Soc.*, 1995, **117**, 11 142.
16 P. Auffinger, S. Louise-May and E. Westhof, *J. Am. Chem. Soc.*, 1996, **118**, 1181.

*Received, 24th December 1996; Com. 6/08603I*

# A dinuclear double-helical complex of potassium ions with a compartmental bridging ligand containing two terdentate N-donor fragments

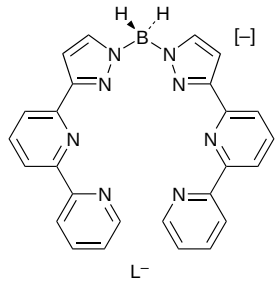
**Elefteria Psillakis, John C. Jeffery, Jon A. McCleverty* and Michael D. Ward***

*School of Chemistry, University of Bristol, Cantock's Close, Bristol, UK BS8 1TS*

**The compartmental bridging ligand bis{3-[6′-(2,2′-bipyridyl)]pyrazol-1-yl}hydroborate ($L^-$), which contains two chelating terdentate N-donor arms linked by an anionic $–BH_2–$ bridge, forms a dinuclear double-helical complex $K_2L_2$ with $K^+$ ions.**

Recently helicates have become a well known structural motif in supramolecular coordination chemistry.[1–4] They are of particular interest not just for their appealing structures but also because of the processes of molecular recognition and self-assembly that are required for their formation. Their formation requires (*i*) ligands which contain several discrete metal-ion binding domains, and (*ii*) metal ions with specific preferences for particular coordination geometries that match the ligand binding sites. It is the appropriate combination of these two factors which dictates the outcome of the self-assembly process. Thus, a ligand which has two terdentate domains might give a double helicate with a transition-metal ion (coordination number six) but a triple helicate with a lanthanide (coordination number nine).[2–5] In contrast, linear oligopyridines can partition themselves according to the dictates of the metal ion, and give different structures with $Cu^I$ (when the ligand is partitioned into bidentate domains) and $Cd^{II}$ or $Ni^{II}$ (when it is split into terdentate domains).[1]

The requirement of the metal ion for a specific geometry or coordination number is principally controlled by charge/size effects: thus $Cu^I$ and $Ag^I$ have a preference for (usually) four-coordination, whereas transition-metal dications generally prefer six-coordination and lanthanides prefer approximately nine-coordination.[1–5] In contrast the use of s-block metals in double helicates is virtually unknown. The only certain example, recently published by Bell and Jousselin, is a 2 : 2 complex of $Na^+$ with a 'heterohelicene' ligand which is preorganised into a helical shape and therefore inevitably imposes a helical structure on its complexes.[6] The complex was characterised by NMR spectroscopy and mass spectrometry, but not crystallographically. It is also possible that the 1 : 1 adduct of 2,2′ : 6′,2″ : 6″,2‴ : 6‴,2⁗-quinquepyridine with $LiClO_4$ is a double helicate.[7] Cram and coworkers recently described a macrocyclic ligand containing two phenanthroline binding sites that was twisted into a helically chiral conformation by virtue of binaphthyl groups incorporated into the cycle; this imposes a helically chiral geometry on alkali-metal cations due to its preorganisation.[8]




We describe here the preparation of the new compartmental bis-terdentate ligand bis{3-[6′-(2,2′-bipyridyl)]pyrazol-1-yl}-hydroborate ($L^-$) as its potassium salt KL, and the crystal structure of this salt which reveals a double-helical complex of stoichiometry $K_2L_2$. The ligand was prepared by reaction of 6-(3-pyrazolyl)-2,2′-bipyridine[9] with $KBH_4$,† which is the usual route for preparing bidentate bis(pyrazol-1-yl)hydroborates[10] and tridentate tris(pyrazol-1-yl)hydroborates[11] from substituted pyrazoles. All of the spectroscopic and analytical data were consistent with formation of KL, in which two terdentate N-donor arms are linked by an anionic $–BH_2–$ fragment. Even using a fourfold excess of the pyrazole, we found that only the bis(pyrazolyl)borate was obtained, and this is the first example of a bis(pyrazolyl)borate functionalised in this manner so that each arm becomes chelating rather than monodentate. The compound was crystallised by slow evaporation from chloroform to give colourless prisms; the crystal structure is in Fig. 1,‡ and reveals that in the solid state the

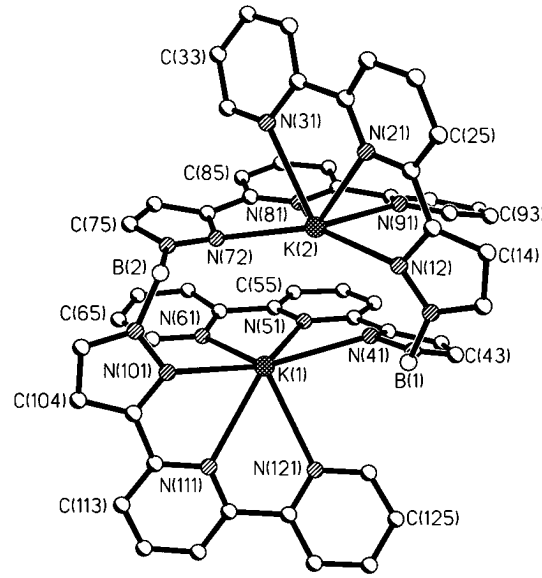



**Fig. 1** Crystal structure of $K_2L_2$. Selected bond lengths (Å) and angles (°): K(1)–N(101) 2.772(5), K(1)–N(41) 2.784(6), K(1)–N(61) 2.816(6), K(1)–N(51) 2.857(5), K(1)–N(111) 2.927(5), K(1)–N(121) 2.956(6), K(2)–N(72) 2.766(6), K(2)–N(12) 2.777(6), K(2)–N(91) 2.802(6), K(2)–N(81) 2.855(6), K(2)–N(31) 2.877(6), K(2)–N(21) 2.890(6), K(1)···K(2) 3.954(2); N(101)–K(1)–N(41) 150.1(2), N(101)–K(1)–N(61) 84.2(2), N(41)–K(1)–N(61) 116.1(2), N(101)–K(1)–N(51) 139.3(2), N(41)–K(1)–N(51) 59.2(2), N(61)–K(1)–N(51) 57.4(2), N(101)–K(1)–N(111) 57.3(2), N(41)–K(1)–N(111) 134.9(2), N(61)–K(1)–N(111) 95.4(2), N(51)–K(1)–N(111) 132.5(2), N(101)–K(1)–N(121) 111.9(2), N(41)–K(1)–N(121) 80.3(2), N(61)–K(1)–N(121) 115.3(2), N(51)–K(1)–N(121) 97.8(2), N(111)–K(1)–N(121) 56.4(2), N(72)–K(2)–N(12) 150.1(2), N(72)–K(2)–N(91) 116.3(2), N(12)–K(2)–N(91) 85.4(2), N(72)–K(2)–N(81) 58.8(2), N(12)–K(2)–N(81) 141.5(2), N(91)–K(2)–N(81) 58.1(2), N(72)–K(2)–N(31) 80.7(2), N(12)–K(2)–N(31) 114.4(2), N(91)–K(2)–N(31) 105.8(2), N(81)–K(2)–N(31) 89.2(2), N(72)–K(2)–N(21) 135.8(2), N(12)–K(2)–N(21) 59.4(2), N(91)–K(2)–N(21) 88.5(2), N(81)–K(2)–N(21) 124.7(2), N(31)–K(2)–N(21) 56.6(2).

compound is in fact a double-helical complex $K_2L_2$. The double-helical structure is emphasised in Fig. 2.

Each $K^+$ ion is coordinated in an irregular six-coordinate environment by two terdentate arms, one from each of the two ligands. The K–N bond distances around K(1) lie in the range 2.77–2.96 Å and those around K(2) lie in the range 2.77–2.89 Å, which are comparable to those found for the $K^+$ complex of one of Bell's cyclic torand ligands based on pyridyl donors[12] and for $[K(phen)_3][BPh_4]$.[13] There are additional weak interactions between K(1) and N(72) [3.469(5) Å] and between K(2) and N(41) [3.437(5) Å], which probably just arise from the steric constraints of the complex and do not represent true bridging behaviour by N(41) and N(71). Each ligand donates one terdentate arm to each of the two metal ions, a binding mode which is facilitated by the flexible $–BH_2–$ 'hinge' at the centre of each ligand. The N–B–N angles are 111.0(6)° at B(1) and 110.3(5)° at B(2), both very close to the ideal tetrahedral value which indicates that this mode of coordination is not imposing any steric strain on the ligands: this is no doubt facilitated by the ability of $K^+$ to tolerate a highly irregular coordination environment. The two terdentate fragments of each ligand are therefore approximately mutually perpendicular.

The structure appears to be stabilised by aromatic π-stacking interactions (3.2–3.6 Å) between near-parallel, overlapping sections of the two ligands. This is a common feature of helical complexes[1–4] but one which is not essential for helicate formation: the matching of metal-ion coordination geometry and ligand donor properties is probably more important.[14] The metal–metal separation [3.954(2) Å] is shorter than that in metallic potassium (4.54 Å) but significantly longer than the sum of two ionic radii for $K^+$ ions (*ca*. 2.7 Å). The crystal contains opposite enantiomers in the unit cell, related by an inversion centre. As with all 'supramolecular' structures based on labile metal ions, the solid-state structure is not necessarily wholly representative of the solution behaviour which could be considerably more complex.

This complex has several unusual features. First, it is to date the only structurally characterised double-helical complex with an s-block metal. Secondly, unlike the helical complexes described by Bell and Jousselin[6] and Cram and coworkers,[8] the helical geometry is not imposed by a preorganised ligand but arises naturally from the assembly of achiral ligands around the metal ions, as normally occurs for the transition-metal and lanthanide based helicates.[1–5] Thirdly, it is an unusual example of alkali-metal coordination by an open-chain nitrogen donor ligand.[13] Although several examples of alkali-metal complexes with exclusively N-donor ligands are known, they usually require highly preorganised ligands such as torands,[12,15] macrocycles[16] and cryptands,[17] where the cavity size is a particularly good match for an alkali-metal cation, and the coordination geometry is particulary unsuited to a transition-metal ion, neither of which is true in $K_2L_2$. It is probable that, considering the predominantly ionic nature of the complex, the affinity of $L^-$ for $K^+$ is enhanced by the negative charge of the ligand.

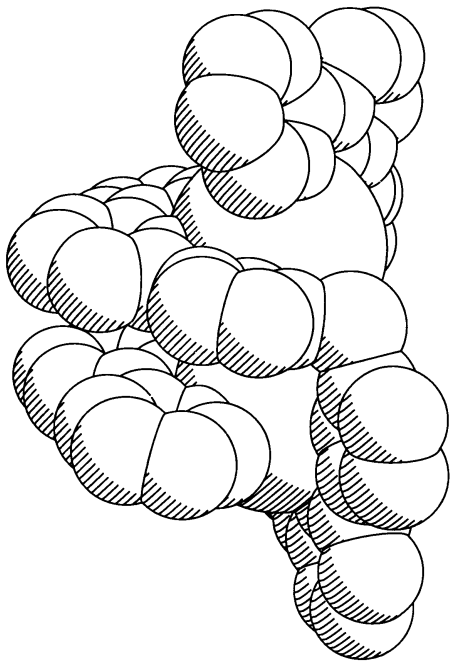


**Fig. 2** Space-filling diagram of $K_2L_2$

## Footnotes

† *Preparation* of $K_2L_2$: a mixture of 6-(3-pyrazolyl)-2,2′-bipyridine (0.25 g, 1.13 mmol) and $KBH_4$ (0.015 g, 0.28 mmol) was finely ground together in a mortar to ensure intimate mixing. The solid mixture was then heated to 190 °C under $N_2$ for 3 h (it melted at *ca*. 120 °C and $H_2$ evolution was observed to start at *ca*. 150 °C). After cooling the mixture the solid was washed with toluene to remove excess unreacted 6-(3-pyrazolyl)-2,2′-bipyridine; the remaining solid was collected by filtration and dried to give KL (0.040 g, 30%). Negative-ion electrospray MS: *m/z* 455 (100%, $L^-$). A satisfactory elemental analysis was obtained.

‡ *Crystal data* for $K_2L_2$: $C_{52}H_{40}B_2K_2N_{16}$, colourless prisms, crystal size 0.40 × 0.25 × 0.10 mm, $M$ = 988.82, triclinic, space group $P\bar{1}$, $a$ = 9.858(2), $b$ = 13.566(2), $c$ = 18.4766(12) Å, α = 87.541(10), β = 85.050(9), γ = 83.102(9)°, $U$ = 2442.5(6) Å$^3$, $Z$ = 2, $D_c$ = 1.345 g cm$^{-3}$, μ(Mo-Kα) = 0.25 mm$^{-1}$. Using a Siemens SMART diffractometer and graphite-monochromated Mo-Kα X-radiation, 11128 data were collected at −100 °C with $2\theta_{max}$ = 46.5°, and merged to give 6871 unique data ($R_{int}$ = 0.067). The data were corrected for absorption effects by an empirical method based on multiple measurements of equivalent reflections. The structure was solved by direct methods, and refined on all $F^2$ data using the SHELX suite of programs (version 5.03). All non-hydrogen atoms were refined with anisotropic thermal parameters. Aromatic C–H hydrogen atoms were included in calculated positions with isotropic thermal parameters 20% higher than those of the parent atoms; the four B–H hydrogen atoms were located directly and their thermal parameters refined freely. Refinement of 665 parameters using 6616 data converged at $R_1$ = 0.088, $wR_2$ = 0.207. Atomic coordinates, bond lengths and angles, and thermal parameters have been deposited at the Cambridge Crystallographic Data Centre (CCDC). See Information for Authors, Issue No. 1. Any request to the CCDC for this information should quote the full literature citation and the reference number 182/364.

## References


1 E. C. Constable, *Prog. Inorg. Chem*., 1994, **42**, 67.
2 D. Philp and J. F. Stoddart, *Angew. Chem., Int. Ed. Engl*., 1996, **35**, 1155.
3 D. S. Lawrence, T. Jiang and M. Levett, *Chem. Rev*., 1995, **95**, 2229.
4 D. B. Amabilino and J. F. Stoddart, *Chem. Rev*., 1995, **95**, 2725.
5 B. Hasenknopf and J.-M. Lehn, *Helv. Chim. Acta*, 1996, **79**, 1643; C. Piguet, J.-C. G. Bünzli, G. Bernardinelli, G. Hopfgartner and A. F. Williams, *J. Am. Chem. Soc*., 1993, **115**, 8197.
6 T. W. Bell and H. Jousselin, *Nature*, 1994, **367**, 441.
7 G. Oepen and F. Vögtle, *Liebigs Ann. Chem*., 1979, 2114.
8 J. K. Judice, S. J. Keipert and D. J. Cram, *J. Chem. Soc., Chem. Commun*., 1993, 1323.
9 J. C. Jeffery, P. L. Jones, K. L. V. Mann, E. Psillakis, J. A. McCleverty, M. D. Ward and C. M. White, *Chem. Commun*., 1997, 175.
10 S. Trofimenko, J. C. Calabrese and J. S. Thompson, *Inorg. Chem*., 1992, **31**, 974 and references therein.
11 S. Trofimenko, *Chem. Rev*., 1993, **93**, 943.
12 T. W. Bell, P. J. Cragg, M. G. B. Drew, A. Firestone and D.-I. A. Kwok, *Angew. Chem., Int. Ed. Engl*., 1992, **31**, 345.
13 G. Bombieri, G. Bruno, M. D. Grillone and G. Polizzotti, *Acta Crystallogr., Sect. C*, 1984, **40**, 2011.
14 E. C. Constable, M. J. Hannon and D. A. Tocher, *J. Chem. Soc., Dalton Trans*., 1993, 1883.
15 T. W. Bell, P. J. Cragg, M. G. B. Drew, A. Firestone, A. D.-I. Kwok, J. Liu, R. T. Ludwig and A. T. Papoulis, *Pure Appl. Chem*., 1993, **65**, 361.
16 E. C. Constable, M. J. Doyle, J. Healy and P. R. Raithby, *J. Chem. Soc., Chem. Commun*., 1988, 1262.
17 J.-M. Lehn and J. B. R. De Vains, *Helv. Chim. Acta*, 1992, **75**, 1221 and references therein.


*Received, 25th November 1996; Com. 6/07984I*

# The first structurally authenticated zerovalent heteroarene complex of a lanthanide; synthesis and X-ray structure of bis(2,4,6-tri-*tert*-butylphosphorin)holmium(O)

**Polly L. Arnold, F. Geoffrey N. Cloke,* Peter B. Hitchcock**

*The Chemistry Laboratory, School of Chemistry, Physics and Environmental Science, University of Sussex, Brighton, E. Sussex, UK BN1 9QJ*

**Holmium vapour reacts with 2,4,6-tri-*tert*-butylphosphorin to afford the zerovalent [Ho(η-$PC_5H_2Bu^t_3$-2,4,6)$_2$], the first structurally characterised complex of this class.**

The organometallic chemistry of the lanthanides has seen huge growth in recent years. Initial employment of ligands utilising purely electrostatic bonding was widespread, but recently the use of anionic and neutral π-ligands has emerged to encompass a wide range of complexes.[1,2] The reports of binding of only neutral ligands still remain predominantly in the field of low-temperature matrix-isolation studies, since the highly electropositive metal centre is difficult to stabilise in very low oxidation states.[3–5] Examples of stable compounds where binding to the lanthanide can be regarded as covalent in nature are the bis(tri-*tert*-butylarene) zerovalent lanthanides.[6] These complexes should not be considered as 'metastable' metal atoms isolated in the arene organic cavity, since thermochemical bond energy measurements supported by theoretical calculations have shown that the complexes which form are indeed thermodynamically stable with respect to their constituent metal atom and arenes, and that there is significant back bonding from the metal frontier orbitals.[7,8] The members of the series of f-element bis(η-1,3,5-tri-*tert*-butylbenzene)metal(O) compounds that have not been isolated at room temperature are either those where the promotion energy from $f^n$ to an $f^{n-1}d^1s^2$ configuration for bonding is prohibitively high, or those in which the atomic radius is presumably simply too large to allow kinetic stability through steric saturation.[6] We have been interested in synthesising further examples of these sandwich compounds using a variety of new ligands to access remaining members of the series, and explore the reactivity thereof.

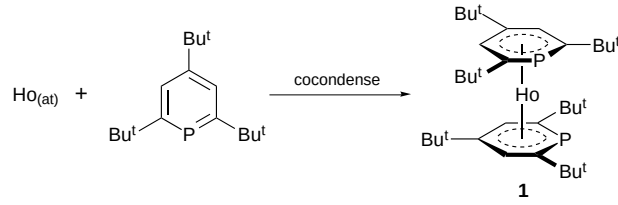
The replacement of a CH moiety by phosphorus is well documented, as is the effect on first-row transition-metal complexes synthesised from the resultant heteroarene.[9] The use of tri-*tert*-butylphosphorin both constrains the mode of bonding interaction to a π-arene type by hindering access to the phosphorus lone pair, and satisfies the requirement of steric saturation at the metal centre for stabilisation of such an electropositive metal.[10–13]

Cocondensation of holmium vapour with an excess of 2,4,6-tri-*tert*-butylphosphorin[14,15] at −196 °C leads to the formation of a dark purple matrix,[16] from which extremely air- and moisture-sensitive purple iridescent crystals of bis(2,4,6-tri-*tert*-butylphosphorin)holmium(O) **1**, can be isolated in gram quantities (45% yield) after work-up and recrystallisation from pentane (Scheme 1).†

The UV–VIS spectrum of **1** shows one absorption at 489 nm, ascribed to ligand-to-metal charge transfer. This is in accordance with prior observations of bathochromic shifts that related heterocyclic systems show with respect to their carbocyclic analogues {$\lambda_{max}$ [Ho(η-$C_6H_3Bu^t_3$-1,3,5)$_2$] = 507 nm}.[17] If the charge-transfer shift to higher energy is taken to imply stronger metal–ligand bonding, then this agrees well with the observation of the capacity of a phosphaarene to act as a better π-electron acceptor but similar electron donor towards a metal.[18,19]

The sandwich complex sublimes ($10^{-5}$ mbar) with around 90% recovery at 160 °C. This remarkable thermal stability enabled single crystals suitable for X-ray structural determination to be grown by vapour-phase diffusion. A Chem 3D representation of the structure is depicted in Fig. 1.‡ It is interesting that although the distortion of the arene from $C_{3v}$ symmetry on inclusion of the large heteroatom is considerable, the *tert*-butyl groups dominate the orientations of crystal packing, thus throughout the molecules in the lattice the phosphorus atoms evenly show 1/3 occupancy and the CH moieties 2/3 occupancy. No preference for *syn* or *anti* conformation of the rings in a single molecule can be inferred. The high solubility of the transition-metal complexes [V(η-$PC_5H_2Bu^t_3$-2,4,6)$_2$] and [Cr(η-$PC_5H_2Bu^t_3$-2,4,6)$_2$] mentioned by Elschenbroich *et al*. frustrated attempts to grow crystals suitable for X-ray structural determination.[13] Extensive disorder meant the data collected for single crystals of the titanium complex synthesised in our laboratory remained insoluble so no meaningful comparisons can be made. Elschenbroich *et al*. showed that in the phosphorus-expanded bis(arene) molecule, a smaller metal fits better if the rings have mutually *syn* rather than *anti* conformations. This is confirmed in our solution studies of the titanium complex, [$r_{cov}$(Ti) = 1.32 Å].[20] The greater size of this metal [$r_{cov}$(Ho) = 1.58 Å][21] is possibly a factor in allowing ready access to all relative conformations of the rings.

It is of interest that twelve of the *tert*-butyl methyl groups are oriented towards the central metal atom providing considerable steric shielding, Fig. 1(*c*), however no significantly short metal–carbon or –hydrogen distances are seen. This geometry was equally noticeable in the structures of [M(η-$C_6H_3Bu^t_3$-1,3,5)$_2$] (M = Ho, Gd, Y)[22] which are isostructural with each other and show little change in ring geometry apart from the expected slight ring C–C bond lengthening upon binding of the ligand. The phosphaarene bond lengths in **1** are consistent with retention of aromaticity in the heteroarene upon complexation, and the rings remain planar apart from the slight inclination of each phosphorus atom towards the metal, bending from the plane described by the five carbon atoms by an angle of 6.7(7)°.




**Scheme 1**

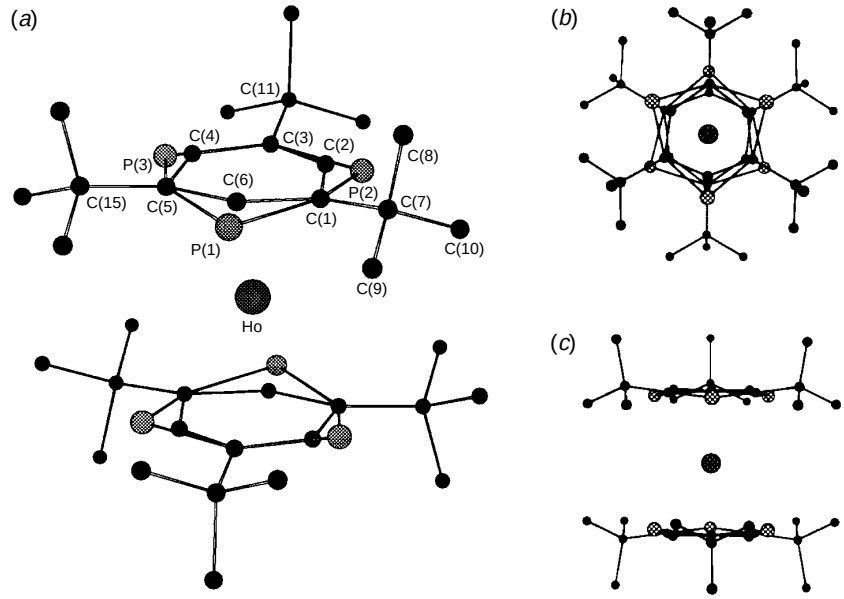



**Fig. 1** (*a*) Chem 3D Representation of the crystal structure of **1**. (*a*) All orientations of P and C have been included, as refined in the structure, allowing for the three-fold disorder: Selected distances (Å) and angles (°): Ho–C(1) 2.649(7), Ho–C(2) 2.587(14), Ho–C(3) 2.633(10), Ho–C(6) 2.58(2), P(1)–C(1) 1.797(10), P(2)–C(1) 1.785(10), P(2)–C(3) 1.760(8), C(1)–C(2) 1.42(2), C(1)–C(6) 1.45(12), C(1)–C(7) 1.495(13), C(2)–C(3) 1.44(2), C(3)–C(4) 1.44(2), C(3)–C(11) 1.52(2), C(7)–C(8) 1.44(2), C(7)–C(9) 1.43(2), C(7)–C(10) 1.39(2); C(1)–P(1)–C(5) 94.1(7), C(1)–P(2)–C(3) 95.9(6), C(2)–C(1)–C(7) 126.1(10), C(2)–C(1)–P(1) 125.8(9), C(7)–C(1)–P(1) 107.8(6), C(1)–C(2)–C(3) 134.0(13), C(4)–C(3)–C(2) 105(2). (*b*) Top view, all disordered atoms refined are included. (*c*) Side view.

The rings are mutually parallel with perfectly staggered *tert*-butyl groups, bent slightly away from the metal (8.8°).

Repeated determinations of the magnetism of a toluene solution of **1** (Evans' method) reproducibly yield an effective magnetic moment of 8.9 $\mu_B$, the solution displaying Curie–Weiss paramagnetism over the temperature range studied (205–355 K) with a value of $\theta = -10.6$ K. This value of the moment is lower than that calculated for the case where spin–spin coupling is small compared to $kT$ (10.75 $\mu_B$), and lower than that found in [Ho($\eta$-$C_6H_3Bu^t_3$-1,3,5)$_2$] (10.10 $\mu_B$) or atomic holmium (9.58 $\mu_B$). The lowering of symmetry of the frontier orbitals inflicted by the heteroatom conceivably allows more extensive degree of distribution of the unpaired electron density away from the metal *via* enhanced spin–orbit coupling; this would lead to the observed lower value for $\mu_{eff}$ in **1** as compared with [Ho($\eta$-$C_6H_3Bu^t_3$-1,3,5)$_2$].

The authors are grateful to Dr A. Abdul-Sada for determination of the mass spectrum of **1** and to the EPSRC for funding.

## Footnotes

† Holmium (0.65 g, 3.9 mmol) was vaporised by resistive heating (alumina crucible, 250 W) and cocondensed with an excess of 2,4,6-tri-*tert*-butylphosphorin (20 g, 76 mmol) at −196 °C. The dark purple matrix was extracted from the vessel at ambient temperature under an argon atmosphere. Removal of free metal by filtration through a bed of Celite and recovery of excess ligand after removal of volatiles under reduced pressure, yielded a dark solid from which extremely air- and moisture-sensitive purple iridescent crystals of bis(2,4,6-tri-*tert*-butylphosphorin)holmium(O) **1**, could be isolated in 45% yield, 1.2 g after recrystallisation from pentane. UV–VIS: $\lambda_{max}$ 489 nm ($\varepsilon$ 1.2 × $10^4$ dm$^3$ mol$^{-1}$). MS (EI): *m/z* 693 (69%) ($M^+$). Elemental analysis: Found C, 56.65; H, 8.47%. $C_{34}H_{58}HoP_2$ requires: C, 58.87; H, 8.43%. The low measured carbon percentage is also found for other complexes of this class, and is attributed to incomplete combustion.

‡ *Crystal data* for **1**: $C_{34}H_{58}HoP_2$, $M$ = 639.7, monoclinic, space group $C2/m$ (no. 12), $a$ = 10.279(3), $b$ = 17.758(3), $c$ = 10.293(2) Å, $\beta$ = 109.70°, $U$ = 1768.9(7) Å$^3$, $T$ = 293(2) K, $Z$ = 2, $D_c$ = 1.30 g cm$^{-3}$, 2 < $\theta$ < 25°, $\mu$(Mo-K$\alpha$) = 2.35 mm$^{-1}$. Dark purple block, crystal size 0.20 × 0.20 × 0.15 mm. Refinement on $F^2$ using SHELXL-93. $R_1$ = 0.048 for 1547 reflections with $I > 2\sigma(I)$, $wR_2$ = 0.126 for all 1621 unique reflections. The molecule lies on a site of 2/*m* symmetry and the $PC_5$ rings show threefold disorder. Atomic coordinates, bond lengths and angles, and thermal parameters have been deposited at the Cambridge Crystallographic Data Centre (CCDC). See Information for Authors, Issue No. 1. Any request to the CCDC for this material should quote the full literature citation and the reference number 182/363.

## References

1 W. J. Evans, *Polyhedron*, 1987, **6**, 803.
2 C. J. Schaverien, *Adv. Organomet. Chem*., 1994, **36**, 283.
3 J. A. Howard, B. Mile, C. A. Hampson and H. Morris, *J. Chem. Soc., Faraday Trans. 1*, 1989, **85**, 3953.
4 J. B. Schilling and J. L. Beauchamp, *J. Am. Chem. Soc*., 1988, **110**, 15.
5 K. J. Klabunde, in *Chemistry of Free Atoms and Particles*, 1980, Academic Press, London, ch. 10, p. 217.
6 F. G. N. Cloke, *Chem. Soc. Rev*., 1993, 17.
7 T. J. Marks, W. A. King, S. DiBella, G. Lanza, K. Khan, D. J. Duncalf, F. G. N. Cloke and I. L. Fragala, *J. Am. Chem. Soc*., 1996, **118**, 627.
8 T. J. Marks, S. DiBella, G. Lanza and I. L. Fragala, *Organometallics*, 1996, **15**, 3985.
9 C. Elschenbroich, M. Notowny, B. Metz, W. Massa, J. Graulich, K. Bieler and W. Sauer, *Angew. Chem., Int. Ed. Engl*., 1991, **30**, 547.
10 H. Lehmkuhl, R. Paul and R. Mynott, *Liebigs Ann. Chem*., 1981, 1139.
11 C. Elschenbroich, M. Notowny, A. Behrendt, W. Massa and S. Wocadlo, *Angew. Chem., Int. Ed. Engl*., 1992, **31**, 1343.
12 H.-D. Amberger and J. Ren, *J. Mol. Struct. (THEOCHEM.)*, 1991, **236**, 231.
13 C. Elschenbroich, F. Bär, E. Bilger, D. Mahrwald, M. Nowotny and B. Metz, *Organometallics*, 1993, **12**, 3373.
14 K. Dimroth and W. Mach, *Angew. Chem., Int. Ed. Engl*., 1968, **7**, 460.
15 G. Märkle, F. Lieb and A Merz, *Angew. Chem., Int. Ed. Engl*., 1967, **6**, 458.
16 M. L. H. Green and F. G. N. Cloke, *J. Chem. Soc., Dalton Trans*., 1981, 1938.
17 K. Khan, D. Phil, Thesis, University of Sussex, 1992.
18 A. J. Ashe III, P. D. Burrow, D. J. Bellville and K. D. Jordan, *J. Am. Chem. Soc*., 1982, **104**, 425.
19 A. J. Ashe III, J. Michl, J. Waluk and H.-D. Klein, *Organometallics*, 1989, **8**, 2804.
20 P. L. Arnold, F. G. N. Cloke, K. Khan and P. Scott, *J. Organomet. Chem*., 1996, in the press.
21 J. Emsley, *The Elements*, Oxford University Press, Oxford, 1989.
22 J. G. Brennan, F. G. N. Cloke, A. A. Samch and A. Zalkin, *J. Chem. Soc., Chem. Commun*., 1987, 1669.

*Received, 18th November 1996; Com. 6/07827C*

# Polycarbon ligand chemistry. Novel behaviour of μ-η¹,η²$_{\alpha,\beta}$-butadiynyls towards metal fragment additions

**Peter Blenkiron,[a] Gary D. Enright[a] and Arthur J. Carty*[a,b]**

[a] *The Steacie Institute for Molecular Sciences, National Research Council of Canada, 100 Sussex Drive, Ottawa, Ontario, Canada K1A OR6*

[b] *Department of Chemistry, University of Ottawa, Ottawa, Ontario, Canada K1N 6N5*

**Reaction of $[Ru_2(CO)_6(\mu\text{-}PPh_2)(\mu\text{-}\eta^1,\eta^2_{\alpha,\beta}\text{-}C{\equiv}C{-}C{\equiv}CR)]$ (R = Bu$^t$ 1a, Ph 1b) with the labile complexes $[Pt(PPh_3)_2(\eta\text{-}C_2H_4)]$, $[Pt(dppb)(\eta\text{-}C_2H_4)]$ and $[Ni(cod)_2]$ or $[Ni(CO)_4]$ leads to the heteronuclear derivatives $[Ru_2Pt(CO)_7(PPh_3)(\mu_3\text{-}\eta^1,\eta^1,\eta^1\text{-}C{=}C{-}C{\equiv}CR)(\mu\text{-}PPh_2)]$ 2a,b, $[Ru_2Pt(CO)_6(dppb)(\mu_3\text{-}\eta^1,\eta^1,\eta^1\text{-}C{=}C{-}C{\equiv}CBu^t)(\mu\text{-}PPh_2)]$ 2c and $[Ru_4Ni(CO)_{12}(\mu\text{-}PPh_2)_2(\mu_4\text{-}\eta^1,\eta^1,\eta^2,\eta^4\text{-}Bu^tC{\equiv}CC_4C{\equiv}CBu^t)]$ 3 resulting from addition of a $PtL_2$ fragment and Ni-assisted stoichiometric coupling of two molecules of 1a respectively; the X-ray crystal structures of 2a and 3 are described.**

The ability of ynyl and polyynyl [–C≡CR, –(C≡C)$_x$–] ligands to link metal centres into linear arrays bearing extended carbon–carbon unsaturation has stimulated the designed synthesis of molecular wires and rod-like new materials.[1] These highly unsaturated, carbon-rich chains possess even greater potential for the construction of two- and three-dimensional multimetallic arrays if the full coordinating capacity of the π systems can be exploited.[2,3] Here, we describe the addition of the reactive Pt and Ni reagents $[Pt(PPh_3)_2(\eta\text{-}C_2H_4)]$, $[Pt(dppb)(\eta\text{-}C_2H_4)]$ [dppb = 1,4-bis(diphenylphosphino)butane], $[Ni(cod)_2]$ and $[Ni(CO)_4]$ to the butadiynyl complexes $[Ru_2(CO)_6(\mu\text{-}PPh_2)(\mu\text{-}\eta^1,\eta^2_{\alpha,\beta}\text{-}C{\equiv}C{-}C{\equiv}CR)]$ (R = Bu$^t$ **1a**, Ph **1b**).

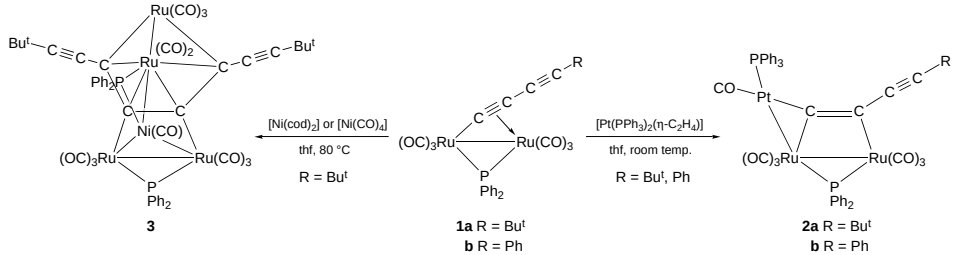
The σ–π butadiynyl complexes **1a** and **1b** react with $[Pt(PPh_3)_2(\eta\text{-}C_2H_4)]$ in thf to give the trinuclear mixed-metal species $[Ru_2Pt(CO)_7(PPh_3)(\mu_3\text{-}\eta^1,\eta^1,\eta^1\text{-}C{=}C{-}C{\equiv}CR)(\mu\text{-}PPh_2)]$ **2** (**2a** 18%, **2b** 22%) (Scheme 1).† The molecular structure of **2a** (Fig. 1)‡ suggest that **2a,b** are formed from the addition of a $Pt(CO)(PPh_3)$ fragment across the Ru–C$_\alpha$ bond of **1**. Thus **2a** contains the $Ru_2(CO)_6(\mu\text{-}PPh_2)$ unit found in **1** and is connected to Pt *via* Ru(1) to give a bent three-metal atom chain [Pt–Ru(1)–Ru(2) 105.837(17)°; Ru(1)–Pt 2.7725(13) Å]. The hydrocarbyl ligand is bound to all three metal atoms [Pt–C(38) 1.969(6), Ru(1)–C(38) 2.266(5), Ru(2)–C(39) 2.151(5) Å] and may be viewed as a metallated, alkynyl-functionalised μ-vinylidene bridging the Ru(1)–Pt bond *via* C(38) [C(38)–C(39) 1.284(8) Å]. The Pt centre is also ligated by a CO group [Pt–C(1) 1.905(7) Å] evidently scavenged from the reaction mixture and a $PPh_3$ ligand [Pt–P(2) 2.2884(13) Å] *trans* disposed to the Ru–Pt bond. The coordination environment about the Pt is approximately square planar and this moiety serves as a 16-electron fragment giving an overall count of 48 valence electrons for **2**, as found for other linear or bent $M_2Pt$ complexes.[4] The transition from a σ–π bonding mode in **1a** to 3σ attachment in **2a** effects a distortion in the C$_4$ ligand [C(38)–C(39)–C(40) 136.3(5)° *cf.* 164. 9(4)° for the corresponding angle in **1a**[5]], although the outer triple bond length is essentially unchanged at 1.170(9) [*cf.* 1.172(6) in **1a**].

A competing process in the reaction of **1** with $[Pt(PPh_3)_2(\eta\text{-}C_2H_4)]$ is phosphine substitution to give $[Ru_2(CO)_{6-n}(PPh_3)_n(\mu\text{-}PPh_2)(\mu\text{-}\eta^1,\eta^2_{\alpha,\beta}\text{-}C{\equiv}C{-}C{\equiv}CR)]$ [$n$ = 1 (R = Bu$^t$, 29%), $n$ = 2 (R = Bu$^t$, 13%)].§ Substitution is inhibited by using the chelating Pt complex $[Pt(dppb)(\eta\text{-}C_2H_4)]$ which reacts rapidly at 293 K with a thf solution of **1a** to give the addition product $[Ru_2Pt(CO)_6(dppb)(\mu_3\text{-}\eta^1,\eta^1,\eta^1\text{-}C{=}C{-}C{\equiv}CBu^t(\mu\text{-}PPh_2)]$ **2c** in 54% yield. X-Ray analysis confirmed **2c** as the analogue of **2a** and **2b**.

An isolobal analogy can be drawn between the reaction of **1** with the 14e moiety $Pt(CO)(PPh_3)$ and the well documented addition of d$^{10}$ $ML_2$ fragments to M=C bonds in mono- and poly-nuclear carbene and vinylidene complexes.[6] The Ru(1)=C$_\alpha$ unsaturation in **1a** presumably derives from a contribution of the canonical form Ru$^-$=C=C=C=C$^+$Bu$^t$ to the bonding in **1**.[5]

**1a** also reacted smoothly with the naked nickel precursor $[Ni(cod)_2]$. After 2 h in refluxing thf, work-up gave a single major product $[Ru_4Ni(CO)_{12}(\mu\text{-}PPh_2)_2(\mu_4\text{-}\eta^1,\eta^1,\eta^2,\eta^4\text{-}Bu^tC{\equiv}CC_4C{\equiv}CBu^t)]$ **3**.

The pentanuclear cluster **3** (Fig. 2) originates from the stoichiometric coupling of two molecules of **1a**, together with the incorporation of a single nickel atom which links the two $Ru_2$ units [Ru(2)–Ni 2.6910(16), Ru(3)–Ni 2.7042(17), Ru(4)–Ni 2.6957(16) Å]. The most outstanding feature of **3** is the head-to-head coupling of two butadiynyl ligands to create a C$_8$ chain which is attached to all four Ru atoms. This gives rise to a ruthenole unit formed from the π coordination of the Ru(1)–C(14)–C(13)–C(18)–C(19) ruthenacyclopentadiene ring to Ru(2). Although terminal, mononuclear butadiynyl ligands have been linked *via* oxidative coupling to generate linear C$_8$ chains,[1a,7] we are unaware of any examples of transition-metal mediated synthesis of C$_8$ ligands from binuclear or polynuclear C$_4$ precursors. The metallacyclopentadiene ring contains one long and two short C–C bonds [C(13)–C(14) 1.411(12), C(13)–C(18) 1.457(11), C(18)–C(19) 1.399(11) Å] in common with other crystallographically characterised examples from group 8, with the long bond bridging the Ru(3)–Ru(4) unit. This limited delocalisation extends to the exocyclic C(14)–C(15)




**3** **1a** R = Bu$^t$ **b** R = Ph **2a** R = Bu$^t$ **b** R = Ph

**Scheme 1**

[1.428(13) Å] and C(19)–C(20) [1.441(12) Å] bonds. Interestingly however, no elongation is apparent in the pendant alkynyl groups which exhibit typical $C_{sp}$–$C_{sp}$ bond distances [C(15)–C(16) 1.182(13), C(20)–C(21) 1.186(13)].

Clearly a key step in the formation of **3** is the incorporation of a Ni(CO) moiety. Thus refluxing a thf solution of **1a** with excess $Ni(CO)_4$ indeed gave **3** as the major product, albeit in slightly lower yield {15% *cf.* 20% with $[Ni(cod)_2]$}, possibly suggesting the role of free nickel [*vs.* Ni(CO)] as an intermediate in the assembly of **3**.

It is perhaps surprising that both **2** and **3** contain uncoordinated triple bonds derived directly from the outer alkyne unit of precursor **1**, particularly considering the propensity of $Pt^0$ and $Ni^0$ reagents to form $\eta^2$-coordination complexes with free alkynes. Since sterically congested alkynes form $\eta^2$-coordination complexes with $Pt^0$ and $Ni^0$, it is unlikely that the presence of Bu$^t$ or Ph substituents on the outer alkyne units of **1** account for the lack of complexation at these sites. However, while we believe this to be the first report detailing metal fragment additions to σ–π-butadiynyl complexes, there is evidence that metal aggregation ('clustering') occurs when fragments such as $PtL_2$ (L = $PR_3$, $L_2$ = cod) add to vinylidene and other hydrocarbyl-ligated species.[6] We suggest therefore that while

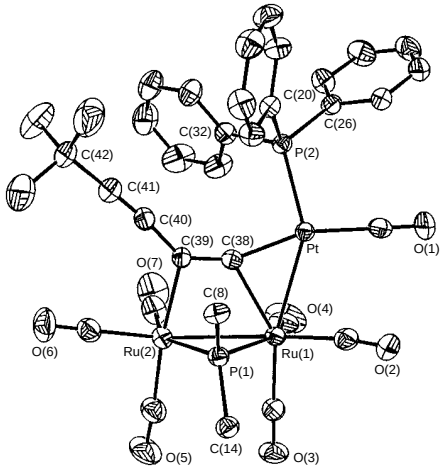



**Fig. 1** Molecular structure of **2a**. For clarity, only the *ipso* carbons of the μ-$PPh_2$ phenyl rings are drawn. Relevant bond parameters: Ru(1)–Ru(2) 2.8407(6), C(39)–C(40) 1.400(8) Å; Ru(1)–P(1)–Ru(2) 74.56(4), Ru(2)–Ru(1)–Pt 105.837(17), Ru(1)–C(38)–Pt 81.46(20), Pt–C(38)–C(39) 153.9(5), C(39)–C(40)–C(41) 172.1(6), C(1)–Pt–C(38) 162.00(24), P(2)–Pt–Ru(1) 149.38(4)°.

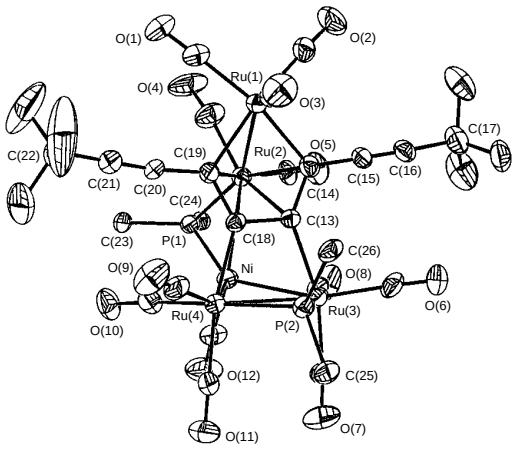



**Fig. 2** Molecular structure of **3**. Relevant bond parameters: Ru(1)–Ru(2) 2.6860(11), Ru(3)–Ru(4) 2.8981(10), Ru(1)–C(14) 2.114(9), Ru(1)–C(19) 2.097(9), Ru(2)–C(13) 2.300(8), Ru(2)–C(14) 2.269(9), Ru(2)–C(18) 2.379(8), Ru(2)–C(19) 2.270(8), Ru(3)–C(13) 2.139(8), Ru(4)–C(18) 2.119(8) Å; Ru(2)–Ni–Ru(3) 91.73(5), Ru(2)–Ni–Ru(4) 100.46(5)°.

**2a**–**c** are likely thermodynamic products and would not rearrange to the expected $\eta^2$-alkyne products, reaction at $C_\alpha$ may be driven by activation associated with μ-$\eta^1$,$\eta^2$ coordination. Such activation also accounts for recently observed regiospecificity in directing nucleophilic attack exclusively at the $C_\alpha$–$C_\beta$ sites[2a,8] in μ-$\eta^1$,$\eta^2$-butadiynyl complexes. These results suggest that metal activation of polyynyl ligands *via* μ-$\eta^1$,$\eta^2$-coordination can direct site specific metal fragment electrophilic attack and new patterns of C–C coupling.

We thank the NRC and NSERC for financial support of this work. We are indebted to G. Lesley and T. B. Marder for a sample of $[Pt(dppb)(C_2H_4)]$.

## Footnotes

† Experimental and spectroscopic data will be made available on the World Wide Web at http://chemistry.rsc.org/rsc/cccpub.htm

‡ *Crystallographic data*: **2a**: crystal grown from $CH_2Cl_2$–*n*-hexane (1 : 4) at –20 °C; $C_{45}H_{34}O_7P_2PtRu_2$, $M$ = 1145.9; monoclinic, space group $P2_1/n$, $a$ = 9.2369(6), $b$ = 23.0550(11), $c$ = 20.7034(8) Å, β = 97.596(5)°, $U$ = 4370.3(4) Å$^3$, $Z$ = 4, $T$ = 295 K, $D_c$ = 1.742 g cm$^{-3}$, $F$(000) = 2211, λ = 1.54056 Å, μ(Cu-Kα) = 12.70 mm$^{-1}$. Intensity data were collected on a crystal of dimensions 0.25 × 0.25 × 0.20 mm mounted on an Enraf-Nonius CAD4 diffractometer using the θ–2θ scan method. The structure was solved (direct methods) and refined (full-matrix least squares) using 6526 observed [$I > 2.5\ \sigma(I)$] reflections to final $R$ and $R_w$ values of 0.031 and 0.041 respectively.

**3**: crystal grown from *n*-hexane at −20 °C; $C_{52}H_{38}O_{12}NiP_2Ru_4$, $M$ = 1379.8; monoclinic, space group $P2_1/c$, $a$ = 11.4833(19), $b$ = 12.460(3), $c$ = 38.055(4) Å, β = 91.016(14)°, $U$ = 5444.3(17) Å$^3$, $Z$ = 4, $T$ = 295 K, $D_c$ = 1.683 g cm$^{-3}$, $F$(000) = 2717, λ = 1.54056 Å, μ(Cu-Kα) = 10.43 mm$^{-1}$. Intensity data were collected on a crystal of dimensions 0.03 × 0.20 × 0.20 mm as for **2a**. The structure was solved (direct methods) and refined (full-matrix least squares) using the 5211 observed [$I > 2.5\ \sigma(I)$] reflections to final $R$ and $R_w$ values of 0.043 and 0.049 respectively. Atomic coordinates, bond lengths and angles, and thermal parameters have been deposited at the Cambridge Crystallographic Data Centre (CCDC). See Information for Authors, Issue No. 1. Any request to the CCDC for this material should quote the full literature citation and the reference number 182/338.

§ Performing the reaction with **1a** under a purge of CO gas inhibited the formation of substitution products but gave exactly the same yield of **2a**. For **1b** using a CO purge, **2b** (22%) and the monophosphine complex $[Ru_2(CO)_5(PPh_3)(\mu\text{-}PPh_2)(\mu\text{-}\eta^1,\eta^2_{\alpha,\beta}\text{-}C{\equiv}C\text{–}C{\equiv}CPh)]$ (36%) were produced.

## References

1 (*a*) T. Bartik, B. Bartik, M. Brady, R. Dembinski and J. A. Gladysz, *Angew. Chem., Int. Ed. Engl.*, 1996, **35**, 414; (*b*) R. W. Lass, P. Steinert, J. Wolf and H. Werner, *Chem. Eur. J.*, 1996, **2**, 19; (*c*) D. Touchard, N. Pirio, L. Toupet, M. Fettouhi, L. Ouahab and P. H. Dixneuf, *Organometallics*, 1995, **14**, 5263; (*d*) M. J. Irwin, G. Jia, N. C. Payne and R. J. Puddephatt, *Organometallics*, 1996, **15**, 51; (*e*) J. Lewis, M. S. Khan, A. K. Kakkar, B. F. G. Johnson, T. B. Marder, H. B. Fyfe, F. Wittmann, R. H. Friend and A. E. Dray, *J. Organomet. Chem.*, 1992, **425**, 165.

2 (*a*) C. J. Adams, M. I. Bruce, E. Horn, B. W. Skelton, E. R. T. Tiekink and A. H. White, *J. Chem. Soc, Dalton Trans.*, 1993, 3299; (*b*) P. Blenkiron, N. J. Taylor and A. J. Carty, *J. Chem. Soc., Chem. Commun.* 1995, 327; (*c*) J. F. Corrigan, S. Doherty, N. J. Taylor and A. J. Carty, *Organometallics*, 1993, **12**, 1365.

3 H. Werner, O. Gevert, P. Steinert and J. Wolf, *Organometallics*, 1995, **14**, 1786; (*b*) W. Weng, A. M. Arif and J. A. Gladysz, *Angew. Chem., Int. Ed. Engl.*, 1993, **32**, 891.

4 P. Braunstein, G. Predieri, F. J. Lahoz and A. Tiripicchio, *J. Organomet. Chem.*, 1985, **288**, C13; D. Moras, J. Dehand and R. Weiss, *C. R. Acad. Sci., Ser. C*, 1968, **267**, 1471.

5 P. Blenkiron, D. Pilette, J. F. Corrigan, N. J. Taylor and A. J. Carty, *J. Chem. Soc., Chem. Commun.*, 1995, 2165; P. Blenkiron, J. F. Corrigan, D. Pilette, N. J. Taylor and A. J. Carty, *Can. J. Chem.*, in the press.

6 F. G. A. Stone, *Angew. Chem., Int. Ed. Engl.*, 1984, **23**, 89.

7 M. Brady, W. Weng and J. A. Gladysz, *J. Chem. Soc., Chem. Commun.*, 1994, 2655.

8 P. Blenkiron, G. D. Enright, N. J. Taylor and A. J. Carty, *Organometallics*, 1996, **15**, 2855.

*Received, 14th August 1996; Com. 6/05711J*

# Hexanuclear hydrolysis products of the uracil nucleobase complex (1,3-dimethyluracil-5-yl)mercury(II) nitrate

**Félix Zamora,[a] Michal Sabat,*[b] Matthias Janik,[a] Christoph Siethoff[c] and Bernhard Lippert*[a]**

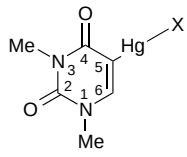
[a] *Fachbereich Chemie, Universität Dortmund, D-44221 Dortmund, Germany*
[b] *Department of Chemistry, University of Virginia, Charlottesville, Virginia 22901, USA*
[c] *Institut für Spektrochemie und angewandte Spektroskopie (ISAS), D-44139 Dortmund, Germany*

**(1,3-Dimethyluracil-5-yl)mercury(II) nitrate undergoes, in aqueous solution, hydrolysis to the tris(1,3-dimethyluracil-5-yl)mercurioxonium salt, which dimerizes in two different ways *via* weak Hg···Hg contacts.**

The propensity of mercury(II) salts to undergo hydrolysis with formation of oligo- and poly-meric $[Hg(OH)]_n^{n+}$ or $[HgO]_n$ species is well established.[1] This feature is maintained in complexes of $Hg^{II}$ containing one firmly bound ligand such as a methyl group. Thus, $[MeHg(H_2O)]^+$ forms, among others, the trismethylmercurioxonium cation, $[(MeHg)_3O]^+$,[2] which represents a very flat trigonal pyramid with the oxygen in the apical position.[3] $[(ClHg)_3O]^+$ has a very similar structure.[4] Here we report on hydrolysis products of an analogous complex with a C-bound uracil nucleobase (1,3-dimethyluracil, dmura) which have dimerized *via* one and two Hg···Hg contacts, respectively, of the $Hg_3O$ to give hexanuclear compounds. This feature is reminiscent of the behaviour of phosphinegold(I) oxonium compounds, $[(R_3PAu)_3O]^+$.[5] This appears to be a consequence of the well known tendency of $Au^I$ compounds to form weak Au–Au bonds and has been termed aurophilicity.[6]

We have recently described several examples of dmura nucleobase complexes containing $Hg^{II}$ bound *via* the C-5 position.[7–9] Mercuriation of this site, although not fully unexpected,[10] was unusual considering previous findings.[11,12]

In the course of an NMR study on ligand exchange reactions of X[8] we observed precipitation of a colourless, crystalline compound from aqueous solution, pH 4 in the presence of $X = NO_3^-$.† X-Ray crystallography‡ revealed that the unit cell of the compound contains two different $[L_3Hg_3O]^+$ cations, **I** and **II** (L = 1,3-dimethyluracil-5-yl), each of which has a centrosymmetrically related counterpart (primed atoms), with which it is connected through weak Hg···Hg contacts. Cation **I** represents a very flat pyramid, whereas cation **II** is virtually planar (Fig. 1). Hg···Hg distances within the triangle of **I** range from 3.4705(5) to 3.5859(5) Å. The short contacts of 3.5620(5) Å between neighbouring cations involve Hg(1) and Hg(2′) as well as Hg(2) and Hg(1′) and generate a chairlike arrangement of the six mercury ions. In cation **II** the Hg···Hg separations range from 3.4552(6) to 3.5974(5) Å within the triangle. The closest intercationic Hg···Hg distance, between Hg(6) and Hg(6′) is only slightly longer, 3.6728(8) Å. All these Hg···Hg separations are significantly longer than those found in dinuclear mercury(I) complexes or in mercury clusters with Hg in the oxidation state zero,[13] but are close to or shorter than the sum of two van der Waals radii (1.7–2.0 Å).[14] Hg–O–Hg angles are within the range 116.0(3)–122.5(3)° and compare with those found in $[(MeHg)_3O]^+$ (116°)[3] and $[(ClHg)_3O]^+$ (118.9°).[4] The Hg–O distances are normal (av. 2.05 Å), as are the Hg–C distances to the nucleobases (2.05 Å[7–9]). Views perpendicular to the $Hg_3$ triangles and their centrosymmetrical counterparts (Fig. 2) clearly show that nucleobase stacking is not taking place, thereby excluding this possibility as a driving force for association of trinuclear entities.




Solid-state Raman spectra of Hdmura, [Hg(dmura-$C^5$)($O_2$CMe)] and $[Hg_6(dmura)_2O_2][NO_3]_2$ were compared.§

The $^1$H NMR spectrum of the title compound in $D_2O$, pH* 4.9 [δ H-6, 7.40, $^3J(^1H–^{199}Hg)$ 189 Hz; δ $CH_3$, 3.40 and 3.30] is consistent with an oxygen donor *trans* to C-5 of dmura,[8] but permits no conclusions concerning the nature of the species in solution (monomer, trimer, hexamer).

However, ESI mass spectra¶ of $D_2O$ and $Me_2SO$ solutions of the title compound establish the formulation as $[Hg_6$-

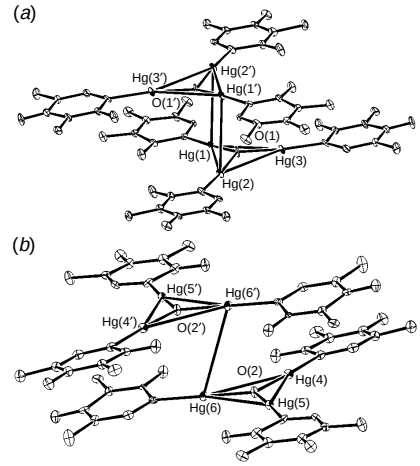



**Fig. 1** Perspective view of centrosymmetrically related cations **I** (*a*) and **II** (*b*) of $[L_3Hg_3O][NO_3]\cdot 2H_2O$ (L = 1,3-dimethyluracil-5-yl). Ellipsoids are at the 30% probability level.

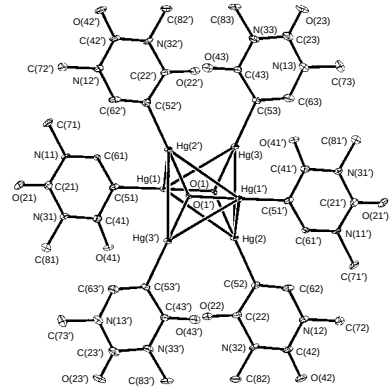


**Fig. 2** View perpendicular to $Hg_3$ triangles of cations **I** indicating that there is no base stacking within pairs of $[L_3Hg_3O]^+$ cations. The situation with cations **II** is similar, but the $Hg_3$ triangles are somewhat shifted.

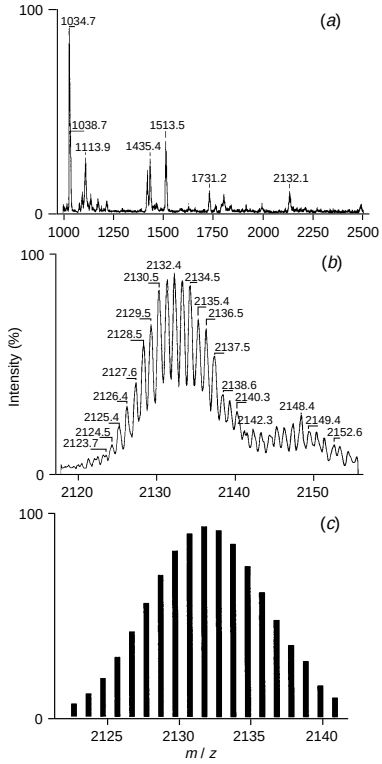



**Fig. 3** Section of ESI mass spectrum of the title compound (*a*), of the $[L_6Hg_6O_2(NO_3)]^+$ peak (*b*) and calculated mass distribution for the latter peak (*c*)

$(dmura)_6O_2][NO_3]_2$ even under the conditions of the experiment: from the mass spectrum recorded of a $Me_2SO$ solution (Fig. 3) the existence of $[Hg_6(dmura)_6O_2(NO_3)]^+$ is evident (*m*/*z* 2132.4), with excellent agreement between observed and calculated isotopic mass distributions. Signals due to $[Hg_3(dmura)_3O]^+$ (*m*/*z* 1034.7) are likewise observed, but the most intense signal centred at *m*/*z* 418.9 corresponds to $[Hg(dmura)(Me_2SO)]^+$. In aqueous solution the parent ion of the hexanuclear species is not observed, but fragments of the latter {$[Hg_4(dmura)_5O]^+$, *m*/*z* 1513.7; $[Hg_5(dmura)_5O_2]^+$, *m*/*z* 1729.5} point to its existence. The trinuclear species gives rise to an intense signal set at *m*/*z* 1035.5.

In conclusion, the solid-state structure of the title compound lends support to the option that $[Hg_3(dmura)_3O]^+$ cations, like $[(R_3PAu)_3O]^+$ cations, undergo association *via* Hg···Hg contacts. These appear to be sufficiently strong to survive ESIMS experiments.

This work was supported by the DFG and the FCI. We thank Dr M. Linscheid, ISAS (Dortmund), for providing the MS facilities, and Dr C. Campana, Siemens Analytical X-Ray Instruments, Inc., Madison, WI, for his help with the data collection and refinement.

## Footnotes

† In a typical experiment [Hg(dmura)($O_2$CMe)] (0.1 mmol) in water (2 ml) was treated with either $KNO_3$ or $AgNO_3$ (0.3 mmol each). From the solution (pH 4), upon standing at room temperature, colourless crystals formed overnight in *ca.* 40% yield. Alternatively, reaction of $Hg(NO_3)_2$ and dmura (1:1, 60 °C, 24 h) in $H_2O$ gave crystals of the title compound in 33% yield. {[Hg(dmura-$C^5$)]$_3$O}$NO_3$·$2H_2O$, $C_{18}H_{25}Hg_3N_7O_{12}$ [Found (Calc.)]: C, 18.9 (19.1); H, 2.2 (2.2); N, 8.6 (8.6) %. IR (KBr) 1341 ν($NO_3^-$), 1617 ν(C=C), 1670 $cm^{-1}$ ν(C=O). $^1$H NMR spectrum [200 MHz, $(CD_3)_2SO$, $SiMe_4$]: δ H-6, 7.35, δ $CH_3$, 3.32 and 3.19; $^3J(^1H–^{199}Hg)$ 190 Hz. $^{199}$Hg NMR [35.79 MHz, $(CD_3)_2SO$, relative to $HgMe_2$] δ −1320.

‡ *Crystal data* for $C_{36}H_{50}Hg_6N_{14}O_{24}$: $M$ = 2266.41, triclinic, space group $P\bar{1}$ (no. 2), $a$ = 10.0050(2), $b$ = 13.7841(2), $c$ = 19.6534(2) Å, α = 99.797(1), β = 95.673(1), γ = 96.313(1) °, $U$ = 2635.48(7) Å$^3$, $Z$ = 2, $D_c$ = 2.86 g $cm^{-3}$, λ(Mo-Kα) = 0.710 73 Å, μ(Mo-Kα) = 175.9 $cm^{-1}$, $F$(000) = 2072, $T$ = 153 K. The structure was solved by direct methods employing the SIR88 program[17] of the teXsan 1.7 software package[18] and refined by using the SHELXTL/PC software package[19] to $R$ = 0.061 ($R_w$ = 0.122) for 14 874 absorption-corrected (empirical corrections; transmission factors 0.23–0.80) reflections with $I > 2\sigma(I)$. A total of 38 024 (26 669 unique, $R_{int}$ = 0.052) reflections were collected in the range $4 \leqslant 2\theta \leqslant 80°$ on a Siemens SMART area detector system using graphite-monochromated Mo-Kα radiation. All non-hydrogen atoms were refined with anisotropic thermal displacement parameters. Atomic coordinates, bond lengths and angles, and thermal parameters have been deposited at the Cambridge Crystallographic Data Centre (CCDC). See Information for Authors, Issue No. 1. Any request to the CCDC for this material should quote the full literature citation and the reference number 182/353.

§ Bands at 215 and 109 $cm^{-1}$ are tentatively assigned to ν[Hg–C(dmura)] and ν(Hg–O). The respective modes for $[(MeHg)_3O]^+$ in $H_2O$ are at 570 and 134 $cm^{-1}$.[15] A band at 198 m $cm^{-1}$ in the spectrum of [Hg(dmura-$C^5$)($O_2$CMe)], absent in the spectrum of Hdmura, is assigned to ν[Hg–C(dmura)] from comparison with ν(Hg–Ph) modes.[16] Raman solution spectra could not be obtained due to insufficient solubility.

¶ Electrospray mass spectrometry (ESIMS) was performed on a Finnigan MAT 90 mass spectrometer equipped with an ESI II interface (Finnigan MAT, Bremen, Germany) operating in the positive mode. The mass spectra were acquired from *m*/*z* 250 to 2500 using scan rates between 5 and 100 s $decade^{-1}$ and a resolution between 1000 and 2500. Water and $Me_2SO$ solutions of the title compound were introduced into the ESI source at a flow rate of 0.5 μl $min^{-1}$. The temperature of the desolvation capillary was set to 200 °C.

## References

1 K. Brodersen and H.-U. Hummel, *Comprehensive Coordination Chemistry*, ed. G. Wilkinson, R. D. Gillard and J. A. McCleverty, Pergamon, Oxford, 1987, vol. 5, pp. 1047–1097.
2 D. L. Rabenstein, *Acc. Chem. Res.*, 1978, **11**, 100.
3 D. Grdenic, B. Kamenar and S. Povec, *Acta Crystallogr., Sect. A*, 1978, **34**, S127.
4 K. Aurivillius, *Arkiv Kemi*, 1964, **22**, 517; 537.
5 A. N. Nesmeyanov, E. G. Perevalova, Yu. T. Struchkov, M. Yu. Antipin, K. I. Grandberg and V. P. Dyadchenko, *J. Organomet. Chem.*, 1980, **201**, 343; Y. Yang, V. Ramamoorthy and P. R. Sharp, *Inorg. Chem.*, 1993, **32**, 1946; K. Angermaier and H. Schmidbaur, *Inorg. Chem.*, 1994, **33**, 2069.
6 H. Schmidbaur, *Gold Bull.*, 1990, **23**, 11; *Interdisc. Sci. Rev.*, 1992, **17**, 213; D. M. P. Mingos, *J. Chem. Soc., Dalton Trans.*, 1996, 561; R. J. Puddephatt, *Comprehensive Coordination Chemistry*, ed. G. Wilkinson, R. D. Gillard and J. A. McCleverty, Pergamon, Oxford, 1987, vol. 5, pp. 861–923.
7 M. Höpp, A. Erxleben, I. Rombeck and B. Lippert, *Inorg. Chem.*, 1996, **35**, 397.
8 F. Zamora, M. Sabat and B. Lippert, *Inorg. Chem.*, 1996, **35**, 4858.
9 F. Zamora, M. Kunsman, M. Sabat and B. Lippert, *Inorg. Chem.*, 1997, in the press.
10 R. M. K. Dale, D. C. Livingston and D. C. Ward, *Proc. Natl. Acad. Sci. USA*, 1973, **70**, 2238. L. Skulski, A. Kujawa and T. M. Kujawa, *Bull. Pol. Acad. Sci. Chem.*, 1987, **35**, 499. P. H. Toma, J. M. Dalla Riva Toma and D. E. Bergstrom, *Acta Crystallogr., Sect. C*, 1993, **49**, 2047.
11 M. Goodgame and K. W. Johns, *Inorg. Chim. Acta*, 1978, **30**, L335; B. A. Cartwright, M. Goodgame, K. W. Johns and A. C. Skapski, *Biochem. J.*, 1978, **175**, 337.
12 J. A. Carrabine and M. Sundaralingam, *Biochemistry*, 1971, **10**, 292.
13 K. Wurst and J. Strähle, *Z. Anorg. Allg. Chem.*, 1991, **595**, 239 and references therein.
14 A. J. Canty and G. B. Deacon, *Inorg. Chim. Acta*, 1980, **45**, L225.
15 D. L. Rabenstein, C. A. Evans, M. C. Tourangean and M. T. Fairhurst, *Anal. Chem.*, 1975, **47**, 338.
16 P. L. Goggin and D. M. McEwan, *J. Chem. Res. (S)*, 1978, 171.
17 M. C. Burla, M. Camalli, G. Cascarano, C. Giacovazzo, G. Polidori, R. Spagna and D. Viterbo, *J. Appl. Crystallogr.*, 1989, **22**, 389.
18 teXsan 1.7, Single Crystal Structure Analysis Software, Molecular Structure Corp., The Woodlands, TX, 1995.
19 G. M. Sheldrick, SHELXTL/PC, Siemens Analytical X-Ray Instruments, Inc., Madison, WI, 1995.

*Received, 21st October 1996; Com. 6/07186D*

# Synthesis, isolation and spectroscopic characterisation of 3-chloro-[6](2,4)-troponophane: the first 2,4-polymethylene-bridged troponoid

**Martin G. Banwell* and Hans M. Schuhbauer**

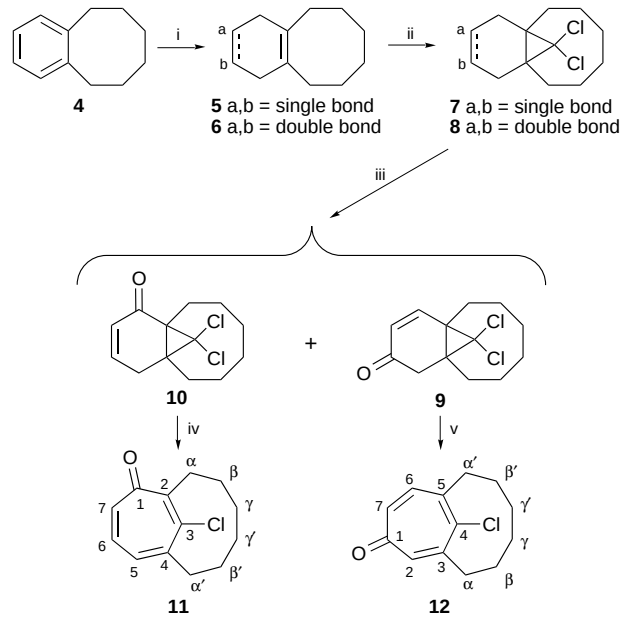
*Research School of Chemistry, Institute of Advanced Studies, The Australian National University, Canberra, ACT 0200, Australia*

**Treatment of the tricyclic enone 10 with perchloric acid results in formation of the title troponophane 11, the first example of a (2,4)-polymethylene bridged troponoid.**

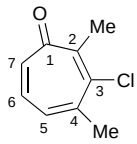
The delocalisation energies per electron within non-benzenoid rings are usually substantially smaller than those associated with comparable benzenoid rings. Consequently, short-bridged non-benzenoid cyclophanes have attracted considerable attention because of the expectation that there is likely to be greater deformation (relative to benzenoid counterparts) of the conjugated carbocyclic ring in accommodating any strain created by the introduction of bridges between non-adjacent ring carbons.[1] There is a further expectation that such deformations will be manifested in unusual reactivity patterns.[1] Studies of troponophanes have been especially interesting in this regard and numerous [*n*](2,7)-troponophanes **1** have been described including trimethylene-bridged systems ($n = 3$).[1,2] Their [*n*](3,5) counterparts **2** are much less common[3] but include a system where $n = 6$.[4] In contrast, [*n*](2,4)-troponophanes **3** remain virtually unknown.[5] Calculations† suggest that for a given value of *n* (where $n \leqslant 6$) the order of stability amongst the '*meta*'-troponophanes is **1** > **2** > **3** meaning that the last system is probably the most strained of the three and, therefore, likely to be the most interesting. Consequently, we now report on the synthesis, isolation, spectroscopic properties and some aspects of the chemistry of the title compound **11**, the first example of a 2,4-polymethylene-bridged troponoid.

The synthesis of compound **11** is outlined in Scheme 1 and follows very much the same strategy as used in the preparation of the isomeric [6](3,5)-troponophane **12**.[4] Thus, Birch reduction of cyclooctene **4**[7] with lithium in liquid ammonia afforded a *ca*. 15 : 1 : 100 mixture of compounds **4**, **5**[8] and **6**[9] which was subjected to reaction with chloroform–potassium *tert*-butoxide in diethyl ether between −30 and 20 °C. In this manner dichlorocarbene adducts **7**[4] (< 1%) and **8** (75% from **4**) (mp 86–88 °C; lit.,[4] mp 87–88 °C) were obtained and these could be separated from one another by fractional crystallisation. Allylic oxidation of alkene **8** was accomplished using the chromium trioxide–3,5-dimethylpyrazole (3,5-DMP) complex,[10] and the enones **9**[4] (44%) and **10**‡ (20%) (mp 97–100 °C) thereby obtained were separated from one another by chromatography on silica.[11] Treatment of a *ca*. 0.3 M chloroform solution of compound **10** with *ca*. 12 equiv. of 70% aq. perchloric acid resulted in its slow (20 h at 20 °C) conversion into the target troponophane **11**§ (71%) which could be isolated by flash chromatography[11] on silica gel ($R_f$ 0.5 in $CH_2Cl_2$) and which was obtained as a light green oil. Enone **9** was subjected to similar conditions in order to provide a sample of the isomeric troponophane **12** which was identical with material obtained previously.[4]

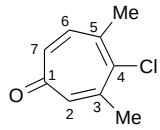
The $^1$H NMR spectrum of compound **11** possessed features strongly suggestive of the presence of a phane system. Thus, the one-proton multiplet at δ 0.43 is assigned to one of the protons associated with $C_\gamma$ of the hexamethylene bridge which is forced to project into the shielding zone of the troponoid ring. In addition, the chemical shifts (δ 3.14–2.93) and the multiplicities of the signals due to three of the four protons attached to $C_\alpha$ and $C_\alpha'$ are reminiscent of those reported for the analogous protons in 13-bromo[7]-metacyclophane[12] and [7](3,7)-tropolonophane.[13] The fourth such proton (attached to $C_\alpha$) resonates upfield, at δ 1.87, by virtue of its projecting into the shielding zone of the adjacent carbonyl group. Spectral comparisons were made with the model compound **13** (mp 52–55 °C)§ (readily prepared by established methods[14] from *o*-xylene). The low field regions in the $^{13}$C NMR spectra of these two compounds were similar although the resonance due to C-1 in troponophane **11** was deshielded by 1.7 ppm relative to its counterpart in tropone **13**, an observation consistent with the expectation that the troponoid ring within the former compound is buckled. In the $^1$H NMR spectra of compounds **11** and **13**, signal multiplicities and coupling constants for the troponoid ring protons were essentially identical but the chemical shifts of the



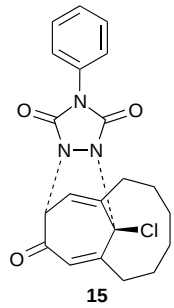

**Scheme 1** *Reagents and conditions*: i, Li (19 mol), $NH_3$, −78 °C then **4** in THF, $Bu^tOH$, −78 to −30 °C, 5.5 h then MeOH; ii, $Bu^tO^-K^+$ (1.6 equiv.), $CHCl_3$ (1.5 equiv.), $Et_2O$, −30 to 20 °C, 16.5 h; iii, $CrO_3$ (30 equiv.), 3,5-DMP (30 equiv.), $CH_2Cl_2$, −20 to −10 °C, 3.5 h; iv, 70% aq. $HClO_4$ (*ca*. 12 equiv.), $CHCl_3$, 20 °C, 20 h; v, 70% aq. $HClO_4$ (*ca*. 12 equiv.), $CHCl_3$, 20 °C, 1 h




**13**




**14**




**15**

**Table 1** Comparison of selected $^1$H NMR spectral parameters for compounds **11**–**14** (acquired in $C_6D_6$ solution at 21.2 °C)

| | δ | | | | Coupling constants/Hz | | |
|---|---|---|---|---|---|---|---|
| | H-2 | H-5 | H-6 | H-7 | $J_{2,7}/J_{7,2}$ | $J_{5,6}/J_{6,5}$ | $J_{6,7}/J_{7,6}$ |
| **11** | | 5.58 | 6.03 | 6.44 | | 6.0 | 11.9 |
| **13** | | 5.90 | 6.03 | 6.65 | | 8.6 | 11.8 |
| Δδ | | −0.32 | 0.00 | −0.21 | | | |
| **12** | 6.13 | | 5.97 | 6.41 | 2.7 | | 12.0 |
| **14** | 6.85 | | 6.03 | 6.63 | 2.7 | | 12.2 |
| Δδ | −0.72 | | −0.06 | −0.22 | | | |

signals due to two of the troponoid ring protons in **11** were shielded relative to their counterparts in model **13**, a situation similar to that observed previously in comparing troponophane **12** with model compound **14**[4] (Table 1).

The behaviour of troponophane **11** towards cycloaddition processes has been examined but we have yet to obtain convincing evidence of the participation of this compound in any such reaction. In contrast, the isomeric troponophane **12** reacts almost instantaneously with 4-phenyl-3,5-dihydro-1,2,4-triazole-3,5-dione (in $CH_2Cl_2$ at 20 °C) to give adduct **15**§ (mp 210–212 °C) in 95% yield. These observations are consistent with semi-empirical calculations† which suggest that troponophane **12** has a higher lying HOMO than isomer **11** ($\Delta E$ = 0.23 eV) and should, therefore, be more reactive towards electron-deficient dienophiles in normal electron demand Diels–Alder cycloaddition processes.

We thank the Institute of Advanced Studies for financial support including the provision of a post-Doctoral Stipend to H. M. S. for the period from June 1996 to the present. The award of a Deutsche Forschungsgemeinschaft (DFG) Fellowship to H. M. S. for the period from June 1995 to May 1996 is also gratefully acknowledged. We thank Professor L. Radom and members of his group (ANU) for assistance with theoretical calculations and Associate Professor D. Ridley (University of Sydney) for CAS Online substructure searching.

## Footnotes

† AM1 semi-empirical calculations (ref. 6) were carried out using the SPARTAN ver. 4.1.1 software package (as provided by Wavefunction Inc., Irvine, CA. 92715) on a Silicon Graphics workstation.

‡ All new compounds had spectroscopic data [IR, UV (where appropriate), NMR and mass spectrum] consistent with the assigned structure. Satisfactory combustion and/or high resolution mass spectral analytical data were obtained for all new compounds. Reported yields refer to isolated materials.

§ *Selected spectral data* for **11**: $^{13}$C NMR (75 MHz, $C_6D_6$): δ 186.4 (C), 151.7 (C), 148.7 (C), 144.4 (C), 136.6 (CH), 132.9 (CH), 121.4 (CH), 34.5 ($CH_2$), 34.3 ($CH_2$), 29.9 ($CH_2$), 28.7 ($CH_2$), 26.8 ($CH_2$) and 26.4 ($CH_2$); $^1$H NMR (300 MHz, $C_6D_6$): δ 6.44 (d, *J* 11.9 Hz, 1 H, H 7), 6.03 (dd, *J* 11.9 and 6.0 Hz, 1 H, H 6), 5.58 (d, *J* 6.0 Hz, 1 H, H 5), 3.14–2.93 (complex m, 3 H), 1.87 (ddd, *J* 13.7, 8.3 and 3.3 Hz, 1 H), 1.76–1.56 (complex m, 2 H), 1.48–1.22 (complex m, 3 H), 1.18–1.02 (complex m, 2 H), 0.43 (m, 1 H); MS *m/z* (El, 30 eV) 225 (3%) 223 (9) [(M + H)$^+$], 224 (16) 222 (50) [M$^+$], 188 (54) [(M + H − Cl·)$^+$], 187 (100) [(M − Cl·)$^+$] and 159 (45) [(M − CO − Cl·)$^+$]; $\nu_{max}$(NaCl)/cm$^{-1}$ 1626 and 1597; $\lambda_{max}$($CHCl_3$)/nm 266 (log ε 3.99) and 354 (3.54) (HRMS: M$^+$, 222.0815. $C_{13}H_{15}{}^{35}ClO$ requires M$^+$, 222.0811). For **13**: $^{13}$C NMR (75 MHz, $C_6D_6$): δ 184.7 (C), 148.4 (C), 145.7 (C), 142.9 (C), 136.3 (CH), 132.5 (CH), 129.4 (CH), 28.0 ($CH_3$) and 21.6 ($CH_3$); $^1$H NMR (300 MHz, $C_6D_6$): δ 6.65 (br d, *J* 11.8 Hz, 1 H, H 7), 6.03 (dd, *J* 11.8 and 8.6 Hz, 1 H, H 6), 5.90 (br d, *J* 8.6 Hz, 1 H, H 5), 2.46 (s, 3 H, $CH_3$) and 1.89 (s, 3 H, $CH_3$); $\nu_{max}$(KBr)/cm$^{-1}$ 1628 and 1576; $\lambda_{max}$($CHCl_3$)/nm 250 (log ε 4.06) and 318 (3.77). For **15**: $^{13}$C NMR (75 MHz, $CDCl_3$): δ 186.2 (C), 168.9 (C), 150.6 (C), 130.6 (C), 129.2 (CH), 128.7 (CH), 125.5 (CH), 125.0 (CH), 118.7 (CH), 84.8 (C), 63.0 (CH), 37.4 ($CH_2$), 31.6 ($CH_2$), 29.7 ($CH_2$), 26.5 ($CH_2$), 24.8 ($CH_2$) and 23.1 ($CH_2$) (two signals obscured or overlapping); $^1$H NMR (300 MHz, $CDCl_3$): δ 7.45–7.35 (complex m, 5 H), 6.26 (d, *J* 7.7 Hz, 1 H, H 6), 5.83 (d, *J* 1.1 Hz, 1 H, H 2), 5.25 (dd, *J* 7.7 and 1.1 Hz, 1 H, H 7), 3.09 (m, 2 H), 2.46 (m, 2 H), 2.28 (m, 1 H), 1.91 (m, 1 H), 1.55 (m, 5 H), 1.23 (m, 1 H); $\nu_{max}$(KBr)/cm$^{-1}$ 1727, 1672 and 1403 (HRMS: M$^+$, 397.1195. $C_{21}H_{20}{}^{35}ClN_3O_3$ requires M$^+$, 397.1193).

## References

1 For general reviews on non-benzenoid cyclophanes, see S. Ito, Y. Fujise and Y. Fukazawa, *Org. Chem. (N.Y.)*, 1983, **45** (Cyclophanes, Vol. 2), 485; S. Ito, *Pure Appl. Chem*., 1982, **54**, 957.

2 E. Kloster-Jensen and C. Rømming, *Acta Chem. Scand.*, 1992, **46**, 309 and references cited therein; Y. Mazaki, Y. Fujise, Y. Fukazawa and S. Ito, *Tetrahedron Lett*., 1987, **28**, 977 and references cited therein; K. Kubo, A. Mori and H. Takeshita, *Heterocycles*, 1993, **36**, 1941.

3 M. G. Banwell, R. W. Gable, J. H. Ryan and M. F. Mackay, *J. Chem. Soc., Chem. Commun*., 1994, 1015; H. Yamaga, Y. Fujise and S. Ito, *Tetrahedron Lett*., 1987, **28**, 585; some evidence for the transient existence of [4](3,5)-troponophanes has been provided: H. J. Lindner, B. Kitschke, M. Liesner and D. Seebach, *Helv. Chim. Acta*, 1977, **60**, 1151.

4 M. G. Banwell and J. H. Ryan, *J. Chem. Soc., Chem. Commun*., 1994, 1603.

5 It has been reported that subjection of α-tropolone to reaction with horseradish peroxidase/hydrogen peroxide affords an oxidatively coupled and tetrameric species which has been assigned a [13](2,4)-troponophane structure (V. Kahn and A. Andrawis, *Phytochemistry*, 1985, **24**, 909). However, in our opinion, this assignment must be viewed with some caution since structural characterisation only involved UV–VIS spectroscopic studies. To the best of our knowledge, this represents the only example of a 2,4-bridged troponoid reported to date.

6 M. J. S. Dewar, E. G. Zoebisch, E. F. Healy and J. J. P. Stewart, *J. Am. Chem. Soc*., 1985, **107**, 3902.

7 R. Huisgen and W. Rapp, *Chem. Ber*., 1952, **85**, 826.

8 V. Dave and J. S. Whitehurst, *Tetrahedron*, 1974, **30**, 745.

9 L. A. Paquette, T. Kakihana, J. F. Hansen and J. C. Phillips, *J. Am. Chem. Soc*., 1971, **93**, 152.

10 W. G. Salmond, M. A. Barta and J. L. Havens, *J. Org. Chem*., 1978, **43**, 2057.

11 W. C. Still, M. Kahn and A. Mitra, *J. Org. Chem*., 1978, **43**, 2923.

12 S. Hirano, H. Hara, T. Hiyama, S. Fujita and H. Nozaki, *Tetrahedron*, 1975, **31**, 2219.

13 H. Saito, Y. Fujise and S. Ito, *Tetrahedron Lett*., 1984, **25**, 4761.

14 M. G. Banwell, *Aust. J. Chem*., 1991, **44**, 1; M. G. Banwell, *J. Chem. Soc., Chem. Commun*., 1982, 847.

*Received, 25th November 1996; Com. 6/07962H*

# Diastereoselective formation of *P* and *M* dicopper(I) double helicates with chiral 2,2′:6′,2″-terpyridines

**Edwin C. Constable,*† Torsten Kulke, Markus Neuburger and Margareta Zehnder**

*Institut für Anorganische Chemie, Spitalstrasse 51, CH-4056 Basel, Switzerland*

**Chiral 2,2′:6′,2″-terpyridines bearing bornyl groups in the 6-position are prepared; these ligands preferentially form *P* or *M* dinuclear double helicates upon coordination to copper(I) which have been structurally characterised.**

Oligopyridines and oligopyridine metal-binding domains are a recurrent feature in metallosupramolecular chemistry.[1] It is now well established that the higher oligopyridines can give multiple helical transition-metal complexes[2] and that 2,2′:6′,2″-terpyridine is a prototype ligand which forms dicopper(I) double helicates.[3] We have recently addressed questions of directionality within helicates assembled from asymmetric ligand threads[4] and now extend these studies to the diastereoselective formation of helicates from chiral ligands. Although preorganised chiral ligands bearing multiple oligopyridine domains have been shown to lead to diastereomeric excesses of multiple helicates,[5,6] this report provides the first fully characterised example of high diastereomeric discrimination in a multi-component self-assembly process.

A pair of enantiomeric 2,2′:6′,2″-terpyridines, $L^1$ and $L^2$, was obtained from the reaction of 6-bromo-6″-methyl-2,2′:6′,2″-terpyridine[7] with the sodium salts of (1*S*)-(−) or (1*R*)-(+)-borneol (prepared *in situ* by reaction of the appropriate alcohols with sodium hydride) in *N*,*N*-dimethylformamide in 52 and 58% yield respectively. These reactions are stereoretentive and allow the facile and selective introduction of functionality from the chiral pool.

The coordination of 2,2′:′,2″-terpyridines to copper(I) in the absence of other good ligands yields dinuclear double-helical $[Cu_2L_2]^{2+}$ species.[3] With the new chiral ligands there are a number of possible double helicates (Fig. 1). Firstly, head-to-head (HH) or head-to-tail (HT) isomers might be expected. Secondly, each double helix is itself chiral and might possess a *P* or an *M* conformation. When chiral ligands are involved, the (*S**)(*S**)-(*M*) and (*S**)(*S**)-(*P*) forms are diastereomers. We hoped that the energy differences between the diastereomers might lead to partial or complete selectivity for the *P* or *M* forms.

The reaction of $L^1$ or $L^2$ with $[Cu(MeCN)_4][PF_6]$ in acetonitrile resulted in the formation of orange–red solutions from which orange solids were precipitated by the addition of $[NH_4][PF_6]$. Mass spectrometric analysis supported the formulation of these solids as $[Cu_2L^1_2][PF_6]_2$ or $[Cu_2L^2_2][PF_6]_2$ respectively. The $^1$H NMR spectra of $CD_3CN$ solutions of the two complexes were similar and indicated, in each case, the presence of two solution species present in a ratio of 6.5 : 1. Molecular modelling studies using parameters derived from structurally characterised $[Cu_2L_2]^{2+}$ double helicates with 2,2′:6′,2″-terpyridines‡ indicated that the enantiomeric (*S*)(*S*)-(*M*)-HT and (*R*)(*R*)-(*P*)-HT helicates should be stabilised with respect to the diastereomers (*R*)(*R*)-(*M*)-HT and (*S*)(*S*)-(*P*)-HT by about 10 kcal mol$^{-1}$ (1 cal = 4.184 J). Furthermore, the modelling studies indicated that the HH isomers would lie very much higher in energy.

Recrystallisation of the crude $[Cu_2L^1_2][PF_6]_2$ or $[Cu_2L^2_2][PF_6]_2$ complexes from acetonitrile by the diffusion of diethyl ether vapour into the solution yielded X-ray quality crystals of compounds shown by $^1$H NMR spectroscopy to contain only the major isomer in each case. Each of the compounds crystallised as bis(acetonitrile) solvates in the non-centrosymmetric space group $P2_12_12$ and the molecular structures of $[Cu_2L^1_2][PF_6]_2\cdot2MeCN$ and $[Cu_2L^2_2][PF_6]_2\cdot2MeCN$ are presented in Fig. 2(*a*) and (*b*).§ The X-ray structural determination confirms the formation of the HT isomers in the solid state and furthermore shows the diastereoselective formation of the predicted (*S*)(*S*)-(*M*)-HT isomer of the $[Cu_2L^1_2]^{2+}$ cation and the (*R*)(*R*)-(*P*)-HT isomer of the $[Cu_2L^2_2]^{2+}$ cation. The solid-state structures of the two enantiomers are identical within experimental error and the gross structural features of the complex cations closely resemble those of previously characterised $[Cu_2L_2]^{2+}$ double helicates with 2,2′:6′,2″-terpyridines[3] although the pitch is dependent on the intermetallic separation; in this case, the copper–copper distance in each of the cations is 2.688(1) Å. The precise coordination geometry in copper(I) tpy double helicates is rather variable,[3] but in this case the two copper centres are equivalent and best described as two-coordinate [Cu(1)–N(1) 1.947(3) Å, Cu(1)–N(3′) 1.940(3) Å, N(1)–Cu(1)–N(3′) 165.2(1)°]. Each copper exhibits longer contacts to N(2) and N(2′) [2.431(2), 2.317(3) Å].

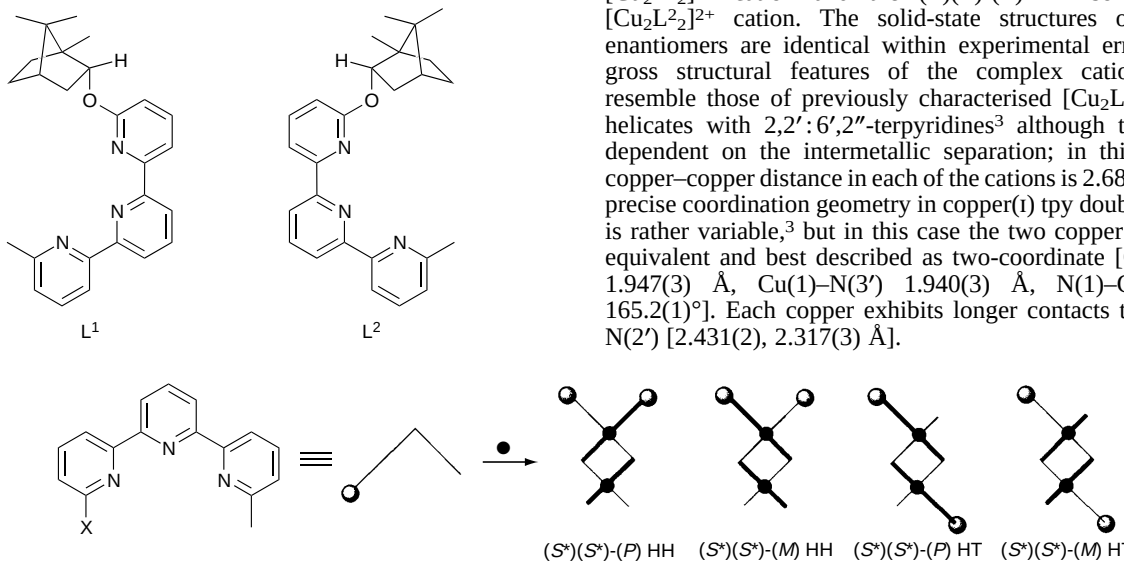



**Fig. 1** The formation of a dinuclear double helicate from the reaction of a chiral 2,2′:6′,2″-terpyridine with copper(I) can yield a pair of diastereomeric HH and a pair of diastereomeric HT compounds. *S** denotes homochiral compounds [*i.e.* either (*S*,*S*) or (*R*,*R*)]; ● = $Cu^I$.

The formation of the HT rather than HH isomers minimises steric interactions between the chiral substituents. The origin of the diastereoselectivity is not so easy to understand; no single interaction appears to be responsible, and, in contrast to previous studies[6] there is no obvious steric destabilisation of the less-favoured helicate. We are currently further studying the origin of this selectivity.

In conclusion, we have unambiguously demonstrated the diastereoselective formation of *P* or *M* helicates upon the coordination of chiral helicands to copper(I). We are currently extending these studies to increase the diastereoselectivity and to observe similar effects with chiral derivatives of higher oligopyridines.

We should like to thank the Schweizerischer Nationalfonds zur Förderung der wissenschaftlichen Forschung (Grant numbers: 21-37325.93 and 20-043359.95), the European community (associated contract CEC ERBCHRXCT 940492/A2) and the University of Basel for support.

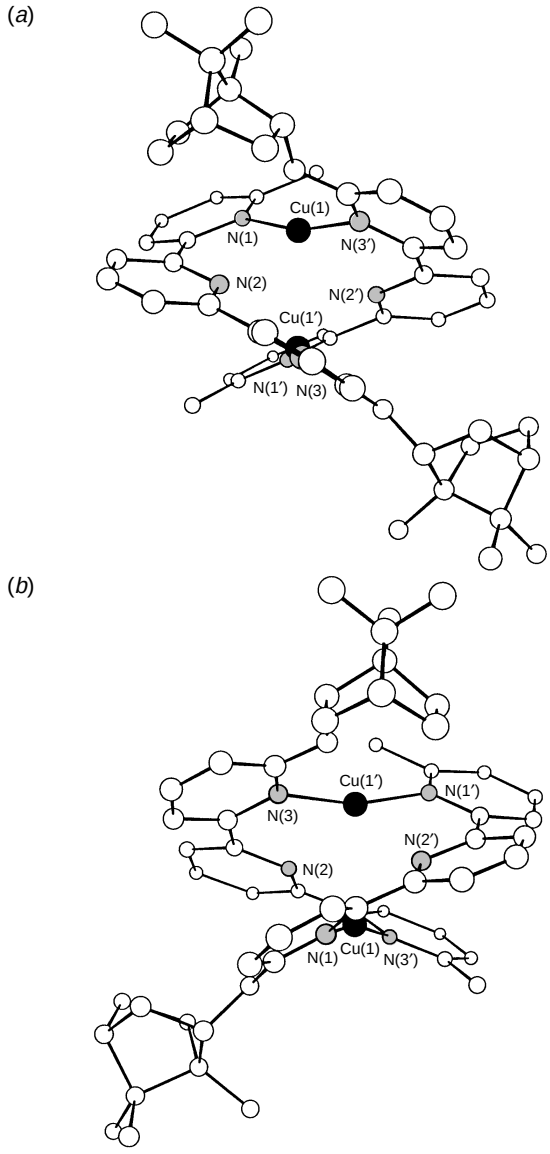



**Fig. 2** Crystal and molecular structures of (*a*) the double-helical cation with *M* chirality in the lattice of $[Cu_2L^1{}_2][PF_6]_2 \cdot 2MeCN$ and (*b*) the double-helical cation with *P* chirality in the lattice of $[Cu_2L^2{}_2][PF_6]_2 \cdot 2MeCN$

## Footnotes

† E-mail: constable@ubaclu.unibas.ch

‡ Modelling studies were initially made using the previous structural determinations[3] as a starting point. Once the structural determinations made in this paper had been made, the Cu–Cu distances were constrained to 2.70 Å. Calculations were made using the MM2 implementation in Chem 3D Pro version 3.5 or the Universal Force Field Implemented in Molecular Simulations Cerius$^{2TM}$ software.

§ *Crystal data*: $[Cu_2L^1{}_2][PF_6]_2 \cdot 2MeCN$: orange crystal, $C_{56}H_{64}Cu_2F_{12}N_8P_2$, $M$ = 1298.18, orthorhombic, space group $P2_12_12$, $a$ = 8.475(1), $b$ = 28.268(2), $c$ = 12.286(1) Å, $U$ = 2943.5(3) Å$^3$, $Z$ = 2, $D_c$ = 1.46 g cm$^{-3}$, $F(000)$ = 1336, λ = 1.54180 Å, μ(Cu-Kα) 2.14 mm$^{-1}$. Intensity data were collected by the ω–2θ scan method (4.2 < 2θ < 154°); for a crystal of dimensions 0.10 × 0.50 × 0.65 mm at room temp.; of 3250 (3238 independent) reflections measured, 2790 [$I \geqslant 3\sigma(I)$] were used in the structure solution. The structure was solved by direct methods using SIR92 (A. Altomare, G. Cascarano, G. Giacovazzo, A. Guagliardi, M. C. Burla, G. Polidori and M. Camalli, *J. Appl. Crystallogr*., 1994, **27**, 435) and refined using CRYSTALS (D. J. Watkin, J. R. Carruthers and P. Betteridge, Chemical Crystallography Laboratory, Oxford, UK) to give final $R$ and $R_w$ values of 0.0513 and 0.0570 respectively (Chebychev polynomial weighting: J. R. Carruthers and D. J. Watkin, *Acta Crystallogr., Sect. A*, 1979, **35**, 698).

$[Cu_2L^2{}_2][PF_6]_2 \cdot 2MeCN$: orange crystal, $C_{56}H_{64}Cu_2F_{12}N_8P_2$, $M$ = 1298.18, orthorhombic, space group $P2_12_12$, $a$ = 8.475(1), $b$ = 28.231(2), $c$ = 12.284(1) Å, $U$ = 2932.7(4) Å$^3$, $Z$ = 2, $D_c$ = 1.47 g cm$^{-3}$, $F(000)$ = 1336, λ = 1.54180 Å, μ(Cu-Kα) 2.15 mm−$^1$. Intensity data were collected by the ω–2θ scan method (4.2 < 2θ < 154°); for a crystal of dimensions 0.10 $^1$ 0.45 × 0.65 mm at room temp.; of 3188 (3174 independent) reflections measured, 2444 [$I \geqslant 3\sigma(I)$] were used in the structure solution. The structure was solved by direct methods using SIR92 and refined using CRYSTALS to give final $R$ and $R_w$ values of 0.0679 and 0.0626 respectively (Chebychev polynomial weighting).

Atomic coordinates, bond lengths and angles, and thermal parameters for both structures have been deposited at the Cambridge Crystallographic Data Centre (CCDC). See Information for Authors, Issue No. 1. Any request to the CCDC for this material should quote the full literature citation and the reference number 182/334.

## References

1 J.-M. Lehn, *Supramolecular Chemistry*, VCH, Weinheim, 1995; E. C. Constable, in *Comprehensive Supramolecular Chemistry*, ed. J.-M. Lehn, Elsevier, 1996, vol. 9; E. C. Constable and D. R. Smith, *The Polymeric Materials Encyclopedia*, CRC Press, Boca Raton, FL, 1996, p. 4237.

2 E. C. Constable, *Tetrahedron*, 1992, **48**, 10 013; *Prog. Inorg. Chem*., 1994, **42**, 67.

3 E. C. Constable, A. J. Edwards, M. J. Hannon and P. R. Raithby, *J. Chem. Soc., Chem. Commun*., 1994, 1991; K. T. Potts, M. Keshavarz-K, F. S. Tham, H. D. Abruña and C. R. Arana, *Inorg. Chem*., 1993, **32**, 4450.

4 E. C. Constable, M. Neuburger, D. R. Smith and M. Zehnder, *Chem. Commun*., 1996, 1917; E. C. Constable, F. R. Heirtzler, M. Neuburger and M. Zehnder, *Supramol. Chem*., 1995, **5**, 197; *Chem. Commun*., 1996, 933; *J. Am. Chem. Soc*., in the press.

5 C. R. Woods, M. Benaglia, F. Cozzi and J. S. Siegel, *Angew. Chem., Int. Ed. Engl*., 1996, **35**, 1830.

6 W. Zarges, J. Hall and J.-M. Lehn, *Helv. Chim. Acta*, 1991, **74**, 1843.

7 This compound was prepared by an analogous route to that reported for 6-bromo-2,2′:6′,2″-terpyridine: R. Chotalia, E. C. Constable, M. J. Hannon and D. A. Tocher, *J. Chem. Soc., Dalton Trans*., 1995, 3571.

*Received, 21st October 1996; Com. 6/07134A*

# Mesoporous zirconia obtained with anionic templates

**G. Pacheco,[a] E. Zhao,[a] A. Garcia,[c] A. Sklyarov[b] and J. J. Fripiat*[a]**

[a] *Department of Chemistry and Laboratory for Surface Studies, and* [b] *Advanced Analysis Facility, University of Wisconsin-Milwaukee, PO Box 413, Milwaukee, WI 53211, USA*

[c] *Materials Department, Instituto Polytechnico Nacional, Zacatenco, Lindavista, CP 07300, Mexico, DF, Mexico*

**Mesoporous zirconia is synthesized with anionic templates.**

The success of Mobil scientists in the surfactant-assisted synthesis of mesoporous molecular sieves[1,2] with hexagonal or cubic ordering of the pore system and high temperature stability has been followed by an enormous amount of research worldwide. An array of cationic surfactants (such as quaternary alkylammonium) with chains containing, typically, twelve carbon atoms interact with an inorganic anionic or cationic oligomer (or polymer) to form a solid in which small-angle X-ray scattering reveals the existence of an ordered system of pores.

The basic principles of these syntheses have been reviewed by Huo *et al*.[3] who have distinguished the interaction between cationic or anionic surfactant with anionic or cationic metal oligomers on the basis of studies involving a large variety of metals other than silicon. Three kinds of structures have been characterized by their X-ray patterns, namely, hexagonal, lamellar and cubic. A high spacing reflection is easily observed in the range 2θ 2–4°, whereas the other Bragg reflections, on which the differentiation between the structures is based, are more difficult to observe because of their intrinsic lower intensity and the broadening due to disorder. Removal of the surfactant does not necessarily keep the hexagonal or cubic structure intact, as desirable for producing high-area solids.

The incorporation of titanium[4] and of zirconium[5] in hexagonal mesoporous silica has been proposed to circumvent the lack of stability of mesoporous titania or zirconia. However, hexagonally packed transition-metal mesoporous molecular sieves of pure niobium, titanium or tantalum oxide have been synthesized with octadecylamine by Antonelli and Ying.[6,7] The preparation of pure mesoporous zirconia with surface area of *ca*. 300 $m^2\ g^{-1}$ at 500 °C has been achieved by Knowles and Hudson[8] using tetramethyl alkylammonium surfactants and zirconyl chloride. Starting from Zr sulfate or propoxide, Schüth[9] and Ciesla *et al*.[10] have obtained a hexagonal mesoporous zirconia of a quality corresponding to that of the silica analogue using alkyl tetramethylammonium surfactants as templates. Reddy and Sayari[11] obtained either hexagonal or lamellar phases of templated zirconia using either quaternary ammonium surfactants or acidified primary alkylamine, respectively. Sachtler and coworkers[12] have used a primary acidified ($C_{16}$) alkylamine. The ordering of the pores was far from perfect but the sulfation of the 'as-synthesized precursor' remarkably stabilizes the structure. After sulfation the X-ray diagram characteristic of tetragonal $ZrO_2$ appears at about 600 °C.

Except in this latter work, the formation of structurally 'ordered' walls has not drawn much attention. Since the stability of tetragonal $ZrO_2$ appears to be driven by particle size,[13,14] the onset of crystallization of the wall in the monoclinic phase could give information on the thickness of the walls between pores. At 500 °C, particles with diameters > 16 nm undergo the tetragonal to monoclinic transformation.[15]

Here, we report on the synthesis of mesoporous zirconia using two anionic surfactants. As far as we know such synthesis has not been achieved up to now and it may be that the elimination of this category of surfactants could be easier. The preparation was as follows. The source of zirconium was a 70% m/m solution of zirconium propoxide in propanol. The two 'straight alkyl chain' surfactants were: $C_{12}H_{25}OP(OH)_2$ ($M$ = 266), abbreviated $P_{12}$ and $C_{12}H_{25}OSO_3Na$ ($M$ = 288), abbreviated $S_{12}$, respectively. The $P_{12}$ solution was left at pH = 3, namely, the original pH of the solution. The initial pH of the $S_{12}$ solution was adjusted by HCl at about 3. The propanolic zirconium alkoxide solution was added slowly to the surfactant solution until the molar ratio S/Zr was 0.16. The mixture was transferred into a hydrothermal bomb where it was heated between 90 and 120 °C for about 12 h. The products of the reaction, called, in short, either $P_{12}$ or $S_{12}$ solids, were dried at 140 °C or calcined at 500 °C.

Low-angle X-ray scattering in the range 2θ 0.8–10° was obtained with a Scintag Θ–Θ X-ray diffractometer (Cu-Kα) fitted with a solid-state detector and the following set of slits: 0.5, 0.3, 0.2 and 0.07°. For medium-angle X-ray scattering (2–70°), the slits were 3, 2, 0.5 and 0.3°. Fig. 1 shows a diffraction line corresponding to spacing at about 47 Å after drying at 140 °C. After calcination at 500 °C, the spacing generally increases, but sometimes, as observed for the $S_{12}$ solid, the ordering disappears.

The $N_2$ adsorption–desorption isotherms were obtained with an automated physisorption instrument operated in a static mode (Omnisorp 100, Coulter Co.). All measurements were performed after outgassing at 150 °C under vacuum down to a residual pressure better than $10^{-4}$ Torr. During calcination in air at 500 °C, all organics were burned as proved by the analysis of residual carbon (Table 1). The typical shape expected for mesoporous solids is observed in Fig. 2(*a*), namely, for the $S_{12}$ and $P_{12}$ solids dried at 140 °C. The *t*-plot specific surface area is in excess of 500 $m^2$. A broad maximum in the porosity distribution function d$V$/d$r$ *vs*. $r$, the radius of the pore, is observed at 2$r$ *ca*. 35 Å. As shown in Table 1, for these solids over 70% of the porous volume is in pores with diameters between 10 and 100 Å, even in $P_{12}$ calcined at 500 °C, in spite of a *ca*. 50% loss in mesoporosity [Fig. 2(*b*)]. The qualitative agreement between the small-angle X-ray scattering data is

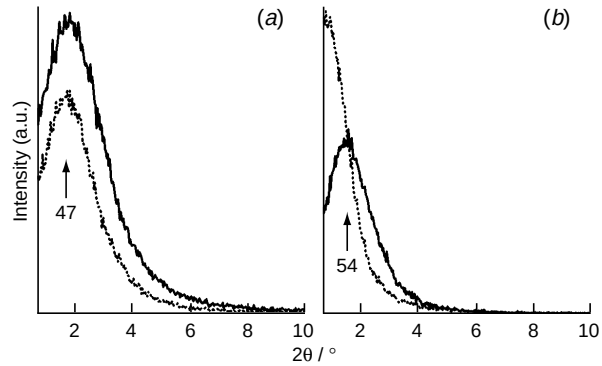



**Fig. 1** Small-angle XRD reflections for the $P_{12}$ (—) and $S_{12}$ (---) solids (*a*) dried at 140 °C or (*b*) calcined at 500 °C

**Table 1** Chemical and physical characteristics of mesoporous zirconias obtained from templating with $P_{12}$ or $S_{12}$ surfactants. The solids are dried at 140 °C or calcined at 500 °C. S/Zr: surfactant to zirconium molar ratio. Porous volume (ml liquid $N_2$ $g^{-1}$) in pores with diameter, $\phi$ < 10 Å or between 10 and 100 Å. $N_2$ desorption branch is used

| | | Pore volume | | |
|---|---|---|---|---|
| | S/Zr | $\phi$ < 10 | 10 ⩽ $\phi$ ⩽ 100 | % Pore volume 10 ⩽ $\phi$ ⩽ 100 |
| $P_{12}$, 140 | 0.12 | 0.007 | 0.538 | 89.0 |
| $S_{12}$, 140 | 0.13 | 0.028 | 0.577 | 74.2 |
| $P_{12}$, 500 | 0 | 0.006 | 0.225 | 81.3 |
| $S_{12}$, 500 | 0 | 0.001 | 0.093 | 37.5 |

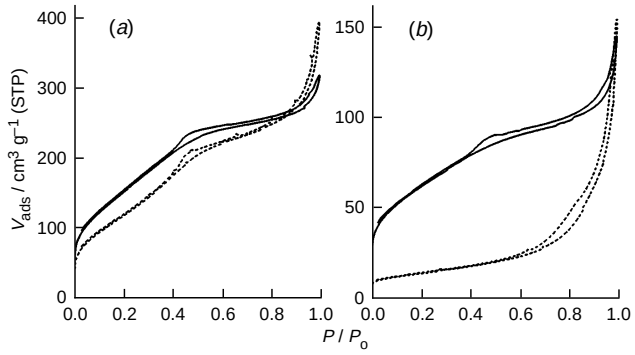



**Fig. 2** $N_2$ adsorption–desorption isotherms for mesoporous zirconia obtained from templating with $P_{12}$ (—) and $S_{12}$(---); (*a*) samples dried at 140 °C or (*b*) samples calcined at 500 °C

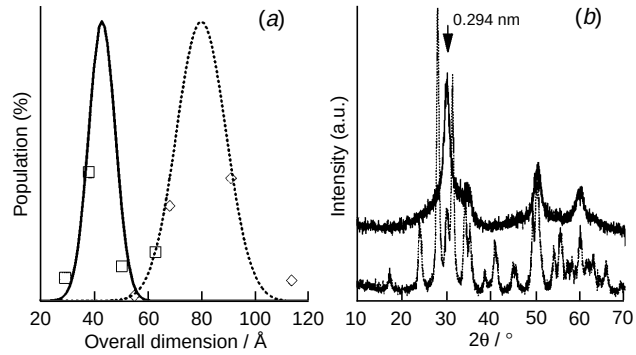



**Fig. 3** (*a*) Gaussian-fitted distribution of the dimension (Å) of the hexagons observed in the HRTEM pictures of the $P_{12}$ and $S_{12}$ solids dried at 140 °C (□, maximum at *ca*. 43 Å). The distribution with maximum at *ca*. 80 Å is observed for $P_{12}$ calcined at 500 °C (◇). (*b*) XRD obtained for $P_{12}$ (—) or for $S_{12}$(---) solids calcined at 500 °C. The reflection at 2.94 Å is characteristic of the trigonal structure.

striking, particularly when comparing the development of macroporosity due to the sintering of $S_{12}$ at 500 °C.

The materials were examined with high-resolution transmission electron microscopy (HTREM, 200 kV). On a microphotograph (Fig. 4) obtained with $P_{12}$ dried at 140 °C, a network of more or less organized pseudo-hexagonal pores is observed. In Fig. 3(*a*), the measured distribution of the overall dimension (Å) of the pseudo-hexagonal pores in $P_{12}$ or $S_{12}$ is fitted to a Gaussian distribution with a maximum at *ca*. 44 Å and a width of 7 Å. Upon calcining $P_{12}$ at 500 °C, the maximum of the distribution shifted towards 80 Å while the width doubled. Again, this is in qualitative agreement with the low-angle scattering data in Fig. 1(*b*) and the isotherms shown in Fig. 2(*b*). The loss of mesoporosity in solid $S_{12}$ calcined at 500 °C is supported by the disappearance of the network of pseudo-hexagons in the corresponding HRTEM picture (not shown). The comparison [Fig. 3(*b*)] of the X-ray scattering data of $P_{12}$

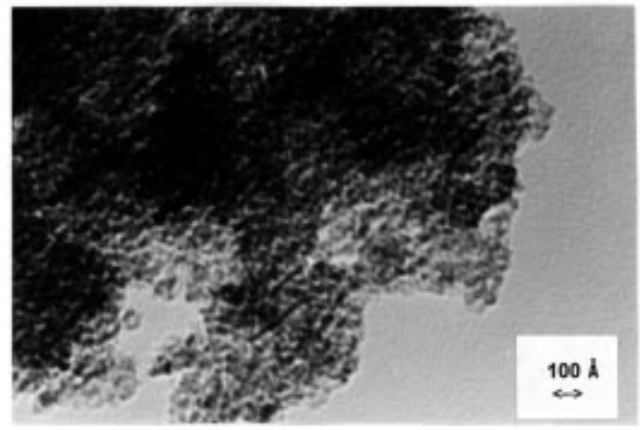



**Fig. 4** HRTEM picture of mesoporous zirconia obtained with $P_{12}$ template

and $S_{12}$ solids calcined at 500 °C provides some insight into the sintering observed for $S_{12}$, since in this sample the phase transformation from a tetragonal to monoclinic structure is evident while $P_{12}$ is at the onset of crystallization. The thickness of the walls between pseudo-hexagons increases from approximately 10 Å to *ca*. 20 Å (HRTEM). $^{31}$P NMR spectroscopy shows that the phosphate remains in the solid after calcination at 500 °C.

Scanning electron microscopy revealed that $P_{12}$ and $S_{12}$ consist mainly of a collection of polygonal particles, of diameter 4–10 μm. Spherical particles in this range of dimensions appear upon sintering $S_{12}$ at 500 °C.

Thus, it may be concluded that mesoporous zirconia can be prepared by hydrolysing the zirconium propoxide in the presence of anionic surfactants (alkyl-phosphate and -sulfate) and subsequent ageing.

The partial support of DOE grant DE-FG02-90 ER1430 is gratefully acknowledged.

## References

1 C. T. Kresge, M. E. Leonowicz, W. J. Roth, J. C. Vartuli and J. S. Beck, *Nature*, 1992, **359**, 710.
2 J. S. Beck, J. C. Vartuli, W. J. Roth, M. E. Leonowicz, C. T. Kresge, K. D. Schmidth, C.T.-W. Chu, D. H. Olson, E. W. Sheppard, S. B. McCullen, J. B. Higgins and J. L. Schlenker, *J. Am. Chem. Soc*., 1992, **116**, 10 836.
3 Q. Huo, D. L. Margoles, V. Ciesla, B. Demuth, P. Feng, T. F. Gier, P. Sieger, A. Firouzi, B. F. Schmelka, F. Schüth and G. D. Stucky, *Chem. Mater*., 1994, **6**, 1176.
4 P. T. Tanev, M. Chibwe and T. J. Pinnavaia, *Nature*, 1996, **368**, 321.
5 S. A. Bagshaw, E. Prouzet and T. J. Pinnavaia, *Science*, 1995, **269**, 1242.
6 D. M. Antonelli and J. Y. Ying, *Chem. Mater*., 1996, **8**, 879.
7 D. M. Antonelli and J. Y. Ying, *Angew. Chem., Int. Ed. Engl*., 1995, **34**, 2014.
8 J. A. Knowles and M. J. Hudson, *J. Chem. Soc., Chem. Commun*., 1995, 2083.
9 F. Schüth, *Ber-Bunsen-Ges. Phys. Chem*., 1995, **99**, 1306.
10 V. Ciesla, S. Schacht, G. D. Stucky, K. K. Unger and F. Schüth, *Angew. Chem., Int. Ed. Engl*., 1996, **35**, 541.
11 J. S. Reddy and A. Sayari, *Catal. Lett*., 1996, **30**, 219.
12 Yin-Yan Huang, T. J. McCarthy and W. M. H. Sachtler, *Appl. Catal. A.: General*, in the press.
13 R. G. Garvie, *J. Phys. Chem*., 1978, **82**, 219.
14 (*a*) A. Chatterjee, S. K. Pradhan, A. Dakka, M. De and D. Chakravorthy, *J. Mater. Res*., 1996, **9**, 263; C. R. Aita, M. D. Wiggins, R. Whig, C. M. Scanlan and M. Gajdardziska-Josifovska, *J. Appl. Phys*., 1994, **79**, 1176.
15 M. Gajdardziska-Josifovska and C. R. Aita, *J. Appl. Phys*., 1994, **79**, 1315.

*Received, 1st November 1996; Com. 6/07438C*

# Epoxide ring opening of α,β-epoxysilanes with prop-2-ynyl sulfide dianion—synthesis of (11*R*,12*S*,5*Z*,7*E*,9*E*,14*Z*)-dihydroxyeicosa-5,7,9,14-tetraenoic acid

**Yuichi Kobayashi, Kiyoshi Shimizu and Fumie Sato***

*Department of Biomolecular Engineering, Tokyo Institute of Technology, 4259 Nagatsuta-cho, Midori-ku, Yokohama 226, Japan*

**A new methodology for synthesis of lipoxygenase metabolites possessing *vic*-diol substructures coupled with the conjugated alkene system is developed and successfully applied to the synthesis of (11*R*,12*S*,5*Z*,7*E*,9*E*,14*Z*)-dihydroxyeicosa-5,7,9,14-tetraenoic acid (DiHETE).**

The biological importance of the lipoxygenase pathways of arachidonic acid metabolism has been repeatedly reviewed.[1] Since these metabolites are available only in minute quantities from biological sources, their total synthesis for further evaluation of their biological properties has attracted much interest.[2] The lipoxygenase metabolites are characterised by monool, *vic*-diol, or epoxide substructures coupled with a conjugated alkene system. So far, a number of syntheses of the monool and epoxide metabolites have been published. However, much less attention has been directed toward the *vic*-diol metabolites (Fig. 1).[3–5]

On the basis of Wicha's finding,[6,7a] we recently reported that reaction of the γ-trimethylsilyl epoxy alcohols **3** and the anions derived from **2**, in which the leaving group (Y) is attached at the α carbon, affords silyl ethers **4** ($R^4$ = $SiMe_3$) or free alcohols **4** ($R^4$ = H) after hydrolysis (Scheme 1).[8] Taking into account these results and the ready availability of optically active **3**[9] (> 99% ee) in large quantities by the kinetic resolution of the corresponding racemic allylic alcohols using the Sharpless epoxidation,[10] we envisaged that, if *anti*,*trans* enyne **6** were prepared by reaction of the *anti* epoxy alcohol **3** and dianion derived from a prop-2-ynylic compound **5** (where L is a leaving group), hydroboration of **6** ($R^3$ = $R^4$ ≠ H) and subsequent palladium-catalysed coupling reaction[11] with *cis* iodide **7** would furnish DiHETE **1** stereoselectively (Scheme 2). We recently applied a similar palladium-catalysed coupling reaction to the highly stereoselective construction of leukotriene $B_4$ ($LTB_4$) and its derivatives.[2b,12] Herein we report the substantiation of our postulate, exemplified by the facile synthesis of (11*R*12*S*)-DiHETE **14**, a metabolite of the 12-lipoxygenase cascade of arachidonic acid.[4a,13]

Requisite *anti* γ-silyl epoxy alcohol **9** (> 99% ee), the enantiomer of the intermediate for synthesis of $LTB_4$,[12a] was prepared by the kinetic resolution of racemic allylic alcohol DL-**8** in 43% yield based on DL-**8**.[9] Since we had no prior knowledge of the leaving group (L) of **5** and the requisite reaction conditions to afford the key intermediate **10** with *trans* alkene geometry, we examined reaction of **9** or the α-ethoxyethyl ether of **9** with the dianion derived from **5** [L = SPh, S(O)Ph] and BuLi. The reaction proceeded smoothly when **9** and 3 equiv. of **5** (L = SPh) were used in THF. However, after hydrolysis of the *vic*-diol monosilyl ethers under acidic conditions, the ratio of the desired enyne **10** and the *cis* isomer **15** incidentally produced was a disappointing 66 : 34 by $^1$H NMR spectroscopy (Table 1, entry 1).

Other prop-2-ynyl sulfides were then tried (entries 2–4) and *tert*-butyl sulfide **5** (L = $SBu^t$) was finally found to show high stereoselectivity. Thus, **9** was added to a THF solution of the dianion of **5** (L = $SBu^t$) generated by using 2 equiv. of BuLi (1 h, −15 °C). The solution was stirred at −15 °C for 2 h and then at room temp. for 12 h to give the product which, upon treatment with dil HCl, furnished **10** and **15** in a ratio of 89 : 11 (entry 4). Both isomers were easily separated by column chromatography on silica gel [$R_f$ values: **10**, 0.67; **15**, 0.57 (hexane–$Et_2O$ = 2:5)] and **10** [$\alpha]_D^{23}$ +1.8 (*c* 0.56, $CHCl_3$)] was isolated in 70% yield. Addition of HMPA resulted in low stereoselection (entry 5).

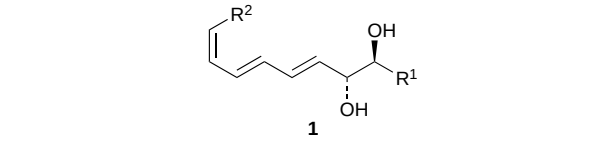
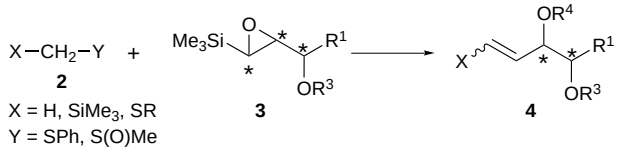
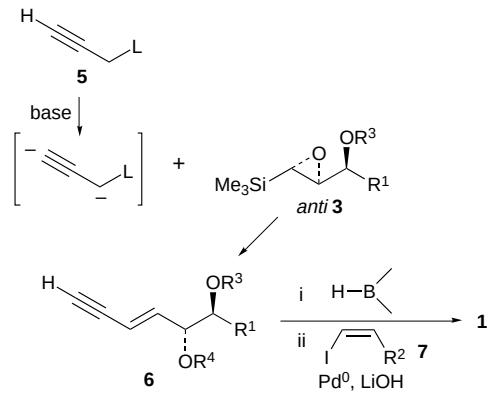



**Fig. 1** General structure of the *vic*-diol metabolites




**Scheme 1**




**Scheme 2**

**Table 1** Reaction of **9** and the dianion generated from **5** and BuLi[a]

| Entry | Sulfide **5** L | Solvent | Ratio[b] **10** : **15** | Yield (%)[c] |
|---|---|---|---|---|
| 1 | SPh | THF | 66 : 34 | 82 |
| 2 | $SC_6H_4$-*p*-OMe | THF | 75 : 25 | —[d] |
| 3 | SBu | THF | 52 : 48 | 74 |
| 4 | $SBu^t$ | THF | 89 : 11 | 79 |
| 5 | $SBu^t$ | THF–HMPA[e] | 60 : 40 | 65 |

[a] Dianion of **5** was generated by using BuLi (2 equiv.) at −15 °C for 1 h. Reaction was carried out at −15 °C to room temp. for 4–14 h and the crude monosilyl ethers were treated with aqueous HCl in MeOH. [b] Determined by $^1$H NMR spectroscopy. [c] Combined yields of **10** and **15** after chromatography on silica gel. [d] Not determined. [e] THF–HMPA = 3 : 1.

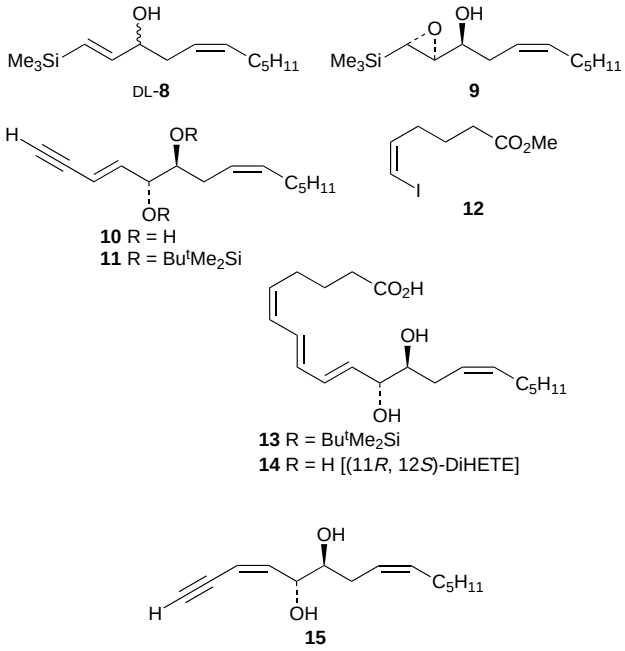


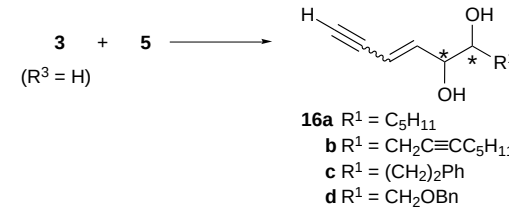

**Table 2** Reaction of **3** ($R^3$ = H) and the dianion derived from **5**[a]

| Entry | Stereochem. of **3** | $R^1$ | L of **5** | Product[b] | *trans* : *cis* | Yield (%)[c] |
|---|---|---|---|---|---|---|
| 1 | *anti* | $C_5H_{11}$ | SBu$^t$ | **16a** | 83 : 17 | 80 |
| 2 | *anti* | $C_5H_{11}$ | SPh | **16a** | 73 : 27 | 84 |
| 3 | *syn* | $C_5H_{11}$ | SBu$^t$ | **16a** | 94 : 6 | 81 |
| 4 | *syn* | $C_5H_{11}$ | SPh | **16a** | 87 : 13 | 84 |
| 5 | *anti* | $CH_2C{\equiv}CC_5H_{11}$ | SBu$^t$ | **16b** | 84 : 16 | 79 |
| 6 | *anti* | $(CH_2)_2Ph$ | SBu$^t$ | **16c** | 90 : 10 | 92 |
| 7 | *anti* | $CH_2OBn$ | SBu$^t$ | **16d** | 89 : 11 | 71 |

[a] See footnote *a* to Table 1. [b] In all cases, *trans* and *cis* isomers were separated by chromatography and characterized by $^1$H NMR. [c] Combined yields of *trans* and *cis* enynes **16** after chromatography.

To complete the synthesis, the hydroxy groups of **10** were protected [Bu$^t$Me$_2$SiCl, imidazole, DMF, 45 °C] to afford the disilyl ether **11** {$[\alpha]_D^{25}$ −2.8 (*c* 1.06, $CHCl_3$)} in 85% yield. Hydroboration of **11** with disiamylborane (1.5 equiv., 0 °C, THF) and subsequent coupling with the iodide **12** (2.3 equiv.) in the presence of $Pd(PPh_3)_4$ (0.1 equiv.) and excess of aqueous LiOH at 35 °C furnished 11,12-DiHETE disilyl ether **13** in 96% yield. Finally, desilylation of **13** with $Bu_4NF$ afforded in 90% yield (11*R*,12*S*)-DiHETE **14** ($^1$H NMR,[4a,13a] UV[4c]), whose chemical purity was > 95% by RP-HPLC.

In the above paragraphs, we described the synthesis of 11,12-DiHETE **14**, in which the key intermediate **10** was synthesized from **9** and the *tert*-butyl sulfide **5** (L = SBu$^t$) (Table 1, entry 4). By using the general strategy proposed in Scheme 2, synthesis of other DiHETEs **1** and their analogues as well as metabolites possessing the DiHETE substructure such as lipoxins should be possible. Thus, stereoselectivity of the key reaction was briefly examined by using various *anti* and/or *syn* γ-silyl epoxy alcohols **3** ($R^3$ = H) and prop-2-ynylic sulfides **5** (L = SBu$^t$, SPh) (Scheme 3) under the reaction conditions described above. Results are summarised in Table 2. With synthetically useful stereoselectivities and good yields were produced *trans* enynes **16a**–**d** in all cases when *tert*-butyl sulfide **5** (L = SBu$^t$) was used (entries 1 *vs.* 2, 3 *vs.* 4, 5–7). In every case, the major *trans* enyne and the minor *cis* isomer were




**Scheme 3**

separated easily by chromatography. Interestingly, higher *trans* selectivity was observed in the case of *syn* **3** ($R^1$ = $C_5H_{11}$, $R^3$ = H) (entries 1 and 3). It is also noteworthy that the sense of the *trans* alkenes afforded as the major product in our system was *opposite* to that reported by Wicha *et al*.[7]

We gratefully acknowledge receipt of the Daiichi Pharmaceutical Award in Synthetic Organic Chemistry, Japan.

## References

1 Recent reviews: W. König, W. Schönfeld, M. Raulf, M. Köller, J. Knöller, J. Scheffer and J. Brom, *Eicosanoids*, 1990, **3**, 1; T. Shimizu and L. S. Wolfe, *J. Neurochem*., 1990, **55**, 1.
2 Reviews: (*a*) J. Rokach, Y. Guindon, R. N. Young, J. Adams and J. G. Atkinson, in *The Total Synthesis of Natural Products*, ed. J. ApSimon, Wiley, New York, 1988, vol. 7, p. 141; (*b*) F. Sato and Y. Kobayashi, *Synlett*, 1992, 849.
3 5,6-DiHETE: K. C. Nicolaou, J. Y. Ramphal, J. M. Palazon and R. A. Spanevello, *Angew. Chem., Int. Ed. Engl*., 1989, **28**, 587; A. Gigou, J.-P. Lellouche, J.-P. Beaucourt, L. Toupet and R. Grée, *Angew. Chem., Int. Ed. Engl*., 1989, **28**, 755; C. Kugel, J.-P. Lellouche, J.-P. Beaucourt, G. Niel, J.-P. Girard and J.-C. Rossi, *Tetrahedron Lett*., 1989, **30**, 4947.
4 11,12-DiHETE: (*a*) P. Westlund, J. Palmblad, J. R. Falck and S. Lumin, *Biochim. Biophys. Acta*, 1991, **1081**, 301; (*b*) A. Gigou, J.-P. Beaucourt, J.-P. Lellouche and R. Grée, *Tetrahedron Lett*., 1991, **32**, 635; (*c*) J. P. Lellouche, A. Gigou-Barbedette and R. Grée, *Bull. Soc. Chim. Fr*., 1992, **129**, 605; (*d*) G. V. M. Sharma and S. M. Rao, *Tetrahedron Lett*., 1994, **35**, 4231.
5 14,15-DiHETE: J. R. Falck, S. Manna, J. Capdevila and J. D. Buynak, *Tetrahedron Lett*., 1983, **24**, 5719; O. Radmark, C. Serhan, M. Hamberg, U. Lundberg, M. D. Ennis, G. L. Bundy, T. D. Oglesby, P. A. Aristoff, A. W. Harrison, G. Slomp, T. A. Scahill, G. Weissmann and B. Samuelsson, *J. Biol. Chem*., 1984, **259**, 13 011.
6 P. Jankowski, P. Raubo and J. Wicha, *Synlett*, 1994, 985.
7 Reaction of epoxy silanes and α-sulfonyl anions affords *cis* allylic alcohols: (*a*) M. Masnyk and J. Wicha, *Tetrahedron Lett*., 1988, **29**, 2497; (*b*) S. Marczak, M. Masnyk and J. Wicha, *Liebigs Ann. Chem*., 1990, 345; (*c*) M. Masnyk and J. Wicha, *Chem. Ber*., 1994, **127**, 677; Attempts to give *trans* allylic alcohols: (*d*) P. Jankowski, S. Marczak, M. Masnyk and J. Wicha, *J. Organomet. Chem*., 1991, **403**, 49; (*e*) B. Achmatowicz, P. Raubo and J. Wicha, *J. Org. Chem*., 1992, **57**, 6593.
8 Y. Kobayashi, T. Ito, I. Yamakawa, H. Urabe and F. Sato, *Synlett*, 1991, 813.
9 Y. Kitano, T. Matsumoto and F. Sato, *Tetrahedron*, 1988, **44**, 4073.
10 M. G. Finn and K. B. Sharpless, in *Asymmetric Synthesis*, ed. J. D. Morrison, Academic, New York, 1985, vol. 5, ch. 8, p. 247.
11 N. Miyaura, K. Yamada, H. Suginome and A. Suzuki, *J. Am. Chem. Soc*., 1985, **107**, 972.
12 (*a*) Y. Kobayashi, T. Shimazaki, H. Taguchi and F. Sato, *J. Org. Chem*., 1990, **55**, 5324; (*b*) T. Shimazaki, Y. Kobayashi, F. Sato, T. Iwama and K. Shikada, *Prostaglandins*, 1990, **39**, 459; (*c*) T. Shimazaki, K. Kawajiri, Y. Kobayashi and F. Sato, *Prostaglandins*, 1993, **45**, 335; (*d*) Y. Kobayashi, T. Shimazaki, K. Kawajiri, T. Shimizu, Y. Seyama and F. Sato, *Biochim. Biophys. Acta*, 1994, **1215**, 280.
13 (*a*) I. Miki, T. Shimizu, Y. Seyama, S. Kitamura, K. Yamaguchi, H. Sano, H. Ueno, A. Hiratsuka and T. Watabe, *J. Biol. Chem*., 1989, **264**, 5799; (*b*) P. Westlund, C. Edenius and J. Å. Lindgren, *Biochim. Biophys. Acta*, 1988, **962**, 105.

*Received, 16th December 1996; Com. 6/08429J*

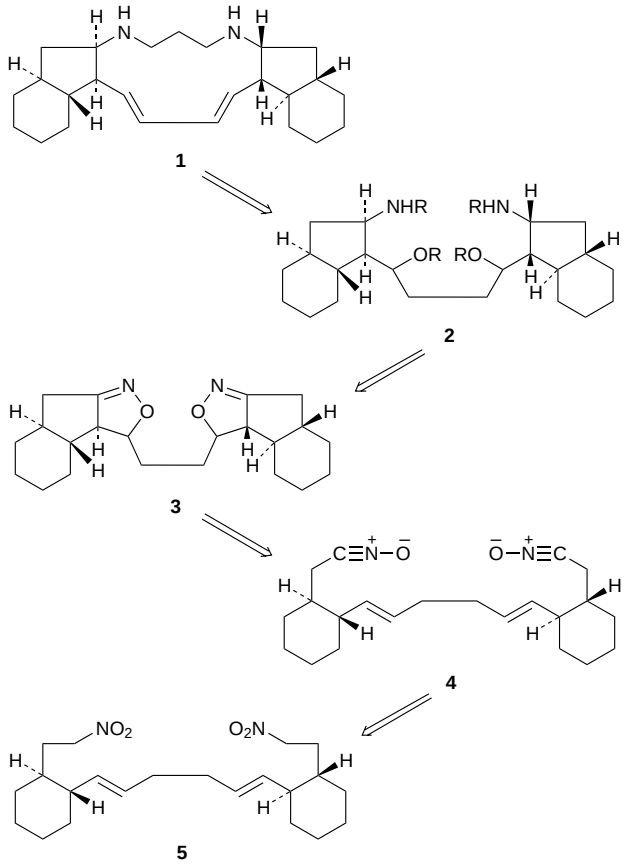
# Novel nitrile oxide cycloaddition approach towards papuamine: stereoselective synthesis of a potentially useful *trans*-hydrindane intermediate

**Arabinda Saha and Anup Bhattacharjya***

*Indian Institute of Chemical Biology, 4 Raja S. C. Mullick Road, Calcutta 700 032, India*

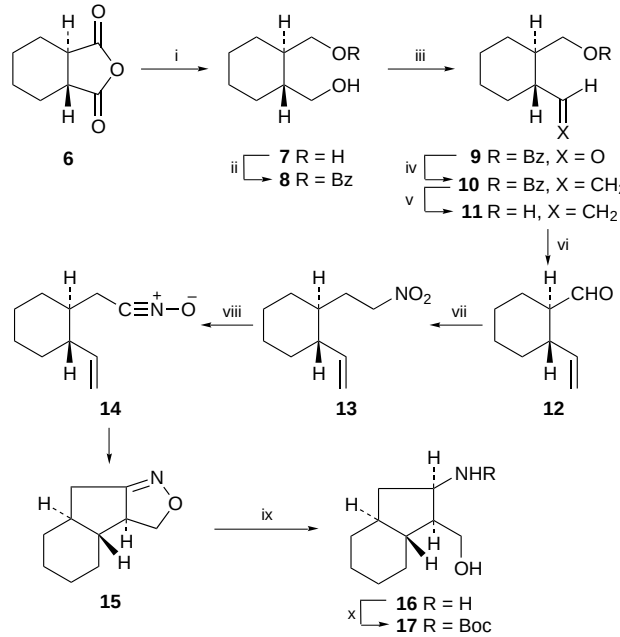
**In a potentially useful approach to the marine alkaloid papuamine 1, a known *trans*-hydrindane intermediate 17 has been synthesised in racemic form using a model sequence of reactions involving a nitrile oxide cycloaddition as a key step.**

Papuamine **1**, a unique $C_2$-symmetric pentacyclic alkaloid, was isolated from the marine sponge *Haliclona sp*.[1,2] The presence of two disubstituted *trans*-hydrindane units of identical chirality and a central diazadiene ring makes papuamine a challenging target for synthesis. A crucial task in such a synthesis is the stereoselective construction of the disubstituted *trans*-hydrindane unit incorporating four chiral centres. Three recent syntheses[3–5] of optically active papuamine have solved this problem either by reductive amination of suitably substituted *trans*-hydrindanone derivatives[3,4] or by utilising a highly stereoselective iminoene reaction.[5] We envisaged a novel and expedient strategy (Scheme 1) towards **1** involving the intramolecular cycloaddition of the bis-nitrile oxide **4** to give a bis-isoxazoline derivative **3**, which could be elaborated to the papuamine skeleton by reductive cleavage to **2** followed by the incorporation of a $C_3$-unit. The future success of this approach is critically dependent on the fidelity of the sequence **4** → **3** → **2**. We herein report an unusually simple but efficient synthesis of a racemic *trans*-hydrindane intermediate **17**, which is the racemate of an intermediate used[3] for papuamine, *via* the model sequence of conversions **14** → **15** → **17** involving a highly stereoselective, intramolecular, nitrile oxide cycloaddition and subsequent reduction of the isoxazoline ring (Scheme 2).




**Scheme 1**

The diol **7**, which was easily obtained from (±)-**6** by reduction with $LiAlH_4$, was monobenzoylated and the resulting alcohol **8**† was oxidised[6] with PCC to the aldehyde **9**. Wittig methylenation of **9** gave the olefinic ester **10**, which on deprotection furnished the alcohol **11**. Oxidation of **11** by PCC led to the aldehyde **12**, which was converted to the nitro compound **13** *via* a known protocol[7] involving reaction with nitromethane, acetylation and reduction with sodium borohydride without purification of any of the intermediate products. The conversion of **6** to **12** was effected *via* the above route in order to adapt this strategy for preparing enantiomerically pure intermediates required for the synthesis of optically active papuamine. The construction of the crucial *trans*-hydrindane skeleton was then achieved by the treatment of **13** with phenyl isocyanate leading to the formation of the nitrile oxide **14**, which underwent cycloaddition to furnish the isoxazoline **15**‡ as the exclusive product. The gross structure of **15** was




**Scheme 2** *Reagents and conditions*: i, $LiAlH_4$, THF, 90%; ii, NaH (1 equiv.), then BzCl (1 equiv.), 82%; iii, PCC, neutral alumina, $CH_2Cl_2$, 96%; iv, $Ph_3PMe^+I^-$, BuLi, THF, 70%; v, NaOH, MeOH, $H_2O$, 96%; vi, PCC, neutral alumina, $CH_2Cl_2$, 92%; vii, $CH_3NO_2$, KF, then $Ac_2O$, then $NaBH_4$, EtOH (68% overall); viii, PhNCO, $C_6H_6$, 72%; ix, $LiAlH_4$, $Et_2O$, 88%; x, $Boc_2O$, EtOAc, 90%

established on the basis of $^1H$ and $^{13}C$ NMR spectral data. The stereochemistry of the newly formed chiral centre in the isoxazoline ring could not be determined unambiguously from the spectral data, although it could be tentatively assigned on the basis of the stereochemical outcome observed in the cycloaddition of analogous nitrile oxides.[8] The unambiguous assignment of the structure of **15** was provided by its reductive cleavage with $LiAlH_4$, resulting in the formation of the amino alcohol **16**, which was isolated as the Boc derivative **17**. A comparison of the IR, $^1H$ and $^{13}C$ NMR spectra of **17** with those of an intermediate reported[3] by Barrett *et al*. established the identity of the two derivatives. The high stereoselectivity observed in the reduction of the isoxazoline ring in **15** was in accord with the results obtained in similar reductions with $LiAlH_4$.[9]

The fact that the corresponding *N*-deprotected *O*-benzylated derivative of **17** was involved in the synthesis[3] of papuamine by Barrett *et al.* indicates the practical importance of the strategy. Moreover, since the work described above established the successful conversion of **13** to **16**, the synthesis of papuamine **1** from **5** appears to be a distinct possibility and is in progress.

We are indebted to Professor A. G. M. Barrett for providing the copies of the IR, $^1H$ and $^{13}C$ NMR spectra of **17**. A. S. gratefully acknowledges the award of a Research Associateship by CSIR, India. We are grateful to Dr A. Patra for the 300 MHz $^1H$ NMR spectrum of **17**. Thanks are due to Mr P. P. Ghosh Dastidar, Dr R. C. Yadav and Dr R. Mukhopadhyay for NMR and mass spectral analyses.

## Footnotes

† All new compounds were liquids and were characterised by GC, IR, mass, and $^1H$ NMR spectral analyses; satisfactory $^{13}C$ NMR spectral data were recorded for **10**, **13**, **15** and **17**. The 300 MHz $^1H$ NMR and a 25 MHz $^{13}C$ NMR spectra of compound **17** were identical with those provided by Professor Barrett.

‡ *Selected spectral data* for **15**: $^1H$ ($CDCl_3$; 100 MHz): δ 2.48–2.84 (m, 1 H), 3.20–3.52 (m, 1 H), 3.80 (dd, *J* 8 and 12 Hz, 1 H) and 4.48 (dd, *J* 8 and 10 Hz, 1 H); $^{13}C$ ($CDCl_3$; 25 MHz): δ 25.8, 25.9, 27.7, 30.7, 31.4, 49.4, 49.9, 61.3 and 170.7.

## References

1 B. J. Baker, P. J. Scheuer and J. N. Shoolery, *J. Am. Chem. Soc.*, 1988, **110**, 965.
2 E. Fahy, T. F. Molinski, M. K. Harper, B. W. Sullivan, D. J. Faulkner, L. Parkanyi and J. Clardy, *Tetrahedron Lett.*, 1988, **29**, 3427.
3 A. G. M. Barrett, M. L. Boys and T. L. Boehm, *J. Org. Chem.*, 1996, **61**, 685.
4 T. S. McDermott, A. A. Mortlock and C. H. Heathcock, *J. Org. Chem.*, 1996, **61**, 700.
5 R. M. Borzilleri, S. M. Weinreb and M. Parvez, *J. Am. Chem. Soc.*, 1995, **117**, 10905.
6 A. Speicher and T. Eicher, *Synthesis*, 1995, 998.
7 A. P. Kozikowski and C.-S. Li, *J. Org. Chem.*, 1985, **50**, 778.
8 A. P. Kozikowski and P. D. Stein, *J. Org. Chem.*, 1984, **49**, 2301.
9 V. Jäger and V. Buss, *Liebigs Ann. Chem.*, 1980, 101.

*Received, 8th January 1997; Com. 7/00182G*

# The first water-soluble hermicarceplexes

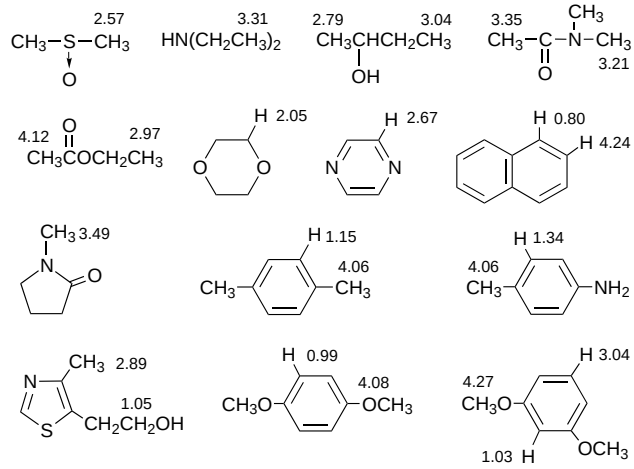
**Juyoung Yoon and Donald J. Cram***

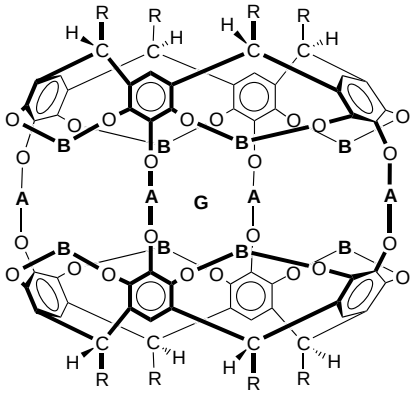
*Department of Chemistry and Biochemistry, University of California, Los Angeles, CA 90095-1569, USA*

**The synthesis of the first water-soluble hemicarcerand and its spectral and binding properties with 14 guests in water are described.**

Many hemicarcerands and hemicarceplexes of general structures **1** and **1**⊙G, respectively, have been reported in which the carbon chains of the bridging A groups, the spanning B groups, the feet (R groups) and guests (G) have been widely varied.[1] The host which binds the largest number and variety of guests is **2** [A = $(CH_2)_4$, B = $CH_2$, R = $CH_2CH_2Ph$].[2] Recently a family of hosts has been synthesized in which A = 3-$CH_2C_6H_4CH_2$, B = $(CH_2)_n$ (*n* = 1–3) and R = $(CH_2)_4Me$.[3] Of the hundreds of known hemicarceplexes,[4] all have been too lipophilic to be soluble in water. If hemicarcerands are to be candidates for drug delivery systems, they should not only bind a wide variety of guests but they and their complexes should be soluble in water not far from physiological pH values. Here we report the synthesis, spectra and host-binding properties toward representative organic guests of the first water-soluble hemicarcerand **4**.†,‡

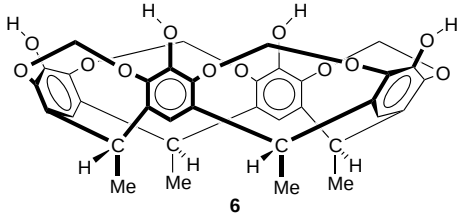
For complexation studies, a stock 1.5 mmol $dm^{-3}$ solution of octaacid **4** in 0.1 mol $dm^{-3}$ deuteriated sodium borate buffer (adjusted to pH 9 with NaOD in $D_2O$)[7] was prepared, and its 400 MHz $^1$H NMR spectrum was recorded. About 10 equiv. of each listed guest were added to the host solution, the pH was again adjusted if necessary, and the $^1$H NMR spectrum of the aqueous solution was taken at 25 °C. The effects of incarceration for 14 guests on important signals in their $^1$H NMR spectra in $D_2O$ at 25 °C are recorded in values of Δδ, which equals $\delta_{free} - \delta_{complexed}$. These Δδ values (ppm) are placed close to their assigned protons in the 14 guest formulas. The fact that the exchange of places of free and incarcerated guest was slow on the NMR time scale allowed the inner-phase guests to be differentiated from those in the bulk phase. Complexation appeared to be complete in a few minutes for all guests formulated except naphthalene, whose limited solubility in $D_2O$ made dissolution of the solid in $D_2O$ the rate-limiting step rather than complexation. The insolubility of naphthalene in $D_2O$ coupled with the 12 h it took for all of the free host to become complexed indicates that complexation was the cause of dissolution of naphthalene in $D_2O$. All complexes were 1 : 1, a conclusion drawn from peak intensity comparisons.



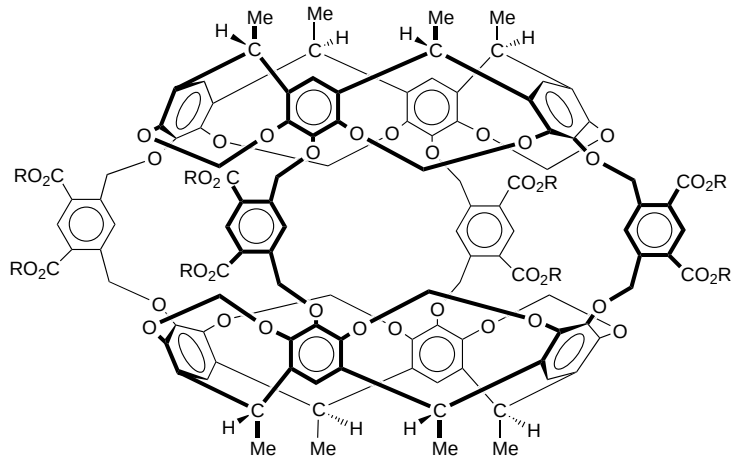




**1** ⊙G, **2**⊙G, A = $(CH_2)_4$, B = $CH_2$, R = $CH_2CH_2Ph$

**3** ⊙G, A = 3-$CH_2C_6H_4CH_2$, B = $CH_2$, R = $CH_2CH_2Ph$

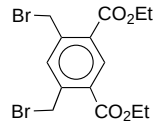


**6**



**4** R = H

**5** R = Et



**7**

The four salts $Me_4NBr$, $PhNMe_3Br$, $BnNMe_3Br$ and 3-$MeC_6H_4CO_2Na$ failed to complex **4** in $D_2O$ buffer, probably because $D_2O$ solvates their charges much better than does the interior of **4**. Although the release of many inner-phase-solvating water molecules for each host and from bulk-phase water for each guest molecule would provide a substantial entropic driving force for complexation of the cations the enthalpic solvation energies of their charges by water appear to be dominant in inhibiting complexation.

The guests formulated that are incarcerated in **4** which is dissolved in $D_2O$ provide a wide range in size, polarity and water solubility. The smallest one is $Me_2SO$ containing 4 heavy atoms (non-hydrogen), which is highly polar, is miscible with $D_2O$ in all proportions, and is a good hydrogen bond acceptor. The next largest are $MeCH(OH)CH_2Me$ and $(MeCH_2)_2NH$ with 5 heavy atoms, which are both moderately polar, good hydrogen bond acceptors and donors, and are rather soluble in $D_2O$. Of the four guests containing 6 heavy atoms, $MeCONMe_2$ and $MeCO_2Et$ are highly polar, $O(CH_2CH_2)_2O$ and $C_4N_2H_4$ (1,4-diazine) are polarizable, all are highly soluble in $D_2O$, and are excellent hydrogen bond acceptors. The only 7-heavy atom guest is $C_5H_9NO$ (*N*-methylpyrrolidinone or NMP), which is very polar, water soluble and a good hydrogen bond acceptor. Of the two guests containing 8 heavy atoms, 4-$MeC_6H_4NH_2$ and 1,4-$(Me)_2C_6H_4$, the former is of intermediate polarity, is somewhat soluble in $D_2O$ and is a good hydrogen bond acceptor and donor, whereas the latter is slightly polarizable, slightly soluble in $D_2O$, and is a poor hydrogen bond acceptor. The only 9-heavy atom guest is 4-methyl-5-(2-hydroxyethyl)thiazole, which is an intermediate in the synthesis of vitamin $B_1$ and is a sedative. This guest is rather polar, is very soluble in water, and is a good donor and acceptor of hydrogen bonds. Of the three 10-heavy atom guests that complexed **4**, 1,4-dimethoxybenzene and 1,3-dimethoxybenzene are relatively nonpolar compounds slightly soluble in $D_2O$ with low hydrogen bond-accepting ability, whereas naphthalene is even less polar, is an even poorer hydrogen bond acceptor, and is essentially insoluble in $D_2O$.

Corey–Pauling–Koltun (CPK) molecular models of the 14 guests listed can be pushed, the larger ones only with difficulty, through the portals of CPK models of **4** containing new atom connectors which survive the encapsulation. Experimentally, the 1 : 1 complexes all appeared stable at ambient temperature in the medium containing excess guest in which they were prepared. It is likely that other guests that complex **3** and are stable in $CDCl_3$ at 25 °C should be stable as complexes of **4** in $D_2O$ at 25 °C, since the hosts' interiors are essentially the same. The only guests common to this study and those involving **3** are 1,4-$Me_2C_6H_4$ and 1,4-$(MeO)_2C_6H_4$, whose complexes with **3** were stable to formation at high temperatures and even isolation, but decomplexed rapidly enough at 25 °C in $CDCl_3$ to inhibit recording reportable $^1$H NMR spectra. Particularly with these two lipophilic guests, we expect hydrophobic binding to contribute more stability to **4**⊙G in $D_2O$ than solvophobic binding in $CDCl_3$ does to **3**⊙G.

The $^1$H NMR results provide the following interesting conclusions. (1) All inner volumes occupied (on average) by guest protons of **4**⊙G are shielding, but vary widely. At the extremes, the β protons of **4**⊙naphthalene (in $D_2O$) give a Δδ value of 4.24, whereas the α protons give 0.80 ppm. Similarly, the six methyl protons of **4**⊙1,3-$(MeO)_2C_6H_4$ provide a Δδ value of 4.27, while the Ar–H flanked by the two MeO groups gives 1.03 ppm. Model examination of both complexes shows that the longer axes of both guests must be aligned along the longer (polar) axis of the inner phase of **4**, and the shorter guest axes along the shorter equatorial axis of **4**. The seven-heavy atom MeOCCCOMe moiety of 1,3-$(MeO)_2C_6H_4$ is the longest axis of this guest. These alignments place the β protons of naphthalene and the methyl protons of 1,3-$(MeO)_2C_6H_4$ in the highly shielding polar caps of **4**, and the α protons of naphthalene and the methoxy-flanked Ar–H protons of 1,3-$(MeO)_2C_6H_4$ in the much lower shielding, bridge region of the inner phase of **4**. The other Δδ values lend themselves to similar analysis. (2) The patterns of Δδ values for the protons of the same guest incarcerated in **2**⊙G and **4**⊙G in eight sets of available comparisons are very similar, although those of **2**⊙G without exception are between 0.02 and 0.38 ppm higher valued than those of **4**⊙G. This reflects the fact that although the cavities of **2** and **4** are similarly shaped, the $O(CH_2)_4O$ bridges of **2** are one atom shorter than the 3-$OCH_2C_6H_4CH_2O$ bridges of **4**. (3) Generally the Δδ values for all the complexes fall into three groups. Values of 1 ± 0.3 are observed for protons that do not terminate chains [*e.g.* $CH_2$ of **4**⊙4-methyl-5-(2-hydroxyethyl)thiazole, Δδ = 0.88, or Ar-H of 1,4-$(MeO)_2C_6H_4$, Δδ = 0.99 ppm], are close to the centre of the guest, and therefore cannot approach closely the generally shielding inner surfaces of the cavities. Values of Δδ = 2–3 ppm are found for protons which are forced to occupy the equatorial regions of the host (*e.g.* $CH_2$ protons of NMP), or are small enough to average many locations by rapid rotations within the host's cavity [*e.g.* protons of $Me_2SO$, $O(CH_2CH_2)_2O$ or 1,4-diazine]. Values of 3.0–4.5 ppm occur for guests whose protons are forced into the faces of the host's aryl groups [*e.g.* the β protons of naphthalene, the Me protons of $MeCO_2Et$ and of $MeCONMe_2$].

The authors warmly thank the NIH for grant GM 12640 which supported this research.

## Footnote

† Tetrol **6**[5] (1 equiv.) was stirred under argon at 25 °C with 2.1 equiv. of dibromide **7**[6] in dry *N*-methylpyrrolidinone (NMP)–$Cs_2CO_3$ for 24 h under high dilution conditions. An additional 1.5 equiv. of **7** were added and the stirring continued at 40 °C for 24 h. The mixture was filtered, the filtrate was evaporated under high vacuum, and the residue was dissolved in $CHCl_3$. The mixture was filtered, the filtrate was evaporated to *ca.* 5 ml and mixed with 100 ml of MeOH which precipitated octaester **5**. This material was filtered and purified by chromatography on a TLC plate (silica gel–$CH_2Cl_2$) to give a 15% yield of **5**. This ester was hydrolysed to give octaacid **4** in THF–1 mol $dm^{-3}$ aqueous KOH–18-crown-6 (4 h at reflux). The solvent was evaporated, and the aqueous solution acidified to pH 1 with 1 mol $dm^{-3}$ aqueous HCl. The octaacid **4** was extracted with EtOAc, the organic layer was dried, and the solvent evaporated to give pure **4** in 90% yield.

‡ New compounds, **4** and **5**, gave elemental analyses within 0.30% of theory, and the expected $^1$H NMR spectra and FABMS (*m/z*, $M^+ + H$).

## References

1 D. J. Cram and J. M. Cram, *Container Molecules and Their Guests*, Monographs in Supramolecular Chemistry, ed. J. Fraser Stoddart, The Royal Society of Chemistry, Cambridge, 1994, pp. 131–216.
2 T. A. Robbins, C. B. Knobler, D. R. Bellew and D. J. Cram, *J. Am. Chem. Soc.*, 1994, **116**, 111.
3 R. C. Helgeson, K. Paek, C. B. Knobler, E. F. Maverick and D. J. Cram, *J. Am. Chem. Soc.*, 1996, **118**, 5590.
4 E. Maverick and D. J. Cram in, ch. 12, *Comprehensive Supramolecular Chemistry*, ed. F. Vögtle, Pergamon, Oxford, 1996, vol. 2, pp. 367–418.
5 D. J. Cram, S. Karbach, H. Kim, C. B. Knobler, E. F. Maverick, J. L. Ericson and R. C. Helgeson, *J. Am. Chem. Soc.*, 1988, **110**, 2229; J. R. Fraser, B. Borecka, J. Trotter and J. C. Sherman, *J. Org. Chem.*, 1995, **60**, 1207.
6 A. Schröder, D. Karbach, R. Güther and F. Vögtle, *Chem. Ber.*, 1992, **125**, 1881.
7 M. A. Petti, T. J. Shepodd, R. E. Barrans, Jr. and D. A. Dougherty, *J. Am. Chem. Soc.*, 1988, **110**, 6825.

*Received, 28th October 1996; Com. 6/07353K*

# Formation of substituted macrocyclic ethers by radical cyclisation

**Athelstan L. J. Beckwith,*[a] Kitty Drok,[a] Bernard Maillard,*[b] Marie Degueil-Castaing[b] and Annie Philippon[b]**

[a] *Research School of Chemistry, Australian National University, Canberra, Australia 0200*
[b] *Laboratoire de Chimie Organique et Organométallique, associé au CNRS URA35, Université Bordeaux 1, F-33405 Talence-Cedex, France*

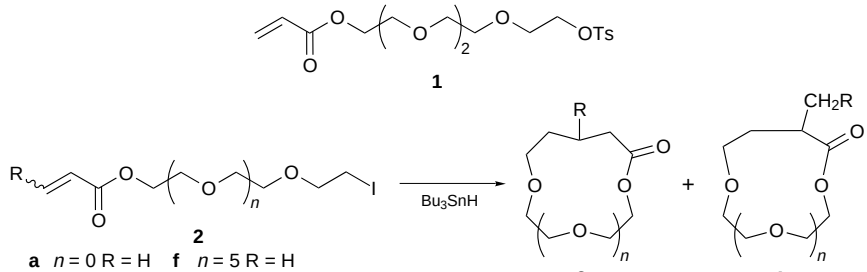
**ω-Iodopolyoxaalkyl acrylates and related compounds undergo radical cyclisation when treated with tributylstannane to afford substituted macrocylic polyethers.**

3-Oxahex-5-enyl radicals ($CH_2$=$CHCH_2OCH_2CH_2$·) undergo *exo* cyclisation about 25 times more rapidly at 80 °C than do hex-5-enyl radicals.[1,2] Similarly the 2-allyloxyphenyl radical cyclises much more rapidly than its all carbon analogue.[3] The effect of an oxygen atom in the chain on the rates of cyclisation of these and related species has been attributed to the decrease in the strain energy of the cyclisation transition structures resulting from the replacement of a carbon atom by oxygen,[1,4] an hypothesis supported by molecular mechanics calculations.[4] These observations suggested that the ring closure of radicals derived from suitable polyether precursors might proceed relatively rapidly. Here we show that such radicals do indeed cyclise more readily than their all-carbon analogues, and that this method provides a viable alternative to ionic reactions as a route to macrocyclic polyethers of potential utility as ionophores.

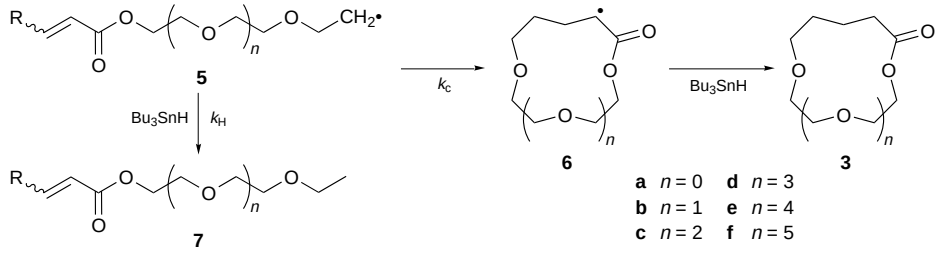
Suitable radical precursors **2a–j** were readily prepared from ethylene glycol oligomers. In a typical example, treatment of the monotosylate of tetraethylene glycol[5] with acryloyl chloride and Hünig's base gave the acrylate **1** (92%) which was converted into the iodide **2c** (95%) on stirring with sodium iodide in acetone. In some cases the oligomeric ethylene glycol was first esterified by treatment with an acid chloride and triethylamine and the iodide was then prepared *via* the mesylate. Heating of each of the compounds **2b–j** with 1.1 molar equivalents of tributylstannane (0.01 mol $dm^{-3}$) and AIBN as catalyst in benzene under reflux for 2 h gave the corresponding cyclic polyethers **3b–j** (and in some cases **4g–j**), but no cyclised product could be obtained from **2a**. Uncyclised products formed by direct hydrogen atom transfer to the initially formed radicals were also detected. Their formation allowed the estimation of the rate constants for cyclisation on the basis of the mechanism shown in Scheme 1. Accurate GC analysis of the product mixtures and treatment of the data in the usual way[6] gave values of $k_c/k_H$ which, when combined with the rate constant for hydrogen transfer from tributylstannane to a primary radical ($k_H$ = 6.3 × $10^6$ $dm^3$ $mol^{-1}$ $s^{-1}$ at 80 °C),[7] gave $k_c$ at 80 °C. The results presented in Table 1 show that the radicals **5b** and **5c**, respectively, cyclise 30 and 10 times faster than their all-carbon-chain analogues ($k_c$ = 4.8 × $10^3$ and 1.2 × $10^4$ $s^{-1}$ at 80 °C, calculated from data in the literature[8]).

Each of the substrates **2b–f** undergoes exclusive *endo* cyclisation to give **3b–f**, but substrates **2g–j** bearing an activating substituent at the remote end of the acrylate double bond also undergo some *exo* cyclisation. Interestingly, the maleate ester **2h** and the corresponding fumarate **2g** cyclise with slightly different *endo* : *exo* ratios of 43 : 57 and 58 : 42, respectively. As measured approximately by NMR the ratio was 1 : 1 for cyclisation of **2i**. In an attempt to improve the *endo* : *exo* selectivity we examined the behaviour of the ester **2j**[9] bearing the bulky *tert*-butyl group. However, once again the **3j** : **4j** ratio was about 1 : 1.

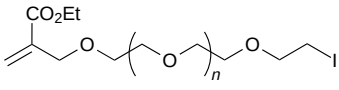
Consideration of the competing reactions available to the various radicals involved in these cyclisations suggested that the



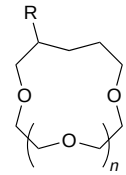

**Scheme 1**



formation of cyclised products should be improved by conducting the experiments with very low concentrations of both the iodoacrylate and $Bu_3SnH$, thus respectively decreasing of the formation of oligomers and the rate of hydrogen atom transfer to uncyclised radicals. Because such high dilution conditions require the use of very large quantities of solvent for the production of small amounts of products, they are of no interest for preparative purposes. However, the same effect was obtained by the separate slow addition with syringe pumps of both $Bu_3SnH$ and iodoacrylate to a solution of AIBN in benzene (method A). Under these conditions cyclised products were isolated in modest to good yield (Table 2). In an alternative procedure the precursors were heated with 1.1 molar equivalents of $Bu_3SnH$ (0.01 mol $dm^{-3}$), AIBN and sodium tosylate (method B). The role of the sodium tosylate is still uncertain but it certainly promotes cyclisation. Each of these methods is suitable for the convenient preparation of macrocyclic polyethers on a gram scale.




**8** $n = 1$
**9** $n = 2$




**10** $n = 1$ R = $CO_2Et$
**11** $n = 2$ R = $CO_2Et$
**12** $n = 2$ R = $CO_2H$
**13** $n = 2$ R = $CH_2OH$

**Table 1** Cylisation rate constants for polyether radicals in benzene at 80 °C

| Radical | $k_c \times 10^{-4}/s^{-1}$ | Radical | $k_c \times 10^{-4}/s^{-1}$ |
|---|---|---|---|
| **5b** | 15 ± 4 | **5c** | 13 ± 1 |
| **5d** | 5.1 ± 0.8 | **5e** | 10 ± 2 |
| **5f** | 3.0 ± 04 | | |

**Table 2** Formation of macrocyclic polyethers by radical cyclisation

| Substrate | Ring size | Products [yield (%)] |
|---|---|---|
| **2a** | 9 | **3a** |
| **2b** | 12 | **3b** (78[a]) |
| **2c** | 15 | **3c** (72[a], 78[b]) |
| **2d** | 18 | **3d** (70[a], 87[b]) |
| **2e** | 21 | **3e** (63[a], 90[b]) |
| **2f** | 24 | **3f** (30[a]) |
| **2g** | 12/11 | **3g** (37[a] **4g** (21[a]) |
| **2h** | 12/11 | **3h** (43[a,c]) **4h** (57[a,c]) |
| **2i** | 15/14 | **3i** (36[d]) **4i** (36[d]) |
| **2j** | 15/14 | **3j** (29[d]) **4j** (29[d]) |

[a] Method A (see text); isolated yields. [b] Method B (see text); yields determined by GC with an internal reference. [c] Relative yield; for this reaction the absolute yield was not determined. [d] Method B; total yield determined by GC; relative yields by NMR.

Finally we examined the preparation of macrocycles that do not contain a lactone group within the ring and hence should be able to survive robust manipulation of the side chain. Thus treatment of the ester **8** with $Bu_3SnH$ in the usual way gave **10** (64%) with a rate constant for cyclisation of $k_c = 2 \times 10^4\ s^{-1}$ at 80 °C, while **9** gave **11** (87%). An advantage of products such as **10** and **11** is that the side chain can be readily converted into functionality suitable for tethering the macrocycle to other ionophores or to fluorescent agents. Thus **11** readily underwent hydrolysis with KOH in methanol to afford the acid **12** (84%) while reduction with LAH in THF gave the alcohol **13** (79%).

In conclusion it appears that, as in the case of simple hexenyl species, the introduction of oxygen atoms into suitable long chain precursors enhances the rate of radical cyclisation sufficiently to allow the preparation of substituted macrocyclic polyethers in modest to good yield under convenient experimental conditions. These results therefore complement those describing other applications of radical macrocyclisation in synthesis.[10,11] Preliminary experiments indicate that some of the macrocyclic polyethers described above may be useful as complexing agents.

We gratefully acknowledge technical assistance from Mr Robert Longmore and the award of a Commonwealth Postgraduate Scholarship to K. D. and of a BDI Scholarship by CNRS and Région Aquitaine to A. P.

## References

1 A. L. J. Beckwith and S. A. Glover, *Aust. J. Chem*., 1987, **40**, 157.
2 A. L. J. Beckwith, V. W. Bowry and G. Moad, *J. Org. Chem*., 1988, **53**, 1632.
3 A. N. Abeywickrema and A. L. J. Beckwith, *J. Chem. Soc., Chem. Commun*., 1986, 464.
4 A. L. J. Beckwith and C. H. Schiesser, *Tetrahedron*, 1985, **41**, 3925.
5 The monotosylate was prepared by the general method previously used for the preparation of the ditosylate: J. Dale and P. O. Kristiansen, *Acta Chem. Scand*., 1972, **26**, 1471.
6 A. L. J. Beckwith and G. Moad, *J. Chem. Soc., Chem. Commun*., 1974, 472.
7 C. Chatgilialoglu, K. U. Ingold and J. C. Scaiano, *J. Am. Chem. Soc*., 1981, **103**, 7739.
8 N. A. Porter and V. H.-T. Chang, *J. Am. Chem. Soc*., 1987, **109**, 4976.
9 **2j** was obtained *via* DCC coupling of mono *tert*-butyl maleate with tetraethylene glycol monotosylate. *tert*-Butyl maleate was prepared by the same general method as that previously used for the preparation of *tert*-butyl phthalate: W. A. Fessler and R. L. Schriner, *J. Am. Chem. Soc*., 1936, **58**, 1384.
10 N. A. Porter, D. R. Magnin and B. T. Wright, *J. Am. Chem. Soc*., 1986, **108**, 2787; N. A. Porter, B. Lacher, V. H.-T. Chang and D. R. Magnin, *J. Am. Chem. Soc*., 1989, **111**, 8309.
11 For some recent examples see: J. Ullrich and D. P. Curran, *Tetrahedron Lett*., 1995, **36**, 8921; E. I. Troyansky, R. F. Ismagilov, V. V. Samoshin, Y. A. Strelenko, D. V. Demchuk, G. I. Nikishin, S. V. Lindeman, V. V. Khrustalyov and Y. T. Struchkov, *Tetrahedron*, 1995, **51**, 11 431; I. Ryu, K. Nagahara, H. Yamazaki, S. Tsunoi and N. Sonoda, *Synlett*, 1994, 643; M. J. Begley, G. Pattenden, A. J. Smithies and D. S. Walter, *Tetrahedron Lett*., 1994, **35**, 2417; K. S. Feldman, H. M. Berven, A. L. Romanelli and M. Parvez, *J. Org. Chem*., 1993, **58**, 6851.

*Received, 19th December 1996; Com. 6/08494J*

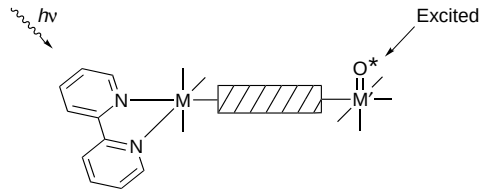
# Synthesis, characterization and photophysical properties of $[OsO_2(mes)_2(NC)Ru(bpy)_2(CN)]$

**Jack Y. K. Cheng, Kung-Kai Cheung and Chi-Ming Che***

*Department of Chemistry, The University of Hong Kong, Pokfulam Road, Hong Kong*

**A novel heterometallic complex comprising of a $d^2$ $OsO_2(mes)_2$ and a $d^6$ $Ru(bpy)_2(CN)_2$ fragment is prepared and characterized by X-ray analysis; its photophysical properties are measured.**

The design of new heterometallic complexes for photoinduced atom transfer reactions has received current interest. One of our approaches is to link a low-valent metal–polypyridine to a high-valent metal–oxo fragment *via* self-assembly reactions.[1] The former would serve as a good light absorber while the latter functions as an oxygen atom transfer agent.




In this context, the cyanide ion, which is known to form stable complexes with metal ions in both high and low oxidation states would be a good bridging ligand.[2] Described herein are the structure and photophysical properties of the first heteronuclear $Ru^{II}Os^{VI}$ $[OsO_2(mes)_2(NC)Ru(bpy)_2(CN)]$ **1** formed by reaction of $[OsO_2(mes)_2]$ (mes = mesityl)[3] with $[Ru(bpy)_2(CN)_2]$ (bpy = 2,2′-bipyridine).[2]

Upon slow evaporation of a solution of $[OsO_2(mes)_2]$ and $[Ru(bpy)_2(CN)_2]$ in dichloromethane–methanol at 0 °C, brown needle crystals† of **1** were obtained (yield 95%) and the structure was characterized by X-ray analysis.‡ Fig. 1 shows a perspective view of the molecule. The osmium atom adopts a distorted square-pyramidal geometry with an average Os–O distance of 1.700 Å and O–Os–O angle of 144.9(2)°. These are comparable to values of 1.720 Å and 147.5(3)° in the related complex $[\{OsO_2(mes)_2\}_2(pyz)]$[4] which has a square-pyramidal geometry at the Os atom. Although the measured N–C–Ru angle of 177.7(4)° is close to 180°, the Os–N–C angle of 160.5(4)° reveals that the Ru–C≡N–Os array is not quite linear. The N–C and Ru–C distances for the bridging cyanide are both 0.04 Å shorter than that of the terminal cyanide. The IR data are in accord with the X-ray structure with ν(C≡N) stretches at 2088.5 and 2072.8 $cm^{-1}$, at higher frequencies relative to $[Ru(bpy)_2(CN)_2]$ [ν(C≡N) 2067.4, 2052.9 $cm^{-1}$]. The ν(Os=O) stretches are at 893.1 and 884.6 $cm^{-1}$, which are comparable to the related value of 900 $cm^{-1}$ for $[\{OsO_2(mes)_2\}_2(\mu\text{-pyz})]$.

Complex **1** is soluble in common organic solvents such as dichloromethane and methanol. Similarly to the reported $[OsO_2(mes)_2L]$ complexes (L = 1,10-phenanthroline or *N*,*N*,*N*′,*N*′-tetramethylethylenediamine),[5] the equilibrium reaction [eqn. (1)] exists in solution and dissociation is suppressed by addition of an excess of $[OsO_2(mes)_2]$.

$$[OsO_2(mes)_2(NC)Ru(bpy)_2(CN)] \rightleftharpoons [OsO_2(mes)_2] + [Ru(bpy)_2(CN)_2] \quad (1)$$

Fig. 2 shows the absorption spectra of solutions of $[Ru(bpy)_2(CN)_2]$ in the presence of various concentrations of $[OsO_2(mes)_2]$. The MLCT band of $[Ru(bpy)_2(CN)_2]$ shifts to a higher energy (461 to 436 nm) upon addition of $[OsO_2(mes)_2]$ (0 to 10-fold excess). A similar experiment with $[Ru(bpy)_3]Cl_2$ has also been done but its MLCT band does not change even in the presence of tenfold excess of $[OsO_2(mes)_2]$. Thus the progressive blue shift is evidence for the formation of the dimeric species **1** in solution.[6]

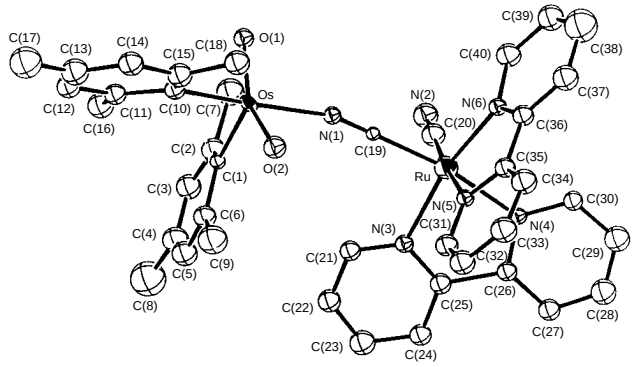



**Fig. 1** A perspective view of **1** (thermal ellipsoids at 40% probability level). Selected bond lengths (Å) and angles (°): Os–O(1) 1.704(3), Os–O(2) 1.696(3), Os–N(1) 2.235(4), Os–C(1) 2.063(5), Os–C(10) 2.108(4), Ru–N(3) 2.064(4), Ru–N(4) 2.113(4), Ru–C(19) 1.972(4), Ru–C(20), 1.992(4), N(1)–C(19) 1.143(6), N(2)–C(20) 1.145(6); O(1)–Os–O(2) 144.9(2), O(1)–Os–N(1) 88.5(1), O(1)–Os–C(1) 110.4(2), O(1)–Os–C(10) 91.5(2), N(1)–Os–C(1) 87.1(2), N(1)–Os–C(10) 173.4(2), C(1)–Os(1)–C(10) 99.1(2), C(19)–Ru–C(20) 89.5(2), Os–N(1)–C(19) 160.5(4), Ru–C(19)–N(1) 177.7(4), Ru–C(20)–N(2) 178.6(4).

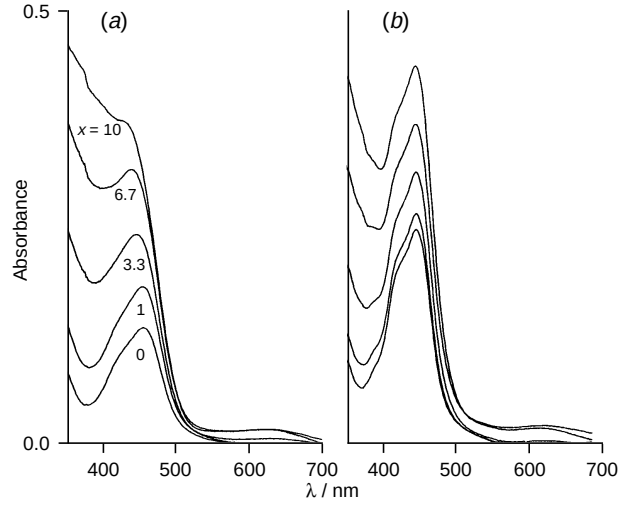



**Fig. 2** UV–VIS absorption spectra of (*a*) $[Ru(bpy)_2(CN)_2]$ ($2.0 \times 10^{-5}$ mol $dm^{-3}$) and (*b*) $[Ru(bpy)_3]Cl_2$ ($2.0 \times 10^{-5}$ mol $dm^{-3}$) at various concentrations of $[OsO_2(mes)_2]$. Ratio of the $OsO_2(mes)_2$ : Ru complexes = 1 : *x*.

Complex **1** in the solid state is non-emissive at 298 and 77 K. In solution, it gives an emission at the same energy as that of $[Ru(bpy)_2(CN)_2]$ measured under similar conditions. However, the lifetime and intensity of the emission are much reduced. Fig. 3 shows $\phi_0/\phi$ and $\tau_0/\tau$ *vs.* [quencher] plots for $[Ru(bpy)_2(CN)_2]$ and $[Ru(bpy)_3]Cl_2$ with $[OsO_2(mes)_2]$ as quencher ($\phi$ and $\tau$ are emission intensity and decay lifetime, respectively). It is interesting that the decay time Stern–Volmer quenching constant, $K_{SV}^{\tau}$ {deduced from the slope of the plot of $\tau_0/\tau$ *vs.* concentration of $[OsO_2(mes)_2]$} for both complexes are similar (1038 and 1098 $dm^3\ mol^{-1}$). The value of the Stern–Volmer quenching constant, $K_{SV}^{\phi}$ {deduced from the slope of the plot of $\phi_0/\phi$ *vs.* concentration of $[OsO_2(mes)_2]$} for $[Ru(bpy)_3]Cl_2$ (1842 $dm^3\ mol^{-1}$) is slightly larger than the $K_{SV}^{\tau}$ value, presumably this is due to the overlap of the absorption spectrum of $[OsO_2(mes)_2]$ with the excitation spectrum of $[Ru(bpy)_2(CN)_2]$. Interestingly, the Stern–Volmer plots for $[Ru(bpy)_2(CN)_2]$ are not linear and exhibits upward curvature characteristic of a system showing both static and dynamic quenching.[7] The static quenching is assigned to ground-state complex formation of $[OsO_2(mes)_2(NC)Ru(bpy)_2(CN)]$ from $[OsO_2(mes)_2]$ and $[Ru(bpy)_2(CN)_2]$ in solution. This heterometallic complex in the solid state is non-emissive suggesting that the long-lived emissive MLCT state of the $Ru(bpy)_2(CN)_2$ chromophore is completely quenched by the $OsO_2(mes)_2$ unit *via* the bridging cyano group. Because the $K_{SV}^{\tau}$ values for $[Ru(bpy)_3]Cl_2$ and $[Ru(bpy)_2(CN)_2]$ are similar, we propose that the dynamic quenching mechanism which represents the collision of $[OsO_2(mes)_2]$ and the excited ruthenium partner through diffusion would be outer sphere in terms of electron- and/or energy-transfer.

Previous studies showed that the $Ru(bpy)_2(CN)_2$ chromophore could be easily functionalized *via* cyanide bridge formation with a suitable choice of adducts [Pt(dien)[2b] or $Ru(NH_3)_5$[2b]] but Ru–CN–M (M = Lewis acid) adduct formation were found not to substantially modify the excited-state properties of the $Ru(bpy)_2(CN)_2$ chromophore.[2b,6] In this work, the excited state of **1** which localizes at the ruthenium centre should be MLCT in nature. This excited state is rapidly quenched by intramolecular energy and/or electron transfer pathways. If intramolecular energy transfer proceeds, the quenching product is $[OsO_2(mes)_2]$*. If intramolecular electron transfer proceeds, the quenching product is either the reduced or oxidized species of $[OsO_2(mes)_2]$. In any case, the energetic or reactive site shifts from ruthenium to the Os–oxo moiety. The rich oxidation chemistry and photochemistry of high-valent osmium–oxo complexes are well documented in literature.[9] Thus formation of an activated five-coordinate osmium–oxo complex through intramolecular electron- and/or energy-transfer would provide an entry to a new class of metal–oxo photooxidants with good light absorbing properties.

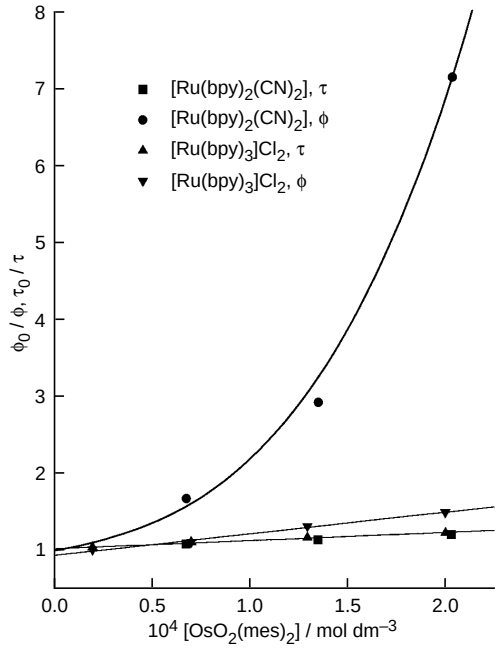



**Fig. 3** Plots of $\phi_0/\phi$ and $\tau_0/\tau$ *vs.* $[OsO_2(mes)_2]$ for complex **1**

We acknowledge support from the University of Hong Kong, the Croucher Foundation, and the Hong Kong Research Grants Council.

## Footnotes

† A mixture of $[OsO_2(mes)_2]$ (60 mg, 0.13 mmol) and $[Ru(bpy)_2(CN)_2]$ (50 mg, 0.11 mmol) in dichloromethane–methanol (1 : 1, 10 ml) was stirred for 1 h. The solvent was slowly evaporated to dryness in a water bath (25 °C) to give a brown microcrystalline solid which was washed with diethyl ether (3 × 10 ml). This was recrystallized by slow evaporation of a dichloromethane–methanol mixture at 0 °C to afford brown needle crystals; yield 97 mg (95%). $^1$H NMR ($CD_3OD$): δ (bpy) 9.61 (d, 2), 8.52 (d, 2), 8.46 (d, 2), 8.09 (t, 2), 7.94 (t, 2), 7.58 (m, 4), 7.29 (t, 2), (mes) 6.92 (s, 4), 2.43, (s, 6), 2.32 (s, 12). IR ν(C≡N) 2088.5s, 2072.8s; ν(Os=O) 893.1s, 884.6s, 849.1m. Anal. Calc. for $C_{40}H_{38}N_6O_2OsRu$: C, 51.88; N, 9.08; H, 4.14. Found: C, 50.91; N, 8.90; H, 3.98%.

‡ *Crystal data*: $[C_{40}H_{38}N_6O_2OsRu{\cdot}2CH_3OH]$; $M_r$ = 990.133, monoclinic, space group $P2_1/c$ (no. 14), $a$ = 17.421(3), $b$ = 10.194(3), $c$ = 23.259(3) Å, β = 95.91(2)°, $U$ = 4108(1) Å$^3$, $Z$ = 4, $D_c$ = 1.601 g cm$^{-3}$, μ(Mo-Kα) = 35.03 cm$^{-1}$, $F$(000) = 1968, $T$ = 301 K. A brown crystal of dimensions 0.25 × 0.20 × 0.30 mm was used for data collection at 28 °C on a MAR diffractometer with a 300 mm image plate detector using graphite-monochromated Mo-Kα radiation (λ = 0.710 73 Å). 7804 unique reflections were obtained from a total of 33 227 measured reflections. 5747 reflections with $I > 3\ \sigma(I)$ were considered observed and used in the structural analysis. All 54 non-H atoms were refined anisotropically. Hydrogen atoms of the methanol molecules were not found but 38 H atoms of the complex molecule at calculated positions with thermal parameters equal to 1.3 times that of the attached C atoms were not refined. Convergence for 487 variable parameters by least-squares refinement on $F$ with $w = 4F_0^2/\sigma^2(F_0^2)$, where $\sigma^2(F_0^2) = [\sigma^2(I) + (0.018\ F_0^2)^2]$ for 5747 reflections with $I > 3\sigma(I)$ was reached at $R$ = 0.035 and $wR$ = 0.043 with a goodness-of-fit of 1.61 $(\Delta/\sigma)_{max}$ = 0.04 for atoms of the complex molecule. The final difference Fourier map was featureless, with maximum positive and negative peaks of 0.66 and 1.24 eÅ$^{-3}$ respectively. Atomic coordinates, bond lengths and angles, and thermal parameters have been deposited at the Cambridge Crystallographic Data Centre (CCDC). See Information for Authors, Issue No. 1. Any request to the CCDC for this material should quote the full literature citation and the reference nubmer 182/350.

## References

1 P. K. K. Ho, K. K. Cheung and C. M. Che, *Chem. Commun.*, 1996, 1197.
2 (*a*) C. A. Bignozzi, S. Roffia and F. Scandola, *J. Am. Chem. Soc.*, 1985, **107**, 1644; (*b*) C. A. Bignozzi and F. Scandola, *Inorg. Chem.*, 1984, **23**, 1540.
3 B. S. McGilligan, J. Arnold, G. Wilkinsin, B. Hussain-Bates and M. B. Hursthouse, *J. Chem. Soc., Dalton Trans.*, 1990, 2465.
4 W. H. Leung, J. Y. K. Cheng, T. S. M. Hun, C. M. Che, W. T. Wong and K. K. Cheung, *Organometallics*, 1996, **15**, 1497.
5 K. F. Chin, Y. K. Cheng, K. K. Cheung, C. X. Guo and C. M. Che, *J. Chem. Soc., Dalton Trans.*, 1995, 2967.
6 C. Bartocci, C. A. Bignozzi, F. Scandola, R. Rumin and P. Courtot, *Inorg. Chim. Acta*, 1983, **76**, L119.
7 J. N. Demas and J. W. Addington, *J. Am. Chem. Soc.*, 1974, **96**, 3663; J. N. Demas, J. W. Addington, S. H. Peterson and E. W. Harris, *J. Phys. Chem.*, 1977, **81**, 1039.
8 A. Vogler and J. Kisslinger, *J. Am. Chem. Soc.*, 1982, **104**, 2311.
9 V. W. W. Yam and C. M. Che, *J. Chem. Soc., Dalton Trans.*, 1990, 3741.

*Received, 5th November 1996; Com. 6/07514B*

# Synthesis and structural characterisation of the first homoleptic organometallic nickel(III) compound

**Pablo J. Alonso, Larry R. Falvello, Juan Forniés,* Antonio Martín, Babil Menjón and Gerardo Rodríguez**

*Instituto de Ciencia de Materiales de Aragón, Facultad de Ciencias, Universidad de Zaragoza-C.S.I.C., Pza. S. Francisco s/n, E-50009 Zaragoza, Spain*

**The homoleptic, square-planar, $d^7$, 15-electron species $[NBu_4][Ni^{III}(C_6Cl_5)_4]$ 2 is obtained by low-temperature oxidation of $[NBu_4]_2[Ni^{II}(C_6Cl_5)_4]$ 1 with $Cl_2$.**

In the last few years the chemistry of $Ni^{III}$ has evolved very rapidly[1,2] partly because of its relevance to some metalloprotein systems.[3,4] In spite of this burgeoning development, organometallic compounds of $Ni^{III}$ are still extremely rare, the only isolated examples of this class of compounds being, to our knowledge, those reported by van Koten and coworkers.[5] They contain a single Ni–C bond and are stabilised by using polydentate ligands. We now report on the synthesis and characterisation of the first homoleptic organometallic nickel(III) compound, which contains four non-assisted Ni–C σ bonds.

Low-temperature chlorination of the substrate $[NBu_4]_2[Ni^{II}(C_6Cl_5)_4]$ **1**[6] renders the complex $[NBu_4][Ni^{III}(C_6Cl_5)_4]$ **2**, which has been isolated as a green solid in good yield.† Complex **2** is air- and moisture-stable but because of its rather limited thermal stability it is best formed and handled at low temperature. At room temperature it readily decomposes both in solution and in the solid state, undergoing reductive elimination of $C_6Cl_5$–$C_6Cl_5$.‡ This observation is of particular interest because of its relevance to the nickel-mediated synthesis of biaryls, which has been shown to proceed in some instances *via* unstable aryl intermediates of $Ni^{III}$.[7]

The **2**–**1** couple is not only chemically but also electrochemically related by a reversible redox process at a remarkably low potential ($E_{1/2}$ = −0.11 V).§ The IR spectrum of **2** shows the absorptions corresponding to the X-sensitive mode of the $C_6Cl_5$ group and to the ν(Pt–C) mode[8] at higher wavenumbers than those observed for the nickel(II) parent compound (*cf.* **1**, 813 and 581 $cm^{-1}$; **2**, 827 and 603 $cm^{-1}$, respectively). This shift can be associated with the increase in the oxidation state of the metal centre in keeping with previous observations in the perhalogenophenyl chemistry of palladium and platinum.[8a,9]

The structure of the anion $[Ni^{III}(C_6Cl_5)_4]^-$ as found in the diethetate **2**·2$Et_2O$ by X-ray diffraction methods is shown in Fig. 1.¶ The Ni atom is in an almost square-planar environment. The $C_6Cl_5$ groups define a helix around the metal centre with two possible orientations, Δ and Λ, both of which are present in the crystal measured (centrosymmetric space group). The mean dihedral angle formed by the $C_6Cl_5$ groups and the coordination plane is 63.2(3)°. The mean Ni–$C_{ipso}$ distance [200.7(8) pm] is slightly longer than found in other pentachlorophenyl derivatives of $Ni^{II}$ (mean value 192.2 pm).[10] This seeming elongation is at variance with the expected dependence of the M–C distance on the oxidation state of M. This difference, however, must be treated with caution because it could merely be due to the recently demonstrated flexibility of bond distances.[11] The EPR spectrum of a powder sample of **2** is given in Fig. 2‖ in which two features can be observed: one at *ca.* 340 mT having a parallel character and the other one at *ca.* 230 mT having a perpendicular character. This spectrum can be interpreted as due to a paramagnetic $S$ = 1/2 entity in an axial symmetry including only an anisotropic electronic Zeeman interaction and can be described with the following spin-Hamiltonian $H = \mu_B[g_\perp(S_xB_x + S_yB_y) + g_\parallel S_zB_z]$, where $\mu_B$ is the Bohr magneton and $g_\parallel$ = 1.92 and $g_\perp$ = 2.84. This would imply a low-spin (strong ligand field) situation for the $3d^7$ ion. Since the $Ni^{III}$ centre in **2** is in a square-planar environment, the unpaired electron should be expected to occupy an $a_{1g}$ ($z^2$) orbital.[12] In terms of the crystal-field approximation, a second order of perturbation for such an ion would give $g_\parallel = g_e$ and $g_\perp = g_e - 6\lambda/\Delta$, where λ is the spin–orbit constant and Δ the difference in energy between the $a_{1g}$ ($z^2$) and $e_g$ (*xz*,*yz*) orbitals. Since $\lambda < 0$ for $Ni^{III}$, the former expression predicts that $g_\perp > g_e$ while $g_\parallel$ lies close to the free-electron value in agreement with our observation.** This behaviour is in keeping with that reported for other nickel(III) species,[13] the only remarkable feature being in our case the high *g* anisotropy observed.

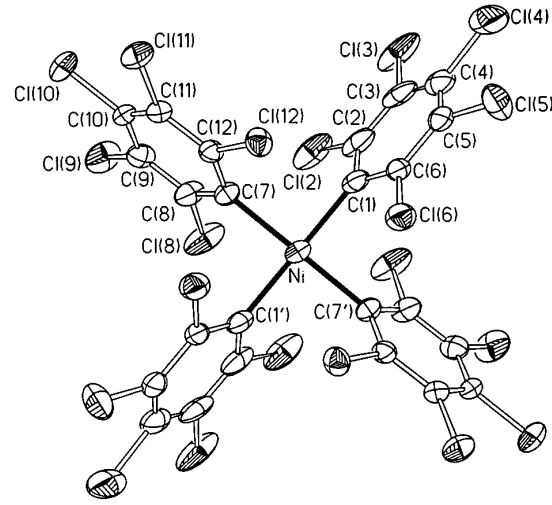



**Fig. 1** Thermal ellipsoid diagram of the anion of **2**. Selected distances (pm) and angles (°): Ni–C(1) 200.1(8), Ni–C(7) 201.4(7); C(1)–Ni–C(7) 90.1(3), C(1)–Ni–C(1′) 178.6(5), C(7)–Ni–C(1′) 90.0(3), C(7)–Ni–C(7′) 178.9(4).

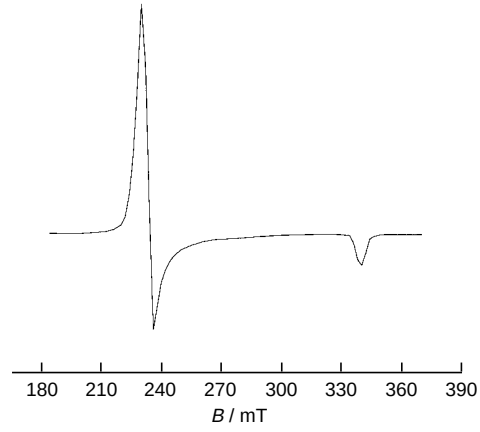



**Fig. 2** EPR spectrum of a powder sample of **2** (X-band, 77.3 K)

It can be concluded that the pentachlorophenyl group is a ligand especially well suited to stabilising unusual oxidation states, at least in the platinum-group metals.[9,14] Studies aimed at testing the reactivity of this unprecedented nickel(III) compound are in progress.

We thank the Dirección General de Enseñanza Superior (Projects PB95-0003-CO2-01 and PB95-0792) for financial support.

## Footnotes

† *Experimental procedure*: to a yellowish suspension of $[NBu_4]_2[Ni^{II}(C_6Cl_5)_4]$ **1** (0.5 g, 0.32 mmol) in $CH_2Cl_2$ (7 $cm^3$) at −40 °C was added $Cl_2$ dissolved in $CCl_4$ (0.18 mmol). The system changed immediately to green and, after addition of MeOH (20 $cm^3$) at −80 °C, the resulting green solid was filtered off in a low-temperature device, subsequently washed with cold $Et_2O$ (3 × 10 $cm^3$) and dried (**2**, 70% yield). Anal. Found: C 36.5, H 2.8, N 1.1; $C_{40}H_{36}Cl_{20}NNi$ requires: C 37.0, H 2.8, N 1.1%. IR(Nujol; $cm^{-1}$): selected absorptions associated with the $C_6Cl_5$ groups:[8] 827vs (X-sensitive vibr.), 675vs, 603s [ν(Pt–C)] and 275m.

‡ The fate of the metal-containing fragment could not be determined so far and hence we still do not know whether this reductive elimination process takes place inter- or intra-molecularly.

§ The cyclic voltammogram of **1** at 100 mV $s^{-1}$ scan rate in 0.1 M $NBu_4PF_6$ shows $E_{pa}$ = −0.055 V and $E_{pc}$ = −0.168 V *vs*. SCE.

¶ *Crystal data* for **2**·2$Et_2O$: $C_{48}H_{56}Cl_{20}NNiO_2$, $M$ = 1446.65, monoclinic, space group $C2/c$ (no. 15), $a$ = 1987.3(2), $b$ = 2167.8(1), $c$ = 1487.2(1) pm, β = 110.026(5)°, $U$ = 6.031(2) $nm^3$, $Z$ = 4, $F$(000) = 2940, $D_c$ = 1.593 g $cm^{-3}$, λ(Mo-Kα) = 71.073 pm, 344 parameters refined with 5300 reflections with $I > 2\sigma(I)$ to $R$ = 0.0736, $R_w$ = 0.1577. Atomic coordinates, bond lengths and angles, and thermal parameters have been deposited at the Cambridge Crystallographic Data Centre (CCDC). See Information for Authors, Issue No. 1. Any request to the CCDC for this material should quote the full literature citation and the reference number 182/365.

‖ EPR data were taken on a Varian E-112 spectrometer working in the X-band. Measurements at liquid-nitrogen temperature (77.3 K) were taken using a quartz immersion Dewar. The magnetic field was measured with a Bruker ER035M gaussmeter. The diphenylpicrylhydrazyl resonance signal [$g$ = 2.0037(2)] was used to determine the microwave frequencies.

** Other contributions such as charge-transfer, covalency, *etc*. can modify the principal $g$-values so as to make the crystal-field description inadequate. In fact, either positive or negative $g$-shifts are observed for square-planar low-spin $d^7$ complexes.[12]

## References

1 A. G. Lappin and A. McAuley, *Adv. Inorg. Chem*., 1988, **32**, 241; L. Sacconi, F. Mani and A. Bencini, in *Comprehensive Coordination Chemistry*, ed. G. Wilkinson, R. D. Gillard and J. A. McCleverty, Pergamon, Oxford, 1987, vol. 5, ch. 50, p. 1; R. I. Haines and A. McAuley, *Coord. Chem. Rev*., 1981, **39**, 77; K. Nag and A. Chakravorty, *Coord. Chem. Rev*., 1980, **33**, 87.

2 K. R. Dunbar, J.-S. Sun and A. Quillevéré, *Inorg. Chem*., 1994, **33**, 3598 and references therein.

3 J. J. G. Moura, M. Teixeira and I. Moura, *Pure Appl. Chem*., 1989, **61**, 915; R. Cammack, *Adv. Inorg. Chem*., 1988, **32**, 297; D. W. Margerum, *Pure Appl. Chem*., 1983, **55**, 23.

4 C. A. Marganian, H. Vazir, N. Baidya, M. M. Olmstead and P. K. Mascharak, *J. Am. Chem. Soc*., 1995, **117**, 1584 and references therein.

5 (*a*) L. A. van de Kuil, Y. S. J. Veldhuizen, D. M. Grove, J. W. Zwikker, L. W. Jenneskens, W. Drenth, W. J. J. Smeets, A. L. Spek and G. van Koten, *J. Organomet. Chem*., 1995, **488**, 191; (*b*) D. M. Grove, G. van Koten, P. Mul, R. Zoet, J. G. M. van der Linden, J. Legters, J. E. J. Schmitz, N. W. Murrall and A. J. Welch, *Inorg. Chem*., 1988, **27**, 2466; (*c*) D. M. Grove, G. van Koten, W. P. Mul, A. A. H. van der Zeijden, J. Terheijden, M. C. Zoutberg and C. H. Stam, *Organometallics*, 1986, **5**, 322; (*d*) D. M. Grove, G. van Koten, R. Zoet, N. W. Murrall and A. J. Welch, *J. Am. Chem. Soc*., 1983, **105**, 1379.

6 R. Usón, J. Forniés, P. Espinet, R. Navarro, F. Martínez and M. Tomás, *J. Chem. Soc., Chem. Commun*., 1977, 789.

7 C. Amatore and A. Jutand, *Organometallics*, 1988, **7**, 2203; T. T. Tsou and J. K. Kochi, *J. Am. Chem. Soc*., 1979, **101**, 7547; 1978, **100**, 1634; M. Almemark and B. Åkermark, *J. Chem. Soc., Chem. Commun*., 1978, 66.

8 (*a*) R. Usón and J. Forniés, *Adv. Organomet. Chem*., 1988, **28**, 219; (*b*) E. Maslowsky Jr., *Vibrational Spectra of Organometallic Compounds*, Wiley, New York, 1977, p. 437; (*c*) J. Casabó, J. M. Coronas and J. Sales, *Inorg. Chim. Acta*, 1974, **11**, 5.

9 J. Forniés, B. Menjón, R. M. Sanz-Carrillo, M. Tomás, N. G. Connelly, J. G. Crossley and A. G. Orpen, *J. Am. Chem. Soc*., 1995, **117**, 4295; R. Usón, J. Forniés, M. Tomás, B. Menjón, R. Bau, K. Sünkel and E. Kuwabara, *Organometallics*, 1986, **5**, 1576.

10 D. Xu, K. Miki, M. Tanaka, N. Kasai, N. Yasuoka and M. Wada, *J. Organomet. Chem*., 1989, **371**, 267; B. Longato, B. Corain, R. Angeletti and G. Valle, *Inorg. Chim. Acta*, 1987, **130**, 243; D. Xu, K. Miki, Y. Kai, N. Kasai and M. Wada, *J. Organomet. Chem*., 1985, **287**, 265; K. Miki, H. Taniguchi, Y. Kai, N. Kasai, K. Nishiwaki and M. Wada, *J. Chem. Soc., Chem. Commun*., 1982, 1178.

11 A. Martín and A. G. Orpen, *J. Am. Chem. Soc*., 1996, **118**, 1464.

12 J. A. Aramburu and M. Moreno, *J. Chem. Phys*., 1983, **79**, 4996.

13 T. J. Collins, T. R. Nichols and E. S. Uffelman, *J. Am. Chem. Soc*., 1991, **113**, 4708; H.-J. Krüger, G. Peng and R. H. Holm, *Inorg. Chem*., 1991, **30**, 734; see also refs. 2, 5(*b*) and 5(*d*).

14 M. P. García, M. V. Jiménez, L. A. Oro, F. J. Lahoz, M. C. Tiripicchio and A. Tiripicchio, *Organometallics*, 1993, **12**, 4660; M. P. García, M. V. Jiménez, L. A. Oro, F. J. Lahoz, J. M. Casas and P. J. Alonso, *Organometallics*, 1993, **12**, 3257; M. P. García, M. V. Jiménez, L. A. Oro, F. J. Lahoz and P. J. Alonso, *Angew. Chem., Int. Ed. Engl*., 1992, **31**, 1527.

*Received, 11th November 1996; Com. 6/07668H*

ChemComm
FEATURE ARTICLE

# Selective transformations of alkynes with ruthenium catalysts

**Christian Bruneau and Pierre H. Dixneuf***

*Laboratoire de Chimie de Coordination et Catalyse, URA CNRS 415, Université de Rennes, Campus de Beaulieu, 35042 Rennes, France*

**The electrophilic activation of terminal alkynes by suitable ruthenium(II) catalyst precursors has provided selective access to enol esters, functional dienes, ketoesters and furans. The step-by-step modification of the ligands of simple complexes such as (arene)$RuCl_2(PR_3)$, $[Ru(\mu\text{-}O_2CH)(CO)_2(PR_3)]_2$ or (diphosphine)$Ru(allyl)_2$, has allowed the determination of efficient catalytic conditions for regio- and stereo-selective additions to alkynes. The utilization of electron-rich ruthenium(II) complexes containing the bulky pentamethylcyclopentadienyl ligand, has made possible the catalytic carbon–carbon bond forming reaction from alkynes and allyl alcohol to give unsaturated aldehydes.**

## Introduction

Transition-metal complexes are powerful catalysts for organic synthesis and polymerization, for when the suitable ligands are associated with the metal centre, they can offer chemio-, regio- or stereo-selectivity under mild conditions. During the last decade, ruthenium catalysts have brought a tremendous contribution to organic synthesis not only for enantioselective hydrogenation with chiral ruthenium complexes[1] or for mild oxidation reactions,[2] but also for the activation of simple unsaturated hydrocarbon molecules to produce functional derivatives[3–5] or polymers,[6] thus avoiding the use of toxic reagents. As ruthenium catalysts tolerate most functional groups they have been used to promote new methods for carbon–heteroatom and carbon–carbon bond formation by combination of two substrates with atom economy.[7]

Our experience in the stoichiometric activation of alkynes by organoruthenium derivatives[8] has offered an evaluation of the electrophilicity of ruthenium(II) precursors in activation processes. These studies have aided progress towards the field of catalysis for the selective transformation of alkynes for which several aspects have been considered: (i) the study of simple catalytic additions to alkynes provided by electrophilic activation with ruthenium(II) complexes in order to achieve excellent regioselectivity and avoid the formation of by-products; (ii) the possibility of step-by-step modification of the catalyst, by using tunable ligands, in order to create activity at the metal centre and favour regioselectivity; and (iii) the formation from alkynes of simple reagents that are useful synthetic intermediates or polymer precursors.

Here, we describe some aspects of ruthenium-catalysed syntheses: the Markovnikov and *anti*-Markovnikov additions to alkynes, the synthesis and uses of the resulting enol esters, the recovery of the ruthenium catalysts, the stereoselective transformation of prop-2-yn-1-ols and the synthesis of functional furans, dienes or unsaturated aldehydes. All these reactions are performed using air-stable ruthenium catalysts which can be easily prepared and used in organic synthesis.

## Ruthenium-catalysed synthesis of enol esters *via* selective addition of carboxylic acids to alkynes

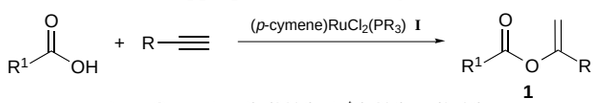
Enol esters have specific industrial applications as monomers for the production of various polymers and copolymers.[9] They are also useful reagents for carbon–carbon and carbon–heteroatom bond formation *via* the generation of enolates or acylation reactions. Although mercury(II)-assisted carboxylation of alkynes[10] constitutes an efficient route to enol esters, an environment-friendly process would be preferred. We have considered the possibility of electrophilic activation of alkynes by ruthenium(II) complexes towards the addition of carboxylates. While $RuCl_3 \cdot xH_2O$ can be used to catalyse the addition of carboxylic acids to phenylacetylene at 120 °C with no regioselectivity,[11] by contrast, (arene)$RuCl_2(PR_3)$ **I** complexes emerged as very efficient catalysts for the regioselective Markovnikov addition of carboxylates to the internal carbon of the triple bond of terminal alkynes, and the production of alk-1-en-2-yl esters **1** (Scheme 1).[11,12] A variety of carboxylic acids can thus be added directly to aliphatic alkynes such as hex-1-yne and propyne at 80–100 °C in toluene.

The ruthenium-catalysed addition of carboxylic acids has been used for the production of functional dienes, the 2-acyloxy-1,3-dienes **2** from conjugated enynes (Scheme 2).[13]

In the presence of (arene)$RuCl_2(PR_3)$ catalysts, these reactions took place under mild conditions and without racemization of the substrates. Thus, the addition of optically pure *N*-protected aminoacids led to optically pure *N*-protected amino acid enol **3**[14] and dienol **4**[13] esters in good yields and high regioselectivity (Scheme 3).

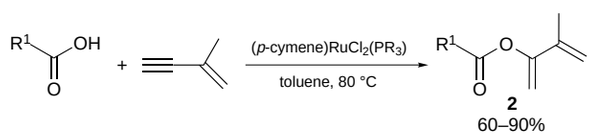
### *Uses of enol esters as acylation reagents*

Enol esters have been used in a variety of reactions involving carbon–carbon bond formation, such as acylation of carbonyl compounds,[15] palladium-catalysed allylation,[16] arylation[17] and aldol-type condensation,[18] cyclopropanation,[19] Diels–Alder cycloaddition[20] and hydroformylation.[21] However, the most widespread use of enol esters in organic synthesis is in the acylation of alcohols and amines,[22] including enzymatic chemistry.[23] Alk-2-enyl esters are much more reactive than alkyl esters and can be used as efficient acylating reagents. In addition, they release a neutral ketone as the only by-product and therefore are appropriate for the acylation of substrates

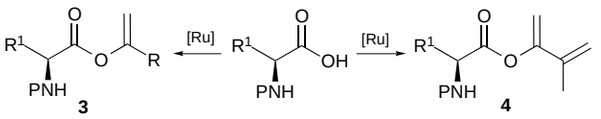



R = *n*-$C_4H_9$; R = Ph (92%), $Bu^t$ (78%), H (94%)
R = Me; R = Ph (87%), $C_6H_4Cl$-*p* (58%)

**Scheme 1**




**Scheme 2**




P = Boc ($Bu^tO_2C$-) or Z ($PhCH_2O_2C$-)

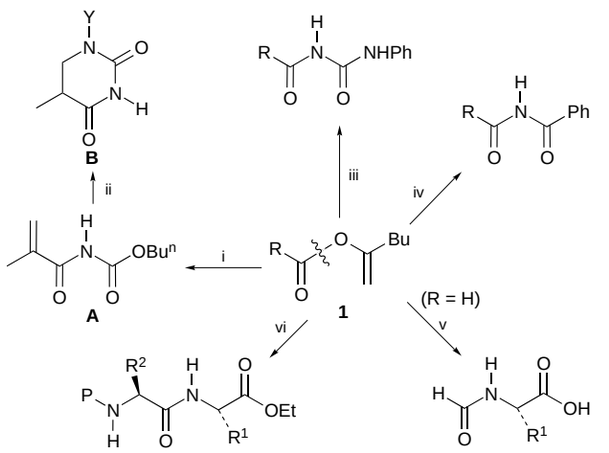
**Scheme 3**

sensitive to acids (from acyl chloride or anhydrides) or bases (such as dimethylaminopyridine).

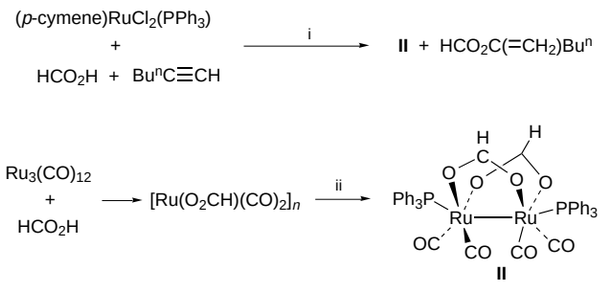
Thus, hex-1-en-2-yl formate is an efficient and easy-to-handle formylating reagent for the preparation of formamides at room temperature from primary and secondary amines, and esters from alcohols at 50 °C in the presence of catalytic amounts of imidazole (Scheme 4).[24] The *N*-formylation of unprotected amino acids was also possible in THF at 70 °C, and formyl-leucine, -alanine, -phenylalanine and -glycine were prepared in 84, 91, 87 and 91% isolated yields, respectively. Esters of amino acids were also efficiently acylated by enol esters derived from *N*-protected amino acids to produce dipeptides.[25] Compounds of the type $H_2NC(O)Y$ (Y = alkyl, aryl, OR, $NR_2$), which could not be acylated by enol esters, react upon the addition of a stoichiometric amount of NaH, allowing the one-pot acylation of amides, carbamates and ureas in high yields.[26] Of special interest is the butyl methacryloylcarbamate **A**, which reacts readily with primary amines to afford dihydropyrimidinediones **B** (Scheme 4).[27]

However, (arene)$RuCl_2(PR_3)$ **I** complexes were not efficient catalysts for the addition of oxalic acid and α-hydroxy acids to terminal alkynes. The use of the binuclear derivative $[Ru(O_2CH)(CO)_2(PPh_3)]_2$ **II**, an easy-to-handle, air-stable ruthenium complex produced by treatment of (*p*-cymene)-$RuCl_2(PPh_3)$ with formic acid in the presence of hex-1-yne or by reaction of $[Ru(O_2CH)(CO)_2]_n$ with $PPh_3$[26] according to Scheme 5, made possible the addition of oxalic acid to hex-1-yne and propyne at 100 °C to afford dihex-1-en-2-yl **5** and diisopropenyl **6** oxalates, respectively (Scheme 6).[28] Compounds **5** and **6** actually led to a variety of α-dicarbonyl compounds by stepwise reactions with alcohols (**C**), amines (**D**) or aminoalcohols (**E**) (Scheme 7).

Mandelic acid could also be added to alkynes in the presence of **II** to afford alk-1-en-2-yl mandelates **7** in THF, whereas




**Scheme 4** Acylation of nucleophiles with enol esters. *Reagents and conditions*: i, NaH, $H_2NCO_2Bu^n$, room temp.; ii, Y-$NH_2$, room temp.; iii, NaH, $H_2NCONHPh$, room temp.; iv, NaH, $H_2NCOPh$, room temp.; v, $H_2NCHR^1CO_2H$, THF, 70 °C; vi, $H_2NCHR^1CO_2Et$, KCN (cat.), room temp.



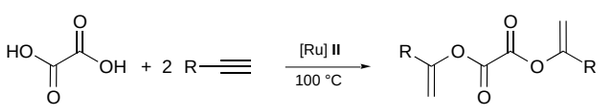

**Scheme 5** Preparation of complex **II**. *Reagents and conditions*: i, 60 °C; ii, $PPh_3$, $Et_2O$, reflux, 4 h.

dioxolanones **8** were formed stereoselectively in toluene *via* a subsequent ruthenium(II) electrophilic activation of the double bond of the enol ester **7** towards the addition of the hydroxy group (Scheme 8).[29]

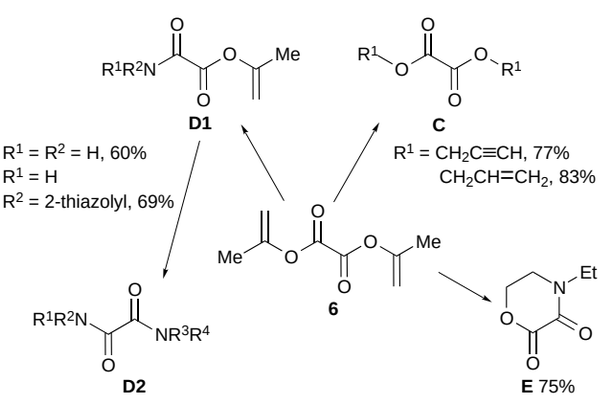
$[Ru(O_2CH)(CO)_2(PR_3)]_2$ complexes appeared to be the best catalysts for the Markovnikov addition of carboxylic acids to unfunctionalized alkynes, especially the terminal unconjugated octa-1,7-diyne which was transformed into the dienyl esters **9** in >80% isolated yields after reaction at 80 °C for 8 h (Scheme 9).

Alkenylruthenium complexes, such as (hexamethylbenzene)RuCl($PMe_3$)[C(OMe)=CHR] **III** (R = Me, Ph), prepared from the reaction of ($\eta^6$-$C_6Me_6$)$RuCl_2(PMe_3)$ with terminal alkynes in the presence of $NaPF_6$ in methanol followed by deprotonation with $Bu^tOK$, also appeared to be very good catalyst precursors. These alkenylruthenium complexes were very efficient for the preparation of dioxolanones **8** with good diastereoselectivity.[30] They were particularly active for the preparation of enol **10** and dienol **11** methacrylates (Scheme 10), both of which are excellent precursors for the preparation of polymers by copolymerization and polycondensation, respectively.[30]

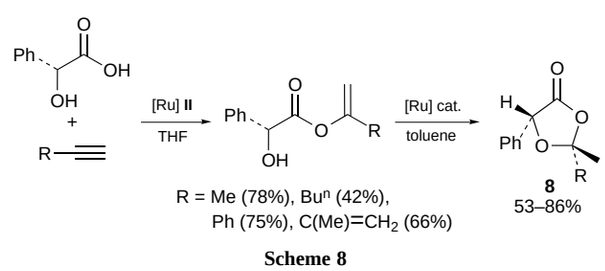
For the above reactions to be economically useful, easy recovery of the ruthenium catalyst is required. A simple solution



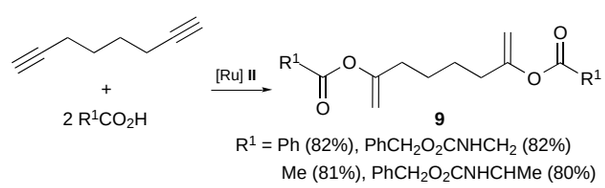

**Scheme 6**




**Scheme 7**




**Scheme 8**




**Scheme 9**

was found to be modification of the solubility of the ruthenium catalyst. The easy coordination of the polymeric diphenylphosphinoalkane $Ph_2P(CH_2CH_2)_nCH_2CH_3$, prepared by BuLi-initiated polymerization of ethene followed by reaction with $Ph_2PCl$, led to the preparation of the binuclear ruthenium complex $[Ru(O_2CH)(CO)_2\{Ph_2P(CH_2CH_2)_nCH_2CH_3\}]_2$.[31] This complex (**IV**; $n$ = 50) was soluble in toluene at 100 °C and catalysed the addition of carboxylic diacids to terminal alkynes (Scheme 11). When the reaction mixture was cooled to room temperature the complex became insoluble, the diester **12** was isolated and the catalyst could be recovered unchanged by simple filtration and used again at least six times without loss of activity and regioselectivity.

### *Mechanism*

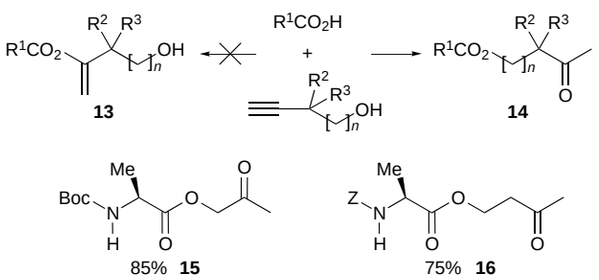
Although the catalytic mechanism has not yet been determined fully, an important feature for the addition of the carboxylate to C(2) of terminal alkynes is the presence of a monophosphine coordinated to the ruthenium centre. The nature of the phosphine does not seem to be crucial, as $PMe_3$, $PBu_3$ and $PPh_3$ led to similar results. We have shown by performing cross-reactions that the carboxylate ligand attached to the ruthenium centre in either $[Ru(O_2CR)(CO)_2(PPh_3)]_2$ or (arene)Ru-$Cl(O_2CR)$ complexes did not add to the alkyne, but only to the carboxylate generated from the free carboxylic acid used as reagent. The fact that the reaction proceeds *via* external attack of the nucleophilic carboxylate to the electrophilically activated alkyne rules out the possibility of insertion of the triple bond into an Ru–O(carboxylate) bond.

### Catalytic synthesis of ketoesters

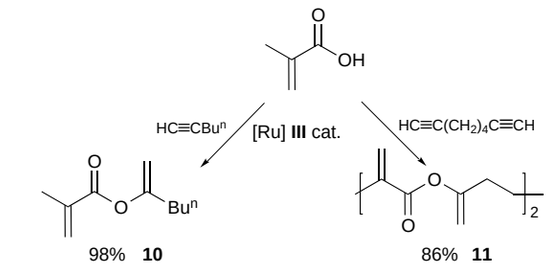
The ruthenium(II)-catalysed addition of carboxylic acids to prop-2-ynylic and but-3-ynylic alcohols did not lead to the expected hydroxy enol esters **13**, but to ketoesters **14** (Scheme 12).[32] At 60 °C, (arene)$RuCl_2(PPh_3)$ complexes catalysed the addition of N-protected amino acids to prop-2-ynylic[33] and but-3-ynylic[32] alcohols to give β-oxopropyl **15** and γ-oxobutyl **16** esters without racemization. For the addition of carboxylic acids to sterically hindered alkynols, the use of $[Ru(O_2CH)(CO)_2(PPh_3)]_2$ **II** was required, as exemplified by the selective transformation of steroids **17** containing both an alkynyl and a hydroxy group attached to C(17). In that case, the addition took place without racemization and with retention of the configuration of C(17) and led to steroids **18** (Scheme 13).[34] The mechanism of this reaction involves the addition of the carboxylate to C(2) of the alkyne followed by internal transesterification. When the geometry of the starting hydroxy alkyne did not allow the intramolecular transesterification, hydroxylated enol esters were formed. This was confirmed by the addition of carboxylic acids to (*E*)-3-methylpent-2-en-4-yn-1-ol, which selectively afforded the hydroxylated 2-carboxy-1,3-dienes **19** in good yields (Scheme 14).[32]

### Catalytic synthesis of furans

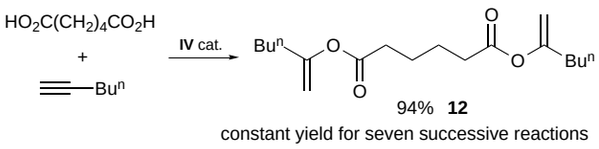
(*Z*)-3-Methylpent-2-en-4-yn-1-ol has suitable geometry for the intramolecular addition of the hydroxy group to the triple bond, under electrophilic ruthenium-catalysis conditions. Indeed, at 60 °C in the presence of a catalytic amount of (*p*-cymene)Ru-$uCl_2(PPh_3)$ **I**, furan **20** was formed selectively (Scheme 15),resulting from cyclization of the starting enynol.[35] This reaction, which took place under neutral conditions, corresponded to the first ruthenium-catalysed Markovnikov intramolecular addition of a hydroxy group to a non-activated terminal triple bond. We have shown that the absence of a base and the relatively low reaction temperature ( < 110 °C) made




**Scheme 12**

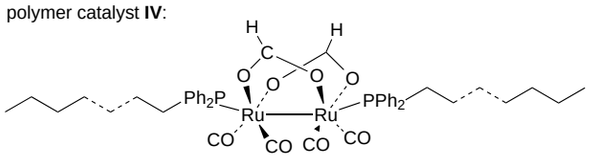



**Scheme 10**

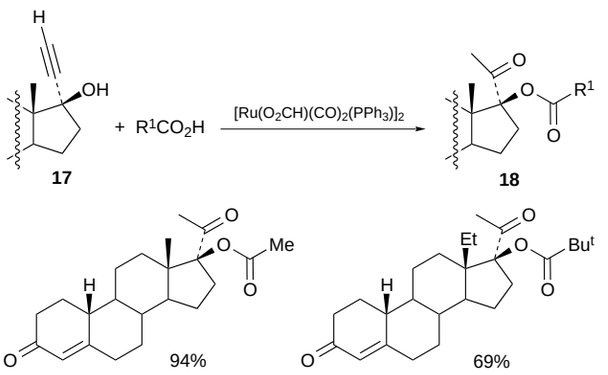



constant yield for seven successive reactions

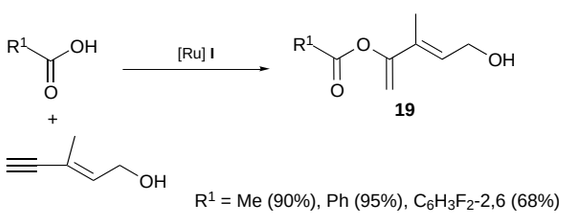
polymer catalyst **IV**:



**Scheme 11**




**Scheme 13**




**Scheme 14**

possible the cyclization of enynols containing trimethylsilylethynyl or cyanide groups,[36] the starting (*Z*)-enynols being easily prepared by reaction of organometallic derivatives with the corresponding (*Z*)-aldehyde resulting from the oxidation of the unsubstituted (*Z*)-enynol.

### Synthesis of (*Z*)-enol esters: *anti*-Markovnikov addition of carboxylic acids to alkynes

After developing the catalytic Markovnikov addition of carboxylic acids to terminal alkynes, it became a challenge to perform the *anti*-Markovnikov addition corresponding to the reverse regioselectivity. The idea was to generate vinylidene–ruthenium species able to make the terminal carbon of the alkyne electrophilic. Such an example of activation of terminal alkynes was shown in the regioselective synthesis of vinylic carbamates **21** by the reaction of secondary amines, $CO_2$ and terminal alkynes in the presence of (arene)$RuCl_2(PR_3)$ catalyst precursor (Scheme 16), which can be explained *via* the formation of a ruthenium–vinylidene [Ru=C=CHR$^1$] active species.[37]

Our approach to the reversal of the regioselectivity of the addition to alkynes was to modify the ruthenium catalysts, first by introducing hydrocarbon ligands, labile under acidic conditions, to provide vacant coordination sites, and secondly by replacing the monophosphine ligands by bidentate diphosphines which are known to stabilize intermediate organometallic catalytic species. New ruthenium complexes containing two allylic ligands and a tunable diphenylphosphinoalkane were prepared according to a known method (Scheme 17).[38]

The step-by-step lengthening of the hydrocarbon chain from one to four carbons between the two diphenylphosphino groups made it possible to observe important differences in the catalytic behaviour of these catalyst precursors. The complex (dppb)Ru(2-methylallyl)$_2$ was shown to be the best catalyst precursor, in terms of reactivity and regioselectivity, for the addition of benzoic acid to the C(1) of terminal alkynes in good yields in toluene at 65 °C (Table 1).[39]

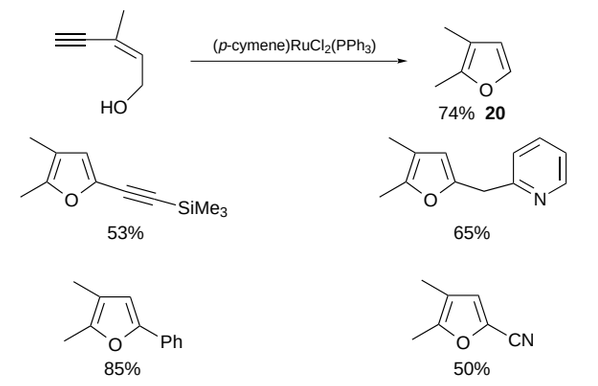
Moreover, the stereoselectivity was excellent and (*Z*)-enol esters of type **22** could be obtained in > 95% stereoselectivity (Scheme 18). The regio- and stereo-selectivities of this addition were very dependent on (i) the bulkiness of both the carboxylic acid and the alkyne, (ii) the reaction temperature, and (iii) the acidity of the carboxylic acid. In general terms, we have shown that the lower the reaction temperature, the higher the regio- and stereo-selectivities, but a minimum temperature had to be found to obtain a reasonable reaction rate.[40]

Saturated and unsaturated aliphatic acids, and substituted aromatic acids have allowed the preparation of a variety of new (*Z*)-enol esters upon addition to hex-1-yne and phenylacetylene. The absence of racemization under mild temperature conditions made it possible to synthesise optically pure (*Z*)-enol amino acid esters **23** from N-protected amino acids. In the presence of catalytic amounts of (dppb)Ru(2-methylpropenyl)$_2$, this reaction could be extended to octa-1,7-diyne to stereoselectively produce (*Z*,*Z*)-1,8-dienyl esters **24**, by contrast to the isomers **9**. This *anti*-Markovnikov addition could be extended to conjugated enynes when bulky carboxylic acids were used. The most efficient catalyst precursor was (dppb)Ru(2-methylallyl)$_2$ which led to 1-carboxy-1,3-dienes **25** at 40–65 °C in good yields and very high stereoselectivity with benzoic and *N*-protected amino acids (Scheme 19).

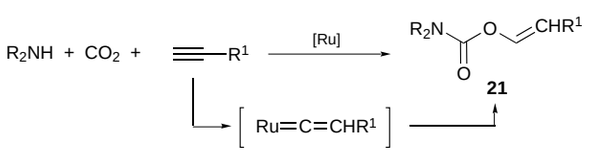
The addition of carboxylic acids to trimethylsilylacetylene was also possible in the presence of (dppb)Ru(2-methylpropenyl)$_2$ as catalyst precursor, but in this special case, the bulkiness of the alkyne allowed a more rapid reaction at 50–60 °C in the presence of (dppe)Ru(2-methylallyl)$_2$ as catalyst, affording functional trimethylsilylated alkenes in > 98% regio- and stereo-selectivity. The same reactivity was observed in the addition to bulky methyl prop-2-yn-1-yl ethers. By using (dppe)Ru(2-methylpropenyl)$_2$ as catalyst precursor, the rate of the reaction could be improved drastically and 81% yield of the (*Z*)-benzoate **26** was obtained with 100% stereoselectivity for the (*Z*)-isomer (Scheme 20).

The presence of an additional functionality close to the triple bond did not affect the reaction; (*Z*,*Z*)-4-methoxybuta-1,3-dienyl esters **27** were prepared at 65 °C in toluene in the presence of (dppb)Ru(2-methallyl)$_2$ as catalyst precursor with stereoselectivities > 97% from (*Z*)-1-methoxybut-1-en-3-yne (Scheme 21).

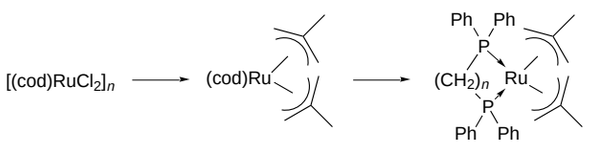
It is noteworthy that (diphosphine)Ru(2-methylpropenyl)$_2$ complexes were not able to promote the regioselective addition of carboxylic acids to the terminal carbon of the triple bond of prop-2-ynylic alcohols. Only ketoesters were formed, indicating that the regioselectivity of the addition of carboxylic acids was influenced by the presence of the hydroxy group as with (*p*-cymene)$RuCl_2(PPh_3)$ or $[Ru(O_2CH)(CO)_2(PPh_3)]_2$. This




**Scheme 15**




**Scheme 16**




**Scheme 17** *Reagents and conditions*: $Ph_2P(CH_2)_nPPh_2$, hexane, reflux, 5 h

**Table 1** Synthesis of hexenyl benzoates: influence of the nature of the diphosphine ligand in (diphosphine)Ru(methallyl)$_2$ catalyst precursors

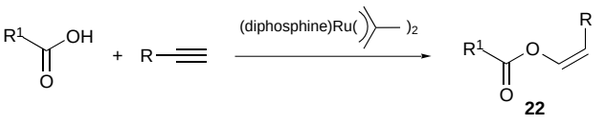
| | | Product selectivity (%) | | |
|---|---|---|---|---|
| Diphosphine | Reaction time/h | Hex-1-en-1-yl benzoate (*Z*) | Hex-1-en-1-yl benzoate (*E*) | Hex-1-en-2-yl benzoate |
| $Ph_2PCH_2PPh_2$ (dppm) | 3 | 16 | 4 | 80 |
| $Ph_2PCH_2CH_2PPh_2$ (dppe) | 24 | 72 | 21 | 7 |
| $Ph_2PCH_2CH_2CH_2PPh_2$ (dppp) | 24 | 69 | 6 | 25 |
| $Ph_2PCH_2CH_2CH_2CH_2PPh_2$ (dppb) | 2.5 | 98 | 2 | 0 |

behaviour clearly exhibited the determinant role of the hydroxy group of alkynols.

This method offers the first stereoselective synthesis of (*Z*)-enol esters in one step from terminal alkynes and carboxylic acids. These (*Z*)-esters are formally masked aldehydes allowing the functionalization at C(1) of terminal alkynes: two equivalents of secondary amines reacted with (*Z*)-enol esters at room temperature to afford (*E*)-enamines **28** in very high yields (Scheme 22). This two-step synthesis of enamines from terminal alkynes and amines represents a complementary method to the mercury-catalysed addition of amines to alkynes which leads to enamines resulting from the addition of the amine to the internal carbon of the triple bond.

### Catalytic synthesis of unsaturated aldehydes and acetals: oxidative coupling of allyl alcohol with alkynes

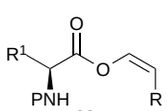
The coupling of terminal alkynes with allyl alcohol promoted by $RuCl(PPh_3)_2(C_5H_5)$–$NH_4PF_6$ to afford unsaturated ketones has been demonstrated to result from the formation of the ruthenium–vinylidene intermediate $[Ru{=}C{=}CHR(PPh_3)(C_5H_5)]^+$, followed by the addition of the alcohol to the electrophilic carbene carbon atom.[41] We have shown that the use of an analogous ruthenium(II) catalyst, $RuCl(cod)(C_5Me_5)$ **V**, which contains a labile ligand (cod = cycloocta-1,5-diene) and an electron-donating, bulky $C_5Me_5$ group led to a quite different reaction. The carbon–carbon coupling of the C≡C and the C=C bonds led to the formation of γ,δ-unsaturated aldehydes **29a** and **29b** (Scheme 23).[42] It is noteworthy that the reaction can be carried out in water (allyl alcohol–water, 1 : 8) to achieve the best yields, and that the formation of the branched isomer was always favoured, it was the only product from the bulky *tert*-butylacetylene (Table 2).



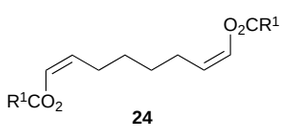

**22**

R = $Bu^n$; $R^1$ = Ph (95%), $Ph_2CH$ (97%), $Bu^tO_2CNHCH(CH_2Ph)$ (97%)
R = Ph; $R^1$ = $Bu^n$ (92%), $CF_3$ (90%), $MeOCH_2$ (96%), 2-HO-$C_6H_4$ (94%)

**Scheme 18**

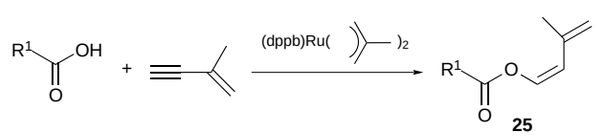


**23**



**24**

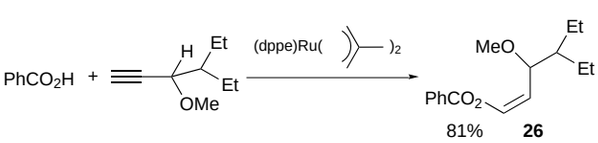
$R^1$ = H (88%), Me (85%), Ph (92%),
$PhCH_2O_2CNHCH_2$ (89%)




**25**

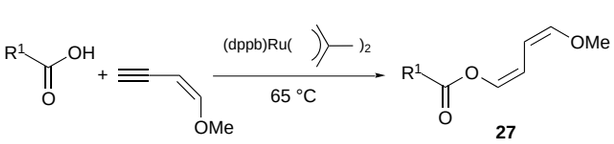
$R^1$ = Ph (92%), *n*-$C_4H_9$ (77%)

**Scheme 19**




81% **26**

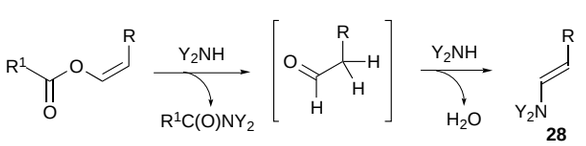
**Scheme 20**




**27**

$R^1$ = Ph (81%), $PhCH_2$ (76%),
$MeOCH_2$ (69%)

**Scheme 21**




**28**

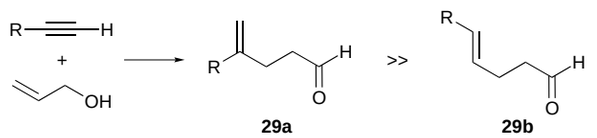
**Scheme 22**

The reaction when applied to symmetrically substituted alkynes, constituted an excellent method for the production of the corresponding γ,δ-unsaturated aldehydes **30** (Scheme 24).[43] Moreover, it showed that the reaction was not restricted to terminal alkynes and did not involve a vinylidene intermediate. The experiments suggested that the mechanism involved the displacement of cod and the oxidative coupling of C≡C and C=C bonds to generate intermediate **F** or **G**. The bulkiness of the R group favoured the formation of **F** and thus that of isomer **29a**.

It is noteworthy that the ruthenium(IV) precursor, $RuCl_2(\eta^3\text{-}CH_2CH{=}CH_2)(C_5Me_5)$, also catalysed the above reaction. However, the precursor was expected to partially form ruthenium(II) species *via* the loss of allyl chloride, but in the presence of ruthenium(IV) species, the aldehydes were transformed into the corresponding acetals with allyl alcohol.

### Conclusion

The selective catalytic reactions described show that slight modifications of ruthenium(II) catalyst precursors allow the activation of alkynes, to achieve high regioselectivity in the

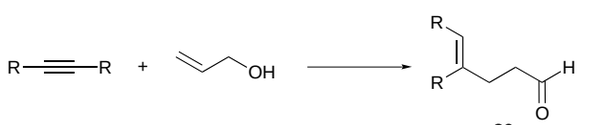


**29a** **29b**

**Scheme 23** *Reagents and conditions*: [$Ru^{II}$] **V** (cat.), room temp., 10–15 min

**Table 2** Formation of γ,δ-unsaturated aldehydes **29**

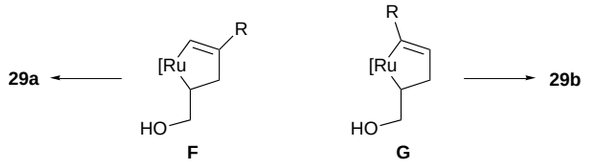
| R | Yield (%) | Branched : linear **29a** : **29b** |
|---|---|---|
| Ph | 85 | 75 : 25 |
| $C_6H_{13}$ | 83 | 80 : 20 |
| $(CH_2)_2OH$ | 75 | 58 : 42 |
| *p*-$MeOC_6H_4$ | 82 | 68 : 32 |
| $Bu^t$ | 60 | 100 : 0 |



**30**

R = Et (89%), Ph (95%)

**Scheme 24**




**F** **G**

**Scheme 25**

formation of carbon–heteroatom bonds. By contrast, the use of electron-rich ruthenium(II) complexes favours the formation of carbon–carbon bonds by oxidative coupling of C≡C and C=C bonds. The tolerance of ruthenium(II) complexes for functional groups, which we observed in the synthesis of enol esters, carboxydienes, ketoesters, steroids, furans and unsaturated aldehydes, may presage an important development of the use of ruthenium complexes in catalysis and polymerization in the near future.

**Christian Bruneau graduated as Engineer in chemistry in Rouen (1974) and obtained his Doctorate degree at the National School of Chemistry in Rennes (ENSCR). He was appointed research engineer at CNRS in 1980, and since 1986 he has been developing his research at the University of Rennes (URA CNRS 415) in the field of homogeneous catalysis by transition-metal complexes. His main research interests are in activation of alkynes, catalytic transformations of $CO_2$ and carbonates and enantioselective hydrogenation.**

**The recent research interests of Pierre Dixneuf are in the fields of activation of molecules by metal complexes, especially ruthenium derivatives, for selective organic catalysis and the design of unsaturated, carbon-rich organometallics. He was born in Anjou and studied in Rennes (Bretagne). He prepared his doctorate with Professor R. Dabard and did postdoctoral research in Brighton with Professor M. F. Lappert. Professor in Rennes since 1978, he is now the head of a Research Unit, associated with the CNRS, on molecular chemistry and electrochemistry: 'Organometallics and catalysis'. He has been honoured by the awards of the A. von Humboldt Foundation and the French Académie des Sciences. He is a 1996 Laureate of the JSPS (Japan) invited fellowship.**

## References


1 R. Noyori, *Asymmetric Catalysis in Organic Synthesis*, Wiley, New York, 1993; S. Akutagawa, *Appl. Catal. A: General*, 1995, **128**, 171.
2 S. H. Murahashi, T. Nota, N. Miyaguchi and T. Nakato, *Tetrahedron Lett.*, 1992, **33**, 6991; S. H. Murahashi and T. Nota, *Synthesis*, 1993, 433.
3 T. Kondo, A. Tanaka, S. Kotachi and Y. Watanabe, *J. Chem. Soc., Chem. Commun.*, 1995; 413, S. W. Zhang, T. Mitsudo, T. Kondo and Y. Watanabe, *J. Organomet. Chem.*, 1995, **485**, 55; T. Mitsudo, S. W. Zhang, M. Nagao and Y. Watanabe, *J. Chem. Soc., Chem. Commun.*, 1991, 598; T. Mitsudo, Y. Hori, Y. Yamakawa and Y. Watanabe, *J. Org. Chem.*, 1987, **52**, 2230.
4 N. Chatani, Y. Fukumoto, T. Ida and S. Murai, *J. Am. Chem. Soc.*, 1993, **115**, 11614; S. Murai, F. Kakiuchi, S. Sekine, Y. Tanaka, A. Kamatani, M. Sonoda and N. Chatani, *Nature (London)*, 1993, **366**, 529; S. Murai, *J. Synth. Org. Chem. Jpn.*, 1994, **52**, 120; F. Kakiuchi, Y. Tanaka, T. Sato, N. Chatani and S. Murai, *Chem. Lett.*, 1995, 679; F. Kakiuchi, Y. Yamamoto, N. Chatani and S. Murai, *Chem. Lett.*, 1995, 681.
5 H. Nishiyama, Y. Itoh, Y. Sugawara, H. Matsumoto, K. Aoki and K. Itoh, *Bull. Chem. Soc. Jpn.*, 1995, **68**, 1247; A. Demonceau, E. Abreu Dias, C. A. Lemoine, A. W. Stumpf and A. F. Noels, *Tetrahedron Lett.*, 1995, **36**, 3519; S. H. Kim, W. J. Zuercher, N. B. Bowden and R. H. Grubbs, *J. Org. Chem.*, 1996, **61**, 1073.
6 D. M. Lynn, S. Kanaoka and R. H. Grubbs, *J. Am. Chem. Soc.*, 1996, **118**, 784; R. H. Grubbs, S. J. Miller and G. C. Fu, *Acc. Chem. Res.*, 1995, **28**, 446; A. W. Stumpf, E. Saive, A. Demonceau and A. F. Noels, *J. Chem. Soc., Chem. Commun.*, 1995, 1127.
7 B. M. Trost, *Angew. Chem., Int. Ed. Engl.*, 1995, **34**, 259.
8 H. Le Bozec, K. Ouzzine and P. H. Dixneuf, *Organometallics*, 1991, **10**, 2768; H. Le Bozec, D. Pilette and P. H. Dixneuf, *New J. Chem.*, 1990, **14**, 793; H. Le Bozec, K. Ouzzine and P. H. Dixneuf, *J. Chem. Soc., Chem. Commun.*, 1989, 219; D. Pilette, S. Moreau, H. Le Bozec, P. H. Dixneuf, J. Corrigan and A. J. Carty, *J. Chem. Soc., Chem. Commun.*, 1994, 409; P. Haquette, N. Pirio, D. Touchard, L. Toupet and P. H. Dixneuf, *J. Chem. Soc., Chem. Commun.*, 1993, 163; D. Touchard, P. Haquette, A. Daridor, L. Toupet and P. H. Dixneuf, *J. Am. Chem. Soc.*, 1994, **116**, 11157; D. Touchard, N. Pirio and P. H. Dixneuf, *Organometallics*, 1995, **14**, 4920.
9 J. P. Monthéard, M. Camps, G. Seytre, J. Guillet and J. C. Dubois, *Makromol. Chem.*, 1978, **72**, 45; A. Seidel, E. Jägers and F. Bylsma, *Eur. Pat.*, 0574725 A1, 1993.
10 E. S. Rothman, S. S. Hecht, P. E. Pfeffer and L. S. Silbert, *J. Org. Chem.*, 1972, **37**, 3551; P. F. Hudrlik and A. M. Hudrlik, *J. Org. Chem.*, 1973, **38**, 4254; R. C. Larock, K. Oertle and K. M. Beatty, *J. Am. Chem. Soc.*, 1980, **102**, 1966; Y. Kita, S. Akai, N. Ajimura, M. Yoshigi, T. Tsugoshi, H. Yasuda and Y. Tamura, *J. Org. Chem.*, 1986, **51**, 4150.
11 C. Ruppin and P. H. Dixneuf, *Tetrahedron Lett.*, 1986, **27**, 6323.
12 C. Bruneau, M. Neveux, Z. Kabouche and P. H. Dixneuf, *Synlett*, 1991, 755.
13 K. Philippot, D. Devanne and P. H. Dixneuf, *J. Chem. Soc., Chem. Commun.*, 1990, 1199.
14 C. Ruppin, P. H. Dixneuf and S. Lécolier, *Tetrahedron Lett.*, 1988, **29**, 5365.
15 E. S. Rothman and G. G. Moore, *Tetrahedron Lett.*, 1969, 2553; E. S. Rothman, G. G. Moore and A. N. Speca, *Tetrahedron Lett.*, 1969, 5205.
16 J. Tsuji, I. Minami and I. Shimizu, *Tetrahedron Lett.*, 1983, **24**, 5205.
17 M. Kosugi, I. Hagiwara, T. Sumiya and T. Migita, *J. Chem. Soc., Chem. Commun.*, 1983, 344.
18 Y. Masuyama, T. Sakai and Y. Kurusu, *Tetrahedron Lett.*, 1993, **34**, 653; Y. Masuyama, T. Sakai, T. Kato and Y. Kurusu, *Bull. Chem. Soc. Jpn.*, 1994, **67**, 2265.
19 A. Demonceau, E. Saive, Y. de Froidmont, A. F. Noels and A. J. Hubert, *Tetrahedron Lett.*, 1992, **33**, 2009; W. B. Motherwell and L. R. Roberts, *J. Chem. Soc., Chem. Commun.*, 1992, 1582.
20 M. E. Jung and J. P. Hudspeth, *J. Am. Chem. Soc.*, 1978, **100**, 4309; L. F. Tietze, A. Montenbruck and C. Schneider, *Synlett*, 1994, 509.
21 N. Sakai, K. Nozaki, K. Mashima and H. Takaya, *J. Am. Chem. Soc.*, 1993, **115**, 7033.
22 J. E. W. van Melick, J. W. Scheeren and R. J. F. Nivard, *Tetrahedron Lett.*, 1971, 2083; Y. Kita, H. Maeda, K. Onari, T. Okuno and T. Tamura, *J. Chem. Soc., Perkin Trans. 1*, 1993, 2999. Y. Kita, S. Akai, M. Yoshigi, Y. Nakajima, H.Yasuda and Y. Tamura, *Tetrahedron Lett.*, 1984, **25**, 6067; D. Villemin, B. Labiad and A. Loupy, *Synth. Commun.*, 1993, **23**, 419.
23 C. Larpent and X. Chasseray, *New J. Chem.*, 1993, **17**, 851; M. Uemura, H. Nishimura, S. Yamada, K. Nakamura and Y. Hayashi, *Tetrahedron Lett.*, 1993, **34**, 6581; Y. Kume and H. Ohta, *Tetrahedron Lett.*, 1992, **33**, 6367; M. Lobell and M. P. Schneider, *Tetrahedron: Asymmetry*, 1993, **4**, 1027.
24 M. Neveux, C. Bruneau and P. H. Dixneuf, *J. Chem. Soc., Perkin Trans. 1*, 1991, 1197.
25 Z. Kabouche, C. Bruneau and P. H. Dixneuf, *Tetrahedron Lett.*, 1991, **32**, 5359.
26 B. Seiller, D. Heins, C. Bruneau and P. H. Dixneuf, *Tetrahedron*, 1995, **51**, 10901.
27 B. Seiller, C. Bruneau and P. H. Dixneuf, *Synlett*, 1995, 707.
28 M. Neveux, C. Bruneau, S. Lécolier and P. H. Dixneuf, *Tetrahedron*, 1993, **49**, 2629.
29 M. Neveux, B. Seiller, F. Hagedorn, C. Bruneau and P. H. Dixneuf, *J. Organomet. Chem.*, 1993, **451**, 133.
30 O. Lavastre and P. H. Dixneuf, *J. Organomet. Chem.*, 1995, **488**, C9.
31 O. Lavastre, P. Bebin, O. Marchaland and P. H. Dixneuf, *J. Mol. Catal. A*, 1996, **108**, 29.
32 C. Bruneau, Z. Kabouche, M. Neveux, B. Seiller and P. H. Dixneuf, *Inorg. Chim. Acta*, 1994, **222**, 155.
33 D. Devanne, C. Ruppin and P. H. Dixneuf, *J. Org. Chem.*, 1988, **53**, 925.
34 C. Darcel, C. Bruneau, P. H. Dixneuf and G. Neef, *J. Chem. Soc., Chem. Commun.*, 1994, 333.
35 B. Seiller, C. Bruneau and P. H. Dixneuf, *J. Chem. Soc., Chem. Commun*., 1994, 493.
36 B. Seiller, C. Bruneau and P. H. Dixneuf, *Tetrahedron*, 1995, **51**, 13089.
37 R. Mahé, Y. Sasaki, C. Bruneau and P. H. Dixneuf, *J. Org. Chem.*, 1989, **54**, 1518.
38 M. Cooke, R. J. Goodfellow, M. Green and G. Parker, *J. Chem. Soc. A*, 1971, 16; J. P. Genêt, S. Mallart, C. Pinel, S. Jugé and J. A. Laffitte, *Tetrahedron: Asymmetry*, 1991, **2**, 43.
39 H. Doucet, J. Höfer, C. Bruneau and P. H. Dixneuf, *J. Chem. Soc., Chem. Commun.*, 1993, 850.
40 H. Doucet, B. Martin-Vaca, C. Bruneau and P. H. Dixneuf, *J. Org. Chem.*, 1995, **60**, 7247.
41 B. M. Trost, G. Dyker and R. J. Kulawiec, *J. Am. Chem. Soc.*, 1990, **112**, 7809.
42 S. Dérien and P. H. Dixneuf, *J. Chem. Soc., Chem. Commun.*, 1994, 2551.
43 S. Dérien, D. Jan and P. H. Dixneuf, *Tetrahedron*, 1996, **52**, 5511.


*6/04112D*

# The trityl group as a removable steric buttress in cycloaddition reactions

**Nandeo Choony, Anjum Dadabhoy and Peter G. Sammes***

*Molecular Probes Unit, Department of Chemistry, Brunel University, Uxbridge, UK UB8 3PJ*

**The trityl group is utilised as an effective, temporary, steric buttress in an intramolecular Diels–Alder reaction between an alkene and furan ring.**

Steric buttresses have been utilised to accelerate intramolecular cycloaddition reactions but those used hitherto have not been readily removed.[1] Herein we report an example of steric buttressing as an aid to a cycloaddition reaction that is otherwise thermodynamically disfavoured; subsequent to the cycloaddition reaction the steric buttress may be removed.

The example involves the attempted cycloaddition of *N*-allylfurfurylamine **1** to the cycloadduct **2**. Heating compound **1** at various temperatures does not show any sign of the cycloadduct product **2**.† This lack of cycloaddition is consistent with several reported attempts at a range of similar intramolecular cycloaddition reactions between isolated alkene bonds and the furan ring.[2] For example, Gshwend *et al.* attempted to prepare the related cycloadduct **3** from the corresponding amide **4** but found that this spontaneously ring opened to form the allyated furfurylamine **5**.[3]

In previous work we have shown that cycloadditions may be encouraged by use of appropriate steric buttressing; an example is with compound **6**, which undergoes cycloaddition to the adduct **8**, whereas the parent compound **7**, in which the methyl buttresses are absent, does not undergo cycloaddition.[4]

We argued that, by restricting the degrees of conformational freedom in the reacting arms of compound **1**, cycloaddition would also be more favourable. The protected amine derivatives **9**–**12** were therefore prepared, using variably sized protecting groups, and their behaviour to cycloaddition examined. Solutions of the protected amines were heated at various temperatures (100–135 °C), monitoring for the appearance of the expected cycloadducts **13**–**16** and thermodynamic equilibration by use of $^1$H NMR spectroscopy.

Of the derivatives, the *N*-trityl derivative **9** showed the greatest degree of cycloaddition (97.5%) (Table 1). The cycloadduct **13** showed a consistent $^1$H NMR spectrum—loss of the allyl group and furan protons and replacement by the higher field protons of the tricyclic product. Use of the smaller benzhydryl protecting group, as in **10**, gave an approximately 50 : 50 ratio of cyclised product **14** to the uncyclised material at equilibrium and use of the benzyl derivatives **11** and **12** gave even less of the required cycloadducts.

The trityl group could be easily removed from the cycloadduct, by brief treatment with warm ethanolic hydrochloric acid,[5] to produce the secondary amine **2**. The latter amine was stable for considerable periods at room temperature but, on heating, reverted to the open form **1**. The stereochemistry about the bridgehead proton suggested the depicted stereoisomer was formed (Fig. 1).

**1** R = H
**9** R = $Ph_3C$
**10** R = $Ph_2CH$
**11** R = Bn
**12** R = 2,4,6-$Me_3C_6H_2CH_2$

**2** R = H
**13** R = $Ph_3C$
**14** R = $Ph_2CH$
**15** R = Bn
**16** R = 2,4,6-$Me_3C_6H_2CH_2$

**6** R = Me
**7** R = H

**8** R = Me

**4** **3** **5**

**Table 1** Thermal equilibration of amines **1**, **9**–**12**

| Starting amine | Product[a] | Yield of product (%) isolated | Cyclisation conditions | Open : cyclic[b] |
|---|---|---|---|---|
| **1** | **2** | 0 | 110 °C, toluene, several days | 100 : 1 |
| **9** | **13** | 85 | 110 °C, toluene, 40 h | 2.5 : 97.5 |
| **10** | **14** | 35 | 135 °C, xylene, 34 h | 50 : 50 |
| **11** | **15** | —[c] | 135 °C, xylene, 60 h | 98 : 2 |
| **12** | **16** | —[c] | 135 °C, xylene, 60 h | 90 : 10 |

[a] Isolated by column chromatography. [b] Estimated by 360 MHz $^1$H NMR spectroscopy after thermal equilibration. [c] Isolation not attempted.

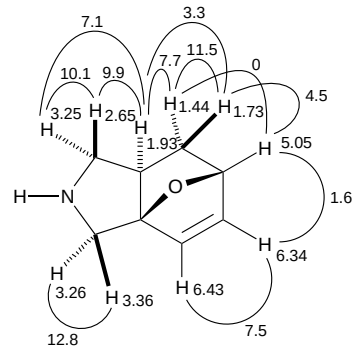



**Fig. 1** Chemical shifts and coupling constants for the amine **2**

As a cross-check, the cyclic amine **2** was also converted into the protected forms **14** and **15**; on heating these the thermal equilibrium between the open and closed forms was re-established.

Molecular models show that the trityl group and its derivatives are particularly bulky, thus restricting the conformational freedom of the diene and dienophile groups into ones where they are forced into close proximity. We are currently studying the use of the trityl group as a steric buttress in other modes of cycloaddition.

We thank the British Council for support of this work (to N. C.).

## Footnote

† All new compounds have been characterised by microanalysis and/or accurate mass measurement.

## References

1 *Cf*. P. G. Sammes and D. J. Weller, *Synthesis*, 1995, 1205.
2 D. D. Sternbach, D. M. Rosanna and K. D. Onan, *Tetrahedron Lett.*, 1985, **26**, 591; K. A. Parker and M. R. Adamchuk, *Tetrahedron Lett.*, 1978, 1689; M. E. Jung and J. Gervay, *J. Am. Chem. Soc.*, 1991, **113**, 224; S. Cauwberghs, P. J. De Clercq, B. Tinant and J. P. Declercq, *Tetrahedron Lett.*, 1988, **29**, 2493; L. L. Klein, *J. Org. Chem.*, 1985, **50**, 1770.
3 H. W. Gschwend, M. J. Hillman, B. Kiss and R. K. Rodebaugh, *J. Org. Chem.*, 1976, **41**, 104.
4 B. S. Orlek, P. G. Sammes and D. J. Weller, *Tetrahedron*, 1993, **49**, 8179.
5 H. E. Applegate, C. M. Cimarusti, J. E. Dolfini, P. T. Funke, W. H. Koster, M. S. Puar, W. A. Slusarchyk and M. G. Young, *J. Org. Chem.*, 1979, **44**, 811.

*Received, 14th January 1997; Com. 7/00313G*

# Approaches towards specifically functionalized cascade macromolecules: dendrimers with incorporated metal binding sites and their palladium(II) and copper(II) complexes

**George R. Newkome,* Jens Groß, Charles N. Moorefield and Barry D. Woosley**

*Center for Molecular Design and Recognition, Department of Chemistry, University of South Florida, Tampa, Florida 33620-5250, USA*

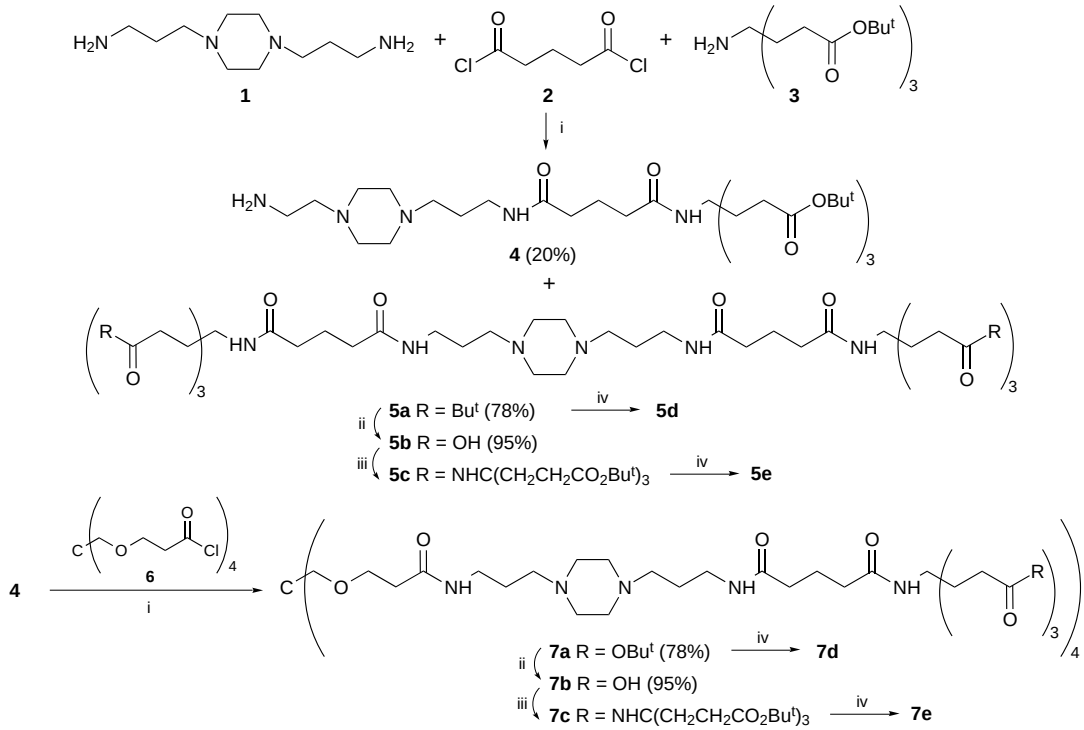
**Construction of ligand functionalized branched building blocks has afforded entrance to a series of dendrimers possessing multiple, internally incorporated piperazine moieties, which readily form $Pd^{II}$ and $Cu^{II}$ complexes.**

Metallodendrimer coordination spheres,[1–6] which are not completely filled, are of particular interest with regard to utilitarian aspects. We herein report the synthesis of related two- (**5a**,**c**) and four-directional (**7a**,**c**) dendrimers possessing specifically localized piperazine subunits and their complexation to afford $Cu^{II}$ and $Pd^{II}$ complexes.

*N*,*N*′-Bis(3-aminopropyl)piperazine **1**, as the metal binding site,[7] and the tris(*tert*-butyl ester)[8] **3** are readily linked in a one-pot reaction with glutaric acid dichloride **2** to form the extended building block **4**† and the colourless, two-directional dendrimer **5a**† in moderate yields (20 and 30%, respectively; Scheme 1). Amidation of **4** with the tetrakis(acyl halide) **6**, prepared from the corresponding tetraacid,[9] afforded (78%) the related four-directional dodecaester dendrimer **7a**† as a colourless solid. Hydrolysis of the *tert*-butyl esters **5a** and **7a** using formic acid generated (> 95%) the corresponding 6- (**5b**)† and 12-acid (**7b**).† Reaction of these polyacids with building block **3** under typical peptide coupling conditions (DCC, 1-BHT)[10] transformed each to the corresponding next higher 18- (**5c**)† and 36-ester (**7c**)† homologues.

Stable, orange microcrystalline $Pd^{II}$ complexes (**5d**,**e**) were formed upon stirring solutions of the 6- (**5a**) and 12-ester (**5c**) in MeCN at 25 °C with added $Pd(MeCN)_2Cl_2$. $^{13}C$ NMR Spectra (Fig. 1) provide direct evidence of a successful complexation at the piperazine binding loci due to the appearance of a new set of signals; titration of the free ligands by controlled addition of the metal salt can be conveniently followed by the observation of these absorptions. Evidence for complexation is provided by significant downfield shifts (3 and 1.2 ppm) for the C1 and C2 piperazine carbon atoms; however, the upfield shift (1.8 and 0.2 ppm) for C4 and C5, respectively, as well as the shift ($\Delta\delta$ = 0.6 ppm) for the innermost amido carbonyls support a further contribution to the coordination sphere. It is postulated that for metal chelation, the piperazine ring adopts the boat conformation[11] facilitating an overall compression of the molecular framework (Fig. 2).

Broadened, equatorial and axial $^1H$ NMR signals of the uncomplexed, rapidly interconverting piperazine ring are enveloped by a triplet assigned to the adjacent aminomethyl moiety (shaded region; Fig. 3). Whereas in the metal-complexed ring, there is a downfield shifted signal attributed to




**Scheme 1** *Reagents and conditions*: i, $EtPr^i_2N$, THF, 25 °C, 24 h; ii, $HCO_2H$, 25 °C, 12 h, then 40–50 °C, 3 h; iii, DCC, 1-HBT, 25 °C, then DMF, amine **3**, 25 °C, 48 h; iv, $Pd(MeCN)_2Cl_2$, MeCN, 25 °C

the equatorial protons ($\Delta\delta$ = 1.4 ppm) with a concomitant upfield shifted signal for the axial protons ($\Delta\delta$ = 0.05 ppm); geminal coupling in each signal suggests a frozen bond configuration in the complex. The triplet assigned to the adjacent methylene moiety is observed to broaden and shift downfield. Further, participation of the more closely juxtaposed amido moiety is evident from an observed upfield shift of the amide proton ($\Delta\delta$ = 0.35 ppm); the more distant amide proton adjacent to the branching centre is only slightly shifted ($\Delta\delta$ = 0.04 ppm downfield) upon complexation.

Similar first order patterns ($^{13}$C NMR) are found for the metal-free four-directional dendrimers **7a** and **7c**; however, upon complexation, only at early stages of the addition of the Pd salt was the spectral data of interest. Compared to the NMR spectra of the two-directional dendrimers, the signals exhibit enhanced broadening attributed to the presence of four competing adjacent binding sites. As the metal : ligand ratio increases above 1.2 equiv. (4 : 1 maximum), the metal complexes become markedly less soluble in diagnostic solvents further inhibiting NMR complexation monitoring. After addition of 4 equiv. of Pd salt, the resultant bright yellow complex precipitates from MeCN.

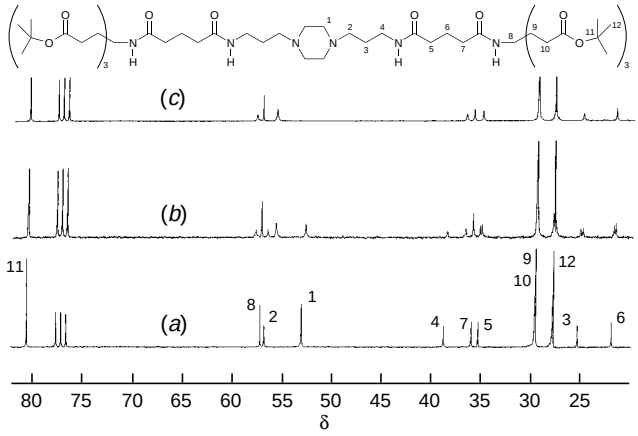



**Fig. 1** (*a*) $^{13}$C NMR Spectrum of the two-directional ligand **5a**; (*b*) with added 0.5 equiv. $PdCl_2(MeCN)_2$; (*c*) with 1 equiv. of $PdCl_2(MeCN)_2$

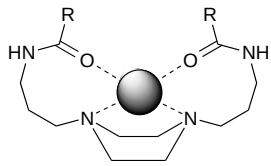



**Fig. 2** Pictorial representation of the metal centre depicting the interaction of the juxtaposed amido groups

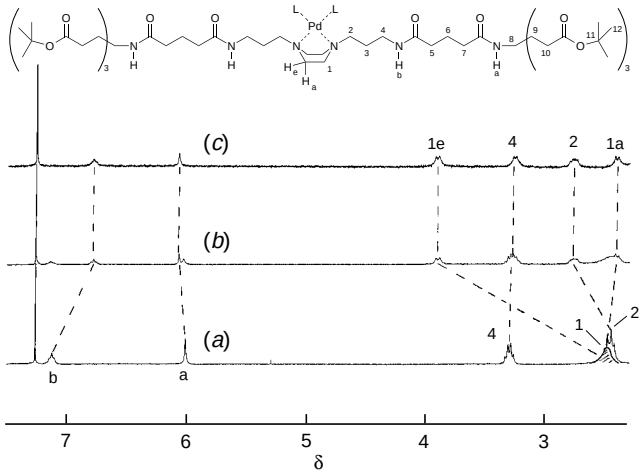



**Fig. 3** (*a*) Partial $^1$H NMR spectrum of ligand **5a** without added metal salt where the shaded region depicts H1 absorption for clarity; (*b*) with 0.7 equiv. of added $PdCl_2(MeCN)_2$; (*c*) with 1 equiv. of added $PdCl_2(MeCN)_2$

The related $Cu^{II}$ complexes were easily obtained by treating absolute EtOH solutions of either **5a,c** or **7a,c** with anhydrous $CuCl_2$ resulting in translucent olive-green solutions that exhibit excellent solubility in common organic solvents (*e.g.* $CHCl_3$). The signals ($^{13}$C NMR) do not significantly shift in contrast to those of the corresponding Pd complexes but significantly broaden and decrease in intensity due to presence of the new paramagnetic metal centre. For hexaester **5a** containing 1 equiv. of $Cu^{II}$ or dodecaester **7a** containing 4 equiv. of $Cu^{II}$, all of the internal carbon resonances disappear, while the outer carbon absorptions identifying the branching portion of these macromolecules remain as sharp, first-order patterns.

These specifically localized metal centres afford insight into their use as metallo-unimolecular micelles and metallospheres and superclusters,[12] as well as suggesting the use of dendrimers for ordered networks. Also, similarly constructed bipyridine-based dendrimers are currently under investigation.

This research (G. R. N.) was supported by the National Science Foundation (92-17331; 96-22609) and the U.S. Army Office of Research (DAAH04-93-0048) and J. G. thanks the Alexander von Humboldt-Stiftung for the Feodor Lynen fellowship.

## Footnote

† All new compounds gave consistent $^1$H and $^{13}$C NMR spectral and analytical data.

## References

1 (*a*) G. R. Newkome, C. N. Moorefield and F. Vögtle, *Dendritic Molecules—Concepts, Syntheses, Perspectives*, VCH, New York, 1996, ch. 8; (*b*) S. Serroni, S. Campagna, G. Denti, A. Juris, M. Venturi and V. Balzani, in *Advances in Dendritic Macromolecules*, ed. G. R. Newkome, JAI Press, Greenwich, 1996, ch. 3.
2 S. Seroni, G. Denti, S. Campagna, A. Juris, M. Ciano and V. Balzani, *Angew. Chem., Int. Ed. Engl.*, 1992, **31**, 1493; G. Denti, S. Campagna, S. Seroni, M. Ciano and V. Balzani, *J. Am. Chem. Soc.*, 1992, **114**, 2944.
3 G. R. Newkome, F. Cardullo, E. C. Constable, C. N. Moorefield and A. M. W. C. Thompson, *J. Chem. Soc., Chem. Commun.*, 1993, 925.
4 G. R. Newkome, R. Guether, C. N. Moorefield, F. Cardullo, L. Echegoyen and E. Pérez-Cordero, *Angew. Chem., Int. Ed. Engl.*, 1995, **34**, 2023.
5 E. C. Constable and P. Harverson, *Chem. Commun.*, 1996, 33.
6 C. D. Eisenbach, U. S. Schubert, G. R. Baker and G. R. Newkome, *J. Chem. Soc., Chem. Commun.*, 1995, 69; G. R. Newkome, R. Güther and F. Cardullo, *Makromol. Symp.*, 1995, **98**, 467; G. R. Newkome and C. N. Moorefield, *Makromol. Symp.*, 1994, **77**, 63.
7 F. G. Mann and H. R. Watson, *J. Chem. Soc.*, 1958, 2772.
8 J. K. Young, G. R. Baker and G. R. Newkome, *Macromolecules*, 1994, **27**, 3463; C. D. Weis and G. R. Newkome, *Org. Prep. Proc. Int.*, 1996, **28**, 485.
9 G. R. Newkome and C. D. Weis, *Org. Prep. Proc. Int.*, 1996, **28**, 242.
10 J. Klausner and B. Bodansky, *Synthesis*, 1972, 453.
11 For a comparable conformation (X-ray): O. Hassel and B. Pedersen, *Proc. Chem. Soc.*, 1959, 394.
12 G. R. Newkome and C. N. Moorefield, U. S. Patents 5 376 690 (Dec. 27, 1994), 5 422 379 (June 06, 1995), 5 516 810 (May 14, 1996) and 5 585 457 (December 17, 1996).

*Received, 6th December 1996; Com. 6/08240H*

# Chiral discrimination in the oxidation of ferrocenes by cytochrome c peroxidase

**Sheila J. Sadeghi,[a] Gianfranco Gilardi,[a] Giovanni Nicolosi[b] and Anthony E. G. Cass[a]†**

[a] *Department of Biochemistry, Imperial College of Science, Technology & Medicine, South Kensington, London, UK SW7 2AY*
[b] *Istituto per lo Studio delle Sostanze Naturali di Interesse Alimentare e Chimico-Farmaceutica, Valverde CT, Italy*

**Cytochrome c peroxidase shows a two-fold difference in its reaction rate with enantiomers of a chiral ferrocene; the enantiomeric selectivity is reversed by a single site specific change in the surface charge of the enzyme.**

Chiral recognition is a fundamental property of many biological molecules and many examples have been reported in the literature, including enzyme–substrate and ligand–receptor interactions.[1–3] Previous reports of chiral discrimination in electron transfer reactions between small redox proteins and chiral metal complexes have described small but significant differences in kinetic enantioselectivity (10–20%) which has been used to probe the pathway(s) of electron transfer.[4–6] Electron transfer between redox enzymes and small molecules has also been extensively studied in the context of electrochemical sensors[7–9] and ferrocenes have been particularly exploited in the role of mediators between enzymes and solid electrodes. Although differences in electron transfer rates are seen with different ferrocenes there does not appear to be a simple relationship between the structure of the mediator and its reactivity.[10] There is a clear dependence of the rate of protein-mediator electron transfer on both the redox potential difference and the nature of the group(s) substituting the cyclopentadienyl rings. One particular feature of ferrocenes that has not been explored with respect to the kinetics of electron transfer is their property of planar chirality when substituted with two different groups on the same cyclopentadienyl ring. Previously it has been shown that lipases can distinguish between two enantiomers in the esterification of ferrocenyl alcohols.[11] We report here the significant chiral discrimination shown by the enzyme cytochrome c peroxidase (CCP) with two ferrocene enantiomers and the reversal of this chiral specificity by a site specific change in the surface charge on the protein.

The yeast CCP used in this work was expressed in *E. coli*, purified by a previously published method[12] and had a turnover number (horse heart cytochrome as the substrate) of 200 $s^{-1}$. The mutation of a surface aspartate residue to a lysine residue employed the polymerase chain reaction and was confirmed by DNA sequencing. The synthesis of both (*S*)- and (*R*)-1-hydroxymethyl-2-dimethylaminomethylferrocene (HMDMF) was as described by Nicolosi *et al.*[13] Rates of reaction between the two enantiomers of HMDMF and CCP were estimated by cyclic voltammetry. Both enantiomeric ferrocenes exhibited quasi-reversible one-electron voltammograms with mid-point potentials of 390 mV (*vs.* SCE), a peak separation of 61 mV, peak currents proportional to the square root of the potential sweep rate. The latter observation confirming that the mass transport of mediator is occurring under conditions of planar diffusion. Upon addition of hydrogen peroxide to a solution of the mediator there was no change in the observed voltammograms showing that hydrogen peroxide does not give rise to significant oxidation currents on glassy carbon in the operating potential region. However, on addition of the CCP to a solution of mediator containing hydrogen peroxide, a characteristic catalytic wave with an enhanced reduction current and no oxidation peak was seen. Both the change in the appearance of the voltammogram and the increased current are consistent with catalytic regeneration of oxidised mediator in the diffusion layer as observed previously with non-chiral ferrocenes.[14,15] The absence of diffusional peaks in the cyclic voltammograms under conditions of enzyme turnover are consistent with the cathodic currents arising from enzymatically generated, rather than electrochemically generated, ferrocenium ions.

Fig. 1 shows the catalytic currents obtained in the system containing CCP and either (*S*)- or (*R*)-HMDMF as diffusional electron transfer mediators in the presence of hydrogen peroxide. It can be seen clearly from Fig. 1 that the *R*-enantiomer acts as a faster electron transfer mediator than the *S*. The catalytic current for (*R*)-HMDMF is about two-fold higher than that of (*S*)-HMDMF.

When the limiting currents in the cyclic voltammograms are plotted against the square root of the enzyme concentration a linear relationship is observed, consistent with the expected behaviour in an enzyme coupled system.[10] For each enantiomer the overall second order rate constant for the reaction between reduced mediator and oxidised enzyme was determined from the scan rate dependence of the catalytic currents at five different enzyme concentrations.[16] The values for the rate constants showed a significant ($P < 0.001$) difference between the two enantiomers with (*R*)-HMDMF reacting approximately twice as fast as (*S*)-HMDMF (Table 1). This difference in rate constants is comparable to that observed by Marx-Tibbon *et al.*[17] for the reaction of *N,N*-dimethyl-1-ferrocenylethylamine

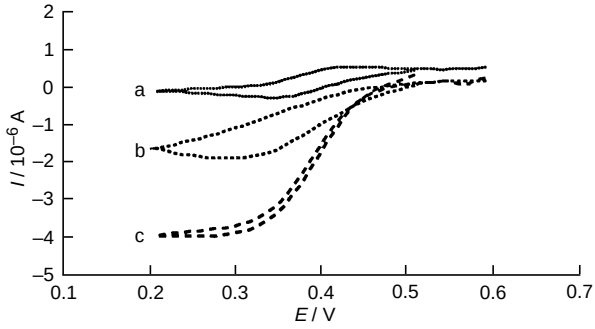



**Fig. 1** Cyclic voltammogram of (*a*) 0.5 mM (*R*)-HMDMF in phosphate buffer (50 mM, pH 6.5) containing 2 mM hydrogen peroxide; (*b*) 0.5 mM (*S*)-HMDMF together with 2 mM hydrogen peroxide after addition of 0.7 μM CCP; and (*c*) 0.5 mM (*R*)-HMDMF together with 2 mM hydrogen peroxide after addition of 0.7 μM CCP. All voltammograms were recorded at 5 mV $s^{-1}$ on a glassy carbon electrode with an area of 0.125 $cm^2$.

**Table 1** Rate constants for the reaction of cytochrome c peroxidase wild type and mutant enzymes with both enantiomers of 1-hydroxymethyl-2-dimethylaminomethylferrocene

| | *R*-Enantiomer | *S*-Enantiomer |
|---|---|---|
| Wild Type CCP | $(2.9 \pm 0.4) \times 10^6$ $dm^3$ $mol^{-1}$ $s^{-1}$ | $(1.6 \pm 0.2) \times 10^6$ $dm^3$ $mol^{-1}$ $s^{-1}$ |
| D34K CCP | $(5.9 \pm 0.5) \times 10^6$ $dm^3$ $mol^{-1}$ $s^{-1}$ | $(14.8 \pm 1) \times 10^6$ $dm^3$ $mol^{-1}$ $s^{-1}$ |

(a ferrocene with a chiral side chain) with glucose oxidase, although this work has recently been the subject of a reinterpretation by Boudillon *et al*.[18]

The rates of reaction of the enantiomers of HMDMF with a mutant of CCP (Aspartate 34 to Lysine) were also determined. Aspartate 34 is a negatively charged residue, situated on the surface of CCP and has been implicated in its reaction with its physiological partner, cytochrome c on the basis of the crystal structure of the complex.[19] When the rate constants for this mutant were evaluated with the artifical ferrocene donor two striking observations were made, firstly the values for both enantiomers were increased, showing that this mutant turned over the ferrocene substrates more rapidly than the wild type enzyme. More interestingly the chiral preference of the enzyme was reversed with the *S*-enantiomer now being the faster substrate. In fact in this mutant the rate of reaction with the *S*-enantiomer is increased by an order of magnitude compared with the wild type. The corresponding rate constants for (*R*)- and (*S*)-HMDMF are also reported in Table 1. We have also investigated the reaction of this mutant with non-chiral ferrocenes[20] and, as might be anticipated, differences in rate are observed reflecting the different interactions of the two forms with the mediator. If however substrate chirality was not implicated in the reaction we should observe that both enantiomers would exhibit the same change in rate, in contrast to the observations here where quite different increases are seen.

These data clearly show that not only is there a specific molecular recognition event occurring between the chiral ferrocenes and CCP but also that this interaction is exquisitely sensitive to a specific surface charge on the CCP. Calculated potential maps were obtained for wild type and D34K CCP using the finite difference method introduced by Sharp and Honig[21] and show large changes in the proteins' electrostatic fields around the site of mutation the analysis of which will be published in detail elsewhere.

We thank Professor T. Poulos for the gift of the pT7CCP plasmid.

## Footnote

† E-mail: t.cass@ic.ac.uk

## References

1 L. Casella and A. Marchesini, *Biochemistry*, 1994, **33**, 6377.
2 R. A. Marushak and T. A. Shields, in *Electron Transfer in Biology and the Solid State*, ed. M. K. Johnson, R. B. King, D. M. Kurtz, C. Kutal, M. L. Norton and R. A. Scott, *ACS Advances in Chemistry 226*, American Chemical Society, Washington DC, 1990.
3 A. Fersht, *Enzyme Structure and Function*, Freeman WH and Co., New York, 1984, 2nd edn., pp. 221–247.
4 K. Bernauer, M. Monzione, P. Schurmann and V. Viette, *Helv. Chim. Acta*, 1990, **73**, 346.
5 J. R. Pladziewicz, M. A. Accola, P. Osvath and A. M. Sargeson, *Inorg. Chem*., 1993, **32**, 2525.
6 J. R. Pladziewicz, S. O. Gullerud and M. A. Accola, *Inorg. Chim. Acta*, 1994, **225**, 151.
7 E. J. D'Costa, I. J. Higgins and A. P. F. Turner, *Biosensors*, 1986, **2**, 71.
8 A. E. G. Cass, G. Davis, G. D. Francis, H. A. O. Hill, W. J. Aston, I. J. Higgins, E. V. Plotkin, L. D. L. Scott and A. P. F. Turner, *Anal. Chem*., 1984, **56**, 667.
9 Z. S. Ali, W.-C. Tsai and A. E. G. Cass, *Bull. Electrochem*., 1992, **28**, 171.
10 E. Liaudet, F. Battaglini and E. J. Calvo, *J. Electroanal. Chem*., 1990, **293**, 55.
11 G. Nicolosi, A. Patti, R. Morrone and M. Piattelli, *Tetrahedron: Asymmetry*, 1994, **5**, 1275.
12 L. A. Fishel, J. E. Villafranca, J. M. Mauro and J. Kraut, *Biochemistry*, 1987, **26**, 351.
13 G. Nicolosi, R. Morrone, A. Patti and M. Piattelli, *Tetrahedron: Asymmetry*, 1992, **3**, 753.
14 J. M. Cooper, J. V. Bannister and C. J. McNeil, *J. Electroanal. Chem*., 1991, **312**, 155.
15 J. E. Frew, M. A. Harmer, H. A. O. Hill and S. I. Libor, *J. Electroanal. Chem*., 1986, **201**, 1.
16 H. A. O. Hill and G. S. Sanghera, in *Biosensors: A Practical Approach*, ed. A. E. G. Cass, IRL Press, Oxford, 1990, pp. 19–46.
17 S. Marx-Tibbon, E. Katz and I. Willner, *J. Am. Chem. Soc*., 1995, **117**, 9925.
18 C. Boudillon, C. Demaille, J. Moiroux and J.-M. Saveant, *Acc. Chem. Res*., 1996, **29**, 529.
19 H. Pelletier and J. Kraut, *Science*, 1992, **258**, 1748.
20 S. J. Sadeghi, PhD Thesis, University of London, 1996.
21 K. A. Sharp and B. Honig, *Ann. Rev. Biophys. Bioeng*., 1990, **19**, 301.

*Received, 7th October 1996; Revised manuscript received 10th January 1997; Com. 7/00243B*

# Alkali metals on nanoporous carbon: new solid-base catalysts

**Mark G. Stevens and Henry C. Foley***

*Center for Catalytic Science and Technology, Department of Chemical Engineering, University of Delaware, Newark, Delaware, USA*

**Caesium entrapped in nanoporous carbon is not pyrophoric, is thermally stable towards desorption up to 773 K, but retains its ability to produce hydrogen from water, and is a strong basic catalyst, providing a greater than 9 : 1 ratio of the less stable *cis*-but-2-ene over the *trans* isomer in the isomerization of but-1-ene at 273 K.**

Materials produced from alkali metals and carbon have been of interest to researchers for many years. Graphite intercalation compounds of alkali metals have been extensively studied[1] and shown to be active basic catalysts in reactions such as side-chain alkylation,[2] but-1-ene isomerization[3] and amine synthesis.[4] Unfortunately, these materials were found to be pyrophoric, had relatively low surface area, and exfoliated at reaction temperature.[5] A catalytically active caesium fulleride, $C_{20}Cs_6$, has been reported, but it was found to be highly air-sensitive.[6]

Carbogenic molecular sieves (CMS) are chemically inert solids that contain nanopores,[7,8] formed from aromatic nanodomains, arranged chaotically in space. Here, we show that alkali metals introduced into a CMS structure adsorb in these nanopore spaces, and that curvature effects within the CMS pores provide for a much higher thermal stability, and that these materials are exceptionally active base catalysts in double-bond migration.

CMS samples were prepared pyrolitically from polyvinylchloride–polyvinyldichloride-, poly(furfuryl alcohol)- and poly(furfuryl alcohol)–poly(ethylene glycol) mixtures.[7–10] A poly(furfuryl alcohol)–poly(ethylene glycol) mixture (PFA–PEG) produces material that forms a nanopore structure similar to the PFA carbons, with a pore-size distribution centred around 0.5 nm. However, the addition of PEG results in the formation of transport porosity[11] with a second distribution centred around 10 nm, that allows access to catalytic sites contained in the nanopores.[12] Cs was chosen as the catalytic metal because it is the most electropositive element and its covalent atomic diameter (0.48 nm) is close to the nanopore size of the CMS (*ca*. 0.5 nm). Since Cs is strongly electropositive, a significant portion of the Cs may be ionized (crystallographic diameter 0.34 nm), which should add to the compound's stability.

The synthesis of the Cs/CMS material was achieved by vapour-phase deposition.† The base-catalysed isomerization of but-1-ene to but-2-ene, which begins with the abstraction of the allylic proton to form the *cis* or *trans* form of the allyl anion,[13] was used to probe for catalytic activity. Since the *cis* form of this intermediate is more stable than the *trans* form, *cis*-but-2-ene is formed predominantly in base catalysis, although *trans*-but-2-ene is more stable thermodynamically.

Samples containing 3–42 mass% Cs in CMS‡ were synthesized. The thermal stability of these materials was demonstrated by heating them in vacuum to temperatures as high as 773 K; the Cs did not desorb from the CMS. In contrast Cs is lost rapidly from Cs/graphite compounds, which exfoliate readily.[5]

Results of magnetic susceptibility and EPR measurements show a significant population of unpaired electrons exists in these materials. When a 17% Cs/CMS sample was exposed to 100% humidity at 288 K it absorbed 850 mg $g^{-1}$ of water. When submerged in oxygen-free water, a 9.2% Cs sample produced sufficient hydrogen to indicate that 26% of the Cs was still active for water reduction.§ Hence, the Cs is active and accessible. Yet, unlike metallic Cs and graphite Cs compounds, Cs/CMS is not pyrophoric, even at 40% Cs loading.

A wholly nanoporous pyrolized polyvinylchloride–polyvinyldichloride carbon impregnated with 14% Cs showed no catalytic activity for but-1-ene isomerization¶ at 298 K, but did show activity at higher temperatures (18% conversion at 523 K). When transport porosity is added to the CMS, making the Cs in the nanopores more accessible, the reaction took place at low temperatures (Table 1). The catalysts were found to be stable, with a reaction turnover of > 30 (30 mol of but-2-ene produced per mol of Cs) before deactivation. To determine the global, first-order rate constant for the reaction we diluted the butene feed to 33 mol% but-1-ene in argon. From differential conversion experiments¶ on a 9% Cs sample we determined an apparent first-order rate constant ($k_a$) of 0.07 $s^{-1}$ $g^{-1}$ and a *cis* : *trans* ratio of 9.1 at 273 K. This combination of high bacisity with reduction activity and the lack of pyrophoricity makes Cs/CMS extraordinarily interesting and useful.

**Table 1** Average conversion on 4.5 g catalyst and *cis*/*trans* ratio of the product gas for the isomerization of 15 $cm^5$ $min^{-1}$ butene to *cis*- and *trans*-but-2-ene at 298 K and 1 bar. Six datapoints (gas chromatography) were collected from the flow reactor over a 2 h period and averaged

| Catalyst | Conversion (%) | *cis*/*trans* ratio |
|---|---|---|
| 3% Cs-PFA–PEG | 13% | 2.3 |
| 10% Cs-PFA–PEG | 75% | 3.3 |
| 11% Cs-PFA–PEG | 60% | 4.9 |
| 18% Cs-PFA–PEG | 90% | 2.8 |
| 21% Cs-PFA–PEG | 87% | 3.7 |

## Footnotes

† After a sample of the CMS was heat-treated in vacuum at 450 °C for 24 h, Cs vapour was introduced into the carbon at moderate temperature (350 °C) at its vapour pressure (*ca*. 10 mmHg). The temperature was held at 350 °C under static vacuum for 24 h.

‡ Galbraith Laboratories, Inc. provided metal analysis *via* plasma emission spectroscopy for the determination of alkai-metal loading.

§ A 2 g sample of catalyst was submerged in 20 ml of deionized, oxygen-free, water, without exposure to air. Gas evolved. The gas was quantified and determined to be hydrogen by gas chromatography. The water and catalyst were titrated with 0.0125 M sulfuric acid to calculate the amount of Cs present as CsOH.

¶ We constructed a computer-controlled, tubular, flow reactor. For the initial experiments: the reactor was loaded in an inert atmosphere with 4.75 g of catalyst. Technical grade but-1-ene (Matheson gas company) flowed at 15 $cm^3$ $min^{-1}$ at atmospheric pressure. For the kinetic experiments: the reactor contained 3.0 g of catalyst. Technical grade but-1-ene flowed at 20 $cm^3$ $min^{-1}$, mixed with 40 $cm^3$ $min^{-1}$ argon at atmospheric pressure. Analysis was performed *via* gas chromatography.

## References

1 N. Bartlet and B. W. McQuillan, in *Intercalation Chemistry*, ed. M. S. Whittingham and A. J. Jacobson, Academic Press, New York, 1982, pp. 19–50 and references therein.

2 W. E. Foster, *US Pat*. 3,160,670, 1964.

3 M. A. M. Boersma, in *Advanced Materials in Catalysis*, ed. J. J. Burton and R. L. Garten, Academic Press, New York, 1977, pp. 67–79.
4 D. Savoia, C. Trombini and A. Umani-Ronchi, *J. Chem. Soc., Perkin Trans. I*, 1977, 123.
5 F. J. Salzano and S. Aronson, *J. Chem. Phys.*, 1966, **45**, 6.
6 S. Serizawa, I. Gabrielova, T. Fujimoto, T. Shido and M. Ichikawa, *J. Chem. Soc., Chem. Commun.*, 1994, 799.
7 H. C. Foley, *Microporous Mater.*, 1995, **4**, 407.
8 H. C. Foley, M. S. Kane and J. F. Goellner, in *Access in Nanoporous Materials*, ed. J. J. Pinnavaia and M. F. Thorpe, Plenum, New York, 1995.
9 D. S. Lafyatis, J. Tong and H. C. Foley, *Ind. Eng. Chem. Res.*, 1994, **30**, 865.
10 R. K. Mariwala and H. C. Foley, *Ind. Eng. Chem. Res.*, 1994, **33**, 607.
11 D. S. Lafayatis, J. Tung and H. C. Foley, *Ind. Eng. Chem. Res.*, 1991, **30**, 865.
12 M. S. Kane, L. C. Kao, R. Mariwala, D. F. Hilscher and H. C. Foley, *Ind. Eng. Chem. Res.*, 1996, **35**, 3319.
13 H. Attori, *Chem. Rev.*, 1995, **95**, 537.

*Received, 14th November 1996; Com. 6/07731E*

# Formation of an intermediate during the hydrothermal synthesis of ULM-5 studied using time-resolved, *in situ* X-ray powder diffraction†

**Robin J. Francis,[a] Stephen J. Price,[a] Stephen O'Brien,[a] Andrew M. Fogg,[a] Dermot O'Hare,*[a]‡ Thierry Loiseau[b] and Gerard Férey[b]**

[a] *Inorganic Chemistry Laboratory, University of Oxford, South Parks Road, Oxford, UK OX1 3QR*
[b] *Institut Lavoisier, IREM UMR C 173, Université de Versailles, 45 Avenue des Etat-Unis, 78035 Versailles, France*

***In situ* energy dispersive X-ray diffraction studies on the hydrothermal synthesis of the oxyfluorinated gallophosphate, ULM-5, show that when orthophosphoric acid is used as a starting material ULM-5 forms rapidly after an initial induction period, whereas when phosphorus pentoxide is used as a starting material a previously unobserved crystalline intermediate is formed, which subsequently reacts to form ULM-5; conditions have been identified in which this intermediate is relatively long lived and this has allowed the subsequent isolation of a pure sample of this intermediate.**

Microporous materials are an academically and industrially important class of materials due to their great utility as catalysts and absorbents.[1,2] These properties arise from their unique three-dimensional open-framework structures which consist of a regular array of uniform pores and channels. ULM-5 is a microporous oxyfluorinated gallophosphate $\{Ga_{16}(HPO_4)_{14}(PO_4)_2(OH)_2F_7{\cdot}4NH_3CH_2CH_2NH_3{\cdot}6H_2O\}$ containing large 16-membered rings and interconnecting 8-membered rings.[3] The 16-membered rings form oval channels with a free aperture of 12.20 × 8.34 Å. ULM-5 is synthesised hydrothermally; gallium oxide, a phosphorus source and hydrofluoric acid are reacted in water at 180 °C in the presence of the templating agent 1,6-diaminohexane.

Over the past few years much interest has focused on the synthesis of new open-framework materials with particular catalytic and ion-exchange properties. Unfortunately, although some mechanistic theories have been proposed,[4,5] the synthesis of new structure types is hampered by the fact that the fundamental processes occurring during hydrothermal syntheses are not well understood, and there is very little knowledge of the transformations occurring during the formation of the product phase. In an effort to gain a greater understanding of these reactions we have recently developed an apparatus capable of studying hydrothermal reactions *in situ*, using time-resolved energy dispersive synchrotron X-ray diffraction (EDXRD).[6,7] As has been pointed out by ourselves and others previously,[6–9] such non-invasive *in situ* measurements offer many advantages over other *ex-situ* techniques, since they allow the direct observation of crystalline intermediate and product phases, which avoids the possibly complicating effects of sample work-up.

As part of our on-going program of studying hydrothermal syntheses of microporous materials *in situ*, we have undertaken a study of the formation of ULM-5 under a variety of synthetic conditions in order to gain a greater understanding of the dynamics of crystal growth and nucleation. Here we report the importance of the phosphorus source on the reaction pathway, and the observation of the formation of a crystalline intermediate phase when phosphorus pentoxide is used as the source.

All reactions were performed using a reaction mixture of initial composition $Ga_2O_3 : P_2O_5 : 2HF : 1,6DAH : 80H_2O$. Using orthophosphoric acid as the phosphorus source there is a short induction period, which presumably is partially due to reactant dissolution and partially due to a build up in pressure, after which pure ULM-5 is observed to rapidly and smoothly crystallise. No crystalline intermediates are observed to form at any stage. A plot of the integrated intensity of the 002 reflection is shown in Fig. 1. The main feature of note is the extremely rapid nature of the crystallisation after the induction period. The half-life of crystallisation at this temperature is under 1 min, and the reaction is essentially over 40 min after the onset of crystallisation. Initial analysis of the kinetic data suggests that the formation of ULM-5 under these conditions is an essentially diffusion limited process. We have also performed this reaction at other temperatures down to 130 °C, and whilst there is a general trend to longer induction times at lower temperatures the crystallisation kinetics after induction are essentially identical over this temperature range.

However, dramatically different behaviour was observed when the reaction was performed under identical conditions except for the replacement of orthophosphoric acid with phosphorus pentoxide as the phosphorus source. Under these conditions a highly crystalline intermediate phase is observed to form which then subsequently reacts to form ULM-5. The course of the reaction at 180 °C is shown as a three-dimensional plot in Fig. 2, and a plot of the integrated intensity of the 13.1 Å reflection and the ULM-5 final product 002 reflection is shown in Fig. 3. As can be seen from Fig. 3 after an induction time of approximately 5 min, the intermediate forms rapidly, the intensity of the diffraction peaks reaching a maximum intensity after just 15 min. The intensity of these peaks then immediately begins to decrease together with concomitant growth of peaks belonging to the product (ULM-5). Although not conclusive, the high degree of correlation between the decay of the intermediate and growth of the product peaks is good evidence for the two phases being related, and the intermediate phase directly converting into the final product. The transformation is much slower than both the initial formation of the intermediate

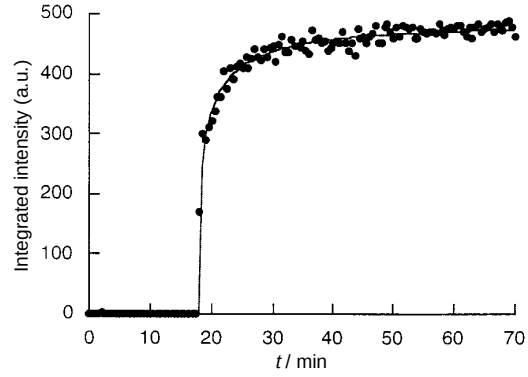



**Fig. 1** Plot of intensity of the (002) Bragg reflection of ULM-5 as a function of time using orthophosphoric acid as a starting material. The solid line is a fit to the Avrami equation $I = A\exp[-k(t - t_0)]^{0.4}$, where $t_0$ is the induction time.

and the formation of ULM-5 when orthophosphoric acid is used as a starting material, taking over 2 h to go to completion.

The same reaction was also performed at lower temperatures. Broadly similar behaviour was observed; an intermediate being formed which converts to the final product. However, although the initial growth occurs at virtually the same rate, the transformation to product was much slower at lower temperatures. At 150 °C the beginnings of a 'plateau' in the intensity of the intermediate peak could be seen, and by 130 °C this plateau in intensity is pronounced, with the intermediate being stable for approximately 30 min. Conversion into the final product does not occur until after 40 min into the reaction at this temperature.

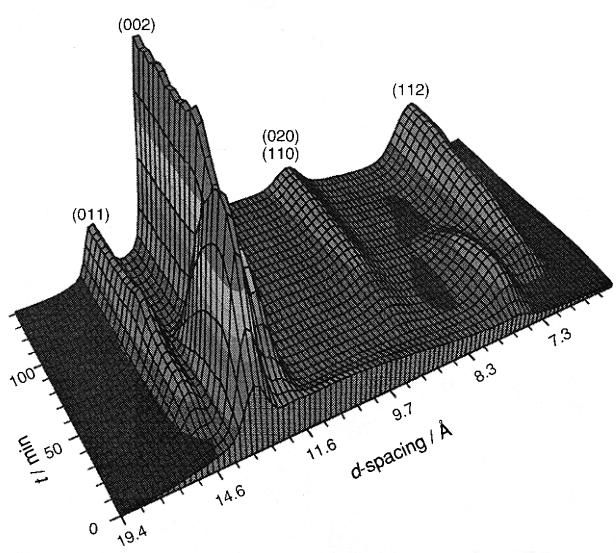



**Fig. 2** Three-dimensional plot showing the EDXRD spectra as a function of time during the synthesis of ULM-5 using phosphorus pentoxide as a starting material. The peak labels correspond to the indices of the Bragg reflections of ULM-5. The experiments were performed on station 16.4 of the UK SRS at Daresbury Laboratory, Warrington. Each spectrum was acquired in 60 s at a diffraction angle of $2\theta = 1.22°$. Details of the experimental apparatus and station design have been published previously.[6,10]

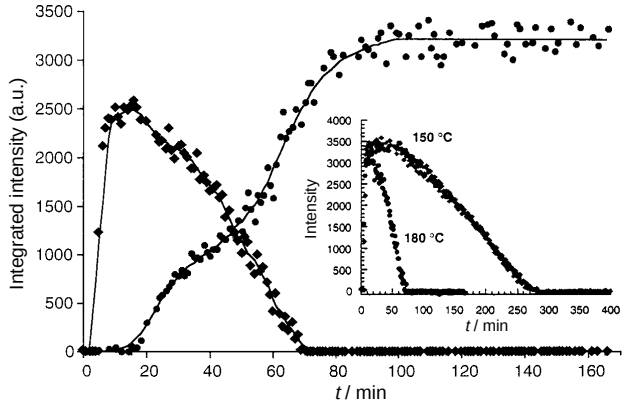



**Fig. 3** Plot of the intensity of the (100) Bragg reflection of the intermediate (◆) and the (002) Bragg reflection (●) of ULM-5 as a function of temperature at 180 °C. Solid lines are for guidance only and have no physical significance. Inset: Plot of intensity of the (100) reflection of the intermediate at 180 and 150 °C.

The determination of conditions in which the intermediate is relatively stable opened up the possibility of isolation of this material by quenching of the reaction during the early stages before the conversion to the final product has begun, assuming that the material does not transform during the quenching procedure. In an attempt to do this another reaction was performed at 150 °C in which the reaction cell was removed from the heating block when the diffraction peaks due to the intermediate were observed to reach the maximum intensity, and the cell was then quenched with cold water. Powder X-ray diffraction of the material obtained from the quenched autoclave showed that the intermediate phase had indeed been successfully isolated. The X-ray diffraction pattern of this isolated phase could be tentatively indexed on the orthorhombic cell with lattice parameters $a = 20.274$, $b = 13.125$, $c = 24.550$ Å. Interestingly, two of these parameters are closely related to two of the cell parameters in ULM-5 which is also orthorhombic with $a = 10.252$, $b = 18.409$ and $c = 24.639$ Å (*i.e.* $a' \approx 2a$ and $c' \approx c$). This suggests that the two materials may be closely structurally related. Structural studies on this material are being carried out in order to determine the relationship between this material and ULM-5, but these have been hampered by the fact that the isolated product is metastable and transforms to another unknown material on standing for a few days at room temperature.

In conclusion, these *in situ* experiments are a dramatic illustration of the complexity of hydrothermal syntheses, and how subtle changes in the reaction conditions, such as the use of slightly different starting materials, can greatly affect the course of these reactions. It also demonstrates the unique ability of *in situ* experiments to gain information not available using other techniques.

We would like to thank DRAL for a CASE studentship (R. J. F.) and the use of the Synchrotron radiation source facility, and Dr S. M. Clarke, and the technical staff at Daresbury Laboratory for helping in the design and construction of the experimental cell.

## Footnotes

† This ChemComm is also available in enhanced multi-media format *via* the World Wide Web: http://chemistry.rsc.org/rsc/cccenha.htm

‡ D. O'Hare is the Royal Society of Chemistry Sir Edward Frankland Fellow.

## References

1 R. M. Barrer, *Hydrothermal Chemistry of Zeolites*, Academic Press, New York, London, 1982.
2 P. B. Venuto, *Microporous Mater*., 1994, **2**, 297.
3 T. Loiseau and G. Ferey, *J. Solid State Chem*., 1994, **111**, 403.
4 S. L. Burkett and M. E. Davis, *Chem. Mater*., 1995, **7**, 920.
5 S. L. Burkett and M. E. Davis, *Chem. Mater*., 1995, **7**, 1453.
6 J. S. O. Evans, R. J. Francis, D. O'Hare, S. J. Price, S. M. Clarke, J. Flaherty, J. Gordon, A. Nield and C. C. Tang, *Rev. Sci. Instrum*., 1995, **66**, 2442.
7 R. J. Francis, S. J. Price, J. S. O. Evans, S. O'Brien, D. O'Hare and S. M. Clark, *Chem. Mater*., 1996, **8**, 2102.
8 J. Munn, P. Barnes, D. Häusermann, S. A. Axon and J. Klinowski, *J. Phase Transitions*., 1992, **39**, 1 29.
9 J. M. Thomas and G. N. Greaves, *Science*, 1994, **265**, 1675.
10 S. M. Clark, R. J. Cernik, A. Grant, S. York, P. A. Atkinson, A. Gallagher, D. G. Stokes, S. R. Gregory, N. Harris, W. Smith, M. Hancock, M. C. Miller, K. Ackroyd, R. Francis and D. O'Hare, *Mater. Sci. Forum*., 1996, **228**–**231**, 213.

*Received, 13th December 1996; Com. 6/08378A*

# Oxidative quenching of excited-state tetrakis(μ-pyrophosphito)diplatinate(II) tetraanion by iodine atom transfer from iodopentacyanocobaltate(III)

**Alexander D. Kirk* and Le-Zhen Cai**

*Department of Chemistry, University of Victoria, PO Box 3065, Victoria, BC, V8W 3V6, Canada*

**Iodopentacyanocobaltate(III) oxidatively quenches excited state tetrakis(μ-pyrophosphito)diplatinate(II) tetraanion *via* iodine atom transfer.**

The bridged binuclear complex $[Pt_2(pop)_4]^{4-}$ (pop = $H_2P_2O_5^{2-}$) has attracted great interest due to its distinctive excited-state properties. The triplet excited state $^3A_{2u}$ {denoted as $[*Pt_2(pop)_4]^{4-}$} is known to be a strong oxidant and reductant, and has biradical character.[1–3] Quenching studies have shown that the excited state can be quenched by energy transfer, electron transfer, or atom transfer mechanisms.[4] The latter mechanism has been observed for organic quenchers, such as RX, ROH (X = Cl, Br, I; R = alkyl, aryl),[5] but quenching by coordination complexes has invariably occurred *via* energy or electron transfer. During a detailed study[6] of salt effects on the quenching interaction between $[Pt_2(pop)_4]^{4-}$ and the anions $[Co(CN)_5X]^{3-}$ (X = I, Br, Cl, $N_3$), we saw evidence for atom transfer in the quenching of $[*Pt_2(pop)_4]^{4-}$ by $[Co(CN)_5I]^{3-}$. The finding provides new insight into the deactivation of excited-state metal complexes and further illustrates the rich photochemistry of this platinum dimer.

In our initial approach, the lifetime of $[Pt_2(pop)_4]^{4-}$ in deaerated 0.500 M KCl–0.010 M $HClO_4$ solution was measured using a nitrogen laser, wavelength shifted† by a separate cell containing quinine sulfate to provide 370 nm, fast decay pulses to excite preferentially $[Pt_2(pop)_4]^{4-}$. The $[Co(CN)_5I]^{3-}$ quencher, dissolved in 0.500 M KCl–0.010 M $HClO_4$ solution, was delivered in μl aliquots from a microburette directly into the $[Pt_2(pop)_4]^{4-}$ solution. The high electrolyte concentration served to promote[6] the anion–anion interaction and the choice of chloride established a chloride–iodide competition required to demonstrate the occurrence of atom transfer. The second-order quenching rate constant $k_q$ was calculated from the Stern–Volmer plot and was found to be $2.1 \times 10^8$ $M^{-1}$ $s^{-1}$ at 22.0 ± 0.1 °C for the above ionic strength.

When a deaerated solution of $2.9 \times 10^{-5}$ M $K_4[Pt_2(pop)_4]$, $1.7 \times 10^{-4}$ M of $K_3[Co(CN)_5I]$ and 0.500 M KCl–0.010 M $HClO_4$ was irradiated by a Hg lamp at 370 nm, the absorption bands at 370 and 262 nm were bleached, accompanied by the development of new bands at 328 and 438 nm (Fig. 1). Reaction terminated when the light source was removed, showing that a genuine photochemical reaction not a thermal or photocatalytic process occurs. The peaks diminished were those of reactant $[Pt_2(pop)_4]^{4-}$, $\lambda_{max}$ (ε) = 369 nm ($3.4 \times 10^4$ $M^{-1}$ $cm^{-1}$), and quencher $[Co(CN)_5I]^{3-}$, $\lambda_{max}$ (ε) = 262 nm ($1.8 \times 10^4$ $M^{-1}$ $cm^{-1}$), and the spectral changes showed that quencher and $[Pt_2(pop)_4]^{4-}$ reacted in a 2 : 1 molar ratio. The product peaks could be attributed to $[Pt_2(pop)_4I_2]^{4-}$. They appeared at 328 and 438 nm which compares well to literature results for $[Pt_2(pop)_4I_2]^{4-}$, $\lambda_{max}$ (ε) = 331 nm ($4 \times 10^4$ $M^{-1}$ $cm^{-1}$) and 438 ($1.7 \times 10^4$),[8] and had the correct ratio, experiment $A_{328}/A_{438}$ = 2.2 (lit.[8] $\varepsilon_{331}/\varepsilon_{438}$ = 2.4). Moreover, the amount of product $[Pt_2(pop)_4I_2]^{4-}$ formed was equal to the amount of $[Pt_2(pop)_4]^{4-}$ consumed, $(\Delta A/\varepsilon)_{[Pt_2(pop)_4I_2]^{4-}}$: $(\Delta A/\varepsilon)_{[Pt_2(pop)_4]^{4-}}$ = 1.0 ± 0.1. It can be concluded that $[*Pt_2(pop)_4]^{4-}$ is oxidatively quenched by $[Co(CN)_5I]^{3-}$ to form $[Pt_2(pop)_4I_2]^{4-}$. The quantum yield for this photooxidation was calculated to be 0.083 ± 0.002.

Formation of $[Pt_2(pop)_4I_2]^{4-}$ in 0.5 M chloride is most unlikely *via* oxidative electron transfer and halide ion scavenging of the resulting mixed-valence Pt dimer. The result suggests a mechanism involving direct I atom transfer from $[Co(CN)_5I]^{3-}$ to form $[Pt^{II}Pt^{III}(pop)_4I]^{4-}$ [eqn. (1)].

$$[*Pt_2(pop)_4]^{4-} + [Co(CN)_5I]^{3-} \xrightarrow{k_{AT}} [Pt^{II}Pt^{III}(pop)_4I]^{4-} + [Co(CN)_5]^{3-} \quad (1)$$

The mixed valence species $[Pt^{II}Pt^{III}(pop)_4I]^{4-}$ can then form the observed $[Pt_2(pop)_4I_2]^{4-}$ product either by disproportionation or by further reaction with $[Co(CN)_5I]^{3-}$. The species $[Co(CN)_5]^{3-}$ will quickly undergo acid-catalysed decomposition to give $Co^{II}$(aq) and HCN under our conditions.[9]

The above mechanistic ambiguity was resolved in our second approach, which also avoided possible mechanistic complications at the high chloride concentration needed for the competition study. A solution of $2 \times 10^{-5}$ M $[Pt_2(pop)_4]^{4-}$ and $2 \times 10^{-4}$ M $[Co(CN)_5I]^{3-}$ in nitrogen-degassed 0.01 M $HClO_4$–saturated $KClO_4$ solution was flash photolysed with a 25 mJ, 10 ns pulse at 355 nm with monitoring of the triplet $[Pt_2(pop)_4]^{4-}$ emission at 514 nm, its excited-state absorption at 460 nm (fast), the $[Co(CN)_5I]^{3-}$ ground-state absorption at 280 nm and the development of $[Pt_2(pop)_4I_2]^{4-}$ product absorption at 460 nm (slow). The absorption and emission from the triplet excited state decayed exponentially with the quenched lifetime, 4.9 and 5.1 μs respectively, while the ground-state absorption of $[Co(CN)_5I]^{3-}$ decreased with the same lifetime (4.7 μs), Fig. 2(*a*). This proves the direct reaction of $[Pt_2(pop)_4]^{4-}$ triplet state with $[Co(CN)_5I]^{3-}$ consistent with eqn. (1). The transient

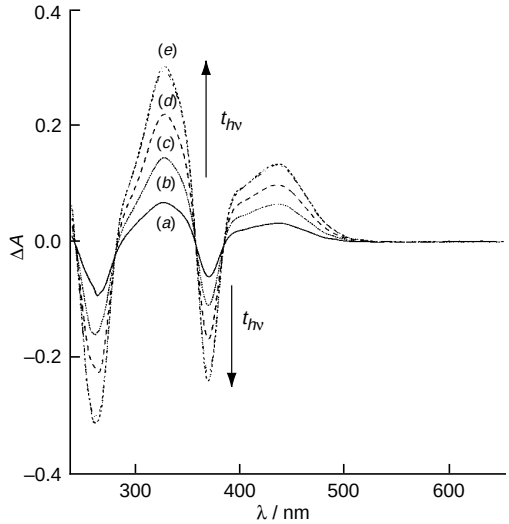



**Fig. 1** Absorbance change with the reaction of $[*Pt_2(pop)_4]^{4-}$ by $[Co(CN)_5I]^{3-}$ in 0.50 M KCl–0.010 M $HClO_4$ solution. Irradiation time: (*a*) 30, (*b*) 60, (*c*) 90, (*d*) 120 s; (*e*) kept in dark for 120 s after (*d*).

that results leads to $[Pt_2(pop)_4I_2]^{4-}$ which grows in with a 0.5 ms lifetime (see below), but no further reaction of $[Co(CN)_5I]^{3-}$ occurs (monitored at 280 nm) as shown in Fig. 2(*b*). This proves that the dominant second step of the reaction is a disproportionation process [eqn. (2)].

$$2[Pt^{II}Pt^{III}(pop)_4I]^{4-} \longrightarrow [Pt_2(pop)_4I_2]^{4-} + [Pt_2(pop)_4]^{4-} \quad (2)$$

not further reaction with $[Co(CN)_5I]^{3-}$ such as a second atom transfer [eqn. (3)].

$$[Pt^{II}Pt^{III}(pop)_4I]^{4-} + [Co(CN)_5I]^{3-} \xrightarrow{k_{AT}} [Pt_2(pop)_4I_2]^{4-} + [Co(CN)_5]^{3-} \quad (3)$$

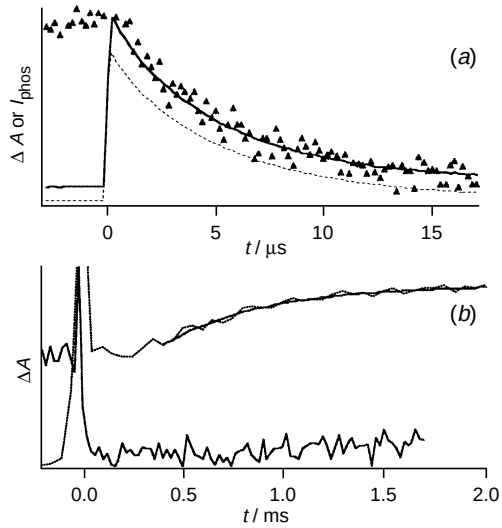



**Fig. 2** Transient signals on flash photolysis of $2 \times 10^{-5}$ M $[Pt_2(pop)_4]^{4-}$ and $2 \times 10^{-4}$ M $[Co(CN)_5I]^{3-}$ in nitrogen-degassed 0.01 M $HClO_4$–saturated $KClO_4$ solution with a 25 mJ, 10 ns pulse at 355 nm. (*a*) (---) $[*Pt_2(pop)_4]^{4-}$ emission at 514 nm; (—) $[*Pt_2(pop)_4]^{4-}$ absorption at 460 nm; (▲) $[Co(CN)_5I]^{3-}$ absorption at 280 nm. (*b*) (—) $[Co(CN)_5I]^{3-}$ absorption at 280 nm; (···) $[Pt_2(pop)_4I_2]^{4-}$ absorption at 460 nm.

The disproportionation step should be simple second order, but given the noise level of the data, Fig. 2(*b*), the time evolution is indistinguishable from an exponential decay with a lifetime of 0.5 ms for these conditions.

In conclusion, both approaches show that direct iodine atom abstraction occurs in this system. A full paper with results on the salt and specific ion effects in the quenching of $[*Pt_2(pop)_4]^{4-}$ by $[Co(CN)_5I]^{3-}$ and other pentacyanocobaltate complexes has been submitted.[6]

## Footnote

† At 337 nm $[Pt_2(pop)_4]^{4-}$ has a much smaller molar absorptivity than $[Co(CN)_5I]^{3-}$. To quench the lifetime of $[Pt_2(pop)_4]^{4-}$ to half of its initial value, the quencher concentration should be about $10^{-3}$ M, while the concentration of $[Pt_2(pop)_4]^{4-}$ should be about $3 \times 10^{-4}$ M to achieve an absorbance of 0.3 at 337 nm. Under such conditions the iodo complex would absorb 90% of the light, possibly leading to the photolysis of the quencher, as well as serious inner filter effects in the Stern–Volmer study. Quinine sulfate has a strong absorption between 320 nm and 340 nm ($\log \varepsilon = 4$) and emits at 370 nm, where $\varepsilon\{[Pt_2(pop)_4]^{4-}\} \gg \varepsilon\{[Co(CN)_5I]^{3-}\}$, and has[7] a fluorescence lifetime of 19.2 ns, short enough to avoid distortion of the 9 μs emission decay curve of $[*Pt_2(pop)_4]^{4-}$.

## References


1 D. C. Smith and H. B. Gray, *Coord. Chem. Rev.*, 1990, **100**, 169.
2 D. M. Roundhill, *Photochemistry and Photophysics of Metal Complexes*, Plenum Press, New York, 1994.
3 D. M. Roundhill, *J. Am. Chem. Soc.*, 1985, **107**, 4354.
4 A. P. Zipp, *Coord. Chem. Rev.*, 1988, **84**, 47.
5 D. M. Roundhill, Z.-P. Shen, C. King and S. J. Atherton, *J. Phys. Chem.*, 1988, **92**, 4088.
6 L.-Z. Cai and A. D. Kirk, unpublished work.
7 S. L. Murov, I. Carmichael and G. L. Hug, *Handbook of Photochemistry*, Marcel Dekker, Inc., New York, 1993.
8 S. A. Bryan, M. K. Dickson and D. M. Roundhill, *Inorg. Chem.*, 1987, **26**, 3878.
9 H. Tagaki and T. W. Swaddle, *Inorg. Chem.*, 1992, **31**, 4669.


*Received, 16th December 1996; Com. 6/08426E*

# A new route to polyselenoether macrocycles. Catalytic macrocyclization of 3,3-dimethylselenatane by $[Re_2(CO)_9]$

**Richard D. Adams* and Kenneth T. McBride**

*Department of Chemistry and Biochemistry, University of South Carolina, Columbia, SC 29208, USA*

**3,3-Dimethylselenatane, $SeCH_2CMe_2CH_2$, DMSe is cyclooligomerized catalytically at 115 °C in the presence of $[Re_2(CO)_9(SeCH_2CMe_2CH_2)]$ to yield three new polyselenoether macrocycles 3,3,7,7-tetramethyl-1,5-diselenacyclooctane, 3,3,7,7,11,11-hexamethyl-1,5,9-triselenacyclododecane, 3,3,7,7,11,11,15,15-octamethyl-1,5,9,13-tetraselenacyclohexadecane and polymer of DMSe; all three macrocycles are characterized crystallographically; in all cases the *gem*-dimethyl groups are directed toward the exterior of the rings; interestingly, some methylene groups are directed to the interior.**

In recent studies we have shown that $[Re_2(CO)_9(NCMe)]$ and other third-row transition-metal carbonyl complexes can serve as effective catalysts for the ring-opening cyclooligomerization of thietanes to polythioether macrocycles.[1] Polythioether macrocycles have attracted attention for their ability to serve as ligands for transition metals.[2] Polyselenoether macrocycles have an equally good potential to serve as ligands,[3] but the number of known polyselenoether macrocycles is very small.[4]

We have now found that $[Re_2(CO)_9(SeCH_2CMe_2CH_2]$ **1** serves as a catalyst for the ring-opening macrocyclization of 3,3-dimethylselenatane, $SeCH_2CMe_2CH_2$, DMSe, to yield three new polyselenoether macrocycles.† 15.0 mg of **1** was dissolved in 0.750 g of DMSe[5] and the solution was heated to 115 °C for 8 h.‡ This yielded a residue of 340 mg after removal of the unreacted DMSe. The products were separated by TLC to yield 4.3 mg of 3,3,7,7-tetramethyl-1,5-diselenacyclooctane **2**, 104.1 mg of 3,3,7,7,11,11-hexamethyl-1,5,9-triselenacyclododecane **3** and 12.0 mg of 3,3,7,7,11,11,15,15-octamethyl-1,5,9,13-tetraselenacyclohexadecane **4**. The remainder is believed to be polymer of DMSe. For **3** this is equivalent to 12.0 turnovers or 1.5 turnovers $h^{-1}$.

All three macrocycles were characterized crystallographically, and structural diagrams of each are shown in Figs. 1–3, respectively.§ In all three structures the *gem*-dimethyl groups are directed toward the exterior of the ring. In the solid state **2** and **4** both contain a crystallographically imposed centre of

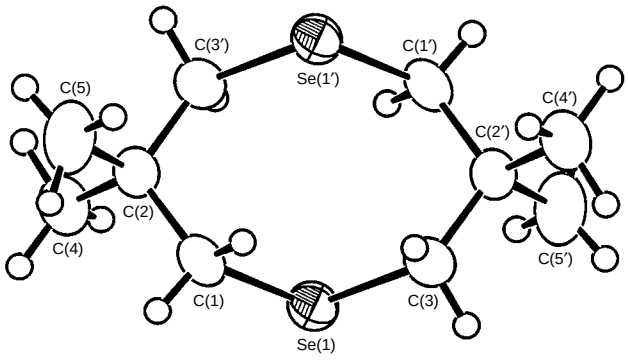



**Fig. 1** An ORTEP diagram of 3,3,7,7-tetraamethyl-1,5-diselenacyclooctane **2**. Selected interatomic distances (Å): Se(1)–C(1) 1.961(8), Se(1)–C(3) 1.974(8), C(1)–C(2) 1.52(1), C(2)–C(3′) 1.52(1).

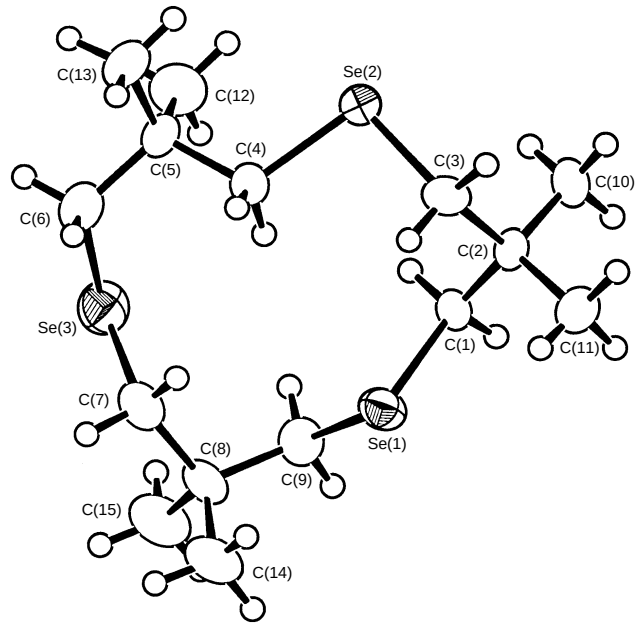



**Fig. 2** An ORTEP diagram of 3,3,7,7,11,11-hexamethyl-1,5,9-triselenacyclododecane **3**. Selected interatomic distances (Å): Se (1)–C(1) 1.965(8), Se(1)–C(9) 1.953(9), Se(2)–C(3) 1.952(9), Se(2)–C(4) 1.957(9), Se(3)–C(6) 1.97(1), Se(3)–C(7) 1.97(1).

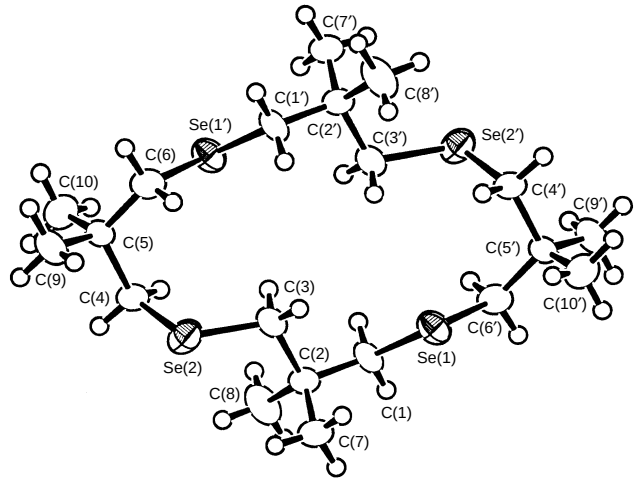
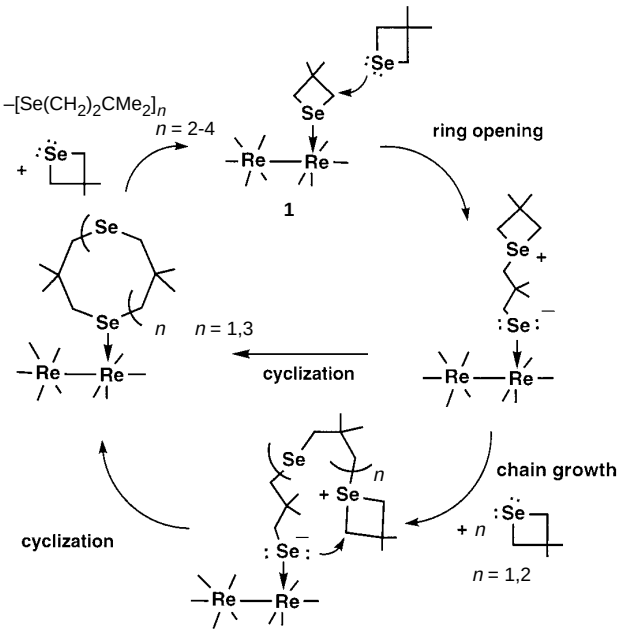



**Fig. 3** An ORTEP diagram of 3,3,7,7,11,11,15,15-octamethyl-1,5,9,13-tetraselenacyclohexadecane **4**. Selected interatomic distances (Å): Se(1)–C(1) 1.961(9), Se(1)–C(6) 1.967(9), Se(2)–C(3) 1.961(9), Se(2)–C(4) 1.956(9), C(1)–C(2) 1.54(1), C(2)–C(3) 1.57(1), C(4)–C(5) 1.55(1), C(5)–C(6) 1.51(1).




**Scheme 1**

symmetry. All Se–C distances are similar, Se(1)–C(1) 1.961(8) and Se(1)–C(3) 1.974(8) Å for **2**; Se(1)–C(1) 1.965(8), Se(1)–C(9) 1.953(9), Se(2)–C(3) 1.952(9), Se(2)–C(4) 1.957(9), Se(3)–C(6) 1.97(1) and Se(3)–C(7) 1.97(1) Å for **3**; and Se(1)–C(1) 1.961(9), Se(1)–C(6) 1.967(9), Se(2)–C(3) 1.961(9) and Se(2)–C(4) 1.956(9) Å for **4** and all are similar to those found in the unsubstituted selenoether macrocycles: [12]ane$S_4$, [18]ane$Se_6$, [16]ane$Se_4$, [24]ane$Se_6$ and [14]ane$Se_4$.[4c] It has been suggested that *gem*-dimethyl groups on the ring of polythioether macrocycles will force the sulfur atoms to turn toward the interior of the ring and enhance their ligand properties.[6] This is only partially supported by the results for the selenium compounds described here. Although conformations of **3** and **4** differ from those of their unsubstituted sulfur and selenium homologues 1,5,9-trithiacyclododecane¶ and 1,5,9,13-tetraselenacyclohexadecane,[4c] the selenium atoms are not directed inward. In fact, it is methylene groups, C(4) on **3** and C(3) on **4**, that are most dramatically turned toward the interior of the macrocycles.

In the absence of **1**, no significant amounts of the macrocycles or polymer are formed from DMSe under these conditions. We feel that the mechanism involves a series of ring opening additions of DMSe to the DMSe ligand in a $Re_2(CO)_9$ complex followed by a recyclization, similar to that established for the macrocyclizations of thietane[1c] and 3-methylthietane,[1f] see Scheme 1. To date, our studies have been limited to DMSe due to the lower stability of the less substituted selenatanes. Efforts to prepare metal complexes of these new macrocycles are now in progress.

These studies were supported by the Division of Chemical Sciences of the Office of Basic Energy Sciences of the US Department of Energy.

## Footnotes

† $[Re_2(CO)_9(\overline{SeCH_2CMe_2CH_2})]$ **1** was obtained in 88% yield from the reaction of $[Re_2(CO)_9(NCMe)]$ with 3,3-dimethylselenatane in hexane at reflux for 2 h.

*Analytical data*: **1**, $^1$H NMR ($CDCl_3$): δ 3.58 (d, 2 H, $J_{HH}$ 9.4 Hz), 3.20 (d, 2 H, $J_{HH}$ 9.7 Hz), 1.41 (s, 3 H), 1.22 (s, 3 H). IR ν(CO)/cm$^{-1}$ (hexane): 2102.2w, 2040.5m, 2016.0w, 1995.0s, 1988.5s, 1976.8m, 1967.1m, 1954.4w, 1933.5m. Anal. Found (Calc.): C 21.99 (21.74), H 1.31 (1.30)%.

‡ **2**, $^1$H NMR ($CDCl_3$), δ 2.90 (s, 8 H), 0.97 (s, 12 H); $^{13}$C NMR, δ 44.46 (2 C), 37.72 (1 C), 28.64 (2 C); $^{77}$Se NMR ($CDCl_3$), δ 56.05; MS ($^{80}$Se), *m/z* 300 [$2^+$], 230 ($2^+ - C_5H_{10}$), 69 ($C_5H_9$).

**3**, $^1$H NMR ($CDCl_3$) δ, 2.81 (s, 12 H), 1.54 (s, 18 H); $^{13}$C NMR 37.91 (2 C), 36.09 (1 C), 28.32 (2 C); $^{77}$Se NMR, δ 54.46 (s, 3 Se); MS ($^{80}$Se), *m/z* 450 [$3^+$], 230 [$3^+ - SeC_{10}H_{20}$], 150 ($3^+ - Se_2C_{10}H_{20}$), 69 ($C_5H_9$). Anal. Calc. for **3** ($Se_3C_{15}H_{30}$): C, 40.28; H, 6.76. Found: C, 40.27; H, 6.65%.

**4**, $^1$H NMR ($CDCl_3$), δ 2.75 (s, 16 H), 1.05 (s, 24 H); $^{13}$C NMR, δ 39.99 (2 C), 36.43 (1 C), 27.69 (2 C); $^{77}$Se NMR, δ 53.90 (s, 4 Se). MS ($^{80}$Se), *m/z* 600 ($4^+$) 300 ($4^+ - Se_2C_{10}H_{20}$), 230 ($4^+ - Se_2C_{15}H_{30}$), 150 ($4^+ - Se_3C_{15}H_{30}$), 69 ($C_5H_9$).

§ *Crystal data*: **2**, $C_{10}H_{20}Se_2$, monoclinic, space group *C*2/*c*, *a* = 10.534(3), *b* = 7.602(2), *c* = 15.612(3) Å, β = 96.88(2)°, *U* = 1241.1(5) Å$^3$, *Z* = 4. 873 unique reflections, $R$ = 0.043, $R_w$ = 0.049 for 631 reflections with $I > 3\sigma(I)$. **3**, $C_{15}H_{30}Se_3$, monoclinic, space group $P2_1/a$, *a* = 11.660(3), *b* = 10.975(2), *c* = 14.578(3) Å, β = 98.57(2)°, *U* = 1860(2) Å$^3$, *Z* = 4. 2570 unique reflections, $R$ = 0.045, $R_w$ = 0.049 for 1697 reflections with $I > 3\sigma(I)$. **4**, $C_{20}H_{40}Se_4$, triclinic, space group $P\bar{1}$, *a* = 8.669(1), *b* = 9.719(2), *c* = 7.402(1) Å, α = 94.23(2), β = 94.72(1), γ = 79.34(2)°, *U* = 1860(2) Å$^3$, *Z* = 1. 1591 unique reflections, $R$ = 0.043, $R_w$ = 0.046 for 1241 reflections with $I > 3\sigma(I)$. For all structures data were collected on a Rigaku AFC6S diffractometer using Mo-Kα radiation. $L_p$ and absorption corrections were applied in all analyses.

Atomic coordinates, bond lengths and angles, and thermal parameters have been deposited with the Cambridge Crystallographic Data Centre (CCDC). See Information for Authors, Issue No. 1. Any request to the CCDC for this material should quote the full literature citation and the reference number 182/376.

¶ The molecular structure of [12]ane$Se_3$ has not yet been determined. Most likely it is similar to that of [12]ane$S_3$.[7] The structures of [16]ane$S_4$ and [16]ane$Se_4$ are similar.[4c]

## References

1 (*a*) R. D. Adams and S. B. Falloon, *Chem. Rev.*, 1995, **95**, 2587; (*b*) *J. Am. Chem. Soc.*, 1994, **116**, 10540; (*c*) R. D. Adams, J. E. Cortopassi and S. B. Falloon, *Organometallics*, 1995, **14**, 1748; (*d*) R. D. Adams and S. B. Falloon, *Organometallics*, 1995, **14**, 4594; (*e*) R. D. Adams, S. B. Falloon, J. Perrin, J. A. Queisser and J. H. Yamamoto, *Chem. Ber.*, 1996, **126**, 313; (*f*) R. D. Adams, J. A. Queisser and J. H. Yamamoto, *Organometallics*, 1996, **15**, 2489.

2 S. R. Cooper, in *Crown Compounds: Toward Future Applications*, ed. S. R. Cooper, VCH, New York, 1992, ch. 15; S. R. Cooper and S. C. Rawle, *Struct. Bonding* (*Berlin*), 1990, **72**, 1; A. J. Blake and M. Schröder, *Adv. Inorg. Chem.*, 1990, **35**, 1.

3 R. J. Batchelor, F. W. B. Einstein, I. D. Gay, J.-H. Gu, B. M. Pinto and X.-M. Zhou, *J. Am. Chem. Soc.*, 1990, **112**, 3706; R. J. Batchelor, F. W. B. Einstein, I. D. Gay, J.-H. Gu and B. M. Pinto, *J. Organomet. Chem.*, 1991, **411**, 147; W. Levason, J. J. Quirk and G. Reid, *J. Chem. Soc., Dalton Trans.*, 1996, 3713; W. Levason, J. J. Quirk, G. Reid and C. S. Frampton, *Inorg. Chem.*, 1994, **33**, 6120; N. R. Champness, P. F. Kelly, W. Levason, G. Reid, A. M. Z. Slawin and D. J. Williams, *Inorg. Chem.*, 1995, **34**, 615.

4 (*a*) E. G. Hope and W. Levason, *Coord. Chem. Rev.*, 1993, **122**, 109; (*b*) I. Cordova-Reyes, E. VandenHoven, A. Mohammed and B. M. Pinto, *Can. J. Chem.*, 1995, **73**, 113; (*b*) R. J. Batchelor, F. W. B. Einstein, I. D. Gay, J.-H. Gu, B. D. Johnston and B. M. Pinto, *J. Am. Chem. Soc.*, 1990, **112**, 1297; (*c*) R. J. Batchelor, F. W. B. Einstein, I. D. Gay, J.-H. Gu, B. D. Johnston and B. M. Pinto, *J. Am. Chem. Soc.*, 1989, **111**, 6582; (*d*) B. M. Pinto, B. D. Johnston, R. J. Batchelor, F. W. B. Einstein and I. D. Gay, *Can. J. Chem.*, 1988, **66**, 2956; (*e*) B. M. Pinto, R. J. Batchelor, B. D. Johnston, F. W. B. Einstein and I. D. Gay, *J. Am. Chem. Soc.*, 1988, **110**, 2990.

5 H. J. Backer and F. S. Winter, *Recl. Trav. Chim. Pays-Bas*, 1937, **56**, 492.

6 R. E. Wolf Jr., J. R. Hartman, J. M. E. Storey, B. M. Foxman and S. R. Cooper, *J. Am. Chem. Soc.*, 1987, **109**, 4328; J. M. Desper and S. H. Gellman, *J. Am. Chem. Soc.*, 1990, **112**, 6732; A. Y. Nazarenko, R. M. Izatt, J. D. Lamb, J. M. Desper, B. E. Matysik and S. H. Gellman, *J. Am. Chem. Soc.*, 1990, **112**, 6732; J. M. Desper and S. H. Gellman, *J. Am. Chem. Soc.*, 1990, **112**, 6732.

7 S. C. Rawle, G. A. Admans and S. R. Copper, *J. Chem. Soc., Dalton Trans.*, 1988, 93.

*Received, 18th December 1996; Com. 6/08481H*

# A supramolecular motif in the solid-state structure of a difunctional thallium(I) amide defined by weak Tl···Tl attractions

**Konrad W. Hellmann, Lutz H. Gade,* Roland Fleischer and Dietmar Stalke**

*Institut für Anorganische Chemie der Universität Würzburg, Am Hubland, D-97074 Würzburg, Germany*

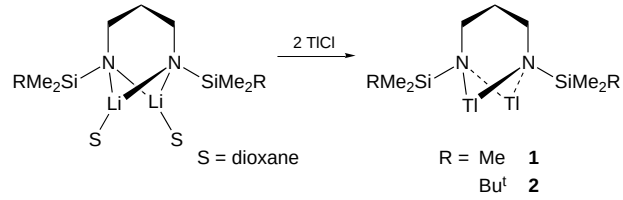
**The crystal structure of the difunctional thallium(I) amide $CH_2[CH_2N(Tl)SiMe_3]_2$ 1 reveals a pattern of aggregation based on weak attractive metal–metal interactions, a situation which appears to be influenced by the degree of exposure of the thallium centres; this is evidenced by the solid-state structure of the more shielded analogue $CH_2[CH_2N(Tl)SiBu^tMe_2]_2$ 2 which features no significant Tl···Tl contacts.**

The utilization of intermolecular interactions which generate specific supramolecular motifs has greatly enhanced the systematic approach to both the understanding and the design of highly organized molecular arrays in solids.[1] Intermolecular hydrogen bonding as well as ionic or dipolar interactions have been the most widely employed 'directional forces' in this context.[2] More recently, the attractive interactions between heavy closed-shell metal centres (with $d^{10}$ or $d^{10}s^2$ configuration) and the way they affect the intermolecular aggregation in solids have been investigated.[3] While compounds of monovalent gold have provided the most spectacular objects of study in this context, the neighbouring metals in the Periodic Table, in particular thallium(I), seem to be equally capable of aggregation through (mainly dispersive) metal–metal attraction.[4] The nature of these weak metal–metal interactions in thallium(I) compounds has been the subject of some debate,[5,6] although there is little doubt about their role in molecular aggregation.

The accessibility of the thallium(I) amides *via* metal exchange with well established alkali-metal analogues[7] prompted us to study their structural chemistry in more detail, in particular, with regard to the modes of aggregation defined by metal–metal interactions. That dispersive thallium(I)··· thallium(I) attractions may indeed strongly influence the solid-state structures of polyfunctional thallium(I) amides was recently demonstrated by the drastic distortions of the ligand framework which the tripodal Tl–amide $MeSi[SiMe_2N(Tl)Bu^t]_3$ displays in its crystal structure.[8] In this case, a highly flexible ligand system permitted rather unpredictable molecular shapes and thus molecular units aggregating in the crystal. In order to study intermolecular structural motifs in a meaningful and more systematic way, we chose a simpler difunctional Tl amide the molecular structure of which did not allow for significant geometrical rearrangement.

Stirring a solution of $CH_2[CH_2N(Li)SiMe_3]_2(dioxane)_2$ with TlCl in dioxane at room temp. for 3 h led to a complete metal exchange. The work up of the crude product mixture by extraction with toluene afforded a deep-orange solution from which a red, highly air-sensitive, crystalline solid could be obtained at −30 °C (yield 70%), the analytical data of which were consistent with its formulation as $CH_2[CH_2N(Tl)SiMe_3]_2$ **1** (Scheme 1). The results of variable-temperature NMR studies and cryoscopic measurements in benzene indicated that the compound is monomeric in solution.† It may also be sublimed at 60 °C and $10^{-2}$ mbar without decomposition. A single-crystal X-ray structure analysis, however, revealed a truly remarkable pattern of molecular packing in the crystal (Fig. 1).‡

As indicated in Scheme 1, the monomeric unit of the difunctional thallium amide has the expected molecular structure in which the two amido-N atoms and the two thallium(I) centres form a puckered four-membered ring, the metal atoms occupying rather exposed positions thus generating the poten-




**Scheme 1** Synthesis of **1** and **2** by Li/Tl exchange

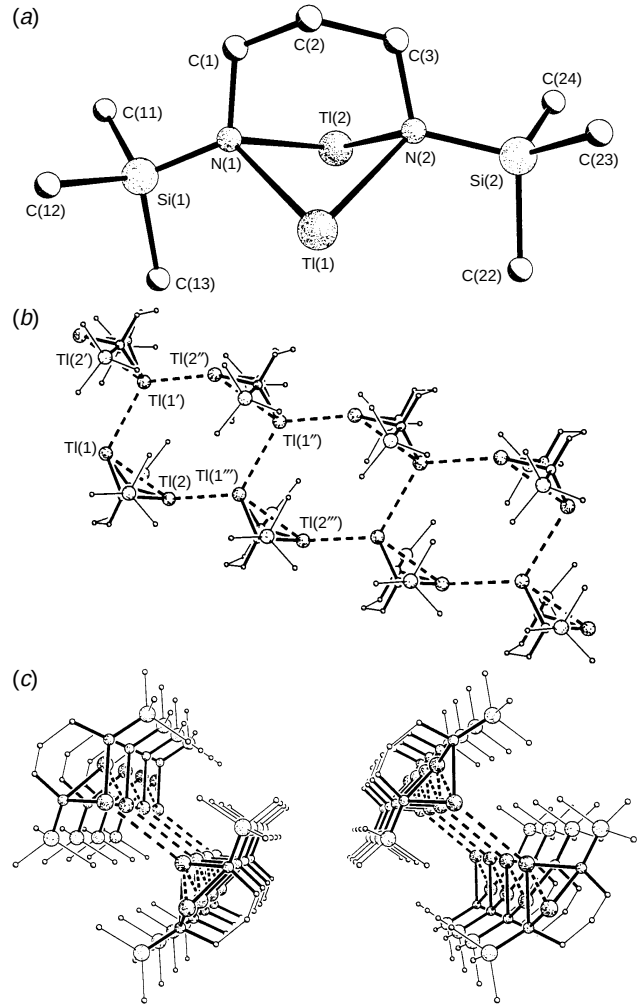



**Fig. 1** Crystal structure of **1**. Molecular structure (*a*) and aggregation in the crystal viewed along the crystallographic *b* axis (*b*) and *a* axis (*c*). Selected bond lengths (Å) and interbond angles (°) of the molecule: Tl(1)···Tl(2) 3.490(3), Tl(1)–N(1) 2.469(14), Tl(1)–N(2) 2.408(13), Tl(2)–N(1) 2.475(12), Tl(2)–N(2) 2.457(13); N(1)–Tl(1)–N(2) 74.8(4), N(1)–Tl(2)–N(2) 73.9(4), Tl(1)–N(1)–Tl(2) 89.8(4), Tl(1)–N(2)–Tl(2) 91.7(4).

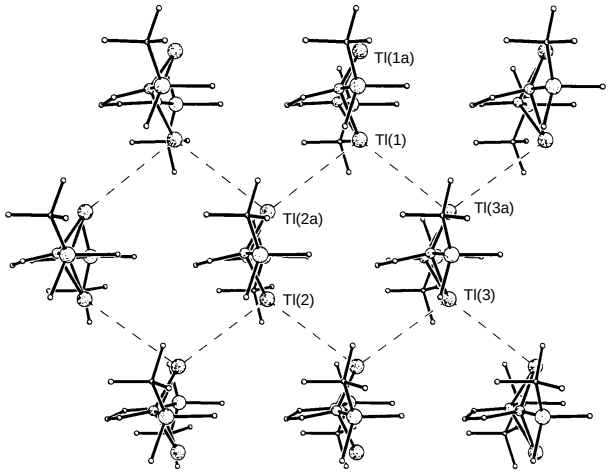



**Fig. 2** Packing of **2** in the crystal viewed along the *c* axis. Selected bond lengths (Å) and interbond angles (°) of the molecule: Tl(1)···Tl(1′) 3.4800(7), Tl(1)–N(1) 2.405(7), Tl(1)–N(1′) 2.481(7); N(1)–Tl(1)–N(1′) 74.7(3), Tl(1)–N(1)–Tl(1′) 90.8, intermolecular Tl···Tl > 4.70.

tially 'sticky ends' for aggregation [Fig. 1(*a*)]. The fairly short Tl···Tl distance of 3.490(2) Å is probably a consequence of the bridging ligands tying the two metals together rather than due to significant bonding interaction although it is rather close to the interatomic distances found in α-thallium (3.408 and 3.457 Å).[9]

In the solid the molecular units of **1** aggregate *via* Tl···Tl contacts to form infinite, double-stranded bands [Fig. 1(*b*,(*c*)]. The two strands consist of monomers facing each other and occupying translationally displaced positions generating a one-dimensional grid consisting of distorted hexagons of metal–metal contacts. In the resulting planar bands one of the two metal atoms in the monomers not only forms a direct contact to its neighbour within a strand [Tl···Tl 3.775(3) Å] but also across to the opposite strand [Tl···Tl 3.697(3) Å].

In order to assess the importance of the relative exposure of the thallium(I) centres in the structure of **1** for the aggregation in the solid the structurally analogous Tl–amide $CH_2[CH_2N(Tl)SiBu^tMe_2]_2$ **2** containing the bulkier silyl substituent $Bu^tMe_2Si$ at the amido functionalities was synthesized using the identical procedure outlined for **1** (yield 74%).† The crystal structure of **2** has revealed a packing in the solid which appears to be entirely dictated by the molecular shape rather than metal–metal contacts as found for **1** (Fig. 2).‡

The shortest intermolecular Tl···Tl distances of over 4.7 Å are testimony to the absence of significant metal–metal interaction in the crystal. With the exception of the somewhat greater shielding of the $Tl_2N_2$-unit in the molecule the overall molecular shapes of **1** and **2** are closely related. This is to be seen in the context of a notion put forward by von Schnering who pointed out that aggregations *via* heavy metals in a molecule may in fact arise from the requirements of crystal packing dictated by the shape of the whole molecule, a situation aptly described as the 'umbrella effect'.[10] The fact that the molecules containing the more exposed metal atoms display structural motifs characterized by metal–metal contacts, while those less favoured in doing so by nature of their more shielded molecular structure do not, supports the relevance of such weak interactions between the heavy metals in the structure of compound **1**.

We thank the Deutsche Forschungsgemeinschaft (Schwerpunktprogramm 'Polyeder'), for financial support and Professor H. Werner (Würzburg) for his continued interest and support of this work.

## Footnotes

† *Selected spectroscopic data*. **1**: $^1$H NMR ($C_6D_6$, 295 K); δ 0.13 [s, 18 H, $Si(CH_3)_3$], 1.70 (m, 2 H, $CH_2C$), 4.32 (br, t, 4 H, $^3J_{HTlH}$ 54.8 Hz, $CH_2N$). $^{13}C\{^1H\}$ NMR ($C_6D_6$, 295 K); δ 0.8 [t, $^3J_{TlC}$ 59.3 Hz, $Si(CH_3)_3$], 37.7 ($CH_2C$), 51.0 (t, $^2J_{TlC}$ 82.5 Hz, $CH_2N$). **2**: $^1$H NMR ($C_6D_6$, 295 K); δ 0.05 [s, 12 H, $Si(CH_3)_2$], 1.02 [s, 18 H, $C(CH_3)_3$], 1.72 (br m, 2 H $CH_2C$), 4.37 (br t, $^3J_{TlH}$ 52 Hz, 4 H, $CH_2N$). $^{13}C\{^1H\}$ NMR ($C_6D_6$, 295 K); δ −3.5 [t, $^3J_{TlC}$ 102 Hz, $Si(CH_3)_2$], 22.4 [s, $(CH_3)_3C$], 28.4 [t, $^4J_{TlC}$ 50 Hz, $C(CH_3)_3$], 37.4 (s, $CH_2C$), 52.4 (t, $^2J_{TlC}$ 86 Hz, $CH_2N$). Correct C, H, N, Tl analyses were obtained.

‡ *Crystal data*: **1**; $[C_9H_{24}N_2Si_2Tl_2]_\infty$, crimson, crystal dimensions 0.4 × 0.3 × 0.2 mm, $M$ = 625.22, triclinic, space group $P\bar{1}$, $a$ = 6.557(5), $b$ = 11.520(7), $c$ = 12.838(8) Å, α = 116.29(4), β = 91.28(4), γ = 104.82(3)°, $U$ = 830.2(10) Å$^3$, $Z$ = 2, $D_c$ = 2.501 Mg m$^{-3}$, μ = 19.509 mm$^{-1}$, $F(000)$ = 564, 4523 reflections collected ($10 \leqslant 2\theta \leqslant 45°$) at 192(2) K, 2132 independent reflections used in the structure refinement [$R_{int}$ = 0.108]; $R_1$ = 0.066 [$I > 2\sigma(I)$], $wR_2$ = 0.175 (all data), 142 parameters, largest difference peak, hole = 3.14, −3.20 e Å$^{-3}$;

**2**; $[C_{15}H_{36}N_2Si_2Tl_2]_\infty$, orange crystal dimensions 0.4 × 0.4 × 0.4 mm, $M$ = 709.38, monoclinic space group $C2/c$, $a$ = 12.7223(3), $b$ = 7.3019(2), $c$ = 24.2444(4) Å, β = 99.9330(3), $U$ = 2218.47 Å$^3$, $Z$ = 4, $D_c$ = 2.124 Mg m$^{-3}$, μ = 14.614 mm$^{-1}$, $F(000)$ = 1320, 13545 reflections collected ($6 \leqslant 2\theta \leqslant 52°$) at 133(2) K, 2237 independent reflections used in the structure refinement [$R_{int}$ = 0.137]; $R_1$ = 0.054 [$I > 2\sigma(I)$], $wR_2$ = 0.136 (all data), 115 parameters and 23 restrains, largest difference peak, hole = 2.82, −3.93 e Å$^{-3}$. The data were collected on a Stoe-Siemens AED four-circle diffractomer (**1**) and on a Stoe-Siemens-Huber diffractometer fitted with a Siemens CCD detector (**2**) (graphite-monochromated Mo-Kα radiation, λ = 0.710 73 Å) equipped with a modified version of the Siemens/Nicolet LTIIa low-temperature device.[11] The structures were solved by direct methods (SHELXS-90)[12] and refined by full-matrix least-squares methods against $F^2$ (SHELXL-96).[13] The central methylene group in **2** was refined by suppressed constraints of the special position required from the twofold axis All data were absorption corrected and the non-H atoms were refined anisotropically. Definition of R values: $wR_2 = [\Sigma[w(F_o^2 - F_c^2)^2]/\Sigma[w(F_o^2)^2]]^{\frac{1}{2}}$, $R_1 = \Sigma\|F_o| - |F_c\|/\Sigma|F_o|$. Atomic coordinates, bond lengths and angles, and thermal parameters have been deposited at the Cambridge Crystallographic Data Centre (CCDC). See Information for Authors, Issue No. 1. Any request to the CCDC for this material should quote the full literature citation and the reference number 182/367.

## References

1 J.-M. Lehn, *Angew. Chem., Int. Ed. Engl*., 1988, **27**, 89; 1990, 29, 1304; F. Vögtle, *Supramolecular Chemistry*, Wiley, Chichester, 1991: ed. H.-J. Schneider and H. Dürr, *Frontiers in Supramolecular Organic Chemistry and Photochemistry*, VCH Weinheim, 1991.
2 See for example: J. A. Zerowski, C. T. Seto and G. M. Whitesides, *J. Am. Chem. Soc*., 1992, **114**, 5473; J.-M. Lehn, M. Mascal, A. DeCian and J. Fischer, *J. Chem. Soc., Chem. Commun*., 1990, 479; Y.-L. Chang, M.-A. West, F. W. Fowler and J. W. Lauher, *J. Am. Chem. Soc*., 1993, **115**, 5991 and references cited.
3 *Unkonventionelle Wechselwirkungen in der Chemie metallischer Elemente*, ed. B. Krebs, VCH Weinheim, 1992.
4 Examples: J. S. Casas, A. Castineiras, I. Haiduc, A. Sanchez, J. Sordo and E. M. Vasques-Lopez, *Polyhedron*, 1994, **13**, 1805; H. Pritzkow and P. Jennische, *Acta Chem. Scand., Ser. A*, 1975, **29**, 60; R. Atencio, J. Barbera, C. Cativiela, F. J. Lahoz, J. L. Serrano and M. M. Zurbano, *J. Am. Chem. Soc*., 1994, **116**, 11558; P. Jutzi, D. Wegener and M. B. Hursthouse, *Chem. Ber*., 1991, **124**, 295; P. Jutzi, J. Schnittger and M. B. Hursthouse, *Chem. Ber*., 1991, **124**, 1693; K. W. Klinkhammer and S. Henkel, *J. Organomet. Chem*., 1994, **480**, 167 and references therein.
5 C. Janiak and R. Hoffmann, *J. Am. Chem. Soc*., 1990, **112**, 5924.
6 P. Schwerdtfeger, *Inorg. Chem*., 1991, **30**, 1660 and references therein; G. Treboux and J.-C. Barthelat, *J. Am. Chem. Soc*., 1993, **115**, 4870.
7 M. Veith, A. Spaniol, J. Pöhlmann, F. Gross and V. Huch, *Chem. Ber*., 1993, **126**, 2625; K. W. Hellmann, L. H. Gade, A. Steiner, D. Stalke and F. Möller, *Angew. Chem., Int. Ed. Engl*., 1997, **36**, 160.
8 K. W. Hellmann, L. H. Gade, I. J. Scowen and M. McPartlin, *Chem. Commun*., 1996, 2515.
9 W. B. Pearson, *Handbook of Lattice Spacings and Structures of Metals*, Pergamon Press, Oxford 1967, vol. 2.
10 Cited in ref. 5 (as personal communication, ref. 132).
11 T. Kottke, R. J. Lagow and D. Stalke, *J. Appl. Crystallogr*., 1996, **29**, 465.
12 G. M. Sheldrick, *Acta Crystallogr., Sect. A*, 1990, **46**, 467.
13 G. M. Sheldrick, SHELXL-96 program for crystal structure refinement, University of Göttingen, 1996.

*Received, 13th November 1996; Com. 6/07701C*

# Synthesis of 2-hydroxybenzoic acid from $CO_2$ and phenol in aqueous heterogeneous photocatalytic systems

**Antonino Sclafani, Leonardo Palmisano and Gianluca Farneti**

*Dipartimento di Ingegneria Chimica dei Processi e dei Materiali, Università di Palermo, Viale delle Scienze, 90128, Palermo, Italy*

**The photocatalytic reaction occurring in aqueous deaereated suspensions saturated with $CO_2$ and containing polycrystalline semiconductors, bare or loaded with Pt or Cu, affords 2-hydroxybenzoic acid and catechol as the main products.**

Many studies[1–6] have reported the photocatalytic reduction of $CO_2$ in both gas–solid and liquid–solid heterogeneous systems using mild experimental conditions and in the presence of $H_2O$. The solids used as photocatalysts were polycrystalline semiconductors, and bare Cu-doped $TiO_2$ (anatase) proved to be the most suitable.[6] Light organic compounds, such as for instance $HCO_2H$, MeOH and $CH_4$, were obtained as the main products and their relative ratios depended on the type of photocatalyst and experimental conditions used.

However, very few studies[7,8] can be found on the insertion of $CO_2$ in organic aromatic substrates using photochemical methods. The heterogeneous photocatalytic insertion of $CO_2$ into aromatic molecules, to the best of our knowledge, has not yet been reported.

Here preliminary results are reported on the production of 2-hydroxybenzoic acid (salicylic acid) by the photocatalytic reaction between $CO_2$ and phenol in aqueous deaerated suspensions containing a polycrystalline semiconductor, bare or loaded with Pt or Cu. Catechol was produced together with 2-hydroxybenzoic acid and its amount depended on the catalyst used.

The experimental runs were performed in a Solarbox manufactured by CO.FO.ME.GRA., Milan, equipped with a 1500 W Xe lamp, simulating the solar spectrum. Pyrex photoreactors (50 ml) containing 25 ml of aqueous phenol (8.2 g $l^{-1}$) solutions at pH = 5.85 saturated with $CO_2$ were used for each run. The photon flux provided by the lamp was measured in the locations of the photoreactors by means of the standard potassium ferrioxalate actinometric method which gave $6.6 \times 10^{-7}$ Einstein $s^{-1}$ with oscillations of only *ca.* 3%. The photocatalyst (2 g $l^{-1}$) was suspended in the phenol solution and magnetically stirred.

The solids used as photocatalysts were: anatase $TiO_2$ (Merck), $TiO_2$ (P25 Degussa), Cu-doped $TiO_2$ (P25 Degussa), Rutile $TiO_2$ (Tioxide), $WO_3$ (Carlo Erba, RPE), Pt-doped $WO_3$ (Carlo Erba, RPE), ZnO (BDH) and $SiO_2$ (BDH). The runs lasted 4 h and samples were withdrawn for HPLC analyses. The analyses were carried out after filtration through 0.45 μm cellulose acetate membrane (HA, Millipore) and subsequent centrifugation. One run lasted 8 h (anatase $TiO_2$ Merck) and it was contemporaneously performed using five identical photoreactors: two of them were used for analyses carried out after 1 and 2 h of illumination, the other three for analyses carried out after 4, 6 and 8 h.

Typically the filtered samples were injected into a chromatograph composed of a Varian model 9010 pump, a Varian 9050 UV–VIS detector and a 10 μm Econosil C18 (Alltech) 250 × 4.6 mm i.d. column. Isocratic elution with methanol–$H_3PO_4$ 0.05 mass% aqueous solution was performed at 1 ml $min^{-1}$. The products were monitored at λ = 254 nm.

The results are shown in Table 1. It can be seen that the most significant formation of 2-hydroxybenzoic acid was obtained by using anatase $TiO_2$ (Merck), while Pt(2 mass%)–$WO_3$ favoured the formation of catechol $TiO_2$ (Degussa P25, *ca.* 80% anatase and 20% rutile) was found to be less photoactive than anatase $TiO_2$ (Merck) which could be due to the higher oxidant properties of $TiO_2$ (Degussa P25) with respect to $TiO_2$ (Merck). The high oxidant properties of $TiO_2$ (Degussa) when used as photocatalyst for degradation reactions of organic molecules carried out in aqueous media are well known. The runs carried out using the other solids showed the formation of significantly smaller amounts of the above compounds. As expected, no 2-hydroxybenzoic acid, only traces of catechol, were found when the insulator oxide $SiO_2$ was used. Moreover, the poor photoactivity of bare $WO_3$ should be noted in comparison with the corresponding sample Pt(2 mass%)–$WO_3$ in the presence of which the biggest production of catechol was observed. The presence of Pt on the surface of $WO_3$ particles modifies the adsorption of the reagents, but in this case the major role consists in enhancing the lifetime of the photoproduced electron–hole pairs, due to its high work function.[9] The electrons migrate from $WO_3$ to Pt, giving rise to reduction reactions. The trend of the photoactivity of the samples is not much different if the BET specific surface areas of the powders reported in Table 1 are considered, *i.e.* if the specific photoactivity of the samples is calculated.

The results suggest that the photoreactivity is strongly influenced by both the surface physico-chemical and the electronic properties of the catalysts. The adsorption phenomena, indeed, are of primary importance for $CO_2$ photoactivation and they are related to several factors such as, for instance, the presence of catalytic metals, the surface acid–base properties, the zero charge potential and the surface hydroxylation.

In Fig. 1 the concentrations of 2-hydroxybenzoic acid and catechol *vs.* illumination time are reported when anatase $TiO_2$ (Merck) is used as photocatalyst.

It can be seen that the production of 2-hydroxybenzoic acid approaches the maximum value asymptotically. This could be

**Table 1** Average 2-hydroxybenzoic acid and catechol concentrations per hour and BET specific surface areas (SA) of the photocatalysts used

| Catalyst | Surface area/ $m^2\ g^{-1}$ | 2-Hydroxybenzoic acid/μmol $l^{-1}\ h^{-1}$ | Catechol/ μmol $l^{-1}\ h^{-1}$ |
|---|---|---|---|
| Anatase $TiO_2$ (Merck) | 10.5 | 371.2 | 44.31 |
| $TiO_2$ (P25 Degussa) | 44 | 64.2 | 3.5 |
| Cu (0.1 mass%)–$TiO_2$ (P25 Degussa) | 50 | 27.9 | 22.7 |
| Rutile $TiO_2$ (Tioxide) | 20 | 13.6 | 8.5 |
| $WO_3$ (Carlo Erba, RPE) | 15.5 | 18.5 | — |
| Pt (2.0 mass%)–$WO_3$ (Carlo Erba, RPE) | 16.4 | 117.7 | 1118.2 |
| ZnO (BDH) | 4 | 9.4 | — |
| $SiO_2$ (BDH) | n.d.[a] | — | traces |

[a] N.d. = not determined.

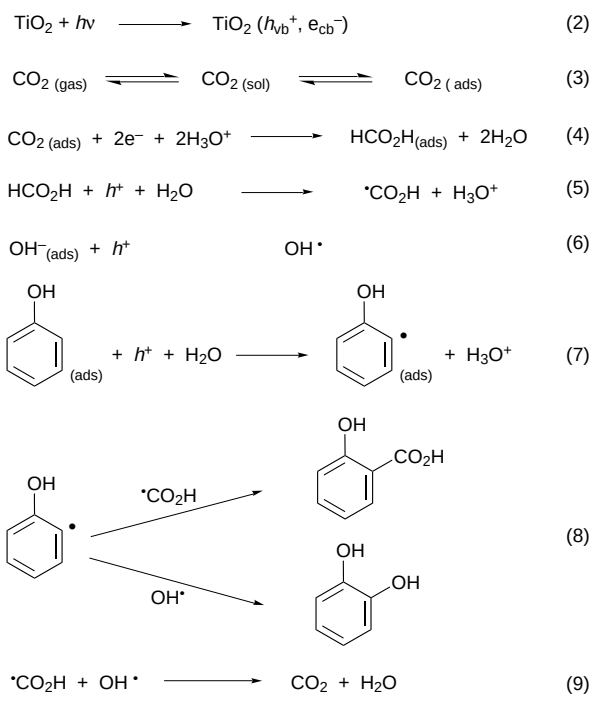
due to a decrease of $CO_2$ concentration in the batch discontinuous reacting system and/or to the competition of the photoreaction affording catechol.

By taking into account the experimental results it is evident that $CO_2$ is reduced by means of a photocatalytic reaction. The reduction process could be given by eqn. (1), where the redox

$$CO_2 + e^- + H_3O^+ \rightarrow \cdot COOH + H_2O \quad (1)$$

potential, $E^0_{redox}$ is −1.52 V *vs*. SHE.[10] Nevertheless the thermodynamic level of the conduction bands of the semiconductors used is more positive than −1.52 V and, even if the adsorption energy of $CO_2$[11] and the formation of surface states is considered, the difference between the thermodynamic level of eqn. (1) and the conduction bands of the used semiconductors is too high and, consequently, the above reduction reaction is not likely.

A more likely hypothesis for the reaction mechanism could be given by eqns. (2)–(9).




The thermodynamic potential of eqn. (4) is in standard conditions equal to −0.11 V *vs*. SHE. This last value is closer to those of the conduction bands of the used semiconductors. Anatase $TiO_2$, for instance, has the thermodynamic level of the conduction band equal to *ca*. −0.1 V *vs*. SHE,[12] while the conduction band of $WO_3$ (no variation is induced by the presence of Pt) is equal to 0.26 V *vs*. SHE (−0.059 V for each pH unity).[13]

The formation of $H_2$ as opposed to $HCO_2H$ according to eqn. (4) is thermodynamically less likely because $E_{H+/H2}$ is equal to −0.34 V *vs*. SHE in our experimental conditions (pH = 5.85). In the above mechanism, moreover, the competion among various adsorbed species for the oxidation process is taken into consideration and the occurrence of this competition could explain the different ratios of 2-hydroxybenzoic acid and catechol obtained by using different oxides.

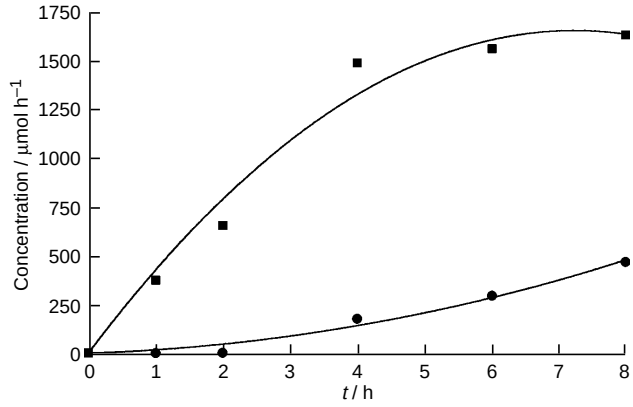



**Fig. 1** Concentration *vs*. illumination time of 2-hydroxybenzoic acid (■) and catechol (●) when anatase $TiO_2$ (Merck) was used

It should be noticed that OH radicals can attack catechol and 2-hydroxybenzoic acid further, giving rise to formation of other oxidation compounds and subsequent opening of the aromatic ring[14,15] and/or to attack methanoic acid with formation of carbon dioxide and water, eqn. (9).

Finally, it is also worth to notice that HPLC analyses indicate the presence of unidentified products and work is in progress to clarify the mechanistic aspects of the photocatalytic reaction.

## References


1 M. Halmann, M. Ulmann and B. Aurian-Blajeni, *Sol. Energy*, 1983, **31**, 429.
2 M. Halmann, V. Katzir, E. Borgarello and J. Kiwi, *Sol. Energy Mat.*, 1984, **10**, 85.
3 M. Anpo and K. Chiba, *J. Mol. Catal*., 1992, **207**, 74.
4 O. Ishitani, C. Inoue, Y. Suzuki and T. Ibusuki, *J. Photochem. Photobiol. A: Chem*., 1993, **72**, 269.
5 T. Mizuno, H. Tsutsumi, K. Ohta, A. Saji and H. Noda, *Chem. Lett*., 1994, 1533.
6 H. Yamashita, H. Nishiguchi, N. Kamada, M. Anpo, Y. Teraoka, H. Hatano, S. Ehara, K. Kikui, L. Palmisano, A. Sclafani, M. Schiavello and M. A. Fox, *Res. Chem. Intermedi*., 1994, **20**, 815 and references cited therein.
7 H. Sugimoto, I. Kawata, H. Taniguchi and Y. Fujiwara, *J. Organomet. Chem*., 1984, **C44**, 266.
8 H. Tagaya, M. Onuki, M. Karasu and K. Chiba, *Proc. The International Symposium on Chemical Fixation of Carbon Dioxide*, December 2–4, Nagoya, Japan, 1991, B10, p. 195.
9 A. Sclafani, L. Palmisano, G. Marcì and A. M. Venezia, unpublished results.
10 K. W. Frese, Jr., in *Electrochemical and Electrocatalytic Reactions of $CO_2$*, ed. K. Christ, E. Guard and B. P. Sullivan, Elsevier, Amsterdam, 1993, p. 148.
11 J. Raskó and F. Solymosi, *J. Phys. Chem*., 1994, **98**, 7147.
12 Y. V. Pleskov, *Solar Energy Conversion*, Springer, Berlin 1990, p. 116.
13 J. Desilvestro and M. Grätzel, *J. Electroanal. Chem*., 1987, **238**, 129.
14 R. W. Matthews, *J. Phys. Chem*., 1987, **91**, 3328.
15 S. Tunesi and M. Anderson, *J. Phys. Chem*., 1991, **95**, 3399.


*Received, 13th November 1996; Com. 6/07705F*

# Non-empirical quantum chemical calculation of Henry and separation constants and heats of adsorption for diatomic gases in faujasite

**J. C. Peirs,[a] F. De Proft,[a] G. Baron,[b] C. Van Alsenoy[c] and P. Geerlings*[a]†**

[a] *Eenheid Algemene Chemie, Faculty of Sciences, Free University of Brussels, Pleinlaan 2, 1050 Brussels, Belgium*
[b] *Department of Chemical Engineering, Faculty of Applied Sciences, Free University of Brussels, Pleinlaan 2, 1050 Brussels, Belgium*
[c] *Department of Chemistry, University of Antwerp (UIA), Universiteitsplein 1, 2610 Antwerp, Belgium*

**The Henry and separation constants and heat of adsorption of $N_2$ and $O_2$ in faujasite are calculated in a non-empirical way; they show fair agreement with experiment taking into account the extreme sensitivity of the configuration integral to small variations in interaction energy values.**

Zeolites are of utmost importance both as catalysts, essentially due to the acidic properties of their bridging hydroxy groups,[1,2] and as adsorbents due to their adsorption properties.[3] Present-day quantum chemistry already allows non-parametrized, highly accurate *ab initio* calculations on the acidic properties using the supermolecule approach yielding interaction energies and spectroscopic properties used as acidity indicator (*e.g.* IR frequency and intensity shifts).[4–6] The calculation of the adsorption behaviour and the thermodynamic quantities associated with it (Henry constant, separation constant, heat of adsorption) was up to now, essentially due to computational reasons, performed using model interaction potentials[7–9] and various models involving adjustable parameters.[10,11]

In this contribution we report the, as far as we know, first *ab initio* calculations of Henry constants, separation constants and heats of adsorption. The methodology is described and applied to the adsorption behaviour of $O_2$ and $N_2$ in the large cavities of a faujasite large cavity for which experimental data are available.[12,13] Its extension to less symmetrical cases and cation distributions will be straightforward.

The starting point in the evaluation of the above mentioned properties is the Henry constant expression, based on an evaluation of the ratio of the partition functions of the free and adsorbed gas.[14,15] Neglecting vibrational corrections upon adsorption and applying the ideal gas law for the non-adsorbed gas one arrives at the following expression for the Henry constant $K$ [eqn. (1)], where $B$ is the number of cavities

$$K = \frac{BI}{aRT} \tag{1}$$

in which the adsorption process can take place per mass zeolite, $R$ the ideal gas constant and $T$ the absolute temperature. The factor $a$‡ = 1 in the case of a monoatomic gas, $4\pi$ for a linear molecule and $8\pi^2$ for a non-linear molecule. $I$ is the configuration integral [eqn. (2)], where $E$ represents the interaction

$$I = \int \exp[-E(\boldsymbol{r},\boldsymbol{\phi})/RT]\mathrm{d}\boldsymbol{r}\ \mathrm{d}\boldsymbol{\phi} \tag{2}$$

energy molecule–zeolite cage when the centre of gravity of the molecule is at position $\boldsymbol{r}$ and the molecular orientation characterized by angles gathered in a vector $\boldsymbol{\phi}$. The integration is performed over all positions $\boldsymbol{r}$ in the faujasite cavity and for each position over all orientations.

The cage was chosen as to represent a faujasite Y zeolite, using hydroxy groups as terminators and showing a Si/Al ratio of 3, with bruto-formula $Na_{16}Si_{36}Al_{12}O_{120}H_{48}$.

Four of the 16 $Na^+$ ions are localized in site II with a tetrahedral orientation towards the centre of the large cavity. The interaction of the molecules ($N_2$ and $O_2$) with the cage were calculated using the 'molecule in point charge environment' approach as often used in the study of molecular crystals.[17] The point charges of the cage atoms were obtained with the ChelpG method[18] at an STO 3G[19] level. A scaling procedure was then introduced in order to account for the change in potential when removing the terminating hydroxy groups in order to be able to fully exploit the symmetry of the cage (*vide infra*): all charges were multiplied by a constant yielding the 'correct' potential at the centre of the cage (*i.e.* the potential at the centre of the cavity with the terminating hydroxy groups still present).§ This procedure is based on the idea that the artificial terminators (hydroxy groups) might perturb the real symmetry of the cage due to the presence of the hydrogen atoms.

Being able to fully exploit the cage symmetry, a cubic grid of points in the cage has been created by selecting points at a 0.5 Å distance along $x$, $y$ and $z$ axis, thereby performing the integration over $\boldsymbol{r}$ in eqn. (2) *via* a numerical procedure of evaluating the interaction energy $E$ of molecules at the centre of each cube, inserting it in the $\exp(-E/RT)$ expression and multiplying it by the elementary volume $\Delta V$ of 0.125 Å.$^3$ The integration over all orientations is ensured by performing the above-mentioned interaction energy calculation once with the molecule aligned along the $x$- as ($E_x$), once along the $y$-axis ($E_y$), and once along the $z$-axis ($E_z$) and multiplying each contribution $\exp(-E_\alpha/RT)$ ($\alpha = x, y, z$) by $4\pi/3$. Symmetry is exploited by considering only 1/24th part of the zeolite cage (*cf.* ref. 7) using a self-developed algorithm to select those grid points contained in a polyhedron with the following vertices: the centre of the cavity and the position of the cations at $S_{II}$, $S_{III}$ and $S_{IV}$.

In this way 321 points were selected and the integral (2) was replaced by the sum given in eqn. (3), where $g_i$ is a weight

$$I \approx \frac{4\pi}{3} \sum_i [\exp(-E_{x,i}/RT) + \exp(-E_{y,i}/RT) + \exp(-E_{z,i}/RT)]\ \Delta V_{gi} \tag{3}$$

factor taking the value 1,4, 12, or 24 for a point at the centre of the cavity, at an edge, on a side, or inside the '1/24' sector.

Moreover those points were rejected for which the distance to the $Na^+$ ions in the sector is smaller than the sum of the equilibrium distance $Na^+\cdots X_2$ (X = N, O) and half of the equilibrium distance of $X_2$ (both values being calculated at a 6-31G* level lead to spheres around the $Na^+$ cation of 2.50 (X = N) and 2.52 Å (X = O) respectively, in order to account for the deficiency in the short-range behaviour of the point charge model. At these distances, the true interaction energy will in most cases be repulsive so that in reality very small terms add to the sum in eqn. (3). We prefer to stick to this approximation rather than introducing a repulsive part in the point-charge potential, which will inevitably lead to some adjustable parameters in the procedure.

All interaction energies were calculated at the HF-631G* level[19] with equilibrium distances for $N_2$ and $O_2$ at the same level (1.0784 and 1.1677 Å respectively) using RHF and UHF[19] procedures for $N_2$ and $O_2$ respectively.

The configuration integrals $I$ (in m$^3$) for $N_2$ and $O_2$ at 298.15 K resulting from (3) were: $1.937\ 10^{-23}$ m$^3$ for $N_2$ and 6.335

$10^{-25}$ m$^3$ for $O_2$. The larger value for $N_2$ is in line with 6-31G* calculated stabilization energy for a linear molecule cation complex, taking basis set superposition errors[21] into account ($\Delta E$ = −6.98 *vs.* −5.11 kcal mol$^{-1}$, 1 cal = 4.184 J).

Using eqn. (1) the following values for Henry constants and the separation constant $\alpha$ [$=K(N_2)/K(O_2)$] were obtained at 298.15 K;¶ $K(N_2)$ = 37.87 × $10^{-6}$ mol kg$^{-1}$ Pa$^{-1}$, $K(O_2)$ = 7.78 × $10^{-6}$ mol kg$^{-1}$ Pa$^{-1}$, $\alpha$ = 4.87: the corresponding experimental values, for an NaY zeolite with an Si/Al ratio of 2.43 are,[12,13] 2.58 × $10^{-6}$, 1.01 × $10^{-6}$ mol kg$^{-1}$ Pa$^{-1}$ and 2.56, respectively.

The theoretical values reproduce the higher value of the Henry constant for $N_2$ as compared to $O_2$ whereas both values are roughly one order of magnitude too large, their ratio (separation constant) being of the correct order.

At this point the extreme sensitivity of $K$ to the interaction energy values appearing in the exponent should be realized. It is easily checked that, assuming a position independent difference between theoretical and experimental values, a difference of only 1.4 kcal mol$^{-1}$ accounts for an order of magnitude difference in $K$ at 298.15. In view of the parameter-free evaluation of $K$ the result is therefore pleasing, certainly when compared with literature results often adjusting interaction potentials to experimental Henry constants.

Moreover, when applying the Van't Hoff's eqn. (4)[15] the

$$\frac{\partial \ln K}{\partial T} = \frac{\Delta H^\circ}{RT^2} \qquad (4)$$

temperature range 250–310 K, recalculating for each temperature $K$ *via* eqn. (1) and (3) an almost perfect linear plot of ln $K$ *vs.* 1/$T$ is found as shown in Fig. 1 for $O_2$. The resulting heats of adsorption, $-\Delta H^\circ$, are 28.8 and 18.0 kJ mol$^{-1}$ respectively, whose order of magnitude and sequence is in reasonable agreement with the experimental values of 19.5 and 16.5 kJ mol$^{-1}$.

In view of the fast increase in computational software and hardware, *e.g.* in the application of density functional theory,[22] to problems of charge distribution[23] we consider the results of these first non-parametrized evaluations of thermodynamic quantities describing adsorption in zeolites as highly promising, offering possibilities in developing tailor-made materials (cations, structure, *etc.*) using computer experiments.[24]

P. G. and G. B. wish to thank their colleague Professor R. Schoonheydt (Laboratory for Surface Science and Catalysis, Catholic University of Leuven) for providing the Cartesian coordinates of the zeolite cage and Professor R. Kieboom of the Mathematics Department of the Free University of Brussels for advice in constructing the algorithm for selecting grid points. Dr G. Destree from the Computer Center of the Free University of Brussels is thanked for help in the automation of the interaction energy calculations. F. D. P. and C. V. A. are indebted to the Belgian National Science Foundation (NFWO) for a post-doctoral research fellow (F. D. P.) and Research Director (C. V. A.) position, respectively.

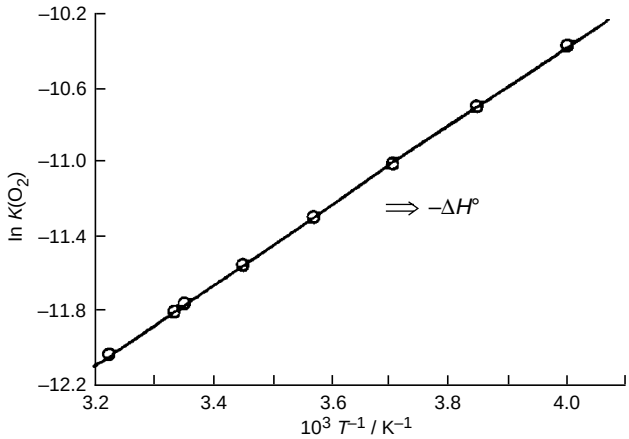



**Fig. 1** Plot of ln $K(O_2)$ *vs.* 1/$T$ calculated for $T$ in the range 250–310 K

## Footnotes

† E-mail: pgeerlin@vnet3.vub.ac.be

‡ Originating from the rotational partition function.

§ In a later stage the cage charges were recalculated at the 3-21G[19] level, using one of the author's MIA method[20] in order to speed up this 2008 basis functions problem. As the linear correlation coefficient $r$ of STO 3G and 3-21G charges amounts to 0.988, no fundamental difference between each result can be expected.

¶ The $B$ value was computed starting from the bruto formula of the unit cell [$Na_{48}$ $(AlO_2)_{48}(SiO_2)_{144}$]: taking into account that eight large cavities are present in the unit cell $B$ = 3.8275 × $10^{20}$ g$^{-1}$.

## References

1 P. A. Jacobs, *Catal. Rev. Sci. Eng.*, 1982, **24**, 415.
2 R. A. Van Santen and G. J. Kramer, *Chem. Rev.*, 1995, **95**, 637.
3 J. Kärger and D. M. Rutven, *Diffusion in Zeolites and other Microporous Solids*, Wiley, New York, 1992.
4 J. Datka, P. Geerlings, W. J. Mortier and P. A. Jacobs, *J. Phys. Chem.*, 1985, **89**, 3488.
5 W. Langenaeker, N. Coussement, F. De Proft and P. Geerlings, *J. Phys. Chem.*, 1994, **98**, 3010.
6 J. Sauer, *Chem. Rev.*, 1994, **94**, 2095.
7 A. G. Bezus, A. V. Kiselev, A. A. Lopatkin and P. Quang Du, *J. Chem. Soc., Faraday Trans. 2*, 1978, **74**, 367.
8 A. Kiselev, *Pure Appl. Chem.*, 1980, **52**, 6161.
9 A. G. Bezus, M. Kocizik, A. V. Kiselev, A. A. Lopatkin and E. A. Vasilyeva, *Zeolites*, 1986, 101.
10 R. J. M. Pellenq and D. Nicholson, *J. Phys. Chem.*, 1995, **98**, 10 175.
11 D. Nicholson, *J. Chem. Soc., Faraday Trans.*, 1996, **92**, 1.
12 M. Van de Voorde, Y. Tavernier, J. Martens, H. Verelst, P. A. Jacobs and G. Baron, in *Gas Separation Technology*, ed. E. F. Vansant and R. Dewolfs, Elsevier, Amsterdam, 1990.
13 J. A. Martens, D. Ghys, M. Van de Voorde, H. Verelst, G. Baron and P. A. Jacobs, in *Separation Technology*, ed. E. Vansant, Elsevier, Amsterdam, 1994.
14 D. M. Rutven, *Principles of Adsorption and Adsorption Processes*, Wiley, New York, 1984, p. 44.
15 P. W. Atkins, *Physical Chemistry*, Oxford University Press, Oxford, 1994, ch. 20.
16 C. Mellot, J. Liquières, P. Pullunbi and R. Guilard, *Rev. Inst. Fran. Pétrole*, 1996, **51**, 81.
17 A. Peeters, C. Van Alsenoy, A. T. R. Lenstra and H. J. Geise, *J. Chem. Phys.*, 1995, **103**, 6608.
18 C. M. Breneman and K. Wiberg, *J. Comput. Chem.*, 1990, **11**, 361.
19 W. J. Hehre, L. Radom, P. v. R. Schleyer and J. A. Pople, *Ab Initio Molecular Orbital Theory*, Wiley, New York, 1986.
20 C. Van Alsenoy, *J. Comput. Chem.*, 1988, **9**, 620; C. Van Alsenoy and A. Peeters, *J. Mol. Struct.* (THEOCHEM), 1993, **286**, 19.
21 S. F. Boys and F. Bernardi, *Mol. Phys.*, 1970, **19**, 553.
22 R. G. Parr and W. Yang, *Density Functional Theory of Atoms and Molecules*, Oxford University Press, New York, 1987.
23 See for example: P. Geerlings, F. De Proft and J. M. Martin, in *Theoretical and Computational Chemistry*, ed. J. Seminario, Elsevier, Amsterdam, 1996, vol. 4, pp. 773–809.

*Received, 28th November 1996; Com. 6/08061H*

# A novel porphyrin based fluorescent chemosensor using a molecular recognition approach

**Francis D'Souza,*† Golapalli R. Deviprasad and Yi-Ying Hsieh**

*Department of Chemistry, The Wichita State University, Wichita, KS 67260-0051, USA*

**Free-base porphyrin covalently linked to quinone exhibits enhanced fluorescence on coupling the quinone with hydroquinone, primarily due to the unfavourable conditions for an electron transfer reaction between the singlet excited porphyrin and the newly formed quinone–hydroquinone entity.**

Fluorescent chemosensors are compounds with a fluorophore, binding site and a well-defined mechanism for communication. In general, these molecular systems possess binding ability coupled with photophysical–photochemical properties.[1] Two types of metal ion sensing chemosensors are known in literature:[1,2] (i) heterocycles bearing chelating arrays of donor atoms, the intrinsic chemosensors and (ii) systems in which the donor atoms remain insulated from the fluorophore π-system, the conjugate chemosensors. Some studies have also reported anion sensing fluorophores which often involve the inherent quenching property of the analyte.[1,3] On the other hand, neutral analyte sensing devices are found to be rare due to the limited availability of systems possessing complementary binding sites with an electrostatic handle on them.[4] Here we report a porphyrin based fluorescent chemosensor, where H-bonds and charge-transfer interactions are primarily responsible for stabilizing the quinone–hydroquinone complex (Fig. 1) and demonstrate enhanced fluorescence emission of porphyrin upon coupling the quinone with hydroquinone.

The quinone appended porphyrin, 5,10,15-triphenyl-20-(3,6-dioxocyclohexa-1,4-dienyl)porphyrin‡ **1a** was synthesized by the chemical oxidation of 5,10,15-triphenyl-20-(2,5-dihydroxyphenyl)porphyrin[5] using an excess of 2,6-dichloro-3,5-dicyano-1,4-benzoquinone (DDQ). The UV–VIS spectrum of **1a** in benzonitrile revealed spectral features similar to that reported for porphyrin–quinone systems in literature.[6] Addition of hydroquinone (10 equiv.) to the solution of **1a** revealed a small red shift of *ca*. 2 nm without any dramatic changes in the ε values, indicating the absence of any interactions between the added hydroquinone and the porphyrin ring. $^1$H NMR studies revealed quinone–hydroquinone coupling. The singlet peak corresponding to the aromatic protons of the free hydroquinone exhibited a multiplet pattern with a net deshielding of nearly 0.1 ppm on forming the quinone–hydroquinone complex, while the porphyrin ring protons experience a small shielding. The binding constant calculated from the $^1$H NMR data is found to be 13.1 dm$^3$ mol$^{-1}$ in $CDCl_3$ at 25 °C.

Compound **1a** is found to be weakly fluorescent ($\phi_f < 0.01$) and this has been ascribed to the photoinduced intramolecular electron transfer from the excited singlet-state porphyrin, the donor, to the appended quinone, the acceptor.[7] Interestingly, as shown in Fig. 2, addition of 1,4-hydroquinone to the solution of **1a** exhibits a drastic enhancement of the porphyrin fluorescence intensity§ and the two bands at 652 and 720 nm correspond to the free-base porphyrin emission.[8] After addition of 8 equiv. of 1,4-hydroquinone, the fluorescence emission reaches a maximum and further addition results in no appreciable changes. At the saturation point, the calculated fluorescence quantum yield,¶ $\phi_f$ is found to be 0.25 and is nearly twice that of the unsubstituted meso-tetraphenylporphyrin,[8] $H_2TPP$ ($\phi_f$ = 0.13).‖

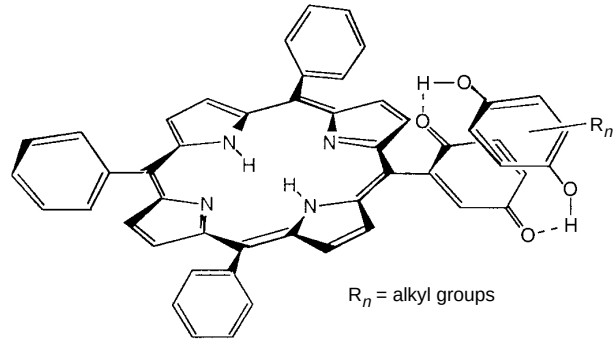



**Fig. 1**

Recently, we demonstrated a hydroquinone–quinone complexation in hydroquinone appended zinc porphyrin with intermolecularly added quinones.[5] Efficient fluorescence quenching of the zinc porphyrin was observed upon coupling the hydroquinone with substituted quinones. Electrochemical studies demonstrated that the reduction potential of the hydroquinone–quinone complexes are negatively shifted by 500–800 mV compared to that of the free quinones used for pairing. Based on the electrochemical reduction potentials of the newly formed hydroquinone–quinone redox couple, the optimum concentration of quenchers needed to saturate the fluorescence intensity and the calculated free-energy change, an excited-state electron transfer was suggested to be the quenching mechanism.[5] The present system, however, differs from the earlier one studied, in that the quinone entity is directly attached to the porphyrin π-system. In addition, it possesses a quinone–hydroquinone pair with a low reduction potential,** a free-base porphyrin with high oxidation potential†† and low energy of singlet-singlet emission compared to that of zinc porphyrin.[8] The net result of this redox tuning and altered photophysical property is the inhibition of fluorescence quenching due to intramolecular electron transfer. The calculated free energy change for an electron transfer from the excited free-base porphyrin to the quinone–hydroquinone complex, using the Rehm and Weller equation,[10] is found to be endergonic by *ca*. 0.33 V. As a result, the added hydroquinone upon complexing with quinone, inhibits the excited-state electron transfer in **1a** and consequently enhances the porphyrin fluorescence emission.[11]

Under normal conditions, one would expect the $\phi_f$ of **1a** in presence of hydroquinone to be close to that of the unsubstituted free-base porphyrin, $H_2TPP$; however, in the present study, the calculated $\phi_f$ is nearly two times that of $H_2TPP$ [see Fig. 2(*h*)]. This additional fluorescence enhancement could be attributed to the mode of attachment of the quinone–hydroquinone to the porphyrin macrocycle and the nature of the charge-transfer interactions. Spectroscopic studies on the hydroquinone–quinone complexes have shown substantial charge-transfer interactions between the hydroquinone as a donor and benzo-

quinone as an acceptor.[12] This suggests that when the linkage is through quinone, the partial negative charge residing on the quinone would interact with the porphyrin π-system and might be responsible for fluorescence enhancement. If this is correct, then one would expect higher $\phi_f$ on fully reducing the quinone of **1a** instead of the partial negative charge of the quinone–hydroquinone complex. The following electrochemical studies suggest that this is more likely the case.

The cyclic voltammogram†† of **1a** in PhCN exhibits four well separated one-electron reductions (Fig. 3). The first two processes corresponding to the reduction of the appended benzoquinone are located at $E_{1/2} = -0.51$ and $-0.93$ V respectively[13] while the latter two processes corresponding to the porphyrin ring reductions[14] are located at $E_{1/2} = -1.41$ and $E_{pc} = -1.83$ V *vs*. SCE respectively at a scan rate of 0.1 V $s^{-1}$. In order to generate a neutral free-base porphyrin linked to quinone anion radical, bulk electrolysis of **1a** was carried out at an applied potential of $-0.75$ V, a potential slightly more negative than the first reduction potential of the appended benzoquinone. After completion of the electrolysis, the fluorescence spectrum of the one-electron reduced product was recorded [see Fig. 2(*i*)]; the emission intensity was nearly 10% more than that observed for **1a** in the presence of excess of hydroquinone, suggesting that the interactions between the partially or fully reduced quinone and the porphyrin macrocycle could be responsible for additional fluorescence enhancement. However, further studies are needed to fully understand the mechanistic details of fluorescence enhancement in this novel system and these studies are in progress.

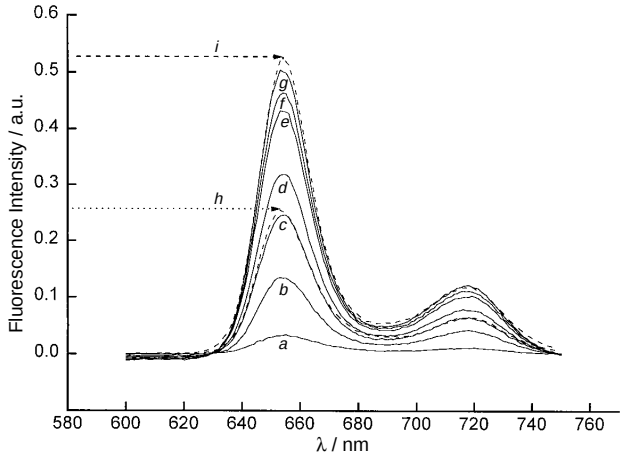



**Fig. 2** Fluorescence emission spectrum of (*a*) compound **1a** (1 μM) in PhCN, $\lambda_{ex}$ = 514 nm. Spectra (*b*)–(*g*) represent the emission spectrum of **1a** on increasing addition of hydroquinone (1 μM aliquots). Spectra (*h*) and (*i*) represent the emission spectrum of $H_2$TPP and the one-electron reduced product of **1a** in PhCN.

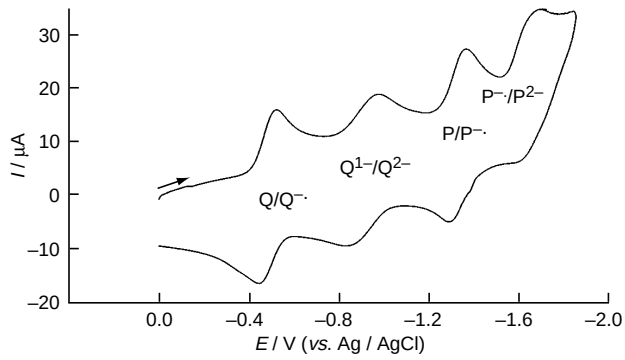



**Fig. 3** Cyclic voltammogram of compound **1a** in benzonitrile, 0.1 M TBAP, scan rate = 0.1 V $s^{-1}$

This work was supported by the National Science Foundation under Grant No. EPS-9550487 and matching support from the State of Kansas.

## Footnotes

† E-mail: dsouza@wsuhub.uc.twsu.edu

‡ $\delta_H(CDCl_3)$ 8.90 (m, 8 H, pyrrole-H), 8.20 (s, 6 H, *ortho*-H of the triphenyl entity), 7.75 (m, 9 H, *meta*- and *para*-H), 7.29, 7.60, 8.38 (d, d and s, 3 H, quinone-H) and −2.78 (s, 2 H, imino-H). $\lambda_{max}$ (PhCN)/nm (log ε) 414.6 (5.85), 511.6 (4.31), 542.2 (3.77), 590.3 (3.75) and 649.8 (3.66).

§ Addition of excess of hydroquinone to a solution of $H_2$TPP resulted in no appreciable changes in the fluorescence emission.

¶ Fluorescence quantum yields were calculated using the method described in ref. 9.

‖ Use of other alkyl substituted hydroquinones resulted in a similar fluorescence enhancement.

** Reduction of the quinone–hydroquinone complex in PhCN occurs at $E_{1/2} = -1.26$ V *vs*. SCE.

†† The first reversible oxidation of **1a** in PhCN, 0.1 M TBAP occurs at $E_{1/2}$ = 1.01 V *vs*. SCE.

‡‡ Cyclic voltammograms were obtained on a EG & G Model 263 A potentiostat using a three-electrode system. A glassy carbon electrode was used as the working electrode. A platinum wire served as the counter electrode, and Ag/AgCl was used as the reference electrode.

## References

1 A. W. Czarnik, *Acc. Chem. Res.*, 1994, **27**, 302; L. R. Sousa, B. Valeur, A. P. de Silva, Bouas, H. Laurent, A. Ueno, T. Bell, R. Y. Tsien, M. Kuhn, D. Masilamani and G. Krafft, in *Fluorescent Chemosensors for Ion and Molecule Recognition*, ed. A. W. Czarnk, American Chemical Society, Washington DC, 1993; R. A. Bissell, A. P. de Silva, H. Q. N. Gunaratne, P. L. M. Lynch, G. E. M. Maguire, C. P. McCoy and K. R. A. S. Sandanayake, *Top. Curr. Chem.*, 1993, **168**, 223.

2 L. R. Sousa and J. M. Larson, *J. Am. Chem. Soc.*, 1977, **99**, 307; P. Nanjappan and A. W. Czarnik, *J. Am. Chem. Soc.*, 1987, **109**, 1826; M. Houston, K. Haider, K and A. W. Czarnik, *J. Am. Chem. Soc.*, 1988, **110**, 4460; A. P. de Silva and S. A. de Silva, *J. Chem. Soc., Chem. Commun.*, 1986, 1709; E. U. Akkaya, M. E. Houston and A. W. Czarnik, *J. Am. Chem. Soc.*, 1990, **112**, 3590; M. E. Houston and A. W. Czarnik, *J. Am. Chem. Soc.*, 1990, **112**, 7054; M.-Y. Chae and A. W. Czarnik, *J. Am. Chem. Soc.*, 1992, **114**, 9704; M.-Y. Chae, X. M. Cherian and A. W. Czarnik, *J. Org. Chem.*, 1993, **58**, 5797; H. A. Godwin and J. M. Berg, *J. Am. Chem. Soc.*, 1996, **118**, 6514; G. K. Walkup and G. Imperiali, *J. Am. Chem. Soc.*, 1996, **118**, 3053.

3 M. E. Houston, E. U. Akkaya and A. W. Czarnik, *J. Am. Chem. Soc.*, 1989, **111**, 8735; D. H. Vance and A. W. Czarnik, *J. Am. Chem. Soc.*, 1994, **116**, 9397.

4 J.-Y. Yoon and A. W. Czarnik, *J. Am. Chem. Soc.*, 1992, **114**, 5874; J.-Y. Yoon and A. W. Czarnik, *Bioorg. Med. Chem.*, 1993, **1**, 267; R. Grigg and W. D. J. A. Morbert, *J. Chem. Soc., Chem. Commun.*, 1992, 1298; P. Tecilla, R. P. Dixon, G. Slobodkin, D. S. Alavi and D. H. Waldeck, *J. Am. Chem. Soc.*, 1990, **112**, 9408; A. Harriman, Y. Kubo and J. A. Sessler, *J. Am. Chem. Soc.*, 1992, **114**, 388; T. Hayashi, T. Miyahara, N. Hashizume and H. Ogoshi, *J. Am. Chem. Soc.*, 1993, **114**, 2049.

5 F. D'Souza, *J. Am. Chem. Soc.*, 1996, **118**, 923.

6 K. Wynne, S. M. LeCours, C. Galli, M. J. Therien and R. M. Hochstrasser, *J. Am. Chem. Soc.*, 1995, **117**, 3749.

7 J. Dalton and L. R. Milgrom, *J. Chem. Soc., Chem. Commun.*, 1979, 609; M. A. Bergkamp, J. Dalton and T. L. Netzel, *J. Am. Chem. Soc.*, 1982, **104**, 253.

8 P. G. Seybold and M. Gouterman, *J. Mol. Spectrosc.*, 1969, **31**, 1; D. J. Quimby and F. R. Longo, *J. Am. Chem. Soc.*, 1975, **97**, 5111.

9 A. Austin and M. Gouterman, *Bioinorg. Chem.*, 1978, **9**, 281.

10 D. Rehm and A. Weller, *Isr. J. Chem.*, 1970, **8**, 529.

11 R. A. Bissell, A. P. De Silva, H. Q. N. Gunaratne, P. L. M. Lynch, G. E. M. Maguire and D. R. A. S. Sandanayake, *Chem. Soc. Rev.*, 1992, **21**, 187.

12 M. A. Slifkin and R. H. Walmsley, *Spectrochim. Acta*, 1970, **26A**, 1237; M. Kubinyi and G. Keresztury, *Spectrochim. Acta*, 1989, **45A**, 421.

13 J. Q. Chambers, in *The Chemistry of Quinonoid Compounds*, ed. S. Patai, Wiley, New York, 1974, ch. 14.

14 K. M. Kadish, *Prog. Inorg. Chem.*, 1986, **34**, 435.

*Received, 29th October 1996; Com. 6/07384K*

# Regioselective palladium-catalysed coupling reactions of vinyl chlorides with carbon nucleophiles

**Manfred T. Reetz,* Klaus Wanninger and Marcus Hermes**

*Max-Planck-Institut für Kohlenforschung, Kaiser-Wilhelm Platz 1, D-45470 Mülheim/Ruhr, Germany*

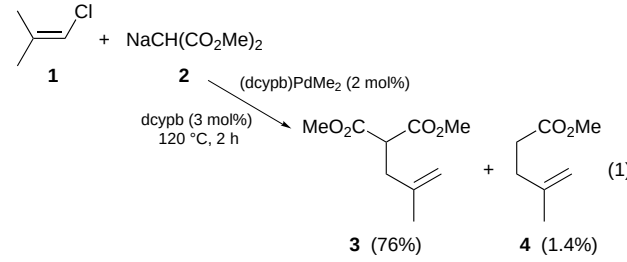
**Vinyl chlorides bearing methyl groups in the 2-position can be activated catalytically by palladium(0)-complexes of 1,4-bis(dicyclohexylphosphino)butane, the process involving vinyl–allyl isomerization *via* CH-activation followed by nucleophilic attack of C-nucleophiles on the intermediate palladium–π-allyl species.**

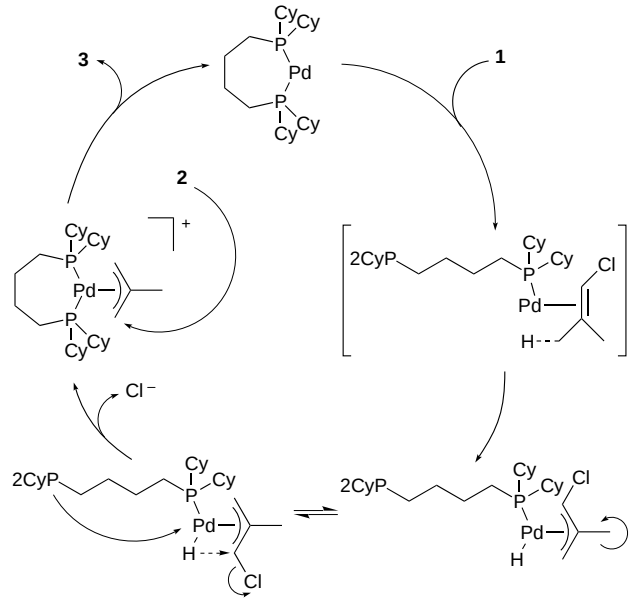
The palladium-catalysed activation of carbon–chlorine bonds in Heck reactions of chloro-aromatics is of great industrial interest because these substrates are much cheaper than the considerably more reactive bromo or iodo analogues.[1] One interesting approach recently published by Milstein makes use of the 1,4-bis(diisopropylphosphino)butane bidentate ligand (dippb), which is believed to open and reclose reversibly with respect to palladium complexation during the catalytic cycle.[2] While the quest for higher efficiency and broader synthetic scope continues in this area, very little is known concerning the catalytic activation of vinyl chlorides.[3] Here we report a serendipitous finding according to which this class of compounds can be induced to undergo unusual C–C bond forming reactions with carbon nucleophiles such as sodium malonates.[4]

In initial attempts to perform a Heck reaction of 1-chloro-2-methylprop-1-ene **1** with styrene, we essentially used the Milstein protocol described for chlorobenzene, except that dippb was replaced by a geometrically and electronically similar ligand which is more readily available, namely 1,4-bis-(dicyclohexylphosphino)butane (dcypb). However, only 5–20% of the Heck coupling product 1,1-dimethyl-4-phenylbutadiene was formed. Speculating that the problem could be due to the formation of a catalytically non-active palladium–π-allyl species following Heck-type C–C bond formation, we repeated the reaction in the presence of sodium dimethylmalonate **2** as a carbon nucleophile in hope of inducing a tandem Heck[5]–allyl substitution process [2 mol% $Pd(OAc)_2$, 5 mol% dcypb, DMF, 150 °C, 18 h]. To our surprise none of the expected tandem reaction product was observed, the major products being 2-methylallylmalonic acid dimethyl ester **3** (55%) and its decarboxylated form **4** (20%). Since styrene is not involved, the reaction was repeated in the absence of this olefin at a lower temperature [2 mol% $Pd(OAc)_2$, 5 mol% dcypb, DMF; 120 °C, 18 h]. Again the methallylated products **3** (70%) and **4** (12%) were formed. Other ligands are less effective, the yields of **3**/**4** being lower, as in the case of $PPh_3$ (8%/3%), 1,2-bis(diphenylphosphino)ethane (4%/5%) and 1,4-bis(diphenylphosphino)butane (32%/26%). In further optimization it was discovered that the best catalyst system is the dimethylpalladium complex of the ligand (dcypb) $PdMe_2$ (2 mol%) in the presence of additional dcypb (3 mol%) at 120 °C, 2 h, leading to products **3** (76%) and **4** (1.4%) eqn. (1).†

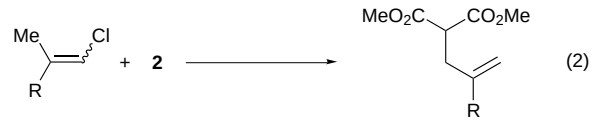
A plausible mechanism involves palladium-catalysed isomerization of the otherwise non-reactive vinyl chloride **1** to methallyl chloride followed by classical palladium-catalysed allylic substitution in which the malonate participates as the carbon nucleophile. Separate NMR experiments revealed that the reaction is initiated by thermolytic decomposition of (dcypb)$PdMe_2$ with formation of (dcypb) Pd° (or its dimer).[4] It is likely that the reactive palladium(0)-catalyst then coordinates to the double bond of **1** and induces CH-activation in one of the methyl groups, the first step in the isomerization. Methallyl chloride may not actually be set free, since palladium can remain coordinated to the π-allyl system, chloride being expelled with intermediate formation of $[Pd\{\eta^3\text{-}(CH_2CMe{=}CH_2)\}(dcypb)]^+$. Indeed, upon heating (dcypb)$PdMe_2$ in the presence of **1** as the sole reaction partner, this cationic palladium–π-allyl species was identified as the major product by NMR spectroscopy; its $BF_4^-$ salt was synthesized by an independent route and its structure proven by X-ray structural analysis.[4] Scheme 1 shows a possible catalytic cycle which is in accord with all of the present data, including the observation that other ligands are less effective.

Regioselectivity and therefore the possibility of two different products becomes relevant in the case of unsymmetrically substituted vinyl chlorides. In order to test whether the reaction is regioselective, substrates **5** [eqn. (2)] were subjected to the isomerization–substitution reaction. In all cases complete regioselectivity was observed in that CH-activation occurs solely at the methyl groups.




**Scheme 1**



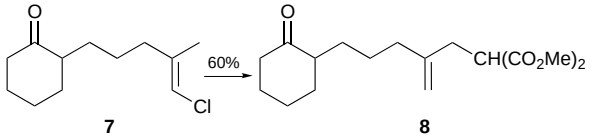

(2)

**5** **6**

**a** *E*, R = cyclo-$C_6H_{11}$ 75%

**b** *Z*, R = cyclo-$C_6H_{11}$ 65%

Finally, more highly functionalized substrates such as **7** [eqn. (3)] are also amenable to the reaction. In this case a small




(3)

**7** **8**

amount of a double bond isomer was also observed (14%). Substrates bearing groups larger than methyl do not react analogously, probably due to steric reasons. The bulky ligands due not tolerate additional alkyl groups in the substrate, *e.g*. in the palladium–π-allyl species (Scheme 1).

In summary, vinyl chlorides having at least one methyl group in the 2-position can be activited catalytically using palladium(0)-complexes of 1,4-bis(dicyclohexylphosphino)butane. The gross features of the mechanism involve vinyl–allyl isomerization *via* CH-activation at the methyl groups followed by classical nucleophilic attack by sodium malonate on the intermediate cationic palladium–π-allyl species. The results suggest that the catalytic activation of otherwise inert vinyl chlorides should be possible in other types of processes using palladium or other transition metal catalysts.

## Footnote

† *Typical procedure*: A dry 25 ml Schlenk tube under an argon atmosphere is charged with **1** (0.5 ml, 5 mmol), (dcypb)$PdMe_2$ (58 mg, 0.1 mmol), dcypb (68 mg, 0.15 mmol), **2** (5 mmol) in DMF (5 ml) and heated to 120 °C for 2 h. The mixture is diluted with ethyl acetate (15 ml), treated successively with 10% HCl solution, water and $NaHCO_3$ and NaCl solutions and dried over $MgSO_4$. Most of the solvent is removed and the residue analysed by gas chromatography. **3** is purified by chromatography (silica, pentane–$Et_2O$ 4 : 1).

## References

1 B. Cornils and W. A. Herrmann, *Applied Homogeneous Catalysis with Organometallic Compounds*, VCH, Weinheim, 1996; A. de Meijere and F. E. Meyer, *Angew. Chem*., 1994, **106**, 2473; *Angew. Chem., Int. Ed. Engl*., 1994, **33**, 2379; V. V. Grushin and H. Alpes, *Chem. Rev*., 1994, **94**, 1047.

2 Y. Ben-David, M. Portnoy, M. Gozin and D. Milstein, *Organometallics*, 1992, **11**, 1995.

3 R. F. Heck, *Palladium Reagents in Organic Syntheses*, Academic, London, 1985; J. Tsuji, *Palladium Reagents and Catalysts: Innovations in Organic Synthesis*, Wiley, Chichester, 1995.

4 K. Wanninger, Dissertation, Universität Bochum, 1995.

5 Heck reactions of vinyl bromides with olefins followed by tandem nucleophilic additions: B. A. Patel and R. F. Heck, *J. Org. Chem*., 1978, **43**, 3898; C. S. Nylund, J. M. Klopp and S. M. Weinreb, *Tetrahedron Lett*., 1994, **35**, 4287.

*Received, 13th December 1996; Com. 6/08371D*

# A novel method of preparing thiol-derivatised nanoparticles of gold, platinum and silver forming superstructures

**K. Vijaya Sarathy, G. U. Kulkarni and C. N. R. Rao***

*Jawaharlal Nehru Centre for Advanced Scientific Research, Jakkur, Bangalore 560 064, India*

**Thiol-derivatised nanoparticles of Au, Pt and Ag (diameter 1–10 nm) forming superstructures, are prepared by the acid-facilitated transfer of well characterized particles in a hydrosol to a toluene layer containing the thiol.**

Nanoparticles of gold and other noble metals are attracting much attention because of their potential applications in microelectronics.[1,2] Several wet chemical methods have been reported in the recent years, for the preparation of colloidal metal sols.[3,4] The methods generally involve the reduction of the relevant metal salt in the presence of a suitable surfactant, the surfactant being useful in the control of the growth of the metal particles. Thiol-derivatised nanoparticles of noble metals are particularly fascinating in that they can be recrystallised from the parent solution; they often self-assemble into cross-linked structures or superlattices on removal of the solvent.[2,5] Since the first report on the synthesis of thiol-derivatised nanoparticles,[6] the common practice is to first extract the metal ions from the aqueous medium to a hydrocarbon (toluene) layer by means of a phase-transfer reagent such as tetraoctylammonium bromide and then to carry out the reduction with $NaBH_4$ in the presence of an alkanethiol. Here, the nucleation and growth of the metal particles as well as the attachment of the thiol molecules occur nearly simultaneously. Metal particles prepared in this manner generally contain nitrogenous surface impurities due to the phase-transfer reagent,[6] which render it difficult to obtain good superstructures. What would be desirable is a procedure wherein one can transfer the well characterized metal nanoparticles from a hydrosol to a non-polar medium containing the thiol. We have indeed found such a direct procedure to be feasible and have successfully prepared thiol-derivatised nanoparticles of Au, Ag and Pt of desired size distributions.

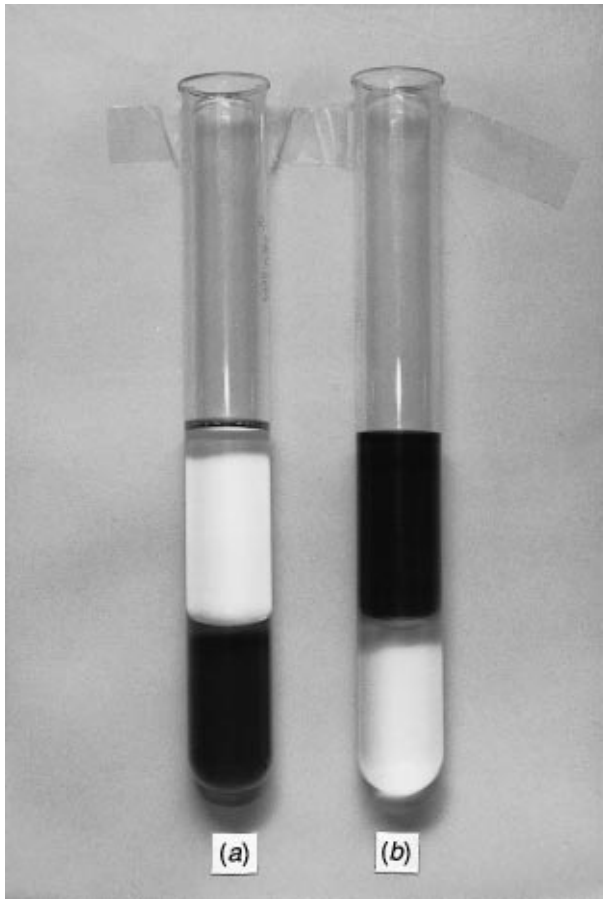



**Fig. 1** Immiscible layers of (*a*) the gold hydrosol (at the bottom) and the clean toluene solution containing the thiol (on top). (*b*) Thiol-derivatised Au sol in toluene (on top) and the clean aqueous solution at the bottom.

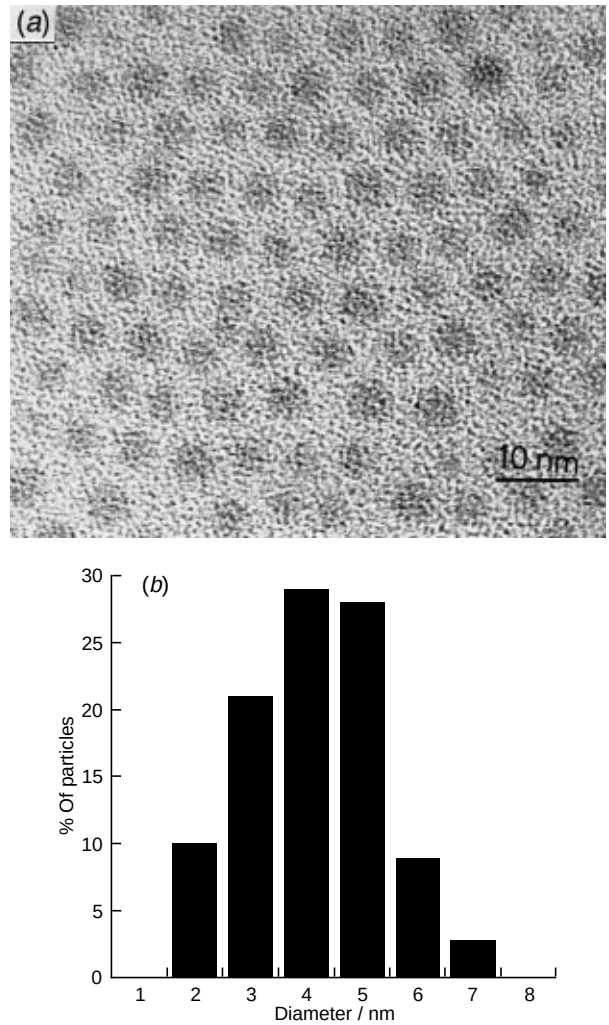



**Fig. 2** (*a*) TEM image of the thiol-derivatised Au nanoparticles forming a superstructure. (*b*) Histogram showing the size distribution.

In a typical preparation, a hydrosol containing small clusters of Au was first prepared by the reduction of chloroaurate ions (2.2 ml of 25 mM aqueous solution) using partially hydrolysed tetrakis(hydroxymethyl) phosphonium chloride (THPC),[7] having prepared the latter by adding 1 ml of a fresh 50 mM solution of THPC in water to 47 ml of 6.38 mM NaOH solution. To the gold sol so obtained, 100 ml of a 0.25 mM solution of dodecanethiol in toluene (Au : S = 2 : 1) was added, to obtain two immiscible layers consisting of the transparent organic phase containing the thiol on the top and the coloured hydrosol at the bottom. To this biphasic mixture, 125 ml of conc. HCl was added under stirring. This resulted in a remarkably swift movement (within 3 min) of the Au nanoparticles to the hydrocarbon layer containing the thiol. Clearly, the gold particles have an inherent attraction to the thiol molecules. This could be seen vividly by the complete transfer of colour across the interface to the hydrocarbon layer as shown in Fig. 1. The gold sol in toluene was shaken with water several times to remove traces of HCl and evaporated to *ca*. 2 ml in a rotary evaporator. The excess thiol was removed by the addition of 350 ml of ethanol (95%). The dark brown solid thus obtained was filtered, washed with ethanol and dispersed in 10 ml of toluene for further investigations. The UV–VIS spectrum of the toluene sol of gold showed a broad band at *ca.* 520 nm due to plasmon absorption just as the hydrosol. The core-level X-ray photoelectron spectrum showed the Au $4f_{7/2}$ binding energy at 84 eV, corresponding to the $Au^0$ state. There was a feature at 163.5 eV due to S 2p showing that the thiol molecules were chemisorbed on the gold surface. There was no evidence of a feature due to P 2p from THPC in the spectrum, unlike in the particles from the hydrosol which showed the feature at *ca*. 133 eV. It appears that the role of HCl in the present procedure is to cleanse the surface of the Au particles and facilitate their transfer to the hydrocarbon layer.

Fig. 2(*a*) shows the transmission electron microscope (TEM) image (recorded with JEOL JEM3010, Japan) of the thiol-derivatised Au nanoparticles obtained by placing a drop of the toluene sol on the holey carbon grid. The particles are nearly spherical with a mean diameter of 4.1 nm. The size distribution obtained, with the help of a Quantimat image analyser, is quite narrow as can be seen from the histogram in Fig. 2(*b*). Furthermore, the nanoparticles assemble into a superstructure as revealed by Fig. 2(*a*). The centre-to-centre nearest-neighbour distance between the nanoparticles is nearly constant at *ca*. 5.5 nm, throughout the superstructure domain. The X-ray diffraction pattern of a film of this material exhibits a low-angle peak corresponding to a *d*-spacing of *ca*. 5 nm. In order to examine whether the individual nanoparticles were crystalline or not, nanoparticles deposited on thin flakes of layered $MoSe_2$ were observed by TEM. The images showed Moiré patterns arising from the interference between the crystallographic planes of $MoSe_2$ and those of the nanoparticles, thereby establishing the crystallinity of the individual particles.

We have been able to prepare thiol-derivatised nanoparticles of Au with different mean diameters in the 1–10 nm range, by varying the concentration of $HAuCl_4$ in the initial hydrosol, by employing the present procedure. We have also prepared Au hydrosols with other reducing agents such as citric acid[8] and thiol-derivatised them by this procedure. The citric acid procedure, however, seems to yield nanoparticles of different shapes (spherical, triangular, pentagonal, hexagonal and rod-like) with varying sizes (*ca*. 25–50 nm).

We have prepared thiol-derivatised nanoparticles of Pt and Ag by the present procedure, by starting with hydrosols obtained with $NaBH_4$ as the reducing agent. Fig. 3(*a*), shows a typical TEM image of thiol-derivatised Pt nanoparticles. These particles are spherical with a narrow size distribution, the mean diameter being 4.4 nm. The figure also reveals a superstructure similar to that of Au in Fig. 2(*a*). A TEM image of thiol-derivatised Ag nanoparticles is shown in Fig. 3(*b*). The image shows that the Ag particles are not as spherical as those of Au and Pt and resemble the Ag particles prepared under vacuum.[9]

The authors thank the Department of Science and Technology for support of this research.

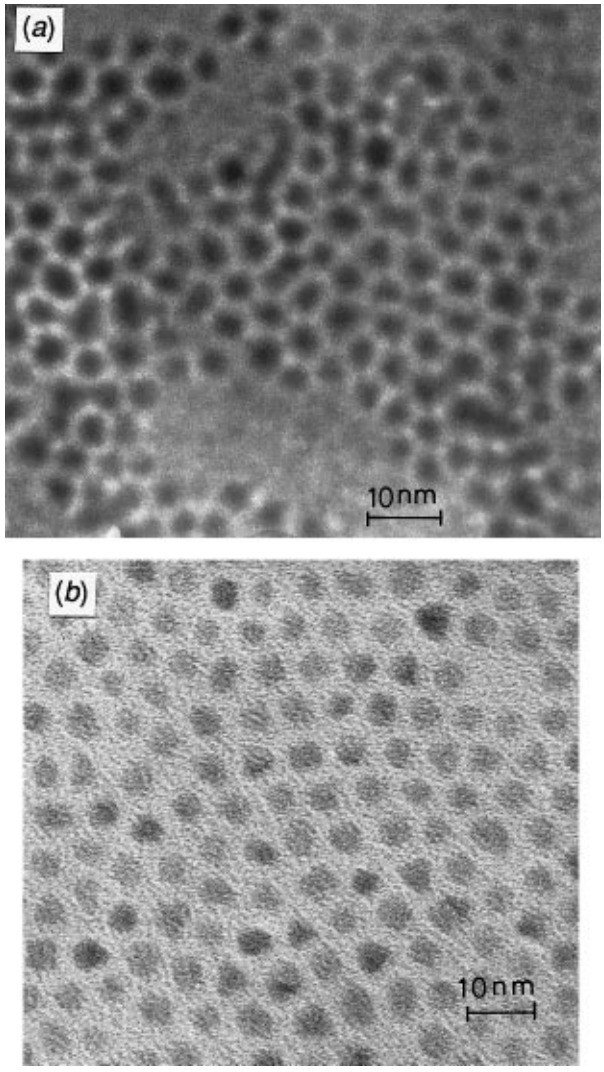



**Fig. 3** TEM images of thiol-derivatised Pt (*a*) and Ag (*b*) nanoparticles

## References

1 G. Schmid, *Chem. Rev*., 1992, **92**, 1709.
2 R. P. Andres, J. D. Bielefeld, J. I. Henderson, D. B. Janes, V. R. Kolagunta, C. P. Kubiak, W. J. Mahoney and R. G. Osifchin, *Science*, 1996, **273**, 1690.
3 J. H. Fendler and F. C. Meldrum, *Adv. Mater*., 1991, **7**, 607.
4 C. N. R. Rao, *Chemical Approaches to the Synthesis of Inorganic Materials*, Wiley, New York, 1994.
5 R. L. Whetten, J. T. Khoury, M. Alvarez, S. Murthy, I. Vezmar, Z. I. Wang, P. W. Stevens, C. L. Cleveland, W. D. Luedtke and U. Landman, *Adv. Mater*., 1996, **8**, 428.
6 M. Brust, M. Walker, D. Bethel, D. J. Schiffrin and R. Whyman, *J. Chem. Soc., Chem. Commun*., 1994, 801.
7 D. G. Duff, A. Baiker and P. P. Edwards, *J. Chem. Soc., Chem. Commun*., 1993, 96.
8 J. Turkevich, P. C. Stevenson and J. Miller, *Discuss. Faraday Soc*., 1951, **11**, 55.
9 S. A. Harfenist, Z. L. Wang, M. M. Alvarez, I. Vezmar and R. L. Whetten, *J. Phys. Chem*., 1996, **100**, 13904.

*Received, 31st January 1997; Com. 7/00738H*

# Synthesis of an iron(II) complex versatile for preparation of iron(II) complexes with novel pentadentate ligands *via* C–C bond formation with various nitriles: 1,3-dimethyl-1,3-propanediylidenebis(2-pyridylmethanamine)iron(II) perchlorate

**Masafumi Goto,*[a] Yoshinobu Ishikawa,[a] Takao Ishihara,[a] Chika Nakatake,[a] Tomoe Higuchi,[a] Hiromasa Kurosaki[a] and the late Virgil L. Goedken[b]**

[a] *Faculty of Pharmaceutical Sciences, Kumamoto University, 5-1 Oe-honmachi, Kumamoto 862, Japan*
[b] *Department of Chemistry, Florida State University, Tallahassee, Florida 32306-3006, USA*

**A bis(acetonitrile)iron(II) complexes with 1,3-dimethyl-1,3-propanediylidenebis(2-pyridylmethanamine) undergoes a nucleophilic addition to the nitrile carbon on addition of triethylamine to a nitrile solution yielding mono(acetonitrile)iron(II) complex with a novel pentadentate polyimine ligand.**

A tetradentate ligand containing a 1,3-diimine moiety, 1,3-dimethyl-1,3-propanediylidenebis(2-pyridylmethanamine), L, which is formally derived from acetylacetone and 2-(aminomethyl)pyridine, is expected to coordinate to metal ions leaving two coordination sites for other ligands. In this report, we describe the synthesis of the iron(II) complex with this ligand and its reaction products with acetonitrile and [$^2H_3$]acetonitrile and their structures obtained by X-ray crystallography.

The iron(II) complex, *trans*-[FeL(MeCN)$_2$][ClO$_4$]$_2$·MeCN **1** was prepared in moderate yield (50–60%) under strict anaerobic and dehydrated conditions by successive additions of precursor tridentate ligand MeCOCH$_2$C(Me)=NHCH$_2$C$_5$H$_4$N and 2-(aminomethyl)pyridine to an acetonitrile solution of [Fe(MeCN)$_6$]$^{2+}$ prepared *in situ*.† These crystals were not stable under air and even stored in a vacuum were potentially explosive.

The structure of **1** was determined by X-ray crystallography and that of the cation is shown in Fig. 1.‡ Two acetonitriles coordinate *trans* to each other to form a distorted octahedral geometry. The six-membered chelate ring of the 1,3-diimine moiety is almost planar with a mean deviation of 0.042 Å and a largest deviation of 0.076(6) Å at C(8). The two pyridine rings swing away from each other in order to evade the intramolecular repulsion between two 6-position hydrogen atoms on each pyridine to give a dihedral angle of 30.95° between two pyridine rings as found for *trans*-bis(bipyridine)palladium complexes.[1]

This complex showed a C≡N stretching band at 2244 cm$^{-1}$ and weak absorption band at 527 nm ($\varepsilon$ = 150 dm$^3$ mol$^{-1}$ cm$^{-1}$) for an acetonitrile solution. The variable-temperature $^1$H NMR spectra of this compound§ exhibited seven signals which obey non-Curie dependency similar to that reported about intersystem crossing polypyridyl ferrous complexes.[2]

The C–C bond formation between a coordinated tetradentate ligand and a (coordinated) acetonitrile occurred at room temperature within 2 h on addition of a small amount of triethylamine to an acetonitrile solution of **1**. Orange crystals of the iron(II) complex of 2-(1-iminoethyl)-1,3-dimethyl-1,3-propanediylidenebis(2-pyridylmethanamine), L′, [FeL′(MeCN)][ClO$_4$]$_2$·thf, **2** were used for crystal structure determination. These are two crystallographically independent molecular ions with almost identical structures and two thf molecules in the asymmetric unit: one of the molecular ions is shown in Fig. 2.‡ The tetradentate moiety adopts *cis*-β coordination and the

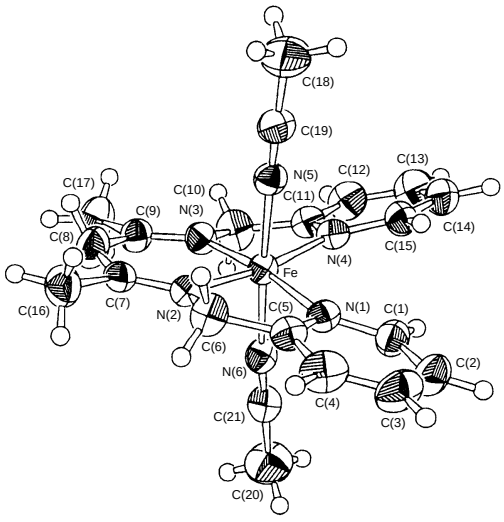



**Fig. 1** Molecular structure of the cation of **1** showing the atom numbering scheme

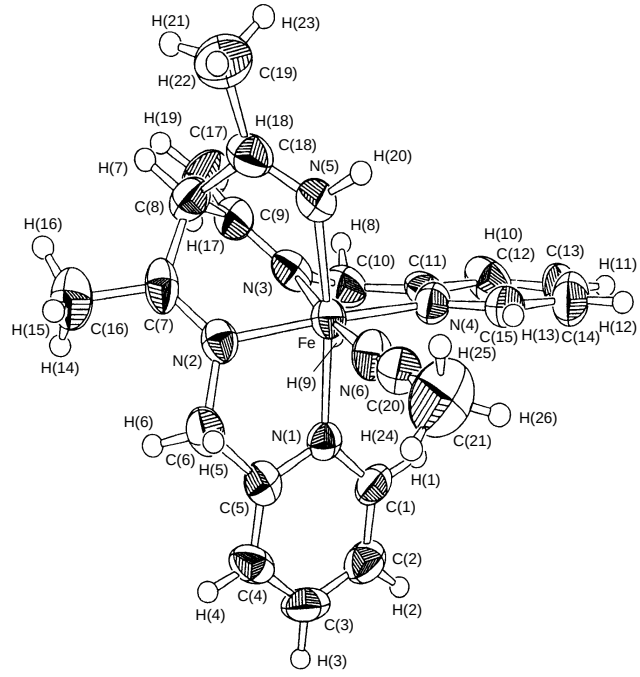



**Fig. 2** Molecular structure of one of the crystallographically independent cations of **2** showing the atom numbering scheme

acetonitrile was fused to the central carbon atoms of the 1,3-diimine moiety. One trigonal face is occupied by the three isolated imines which are linked to the tetrahedral C(8) and the C=N bond distances are N(2)–C(7) 1.31(1), N(3)–C(9) 1.28(1) and N(5)–C(18) 1.29(1) Å. The six-membered chelate rings of FeN(2)C(7)C(8)C(9)N(3) changed to a boat conformation due to the tethering methylimino group. The two pyridine rings coordinate *cis* to each other and the dihedral angle between the two pyridine planes was 94.07°.

Complex **2** gave broad $^1$H NMR spectra at room temperature but the spectra showed sharp signals at −10 °C. A new signal at δ 11.14 is assigned to the coordinated C=NH. The complex prepared from [$^2H_3$]acetonitrile in place of acetonitrile showed a spectrum which lacked the methyl signal at δ 2.48.§

The addition reaction of acetonitrile closely related to this has been reported by Riley and Busch.[3] The reaction conditions for preparation of acetonitrile adducts of macrocyclic tetraimine iron(II) complexes preclude the use of nitriles other than acetonitrile. However, the isolation of **1** allows the reaction with other nitriles as solvents, in place of acetonitrile, *e*.g. [$^2H_3$]acetonitrile in this experiment. The reaction mechanism may be *via* nucleophilic attack of a carbanion formed at the central carbon of the 1,3-diimine moiety either to the acetonitrile coordinated to the apical position and activated by the iron(II) centre as proposed by Riley *et al*. or to a bulk acetonitrile followed by coordination of imine nitrogen to the apical position. This can be resolved by the kinetics of this reaction. The use of a variety of nitriles for the preparation of iron(II) complexes with this new class of pentadentate ligands are now under study.

## Footnotes

† *Experimental procedure*: **1**; $Fe(ClO_4)_2\cdot 6H_2O$ (8.02 g, 95%, 0.021 mol) was placed in a 250 ml Schrenck and a mixture of orthoethylformate (23 ml) and acetonitrile (46 ml) was added. The mixture was stirred at 50 °C overnight. $MeCOCH_2C(Me)=NHCH_2C_5H_4N$ (3.99 g, 0.021 mol) and 2-(aminomethyl)pyridine (2.16 g, 0.019 mol) were added successively. After the mixture was stirred for 2 h at 50 °C, the mixture was cooled and dehydrated diethyl ether was added. Pale-red crystals were obtained which were stored *in vacuo*. Yield, 6.97 g (0.11 mol), 53.8%.

**2**; five drops of triethylamine was added through a syringe to an acetonitrile (8 ml) solution of **1** (266 mg, 0.404 mmol). After stirring at room temp. for 2 h, the reaction mixture was concentrated to dryness. The remaining orange solid was dissolved in 5 ml of acetonitrile, thf (40 ml) was added and the separated orange crystals were collected and stored *in vacuo*. Yield, 235 mg (84.4%). Anal. Calc. for $C_{21}H_{26}Cl_2FeN_6O_8\cdot C_4H_8O$: C, 43.56; H, 4.97; N, 12.19. Found: C, 43.04; H, 4.79; N, 12.02%.

‡ *Crystal data* for **1** and **2**: reflections were collected on a Rigaku AFC7R diffractometer using graphite-monochromated Mo-Kα radiation (λ = 0.710 69 Å), at $T$ = 293 K to $2\theta_{max}$ = 55.0°. **1**; $C_{23}H_{29}Cl_2FeN_7O_8$, $M$ = 658.28, triclinic, space group $P\bar{1}$, $a$ = 12.361(3), $b$ = 12.415(2), $c$ = 10.472(2) Å, α = 94.68(1), β = 112.19(1), γ = 80.41(2)°, $U$ = 1467.1(6) Å$^3$, $Z$ = 2, $D_c$ = 1.490 g cm$^{-3}$, $F(000)$ = 680, μ = 7.53 cm$^{-1}$. Data were corrected for absorption and extinction. $R_w = \{\Sigma w(F_o - F_c)^2/\Sigma wF_o^2)\}^{1/2}$ = 0.055, $R = \Sigma|F_o - F_c|/\Sigma|F_o|$ = 0.050 for 3399 reflections with $I/\sigma(I) > 3.0$.

**2**: $C_{25}H_{34}Cl_2FeN_6O_9$, $M$ = 689.33. monoclinic, space group $P2_1/a$, $a$ = 19.235(2), $b$ = 16.044(3), $c$ = 20.732(3) Å, β = 102.91(1)°, $U$ = 6236(1) Å$^3$, $Z$ = 8, $D_c$ = 1.468 g cm$^{-3}$, $F(000)$ = 2864.00, μ = 7.13 cm$^{-1}$. Data were corrected for absorption and extinction. $R_w$ = 0.068, $R$ = 0.082 for 7115 reflections with $I/\sigma(I) > 3.0$. Atomic coordinates, bond lengths and angles, and thermal parameters have been deposited at the Cambridge Crystallographic Data Centre (CCDC). See Information for Authors, Issue No. 1. Any request to the CCDC for this material should quote the full literature citation and the reference number 182/368.

§ *Selected spectroscopic data*: **1**; $^1$H NMR ($CD_3CN$, 298 K) δ 10.59 [C(1)H], 8.53[C(4)H], 8.26[C(2)H], 7.86[C(3)H], 6.35[$C(6)H_2$], 3.98[$C(8)H_2$], 2.61[$C(16)H_3$]. **2**; the HMQC and HMBC spectra (500 MHz) at −10 °C uniquely determined the $^{13}$C and $^1$H signals (δ): C(1), 152.51; C(2), 125.03; C(3), 138.90; C(4), 121.92; C(5), 165.70; C(6), 61.06; C(7); 176.96; C(8), 69.35; C(9), 177.78; C(10), 60.39; C(11), 165.13; C(12), 122.60; C(13), 139.19; C(14), 125.27; C(15), 156.01; C(16), 24.39; C(17), 24.28; C(18), 184.70; C(19), 29.15.

H(1), 7.10; H(2), 7.18; H(3), 7.82; H(4), 7.49; H(5), H(6), 5.24, 5.49 (AB); H(7), 5.66; H(8), H(9), 4.79, 5.33 (AB); H(10), 7.63; H(11), 8.02; H(12), 7.57; H(13), 9.03; H(14)–(16), 2.58; H(17)–(19), 2.40; H(20), 11.14; H(21)–(23), 2.48.

## References


1 A. J. Carty and P. C. Chieh, *J. Chem. Soc., Chem. Commun*., 1972, 158; M. Hinamoto, S. Ooi and H. Kuroya, *J. Chem. Soc., Chem. Commun*., 1972, 356.

2 J. K. McCusker, K. N. Walda, R. C. Dunn, J. D. Simon, D. Magde and D. N. Hendrickson, *J. Am. Chem. Soc*., 1993, **115**, 298; H. Toftlund and S. Yde-Andersen, *Acta Chem. Scand. Ser. A*, 1981, **35**, 575; H.-R. Chang, J. K. McCusker, H. Toftlund, S. R. Wilson, A. X. Trautwein, H. Winkler and D. N. Hendrickson, *J. Am. Chem. Soc*., 1990, **112**, 6814.

3 D. P. Riley, J. A. Stokes and D. H. Busch, *J. Am. Chem. Soc*., 1976, **98**, 1752; D. P. Riley, J. A. Stokes and D. H. Busch, *J. Am. Chem. Soc*., 1977, **99**, 767; K. B. Mertes, P. W. R. Corfield and D. H. Busch, *Inorg. Chem*., 1977, **16**, 3226.



*Received, 13th January 1997; Com. 7/00283A*

# Self-assembly and X-ray structure of a ten-component, three-dimensional metallosupramolecular cage

**Chris M. Hartshorn and Peter J. Steel***

*Chemistry Department, University of Canterbury, Christchurch, New Zealand*

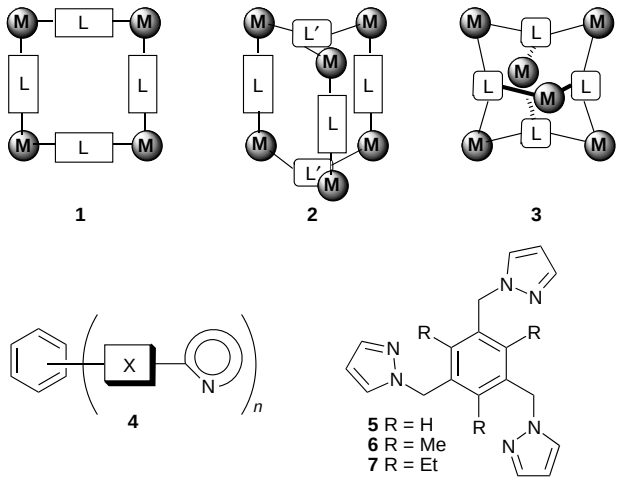
**Reaction of 1,3,5-tris(pyrazol-1-ylmethyl)-2,4,6-triethylbenzene 7 with palladium chloride results in the self-assembly of a three-dimensional cage; an X-ray crystal structure determination shows that the cage is comprised of an octahedral arrangement of six palladium atoms bridged by a tetrahedral network of four molecules of the ligand and contains a (disordered) guest molecule of dimethyl sulfoxide.**

The use of metal ions to control the self-assembly of multicomponent supramolecular structures of varying architecture is a subject of much current investigation;[1] particular recent attention has focused on the formation of species with internal cavities.[2] Since 1990, several groups have reported the construction of various molecular squares, represented schematically by structure **1**.[3] Lehn and coworkers[4] subsequently reported the formation of a three-dimensional cylindrical molecular box **2**, comprised of six metal ions and two types of bridging ligand. Fujita *et al.* have since reported the assembly of a five-component molecular cage[5] and, most recently, a ten-component adamantanoid-type cage **3** comprised of six metals with four identical bridging ligands.[6] We now report the formation and X-ray structure of a constitutionally similar but topologically different $M_6L_4$ cage.

We are currently engaged in a detailed study[7] of the coordination chemistry of a series of polyheteroaryl-substituted arenes **4**, which consist of various heterocyclic rings attached *via* spacer groups, X, to a central arene core, and have reported the syntheses of a number of poly(pyrazolylmethyl)benzenes.[8] We have also shown that the mesitylene-derived ligands **5** and **6** are able to encapsulate an octahedral metal atom, with simultaneous $\eta^6$-arene coordination and tripodal chelation to the pyrazole rings.[9] We have now extented this study to examine the complexes of these ligands with metal ions of different coordination geometry. In an effort to pre-organise the three pyrazole rings on the same side of the benzene ring,[10] we have now synthesised the triethyl analogue **7**, by trisbromomethylation[11] of 1,3,5-triethylbenzene, and subsequent phase-transfer-catalysed reaction with pyrazole.†

Reaction of **7** with palladium chloride gave immediate precipitation of an orange product,‡ which, on dissolution in $Me_2SO$, gave a $^1H$ NMR spectrum that showed significantly different chemical shifts from those of **7**, but retained the threefold symmetry. This was difficult to explain in terms of a square-planar palladium complex of low-nuclearity. Single crystals of this compound were grown by diffusion of acetone into an $Me_2SO$ solution of the solid, but these decomposed instantaneously upon removal of the solvent. After many attempts, a crystal was successfully tranferred to the low-temperature stream of a four-circle diffractometer with only minor decomposition.§

Fig. 1 shows a perspective view of the major component of the contents of the asymmetric unit of this structure.¶ It consists of a ten-component, three-dimensional metallosupramolecular cage comprised of six *trans*-dichloropalladium units bridged by four molecules of **7**. The six palladium atoms are arranged in a pseudo-octahedral array, while the four molecules of **7** form a tetrahedrally disposed internal core of benzene rings of approximately 4.7 Å internal radius. Within this core resides a single (disordered) $Me_2SO$ molecule (not shown in Fig.1). The potential $T_d$ symmetry is not crystallographically imposed, and is destroyed by differing conformations of the ethyl groups; specifically, one of the ligands has all three terminal methyl groups directed towards the internal core, while the other three ligands have one methyl group directed outside the core. This, along with the presence of the $Me_2SO$ guest and intermolecular interactions, results in a significant reduction in symmetry



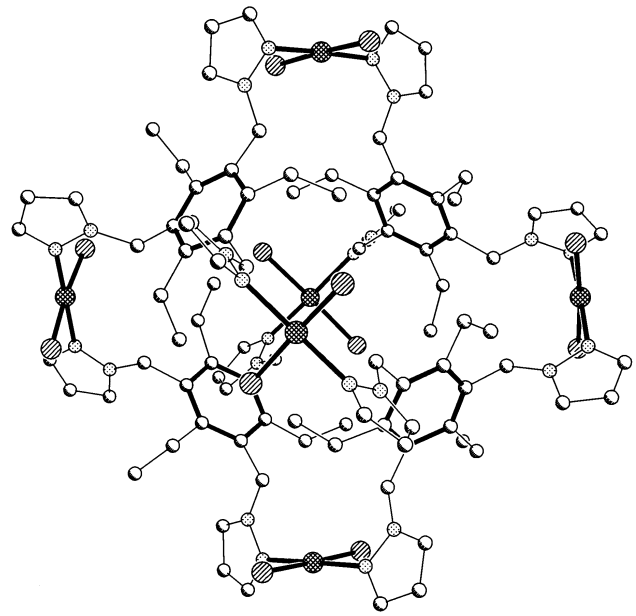



**Fig. 1.** Perspective view of the X-ray crystal structure; hydrogen atoms and solvate molecules not shown for clarity

in the solid state. For example, the diagonally opposite palladium atoms have separations ranging from 13.26 to 15.54 Å (Fig. 2). We believe that this cage structure is maintained in solution, which explains the symmetry observed in the NMR spectra and the slight broadening of the signals due to the methyl and methylene protons.

This molecule represents the second example of a $M_6L_4$ supramolecular adamantanoid cage, and serves to demonstrate the generality of such assembly processes; examples are also known of stoichiometrically inverted $M_4L_6$ compounds.[12] It is also the first X-ray structure of a free cage of this sort; in the previous example,[6] a low-precision X-ray structure of a clathrate complex with four adamantanyl carboxylate ions was determined. Although constitutionally similar to the previously reported $M_6L_4$ cage, the present structure is topologically quite different in shape. This is primarily a consequence of the different coordination geometries of the palladium atoms in the two compounds. In the only other example,[6] the bridging ligands were obligatorily *cis*-coordinated to the palladiums, due to the presence of chelating ethylenediamine ancillary ligands; in the present case, the ligands are *trans*- coordinated, which has the effect of making the palladiums more exposed on the surface of the cage. Furthermore, the methylene spacer groups in **7** impart greater flexibility to the ligand and, combined with the fact that the coordinating nitrogen is adjacent to the spacer group, allows for more compact packing within the cage; in the earlier case[6] the diagonally opposite palladiums were separated by *ca*. 19 Å.

The internal core of four tetrahedrally arranged benzene rings is reminiscent of that in the recently synthesised $C_{36}H_{36}$ spheriphane molecule which has covalently bonded ethylene bridges linking the benzenes and a radius of the internal cavity (as measured from the centroids of the rings) of 2.84 Å.[13] In the present case, the nature of the bridges expands this core to a radius of approximately 4.7 Å and allows for the incorporation of an $Me_2SO$ guest molecule. The octahedral arrangement of the six metals is also related to that in the hexacoordinated palladium and platinum complexes of $C_{60}$, wherein the diagonally opposite metals are separated by *ca*. 11.2 Å and the internal core has a diameter of only 3.51 Å.[14]

In conclusion, we have shown that, upon reaction with palladium chloride, the ligand **7** self-assembles into a ten-component metallosupramolecular cage. Studies directed towards the assembly of related structures employing other bridging ligands, including dissymmetric and asymmetric examples, are currently in progress.

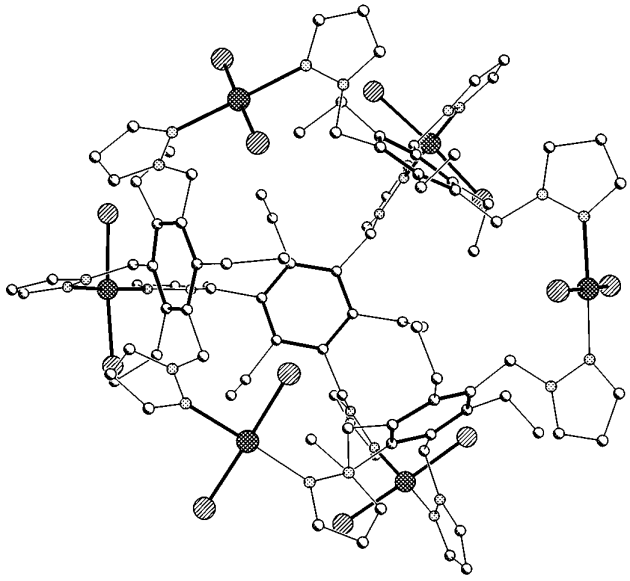


**Fig. 2.** View perpendicular to one benzene ring showing the reduction from $T_d$ symmetry, in the solid state

## Footnotes

† *Selected data* for **7**: isolated yield 60%, mp 125–126 °C (light petroleum). Found: C, 71.89; H, 7.73; N, 20.69. $C_{24}H_{30}N_6$ requires C, 71.61; H, 7.51; N, 20.88%. $^1$H NMR ($CDCl_3$): δ 0.96 (9 H, t, $CH_3$), 2.70 (6 H, m, 2,4,6-$CH_2$), 5.45 (6 H, s, 1,3,5-$CH_2$), 6.20 (3 H, t, H 4′), 6.98 (3 H, d, H5′), 7.55 (3 H, d, H3′). $^1$H NMR [$(CD_3)_2SO$]: δ 0.88 (9 H, t, $CH_3$), 2.88 (6 H, m, 2,4,6-$CH_2$), 5.47 (6 H, s, 1,3,5-$CH_2$), 6.32 (3 H, t, H4′), 7.53 (3 H, d, H5′), 7.57 (3 H, d, H3′).

‡ *Selected data*: isolated yield 87%, mp > 295 °C (decomp.) Found: C, 41.09; H, 4.92; N, 11.37; Cl, 14.93. $C_{96}H_{120}Cl_{12}N_{24}$ $Pd_6{\cdot}2C_2H_6OS{\cdot}4H_2O$ requires C, 41.38; H, 4.86; N, 11.58; Cl, 14.66%. $^1$H NMR [$(CH_3)_2SO$]: δ 1.23 (9 H, br t, $CH_3$), 2.50 (6 H, br m, 2,4,6-$CH_2$), 6.50 (6 H, br s, 1,3,5-$CH_2$), 6.65 (3 H, t, H4′), 7.93 (3 H, d, H5′), 8.15 (3 H, d, H3′).

§ *Crystal data* for $(PdCl_2)_6$(**7**)$_4{\cdot}8Me_2SO{\cdot}8H_2O$: $C_{112}H_{184}Cl_{12}N_{24}O_{16}Pd_6S_8$, $M_w$ = 3443.1, triclinic, space group $P\bar{1}$, $a$ = 19.648(6), $b$ = 19.730(5), $c$ = 24.995(5) Å, $\alpha$ = 97.94(1), $\beta$ = 108.88(1), $\gamma$ = 95.17(2)°, $U$ = 8986(4) Å$^3$, $Z$ = 2, $D_c$ = 1.273 g cm$^{-3}$, $\mu$ = 0.91 mm$^{-1}$, $F(000)$ = 3520, $T$ = -105 °C. Cell parameters were determined by least-squares refinement of 35 accurately centred reflections. A yellow block (0.44 × 0.30 × 0.17 mm) was used to collect (Siemens P4s diffractometer, Mo-Kα radiation, ω scans) 21966 independent reflections with $4 < 2\theta < 44°$, with significant crystal decomposition during data collection. The structure was solved by a combination of Patterson and difference Fourier methods and refined on $F^2$, using all data, to $R$ = 0.0692, $R_w$ = 0.1849 for 1654 parameters.

Atomic coordinates, bond lengths and angles, and thermal parameters have been deposited at the Cambridge Crystallographic Data Centre (CCDC). See Information for Authors, Issue No. 1. Any request to the CCDC for this material should quote the full literature citation and the reference number 182/372.

¶ In addition to the atoms shown in Fig. 1, the asymmetric unit contains a $Me_2SO$ guest in the cavity of the cage which has the sulfur atom disordered over two sites, and, external to the cage, seven $Me_2SO$ and eight water solvate molecules, many of which are also disordered.

## References


1 D. S. Lawrence, T. Jiang and M. Levett, *Chem. Rev.*, 1995, **95**, 2229 and references therein.
2 C. Seel and F. Vögtle, *Angew. Chem., Int. Ed. Engl.*, 1992, **31**, 529; C. A. Hunter, *Angew. Chem., Int. Ed. Engl.*, 1995, **34**, 1079.
3 M. Fujita, O. Sasaki, T. Mitsuhashi, T. Fujita, J. Yazaki, K. Yamaguchi and K. Ogura, *Chem. Commun.*, 1996, 1535; M. Fujita and K. Ogura, *Coord. Chem. Rev.*, 1996, **148**, 249; *Bull. Chem. Soc. Jpn.*, 1996, **69**, 1471 and references therein; R. V. Slone, J. T. Hupp, C. L. Stern and T. E. Albrecht-Schmitt, *Inorg. Chem.*, 1996, **35**, 4096; B. Olenyuk, J. A. Whiteford and P. J. Stang, *J. Am. Chem. Soc.*, 1996, **118**, 8221 and references therein.
4 P. Baxter, J.-M. Lehn, A. DeCian and J. Fischer, *Angew. Chem., Int. Ed. Engl.*, 1993, **32**, 69.
5 M. Fujita, S. Nagao and K. Ogura, *J. Am. Chem. Soc.*, 1995, **117**, 1649.
6 M. Fujita, D. Oguro, M. Miyazawa, H. Oka, K. Yamaguchi and H. Ogura, *Nature*, 1995, **378**, 469.
7 C. M. Hartshorn and P. J. Steel, *Inorg. Chem.*, 1996, **35**, 6902.
8 C. M. Hartshorn and P. J. Steel, *Aust. J. Chem.*, 1995, **48**, 1587.
9 C. M. Hartshorn and P. J. Steel, *Angew. Chem., Int. Ed. Engl.*, 1996, **35**, 2655.
10 For a related strategy in a different context see: C. Walsdorff, W. Saak and S. Pohl, *J. Chem. Res. (S)*, 1996, 282.
11 A. W. van der Made and R. H. van der Made, *J. Org. Chem.*, 1993, **58**, 1262.
12 R. W. Saalfrank, R. Burak, A. Breit, D. Stalke, R. Herbst-Irmer, J. Daub, M. Porsch, E. Bill, M. Muther and A. X. Trautwein, *Angew. Chem., Int. Ed. Engl.*, 1994, **33**, 1621; T. Beissel, R. E. Powers and K. N. Raymond, *Angew. Chem., Int. Ed. Engl.*, 1996, **35**, 1084.
13 F. Vögtle, J. Gross, C. Seel and M. Nieger, *Angew. Chem., Int. Ed. Engl.*, 1992, **31**, 1069.
14 P. J. Fagan, J. C. Calabrese and B. Malone, *J. Am. Chem. Soc.*, 1991, **113**, 9408; *Acc. Chem. Res.*, 1992, **25**, 134.


*Received, 29th November 1996; Com. 6/08081B*

# Polymerized gels and 'reverse aerogels' from methyl methacrylate or styrene and tetraoctadecylammonium bromide as gelator

**Weiqiang Gu,[a] Liangde Lu,[a] George B. Chapman[b] and Richard G. Weiss*[a]**

*Departments of Chemistry[a] and Biology,[b] Georgetown University, Washington, DC 20057-1227, USA*

**The low molecular mass gelator, tetraoctadecylammonium bromide, can be removed from polymerized gels of methyl methacrylate or styrene to leave mesoscopic channels with submicrometre diameters.**

Recently, we observed that very small concentrations of several tetraalkylammonium salts, some containing a cholesteryl or aromatic unit[1] and others having four *n*-alkyl chains,[2] gel a variety of organic liquids in a thermo-reversible fashion. Subsequently, we discovered that methyl methacrylate (MMA) and styrene (STY) are among them. Here, we report (*i*) the polymerization of gels of MMA and STY in which the gelator is tetraoctadecylammonium bromide (TOAB),[2] (*ii*) a comparison of the gel properties before and after polymerization, and (*iii*) the successful removal of the gelator molecules, leaving the polymerized matrix with vacant submicron cross-sectional channels.

Typically, low molecular mass gelators organize into long, thin strands that assemble into colloids.[3] When the colloids fill the sample volume and are in contact with each other, the liquid component is immobilized on a macroscopic scale by surface tension, but remains isotropic on a microscopic (molecular) scale.[4] Gels can be converted to aerogels by evaporation of the liquid when the gelator strands have sufficient mechanical strength not to collapse under the force of gravity. This case is usually limited to high molecular mass (*i.e.* polymeric), inorganic gelators;[5] collapsed aerogels (*i.e.* xerogels) are usually obtained from gels with low molecular mass gelators.[6] The sizes of the channels created in an aerogel are dependent upon how extensive is the gelator network, but they are not uniform.[7]

If, instead, the gelator strands were removed and the liquid component were frozen in place, reverse aerogels, in which the cross-sections of channels are more uniform and less dependent upon the gelator concentration, would result. We report the formation of reverse organoaerogels from TOAB gels after polymerization of the liquid component.

The recipe for gels with monomeric liquid components is MMA or STY containing 8 vol% divinylbenzene (DVB, a cross-linking agent), 7 vol% ethylvinylbenzene, 1 mass% benzoin ethyl ether (the photoinitiator), and 0.1–2.0 mass% of TOAB.† The mixtures were flame-sealed under vacuum in 0.4 × 4.0 mm (id) × *ca.* 2 cm Kimax flattened-capillary tubes after being degassed by two freeze–pump–thaw cycles. The capillaries were heated in a hot water-bath (near 90 °C) until the solids dissolved. After agitating the solutions to homogenize the components, they were cooled either by quenching in an ice/water–bath or by placing them in the air; the cooling protocol was important in determining the sizes of the strands and their colloids (*vide infra*). Below *ca.* 1 mass% of TOAB, the samples were viscous, partially gelled materials that are better described as sols (or fracture gels). Polymerization was effected by irradiation of the capillaries in a water-bath (to maintain a near ambient temperature) at 320–360 nm for 5 h (MMA) or 14 h (STY). The stiff, solid samples were removed by breaking the capillary tubes with a metal object.

The unpolymerized and polymerized gels in the capillaries were examined by optical microscopy (× 50; *ca.* × 83 including photo to negative size ratio) between crossed polars using a full-wave plate for enhanced contrast. At 2 mass% TOAB, it is possible to detect colloids (*ca.* 500 μm in diameter) of the slower cooled MMA gels [Fig. 1(*a*)]. In general, their appearance was not affected markedly by polymerization [Figs. 1(*a*) and (*b*)]. Although the strands are less extensive in samples with lower concentrations of TOAB, there is no apparent concentration dependence on their cross-sectional dimensions when the same cooling procedure was followed [Fig. 2(*a*) and (*b*)]. The strand cross-sections are smaller and the strand lengths are shorter when samples are cooled more rapidly [Figs. 1(*a*) and 3].

Since the long axes of strands of other gels have been oriented by allowing gelation to occur in strong magnetic fields,[8,9] we reheated (unpolymerized) STY and MMA gels (with 0.5 or 1.0 mass% TOAB) to 87 °C, far above the gel–liquid phase transition temperature, in a 6.3 T magnetic field and allowed them to cool slowly to room temperature. By optical microscopy, the strand networks seemed more homogeneously dispersed (probably due to more careful and slower cooling), but there was no indication of alignment.

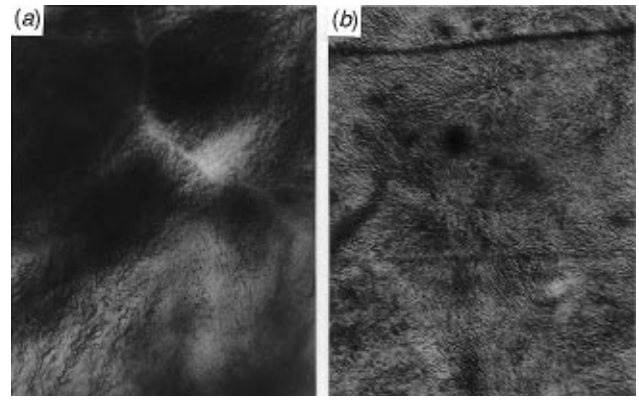



**Fig. 1** Optical micrographs of a 2 mass% TOAB/MMA gel prepared by the slower cooling method before (*a*) and after (*b;*) polymerization

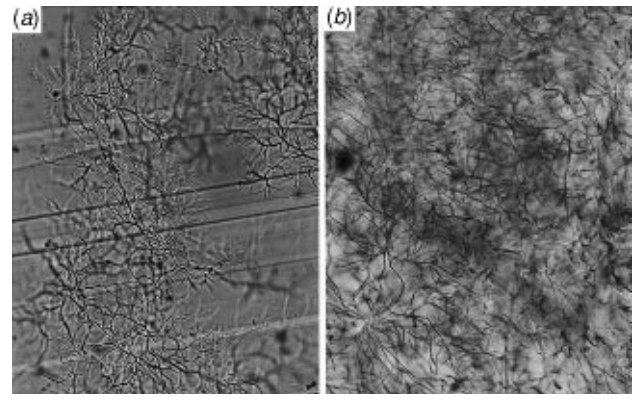



**Fig. 2** Optical micrographs of 0.1 (*a*) and 2.0 mass% (*b*) TOAB/STY gels prepared by the slower cooling method and polymerized

Polymerized MMA and STY gels with 2 mass% TOAB were heated and cooled between crossed polars while being observed under an optical microscope. Since the glass transition temperatures ($T_g$) of non-cross-linked MMA and STY are $\geqslant$100 °C,[10] and $T_g$ of a polymerized cross-linked STY gel was found to be *ca*. 130 °C by DSC, the TOAB, mp 97–102 °C, should melt before its polymer matrix becomes malleable. The birefringence associated with the TOAB strands of the polymerized MMA gel was lost between 89 and 94 °C. Cooling from 100 °C resulted in reappearance of birefringence in most of the strands near 90 °C. During the second heating, the birefringence was lost at a slightly higher temperature range and only about half reappeared upon cooling. Very similar results were obtained with a polymerized STY gel. In both cases, we suspect that gelator molecules from some strands merge, leading to larger but fewer domains. Based upon the proximity of the melting points, we conjecture that TOAB molecules are packed in similar fashions in bulk crystalline and strand phases. This is not always the case with low molecular mass gelators.[11]

When refluxed in *tert*-butyl alcohol (bp 83 °C), a polymerized STY gel lost a large fraction, but not all, of the TOAB molecules in its strands. Residual TOAB strands were evident by optical microscopy, even when no more could be leached from the gel; refluxing with fresh aliquots of alcohol was continued until no precipitate was detected upon addition of $AgNO_3$. Thus, some of the strands are in environments that have no contact with the surface of the polymerized sample through other strands.

All of the TOAB was removed rapidly and at room temperature from 1 or 2 μm thick slabs of the polymer (cut from the bulk with a diamond knife) placed in *tert*-butyl alcohol. Cross-sectional diameters of the strands (before TOAB removal) appeared to be the same as the channels (after TOAB removal). However, when the slabs were refluxed in *tert*-butyl alcohol, the channels were slightly wider than the strands. Widening of the channels may be due to coincidental loss of some unpolymerized liquid-component molecules with the TOAB. The average strand sizes in MMA and STY polymerized gels as a function of TOAB concentration and cooling protocol (during initial gel formation) are shown in Table 1. The data, from optical microscopic observations ($\times$ 645) of the narrowest and widest strands in 1 μm slabs, demonstrate that the cross-sections are not uniform, but can be made to diameters that are within a small range. It is unclear as yet whether the strands are twined multiples of a smaller unit or are the result of stochastic nucleation processes. In other studies, we[4] and others[3] have found that the former is the norm. It is also possible that the strands were distorted somewhat during the sectioning into slabs or may have suffered much more severe changes due to friction of the knife (*e.g*. local heating to above the polymer $T_g$ or tearing of the strand borders): even at 2 mass% TOAB, strands were not visible by optical microscopy in the faster cooled (polymerized) MMA gels before cutting; however, strands (or strand-like objects) were easily detected in the slabs. Since the MMA was gelled, strands must have been present, but may have been too small to be seen at the highest magnification of our optical microscope. Regardless, the data indicate that fast-cooling leads to somewhat narrower strands.

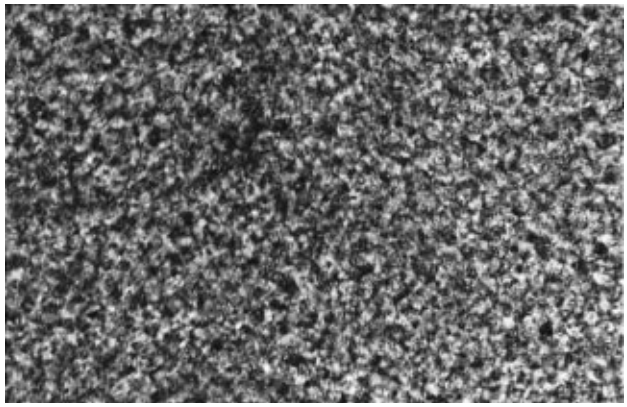


**Fig. 3** Optical micrograph of a 2 mass% TOAB/MMA gel prepared by the faster cooling method before polymerization

**Table 1** Approximate range of strand cross-sections in 1 μm thick slabs of polymerized gels as a function of TOAB concentration and cooling protocol (see text) of the unpolymerized samples from the isotropic to the gel phase

| TOAB (mass%) | Monomer | Cooling protocol | Cross-sectional range/μm |
|---|---|---|---|
| 2.0 | STY | Faster | 0.24–0.5 |
| 2.0 | STY | Slower | 0.5–1.5 |
| 0.5 | STY | Faster | 0.5–1.0 |
| 0.5 | STY | Slower | 0.5–1.0 |
| 0.1 | STY | Faster | 0.5–0.7 |
| 0.1 | STY | Slower | 0.5–1.0 |
| 2.0 | MMA | Faster | 0.3–0.5 |
| 2.0 | MMA | Slower | 0.4–1.0 |
| 0.5 | MMA | Faster | 0.24 |
| 0.5 | MMA | Slower | 0.24–1.2 |
| 0.1 | MMA | Faster | –[a] |
| 0.1 | MMA | Slower | 0.24–1.4 |

[a] No objects clearly identifiable as strands were observed.

The slabs with vacated channels have potential applications as membranes, and the bulk polymers, even with partial removal of the gelator molecules, may be useful as selective adsorbers and complexing agents for chromatography[12] and selective guest reactions.[13] Future efforts will be directed to make reverse aerogels whose channels are narrower and have greater cross-sectional uniformity (*i.e*. organic zeolites).

The authors from the Chemistry Department thank the National Science Foundation for its support of this research. We are also grateful to Professors M. C. Feiters and R. J. M. Nolte of Katholieke Universiteit Nijmegen who agreed to concurrent publication of their work[14] and ours.

## Footnote

† MMA, STY, and DVB (a mixture of *meta* and *para* isomers containing *ca*. 45% ethylvinylbenzene) from Aldrich were distilled under vacuum prior to use. Benzoin ethyl ether (99%) and TOAB (98%) from Aldrich were used as received.

## References

1 L. Lu and R. G. Weiss, *Langmuir*, 1995, **11**, 3630.
2 L. Lu and R. G. Weiss, *Chem. Commun*., 1996, 2029.
3 P. Terech, in *Specialist Surfactants*, ed. I. Robb, Blackie, Chapman & Hall, London, 1997, ch. 8.
4 Y.-c. Lin, B. Kachar and R. G. Weiss, *J. Am. Chem. Soc*., 1989, **111**, 5542.
5 V. S. Fajnor and K. Jesenak, *Chemicke Listy*, 1994, **88**, 24.
6 P. Terech, V. Rodriguez, J. D. Barnes and G. B. McKenna, *Langmuir*, 1994, **10**, 3406.
7 S. Q. Zeng, A. J. Hunt, W. Cao and R. Greif, *J. Heat Transfer*, 1994, **116**, 756.
8 P. Terech and C. Berthet, *J. Phys. Chem*., 1988, **92**, 4269.
9 P. Terech, *J. Surf. Sci. Technol*., 1989, **5**, 163.
10 O. G. Lewis, *Physical Constants of Linear Homopolymers*, Springer-Verlag, New York, 1968.
11 E. Ostuni, P. Kamaras and R. G. Weiss, *Angew. Chem., Int. Ed. Engl*., 1996, **35**, 1324.
12 F. Svec and J. M. J. Frechet, *Chem. Mater*., 1995, **7**, 707.
13 R. G. Weiss, V. Ramamurthy and G. S. Hammond, *Acc. Chem. Res*., 1993, **26**, 530.
14 R. J. H. Hafkamp, B. P. A. Kokke, I. M. Danke, H. P. M. Geurts, A. E. Rowan, M. C. Feiters and R. J. M. Nolte, *Chem. Commun*., following paper.

*Received, 20th November 1996; Com. 6/07868K*

# Organogel formation and molecular imprinting by functionalized gluconamides and their metal complexes

**Rudi J. H. Hafkamp,[a] Bas P. A. Kokke,[a] Iris M. Danke,[a] Hubertus P. M. Geurts,[b] Alan E. Rowan,[a] Martinus C. Feiters[a] and Roeland J. M. Nolte*[a]**

[a] *Department of Organic Chemistry, NSR Centre, University of Nijmegen, Toernooiveld, NL-6525 ED Nijmegen, The Netherlands*
[b] *Central Electron Microscopy Facility, University of Nijmegen, Toernooiveld, NL-6525 ED Nijmegen, The Netherlands*

**Functionalized gluconamides and their metal complexes are shown to give supramolecular assemblies, in some cases chiral, and to form organogels in a large variety of organic solvents, *e.g.* methacrylate mixtures which can be polymerized, as well as *o*-xylene, chloroform, ethyl acetate, ethanol and tetrahydrofuran.**

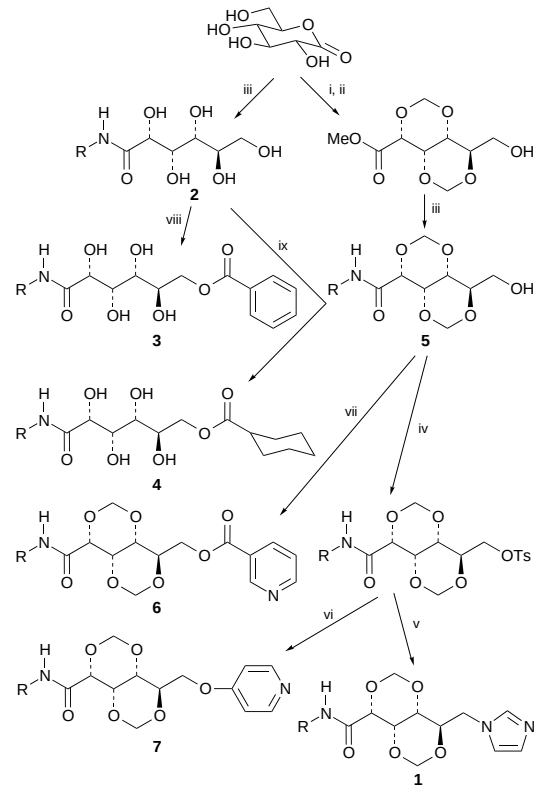
Gluconamides are known to form suprastructures in water.[1] We have recently shown[2] that the self-assembly behaviour of the imidazole-functionalized *N*-octylgluconamide **1a** in water can be tuned. Dispersion of the compound in water at pH 8.5 results in fibres and hollow tubuli, whereas at low pH vesicles are formed. We report here that further functionalization of gluconamides with different head-groups and the addition of metal ions result in diverse suprastructures which induce gelation in a large variety of organic solvents.

In recent years, a relatively broad range of compounds has been found to gelate organic solvents.[3] Gluconamide **2a** has been reported to aggregate into bilayer scrolls and form an unstable organogel in *o*-xylene.[4] We find, however, that a number of ester derivatives of **2a**, *viz*. the benzoate **3a** and the cyclohexanoate **4a** (*cf.* Scheme 1 for structures and outline of preparations)† form stable organogels in a number of solvents, *e.g.* *o*-xylene, chloroform, and ethyl acetate (Table 1). In chloroform, **3a** yields fibres or bundles of fibres which do not exhibit chirality [Fig. 1(*a*), (*b*)]. In contrast, **4a** in ethyl acetate [Fig. 1(*c*)] is able to express its molecular chirality in the suprastructure, resulting in helical fibres. From electron microscopic investigations, we propose that these fibres consist of double and multiple-stranded helices, and that the knobs at the end of the fibres represent hairpin-like turns of these helices.

In contrast to the functionalized gluconamides with free hydroxy groups, most of the bis-methylene protected *N*-*n*-octylgluconamide derivatives investigated, including the imidazolyl derivative **1a** as well as the 6-hydroxy analogue **5a** and the benzoate and picolinate (**6**) esters thereof, did not form organogels (Table 1). We decided to investigate the palladium(II)[8] and platinum(II) complexes of the pyridine-functionalized gluconamides **6** and **7**. *trans*-[Pd(**7b**)$_2$Cl$_2$] was soluble in chloroform but precipitated in water. In thf a rigid gel was obtained, which showed helical ribbons (width 36 nm) with a regular twist (pitch 110 nm) and a (maximum) aspect ratio of 25 [*cf.* Fig. 1(*d*)].

*trans*-[Pd(**6b**)Cl$_2$] dissolved in thf without giving a gel. It is not clear why [Pd(**7b**)$_2$Cl$_2$] forms an organogel in thf and [Pd(**6b**)$_2$]Cl$_2$ does not. A slight difference is expected between the conformations of [Pd(**7b**)$_2$Cl$_2$] and [Pd(**6b**)$_2$Cl$_2$], because in the latter compound the pyridyl ring is *meta*-substituted and the connection to the carbohydrate is *via* an ester group. These differences can cause a bend in the overall shape of the molecule which is not favourable for gelating solvents according to the rule of thumb: 'gelators of organic fluids should have the capability of adopting rodlike shapes in their extended conformations'.[9] We have also prepared the Pt complex, *trans*-[Pt(**7b**)$_2$Cl$_2$], and find that it gelates thf, toluene, and methanol at concentrations of 1, 2, and 5 mg ml$^{-1}$, respectively. For all gels, TEM showed fibres with approximately the same diameters as **7a**, but without a helical twist. In toluene, these non-helical fibres in turn self-assemble in a hierarchical process to give μm-sized twisted superstructures [Fig. 1(*e*)].

We were interested in using the organogels to prepare membranes with pores by the technique of 'imprinting'.[10] Using this approach, **3a** and **4a** (1% m/v) were dissolved in a warm mixture of methyl methacrylate and *n*-butyl methacrylate (1 : 4, v/v) containing 0.5% (m/v) polymerization catalyst (benzoin ethyl ether), as adapted from the literature.[11] Well defined aggregates with high aspect ratios were formed and gelated this solvent mixture. The organogel was transferred into gelatin cups and readily polymerized overnight with UV light (λ = 365 nm) in a refrigerator (5 °C), yielding a rigid polymer matrix. Using a glass knife and a diamond microtome, slabs of this polymer matrix were sliced in thin coupes (90 nm) which were allowed to float on a water surface before they were transferred




**Scheme 1** R = *n*-octyl **a** or *n*-hexadecyl **b**. Outline of syntheses of gluconamide derivatives from gluconolactone. *Reagents and conditions*: i, trioxane, $H_2O$–$H^+$;[6] ii, $H^+$-MeOH;[7] iii, excess alkylamine;[1] iv, TsCl in pyridine, 0 °C; v, imidazole, $CHCl_3$, 15 kbar, 50 °C; vi, 4-hydroxypyridine, triethylamine, 115 °C; vii, picolinoyl chloride, $CHCl_3$, 0 °C; viii, benzoyl chloride, pyridine, 0 °C; ix, $C_6H_{11}C(O)Cl$, 0 °C.

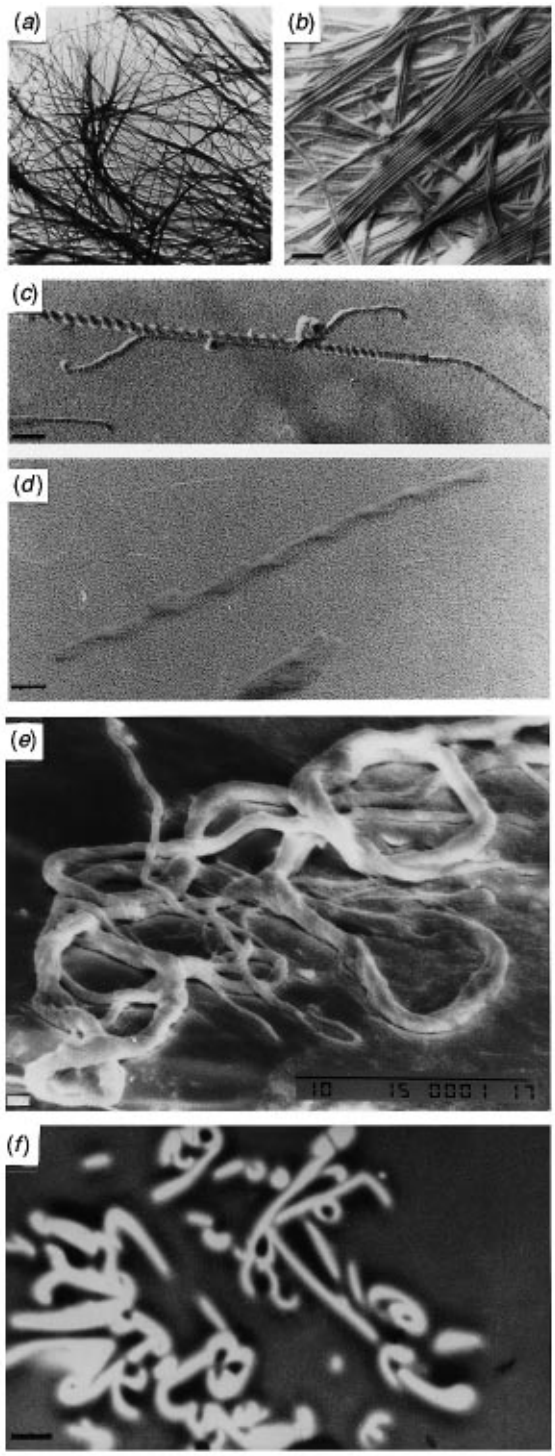



**Fig. 1** TEM pictures (Pt shadowing) of a dried gel of **3a** in chloroform: (*a*) network of fibres (bar 1.5 μm), (*b*) bundles of whisker-type fibres (bar 240 nm), (*c*) TEM picture (Pt shadowing, bar 110 nm) of a dried gel of **4a** in ethyl acetate, (*d*) TEM picture (Pt shadowing, bar 63 nm) of a helical ribbon formed by the complex $[Pd(\mathbf{7b})_2Cl_2]$ in thf, (*e*) SEM picture (Au coated, white bar 1 μm) of super helices formed on slowly cooling a gel of $[Pt(\mathbf{7b})_2Cl_2]$ in toluene (*f*) TEM pictures of imprinted pores of **4a** (bar 1.35 μm)

to electron microscopy grids. According to TEM the coupes show well defined pores [Fig. 1(*f*)]. Apparently, the gluconamide suprastructures disassemble and are removed from the polymeric matrix in water. Although dispersions of compound **4a** form helical aggregates [Fig. 1(*c*)], the pores observed in the polymeric matrix did not have helical charcter [Fig. 1(*f*)]. It should be noted that the size of the pores is approximately one

**Table 1** Gelation behaviour of functionalized gluconamides in organic solvents[a]

| Compound/ solvent | *o*-Xylene | $CHCl_3$ | EtOAc | EtOH |
|---|---|---|---|---|
| **1a** | R | S | S | S |
| **2a** | G | I | I | R |
| **3a**[b] | G | G | G | G |
| **4a** | G | G | G | S |
| **5a** | T | S | S | S |
| **6a** | S | S | S | S |

[a] G, gelates forming a high-viscosity mixture upon cooling; I, insoluble; R, recrystallizes within 1 h upon cooling; S, dissolves without gelation; T, gives a turbid mixture with slightly increased viscosity upon cooling. [b] Compound **3a** also forms gel in methanol, acetonitrile, acetone, dioxane, dichloromethane, toluene and benzene. It recrystallizes from water, dissolves without gelation in thf, and is insoluble in *n*-hexane and in diethyl ether.

order of magnitude larger than that of the helical fibres. The increase in size as well as the loss of chirality are probably due to shrinking of the methacrylate gel during polymerization.

In conclusion, we have shown that functionalized gluconamides and their metal complexes form a variety of chiral and non-chiral aggregates in a large variety of organic solvents and polymerizable methacrylate mixtures, and that it is possible to make imprints of the gluconamide assemblies.

We thank Professor R. G. Weiss (Georgetown, USA) for discussing his results with us prior to publication, and agreeing to concurrent publication of their work[12] and ours.

## Footnote

† The preparations of 6-deoxy-6-(1-imidazolyl)-*N*-*n*-octyl-D-gluconamide **1a**,[2] *N*-*n*-octyl-D-gluconamide **2a**,[1a] and 2,4 : 3,5-dimethylene-*N*-*n*-octyl-D-gluconamide **5**[2] are in the literature. The syntheses and characterizations of *N*-*n*-octyl-D-gluconamide-6-benzoate **3a**, *N*-*n*-octyl-D-gluconamide-6-cyclohexanoate **4a**, 2,4;3,5-dimethylene-*N*-*n*-hexadecyl-D-gluconamide-6-pyridylcarboxylic acid ester **6b** and 6-(4-pyridyl)-2,4;3,5-dimethylene-*N*-*n*-hexadecyl-D-gluconamide **7b**, and their $Pd^{II}$ and $Pt^{II}$ complexes are described elsewhere.[5] The purity and assigned structures of all compounds are fully supported by spectroscopy and elemental analyses.

## References

1 (*a*) B. Pfannemüller and W. Welte, *Chem. Phys. Lipids*, 1985, **37**, 227; (*b*) J.-H. Fuhrhop, P. Schnieder, J. Rosenberg and E. Boekema, *J. Am. Chem. Soc.*, 1987, **109**, 3387.
2 R. J. H. Hafkamp, M. C. Feiters and R. J. M. Nolte, *Angew. Chem.*, 1994, **33**, 986.
3 R. J. Twieg, T. P. Russell, R. Siemens and J. F. Rabolt, *Macromol.*, 1985, **18**, 1361; Y.-C. Lin and R. G. Weiss, *Macromol.*, 1987, **20**, 414; R. Scartazzini and P. L. Luisi, *J. Phys. Chem.*, 1988, **92**, 829; K. Hanabusa, K. Okui, K. Karaki, T. Koyama and H. Shirai, *J. Chem. Soc., Chem. Commun.*, 1992, 1371; E. J. de Vries and R. M. Kellogg, *J. Chem. Soc., Chem. Commun.*, 1993, 238.
4 J.-H. Fuhrhop, P. Schnieder, E. Boekema and W. Helfrich, *J. Am. Chem. Soc.*, 1988, **110**, 2861; J. Köning, C. Boettcher, H. Winkler, E. Zeitler, Y. Talmon and J.-H. Fuhrhop, *J. Am. Chem. Soc.*, 1993, **115**, 693.
5 R. J. H. Hafkamp, PhD Thesis, University of Nijmegen, 1996.
6 M. Zief and A. Scattergood, *J. Am. Chem. Soc.*, 1947, **69**, 2132.
7 C. L. Mehltretter, R. L. Mellies, C. E. Rist and G. E. Hilbert, *J. Am. Chem. Soc.*, 1947, **69**, 2130.
8 S. A. Hudson and P. M. Maitlis, *Chem. Rev.*, 1993, **93**, 861.
9 Y.-C. Lin, B. Kachar and R. G. Weiss, *J. Am. Chem. Soc.*, 1989, **111**, 5542.
10 K. J. Shea, E. A. Thompson, S. D. Pandey and P. S. Beauchamp, *J. Am. Chem. Soc.*, 1980, **102**, 2140; G. Wulff, *Pure Appl. Chem.*, 1982, 2093.
11 E. Carlemalm, R. M. Garavito and W. Villiger, *J. Microsc.*, 1982, **126**, 123; H. Gankema, M. A. Hempenius and M. Möller, *Recl. Trav. Chim. Pays-Bas*, 1994, **113**, 241.
12 W. Gu, L. Lu, G. B. Chapman and R. G. Weiss, *Chem. Commun.*, preceding paper.

*Received, 9th December 1996; Com. 6/08266A*

# A novel hydride rearrangement of the acetal group of tetraacetal tetraoxa-cages mediated by Lewis acids

**Hsien-Jen Wu* and Jyh-Haur Chern**

*Department of Applied Chemistry, National Chiao Tung University, Hsinchu, Taiwan, China*

**Treatment of tetraoxa-cages 1a–f with Lewis acids such as $TiCl_4$, $AlCl_3$, $BF_3{\cdot}OEt_2$ and $MeSO_3H$ in dichloromethane at 25 °C gives the rearrangement products 2a–f in 90% yields regioselectively and stereoselectively; a novel hydride rearrangement of the acetal group of tetraacetal tetraoxa-cages mediated by Lewis acids.**

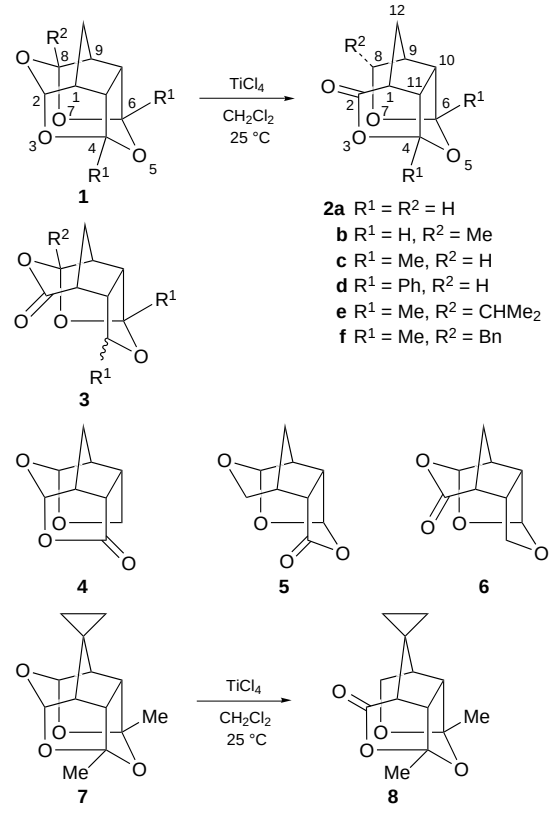
The reaction chemistry of acetals has been greatly expanded by the use of Lewis acidic promoters, particularly in conjunction with silicon-containing nucleophiles.[1,2] Usually, acyclic and monocyclic acetals, especially the acetal groups in monosaccharide derivatives, are the objects for study. Recently, we accomplished the synthesis of novel oxa-cage compounds, such as diacetal trioxa-cages,[3] triacetal trioxa-cages,[4] tetraacetal tetraoxa-cages,[5] tetraacetal pentaoxa-cages[6] and pentaacetal pentaoxa-cages (the pentaoxa[5]peristylanes).[7] All these oxa-cages contain acetal and ketal groups. As part of a program that involves the synthesis, chemistry and applications of new heterocyclic cages, we report here a novel hydride rearrangement of the acetal group of the tetraacetal tetraoxa-cages **1** mediated by Lewis acids.

Reaction of the tetraacetal tetraoxa-cages **1a–f** with two equivalents of Lewis acids, such as $TiCl_4$, $AlCl_3$, $BF_3{\cdot}OEt_2$ and $MeSO_3H$ in dichloromethane at 25 °C for 3 h gave the novel hydride rearrangement products **2a–f** in 90–95% yields regioselectively and stereoselectively (Scheme 1). No detectable amount of the other regioisomer **3** was obtained. In the case of the unsubstituted (parent) compound **1a**, no detectable amount of the other regioisomers **4**, **5** or **6** was obtained. We attribute the high regioselectivity of the hydride rearrangement to the angle strain of the unusually large bond angle of C(2)–O(13)–C(8) of the tetraoxa-cages **1a–f**. While the other C–O–C bond angles of the tetraoxa-cages **1** are between 111°–108°, the C(2)–O(13)–C(8) bond angle is 117.5°, remarkably larger than ordinary bond angles about $sp^3$-hybridized atoms.[5a] In the cases of both **1a** and **1b**, with no alkyl substituents on C(4) and C(6), the hydride rearrangement still took place regioselectively between C(2) and C(8). Thus, a steric hindrance factor for the regioselective hydride rearrangement of **1** to **2** was excluded. Treatment of the tetraoxa-cage **7** with $TiCl_4$ under the same reaction conditions gave **8** in 90% yield. A three-membered spiro ring on the apical carbon did not interfere with the hydride rearrangement.

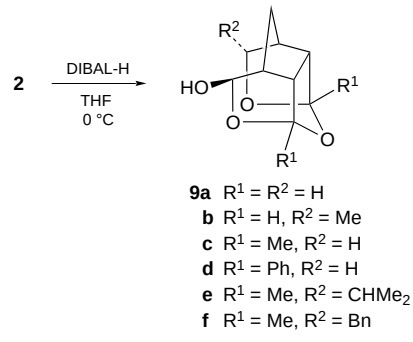
The IR spectra of **2a–f** showed strong absorption at 1770 $cm^{-1}$ for the five-membered lactone carbonyl group. The $^1H$ NMR spectrum of **2a** revealed two doublets at δ 6.04 and 5.97 for the two acetal protons on C(4) and C(6) and two doublets of doublets at δ 4.13 and 3.50 for the methylene protons on C(8). The $^{13}C$ NMR spectrum of **2a** diplayed a singlet at δ 179.09 for the lactone carbonyl, two peaks at δ 112.31 and 106.38 for the acetal carbons C(4) and C(6) and one peak at δ 71.59 for the methylene carbon C(8).

The stereochemistry of the alkyl group on C(8) of **2b**, **2e** and **2f** was assigned on the basis of the following chemical transformation of **2a–f** and NOE experiments of **2b**. Irradiating the methyl group on C(8) of **2b** gives 8.6% enhancement of the intensity of the C(9) proton. Reduction of **2a–f** with DIBAL-H in dry THF at 0 °C gave compounds **9a–f** stereoselectively in 85–90% yields (Scheme 2). The stereochemistry of the hydroxy group and the alkyl substituent on C(8) was proven by X-ray analysis of the crystalline compound **9b** (Fig. 1).† Hence, the stereochemistry of the alkyl substituent on C(8) of **2b**, **2e** and **2f** was confirmed.

A reaction mechanism is proposed for the hydride rearrangement from **1** to **2** (Scheme 3). Coordination of $TiCl_4$ to the oxygen atom O(13) of **1** followed by cleavage of the C(8)–O(13) bond gives the oxonium ion **10**. Fragmentation of **10** to a monocyclic species **11** followed by zipping back up to




**Scheme 1**




**Scheme 2**

the stereoisomer **12** and a subsequent (fast) intramolecular hydride transfer gives **2**.

In summary, we have discovered a novel hydride rearrangement of the acetal group of tetraacetal tetraoxa-cages mediated by Lewis acids. The hydride rearrangement is found to be regio- and stereo-selective. We attribute the highly regioselective hydride rearrangement to the unusually large bond angle of C(2)–O(13)–C(8) of the tetraoxa-cages **1**.

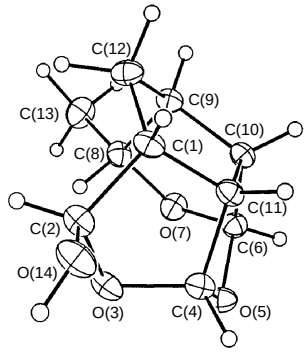
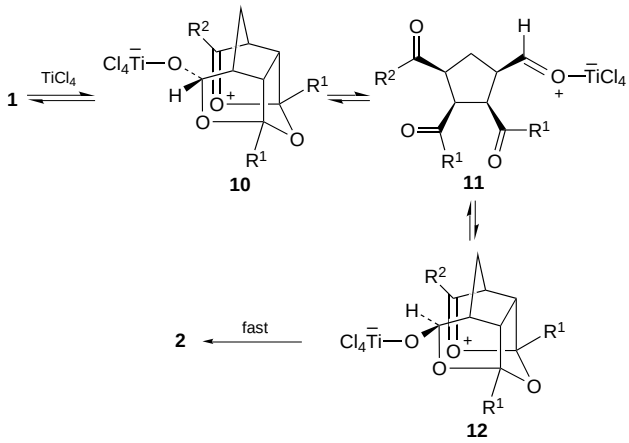



**Fig. 1** ORTEP diagram of **9b**




**Scheme 3**

Financial support from the National Science Council of the Republic of China is gratefully acknowledged. We thank Miss F. L. Liao and Dr S. L. Wang (at the Department of Chemistry, National Tsing Hua University) for their help in carrying out the X-ray crystallographic analysis.

## Footnote

† *Crystal data*: for **9b**: $C_{10}H_{14}O_4$, $M$ = 198.2, monoclinic, space group $P2_1/n$, $a$ = 5.4843(2), $b$ = 13.6462(7), $c$ = 12.2570(6) Å, β = 91.865(2)°, $U$ = 916.8(4) Å$^3$, $Z$ = 4, $R$ = 0.0422, $Rw$ = 0.0517. Atomic coordinates, bond lengths and angles, and thermal parameters have been deposited at the Cambridge Crystallographic Data Centre (CCDC). See Information for Authors, Issue No. 1. Any request to the CCDC for this material should quote the full literature citation and the reference number 182/371.

## References

1 Reviews: T. Mukaiyama and M. Murakami, *Synthesis*, 1987, 1043; A. Hosomi, M. Endo and H. Sakurai, *Chem. Lett*., 1976, 941.

2 T. Mukaiyama and M. Hayashi, *Chem. Lett*., 1974, 15; A. Hosomi, M. Endo and H. Sakurai, *Chem. Lett*., 1976, 941; A. Hosomi, H. Hashimoto and H. Sakurai, *Tetrahedron Lett*., 1980, **21**, 951; T. Mukaiyama, H. Ishihara and K. Inomata, *Chem. Lett*., 1975, 527; A. S. Kende, S. Johnson, P. Sanfilippo, J. C. Hodges and L. N. Jungheim, *J. Am. Chem. Soc*., 1986, **108**, 3513; I. Mori, K. Ishihara, L. A. Flippin, K. Nozaki, H. Yamamoto, P. A. Bartlett and C. H. Heathcock, *J. Org. Chem*., 1990, **55**, 6107; A. Mori, K. Ishihara and H. Yamamoto, *Tetrahedron Lett*., 1986, **27**, 987; S. E. Denmark and N. G. Almstead, *J. Am. Chem. Soc*., 1991, **113**, 8089; S. E. Denmark and N. G. Almstead, *J. Org. Chem*., 1991, **56**, 6458.

3 H. J. Wu, S. H. Tsai and W. S. Chung, *Tetrahedron Lett*., 1996, **37**, 8209; S. H. Tsai, H. J. Wu and W. S. Chung, *J. Chinese Chem. Soc*., 1996, **43**, 445.

4 C. Y. Wu, C. C. Lin, M. C. Lai and H. J. Wu, *J. Chinese Chem. Soc*., 1996, **43**, 187; H. J. Wu, C. Y. Wu and M. C. Lai, unpublished results.

5 (*a*) H. J. Wu and C. C. Lin, *J. Org. Chem*., 1995, **60**, 7558; (*b*) H. J. Wu and C. C. Lin, *J. Org. Chem*., 1996, **61**, 3820; (*c*) C. C. Lin and H. J. Wu, *Tetrahedron Lett*., 1995, **36**, 9353; (*d*) H. J. Wu, F. J. Huang and C. C. Lin, *J. Chem. Soc., Chem. Commun*., 1991, 770; (*e*) C. C. Lin and H. J. Wu, *J. Chinese Chem. Soc*., 1995, **42**, 815; (*f*) C. C. Lin, F. J. Huang, J. C. Lin and H. J. Wu, *J. Chinese Chem. Soc*., 1996, **43**, 177; (*g*) R. L. Lin, C. Y. Wu, J. H. Chern and H. J. Wu, *J. Chinese Chem. Soc*., 1996, **43**, 289; (*h*) H. J. Wu, J. H. Chern and C. Y. Wu, *Tetrahedron*, 1997, in the press.

6 C. C. Lin and H. J. Wu, *Synthesis*, 1996, 715.

7 H. J. Wu and C. Y. Wu, unpublished results.

*Received, 30th October 1996; Com. 6/07403K*

# Preparation of α-(2,2-diphenylhydrazino)- and α-(benzyloxyamino)-lactones by radical cyclization: use of glyoxylic acid diphenylhydrazone and glyoxylic acid *O*-benzyloxime

**Derrick L. J. Clive* and Junhu Zhang**

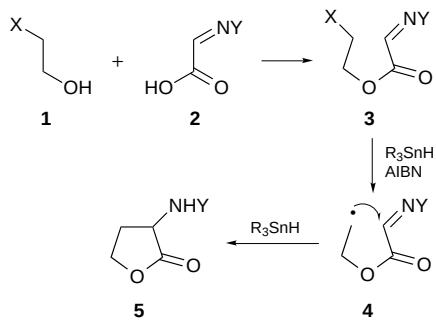
*Chemistry Department, University of Alberta, Edmonton, Alberta, Canada T6G 2G2*

**Glyoxylic acid diphenylhydrazone (2, Y = $NPh_2$) and the corresponding *O*-benzyloxime (2, Y = OBn) are easily esterified in high yield by β-bromo alcohols, and the resulting esters undergo radical cyclization to α-(2,2-diphenylhydrazino) or α-(benzyloxyamino) lactones on treatment with tributyltin hydride; the initial radical can be formed by homolysis of a carbon–selenium bond as well as a carbon–bromine bond and, when applied to appropriate alcohols, the esterification–radical closure sequence can also be used to make six- or seven-membered lactones.**

We report here the synthesis of α-hydrazino lactones (**5**, Y = $NPh_2$) and the corresponding *O*-benzylhydroxylamines (**5**, Y = OBn) by the radical cyclization process summarized in Scheme 1 (X = Br, SePh). The radical precursors **3** are readily accessible by DCC-mediated coupling of glyoxylic acid diphenylhydrazone (**2**, Y = $NPh_2$)[1] or *O*-benzyloxime (**2**, Y = OBn)[2] with β-bromo or β-(phenylselanyl) alcohols (**1**, X = Br or SePh), themselves easily made from alkenes (NBS–$H_2O$,[3] PhSeX[4]) or epoxides ($Me_2BBr$,[5] PhSeNa[6]). The glyoxylic acids **2** (Y = $NPh_2$ or OBn) are stable, crystalline reagents, formed in high yield (90–96%) from glyoxylic acid.†

Both the coupling reaction (**1** + **2** → **3**) and the radical closure (**3** → **4** → **5**) generally proceed in good yield. Most of our work has been done with hydrazone acid **2** (Y = $NPh_2$), but related experiments with the *O*-benzyloxime acid **2** (Y = OBn) were also successful; however, we have not made a sufficiently extensive comparison to identify which series (hydrazone or oxime) is generally more efficient. Likewise, the superiority of bromides over selenides for the radical closure step has also not yet been firmly established.

Formation of carbocycles — specially five-membered rings — by radical closure onto a carbon–nitrogen double bond is well-established with oxime ethers,[7] but to a much lesser extent with diphenylhydrazones.[8,9] In the case of hydrazones there is evidence to suggest[8a] that hydrazone amides and semicarbazides **6** (Y = NHCOPh or $NHCONHNH_2$) close more efficiently than do the corresponding diphenylhydrazones; however, in this preliminary work we used diphenylhydrazones. The ring closure shown for **4** (Scheme 1) requires the indicated proximity of the carbon radical and the carbon–nitrogen double bond; this conformation is adequately accessible because of the sufficiently low rotational barrier about ester C(O)–O single bonds.[10]




X = Br, SePh, Y = $NPh_2$, OBn

**Scheme 1**

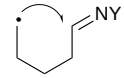
Our reaction produces lactones bearing an α-nitrogen substituent (Table 1). When the starting alcohol **1** is cyclic, the stereochemical outcome at the newly-created ring junction is determined by the stereochemistry of the original hydroxy-bearing carbon in **1**, but for both cyclic and non-cyclic starting alcohols the degree of stereoselectivity α to the lactone carbonyl is low,[11] at least under the thermal conditions we have used (see footnotes to Table 1).

Experiments with indane derivative **15a** (see Table 1) revealed the intervention of a 1,2-acyl migration[12] which, in this case, must be especially fast because of the fact that it leads—*via* a readily accessible and favourable geometry—to a benzylic radical. Entry 6 of Table 1 shows an application to carbohydrates, and also serves as an example of 7-*exo* closure. Presumably, favourable geometrical constraints are operating in this case, but are absent in **9a** (6-*exo* closure), where an appreciable amount of reduction occurs before cyclization.

All the coupling experiments to generate the radical precursors **3** were done by addition of DCC (5.5 mmol) and DMAP (0.5 mmol) to a solution of the appropriate alcohol (5.5 mmol) and reagent **2** (Y = $NPh_2$ or OBn) (5 mmol) in $CH_2Cl_2$. After 6–12 h at room temperature, the esters could be isolated in the yields shown. The radical cyclizations were conducted by simultaneously adding toluene solutions‡ (double syringe pump, 9-10 h) of $Bu_3SnH$ (1.73 mmol, 0.173 M) and AIBN (0.12 mmol, 0.012 M) to a refluxing solution of the substrate (1.15 mmol, 0.016 M) in the same solvent. At the end of the addition refluxing was continued for an arbitrary period of 2–3 h (except for **8a**, where this period was 5 h).

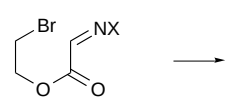
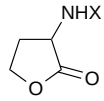
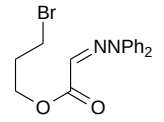
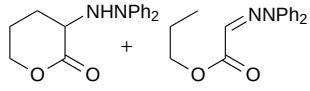
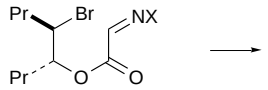
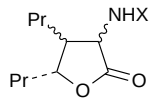
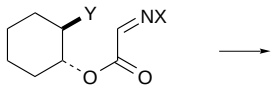
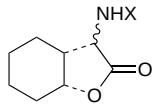
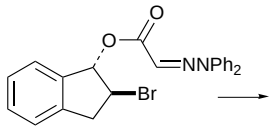
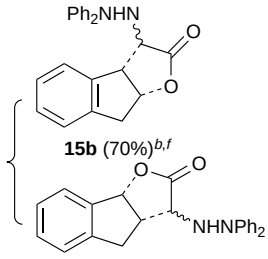
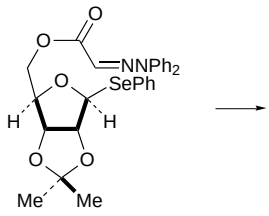
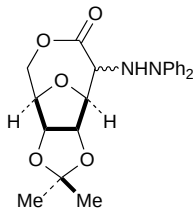
α-Hydrazino- and α-(hydroxyamino)-γ-lactones (*cf.* substructure **5**) are not well-known; neither are the corresponding δ-lactones.[13] In principle, these α-substituted lactones can be modified in various ways and, in the case of **7b** for example, hydrogenolysis (10% Pd–C, THF-aqueous HCl 6 M) gave homoserine γ-lactone hydrochloride[14] (81% after crystallization from acetone).

All new compounds were characterized by spectroscopic methods, including accurate mass measurements. The isomers of **11b** (four), **14b** (two) and **15b** (two) were chromatographic-




**6** Y = NHCOPh, $NHCONHNH_2$

**Table 1** Yields for coupling reaction to form hydrazones or oximes, and for radical cyclization

| Hydrazone or oxime (yield) | Lactone (yield) |
|---|---|
| 1  **7a** X = $NPh_2$ (80%) **8a** X = OBn (82%) |  **7b** X = $NPh_2$ (75%) **8b** X = OBn (51%) |
| 2  **9a** (72%) |  **9b** (50%) **9b** (20%) |
| 3  **10a** X = $NPh_2$ (98%) **11a** X = OBn (*ca.* 100%) |  **10b** X = $NPh_2$ (82%)[a] **11b** X = OBn (78%)[b,c] |
| 4  **12a** X = $NPh_2$, Y = Br (90%) **13a** X = $NPh_2$, Y = SePh (85%) **14a** X = OBn, Y = Br (88%) |  **12b** X = $NPh_2$ (70%)[d] **13b** X = $NPh_2$ (*ca.* 20%)[d] **14b** X = OBn (64%)[b,e] |
| 5  **15a** (82%) |  **15b** (70%)[b,f] **15c** (<10%)[g] |
| 6  **16a** (92%) |  **16b** (64%)[d] |

[a] Isomers not chromatographically separable; ratio ($^1$H NMR) *ca.* 2 : 3 : 2 : 3. [b] The individual isomers were separated and the relative stereochemistry of each was established by NOE measurements. [c] Taking the nitrogen function of C(2) to be on the α-face, the stereochemistry of the C(3) and C(4) substituents, in that order, can be defined as α (same face as the nitrogen function) and β. The isomer ratio ($^1$H NMR) was αα : αβ : ββ : βα : : 1 : 2 : 2.3 : 3. [d] Isomer ratio ($^1$H NMR) *ca.* 1 : 1. [e] Isomer ratio (isolation) 1 : 1. [f] Isomer ratio (isolation) 1 : 1.2. [g] Tentative structural assignment; the material was obtained mixed with **15b**. Isomer ratio ($^1$H NMR) *ca.* 1 : 1.

ally separable, and the relative stereochemistry of each was established by NOE measurements.

Acknowledgment is made to the Natural Sciences and Engineering Research Council of Canada for financial support.

## Footnotes

† We used the procedure of ref. 2 for both reagents, but simply filtered off the product, without extraction into $CH_2Cl_2$, in the case of the hydrazone. ‡ For **16a** → **16b**, benzene was used, in order to demonstrate that the reaction works also at the reflux temperature of this solvent.

## References


1 H. J. Barber and E. Lunt, *J. Chem. Soc*., 1965, 1468.
2 J. D. M. Herscheid, J. H. Colstee and H. C. J. Ottenheijm, *J. Org. Chem*., 1981, **46**, 3346.
3 *E.g.* D. Van Ende and A. Krief, *Tetrahedron Lett*., 1975, 2709; C. O. Gus and R. Rosenthal, *J. Am. Chem. Soc*., 1955, **77**, 2549; D. R. Dalton, V. P. Dutta and D. C. Jones, *J. Am. Chem. Soc*., 1968, **90**, 5498.
4 *E.g.* D. L. J. Clive, *J. Chem. Soc., Chem. Commun*., 1974, 100; K. C. Nicolaou, D. A. Claremon, W. E. Barnette and S. P. Seitz, *J. Am. Chem. Soc*., 1979, **101**, 3704.
5 Y. Guindon, M. Therien, Y. Girard and C. Yoakim, *J. Org. Chem*., 1987, **52**, 1680; R. C. Larock, *Comprehensive Organic Transformations*, VCH, New York, 1989, p. 508.
6 *E.g.* K. B. Sharpless and R. F. Lauer, *J. Am. Chem. Soc*., 1973, **95**, 2697.
7 P. A. Bartlett, K. L. McLaren and P. C. Ting, *J. Am. Chem. Soc*., 1988, **110**, 1633; E. J. Enholm, J. A. Burroff and L. M. Jaramillo, *Tetrahedron Lett*., 1990, **31**, 3727; N. S. Simpkins, S. Stokes and A. J. Whittle, *J. Chem. Soc., Perkin Trans. 1*, 1992, 2471; G. Pattenden and D. J. Schultz, *Tetrahedron Lett*., 1993, **34**, 6787; A. H. Ingall, P. R. Moore and S. M. Roberts, *J. Chem. Soc., Chem. Commun*., 1994, 83; S. E. Booth, P. R. Jenkins, C. J. Swain and J. B. Sweeney, *J. Chem. Soc., Perkin Trans. 1*, 1994, 3499; K. A. Parker and D. Fokas, *J. Org. Chem*., 1994, **59**, 3927; T. Naito, K. Tajiri, T. Harimoto, I. Ninomiya and T. Kiguchi, *Tetrahedron Lett*., 1994, **35**, 2205; T. Kiguchi, K. Tajiri, I. Ninomiya, T. Naito and H. Hiramatsu, *Tetrahedron Lett*., 1995, **36**, 253. M. Santagostino and J. D. Kilburn, *Tetrahedron Lett*., 1995, **36**, 1365; G. E. Keck, S. F. McHardy and J. A. Murry, *J. Am. Chem. Soc*., 1995, **117**, 7289; J. L. Chiara, J. Marco-Contelles, N. Khiar, P. Gallego, C. Destabel and M. Bernabé, *J. Org. Chem*., 1995, **60**, 6010; J. Marco-Contelles, C. Destabel, P. Gallego, J. L. Chiara and M. Bernabé, *J. Org. Chem*., 1996, **61**, 1354.
8 (*a*) Closures onto various hydrazones: W. R. Bowman, P. T. Stephenson, N. K. Terrett and A. R. Young, *Tetrahedron*, 1995, **51**, 7959; (*b*) C. F. Sturino and A. G. Fallis, *J. Am. Chem. Soc*., 1994, **116**, 7447; (*c*) C. F. Sturino and A. G. Fallis, *J. Org. Chem*., 1994, **59**, 6514.
9 *Cf.* Closures onto imines: W. R. Bowmann, P. T. Stephenson and A. R. Young, *Tetrahedron*, 1996, **52**, 11 445; Closures onto special hydrazones; S. Kim, J. H. Cheong and K. S. Yoon, *Tetrahedron Lett*., 1995, **36**, 6069 and references cited therein.
10 E. L. Eliel and S. H. Wilen, *Stereochemistry of Organic Compounds*, Wiley, New York, 1994, p. 618.
11 *Cf.* D. L. J. Clive and P. L. Beaulieu, *J. Chem. Soc., Chem. Commun*., 1983, 307.
12 D. Crich, A. L. J. Beckwith, G. F. Filzen and R. W. Longmore, *J. Am. Chem. Soc*., 1996, **118**, 7422 and references cited therein.
13 A CASONLINE substructure search identified the following references: α-hydrazino compounds: *Chem. Abstr*., 1992, **119**, 226 330; G. G. Black and M. Sainsbury, *J. Chem. Res., Synop*., 1986, 332; B. Petersen, *Acta. Chem. Scand., Ser. B*, 1980, **34**, 429; H. Paulsen and H. Kuhne, *Carbohydr. Res*., 1970, **13**, 289; α-Hydroxyamino-γ-butyrolacetone: *Chem. Abstr*., 1970, **72**, 43 314.
14 H. R. Snyder, J. H. Andreen, G. W. Cannon and C. F. Peters, *J. Am. Chem. Soc*., 1942, **64**, 2082.


*Received, 6th December 1996; Com. 6/08236J*

# Chlorination of enantiomerically pure 1,1′-bis(hydroxyalkyl)-3,3′-biindolizines: conservation of chirality by thermal treatment

**Helmut Sonnenschein,*† Fritz Theil, Thomas Kreher and Angela Köckritz**

*Institut für Angewandte Chemie Berlin-Adlershof, Abt. Organische Synthese, Rudower Chaussee 5, D-12484 Berlin, Germany*

**Enantiomerically pure 1,1′-bis(hydroxyalkyl)-3,3′-biindolizines 1 racemize unexpectedly by reaction with tetrachloromethane–triphenylphosphine at room temperature affording the corresponding dichloro compounds 2, whereas the chirality is preserved at higher reaction temperatures.**

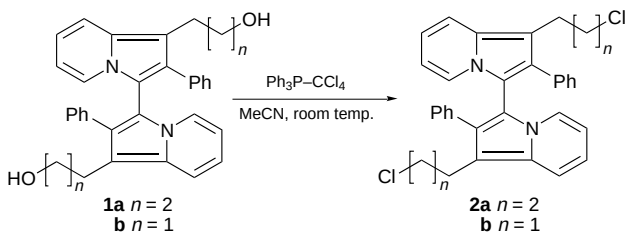
Axial-chiral ligands, especially binaphthyls, play an important role in asymmetric synthesis.[1] Recently, we reported the chirality of biindolizines[2] and the enzyme-catalysed kinetic resolution of racemic bis(hydroxyalkyl)biindolizines.[3] To further extend the utility of this new chiral source, *e.g.* as chiral modifiers and complex ligands in homogeneous catalysis, we attempted the preparation of derivatives of the non-racemic chiral diols **1a** and **1b**.

First attempts using the racemic diols (±)-**1a** and (±)-**1b** showed that the chlorination with triphenylphosphine and tetrachloromethane[4] is a useful method for the synthesis of the corresponding racemic bis(chloroalkyl)biindolizines (±)-**2a** and (±)-**2b**, respectively. By addition of acetonitrile to the reaction mixture the conversion takes place at room temperature.

Application of these mild conditions to the conversion of the enantiomerically pure diols (−)-**1a** and (+)-**1b** to the corresponding dichloro compounds surprisingly resulted in complete racemization‡ affording (±)-**2a** and (±)-**2b**, respectively, despite the fact that there are four or five bonds between the chirality axis and the reacting carbon atom.

The reaction at higher temperatures revealed an unusual and unexpected behaviour of the enantiomerically pure diols (−)-**1a** and (+)-**1b** depending on the reaction conditions. Reaction of (−)-**1a** with an ee of 98% in refluxing tetrachloromethane in the absence of acetonitrile furnished the dichloro compound (−)-**2a**§ with an ee of 96%. In order to investigate the influence of acetonitrile on the outcome of the reaction, acetonitrile was added to the refluxing solution of the diol (−)-**1a** and triphenylphosphine in tetrachloromethane. This treatment did not influence the enantiomeric excess of the dichloro compound (−)-**2a** (ee 98%) formed, but as expected, the reaction rate was drastically increased.

In comparison with (±)-**1a** the diol (±)-**1b** is less reactive. Only in the presence of acetonitrile does the chlorination proceed in good yields. In contrast to the results described before, the conversion of the diol (+)-**1b** with an ee of 98% led, in the presence of triphenylphosphine in refluxing tetrachloromethane and subsequent addition of acetonitrile, to a partial racemization affording the dichloro compound (+)-**2b**§ with an ee of only 63%. Therefore, it seemed promising to enhance the reaction temperature to suppress further racemization. This was realised by addition of triphenylphosphine to a refluxing solution of (+)-**1b** in tetrachloromethane–toluene–acetonitrile (2:5:1) yielding (+)-**2b** with an ee of 87%. These results clearly demonstrate that increased reaction temperatures suppress the racemization during the chlorination of (−)-**1a** and (+)-**1b** to (−)-**2a** and (+)-**2b**, respectively, under the described conditions. The results are summarized in Table 1.




**1a** *n* = 2
**b** *n* = 1

**2a** *n* = 2
**b** *n* = 1

**Scheme 1** Chlorination of **1a** and **1b** by $PPh_3$–$CCl_4$

Results published recently by K. Fuji *et al*. on the unexpected racemization of 8-diphenylphosphinoyl-8′-methoxy-1,1′-binaphthyl[5] illustrate the difficulties in explaining such a surprising loss of axial chirality. Based on the crystal structure, the authors suggest that a strong destabilisation of the ground state of this compound is responsible for the racemization.

The different substitution of the biindolizines **1** and **2** should not have an influence on the configurational stability as a result of the different torsion angles between the coupled heterocyclic systems. Each enantiomer of **2a** and **2b** exists independently. There is every indication that in our case both the twisted and normally rotation-hindered aromatic systems are each forced to occupy coplanar configurations during the time-scale of the conversion of the biindolizines. Such a coplanar transition state or intermediate could be explained by intramolecular interactions between the 'α- and ω-end' of the molecule. Particularly, a strong strained cyclic species is imaginable, cancelling the twisting of the coupled indolizines.

We have no evidence concerning the nature of such a cyclic species and thus can only speculate. Possibly, the low reactivity of **1a** and **1b** is responsible for the formation of a cyclic transition state or intermediate. Therefore, only the bifunctional intermediate $Ph_3P^+CCl_2P^+Ph_3$, $2Cl^-$ **3**[4] reacts with the diol to give the dichloro compounds **2a** and **2b** quickly at room temperature. Fig. 1 shows the imaginable addition product **4**—formed by reaction of the diol **1b** with the described dication **3**—causing a small torsion angle between the two heterocyclic systems. At higher temperatures this intermediate is unfavoured because the system reacts before **4** is formed. This assumption is in accordance with our observation that the less reactive diol **1b** tends to racemize even at higher temperatures. Obviously, even in refluxing tetrachloromethane the reaction partially takes place *via* a coplanar intermediate such as **4**. Only more drastic conditions allowed an almost complete chirality conservation.

**Table 1** The influence of the reaction conditions on the degree of racemization by chlorination of non-racemic **1a** and **1b**

| | | Product ees under various reaction conditions (%) | | |
|---|---|---|---|---|
| Product **2** | Ee of starting material (%) | $CCl_4$–MeCN (5:1), room temperature | $CCl_4$–MeCN (30:1), reflux | $CCl_4$–MeCN–PhMe (2:1:5), reflux |
| **a** | 98 | 0 | 98 | — |
| **b** | 98 | 0 | 63 | 87 |

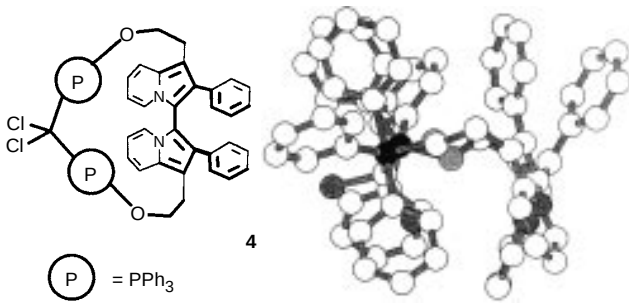



**Fig. 1** Structures of the assumed cyclic intermediate **4** generated through HYPERCHEM (release 4, $MM^+$, optimised by Polak-Ribiere)

Nevertheless, we have found a possible method to prevent the unexpected racemization and to obtain the 1,1′-bis(chloroalkyl)-3,3′-biindolizines **2a** and **2b** in high enantiomeric excess. We are also looking for other chlorination methods to obtain enantiomerically pure dichloro compounds.

## Footnotes

† E-mail: theil@aca.fta-berlin.de

‡ The ee was determined by HPLC on Chiralpak AD with heptane–propan-2-ol (95 : 5).

§ The dichlorides were successfully characterised by $^1H$ and $^{13}C$ NMR spectroscopy, MS and elemental analysis. *Selected data* (NMR in $CDCl_3$/$SiMe_4$, *J* in Hz): for (±)-**2a**: $^1H$ NMR δ 7.46 (d, *J* 9.1, 2 H), 7.24 (d, *J* 6.4, 2 H), 7.08 (m, 6 H), 6.79 (dd, *J* 7.8 and 1.7, 4 H), 6.70 (dd, *J* 8.6 and 6.8, 2 H), 6.37 (ddd, *J* 6.8 and 0.9, 2 H), 3.40 (t, *J* 6.5, 4 H), 2.97 (t, *J* 7.3, 4 H) and 1.92 (t, *J* 7.3, 4 H). $^{13}C$ NMR δ 135.2 (s), 131.4 (s), 130.9 (s), 129.7 (d), 127.9 (d), 126.2 (d), 122.9 (d), 117.3 (d), 116.9 (d), 111.5 (s), 110.5 (d), 109.9 (s), 44.7 (t), 33.9 (t) and 21.3 (t). *m/z* (CI): 536 [$(M + H)^+$, 100%]. (−)-**2a**: $[\alpha]_D^{20}$ −4.5, (*c* 0.4, THF), 96% ee. For (±)-**2b**: $^1H$ NMR δ 7.46 (td, *J* 9.0 and 1.0, 2 H), 7.26 (td, *J* 6.9 and 1.0, 2 H), 7.10 (m, 4 H), 6.76 (m, 6 H), 6.42 (dt, *J* 6.8 and 1.2, 4 H), 3.52 (m, 4 H) and 3.25 (m, 4 H). $^{13}C$ NMR δ 134.6 (s), 131.8 (s), 131.2 (s), 129.0 (d), 128.0 (d), 126.5 (d), 123.1 (d), 117.5 (d), 117.2 (d), 111.6 (s), 110.9 (d), 107.4 (s), 44.5 (t) and 28.2 (t). *m/z* (FAB-MS): 508 [$M + H^+$), 100%]. (+)-**2b**: $[\alpha]_D^{20}$ + 17.2, (*c* 1, THF), ee 87%.

## References

1 C. Rosini, L. Franzini, A. Raffaeli and P. Salvadori, *Synthesis*, 1992, 503; R. Noyori, *Asymmetric Catalysis in Organic Chemistry*, Wiley, New York, 1994.
2 H. Sonnenschein, T. Kreher, E. Gründemann, R.-P. Krüger, A. Kunath and V. Zabel, *J. Org. Chem*., 1996, **61**, 710.
3 F. Theil, H. Sonnenschein and T. Kreher, *Tetrahedron: Asymmetry*, 1996, **7**, 3365.
4 R. Appel, *Angew. Chem*., 1975, **87**, 863; *Angew. Chem., Int. Ed. Engl*., 1975, **14**, 801; B. R. Castro, *Org. React*., 1983, **29**, 1.
5 K. Fuji, M. Sakurai, N. Tohkai, A. Kuroda, T. Kawabata, Y. Fukazawa, T. Kinoshita and T. Tada, *Chem. Commun*., 1996, 1609.

*Received, 13th November 1996; Com. 6/07703J*

# Concurrent reduction and modification of polyaniline emeraldine base with pyrrolidine and other nucleophiles

**Chien-Chung Han* and Rong-Chyuan Jeng**

*Department of Chemistry, National Tsing Hua University, Hsinchu, Taiwan 300, Republic of China*

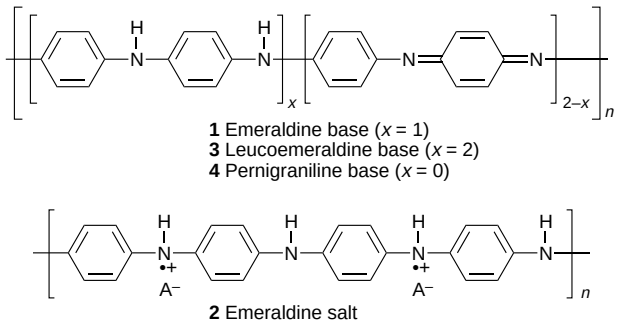
**Polyaniline emeraldine base 1 can be easily modified by pyrrolidine and other nucleophiles, *e.g.* piperidine, morpholine, alkane-1-thiols and mercaptoacetic acid, presumably *via* a concurrent reduction and substitution mechanism.**

Among other conducting polymers, polyanilines are of particular interest in light of their unique electro-optical properties and market potential.[1,2] Although undoped (neutral) polyaniline, *i.e.* the emeraldine base **1** (Scheme 1), can be solution processed more easily than other conducting polymers, doped (conductive) polyanilines, *i.e.* the emeraldine salts **2**, cannot be processed easily. The difficulty encountered in solution processing the emeraldine salts **2** has recently been alleviated by an *in situ* de-doping and re-doping process,[3,4] and also by a counter-ion induced solubility approach.[4–6] In our previous attempt to develop the *in situ* de-doping and re-doping solution processing chemistry,[7] we found that many Lewis base solvents, *e.g.* pyrrolidine, piperidine and morpholine, are highly effective solvents for emeraldine salts[8] and emeraldine base.[9] Highly conductive coatings with good optical quality can be directly prepared from the fresh pyrrolidine solutions of emeraldine base **1** or emeraldine salts **2**. In those previous works, we also found some mysterious aging phenomena happened to those cyclic amine solutions. The polyaniline coatings prepared from such aged solutions were somehow less conductive.

In this work, we explore the nature of this aging chemistry to find possible means for prevention. These results actually suggest a very interesting concurrent reduction and substitution chemistry between polyaniline and nucleophiles. This new chemistry provides a facile approach for modifying a polyaniline backbone with various electron-donating groups, *e.g.* amino, alkylthio and alkoxy.

When polyaniline emeraldine base **1** was stirred in pyrrolidine for 96 h, the solution's colour gradually changed from blue to purple, and finally to purple–brown. The resultant polymer was precipitated with a large amount of $Et_2O$, collected, rinsed with copious amounts of acetone, and then dried at 90 °C under dynamic vacuum for 12 h to remove any solvent residues. The obtained polymer sample was free of the strong odour of pyrrolidine and had no weight loss up to 130 °C by thermogravimetric analysis. The solid state $^{13}C$ CPMAS (cross-polarization magic angle spinning) NMR spectrum of the resultant polymer, Fig. 1, strongly suggests that emeraldine base **1** has been reduced and the pyrrolidino substituents subsequently added. The new $sp^3$ carbon signals at *ca.* δ 25 and 52 are similar to those chemical shifts of pyrrolidine,† confirming the presence of pyrrolidino fragments. Correspondingly, a decrease in the peak intensity of *ca.* δ 157 (the characteristic peaks of the imine quinoid rings assigned by Kaplan *et al.*[10]) and an increase at *ca.* δ 135 and 120 (characteristic peaks of the amine benzenoid rings[10]) confirmed the reduction of polyaniline. These results suggest that some of the imine quinoid rings are converted to amine benzenoid rings while introducing pyrrolidino substituents. Except for no $sp^3$ carbons, similar NMR signal variation behaviour in the aromatic region [Fig. 1(*d*)] was observed when emeraldine base **1** was reduced by hydrazine to form leucoemeraldine base **3**. Our NMR results clearly indicated that the amounts of new $sp^3$ carbons and the degrees of reduction of emeraldine base **1** simultaneously increased with reaction time. Thus, the above results strongly suggest that the reduction and substitution events were actually concurrent.

The IR spectroscopic results in Fig. 2 also verify the presence of pyrrolidino substituents. The intensity of the newly appeared $sp^3$ C–H stretching peaks among 2800–3000 $cm^{-1}$, as caused by the pyrrolidino attachment, increased with the reaction time.




**Scheme 1**

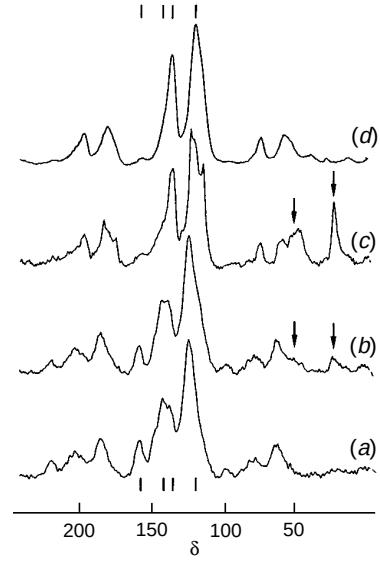



**Fig. 1** Solid state $^{13}C$ CPMAS NMR spectra for various polyanilines measured at 50.3 MHz at a spinning speed of about 3 kHz. The NMR spectrum (*a*) is for emeraldine base; (*b*) and (*c*) are for emeraldine bases after reacting with pyrrolidine for 10 min and 96 h, respectively; and (*d*) is for leucoemeraldine base. Vertical bars are placed at δ 157, 143, 135 and 120. Arrow marks are placed at δ 52 and 25.

Also, the relative degrees of reduction of the resulted polyanilines increased simultaneously with reaction time, as indicated by the increase in intensity at around 1500 $cm^{-1}$ (C=C stretching vibration of amine benzenoid rings) relative to that at 1600 $cm^{-1}$ (C=C stretching vibration of imine quinoid rings).[11] The new peaks at 960 $cm^{-1}$ and the shoulder at 925 $cm^{-1}$ might be caused by the newly formed 1,2,4-trisubstituted benzene ring.[12] The reduction phenomenon of emeraldine base **1** induced by pyrrolidine has also been confirmed by UV–VIS spectroscopy. The fact that polyaniline emeraldine **1** was slowly reduced by pyrrolidine toward the less conductive leucoemeraldine form explains why the polyaniline coatings prepared from the aged solutions were less conductive.

The same concurrent reduction and substitution chemistry is applicable to other cyclic amine systems, *e.g.* piperidine and morpholine. In both cases, $^{13}C$ CPMAS NMR and IR spectroscopy confirmed that the resultant polymers (after thoroughly washed and dried) were partially reduced and substituted with piperidino and morpholino fragments, respectively. The $^{13}C$ NMR for the piperidine-treated polyaniline showed new $sp^3$ carbons at *ca.* δ 25 and 52 and those for the morpholine-treated polyaniline at *ca.* δ 52 and 68, similar to those chemical shifts of piperidine and morpholine, respectively.† A model compound, *N,N′*-diphenylphenylene-1,4-diimine, also reacted with pyrrolidine *via* the same reductive substitution chemistry, yielding a pyrrolidino-substituted *N,N′*-diphenylphenylene-1,4-diamine.‡

This chemistry can also be extended to other nucleophile systems, *e.g.* thiols and alcohols. Our preliminary results indicate that alkanethiols, such as dodecane-1-thiol and butane-1-thiol, react at a much higher rate (*ca.* 1000 times faster) than amines. Since dodecane-1-thiol contains greater number of $sp^3$ carbons, the IR spectrum for the dodecanethiol-treated polyaniline, Fig. 2(*d*), showed much stronger $sp^3$ C–H stretching vibration signals among 2800–3000 $cm^{-1}$. Although the above polymer was identified by elemental analysis to contain 20.7 mol% of dodecylthio group basing on aniline repeat unit, it was free of any odour of thiol. The cyclic voltammograms of the resultant polymers did not behave any more like the unsubstituted polyaniline, but rather resembled to the polyanilines substituted with electron-donating groups, such as polyanisidine and polyphenetidine. The nature of the S atoms in the sample was characterized by X-ray photoelectron spectroscopy. The S 2p line was measured to be at 163.5 eV, confirming the formation of sulfide, but not disulfide or thiol.§ These dodecylthio-substituted leucoemeraldine bases can be converted back to their corresponding emeraldine forms by oxidaton with *m*-chloroperoxybenzoic acid. Additional dodecylthio groups can be attached by repeating the reductive substitution chemistry with dodecane-1-thiol. We have found that the multiple reduction–oxidation modification cycles can be most conveniently carried out by an electrochemical process. In another example, we have also succeeded in attaching mercaptoacetic acid to the backbone of polyaniline, forming a self-doping polyaniline. The carboxylic acid groups remained at the polyaniline backbones even after thorough de-doping treatments with bases.

A possible reaction mechanism is as follows. Protonation of the imine nitrogen could possibly promote the nucleophilic attack of pyrrolidine (and other nucleophiles) at the *meta*-position of the protonated quinoid ring, followed by a 1,3-proton shift of the *meta*-proton to the *para*-imine nitrogen and, ultimately, a conversion of the less stable quinoid ring to the more stable benzenoid.

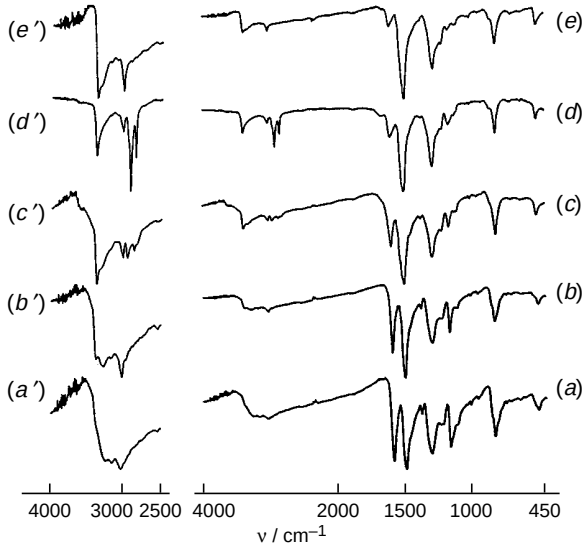



**Fig. 2** IR spectra for various polyanilines are obtained in the transmission mode using KBr pellets at a nominal resolution of 8 $cm^{-1}$ and co-adding 16 scans, IR trace (*a*) is for emeraldine base; (*b*) and (*c*) are for the emeraldine bases after reacting with pyrrolidine for 10 min and 96 h, respectively; and (*e*) is for leucoemeraldine base. Trace (*d*) is for the dodecanethiol-modified emeraldine base. Those corresponding blowup spectra for the 2500–4000 $cm^{-1}$ regions (with arbitrary magnifications) are displayed in traces (*a′*)–(*e′*).

## Footnotes

† For pyrrolidine, $\delta_C$ 25.64 and 47.20; for piperidine, $\delta_C$ 25.21, 27.32 and 47.53; for morpholine, $\delta_C$ 46.61 and 68.15.

‡ $^{13}C$ NMR data for pyrrolidino-substituted *N,N′*-diphenylphenylene-1,4-diamine, $\delta_C$ 24.8, 47.5, 112.3, 113.6, 117, 122.5, 128.9, 131.1, 143.7 and 146.5; for *N,N′*-diphenylphenylene-1,4-diamine, $\delta_C$ 115, 118.2, 119.6, 128.93, 136.4, and 144.8. For *N,N′*-diphenylphenylene-1,4-diimine, $\delta_C$ 120.25, 120.38, 124.35, 125.04, 125.08, 125.29, 136.39, 137.7, 149.8, 149.83, 157.84 and 157.9, complicated by the presence of both *E* and *Z* forms (ref. 13).

§ The S 2p line was reported to be 163.66 eV for poly(phenylene sulfide) and 163.50 eV for poly(ethylene sulfide); 164.4 eV for phenyl disulfide and 164.1 eV for butyl disulfide; 163.1 eV for thiophenol and 161–163 eV for alkanethiols (ref. 14).

## References


1 *Handbook of Conducting Polymers*, ed. T. A. Skotheim, Marcel Dekker, New York and Basel, 1986, vols. 1 and 2.
2 E. M. Genies, A. Boyle, M. Lapkowski and C. Tsintavis, *Synth. Met.*, 1990, **36**, 139.
3 C. C. Han, L. W. Shacklette and R. L. Elsenbaumer, *Solution Processing of Conductive Polyaniline*, at MRS meeting, Dec. 1991, Boston, MA.
4 C. C. Han, *Solution Processing of Conductive Polyaniline*, in Chemistry Colloquium at University of Polytech, Brooklyn, New York City, Dec. 1991 and University of Rhode Island, April 1992.
5 C. C. Han, *Solubility Modification of Conductive Conjugated Backbone Polymers* Via *Dopant Moieties*, WO 9 305 519 A1 930 318 (1993) and EP 0601 105 A1 940 615 (1994).
6 Y. Cao, P. Smith and A. J. Heeger, *Synth. Met.*, 1992, **48**, 91.
7 C. C. Han, R. L. Elsenbaumer, L. W. Shacklette and G. G. Miller, WO 9 211 644 A1 92 0709 (1992).
8 C. C. Han, R. L. Elsenbaumer and L. W. Shacklette, WO 9 211 645 A1 920 709 (1992).
9 C. C. Han, L. W. Shacklette and R. L. Elsenbaumer, WO 9 218 572 A2 921 029 (1992).
10 S. Kaplan, E. M. Conwell, A. F. Richter and A. G. MacDiarmid, *Synth. Met.*, 1989, **29**, E235.
11 F. Wudl, R. O. Angus Jr., P. M. Allemand, D. J. Vachon, M. Norwak, Z. X. Liu and A. J. Heeger, *J. Am. Chem. Soc.*, 1987, **109**, 3677.
12 F. Lux, E. J. Samuelsen and E. T. Kang, *Synth. Met.*, 1995, **69**, 167.
13 T. Hjertberg and M. Sandberg, *Synth. Met.*, 1989, **29**, E257.
14 G. Beamson and D. Briggs, *High Resolution XPS of Organic Polymers*, Wiley, New York, 1992; *Handbook of X-ray Photoelectron Spectroscopy*, Perkin-Elmer Corporation and references cited therein.


*Received, 29th November 1996; Com. 6/08079K*

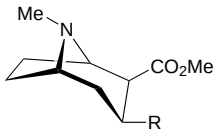
# Synthesis of the isomers of (1*R*)-3-(phenylthio)tropane-2-carboxylic acid methyl ester. A new class of ligands for the dopamine transporter

**Mohan Thiruvazhi,[a] Philip Abraham,[a] Michael J. Kuhar[b] and F. Ivy Carroll[a*]**

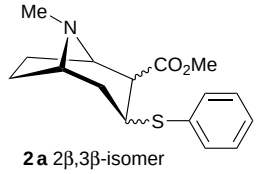
[a] *Chemistry and Life Sciences, Research Triangle Institute, Post Office Box 12194, Research Triangle Park, NC 27709, USA*
[b] *National Institute on Drug Abuse, Addiction Research Center, Post Office Box 5180, Baltimore, MD 21224, USA*

**The syntheses of all four isomers of (1*R*)-3-(phenylthio)tropane-2-carboxylic acid methyl ester are described; the 2β,3β-isomer shows high affinity for the cocaine binding site on the dopamine transporter.**

The behavioural and reinforcing properties of (−)-cocaine **1a** are attributed to its inhibition of dopamine (DA) reuptake.[1,2] We and others have reported that analogues of 3β-(phenyl)tropane-2β-carboxylic acid methyl ester **1b** (WIN 35,065-2) were more potent than cocaine in inhibiting radioligand binding to the cocaine binding site on the dopamine transporter (DAT).[3] However, to the best of our knowledge cocaine analogues possessing a sulfur substituent directly attached to the C-3 position on the tropane ring have not been reported.



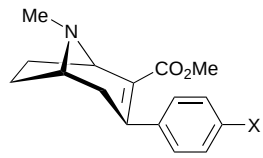

**1a** R = OC(O)Ph
**b** WIN 35,065-2: R = Ph



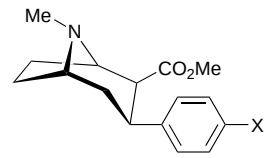

**2 a** 2β,3β-isomer
**b** 2α,3β-isomer
**c** 2β,3α-isomer
**d** 2α,3α-isomer

Here we describe the synthesis of the four possible isomers of (1*R*)-3-(phenylthio)tropane-2-carboxylic acid methyl ester **2a**–**d**. Compound **2a** has the same stereochemistry as **1b** and differs from **1b** by having a sulfur atom between the 3β-phenyl group and the tropane ring system.

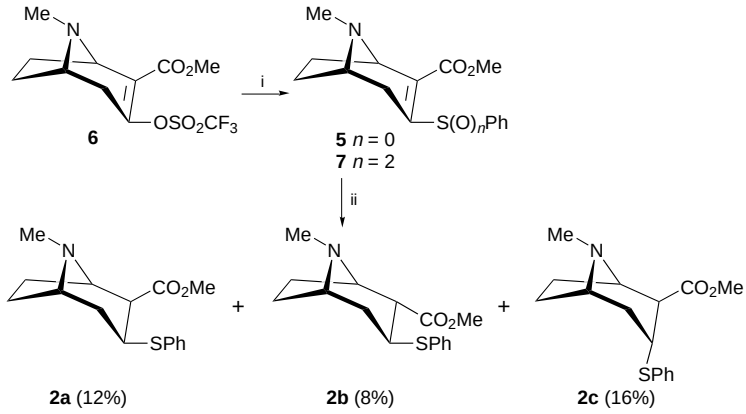
We recently reported that samarium iodide reduction of tropene **3** provided a new synthesis of **4**.[4] This result suggested that the synthesis of (1*R*)-3-(phenylthio)trop-2-ene-2-carboxylic acid methyl ester **5** followed by its reduction with samarium iodide[4,5] might afford the 2β,3β isomer **2a**. We found that treatment of (1*R*)-3-(trifluoromethylsulfonyloxy)trop-2-ene-2-carboxylic acid methyl ester **6**[4] with the sodium salt of thiophenol in THF gave **5** in 86% yield (Scheme 1).† We also found that the sodium salt of benzenesulfinic acid displaced the trifluoromethylsulfonyloxy substituent from **6** to afford the 3-(phenylsulfonyl)trop-2-ene-2-carboxylic acid methyl ester **7** in 78% yield.[6] At −78 °C, slow syringe-pump addition of a methanolic solution of **5** to samarium iodide in THF gave 85%



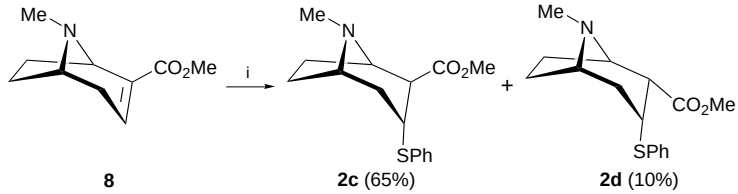

**3**




**4**




**Scheme 1** *Reagents and conditions*: i, for **5**: NaSPh, THF (86%); for **7**: benzenesulfinic acid sodium salt, DMF (78%); ii, $SmI_2$, inverse addition, MeOH −78 °C




**Scheme 2** *Reagents*: i, PhSH, $Et_3N$

of a 15 : 3 : 1 ratio of **2a**, **2b** and **2c**, respectively. None of the 2α,3α isomer **2d** was produced. Silica gel flash column chromatography[7] [$Et_3N$–$Et_2O$–hexanes (1 : 9 : 10)] was used to separate **2b** ($R_f$ 0.25, 8%) from **2a** and **2c** ($R_f$ 0.35). The **2a** and **2c** isomers were separated by HPLC on a silica gel column using $Et_3N$–$Pr^iOH$–hexanes (1 : 99 : 1900) as the eluent system to afford individual isomers **2a** and **2c** in 12 and 16% yields, respectively. The 2β,3β isomer **2a** had mp 55–57 °C (fusion) and $[\alpha]_D$ −83.19 (*c* 0.47, MeOH) for its (+)-tartrate salt. The (+)-tartrate salt of compound **2b** had mp 143–144 °C and $[\alpha]_D$ +49.9 (*c* 0.22, MeOH), and **2c** (+)-tartrate had mp 53–58 °C (fusion) and $[\alpha]_D$ of −37.17 (*c* 0.955, MeOH).

The 2α,3α isomer **2d** was prepared as shown in Scheme 2. Nucleophilic addition of thiophenol to anhydroecgonine methyl ester **8**[8] in the presence of $Et_3N$ gave, after 24 h, the 2β,3α isomer **2c** and 2α,3α isomer **2d**. Silica gel flash chromatography using $Et_3N$–$Et_2O$ (1 : 4) gave **2c** ($R_f$ 0.91, 65%) and **2d** ($R_f$ 0.29, 10%), respectively. Compound **2d** had mp 179–180 °C and an $[\alpha]_D$ +60.4 (*c* 0.106, MeOH) for its hydrochloride salt. Reaction times of several days afforded, after purification, a 1.2:1 ratio of **2c** and **2d** in 75% overall yield. In either case, the nucleophile shows complete preference for an α-face attack on **8**, possibly due to steric hindrance provided by the *N*-methyl group. The formation of two products may be a consequence of complete facial bias during protonation of the intermediate enol ester to give **2c** followed by partial base-catalysed epimerization of H-2 to afford **2d**. Again, the base-catalysed epimerization of **2c** at C-2 could be forced by an unfavourable steric repulsion between the *N*-methyl and the 2-methoxycarbonyl group. Basic conditions encourage facile elimination of thiophenol from **2d** to give **8**. Neither of the isomers **2a** or **2b** were observed in the above reaction when the sodium salt of thiophenol was replaced by the lithium or magnesium salts.

Two dimensional NMR experiments (COSY and HETCOR) aided in chemical shift assignments, while the *J* values and NOESY experiments were used to decipher the stereochemical relationship of the C-2 and C-3 substituents in the **2a**–**d** isomers. For example, **2b** has a large $J_{2,3}$ value of 12.0 Hz, expected for their *anti* disposition. On the contrary, $J_{2,3}$ for **2a**, **2c** and **2d**, were 5.2, 1.1 and 6.9 Hz, respectively. Most importantly, H-2 in **2b** showed an NOE with N-Me and H-$4_{ax}$, while H-3 showed an NOE with H-$6_{ax}$ and H-$7_{ax}$. The observed NOE results are possible *only if* **2b** exists in a chair conformation with H-2 and H-3 in diaxial positions (Fig. 1). Using similar arguments, **2a**, **2c** and **2d** were shown to possess the relative stereochemistry and conformation as displayed in their corresponding structures. It was also interesting to note that the proton spectra patterns of **2a**–**d** resemble those of the corresponding cocaine isomers.[9]

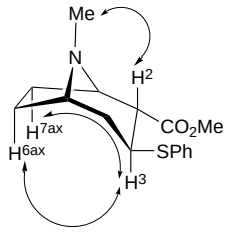



**Fig. 1** Structure of **2b** with selected NOE effects

Binding data on **2a**–**d** revealed that the 2β,3β isomer **2a** was the most potent ($IC_{50}$ 14.3 nm $dm^{-3}$) at the cocaine binding site of the dopamine transporter. The other isomers **2c** ($IC_{50}$ 183 nm $dm^{-3}$), **2d** ($IC_{50}$ 222 nm $dm^{-3}$) and **2b** ($IC_{50}$ 613 nm $dm^{-3}$) were only moderately potent. It is interesting to note that **2a** is slightly more potent than the lead compound, WIN 35065-2 ($IC_{50}$ 23 nm $dm^{-3}$). Since substitution of the phenyl group of the WIN 35,065-2 series was found to increase potency,[3] substituted phenyl analogues of **2a**, and even **2c**–**d**, may be more potent. Studies along this line are underway, and results will be reported in due course.

This research was supported by the National Institute on Drug Abuse, Grant DA05477. We thank Dr Jason P. Burgess for performing the two dimensional NMR experiments, and Dr Pravin Kotian and Dr Yigong Gao for help in the synthesis of **2d**.

## Footnote

† All new compounds showed satisfactory elemental analyses.

## References

1 F. I. Carroll, A. H. Lewin, J. W. Boja and M. J. Kuhar, *J. Med. Chem*., 1992, **35**, 969.
2 M. J. Kuhar, M. C. Ritz and J. W. Boja, *Trends Neurosci*., 1991, **14**, 299.
3 F. I. Carroll, A. H. Lewin and M. J. Kuhar, *Neurotransmitter Transporters: Structure, Function, and Regulation*, ed. M. E. A. Reith, Humana Press Inc., Totowa, NJ, 1997, p. 263.
4 K. I. Keverline, P. Abraham, A. H. Lewin and F. I. Carroll, *Tetrahedron Lett*., 1995, **36**, 3099.
5 P. Girard, J. L. Namy and H. B. Kagan, *J. Am. Chem. Soc*., 1980, **102**, 2693.
6 For another incident of such an addition-displacement reaction, see T. A. Crowell, B. D. Halliday, J. H. McDonald, III, J. M. Indelicato, C. E. Pasini and E. C. Y. Wu, *J. Med. Chem*., 1989, **32**, 2436.
7 W. C. Still, M. Kahn and A. Mitra, *J. Org. Chem*., 1978, **43**, 2923.
8 R. L. Clarke, S. J. Daum, A. J. Gambino, M. D. Aceto, J. Pearl, M. Levitt, W. R. Cumiskey and E. F. Bogado, *J. Med. Chem*., 1973, **16**, 1260.
9 F. I. Carroll, M. L. Coleman and A. H. Lewin, *J. Org. Chem*., 1982, **47**, 13.

*Received, 6th December 1996; Com. 6/08238F*

# Synergistic oxidation of cyclohexane and hydrogen sulfide under Gif conditions

**Derek H. R. Barton,* Tingsheng Li and John MacKinnon**

*Department of Chemistry, Texas A&M University, College Station, TX 77843-3255 USA*

**Saturated hydrocarbons and hydrogen sulfide can be synergistically oxidised by oxygen (or air) to give efficiently ketones (and the corresponding alcohols) and sulfur in the presence of a Gif catalyst based on $Fe^{II}$, picolinic acid and 4-*tert*-butylpyridine with acetonitrile as solvent at room temperature and nearly neutral pH.**

We report an unusual reaction in which cyclohexane is oxidised to cyclohexanol and cyclohexanone whilst at the same time hydrogen sulfide is converted to sulfur. The only oxidant needed is oxygen or air.

In recent publications[1,2] we have presented a coherent theory of Gif ketonization chemistry. From the practical point of view the selective functionalization of hydrocarbons to furnish ketones, or other derivatives selectively substituted at secondary positions, requires the right kind of carboxylate ligands as, for example, in picolinic acid.[1] Exactly two picolinic acids are bonded to $Fe^{III}$ as determined by quantitative $^{13}C$ NMR studies.[3] There is also an essential need for a certain kind of pyridine ligand as, for example, in 4-*tert*-butylpyridine or in pyridine itself. One of these ligands[2] is bonded to $Fe^{III}$. In practise, about 15 equiv. per $Fe^{III}$ of the pyridine base give optimal results. As solvent the inert acetonitrile is satisfactory.

There are two ways in which the activated iron species can be formed.[1] The first is by addition of superoxide to $Fe^{II}$. This has been well established by electrochemical studies.[4] The second is by substitution chemistry on $Fe^{III}$ by $H_2O_2$.

It occurred to one of us (D.H.R.B.) that if $Fe^{II}$ and $O_2$ would furnish superoxide (and $Fe^{III}$) then the latter would react with more $Fe^{II}$ to make the activated iron species and hence permit entry to Gif ketonization chemistry. If the $Fe^{III}$ formed in the first step could be reduced by $H_2S$ to give $Fe^{II}$ and sulfur then it should be possible to concert the oxidation of saturated hydrocarbons to ketone (and alcohol) with the oxidation $H_2S$ to sulfur. Indeed we have recently established that $Fe^{III}$ is rapidly reduced to $Fe^{II}$ by $H_2S$.[5]

In this way we would be able to coordinate the oxidation of (say) cyclohexane to cyclohexanone (and alcohol) with the removal of toxic hydrogen sulfide from (say) natural gas. The methane and ethane in the natural gas would not react under Gif conditions as evidenced by prior experiments.

For those not initiated into the unusual reactivity seen in Gif chemistry (the Gif paradox) the above sequence might seem improbable.[6] However, whatever oxidation species is present does have a special affinity for saturated hydrocarbons. The latter activates the iron reagent to attack the secondary position and make a species which is not a radical. We still formulate this as an iron–carbon bond.[7]

Be all this as it may, the experimental facts confirm the hypothesis. Using hydrogen sulfide and oxygen, cyclohexane is converted to cyclohexanone and cyclohexanol at the same time that hydrogen sulfide is oxidised to sulfur (see Table 1).

In contrast to our prior work[6] there is no limitation on the conversion. The formation of ketone and alcohol remains quantitative even up to a conversion of 36%. In blank experiments cyclohexanone is not transformed into any other derivatives as it is in prior Gif chemistry.[8] Thus the limit of 20–30% on the convertion previously observed[6] no longer pertains. Cyclohexanol is slowly converted into cyclohexanone. It did not seem likely that carbon radicals would be playing a role in the presence of excess $H_2S$ and its derived radical H–S·. Indeed the addition of excess LiCl afforded no trace of cyclohexyl chloride. Of course, a blank experiment showed that cyclohexyl chloride did not react under the conditions of the oxidation. In agreement with Minisci[9] we accept that carbon radicals react rapidly with $Fe^{III}$–Cl species to make chloride.

As an industrial process, the selective oxidation of hydrocarbons is known to be very inefficient. The Dupont process converts cyclohexane to cyclohexanol and cyclohexanone in a 4% yield with 80% selectivity. The remaining 16% consists of various ring cleavage products and over oxidation products. The conversion is carried out at high temperatures (160 °C) and pressure (15 bar).[8] In this new system the reaction is carried out at room temperature and atmospheric conditions. Hydrogen sulfide (2–2.5 ml $min^{-1}$) and oxygen (25 ml $min^{-1}$) were simultaneously passed through a standard solution containing $Fe^{III}Cl_3$ (1 mmol), picolinic acid or its *N*-oxide (PA-N-oxide) (4 mmol), cyclohexane (20 mmol) and 4-*tert*-butylpyridine (15 mmol) in acetonitrile (33 ml). After a period of time the solution was filtered from the sulfur deposited and the mixture analysed. The efficiencies of the hydrocarbon oxidation are summarized in (Table 1).

Cyclohexane was oxidised to cyclohexanol and cyclohexanone with a 36% conversion after 9 h (Table 1, entry 3). When PA-N-oxide was used as a ligand, a conversion of 33% was achieved in 6 h (Table 1, entry 6). This oxidation procedure can be applied to different hydrocarbons (Table 1, entries 7 and 8).

**Table 1** Efficiency of oxidation of hydrocarbons with hydrogen sulfide and oxygen

| Entry | Hydrocarbon | mmol | Ligand | *t*/h | Ketone[a]/ mmol | Alcohol[a]/ mmol | Conversion (%) |
|---|---|---|---|---|---|---|---|
| 1 | Cyclohexane | 20 | Picolinic acid | 3 | 2.10 | 1.87 | 19.9 |
| 2 | Cyclohexane | 20 | Picolinic acid | 6 | 2.76 | 2.57 | 26.7 |
| 3 | Cyclohexane | 20 | Picolinic acid | 9 | 3.00 | 4.13 | 35.7 |
| 4 | Cyclohexane | 30 | PA-N-oxide | 2 | 2.65 | 3.15 | 19.3 |
| 5 | Cyclohexane | 30 | PA-N-oxide | 4 | 4.18 | 4.52 | 29.0 |
| 6 | Cyclohexane | 30 | PA-N-oxide | 6 | 4.97 | 4.90 | 32.9 |
| 7 | Cyclododecane | 20 | Picolinic acid | 6 | 4.01 | 2.41 | 32.1 |
| 8 | Cyclododecane | 20 | PA-N-oxide | 4 | 2.47 | 1.97 | 22.2 |

[a] The products were analysed by GC, naphthalene was used as internal standard.

Cyclododecane was converted to cyclododecanone and cyclododecanol with a 32% conversion after 6 h. Elemental sulfur was also formed and filtered.

A major limitation with hydrocarbon oxidation was over oxidation of the oxygenated products.[6,10] Blank experiments were carried out to investigate the inherent stability of the products of oxidation. The results are summarized in Table 2.

Both cyclohexanone and cyclododecanone were stable under the oxidative conditions outlined above. It was also shown that the ketone produced as the major oxidation product (Table 1) was not the result of over oxidation of the alcohol. Since essentially no over oxidation occurs over 36 h the possibility of nearly 100% conversion of the hydrocarbon is now a realistic target.

**Table 2** Stability of oxygenated products in hydrogen sulfide Gif oxidation[a]

| Starting material | Recovered ketone (%) | Recovered alcohol (%) | Others (%) |
|---|---|---|---|
| Cyclohexanone | 98.6 | — | —[a] |
| Cyclohexanol | 1.5 | 98.5 | —[b] |
| Cyclododecanone | 95.6 | — | 4.4[c] |

[a] $Fe^{III}Cl_3 \cdot 6H_2O$ (1 mmol), ligand (4 mmol), ketone or alcohol (20 mmol), 4-*tert*-butylpyridine (15 mmol), MeCN (33 ml). Oxygen and hydrogen sulfide were passed through the homogeneous solution for 4 h. The products were analysed by GC, naphthalene was used as internal standard. [b] Not detected. [c] Four diketones in minor amounts.

**Table 3** Conversion of cyclohexane to oxygenated products on a 784 mmol scale[a]

| Entry | *t*/h | Cyclohexanone/ mmol | Cyclohexanol/ mmol | Total/ mmol | Conversion (%) |
|---|---|---|---|---|---|
| 1 | 4 | 15.97 | 4.91 | 20.88 | 2.66 |
| 2 | 8 | 22.43 | 8.39 | 30.82 | 3.93 |
| 3 | 12 | 31.57 | 10.30 | 41.87 | 5.34 |
| 4 | 16 | 34.90 | 12.05 | 46.95 | 5.99 |
| 5 | 20 | 43.08 | 17.00 | 60.08 | 7.66 |
| 6 | 24 | 47.66 | 18.91 | 66.57 | 8.49 |
| 7 | 28 | 55.32 | 22.06 | 77.38 | 9.87 |
| 8 | 36 | 78.97 | 33.35 | 112.32 | 14.33 |

[a] $Fe^{III}Cl_3 \cdot 6H_2O$ (20 mmol), ligand (60 mmol), cyclohexane (784 mmol), 4-*tert*-butylpyridine (150 mmol), MeCN (80 ml). Oxygen and hydrogen sulfide were passed through the homogeneous solution. The solution was filtered to remove the sulfur deposited and the products were analysed by GC, naphthalene was used as internal standard.

**Table 4** Effect of the amount of $H_2S$ and $O_2$ on ketone/alcohol formation in presence of $Fe^{II}$[a]

| Entry | $H_2S$/ mmol | $O_2$/ ml $min^{-1}$ | *t*/h | Ketone/ mmol | Alcohol/ mmol | Sulfur/ mmol |
|---|---|---|---|---|---|---|
| 1 | 35 | 25 | 8 | 1.23 | 0.79 | 17 |
| 2 | 35 | 50 | 8 | 1.55 | 1.27 | 30 |
| 3 | 35 | 100 | 4 | 2.16 | 1.45 | 28 |
| 4 | 35 | 120 | 4 | 2.17 | 1.98 | 30 |
| 5 | 25 | 100 | 4 | 1.24 | 0.55 | 21 |
| 6 | 25 | 50 | 8 | 1.07 | 0.97 | 20 |
| 7 | 25 | 25 | 8 | 0.75 | 0.61 | 19 |
| 8 | 15 | 100 | 4 | 0.56 | 0.38 | 11 |
| 9 | 15 | 50 | 4 | 0.87 | 0.78 | 11 |
| 10 | 15 | 25 | 4 | 0.71 | 0.65 | 10 |
| 11 | 15 | 15 | 4 | 0.60 | 0.36 | 11 |

[a] $Fe^{II}Cl_2 \cdot 4H_2O$ (1 mmol), ligand (3 mmol), hydrocarbon (20 mmol), 4-*tert*-butylpyridine (15 mmol), MeCN (33 ml). Oxygen and hydrogen sulfide were passed through the homogeneous solution for 4–8 h. The products were analysed by GC, naphthalene was used as internal standard. The $H_2S$ is the total passed.

The oxidation of cyclohexane was not only limited to a 20 mmol scale. A large scale experiment was carried out (Table 3).

After 36 h the conversion of the hydrocarbon to ketone and alcohol was 14.33%. The lower conversion value was a result of a decrease in the rate of the reaction due to the increased hydrocarbon to solvent ratio. After filtration of the reaction mixture, 625 mmol of sulfur was obtained. In other experiments using variable $H_2S$ and $O_2$ flow rates the sulfur formed was quantified (Table 4).

When the flow rates of one or both of $H_2S$ and $O_2$ were varied from that of the standard flow rate (Table 4, entry 4), the total amount of ketone and alcohol decreased. A reasonable correlation between the amount of $H_2S$ used and that of sulfur obtained was seen.

We have developed an efficient new procedure for the selective oxidation of hydrocarbons to the corresponding ketone and alcohol by simply passing through a stream of oxygen and hydrogen sulfide. At the same time we have provided an efficient route to dispose of hydrogen sulfide gas. This synergistic oxidation of hydrocarbons and removal of hydrogen sulfide provides a route for the nearly quantitative conversion of hydrocarbons to their oxygenated products. It is a significant improvement on our original work.[10]

Although there is considerable prior work on the oxidation of saturated hydrocarbons by non-haem systems[11] the normal substitution pattern according to the C–H bond strength is followed. Gif chemistry is a separate subject.[1,6,12] In the present work, as in general,[1] if the picolinic acid or the pyridine base are omitted from the system then very little oxidation takes place. A detailed mechanistic discussion has not been presented. The reactions differ from normal only in the enhancement of alcohol relative to ketone.

We thank Quest International, the Welch Foundation, the N.S.F and the Schering Plough Corporation for the support of this work.

## References

1 D. H. R. Barton, B. Hu, D. K. Taylor and R. U. Rojas Wahl, *J. Chem. Soc., Perkin Trans. 2*, 1996, 1031.
2 D. H. R. Barton, B. Hu, T. Li and J. MacKinnon, *Tetrahedron Lett.*, 1996, **37**, 8329.
3 D. H. R. Barton; B. Hu, D. K. Taylor and R. U. Rojas Wahl, *New. J. Chem.*, 1996, **20**, 121.
4 D. H. R. Barton and A. Sobkowiak, *New J. Chem.*, 1996, **20**, 929 and references there cited.
5 D. H. R. Barton and B. Chabot, *Tetrahedron*, 1996, **52**, 10287.
6 D. H. R. Barton and D. Doller, *Acc. Chem. Res*., 1992, **25**, 504.
7 D. H. R. Barton, M. Costas and J. MacKinnon, unpublished results.
8 V. Schuchardt, W. A. Carvalho and E. V. Spinace, *Synlett*, 1993, 713.
9 F. Minisci, F. Fontana, S. Araneo and F. Recupero, *J. Chem. Soc., Chem. Commun.*, 1994, 1823; *Tetrahedron Lett*., 1994, **35**, 3759; F. Minisci and F. Fontana, *Tetrahedron Lett.*, 1994, **35**, 1427.
10 D. H. R. Barton, M. J. Gastiger and W. B. Motherwell, *J. Chem. Soc., Chem. Commun*., 1983, 41.
11 See, for example, G. K. Cook and J. M. Mayer, *J. Am. Chem. Soc*. 1995, 117, 7139.
12 W. Nam and J. S. Valentine, *New J. Chem*, 1989, **13**; C. Sheu, A. Sobkowiak, L. Zhang, N. Ozbalik, D. H. R. Barton and D. T. Sawyer, *J. Am. Chem. Soc*., 1989, **111**, 8030; C. Sheu, A. Sobkowiak, S. Jeon and D. T. Sawyer, *J. Am. Chem. Soc*., 1990, **112**, 879; C. Sheu, S. A. Rickert, P. Cofre, B. Ross, A. Sobkowiak, D. T. Sawyer and J. R. Kanofsky, *J. Am. Chem. Soc*., 1990, **112**, 1936; C. Sheu and D. T. Sawyer, *J. Am. Chem. Soc*., 1990, **112**, 8212, and later papers from the Sawyer group. Summarising article: V. Schuchardt, W. A. Carvalho and E. V. Spinace, *Synlett*, 1993, 713, and earlier papers there cited B. Singh, J. R. Long, G. C. Papaefthymiou and P. Stavropoulos, *J. Am. Chem. Soc.*, 1996, **118**, 5824.

*Received, 12th November 1996; Com. 6/07700E*

# New reaction mode of the Horner–Wadsworth–Emmons reaction using $Sn(OSO_2CF_3)_2$ and *N*-ethylpiperidine

**Shigeki Sano, Kenji Yokoyama, Mari Fukushima, Tetsuo Yagi and Yoshimitsu Nagao***

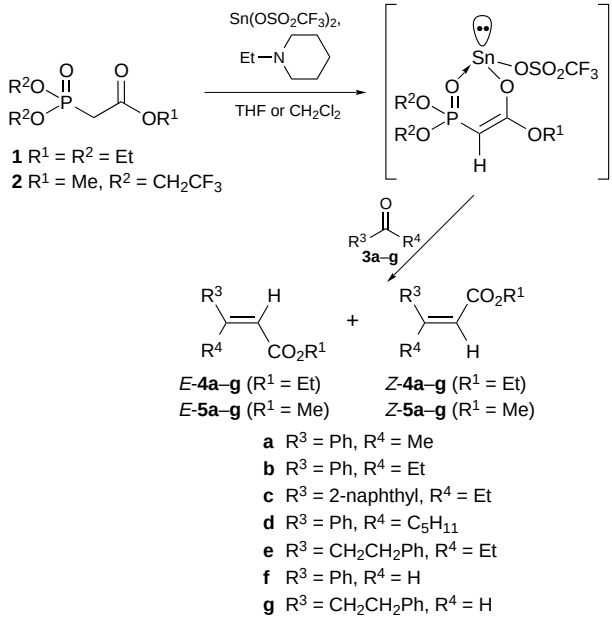
*Faculty of Pharmaceutical Sciences, The University of Tokushima, Sho-machi, Tokushima 770, Japan*

**Excellent *Z* or *E* selectivity is observed in the Horner–Wadsworth–Emmons reactions of methyl bis(trifluoroethyl)phosphonoacetate 2 with aryl alkyl ketones 3a–d or aldehydes 3f,g using $Sn(OSO_2CF_3)_2$ in the presence of *N*-ethylpiperidine, which should have a different reaction mode to those using sodium hydride.**

The Horner–Wadsworth–Emmons (HWE) reaction is one of the most efficient methods for the preparation of α,β-unsaturated esters.[1] The reactions of aldehydes with phosphonates bearing α-substituents that stabilise the carbanion preferentially furnish the corresponding *E*-alkenes. Various bases such as sodium hydride, butyllithium and sodium ethoxide have been employed in order to generate the phosphonate carbanions. In similar HWE reactions, mild olefination procedures using lithium and magnesium salts[2] in the presence of tertiary amines or with lithium hydroxide[3] are also available. Interestingly, the reactions of methyl bis(trifluoroethyl)phosphonoacetate **2**[4] or ethyl diphenylphosphonoacetate[5] with aldehydes selectively yield *Z*-alkenes. However, the stereoselectivity of their HWE reactions with ketones has never been investigated in detail because of their low reactivity and low stereoselectivity.[6]

Herein we describe the stereochemical outcome in the HWE reactions of ethyl diethylphosphonoacetate **1** and methyl bis(trifluoroethyl)phosphonoacetate **2** with some aryl alkyl ketones **3a**–**e** and aldehydes **3f**,**g** using $Sn(OSO_2CF_3)_2$ in the presence of *N*-ethylpiperidine, as shown in Scheme 1.† The results are shown in Tables 1–3.‡

The conventional HWE reactions of aryl alkyl ketones **3a**–**d** with phosphonate **1** in the presence of sodium hydride in THF at 0 °C and then at room temperature gave the corresponding α,β-unsaturated esters **4a**–**d** with modest *E* selectivity (Table 1, entries 1–4). On the other hand, treatment of **3b**–**d** and **1** with $Sn(OSO_2CF_3)_2$ in the presence of *N*-ethylpiperidine in THF at 0 °C afforded *Z*-alkenes **4b**–**d**, respectively, in a highly selective fashion (Table 2, entries 2–4). Under both sets of reaction conditions described above, the HWE reactions of aldehydes **3f**,**g** with **1** gave **4f**,**g** in the usual highly *E*-selective manner (Table 1, entries 6 and 7; Table 2, entries 6 and 7). Poor stereoselectivity was observed in both reaction systems for ketone **3e** (Table 1, entry 5; Table 2, entry 5). A significant




**Scheme 1**

**Table 1** NaH/THF mediated Horner–Wadsworth–Emmons reactions of **1** and **2** with ketones **3a**–**e** and aldehydes **3f**,**g**[a]

| Entry | Phosphono-acetate | Ketone or aldehyde | *t*/h | Yield (%)[b] | Alkene (*E*/*Z*)[c] |
|---|---|---|---|---|---|
| 1 | **1** | **3a** | 66 | 100 | **4a** (85:15) |
| 2 | **1** | **3b** | 72 | 100 | **4b** (62:38) |
| 3 | **1** | **3c** | 72 | 86 | **4c** (57:43) |
| 4 | **1** | **3d** | 72 | 88 | **4d** (51:49) |
| 5 | **1** | **3e** | 72 | 93 | **4e** (53:47)[d] |
| 6 | **1** | **3f** | 1 | 100 | **4f** (100:0) |
| 7 | **1** | **3g** | 1 | 79 | **4g** (97:3) |
| 8 | **2** | **3a** | 23 | 100 | **5a** (45:55) |
| 9 | **2** | **3b** | 23 | 93 | **5b** (39:61) |
| 10 | **2** | **3c** | 24 | 82 | **5c** (36:64) |
| 11 | **2** | **3d** | 24 | 91 | **5d** (35:65) |
| 12 | **2** | **3e** | 23 | 52 | **5e** (38:62)[d] |
| 13 | **2** | **3f**[e] | 3 | 100 | **5f** (15:85) |
| 14 | **2** | **3g**[e] | 3 | 94 | **5g** (8:92) |

[a] Conditions: THF, 0 °C to room temp., **1** or **2**/NaH/**3** (1.7 : 1.5 : 1). [b] Isolated yields. [c] $^1$H NMR (400 MHz, $CDCl_3$) analysis. [d] HPLC analysis (TSK-GEL Silica 60, hexane–propan-2-ol. [e] −78 °C.

**Table 2** $Sn(OSO_2CF_3)_2$/*N*-ethylpiperidine/THF mediated Horner–Wadsworth–Emmons reactions of **1** and **2** with ketones **3a–e** and aldehydes **3f,g**[a]

| Entry | Phosphono-acetate | Ketone or aldehyde | *t*/h | Yield (%)[b] | Alkene (*E*/*Z*)[c] |
|---|---|---|---|---|---|
| 1 | **1** | **3a** | 21 | —[d] | — |
| 2 | **1** | **3b** | 72 | 44 | **4b** (7:93) |
| 3 | **1** | **3c** | 19 | 38 | **4c** (6:94) |
| 4 | **1** | **3d** | 80 | 36 | **4d** (6:94) |
| 5 | **1** | **3e** | 19 | 4 | **4e** (58:42)[e] |
| 6 | **1** | **3f** | 20 | 47 | **4f** (100:0) |
| 7 | **1** | **3g** | 18 | 31 | **4g** (100:0) |
| 8 | **2** | **3a** | 18 | 95 | **5a** (16:84) |
| 9 | **2** | **3b** | 17 | 100 | **5b** (16:84) |
| 10 | **2** | **3c** | 16 | 92 | **5c** (13:87) |
| 11 | **2** | **3d** | 17 | 95 | **5d** (12:88) |
| 12 | **2** | **3e** | 17 | 65 | **5e** (36:64)[e] |
| 13 | **2** | **3f**[f] | 20 | 62 | **5f** (89:11) |
| 14 | **2** | **3g**[f] | 20 | 44 | **5g** (95:5) |

[a] Conditions: THF, 0 °C, **1** or **2**/$Sn(OSO_2CF_3)_2$/*N*-ethylpiperidine/**3** (1.4 : 1.68 : 1.54 : 1). [b] Isolated yields. [c] $^1$H NMR (400 MHz, $CDCl_3$) analysis. [d] Aldol product (78% yield). [e] HPLC analysis (TSK-GEL Silica 60, hexane–propan-2-ol. [f] −78 °C.

**Fig. 1**

**Table 3** $Sn(OSO_2CF_3)_2$/*N*-ethylpiperidine/$CH_2Cl_2$ mediated Horner–Wadsworth–Emmons reactions of **2** with ketones **3a–e** and aldehydes **3f,g**[a]

| Entry | Ketone or aldehyde | *t*/h | Yield (%)[b] | Alkene (*E*/*Z*)[c] |
|---|---|---|---|---|
| 1 | **3a** | 15 | 84 | **5a** (2 : 98) |
| 2 | **3b** | 18 | 90 | **5b** (< 1 : > 99) |
| 3 | **3c** | 18 | 95 | **5c** (2 : 98) |
| 4 | **3d** | 18 | 98 | **5d** (1 : 99) |
| 5 | **3e** | 15 | 59 | **5e** (40 : 60)[d] |
| 6 | **3f**[e] | 23 | 29 | **5f** (94 : 6) |
| 7 | **3g**[e] | 24 | —[f] | — |

[a] Conditions: $CH_2Cl_2$, 0 °C, **2**/$Sn(OSO_2CF_3)_2$/*N*-ethylpiperidine/**3** (1.4 : 1.68 : 1.54 : 1). [b] Isolated yields. [c] $^1H$ NMR (400 MHz, $CDCl_3$) analysis. [d] HPLC analysis (TSK-GEL Silica 60, hexane–propan-2-ol. [e] −78 °C. [f] No reaction.

improvement in the selectivity and yield was found when Still's reagent, methyl bis(trifluoroethyl)phosphonoacetate **2**, was used under the $Sn^{II}$-promoted (Tables 2 and 3). In particular, the reactions of **3a–d** with **2** employing $Sn(OSO_2CF_3)_2$ and *N*-ethylpiperidine in $CH_2Cl_2$ at 0 °C afforded the corresponding *Z*-alkenes **5a–d** in a more highly selective manner (Table 3, entries 1–4) than those carried out in THF (Table 2, entries 8–11). The reactions using the NaH procedure resulted in low *Z*-selectivity (Table 1, entries 8–11). The HWE reactions of aldehydes **3f,g** with **2** in the presence of NaH in THF at −78 °C gave *Z*-**5f,g** with similar good selectivity to that using Still's reagent (Table 1, entries 13 and 14). The same reactions employing $Sn(OSO_2CF_3)_2$ and *N*-ethylpiperidine in THF or $CH_2Cl_2$ at −78 °C, on the contrary, gave *E*-**5f,g** with fairly good selectivity, as we anticipated (Table 2, entries 13 and 14; Table 3, entry 6). Surprisingly the stereoselectivity of **5f,g** in the $Sn^{II}$-promoted reactions of **3f,g** with **2** [THF, 20–22 h, **2**/$Sn(OSO_2CF_3)_2$/*N*-ethylpiperidine/**3f** or **3g** (1.4 : 1.68 : 1.54 : 1)] was variable depending on the reaction temperatures as follows; *E* : *Z* ratio (temperature, yield) of **5f** = 33 : 67 (0 °C, 90%), 19 : 81 (−30 °C, 72%), 12 : 88 (−45 °C, 68%), 26 : 74 (−56 °C, 62%), 71 : 29 (−65 °C, 57%) and 89 : 11 (−78 °C, 62%); *E* : *Z* ratio (temperature, yield) of **5g** = 6 : 94 (0 °C, 85%), < 1 : > 99 (−40 °C, 53%) and 95 : 5 (−78 °C, 44%). However, the similar $Sn^{II}$-promoted reaction of **3f** in $CH_2Cl_2$ always afforded the *E*-alkene **5f** (*E* : *Z* = 78 : 22 to 94 : 6) irrespective of the reaction temperature (room temperature to −78 °C). The NaH-promoted reactions of **3f,g** in THF also always gave the corresponding *Z*-alkenes **5f** [*E* : *Z* = 28 : 72 (0 °C) and 15 : 85 (−78 °C)] and **5g** [*E* : *Z* = 18 : 82 (0 °C) and 8 : 92 (−78 °C)], respectively.

On the basis of the experimental results described above, the high *Z*-selectivity in the $Sn(OSO_2CF_3)_2$-mediated HWE reactions of ketones **3a–d** with **1** and **2** can be rationalised in terms of six-membered transition state **A** (*e.g.* **3b**) involving $Sn^{II}$ chelation (Fig. 1). Another possible transition state **B** favouring *E*-selectivity will be disadvantageous due to 1,3-diaxial steric repulsion between the ethyl (or other alkyl) group and the $R^1O$ group. This speculative consideration is supported by the fact that 1-methyl-1-phenylcyclohexane exhibits an axial preference for the phenyl group in spite of the relatively large *A* value of the phenyl group (2.87 kcal $mol^{-1}$) compared with the ethyl group (1.8 kcal $mol^{-1}$).[7] The *E*-selectivity in the $Sn(OSO_2CF_3)_2$-mediated HWE reactions of aldehydes **3f,g** with **1** in THF at 0 °C, with **2** in THF at −65 to −78 °C and with **2** in $CH_2Cl_2$ at room temperature to −78 °C may also be explained in terms of six-membered transition state **C** (*e.g.* **3f**). The $Sn^{II}$-promoted HWE reactions of the reactive reagent **2** with aldehydes **3f,g** in THF at higher reaction temperatures than −65 °C seem to proceed in a non-chelation-controlled manner like the case of NaH.

## Footnotes

† Presented in part at the 114th Annual Meeting of the Pharmaceutical Society of Japan, Tokyo, March 29–31, 1994; abstract paper 2, p. 79.
‡ Full characterisation will be published as part of a forthcoming paper.

## References


1 B. E. Maryanoff and A. B. Reitz, *Chem. Rev.*, 1989, **89**, 863 and references cited therein.
2 M. A. Blanchette, W. Choy, J. T. Davis, A. P. Essenfeld, S. Masamune, W. R. Roush and T. Sakai, *Tetrahedron Lett.*, 1984, **25**, 2183; M. W. Rathke and M. Nowak, *J. Org. Chem.*, 1985, **50**, 2624; M. W. Rathke and E. Bouhlel, *Synth. Commun.*, 1990, **20**, 869.
3 F. Bonadies, A. Cardilli, A. Lattanzi, L. R. Orelli and A. Scettri, *Tetrahedron Lett.*, 1994, **35**, 3383.
4 W. C. Still and C. Gennari, *Tetrahedron Lett.*, 1983, **24**, 4405.
5 K. Ando, *Tetrahedron Lett.*, 1995, **36**, 4105.
6 S. K. Thompson and C. H. Heathcock, *J. Org. Chem.*, 1990, **55**, 3386.
7 N. L. Allinger and L. A. Freiberg, *J. Org. Chem.*, 1966, **31**, 894; N. L. Allinger and M. T. Tribble, *Tetrahedron Lett.*, 1971, 3259; E. L. Eliel and M. Manoharan, *J. Org. Chem.*, 1981, **46**, 1959.



*Received, 19th December 1996; Com. 6/08495H*

# Regio- and enantio-selective allylic alkylation catalysed by a chiral monophosphine–palladium complex

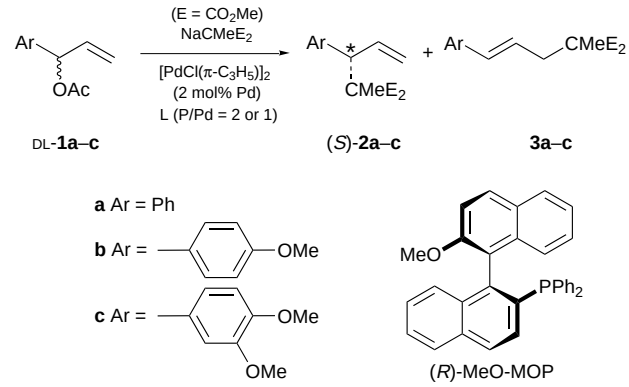
**Tamio Hayashi,* Motoi Kawatsura and Yasuhiro Uozumi**

*Department of Chemistry, Faculty of Science, Kyoto University, Sakyo, Kyoto 606-01, Japan*

**Allylic alkylation of racemic 1-arylprop-2-enyl acetates [ArCH(OAc)CH=$CH_2$] with the sodium enolate of dimethyl methylmalonate in the presence of a palladium catalyst coordinated with (*R*)-2-diphenylphosphino-2′-methoxy-1,1′-binaphthyl [(*R*)-MeO-MOP] proceeds with high branch selectivity (90%) to give chiral products [ArC*H(Nu)CH=$CH_2$] of up to 87% ee.**

Palladium-catalysed allylic substitution reactions including catalytic asymmetric reactions have attracted considerable attention owing to their synthetic utility and mechanistic interest.[1] One of the major problems in developing catalytic asymmetric allylic substitutions is undesirable regiochemistry which limits the substitution patterns of allylic substrates. As a typical example, the substitution with soft carbon nucleophiles that proceeds through π-allylpalladium intermediates containing one substituent at the C-1 position produces the linear isomer rather than the branch isomer.[1] It follows that the reaction cannot be extended to asymmetric synthesis because the linear isomer lacks the chiral carbon centre. The regioselectivity in forming the branch isomer is usually very low except when methyl is the substituent.[2] Here we report that the use of 2-diphenylphosphino-2′-methoxy-1,1′-binaphthyl (MeO-MOP),[3] which is a sterically bulky chiral monophosphine ligand, for the allylic alkylation of 1-arylprop-2-enyl acetates **1** reversed the regiochemistry to give branch isomers **2** with high selectivity and up to 87% ee in this new allylic alkylation system.

The results obtained for the allylic substitution of racemic 1-arylprop-2-enyl acetates DL-**1** in the presence of palladium–phosphine complexes (Scheme 1) are summarized in Table 1. The reaction of DL-1-phenylprop-2-enyl acetate **1a** with the sodium salt of dimethyl methylmalonate in THF at −20 °C in the presence of 2 mol% of palladium catalyst generated from $[PdCl(\pi\text{-}C_3H_5)]_2$ and 1,2-bis(diphenylphosphino)ethane (dppe) gave linear isomer (*E*)-**3a** with 93% regioselectivity (entry 1). The linear selectivity (79–85% regioselectivity) was also observed in the reaction with a palladium catalyst coordinated with triphenylphosphine (entries 2 and 3). It is noteworthy that the reaction catalysed by palladium–$PPh_3$ requires 2 equiv. of triphenylphosphine (to Pd) for the allylic substitution to proceed smoothly. With 1 equiv. of triphenylphosphine, the reaction stops at about 60% conversion. The opposite regioselectivity was observed in the same substitution reaction of **1a** by use of MeO-MOP as a ligand, which gave branch isomer **2a** with 79% regioselectivity at −20 °C (entries 4 and 5). With the palladium–MeO–MOP catalyst, the ratio of phosphine to palladium did not affect either the catalytic activity or the regioselectivity. Higher regioselectivity in forming the branch isomer was observed in the reaction of 1-arylprop-2-enyl




**Scheme 1**

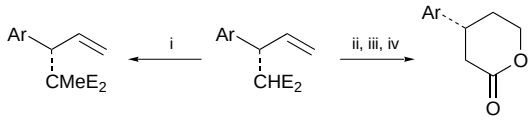
**Table 1** Regio- and enantio-selective allylic alkylation of acetate **1** catalysed by palladium–phosphine complexes[a]

| Entry | Allyl ester | Ligand (ratio P : Pd) | Conditions | | Yield (%)[b] **2** and **3** | Ratio[c] **2** : **3** | Ee (%) of **2** (config.) |
|---|---|---|---|---|---|---|---|
| | | | *T*/°C | *t*/h | | | |
| 1 | **1a** | dppe (2 : 1) | −20 | 4 | 92 | 7 : 93 | — |
| 2 | **1a** | $PPh_3$ (2 : 1) | −20 | 4 | 99 | 15 : 85 | — |
| 3 | **1a** | $PPh_3$ (1 : 1) | −20 | 24 | 63 | 21 : 79 | — |
| 4 | **1a** | (*R*)-MeO-MOP (2 : 1) | −20 | 6 | 99 | 79 : 21 | 68[d] |
| 5 | **1a** | (*R*)-MeO-MOP (1 : 1) | −20 | 6 | 99 | 79 : 21 | 68[d] |
| 6 | **1a** | (*R*)-MeO-MOP (1 : 1) | −30 | 6 | 97 | 82 : 18 | 86[d,e] |
| 7 | **1b** | dppe (2 : 1) | −20 | 2 | 96 | 27 : 73 | — |
| 8 | **1b** | $PPh_3$ (2 : 1) | −20 | 6 | 97 | 30 : 70 | — |
| 9 | **1b** | $PPh_3$ (1 : 1) | −20 | 24 | 58 | 28 : 72 | — |
| 10 | **1b** | (*R*)-MeO-MOP (2 : 1) | −20 | 2 | 97 | 86 : 14 | 76[f] (*S*) |
| 11 | **1b** | (*R*)-MeO-MOP (1 : 1) | −20 | 2 | 99 | 85 : 15 | 76[f] (*S*) |
| 12 | **1b** | (*R*)-MeO-MOP (1 : 1) | −30 | 2 | 96 | 90 : 10 | 87[f] (*S*)[e] |
| 13 | **1c** | (*R*)-MeO-MOP (1 : 1) | −30 | 2 | 99 | 89 : 11 | 85[g,e] |

[a] All reactions were carried out in THF under nitrogen: THF (1.0 ml), allylic acetate (0.20 mmol), $NaCMe(CO_2Me)_2$ (0.40 mmol), $[PdCl(\pi\text{-}C_3H_5)]_2$ (0.002 mmol) and phosphine ligand. [b] Isolated yield by silica gel column chromatography. [c] The ratio was determined by $^1H$ NMR analysis of the products. [d] Determined by GLC analysis with CP Cyclodex β236M after demethoxycarbonylation of one of the two methoxycarbonyl groups. [e] Specific rotations of **2a** (entry 6), **2b** (entry 12) and **2c** (entry 13) were $[\alpha]_D^{20}$ +46.4, +50.3 and +45.0 (*c* 1.1–1.8, $CHCl_3$), respectively. [f] Determined by HPLC analysis with Chiralpak AD (hexane–propan-2-ol = 9 : 1). [g] Determined by HPLC analysis with Chiralcel OD-H (hexane–propan-2-ol = 9 : 1).

acetates **1b** and **1c** which contain methoxy group(s) on the aromatic ring (entries 10–13). At the reaction temperature of −30 °C, 1-(4-methoxyphenyl)prop-2-enyl acetate **1b** gave branch isomer **2b** with 90% regioselectivity (entry 12). The enantiomeric purity of **2b** determined by a chiral stationary phase column (Chiralpak AD) was 87% ee and its absolute configuration was assigned to be (+)-(*S*) by correlation with known (*R*)-(−)-4-(4-methoxylphenyl)tetrahydro-2*H*-pyran-2-one[4] **4** by way of (*R*)-(+)-dimethyl (1-arylprop-2-enyl)malonate **5** (Scheme 2). Here again the palladium catalyst containing dppe or triphenylphosphine gave linear isomer **3b** preferentially (entries 7–9). The reaction of allylic acetate **1c** in the presence of MeO-MOP at −30 °C also gave the corresponding alkylation product **2c** of 85% ee with high branch selectivity (entry 13). Thus, chiral monodentate phosphine ligand, MeO-MOP, is playing a key role on the high branch selectivity in the catalytic allylic alkylation of 1-arylprop-2-enyl acetates. This type of asymmetric alkylation is considered to be difficult with chelating bisphosphine ligands so far used mostly for the asymmetric allylic alkylation which proceeds by way of palladium intermediates containing 1,3-disubstituted π-allyl moieties such as 1,3-diphenyl.[1,5]

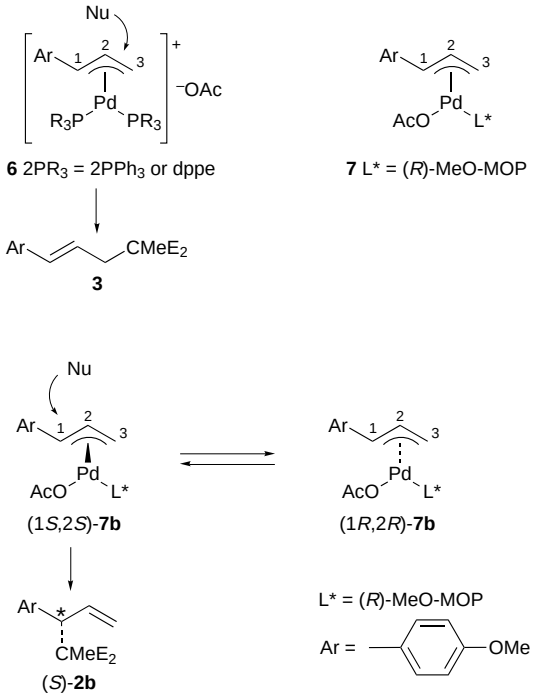
The preferential formation of linear isomers in the allylic alkylation of **1** catalysed by palladium–dppe or palladium–$PPh_3$ is as expected because cationic [π-(1-aryl)allyl]bis-(phosphine)palladium(II) intermediate **6** formed by oxidative addition of **1** to bis(phosphine)palladium(0) will undergo nucleophilic attack on the less hindered end of the π-allyl, namely, C-3 position of π-(1-aryl)allyl group (Scheme 3). It gives the thermodynamically more stable product **3** where the double bond is conjugated with aromatic ring. On the other hand, the reaction with MeO-MOP ligand should proceed *via* neutral [π-(1-aryl)allyl](acetato)(phosphine)palladium(II) intermediate **7** because the steric bulkiness of the MOP ligand does not allow the palladium to form a cationic bis(phosphine) complex which is analogous to **6**.




Ar = 4-$MeOC_6H_4$, E = $CO_2Me$

(*S*)-(+)-**2b** (*R*)-(+)-**5** (*R*)-(−)-**4**

**Scheme 2** *Reagents and conditions*: i, (*R*)-(+)-**5** {$[\alpha]_D^{20}$ + 15.9 (*c* 1.0, $CHCl_3$)}, MeI, NaOMe, MeOH, reflux, 86% {$[\alpha]_D^{20}$ + 40.7 (*c* 1.7, $CHCl_3$)}; ii, LiCl, $Me_2SO$, $H_2O$ 120 °C, 79%, iii, $BH_3$·THF, 77%; iv, *p*-TsOH, benzene, 96% {$[\alpha]_D^{20}$ −6.2 (*c* 1.0, $CHCl_3$)}




**6** 2$PR_3$ = 2$PPh_3$ or dppe **7** L* = (*R*)-MeO-MOP

**3**

**Scheme 3**

The π-allylpalladium complex **7b** (Ar = 4-$MeOC_6H_4$) was prepared by mixing the [π-(1-aryl)allyl](acetato)palladium(II) dimer with 1 equiv. (to Pd) of (*R*)-MeO-MOP and it was characterized by $^{31}P$ and $^1H$ NMR spectra. In $CDCl_3$ at −50 °C the complex exists as a mixture of isomers in a ratio of 9 : 1.† The main isomer has substituted carbon (C-1) of the π-allyl *trans* to the phosphorus atom of MeO-MOP and the unsubstituted carbon (C-3) *cis* to phosphorus, which is determined by a large coupling constant ($J$ = 8.2 Hz) between C-1 proton and phosphorus and no couplings between C-3 protons and phosphorus. Our structural studies of related PdCl(π-allyl)-(MeO-MOP) complexes[6] also showed that the unsubstituted π-allyl carbon adopts the *cis* position to phosphorus. The nucleophile attacks the C-1 carbon which is more weakly bonded to palladium due to a stronger *trans* influence of phosphine ligand to give branch product preferentially. The stoichiometric reaction of π-allylpalladium complex **7b** with the sodium enolate of dimethyl methylmalonate in THF at −20 °C gave (*S*)-**2b** of 90% ee with 88% regioselectivity, which is in good agreement with the catalytic reactions in terms of both regio- and enantio-selectivity.

We thank the Ministry of Education, Japan, for a Grant-in-Aid for Scientific Research for partial financial support of this work.

## Footnote

† *Selected NMR data* for the major isomer of **7b**: $^1H$ NMR ($CDCl_3$ at −50 °C) δ 1.51 (s, 3 H), 1.56 (d, $J$ = 11.6 Hz, 1 H, *anti*-H on C-3), 2.66 (d, $J$ = 6.3 Hz, 1 H, *syn*-H on C-3), 3.03 (s, 3 H), 3.28 (m, 1 H, H on C-2), 3.89 (s, 3 H), 5.41 (dd, $J_{H-H}$ = 13.5 Hz, $J_{H-P}$ = 8.2 Hz, 1 H, H on C-1), 6.87–8.10 (m, 26 H). $^{31}P$ NMR ($CDCl_3$ at −50 °C) δ 23.2 (s). $^{31}P$ NMR for minor isomer of **7b**: δ 24.8 (s).

## References

1 For reviews on catalytic asymmetric allylic substitutions: B. M. Trost and D. L. Van Vranken, *Chem. Rev*., 1996, **96**, 395; T. Hayashi, in *Catalytic Asymmetric Synthesis*, ed. I. Ojdima, VCH, New York, 1993; p. 325; C. G. Frost, J. Howarth and J. M. J. Williams, *Tetrahedron: Asymmetry*, 1992, **3**, 1089; G. Consiglio and M. Waymouth, *Chem. Rev*., 1989, **89**, 257.

2 For examples: T. Hayashi, K. Kishi, A. Yamamoto and Y. Ito, *Tetrahedron Lett*., 1990, **31**, 1743; B. M. Trost, M. J. Krische, R. Radinov and G. Zanoni, *J. Am. Chem. Soc*., 1996, **118**, 6297.

3 Y. Uozumi and T. Hayashi, *J. Am. Chem. Soc*., 1991, **113**, 9887; Y. Uozumi, A. Tanahashi, S.-Y. Lee and T. Hayashi, *J. Org. Chem*., 1993, **58**, 1945; Y. Uozumi, N. Suzuki, A. Ogiwara and T. Hayashi, *Tetrahedron*, 1994, **50**, 4293.

4 D. Enders and B. E. M. Rendenbach, *Chem. Ber*., 1987, **120**, 1223.

5 For recent examples: B. M. Trost and R. C. Bunt, *Angew. Chem., Int. Ed. Engl*., 1996, **35**, 99; G. Zhu, M. Terry and X. Zhang, *Tetrahedron Lett*., 1996, **37**, 4475; W. Zhang, T. Kida, Y. Nakatsuji and I. Ikeda, *Tetrahedron Lett*., 1996, **37**, 7995; N. Nomura, Y. C. Mermet-Bouvier and T. V. RajanBabu, *Synlett*, 1996, 745; H. C. L. Abbenhuis, U. Burckhardt, V. Gramlich, C. Kollner, P. S. Pregosin, R. Salzmann and A. Togni, *Organometallics*, 1995, **14**, 759.

6 T. Hayashi, H. Iwamura, M. Naito, Y. Mausumoto, Y. Uozumi, M. Miki and K. Yanagi, *J. Am. Chem. Soc*., 1994, **116**, 775; T. Hayashi, H. Iwamura, Y. Uozumi, Y. Matsumoto and F. Ozawa, *Synthesis*, 1994, 526.

*Received, 2nd January 1996; Com. 7/00045F*

# Actinide (uranyl) hydrolysis of phosphodiesters

**Robert A. Moss,* Kathryn Bracken and Jing Zhang**

*Department of Chemistry, Rutgers University New Brunswick, New Jersey 08903, USA*

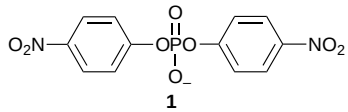
**Uranyl ($UO_2^{2+}$) cations mediate the hydrolysis of aggregated and non-aggregated *p*-nitrophenyl phosphodiesters in mildly acidic aqueous solutions (pH 4.9) with rate enhancements > 1000 at 37 °C.**

The past several years have witnessed intensive study of the lanthanide ion catalysis of phosphodiester hydrolysis, stimulated by the drive to develop synthetic nucleases.[1] The activated phosphodiester, bis(*p*-nitrophenyl) phosphate **1** (BNPP), has been a favourite model substrate,[2–4] although lanthanides and their complexes have also cleaved DNA,[5,6] phosphonates[7] and phosphate monoesters.[8] RNA, and the RNA model substrate **2**, have also been catalytically cleaved by lanthanides[1] and other metal cations.[9–11]

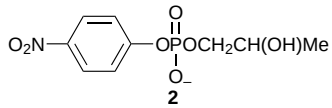
Recently, we reported that the $Eu^{3+}$ or $La^{3+}$–$H_2O_2$ cleavages of liposomal phosphodiester **3** were accelerated 50–70 times, relative to the non-aggregated model phosphodiester **4** (PNP = *p*-nitrophenyl).[12] Binding of the cationic lanthanide ions to the anionic liposomes afforded additional catalysis above that normally expected from the lanthanides.

Although many lanthanide and transition metal cations have been examined as catalysts for the hydrolysis of phosphodiesters, the actinide uranyl ($UO_2^{2+}$) cation has not.† This is surprising because $UO_2^{2+}$ is known to bind strongly to various nucleotides,[14] as well as DNA,[15] with P–O–U bonding a key feature.[14] Indeed, $UO_2^{2+}$ bound between the phosphate groups of stacked DNA strands mediates photolytic, oxidative cleavage of the DNA.[15] Moreover, $UO_2^{2+}$ catalyses the oligomerization of nucleotide 5′-phosphoroimidazolides and 5′-thiophosphoroimidazolides *via* U–O–P–Im complexes in which the electrophilic uranium activates the substrate to nucleophilic attack at P by an incoming 2′-OH nucleophile.[16]‡

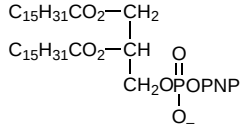
The clear implication is that $UO_2^{2+}$ should bind activated phosphodiesters and predispose these substrates to hydrolytic cleavage. Here, we report that this inference is correct: substrates **1**–**4**, as well as the micellar phosphodiester **5**, are indeed hydrolysed by $UO_2^{2+}$ in mildly acidic aqueous solutions, with additional catalysis apparent for the aggregated substrates **3** and **5**. These are the initial examples of phosphodiester hydrolysis mediated by uranyl cations, and also feature the first metal ion cataysed hydrolysis of a micellar phosphodiester **5**.



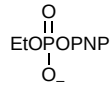

**1**



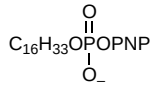

**2**




**3**




**4**




**5**

The RNA model, 2-hydroxypropyl *p*-nitrophenyl phosphate **2**,[18] was efficiently hydrolysed in the presence of excess $UO_2^{2+}$ at 37 °C, pH 4.9±0.1.§ The exact conditions appear in Table 1, where kinetic data for comparable hydrolyses mediated by the lanthanide cations, $Eu^{3+}$ and $Tm^{3+}$, are also collected. Note that these comparisons are under identical conditions in the absence of buffer ions.¶

$UO_2^{2+}$ mediates the quantitative (UV, HPLC) cleavage of substrate **2** with an observed rate constant ($2.2\times10^{-4}$ $s^{-1}$) that is at least 6700 times greater than that for the uncatalysed reaction, where the rate constant for the uncatalysed hydrolysis of **2** is determined at pH 7,[1a] and must be presumed to exceed the value at pH 4.9. (Hydrolysis was not observed over 4 days in the absence of $UO_2^{2+}$ at pH 4.9.) The $k_{rel}$ values in Table 1 are therefore minima. Moreover, the uranyl-catalysed hydrolysis is also 3.5–4.5 times faster than lanthanide cleavage brought about by Eu or Tm cations under these conditions.

Hydrolysis of **2** involves cyclization with displacement of the leaving group by intramolecular OH attack[1] on the metal-bound and activated phosphate. Accordingly, $UO_2^{2+}$ cleavage of ethyl *p*-nitrophenyl phosphate, **4**,[12] which lacks the neighbouring hydroxy is *ca.* 16 times slower ($k_{obs} = 1.4 \times 10^{-5}$ $s^{-1}$) than the hydrolysis of **2** under the conditions of Table 1. Nevertheless, cleavage of **4** is at least 420 times faster than the uncatalysed hydrolysis of **2** at pH 7.

Interestingly, the $UO_2^{2+}$-mediated hydrolyses of **2** and **4** are *ca.* 3.7 times faster than analogous $Eu^{3+}$-catalysed processes (Table 1 and ref. 12). At the low pH used in the present reactions, the lanthanides ($pK_a \sim 8.0$)[19] bear $H_2O$ rather than OH groups and most likely express only electrophilic catalysis due to P–$O^-$ binding; nucleophilic assistance from M–OH would be suppressed. However, $UO_2^{2+}$ has $pK_a$ *ca.* 4.2–6.1 in aqueous solution, depending on ionic strength, added salts and ligand association.[19] Therefore, both electrophilic ($M^+$, external $H_2O$) and nucleophilic (M–OH) components may contribute to uranyl cation catalysis at pH 5.

$UO_2^{2+}$ precipitates with BNPP **1** or the aggregated substrates **3**[12] or **5**.‖ However, addition of 0.1 equivalents of *N*-hexadecyl-*N*,*N*′,*N*′-trimethylethylenediamine (HTMED)[12,20] solubilizes the uranyl cations, presumably in a mixed HTMED-substrate aggregate, thus making it possible to obtain stable $UO_2^{2+}$-substrate solutions. Neither tetramethylethylene diamine nor cetyltrimethylamine solubilizes $UO_2^{2+}$ under our conditions; only a long-chain diamine succeeds, indicating the dependence of solubilization on both cation chelation and HTMED

**Table 1** Kinetics of the metal ion catalysed hydrolysis of **2**[a]

| Catalyst | $k_{obs}/s^{-1}$ | $k_{rel}$ | % Cleaved at 20 h |
|---|---|---|---|
| None[b] | $3.3 \times 10^{-8}$ | 1.0 | — |
| $UO_2(NO_3)_2$ | $2.2 \times 10^{-4}$ | 6700 | 100 |
| $EuCl_3$ | $4.8 \times 10^{-5}$ | 1450 | 75 |
| $TmCl_3$ | $6.2 \times 10^{-5}$ | 1900 | 78 |

[a] Conditions: [**2**] = $1 \times 10^{-4}$ mol $dm^{-3}$, [catalyst] = $1 \times 10^{-3}$ mol $dm^{-3}$, 0.01 mol $dm^{-3}$ aq. KCl, pH 4.9 ± 0.1, 37 °C. [b] Data from ref. 1(*a*) at pH 7.0, 37 °C.

**Table 2** Kinetics of the uranyl ion catalysed hydrolysis[a]

| Substrate | $k_{obs}/s^{-1}$ | $k_{rel}$ | % Cleaved at 20 h |
|---|---|---|---|
| **1** | $9.5 \times 10^{-6}$ | 5.6 | 84 |
| **2** | $1.5 \times 10^{-5}$ | 8.8 | 95 |
| **3** | $1.1 \times 10^{-4}$ | 65 | 95 |
| **4** | $1.7 \times 10^{-6}$ | 1.0 | 72 |
| **5** | $1.1 \times 10^{-4}$ | 65 | 92 |

[a] Conditions: [substrate] = $1 \times 10^{-4}$ mol dm$^{-3}$, [HTMED] = $1 \times 10^{-4}$ mol dm$^{-3}$, [$UO_2^{2+}$] = $1 \times 10^{-3}$ mol dm$^{-3}$, $2 \times 10^{-3}$ mol dm$^{-3}$ HEPES buffer, 0.01 mol dm$^{-3}$ KCl, pH 4.9 ± 0.1, 37 °C. Kinetic data were obtained at 317 nm.

coaggregation. We are thus able to measure the $UO_2^{2+}$ hydrolytic rate constants collected in Table 2.**

Note first that the $UO_2^{2+}$ catalysed cleavages of **2** and **4** are slower by factors of *ca.* 15 and 8, respectively, relative to reactions in the absence of HTMED (*cf.* Table 1 and above), presumably because the electrophilic character of the uranyl cation is attenuated by chelation with HTMED. Most importantly, however, Table 2 reveals the additional reactivity inherent in the liposomal **3** and micellar **5** phosphodiester substrates, both of which are hydrolysed 65 times more rapidly than **4** in the presence of $UO_2^{2+}$. This aggregate catalysis is undoubtedly due to the binding of the metal cations to the anionic aggregates, assisted by the HTMED which probably forms part of a coaggregate. The cleavage of liposomal **3** by the lanthanide, $Eu^{3+}$, is similarly enhanced by a factor of 56, relative to **4**.[12]

The $UO_2^{2+}$-mediated hydrolyses of **3** and **5** at pH 5 (Table 2) occur at similar rates to the $Eu^{3+}$ reaction with **3** ($k_{obs}$ = $2 \times 10^{-4}$ s$^{-1}$, pH 5.6, 25 °C) at similar reactant concentrations.[12] Relative to substrate **2** in the absence of $UO_2^{2+}$ (Table 1), the actinide plus aggregate catalysis affords a kinetic advantage of > 3300 in the hydrolysis of substrates **3** and **5**.

Finally, we note that both the *exo*- and *endo*-liposomal *p*-nitrophenylphosphate functional groups of **3** are quantitatively cleaved by $UO_2^{2+}$-HTMED in a uniphasic kinetic process at both 25 and 37 °C ($T_c$ of **3** is 42 °C[12]); there is no evidence of the *exo*-liposomal-specific cleavage observed with 'naked' $Eu^{3+}$ at 25 °C.[12] Presumably, the difference originates in the obligatory presence of HTMED, which can chelate $UO_2^{2+}$ and rapidly ($> k_{hydrol}$) transport it across the liposomal bilayer to mediate *endo*-liposomal cleavage. Alternatively, the HTMED molecules could disrupt the integrity of the liposomal membrane, permitting uranyl cation permeation. $Eu^{3+}$ cleavage of liposomal **3** also becomes complete and uniphasic in the presence of HTMED for related reasons.[12]

We are grateful to Professor Paolo Scrimin (University of Padua) for a gift of HTMED, and to both Professors Scrimin and John Brennan (Rutgers University) for helpful discussions. We thank the U.S. Army Research Office for financial support.

## Footnotes

† Martell (ref. 13) reported the rapid cleavage of the fluorophosphonate Sarin by the 1,8-dihydroxynaphthalene-3,6-disodium sulfonate (DNS) complex of $UO_2^{2+}$. Phosphodiester substrates, however, are much less reactive than fluorophosphonates. Indeed, we find substrates **2** and **3** to be quite unreactive to the $UO_2^{2+}$–DNS complex at either pH 5 or 7 ($k_{hydrol} \ll 1x10^{-6}$ s$^{-1}$), with hydrolysis < 50% complete after 5 days at 37 °C.

‡ After our current work had been completed, it was reported that the actinide $Th^{4+}$ accelerates the hydrolyses of various nucleotide phosphomonoester and -diester bonds in acidic aqueous solutions (ref. 17).

§ $UO_2^{2+}$ precipitates as polynuclear metal hydroxide gels at pH ≥ 5.3 (ref. 19) restricting us to pH *ca.* 5.0. Below pH 4.0, no hydrolysis of the phosphodiester substrates was observed over 24 h.

¶ Hydrolyses were followed spectrophotometrically between 200–600 nm; and kinetics were measured at both 290 nm (disappearance of substrate) and 317 nm (appearance of *p*-nitrophenol). Pseudo-first-order rate constants (measured over 20 h) are reported as means of 2 or 3 runs ($r > 0.997$), with reproducibility within ±10%. The pH, adjusted with 0.1 mol dm$^{-3}$ HCl, was buffered by the metal cations and varied no more than 0.2 pH units during the course of reaction. The percentage cleavage was determined from the concentration of liberated *p*-nitrophenoxide ion, measured at pH 12 (400 nm), after 20 h of reaction.

‖ Substrate **5** (mp 165 °C, decomp.) was prepared by phosphorylation of hexadecanol with 4-nitrophenyl phosphorodichloridate ($CH_2Cl_2$, $Et_3N$, 0–25 °C, 3.5 h), followed by methanolysis to hexadecyl methyl *p*-nitrophenyl phosphate. The methyl group was removed by reaction with LiBr in refluxing acetone (48 h), affording white crystalline **5** (Li salt), which was characterized by NMR and elemental analysis.

** HEPES buffer (2 mmol dm$^{-3}$) is present in these runs because it is necessary in the preparation of liposomal **3** (ref. 12). The buffer alone does not solubilize $UO_2^{2+}$ in the presence of substrates **1**, **3** or **5**, nor does it alter the reactivity of the cation toward **2** or **4**. Control experiments also show that HTMED alone does not induce cleavage of the substrates.

## References

1 (*a*) R. Breslow and D.-L. Huang, *Proc. Natl. Acad. Sci. USA*, 1991, **88**, 4080; (*b*) J. R. Morrow, L. A. Buttrey and K. A. Berback, *Inorg. Chem.*, 1992, **31**, 16 and references cited therein.
2 H.-J. Schneider, J. Rammo and R. Hettich, *Angew. Chem., Int. Ed. Engl.*, 1993, **32**, 1716; K. G. Ragunathan and H.-J. Schneider, *Angew. Chem., Int. Ed. Engl.*, 1996, **35**, 1219; J. R. Morrow, K. Aures and D. Epstein, *J. Chem. Soc., Chem. Commun.*, 1995, 2431.
3 B. K. Takasaki and J. Chin, *J. Am. Chem. Soc.*, 1993, **115**, 9337; R. Breslow and B. Zhang, *J. Am. Chem. Soc.*, 1994, **116**, 7893; B. K. Takasaki and J. Chin, *J. Am. Chem. Soc.*, 1995, **117**, 8582.
4 N. Takeda, M. Irisawa and M. Komiyama, *J. Chem. Soc., Chem. Commun.*, 1994, 2773.
5 S. Hashimoto and Y. Nakamura, *J. Chem. Soc., Chem. Commun.*, 1995, 1413; J. Rammo, R. Hettich, A. Roigk and H.-J. Schneider, *Chem. Commun.*, 1996, 105.
6 B. K. Takasaki and J. Chin, *J. Am. Chem. Soc.*, 1994, **116**, 1121; M. Komiyama, N. Takeda, Y. Takahashi, H. Uchida, T. Shiiba, T. Kodama and M. Yashiro, *J. Chem. Soc., Perkin Trans. 2*, 1995, 269; N. Takeda, T. Imai, M. Irisawa, J. Sumaoka, M. Yashiro, H. Shigekawa and M. Komiyama, *Chem. Lett.*, 1996, 599.
7 A. Tsubouchi and T. C. Bruice, *J. Am. Chem. Soc.*, 1994, **116**, 11 614; *J. Am. Chem. Soc.*, 1995, **117**, 7399.
8 S. J. Oh, K. H. Song and J. W. Park, *J. Chem. Soc., Chem. Commun.*, 1995, 575.
9 M. Irisawa, N. Takeda, and M. Komiyama, *J. Chem. Soc., Chem. Commun.*, 1995, 1221.
10 N. H. Williams and J. Chin, *Chem. Commun.*, 1996, 131.
11 B. Linkletter and J. Chin, *Angew. Chem., Int. Ed. Engl.*, 1995, **34**, 472; J. Chin, *Acc. Chem. Res.*, 1991, **24**, 145.
12 R. A. Moss, B. D. Park, P. Scrimin and G. Ghirlanda, *J. Chem. Soc., Chem. Commun.*, 1995, 1627.
13 R. C. Courtney, R. L. Gustafson, S. J. Westerback, H. Hyytiainen, S. C. Cheberek, Jr. and A. E. Martell, *J. Am. Chem. Soc.*, 1957, **79**, 3030.
14 M. Kainosho and M. Takahashi, *Nucleic Acid Res. Symp. Ser.*, 1983, **12**, 181; K. E. Rich, R. T. Agarwal and I. Feldman, *J. Am. Chem. Soc.*, 1970, **92**, 6818; I. Feldman and K. E. Rich, *J. Am. Chem. Soc.*, 1970, **92**, 4559.
15 P. E. Nielsen, C. Hiort, S. H. Sonnichsen, O. Buchardt, O. Dahl and B. Norden, *J. Am. Chem. Soc.*, 1992, **114**, 4967; N. E. Mollegaard, A. I. H. Murchie, D. M. J. Lilley and P. E. Nielsen, *EMBO J.*, 1994, **13**, 1508
16 M. Shimazu, K. Shinozuka and H. Sawai, *Angew. Chem., Int. Ed. Engl.*, 1993, **32**, 870; H. Sawai, K. Higa and K. Kuroda, *J. Chem. Soc., Perkin Trans. 1*, 1992, 505.
17 T. Ihara, H. Shimura, K. Ohmori, H. Tsuji, J. Takeuchi and M. Takagi, *Chem. Lett.*, 1996, 687.
18 D. M. Brown and D. A. Usher, *J. Chem. Soc.*, 1965, 6558.
19 J. Burgess, *Metal Ions in Solution*, Halsted Press, New York, 1978, pp. 267–270.
20 P. Scrimin, P. Tecilla and U. Tonellato, *Tetrahedron*, 1995, **51**, 217; Y. Y. Lim, E. H. L. Tan and L. H. Gan, *J. Coll. Interface Sci.*, 1993, **157**, 442; F. M. Menger, L. H. Gan, E. Johnson and H. D. Durst, *J. Am. Chem. Soc.*, 1987, **109**, 2800.

*Received, 10th January 1997; Com. 7/00260B*

# Use of lithium (α-methylbenzyl)allylamide for a formal asymmetric synthesis of thienamycin

**Stephen G. Davies* and David R. Fenwick**

*The Dyson Perrins Laboratory, University of Oxford, South Parks Road, Oxford, UK OX1 3QY*

**The highly stereoselective conjugate addition of lithium (α*R*)-(α-methylbenzyl)allylamide 3 to (*E*)-*tert*-butyl penta-2,4-dienoate 4, followed by a stereoselective aldol reaction with acetaldehyde, are the key steps in the synthesis of the known β-lactam intermediate, (3*S*,4*R*)-3-[(*R*)-1-(*tert*-butyldimethylsilyloxy)ethyl]-4-vinylazetidin-2-one 2, for elaboration to thienamycin and its derivatives.**

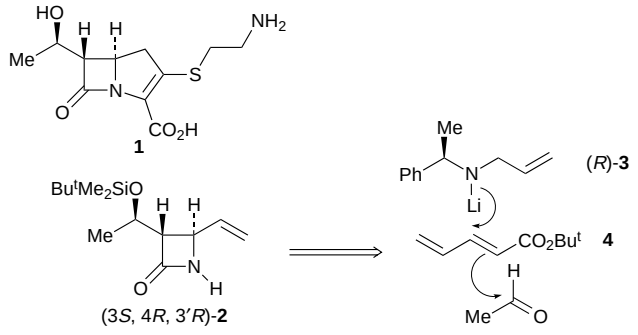
The carbapenems are an important class of β-lactam antibiotics with broad-spectrum potency and stability to β-lactamases. (+)-Thienamycin **1**, the first member of the family to be discovered,[1] has been the subject of numerous syntheses, with the *trans* stereochemistry of the protons in the β-lactam ring and the 3-[(*R*)-1-hydroxyethyl] side chain presenting a considerable synthetic challenge.[2] This key β-lactam framework is also found in the 1β-methylcarbapenems[3] and the tribactams,[4] antibiotics of current interest due to their enhanced chemical and metabolic stabilities.

A concise approach to this β-lactam framework is *via* a conjugate addition-aldol condensation strategy. Yamamoto *et al*. have used lithium *N*-benzyltrimethylsilylamide to give a key β-lactam intermediate as a single diastereomer,[5] but with the wrong absolute stereochemistry, and lithium (α-methylbenzyl)benzylamide,[6] developed in our laboratories, to give a β-lactam with the correct absolute stereochemistry but, due to the requirement of removing the *N*-benzyl groups by hydrogenation, without the possibility of incorporating an unsaturated side chain necessary for further synthetic elaboration.[7]

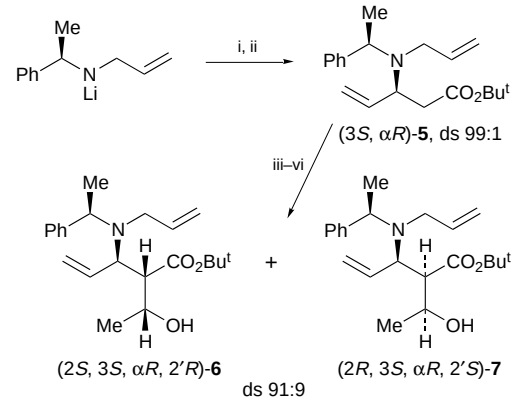
We have recently developed lithium (α*R*)-(α-methylbenzyl)allylamide **3** specifically for the synthesis of homochiral β-amino acids and β-lactams[8] and its application to the synthesis of carbapenem intermediates has already been demonstrated.[9] In particular, the use of this reagent to generate β-lactams with unsaturated side chains suggested its application in the synthesis of the known β-lactam intermediate, (3*S*,4*R*)-3-[(*R*)-1-(*tert*-butyldimethylsilyloxy)ethyl]-4-vinylazetidin-2-one **2**[10,11] for the synthesis of thienamycin, *via* a conjugate addition–aldol condensation approach (Scheme 1).

Addition of lithium (α-methylbenzyl)allylamide (*R*)-**3** to (*E*)-*tert*-butyl penta-2,4-dienoate **4**,† followed by quenching with aqueous ammonium chloride, gave the β-amino adduct (3*S*,α*R*)-**5** in 87% yield with no 1,2- nor 1,6-addition being observed (Scheme 2). Analysis of the 500 MHz $^1$H NMR spectrum of the crude addition product showed the diastereoselectivity (ds) to be 99 : 1. Treatment of the adduct (3*S*, α*R*)-**5** with LDA in THF at 0 °C for 2 h followed by cooling to −78 °C and quenching with acetaldehyde gave only two of the four possible diastereomeric aldol products, (2*S*,3*S*,α*R*,2′*R*)-**6** and (2*R*,3*S*,α*R*,2′*S*)-**7**, in a 4 : 1 ratio by analysis of the 500 MHz $^1$H NMR spectrum of the crude reaction mixture. To improve the stereoselectivity of the aldol reaction a series of transmetallating reagents were investigated. The best selectivity was achieved using trimethyl borate, giving the same two diastereomers but with an improved ratio of 91 : 9 (Scheme 2), in accordance with the results from Asao *et al*. using lithium (α-methylbenzyl)benzylamide,[7] attesting to the structural similarity of the intermediate enolates. These were separable by flash chromatography to give (2*S*,3*S*,α*R*,2′*R*)-**6** as a single diastereomer in 75% yield.

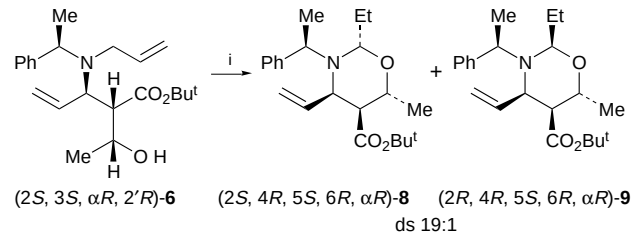
The absolute stereochemistry of (2*S*,3*S*,α*R*,2′*R*)-**6** was determined by treatment with tris(triphenylphosphine)rhodium(I) chloride in toluene under anhydrous conditions. This gave cyclisation to a 19:1 mixture of the perhydro-1,3-oxazines, (2*S*,4*R*,5*S*,6*R*,α*R*)-**8** and (2*R*,4*R*,5*S*,6*R*,α*R*)-**9**, diastereomeric at the newly formed C2 aminol centre, in 90% yield (Scheme 3). The cyclisation presumably occurs by intramolecular trapping of an intermediate imminium species, in equilibrium with the enamine generated in the isomerisation of the allyl double bond, by the 2′-hydroxy group.‡ Analysis of the coupling constants in the 500 MHz $^1$H NMR spectrum of the major diastereomer




**Scheme 1**




**Scheme 2** *Reagents and conditions*: i, $CH_2$=CHCH=$CHCO_2Bu^t$ **4**, ii, aq. $NH_4Cl$, 87%; iii, LDA, iv, $B(OMe)_3$, v, MeCHO, vi, aq. $NH_4Cl$, 82%




**Scheme 3** *Reagents and conditions*: i, $(PPh_3)_3RhCl$, 90%

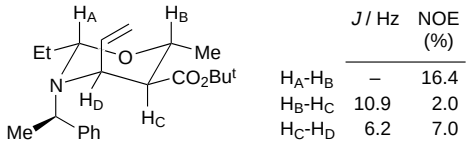
(2*S*,4*R*,5*S*,6*R*,α*R*)-**8** allowed determination of the two stereocentres formed in the aldol reaction ($H_B$-$H_C$, *J* 10.9 Hz, ax–ax coupling; $H_C$-$H_D$ *J* 6.2 Hz, ax–eq coupling) and NOE analysis verified the expected equatorial stereochemistry of the ethyl group at the aminol centre ($H_A$–$H_B$, 16.4%) (Fig. 1).

Although treatment of this mixture of perhydro-1,3-oxazines with aqueous hydrochloric acid gave only the desired β-amino acid (2*S*,3*S*,α*R*,2′*R*)-**10** in 92% yield, verifying that they were diastereomeric only at C2, it proved more efficient to first remove the allyl group from the aldol product (2*S*,3*S*,α*R*,2′*R*)-**6** with tetrakis(triphenylphosphine)palladium(0) and *N*,*N*-dimethylbarbituric acid[12] to give the deallylated product in 98% yield. Since the deprotection proceeds *via* a π-allyl cation there is no opportunity for cyclisation to a perhydro-1,3-oxazine. Hydrolysis of the *tert*-butyl ester with trifluroacetic acid then gave the β-amino acid (2*S*,3*S*,α*R*,2′*R*)-**10** in 97% yield (Scheme 4). Despite its polar nature and the possibility of a zwitterionic form the acid was readily extracted into ethyl acetate, presumably because of its ability to intramolecularly hydrogen bond.

Treatment of β-amino acid (2*S*,3*S*,α*R*,2′*R*)-**10** with 2,2′-dipyridyl disulfide and triphenylphosphine[13] gave cyclisation to the β-lactam (3*S*,4*R*,α*R*,3′*R*)-**11** in 98% yield (Scheme 4). Protection of the hydroxy group with *tert*-butyldimethylsilyl chloride proceeded in 98% yield and was followed by removal of the *N*-α-methylbenzyl group using sodium in liquid ammonia[14] to give the known intermediate (3*S*,4*R*,3′*R*)-**2** in 95% yield. The specific rotation, $[\alpha]_D^{22}$ −25.9 (*c* 1.06, $CHCl_3$), of (3*S*,4*R*,3′*R*)-**2**, was in excellent agreement with the literature value, $[\alpha]_D^{25}$ −24.5 (*c* 1.05, $CHCl_3$), as was the spectroscopic data.§

In summary, the key β-lactam intermediate (3*S*,4*R*,3′*R*)-**2** for the synthesis of thienamycin and its derivatives has been synthesised in seven steps and 58% overall yield from lithium (α-methylbenzyl)allylamide (*R*)-**3** and (*E*)-*tert*-butyl penta-2,4-dienoate **4**. The highly diastereoselective conjugate addition of the lithium amide (*R*)-**3** to the unsaturated ester **4**, followed by a selective aldol reaction with acetaldehyde, constructed all three stereocentres with the correct absolute stereochemistry in two steps. Since the conjugate addition of the lithium amide has been shown to be highly selective to a wide range of α,β-unsaturated esters this methodology can be applied to the synthesis of the key β-lactam frameworks of a variety of carbapenems.

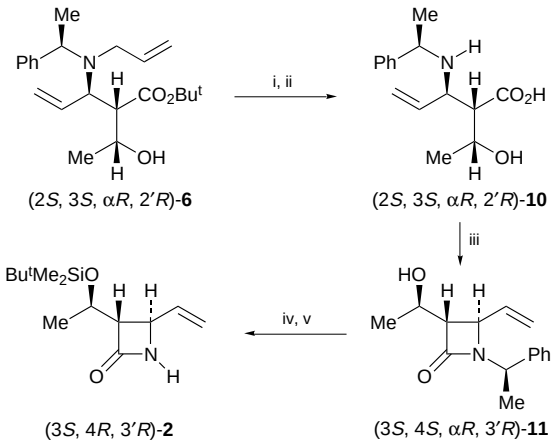
We thank the EPSRC, FMC Ltd and Oxford Asymmetry Ltd for support (to D. R. F.) through a CASE award.




| | *J* / Hz | NOE (%) |
|---|---|---|
| $H_A$-$H_B$ | – | 16.4 |
| $H_B$-$H_C$ | 10.9 | 2.0 |
| $H_C$-$H_D$ | 6.2 | 7.0 |

(2*S*, 4*R*, 5*S*, 6*R*, α*R*)-**8**

**Fig. 1**




(2*S*, 3*S*, α*R*, 2′*R*)-**6**

(2*S*, 3*S*, α*R*, 2′*R*)-**10**

(3*S*, 4*R*, 3′*R*)-**2**

(3*S*, 4*S*, α*R*, 3′*R*)-**11**

**Scheme 4** *Reagents and conditions*: i, $Pd(PPh_3)_4$, NDMBA, 98%, ii, TFA, 97%; iii, $(PyS)_2$–$PPh_3$, 98%; iv, $Bu^tMe_2SiCl$, 98%; v, Na, $NH_3$ (l), 95%

## Footnotes

† (*E*)-penta-2,4-dienoic acid was prepared by the Knoevenagel-type reaction of malonic acid with acrolein in the presence of pyridine, see: P. J. Jessup, C. B. Petty, J. Roos and L. E. Overman, *Org. Synth.*, 1988, **Coll. Vol. 6**, 95. The *tert*-butyl ester **4** was preapred from the acid using isobutylene and a catalytic amount of concentrated sulfuric acid. This bulky ester group prevents 1,2-addition of the lithium amide.

‡ An analagous cyclisation to form acetals has been observed in the isomerisation of allyl ethers to prop-1-enyl ethers using tris(triphenylphosphine)rhodium(I) chloride, R. Gigg and C. D. Warren, *J. Chem. Soc. C*, 1968, 1903.

§ (3*S*,4*R*)-3-[(*R*)-1-(*tert*-butyldimethylsilyloxy)ethyl]-4-vinylazetidin-2-one **2** was isolated as a white crystalline solid; mp 62–63 °C; $[\alpha]_D^{21}$ −25.9 (*c* 1.06, $CHCl_3$); (Found: C, 61.24; H, 9.85; N, 5.17. $C_{13}H_{25}NO_2Si$ requires C, 61.13; H, 9.87; N, 5.48%); $\nu_{max}$($CHCl_3$/cm$^{-1}$ 3415m (N–H), 2957m (C–H), 1762s (C=O); $\delta_H$ (300 MHz; $CDCl_3$) 6.02 (1 H, br s, NH), 5.96 (1 H, ddd, *J* 17.1, 10.3 and 6.8, C*H*=$CH_2$), 5.32 (1 H, d, *J* 17.1, *trans* CH=C*H*$_2$), 5.17 (1 H, d, *J* 10.3, *cis* CH=C*H*$_2$), 4.10–4.30 (2 H, m, CHOSi, NC*H*CH), 2.89 (1 H, dd, *J* 4.4 and 2.4, NCHC*H*), 1.22 (3 H, d, *J* 6.3, $CH_3$CO), 0.88 [9 H, s, ($CH_3$)$_3$CSi], 0.08 [6 H, s, ($CH_3$)$_2$Si]; $\delta_C$ (50 MHz) 169.1 (C=O), 137.8 (*C*H=$CH_2$), 116.5 (CH=*C*H$_2$), 65.8, 65.3 (CHOSi, NCH), 52.2 (CHCO), 25.6 [C(*C*H$_3$)$_3$], 22.2 (*C*H$_3$CO), 17.8 [*C*(CH$_3$)$_3$], −4.4, −5.2 [Si(CH$_3$)$_2$]; *m*/*z* (CI, $NH_3$) 256 ($MH^+$, 100%). For comparative data see ref. 11. All other compounds exhibited satisfactory analytical and spectroscopic data.

## References

1 H. Kropp, J. S. Kahan, F. M. Kahan, J. Sanderof, G. Darland and J. Birnbaum, Abstract 228, *16th Intersci. Conf. Antimicrob. Agents and Chemother*., Chicago 1976; J. S. Kahan, F. M. Kahan, R. Goegelman, S. A. Currie, M. Jackson, E. O. Stapley, T. W. Miller, A. K. Miller, D. Hendlin, S. Mochales, S. Hernandez, H. B. Woodruff and J. Birnbaum, *J. Antibiot*., 1979, **32**, 1; G. Albers-Schönberg, B. H. Arison, O. D. Hensens, J. Hirshfield, K. Hoogsteen, E. A. Kaczka, R. E. Rhodes, J. S. Kahan, F. M. Kahan, R. W. Ratcliffe, E. Walton, L. J. Ruswinkle, R. B. Morin and B. G. Christensen, *J. Am. Chem. Soc*., 1978, **100**, 6491.

2 For reviews, see: R. C. Thomas, in *Recent Progress in the Chemical Synthesis of Antibiotics*, ed. G. Lukacs and M. Ohno, Springer-Verlag, Berlin, 1990; R. J. Ternansky and J. M. Morin Jr., in *The Organic Chemistry of ß-Lactams*, ed. G. I. Georg, VCH, New York, 1993.

3 D. H. Shih, F. Baker, L. Cama and B. G. Christensen, *Heterocycles*, 1984, **21**, 29: D. R. Bender, A. M. DeMarco, D. G. Melillo, S. M. Riseman and I. Shinkai, *J. Org. Chem*., 1992, **57**, 2411.

4 C. Bismara, R. Di Fabio, d. Donati, T. Rossi and R. J. Thomas, *Tetrahedron Lett*., 1995, **36**, 4283 and references cited therein.

5 Y. Yamamoto, N. Asao and T. Uyehara, *J. Am. Chem. Soc*., 1992, **114**, 5427.

6 S. G. Davies and O. Ichihara, *Tetrahedron: Asymmetry*, 1991, **2**, 183.

7 N. Asao, N. Tsukada and Y. Yamamoto, *J. Chem. Soc., Chem. Commun*., 1993, 1660.

8 S. G. Davies and D. R. Fenwick, *J. Chem. Soc., Chem. Commun*., 1995, 1109.

9 S. G. Davies, C. J. R. Hedgecock and J. M. McKenna, *Tetrahedron: Asymmetry*, 1995, **6**, 827; 1995, **6**, 2507.

10 K. Hattori, M. Miyata and H. Yamamoto, *J. Am. Chem. Soc*., 1993, **115**, 1151.

11 Y. Ito, Y. Kobayashi, T. Kawabata, M. Takase and S. Terashima, *Tetrahedron*, 1989, **45**, 5767.

12 F. Garro-Helion, A. Merzouk and F. Guibé, *J. Org. Chem*., 1993, **58**, 6109.

13 S. Kobayashi, T. Iimori, T. Izawa and M. Ohno, *J. Am. Chem. Soc*., 1981, **103**, 2406.

14 S. T. Hodgson, D. M. Hollinshead and S. V. Ley, *Tetrahedron*, 1985, **41**, 5871.

*Received, 9th January 1997; Com. 7/00216E*

# A supramolecular carpet formed *via* self-assembly of bis(4,4′-dihydroxyphenyl) sulfone†

**Caitlin Davies,[a] Richard F. Langler,*[a] C. V. Krishnamohan Sharma[b] and Michael J. Zaworotko*[b]**

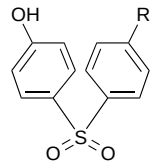
[a] *Department of Chemistry, Mount Allison University, Sackville, New Brunswick, Canada E0A 3C0*
[b] *Department of Chemistry, Saint Mary's University, Halifax, Nova Scotia, Canada B3H 3C3*

**Bis(4,4′-dihydroxyphenyl) sulfone 1 exploits its tetrahedrally disposed complementary hydrogen bonding sites to generate a unique doubly interwoven molecular carpet architecture in the solid state.**

The concept of rational design of 2D and 3D frameworks has evoked considerable interest in recent years as many functional properties of solids are dependent on crystal packing.[1,2] A particularly interesting and relevant problem that has been addressed by several groups concerns the preparation of open cage and/or interwoven networks.[3–5] While the former is desired in the context of porous solids, the latter is an associated phenomenon which invariably occurs if > 50% of a solid would otherwise be empty. Such interpenetration (or catenation) is appreciated for its aesthetic appeal and offers potential host materials if guest molecules can be exploited to prevent interpenetration.[6] Understanding and predicting interpenetration patterns therefore constitutes an important aspect of crystal engineering.

Self-assembly can be an effective strategy for crystal engineering but it requires careful control over molecular symmetry and functionality.[3] In general, tetrahedral molecules with rigid complementary hydrogen bonding sites adapt diamondoid architecture with levels of interpenetration based on the relative size of superdiamondoid cage and the volume of the tecton.[7] We report herein an alternate motif for such compounds which occurs if there is flexibility present in the tecton: interwoven 2D square grids.[8]

A solution of bis(4-chlorophenyl) sulfone (4.0 g) and sodium hydroxide (4.0 g) in $Me_2SO$ (160 ml) and water (40 ml) was maintained at 100 °C for two months. Extractive workup with diethyl ether furnished a mixture of unchanged chloro sulfone, bis(4-hydroxyphenyl) sulfone **1** and 4-chlorophenyl (4′-hydroxyphenyl) sulfone **2**. Chloroform elution on silica gel furnished pure **1** (2%) and **2** (50%).




**1** R = OH
**2** R = Cl

Non-centrosymmetric crystals of **1** were obtained from acetone–$CHCl_3$ (mp 247–249 °C). The crystal structure‡ reveals an infinite 2D hydrogen bonded network sustained by interaction between hydroxy and sulfone groups (O···O 2.705(7), 2.800(3) Å, Fig. 1). The network generates square cavities with *ca.* 8 × 10 Å dimensions, large enough to facilitate generation of a 2-fold interwoven molecular carpet (Fig. 2). The entangled 2D grids are stabilized by van der Waals and herringbone interactions. A 3D diamondoid architecture is also feasible but presumably packs less efficiently in the absence of an appropriate guest.

The molecular carpet architecture of **1** demonstrates how molecules with flexible hydrogen bonding sites can self-assemble to yield 2D interwoven networks as an alternative to 3D diamondoid architectures. Such networks would be expected to have clay-like intercalation properties and, if appropriate guests can be used to eschew interpenetration, large cavities within the grid.[9] The critical importance of complementarity amongst the hydrogen bonding sites is illustrated by what happens if one hydroxy substituent of **1** is replaced by a chloro substituent. 4-chlorophenyl (4′-hydroxyphenyl) sulfone **2** exhibits a less predictable but nonetheless intriguing crystal structure.§ Compound **2** crystallizes from $CHCl_3$ (mp 150–151 °C) in the non-centrosymmetric space group *P*1 with, remarkably, four molecules in the asymmetric unit. There are two discrete hydrogen bonding motifs: i, simple linear hydrogen bonding between sulfone and hydroxy groups [2.898(6) Å]; ii, cyclic hydrogen bonding involving two of the sulfone O atoms and three hydroxy groups, possibly with two of the hydroxy groups being disordered [Scheme 1, O···O: 2.838(6), 2.881(6),

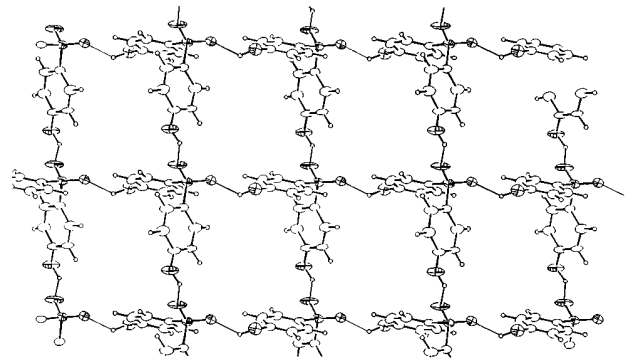


**Fig. 1** ORTEP diagram of **1** illustrating a single hydrogen bonded network

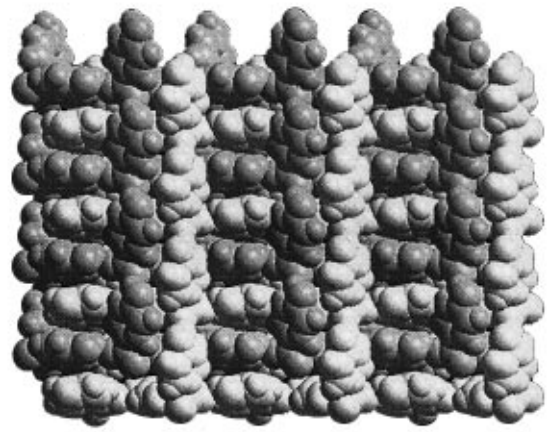
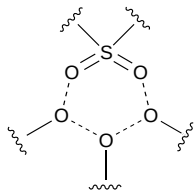


**Fig. 2** A space filling diagram of the interwoven supramolecular carpet architecture of **1**. The two independent grids are colour coded for clarity.



**Scheme 1**

3.019(6), 2.913(6) Å]. Furthermore, there are two different kinds of aryl–aryl stacking interactions: between chlorophenyl and hydroxyphenyl groups and between adjacent chlorophenyl groups. The mean interplanar distances and dihedral angles of these two stacking interactions are 3.74 and 3.60 Å, 2.9 and 3.4° respectively.

Compounds **1** and **2** illustrate clearly the importance of self-assembly to crystal engineering. Compound **1** demonstrates how tetrahedral moieties with complementary hydrogen bonding sites are capable of self-assembling into a predictable 2D motif if the hydrogen bonding sites are robust and flexible. However, **2** demonstrates how even minor changes in functionality can lead to unusual and unpredictable crystal packing.

## Footnotes

† This ChemComm is also available in enhanced multi-media format *via* the World Wide Web: http://chemistry.rsc.org/rsc/cccenha.htm

‡ *Crystal Data* for **1**: 4,4′-Dihydroxyphenyl sulfone, $M$ = 249.26, orthorhombic, *C*2*cb*, $a$ = 8.1572(10), $b$ = 19.2757(21), $c$ = 15.0471(20) Å, $V$ = 2365.9(5) Å$^3$, $Z$ = 8, $D_{calc}$ = 1.40 Mg m$^{-3}$, λ = 0.70930 Å, $F$(000) = 1032.921 reflections with $I_{net} > 3\sigma(I_{net})$ out of 1121 unique reflections measured at 290 K for a crystal of dimensions 0.3 × 0.2 × 0.4 mm on an Enraf-Nonius CAD4 diffractometer using the ω scan mode ($4 < 2\theta < 50°$) afforded, on convergence, final values of $R_f$ = 0.077 and $R_w$ = 0.089. The H atom of one of the two OH groups was found *via* difference Fourier map inspection. Other H atoms were placed in calculated positions (C–H = 1.0 Å). All non-hydrogen atoms were anisotropically refined. The crystallographic calculations were carried out using NRCVAX program package. Atomic coordinates, bond lengths and angles, and thermal parameters for both **1** and **2** (see below) have been deposited at the Camrbidge Crystallograpic Centre (CCDC). See Information for Authors, Issue No. 1. Any request to the CCDC for this material should quote the full literature citation and the reference number 182/360.

Since submission of this article an account of the structure of **1** has been published. See G. Ferguson and C. Glidewell, *Acta Crystallogr., Sect. C*, 1996, **52**, 2528.

§ *Crystal Data* for **2**: As for **1** but 4-hydroxyphenyl, 4′-chlorophenyl sulfone, $M$ = 267.96, triclinic, $P1$, $a$ = 7.6401(11), $b$ = 9.2850(11), $c$ = 17.6630(13) Å, α = 93.04(2), β = 91.51(3), γ = 108.64(2), $V$ = 1184.35(24) Å$^3$, $Z$ = 4, $D_{calc}$ = 1.503 Mg m$^{-3}$, λ = 0.70930 Å, $F$(000) = 552. 3591 reflections with $I_{net} > 3\sigma(I_{net})$ out of 4149 unique reflections measured at 290 K for a crystal of dimensions 0.4 × 0.2 × 0.2 mm afforded values of $R_f$ = 0.042 and $R_w$ = 0.047.

## References


1 G. R. Desiraju, *Crystal Engineering: The Design of Organic Solids*, Elsevier, Amsterdam, 1989.

2 B. F. Abrahams, B. F. Hoskins and R. Robson, *J. Am. Chem. Soc.*, 1991, **113**, 3603.

3 M. J. Zaworotko, *Chem. Soc. Rev.*, 1994, 283.

4 G. B. Gardner, D. Venkataraman, J. S. Moore and S. Lee, *Nature*, 1995, **374**, 792; O. M. Yaghi, G. Li and H. Li, *Nature*, 1995, **378**, 703; M. E. Brown and M. D. Hollingsworth, *Nature*, 1995, **376**, 323; S. V. Kolotuchin, E. E. Fenlon, S. R. Wilson, C. J. Loweth and S. C. Zimmerman, *Angew. Chem., Int. Ed. Engl.*, 1995, **34**, 2654; S. Subramanian and M. J. Zaworotko, *Angew. Chem., Int. Ed. Engl.*, 1995, **34**, 2127; M. Munakata, L. P. Wu, M. Yamamoto, T. Kuroda-Sowa and M. Maekawa, *J. Am. Chem. Soc.*, 1996, **118**, 3117.

5 D. B. Amabilino and J. F. Stoddart, *Chem. Rev.*, 1995, **95**, 2725; D. S. Reddy, D. C. Craig, A. D. Rae and G. R. Desiraju, *J. Chem. Soc., Chem. Commun.*, 1994, 1457; D. M. Goodgame, S. Menzer, A. M. Smith and D. J. Williams, *J. Chem. Soc., Chem. Commun.*, 1995, 1975; L. Carlucci, G. Ciani, D. M. Proserpio and A. Sironi, *J. Chem. Soc., Chem. Commun.*, 1994, 2755; P. M. V. Calcar, M. M. Olmstead and A. Balch, *J. Chem. Soc., Chem. Commun.*, 1995, 1723; L. R. MacGillivray, S. Subramanian and M. J. Zaworotko, *J. Chem. Soc., Chem. Commun.*, 1994, 1325.

6 F. H. Herbstein, M. Kapon and G. M. Reisner, *J. Inclusion Phenom.*, 1987, **5**, 211.

7 O. Ermer, *J. Am. Chem. Soc.*, 1988, **110**, 3747; O. Ermer, *Angew. Chem., Int. Ed. Engl.*, 1988, **27**, 829; X. Wang, M. Simard and J. D. Wuest, *J. Am. Chem. Soc.*, 1994, **116**, 12119.

8 Supramolecular carpets from multiple components were reported by us earlier: S. B. Copp, S. Subramanian and M. J. Zaworotko, *Angew. Chem., Int. Ed. Engl.*, 1993, **32**, 706; C. V. K. Sharma and M. J. Zaworotko, *Chem. Commun.*, 1996, 2655. Related coordination polymers have also been encountered: D. M. L. Goodgame, S. Menzer, A. M. Smith and D. J. Williams, *Angew. Chem., Int. Ed. Engl.*, 1995, **34**, 574.

9 A. Muller, H. Reuter and S. Dillinger, *Angew. Chem., Int. Ed. Engl.*, 1995, **34**, 2328; S. B. Copp and M. J. Zaworotko, unpublished results.



*Received, 17th May 1996; Revised manuscript received, 15th January 1997; Com. 7/00363C*

# Bandgap control through reduction of bond length alternation in bridged poly(diethienylethylene)s

**Hugues Brisset, Philippe Blanchard, Bertrand Illien, Amédée Riou and Jean Roncali***

*Ingénierie Moléculaire et Matériaux Organiques, CNRS UMR 6501, Université d'Angers, 2 Bd Lavoisier, F-49045 Angers, France*

**X-Ray structure analysis of a new rigid dithienylethylene shows that the observed reduction of the HOMO–LUMO gap results from a relaxation of bond length alternation.**

In recent years, the control of the bandgap (*E*g) of linearly π-conjugated systems has become one of the main challenges for synthetic chemists involved in the field of organic conductors. Since *E*g governs the intrinsic electronic properties of the π-conjugated system, progress in this area constitutes the key to many fundamental and technological problems and in the longer term to the possible achievement of intrinsic metallic conductivity.

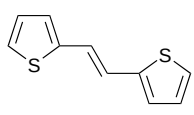
In addition to the degree of coplanarity of the π-conjugated backbone, the degree of bond length alternation (BLA) related to the difference between the average length of single and double bonds (δ*r*) represents the main contribution to the existence of a finite bandgap in π-conjugated polymers.[1]

Poly(isothianaphthene) was one of the earliest and most successful attempts at reducing *E*g in poly(heterocyclic) conjugated polymers.[2] The fusion of the benzene and thiophene rings leads to an increase in the quinoid character of the poly(thiophene) backbone, to the detriment of its aromaticity. This results in a relaxation of BLA accompanied with a reduction of *E*g from 2.0–2.2 eV for poly(thiophene)[3] to 1.1 eV.[4] While this approach is still widely used,[5] recent years have witnessed the emergence of other strategies, such as the introduction of electron-withdrawing groups at selected positions of the π-conjugated backbone[6] or the rigidification of the π-conjugated system.[7]

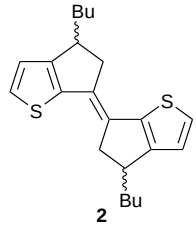
Recently, we have shown that the covalent bridging of the thiophene rings with the central double bond of dithienylethylene **1** leads to a reduction of the bandgap of the corresponding electrogenerated polymer from 1.80 to 1.40 eV.[8] However, the origin of this decrease in *E*g was not clearly identified.

We report here the synthesis and X-ray structural characterization of a new substituted bridged DTE **2**.† Experimental and theoretical data show unequivocally that the observed narrowing of the HOMO–LUMO gap results from a reduction of BLA induced by the rigidification of the DTE molecule.

The synthesis of 6,6′-bis(4-butyl-4,5-dihydro-6*H*-cyclopenta-[*b*]thienylidene) **2** is depicted in Scheme 1. 3-Pentanoylthiophene **6** was obtained by reaction of butylmagnesium bromide with thiophene-3-carbaldehyde **7** followed by oxidation of the resulting secondary alcohol with chromium trioxide. Wittig–Horner olefination of **6** with ethyl diethylphosphonoacetate gave a mixture of *Z* and *E* isomers of the α-unsaturated ester **5**. Saponification of **5** followed by reduction of the double bond with sodium amalgam and acidification gave carboxylic acid **4**.



**1**

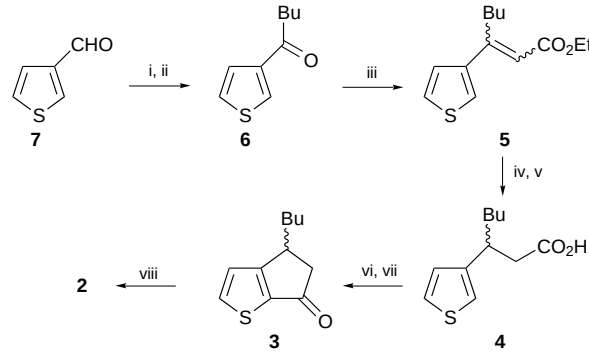


**2**

Conversion of **4** into the corresponding acid chloride and intramolecular Friedel–Crafts acylation yielded cyclic ketone **3** as a racemic mixture. The target compound **2** was then obtained as a mixture of diastereomers by McMurry dimerization of **3**.‡

Fig. 1 shows the ORTEP view of the *meso* form of 2.§ Molecules **1**[9] and **2** belong to the $C_i$ molecular point group. In both cases the thiophene ring is almost planar and there is a dihedral angle value of 3° between the thiophene ring average plane and the C1–C1′ double bond. The invariance of this angle shows that the reduction of *E*g observed for the polymers derived from bridged precursors[8] is not related to an enhancement of the planarity of the DTE moiety.

Comparison of the bond distances along the conjugated path for **1** and **2** (Table 1) shows that the bridging of the DTE molecule induces a deformation of the thiophene ring with a 0.031 and 0.044 Å shortening of the C5–C6 and C3–C6 bonds,




**Scheme 1** *Reagents*: i, BuMgBr; ii, $CrO_3$; iii, $(EtO)_2P(O)CH_2CO_2Et$, BuLi; iv, NaOH–EtOH; v, Na/Hg then HCl; vi, $SOCl_2$; vii $AlCl_3$; viii, $TiCl_4$–Zn

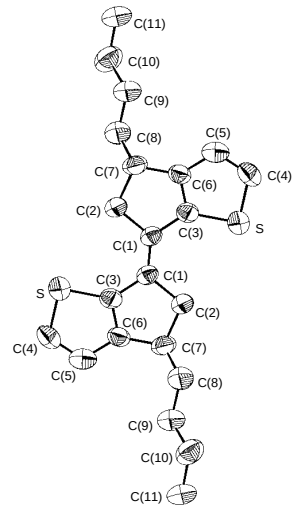



**Fig. 1** ORTEP view of **2**. H atoms omitted, ellipsoids drawn at 2.5% probability level

**Table 1** Selected bond lengths for compounds **1** and **2** along the conjugated path

| | Length/Å | |
|---|---|---|
| Bond | **1** | **2** |
| C4–C5 | 1.351(8) | 1.350(1) |
| C5–C6 | 1.44(1) | 1.409(8) |
| C6–C3 | 1.40(1) | 1.356(8) |
| C3–C1 | 1.457(7) | 1.440(7) |
| C1–C1′ | 1.309(8) | 1.335(6) |
| δ*r*/Å | 0.095 | 0.078 |

**Table 2** Anodic peak potentials[a] and computed HOMO–LUMO gaps for **1** and **2**

| Compound | *E*pa/V | $E_{HOMO}$/eV | $E_{LUMO}$/eV |
|---|---|---|---|
| **1** | 1.10 | −8.58 | −0.63 |
| **2** | 0.72 | −8.16 | −0.59 |

[a] Substrate ($10^{-3}$ M) in $Bu_4NPF_6$–MeCN (0.1 M), scan rate 100 mV $s^{-1}$, Pt electrodes, saturated calomel electrode.

respectively. On the other hand, the length of the C3–C1 single bond in the linker group decreases by 0.017 Å while that of the C1–C1′ central double bond increases by 0.026 Å. These various bond length modifications lead to a decrease of δ*r* from 0.095 Å for **1** to 0.078 Å for **2**.

Table 2 lists the values of the anodic peak potentials (*E*pa) for **1** and **2** together with the computed values of the HOMO and LUMO energies.¶ As for the parent unsubstituted analogue of **2**, the bridging of the DTE molecule leads to a *ca*. 0.40 V negative shift of *E*pa.[8] This difference, which nicely agrees with the 0.42 eV increase in $E_{HOMO}$, shows that the smaller HOMO–LUMO gap of bridged DTEs is related to an increase in $E_{HOMO}$.

These results, which confirm the efficiency of the rigidification approach for controlling *E*g, provide the first conclusive evidence that the bandgap of conjugated polymers is adjustable *via* bond length control.

## Footnotes

† The synthesis and characterization of poly(**2**) and other small bandgap polymers derived from substituted bridged DTEs will be published elsewhere.

‡ Satisfactory analytical and spectroscopic data were obtained.

§ *Crystal data* for **2**: $C_{22}H_{28}S_2$, $M_W$ = 356.58, monoclinic, *P*21/*n*, *Z* = 2, *a* = 11.891(7), *b* = 5.284(15), *c* = 15.89(2) Å, β = 100.98(7)°, *V* = 980(3) Å$^3$, λ = 0.71069 Å. Data collection: Data collection was carried out by zig-zag ω scan technique (2.5 ⩾θ⩾ 30°) on an Enraf-Nonius Mach III diffractometer. Conditions of measurements were $t_{max}$ = 40 s, range *h*, *k*, *l* (*h* 0,16; *k*, 0,7; *l*, −22,22). Intensity control reflections were measured every 2 h without appreciable Decay (0.15%). 3182 Independent reflections were collected from which 1071 correspond to $I > 3\sigma(I)$. Structure refinement: After Lorentz and polarisation corrections the structure was solved by direct methods (SIR) which reveal all the non-hydrogen atoms. After anisotropic refinement of all the C and S atoms, the coordinates of H atoms were determined from the HYDRO program. The whole structure was refined by full-matrix least-square techniques {refinement on *F*, *x*, *y*, *z*, $U_{ij}$ for S and C atoms, *x*, *y*, *z* and *U* fixed for H atoms; 109 variables and 1071 observations, weighting scheme: non-Poisson contribution with $w = 1/\sigma(F_0)^2 = 4F_0^2/[\sigma(I)^2 + (0.04\ F_0^2)^2]$· with the resulting *R* = 0.078, *R*w = 0.090}. All calculations were performed using the MolEN package.

Atomic coordinates, bond lengths and angles, and thermal parameters have been deposited at the Cambridge Crystallographic Data Centre (CCDC). See Information for Authors, Issue No. 1. Any request to the CCDC for this material should quote the full literature citation and the reference number 182/362.

¶ AM1 (ref. 10) calculations have been based on X-ray structures, however, since some hydrogen atoms were not experimentally defined, hydrogen atoms of all molecules were optimized at the AM1/RHF level using VAMP 5.51, (Oxford Molecular Ltd. England).

## References


1 J. L. Brédas, *J. Chem. Phys*., 1985, **82**, 3808; J. L. Brédas, G. B. Street, B. Thémans and J. M. André, *J. Chem. Phys*., 1985, **83**, 1323; O. Wennerström, *Macromolecules*, 1985, **18**, 1977; M. Kertesz and Y.-S. Lee, *J. Phys. Chem*., 1987, **91**, 2690.

2 F. Wudl, M. Kobayashi and A. J. Heeger, *J. Org. Chem*., 1984, **49**, 3382.

3 J. Roncali, *Chem. Rev*., 1992, **92**, 711.

4 J. L. Brédas, A. J. Heeger and F. Wudl, *J. Chem. Phys*., 1986, **85**, 4673.

5 D. Lorcy and M. P. Cava, *Adv. Mater*., 1992, **4**, 562; P. Bäuerle, G. Götz, P. Emerle and H. Port, *Adv. Mater*., 1992, **4**, 564.

6 T. M. Lambert and J. P. Ferraris, *J. Chem. Soc., Chem. Commun*., 1991, 752; E. E. Havinga, W. Ten Hoeve and H. Wynberg, *Synth. Met*., 1993, **55**–**57**, 299; M. Karikomi, C. Kitamura, S. Tanaka and Y. Yamashita, *J. Am. Chem. Soc*., 1995, **117**, 6791; H. A. Ho, H. Brisset, P. Frère and J. Roncali, *J. Chem. Soc., Chem. Commun*., 1995, 2309.

7 H. Brisset, C. Thobie-Gautier, A. Gorgues, M. Jubault and J. Roncali, *J. Chem. Soc., Chem. Commun*., 1994, 1305; H. Brisset, C. Thobie-Gautier, A. Gorgues, M. Jubault and J. Roncali, *J. Chem. Soc., Chem. Commun*., 1994, 1765; J. Roncali and C. Thobie-Gautier, *Adv. Mater*., 1994, **6**, 841.

8 J. Roncali, C. Thobie-Gautier, E. Elandaloussi and P. Frère, *J. Chem. Soc., Chem. Commun*., 1994, 2249.

9 G. Ruban and D. Zobel, *Acta Crystallogr., Sect. B*., 1975, **31**, 2632.

10 M. I. S. Dewar, E. G. Zoebish, E. F. Healy and J. J. P. Stewart, *J. Am. Chem. Soc*., 1985, **107**, 3902.


*Received, 21st November 1996; Com. 6/07890G*

# Oxidation of 2-phenylhydrazono-γ-butyrolactone: a novel ring expansion rearrangement leading to tetrahydro-1,3-oxazine-2,4-dione derivatives

**Derek H. R. Barton* and Wansheng Liu***

*Department of Chemistry, Texas A&M University, College Station, Texas 77843, USA*

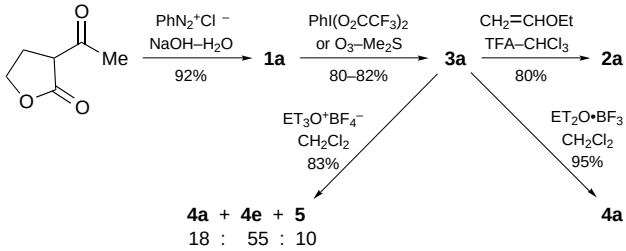
**2-Hydroxy-2-phenylazo-γ-butyrolactone 3a, prepared from oxidation of phenylhydrazone 1a, either decomposes to form α-keto-γ-butyrolactone 2a in 80% yield or rearranges to tetrahydro-1,3-oxazine-2,4-dione derivative 4a in 95% yield under different conditions.**

The chemistry of 1,3-oxazines has been of interest since the 1950s.[1] Preparative schemes for many 1,3-oxazine derivatives, especially tetrahydro-1,3-oxazines, were patented mainly as a result of their interesting biological activities. In addition to the synthetic utility of 5,6-dihydro-4*H*-1,3-oxazines,[2] another fact which makes 1,3-oxazine chemistry important is that some antibiotics contain the 1,3-oxazine ring.[1,3,4]

Tetrahydro-1,3-oxazine-2,4-diones are normally synthesized from β-hydroxy acids by reaction with sodium cyanate, followed by cyclization with thionyl chloride.[5] Alternative preparations utilize the reaction of oxetanes with either isocyanates or *S*-alkylthioureas. Here we report an unexpected rearrangement reaction leading to tetrahydro-1,3-oxazine-2,4-dione derivatives.

During the synthetic studies of 3-deoxy-D-*manno*-2-octulosonic acid (KDO), we encountered the sugar derivative 2-phenylhydrazono-γ-lactone **1b**.[6] Many failed attempts at the conversion of **1b** to KDO precursor **2b** prompted us to study oxidation of 2-phenylhydrazono-γ-butyrolactone **1a** (Scheme 1).[7] When **1a** was oxidized with bis(acetoxy)iodobenzene in ACOH, 2-acetoxy-2-phenylazo-γ-butyrolactone **3b**† was isolated as a bright yellow oil in 98% yield. Oxidation with bis(trifluoroacetoxy)iodobenzene (BTIB) in TFA afforded 2-trifluoroacetoxy-2-phenylazo-γ-butyrolactone **3c**, which hydrolysed with facility when exposed to air at room temperature. When the oxidation of **1a** by BTIB was carried out in MeCN–MeOH (5 : 1), crystalline 2-methoxy-2-phenylazo-γ-butyrolactone **3d** was obtained in 63% yield.

When **1a** was oxidized by BTIB in MeCN–MeOH (5 : 1), aqueous work-up with sodium hydrogen carbonate furnished 2-hydroxy-2-phenylazo-γ-butyrolactone **3a** in 80% yield after column chromatography. Ozonolysis of **1a** in methanol at −50 °C for 30 min followed by $Me_2S$ work-up also afforded **3a** in 82% yield. This intermediate behaved differently from the acyclic counterparts.[8] At room temp. **3a** decomposed to form two products, *i.e.* the expected 2-keto-γ-butyrolactone (so-called α-tetronic acid[9]) in the 2-enol tautomeric form **2a** by $^1$H and $^{13}$C NMR spectroscopy, and an unexpected rearrangement product tetrahydro-1,3-oxazine-2,4-dione derivative **4a**.

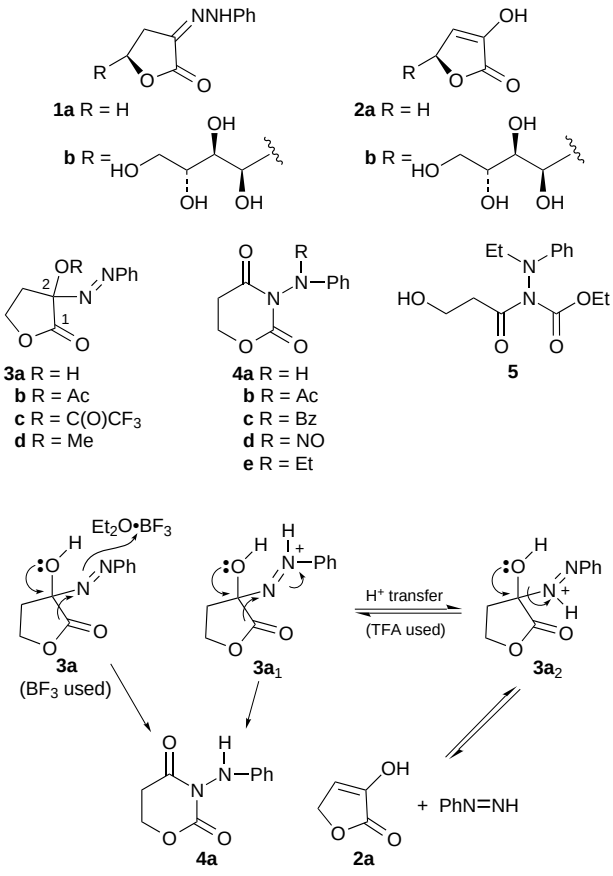



**Scheme 1**

The intermediate **3a** was surprisingly stable in the presence of $Et_3N$. By $^1$H NMR, only 10% decomposition was observed ten days after $Et_3N$ had been added to a $CDCl_3$ solution of **3a** at room temp. This suggested that **3a** does not readily decompose by loss of $PhN{=}N^-$ anion.[10] A simple explanation is that the formation of a carbonyl group in a five-membered ring α- to another carbonyl group is disfavoured by the strong dipole–dipole interaction. In contrast, in open chain compounds this transformation takes place easily[8] since the opposed dipole moments in the product cancel each other.

In $CDCl_3$, **3a** decomposed very rapidly to **2a** and **4a** when catalysed by TFA. The decomposition was much slower in both $Me_2CO$ and MeOH than in $CHCl_3$. The formation of phenyldiazene or the protonated congeners was readily observed by $^1$H NMR. When 1,4-benzoquinone, which is known to aid the decomposition by electron transfer of phenyldiazene,[11] was used with TFA, **2a** became the major product.

The above results suggested that a high concentration of TFA favoured rearrangement, whereas 1,4-benzoquinone promoted fragmentation. We propose that two different protonated forms of **3a**, *i.e.* $\mathbf{3a}_1$ and $\mathbf{3a}_2$, resulted in molecular rearrangement and elimination of phenyldiazene, respectively (Scheme 2). Re-




**Scheme 2**

moval of phenyldiazene by 1,4-benzoquinone drove the equilibrium between **3a**$_1$ and **3a**$_2$ towards the formation of **2a**. It is known that phenyldiazene reacts with 1,4-benzoquinone in a stoichiometry of approximately 2:1.[12] This is supported by the observation that half an equiv. of 1,4-benzoquinone produced a higher **2a** : **4a** ratio. Apparently, 1,4-benzoquinone reduced the formation of benzene. In addition to quinones, ethyl vinyl ether in the presence of TFA was found to be highly effective in favouring the formation of **2a**. It was assumed that the driving force came from the trapping of phenyldiazene by the carbocation $EtO^+Me$, which is generated by the reaction of ethyl vinyl ether and TFA. A preparative experiment gave crystalline **2a** in 80% yield when **3a** was treated with TFA in the presence of excess ethyl vinyl ether in $CHCl_2$. Considering the difficulties encountered by others in attempts to convert 2-oximino-γ-butyrolactone to **2a**,[9] we conclude that the present procedure from the phenylhydrazone provides an attractive alternative. In principle it constitutes an efficient method of preparing 2-keto-γ-butyrolactones from simple, commercially available starting materials.[13]

Interestingly, **3a** readily rearranged to crystalline **4a** in 95% yield when treated with $BF_3{\cdot}Et_2O$ in $CH_2Cl_2$ at room temp. To our knowledge, this seems to be the first example of a 1,2-migration of an oxycarbonyl group from carbon to azo-nitrogen. Similarly, when **3a** was treated with Meerwein's salt ($Et_3O^+BF_4^-$),[14] three products were isolated: **4a** (18%), *N*′-ethylated derivative **4e** (55%), and *N*′,*O*-bis-ethylated derivative **5** (10%). When the reaction between **3a** and $BF_3{\cdot}Et_2O$ was carried out in $CDCl_3$ and followed by NMR, it was observed that an intermediate formed immediately when $BF_3$ was added, and then gradually decomposed to **4a** at room temp. The proposed mechanism is illustrated in Scheme 2.

Compound **4a** was readily acylated and nitrosated at the *N*′-position to give crystalline derivatives. Although the reaction between **4a** and $Ac_2O$–pyridine–DMAP was very sluggish even at elevated temperatures, the *N*′-acetyl derivative **4b** was readily obtained in quantitative yield at room temp. when **4a** reacted with neat acetyl chloride. The benzoyl derivative **4c** was also obtained quantitatively when benzoyl chloride was used at 60 °C. When **4a** was treated with isoamyl nitrite in $CH_2Cl_2$ at room temp., *N*′-nitroso compound **4d** was obtained quantitatively after 10 min.

Reduction of the *N*′-nitroso derivative **4d** by zinc in AcOH gave **4a** and unsubstituted tetrahydro-1,3-oxazine-2,4-dione[15] in a 1:1 ratio. The NMR and GC–MS spectra of the latter were in agreement with the literature data. This supported the proposed structure of **4a**. When **4d** was treated with zinc in AcHO–pyridine at 0 °C, **4a** was obtained in 66% yield after 30 min.

The structure of **4a** was further verified through degradation reactions. Hydrolysis of **4a** by NaOH in MeOH furnished methyl β-(hydroxypropionyloxy)propionate [$HO(CH_2)_2$-$CO_2(CH_2)_2CO_2Me$] in 61% yield. The product was identical by IR, $^1$H, and $^{13}$C NMR to an authentic sample prepared from β-propiolactone.[16] Similarly, methanolysis of **4b** in the presence of potassium carbonate gave *N*-acetylphenylhydrazine [$PhN(Ac)NH_2$[17]] in 62% yield.

In conclusion, a novel rearrangement reaction provided efficient entry to interesting *N*-substituted tetrahydro-1,3-oxazine-2,4-dione derivatives. It is conceivable that the reaction may be extended to the construction of other related heterocyclic compounds.

Financial support from the National Institutes of Health and the Schering-Plough Corporation is gratefully acknowledged.

## Footnote

† All new compounds gave satisfactory $^1$H and $^{13}$C NMR spectra, and microanalytical data.

## References

1 Z. Eckstein and T. Urbanski, *Adv. Heterocycl. Chem.*, 1963, **2**, 311; Z. Eckstein and T. Urbanski, *Adv. Heterocycl. Chem.*, 1978, **23**, 1; T. Kato, N. Katagiri and Y. Yamamoto, *Heterocycles*, 1980, **14**, 1333.
2 A. I. Meyers, *Heterocycles in Organic Synthesis*, Wiley, New York, 1974, pp. 160–266; R. R. Schmidt, *Synthesis*, 1972, 333.
3 T. Haneishi, T. Okazaki, T. Hata, C. Tamuta, M. Namura, A. Naito, I. Seki and M. Arai, *J. Antibiot.*, 1971, **24**, 797; K. Sasaki, Y. Kusakabe and S. Esumi, *J. Antibiot.*, 1972, **25**, 151; Y. Kusakabe, J. Nagatsu, M. Shibuya, O. Kawaguchi, C. Hirose and S. Shirato, *J. Antibiot.*, 1972, **25**, 44; D. B. Silvano and W. Manfred, *J. Org. Chem.*, 1972, **42**, 109.
4 M. S. von Wittenau and H. Els, *J. Am. Chem. Soc.*, 1961, **83**, 4678.
5 M. Sainsbury, in *Comprehensive Heterocyclic Chemistry*, ed. A. R. Katritzky and C. W. Rees, Pergamon, New York, 1984, vol. 3, pp. 995–1038.
6 D. H. R. Barton, J. C. Jaszberenyi, W. Liu and T. Shinada, *Tetrahedron*, 1996, **52**, 2717.
7 R. H. Harradence and F. Lions, *J. Proc. Royal Soc. N. S. Wales*, 1938, **72**, 221.
8 D. H. R. Barton, J. Cs. Jaszberenyi, W. Liu and T. Shinada, *Tetrahedron*, 1996, **52**, 14 673.
9 L. Kletz and A. Lapworth, *J. Chem. Soc.*, 1915, **107**, 1254.
10 P. C. Huang and E. M. Kosower, *J. Am. Chem. Soc.*, 1968, **90**, 2354.
11 E. M. Kosower, *Acc. Chem. Res.*, 1971, **4**, 193.
12 P. C. Huang and E. M. Kosower, *J. Am. Chem. Soc.*, 1968, **90**, 2367.
13 H. Schinz and M. Hinder, *Helv. Chim. Acta*, 1947, **30**, 1349; C. G. Wermuth, *Bull. Soc. Chim. Fr.*, 1966, 1435; H. H. Wasserman and J. L. Ives, *J. Org. Chem.*, 1978, **43**, 3238; I. Tapia, V. Alcazar, J. R. Moran, C. Caballero and M. Grande, *Chem. Lett.*, 1990, 697.
14 H. Meerwein, *Org. Synth.*, 1973, **Coll. Vol. 5**, 1080.
15 S. Ozaki and T. Kato, *J. Polym. Sci., C*, 1968, 695.
16 T. L. Gresham, J. E. Jansen, F. W. Shaver, J. T. Gregory and W. L. Beears, *J. Am. Chem. Soc.*, 1948, **70**, 1004.
17 H. Yamamoto, *J. Org. Chem.*, 1967, **32**, 3693.

*Received, 15th November 1996; Com. 6/07830C*

# Bis(amido)calix[4]arenes in the pinched cone conformation as tuneable hydrogen-bonding anion receptors

**Beth R. Cameron and Stephen J. Loeb*†**

*Department of Chemistry and Biochemistry, University of Windsor, Windsor, Ontario, Canada N9B 3P4*

**Calix[4]arene units functionalized at the 1,3-positions of the upper rim with amido groups, –NHC(O)X, act as neutral, hydrogen-bonding receptors for hydrogen sulfate, dihydrogen phosphate, acetate, benzoate, nicotinate, oxalate, terephthalate, isophthalate and fumarate with binding strength and selectivity tunable by varying the electron-withdrawing ability of the terminal substituent X (X = $CH_2Cl$, $CHCl_2$, $CCl_3$).**

Increased interest in the molecular recognition of anionic substrates has led to the synthesis and evaluation of a variety of anion receptors.[1] The most common employ ammonium or guanidinium binding sites while recently electron-deficient, Lewis acid centres such as tin,[2] boron,[3] mercury,[4] silicon[5] and the uranyl ion[6] have received attention. Although some of these systems are quite efficient receptors, it is interesting to note that anion binding by proteins is most commonly achieved *via* neutral amide functions employing the hydrogen-bond accepting properties of the amido NH group.[7] Indeed, some very efficient anion ($Cl^-$, $H_2PO_4^-$) receptors containing both Lewis acidic centres and amide binding sites have been reported recently.[6,8]

A major disadvantage to employing the amide function –NHC(O)– is the rigid directionality of the NH group which makes if difficult to incorporate into a highly structured framework such as a macrocycle.[9] This problem can be overcome by including the amide function as a terminal group on the upper-rim of a calix[4]arene framework.[10] We report herein the syntheses of bis(amido)calix[4]arene-based anion receptors which exhibit a selectivity for carboxylate ions, particularly benzoate derivatives, over tetrahedral oxyanions.

Receptors **2** and **3** were prepared by the reaction of 5,17-bis-(amino)-25,26,27,28-tetrapropoxycalix[4]arene with 2.5 equiv. of dichloroacetyl chloride or trichloroacetyl chloride in a manner similar to the published procedure for **1**.[11]‡§

Initially, the anion complexation properties of receptor **1** were investigated using $^1$H NMR spectroscopy and association constants were measured for a variety of simple anions (Table 1). In each case, the anion–receptor stoichiometry was confirmed to be 1 : 1 by a Job plot. These results indicate a preference for the Y-shaped carboxylate anions acetate and benzoate over tetrahedral-shaped anions, $H_2PO_4^-$, $ReO_4^-$ and $HSO_4^-$. For example, addition of 1 equiv. of $[Bu_4N^+][C_6H_5CO_2^-]$ to a $10^{-3}$ mol $dm^{-3}$ solution of **1** in $CDCl_3$ resulted in a dramatic downfield shift of 1.33 ppm for the amide NH proton and a moderate downfield shift of 0.12 ppm for the $CH_2Cl$ resonance. Whereas, the same experiment using $H_2PO_4^-$ resulted in much smaller downfield shifts of 0.90 and a 0.07 ppm for the NH and $CH_2Cl$ resonances.

It is reasonable to assume that increasing the acidity of the amide proton by introducing more effective electron-withdrawing groups in the terminal position would enhance anion binding. This was investigated by measuring the binding of benzoate ion with a series of receptors differing only in the terminal substituent X, in the NHC(O)X group (X = $CH_2Cl$, $CHCl_2$, $CCl_3$) (Table 2). Receptor **2** exhibits the highest association constant with downfield shifts of 2.38 and 0.73 ppm observed for the NH and $CHCl_2$ resonances in the $^1$H NMR spectrum of **2** upon addition of 1 equiv. of benzoate anion. The replacement of hydrogen by chlorine results in a *ca*. 50-fold increase in association constant.

The benzoate anion binds in a bidentate fashion to the two amide protons present on the upper rim of the calix[4]arene (Fig. 1). In order for this to occur, the calix[4]arene must exist in the pinched cone conformation in which the rings bearing the amide groups are essentially parallel. This is clearly demonstrated by observed changes in the $^1$H NMR spectra upon anion binding. The $^1$H NMR spectrum of **2** exhibits a singlet for the four aromatic protons on the amido substituted rings and an unresolved multiplet for the six protons on the unsubstituted rings. Addition of benzoate ion results in an upfield shift of the substituted ring protons and a downfield shift and resolution of

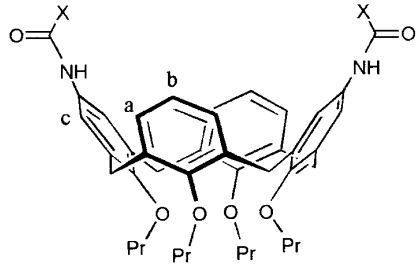
**Table 1** $K_{ass}$ Values of receptor **1**

| Anion | $H_2PO_4^-$ | $HSO_4^-$ | $ReO_4^-$ | $CH_3CO_2^-$ | $C_6H_5CO_2^-$ |
|---|---|---|---|---|---|
| $K_{ass}$ 1 | 22 | 27 | < 10 | 88 | 107 |

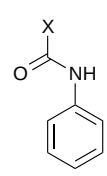
**Table 2** $K_{ass}$ Values of benzoate anion with receptors **1**–**6**

| Receptor | **1** | **2** | **3**[a] | **4** | **5** | **6**[a] |
|---|---|---|---|---|---|---|
| $K_{ass}$ 1 | 107 | 5160 | — | 81 | 210 | — |

[a] No binding is observed.




**1** X = $CH_2Cl$
**2** X = $CHCl_2$
**3** X = $CCl_3$




**4** X = $CH_2Cl$
**5** X = $CHCl_2$
**6** X = $CCl_3$

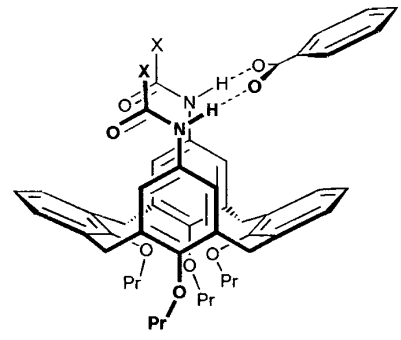


**Fig. 1**

the protons on the unsubstituted ring. Also, the $OCH_2$ resonances which overlap in **2** resolve into two distinct triplets and the $CHCl_2$ protons are systematically shifted downfield upon anion binding (Fig. 2). These changes can be attributed to a perturbation of the see-saw motion between the two pinched cone conformers of the calix[4]arene skeleton. This conformational isomerism is usually ignored in calix[4]arene chemistry, although the energy barrier to this interconversion was measured to be *ca*. 40 kJ $mol^{-1}$.[12] Thus, anion coordination freezes the calixarene unit in the pinched cone conformation with the substituted rings parallel and allows for two linear hydrogen bonding interactions between receptor and anion.

Surprisingly, the presence of three chloro substituents results in absolutely no binding of the anion as is evident from the absence of any change in the $^1$H NMR spectrum. Since the model compound **6** also showed no change in the $^1$H NMR spectrum with the addition of 10 equiv. of benzoate anion, it is likely that the amide protons in receptors **3** and **6** are inaccessible for the approach of the anion due to steric crowding of the trichloromethyl substituents rather than an inability of **3** to achieve the appropriate pinched cone conformation.

Association constants for various other mono-carboxylate anions with receptor **2** are given in Table 3 These results demonstrate that receptor **2** is not only selective for carboxylate ions but has a particular affinity for the benzoate ion. Examination of CPK models suggested a more open conformation might provide a suitable geometric fit for some dicarboxylates. The binding of receptor **2** with dicarboxylate ions was investigated and results are also given in Table 3.

A Job plot of receptor **2** with oxalate anion showed 1 : 1 complexation. The changes evident in the aromatic region of the spectrum of **2** are opposite to those demonstrated with the benzoate anion. This suggests that the calix[4]arene exists in a pinched cone conformation in which the unsubstituted rings are parallel. This allows accommodation of the dianion and still maintains a 1 : 1 stoichiometry. In contrast, the larger dicarboxylate anions (isophthalate, terephthalate, fumarate) were found by Job plots to bind with an anion–receptor ratio of 1 : 2. $^1$H NMR Spectra show the same trends observed for benzoate and suggest that the calixarene receptors can be assembled around the anion with a similar coordination mode for each carboxylate group.

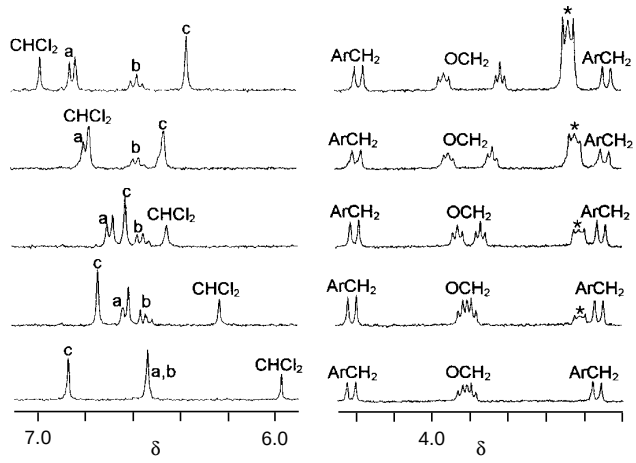



**Fig. 2** $^1$H NMR spectra of stepwise addition of 0.0 (bottom), 0.25, 0.50, 1.0 and 2.0 equiv. of $[Bu_4N][C_6H_5CO_2]$ to receptor **2** (* = peak due to $Bu_4N^+$ cation). Aromatic H-atoms a, b and c are assigned as in Fig. 1.

**Table 3** $K_{ass}$ Values of **2** with monocarboxylate and dicarboxylate anions

| Anion | Benzoate[a] | Nicotinate[a] | Acetate[a] | Oxalate[a] | Isophthalate[b] | Terephthalate[b] | Fumarate[b] |
|---|---|---|---|---|---|---|---|
| $K_{ass}$ 1 | 5160 | 821 | 609 | 707 | $> 10^6$ | $> 10^6$ | $> 10^6$ |

[a] Stoichiometry is 1 : 1. [b] Stoichiometry is 1 : 2 and values are $\beta(K_1K_2)$.

In summary, neutral, hydrogen-bonding anion receptors can be derived from a pair of terminal amido groups built into a calix[4]arene framework. The pinched cone conformation is flexible enough to allow for the binding of a variety of anions and the acceptor properties of the amido group can be tuned by varying the electron-withdrawing nature of the terminal substituent. These new receptors are selective for Y-shaped carboxylate ions over tetrahedral anions and show a particular preference for benzoate derivatives.

We thank the Natural Science and Engineering Council of Canada and the Petroleum Research Fund administered by the American Chemical Society for financial support of this research.

## Footnotes

† E-mail: loeb@uwindsor.ca

‡ All new compounds were successfully characterized by $^1$H and $^{13}$C NMR spectroscopy, LSIMS and elemental analysis. $^1$H NMR Titrations: varying amounts of stock solutions of anionic guests (0.0125 mol $dm^{-3}$) were added to 0.1 $cm^3$ aliquots of host solutions (0.005 mol $dm^{-3}$ stock solutions) and were made up to 0.5 $cm^3$ with solvent to maintain a constant volume and thus a constant host concentration of 0.001 mol $dm^{-3}$. Anion–receptor ratios were varied from 0.1–10. $K_{ass}$ Values were determined using the chemical shift of the amide proton as the probe. Values were fitted using the program EQNMR[13] with errors < 10% for $K_{ass}$ > 100 and errors < 5% for $K_{ass}$ < 100.

§ *Selected data* for **2**: $^1$H NMR ($CDCl_3$) δ 7.87 (s, NH, 2 H), 6.87 (s, ArH, 4 H), 6.54 (s, ArH, 6 H), 5.97 (s, $CHCl_3$, 2 H), 4.43 (d, $ArCH_2$, 4 H), 3.82 (m, $OCH_2$, 8 H), 3.13 (d, $ArCH_2$, 4 H), 1.91 (m, $CH_2$, 8 H), 0.97 (m, Me, 12 H); $^{13}$C NMR ($CDCl_3$) δ 161.62, 156.10, 154.90, 136.24, 134.07, 129.87, 128.14, 122,36, 121.29, 76.84, 66.96, 31.00, 23.23, 23.14, 10.36, 10.20; LSIMS *m/z* $[M + H]^+$ = 845. For **3**: $^1$H NMR ($CDCl_3$) δ 8.23 (s, NH, 2 H), 7.19 (s, ArH, 4 H), 6.37 (m, ArH, 6 H), 4.45 (d, $ArCH_2$, 4 H), 3.95 (t, $OCH_2$, 4 H), 3.73 (t, $OCH_2$, 4 H), 3.15 (d, $ArCH_2$, 4 H), 1.91 (m, $CH_2$, 8 H), 1.05 (t, Me, 6 H), 0.92 (t, $CH_3$, 6 H); $^{13}$C NMR ($CDCl_3$) δ 159.15 (CO), 155.61, 155.59, 137.27, 133.21, 129.65, 127.87, 122.43, 120.98 (ArC), 93.06 ($CCl_3$), 77.05, 76.85 ($OCH_2$), 31.08 ($ArCH_2$), 23.45, 23.08 ($CH_2$), 10.67, 10.05 ($CH_3$); LSIMS *m/z* $[M]^+$ = 913.

## References

1 B. Dietrich, *Pure Appl. Chem.*, 1993, **65**, 1457; C. Seel and J. de Mendoza, in, *Comprehensive Supramolecular Chemistry*, ed. F. Vogtle, Elsevier Science, New York, 1996, vol. 2, ch. 17, pp. 519–552.
2 M. Newcomb, J. H. Horner, M. T. Blanda and P. J. Squattrito, *J. Am. Chem. Soc.*, 1989, **111**, 6294.
3 M. T. Reetz, C. M. Niemeyer and K. Harms, *Angew. Chem., Int. Ed. Engl.*, 1991, **30**, 1472.
4 X. Yang, C. B. Knobler and M. F. Hawthorne, *Angew. Chem., Int. Ed. Engl.*, 1991, **30**, 1507.
5 H. E. Katz, *J. Am. Chem. Soc.*, 1986, **108**, 7640.
6 D. M. Rudkevich, W. Verboom, Z. Brzozka, M. J. Palys, W. P. R. V. Stauthamer, G. J. van Hummel, S. M. Franken, S. Harkema, J. F. J. Engbersen and D. N. Reinhoudt, *J. Am. Chem. Soc.*, 1994, **116**, 4341.
7 D. Voet and J. G. Voet, *Biochemistry*, Wiley, New York, 1995.
8 P. D. Beer, *Chem. Commun.*, 1996, 689; D. M. Rudkevich, J. D. Mercer-Chalmers, W. Verboom, R. Ungaro, F. de Jong and D. N. Reinhoudt, *J. Am. Chem. Soc.*, 1995, **117**, 6124.
9 S. Valiyaveettil, J. F. J. Engbersen, W. Verboom and D. N. Reinhoudt, *Angew. Chem., Int. Ed. Engl.*, 1993, **32**, 900.
10 Y. Morzherin, D. M. Rudkevich, W. Verboom and D. N. Reinhoudt, *J. Org. Chem.*, 1993, **58**, 7602; J. Scheerder, J. P. M. van Duynhoven, J. F. J. Engbersen and D. N. Reinhoudt, *Angew. Chem., Int. Ed. Engl.*, 1996, **35**, 1090.
11 D. M. Rudkevich W. Verboom and D. N. Reinhoudt, *J. Org. Chem.*, 1994, **59**, 3683.
12 A. Arduini, M. Fabbi, M. Mantovani, L. Mirone, A. Pochini, A. Secchi and R. Ungaro, *J. Org. Chem.*, 1995, **60**, 1454.
13 M. J. Hynes, *J. Chem. Soc., Dalton Trans.*, 1993, 311.

*Received, 13th November 1996; Com. 6/07726I*

# Mesoporous aluminoborates

**S. Ayyappan and C. N. R. Rao***

*CSIR Centre of Excellence in Chemistry and Materials Research Centre, Indian Institute of Science, Bangalore 560 012, India and Jawaharlal Nehru Centre for Advanced Scientific Research, Jakkur, Bangalore 560 064, India*

**Hexagonal, cubic and lamellar aluminoborate mesophases containing octahedral aluminium and tetrahedral boron are prepared and characterized for the first time.**

Since the first synthesis of mesoporous silica,[1] there has been intense activity in the design and synthesis of a variety of mesoporous solids.[2–4] These studies have also unravelled the mechanism of formation of these materials by means of supramolecular templating involving an unusual combination of surfactant aggregates and anionic silicate species.[4,5] By varying the pH or the surfactant to silica ratio, hexagonal, cubic and lamellar forms of silica mesophases have been prepared.[6] Besides ionic surfactants, neutral amines[7] and polyalkene oxides[8] have been employed to synthesise the mesophases. The strategy to prepare silica-based mesophases has been extended to prepare a variety of mesoporous metal oxides such as $Al_2O_3$,[8] $TiO_2$[9,10] and $ZrO_2$[11] and $Nb_2O_5$.[12] $AlPO_4$ which is isoelectronic with $SiO_2$ has provided the basis for a distinct family of microporous materials.[13] However, efforts to make hexagonal mesoporous $AlPO_4$ have not been successful; instead, only lamellar $AlPO_4$ has been obtained.[14] We considered it most worthwhile to explore the synthesis of the mesoporous phases of the analogous aluminoborates containing the $AlBO_4^{2-}$ species. There has been some effort[15] to make microporous aluminoborates with different B/Al ratios, but the products do not seem to have been adequately characterized. Here, we report the first successful synthesis and characterization of mesoporous aluminoborate phases in hexagonal, cubic and lamellar forms. It has been possible to remove the surfactant from the hexagonal phase and expand the pore size of the hexagonal phase by using aliphatic hydrocarbons as solubilizing agents.

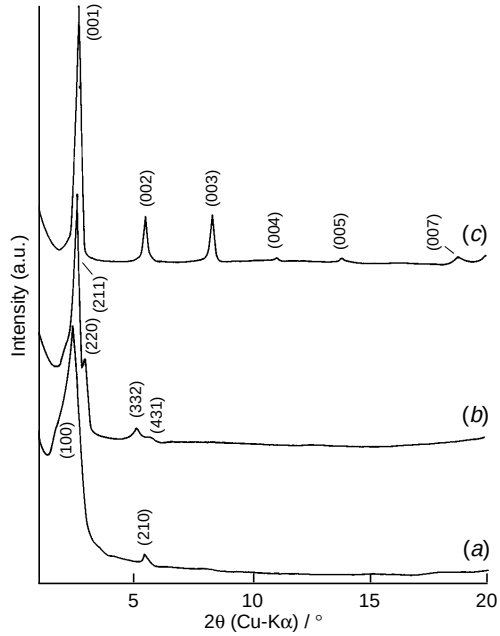



**Fig. 1** X-Ray diffraction patterns of the aluminoborate mesophases: (*a*) hexagonal, (*b*) cubic and (*c*) lamellar

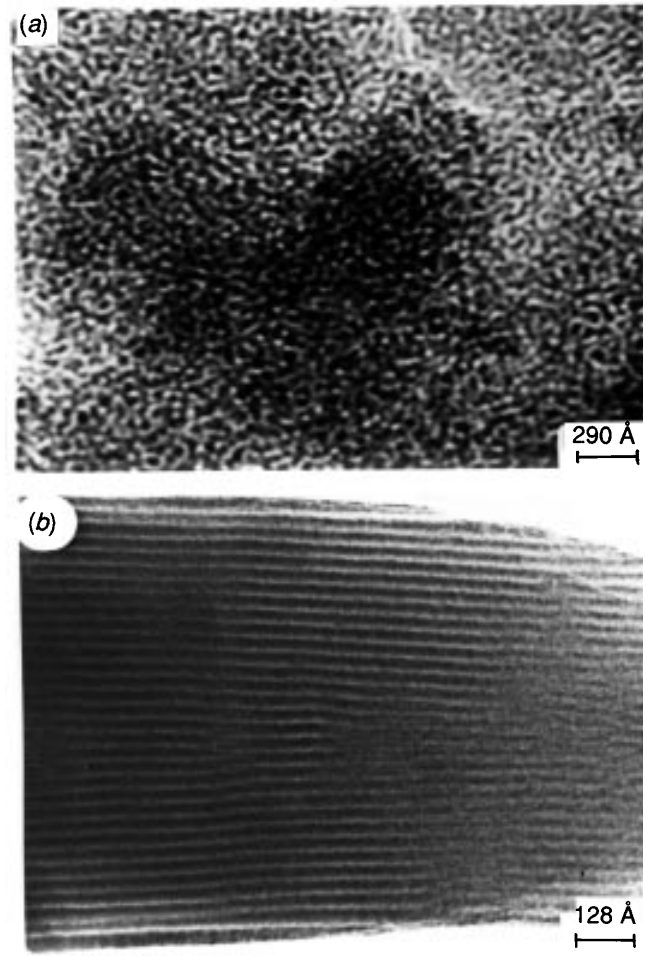



**Fig. 2** TEM images of (*a*) hexagonal and (*b*) lamellar aluminoborate mesophases

Mesoporous aluminoborate phases could not be obtained when cationic surfactants or long-chain amines were employed for the synthesis. They could however be prepared by employing sodium dodecyl sulfate (SDS) as the surfactant. In a typical preparation, to a solution containing Ca, Al and B in 1 : 1 : 1 molar ratio, prepared by dissolving appropriate quantities of CaO and $Al(NO_3)_3$ and boric acid in aqueous nitric acid, sodium dodecyl sulfate (1.0 mol with respect to Ca or Al) was added under stirring. Ammonia was added to the resulting turbid solution under constant stirring to reach the desired value of pH. The resultant gel was maintained at room temperature for 48 h. The product so obtained was washed several times with distilled water and dried at 100 °C in a hot air oven. X-Ray diffraction (XRD) patterns of the dried solids were recorded with a Rich–Seifert (model XRD 3000TT) instrument. Fig. 1 shows the XRD patterns of the products obtained at different pH values. The XRD pattern of the product obtained at pH 2 [Fig. 1(*a*)] is characteristic of a hexagonal phase with a $d_{100}$ value of 36.1 Å ($a_0$ = 41.7 Å). The XRD pattern of the product

obtained at a pH of 3.5 [Fig. 1(*b*)] corresponds to that of a cubic phase. This pattern could be indexed with $a$ = 83.5 Å. The XRD pattern of the product obtained at pH *ca*. 5.5 [Fig. 1(*c*)] is characteristic of a lamellar phase and accordingly exhibits the various 00*l* reflections ($d_{001}$ = 32.5 Å). The scanning electron micrographs of the hexagonal and lamellar phases exhibit characteristic differences in morphology, the lamellar form showing the flaky structure. The transmission electron microscope (TEM) image (recorded with a JEOL JEM 3010 microscope) reveals the presence of disordered hexagonal pores with an opening of *ca*. 32 Å with a wall thickness of *ca*. 11 Å [Fig. 2(*a*)]. The TEM image of the lamellar phase shows an interlayer separation of *ca*. 32 Å [Fig. 2(*b*)].

EDAX analysis of the aluminoborate mesophases showed the Ca : Al molar ratio to be 1 : 1, while an ICP analysis gave a Al : B molar ratio of 1 : 1. Thermogravimetry showed the loss of water by 150 °C and of the surfactant by 600 °C. Based on the mass loss data and assuming the Ca : Al : B molar ratio to be 1 : 1 : 1, the composition of the aluminoborate–surfactant adduct works out to be $CaO{\cdot}0.5Al_2O_3{\cdot}0.5B_2O_3{\cdot}0.6SDS{\cdot}1.5H_2O$. The %mass of boron from the ICP analysis (3.15 ± 0.25%) is also consistent with the theoretical value of 3.2% based on the empirical formula. The IR spectrum of this adduct showed a boron–oxygen stretching band in the region 900–1100 $cm^{-1}$ due to $BO_4$ tetrahedra. The IR band characteristic of $BO_3$ units in the region 1200–1400 $cm^{-1}$ was absent. Significant structural information was obtained by means of $^{27}Al$ and $^{11}B$ MAS NMR spectra (recorded with a Bruker MSL-300 spectrometer) of the hexagonal aluminoborate mesophase. The $^{27}Al$ NMR signal is centred around δ 0.0 [Fig. 3(*a*)], characteristic of an octahedral environment of Al.[16] The $^{11}B$ NMR signal is also centred around δ 0.0 [Fig. 3(*b*)] suggesting a tetrahedral environment for boron.[17]

By heating the as-prepared hexagonal mesophase to 300 °C, we could remove some of the surfactant without destroying the structure. Thus, the XRD pattern of the resulting product shows the mesoporous structure with a $d_{100}$ value of 35.2 Å. We could however remove the surfactant by refluxing the hexagonal mesophase with acidified ethanol for 3 h. The removal of the template was confirmed by the absence of mass loss over the temperature range where the template is normally removed as well as by the XRD pattern. The removal of the surfactant from the hexagonal phase was confirmed by the IR spectra,which showed the near-absence of bands arising from $CH_2$ groups. Accordingly, the surface area of the hexagonal aluminoborate obtained by calcination was *ca*. 100 $m^2\ g^{-1}$ and that of the sample obtained by alcohol extraction was 470 $m^2\ g^{-1}$; their XRD patterns were not identical.

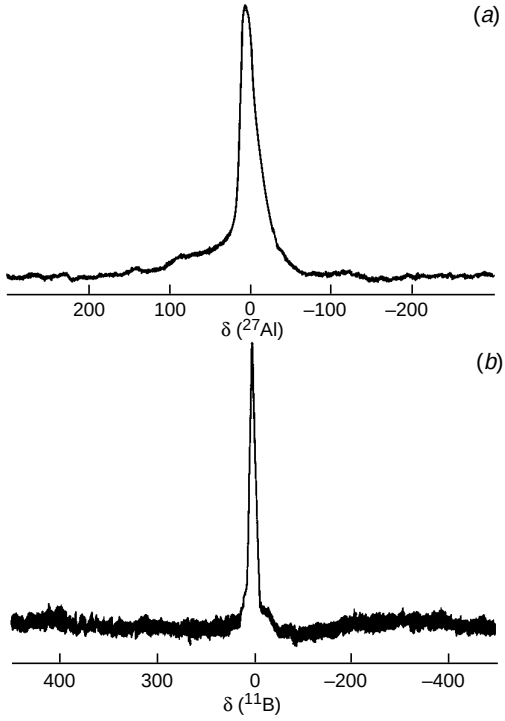



**Fig. 3** MAS NMR spectra of mesoporous aluminoborate: (*a*) $^{27}Al$ spectrum and (*b*) $^{11}B$ spectrum

We have been able to expand the pore size of the hexagonal mesoporous aluminoborate by the use of *n*-alkanes as solubilizing agents. For this purpose, we added the alkane along with the surfactant solution to the acidic solution containing Ca, Al and B, maintaining the molar ratio of the alkane to the surfactant to be 1 : 1. This molar ratio was found to be optimal for expanding the pore size. The XRD patterns gave $d_{100}$ values of 49.0 and 56.6 Å respectively with *n*-octane and *n*-hexadecane, compared to the value of 36.1 Å obtained in the absence of the alkanes.

We have also varied the Al : B ratio and obtained hexagonal mesoporous phases with Al : B ratios down to 0.5 : 1.5. By using $Na^+$ as the cation instead of $Ca^{2+}$, a hexagonal mesoporous phase with a Na : Al : B ratio of 2 : 1 : 1 was obtained with a $d_{100}$ value of 35.5 Å.

## References


1 J. S. Beck, J. C. Vartuli, W. J. Roth, M. E. Leonowicz, C. T. Kresge, K. D. Schmitt, C. T. W. Chu, D. H. Olson, E. W. Sheppard, S. B. McCullen, J. B. Higgins and J. L. Schlenker, *J. Am. Chem. Soc.*, 1992, **114**, 10 834.

2 P. Behrens and G. D. Stucky, *Angew. Chem., Int. Ed. Engl.*, 1993, **32**, 696.

3 P. Behrens, *Angew. Chem., Int. Ed. Engl.*, 1996, **35**, 515.

4 J. S. Beck and J. C. Vartuli, *Curr. Opinion Solid State Mater. Sci.*, 1996, **1**, 76.

5 Q. Huo, D. I. Margolese, U. Ciesla, D. G. Demuth, P. Feng, T. E. Gier, P. Sieger, A. Firouzi, B. F. Chmelka, F. Schüth and G. D. Stucky, *Chem. Mater.*, 1994, **6**, 1176; Q. Huo, D. Margolese and G. D. Stucky, *Chem. Mater.*, 1996, **8**, 1147.

6 A. Monnier, F. Schüth, Q. Huo, D. Kumar, D. Margolese, R. S. Maxwell, G. D. Stucky, M. Krishnamurty, P. Petroff, A. Firouzi, M. Janicke and B. F. Chmelka, *Science*, 1993, **261**, 1299; J. C. Vartuli, K. D. Schmitt, C. T. Kresge, W. J. Roth, M. E. Leonowicz, S. B. McCullen, S. D. Helbring, J. S. Beck, J. S. Schlenker, D. H. Olson and E. W. Sheppard, *Chem. Mater.*, 1994, **6**, 2317.

7 P. T. Tanev and T. J. Pinnavaia, *Science*, 1995, **267**, 365.

8 S. A. Bagshaw and T. J. Pinnavaia, *Angew. Chem., Int. Ed. Engl.*, 1996, **35**, 1102.

9 D. M. Antonelli and J. Y. Ying, *Angew. Chem., Int. Ed. Engl.*, 1995, **34**, 2014.

10 N. Ulagappan and C. N. R. Rao, *Chem. Commun.*, 1996, 1685.

11 U. Ciesla, S. Schacht, G. D. Stucky, K. K. Unger and F. Schüth, *Angew. Chem., Int. Ed. Engl.*, 1996, **35**, 426; N. Ulagappan, Neeraj, B. V. N. Raju and C. N. R. Rao, *Chem. Commun.*, 1996, 2243.

12 D. M. Antonelli and J. Y. Ying, *Angew. Chem., Int. Ed. Engl.*, 1996, **35**, 426.

13 S. T. Wilson, B. M. Lok, C. A. Messina, T. R. Connan and E. M. Flanigan, *J. Am. Chem. Soc.*, 1982, **104**, 1176.

14 A. Sayari, V. R. Karra, J. S. Reddy and I. L. Moudrakovski, *Chem. Commun.*, 1996, 411.

15 J. Wang, S. Feng and R. Xu, *J. Chem. Soc., Chem. Commun.*, 1989, 265; J. Yu, K. Tu and R. Xu, in *Zeolites and Related Microporous Materials: State of the Art*, ed. J. Weitkamp, H. G. Karge, H. Pfeifer and W. Hölderich, Elsevier, Amsterdam, 1994.

16 C. A. Fyfe, G. C. Gobbi, J. Klinowski, J. M. Thomas and S. Ramdas, *Nature*, 1982, **96**, 530.

17 C. A. Fyfe, L. Berni, H. G. Clark, J. A. Davies, G. C. Cobbi, J. S. Hartman, P. J. Hayes and R. E. Wasilyshen, *Adv. Chem. Ser.*, 1983, **211**, 405.


*Received, 18th November 1996; Com. 6/07782J*

# Preparation of porous hafnium oxide in the presence of a cationic surfactant

**Ping Liu,[a] Jun Liu[b] and Abdelhamid Sayari*[a]**

[a] *Department of Chemical Engineering and CERPIC, Université Laval, Ste-Foy, Qc, Canada, G1K 7P4*
[b] *Pacific Northwest National Laboratory, Richland, WA 99352, USA*

**A thermally stable mesostructured hafnium oxide is synthesized for the first time.**

Shortly after the discovery of M41S mesoporous materials,[1] the supramolecular templating approach was extended to the synthesis of non-silica based materials.[2] Stucky and coworkers[2,3] synthesized a variety of oxides of Pd, W, Mo and Fe, but obtained only a limited number of three-dimensional mesostructures. However, the surfactants in these materials could not be removed without the collapse of the structure. Recently, Antonelli *et al.*[4–6] successfully synthesized mesoporous niobium and tantalum oxides using a ligand-assisted templating approach. The surfactant was removed by solvent extraction using a mixture of nitric acid and isopropyl alcohol. Mesoporous alumina has also been obtained by using either non-ionic polymer surfactants[7] or long-chain carboxylic acids[8] as templates.

Hexagonal mesoporous zirconium oxide has been synthesized by Sayari and coworkers.[9,10] While the as-synthesized material was not stable upon removal of the surfactant, it was successfully stabilized by a post-synthesis treatment with potassium phosphate. After air calcination, a Zr–P oxide with a surface area as high as 500 $m^2\ g^{-1}$ was obtained. Independently, Ciesla *et al.*[11] reported similar results. In addition, they obtained a pure zirconium oxide with a surface area of 280 $m^2\ g^{-1}$ using zirconium isopropoxide in the presence of large amounts of ammonium sulfate and hydrochloric acid.

Hafnium oxide is useful for the preparation of strong acid catalysts similar to sulfated zirconia.[12] Here, we report the first synthesis of porous hafnium oxide, using the surfactant templating approach. In a typical synthesis, 2.68 g of $HfCl_4$ was hydrolysed in 10 g of water. To this solution, 0.82 g of cetyltrimethylammonium bromide (CTAB) in 8 g of water was added followed by a solution of 4.4 g of $(NH_4)_2SO_4$ in 24 g of water. After stirring for 10 min, the pH of the solution was adjusted to 2.1 by adding 1.4 g of 30 mass% ammonia. The gel was then stirred for 30 min before being transferred to a Teflon-lined autoclave and heated statically for 24 h at 373 K. The solid was recovered by filtration and washed with large amounts of water, followed by drying at room temperature for 24 h.

X-Ray powder diffraction was performed on a Siemens D5000 diffractometer. The XRD pattern of the solid shows an intense peak at a low angle ($d \gg 4.0$ nm) along with a shoulder [Fig. 1(*a*)]. This pattern is characteristic of a mesophase with a pore system lacking long-range order. Fig. 2(*a*) shows the transmission electron microscopy (TEM) image of the as-synthesized material. As seen, the pore structure has no long-range order which is consistent with the XRD data. This is reminiscent of HMS[13] and MSU[14] mesoporous materials.

FTIR and EDX showed that the material calcined in air at 773 K for 2 h was carbon free. Its surface area as determined from $N_2$ adsorption isotherm (Fig. 1, insert) was 204 $m^2\ g^{-1}$. Taking the molecular mass difference between $HfO_2$ and $ZrO_2$ (104 *vs.*

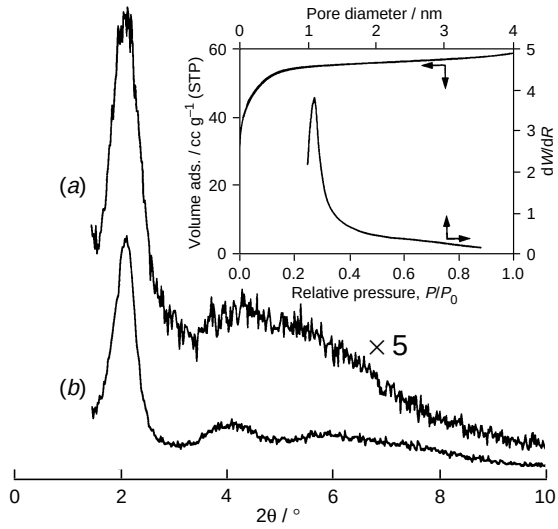



**Fig. 1** Powder X-ray diffraction patterns of mesostructured hafnium oxide prepared at (*a*) 373 K and (*b*) room temperature. Insert: nitrogen adsorption–desorption isotherm and pore size distribution for the sample prepared at 373 K.

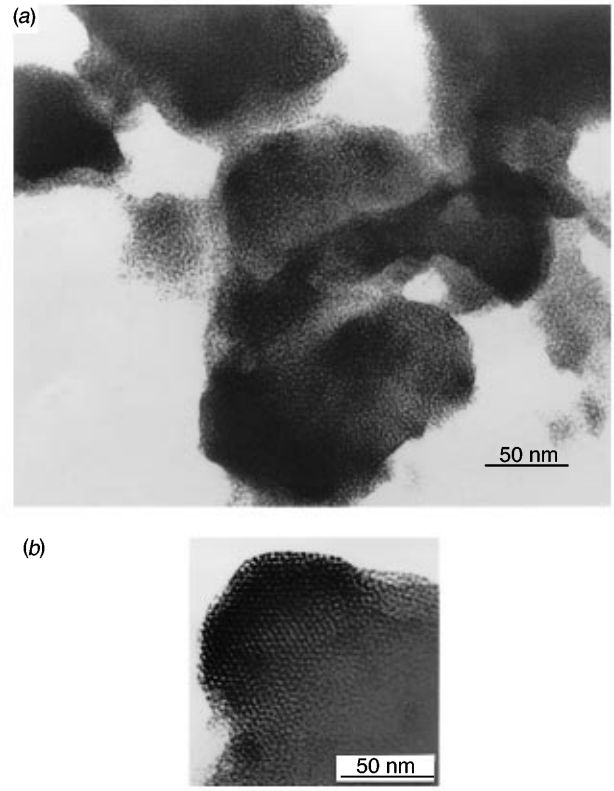



**Fig. 2** Transmission electron micrographs of as-synthesized samples prepared at (*a*) 373 K and (*b*) room temperature

72) into account, this surface area is comparable to that obtained for pure zirconium oxide (280 $m^2$ $g^{-1}$).[11] The pore diameter calculated from the adsorption isotherm using the Horvath–Kawazoe model[15] was *ca*. 1.1 nm (Fig. 1, insert). This is also comparable to the pore diameter of $ZrO_2$.[9] An extensive contraction of the inorganic structure took place during the removal of the surfactant at high temperature.

The effects of pH and synthesis temperature on the final morphology were also investigated. It was found that a pH higher than 1.5 is essential for the formation of the mesostructure. Mesostructured $HfO_2$ can also be prepared at room temperature. In one synthesis, 2.68 g of $HfCl_4$ was hydrolysed in 10 g of water. A solution of 0.82 g of CTAB in 8 g of water was added followed by 4.4 g of $(NH_4)SO_4$. The mixture was stirred for 10 min before adding 1.2 g of 30 mass% ammonia. After stirring for 30 min, 30 g of water was added and the gel was stirred for 10 min. The pH of the final mixture was around 1.6. As inferred from XRD data [Fig. 1(*b*)] and confirmed by TEM [Fig. 2(*b*)], this mesostructure is much more ordered and the hexagonal pore structure can be easily seen. However, the materials thus obtained were found to be thermally unstable. This indicates that hydrothermal treatment at 373 K or a higher pH of the synthesis gel enhances the polymerization of the inorganic species and improves the stability.

In conclusion, we have for the first time synthesized a thermally stable porous hafnium oxide. The high surface area of this material would be useful for the preparation of strong acid catalysts.

## References


1 C. T. Kresge, M. E. Leonowicz, W. J. Roth, J. C. Vartuli and J. S. Beck, *Nature*, 1992, **359**, 710.
2 Q. Huo, D. I. Margolese, U. Ciesla, D. G. Demuth, P. Feng, T. E. Gier, P. Sieger, A. Firouzi, B. F. Chmelka, F. Schüth and G. D. Stucky, *Chem. Mater.*, 1994, **6**, 1176.
3 U. Ciesla, D. Demuth, R. Leon, P. M. Petroff, G. Stucky, K. Unger and F. Schüth, *J. Chem. Soc., Chem. Commun.*, 1994, 1387.
4 D. M. Antonelli and J. Y. Ying, *Angew. Chem., Int. Ed. Engl.*, 1996, **35**, 426.
5 D. M. Antonelli and J. Y. Ying, *Chem. Mater.*, 1996, **8**, 874.
6 D. M. Antonelli, A. Nakahira and J. Y. Ying, *Inorg. Chem.*, 1996, **35**, 3126.
7 S. A. Bagshaw and T. J. Pinnavaia, *Angew. Chem., Int. Ed. Engl.*, 1996, **35**, 1102.
8 F. Vaudry, S. Khodabandeh and M. E. Davis, *Chem. Mater.*, 1996, **8**, 1451.
9 P. Liu, J. S. Reddy and A. Sayari, *Mater. Res. Soc. Symp. Proc.*, 1996, **431**, 101.
10 J. S. Reddy and A. Sayari, *Catal. Lett.*, 1996, **38**, 219.
11 U. Ciesla, S. Schacht, G. D. Stucky, K. K. Unger and F. Schüth, *Angew. Chem., Int. Ed. Engl.*, 1996, **35**, 541.
12 X. Song and A. Sayari, *Catal. Rev. Sci. Eng.*, 1996, **38**, 329.
13 P. T. Tanev and T. J. Pinnavaia, in *Access in Nanoporous Materials*, ed. T. J. Pinnavaia and M. F. Thorpe, Plenum, New York, 1995, p. 13.
14 S. A. Bagshaw, E. Prouzet and T. J. Pinnavaia, *Science*, 1995, **269**, 1242.
15 G. Horvath and K. Kawazoe, *J. Chem. Eng. Jpn.*, 1983, **16**, 470.



*Received, 25th November 1996; Com. 6/07988A*

# Correlation between optical rotation sign and conformation of γ-butyrolactones

**Fu-An Kang* and Cheng-Lie Yin**

*Department of Chemistry, Beijing Normal University, Beijing 100875, PRC*

***trans*-4,5-Disubstituted-γ-butyrolactones are found to adopt different conformations by NMR spectroscopy; their optical rotation signs are found to depend on the conformations they assume.**

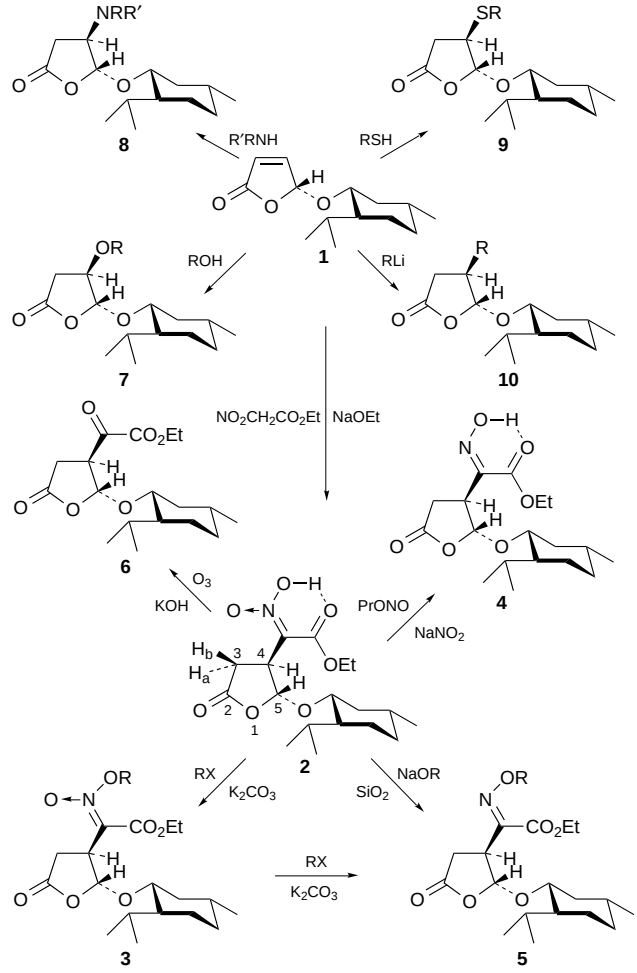
Since the beginning of the study of optically active substances, many attempts have been made to devise a method for calculating optical activity or at least to learn how to predict the sign of rotation. Although some empirical rules[1] concerning the optical activities have been found, the nature of optical activity of chiral molecules is still a problem that has not been solved. Empirical methods[2] for the prediction of the sign and amount of rotation based on bond refractions and polarizabilities of groups in a molecule have been suggested, which has given fairly good results in quite a few cases. Here we report our discovery of the correlation between optical rotation sign and conformation of *trans*-4,5-disubstituted-γ-butyrolactones.

Recently, in the study of the physical and spectral properties of a series of *trans*-4,5-disubstituted-γ-butyrolactones **2**–**10** derived from (*R*)-(−)-5-[(1*R*)-menthyloxy]furan-2(5*H*)-one[3] **1** (Scheme 1), we found that the optical rotation signs of the γ-butyrolactones correlate strictly with the relative order of the chemical shifts of the $C_3$ methylene protons $H_{3a}$ and $H_{3b}$ in the range of δ 2.0–3.0, as the substituent on the $C_4$ atom changes from one series to another. That is, the optical rotation signs of compounds **2**,[4] **3**,[4] **4**,[5] **5**[4] are all positive, where $H_{3a}$ resonates at higher magnetic field than $H_{3b}$, or δ $H_{3a}$ < δ $H_{3b}$; while the optical rotation signs of compounds **6**,[5] **7**,[5] **8**,[6] **9**,[7] **10**[8] are all negative, where $H_{3a}$ resonates at lower magnetic field than $H_{3b}$, or δ $H_{3a}$ > δ $H_{3b}$ (Table 1). This phenomenon appears somewhat confusing and unlikely considering that there is only one difference, the $C_4$ substituent, among these compounds. The possibility of the anisotropic effects of the $C_4$ substituents can be removed, because, although compounds **2**–**5** and compound **6** all have double bonds (C=N or C=O bonds), they still lead to a different relative order of the chemical shifts of $H_{3a}$ and $H_{3b}$.

There seems to be only one interpretation for the interesting transposition of the chemical shifts of the $C_3$ methylene protons $H_{3a}$ and $H_{3b}$, which is that the two series of compounds **2**–**5** and compounds **6**–**10** assume different conformations, respectively. γ-Butyrolactone is a five-membered ring and it is not surprising that it should adopt an envelope conformation. The preference for coplanarity of the lactone group[9] implies that the stable conformations of the γ-butyrolactone are restricted to an enantiomeric pair, in which the $C_4$ atom is either below (conformation I) or above (conformation II) the lactone plane (Fig. 1). The hydrogens or substituents at $C_3$, $C_4$ and $C_5$ atoms are expected to adopt quasi-axial or quasi-equatorial positions.[10]

In conformation I, $H_{3b}$, $H_4$ and $H_5$ are quasi-axial protons, while $H_{3a}$, menthyloxy and $R^1$ adopt the quasi-equatorial positions. On the contrary, in conformation II, $H_{3a}$, menthyloxy and $R^2$ assume the quasi-axial positions, while $H_{3b}$, $H_4$ and $H_5$ are quasi-equatorial protons. According to the proposed model[11] of the anisotropic effect of the carbonyl group, the quasi-equatorial protons of the $C_3$ methylenes in both conformations I and II should be in the shielding region of the $C_2$ carbonyl group while the corresponding quasi-axial protons should be in the deshielding region. As a result, in the two conformations I and II, the quasi-axial proton on the $C_3$ methylene is expected to resonate at lower magnetic field than the corresponding quasi-equatorial proton. Since for compounds **2**–**5** the relative order of the chemical shifts of $H_{3a}$ and $H_{3b}$ is δ $H_{3a}$ < δ $H_{3b}$, it is self-evident that compounds **2**–**5** all assume conformation I. And because, for compounds **6**–**10**, the relative order of the chemical shifts of $H_{3a}$ and $H_{3b}$ is δ $H_{3a}$ > $H_{3b}$, it can also be seen that compounds **6**–**10** all adopt conformation II. Apparently, this result agrees with the previous observations that in steroidal α-acetoxy ketones,[12] α-halo ketones[13] and α-bromo cyclohexanones,[14] the α-protons of the carbonyl groups resonate at lower magnetic fields when axial than when equatorial.

In both conformations I and II, the geminal coupling constants of the $C_3$ methylene protons $H_{3a}$ and $H_{3b}$ alter in a narrow range, or $^2J_{3a,3b}$ = 15–18 Hz. $H_{3a}$, $H_{3b}$ and $H_4$ protons

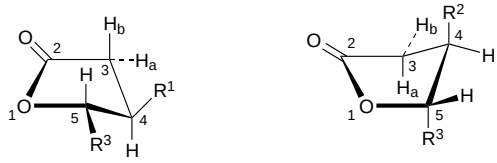



**Scheme 1**

**Table 1**

| Compound | R | Mp/°C | [α] (*c*, solvent)[a] | $\delta H_{3a}$ | $\delta H_{3b}$ | $\Delta\delta$[c] | *J*/Hz 3a,3b | 3a,4 | 3b,4 | 4,5 | Ref. |
|---|---|---|---|---|---|---|---|---|---|---|---|
| **2** | | 146–147 | +52 (1.0, $CHCl_3$) | 2.64 | 2.94 | −0.30 | 17.4 | 11.5 | 3.3 | 0 | 4 |
| **3a** | Me | 93–94 | +64 (1.0, $CHCl_3$) | 2.58 | 2.86 | −0.28 | 16.6 | 11.5 | 3.4 | 0 | 4 |
| **3b** | Et | 71.5–72.5 | +68 (1.0, $CHCl_3$) | 2.55 | 2.83 | −0.28 | 16.6 | 11.2 | 3.4 | 0 | 4 |
| **4** | | 121–122 | +118 (1.0, $CHCl_3$) | 2.36 | 2.88 | −0.52 | 17.2 | 11.5 | 3.2 | 0 | 5 |
| **5a** | $C_5H_9$ | oil | +104 (2.18, hexane) | 2.36 | 2.76 | −0.40 | 16.0 | 10.8 | 3.7 | 1.8 | 4 |
| **5b** | $C_6H_{11}$ | oil | +94 (0.72, hexane) | 2.36 | 2.76 | −0.40 | 16.0 | 10.8 | 3.7 | 1.8 | 4 |
| **6** | | 58–61 | −134 (0.83, $CH_2Cl_2$)[b] | 2.97 | 2.78 | +0.19 | 18.0 | 9.4 | 4.8 | 2.2 | 5 |
| **7a** | Et | 93–94 | −146 (1.1, $CHCl_3$) | 2.79 | 2.45 | +0.34 | 17.8 | 6.0 | 1.4 | 0 | 5 |
| **7b** | Pr | 92–93 | −132 (0.86, $CHCl_3$) | 2.77 | 2.45 | +0.32 | 18.0 | 6.0 | 1.6 | 0 | 5 |
| **8a** | H, Bn | 100.6–102.7 | −101 (1.0, $CHCl_3$)[b] | 2.8 | 2.3 | +0.5 | 15 | 7 | 3 | 0 | 6 |
| **8b** | Me, Bn | oil | −109 (1.0, $CHCl_3$)[b] | 2.7 | 2.1 | +0.6 | 15 | 8 | 2 | 0 | 6 |
| **9** | Ph | 77.8–78 | −62 (1.0, $CHCl_3$)[b] | 3.04 | 2.38 | +0.66 | 15 | 8 | 3 | 0 | 7 |
| **10** | Me | 78.2–79.8 | −147 (0.9, $CHCl_3$)[b] | 2.82 | 2.09 | +0.73 | 17.6 | 8.2 | 4.0 | 2.2 | 8 |

[a] Unless otherwise indicated, the specific rotations were measured at 578 nm at 25 °C. [b] Determined at 589 nm at 20 or 25 °C. [c] $\Delta\delta = \delta H_{3a} - \delta H_{3b}$.




$R^1$ = $C(NO_2H)CO_2Et$, $C(NO_2R)CO_2Et$, $C(NOH)CO_2Et$, $C(NOR)CO_2Et$
$R^2$ = $COCO_2Et$, OR, NRR′, SR, R
$R^3$ = menthyloxy

**Fig. 1**

constitute a typical ABX coupling system with the vicinal coupling constants $^3J_{3a,4}$ = 10.8–11.5 and $^3J_{3b,4}$ = 3.2–3.7 Hz in conformation I, and $^3J_{3a,4}$ = 5.8–9.4 and $^3J_{3b,4}$ = 1.2–1.8 Hz in conformation II. In both cases, the quasi-axial proton is deshielded 0.2–0.7 ppm by the $C_2$ carbonyl group with respect to the quasi-equatorial proton, which is in contrast to the situation of a six-membered ring where an equatorial proton is generally deshielded 0.1–0.7 ppm by the C–C bonds with respect to the corresponding axial proton.[15]

The conformational analysis of the *trans*-4,5-disubstituted-γ-butyrolactones described above is partially confirmed by the X-ray analysis of (4*R*,5*R*)-(−)pyrrolidin-4-yl-5-[(1*R*)-menthyloxy]-γ-butyrolactone, mp 134.6–134.8 °C, $[\alpha]^{20}_D$ −150 (*c* 1.0, $CHCl_3$).[6] Its ORTEP plot shows that it adopts an envelope conformation with the $C_4$ atom deviating above the lactone plane and $H_{3a}$, menthyloxy and pyrrolidinyl assuming the quasi-axial positions, which is exactly consistent with the predicted conformation II.

If the substituents $R^1$, $R^2$ and $R^3$ were displaced with hydrogens, it would be obvious that conformer I and conformer II should be enantiomers, or that one is the mirror image of the other. Since the absolute configuration of the $C_4$ and $C_5$ atoms are the same in both conformations I and II, therefore it appears to be significant that the optical rotation signs of the γ-butyrolactones depend on the conformations they assume rather than on the substituents on the lactone ring, in other words, conformer I creates a right-handed rotation, while conformer II results in a left-handed rotation. Because of the widespread occurrence of γ-butyrolactone rings in nature, *e.g.* in carbohydrates, steroids, alkaloids, nucleic acids and many other natural products, we think the conformational analysis of γ-butyrolactones by NMR spectroscopy and the correlation between optical rotation sign and conformation of γ-butyrolactones will be useful for prediction of optical activity and conformation of such compounds.

We thank Professor Yu-Ying Yin for helpful discussions. Financial support provided by the National Science Foundation and the Doctoral Program Foundation of the State Education Commission is gratefully acknowledged.

## References

1 V. M. Potapov, *Stereochemistry*, Mir, Moscow, 1978, pp. 200–207; J. A. Mills and W. Klyne, *Prog. Stereochem.*, 1954, **1**, 204; W. Klyne and P. M. Scopes, *Prog. Stereochem.*, 1969, **4**, 97; E. L. Eliel, *Stereochemistry of Carbon Compounds*, McGraw-Hill, New York, 1962, pp. 110–114; H. B. Kagan, *Determination of Configuration by Chemical Methods*, Thieme, Stuttgart, 1977, vol. 3; W. Schlenk, *Angew. Chem., Int. Ed. Engl.*, 1965, **4**, 139.
2 J. H. Brewster, *Top. Stereochem.*, 1967, **2**, 1; J. H. Brewster, *J. Am. Chem. Soc.*, 1959, **81**, 5475; 5483; 5493; D. D. Davis and F. R. Jensen, *J. Org. Chem.*, 1970, **35**, 3410; J. Applequist, *J. Am. Chem. Soc.*, 1973, **95**, 8255; 8258.
3 B. L. Feringa and J. C. De Jong, *J. Org. Chem.*, 1988, **53**, 1125.
4 F.-A. Kang, C.-L. Yin and S.-W. She, *J. Org. Chem.*, 1996, **61**, 5523.
5 F.-A. Kang, Ph.D. Dissertation, Beijing Normal University, 1996.
6 B. De Lange, F. Van Bolhuis and B. L. Feringa, *Tetrahedron*, 1989, **45**, 6799.
7 B. L. Feringa and B. De Lange, *Tetrahedron*, 1988, **44**, 7213.
8 J. Jansen and B. L. Feringa, *Synth. Commun.*, 1992, **22**, 1367.
9 A. McL. Mathieson, *Tetrahedron Lett.*, 1963, 81.
10 G. M. Loudon, *Organic Chemistry*, Addison-Wesley, New York, 1984, p. 255.
11 G. J. Karabatsos, G. C. Sonnichsen, N. Hsi and D. J. Fenoglio, *J. Am. Chem. Soc.*, 1967, **89**, 5067.
12 K. L. Williamson and W. S. Johnson, *J. Am. Chem. Soc.*, 1961, **83**, 4623.
13 A. Nickon, M. A. Castle, R. Harada, C. E. Berkoff and R. O. Williams, *J. Am. Chem. Soc.*, 1963, **85**, 2185.
14 E. W. Garbish, *J. Am. Chem. Soc.*, 1964, **86**, 1780; K. M. Wellman and F. G. Bordwell, *Tetrahedron Lett.*, 1963, 1703.
15 R. M. Silverstein, G. C. Bassler and T. C. Morrill, *Spectrometric Identification of Organic Compounds*, Wiley, New York, 1981.

*Received, 2nd January 1997; Com. 7/00073A*

# Fluorescent sensor of imidazole and histidine

**Luigi Fabbrizzi,* Giancarlo Francese, Maurizio Licchelli, Angelo Perotti and Angelo Taglietti**

*Dipartimento di Chimica Generale, Università di Pavia, via Taramelli 12, 27100 Pavia, Italy*

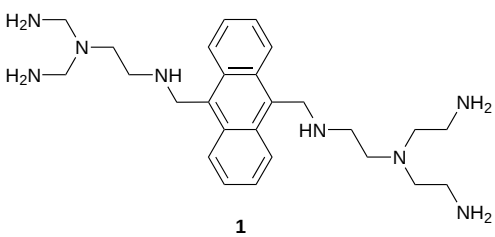
**The dizinc(II) complex of an octamine containing the anthracene subunit binds both the imidazolate anion and the imidazolate moiety of L-histidine, and signals the binding through the fluorescence quenching of the fluorophore.**

The design of multicomponent fluorescent systems able to detect the presence and monitor concentration changes of biologically active small molecules, in particular natural amino acids, is highly desirable. A fluorescent sensor of γ-amino-buyric acid has recently been reported.[1]

We have recently developed a receptor capable of recognising histidine in the presence of any other natural amino acid.[2] The receptor contains two $Cu^{II}$ ions prepositioned within a poly-aza macrocycle. Recognition is based on the fact that the imidazole residue of histidine, in an aqueous solution adjusted to pH 9, deprotonates and bridges the metal centres. This situation is in some ways reminiscent of Cu-Zn superoxide dismutase (CuZn-SOD), in which a $Cu^{II}$ and a $Zn^{II}$ ion are bridged by the imidazolate residue of a histidine fragment.

We considered that the octamine **1**† could provide a convenient framework for the construction of a fluorosensor for histidine, as (i) it offers two quadridentate binding sites for $Cu^{II}$ ions, leaving each metal centre coordinatively unsaturated and an open position for a further ligand (*i.e.* one of the two nitrogen atoms of an imidazolate subunit) and (ii) the anthracene fragment linking the tetraamine subunits gives an intense and characteristically structured fluorescent emission, suitable for signalling the occurrence of the receptor–substrate interaction.

The pH titration experiments were carried out on an aqueous solution containing **1** (1 equiv.) and $Cu^{2+}$ (2 equiv.), in the absence and in the presence of 1 equiv. of imidazole (imH). Non-linear fitting of the titration curve in the absence of imH indicated the formation of the dimetallic species $[Cu^{II}_2L]^{4+}$ at pH 4. This is present as the major species in the 5–7 pH interval; at higher pH, hydroxide-containing species form. In the presence of imH, an imidazolate-containing dimetallic species $[Cu^{II}L(im)]^{3+}$ formed as a major species between pH 7–11. However, whereas the $[Cu^{II}_2L]^{4+}$ system appears to be an excellent receptor for imidazole, it cannot function as a fluorosensor since the $Cu^{II}$ ions fully quench anthracene fluorescence in both the $[Cu^{II}_2L]^{4+}$ and the $[Cu^{II}L(im)]^{3+}$ complexes, and thus any monitoring of the recognition process through the variation of the fluorescent emission is prevented. Thus, we considered the use of a pair of $Zn^{II}$ ions as binding sites for imidazole in the octamine receptor **1**. $Zn^{II}$ is photophysically inactive and is expected to display some affinity towards a bridging imidazolate fragment, as it shows in the CuZn-SOD enzyme.




**1**

Further pH titration experiments were carried out on an aqueous solution containing **1** (1 equiv.) and $Zn^{2+}$ (2 equiv.), in the absence and in the presence of 1 equiv. of imH. Non-linear fitting of the titration curve in the absence of imH indicated the formation of stable dimetallic complexes at pH ⩾5. In particular, the complex of the neutral ligand $[Zn^{II}_2L]^{4+}$ forms at pH 5.5 and is present as the major species between pH 7–8.5. At pH ⩾9, hydroxide-containing complexes dominate: $[Zn^{II}_2L(OH)]^{3+}$ and $[Zn^{II}_2L(OH)_2]^{2+}$. Each hydroxide ion should be bound to the $Zn^{II}$ centre and should result from the deprotonation of a coordinated water molecule.

Fig. 1 displays the distribution diagram of the species present at equilibrium in the system containing 1 equiv. of **1**, 2 equiv. of $Zn^{II}$ and 1 equiv. of imH.‡ It is seen that at pH 7 the imidazolate-containing species $[Zn^{II}_2L(im)]^{3+}$ forms and exists as the dominant species in the pH 9–10 interval (60%), prevailing over the $[Zn^{ii}_2L(OH)]^{3+}$ complex (20%). A titration experiment was then carried out in a spectrofluorimetric cuvette, by adding standard NaOH to a solution containing 1 equiv. of **1**, 2 equiv. of $Zn^{II}$, 1 equiv. of imidazole and excess acid. The variation of the relative fluorescence intensity $I_F$ (%) with the increasing pH profile is shown in Fig. 1 and can be explained as follows: in the pH 2–4 interval, **1** is present exclusively as $LH_6^{6+}$ species. It is suggested that in each tetramine subunit of **1** the three peripheral amine groups (two primary and one secondary) are protonated and the central tertiary nitrogen atom is not. This situation would minimize electrostatic repulsions. In these circumstances, it seems possible that an electron transfer (eT) process from the lone pair of the tertiary nitrogen atom of each tren subunit to the excited anthracene moiety (An*) takes place, thus competing with radiative deactivation and partially quenching fluorescence. On addition of standard base (pH 4–5), the two secondary amine groups which are close to the anthracene subunit deprotonate, making the electron transfer to An* more effective and thus inducing a progressive $I_F$ decrease. However, at pH 5, zinc-containing species begin to form (see the corresponding distribution curve in Fig. 1) and the $Zn^{II}$-bound

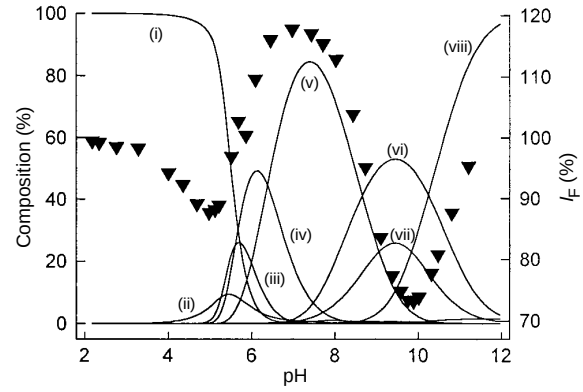
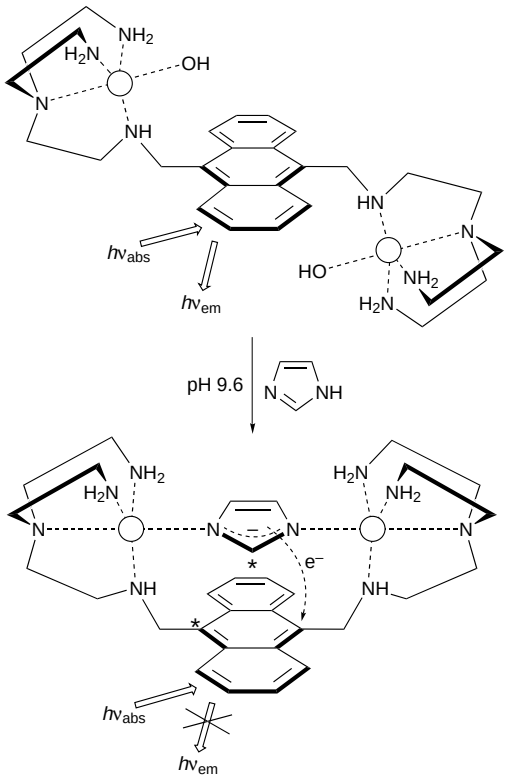



**Fig. 1** Left vertical axis, pH dependence of the concentration of species present at equilibrium for the system **1** (L, 1 equiv.)–$Zn^{II}$ (2 equiv.)–imidazole (imH) in aqueous 0.1 M $NaClO_4$ at 25 °C: (i) $[LH_6]^{6+}$; (ii) $[LH_5]^{5+}$; (iii) $[Zn^{II}_2(LH_2)]^{6+}$; (iv) $[Zn^{II}_2(LH)]^{5+}$; (v) $[Zn^{II}_2L]^{4+}$; (vi) $[Zn^{II}_2L(Im)]^{3+}$; (vii) $[Zn^{II}_2L(OH)]^{3+}$; (viii) $[Zn^{II}_2L(OH)_2]^{2+}$. Right vertical axis (full triangles), pH dependence of the fluorescence intensity of the solution ($I_F$).




**Scheme 1**

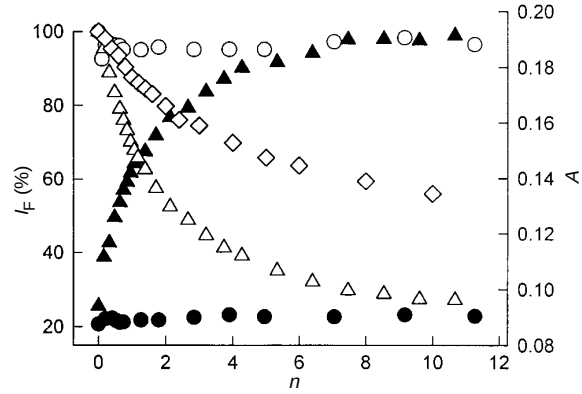



**Fig. 2** Variation of the relative fluorescence intensity ($I_F$, left vertical axis) and of the absorbance at 300 nm ($A$, right vertical axis) during the titration of $9 \times 10^{-6}$ M $[Zn^{II}_2L]^{2+}$, buffered at pH 9.6, with imidazole, histidine and acetate: (△) $I_F$ (imidazole); (▲) $A$ (imidazole); (○) $I_F$ (acetate); (●) $A$ (acetate); (◇) $I_F$ (L-histidine). $n$ = number of equivalents of the added substrate.

lone pairs of the anthrylamine groups (the secondary and the tertiary ones, in particular) are no longer available for the eT quenching mechanism, allowing fluorescence to revive. At pH 7.0–7.5, where $[Zn^{II}_2L]^{4+}$ is present as a major species, $I_F$ reaches its maximum value. The formation of the imidazolate bridged complex $[Zn^{II}_2L(im)]^{3+}$ then induces a substantial fluorescence quenching. In particular, the minimum of the anthracene emission intensity corresponds to the maximum concentration of $[Zn^{II}_2L(im)]^{3+}$, at around pH 10. We ascribe this effect to the occurrence of an eT process from a π-orbital of the electron rich $im^-$ moiety to a π-orbital of the photo-excited anthracene fragment within the $[Zn^{II}_2L(im)]^{3+}$ adduct. The photophysical effects associated with $im^-$ binding by the $[Zn^{II}_2L]^{2+}$ receptor are outlined in Scheme 1.

Molecular modelling indicates that the imidazolate and anthracene fragments in the $[Zn^{II}_2L(im)]^{3+}$ adduct are quite close. In particular, a distance of 3.2 Å is calculated between the closest atoms of the two subunits; these are labelled with an asterisk in Scheme 1.

The fluorescence quenching that follows $im^-$ binding opens the way to fluorescent sensing of imH and of any molecule bearing an imidazole residue. To demonstrate this, an aqueous solution containing 1 equiv. of **1** and 2 equiv. of $Zn^{II}$ was adjusted to pH 9.6 with CHES buffer and was titrated with a solution of imH. Anthracene fluorescence was observed to decrease according to the profile displayed in Fig. 2. Non-linear fitting of the $I_F$ *vs.* equiv. substrate curve indicates the formation of a 1 : 1 receptor–substrate adduct, *i.e.* $[Zn^{II}_2L(im)]^{3+}$, with a conditional constant of 3.65 ± 0.04 log units. The formation of the $[Zn^{II}_2L(im)]^{3+}$ adduct could also be followed spectrophotometrically, by monitoring an increase of the absorption band at 300 nm. The absorbance *vs.* equiv. substrate profile, shown in Fig. 2, is specularly symmetric to the $I_F$ *vs.* equiv. substrate profile and gives the same log$K$ value (3.65 ± 0.09). It should be noted that titration with 1-methylimidazole, which *cannot* undergo deprotonation, did not induce any modification of the anthracene fluorescent emission, confirming that signalling is promoted by Zn–Zn bridging of the $im^-$ fragment.

Spectrofluorimetric titration of $[Zn^{II}_2L]^{2+}$ with L-histidine induced a fluorescence quenching similar to that produced by imidazole (see Fig. 2): the shallower $I_F$ *vs.* equiv. substrate profile corresponds to a lower value for the binding constant (log$K$ = 2.92 ± 0.01), which may reflect the existence of some steric repulsions between by the imidazole-appended amino acid fragment and the receptor framework. Interestingly, the titration profile is not modified when the solution contains an excess of any other amino acid. As an example, addition of L-histidine to a solution buffered at pH 9.6 and containing the receptor $[Zn^{II}_2L]^{2+}$ plus 10 equiv. of L-glycine produced an $I_F$ *vs.* equiv. substrate profile superimposable onto that given in Fig. 2. The lack of interference may be due to the fact that the only anionic group any amino acid other than histidine can offer, *i.e.* the carboxylate fragment, does not display bridging tendencies towards the dimetallic core of $[Zn^{II}_2L]^{2+}$. Indeed, titration of a solution of $[Zn^{II}_2L]^{2+}$ with acetate did not induce any decrease of the fluorescent emission and did not cause any change of the absorbance at 300 nm nor at any other wavelength in the UV–VIS region. Thus, $[Zn^{II}_2L]^{2+}$ recognizes and senses L-histidine in the presence of any other natural amino acid.

This work was supported by the Italian National Council of Research (CNR: Progetto Strategico: Tecnologie Chimiche Innovative) and by the European Union (HCM program: Network Contract No. ERBCHRXCT940492).

## Footnotes

† The octamine **1** was prepared as follows: 9,10-dichloromethylanthracene[3] (1.5 g, 5.4 mmol) and tris(2-aminoethyl)amine (tren, 4.73 g, 32.4 mmol) were dissolved in toluene (50 ml) and the solution was refluxed under magnetic stirring for 6 h. After cooling to room temperature, the resulting yellow–orange solution was filtered, then the solvent and the excess tren were distilled off at reduced pressure, giving **1** as an orange oil (72%); $^1$H NMR (400 MHz, $CDCl_3$, 25 °C): δ 1.85 (br s, NH and $NH_2$), 2.3–2.9 (m, 24 H, $CH_2N$), 4.67 (s, 4 H, benzylic), 7.2–7.5 (m, 4 H, aromatic), 8.1–8.4 (m, 4 H, aromatic).

‡ The equilibrium constants were obtained by processing data of pH titration experiments with the non-linear least-squares program HYPERQUAD[4] and were used to calculate the distribution curves shown in Fig. 1.

## References

1 A. P. de Silva, H. Q. N. Gunaratne, C. McVeigh, G. E. M. Maguire, P. R. S. Maxwell and E. O'Hanlon, *Chem. Commun.*, 1996, 2191.
2 L. Fabbrizzi, P. Pallavicini, L. Parodi, A. Perotti and A. Taglietti, *J. Chem. Soc., Chem. Commun.*, 1995, 2439.
3 M. W. Miller, R. W. Amidon and P. O. Tawney, *J. Am. Chem. Soc.*, 1955, **77**, 2845.
4 A. Sabatini, A. Vacca and P. Gans, *Coord. Chem. Rev.*, 1992, **120**, 389.

*Received, 23rd December 1996; Com. 6/08531H*

# Metal selection of ligand functionality in $[(mes)_2P(=O)_2Li\cdot 2thf]_2$ and $[\{(Me_3Si)_2N\}Cd\{(mes)_2P=O\}_2Li\cdot 2thf]$ (mes = $C_6H_2Me_3$-2,4,6)

**Michael A. Beswick, Natalie L. Cromhout, Christopher N. Harmer, Julie S. Palmer, Paul R. Raithby, Alexander Steiner, Kerry L. Verhorevoort and Dominic S. Wright***

*Chemistry Department, University of Cambridge, Lensfield Road, Cambridge, UK CB2 1EW*

**The reaction of LiBu$^n$ with $[(mes)_2P(H)=O]$ affords the diorganophosphinate complex $[(mes)_2P(=O)_2Li\cdot 2thf]$ 1 and $[(mes)_2PLi]$, however, addition of $[Cd\{N(SiMe_3)_2\}_2]$ to the mixture gives the diorganophosphinite complex $[\{(Me_3Si)_2N\}Cd\{(mes)_2P=O\}_2Li\cdot 2thf]$ 2; the formation of these complexes illustrates that the ligand functionality of 1 can be controlled by the character of the coordinated metal ion.**

Although a large number of transition- and main-group metal complexes containing diorganophosphinate ligands, $[R_2P(=O)_2]^-$, have been structurally characterised,[1] only transition-metal complexes of the diorganophosphinites, $[R_2P=O]^-$, have so far been investigated.[2,3] In comparison to the variety of metal coordination modes observed for $[R_2P(=O)_2]^-$ [terminal metal–O, bridging (μ-O, μ-O), and bidentate], almost all of the structurally characterised $[R_2P=O]^-$ complexes contain a (μ-O, μ-P) metal bridging mode. Our current interest in this ligand set is in its potential for forming stabilised main-group metal–P bonded complexes and heterobimetallic systems. As a prelude to more extensive studies, we embarked on an investigation of the influence of the character of main-group metal ions on the coordination mode of the $[R_2P=O]^-$ ligand.

We report here the surprising finding that lithiation of $[(mes)_2P(H)=O]$ with LiBu$^n$ (1:1 equiv.) in thf affords the diorganophosphinate complex $[(mes)_2P(=O)_2Li\cdot thf]_2$ **1**. However, addition of $[Cd\{N(SiMe_3)_2\}_2]$ to the $[(mes)_2P(H)=O]$–LiBu$^n$ mixture gives the heterobimetallic diorganophosphinite complex $[\{(Me_3Si)_2N\}Cd\{(mes)_2P=O\}_2Li\cdot 2thf]$ **2**.† The very different ligand functionalities exhibited appear to stem from the disproportionation reaction of the diorganophosphinite anion to the diorganophosphinate anion in solution (Scheme 1).‡ Although this disproportionation may be implicated in the formation of $[R_2PH]$ and $[R_2P(OH)=O]$ during base hydrolysis of $[R_2PCl]$,[4] the metal-dependent selection of these ligands (observed in **1** and **2**) has not previously been reported.

A low-temperature X-ray crystallographic study of **1**§ (Fig. 1) shows that the complex has the dimeric structure $[(mes)_2P(=O)_2Li\cdot 2thf]_2$, composed of planar eight-membered $[LiO_2P]_2$ rings. The Li–O bond lengths in **1** are similar to those occurring in lithium alkoxides and related compounds (Li–O av. 1.881 Å; *cf.* range 1.80–2.10 Å for other Li–O bonds).[5] The bridging mode of the $[(mes)_2P(=O)_2]^-$ anion and the dimeric structure of **1** are typical of a variety of diorganophosphinate complexes containing a range of main-group and transition metals.[1]

A low-temperature X-ray crystallographic study of **2**§ shows it to have the heterobimetallic structure $[\{(Me_3Si)_2N\}Cd\{(mes)_2P=O\}_2Li\cdot 2thf]$ (Fig. 2). Molecules of **2** are composed of puckered heterocyclic $[Cd(PO)_2Li]$ rings, resulting from the bridging of the Cd and Li centres by the two $[(mes)_2P(=O)]^-$ ligands. The trigonal-planar Cd centre is attached slightly unsymmetrically to the P atoms of these bridging ligands [Cd–P(1) 2.579(5), Cd(1)–P(2) 2.609(3) Å] and to a terminal $(Me_3Si)_2N$ group [Cd–N(1) 2.136(7) Å]. Presumably, the distortion of the $[Cd(PO)_2Li]_2$ ring occurs principally in order to facilitate complexation of the pseudo-tetrahedral $Li^+$ cation by the O atoms of the $[(mes)_2PO]^-$ ligands [1.90(2) Å] (while at the same time minimising the steric confrontation between the mesityl groups and the Li-attached thf ligands). Although a number of transition-metal complexes containing $[R_2P=O]^-$ ligands have been structurally characterised,[2,3] **2** is the first non-transition-metal example and, to our knowledge, the first containing a $P^V$–Cd bond.[6]

The occurrence of the $[(mes)_2P(=O)_2]^-$ anion in **1** and the $[(mes)_2P=O]^-$ anion in **2** can be interpreted in terms of the way in which the underlying thermodynamics of metal–ligand bond formation affects the equilibrium between these anions. The presence of the small, highly charged $Li^+$ cation will tend to shift this reaction towards the diorganophosphinate, with strong Li–O bonding being maximised in **1**. In **2**, the scales are tipped towards the diorganophosphinite anion since the P/O donor set offered will provide optimum bonding with the soft Cd and hard Li metal cations. It is interesting, in the light of this current work, that the few synthetic studies of the oxidation of metal diorganophosphides indicate that the hardness or softness of the metal present has some bearing on the phosphorus oxyanions produced. Thus, oxidation of $[Me_2In(PPh_2)]_2$ with pyridine-*N*-oxide gives the diorganophosphinate $[Me_2In\{(O)_2PPh_2\}]_2$,[1l] whereas the $O_2$ oxidation of $[Pd(\mu\text{-}PBu^t_2)(P\text{-}Bu^t_2H)_2]$ gives the mixed-ligand complex $[Pd(Bu^t_2PO_2)(Bu^t_2\text{-}PO)_2H]$.[1o]

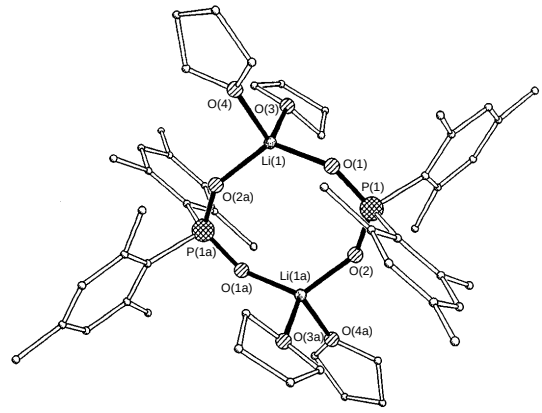
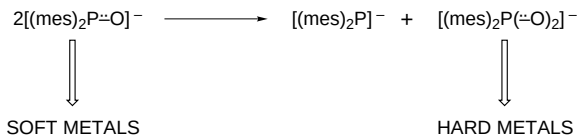



**Fig. 1** Molecular structure of **1**. Hydrogen atoms have been omitted for clarity. Selected bond lengths (Å) and angles (°): P(1)–O(1) 1.501(2), P(1)–O(2) 1.496(2), Li(1)–O(1) 1.878(4), Li(1)–O(2a) 1.884(4), Li(1)–O(3,4) 2.05; O(1)–P(1)–O(2) 117.39(9), av. angles about P 109.4, P(1)–O(1)–Li(1) 140.2(1), P(1)–O(2)–Li(1a) 143.4(1), O(1)–Li(1)–O(2a) 124.4(2), av. angles about Li 107.9.




**Scheme 1**

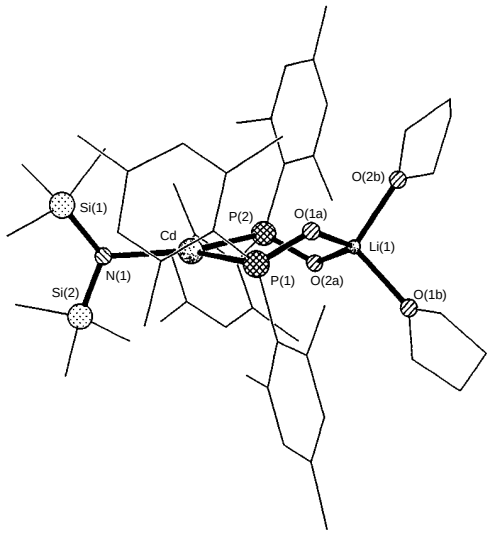



**Fig. 2** Core structure of **2**. Hydrogen atoms have been omitted for clarity. Selected bond lengths (Å) and angles (°): Cd–N(1) 2.136(7), Cd–P(1) 2.579(3), Cd–P(2) 2.609(3), P(1)–O(1a) 1.512(8), P(1)–O(2a) 1.526(8), Li(1)–O(1a) 1.90(2), Li(1)–O(2a) 1.90(2), Li(1)–O(1b) 1.95(2), Li(1)–O(2b) 1.92(2), P(1)–Cd–P(2) 99.9, N(1)–Cd–P(1,2) (av.) 129.9, Cd–P(1,2)–O(1a,2a) (av.) 106.7, P(1,2)–O(1a,2a)–Li(1) (av.) 122.4, O(1a)–Li(1)–O(2a) 118(1); av. angles about Li 109.3.

We gratefully acknowledge the EPSRC (M. A. B., C. N. H., J. S. P., P. R. R., D. S. W.), the European Union (Fellowship for A. S.), and The ORS and The Commonwealth Trust (N. L. C.) for financial support.

## Footnotes

† [(mes)$_2$PH=O] was prepared by an alternative method to that reported in the literature, by the direct hydrolysis of [(mes)$_2$PCl] [generated *in situ* from (mes)MgBr and $PCl_3$ (2 : 1 equiv.) in $Et_2O$] with $H_2O$. The crystalline phosphinous acid was obtained in 72% yield.

*Syntheses*: **1**: a solution of [(mes)$_2$P(H)=O] (0.57 g, 2.0 mmol) in thf (10 ml) was reacted with LiBu$^n$ (1.3 ml, 2.0 mmol, 1.6 mol dm$^{-3}$ in hexanes) under argon. The yellow solution was reduced to dryness under vacuum, leaving a white solid. The solid was redissolved in hexane (10 ml) and a few drops of thf (*ca*. 0.5 ml). Storage at 20 °C (72 h) gave (reproducably) large crystalline blocks of **1** {first batch, 0.14 g, 16%, based on [(mes)$_2$P(H)=O] consumed}.

**2**: a solution of [(mes)$_2$P(H)=O] (1.43 g, 5.0 mmol) in thf (10 ml) was reacted with LiBu$^n$ (6.3 ml, 5.0 mmol, 1.6 mol dm$^{-3}$ in hexanes) under argon. To the yellow solution produced was added neat [Cd{N(SiMe$_3$)$_2$}] (1.0 ml, 5 mmol). Stirring at room temp. (15 min) gave a colourless solution which was reduced *in vacuo* to *ca*. 10 ml. Storage at 5 °C (24 h), gave air-sensitive crystalline cuboids of **2** (2.00 g, 80%).

‡ Variable-temperature $^{31}$P NMR studies show that the composition of the LiBu$^n$–[(mes)$_2$P(H)=O] reaction mixture is far from simple and that it changes with ageing. However, the intermediate formation of [(mes)$_2$POLi] is confirmed by the observation of a weak 1 : 1 : 1 : 1 quartet (δ *ca*. −71.0) at −80 °C ($^1J_{^{31}P^7Li}$ *ca*. 75 Hz). Storage under argon at 20 °C results in gradual broadening of the resonances originally at δ *ca*. −41 and another peak at δ −182.4 starts to predominate (after *ca*. 72 h). This is consistent with the formation of [(mes)$_2$PLi], produced by the reaction shown in Scheme 1.

§ *Crystal data*: **1**: $C_{52}H_{76}Li_2O_8P_2$, $M$ = 904.95, triclinic, space group $P\bar{1}$, $a$ = 9.934(3), $b$ = 11.423(4), $c$ = 13.084(5) Å, α = 68.04(4), β = 68.91(4), γ = 71.09(4)°, $U$ = 1233.6(8) Å$^3$, $Z$ = 1, $D_c$ = 1.199 Mg m$^{-3}$, λ = 0.710 73 Å, $T$ = 153(2) K, μ(Mo-Kα) = 0.138 mm$^{-1}$. Data were collected on a Siemens-Stoe AED diffractometer using an oil-coated rapidly cooled crystal[8] of dimensions 0.5 × 0.5 × 0.3 mm by the θ–ω method (3.69 ⩽ θ ⩽ 25.02°). Of a total of 5998 collected reflections, 4331 were independent. The structure was solved by direct methods and refined by full-matrix least-squares on $F^2$ to final values of $R_1$ [$F > 4\sigma(F)$] = 0.045 and $wR_2$ = 0.123 (all data);[9] largest peak, hole in the final difference map = 0.285, −0.321 e Å$^{-3}$.

**2**: $C_{50}H_{78}CdLiNO_4P_2Si_2$, $M$ = 994.59, monoclinic, space group $C2/c$, $a$ = 14.683(5), $b$ = 22.611(5), $c$ = 17.538(5) Å, β = 114.244(5)°, $U$ = 5374(3) Å$^3$, $Z$ = 4, $D_c$ = 1.229 Mg m$^{-3}$, λ = 0.710 73 Å, $T$ = 153(2) K, μ(Mo-Kα) = 0.550 mm$^{-1}$. The procedure was identical to that for **1** with crystal dimensions 0.3 × 0.2 × 0.2 mm (2.50 ⩽ θ ⩽ 22.49°). Of a total of 4426 collected reflections, 3518 were independent. The structure was solved by direct methods and refined by full-matrix least-squares on $F^2$ to final values of $R_1$ [$F > 4\sigma(F)$] = 0.064 and $wR_2$ = 0.179 (all data). Largest peak, hole in the final difference map = 0.805, −1.788 e Å$^{-3}$. Atomic coordinates, bond lengths and angles, and thermal parameters have been deposited at the Cambridge Crystallographic Data Centre (CCDC). See Information for Authors, Issue No. 1. Any request to the CCDC for this material should quote the full literature citation and the reference number 182/377.

## References

1 For examples, see: (*a*) P. Colamarino, P. L. Orioli, W. D. Benzinger and H. D. Gillman, *Inorg. Chem*., 1976, **15**, 800; (*b*) H.-H. Detjen, E. Lindner and J. Strahle, *Chem. Ber*., 1978, **111**, 2067; (*c*) A.-F. Shihada and F. Weller, *Z. Anorg. Allg. Chem*., 1981, **472**, 102; (*d*) K. W. Oliver, S. J. Rettig, R. C. Thomas and J. Trotter, *Can. J. Chem*., 1982, **60**, 2017; (*e*) R. Cini, P. Orioli, M. Sabat and H. D. Gillman, *Inorg. Chim. Acta*, 1982, **59**, 225; (*f*) S. Blosl, W. Schwarz and A. Schmidt, *Z. Naturforsch., Teil B*, 1983, **38**, 143; (*g*) J. Haynes, K. W. Oliver, S. J. Rettig, R. C. Thomson and J. Trotter, *Can. J. Chem*., 1984, **62**, 891; (*h*) R. O. Day, J. M. Holmes, V. Chaudrasekhar and R. R. Holmes, *J. Am. Chem. Soc*., 1987, **109**, 940; (*i*) R. R. Holmes, K. C. K. Swamy, C. G. Schmid and R. O. Day, *J. Am. Chem. Soc*., 1988, **110**, 7060; (*j*) P. Betz and A. Bino, *Inorg. Chim. Acta*, 1988, **147**, 109; (*k*) R. O. Day, V. Chadrasekhar, K. C. K. Swamy, J. M. Holmes, S. D. Burton and R. R. Holmes, *Inorg. Chem*., 1988, **27**, 2887; (*l*) A. M. Arif and A. R. Barron, *Polyhedron*, 1988, **7**, 2091; (*m*) F. E. Hahn, B. Schneider and F.-W. Reier, *Z. Naturforsch., Teil B*, 1990, **45**, 134; (*n*) K. C. K. Swamy, R. O. Day and R. R. Holmes, *Inorg. Chem*., 1992, **31**, 4184; (*o*) P. Leoni, F. Marchett and M. Pasquali, *J. Organomet. Chem*., 1993, **451**, C25.

2 Homonuclear examples, see: G. Munding, B. Schilling, M. Weishaupt, E. Lindner and J. Strahle, *Z. Anorg. Allg. Chem*., 1977, **437**, 169; S. Hoehne, E. Lindner and B. Schilling, *J. Organomet. Chem*., 1977, **139**, 315; D. E. Berry, K. A. Beveridge, J. Browning, G. W. Bushnell and K. K. Dixon, *Can. J. Chem*., 1986, **64**, 1903; D. E. Fogg, N. J. Taylor, A. Meyer and A. J. Carty, *Organometallics*, 1987, **6**, 2252; N. W. Alcock, P. Bergamini, T. M. Gomes-Carniero, R. D. Jackson, J. Nicholls, A. G. Orpen, P. G. Pringle, S. Sostero and O. Traverso, *J. Chem. Soc., Chem. Commun*., 1990, 980; H. Brunner, R. Eder, B. Hammer and U. Klement, *J. Organomet. Chem*., 1990, **394**, 555; I. J. B. Lin, T. S. Lai, Ling-Kang Liu and Y. S. Wen, *J. Organomet. Chem*., 1990, **399**, 361; D. Matt, F. Ingold, F. Balegronne and D. Grandjean, *J. Organomet. Chem*., 1990, **339**, 349; R. O. Day, P. R. Holmes, A. Schmidpeter, K. Stoll and L. Howe, *Chem. Ber*., 1991, **124**, 2443; A. Beguin, H.-C. Bottcher, M. C. Dai, G. Rheingold, H. Stoeckli-Evans, G. Suss-Fink and B. Watther, *Chimia*, 1993, **47**, 192; U. Florke and H.-J. Haupte, *Z. Kristallogr*., 1993, **205**, 119; V. Riera, M. A. Ruiz, F. Willafane, C. Bois and Y. Jeannin, *Organometallics*, 1993, **12**, 124.

3 Heteronuclear examples, see: J. R. Allen, G. H. W. Milburn, L. Sawyer and V. K. Shah, *Acta Crystallogr., Sect. C*, 1985, **41**, 58; J. R. Allen, J. Halfpenny, G. H. W. Milburn and P. M. Veitch, *J. Chem. Res*., 1986, **279**, 2601; P. M.Veitch, J. R. Allen, A. J. Blake and M. Schroder, *J. Chem. Soc., Dalton Trans*., 1987, 2853; D. M. Anderson, A. J. Blake, J. D. Fotheringham, T. A. Stephenson, J. R. Allen and P. M. Veitch, *Acta. Crystallogr., Sect. C*, 1988, **44**, 1305; U. Kolle, G. Flunkert, R. Gorissen, M. U. Schmidt and U. Englert, *Angew. Chem., Int. Ed. Engl*., 1992, **31**, 440.

4 (a) *Methoden der Organischen Chemie* (Houben-Weyl), *Phosphor-Verbindungen I*, Georg Theime Verlag, Stuttgart, 1982, vol. E1, p. 242; H.-J. Kleiner, *Liebig Ann. Chem*., 1974, 751; Fabw. Hoeschst., Erif: H.-J. Kleiner and K. Schimmelshmidt, *Chem. Abstr*., 74 88129K, 1971.

5 *Lithium Chemistry—A Theoretical and Experimental Overview*, ed. A.-M. Sapse and P. von Rague Schleyer, Wiley, New York, 1995, ch. 9 and references therein.

6 There are only a few structurally characterised cadmium diorgano-phosphide complexes (containing $R_2P$–Cd), see M. A. Matchett, M. Y. Chiang and W. E. Burho, *Inorg. Chem*., 1994, **33**, 1109; S. C. Goel, M. Y. Chiang, D. J. Rauscher and W. E. Burho, *J. Am. Chem. Soc*., 1993, **115**, 160; B. L. Benac, A. H. Cowley, R. A. Jones, C. M. Nunn and T. C. Wright, *J. Am. Chem. Soc*., 1989, **111**, 4986; A. Eichöfer, J. Eisenmann, D. Fenske and F. Simon, *Z. Anorg. Allg. Chem*., 1993, **691**, 1360.

7 E. Lindner and G. Frey, *Chem. Ber*., 1980, **113**, 2769; 3261.

8 T. Kottke and D. Stalke, *J. Appl. Crystallogr*., 1993, **26**, 615.

9 G. M. Sheldrick, SHELXL-93, Göttingen, 1993.

*Received, 4th December 1996; Com. 6/08202E*

# Tetrakis(cyclopentamethylenedithiocarbamate-*S*,*S*′)technetium(v) bromide, an unusual eight-coordinate complex of technetium(v)

**Russell A. Bell,*† James F. Britten, Alan Guest, the late Colin J. L. Lock and John F. Valliant**

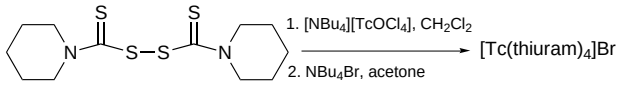
*Department of Chemistry, McMaster University, ABB-420, Hamilton, ON, Canada L8S 4M1*

**Reaction of the ligand dicyclopentamethylenethiuram disulfide with [$NBu_4$][$TcOCl_4$] results in the formation of a unique eight-coordinate technetium(v) species.**

The use of the metastable isotope of technetium ($^{99m}$Tc) in diagnostic imaging is well documented.[1] Technetium forms complexes in a variety of oxidation states, of which $Tc^{V}$ is the best characterized. One of the reoccurring features of the $Tc^{V}$ oxidation state is the stability of the $TcO^{3+}$ unit, which can be transferred from compound to compound. We examined the reaction of $TcOCl_4^-$ anion with the ligand dicyclopentamethylenethiuram disulfide (Scheme 1) to determine if carbamates would be useful functional groups to include in a new class of technetium(v) chelants.

To our surprise the product was a stable eight co-ordinate cation **1** (Fig. 1) in which the oxygen had been removed from the technetium. Even more puzzling, the oxidation state of the metal had not changed. Four cyclopentamethylenedithiocarbamate groups from the cleaved ligand became bound, to give the large cation. Although eight coordination is known for rhenium(v),[2] eight-coordinate $Tc^{V}$ is uncommon.[3,4]

The reaction of morpholine-*N*-carbodithioate anion with [$NBu_4$][$TcOCl_4$] gives tetrakis(morpholine-*N*-carbodithioato-*S*,*S*′)technetium(IV).[4] The formation of this paramagnetic compound occurs by the ligand anion acting as a reducing agent and formation of the ligand disulfide. The compound was remarkably stable and attempts to oxidize it to a cation of $Tc^{V}$, of the type reported here, were unsuccessful. Under somewhat different conditions $TcOCl_4^-$ reacts with dialkyldithiocarbamates (dtc) to give the substitution, and hydrolysis products [$Tc_2O_3$(dtc)$_4$].[5] Xanthate complexes of $Tc^{III}$ are known in which the technetium is surrounded by three xanthate ligands and one triphenylphosphine.[6] Baldas *et al.*[7] synthesised a compound similar to the xanthate species, demonstrating that pertechnetate could be reduced in the presence of sodium diethyldithiocarbamate to give a tris(diethyldithiocarbamato)technetium(III) species in which carbon monoxide is coordinated on the technetium. Until now there has been no solid evidence for eight-coordinate dithiocarbamatetechnetium(v) species.




**Scheme 1** Synthesis of **1**

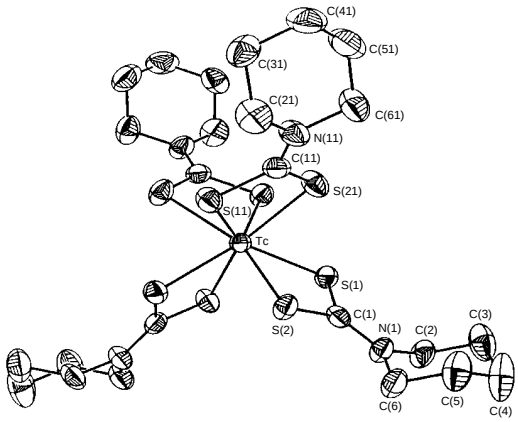



**Fig. 1** 50% thermal ellipsoid diagram of **1**. Hydrogen atoms have been omitted for clarity. Selected bond lengths (Å) and angles (°): Tc–S(1) 2.491(2), Tc–S(2) 2.463(2), Tc–S(21) 2.482(2), Tc–S(11) 2.494(2); S(2)–C(1)–S(1) 109.0(4), S(2)–Tc–S(1) 77.30(6), S(21)–C(11)–S(11) 109.3(4), S(21)–Tc–S(11) 79.57(7).

Compound **1** was obtained by addition of a dichloromethane solution of [$NBu_4$][$TcOCl_4$][8] to a dichloromethane solution of the ligand. The product was crystallized from acetone as a bromide salt. Slow evaporation of the acetone solution of the bromide salt provided large, dark red X-ray quality crystals in reasonable yield (67%).‡

Compound **1** co-crystallized with its bromide counter ion, which was confirmed by neutron activation analysis, and a disordered acetone molecule. Its shape is a distorted square antiprism with Tc–S distances ranging between 2.463(2) and 2.494(2) Å which are consistent with other technetium thiocarbamates. The four S–Tc–S angles range between 77.30 and 79.57° and the S–Tc–S angles are all approximately 109°.

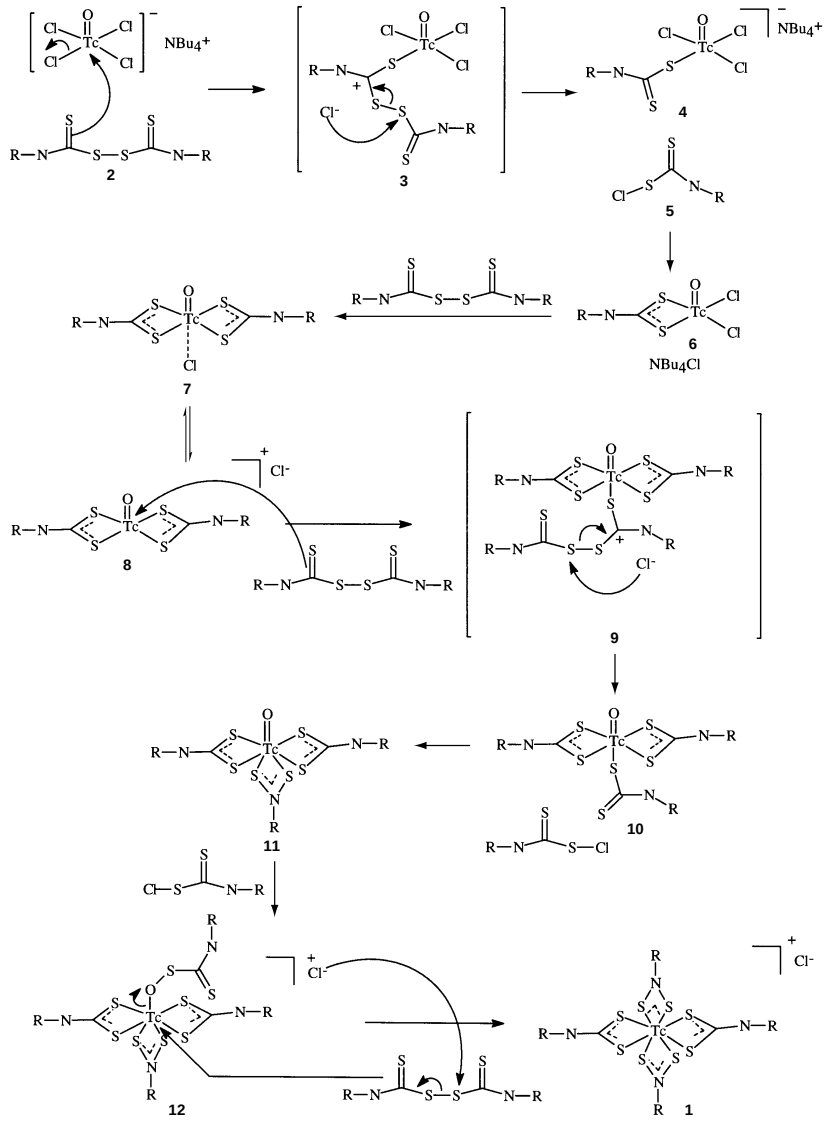
The electrospray mass spectrum of **1** contained the parent peak as well as fragmentation peaks which corresponded to sequential losses of carbamate groups. The $^1$H and $^{13}$C NMR spectra of compound **1** were relatively simple, with the $^{13}$C NMR spectrum showing only four signals.

A possible mechanism for the formation of **1** is shown in Scheme 2. The driving force for this process is the formation of Tc–S bonds coupled with the cleavage of relatively weak S–S bonds by nucleophilic chloride ion. The first step of the proposed mechanism involves nucleophilic attack of the dithiocarbamate disulfide **2** on $TcOCl_4^-$. Because of the aprotic solvent nucleophilic chloride ion may react with the disulfide of intermediate **3** to give the technetium(v) species **4** and compound **5**; the cyano analogue of **5** has been reported.[9] Intermediate **4** converts to **6**, a typical reaction for dithiocarbamates. The sequence is repeated until species **7** is formed. We have prepared the rhenium analogue of **7** and observed that it equilibrates in solution to the cation **8**.[10] Intermediate **8** reacts with another dithocarbamate to form the neutral species **10** which converts to **11**. Because of the electron density supplied by the three dithiocarbamate ligands, the Tc–O bond should be sufficiently polarized to react with a molecule of the reactive species **5**. The resulting species **12** would then be susceptable to nucleophilic attack by another molecule of **2** to give the title compound **1**.

## Footnotes

† E-mail: Bell@Mcmail.cis.mcmaster.ca

‡ *Crystal data for* **1**: [$Tc(C_6H_{10}NS_2)_4$]Br·$C_3H_6O$, $M$ = 877.07, monoclinic, space group $C2/c$, $a$ = 12.343(2), $b$ = 20.557(3), $c$ = 15.133(2) Å, β = 103.42(1)°, $U$ = 3735(1) Å$^3$, $Z$ = 4, $D_c$ = 1.56 g cm$^{-3}$, $F$(000) = 1808, μ(Mo-Kα) = 1.931 mm$^{-1}$, 4012 reflections collected in the range 1.96 < θ < 25.00°; of these 3279 were unique, $R$ = 0.0919,



**Scheme 2** Proposed mechanism for the formation of **1**

$R_w$ = 0.1320 for 188 parameters. Atomic coordinates, bond lengths and angles, and thermal parameters have been deposited at the Cambridge Crystallographic Data Centre (CCDC). See Information for Authors, Issue No. 1. Any request to the CCDC for this material should quote the full literature citation and the reference number 182/375.

§ *Preparation* of **1**. $[NBu_4][TcOCl_4]$ (50 mg, 0.10 mmol) in dichloromethane (2 ml) was added to dicyclopentamethylenethiuram disulfide (0.128 g, 0.4 mmol) in dichloromethane (4 ml) with stirring. After 2 h at room temp., acetone (4 ml) was added and the whole filtered after a further 2 h with an acetone wash (10 ml). $[NBu_4][Br]$ (65 mg, 0.20 mmol) was added to the filtrate giving **1** as deep red crystals (48 mg, 67%). Mp 188 °C (decomp.); $^1$H NMR ($CD_3OD$) δ 3.752–3.715 (m, 4 H, *o*-H), 1.796–1.781 (m, 2 H, *p*-H), 1.680–1.663 (m, 4 H, *m*-H); $^{13}$C NMR ($CD_3OD$) δ 195.96 ($CS_2$), 47.31 ($C_\alpha$), 26.34 ($C_\beta$), 24.99 ($C_\gamma$); ESIMS (+ve ion) *m/z* (%), 739 {55, $[Tc\{S_2CN(CH_2)_5\}_4]^+$}, 579 {100, $[Tc\{S_2CN(CH_2)_5\}_3]^+$}, 517 {4, $[Tc\{HO_3SCSN(CH_2)_5\}_2]^+$}, 435 {18, $[TcO\{S_2CN(CH_2)_5\}_2]^+$}, 210 {3, $[(CH_2)_5NCSSO_3H_2]^+$}.

## References


1 S. Baum and R. Bramlet, *Basic Nuclear Medicine*, Appleton-Century-Crofts, New York, 1975.

2 *Comprehensive Coordination Chemistry*, ed. G. Wilkinson, R. D. Gillard and J. A. McCleverty, Pergamon, Oxford, 1987, vol. 4, ch. 43.

3 K. A. Glavan, R. Whittle, J. F. Johnson, R. C. Elder and E. Deutsch, *J. Am. Chem. Soc.*, 1980, **102**, 2103.

4 J. G. H. DuPreez, T. I. A. Gerber and O. Knoesen, *Inorg. Chim. Acta*, 1985, **109**, L17.

5 H. S. Trop, Ph.D. Thesis, Massachusetts Institute of Technology, 1979.

6 T. Nicholson, J. Thornback, L. O'Connell, G. Morgan and A. Davison, *Inorg. Chem.*, 1990, **29**, 89.

7 J. Baldas, J. Bonnyman, P. M. Pojer, G. A. Williams and M. F. Mackay, *J. Chem. Soc., Dalton Trans.*, 1992, 451.

8 F. A. Cotton, A. Davison, V. W. Day, L. Gage and H. S. Trop, *Inorg. Chem.*, 1979, **18**, 3024.

9 J. von Braun and F. Stechele, *Chem. Ber.*, 1903, **36**, 2275.

10 R. A. Bell, M. Dugal, C. J. L. Lock and J. F. Valliant, unpublished work.



*Received, 29th October 1996; Com. 6/07382D*

# Metal hurdling in transition-metal complexes of 2,4,6-tris(2-pyridyl)-1,3,5-triazine (tpt) and 2,4,6-tris-(2-pyridyl)pyrimidine (tpp)

**Andrew Gelling, Matthew D. Olsen, Keith G. Orrell,* Anthony G. Osborne and Vladimir Šik**

*Department of Chemistry, The University, Exeter, Devon, UK EX4 4QD*

**$^1$H NMR two-dimensional exchange spectroscopy (EXSY) reveals that in palladium(II) and platinum(II) complexes of the ligands 2,4,6-tris(2-pyridyl)-1,3,5-triazine (tpt) and 2,4,6-tris(2-pyridyl)pyrimidine (tpp), a highly novel type of fluxion occurs in which the metal moiety hurdles a C–C bond and moves from one edge of the central ligand ring to an adjacent edge; this process is accompanied by 1,4 metallotropic shifts analogous to those found in complexes of 2,2′:6′,2″-terpyridine.**

Since our discovery that 2,2′:6′,2″-terpyridine (terpy) acts as a fluxional bidentate ligand to certain metals[1–4] we have revealed analogous 1,4 metallotropic shifts in a range of rhenium(I) or platinum(IV)[5–7] complexes of N,N,N-ligands based on combinations of pyridine, pyrazole, pyrimidine and 1,3,5-triazine rings. Recently we have presented NMR evidence that the metallotropic shift in 2,2′:6′,2″-terpyridine complexes occurs through a purely associative process.[8] We have now turned our attention to transition-metal complexes of the related trigonal planar ligands 2,4,6-tris(2-pyridyl)-1,3,5-triazine (tpt) and 2,4,6-tris(2-pyridyl)pyrimidine (tpp).

The presence of more than one N heteroatom in the central ring in these ligands allows for much greater variety of fluxionality compared to terpy complexes. In the $^1$H two-dimensional EXSY spectrum of the complex [Pt($C_6F_4CF_3$-*p*)$_2$(tpt)] at 393 K, in addition to the exchanges of $H_A$–$H_D$ (ring 1) with $H_E$–$H_H$ (ring 2) associated with the 1,4 metallotropic shift, exchange of $H_E$–$H_H$ (ring 2) with $H_I$–$H_L$ (ring 3) was also observed (Fig. 1 and Scheme 1). This second exchange between uncoordinated pyridyls can only be rationalised by a movement of the metal moiety from one side of the pyridyl–triazine C–C bond of the chelate ring to the other. Such 'hurdling' of the C–C bond by the metal moiety can be achieved in two ways, either by full dissociation of the metal centre from the ligand followed by recombination, or, by partial dissociation, by the breaking of a single metal–nitrogen bond (that to the triazine), followed by 180° rotation of the metal-bound pyridyl about the pyridyl–triazine bond, followed by recombination of the metal to the new triazine nitrogen. The first process would lead to an equal probability of the metal recoordinating at nitrogens on any pair of adjacent rings, and hence exchange between hydrogens of all pyridine rings would occur with equal rates. As this is not seen, in fact no exchange between the hydrogens of rings 1 and 3 (Scheme 1 and Fig. 1) is observed, we conclude that the second partially dissociative process occurs with the metal effectively hurdling the pyridyl–triazine bond and recoordinating to the triazine.

Rates of the metallotropic shift and rotational hurdling processes were found, by high-temperature quantitative $^1$H two-dimensional EXSY experiments, to be comparable. A combination of the two processes enables the metal moiety to move completely round the outside of the triazine ring passing through structures **i**–**vi** (Scheme 1). The rate of the metallotropic shift relative to that of the rotation was found to increase more rapidly with temperature leading to a slightly higher activation energy ($\Delta G^{\ddagger}$) than for the hurdling process (Table 1).

In the complex [Pd($C_6F_4CF_3$-*p*)$_2$(tpt)] metallotropic shifts and metal hurdling processes occur at measurable rates at ambient temperatures. Consequently, $^{19}$F one-dimensional bandshape analysis (of $CF_3$ signals) over a temperature range 293–403 K enabled the metallotropic shift to be monitored, and a $^1$H two-dimensional EXSY experiment at room temperature provided an estimate of the activation energy for the hurdling process (Table 1).

Metal complexes of the pyrimidine-based ligand tpp differ in two fundamental ways from those of tpt. Firstly, while all tpt chelate complexes are degenerate with equal populations of coordination species, in tpp complexes the two coordination species are chemically different and so differing populations are expected. Surprisingly, there was a very great imbalance in populations, namely 99 : 1. It is known that in the X-ray crystal structure of terpyridine the nitrogens adopt a *trans*,*trans* configuration,[9] and, by analogy, this will be the preferred configuration in tpp. This can be achieved by rotation of the pyridyls attached to the 4- and 6-positions of the pyrimidine ring. However, when the 2-position pyridyl ring is coplanar with the other rings, its nitrogen donor is inevitably *cis* to one of the pyrimidine nitrogens and thus ideally placed to effect metal chelation. Thus, in Scheme 1, complexes **i** and **ii** are strongly preferred over **iii** and **vi**. The second major difference from the tpt complexes is that no combination of metallotropic shifts and rotational hurdling will allow the metal to move completely round the ligand. Only one rotation and two 1,4 shifts are

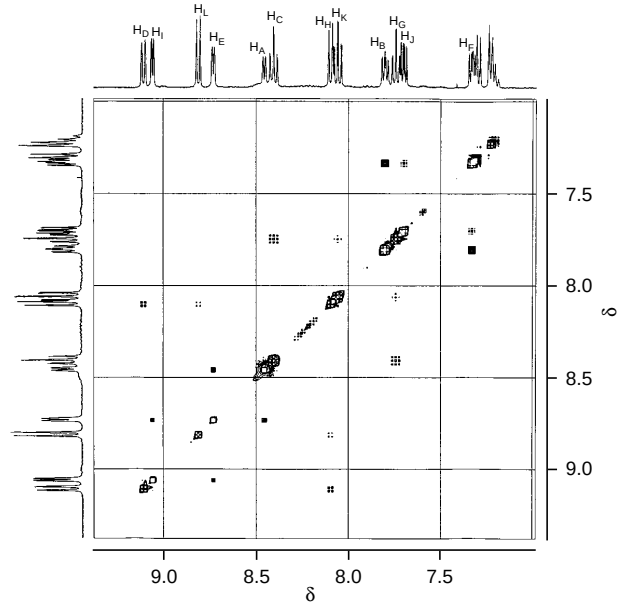
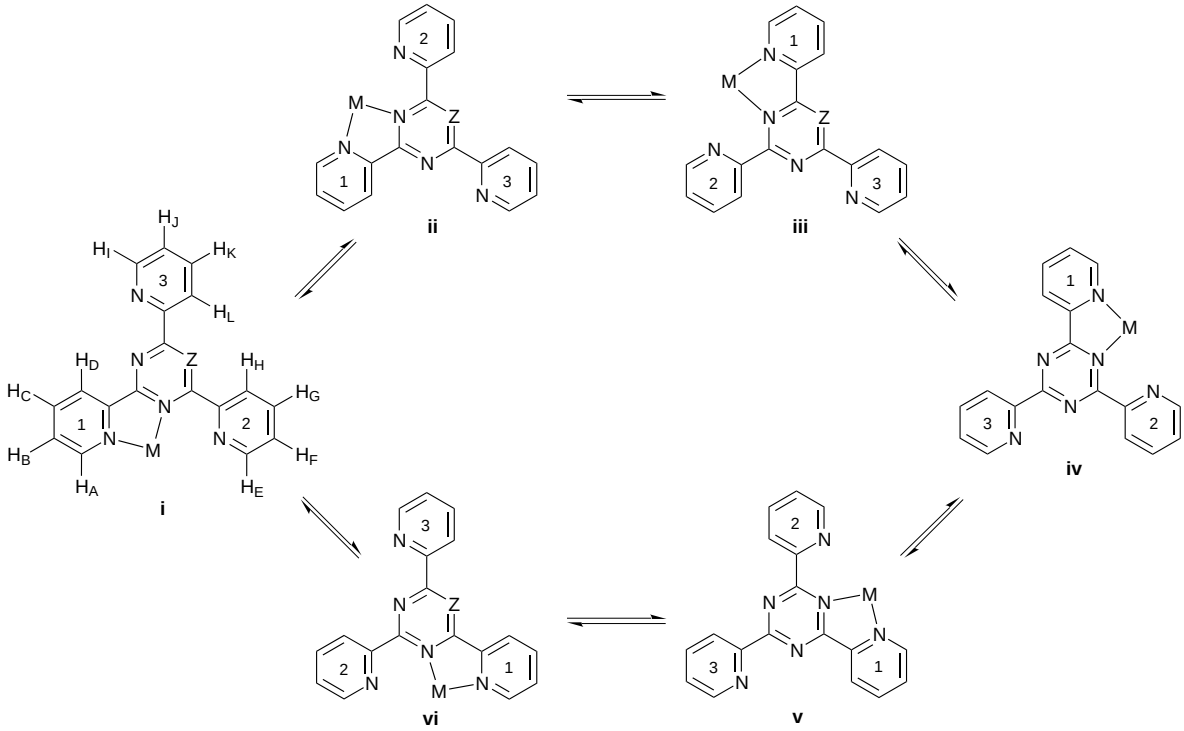



**Fig. 1** $^1$H NMR two-dimensional EXSY spectrum (at 393 K, mixing time 0.8 s) of [Pt($C_6F_4CF_3$-*p*)$_2$(tpt)] in $CDCl_2$, $CDCl_2$ showing exchanges due to both the 1,4 metallotropic shift ($H_A$–$H_D$ ⇌ $H_E$–$H_H$) and the rotational hurdling process ($H_E$–$H_H$ ⇌ $H_I$–$H_L$). The unlabelled signals at δ 7.2–7.3 are due to an unknown impurity.



**Scheme 1** The exchange pathways for both the 1,4 metallotropic shift and rotational hurdling processes in [M($C_6F_4CF_3$-*p*)$_2$L] complexes [M = Pt or Pd; L = tpt (Z = N) or tpp (Z = CH). Individual rings are numbered to show how exchange affects their chemical environments. In the case of L = tpt the metal can travel completely round the ligand exchanging all six structures **i**–**vi** while in the L = tpp complexes this motion is restricted to only four of them **i**–**iii** and **vi** as coordination to Z = CH is impossible.

**Table 1** Activation energy data for both the 1,4 metallotropic shift and hurdling rotation

| Complex | $\Delta G^{\ddagger}$ (1,4 shift)[a]/ kJ mol$^{-1}$ | $\Delta G^{\ddagger}$ (hurdling)/ kJ mol$^{-1}$ |
|---|---|---|
| [Pt($C_6F_4CF_3$-*p*)$_2$(tpt)] | 102.7 ± 0.4[b] | 92.5[c] |
| [Pd($C_6F_4CF_3$-*p*)$_2$(tpt)] | 72.0 ± 0.2[d] | 73.7[e] |
| [Pt($C_6F_4CF_3$-*p*)$_2$(tpp)] | 117.7[f,g] | 113.0[g] |
| [Pd($C_6F_4CF_3$-*p*)$_2$(tpp)] | 69.0[f,h] | —[i] |

[a] At 298 K unless otherwise stated. [b] Based on results of two-dimensional EXSY experiments. [c] Calculated at 298 K from high-temperature two-dimensional EXSY experiments. [d] Based on bandshape analysis of one-dimensional $^{19}$F spectra (*p*-$CF_3$ groups). [e] Based on two-dimensional EXSY at 303 K. [f] For major → minor exchange pathway. [g] Based on two-dimensional EXSY at 413 K. [h] Based on bandshape analysis of one-dimensional $^1$H spectra (pyrimidyl hydrogens). [i] Not measured.

possible, since complexes of type **iv** and **v** in Scheme 1 do not exist for tpp complexes.

The $^1$H two-dimensional EXSY spectrum of the complex [Pt($C_6F_4CF_3$-*p*)$_2$(tpp)] at 413 K shows exchange of the signals $H_E$–$H_H$ (ring 2) with $H_I$–$H_L$ (ring 3); such an exchange between signals of major solution species can only be due to the presence of the rotational hurdling process as the 1,4 metallotropic shift would exchange signals of major and minor species. Despite the very low populations of the minor species and the fact that not all their signals could be unambiguously detected in the one-dimensional spectrum, all exchange cross peaks due to the 1,4 metallotropic shift could be observed in the two-dimensional EXSY spectrum leading to the identification of the chemical shifts of all hydrogens in the minor species. Rates of metallotropic shift and rotational hurdling are again of comparable magnitude, although the calculated activation energies are slightly higher than for the tpt complexes (Table 1), presumably reflecting the differing basicities of the pyrimidine and triazine centres.

Both metal hurdling and 1,4-shifting processes were also detected in [Pd($C_6F_4CF_3$-*p*)$_2$(tpp)], this time at room temperature as in the case of the Pd$^{II}$–tpt complex. In contrast, no evidence of the metal hurdling process was found for the octahedral complex [ReBr(CO)$_3$(tpt)]; only the 1,4-shift process occurs. This implies that axial ligands on the metal sterically prevent the metal moiety from rotating over (or under) the pyridyl–triazine C–C bond. Presumably the same negative result would be found for the isoelectronic metal moiety $PtBrMe_3$.

We thank the EPSRC for a postdoctoral research fellowship (to A. G.) and for a research studentship (to M. D. O.).

## References

1 E. W. Abel, N. J. Long, K. G. Orrell, A. G. Osborne, H. M. Pain and V. Šik, *J. Chem. Soc., Chem. Commun.*, 1992, 303.
2 E. W. Abel, V. S. Dimitrov, N. J. Long, K. G. Orrell, A. G. Osborne, V. Šik, M. B. Hursthouse and M. A. Mazid, *J. Chem. Soc., Dalton Trans.*, 1993, 291.
3 E. W. Abel, V. S. Dimitrov, N. J. Long, K. G. Orrell, A. G. Osborne, H. M. Pain, V. Šik, M. B. Hursthouse and M. A. Mazid, *J. Chem. Soc., Dalton Trans.*, 1993, 597.
4 E. W. Abel, K. G. Orrell, A. G. Osborne, H. M. Pain and V. Šik, *J. Chem. Soc., Dalton Trans.*, 1994, 111.
5 M. Angeles M. Garcia, A. Gelling, D. R. Noble, K. G. Orrell, A. G. Osborne and V. Šik, *Polyhedron*, 1996, **15**, 371.
6 A. Gelling, D. R. Noble, K. G. Orrell, A. G. Osborne and V. Šik, *J. Chem. Soc., Dalton Trans.*, 1996, 3065.
7 A. Gelling, K. G. Orrell, A. G. Osborne and V. Šik, *J. Chem. Soc., Dalton Trans.*, 1996, 3371.
8 E. W. Abel, A. Gelling, K. G. Orrell, A. G. Osborne and V. Šik, *Chem. Commun.*, 1996, 2329.
9 C. A. Bessel, R. F. See, D. L. Jameson, M. R. Churchill and K. J. Takeuchi, *J. Chem. Soc., Dalton Trans.*, 1992, 3223.

*Received, 3rd January 1997; Com. 7/00090A*

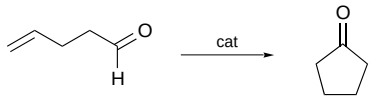
# Asymmetric catalytic intramolecular hydroacylation of 4-substituted pent-4-enals to β-substituted cyclopentanones

**Richard W. Barnhart, David A. McMorran and B. Bosnich**

*Department of Chemistry, The University of Chicago, 5735 South Ellis Avenue, Chicago, Illinois 60637, USA*

**The catalyst, [Rh(*S*,*S*-Me-duphos)(acetone)$_2$]$^+$, rapidly and efficiently converts 4-substituted pent-4-enals bearing primary and secondary substituents to the corresponding cyclopentanones and for a variety of substituents the ee was found to range from 93 to 96% at 25 °C.**

Asymmetric catalytic intramolecular hydroacylation involving the conversion of pent-4-enals to cyclopentanones (eqn. 1) is




(1)

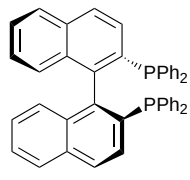
potentially an important transformation because it provides pivotal precursors for the generation of elaborate molecules. Generally, cationic rhodium(I) complexes bearing chelating diphosphines provide catalysts which have high turnover frequencies and numbers.[1,2] In contrast, analogous complexes bearing unidentate phosphines give poor turnover numbers[3] because decarbonylation of the substrate leads to the formation of stable monocarbonyl rhodium complexes which are catalytically inactive. In order to achieve efficient catalysis with chelating diphosphine rhodium(I) complexes, two vacant or virtually vacant coordination positions are required in order to allow ready access of the substrate to the metal.[1,2] This is usually achieved by hydrogenation of the dialkene (norbornadiene or cycloocta-1,4-diene) complex to produce the cationic disolvento catalyst. Weakly bound solvento complexes give the highest rates. Generally, high yields and rapid turnover frequencies are observed for substrates bearing substituents at the 3- and 4-positions whereas substituents at the 2- and 5-positions hinder the rate of hydroacylation.

We recently reported that the *S*-binap (**1**) catalyst, [Rh(*S*-binap)(solvent)$_2$]$^+$, where solvent is dichloromethane or acetone, is a very efficient and highly enantioselective catalyst for certain 4-substituted pent-4-enals **2**.[4] In particular, when R is a tertiary carbon or tertiary silicon group, cyclopentanone products are produced in > 99% ee and in quantitative chemical yield. Similarly, when R is an ester group, essentially enantiomerically pure products are also produced and when R is a ketone, very high ees are observed. Significantly, all of these high enantioselectivities occur at 25 °C and at low catalyst loadings and given the consistency of the results, it would appear that the binap catalyst will give essentially enantiomerically pure cyclopentanones for any tertiary or ester R group and will give high ees for ketonic substituents.

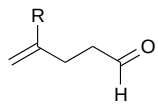
The binap catalyst, however, gives modest ees for substrates bearing a primary or secondary R group and we sought to find a catalyst which would serve to produce consistently high ees for these substituents. The rhodium(I) complex incorporating *S*,*S*-Me-duphos, **3**, proved to be effective for these substrates. The catalytic precursor, [Rh(*S*,*S*-Me-duphos)(NBD)]$PF_6$, where NBD is norbornadiene, was isolated as crystals and the catalyst, [Rh(*S*,*S*-Me-duphos)(acetone)$_2$]$PF_6$, was generated by hydrogenation of the NBD ligand in acetone solution. Addition of the 4-substituted pent-4-enals at 25 °C to these solutions causes rapid catalysis in nearly all cases and quantitive chemical yields are observed.

In Table 1, we list the results obtained for a variety of substrates, one class where primary alkyl groups are present α to the vinyl group (entries 1–6) and the other where a secondary carbon is bound to the vinyl group (entries 7–10). All reactions were carried out in acetone, with substrate concentrations of 0.15–0.2 mol dm$^{-3}$, and the time to completion data are listed for 5 mol% catalyst loadings. The times listed in Table 1 were obtained from $^1$H NMR spectroscopy and no side products were detected. For large scale experiments, 2 mol% catalyst loadings were employed and the % ee was determined by $^{13}$C NMR spectra of the Samp[5] derivatives **4**. The absolute configurations were determined by comparing the optical rotations with those reported. Where the absolute configuration was unknown, it was assumed that the $^{13}$C NMR chemical shifts of the Samp diastereoisomers would be consistent throughout as they were found to be for those cyclopentanones of known configuration.[6]

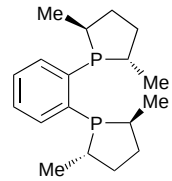
Aside from entry 6 where the substrate carries a phenyl group, all of the reactions are essentially complete upon mixing at 25 °C. It will be noted that all of the products have the same absolute configuration, that all ees are consistently high and vary very little over a variety of substituents. It seems reasonable to conclude that the Me-duphos catalyst is likely to provide high enantioselectivity for any 4-substituted pent-4-enal bearing a primary or secondary carbon atom substituent. Using the Et-duphos catalyst gave similar ees for these substrates. Because the catalytic turnover frequency is so high for most of the substituents, we investigated the enantioselectivity at −10 °C for two substrates. The time of reaction and the ees are given in the square brackets (Table 1). At −10 °C, the ee is raised to 98% in both cases, suggesting that essentially optically pure products are accessible by manipulation of the catalytic conditions. Further, catalysis proceeds even at 0.5 mol% loading, although at 25 °C, 2 h were required for complete conversion of the butyl substrate (entry 3). No side products were observed. It is probable that the low turnover frequency for the phenylated substrate (entry 6) is due to the formation of the catalytically inactive π-aryl complex of the catalyst.[7]



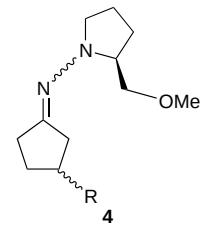

**1**




**2**

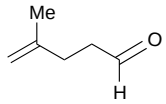
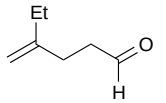
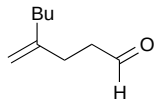
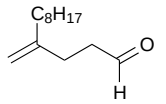
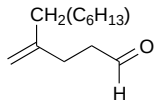
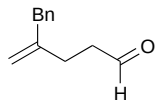
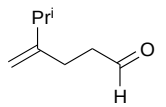
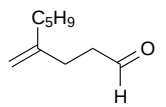
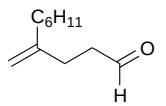



**3**




**4**

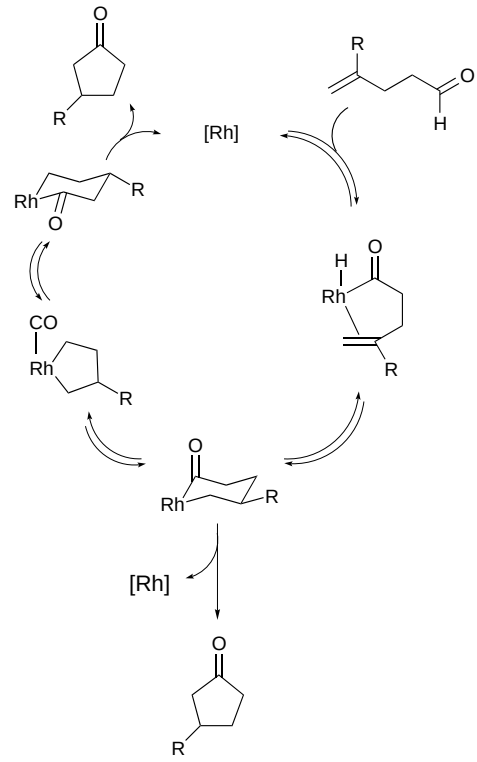
**Table 1** Asymmetric catalytic intramolecular hydroacylation of 4-substituted pent-4-enals using 5 mol% of the [Rh(*S*,*S*-Meduphos) (acetone)$_2$]$PF_6$ catalyst in acetone solution

| Entry | Substrate | *t*/min[a] | Ee (%) (abs. config.) |
|---|---|---|---|
| 1 |  | < 5 | 94 (*S*) |
| 2 |  | < 5 | 95 (*S*) |
| 3 |  | < 5<br>[60][b] | 94 (*S*)<br>[98][b] |
| 4 |  | < 5 | 93 (*S*) |
| 5 |  | < 5 | 93 (*S*) |
| 6 |  | 180 | 94 (*S*) |
| 7 |  | < 5 | 96 (*S*) |
| 8 |  | < 5 | 96 (*S*) |
| 9 |  | < 5<br>[60][b] | 94 (*S*)<br>[98][b] |

[a] For > 95% completion. [b] Results obtained at −10 °C, all other entries refer to 25 °C.

In the context of the consistency of the results listed in Table 1 and those reported for the binap catalyst, it is interesting that the Me-duphos catalyst gives modest ees at 25 °C for substrates bearing tertiary groups. Thus, when the R substituent in the substrate **2** is Bu$^t$, $Me_3Si$ or $PhMe_2Si$, the Me-duphos catalyst gives the corresponding *S*-cyclopentanones with ees of 44, 64 and 61%, respectively. As for the case of the binap catalyst, the Me-duphos catalyst gave moderate ees for 4-aryl substituted pent-4-enals. It was found that for the substrates where R = phenyl, *p*-tolyl, *p*-methoxyphenyl and *o*-methoxyphenyl, the ees were 46 (*R*), 72 (*R*), 70 (*R*) and 54% (*S*), respectively, using the *S*,*S*-Me-duphos catalyst. The chiraphos catalyst remains the most effective for these aryl bearing substrates where the ees range from 65 to 78%.[4]

The probable mechanism for hydroacylation is outlined in Scheme 1.[8] Except for the final reductive elimination step to produce the product, all of the steps are reversible. As was shown previously,[8] however, these reversible steps are not at equilibrium but the enantioselectivity is to some extent controlled by these steps. Thus the enantioselectivity is controlled by a complex mix of rate constants and it is not possible to identify a particular intermediate which determines the ee, and, consequently, there is no guiding principle that can be postulated for the origins of the enantioselection.




This work was supported by grants from the NIH.

## References


1 D. P. Fairlie and B. Bosnich, *Organometallics*, 1988, **7**, 936.
2 D. P. Fairlie and B. Bosnich, *Organometallics*, 1988, **7**, 946.
3 K. Sakai, J. Ide, O. Oda and N. Nakamura, *Tetrahedron Lett.*, 1972, 1287; C. F. Lochow and R. G. Miller, *J. Am. Chem. Soc.*, 1976, **98**, 1281; R. E. Campbell, C. F. Lochow, K. P. Vora and R. G. Miller, *J. Am. Chem. Soc.*, 1980, **102**, 5824; J. W. Suggs, *J. Am. Chem. Soc.*, 1978, **100**, 640; R. C. Larock, K. Oertle and G. F. Potter, *J. Am. Chem. Soc.*, 1980, **102**, 190; K. P. Vora, C. F. Lachow and R. G. Miller, *J. Org. Chem.*, 1980, **192**, 257; R. E. Campbell and R. G. Miller, *J. Org. Chem.*, 1980, **186**, C27; D. Milstein, *J. Chem. Soc., Chem. Commun.*, 1982, 1357; B. R. James and C. G. Young, *J. Chem. Soc., Chem. Commun.*, 1983, 1215; K. Sakai, Y. Ishiguor, K. Funakoshi, K. Ueno and H. Suemune, *Tetrahedron Lett.*, 1984, **40**, 961; B. R. James and C. G. Young, *J. Org. Chem.*, 1985, **285**, 321; J. W. Suggs and M. J. Wovkulich, *Organometallics*, 1985, **4**, 1101; Y. Taura, M. Tanaka, K. Funakoshi and K. Sakai, *Tetrahedron Lett.*, 1989, **30**, 6349; K. P. Gable and G. A. Benz, *Tetrahedron Lett.*, 1991, **32**, 3473; Y. Taura, M. Tanaka, X. Wu, K. Funakoshi and K. Sakai, *Tetrahedron*, 1991, **47**, 4879; X. Wu, K. Funakoshi and K. Sakai, *Tetrahedron Lett.*, 1992, **33**, 6331; X. Wu, K. Funakoshi and K. Sakai, *Tetrahedron Lett.*, 1993, **34**, 5927; P. Eilbrach, A. Gersmeier, D. Lennartz and T. Huber, *Synthesis*, 1994, 330.
4 R. W. Barnhart, X. Wang, P. Noheda, S. H. Bergens, J. Whelan and B. Bosnich, *J. Am. Chem. Soc.*, 1994, **116**, 1821.
5 D. Enders and H. Eichenauer, *Tetrahedron Lett.*, 1977, 191.
6 For R = Me and Pr$^i$, see: G. H. Posner, L. L. Frye and M. Hulce, *Tetrahedron*, 1984, **40**, 1401; D. F. Taber and K. Raman, *J. Am. Chem. Soc.*, 1983, **105**, 5935; G. H. Posner and M. Hulce, *Tetrahedron Lett.*, 1994, **25**, 379.
7 P. Albano, M. Aresta and M. Manassero, *Inorg. Chem.*, 1980, **19**, 1069.
8 R. W. Barnhart and B. Bosnich, *Organometallics*, 1995, **14**, 4343.


*Received, 23rd December 1996; Com. 7/00076F*

# Substrate directed diastereoselective hydroformylation of acyclic homomethallylic alcohols

**Bernhard Breit**

*Fachbereich Chemie, Philipps-Universität Marburg, Hans-Meerweinstr., D-35043 Marburg, Germany*

**Diastereoselective hydroformylation of acyclic homomethallylic alcohols with the aid of a catalyst directing group is achieved and the stereochemical outcome of this reaction is rationalized by analysing the preferred substrate conformation in solution.**

Transition metal catalysed C–C bond forming reactions provide efficient ways to build carbon backbones in organic synthesis. These reactions also allow the generation of stereogenic centres, be it with the aid of a chiral catalyst[1] or by substrate based asymmetric induction.[2] The latter approach is not frequently utilized,[3] but its potential may be enhanced by the introduction of a catalyst directing group, a group that binds reversibly to the catalytically active metal species, and positions it selectively at one of the diastereotopic faces of the substrate.[4,5]

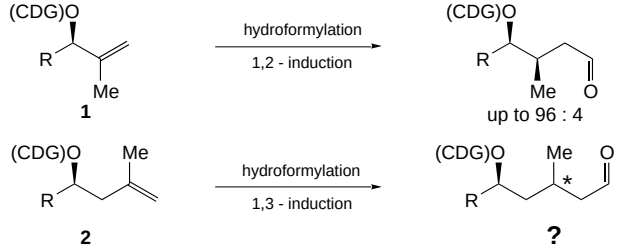
We recently found that *o*-diphenylphosphinobenzoic acid may be used as an effective catalyst directing group in stereoselective hydroformylation of methallylic alcohols **1** (Scheme 1).[5] In this process high 1,2-asymmetric induction is realized by means of the catalyst directing group. We report now that this approach allows also for high 1,3-asymmetric induction in the hydroformylation of homomethallylic alcohols **2** by use of the same catalyst directing group.

To probe 1,3-asymmetric induction homomethallylic alcohols seemed to be particularly interesting substrates, because hydroformylation delivers an acyclic structural fragment with hydroxy and methyl substituted stereocentres in a 1,3 relation. Such a structural motif is widespread, especially in polyketide natural products, and therefore of significant synthetic importance.[6]

Starting from readily available homomethallylic alcohols[7] we introduced the catalyst directing *o*-DPPB group employing the DCC–DMAP coupling method.[8] The resulting homomethallylic *o*-DPPB esters **3** were subjected to hydroformylation conditions using 0.7 mol% of $Rh(CO)_2acac$–$P(OPh)_3$ as the catalyst. The hydroformylation proceeded smoothly to give the corresponding aldehydes **4** in good to excellent yields and with *anti*-diastereoselectivities of up to 91%.†‡

Interestingly a significant dependence of the diastereoselectivity on the reaction temperature was observed. Thus the isopropyl derivative **3a** at 90 °C gave only a 70 : 30 ratio (entry 3). Lowering the reaction temperature to 70 °C and even further to 50 °C improved the diastereomeric ratio from 87 : 13 to 91 : 9 favouring the *anti*-aldehyde (entries 1 and 2). Furthermore no significant influence of the diastereoselectivity on the nature of the substituent R could be detected. Thus primary and secondary alkyl as well as aryl substituents were tolerated and gave diastereomer ratios independant on the nature of R of *ca.* 91 : 9. Remarkable is the hydroformylation of the alkenyl substituted derivative **3f**, in which a 1,1-disubstituted alkene could be reacted chemo-, regio- and stereo-selectively in the presence of a trisubstituted alkene to give the *anti*-aldehyde **4f** in 85% yield and a diastereomeric ratio of 90 : 10 (entry 8).

The observed independence of the diastereoselectivity on the nature of the substituent R seemed to indicate that a conformational preference inherent to the homomethallylic system itself might be the origin of the observed 1,3 asymmetric induction. To test this hypothesis we examined the preferred conformation of the homomethallylic *o*-DPPB ester substrate **3a** in solution at 25 °C. Determination of coupling constants as well as 2D-NOESY spectra showed compound **3a** to have a preferred conformation **A** (Scheme 3) in agreement with MM3 calculations. The driving force for this conformation is the minimization of 1,3-allylic strain and the avoiding of *syn*-pentane interactions.[9] If we assume a coordination of the rhodium catalyst between the catalyst directing group and the alkene as indicated (Scheme 3), hydroformylation would provide the

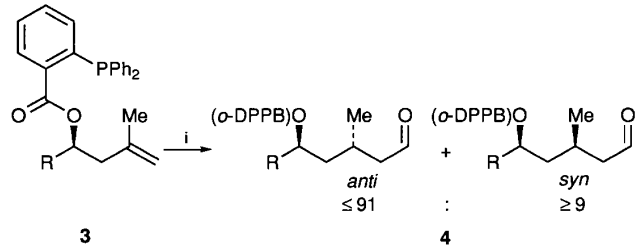



**Scheme 1** CDG = Catalyst directing group

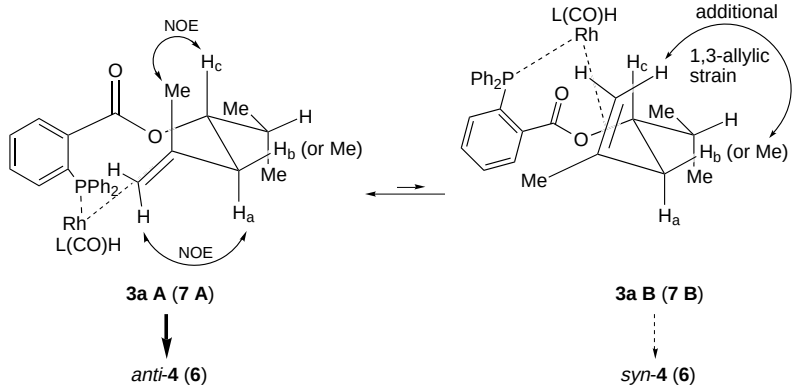
**Table 1** Results of the diastereoselective hydroformylation of homomethallylic *o*-DPPB esters **3**

| Entry[a] | Compound **3** | R | *T*/°C | *t*/h | Yield (%)[b] | *anti* : *syn*[c] |
|---|---|---|---|---|---|---|
| 1 | **a** | $Pr^i$ | 50 | 72 | 93 | 91 : 9 |
| 2 | **a** | $Pr^i$ | 70 | 24 | 99 | 87 : 13 |
| 3 | **a** | $Pr^i$ | 90 | 24 | 99 | 70 : 30 |
| 4 | **b** | *c*-Hex | 50 | 72 | 90 | 91 : 9 |
| 5 | **c** | Hex | 30 | 168 | 81 | 90 : 10 |
| 6 | **d** | Ph | 30 | 120 | 72 | 90 : 10 |
| 7 | **e** | *o*-$MeOC_6H_4$ | 30 | 240 | 78 | 90 : 10 |
| 8 | **f** | (*E*)-EtCH=CMe | 30 | 168 | 85 | 90 : 10 |

[a] For a general experimental procedure see ref. 5. [b] Isolated yields after column chromatography. [c] Determined by NMR spectroscopy of the crude reaction mixture.



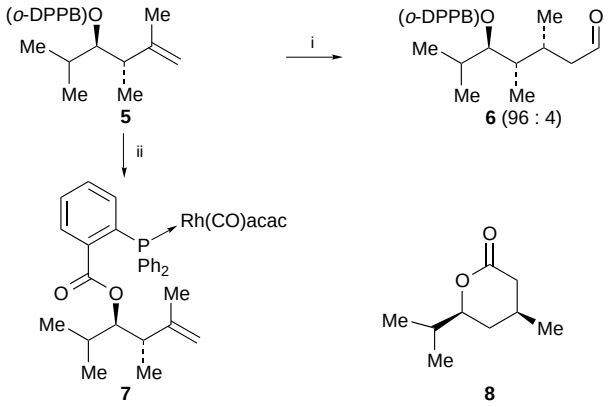

**Scheme 2** *Reagents and conditions*: i, 0.7 mol% $[Rh(CO)_2acac/4\ P(OPh)_3]$, 20 bar $H_2$–CO (1 : 1), toluene, *o*-DPPB = *ortho*-diphenylphosphinobenzoate




**3a A** (**7 A**) **3a B** (**7 B**)

*anti*-**4** (**6**) *syn*-**4** (**6**)

**Scheme 3** Preferred conformation for **3a** and **7** in $CDCl_3$ solution at 25 °C determined by 2D-NOESY NMR spectra and selective $^1H$ NMR decoupling experiments. The indicated coordination of the rhodium catalyst to phosphine and alkene is hypothetic.




**Scheme 4** *Reagents and conditions*: i, 0.7 mol% $[Rh(CO)_2acac/4\ P(OPh)_3]$, 20 bar $H_2$–CO (1 : 1), toluene, 50 °C, 7 d, 91%; ii, $Rh(CO)_2acac$, benzene, 25 °C, 15 min, 99%

*anti*-aldehyde **4** as was found experimentally. The less preferred conformation **B** should give rise to complexation of the opposite diastereotopic alkene face, *i.e.* to the formation of the corresponding *syn*-aldehyde **4**.§

Consequently the replacement of $H_b$ in **3a** by a methyl substituent should favour conformation **A** even more, because the alternative conformation **B** would develop, in addition to the *syn*-pentane interaction between the alkenic methyl substituent and the oxygen substituent, a repulsive 1,3-allylic strain between the additional methyl substituent and the $sp^2$-hybridized $CH_2$-fragment. To investigate such a conformational situation as close as possible to hydroformylation catalysis, we prepared the rhodium complex **7** by reacting alcohol **5** with stoichiometric amounts of $Rh(CO)_2acac$. 2D-NOESY and selective proton decoupling experiments showed rhodium complex **7** to have preferentially the conformation **A** at 25 °C in $CDCl_3$ (Scheme 3).

When **5** was hydroformylated at 50 °C, the *anti*-aldehyde **6** was obtained in 91% yield with a diastereomeric ratio of 96 : 4 (Scheme 4). Thus the additional methyl substituent, which disfavours conformer **B**, gives rise to a significantly higher diastereoselectivity in agreement with our model.

This work was supported by the Fonds der Chemischen Industrie (Liebig stipend for B. B.), the Otto Röhm Gedächtnisstiftung and by the Deutsche Forschungsgemeinschaft (SFB 260). We thank Professor R. W. Hoffmann for his generous support, BASF and Degussa for their gifts of chemicals and M. Dauber for his skilful experimental assistance.

## Footnotes

† For a general procedure see ref. 5.

‡ All compounds were characterized by NMR spectroscopy and elemental analyses. The relative stereochemistry was assigned for **4a** by transformation to the known lactone **8** (ref. 10).

§ On going from 30 to 90 °C the vicinal coupling constants for $H_aH_c$ and $H_bH_c$ change from 9.0/4.1 Hz to 8.4/4.6 Hz. These data indicate a change in conformer populations for **3a** when going to the higher temperatures, which is reflected in the temperature dependence of the diastereoselectivities of the hydroformylation reaction.

## References

1 M. Sakai, S. Mano, K. Nozaki and H. Takaya, *J. Am. Chem. Soc*., 1993, **115**, 7033; B. M. Trost, *Acc. Chem. Res.*, 1996, **29**, 355; *Catalytic Asymmetric Synthesis*, ed. I. Ojima, VCH, Weinheim, 1993.

2 A. H. Hoveyda, D. A. Evans and G. C. Fu, *Chem. Rev.*, 1993, **93**, 1307.

3 A. H. Hoveyda and Z. Xu, *J. Am. Chem. Soc.*, 1991, **113**, 5079; A. H. Hoveyda, Z. Xu, J. P. Morken and A. F. Houri, *J. Am. Chem. Soc.*, 1991, **113**, 8950 as well as refs. 4 and 5.

4 S. D. Burke and J. E. Cobb, *Tetrahedron Lett.*, 1986, **27**, 4237; W. R. Jackson, P. Perlmutter and E. E. Tasdelen, *J. Chem. Soc., Chem. Commun.*, 1990, 763; M. T. Didiuk, J. P. Morken and A. H. Hoveyda, *J. Am. Chem. Soc.*, 1995, **117**, 7273.

5 B. Breit, *Angew. Chem.*, 1996, **108**, 3021; *Angew. Chem., Int. Ed. Engl.*, 1996, **35**, 2835.

6 H. Tanaka, A. Kuroda, H. Marusawa, H. Hatanaka, T. Kino, T. Goto, M. Hashimoto and T. Taga, *J. Am. Chem. Soc.*, 1987, **109**, 5031; T. Kino, H. Hatanaka, M. Hashimoto, M. Nishiyama, T. Goto, M. Okuhara, M. Kohsaka, H. Aoki and H. Imanaka, *J. Antibiot.*, 1987, **40**, 1249; Aplyronine A/B/C: K. Yamada, M. Ojika, T. Ishigaki, Y. Yoshida, H. Ekimoto and M. Arakawa, *J. Am. Chem. Soc.*, 1993, **115**, 11 020; Palytoxin: J. K. Cha, W. J. Christ, J. M. Finan, H. Fujioka, Y. Kishi, L. L. Klein, S. S. Ko, J. Leder, W. W. McWhorter Jr., K.-P. Pfaff, M. Yonaga, D. Uemura and Y. Hirata, *J. Am. Chem. Soc.*, 1982, **104**, 7369; Herbimycin: S. Omura, A. Nakagawa and N. Sadakane, *Tetrahedron Lett.*, 1979, 4323; side chain of Maitotoxin: M. Sasaki, N. Matsumori, T. Maruyama, T. Nonomura, M. Murata, K. Tachibana and T. Yasumoto, *Angew. Chem.*, 1996, **108**, 1782; AAL-Toxin TA1: A. T. Bottini and D. G. Gilchrist, *Tetrahedron Lett.*, 1981, **22**, 2719; Fumonisin B1: S. C. Bezuidenhout, W. C. A. Gelderblom, C. P. Gorst-Allman, R. M. Horak, W. F. O. Marasas, G. Spiteller and R. Vleggaar, *J. Chem. Soc., Chem. Commun.*, 1988, 743.

7 T. Imai and S. Nishida, *Synthesis*, 1993, 395.

8 G. Höfle, W. Steglich and H. Vorbrüggen, *Angew. Chem.*, 1978, **90**, 602; *Angew. Chem., Int. Ed. Engl.*, 1978, **17**, 569.

9 R. W. Hoffmann, *Chem. Rev.*, 1989, **89**, 1841; R. W. Hoffmann, *Angew. Chem.*, 1992, **104**, 1147; *Angew. Chem., Int. Ed. Engl.*, 1992, **31**, 1124; R. Göttlich, C. Kahrs, J. Krüger and R. W. Hoffmann, *Chem. Commun.*, 1997, 247.

10 B. Bardili, H. Marschall-Weyerstahl and P. Weyerstahl, *Liebigs Ann. Chem.*, 1985, 275.

*Received, 24th December 1996; Com. 6/08612H*

# Crystal structures and electrical conductivities of cation-radical salts of a tellurium-containing donor: 3,4-dimethylanthra [1,9-*cd* : 4,10-*c′d′*]bis[1,2]-ditellurole

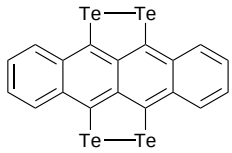
**Masahiro Nakata,[a] Akiko Kobayashi,*[a] Taro Saito,[a] Hayao Kobayashi,[b] Kazuo Takimiya,[c] Tetsuo Otsubo[c] and Fumio Ogura[d]**

[a] *Department of Chemistry, School of Science, The University of Tokyo, Hongo, Bunkyo-ku, Tokyo 113, Japan*
[b] *Institute for Molecular Science, Myodaiji, Okazaki 444, Japan*
[c] *Department of Applied Chemistry, Faculty of Engineering, Hiroshima University, Kagamiyama, Higashi-Hiroshima 739, Japan*
[d] *Department of Industrial Chemistry, Faculty of Engineering, Kinki University, Umenobe-1, Takaya, Higashi-Hiroshima 739-21, Japan*

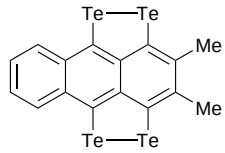
**The crystal structures and conducting properties of various cation-radical salts of a tellurium-containing polyacene donor molecule, 3,4-dimethylanthra[1,9-*cd* : 4,10-*c′d′*]bis-[1,2]ditellurole, are described; the $Br^-$ salt shows a relatively high conductivity at room temperature.**

In the field of molecular conductors, systems based on tellurium-containing donor molecules have not received as much attention as systems based on sulfur- or selenium-containing donors.[1] Only a few conducting complexes with tellurium-containing donors have been reported, including the cation-radical salts of hexamethylenetetratellurafulvalene (HMTTeF)[2] and the tetratellurafulvalene (TTeF)–TCNQ complex.[3] By incorporating heavy chalcogen atoms such as tellurium into donor molecules, a new metallic system with a wider bandwidth and a higher dimensionality is expected to appear.[1] In particular, a polyacene donor molecule containing *peri*-ditellurium bridges might reflect the atomic character of tellurium more directly than a donor with a tetratellurafulvalene framework, and is expected to show novel physical properties. Tetratellurotetracene (TTeT) is well known as a donor molecular containing *peri*-ditellurium bridges,[4] but few cation-radical salts or charge transfer complexes of TTeT have been reported because of its extremely poor solubility.[5] We report here the first examples of cation radical salts of a polyacene donor with *peri*-ditellurium bridges, 3,4-dimethylanthra-[1,9-*cd* : 4,10-*c′d′*]bis[1,2]ditellurole (2,3-dimethyltetratel-luroanthracene: 2,3-DMTTeA), the synthesis of which was first reported by Takimiya and co-workers.[6] 2,3-DMTTeA is an unsymmetrical polyacene molecule with an anthracene framework, two Te–Te bridges and two methyl groups. The solubility of 2,3-DMTTeA in organic solvents is high due to the two methyl groups. Therefore, we can examine the complexes of this donor with the usual chemical or electrochemical methods using organic solvents.

Single crystals of the cation-radical salts were obtained by electrochemical oxidation of 2,3-DMTTeA in a THF solution of $Bu_4N$ (Table 1). A standard H-shaped cell and platinum electrodes were used and a constant current (0.1–1.0 μA) was applied for 7–15 days. Needle- or plate-shaped black crystals grew on the anode.



TTeT



2,3-DMTTeA

The electrical resistivities of the salts were measured by a four-probe method along the donor-stacking axes of the single crystals. The resistivities of all the salts showed semiconducting temperature dependence. However, the $Br^-$ salt has quite a high room temperature conductivity ($1.3 \times 10^3$ S cm$^{-1}$) and a very low activation energy (0.010 eV) (Fig. 1). Room temperature conductivities, activation energies and stoichiometries of the salts are listed in Table 1.

X-ray structure analyses were performed on neutral 2,3-DMTTeA and its cation-radical salts with $ClO_4^-$, $BF_4^-$, $ReO_4^-$, $PF_6^-$, $AsF_6^-$ and $Br^-$ counter anions.†,‡ The $BF_4^-$ and $ReO_4^-$ salts are isomorphous with the $ClO_4^-$ salt, and the $PF_6^-$ salt is isomorphous with the $AsF_6^-$ salt. The common feature to all the structures is the disorder of the donor molecules caused by their unsymmetrical shape, which makes the 2,3-DMTTeA molecules appear as if they have a tetracene framework instead of their actual anthracene framework. One possible reason why the donor molecules have this orientational disorder is that the formation of the Te···Te network is dominant in the construction

**Table 1** Composition and electrical conductivities of 2,3-DMTTeA salts

| Anion | Donor : anion ratio | Form | $\sigma_{293}$/S cm$^{-1}$ | $E_a$/eV |
|---|---|---|---|---|
| $ClO_4^-$ | 3 : 2[a] | plate | $7.1 \times 10^{-3}$ | 0.16 |
| $BF_4^-$ | 3 : 2[a] | plate | $9.7 \times 10^{-3}$ | 0.17 |
| $ReO_4^-$ | 3 : 2[a] | plate | $5.5 \times 10^{-3}$ | 0.16 |
| $PF_6^-$ | 5 : 1[b] | plate | $5.6 \times 10^{-2}$ | 0.077 |
| $AsF_6^-$ | 5 : 1[b] | plate | $1.2 \times 10^{-1}$ | 0.068 |
| $Br^-$ | 2 : 1[b] | needle | $1.3 \times 10^{3}$ | 0.010 |

[a] Determined from the X-ray crystal structure analysis. [b] Determined by elemental analysis.

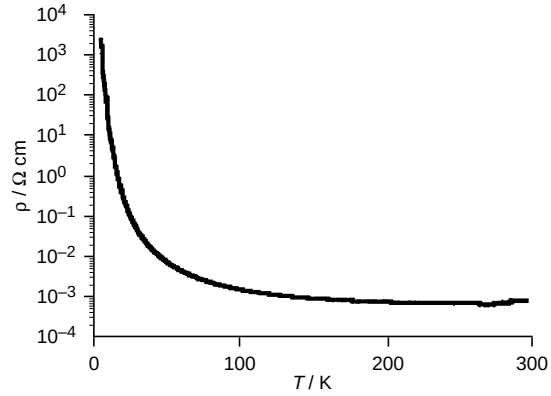


**Fig. 1** Electrical resistivity of $(2,3\text{-DMTTeA})_2Br$

of the crystal structures. This disorder, which is absent from the sulfur or selenium isologue of 2,3-DMTTeA,[6b] is considered to reflect the character of tellurium atoms. In addition, the anions are also disordered in the $AsF_6^-$ and $Br^-$ salts. In spite of their disordered structures, however, all were refined with *R* factors of 3–9%, because the donor molecules contain heavy tellurium atoms.

The structure of $(2,3\text{-DMTTeA})_3(ClO_4)_2$ is shown in Fig. 2. There are donor stacks along the *c* axis, and in each stack, two crystallographically independent donor molecules, A and B in Fig. 2, overlap with their long axis 90° rotated. This rotated overlapping arrangement causes the very small value of the calculated intermolecular overlap integral§ between A and B ($< 1 \times 10^{-3}$). On the other hand, B and B′, which are crystallographically equivalent, are almost eclipsed and the overlap integral between them is $10 \times 10^{-3}$, so they may be regarded as forming a dimer. The weak interaction between A and B causes the dimer to be isolated, which causes the poor conductivity of this salt.

The $AsF_6^-$ salt has donor stacks along the *a* axis. There is a short interstack Te···Te contact (3.83 Å) which is shorter than the intermolecular Te···Te distance within the stack (4.16 Å). Therefore, two-dimensional character is expected in its conducting properties.

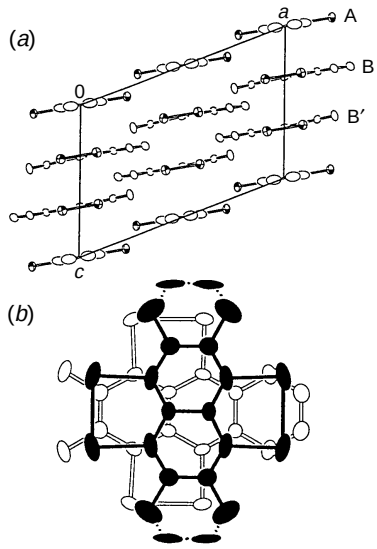



**Fig. 2** (*a*) Crystal structure of $(2,3\text{-DMTTeA})_3(ClO_4)_2$ projected onto the *ac* plane. $ClO_4^-$ anions are omitted for clarity. (*b*) Overlapping mode of the donor molecules of $(2,3\text{-DMTTeA})_3(ClO_4)_2$ projected onto the molecular plane. While molecule A (coloured black) has a disordered tetracene structure, molecule B (coloured white), is not disordered.

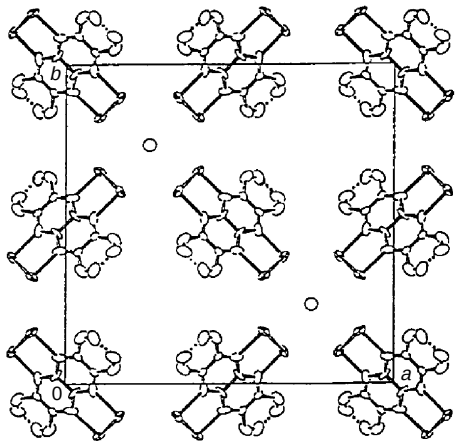



**Fig. 3** Crystal structure of $(2,3\text{-DMTTeA})_2Br$ projected onto the *ab* plane

In the $Br^-$ salt (Fig. 3), the donor stacking structure is isomorphous with the tetragonal structure of $(TSeT)_2Cl$, reported by Shibaeva and Kaminskii in 1978 (TSeT = tetraselenotetracene).[7] There exist donor stacks along the *c* axis, and in each stack there are very close Te···Te intermolecular contact (3.70 Å). Between neighbouring stacks, however, no short contacts are found. Therefore, this structure may be called quasi-one-dimensional. In addition, the $Br^-$ anions are disordered along the *c* axis, which is responsible for the semiconducting property of this salt.

We have obtained the first single crystals of the molecular conductors based on a donor molecule with *peri*-ditellurium bridges. The higher conductivity of the $Br^-$ salt suggests the possibility of molecular metals with novel tellurium-based conduction passways, if the disorder in the crystal structure can be eliminated.

## Footnotes

† *Crystal data* for 2,3-DMTTeA: monoclinic, space group $P2_1/c$, $a$ = 9.976(5), $b$ = 5.137(1), $c$ = 16.186(1) Å, β = 104.28(2)°, $V$ = 803.8(3) Å$^3$, $Z$ = 2, $D_c$ = 2.944 g cm$^{-3}$, $R$ = 0.057 for 1200 reflections. For $(2,3\text{-DMTTeA})_3(ClO_4)_2$: monoclinic, space group $C2/m$, $a$ = 16.538(3), $b$ = 14.681(2), $c$ = 11.612(4) Å, β = 111.48(2)°, $V$ = 2623(1) Å$^3$, $Z$ = 2, $D_c$ = 2.958 g cm$^{-3}$, $R$ = 0.037 for 2568 reflections. For $(2,3\text{-DMTTeA})(AsF_6)_{0.2}$: monoclinic, space group $P2_1/a$, $a$ = 4.155(2), $b$ = 19.898(3), $c$ = 11.572(7) Å, β = 94.85(9)°, $V$ = 953.3(6) Å$^3$, $Z$ = 2, $D_c$ = 2.614 g cm$^{-3}$, $R$ = 0.066 for 1400 reflections. For $(2,3\text{-DMTTeA})_2Br$: tetragonal, space group $P4_2/ncm$, $a$ = 18.655(2), $c$ = 5.438(3) Å, $V$ = 1892(1) Å$^3$, $Z$ = 2, $D_c$ = 2.641 g cm$^{-3}$, $R$ = 0.093 for 578 reflections.

The data were collected on a Rigaku automated four-circle diffractometer (AFC5R, AFC7R) with graphite monochromated Mo-Kα radiation. The structures were solved by direct methods (SHELX86, SIR92) and refined by full-matrix least-squares methods using reflections with $I \geqslant 3\sigma(I)$.

Atomic coordinates, bond lengths and angles, and thermal parameters have been deposited at the Cambridge Crystallographic Data Centre (CCDC). See Information for Authors, Issue No. 1. Any request to the CCDC for this material should quote the full literature citation and the reference number 1822/382.

‡ Intramolecular bond lengths of the neutral 2,3-DMTTeA: Te–Te = 2.664(2), C–Te = 2.11(1) Å.

§ Intermolecular overlap integrals were calculated using the HOMO obtained by the extended Hückel MO calculation.

## References


1 D. O. Cowan and A. Kini, *The Chemistry of Organic Selenium and Tellurium Compounds*, ed. S. Patai, Wiley, London, 1987, vol. 2, pp. 463–494; D. O. Cowan, R. McCullough, A. Bailey, K. Lerstrup, D. Talham, D. Herr and M. Mays, *Phosphorus, Sulfur Silicon Relat. Elem*., 1992, **67**, 277.

2 K. Kikuchi, K. Yakushi, H. Kuroda, I. Ikemoto, K. Kobayashi, M. Honda, C. Katayama and J. Tanaka, *Chem. Lett*., 1985, 419; Z. S. Li, S. Matsuzaki, R. Kato, H. Kobayashi, A. Kobayashi and M. Sano, *Chem. Lett*., 1986, 1105.

3 D. O. Cowan, M. D. Mays, T. J. Kistenmacher, T. O. Poehler, M. A. Beno, A. M. Kini, J. M. Williams, Y. K. Kwok, K. D. Carlson, L. Xiao, J. J. Novoa and M. H. Whangbo, *Mol. Cryst. Liq. Cryst*., 1990, **181**, 43.

4 D. J. Sandman, J. C. Stark and B. M. Foxman, *Organometallics*, 1982, **1**, 739.

5 R. Kato, H. Kobayashi and A. Kobayashi, *Physica B + C*, 1986, **143**, 304.

6 (*a*) K. Takimiya, Y. Aso, T. Otsubo and F. Ogura, *Bull Chem. Soc. Jpn*., 1991, **64**, 2091; (*b*) For the sulfur and the selenium isologues of 2,3-DMTTeA, see K. Takimiya, A. Ohnishi, Y. Aso, T. Otsubo, F. Ogura, K. Kawabata, K. Tanaka and M. Mizutani, *Bull. Chem. Soc. Jpn*., 1994, **67**, 766.

7 R. P. Shibaeva and V. F. Kaminskii, *Sov. Phys. Crystallogr. Engl. Transl*., 1978, **23**, 669; I. F. Shchegolev and E. B. Y. Yagubskii, *Extended Linear Chain Compounds*, ed. J. S. Miller, Plenum Press, New York, 1982, vol. 2, pp. 385–434.


*Received, 23rd December 1996; Com. 6/08589J*

# Reaction control and potential tuning in a supercritical fluid

**Anthony A. Clifford,* Kate Pople, William J. Gaskill, Keith D. Bartle and Christopher M. Rayner**

*School of Chemistry, University of Leeds, Leeds, UK LS2 9JT*

**A maximum is found in the ratio of *endo*- to *exo*- products *vs.* density in the Diels–Alder reaction between cyclopentadiene and methyl acrylate in supercritical carbon dioxide and is explained by the adjustment of the position of the nearest-neighbour solvent molecules with respect to the transition states.**

There have been a number of previous investigations of product ratio in supercritical fluids and these have been reviewed in a recently published study.[1] Many of these have concentrated on the critical region. In some cases, the lowering of diffusion coefficients in the critical region at finite concentrations can give rise to rapid changes of product ratio with density, as has been observed in the photo-Fries rearrangement of naphthyl acetate in supercritical carbon dioxide.[2] In other cases, rapid changes are seen as a function of pressure, but these largely reflect the rapid change in density with pressure, and as a function of density changes in product ratio are less dramatic. In this study we report an interesting maximum in product ratio, which occurs at a density rather higher than the critical density.

Experimental measurements on the Diels–Alder reaction between methyl acrylate and cyclopentadiene were carried out at 308 and 313 K in carbon dioxide at various pressures. A 50 ml vessel (Autoclave Engineers) with a magnetically coupled stirrer was used, which was modified in-house to improve the temperature control and pressure measurement. $CO_2$ was added from an HPLC pump with a cooled head and an injection valve in the supply line (Rheodyne) for adding reagents. Connecting tubes were heated to the reaction temperature to prevent condensation in them. For each experiment 200 μl of methyl acrylate was added at the beginning, the vessel pressurised with $CO_2$ and allowed to reach temperature equilibrium over half an hour. 100 μl of cyclopentadiene, prepared just beforehand from the dimer, was then added through the injection valve and more $CO_2$ added to raise the pressure another 4–5 bar. The reaction was then carried out for 4 h, after which the reaction mixture was released, trapped in HPLC grade acetone, kept at 195 K and analysed by GC. The reactions were carried out at lower dilutions than some previous experiments[3] to avoid the danger of two phases being present.

We now consider a system in which there are two competing bimolecular reactions in which the two products are stereo-isomers. The ratio of products obtained is equal to the ratio of rate coefficients, defined in terms of mole fractions, $k_x'/k_x''$. By manipulating the equations for transition-state theory applied to supercritical fluids[5] it can be shown that the partial derivative of the logarithm of this ratio with molar volume, $V$, at constant temperature and composition is given by eqn. (1).

$$RT\left(\frac{\partial \ln\left(k_x'/k_x''\right)}{\partial V}\right)_{T,x} = \left(\frac{\partial p}{\partial x_2}\right)'_{T,V} - \left(\frac{\partial p}{\partial x_2}\right)''_{T,V} \qquad (1)$$

The quantities $(\partial p/\partial x_2)_{T,V}$, which do not come under the definition of partial molar quantities, but which can be conveniently called tuning functions, are partial derivatives of the pressure with respect to the mole fraction of the appropriate transition state. Equations for the variation with $V$ of other equilibria and individual reaction rates can also be written in terms of these functions.

Expressions for the tuning functions can be obtained in terms of an equation of state. The van der Waals equation is used below for analysing the experimental data. These tuning functions pass from negative at low density to positive at high density as the mean distance between the transition states and their nearest-neighbour solvent molecules moves from the attractive region of their mutual pair potential, through its minimum to its repulsive region. The functions therefore describe the manipulation of the transition-state solvation energy *via* the density. In the case of competing reactions, a difference in two tuning functions is important, as shown in eqn. (1). This difference is related to the change in pressure as one transition state is replaced by the other and represents the difference of the potential tuning behaviour of the two transition states.

Experimental data for the ratio of *endo*- to *exo*- product are plotted against the solution density in Fig. 1. The range of values of the ratio is no different than that which can be obtained by changing the solvent in the liquid-phase reaction.[5] However, by controlling the density, this range can be obtained in a single solvent. At the temperatures of this study, 1, 4 and 9 K above the critical temperature of carbon dioxide, inaccuracies in pressure measurement and fluctuations in pressure because of temperature instability cause large errors in the estimation of the density. Estimations of this effect are shown by horizontal error bars, which are large near the critical density, but are smaller than the point sizes at higher densities. Further errors in the measurement of the product ratio of 5%, or 0.2, are not shown.

The curves shown in Fig. 1 are theoretical curves obtained from eqn. (1) using tuning functions calculated from the van der Waals equation of state, with simple combination rules for the parameters, to give a ratio of the rate constants, eqn. (2),

$$\frac{k_x'}{k_x''} = \left(\frac{k_x'}{k_x''}\right)_0 \exp\left(-\frac{b_2' - b_2''}{V - b_1} - \frac{2\sqrt{a_1}\left(\sqrt{a_2'} - \sqrt{a_2''}\right)}{RTV}\right) \qquad (2)$$

where $a_1$ and $b_1$ are the van der Waals parameters for the solvent, $a_2'$, $b_2'$, $a_2''$ and $b_2''$ are those for the two transition states and $(k_x'/k_x'')_0$ is the rate coefficient ratio in ideal gas conditions as $V \rightarrow \infty$. Thus the equation has three unknown parameters: $(k_x'/k_x'')_0$, $(b_2' - b_2'')$ and $[\sqrt{a_1}(\sqrt{a_2'} - \sqrt{a_2''})]$, which were obtained by fitting the data at 313 K. A value for $b_1$ for $CO_2$ of $31.33 \times 10^{-6}$ m$^3$ mol$^{-1}$, obtained from its critical volume, was used. The same three parameters obtained were then used to produce curves for both temperatures in Fig. 1, on the assumption that $(k_x'/k_x'')_0$ will not change significantly between the two temperatures, as is expected from reaction behaviour in the liquid phase.[5]

The rising part of the curve at lower densities is associated with the difference between the attractive forces of the two transition states and the steeper falling part with repulsion differences. A more physically transparent investigation can be made using the virial theorem of Clausius, which leads to the same relationship between tuning functions and the inter-molecular pair potential, as will be reported later. The interpretations can be summarised as follows. In a compressible medium such as a supercritical fluid it may often be possible, by controlling the density, to vary the mean distance between a

solute species and its nearest-neighbour solvent molecules within a range where their mutual pair potential energy is changing significantly. This statement is substantiated by calculations of the naphthalene–carbon dioxide pair correlation function in a supercritical fluid.[6] The solvation energy of the solute can therefore be controlled by the density of the medium and this will cause variations in a physical or chemical equilibrium or, if the species is a transition state, the rate of a chemical reaction. We suggest that the present study demonstrates that the effect of this 'potential tuning' is significant and observable for two competing reactions under accessible conditions. Recent results on absolute rate constants, which show a minimum in the reaction rate *vs.* density,[7] can also be explained by this effect, which is not particularly associated with the region around a critical point or line or with the critical density.

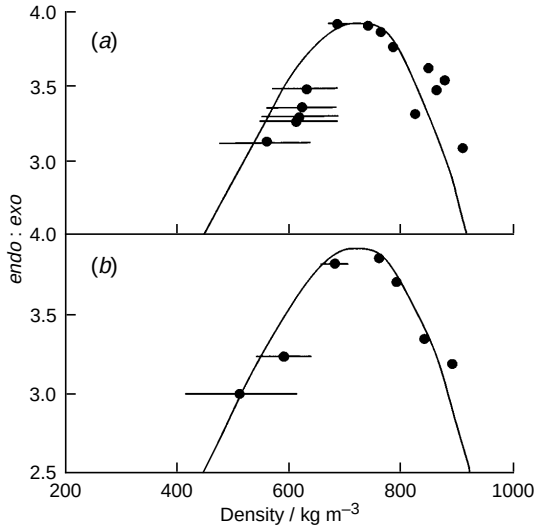



**Fig. 1** Experimental data (points) for the ratio of *endo*- to *exo*- product from the reaction of methyl acrylate and cyclopentadiene in carbon dioxide at (*a*) 308 and (*b*) 313 K. The curve shows predictions from the van der Waals equation, fitted to the experimental points at 313 K. Horizontal bars show errors in the calculated density, which are large near the critical density of 466 kg $m^{-3}$.

The authors would like to acknowledge discussions with Professor J. S. Rowlinson and financial support from EPSRC (UK)

## References

1 B. L. Knutson, A. K. Dillow, C. L. Liotta and C. A. Eckert, in *Innovations in supercritical fluids*, ACS Symposium Series 608, ed. K. W. Hutchenson and N. R. Foster, American Chemical Society, Washington, 1995, p. 166.
2 D. Andrew, B. T. Des Islet, A. Margaritis and A. C. Weedon, *J. Am. Chem. Soc*., 1995, **117**, 6132.
3 S. Kim and K. P. Johnston, *Chem. Eng. Commun*., 1988, **63**, 49.
4 A. A. Clifford, in *Supercritical fluids*, ed. E. Kiran and J. M. H. Levelt Sengers, Kluwer, Amsterdam, 1994, 449.
5 J. A. Berson, Z. Hamlet and W. A. Mueller, *J. Am. Chem. Soc*., 1962, **84**, 297.
6 H. D. Cochran and L. L. Lee, in *Supercritical fluid science and technology*, ACS Symposium Series 406, ed. K. P. Johnston and J. M. L. Penninger, American Chemical Society, Washington, 1988, p. 27.
7 R. D. Weinstein, A. R. Renslow, R. L. Danheiser, J. G. Harris and J. W. Tester, *J. Phys. Chem*., 1996, **100**, 12337.

*Received, 26th November 1996; Com. 6/08066I*

# A squaraine-based near-infrared absorbing sensor for the selective detection of transition and other metal ions in aqueous media†

**K. George Thomas, K. J. Thomas, S. Das* and M. V. George**

*Photochemistry Research Unit, Regional Research Laboratory (CSIR), Trivandrum 695 019, India*

**A near infrared absorbing cationic squaraine dye 1 is shown to be capable of detecting trace amounts of transition and lanthanide metal ions in aqueous media, even in the presence of alkali and alkaline earth metal ions.**

Design of fluorescent or chromogenic chemosensors for the selective detection of low concentrations of ions is an active area of research.[1–6] With a few exceptions,[3,4] most of the studies have been concerned with non-aqueous solutions of ions. Moreover, most of the chromophores hitherto reported suffer from the requirement of short wavelength excitation. For detection of metal ions in naturally occurring systems, particularly for intracellular applications, near-infrared absorbing water soluble chemosensors would be highly desirable.[2] In the course of our studies on the design of squaraine-based fluoro- and chromo-ionophores,[6] we have observed that a newly reported[7] squaraine dye, **1**, is highly suited for such applications. This dye is water soluble, has a very strong absorption in the near-infrared region and is capable of quantitatively and selectively detecting trace amounts of metal ions.‡ Complexation of **1** by different metal ions gives rise to a new absorption band, which in most cases is characteristic of the metal ion involved. Using this simple procedure, trace amounts of metal ions such as $Cu^{2+}$, $Hg^{2+}$, $Pb^{2+}$, $Mn^{2+}$, $La^{3+}$, $Eu^{3+}$, $Tb^{3+}$, $Gd^{3+}$ and $Lu^{3+}$ can be detected selectively.

The cationic dye **1** possesses two absorption maxima centred around 790 and 640 nm in a mixture (4 : 1) of water and acetonitrile at pH 6.7. Lowering the pH of the solution leads to a decrease in the intensities of these bands which is accompanied with the formation of a new band centred around 690 nm. The p$K_a$ of **1** has been evaluated as 4.9, based on these pH dependent spectral changes and the probable structures of the acid/base species in equilibrium with each other are shown in Scheme 1.

Addition of low concentrations of copper ions to a solution of **1** in a mixture (4 : 1) of water and acetonitrile at pH 6.7, where the dye is predominantly in its deprotonated form, led to a decrease in the intensities of the absorption maxima at 790 and 640 nm, which was accompanied by the formation of a sharp new band around 670 nm (Fig. 1). It has been observed that even addition of 50 nM (4 ppb) of $Cu^{2+}$ leads to a notable change in the absorption spectrum. Benesi–Hildebrand analysis of the complex formation, studied by following the changes in absorption spectra on addition of copper ions, indicated a 1 : 1 dye to metal stoichiometry with a stability constant of $1.5 \times 10^5$ $dm^3\ mol^{-1}$. Similarly, complexation of **1** with other metal ions leads to the formation of a new absorption band characteristic of the metal ion involved. It may be noted that the pH of the solution remains unchanged on addition of metal ions. The absorption maxima and equilibrium constants measured for different metal ions are shown in Table 1. With the exception of the complexes of $Hg^{2+}$ and $Cu^{2+}$ which have a maximum at 670 nm, the other complexes have their own characteristic absorption maxima. This is specially important with reference to the lanthanides investigated, since it is known that lanthanides when complexed with most chromogenic agents have similar absorption spectra and are therefore difficult to distinguish.[8] In the present study, however, there is a marked difference in the absorption maxima of the complexes of the dye with the various lanthanides studied (Table 1). The minimum concentration detectable for $Cu^{2+}$, $La^{3+}$, $Eu^{3+}$, $Tb^{3+}$, $Gd^{3+}$ and $Lu^{3+}$ is > 50–80 nM, for $Hg^{2+}$ is > 2 μM, for $Pb^{2+}$ is > 20 μM and for $Mn^{2+}$ is > 50 μM.

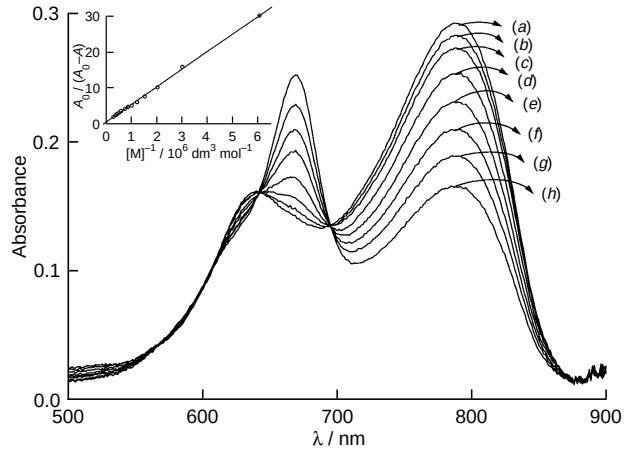
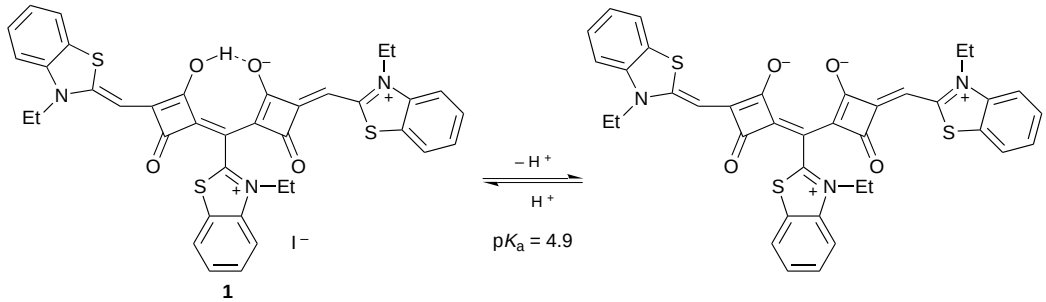



**Fig. 1** Effect of $Cu^{2+}$ concentrations on the absorption spectrum of **1** (4.7 μM) in $H_2O$–MeCN (4 : 1): $[Cu^{2+}]$ (*a*) 0, (*b*) 0.15, (*c*) 0.3, (*d*) 0.6, (*e*) 1.2, (*f*) 1.8, (*g*) 2.4, (*h*) 3.0 μM. Inset shows the plot of $A_0/(A_0 - A)$ *vs.* $1/[Cu^{2+}]$




**1**

**Scheme 1**

**Table 1** Complexation properties of **1** with various metal cations in $H_2O$–MeCN (4 : 1)

| Cation | $Cu^{2+}$ | $Hg^{2+}$ | $Pb^{2+}$ | $Mn^{2+}$ | $Zn^{2+}$ | $La^{3+}$ | $Eu^{3+}$ | $Gd^{3+}$ | $Tb^{3+}$ | $Lu^{3+}$ |
|---|---|---|---|---|---|---|---|---|---|---|
| $\lambda_{max}$/nm | 670 | 670 | 732 | 720 | 718 | 735 | 733 | 727 | 724 | 732 |
| log $K_s$[a,b] | 5.19 | 3.90 | 3.52 | 2.87 | — | 5.90 | 5.75 | 5.44 | 5.23 | 5.24 |
| Charge density | 2.778 | 1.818 | 1.667 | 2.500 | 2.703 | 2.953 | 3.158 | 3.198 | 3.250 | 3.529 |

[a] Benesi–Hildebrand equation for 1 : 1 complex formation between dye and metal ion, $A_0/(A_0 - A) = [E_L/(E_L - E_{mL})]\ \{1/(K_s[M]) + 1\}$, was used for determining the stability constant. $K_s$ is the stability constant, $A_0$ and $A$ are the absorbance of dye solution (790 nm band was followed) in the absence and presence of metal ions, $[M^{n+}]$. $E_L$ and $E_{mL}$ are the molar extinction coefficient of the free ligand and the complex respectively. All the $K_s$ values reported are within the experimental error of ±5%. [b] Complexes of all the metal ions studied except with $Cu^{2+}$ and $Mn^{2+}$ are stable in $H_2O$–MeCN (4 : 1) and the solutions were kept for 15 min for equilibration before carrying out the measurements. In the case of $Cu^{2+}$ and $Mn^{2+}$, the measurements were carried out immediately after the addition of the metal ions.

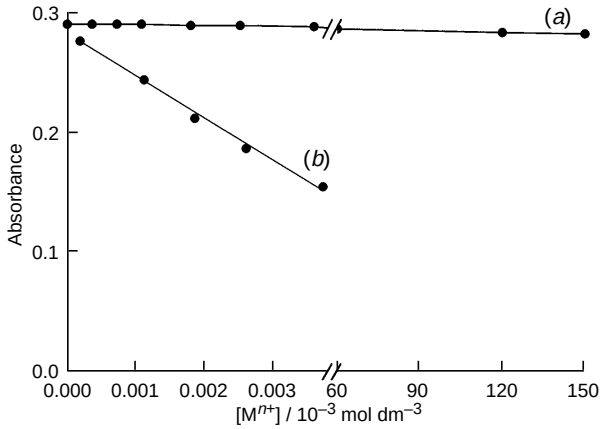



**Fig. 2** Determination of $Cu^{2+}$ in the presence of $Na^+$ using **1** (4.7 μM) in $H_2O$–MeCN (4 : 1) following the absorbance at 790 nm: (*a*) effect of addition of $Na^+$ (up to 150 mM); (*b*) effect of addition of $Cu^{2+}$ containing 150 mM of $Na^+$

An interesting feature of this extremely simple method of detecting trace amounts of metal ions is that although $Hg^{2+}$ and $Cu^{2+}$ complexes absorb at the same wavelengths, the differences in equilibrium constants for complex formation permit the analysis of low concentrations of $Cu^{2+}$ (> 50 nM) even in the presence of 1 μM of $Hg^{2+}$. The equilibrium constants listed in Table 1 indicate that the selectivity among the heavy metal ions is relatively high whereas within the lanthanide series it is not appreciable. The absorption spectrum of **1** was found to be unaffected by the addition of alkali and alkaline earth metal ions. For example, Fig. 2, curve (*a*) shows that addition of $Na^+$ ions up to 150 mM does not have any significant effect on the absorption spectrum of **1**. However, addition of even nM quantities of $Cu^{2+}$ (> 50 nM) to the above solution containing 150 mM of $Na^+$ [curve (*b*)] causes a decrease in the intensities of absorption of the dye accompanied by the formation of the 670 nm band characteristic of $Cu^{2+}$–dye complex. Thus, trace amounts (*ca.* 50 nM) of metal ions like $Cu^{2+}$ can be detected even in the presence of mM concentrations of $Na^+$, $Li^+$, $K^+$ and $Ca^{2+}$ (Fig. 2).

In the anionic form of the dye **1**, the oxygen atoms of the two cyclobutane rings are ideally located to yield the suitable geometry for strong complexation with metal ions. The intense absorption band observed in the NIR region of squaraines is essentially due to the intramolecular charge transfer transition which is primarily confined to the $C_2O_4$ unit.[9] The hypsochromic shift in the absorption spectra, upon complexation, can therefore be attributed to a reduction in the electron-donating ability of the $O^-$ atoms on complexation by the metal ions. Comparison of the shift in absorption maxima with charge density of the metal ions within the lanthanide series as well as between other metal ions (Table 1) indicate that, with the exception of $Cu^{2+}$ and $Hg^{2+}$, the hypsochromic shift does indeed increase with increasing charge density of the metal ion.

In conclusion, we have observed that the cationic squaraine dye **1** can act as a near-infrared absorbing chromogen for detecting trace amounts of toxic and environmentally hazardous metal cations such as $Cu^{2+}$, $Hg^{2+}$, $Pb^{2+}$ and $Mn^{2+}$ as well as several lanthanide metal ions in aqueous media. We are currently working on the synthesis and study of newer derivatives of the cationic squaraine dye, which can potentially yield a new class of chromogens for the selective and quantititative detection of metal ions, both for biological and environmental applications.

We thank the Council of Scientific and Industrial Research and the Department of Science and Technology, Government of India, for support.

## Footnotes

† This is contribution No. RRLT-PRU-70 from the Regional Research Laboratory, Trivandrum.

‡ Since the dye and dye–metal ion complexes undergo a slow precipitation and loss in absorption in aerated aqueous media all experiments were carried out in argon-purged 4 : 1 water–acetonitrile mixtures.

## References

1 J. C. Lockhart, *Comprehensive Supramolecular Chemistry*, ed. G. W. Gokel, Pergamon, 1996, vol. 1, 605; T. Hayashita and M. Takagi, *Comprehensive Supramolecular Chemistry*, ed. G. W. Gokel, Pergamon, 1996, vol. 1, p. 635; P. D. Beer, *Chem. Commun.*, 1996, 689.

2 *Topics in Fluorescence Spectroscopy, Vol. 4: Probe Design and Chemical Sensing*, ed. J. R. Lakowicz, Plenum, New York, 1994; *Fluorescent Chemosensors for Ion and Molecule Recognition*, ed. A. W. Czarnik, ACS Symposium Series 538, Washington DC, 1993.

3 R. A. Bisell, A. P. de Silva, H. Q. N. Gunaratne, P. L. M. Lynch, G. E. M. Maguire and K. R. A. S. Sandanayake, *Chem. Soc. Rev.*, 1992, 187; A. W. Czarnik, *Acc. Chem. Res.*, 1994, **27**, 302; L. Fabbrizzi and A. Poggi, *Chem. Soc. Rev.*, 1995, 197.

4 A. P. de Silva, H. Q. N. Gunaratne and C. P. McCoy, *Nature*, 1993, **364**, 42; A. P. de Silva, H. Q. N. Gunaratne and G. E. M. Maguire, *J. Chem. Soc., Chem. Commun.*, 1994, 1213; A. P. de Silva, H. Q. N. Gunaratne, T. Gunnlaugsson and M. Nieuwenhuizen, *Chem. Commun.*, 1996, 1967; G. K. Walkup and B. Imperiali, *J. Am. Chem. Soc.*, 1996, **118**, 3053; D. Y. Sasaki, D. R. Shnek, D. W. Pack and F. H. Arnold, *Angew. Chem., Int. Ed. Engl.*, 1995, **34**, 905.

5 I. O. Sutherland, *Crown Compounds Toward Future Applications*, ed. S. R. Cooper, VCH, New York, 1992, p. 235; A. Mason, A. Sheridan, I. O. Sutherland and A. Vincent, *J. Chem. Soc., Chem. Commun.*, 1994, 2627.

6 S. Das, K. G. Thomas, K. J. Thomas, P. V. Kamat and M. V. George, *J. Phys. Chem.*, 1994, **98**, 9291; S. Das, K. G. Thomas, K. J. Thomas, M. V. George, I. Bedja and P. V. Kamat, *Anal. Proc.*, 1995, **32**, 213.

7 H. Nakazumi, K. Natsukawa, K. Nakai and K. Isagawa, *Angew. Chem., Int. Ed. Engl.*, 1994, **33**, 1001.

8 V. Bhagavathy, T. P. Rao and A. D. Damodaran, *Handbook on the Physics and Chemistry of Rare Earths*, ed. K. A. Gschneidner Jr. and L. Eyring, Elsevier, Amsterdam, 1995, vol. 21, p. 367.

9 R. W. Bigelow and H.-J. Freund, *Chem. Phys.*, 1986, **107**, 159; K.-Y. Law, *J. Phys. Chem.*, 1987, **91**, 5184; P. V. Kamat, S. Das, K. G. Thomas and M. V. George, *J. Phys. Chem.*, 1992, **96**, 195.

*Received, 16th December 1996; Com. 6/08397H*

# Fluorinative α-cleavage of cyclic ketoximes with diethylaminosulfur trifluoride: an efficient synthesis of fluorinated carbonitriles

**Masayuki Kirihara, Kanako Niimi and Takefumi Momose***

*Faculty of Pharmaceutical Sciences, Toyama Medical and Pharmaceutical University, Sugitani 2630, Toyama 930-01, Japan*

**Diethylaminosulfur trifluoride effects ready cleavage of cyclic ketoximes to fluorinated carbonitriles.**

Fluorinated organic compounds are widely used in scientific and industrial fields. Since the preparative methods for organofluorine compounds remain limited to a few procedures, new fluorinating agents and methodology are required.[1] Since diethylaminosulfur trifluoride (DAST), a reagent converting aliphatic alcohols into alkyl fluorides, has been introduced into organic synthesis,[2] there have been several reports concerning new fluorinating methods.[3–9] Among the methods, we reported the reaction of DAST with tertiary cyclopropyl silyl ethers causing ring opening to give allylic fluorides.[10]

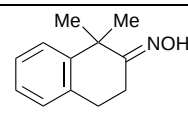
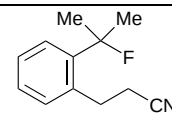
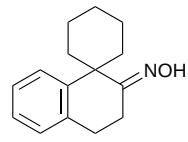
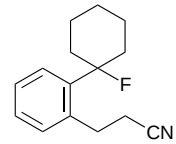
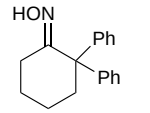
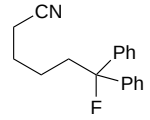
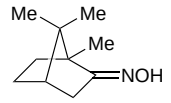
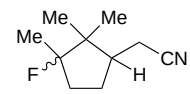
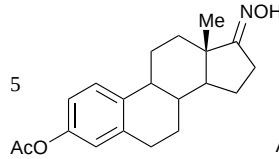
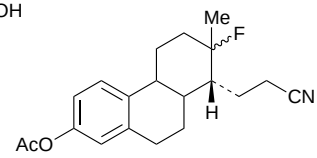
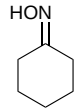
Here we describe a novel reaction involving the treatment of cyclic ketoximes **1** with DAST to cause a ring fragmentation resulting in the formation of fluorinated carbonitriles **2**.† The methodology has also provided an efficient route to tertiary fluorides or fluoroalkenes. The results are summarized in Table 1.

The presence of substituent(s) capable of stabilising a carbocation at the position α to the oximino carbon is essential to obtain fluorinated carbonitriles. An oxime lacking such substituents afforded a complex mixture (*e.g.* run 6 in Table 1). In the cases of runs 4 and 5, the products were a 1 : 1 mixture of stereoisomers. The results suggest that the reaction is a kind of Beckmann fragmentation (abnormal Beckmann rearrangement)[11] involving a carbocation intermediate.

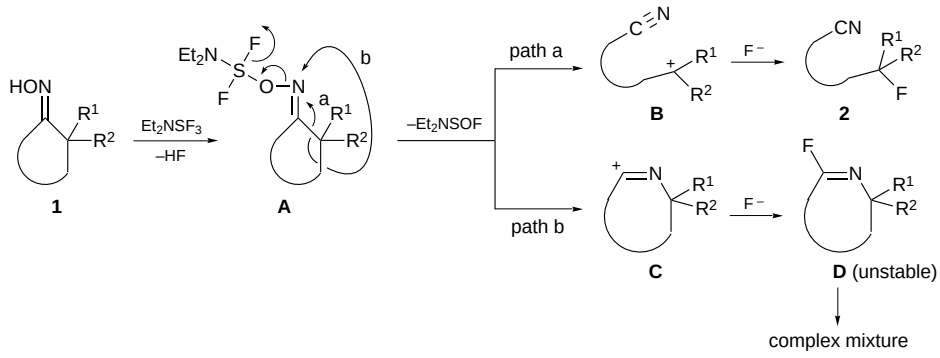
A postulated reaction mechanism is depicted in Scheme 1. The first step is the nucleophilic displacement of a fluorine in DAST by the oxygen of the oximino substrate **1** with elimination of hydrogen fluoride. Next, the elimination of diethylaminosulfino fluoride from the intermediate **A** causes the bond cleavage and gives a carbocation intermediate **B**. Finally, the fluoride ion attacks **B** to afford the fluorinated carbonitrile **2** (path a). In the case of compounds lacking substituents to stabilise the α-carbocation, the reaction proceeds through a mechanism similar to that of the 'normal' Beckmann rearrangement. The carbon–carbon bond *anti* to the oximino leaving group in the intermediate **A** migrates to the nitrogen atom to afford the carbocation **C**. The fluoride ion attacks **C** to give an unstable compound **D**, which leads to a complex mixture (path b).

Compounds bearing a sulfur functionality **3** at the position α to the oximino carbon reacted with DAST to cause the fragmentation efficiently leading to α-fluoro sulfides **4**. Since α-fluoro sulfides **4** were not stable, they were subjected, without purification, to oxidation with MCPBA. The resulting sulf-

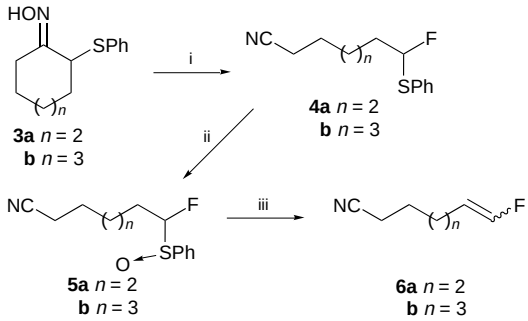
**Table 1**

| Run | Starting material[a] | Product[b] | Yield (%) |
|---|---|---|---|
| 1 |  |  | 77 |
| 2 |  |  | 91 |
| 3 |  |  | 75 |
| 4 |  |  | 69[c] |
| 5 |  |  | 63[c] |
| 6 |  | complex mixture | — |

[a] Oximes were prepared from ketones by reaction with hydroxylamine. [b] All compounds were characterised on the basis of mass, IR, $^1$H and $^{19}$F NMR spectral data. [c] A 1 : 1 mixture of stereoisomers.




**Scheme 1**




**Scheme 2** *Reagents and conditions*: i, DAST, $CH_2Cl_2$, −78 °C, ii, MCPBA, $CH_2Cl_2$ (**5a** : 51%, **5b**: 75%, in 2 steps), iii, 160 °C, $C_6H_6$, heated in a sealed tube (**6a** : 91%, **6b** : 97%)

oxides **5** were heated in a sealed tube at 160 °C to afford fluoroalkenes **6** in high yields (Scheme 2).

## Footnote

† A typical experimental procedure is as follows: to a solution of oxime (1.0 mmol) in dichloromethane (3 ml) was added DAST (1.0 mmol) at −78 °C under an inert atmosphere, and the reaction mixture was stirred for 30 min. A saturated sodium hydrogen carbonate solution was added to the reaction mixture, and the resulting mixture was extracted with dichloromethane. The extract was dried over anhydrous sodium sulfate, filtered, and evaporated to afford the crude product. Purification by chromatography (silica gel, hexane–dichloromethane) gave a pure sample.

## References

1 O. A. Mascaretti, *Aldrichim. Acta*, 1993, **26**, 47; J. A. Wilkinson, *Chem. Rev.*, 1992, **92**, 505.
2 M. Hudlicky, *Org. React.* (*N.Y.*), 1988, **35**, 513.
3 J. R. McCarthy, N. P. Peet, M. E. LeTourneau and M. Inbasekaran, *J. Am. Chem. Soc.*, 1985, **107**, 735.
4 S. F. Wnuk and M. J. Robins, *J. Org. Chem.*, 1990, **55**, 4757.
5 Y. Kikugawa, K. Matsumoto, K. Mitsui and T. Sakamoto, *J. Chem. Soc., Chem. Commun.*, 1992, 921.
6 G. Neef, G. Ast, G. Michl, W. Schwede and H. Vierhufe, *Tetrahedron Lett.*, 1994, **35**, 8587.
7 M. Kuroboshi, S. Furuta and T. Hiyama, *Tetrahedron Lett.*, 1995, **36**, 6121.
8 A. J. Ratcliffe and I. Warner, *Tetrahedron Lett.*, 1995, **36**, 3881.
9 S. Bildstein, J. Ducep, D. Jacobi and P. Zimmermann, *Tetrahedron Lett.*, 1996, **37**, 4941.
10 M. Kirihara, T. Kambayashi and T. Momose, *Chem. Commun.*, 1996, 1103.
11 R. E. Gawley, *Org. React.* (*N.Y.*), 1988, **35**, 1.

*Received, 15th November 1996; Com. 6/07749H*

# Supported BINOLate salts as base catalysts. Preparation and use in the Michael reaction

**Duncan J. Macquarrie†**

*Department of Chemistry, University of York, Heslington, York, UK YO1 5DD*

**Two silica supported BINOL complexes are prepared, both of which are active catalysts in the Michael reaction.**

The use of derivatives of 1,1′-naphthalene-2,2′-diol (BINOL) as base catalysts has recently been disclosed.[1,2] In particular, the use of podand-substituted salts of BINOL has led to efficient base catalysts for the Michael reaction.[2] As part of a programme aimed at the development of heterogenised base catalysts for use in the synthesis of fine chemicals, we have prepared two BINOL derivatives supported on silica **1** and **2**, and evaluated them in the Michael reaction.

The first catalyst, **1**, was prepared from γ-aminopropylsilica[3] (AMPS, **3**) and **4**, prepared by known methods[4,5] from the commercially available poly(ethylene glycol) methacrylate (Aldrich, $M_n$ = 306) by tosylation, displacement with the Na salt of BINOL, hydrolysis of the methacrylate, retosylation and displacement of the tosylate with **3** under reflux in toluene overnight (Fig. 1). Deprotonation of the BINOL unit was achieved by stirring with 1.5 equiv. NaOH in methanol (0.05 mol dm$^{-3}$) for 4 h, followed by exhaustive washing with methanol to remove excess base and physisorbed material. Thermogravimetric analysis (TGA) and elemental analysis were in agreement and indicated a loading of 0.2 mmol g$^{-1}$. The product was further analysed by $^{13}$C–CPMAS (300 MHz, δ 8.67, 18.00, 42.93 aminopropyl; 69.57 PEG, 127.04 + weak signal at 137–140 BINOL unit). The Diffuse Reflectance FTIR (DRIFT) spectrum of the product displayed the expected peaks for the BINOL unit at 1603, 1579 and 1510 cm$^{-1}$.

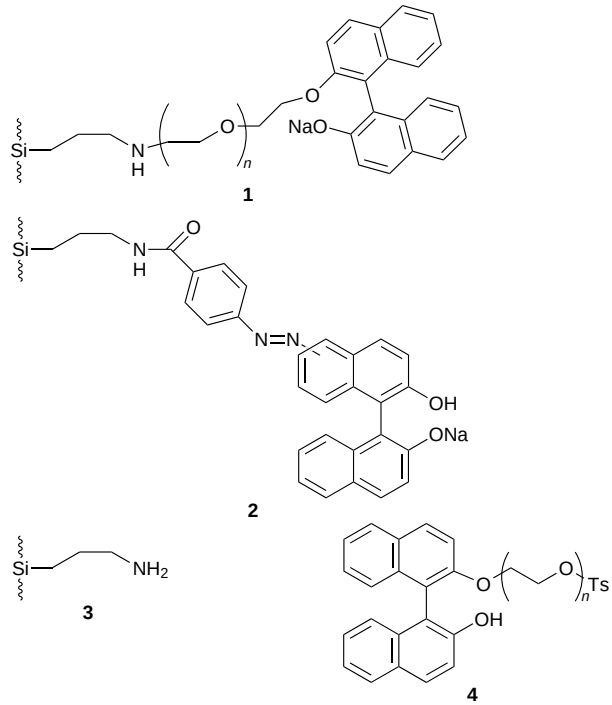
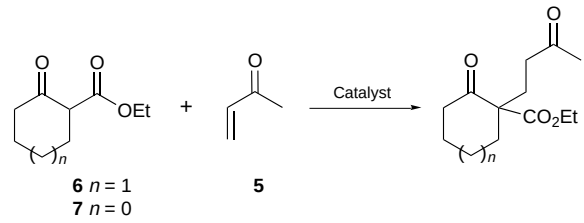



**Fig. 1** structures of the silica supported catalysts and precursor

The second catalyst, **2**, was prepared, also from **3**, in four steps (amide formation with 4-aminobenzoic acid,[3] diazotisation[6] and coupling with BINOL at pH 7, followed by deprotonation). The deprotonation procedure was the same for both catalysts. Elemental analysis was consistent with the proposed catalyst structure at a loading of 0.3 mmol g$^{-1}$, in accordance with weight loss as measured by TGA. Diffuse reflectance UV–VIS (DRUV) spectroscopy indicated a peak at 520 nm, which corresponds well to the diazo coupling product from 4-aminobenzoic acid and BINOL after physisorption on silica. Diffuse reflectance IR spectroscopy showed peaks at 1653 and 1565 cm$^{-1}$ (amide) and 1600, 1585 and 1506 cm$^{-1}$ (aromatics). The position of attachment of the N=N unit to the BINOL ring system is, as yet, unknown.

The products were evaluated as catalysts in the reaction of but-3-en-2-one **5** with the β-diketones ethyl cyclohexanone 2-carboxylate **6** and ethyl 2-oxocyclopentane-2-carboxylate **7** (Scheme 1). The catalyst (0.25 g), was added to a solution of diketone (10 mmol) and but-3-en-2-one (14 mmol) in solvent (15 ml). The reaction was stirred at room temp. and monitored




**Scheme 1** Michael addition between β-diketones and but-3-en-2-one, catalysed by supported BINOL catalysts

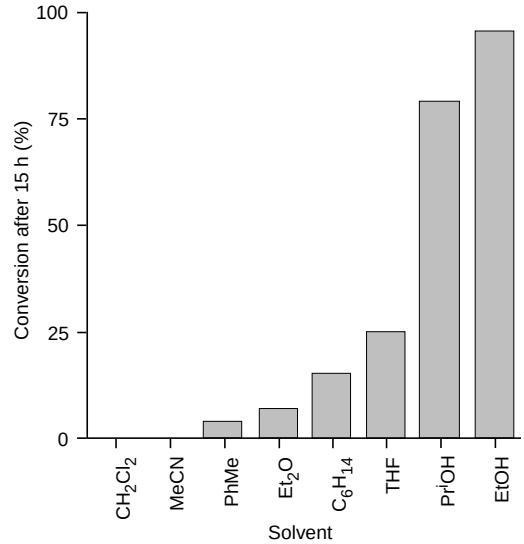



**Fig. 2** Solvent dependence in the reaction between **5** and **6** at room temp. (15 ml solvent, 0.2 g dodecane as internal standard, 14 mmol **5** and 10 mmol **6**). The reaction in isopropanol was complete after 24 h.

by GC using dodecane as internal standard. The reaction of **6** using **1** as catalyst was evaluated first and displayed a remarkable solvent dependence (Fig. 2). No reaction takes place in dichloromethane or in acetonitrile, with no product being detected even after 72 h. This is remarkable since the homogeneous version of this catalyst is used in dichloromethane.[2] Toluene is poor, and ethers (diethyl ether and THF) are slightly better. The best solvents by far are alcohols, with ethanol being particularly effective, complete reaction being achieved after 15 h (Fig. 2). It is possible that the oxygen-containing solvents are better able to interact with the PEG chain, particularly the hydrogen-bonding alcohols. The relatively good performance of hexane is puzzling (we have recently observed such anomalous behaviour in different systems[7]), and it may be due to partitioning effects. Isopropanol effected complete transesterification of the product under the reaction conditions. The product can be isolated by filtration of the catalyst and normal work-up, in yields typically 5–8% lower than the GC yield. Reuse of catalyst (after decantation of the supernatant) has been studied (Table 1), and there is a gradual slowing of reaction with repeated reuse (up to four uses). Conversions are close to complete and fall off only slightly with reuse. Compound **7** reacts more rapidly under the same conditions, reaction being complete after 8 h, as opposed to 15 h with **6**. Similar slowing of reaction was observed upon reuse.‡

Compound **2** was also evaluated in the above reactions, and was found to be slightly less active [reactions took 28 h (**6**) and 15 h (**7**) respectively]. Reuse was also successful, with less reduction in performance being observed than with **1**. While a thorough solvent study has not yet been carried out on this catalyst, reaction in dichloromethane does proceed, albeit slowly, to the extent of 8% in 24 h.§

Future work will concentrate on further optimisation of the systems and extension of the methodology to other phenols, Michael reactions and to enantioselective chiral BINOL systems.

D. J. M. thanks the Royal Society for the award of a University Research Fellowship.

**Table 1** Catalyst reuse in the reaction of **5** with **6** and **7**[a]

| Catalyst | Substrate | Conversion (%) | *t*/h |
|---|---|---|---|
| **1** | **6** | 97 | 15 |
| **1** (1 reuse) | **6** | 98 | 16 |
| **1** (2 reuses) | **6** | 99 | 19 |
| **1** (3 reuses) | **6** | 96 | 23 |
| **1** | **7** | 99 | 8 |
| **2** | **6** | 98 | 28 |
| **2** (1 reuse) | **6** | 98 | 29 |
| **2** (2 reuses) | **6** | 96 | 28 |
| **2** (3 reuses) | **6** | 97 | 30 |
| **2** | **7** | 99 | 15 |

[a] Reactions were carried out in 15 ml ethanol at room temp. with dodecane as internal standard, using 0.25 g catalyst, 10 mmol keto ester and 14 mmol enone. Isolated yields were 3–8% lower than the reported GC yields.

## Footnote

† E-mail address: djm13@york.ac.uk

‡ Turnover numbers for **1** and **2** can thus be estimated to be of the order of 800 and 530, respectively.

§ Leaching does not appear to be a problem with either catalyst, since reactions which were interrupted before completion by removal of catalyst did not procceed after removal of the catalyst.

## References

1 H. Sasai, T. Arai, Y. Satow, K. N. Houk and M. Shibasaki, *J. Am. Chem. Soc*., 1995, **117**, 6194; K. Iseki, S. Oishi, H. Sasai and M. Shibasaki, *Tetrahedron Lett*., 1996, **37**, 9081.
2 Y. Tamai, A. Kamifuku, E. Koshiishi and S. Miyano, *Chem. Lett*., 1995, 957.
3 V. A. Basiuk and A. A. Chuiko, *J. Chromatogr*., 1990, **521**, 29.
4 Y. Tamai, S. Koike, A. Ogura and S. Miyano, *J. Chem. Soc., Chem. Commun*., 1991, 799.
5 Y. Tamai, M. Akiyama, A. Okamura and S. Miyano, *J. Chem. Soc., Chem. Commun*., 1992, 687.
6 V. A. Basiuk and E. G. Khil'chevskaya, *Anal. Chem. Acta*, 1991, **255**, 197.
7 D. J. Macquarrie, A. Lambert, A. Priest and J. Mdoe, unpublished results; J. H. Clark, D. J. Macquarrie and J. C. Ross, unpublished results.

*Received, 10th January 1997; Com. 7/00261K*

# Stereospecific propene polymerisation catalysis using an organometallic modified mesoporous silicate

**Jonathan Tudor and Dermot O'Hare*†**

*Inorganic Chemistry Laboratory, University of Oxford, South Parks Road, Oxford, UK OX1 3QR*

**The mesoporous silicate, MCM-41 is modified by grafting the chiral alkene polymerisation catalyst *rac*-ethenebis(indenyl)zirconium dichloride onto the surfaces of the mesopore and used to produce highly isotactic polypropene with a unique spherulite morphology.**

Since homogeneous catalysts for alkene polymerisation were first reported in 1957,[1] there has been much interest both in academic and industrial circles in the application and evolution of new catalytic systems. Polypropene is probably the most marketable and versatile of the polyalkenes produced industrially and is found in many industries from the automotive trade to the leisure industry. Of the three forms of polypropene, the highly ordered, high molecular mass isotactic form is the most important. Under homogeneous conditions isotactic polypropene can be produced by chiral *ansa*-metallocenes such as *rac*-EBI–zirconium dichloride {EBI = 1,2-bis(inden-1-yl)-ethane} in combination with a co-catalyst, methylaluminoxane (MAO). Compared to polypropenes produced by classical heterogeneous Ziegler–Natta catalysts, molecular masses and melting points are low, making their products of little commercial worth for most technical applications. Kaminsky reported a silica-supported metallocene catalyst which yielded isotactic polypropene with high molecular masses and high melting points.[2] This is in contrast to previous studies of metallocenes supported on silica, where high activities for polymerisation were reported, but with low molecular masses and low melting points.

We have recently reported that the cationic zirconocenium alkene polymerisation catalyst, $[Zr(\eta\text{-}C_5H_5)_2Me(thf)]BPh_4$ can be readily ion-exchanged into modified charged 2 : 1 layered silicates.[3] With propene, the catalyst system produces atactic polymer with molecular masses some 25% greater than the homogeneous analogues, but with significantly lower activities. In an effort to produce new propene polymerisation catalyst systems which yield high molecular mass polypropylene with even greater specific isotacticities we have investigated the catalytic activity of mesoporous silicates with included chiral *ansa*-metallocenes.

As an alternative host support material we have investigated the use of the siliceous mesoporous material MCM-41.[4] The internal walls of MCM-41 are lined with silanol groups, the chemistry of which the chemist can exploit to develop modified materials; there has already been reports in the literature of the encapsulation of organometallic species inside the host channels.[5–7]

Incorporation of *rac*-[$ZrCl_2$(EBI)] into MCM-41 was achieved by heating a saturated solution of *rac*-[$ZrCl_2$(EBI)] with a suspension of a pre-treated MCM-41 suspension. The pre-treatment involves initial dehydration of the as-prepared materials and then subsequent treatment of the anhydrous material with an excess of a toluene solution of MAO at 50 °C for 24 h, followed by filtration, washing with toluene and drying under vacuum to give a white, air sensitive mesoporous material. The Al content as determined by elemental microanalysis, gave a loading of 6.1 mmol (Al) $g^{-1}$ of silicate, the C : H : Al ratio being 2.50 : 2.95 : 1. The final organometallic–silicate complex has a Zr loading of 0.35 mmol $g^{-1}$‡ as evidenced by elemental microanalysis. Inspection of the powder X-ray diffraction pattern after modification of the MCM-41 with MAO and then with *rac*-[$ZrCl_2$(EBI)] reveals that the reactions do not destroy the hexagonal framework of the mesoporous material; although the peak width at half maximum suggests a slight loss in crystallinity.

The material has been successfully used in the polymerisation of propene to yield highly isotactic polypropene. The results of polymerisation runs are outlined in Table 1; to serve as a comparison, polymerisation tests were also undertaken on the homogeneous system, *rac*-[$ZrCl_2$(EBI)] and *rac*-[$ZrCl_2$(EBI)] supported on a MAO modified clay.§ From the data it appears that the polymer properties are little affected by grafting the metallocene to the mesopore. This implies that during the course of the reaction between metallocene and the MCM-41 support, the metallocene has remained essentially structurally intact on the mesoporous material. However, due to the nature of the support, the possibility of there being active sites on the external surfaces of the mesopore which could be responsible for the polymerisation cannot be ignored.

Inspection of Table 1 reveals several interesting properties of the isotactic polypropene produced by the three different forms of *rac*-[$ZrCl_2$(EBI)]. With respect to activity, the homogeneous system proves to be the most active. Out of the two supported catalysts, the clay support proves to be more active than the mesoporous support by about threefold. A diffusion limiting effect could be partly responsible for the lower activity; whereby active metal centres located toward the centre of the mesoporous channels are effectively screened from approaching monomer units by active centres closer to the channel ends, which harbour growing polymer chains. The number average molecular masses ($M_n$) also vary for each sample. The clay-supported catalyst produced the highest $M_n$ value, with the values for the MCM-41 support slightly lower, but both of these showed an approximate fourfold increase in the number average molecular mass of the polypropene relative to the homogeneous system. The isotacticity of the three polymer samples has been investigated using $^{13}C$ solution NMR spectroscopy. The homogeneously produced polymer is the least isotactic, the two supported samples producing similar spectra indicative of highly isotactic polypropene. Differential scanning calorimetry of the polymer samples reveals that the MCM-41 produced material has the highest melting point of the three polymers at 141 °C, compared to melting points of 128 °C for polymer

**Table 1** Propene polymerisation activities and polymer properties

| Material[a] | Loading mmol (Zr) $g^{-1}$ | Activity Kg mol (Zr h)$^{-1}$ | $\bar{M}_n$[b]/(GPC) | Polydispersity |
|---|---|---|---|---|
| 1 | 0.35 | 1163 | 11849 | 1.95 |
| 2 | 2.39 | 4941 | 3110 | 1.91 |
| 3 | 0.14 | 3033 | 14038 | 1.92 |

[a] 1 = MCM-41–MAO–*rac*-[$ZrCl_2$(EBI)], 2 = *rac*-[$ZrCl_2$(EBI)], 3 = clay–*rac*-[$ZrCl_2$(EBI)]. [b] GPC *vs.* polystyrene, 140 °C in 1,2-dichlorobenzene, ratio of Zr : MAO was 1 : 1000 in each case.

produced homogeneously and 135 °C for the polymer produced by *rac*-[$ZrCl_2$(EBI)] supported on a layered silicate clay.

To assess morphological differences between the three isotactic polymer samples, scanning electron microscopy (SEM) was used. Figs. 1 and 2 show micrographs of homogeneously and MCM41 produced polymer samples, respectively. Inspection of the micrographs reveals striking differences between the two samples. The polymer produced by the homogeneous system (Fig. 1) consists of particles with a very porous open structure and appears to be composed entirely of sub-particles around 1 μm. A similar structure is observed for polymer produced by the clay support, except that the average particle size is much larger at *ca*. 10 μm. The micrograph also reveals the plate-like morphology of the clay material has been replicated in the polymer. The SEM micrograph for the MCM-41 produced IPP (Fig. 2) exhibits some quite remarkable

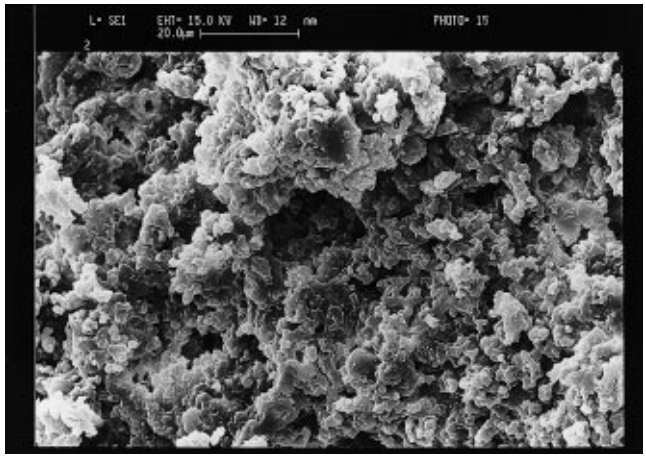



**Fig. 1** SEM micrograph of isotactic polypropene produced by a homogeneous solution of [$ZrCl_2$(EBI)]

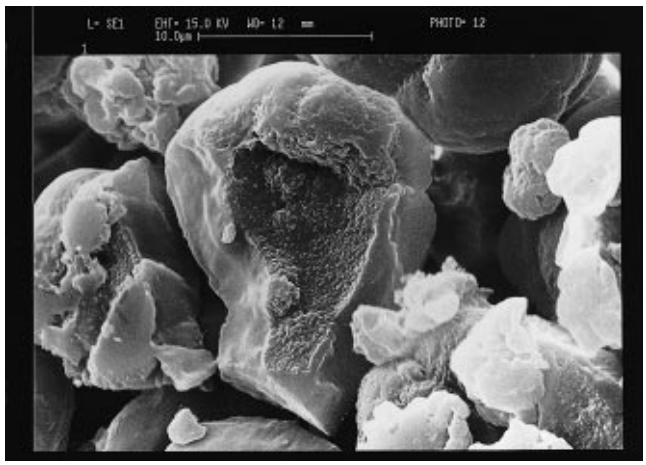



**Fig. 2** SEM micrograph of isotactic polypropene produced by MCM-41 supported [$ZrCl_2$(EBI)] showing the spherulite structure. The internal structure of the spherulites can be seen by examining a crushed particle.

features. The catalyst produces spherulite particles of approximate diameter 10 μm. The internal structure of the polymer grains can also be probed by crushing it at −120 °C and then re-examining the sintered particles with SEM. The micrograph of such a broken particle is shown in Fig. 2. This clearly shows that the very fine scale of the internal structure of the polymer is substantially different from the external structure; suggesting that the polymer consists of a distinct core and shell arrangement, a feature which is atypical for most homogeneously produced polymers. Similar freezing and sheering of the homogeneous and clay samples shows no difference between their internal and external morphology. The MCM-41 produced polymer was also studied under crossed polarising microscope. From the optical micrograph the sphericular nature of the polymer becomes clear from the large birefringent regions of the central particle. Spherulites are a morphological feature of bulk crystallised polymers with a large number of lamellar crystallites radiating in all directions from one central nucleus with well defined boundaries. The observation of birefringence in the optical measurement indicates a general tangential arrangement of the chains within the spherulites.

In conclusion, we have demonstrated the effectiveness of MCM-41 in providing a solid support for the homogeneous chiral catalyst *rac*-[$ZrCl_2$(EBI)] and its application toward controlling polymer morphology. Hence, polypropene produced by the MCM-41 derived catalyst consists of entirely of spherulite particles, with a distinct shell and core morphology. The polymer is highly isotactic and exhibits higher melting points than the corresponding homogeneous and clay supported system.

We would like to thank V. Murphy for polymer analysis, and Shell UK for financial assistance.

## Footnotes

† D. O'Hare is the Royal Society of Chemistry Sir Edward Frankland Fellow.

‡ Exact Al and Zr loadings vary with MCM-41 batch, the values given reflect a typical value.

§ The clay used was the synthetic smectite, LaponiteRD, $Na_{0.46}Mg_{5.42}Si_8O_{20}(OH)_4$.

*Note added in proof*: Following submission of this article, a related study on *rac*-EBI-$ZrCl_2$/MCM-41 has been published. Y. S. Ko, T. K. Han, J. W. Park and S. I. Woo, *Macromol. Rapid Commun.*, 1996, **17**, 749.

## References

1 D. S. Breslow and N. R. Newburg, *J. Am. Chem. Soc.*, 1957, **79**, 5072.
2 W. Kaminsky and F. Renner, *Makromol. Chem. Rapid Commun.*, 1993, **14**, 239.
3 J. Tudor, L. Willington, D. O'Hare and B. Royan, *Chem. Commun.*, 1996, 2031.
4 C. T. Kresge, M. E. Leonowitz, W. J. Roth, J. C. Vartulli and J. S. Beck, *Nature*, 1992, **359**, 710.
5 R. Ryoo, C. H. Ko, J. M. Kim and R. Howe, *Catal. Lett.*, 1996, **37**, 29.
6 T. Maschmeyer, F. Rey, G. Sankar and J. M. Thomas, *Nature*, 1995, **378**, 159.
7 C. Huber, K. Moller and T. Bein, *J. Chem. Soc., Chem. Commun.*, 1994, 2619.

*Received, 21st November 1996; Com. 6/07886I*

# Conformational change of protein cytochrome b-562 adsorbed on colloidal gold particles; absorption band shift

**H. S. Zhou,*[a] S. Aoki,†[b] I. Honma,[c] M. Hirasawa,[b] T. Nagamune[b] and H. Komiyama[b]**

[a] *Nanophotonics Laboratory, Frontier Research Program, The Institute of Physical and Chemical Research (RIKEN), Hirosawa 2-1, Wako-shi, Saitama 351-01, Japan*
[b] *Department of Chemical System Engineering, Faculty of Engineering, University of Tokyo, 7-3-1 Hongo, Bunkyo-ku, Tokyo, Japan*
[c] *Electrotechnical Laboratory (ETL) 1-1-4, Umezono, Tsukuba, Ibaraki 305, Japan*

**An enormous and continuous shift of a surface plasmon resonance of gold particles is observed when protein cytochrome b-562 is adsorbed on to the surface.**

Organic–inorganic nanostructured composites provide a rich source of new functional materials for fundamental research and applications.[1–5] Examples include ordered mesoporous molecular sieves synthesized *via* a liquid-crystal surfactant template;[1,2] a low-cost, high-efficiency solar cell system of nanocrystallites covered by a chlorophyll derivative or related natural porphyrins;[3,4] and a polydiacetylene shell layer synthesized on a template of nanosized gold particles.[5] Although many interesting functional materials have been synthesized, it is still not clear how these organic functional molecules are deposited on, or affected by a solid boundary surface of nanoparticles; or what conformations and orientations are adopted. If the mechanism by which organic molecules are adsorbed on the solid surface of nanoparticles is clarified, it will open a wide opportunity in studying the basic physics and chemistry of nanostructure composite materials.

Here, we disclose our recent findings for optical coupling in an organic–inorganic nanostructure composite system of the protein cytochrome b-562 and colloidal gold particles. Although many studies, especially surface enhanced Raman scattering (SERS),[6–8] have been carried out for protein adsorption on solid surfaces, direct optical measurement at the protein's molecular level and conformational study of the protein on the surface of gold particles has scarcely been reported.

An aqueous gold colloidal solution was prepared by reduction of $HAuCl_4$ ($5 \times 10^{-3}$ mass%, solution 1) with citric acid (0.15 mass%, solution 2).[9] Solution 1 (750 ml) was heated at 100 °C for 12 min in an oil bath, and then solution 2 (37.5 ml) added. After *ca*. 2 min the boiling solution turned blue, and after 3 min became reddish purple. At this stage, the mean particle size was 31.0 nm with a narrow size distribution according to both transmission electron microscopy (TEM) and dynamic light scattering.[10,11] The dynamic light scattering method is a useful tool for measuring particle sizes in the range from 10 nm to several μm.

Cytochrome b-562 solutions of various concentrations were prepared (0.0003–0.16 g $l^{-1}$). The solution (0.2 ml) was added to the gold colloidal solution (20 ml) with vigorous stirring. Cytochrome b-562 is a small cylindrical[12] haem protein (height 5.0 nm, diameter 2.5 nm; Fig. 1) found in the periplasm of *Escherichia coli* with a chromophore (protohaem IX) about 3.5 nm from the base. A significant absorption occurs at 418 nm and smaller absorbances at 530 and 560 nm.

The surface plasma resonant absorption band of gold particles is located at *ca*. 530 nm.[13] The plasmon absorption band (at 530 nm) of the original 31.0 nm gold colloidal suspension was red-shifted and broadened upon adsorption of the protein. When only a small amount of the protein was added, much less than for full monolayer coverage, the interaction is weak and only a small shoulder emerged at *ca*. 650 nm. However, with increasing quantity of the protein, the interaction becomes stronger and the new peak is broadened and shifted to long wavelength (up to 750 nm).

Upon further addition of protein the absorption spectrum unexpectedly returned to that of the original colloidal solution and the absorption peak of isolated cytochrome b-562 appeared at *ca*. 418 nm arising from solution-phase protein. At this stage, composite particles and isolated protein co-exist and interaction between them becomes weak eventually non-existant at high protein concentration.

We introduce the concept of effective coverage to describe the status of adsorbed protein cytochrome b-562 on the surface of gold particles taking into account factors such as the shape of the protein and the protein electrostatic repulsive force to effect full coverage.

The effective coverage $\beta = 1.0$ and $\beta = 2.0$ refer to full coverage of cytochrome b-562 on the surface of gold particles in 'side-on' and 'tail-on' conformations respectively.

Fig. 2 shows the shifting of the long-wavelength absorption peak position as a function of the protein's effective coverage β. In the present experiment, as all of the protein is adsorbed on the particle surfaces, the surface coverage is linearly proportional to the amount of protein added to the solution. As the protein

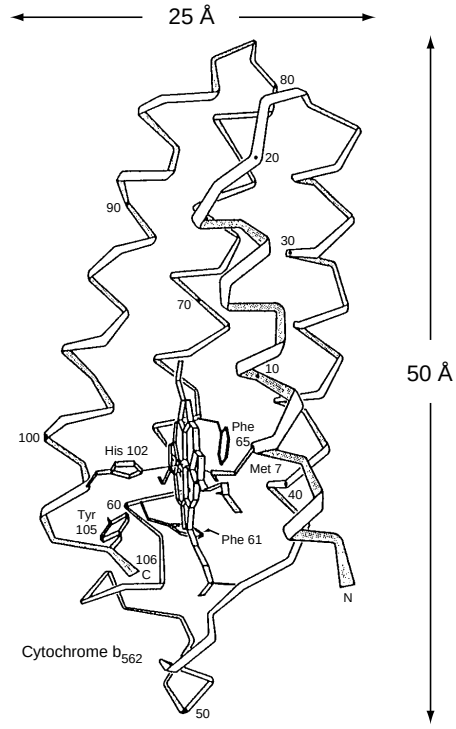



**Fig. 1** Schematic structure of cytochrome b-562

coverage increases, the peak position moves to longer wavelength until it reaches 750 nm and the effective coverage β at this point is 1.0, where the particle surface is covered by proteins in a 'side-on' conformation. The expected size of such a structure is verified by dynamic light scattering measurements. Further addition of the protein moves the peak back to its original position at 530 nm, although the composite particle size increases monotonously with the protein coverage. This indicates that the phenomenon of $\lambda_{max}$ moving back to its original value is not a consequence of separation of the protein and gold particles. We propose that the protein's adsorption conformation on the surface changes at a certain concentration. A model is proposed which considers two adsorption conformations of cytochrome b-562 on the gold surface. Namely, the 'side-on' conformation predominates at low concentrations ($\beta < 1.0$) while the 'tail-on' conformation predominates at high concentrations ($1 < \beta < 2$).

Different conformations of the protein lead to differences in the interaction distance between the gold surface and the interior chromophore of cytochrome b-562. In other words, the interaction between the gold particles and cytochrome b-562 depends strongly on the distance between the surface and the chromophore. The red-shift to 750 nm and spectral broadening occurred only for the 'side-on' conformation because the short separation in this case.

The model of the conformation change of the protein was supported by particle size measurement as determined by dynamic light scattering. Initially the diameter of the gold particles is 31.0 nm and it increases with protein coverage (Fig. 2). The composite particle size was 36 nm at the maximum spectral shift of the plasmon absorption band. At this stage, the protein b-562 is in a 'side-on' conformation on the gold surface. Since in such a conformation the width of the protein is 2.5 nm the value of 36 nm ($= 31 + 2 \times 2.5$ nm) is as expected for monolayer coverage. As the concentration is raised further the absorbed protein molecules start shifting conformation and eventually at a particle size of 40 nm, the interaction was so weak that the optical absorption spectrum was almost the same as the intrinsic absorption spectrum of the gold particles. The effective coverage β at this stage is 2.0 corresponding to effective full coverage of cytochrome b-562 on the surface of the gold particles in the 'tail-on' conformation. A size of 40 nm is also in accord with such a conformation. Further addition of protein leads to no change and no second layer coverage is observed with the additional protein isolated in solution as reflected by the absorption band od 418 nm.

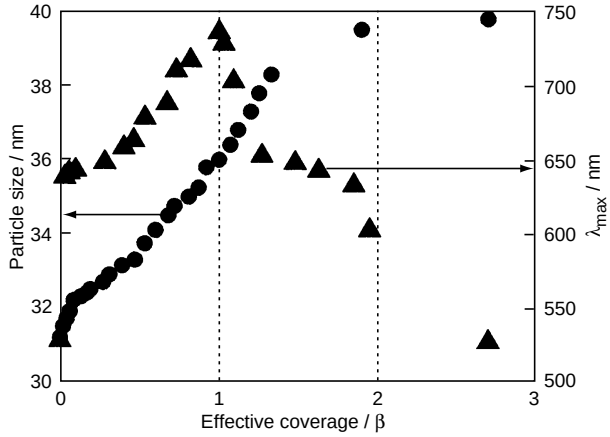



**Fig. 2** Changes of particle size and peak position of the longer wavelength plasmon band with surface protein effective coverage β

To summarise, changes in conformation of adsorbed protein have been optically detected, for the first time, by the shift of the resonant plasmon absorption arising from the distance-sensitive dielectric interaction between the protohaem within the protein and the gold surface.

## Footnote

† *Present address*: Electric Materials and Equipment Section 3, Sumitomo Corporation, 1-2-2, Hitotsubashi, Chiyoda-ku, Tokyo, 100 Japan.

## References


1 C. T. Kresge, M. E. Leonowicz, W. J. Roth, J. C. Vartuli and J. S. Beck, *Nature*, 1992, **359**, 710.
2 P. V. Braun, P. Osenar and S. I. Stupp, *Nature*, 1996, **380**, 325.
3 B. O'Regan and M. Gratzel, *Nature*, 1991, **353**, 737.
4 A. Kay and M. Gratzel, *J. Phys. Chem.*, 1993, **97**, 6272.
5 H. S. Zhou, T. Wada and H. Sasabe, *J. Chem. Soc., Chem. Commun.*, 1995, 1525.
6 I. M. Fleischman, P. J. Hendra and A. McQuillan, *J. Chem. Phys. Lett.*, 1974, **26**, 163.
7 *Surface Enhanced Raman Scattering*, ed. R. K. Chang and T. E. Furtake, Plenum, New York, 1982.
8 I. Pockrand and J. D. Swalen, *J. Opt. Soc. Am.*, 1978, **68**, 1147.
9 G. Frens, *Nature*, 1973, **241**, 20.
10 B. E. Dahneke and D. K. Hutchins, *J. Chem. Phys.*, 1994, **100**, 7890; 7903.
11 C. L. Gettinger, A. J. Heeger, D. J. Pine and Y. Cao, *Synth. Met.*, 1995, **74**, 81.
12 P. C. Weber, F. R. Salemme, F. S. Mathews and P. H. Bethge, *J. Biol. Chem.*, 1981, **256**, 7702; A. P. Brunet, E. S. Huang, M. E. Huffine, J. E. Loeb, R. J. Weltman and M. H. Hecht, *Nature*, 1993, **364**, 355.
13 U. Kreibig and M. Vollmer; *Optical Properties of Metal Clusters*, Springer, 1995.


*Received, 1st November 1996; Com. 6/07451K*

# Intramolecular electron transfer from coordinated manganese(II) to photogenerated ruthenium(III)

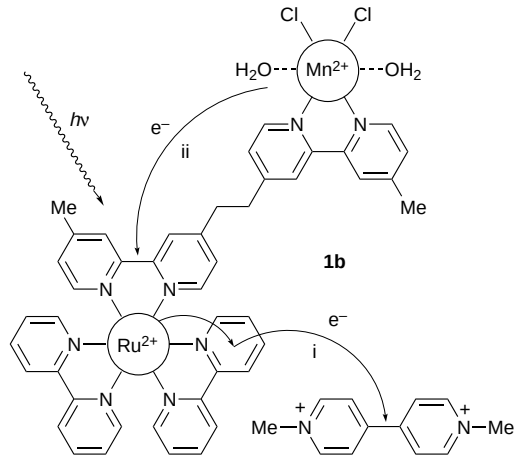
**Licheng Sun,[a] Leif Hammarström,[b] Thomas Norrby,[a] Helena Berglund,[b] Roman Davydov,[c] Mikael Andersson,[b] Anna Börje,[a] Peter Korall,[a] Christian Philouze,[a] Mats Almgren,*[b] Stenbjörn Styring*[c] and Björn Åkermark*[a]**

[a] *Royal Institute of Technology, Department of Chemistry, Organic Chemistry, S-100 44 Stockholm, Sweden*
[b] *Department of Physical Chemistry, Uppsala University, PO Box 532, S-751 21 Uppsala, Sweden*
[c] *Department of Biochemistry, Center for Chemistry and Chemical Engineering, University of Lund, PO Box 124, S-221 00 Lund, Sweden*

**A binuclear ruthenium–manganese complex is synthesised; upon illumination the ruthenium transfers an electron to an external acceptor, then retrieves it by intramolecular electron transfer from the manganese.**

A key enzyme in green plant photosynthesis is Photosystem II (PSII).[1] Upon illumination, the chlorophyll $P_{680}$ in PSII transfers an electron to a series of acceptors, to give the $P_{680}^{+}$ cation which is then reduced back to $P_{680}$ by electron transfer (ET) (mediated by tyrosine-z) from a cluster of four manganese ions. After four consecutive ET events, the cluster recovers all four electrons in one step by oxidizing two water molecules to molecular oxygen.[2] We decided to study if simple model systems could be prepared, where a ruthenium(II) tris bipyridyl type complex on illumination transfers an electron to an external acceptor,[3,4] then recovers an electron by internal ET from a coordinated manganese ion. The bimetallic ruthenium(II) manganese(II) complex **1b** (Scheme 1) was found to be one model system of this type, and a suitable starting point for the development of multinuclear $RuMn_n$ complexes.

Our synthetic route started with the bridging ligand 1,2-bis[4-(4′-methyl-2,2′-bipyridyl)]ethane (Mebpy–Mebpy),[5] which was first treated with $[Ru(bpy)_2Cl_2]$[6] in refluxing methanol to give $[Ru(bpy)_2(Mebpy–Mebpy)]Cl_2$ **1a**.[7] On treatment with $MnCl_2$ in acetonitrile, **1a** gave the binuclear $Mn^{II}Ru^{II}$ complex **1b**. Complex **1b** was characterized by electrospray ionization mass spectrometry (ESIMS), elemental analysis and X-band electron paramagnetic resonance (EPR) techniques. The distance between $Mn^{II}$ and $Ru^{II}$ in **1b** was estimated by molecular mechanics calculations to *ca.* 13 Å for the most extended conformation, which should allow efficient electron transfer.[8]




**Scheme 1** Proposed pathway for the electron transfer following irradiation of **1b** in the presence of $MV^{2+}$ in acetonitrile solution; (*i*) photoinduced intermolecular electron transfer, generating $Ru^{III}$ and $MV^{+\cdot}$; (*ii*) intramolecular electron transfer from $Mn^{II}$ to $Ru^{III}$

Comparison of the emission spectra of **1b**, **1a** and $[Ru(bpy)_3]^{2+}$[9] in acetonitrile solution showed that the wavelength of the emission maximum (*ca.* 615 nm) was essentially the same in all three cases, but the emission was considerably quenched in **1b** ($\tau \approx 260$ ns) compared to **1a** ($\tau \approx 980$ ns) and $[Ru(bpy)_3]^{2+}$. The manganese thus interacts with the excited state of ruthenium complex, but it does not quench the emission completely.

Flash photolysis experiments in the presence of 5–10 mM of an acceptor, methyl viologen ($MV^{2+}$), were performed in an acetonitrile solution of **1a**, **1b** and $[Ru(bpy)_3]^{2+}$, respectively. Following a laser flash ($\lambda_{ex} = 458$ nm), a rapid electron transfer from $Ru^{II}$* to $MV^{2+}$ took place[4] (Scheme 1, step i) with a lifetime of *ca.* 200 ns for complex **1a**. The regeneration of $Ru^{II}$ (monitored by the absorption at 452 nm) and the decay of the $MV^{+\cdot}$ radicals (monitored by the absorption at 600 nm) followed similar second-order kinetics with rate constants of *ca.* $5.0 \times 10^9$ dm$^3$ mol$^{-1}$ s$^{-1}$. Thus the products of the charge separation recombine on the timescale of a few hundred μs when a few μM of the products were created. The behaviour of $[Ru(bpy)_3]^{2+}$ was identical. For the bimetallic $Mn^{II}Ru^{II}$ complex **1b**, the $MV^{+\cdot}$ radical was generated, and decayed with the same rate as in the experiments with **1a** and $[Ru(bpy)_3]^{2+}$.† In contrast, the regeneration of $Ru^{II}$ from the photoproduced $Ru^{III}$ was found to be one order of magnitude faster than for **1a** and $[Ru(bpy)_3]^{2+}$. This means that the photo-oxidized $Ru^{III}$ moiety in **1b** must have received an electron from another source than $MV^{+\cdot}$, and one that is not present in **1a** and $[Ru(bpy)_3]^{2+}$.

Analysis of the transient absorbance recovery traces for **1b** over the concentration range examined {[**1b**] = $(2–10) \times 10^{-5}$ M} revealed a concentration independant first-order kinetic process with a rate constant $k = 1.5 \times 10^5$ s$^{-1}$. This we ascribe to the intramolecular ET from the $Mn^{II}$ moiety to the photogenerated $Ru^{III}$ moiety (Scheme 1, step ii). Separate experiments were performed in order to prove that the $Mn^{II}$ moiety could be oxidized to $Mn^{III}$ by $Ru^{III}$. Both manganese(II) ($S = 5/2$) and ruthenium(III) species give rise to distinct EPR spectra. When equimolar amounts of $[Ru(bpy)_3]^{3+}$ and complex **1b**, which contains $Mn^{II}$, were reacted, both EPR signals disappeared, showing that the reactants had been converted completely to the corresponding ruthenium(II) and manganese(III) species. The decay of $MV^{+\cdot}$ radical in the photolysis experiment with **1b** was probably due to recombination with $Mn^{III}$.

We would like to thank the Swedish Natural Science Research Council and the Knut and Alice Wallenberg Foundation for supports and Drs G. Stenhagen and J. Mårtensson, Chalmers University of Technology, for ESIMS measurements.

## Footnote

† In experiments without $MV^{2+}$ no products of the Ru-quenching by Mn were seen. Thus, even if the quenching mechanism could be reductive, the $Mn^{III}$–$Ru^{I}$ recombination would be much faster, so that the production of $MV^{+\cdot}$ *via* diffusional encounter with $Ru^{I}$ would be negligible.

## References


1 J. Barber and B. Andersson, *Nature*, 1994, **370**, 31; B. Andersson and S. Styring, in *Curr. Top. Bioenerg*., 1991, **16**, 1.
2 V. K. Yachandra, V. J. DeRose, M. J. Latimer, I. Mukerji, K. Sauer and M. P. Klein, *Science*, 1993, **260**, 675; H. Dau, J. C. Andrews, T. A. Roelofs, M. Latimer, W. Liang, V. K. Yachandra, K. Sauer and M. P. Klein, *Biochemistry*, 1995, **34**, 5274; G. N. George, R. C. Prince and S. P. Cramer, *Science*, 1989, **243**, 789.
3 I. Willner and B. Willner, *Top. Curr. Chem*., 1991, **159**, 153; V. Balzani and F. Scandola, *Supramolecular Photochemistry*, Ellis Horwood, Chichester, 1991; T. J. Meyer, *Acc. Chem. Res*., 1989, **22**, 163; A. Juris, V. Balzani, F. Barigelletti, S. Campagna, P. Belser and A. von Zelewsky, *Coord. Chem. Rev*., 1988, **84**, 85; V. Balzani, A. Juris, M. Venturi, S. Campagna and S. Serroni, *Chem. Rev*., 1996, **96**, 759.
4 K. Kalyanasundaram, *Photochemistry of Polypyridine and Porphyrin Complexes*, Acadmic, London, 1992, ch. 6.
5 C. M. Elliott, R. A. Freitag and D. D.Blaney, *J. Am. Chem. Soc*., 1985, **107**, 4647.
6 B. P. Sullivan, D. J. Salmon and T. J. Meyer, *Inorg. Chem*., 1978, **17**, 3334.
7 S. L. Larson, S. M. Hendrickson, S. Ferrere, D. L. Derr and C. M. Elliott, *J. Am. Chem. Soc*., 1995, **117**, 5881.
8 V. Balzani and F. Scandola, *Supramolecular Photochemistry*, Ellis Horwood, Chichester, 1991, ch. 5.
9 J. A. Broomhead and C. G. Young, *Inorg. Synth*., 1990, **28**, 338.



*Received, 6th January 1997; Com. 7/00100B*

# Facile α-C–H activation in 14-electron zirconium half-sandwich compounds: evidence for a new catalyst deactivation pathway

**Gerardo Jimenéz Pindado, Mark Thornton-Pett and Manfred Bochmann***

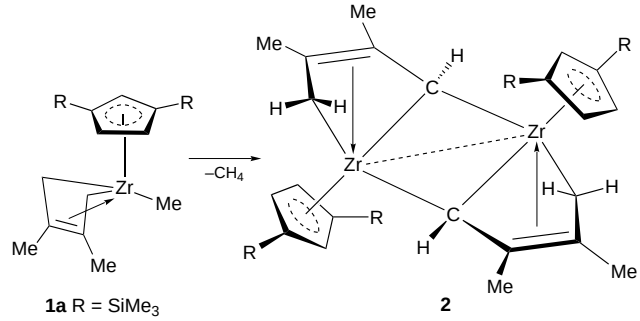
*School of Chemistry, University of Leeds, Leeds, UK LS2 9JT*

**The electron-deficient zirconium diene complex [Zr(Cp″)Me($C_4H_4Me_2$-2,3)] [Cp″ = $C_5H_3(SiMe_3)_2$-1,3] cleanly eliminates methane to give an unusual dinuclear dienyl complex [Zr(Cp″)(μ-η¹ : η⁴-$C_4H_3Me_2$-2,3)]$_2$, characterised by a new type of μ-η¹ : η⁴-butadienyl coordination mode; the complex and its zwitterionic reaction product with $B(C_6F_5)_3$ provide support for catalyst deactivation processes involving alkane elimination reactions.**

Electron deficient group 4 metallocene and half-sandwich complexes are known to give rise to extremely active alkene polymerisation catalysts.[1] The activity profile of these catalysts typically shows a very high initial activity, followed by an exponential decay to a lower steady-state level after some time. Little is known however about the nature of the deactivation processes involved. The kinetics of propene polymerisation with [Zr(η-$C_5H_5)_2Cl_2$]–methylaluminoxane catalysts suggest a catalyst deactivation process which is second order in [Zr].[2] We have previously shown two types of C–H activation processes which may be relevant in this context: α-C–H activation leading to dinuclear cationic μ-$CH_2$ zirconium fulvalene complexes,[3] and the formation of μ-$C_2H_4$-bridged species by a β-elimination process.[4] We report here the facile decomposition of a neutral catalyst precursor *via* an α-C–H activation process, to give a dinuclear dienyl complex exhibiting a novel μ-η¹ : η⁴-butadienyl coordination mode.

The reaction of [Zr(Cp″)Cl(η⁴-2,3-dimethylbutadiene)] [Cp″ = $C_5H_3(SiMe_3)_2$-1,3] with methyllithium in diethyl ether affords the methyl complex [Zr(Cp″)Me(η⁴-2,3-dimethylbutadiene)] **1a** which can be isolated at room temperature as a red solid in > 80% yield. The analogous hafnium complex **1b** is similarly obtained as a spectroscopically pure yellow oil.† These isolated compounds are thermally more stable than related $C_5Me_5$ derivatives which have to be kept below 0 °C.[5] However, monitoring the behaviour of **1a** by NMR spectroscopy over a period of time revealed a slow clean transformation to a new product at room temperature, with elimination of methane. Attempts to recrystallise **1a** from light petroleum at −16 °C led to the isolation of deep red crystals of [Zr(Cp″)(μ$_2$-η¹ : η⁴-$C_4H_3Me_2$-2,3)]$_2$ **2** in *ca.* 40% yield, evidently formed by abstraction of a methylene hydrogen from the diene ligand (Scheme 1).

Compound **2** was identified spectroscopically† and shows a characteristic $^{13}C$ NMR resonance at δ 175 for the μ-CHR carbon. Single-crystal X-ray diffraction‡ confirmed the dinuclear structure of **2** and revealed the novel coordination mode of the butadienyl ligand (Fig. 1). Each half of the molecule forms a (cyclopentadienyl)zirconium(butadienyl) sandwich with an almost symmetrical μ-CHR bridge [Zr(1)–C(6) 2.216(2), Zr(1)–C(6′) 2.191(2) Å]. The four sp²-hydridised carbon atoms of the butadienyl moiety are coplanar and η⁴-coordinated. As in mononuclear diene complexes[6] the bonding in the dienyl moiety may be described by two resonance structures **A** and **B**, with a significant contribution of a zirconacyclopentene resonance structure **B** to account for the bond length distribution within the $C_4$ unit. The [Zr(dienyl)]$_2$ moiety in **2** closely resembles the 'envelope' structure of a Zr(diene) complex in which one diene α-hydrogen is replaced by a zirconium atom. The geometry of the butadienyl ligand in **2** contrasts sharply with that in the zwitterionic 16-electron metallocene complex [{($C_6F_5)_3BC_5H_4$}(η-$C_5H_5$)Zr($C_4HMe_4$-1,2,3,4)] where the dienyl ligand is η¹-bonded, with a long C(2)–C(3) single and short C(1)–C(2) and C(3)–C(4) double bonds (**C**), and where coordination of an *o*-F atom of a $C_6F_5$ unit is favoured over the interaction of the diene with the metal centre.[7] The Zr–Zr distance of 3.1516(5) Å in **2**, with a formal electron count of 14 per Zr centre, is short compared to the metal–metal distance in 16 electron metallocene dimers such as [($C_5H_4Me)_2$ZrH(μ-H)]$_2$ (3.46 Å);[8] to our knowledge there are




**Scheme 1**

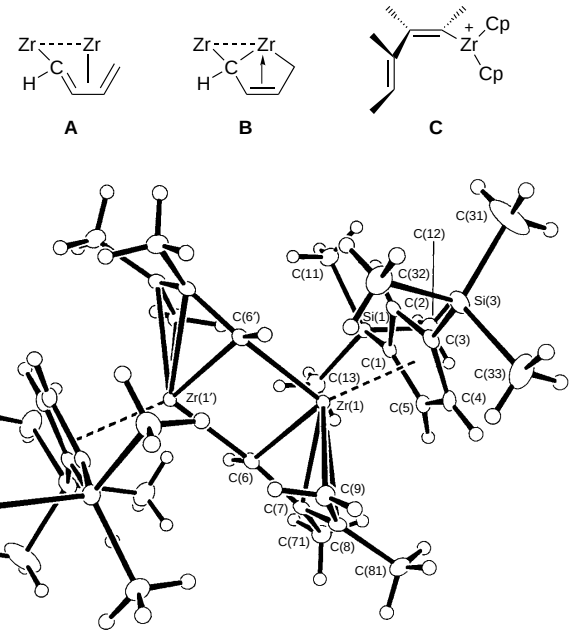
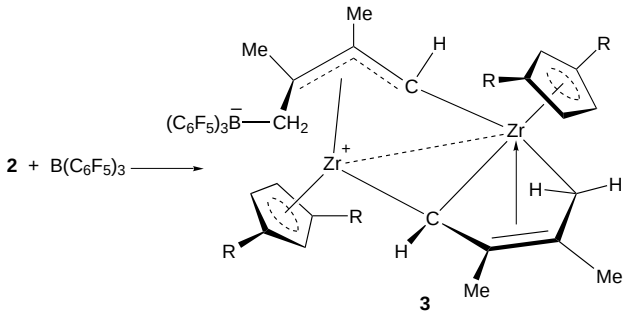



**Fig. 1** Crystal structure of **2** (H atoms omitted for clarity). Selected bond lengths (Å) and angles (°): Zr(1)–Zr(1′) 3.1516(5), Zr(1)–C(1) 2.497(2), Zr(1)–C(2) 2.501(2), Zr(1)–C(3) 2.556(2), Zr(1)–C(4) 2.558(2), Zr(1)–C(5) 2.520(2), Zr(1)–C(6′) 2.191(2), Zr(1)–C(6) 2.216(2), Zr(1)–C(7) 2.470(2), Zr(1)–C(8) 2.480(2), Zr(1)–C(9) 2.289(2), C(6)–C(7) 1.435(3), C(7)–C(8) 1.409(3), C(8)–C(9) 1.443(3) Å; C(6)–Zr(1)–C(6′) 88.69(8), Zr(1)–C(6)–Zr(1′) 91.31(4°), H(6)–C(6)–C(7) 115(2)°, C(6)–C(7)–C(8) 122.1(2)°, C(7)–C(8)–C(9) 123.7(2)°.




**Scheme 2** R = $SiMe_3$

only two previous examples of dinuclear 14-electron complexes with comparable Zr–Zr bond lengths.[9] Evidently electron deficiency significantly favours metal–metal interactions. The hafnium compound **1b** decomposes less cleanly than **1a**, to give a mixture of products which could not be separated. There was, however, no evidence for the formation of a dinuclear hafnium analogue of **2**.

Treatment of **2** with $B(C_6F_5)_3$ leads to the zwitterionic complex **3** (Scheme 2). Only one of the two butadienyl ligands is attacked by the borane, even in the presence of an excess of $B(C_6F_5)_3$. At −50 °C the $^{19}F$ NMR spectrum shows six signals for the *o*-F atoms of three different $C_6F_5$ substituents, indicative of hindered rotation; there is however no evidence for an *ortho*-F···Zr coordination, unlike in the structurally related zwitterionic allyl complex $[Zr(\eta\text{-}C_5H_5)_2(\eta^3\text{-}CH_2CHCHCH_2\text{-}B(C_6F_5)_3]$.[10]

Toluene solutions of **1a** do not react with ethene (1 bar) at 0 °C§ but on addition of 1 equiv. of $B(C_6F_5)_3$ catalyse the polymerisation of ethene with a productivity of $3 \times 10^4$ g PE (mol Zr)$^{-1}$h$^{-1}$. Related allyl complexes $[Zr(Cp'')(\eta^3\text{-allyl})(\text{diene})]$ are similarly active.[11] By contrast, complex **3** is inactive under identical conditions, though some polymerisation takes place on warming to 64 °C. These findings support the notion that, apart from hydrolysis reactions and the intervention of nucleophilic impurities, deactivation of metallocene-type polymerisation catalysts is linked to the formation of dinuclear products as a result of a number of C–H activation pathways.

We thank the EPSRC and the Science and Education Ministry of Spain for support of this work.

## Footnotes

† *NMR spectroscopic data*: **1a**; $^1H$ ($C_6D_6$, 300 MHz, 25 °C) δ −0.30 (br s, 3 H, ZrMe), 0.27 (s, 18 H, SiMe), 0.45 (d, 2 H, *J* 9.6 Hz, $=CH_2$ *anti*); 2.00 (s, 6 H, diene-Me), 2.34 (d, 2 H, *J* 9.6 Hz, $=CH_2$ *syn*), 6.04 (br s, 2 H,, 4,5-$C_5H_3$) 7.10 (br s, 1 H, 2-$C_5H_3$). $^{13}C$ ($C_6D_6$, 75.4 MHz, 25 °C) δ 0.11 (q, *J* 119.0 Hz, SiMe), 23.3 (q, *J* 126.1 Hz, diene-Me), 45.2 (br q, *J* 113.2 Hz, ZrMe), 63.2 (t, *J* 142.3 Hz, $=CH_2$), 117.4 (d, *J* 169.8 Hz, 4,5-$C_5H_3$), 122.6 (d, *J* 167.5 Hz, 2-$C_5H_3$), 123.4 (m, =*C*Me) 119.84 (m, 1,3-$C_5H_3$). **1b**; $^1H$ ($C_6D_6$, 300 MHz, 25 °C) δ −0.65 (s, 3 H, HfMe), −0.21 (d, 2 H, *J* 11.4 Hz, $=CH_2$ *anti*), 0.25 (s, 18 H, SiMe), 2.11 (s, 6 H, diene-Me), 2.33 (d, 2 H, *J* 11.4 Hz, $=CH_2$ *syn*), 6.0 (d, 2 H, *J* 1.8 Hz, 4,5-$C_5H_3$), 6.91 (t, 1 H, *J* 1.8 Hz, 2-$C_5H_3$). $^{13}C$ ($C_6D_6$, 25 °C) δ 0.7 (q, *J* 119.1 Hz, SiMe), 23.2 (q, *J* 126.1 Hz diene-Me), 53.4 (q, *J* 111.4 Hz, HfMe), 68.0 (t, *J* 139.5 Hz, $=CH_2$), 117.2 (d, *J* 169.0 Hz, 4,5-$C_5H_3$), 122.4 (d, *J* 168.3 Hz, 2-$C_5H_3$), 123.7 (m, =*C*Me), 126.8 (m, 1,3-$C_5H_3$). **2**; $^1H$ ($C_6D_6$, 300 MHz, 25 °C) δ 0.06, 0.52 (s, 9 H, SiMe), 1.50 (s, 1 H, ZrCHZr), 1.80, 1.85 (s, 3 H, diene-Me), 2.03, 3.78 (d, 1 H, *J* 5.7 Hz, $=CH_2$), 4.58, 6.20 (dd, 1 H, *J* 2.9, 1.9 Hz, 4,5-$C_4H_3$), 6.60 (t, 1 H, *J* 1.9 Hz, 2-$C_5H_3$). $^{13}C$ ($C_6D_6$, 25 °C) δ 0.7, 0.8 (q, *J* 119.0 Hz, SiMe), 24.0 (q, *J* 126.0 Hz, diene-Me), 25.4 (q, *J* 126.2 Hz, diene-Me), 65.6 (t, *J* 144.5 Hz, $=CH_2$), 116.0, 116.7 (d, *J* 168.3 Hz, 4,5-$C_5H_3$), 116.9 (d, *J* 169.0 Hz, 2-$C_5H_3$), 111.8, 115.2, 118.6, 127.5 (m, 1,3-$C_5H_3$ and =*C*Me), 174.9 (d, *J* 111 Hz, ZrCHZr); **3**; $^1H$ ($CD_2Cl_2$, 300 MHz, −20 °C) δ 0.31, −0.08, 0.16, 0.48 (s, 9 H, SiMe), 0.58, 2.78 (s, 1 H, ZrCHZr), 1.23, 3.17 (d, 1 H, *J* 6.3 Hz, $=CH_2$), 1.66, 1.81, 1.97 (s, 6 H, 3 H, 3H diene-Me), 1.69 and 1.98 (two s, 1 H each, $CH_2B$. These signals overlap with those for diene-Me and were identified from difference spectra), 5.29, 5.63, 6.48, 6.55 (m, 1 H each, Cp″), 6.61 (m, 2 H, Cp″). $^{13}C\{^1H\}$ ($CD_2Cl_2$, 75.4 MHz, −50 °C) δ −0.9, −0.6, −0.3, 0.2 (SiMe), 18.9, 23.4, 24.7, 27.0 (diene-Me), 29.8 (br, $BCH_2$), 67.6 (br, $=CH_2$), 106.8, 112.4, 115.7, 119.7, 119.9, 122.7, 123.0, 123.9, 124.5, 131.1, 133.7, 146.6, 149.9, (Cp″, =*C*Me), 180.4, 179.2 (ZrCHZr). $^{11}B\{^1H\}$ ($CD_2Cl_2$, 96.25 MHz, −70 °C) δ −12.0. $^{19}F$ ($CD_2Cl_2$, 2.82 MHz, −50 °C) δ −129.0, −129.3, −130.7, −132.8, −133.08, −135.0 (*o*-F of $C_6F_5$), −160.9 (2 F, *p*-F of $C_6F_5$), −161.54 (1 F, *p*-F of $C_6F_5$), −165.0, −165.35, −165.7 (2 F each, *m*-F of $C_6H_5$).

‡ *Crystal data* for **2**: $C_{34}H_{60}Si_4Zr_2$, $M$ = 763.62, crystal size 0.38 × 0.26 × 0.19 mm, triclinic, space group $P\bar{1}$, $a$ = 8.957(2), $b$ = 10.105(2), $c$ = 12.1262(14) Å, α = 86.249(12), β = 76.699(12), γ = 66.353(14)°, $U$ = 978.0(3) Å$^3$, $Z$ = 1, $D_c$ = 1.297 Mg m$^{-3}$, $F(000)$ = 400, μ = 0.676 mm$^{-1}$, $T$ = 160 K. 3434 reflections were collected on a Stoe STADI4 4-circle diffractometer using graphite monochromated Mo-Kα radiation (λ = 0.710 73 Å) and ω–θ scans. Data were corrected for absorption empirically using azimuthal ψ-scans. The structure was solved by heavy-atom methods[12] and was refined by full-matrix least-squares analysis on $F^2$ using all 3434 reflections.[13] $R_w$ = $\{\Sigma[w(F_o^2 - F_c^2)^2/\Sigma\{w(F_o^2)^2]\}^{1/2}$ = 0.0608 for all data, conventional $R$ [on $F$ values of 3173 reflections with $R_o^2 > 2\sigma(F_o^2)$] = 0.0232, goodness of fit $S$ 1.141 on all $F^2$ for 201 parameters. All non-hydrogen atoms were refined with anisotropic displacement parameters. All hydrogen atoms were constrained to idealised positions with fixed isotropic displacement parameters of $nU_{eq}$ (where $n$ was 1.5 for methyl and 1.2 for all others) except those on atoms C(6) and C(9) which were located on a Fourier difference synthesis and were freely refined with individual isotropic displacement parameters. Atomic co-ordinates, bond lengths and angles, and thermal parameters have been deposited at the Cambridge Crystallographic Data Centre. See Information for Authors, Issue No. 1. Any request to the CCDC for this material should quote the full literature citation and the reference number 182/381.

§ After the submission of this article the oligomerisation of ethene by the related complex $[Zr(\eta\text{-}C_5Me_5(C_6H_{10})Bu^n]$ in the absence of $B(C_6F_5)_3$ has been reported: B. Hessen and H. van der Heijden, *J. Am. Chem. Soc.*, 1996, **118**, 11670.

## References

1 H. H. Brintzinger, D. Fischer, R. Mülhaupt, B. Rieger and R. Waymouth, *Angew Chem.*, 1995, **107**, 1255; *Angew. Chem., Int. Ed. Engl.*, 1995, **34**, 1143; M. Bochmann, *J. Chem. Soc., Dalton Trans.*, 1996, 255.
2 D. Fischer and R. Mülhaupt, *J. Organomet. Chem.*, 1991, **417**, C7; D. Fischer, S. Jüngling and R. Mülhaupt, *Makromol. Chem. Macromol. Symp.*, 1993, **66**, 191.
3 M. Bochmann, T. Cuenca and D. T. Hardy, *J. Organomet. Chem.*, 1994, **484**, C10. For methane elimination in MAO-activated metallocene catalysts see also: W. Kaminsky and R. Steiger, *Polyhedron*, 1988, **7**, 2375.
4 S. J. Lancaster, O. B. Robinson, M. Bochmann, S. J. Coles and M. B. Hursthouse, *Organometallics*, 1995, **14**, 2456; W. Kaminsky and H. Sinn, *Liebigs Ann.*, 1975, 438; W. Kaminsky, J. Kopf, H. Sinn and H. J. Vollmer, *Angew. Chem.*, 1976, **88**, 688; *Angew. Chem., Int. Ed. Engl.*, 1976, **15**, 629.
5 J. Blenkers, B. Hessen, F. van Bolhuis, A. J. Wagner and J. H. Teuben, *Organometallics*, 1987, **6**, 459.
6 M. Bochmann, in *Comprehensive Organometallic Chemistry II*, ed. E. W. Abel, F. G. A. Stone and G. Wilkinson, Pergamon, Oxford, 1995, vol. 4, p. 221ff; G. Erker, K. Berg, C. Krüger, G. Müller, K. Angermund, R. Benn and G. Schroth, *Angew. Chem., Int. Ed. Engl.*, 1984, **23**, 455; G. Erker, C. Krüger and G. Müller, *Adv. Organomet. Chem.*, 1985, **24**, 1; H. Yamamoto, H. Yasuda, K. Tatsumi, K. Lee, A. Nakamura, J. Chen, Y. Kai and N. Kasai, *Organometallics*, 1989, **8**, 105.
7 J. Ruwwe, G. Erker and R. Fröhlich, *Angew. Chem.*, 1996, **108**, 108; *Angew. Chem., Int. Ed. Engl.*, 1996, **35**, 80.
8 S. B. Jones and J. L. Petersen, *Inorg. Chem.*, 1981, **20**, 2889. See also: K. P. Reddy and J. L. Petersen, *Organometallics*, 1989, **8**, 547; R. Choukroun, F. Dahan, A. M. Larsonneur, E. Samuel, J. Petersen, P. Meunier and C. Sornay, *Organometallics*, 1991, **10**, 374.
9 D. J. Arney, M. A. Bruck, S. R. Huber and D. E. Wigley, *Inorg. Chem.*, 1992, **31**, 3749; M. Bochmann, S. J. Lancaster, M. B. Hursthouse and M. Mazid, *Organometallics*, 1993, **12**, 4718.
10 B. Temme, G. Erker, J. Karl, H. Luftmann, R. Fröhlich and S. Kotila, *Angew. Chem.*, 1995, **107**, 1867; *Angew. Chem., Int. Ed. Engl.*, 1995, **34**, 1755; B. Temme, J. Karl and G. Erker, *Chem. Eur. J.*, 1996, **2**, 919.
11 G. Jimenéz Pindado and M. Bochmann, manuscript in preparation.
12 G. M. Sheldrick, *Acta Crystallogr., Sect. A*, 1990, **46**, 467.
13 G. M. Sheldrick, SHELXL-93, Program for refinement of crystal structures, University of Göttingen, 1993.

*Received, 26th November 1996; Com. 6/08014F*

# Synthesis and Diels–Alder reactions of α,β-unsaturated γ-sultone

**Albert W. M. Lee,* W. H. Chan,* L. S. Jiang and K. W. Poon**

*Department of Chemistry, Hong Kong Baptist University, Kowloon Tong, Kowloon, Hong Kong*

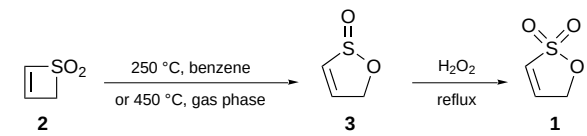
**An efficient synthesis of prop-1-ene 1,3-sultone 1 and its Diels–Alder reactions are reported; ring-opening reactions of the cycloadducts with nucleophiles and transformations to the sultams were also investigated.**

Sultones are cyclic esters of the corresponding hydroxysulfonic acid, the sulfur analogues of lactones. The preparation and chemistry of saturated sultones of 4- to 6-membered ring sizes are relatively well studied.[1] However, there is less investigation of the chemistry of the unsaturated sultones, in particular, the α,β-unsaturated γ-sultone prop-1-ene 1,3-sultone **1**. We have long been interested in the uses of sulfur-containing functional groups for the activation of acetylenic or vinyl moieties resulting in useful synthons for organic synthesis.[2] We here report a synthesis of **1**, its Diels–Alder reactions and some further transformations of the cycloadducts.

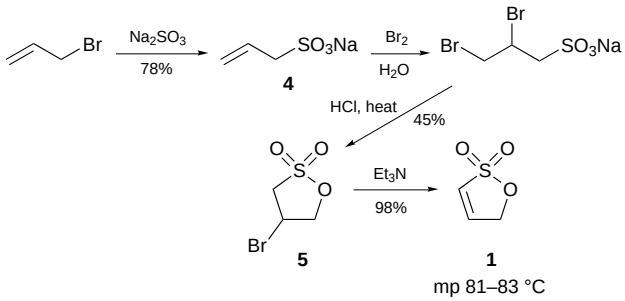
There are only limited accounts in literature for the synthesis of **1**. Thermolysis of thiete 1,1-dioxide **2** yielded sultine **3** which could be oxidized to **1** (Scheme 1).[3] It had also been reported that distillation of 3-hydroxyprop-1-ene-1-sulfonic acid, which was synthesized from prop-2-ynyl alcohol *via* free radical sulfitation, also afforded **1**.[4] These reported procedures were not efficient and practical enough for the laboratory synthesis of the compound. Our synthesis of **1** is shown in Scheme 2. Sodium prop-2-enesulfonate **4** could be prepared from allyl bromide and sodium sulfite in good yield.[5] Bromination of **4** in water gave the dibromide which was not isolated. Vacuum distillative cyclization of the dibromide under acidic conditions afforded β-bromo sultone **5** in 45% isolated yield from **4**. Treatment with amine base in benzene solution at room temperature afforded **1**† as a white crystalline solid in good yield.

The dienophilicity of unsaturated sultone **1** in the Diels–Alder reaction was investigated. Sulfonate has been used as an activating group for olefinic dienophiles, for example, vinyl sulfonates were found to be reactive dienophiles in both intermolecular[6] and intramolecular[7] Diels–Alder reactions. The results of Diels–Alder reactions of **1** towards a series of simple dienes are summarized in Table 1.‡ For a reactive diene such as cyclopentadiene, despite the slow reaction rate, reaction with **1** could take place at room temperature with moderate *endo* : *exo* selectivity. At a higher temperature, the reaction could be completed in 4 h. The *endo*-**6** and *exo*-**7** isomers could be easily separated by column chromatography. For less reactive dienes, elevated temperature or sealed tube conditions were used. In the cases of cyclohexa-1,3-diene and 2,3,4,5-tetrachloro-1,1-dimethoxycyclopentadiene, the *endo*-isomers were the only isolated products. For unsymmetrical dienes, 1 : 1 inseparable mixture of regioisomers resulted.

The sultone cycloadduct could be further manipulated by ring-opening with various nucleophiles such as alcohols, amines and thiols at the γ-position. Selected examples are depicted in Schemes 3 and 4. The alkoxide reacted smoothly with cycloadducts **6** and **8** at room temperature to afford the ring opening products **9a**,**b** in quantitative yields. Similarly, amine and thio compounds also reacted with the cycloadducts in

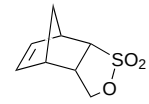
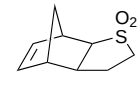
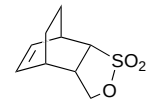
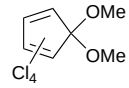
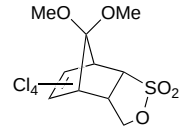
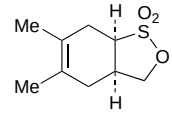
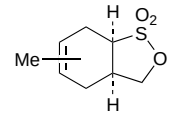
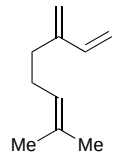
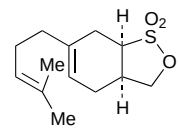
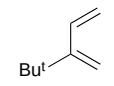
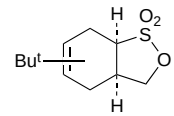



**Scheme 1**

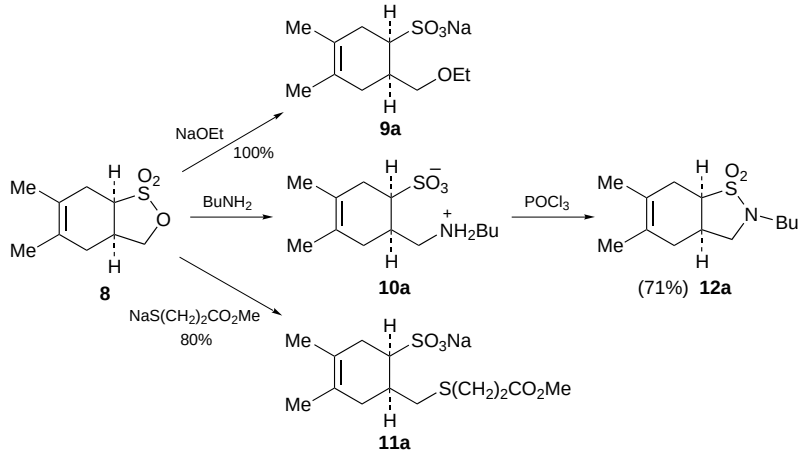



**Scheme 2**

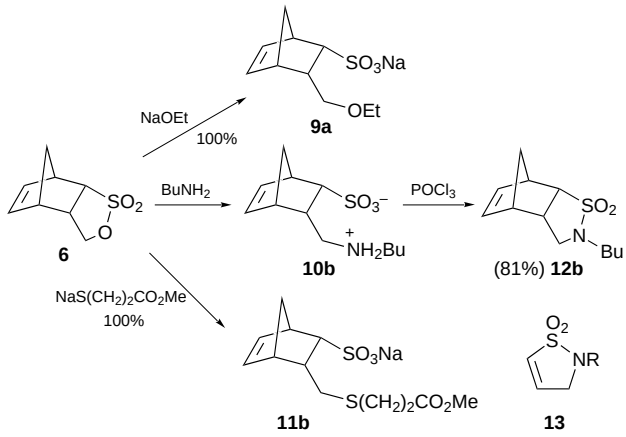
**Table 1** Diels–Alder reactions of α,β-unsaturated γ-sultone

| Dienes | Solvent; *T*/°C; *t*/h | Adduct (% yield) | |
|---|---|---|---|
|  | |  **6** |  **7** |
| | $CH_2Cl_2$; 20; 168 | 84 | : 16 (quant) |
| | Toluene; 120[a]; 4 | 73 | : 27 (96%) |
|  | Toluene; 150[a]; 18 |  | *endo* only (96%) |
|  | Xylene; reflux; 20 |  | *endo* only (72%) |
|  | Toluene; 150[a]; 18 |  **8** | (96%) |
|  | Toluene; 140[a]; 13 |  | (84%)[b] |
|  | Xylene; reflux; 20 |  | (75%)[b] |
|  | Benzene; 110[a]; 18 |  | (89%)[b] |

[a] Sealed tube. [b] Mixture of regioisomers.




**Scheme 3**




**Scheme 4**

methanol solution to afford the ring-opening products **10** and **11**, respectively. Compounds **10a** and **10b** were further cyclized to sultams **12a** and **12b** in good yield upon treatment with $POCl_3$ in THF. In this regard, unsaturated sultone **1** could be viewed as the synthetic equivalent of unsaturated sultam **13**[8] as dienophile in the Diels–Alder reaction.

Financial support from the Research Grant Council (HKBC 136/94P) is gratefully acknowledged.

## Footnotes

† Prop-1-ene 1,3-sultone **1**: mp 81–83 °C; $^1$H NMR ($CDCl_3$, 270 MHz) δ 5.12 (dd, 2 H, $J$ = 2.43, 1.89 Hz), 6.83 (dt, 1 H, $J$ = 6.62, 2.43 Hz), 7.08 (dt, 1 H, $J$ = 6.62, 1.89 Hz); $^{13}$C NMR δ 72.5, 123.9, 137.3; IR (KBr) ν/cm$^{-1}$ 3214, 3115, 3095, 1610, 1323, 1179; MS *m/z* (relative intensity), 120 ($M^+$, 65), 91 (38), 66 (100), 56 (17); Analysis for $C_3H_4O_3S$. Found: C, 30.08%, H, 3.39%. Calculated C, 30.00%, H, 3.36%.

‡ All new compounds are characterized by spectroscopic methods [IR, $^1$H (270 MHz) and $^{13}$C NMR, HRMS and/or elemental analysis].

## References

1 Recent reviews: D. W. Roberts and D. L. Williams, *Tetrahedron*, 1987, **43**, 1027; A. J. Buglass and J. G. Tillett, in *The Chemistry of Sulphonic Acids, Esters and their Derivatives*, ed. S. Patai and Z. Rappoport, Wiley, New York, 1991, pp. 789.
2 A. W. M. Lee and W. H. Chan, *Top. Curr. Chem.*, in the press.
3 J. F. King, P. de Mayo, C. L. McIntosh, K. Piers and D. J. H. Smith, *Can. J. Chem.*, 1970, **48**, 3704.
4 J. H. Hellberger and G. Muller, *Ger.*, 1963, **1**, 146, 870; *Chem. Abstr.*, 1963, **59**, 11259d.
5 F. Püschel and C. Kaiser, *Chem. Ber.*, 1964, **97**, 2926.
6 L. L. Klein and T. M. Deeb, *Tetrahedron Lett.*, 1985, **26**, 3935.
7 P. Metz, M. Fleischr and R. Fröhlich, *Tetrahedron*, 1995, **51**, 711.
8 Recently, the use of sulfonamide as an activator for vinyl dieneophiles in intramolecular Diels–Alder reactions was reported: P. Metz, D. Seng, R. Fröhlick and B. Wibbeling, *Synlett*, 1996, 741.

*Received in Cambridge, UK, 29th January 1997; Com. 7/00656J*

# Lanthanide(III) triflates as recyclable catalysts for atom economic aromatic nitration

**Francis J. Waller,*[a] Anthony G. M. Barrett,*[b] D. Christopher Braddock[b] and Dorai Ramprasad[a]**

[a] *Air Products and Chemicals, Inc., 7201 Hamilton Boulevard, Allentown, PA 18195-1501, USA*
[b] *Department of Chemistry, Imperial College of Science, Technology and Medicine, South Kensington, London, UK SW7 2AY*

**Lanthanide(III) triflates catalyse (1–10 mol%) the nitration of a range of simple aromatic compounds in good to excellent yield using stoichiometric quantities of 69% nitric acid; the only by-product is water and the catalyst can be readily recycled by simple evaporation.**

Nitration of aromatic compounds is an immensely important industrial process.[1] The nitroaromatic compounds so produced are themselves widely utilised and act as chemical feedstocks for a great range of useful materials such as dyes, pharmaceuticals, perfumes and plastics. Unfortunately nitrations typically require the use of potent mixtures of concentrated or fuming nitric acid with sulfuric acid leading to excessive acid waste streams and added expense. Alternatively, nitric acid may be used in conjunction with strong Lewis acids such as boron trifluoride.[2] The Lewis acid is used at or above stoichiometric quantities and is destroyed in the aqueous quench liberating large amounts of strongly acidic by-products. With chemists under increasing pressure to perform atom economic processes[3] with minimal or no environmentally unfriendly by-products, development of novel catalyst systems that facilitate aromatic nitrations in this manner should be of great importance.[4]

Lanthanides have found increasing use as mild and selective reagents in organic synthesis.[5] In particular, lanthanide(III) triflates[6,7] have been used to good effect as Lewis acids in Diels–Alder,[8] Michael,[9] Friedel–Crafts[10] and Mukaiyama[11] reactions. For the Mukaiyama reaction the optimum solvent system was found to be aqueous THF; the catalyst was recycled *via* aqueous work-up and used repeatedly with little detriment to rate or yield. The compatibility of lanthanide(III) triflate salts with water and yet their apparent ability to function as strong Lewis acids is somewhat paradoxical. We sought to harness this water tolerant Lewis acidity and herein report the use of catalytic quantities of lanthanide(III) triflates for the nitration of a range of simple aromatic compounds in good to excellent yield using a stoichiometric amount of 69% nitric acid where the only by-product is water. Furthermore the catalyst is readily recycled by a simple evaporative process.

Ytterbium(III) triflate was selected as the most promising candidate for the proposed nitrations. Accordingly a range of simple aromatic compounds were treated with 1 equiv. of 69% nitric acid in 1,2-dichloroethane heated at reflux in the presence of 10 mol% ytterbium(III) triflate.The results are shown in Table 1. No dinitrated products were observed in any case and in accord with this the system failed to nitrate nitrobenzene. In the control experiments with no catalyst, only slow reaction occurred and no more than 10% of nitrated products were observed. Ytterbium triflate was found to be effective even at catalyst loadings as low as 1 mol% and with *m*-xylene the reaction had proceeded to 80% conversion after 12 h.

The following procedure is representative. Nitric acid (69%; 192 μl, 3.0 mmol) was added to a stirred suspension of ytterbium(III) triflate (186 mg, 0.30 mmol) in 1,2-dichloroethane (5 ml). The suspension dissolved to give a two phase system in which the aqueous phase was the more dense. Toluene (240 μl, 3.0 mmol) was added and the stirred mixture was heated at reflux for 12 h. During the reaction a white solid precipitated and the organic phase became yellow, and after 12 h no phase boundary was apparent. The solution was allowed to cool and diluted with water. The yellow organic phase was dried ($MgSO_4$) and evaporated to give nitrotoluene (390 mg, 95%). The colourless aqueous phase was evaporated to give ytterbium(III) triflate as a white free-flowing solid (183 mg, 98%).

A series of other metal triflate salts were screened for catalytic activity (Table 2). Scandium triflate was found to have comparable catalytic activity to that of the corresponding ytterbium salt, but praseodymium, europium and lanthanum triflates, although active, were found to be somewhat less effective.

The recovered catalyst was found to be active for further nitrations with no reduction in rate or yield and with no change in selectivity. The results from four successive nitrations with *m*-xylene are shown in Table 3. On one occasion the white precipitate obtained from the nitration mixture with lanthanum(III) triflate consisted of crystals of the known lanthanum(III) triflate nonahydrate.[12]† These crystals were also found to have an identical diffuse reflectance IR spectrum to that of the amorphous recovered material and also that of the commercial

**Table 1** Nitration of aromatics in the presence of ytterbium(III) triflate[a]

| Arene | Conversion (%)[b,c] | Product distribution (%)[c] | | |
|---|---|---|---|---|
| | | *ortho* | *meta* | *para* |
| PhH | > 75 (75) | — | — | — |
| PhMe | > 95 (95) | 52 | 7 | 41 |
| PhPh | 89 | 38 | trace | 62 |
| PhBr | 92 | 44 | trace | 56 |
| $PhNO_2$ | 0 | — | — | — |
| *p*-xylene | > 95 | — | — | — |
| *p*-dibromobenzene | 8 | — | — | — |
| *m*-xylene | > 95 | 4-$NO_2$: 85 | | 2-$NO_2$: 15 |
| naphthalene | > 95 | 1-$NO_2$: 91 | | 2-$NO_2$: 9 |

[a] All reactions carried out on a 3 mmol scale with 10 mol% ytterbium(III) triflate and 1 equiv. of 69% nitric acid in refluxing 1,2-dichloroethane (5 ml) for 12 h. [b] Isolated yields in parenthesis. [c] GC and/or $^1H$ NMR analysis.

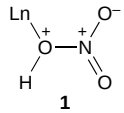
**Table 2** Effect of lanthanide(III) triflate on nitration of *m*-xyelene[a]

| $M(OTf)_3$[b] | Conversion (%)[c] | Product distribution (%)[c] | |
|---|---|---|---|
| | | 4-$NO_2$ | 2-$NO_2$ |
| La | 22 | 86 | 14 |
| Eu | 36 | 86 | 14 |
| Pr | 65 | 88 | 12 |
| Sc | 85 | 85 | 15 |
| Yb | 88 | 85 | 15 |

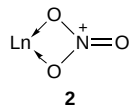
[a] All reactions performed with 10 mol% lanthanide(III) triflate, 1 equiv. each of *m*-xylene and 69% nitric acid in refluxing dichloromethane (15 ml) for 18 h. [b] Commercially available hydrated forms. [c] GC analysis.

available lanthanide salt.‡ As expected the crystals were found to catalyse the nitration reaction.

The nature of the *de facto* nitration agent is not known at present. The different rates with various lanthanide triflates indicate that the metal centre is involved. Nitric acid–triflic acid mixtures are known to effect nitration[13] but free triflic acid seems unlikely in our system since ytterbium(III) triflate yields a near-neutral solution when dissolved in water.§ The relative ratios of the various nitroaromatic isomers produced are fully consistent with electrophilic attack by $NO_2^+$ or more probably an $NO_2^+$ carrier of the type **1**[1]. However, bidentate lanthanide nitrates **2** are well characterised compounds,[14] and nitration




**1**




**2**

may proceed *via* direct attack of such a (protonated) species. Bidentate metal nitrates have been implicated in nitrations with titanium tetranitrate[15] and ceric ammonium nitrate[16] where the arene is thought to attack the metal bound nitrate species directly.

In conclusion, we have demonstrated the catalytic use of lanthanide(III) triflates for the atom economic nitration of simple aromatic substrates where the only by-product is water. The catalyst is readily recyclable and we believe this to be a major step forward in the area of clean technology for aromatic nitration.

The Imperial College group thank Air Products and Chemicals, Inc. for support of our research under the auspices of the joint Strategic Alliance, Glaxo Group Research Ltd. for the most generous endowment (to A. G. M. B), the Wolfson Foundation for establishing the Wolfson Centre for Organic Chemistry in Medical Science at Imperial College, the EPSRC and Dr David Williams and Dr Andrew J. P. White for the single crystal X-ray structure determination of lanthanum(III) triflate nonahydrate.

**Table 3** Recycled ytterbium(III) triflate[a]

| Run | Conversion (%)[b] | Mass of catalyst/mg[c] |
|---|---|---|
| 1 | 89 | 190 ( > 100) |
| 2 | 81 | 152 (82) |
| 3 | 90 | 127 (68) |
| 4 | 88 | 115 (62) |

[a] All runs performed with 3 mmol *m*-xylene, 10 mol% ytterbium triflate (run 1) and 1 equiv. of nitric acid in refluxing 1,2-dichloroethane (5 ml) for 5 h. [b] GC analysis. The isomeric ratio of 4- and 2-nitroxylene was unchanged throughout (85:15 respectively). [c] Mass of ytterbium(III) triflate recovered from each run. The figures in parenthesis indicate the percentage recovery which were not optimised.

## Footnotes

† A single crystal X-ray diffraction showed the material to be identical with the known lanthanum(III) triflate nonahydrate where the nine water molecules occupy the first co-ordination sphere in a tricapped trigonal prism arrangement with triflate counterions

‡ Aldrich chemical company

§ The pH of a 0.08 M solution of ytterbium(III) triflate in water was determined to be 6.40.[7]

## References

1 G. A. Olah, R. Malhotra and S. C. Narang, *Nitration: Methods and Mechanisms*, VCH, New York, 1989; C. K. Ingold, *Structure and Mechanism in Organic Chemistry*, Cornell University Press, Ithaca, New York, 2nd edn., 1969; G. A. Olah and S. J. Kuhn, in *Friedel-Crafts and Related Reactions*, ed. G. A. Olah, Wiley-Interscience, New York, 1964, vol. 2; K. Schofield, *Aromatic Nitrations*, Cambridge University Press, Cambridge, 1980.

2 R. J. Thomas, W. F. Anzilotti and G. F. Hennion, *Ind. Eng. Chem.*, 1940, **32**, 408; G. F. Hennion, US Pat., 2 314 212, 1943.

3 B. M. Trost, *Angew. Chem., Int. Ed. Engl.*, 1995, **34**, 259.

4 For a recent nitration using clean methodology, see K. Smith, A. Musson and G. A. DeBoos, *Chem. Commun.*, 1996, 469. However this method suffers from the disadvantage of stoichiometric quantities of acidic by-products.

5 T. Imamaoto, in *Lanthanides in Organic Synthesis*, Academic Press, London, 1994.

6 R. W. Marshmann, *Aldrichim. Acta*, 1995, **28**, 77.

7 S. Kobayashi, *Synlett*, 1994, 689.

8 S. Kobayashi and H. Ishitani, *J. Am. Chem. Soc.*, 1994, **116**, 4083; I. E. Marko and G. R. Evans, *Tetrahedron Lett.*, 1994, **35**, 2771.

9 S. Kobayashi, I. Hachiya, T. Takakori, M. Akida and H. Ishitani, *Tetrahedron Lett.*, 1992, **33**, 6815.

10 A. Hachiya, M. Moriwaki and S. Kobayashi, *Bull. Chem. Soc. Jpn.*, 1995, **68**, 2053; A. Kawada, S. Mitamura and S. Kobayashi, *Chem. Commun.*, 1996, 183; A. Kawada, S. Mitamura and S. Kobayashi, *Synlett*, 1994, 545; A. Kawada, S. Mitamura and S. Kobayashi, *J. Chem. Soc., Chem. Commun.*, 1993, 1157.

11 S. Kobayashi and I. Hachiya, *J. Org. Chem.*, 1994, **59**, 3590 and references cited therein.

12 J. M. Harrowfield, D. L. Kepert, J. M. Patrick and A. H. White, *Aust. J. Chem.*, 1983, **36**, 483; A. Chatterjee, E. N. Maslen and K. J. Watson, *Acta Crystallogr., Sect. B,*, 1988, **44**, 381.

13 C. L. Coon, W. G. Blucher and M. E. Hill, *J. Org. Chem.*, 1973, **38**, 4243.

14 F. A. Cotton and G. Wilkinson, *Advanced Inorganic Chemistry*, Wiley, New York, 4th edn., 1980, pp. 173, 981–1004.

15 D. W. Amos, D. A. Baines and G. W. Flewett, *Tetrahedron Lett.*, 1973, 3191.

16 S. Dincturk and J. H. Ridd, *J. Chem. Soc., Perkin Trans. 2*, 1982, 961.

*Received, 23rd January 1997; Com. 7/00546F*

# 1,4-Asymmetric induction in the formation of cyclohexadienones by chirality transfer from a transiently installed chromium–stereospecific electrocyclic ring closure of a metal complexed vinyl ketene

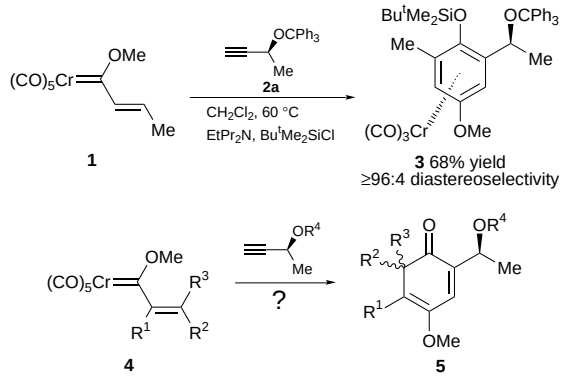
**Richard P. Hsung,[a] John F. Quinn,[a] Brian A. Weisenberg,[a] William D. Wulff,*[a] Glenn P. A. Yap[b] and Arnold L. Rheingold[b]**

[a] *Department of Chemistry, Searle Chemistry Laboratory, The University of Chicago, Chicago, Illinois 60637, USA*
[b] *Department of Chemistry, University of Delaware, Newark, Delaware 19716, USA*

**The cyclohexadienone annulation of a β,β-disubstituted vinyl chromium carbene complex and a chiral prop-2-ynylic ether results in high 1,4-asymmetric induction at the newly formed quaternary carbon; the stereochemical information from the prop-2-ynylic ether is initially transfered to the chromium coordination sphere and then to the quaternary carbon of the cyclohexa-2,4-dienone.**

We recently reported the first examples of an asymmetric synthesis of an arene chromium tricarbonyl from a benzannulation reaction.[1,2] The formation of the arene complex **3** occurs *via* 1,2-induction from the prop-2-ynylic carbon to the chiral centre of the complexed arene (Scheme 1). This success prompted us to investigate the cyclohexadienone annulation of β,β-disubstituted vinyl carbene complexes **4** with chiral prop-2-ynyl ethers.[3] We report here that this reaction occurs with significant 1,4-asymmetric induction and that the sense of induction provides the first experimental determination of the stereoselectivity associated with the elctrocyclic ring closure of a metal complexed vinyl ketene intermediate.

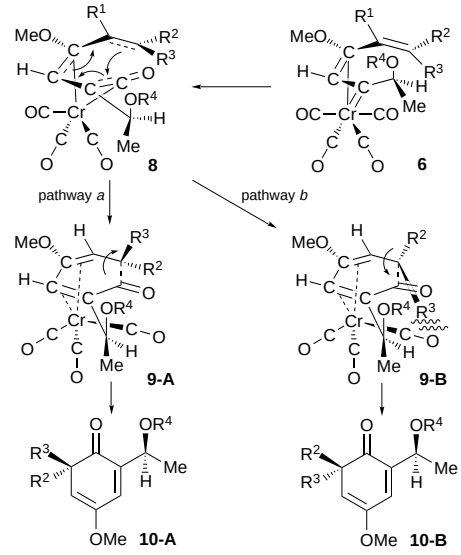
The expectation that a 1,4-asymmetric induction would occur with high fidelity was not at all clear for several reasons. First, the vinyl carbene complex **4** may undergo *cis–trans* isomerization. Although rates of isomerization for β,β-disubstituted complexes have not been reported, it is known that the *cis*-propenyl complex (**4**, $R^3$ = Me, $R^2$, $R^1$ = H) will isomerize to the *trans*-propenyl complex **1** at a rate competitive with its reaction with pent-1-yne.[4] This unpropitious result does not bode well for the stereoselective synthesis of the cyclohexadienone **5**. Additionally, the stereochemistry associated with the electrocyclic ring closure of the vinyl ketene complex has not been previously discussed or examined experimentally.[5] According to the most likely mechanism,[5,6] the ring closure occurs *via* a six electron electrocyclic reaction of the vinyl ketene complex **8** (Scheme 2). However, since the arene complex **3** must be derived from the vinyl carbene intermediate **6** and not its diastereoisomer **7** (not shown), and since only a single diastereoisomer of **3** is formed, it is likely that only one diastereoisomer of the vinyl ketene complex is formed. Therefore, while the selective formation of **3** reveals that the chiral centre on the prop-2-ynylic alkyne must induce a stereoselective coordination of the chromium, the selective formation of cyclohexadienone **5** requires that the chromium in ketene complex **8** induces a selective electrocyclic ring closure. This could occur by either pathway *a* or *b* as indicated in Scheme 2.




**Scheme 1**

The reactions of carbene complexes **11** and **12** with alkyne **2** are both stereoselective and stereospecific (Table 1). Complex *E*-**11** gives cyclohexadienone **13** with an α-ethyl group (92 : 8) while the *Z*-isomer gives cyclohexadienone **14** with a β-ethyl group (91 : 9). The reaction of complex **12** is also stereospecific. The isomerically pure *E*-**12** gave a 90 : 10 mixture of **15** and **16** and a 60 : 40 mixture[8] of *E*-**12** and *Z*-**12** gave a 68 : 32 mixture of **15** and **16**. In both cases, the substituent $R^3$ *syn* to the carbene unit is selectivity incorporated *syn* to the trityloxy group when the product is drawn as shown. If the alkoxy substituent $R^4$ is changed from $CPh_3$ to TBS the selectivity drops from 9 : 1 to 4.6 : 1. This appears to be due to electronics rather than sterics.[1,9] When a heptane solution of *E*-**11** was heated at 90 °C for 14 h no isomerization could be detected. Likewise, when *E*-**12** was heated in heptane at 85 °C for 11 h no isomerization could be detected. These results suggest that the carbene complexes do not isomerize under the reaction conditions.

The stereochemical assignments for the dienones were made on the basis of an X-ray structure of dienone **15a**.† Correlation of the $^1$H NMR spectra of **15a** and **16a** with **13** and **14** then leads to the assignment of the major product from the reaction of complex *E*-**11** as the cyclohexadienone **13**. In a similar fashion




**Scheme 2**

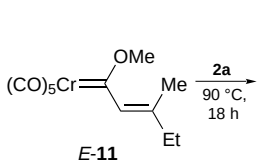
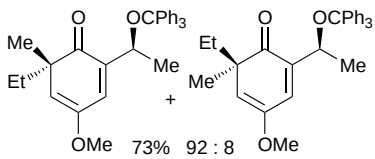
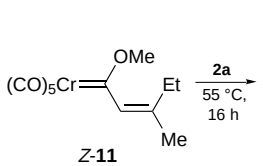
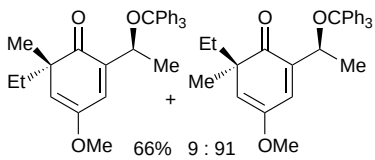
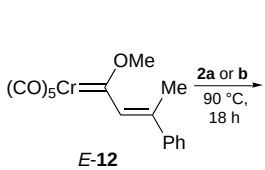
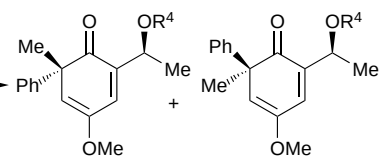
the stereochemistry of the major product from the reaction of *E*-**12** with **2b** was assigned as **15b**. The stereochemistry of the cyclohexadienone products allows for an assignment of the direction of the electrocyclic ring closure. The favoured pathway is thus with the rotation of the substituent $R^3$ up and away from the metal centre in the vinyl ketene complex **8** to give the cyclohexadienone metal complex **9**-**A**. Downward rotation of $R^3$ (pathway *b*) is apparently disfavoured due to severe close-contacts with the metal and its ligands. The overall stereo-induction begins with the prop-2-ynylic chiral centre which leads to a stereospecific coordination of the chromium to the lower face of the vinyl ketene complex **8**. This in turn leads to stereo-induction in the formation of the quaternary carbon centre formed in the ring closing step. This represents an overall 1,4-induction with a stereochemical relay *via* a transiently installed metal centre.

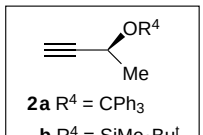
An alternative mechanism for the observed stereo-induction involves a 16 $e^-$ $\eta^2$-vinyl carbene complex which could be derived from decoordination of the double bond in **6**, followed by the formation of the vinyl ketene complex **8** according to the allochemical mechanism.[10] This would involve a 1,2-induction in the formation of an $\eta^2$-coordinated vinyl ketene complex. This possibility is not considered here because of evidence which suggests that the allochemical mechanism is not operative when hexane is the solvent.[6a] The less than complete stereoselection observed in these reactions may not necessarily be due to rotation of $R^3$ through the metal centre in the vinyl ketene complex **8**. Rather, it may reflect the level of stereoselection associated with the introduction of the metal to a particular face of the vinyl carbene species in intermediate.‡

In the light of the synthetic importance of both the benzannulation reaction and the cyclohexadienone annulation, further studies on the mechanism of these reactions are being pursued. Additionally, synthetic applications for the stereospecific cyclohexadienone annulation are being explored.

This was supported by the National Institutes of Health (GM 33589)

**Table 1** 1,4-Induction with stereoisomerically pure vinly carbene complexes[a2]

| Carbene complex[b] | Cyclohexadienones |
|---|---|
|  *E*-**11** (68%) |  **13** 73% 92 : 8 **14** |
|  *Z*-**11** (56%) |  **13** 66% 9 : 91 **14** |
|  *E*-**12** (57%) |  **15** **16** |




72% 90 : 10 $R^4$ = $CPh_3$
68% 80 : 20[c] $R^4$ = $CPh_3$
65% 68 : 32[d] $R^4$ = $CPh_3$
73% 82 : 18 $R^4$ = $SiMe_2Bu^t$
49% 66 : 34[c] $R^4$ = $SiMe_2Bu^t$

[a] Reaction carried out under argon with carbene complex (0.01 mol $dm^{-3}$) and alkyne (1.3 equiv.) in heptane; *E*-**11** 90 °C, 18 h; *Z*-**11** 55 °C, 16 h; *E*-**12** 90 °C, 18 h. [b] Made from the corresponding vinyl iodides in the indicated yields. The vinyl iodides were made by the method of Negishi (ref. 7) each with greater than 98% diastereoisomeric purity as determined by capillary GC and $^1$H NMR spectroscopy. The isomeric purity of the carbene complexes was determined by $^{13}$C NMR spectroscopy to be ≥ 98% for *E*-**11** and *Z*-**11** and ≥ 97% for *E*-**12**. [c] Reaction performed in the presence of 3.0 equiv. of $Bu_3P$. [d] Reaction of a 60 : 40 mixture of *E* and *Z* isomers of complex **12** which was prepared in 8% yield by Michael addition in a manner similar to that reported for a related complex, ref. 8.

## Footnotes

† *Crystal data* for **15a**: $C_{35}H_{32}O_3$, monoclinic, $a$ = 17.457(7), $b$ = 8.689(3), $c$ = 21.408(9) Å, space group $C2$, $V$ = 3082(2) Å$^3$, $Z$ = 4, $D_c$ = 1.079 g $cm^{-3}$, crystal dimensions 0.2 × 0.2 × 0.2 mm, radiation: Mo-Kα (λ = 0.71073 Å), 2θ scan range 4.0–42.0°, standard reflection: 3 standards, 197 reflections; independent reflections: 1793; $R$ = 0.1108, $R_w$ = 0.1395, GOF 1.84. Atomic coordinates, bond lengths and angles, and thermal parameters have been deposited at the Cambridge Crystallographic Data Centre (CCDC). See Information for Authors, Issue No. 1. Any request to the CCDC for this material should quote the full literature citation and the reference number 182/289.

‡ The cyclohexadienone **13** does not isomerize under the reaction conditions. A sample of **13** and **14** (84.3 : 15.7) was heated in heptane for 23 h at 85 °C and recovered quantitatively with no change in composition (84.1 : 15.9).

## References

1 R. P. Hsung; W. D. Wulff and A. L. Rheingold, *J. Am. Chem. Soc*., 1994, **116**, 6449.
2 For subsequent examples, see: R. Neidlein, S. Gürtler and C. Krieger, *Helv. Chim. Acta*., 1994, **77**, 2303; R. L. Beddoes, J. D. King and P. Quayle, 1995, **36**, 3027; K. H. Dotz, C. Stinner and M. Nieger, *J. Chem. Soc., Chem. Commun*., 1995, 2535; R. P. Hsung, W. D. Wulff and C. A. Challener, *Synthesis*, 1996, 773.
3 P. C. Tang and W. D. Wulff, *J. Am. Chem. Soc*., 1984, **106**, 1132.
4 W. D. Wulff, K. S. Chan and P. C. Tang, *J. Org. Chem*., 1984, **49**, 2293; The corresponding *cis*-propenyl tungsten complex does not isomerize as rapidly: W. D. Wulff, W. E. Bauta, R. W. Kaesler, P. J. Lankford, R. A. Miller, C. K. Murray and D. C. Yang, *J. Am. Chem. Soc*., 1990, **112**, 3642.
5 For reviews on the synthetic applications of Fischer carbene complexes, see: W. D. Wulff, *Comprehensive Organometallic Chemistry II*, ed. E. W. Abel, F. G. A. Stone and G. Wilkinson, Pergamon, 1995, vol 12; L. S. Hegedus, in *Comprehensive Organometallic Chemistry II*, ed. E. W. Abel, F. G. A. Stone and G. Wilkinson, Pergamon, 1995, vol 12; M. Doyle, in *Comprehensive Organometallic Chemistry II*, ed. E. W. Abel, F. G. A. Stone and G. Wilkinson, Pergamon, 1995, vol 12.
6 For discussions of, and recent citations to mechanistic issues, see (*a*) W. D. Wulff, B. M. Bax, T. A. Brandvold, K. S. Chan, A. M. Gilbert, R. P. Hsung, J. Mitchell and J. Clardy, *Organometallics*, 1994, **13**, 102; (*b*) J. Christoffers and K. H. Dötz, *Chem. Ber*., 1995, **128**, 157; (*c*) J. W. Herndon and A. Hayford, *Organometallics*, 1995, **14**, 1556; (*d*) M. F. Gross and M. G. Finn, *J. Am. Chem. Soc*., 1994, **116**, 10 921; (*e*) J. Barluenga, F. Aznar, A. Martin, S. Garcia-Granda and E. Perez-Carreno, *J. Am. Chem. Soc*., 1994, **116**, 11 191; (*f*) D. F. Harvey, E. M. Grenzer and P. K. Gantzel, *J. Am. Chem. Soc*., 1994, **116**, 6719; (*g*) M. Duetsch, S. Vidoni, F. Stein, F. Funke, M. Noltemeyer and A. de Meijere, *J. Chem. Soc., Chem. Commun*., 1994, 1679; (*h*) C. Bouancheau, A. Parlier, M. Rudler, H. Rudler, J. Vaissermann and J.-C. Daran, *Organometallics*, 1994, **13**, 4708; (*i*) J. R. Knorr and T. L. Brown, *Organometallics*, 1994, **13**, 2178; (*j*) W. D. Wulff, A. M. Gilbert, R. P. Hsung and A. Rahm, *J. Org. Chem*., 1995, **60**, 4566.
7 E. Negishi, D. E. Van Horn and T. Yoshida, *J. Am. Chem. Soc*., 1985, **107**, 6639.
8 H. Fischer, T. Meisner and J. Hofmann, *Chem. Ber*., 1990, **123**, 1799.
9 B. A. Lorsbach, A. Prock and W. P. Giering, *Organometallics*, 1995, **14**, 1694.
10 M. E. Bos, W. D. Wulff, R. A. Miller, S. Chamberlin and T. A. Brandvold, *J. Am. Chem. Soc*., 1991, **113**, 9293.

*Received, 5th July 1996; Com. 6/04742D*

# Absolute kinetics of mesitylmethylchlorocarbene reactions

**Robert A. Moss* and Dina C. Merrer**

*Department of Chemistry, Rutgers, The State University of New Jersey, New Brunswick, New Jersey 08903, USA*

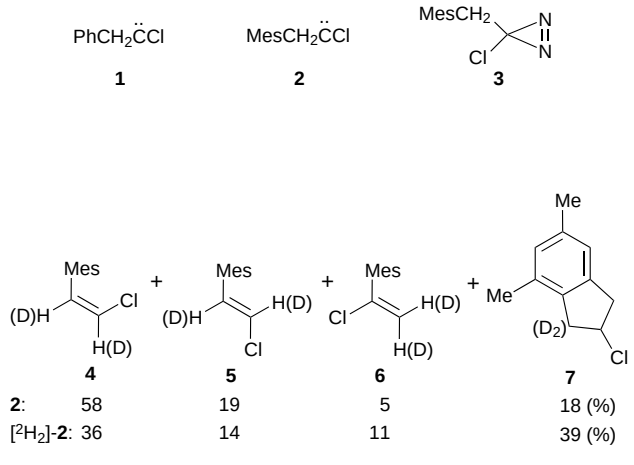
**Absolute rate constants were determined for reactions of mesitylmethylchlorocarbene, which affords intramolecular products derived from 1,2-H migration, 1,2-mesityl migration, and C–H insertion; at −35 or −70 °C, however, the intrusion of intermolecular channels affords azine and carbene dimer, complicating interpretations of the kinetics.**

Over the past dozen years, the chemistry of benzylchlorocarbene, **1**, has provided a rich complement of contemporary puzzles in carbene chemistry.[1] Continuing kinetics studies have raised questions about the relevance of carbene/alkene complexes,[2] excited carbene precursors[3] and quantum mechanical tunnelling[4] during the 1,2-H migration of **1**, as well as the origin(s) of curved Arrhenius correlations[4b,c,5] and abnormal kinetic isotope effects[4] in these same rearrangements.

Our own interest in these matters[1b,d] impelled us to open a new investigation from the perspective of the related mesitylmethylchlorocarbene, **2**. Although our results partly accord with findings in the benzyl system, they raise important questions concerning the influence of competitive intermolecular carbene reactions at moderately low temperatures.

Carbene **2** and [α,α-$^2H_2$]-**2** were generated by photolysis or thermolysis of the corresponding diazirine precursors,[6] **3** and [α,α-$^2H_2$]-**3**: $\lambda_{max}$ (pentane) 342, 348 (346 for [$^2H_2$]-**3**), 358 nm; $\varepsilon_{342}$ = 50 dm$^3$ mol$^{-1}$ cm$^{-1}$ ($CDCl_3$). For the generation of **2**, we initially employed diazirine solutions with $A_{342}$ *ca.* 1.0–1.1; [**3**] *ca.* 0.02 mol dm$^{-3}$. Photolysis of **3** (isooctane, 25 °C, λ > 300 nm) was continued until the diazirine was destroyed, and afforded products **4**–**7**, attributed to carbene **2** in > 96% yield.

The product distributions from carbenes **2** and [$^2H_2$]-**2** were determined relative to an internal decane standard (±2%) and appear below. We obtained 1,2-H-rearranged alkenes *Z*- and *E*-(2-chloroethenyl)mesitylene (**4** and **5**), 1,2-mesityl shifted (1-chloroethenyl)mesitylene (**6**) and methyl insertion product 2-chloro-1,3-dihydro-4,6-dimethylindane (**7**). Thermolysis [pentane, sealed tube, 80 °C (**3**) or 100 °C ([$^2H_2$]-**3**), 36 h] led to distributions that were quite similar to those from photolysis. Comparison of the yields of (**4** + **5**) *vs.* (**6** + **7**) from **2** and its [α,α-$^2H_2$] analogue point to a substantial primary kinetic isotope effect (KIE) associated with the H(D) shift. This is discussed below.




| | **4** | **5** | **6** | **7** |
|---|---|---|---|---|
| **2**: | 58 | 19 | 5 | 18 (%) |
| [$^2H_2$]-**2**: | 36 | 14 | 11 | 39 (%) |

Photolyses of **3** in the presence of 2-methylbut-1-ene led to **4**–**7** and the carbene/alkene addition products, *Z*- and *E*-1-chloro-1-mesitylmethyl-2-ethyl-2-methylcyclopropanes. When photolyses of **3** or [$^2H_2$]-**3** were performed in the presence of increasing concentrations of the alkene in isooctane, correlations of (addition/intramolecular products) *vs.* [alkene] were curved for each of the intramolecular products. However, the inverse correlations of (intramolecular/addition products) *vs.* 1/[alkene] were each linear.

If we assume that the second product-forming intermediate (in addition to carbene **2**) demanded by these results is excited diazirine **3***,[3] rather than a carbene/alkene complex,[2] then the *y*-intercepts of the inverse correlations give the partitions of **3*** between $N_2$-loss to **2** or direct formation of **4**–**7**.[1b,c,3] Product formation from **3*** is then (**4** + **5**) 17.5; **6**, 1.4; and **7**, 4.7%. From [$^2H_2$]-**3***, the corresponding values are 24.5, 3.4 and 10.6%, respectively. The balance of each product comes from the carbene, and the 'raw' product yields can be 'corrected' and renormalized to afford carbene-only distributions:[7] (from **2**) (**4** + **5**), 74.3; **6**, 5.7; **7**, 20.0%; (from [$^2H_2$]-**2**) (**4** + **5**), 45.4; **6**, 12.7; **7**, 41.9%. These data are used below to partition the global rate constants for carbene decay.

Global rate constants for the disappearance of carbenes **2** or [$^2H_2$]-**2** were obtained by laser flash photolysis (LFP) at 351 nm of the diazirines in isooctane. Carbene decay was followed directly at 310–313 nm and from −70 to 47 °C. Rate constants are considered accurate to ±10%.

Fig. 1 illustrates the Arrhenius correlations of ln *k vs.* $T^{-1}$ for the carbene decays. Linearity is observed for **2** down to *ca.* −40 °C, and for [$^2H_2$]-**2** to *ca.* −20 °C, after which the observed rate constants begin to level off with convergence at *k ca.* 9 × 10$^5$ s$^{-1}$ (ln *k ca.* 13.7). This behaviour resembles that of **1** and

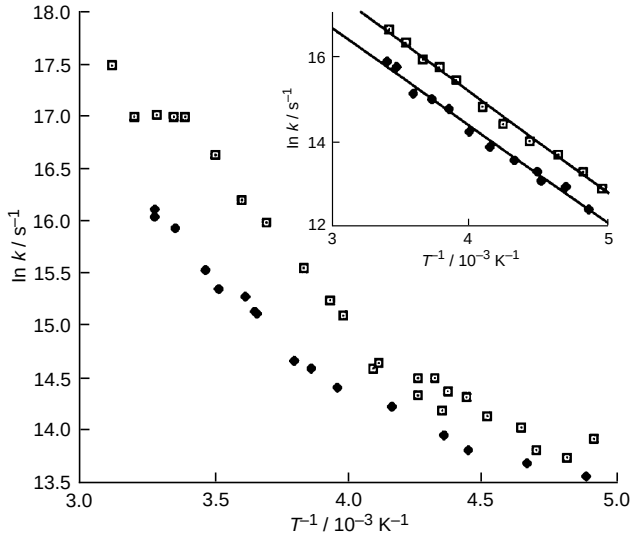


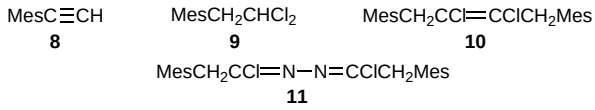

**Fig. 1** Arrhenius correlations for the decays of carbenes **2** (□) and [α,α-$^2H_2$]-**2** (◆); $A_{342}$ *ca.* 1.0. Inset: Arrhenius correlations for the decays of carbenes **2** (□) and [α,α-$^2H_2$]-**2** (◆); $A_{342}$ *ca.* 0.5.

[$^2H_2$]-**1**, where leveling occurs at −40 and −10 °C, respectively, with convergence at *k ca.* $1.2 \times 10^7$ $s^{-1}$.[4b] Note, in both cases, that Arrhenius curvature begins at a higher temperature for the [α,α-$^2H_2$] carbene.

At 25 °C, the global rate constant for decay of **2** is $2.4 \times 10^7$ $s^{-1}$, which can be partitioned as $1.8 \times 10^7$ $s^{-1}$ for H-shift to **4**/**5**, $1.4 \times 10^6$ $s^{-1}$ for 1,2-mesityl shift to **6**, and $4.8 \times 10^6$ $s^{-1}$ for insertion to **7**. For [$^2H_2$]-**2**, the corresponding total rate constant is $8.2 \times 10^6$ $s^{-1}$, and the partitioned rate constants are $3.7 \times 10^6$ $s^{-1}$ (1,2-D shift), $1.0 \times 10^6$ $s^{-1}$ (1,2-mesityl shift), and $3.4 \times 10^6$ $s^{-1}$ (insertion). The global rate constants are somewhat smaller than those reported for **1** ($6.2 \times 10^7$ $s^{-1}$) and [$^2H_2$]-**1** ($2.1 \times 10^7$ $s^{-1}$) at 25 °C.[4b]

Our partitioned rate constants afford a large KIE for 1,2-H or 1,2-D shifts of **2** at 25 °C; $k_H/k_D$ = 4.8. Product distributions were not corrected for incursion of **3*** at other temperatures, so that those global rate constants cannot be accurately partitioned to reflect carbene-only product formation. From the global rate constants for decay of **2** or [$^2H_2$]-**2** (Fig. 1), $k_H/k_D$ appears to decrease with decreasing temperature, as was reported for **1**.[4b] As shown below, however, this picture is deceptive.

Thus far, the chemistry of mesitylmethylchlorocarbene closely parallels that of benzylchlorocarbene.[1a,2,4a,b] An important divergence occurs, however, for product formation at low temperature. Photolyses of **3** and [$^2H_2$]-**3** were carried out at 30, 0, −35 and −70 °C. At the two higher temperatures, **4**–**7** accounted for > 96% of the products from either **2** or [$^2H_2$]-**2**. However, at −35 or −70 °C, product mixtures became increasingly complex, with up to six new products formed. Of these, we have identified **8**–**11**.




Acetylene **8**, also present in 2% yield in the 25 °C photolysis of **3**, appears to be an elimination product of **4**, **5** or **6**. Dichloride **9** results from reaction of **2** with HCl. The chromatographically inseparable mixture of 15 : 85 carbene dimer **10** and azine **11** (from **2** + **3**) was identified by NMR, GC–MS, microanalysis and exact mass measurements. Yields of **8** and **9** were low (⩽2%) under all conditions; whereas (**10** + **11**) constituted 2.5 and 11.2% of the products at −35 and −70 °C, respectively. For [$^2H_2$]-**2**, dimer/azine formation was already apparent at 0 °C (2.1%), and increased to 8.5 and 16% at −35 and −70 °C. Analogous azine formation has also been observed from benzylfluorodiazirine and benzylfluorocarbene.[8]

Azine formation was discounted as a complicating factor in the chemistry of carbene **1**,[4b] but it cannot be ignored here. Moreover, azine formation will be more marked, and commence at higher temperatures with [$^2H_2$]-**2**, which has a threefold lower rate constant for decay at 25 °C than does **2**; intramolecular reactions compete less efficiently with intermolecular reactions for the deuteriated carbene.

Azine (and dimer) formation are initially observed for **2** at −35 °C and for [$^2H_2$]-**2** at 0 °C. Arrhenius curvature (Fig. 1) becomes apparent at similar temperatures (−40 and −20 °C). These correspondences are not coincidental; with decreasing temperature the intramolecular reactions of the carbenes are slowed sufficiently so that the effectively temperature independent intermolecular azine formation gains in importance, causing significant curvature and levelling in the Arrhenius correlations. Consistent with this explanation, we find that twofold dilution of diazirines **3** and [$^2H_2$]-**3** ($A_{342}$ = 0.5 in isooctane, [diazirine] *ca.* 0.01 mol $dm^{-3}$) leads to Arrhenius correlations for both carbenes that are linear to −70 °C (inset, Fig. 1).

These new correlations afford $E_a$ = 4.8 kcal $mol^{-1}$ (1 cal = 4.184 J), log *A* = 10.7 $s^{-1}$ and $\Delta S^*(298)$ = −11.4 e.u. for **2**, and analogous values of 4.6 kcal $mol^{-1}$, 10.2 $s^{-1}$ and −13.7 e.u. for [$^2H_2$]-**2**. Of course, these data contain contributions from all carbene decay channels, but they are similar to the activation parameters determined for carbene **1**.[4b] Importantly, with the disappearance of Arrhenius curvature, the temperature dependence of the KIE for **2**/[$^2H_2$]-**2** no longer exhibits a marked decrease with decreasing temperature. It is also interesting to note from the activation parameters that $k_H/k_D$ for the disappearance of **2**/[$^2H_2$]-**2** (at least from the global rate constants) is controlled by entropic, not enthalpic factors.

In the cases of **1** and [$^2H_2$]-**1**, Arrhenius curvature was attributed to increasing intervention of carbenic reaction with the isooctane solvent and/or 1,2-H shift tunnelling.[4b] However, no products of carbene/isooctane reactions were observed.[4b] Moreover, in preliminary experiments, we have observed the formation of azine (up to 30%) in photolyses of benzylchlorodiazirine ($A_{344}$ = 0.7) at −70 °C in isooctane, under conditions analogous to those used in the photolysis of **3**. In the light of our findings with carbene **2**, it seems likely that azine formation is a major cause of the Arrhenius curvature observed in the H-shift reactions of **1**.

We do not exclude tunnelling as a contributory factor to the Arrhenius curvature. Tunnelling is surely involved in the rearrangements of **1** in argon matrices at 20–30 K,[4a] and may be important in the rearrangements of $CH_3CCl$ and $CD_3CCl$ at temperatures that are much closer to ambient.[4c,d]

In conclusion, the intramolecular chemistry of mesitylmethylchlorocarbene parallels that of benzylchlorocarbene, but the increasing product complexity and azine formation at low temperatures suggest important revisions to previous interpretations of the rearrangement kinetics of the latter carbene. We are continuing our studies of carbenes **1**, **2** and their fluoro analogues.

We are grateful to the National Science Foundation for financial support, to Professors J. L. Goodman, M. T. H. Liu and M. S. Platz for helpful discussions, and to Dr L. Maksimovic for technical assistance.

## References

1 Reviews: (*a*) M. T. H. Liu, *Acc. Chem. Res.*, 1994, **27**, 287; (*b*) R. A. Moss, in *Advances in Carbene Chemistry*, vol. 1, ed. U. H. Brinker, JAI Press, Greenwich, 1994, p. 59; (*c*) J. E. Jackson and M. S. Platz, p. 89; (*d*) R. A. Moss, *Pure Appl. Chem.*, 1995, **67**, 741.

2 (*a*) H. Tomioka, N. Hayashi, Y. Izawa and M. T. H. Liu, *J. Am. Chem. Soc.*, 1984, **106**, 454; (*b*) M. T. H. Liu, *J. Chem. Soc., Chem. Commun.*, 1985, 982; (*c*) R. Bonneau, M. T. H. Liu, K. C. Kim and J. L. Goodman, *J. Am. Chem. Soc.*, 1996, **118**, 3829 and references cited therein.

3 J. A. LaVilla and J. L. Goodman, *Tetrahedron Lett.*, 1990, **31**, 5109; W. R. White III and M. S. Platz, *J. Org. Chem.*, 1992, **57**, 2841; D. A. Modarelli, S. Morgan and M. S. Platz, *J. Am. Chem. Soc.*, 1992, **114**, 7034; R. A. Moss and W. Liu, *J. Chem. Soc., Chem. Commun.*, 1993, 1597.

4 (*a*) S. Wierlacher, W. Sander and M. T. H. Liu, *J. Am. Chem. Soc.*, 1993, **115**, 8943; (*b*) M. T. H. Liu, R. Bonneau, S. Wierlacher and W. Sander, *J. Photochem. Photobiol. A: Chem.*, 1994, **84**, 133; (*c*) E. J. Dix, M. J. Herman and J. L. Goodman, *J. Am. Chem. Soc.*, 1993, **115**, 10 424; (*d*) J. W. Storer and K. N. Houk, *J. Am. Chem. Soc.*, 1993, **115**, 10 426.

5 M. T. H. Liu and R. Bonneau, *J. Am. Chem. Soc.*, 1990, **112**, 3915.

6 R. A. Moss, W. Ma, D. C. Merrer and S. Xue, *Tetrahedron Lett.*, 1995, **36**, 8761.

7 R. A. Moss and G.-J. Ho, *J. Phys. Org. Chem.*, 1993, **6**, 126.

8 L. Maksimovic, unpublished work in this laboratory.

*Received, 4th November 1996; Com. 6/07552E*

# A hydrodynamic AFM flow cell for the quantitative measurement of interfacial kinetics

**Barry A. Coles,* Richard G. Compton, Jonathan Booth, Qi Hong and Giles H. W. Sanders**

*Physical and Theoretical Chemistry Laboratory, Oxford University, South Parks Road, Oxford, UK OX1 3QZ*

**A novel liquid flow cell is developed which allows atomic force microscopy images to be obtained under defined and modelled hydrodynamic flow conditions, enabling measured reaction fluxes to be compared with those calculated from proposed heterogeneous reaction mechanisms.**

AFM of reacting surfaces has been carried out without defined flow conditions, for example by Hansma and coworkers[1] who observed that steps on a calcite surface under aqueous solution moved laterally as dissolution proceeded. This technique is extremely powerful since it can identify key structural features, for example steps or etch pits, which contribute to the dissolution process. This approach remains qualitative since no attempts have been reported in which quantitative measures of the reaction flux are related to a chemical model of the interfacial reaction. The latter dictates defined hydrodynamics and mass transport so that the variations of concentrations in space and time above the surface can be modelled.

The value of defined hydrodynamic conditions has been demonstrated by measurements in channel flow cells[2] in which a laminar flow of solution passed through a rectangular channel with a calcite crystal forming part of one wall. The reaction was monitored electrochemically by an electrode flush with the wall and immediately downstream of the calcite surface. Precise knowledge of the flow pattern enabled it to be shown that the reaction between $H^+$ and calcite was a first-order heterogeneous reaction of $H^+$. However, the channel geometry does not facilitate simultaneous observation of the changes in surface topography or a direct physical measurement of the rate of surface dissolution, since the insertion of a scanning probe would invalidate the analytic expression for flow velocities.

We have developed a novel flow cell, based on the standard Topometrix[3] Discoverer liquid immersion cell, in which AFM images may be obtained in the presence of a flowing liquid and in which the flow pattern may be calculated. The standard cell has tangential inlet and outlet ports at the periphery of a large irregular volume, so that the flow in the vicinity of the scanning cantilever is unpredictable. We have redesigned the cell by the addition of a new inlet port so that solution can be delivered through a precisely shaped and positioned stainless-steel duct directly to the front of the cantilever chip (Fig. 1). The liquid jet is aligned parallel to the front of the cantilever support chip and transverse to the cantilever. This gives a partly free field flow, not confined except by the sample below and the cantilever chip to one side, so the flow pattern is complex and is not amenable to an analytic solution. Such flow fields can however be solved using computational fluid-dynamics programs.

We report here preliminary studies in which the flow field was calculated by two-dimensional simulations, together with experimental data to demonstrate the validity of this design. Initial studies of an inclined jet using the FLOTRAN[4] and subsequently FIDAP[5] programs showed that a satisfactory flow field would be set up. In particular, it was confirmed that all of the solution reaching the surface of the sample will be fresh solution from the jet with no mixture or entrainment of the surrounding bulk solution, which is an essential requirement for full characterisation. Initial tests of the cell using a gold calibration microgrid also confirmed that AFM images could be obtained under flow conditions without detectable deterioration of image quality up to the highest flow rates used.

In the first study, the flow behaviour has been confirmed over a wide range of flow rates by determining the limiting current at a $1 \times 1$ mm platinum electrode which was placed in the sample position, Fig. 2. An aqueous solution of 5 mM potassium hexacyanoferrate(II) with 1 M KCl was used, and the limiting current for the reversible one-electron oxidation to hexacyanoferrate(III) determined for volume flow rates in the range 0.029 to $1.4 \times 10^{-5}$ cm$^3$ s$^{-1}$, with a stainless-steel jet of internal dimensions $0.057 \times 0.057$ cm.

The FIDAP simulation was based on a two-dimensional finite element model of a section of fluid $5.86 \times 3.06$ mm, including the cross-section of the jet tube and bounded below by the sample surface. The remaining boundaries represented the bulk fluid in the cell and permitted free flow. The model comprised 6564 elements of graded size, with a fine element mesh in regions of high gradients of velocity or of concentration, such as at the edges of the electrode. The simulation for a flow rate of 0.0014 cm$^3$ s$^{-1}$ is shown in Fig. 2 as a streamline contour plot,

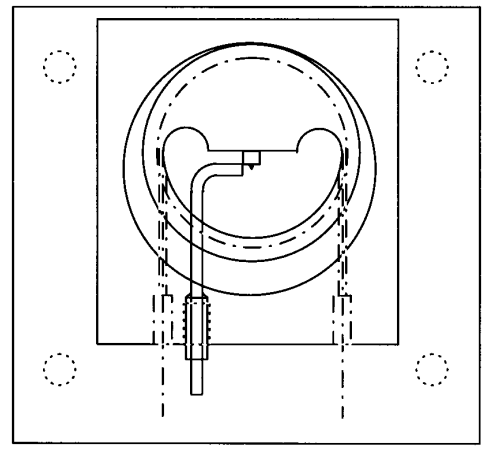


**Fig. 1** Top view of the Topometrix sample cell showing the new inlet duct

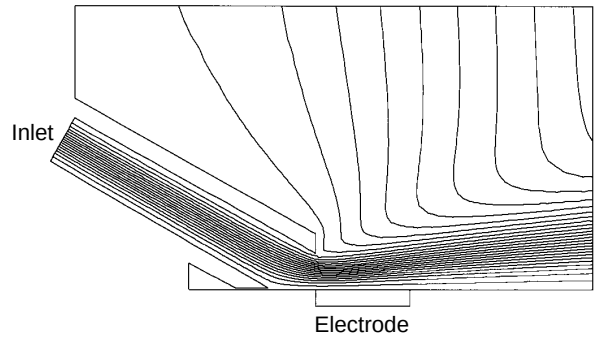



**Fig. 2** The two-dimensional cross-section of solution modelled with FIDAP, showing jet and electrode positions, with streamline contours for a flow rate of 0.0014 ml s$^{-1}$

indicating that the jet flows near to the surface, moving away from it at a fairly shallow angle; as the flow rate is lowered, this angle increases and the jet broadens. The flux of hexacyanoferrate(II) to the electrode was calculated using FIDAP, by setting concentration boundary conditons of 5 mM at the inlet to the jet tube, and of zero, corresponding to the limiting current condition, at the electrode surface. Fig. 3 shows the simulated and the experimental limiting currents as a function of (flow rate)$^{1/2}$. For this two-dimensional approximation, it was assumed that the effective electrode width was 0.45 mm due to the narrower jet. On this basis good agreement was obtained over more than three orders of magnitude of flow rate, broadly confirming the simulated behaviour.

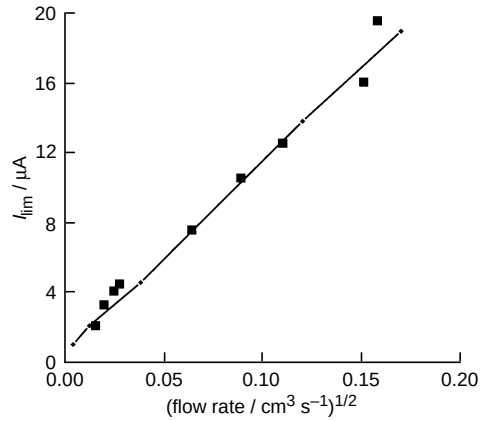



**Fig. 3** Experimental (■) and simulated (—) limiting currents as a function of (flow rate)$^{1/2}$

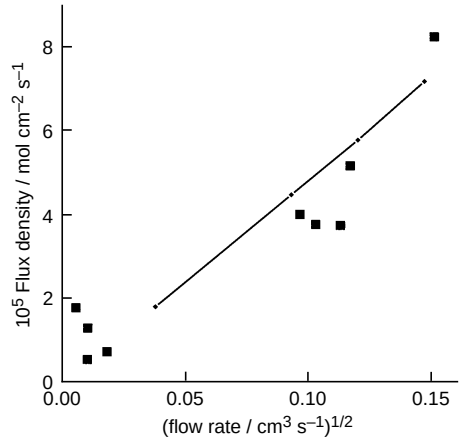



**Fig. 4** Dissolution rate of calcite determined by AFM (■) and simulated (—) as a function of (flow rate)$^{1/2}$

The second study was the dissolution of a calcite surface in 0.98 mM aqueous HCl as a function of flow rate. By monitoring the change of the Z-piezo voltage during successive scans of the AFM image, the rate of recession of the surface and hence the flux of reacted material could be determined for different flow rates assuming a density of 2.71 g cm$^{-3}$ for calcite. For the simulation (again two-dimensional), the dissolution reactions were expressed by eqns. (1)–(3) and the reaction flux at the scan location was calculated using the backward implicit finite difference (BIFD) method[6] with the rate constants $K_{H_2CO_3} = 1.72 \times 10^{-4}$ M (this value is corrected for activity coefficients[2]), $k_3 = 20$ s$^{-1}$, and variable $k_1$, and with the fluid velocities taken from a FIDAP simulation. Fig. 4 shows the AFM determined flux rates together with the FIDAP/BIFD simulated values plotted against (flow rate)$^{1/2}$ for the case of $k_1 = 0.035$ cm s$^{-1}$.

$$H^+(aq) + CaCO_3(s) \rightarrow Ca^{2+}(aq) + HCO_3^-(aq) \quad (1)$$

$$H^+(aq) + HCO_3^-(aq) \rightleftharpoons H_2CO_3(aq) \quad (2)$$

$$H_2CO_3(aq) \rightarrow H_2O + CO_2(aq) \quad (3)$$

This is in excellent agreement with the value (0.043 ± 0.015) cm s$^{-1}$ deduced from independent channel flow cell experiments[2] and confirms the validity of the hydrodynamic AFM approach.

We have shown that this novel design for an AFM flow cell is practicable and gives good agreement between experimental and calculated results using a two-dimensional finite element fluid-dynamics simulation of the complex flow field. A full three-dimensional flow simulation, while requiring substantial computer resources, should further improve accuracy, and work on this is in progress. This new cell should prove of value to AFM users for mechanistic investigations in many areas of solid/liquid reactions, allowing physical and structural changes to the surface to be related directly to proposed reaction mechanisms and rate constants.

We thank EPSRC for support *via* ROPA, Zeneca and EPSRC for a CASE studentship for J. B., and Glaxo for a studentship for G. H. W. S.

## References

1 P. E. Hillner, S. Manne, A. J. Gratz and P. K. Hansma, *Ultramicroscopy*, 1992, **42**, 1387.
2 R. G. Compton and P. R. Unwin, *Philos. Trans. R. Soc. London, Ser. A*, 1990, **330**, 1.
3 Topometrix Corporation, Santa Clara, CA.
4 FLOTRAN, Ansys Inc., Houston, PA, 1992.
5 FIDAP, FDI Inc., Evanston, IL, 1995.
6 R. G. Compton, M. B. G. Pilkington and G. M. Stearn, *J. Chem. Soc., Faraday Trans. 1*, 1988, **84**, 2155.

*Received, 29th November 1996; Com. 6/08133I*

# Synthesis of organic sulfides using Ce-exchanged NaY catalyst

**T. Indrasena Reddy and Rajender S. Varma***

*Department of Chemistry and Texas Regional Institute for Environmental Studies (TRIES), Sam Houston State University, Huntsville, TX 77341-2117, USA*

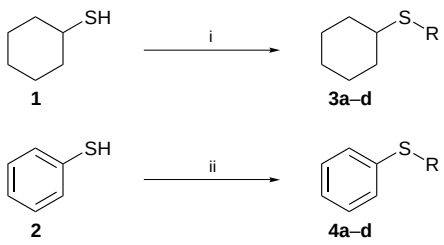
**Synthesis of organic sulfides from thiols and alkyl halides is achieved using Ce-exchanged zeolite catalyst, Ce(72%)NaY.**

While investigating the chemoselectivity aspects of oxidation reactions utilizing titanium silicates, we required various sulfides bearing unsaturated functionalities. There are few general methods available for the preparation of organic sulfides; however those available include phase-transfer procedures[1,2] and reactions using supported reagents on alumina.[3] Sodium sulfide impregnated on alumina facilitates the synthesis of symmetrical sulfides,[3] whereas base-catalysed alkylation of thiols using sodium hydroxide 'doped' alumina gives unsymmetrical sulfides.[3] 3-Aminopropyl(triethoxy)silane-modified basic montmorillonite clay has been used to catalyse the reaction of benzyl chloride with various thiols to produce unsymmetrical sulfides.[4] Recently, another approach has been described that uses a Pd catalyst with aryl thiocyanate-derived samarium thiolates for the synthesis of unsymmetrical sulfides.[5]

In continuation of our efforts to develop environmentally benign synthetic protocols using microwave (MW) irradiation[6] and zeolite materials,[7] we explored the synthesis of the requisite sulfides with unsaturated functionalities on solid supports. Since our attempts with sodium hydroxide 'doped' alumina and other solid supports produced only poor yields of unsaturated sulfides,[6] we focused our efforts on zeolite molecular sieves, particularly metal-exchanged Y zeolites which are weakly basic.[7a,8]

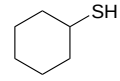
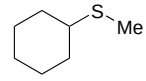
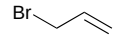
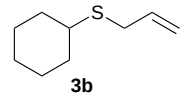
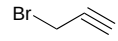
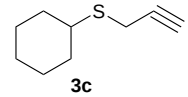
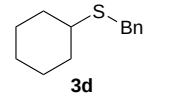
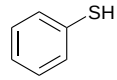
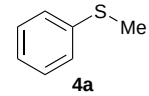
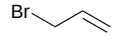
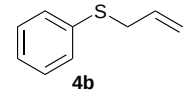
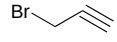
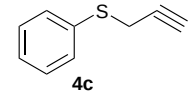
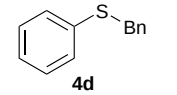
The use of various zeolite catalysts in organic transformations is a growing area of interest.[9,10] The Na form of faujasites (ex. X and Y), a class of zeolite catalyst, is almost neutral in nature. However, a basic character can be introduced by increasing the alumina content of the catalyst framework, thereby increasing the population of counter cations and their radii.[7a,11,12] Furthermore, the electrostatic interaction between the metal cation and the organic guests within the zeolite supercage has been well studied.[13,14] In this context, we have initiated a program exploiting the interactions of exchanged rare-earth cations of the faujasites with the included organic guest molecules in the supercages. Our main aim is to identify the conditions in which such an interaction could create sufficient polarization of the organic guests inside the supercages to facilitate chemical transformations. In line with our expectations, when a hexane solution of thiophenol **2** and benzyl bromide was refluxed in the presence of cerium-exchanged NaY (or NaX) zeolite, the benzyl phenyl sulfide was produced in 92% yield† (Scheme 1). These encouraging results prompted us to explore the use of the cerium-exchanged NaY zeolite, Ce(72%)NaY, for the synthesis of unsymmetrical sulfides.

Briefly, the preparation of the Ce-exchanged catalyst involved the treatment of zeolite NaY[15]‡ with aqueous cerium chloride solution (prepared using double distilled and deionized water with pH adjusted to 5.0) at 95 °C for 8 h. After cooling to room temperature, the exchanged catalyst was filtered off and washed with water. The percentage of $Na^+$ exchange was determined (35%) by conventional gravimetric analysis of the aqueous filtrate; this procedure is repeated twice, resulting in a maximum exchange of 72%. The Ce(72%)NaY was dried at




**Scheme 1** *Reagents and conditions*: i, RX, hexane, Ce(72%)NaY, reflux, 14–16 h; ii, RX, hexane, Ce(72%)NaY, reflux, 8–10 h

**Table 1** Synthesis of unsymmetrical sulfides using zeolite catalyst Ce(72%)NaY†

| Entry | Thiols | Alkyl halides | Sulfides[a] | Yield (%)[b] |
|---|---|---|---|---|
| 1 |  **1** | MeI |  **3a** | 75 |
| 2 | |  |  **3b** | 83 |
| 3 | |  |  **3c** | 77 |
| 4 | | BnBr |  **3d** | 84 |
| 5 |  **2** | MeI |  **4a** | 82 |
| 6 | |  |  **4b** | 85 |
| 7 | |  |  **4c** | 79 |
| 8 | | BnBr |  **4d** | 92 |

[a] Products exhibited spectral data compatible with assigned structures. [b] Isolated and unoptimised yields.

120 °C for 4 h and its crystalline structural integrity was discerned by X-ray analysis.[8a]

The freshly activated Ce(72%)NaY§ was used for the alkylation of cyclohexanethiol **1** and thiophenol **2** with a variety of alkyl halides such as iodomethane, allyl bromide, prop-2-ynyl bromide and benzyl bromide to provide corresponding sulfides in high yields (Table 1). The heterogeneous catalytic method described herein is attractive since it compares favourably with other reported protocols[2–4] in terms of yield. The reactions with thiophenol require 8–10 h to reach completion, whereas in the case of aliphatic compounds such as cyclohexanethiol, a relatively longer time period of 14–16 h is necessary.

In conclusion, we have demonstrated the versatility of cerium-exchanged NaY zeolite as an efficient catalyst for the synthesis of organic sulfides. These thermally stable crystalline inorganic materials are safe to handle and environmentally benign. Their recyclable nature and ease of manipulation, entailing a simple filtration step, illustrate some of the added advantages of zeolite catalysts.

We are grateful to the Texas Advanced Research Program (ARP) in Chemistry (Grant no. 003606-023) and the Retina Research Foundation, Houston for generous support.

## Footnotes

† Typical experimental procedure: Thiophenol (200 mg, 1.81 mmol), benzyl bromide (373 mg, 2.18 mmol) and freshly activated catalyst (40 mg, 20 mass% of thiophenol) in hexane (15 ml) was stirred for 12 h at reflux temperature to complete conversion. The progress of the reaction was monitored by TLC. The reaction mixture was cooled to room temperature, the catalyst was filtered off and washed it with hexane (3 × 10 ml). The combined solution was concentrated at reduced pressure to afford benzyl phenyl sulfide in 92% (330 mg, mp 45–47 °C).

‡ Zeolites NaX and NaY were obtained from Union Carbide Corporation, USA. The $SiO_2/Al_2O_3$ ratio is 2.52 in NaX and 4.20 in NaY.

§ These reactions have also been carried out using Ce(72%)NaX catalyst with almost equal efficiency.

## References

1 D. Landini and F. Rolla, *Synthesis*, 1974, 565.
2 A. W. Herriott and D. Picker, *Synthesis*, 1975, 447.
3 B. Czech, S. Quici and Q. S. Regen, *Synthesis*, 1980, 113.
4 P. Kannan, K. Pitchumani, S. Rajagopal and C. Srinivasan, *Chem. Commun.*, 1996, 369.
5 I. W. J. Still and F. D. Toste, *J. Org. Chem.*, 1996, **61**, 7677 and reference cited therein.
6 R. S. Varma, J. B. Lamture and M. Varma, *Tetrahedron Lett.*, 1993, **34**, 3029; R. S. Varma, A. K. Chatterjee and M. Varma, *Tetrahedron Lett.*, 1993, **34**, 3207; R. S. Varma, A. K. Chatterjee and M. Varma, *Tetrahedron Lett.*, 1993, **34**, 4603; R. S. Varma, M. Varma and A. K. Chatterjee, *J. Chem. Soc., Perkin Trans. 1*, 1993, 999.
7 (*a*) T. I. Reddy and R. S. Varma, *Tetrahedron Lett.*, in the press; (*b*) T. I. Reddy and R. S. Varma, *Chem. Commun.*, in the press; (*c*) T. I. Reddy, M. Sasidharan and R. S. Varma, unpublished results.
8 For the exchange of $Na^+$ ions by other metal ions, see: (*a*) V. P. Shiralkar and S.B. Kulkarni, *Indian J. Chem.*, 1978, **16A**, 665; (*b*) T. I. Reddy, Ph.D. Thesis, University of Poona, Pune, 1993; (*c*) J. W. Ward, *J. Catal.*, 1969, **13**, 321.
9 M. E. Davis, *Acc. Chem. Res.*, 1993, **26**, 111; W. M. H. Sachtler, *Acc. Chem. Res.*, 1993, **26**, 383; S. L. Suib, *Chem. Rev.*, 1993, **93**, 803; A. Corma, *Chem. Rev.*, 1995, **95**, 559; A. Corma and A. Martinez, *Adv. Mater.*, 1995, **7**, 137; W. F. Holderich, M. Hesse and F. Naumann, *Angew. Chem., Int. Ed. Engl.*, 1988, **27**, 226.
10 For selected reviews on photochemistry in zeolites, see V. Ramamurthy, D. F. Eaton and J. V. Caspar, *Acc. Chem. Res.*, 1992, **25**, 299; V. Ramamurthy, in *Photochemistry in Organized and Constrained Media*, ed. V. Ramamurthy, VCH, New York, 1991, ch. 10; N. J. Turro, *Pure Appl. Chem.*, 1986, **58**, 1219.
11 *Innovation in Zeolite Material Science*, ed. D. Barthomeuf, A. Mallmann and P. J. Grobet, Elsevier, Amsterdam, 1988; D. Barthomeuf, *J. Phys. Chem.*, 1984, **88**, 42; A. Corma, V. Fornes, R.M. Martin-Aranda, H. Garcia and J. Primo, *Appl. Catal.*, 1990, **59**, 237.
12 A. R. A. S. Deshmukh, T. I. Reddy, B. M. Bhawal, V. P. Shiralkar and S. Rajappa, *J. Chem. Soc., Perkin Trans. 1*, 1990, 1217; T. I. Reddy, B. M. Bhawal and S. Rajappa, *Tetrahedron*, 1993, 2101; T. I. Reddy and S. Rajappa, unpublished observations.
13 M. Czjzek, T. Vogt and H. Fuess, *Angew. Chem., Int. Ed. Engl.*, 1989, **28**, 770; H. Jobic, A. Renouprez, A. N. Fitch and H. J. Lauter, *J. Chem. Soc., Faraday Trans.*, 1987, **83**, 3199; A. N. Fitch, H. Jobic and A. Renouprez, *J. Phys. Chem.*, 1986, **90**, 1311.
14 M. A. Hepp, V. Ramamurthy, D. R. Corbin and C. Dybowski, *J. Phys. Chem.*, 1992, **96**, 2629.
15 For background information on faujasite zeolites, see D. W. Breck, *Zeolite Molecular Sieves: Structure, Chemistry and Use*, Wiley, New York, 1974; S. M. Csicsery, *Zeolite Chemistry and Catalysis*, ed. J. A. Rabo, ACS Monograph 171, Washington, DC, 1976, p. 680ff; W. F. Holderich and H. van Bekkum, in *Introduction to Zeolite Science and Practice*, ed. H. van Bekkum, E. M. Flanigen and J. C. Jansen, *Stud. Surf. Sci. Catal.*, 1991, **58**, 631; A. Dyer, *An Introduction to Zeolite Molecular Sieves*, Wiley, New York, 1988.

*Received, 18th December 1996; Com. 6/08493A*

# Highly luminescent neutral *cis*-dicyano osmium(II) complexes

**Jack Y. K. Cheng, Kung-Kai Cheung and Chi-Ming Che***

*Department of Chemistry, The University of Hong Kong, Pokfulam Road, Hong Kong*

**Two highly luminescent neutral *cis*-dicyanoosmium(II) complexes are prepared by photoinduced oxygen atom transfer reactions of *trans*-$[OsO_2(CN)_2(dpphen)]$ with $PPh_3$ and $Me_2SO$; their MLCT excited states are emissive with long lifetimes (0.20–1.99 μs) and high quantum yields [(40–1.8) $\times 10^{-2}$] and the emission maxima show pronounced solvatochromism.**

Luminescent metal complexes with high emission quantum yields and which could function as molecular building blocks for polynuclear metal complexes find useful applications in supramolecular chemistry and photocatalysis.[1] However, examples of these complexes are sparse in literature. In this context, we were attracted to the wide applications of $[RuL_2(CN)_2]^2$ (L = 2,2′-bipyridine or 1,10-phenanthroline) as building blocks for polynuclear cyano-bridged metal complexes and the striking luminescent properties of $[Os^{II}L_x(P–P)_{3-x}]^{2+}$ (P–P = diphosphine, $x$ = 1 or 2).[3] Herein is described the formation of highly luminescent neutral cyanoosmium(II) complexes which have the combined features and properties of both $[RuL_2(CN)_2]$ and $[Os^{II}L_x(P–P)_{3-x}]^{2+}$. These complexes are anticipated to provide a new entry to supramolecular photochemistry.

$[OsO_2(CN)_2(dpphen)]$ **1** (dpphen = 4,7-diphenyl-1,10-phenanthroline) was prepared from dpphen and $[OsO_2(CN)_2(OH)_2]^{2-}$ following the reported literature method.[4] As with other dioxoosmium(VI) complexes,[4,5] it has a long-lived and emissive excited state [lifetime 1 μs; quantum yield $5 \times 10^{-4}$; $\lambda_{max,\,em}$ 650 nm].

Under UV irradiation, complex **1** oxidizes $PPh_3$ and $Me_2SO$ to give $OPPh_3$ and $Me_2SO_2$, respectively. For the photoreaction of **1** in neat $Me_2SO$, removal of the solvent after photolysis gave an orange solid, which was recrystallized from MeOH–$Et_2O$ to give $[Os(CN)_2(Me_2SO)_2(dpphen)]\cdot 2H_2O$ **2**. Similar photoreaction with $PPh_3$ gave $[Os(CN)_2(PPh_3)_2(dpphen)]$ **3**.†

Fig. 1 shows a perspective view of **2**.‡ The structure features a rare example of $Os^{II}$–CN and $Os^{II}$–$Me_2SO$ complexes. The coordination geometry of the Os atom is slightly distorted octahedral with the cyanide ligands *cis* to each other. The Os–C bond of 2.00(1) Å is comparable to that of 2.023 Å in $[AsPh_4]_2[Os(PPh_3)_2(CN)_4]\cdot 2MeCN\cdot 2H_2O$.[6] The two $Me_2SO$ ligands are S-bonded to the Os atom. They are *trans* to each other with S–Os–S angle of 174.1(2)°. The Os–S distance of 2.293(3) Å is similar to the related distances of 2.31(2) Å in $[Os(S_7)(PMe_3)_3]$[7] and 2.261 Å in $[Ru(Me_2SO)_3Cl_3]^-$ (S-coordinated).[8] To our knowledge, no X-ray structure of an $Os^{II}$–$Me_2SO$ complex has been reported in the literature. $[Os(Me_2SO)_3Cl_3]$[9] has been proposed to be O- and S-coordinated while the structure of $[Os(bpy)_2(MeSO)_2]^{2+}$ is unknown.[3b]

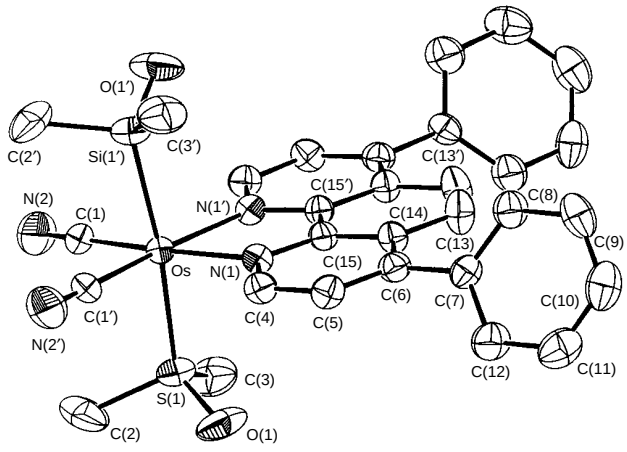



**Fig. 1** A perspective view of **2** (40% probability ellipsoids): Os–S(1) 2.293(3), Os–N(1) 2.111(8), Os–C(1) 2.00(1); S(1)–Os–S(1′) 174.1(2), S(1)–Os–C(1) 87.7(3), S(1)–Os–N(1) 91.1(2), N(1)–Os–C(1) 94.5(4), C(1)–Os–C(1′) 94.6(6)

Complexes **2** and **3** are luminescent in the solid state and in solution with emission maxima ranging from 710 to 564 nm. The spectral data are listed in Table 1. The two complexes display a strong absorption band in the UV region ($\lambda_{max}$ *ca*. 300 nm, $\varepsilon > 10^5$ dm$^3$ mol$^{-1}$ cm$^{-1}$) and a moderate intense absorption band at the visible region ($\lambda_{max}$ *ca*. 440 nm, $\varepsilon > 10^3$ dm$^3$ mol$^{-1}$ cm$^{-1}$) with a tailing at 500–600 nm, the latter is ascribed to the Os $d_\pi$–$\pi^*$ MLCT transition.[10] Both the absorption and emission spectra are strongly affected by the solvent and both the emission lifetime and quantum yield decrease as the solvent polarity decreases.

Plots of 1n $k_{nr}$ *vs*. $E_{em}$ for complexes **2** and **3** in various solvents are shown in Fig. 2. Except for the data of **2** in protic solvents, a linear correlation between 1n $k_{nr}$ and $E_{em}$ values is observed suggesting that the non-radiative decay is governed by the energy-gap law.[11] The slope of $-6.8$ eV$^{-1}$ and intercept of

**Table 1** Spectroscopic data for complexes **2** and **3**

| | Solvent (AN[a]) | $\lambda_{max,\,em}$ ($\lambda_{max,\,abs}$)[b]/nm | Lifetime/μs (quantum yield) |
|---|---|---|---|
| **2** | $C_6H_6$ (8.2) | 629 (377) | 1.12 (0.24) |
| | $C_6H_5Me$ (8.2) | 630 (375) | 1.09 (0.23) |
| | $Me_2CO$ (12.5) | 635 (369) | 0.92 (0.17) |
| | dmf (16.0) | 630 (359) | 0.95 (0.17) |
| | $C_2H_4Cl_2$ (16.7) | 616 (361) | 1.45 (0.39) |
| | $Me_2SO$ (19.3) | 630 (364) | 1.04 (0.20) |
| | MeCN (19.3) | 625 (359) | 1.10 (0.18) |
| | $CH_2Cl_2$ (20.4) | 613 (359) | 1.45 (0.34) |
| | $CHCl_3$ (23.1) | 597 (357) | 1.99 (0.49) |
| | EtOH (37.1) | 600 (344) | 1.42 (0.28) |
| | $HCONH_2$ (39.8) | 594 (341) | 1.43 (0.34) |
| | MeOH (41.3) | 595 (340) | 1.34 (0.25) |
| | MeOH–$H_2O$ | 575 (332) | 1.62 (0.04) |
| | $H_2O$ (54.8) | 564 (327) | 1.37 (0.08) |
| **3** | $C_6H_6$ (8.2) | 710 (438) | 0.33 (0.03) |
| | $Me_2CO$ (12.5) | 700 (420) | 0.42 (0.04) |
| | Py (14.2) | 681 (420) | 0.48 (0.06) |
| | dmf (16.0) | 675 (418) | 0.55 (0.09) |
| | $Me_2SO$ (19.3) | 673 (414) | 0.57 (0.08) |
| | MeCN (19.3) | 660 (409) | 1.39 (0.05) |
| | $CH_2Cl_2$ (20.4) | 672 (418) | 0.62 (0.09) |
| | $CHCl_3$ (23.1) | 595 (379) | 3.72 (0.33) |
| | EtOH (37.1) | 645 (399) | 0.79 (0.13) |
| | $HCONH_2$ (39.8) | 632 (387) | 1.09 (0.17) |
| | MeOH (41.3) | 639 (396) | 0.94 (0.11) |

[a] Gutmann's solvent acceptor number.[14b] Measurements at room temperature. [b] Spin-allowed MLCT absorption maximum.

27 agree with similar values of *ca.* −7.5 $eV^{-1}$ (slope) and 28–30 (intercept) of complexes $[OsX_4L]$ and $[OsX_2L_2]$ (X ≠ CO) in which cases the non-radiative decay is dominated by the ligand-based C–C vibrational stretch modes (*ca.* 1350 $cm^{-1}$).[12] Complex **2** shows derivation from the linear correlation in protic solvents. Presumably, a change of dominant acceptor vibration for non-radiative decay is attributed to the hydrogen-bonding interaction between the solvent and $Me_2SO$.[2c]

For both complexes, the plots of absorption and emission energy *versus* Gutmann's solvent acceptor number, AN, are shown in Fig. 3. Good linear relationship is observed in each case. The absorption and emission spectra shift to higher energy with increasing AN. This implies the donor–acceptor interaction between the solvent and the complexes. The donor–acceptor interaction results in decrease of the σ-donating ability of the cyanide ligand (and/or $Me_2SO$ ligand).

Most osmium(II) polypyridine complexes are known to be stable towards photosubstitution reaction. However, it has been noted that the $[Os(bpy)_2(Me_2SO)_2]^{2+}$ complex is photochemically unstable and this has been ascribed to its MLCT and low-lying d–d states being close in energy.[3b] Complexes **2** and **3** were found to be stable even after photolysis in acetonitrile for 2 days. Presumably, the $Os^{II}\rightarrow CN$ π-back bonding increases the d–d state energy relative to the MLCT emitting state.[13]

We acknowledge support from the University of Hong Kong, the Croucher Foundation, and the Hong Kong Research Grants Council.

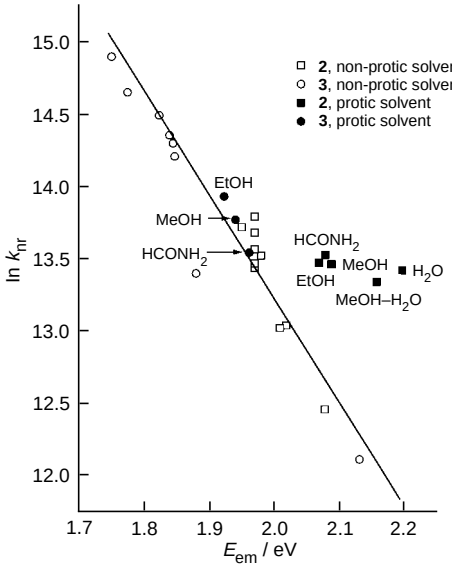



**Fig. 2** A plot of 1n $k_{nr}$ *vs.* $E_{em}$ for complexes **2** and **3**

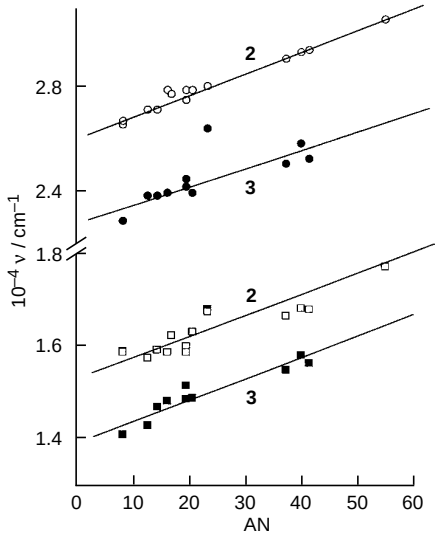



**Fig. 3** Plots of $\nu_{abs}$ (circles) and $\nu_{em}$ (squares) *vs.* Gutmann's acceptor number (AN) for complexes **2** and **3**

## Footnotes

† **2** $^1$H NMR ($CDCl_3$) δ 10.01 (d, 2 H), 8.06 (s, 2 H), 7.84 (d, 2 H), 7.67–7.59 (m, 10 H), 3.39 (s, 12 H, $OSMe_2$). UV–VIS (MeCN) $\lambda_{max}$/nm (ε $dm^3$ $mol^{-1}$ $cm^{-1}$): 269 (34 721), 287 (32 589), 359 (10 457), 405 (sh) (6498), 450 (sh) (1427). ($H_2O$): 257 (18 400), 287 (33 098), 327 (13 814), 385 (sh) (5697). **3** $^1$H NMR ($CDCl_3$) δ 8.34 (d, 2H), 8.17 (d, 2H), 7.62–7.58 (m, 4H), 7.50–7.41 (m, 18H), 7.17–7.04 (m, 18H), 6.72 (dd, 2H). UV–VIS (MeCN) $\lambda_{max}$/nm (ε/$dm^3$ $mol^{-1}$ $cm^{-1}$): 282 (36 590), 410 (7454), 440 (6445), 515 (sh) (1185).

‡ *Crystal data*: $[OsS_2O_2N_4C_{30}H_{28}\cdot 2H_2O]$, $M_r$ = 766.93, monoclinic, space group *C*2/*c* (no. 15), *a* = 19.180(5), *b* = 19.902(5), *c* = 9.471(3) Å, β = 118.18(3)°, *U* = 3186(1) Å$^3$, *Z* = 4, $D_c$ = 1.598 g $cm^{-3}$, μ = 41.69 $cm^{-1}$, *F*(000) = 1520, *T* = 301 K. An orange–brown crystal of dimensions 0.15 × 0.10 × 0.25 mm, was used for data collection on a Rigaku AFC7R diffractometer with graphite-monochromated Mo-Kα radiation (λ = 0.71073 Å). 2905 unique reflections measured, 2117 of which [with $I > 3\sigma(I)$] were considered observed. The structure was solved by the Patterson method and refined by full-matrix least-squares. Convergence for 186 variable parameters by least-squares refinement on *F* with $w = 4F_o^2/\sigma(F_o^2)$ where $\sigma^2(F_o^2) = [\sigma^2(I) + (0.014F_o^2)^2]$ for 2117 unique reflections was reached at $R$ = 0.040, $R_w$ = 0.057, G.O.F. = 1.89. The final difference Fourier map was featureless, with maximum positive and negative peaks of 1.38 and −0.81 e Å$^{-3}$ respectively. Atomic coordinates, bond lengths and angles, and thermal parameters have been deposited at the Cambridge Crystallographic Data Centre (CCDC). See Information for Authors, Issue No. 1. Any request to the CCDC for this material should quote the full literature citation and the reference number 182/370.

## References

1 V. Balzani and F. Scandola, *Supramolecular Photochemistry*, Ellis Horwood, Chichester, 1991.
2 (*a*) C. A. Bignozzi and F. Scandola, *Inorg. Chem.*, 1984, **23**, 1540; (*b*) C. A. Bignozzi, C. Chiorboli, M. T. Indelli, M. A. Rampi Scandola, G. Varani and F. Scandola, *J. Am. Chem. Soc.*, 1986, **108**, 7872; (*c*) N. Kitamura, M. Sato, H. B. Kim, R. Obata and S. Tazuke, *Inorg. Chem.*, 1988, **27**, 651.
3 (*a*) E. M. Kober, B. P. Sullivan, W. J. Dressick, J. V. Caspar and T. J. Meyer, *J. Am. Chem. Soc.*, 1980, **102**, 7383; (*b*) E. M. Kober, J. L. Marshall, W. J. Dressick, B. P. Sullivan, J. V. Caspar and T. J. Meyer, *Inorg. Chem.*, 1985, **24**, 2755; (*c*) E. M. Kober, J. V. Caspar, B. P. Sullivan and T. J. Meyer, *Inorg. Chem.*, 1988, **27**, 4587.
4 K. F. Chin, Y. K. Cheng, K. K. Cheung, C. X. Guo and C. M. Che, *J. Chem. Soc., Dalton Trans.*, 1995, 2967.
5 V. W. W. Yam and C. M. Che, *New J. Chem.*, 1989, **13**, 707; *Coord. Chem. Rev.*, 1990, **97**, 93.
6 V. W. W. Yam, PhD Thesis, The University of Hong Kong, 1988.
7 J. Gotzig, A. L. Rheingold and H. Werner, *Angew. Chem., Int. Ed. Engl.*, 1984, **23**, 814.
8 R. S. McMillan, A. Mercer, B. R. James and J. Trotter, *J. Chem. Soc., Dalton Trans.*, 1975, 1006.
9 P. G. Antonov, Y. N. Kukushkin, V. I. Konnov and B. I. Ionin, *Russ. J. Inorg. Chem. (Engl. Transl.)*, 1978, **23**, 245.
10 B. J. Pankuch, D. E. Lacky and G. A. Crosby, *J. Phys. Chem.*, 1980, **84**, 2061; D. E. Lacky, B. J. Pankuch and G. A. Crosby, *J. Phys. Chem.*, 1980, **84**, 2068.
11 J. V. Casper and T. J. Meyer, *J. Phys. Chem.*, 1983, **87**, 952.
12 E. M. Kober, J. V. Caspar, R. S. Lumpkin and T. J. Meyer, *J. Phys. Chem.*, 1986, **90**, 3722.
13 L. A. Sacksteder, J. N. Demas and B. A. DeGraff, *Inorg. Chem.*, 1989, **28**, 1787.
14 V. Gutmann, *The Donor-Acceptor to Molecular Interactions*, Plenum, New York, 1978, ch. 2.

*Received, 2nd January 1997; Com. 7/00051K*

# Investigation of the inframolecular acid–base properties of D-*myo*-inositol 1,3,4,5-tetrakisphosphate and DL-*myo*-inositol 1,2,4,5-tetrakisphosphate

**Philippe Guédat,[a] Gilbert Schlewer,[a] Elisabeth Krempp,[a] Andrew M. Riley,[b] Barry V. L. Potter[b] and Bernard Spiess[a,b]**

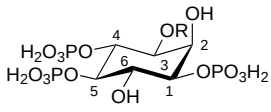
[a] *Laboratoire de Pharmacochimie Moléculaire, UPR 421 du CNRS, Faculté de Pharmacie, 74, route du Rhin, B.P. 24, 67401 Illkirch Cedex, France*

[b] *Department of Medicinal Chemistry, School of Pharmacy and Pharmacology, University of Bath, Claverton Down, Bath, UK BA2 7AY*

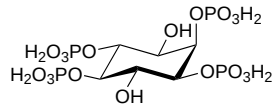
**The protonation processes of the individual phosphate groups in two regioisomeric inositol polyphosphates, D-*myo*-inositol 1,3,4,5-tetrakisphosphate and DL-*myo*-inositol 1,2,4,5-tetrakisphosphate, have been investigated by $^{31}$P NMR titration experiments; the results are compared to those from D-*myo*-inositol 1,4,5-trisphosphate.**

D-*myo*-Inositol 1,4,5-trisphosphate [Ins(1,4,5)$P_3$] **1** (Fig. 1) produced in response to stimulation of a wide variety of cellular membrane receptors, exhibits well-known second messenger properties.[1,2] Besides Ins(1,4,5)$P_3$ a host of inositol polyphosphates, among them D-*myo*-inositol 1,3,4,5-tetrakisphosphate [Ins(1,3,4,5)$P_4$] **2**, have also been characterised in the cytoplasm of many cell types. While the role of Ins(1,4,5)$P_3$ and its calcium mobilising ability is well-defined in many tissues, the physiological role of Ins(1,3,4,5)$P_4$ remains a matter of much debate and controversy. In some cases Ins(1,3,4,5)$P_4$ potentiates the Ins(1,4,5)$P_3$-induced response,[3,4] while in others it inhibits calcium signalling.[5] A main route to resolving the precise function of Ins(1,3,4,5)$P_4$ is to identify the molecular nature of its receptor[6,7] and recently a specific Ins(1,3,4,5)$P_4$ binding protein has been characterised and denoted as GAP1$^{IP4BP}$.[8] A complementary method is to focus on the ligand itself and to compare its physico-chemical properties with those of Ins(1,4,5)$P_3$. In this respect, Ins(1,2,4,5)$P_4$ **3**, a regioisomer of Ins(1,3,4,5)$P_4$ and a potent analogue of Ins(1,4,5)$P_3$,[9,10] is also worthy of consideration. A fundamental difference in the binding of both Ins(1,4,5)$P_3$ and Ins(1,3,4,5)$P_4$ to their specific or putative receptors respectively is the effect of pH. The affinity of the former for its receptor is increased by raising the pH,[11] whereas the inverse occurs for the latter.[6] A consideration of the acid–base properties of these ligands is of prime importance in gaining reliable knowledge of the binding mechanisms and we have therefore chosen for investigation two regioisomeric inositol tetrakisphosphates, differing only in the substitution position of a single phosphate group, but with strikingly different biological properties.

Herein we present the protonation constants as well as a picture of the protonation process of the individual phosphate groups for Ins(1,3,4,5)$P_4$ and Ins(1,2,4,5)$P_4$ (IP4s). The results will further be compared to the acid–base behaviour of Ins(1,4,5)$P_3$.[12,13] The study was performed in 0.2 mol dm$^{-3}$ KCl at 37 °C, a medium that mimics the ionic strength and temperature conditions encountered in the cell.




R = H, Ins(1,4,5)$P_3$ **1**
R = $PO_3H_2$, Ins(1,3,4,5)$P_4$ **2**




Ins(1,2,4,5)$P_4$ **3**

**Fig. 1** Structure of inositol polyphosphates (D-isomers are shown)

The logarithms of the stepwise protonation constants for the studied ligands ($L^{n-}$), $K_y$, referring to the equilibria $H_{y-1}L^{(n-y+1)-} + H^+ \Leftrightarrow H_yL^{(n-y)-}$ are listed in Table 1. In comparison with the constants determined for Ins(1,4,5)$P_3$,[13] an additional phosphate group raises the first protonation constant by two orders of magnitude. This is clearly the result of the increase in negative charge density on the *myo*-inositol ring phosphates that electrostatically stabilises the binding of the first proton. However, by considering the values in Table 1, it can be observed that both IP4s display nearly the same overall basicities, Ins(1,3,4,5)$P_4$ showing only a slightly more pronounced basic character over Ins(1,2,4,5)$P_4$. While a simple examination of these macroscopic protonation constants seems to indicate a similar acid–base behaviour it is therefore necessary to investigate the protonation process of the two IP4s at an 'inframolecular' level, *i.e.* at each individual phosphate group.

In a previous work[14] we showed that $^{31}$P NMR spectroscopy gives easy access to the protonated fraction $f_{i,p}$ of a phosphate group in position *i* on the inositol ring if the observed chemical shift for the resonance $\delta_i^{obs}$ depends on the electronic effects accompanying the deprotonation of this group. The value of $f_{i,p}$ can then be calculated from eqn. (1),

$$f_{i,p} = \frac{\delta_i^{obs} - \delta_{i,d}}{\delta_{i,p} - \delta_{i,d}} \quad (1)$$

where $\delta_{i,p}$ and $\delta_{i,d}$ correspond to the chemical shifts of the protonated and deprotonated fractions of the phosphates in position *i*, respectively. The previous condition can be checked by the superimposition of the $\bar{p} = f(pH)$ curves calculated from both the potentiometric and NMR data according to eqns. (2) and (3), respectively.

$$\bar{p} = \frac{C_H - [H^+] + [OH^-]}{C_L} \quad (2)$$

**Table 1** Logarithms of the stepwise protonation constants for D-Ins(1,3,4,5)$P_4$ and DL-Ins(1,2,4,5)$P_4$ in KCl 0.2 mol dm$^{-3}$ ($H_2O$) at 37 °C[a]

| log $K_y$ | Ins(1,4,5)$P_3$ | Ins(1,3,4,5)$P_4$ | Ins(1,2,4,5)$P_4$ |
|---|---|---|---|
| $y$ = 1 | 7.85 | 9.92 ± 0.02 | 9.39 ± 0.02 |
| $y$ = 2 | 6.40 | 7.66 ± 0.02 | 7.65 ± 0.02 |
| $y$ = 3 | 5.31 | 6.36 ± 0.02 | 6.06 ± 0.02 |
| $y$ = 4 | – | 5.23 ± 0.02 | 5.23 ± 0.02 |
| $N(n)$ | – | 4(221) | 2(198) |

[a] These constants were determined by potentiometry (see ref. 12) where the pH measurements are processed by the program SUPERQUAD (ref. 16). The constants are the result of $N$ experiments including a total number of $n$ observations. The standard deviations are given by SUPERQUAD. The values for Ins(1,4,5)$P_3$ were taken from ref. 13.

$$\bar{p} = \sum_{i=1}^{i=N} f_{i,\mathrm{p}} \qquad (3)$$

In these eqns., $\bar{p}$ is the mean number of protons bound per mole of IP4 and $C_H$ and $C_L$ correspond to the analytical concentrations of the acid and IP4, respectively.

For Ins(1,3,4,5)$P_4$ and Ins(1,2,4,5)$P_4$ both potentiometric and NMR $\bar{p} = f(\mathrm{pH})$ curves superimpose well from pH 2 to 8.5 (curves not shown). Above this pH a slight difference is noted indicating that $\delta_i^{obs}$ comprises, in addition to the protonation effect, another effect presumably due to conformational changes. Consequently, the $f_{i,\mathrm{p}} = f(\mathrm{pH})$ curves strictly describe $f_{i,\mathrm{p}}$ below pH 8.5 and give a good approximation of it above this pH.

The $f_{i,\mathrm{p}} = f(\mathrm{pH})$ curves for the studied IP4s are shown in Fig. 2. It can be seen that, even though the overall basicities of the IP4s are similar, the protonation fraction curves differ markedly indicating distinct protonation processes. Ins(1,2,4,5)$P_4$ exhibits almost monophasic (P1 and P2) and biphasic (P4 and P5) curves which resemble those of the corresponding bisphosphates. The general pattern of these curves attests to the independence of the two bisphosphate moieties. However, compared to Ins(1,4,5)$P_3$, the basicities of P4 and P5 appear inverted. The $f_{i,\mathrm{p}} = f(\mathrm{pH})$ curves for Ins(1,3,4,5)$P_4$ are much more complicated due to the strong interaction between phosphates P3, P4 and P5. As expected, P3 and P5 behave similarly, whereas P4, which experiences the highest density of negative charge, shows a very peculiar protonation process already observed for P5 in Ins(4,5,6)$P_3$.[15] The monophasic appearance retained by the P1 curve attests to the independence of this phosphate group. Consideration of the protonation fraction curves allows a detailed investigation of the protonation state of each individual phosphate group at any pH. Thus, at a near physiological pH (7.50), for Ins(1,3,4,5)$P_4$ and Ins(1,2,4,5)$P_4$ the percentage of protonated phosphates are P1 (5%), P3 (50%), P4 (60%), P5 (60%) and P1 (60%), P2 (15%), P4 (70%), P5 (35%), respectively. Large differences can be observed, especially in the basicity of P1 and P5 which are common to both IP4s. The observation that P5 is much more basic for Ins(1,3,4,5)$P_4$ than Ins(1,2,4,5)$P_4$ may be of biological significance. Indeed, it has been suggested that the increase in affinity of Ins(1,4,5)$P_3$ for its receptor when the pH rises may be caused by the ionization of the P5 phosphate group.[12] Therefore, binding of Ins(1,2,4,5)$P_4$ to the Ins(1,4,5)$P_3$ receptor could also be favoured by a low protonation state of the P5 phosphate at physiological pH. In constrast to Ins(1,4,5)$P_3$, for Ins(1,3,4,5)$P_4$, specific binding decreases steadily from pH 5.5 to 9.0. Moreover, these specific binding data *vs*. pH could be roughly superimposed on the P3 and P5 NMR titration curves (*e.g*. at pH 7.5, $f_{5,\mathrm{p}}$ *ca*. 60% and specific binding *ca*. 65%).[6] It is therefore likely that, if the protonation state of Ins(1,3,4,5)$P_4$ is involved in its binding to a specific protein, the observed high basicity of P5 will undoubtedly advantage such a binding. The results described herein which demonstrate the acid–base requirements needed for the observation of either an Ins(1,2,4,5)$P_4$ type or an Ins(1,3,4,5)$P_4$ type of biological activity may be of great help to chemists who aim at the synthesis of potent analogues. Further studies on the influence of the ionic environment of the IP4s on their acid–base and conformational properties are in progress and will be reported in due course.

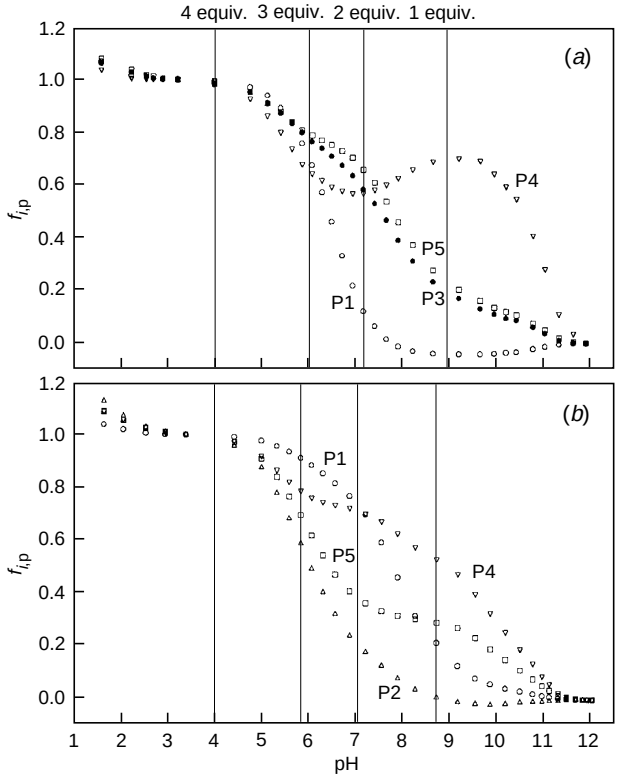



**Fig. 2** Protonation fraction curves $f_{i,\mathrm{p}}$ as a function of pH in KCl 0.2 mol $dm^{-3}$ (99.9% $D_2O$) at 37 °C for D-Ins(1,3,4,5)$P_4$ (*a*) and DL-Ins(1,2,4,5)$P_4$ (*b*). The vertical lines correspond to the theoretical addition of 1–4 equiv. of protons. These curves were calculated according to eqn. (1) from $^{31}P$ NMR titrations carried out at 121.497 MHz on a Bruker 300 DPX FT spectrometer. Chemical shifts were measured relative to an external 85% orthophosphoric reference. Resonance peaks of D-Ins(1,3,4,5)$P_4$ and DL-Ins(1,2,4,5)$P_4$ were assigned by performing proton phosphorus 2D correlation experiments at pH 1.62, 2.25, 7.92, 12.00 and 1.65, 5.93, 7.90, 11.65, respectively. The assignment of the proton resonances was done on the basis of the chemical shifts and the coupling patterns confirmed by $^1H$–$^1H$ COSY experiments. The titrations were performed as previously indicated[14] but on a volume of 0.45 ml instead of 2 ml. Ins(1,2,4,5)$P_4$ was prepared as described in ref. 9 and the synthesis of Ins(1,3,4,5)$P_4$ will be published elsewhere.

## References


1 M. J. Berridge, *Nature*, 1993, **361**, 315.
2 M. J. Berridge, *Ann. N. Y. Acad. Sci*., 1996, 31.
3 L. B. Zhang, M. E. Bradley and I. L. O. Buxton, *Int. J. Biochem. Cell Biol*., 1995, **27**, 1231.
4 J. W. Loomishusselbee, P. J. Cullen, U. E. Dreikhausen, R. F. Irvine and A. P. Dawson, *Biochem. J*., 1996, **314**, 811.
5 G. S. J. Bird and J. W. Putney, *J. Biol. Chem*., 1996, **271**, 6766.
6 P. J. Cullen, S. K. Chung, Y. T. Chang, A. P. Dawson and R. F. Irvine, *FEBS Lett*., 1995, **358**, 240.
7 B. Huisamen and A. Lochner, *Mol. Cell. Biochem*., 1996, **157**, 229.
8 P. J. Cullen, J. J. Hsuan, O. Truong, A. J. Letcher, T. R. Jackson, A. P. Dawson and R. F. Irvine, *Nature*, 1995, **376**, 527.
9 M. Hirata, N. Narumoto, Y. Watanabe, T. Kanematsu, T. Koga and S. Ozaki, *Mol. Pharmacol*., 1994, **45**, 271.
10 R. A. Wilcox, S. T. Safrany, D. Lampe, S. J. Mills, S. R. Nahorski and B. V. L. Potter, *Eur. J. Biochem*., 1994, **223**, 115.
11 P. F. Worley, J. M. Baraban, S. Supattapone, V. S. Wilson and S. H. Snyder, *J. Biol. Chem*., 1987, **262**, 12 132.
12 L. Schmitt, P. Bortmann, G. Schlewer and B. Spiess, *J. Chem. Soc., Perkin Trans. 2*, 1993, 2257.
13 L. Schmitt, G. Schlewer and B. Spiess, *Biochim. Biophys. Acta*, 1991, **1075**, 139.
14 K. Mernissi Arifi, L. Schmitt, G. Schlewer and B. Spiess, *Anal. Chem*., 1995, **67**, 2567.
15 L. Schmitt, B. Spiess and G. Schlewer, *Bioorg. Med. Chem. Lett*., 1995, **5**, 1225.
16 P. Gans, A. Sabatini and A. Vacca, *J. Chem. Soc., Dalton Trans*., 1985, 1195.


*Received, 12th December 1996; Com. 6/08347A*

# Synthesis and characterisation of the potassium 1,1-dithiolate $C_{12}H_{20}N_2S_2K_2$: a novel $K_{12}S_{12}$ cluster compound

**Norbert Kuhn,*[a] Gerd Weyers[a] and Gerald Henkel[b]**

[a] *Institut für Anorganische Chemie der Universität Tübingen, Auf der Morgenstelle 18, D-72076 Tübingen, Germany*
[b] *Fachbereich 6 (Chemie) der Universität-GH Duisburg, Lotharstr. 1, D-47048 Duisburg, Germany*

**The carbene adduct 1 reacts with potassium to give the potassium 1,1-dithiolate 2; its tetrahydrofuran adduct exhibits a cage structure consisting of a hexagonal $K_6S_6$ prism incorporated into a twelve-membered $K_6S_6$ ring connected both by direct K–S bonds and vinylidene type bridges.**

Organoalkali-metal compounds are generally made up of ring- and ladder-type fragments.[1] Although a limited number of one- and multi-dimensional ladder structures have been identified for potassium thiolates,[2] compounds of this class containing ring fragments were previously unknown.

By reduction of the carbene adduct **1**[3] with potassium in tetrahydrofuran we have now obtained† the potassium 1,1-dithiolate **2** as a yellow air-sensitive solid. A single-crystal X-ray structural analysis‡ of the solvate complex $\mathbf{2}\cdot 2C_4H_8O\cdot 1/3K_2S_2$ revealed the presence of a hexagonal prism with the composition $K_6S_6$ as the central unit surrounded by a twelve-membered $K_6S_6$ ring consisting of alternating potassium and sulfur atoms (Fig. 1). Hexagonal prisms have frequently been observed in $Li_6X_6$ compounds (X = C, N, O, Si, Te)[1] but for potassium they have to date only been realised in a single structure with a $K_6O_6$ core.[4] Previously, hexagonal prisms of the $M_6S_6$ type were only known in the chemistry of the transition metals.[5] Of the two sulfur atoms of each dithiolate ligand, one is part of the twelve-membered ring while the second sulfur atom is incorporated into the hexagonal prism. Therefore, the rings and the prisms are connected both through vinylidene bridges and direct K–S bonds. The observed potassium–sulfur contacts (3.023–3.308 Å) are in the expected range. In the hexagonal prism, alternating K–S bond lengths are observed [K(1)–S(1a) 3.023(3), K(1)–S(1b) 3.192(3) Å] for the six-membered rings. Their mean value corresponds well both to the distance of the two six-membered rings in the prism [K(1)–S(1) 3.107(4) Å] as well as to the K–S bond lengths of the surrounding $K_6S_6$ ring [K(2)–S(2) 3.115(3), K(2)–S(2b) 3.098(3) Å]. The longest K–S distance is observed for the connection of the $K_6S_6$ ring and prismatic fragments [K(2)–S(1) 3.308(5) Å]. In comparison to the metal structure,[6] the metal–metal separations are, in part, shortened by up to 0.75 Å and for K(1)–K(2) (3.937 Å) reach the calculated and observed bond lengths for $K_2$.[7] Even under the aspects of electrostatic K–S interactions,[8] however, such a close approach is not unusual.[9]

A comparison of the 1,1-dithiolate fragment in **2** (Fig. 2) with the structure of the carbene adduct **3**[3] reveals a markedly changed distribution of the π electrons; the coplanar orientation of the $CS_2$ fragment in **2** to the five-membered ring, the significant shortening of the C(1)–C(2) bond [1.375(13) Å] by about 0.12 Å in comparison to that of **3**, and the lengthening of the C–S bonds [C(12)–S(1) 1.803(8) Å, C(12)–S(2) 1.764(11) Å] by the same order of magnitude are all indications of the presence of an exocyclic C–C double bond in **2**. This is further substantiated by the relative widening of the angle N(1)–C(1)–

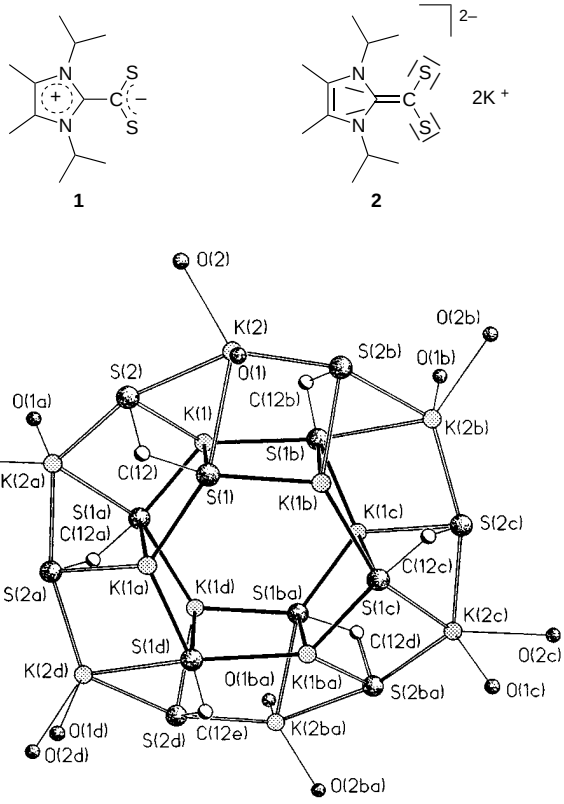



**Fig. 1** The $K_{12}S_{12}O_{12}$ core in crystals of $\mathbf{2}\cdot 2C_4H_8O\cdot 1/3K_2S_2$. Selected bond lengths (Å): K(1)···K(2) 3.937(4), K(1)···K(1a) 4.105(4), K(1)···K(1b) 4.105(4), K(1)···K(2a) 4.212(4), K(1)–S(1) 3.107(4), K(1)–S(2) 3.193(4) K(1)–S(1a) 3.023(3), K(1)–S(1b) 3.192(3), K(2)–S(1) 3.308(5), K(2)–S(2) 3.115(3), K(2)–K(2b) 3.098(3), K(2)–O(1) 2.782(13), K(2)–O(2) 2.810(13).

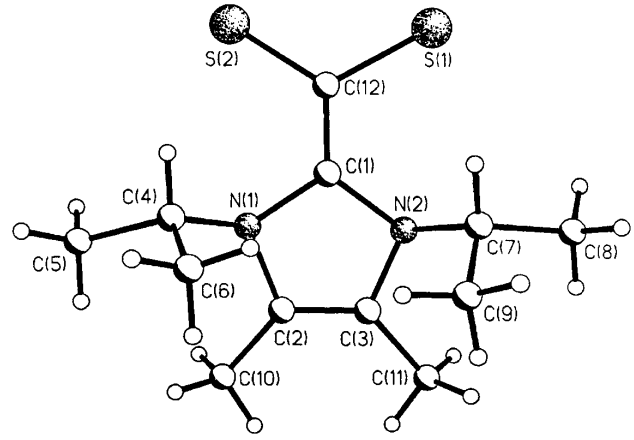
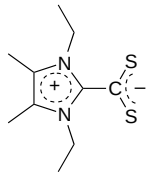
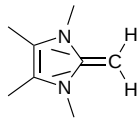



**Fig. 2** The structure of the 1,1-dithiolate anion in crystals of $\mathbf{2}\cdot 2C_4H_8O\cdot 1/3K_2S_2$. Selected bond lengths (Å) and angles (°): C(1)–C(12) 1.375(13), C(12)–S(1) 1.803(8), C(12)–S(2) 1.764(11), C(1)–N(1) 1.455(10), N(1)–C(2) 1.454(15), C(2)–C(3) 1.310(16), C(3)–N(2) 1.428(11), N(2)–C(1) 1.428(15); S(1)–C(12)–S(2) 117.6(5), S(1)–C(12)–C(1) 118.0(8), S(2)–C(12)–C(1) 124.4(7).



**3**



**4**

N(2) [109.3(7)°] and, above all, by the marked contraction by around 12° of the angle S(1)–C(12)–S(2) [117.6(5)°]. The ethylene structure causes a strong steric interaction between the isopropyl substituents and the sulfur atoms which results in a pronounced protrusion of the carbon atoms C(4) and C(7) by 1.112 and 1.023 Å, respectively, out of the plane defined by the five-membered ring. As a consequence from steric hindrance, the methyl protons of the isopropyl substituents appear as two broad signals in the NMR spectrum. We consider this reorientation of the $CS_2$ fragment upon reduction of the carbene adduct (in **3** the planes of the ring and the $CS_2$ fragment are perpendicular to each other) to be in a causal relationship with the quasireversibility that can be recognized in cyclovoltammetric studies.[10] It certainly proceeds in concert with the electron transfer and increases the activation barrier. The close analogy to the structure of the methyleneimidazoline **4**,[11] which reacts similarly to an ylide, excludes the take-up of π-electron density by the five-membered ring as is typical for conventional 1,1-dithiolates and makes the electronic argument for the bending of the isopropyl groups ($sp^3$ hybridisation of the nitrogen atoms) less favourable.

The geometry of **2** is indicative of a bonding situation that can be intepreted with regard to the electron distribution as an '*umpolung*' in comparison to conventional 1,1-dithiolates. We will report elsewhere on the results of cyclic voltammetry and the chemical properties of **2** which all support this hypothesis.

## Footnotes

† All reactions were performed under anaerobic and anhydrous conditions; **1** was prepared by a published procedure.[3]

To a suspension of 1.026 g (4 mmol) **1** in 30 ml tetrahydrofuran 0.20 g (5.12 mmol) potassium were added. The mixture was stirred for 16 h at room temperature. After separation of excess potassium and reducing to a small volume *in vacuo*, 30 ml diethyl ether were added. The resulting yellow solid was filtered off and washed three times with 20 ml of diethyl ether to give 1.562 g (81%) $C_{20}H_{40}K_2N_2O_2S_2$ (**2**·2$Et_2O$), identified by potassium and sulfur analysis. $^1H$ NMR (250 MHz, [$^2H_8$]tetrahydrofuran, $SiMe_4$ ext.): δ 4.74 [m, 2 H, C*H*$(CH_3)_2$], 1.72 [s, 6 H, 4,5-$CH_3$], 1.24, 1.05 [2 br s, 12 H, CH(C*H*$_3)_2$]; in addition, signals at δ 3.38 (q) and 1.10 (t) are observed arising from 2 equiv. of $Et_2O$. The compound decomposes readily in polar solvents like acetone and acetonitrile. At *ca.* 90 °C, potassium sulfides and unidentified organic compounds are formed. Crystals of **2**·2$C_4H_8O$·1/3 $K_2S_2$ have been obtained by slow evaporation of a tetrahydrofuran solution of **2**·2$Et_2O$.

‡ *Crystal data* for $C_{20}H_{36}K_{2.667}N_2O_2S_{2.667}$ (**2**·2$C_4H_8O$·1/3$K_2S_2$), $M$ = 526.27, trigonal, space group $P\bar{3}$, $a$ = 19.145(8), $c$ = 13.753(6) Å, $U$ = 4365.55 Å$^3$, $Z$ = 6, $D_c$ = 1.201 g cm$^{-3}$, μ(Mo-Kα) = 0.63 mm$^{-1}$, Siemens P4RA four-circle diffractometer, rotating anode generator, Mo-Kα radiation (λ = 0.710 73 Å), graphite monochromator, scintillation counter, $T$ = 150 K, empirical absorption corrections; direct methods, full matrix least-squares refinements, non-hydrogen atoms anisotropic, H atoms at idealized positions, one common isotropic temperature factor for H within each residue, one extinction parameter, one scaling factor; transmission range 0.714–0.516, $2\theta_{max}$ = 48°, ω scan, crystal dimensions *ca.* 0.75 × 0.65 × 0.21 mm, 3556 unique reflections, $R(R_w)$ = 0.0884 (0.0857) for 2358 reflections with $I > 2\sigma(I)$, 287 variables. The atomic displacement parameters indicate a possible disorder of the $C_4H_8O$ molecules which could not be resolved in terms of a physically meaningful superposition. Atomic coordinates, bond lengths and angles, and thermal parameters have been deposited at the Cambridge Crystallograpic Data Centre (CCDC). See Information for Authors, Issue No. 1. Any request to the CCDC for this material should quote the full literature citation and the reference number 182/383.

## References


1 D. S. Wright and M. A. Beswick, *Comprehensive Organometallic Chemistry II*, ed. E. W. Abel, F. G. A. Stone, G. Wilkinson and C. E. Housecroft, Pergamon Elsevier, Oxford, 1995, vol. 1; A.-M. Sapse and P. von R. Schleyer, *Lithium Chemistry*, Wiley, New York, 1995; K. Gregory, P. von R. Schleyer and R. Snaith, *Adv. Inorg. Chem.*, 1994, **37**, 47; E. Weiss, *Angew. Chem., Int. Ed. Engl.*, 1993, **32**, 1501; R. E. Mulvey, *Chem. Soc. Rev.*, 1991, **20**, 167; M. Veith, *Chem. Rev.*, 1990, **90**, 3.

2 S. Brooker, F. T. Edelmann, T. Kottke, H. W. Roesky, G. M. Sheldrick, D. Stalke and K. H. Whitmire, *J. Chem. Soc., Chem. Commun.*, 1991, 144; K. Ruhlandt-Senge and U. Englich, *Chem. Commun.*, 1996, 147.

3 N. Kuhn, H. Bohnen and G. Henkel, *Z. Naturforsch., Teil B*, 1994, **49**, 1473.

4 P. G. Willard and G. B. Carpenter, *J. Am. Chem. Soc.*, 1986, **108**, 462.

5 J. K. Stalick, A. R. Siedle, A. D. Mighell and C. R. Hubbard, *J. Am. Chem. Soc.*, 1979, **101**, 2903; M. G. Kanatzidis, W. R. Hagen, W. R. Dunham, R. K. Lester and D. Coucouvanis, *J. Am. Chem. Soc.*, 1985, **107**, 953; K. Tatsumi, Y. Inoue, H. Kawaguchi, M. Kohsaka, A. Kakamura, R. E. Cramer, W. VanDoorne, G. J. Taogoshi and P. N. Richmann, *Organometallics*, 1993, **12**, 352.

6 A. F. Wells, *Structural Inorganic Chemistry*, Oxford Science Publication, 5th edn., 1984.

7 J. Heinze, U. Schühle, F. Engelke and C. D. Caldwell, *J. Chem. Phys.*, 1987, **87**, 45; E. Ilyabaev and U. Kaldor, *J. Chem. Phys.*, 1993, **98**, 7126; G. Jong, L. Li, T.-J. Whang, W. C. Stwalley, J. A. Coxon, M. Li and A. M. Lyyra, *J. Mol. Spectrosc.*, 1992, **155**, 115.

8 C. Lambert and P. von R. Schleyer, *Angew. Chem., Int. Ed. Engl.*, 1994, **33**, 1129.

9 The shortest K–K distance (3.22 Å) has been detected in $K_2O$: E. Zintl, A. Harder and B. Dauth, *Z. Elektrochem.*, 1934, **40**, 588.

10 B. Speiser, personal communication.

11 N. Kuhn, H. Bohnen, J. Kreutzberg, D. Bläser and R. Boese, *J. Chem. Soc., Chem. Commun.*, 1993, 1136.



*Received, 18th November 1996; Com. 6/07828A*

# Methods for attaching metal-capped sp carbon chains to metal clusters: synthesis, structure and reactivity of rhenium–triosmium carbon complexes $[(\eta^5\text{-}C_5Me_5)Re(NO)(PPh_3)(CC)_nOs_3(CO)_{10}H]$

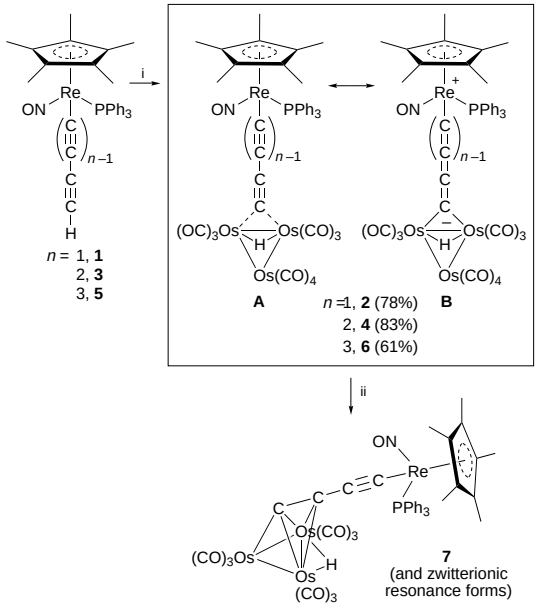
**Stephen B. Falloon, Atta M. Arif and J. A. Gladysz***

*Department of Chemistry, University of Utah, Salt Lake City, Utah 84112, USA*

**Reactions of $[(\eta^5\text{-}C_5Me_5)Re(NO)(PPh_3)\{(C{\equiv}C)_nH\}]$ and $[Os_3(CO)_{10}(NCMe)_2]$ give the title $Re(CC)_nOs_3$ complexes ($n$ = 1–3, 83–61%); a crystal structure ($n$ = 1), and IR and NMR properties, indicate contributions by neutral Re–$(C{\equiv}C)_n$–$(Os_3)$ and zwitterionic $^+Re{=}(C{=}C)_n{=}(Os_3)^-$ resonance forms.**

There has been much recent interest in unsupported sp carbon chains that span two transition metals.[1–4] These wire-like assemblies offer intriguing possibilities for molecular-level devices.[5] To date, nearly all such compounds feature monometallic endgroups. However, polymetallic endgroups might confer special attributes, including enhanced electronic coupling or communication between the termini, or greater capacitance in the case of good electron reservoirs. Indeed, two-dimensional superlattices of alkynyl- and aryl-linked metal clusters are under active pursuit in other laboratories, with the ultimate aim of nanoelectronic digital circuits.[6]

We were attracted by the architectural versatility of trimetallic clusters, which allow three $\eta^1$ modes of carbon chain attachment: (*i*) a $\mu_1$ link to one metal; (*ii*) an edge-bridging $\mu_2$ link to two metals; (*iii*) a face-bridging $\mu_3$ link to three metals. In the second and third modes, the ligating carbon does not necessarily remain sp hybridized. It should also be emphasized that there is extensive literature on metal cluster carbide complexes,[7] some of which provide models for surface-bound intermediates in heterogeneously catalysed commodity chemical processes. However, only a few contain sp carbon segments that span otherwise unconnected polymetallic termini.[3d,8–10]




**Scheme 1** Syntheses of $Re(CC)_nOs_3$ complexes. *Reagents and conditions*: i, $Os_3(CO)_{10}(NCMe)_2$, $CH_2Cl_2$, 20 °C; ii, $n$ = 2, hexane, reflux.

As shown in Scheme 1, the chiral, racemic rhenium ethynyl complex **1**[11] and triosmium complex $[Os_3(CO)_{10}(NCMe)_2]$ were reacted in $CH_2Cl_2$ at room temperature. After 3 h, chromatography gave an orange, air-stable product **2** (78%). The labelled complex $[^{13}C_2]$**2** was similarly prepared.† Spectroscopic data suggested the composition $[(\eta^5\text{-}C_5Me_5)Re(NO)(PPh_3)(CC)Os_3(CO)_{10}H]$. In particular, a diagnostic hydride ligand $^1H$ NMR signal (δ −16.7), and ten terminal CO $^{13}C$ NMR signals (δ 184–171), were observed. However, the ReC $^{13}C$ signal was between those of **1** and the cationic vinylidene complex[12] $[(\eta^5\text{-}C_5Me_5)Re(NO)(PPh_3)(=C{=}CH_2)]BF_4$ [δ 245.4 *vs.* 98.0 and 330.4, $J_{CP}$ 8.8 *vs.* 15.8 and 9.5 Hz ($CH_2Cl_2$, $C_6D_6$, $CH_2Cl_2$]; Re*C*C at δ 124.2 *vs.* 116.0 and 116.1). The IR $\nu_{NO}$ value showed a similar relationship (1667 *vs.* 1637–1629 and 1728–1711 $cm^{-1}$).

Many reactions of terminal alkynes and triosmium complexes $[Os_3(CO)_{10}L(L')]$ (L/L′ = CO or NCMe) have been reported.[13] However, to our knowledge no adducts analogous to **2** have previously been isolated. Thus, a crystal structure was determined.‡ The molecular structure, and key metrical parameters, are given in Fig. 1. The hydride and ReCC terminus symmetrically bridge the same two osmiums, with the $Os_3$ and $ReOs_2$ planes roughly orthogonal (105°). The rhenium–carbon bond [1.964(9) Å] is shorter than in complexes of formula $[(\eta^5\text{-}C_5Me_5)Re(NO)(PPh_3)(C{\equiv}CX)]$ [2.079(9), 2.037(5), 2.032(7) Å],[2a,c,d] but longer than in analogous cationic species with $Re{=}C(=C)_n$ linkages [1.909(7), 1.91(1), 1.916(7) Å].[2d,4a] Also, the carbon–carbon bond is longer than those in disubstituted organic alkynes and alkynyl complexes [1.252(12) Å *vs.* mean values of 1.192(12) and 1.210(13) Å].[14]

To help clarify these bonding issues, the IR spectra of **2** and $[^{13}C_2]$ **2** were compared. A 1705 $cm^{-1}$ band shifted to 1632 $cm^{-1}$ (calc for $\nu_{^{13}C^{13}C}$, 1637 $cm^{-1}$). Other absorptions in the 2100–1600 $cm^{-1}$ region were unaffected. These $\nu_{CC}$ values confirm that the $C_2$ bridge has appreciable double bond character. Hence, **2** is best described as a hybrid of the neutral and zwitterionic resonance forms **A** and **B** in Scheme 1. Also,

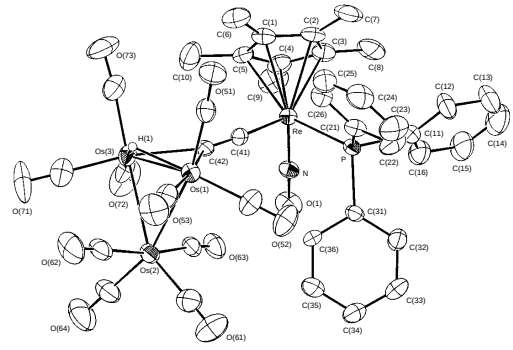


**Fig. 1** Molecular structure of **2**·0.5$C_6H_{14}$. Selected bond distances (Å) and angles (°): Re–P 2.395(2), Re–N 1.757(7), Re–C(41) 1.965(9), Os(1)–Os(3) 2.7933(7), Os(1)–H(1) 1.79(9), Os(3)–H(1) 1.82(9), Os(1)–C(42) 2.150(9), Os(3)–C(42) 2.164(9), C(41)–C(42) 1.252(12); N–Re–P 90.5(2), N–Re–C(41) 97.5(3), C(41)–Re–P 94.4(2), C(42)–C(41)–Re 174.2(7), C(42)–C(41)–Os(1) 139.3(7), C(42)–C(41)–Os(3) 140.0(7).

the P–Re–C(41) and C(42)–Os(1)–Os(3) units were nearly coplanar [angle 14.5(5)°], consistent with a frontier-orbital-derived conformational minimum as commonly observed for $^{+}$Re=C adducts such as **B**.[2d]

The extension of this simple procedure to higher carbon chains was investigated (Scheme 1). A similar reaction of the butadiynyl complex **3**[2a] and $[Os_3(CO)_{10}(NCMe)_2]$ gave the $ReC_4Os_3$ species **4** (83%) as a red–orange powder.† A low-temperature reaction of the hexatriynyl complex **5**[2b] afforded the corresponding $ReC_6Os_3$ species **6** (62%) as a thermally labile red–brown powder. However, the analogous octatetraynyl complex[2b] gave a multitude of products. Mass spectra of **4** and **6** showed intense molecular ions, and many NMR and IR properties were close to those of **2** (NMR: OsH δ −13.10, −15.90; ReC δ 242.9, 204.9; $PPh_3$ δ 21.6, 22.3 *vs.* 21.0; IR $\nu_{NO}$ 1662, 1663 $cm^{-1}$). Low-temperature $^{13}C$ NMR spectra were complicated by decoalescence phenomena, and practical routes to labelled $^{13}C_4$ or $^{13}C_6$ derivatives are unavailable. Thus, most $C_x$ NMR signals could only be provisionally assigned.

The stabilities of **2**, **4** and **6** decreased with increasing chain length. We sought to probe the nature of these decomposition pathways. When **4** was refluxed in hexane, CO was evolved. Work-up gave the nonacarbonyl complex $[(\eta^5\text{-}C_5Me_5)Re(NO)(PPh_3)(CCCC)Os_3(CO)_9(H)]$ **7** in 57% yield. Although material suitable for a crystal structure could not be obtained, the formulation was supported by microanalysis, mass spectrometry, NMR [(OsH δ δ22.34; ReC 242.9 (d, $J_{CP}$ 11.5 Hz)] and IR ($\nu_{NO}$ 1663 $cm^{-1}$).† A structure consistent with these data is given in Scheme 1. Analogous adducts of $Os_3(CO)_9H$ and other CCR ligands (R = H, $Me_3$, *etc.*) have been previously characterized.[13,15] All exhibit OsH NMR signals near δ −23, and IR $\nu_{CO}$ band patterns similar to **7**.

Additional properties of **2**, **4**, and **6** were compared. UV–VIS spectra showed progressive red shifts of the longest wavelength band [λ/nm, hexane (ε/$dm^3$ $mol^{-1}$ $cm^{-1}$): **2**, 316 (20 000), 350 (21 000), 384 (18 000); **4**, 296 (20 000), 388 (7500), 500 (4900); **6**, 306 (18 000), 516 (3600)]. No absorptions were significantly solvatochromic (hexane, $CH_2Cl_2$, acetonitrile). Cyclic voltammograms ($CH_2Cl_2$–$NBu_4BF_4$, 100 mV $s^{-1}$) showed partially reversible oxidations with $E°$ values of 0.78, 0.43, and 0.44 V, respectively (ferrocene standard, $E°' = 0.46$ V). These have no counterparts in triosmium complexes $[Os_3(CO)_{10}L_2]$, and are much less favourable thermodynamically than oxidations of $[(\eta^5\text{-}C_5Me_5)Re(NO)(PPh_3)(C{\equiv}CX)]$ complexes.[2] This may be due to the zwitterionic character.

While this work was in progress, the reaction of the tungsten butadiynyl complex $[(\eta^5\text{-}C_5H_5)W(CO)_3(C{\equiv}CC{\equiv}CH)]$ and triruthenium complex $[Ru_3(CO)_{10}(NCMe)_2]$ was briefly described.[16] In contrast to Scheme 1, a π adduct of the C≡CH moiety formed. This rearranged in refluxing benzene to a $[WC_4Ru_3(CO)_9H]$ complex analogous to **7**. Tungsten alkynyl complexes $[(\eta^5\text{-}C_5R_5)W(CO)_3(C{\equiv}CR')]$ and $[Os_3(CO)_{10}(NCMe)_2]$ react in refluxing toluene to give tetranuclear products of formula $(\eta^5\text{-}C_5R_5)WOs_3(CO)_{11}(C{\equiv}CR')$].[17]

We have demonstrated that sp carbon chains with $Os_3(CO)_{10}$ endgroups are easily constructed. However, the $\eta^1,\mu_2$ assemblies are labile. From some standpoints this is desirable, as other architecturally interesting carbon complexes can be readily accessed. However, from the perspective of long-lived molecular devices, this is undesirable. Hence, future efforts would be best directed at trimetallic systems with less dissociable spectator ligands, a more restricted set of binding modes, and higher kinetic barriers. Regardless, the new $Re(CC)_nOs_3$ complexes described above have numerous interesting properties, and further investigations are ongoing.

We thank the Department of Energy for support of this research.

## Footnotes

† All new complexes were characterized by IR and NMR ($^1H$, $^{13}C$, $^{31}P$) spectroscopy, as summarized (with crystallographic data) in supplementary material provided to the reviewers and available from the author. Solid samples showed a marked tendency to retain hexane, even after vacuum drying. Correct microanalyses could be obtained for solvates of **2**, **6** and **7**. *Representative data*: IR ($cm^{-1}$, hexane) 2091m, 2054s, 2039m, 2005vs, 1981m, (sh) 1969m, 1705m, 1667m. NMR (δ, $CD_2Cl_2$): $^1H$ 7.99, 7.40, 7.26 (m, 3 Ph), 1.74 (s, $C_5Me_5$), −16.70 (s, OsH); $^{13}C\{^1H\}$ {for [$^{13}C_2$] **2**} 245.4 (dd, $J_{CP}$ 8.8, $J_{CC}$ 64.5 Hz ReC), 183.9, 183.8, 182.8, 181.9, 179.4, 178.4, 175.3, 172.8, 172.4, 170.7 (s, 10 CO), 135.6 (br d, *o*-Ph), 132.1 (br d, *ipso*-Ph), 129.3 (s, *p*-Ph), 128.5 (br d, *m*-Ph), 124.2 (d, $J_{CC}$ 64.5 Hz, ReCC), 104.8 [s, $C_5(CH_3)_5$], 10.2 [s, $C_5(CH_3)_5$]; $^{31}P\{^1H\}$ 21.0s.

‡ Atomic coordinates, bond lengths and angles, and thermal parameters have been deposited at the Cambridge Crystallographic Data Centre (CCDC). See Information for Authors, Issue No. 1. Any request to the CCDC for this material should quote the full literature citation and the reference number 182/373.

## References


1 General reviews or perspectives: W. Beck, B. Niemer and M. Wieser, *Angew. Chem., Int. Ed. Engl.*, 1993, **32**, 923; H. Lang, *Angew. Chem., Int. Ed. Engl.*, 1994, **33**, 547; U. Bunz, *Angew. Chem., Int. Ed. Engl.*, 1996, **35**, 969.

2 (*a*) W. Weng, T. Bartik, M. Brady, B. Bartik, J. A. Ramsden, A. M. Arif and J. A. Gladysz, *J. Am. Chem. Soc.*, 1995, **117**, 11 922; (*b*) T. Bartik, B. Bartik, M. Brady, R. Dembinski and J. A. Gladysz, *Angew. Chem., Int. Ed. Engl.*, 1996, **35**, 414, and references therein; (*c*) B. Bartik, R. Dembinski, T. Bartik, A. M. Arif and J. A. Gladysz, *New J. Chem.*, 1996, in the press; (*d*) M. Brady, W. Weng, Y. Zhou, J. W. Seyler, A. J. Amoroso, A. M. Arif, M. Böhme, G. Frenking and J. A. Gladysz, *J. Am. Chem. Soc.*, 1997, **119**, 775.

3 (*a*) N. Le Narvor, L. Toupet and C. Lapinte, *J. Am. Chem. Soc.*, 1995, **117**, 7129; (*b*) F. Coat and C. Lapinte, *Organometallics*, 1996, **15**, 477; (*c*) M. I. Bruce, L. I. Densiovich, P. J. Low, S. M. Peregudova and N. A. Ustynyuk, *Mendeleev Commun.*, 1996, 200; (*d*) M. I. Bruce, M. Ke and P. J. Low, *Chem. Commun.*, 1996, 2405.

4 (*a*) W. Weng, A. M. Arif and J. A. Gladysz, *Angew. Chem., Int. Ed. Engl.*, 1993, **32**, 891; (*b*) W. Weng, T. Bartik and J. A. Gladysz, *Angew. Chem., Int. Ed. Engl.*, 1994, **33**, 2119 and references therein.

5 M. D. Ward, *Chem. Soc. Rev.*, 1995, 121; *Chem. Ind.*, 1996, 568; V. Grosshenny, A. Harriman, M. Hissler and R. Ziessel, *Platinum Met. Rev.*, 1996, **40**, 26; 72.

6 R. P. Andres, J. D. Bielefeld, J. I. Henderson, D. B. Janes, V. R. Kolagunta, C. P. Kubiak, W. J. Mahoney and R. G. Osifchin, *Science*, 1996, **273**, 1690.

7 J. S. Bradley, *Adv. Organomet. Chem.*, 1983, **22**, 1; (*b*) Review of $C_2$ complexes: M. Akita and Y. Moro-oka, *Bull. Chem. Soc. Jpn.*, 1995, **68**, 420.

8 Tricobalt clusters $Co_3(CO)_9$ have been joined by $\eta^1,\mu_3$ carbon chains. For leading references, see G. H. Worth, B. H. Robinson and J. Simpson, *Organometallics*, 1992, **11**, 3863; D. Osella, O. Gambino, C. Nevi, M. Ravera and D. Bertolino, *Inorg. Chim. Acta*, 1993, **206**, 155.

9 Dicobalt clusters $Co_2(CO)_6$ have been joined by $\eta^2,\mu_2$ linkages to a cyclic carbon chain. See: F. Diederich, Y. Rubin, O. L. Chapman and N. S. Goroff, *Helv. Chim. Acta*, 1994, **77**, 1441.

10 For topologically related complexes in which metal clusters are joined by non-sp hybridized $C_x$ moieties, see C. J. Adams, M. I. Bruce, E. Horn, B. W. Skelton, E. R. T. Tiekink and A.H. White, *J. Chem. Soc., Dalton Trans.*, 1993, 3299; 3313; D. M. Norton, C. L. Stern and D. F. Shriver, *Inorg. Chem.*, 1994, **33**, 2701.

11 J. A. Ramsden, W. Weng and J. A. Gladysz, *Organometallics*, 1992, **11**, 3635.

12 W. Weng, T. Bartik, M. T. Johnson, A. M. Arif and J. A. Gladysz, *Organometallics* 1995, **14,** 889.

13 A. K. Smith, in *Comprehensive Organometallic Chemistry II*, ed. E. W. Abel, F. G. A. Stone and G. Wilkinson; vol. ed. D. F. Shriver and M. I. Bruce, Pergamon, New York, 1995; vol. 7, ch. 13.1–13.2.

14 J. Manna, K. D. John and M. D. Hopkins, *Adv. Organomet. Chem.*, 1995, **38**, 79.

15 A. J. Deeming, S. Hasso and M. Underhill, *J. Chem. Soc., Dalton Trans.*, 1975, 1614.

16 M. I. Bruce, B. W. Skelton, A. H. White and N. N. Zaitseva, *J. Chem. Soc., Dalton Trans.*, 1996, 3151. Related reactions are mentioned in the very recent ref. 3(*d*).

17 P.-C. Su, S.-J. Chiang, L.-L. Chang, Y. Chi, S.-M. Peng and G.-H. Lee, *Organometallics*, 1995, **14**, 4844 and references therein.


*Received, 21st November 1996; Com. 6/07884B*

# Self-assembly of a three-dimensional network from two-dimensional layers *via* metallic spacers: the (3,4)-connected frame of $[Ag_3(hmt)_2][ClO_4]_3\cdot 2H_2O$ (hmt = hexamethylenetetramine)

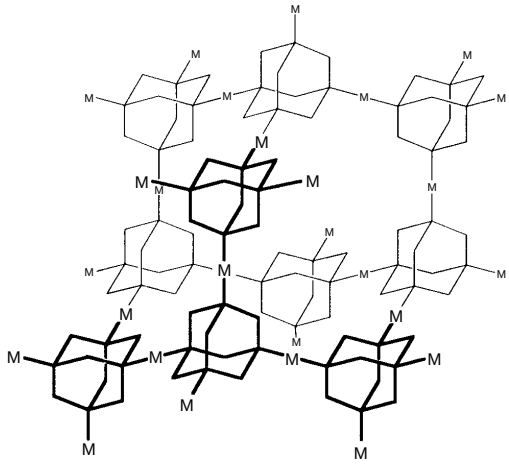
**Lucia Carlucci, Gianfranco Ciani,* Dorothea W. v. Gudenberg, Davide M. Proserpio and Angelo Sironi**

*Dipartimento di Chimica Strutturale e Stereochimica Inorganica and Centro CNR, Via G. Venezian 21, 20133 Milano, Italy*

**$AgClO_4$ reacts with hexamethylenetetramine (hmt) in ethanol–$CH_2Cl_2$ in the ratio 1 : 1 to yield the two-dimensional polymer [Ag(hmt)] $ClO_4$, consisting of hexagonal meshed layers, while a twofold excess of $AgClO_4$ produces $[Ag_3(hmt)_2]ClO_4]_3\cdot 2H_2O$, in which $Ag^I$ ions intercalate between the sheets of the two-dimensional polymer, joining them as spacers to give a three-dimensional (3,4)-connected open network of uncommon topological type.**

The recent efforts in the field of crystal engineering of networked materials based on polymeric coordination compounds[1,2] have been devoted to the use of novel polydentate ligands. In contrast to the more common frameworks based on metal centres and bidentate organic rods, the presence of polyhapto bases also introduces organic centres in addition to the metallic ones, which can give rise to new and varied topological types. Very interesting frames have been assembled with large trihapto trigonal ligands, such as 2,4,6-tris(4-pyridyl)-1,3,5-triazine,[3] 1,3,5-tris(4-ethynylbenzonitrile)-benzene[4] and tricyanomelamine.[5] With polydentate bases L (of hapticity greater than two) the topology of the array may also be entirely determined by the ligands, when the metals (such as diagonal $Ag^I$ and $Cu^I$) do not occupy nodes of the net, but work as simple spacers (L–M–L metallic synthons).† In this concern a potentially tetradentate ligand such as hexamethylenetetramine (hmt) seems quite suitable for the preparation of supertetrahedral networks with metallic synthons (see Scheme 1), paralleling the supramolecular organic chemistry of adamantyl templates with different synthons,[6] well exemplified by the fivefold interpenetrated frame of the adamantane-1,3,5,7-tetracarboxylic acid.[7]

Working on these lines we have reacted hmt with different $Ag^I$ salts of non-coordinating anions and we have recently described the polymeric $[Ag(hmt)]PF_6\cdot H_2O$,[8] containing a three-dimensional triconnected frame topologically related to the prototypal $SrSi_2$. We report here that hmt reacts with $AgClO_4$ in the ratio 1 : 1 to yield the two-dimensional polymer $[Ag(hmt)]ClO_4$ **1**, while a twofold excess of $AgClO_4$ gives $[Ag_3(hmt)_2][ClO_4]_3\cdot 2H_2O$ **2**, in which metal ions (with their counter-ions and water molecules) intercalate between sheets like those of **1**, joining them (as spacers) to give a three-dimensional (3,4)-connected network of uncommon topological type.




**Scheme 1**

Compound **1** can be obtained in large yields, as needle shaped colourless crystals, on layering over a $CH_2Cl_2$ solution of hmt an ethanolic solution of $AgClO_4$ (molar ratio 1 : 1). The crystal structure of **1**‡ consists of two-dimensional infinite layers of hexagonal meshes formed by alternate triconnected silver ions and hmt molecules [Fig. 1(*a*)]. These layers are similar to those present in the polymeric $[Ag(hmt)]NO_3$),[9] the main difference being the stronger Ag–O($NO_3^-$) interactions, 2.593(8) and 2.62(1) Å, *vs*. the Ag···O($ClO_4^-$) ones in **1**, 2.796(5) Å. It is noteworthy that the rings in the sheets present a rare conformation of the boat type [see Fig. 2 (*a*)], instead of the usual chair conformation (grey arsenic-like or black phosphorus-like layers).

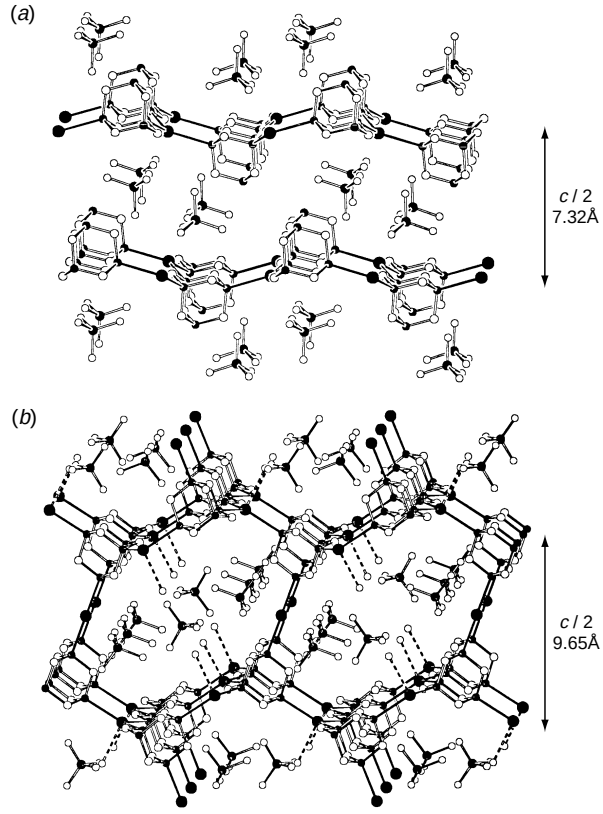



**Fig. 1** A SCHAKAL view of the stacking of the two-dimensional layers in compounds **1** (*a*) and **2** (*b*). In **2** only one of the two locations of the statistically disordered $ClO_4^-$ and $H_2O$ (see text) is shown for clarity.

On performing the above reaction with an $AgClO_4$ : hmt ratio of 2 : 1 we have observed the initial formation of crystals of **1**, but on allowing the solution to concentrate by evaporation the reaction further proceeds giving fine multifaced crystals of **2**, investigated by X-ray diffraction analysis.‡

The structure of **2** consists of an open three-dimensional cationic network formed by [Ag(hmt)] hexagonal layers as in **1**, joined by biconnected silver ions, which coordinate to the free N atoms of the hmt ligands [Fig. 1(*b*)]. The Ag–N bond lengths for these spacers, 2.223(5) Å, are shorter than those involving the other silver ions, 2.355(5)–2.396(4) Å [2.326(5)–2.373(4) Å in **1**]. On passing from **1** to **2** a relative sliding of the layers takes place, together with a change of the ring conformation from boat to chair (to give black phorphorus-like layers) and, what is particularly interesting, the interlayer separation increases from 7.32 to 9.65 Å. Guest water molecules occupy the large, approximately hexagonal, channels [Fig. 1(*b*)] and interact with the silver ions of the layers [Ag–O bond lengths of 2.467(10) Å]. Thermal analyses have shown that these water molecules can be reversibly removed from the crystals by thermal activation.§

From the topological point of view the three-dimensional framework of **2** is a (3,4)-connected net, comprised of triconnected (silver ions of the layers) and tetraconnected (hmt molecules) centres in the ratio 1 : 1 [Fig. 2,(*b*)]. The topological type can be assigned, following the pioneering ideas of Wells,[10] on considering that the shortest circuits starting and ending on each centre are all three 6-gons for the triconnected silver ions and 6-gons and 8-gons in the ratio 5 : 1 for the hmt ligands, hence $(6^3)(6^5,8)$. Wells has described four nets with this connectivity and has classified that one here reported as $(6^3)(6^5,8)$-b,[10] space group *Pnnm*, in its highest symmetry. Though this seems to be one of the more simple (3,4)-connected nets we have been able to find only one net with the same topology, namely InS (triconnected S and tetraconnected In).[12]

We have not isolated the supertetrahedral $[Ag_2(hmt)]$ hypothetical frame of Scheme 1, but compound **2** represents at least a step in that direction. Factors such as, *inter alia*, the tendency of the metal ions to achieve coordination numbers higher than two and that of hmt to be less than tetradentate, as in **1** and in $[Ag(hmt)]PF_6 \cdot H_2O$, can operate against the desired goal. Nevertheless, interesting networks joined exclusively *via* metallic synthons will probably assume some relevance in the near future.

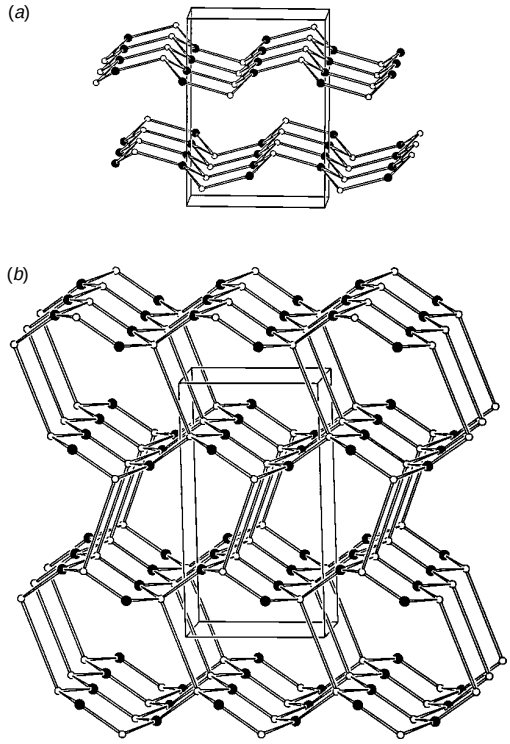



**Fig. 2** A schematic view, approximately down the **a** axis, of the two-dimensional layers in **1** (*a*) and of the three-dimensional network $(6^3)(6^5,8)$-b in **2** (*b*). Filled spheres = $Ag^I$ open spheres = baricentres of the hmt molecules.

## Footnotes

† We call metallic synthon, extending the term used for the supramolecular interactions in organic systems by Desiraju,[6] the interaction of two polydentate organic bases mediated by a metal ion (or complex) which, dedicating only two coordination sites to the net, does not influence its topology. Hoskins and Robson have previously considered this kind of interaction.[1a] However, the networks exclusively based on organic molecules (as centres) and metallic synthons are quite rare.

‡ *Crystal data*: **1**; orthorhombic, *Pmcn* (no. 62), $a$ = 6.484(2), $b$ = 10.636(3), $c$ = 14.651(3) Å, $U$ = 1010.4(5) Å$^3$, $Z$ = 4, $D_c$ = 2.285 Mg m$^{-3}$, Mo-K$\alpha$ radiation ($\lambda$ = 0.710 73 Å). The data collection was performed at 293 K on an Enraf-Nonius CAD-4 diffractometer, by the $\omega$-scan method, within the limits $3 < \theta < 25°$. The structure was solved by direct methods (SIR92) and refined by full-matrix least-squares analysis (SHELX93). The final agreement index $R$ was 0.0274 for 674 independent significant [$I > 3\sigma(I)$] absorption corrected data. Anisotropic thermal factors were assigned to all the non-hydrogen atoms.

**2**; orthorhombic, *Pnnm* (no. 58), $a$ = 6.533(2), $b$ = 10.453(2), $c$ = 19.293(8) Å, $U$ = 1317.5(7) Å$^3$, $Z$ = 2, $D_c$ = 2.365 Mg m$^{-3}$. The structure was solved by direct methods and refined by full-matrix least-squares analysis. One of the perchlorato anions and the solvated water molecule, which is hydrogen bonded to it, form a pair statistically disordered about a mirror plane. The final agreement index $R$ was 0.0453 for 1158 independent significant [$I > 3\sigma(I)$] absorption corrected data. Other experimental features are as in **1**.

Atomic coordinates, bond lengths and angles, and thermal parameters have been deposited at the Cambridge Crystallographic Data Centre (CCDC). See Information for Authors, Issue No. 1. Any request to the CCDC for this material should quote the full literature citation and the reference number 182/378.

§ Differential scanning calorimetry (DSC) shows an endothermic peak at *ca.* 120 °C and thermogravimetric analysis (TGA) gives a mass loss in the range 70–130 °C corresponding to two water molecules per formula unit. Decomposition of the compound begins above 200 °C. Samples heated to 140 °C and left in air for a few hours display again the same DSC peak.

## References


1 B. F. Hoskins and R. Robson, *J. Am. Chem. Soc*., 1990, **112**, 1546; R. Robson, B. F. Abrahams, S. R. Batten, R. W. Gable, B. F. Hoskins and J. Liu, *Supramolecular Architecture*, ACS publications, Washington, 1992, ch. 19.

2 C. L. Bowes and G. A. Ozin, *Adv. Mater*., 1996, **8**, 13.

3 S. R. Baten, B. F. Hoskins and R. Robson, *Angew. Chem., Int. Ed. Engl*., 1995, **34**, 820; *J. Am. Chem. Soc*., 1995, **117**, 5385; B. F. Abrahams, S. R. Baten, H. Hamit, B. F. Hoskins and R. Robson, *Chem. Commun*., 1996, 1313; B. F. Abrahams, S. R. Baten, H. Hamit, B. F. Hoskins and R. Robson, *Angew. Chem., Int. Ed. Engl*., 1996, **35**, 1690.

4 G. B. Gardner, D. Venkataraman, J. S. Moore and S. Lee, *Science*, 1995, **374**, 792; D. Venkataraman, S. Lee, J. S. Moore, P. Zhang, K. A. Hirsch, G. B. Gardner, A. C. Covey and C. L. Prentice, *Chem. Mater*., 1996, **8**, 2030.

5 B. F. Abrahams, S. J. Egan, B. F. Hoskins and R. Robson, *Chem. Commun*., 1996, 1099.

6 G. R. Desiraju, *Angew. Chem., Int. Ed. Engl*., 1995, **34**, 2311.

7 O. Ermer, *J. Am. Chem. Soc*., 1988, **110**, 3747.

8 L. Carlucci, G. Ciani, D. M. Proserpio and A. Sironi, *J. Am. Chem. Soc*., 1995, **117**, 12 861.

9 A. Michelet, B. Voissat, P. Khodadad and N. Rodier, *Acta Crystallogr., Sect. B*, 1981, **37**, 2171.

10 A. F. Wells, *Further Studies of Three-dimensional Nets*, ACA Monograph No. 8, 1979.

11 K. Schubert, E. Doerre and E. Guenzel, *Naturwissenschaften*, 1954, **41**, 448; R. Walther and H. J. Deiseroth, *Z. Krystallogr*., 1995, **210**, 360.



*Received, 20th January 1997, Com. 7/00446J*

# A combinatorially developed reducing agent

**Fredric M. Menger,* Craig A. West and Julia Ding**

*Department of Chemistry, Emory University, Atlanta, Georgia 30322, USA*

**An automated search of thousands of combinatorially-functionalized polymers bearing dihydropyridine groups defines a few active examples that can reduce a ketone in water.**

Recently we introduced a new approach to reaction dynamics in which a huge library of randomly-functionalized polymers was screened for catalytic activity toward phosphate ester hydrolyses.[1] Rate enhancements as large as $3 \times 10^4$ were thereby uncovered (exceeding those reported for a corresponding catalytic antibody). It was argued that the approach provides an alternative to the classical method of synthesizing enzyme models in which multiple functional groups are in the proper juxtaposition to effect catalysis. Such synthetic work can be extremely time consuming, and there is no guarantee, even when the desired compound is in hand, that it will perform as hoped.

The details are simple. Two commercially available polymers, poly(allylamine) (PAA, MW = 50–60 kD) and poly(ethylenimine) (PEI, MW = 25 kD), were randomly derivatized, *via* amide bonds, by a mixture of three or four carboxylic acids selected from Fig. 1. EDCI, a water-soluble carbodiimide, was used as the coupling agent. From 20–60% of the polymer amino groups were functionalized, the remainder being left untouched. For example, a polymer might be constructed with 10% naphthyl groups, 15% imidazole groups, 5% octyl groups and 5% butanol groups (using Nap, Imi, Oct and BuOH in Fig. 1, respectively). All kinetic runs were carried out at pH 7.2 where the free amino groups, being largely protonated, solubilize the polymer in water. In addition, any unprotonated amino groups could act as ligands for metals (*e.g.* $Cu^{+2}$) that were added to the system.

Aqueous solutions of polymer, EDCI, and the various carboxylic acids were made available to an automatic pipeting device. A computer program directed the device to dispense the reactants (including 96 different concentration ratios of carboxylic acids) into a set of test tubes for a 24 h incubation at 55–60 °C. No unreacted carboxylic acid was detected by TLC after this time. The resulting polymers were 'randomly' substituted in the sense that no control was exercised over the functionalizations. In actual fact, however, the positioning of the four substituents, and the subsequently added metal ion, may not be 'random' in the strict meaning of the word. For example, when one amino group is derivatized with an octanoyl group, the adjacent amino groups may become more prone to receiving other octanoyl groups owing to hydrophobic attraction. To preclude confusion about the meaning of 'random', compounds will henceforth be called 'combinatorial polymers'. Each combinatorial polymer is, of course, a complex system[2] composed of a mixture of polymeric variations that is impossible to separate. Even if we could isolate a pure component, it would be extremely difficult to sequence it because (unlike proteins) the polymer chain cannot be subdivided. Fortunately, our goals are directed primarily toward function. A polymer system that serves a useful function is of great interest even in the absence of detailed structural information.

It was clear that, in order for combinatorial polymers to become something other than a curiosity, they must be able to do more than catalyse the ever-popular ester hydrolysis. For this reason we have been examining eliminations, condensations and redox systems of synthetic utility. This article focuses on the conversion of ketones to alcohols *via* combinatorial polymers having a reductive capacity. Reducing capabilities were imparted to the polymers by incorporating (simultaneously with the other diverse functionalities) a 5 or 10% content of the dihydropyridine DHP. Dihydropyridines are well known from NADH models[3–8] to convert activated ketones into alcohols. The hope, therefore, was to construct active sites that promote enzyme-like reductions within their confines.

Combinatorial polymers were screened for their ability to homogeneously reduce benzoylformic acid ($PhCOCO_2^-$) to

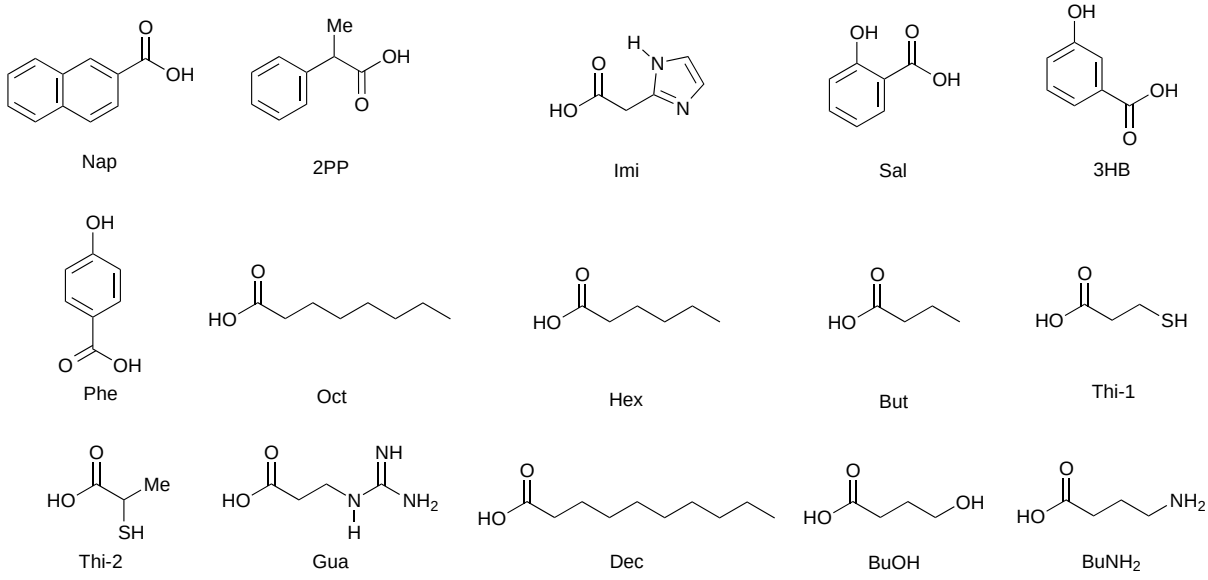



**Fig 1** Carboxylic acids used to derivatize the polyamines

**Table 1** Five active polymers taken from a library of over 8000, most of which were inactive[a]

| Polymer | Side-chains[b] | Activity (%) |
|---|---|---|
| PEI | 2.5% Imi, 5% Hex, 7.5% Nap, 2.5% Thi-1, 5% $Zn^{+2}$ | 30 |
| PEI | 15% Hex, 2.5% Gua, 2.5% BuOH, 5% $Mg^{+2}$ | 33 |
| PEI | 2.5% Imi, 15% Nap, 2.5% Hex, 5% $Mg^{+2}$ | 34 |
| PAA | 10% Imi, 2.5% Hex, 10% Nap, 10% Thi-2, 10% $Zn^{+2}$ | 42 |
| PAA | 2.5% Gua, 7.5% Hex, 7.5% Nap, 2.5% Thi-2, 10% $Cu^{+2}$ | 28 |

[a] Each activity is an average from three polymers created *de nova*. The uncertainty in the values is 6 in absolute %. [b] Symbols are defined in Fig. 1. Percentages represent the composition of solutions from which the polymers were made.

mandelic acid [$PhCH(OH)CO_2^-$]. A total of 96 runs at a time were carried out side-by-side within the 400 μl wells of a microtiter plate. Each well contained the following components dissolved in a pH 7.2 TRIS buffer at 24 °C: 50 μl of a functionalized polymer (corresponding to 2.4 mM of the dihydropyridine); 100 μl of 1.25 mM $Cu^{+2}$, $Mg^{+2}$ or $Zn^{+2}$; and 150 μl of 0.021 M benzoylformic acid. Reactions were monitored periodically, with an ICN MCC/340 scanner, at 340 nm for the disappearance of the dihydropyridine chromophore. Data, recorded as percentage yield, refer to the percent of oxidized dihydropyridine after 5 days when all the reactions had ceased. The percentage yield varied from 0–50% depending upon the polymer functionalization. A yield of 23%, for example, indicates that 23% of the 25–100 dihydropyridine sites per polymer chain were active. A larger scale reaction, worked up by column chromatography on silica (MeOH–$CHCl_3$–$H_2O$, 30 : 60 : 4) gave a product identified as mandelic acid by $^1H$ NMR spectroscopy. GLC analysis of mandelic acid (as the methyl ester) gave a percentage yield that corresponded to that calculated from the dihydropyridine chromophore.

Among a total of 8198 polymers tested, 92% were considered inactive ( < 10% yield). Activities of 10–20, 20–40 and > 40%, were found in 7, 1 and 0.3% of the polymer population, respectively. Two of the most active polymers ( > 25%) were: (*a*) PEI; 5% DHP; 2.5% Imi; 15% Nap; 2.5% Thi-1; 5% $Zn^{+2}$. (*b*) PAA; 10% DHP; 10% Imi; 2.5% Hex; 10% Nap; 10% Thi-2; 10% $Zn^{+2}$. By contrast, the following two were inactive: (*a*) PEI; 5% DHP; 5% Imi; 5% BuOH; 5% Nap; 5% Sal; 5% $Zn^{+2}$ or 5% $Mg^{+2}$; (*b*) PAA; 10% DHP; 5% Dec; 5% Gua; 7.5% 2PP; 5% Sal; 10% $Zn^{+2}$. Table 1 lists five additional reactive polymers; note that recipes for PAA and PEI are, in general, not the same.

The multitude of inactive systems can be regarded as 'controls' in that, apart from polymer composition, they duplicate the reaction conditions. Moreover, mixtures of individual components that simulated the high-activity polymers were all found to be inert. Thus, a polymer was functionalized only with the DHP. No reducing capabilities were observed with this polymer when (after purification from EDCI by GPC) it was mixed with an appropriate combination of free acids in Fig. 1 plus a metal ion. Clearly, a polymeric ensemble of functionalities is necessary for activity. Lack of disappearance of the DHP chromophore in the control also demonstrated the stability of DHP to hydrolysis. A single run with poly(ethylenimine) of low molecular weight (7 kD) was also carried out. This polymer, endowed with a 'favourable' substituent ratio with respect to the 25 kD polymer, gave no reaction. Although a useful combinatorial polymer of low molecular weight might well exist, one would have to discover its recipe in a separate and distinct set of screenings.

To assess the reproducibility of the combinatorial polymers, two people each prepared the ten best polymers discovered by the other. Yields were reproduced within a factor of two and usually much better. The same was true when duplicating a full set of 96. Although not all the variables affecting the polymer functionalizations have been systematically investigated, it is known that the reaction conditions are critical. For example, the presence of a dioxane cosolvent in the functionalization mixtures has a profound effect upon the activity of the resulting polymer. This is hardly surprising; polymer sequences would be expected to have a high solvent sensitivity. Sequences could also be sensitive to the order in which functionalities are placed onto the polymer, but this point has not yet been tested.

Thousands of activity data are best summarized by the following generalizatons. (*a*) A metal ion is necessary for activity. (*b*) All high-activity polymers possess at least one hydrophobic side-chain (Nap Oct, *etc.*). (*c*) Imi or Gua is found in most but not all reactive polymers. (*d*) Percentages within a single set of functionalities can be important. For example, PEI with 2.5% Imi, 15% Nap and 2.5% Thi-1 (plus 10% $Mg^{2+}$) had an activity of 40%. The same system but with 10% Imi, 2.5% Nap, and 7.5% Thi-1 had an activity of only 1.3%. (*e*) No active poly(allylamines) were observed when they contained oxalic or malonic acid even in concert with other seemingly 'beneficial' combinations. (*f*) A thiol or hydroxy group often assists the reduction. Coincidentally, no doubt, alcohol dehydrogenase also requires a dihydropyridine (NADH), a metal ion ($Zn^{2+}$ coordinated to two thiolates), a histidine and a serine.[9]

The half-life of our better reductions is about 2 h. This is fast relative to many other 'NADH models'[3] which, in order to obtain any reaction at all, require aprotic solvents rather than water, as used in our experiments.

The potential for combinatorial reactivity seems unlimited. In the specific case at hand, one can contemplate: (*a*) achieving true catalysis *via* an external reducing agent that regenerates the dihydropyridine units of high-activity polymers; (*b*) discriminating between two ketones (*e.g.* reducing $PhCOCO_2^-$ but not $PhCOCO_2Me$) or between two similar ketones in the same molecule [*e.g.* reducing $MeCO(CH_2)_2CO(CH_2)_3Me$ to $MeCO(CH_2)_2CHOH(CH_2)_3Me$]; (*c*) stereoselectively reducing ketones with chiral polymers (*e.g.* polymers based on poly-L-lysine or on PAA with chiral substituents).

Low cost is an important virtue of combinatorial polymers. Once an active polymer is discovered, it can be prepared in large amounts and in a single step without specialized biochemical methods.

We thank the National Science Foundation for support of this work.

## References

1 F. M. Menger, A. V. Eliseev and V. A. Migulin, *J. Org. Chem.*, 1995, **60**, 6666.
2 F. M. Menger, *Angew. Chem., Int. Ed. Engl.*, 1991, **30**, 1086.
3 P. M. T. de Kok, L. A. M. Bastiaansen, P. M. van Lier, J. A. J. M. Vekesnans and H. M. Buck, *J. Org. Chem.*, 1989, **54**, 1313.
4 M. Seki, N. Baba, J. Oda and Y. Inouye, *J. Org. Chem.*, 1983, **48**, 1370.
5 K. Skog and O. Wennerström, *Tetrahedron Lett.*, 1992, **33**, 1751.
6 J. F. J. Engbersen, A. Koudijs and H. C. van der Plas, *J. Org. Chem.*, 1990, **55**, 3647.
7 A. G. Talma, P.Jouin, J. G. DeVries, C. B. Troostwijk, G. H. W. Buning, J. K. Waninge, J. Visscher and R. M. Kellogg, *J. Am. Chem. Soc.*, 1985, **107**, 3981.
8 Y. Murakami, J. Kikuchi, K. Nishida and A. Nakano, *Bull. Chem. Soc. Jpn.*, 1984, **57**, 1371.
9 H. Eklund, B. V. Plapp, J. P. Samama and C. I. Braenden, *J. Biol. Chem.*, 1982, **257**, 14 349.

*Received, 8th January 1997; Com. 7/00259I*

# Asymmetric hydroformylation catalysed by platinum complexes of new chiral bisphosphites

**Stefánia Cserépi-Szücs and József Bakos***

*Department of Organic Chemistry, University of Veszprém, H-8201 Veszprém, PO Box 158, Hungary*

**Asymmetric hydroformylation of styrene using bis(phosphite)$PtCl_2$–$SnCl_2$ systems gives branched aldehydes with high enantioselectivity (up to 91%).**

Asymmetric hydroformylation is a convenient synthetic method for obtaining optically active aldehydes from olefinic substrates.[1] These aldehydes are attractive building blocks in organic synthesis.[2] Most compounds which have been developed for chiral modification of catalysts are chiral derivatives of aryl- or alkyl-phosphines; less work has been done with less electron-rich ligands such as phosphites. For asymmetric hydroformylation of olefins, chiral diphosphine–$Rh^{I}$,[3] diphosphine–$Pt^{II}$,[4] bisphosphite–$Rh^{I}$[5] or phosphinephosphite–$Rh^{I}$[6] have mostly been used. Surprisingly, however, there have been no reports on the application of bisphosphite–$Pt^{II}$–$SnCl_2$ complexes for asymmetric hydroformylation. This system may reasonably be expected to represent an alternative to the diphosphine system because the less electron-rich phosphites may cause dramatic changes in the reactivity and selectivity.

Here we report the synthesis and spectroscopic characterization of new bisphoshites, which afforded highly active platinum catalysts for asymmetric hydroformylation. The highest enantioselectivity (91%) was obtained with the platinum(II)–$SnCl_2$ catalytic system associated with (2*S*,4*S*)-bis(*S*)-**1** and its enantiomer (2*R*,4*R*)-bis(*R*). These ligands are of particular interest, because they contain a chiral centre in the backbone and a chiral axis in the terminal groups. In this regard, these model ligands show the exploration of chiral cooperativity.

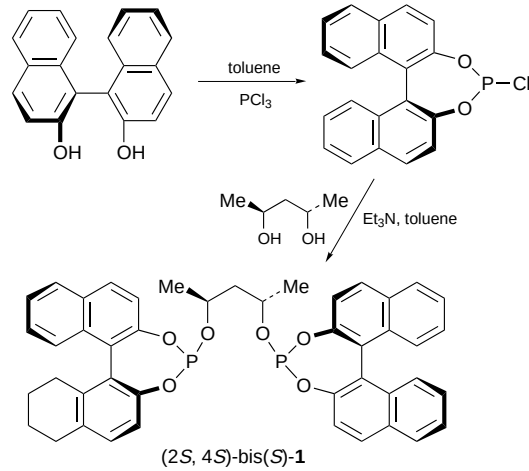
The reaction of racemic 1,1′-bi-2-naphthol with excess $PCl_3$ in toluene catalysed by 1-methylpyrrolidin-2-one gave phosphorochloridite (*S*,*R*)-6-chlorodinaphtho[*d*,*f*][1,3,2]dioxaphosphepine. Two equivalents of the racemic dioxaphosphepine were reacted with optically pure (2*R*,4*R*)-pentane-2,4-diol in the presence of triethylamine to give a diastereoisomeric mixture of 2,4-bis[dinaphtho[*d*,*f*][1,3,2]dioxaphosphepin-6-yloxy]-pentane. Diastereoisomers were obtained in a 1 : 2 : 1 ratio showing that the chiral pentanediol does not induce diastereoselectivity in the bisphosphite formation. Separation of the diastereoisomers was not successful.

In the $^{31}P$ NMR{$^{1}H$} spectrum of the product at ambient temperature, six lines are observed with relative intensities and splitting consistent with the expected three diastereoisomers. An explanation is that four resonances arise from the *meso* form, (2*R*,4*R*)-(*S*,*R*) = (2*R*,4*R*)-(*R*,*S*). The 2D homonuclear $^{31}P$ COSY NMR spectrum of the product confirms the existence of coupling ($^{6}J_{P–P}$ 9.5 Hz) between the P atoms (δ 149.0 and 153.6) six bonds apart.[7] Two singlets [δ 153.6 for (2*R*,4*R*)-bis(*R*)-**1** and 147.1 for (2*R*,4*R*)-bis(*S*)-**2**]) are attributed to the presence of the other two diastereoisomers. This was supported by the NMR spectra of the optically pure diastereoisomers obtained from (*S*)-6-chlorodinaphtho[*d*,*f*]-[1,3,2]dioxaphosphepine and (2*S*,4*S*)- (Scheme 1) or (2*R*,4*R*)-pentane-2,4-diol, respectively. In these cases the other two diastereoisomers were not detected by $^{31}P$ NMR. This implies that the diastereoisomers (**1** and **2**) were obtained in optically pure form. Optical resolution of 1,1′-bi-2-naphthol was carried out by using (*R*,*R*)-(+)-2,3-dimethoxy-*N*,*N*,*N*′,*N*′-tetramethylsuccinamide as a host compound[8] or (8*S*,9*R*)-(−)-*N*-benzylcinchonidium chloride as a resolving agent.[9]

Phosphites **1** and **2** in $CD_2Cl_2$ form phosphite–platinum complexes. The $^{31}P$ NMR{$^{1}H$} spectrum of $PtCl_2$[(2*S*,4*S*)-bis(*S*)-**1**] yields a characteristic satellite 'triplet' pattern (δ 87.5, $J_{Pt–P}$ = 5672 Hz) and of $PtCl(SnCl_3)$[2*S*,4*S*)-bis(*S*)-**1**] exhibits a P–P coupling pattern ($J_{P–P}$ = 20 Hz) with well separated chemical shifts (δ 98.0 and 89.1) and large inequivalent P–Pt coupling constants (5580 and 4420 Hz) as expected for inequivalent P atoms in positions *trans* to the chloro and $SnCl_3$ ligands, respectively. Reaction of $PtCl_2(PhCN)_2$ with both **1** and **2** afforded only the expected *cis* mononuclear eight-membered complexes without any oligomeric species. Oligomeric platinum complexes of diphospholes, dibenzophospholes and bisbinaphthophospholes have been reported with *trans* P–Pt–P disposition.[10]

In a typical experiment the autoclave was filled with solvent, alkene and the catalyst precursor. Catalysts were prepared *in situ* by simple mixing $PtCl_2(PhCN)_2$ in toluene or in dichloromethane with the ligands, while anhydrous $SnCl_2$ was used as co-catalyst. It was then purged with syn gas [$CO–H_2$ (1 : 1)] and pressurised. Catalytic reactions were carried out under classical conditions to give a mixture of the branched (*b*, 2-phenylpropanal) and the normal (*n*, 3-phenylpropanal) regioisomers and hydrogenated (ethylbenzene) products. At the end of the reaction the autoclave was cooled and depressurised. The reaction mixture was directly vacuum distilled to remove the catalyst. The reaction mixture and the distilled products were analysed by GC. The enantiomeric excess was determined by GC using a chiral capillary column.

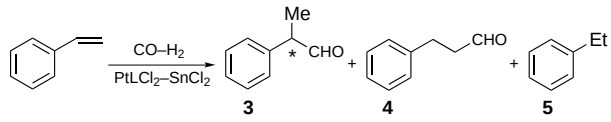
Some representative results are given in Table 1. When **1** or **2** was used as the ligand in platinum catalysed asymmetric hydroformylation of styrene, the absolute configuration of central chirality in the bridge is of primary importance in asymmetric induction (Table 1). In the case of (2*S*,4*S*)-bis(*S*)-**1**, there is a cooperative effect of the axial chirality of the terminal 1,3,2-dioxaphosphepine groups and the central chirality of the




(2*S*, 4*S*)-bis(*S*)-**1**

**Scheme 1**

**Table 1** Enantioselective hydroformylation of styrene catalysed by bis(phosphite)$PtCl_2$-$SnCl_2$ complex [100 atm. of $H_2$–CO (1 : 1), P/Pt: 2.05, $SnCl_2$/Pt: 1.0][a]




**3** **4** **5**

| Ligand | *t*/h | *T*/°C | Solvent | Substr/Pt | Conv. (%)[b] | **5** (%)[b] | (*b*/*n*)[b] | Ee of **3** (%)[c] | Config.[d] |
|---|---|---|---|---|---|---|---|---|---|
| **2** | 10 | 60 | PhMe | 2000 | 65 | 59 | 62/38 | 14 | *S* |
| **1** | 67 | 17 | PhMe | 2000 | 76 | 55 | 58/42 | 88 | *R* |
| **1** | 2 | 60 | PhMe | 2000 | 100 | 55 | 60/40 | 73 | *R* |
| **1** | 2 | 100 | PhMe | 2000 | 100 | 59 | 59/41 | 62 | *R* |
| **1** | 70 | 17 | $CH_2Cl_2$ | 5000 | 90 | 54 | 60/40 | 91 | *R* |
| **1** | 4 | 60 | $CH_2Cl_2$ | 5000 | 96 | 47 | 58/42 | 75 | *R* |
| **1** | 22 | 17 | — | 5000 | 50 | 48 | 58/42 | 89 | *R* |

[a] Reactions were carried out in the given solvent [*ca.* 2.5 mol $dm^{-3}$, except in $CH_2Cl_2$ (8.35 mol $dm^{-3}$)] in a 20 ml stainless-steel autoclave under an atmosphere of $H_2$ and CO (1 : 1) at 100 atm. initial total pressure. [b] Conversions and composition of the reaction mixture (*b* : *n* : *h* branched : normal : hydrogenated) were determined by GC (SPB-1) using decane as an internal standard. [c] Determined by GC analysis (β-DEX, 30 m, id. 0.25 mm) of the corresponding acid. [d] Determined by the sign of optical rotation of the corresponding aldehyde.

backbone. The highest enantioselectivity (91% *R*) was obtained with the platinum(II)–$SnCl_2$ catalytic system associated with (2*S*,4*S*)-bis(*S*)-**1** and its enantiomer (2*R*,4*R*)-bis(*R*)-**1** (matched constellation).[11] Reactions with (2*R*,4*R*)-bis(*S*)-**2** (mismatched constellation) resulted in much lower enantioselectivities. Up until now the highest enantioface discrimination (86.3% ee) has been reported[4b] for the hydroformylation of styrene to hydratropaldehyde with the platinum–Sn system [(*R*,*R*)-BCO-DBP]$PtCl_2$ [BCO-DBP = 5,5′-(bicyclo[2.2.2]octane-2,3-diyldimethyl)bis(5*H*-benzo[*b*]phosphindole)].

Addition of $SnCl_2$ is essential for catalytic activity. The role of the $SnCl_2$ co-catalyst in promoting the key steps of Pt–Sn-catalysed hydroformylation, such as the alkene insertion, the CO insertion and the hydrogenolysis of acyl complexes, has been thoroughly investigated.[12] A dramatic increase in reaction rate and a slight decrease in enantioselectivity were found when the reaction temperature was increased. Regioselectivity was almost independent of reaction temperature.

In spite of the high hydrogenation activity of the catalyst, we were able to find a catalytic system with remarkably high hydroformylation activity. For example, in dichloromethane at 60 °C, hydroformylation rates of *ca.* 1100 and 530 turnovers $h^{-1}$ at 54 and 88% of conversion were observed in combination with high enantioselectivity (75% ee), respectively. Surprisingly when $Rh(CO)_2(acac)$ was used as a catalytic precursor (100 atm. and 60 °C) both diastereoisomers afforded the same preferred *R* enantiomer in the product with the same regioselectivity (81 : 19 *b*/*n*), enantioselectivity (16% ee) and with complete chemoselectivity.

Financial support from the Hungarian National Science Foundation (OTKA-T016269) and the Ministry of Culture and Education (MDM-698/95) is gratefully acknowledged. We are grateful to Mr Béla Édes for skillful assistance in the catalytic experiments.

## Footnote

* E-mail: bakos@almos.vein.hu

## References

1 Recent reviews, see S. Gladiali, J. C. Bayón and C. Claver, *Tetrahedron: Asymmetry*, 1995, **7**, 1453; M. Beller, B. Cornils, C. D. Frohning and V. W. Kohlpainter, *J. Mol Catal.*, 1995, **104**, 17; F. Agbossou, J.-F. Carpentier and A. Mortreux, *Chem. Rev.*, 1995, **95**, 2485; G. Consiglio, in *Catalytic Asymmetric Syntheses*, ed. I. Ojima, Weinheim, 1993, p. 273.
2 C. Botteghi, S. Paganelli, A. Schionato and M. Marchetti, *Chirality*, 1991, **3**, 355.
3 A. M. Masdeu-Bultó, A. Orejon, A. Castellanos, S. Castillón and C. Claver, *Tetrahedron: Asymmetry*, 1996, **7**, 1834.
4 (*a*) J. K. Stille, H. Su, P. Brechot, G. Parenillo and L. S. Hegedus, *Organometallics*, 1991, **10**, 1183; (*b*) G. Consiglio, S. C. A. Nefkens and A. Borer, *Organometallics*, 1991, **10**, 2046; (*c*) A. Scrivanti, S. Zeggio, V. Beghetto and U. Matteoli, *J. Mol. Catal.*, 1995, **101**, 217.
5 J. E. Babin and G. T. W. O. Whiteker, USP 911 518, 1992; G. J. H. Buisman, P. C. J. Kamer and P. W. N. M. van Leeuwen, *Tetrahedron: Asymmetry*, 1993, **4**, 1625; G. J. H. Buisman, M. E. Martin, E. J. Vos, A. Klootwijk, P. C. J. Kamer and P. W. N. M. van Leeuwen, *Tetrahedron: Asymmetry*, 1995, **7**, 719.
6 N. Sakai, K. Nozaki, K. Mashima and H. Takaya, *Tetrahedron: Asymmetry*, 1992, **3**, 583; N. Sakai, S. Mano, K. Nozaki and H. Takaya, *J. Am. Chem. Soc.*, 1993, **115**, 7033; T. Horiuchi, T. Ohta, K. Nozaki and H. Takaya, *Chem. Commun.*, 1996, 155.
7 G. Szalontai, J. Bakos, I. Tóth and B. Heil, *Magn. Reson. Chem.*, 1987, **25**, 761.
8 F. Toda and K. Tanaka, *J. Org. Chem.*, 1988, **53**, 3607.
9 Q.-S. Hu, D. Vitharana and L. Pu, *Tetrahedron: Asymmetry*, 1995, **6**, 2123.
10 J. J. Brunet, M. Gòmez, H. Hajouji and D. Neibecker, *J. Organomet. Chem.*, 1993, **463**, 205; G. Consiglio, S. C. A. Nefkens, *Tetrahedron: Asymmetry*, 1990, **1**, 417; S. Gladiali, D. Fabri and L. Kollár, *J. Organomet. Chem.*, 1995, **491**, 91.
11 S. Masamune, W. Choy, J. S. Petersen and L. R. Sita, *Angew. Chem., Int. Ed. Engl.*, 1985, **24**, 1.
12 G. K. Anderson, H. C. Clark and J. A. Davies, *Organometallics*, 1982, **1**, 64; P. J. Stang, Z. Zhong and A. M. Arif, *Organometallics*, 1992, **11**, 1017; I. Tóth, T. Kégl, C. J. Elseiver and L. Kollár, *Inorg. Chem.*, 1994, **33**, 5708 and references cited therein.

*Received, 17th December 1996; Com. 6/08436B*

# Application of 7-*endo*, 8-*endo* and 9-*endo* radical cyclisations to the synthesis of conformationally constrained amino acids and comparison with the corresponding Heck reactions

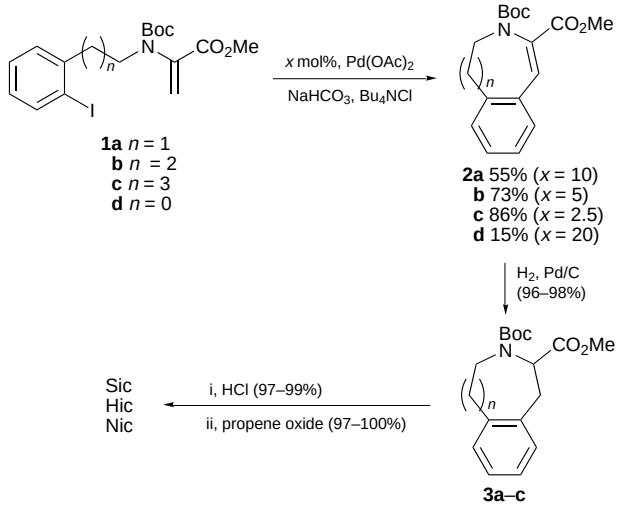
**Susan E. Gibson (née Thomas),[a]† Nathalie Guillo[a] and Matthew J. Tozer[b]**

[a] *Department of Chemistry, Imperial College of Science, Technology and Medicine, South Kensington, London, UK SW7 2AY*
[b] *James Black Foundation, 68 Half Moon Lane, London, UK SE24 9JE*

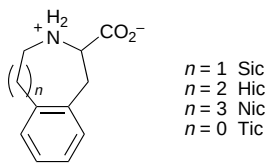
**Radical cyclisation of substrates 1a–c proceeds smoothly to give seven-, eight- and nine-membered rings 3a–c in 73, 71 and 52% yield respectively; comparison of these results with those obtained using the intramolecular Heck reactions suggests that the two cyclisation methods provide complementary approaches to medium-sized rings.**

The formation of seven-, eight- and nine-membered rings *via* radical cyclisation methods is generally believed to be difficult and hence of marginal synthetic use.[1] Indeed, whilst there are several hundred examples of high-yielding radical-based five- and six-membered ring-forming reactions,[1a] examples of the formation of seven-membered rings by this approach are relatively rare,[1a,2] and most of them proceed in moderate yield. A mere handful of eight-membered ring syntheses have been reported,[1a,3] and, to the best of our knowledge, there are only two reports to date of radical-mediated nine-membered ring-forming reactions.‡,[3c,4]

We recently synthesised Sic, Hic and Nic,[6] novel analogues of the well-established and readily-available conformationally constrained phenylalanine analogue Tic. Our approach to Sic, Hic and Nic utilised an intramolecular Heck reaction on substrates **1a–c** to create the required seven-, eight- and nine-membered rings in 55, 73 and 86% yield catalysed by 10, 5 and 2.5 mol% of palladium acetate respectively (Scheme 1),



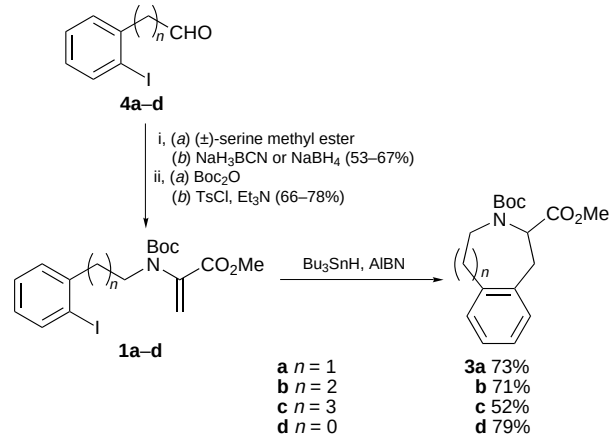

**Scheme 1**




reactions which represent rare examples of the use of the Heck reaction to create seven-, eight- and nine-membered rings.[7] The products of the Heck reaction (**2a–c**) were hydrogenated to **3a–c** which in turn were deprotected to give the required amino acids. Subsequent incorporation of Tic, Sic, Hic and Nic into a cholecystokinin-B/gastrin receptor antagonist revealed a significant difference in biological activity between the Nic-containing ligand and the other ligands,[8] the source of which is currently being actively pursued.

In view of the moderate yield and high catalyst loading of the reaction used to synthesise the seven-membered ring and the current interest in comparing the outcome of radical cyclisations and Heck reactions on a given substrate,[2d,9] we decided to explore the possibility of using radical reactions to create the required rings. Despite the poor precedent for the use of radical cyclisations to generate seven-, eight- and nine-membered rings, we were somewhat encouraged by the relatively high cyclisation rates observed for aryl radicals[1] and the established ability of captodative radicals to influence the *endo*/*exo* selectivity of radical reactions,[2a] and thus the radical cyclisation of substrates **1a–c** was attempted.

Substrates **1a–c** were synthesised as described previously[6] from the iodo aldehydes **4a–c** and (±)-serine methyl ester. Preliminary experiments indicated that slow addition of $Bu_3SnH$ to the aryl iodide was the preferred experimental procedure and thus a mixture of $Bu_3SnH$ (1.1 equiv.) and AIBN (0.1 equiv.) in nitrogen-saturated benzene was added over 1 h to a solution of **1a** and AIBN (0.1 equiv.) in nitrogen-saturated benzene maintained at 80 °C to give a reaction mixture 0.008 M in **1a**. The reaction mixture was heated under reflux for a further 1 h. Subsequent solvent removal, addition of DBU in diethyl ether, titration with etheral iodine (0.1 M), silica gel filtration[10] and column chromatography gave a colourless oil which was identified as the cyclic product **3a** by microanalysis and comparison of its $^1H$ and $^{13}C$ NMR spectra with those of a fully




**Scheme 2**

characterised sample of **3a** prepared previously.[6] Encouraged by the 73% yield obtained for **3a**, which represents a considerable improvement on the Heck approach to **3a**, an identical procedure was applied to substrates **1b** and **1c**. Gratifyingly, these reactions proceeded surprisingly smoothly to give the eight-membered ring **3b** in 71% yield and the nine-membered ring **3c** in 52% yield (Scheme 2).

In order to provide a fuller comparison between the intramolecular Heck reaction and the radical cyclisation method, the palladium-catalysed and the $Bu_3SnH$-promoted reactions of substrate **1d** were examined. As anticipated from the results described above, the Heck reaction required large quantities of palladium catalyst (20 mol%) to produce a poor yield (15%) of the six-membered ring **2d** (obtained as an inseparable 1 : 1 mixture with 1-methoxycarbonyl-1-methyl-2-(*tert*-butoxycarbonyl)-1,2,3-trihydroisoindole, a product of the *exo* mode of cyclisation), whilst the radical cyclisation proceeded much more smoothly to give a high yield (79%) of the novel Tic precursor **3d**.

In conclusion, 6-*endo*, 7-*endo*, 8-*endo* and 9-*endo* radical cyclisations have been used to synthesise precursors to conformationally constrained amino acids. Furthermore, comparison of the yields obtained and the catalyst loadings used for the conversion of **1** to **2** with the yields obtained for the conversion of **1** to **3** suggests that radical cyclisations and intramolecular Heck reactions provide complementary approaches to the synthesis of medium-sized rings.

We gratefully acknowledge financial support from the James Black Foundation.

## Footnotes

† E-mail: s.gibson@ic.ac.uk

‡ In addition, an elegant tandem 9-*endo*-5-*exo* radical cyclisation to form a 5,6-fused bicyclic ketone is of note (ref. 5).

## References

1 (*a*) B. Giese, B. Kopping, T. Göbel, J. Dickhaut, G. Thoma, K. J. Kulicka and F. Trach, *Org. React.* (*N.Y.*), 1996, **48**, 315; (*b*) W. B. Motherwell and D. Crich, *Free Radical Chain Reactions in Organic Synthesis*, Academic Press, London, 1992, p. 242; (*c*) A. L. J. Beckwith and C. H. Schiesser, *Tetrahedron*, 1985, **41**, 3925.

2 For recent examples, see (*a*) L. Colombo, M. Di Giacomo, G. Papeo, O. Caringo, C. Scolastico and L. Manzoni, *Tetrahedron Lett.*, 1994, **35**, 4031; (*b*) C. D. S. Brown, A. P. Dishington, O. Shishkin and N. S. SImpkins, *Synlett*, 1995, 943; (*c*) C. J. Moody and C. L. Norton, *Tetrahedron Lett.*, 1995, **36**, 9051; (*d*) A. K. Mohanakrishnan and P. C. Srinivasan, *Tetrahedron Lett.*, 1996, **37**, 2659.

3 For recent examples, see (*a*) G. A. Molander and J. A. McKie, *J. Org. Chem.*, 1994, **59**, 3186; (*b*) K. Ghosh, A. K. Ghosh and U. R. Ghatak, *J. Chem. Soc., Chem. Commun.*, 1994, 69; (*c*) F. O. H. Pirrung, H. Hiemstra, W. N. Speckamp, B. Kaptan and H. E. Schoemaker, *Synthesis*, 1995, 458; (*d*) G. A. Russell and C. Li, *Tetrahedron Lett.*, 1996, **37**, 2557; (*e*) E. Lee and C. H. Yoon, *Tetrahedron Lett.*, 1996, **37**, 5929.

4 K. Ghosh and U. R. Ghatak, *Tetrahedron Lett.*, 1995, **36**, 4897.

5 G. Pattenden, A. J. Smithies, D. Tapolczay and D. S. Walters, *J. Chem. Soc., Perkin Trans. 1*, 1996, 7.

6 (*a*) S. E. Gibson (née Thomas), N. Guillo, R. J. Middleton, A. Thuilliez and M. J. Tozer, *J. Chem. Soc., Perkin Trans. 1*, 1997, 447; (*b*) S. E. Gibson (née Thomas) and R. J. Middleton, *J. Chem. Soc., Chem. Commun.*, 1995, 1743.

7 See ref. 6(*b*) and references cited therein and S. Ma and E. Negishi, *J. Am. Chem. Soc.*, 1995, **117**, 6345.

8 S. E. Gibson (née Thomas), N. Guillo, S. B. Kalindjian and M. J. Tozer, unpublished results.

9 (*a*) A. Ali, G. B. Gill, G. Pattenden, G. A. Roan and T.-S. Kam, *J. Chem. Soc., Perkin Trans. 1*, 1996, 1081; (*b*) J. H. Rigby and M. N. Qabas, *J. Org. Chem.*, 1993, **58**, 4473.

10 D. P. Curran and C.-T. Chang, *J. Org. Chem.*, 1989, **54**, 3140.

*Received, 20th January 1997; Com. 7/00450H*

# Activation of water by permethyltungstenocene; evidence for the oxidative addition of water

**Myungok Yoon and David R. Tyler***

*Department of Chemistry, University of Oregon, Eugene, Oregon 97403-1253, USA*

**Water oxidatively adds to photogenerated [W($\eta^5$-$C_5Me_5$)$_2$] to form [WH(OH)($\eta^5$-$C_5Me_5$)$_2$]; continued irradiation converts [WH(OH)($\eta^5$-$C_5Me_5$)$_2$] to [WO($\eta^5$-$C_5Me_5$)$_2$].**

Oxidative addition is a potentially important reaction for the activation of water in solar energy conversion schemes and in other homogeneous catalytic cycles involving water.[1–3] Here, we report the oxidative addition of water to [W($\eta^5$-$C_5Me_5$)$_2$] and, by analogy, to [Mo($\eta^5$-$C_5H_5$)$_2$]. Oxidative addition reactions of water are uncommon for both thermodynamic and kinetic reasons.[4] In fact, only a few well characterized systems involving oxidative addition of water to organometallic complexes have been reported. For example, Milstein *et al.*[2] demonstrated the oxidative addition of water to several iridium(I) complexes [eqn. (1)] and Yoshida[1] reported the oxidative addition of water to rhodium(I) hydrido complexes [*e.g.* eqn. (2)].

$$[Ir(PMe_3)_4]^+ + H_2O \rightarrow \textit{cis}\text{-}[Ir(PMe_3)_4(H)(OH)]^+ \quad (1)$$

$$[RhH(PPr^i_3)]_3 + H_2O \xrightarrow{py} [RhH_2(py)_2(PPr^i_3)_2(OH)] \quad (2)$$

Oxidative addition of water has been proposed in several other studies,[3,5] generally as part of longer reaction pathways, but these reactions are not understood mechanistically, and oxidative addition has not been established with certainty in these systems.

Our interest in the oxidative addition of water to [Mo($\eta^5$-$C_5H_5$)$_2$] was piqued when, as part of a water-splitting project, we found that irradiation of [MoH$_2$($\eta^5$-$C_5H_5$)$_2$] in acetonitrile–water formed [MoO($\eta^5$-$C_5H_5$)$_2$] and $H_2$ in quantitative yield.[6]

$$[MoH_2(\eta^5\text{-}C_5H_5)_2] + H_2O \xrightarrow[MeCN]{h\nu} [MoO(\eta^5\text{-}C_5H_5)_2] + 2H_2 \quad (3)$$

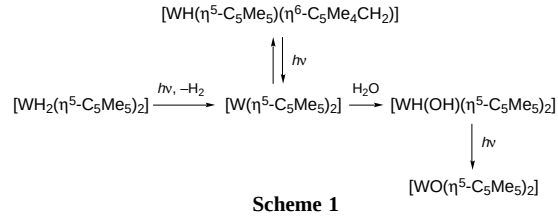
It is well established that irradiation of [MH$_2$($\eta^5$-$C_5H_5$)$_2$] (M = Mo, W) forms $H_2$ and [M($\eta^5$-$C_5H_5$)$_2$],[7] and a consideration of possible mechanisms for reaction (3) led us to hypothesize that oxidative addition of water to [Mo($\eta^5$-$C_5H_5$)$_2$] was involved. In order to investigate this hypothesis, we studied the photochemistry of the related [WH$_2$($\eta^5$-$C_5Me_5$)$_2$] molecule rather than [MoH$_2$($\eta^5$-$C_5H_5$)$_2$] because [WH(OH)($\eta^5$-$C_5Me_5$)$_2$] is a relatively stable molecule, whereas [MoH(OH)($\eta^5$-$C_5H_5$)$_2$] has not been reported.[8] {Note that the[WH(OH)($\eta^5$-$C_5Me_5$)$_2$] was prepared by $LiAlH_4$ reduction of [WO($\eta^5$-$C_5Me_5$)$_2$], not by reaction of water with the [W($\eta^5$-$C_5Me_5$)$_2$] intermediate.}

Irradiation of [WH$_2$($\eta^5$-$C_5Me_5$)$_2$] in $CD_3CN$ (37 mM; $\lambda$ > 340 nm) in the presence of water (3.7 M) for 7.5 h caused a colour change from yellow to yellow–green.†‡ $^1H$ and $^{13}C$ NMR analysis (Table 1) of the solution showed the presence of the oxidative addition product [WH(OH)($\eta^5$-$C_5Me_5$)$_2$] (12%), as well as [WO($\eta^5$-$C_5Me_5$)$_2$] (12%), [WH($\eta^5$-$C_5Me_5$)$_2$($\eta^6$-$C_5Me_4CH_2$)] (9%), and unreacted [WH$_2$($\eta^5$-$C_5Me_5$)$_2$] (67%), eqn. (4) and Scheme 1. [WH($\eta^5$-$C_5Me_5$)($\eta^6$-$C_5Me_4CH_2$)] is the known intramolecular C–H oxidative addition product that forms from the [W($\eta^5$-$C_5Me_5$)$_2$] intermediate.§ The formation of this product indicates that [W($\eta^5$-$C_5Me_5$)$_2$] is forming as an intermediate in the reaction, as planned. Continued irradiation of the reaction solution for a total of 15 h caused the solution to turn green ($\lambda_{max}$ = 596 nm), at which point $^1H$ and $^{13}C$ NMR analysis showed [WH(OH)($\eta^5$-$C_5Me_5$)$_2$] (27%), an increased amount of [WO($\eta^5$-$C_5Me_5$)$_2$] (59%), and unreacted [WH$_2$($\eta^5$-$C_5Me_5$)$_2$] (14%).

$$[WH_2(\eta^5\text{-}C_5Me_5)_2] \xrightarrow[CD_3CN\text{–}H_2O]{h\nu} [WH(OH)(\eta^5\text{-}C_5Me_5)_2] + [WO(\eta^5\text{-}C_5Me_5)_2] + [WH(\eta^5\text{-}C_5Me_5)(\eta^6\text{-}C_5Me_4CH_2)] \quad (4)$$

The results above show that water oxidatively adds to the photogenerated [W($\eta^5$-$C_5Me_5$)$_2$] intermediate, and they also suggest that [WH(OH)($\eta^5$-$C_5Me_5$)$_2$] is an intermediate on the pathway from [WH$_2$($\eta^5$-$C_5Me_5$)$_2$] to [WO($\eta^5$-$C_5Me_5$)$_2$]. Consistent with this latter hypothesis, irradiation of [WH(OH)($\eta^5$-$C_5Me_5$)$_2$]¶ (28 mM; $\lambda$ > 340 nm) in $CD_3CN$–$H_2O$ ([$H_2O$] = 3.7 M) for 7.5 h gave [WO($\eta^5$-$C_5Me_5$)$_2$] as the only product {38% yield with 62% [WH(OH)($\eta^5$-$C_5Me_5$)$_2$] still unreacted}, eqn. (5).

$$[WH(OH)(\eta^5\text{-}C_5Me_5)_2] \xrightarrow[CD_3CN\text{–}H_2O]{h\nu} [WO(\eta^5\text{-}C_5Me_5)_2] \quad (5)$$




**Scheme 1**

**Table 1** $^1H$ NMR chemical shifts in various solvents

| | Assignment | [WH$_2$($\eta^5$-$C_5Me_5$)$_2$] | [WO($\eta^5$-$C_5Me_5$)$_2$] | [WH(OH)-($\eta^5$-$C_5Me_5$)$_2$] | [WH($\eta^5$-$C_5Me_5$)-($\eta^6$-$C_5Me_4CH_2$)][a] |
|---|---|---|---|---|---|
| $C_6D_6$ | $C_5Me_5$ | 1.98 | 1.87 | 1.81 | 1.86 |
| | W–OH | | | −0.51 | |
| | W–H | −11.25 | | −11.05 | −11.94 |
| $CD_3CN$ | $C_5Me_5$ | 1.95 | 1.90 | 1.82 | 1.87 |
| | W–OH | | | −0.88 | |
| | W–H | −11.86 | | −11.47 | −12.39 |
| $CD_3CN$–$H_2O$ | $C_5Me_5$ | 1.95 | 1.92 | 1.85 | 1.87 |
| (15/1) | W–H | −12.01 | | −11.57 | −12.43 |

[a] For comparison to the other complexes, only the $C_5Me_5$ and hydride resonances are reported in this Table. For the complete spectrum, see footnote ¶.

Also consistent with the hypothesis, irradiation ($\lambda > 340$ nm; 7.5 h) of $[WH(OH)(\eta^5\text{-}C_5Me_5)_2]$ (22 mM) in dry $CD_3CN$ gave $[WO(\eta^5\text{-}C_5Me_5)_2]$ (19%), $[WH_2(\eta^5\text{-}C_5Me_5)_2]$ (10%), and a small amount of $[WH(\eta^5\text{-}C_5Me_5)(\eta^6\text{-}C_5Me_4CH_2)]$ (1%), with 70% of $[WH(OH)(\eta^5\text{-}C_5Me_5)_2]$ still unreacted.‖

$$[WH(OH)(\eta^5\text{-}C_5Me_5)_2 \xrightarrow[CD_3CN]{h\nu} [WO(\eta^5\text{-}C_5Me_5)_2] + [WH_2(\eta^5\text{-}C_5Me_5)_2] + [WH(\eta^5\text{-}C_5Me_5)(\eta^6\text{-}C_5Me_4CH_2)] \quad (6)$$

Several additional experiments provided further insights into the reactions presented in Scheme 1. Irradiation ($\lambda > 340$ nm) of $[WH_2(\eta^5\text{-}C_5Me_5)_2]$ (37 mM) for 7.5 h in $CD_3CN$ containing only small amounts of water (59 mM) gave $[WH(\eta^5\text{-}C_5Me_5)(\eta^6\text{-}C_5Me_4CH_2)]$ (58%) as the major product along with a small amount of $[WO(\eta^5\text{-}C_5Me_5)_2]$ (3%) and unreacted $[WH_2(\eta^5\text{-}C_5Me_5)_2]$ (39%). {Irradiation ($\lambda > 340$ nm) of $[WH_2(\eta^5\text{-}C_5Me_5)_2]$ (22 mM) for 23 h in dry $CD_3CN$ gave $[WH(\eta^5\text{-}C_5Me_5)(\eta^6\text{-}C_5Me_4CH_2)]$ as the only product.} The formation of $[WH(\eta^5\text{-}C_5Me_5)(\eta^6\text{-}C_5Me_4CH_2)]$ was reversible, however, as irradiation of this compound in $CD_3CN$ (16 mM; $\lambda > 340$ nm) for 7.5 h in the presence of a large excess of water (3.7 M) gave $[WH(OH)(\eta^5\text{-}C_5Me_5)_2]$ (21%) and $[WO(\eta^5\text{-}C_5Me_5)_2]$ (79%). Continued irradiation for a total of 18 h gave complete conversion to $[WO(\eta^5\text{-}C_5Me_5)_2]$. In the reverse reaction, it is suggested that reductive elimination of a C–H bond occurs to give $[W(\eta^5\text{-}C_5Me_5)_2]$, which then reacts with $H_2O$ to form $[WH(OH)(\eta^5\text{-}C_5Me_5)_2]$ and then $[WO(\eta^5\text{-}C_5Me_5)_2]$.

The mechanism for the conversion of $[WH(OH)(\eta^5\text{-}C_5Me_5)_2]$ to $[WO(\eta^5\text{-}C_5Me_5)_2]$ is uncertain. One possibility is a mechanism suggested by Bercaw and Parkin for the thermal conversion of $[WH(OH)(\eta^5\text{-}C_5Me_5)_2]$ to $[WO(\eta^5\text{-}C_5Me_5)_2]$ (at 80 °C).[10] Their mechanism is shown in reactions (7) and (8).

$$2\,[WH(OH)(\eta^5\text{-}C_5Me_5)_2] \rightarrow [WH_2(\eta^5\text{-}C_5Me_5)_2] + [W(OH)_2(\eta^5\text{-}C_5Me_5)_2] \quad (7)$$

$$2\,[W(OH)_2(\eta^5\text{-}C_5Me_5)_2] \rightarrow [WO(\eta^5\text{-}C_5Me_5)_2] + H_2O \quad (8)$$

The products of reaction (6) are consistent with this pathway. According to this mechanism $[WH(\eta^5\text{-}C_5Me_5)(\eta^6\text{-}C_5Me_4CH_2)]$ is formed in a secondary photolysis by irradiation of $[WH_2(\eta^5\text{-}C_5H_5)_2]$, not by a route involving reductive elimination of water from $[WH(OH)(\eta^5\text{-}C_5Me_5)_2]$. It is not obvious, however, why the mechanism would be photochemically activated. Another possible mechanism is a 1,2-elimination of $H_2$ from $[WH(OH)(\eta^5\text{-}C_5Me_5)_2]$. Consistent with this pathway is the observation that $[WO(\eta^5\text{-}C_5Me_5)_2]$ is the only product formed by irradiation of $[WH(OH)(\eta^5\text{-}C_5Me_5)_2]$ in the presence of an excess of water [eqn. (5)]. However, the formation of $[WH_2(\eta^5\text{-}C_5Me_5)_2]$ in eqn. (6) is not accounted for by this mechanism.

In summary, the spectroscopic observation of $[WH(OH)(\eta^5\text{-}C_5Me_5)_2]$ provides convincing evidence for the oxidative addition of water to $[W(\eta^5\text{-}C_5Me_5)_2]$ and by analogy to $[Mo(\eta^5\text{-}C_5H_5)_2]$. The $[WH(OH)(\eta^5\text{-}C_5Me_5)_2]$ molecule is photoreactive and it is converted to $[WO(\eta^5\text{-}C_5Me_5)_2]$. We are continuing to investigate the mechanisms of these reactions and their applications to water splitting.

Acknowledgment is made to the Department of Energy for the support of this research.

## Footnotes

† $[WH_2(\eta^5\text{-}C_5Me_5)_2]$ and $[WO(\eta^5\text{-}C_5Me_5)_2]$ were prepared by literature procedures.[8]

*Spectroscopic data*: $[WH_2(\eta^5\text{-}C_5Me_5)_2]$ (see also Table1 and refs. 8 and 9). $^{13}C\{^1H\}$ NMR ($C_6D_6$, 300 MHz, in ppm relative to $SiMe_4$): δ 12.40 (s, $CH_3$), 90.09 (s, $CCH_3$). $^{13}C\{^1H\}$ NMR ($CD_3CN$): δ 12.42 (s, $CH_3$), 91.05 (s, $CCH_3$). $^{13}C\{^1H\}$ NMR ($CD_3CN$–$H_2O$; 15 : 1): δ 12.10 (s, $CH_3$), 90.96 (s, $CCH_3$). EIMS (70 eV): *m/z* 454 ($M^+ - 2$, 100% with correct isotope pattern). UV–VIS (MeCN) $\lambda_{max}$ = 281 nm (ε = 7221 $dm^3\ mol^{-1}\ cm^{-1}$).

$[WO(\eta^5\text{-}C_5Me_5)_2]$ (see also Table 1). $^{13}C\{^1H\}$ NMR ($CD_3CN$): δ 11.72 (s, $CH_3$), 99.02 (s, $CCH_3$). $^{13}C\{^1H\}$ NMR ($CD_3CN$–$H_2O$; 15 : 1): δ 11.49 (s, $CH_3$), 99.38 (s, $CCH_3$). UV–VIS (MeCN) $\lambda_{max}$ = 596 nm (ε = 113 $dm^3\ mol^{-1}\ cm^{-1}$). In addition to the NMR spectra, the band at 596 nm was a useful diagnostic that indicates the formation of $[WO(\eta^5\text{-}C_5Me_5)_2]$ in a reaction.

‡ A typical photolysis experiment was performed as follows. To an NMR tube attached to a stopcock was loaded 10 mg of $[WH_2(\eta^5\text{-}C_5Me_5)_2]$ (21.9 μmol) and $CD_3CN$ (0.6 ml) in a dry box. Distilled water (40 μl, 2.2 mmol), which had been degassed by three freeze–pump–thaw (FPT) cycles, was syringed into the tube under $N_2$. After the resulting solution was degassed by two FPT cycles, the tube was flame-sealed. During the photolysis, the solution in the NMR tube was cooled with ice–water and shaken frequently. The solutions were irradiated using a high-pressure Hg arc lamp (200 W) fitted with a water filter and a UV cutoff filter (Corning Glass CS 0-52). When the chemical resonances of $[WH_2(\eta^5\text{-}C_5Me_5)_2]$ overlapped with those of solvents, the amount of $[WH_2(\eta^5\text{-}C_5Me_5)_2]$ was estimated by subtracting integrations corresponding to solvent, which in turn were calculated using their ratios to added $SiMe_4$ in stock NMR solvents.

§ The complex $[WH(\eta^5\text{-}C_5Me_5)(\eta^6\text{-}C_5Me_4CH_2)]$ was reported to form from $[W(\eta^5\text{-}C_5Me_5)_2]$ in (*a*) photolysis of $[WH_2(\eta^5\text{-}C_5Me_5)_2]$ in pentane,[9] (*b*) reaction of $[W(H)Cl(\eta^5\text{-}C_5Me_5)_2]$ with MeLi in toluene at 100 °C,[8] (*c*) reaction of $[WCl_2(\eta^5\text{-}C_5Me_5)_2]$ with MeLi in $C_6D_6$ at 80 °C,[8] and (*d*) reaction of $[WCl_2(\eta^5\text{-}C_5Me_5)_2]$ with Na–Hg in thf.[9b]

¶ The preparation of $[WH(OH)(\eta^5\text{-}C_5Me_5)_2]$ was modified from the literature procedure[8] as follows. Diethyl ether (20 ml) was added to a mixture of $[WO(\eta^5\text{-}C_5Me_5)_2]$ (240 mg; 0.51 mmol) and $LiAlH_4$ (180 mg; 4.75 mmol) at −77 °C. The reaction mixture was warmed to room temp. and stirred for 2 h, producing an orange–brown solution. After unreacted $LiAlH_4$ was filtered off, and solvent was removed, the residual solid was chromatographed on basic alumina.[6b] The first fraction (hexanes) was $[WH(\eta^5\text{-}C_5Me_5)(\eta^6\text{-}C_5Me_4CH_2)]$ (45.9 mg, 0.10 mmol, 19.6%). The second fraction (hexanes–ether = 1 : 1) was $[WH_2(\eta^5\text{-}C_5Me_5)_2]$ (9.3 mg, 0.02 mmol, 3.9%), and the third fraction was a negligible amount of unreacted $[WO(\eta^5\text{-}C_5Me_5)_2]$. The last fraction (ether–thf = 1 : 1) was $[WH(OH)(\eta^5\text{-}C_5Me_5)_2]$ (51.5 mg, 0.11 mmol, 21.4%). $^1H$ NMR data for $[WH(\eta^5\text{-}C_5Me_5)(\eta^5,\eta^1\text{-}C_5Me_4CH_2)]$ in $CD_3CN$: δ 1.87 [15 H, s, $C_5(Me)_5$], 1.51, 1.80 and 2.06 [each 3 H, s, $C_5(Me)_4CH_2$], 2.01 [3H, d, $C_5(Me)_4CH_2$, $J_{HW(H)}$ = 3 Hz], 2.87 and 3.08 [each 1 H, m, $C_5(Me)_4CH_2$], −12.39 (1 H, br m, $J_{WH}$ = 93 Hz). Spectroscopic data for $[WH(OH)(\eta^5\text{-}C_5Me_5)_2]$ (see also Table 1). $^{13}C\{^1H\}$ NMR ($CD_3CN$): δ 13.14 (s, $CH_3$), 108.43 (s, $CCH_3$). $^{13}C\{^1H\}$ NMR ($CD_3CN$–$H_2O$; 15 : 1): δ 13.36 (s, $CH_3$), 109.30 (s, $CCH_3$). IR (KBr pellet, $cm^{-1}$): 2973m, 2904s, 2860m, 2725w, 1906m (WH), 1378s, 1265m, 1102w, 1070w, 1024m, 934w, 872m, 801m, 692w. The resonance of the OH proton could be located at δ −0.51 ($C_6D_6$), which broadens upon addition of a stoichiometric amount of water or ethanol, and disappears with addition of an excess of water.

‖ Further irradiation for a total of 30 h produced a solution containing a decreased amount of $[WH_2(\eta^5\text{-}C_5Me_5)_2]$ (1%), an increased amount of $[WH(\eta^5\text{-}C_5Me_5)(\eta^6\text{-}C_5Me_4CH_2)]$ (18%), $[WO(\eta^5\text{-}C_5Me_5)_2]$ (49%), and unreacted $[WH(OH)(\eta^5\text{-}C_5Me_5)_2]$ (42%).

## References


1 T. Yoshida, T. Okano, K. Saito and S. Otsuka, *Inorg. Chim. Acta*, 1980, **44**, L135.
2 D. Milstein, J. C. Calabrese and I. D. Williams, *J. Am. Chem. Soc.*, 1986, **108**, 6387.
3 G. L. Hillhouse and J. E. Bercaw, *J. Am. Chem. Soc.*, 1984, **106**, 5472.
4 P. E. M. Siegbahn, R. A. Blomberg and M. Svensson, *J. Phys. Chem.*, 1993, **97**, 2564.
5 M. A. Bennett and T. Yoshida, *J. Am. Chem. Soc.*, 1978, **100**, 1750; M. M. T. Khan, S. B. Halligudi and S. Shukla, *Angew. Chem., Int. Ed. Engl.*, 1988, **27**, 1735.
6 (*a*) G. T. Baxley, T. M. Aukett and D. R. Tyler, manuscript in preparation; (*b*) N. D. Silavwe, M. R. M. Bruce, C. E. Philbin and D. R. Tyler, *Inorg. Chem.*, 1988, **27**, 4669.
7 G. L. Geoffroy and M. S. Wrighton, *Organometallic Photochemistry*, Academic Press, New York, 1979, p. 279.
8 G. Parkin and J. E. Bercaw, *Polyhedron*, 1988, **7**, 2053.
9 (*a*) F. G. N. Cloke, J. C. Green, M. L. H. Green and C. P. Morley, *J. Chem. Soc., Chem. Commun.*, 1985, 945; (*b*) F. G. N. Cloke, J. P. Day, J. C. Green, C. P. Morley and A. C. Swain, *J. Chem. Soc., Dalton Trans.*, 1991, 789.
10 G. Parkin and J. E. Bercaw, *Organometallics*, 1989, **8**, 1172.


*Received, 3rd January 1997; Com. 7/00087A*

# Modification of MCM-41 *via* ring opening of a strained [1]ferrocenophane

**Stephen O'Brien, Jonathan Tudor, Stephen Barlow, Mark J. Drewitt, Stephen J. Heyes and Dermot O'Hare*†**

*Inorganic Chemistry Laboratory, South Parks Road, Oxford, UK OX1 3QR*

**The walls of the mesoporous silicate MCM-41 can be functionalised with ferrocenyl end groups by reaction with an alkane solution of (1,1′-ferrocenediyl)dimethylsilane; the product is studied by solid-state NMR and EXAFS spectroscopies.**

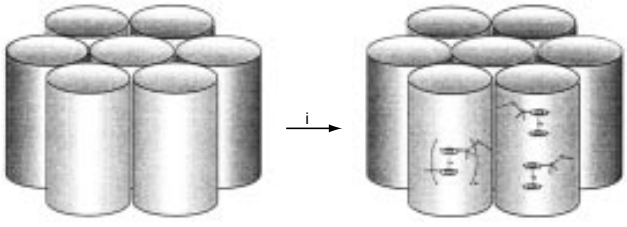
The synthesis, characterisation and potential uses of the new generation of mesoporous silicates has attracted considerable interest in recent years.[1,2] The size of the channels (diameters of 20–100 Å) allows the catalytic conversion of substrates much larger than previously possible using zeolites. The immobilisation of transition-metal catalysts on the surface is possible by utilising the reactivity of the hydroxy groups on the pore walls (an estimated 8–27% of the silicons are silanols in MCM-41[3,4]).

Bein and coworkers reported the surface attachment of a trimethylstannyl complex in MCM-41,[5] and Thomas and coworkers successfully achieved the inclusion of titanium dioxide nanoparticles inside the channels of MCM-41 using an organotitanium precursor.[6]

Here we report on the use of the ring-opening reaction of the strained metallocenophane [Fe{(η-$C_5H_4$)$_2$$SiMe_2$}][7,8] as a high-yield, low-temperature method of functionalising mesoporous silicates.

The functionalisation of a silica surface with (1,1′-ferrocenediyl)dimethylsilane, was first reported by Wrighton and coworkers[7] and utilises the susceptibility of [1]ferrocenophanes to nucleophilic attack by the hydroxy groups on the surface of the silica wall. It has been found previously that reaction of [1]ferrocenophanes with nucleophiles can lead, depending on the reaction conditions, to oligomeric and high molecular mass species[8,9] as well as stoichiometrically ring-opened species.

MCM-41 was prepared according to the published procedure.[10] It was activated at 540 °C for 8 h and then heated to 150 °C under a vacuum of $10^{-4}$ Torr for 6 h. Treatment with a pentane solution of [Fe{($C_5H_4$)$_2$$SiMe_2$}] for 24 h under nitrogen gave an orange powder (Scheme 1). The orange solid was then washed repeatedly with dry pentane until the pentane extracted remained colourless. Trace amounts of ferrocene were recovered from the pentane washings. The proportion of [1]ferroceneophane converted to ferrocene was 4–5%, while the rest was immobilised within the host. Elemental analysis indicated that a high loading of the organometallic guest into the silicate had been achieved, typical analysis gives 8.28 mass% Fe. XRD showed the product to be a slightly less well defined hexagonal phase than the original MCM-41 used, with a lattice constant, $a$ = 45.8 Å. Reaction with iodine vapour under vacuum immediately turned the solid green, indicating facile oxidation of the ferrocenyl units.




**Scheme 1** *Reagents and conditions*: i [Fe{(η-$C_5H_4$)$_2$$SiMe_2$}] in pentane, room temp., 24 h

The ferrocenyl-functionalised MCM-41 **1** was investigated using $^{13}C$ and $^{29}Si$ solid-state NMR and Fe K-edge EXAFS spectroscopy. The room-temperature solid-state CP MAS $^{29}Si$ NMR is shown in Fig. 1(*b*). Four resonances can be observed, the two closely spaced signals at δ −101.1 and −108.0 can be assigned as two convoluted broad signals representative of the silica framework, consisting mainly of $Q_3$ and $Q_4$ units with the presence of a very little $Q_2$ [where $Q_n$ is defined as $Si(OSi)_n(OH)_{4-n}$]. A comparison with the $^{29}Si$ NMR of the original mesoporous silicate showed that the intensities of $Q_2$ and $Q_3$ had decreased significantly. This was confirmed by a significant decrease in the ν(OH) adsorptions in the IR spectrum. The signal at δ 7.0 can be assigned as an $(O)_3SiR$ (R = alkyl) in accordance with previously reported chemical shifts for such species.[1,11] The remaining narrow signal at δ −6.5 has a longer relaxation than its neighbours, and hence some ring-down can be observed at this acquisition time. This resonance has been assigned to the bridging silicon atoms present in small oligomeric units of poly(ferrocenylsilane) with the first unit

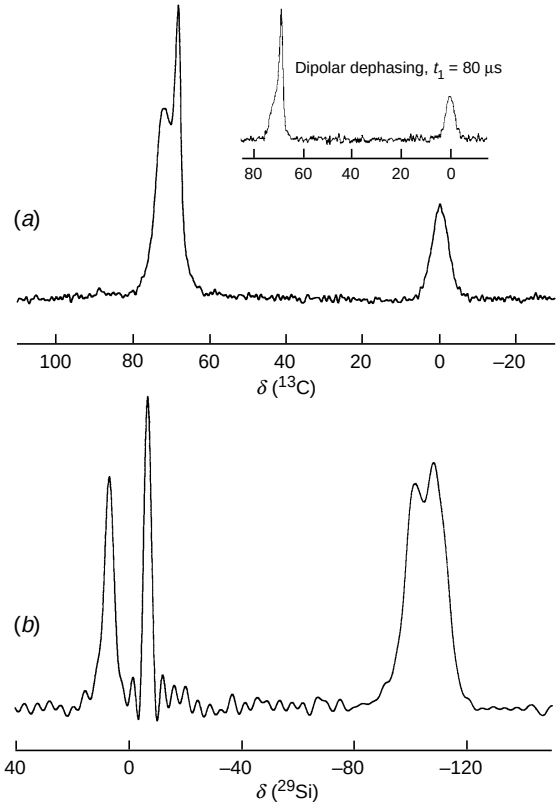



**Fig. 1** (*a*) Room-temperature 50.32 MHz solid-state $^{13}C$ CP MAS NMR spectra of [Fe{(η-$C_5H_4$)$_2$$SiMe_2$}]/MCM-41 **1** with spinning rate of 2.66 kHz. Contact times were 1 ms and recycle delay 2 s. (*b*) Room-temperature 39.76 MHz solid-state $^{29}Si$ CP MAS NMR spectrum of [Fe{(η-$C_5H_4$)$_2$$SiMe_2$}]/MCM-41 **1** at a spinning rate of 2.47 kHz. Contact time 2 ms and recycle delay 3 s. Recorded on a Bruker MSL200.

bound to the channel wall by comparison to the value of δ −6.4 quoted for the shift of poly(ferrocenylsilane) in $C_6D_6$ solution.[8] The narrower linewidth, suggesting longer spin–spin relaxation time, is consistent with a model of a molecule that exhibits more motional averaging relative to its counterparts, and this would be possible through rotation about a bond to the silicon atom.

The room-temperature solid-state $^{13}C$ CP MAS NMR spectrum of **1** is shown in Fig. 1(*a*). Three broad resonances are observed, all of which are broader than those of the related crystalline ferrocene compounds. The broadness is due to the range of chemically different environments in which the molecules are located, giving rise to an envelope of peaks with very similar chemical shifts. The isotropic chemical shifts are at δ −0.1, 68.6 and 72.1 with full widths at half maximum (FWHM) of 234, 105 and 220 Hz respectively. The widths can be compared with those of the solid-state NMR of the [1]ferrocenophane which were measured as 180.7 Hz (δ 77–79.5, $C_5H_4$), 30.3 Hz (δ 34.4, cyclopentadienyl C–Si) and 58.3 Hz (δ −2.5, $CH_3$). The signal at δ −0.1 can be assigned to the methyl carbons attached to bridging silicon atoms, be they bonded to the wall of the silicate *via* an oxygen or to another ferrocenyl unit (expected chemical shifts of δ *ca*. 0.4 and −0.5, respectively). The set of peaks downfield is due to cyclopentadienyl carbons of the modified ferrocene analogue. The sharper, more clearly defined peak at δ 68.6 is the free $C_5$ ring comparable to the chemical shift observed for the cyclopentadienyl ring formed from the ring-opening reaction of (1,1′-ferrocenediyl)dimethylsilane with $CD_3OD$. Cross-polarization and dephasing techniques (described by Alemany *et. al.*[12]) were employed to discern between the carbon atoms in the system. These experiments showed that the broad peak at δ 72.1 exhibited rapid dephasing [see Fig. 1(*a*), inset] and so we assign this signal to the CH groups of the static cyclopentadienyl ring grafted to the walls. Dephasing was slower for the neighbouring signal, indicating an attenuated $^{13}C$–$^{1}H$ dipolar coupling, as a result of greater motional freedom in the form of ring rotation. The methyl carbons attached to the silicon demonstrated an attenuation of effective $^{13}C$–$^{1}H$ coupling owing to rapid rotational motion.

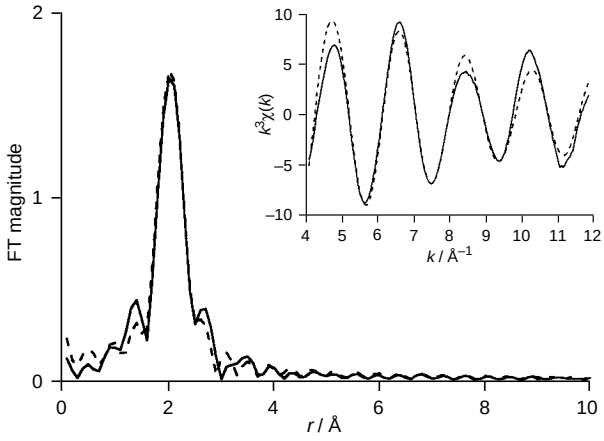



**Fig. 2** Fourier transform of the K-edge transmission EXAFS spectrum (shown in inset) for the [Fe{(η-$C_5H_4$)$_2$$SiMe_2$}]/MCM-41 **1**, together with best fit (—) experiments, (---) theory. Data was collected on station 8.1 [equipped with a Si(220) monochromator and ion chambers for obtaining data in transmission mode] of the CLRC synchrotron radiation source, Daresbury (2 GeV with typical current ranging from 150 to 250 mA). Data analysis was carried out using curved-weight theory[13] to obtain the structural parameters outlined in Table 1.

**Table 1** EXAFS structural parameters for [Fe{(η-$C_5H_4$)$_2$$SiMe_2$}]/MCM-41 **1**[a]

| Atom type | $N^b$ | $r^c$/Å | Error (%) | $\sigma^{2\,d}$/Å$^2$ | Error (%) |
|---|---|---|---|---|---|
| C | 10 | 2.045 | 0.1 | 0.0073 | 1 |
| C | 2 | 2.555 | 1 | 0.0098 | 4 |

[a] $R$ factor for refinement = 22.0 defined as $R = \int|\chi^T - \chi^E|k^3dk / \int|\chi^E|k^3dk \times 100\%$ (T = theory, E = Experiment). [b] $N$ = coordination number. [c] $r$ = interatomic distance. [d] σ = Debye–Waller factor.

The Fe K-edge EXAFS of **1** was recorded on Station 8.1 at the SRS Daresbury Laboratory. Fig. 2 shows the observed and best fit to the model described below. The analysis was initially conducted by postulating a model of ferrocene for the Fe centre, and therefore selecting a single shell (coordination sphere) of ten carbon atoms using standard scattering treatment of the EXAFS data.[13] Refinement gave a bond distance appropriate and comparable to that observed in crystals of ferrocene (Fe–$C_{av}$ 2.045 Å). The best fitting was achieved by including an additional second shell of two carbon atoms. This shell is thought to arise from neighbouring rather than bonding carbon atoms (most likely from methyl groups attached to the silicon atoms) or as result of multiple scattering complications due to collinearity of the cyclopentadienyl carbons.

In conclusion, we have demonstrated the use of strained ferrocenophanes to functionalise mesoporous silicates. Both solid-state NMR and EXAFS spectroscopy indicate that the organometallic guest has remained intact within the silicate structure and is tethered to the silicate wall *via* Si–O linkages.

We thank the EPSRC for access to the SRS, Daresbury Laboratory and Dr Mosselmans for his help with the EXAFS experiments. We also thank EPSRC for studentships (S. O'B., J. T., S. B.).

## Footnote

† D. O'Hare is the Royal Society of Chemistry Sir Edward Frankland Fellow.

## References

1 J. S. Beck, J. C. Vartuli, W. J. Roth, M. E. Leonowicz, C. T. Kresge, K. D. Schmitt, C. T.-W. Chu, D. H. Olson, E. W. Sheppard, S. B. McCullen, J. B. Higgins and J. L. Schlenker, *J. Am. Chem. Soc*., 1992, **114**, 10 834.
2 P. T. Tanev, M. Chibwe and T. J. Pinnavaia, *Nature*, 1994, **368**, 321.
3 B. P. Feuston and J. B. Higgins, *J. Phys. Chem*., 1994, **98**, 4459.
4 C.-Y. Chen, S. L. Burkett, M. E. Davis and H. X. Li, *Microporous Mater*., 1993, **2**, 17.
5 C. Huber, K. Moller and T. Bein, *J. Chem. Soc., Chem. Commun*., 1994, 2619.
6 T. Maschmeyer, F. Rey, G. Sankar and J. M. Thomas, *Nature*, 1995, **378**, 159.
7 A. B. Fischer, J. B. Kinney, R. H. Staley and M. S. Wrighton, *J. Am. Chem. Soc*., 1979, **101**, 6501.
8 D. A. Foucher, R. Ziembinski, B.-Z. Tang, P. M. MacDonald, J. Massey, C. R. Jaeger, G. J. Vansco and I. Manners, *Macromolecules*, 1993, **26**, 2878.
9 R. Rulkens, A. J. Lough and I. Manners, *J. Am. Chem. Soc*., 1994, **116**, 797.
10 C. T. Kresge, M. E. Leonowicz, W. J. Roth, J. C. Vartuli and J. S. Beck, *Nature*, 1992, **369**, 710.
11 D. W. Sindorf and G. E. Maciel, *J. Am. Chem. Soc*., 1994, **116**, 797.
12 L. B. Alemany, D. M. Grant, T. D. Alger and R. J. Pugmire, *J. Am. Chem. Soc*., 1983, **105**, 6697.
13 N. Binstead, J. W. Campbell, S. J. Gurman and P. Stephenson, EXCURV92-Program, SERC Daresbury Labs., 1992.

*Received, 8th January 1997; Com. 7/00176B*

# Formation of a vanadium(v) bicyclic carbene–amide complex *via* insertion of alkyne into a V–C bond

**Mark Moore,[a] Sandro Gambarotta,*[a] Glenn Yap,[b] Louise M. Liable-Sands[b] and Arnold L. Rheingold*[b]**

[a] *Department of Chemistry, University of Ottawa, Ottawa, Ontario K1N 6N5, Canada*
[b] *Department of Chemistry and Biochemistry, University of Delaware, Newark, DE 19716, USA*

**Reaction of $[(Me_3Si)_2N]_2V(thf)(BH_4)$ with excess diphenylacetylene leads to the formation of the bicyclic carbene complex $(Me_3Si)_2NVN(SiMe_3)SiMe_2CH_2C(Ph)C(Ph)C(Ph)C(Ph)$ 1 which is isolated as brown diamagnetic crystals cocrystallized with *trans*-stilbene; the same compound *trans*-stilbene-free is also prepared *via* reaction of $\{[(Me_3Si)_2N]V[\mu\text{-}CH_2SiMe_2N(SiMe_3)]\}_2$ with 4 equiv. of diphenylacetylene.**

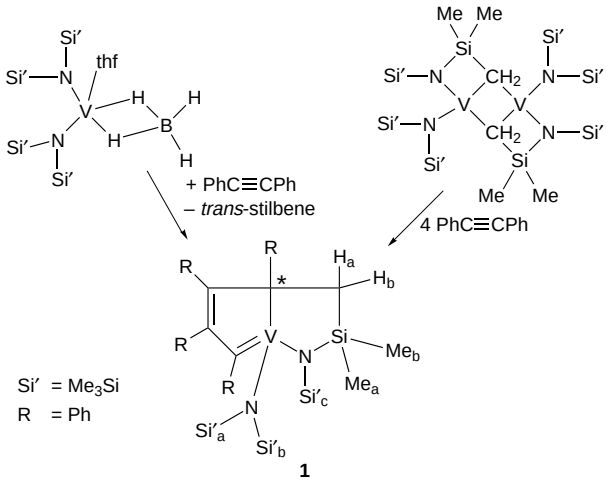
A very large part of the organometallic chemistry of vanadium has been developed with the utilization of cyclopentadienyl ligands[1] with which it is possible to stabilize reactive functions such as carbenes[2] and hydrides.[3] Nitrogen donor based ligands (amides, amidinates) provide a convenient and accessible alternative to the cyclopentadienyl ligand systems, since they significantly enhance the reactivity of the vanadium centre,[4] stabilize rare vanadium species such as dinitrogen,[5] azide,[6] nitride,[7] metallacyclic[8] and alkyl complexes[9] or assist the metal in hydrogen-transfer reactions.[5c,10]

Here we describe the formation and the unusual NMR feature of a unique bicyclic vanadium(v) derivative supported by silazanate ligand, which is also a rare example of a vanadium carbene complex.[2]

According to Scheme 1, the reaction of $[(Me_3Si)_2N]_2V(thf)(BH_4)$[11] with diphenylacetylene in hexane proceeds rapidly at room temperature to yield a brown solution from which dark diamagnetic crystals of **1** were isolated in low yield.† The presence of *trans*-stilbene in the lattice in the ratio 2 : 1, as shown by the X-ray crystal structure,‡ was confirmed by $^1H$ NMR spectroscopy.

The complex is monomeric and features a distorted tetrahedral geometry around the vanadium atom which is combined in two fused five-membered metallacycles (Fig. 1). One intact amide group occupies the fourth coordination site of vanadium. One metallacycle is formed *via* linkage of a $CH_2$ unit from a trimethylsilylamide function with a carbon atom at one end of the coupled tolane units. The second metallacycle is composed of two diphenylacetylene units forming a tetraphenylvanadacyclopentadiene ring. The geometry around three of the four carbon atoms is trigonal planar, suggesting an $sp^2$ hybridization for these atoms. Conversely, the fourth carbon atom shared with the first ring is tetrahedral and chiral. The vanadium atom is also chiral and the enantiomer is present as a second molecule in the triclinic cell together with one molecule of stilbene.

At this stage, we are unable to provide a non-speculative explanation for the formation of **1**. However, the production of *trans*-stilbene during the formation of **1** suggests that the first step of the reaction is probably the hydrogenation of diphenylacetylene Complex **1** could also be prepared without *trans*-stilbene and in significantly higher yield (44%)† by reacting the previously reported dinuclear vanadacycloazabutane $\{[(Me_3Si)_2N]V[\mu\text{-}CH_2SiMe_2N(SiMe_3)]\}_2$[8] with 4 equiv. or an excess of diphenylacetylene. In this case, the formation of **1** is simply the result of the insertion of two molecules of diphenylacetylene into the $V–CH_2$ bond of the metallacycle followed by a tautomeric reorganization of the macrocycle into the bicyclic structure. The formation of **1** from both reactions suggests that perhaps $\{[(Me_3Si)_2N]V[\mu\text{-}CH_2SiMe_2N(SiMe_3)]\}_2$ is produced as a transient intermediate of the reaction of $(Me_3Si)_2N]_2V(thf)(BH_4)$ with diphenylacetylene after the initial formation of *trans*-stilbene. The addition of only




**1**

**Scheme 1**

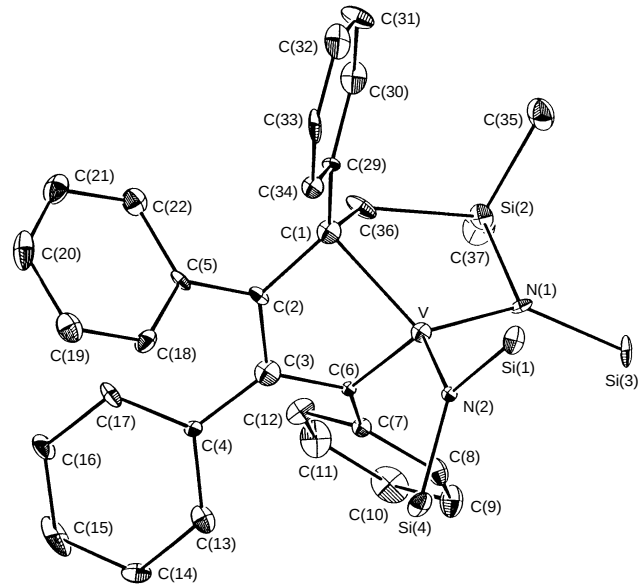



**Fig. 1** ORTEP plot of **1**. Thermal ellipsoids are drawn at the 50% probability level. Selected bond distances (Å) and angles (°): V–N(1) 1.849(5), V–N(2) 1.889(5), V–C(1) 2.092(7), V–C(6) 1.876(7), N(1)–Si(2) 1.729(5), Si(2)–C(36) 1.918(7), C(1)–C(36) 1.541(9), C(1)–C(2) 1.467(9), C(2)–C(3) 1.43(1), C(3)–C(6) 1.406(9); V–N(1)–Si(2) 99.3(3), V–C(1)–C(36) 85.4(4), V–C(1)–C(2) 90.5(4), N(1)–V–N(2) 111.9(2), N(2)–V–C(6) 116.4(3), V–C(6)–C(3) 100.1(5), Si(2)–C(36)–C(1) 123.4(5), C(2)–C(3)–C(6) 117.0(6), C(1)–C(2)–C(3) 119.0(6).

1 equiv. of tolane to $\{[(Me_3Si)_2N]V[\mu\text{-}CH_2SiMe_2N(SiMe_3)]\}_2$ still gave the diamagnetic and pentavalent **1** albeit in lower yield. This behaviour is remarkably different from that of the monomeric pyridine adduct $[(Me_3Si)_2N]V[\mu\text{-}CH_2SiMe_2N(SiMe_3)](py)$, which reacts with diphenylacetylene to give a monoinserted vanadium(III) paramagnetic species.[10]

The diamagnetism of **1** indicates a formal oxidation state (+5) for the vanadium centre, which implies the existence of a formal V–C double bond. Since the rigid structure observed in the solid state is reasonably expected to be maintained in solution, the crystal structure also provides the key to interpreting the remarkable NMR features of complex **1**. The intact group features two sharp singlets ($Si'_a$ and $Si'_b$) at δ 0.63 and 0.61, consistent with the fact that the two $SiMe_3$ groups point respectively above and below the folded molecular plane. The $SiMe_3$ of the second amide group ($Si'_c$) exhibits a rather broad singlet centred at δ −0.05. Remarkably, the two methyl groups of the silicon atom engaged in the formation of the first metallacycle ($CH_{3a}$ and $CH_{3b}$) give rise to two widely separated signals at δ 0.32 and −0.82. Even more surprising, the two enantiotopic hydrogens of the methylene group ($H_a$ and $H_b$) produce two doublets positioned far apart from each other at δ 2.85 and −1.43. HQMC experiments clearly indicate that these two protons are attached to the same carbon atom resonating at δ 20.4 in the $^{13}C$ NMR spectrum. The $^{51}V$ NMR resonance was located as a rather broad line (1800 Hz) at δ +1318.8.[12] Variable-temperature spectra show the expected broadening of the line (4300 Hz at 210 K) but also a significant downfield shift of about 100 ppm. Some of the hydrogen lines of the $^1H$ NMR spectrum also significantly broaden and shift at low temperature, suggesting the presence of fluxionality. At low temperature, the line at δ −0.05, attributed to the three methyl groups of the $Si'_c$ group, collapsed and resolved into three sharp resonances at δ 0.39, −0.18 and −0.51. However, under the same conditions, the resonances arising from $CH_{3a}$ and $CH_{3b}$ and the two enantiotopic methylene protons ($H_a$ and $H_b$) broadened only slightly. In contrast to the minor line broadening, the resonance at δ 2.85 shifted by about 1 ppm to higher field while the resonance at δ −0.82 shifted by only 0.3 ppm in the same direction. The crystal structure showed that one of these two enantiotopic protons is considerably closer to the vanadium centre than the other [V–H(59) 2.73, V–H(60) 3.11 Å]. A similar feature has been observed with the two methyl groups $CH_{3a}$ and $CH_{3b}$. However, no significant variation of the chemical shift was found over a range of temperature for these two methyl groups.

This work was supported by the National Science and Engineering Council of Canada (NSERC) through a strategic and operating grant. We are grateful to Professor D. Rehder (Hamburg) for helpful discussions.

## Footnotes

† *Synthesis and characterisation*: *Method A.* A blue solution of $[(Me_3Si)_2N]_2V(thf)(BH_4)$ (6.26 mmol) in hexane (70 ml) was treated with diphenylacetylene (20.56 mmol) at room temp. The resulting brown mixture was stirred overnight. A light brown material was removed by filtration and the resulting dark brown solution was kept at −30 °C for several weeks. Dark crystals of $\mathbf{1}\cdot 0.5\ C_{14}H_{12}$ were obtained (0.2 g, 0.7 mmol, 8%). Anal. Calc. (found) for $C_{47}H_{61}N_2Si_4V$: C 69.07 (70.40), H 7.52(7.63), N 3.43 (3.20)%.

*Method B.* A suspension of $\{[(Me_3Si)_2N]V[\mu\text{-}CH_2SiMe_2N(SiMe_3)]\}_2$ (2.0 g, 2.6 mmol) in hexane (50 ml) was reacted with diphenylacetylene (1.86 g, 10.4 mmol) at room temperature. The mixture was stirred overnight at room temperature, during which time the colour had changed to brown. After 24 h, the mixture was filtered to eliminate a small amount of brown insoluble material. The resulting intense red–brown solution was concentrated to approximately 15 ml until incipient crystallization of a brown material. The solution was allowed to stand overnight at 4 °C to yield a crop of brown crystals of $\mathbf{1}\cdot 0.5C_6H_{14}$ (1.66 g, 2.1 mmol, 44%). Spontaneous loss of hexane prevented accurate and reproducible analytical data from being obtained. IR (Nujol, KBr plates) ν/cm$^{-1}$: 1593s, 1491vs, 1252s, 1112m, 1088m, 1029s, 955vs, 889vs, 870s, 849s, 799s, 700m. Samples were pumped *in vacuo* to eliminate the hexane resonances from the NMR spectra. $^{51}V$ NMR ($C_6D_6$, 131.4 MHz, 25 °C: δ 1318.8. $^1H$ NMR ($C_6D_6$, 500 MHz, 25 °C): δ 7.59–6.60 (series of m, 20 H, phenyl), 2.85 (d, 1 H, $H_a$), 0.63 (s, 9 H, $Me_3Si_a$), 0.61 (s, 9 H, $Me_3Si_b$), 0.32 (s, 3 H, $CH_{3a}$), −0.05 (s, 9 H, $Me_3Si_c$), −0.82 (s, 3 H $CH_{3b}$), −1.43 (d, 1 H, $H_b$). $^{13}C$ NMR ($C_6D_6$, 125 MHz, 25 °C): δ 318.17 (quat. carbene), 145.95 (quat. C ring), 140.87 (quat. C ring), 135–123 (Ph), 90.10 (quat. chiral C), 20.45 ($CH_AH_B$), 5.64 ($Me_3Si_A$, $Me_3Si_B$), 5.46 ($Me_3Si_C$), 3.30 ($CH_{3A}$), 0.47 ($CH_{3B}$).

‡ *Crystal data*: $\mathbf{1}\cdot 0.5C_{14}H_{12}$: $C_{47}H_{61}N_2Si_4V$, $M$ = 817.30, triclinic, space group $P\bar{1}$, $a$ = 11.505(2), $b$ = 21.527(1), $c$ = 10.228(2) Å, α = 100.39(2), β = 114.72(1), γ = 85.58(3)°, $U$ = 2236(1) Å$^3$, $Z$ = 2, $D_c$ = 1.199 g cm$^{-3}$, $F(000)$ = 872, μ = 31.23 cm$^{-1}$, Cu-Kα (λ = 1.541 78 Å), $T$ = −150 °C, $R$ = 0.065, $R_w$ = 0.077 GOF = 2.69 for 472 parameters and 3929 reflections out of 4668 unique. Non-hydrogen atom positions were located and refined anisotropically with the exception of N(2), C(6) and C(7). Hydrogen atoms were introduced at their idealized positions. Absorption corrections (DIFABS) were applied to the data.

$\mathbf{1}\cdot 0.5C_6H_4$: $C_{40}H_{55}N_2Si_4V$, $M$ = 770.25, triclinic, space group $P\bar{1}$ $a$ = 10.267(1), $b$ = 11.569(1), $c$ = 21.133(2) Å, α = 78.48(1), β = 87.43(1), γ = 65.45(1)°, $U$ = 2235.2(5) Å$^3$, $Z$ = 2, $D_c$ = 1.144 g cm$^{-3}$, μ = 3.60 cm$^{-1}$, Mo-Kα (λ = 0.710 73 Å), $T$ = 298 K, $R$ = 0.057, for 3070 observed independent reflections ($4 \leqslant 2\theta \leqslant 43°$) contributions except those on the solvent molecule which were ignored.

Atomic coordinates, bond lengths and angles, and thermal parameters have been deposited at the Cambridge Crystallographic Data Centre (CCDC). See Information for Authors, Issue No. 1. Any request to the CCDC for this material should quote the full literature citation and the reference number 182/384.

## References

1 P. Berno, S. Gambarotta and D. Richeson, in *Comprehensive Organometallic Chemistry II*, ed. E. W. Abel, F. G. A. Stone and G. Wilkinson, Oxford, 1995.
2 B. Hessen, A. Meetsma and J. H. Teuben, *J. Am. Chem. Soc*., 1989, **111**, 5977.
3 K. Jonas, V. Wiskamp, Y. H. Tsay and C. Kruger, *J. Am. Chem. Soc*., 1983, **105**, 5480; B. Hessen, F. van Bolhuis and J. H. Teuben, *J. Am. Chem. Soc*., 1988, **110**, 295.
4 C. C. Cummins, R. R. Schrock and W. M. Davis, *Organometallics*, 1992, **11**, 1452.
5 (*a*) S. Hao, P. Berno, R. Minhas and S. Gambarotta, *Inorg. Chim. Acta*, in the press; (*b*) P. Berno, S. Hao, R. Minhas and S. Gambarotta, *J. Am. Chem. Soc*., 1994, **116**, 7417; (*c*) J. I. Song, P. Berno and S. Gambarotta, *J. Am. Chem. Soc*., 1994, **116**, 6927; (*d*) N. Demangles, H. Jenkins, K. B. Ruppa and S. Gambarotta, *Inorg. Chim. Acta*, submitted for publication.
6 M. G. Fickes, W. M. Davis and C. C. Cummins, *J. Am. Chem. Soc*., 1995, **117**, 6384.
7 P. Berno and S. Gambarotta, *Angew. Chem., Int. Ed. Engl*., 1995, **34**, 822; J. I. Song and S. Gambarotta, *Chem. Eur. J*., in the press; J. Jubb, H. Jenkins and S. Gambarotta, *Chem. Eur. J*., in the press.
8 P. Berno, R. Minhas, S. Hao and S. Gambarotta, *Organometallics*, 1994, **13**, 1052; P. Berno and S. Gambarotta, *J. Chem. Soc., Chem. Commun*., 1994, 2419.
9 A. R. Willis and P. G. Edwards, *J. Chem. Soc., Dalton Trans*., 1989, 1253; H. O. Frölich, C. Kälber and V. Stirnweiss, *Z. Anorg. Allg. Chem*., 1979, **458**, 89; H. O. Frölich and H. Kacholdt, *Z. Chem*., 1975, **15**, 233.
10 P. Berno and S. Gambarotta, *Organometallics*, 1994, **13**, 2569.
11 P. Berno, M. Moore, R. Minhas and S. Gambarotta, *Can. J. Chem*., in the press.
12 D. Rehder, *Coord. Chem. Rev*., 1991, **110**, 161; in *Advanced Applications of NMR to organometallic Chemistry*, ed. B. Wrackmeyer, M. Gielen and R. Willem, Wiley, New York, in the press.

*Received, 8th October 1996; Com. 6/06904E*



Typeset and printed by Black Bear Press Limited, Cambridge, England

ChemComm
FEATURE ARTICLE

# Some influences of fluorine in bioorganic chemistry

**David O'Hagan[a]† and Henry S. Rzepa[b]‡**

[a] *Department of Chemistry, Science Laboratories, South Road, Durham, UK DH1 3LE*
[b] *Department of Chemistry, Imperial College of Science Technology and Medicine, London, UK SW7 2AY*

**The stereochemical outcome on processing fluorinated substrate analogues by enzymes can often be controlled by electronic and stereoelectronic factors associated with the fluorine atom.**

Substitution of a hydrogen atom or a hydroxy group by fluorine in enzyme substrate analogues has been widely practised in various arenas of bioorganic and medicinal chemistry. It is very difficult however to generalise on the relative abilities of fluorine to act as a hydrogen or hydroxy group mimic and various factors have to be considered in each circumstance. The van der Waals radii of fluorine (1.47 Å) lies between oxygen (1.57 Å) and hydrogen (1.2 Å)[1] and thus fluorine appears to have a particularly close isosteric relationship to oxygen while being larger than hydrogen. However, in solid state X-ray structures, fluorine and hydrogen often interchange, and scanning tunnelling microscopy analyses of monofluorinated stearic acids deposited on graphite show very little distortion in two dimensional packing, suggesting a very close isosteric relationship between hydrogen and fluorine.[2] Consistent with this, the steric impact of replacing hydrogen by fluorine is never too great and binding of analogues to target proteins is not normally impeded. Thus despite the size anomoly fluorine emerges as a reasonable hydrogen mimic.

The ability of fluorine to act as a hydroxy group mimic is less clear and is discussed at some length below. Despite a good size correlation between fluorine and oxygen the electrostatic influence of fluorine is much weaker than that of oxygen, and this compromises its hydrogen bonding ability, a limitation of particular significance in enzyme substrate binding.

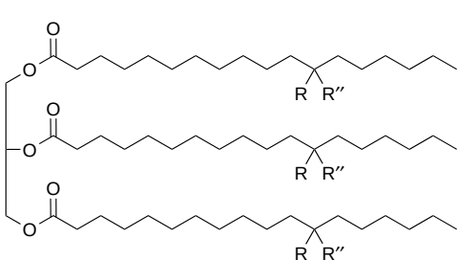
Our work has focused on exploring the behaviour of organofluorine compounds in the bioorganic arena, with a particular emphasis on investigating geometric and stereoelectronic effects which emerge as a consequence of replacing fluorine for hydrogen or oxygen. Stereoelectronic effects, which are generally lower energy phenomenon, are considerably attenuated by indiscriminate solvent interactions (H-bonding, electrostatic, dipolar *etc.*) in solution. The anomeric effect serves as a good example.[3] However the enzyme environment is significantly less polar than aqueous solvent[4] where relative permittivities in the range 15–20 have been estimated and can be compared to 78.5 for water.[5] After binding, the substrate is largely desolvated, with the substrate reaction centre proximate[6,7] and exposed to the cofactor, enzyme or second substrate without intervening solvent. Indeed it has been argued,[8] in the extreme, that enzyme reactions are more closely modelled in the gas phase rather than in the solution state due to these factors. Thus the low polarity of the enzyme active site and the possibilities of conformational control offer an attractive environment in which to assess the stereoelectronic influence of the fluorine atom.

## 1 Steric and geometric effects in CF, $CF_2$ and $CF_3$ systems

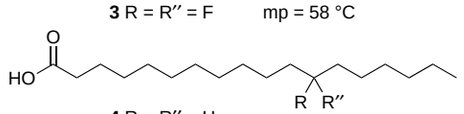
### *1.1 The CF for CH and $CF_2$ for $CH_2$ replacement*

Despite the larger van der Waals radii for fluorine over hydrogen, the experimental evidence suggests that, in general terms, the substitution of a single fluorine for a hydrogen atom introduces only small steric and geometric perturbations relative to the hydrocarbon counterpart.[2] Dehydrofluorinated (CH for CF) enzyme substrate analogues usually have a high affinity for their target protein. For example selectively β-fluorinated α-amino acids have been widely explored as suicide substrates[9–11] for decarboxylases, racemases and transaminases, and other fluorinated amino acids are assimilated biochemically into proteins.[12] Fluoroacetyl-CoA is an excellent acetyl-CoA mimic for citrate and malate synthases (see section 3.4) and fluoropyruvate is a pyruvate surrogate for L-lactate dehydrogenase.[13] Thus the fluorine for hydrogen substitution is not generally detrimental to binding, however the high electronegitivity of fluorine can have dramatic mechanistic consequences which can lead to mechanistic deviations and enzyme inhibition.[9–11]

Replacement of a methylene for a difluoromethylene group ($CH_2$ for $CF_2$) can be much more dramatic than the single substitution. In a recent study[14] in Durham we have compared the physical properties of tristearins **2** and **3** containing one and two fluorine atoms substituted for the C-12 methylene hydrogens of the hydrocarbon chain. The melting points of these tristearins are shown in Fig. 1. Substitution of one fluorine atom at C-12, in **2**, has very little effect on the melting point, polymorphic phase behaviour and X-ray powder diffraction pattern (data not shown) when compared to tristearin **1** itself, however introduction of the second fluorine atom in **3** leads to a significant lowering of the melting point (72 *vs*. 58 °C) and the polymorphic phase behaviour and X-ray powder diffraction pattern become quite different. The stability of Langmuir films of the corresponding fluorinated stearic acids **4**–**6** was also investigated. 12-Fluorostearic acid **5**, like stearic acid **4**, formed a stable monolayer on the surface of aqueous subphase, however the monolayer of 12,12-difluorostearic acid **6** was unstable and susceptible to collapse/reorganisation at comparable surface pressures, indicative of significant conformational disorder.




**1** R = R″ = H mp = 72 °C
**2** R = H, R″ = F mp = 73 °C
**3** R = R″ = F mp = 58 °C




**4** R = R″ = H
**5** R = H, R″ = F
**6** R = R″ = F

**Fig. 1** Melting points of tristearins

A similar lowering in the melting points (by *ca*. 6–10 °C) of $CF_2$-labelled diacylphosphatidylcholines relative to their hydrocarbon counterparts has also been noted[15] and the phenomenon appears to be general. We attribute this to an increased conformational flexibility of the hydrocarbon as a consequence of $CF_2$ substitution (Fig. 2). Crystallographic[16] and theoretical evidence[17] support a widening of the C–$CX_2$–C angle from the $sp^3$ tetrahedral angle (109.5°) in the hydrocarbon to *ca*. 115–119° in the $CF_2$-hydrocarbon systems. This angle widening is also apparant from the structures of C–$CH_2$–P, C–CHF–P and C–$CF_2$–P phosphonates where the C–C–P angles are 112, 113 and 116° respectively (see section 2.2). The extended zig-zag conformation is favoured in a hydrocarbon chain as disfavoured *gauche* conformations bring 1,4-hydrogens into close contact (*ca*. 1.8 Å) (Fig 3).[18] However, angle widening at the substituted carbon in the $CF_2$-containing hydrocarbon chains results in increasing this 1,4-H···H distance and in turn lowers the energy of attainment of a *gauche* conformation. A complementary situation occurs when sulfur[19] (but not oxygen) is introduced into a hydrocarbon as the increased C–S bond length (1.8 Å) over that for C–C (1.5 Å) or C–O (1.4 Å) increased the 1,4-hydrogen distance to 2.4 Å and relaxes this interaction.

### *1.2 The $CF_3$ for $CH_3$ replacement*

It is generally appreciated that the methyl and trifluoromethyl groups bear very little steric resemblance. A comparison of the molar volumes of a series of related compounds[20] with various substituents, and with a $CF_3$ group, reveals a size closer to the isopropyl rather than methyl group. Seebach has argued[21] that the $CF_3$ group is between two and three times larger than $CH_3$ when the van der Waals hemispheres of these groups are considered (Fig 4). Other assessments[22] suggest a steric influence close to that of an isopropyl group. However there are several cases in asymmetric synthesis[23] where the directing influence of the $CF_3$ group has been assessed relative to other substituents and a close analogy with the phenyl ring or even a *tert*-butyl group has been found. Of course the origin of this apparantly gross steric effect must be attributed in no small part to polar and electrostatic influences, in a given situation. Such factors are discussed below (section 2.3) in an assessment of lipase resolutions of $CF_3$ containing compounds. On balance the various lines of evidence place $CF_3$ significantly larger than methyl and a good upper estimate would equate it with the isopropyl group. Thus the substitution of one, two and three hydrogen atoms on carbon, by fluorine, becomes increasingly distorted in maintaining an isogeometric profile between the fluoro- and hydro-carbon series.

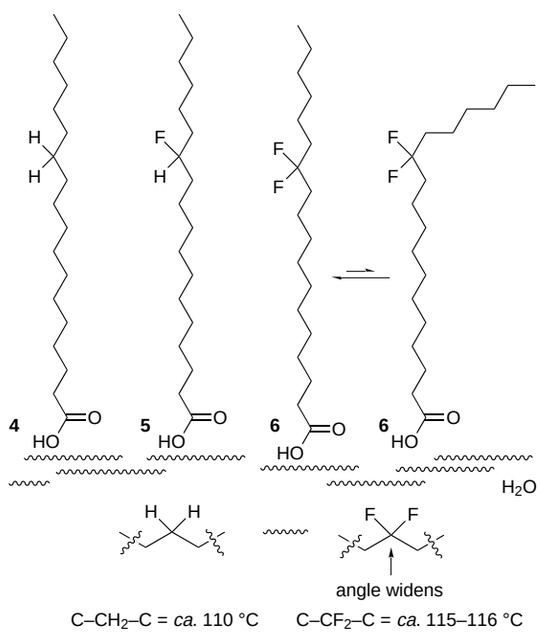



**Fig. 2** Schematic representation of C-12 fluorinated stearic acids on the surface of water. The $CF_2$ stearate **6** posesses significant conformational disorder.

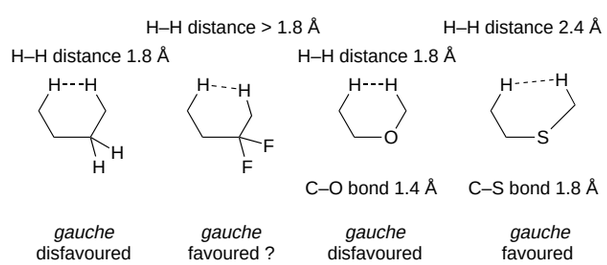



**Fig. 3** Schematic representation of 1,4-hydrogen interactions and the preference for *gauche* or zig-zag conformations

## 2 Electrostatic effects

Despite one extra lone pair, the higher electronegativity and lower polarisibility of fluorine attenuate its electrostatic influence in comparison with oxygen. So despite their apparent similarity in size, electrostatics emerge as a significant factor underlying the limited ability of fluorine to mimic a hydroxy group. In bioorganic chemistry hydrogen bonding is probably the most significant area in which electrostatic interactions are involved, certainly when considering enzyme substrate binding interactions.

### *2.1 Fluorine as a hydrogen bonding acceptor*

The capacity of organically bound fluorine to act as an oxygen surrogate (*e.g.* an OH mimic) and enter into hydrogen bonding as an acceptor has been widely discussed.[24,25] Recent theoretical calculations[26] have measured the strength of an optimum F··H bond (1.9 Å) to be 2.38 kcal $mol^{-1}$ in an adduct between fluoromethane ($CH_3F$) and water as shown in Fig. 5. Interestingly, the strength of the optimum interaction (1.95 Å) between fluoroethene ($CH_2$=CHF) and water was only 1.48 kcal $mol^{-1}$, suggesting that the C($sp^3$)–F··H interaction is stronger than the C($sp^2$)–F··H interaction. In strength therefore, F··H hydrogen bonds are clearly weaker than O··H hydrogen bonds, which are conservatively estimated[27] to be *ca*. 5 kcal $mol^{-1}$, but are stronger than O/NH–π interactions.[28,29] The weaker F··HO over O··HO interaction appears to be due to the higher nuclear charge on the F nucleus compacting the surrounding lone pairs.

Calculations[30] measuring the difference in electrostatic potentials around methanol and fluoromethane (Fig. 6) with distance from the nucleus reinforce the view that the C($sp^3$)–

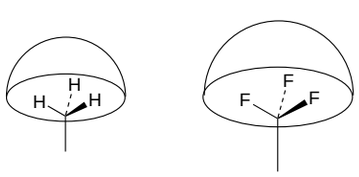



**Fig. 4** Van der Waals hemisphere volumes comparing $CH_3$ and $CF_3$ (ref. 21)

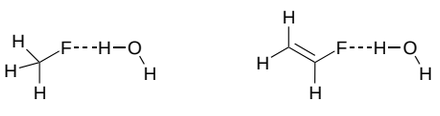



**Fig. 5** Calculated strengths of C($sp^3$)–FH··H and C($sp^2$)–F··H bonds

F···H bond strength is half that of the H···O value. The reduced electrostatic influence of fluorine requires that an incoming hydrogen bond donor must approach the fluorine nucleus more closely than oxygen, and the resulting increase in the nuclear–nuclear repulsions does not allow a strong hydrogen bond to be formed. Thus a best case scenario suggests that fluorine can contribute up to about one half of the binding energy of a hydrogen bond to oxygen. A recent[31] and controversial discussion[32] on low barrier hydrogen bonding (LBHB) suggests that in transition states of enzyme mediated reactions, O···H···O bonds can contribute upto 10–20 kcal mol$^{-1}$ although these arguments appear increasingly tenuous.[33] However if this latter situation is close to reality then the replacement of OH for fluorine would be inadequate if a hydrogen bond was important in stabilising a transition state on the enzyme surface.

Surveys[34] of the organofluorine compounds logged in the Cambridge Crystallographic Data Centre (CCDC) have revealed relatively few situations where fluorine is involved in short contacts to hydrogens. Short contacts between fluorine and less acidic H–C protons are most common whereas those between fluorine and the more acidic O–H or N–H protons are rare, clearly for statistical reasons (*i.e.* more CHs than OH or NHs) but also, acidic hydrogens prefer to find an oxygen or nitrogen acceptor in preference of fluorine. Thus the theoretical and crystallographic evidence force the conclusion that fluorine is a poor hydrogen bond acceptor with only a moderate capacity to replace oxygen (or nitrogen) in this role. In a desolvated and preorganised enzyme cavity, where the fluorine atom is predisposed towards an acidic hydrogen (donor) then these circumstances may amount to an optimal situation for F···H bonding. There are examples in the bioorganic literature which clearly suggest that fluorine is replacing OH as a hydrogen bond acceptor, however they are few and more often than not the substitution proves detrimental.[35]

### *2.2 $CF_2$-phosphonates*

Phosphate groups are susceptable to hydrolysis by the action of phosphatase enzymes; thus phosphonates, where the bridging oxygen is replaced by carbon, have been explored as phosphatase stable phosphate mimics.[36] A particular refinement of this strategy has been developed by Blackburn[37] and involves the replacement of the bridging oxygen atom by a $CF_2$ substituent. This is attractive as the fluorine atoms reintroduce the electronegativity lost on removal of the oxygen atom. The degree of electronegativity can be assessed from the p$K_a$ values of the second deprotonation of the phosphonate groups. These values are summarised for the phosphate and various phosphonates in Fig. 7. The $CF_2$-phosphonate (p$K_a$ = *ca.* 5.64) is approximately one p$K_a$ unit more acidic than the phosphate group it is designed to mimic. The CHF-phosphonate value (p$K_a$ = *ca.* 6.2) is much more closely matched and the $CH_2$-phosphonate (p$K_a$ = 7.6) is a p$K_a$ unit less acidic. It is generally assumed that the phosphate unit will be fully ionised on protein binding, thus the increased acidity of the $CF_2$-phosphonate is not judged detrimental in this respect and often $CF_2$-phosphonates emerge as excellent phosphate surrogates.

Crystal structures[16,38] of the aminophosphonic acids **7**, **9** and **10** reveal that the P–C–C angle of the $CF_2$-phosphonate (116°) is closer than that of the $CH_2$- (112°) and CHF- (113°) phosphonates to the C–O–P angle (118°) of the phosphate group of **8**. Thus the $CF_2$-phosphonate appears to approximate the geometry of the phosphate group most closely in the series, at least in the ground state. Therefore on geometric and ionic grounds the $CF_2$-phosphonate emerges as a good phosphate mimic. On the other hand the substitution of oxygen for $CF_2$ will have an increased steric impact, as the fluorine atoms are resident in the space previously occupied by the lone pairs of oxygen.

The electrostatic profile of the CHF and $CF_2$ groups in comparison to oxygen must also be considered when evaluating these systems. A recent theoretical analysis by Thatcher and Campbell[39] compared the negative electrostatic profile of the phosphate group with the CHF-phosphonate by superimposing the two. Fluorine has a suppressed electrostatic influence relative to oxygen, but placing it one C–F bond length out from the oxygen extends the centre of its electrostatic influence a little beyond that of oxygen when comparing oxygen and C–F. Also the area of maximum negative density for CHF-system is asymmetrically displaced from that of oxygen in the phosphate, by about 1 Å, due to the stereogenic centre. Although the comparison did not extend to the $CF_2$ system, an extrapolation of Thatcher's results suggests that the $CF_2$ group will have at least a similar, and possibly greater, electrostatic influence than the phosphate oxygen. Comparative molecular electrostatic potentials (MEPs) of the CHF- and $CF_2$-phosphonates of the aminophosphonic acids **11** and **12** respectively were evaluated by one of us[40] and reinforces the notion that the $CF_2$ phosphonate has a significant electrostatic influence (see Fig. 8), in this case on chiral recognition of the substrate *via* the asymmetric binding of the aryl group into a cyclodextrin cavity.

In the case of the CHF-phosphonate **11** the presence of fluorine induces an asymmetric negative potential (red area) on one side of the aryl π-face. This asymmetry is much less evident for the $CH_2$-phosphonate **13**.[40]

In a recent study[38,41] at Durham, using phosphonates as phosphate mimics, we have drawn the conclusion that an electrostatic interaction between an enzyme and its substrate emerges as an important factor in binding. The $CH_2$ and CHF-phosphonate analogues **15** and **16** of *sn*-glycerol-3-phosphate **14** have a greater affinity than the $CF_2$-phosphonate analogue **17** for the enzyme glycerol-3-phosphate dehydrogenase. The enzyme is NAD dependant and oxidised the secondary alcohol of each of the phosphonates to their corresponding dihydrox-

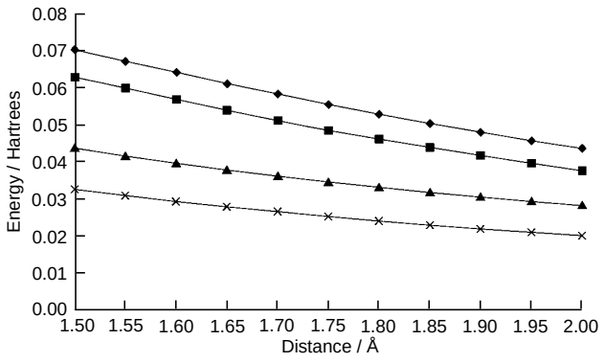



**Fig. 6** A plot of calculated electrostatic potential values at the B3LYP/6-31G(d,p) level for methanol (◆), hydroxyethene (■), fluoromethane (▲) and fluoroethene (X) as a function of distance (Å) from the F/O nucleus. The maximum value of the potential at this distance is shown.

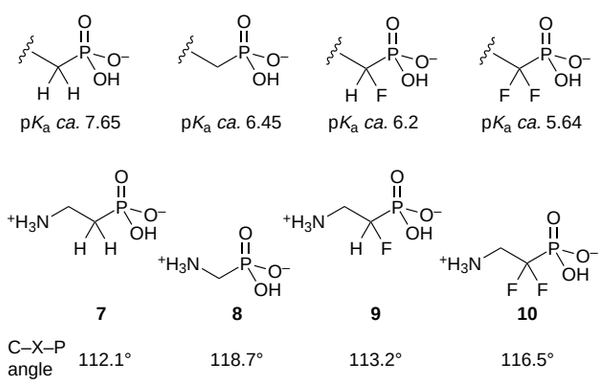



**Fig. 7** Phosphate/phosphonate acidity (second deprotonation) and C–X–P angles as obtained from the X-ray structures of compounds **7**–**10**

yacetone phosphate analogues. The relative $V_{max}$ and $K_m$ values are given in Fig. 9. The maximal rates are similar for each substrate, but the $K_m$ value for the CHF-phosphonate analogue is significantly lower than the natural phosphate substrate **14** (0.17 *vs*. 0.29 mM). This low value correlates with previous data[42] on the $CH_2$-phosphonate **15** and it is perhaps surprising that replacing the bridging oxygen of the phosphate, by carbon, leads to a higher binding affinity. Intriguingly glycerol-3-phosphate dehydrogenase appears to be unoptimised in its binding of the phosphate group of the natural substrate **14**, revealing a sensitivity to the electrostatic influence of oxygen, a situation that relaxes with the $CH_2$- and CHF-phosphonate analogues. The poorer performance of the $CF_2$-phosphonate **17** analogue, now with two fluorine atoms, is consistent with an even greater electrostatic influence impacting on the surface of the protein.

Phosphonate analogues of phosphotyrosine have been prepared and incorporated into peptides as phosphatase resistant SH-2 domain inhibitors, in the only other example[43] where $CH_2$-, CHF- and $CF_2$-phosphonates have been compared directly in a biological system. The ability of phosphotyrosine residues to bind such domains is important in signal-transducing molecules. A series of pentapeptide analogues (Gly-pX-Tyr-Val-Pro-Met-Leu) were assessed for their ability to bind the C-terminal SH-domain of phosphatidylinositol-3-kinase and were found to bind in the following order; CHOH < $CH_2$ < CHF < $CF_2$ = O where the $CF_2$-phosphonate was the optimal phosphate mimic in this case. Different biological systems respond differently to the CHF- and $CF_2$-phosphonate analogues and clearly each has to be assessed individually.

### *2.3 Electrostatic or steric influences in lipase resolutions?*

Lipases and other hydrolytic enzymes have been widely used for the kinetic resolution of ester racemates.[44] In general terms the effectiveness of such resolutions is interpreted on the basis of steric interactions between the surface of the protein and the substrate. Indeed steric models for the more widely used lipases have been proposed and refined by identifying hydrophobic and hydrophilic compatible regions.[44] Pig liver esterase is a good example.[45] Such models are used successfully in a predictive way to assess the viability and stereochemical preference of a particular resolution. On the other hand, the kinetic resolution of some $CF_3$ containing substrates are not so easily rationalised by steric models. For example the *Candida rugosa* lipase (formerly *C. cyclindracea* and also MY-Lipase) esterifies/desterifies the *R*-enantiomer of phenethanol **18** in preference to the *S*-enantiomer.[46]

For trifluorophenethanol however the enzyme prefers alcohol (*R*)-**19** of the opposite configuration (**19** also posesses the *R*-configuration due to a change is assignment priorities).[47] A steric interpretation then suggests that the $CF_3$ group is larger than the phenyl ring, however as discussed above (section 1.3), various methods of comparison reinforce the trend Ph > $CF_3$ > $CH_3$ > H for the steric influence of these substituents. The $CF_3$ group is larger than the methyl group and will compete more




**11** X = CHF
**12** X = $CF_2$
**13** X = $CH_2$

**Fig. 8** *Ab initio* electrostatic potential map at the B3LYP/6-31G level for (*a*) the phosphonate **11**, contoured at 0.025 Hartree and (*b*) the F-epimer of **11**. An active three dimensional view of these diagrams encoded in VRML is available *via* the enhanced electronic version of this article. See http://chemcomm.clic.ac.uk/ for further details.

favourably than $CH_3$ with Ph in steric terms, however it is still smaller than Ph. Thus steric factors alone cannot account for this reversal phenomenon with **19**. If the electrostatic influence of the various substituents is considered then the trend $CF_3$ > Ph > $CH_3$ emerges. The electrostatic influence of the $CF_3$ group is of course greater than $CH_3$ and it will exert greater repulsion on for example an alkoxide nucleophile (on the enzyme), or on another area of negative density on the protein surface. Also, in an intriguing interplay the $CF_3$ group in **19** is predicted to reduce the electrostatic influence on one face of the aromatic ring. This was shown in a study by one of us on the chiral resolving agent (*S*)-2,2,2-trifluoro-1-(9-anthranyl)ethanol (Pirkle's reagent).[48,29]

The X-ray structure of **20** shown in Fig. 10 has the $CF_3$ group lying perpendicular to the plane of the anthracene ring. A molecular electrostatic potential map calculated for **20** also shown in Fig. 10 revealed a distinct difference in the negative potential of the two π-faces of the aromatic. The face *anti* to the $CF_3$ group is reduced in electron density relative to the face *syn* to the $CF_3$ group (Fig. 2). The decreased electrostatic potential on the *anti* face is rationalised by negative hyperconjugation due to overlap of the π-orbital system with the σ*-orbital

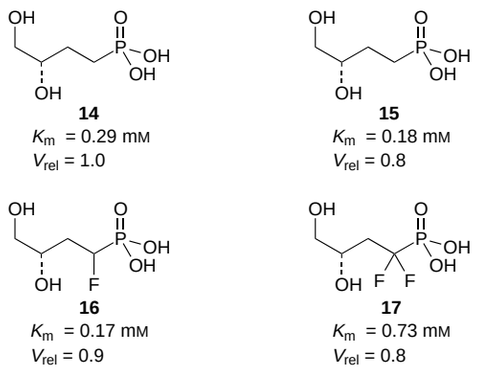
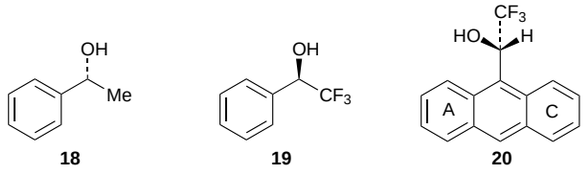



**Fig. 9** Kinetic data on **14**–**17** as substrates for glycerol-3-phosphate dehydrogenase[41]



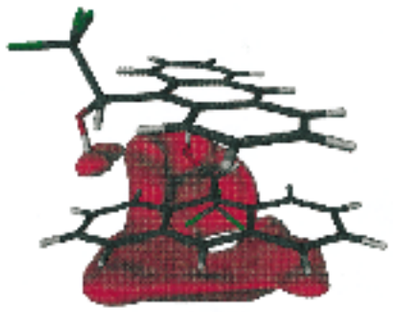



**Fig. 10** The X-ray structure of **20** showing the dimeric self-interaction, with a superimposed negative electrostatic potential computed (B3LYP/6-31G, contoured at 0.0175 Hartree) for a single molecule shown in red. The +ve potential is not shown. Note in particular the asymmetry of the π-system, and the coincidence of the residual −ve potential on one face with the position of the πH–O interaction from the second molecule. An active three dimensional view of this diagram encoded in VRML is avaialble *via* the enhanced electronic version of this article. See http://chemcomm.clic.ac.uk/ for further details.

associated with the C–$CF_3$ bond. Thus the $CF_3$ group has a synergic effect in possessing a significant electrostatic influence of its own and also depleting that on one face of the aromatic ring. The induced asymmetry extends not only to the two π-faces, but to differentiating between rings A and C on the aromatic system, as a consequence of further interaction between the $CF_3$ group and the adjacent OH group. The crystal structure shows a OH··π hydrogen bond to the edge of ring A, precisely where the maximum in the negative electrostatic potential on this face is computed to occur. Thus the role of the $CF_3$ group could be regarded as focusing the role of the two aromatic faces into a π-stacking side and hydrogen bond accepting side. A similar directing influence of a $CF_3$ group towards an electrophile was observed in the π-facially stereoselective epoxidation of phenyltrifluoromethylpropenol.[49]

In the case of the $CH_3$- and $CF_3$-phenethanols **18** and **19** the combined steric, but particularly electrostatic impact of the substituents is now predicted to follow $CF_3$ > $Ph_{CH_3}$ > $Ph_{CF_3}$ > $CH_3$. This trend is entirely consistent with the observed stereochemical preferences of the *Candida rugosa* lipase for **18** and **19**.

## 3 Stereoelectronic effects

### *3.1 The Fluorine anomeric and Anh–Eisenstein effects*

The anomeric effect[50] which in carbohydrates recognises the preference for an axial over an equatorial conformation at the O–C–O anomeric carbon, extends to O–C–F and N–C–F systems.[51] The molecular orbital explanation for the anomeric effect suggests that the lone pair on oxygen lying *anti*-parallel to the C–X bond donates electron density into the $\sigma^*_{C-X}$ orbital in a stabilising hyperconjugative interaction as illustrated in Fig. 11. Theoretical studies on fluoromethanol ($HOCH_2F$),[51] fluoromethyl methyl ether ($MeOCH_2F$)[52,53] and fluoromethylamine ($FCH_2NH_2$)[54] suggest a stabilisation of around 6.0 kcal $mol^{-1}$ and X-ray structure data of appropriate compounds[51,52] indicate a consequent shortening of the C–O bond and lengthening of the C–F bond consistent with the hyperconjugation hypothesis.

Anh and Eisenstein,[55] in a theoretical study investigating transition states for hydride attack to 2-chloropropionaldehyde, have suggested that the most stable transition state will have the HOMO of the nucleophile approaching the carbonyl LUMO where the p-orbitals are co-aligned with the σ*-orbital of the vicinal C–Cl bond. An *anti*-parallel approach of the nucleophile to the C–Cl bond is preferred to accommodate mixing of the developing σ-bond electrons with the σ*-orbital of the C–Cl bond and relaxation of any electrostatic repulsion between the halogens, as shown in Fig. 12. This set-up allows negative hyperconjugation where the electron density of the nucleophile is accommodated in the antibonding orbital (σ*-LUMO) associated with the C–Cl bond. The effect was further

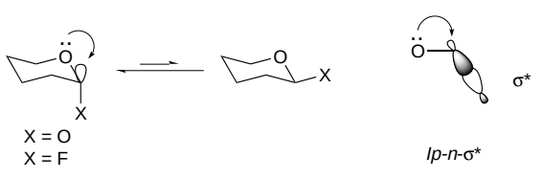



**Fig. 11** A molecular orbital representation of the anomeric effect

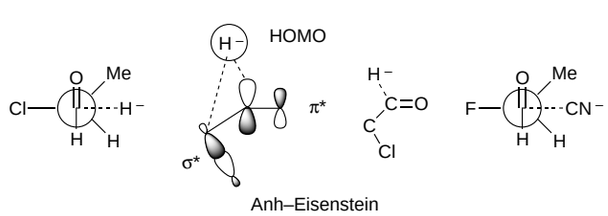



**Fig. 12** A molecular orbital description of Anh–Eisenstein type stabilisation of a nucleophile approaching an α-haloaldehyde

evaluated[56] for fluorine in a theoretical study by Wong and Paddon-Row, on transition state geometries of cyanide attack to 2-fluoropropionaldehyde. This effect emerges as an important one in interpreting the stereoselective processing of fluorinated substrates in certain enzyme reactions and is discussed in the next section.

### *3.2 Anh–Eisenstein stabilisation in enzyme reactions*

The ability of lipases to mediate kinetic resolutions by hydrolysis of racemic or *meso* esters has been widely practiced.[45] Active site models have been mapped for the common lipases which identify areas of hydrophobicity and regions that can accommodate small medium and large groups.[44] In general the lipase active site is considered to accommodate a particular substrate enantiomer on the basis of fit and electronic compatibility to the surface of the protein, and this in turn leads to preferential binding and hydrolysis of a single enantiomer. However the lipase resolutions[57,58] of α-fluoro esters shown in Fig. 13 illustrate that in each case the lipase can distinguished completely between the fluorine and hydrogen atoms. This is difficult to reconcile on the basis of a spacial active site model, as the steric influence of fluorine over hydrogen would not be expected to lead to such a high level of selectivity.

On the other hand we have proposed[59] that these resolutions can be rationalised on the basis of Anh–Eisenstein type stabilisation. Each of the enantiomers of the α-fluoro ester give rise to one of two diastereoisomeric transition states where the serine alkoxide nucleophile of the lipase attacks the ester carbonyl. The nucleophile can either approach *anti* to the C–F bond in one case (as shown in Fig. 13) or *gauche* to the C–F bond for the other enantiomer (interchange H for F). *Ab initio* calculations have been used to model the transition states of these hydrolytic reactions. Methoxide was selected as the nucleophile (serine hydroxide surrogate) and methyl 2-fluoropropionate as the substrate ester. It emerged that the transition state with the nucleophile approaching *anti* to the C–F bond, is more stable by up to 2.8 kcal $mol^{-1}$ than the diastereomeric transition state where the hydrogen and fluorine atoms are interchanged. The energy differential between these transition states is sufficient to give 100 : 1 selectivity and can fully account for the observed high enantioselectivities (99% ee).

In a further exploration of Ahn–Eisenstein type stabilisation in an enzyme reaction we have investigated the selectively fluorinated substrate analogue **23** for the enzyme cyclohexenylcarbonyl-CoA reductase.[60] This NADPH dependant enzyme was isolated from *Streptomyces collinus* and operates on the biosynthetic pathway to the antibiotic ansatrienin.[61] The enzyme reduces cyclohexenylcarbonyl-CoA **21** to the corresponding cyclohexane ring product **22**, and offers an ideal framework in which to explore stereoelectronic effects. Hydrogen is added in an *anti* manner across the double bond with hydride from the co-factor delivered to the *si*-face as illustrated in the Fig. 14. In substrate **23** the fluorine at C-3 can occupy two sites. The diastereoisomer where fluorine is sited at C-3 antiperiplanar to the incoming hydride should accommodate the nucleophile, due to Anh–Eisenstein type stabilisation, relative to the diastereisomeric transition state with fluorine in a *gauche* position.

The requisite C-3 fluorinated substrate analogue was synthesised as a 1 : 1 epimeric mixture at C-3.[60] A number of interesting features emerged from the kinetic analysis of this system. The fluorinated substrate had a $K_m$ value of 44 μM indicating a good affinity for the enzyme relative to the natural substrate ($K_m$ = 25 μM). Intriguingly the $V_{max}$ of the fluorinated substrate was five times greater than that of the natural substrate. This observation can be rationalised by the electronegative fluorine atom rendering the site of hydride delivery more electropositive and lowering the transition state energy. This conclusion was reinforced by kinetic isotope data utilising deuterium labelled cofactor (NADP$^2$H). The natural substrate displayed a kinetic isotope effect of $k_H/k_D$ = 3 consistent with hydride delivery as the rate limiting step in the reaction. However this isotope effect was reduced to $k_H/k_D$ = 1.3 with the fluorinated substrate. Thus the transition state energy for hydride delivery, the highest barrier on the reaction course, is lowered as a result of fluorine substitution at C-3, and hydride delivery is now competing with another step (*e.g.* co-factor binding/debinding) as the rate limiting step.

On the issue of Anh–Eisenstein stabilisation, the enzymatic reduction of the fluorinated substrate was monitored by $^{19}$F NMR spectroscopy. The stereospecificity of the enzyme reaction, and the preference of the SCoA group to adopt an equatorial conformation, dictate that (3*R*)-**23** will deliver the product **24** with the fluorine atom axial, and (3*S*)-**23** will deliver **24** with the fluorine atom equatorial. Thus the diastereoisomeric products can be distinguished readily by $^{19}$F NMR spectroscopy. In the early stages of the reaction there was indeed a small but significant bias in favour of the axial over the equatorial product as predicted *i.e.* at 20% conversion the axial–equatorial ratio was 1.3 (*ax–eq* = 1.3) (see Fig. 5). As the reaction progressed towards > 50% conversion then this ratio reduced to *ax–eq* = 1.0 as expected, as both diastereoisomers of **23** are progressed through the reaction. The stereochemical bias in the early stages of the reaction is consistent with Anh–Eisenstein type hyperconjugation favouring the product **24**, with fluorine in an axial position.

### *3.3 The* gauche *and* cis *effects*

Perhaps the most widely discussed stereoelectronic effects associated with organofluorine compounds are the *gauche*[62,63]

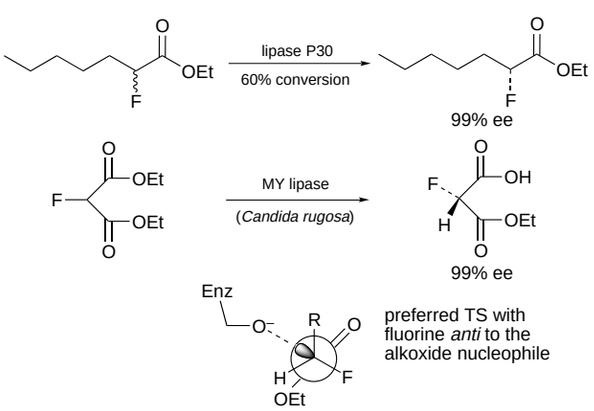



**Fig. 13** The high stereospecificity displayed in the resolution of α-fluoro esters is rationalised by Anh–Eisenstein type stabilisation in the transition state

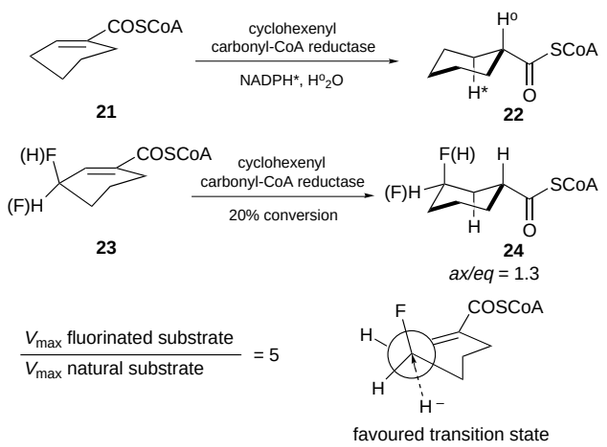



**Fig. 14** Cyclohexenylcarbonyl-CoA reductase. Processing of the fluorinated substrate **23** displays a stereochemical bias favouring **24** with fluorine in an axial position.

and *cis* effects.[64] The *gauche* effect recognises that the lowest energy conformation for 1,2-difluoroethane has the fluorine atoms *gauche* rather than *anti* parallel to each other as illustrated in Fig. 15. The *cis* effect is probably related in origin, and recognises that the *cis* geometric isomer is more stable than the *trans* by about 1–2 kcal mol$^{-1}$. Various hypotheses[65,66] exist to rationalise these observations.[67]

### *3.4 The* cis *effect in enzyme chemistry; citrate synthase*

Citrate synthase, an enzyme of the Kreb's cycle, catalyses the reaction between acetyl-CoA and oxaloacetate to generate citric acid. Fluoroacetyl-CoA, where one hydrogen of the methyl group of acetyl-CoA is replaced by a fluorine atom, is an excellent substrate for the enzyme, generating (2*F*,3*R*)-fluorocitrate **25** as a single stereoisomer[68] as illustrated in Fig. 16. It is this reaction which accounts for the toxicity of fluoroacetate,[69] where the resultant (2*R*,3*R*)-fluorocitrate inhibits aconitase, the next reaction of the Kreb's cycle, and also impedes citrate transport across mitochondrial membranes. The high stereospecificity of this reaction attracted our interest, particularly as a related reaction mediated by malate synthase does not show the same level of stereochemical discrimination. Malate synthase also utilises fluoroacetyl-CoA in place of acetyl-CoA and mediates a condensation with glyoxal to generate two diastereoisomers (2*R*,3*R*) and (2*R*,3*S*) of 3-fluoromalate in an approximately a 3 : 4 ratio.[70,71] Thus in this case the enzyme does not control the stereochemistry of the new chiral centre generated as a consequence of fluorine substitution. These aldol reactions must proceed *via* enzyme bound enol or enolate intermediates of fluoroacetyl-CoA, and clearly these enols can have *Z* or *E* geometries. The high level of stereospecificity, delivering the *R* absolute stereochemistry to C-2 of fluorocitrate **25**, dictates that the *E* enol or enolate of fluoroacetyl-CoA is generated exclusively by citrate synthase, whereas for malate synthase the enzyme appears unable to control this *E*/*Z* geometry to the same extent.

We have calculated[72] the relative energies of such enols and enolates by computational methods. High level *ab initio* calculations demonstrate a significant difference (*ca*. 4 kcal mol$^{-1}$) in the relative energies of the neutral *E* and *Z* enols generated in a model system from $FCH_2C(O)SH$, whereas this differential was significantly reduced (*ca*. 1.8 kcal mol$^{-1}$) when the charged enolate intermediates were considered. Thus it would appear that the (2*R*)-stereochemistry in the resultant (2*R*,3*R*)-fluorocitrate arises because the enzyme acts as a general acid and protonates the developing enolate to generate an enzyme bound enol. The intermediacy of a neutral enol in citrate synthase has previously been proposed[73] and is supported by X-ray structure[74] and experimental evidence.[75] X-Ray structural analysis of the enzyme has identified His-274 as the most likely candidate for this general acid as shown in Fig. 17.

The increased stability of the *E* over the *Z* enol in the model system does not have its exclusive origin in an intramolecular bridging hydrogen bond between oxygen and fluorine, as the enol energy is not significantly perturbed when the hydrogen is bridging or turned away from the fluorine atom. Alternatively the stabilisation would appear to be an example of the *cis* effect where the harder fluorine and oxygen atoms pair in preference to the hard/soft interaction between fluorine and sulfur. A corollary of this analysis is that malate synthase, which is less able to control the stereochemistry at the new fluorogenic centre, will have an intermediate with more enolic than enol character. This however remains to be determined.

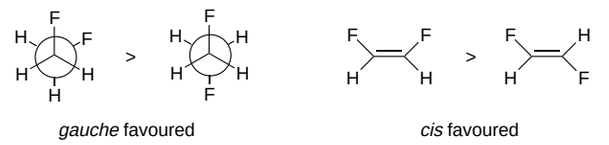



**Fig. 15** The *gauche* and *cis* effects favour a *syn* relationship between vicinal fluorine atoms

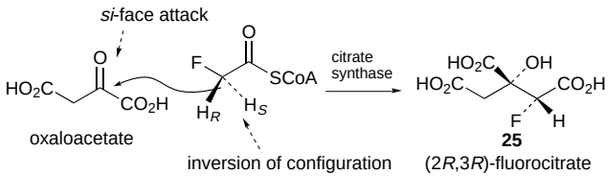



**Fig. 16** Citrate synthase generates (2*R*,3*R*)-fluorocitrate **25** as a single stereoisomer after condensation of oxaloacetate and fluoroacetyl-CoA

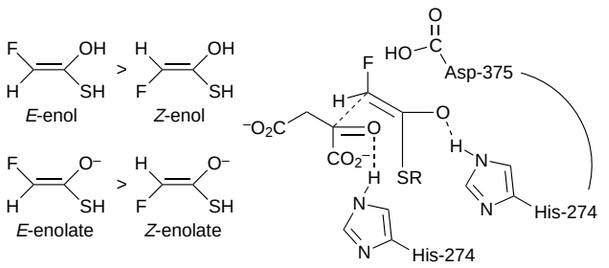



**Fig. 17** The *E* enol of $FCH_2C(O)SH$ is more stable than the *Z* enol which is in turn more stable than the *E* enolate followed by the *Z* enolate. This suggests that the high stereochemical control exhibited by citrate synthase in processing fluoroacetyl-CoA involves an enzyme bound *E* enol intermediate.

## 4 Summary

We have rationalised that the stereoelectronic influence of fluorine can control completely, or influence partially, the stereochemical outcome of given enzyme reactions after an F for H replacement. Interpreting or predicting the behaviour of fluorinated compounds is complex and has led to the term flustrates (fluorine containing substrates) being coined.[21,76] However, a greater appreciation of the electronic and stereoelectronic properties of organic fluorine renders the behaviour of these compounds more interpretable.


## Acknowledgements

The studies over the last few years have involved many coworkers and we thank them warmly for their collaboration.



**David O'Hagan was born in Glasgow in 1961 and received his BSc from the University of Glasgow in 1982. After graduating with a PhD from the University of Southampton with J. A. Robinson in 1985 he spent a post-doctoral year at the Ohio State University with H. G. Floss. He moved to the University of Durham in 1986 where he is now a Senior Lecturer. His research interests include bioorganic fluorine chemistry, biotransformations and investigations into the biosynthesis of plant, fungal and bacterial secondary metabolites.**

**Henry S. Rzepa was born in London in 1950, and received both his BSc and PhD degrees from Imperial College, in 1971 and 1974. Following a post-doctoral period with Michael Dewar at the University of Texas, Austin, he returned to Imperial College, where he is now a Reader in Organic Chemistry. His research interests include the theoretical study of stereoelectronic effects, structural studies of unusual forms of hydrogen bonding such as π-facial interactions and those responsible for chiral recognition, and novel applications of the Internet to chemistry.**

## Footnotes

† E-mail: david.o'hagan@dur.ac.uk
‡ E-mail: rzepa@ic.ac.uk

## References

1 A. Bondi, *J. Phys. Chem.*, 1964, **68**, 441.
2 A. Stabel, L. Dasaradhi, D. O'Hagan and J. P. Rabe, *Langmuir*, 1995, **11**, 1427.
3 H. Booth, T. B. Grindley and K. A. Khedhair, *J. Chem. Soc., Chem. Commun.*, 1982, 1047.
4 A. Warshel and J. Aqvist, *Annu. Rev. Biophys. Biophys. Chem.*, 1991, **20**, 267; A. Warshel and M. Levitt, *J. Mol. Biol.*, 1976, **103**, 227.
5 J. P. Guthrie and R. Kluger, *J. Am. Chem. Soc.*, 1993, **115**, 11 569.
6 T. C. Bruice, *Annu. Rev. Biochem.*, 1976, **45**, 331.
7 F. M. Menger, *Acc. Chem. Res.*, 1993, **26**, 206.
8 M. J. S. Dewar, *Enzyme*, 1986, **36**, 8.
9 J. Mann, *Chem. Soc. Rev.*, 1987, **16**, 318.
10 C. Walsh, *Tetrahedron*, 1982, **38**, 871.
11 C. Walsh, *Adv. Enzymol.*, 1982, **55**, 197.
12 S. E. Chambers, E. Y. Lau and J. T. Gerig, *J. Am. Chem. Soc.*, 1994, **116**, 3603; D. H. Gregory and J. T. Gerig, *Biopolymers*, 1991, **31**, 845.
13 E. A. Wang and C. Walsh, *Biochemistry*, 1981, **20**, 7539.
14 L. Dasaradhi, D. O'Hagan, M. C. Petty and C. Pearson, *J. Chem. Soc., Perkin Trans. 2*, 1995, 221.
15 B. McDonough, P. M. Macdonald, B. D. Sykes and R. N. McElhaney, *Biochemistry*, 1983, **22**, 5097; K. J. Longmuir, R. A. Capaldi and F. W. Dahlquist, *Biochemistry*, 1977, **16**, 5746.
16 R. D. Chambers, D. O'Hagan, B. Lamont and S. C. Jain, *J. Chem. Soc., Chem. Commun.*, 1990, 1053.
17 B. E. Smart, *Molecular Structure and Energetics*, VCH, 1986, vol. 3, p. 141; N. C. Baird, *Can. J. Chem.*, 1983, **61**, 1567; L. Radom and P. J. Styles, *Tetrahedron Lett.*, 1975, 789.
18 J. E. Mark and P. J. Florey, *J. Am. Chem. Soc.*, 1965, **87**, 1415.
19 R. E. Wolf, J. R. Hartmann, J. M. E. Storey, B. M. Foxman and S. R. Cooper, *J. Am. Chem. Soc.*, 1987, **109**, 4328.
20 G. Bott, L. D. Field and S. Sternhill, *J. Am. Chem. Soc.*, 1980, **102**, 5618.
21 D. Seebach, *Angew Chem., Int. Ed. Engl.*, 1990, **29**, 1320.
22 H. S. Mosher, J. E. Stevenot and D. O. Kimble, *J. Am. Chem. Soc.*, 1956, **78**, 4374.
23 For an excellent overview see: P. V. Ramachandran, A. V. Teodorovic and H. C. Brown, *Tetrahedron*, 1993, **49**, 1725.
24 B. E. Smart, *Characteristics of C–F Systems*, in *Organofluorine Chemistry: Principals and Commercial Applications*, ed. R. E. Banks, Plenum, New York, 1994.
25 D. A. Dixon and B. E. Smart, *J. Phys. Chem.*, 1991, **95**, 1609; D. A. Dixon and B. E. Smart, *The Effect of Fluorination on Polyacetylene and the Role of Internal Hydrogen Bonds to Fluorine*, in *Selective Fluorination in Organic and Bioorganic Chemistry*, ACS Symposium Series, 456, ed. J. T. Welch, Washington DC, 1991; L. A. Curtiss, D. J. Frurip and M. Blander, *J. Am. Chem., Soc.*, 1978, **100**, 79.
26 J. A. K. Howard, V. J. Hoy, D. O'Hagan and G. T. Smith, *Tetrahedron*, 1996, **53**, 12 613.
27 A. Fersht, *Enzyme Structure and Mechanism*, W. H. Freeman and Co, New York, 2nd edn., 1984, p. 298.
28 H. Adams, K. D. M. Harris, G. A. Hembury, C. A. Hunter, D. Livingstone and J. F. McCabe, *Chem. Commun.*, 1996, 2531.
29 H. S. Rzepa, M. H. Smith and M. L. Webb, *J. Chem. Soc., Perkin Trans 2*, 1994, 703.
30 C. S. Page and H. S. Rzepa, to be published.
31 W. Cleland and M. Kreevoy, *Science*, 1994, **264**, 1887; P. A. Frey, S. A. Whitt and J. B. Tobin, *Science*, 1994, **264**, 1927.
32 A. Warshel, A. Papazyan and P. A. Kollman, *Science*, 1995, **269**, 102; W. W. Cleland and M. Kreevoy, *Science*, 1995, **269**, 104; P. A. Frey, *Science*, 1995, **269**, 104.
33 J. P. Guthrie, *Chem. Biol.*, 1996, **3**, 163.
34 L. Shimoni and J. P. Glusker, *Struct. Chem.*, 1994, **5**, 383; P. Murray-Rust, W. C. Stallings, C. T. Monti, K. R. Preston and J. P. Glusker, *J. Am. Chem. Soc.*, 1983, **105**, 3206.
35 J. D. McCarter, M. J. Adam and S. G. Withers, *Biochem. J.*, 1992, **286**, 721.
36 R. Engel, *Chem. Rev.*, 1977, **77**, 349.
37 G. M. Blackburn, D. L. Jakeman, A. J. Ivory and M. P. Williamson, *Bioorg. Med. Chem. Lett.*, 1994, **4**, 2573; G. M. Blackburn, D. E. Kent and F. Kolkmann, *J. Chem. Soc., Perkin Trans. 1*, 1984, 1119; G. M. Blackburn, *Chem. Ind.* (*London*), 1981, 134.
38 J. Nieschalk, A. S. Batsanov, D. O'Hagan and J. A. K. Howard, *Tetrahedron*, 1996, **52**, 165.
39 G. R. J. Thatcher and A. S. Campbell, *J. Org. Chem.*, 1993, **58**, 2272.
40 P. Camilleri, A. J. Edwards, H. S. Rzepa and S. M. Green, *J. Chem. Soc., Chem. Commun.*, 1992, 1122.
41 J. Nieschalk and D.O'Hagan, *J. Chem. Soc., Chem. Commun.*, 1995, 719.
42 P. R. Adams and R. Harrison, *Biochem. J.*, 1974, **141**, 729; P.-J. Cheng, R. Hickey, R. Engel and B. E. Tropp, *Biochem. Biophys. Acta*, 1974, **341**, 85.
43 T. R. Burke, M. S. Smith, A. Otaka, M. Nomizu, P. R. Roller, G. Wolf, R. Case and S. E. Shoelson, *Biochemistry*, 1994, **33**, 6490.
44 K. Faber, *Biotransformations in Organic Chemistry*, Springer, 2nd edn., 1995; *Preparative Biotransformations; Whole Cell and Isolated Enzymes in Organic Synthesis*, ed. S. M. Roberts, Wiley, Chichester, 1993.
45 L. Provencher, H. Wynn, J. B. Jones and A. R. Krawczyk, *Tetrahedron: Asymmetry*, 1993, **4**, 2025.
46 C.-S. Chen and C. J. Sih, *Angew. Chem., Int. Ed. Engl.*, 1989, **28**, 695.
47 J. T. Lin, T. Yamazaki and T. Kitazume, *J. Org. Chem.*, 1987, **52**, 3211.
48 H. S. Rzepa, M. L. Webb, A. M. Z. Slawin and D. J. Williams, *J. Chem. Soc., Chem. Commun.*, 1991, 766.
49 O. Casher, D.O'Hagan, C. A. Rosenkranz, H. S. Rzepa and N. A. Zaidi, *J. Chem. Soc., Chem. Commun.*, 1993, 1337.
50 A. J. Kirby, *The Anomeric Effect and Related Stereoelectronic Effects at Oxygen*, Springer Verlag, Berlin, 1983.
51 H. Senderowitz, P. Aped and B. Fuchs, *Tetrahedron*, 1993, **49**, 3879.
52 G. A. Geffrey and J. H. Yates, *J. Am. Chem. Soc.*, 1979, **101**, 820.
53 M. Hayashi and H. Kato, *Bull. Chem. Soc. Jpn.*, 1980, **53**, 2701.
54 J. J. Irwin, T.-K. Ha and J. Dunitz, *Helv. Chim. Acta.*, 1990, **73**, 1805.
55 N. T. Anh and O. Eisenstein, *Nouv. J. Chim.*, 1977, **1**, 61.
56 S. S. Wong and M. N. Paddon-Row, *J. Chem. Soc., Chem. Commun.*, 1990, 456.
57 P. Kalaritis, R. W. Regenye, J. J. Partridge and D. L. Coffin, *J. Org. Chem.*, 1990, **55**, 812.
58 T. Kitazume, K. Murata and T. Ikeya, *J. Fluorine Chem.*, 1986, **31**, 143.
59 D. O'Hagan and H. S. Rzepa, *J. Chem. Soc., Perkin Trans. 2*, 1994, 3.
60 C. F. Bridge, D. O'Hagan, K. A. Reynolds and K. K. Wallace, *J. Chem. Soc., Chem. Commun.*, 1995, 2329.
61 K. A. Reynolds, P. Wang, K. M. Fox, M. K. Speedie, Y. Lam and H. G. Floss, *J. Bacteriol.*, 1992, **14**, 3850.
62 S. Wolfe, *Acc. Chem. Res.*, 1972, **5**, 102.
63 R. D. Amos, N. C. Handy, P. G. Jones, A. J. Kirby, J. K. Parker, J. M. Percy and M. D. Su, *J. Chem. Soc., Perkin Trans. 2*, 1992, 549.
64 N. C. Craig, L. G. Piper and V. L. Wheeler, *J. Phys. Chem.*, 1971, **75**, 1453; N. C. Craig and E. A. Entemann, *J. Am. Chem. Soc.*, 1961, **83**, 3047.
65 N. D. Epiotis, W. R. Cherry, S. Shaik, R. L. Yates and F. Bernardi, *Top. Curr. Chem.*, 1977, **70**, 1.
66 R. C. Bingham, *J. Am. Chem. Soc.*, 1976, **98**, 535.
67 For a good discussion, see: E. L. Eliel and S. H. Wilen, *Stereochemistry of Organic Compounds*, Wiley, 1994.
68 D. W. Fanshier, L. K. Gottwald and E. Kun, *J. Biol. Chem.*, 1964, **239**, 425.
69 D. B. Harper and D. O'Hagan, *Nat. Prod. Rep.*, 1994, **11**, 123.
70 R. Keck, H. Haas and J. Retey, *FEBS Lett.*, 1980, **114**, 287.
71 M. A. Marletta, P. A. Srere and C. Walsh, *Biochemistry*, 1981, **20**, 3719.
72 D. O'Hagan and H. S. Rzepa, *J. Chem. Soc., Chem. Commun.*, 1994, 2029.
73 M. Karpusas, D. Holland and S. J. Remington, *Biochemistry*, 1991, **30**, 6024.
74 M. Karpusas, B. Branchaud and S. J. Remington, *Biochemistry*, 1990, **29**, 2213.
75 K. C. Usher, S. J. Remington, D. P. Martin and D. G. Drueckhammer, *Biochemistry*, 1994, **33**, 7753; D. P. Martin, R. T. Bibart and D. G. Drueckhammer, *J. Am. Chem. Soc.*, 1994, **116**, 4660.
76 M. Gautschi and D. Seebach, *Angew. Chem., Int. Ed. Engl.*, 1992, **31**, 1083.

*6/04140J*

# Synthesis, structural characterisation and preliminary magnetic studies of a tetraicosanuclear cobalt coordination complex

**Euan K. Brechin, Steven G. Harris, Andrew Harrison, Simon Parsons, A. Gavin Whittaker and Richard E. P. Winpenny***

*Department of Chemistry, The University of Edinburgh, West Mains Road, Edinburgh, UK EH9 3JJ*

**The highest nuclearity complex containing cobalt consists of cubic-close packed planes of hydroxide, methoxide or chloride anions, bridging cobalt(II) centres; preliminary magnetic studies indicate a high-spin ground state and the possibility of superparamagnetic behaviour.**

Polymetallic compounds of metals in high oxidation states have been reported which contain as many as 154 metal centres.[1] High-nuclearity clusters of low oxidation states rival these species in size, with chalcogenide bridged complexes involving 146 metals structurally characterised.[2] Complexes where the metals are in moderate oxidation states do not approach these behemoths in nuclearity, with the largest reported being an $Fe_{40}$ compound.[3]

The route to one of the largest of these complexes, Powell's $Fe_{19}$ 'crust' **2**,[4] involves arresting the formation of iron hydroxide in an aqueous solution by addition of a polydentate ligand; the rate of nucleation can be controlled by pH and by the iron : ligand ratio. We reasoned that an alternative procedure would be to perform reactions in solvents with a known propensity for absorbing atmospheric moisture which might thus serve as a source of bridging hydroxides. The solvent we chose for these experiments was ethyl acetate, from which an $Fe_{17}$ complex has previously been synthesised using this approach.[5] Ethyl acetate can contain up to 3% by mass of dissolved water; in these experiments the water content is around 0.1%.

Reaction of $CoCl_2$ (3.9 mmol) with Na(mhp) (Hmhp = 2-methyl-6-hydroxypyridine) (8 mmol) in MeOH (40 ml) for 24 h at 290 K, followed by evaporation to dryness gives an uncharacterised purple paste. Dissolution of this paste in ethyl acetate, followed by filtration, gave purple crystals† in 3 days. The synthesis is reproducible, however the yield varies between 5 and 20%, possibly depending on the exact water content of the EtOAc used. Structural analysis‡ reveals a complex of formula $[Co_{24}(\mu_3\text{-}OH)_{14}(\mu\text{-}OH)_4(\mu_3\text{-}OMe)_2(\mu_3\text{-}Cl)_2Cl_4(mhp)_{22}]$ **1** (Fig. 1) which has a centrosymmetric structure related to many minerals, and indeed to **2**.[4] The cages pack parallel to the crystallographic *ab*-plane.

The structure is based on $[Co_3(OH)_4]^{2+}$ cubes with one corner missing, and in some cases with one of the hydroxide vertices occupied by methoxide or chloride groups. The array is therefore held together by OH bridges. Of the twelve crystallographically independent Co sites, five [Co(1), Co(2), Co(3), Co(4), Co(5)] have a coordination geometry close to a regular octahedron. There are no chelating ligands attached to these metal sites. Three further sites [Co(6), Co(7), Co(8)] have one chelating ligand and four monodentate ligands attached, and have more distorted octahedral geometries. Co(12) also has one chelating ligand and three further contacts, and is probably best described as based on a distorted tetrahedral geometry [four bonds between 1.971(5) and 2.265(3) Å] with one much longer contact [2.884(5) Å]. The final three distinct sites [Co(9), Co(10), Co(11)] each have two chelating mhp ligands attached, with in each case the bond to the O-donor much longer than the bond to the N-donor of the group. Two further monodentate ligands lead to a coordination geometry best described as involving four short contacts in a distorted tetrahedral array [1.971(5)–2.282(3) Å] and two longer contacts [2.310(5)–3.022(5) Å]. The shortest Co···Co contact observed in **1** is 3.014(3) Å between Co(7) and Co(11).

The exterior of the molecule is covered by twenty-two pyridonate ligands. These adopt three distinct bonding modes: binucleating, binding to differing Co atoms through the N- and O-donors; chelating to one Co atom and then bridging to a second Co through the exocyclic O atom; trinucleating, binding to one Co through the ring nitrogen only, and bridging two further Co centres through the oxygen. Such behaviour is typical for these ligands, and perhaps explains why such a simple bridging ligand can stabilise such a large metal–hydroxide structure where previously it has been suggested a polydentate ligand is required.

Preliminary magnetic studies§ of **1** have been performed [Fig. 2(*a*)]. At room temperature the value of the product $\chi_m T$ is *ca*. 63 emu K mol$^{-1}$ ($\chi_m$ is the molar magnetic susceptibility). We assume that this value corresponds to that for 24 non-interacting $S = 3/2$ centres, which would lead to a calculated value of 64.8 emu K mol$^{-1}$ [assuming $g = 2.4$, which is reasonable for high-spin $Co^{II}$]. $\chi_m T$ declines steadily until 30 K where it increases sharply to a value of 62 emu K mol$^{-1}$ at 8 K.

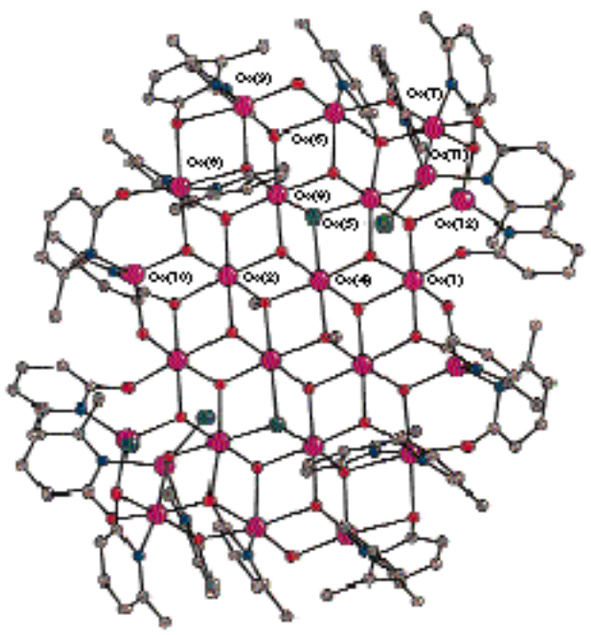



**Fig. 1** The structure of **1** in the crystal. Selected bond length ranges (Å): Co–O(hydroxide) 1.971–2.194, Co–O(methoxide), 2.054–2.120, Co–O(mhp), 2.019–2.376, Co–N(mhp), 2.024–2.246, Co–Cl, 2.265–2.608 Å (av. esd 0.005 Å). These ranges treat Co(9)–Co(12) as four-coordinate and exclude the longer contacts. (Co, magenta; O, red; N, blue; Cl, green; C, grey. Figure drawn using CAMERON.[9])

Below this temperature it falls again, possibly due to intermolecular interactions or zero-field splitting within the spin ground state. If the 8 K value is due to a non-degenerate spin state we can estimate that this is approximately an $S = 9$ state, however further experiments are required to confirm this estimation. Given the structural resemblance between **1** and **2**,[4] a high-spin state would be unsurprising as the latter has a ground state of at least $S = 33/2$. More exciting are differences observed between the field-cooled and zero-field cooled *M/H* curves of **1** [Fig. 2(*b*)] (*M* = magnetisation, *H* = applied field). This provides evidence for freezing of the spins and may be an indication of superparamagnetic behaviour. Such behaviour has been observed for nanoscale cobalt particles prepared in inverse micelles[10] and for a dodecanuclear manganese complex.[11]

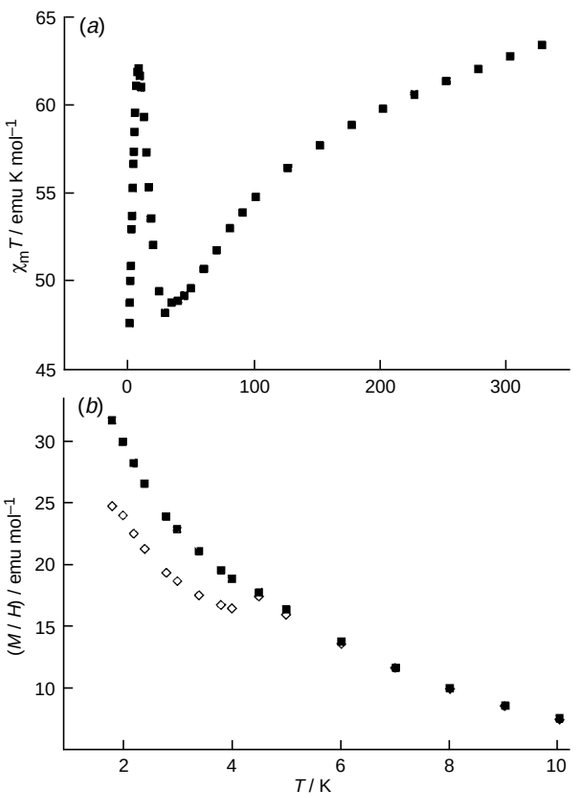



**Fig. 2** (*a*) Plot of $\chi_m T$ *vs*. *T* for **1** measured in a 1000 G field. (*b*) Plot of *M/H vs*. *T* for **1** measured in a 100 G field; zero-field cooled *M/H* shown as open diamonds, field-cooled as filled squares. (*M/H* = $\chi_m$ if *M* is linear with *H*).

Further studies are being undertaken to confirm this behaviour.

We thank the EPSRC for funding for a diffractometer and SQUID suspectometer, for a post-doctoral fellowship (to A. G. W.) and for studentships (for E. K. B. and S. G. H.).

## Footnotes

† Elemental analysis for **1**: Found: C, 37.3; H, 3.7; N, 7.0. Calc., C, 36.8; H, 3.6; N, 7.0%.

‡ *Crystal data* for $C_{134}H_{156}Cl_6Co_{24}N_{22}O_{42}\cdot C_4H_8O_2$ **1**: triclinic, space group $P\bar{1}$, $a = 15.459(6)$, $b = 18.619(8)$, $c = 21.402(9)$ Å, $\alpha = 76.43(3)$, $\beta = 70.04(2)$, $\gamma = 72.70(2)°$, $U = 5467(4)$ Å$^3$, $M = 4461.9$, $Z = 1$ (the molecule lies on an inversion centre), $T = 220.0(2)$ K, $R_1 = 0.0572$. Data collection, structure solution and refinement were performed as detailed in ref. 5 using programs SHELXS-86,[6] SHELXL-93[7] and PLATON.[8] Atomic coordinates, bond lengths and angles, and thermal parameters have been deposited at the Cambridge Crystallographic Data Centre (CCDC). See Information for Authors, Issue No. 1. Any request to the CCDC for this material should quote the full literature citation and the reference number 182/412.

§ Variable-temperature magnetic measurements on **1** in the region 1.8–325 K were made using a SQUID magnetometer (Quantum Design) with samples sealed in gelatine capsules. Field-cooled/zero-field cooled measurements were made in a 100 G field, all other measurements in a 1000 G field. The data have not been adjusted for the diamagnetism of the sample. Compound **1** was also studied embedded in silicon grease to confirm that crystallite orientation was not playing a significant part in the observed behaviour. The magnetic data are available as supplementary material from the authors on request.

## References

1 A. Müller, K. Krickemeyer, J. Meyer, H. Bögge, F. Peters, W. Plass, E. Diemann, S. Dillinger, F. Nonenbruch, M. Randerath and C. Menke, *Angew. Chem., Int. Ed. Engl.*, 1995, **34**, 2122.
2 H. Krautscheid, D. Fenske, G. Baum and M. Semmelmann, *Angew. Chem., Int. Ed. Engl.*, 1993, **32**, 1303.
3 J.-F. You, G. C. Papafethymiou and R. C. Holm, *J. Am. Chem. Soc.*, 1992, **114**, 2697.
4 A. K. Powell, S. L. Heath, D. Gatteschi, L. Pardi, R. Sessoli, G. Spina, F. Del Giallo and F. Pieralli, *J. Am. Chem. Soc.*, 1995, **117**, 2491.
5 S. Parsons, G. A. Solan and R. E. P. Winpenny, *J. Chem. Soc., Chem. Commun.*, 1995, 1987.
6 G. M. Sheldrick, *Acta Crystallogr., Sect. A*, 1990, **46**, 467.
7 G. M. Sheldrick, SHELXL-93, University of Göttingen, 1993.
8 P. van der Sluis and A. L. Spek, *Acta Crystallogr., Sect. A*, 1990, **46**, 194.
9 L. J. Pearce, C. K. Prout and D. J. Watkin, CAMERON: a program for graphical representation of structural data, Chemical Crystallography Laboratory, University of Oxford, 1994.
10 J. P. Chen, C. M. Sorensen, K. J. Klabunder and G. C. Hadjipanayis, *J. Appl. Phys.*, 1994, **78**, 6318.
11 R. L. Sessoli, H.-L. Tsai, A. R. Schake, S. Wang, J. B. Vincent, K. Folting, D. Gatteschi, G. Christou and D. N. Hendrickson, *J. Am. Chem. Soc.*, 1993, **115**, 1804.

*Received, 29th October 1996; Com. 6/07355G*

# Self-assembly of a tetranuclear macrocyclic copper(II) complex

**Paul V. Bernhardt* and Lathe A. Jones**

*Department of Chemistry, University of Queensland, Brisbane, 4072, Australia*

**A dinuclear macrocyclic complex is synthesized *via* the one-pot reaction of dipotassium nitroacetate, formaldehyde and a linear tetraamine copper(II) complex; the X-ray crystal structure of the product reveals an association of two dinuclear complexes to form a novel tetracopper(II) species.**

Reactions of metal templates such as $[M(en)_2]^{2+}$ or $[M(2,3,2\text{-tet})]^{2+}$ (M = $Ni^{II}$, $Cu^{II}$; en = ethane-1,2-diamine, 2,3,2-tet = 1,4,8,11-tetraazaundecane) with formaldehyde and a nitroalkane 'locking' fragment have emerged as versatile and effective synthetic routes toward pendant-armed macrocycles.[1] More recently, the range of locking fragments has been extended to include primary amines,[2] amides and sulfonamides[3] and heterocycles.[4] These molecules effect ring closure after reaction of formaldehyde with the coordinated primary amines to produce 14-membered macrocyclic rings based upon the well known cyclam (1,4,8,11-tetraazacyclotetradecane) framework, with the pendant groups arising from substituents on the locking fragments. In principle, this approach may be extended to bifunctional locking groups to generate alkyl-bridged dinuclear complexes, and one report of this type of chemistry is known using dinitro alkanes in this role.[5]

Here we report a new method of generating binuclear complexes *via* one-pot metal-directed reactions of dipotassium nitroacetate, formaldehyde and a tetraaminecopper(II) complex. An aqueous solution of $Cu(NO_3)_2{\cdot}3H_2O$ was stirred while an equimolar amount of 2,3,2-tet was added dropwise. To the resulting purple solution was added aqueous formaldehyde (2 equiv.) and $K_2(O_2CCHNO_2)$ (1 equiv.). The mixture was heated with stirring at 50 °C for 20 h before being filtered. Ion-exchange chromatography of the reaction mixture yielded two products; the first being the mononuclear complex $[CuL^2][ClO_4]_2$ ($\lambda_{max}$ = 518 nm, $\varepsilon$ = 84.2 $dm^3\ mol^{-1}\ cm^{-1}$) followed by the major product, the dimeric $[Cu_2L^1]_2[ClO_4]_3Cl_3$ ($\lambda_{max}$ = 510 nm, $\varepsilon$ = 137 $dm^3\ mol^{-1}\ cm^{-1}$ per Cu centre). The first crop of $[Cu_2L^1]_2[ClO_4]_3Cl_3$ was obtained in 13% yield (of solid compound), but further crops precipitated on standing. The solution properties of both products are typical of cyclam-type complexes of $Cu^{II}$, with respect to their visible electronic maxima and resistance to acid catalysed dissociation (3 M HCl) over a period of several weeks.

X-Ray quality crystals† of the dimer $[Cu_2L^1]_2[ClO_4]_3Cl{\cdot}6H_2O$ were obtained by slow evaporation of an aqueous solution of the complex containing an excess of $NaClO_4$ and NaCl. The crystal structure analysis shows that two dicopper(II) complexes have assembled into a dimeric tetranuclear species (Fig. 1). The pairs of covalently linked macrocyclic planes are twisted relative to each other by an approximate angle of 50° and the Cu···Cu distance is 11.32 Å. Interestingly, the central C atom [C(12)] is deprotonated and the resulting nitronate group forms an intermolecular coordinate bond to an adjacent $Cu^{II}$ centre [2.412(6) Å]. The geometry of each unique $Cu^{II}$ ion is best described as distorted tetragonally elongated octahedral, with anions occupying the remaining coordination sites. The nitronate group and adjacent atoms $[C(C)CNO_2]$ form a planar structure. In addition, a lengthening of the N–O bonds (*ca.* 0.1 Å) and shortening of the C–N bond (*ca*. 0.2 Å) relative to the nitro groups appended to each macrocyclic ring was found. These observations lead to the conclusion that the C–N bond in this functional group has essentially double-bond character.

The formation of $[Cu_2L^1]^{3+}$, and its crystallisation as a dimeric tetranuclear complex, is remarkable, and was unexpected. The crystallisation of $[Cu_2L^1]_2^{6+}$ involves the assembly of 22 different molecules {4 × $[Cu(2,3,2\text{-tet})]^{2+}$, 6 × $(O_2CCHNO_2)^{2-}$, 12 × $CH_2O$} into one supramolecular unit in a one-pot reaction, which illustrates the efficiency of metal-directed reactions of this kind. Dipotassium nitroacetate $K_2(O_2CCHNO_2)$ and its derivatives are unstable toward decarboxylation in aqueous solution.[8] In this case, condensation of three $(O_2CCHNO_2)^{2-}$ ions with two equivalents of formaldehyde followed by decarboxylation generates the molecule 1,3,5-trinitropentane *in situ*. Decarboxylation may occur either before or after the formaldehyde/nitroacetate condensation. The latter mechanism is more likely, *i.e.* 1,3,5-trinitropentane-1,3,5-tricarboxylate is initially formed as an intermediate, since metal-directed reactions of nitromethane (the decarboxylation product of nitroacetate) with formaldehyde under similar conditions do not lead to macrocyclic species. Similarly, the formation of $[CuL^2]^{2+}$ most likely involves the nitrocarboxylate substituted macrocycle as an intermediate which decarboxylates in the final step. Analogous processes have been observed in *gem*-diacid substituted tetraamine complexes.[9]

The electron paramagnetic resonance (EPR) spectra of $[CuL^2]^{2+}$ and $[Cu_2L^1]^{3+}$ [Fig. 2(*a*) and (*c*)] as frozen solutions are quite different, with the latter being consistent with a weakly

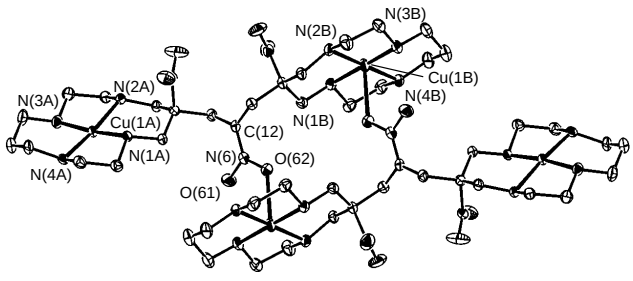
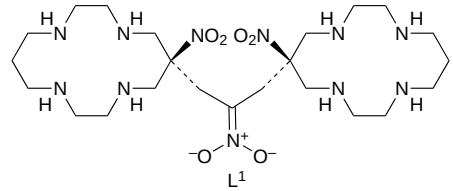
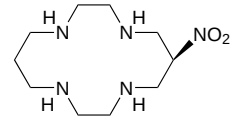



**Fig. 1** Drawing of the $[Cu_2L^1]_2^{6+}$ cation (anions and H-atoms omitted); ellipsoids are drawn at the 30% probability level




$L^1$




$L^2$

dipole–dipole coupled dicopper(II) complex. Simulation of the EPR spectrum of $[Cu_2L^1]^{3+}$ [Fig. 2(*b*), $g_{\|} = 2.17$, $A_{\|} = 205$ G; $g_{\perp} = 2.035$, $A_{\perp} = 50$ G] was achieved with the program DISSIM,[10] which also yielded a Cu···Cu separation of 11.0 Å and a twist angle between the two macrocyclic planes of 80°. The simulation indicates that the compound exists as discrete dicopper(II) complexes in solution and not as the tetranuclear dimer identified in the solid-state structure. In addition, the relative twist angle between the two macrocycles derived from the simulation is *ca*. 30° greater than that identified in the X-ray crystal structure. That is, formation of the tetranuclear dimer perturbs slightly the relative positions of the two covalently linked macrocyclic planes. The EPR spectrum of the mononuclear analogue $[CuL^2]^{2+}$ [Fig. 2(*a*)] is better resolved and typical of an isolated $d^9$ complex in a pseudo-axial ligand field. The similarity between the spectra of $[Cu_2L^1]^{3+}$ and $[CuL^2]^{2+}$ indicates that the two metal centres in $[Cu_2L^1]^{3+}$ are only weakly interacting at this internuclear separation (11 Å), and that dipole–dipole coupling merely acts to broaden what is essentially a mononuclear spectrum.

We have shown that the nitroacetate dianion is a potentially useful synthetic intermediate which, in conjunction with formaldehyde, may generate multifunctional carbon acids *in situ* capable of simultaneously cyclising and bridging two metal centres. Furthermore, this reagent offers a route towards mono-C-substituted ($–NO_2$) macrocycles such as $[CuL^2]^{2+}$ which have been much more difficult to prepare than disubstituted ($–NO_2$, –Me) analogues derived from nitroethane and formaldehyde. Further work is continuing utilising this novel reagent to effect macrocyclic ring closure.

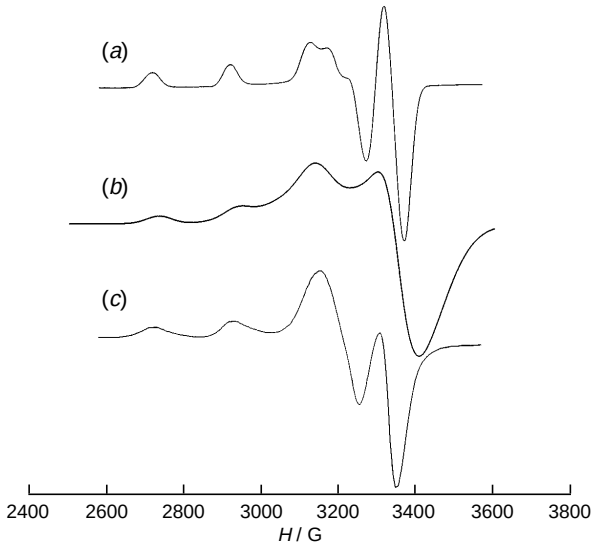



**Fig. 2** (*a*) Experimental EPR spectrum of $[CuL^2]^{2+}$, (*b*) simulated EPR spectrum of $[Cu_2L^1]^{3+}$ and (*c*) experimental EPR spectrum of $[Cu_2L^1]^{3+}$; frequency = 9.272 GHz, $T = 77$ K, solvent water–dimethylformamide (2 : 1)

We gratefully acknowledge Mr David Hunter for his assistance with the EPR spectral measurements and we thank the Energy Research and Development Corporation and the University of Queensland for financial support.

## Footnote

† *Crystal data*: $[Cu_2L^1]_2[ClO_4]_3Cl_3·6H_2O$, $C_{46}H_{108}Cl_6Cu_4N_{22}O_{30}$, $M = 1916.4$, triclinic, space group $P\bar{1}$, $a = 9.677(1)$, $b = 13.354(1)$, $c = 15.583(2)$ Å, $\alpha = 92.170(9)$, $\beta = 90.94(1)$, $\gamma = 99.14(1)°$, $U = 1986.2(4)$ Å$^3$, $Z = 1$, $D_c = 1.602$ g cm$^{-3}$, $\mu$(Mo-K$\alpha$) = 13.49 cm$^{-1}$, $F(000) = 996$, $T = 293$ K, final $R_1 = 0.0683$, $wR_2 = 0.1797$ for 3789 observed reflections [$|F_o| > 2\sigma|F_o|$, $2\theta < 50°$], $w^{-1} = \sigma^2(F_o^2) + (0.1203P)^2 + 4.65P$, where $P = (F_o^2 + 2F_c^2)/3$. Data were collected on an Enraf-Nonius CAD4 diffractometer using graphite-monochromated Mo-K$\alpha$ radiation and employing the $\omega$–$2\theta$ scan method. The structure was solved by direct methods with SHELXS-86[6] and refined by full-matrix least squares on $F^2$ with SHELXL-93.[7] All non-H atoms were refined with anisotropic thermal parameters, whereas H-atoms were constrained at estimated positions.

Atomic coordinates, bond lengths and angles, and thermal parameters have been deposited at the Cambridge Crystallographic Data Centre (CCDC). See Information for Authors, Issue No. 1. Any request to the CCDC for this material should quote the full literature citation and the reference number 182/386.

## References

1 P. V. Bernhardt and G. A. Lawrance, *Coord. Chem. Rev.*, 1990, **104**, 297.
2 L. Fabbrizzi, A. M. M. Lanfredi, P. Pallavicini, A. Perotti, A. Taglietti and F. Ugozzoli, *J. Chem. Soc., Dalton Trans.*, 1991, 3264.
3 A. De Blas, G. De Santis, L. Fabbrizzi, M. Lichelli, A. M. M. Lanfredi, P. Morosini, P. Pallavicini and F. Ugozzoli, *J. Chem. Soc., Dalton Trans.*, 1993, 1411.
4 Y. D. Lampeka, A. I. Prikhod'ko, A. Y. Nazarenko and E. B. Rusanov, *J. Chem. Soc., Dalton Trans.*, 1996, 2017.
5 P. Comba and P. Hilfenhaus, *J. Chem. Soc., Dalton Trans.*, 1995, 3269.
6 G. M. Sheldrick, *Acta Crystallogr., Sect. A*, 1990, **46**, 467.
7 G. M. Sheldrick, SHELXL-93, A Program for Crystal Structure Determination, University of Göttingen, 1993.
8 M. T. Shipchandler, *Synthesis*, 1979, 666.
9 P. V. Bernhardt, G. A. Lawrance, B. W. Skelton and A. H. White, *Aust. J. Chem.*, 1990, **43**, 399.
10 J. R. Pilbrow and T. D. Smith, *Coord. Chem. Rev.*, 1974, **13**, 173.

*Received, 9th January 1997; Com. 7/00213K*

# Synergetic effect of nickel and platinum supported on silica in catalytic methanol decomposition

**Yasuyuki Matsumura,[a] Kenkichi Kagawa,[b] Yoshikazu Usami,[b] Masanobu Kawazoe,[b] Hiroaki Sakurai[a] and Masatake Haruta[a]**

[a] *Osaka National Research Institute, AIST, Midorigaoka, Ikeda, Osaka 563, Japan*
[b] *Mechanical Engineering Laboratory, Daikin Industries Ltd., Kanaoka-cho, Sakai, Osaka 591, Japan*

**Alloy formation of nickel and platinum leads to a synergetic effect in the decomposition of methanol to carbon monoxide and hydrogen over silica supported metal catalysts.**

Methanol is recognized as an alternative energy carrier as well as an important chemical feedstock. Methanol decomposition to hydrogen and carbon monoxide is very beneficial in saving energy because the industrially produced waste heat can be utilized to increase the heating value of a fuel. Methanol decomposition is also applicable in vehicles (on-board reforming) to increase the fuel efficiency and reduce the amount of formaldehyde by-product.[1] Catalysts containing nickel have been reported to be active for this reaction,[2–6] however, further improvement is still necessary especially for the application to the recovery of waste heat. Studies on the surface science of the nickel–platinum single-crystal alloy suggest a synergetic effect of the alloy towards some catalytic reactions such as hydrogenation,[7–9] although the effect was not evident on a nickel–platinum alloy supported on alumina.[10] Here, we show the coexistence of nickel and platinum on silica results in a significant improvement in the catalytic activity of methanol decomposition.

Catalysts were prepared by the impregnation technique from an aqueous solution of $Ni(NO_3)_2{\cdot}6H_2O$ (Mitsuwa Chemical, GR grade) and/or $H_2PtCl_6$ (Kanto Chemical, GR grade) using silica (Fuji Silicia, ID G) as a support. The resulting solids were calcined in air at 500 °C for 5 h after being vacuum-dried for 1 day. The samples were further washed five times in boiling water for 1 h to remove chloride ion, and dried at 300 °C for 5 h. The residual chlorine content in the catalysts was found to be < 40 ppm (emission spectral analysis). The prepared catalysts listed in Table 1 all contain 10% Ni by mass.

Catalytic experiments were performed in a fixed-bed continuous flow reactor operated under atmospheric pressure at 250 °C. The catalyst was sandwiched with quartz wool plugs in a quartz tube reactor (i.d., 10 mm) whose contribution to the reaction was negligible. After reducing the sample (0.50 g) in a flow of 10 vol.% hydrogen in argon at 500 °C for 1 h, methanol was fed in an argon carrier stream at a concentration of 20 vol.% with a total flow rate of 2.5 $dm^3\ h^{-1}$. The reactant and products were analysed with two on-stream Ohkura 802T gas chromatographs equipped with TC detectors. An activated carbon (2 m, Ar carrier) column and a Porapak T (2 m, He carrier) column were employed in the analyses.

The surface areas of the catalysts were measured by the conventional BET nitrogen adsorption method. Powder X-ray diffraction (XRD) patterns of the catalysts removed from the reactor after reaction were recorded on a Rigaku Rotaflex 20 diffractometer using nickel-filtered Cu-Kα radiation. X-Ray photoelectron spectra (XPS) of the catalysts after reaction were recorded on a Shimadzu ESCA 750 instrument. The samples were sputtered with argon ions (2 kV, 0.5 min) prior to measurement to eliminate surface contaminants. Charge correction of the XPS data was accomplished by assuming that the binding energy of the C 1s peak is 284.6 eV.

Methanol was decomposed mainly to carbon monoxide and hydrogen with methane detected as a by-product over the catalysts containing nickel and/or platinum at 250 °C (Table 1). The specific surface areas of the catalysts were in the range 172–191 $m^2\ g^{-1}$. The catalysts containing both nickel and platinum were more active than those containing only one of the metals revealing a significant synergetic effect between nickel and platinum. The catalytic activity was 95.3% at 3 mass% loading of Pt.

XRD peaks attributed to metallic nickel were recorded in the pattern of $Ni/SiO_2$ at $2\theta = 44.1°$ [Ni(111)] and 51.4° [Ni(200)].[11] The lattice parameter, *a* of 0.355 nm (*Fm*3*m*) is slightly larger than that for nickel metal (0.352–0.354 nm).[12] In the case of $Pt/SiO_2$ XRD peaks at $2\theta = 39.7$ and 46.2° were observed.[11] Although 1- and 2-$PtNi/SiO_2$ contained platinum, no peaks attributable to platinum could be been in the patterns which were very similar to that of $Ni/SiO_2$. However, the patterns for 3- and 4-$PtNi/SiO_2$ were significantly different from the samples containing lower amounts of platinum. Peaks for nickel were shifted to lower values at $2\theta = 43.5 \pm 0.3°$ and $50.8 \pm 0.3°$ with considerably lower intensities and with broad and asymmetric shapes. The stronger peak at $2\theta = 43.5°$ can be deconvoluted into two peaks at 43.2 and 43.7°, showing that

**Table 1** Catalytic activity and surface properties of catalysts containing nickel and/or platinum

| Catalyst | Content (mass%) Ni | Pt | MeOH Conv. (%) | Selectivity (%) CO | $CH_4$ | $S_{BET}$[a]/ $m^2\ g^{-1}$ | $E_b$[b]/eV Pt $4f_{7/2}$ | Ni $2p_{3/2}$ | Pt/Ni : surface atomic ratio[c] |
|---|---|---|---|---|---|---|---|---|---|
| $Ni/SiO_2$ | 10 | 0 | 56.8 | 96.6 | 3.4 | 180 | — | 852.8 | |
| 1-$PtNi/SiO_2$ | 10 | 1 | 79.3 | 94.4 | 5.6 | 174 | 71.1 | 853.0 | 0.05 (0.06) |
| 2-$PtNi/SiO_2$ | 10 | 2 | 78.1 | 94.6 | 5.4 | 178 | 71.1 | 852.9 | 0.09 (0.11) |
| 3-$PtNi/SiO_2$ | 10 | 3 | 95.3 | 92.1 | 7.9 | 172 | 71.4 | 852.7 | 0.11 (0.17) |
| 4-$PtNi/SiO_2$ | 10 | 4 | 78.9 | 95.0 | 5.0 | 177 | 71.3 | 853.5 | 0.11 (0.22) |
| $Pt/SiO_2$ | 0 | 2 | 5.2 | 100.0 | 0.0 | 191 | 70.7 | — | |

[a] BET surface area. [b] Binding energy. [c] Atomic ratio calculated from the XPS peak areas using atomic sensitivity factors of 3.0 for Ni $2p_{3/2}$ and 4.4 for Pt 4f.[14] Atomic ratios calculated from the chemical composition are given in parentheses.

there are two crystalline phases in the metal. The lattice parameters (*a*) are tentatively calculated as 0.362 and 0.358 nm, respectively. Deconvolution of the peak at 50.5° was impossible because of its weak intensity. The *a* parameter for $Ni_{23}Pt_2$ is 0.3564 nm (*Fm*3*m*) which is discernibly smaller than the above values,[12] and the change in the XRD pattern suggests that a phase transition of a Ni–Pt alloy such as $Ni_{23}Pt_2$ to new phases such as $Ni_3Pt$ (space group *Pm*3*m*) occurs at high platinum content.[12,13] It should be noted that the surface atomic ratio of Pt/Ni for 3- or 4-PtNi/$SiO_2$ obtained by XPS analyses was considerably lower than the ratio calculated from the chemical composition while the value for 1- or 2-PtNi/$SiO_2$ was close to that expected from the composition (Table 1). This implies that the concentration of platinum in the bulk of 3- or 4-PtNi/$SiO_2$ is higher than the chemical composition (Pt/Ni ratio = 0.17 and 0.22, respectively) and formation of $PtNi_3$ may well be possible in the bulk.

The binding energy of Pt $4f_{7/2}$ in the XPS of Pt/$SiO_2$ was 70.7 eV, but PtNi/$SiO_2$ were appreciably higher in energy (Table 1). This shows that platinum in PtNi/$SiO_2$ is not present as a separate single phase on the surface of silica but rather interacts with nickel. The difference in the binding energies of Pt $4f_{7/2}$ between 1- and 2-PtNi/$SiO_2$ and those for 3- and 4-PtNi/$SiO_2$ reflect more clearly on the difference in the catalytic activity than does the change in the XRD patterns. Hence, it is strongly indicated that platinum and nickel form an alloy on the surface of silica and this is the active phase for methanol decomposition. The binding energy of Ni $2p_{3/2}$ for all the samples was at 852.8 ± 0.2 eV except for 4-PtNi/$SiO_2$ for which it was at 853.5 eV. This higher binding energy may account for the lower catalytic activity of 4-PtNi/$SiO_2$ relative to 3-PtNi/$SiO_2$. Binding energies for Si 1s and O 1s were 103 ± 0.2 and 532.8 ± 0.2 eV, respectively, for all the samples.

K. K., Y. U. and M. K. gratefully acknowledge financial support from the New Energy and Technology Development Organization.

## References

1 National Research Council, *Catalysis Looks to the Future*, National Academy Press, Washington, DC, 1992.
2 Y. Matsumura, N. Tode, T. Yazawa and M. Haruta, *J. Mol. Catal. A*, 1995, **99**, 183.
3 B. Chen and J. L. Falconer, *J. Catal*., 1993, **144**, 214.
4 O. Tokunaga, T. Satoh, T. Fukushima and S. Ogasawara, *Sekiyu Gakkaishi*, 1990, **33**, 173.
5 H. Imamura, T. Takada, S. Kasahara and S. Tsuchiya, *Appl. Catal*., 1990, **58**, 165.
6 A. Tada, Y. Watarai, K. Takahashi, Y. Imizu and H. Itoh, *Chem. Lett*., 1990, 543.
7 J. C. Bertolini, J. Massardier, P. Ruiz and B. Tardy, *Surf. Sci*., 1989, **211/212**, 1053.
8 M. Abon, J. Massardier, B. Tardy and J. C. Bertolini, *Surf. Sci*., 1987, **189/190**, 880.
9 J. Massardier and J. C. Bertolini, *J. Catal*., 1984, **90**, 385.
10 S. S. Mahmoud, *Indian J. Technol*., 1993, **31**, 709 *Chem. Abstr*., (121(12)134838e).
11 JCPDS files, 4-0850, 4-0802.
12 *Pearson's Handbook of Crystallographic Data for Intermetallic Phases*, ed. P. Villars and L. D. Calvert, The Materials Information Society, Materials Park, Ohio, 1985, vol. 4.
13 *Binary Alloy Phase Diagrams*, ed. T. B. Massalski, J. L. Murray, L. H. Bennett and H. Baker, American Society for Metals, Ohio, 1986, vol. 2.
14 *Practical Surface Analysis*, ed. D. Briggs and M. P. Seah, Wiley, New York, 2nd edn., 1990, vol. 1.

*Received, 28th October 1996; Com. 6/07301H*

# The first Diels–Alder adduct of [60]fullerene with a tetrathiafulvalene

**Josep Llacay,[a] Montserrat Mas,[a] Elies Molins,[a], Jaume Veciana,[a] Dave Powell[b] and Concepció Rovira*[a]**

[a] *Institut de Ciència de Materials de Barcelona, (C.S.I.C.), Campus de la U. A. B., 08193, Bellaterra, Spain*
[b] *Department of Chemistry, University of Florida, Gainesville, FL 32611-7200, USA*

**A Diels–Alder adduct of [60]fullerene and a tetrathiafulvalene (TTF) derivative is synthesised by direct reaction of [60]fullerene with a TTF diene precursor; the crystal structure of the formal intermediate 1,3-dithiole-2-thione derivative of [60]fullerene reveals short contacts between the [60]fullerene and 1,3-dithiole-2-thione moieties.**

In the search for intramolecular energy and electron transfer phenomena in [60]fullerene donor-containing molecules, some electron donor fragments have been covalently linked to the fullerene core.[1–5] Only in very few cases has reliable evidence of thermal or photoinduced intramolecular electron-transfer processes been reported.[3–5] One of the strongest donors that can be attached to the [60]fullerene skeleton is tetrathiafulvalene (TTF). This attachament has been achieved for some compounds, in which the donor TTF moiety is linked by only one single bond to the [60]fullerene through a pyrrolidine bridge, but no electron transfer process has been observed.[6] With the aim of promoting an intramolecular electron transfer we sought to develop a novel type of TTF derivative of [60]fullerene in which the TTF core is directly attached by two σ-bonds to the ball giving rise to a different and more rigid spatial orientation of the HOMO of the TTF addend with respect to the LUMO of [60]fullerene.

Diels–Alder functionalisation of [60]fullerene was chosen in order to reach our goal, since it has been one of the most successful methods for a double attachment of a large variety of substituents[2,7] and it has recently been demonstrated that some Diels–Alder bichromophoric systems undergo energy and electron-transfer phenomena.[5] As a first approach, the thione **1** with a thermolabile sulfone group was used as a diene precursor. We synthesised the compound **1**† by the same procedure used in the synthesis of the parent selenone,[8] and the adduct formation with [60]fullerene was achieved by refluxing a two-fold excess of [60]fullerene with **1** in chlorobenzene–benzonitrile (10 : 1). Chromatographic separation on silica gel ($CS_2$–$CHCl_3$, 10 : 1) afforded the target compound, the Diels–Alder adduct **2**,† as a 1 : 1 clathrate with $CS_2$ in a 41% yield.

The crystallisation of **2**·$CS_2$ by vapour diffusion of pentane into an *o*-dichlorobenzene solution surprisingly gave the **2**·$CS_2$ clathrate back as brilliant dark plates, indicating the very high stability of this clathrate.‡ The crystal structure of thione **2** is shown in Fig. 1.§ As for other adducts,[9] the cyclohexene ring formed by the cycloaddition of the diene derived from thione **1** to the reactive 6,6-ring junction of [60]fullerene shows a boat conformation [Fig. 1(*a*)]. Nevertheless, the angle determined by the two mean planes defined by C(1)–C(2)–C(61)–C(65) and C(61)–C(65)–C(62)–C(64) is smaller (109.2 (4)°) than those found (*ca* 130°) in three other related compounds for which the X-ray structure has been solved so far.[2,9] This small angle gives rise to short intramolecular S···C distances (3.915–4.036 Å) between the sulfur atoms S(1) and S(3) of the addend and C(1), C(2), C(3) and C(6) of the [60]fullerene moiety. If similar short

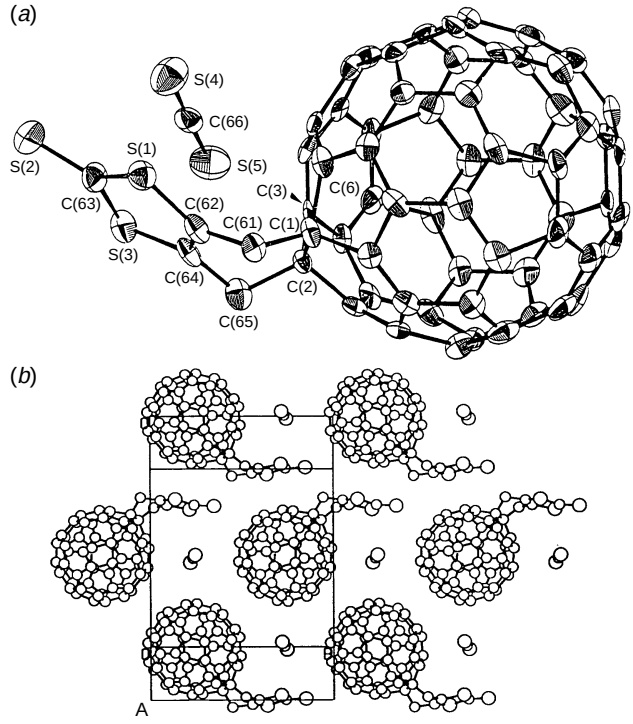
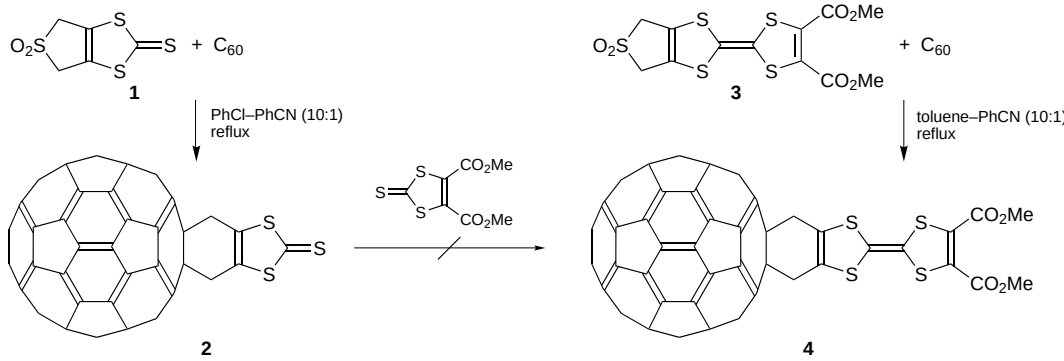



**Fig. 1** Molecular and X-ray crystal structure of **2**·$CS_2$: (*a*) asymmetric unit and, (*b*) crystal packing of **2**·$CS_2$, view perpendicular to the *bc* plane




**Scheme 1**

**Table 1** $E_{1/2}$ Values (V *vs.* $Fc^+/Fc$) of the redox couples of [60]fullerene and compounds **2**–**4** in $CH_2Cl_2$ solutions (0.1 M, $TBAPF_6$), room temp., Pt working and counter eletrodes

| Redox couple | $E^{0/1-}$ | $E^{1-/2-}$ | $E^{2-/3-}$ | $E^{0/1+}$ | $E^{1+/2+}$ |
|---|---|---|---|---|---|
| $C_{60}$ | −0.98 | −1.36 | −1.83 | — | — |
| **2** | −1.03 | −1.41 | −1.93 | — | — |
| **4** | −1.08 | −1.46 | −1.97 | 0.18 | 0.65 |
| **3** | — | — | — | 0.33 | 0.63 |

distances are maintained in the corresponding [60]fullerene–TTF derivatives an intramolecular electron-transfer phenomenon could be expected. The crystal packing of **2**·$CS_2$ consists of parallel intercalated planes (along *a*) of connected chains of molecules along the *b* axis formed by intermolecular close contacts [3.45(3) Å] between sulfur atoms of the thiocarbonyl group and carbon atoms of the contiguous [60]fullerene [Fig. 1(*b*)]. Solvent molecules show some short S···C contacts with two surrounding adduct molecules in addition to the contacts with the adduct inside the asymmetric unit.

Unfortunately, all attempts to perform a phosphite-mediated coupling of thione **2** in order to synthesise [60]fullerene–TTF derivatives have so far been unsuccessful.¶ So, we moved to the key compound **3** as a TTF diene precursor. The asymmetric TTF derivative **3**† was synthesised by a Wittig based methodology[10] in acceptable yield and the corresponding diene indeed undergoes a Diels–Alder addition to [60]fullerene yielding our target compound **4**† as a dark brown solid (47%).

All electroactive compounds here described were studied by cyclic voltammetry. The results are reported in Table 1. In the experimental conditions employed, compounds **2** and **4** show three one-electron reversible reduction waves due to the stepwise reduction of the fullerene moiety. The first reduction potentials of both compounds are slightly shifted cathodically compared to those of [60]fullerene, as observed in many [60]fullerene adducts in which one double bond has been saturated.[11] As expected, compound **4** shows two additional reversible oxidation processes corresponding to the formation of radical cation and dication of the TTF moiety.

The UV–VIS spectra of compounds **2** and **4** clearly show a weak band around 430 nm characteristic of [60]fullerene cycloderivatives.[12] For compound **4** an additional weak and broad band appears at 482 nm (log ε = 3.43) which is not shifted significatively with the modification of the solvent polarity**.** The last result, together with the normal shift of the first reduction potential of **4** in relation with [60]fullerene, does not permit us to assign the extra band to an intramolecular electron-transfer process, as occurs in the case of 1,3-diphenylpyrazolo[4′,5′:1,2][60]fullerene.[3]

We have already synthesised some other TTF derivatives containing the sulfone group precursor of diene group on one side of the TTF core and different atoms (H, Me) on the other side. These compounds have better donor properties than compound **3**‖ and the synthesis and characterization of their corresponding [60]fullerene adducts has been recently performed in our laboratory with the aim of tuning the energy gap between the HOMO of the TTF addend and the LUMO of the [60]fullerene moiety. The study of the photoinduction of electron transfer in [60]fullerene adducts is being pursued.

This work was supported by grants from the Programa Nacional de Química Fina, (CIRIT-CICyT, grant, QFN95-00507-C01), the Acción especial Fullerenos (C.S.I.C) and by the Generalitat de Catalunya (GRP93-8028). J. L. thanks the CIRIT for a fellowship.

## Footnotes

† Satisfactory spectroscopic and analytical data were obtained for all new compounds: **1**, **2**, **3** and **4**. *Selected analytical and spectroscopic data* for **2**: calc. for $C_{65}H_4S_3$: C, 88.6; H, 0.4; S, 10.9. Found: C, 88.1; H, 0.4; S, 10.8%. $^1$H NMR (300 MHz, $CDCl_3$) δ 4.56. $^{13}$C NMR [75.42 MHz, $CS_2$–$CDCl_3$, 1 : 1, $Cr(acac)_3$] δ 40.33 ($CH_2$), 64.50 ([60]fullerene $C_{sp^3}$), 128.54 ($C_{sp^2}$), 135.42, 138.24, 139.97, 141.36, 141.77, 142.36, 142.71, 143.87, 144.28, 144.61, 145.20, 145.33, 145.98, 146.28, 147.53, 154.05, 219.25 (C=S). $\lambda_{max}(CHCl_3)$/nm (log ε): 257 (5.02), 316 (4.41), 383 (4.41), 433 (3.58). *m/z* 880 (7%, $M^+$), 720 (100, $[M - C_3H_4S_3]^+$). For **4**: Calc. for $C_{72}H_{10}S_4O_4$: C, 81.0; H, 0.9; S, 12.0. Found: C, 81.0; H, 1.1; S, 11.9%. $^1$H NMR (300 MHz, $CS_2$–$CDCl_3$, 1 : 1) δ 4.37 (s, 4 H, $CH_2$), 3.89 (s, 6 H, $CH_3$). $^{13}$C NMR (75.42 MHz, $CS_2$–$CDCl_3$, 1 : 1) δ 41.06 ($CH_2$), 53.25 ($CH_3$), 65.95 ([60]fullerene $C_{sp^3}$), 125.40 ($C_{sp^2}$), 132.38 ($C_{sp^2}$), 135.85, 140.34, 141.73, 142.16, 142.30, 142.78, 143.20, 144.71, 144.97, 145.59, 145.67, 145.81, 146.36, 146.64, 147.80, 155.04, 159.80 (C=O). $\lambda_{max}(CHCl_3)$/nm (log ε): 256 (4.91), 313 (4.56), 432 (3.65), 482 (3.43). HRMS (FAB) calc. for $C_{72}H_{10}O_4S_4$: 1065.946. Found: 1065.951.

‡ Thermogravimetric analysis reveals that the loss of solvent takes place between 120 and 190 °C giving rise to the solvent free adduct **2** that is completely stable up to 390 °C.

§ *Crystal data* for **2**: $C_{68}H_3S_3{\cdot}CS_2$, $M$ = 956.9; monoclinic, $P2_1/n$, $a$ = 15.167(2), $b$ = 13.670(2), $c$ = 17.701(2) Å; β = 105.76(2)°; $V$ = 3532.0(8) Å$^3$; $Z$ = 4; $D_c$ = 1.80 g cm$^{-3}$; μ(Mo-Kα) = 3.9 cm$^{-1}$, $2\theta_{max}$ = 47.4°, giving 5342 unique reflections. A dark brown plate of dimensions 0.29 × 0.12 × 0.08 mm was used. The structure was solved by direct methods (SHELXS-86) yielding $R$ = 0.056, $R_w$ = 0.127 for 1838 independent reflexions with $F > 4\sigma(F)$. Atomic coordinates, bond lengths and angles, and thermal parameters have been deposited at the Cambridge Crystallographic Data Centre (CCDC). See Information for Authors, Issue No. 1. Any request to the CCDC for this material should quote the full literature citation and the reference number 182/385.

¶ Besides homocoupling of **2**, heterocoupling with distinct thiones and ketones similar to **1** using a variety of different phosphites and solvents, have been performed. In all cases compound **2** was recovered almost quantitatively.

‖ First oxidation potentials (*vs* $Fc^+/Fc$) are $E^{1/2}$ = 0.01 V for the donor with Me substituents and $E^{1/2}$ = 0.02 V for the donor with no substituents.

## References

1 T. Drovestkaya, Ch. A. Reed and P. Boyd, *Tetrahedron Lett.*, 1995, **36**, 7971; M. Maggini, A. Karlsson, G. Scorrano, G. Sandonà, G. Farina and M. Prato, *J. Chem. Soc., Chem. Commun.*, 1994, 598.
2 J. M. Lawson, A. M. Oliver, D. F. Rothenfluh, Y-Z. An, G. A. Ellis, M. G. Ranasinghe, S. I. Khan, A. G. Franz, P. S. Ganapathi, M. J. Shephard, M. N. Paddon-Row and Y. Rubin, *J. Org. Chem.*, 1996, **61**, 5032.
3 Y. Matsubara, H. Tada, S. Nagase and Z. Yoshida, *J. Org. Chem.*, 1995, **60**, 5372.
4 H. Imahori, K. Hagiwara, T. Akiyama, S. Taniguchi, T. Okada and Y. Sakata, *Chem. Lett.*, 1995, 265; R. M. Williams, J. M. Zwier and J. W. Verhoeven, *J. Am. Chem. Soc.*, 1995, **117**, 4093; Y. Nakamura, T. Minowa, S. Tobita, H. Shizuka and J. Nishimura, *J. Chem. Soc., Perkin Trans. 2*, 1995, 2351.
5 R. M. Williams, M. Kroeberg, J. M. Lawson, Y.-Z. An, Y. Rubin, M. N. Paddon-Row and J. W. Verhoeven, *J. Org. Chem.*, 1996, **61**, 5055.
6 M. Prato, M. Maggini, C. Giacometti, G. Scorrano, G. Sandonà and G. Farina, *Tetrahedron*, 1996, **52**, 5221; N. Martín, L. Sánchez, C. Seoane, R. Andreu, J. Garín and J. Orduna, *Tetrahedron Lett.*, 1996, **33**, 5979.
7 A. Hirsch, *The Chemistry of the Fullerenes*, Thieme, Stuttgart, 1994; F. Diederich and C. Thilgen, *Science*, 1996, **271**, 317
8 J. Veciana, C. Rovira and D. O. Cowan, *Tetrahedron Lett.*, 1988, **29**, 3467.
9 Y. Rubin, S. Khan, D. I. Freedberg and C. Yeretzian, *J. Am. Chem. Soc.*, 1993, **115**, 334; F. Diederich, U. Jonas, V. Gramlich, A. Hermann, H. Ringsdorf and C. Thilgen, *Helv. Chim. Acta*, 1993, **76**, 2445; P. Belik, A. Gügel, A. Kraus, J. Spikermann, V. Enkelmann, G. Frank and K. Müllen, *Adv. Mater.*, 1993, **5**, 854.
10 A. J. Moore and M. R. Bryce, *Synthesis*, 1991, 26.
11 T. Suzuki, Y. Maroyama, T. Akasaba, W. Ando, K. Kobayashi and S. Nagasane, *J. Am. Chem. Soc.*, 1994, **116**, 1359.
12 M. Ohno, T. Azuma and S. Eguchi, *Chem. Lett.*, 1993, 1833; T. G. Linssen, K. Dürr, M. Hanack and A. Hirsch, *J. Chem. Soc., Chem. Commun.*, 1995, 103.

*Received, 19th November 1996; Com. 6/07857E*

# Biosynthesis of tetraponerine-6. Evidence that two different pathways are operating in the biosynthesis of the two tetraponerine skeletons

**C. Devijver,[a] J. C. Braekman,[a] D. Daloze[a] and J. M. Pasteels[b]**

[a] *Laboratory of Bio-organic Chemistry, Faculty of Sciences, CP160/07, University of Brussels, Av. F. D. Roosevelt, 50, B-1050 Brussels, Belgium*

[b] *Laboratory of Animal and Cellular Biology, Faculty of Sciences, CP 160/12, University of Brussels, Av. F. D. Roosevelt, 50, B-1050 Brussels, Belgium*

**Evidence is presented showing that tetraponerine-6 2a from *Tetraponera* sp. ants is biosynthesized from two molecules of putrescine and a seven-carbon moiety coming from an eight-carbon polyacetate chain through decarboxylation, in contrast with tetraponerine-8 1a, which derives from one putrescine unit and a twelve-carbon polyacetate precursor.**

The tetraponerines are a group of eight tricyclic alkaloids isolated from the poison gland of the Neo Guinean ant *Tetraponera* sp.[1] Structural and synthetic work from our laboratories[2–4] showed that these compounds are distributed into two families, which are based either on the 5-alkyldecahydropyrido[1,2-*c*]pyrrolo[1′,2′-*a*]pyrimidine† skeleton **1** (tetraponerines-3, -4, -7 and -8) or on the 5-alkyldecahydrodipyrrolo[1,2-*a*:1′,2′-*c*]pyrimidine† skeleton **2** (tetraponerines-1, -2, -5 and -6) (Fig. 1). In each family, the compounds differ from each other by the length of the alkyl chain (propyl or pentyl) and (or) by the configuration of the carbon atom to which it is attached.

Incorporation experiments with *Tetraponera* sp. ants using sodium [1-$^{14}$C]- and [2-$^{14}$C]-acetate, L-[U-$^{14}$C]glutamic acid, L-[U-$^{14}$C]ornithine hydrochloride, and [1,4-$^{14}$C]putrescine dihydrochloride, followed by chemical degradation of radioactive tetraponerine-8 (T-8) **1a**, the major alkaloid of the venom, allowed us to propose a biosynthetic pathway for this alkaloid.[5] It was found that acetate is a precursor of the entire carbon skeleton of T-8, but it is incorporated through two different pathways: the pyrrolidine ring of T-8 comes from acetate by its conversion, *via* the tricarboxylic acid cycle, into L-glutamic acid **3**, L-ornithine **4** and putrescine **5**, whereas the twelve remaining carbon atoms appear to be derived from a polyacetate precursor, for which a compound such as **6** is a likely candidate (Scheme 1).

The presence of alkaloids based on two different, albeit closely related, skeletons in one and the same organism is intriguing, particularly with respect to their biosynthesis. We now report our results from biosynthetic studies conducted on tetraponerine-6 (T-6) **2a**, which show that the two tetraponerine skeletons **1** and **2** are assembled *via* two different pathways.

We had to repeat the incorporation experiments with [1,4-$^{14}$C]putrescine dihydrochloride, since the sample of T-6 **2a** isolated from the first experiment[5] decomposed before it could be submitted to chemical degradation. Thus, 1000 *Tetraponera* sp. ants were starved for three days, then fed with a 1 mol dm$^{-3}$ sucrose solution containing [1,4-$^{14}$C]putrescine dihydrochloride (specific activity: 114 Ci mol$^{-1}$; total activity: 50 μCi). They were killed ten days later by dropping them into methanol. Using the already described[2] extraction and purification scheme, four of the tetraponerines (T-8 **1a**, T-4 **1b**, T-6 **2a** and T-5 **2c**) could be isolated in pure state. All were radioactive. Their specific activity and specific incorporation rate (SIR) are reported in Table 1 (experiment 2), together with the values measured from the first incorporation experiment[5] for T-8 (experiment 1). Table 1 shows that the specific incorporation rates of the four alkaloids isolated from experiment 2 are of the same order of magnitude as that of T-8 **1a** from the first experiment.[5] A closer inspection, however, shows that, in experiment 2, the specific incorporation rates of T-6 **2a** and T-5 **2c** are nearly twice that of T-8. Compound T-6 **2a** (6.50 mg), which in this experiment was found to be the major alkaloid of the venom, was then diluted with racemic synthetic[4] material (23.91 mg) as carrier, and divided into two parts, each of which was separately submitted to a degradation scheme analogous to that devised for T-8[5] (Scheme 2). This procedure allowed us to split the molecule into three moieties:‡ *N*-methylpyrrolidine **9**, comprising C-4 to C-7, *N*-tosyl-*p*-bromophenacylprolinate **10**, comprising C-1 to C-3, C-9 and C-10, and *p*-bromophenacylhexanoate **11**, comprising C-8 and C-11 to C-15 of T-6 (Scheme 2). The specific activities and relative specific activities (RSA) of compounds **9** to **11**, and of the two

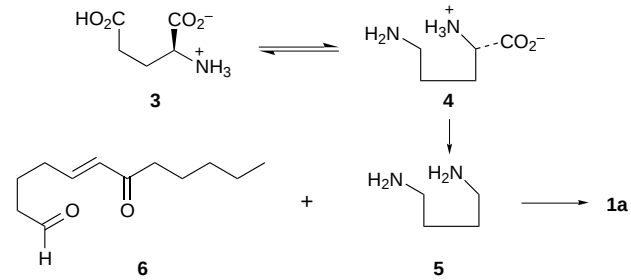


**1a** 9β-H; R = $C_5H_{11}$ (T-8)
**b** 9β-H; R = $C_3H_7$ (T-4)
**c** 9α-H; R = $C_5H_{11}$ (T-7)
**d** 9α-H; R = $C_3H_7$ (T-3)



**2a** 9β-H; R = $C_5H_{11}$ (T-6)
**b** 9β-H; R = $C_3H_7$ (T-2)
**c** 9α-H; R = $C_5H_{11}$ (T-5)
**d** 9α-H; R = $C_3H_7$ (T-1)

**Fig. 1** Structures of the eight tetraponerines

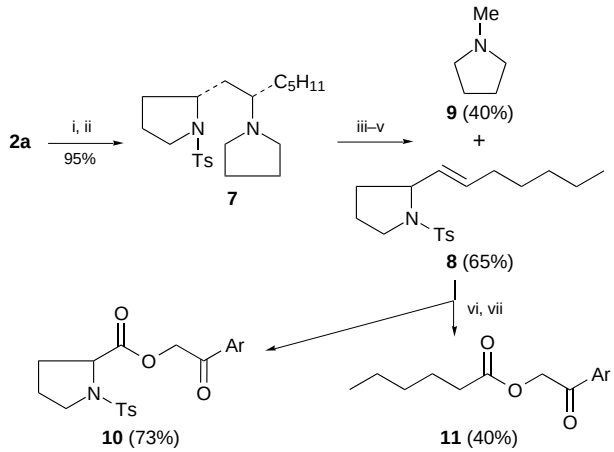


**Scheme 1** Biogenetic scheme proposed for tetraponerine-8 **1a**

**Table 1** Incorporation of [1,4-$^{14}$C] putrescine (50 μCi, 114 Ci mol$^{-1}$) into the tetraponerines

| Experiment | Compound | Amount/mg | TA[a]/μCi | $10^2$ SA[b]/Ci mol$^{-1}$ | $10^2$ SIR[c] (%) |
|---|---|---|---|---|---|
| 1 | **1a** (T-8) | 6.4 | 1.01 | 4.0 | 3.7 |
| 2 | **1a** (T-8) | 5.70 | 0.68 | 3.0 | 2.6 |
| 2 | **2a** (T-6) | 6.70 | 1.44 | 5.1 | 4.5 |
| 2 | **1b** (T-4) | 0.81 | 0.12 | 3.3 | 2.9 |
| 2 | **2c** (T-5) | 0.22 | 0.05 | 4.9 | 4.3 |

[a] Total activity. [b] Specific activity. [c] Specific incorporation rate.




**Scheme 2** Degradation scheme of tetraponerine-6 **2a**. *Reagents and conditions*: i, $H_2$, $PtO_2$, EtOH, HCl; ii, TsCl, pyridine; iii, MeI, MeCN; iv, $OH^-$; v, 160 °C, 3 h; vi, $KMnO_4$, $NaIO_4$, 24 h; vii, *p*-$BrC_6H_4COCH_2Br$, MeCN, reflux, 1 h (Ts = *p*-$MeC_6H_4SO_2$, Ar = 4-$BrC_6H_4$).

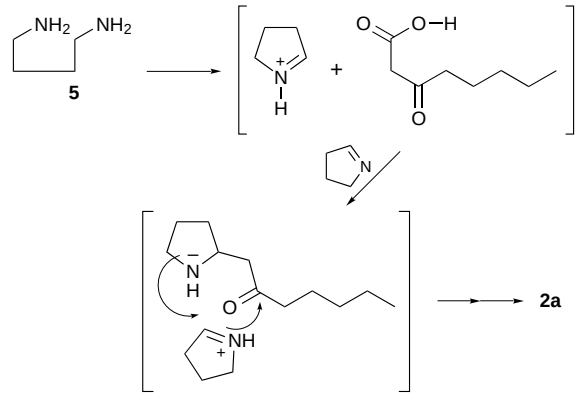
**Table 2** Observed distribution of label within the degradation products of T-6 **2a**[a]

| Compound | $10^3$ SA/ Ci $mol^{-1}$ | RSA[b] (%) |
|---|---|---|
| **2a**[c] | 10.9 | – |
| **7** | 10.7 | 100.0 |
| **8** | 5.0 | 47.5 |
| **9** | 5.0 | 46.5 |
| **10** | 4.7 | 44.5 |
| **11** | 0 | 0 |

[a] Mean of two separate experiments. [b] Relative specific activity, that of **7** being taken as 100%. [c] 6.50 mg diluted with 23.91 mg of cold synthetic (±)-**2a**.

degradation intermediates **7** and **8** (Scheme 2), calculated by using a 100% value for the RSA of **7**, are reported in Table 2.

Surprisingly, the radioactivity of T-6 **2a** was equally divided between *N*-methylpyrrolidine **9** and the olefin **8**. This was in complete contrast with our previous results on putrescine incorporation in T-8 **1a** (experiment 1),[5] where the olefin corresponding to **8** was not labelled at all. Moreover, after oxidative cleavage of the double bond of **8**, only the *N*-tosyl-*p*-bromophenacylprolinate **10** was found to be radioactive, whereas no activity was found in **11**. It turns out that, during the biosynthesis of T-6 **2a**, putrescine serves as precursor to both pyrrolidine rings. To confirm that different pathways are indeed operating in the biosynthesis of T-6 and T-8, the sample of T-8 **1a** (5.70 mg) isolated from the second incorporation experiment was also diluted with cold synthetic material,[6] and submitted to the usual degradation scheme. The results obtained were in complete agreement with those already reported for this alkaloid,[5] confirming that all the label from putrescine was located in the pyrrolidine ring of T-8, with no radioactivity detected at any other position of the molecule.




**Scheme 3** Biogenetic scheme proposed for tetraponerine-6 **2a**

These results allow us to propose a biogenetic hypothesis for the formation of tetraponerine skeleton **2** in *Tetraponera* sp. ants. Thus, whereas skeleton **1** presumably originates from the condensation of a twelve-carbon polyacetate precursor with one putrescine unit (Scheme 1), skeleton **2** is formed by reaction of two putrescine units with an eight-carbon polyacetate chain, with concomitant decarboxylation (possibly under enzyme control, Scheme 3).

This work was supported by grants from the Belgian Fund for Basic Research (Grant 2.4513.90-96) and the French Community of Belgium (ARC 93/98-137). C. D. gratefully acknowledges the 'Institut pour l'Encouragement de la Recherche Scientifique dans l'Industrie et l'Agriculture' (IRSIA) for financial support. We thank Dr R. Ottinger for the NMR spectra and Mr C. Moulard for the mass spectra. This paper represents contribution No 339 of King Leopold III Biological Station, Laing Island, Papua New Guinea.

## Footnotes

† IUPAC numbering. For convenience, we will use the numbering of earlier publications.

‡ All compounds isolated from the degradation scheme were characterized by EIMS, $^1H$ NMR, $^{13}C$ NMR and IR spectroscopy, and, in some cases, by HREIMS.

## References

1 J. C. Braekman, D. Daloze, J. M. Pasteels, P. Vanhecke, J. P. Declercq, V. Sinnwell and W. Francke, *Z. Naturforsch., C Biosci*., 1987, **42**, 627.
2 P. Merlin, J. C. Braekman, D. Daloze and J. M. Pasteels, *J. Chem. Ecol*., 1988, **14**, 517.
3 P. Macours, J. C. Braekman and D. Daloze, *Tetrahedron*, 1995, **51**, 1415.
4 C. Devijver, J. C. Braekman and D. Daloze, *Tetrahedron*, 1995, **51**, 10 913.
5 B. Renson, P. Merlin, D. Daloze, J. C. Braekman, Y. Roisin and J. M. Pasteels, *Can. J. Chem*., 1994, **72**, 105.
6 P. Merlin, J. C. Braekman and D. Daloze, *Tetrahedron*, 1991, **47**, 3805.

*Received, 4th December 1996; Com. 6/08180K*

# Synthesis of ferrisilicate with the MCM-22 structure

**Peng Wu, Hong Lin, Takayuki Komatsu and Tatsuaki Yashima***

*Department of Chemistry, Tokyo Institute of Technology, Ookayama 2-12-1, Meguro-ku, Tokyo, 152, Japan*

**A new ferrisilicate molecular sieve with the MCM-22 structure is synthesized in Al-free form and exhibits low activity as a solid-acid catalyst and significant activity for the selective catalytic reduction of NO with $NH_3$.**

A new zeolite MCM-22 patented recently[1] has been proposed to contain two independent pore systems, both of which are accessed through rings composed of ten tetrahedral (T) atoms.[2] One of these pore systems consists of large supercages of 12-membered rings. This unique pore structure of the aluminosilicate MCM-22 means it is an interesting catalyst for a wide variety of acid-catalysed reactions.[3–5]

Isomorphous substitution of other elements for Si or Al into the silica based zeolite framework to prepare the corresponding metallosilicates is an effective way to modify the activity and selectivity of zeolite catalysts. Isomorphous substitution of Ga, Fe, As, Ti, V, Sn, *etc.* into the framework has already been reported. Among these metallosilicates, ferrisilicates have been used as both solid-acid catalysts and oxidation catalysts. The acid strength of MFI type (ZSM-5 type) ferrisilicate is moderate and weaker than that of the Ga and Al analogues.[6] More importantly, we have reported that MFI type ferrisilicate is a more selective catalyst than $Fe^{3+}$-exchanged ZSM-5 and iron oxide supported on silicalite in the oxidative dehydrogenation of alkanes,[7] and that it is also an active catalyst for the selective catalytic reduction (SCR) of NO with $NH_3$ in the presence of $O_2$.[8] Ferrisilicates have been synthesized for MFI,[6] beta,[9] MOR (mordenite),[10] FER (ferrierite), *etc.*,[11] but, as yet, not for the MCM-22 topology. Here, we report for the first time, the synthesis of iron-substituted MCM-22 zeolite and its physicochemical and catalytic properties.

MCM-22 type ferrisilicate (Fe-MCM-22) was synthesized using fumed silicon dioxide (Cab-o-sil M7D) as the source of silicon to obtain an Al-free material (Si/Al > 10 000). Hexamethyleneimine (HM) and $Fe(NO_3)_3 \cdot 9H_2O$ were used as the template and iron source, respectively. In a typical synthesis, silicon dioxide and sodium hydroxide were dissolved in an aqueous solution of HM with stirring for 2 h. The resultant mixture was then added dropwise into an aqueous solution of $(Fe(NO_3)_3$. The mixture was stirred for another 2 h to obtain a clear gel. The pH of the final gel was *ca*. 12 and its molar composition was $SiO_2 : 0.03\ Fe_2O_3 : 0.15\ Na_2O : 45\ H_2O$. The gel was then transferred into a Teflon autoclave and heated at 408 K for 11 days under stirring (60 rpm). The resultant solid product was filtered and washed thoroughly with deionized water, dried at 403 K and calcined in air at 753 K for 5 h to remove the template. The Na form of the zeolite thus obtained was transformed into the H form by ion exchange with 0.1 M $NH_4NO_3$ followed by calcination in air at 723 K for 2 h. A reference sample of the Al analogue, Al-MCM-22, was synthesized according to ref. 12. These two samples were characterized with XRD, IR, $N_2$ adsorption and catalytic studies.

Fe-MCM-22 was nearly white, indicating the absence of iron oxides within the crystals. The XRD pattern of Fe-MCM-22 was very similar to that of its aluminosilicate analogues reported previously[12] except that the relative peak intensities were somewhat different (Fig. 1). Its framework IR spectrum was also similar to that of Al-MCM-22. Upon substitution of Fe for Al, some vibration bands were shifted to lower wavenumbers which can be taken as evidence that Fe ions are present in the tetrahedral framework sites since Si–O–Fe vibrations are weaker than those of Si–O–Al. The internal asymmetric vibration has been reported to show a larger shift than the external one upon the substitution of Fe for Al in beta and MOR.[9,10] However, the extent of the shift of these two vibrations was reversed for MCM-22 (Table 1), which may be due to the unique structure of the MCM-22 zeolite. From $N_2$ adsorption experiments, Fe-MCM-22 had a comparable micropore volume and specific surface area to Al-MCM-22. These data were also similar to those reported for MCM-22 aluminosilicates[4] and is a clear indication that Fe-MCM-22 has a high degree of crystallinity.

If trivalent $Fe^{3+}$ ions are incorporated into the silicate framework, Si(OH)Fe hydroxy groups must be generated when Fe-MCM-22 was exchanged into the H form. Fig. 2 shows IR spectra of both H-form Fe-MCM-22 and H-form Al-MCM-22 in the hydroxy region. For Al-MCM-22 [Fig. 2(*a*)], the bands at 3748 $cm^{-1}$ (external silanols), 3730 $cm^{-1}$ (internal silanols), 3663 $cm^{-1}$ (associated with extraframework Al species) and 3621 $cm^{-1}$ [the structural Si(OH)Al hydroxy groups] were

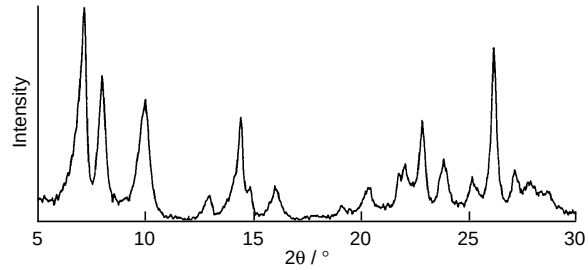



**Fig. 1** X-Ray diffraction pattern of Fe-MCM-22

**Table 1** Physicochemical and catalytic properties of Fe-MCM-22 and Al-MCM-22

| | | $N_2$ adsorption | | $\nu_{asym}/cm^{-1}$ | | Catalytic activity/mol% | |
|---|---|---|---|---|---|---|---|
| | Si/M ratio in gel | Micropore/ ml $g^{-1}$ | Surface area/ $m^2\ g^{-1}$ | External | Internal | *o*-Xylene[a] isomerization | Toluene[b] methylation |
| Fe-MCM-22 | 15 | 0.197 | 544 | 1229 | 1089 | 6.1 | 23.9 |
| Al-MCM-22 | 15 | 0.203 | 551 | 1244 | 1092 | 67.5 | 81.6 |

[a] *o*-Xylene isomerization: cat., 0.4 g; *W/F* = 7.2 g h $mol^{-1}$; *T* = 573 K; He, 20 ml $min^{-1}$; time on stream (TOS) = 1 h. [b] Toluene methylation: cat., 0.4 g; *W/F* = 6.8 g h $mol^{-1}$; *T* 573 K; MeOH–toluene molar ratio = 2 : 1; He, 20 ml $min^{-1}$; TOS = 1 h.

clearly distinguished. Fe-MCM-22 [Fig. 2(*b*)] exhibited a characteristic band at 3637 $cm^{-1}$. This band was removed completely after pyridine adsorption followed by desorption at 423 K, while a band due to pyridinium ions was observed at 1550 $cm^{-1}$. This allows us to assign the band at 3637 $cm^{-1}$ to structural Si(OH)Fe groups with Brønsted acidity. Hence, the above results are considered as strong proof of the incorporation of $Fe^{3+}$ ions in the framework. The higher wavenumber of Si(OH)Fe groups suggests that the Brønsted acidity of Fe-MCM-22 is much weaker than that of Al-MCM-22 and Fe-MCM-22 showed very low activity for *o*-xylene isomerization (catalysed by Brønsted-acid sites having at least medium strength), while it exhibited a relatively higher activity for toluene methylation (proceeds even over weak Brønsted-acid sites) at the same reaction temperature (Table 1).

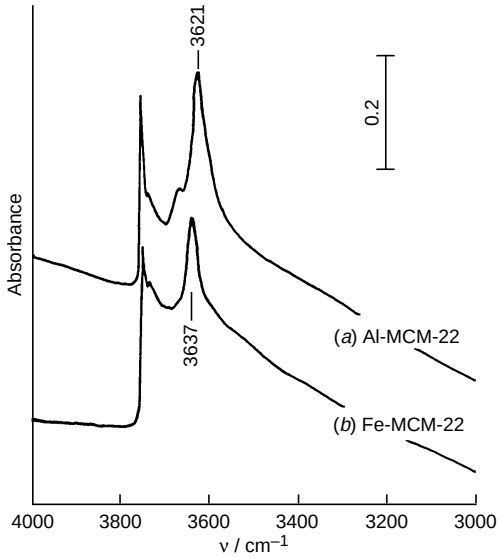



**Fig. 2** IR spectra in the hydroxy region

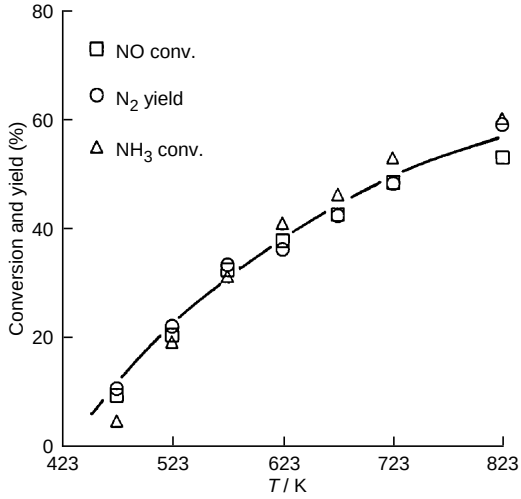



**Fig. 3** NO reduction over Fe-MCM-22 with $NH_3$ in the presence of $O_2$. *Reaction conditions*: cat. 0.1 g; feed, NO (0.1%), $NH_3$ (0.1%), $O_2$ (2%), He (balance); total flow rate, 500 ml $min^{-1}$.

Further, Fe-MCM-22 was also tested for the selective catalytic reduction of NO with $NH_3$ in the presence of $O_2$. It is obvious from Fig. 3 that Fe-MCM-22 is an effective catalyst for NO reduction with $NH_3$ as a reductant. The activity of Fe-MCM-22 was even *ca*. 10% higher than that of MFI-type ferrisilicate (Si/Fe = 25) below 600 K (the temperature region where NO reduction occurred selectively for MFI-type ferrisilicate). It should be noted that Al-MCM-22 only showed NO conversion of less than 5% at the temperatures studied. Thus, the active sites must be the framework $Fe^{3+}$ ions, as reported previously for MFI type ferrisilicate.[8] NO conversion, $N_2$ yield and $NH_3$ conversion correlated well with each other even at high temperatures, indicating that the reduction of NO by $NH_3$ occurred selectively. This result also verifies that extraframework Fe species are negligible in Fe-MCM-22 since we have observed that iron oxide species supported on MFI type silicalite exhibits activity for the oxidation of $NH_3$ by $O_2$ to form NO but no activity for the reduction of NO.[8] As Fe-MCM-22 can be synthesized with relatively high Fe content (Si/Fe = 15), it is anticipated that more active catalysts for SCR of NO can be obtained by exchange with other transition-metal ions into Fe-MCM-22.

To summarize, a new ferrisilicate possessing the MCM-22 structure has been hydrothermally synthesized. Fe-MCM-22 is a weak solid acid but is an effective catalyst for the selective reduction of NO.

## Footnote

* E-mail: Komatsu@chem.titech.ac.jp

## References

1 M. K. Rubin and P. Chu, *US Pat.*, 4439409, 1990.
2 M. E. Leonowicz, J. A. Lawton, S. L. Lawton and M. K. Rubin, *Science*, 1996, **264**, 1910.
3 K. J. Del Rossi and Jr. Huss, *US Pat.*, 5107047, 1992; Jr. A. Huss, G. W. Kirker, K. M. Keville and R. T. Thomson, *US Pat.*, 4992615, 1991.
4 R. Ravishankar, T. Sen, V. Ramaswamy, H. S. Soni, S. Ganapathy and S. Sivasanker, *Stud. Surf. Sci. Catal.*, 1994, **84**, 331.
5 M. A. Asensi, A. Corma and A. Martínez, *J. Catal.*, 1996, **158**, 561.
6 C. T.-W. Chu and C. D. Chang, *J. Phys. Chem.*, 1985, **89**, 1569.
7 Md. A. Uddin, T. Komatsu and T. Yashima, *J. Catal.*, 1994, **146**, 468; Md. A. Uddin, T. Komatsu and T. Yashima, *J. Catal.*, 1994, **150**, 439.
8 Md. A. Uddin, T. Komatsu and T. Yashima, *J. Chem. Soc., Faraday Trans.*, 1995, **91**, 3275.
9 R. Kumar, A. Thangaraj, R. N. Bhat and P. Ratnasamy, *Zeolites*, 1991, **11**, 42.
10 A. J. Chandwadkar, R. N. Bhat and P. Ratnasamy, *Zeolites*, 1990, **10**, 85.
11 R. B. Borade and A. Clearfield, *Chem. Commun.*, 1996, 2267.
12 A. Corma, C. Corell and J. Pérez-Pariente, *Zeolites*, 1995, **15**, 2.

*Received, 18th November 1996; Com. 6/07769B*

# Calix[4]pyrroles: *C*-rim substitution and tunability of anion binding strength

**Philip A. Gale, Jonathan L. Sessler,* William E. Allen, Nicolai A. Tvermoes and Vincent Lynch**

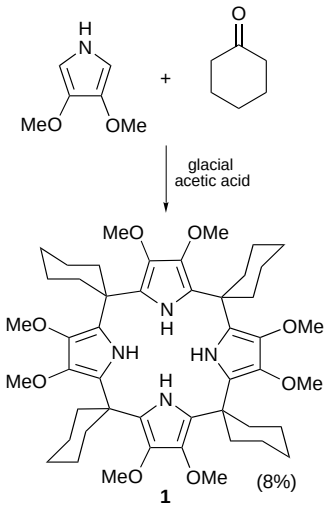
*Department of Chemistry and Biochemistry, University of Texas at Austin, Austin, Texas 78712-1167, USA*

**Electron-rich and electron-deficient *C*-rim substituted calix[4]pyrroles 1–4 are synthesised and the anion binding ability of these receptors is found to be dependent upon the *C*-rim substituents.**

Stimulated by how nature utilises anions in numerous biochemically important systems such as chloride channels,[1] proteins[2] and as polyanions for the storage and transmission of genetic information,[3] the molecular recognition of anionic guest species is an area of coordination chemistry attracting increasing interest.[4–7] As part of a programme aimed at the synthesis of new easy-to-make anion binding agents, and exploiting our recent discovery that calix[4]pyrroles (*meso*-octaalkylporphyrinogens; first synthesised in 1886 by Baeyer[8]) are effective and selective anion binding agents both in solution and in the solid state,[9,10] we decided to investigate whether the anion binding ability of these latter materials could be tuned by appending functional groups to the carbon rim (*C*-rim) of the calixpyrrole. Previously, Jacoby *et al*. have investigated modification of the *meso*-octaakylporphyrinogen skeleton using organometallic methodologies.[11] We adopted two strategies for the synthesis of *C*-rim calix[4]pyrroles: firstly, synthesis from 3,4-disubstituted pyrroles and ketones, and secondly, direct modification of the *C*-rim of a pre-synthesised calix[4]pyrrole.

Using the first strategy, 3,4-dimethoxypyrrole[12] was condensed with cyclohexanone in glacial acetic acid. Removal of the acid *in vacuo* and subsequent purification of the residue by column chromatography (silica gel, $CH_2Cl_2$ eluent) afforded the novel β-octamethoxy-*meso*-tetraspirocyclohexylcalix[4]-pyrrole **1** as a white powder in 8% yield (Scheme 1).

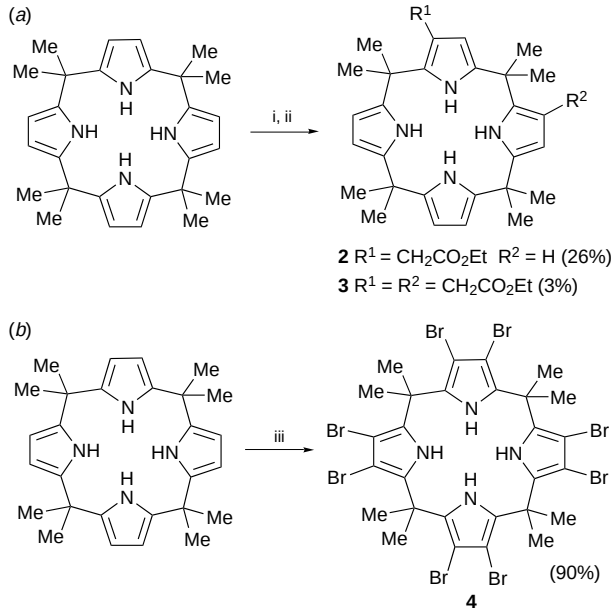
Following the second strategy, *meso*-octamethylcalix[4]pyrrole was dissolved with stirring in dry THF under an Ar atmosphere, and the flask cooled to −78 °C. A solution of butyllithium in hexanes (4.0 equiv.) was added dropwise to the calixpyrrole solution and after 30 min, 4.0 equiv. of ethyl bromoacetate were also added. The reaction was stirred for a further 1 h at −78 °C and then allowed to warm to room temperature. Purification by column chromatography (silica gel, $CH_2Cl_2$ eluent) afforded two isolable products. The first proved to be *C*-rim monoester **2** (formed in 26% yield) and the second the diester **3** (3% yield) [Scheme 2(*a*)]. Surprisingly, $^1$H and $^{13}$C NMR experiments showed that the diester **3** present in the fraction collected was a single isomer. Support for the proposed 1,3-substitution pattern of **3** was obtained from X-ray crystallographic analysis even though the quality of the crystals did not permit a complete refinement.




**Scheme 1**

β-Octabromo-*meso*-octamethylcalix[4]pyrrole **4** was synthesised in 90% yield by reaction of *meso*-octamethylcalix[4]pyrrole with *N*-bromosuccinimide (NBS) in dry THF heated at reflux [Scheme 2(*b*)]. Single crystals of compound **4** were grown by slow evaporation of a dilute dichloromethane solution of the macrocycle (Fig. 1).† The structure reveals that compound **4** exists in a chair-like flattened 1,2-alternate conformation in the solid state (*i.e*. the dihedral angles between pyrrole rings and plane through the calixpyrrole *meso*-carbon atoms are 66.8, 5.8, −66.8 and −5.8°).

Analyses of the solution phase anion binding properties of calix[4]pyrroles **1**, **2** and **4** were made using $^1$H NMR spectroscopic titrations carried out in $CD_2Cl_2$. Data analysis and stability constant determinations were then made using the EQNMR computer program fitting the binding profiles to a 1 : 1 calixpyrrole–anion solution complex model.[13] The results are summarised in Table 1. Compound **1** has lower stability constants with fluoride and chloride than *meso*-tetraspirocyclohexylcalix[4]pyrrole.[9] This may be due to the electron-donating ability of the eight *C*-rim methoxy groups causing a decrease in the acidity of the pyrrole NH protons and hence reducing anion binding ability. Likewise compound **2** shows lower stability constants for the complexation of fluoride, chloride and dihydrogen phosphate anions than does *meso*-




**Scheme 2** *Reagents*: i, BuLi (4 equiv.), THF; ii, $BrCH_2CO_2Et$ (4 equiv.); iii, NBS, THF

octamethylcalix[4]pyrrole.[9] In this case the reduction in anion binding strength (with the respect to *meso*-octamethylcalix[4]pyrrole) may be due to unfavourable interactions between the bound anion and the lone pair electrons on the oxygen atoms of the *C*-rim ester group.

In contradistinction to receptors **1** and **2**, compound **4** exhibits higher stability constants for the binding of fluoride, chloride and dihydrogen phosphate anions than does *meso*-octamethylcalix[4]pyrrole under the same conditions. This may be due to the electron-withdrawing nature of the eight *C*-rim bromine atoms increasing the acidity of the pyrrole NH protons and thus enhancing anion binding ability.

In summary, we have shown that the anion binding ability of the calix[4]pyrroles can be tuned by appending different groups to the carbon or *C*-rim of the calixpyrrole. Receptors with an increased anion binding ability such as **4** may have potential uses as anion sequestering agents (*e.g.* in removal of phosphate pollutants from aqueous environments) while those with decreased anion binding ability (compounds **1** and **2**) could prove useful as HPLC column media since in this latter application low affinity constants and fast complexation–decomplexation rates generally lead to efficient separation of substrates.[14] In any event the fact that compounds **2** and **3** come 'prefunctionalised' with ester groups should facilitate the attachment of other substituents, making it easier to use the calix[4]pyrroles in a range of applications.

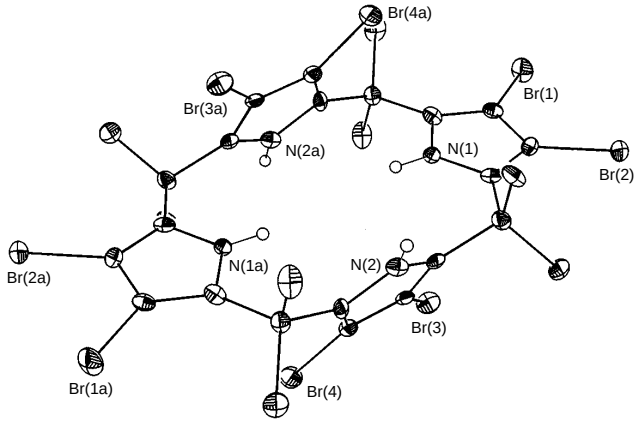



**Fig. 1** View of $C_{28}H_{28}N_4Br_8$ **4** showing the flattened 1,2-alternate conformation. Thermal ellipsoids are scaled to the 30% probability level.

**Table 1** Stability constants for compounds **1**, **2** and **4** with anionic substrates[a] in $CD_2Cl_2$ at 298 K

| | Stability constant/dm$^3$ mol$^{-1}$ | | |
|---|---|---|---|
| Anion | **1** | **2** | **4** |
| Fluoride | 1.7 (±0.2) × $10^2$ | 1.1 (±0.2) × $10^3$ | 2.7 (±0.4) × $10^4$[b] |
| Chloride | < 10 | 47 (±1) | 4.3 (±0.6) × $10^3$ |
| Dihydrogen-phosphate | —[c] | < 10 | 6.5 (±0.4) × $10^2$ |

[a] Anions were added as 0.03 M $CD_2Cl_2$ solutions of their tetrabutylammonium salts to 3 mM solutions of the receptor in $CD_2Cl_2$ with concentration changes being accounted for by EQNMR (ref. 13). In determining the stability constants, the possible effects of ion pairing (if any) were ignored. [b] Estimated value. The NH proton resonance broadened considerably during the titration, forcing the frequency of the resonance to be noted manually. This value should, therefore, be treated with caution. [c] Not determined.

Financial support from NIH (Grant AI33577), NSF (Grant CHE9122161) and Pharmacyclics Inc. to J. L. S. is gratefully acknowledged. P. A. G. and W. E. A. thank the Fulbright Commission and the American Cancer Society, respectively, for post-doctoral research fellowships.

## Footnotes

* E-mail: Sessler@mail.utexas.edu

† *Crystal data* for $C_{28}H_{28}N_4Br_8$: Large, colourless prisms were grown by slow evaporation from $CH_2Cl_2$. Crystals were monoclinic, $P2_1/n$, $Z$ = 2, $a$ = 10.819(4), $b$ = 12.042(4), $c$ = 12.746(4) Å, β = 99.01(2)°, $V$ = 1640.1(10) Å$^3$, $D_c$ = 2.15 g cm$^{-3}$, μ = 98.07 cm$^{-1}$, $F$(000) = 1008. A total of 7416 reflections were measured, 3763 unique [$R_{int}(F^2)$ = 0.091] on a Siemens P3 diffractometeer using graphite monochromatised Mo-Kα radiation (λ = 0.71073 Å) at −75 °C. The structure was refined on $F^2$ using SHELXTL/PC (ver. 5.03, Siemens Analytical X-ray Instruments, Madison, WI, USA) to an $R_w$ = 0.131, with a conventional $R$ = 0.0575 (2231 reflections with $F_0 > 4[\sigma(F_0)]$), and a goodness-of-fit = 1.105 for 182 refined parameters. The molecule lies on a crystallographic inversion centre at 0,0,0. Atomic coordinates, bond lengths and angles, and thermal parameters have been deposited at the Cambridge Crystallographic Centre (CCDC). See Information for Authors, Issue No. 1. Any request to the CCDC for this material should quote the full literature citation and the reference number 182/395.

## References

1 M. A. van Kuijck, R. A. M. H. van Aubel, A. E. Busch, F. Lang, F. G. M. Russel, R. J. M. Bindels, C. H. van Os and P. M. T. Deen, *Proc. Natl. Acad. Sci. U.S.A.*, 1996, **93**, 5401.
2 P. Chakrabarti, *J. Mol. Biol.*, 1993, **234**, 463.
3 B. J. Calnan, B. Tidor, S. Biancalana, D. Hudson and A. D. Frankel, *Science*, 1991, **252**, 1167.
4 F. P. Schmidtchen, *Nachr. Chem., Tech. Lab.*, 1988, **36**, 8.
5 H. E. Katz, in *Inclusion Compounds*, ed. J. L. Atwood, J. E. D. Davies and D. D. MacNicol, Academic Press, New York, 1991, vol. 4, p. 391.
6 B. Dietrich, *Pure Appl. Chem.*, 1993, **65**, 1457.
7 P. D. Beer, *Chem. Commun.*, 1996, 689 and references cited therein.
8 A. Baeyer, *Ber. Dtsch. Chem. Ges.*, 1886, **19**, 2184.
9 P. A. Gale, J. L. Sessler, V. Král and V. Lynch, *J. Am. Chem. Soc.*, 1996, **118**, 5140.
10 J. L. Sessler, A. Andrievsky, P. A. Gale and V. Lynch, *Angew. Chem., Int. Ed. Engl.*, 1996, **35**, 2782.
11 D. Jacoby, S. Isoz, C. Floriani, A. Chiesi-Villa and C. Rizzoli, *J. Am. Chem. Soc.*, 1995, **117**, 2805.
12 A. Merz, R. Schropp and J. Lex, *Angew. Chem., Int. Ed. Engl.*, 1993, **32**, 291.
13 M. J. Hynes, *J. Chem. Soc., Dalton Trans.*, 1993, 311.
14 J. L. Sessler, P. A. Gale and J. W. Genge, unpublished results.

*Received in Corvallis, OR, USA, 29th January 1997; Com. 7/00685C*

# Ruthenium catalysed hydrogenation of dimethyl oxalate to ethylene glycol

**Herman T. Teunissen and Cornelis J. Elsevier***

*Anorganisch Chemisch Laboratorium, J. H. van't Hoff Research Instituut, Universiteit van Amsterdam, Nieuwe Achtergracht 166, NL-1018 WV Amsterdam, The Netherlands*

**Dimethyl oxalate is efficiently hydrogenated to ethylene glycol under mild conditions [$p(H_2)$ 70 bar; 100 °C] using a ruthenium catalyst based on $Ru(acac)_3$ and $MeC(CH_2PPh_2)_3$.**

The homogeneous hydrogenation of esters to alcohols is a difficult process and only a few papers dealing with this subject have appeared.[1–3] Anionic ruthenium hydride catalysts have been described by Grey *et al.*[1] and neutral ruthenium catalysts were reported by Matteoli *et al.*[2,3] In general, drastic conditions are required for the efficient conversion of an ester to the corresponding alcohol, unless the ester is activated by electron-withdrawing substituents. Thus, the hydrogenation of methyl glycolate (MGL) to ethylene glycol [EGL, eqn. (1)] requires drastic conditions [$p(H_2)$ 200 bar; 180 °C][2] while dimethyl oxalate (DMO) is relatively easily reduced to MGL [eqn.(2)].

$$MeO_2CCH_2OH + 2\ H_2 \rightarrow HOCH_2CH_2OH + MeOH \quad (1)$$

$$MeO_2CCO_2Me + 2\ H_2 \rightarrow MeO_2CCH_2OH + MeOH \quad (2)$$

We report a ruthenium based homogeneous catalyst which is able to homogeneously catalyse the hydrogenation of DMO to EGL under substantially milder conditions.

Exploratory experiments were based on the $Ru(acac)_3$ system, described by Hara and Wada for the hydrogenation of anhydrides to lactones.[4] These experiments revealed that an active catalyst can be generated *in situ* from $Ru(acac)_3$ and a donor ligand in MeOH in the presence of zinc. Zinc was added to initiate a fast reduction of the acetylacetonate complex. The influence of ligands on the catalytic activity of this system was explored in detail and is shown in Table 1.†

From Table 1 it is evident that ruthenium catalysts with phosphine ligands (except tricyclohexylphosphine, entry 7) show a higher activity than with the nitrogen or arsenic compounds (entries 3–6). The applied phosphine ligands induced remarkable differences in terms of catalytic activity as a function of their coordination properties. More specifically, the activity of the ruthenium–phosphine catalysts in the hydrogenation of DMO (expressed as turnover frequency) increases in the order $P(C_6H_{11})_3 < Ph_2PC_2H_4PPh_2 < PPh_3 < PhP(C_2H_4PPh_2)_2 \approx [CH_2P(Ph)C_2H_4PPh_2]_2 \ll MeC(CH_2PPh_2)_3$. The extraordinary effect of the $MeC(CH_2PPh_2)_3$ ligand[5] on the catalytic activity is evident from the formation of EGL in high yield which was not observed in any previous experiment. (Note that the hydrogenation of MGL to EGL is not as activated by an electron-withdrawing substituent as the hydrogenation of DMO to MGL, *vide supra*.) Our catalytic system consisting of $Ru(acac)_3$ and the tridentate ligand $MeC(CH_2PPh_2)_3$ (entry 11) is considerably better with respect to the selectivity of EGL formation and the turnover frequency when compared with the catalytic properties of the best known system so far, *i.e.* $Ru(CO)_2(AcO)_2(PBu_3)_2$.[2] Furthermore, our system displays catalytic activity under relatively mild conditions. The catalytic properties of the ruthenium catalyst derived from $MeC(CH_2PPh_2)_3$ indicate that a ruthenium complex with a *fac* coordinating ligand is essential for high catalytic activity. This conjecture is supported by the relatively low catalytic activity of the $PhP(C_2H_4PPh_2)_2$ and $[CH_2P(Ph)C_2H_4PPh_2]_2$ derived systems, in which the ligands can coordinate either in a *fac* or *mer* fashion to ruthenium.

The $Ru(acac)_3$–$MeC(CH_2PPh_2)_3$ system was explored in more detail with respect to the influence of the hydrogen pressure, the substrate to catalyst ratio, and the role of zinc. From Table 2 it is clear that the turnover number increases from 160 (entry 1) to 642 (entry 3) when the Ru : DMO ratio decreases from 1.19 to 0.18%. As is seen from entries 8 and 9, decreasing the Ru : DMO ratio from 0.20 to 0.15 leads to significantly lower catalytic activity; the turnover frequency decreases from 53.5 to 15.5 $h^{-1}$.

As expected, the $H_2$ pressure has a significant influence on the turnover number and turnover frequencies. Decreasing the $H_2$ pressure from 70 to 20 bar (entries 3–5) leads to a decrease of the turnover frequency by a factor 3.6. Comparing the experiments in entries 3 and 6 (and 7 and 8), the influence of

**Table 1** Influence of the ligand in the ruthenium catalysed hydrogenation of DMO to MGL and ethylene glycol (EGL)[a]

| Entry | DMO/ mmol | Ligand | Ru : DMO (%) | Ligand : Ru (%) | Zn : DMO (%) | Conversion DMO (%) | Yield MGL (%) | Selectivity MGL (%) | Yield EGL (%) | Selectivity EGL (%) | Turnover number | Turnover freq./ $h^{-1}$ |
|---|---|---|---|---|---|---|---|---|---|---|---|---|
| 1 | 0.96 | None[b] | 1.64 | 0.00 | 0.27 | 18 | 2 | 10 | 0 | 0 | 1 | 0 |
| 2 | 0.99 | $PPh_3$ | 1.98 | 5.88 | 1.32 | 73 | 36 | 49 | 0 | 0 | 18.1 | 0.9 |
| 3 | 1.41 | $AsPh_3$ | 1.19 | 8.91 | 0.57 | 1 | 0 | 0 | 0 | 0 | 0 | 0 |
| 4 | 1.04 | 1,10-Phenanthroline | 1.96 | 6.39 | 0.33 | 20 | 0 | 0 | 0 | 0 | 0 | 0 |
| 5 | 0.89 | 2,2′:6′,2″-Terpyridine | 1.74 | 1.79 | 0.38 | 11 | 0 | 0 | 0 | 0 | 0 | 0 |
| 6 | 9.25 | Pyrazolyl ligand[c] | 0.21 | 2.32 | 0.06 | 14 | 1 | 4 | 0 | 0 | 2.9 | 0.2 |
| 7 | 0.89 | $P(C_6H_{11})_3$ | 2.18 | 4.63 | 0.25 | 7 | 1 | 18 | 0 | 0 | 0.5 | 0 |
| 8 | 0.88 | $Ph_2PC_2H_4PPh_2$ | 1.82 | 2.94 | 0.42 | 18 | 11 | 60 | 0 | 0 | 5.9 | 0.4 |
| 9 | 1.14 | $PhP(C_2H_4PPh_2)_2$ | 1.75 | 1.68 | 0.36 | 76 | 67 | 89 | 0 | 0 | 38.2 | 2.5 |
| 10 | 0.96 | $[CH_2P(Ph)C_2H_4PPh_2]_2$ | 2.38 | 1.02 | 0.33 | 91 | 85 | 93 | 0 | 0 | 35.7 | 2.2 |
| 11 | 1.77 | $MeC(CH_2PPh_2)_3$ | 1.19 | 1.37 | 0.26 | 100 | 1 | 1 | 95 | 95 | 160 | 10 |
| 12 | 11.00 | $Ru(CO)_2(OAc)_2(PBu_3)_2$[d] | 1.34 | 4.00 | 0.00 | 100 | 18 | 18 | 82 | 82 | 136 | 0.9 |

[a] Conditions (unless otherwise indicated): $Ru(acac)_3$, 100 °C, $p(H_2)$ = 70 bar, 16 h, MeOH (12 ml), used as received. [b] Reaction time 41 h. [c] Tris(3,5-dimethylpyrazol-1-yl)borohydride. [d] From ref. 2; reaction at 180 °C in MeOH, $p(H_2)$ = 200 bar, 144 h.

**Table 2** Influence of zinc, $p(H_2)$ and MeOH quality on the catalytic properties of the $Ru(acac)_3$–$MeC(CH_2PPh_2)_3$ system[a]

| Entry | DMO/ mmol | Ru : DMO (%) | Zn : DMO (%) | MeOH (12 ml) | Conversion DMO (%) | Yield MGL (%) | Selectivity MGL (%) | Yield EGL (%) | Selectivity EGL (%) | Turnover number | Turnover freq./$h^{-1}$ |
|---|---|---|---|---|---|---|---|---|---|---|---|
| 1 | 1.77 | 1.19 | 0.26 | comm.[b] | 100 | 1 | 1 | 95 | 95 | 160 | 10 |
| 2 | 3.36 | 0.74 | 0.18 | comm. | 100 | 0 | 0 | 94 | 94 | 255 | 16 |
| 3 | 10.19 | 0.18 | 0.06 | comm. | 80 | 15 | 18 | 52 | 65 | 642 | 40.1 |
| 4 | 8.29 | 0.25 | 0.06 | comm. | 59[c] | 24 | 41 | 10 | 17 | 180 | 11.6 |
| 5 | 8.21 | 0.19 | 0.09 | comm. | 35[d] | 19 | 55 | 2 | 5 | 120 | 7.7 |
| 6 | 9.67 | 0.19 | 0.00 | comm. | 56 | 24 | 42 | 22 | 40 | 363 | 23.4 |
| 7 | 8.75 | 0.22 | 0.00 | dry[e] | 88 | 10 | 12 | 63 | 71 | 607 | 36.8 |
| 8 | 9.21 | 0.20 | 0.07 | dry | 100 | 0 | 0 | 84 | 84 | 857 | 53.5 |
| 9 | 14.32 | 0.15 | 0.05 | dry | 50 | 17 | 34 | 10 | 20 | 246 | 15.4 |

[a] Conditions: 100 °C, $p(H_2)$ = 70 bar, 16 h, ligand (1.1–1.6 equiv.). [b] Used as received (commercial quality). [c] $p(H_2)$ = 38 bar. [d] $p(H_2)$ = 20 bar. [e] Distilled from $CaH_2$ under nitrogen.

zinc in obtaining reasonable to good yields of EGL and high turnover numbers is demonstrated; the turnover number decreases by a factor 1.8 when zinc is omitted.‡ Finally, the methanol quality is important for the catalytic activity of our system (entries 7–9). Comparing the experiments of entries 3 and 8 on the one hand and the experiments of entries 6 and 7 on the other shows that the highest catalytic activity is observed in dry methanol, regardless of the presence of zinc. Altogether, a turnover frequency of 53.5 is reached with our catalytic system in the presence of zinc in dry MeOH.

In conclusion, we have demonstrated that a highly reactive catalyst for the hydrogenation of dimethyl oxalate to ethylene glycol can be generated *in situ* from $Ru(acac)_3$ and $MeC(CH_2PPh_2)_3$ in methanol under $H_2$ pressure, which is the most efficient homogeneous catalyst for the hydrogenation of dimethyl oxalate to ethylene glycol.

We are grateful to the Innovation Oriented Research Programme (IOP-katalyse) for their financial support of this research. Dr J. G. de Vries (DSM) and Dr M. J. Doyle (SRTCA) are gratefully acknowledged for stimulating discussions.

## Footnotes

* Email: else4@anorg.chem.uva.nl

† *General procedure*: a home-built stainless steel autoclave was charged with the amount of ruthenium precursor, ligand, zinc and substrate indicated. The autoclave was then flushed with nitrogen several times, after which the solvent was introduced *via* a cannula. Subsequently, the autoclave was pressurized with hydrogen and heated for a specific period (see Tables). The values of the $H_2$ pressure are given at room temperature. The reaction products were characterized by GC–MS while the yields were determined by GC with an internal standard.

‡ Employing zinc in the absence of $Ru(acac)_3$ gave no hydrogenation of DMO whatsoever.

## References

1 R. A. Grey, G. P. Pez and A. Wallo, *J. Am. Chem. Soc*., 1981, **103**, 7536.
2 U. Matteoli, G. Menchi, M. Bianchi and F. Piacenti, *J. Mol. Catal*., 1988, **44**, 347.
3 U. Matteoli, G. Menchi, M. Bianchi, F. Piacenti, S. Ianelli and M. Nardelli, *J. Organomet. Chem*., 1995, **498**, 177 and references cited therein.
4 Y. Hara and K. Wada, *Chem. Lett*., 1991, 553.
5 For the use of $MeC(CH_2PPh_2)_3$ in catalysis, see C. Bianchini, A. Meli, M. Peruzzini, F. Vizza and F. Zanobini, *Coord. Chem. Rev*., 1992, **120**, 193.

*Received in Cambridge, UK, 6th February 1997; Com. 7/00862G*

# Tyrosine nitration and peroxonitrite (peroxynitrite) isomerisation: $^{15}$N CIDNP NMR studies

**A. R. Butler,*[a] T. J. Rutherford,[a] D. M. Short[a] and J. H. Ridd[b]**

[a] *School of Chemistry and Centre for Biomolecular Sciences, University of St. Andrews, Fife, UK KY16 9ST*
[b] *Chemistry Department, University College London, 20 Gordon Street, London, UK WC1H 0AJ*

**In the presence of tyrosine, peroxonitrous acid forms nitrite, nitrate and 3-nitrotyrosine by radical processes.**

One of the most interesting developments in our understanding of the role of nitric oxide in animal physiology is the emergence of peroxonitrite ($ONOO^-$, sometimes called peroxynitrite), formed by reaction of nitric oxide with superoxide, as an important cytotoxic agent.[1] Also, peroxonitrite appears to bring about tyrosine nitration[2] which may have consequences for the process of tyrosine phosphorylation. The presence of nitrated tyrosine residues has been suggested as a marker for peroxonitrite activity.[3] The formation of $NO_2^+$ has been proposed as an essential step in tyrosine nitration by peroxonitrite[4] but, for a substrate as activated towards electrophiles as tyrosine, there are well established alternative pathways. For example, we have observed that the nitration of *N*-acetyltyrosine by dilute nitric acid is a nitrous acid catalysed process and must occur either by nitrosation followed by oxidation or by a radical mechanism. The use of the CIDNP has proved very useful in probing further the mechanisms of such reactions.[5] Nitration of tyrosine with $^{15}$N-labelled nitric acid containing catalytic quantities of nitrite, and examination of the $^{15}$N NMR spectrum immediately after reaction, gave a very large inverted signal for 3-nitrotyrosine, which slowly changed to the normal signal. It is possible to make a number of mechanistic deductions from this observation but it is sufficient, in this preliminary communication, to note that there must be a substantial radical pathway in the formation of 3-nitrotyrosine. We now turn to an examination of nitration by peroxonitrite where both radical and ionic pathways have been suggested.

$^{15}$N-labelled peroxonitrite in alkaline solution was prepared by the method of Leis *et al.*[6] and allowed to react with tyrosine at 25 °C and pH 12. EDTA was present to prevent complications due to a metal-catalysed decomposition pathway.[7] The reaction was followed from changes in the $^{15}$N NMR spectrum using a 500 MHz Varian Unity instrument. The quoted chemical shifts are downfield from liquid ammonia at 25 °C and were measured relative to [$^{15}$N]nitrobenzene ($\delta_N$ 370.3) as an external standard. The identification of the signals was carried out by spiking with authentic samples of $^{15}$N-labelled material.

The initial signal from peroxonitrite ions at $\delta_N$ 554.6 decreased exponentially with time, showing no sign of nuclear polarisation, and two product signals appeared: one from nitrite ions at $\delta_N$ 609.1 in emission and one from nitrate ions at $\delta_N$ 375.9 showing evidence of enhanced absorption (Fig. 1). The UV–VIS spectra of the solutions showed the formation of 3-nitrotyrosine; this absorbs at $\delta_N$ 375.3 (very close to nitrate ions) under these conditions but the amount formed is insufficient to contribute significantly to that signal. When tyrosine is absent or replaced by *O*-methyltyrosine, the only reaction observed is the slow conversion of peroxonitrite ions to nitrate ions without any evidence of nuclear polarisation.

The main features of these observations can be explained by the reaction pathway shown in Scheme 1. The absence of nuclear polarisation in the peroxonitrite ions suggests that the initial homolysis of peroxonitrite is essentially irreversible; this also accords with AMI calculations on the relative energies of the possible transition states. The fact that the nitrate and nitrite ions show nuclear polarisation of opposite phase indicates that one product is derived from reaction within the $NO_2^{\bullet}$–$^{\bullet}OH$ encounter pair and the other from reaction after dissociation of this radical pair. From Kaptein's rules[8] as applied to the $^{15}$N nucleus[9] and from the *g*-values of the $NO_2^{\bullet}$ and $^{\bullet}OH$ radicals,[10] it follows that the reaction within the encounter pair should give an enhanced absorption signal and that from the dissociated radicals should give an emission signal; this accords with the observed spectra of the nitrate and nitrite ions. Tyrosine appears to be involved in two ways: first, the conjugate base of tyrosine reduces the dissociated radicals by an electron transfer reaction and, secondly, the tyrosyl radical so formed reacts directly with the $NO_2^{\bullet}$ and $^{\bullet}OH$ radicals. The relatively low yield of 3-nitrotyrosine may be a consequence of the high reactivity of $^{\bullet}OH$ radicals towards tyrosyl radicals. In the absence of tyrosine, the dissociated $NO_2^{\bullet}$ and $^{\bullet}OH$ radicals are considered to recombine to form nitrate ions and, since only one product is formed, nuclear polarisation would not be expected.

The scheme is similar to that proposed by Pryor and Squadrito.[11] Nitrophenols are known to be formed by the reaction of phenoxy radicals with nitrogen dioxide[12] and aromatic hydroxylation by peroxonitrite ions has been des-

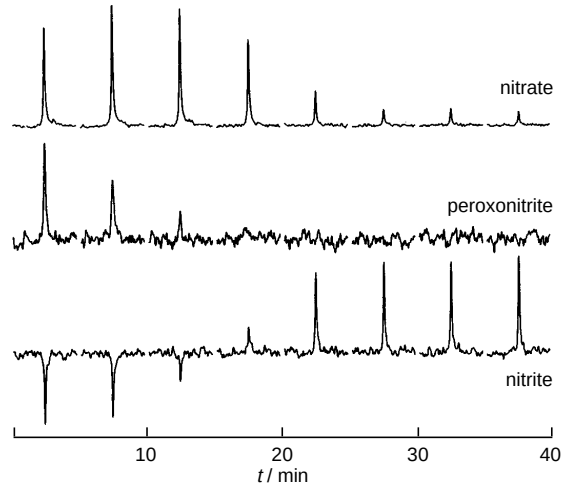
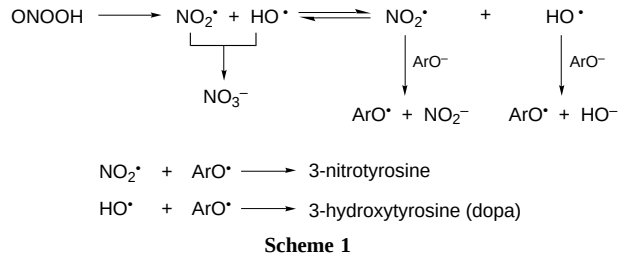



**Fig. 1** Variation of signals with time in the $^{15}$N NMR spectrum for the reaction of peroxonitrite (0.1 mol dm$^{-3}$) with L-tyrosine (0.025 mol dm$^{-3}$). [NaOH] = 0.15 mol dm$^{-3}$.




**Scheme 1**

cribed previously.[13] It is clear from our observations that one pathway, perhaps the only pathway, in the reaction of peroxonitrite ions with tyrosine in alkaline solution is a radical one. The small concentration of nitrotyrosine formed unfortunately precludes any observation of nuclear polarisation in this product but it is reasonable to infer that this nitration is also a radical reaction.

We thank the Wellcome Trust for NMR facilities, the BBSRC for a studentship to D. M. S. and the Rollo Trust for consumables.

## Footnote

* E-mail: arb3@st-andrews.ac.uk

## References

1 H. Ischiropoulos, L. Zhu and J. S. Beckman, *Arch. Biochem. Biophys.*, 1992, **298**, 446.
2 E. Halfpenny and P. L. Robinson, *J. Chem. Soc.*, 1952, 939.
3 W. Maruyama, Y. Hashizume, K. Matsubara and M. Naoi, *J. Chromatogr., Sect. B*, 1996, **676**, 153.
4 H. Ischiropoulos, L. Zhu, J. Chen, M. Tsai, J. C. Martin, C. D. Smith and J. S. Beckman, *Arch. Biochem. Biophys.*, 1992, **298**, 431.
5 J. H. Ridd, *Chem. Soc. Rev.*, 1991, **20**, 149.
6 J. R. Leis, M. E. Peña and A. Rìos, *J. Chem. Soc., Chem. Commun.*, 1993, 1298.
7 M. N. Hughes and H. G. Nicklin, *J. Chem. Soc. A*, 1970, 925.
8 R. Kaptein, *J. Chem. Soc., Chem. Commun.*, 1971, 732.
9 N. A. Porter, G. R. Dubay and J. G. Green, *J. Am. Chem. Soc.*, 1978, **100**, 920.
10 A. H. Clemens, J. H. Ridd and J. P. B. Sandall, *J. Chem. Soc., Perkin Trans. 2*, 1984, 1659; Landolt-Bornstein, *Numerical Data and Functional Relationships in Science and Technology*, ed. H. Fischer, Springer-Verlag, Berlin, 1987, New Series Group 2, vol. 17, part a, pp. 54–55.
11 W. A. Pryor and G. L. Squadrito, *Am. J. Physiol.*, 1995, **268**, L699.
12 R. G. Coombes, A. W. Diggle and S. D. Kempsell, *Tetrahedron Lett.*, 1994, **35**, 6373.
13 A. van der Vliet, C. A. O'Neill, B. Halliwell, C. E. Cross and H. Kaur, *FEBS Lett.*, 1994, **339**, 89.

*Received, 29th January 1997; Com. 7/00676D*

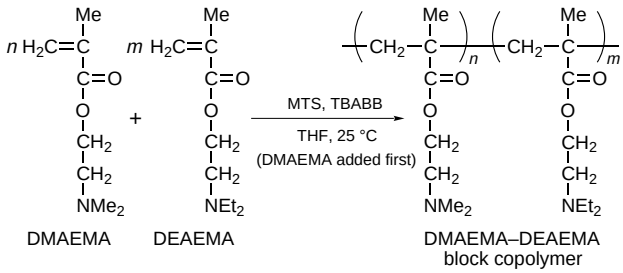
# Synthesis and aqueous solution properties of novel hydrophilic–hydrophilic block copolymers based on tertiary amine methacrylates

**V. Bütün, N. C. Billingham and S. P. Armes***

*School of Chemistry, Physics and Environmental Science, University of Sussex, Falmer, Brighton, UK BN1 9QJ*

**A series of near-monodisperse novel diblock copolymers based on tertiary amine methacrylates has been synthesised using group transfer polymerisation chemistry; subtle differences in basicity between the two blocks lead to interesting aqueous solution behaviour, including pH-induced micellisation and very high surface activity.**

Over the last decade or so group transfer polymerisation[1,2] has become recognised as an excellent method for the synthesis of methacrylate (co)polymers of controlled structure and narrow molecular weight distribution. Recently we have used this technique to prepare well-defined homopolymers and block copolymers based on 2-(dimethylamino)ethyl methacrylate (DMAEMA).[3,4] DMAEMA homopolymer is a weak polybase which is soluble at neutral pH or in acidic media due to protonation of the tertiary amine groups. Functionalisation of the DMAEMA residues is possible: for example, quantitative derivatisation under mild conditions has been recently achieved using propane-1,3-sultone to yield near-monodisperse polysulfopropylbetaines.[5] Here we describe the block copolymerisation of DMAEMA with a related tertiary amine methacrylate, 2-(diethylamino)ethyl methacrylate (DEAEMA) (Scheme 1). Although structurally very similar to DMAEMA, the DEAEMA monomer is immiscible in water and DEAEMA homopolymers are completely insoluble at neutral pH. On the other hand, DEAEMA homopolymers readily dissolve in acidic aqueous solution (*ca*. pH 2) due to protonation of the tertiary amine residues. Here it is demonstrated that the subtle difference in chemical structure between these two tertiary methacrylate comonomers has profound implications for the aqueous solution behaviour of DMAEMA–DEAEMA block copolymers.




**Scheme 1**

A series of DMAEMA–DEAEMA block copolymers was prepared using group transfer polymerisation under similar conditions to those previously described.[4] All copolymerisations were carried out using 1-methoxy-1-trimethylsilyloxy-2-methylprop-1-ene (MTS) as initiator and tetrabutylammonium bibenzoate (TBABB) catalyst at 25 °C in dry THF using Schlenk techniques. The DMAEMA monomer was polymerised first and quantitative yields were obtained in all syntheses. The molecular weights, polydispersities and copolymer compositions of the resulting block copolymers are summarised in Table 1. Narrow molecular weight distributions were obtained in all cases ($M_w/M_n \leqslant 1.15$) as judged by gel permeation chromatography (THF eluent, PMMA standards, RI detector). The actual copolymer compositions as determined by $^1$H NMR spectroscopy corresponded closely (within experimental error) to those expected from the comonomer feeds. As far as we are aware, these are the first reported examples of diblock copolymers in which both block components are polybases.

For reasons outlined above, these DMAEMA–DEAEMA copolymers behave as hydrophilic–hydrophobic blocks in aqueous solution at neutral pH. One of the problems in studying the micellisation behaviour of such copolymers is that water-miscible co-solvents (THF, alcohols, DMF *etc.*) are normally required for efficient dissolution in aqueous solution. Even then, the hydrophobic component usually ensures that the majority of the copolymer chains exist as micellar aggregates, rather than as molecularly dissolved chains. Thus there is little opportunity to study the kinetics of micellisation under true equilibrium conditions. Recently there have been several reports[6–8] of the

**Table 1** A summary of the molecular weights, polydispersities and copolymer compositions of the tertiary amine methacrylate block copolymers determined using gel permeation chromatography and $^1$H NMR spectroscopy, respectively

| Polymer | Theoretical DMAEMA content (mol%) | Actual DMAEMA content[a] (mol%) | Theoretical $M_n$/g mol$^{-1}$ | Actual[b] $M_n$/g mol$^{-1}$ | $M_w/M_n$ |
|---|---|---|---|---|---|
| PDMAEMA | 100 | 100.0 | 10 100 | 12 400 | 1.07 |
| PDEAEMA | — | — | 9 700 | 11 000 | 1.06 |
| DMAEMA-b-DEAEMA | 80 | 77.8 | 10 400 | 12 400 | 1.10 |
| DMAEMA-b-DEAEMA | 74 | 72.0 | 9 000 | 11 400 | 1.10 |
| DMAEMA-b-DEAEMA | 66 | 63.9 | 9 900 | 9 700 | 1.12 |
| DMAEMA-b-DEAEMA | 49 | 48.7 | 10 600 | 9 600 | 1.15 |
| DMAEMA-b-DEAEMA | 35 | 36.0 | 9 900 | 11 900 | 1.09 |
| DMAEMA-b-DEAEMA | 22 | 24.0 | 9 900 | 9 500 | 1.10 |
| DMAEMA-b-DEAEMA | 68 | 66.9 | 18 900 | 21 600 | 1.09 |

[a] As determined by $^1$H NMR spectroscopy in $CDCl_3$. [b] As determined by GPC in THF [RI detector; calibrated with poly(methyl methacrylate) standards].

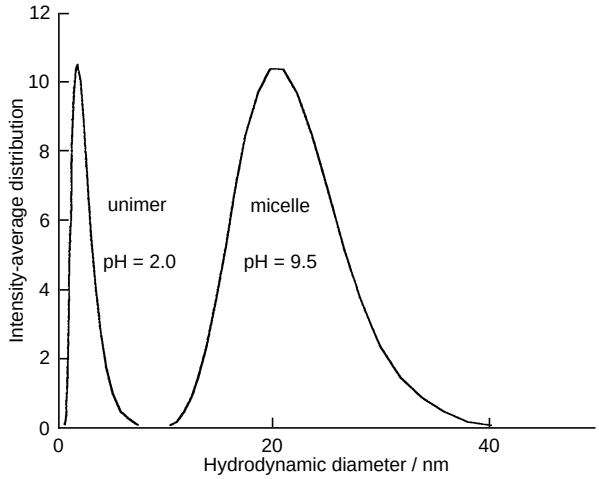



**Fig. 1** Hydrodynamic size of a 72:28 DMAEMA–DEAEMA block copolymer (dissolved in dilute HCl as a 1.0% w/v solution at 25 °C and then tritated to pH 9.5 using KOH)

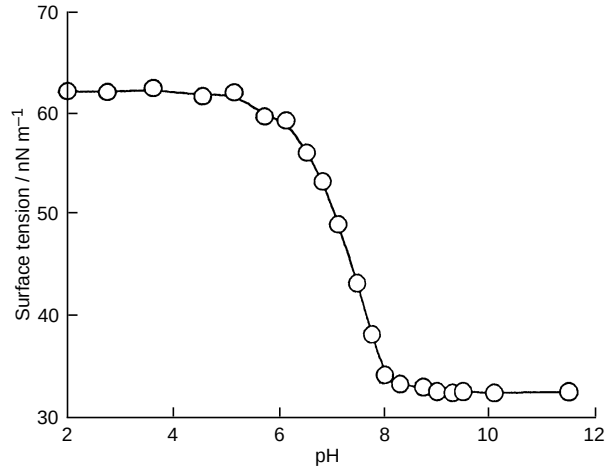



**Fig. 2** Variation of surface tension with solution pH for a 1.0% w/v aqueous solution of a 72:28 DMAEMA–DEAEMA block copolymer. The block copolymer was first dissolved in dilute HCl and the solution pH was then adjusted by addition of KOH.

synthesis of hydrophilic–hydrophilic block copolymers which can be dissolved as unimers in aqueous solution and then aggregated into micelles. One way of inducing micellisation is by raising the solution temperature to the cloud point of the least hydrophilic block component. Alternatively, Martin *et al.*[8] have shown that poly(2-vinylpyridine-block-ethylene oxide) copolymers can be molecularly dissolved in acidic media (hydrophilic protonated 2-vinylpyridine residues) and then aggregated into micelles by adding base (hydrophobic deprotonated 2-vinylpyridine residues). The DMAEMA–DEAEMA blocks described here exhibit similar behaviour but their synthesis is much more controlled, with only minimal levels ( < 5%) of DMAEMA homopolymer contamination indicated by GPC analyses. In contrast, Martin *et al.* reported that the single block copolymer example synthesised in their laboratory contained 30% poly(2-vinylpyridine) homopolymer. In this latter case the homopolymer contaminant is the less hydrophilic block, which profoundly affects the micellisation behaviour of the block copolymer.

Examination of a 1.0% w/v solution of the 72:28 DMAEMA–DEAEMA block in dilute HCl (pH 2) by dynamic light scattering confirmed very weak light scattering and unimer sizes (see Fig. 1). However, adjusting this solution to pH 9.5 with KOH produced much more intense light scattering due to the formation of micelles of around 20 nm diameter with a narrow size distribution. We believe that the DEAEMA block becomes hydrophobic and forms the micelle core, with the still-solvated DMAEMA chains forming the micellar corona. This micellisation proved to be completely reversible: the subsequent addition of acid resulted in complete dissolution of the micelles. Preliminary surface tension *vs.* pH data for the same 72:28 copolymer obtained using a Kruss K10ST surface tensiometer (very similar results were obtained using both plate and ring methods) are shown in Fig. 2. As the solution pH is increased the block copolymer becomes significantly more surface active. Presumably the deprotonated hydrophobic DEAEMA block becomes adsorbed strongly at the air–water interface, thus lowering the surface tension of the solution. Above pH 8 the limiting surface tension of this solution is approximately 32–33 mN $m^{-1}$ (gentle agitation produces a large volume of long-lasting foam), which is similar to that obtained with small molecule surfactants but relatively low compared to most other synthetic water-soluble block copolymers. For example, Baines *et al.*[3] reported that the limiting surface tension obtained for a 1.0% w/v aqueous solution of an 80:20 DMAEMA–methyl methacrylate block copolymer of comparable molecular weight was only 46 mN $m^{-1}$. Similarly, a surface tension plateau of *ca.* 42 mN $m^{-1}$ was observed by Teyssie and co-workers[9] for a sulfonated glycidyl methacrylate–methyl methacrylate block copolymer with a similar hydrophilic–hydrophobic balance.

Provided that the DMAEMA content of the copolymer is greater than approximately 50 mol% these DMAEMA–DEAEMA block copolymers can be dispersed directly into water at around neutral pH to form micelles of around 15 nm diameter. However, DEAEMA-rich block copolymers are insoluble under these conditions. In this context it is noteworthy that the limiting surface tension obtained with the 72:28 DMAEMA–DEAEMA block dissolved directly into water is *ca.* 33 mN $m^{-1}$ at a copolymer concentration of 0.15% w/v. These surface tension data suggest that such hydrophilic–hydrophilic block copolymers may have interesting applications as novel surfactants or emulsifiers.

In summary, a series of new polybase block copolymers has been synthesised using GTP chemistry. These copolymers can be molecularly dissolved in aqueous solution without the use of co-solvents. They exhibit reversible pH-induced micellisation and are remarkably surface active at around neutral pH.

We wish to thank the Turkish government for funding a studentship for V. B. and Sussex University for project consumables support. An EPSRC ROPA grant (GR/K86855) was used to purchase the argon ion laser for the dynamic light scattering studies.

## References

1 O. W. Webster, W. R. Hertler, D. Y. Sogah, W. B. Farnham and T. V. RanjanBabu, *J. Am. Chem. Soc.*, 1983, **105**, 5706.
2 I. B. Dicker, G. M. Cohen, W. B. Farnham, W. R. Hertler, E. D. Langanis and D. Y. Sogah, *Macromolecules*, 1990, **23**, 4034.
3 F. L. Baines, S. P. Armes and N. C. Billingham, *Macromolecules*, 1996, **29**, 3416.
4 F. L. Baines, S. P. Armes, N. C. Billingham and Z. Tuzar, *Macromolecules*, 1996, **29**, 8151.
5 A. B. Lowe, S. P. Armes and N. C. Billingham, *Chem. Commun.*, 1996, 1555.
6 C. Forder, C. S. Patrickios, N. C. Billingham and S. P. Armes, *Macromolecules*, 1996, **29**, 8160.
7 C. Forder, C. S. Patrickios, N. C. Billingham and S. P. Armes, *Chem. Commun.*, 1996, 883.
8 T. J. Martin, K. Prochazka, P. Munk and S. E. Webber, *Macromolecules*, 1996, **29**, 6071.
9 L. Leemans, R. Fayt and P. Teyssie, *J. Polym. Sci., Part A: Polym. Chem.*, 1990, **28**, 1255; L. Leemans, R. Fayt, P. Teyssie and N. C. DeJaeger, *Macromolecules*, 1991, **24**, 5922.

*Received in Bath, 22nd January 1997; Com. 7/00772H*

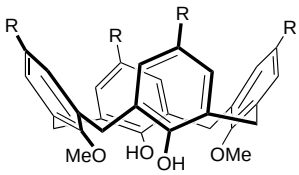
# Synthesis and receptor properties of calix[4]arene–bisphenol-A copolymers

**Alessandro Dondoni,*[a] Chiara Ghiglione,[a] Alberto Marra[a] and Marco Scoponi[b]**

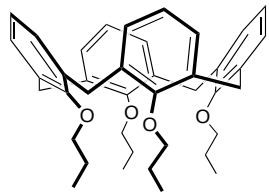
[a] *Dipartimento di Chimica, Laboratorio di Chimica Organica, Università, Ferrara, Italy*
[b] *Centro di Studio su Fotoreattività e Catalisi del CNR, Dipartimento di Chimica, Università, Ferrara, Italy*

**The synthesis of 1,3-dimethyl calix[4]arene–bisphenol-A copolyethers and copolyesters with variable amounts of the macrocycle in the chain is described; the receptor ability of the copolyethers 4 toward silver(I) ions was one hundred-fold that of calix[4]arene tetrapropyl ether 3.**

Compared with the considerable interest during recent years in the use of calixarene monomers as platforms for the construction of supramolecular receptor assemblies,[1] there are few studies on calixarene-containing polymers, most of which exhibit the macrocycle moiety as an appendage of the polymer chain.[2] This issue has been addressed in recent reports. One of these describes the synthesis and the cation receptor properties of low molecular weight calixcrown telomers with different chain backbones such as ether, ester, amide and siloxane;[3] a second deals with the synthesis of oligomers by ruthenium-catalysed metathesis of alkenyl substituted calixarenes;[4] and the third describes the optical properties produced by the incorporation of an upper-rim derivatized calix[4]arene in a water-soluble antenna polyacrylate.[5] It thus appears that calixarene insertion in a polymer chain may give rise to new materials where the intrinsic properties of the macrocycle are enhanced and efficiently exploited. Among the broad range of applications of calixarene-based polymers, one can foresee their use as sensors for chemical and biochemical species,[6] as substrates for the construction of membranes for selective transport of ions,[7] and as antioxidant additives of other polymeric materials.[8] We report here the first synthesis of high molecular weight copolyethers and copolyesters incorporating 1,3-(distal)calix[4]arene and bisphenol-A moieties in the chains in different ratios and describe preliminary studies of the receptor properties of these materials.[9]



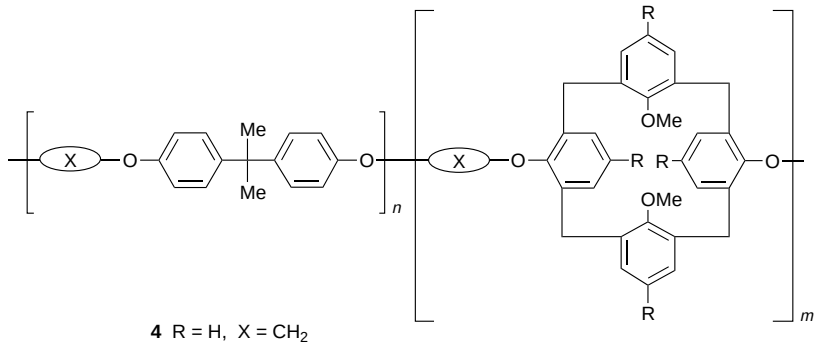

**1** R = H
**2** R = Bu$^t$




**3**

A mixture of 1,3-dimethyl calix[4]arene **1**, bisphenol-A and NaH in a minimum amount of anhydrous THF was stirred at room temperature for 0.5 h, then concentrated. The suspension of the sodium salts in toluene was treated with tetrabutylammonium hydrogensulfate and dibromomethane (10 equiv.) at 60–80 °C for 16 h to give the copolyether **4** (50–60% yield) after reprecipitation from a large volume of acidified methanol. The $M_w$ of this material ranged between 15 000 and 24 000 (determined by GPC analysis referenced to polystyrene standards) depending on the reaction temperature and the amount of the phase transfer reagent (40–80 mol%), and the polydispersity ($M_w/M_n$) was between 4 and 8. $^1$H NMR analysis revealed that the calixarene content in the polymer chains varied depending on the phenolic monomers ratio. Typically a 0.5 : 1 molar ratio of **1** and bisphenol-A led to a copolyether containing 25% of **1** with respect to bisphenol-A whereas a 1:1 ratio gave 50% content.† Higher ratios (2 : 1 up to 10 : 1) did not increase the calixarene content but produced a substantial decrease in yield of the isolated material (20%). Copolyether **5** ($M_w$ 10 000, *ca.* 60% yield) was prepared from 1,3-dimethyl *p-tert*-butylcalix[4]arene **2** by the same procedure. This calixarene proved to be less reactive than **1** in the copolymerization process, thus resulting in low incorporation in the polymer chains to a 20% maximum content. Copolyethers **4** and **5** were semicrystalline materials with a melting temperature range of 210–250 °C and were soluble in chloroform and toluene at room temperature. These copolyethers showed glass transition temperatures between 80 and 120 °C depending on the molecular weight. They showed rather complex $^1$H NMR spectra both at low (−40 °C) and high temperatures (120 °C) indicating that the calixarene units exist in numerous statistical conformations, each one being determined by its adaptability to the complex arrangement of the polymer chains in solution.

Treatment of the mixture of the sodium salts of **1** (0.5 equiv.) and bisphenol-A (1 equiv.) with terephthaloyl chloride (1 equiv.) under the above conditions (toluene, $Bu_4NHSO_4$, 60 °C, 16 h) gave, after a similar purification, the copolyester **6** in 66% yield. The soluble fraction of the recovered material (*ca.* 20% in $CHCl_3$ at room temperature) showed a $M_w$ of *ca.* 21 000 (GPC




**4** R = H, X = $CH_2$
**5** R = Bu$^t$, X = $CH_2$
**6** R = H, X = *p*-CO($C_6H_4$)CO

analysis). The calixarene content appeared to be 24% from its $^1$H NMR spectrum. This content increased to 50% in the copolymer obtained under the same conditions but starting from a 1 : 1 ratio of the phenolic monomers.‡ Both polymers were soluble only in 1,1,2,2-tetrachloroethane at 120 °C.

The $Ag^+$ binding properties of the calixarene containing copolyether **4** were compared with those of the known[10] calix[4]arene tetrapropyl ether **3** using the picrate extraction procedure[11] originally described by Cram and coworkers.[12] Recent work by Ikeda *et al.*[13] has demonstrated that $Ag^+$ is bound to cone and partial-cone calixarenes by π-donor participation of the phenyl rings. Results of two-phase extraction measurements with **4** at 50% calixarene content showed linear correlations between the calixarene concentration and the picrate exchange between the aqueous and organic phase (Fig. 1). We noted also that the extraction by the calixarene in the copolymer is about one hundred-fold that of the tetrapropoxy derivative **3**.§ The involvement of the calixarene in the picrate extraction was proved by the same efficiency shown by a two-fold more concentrated solution of the copolyether **4** at 25% calixarene content.¶ Finally, the decreased concentration of $Ag^+$ in the aqueous layer was confirmed by atomic absorption spectroscopy.

The more pronounced extraction of $Ag^+$ by the calixarene moiety in the copolyether **4** than in the compound **3** suggests that in the former there are more units of the macrocycle with the required conformation for cation–π-interaction. Unfortunately the complexity of the NMR spectra of the polymeric materials did not allow more detailed study. The binding properties of the copolyester **6** could not be studied because of its low solubility in organic solvents at room temperature.

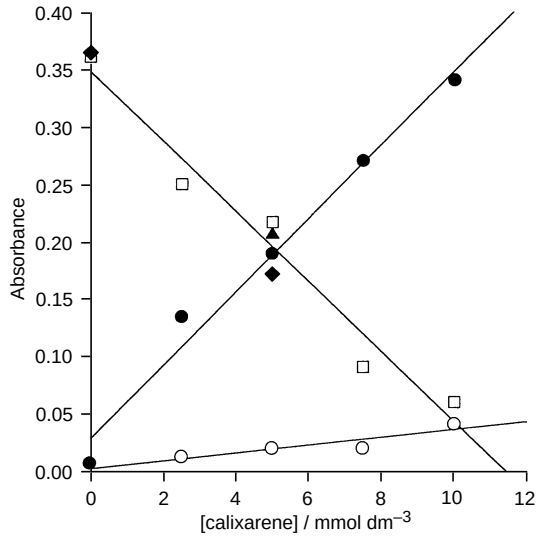



**Fig. 1** Absorbance changes of: (*a*) aqueous solution of $AgNO_3$ ($10^{-2}$ M) and picric acid (2.38 $10^{-3}$ M) extracted with the $CHCl_3$ solutions of **4** with (□) 50% and (◆) 25% calixarene content; (*b*) the corresponding $CHCl_3$ solutions of **4** with (●) 50% and (▲) 25% calixarene content; (*c*) $CH_2Cl_2$ solution of compound **3** (○) after extraction of the above aqueous solution (λ = 356 nm)

We acknowledge the Consiglio Nazionale delle Ricerche (Rome) and the Ministero della Ricerca Scientifica e Tecnologica (Italy) for support of this research.

## Footnotes

* E-mail: ADN@DNS.UNIFE.IT

† *Selected data* for copolyether **4** (from a 1 : 1 ratio of the phenolic monomers); $^1$H NMR (300 MHz, $CDCl_3$, 20 °C): δ 7.13 and 6.96 (2 d, 8 H, $J$ = 9.0 Hz, 2 Ar of bisphenol-A), 6.55–6.29 (m, 12 H, 4 Ar of calixarene), 5.58 (s, 4 H, 2 $OCH_2O$), 4.55–2.80 (m, 14 H, 4 $ArCH_2Ar$, 2 $OCH_3$), 1.61 (s, 6 H, 2 $CH_3$).

‡ *Selected data* for copolyester **6** (from a 1 : 1 ratio of the phenolic monomers); $^1$H NMR (300 MHz, $CDCl_3$, 20 °C): δ 8.30 (s, 8 H, 2 *p*-$COC_6H_4CO$), 7.32 and 7.15 (2 d, 8 H, $J$ = 9.0 Hz, 2 Ar of bisphenol-A), 6.80–6.20 (m, 12 H, 4 Ar of calixarene), 4.20–2.80 (m, 14 H, 4 $ArCH_2Ar$, 2 $OCH_3$), 1.72 (s, 6 H, 2 $CH_3$).

§ Copolyethers **4** are not soluble in $CH_2Cl_2$, therefore their binding properties were evaluated using $CHCl_3$ as a solvent.

¶ Polyethers not incorporating calixarene units (*i.e.* **4** where $m$ = 0) did not display any complexation of silver(I) cations.

## References

1 For recent reviews, see V. Böhmer, *Angew. Chem., Int. Ed. Engl.*, 1995, **34**, 713; M. Takeshita and S. Shinkai, *Bull. Chem. Soc. Jpn.*, 1995, **68**, 1088; C. D. Gutsche, *Aldrichim. Acta*, 1995, **28**, 3; A. Pochini and R. Ungaro, *Comprehensive Supramolecular Chemistry*, Pergamon, Oxford, 1996.

2 S. Shinkai, H. Kawaguchi and O. Manabe, *J. Polym. Sci., Polym. Lett.*, 1988, **26**, 391; S. J. Harris, G. Barrett and M. A. McKervey, *J. Chem. Soc., Chem. Commun.*, 1991, 1224; J. D. Glennon, K. O′Connor, S. Srijaranai, K. Manley, S. J. Harris and M. A. McKervey, *Anal. Lett.*, 1993, **26**, 153.

3 Z.-L. Zhong, C.-P. Tang, C.-Y. Wu and Y.-Y. Chen, *J. Chem. Soc., Chem. Commun.*, 1995, 1737.

4 M. A. McKervey and M. Pitarch, *Chem. Commun.*, 1996, 1689.

5 D. M. Gravett and J. E. Guillet, *Macromolecules*, 1996, **29**, 617.

6 D. W. M. Arrigan, G. Svehla, S. J. Harris and M. A. McKervey, *Electroanalysis*, 1995, **6**, 97; D. Diamond and M. A. McKervey, *Chem. Soc. Rev.*, 1996, 15.

7 W. F. Nijenhuis, E. G. Buitenhuis, F. De Jong, E. J. R. Sudhölter and D. N. Reinhoudt, *J. Am. Chem. Soc.*, 1991, **113**, 7963.

8 S. D. Pastor and P. Odorisio, USP 4617336/1986 (*Chem. Abstr.* 1987, **106**, 6038x); K. Seiffarth, M. Schulz, G. Görmar and J. Bachmann, *Poly. Deg. Stab.*, 1989, **24**, 73.

9 For recent work of two of us in the synthesis of carbohydrate containing calix[4]arene, see A. Marra, M.-C. Scherrmann, A. Dondoni, A. Casnati, P. Minari and R. Ungaro, *Angew. Chem., Int. Ed. Engl.*, 1994, **33**, 2479; A. Marra, A. Dondoni and F. Sansone, *J. Org. Chem.*, 1996, **61**, 5155.

10 A. Ikeda, T. Nagasaki, K. Araki and S. Shinkai, *Tetrahedron*, 1992, **48**, 1059.

11 For examinations of calixarene-based ionophores with this procedure, see ref. 3 and C. A. Gleave and I. O. Sutherland, *J. Chem. Soc., Chem. Commun.*, 1994, 1873.

12 J. M. Timko, S. S. Moore, D. M. Walba, P. C. Hiberty and D. J. Cram, *J. Am. Chem. Soc.*, 1977, **99**, 4207; S. S. Moore, T. L. Tarnowski, M. Newcomb and D. J. Cram, *J. Am. Chem. Soc.*, 1977, **99**, 6398; G. M. Lein and D. J. Cram, *J. Am. Chem. Soc.*, 1985, **107**, 448.

13 A. Ikeda, H. Tsuzuki and S. Shinkai, *J. Chem. Soc., Perkin Trans. 2*, 1994, 2073.

*Received in Cambridge, UK, 8th January 1997; Com. 7/00184C*

# The ′onium butyltriphenylborates as novel donor–acceptor initiators for free radical photopolymerization

**Yasumasa Toba,[a]† Madoka Yasuike[b] and Yoshiharu Usui[a]***

[a] *Graduate School of Science and Engineering, Ibaraki University, 2-1-1 Bunkyo, Mito, Ibaraki 310, Japan*
[b] *Tsukuba Research Laboratories, Toyo Ink Mfg. Co., Ltd., 27 Wadai, Tsukuba, Ibaraki 300-42, Japan*

**Novel donor-acceptor initiators, ′onium butyltriphenylborates, containing both an ′onium cation (electron-accepting radical generator) and a butyltriphenylborate anion (electron-donating radical generator) within the same molecule, are synthesized and investigated for the photopolymerization of an acrylic monomer mixture.**

In order to obtain an efficient free radical generating system for many areas of photosensitive materials research, a more efficient initiator or initiator system (*i.e.* a combination of sensitizer and initiator) which generates free radicals for polymerization is required. Many such initiators or initiator systems have been investigated.[1]

Most well known initiator systems are based on photoinduced electron-transfer reactions and are either electron-donating sensitizer/electron-accepting initiators (*e.g.* ′onium salts)[2,3] or electron-accepting sensitizer/electron-donating initiators (*e.g.* borates or amines).[3,4]

The above initiator systems generate the free radical after a photo-induced electron-transfer from the electron-donating sensitizer to the electron-accepting initiator (or from electron-donating initiator to electron-accepting sensitizer) by light irradiation. The free radical comes from decomposition of the initiator and produces polymerization.

The cation radical (or anion radical) of a sensitizer produced by the reaction is usually inert to free radical polymerization. However, if one utilizes the inert cation radical (or anion radical) of the sensitizer, generating an active free radical for radical polymerization, the quantum efficiencies of the radical generation will be increased, and furthermore, the resulting polymerization will be extremely efficient.

Herein we report the discovery that the ′onium butyltriphenylborates containing both an ′onium cation (electron-accepting radical generator) and a borate anion (electron-donating radical generator) within the same molecule are novel donor–acceptor initiators for extremely efficient free radical photopolymerization.

The novel donor–acceptor initiators diphenyliodonium butyltriphenylborate **1** or dimethylphenacylsulfonium butyltriphenylborate **2** were prepared by the reactions of diphenyliodonium chloride or dimethylphenacylsulfonium bromide with lithium butyltriphenylborate,[5] respectively.‡ Both the ′onium borates were characterized by spectroscopic data and elemental analyses.§

The absorption spectra of **1** in $CH_2Cl_2$ and MeCN are shown in Fig. 1. For comparison, the absorption spectra of tetrabutylammonium butyltriphenylborate **3**, an electron-donating initiator, and diphenyliodonium hexafluorophosphate **4**, an electron-accepting initiator, in $CH_2Cl_2$ are also presented.

Compound **1** in $CH_2Cl_2$ exhibits a weak absorption in the 320–400 nm region, while **3** and **4** in $CH_2Cl_2$ do not exhibit absorption in the same region. The weak absorption is not observed in MeCN which is a polar solvent. It is important that the enhanced absorptivity of **1** in $CH_2Cl_2$ is reproducible and is quite clearly unique to **1** in the non-polar solvent.

We attribute the weak absorption observed for **1** in $CH_2Cl_2$ to an ion-pair charge transfer transition from the butyltriphenylborate anion to the diphenyliodonium cation. Also the spectrum of **2** in $CH_2Cl_2$ showed a slightly greater absorptivity in the 270–350 nm region, in contrast to **3** and dimethylphenacylsulfonium tetrafluoroborate **5** which do not exhibit transitions in the same region. However, both ′onium borates **1** and **2** exist primarily as ion-pairs in $CH_2Cl_2$ and as free ions in MeCN.

In order to reveal the capability of the ′onium borates as free radical polymerization initiators, we carried out the photopolymerization of tetrahydrofurfuryl acrylate (THFA). 4,4′-Bis(dimethylamino)benzophenone (MK), 2-chlorothioxanthone (CTX) and 3,3′-carbonylbis(7-diethylaminocoumarin) (KCD) were used as the sensitizers. The photopolymerization was monitored in IR spectroscopy.[6] To obtain the percentage of double bond conversion ($\gamma$), the initiator, sensitizer, THFA and solvent were placed in a sealed KBr cell. The sample was irradiated with light (365 nm) from a high pressure mercury lamp passed through a band pass filter. The IR spectra were taken before and after the irradiation and the absorbances corresponding to an acrylic bending mode at 810 $cm^{-1}$ were used for the calculations of $\gamma$ [eqn. (1)], where $A_0$ and $A_t$

$$\gamma = (A_0 - A_t)/A_0 \quad (1)$$

are the absorbances corresponding at 810 $cm^{-1}$ before and after the irradiation, respectively. The rate of polymerization ($R_p$) was obtained from the slope ($\Delta\gamma/\Delta t$) of the linear part of the time–$\gamma$ curve measured by this setup [eqn. (2)]. The values of $R_p$ were measured below a $\gamma$ of 10%. $[THFA]_0$ is the THFA concentration before the light exposure.

$$R_p = [THFA]_0 (\Delta\gamma/\Delta t) \quad (2)$$

The relative rates of polymerization, calculated using eqns.(1) and (2), are summarized in Table 1. The ′onium borates **1** or **2** clearly show much higher performances as initiators for the polymerization of THFA than **3**, **4** or **5** with any of the sensitizers.

The most pronounced difference was observed with the results of $R_p$ in $CH_2Cl_2$. The $R_p$ in $CH_2Cl_2$ increased about

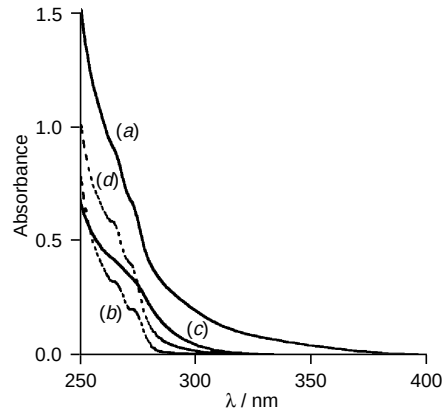
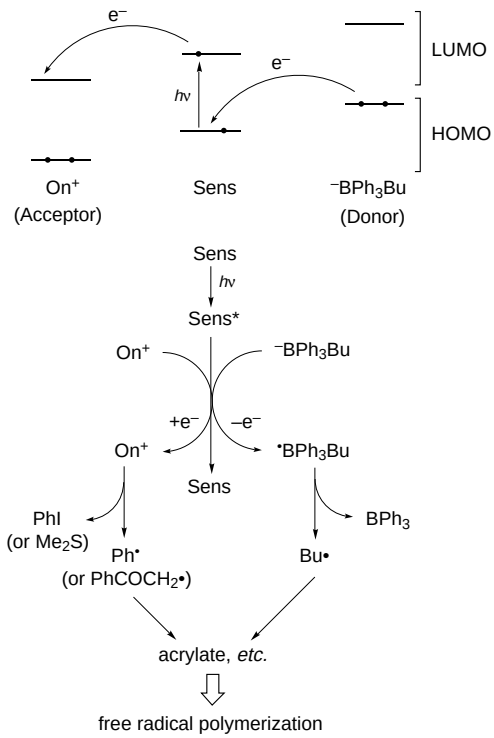



**Fig. 1** UV–VIS absorption spectra of (*a*) **1**, (*b*) **3**, (*c*) **4** in $CH_2Cl_2$ and (*d*) **1** in MeCN. Solution concentrations = $1.0 \times 10^{-4}$ mol $dm^{-3}$.

**Table 1** Rate of photopolymerization of THFA with various sensitizers and initiators in MeCN[a]

| Run | Sensitizer[b] | Initiator | $R_p$[c]/mol dm$^{-3}$ s$^{-1}$ |
|---|---|---|---|
| 1 | MK | **1** | 5.1 (16)[d] |
| 2 | | **2** | 4.6 (15)[d] |
| 3 | | **3** | 0.58 (0.69)[d] |
| 4 | | **4** | 0.21 (0.26)[d] |
| 5 | | **5** | 0.062 |
| 6 | CTX | **1** | 15 |
| 7 | | **2** | 11 |
| 8 | | **3** | 4.0 |
| 9 | | **4** | 2.2 |
| 10 | | **5** | 0.26 |
| 11 | KCD | **1** | 0.29 |
| 12 | | **2** | 0.26 |

[a] Radiant power of the light emission at 365 nm was 1.6 mW cm$^{-2}$; $[THFA]_0 = 9.18 \times 10^{-1}$ mol dm$^{-3}$; $[Initiator]_0 = 1.43 \times 10^{-2}$ mol dm$^{-3}$. [b] [Sensitizer] corresponds to the amount required for 50% transmittance at 365 nm. [c] Rate of polymerization. [d] In $CH_2Cl_2$.




**Scheme 1**

three-fold over the $R_p$ in MeCN (runs 1 and 2) with the ′onium borate initiators. The reason is that both the ′onium borates exist primarily as ion-pairs in $CH_2Cl_2$ and as free ions in MeCN. The photo-induced electron-transfer reaction between the sensitizer and the ′onium borate in $CH_2Cl_2$ occurs more efficiently than does the reaction in MeCN. CTX is a more effective sensitizer than MK or KCD. The photopolymerization with KCD and **3**, **4** or **5** were too poor to measure $R_p$ using this apparatus.

Our postulated reaction mechanism for the sensitizer and the ′onium borate in MeCN is depicted in Scheme 1. Thus, the sensitizer absorbs light at 365 nm which initially generates the excited state of the sensitizer (Sens*). Next, Sens* accepts an electron from a butyltriphenylborate in the ′onium borate, and at the same time, donates an electron to an ′onium cation in the ′onium borate. Consequently, the produced butyltriphenylboranyl radical and ′onium radical decompose to form the butyl radical and phenyl (or phenacyl) radical. These radicals initiate polymerization in the presence of a suitable monomer (*e.g.* THFA). This is also supported by the analysis of the products from the photolysis of the ′onium borates. Conversely, the reaction in $CH_2Cl_2$ would occur as the ion-pair complex of ′onium borates.

Thus, we have demonstrated not only that the ′onium borates are efficient donor–acceptor initiators for free radical photopolymerization but also the generating procedure for the free radicals.

## Footnotes

* E-mail: yusui@mito.ipc.ibaraki.ac.jp
† On leave from Tsukuba Research Laboratories, Toyo Ink Mfg. Co., Ltd., 27 Wadai, Tsukuba, Ibaraki 300-42, Japan.
‡ *General procedure*: A 100 ml round-bottom flask equipped with a Teflon-covered magnetic stirring bar was charged with diphenyliodonium chloride or dimethylphenacylsulfonium bromide (20 mmol) dissolved in water (10 ml). To the flask, lithium butyltriphenylborate (20 mmol) was added with stirring. Diphenyliodonium butyltriphenylborate **1** or dimethylphenacylsulfonium butyltriphenylborate **2** rapidly precipitated. Compound **1** or **2** was collected by filtration and recrystallized from a $CH_2Cl_2$– heptane (1 : 4). The yields were 43% for **1** and 87% for **2**, respectively.
§ Satisfactory elemental analyses have been obtained. *Selected spectroscopic data* for **1**: $\delta_H$ [270 MHz; $(CD_3)_2SO$; $Me_4Si$] 0.68–1.00 (m, 7 H, *Pr*$CH_2B^-$), 1.11–1.27 (m, 2 H, $CH_2B^-$), 6.68–6.78 (m, 3 H, *p*-PhB$^-$), 6.84–6.94 (m, 6 H, *m*-PhB$^-$), 7.14–7.24 (m, 6 H, *o*-PhB$^-$), 7.47–7.57 (m, 4 H, *o*-PhI$^+$), 7.60–7.70 (m, 2 H, *p*-PhI$^+$), 8.17–8.27 (m, 4 H, *m*-PhI$^+$); For **2**: $\delta_H$ [270 MHz; $(CD_3)_2SO$; $Me_4Si$] 0.68–1.00 (m, 7 H, *Pr*$CH_2B^-$), 1.11–1.27 (m, 2 H, $CH_2B^-$), 2.94 (s, 6 H, $Me_2S^+$), 5.40 (s, 2 H, $COCH_2S^+$), 6.68–6.78 (m, 3 H, *p*-PhB$^-$), 6.84–6.94 (m, 6 H, *m*-PhB$^-$), 7.14–7.24 (m, 6 H, *o*-PhB$^-$), 7.58–7.68 (m, 2 H, *m*-PhCO), 7.73–7.83 (m, 1 H, *p*-PhCO), 7.97–8.07 (m, 2 H, *o*-PhCO).

## References

1 For example: S. P. Pappas, in *New Trends in the Photochemistry of Polymers*, ed. N. S. Allen and J. F. Rabek, Elsevier Applied Science, London, 1985, pp. 99–111; R. S. Davidson, *J. Photochem. Photobiol. A: Chem.*, 1993, **73**, 81 and references cited therein.
2 J. P. Fouassier, D. Burr and J. V. Crivello, *J. Photochem. Photobiol., A: Chem.*, 1989, **49**, 317; G. Manivannan, J. P. Fouassier and J. V. Crivello, *J. Polym. Sci. Part A: Polym. Chem.*, 1992, **30**, 1999; K. Ichimura, A. Kameyama and K. Hayashi, *J. Appl. Polym. Sci.*, 1987, **34**, 2747.
3 J. P. Fouassier and S. K. Wu, *J. Appl. Polym. Sci.*, 1992, **44**, 1779.
4 E. Klimtchuk, M. A. J. Rodgers and D. C. Neckers, *J. Phys. Chem.*, 1992, **96**, 9817; A. M.Sarker, A. Y. Polykarpov, A. M. DeRaaff, T. L. Marino and D. C. Neckers, *J. Polym. Sci. Part A: Polym. Chem.*, 1996, **34**, 2817; G. Amirzadeh and W. Schnabel, *Makromol. Chem.*, 1981, **182**, 2821.
5 R. Domico, *J. Org. Chem.*, 1964, **29**, 1971.
6 C. Decker and K. Moussa, *Makromol. Chem.*, 1988, **189**, 2381; T. Tanabe, A. T-Filho and D. C. Neckers, *J. Polym. Sci. Part A: Polym. Chem.*, 1995, **33**, 1691.

*Received in Cambridge, UK, 24th January 1997; Com. 7/00579B*

# Hydrolytic cleavage of DNA by a novel copper(II) complex with *cis,cis*-1,3,5-triaminocyclohexane

**Toyofumi Itoh, Hiroyuki Hisada, Tomoyuki Sumiya, Masami Hosono, Yoshiharu Usui and Yuki Fujii***

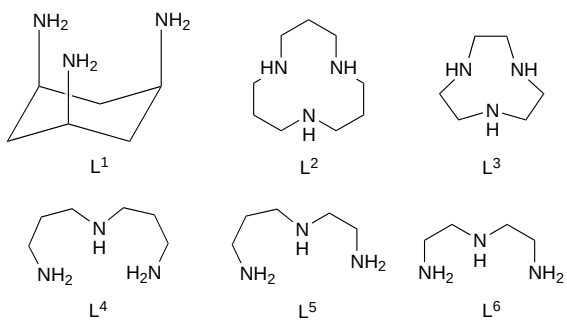
*Graduate School of Science and Engineering, Ibaraki University, 2-1-1, Bunkyo, Mito, Ibaraki 310, Japan*

**Copper(II) complex with *cis,cis*-1,3,5-triaminocyclohexane effectively promotes the hydrolytic cleavage of phage DNA with a rate constant of 4.34 ± 0.77 $h^{-1}$ at pH 8.1 and 35 °C.**

The development of reagents which hydrolytically cleave nucleic acids under mild conditions is currently attracting great interest in the field of artificial nucleases,[1–3] as such a process has the advantage that it produces fragments which may be religated enzymatically. Recently, it has been demonstrated that many chelate compounds of transition metals ($Fe^{2+}$, $Co^{3+}$, $Cu^{2+}$, $Zn^{2+}$) and lanthanides ($La^{3+}$, $Ce^{4+}$, $Eu^{3+}$, $Tm^{3+}$, $Yb^{3+}$, $Lu^{3+}$) are capable of promoting the hydrolytic cleavage of RNA[2,4] and DNA;[2,5–7] however, DNA hydrolysis is much slower compared with RNA hydrolysis. This is mainly because the phosphate diester linkage of DNA is kinetically more stable than that of RNA toward hydrolysis.[8] The best enhanced rate constant for DNA hydrolysis by a metal chelate is in the range 0.18–0.25 $h^{-1}$,[7] and a more active metal chelate is therefore required.

Recently, Burstyn and coworkers reported that copper(II)–macrocyclic triamine ($L^3$) complexes promote the hydrolytic cleavage of plasmid DNA,[6] however, the rate constant is estimated to be 0.04–0.09 $h^{-1}$ at 50 °C from the half life of the hydrolysis.[6a] In order to improve the DNA hydrolysis capacity of copper(II) complexes, we have studied the hydrolysis of lithium 2,4-dinitrophenyl ethyl phosphate (DEP) and phage φx174 DNA† by copper(II) complexes of triamine ligands ($L^1$–$L^6$), and found that a novel copper(II) complex of *cis,cis*-1,3,5-triaminocyclohexane[9,10] ($CuL^1$) has a high potential for DNA hydrolysis: the hydrolysis rate constant reached 4.3 $h^{-1}$ at 35 °C.

Fig. 1 shows agarose gel electrophoresis patterns for the cleavage of φx174 DNA after treated with $CuL^1$ at pH 8.1 and 35 °C for 5 h. The initial concentration of DNA was set at 7 μmol $dm^{-3}$ base pairs, and the concentration of $CuL^1$ was varied from 0 to 70 μmol $dm^{-3}$. The conversion of form I (supercoiled) to form II (nicked) was observed with the increase in concentration of $CuL^1$, and the formation of form III appeared in the presence of 35 and 70 μmol $dm^{-3}$ $CuL^1$ (lanes 6 and 7). The complete disappearance of form I was observed in lanes 5–7 (14–70 μmol $dm^{-3}$ $CuL^1$). On the other hand, $CuL^2$–$CuL^6$ were mostly ineffective under the conditions employed, indicating that only $CuL^1$ effectively enhances the cleavage of φx174 DNA.




A typical time course for DNA cleavage by $CuL^1$ is shown in Fig. 2. The cleavage products were separated by agarose gel electrophoresis and quantified by densitometry after staining with ethidium bromide. The decrease of form I fitted well to a single exponential decay curve. The increase of form II also fitted to a single exponential curve, although the deviation of form II was somewhat larger than that of form I. From these curve fits, the hydrolysis rate constants at a complex concentration of 70 μmol $dm^{-3}$ were estimated to be 1.46 ± 0.22 $h^{-1}$ ($R^2$ = 0.954) for the decrease of form I and 1.82 ± 0.33 $h^{-1}$ ($R^2$ = 0.939) for the increase of form II. Similarly, the hydrolysis rate constants for φx174 DNA in the presence of 7, 14, 140, 210 and 280 mmol $dm^{-3}$ $CuL^1$ were obtained, and are plotted in Fig. 3.

The plots of the rate constants against the concentrations of $CuL^1$ allowed a Michaelis–Menten analysis for φx174 DNA, and gave $k$ = 4.34 ± 0.77 $h^{-1}$, $K_m = 9.55 \times 10^{-5}$ mol $dm^{-3}$ for the decrease of form I, and $k$ = 4.16 ± 0.44 $h^{-1}$, $K_m = 5.75 \times 10^{-5}$ mol $dm^{-3}$ for the increase of form II. The obtained rate constants were similar to each other, and are about twenty times higher than the highest values reported previously for the rate

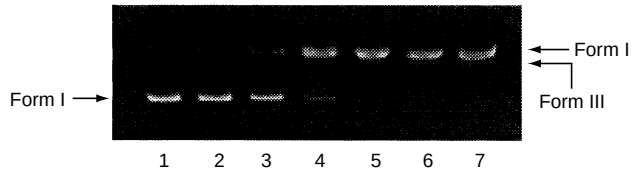



**Fig. 1** Agarose gel electrophoresis patterns for the cleavage of φx174 DNA by $CuL^1$. Conditions: 7 μmol $dm^{-3}$ DNA base pairs; 0–70 μmol $dm^{-3}$ $CuL^1$; 10 mmol $dm^{-3}$ HEPES buffer; pH 8.1; 35 °C; reaction time, 5 h. Lane 1: DNA control. Lane 2: DNA + 0.7 μmol $dm^{-3}$ $CuL^1$. Lane 3: DNA + 3.5 μmol $dm^{-3}$ $CuL^1$. Lane 4: DNA + 7 μmol $dm^{-3}$ $CuL^1$. Lane 5: DNA + 14 μmol $dm^{-3}$ $CuL^1$. Lane 6: DNA + 35 μmol $dm^{-3}$ $CuL^1$. Lane 7: DNA + 70 μmol $dm^{-3}$ $CuL^1$.

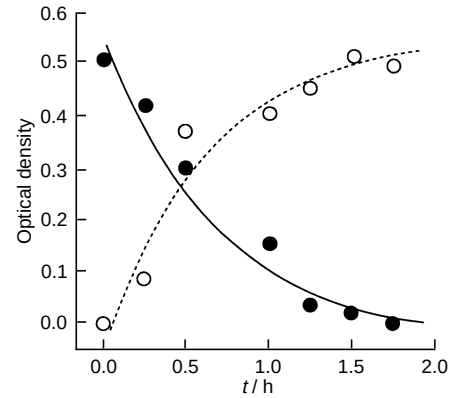



**Fig. 2** Time course of DNA cleavage by $CuL^1$ at pH 8.1 (10 mmol $dm^{-3}$ HEPES buffer) and 35 °C in the presence of 7 μmol $dm^{-3}$ φx174 DNA and 70 μmol $dm^{-3}$ $CuL^1$: (●) form I; (○) form II; solid line, single exponential curvefit for the decrease of form I; dashed line, single exponential curvefit for the increase of form II

constant for DNA hydrolysis by a metal chelate,[7] although the metal and experimental conditions, including employed DNA, were not necessarily the same as those of our experiment.

In Table 1 are summarized the results of the hydrolysis of the phosphate diester DEP by $CuL^1$–$CuL^6$. The hydrolysis of DEP was followed by monitoring the increase in the visible absorbance at 400 nm caused by the release of 2,4-dinitrophenolate ion at pH 8.1 (50 mmol $dm^{-3}$ HEPES buffer) and 25 °C, and analysed by using a reference method.[10] The hydrolysis rate was first order with respect to the concentration of both DEP and CuL. The apparent second order rate constants thus obtained are listed in Table 1.

Table 1 shows that all of the investigated CuL complexes are capable of hydrolysing the phosphate diester linkage, and that $CuL^1$ has a high hydrolysing capacity.‡ In addition, we observed that DNA cleavage by $CuL^1$ is not affected by the presence or absence of $O_2$. This fact indicates that no oxidative process is involved.[6] Hence, these data strongly support the suggestion that DNA cleavage by $CuL^1$ proceeds *via* a hydrolysis mechanism. On the other hand, we found the following discrepancies between DEP and DNA hydrolysis: (i) the former is first order-dependent on complex concentration, but the latter is saturation-dependent on complex concentration; (ii) the former is greatly enhanced by not only $CuL^1$ but also $CuL^2$ and $CuL^3$, but the latter is specific toward $CuL^1$.

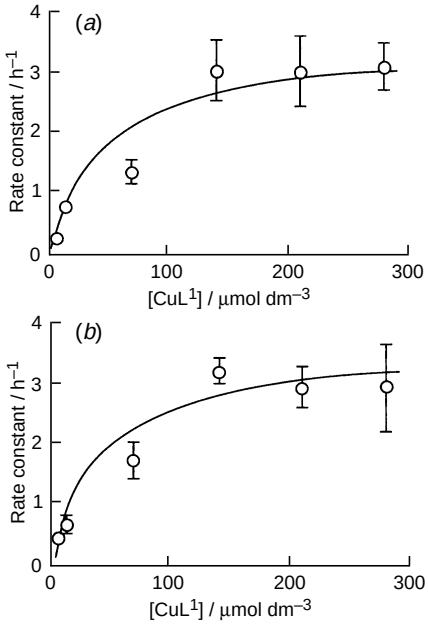



**Fig. 3** Saturation kinetics for cleavage of φx174 DNA by 7–280 μmol $dm^{-3}$ $CuL^1$ at pH 8.1 and 35 °C: (*a*) decrease of form I; (*b*) increase of form II

**Table 1** Rate constants ($k_{app}$) of hydrolysis of DEP by $CuL^1$–$CuL^6$ at pH 8.1 (50 mmol $dm^{-3}$ HEPES), ionic strength = 0.1 M ($NaClO_4$) and 25 °C

| Complex | $k_{app}$/$dm^3$ $mol^{-1}$ $s^{-1}$ |
|---|---|
| $CuL^1$ | $(1.2 \pm 0.1) \times 10^{-2}$ |
| $CuL^2$ | $(1.4 \pm 0.1) \times 10^{-2}$ |
| $CuL^3$ | $(7.1 \pm 0.2) \times 10^{-3}$ |
| $CuL^4$ | $(0.4 \pm 0.1) \times 10^{-4}$ |
| $CuL^5$ | $< 10^{-4}$ |
| $CuL^6$ | $< 10^{-4}$ |

Although we have no clear explanation for these data, one explanation is the possibility of a polymer effect for DNA, with specific reaction sites for $CuL^1$.

We thank Professor M. Kodama (Hirosaki University) and Professor M. Chikira (Chuo University) for their helpful suggestions. This work was partly supported by a Grant-in-Aid for Scientific Research No. 0764735 from the Ministry of Education, Science and Culture of Japan.

## Footnotes

† Phage φx174 RFI DNA was purchased from Sigma Co. Ltd.

‡ We also confirmed the following facts: (i) free copper(II) ions produce almost no cleavage of φx174 DNA at concentrations below 2 μmol $dm^{-3}$ of copper(II) ion under the employed conditions, and (ii) the concentration of free copper(II) ion is less than 1.1 μmol $dm^{-3}$ under our experimental conditions [copper(II) ion exists as over 97.5% $CuL^1$ and $CuL^1$ (OH) species] on the basis of the calculation using the following deprotination and stability constants determined by potentiometric titration at 35 °C; $K_1 = [H^+][H_2L^{2+}]/[H_3L^{3+}] = 10^{-6.94}$, $K_2 = [H^+][HL^+]/[H_2L^{2+}] = 10^{-8.69}$, $K_3 = [H^+][L]/[HL^+] = 10^{-9.75}$, $K_{ML} = [CuL^{2+}]/[Cu^{2+}][L] = 10^{10.55}$, $K_{MHL} = [CuHL^{3+}]/[Cu^{2+}][HL^+] = 10^{6.47}$, $K_a = [CuL(OH)^+][H^+]/[CuL^{2+}] = 10^{-8.40}$.

## References

1 D. S. Sigman, *Biochemistry*, 1990, **29**, 9097; D. S. Sigman, A. Mazumder and D. M. Perrin, *Chem. Rev.*, 1993, **93**, 2295.
2 M. Komiyama, *J. Biochem.*, 1995, **118**, 665.
3 K. Shinozuka, K. Shimizu, Y. Nakashima and H. Sawai, *Bioorg. Med. Chem. Lett.*, 1994, **4**, 1979; R. Male, V. M. Fosse and K. Kleppe, *Nucleic Acids Res.*, 1982, **10**, 6305; A. Fkyerat, M. Demeunynck, J.-F. Constant, P. Michon and J. Lhomme, *J. Am. Chem. Soc.*, 1993, **115**, 9952; A. Fkyerat, M. Demeunynck, J.-F. Constant and J. Lhomme, *Tetrahedron*, 1993, **49**, 11 237; A. Rodger, I. S. Blagbrough, G. Adlam and M. L. Carpenter, *Biopolymers*, 1994, **34**, 1583; G. Adlam, I. S. Blagbrough, S. Taylor, H. C. Latham, I. S. Haworth and A. Rodger, *Bioorg. Med. Chem. Lett.*, 1994, **4**, 2435.
4 K. Matsumura, M. Endo and M. Komiyama, *J. Chem. Soc., Chem. Commun.*, 1994, 2019; M. Endo, K. Hirata, T. Ihara, S. Sueda, M. Takagi and M. Komiyama, *J. Am. Chem. Soc.*, 1996, **118**, 5478; M. Irisawa, N. Takeda and M. Komiyama, *J. Chem. Soc., Chem. Commun.*, 1995, 1221; M. Yashiro, A. Ishikubo and M. Komiyama, *J. Chem. Soc., Chem. Commun.*, 1995, 1793; M. J. Young and J. Chin, *J. Am. Chem. Soc.*, 1995, **117**, 10 577; J. K. Bashkin and L. A. Jenkins, *J. Chem. Soc., Dalton Trans.*, 1993, 3631; S. Kuusela, A. Azhayev, A. Guzaev and H. Lönnberg, *J. Chem. Soc., Perkin Trans. 2*, 1995, 1197; T. P. Prakash and K. N. Ganesh, *J. Chem. Soc., Chem. Commun.*, 1994, 1357.
5 M. Komiyama, N. Takeda, Y. Takahashi, H. Uchida, T. Shiiba, T. Kodama and M. Yashiro, *J. Chem. Soc., Perkin Trans. 2*, 1995, 269; M. Komiyama, T. Shiiba, T. Kodama, N. Takeda, J. Sumaoka and M. Yashiro, *Chem. Lett.*, 1994, 1025; S. Hashimoto and Y. Nakamura, *J. Chem. Soc., Chem. Commun.*, 1995, 1413; B. K. Takasaki and J. Chin, *J. Am. Chem. Soc.*, 1994, **116**, 1121; L. M. T. Schnaith, R. S. Hanson and L. Que, Jr., *Proc. Natl. Acad. Sci. USA*, 1994, **91**, 569. L. A. Basile, A. L. Raphael and J. K. Barton, *J. Am. Chem. Soc.*, 1987, **109**, 7550.
6 (*a*) E. L. Hegg and J. N. Burstyn, *Inorg. Chem.*, 1996, **35**, 7474; (*b*) J. N. Burstyn and K. A. Deal, *Inorg. Chem.*, 1993, **32**, 3585; (*c*) K. A. Deal, A. C. Hengge and J. N. Burstyn, *J. Am. Chem. Soc.*, 1996, **118**, 1713; (*d*) K. A. Deal and J. N. Burstyn, *Inorg. Chem.*, 1996, **35**, 2792.
7 J. Rammo, R. Hettich, A. Roigk and H.-J. Schneider, *Chem. Commun.*, 1996, 105; N. E. Dixon, R. J. Geue, J. N. Lambert, S. Moghaddas, D. A. Pearce and A. M. Sargeson, *Chem. Commun.*, 1996, 1287.
8 F. H. Westheimer, *Science*, 1987, **235**, 1173.
9 U. Brand and H. Vahrenkamp, *Inorg. Chim. Acta*, 1992, **198**–**200**, 663; B. Greener, L. Cronin, G. D. Wilson and P. H. Walton, *J. Chem. Soc., Dalton Trans.*, 1996, 401; B. Greener, M. H. Moore and P. H. Walton, *J. Chem. Soc., Dalton Trans.*, 1996, 27; J. E. Bollinger, W. A. Banks, A. J. Kastin and D. M. Roundhill, *Inorg. Chim. Acta*, 1996, **244**, 201.
10 T. Itoh, Y. Fujii, T. Tada, Y. Yoshikawa and H. Hisada, *Bull. Chem. Soc. Jpn.*, 1996, **69**, 1265.

*Received, 2nd January 1997; Com. 7/00001D*

# Substituted α,β,γ-triazatetrabenzcorrole: an unusual reduction product of a phthalocyanine

**Junzhong Li, Lakshminarayanapuram R. Subramanian and Michael Hanack***

*Institut für Organische Chemie, Lehrstuhl für Organische Chemie II, Universität Tübingen, Auf der Morgenstelle 18, D-72076 Tübingen, Germany*

**4,5-Dipentyldiiminoisoindoline 1 reacts with hexachlorodisilane ($Si_2Cl_6$) to give the ring-contracted hydroxysilicon-α,β,γ-triazatetrabenzcorrole 4 which in solution photolyses giving the ring cleavage compounds 5 and 6; the stability of triazatetrabenzcorroles 4 and 7 with silicon and germanium as central elements is studied by UV–VIS spectroscopy.**

Many of the properties of metallophthalocyanines (PcM) such as semiconductivity, photoconductivity and catalytic properties rely upon the redox properties of the PcM species.[1,2] As a result, the redox chemistry of PcM has been investigated in detail, both by chemical and electrochemical methods with phthalocyanines containing redox inactive as well as redox active metals centres.[3–5] Accordingly, negative ions of Pc or PcM with low valent state metals such as $PcCo^{I}$ and $PcSn^{II}$ have been found,[6–8] however, the basic structure of the resulting reduced macrocycle remained the same.

In 1986, Fujiki *et al.*[9] ascertained for the first time that the earlier reported $PcGe^{II}$,[10] produced by reducing $PcGeCl_2$ with $NaBH_4$, did not retain the phthalocyanine moiety but was a phthalocyanine-like tetrapyrrole macrocycle, namely hydroxygermanium(IV)-α,β,γ-triazatetrabenzcorrole (TBCGeOH) **2**. However, probably due to the report[9] that the stability of TBC complexes with different central elements follows the sequence TBCGeOH **2** ≫ TBCSiOH **3** > TBCAl > TBCGa, and also that the authors[9] succeeded in obtaining only the pure TBCGeOH **2**, no further reports on TBC macrocycles could be found to date.

As part of our ongoing studies to synthesize precursors for polymers containing Pc units,[1,2,11,12] 4,5-dipentyldiiminoisoindoline **1** was treated with $Si_2Cl_6$ to examine the potential of producing phthalocyanine dimers with an Si–Si bond. Unexpectedly, during purification of the reaction mixture by flash chromatography (silica gel, $CHCl_3$), besides obtaining $(C_5H_{11})_8PcSi(OH)_2$, a deep green solid was also isolated which displayed a very sharp absorption at 448 nm (Soret band) with an intensity nearly twice that of the Q band in its electronic spectrum (Fig. 1), which was later found to be the typical UV–VIS spectrum of TBC macrocycles.[9] The mass spectral, $^1H$ NMR, IR and elemental analysis further proved that the compound obtained in this reaction is hydroxysilicon 4,5,11,12,18,19,25,26-octapentyl-α,β,γ-triazatetrabenzcorrole (PTBCSiOH) **4**.† Further studies carried out by treating $Si_2Cl_6$ with **1** in different ratios indicated that if the ratio reached *ca.* 1 : 1, only PTBCSiOH **4** was obtained in 35% yield (Scheme 1). It seems that the excess of $Si_2Cl_6$ reacted with an intermediate phthalocyanine to form the TBC derivative **4** (*vide infra*).

The mechanism for the formation of the TBC macrocycles by reaction of a reducing agent such as $NaBH_4$ with, for example, $PcGeCl_2$ has not been proven experimentally, although in the original work[9] a mechanism for the Pc ring contraction was proposed. $Si_2Cl_6$ is a known deoxygenating reagent, for example, it has been used to produce phosphine from phosphine oxide[13] and phosphine sulfides.[14] On the other hand, $Si_2Cl_6$ is very sensitive to water, affording products in which the Si–Si bond is broken or an oxygen is inserted into the Si–Si bond. As a result, during the reaction of **1** with $Si_2Cl_6$ the dihydroxysilicon phthalocyanine $(C_5H_{11})_8PcSi(OH)_2$ and/or μ-oxo dimers $[(C_5H_{11})_8PcSi(OH)]_2O$ will be produced first, and then reduced by an excess of $Si_2Cl_6$ to form PTBCSiOH **4**. Indeed, in the reaction of $Si_2Cl_6$ with the isoindoline **1** in a ratio of 1 : 2, $(C_5H_{11})_8PcSi(OH)_2$ was isolated by flash chromatography. The assumption that $(C_5H_{11})_8PcSi(OH)_2$ was formed first and then reduced by $Si_2Cl_6$ was confirmed by reacting $(C_5H_{11})_8PcSi(OH)_2$ with $Si_2Cl_6$ in quinoline and isolating PTBCSiOH **4** from the reaction mixture.

PTBCSiOH **4** is stable in the solid state under ambient conditions. However, air saturated solutions of **4** are found to be light sensitive. Of particular interest is that the green solution of **4** in, for example, $CHCl_3$ changed from green to red under light after some time. The resulting 'photolysis' products were separated on silica gel with a mixture of $CHCl_3$ and $CH_2Cl_2$ (v:v, 3:2) as eluent to give a purple and a red compound. Based on mass spectroscopy, IR, UV–VIS and $^1H$ NMR data, the purple **5**‡ and the red **6**† compounds were characterized as cleavage products of the 1,2-double bond of compound **4**. As a result, the central coordinated element is lost. The overall reaction is shown in Scheme 1.

The UV–VIS spectra of PTBCSiOH **4** (Fig. 1) and PTBCGeOH **7** [produced by reducing $(C_5H_{11})_8PcGeCl_2$ with $NaBH_4$ according to a literature method[9]] (Fig. 2) in $CHCl_3$ under air with irradiation at different times were determined in order to investigate the influence of the central element on the stability of TBC complexes under these conditions. In contrast to the earlier report,[9] it is evident both from the decrease in intensity of the Soret and the Q bands that PTBCSiOH **4** is more stable than the germanium complex **7** under the same conditions. As a ring contracted entity of Pc, the TBC ring will prefer the central element with a smaller radius than that of Pc. Obviously Si, with a smaller radius than Ge, forms a more stable complex with the TBC macrocycle than Ge, though the accurate radius of the internal hole of the TBC ring is not known. Fujiki *et al.*[9] did not succeed in producing pure unsubstituted

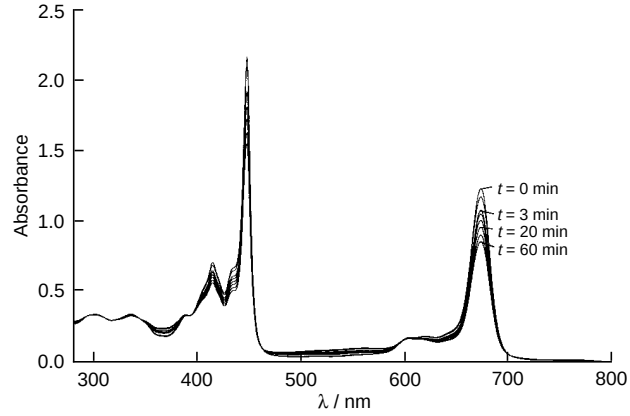
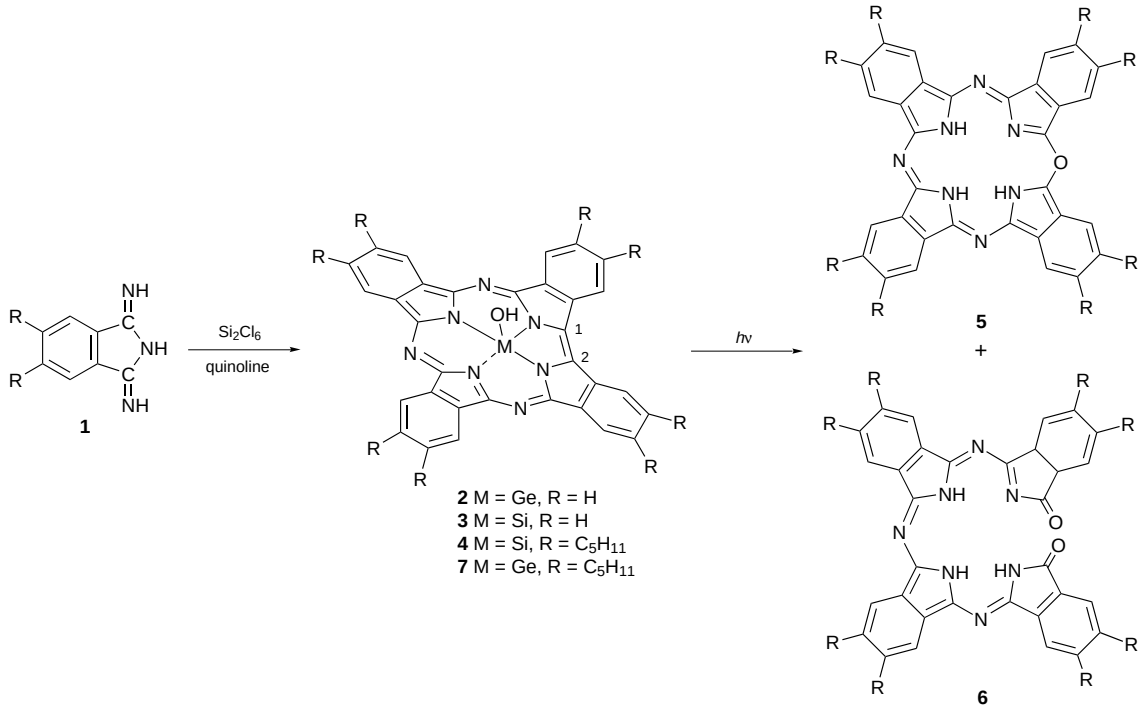



**Fig. 1** Changes in the electronic absorption spectra of PTBCSiOH **4** in $CHCl_3$ under air upon irradiation with light (λ = 650–730 nm) at room temperature




**Scheme 1** Synthetic scheme for PTBCSiOH and its photolysis products

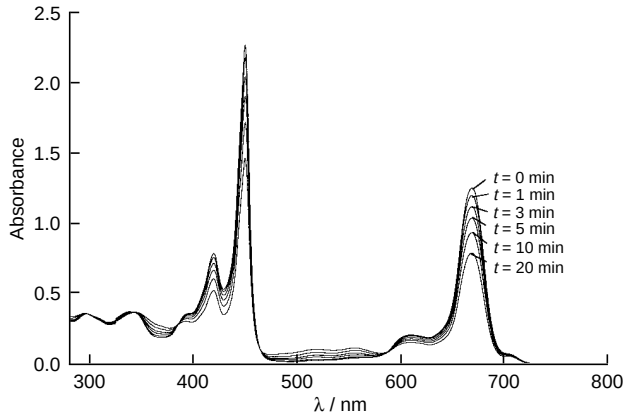



**Fig. 2** Changes in the electronic absorption spectra PTBCGeOH **7** in $CHCl_3$ under air upon irradiation with light (λ = 650–730 nm) at room temperature

TBCSiOH **3** by reducing $PcSiCl_2$ with $NaBH_4$, however, pure substituted PTBCSiOH **4** was obtained by using $Si_2Cl_6$, which shows that reducing agents have an influence on the formation of TBC derivatives from the corresponding Pc complexes. The reason for the conflicting results of Fujiki *et al.*[9] and ourselves on the stability of TBC complexes of Si and Ge might be due to the use of an unsubstituted **3** and a substituted **4** respectively in illumination experiments.

## Footnotes

* E-mail: hanack@uni-tuebingen.de

† *Selected data* for **4**: IR ν/cm$^{-1}$ (KBr) 2955, 2928, 1626, 1462, 1416, 1377, 1261, 1111, 1020, 887, 804, 733. UV–VIS ($CHCl_3$) $\lambda_{max}$/nm (relative absorbance) 295(0.27), 342(0.24), 416(0.39), 434(0.35), 448(1.00), 620(0.12), 675(0.56). $\delta_H$ (250 MHz, [$^2H_8$]THF) 9.35 (s, 2 H, $H_{arom.}$), 9.25 (s, 2 H, $H_{arom.}$), 8.69 (s, 2 H, $H_{arom.}$), 7.98 (s, 2 H, $H_{arom.}$), 3.38 (m, 8 H, $CH_2$), 2.85 (m, 8 H, $CH_2$), 2.16–1.64 (m, 48 H, $CH_2$), 1.15 (m, 24 H, $CH_3$), −1.54 (s, 1 H, OH). MS(FD) *m/z*: 1104.1 ($M^+$). Anal. calc. for $C_{72}H_{97}N_7SiO$(1103.8): C, 78.28; H, 8.85; N, 8.88. Found: C, 77.38; H, 8.60; N, 8.48%. For **5**: IR ν/cm$^{-1}$ (KBr) 2959, 2928, 2856, 1744, 1730, 1609(s), 1468, 1261, 1221, 1096, 1028, 804, 730. UV–VIS ($CHCl_3$) $\lambda_{max}$/nm (relative absorbance) 366(0.86), 519(0.81), 553(1.00), 597(0.70). $\delta_H$ (250 MHz, $CDCl_3$) 11.68 (s, 3 H, NH), 8.30 (s, 2 H, $H_{arom.}$), 7.95 (s, 2 H, $H_{arom.}$), 7.80 (s, 2 H, $H_{arom.}$), 7.73 (s, 2 H, $H_{arom.}$), 2.79 (m, 16 H, $CH_2$), 1.69 (m, 16 H, $CH_2$), 1.23 (m, 32 H, $CH_2$), 0.93 (m, 24 H, $CH_3$). MS(FD and FAB) *m/z*: 1078.5 ($M^+$). For **6**: IR ν/cm$^{-1}$ (KBr) 2955, 2928, 1744, 1674, 1614, 1564, 1477, 1468, 1209, 1138. UV–VIS ($CHCl_3$) $\lambda_{max}$/nm (relative absorbance) 337(0.59), 515(1.00), 554(0.88). $\delta_H$ (250 MHz, $CDCl_3$) 11.41 (s, 1 H, NH), 11.35 (s, 1 H, NH), 9.35 (s, 1 H, NH), 8.45 (s, 1 H, $H_{arom.}$), 8.33 (s, 1 H, $H_{arom.}$), 8.16 (s, 1 H, $H_{arom.}$), 7.90 (s, 1 H, $H_{arom.}$), 7.87 (s, 1 H, $H_{arom.}$), 7.79 (s, 1 H, $H_{arom.}$), 7.66 (s, 1 H, $H_{arom.}$), 7.57 (s, 1 H, $H_{arom.}$), 2.74 (m, 16 H, $CH_2$), 1.67 (m, 16 H, $CH_2$), 1.24 (m, 32 H, $CH_2$), 0.88 (m, 24 H, $CH_3$). MS(FD) *m/z*: 1093.3 ($M^+$).

## References

1 M. Hanack, S. Deger and A. Lange, *Coord. Chem. Rev.*, 1988, **83**, 115.
2 M. Hanack and M. Lang, *Adv. Mater.*, 1994, **6**, 819.
3 A. B. P. Lever, E. R. Milaeva and G. Speier, in *Phthalocyanine: Properties and Applications*, ed. C. C. Leznoff and A. B. P. Lever, VCH, Weinheim, 1989, p. 1.
4 D. W. Clack and Y. R. Yandle, *Inorg. Chem.*, 1972, **11**, 1738.
5 R. Behnisch and M. Hanack, *Synth. Met.*, 1990, **36**, 387.
6 D. W. Clack, N. S. Hush and I. S. Woolsey, *Inorg. Chim. Acta*, 1976, **19**, 129.
7 M. J. Stillman and A. J. Thompson, *J. Chem. Soc., Faraday Trans. 2*, 1974, 805.
8 W. J. Kroenke and M. E. Kenney, *Inorg. Chem.*, 1964, **3**, 251.
9 M. Fujiki, H. Tabei and K. Isa, *J. Am. Chem. Soc.*, 1986, **108**, 1532.
10 R. L. Stover, C. L. Thrall and R. D. Joyner, *Inorg. Chem.*, 1975, **10**, 2335.
11 H. Schultz, H. Lehmann, M. Rein and M. Hanack, *Struct. Bonding* (*Berlin*), 1990, **74**, 41.
12 M. Hanack, A. Datz, R. Fay, K. Fischer, U. Keppeler, J. Koch, J. Metz, M. Mezger, O. Schneider and H. J. Schulze, in *Handbook of Conducting Polymers*, ed. T. A. Skotheim, Marcel Dekker, New York, 1986, p. 133.
13 K. Naumann, G. Zon and K. Mislow, *J. Am. Chem. Soc.*, 1969, **91**, 7012.
14 G. Zon, K. E. Debruin, K. Nauman and K. Mislow, *J. Am. Chem. Soc.*, 1969, **91**, 7023.

*Received, 23rd January 1997; Com. 7/00532F*

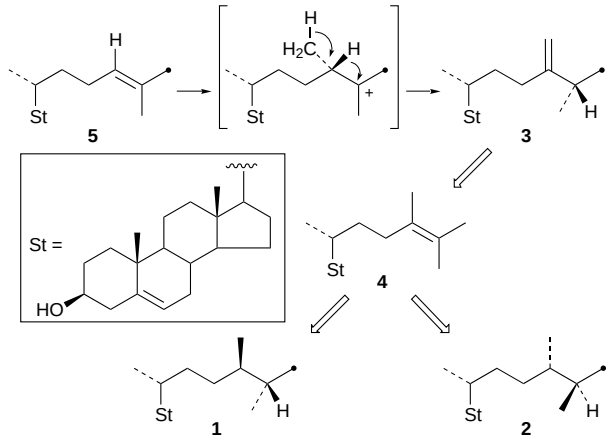
# Stereochemistry of the reduction of 24-methyldesmosterol to campesterol and dihydrobrassicasterol in higher plants

**Yoshinori Fujimoto,*[a]† Naoko Sato,[a] Keisuke Iwai,[b] Hiroki Hamada,[b] Junko Yamada,[c] and Masuo Morisaki[c]**

[a] *Department of Chemistry, Tokyo Institute of Technology, O-okayama, Meguro-ku, Tokyo 152, Japan*
[b] *Department of Applied Science, Okayama University of Science, Ridai-cho, Okayama 700, Japan*
[c] *Kyoritsu College of Pharmacy, Shibakoen, Minato-ku, Tokyo 105, Japan*

**Feeding of chemically synthesized [26-$^{13}$C]- and [27-$^{13}$C]-labelled 24-methyldesmosterols to tissue cultures of *Oryza satiba* and *Catharanthus roseus* followed by $^{13}$C NMR analysis of the biosynthesized sterols reveals that reduction of the 24(25)-double bond giving either campesterol or dihydrobrassicasterol takes place in an *anti*-manner.**

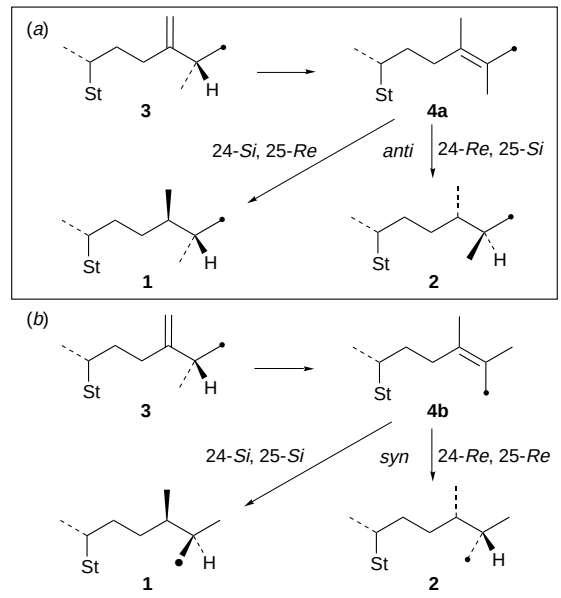
Plant sterols are characterized by a C-24 alkyl substituent (methyl, ethyl, methylene or ethylidene) which originates from *S*-adenosylmethionine by a single or double *trans*-methylation reaction with an olefinic precursor.[1] Accumulated evidence suggests that the final step of the side chain biosynthesis of 24-methylsterols, campesterol **1** and dihydrobrassicasterol **2**, in higher plants is the reduction of 24-methyl-$\Delta^{24(25)}$-sterol (*e.g.* 24-methyldesmosterol **4**).[1,2] The $\Delta^{24(25)}$-sterol is proposed to be formed by the isomerization of 24-methyl-$\Delta^{24(28)}$-sterol (*e.g.* 24-methylenecholesterol **3**) which in turn is produced by the transfer of the methyl group of *S*-adenosylmethionine to a $\Delta^{24(25)}$-sterol such as desmosterol **5** (Scheme 1).[1] Similar reduction of 24-ethyl-$\Delta^{24(25)}$-sterol is proposed for sitosterol biosynthesis. Recently, we offered evidence supporting an intermediary role of 24-methyl-$\Delta^{24(25)}$-sterol in the biosynthesis of campesterol as well as dihydrobrassicasterol in tissue cultures of *Catharanthus roseus* and *Oryza sativa*.[3] Furthermore, we assigned the $^{13}$C NMR chemical shifts of the C-26 and -27 diastereotopic methyl groups of **3** and showed that the isopropylidene (*E*)- and (*Z*)-methyl groups of **5** *pro-S* and *pro-R* methyl groups of **3**, respectively, in the above two tissue cultures.[4] The same steric course in the conversion of lanosterol into 24-methylenelanosterol was reported with *Zea mays*.[5] On the other hand, the C-2 of mevalonate [*via* (*E*)-methyl group of **5**] turns the *pro-S* methyl group of **1** and *pro-R* methyl groups of **2**, whereas C-6 of mevalonate [*via* the (*Z*)-methyl group of **5**] becomes the *pro-R* methyl group of **1** and *pro-S* methyl groups of **2** with cultured cells of *Physalis perviana*[6] and *Amsonia elliptica*.[2] We also obtained the same results on the origin of the diastereotopic methyl groups of **1** and **2** by feeding (*E*)- and (*Z*)-Me $^{13}$C-labelled desmosterols to cultured cells of *C. roseus* and *O. sativa*. Thus, the biosynthetic pathway of 24-methylcholesterols in higher plants can be summarized as depicted in Scheme 1.



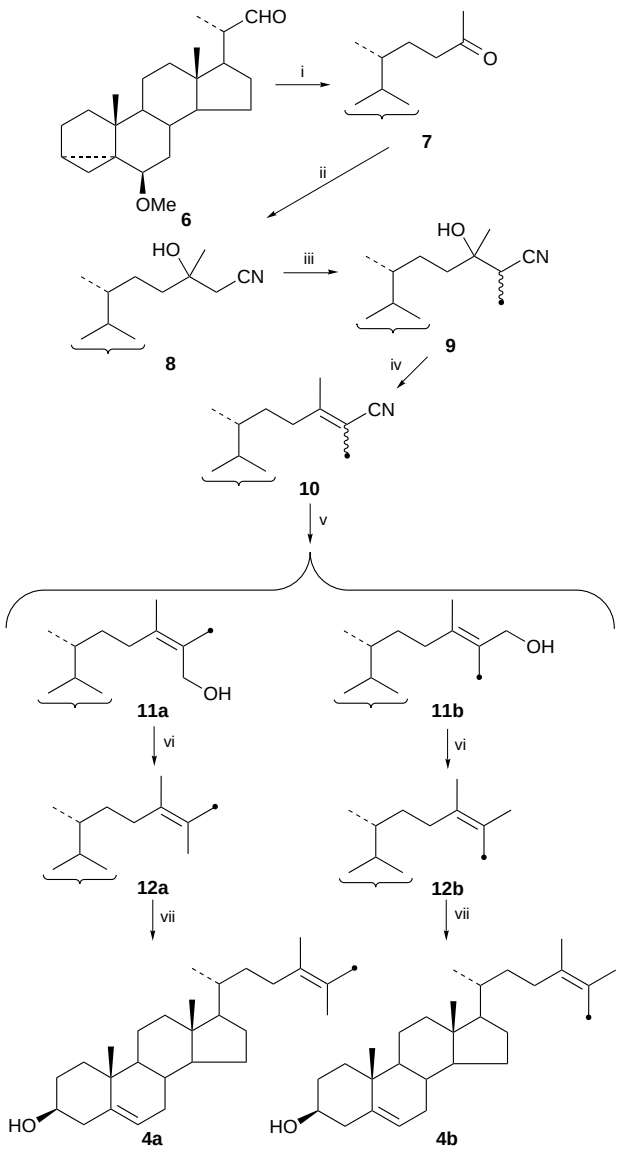

**Scheme 1** Proposed biosynthetic pathway of 24-methylcholesterols. The dots indicate the carbon derived from C-2 of mevalonate.

The steric course of the isomerization from $\Delta^{24(28)}$ to $\Delta^{24(25)}$ (**3** → **4**) and the stereochemistry of the subsequent reduction of $\Delta^{24(25)}$ (**4** → **1** and **2**) remain unclear. Two possible mechanisms can be drawn for the conversion of **3** to **1** and **2**: (*a*) *pro-S*-Me at C-25 of **3** becomes (*E*)-Me of **4** in the double bond isomerization reaction and the reduction proceeds in an *anti*-mode; (*b*) *pro-S*-Me at C-25 of **3** becomes (*Z*)-Me of **4** and the reduction occurs in a *syn*-mode (Scheme 2). We now report that mechanism (*a*) operates in tissue cultures of *O. sativa* and *C. roseus*.

(*E*)-Me $^{13}$C-labelled **4a** and (*Z*)-Me $^{13}$C-labelled **4b** 24-methyldesmosterols were prepared (Scheme 3). Methyl ketone **7** was obtained from well known C-22-aldehyde **6**[7] in four steps. Reactions of **7** with the MeCN anion gave adduct **8**. Methylation of the adduct using $^{13}CH_3I$ (99% $^{13}$C) afforded $^{13}$C-labelled **9** which was dehydrated to give a mixture of (*E*)- and (*Z*)-tetrasubstituted olefin **10**. Stepwise reduction of the olefin mixture with DIBAL-H *via* the corresponding aldehyde gave a mixture of allyic alcohols **11a**,**b**. The geometric isomers were separated by a silica gel Lobar column, affording the less polar (*E*)-alcohol **11a** and the more polar (*Z*)-isomer **11b**. The (*E*)-geometry of **11a** was determined by NOE studies in which irradiation of 28-$H_3$ (δ 1.67) caused the enhancement of the signal intensity of the $CH_3$ resonance at δ 1.73 (d, $J$ = 126 Hz). Similarly, irradiation of 28-$H_3$ (δ 1.71) of **11b** resulted in the enhancement of the intensity of oxymethylene proton signal at




**Scheme 2** Two possible routes for the formation of 24-methylcholesterol




**Scheme 3** Synthesis of regiospecifically labelled 24-methyl-$\Delta^{24(25)}$-cholesterols **4a** and **b**. *Reagent and conditions*: i, acetone, LDA, then MsCl, $Et_3N$, then DBU, then $H_2$, Pd–C (50%); ii, LDA, MeCN (91%); iii, LDA, $^{13}CH_3I$ (41%); iv, $SOCl_2$ (100%); v, DIBAL-H (19% **11a**, 25% **11b**); vi, MsCl, LiCl, lutidine; LAH (70%); vii, TsOH, $H_2O$ (80%).

δ 4.11 (d, $J$ = 4.6 Hz), thus establishing the (*Z*)-geometry for **11b**. The alcohols **11a**,**b** were converted into the (*E*)-Me and (*Z*)-Me $^{13}$C-labeled sterols **4a** ($\delta_C$ 20.51) and **4b** ($\delta_C$ 19.98), respectively, *via* **12a** and **12b**.

Feeding of **4a** to cultured cells of *O. sativa* was carried out as described previously.[3] HPLC separation of the resulting sterol fraction gave a mixture of campesterol and dihydrobrassicasterol. The partial $^{13}$C NMR spectrum of the mixture is shown in Fig. 1. Compound **4b** was similarly incubated to give the same 24-methylcholesterol mixture (Fig. 1).

$^{13}$C Assignments of the diastereotopic methyl groups of **1** and **2** were established previously.[8] Thus, it is evident from Fig. 1 that the (*E*)-methyl of **4** becomes the *pro-S*-methyl of **1** and the *pro-R*-methyl of **2**, whereas the (*Z*)-methyl of **4** becomes the *pro-R*-methyl group of **1** and the *pro-S*-methyl group of **2**. Similar feeding experiments of **4a**,**b** using cultured cells of *C. roseus* led to the same results for the metabolic fates of the isopropylidene methyl groups (data not shown).

These findings demonstrate for the first time that stereospecific hydrogen attack on 24-*Si*, 25-*Re* face of 24-methyldesmosterol **4** affords campesterol **1**, whereas dihydrobrassicasterol **2** is produced by 24-*Re*, 25-*Si* attack of hydrogen on the same 24(25)-olefin **4**. It should be noted that an *anti*-mode of hydrogen addition occurs in both cases.

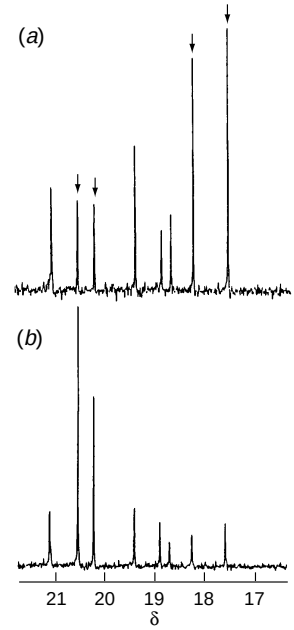



**Fig. 1** $^{13}$C NMR spectra (part) of metabolically formed 24-methylcholesterol fractions. (*a*) [(*E*)-Me-$^{13}$C]-**4a**, (*b*) [(*Z*)-Me-$^{13}$C]-**4b**. Signals indicated by arrows: *pro-S*-Me (δ 18.26) and *pro-R*-Me (δ 20.19) of **1**, *pro-S*-Me (δ 20.50) and *pro-R*-Me (δ 17.60) of **2**.

These results imply that the double bond migration from **3** to **4** should proceed in such a manner that the *pro-R* methyl of **3** becomes (*Z*)-methyl group of **4** while the *pro-S* methyl of **3** becomes (*E*)-methyl group of **4** [Scheme 2(*a*)]. The metabolic correlation of C-26 and C-27 in 24-methylcholesterol biosynthesis in *O. sativa* and *C. roseus* can be summarized as: C-2 of mevalonate → (*E*)-Me of **5** → *pro-S*-Me of **3** → (*E*)-Me of **4** → *pro-S*-Me of **1** and *pro-R*-Me of **2**; C-6 of mevalonate → (*Z*)-Me of **5** → *pro-R*-Me of **3** → (*Z*)-Me of **4** → *pro-R*-Me of **1** and *pro-S*-Me of **2** (Scheme 1).

It has been reported that one of the olefinic methyl groups of **4**, which appeared at higher field [δ 19.93, now assigned to (*Z*)-methyl group] in the $^{13}$C NMR spectrum, was derived from an intact [$^{13}C_2$]acetate molecule with tissue cultures of *P. periviana*,[6] which coincides with our present results.

## Footnote

† E-mail: fujimoto@chem.titech.ac.jp

## References

1 G. G. Janssen, M. Kalinowska, R. A. Norton and W. D. Nes, *Physiology and Biochemistry of Sterols*, ed. G. W. Patterson and W. R. Nes, American Oil Chemists' Society, Champain, 1991, p. 83.
2 S. Seo, A. Uomori, Y. Yoshimura, K. Takeda, H. Noguchi, Y. Ebizuka, U. Sankawa and H. Seto, *J. Chem. Soc., Perkin Trans. 1*, 1992, 569.
3 J. Yamada, M. Morisaki, K. Iwai, H. Hamada, N. Sato and Y. Fujimoto, *Tetrahedron*, in the press.
4 Y. Fujimoto, K. Ohyama, N. Sato, J. Yamada and M. Morisaki, *Chem. Pharm. Bull.*, 1997, **53**, 877.
5 D. Guo, Z. Jia and W. D. Nes, *J. Am. Chem. Soc.*, 1996, **118**, 8507.
6 S. Seo, A. Uomori and K. Takeda, *J. Chem. Soc., Chem. Commun.*, 1984, 1174; A. Oomori, S. Seo, Y. Yoshimura and K. Takeda, *J. Chem. Soc., Chem. Commun.*, 1984, 1176.
7 G. D. Anderson, T. J. Powers, C. Djerassi, J. Fayos and J. Clardy, *J. Am. Chem. Soc.*, 1975, **97**, 388.
8 D. Colombo, F. Ronchetti, G. Russo and L. Toma, *J. Chem. Soc., Chem. Commun.*, 1990, 263.

*Received, 21st January 1997; Com. 7/00492C*

# Monohydroxy terminally functionalised poly(methyl methacrylate) from atom transfer radical polymerisation

**David M. Haddleton,*† Carl Waterson, Peter J. Derrick, Christina B. Jasieczek and Andrew J. Shooter**

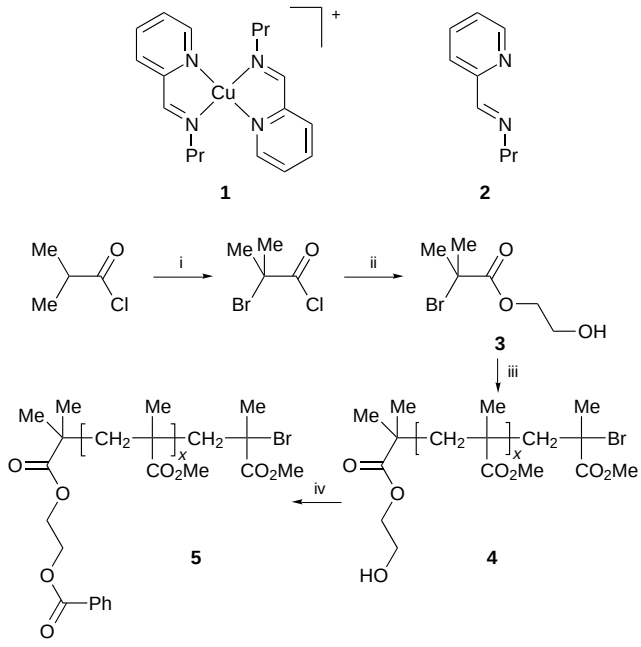
*Department of Chemistry, University of Warwick, Coventry, UK CV4 7AL*

**Atom transfer radical polymerisation (ATRP) of methyl methacrylate with a pyridinecarbaldehyde imine copper(I) catalyst and hydroxy functional alkyl bromide initiator leads to α-hydroxy functional PMMA with controlled $M_n$ and PDI < 1.20 without the use of protecting group chemistry.**

Atom transfer radical polymerisation (ATRP) is a rapidly emerging method of obtaining pseudo-living polymerisation of vinyl monomers with controlled $M_n$ and narrow molecular weight distribution (MWD).[1–5]

It has been developed from atom transfer chemistry in organic synthesis, *e.g*. intramolecular cyclisation, and is a development of the Kharash reaction.[6] Complexes of a range of metals have been demonstrated to be useful including $Ru(PPh_3)_3Br_2$,[1] CuBr–bipyridine[2,3] and $Ni[C_6H_3(CH_2NMe_2)_2$-2,6]Br.[7] In a previous communication we have demonstrated that pyridine-2-carbaldehyde imine copper(I) complexes such as **1** are very effective for ATRP of methyl methacrylate (MMA) in conjunction with ethyl 2-bromoisobutyrate.[8] The objective of this work was to replace the initiator, ethyl 2-bromoisobutyrate, with a hydroxy containing alkyl bromide so as to produce α-hydroxy terminally functionalised PMMA without the need to employ protecting group chemistry.

2-Hydroxyethyl 2′-methyl-2′-bromopropionate‡ **3** was prepared as shown in Scheme 1. Atom transfer radical polymerisation of MMA using **3** as initiator in conjunction with **2** and CuBr was carried out at 90 °C in xylene, MMA : **3** = 20 : 1, **2** : CuBr : **3** = 3 : 1 : 1, to give PMMA of structure **4**. Polymerisation was stopped at low conversion, 7.65%, after 70 min, so as to reduce the amount of termination by radical–radical reactions (reaction A; Table 1). $^1$H NMR data (Fig. 1), clearly shows the presence of the hydroxyethyl ester group, originating from **2** and the methoxy α to the bromo group at the propagating end at δ 4.18, 3.82 and 3.74 respectively. The number average molecular mass, $M_n$, can be calculated directly from NMR which gives a value of 2430 which compares excellently with that obtained from size exclusion chromatography against PMMA standards of 2320, PDI = 1.12 (when precipitated into hexanes $M_n$ = 2960, PDI = 1.12). This excellent agreement indicates that the product has structure **4**. This is confirmed by matrix-assisted laser desorption-ionisation time of flight mass spectrometry, Fig. 2. We see one series of peaks in the MALDI-




**Scheme 1** *Reagents and conditions*: i, $Br_2$–P;‡ ii, ethylene glycol;‡ iii, CuBr, MMA;§ iv, benzoyl chloride§

**Table 1**

| Reaction[a] | **3**/ $10^4$ mol | MMA/ mol | *t*/min | Conversion (%)[d] | $M_n$ SEC | PDI SEC |
|---|---|---|---|---|---|---|
| A[b] | 9.61 | 0.187 | 70 | — | 2530 | 1.10 |
| B[c] | 9.72 | 0.047 | 120 | — | 4540[e] | 1.22[e] |
| C[c] | 9.72 | 0.047 | 120 | — | 3130 | 1.22 |
| D[b] | 9.61 | 0.187 | 60 | 0.21 | — | — |
| E[b] | 9.61 | 0.187 | 120 | 2.27 | — | — |
| F[b] | 9.61 | 0.187 | 180 | 15.74 | 4980 | 1.21 |
| G[b] | 9.61 | 0.187 | 240 | 48.20 | 12 330 | 1.26 |
| H[b] | 9.61 | 0.187 | 300 | 59.75 | 15 580 | 1.29 |
| I[b] | 9.61 | 0.187 | 360 | 66.18 | 17 920 | 1.27 |
| J[b] | 9.61 | 0.187 | 420 | 72.11 | 19 500 | 1.27 |
| K[b] | 9.61 | 0.187 | 480 | 75.05 | 20 100 | 1.28 |
| L[b] | 9.61 | 0.187 | 480 | — | 19 427[e] | 1.31[e] |

[a] All reactions carried out with **2** : CuBr : **3** = 3 : 1 : 1. [b] 20 ml MMA in 40 ml xylene, [c] 5 ml MMA in 6 ml xylene. [d] From gravimetry. [e] After precipitation, otherwise as taken from reaction flask.

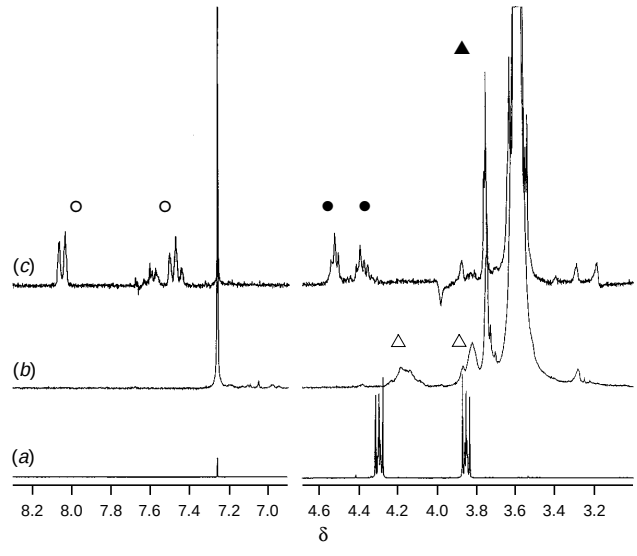



**Fig. 1** Selected region from the $^1$H NMR spectra of (*a*) **3**, (*b*) **4** (△ = $CH_2O$ groups and ▲ = OMe α to Br), (*c*) **5** (● = $CH_2O$ groups, ▲ = OMe α to Br and ○ = aromatic protons from benzoyl group)

TOF MS indicating only one predominant structure, *i.e*. **4**. For example, the peaks at *m/z* 1319.0 and 1419.2 correspond to lithium adducts of **4** where $x$ = 10 and 11 respectively, calculated *m/z* 1318.3 and 1418.4. Control over $M_n$ and PDI is obviously not affected detrimentally by the presence of the primary alcohol group present in the initiator, which might have been expected to complicate the reaction by coordination to the copper catalyst. Indeed the PDI is narrower and the rate of polymerisation faster with **3** than that obtained using a non-functional initiator. Thus ATRP with **1** as catalyst can be utilised to give PMMA of structure **4** as the only detectable product under these conditions. The hydroxy group can be further reacted with benzoyl chloride to give **5** quantitatively.

The terminal benzoyl group of **5** is observed by $^1$H NMR, Fig. 1(*c*), and is detected by SEC with UV detection at 200 nm, **4** shows no absorption at this wavelength. MALDI-TOF MS shows a new series of peaks corresponding to **5**, *e.g*. peaks are

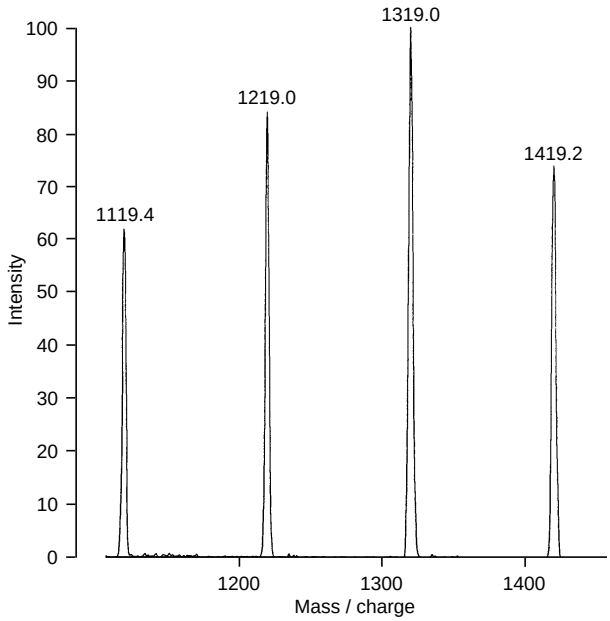



**Fig. 2** Partial MALDI-TOF MS of **3** between $x$ = 8 and 11, peaks correspond to lithium adducts of molecular ions with no observable fragmentation

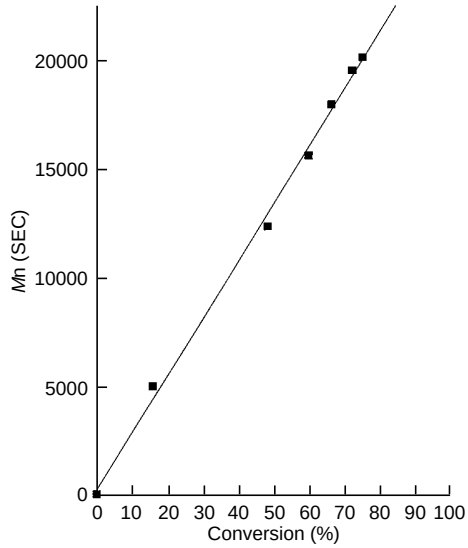



**Fig. 3** Plot showing how $M_n$ from SEC increases with conversion for experiments D–K

now observed at *m/z* 1423.0 and 1522.8 for $x$ = 10 and 11, calculated *m/z* 1422.3 and 1522.4; this reaction is quantitative and no peaks from residual **4** are observed. When the reaction is carried out at a higher MMA : **3** ratio for 120 min a higher molecular weight polymer is produced, *M*n = 4540, PDI = 1.22, as expected (reactions B and C). Again analysis shows terminal hydroxy functionality.

Living or pseudo-living polymerisations have a low rate of termination relative to rate of propagation. This is demonstrated by following a reaction with time (reactions D–K; L is the final product from this reaction). Fig. 3 shows that $M_n$ increases linearly with conversion, up to approx. 80%, whilst PDI remains narrow for reaction with MMA : **3** = 200. In this case the expected $M_n$(theory) at 100% conversion = [100/1 × 100.14 (mass of MMA)] + 220 (mass of end groups) = 20 248. The PDI is broader than would be expected for a true living polymerisation with fast initiation (theoretically 1 + 1/DP). However, PDI does not increase with increasing conversion as would be expected for a reaction with significant termination and this is most probably due to slow initiation relative to propagation.[9]

In summary, atom transfer radical polymerisation with **1** as catalyst and **3** as initiator leads to α-hydroxy functional PMMA. The presence of the hydroxy group during the polymerisation does not reduce the control over the polymerisation, and a narrow PDI polymer with controlled $M_n$ is obtained.

We thank the EPSRC (C. W. GR/K65652, C. B. J. GR/K04606, A. J. S. CASE award) and Courtaulds for funding. We also thank the late Dr Andrew McCamley who proved a source of inspiration and ideas during this work.

## Footnotes

† E-mail: msrgs@csv.warwick.ac.uk

‡ 0.25 g of red phosphorus ($8.06 \times 10^{-3}$ mol) were added to 35.4 ml (0.338 mol) of isobutyryl chloride. The mixture was placed under gentle reflux and 20 ml of bromine (0.388 mol) were added slowly over 8 h. The mixture was refluxed for a further 4 h and the crude reaction mixture added slowly to 350 ml of anhydrous ethylene glycol (6.27 mol). The reaction mixture was refluxed for 4 h, filtered into 500 ml of distilled water and the product extracted into chloroform. After washing with water and sodium hydrogen carbonate and drying over magnesium sulfate the product was isolated as a colourless liquid after the removal of solvent and vacuum distillation at 64.5 °C and 0.1 Torr. $^1$H NMR ($CDCl_3$, 373 K, 250.13 MHz) δ 4.30 (t, *J* 9.6 Hz, 2 H), 3.85 (t, *J* 9.6 Hz, 2 H), 1.94 (s, 6 H): $^{13}$C{$^1$H} NMR ($CDCl_3$, 373 K, 100.6 MHz) δ 171.83, 67.30, 60.70, 55.72, 30.59. IR (NaCl, film) 3436 (br), 2977, 1736 (s), 1464, 1391, 1372, 1278, 1168, 1112, 1080, 1023, 950, 644. EI MS: 213, 211 (mass peaks), 169. 167, 151, 149, 123, 121.

§ *Typical polymerisation procedure*. 0.1376 of copper(I) bromide (98%, 9.6 × 10− 4 mol) were added to 40 ml of xylene and 20 ml of methyl methacrylate (0.187 mol). 0.4272 g of **2** ($2.89 \times 10^{-3}$ mol) were added and the mixture deoxygenated by one freeze-pump-thaw cycle prior to the addition of 0.2029 g of **3** ($9.61 \times 10^{-4}$ mol) at room temperature. The deep red solution was heated at 90 °C for 70 min. The final product was isolated by precipitation into hexanes.

## References

1 M. Kato, M. Kamigaito, M. Sawamoto, and T. Higashimura, *Macromolecules*, 1995, **28**, 1721.
2 K. Matyjaszewski and J.-S. Wang, *Macromolecules*, 1995, **28**, 7901.
3 K. Matyjaszewski, *2nd IUPAC Symp. Free Radical Polym. Kinetics and Mechanism, Preprints*, 1996, 22.
4 V. Perced, B. Barboui, A. Neumann, J. C. Ronda and M. Zhao, *Macromolecules*, 1996, **29**, 3665.
5 V. Percec and B. Barboui, *Macromolecules*, 1995, **28**, 7970.
6 D. Bellus, *Pure Appl. Chem*., 1985, 1827.
7 C. Granel, P. Dubois, R. Jerone, P. Teyssie, *Macromolecules*, 1996, **29**, 8576.
8 D. M. Haddleton, C. B. Jasieczek, M. J. Hannon and A. J. Shooter, *Macromolecules*, in the press.
9 K. Matyjaszewski, *J. Phys. Org. Chem*., 1995, **197**, 8.

*Received, 29th January 1997; Com. 7/00677B*

# $^{13}$C MAS NMR observation of photoproducts in zeolites and their further reaction on acid sites

**Jinhua Zhang, Thomas R. Krawietz, Timothy W. Skloss and James F. Haw***

*Laboratory for Magnetic Resonance and Molecular Science, Department of Chemistry, Texas A&M University, College Station, Texas 77843, USA*

***In situ* $^{13}$C MAS NMR characterization following UV irradiation of two FAU zeolites with adsorbed benzaldehyde or acetophenone and toluene allows observation of photoproducts and subsequent acid-catalysed chemistry.**

Photochemistry of organic compounds included in zeolites and other constrained media is of continuing interest. Many previous investigations have focused on the influence of framework topology and the charge compensating cation of the zeolite on the resulting photoproduct yield and distribution.[1–9] The zeolite is typically selected so as to be otherwise unreactive toward the reactants or photoproducts. Procedures used in diverse, published reports naturally vary; however, in many of the previous studies, the zeolite was irradiated in a slurry of excess reactant, and the products identified *ex situ* following liberation by extraction or destruction of the framework. Here we report $^{13}$C MAS NMR characterization of the photoproducts of benzaldehyde or acetophenone with toluene in two FAU type zeolites, with topologies dominated by 13 Å supercages interconnected through 7.4 Å pore openings.

[α-$^{13}$C]Benzaldehyde and [α,β-$^{13}C_2$]acetophenone were obtained from Isotec, [α-$^{13}$C]toluene from Cambridge Isotope Labs and spectrophotometric grade toluene from Spectrum Chemicals. The zeolite catalysts, USY (ultrastable-Y in the acid form, UOP, Si/Al = 5.5) and NaY (Strem, Si/Al = 2.6), were loaded inside a quartz reaction tube (18 mm diameter, 250 mm length, with an axial valve on one end) and were activated using a previously described procedure.[10] The carbonyl-containing reagent was adsorbed at a loading of one molecule per zeolite supercage. The catalyst was then exposed to an excess of toluene vapour for 30 min to achieve saturation coverage (*ca*. 4 molecules per supercage). The sample container was then sealed, dismounted from the vacuum line, and set up for UV irradiation.

Ultraviolet light from a 500 W mercury vapour arc lamp system (Oriel, Stratford, CT) was filtered by a dichroic mirror to attenuate wavelengths longer than 400 nm then passed through a safety shutter and into a liquid filter (0.85 M aqueous $CoSO_4$). Estimated filtered UV light intensity calculated from the Oriel optical handbook was 37 mW nm$^{-1}$ near the peak at 254 nm, with a total intensity of 250 mW between 245 and 265 nm. The axis of the quartz reaction tube was placed normal to the path of filtered UV light and positioned with the sample in the centre of the beam. During UV exposure, the sample was rotated with one end angled down, at one revolution per second. No significant thermal heating was observed. Published NMR studies of benzaldehyde,[11] other ketones[12] and aldehydes[13] on zeolites suggest little or no thermal reactivity at 298 K for the species studied here.

Fig. 1 reports the $^{13}$C MAS NMR spectra of [α-$^{13}$C]benzaldehyde and [α-$^{13}$C]toluene on zeolites NaY and USY after UV irradiation. On zeolite NaY, chemical shifts of δ 77 and 43 indicate that the major photoproduct is the asymmetric coupling product 1,2-diphenylethanol **1** which forms from hydrogen abstraction between benzaldehyde and toluene.[14] Compound **1** is not stable in an acidic environment, and on zeolite USY undergoes a Friedel–Crafts reaction with a second toluene molecule, forming the isomeric triphenylethanes **2** and **3**, with resonances at δ 54 and 41, respectively.

Representative $^{13}$C MAS NMR spectra of [α,β-$^{13}C_2$]acetophenone and natural abundance toluene on zeolites NaY and USY are shown in Fig. 2. In analogy to the benzaldehyde reaction, the major photoproduct of acetophenone and toluene on NaY was 1,2-diphenylpropan-2-ol **4** (δ 75). In the acidic zeolite, however, further reaction led not to Friedel–Crafts products analogous to **2** and **3**, but rather 1,2-diphenylpropane **5**, and other products by the reaction of a (formal) benzyl cation

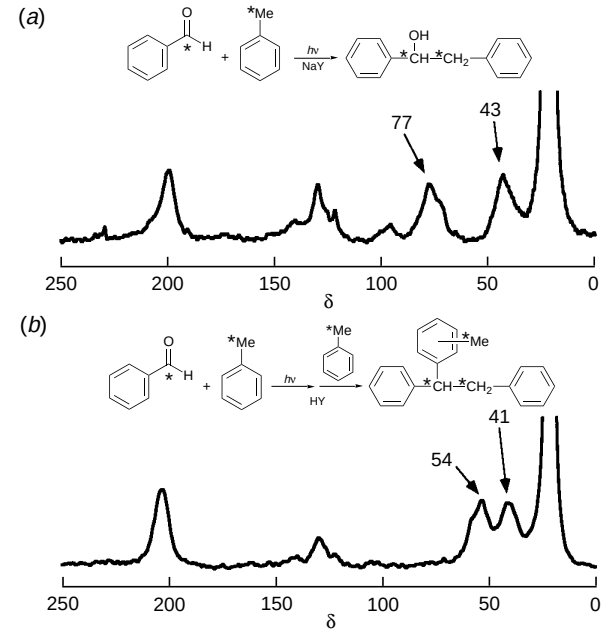
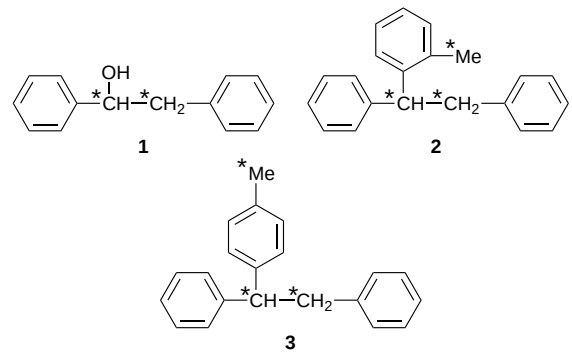



**Fig. 1** 50.1 MHz $^{13}$C CPMAS NMR spectra of the products of [α-$^{13}$C]benzaldehyde and [α-$^{13}$C]toluene on FAU zeolites measured at 298 K following 4 h of UV irradiation (also at 298 K). (*a*) Spectrum of product on zeolite NaY acquired with 5000 transients at a spinning speed of 5000 Hz. (*b*) Spectrum of products on zeolite USY acquired with 4000 transients at a spinning speed for 5000 Hz. (★ Denotes $^{13}$C labelled atoms.)



with toluene. The latter included triphenylmethane as established by other experiments with labeled toluene.

For the cases studied here, the photoproducts observed in the zeolite by NMR were identical to those found *ex situ* in previous studies, but this need not be the case in future work where acid digestion of the zeolite might cause degradation of the photoproducts. Additionally, by matching the acid zeolites with non-acidic controls, we were able to characterize the combination of photochemistry and thermally-activated processes on acid sites. The possibility exists for using photochemistry to synthesize otherwise sterically-excluded adsorbates specifically for the study of carbenium ions or other intermediates[15] formed in a second thermal step.[16] Application of *in situ* NMR methodology to the emerging area of photocatalysis[17,18] should expand research of highly reactive photoproducts.

We acknowledge the National Science Foundation (Grant No. CHE-9528959) for financial support of this work.

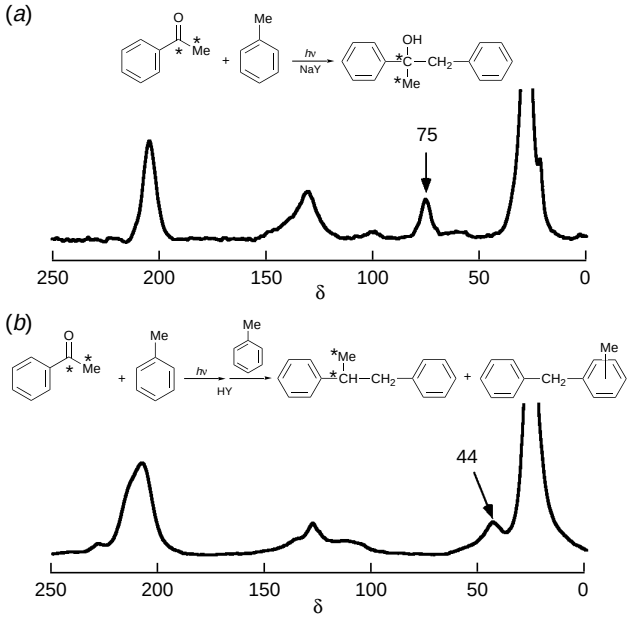



**Fig. 2** 50.1 MHz $^{13}C$ CP MAS NMR spectra of [α,β-$^{13}C_2$]acetophenone and natural abundance toluene on FAU zeolites measured at 298 K after 4 h of UV irradiation (also at 298 K). (*a*) Spectrum of product on zeolite NaY acquired with 1200 transients at a spinning speed of 3600 Hz. (*b*) Spectrum of product on zeolite USY acquired with 1200 transients at a spinning speed of 4500 Hz. The resonance at δ 44 did not survive 50 μs of dipolar dephasing (not shown) supporting the assignment indicated. (★ Denotes $^{13}C$ labeled atoms.)

**4** **5**

## Footnote

* E-mail: haw@chemvx.tamu.edu

## References

1 V. Ramamurthy, *Photochemistry in Organized and Constrained Media*, VCH, New York, 1991.
2 N. J. Turro, A. L. Buchachenko and V. F. Tarasov, *Acc. Chem. Res*., 1995, **28**, 69.
3 V. Ramamurthy, D. F. Eaton and J. V. Caspar, *Acc. Chem. Res*., 1992, **25**, 299.
4 R. G. Weiss, V. Ramamurthy and G. S. Hammond, *Acc. Chem. Res*., 1993, **26**, 530.
5 N. J. Turro, N. Han, X.-G. Lei, J. R. Fehlner and L. Abrahms, *J. Am. Chem. Soc*., 1995, **117**, 4881.
6 V. Ramamurthy, *J. Am. Chem. Soc*., 1994, **116**, 1345.
7 N. J. Turro, C.-C. Cheng, X.-G. Lei and E. M. Flanigen, *J. Am. Chem. Soc*., 1985, **107**, 3739.
8 F. L. Cozens, H. Garcia and J. C. Scaiano, *J. Am. Chem. Soc*., 1993, **115**, 11 134.
9 V. Ramamurthy, D. R. Corbin, C. V. Kumar and N. J. Turro, *Tetrahedron Lett*., 1990, **31**, 47.
10 J. F. Haw, B. R. Richardson, I. S. Oshiro, N. L. Lazo and J. A. Speed, *J. Am. Chem. Soc*., 1989, **111**, 2052.
11 T. Xu, J. Zhang and J. F. Haw, *J. Am. Chem. Soc*., 1995, **117**, 3171.
12 T. Xu, E. J. Munson and J. F. Haw, *J. Am. Chem. Soc*., 1994, **116**, 1962.
13 E. J. Munson and J. F. Haw, *Angew. Chem., Int. Ed. Engl*., 1993, **32**, 615.
14 X. Lei and N. J. Turro, *J. Photochem. Photobiol. A: Chem*., 1992, **69**, 53.
15 J. F. Haw, J. B. Nicholas, T. Xu, L. W. Beck and D. B. Ferguson, *Acc. Chem. Res*., 1996, **29**, 259.
16 T. Xu and J. F. Haw, *J. Am. Chem. Soc*., 1994, **116**, 10 188.
17 A. L. Linsebigler, G. Lu and J. T. Yates, *Chem. Rev*., 1995, **95**, 735.
18 M. A. Fox and M. T. Dulay, *Chem. Rev*., 1993, **93**, 341.

*Received in Corvallis, OR, USA, 20th December 1996; Com. 6/08523G*

# $^7$Li NMR studies on a lithiated non-graphitizable carbon fibre at low temperatures

**K. Tatsumi,*[a] J. Conard,[b] M. Nakahara,[c] S. Menu,[b] P. Lauginie,[b] Y. Sawada[a] and Z. Ogumi[d]**

[a] *Osaka National Research Institute, 1-8-31 Midorigaoka, Ideka, Osaka 563, Japan*
[b] *CRMD-CNRS, 1b, rue de la Férollerie, 45071 Orléans Cedex 2, France*
[c] *Institute for Chemical Research, Kyoto University, Gokasyo, Uji, Kyoto 611, Japan*
[d] *Graduate School of Engineering, Kyoto University, Sakyo-ku, Kyoto 606-01, Japan*

**$^7$Li NMR spectra of a lithiated non-graphitizable carbon fibre measured at temperatures below 200 K display three different signals and the NMR shift of one of the signals is larger than that of Li metal below 163 K.**

Much attention has been focused on carbonaceous materials, *e.g.* graphite, petroleum cokes and carbon fibres, as a host for the $Li^+$ ion, because carbon is one of the most promising anodes for secondary lithium batteries.[1,2] Both electrode potential and capacity of carbon anodes in organic electrolytes are dependent on the nature of the carbon used. Artificial carbon materials are classified into graphitizable (soft) and non-graphitizable (hard) carbons according to the degree of crystallinity by heat treatment.[3] In graphitizable carbons, graphite and carbons having the graphite-like stacking sequence of graphene layers to some extent give the lowest electrode potential (0–0.3 V *vs.* $Li/Li^+$) during electrochemical insertion of $Li^+$ ion.[4–7] The electrochemical capacity of graphite is limited to one lithium atom per six carbon atoms, *i.e.* $LiC_6$.[2,4]

On the other hand, non-graphitizable carbons heat-treated between 1000 and 1300 °C give a capacity higher than $LiC_6$. In addition, the carbons have a significant capacity in the potential range between 0 and 0.1 V, though the carbons have little amount of crystallites of the graphite-like stacking sequence.[8–10] Therefore, non-graphitizable carbons have been thought to have lithium storage sites different from the sites of lithium insertion into graphitizable carbons. $^7$Li NMR methods have been used for analyses of Li in carbon materials.[5,8,11–13] Yamazaki *et al.* reported that lithium species in a non-graphitizable carbon, which showed a band at δ 90 in $^7$Li NMR measurements at room temperature, consist of two species of lithium (δ *ca.* 190 and 20 at 140 K).[13] In the previous work,[8] it was shown that non-graphitizable carbon fibres also give capacity higher than $LiC_6$ with a significant capacity below 0.1 V. Here, we report the first $^7$Li NMR data indicating three different lithium species in a non-graphitizable carbon fibre. Furthermore one of the lithium species gave a NMR shift larger than that of Li metal at temperatures below 163 K.

The non-graphitizable carbon fibre (FIP Petoca, nominal diameter 10 μm) prepared from an isotropic petroleum pitch was heat-treated at 1200 °C under a nitrogen atmosphere. The reversible capacity of the carbon fibre between 0 and 2.5 V was $x = 1.25$ for $Li_xC_6$ with a significant capacity, $x = 0.73$, between 0 and 0.1 V. The carbon fibre electrode was dried at 130 °C under vacuum for 24 h and then electrochemically reduced to 0 V in 1 mol $dm^{-3}$ solution of $LiClO_4$† in ethylene carbonate (EC)–diethylcarbonate (DEC) (1 : 1, v/v) according to the procedure previously reported.[8] The carbon fibre fully lithiated to 0 V was washed with DEC and dried under vacuum for 15 min and then put into a NMR sample tube; the sample tube was sealed by an epoxy resin. All procedures for sample preparation were performed in an Ar-filled dry box. The sample was served for $^7$Li NMR measurements using a wide line probe of a NMR spectrometer (CMX-200H Chemagnetics). NMR shift was measured in ppm against LiCl (δ 0) used as an external standard.

The fully lithiated carbon fibre (reversible capacity $Li_{1.25}C_6$) showed a signal at δ 111 in the $^7$Li NMR spectrum at 298 K [Fig. 1(*a*)]. The lithium species at δ 111 is quite different from those in graphitizable carbons, which give a peak between δ 7 and 45.[5,11] The shift of the signal at δ 111 (298 K) was independent of temperature from 298 to 243 K, whereas the shift increased with a temperature drop from 243 to 123 K. A new band appeared at δ 18 at temperatures lower than 243 K. The intensity markedly increased with lowering temperature. In addition, the spectra below 163 K showed a very broad signal at δ *ca.* 270.

The spectra below 203 K can be simulated by three Lorentzian peaks. The deconvoluted components for the spectrum at 143 K consisted of three signals at δ 18, 192 and 281 (Fig. 2). As seen in Fig. 1, the spectra showed high reversibility between cooling and heating; no spectral hysteresis was detected during a cyclic change of temperature. Moreover, all the signals were deconvoluted to Lorentzian line shapes. Since NMR peaks fitting to Lorentzian lines are observed for liquid- or gas-phase species, the present results suggest that

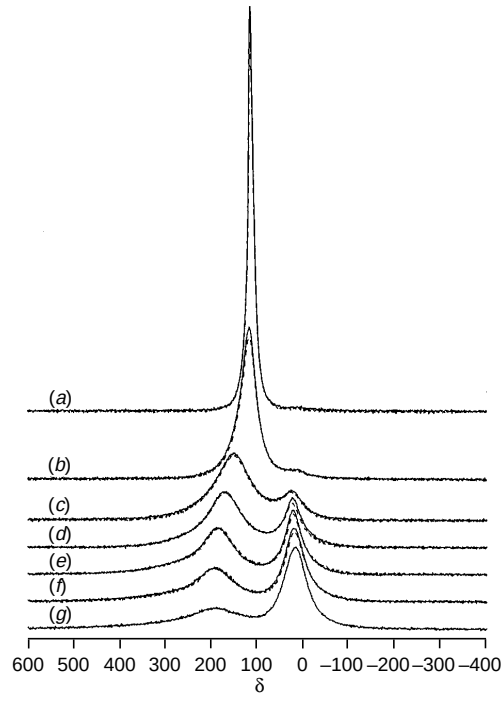



**Fig. 1** $^7$Li NMR (77.8375 MHz, relative to LiCl, δ 0) spectra for the fully lithiated carbon fibre recorded at (*a*) 298, (*b*) 243, (*c*) 203, (*d*) 183, (*e*) 163, (*f*) 143 and (*g*) 123 K; solid line, at the direction of cooling; dashed line, heating

lithium atoms in the carbon fibre are diffusive. These results thus indicate that the variation observed in the spectra is likely ascribed not to a crystalline phase transformation but to exchange of lithium nuclei among lithium atoms at different sites, and that the rate of exchange is slowed down on the timescale of NMR observation at low temperature, in agreement with the observed line broadening. The $^7$Li NMR spectra at low temperature indicate that the fully lithiated non-graphitizable carbon fibre contains three different lithium species.

$^7$Li NMR shift of the signals determined by the curve fitting simulations is plotted as a function of temperature in Fig. 3. In general, $^7$Li NMR shift for a lithium species in graphene layers is independent of temperature[11] as well as lithium metal,[14] and the shift for lithium in the fully lithiated graphitizable carbon heat-treated at 1000 °C was δ 18.[5] Although the peak position

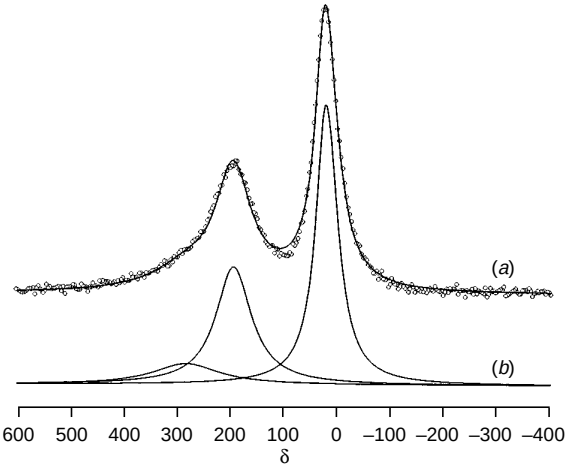



**Fig. 2** $^7$Li NMR spectra of the fully lithiated carbon fibre at 143 K: (*a*) experimental (○) and simulated (solid line) spectra; (*b*) deconvoluted spectra

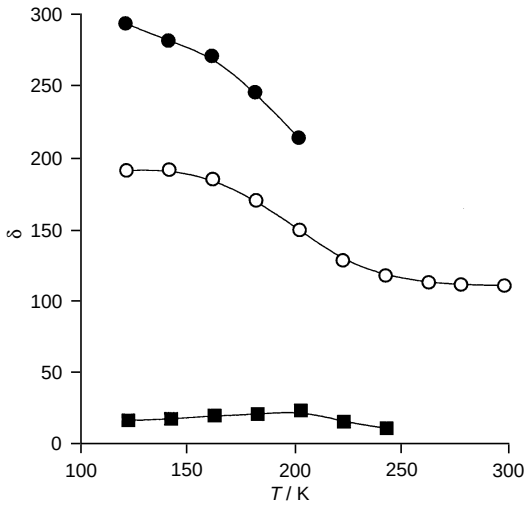



**Fig. 3** $^7$Li NMR shift of the signals determined by the curve fitting simulations as a function of temperature: the signals in the highest (●), the middle (○) and the lowest (■) fields in Fig. 2

in the lowest field in Fig. 2 showed considerable temperature dependence, the signal at δ 18 is inferred to be ascribed to the lithium species in crystalline graphene layers in the carbon fibre. On the other hand, the other signals are quite novel because NMR shift of the two signals increased with lowering temperature below 243 K. Furthermore, the shift of the signal in the highest field is higher than that of lithium metal (δ 262)[14] at low temperatures below 163 K. Although the structure of the lithium species of each peak is not clear at present, high shifts of the signals are explained as a Knight shift and correspond to lithium species with metallic character. Non-graphitizable carbons are considered to have microcavities between the crystalline grains.[3] Therefore, lithium species corresponding to the signals in the middle and the highest fields are inferred to be ascribed to lithium clusters formed in the microcavities of the non-graphitizable carbon fibre. The existence of the lithium species with metallic character is consistent with the result that the carbon fibre showed a significant capacity near 0 V. These features of the non-graphitizable carbon fibre are attractive as an anode material for advanced lithium-ion batteries.

The authors are grateful to Drs Toshifumi Kawamura and Tomiji Hosotubo, Petoca Co. Ltd., for preparing the non-graphitizable carbon fibre.

## Footnotes

* E-mail: tatsumi@onri.go.jp

† Although there have been no reports informing explosion of $LiClO_4$–EC–DEC electrolytes, a cell using $LiClO_4$ electrolyte should not be shocked and overdischarged to voltages lower than 0 V at high current density in order to prevent the risk of explosion (see, *e.g.* G. H. Newman, R. W. Francis, L. H. Gaines and B. M. L. Rao, *J. Electrochem. Soc.*, 1980, **127**, 2025).

## References

1 J. R. Dahn, A. K. Sligh, Hang Shi, B. M. Way, W. J. Weydanz, J. N Reimers, Q. Zhong and U. von Sacken, in *Lithium Batteries: New Materials, Developments and Perspectives*, ed. G. Pistoia, Elsevier, Amsterdam, 1994, p. 1.
2 D. Billaud, A. Naji and P. Willmann, *J. Chem. Soc., Chem. Commun.*, 1995, 1867.
3 R. E. Franklin, *Proc. R. Soc., London, Ser. A*, 1951, **209**, 196.
4 T. Ohzuku, Y. Iwakoshi and K. Sawai, *J. Electrochem. Soc.*, 1993, **140**, 2490.
5 K. Tatsumi, T. Akai, T. Imamura, K. Zaghib, N. Iwashita, S. Higuchi and Y. Sawada, *J. Electrochem. Soc.*, 1996, **143**, 1923.
6 J. R. Dahn, A. K. Sleigh, H. Shi, J. N. Reimers, Q. Zhong and B. M. Way, *Electrochim. Acta*, 1993, **38**, 1179.
7 M. Inaba, H. Yoshida, Z. Ogumi, T. Abe, Y. Mizutani and M. Asano, *J. Electrochem. Soc.*, 1995, **142**, 20.
8 K. Tatsumi, T. Kawamura, T. Hosotubo and Y. Sawada, *J. Power Sources*, in the press.
9 J. S. Xue and J. R. Dahn, *J. Electrochem. Soc.*, 1995, **142**, 3668.
10 Y. Liu, J. S. Xue, T. Zheng and J. R. Dahn, *Carbon*, 1996, **34**, 193.
11 J. Conard and H. Estrade, *Mater. Sci. Eng.*, 1977, **31**, 173.
12 K. Sato, M. Noguchi, A. Demachi, N. Oki and M. Endo, *Science*, 1994, **264**, 556.
13 S. Yamazaki, T. Hashimoto, T. Iriyama, Y. Mori, H. Siroki and N. Tamura, *Proc. Soc. Solid-State NMR Mater.*, 1996, **20**, 39.
14 G. C. Carter, L. H. Bennett and D. J. Kahan, in *Metallic Shifts in NMR, Part I*, Pergamon Oxford, 1977, p. 239.

*Received in Cambridge, UK on 9th January 1997; Com. 7/00221A*

# Diboration of alkenes with bis(pinacolato)diboron catalysed by a platinum(0) complex†

**Tatsuo Ishiyama, Masafumi Yamamoto and Norio Miyaura***

*Division of Molecular Chemistry, Faculty of Engineering, Hokkaido University, Sapporo 060, Japan*

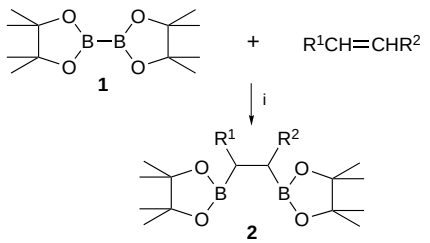
**Bis(pinacolato)diboron selectively adds to terminal alkenes and cyclic alkenes having internal strain to provide bis(boryl)alkanes in 76–86% yields in the presence of a catalytic amount of $Pt(dba)_2$ at 50 °C.**

Increasing attention has been recently focused on the transition-metal-catalysed addition reactions of boron–heteroatom reagents, such as thioboranes,[1] stannylboranes,[2] or silylboranes[3] to alkenes or alkynes, as a direct procedure for preparing organoboron compounds from unsaturated hydrocarbons. We have recently reported the platinum(0)-catalysed addition of bis(pinacolato)diboron **1** to alkynes[4,5] and the conjugated addition to alka-1,3-dienes.[6] The proposed mechanism *via* the oxidative addition of **1** to the platinum(0) complex followed by insertion of an unsaturated C–C bond into the B–Pt–B complex was fully substantiated by Marder and coworkers[7] and Iverson and Smith.[8] However, the extension of this protocol to alkenes has been somewhat troublesome. Phosphine-based platinum(0) catalysts failed because the insertion of an alkene into the B–Pt bond is too slow to develop the catalytic cycle, and rhodium(I) catalysts suffered from side-reactions resulting from β-hydride elimination.[9] In 1995, Baker *et al*. first demonstrated a practical method for the diboration of styrene derivatives with a phosphine–gold(I) catalyst.[9] However, the previous observation,[6] that $Pt(dba)_2$ (dba = dibenzylideneacetone) exhibits much higher catalytic activity than $Pt(PPh_3)_4$ in diboration of 1,3-dienes, prompted us to investigate the platinum(0)-catalysed diboration of alkenes (Scheme 1). The platinum(0) complex $Pt(dba)_2$ is found to be an excellent catalyst allowing alkene insertion into the B–Pt bond under mild conditions.

The diboration of aliphatic and aromatic terminal alkenes, and some cyclic alkenes having internal strain was readily achieved with $Pt(dba)_2$ (Table 1).‡ When dec-1-ene (1.5 equiv.) was allowed to react with **1** (1.0 equiv.) in toluene at 50 °C in the presence of 3 mol% $Pt(dba)_2$, the addition proceeded to completion within 1 h to afford the desired 1,2-bis(boryl)decane **2a** in 82% yield together with two unidentified products (4 : 1 ratio, *ca*. 15%), presumably arising from the β-hydride elimination reported in the rhodium(I)-catalysed diboration of styrene.[9] Among the platinum catalysts we examined, $Pt(dba)_2$ was the most efficient; combination with other ligands such as $PPh_3$, $AsPh_3$ or $P(C_6H_{11})_3$ showed no advantages over $Pt(dba)_2$ itself.

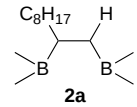
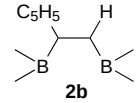
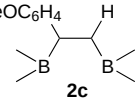
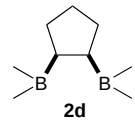
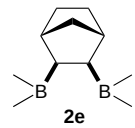
Styrene and 4-methoxystyrene provided **2b** and **2c** with accompanying by products (*ca*. 10%). The addition to 4-methoxystyrene was apparently slower than to styrene itself, the order of which is consistent with the relative reactivity observed on the insertion of arylacetylenes to the B–Pt–B complex.[8]

Cyclopentene (1.5 equiv.) and norbornene (3.0 equiv.) underwent a clean reaction with no byproducts. The *cis*-addition of **1** was established from the $^1H$ NMR spectrum of **2d** and its oxidation to *cis*-cyclopentane-1,2-diol. However, additions to other internal alkenes were slow, as anticipated from the order of alkene reactivity in transition-metal-catalysed reactions. Cyclooctene gave 1,2-bis(boryl)cyclooctane in low yield, but all attempts in the diboration of oct-4-ene, stilbene, cyclohexene or 2-methylpropene were unsuccessful.

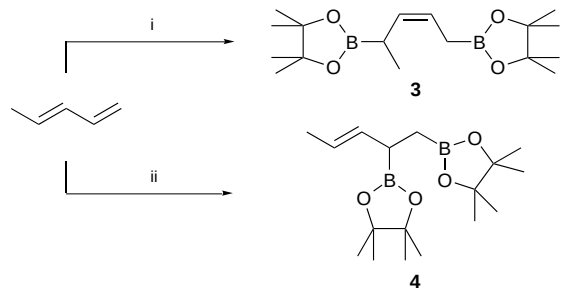



**Scheme 1** *Reagents and conditions*; i, $Pd(dba)_2$, toluene, 50 °C, 1 h

**Table 1** $Pt(dba)_2$-catalysed diboration of alkenes[a]

| Alkene | Product | Yield (%)[b] |
|---|---|---|
| Dec-1-ene |  **2a** | 82 |
| Styrene |  **2b** | 86 |
| 4-Methoxystyrene |  **2c** | 76[c] |
| Cyclopentene |  **2d** | 85 |
| Norbornene |  **2e** | 85[c] |

[a] All reactions were carried out at 50 °C for 1 h with $Pt(dba)_2$ (3 mol%), **1** (1.0 equiv.), alkene (1.5 equiv.), and toluene (6 ml), unless otherwise noted. [b] Isolated yields based on **1**. [c] 3.0 equiv. of alkene was used.




**Scheme 2** *Reagents and conditions*: i, **1**, $Pt(PPh_3)_4$, toluene, 80 °C, 84%; ii, **1**, $Pt(dba)_2$, toluene, room temp., 92%

It is interesting that $Pt(dba)_2$ directed 1,2-addition to certain conjugated dienes, whereas 1,4-addition through a π-allylplatinum(II) intermediate is an energetically more favourable process. The 1,4-addition to penta-1,3-diene at 80 °C with $Pt(PPh_3)_4$ to give **3** was consistent with our previous report,[6] but the same reaction with $Pt(dba)_2$ selectively produced the 1,2-addition product **4** at room temperature (Scheme 2).

Further studies are in progress to elucidate the mechanism and possible synthetic applications.

## Footnotes

* E-mail: miyaura@organ.hokudai.ac.jp

† Preliminary results were discussed at the 43rd Symposium on Organometallic Chemistry, Japan, October 31, 1996.

‡ *A representative procedure* for **2**: a flask was charged with $Pt(dba)_2$ (0.03 mmol) and **1** (1.0 mmol), and flushed with nitrogen. Toluene (6 ml) and dec-1-ene (1.5 mmol) were successively added, and the resulting solution was stirred at 50 °C for 1 h. Concentration and Kugelrohr distillation at 135 °C (0.1 mmHg) gave **2a**: $^1$H NMR (400 MHz, $CDCl_3$), δ 0.79 (dd, 1 H, *J* 6.0, 15.6 Hz), 0.87 (t, 3 H, *J* 6.8 Hz), 0.87 (dd, 1 H, *J* 9.5, 15.6 Hz), 1.0–1.5 (m, 15 H), 1.22 (s, 12 H), 1.23 (s, 12 H); $^{13}$C NMR (100 MHz, $CDCl_3$), δ 14.10, 22.69, 24.73, 24.77, 24.83, 24.90, 28.86, 29.28, 29.56, 29.86, 31.91, 33.83, 82.71, 82.78; $^{11}$B NMR (128 MHz, $CDCl_3$), δ 34.14.

## References

1 T. Ishiyama, K.-i. Nishijima, N. Miyaura and A. Suzuki, *J. Am. Chem. Soc*., 1993, **115**, 7219.
2 S.-Y. Onozawa, Y. Hatanaka, T. Sakakura, S. Shimada and M. Tanaka, *Organometallics*, 1996, **15**, 5450.
3 M. Suginome, H. Nakamura and Y. Ito, *Chem. Commun*., 1996, 2777.
4 T. Ishiyama, N. Matsuda, N. Miyaura and A. Suzuki, *J. Am. Chem. Soc*., 1993, **115**, 11 018.
5 T. Ishiyama, N. Matsuda, M. Murata, F. Ozawa, A. Suzuki and N. Miyaura, *Organometallics*, 1996, **15**, 713.
6 T. Ishiyama, M. Yamamoto and N. Miyaura, *Chem. Commun*., 1996, 2073.
7 G. Lesley, P. Nguyen, N. J. Taylor, T. B. Marder, A. J. Scott, W. Clegg and N. C. Norman, *Organometallics*, 1996, **15**, 5137.
8 C. N. Iverson and M. R. Smith III, *Organometallics*, 1996, **15**, 5155.
9 R. T. Baker, P. Nguyen, T. B. Marder and S. A. Westcott, *Angew. Chem., Int. Ed. Engl*., 1995, **34**, 1336.

*Received in Cambridge, UK, 6th February 1996; Com. 7/00878C*

# Synthetic studies towards peptidyl nucleoside antibiotics: first synthesis of a polyoxamic acid derivative enabling direct coupling with α-amino acid esters

**Claudio Palomo,* Mikel Oiarbide and Aitor Esnal**

*Departamento de Química Orgánica, Facultad de Química, Universidad del País Vasco, Apdo. 1072, 20080 San Sebastián, Spain*

**The reaction of the Mukaiyama's aldehyde-derived *N*-benzyl imine with an hydroxyketene equivalent followed by exposure of the resulting α-hydroxy β-lactam to NaOCl and 2,2,6,6-tetramethylpiperidinyl-1-oxyl (TEMPO) provides a novel α-amino acid *N*-carboxy anhydride formally derived from polyoxamic acid.**

The polyoxin **1** family of nucleoside antibiotics, Fig. 1, has as a common structural feature a dipeptide comprised of an unusual hydroxylated α-amino acid, commonly named polyoxamic acid **2**, linked to one of the related nucleoside α-amino acids.[1] As a consequence of the potent antifungal activity associated with this type of peptidyl nucleosides[1,2] many methods for the preparation of **2** have been proposed over the last few years.[3] However, most of them involve a large number of steps and, therefore, a practical short route to this amino acid still remains of interest. On the other hand, and most important, all of these methods deal with the synthesis of the amino acid in its free form rather than with the generation of a simultaneously amino-protected and carboxy-activated species ready for a subsequent acylation reaction. Consequently, it would be more desirable and also a conceptually new approach to peptidyl nucleoside antibiotics if the synthesis of the polyoxamic moiety could be combined with a peptide coupling step.[4] Here we disclose our initial results on the first synthesis of polyoxamic acid that fulfils all of these requirements.

As Scheme 1 illustrates, the approach takes advantage of the facile construction of an α-hydroxy β-lactam *via* standard [2 + 2] cycloaddition of hydroxyketene equivalents with imines,[5] followed by its quantitative conversion into an α-amino acid *N*-carboxy anhydride (NCA) according to our recently reported method.[6] For the first step of the synthesis we elected to use the imine **3** derived from Mukaiyama's aldehyde, already incorporating the trihydroxylated subunit of the desired amino acid and, at the same time, providing chirality to the corresponding NCA precursor.† Thus, the cycloaddition reaction of acetoxyketene, generated from acetoxyacetyl chloride and triethylamine, with the imine **3** and subsequent saponification of the acetoxy group of the resulting crude product furnished the crystalline α-hydroxy β-lactam **4** [mp 98–102 °C, $[\alpha]_D^{25}$ −12.9 ($CH_2Cl_2$, *c* 1.0)] in 90% yield over the two steps. Likewise, the reaction of benzyloxyketene, generated from benzyloxyacetyl chloride and triethylamine, with the imine **3** gave **5** [mp 74–76 °C, $[\alpha]_D^{25}$ +1.6 ($CH_2Cl_2$, *c* 1.0)] in 85% yield. In each case a single diastereoisomer was produced as judged by $^1$H NMR analysis of the crude reaction products. The relative *cis*-disposition of the substituents at the $C_3$ and the $C_4$ positions of the β-lactam ring was determined by the value of the proton NMR coupling constant ($J_{3,4}$ = 5 Hz) and the absolute configuration of both β-lactams **4** and **5** was primarily established by the assumption of an uniform stereochemical outcome with regard to that observed in closely related reactions.[7,8] Further, chemical correlation of both **4** and **5** with the known 4-formyl derivative **6**[8] confirmed the assignment.

To complete the synthesis of the polyoxamic acid skeleton the 3-hydroxy β-lactam **4** was converted into the NCA **7** by using a solution of commercial bleach and a catalytic amount of 2,2,6,6-tetramethylpiperidinyl-1-oxyl (TEMPO). The transformation occurred almost instantaneously (1–2 min)‡ *via* an intermediate α-keto β-lactam which underwent chemoselective Baeyer–Villiger rearrangement to produce **7** in almost quantitative yield in a single pot operation. That is, from the readily available imine **3** a simultaneously amino-protected and carboxy-activated form of polyoxamic acid is obtained in 90% overall yield. From this approach two key elements are especially noteworthy. First, the creation of the α-amino stereogenic centre of the polyoxamic acid with virtually complete diastereoselectivity as compared with the reported procedures employing Mukaiyama's aldehyde as the starting

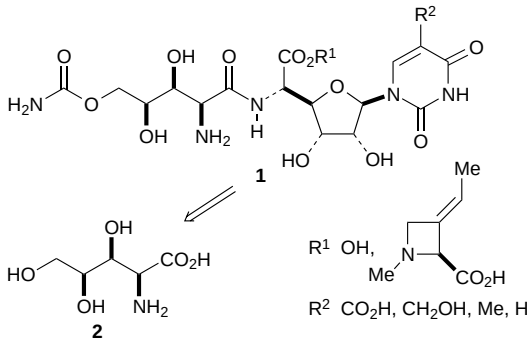
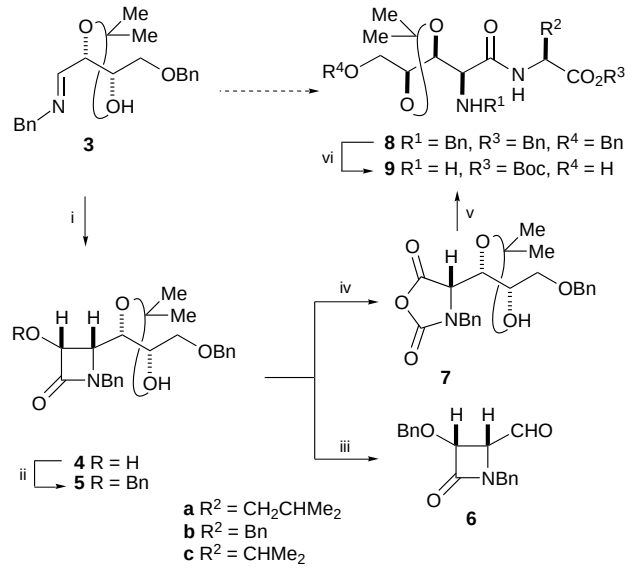



**Fig. 1**




**Scheme 1** *Reagents and conditions*: i, $AcOCH_2COCl$, $Et_3N$, $CH_2Cl_2$, 0 °C → room temp., 16 h then LiOH (6 equiv.), $H_2O_2$ (18 equiv.), THF–$H_2O$, 0 °C, 3 h, 90% or $BnOCH_2COCl$, $Et_3N$, $CH_2Cl_2$, 0 °C → room temp., 16 h, 85%; ii, BnBr, NaH, DMF, −20 °C; iii, **5** with $HO_4Cl$, wet THF, room temp., 2–4 h, then $NaIO_4$, $H_2O$–$Me_2CO$, 0 °C, 2 h; iv, **4** with NaOCl, $CH_2Cl_2$, TEMPO (cat.), $NaHCO_3$, KBr, $KH_2PO_4$–$K_2HPO_4$ (pH 7.0), 0 °C, 1 min; v, (*S*)-$H_2NCH(R^2)CO_2Bn$, $CH_2Cl_2$, room temp., 24 h; vi, $H_2$, Pd–C (10% w/w), $(Boc)_2O$, EtOH, room temp., 24 h

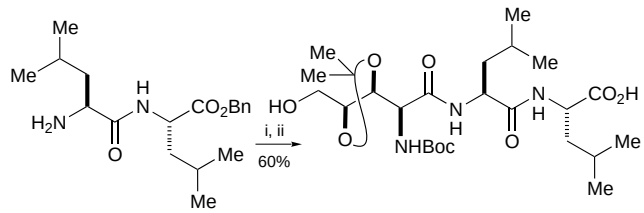
material[3c–g] and, second, the generation, for the first time, of the polyoxamic acid **2** as an active species allowing further coupling reactions. On pursuing this latter aspect, however, the coupling of **7** with an α-amino acid ester was essentially a question of whether epimerization at the α-centre of the NCA **7** could take place; if not, the approach would open up a new and short route to peptidyl nucleoside antibiotics. We were gratified to observe that the reaction of freshly prepared **7** with (*S*)-leucine benzyl ester in dichloromethane as solvent at room temperature for 24 h proceeded with no appreciable epimerization§ to give the desired peptide **8** in 85% yield. The reaction of **7** with both (*S*)-phenylalanine and (*S*)-valine benzyl ester also led to the formation of the corresponding coupling peptides in 86 and 90% yield, respectively. The peptide products were then transformed into their Boc-derivatives **9** for characterization purposes.

The reaction time for the coupling process could be shortened by using a more polar solvent such as DMF, but under these conditions isomerization at the $C_\alpha$ of the NCA occurred¶ giving rise to an equimolar mixture of epimers. This observation prompted us to examine further the influence of the nature of the solvent upon the degree of isomerization. To this end we carried out parallel experiments using an array of common solvents with different polarities. As the results in the Table 1 show, an increase of μ, the dipolar moment of the solvent, leads to increased isomerization, the largest isomerization being when the coupling was performed in HMPA. It thus appears that dipeptide products with the unnatural configuration at the $C_\alpha$ position of the polyoxamic acid might also be obtained from this approach, albeit some further improvement would be required. Finally, as Scheme 2 illustrates, the method can also be applied to the synthesis of tripeptides containing the polyoxamic framework as part of the backbone. Therefore, it is expected that more complex amino acid derived peptides could be made accessible from this approach without the necessity to previously prepare each individual non-proteinogenic α-amino acid.

**Table 1** Solvent effect on the coupling of **7** with (*S*)-LeuOBn[a]

| Entry | Solvent | μ[b] | **8** : *epi*-**8**[c] |
|---|---|---|---|
| 1 | $Et_2O$ | 4.34 | 100 : 0[d] |
| 2 | $CH_2Cl_2$ | 5.17 | 100 : 0[d] |
| 3 | MeCN | 11.48 | 85 : 15 |
| 4 | $MeNO_2$ | 11.88 | 92 : 8 |
| 5 | DMF | 12.88 | 50 : 50 |
| 6 | $Me_2SO$ | 13.00 | 51 : 49 |
| 7 | HMPA | 18.48 | 28 : 72 |

[a] Reactions conducted on a 0.25 mmol scale at room temp. for 24 h in the corresponding solvent (2.5 ml); **7** : (*S*)-LeuOBn, 1 : 2. [b] From C. Reichardt in *Solvent Effects in Organic Chemistry*, ed. H. F. Ebel, Verlag Chemie Gmbh, Weinheim, 1979, p. 270. [c] Determined by $^1$H NMR analysis of the crude products. [d] Corroborated by HPLC analysis.




**Scheme 2**. *Reagents and conditions*: i, **7**, $CH_2Cl_2$, room temp., 24 h, 80%; ii, $H_2$, Pd–C (10% w/w), $Boc_2O$, EtOH, room temp., 24 h, 75%

This work has been supported by Ministerio de Educación y Ciencia (MEC) of the Spanish Government (Project SAF: 95/0749) and in part by the Basque Government (Project: PI95/93). A grant from the Basque Government to A. E. is gratefully acknowledged.

## Footnotes

† For a conceptually different β-lactam route to the unnatural enantiomer of polyoxamic acid, see ref. 3(*k*).

‡ Prolonged exposure of **4** to the reaction conditions causes a reduction in chemical yield.

§ Under these reaction conditions the degree of isomerization was determined to be less than 0.5% by HPLC analysis of the crude reaction nature and comparison with the chromatogram of a sample containing the mixture of epimers, the latter prepared by carrying out the coupling reaction in DMF as solvent, see text.

¶ The possibility of the isomerization of the other labile Cα stereocentre of the amino ester residue under these reaction conditions was ruled out by comparison of the HPLC retention times and NMR spectra of the crude product obtained by coupling of the NCA **7** with both optically pure and racemic amino esters.

## References

1 For reviews on this subject, see K. Isono, *J. Antibiot.*, 1988, **41**, 1711; K. Isono, *Pharm. Ther.*, 1991, **52**, 269.

2 A. B. Cooper, J. Desai, R. G. Lovey, A. K. Saksena, V. M. Girijavallabhan, A. K. Ganguly, D. Loebenberg, R. Parmegiani and A. Cacciapuoti, *Bioorg. Med. Chem. Lett.*, 1993, **3**, 1079 and references cited therein.

3 For reviews, see (*a*) P. Garner, in *Studies in Natural Products Chemistry*, ed. Atta-Ur Rahman, Elsevier, Amsterdam, 1988, vol. 1, part A, p. 397; (*b*) G. Casiraghi, F. Zanardi, G. Rassu and P. Spanu, *Chem. Rev.*, 1995, **95**, 1677. For recent methods, see (*c*) A. K. Saksena, R. G. Lovey, V. M. Girigavallabhan and A. K. Ganguly, *J. Org. Chem.*, 1986, **51**, 5024; (*d*) I. Savage and E. J. Thomas, *J. Chem. Soc., Chem. Commun.*, 1989, 717; (*e*) T. Mukaiyama, K. Suzuki, T. Yamada and F. Tabuga, *Tetrahedron*, 1990, **46**, 265; (*f*) A. Dondoni, S. Franco, F. L. Merchán, P. Merino and T. Tejero, *Tetrahedron Lett.*, 1993, **34**, 5479; (*g*) R. F. W. Jackson, N. J. Palmer, M. J. Wythes, W. Clegg and M. R. J. Elsegood, *J. Org. Chem.*, 1995, **60**, 6431; (*h*) P. Garner and J. M. Park, *J. Org. Chem.*, 1988, **53**, 2979; (*i*) A. Dureault, F. Carreaux and J. C. Depezay, *Synthesis*, 1991, 150; (*j*) M. Irama, H. Hioki and S. Ito, *Tetrahedron Lett.*, 1988, **29**, 3125; (*k*) B. K. Banik, M. S. Manhas and A. K. Bose, *J. Org. Chem.*, 1993, **58**, 307; (*l*) M. M. Paz and F. J. Sardina, *J. Org. Chem.*, 1993, **58**, 6990; (*m*) F. Matsuura, Y. Hamada and T. Shiori, *Tetrahedron Lett.*, 1994, **35**, 733; (*n*) B. M. Trost, A. C. Krueger, R. C. Bunt and J. Zambrano, *J. Am. Chem. Soc.*, 1996, **118**, 6520; (*o*) S. H. Kang and H.-W. Choi, *Chem. Commun.*, 1996, 1521.

4 For a recent review on the synthesis of complex nucleoside antibiotics, see S. Knapp, *Chem. Rev.*, 1995, **95**, 1859. For recent total synthesis of (+)-polyoxin J, see N. Chida, K. Koizumi, Y. Kitida, C. Yokoyama and S. Ogawa, *J. Chem. Soc., Chem. Commun.*, 1994, 111; A. Dondoni, F. Junquera, F. L. Merchán, P. Merino and T. Tejero, *J. Chem. Soc., Chem. Commun.*, 1995, 2127.

5 For reviews, see G. I. Georg and V. T. Ravikumar, in *The Organic Chemistry of β-Lactams*, ed. G. I. Georg, VCH, New York, 1993, p. 295; J. Backes, in *Houben-Weyl Methoden der Organischen Chemie*, ed. E. Muller and O. Bayer, Band E16B, Theime, Stuttgart, 1991, p. 31.

6 C. Palomo, J. M. Aizpurua, C. Cuevas, R. Urchegui and A. Linden, *J. Org. Chem.*, 1996, **61**, 4400.

7 For cycloadditions of glyceraldehyde imines, see C. Hubschwerben and G. Schmid, *Helv. Chim. Acta*, 1983, **66**, 2206; D. R. Wagle, G. Garai, J. Chiang, M. S. Manhas and A. K. Bose, *J. Org. Chem*, 1988, **29**, 5065; S. Saito, T. Ishikawa and T. Moriwake, *Synlett.*, 1993, 139.

8 C. Palomo, F. P. Cossío, C. Cuevas, B. Lecea, A. Mielgo, P. Román, A. Luque and M. J. Martínez-Ripoll, *J. Am. Chem. Soc.*, 1992, **114**, 9360; M. Jayaraman, A. R. A. S. Deshmukh and B. M. Bahawal, *J. Org. Chem.*, 1994, **59**, 932.

*Received in Cambridge, UK, 4th February 1997; Com. 7/00815E*

# Novel two-phase oxidative cross-coupling of the two-component molecular crystal of 2-naphthol and 2-naphthylamine

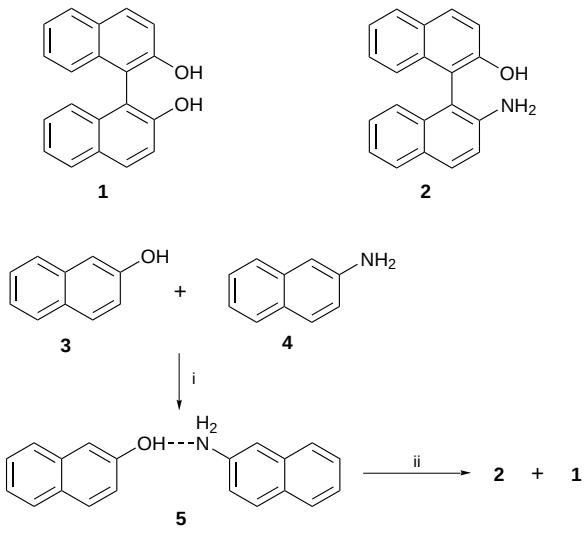
**Kuiling Ding,*[a] Qiguo Xu,[a] Yang Wang,[a] Jinxia Liu,[a] Zhengyan Yu,[a] Baoshi Du,[a] Yangjie Wu,*[a] Hideko Koshima[b] and Teruo Matsuura[b]**

[a] *Department of Chemistry, Zhengzhou University, Zhengzhou 450052, P. R. China*
[b] *Department of Materials Chemistry, Faculty of Science and Technology, Ryukoku University, Seta, Otsu 520-21, Japan*

**Two-phase reaction of a two-component molecular crystal of 2-naphthol and 2-naphthylamine suspended in aqueous $Fe^{3+}$ solutions gives a cross-coupling product, 2-amino-2′-hydroxy-1,1′-binaphthalene, with good selectivity.**

Solid-state organic reactions occurring in the ground state have attracted recent attention in organic synthesis.[1] For example, Toda *et al*. reported that a powdered mixture of 2-naphthol and $FeCl_3·6H_2O$ gave 1,1′-bi-2-naphthol **1** in 95% yield.[2] We have developed a two-phase (solid–liquid) oxidative coupling reaction of 2-naphthol and 6-bromo-2-naphthol suspended in aqueous $Fe^{3+}$ solutions which gives the corresponding 1,1′-bi-2-naphthols in up to 95% yield.[3] Here we report a novel oxidative cross-coupling reaction using a two-component molecular crystal composed of 2-naphthol and 2-naphthylamine *via* a similar solid–liquid process leading to 2-amino-2′-hydroxy-1,1′-binaphthalene **2**, which is a key catalytic ligand for asymmetric synthesis.[4] The present method is the first example of the ground-state reaction using two-component molecular crystals, in contrast to their known excited-state (photo)reactions.[5]

The molecular crystal **5** was obtained by the slow evaporation of an equimolar solution of 2-naphthol **3** and 2-naphthylamine **4** in methanol–acetone (1 : 1, v/v) at room temperature or by melting a 1 : 1 molar mixture of the component compounds followed by resolidification of the melt. Elemental analysis of **5** showed the composition of 2-naphthol and 2-naphthylamine present to be 1 : 1. The melting point of **5** is 127–129 °C which is higher than those of 2-naphthol (120–123 °C) and 2-naphthylamine (108–110 °C). Powder X-ray diffraction (PXD) results and the IR spectra of crystal **5** are quite different from those of the sum of the component compounds. All these results indicate the formation of a molecular compound between 2-naphthol and 2-naphthylamine. Particularly, the $\nu_{NH}$ absorptions at 3375, 3290 and 3170 $cm^{-1}$ in the IR spectrum of 2-naphthylamine become two absorption bands at 3350 and 3260 $cm^{-1}$ in the molecular compound **5** and the $\nu_{OH}$ absorption at 3250 $cm^{-1}$ for 2-naphthol disappears in the spectrum of **5**. It can be deduced that the formation of the molecular compound was caused by hydrogen bonding between the OH and $NH_2$ groups.




**Scheme 1** *Reagents and conditions*: i, acetone–methanol, evaporation, room temp; ii, $Fe^{3+}$–$H_2O$, 55 °C

The oxidative coupling of 2-naphthol **3** reported previously was carried out using a suspension of the substrate in aqueous $Fe^{3+}$ solution.[3] We applied this method to the synthesis of 2-amino-2′-hydroxy-1,1′-binaphthalene **2** *via* oxidative cross-coupling of molecular crystal **5**. In a typical run, a suspension of finely powdered **5** (2.87 g, 10 mmol) in water (50 ml) containing $FeCl_3·6H_2O$ (10.80 g, 40 mmol) was stirred at 55 °C for 6 h under an argon atmosphere. After cooling, the solid material was collected quantitatively by filtration and washed with distilled water to remove $Fe^{3+}$ and $Fe^{2+}$. The solid was chromatographed on an activated charcoal column (100 × 18 mm, 10 g of activated charcoal) using acetone as eluent. The eluent was evaporated and the residual solid was recrystallized from benzene to afford pure **2** (2.0 g, 70%) as colourless needles. Elemental analysis, IR, $^1H$ NMR and $^{13}C$ NMR data were consistent with the structure **2**. This procedure was also applied to the large-scale synthesis of **2**, using **5** (11.5 g, 40 mmol), $FeCl_3·6H_2O$ (43.2 g, 160 mmol) and water (200 ml) at 55 °C for 6 h, to gave 7.15 g of **2** (65% isolated yield).

The selectivity and efficiency of the reaction under various conditions were also examined. The results obtained by the HPLC analysis of the products are summarized in Table 1. In a typical run carried out at 55 °C for 6 h (entry 1), the conversion of 2-naphthol **3** was quantitative and the yield of cross-coupling product **2** was highest. When the reaction was conducted at

**Table 1** Oxidative cross-coupling of **5**

| Entry | $Fe^{3+}$ : **5** | *T*/°C | *t*/h | Conversion of **3** (%) | Yield (%)[a] **2** | **1** |
|---|---|---|---|---|---|---|
| 1 | 4 : 1 | 55 | 6 | 100 | 82 | 14 |
| 2 | 4 : 1 | 55 | 3 | 98.0 | 79 | 13 |
| 3 | 4 : 1 | room temp. | 6 | 98.4 | 71 | 14 |
| 4 | 2.2 : 1 | 55 | 3 | 94.8 | 71 | 19 |
| 5[b] | 4 : 1 | 55 | 3 | 97.0 | 63 | 19 |
| 6[c] | 4 : 1 | 55 | 3 | 81.8 | 31 | 23 |
| 7[c] | 4 : 1 | 55 | 3 | 77.2 | 42 | 30 |
| 8[c] | 4 : 1 | 55 | 3 | 96.8 | 57 | 18 |
| 9[d] | 4 : 1 | 55 | 5 | 100 | 39 | 39 |
| 10[e] | 4 : 1 | 55 | 3 | 96.4 | 78 | 20 |

[a] Yields were obtained by HPLC and based on the amount of consumed **3**. [b] Ultrasound (25 KHz) was applied. [c] $Fe_2(SO_4)_3·9H_2O$, $NH_4Fe(SO_4)_2·12H_2O$ and $NH_4FeCl_4·6H_2O$ were used as oxidants. [d] The reaction was conducted in the solid state. [e] **3** and **4** were added to aqueous $FeCl_3$ solution separately.

room temperature for 6 h (entry 3), the yield and the selectivity for the formation of **2** apparently decreased in comparison with those at 55 °C. At the lower molar ratio of $FeCl_3 \cdot 6H_2O$ to **5** (entry 4) the yields of **2** and **1** were unaltered. Under ultrasonic application (entry 5) no improvement of the yield and selectivity of the formation of **2** were observed. Although three other kinds of $Fe^{3+}$ salts were also used as oxidants (entries 6, 7 and 8), the yield and the selectivity for the formation of **2** were poor in every case. A total solid-state reaction was carried out by grinding a mixture of $FeCl_3 \cdot 6H_2O$ and **5** (4 : 1) in a mortar at 55 °C for 5 h (entry 9), the conversion of 2-naphthol **3** was quantitative, but the yield and the selectivity of the formation of **2** were low. This is interpreted by the fact that with the progress of the reaction the powdered mixture became glassy, a state in which the original arrangement of the component molecules in the crystal lattice may be altered.

It is interesting to note that when the crystals of 2-naphthol **3** and 2-naphthylamine **4** were separately added to the solution of $FeCl_3 \cdot 6H_2O$ in water and the suspension was stirred at 55 °C for 3 h (entry 10), the yield of **2** was comparable to that obtained by the reaction of molecular **5** (entry 2). In order to clarify this phenomenon, a suspension of a mixture of 2-naphthol and 2-naphthylamine in water without the presence of oxidant was stirred at 55 °C for 1 h. The solid collected by filtration showed the same melting point and IR spectrum as those of **5**. It can be concluded that in the case of entry 10 the actual reacting species is molecular **5** and as a result it gave the same yield and selectivity of the product as those obtained from the reaction of **5**.

We are grateful to the Research Foundation of National Education Committee and the Natural Science Foundation of Henan Province for Outstanding Young Scientists for financial support of this work.

## References

1 F. Toda, *Synlett*, 1993, 303.
2 F. Toda, K. Tanaka and S. Iwata, *J. Org. Chem.*, 1989, **54**, 3007.
3 K. Ding, Y. Wang, L. Zhang, Y. Wu and T. Matsuura, *Tetrahedron*, 1996, **52**, 1005.
4 E. Carreira, R. A. Singer and W. Lee, *J. Am. Chem. Soc.*, 1994, **116**, 8837; E. Carreira, W. Lee and R. A. Singer, *J. Am. Chem. Soc.*, 1995, **117**, 3649; R. A. Singer and E. Carreira, *J. Am. Chem. Soc.*, 1995, **117**, 12360; H. J. Knolker and H. Hermann, *Angew. Chem., Int. Ed. Engl.*, 1996, **35**, 341; D. J. Berrisford and C. Bolm, *Angew. Chem., Int. Ed. Engl.*, 1995, **34**, 1717.
5 H. Koshima and T. Matsuura, *Kokagaku*, 1995, **19**, 10; H. Koshima, Y. Chisaka, Y. Wang, X. Yao, H. Wang, R. Wang, A. Maeda and T. Matsuura, *Tetrahedron*, 1994, **50**, 13 617; H. Koshima, K. Ding and T. Matsuura, *J. Chem. Soc. Chem Commun.*, 1994, 2053; H. Koshima, K. Ding, Y. Chisaka and T. Matsuura, *Tetrahedron: Asymmetry*, 1995, **6**, 101; H. Koshima, K. Ding, Y. Chisaka, T. Matsuura, Y. Ohashi and M. Mukasa, *J. Org. Chem.*, 1996, **61**, 2352; H. Koshima, K. Ding, Y. Chisaka and T. Matsuura, *J. Am. Chem. Soc.*, 1996, **118**, 12 059.

*Received, 9th December 1996; Com. 6/08256D*

# Synthesis of 7-deaza-8-bromo cyclic adenosine 5′-diphosphate ribose: the first hydrolysis resistant antagonist at the cADPR receptor

**Victoria C. Bailey,[a] Jaswinder K. Sethi,[b] Antony Galione[b] and Barry V. L. Potter*[a]**

[a] *Department of Medicinal Chemistry, School of Pharmacy and Pharmacology, University of Bath, Claverton Down, Bath, UK BA2 7AY*

[b] *Department of Pharmacology, University of Oxford, Mansfield Road, Oxford, UK OX1 3QT*

**7-Deaza-8-bromo cyclic adenosine 5′-diphosphate ribose is synthesised from 7-deazaadenosine *via* 7-deaza-8-bromo nicotinamide adenine dinucleotide; it is both a more potent antagonist than the 8-bromo derivative and has the advantage of chemical and enzymatic hydrolytic stability.**

Cyclic adenosine 5′-diphosphate ribose (cADPR, **1**, Fig. 1) is a $Ca^{2+}$-mobilising agent known to act *via* ryanodine receptors to release internal stores of $Ca^{2+}$ in a wide variety of cell types,[1–3] independent of the second messenger *myo*-inositol 1,4,5-trisphosphate.[4] The role of cADPR is not yet fully understood, but it may act as a second messenger for a number of receptor agonists, including nitric oxide.[5] The binding protein for cADPR is unknown, and there is doubt whether cADPR acts directly at the ryanodine receptor, although its action involves calmodulin.[6] Hence it is important to build up a structure–activity profile for cADPR in relation to $Ca^{2+}$ release and to design molecules to probe its biological role.

Analogues substituted at the 8-position including the 8-bromo **2** and 8-amino **3** derivatives are documented as antagonists at the cADPR receptor.[7] Importantly, 8-amino-cADPR inhibits cardiac excitation–contraction coupling.[8] Recently, we reported 7-deaza-cADPR **4** as the first partial agonist, highlighting the N-7 position as an essential motif for effective $Ca^{2+}$ release.[9] Furthermore, 7-deaza-cADPR is resistant to both chemical and enzymatic hydrolytic attack, a property desirable to confer upon an antagonist, to improve its physiological value. We have combined these two modifications and we now report 7-deaza-8-bromo-cADPR **5** as the first hydrolysis resistant cADPR antagonist.

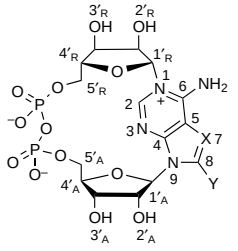
There is no effective chemical synthesis of cADPR, the only published route produces the correct stereoisomeric product in very low yield.[10] We, like others, have relied upon a chemoenzymatic route to develop structural diversity[7,11] utilising *Aplysia* ADP-ribosyl cyclase.[12] The enzyme is extremely flexible in its substrate specificity.[11–13]

7-Deazaadenosine (Tubercidin, **6**) was selectively brominated at the pseudo-8-position (6-position) using *N*-bromosuccinimde (Scheme 1). After chromatography, dry **7** was phosphorylated at the 5′-hydroxy group using essentially the general method described by Yoshikawa *et al.*[15] The novel **8**‡ was purified by ion exchange chromatography using triethylammonium hydrogen carbonate buffer (TEAB). Owing to the increased hydrophobic nature of the modified purine ring (an extra CH group and the bromo substituent), **8** eluted at a higher concentration of buffer than expected, namely 250–300 mM TEAB as opposed to the 200–250 mM observed for adenosine 5′-monophosphate, and was not contaminated by inorganic phosphate, often a problem with this method.

Dicyclohexylcarbodiimide coupled **8** to nicotinamide mononucleotide (NMN).[16] The novel pyrophosphate **9**† was purified from monophosphates and symmetrical pyrophosphates by ion exchange chromatography. 7-Deaza-8-bromo-$NAD^+$ eluted at 120–150 mM TEAB as its triethylammonium salt.

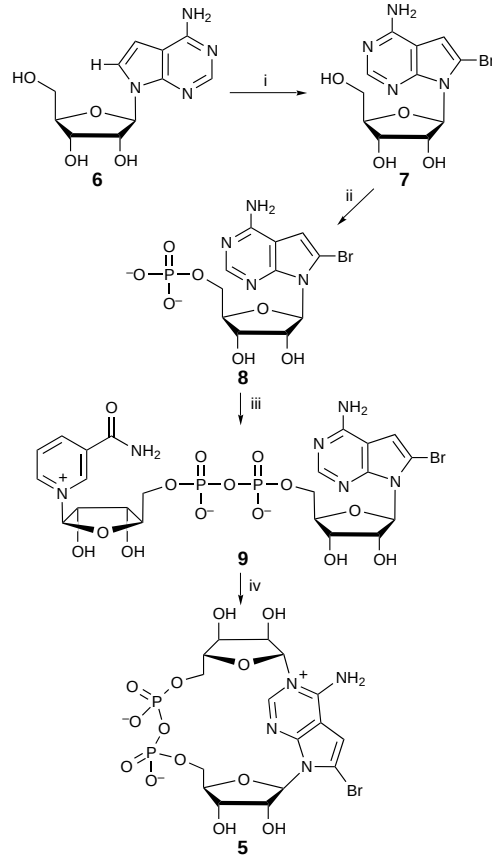
Finally, the $NAD^+$ analogue was cyclised using the *Aplysia* enzyme.[11] 7-Deaza-8-bromo-$NAD^+$ cyclised at a similar rate to cADPR. The product was purified by ion exchange chromatography, at 130–150 mM TEAB, as the triethylammonium salt.

Phosphates **8**, **9** and **5**‡ were quantified using total phosphate analysis[9,17] from which the extinction coefficients were calcu-



**1** X = N, Y = H, cADPR
**2** X = N, Y = Br, 8-Bromo-cADPR
**3** X = N, Y = $NH_2$, 8-Amino-cADPR
**4** X = CH, Y = H, 7-Deaza-cADPR
**5** X = CH, Y = Br, 7-Deaza-8-bromo-cADPR

**Fig. 1** Structures of cADPR **1**, 8-bromo-cADPR **2**, 8-amino-cADPR **3**, 7-deaza-cADPR **4** and 8-bromo-7-deaza-cADPR **5**



**Scheme 1** *Reagents and conditions*: i, NBS, KOAc, DMF, 10 min, 40%; ii, $PO(OEt)_3$ 50 °C, 15 min, then $POCl_3$ (1.5 equiv.), 0 °C, 2 h, then $H_2O$, 44%; iii, DCC, NMN, pyridine–$H_2O$ (4 : 1), 7 d, 28%; iv, 1.5 mM solution in 25 mM HEPES, ADP-ribosyl cyclase, 30 min, 31%

lated, and used to quantify reaction yields and solutions for the biological evaluation of **5**.

The pharmacology of **5** was investigated using sea urchin egg homogenate.[18] 7-Deaza-8-bromo-cADPR antagonised the action of 100 nM cADPR-induced $Ca^{2+}$ release (Fig. 2), desensitised the receptor, and was apparently more potent and efficacious than 8-bromo-cADPR ($IC_{50}$ values of 0.73 ± 0.05 and 0.97 ± 0.04 μM respectively). Furthermore, it was resistant to chemical hydrolysis and induced antagonism even after being incubated in buffer at 85 °C for 90 min. HPLC analysis of a control incubation showed that 7-deaza-8-bromo-cADPR was still present confirming that cyclic material, and not a metabolite, caused antagonism even after heat treatment. In contrast, after identical treatment, 8-bromo-cADPR was no longer able to induce antagonism and HPLC showed no cyclic material remaining. Resistance to enzymatic hydrolysis was tested by pre-incubating the antagonist with homogenate overnight, when an aliquot was removed and its ability to antagonise cADPR-induced $Ca^{2+}$ was tested. Whilst the 8-bromo-cADPR antagonism had reduced significantly, 7-deaza-8-bromo-cADPR was still a significant antagonist. Full biological details will be reported elsewhere.

In 7-deaza analogues of adenosine the glycosidic bond is more resistant to acid catalysed hydrolysis than in adenosine.[19] Similarly, the increased hydrolytic resistance of 7-deaza analogues of cADPR is thought to arise from increased stability of the N1 ribosyl linkage. The N1 position of 7-deazaadenosine is more basic than that of adenosine ($pK_a$ = 5.2 and 3.6 respectively[20]) and similarly this position is more basic in the 8-bromo substituted analogues than in adenosine ($pK_a$ = 4.02 for 8-bromoadenosine[21]). The combination of modifications, therefore, makes the heterocycle substantially more basic at N1 than in adenine. Hydrolysis of the N1 ribosyl linkage probably involves participation of a ribosyl oxygen lone pair to form a carbocation which is then captured by water. The ability of the N1-ribosyl linkage to be hydrolysed should therefore depend upon the leaving group ability of the purine. The more acidic the purine, the better leaving group it will be and, conversely, with the more basic character of N1 in 7-deaza-8-bromo-cADPR, the harder it will be to cleave the N1 ribosyl bond.

Combined modifications at the 7 and 8 positions of cADPR thus produce slightly better antagonistic properties, with the marked added advantage of hydrolytic resistance. One of the most commonly employed antagonists, 8-amino-cADPR, is unsuitable for microinjection work due to its chemical instability.[22] 7-Deaza-8-bromo-cADPR, resistant to both chemical and enzymatic hydrolysis, should be a powerful tool to investigate the cADPR signalling pathway and complements our poorly hydrolysable agonist, cyclic aristeromycin diphosphate ribose.[13]

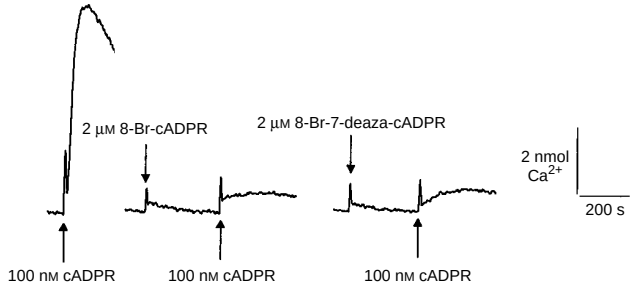



**Fig. 2** *Lytechinus pictus* egg homogenates (2.5% v/v) (ref. 18) containing Fluo-3 (3 μM) were incubated at 17 °C. Homogenate (500 μl) was challenged with cADPR (final concentration 100 nM). $Ca^{2+}$ release was monitored by a change in fluorescence. 7-Deaza-8-bromo-cADPR was tested for its antagonism by pre-treating the homogenate (500 μl) with the sample (final concentration 2 μM) 3 min prior to addition of cADPR (final concentration 100 nM). A subsequent addition of cADPR (100 nM) demonstrated the desensitisation of the $Ca^{2+}$ release mechanism. The traces shown are representative of several such experiments.

We thank the Medical Research Council for a Project Grant (A. G., B. V. L. P.) and two studentships (V. C. B., J. K. S.). A. G. is a Wellcome Trust Fellow and B. V. L. P. is a Lister Institute Research Professor.

## Footnotes

* E-mail: B.V.L.Potter@bath.ac.uk

† *Spectroscopic data* for **8**: $\delta_H$ (400 MHz, $D_2O$): 4.08–4.15 (3 H, m, H4′ and H5′), 4.53 (1 H, dd, *J* 5.7, 5.8 Hz, H3′), 5.07 (1 H, dd, *J* 5.3, 5.8 Hz, H2′), 6.04 (1 H, d, *J* 5.3 Hz, H1′), 6.42 (1 H, s H7), 7.92 (1 H, s, H2). $\delta_P$ (161.7 MHz, $D_2O$): 2.35 broadens when proton coupled. $\delta_C$ (100.4 MHz, $D_2O$): 65.2 (d, $J_{CP}$ 3.7 Hz, C5′), 70.3 (C3′), 72.1 (C2′), 83.6 (d, $J_{CP}$ 7.4 Hz, C4′), 89.8 (C1′), 104.0 (C5), 105.2 (C7), 110.4 (C8), 149.9 (C4), 150.0 (C2), 154.5 (C6). $\lambda_{max}$ 276 nm, ε = 13.3 × $10^3$ $dm^3$ $mol^{-1}$ $cm^{-1}$. *m/z* ($FAB^+$) 425, 427 $(M + H)^+$, ($FAB^-$) 422, 424 $(M - H)^-$, 341 $(M - H - Br)^-$.

For **9**: $\delta_H$ (400 MHz, $D_2O$): 4.03–4.32 (8 H, m, $H_N2'$, $H_N3'$, $H_A4'$, $H_N4'$, $H_A5'$ $H_N5'$), 4.56 (1 H, dd, *J* 5.8, 5.3 Hz, $H_A3'$), 5.16 (1 H, dd, *J* 5.9, 5.8 Hz, $H_A2'$), 5.99 (1 H, d, *J* 4.4 Hz, $H_N1'$), 6.06 (1 H, d, *J* 5.9 Hz, $H_A1'$), 6.60 (1 H, s, $H_A7$), 8.05 (1 H, s, $H_A2$), 8.14 (1 H, dd, *J* 8.3, 6.4 Hz, $H_N3$), 8.73 (1 H, d, *J* 8.3 Hz, $H_N4$), 9.09 (1 H, d, *J* 6.4 Hz, $H_N6$), 9.25 (1 H, s, $H_N2$). $\delta_P$ (161.7 MHz, $D_2O$): −10.5, −10.9 (2d, $J_{PP}$ 20.1 Hz). $\delta_C$ (100.4 MHz, $D_2O$): 65.7 (d, *J* 3.7 Hz, $C_A5'$), 66.5 ($C_N5'$), 70.0 ($C_A3'$), 71.4 ($C_N3'$), 71.9 ($C_A2'$), 78.5 ($C_N2'$), 83.5 (d, *J* 9.2 Hz, $C_A4'$), 87.8 (d, *J* 9.2 Hz, $C_N4'$), 89.8 ($C_A1'$), 100.9 ($C_N1'$), 104.3 ($C_A5$), 105.0 ($C_A7$), 110.5 ($C_A8$), 129.6 ($C_N4$), 140.6 ($C_N5$), 143.1 ($C_N6$), 146.3 ($C_N2$), 150.4 ($C_A2$), 150.7 ($C_A4$), 155.5 ($C_A6$), 166.1 (CO). $\lambda_{max}$ 270 nm, ε = 13.3 × $10^3$ $dm^3$ $mol^{-1}$ $cm^{-1}$. *m/z* (electrospray$^+$) 741, 743 $(M + H)^+$, (electrospray$^-$) 739, 741 $(M - H)^-$.

For **5**: $\delta_H$ (400 MHz, $D_2O$): 3.89–3.93 (1 H, m, $H_A5'$), 3.98–4.03 (1 H, m, $H_R5'$), 4.15–4.20 (1 H, m, $H_A4'$), 4.23–4.27 (1 H, m, $H_R5'$), 4.30–4.40 (2 H, m, $H_A5'$, $H_R3'$), 5.44 (1 H, dd, *J* 5.2, 6.1 Hz, $H_A2'$), 5.97 (1 H, d, *J* 4.0 Hz, $H_R1'$), 6.03 (1 H, d, *J* 6.1 Hz, $H_A1'$), 6.91 (1 H, s, $H_A7$), 8.75 (1 H, s, $H_A2$), all other protons are obscured by the water peak at δ 4.8. $\delta_P$ (161.7 MHz, $D_2O$): −10.8, −11.6 (2d, $J_{PP}$ 18 Hz). $\lambda_{max}$ = 277 nm, ε = 10.85 × $10^3$ $dm^3$ $mol^{-1}$ $cm^{-1}$. *m/z* (electrospray$^+$) 619, 621 $(M + H)^+$, (electrospray$^-$) 617, 619 $(M - H)^-$, 79, 81 $(Br)^-$.

## References

1 H. C. Lee and R. Aarhus, *Cell Reg.*, 1991, **2**, 203.
2 S. Takasawa, K. Nata, H. Yonekura and H. Okamoto, *Science*, 1993, **259**, 370.
3 A. H. Guse, C. P. DaSilva, F. Emmrich, G. A. Ashamu, B. V. L. Potter and G. W. Mayr, *J. Immunol.*, 1995, **155**, 3353.
4 A. Galione, *Trends Pharmacol. Sci.*, 1992, **13**, 304.
5 N. J. Willmott, J. K. Sethi, T. F. Walseth, H. C. Lee, A. M. White and A. Galione, *J. Biol. Chem.*, 1996, **271**, 3699.
6 H. C. Lee, R. Aarhus, R. M. Graeff, M. E. Gurnack and T. F. Walseth, *Nature*, 1994, **370**, 307.
7 T. F. Walseth and H. C. Lee, *Biochim. Biophys. Acta*, 1993, **1178**, 235.
8 S. Rakovic, A. Galione, G. A. Ashamu, B. V. L. Potter and D. A. Terrar, *Curr. Biol.*, 1996, **6**, 989.
9 V. C. Bailey, J. K. Sethi, S. M. Fortt, A. Galione and B. V. L. Potter, *Chem. Biol.*, 1997, **4**, 51.
10 S. Yamada, Q.-M. Gu and C. J. Sih, *J. Am. Chem. Soc.*, 1994, **116**, 10 787.
11 G. A. Ashamu, A. Galione and B. V. L. Potter, *J. Chem. Soc., Chem. Commun.*, 1995, 1359; 1929.
12 H. C. Lee and R. Aarhus, *Cell Reg.*, 1991, **2**, 203.
13 V. C. Bailey, S. M. Fortt, R. J. Summerhill, A. Galione and B. V. L. Potter, *FEBS Lett.*, 1996, **379**, 227.
14 D. E. Bergstrom and A. Brattesani, *Nucleic Acids Res.*, 1980, **8**, 6213.
15 M. Yoshikawa, T. Kato and T. Takenishi, *Bull. Chem. Soc. Jpn.*, 1969, **42**, 3505.
16 N. H. Hughes, G. W. Kenner and A. Todd, *J. Chem. Soc.*, 1957, 3733.
17 A. Briggs, *J. Biol. Chem.*, 1922, **53**, 13.
18 D. L. Clapper, T. F. Walseth, P. J. Dargie and H. C. Lee, *J. Biol. Chem.*, 1987, **262**, 9561.
19 J. E. Pike, L. Slechta and P. F. Weley, *J. Heterocycl. Chem.*, 1964, **1**, 159.
20 L. Ji, N. A. Corfu and H. Sigel, *J. Chem. Soc., Dalton Trans.*, 1991, 1367.
21 E. R. Garrett and P. J. Mehta, *J. Am. Chem. Soc.*, 1972, **94**, 8532.
22 C. M. Perez-Terzic, E. N. Chini, S. S. Shen, T. D. Dousa and D. E. Clapham, *Biochem. J.*, 1995, **312**, 955.

*Received, 14th January 1997; Com. 7/00336F*

# Synthesis and structure of a new layered organic–inorganic compound containing unique chains of $PbI_2$

**Vijayashree Chakravarthy and Arnold M. Guloy***

*Department of Chemistry and Texas Center for Superconductivity, University of Houston, Houston, Texas 77204-5641, USA*

**Synthesis and crystal structure of $[C_6H_{10}N_2]Pb_2I_6{\cdot}3thf$ which contains a novel lead iodide polymeric anion with a double-chain structure.**

There is increasing interest in the study of magnetic, electronic and optoelectronic properties of low-dimensional organic–inorganic hybrid compounds.[1–3] Studies suggest that complex systems consisting of organic and inorganic components have great potential for the creation of functional materials utilizing the wide variety of properties associated with each component.[4,5] Lead(II) iodide compounds are of particular interest due to their significant third-order optical non-linear properties.[6–9]

Although there is significant interest in the physical properties of low-dimensional lead iodide compounds, relevant information regarding their crystal structure, properties and synthesis is limited.[10–12] Our current research is focused on the synthesis of low-dimensional organic–inorganic post-transition-metal iodides with the possibility of incorporating interesting properties associated with the organic and inorganic moieties. This research is motivated by the possibility of tuning properties of inorganic solid-state materials by incorporating polarizable organic moieties. Moreover, important structure–property relationships between low-dimensional structural derivatives and their parent inorganic material can be established.

The compound $[C_6H_{10}N_2]Pb_2I_6{\cdot}3thf$ **1** was prepared by reacting *p*-nitroaniline and $PbI_2$ in solution. The synthesis of **1** starts with dissolving *p*-nitroaniline (0.59 g, 4.33 mmol) and lead(II) iodide (1.00 g, 2.17 mmol) in 8 ml of concentrated 57 mass% aqueous hydriodic acid diluted with acetonitrile. The addition of hydriodic acid increases the solubility of $PbI_2$ in polar organic solvents. The resulting solution was warmed to 60 °C and slowly cooled to 20 °C during which the solution turns dark red-brown, and the formation of a brown precipitate was observed. The precipitate was collected and redissolved in tetrahydrofuran (thf) at 60 °C. The resulting clear red–brown solution was allowed to slowly cool, from 60 to −10 °C over 7 days, and orange parallelepiped crystals were formed. The air-sensitive orange crystals were preserved in the mother-liquor. All reactions were carried out under nitrogen atmosphere and all solvents were degassed before use. Direct reaction of *p*-phenylenediammine and $PbI_2$ in acetonitrile–HI and/or thf does not lead to the formation of compound **1** and could be attributed to the low solubility of the diamine in the organic–HI solvents.

Compound **1** crystallizes in space group $P\bar{1}$.† The asymmetric unit was found to consist of a $[Pb_2I_6]^{2-}$ unit (part of a polymeric chain), two half-molecules of *p*-phenylenediammonium dications, $[C_6H_{10}N_2]^{2+}$, situated about inversion centres, and three molecules of thf solvent. One of the thf molecules was found to be significantly disordered over two distinct sites, with population factors of 70 : 30. The crystal structure of **1** features double chains of *cis*-edge-sharing $PbI_6$ octahedra, $[Pb_2I_6^{2-}]_\infty$, that run along the *a* axis, as shown in Fig. 1. There are three types of I atoms defined by their connectivity to Pb: terminal [I(5), I(6)], double bridged [I(3), I(4)] and triple bridged [I(1), I(2)]. Also, there are two types of Pb atoms, defined by their location in the chain: 'outer' [Pb(1)], bonded to terminal iodides; and 'inner' [Pb(2)] bonded only to bridging iodides. The shortest Pb–I distances (3.05, 3.13 Å) are those between the terminal iodides and Pb(1). The I–Pb–I angles are nearly perpendicular around Pb(1) (84.7–94°) and Pb(2) (83.1–91.4°) with the 'outer' $PbI_6$ octahedra exhibiting the largest deviation from ideal symmetry. The structure of the polymeric anion, $[Pb_2I_6^{2-}]_\infty$, can be regarded as a $<110>$ section of the layered $CdI_2$ type structure. The lead iodide chain is reminiscent of the antimony iodide chains in $[PPh_4]Sb_3I_{10}$ and $[(Me_2N)_3C_3]Sb_3I_{10}$.[13] These $[Sb_3I_{10}^{1-}]_\infty$ complex chains are structural derivatives of the $CdI_2$ type structure but differ in the way the layered structure is excised into chains. The lead iodide double chains in **1** correspond to the higher-order double chain $[M_2I_6]_\infty$ which has not been previously observed. It is important to note that the polymeric anion chain in **1** constitutes a direct structural link between molecular lead iodide complexes to the inorganic solid compound $PbI_2$ ($CdI_2$ type).

An important aspect of the crystal structure of **1** is its organic–inorganic heterostructure. It is dominated by cooperative hydrogen bonding between *p*-phenylenediamine dications with terminal and double-bridging iodines of the inorganic double chain as shown in Fig. 2. The hydrogen bond distances range from 3.56 to 3.83 Å suggesting that any interaction between them is not very strong.[14] The two half-molecules of organic dications in the asymmetric unit generate two inequivalent dications. One type of dication acts as bridge between nearest neighbouring $[Pb_2I_6]^{2-}$ double chains through hydrogen bonding interactions between the amino group and the terminal iodides. These extended interactions result in stair-like layers formed by hydrogen-bonded dications and $[Pb_2I_6^{2-}]_\infty$ chains. The stair-like layered organic–inorganic heterostructure lies nearly parallel to the $<011>$ plane as shown in Fig. 3. The remaining *p*-phenylenediamine dications and solvent molecules (thf) lie between the layers of hydrogen-bonded organic cations and inorganic chains.

During the initial stages of this research, our intention was to introduce push–pull type cations and molecules like *p*-nitroaniline into $PbI_2$. However, in addition to the protonation of the amine groups, we observe that *p*-nitroaniline is reduced to

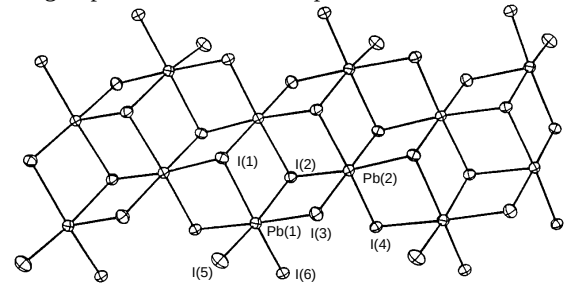



**Fig. 1** ORTEP representation of the structure of the linear polymeric chain in **1** (ellipsoids are drawn at 50% probability). Important distances (Å) and angles (°) are: Pb(1)–I(1) 3.378(1); Pb(1)–I(2) 3.458(1), Pb(1)–I(3) 3.178(2), Pb(1)–I(5) 3.052 (2), Pb(1)–I(6) 3.126(1), Pb(2)–I(2) 3.264(2), Pb(2)–I(3) 3.178(2), Pb(2)–I(4) 3.154(1), I(1)–Pb(1)–I(2) 86.4(1), I(1)–Pb(1)–I(3) 93.3(1), I(1)–Pb(1)–I(5) 87.9(1), I(1)–Pb(1)–I(6) 169.3(1), I(2)–Pb(1)– I(3) 84.1(1), I(2)–Pb(1)–I(5) 174.1(1), I(2)–Pb(1)–I(6) 85.7(1), I(3)–Pb(1)–I(6) 93.1(1), I(2)–Pb(2)–I(3) 88.0(1), I(2)–Pb(2)–I(4) 91.4(1), I(3)–Pb(1)–I(5) 94.0(1).

*p*-phenylenediamine in the presence of hydriodic acid and $PbI_2$. The well known reduction of nitroarenes to primary arylamines in the presence of metal (Sn, Zn, or Fe) and acid (HCl) involves the oxidation of the metals.[15] In this work, the reduction of the nitro group involves oxidation of the iodide ions ($2I^- \rightarrow I_2$). The formation of $I_2$ is observed from the dark red colour of the solution upon the reaction of the inorganic and organic components. Furthermore, the observed reduction of the nitro group by iodide is catalysed by the metal iodide, $PbI_2$. This is indicated by several follow-up experiments wherein catalytic amounts of the metal iodide were needed to initiate the nitro reduction/iodide oxidation reaction. An examination of known oxidation potentials of $Pb^{II}$ and $I^-$ ($Pb^{2+} \rightarrow Pb^{4+} + 2e^-$, $E° = -1.69$ V; $2I^- \rightarrow I_2 + 2e^-$, $E° = -0.53$ V)[16] further supports the better reducing ability of $I^-$. The overall nitroaniline/$I^-$ redox reaction is given by eqn. (1).

$$p\text{-}H_2NC_6H_4NO_2 + 6HI \rightarrow p\text{-}H_2NC_6H_4NH_2 + 3I_2 + 2H_2O \quad (1)$$

The IR spectrum of **1** recorded in KBr contains characteristic bands associated with the phenyl group and a very broad band at 3200 $cm^{-1}$ indicating the presence of protonated amine groups. Furthermore, the characteristic band associated with the aromatic nitro group, around 1300 $cm^{-1}$, is not observed.

The synthesis of **1**, a direct structural derivative of $PbI_2$, is just the first member of a family of compounds with low-dimensional chain structures derived from the layered $PbI_2$ structure. Its novel layered heterostructure attests to the importance of cooperative hydrogen bonding in the crystal structures of organic–inorganic halides. Studies are under way to relate the optical properties of **1** to the unique properties of $PbI_2$.

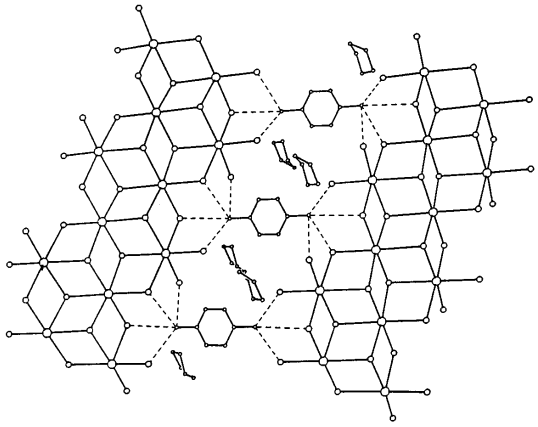


**Fig. 2** View of two nearest neighbouring $[Pb_2I_6^{2-}]\infty$ chains and the bridging *p*-phenylenediamine dications. Hydrogen-bonding interactions, represented by the nearest N···I distances that range between 3.65 and 3.83 Å, are indicated by dashed lines.

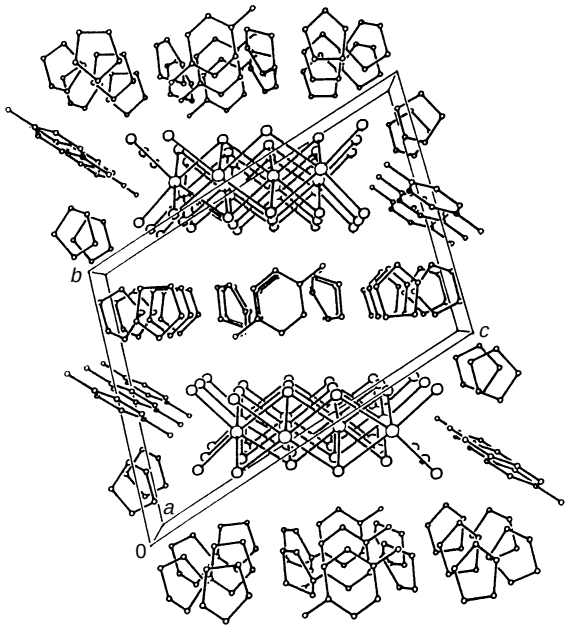



**Fig. 3** A plot of the structure showing the unit-cell packing as viewed into the *a* axis. Only the major orientation of the disordered thf is shown.

This material is based in part on work supported by the Robert A. Welch Foundation and the Texas Center for Superconductivity at the University of Houston. We thank Dr James Korp for help with crystallography.

## Footnotes

* E-mail: aguloy@uh.edu

† Single-crystal X-ray analysis was carried out on a crystal with dimensions *ca.* 0.12 × 0.16 × 0.32 mm mounted in a stream of dry $N_2$ gas at −50 °C. Monochromated Mo-Kα radiation was used and intensities were measured using the θ–2θ scan technique. The intensities of standard reflections were monitored and they showed no significant changes. Lorentz and polarization corrections, and absorption corrections based on 10 ψ-scans were applied.

*Crystal data*: $M$ = 1502.32, $a$ = 8.322(1), $b$ = 13.076(2), $c$ = 17.037(4) Å, $\alpha$ = 70.64(1), $\beta$ = 83.86(1), $\gamma$ = 72.31(1)°, $U$ = 1666 $Å^3$; $Z$ = 2; $D_c$ = 2.99 g $cm^{-3}$, $\mu$ = 156.9 $cm^{-1}$, $\lambda$ = 0.710 73 Å, $2\theta_{max}$ = 45°; total data collected = 4321, reflections observed = 3180 ($I > 3\sigma I$); 259 variables; $R$ = 0.041, $R_w$ = 0.041. All calculations were made using the Nicolet SHELXTL PLUS (1987) crystallographic package. Hydrogens could not be located in difference maps, and no attempt was made to include them in ideal positions. Atomic coordinates, bond lengths and angles, and thermal parameters have been deposited at the Cambridge Crystallographic Data Centre (CCDC). See Information for Authors, Issue No. 1. Any request to the CCDC for this material should quote the full literature citation and the reference number 182/400.

## References

1 See for example: T. Ishihara, J. Takahashi and T. Goto, *Phys. Rev. B*, 1990, **42**, 11 099; M. E. Thomson, *Chem. Mater*., 1994, **6**, 1168; D. W. Bruce and D. O'Hare, *Inorganic Materials*, Wiley, New York; P. Delhase and M. Drillon, *Organic and Inorganic Low Dimensional Crystalline Materials*, Reidel, Dordrecht, 1987, T. E. Gier and G. D. Stucky, *Nature*, 1991, **349**, 508; S. R. Marder, J. E. Sohn and G. D. Stucky, *Materials for Nonlinear Optics*, ACS Symp. Ser. No. 455, 1991.

2 D. B. Mitzi, S. Wang, C. A. Feild, C. A. Chess and A. M. Guloy, *Science*, 1995, **267**, 1473; D. B. Mitzi, S. Wang, C. A. Feild, W. T. A. Harrison and A. M. Guloy, *Nature*, 1994, **364**, 46.

3 P. G. Lacroix, R. Clement, K. Nakatani, J. Zyss and I. Ledoux, *Science*, 1994, **263**, 658.

4 J. Takada, H. Awaji, M. Koshioka, A. Nakajima and W. A. Nevin, *Appl. Phys. Lett*., 1992, **61**, 2184.

5 P. Day, *Phil. Trans. R. Soc. London A*, 1985, **314**, 145.

6 J. Calabrese, N. L. Jones, R. L. Harlow, N. Herron, D. L. Thorn and Y. Wang, *J. Am. Chem. Soc*., 1991, **113**, 2328.

7 T. Ishihara and T. Goto, in *Nonlinear Optics of Organics and Semiconductors*, ed. T. Kobayashi, Springer-Verlag, Berlin, 1989, vol. 36, p. 72.

8 E. Lifshitz, M. Yassen, L. Bykov, and I. Dag, in *Nanophase Materials Synthesis–Properties–Applications*, ed. G. C. Hadjipayanis and R. W. Siegel, NATO ASI Series, Kluwer Academic, Dordecht, 1994, vol. 260, p. 503.

9 G. C. Papavassiliou, A. P. Patsis, D. J. Lagouvardos and I. B. Koutselas, *Synth. Met*., 1993, **55**–**57**, 3887.

10 J. G. Contreras, G. V. Seguel, B. Ungerer, W. F. Maier and F. J. Hollander, *J. Mol. Struct*., 1983, **102**, 295.

11 S. Wang, D. Mitzi, C. A. Field and A. Guloy, *J. Am. Chem. Soc*., 1995, **117**, 5297.

12 H. Krautscheid and F. Vielsack, *Angew. Chem., Int. Ed. Engl*., 1995, **34**, 2035.

13 S. Pohl, W. Saak, and D. Haase, *Z. Naturforsch., Teil B*, 1987, **42**, 1493.

14 J. Trotter and J. K. Fawcett, *Acta Crystallogr*., 1996, **21**, 366.

15 A. I. Vogel, *Textbook of Practical Organic Chemistry*, Longman Scientific & Technical, London, 4th edn., 1978, p. 657.

16 A. J. Bard, R. Parsons and J. Jorden, *Standard Potentials in Aqueous Solution*, Marcel Dekker, New York and Basel, 1985, p. 220.

*Received in Bloomington, IN, USA on 16th December 1996; Com. 6/08415J*

# Molecular structure of diphenylbis(9,10-phenanthrenesemiquinonate)tin(IV), an organometallic diradical complex

**Andrei S. Batsanov,[a] Judith A. K. Howard,[a] Martyn A. Brown,[b] Bruce R. McGarvey[b] and Dennis G. Tuck*[b]**

[a] *Department of Chemistry, University of Durham, South Road, Durham, UK DH1 3LE*
[b] *Department of Chemistry and Biochemistry, University of Windsor, Windsor, Ontario, Canada N9B 3P4*

**The title compound, formed in the reaction between hexaphenylditin and 9,10-phenanthrenequinone, is shown to be an organotin(IV) diradical; its X-ray structure and EPR spectra are reported.**

Substituted *ortho*-quinones can oxidize main-group elements or their low-oxidation state compounds, yielding semiquinone or catecholate complexes, characterised chemically and crystallographically.[1] The oxidation has been shown to proceed *via* successive one-electron transfer reactions,[2] involving semiquinone derivatives as important intermediates, conveniently detectable by electron paramagnetic resonance (EPR) spectroscopy. Some more unusual products were isolated, *e.g.* an oxygen-bridged tetrachlorocatecholate derivative $[(Cl_4C_6O_2)TePh]_2O$ from the reaction between $Ph_2Te$ and $Cl_4C_6O_2$.[3]

The present work is a part of our study of reactions of $Sn_2Ph_6$ with various *o*-quinones and of $Ph_2SnCl_2$ or $Ph_3SnCl$ with sodium semiquinonates,[4] and of the redistribution processes which follow these reactions. The resulting systems comprise $SnPh_4$ and various radical and diradical species, identified by their EPR spectra. In particular, the reaction between equimolar amounts of $Sn_2Ph_6$ and 9,10-phenanthrenequinone (pq) in refluxing dichloromethane (1 h) yielded a brown solid, identified as $Ph_3Sn(psq)$ (psq = 9,10-phenanthrenesemiquinone). The residual solution (strongly EPR active) after about 5 days at room temperature deposited dark brown shiny crystals suitable for an X-ray diffraction study,† which proved them to be $Ph_2Sn(psq)_2$ **1**.‡ On the available evidence we believe that the primary reaction is given by eqn. (1), and the subsequent

$$Sn_2Ph_6 + pq \rightarrow Ph_3Sn(psq) + Ph_3Sn^{\cdot} \qquad (1)$$

processes include ligand redistribution to give the diradical.

The tin atom in **1** has a distorted *cis*-octahedral coordination (Fig. 1). The sensitive indicators of the oxidation state of the chelating ligand are known[2,5] to be the lengths of the C–O bonds (av. 1.23, 1.29 and 1.35 Å for the *o*-benzoquinone, *o*-semiquinone and catecholate) and the intervening C–C bond (1.53, 1.44 and 1.40 Å, respectively). Thus, the corresponding C–O and C–C distances in **1** [mean 1.291(6) and 1.44(1) Å] characterise it unequivocally as a semiquinone complex of tin(IV). The Sn–C distances in **1** (2.16 Å) are essentially equal and within the range (2.09–2.19 Å) observed in other $R_2Sn(O–O)_2$ complexes, *viz*. R = Me, O–O = tropolonate (**2**);[6,7] R = Me, O–O = kojate (6-hydroxymethyl-4*H*-pyran-4-on-3-olate) (**3**);[7] R = Me, O–O = maltolate (3-hydroxy-2-methyl-4*H*-pyran-4-oate) (**4**)[8] and R = Ph, O–O = maltolate (**5**).[8] On the other hand, Sn–O bonds formed by each semiquinone ligand show considerable non-equivalence (Δ) in length. Formally, such a ligand forms one covalent and one dative bond, and their unequal contribution can explain this difference. As Haaland[9] pointed out, a dative bond can have half the enthalpy of the corresponding covalent one and be 0.2 Å (or more) longer. Its length is also very sensitive to inductive effects of other ligands, increasing with their electron donating ability. Indeed, Δ in diphenyl complexes (0.08 Å in **1**, 0.16 Å in **4**) is much smaller than in dimethyl ones (0.34 Å in **3**, 0.28 Å in **5**) in accordance with the values of $\sigma_I$, −0.01 for Me and 0.12 for Ph.[10] However, in both polymorphs of **2**, Δ is only 0.04 Å, probably due to electron-poor character of the tropilium ring itself. It is noteworthy that the shorter Sn–O bonds are invariably in *trans*-positions to the less polar (Sn–C) ones, while exactly the opposite is observed in psq complexes of transition metals,[11] in accordance with the view[12] that in Sn complexes, less electronegative ligands exercise *cis*-influence, rather than *trans* (as for d elements).

The EPR spectra of the solution obtained finally in the reaction of $Sn_2Ph_6$ and pq show the presence of three species. The room temperature solution spectrum which shows hyperfine structure is predominantly that of the primary reaction product identified as the $Ph_3Sn(psq)$ monoradical, but the frozen solution spectrum showed, in addition to the $S = 1/2$ resonance ($g = 2.07$), both a fine structure and a resonance at half-field, indicating the presence of diradical species. The fine structure of the central resonance showed the presence of two such species, with $D = 63$ and $104 \times 10^{-4}$ cm$^{-1}$ respectively. The lower $D$ value is very close to that of *trans*-$Cl_2(dbsq)SnSn(dbsq)Cl_2$ ($dbsq^{\cdot-}$ = 3,5-di-*tert*-butylorthosemiquinonate anion)[1a] and is presumably from the analogous $Ph_2(psq)SnSn(psq)Ph_2$ compound with a Sn–Sn bond. The higher $D$ value can be assigned to **1**. It is of the same order as those observed for $Cd(dbsq)_2L$ (L = py, tmen, bipy) and related

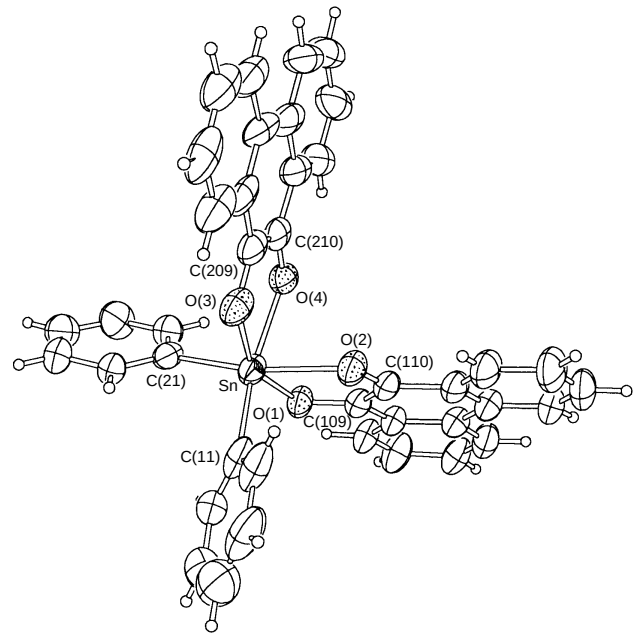



**Fig. 1** Molecular structure of $Ph_2Sn(psq)_2$ **1**, showing 50% probability ellipsoids. Selected bond distances (Å) and angles (°): Sn–O(1) 2.127(5), Sn–O(2) 2.210(5), Sn–O(3) 2.137(5), Sn–O(4) 2.214(5), Sn–C(11) 2.160(9), Sn–C(21) 2.157(7), O(1)–C(109) 1.298(8), O(2)–C(110) 1.284(9), O(3)–C(209) 1.296(10), O(4)–C(210) 1.287(9), C(109)–C(110) 1.446(10), C(209)–C(210) 1.430(12); O(1)–Sn–O(2) 75.8(2), O(3)–Sn–O(4) 76.0(2), C(11)–Sn–O(4) 164.7(3), C(21)–Sn–O(2) 163.8(3).

molecules,[13] but slightly smaller; the difference may be due to the larger size of psq$^{\cdot-}$ compared with dbsq$^{\cdot-}$.

This research was supported in part by grants from the National Sciences and Engineering Research Council of Canada (to B. R. M. and D. G. T.) and EPSRC of the UK (to A. S. B.).

## Footnotes

* E-mail: dgtuck@uwindsor.ca

† The diffraction experiment at $T$ = 150 K on a Siemens three-circle diffractometer with a CCD area detector (graphite-monochromated Mo-K$\alpha$ radiation, $\bar{\lambda}$ = 0.71073 Å, $\omega$ scan mode, $2\theta \leqslant 52°$); structure solution by Patterson method, refinement against $F^2$ of all data (SHELXTL software). The structure contains large cavities with highly disordered solvent of crystallisation, approximated by arbitrary C atoms at electron density peaks; no chemically sensible model could be found. *Crystal data* (neglecting the solvent): $C_{40}H_{26}O_4Sn$, $M$ = 689.3, monoclinic, space group $C2/c$ (no. 15), $a$ = 31.962(1), $b$ = 12.402(1), $c$ = 20.838(1) Å, $\beta$ = 120.20(1)°, $U$ = 7138.9(7) Å$^3$, $Z$ = 8, $D_c$ = 1.28 g cm$^{-3}$, $\mu$ = 7.5 cm$^{-1}$, crystal size 0.35 × 0.2 × 0.2 mm, 15612 reflections total, 6026 unique, 4224 observed, $R_{int}$ = 0.068, 459 variables, final $R(F$, obs. data) = 0.066, $R(F^2$, all data) = 0.188, goodness-of-fit 1.14, max. residual $\Delta\rho$ = 0.84 e Å$^{-3}$. Atomic coordinates, bond lengths and angles, and thermal parameters have been deposited at the Cambridge Crystallographic Data Centre (CCDC). See Information for Authors, Issue No. 1. Any request to the CCDC for this material should quote the full literature citation and the reference number 182/399.

‡ Elemental analysis. Calc. for $C_{40}H_{26}O_4Sn$, C 69.7, H 3.8. Found C 69.8, H 4.0%. Yield *ca.* 9%.

## References

1 (*a*) T. A. Annan, R. K. Chadha, D. G. Tuck and K. D. Watson, *Can. J. Chem.*, 1987, **65**, 2670; (*b*) T. A. Annan, B. R. McGarvey, A. Ozarowski, D. G. Tuck and R. K. Chadha, *J. Chem. Soc., Dalton Trans.*, 1989, 439; (*c*) T. A. Annan, R. K. Chadha, P. Doan, D. H. McConville, B. R. McGarvey, A. Ozarowski and D. G. Tuck, *Inorg. Chem.*, 1990, **29**, 3936; (*d*) M. A. Brown, B. R. McGarvey, A. Ozarowski and D. G. Tuck, *Inorg. Chem.*, 1996, **35**, 1560.
2 D. G. Tuck, *Coord. Chem. Rev.*, 1992, **112**, 215.
3 Z. Tian and D. G. Tuck, *J. Organomet. Chem.*, 1993, **462**, 125.
4 M. A. Brown, B. R. McGarvey, A. Ozarowski and D. G. Tuck, *J. Organomet. Chem.*, in the press.
5 R. M. Buchanan and C. G. Pierpont, *Coord. Chem. Rev.*, 1981, **38**, 45; O. Carugo, C. B. Castellani, K. Djinovic and M. Rizzi, *J. Chem. Soc., Dalton Trans.*, 1992, 837; B. R. McGarvey, A. Ozarowski and D. G. Tuck, *Inorg. Chem.*, 1993, **32**, 4474.
6 I. Waller, T. Hadler, W. Scwarz and J. Weidlein, *J. Organomet. Chem.*, 1982, **232**, 99.
7 T. P. Lockart and F. Davidson, *Organometallics*, 1987, **6**, 2471.
8 S. Bhattacharya, N. Seth, V. D. Gupta, H. North, K. Polborn, W. Thomann and H. Schwenk, *Chem. Ber.*, 1994, **127**, 1895.
9 A. Haaland, *Angew. Chem., Int. Ed. Engl.*, 1989, **28**, 992.
10 M. Charton, *Prog. Phys. Org. Chem.*, 1981, **13**, 119.
11 M. W. Lynch, R. M. Buchanan, C. G. Pierpont and D. N. Hendrickson, *Inorg. Chem.*, 1981, **20**, 1038; R. B. Lauffer, R. H. Heistand II and L. Que Jr., *Inorg. Chem.*, 1983, **22**, 50.
12 Yu. A. Buslaev, E. A. Kravchenko, M. Yu. Burtev and L. A. Aslanov, *Coord. Chem. Rev.*, 1989, **93**, 185.
13 A. Ozarowski, B. R. McGarvey, C. Peppe and D. G. Tuck, *J. Am. Chem. Soc.*, 1991, **113**, 3288.

*Received in Cambridge, UK, on 13th December 1996; Com. 6/08391I*

# Formation of platinum nanorods and nanoparticles in uniform carbon nanotubes prepared by a template carbonization method

**Takashi Kyotani,* Li-fu Tsai and Akira Tomita**

*Institute for Chemical Reaction Science, Tohoku University, 2-1-1 Katahira, Sendai 980-77 Japan*

**Template technique makes it possible to prepare Pt metal-filled uniform carbon nanotubes in which the metal is present as either nanorods or nanoparticles.**

Carbon tubes at the nanometre level have now been characterized as a new carbon material. Specifically, metal-filled carbon nanotubes could have a variety of industrial applications, as reviewed by Freemantle.[1] Thus the preparation and application of such filled nanotubes are now becoming a very challenging area of research. Carbon nanotubes have been prepared thus far mainly using an arc-discharge evaporation technique[2,3] or by thermal decomposition of benzene vapour,[4] and there have been several attempts to insert metal into the tubes prepared by the arc-discharge evaporation technique.[5–8] Recently, we have prepared carbon nanotubes by a template carbonization technique using an anodic aluminium oxide film,[9,10] which has an array of parallel and straight channels with a diameter of nanometre level and has been often utilized as a template to synthesize nanomaterials.[11–17] The most striking feature of our carbonization method is that it allows one to produce monodisperse carbon nanotubes with uniform length, diameter and thickness. Here, we attempt to prepare Pt metal-filled uniform carbon nanotubes with the template method using an anodic oxide film.

An oxide film was prepared by electro-oxidation of an aluminium plate (purity 99.99%) at a cell voltage of 20 V in sulfuric acid. The diameter and thickness of the resulting film were 15 mm and 75 μm, respectively, and its channel diameter was found to be *ca*. 30 nm. The film was placed in a vertical quartz reactor. The reactor temperature was raised to 800 °C under $N_2$ flow and then propene gas (2.5% in $N_2$) was passed through the reactor. The thermal decomposition of propene in the uniform straight channels of the anodic oxide film resulted in carbon deposition on the channel walls. After 3 h decomposition the reactor was cooled to room temp. and the film was taken out. Pt was loaded on this carbon-deposited film by the following evaporation method. The film was impregnated with an ethanol solution of hexachloroplatinic acid ($H_2PtCl_6 \cdot 6H_2O$) at room temp. for 3 h and then ethanol was evaporated at 80 °C under an $N_2$ flow with the film immersed in the solution. The reduction of chloroplatinic acid in the channels was performed by the following two methods; heat treatment at 500 °C under $H_2$ flow or stirring with an excess of a 0.1 M $NaBH_4$ aqueous solution at room temperature. After the reduction, the carbon-deposited film was washed with an excess of a 46% HF solution at room temp. to dissolve the anodic aluminium oxide template. As a result, a Pt metal/carbon nanotube composite was obtained as the insoluble fraction.

Fig. 1(*a*) and (*b*) show bright-field TEM images at different magnifications for the Pt/carbon tube composite prepared at 500 °C. These two images indicate the presence of uniform carbon nanotubes and their outer diameter and wall thickness can be estimated to be 30 nm and *ca.* 5 nm, respectively. Although some of the tubes are empty, the others are filled with many rod-like materials which are observed as dark images. The low-magnification TEM image [Fig. 1(*a*)] indicates that these nanorods are more abundant in the end of the tube hollows, where some of them are > 1 μm in length. Their structure was investigated by electron diffraction and X-ray powder diffraction (XRD). Fig. 1(*c*) shows the electron diffraction pattern which was taken from the TEM image [Fig. 1 (*b*)]. The pattern presents the diffraction from Pt metal crystallites as clear spots together with carbon 002 diffraction as a pair of strong arcs. Some of the spots from the fcc structure of Pt metal and carbon 002 arcs are labelled in the figure. This pattern confirms the dark material to be Pt metal. The appearance of the diffraction for Pt as clear spots, not as rings, indicates the high crystallinity of the Pt nanorods. The small number of these diffraction spots suggests the presence of only a few Pt crystallites in the area of Fig. 1(*b*). The XRD analysis also confirmed the reduction of chloroplatinic acid to Pt metal. From the peak width of the Pt(111) diffraction, the average crystallite size was calculated to be *ca.* 30 nm.

The TEM photographs of the composite reduced by $NaBH_4$ solution at room temp. are displayed in Fig. 2. Like the composites reduced at 500 °C, Pt metal is observed only in the carbon tube hollows and some tubes appear to be completely

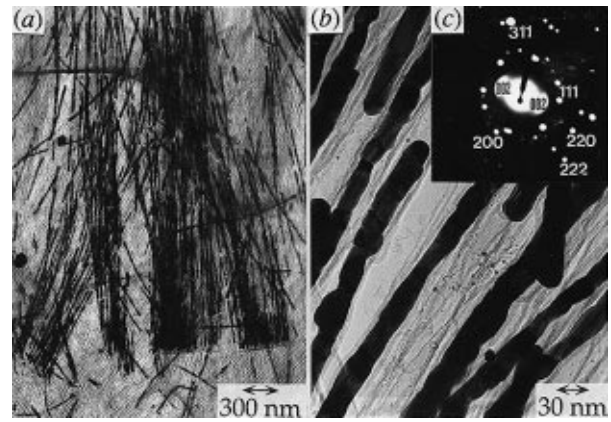



**Fig. 1** (*a*), (*b*) TEM photographs for Pt/carbon tube composites reduced at 500 °C; (*c*) electron diffraction pattern taken from the TEM image (*b*)

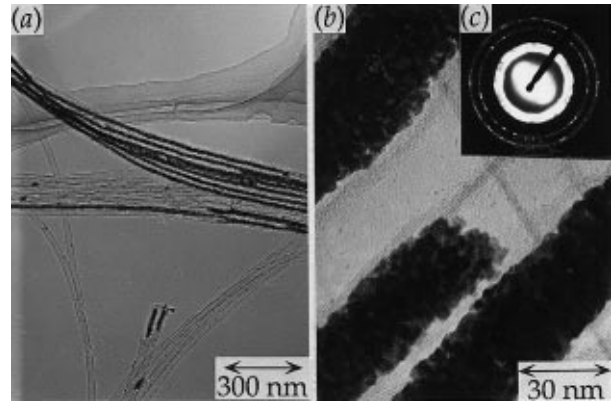



**Fig. 2** (*a*), (*b*) TEM photographs for Pt/carbon tube composites reduced at room temp; (*c*) electron diffraction pattern taken from the TEM image (*b*)

filled with the metal. There is, however, some difference in microscopic features between the two Pt metals prepared at different temperatures [Figs. 1(*b*) and 2(*b*)]. The Pt metal reduced at room temp. appears to consist of very fine particles of size 2–5 nm, which is in good agreement with the calculated value from the XRD analysis. The electron diffraction pattern of the Pt metal gives further information on its structure. The pattern [Fig. 2(*c*)] exhibits a set of diffraction rings from Pt metal (these rings can be indexed [from the inside as] 111, 200, 220, 311 reflectance fcc Pt), together with a pair of carbon 002 arcs. It is noteworthy that the diffraction from Pt metal did not appear as clear spots, but as concentric rings, each of which consists of a large number of very small spots. This finding suggests that the metal reduced by $NaBH_4$ solution is comprised of many fine crystallites, which accords with the microscopic difference between the two types of Pt metal.

For the above two types of composites, Pt was loaded by the evaporation to dryness method. On the other hand, when the impregnated film was removed from the chloroplatinic acid solution and then dried, less Pt was loaded in the carbon tubes Fig. 3 shows the bright-field TEM image of the composite prepared by this loading method, where the reduction of Pt was performed with $NaBH_4$ solution at room temp. The image does not reveal rod-like Pt metal, but rather, very fine Pt particles in the hollows. Some of Pt particles form agglomerates with each other and the size varies from 1 to 4 nm.

Although the carbon nanotubes prepared by our template technique are not structurally perfect, their length, diameter and thickness are controllable and monodisperse. Here, by applying the template technique, we have succeeded in preparing Pt metal-filled uniform carbon nanotubes in which the metal is present as either nanorods or nanoparticles. It should be noted that no Pt metal was observed on the outside wall of the tubes. This is due to the preparation procedure, *viz*., chloroplatinic acid as the Pt metal precursor was loaded into the carbon-deposited alumina film before dissolution of the alumina by HF; thus there is no other space for Pt to be loaded except within the channels.

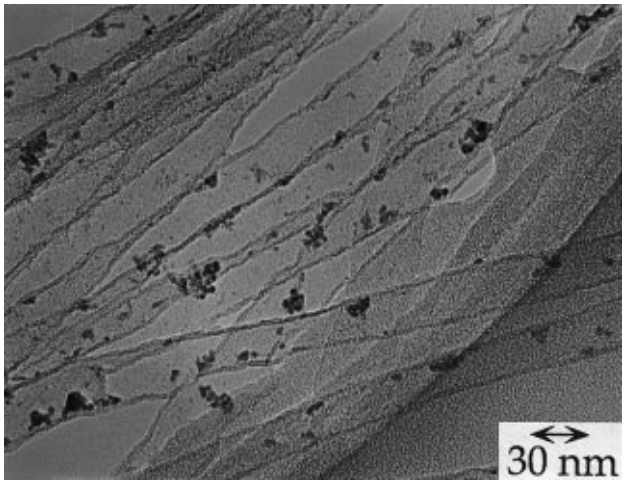



**Fig. 3** Bright-field TEM image of Pt nanoparticles in carbon tubes

We thank the High Voltage Electron Microscope Laboratory of Tohoku University for microscopical analysis. This study was partly supported by Special Coordination Funds for Promising Science and Technology from Science and Technology Agency, Japan, the Ministry of Education, Science, Sports and Culture of Japan (07650777) and the Mitsubishi Foundation.

## Footnote

* E-mail: kyotani@icrs.tohoku.ac.jp

## References

1 M. Freemantle, *Chem. Eng. News*, 1996, **74**, 62.
2 S. Iijima, *Nature*, 1991, **354**, 56.
3 T. W. Ebbesen and P. M. Ajayan, *Nature*, 1992, **358**, 220.
4 M. Endo, K. Takeuchi, S. Igarashi, K. Kobori, M. Shiraishi and H. W. Kroto, *J. Phys. Chem. Solids*, 1993, **54**, 1841.
5 P. W. Ajayan and S. Iijima, *Nature*, 1993, **361**, 333.
6 S. C. Tsang, Y. K. Chen, P. J. F. Harris and M. L. H. Green, *Nature*, 1994, **372**, 159.
7 R. M. Largo, S. C. Tsang, K. L. Lu, Y. K. Chen and M. L. H. Green, *J. Chem. Soc., Chem. Commun.*, 1995, 1355.
8 B. C. Satishkumar, A. Govindaraj, J. Mofokeng, G. N. Subbanna and C. N. R. Rao, *J. Phys. B: At. Mol. Opt. Phys.*, 1996, **29**, 4925.
9 T. Kyotani, L. Tsai and A. Tomita, *Chem. Mater*., 1995, **7**, 1427.
10 T. Kyotani, L. Tsai and A. Tomita, *Chem. Mater*., 1996, **8**, 2109.
11 W. Liang and C. R. Martin, *J. Am. Chem. Soc.*, 1990, **112**, 9666.
12 C. J. Brumlik and C. R. Martin, *J. Am. Chem. Soc*., 1991, **113**, 3174.
13 J. D. Klein, R. D. Herrick II, D. Palmer, M. J. Sailor, C. J. Brumlik and C. R. Martin, *Chem. Mater*., 1993, **5**, 902.
14 C. R. Martin, *Science*, 1994, **266**, 1961.
15 B. Xiaohua, L. Feiyue and R. M. Metzger, *J. Appl. Phys.*, 1996, **79**, 4866.
16 P. Hoyer, *Langmuir*, 1996, **12**, 1411.
17 R. V. Parthasarathy, K. L. N. Phani and C. R. Martin, *Adv. Mater*., 1995, **7**, 896.

*Received in Cambridge, UK on 17th December 1996; Com. 6/08439G*

# The novel heterometallic polymeric helical chain cluster $\{[W_3Ag_3S_{12}]\}_n[Nd(Me_2SO)_8]_n$

**Qun Huang, Xintao Wu* and Jiaxi Lu**

*State Key Laboratory of Structural Chemistry, Fujian Institute of Research on the Structure of Matter, Chinese Academy of Sciences, Fuzhou, Fujian 350002, P.R. China*

**$\{[W_3Ag_3S_{12}]\}_n[Nd(Me_2SO)_8]_n$, showing a novel helical chain configuration and derived from the influence of the dimension of the cation on the self-assembly of $[WS_4]^{2-}$ and $Ag^+$, is described.**

Polymeric transition-metal chalcogenides have attracted much attention because of their possible properties directly derived from their peculiar solid-state structures.[1,2] For example, low-dimensional chalcogenides with the general formula $MCu_{2n}S_{n+1}$ (where M is a monovalent metal) were found to have relatively high conductivity, and furthermore an interesting structural relationship also found.[3,4] The general polymeric configuration of W(Mo)–Ag–S complexes is linear, such as in $(PPh_4)AgMoS_4$,[5] $\{[AgMS_4]\}_n[4\text{-Hmpy}]_n$[6] and $\{[AgWS_4]\}_n[H_3NC(CH_2OH)_3]_n[dmf]_{2n}$.[7] Recently, we have found that the self-assembly of ammonium tetrathiotungstate and silver nitrate is subject to the appropriate small molecules and the valence state of the cation, which is very rare for polymeric transition-metal chalcogenides; for example, water molecules are conducive to the transformation of the single linear chain $\{[WS_4Ag]\}_n[H_3NC(CH_2OH)_3]_n[dmf]_{2n}$[7] to the double chain $\{[WS_4Ag]\}_n[H_3NC(CH_2OH)_3]_n[H_2O]_n$,[7] and the divalent cation $[Ca(Me_2SO)_6]^{2+}$ and the trivalent cation $[Nd(dmf)_8]^{3+}$ are conducive to the zigzag chain $\{[W_4S_{16}Ag_4]\}_n[Ca(Me_2SO)_6]_n$[8] and the one-dimensional chain $\{[W_4S_{16}Ag_5]\}_n[Nd(dmf)_8]_n$,[9] respectively. Herein, the synthesis and crystal structure of the polymeric cluster complex $\{[W_3Ag_3S_{12}]\}_n[Nd(Me_2SO)_8]_n$ **1** with a novel helical chain configuration are reported, which is derived from the influence of the dimension of the cation on the self-assembly of ammonium tetrathiotungstate and silver nitrate.

The reaction of $(NH_4)_2[WS_4]$ and $AgNO_3$ in the presence of $Nd^{3+}$ in $Me_2SO$–MeCN solution (molar ratio of 2 : 4 : 1) leads to orange crystals of complex **1** in 45% yield after allowing the orange–red filtrate to stand in air for one day.† As in the synthesis of $\{[W_4S_{16}Ag_5]\}_n[Nd(dmf)_8]_n$,[9] the trivalent lanthanide cations $Nd^{3+}$, which are oxygenphilic, were also employed as complementary cations. The resulting larger complex cations $[Nd(Me_2SO)_8]^{3+}$ are smaller than the cations $[Nd(dmf)_8]^{3+}$ of the one-dimensional polymeric cluster $\{[W_4S_{16}Ag_5]\}_n[Nd(dmf)_8]_n$. As a consequence of their smaller size, the cations $[Nd(Me_2SO)_8]^{3+}$ induce $WS_4^{2-}$ and $Ag^+$ to self-assemble into $[(W_3Ag_3S_{12})^{3-}]_n$ helical chains rather than $[(W_4S_{16}Ag_5)^{3-}]_n$ one-dimensional chains. The synthesis of complex **1** clearly shows that the self-assembly of $WS_4^{2-}$ and $Ag^+$ is very flexible and subject to the size of the complex cation.

Complex **1** crystallizes in the monoclinic system with space group $P2_1/n$.‡ An ORTEP drawing of a portion of the anion is shown in Fig. 1. The configuration of the polymeric anion can be viewed as a helical chain which is propagated along the crystallographic *b* axis. For clarity, the simplified diagram is shown (Fig. 2) with S atoms omitted. It is seen that the chain turns at each W atom.

All the W atoms are coordinated by one terminal S, two μ-S and one $\mu_3$-S atoms with an approximately tetrahedral geometry [106.7(2)–113.2(2)°]. However, the coordination tetrahedron around the Ag atoms, formed by two μ-S and two $\mu_3$-S atoms, is much more distorted, the coordination angles ranging from 88.4(2) to 143.8(2)°. The average W–Ag–W and Ag–W–Ag angles are 167.63(7) and 93.26(5)°, respectively. The bond lengths W–$S_t$, W–μ-S and W–$\mu_3$-S differ with average values being 2.136, 2.201 and 2.235 Å, respectively. By comparison, the W–$S_t$, W–μ-S and W–$\mu_3$-S bond lengths are 2.128, 2.190 and 2.248 Å in $\{[W_4S_{16}Ag_5]\}_n[Nd(dmf)_8]_n$,[9] 2.146, 2.199 and 2.250 Å in $\{[W_4S_{16}Ag_4]\}_n[Ca(Me_2SO)_6]_n$,[8] and 2.144, 2.217

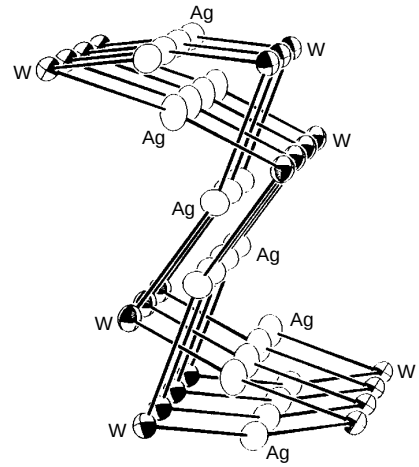



**Fig. 2** Simplified diagram of the anionic helical chain. For clarity, the sulfur atoms are omitted.

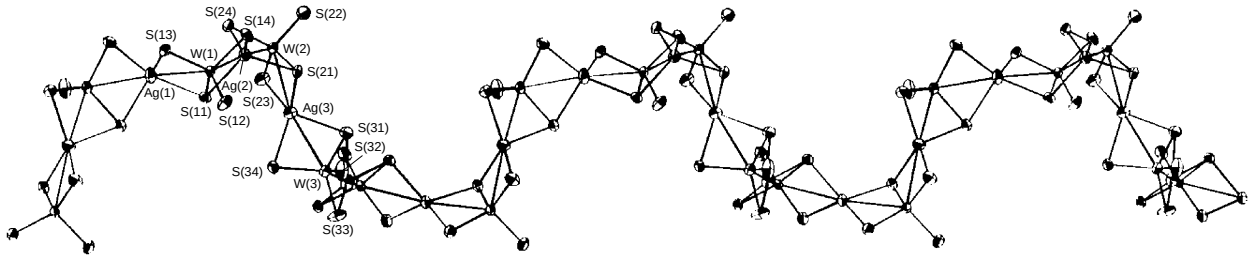



**Fig. 1** ORTEP drawing of a portion of the anion of $\{[W_3Ag_3S_{12}]\}_n[Nd(Me_2SO)_8]_n$ with atomic labelling (20% displacement ellipsoids)

and 2.242 Å in $[\{Ag(PPh_3)\}_3WS_4\{S_2P(OEt)_2\}]$,[10] respectively. The average Ag–S length of 2.564 Å is comparable to the values observed in other polymeric complexes, such as 2.548 Å in $\{[W_4S_{16}Ag_4]\}_n[Ca(Me_2SO)_6]_n$,[8] 2.565 Å in $\{[WS_4Ag]\}_n[H_3NC(CH_2OH)_3]_n[H_2O]_n$,[7] and 2.543 Å in $\{[W_4S_{16}Ag_5]\}_n[Nd(dmf)_8]_n$.[9] However, the average W–Ag length of 2.970 Å is longer than those found in the linear chain complexes $\{[WS_4Ag]\}_n[H_3NC(CH_2OH)_3]_n[dmf]_{2n}$[7] (2.931 Å) and $\{[WS_4Ag]\}_n[NH_4]_n$[9] (2.928 Å), but comparable to those in $\{[W_4S_{16}Ag_5]\}_n[Nd(dmf)_8]_n$[9] (2.964 Å) and in $\{[W_4S_{16}Ag_4]\}_n$-$[Ca(Me_2SO)_6]_n$[8] (2.969 Å).

The single-crystal diffraction analysis shows that one trivalent cation $[Nd(Me_2SO)_8]^{3+}$ is related with the cyclic anionic unit $[W_3Ag_3S_{12}]^{3-}$. The trivalent cations $[Nd(Me_2SO)_8]^{3+}$ are arrayed among the anionic helical chains; these cations are well separated from each other and from the anionic chains. The packing diagram of the unit cell is shown in Fig. 3. Each $Nd^{III}$ atom is coordinated by eight $Me_2SO$ molecules. The average Nd–O bond length is 2.41 Å, and the O–Nd–O angles vary between 64.8(7) and 146.1(6)°; these are comparable to those of another trivalent complex cation $[Nd(dmf)_8]^{3+}$ (average Nd–O lengths of 2.43 Å and O–Nd–O angles between 70.4 and 144.8°) in $\{[W_4S_{16}Ag_5]\}_n[Nd(dmf)_8]_n$.[9] The shortest distance between two Nd atoms is 11.01 Å.

Financial support from the State Key Laboratory of Structural Chemistry, from Fujian Institute of Research on the Structure of Matter, Chinese Academy of Sciences, from the NNSF of China and from the NSF of the Province of Fujian is gratefully acknowledged.

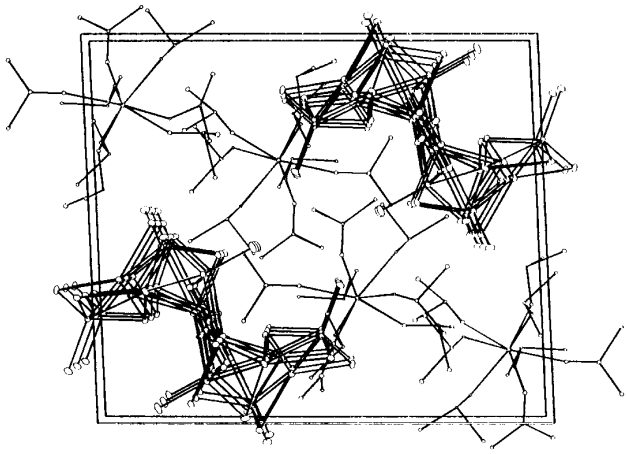


**Fig. 3** Packing drawing of the unit cell viewed down the *b* axis

## Footnotes

* E-mail: wxt@ms.fjirsm.ac.cn

† Complex **1** is only slightly soluble in $Me_2SO$. Elemental analysis. Found: C, 9.52; H, 2.34; S, 31.51; W, 27.24. Calc.: C, 9.47; H, 2.38; S, 31.60; W, 27.18%. IR (KBr pellet, $cm^{-1}$): S=O 1004.9, 954.7 and 935.4; 489.9 (W–$S_t$), 439.7 (W–μ-S), 422.4 and 407.2 (W–$\mu_3$-S).

‡ *Crystal data* for **1**. $Ag_3S_{12}W_3{\cdot}C_{16}H_{48}NdO_8S_8$, $M$ = 2029.24, monoclinic, space group $P2_1/n$; 0.30 × 0.20 × 0.10 mm; $a$ = 15.3985(1), $b$ = 20.0716(2), $c$ = 17.7791(3) Å, β = 92.54(1)°, $U$ = 5489.65(11) $Å^3$, $Z$ = 4, $D_c$ = 2.453 g $cm^{-3}$, λ(Mo-Kα) = 0.71069 Å, μ(Mo-Kα) = 91.26 $cm^{-1}$. The intensity data were collected at room temperature on a Siemens Smart CCD diffractometer. 6070 Absorption-corrected reflections with $I > 2.0\sigma(I)$ of the unique 7875 reflections were used to solve the structure using the SHELXTL-93 program. Except for the sulfur atoms of the $Me_2SO$ groups, metal and other sulfur atoms were refined anisotropically. No attempt was made to locate hydrogen atoms. The final cycle of full-matrix least-squares refinement was converged with $R = \Sigma(||F_o| - |F_c||)/\Sigma|F_o| = 0.056$ and $wR = \{\Sigma w[(F_o^2 - F_c^2)^2]/\Sigma w[(F_o^2)^2]\}^{\frac{1}{2}} = 0.13$ $\{w = [\sigma^2(F_o^2) + (0.0584\,P)^2 + 108.1857P]^{-1}\}$. Atomic coordinates, bond lengths and angles, and thermal parameters have been deposited at the Cambridge Crystallographic Data Centre (CCDC). See Information for Authors, Issue No. 1. Any request to the CCDC for this material should quote the full literature citation and the reference number 182/401.

## References

1 D. W. Murphy and P. A. Christian, *Science*, 1979, **205**, 651; M. S. Whittingham, *Prog. Solid State Chem*., 1978, **12**, 41.
2 R. R. Chianelli, T. A. Pecoraro, T. R. Halbert, H. W. Pan and E. I. Stiefel, *J. Catal*., 1984, **86**, 226.
3 G. V. Vajenine and R. Hoffmann, *Inorg. Chem*., 1996, **35**, 451.
4 R. Berger, R. Dronskowski and L. Norén, *J. Solid State Chem*., 1994, **112**, 120; R. Berger, *J. Less-Common Met*., 1989, **147**, 141; B. P. Ghosh, M. Chaudhury and K. Nag, *J. Solid State Chem*., 1983, **47**, 307.
5 A. Müller, W. Jaegermann and W. Hellmann, *J. Mol. Struct*., 1983, **100**, 559; A Müller and W. Hellmann, *Spectrochim. Acta, Part A*, 1985, **41**, 359.
6 J.-P. Lang, J.-G. Li, S. Bao and X.-Q. Xin, *Polyhedron*, 1993, **12**, 801.
7 Q. Huang, X.-T. Wu, T.-L. Sheng and Q.-M. Wang, *Inorg. Chem*., 1995, **27**, 4931.
8 Q. Huang, X.-T. Wu and J.-X. Lu, *Inorg. Chem*., in the press.
9 Q. Huang, X.-T. Wu, Q.-M. Wang, T.-L. Sheng and J.-X. Lu, *Angew. Chem*., 1996, **108**, 985; *Angew. Chem., Int. Ed. Engl*., 1996, **35**, 868.
10 S.-W. Du, N.-Y. Zhu, P.-C. Chen and X.-T. Wu, *J. Mol. Struct*., 1993, **291**, 167.

*Received in Cambridge, UK on 4th February 1997; Com. 7/00818J*

# Molecular and electronic structure of a mixed-valent class II, dinuclear complex containing a linear $[Fe^{II}–O–Fe^{III}]^{3+}$ core

**Michael Müller, Eckhard Bill, Thomas Weyhermüller and Karl Wieghardt***

*Max-Planck-Institut für Strahlenchemie, PO Box 101365, D-45413 Mülheim an der Ruhr, Germany*

**One-electron reduction of $[\{LFe^{III}(Ph_2acac)\}_2(\mu\text{-}O)][BPh_4]_2$ $\mathbf{1}[BPh_4]_2$ (L = 1,4,7-trimethyl-1,4,7-triazacyclononane, $Ph_2acac^-$ = 1,3-diphenylpropane-1,3-dionate) in $CH_2Cl_2$–toluene by 1 equiv. of cobaltocene produces the mixed-valent complex $[\{LFe(Ph_2acac)\}_2(\mu\text{-}O)][BPh_4]\cdot C_6H_5Me$ $\mathbf{2}[BPh_4]\cdot C_6H_5Me$ which is characterized by X-ray crystallography; 2 has an $S = \frac{1}{2}$ ground state (antiferromagnetically coupled high-spin $Fe^{III}$ and high-spin $Fe^{II}$ with $J = -65$ cm$^{-1}$) and exhibits class II behaviour according to the Robin and Day classification.**

Mixed-valent $Fe^{II}Fe^{III}$ forms have been spectroscopically identified for the non-haem metalloproteins hemerythrin, the R2 subunit of ribonucleotide reductase and methane monooxygenase.[1] In their active sites an antiferromagnetically exchange coupled pair of a high-spin iron(II) and a high-spin iron(III) bridged by a μ-hydroxo or a μ-oxo group give rise to a characteristic, EPR-active $S = \frac{1}{2}$ ground state with $g$ values $< 2.0$. We have recently reported the first μ-hydroxo bridged, mixed-valent complex $[L_2Fe_2(\mu\text{-}OH)(\mu\text{-}O_2CBu^t)_2][ClO_4]_2$ (L = 1,4,7-trimethyl-1,4,7-triazacyclononane) which displays a rhombic EPR signal at 10 K with $g$ values of 1.95, 1.52 and 1.43.[2] A structurally characterised dincuclear complex containing a linear $[Fe^{II}–O–Fe^{III}]^{3+}$ core has not been described to date. Here we report the molecular and electronic structure of such a species.

The reaction† of $[LFe^{III}Cl_3]$[3] and potassium 1,3-diphenylpropane-1,3-dionate (1 : 1) in MeCN–$H_2O$ (8 : 1) yields upon addition of $NEt_3$ and $NaClO_4$ orange crystals of $[\{LFe^{III}(Ph_2acac)\}_2(\mu\text{-}O)][ClO_4]_2$ $\mathbf{1}[ClO_4]_2$ which was converted to $\mathbf{1}[BPh_4]_2$ by metathesis. One-electron reduction of $\mathbf{1}[BPh_4]_2$ in dry $CH_2Cl_2$–toluene by 1 equiv. of cobaltocene† afforded deep-green microcrystals of $[\{LFe(Ph_2acac)\}_2(\mu\text{-}O)]BPh_4\cdot C_6H_5Me$ $\mathbf{2}[BPh_4]\cdot C_6H_5Me$ which crystallises in the triclinic space group $P\bar{1}$ with two formula units per unit cell.‡ Two independent μ-oxo atoms [O(1) and O(4)] lie on a crystallographic centre of symmetry and, consequently, both $Fe^{II}$–O–$Fe^{III}$ cores are linear. The methylene carbon atoms C(1)–C(6) of the macrocyclic amine coordinated to Fe(1) and Fe(1′) display small, 'normal' anisotropic thermal parameters ($U_{eq} \approx 0.029$ Å$^2$) whereas those of the corresponding atoms of the macrocycle coordinated to Fe(2) and Fe(2′) are significantly larger ($U_{eq} \approx 0.062$ Å$^2$). The five-membered Fe–N–C–C–N chelate rings adopt either (λλλ) or (δδδ) conformation. In the monocation composed of Fe(1) and Fe(1′) these two conformations are related by a crystallographic inversion centre and the resulting achiral *meso* isomer is ordered (Fig. 1). In contrast, the other cation comprising Fe(2) and Fe(2′) shows a static disorder because the two enantiomeric forms, (λλλ)FeFe(λλλ) and (δδδ)FeFe(δδδ), occupy this position. Note that a statistical ratio of the two diasteriomeric forms of 1 : 1 is expected from the synthesis. The $Fe–O_{oxo}$ distances at 1.877(1) and 1.901(1) Å are slightly longer than in oxo-bridged diiron(III) complexes (*ca.* 1.80 Å).[4]

The cyclic voltammogram of $\mathbf{1}[ClO_4]_2$ in MeCN (0.1 M $NBu_4PF_6$) in the potential range +1.3 to −1.8 V *vs.* $Fc^+$–Fc displays one reversible one-electron transfer wave at $E_{1/2} = -0.966$ V *vs.* $Fc^+$–Fc which is assigned to the couple **1**–**2**.

From temperature-dependent magnetic susceptibility measurements using a SQUID magnetometer (4–300 K) an $S = 0$ ground state was established for $\mathbf{1}[ClO_4]_2$ with $J = -95$ cm$^{-1}$, $g = 2.0$ (fixed) and a paramagnetic impurity ($S = 5/2$) of 2,6% ($H = -2J\cdot S_1\cdot S_2$, $S_1 = S_2 = 5/2$). This antiferromagnetic coupling is typical for complexes with a linear $[Fe^{III}–O–Fe^{III}]^{4+}$ core.[4] For $\mathbf{2}[BPh_4]\cdot C_6H_5Me$ a similar antiferromagnetic coupling was detected yielding an $S = \frac{1}{2}$ ground state with $J = -65$ cm$^{-1}$, $g = 2.0$ (fixed) ($S_1 = 5/2$, $S_2 = 2$) and a weakly coupled ($J = -10$ cm$^{-1}$) dincuclear $Fe^{II}_2$ impurity of 5% which most probably corresponds to the fully reduced, μ-OH bridged form of **2**.

The $S = \frac{1}{2}$ ground state for $\mathbf{2}[BPh_4]\cdot C_6H_5Me$ was confirmed by its X-band EPR-spectrum measured at 4 K in $CH_2Cl_2$. A rhombic signal is observed (Fig. 2) at $g$-values of 1.99, 1.93 and 1.84. In contrast, $\mathbf{1}[ClO_4]_2$ is EPR silent.§ The rhombic signal of **2** displays a significantly narrower spread of $g$-values as compared to the μ-hydroxo bridged $Fe^{II}Fe^{III}$ species in ref. 1. This observation agrees nicely with spectra reported for the mixed-valent μ-oxo- and μ-hydroxo-bridged mixed-valent forms of the R2 subunit of ribonucleotide reductase, methane monooxygenase and hemerythrin.[1]

The electronic spectrum of $\mathbf{2}[BPh_4]$ in $CH_2Cl_2$ solution displays an intervalence absorption maximum at 635 nm ($\varepsilon = 1.2 \times 10^3$ M$^{-1}$ cm$^{-1}$) which is absent in the spectrum of **1**. A similar but much weaker maximum has been observed at 1350 nm ($\varepsilon = 138$ M$^{-1}$ cm$^{-1}$) for the μ-hydroxo bridged analogue.[2]

Temperature-dependent zero-field Mössbauer spectra of crystalline samples of $\mathbf{1}[ClO_4]_2$ and $\mathbf{2}[BPh_4]\cdot C_6H_5Me$ characterise **2** as a class II mixed-valent species.

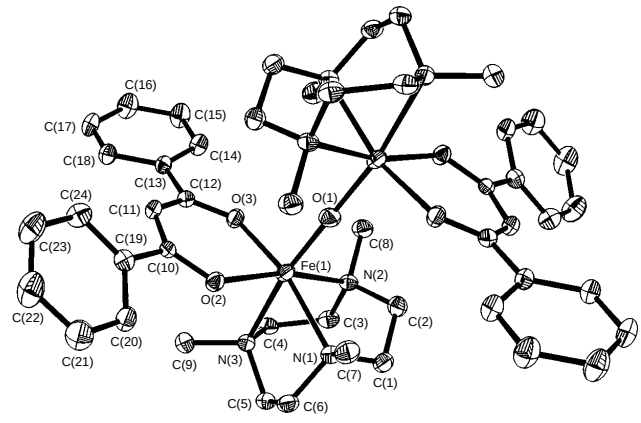



**Fig. 1** Structure of one of the monocations in crystals of $\mathbf{2}[BPh_4]\cdot C_6H_5Me$ at 100(2) K (the ordered *meso* form is shown). Selected bond lengths (Å) and angles (°) with estimated standard deviations in parentheses: Fe(1)–O(1) 1.877(1), Fe(1)–O(2) 2.063(2), Fe(1)–O(3) 2.056(2), Fe(1)–N(1) 2.232(3), Fe(1)–N(2) 2.234(3), Fe(1)–N(3) 2.341(3); Fe(1)–O(1)–Fe(1′) 180.

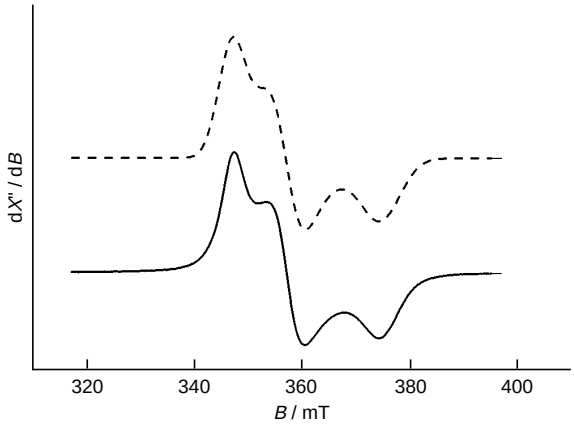



**Fig. 2** X-Band EPR spectrum of **2**[$BPh_4$]·$C_5H_5Me$ in $CH_2Cl_2$ at 4 K: the solid line represents the experimental spectrum and the dashed line is a simulation with $g_x$ = 1.99, $g_y$ = 1.93, $g_z$ = 1.84 (with linewidths: $w_x$ = 2.93, $w_y$ = 3.30, $w_z$ = 4.12 mT).

At temperatures > 200 K the spectra of **2** consist of a symmetric quadrupole doublet with isomer shift δ = 0.78 mm $s^{-1}$ and quadrupole splitting $\Delta E_Q$ = 0.37 mm $s^{-1}$. This value of δ is intermediate between that of **1** (δ = 0.48 mm $s^{-1}$, $\Delta E_Q$ = 1.30 mm $s^{-1}$ at 80 K) and that of the diiron(II) reference compound [$L_2Fe^{II}_2$(μ-OH)(μ-$O_2$CMe)$_2$][$ClO_4$][5] (δ = 1.15 mm $s^{-1}$ at 77 K). Due to the observed temperature-dependent line broadening in the spectrum of **2** we propose that this species exhibits class-II type[6] dynamic valence detrapping of the [$Fe^{II}$–O–$Fe^{III}$]$^{3+}$ core with electron hopping at 200 K being fast on the Mössbauer timescale ($10^{-7}$ s) rather than quantum-mechanical valence delocalisation (class III).[7] The Mössbauer linewidths of **2** increase drastically with decreasing temperature (Γ = 0.47 mm $s^{-1}$ at 200 K, 0.76 mm $s^{-1}$ at 160 K and 1.16 mm $s^{-1}$ at 120 K). Further lineshape distortions at temperatures < 40 K can be assigned to the onset of spin-relaxation processes. Therefore, it is not possible to record unperturbed quadrupole spectra in the slow limit of electron hopping at cryogenic temperatures (< 10 K).

## Footnotes

* E-mail: wieghardt@mpi-muelheim.mpg.de

† *Preparation of complexes*: To a mixture of MeCN (80 ml) and water (10 ml) was added [$LFe^{III}Cl_3$] (1.0 g, 3.0 mmol) and K[$Ph_2$acac] (1.0 g, 3.8 mmol) with stirring at ambient temperature. To the deep-red solution were added a few drops of $NEt_3$. After 2 h of stirring the orange–yellow solution was filtered and $NaClO_4$ (1.0 g) was added. Within a few days orange crystals of **1**[$ClO_4$]$_2$ were obtained in 67% yield (1.10 g). **1**[$BPh_4$]$_2$ was prepared from an acetone solution of **1**[$ClO_4$]$_2$ by adding $NaBPh_4$.

The following reduction was performed under strictly anaerobic conditions (argon) using Schlenk glassware. A solution of **1**[$BPh_4$]$_2$ (0.3 g, 0.20 mmol) and [Co(η-$C_5Me_5$)$_2$] (0.05 g, 0.25 mmol) in dry, deoxygenated $CH_2Cl_2$ (40 ml) was stirred at room temp. for 30 min. From the deep-green solution yellow microcrystals of [Co(η-$C_5H_5$)$_2$][$BPh_4$] precipitated which were filtered off under argon. After addition of dry, $O_2$-free toluene (40 ml) and reduction of the reaction volume by slow evaporation deep-green crystals of **2**[$BPh_4$]·$C_6H_5Me$ precipitated (0.05 g, 20%) which were suitable for X-ray crystallography. Satisfactory elemental analyses for all complexes were obtained.

UV–Vis spectra: **1**[$ClO_4$]$_2$ in MeCN: $\lambda_{max}$ = 283 nm (ε = 3.9 × $10^4$ $M^{-1}$ $cm^{-1}$), 367 (2.9 × $10^4$), 432 (1.65 × $10^4$), 510 (2.2 × $10^3$).

**2**[$BPh_4$]·$C_6H_5Me$ in $CH_2Cl_2$: $\lambda_{max}$ = 228 nm (2.5 × $10^4$ $M^{-1}$ $cm^{-1}$), 362 (1.7 × $10^4$), 635 (1.2 × $10^3$).

‡ *Crystal data*: $C_{79}H_{92}BFe_2N_6O_5$ **2**[$BPh_4$]·$C_6H_5Me$, $M$ = 1328.1, triclinic, space group $P\bar{1}$, $a$ = 11.193(2), $b$ = 15.181(3), $c$ = 22.123(3) Å, α = 83.30(2), β = 88.76(2), γ = 69.77(2)°, $U$ = 3502.5(10) $Å^3$, $Z$ = 2, $D_c$ = 1.259 g $cm^3$, λ(Mo-Kα) = 0.710 73 Å, $F$(000) = 1410, μ = 0.47 $mm^{-1}$, $T$ = 100(2) K, 11311 independent reflections were used in the refinement of which 7254 were observed [$F_0 > 4\sigma(F_0)$]; $R$ = 0.053.

Atomic coordinates, bond lengths and angles, and thermal parameters have been deposited at the Cambridge Crystallographic Data Centre (CCDC). See Information for Authors, Issue No. 1. Any request to the CCDC for this material should quote the full literature citation and the reference number 182/391.

§ The sample investigated displayed a weak signal at $g$ = 4.3 at 10 K due to the mononuclear impurity ($S$ = 5/2).

## References

1 For a leading recent reference to this literature see: R. Davidov, S. Kuprin, A. Gräslund and A. Ehrenberg, *J. Am. Chem. Soc.*, 1994, **116**, 11 120.
2 U. Bossek, H. Hummel, T. Weyhermüller, E. Bill and K. Wieghardt, *Angew. Chem., Int. Ed. Engl.*, 1995, **34**, 2642.
3 K. Wieghardt, K. Pohl and D. Ventur, *Angew. Chem., Int. Ed. Engl.*, 1985, **24**, 392.
4 D. M. Kurtz, Jr., *Chem. Rev.*, 1990, **90**, 585.
5 J. A. R. Hartman, R. L. Rardin, P. Chaudhuri, K. Wieghardt, B. Nuber, J. Weiss, G. C. Papaefthymiou, R. B. Frankel and S. J. Lippard, *J. Am. Chem. Soc.*, 1987, **109**, 7387.
6 M. B. Robin and P. Day, *Adv. Inorg. Chem. Radiochem.*, 1967, **10**, 247.
7 X.-Q. Ding, E. L. Bominaar, E. Bill, H. Winkler, A. X. Trautwein, S. Drüeke, P. Chaudhuri and K. Wieghardt, *J. Chem. Phys.*, 1990, **92**, 178.

*Received in Basel, Switzerland on 3rd December 1996; Com. 6/08159B*

# Formation of $H_2SO_4$ from $SO_3$ and $H_2O$, catalysed in water clusters

**E. V. Akhmatskaya, C. J. Apps, I. H. Hillier, A. J. Masters, N. E. Watt and J. C. Whitehead***

*Chemistry Department, University of Manchester, Manchester, UK M13 9PL*

**Computer simulations predict the facile conversion of $SO_3$ to $H_2SO_4$ in small water clusters having in excess of about twelve solvent molecules, in line with experiment.**

The gas-phase reaction of $SO_3$ with water vapour is considered to be the final stage in the tropospheric oxidation of $SO_2$ to form acid rain and sulfuric acid aerosols. These are important in heterogeneous stratospheric chemistry and ozone depletion, and also in climatology through the nucleation of cloud droplets in the lower troposphere which can scatter both incoming solar radiation and IR radiation from the Earth's surface.

Recent *ab initio* calculations[1] have shown that the barrier for the 1 : 1 reaction of $H_2O + SO_3$ is quite high (32 kcal $mol^{-1}$, cal = 4.184 J), and is considerably lowered (to 11.5 kcal $mol^{-1}$) by the catalytic effect of a second water molecule, enabling a six-membered transition state to be achieved. It is of interest from the point of view of atmospheric chemistry to know the minimum number of water molecules, in a water cluster containing $SO_3$, needed to allow for the facile formation of sulfuric acid.

Studies of reactions using aqueous clusters are a convenient way to study the transition from the gas phase to the condensed liquid phase and thereby investigate the effect of solvation on the dynamics of a reaction in a controlled and systematic manner. Hofmann–Sievert and Castleman[2] have studied the gas-phase reaction of $SO_3$ with small water clusters ($n$ = 2–10) and we first report here an experimental study of the reactivity of $SO_3$ attached to larger water clusters ($n \approx 200$). The details of the experiment have been fully described previously.[3,4] Briefly, a single $SO_3$ molecule is deposited using the pick-up method onto a large water cluster formed by a supersonic molecular beam expansion of pure water vapour at *ca* 1.2 bar. Downstream from the expansion region the beam is detected by an electron-impact ionisation quadrupole mass spectrometer after a flight time of *ca*. 0.5 ms. The mass spectrum (Fig. 1) of pure gas-phase $SO_3$ and of the $SO_3(H_2O)_{200}$ cluster, clearly show the $SO_3$ to be converted into $H_2SO_4$ by reaction with the cluster. A similar behaviour was found by Hofmann-Sievert and Castleman[2] for the smaller clusters and the identity of the reaction product confirmed with electric deflection studies.

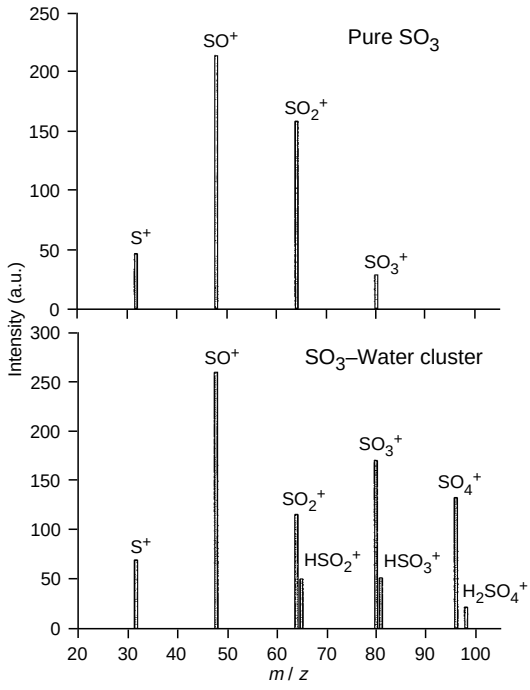



**Fig. 1** Comparison of the mass spectrum for gas-phase $SO_3$ (upper panel) with $SO_3$ attached to a water cluster. The pick-up source pressure was 7 mbar and the water clusters were formed at a stagnation pressure of *ca*. 1.2 bar.

Thus the cluster beam studies show that the conversion to sulfuric acid is a facile process, although the theoretical study with just two water molecules suggests a considerable barrier for the reaction in the $SO_3(H_2O)_2$ cluster. To understand the extent to which further solvation of the $SO_3(H_2O)_2$ cluster may affect the barrier height we have carried out Monte Carlo simulations of the $SO_3(H_2O)_{2+n}$ cluster, in which the calculated ground- and transition-states of the $SO_3(H_2O)_2$ cluster are solvated by a further $n$ water molecules described by a molecular mechanical potential. In brief, the structures of the $SO_3(H_2O)_2$ moiety, predicted from the *ab initio* calculations are kept fixed, the appropriate atomic charges for them are obtained by the usual CHELPG method,[5] using a 6-311 + G(d,p) basis, and the $n$ solvating water molecules are described by a TIP3P potential.

The calculated charge distribution of the $SO_3(H_2O)_2$ entities predicts a greater polarity for the transition state, leading to a correspondingly greater average intermolecular interaction in the $SO_3(H_2O)_2(H_2O)_n$ cluster containing the transition state compared to reactant. With ten additional water molecules we find this differential transition-state stabilisation to be 10.0 kcal $mol^{-1}$, from the Monte Carlo simulation. This quantity will essentially counterbalance the internal energy difference (11.5 kcal $mol^{-1}$) identified by the *ab initio* calculations on $SO_3(H_2O)_2$. Thus we predict that $SO_3$, solvated by approximately twelve water molecules will be converted to sulfuric acid with little or no energy barrier.

Thus, although it has long been recognised that bulk solvent can have profound effects on the rate of chemical reactions, we here show that in fact large catalytic effects can be achieved in quite small solvent clusters.

We thank EPSRC and NERC for support of the research.

## Footnote

* E-mail: j.c.whitehead@man.ac.uk

## References

1 K. Morokuma and C. Muguruma, *J. Am. Chem. Soc.*, 1994, **116**, 10316.
2 R. Hofmann-Sievert and A. W. Castleman, *J. Phys. Chem. A*, 1984, **88**, 3329.
3 M. Ahmed, C. J. Apps, C. Hughes, N. E. Watt and J. C. Whitehead, *J. Phys. Chem. A*, 1977, **101**, 1250.
4 M. Ahmed, C. J. Apps, R. Buesnel, C. Hughes, I. H. Hillier, N. E. Watt and J. C. Whitehead, *J. Phys. Chem. A*, 1997, **101**, 1254.
5 C. M. Breneman and K. B. Wiberg, *J. Comput. Chem.*, 1990, **11**, 361.

*Received in Exeter, UK on 1st February 1997; Com. 7/00802C*

# Excited state carbon acids: irreversible photodeprotonation of the benzylic protons of 10-methyl- and 10-phenyl-thioxanthenium salts

**Darryl Brousmiche, Deepak Shukla and Peter Wan***

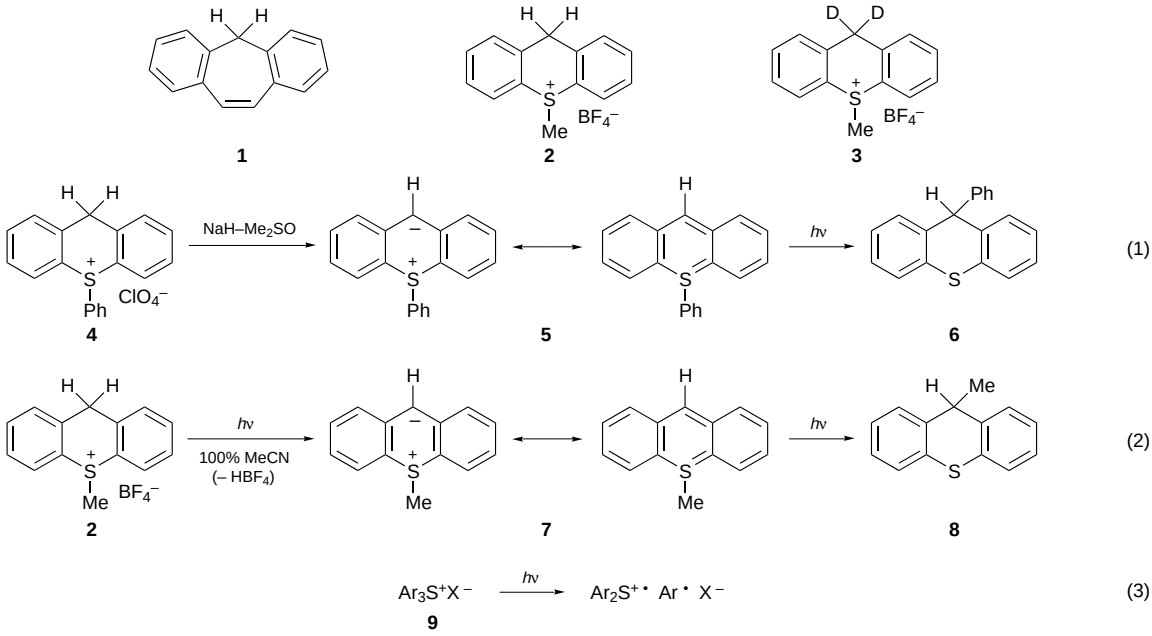
*Department of Chemistry, Box 3065, University of Victoria, Victoria, British Columbia, Canada V8W 3V6*

**The first examples of irreversible photodeprotonation of a C–H bond to generate a formal carbanion, *via* photolysis of thioxanthenium salts, is reported, which gives the corresponding sulfonium ylide (thiaanthracene) and acid ($HBF_4$ or $HClO_4$).**

Carbanions and their associated carbon acids are of fundamental importance in chemistry. Carbanions are most commonly generated *via* deprotonation of the corresponding carbon acid although this process is generally slow.[1] We have reported[2] that the benzylic protons of dibenzosuberene **1** and related compounds are vastly more acidic in the excited singlet state than in the ground state, and hence can be deprotonated efficiently by water (in MeCN; $k_d$ *ca.* $2 \times 10^8$ $dm^3$ $mol^{-1}$ $s^{-1}$) on excitation, to give a formally antiaromatic (8π) carbanion. Photodeprotonation rates approaching the diffusion controlled limit have been measured using primary amines such as ethamine as deprotonating base.[3] However, in all cases reported so far the deprotonation is entirely reversible; direct evidence for carbanion formation was obtained by observation of deuterium exchange of the methylene protons with deuteriated solvent in recovered substrate. Attempts to detect the intermediate carbanion by nanosecond laser flash photolysis have so far been unsuccessful, presumably due to the very short lifetimes (in the ground state) of these photogenerated, formally anti-aromatic, (8π) carbanions. One approach in making the photodeprotonation step irreversible is to make the incipient carbanion longer lived or designing a carbanion that once formed rearranges to a stable product. To this end, we have chosen to study the potential excited state carbon acid behaviour (of the benzylic protons) of 10-methylthioxanthenium tetrafluoroborate, **2** and **3**, and 10-phenylthioxanthenium perchlorate **4**, systems that have the required 8π (anti-aromatic) electron count in the internal cyclic π-array for the incipient carbanion.† We show that photolysis of these compounds in MeCN results in efficient deprotonation of the benzylic proton, giving rise to a long-lived formal carbanion (an ylide), and formation of $HBF_4$ or $HClO_4$. As such, these are the first examples of excited state carbon acids that undergo irreversible dissociation of the C–H proton, with detectable formation of acid.

The thioxanthenium salts **2**–**4** were made according to procedures published by Mislow and co-workers.[4] Treatment of **2** and related thioxanthenium salts with available benzylic protons with a strong base (*e.g.* NaH–$Me_2SO$ or an organometallic reagent) is known to result in deprotonation of the benzylic proton, to give the unstable but highly coloured thiaanthracene **5** ($\lambda_{max}$ = 388 and 497 nm), which subsequently rearranges to the corresponding stable 9-substituted thioxanthene **6** [eqn. (1)].[4,5] The half-lives of some thiaanthracenes generated in basic $Me_2SO$ range from 1 min to several hours at 22 °C.[4b] These results indicate that the p$K_a$s of the benzylic protons of these compounds are significantly lower than those of thioxanthene or dibenzosuberene **1**, which have estimated p$K_a$s in the 30–35 range.[2]

Photolysis of initially colourless $10^{-3}$ M solutions of **2**–**4** in dry MeCN (254 nm; argon-purged solutions) gave deep orange solutions, with visible absorption bands at *ca.* 380 and 485 nm (Fig. 1). No changes were observed without photolysis. These visible bands are identical to those observed for known thiaanthracenes (*e.g.* **5**).[4] However, whereas thermally generated thiaanthracenes in basic media are relatively short-lived, when photogenerated in 100% MeCN, they show no evidence of decay for several days. Additional evidence that thiaanthracenes are indeed photogenerated was obtained by taking the



$^1$H (300 MHz) NMR spectrum of an exhaustively photolysed sample of **2** in $CD_3CN$ (254 or 300 nm; 45–60 min), which showed formation of **8** with yields of up to 60% [eqn. (2)]. The thermal rearrangement of thiaanthracenes under basic conditions to the more stable 9-substituted thioxanthenes is well-known, as discussed above. It seems reasonable to propose that formation of **8** from **7** in an exhaustively photolysed sample of **2** is due to secondary photolysis of **7**. Indeed, the UV–VIS absorption bands of **7** (Fig. 1) was readily bleached when irradiated at 366 nm. A quantum yield of *ca.* 0.1 was measured (at low conversion) for the formation of **7** from **2** in MeCN using UV–VIS spectrophotometry to monitor the progress of the reaction ($\lambda_{excit}$ = 280 nm; potassium ferrioxalate actinometry).

Formation of **7** from photolysis of **2** in 100% MeCN‡ implies loss of a proton from the benzylic position to form $HBF_4$. The increase in acidity of a photolysed solution in 100% MeCN was monitored by diluting aliquots at various photolysis times (at 254 nm) with an equal volume of $H_2O$ and measuring the pH. An initial pH of 4.5 was observed which decreased to pH 3.4 after 5 min of photolysis, which represents about 50% conversion. No changes in pH were observed without photolysis. These results are consistent with excited state carbon acid deprotonation of the benzylic protons of **2**. That this deprotonation step is in fact the product forming step was the finding that the corresponding deuteriated substrate **3** gave a reduced amount of **7**, as monitored by UV–VIS spectrophotometry. This can be quoted as an isotope effect on the quantum yield for forming **7**, *viz.* $\Phi_H/\Phi_D$ = 1.39 ± 0.05, which is a small primary isotope effect for C–H(D) bond cleavage. We have observed a similarly small primary isotope effect for benzylic C–H(D) bond cleavage for dibenzosuberene **1** using ethanolamine as deprotonating base in which the rate is close to the diffusion controlled limit.[3] The small isotope effect was interpreted as being due to an earlier transition state for proton removal by ethanolamine compared to water as base.[3] In the present case, we believe thioxanthenium salts **2**–**4** have early transition states for photodeprotonation of the C–H bond although additional studies are warranted to substantiate this claim.

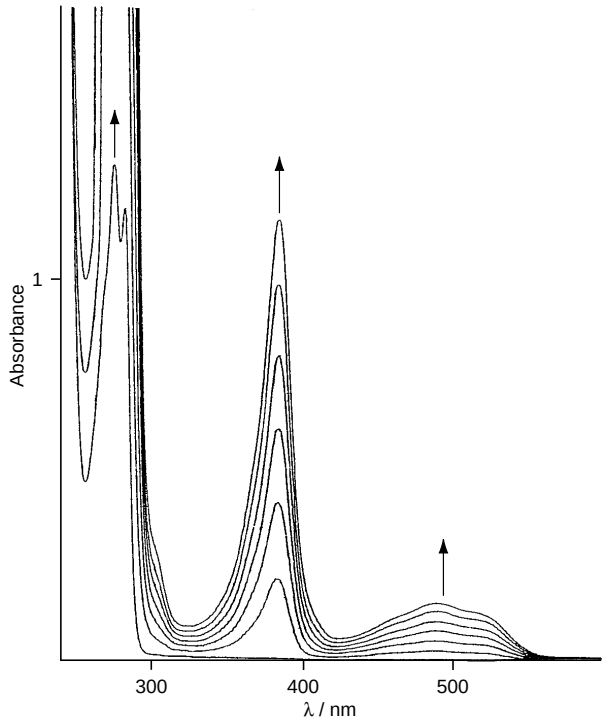



**Fig. 1** UV–VIS traces showing formation of thiaanthracene **7** (visible bands at 383 and 485 nm) from photolysis of **2** in 100% MeCN ($\lambda_{excit}$ = 254 nm; each trace represents about 15 s photolysis)

Recent intense interest in the photochemistry of triaryl and trialkyl sulfonium salts is due to the fact that photolysis of many of these compounds results in efficient generation of a strong Brønsted acid which effectively initiates cationic polymerization and is therefore useful in photoimaging systems and related applications.[6] The commonly accepted mechanism[6] for Brønsted acid production in the photochemistry of triarylsulfonium salts **9** (and for some mixed alkylaryl systems) is the initial aryl–sulfur bond homolysis, to generate an aryl (or alkyl) radical and a diarylsulfinium radical cation [eqn. (3)].§ Subsequent transformations of these species gives rise to the observed Brønsted acid. For example, intramolecular recombination of the radical pair *via* radical attack of Ar· onto one of ring positions of $Ar_2S^{+\cdot}$ results in overall loss of a proton from that ring position.[6a,b] Indeed, we are aware of two reports[6e,f] which show that photolysis of **2** and **4** results in generation of acid *via* the commonly accepted mechanism discussed above for triarylsulfonium salts. However, the results of our study demonstrate that photoacid production from these compounds arises from excited state carbon acid dissociation which may be regarded as a new mechanism for the production of Brønsted acid from photolysis of triarylsulfonium salts.

We acknowledge support of this research by the Natural Sciences and Engineering Research Council (NSERC) of Canada. D. B. thanks the University of Victoria for a graduate fellowship.

## Footnotes

† All dissociating excited state carbon acids reported by us[2,3] so far require an incipient carbanion that is cyclically delocalized with 8π electrons. One of the lone pairs of the sulfur atom of **2**–**4** is used for bonding with the methyl or phenyl group while the second lone pair of electrons can come into π conjugation on deprotonation of the benzylic proton giving rise to an 8π system, which is formally an ylide or a thiaanthracene.

‡ We have avoided photolysis in aqueous MeCN and other protic solvents owing to the possibility of thermal solvolytic decomposition of the substrates.

§ However, Crivello and Lam[6d,g–i] and Crivello and Lee[6d,j] have shown that the mechanisms for photoacid generation from dialkylphenacylsulfonium and dialkyl-4-hydroxyphenylsulfonium salts involve formal loss of a C–H and O–H proton, respectively, rather than *via* the standard mechanism shown in eqn. (3). The mechanism for the deprotonation from the C–H bond in the former does not appear to involve an excited state carbon acid.[6d,j]

## References

1 A. J. Kresge, *Acc. Chem. Res.*, 1978, **8**, 354.
2 (*a*) P. Wan, E. Krogh and B. Chak, *J. Am. Chem. Soc.*, 1988, **110**, 4073; (*b*) P. Wan, D. Budac, M. Earle and D. Shukla, *J. Am. Chem. Soc.*, 1990, **112**, 8048; (*c*) P. Wan and D. Budac, *J. Org. Chem.*, 1992, **57**, 887; (*d*) P. Wan and D. Shukla, *Chem. Rev.*, 1993, **93**, 571; (*e*) D. Budac and P. Wan, *Can. J. Chem.*, 1996, **74**, 1447.
3 D. Budac and P. Wan, *J. Photochem. Photobiol. A*, 1996, **98**, 27.
4 (*a*) B. E. Maryanoff, J. Stackhouse, G. H. Senkler, Jr. and K. Mislow, *J. Am. Chem. Soc.*, 1975, **97**, 2718; (*b*) F. Ogura, W. D. Hounsell, C. A. Maryanoff, W. J. Ritcher and K. Mislow, *J. Am. Chem. Soc.*, 1976, **98**, 3615.
5 (*a*) M. Hori, T. Kataoka, H. Shimizu, H. Hori and S. Sugai, *Chem. Pharm. Bull.*, 1974, **22**, 2754; (*b*) M. Hori, T. Kataoka, H. Shimizu, M. Ikemori and Y. Aoyama, *J. Chem. Soc., Perkin Trans. 1*, 1988, 1209.
6 (*a*) F. D. Saeva, *Top. Curr. Chem.*, 1990, **156**, 59; (*b*) J. L. Dektar and N. P. Hacker, *J. Chem. Soc., Chem. Commun.*, 1987, 1591; (*c*) J. D. Coyle, *The Chemistry of the Sulphonium Group*, Part 1, ed. C. J. M. Stirling, Wiley, Chichester, 1981, ch. 5; (*d*) J. V. Crivello, *Adv. Polym. Sci.*, 1984, **62**, 1; (*e*) J. V. Crivello and J. H. W. Lam, *J. Polym. Sci., Polym. Chem. Ed.*, 1979, **17**, 977; (*f*) R. S. Davidson and J. W. Goodin, *Eur. Polym. J.*, 1982, **18**, 589; (*g*) J. V. Crivello and J. H. W. Lam, *J. Polym. Sci., Polym. Chem. Ed.*, 1979, **17**, 2877; (*h*) *J. Polym. Sci., Polym. Chem. Ed.*, 1980, **18**, 1021; (*i*) *J. Polym. Sci., Polym. Chem. Ed.*, 1980, **18**, 2697; (*j*) J. V. Crivello and L. J. Lee, *Macromolecules*, 1983, **16**, 864.

*Received, 16th December 1996; Com. 6/08434F*

# Structure of the centred icosahedral samarium cluster formed by bis(L-prolinato)nickel(II) ligands

**Yasuhiko Yukawa,*[a] Satoshi Igarashi,[a] Akihito Yamano[b] and Shoichi Sato[b]**

[a] *Department of Environmental Science, Faculty of Science, Niigata University, 8050 Ikarashi Nino-cho, Niigata 950-21, Japan*
[b] *X-ray Research Laboratory, Rigaku Corporation, 3-9-12 Matsubara-cho, Akishima-shi, Tokyo 196, Japan*

**The centred icosahedral twelve-coordinate samarium cluster formed by six bis(L-prolinato)nickel(II) ligands is synthesized and its crystal structure determined.**

Heteronuclear and/or polynuclear complexes are interesting materials due to their structures and properties. Various preparation methods have been proposed in order to obtain such polynuclear complexes. One such method was the preparation of complexes from the interaction of two or more moles of *cis*-$[M(am)_4(OH)_2]^+$ [where $(am)_4$ is a single tetradentate amine ligand, two bidentate amines, or four monodentate amines] with metal halides; [1–4] the bis-hydroxo complexes which are used as ligands can be coordinated to the other metals *via* the hydroxo oxygen atoms. Recently Winpenny and coworkers have reported studies where they have attempted to link mononuclear and/or small polynuclear compounds into larger units; especially, they have been exploring the coordination chemistry of ligands derived from 2-hydroxypyridine (2-pyridone) with first-row transition metals.[5–12] In this work, an amino acid complex was used as a ligand in order to synthesize a new heteronuclear complex.

Amino acids have two or more types of coordination atoms and can act as various bridging ligands.[13–19] Taking advantage of the properties of the amino acid ligands, the synthesis of an amino acid bridging heterometal complex was applied. A lanthanoid ion, a hard acid, and a bis-amino acidato complex were chosen for the purpose of preparing the heterometal complex, and they were mixed in a non-aqueous solvent with poor coordination ability.

The samarium–nickel complex containing bis(L-prolinato)-nickel(II) moieties $[Ni(pro)_2]$: synthesized according to a modified published procedure for $Cu(pro)_2$ [20]] was prepared by reacting 1 mmol of samarium perchlorate dissolved in 20 $cm^3$ of methanol with a six-fold excess of $[Ni(pro)_2]$. Evaporation of the solvent gave purple tetrahedral crystals of $[Sm\{Ni(pro)_2\}_6][ClO_4]_3\cdot 6MeOH$.†

Four $ClO_4^-$ ion sites must exist in the unit cell, since the crystals are cubic (space group: $F23$) and the $ClO_4^-$ ions lie on the three-fold axes. However, this contradicts the result of gravimetric analysis for $ClO_4^-$ using tetraphenylarsonium chloride [Found: 12.33%. Calc. for $[Sm\{Ni(pro)_2\}_6][ClO_4]_3\cdot 6MeOH$, 12.63%]. Therefore, the occupancy of each $ClO_4^-$ site was fixed at 0.75 when the structure was refined.

The methanol molecules are considered to be loosely trapped in the lattice, as revealed by their extremely large thermal parameters, which leads to immediate decomposition upon filtering.

The coordination environments around the Sm and Ni atoms in the complex is shown in Fig. 1 and a stereoscopic view is shown in Fig. 2. Each nickel atom is surrounded by six atoms: two amino nitrogens, two carboxylate oxygens, which form chelate rings with the nitrogen atoms, and two carboxylate oxygen atoms which link the neighbouring nickel atoms. The samarium atom is coordinated to twelve oxygen atoms. The six $Ni(pro)_2$ units are coordinated to the icosahedral metal centre *via* two chelating carboxylate oxygen atoms.

By contrast to most twelve-coordinate complexes which are distorted icosahedral owing to restricted ligand bite size, $[Sm\{Ni(pro)_2\}_6]^{3+}$ shows icosahedral geometry, owing to the larger bite size of the $Ni(pro)_2$ moieties. All the Sm–O bond lengths are 2.691(3) Å, while the average of the nearest neighbouring O···O is 2.83 Å (ratio O···O/Sm–O = 1.05); angles between two adjacent metal–ligand bonds are in the range 62.8(3)–65.1(1)° (av. = 63.4°); *cf.* ideal icosahedral angle between two adjacent metal(M)–ligand(L) bonds of 63.43° and ideal ratio of L–L/M–L of 1.0515.[21] Lanthanoid ions capable of forming twelve-coordinate compounds are $La^{3+}$,[22]

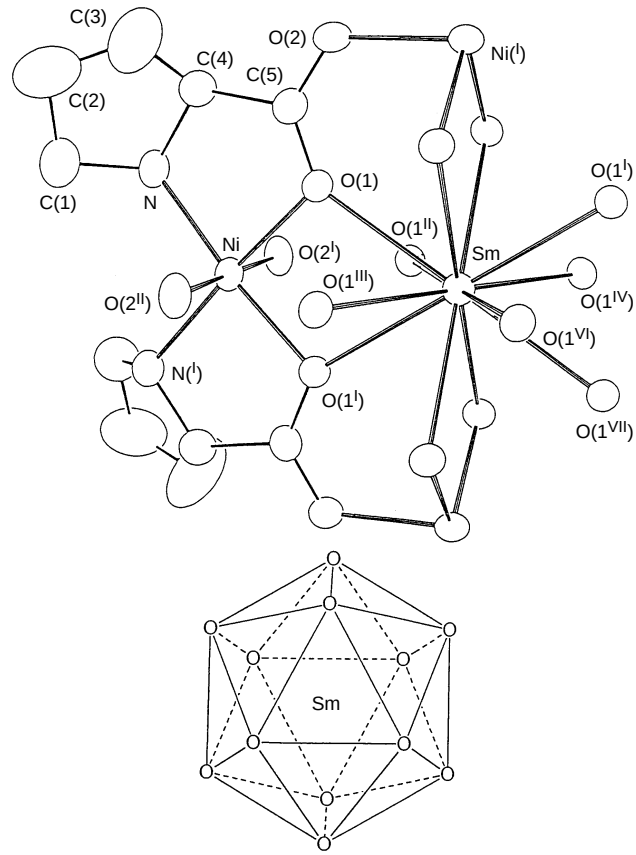



**Fig. 1** ORTEP plot around the Sm and Ni atoms in $[Sm\{Ni(pro)_2\}_6]^{3+}$ showing 50% thermal ellipsoids in the atom numbering scheme. Selected bond distances (Å) and angles (°): Sm–O(1) 2.688(3), Ni–O(1) 2.026(3), Ni–O(2) 2.053(4), Ni–N 2.060(5), O(1)–C(5) 1.295(7), O(2)–C(5) 1.234(7), N–C(1) 1.57(1), N–C(4) 1.496(8), C(1)–C(2) 1.46(2), C(2)–C(3) 1.43(2), C(3)–C(4) 1.37(3), C(4)–C(5) 1.514(8), O(1)–O(1I) 2.874(7), O(1)–O(1II) 2.77(2), O(1)–O(1III) 2.86(2); O(1)–Sm–O(1I) 64.6(1), O(1)–Sm–O(1II) 62.0(4), O(1)–Sm–O(1III) 64.3(4), O(1)–Sm–O(1IV) 116.6(1), O(1)–Sm–O(1V) 115.4(1), O(1)–Sm–O(1VI) 117.11(9), O(1)–Sm–O(1II) 178.5(5), O(1)–Ni–O(1I) 90.4(2), O(1)–Ni–O(2I) 90.1(4), O(1)–Ni–O(2II) 89.1(4), O(1)–Ni–N 84.4(2), O(1)–Ni–NI 172.5(4), O(2II)–Ni–N 85.4(5), O(2II)–Ni–NI 95.2(5), N–Ni–NI 101.2(3), Ni–O(1)–C(5) 114.5(4), NiI–O(2)–C(5) 123.5(3), O(1)–C(5)–O(2) 126.3(5).

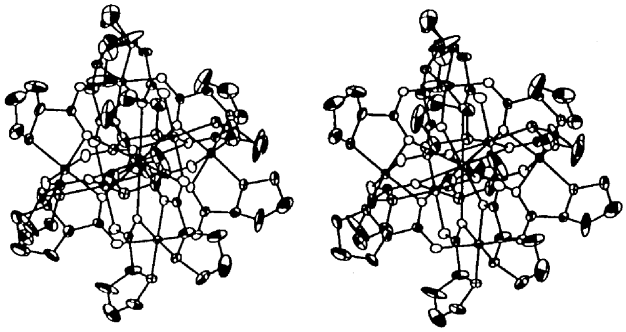


**Fig. 2** Stereoscopic view of $[Sm\{Ni(pro)_2\}_6]^{3+}$

$Ce^{3+}$,[23] $Ce^{4+}$,[24] $Pr^{3+}$,[25] and $Nd^{3+}$[26] whereas it is very difficult to prepare twelve-coordinate complexes of samarium even with $NO_3^-$. Very recently a 'twelve-coordinate' Sm complex with tris[3-(2-pyridyl)pyrazol-1-yl]hydroborate (L), $[SmL_2]BPh_4$, was reported.[27] However, half of the twelve Sm–N bond lengths in the complex are extremely long: av. 2.95 Å *cf.* 2.66 Å (av.) for the shorter set of bonds. Therefore, the complex reported here is very novel. The samarium–oxygen bond lengths in the present complex, 2.691(3) Å, are a little longer than in other eleven- and ten-coordinate samarium complexes,[28–30] which may arise from restriction imposed by the $6[Ni(pro)_2]$ cage structure and the high coordination number.

It was confirmed that the icosahedral cluster structure was retained after loss of methanol molecules from the crystals, based on diffraction data of slightly decayed crystals. Moreover, the structure was also retained in alcohol and acetonitrile solutions; UV–VIS spectra of solutions are perfectly consistent with the powder diffuse reflection spectrum. Cyclic voltammetry‡ of the complex in acetonitrile exhibited reversible waves at *ca.* −1.5 V and complicated irreversible waves at > 0.5 V. The reversible waves imply that $Sm^{3+}$ in the complex shows a Nernstian reduction. The complicated irreversible waves suggest that the nickel atoms interact with each other and that the icosahedral cluster structure may decompose when $Ni^{2+}$ is oxidized to $Ni^{3+}$ in the $Ni(pro)_2$ units.

Future work will be aimed at investigating the magnetochemistry of this complex.

We wish to express our gratitude to Professor F. S. Howell of Sophia University for correcting the manuscript. The present work was supported by Grants-in-Aid for Scientific Research on Priority Area 'New Development of Rare Earth Complexes' Nos. 08220224, 07230230, and 06241228 from the Ministry of Education, Science, Sports and Culture.

## Footnotes

* E-mail:yukawa@geb.ge.niigata-u.ac.jp

† *Crystal data* for $[Sm\{Ni(pro)_2\}_6][ClO_4]_3\cdot 6CH_3OH$: purple, tetrahedron, $C_{66}H_{120}Cl_3N_{12}Ni_6O_{42}Sm$, $M_w$ = 2363.05, cubic, space group *F*23 (no. 196), $a$ = 21.335(2) Å, $U$ = 9710(1) Å$^3$, $D_m$ = 1.64 g cm$^{-3}$, $D_c$ = 1.62 g cm$^{-3}$, $Z$ = 4. Based on the systematic absences (*hkl*: $h + k$, $k + l$, $h + l \neq 2n$), packing considerations, a statistical analysis of the intensity distribution, and the successful solution and refinement of the structure, the space group was determined. Since the absolute configuration of L-Hpro was known, the structure analysis was based on this configuration. A crystal having approximate dimensions of 0.40 × 0.30 × 0.40 mm was mounted in a glass capillary. All measurements were made on a Rigaku AFC5R diffractometer using the ω–2θ scan technique to a maximum 2θ value of 60°, with graphite monochromated Mo-Kα (λ = 0.710 69 Å) radiation at 20 °C. Scans of (1.55 + 0.30 tan θ)° were made at a speed of 16.0° min$^{-1}$ (in ω). Of the 2048 reflections which were collected, 1296 were unique ($R_{int}$ = 0.053); equivalent reflections were merged. The linear absorption coefficient, μ, was 19.1 cm$^{-1}$. An empirical absorption correction based on azimuthal scans of several reflections was applied. This resulted in transmission factors ranging from 0.8920 to 0.9963. The data were corrected for Lorentz and polarization effects. A correction for secondary extinction was applied (coefficient = 1.53190 × 10$^{-7}$). The structure was solved by heavy-atom Patterson methods and expanded using Fourier techniques. The non-hydrogen atoms were anisotropically refined. The final cycle of full-matrix least-squares refinement was based on 769 observed reflections [$I > 3.0\sigma(I)$] and 121 variable parameters and converged at $R$ = 0.033 and $R_w$ = 0.039. At the final stage of refinement, the difference Fourier map showed minimum and maximum peaks between −0.26 and +0.22 e Å$^{-3}$. Atomic coordinates, bond lengths and angles, and thermal parameters have been deposited at the Cambridge Crystallographic Data Centre (CCDC). See Information for Authors, Issue No. 1. Any request to the CCDC for this material should quote the full literature citation and the reference number 182/398.

‡ 5 mmol dm$^{-3}$ $[Sm\{Ni(pro)_2\}_6]^{3+}$ in 0.1 mol dm$^{-3}$ tetraethylammonium perchlorate–acetonitrile solution at a glassy carbon disk electrode (scan rate = 200 mV s$^{-1}$).

## References

1 D. J. Hodgson, L. Michelsen, E. Pedersen and D. K. Towle, *J. Chem. Soc., Chem. Commun*., 1988, 426.
2 D. J. Hodgson, K. Michelsen and E. Pedersen, *J. Chem. Soc., Chem. Commun*., 1988, 1558.
3 D. J. Hodgson, L. Michelsen, E. Pedersen and D. K. Towle, *Inorg. Chem*., 1991, **30**, 815.
4 J. Glerup, P. A. Goodson, D. J. Hodgson, M. H. Lynn and K. Michelsen, *Inorg. Chem*., 1992, **31**, 4785.
5 A. J. Blake, V. A. Cherepanov, A. A. Dunlop, C. M. Grant, P. E. Y. Milne, J. M. Rawson and R. E. P. Winpenny, *J. Chem. Soc., Dalton Trans.*, 1994, 2719.
6 T. F. Carlson, J. P. Fackler, Jr., R. J. Staples and R. E. P. Winpenny, *Inorg. Chem*., 1995, **34**, 426.
7 A. J. Blake, C. M. Grant, S. Parsons and R. E. P. Winpenny, *J. Chem. Soc., Dalton Trans.*, 1995, 1765.
8 A. J. Blake, E. K. Brechin, A. Codron, R. O. Gould, C. M. Crant, S. Parsons, J. M. Rawson and R. E. P. Winpenny, *J. Chem. Soc., Chem. Commun*., 1995, 1983.
9 J. M. Rawson and R. E. P. Winpenny, *Coord. Chem. Rev.*, 1995, **139**, 313.
10 C. Benelli, A. J. Blake, P. E. Y. Milne, J. M. Rawson and R. E. P. Winpenny, *Chem. Eur. J*., 1995, **1**, 614.
11 A. J. Blake, L. M. Gilby, S. Parsons, J. M. Rawson, D. Reed, G. A. Solan and R. E. P. Winpenny, *J. Chem. Soc., Dalton Trans*. 1996, 3575.
12 E. K. Brechin, S. G. Harris, S. Parsons and R. E. P. Winpenny, *Chem. Commun*., 1996, 1439.
13 Y. Yukawa, Y. Inomata, T. Takeuchi, M. Shimoi and A. Ouchi, *Bull. Chem. Soc. Jpn*., 1982, **55**, 3135.
14 Y. Yukawa, Y. Inomata and T. Takeuchi, *Bull. Chem. Soc. Jpn*., 1983, **56**, 2125.
15 Y. Yukawa, N. Yasukawa, Y. Inomata and T. Takeuchi, *Bull. Chem. Soc. Jpn.*, 1985, **58**, 1591.
16 S. Itoh, Y. Yukawa, Y. Inomata and T. Takeuchi, *Bull. Chem. Soc. Jpn*., 1987, **60**, 899.
17 M. Nagase, Y. Yukawa, Y. Inomata and T. Takeuchi, *Bull. Chem. Soc. Jpn*., 1988, **61**, 775.
18 Y. Yukawa, S. Nakagome, H. Yamaguchi, Y. Inomata and T. Takeuchi, *Bull. Chem. Soc. Jpn*., 1989, **62**, 1057.
19 Y. Yukawa, *J. Chem. Soc., Dalton Trans*., 1992, 3217.
20 T. Yasui, *Bull. Chem. Soc. Jpn*., 1965, **38**, 1746.
21 M. C. Favas and D. L. Kepert, *Prog. Inorg. Chem*., 1981, **28**, 309.
22 M. R. Anderson, G. T. Jenkin and J. W. White, *Acta Crystallogr., Sect. B*, 1977, **33**, 3933.
23 A. Zalkin, J. D. Forester and D. H. Templeton, *J. Chem. Phys*., 1963, **39**, 2881.
24 T. A. Beineke and J. Delgaudio, *Inorg. Chem*., 1968, **7**, 715.
25 A. Clearfield, R. Gopal and R. W. Olsen, *Inorg. Chem*., 1977, **16**, 911.
26 J.-C. G. Bünzli, B. Klein and D. Wessner, *Inorg. Chim. Acta*, 1980, **44**, L147.
27 A. J. Amoroso, J. C. Jeffery, P. L. Jones, J. A. McCleverty, L. Rees, A. L. Rheingold, Y. Sun, J. Takats, S. Trofimenko, M. D. Ward and G. P. A. Yap, *J. Chem. Soc., Chem. Commun*., 1995, 1881.
28 M. Ciampolini, N. Nardi, R. Cini, S. Mangani and P. Orioli, *J. Chem. Soc., Dalton Trans*., 1979, 1983.
29 S. M. Bowen, E. N. Duesler and R. Paine, *Inorg. Chim. Acta*, 1982, **61**, 155.
30 V. Chebolu and R. R. Whittle, *Inorg. Chem*., 1985, **24**, 3082.

*Received in Cambridge, UK, on 3rd December 1996; Com. 6/08148G*

# A new approach to identifying substrate binding sites on isolated FeMo-cofactor of nitrogenase

**Karin L. C. Grönberg, Carol A. Gormal, Barry E. Smith and Richard A. Henderson***

*Nitrogen Fixation Laboratory, John Innes Centre, Norwich Research Park, Colney, Norwich, UK NR4 7UH*

**A kinetic method is described which is capable of detecting the binding of molecules and ions such as $CN^-$, $N_3^-$, $Bu^tNC$, imidazole and $H^+$ to the isolated FeMo-cofactor of nitrogenase, and indicates where on the cofactor these species bind.**

The Mo-based nitrogenase converts dinitrogen to ammonia by a sequence of electron- and proton-transfer reactions, and a variety of other small, unsaturated molecules are similarly transformed. There is strong evidence that these substrates are converted into products at a $MoFe_7S$(homocitrate) cluster: the FeMo-cofactor[1,2] (Fig. 2) which can be extracted into *N*-methylformamide (NMF), free from the polypeptide. Fundamental to the understanding of nitrogenase is identification of where these substrates bind on this cluster.[3] Herein, we report the novel approach of using kinetics to detect the binding of a variety of molecules (including some of the substrates of nitrogenase) on extracted cofactor. This approach also indicates where on the cluster this binding occurs.

The principle reaction used in our approach is a simple substitution reaction. Extracted cofactor[4] in the $S = 3/2$ state reacts with one $PhS^-$/FeMo-co.† It is likely that this reaction occurs at tetrahedral Fe and involves displacement of NMF by $PhS^-$. When studied on a stopped-flow spectrophotometer, this substitution is associated with an exponential absorbance increase ($\lambda$ = 400–500 nm), and the rate of the reaction is independent of $[PhS^-]$, with $k_1^{NMF} = 50 \pm 5\ s^{-1}$. These observations are consistent with a mechanism involving rate-limiting dissociation of NMF.

Binding other molecules (L) anywhere on the cluster will perturb the overall electron distribution and would be expected to affect the lability of the Fe–NMF bond. The magnitude of this labilisation gives information about where L binds relative to the site of $PhS^-$ substitution: a large perturbation would be expected from binding close to (or at) the tetrahedral Fe, whereas a small perturbation is expected from binding close to (or at) the remote Mo.[4]

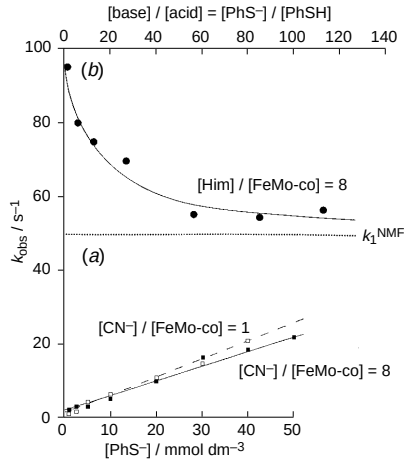



**Fig. 1** (*a*) Effect of $[PhS^-]$ on the rate of the reaction with $CN^-$ and FeMo-cofactor and (*b*) effect of $[PhS^-]_f/[PhSH]_f[PhSH]_f$ ($[PhS^-]_0$ = 0–50 mmol $dm^{-3}$) on the rate of the reaction of $PhS^-$ with imidazole and FeMo-cofactor. The value of $k_1^{NMF}$ is shown as a dotted line at $k_{obs} = 50\ s^{-1}$.

The addition of L = $C_2H_2$ or CO to the cofactor has no effect on the rate of the reaction with $PhS^-$, and it must be concluded that these molecules do not bind to the cofactor in the $S = 3/2$ state. However, for all other species studied (L = $N_3^-$, $Bu^tNC$, $CN^-$, imidazole or $H^+$) perturbations to the rate are observed.

Addition of $CN^-$ to the cofactor ($[CN^-]/[FeMo\text{-}co] = 1.0$) affects the reaction with $PhS^-$ in two ways (Fig. 1). First, the substitution reaction is slower ($k_1^{NMF}/k_1^{CN} = 62.5$). Secondly, the rate law contains two terms: one exhibits a first-order dependence on $[PhS^-]$ the other is independent of $PhS^-$. These observations are consistent with $CN^-$ being bound to tetrahedral Fe and displacement by $PhS^-$ occurring *via* the associative ($k_2^{CN}$) and dissociative ($k_1^{CN}$) pathways shown in Fig. 2.

The addition of excess $CN^-$ ($[CN^-]/[FeMo\text{-}co] \geqslant 2$) leads to further perturbations of the rate: $k_1^{CN}$ is increased by a factor of 1.7, whilst $k_2^{CN}$ is decreased by a factor of 1.2. These small effects are consistent with: (*a*) binding of an additional $CN^-$ remote from the tetrahedral Fe (probably at Mo); (*b*) the presence of this cyanide being transmitted through the cluster. Our interpretation that $CN^-$ binds at both the tetrahedral Fe and the Mo is consistent with EPR studies[5] (which indicate that cofactor can bind more than one $CN^-$) and EXAFS studies[6] (which indicate that when $[CN^-]/[FeMo\text{-}co] = 4$, cyanide is bound to Mo). Of all the molecules studied here, $CN^-$ is the only one which shows binding to more than one site.

The rate of $PhS^-$ substitution is only slightly perturbed on addition of L = $N_3^-$ or $Bu^tNC$ to cofactor (Table 1) which is consistent with these species binding at the Mo end. $N_3^-$ accelerates and $Bu^tNC$ inhibits the rate of reaction with $PhS^-$, presumably as a consequence of the relative electron-releasing and -withdrawing properties of these coordinated molecules.

In the protein, Mo is bound to the polypeptide by the imidazole group of His-442. Consistent with this, our kinetic approach indicates that imidazole binds at the Mo end of extracted cofactor since in the presence of this molecule the rate of the $PhS^-$ substitution reaction is only slightly perturbed. Interestingly, at

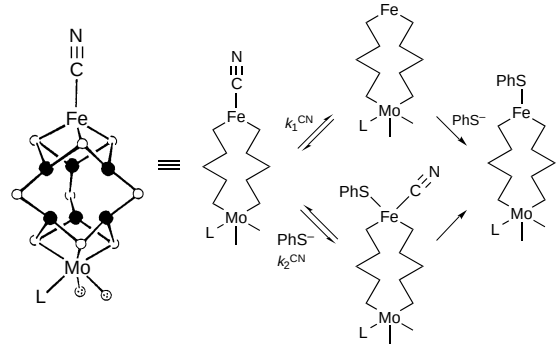



**Fig. 2** ● = three-coordinate Fe, ☉ = O (from homocitrate ligand), ○ = S. Proposed pathways for the reaction between FeMo-cofactor (only skeleton shown for clarity) and $PhS^-$ in the presence of $CN^-$. Rate law: $-d[\text{FeMo-co}]/dt = \{k_1^{CN} + k_2^{CN}[PhS^-]\}[\text{FeMo-co}]$; when $[CN^-]/[\text{FeMo-co}] = 1$, L = NMF, $k_1^{CN} = 0.8\ s^{-1}$, $k_2^{CN} = 5.1 \times 10^2\ dm^3\ mol^{-1}\ s^{-1}$; when $[CN^-]/[\text{FeMo-co}] \geqslant 2$, L = CN, $k_1^{CN} = 1.35\ s^{-1}$, $k_2^{CN} = 4.3 \times 10^2\ dm^3\ mol^{-1}\ s^{-1}$.

**Table 1** Indicated substrate binding sites on FeMo-cofactor in $S = 3/2$ state[a]

| Substrate (L) | $k_1^{NMF}/k_1^{L}$ | Binding site | Spectroscopic information |
|---|---|---|---|
| CO | 1.0 | No binding | No change in $^{19}F$ NMR spectrum of *p*-$CF_3C_6H_4S$–FeMo-co in the presence of CO.[8] |
| $C_2H_2$ | 1.0 | No binding | |
| $CN^-$ | | | |
| $[CN^-]/[FeMo\text{-}co] = 1$ | 62.5 | Fe | Large changes in EPR spectrum.[5] |
| $[CN^-]/[FeMo\text{-}co] \geqslant 2$ | 37 | Mo | EXAFS shows $CN^-$ bound to Mo when $[CN^-]/[Mo] = 4$.[6] |
| | | | $CN^-$ affects relaxation time of *p*-$CF_3C_6H_4S$–FeMo-co.[8] |
| | | | Stoichiometry experiments using EPR indicates more than one $CN^-$ can bind to FeMo-co.[5] |
| $N_3^-$ | 0.83 | Mo | EPR spectrum of FeMo-co[9] sharpens in presence of $N_3^-$. |
| $Bu^tNC$ | 1.21 | Mo | MeNC affects relaxation time of *p*-$CF_3C_6H_4S$–FeMo-co.[8] |
| Him | 0.52 | Mo | EPR spectrum of FeMo-co[9] sharpens in the presence of Him. |
| $H^+$ | 0.16 | S | Both EPR spectrum and electrochemistry indicated |

[a] After several weeks storage of FeMo-co in an anaerobic box the experimental value of $k_1^{NMF}$ gradually increased although activity of FeMo-co is retained. This we attribute to an increase in the concentration of protons in solution due to dithionite decomposition. $k_1^{L}$ is the rate constant when the substrate L is present, and $k_1^{NMF}$ is the rate constant in the absence of L, determined on the same day.

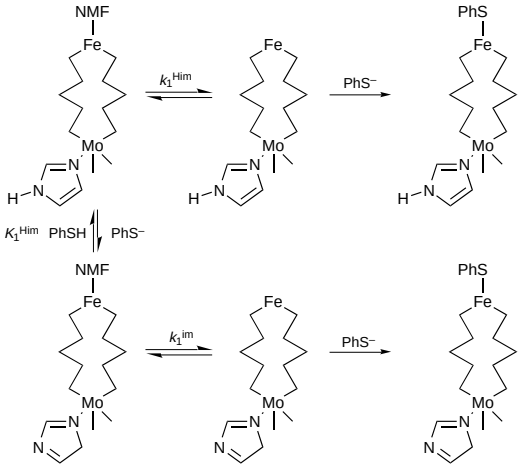



**Fig. 3** Proposed pathways for the reaction between FeMo-cofactor (only skeleton shown) and $PhS^-$ in the presence of imidazole. Rate law:

$$\frac{-d[\text{FeMo-co}]}{dt} = \frac{\{k_1^{Him} + k_1^{im}K^{Him}[PhS^-]_f/[PhSH]_f\}[\text{FeMo-co}]}{1 + K_1^{Him}[PhS^-]_f/[PhSH]_f}$$

where $k_1^{Him} = 95\ s^{-1}$, $k_1^{im} = 50\ s^{-1}$ and $K_1^{Him} = 8 \times 10^{-2}$. The subscript 'f' denotes the concentration of 'free' reactant, having made allowance for the protolytic reaction between uncoordinated imidazole and $PhS^-$: $ImH + PhS^- \rightleftharpoons Im^- + PhSH$. If $[PhS^-]_0 > [Him]_0$ and this reaction goes to completion, (where subscript 0 denotes total concentration of the reagent) $[PhS^-]_f = [PhS^-]_0 - [Him]_0$ and $[PhSH]_f = [Him]_0$.

low $[PhS^-]$ the reaction is accelerated ($k_1^{NMF}/k_1^{Him} = 0.52$), whilst at higher concentrations of $PhS^-$ the acceleration is less marked (Fig. 1). This behaviour is consistent with $PhS^-$ acting not only as a nucleophile to cofactor, but also as a base which can deprotonate imidazole and that the rate of the substitution reaction with $PhS^-$ is sensitive to the state of protonation of the coordinated imidazole. The proposed mechanism is shown in Fig. 3.

Studies on a variety of synthetic Fe/S-based clusters have shown that invariably protons bind to μ-S atoms and increase the substitution reactivity of the cluster.[7] FeMo-cofactor exhibits analogous behaviour with the rate of the $PhS^-$ substitution being faster in the presence of $[NHEt_3]BPh_4$ ($k_1^{NMF}/k_1^{H} = 0.16$).‡ This large acceleration in rate makes it likely that protonation is at a μ-S close to the tetrahedral Fe.[7]

Table 1 shows that the results of our kinetic studies are consistent with earlier studies on binding of molecules at extracted FeMo-cofactor. However, our kinetic approach is more versatile since it circumvents the problem of poor spectroscopic response associated with binding of molecules to cofactor.

This study indicates that various nitrogenase substrates can exhibit a marked selectivity for different sites on cofactor and that there are at least three sites at which substrates can bind. (*i*) The Mo (or a site at this end of the cluster) at which all anionic and neutral substrates bind, (*ii*) tetrahedral Fe at which cyanide prefers to bind, and (*iii*) μ-S where protons bind.

We acknowledge the BBSRC for supporting this work and John Innes Foundation for a studentship to K. L. C. G.

## Footnotes

† FeMo-cofactor from wild type *Klebsiella pneumoniae* M5al was extracted into an NMF solution containing sodium dithionite and sodium phosphate buffer, pH 8, using a modification of the method of P. A. McLean, D. A .Wink, S. K. Chapman, A. B. Hickman, D. M. McKillop and W. H. Orme-Johnson. (*Biochemistry*, 1989, **28**, 9402). In NMF solution, the cluster-protein ligands His-442 and Cys-275 are most likely replaced by solvent molecules. In the kinetic experiments, cofactor was diluted to *ca.* $1 \times 10^{-4}$ mol $dm^{-3}$ in NMF and reacted with $[NEt_4]SPh$ (0–50 mmol $dm^{-3}$). In studies with $L = CN^-$, $N_3^-$, $Bu^tNC$, CO, $C_2H_2$ and imidazole, the substrate was added to a solution of FeMo-cofactor (gases added by syringe), such that (for instance) $[L]/[FeMo\text{-}co] = 8$.

‡ The kinetics of this reaction exhibit a dependence on the ratio, $[NHEt_3^+]_f/[NEt_3]_f$:

$$\frac{-d[\text{FeMo-co}]}{dt} = \frac{\{k_1^{H}K^{H}[NHEt_3^+]_f/[NEt_3]_f\}[\text{FeMo-co}]}{1 + K^{H}[NHEt_3^+]_f/NEt_3]_f}$$

The concentration of 'free' reactants, has made allowance for the protolytic equilibrium: $[NHEt_3]^+ + PhS^- \rightleftharpoons NEt_3 + PhSH$.

Since this reaction goes to completion when $[NHEt_3{}^+]_0 > [PhS^-]_0$, $[NHEt^{3+}]_f = [NHEt_3^+]_0 - [PhS^-]_0$ and $[NEt_3]_f = [PhS^-]_0$.

These kinetics describe a mechanism involving rapid protonation of the cofactor ($K^H = 5.6 \times 10^{-2}$), followed by rate-limiting dissociation of the Fe–NMF bond ($k_1^H = 312\ s^{-1}$).

## References

1 T. R. Hawkes, P. A. McLean and B. E. Smith, *Biochem. J.*, 1984, **217**, 317.
2 B. K. Burgess, *Chem. Rev.*, 1990, **90**, 1377.
3 M. K. Chan, J. Kim and D. C. Rees, *Science*, 1993, **260**, 792.
4 Related effects are observed when small molecules (such as halide, CO, $N_3^-$ and $CN^-$) bind to synthetic clusters such as $[\{MoFe_3S_4(SEt)_3\}_2(\mu\text{-}SEt)_3]^{3-}$; R. A. Henderson and K. E. Oglieve, *J. Chem. Soc., Dalton Trans.*, 1993, 1473 and references therein.
5 A. J. M. Richards, D. J. Lowe, R. L. Richards, A. J. Thomson and B. E. Smith, *Biochem. J.*, 1994, **297**, 373.
6 H. I. Liu, A. Filipponi, N. Gavini, B. K. Burgess, B. Hedman, A. Di Cicco, C. R. Natoli and K. O. Hodgson, *J. Am. Chem. Soc.*, 1994, **116**, 2418.
7 K. L. C. Grönberg and R. A. Henderson, *J. Chem. Soc., Dalton Trans.*, 1996, 3667 and references therein.
8 S. D. Conradson, B. K. Burgess, S. A. Vaughn, A. L. Roe, B. Hedman, K. O. Hodgson and R. H. Holm, *J. Biol. Chem.*, 1989, **264**, 15 967 and references therein.
9 A. J. M. Richards, PhD Thesis, University of East Anglia, 1986.
10 F. A. Schultz, B. J. Feldman, S. F. Gheller and W. E. Newton, *Inorg. Chim. Acta*, 1990, **170**, 115; W. E.Newton, S. F. Gheller, B. J. Feldman, W. R. Dunham and F. A. Schultz, *J. Biol. Chem.*, 1989, **264**, 1924.

*Received, 12th December 1996; Com. 6/08362E*

# Cycloaddition of aromatic imines to a ruthenium butatrienylidene complex: synthesis of 4-ethynylquinoline and 1-azabuta-1,3-diene complexes

**Michael I. Bruce,*[a] Peter Hinterding,[a] Mingzhe Ke,[a] Paul J. Low,[a] Brian W. Skelton[b] and Allan H. White[b]**

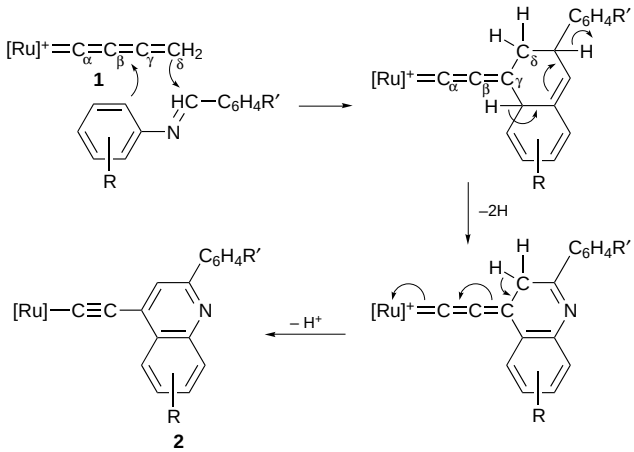
[a] *Department of Chemistry, University of Adelaide, Adelaide, South Australia 5005, Australia*
[b] *Department of Chemistry, University of Western Australia, Nedlands, Western Australia 6907, Australia*

**Reactions of aromatic imines with the putative butatrienylidene–ruthenium cation $[Ru(C{=}C{=}C{=}CH_2)(PPh_3)_2(\eta\text{-}C_5H_5)]^+$ gives complexes containing either 4-ethynylquinoline or 1-azabuta-1,3-diene ligands; the molecular structures of $[Ru(C{\equiv}CC_9H_4MeN)(PPh_3)_2(\eta\text{-}C_5H_5)]$ and $[Ru\{C{\equiv}CC(CH{=}CHPh){=}N(C_6H_4NO_2\text{-}3)\}(PPh_3)_2(\eta\text{-}C_5H_5)]$ are reported.**

We have recently described the formation of an intermediate cationic complex from the reaction between buta-1,3-diyne and $[Ru(thf)(PPh_3)_2(\eta\text{-}C_5H_5)]^+$ which, from its method of formation and subsequent reactions, is proposed to be the butatrienylidene cation $[Ru(C{=}C{=}C{=}CH_2)(PPh_3)_2(\eta\text{-}C_5H_5)]^+$ **1**.[1] We showed that its reactivity is characterised by nucleophilic attack at $C_\gamma$, as predicted by theoretical studies.[2]

The availability of **1**, in which the outer carbons of the four-carbon unsaturated ligand are not sterically protected by the bulky $PPh_3$ ligands as are atoms $C_\alpha$ and $C_\beta$, encouraged us to study its chemistry in more detail. In particular, we were interested in the possibility of cycloaddition to the unsaturated $C_4$ chain through reactions which might involve successive electro- and nucleo-philic attack on a suitable substrate. We chose to examine first *N*-benzylideneaniline and were pleased to discover that the sought-after reaction occurred readily and in high yield.

Thus, addition of *N*-benzylideneaniline (2 equiv.) to a solution of **1** in thf at −50 °C resulted in an immediate colour change to orange–red. Work up by preparative thin layer chromatography (TLC) afforded the yellow complex **2a** (Scheme 1), which was initially characterised as a 1 : 1 adduct by mass spectrometry.† The reaction can be extended to other imines containing substituted C-bonded aryl groups and/or electron-donating substituents on the N-bonded aryl group. The X-ray determined structure of **2b**, obtained from **1** and $PhCH{=}NC_6H_4Me$-4, is shown in Fig. 1 and important bond parameters are collected in the caption. A conventional $Ru(PPh_3)_2(\eta\text{-}C_5H_5)$ fragment is attached by an Ru–C σ bond to an acetylenic ligand of which the other substituent is a 4-quinolinyl group. Structural characteristics of this ligand are not exceptional and further discussion will be deferred until the full report. Similar tricyclic heterocycles are obtained with naphthylimines.




**Scheme 1** R = H, 4-Me, 4-OMe; R′ = H, 3- or 4-$NO_2$ [Ru] = $Ru(PPh_3)_2(\eta\text{-}C_5H_5)$

A remarkable property of complexes **2** is their extreme sensitivity towards protonation, traces of water being sufficient to form to deep claret coloured cations, $[Ru(C{\equiv}CC_9H_4RNH)(PPh_3)_2(\eta\text{-}C_5H_5)]^+$ **3**,† also characterised by an X-ray study for R = H, full details of which will be reported elsewhere.‡ N-Methylation can be achieved using methyl triflate. Complexes **2** and **3** form a readily reversible base–acid system, but in contrast with the well known acetylide–vinylidene systems,[3] there is no evidence for protonation occurring at the acetylide β-carbon.

A likely pathway for this reaction is (*i*) attack of $C_\delta$ of cation **1** on the electron-deficient carbon of the imine, (*ii*) electrophilic attack of $C_\gamma$ on the N-bonded aryl group (Scheme 1). The resulting dihydroquinoline is dehydrogenated to form **2** by a second molecule of imine which is thereby reduced to the corresponding benzylamine, which has been isolated and characterised. Consequently, optimum yields are obtained from reactions between **1** and 2 equiv. of imine.

The presence of electron-withdrawing substituents on the N-bonded aryl group results a different reaction course being followed. Thus, the reaction between **1** and $PhCH{=}N(C_6H_4NO_2\text{-}3)$ gives **4** (Scheme 2)† which was also fully characterised by a single-crystal X-ray study.‡ A molecule of **4** is shown in Fig. 2 and significant bond parameters are included in the caption. Again an $Ru(PPh_3)_2(\eta\text{-}C_5H_5)$-substituted alkynyl fragment is present, now attached to a 1-azabuta-1,3-diene ligand through C(3). No cyclisation involving either aryl group is found in this case, nor does any dehydrogenation take place. Similar complexes have been obtained from

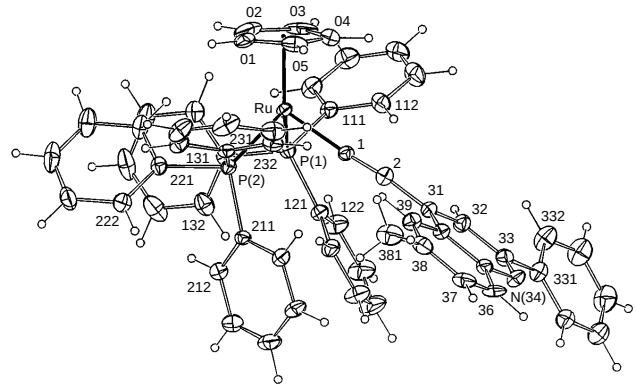
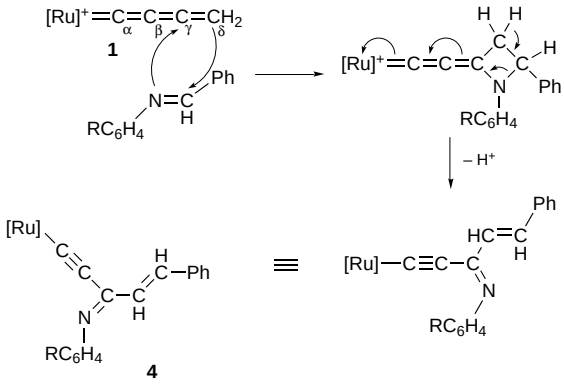



**Fig. 1** Plot of a molecule of $[Ru(C{\equiv}CC_9H_4MeN)(PPh_3)_2(\eta\text{-}C_5H_5)]$ **2b** showing the atom numbering scheme; carbon atoms are designated by number only. In both Figures, non-hydrogen atoms are shown as 20% thermal ellipsoids; hydrogen atoms have arbitrary radii of 0.1 Å. Significant bond parameters: Ru–P(1) 2.308(2), Ru–P(2) 2.300(2), Ru–C(1) 1.997(7), C(1)–C(2) 1.19(1), C(2)–C(31) 1.42(1) Å; Ru–C(1)–C(2) 175.6(7), C(1)–C(2)–C(31) 170.2(8)°.

reactions between **1** and PhCH=N($C_6H_4$R-4) (R = $NO_2$, $CO_2$Et) and PhCH=N(1-$C_{10}H_7$).

In this variant, we propose that a formal [2 + 2] cycloaddition of the $C_\gamma$=$C_\delta$ double bond in **1** to the N=CH of the imine occurs, possibly by attack of the imine N atom on $C_\gamma$ rather than the aryl carbon, after initial $C_\delta$–C(imine) bond formation as in (*i*) above. There is little precedent for this reaction, although it resembles the [2 + 2] cycloadditions of tetracyanoethene (tcne) to transition-metal σ acetylide complexes.[4] In the present case, we do not observe any deep coloured intermediates, but nevertheless, it is unlikely that a concerted addition occurs (which would contravene the Woodward–Hoffmann rules). The initial four-membered $C_3N$ ring formed in such a reaction could undergo ring cleavage (also found with the alkyne–tcne cycloadducts) to give the observed products (Scheme 2).




**Scheme 2** R = $NO_2$-3 or -4, $CO_2$Et-4; [Ru] = Ru($PPh_3$)$_2$(η-$C_5H_5$)

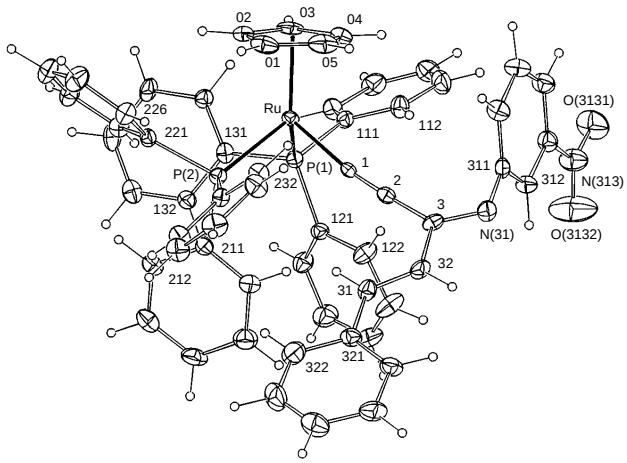



**Fig. 2** Plot of a molecule of [Ru{C≡CC(CH=CHPh)=N($C_6H_4NO_2$-3)}($PPh_3$)$_2$(η-$C_5H_5$)] **4** showing the atom numbering scheme. Significant bond parameters: Ru–P(1) 2.319(2), Ru–P(2) 2.293(2), Ru–C(101) 1.978(8), C(1)–C(2) 1.22(1), C(2)–C(3) 1.43(1), C(3)–C(32) 1.48(1), C(3)–N(31) 1.280(9), C(31)–C(32) 1.32(1) Å; Ru–C(1)–C(2) 171.2(6), C(1)–C(2)–C(3) 176.9(6)°.

Preliminary studies show that other 1,3-dynyl complexes undergo similar reactions. Further discussion of these interesting transformations will be given in the full report.

We thank the Australian Research Council for support of this work and the Deutsche Forschunsgemeinschaft for a Fellowship (P. H); P. J. L. held an Australian Postgraduate Award.

## Footnotes

* E-mail: mbruce@chemistry.adelaide.edu.au

† *Selected spectroscopic data*: for **2b**. IR: ν(C≡C) 2051 $cm^{-1}$. $^1$H NMR: δ 2.36 (Me), 4.43 ($C_5H_5$), 7.05–8.24 (aromatics). FABMS: *m/z* 933, $M^+$; 671, [M − $PPh_3$]$^+$; 429, [Ru($PPh_3$)($C_5H_5$)]$^+$. For **4**. IR: 2048s (C≡C), 1530, 1351s (NO), 831 (CN). $^1$H NMR: δ 4.56 (s, 5 H, $C_5H_5$), 7.0–8.3 (m, 41 H, atomatic). FABMS: *m/z* 966, $M^+$; 702, [M − 2 H − $PPh_3$]$^+$; 429, [Ru($PPh_3$)($C_5H_5$)]$^+$.

‡ *Crystal data and refinement details*: **2b**; [Ru(C≡$CC_9H_4$MeN)($PPh_3$)$_2$(η-$C_5H_5$)]≡$C_{59}H_{47}NP_2$Ru, $M$ = 933.1; triclinic, space group $P\bar{1}$ ($C_i^1$, no. 2), $a$ = 18.067(9), $b$ = 11.472(3), $c$ = 11.279(8) Å, α = 86.08(4), β = 82.47(5), λ = 87.06(3)°, $U$ = 2310 Å$^3$, $Z$ = 2. $D_c$ = 1.34 g $cm^{-3}$; $F$(000) = 964. μ(Mo-Kα) 4.5 $cm^{-1}$; specimen: 0.18 × 0.65 × 0.04 mm; $A$*(min., max.) = 1.02, 1.08.

**4**: [Ru{C≡CC(CH=CHPh)=N($C_6H_4NO_2$-3)}($PPh_3$)$_2$(η-$C_5H_5$)]≡$C_{58}H_{46}N_2O_2P_2$Ru, $M$ = 966.0; triclinic, space group $P\bar{1}$, $a$ = 19.787(8), $b$ = 11.684(3), $c$ = 10.688(3) Å, α = 98.26(2), β = 101.18(2), γ = 101.39(3)°, $U$ = 2333 Å$^3$, $Z$ = 2. $D_c$ = 1.37$_5$ g $cm^{-3}$; $F$(000) = 966. μ(Mo-Kα) 4.5 $cm^{-1}$; specimen: 0.40 × 0.12 × 0.24 mm; $A$*(min., max.) = 1.06, 1.15.

Unique data sets were measured at *ca*. 295 K within the limit $2\theta_{max}$ = 50° using an Enraf-Nonius CAD4 diffractometer (2θ–θ scan mode; monochromatic Mo-Kα radiation, λ = 0.7107$_3$ Å); for **2b**, 7404 independent reflections were obtained [8225 for **4**], 4645 [4544] with $I > 3\sigma(I)$ being considered 'observed' and used in the full-matrix least-squares refinement after gaussian absorption correction. Anisotropic thermal parameters were refined for the non-hydrogen atoms; ($x$, $y$, $z$, $U_{iso}$)$_H$ were included constrained at estimated values. Conventional residuals $R$, $R'$ on $|F|$ are 0.058, 0.059 (for **2b**) and 0.059, 0.058 (for **4**), statistical weights derivative of $\sigma^2(I) = \sigma^2(I_{diff}) + 0.0004\sigma^4(I_{diff})$ being used. Computation used the XTAL 3.0 program system[5] implemented by S. R. Hall; neutral atom complex scattering factors were employed.

Atomic coordinates, bond lengths and angles, and thermal parameters have been deposited at the Cambridge Crystallographic Data Centre (CCDC). See Information for Authors, Issue No. 1. Any request to the CCDC for this material should quote the full literature citation and the referenece number 182/387.

## References

1 M. I. Bruce, P. Hinterding, P. J. Low, B. W. Skelton and A. H. White, *Chem. Commun*., 1996, 1009.
2 B. E. R. Schilling, R. Hoffmann and D. L. Lichtenberger, *J. Am. Chem. Soc*., 1979, **101**, 585.
3 A. Davison and J. P. Selegue, *J. Am. Chem. Soc*., 1978, **100**, 7763; M. I. Bruce and R. C. Wallis, *J. Organomet. Chem*., 1978, **161**, C1.
4 M. I. Bruce, T. W. Hambley, M. R. Snow and A. G. Swincer, *Organometallics*, 1985, **4**, 501.
5 *XTAL Users' Manual, Version 3.0*, ed. S. R. Hall and J. M. Stewart, Universities of Western Australia and Maryland, 1990.

*Received in Cambridge, UK on 29th January 1997; Com. 7/00663B*

# Structural interconversion facilitated by a bifunctional ligand: a covalently linked 2D $Cu^{II}$ sheet $[Cu(3\text{-}pyOH)_2(O_2CCF_3)_2]_n$ and a hydrogen-bond linked 2D $Cu^{II}$ sheet $[Cu(3\text{-}pyOH_2)(O_2CCF_3)_2(thf)_2]_n$

**Satoshi Kawata,[a] Steven R. Breeze,[a] Suning Wang,*[a] John E. Greedan[b] and N. P. Raju[b]**

[a] *Department of Chemistry, Queen's University, Kingston, Ontario, Canada K7L 3N6*
[b] *Department of Chemistry, McMaster University, Hamilton, Ontario, Canada L8S 4M1*

**A covalently linked 2D $Cu^{II}$ compound, $[Cu(O_2CCF_3)_2(3\text{-}pyOH)_2]_n$ 1 (3-pyOH = 3-hydroxypyridine), when dissolved in thf, undergoes conversion to a hydrogen-bond linked 2D $Cu^{II}$ compound, $[Cu(O_2CCF_3)_2(3\text{-}pyOH)_2(thf)_2]$ 2, which upon heating or standing at 23 °C for a few hours is converted back to compound 1 by losing the coordinated thf molecule; weak ferromagnetic interactions between $Cu^{II}$ centres dominate in both compounds.**

There has been an increasing interest in metal complexes containing paramagnetic metal ions and exhibiting extended structures because of their potential applications in molecular magnetic materials.[1] One commonly used strategy in building metal complexes with extended structures is to employ appropriate bridging ligands which are capable of binding to several metal centres through direct bond formation and promoting magnetic interactions as well. The drawback of this strategy is that the complexes tend to have a poor solubility in common solvents which makes them difficult to characterize and fabricate. In contrast, compounds which have hydrogen-bond linked extended structures usually have a good solubility in common solvents. The shortcoming of hydrogen-bonded systems is that the magnetic interactions between the metal centres are usually weak and sometimes the compound undergoes irreversible dissociation when dissolved.[2,3] It is conceivable that if one can use both covalent and hydrogen bonds in building the extended structures, the compounds may have the desired magnetic properties and solubility. In fact, such a strategy has been adapted either by serendipity or by design in a number of magnetic metal complexes where the extended structures are dictated by both covalent and hydrogen bonds.[3,4] We have been interested in building extended structures by using bifunctional ligands (ligands that are capable of forming both metal–ligand bonds and hydrogen bonds).[4] We report herein an unusual structural interconversion, facilitated by the bifunctional ligand, 3-hydroxypyridine (3-pyOH), between a novel $Cu^{II}$ complex $[Cu(O_2CCF_3)_2(3\text{-}pyOH)_2]_n$ **1**, exhibiting a two-dimensional covalently linked extended structure and weak ferromagnetic exchange, and a hydrogen-bonded 2D $Cu^{II}$ complex[4] $[Cu(O_2CCF_3)_2(3\text{-}pyOH)_2(thf)_2]_n$ **2**.

Compound **1** was obtained from the reaction of $Cu(OMe)_2$ with 2 equiv. of trifluoroacetic acid and 3-hydroxypyridine in either 1,4-dioxane or MeCN as a royal blue crystalline solid. The molecular structure of **1** (Fig. 1), established by single-crystal X-ray diffraction analysis,† has an inversion centre. The 3-pyOH ligand acts as a bridging ligand to two $Cu^{II}$ *via* the nitrogen and the oxygen atoms. The $Cu^{II}$ centre in **1** is an elongated octahedron with two nitrogen atoms of the 3-pyOH ligands and two oxygen atoms of the trifluoroacetate ligands occupying the basal positions and two oxygen atoms of the 3-pyOH ligands from the neighbouring molecules occupying the axial positions. The H(5) atom of the 3-pyOH ligand forms a hydrogen bond with the non-coordinated oxygen atom of the trifluoroacetate ligand [O(1′)···O(3) 2.65(2) Å]. As a consequence of the 3-pyOH bridge, compound **1** has an extended 2D sheet structure as shown in Fig. 2. Each mononuclear $Cu^{II}$ unit in the 2D sheet is linked to four other identical mononuclear $Cu^{II}$ units by four 3-pyOH ligands, related by inversion centres with a Cu···Cu separation of 7.27 Å. The two pyridyl rings from two neighbouring mononuclear units are partially stacked with

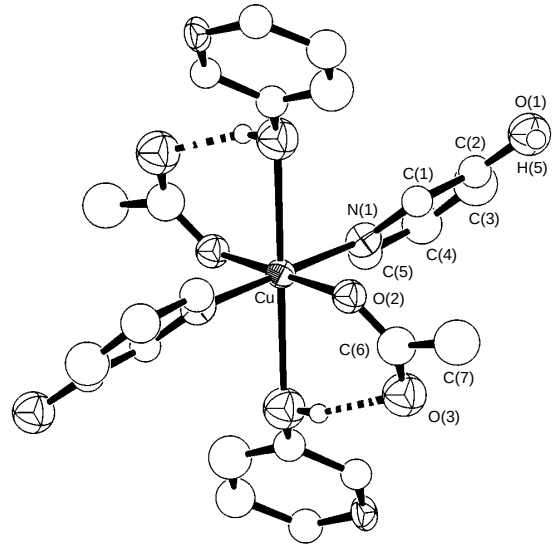



**Fig. 1** An ORTEP diagram showing the mononuclear unit of **1** with 50% ellipsoids and labelling scheme. The fluorine atoms are omitted for clarity. Important bond distances (Å) and angles (°): Cu–O(1′) 2.63(1), Cu–O(2) 1.95(1), Cu–N(1) 1.99(1); N(1)–Cu–O(2) 89.9(5), N(1)–Cu–O(1′) 85.1(4), N(1′)–Cu–O(1′) 94.9(4).

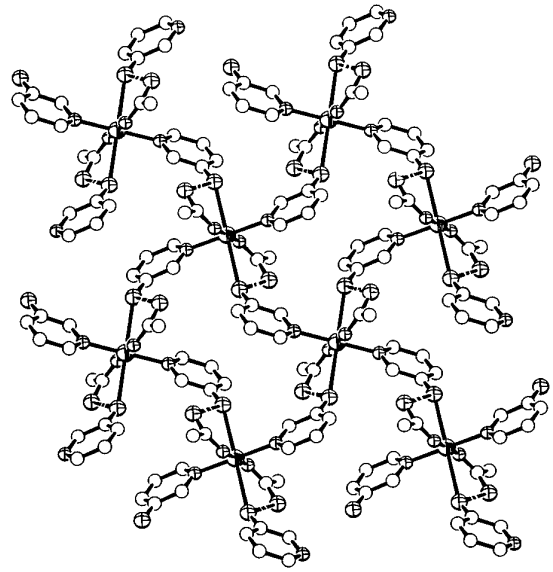


**Fig. 2** A diagram showing the two-dimensional structure of **1** projected down the *a* axis. The fluorine atoms are omitted for clarity.

the shortest atomic separation distance being 3.67 Å. The 2D sheets of **1** stack along the *a* axis with the interlayer Cu···Cu distance being 8.99 Å.

Compound **1** is closely related to $[Cu(O_2CCF_3)_2(3\text{-pyOH})_2(thf)_2]_n$ **2** where the axial positions are occupied by two thf ligands and the mononuclear $Cu^{II}$ units are linked together to form a 2D sheet through intermolecular hydrogen bonds between 3-pyOH and trifluoroacetate ligands (Fig. 3). The separation distance[4] between two neighbouring $Cu^{II}$ ions in the 2D sheet of **2** is 8.04 Å, much longer than that in **1**. Compound **1** is insoluble in solvents such as $CH_2Cl_2$ and MeCN, but very soluble in thf. Upon dissolving in thf, the hydroxy groups at the axial positions in **1** are replaced by two thf molecules and compound **1** is converted to compound **2**. Upon heating or standing at 23 °C for a few hours, compound **2** is converted back to compound **1** in the solid state, accompanied by the loss of thf, as confirmed by X-ray powder diffraction, TGA and DSC analyses. The thf ligand in **2** is replaced by the hydroxy group of the 3-pyOH ligand from a neighbouring $Cu^{II}$ centre in the 2D sheet. The bifunctionality of the 3-pyOH ligand clearly facilitated the conversion process. In **2**, the hydroxy group of the 3-pyOH ligand forms a hydrogen bond only to link the mononuclear units together while in **1** it forms a new weak Cu–O bond, retaining the hydrogen bond, to link the mononuclear units together. It is conceivable that such a structural interconversion is common occurrence among complexes where the metal centres are bound by weak donor ligands and bifunctional ligands. However, to our knowledge, the reversible interconversion between a covalently bonded and a hydrogen-bonded inorganic 2D structure, as observed in **1** and **2**, has not been reported previously. We believe that this interconversion process is important because it provides a mechanism for switching between a soluble and an insoluble phase.

Interestingly, despite the dramatic bonding difference between **1** and **2**, both compounds display similar magnetic properties. For example, the EPR spectrum of the powder sample of **1** at 77 K has a broad signal with $g_\perp = 2.077$ and $g_\parallel = 2.223$, consistent with the elongated octahedral geometry,[5] and a weak half-field transition band at $g = 4.240$, indicative of the presence of magnetic exchange between the $Cu^{II}$ centres.[5] The EPR spectrum of the powder sample of **2** at 77 K resembles that of **1** with $g_\perp = 2.080$ and $g_\parallel = 2.221$ and a weak half-field transition peak at $g = 4.200$. The nature of magnetic exchange in **1** and **2** was established by magnetization and magnetic susceptibility measurements. The effective magnetic moment of **1** increases steadily with the decrease of temperature in the range of 2–10 K, suggesting the presence of ferromagnetic exchange.[6] The magnetization of **1** at 2 K increases rapidly with increasing field strength and reaches 6105 emu G $mol^{-1}$ (1.095 $\mu_B$) at 55 kG, in good agreement with the theoretical magnetization saturation $M_s = 5950$ emu G $mol^{-1}$ (1.065 $\mu_B$) for an $S = 1/2$ and $g_{av} = 2.13$ system.[6] The magnetization curve at 2 K is above the curve of Brillouin function[6] for an $S = 1/2$ and $g_{av} = 2.13$ system, consistent with the presence of weak ferromagnetic interactions. Because all the mononuclear $Cu^{II}$ units in the 2D sheet of **1** are identical and related to each other by inveresion centres, the ferromagnetic interaction is likely to be two dimensional. The low temperature susceptibility data $\chi_m$ and $\chi_m T$ (2 K–10 K) were fitted successfully by using a 2D, spin = 1/2 Heisenberg model,[7] yielding $g = 2.137$ and $J = 0.020(2)$ $cm^{-1}$ from the $\chi_m T$ data and $g = 2.138$ and $J = 0.018(2)$ $cm^{-1}$ from the $\chi_m$ data, supporting the presence of weak 2D ferromagnetic exchange. Preliminary data indicated that **2** is also a weak ferromagnetic interaction dominated system, as evidenced by the positive intercept ($\theta = 1.25$ K) on the *T* axis obtained by the extrapolation of the $C/\chi_M$ data of **2** (5 K–280 K). We have not been able to obtain data below 5 K for **2** due to its poor stability under high vacuum.

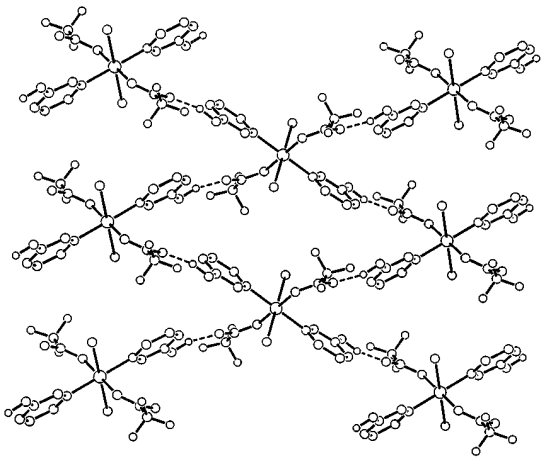


**Fig. 3** A diagram showing the two-dimensional structure of **2**. The carbon of thf were omitted for clarity.

The 3-pyOH ligand in **1** binds to a $d_{z^2}$ and a $d_{x^2-y^2}$ orbitals located at two $Cu^{II}$ centres, respectively, thus makes the interaction of the two $d_{x^2-y^2}$ magnetic orbitals *via* a σ pathway impossible. Therefore, if the σ orbital interaction dictates the spin exchange, one can predict that the magnetic interaction within the 2D sheet of **1** would be either paramagnetic or ferromagnetic.[1,6,8] The π orbitals of the 3-pyOH ligand are essentially orthogonal to the $d_{x^2-y^2}$ orbital. Consequently, the π superexchange pathway, which may yield antiferromagnetic exchange, also becomes impossible. We therefore believe that the weak ferromagnetic exchange observed in **1** is likely caused by orbital orthogonality imposed by the geometric constraint of the 3-pyOH ligand. Dipole–dipole interactions may also contribute since the magnitude of the spin interaction in **1** is very small.

We thank the NSERC (Canada) for financial support and Professor C. V. Stager for use of the magnetometer.

## Footnotes

* E-mail: wangs@chem.queensu.ca

† *Crystal data* for **1**: monoclinic, $P2_1/c$, $a = 8.986(4)$, $b = 9.620(6)$, $c = 10.908(4)$ Å, $\beta = 104.80(3)°$, $Z = 2$, $U = 911.7(7)$ Å$^3$. Final residuals $R = 0.076$ and $R_w = 0.062$. Atomic coordinates, bond lengths and angles, and thermal parameters have been deposited at the Cambridge Crystallographic Data Centre (CCDC). See Information for Authors, Issue No. 1. Any request to the CCDC for this material should quote the full literature citation and the reference number 182/390.

## References

1 D. Gatteschi, *Adv. Mater.*, 1994, **6**, 635; M. Kinoshita, *Jpn. J. Appl. Phys.*, 1994, **33**, 5718; H. O. Stumpf, L. Ouahab, Y. Pei, D. Grandjean and O.Kahn, *Science*, 1993, **261**, 447.

2 J. A. Bertrand, E. Fujita and D. G. VanDerveer, *Inorg. Chem.*, 1980, **19**, 2022; J. A. Bertrand and F. T. Helm, *J. Am. Chem. Soc.*, 1973, **95**, 8184.

3 Y. Pei, M. Verdaguer, O.Khan, J. Sletten and J. P. Renard, *Inorg. Chem.*, 1987, **26**, 138; G. de Munno, D. Viterbo, A. Caneschi, F. Lloret and M. Julve, *Inorg. Chem.*, 1994, **33**, 1585; S. Wang, S. Trepanier, J. C. Zheng and M. J. Wagner, *Inorg. Chem.*, 1992, **31**, 2118; S. Wang, Z. Pang, K. D. L. Smith and M. J. Wagner, *J. Chem. Soc., Dalton Trans.*, 1994, 955.

4 S. R. Breeze and S. Wang, *Inorg. Chem.*, 1993, **32**, 5981.

5 R. S. Drago, *Physical Methods in Chemistry*, W. B. Saunders Co., Philadelphia, 1977; A. Benchini and D. Gatteschi, *EPR of Exchange Coupled Systems*, Springer-Verlag, Berlin, 1992.

6 R. L. Carlin, *Magnetochemistry*, Springer-Verlag, Berlin, 1986.

7 G. A. Baker, Jr. H. E. Gilbert, J. Eve and G. S. Rushbrooke, *Phys. Lett. A*, 1967, **25**, 207.

8 W. E. Hatfield, in *Magneto-Structural Correlations in Exchange Coupled Systems*, ed. R. D. Willett, D. Gatteschi and O. Kahn, NATO ASI, Reidel, Dordrecht, 1985, p. 555.

*Received in Cambridge, UK, 4th December 1996; Com. 6/08178I*

# Experimental study of hydrogen bonding by mutual diffusion

**Nong Chen and T. C. Chan***

*Department of Applied Biology and Chemical Technology, The Hong Kong Polytechnic University, Hung Hom, Kowloon, Hong Kong*

**The use of diffusion data to determine the relative strength of hydrogen bonding and the number of solvent molecules associated with a pseudo-planar solute is demonstrated; the solvation numbers are found to be approximately equal for solutes containing the same polar group in ethanol at 298.2 K.**

Hydrogen bonding is one of the most common and important molecular phenomena which has received intense attention from the earliest days of the subject. Although experimental and theoretical publications on hydrogen bonding abound,[1] however, our knowledge of this phenomenon in liquids is still in its relative infancy. In particular, the nature and consequences of solute–solvent interactions involving hydrogen bonding in very dilute solutions are not well known. This may be due largely to the fact that hydrogen bonding in very dilute solutions is difficult to study by current experimental methods. Nonetheless, the lack of such information may hinder further understanding of the behaviour of many drugs and biological molecules.

Previously, we have found[2] that a linear relationship exists between the reciprocal of the limiting mutual diffusion coefficients ($1/D_{12}$) and the molecular volume ($V$) of non-associated solutes with similar shape. In a preliminary report,[3] we have recently shown evidence of the effect of strong solute–solvent interactions on diffusion and also that the effect can be quantified. This has prompted us to measure more diffusion data, with the primary aim to understand the transport properties of associated molecules. Also, we believe that diffusion measurements can be alternatively designed to probe information about hydrogen bonding. Here, we report the limiting mutual diffusion coefficients of aromatic solutes containing one polar functional group capable of hydrogen bonding in ethanol at 298.2 K. All solutes studied are pseudo-planar in shape. The purpose of this work is to demonstrate how hydrogen bonding in dilute solution can be studied by diffusion data.

Mutual diffusion coefficients at trace concentrations were measured by the Taylor dispersion method, known also as the chromatographic peak-broadening technique. The apparatus and procedures used in the experiment were the same as those described before.[2,3] In this work, the solvent ethanol (99.9%+, E. Merck) was filtered before use with 20 μm stainless-steel HPLC solvent filter. The solute mesitylene (98%, Riedel-de Haen) was purified by fractional distillation; aniline (99.5%+, Aldrich), *p*-chloroaniline (99%+, Fluka), *p*-toluidine (99.9%, Aldrich), 4-chloro-2-methylaniline (99%, Aldrich), 1-naphthylamine (99%+, E. Merck), phenol (99.5%, E. Merck), *p*-chlorophenol (99.5%+, BDH), *p*-cresol (99%+, Fluka), 1-naphthol (99%+, Aldrich), 2-naphthol (99%, Aldrich), biphenyl-2-ol (99%+, E. Merck), anisole (99%+, E. Merck), *p*-chloroanisole (98%+, Fluka), *p*-methylanisole (99%+, E. Merck), 2-methoxynaphthalane (99%, Aldrich), acetophenone (99%, Aldrich), propiophenone (99%+, E. Merck), and 2-acetylnaphthalene (99%+, E. Merck) were used as received. All data were measured at 298.15 ± 0.02 K.

The limiting mutual diffusion coefficients as determined by the Taylor dispersion method are summarized in Table 1. These values are the averages resulting from three or more diffusion measurements. The uncertainty listed is the average absolute error. The reproducibility of data here is consistent with those reported in our previous works using the same technique.[2–5] Also shown in the table are values of the van der Waals volume of the solute monomers, which are calculated from group increments given in the literature.[6–9] When $1/D_{12}$ was plotted against $V$ of the non-associated pseudo-planar solutes, a linear relationship was obtained. The linear regression line is shown in Fig. 1. Also presented in this figure are values for other solutes given in Table 1. Except for aromatic ethers, all $1/D_{12}$ data of these solutes deviate positively from the 'non-associated' line. The deviations indicate that the diffusivities of the solutes are retarded by the volume increase due to hydrogen bonding with the solvent molecules. In this study, the increase in solute size cannot be attributed to solute–solute interaction because the solutions are very dilute and the solvent ethanol is polar. In fact, experimental evidence has already shown that aniline molecules are not even self-associated in non-polar *n*-tetradecane.[3] It is

**Table 1** Limiting mutual diffusion coefficients ($D_{12}$) of aromatic compounds in ethanol at 298.2 K.

| | $V^a$/Å$^3$ | $10^9\ D_{12}$/m$^2$ s$^{-1}$ |
|---|---|---|
| Non-associated solutes | | |
| Benzene | 81.1 | 1.79 ± 0.01[b] |
| Chlorobenzene | 97.2 | 1.61 ± 0.01[b] |
| Toluene | 97.6 | 1.62 ± 0.02[b] |
| Ethylbenzene | 113.8 | 1.45 ± 0.01[b] |
| Naphthalene | 125.4 | 1.32 ± 0.01[b] |
| 1,2,4-Trichlorobenzene | 129.3 | 1.28 ± 0.01[b] |
| Propylbenzene | 130.0 | 1.32 ± 0.02[b] |
| Mesitylene | 130.7 | 1.33 ± 0.02 |
| Biphenyl | 152.4 | 1.19 ± 0.01[b] |
| Phenols | | |
| Phenol | 89.6 | 0.878 ± 0.009 |
| *p*-Chlorophenol | 105.7 | 0.827 ± 0.009 |
| *p*-Cresol | 106.2 | 0.845 ± 0.007 |
| 1-Naphthol | 133.9 | 0.765 ± 0.008 |
| 2-Naphthol | 133.9 | 0.752 ± 0.008 |
| Biphenyl-2-ol | 160.9 | 0.716 ± 0.007 |
| Aromatic amines | | |
| Aniline | 93.8 | 1.19 ± 0.01[c] |
| *p*-Chloroaniline | 109.9 | 1.10 ± 0.01 |
| *p*-Toluidine | 110.4 | 1.11 ± 0.01 |
| 4-Chloro-2-methylaniline | 126.4 | 1.03 ± 0.01 |
| 1-Naphthylamine | 138.1 | 0.991 ± 0.008 |
| Phenones | | |
| Acetophenone | 117.0 | 1.29 ± 0.01 |
| Propiophenone | 133.2 | 1.22 ± 0.01 |
| 2-Acetylnaphthalene | 161.3 | 1.04 ± 0.01 |
| Aromatic ethers | | |
| Anisole | 106.2 | 1.54 ± 0.01 |
| *p*-Chloroanisole | 122.3 | 1.43 ± 0.02 |
| *p*-Methylanisole | 122.7 | 1.44 ± 0.01 |
| 2-Methoxynaphthalene | 150.5 | 1.20 ± 0.01 |

[a] van der Waals volumes are averages from refs. 6–9. [b] From ref. 2. [c] From ref. 3.

interesting that linear relationships also exist between $1/D_{12}$ and $V$ of all pseudo-planar solutes containing the same polar group. The regression lines for phenols, aromatic amines and phenones are shown also in Fig. 1. Remarkably, the slopes for all straight lines in the figure are nearly the same. From Fig. 1, it can be seen that aromatic ethers behave practically as non-associated solutes, and that the strengths of polar groups associated with the solvent through hydrogen bonding decrease in the sequence –OH > $–NH_2$ > –C(O)–.

The increase in size of a polar solute after association can be evaluated from the deviation of its $1/D_{12}$ value from the 'non-associated' line at the same monomeric solute volume in Fig. 1. This is equivalent to the increase in the van der Waals volume that produces such amount of $1/D_{12}$ deviation on the 'non-associated' line. That the linear regression lines of solutes containing –OH, $–NH_2$ and —C(O)– groups are nearly parallel with those of the non-associated solutes indicates that the increased sizes are approximately equal for all solutes containing the same polar group. The average number of ethanol molecules associated with a solute can be determined subsequently from the solute volume increased and the van der Waals volume of the ethanol monomer. The solvation numbers thus calculated for phenols, aromatic amines and phenones are given in Table 2. From this table, it is clear that all phenols on average diffuse together with *ca*. 2.5 ethanol molecules and all aromatic amines with *ca*. one. Phenones are nonetheless only weakly associated with ethanol. The fact that there is little association between phenones (also aromatic ethers) and ethanol is not surprising as the solutes have to compete with other ethanol molecules for forming hydrogen bonds with the solvent. Due to steric hindrance and lack of a proton contribution to form hydrogen bonds, phenones and aromatic ethers are expected to be less competitive in this respect. It should be noted that ethanol is self-associated with an association number of 2.8 in the liquid state at 298.2 K.[10,11] Although solvation numbers can also be calculated[12] from the well known Stokes–Einstein equation, however, the applicability of this equation is not valid for non-spherical solute molecules and for solute molecules small in size compared to the solvent molecules.[13–16] The effects of shape on mutual diffusion have been shown[2] to be as large as 26% in the case of *n*-tetradecane as solvent at 298.2 K.

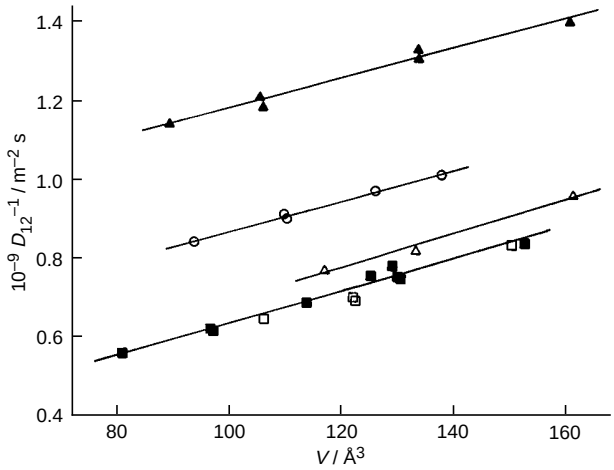



**Fig. 1** Variation of $1/D_{12}$ with molecular volume of solutes diffusing in ethanol at 298.2 K: (■) non-associated solutes, (□) aromatic ethers, (△) phenones, (○) aromatic amines and ( ▲ ) phenols

**Table 2** Solvation numbers (*n*) for solutes in ethanol

| | *n* |
|---|---|
| Phenols | |
| Phenol | 2.6 ± 0.2 |
| *p*-Chlorophenol | 2.6 ± 0.2 |
| *p*-Cresol | 2.5 ± 0.2 |
| 1-Naphthol | 2.5 ± 0.2 |
| 2-Naphthol | 2.6 ± 0.2 |
| Biphenyl-2-ol | 2.4 ± 0.2 |
| Aromatic amines | |
| Aniline | 1.1 ± 0.1 |
| *p*-Chloroaniline | 1.1 ± 0.1 |
| *p*-Toluidine | 1.1 ± 0.1 |
| 4-Chloro-2-methylaniline | 1.1 ± 0.1 |
| 1-Naphthylamine | 1.0 ± 0.1 |
| Phenones | |
| Acetophenone | 0.3 ± 0.1 |
| Propiophenone | 0.2 ± 0.1 |
| 2-Acetylnaphthalene | 0.3 ± 0.1 |

It is interesting that the diffusion coefficients of *p*-chloroaniline (*p*-$ClC_6H_4NH_2$) and *p*-toluidine (*p*-$MeC_6H_4NH_2$) are approximately equal. These two solutes are of similar size and shape. The close resemblance in size between a chloride group and a methyl group has already been discussed.[17] The two solutes are nevertheless different in molecular mass by 19%. Similar results are observed for *p*-chlorophenol (*p*-$ClC_6H_4OH$) and *p*-cresol (*p*-$MeC_6H_4OH$) as well as for *p*-chloroanisole (*p*-$ClC_6H_4OMe$) and *p*-methylanisole (*p*-$MeC_6H_4OMe$). The present data thus further indicate that solvation numbers are insensitive to the mass as well as the size of the monomeric solutes but dependent only on the type of polar group attached.

The authors wish to thank M. L. Chan and K. W. Fong for their technical assistance. This work was supported partially by the Hong Kong Polytechnic University under Grant 350/410, and partially by the Hong Kong Research Grants Council under Grant HKP 88/94P.

## References

1 For reviews, see: G. A. Jeffrey and W. Saenger, *Hydrogen Bonding in Biological Structures*, Springer-Verlag, Berlin, 1991; *Modeling the Hydrogen Bond*, ed. D. A. Smith, *ACS Symp. Ser*., 569, American Chemical Society, Washington, DC, 1994; *The Hydrogen Bond*, ed. P. Schuster, North-Holland Publishing Co., Amsterdam, 1976.
2 T. C. Chan and M. L. Chan, *J. Chem. Soc., Faraday Trans.*, 1992, **88**, 2371; 1993, **89**, 867.
3 M. L. Chan and T. C. Chan, *J. Phys. Chem*., 1995, **99**, 5765.
4 T. C. Chan, *J. Chem. Phys*., 1984, **80**, 5862.
5 T. C. Chan, *J. Chem. Phys*., 1983, **79**, 3591.
6 A. Bondi, *J. Phys. Chem*., 1964, **68**, 441.
7 J. T. Edward, *Chem. Ind. (London)*, 1956, 774.
8 A. I. Kitaigorodskii, *Organic Chemical Crystallography*, Consultants Bureau, New York, 1961.
9 A. E. Luzkii, *Russ. J. Phys. Chem*., 1954, **28**, 204.
10 A. H. Narten and A. Habenschuss, *J. Chem. Phys*., 1984, **80**, 3387.
11 C. K. J. Sun and S. H. Chen, *AIChE J*., 1986, **32**, 1367.
12 L. G. Longsworth, *J. Phys. Chem*., 1963, **67**, 689.
13 D. F. Evans, T. C. Chan and B. C. Lamartine, *J. Am. Chem. Soc*., 1977, **99**, 6492.
14 D. F. Evans, T. Tominaga and T. C. Chan, *J. Solution Chem*., 1979, **8**, 461.
15 D. F. Evans, T. Tominaga and H. T. Davis, *J. Chem. Phys*., 1981, **74**, 1298.
16 S. H. Chen, H. T. Davis and D. F. Evans, *J. Chem. Phys*., 1982, **77**, 2540.
17 S. J. Bertucci and W. H. Flygare, *J. Chem. Phys*., 1975, **63**, 1.

*Received in Cambridge, UK, on 3rd December 1996; Com. 6/08147I*

# Oligonuclear zinc complexes of 2-pyridylmethanol

**Markus Tesmer, Bodo Müller and Heinrich Vahrenkamp***

*Institut für Anorganische und Analytische Chemie der Universität Freiburg, Albertstr. 21, D-79104 Freiburg, Germany*

**The title ligand HL leads to the zinc complexes $[(HL)_2Zn(\mu\text{-}Cl)_2Zn(HL)_2]ZnCl_4$ 1 and $[Zn(ZnL_2)_6]Cl_2$ 2; the ligand arrangement and core structure of 2 make the self-assembly of this complex understandable and show its topological relation to the cadmium iodide structure.**

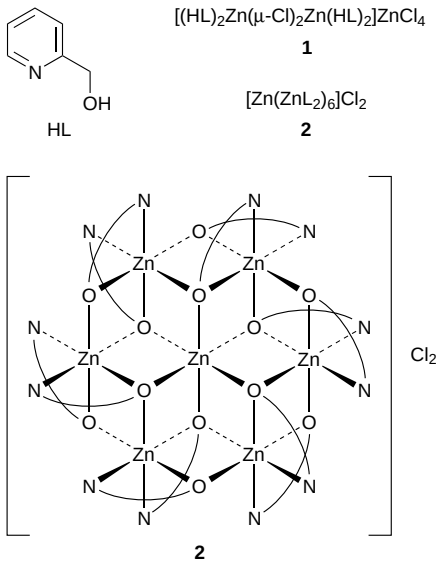
Metal alkoxides, specifically those of zinc, are oligomeric or polymeric,[1] and it is actually difficult to obtain simple mononuclear zinc alkoxide complexes like $[Zn(OR)_2L_2]$ or $[Zn(OR)L_3]$.[2] Such complexes seem attractive either as precursors of new ZnO-containing materials[3] or as models of the enzyme–substrate combination in horse-liver alcohol dehydrogenase (ADH).[4] We therefore tried to obtain such species in a more stable form by making use of the chelate effect, combining the L and OR functions in one ligand molecule. Our ligand of choice was 2-pyridylmethanol whose alkoxide anion can form a five-membered chelate ring. We found that chelation takes place when the ligand is combined with zinc and chloride. The resulting complexes, however, had the unexpected compositions $Zn_3(HL)_4Cl_6$ and $Zn_7L_{12}Cl_2$,† which were found by X-ray analysis to belong to compounds **1** and **2**.‡

Compound **1** resulted from $ZnCl_2$ and HL in diethyl ether. Its strong tendency of formation under these circumstances is obvious from the fact that the reactions were quantitative with respect to HL for stoichiometric ratios ranging from 3 : 4 to 3 : 2. Complex **1** is soluble only in strong donor solvents, and crystals were obtained by diffusion of hexane into a thf solution. Their structure determination (see Fig. 1) revealed the ionic nature of **1** containing the centrosymmetrical dinuclear dications comprised of two $(HL)_2ZnCl$ units. Being a five-membered chelate ring ligand, HL favours octahedral coordination of zinc, as it does for copper in the only other structurally characterized HL complex of a transition metal, $[Cu(HL)_2(salicylate)_2]$.[5]

As $ZnCl_2$–HL combinations, either with or without additional base, did not lead to pyridylmethanolato complexes, a non-polar approach to them was attempted by reacting $Zn[N(SiMe_3)_2]_2$ with HL. In hydrocarbon solvents this produced a precipitate of approximate composition $ZnL_2$. Attempts to purify this by crystallization from strong donor solvents failed, and surprisingly it reacted with $CHCl_3$ or $CH_2Cl_2$ incorporating chlorine with formation of **2** which is soluble in these solvents from which it crystallizes upon diffusion of hexane into the solution. Subsequently it was found that **2** results directly from $Zn[N(SiMe_3)_2]_2$ and HL in $CH_2Cl_2$. At the moment we can only speculate on the course of this reaction which seems to take part of its driving force from the ideal geometry of the resulting $Zn_7L_{12}$ cation (see below).

The formula drawing of **2** in which the chelate ligands are indicated only symbolically indicates the highly symmetrical nature of the complex dication comprised of a central $ZnO_6$ unit surrounded in a disk-like fashion by six $ZnO_4N_2$ units. This is the first such heptametal arrangement for zinc, and it bears no relation to the double cubane arrangement in $[Zn_7Me_6(OMe)_8]$.[6] Its stability and preferred formation become understandable when viewing a space filling model of it, Fig. 2. The six aromatic rings on each side of the $Zn_7O_{12}N_{12}$ scaffold are stacked in triples of pairs such that they perfectly encapsulate the polar inner structure of the cation. The hydrophobic exterior of the cation offers no point of attachment for the chloride anions or the solvating dichloromethane molecules, and it is the reason for the good solubility of **2**. We can think of no other chelate ligand arrangement or core structure of a $Zn_xL_y$ complex derived from 2-pyridylmethanol that would lead to such a perfect match. Thus the cations of **2** are an illustrative example of self-assembly.

When looking at the inorganic core of **2** alone (Fig. 3), another general feature of this complex becomes visible. To a good approximation the O and N atoms form two layers of a close packed array, and of the octahedral interstices in this array one half are filled with zinc ions. Thus the cations of **2** represent fragments of the cadmium iodide or brucite structure inside an organic ligand environment. In this respect **2** is a topological equivalent of the $Fe_{17}$ and $Fe_{19}$ complexes of the tetradentate



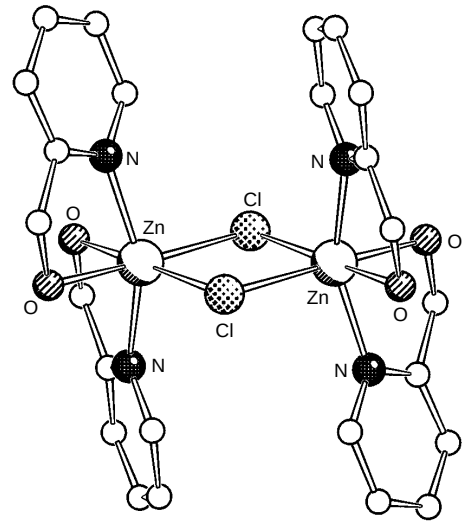




**Fig. 1** Atomic arrangements (bond lengths in Å) in the dication of **1**: Zn–O 2.214(3), 2.217(3); Zn–N 2.075(4), 2.083(3); Zn–Cl 2.409(2), 2.459(2) Å

HEIDI ligand.[8] In both cases the same assembly principle, *i.e.* matching of the ligands' and the core's spatial requirements, is operative.

One would assume that complexes like **2** should exist for pyridylmethanolato complexes of other transition metals. But while the oligonucleating ability of this ligand is well documented,§ we found no other complex like **2** and no other complex with a $M_7X_{24}$ core like in **2** in the literature.

While Fig. 3 points to the materials aspect of these complexes, the aspect of modelling zinc-coordinated intermediates of ADH-catalysed alcohol oxidation lies in the bonding type of the 2-pyridylmethyl-derived ligands. Complex **1** corresponds to the zinc-bound alcohol, **2** to the zinc-bound alkoxide, and the complex $[Zn_2Cl_4(2\text{-pyridylcarbaldehyde})_2]\cdot H_2O$ previously reported by us[9] represents aldehyde coordination by the same type of chelating ligand. Although all three species are zinc chloride compounds as well, their compositions and structures differ so much that a comparative discussion must await the further development of the zinc complex chemistry of these ligands.

This work was supported by the Deutsche Forschungsgemeinschaft.

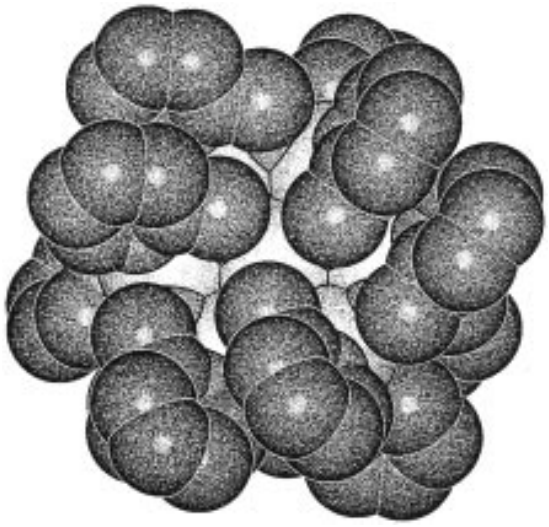


**Fig. 2** SCHAKAL plot[7] of the $[Zn(ZnL_2)_6]$ cation of **2**

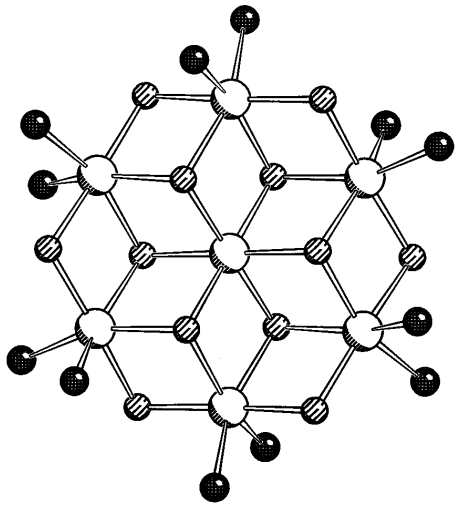


**Fig. 3** The $Zn_7O_{12}N_{12}$ arrangement (bond lengths in Å) in the $[Zn(ZnL_2)_6]$ unit of **2** (Zn colourless, O striped, N dark): for the central zinc Zn–($\mu_3$-O) 2.089(3)–2.127(3); for the peripheral zinc ions Zn–($\mu_3$-O) 2.110(3)–2.186(3), Zn–($\mu$-O) 2.012(3)–2.066(3), Zn–N 2.132(3)–2.182(3)

## Footnotes

† Both compounds yielded satisfactory analytical data. *Selected spectroscopic data*: **1**: IR (KBr) 3732w, 3421s, br (OH), 1611m, 1572w (ring), $^1$H NMR {[$^2H_8$]thf–$(CD_3)_2SO$, 20 : 1} 4.62 (s, br, 2 H, $CH_2$), 5.26 (s, br, 1 H, OH). **2**; IR (KBr) 1603s, 1571m (ring), $^1$H NMR ($CDCl_3$) 4.44–4.77 (m, 2 H, $CH_2$), 5.29 (d, $^2J$ 6.8 Hz, 1 H, $CH_2$), 5.39 (d, $^2J$ 6.9 Hz, 1 H, $CH_2$).

‡ *Crystal data*: **1**: $C_{12}H_{14}Cl_3N_2O_2Zn_{1.5}$, $M$ = 422.68, monoclinic, space group $C2/c$, $a$ = 19.144(2), $b$ = 8.546(5), $c$ = 20.654(4) Å, $\beta$ = 103.00(4)°, $U$ = 3293(3) Å$^3$, $Z$ = 8, $D_c$ = 1.71 g cm$^{-3}$, $R$ = 0.054, $wR_2$ = 0.197 for 3212 reflections. **2**: $C_{36}H_{36}ClN_6O_6Zn_{3.5}\cdot 2CH_2Cl_2$, $M$ = 1082.85, triclinic, space group $P\bar{1}$, $a$ = 12.380(6), $b$ = 14.286(4), $c$ = 14.671(5) Å, $\alpha$ = 61.40(2), $\beta$ = 72.95(3), $\gamma$ = 74.91(3)°, $Z$ = 2, $D_c$ = 1.67 g cm$^{-3}$, $R$ = 0.037, $wR_2$ = 0.087 for 6741 reflections.

*Common data*: data were taken at 183(2) K with Mo-K$\alpha$ radiation on a Nonius CAD4 diffractometer. The structures were solved by direct methods and refinement against $F^2$ using the SHELX program suite.

Atomic coordinates, bond lengths and angles, and thermal parameters have been deposited at the Cambridge Crystallographic Data Centre (CCDC). See Information for Authors, Issue No. 1. Any request to the CCDC for this material should quote the full literature citation and the reference number 182/379.

§ The Cambridge Crystallographic Data File contains 6 dinuclear, 1 trinuclear, 4 tetranuclear, and 1 hexanuclear pyridylmethanolato complexes.

## References

1 M. H. Chisholm and I. P. Rothwell, in *Comprehensive Coordination Chemistry*, ed. G. Wilkinson, R. D. Gillard and J. McCleverty, Pergamon, Oxford, 1987, vol. 2, p. 335; R. C. Mehrotra, A. Singh and U. M. Tripathi, *Chem. Rev*., 1991, **91**, 1287; K. G. Caulton and L. G. Hubert-Pfalzgraf, *Chem. Rev*., 1990, **90**, 969.

2 R. H. Prince, in *Comprehensive Coordination Chemistry*, ed. G. Wilkinson, R. D. Gillard and J. McCleverty, Pergamon, Oxford, 1987, vol. 5, p. 925; M. Melnik, K. Györyova, J. Skorsepa and C. E. Holloway, *J. Coord. Chem*., 1995, **35**, 179.

3 D. C. Bradley, *Chem. Rev*., 1989, **89**, 1317.

4 A. Eklund, A. Jones and G. Schneider, in *Zinc Enzymes*, ed. I. Bertini, C. Luchinat, W. Maret and M. Zeppezauer, Birkhäuser, Boston, 1986, p. 377.

5 N. N. Hoang, F. Valach, M. Dunaj-Jurco and M. Melnik, *Acta Crystallogr., Sect. C*, 1992, **48**, 443.

6 M. L. Ziegler and J. Weiss, *Angew. Chem*., 1970, **82**, 931; *Angew. Chem., Int. Ed. Engl*., 1970, **9**, 905.

7 E. Keller, SCHAKAL-93, Universität Freiburg, 1993.

8 S. L. Heath and A. K. Powell, *Angew. Chem*., 1992, **104**, 191; *Angew. Chem., Int. Ed. Engl*., 1992, **31**, 191.

9 B. Müller, M. Ruf and H. Vahrenkamp, *Angew. Chem*., 1994, **106**, 2164; *Angew. Chem., Int. Ed. Engl*., 1994, **33**, 2089.

*Received, 25th November 1996; Com. 6/07985G*

# Common factors in the mode of action of vancomycin group antibiotics active against resistant bacteria

**Gary J. Sharman and Dudley H. Williams***

*Cambridge Centre for Molecular Recognition, University Chemical Laboratory, Lensfield Road, Cambridge, UK CB2 1EW*

**It is shown that a semisynthetic glycopeptide, with activity against vancomycin resistant bacteria, possesses (as do other glycopeptides active in this way) features which promote its dimerisation and membrane anchoring.**

Vancomycin resistance is a growing problem in the treatment of bacterial infection.[1–5] It arises as a result of a modification of the bacterial cell wall in which the C-terminal D-alanine of cell-wall peptides, to which the antibiotic normally binds, is replaced by D-lactate.[6–8] This results in a repulsive interaction between ligand and antibiotic, and consequently a large decrease in affinity for cell-wall peptides. However, a number of semi-synthetic glycopeptides have recently been developed which show remarkable activity against vancomycin-resistant bacteria.[9] In recent work,[10] we have provided evidence that one such antibiotic, biphenylchloroeremomycin (BCE) or LY307599, developed by researchers at Eli Lilly & Co. in Indianapolis, owes its activity against vancomycin-resistant bacteria to its ability to dimerise and anchor to bacterial cell membranes. We have demonstrated that these two locating devices, which we have previously identified as being important in the mode of action of glycopeptides,[11,12] act cooperatively together to greatly increase the low, intrinsic free solution binding of ligands terminating in D-lactate. We now show that a second semisynthetic glycopeptide (MDL 63246) with activity against vancomycin-resistant bacteria, developed independently by researchers at Lepetit, also appears to share the same locating devices.

MDL 63246 (Fig. 1) is prepared semisynthetically from the antibiotic A40926,[13,14] a relative of the clinically important teicoplanin.[15] Teicoplanin (Fig. 1) shows no evidence of

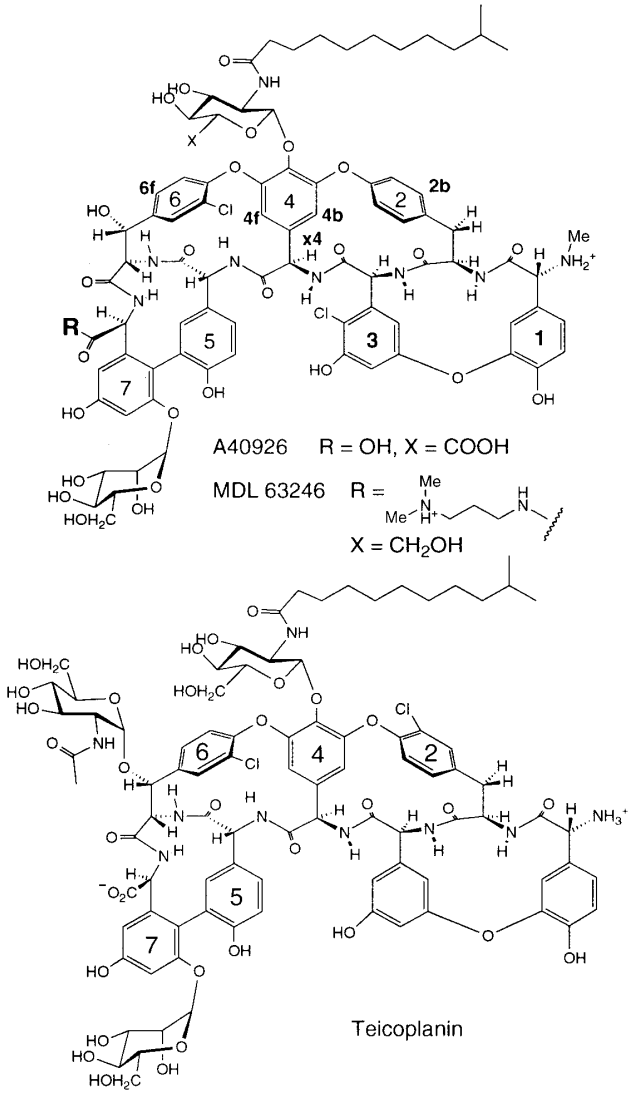



**Fig. 1** Structure of the glycopeptide antibiotics teicoplanin, A40926 and MDL 63246

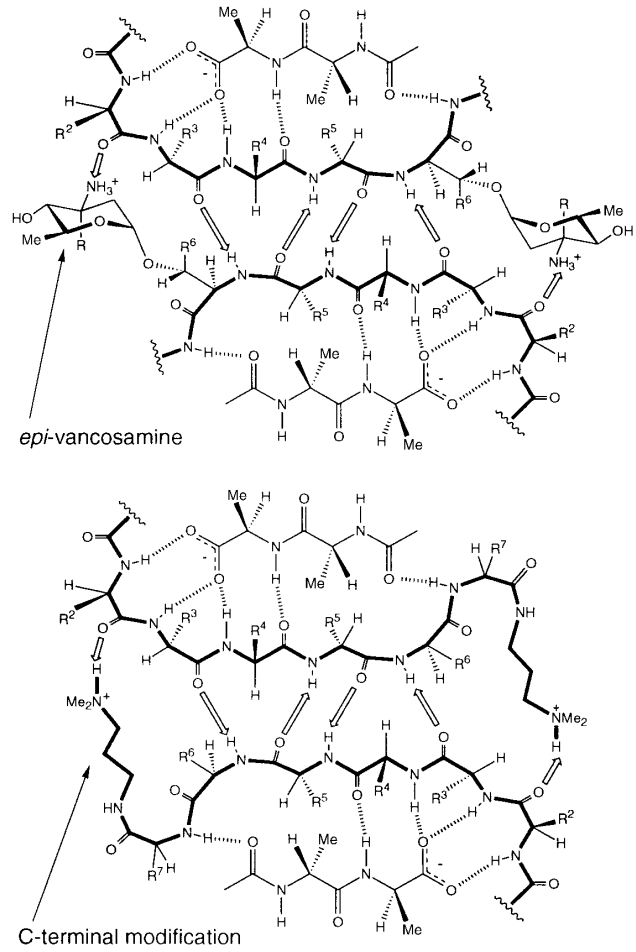



**Fig. 2** Structure of the dimer interface of MDL 63246 and eremomycin, showing how the C-terminal diamine of the former can fulfil a similar role to the *epi*-vancosamine sugar of the latter

dimerisation, but it does possess a membrane anchoring $C_{11}$ chain attached *via* the ring 4 sugar,[16] a feature shared by A40926. However, there are a number of structural differences between A40926 and teicoplanin. A40926 has a ring 3 chlorine, lacks a ring 2 chlorine, and perhaps most importantly in the present context, lacks the acetylated ring 6 sugar found in teicoplanin. The acetylated ring 6 sugar is thought to be the main factor which prevents teicoplanin from dimerising, as it would lead to an unfavourable steric interaction in the dimer structure. It was thus hypothesised that A40926 might dimerise to a limited extent. The structures of the dimers formed by several members of the vancomycin group have been determined by X-ray crystallography[17,18] and two dimensional NMR spectroscopy.[19,20] The use of a CPK model revealed that the diamine present on the C-terminus of MDL 63246 could stabilise such a dimer structure in a similar manner to the *epi*-vancosamine sugar of the antibiotic eremomycin, which increases the dimerisation constant by a factor of *ca*. 100.[21] This increase is due, at least in part, to the formation of a hydrogen bond between the ammonium ion of the *epi*-vancosamine with an amide carbonyl on the other side of the dimer. It further promotes dimerisation in complexes with cell-wall analogues due to an extended salt bridge, mediated through this amide between ammonium ion on one side of the dimer and carboxylate of the cell-wall peptide in the binding pocket of the other side of the dimer (Fig. 2).[19] Thus it was hypothesised that MDL 63246 might dimerise, and that its activity could be explained on the basis of the combined effect of dimerisation and membrane anchoring, exactly as for BCE.

To test this hypothesis, evidence was sought that MDL 63246 did indeed dimerise. When glycopeptide antibiotics dimerise, many $^1$H NMR resonances change their chemical shift in a characteristic way and these shifts are thus indicative of dimerisation. The α-proton of residue 4 (x4) is particularly useful in this respect, as it shifts from *ca*. δ 5.5 in monomer to *ca*. δ 6.5 in dimer. Hence, where the process of dimerisation is in fast exchange, the chemical shift of x4 increases as the antibiotic concentration and proportion of dimer increase.[21] As x4 moves through a region of the spectrum which is relatively uncluttered by other peaks, it serves as an excellent probe for dimerisation. A 3 mM sample of the parent compound A40926 was thus prepared with the ligand di-*N*-Ac-Lys-D-Ala-D-Ala. The $^1$H NMR spectrum was assigned from DQF-COSY, NOESY and TOCSY spectra. The chemical shift of x4 was δ 5.61. On dilution to 0.5 mM, x4 did shift upfield, but only very slightly (< 0.05 ppm), suggesting very weak dimerisation. However, for MDL 63246, a 3 mM solution gave an x4 shift of δ 6.12, changing to δ 5.84 at 0.5 mM. This concentration dependent x4 chemical shift strongly suggested that dimerisation was taking place. A plot of x4 chemical shift versus antibiotic concentration was therefore used to calculate the dimerisation constant by fitting the curve to the expression for dimerisation using a least squares algorithm. Such a plot yielded a dimerisation constant, $K_{dim}$, of 600 dm$^3$ mol$^{-1}$ for MDL 63246 (Fig. 3).

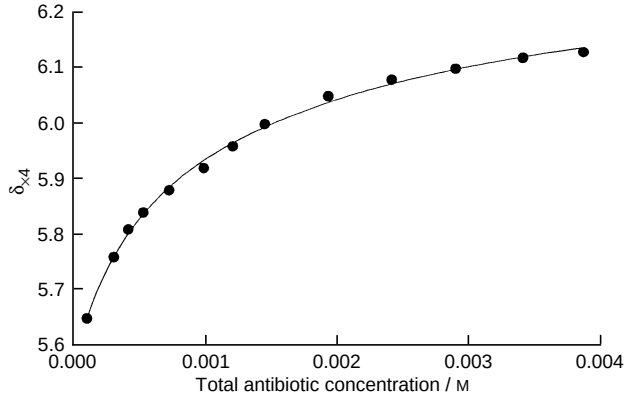



**Fig. 3** Plot of x4 chemical shift against total MDL 63246 concentration. This curve yields a dimerisation constant of 600 ± 100 dm$^3$ mol$^{-1}$.

The dimer structure was investigated further by two dimensional NMR spectroscopy. DQF-COSY, TOCSY and NOESY experiments were used to assign the structure and study its conformation. Several NOE enhancements were observed which were inconsistent with the covalent structure of the antibiotic, but which were indicative of a dimer. These included NOEs between x4 and 6f, an aromatic proton on residue 6 of the antibiotic, and between 6f and 4b (Fig. 1). An NOE enhancement was also observed between 2b and the *N*-methyl groups of the C-terminal diamine, suggesting the diamine was in a position where it could hydrogen bond to the amide between residues 2 and 3, and participate in an extended salt bridge in the presence of cell wall peptides (Fig. 2).

The second example of an antibiotic which dimerises and possesses a membrane anchor, and which exhibits enhanced activity, lends further support to the hypothesis that these two locating devices act cooperatively to enhance binding at the surface of the bacteria. In the case of MDL 63246, it may be possible to improve activity further by modifications which improve dimerisation. This could be achieved in a number of ways, such as optimisation of the C-terminal diamine, through changes in length or removal of rotors. Use of a different base antibiotic, such as teicoplanin with the ring 6 sugar removed, could also improve dimerisation; this antibiotic possesses a ring 2 chlorine, a feature known to enhance dimerisation.[21]

We would like to thank Gruppo Lepetit, Gerenzano, Italy, for kindly supplying samples of MDL 63246 and A40926 and Dr E. Selva (Gruppo Lepetit) for helpful comments. We also thank the EPSRC for financial support.

## References

1 A. P. Johnson, A. H. C. Uttley, N. Woodford and R. C. George, *Clin. Microbiol. Rev*., 1990, **3**, 280.
2 G. M. Eliopoulos, *Eur. J. Clin. Microbiol. Infect. Dis*., 1993, **12**, 409.
3 P. Courvalin, *Antimicrob. Agents Chemother*., 1990, **34**, 2291.
4 S. Dutka-Malen, B. Blaimont, G. Wauters and P. Courvalin, *Antimicrob. Agents Chemother*., 1994, **38**, 1675.
5 Hospital Infection Control Practices Advisory Commitee, *Infect. Control Hosp. Epidemiol*., 1995, **16**, 105.
6 C. T. Walsh, *Science*, 1993, **261**, 308.
7 C. T. Walsh, S. L. Fisher, I.-S. Park, M. Prahalad and Z. Wu, *Chem. Biol*., 1996, **3**, 21.
8 G. D. Wright and C. T. Walsh, *Acc. Chem. Res*., 1992, **25**, 468.
9 T. I. Nicas, D. L. Mullen, J. E. Flokowitsch, D. A. Preston, N. J. Snyder, M. J. Zweifel, S. C. Wilkie, M. J. Rodriguez, R. C. Thompson and R. D. G. Cooper, *Antimicrob. Agents Chemother*., 1996, **40**, 2194.
10 G. J. Sharman, A. C. Try, R. J. Dancer, A. J. Maguire, M. A. Cooper and D. H. Williams, unpublished work.
11 J. P. Mackay, U. Gerhard, D. A. Beauregard and D. H. Williams, *J. Am. Chem. Soc*., 1994, **116**, 4581.
12 D. A. Beauregard, D. H. Williams, M. N. Gwynn and D. J. C. Knowles, *Antimicrob. Agents Chemother*., 1995, **39**, 781.
13 A. Malabarba, R. Ciabatti, R. Scotti, B. P. Goldstein, P. Ferrari, M. Kurz, B. P. Andreini and M. Denaro, *J. Antibiot*., 1995, **48**, 869.
14 J. P. Waltho, D. H. Williams, E. Selva and P. Ferrari, *J. Chem. Soc., Perkin Trans. 1*, 1987, 2103.
15 J. C. J. Barna, D. H. Williams, D. J. M. Stone, T. C. Leung and D. M. Doddrell, *J. Am. Chem. Soc*., 1984, **106**, 4895.
16 M. S. Westwell, U. Gerhard and D. H. Williams, *J. Antibiot*., 1995, **48**, 1292.
17 M. Schafer, T. R. Schneider and G. M. Sheldrick, *Structure*, 1996, **4**, 1509.
18 G. M. Sheldrick, E. Paulus, L. Vértesy and F. Hahn, *Acta Crystallogr., Sect. B*, 1995, **51**, 89.
19 P. Groves, M. S. Searle, J. P. Mackay and D. H. Williams, *Structure*, 1994, **2**, 747.
20 J. P. Waltho and D. H. Williams, *J. Am. Chem. Soc*., 1989, **111**, 2475.
21 U. Gerhard, J. P. Mackay, R. A. Maplestone and D. H. Williams, *J. Am. Chem. Soc*., 1993, **115**, 232.

*Received, 18th December 1996; Com. 6/08477J*

ChemComm
FEATURE ARTICLE

# Unrolling the hydrogen bond properties of C–H···O interactions†

**Thomas Steiner**

*Institut für Kristallographie, Freie Universität Berlin, Takustrasse 6, D-14195 Berlin, Germany*

**It has long been known that C–H groups may form weak hydrogen bonds. The characteristics of these interactions, however, have been explored systematically only recently. Currently, a qualitative understanding is being replaced by quantitative insight into the general properties and functions of weak hydrogen bonds like C–H···O. The current state is reviewed here, with a focus on results obtained by crystal correlation studies.**

## Introduction

The idea that C–H groups may be involved in attractive electrostatic interactions of appreciable strength is usually attributed to Glasstone:[1] in 1937, he explained the formation and the physical properties of liquid complexes like 1 : 1 chloroform–acetone by dimer association, as shown in Fig. 1.

Vibrational spectroscopists soon classified this interaction as a C–H··O 'hydrogen bond', with similar properties to O–H··O or N–H··O hydrogen bonds but lower bond energy. In the following 50 years, however, progress in the field was slow and in some periods even stagnant. Despite conclusive spectroscopic[2] and crystallographic[3] evidence for the structural importance of C–H··O interactions, they were widely neglected or their existence even denied.[4]

Only recently, a wave of interest in weak hydrogen bonding emerged in the different fields of structural chemistry[5] and biology.[6] It is now well documented that C–H··O interactions (and other types of weak hydrogen bonds) are important as secondary interactions, and in many instances even play dominant roles in determining crystal packing[7] and molecular conformation,[8] in molecular recognition processes,[9] in the stabilisation of inclusion complexes[10] and in the stability and possibly even in the activity of biological macromolecules.[11] Most of these studies have concentrated on the *function*, not the *nature*, of weak hydrogen bonds.

The analyses of individual systems were paralleled by detailed investigations on the general characteristics of C–H··O interactions. It turned out that the 'crystal correlation' technique is particularly fruitful in this context. This statistical method is essentially based on comparative analysis of large amounts of published structural data,[12] and can reveal geometrical characteristics and structural preferences that cannot be shown from individual crystal structures alone. In particular, if the studied characteristics are soft, as is normally the case for effects from weak interactions, crystal correlation is often the only suitable access to the problem. The most frequently used source of structural data is the Cambridge Structural Database[13] (CSD), where currently over 160 000 organic and organometallic crystal structures are archived, which offers powerful data retrieval and analysis software. Recent statistical studies on C–H··O interactions will be briefly reviewed here. It will be necessary to point at the limitations of our models (which are narrower than is often assumed), and *caveat* to simplified views must be stated.

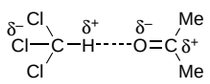



**Fig. 1** Chloroform–acetone dimer

## Some fundamentals

In 1963, Allerhand and Schleyer[14] qualitatively concluded from vibrational spectroscopic experiments that the ability of a C–H group to donate hydrogen bonds depends on the C hybridisation, as C($sp^1$)–H > C($sp^2$)-H > C($sp^3$)–H, and increases with the number of adjacent electron-withdrawing groups. The enhancement of the C–H donor strength by neighbouring electronegative groups is often called 'activation' of C–H. This effect can make even C($sp^3$)–H a relatively strong hydrogen bond donor; examples are $CHCl_3$ and $CH(NO_2)_3$. Particularly strong donors are obtained if C($sp^1$)–H is further activated by neighbouring electronegative atoms, such as in N≡C–H.

Hydrogen bonds in general are composed of different types of interactions.[6] As for all intermolecular interactions, there is a non-directional 'van der Waals' contribution, which is weakly bonding at long distances (by dispersion forces) and strongly non-bonding at short distances (by exchange repulsion). At their optimal geometry, van der Waals interactions contribute some tenths of a kcal $mol^{-1}$ to the hydrogen bond energy. An electrostatic component (dipole–dipole, dipole–charge, *etc.*) is directional and bonding at all distances. It reduces with increasing distance and with reducing dipole moments or charges involved. For donors like O–H or N–H, the electrostatic component is the dominant one in a hydrogen bond (several kcal $mol^{-1}$). This is also true for strongly polarized C–H groups (up to 2 kcal $mol^{-1}$, see below), whereas for weakly polarized C–H groups the electrostatic component is of similar magnitude to the van der Waals contribution. Only for the strongest types of hydrogen bonds does a charge-transfer component become important;[6] it does not play a relevant role for weak C–H··O interactions. The above circumstances carry eminent implications. (i) Electrostatic forces vary smoothly with varying geometry, and diminish only slowly with increasing distance; this leads to a pronounced softness of the hydrogen bond geometry. C–H··O interactions can be easily stretched, compressed and bent from optimal geometry. (ii) The bonding situation is strongly dependent on the donor and acceptor polarisations; therefore, weak hydrogen bonds involving polarizable groups can be critically influenced by their surroundings. (iii) With falling C–H polarisation, the directional electrostatic component is reduced, whereas the isotropic van der Waals component is unaffected; the net interaction therefore loses directionality. (iv) Upon compression, the van der Waals contribution becomes repulsive and might even result in a positive (*i.e.* non-bonding) net energy; this will be more important the smaller the electrostatic component is.

In C–H··O bonds, the net charge on carbon may be negative; this is the classical hydrogen bonding situation ($C^{\delta-}$–$H^{\delta+}$··$O^{\delta-}$). Carbon may also carry a positive partial charge ($C^{\delta+}$–$H^{\delta+}$··$O^{\delta-}$); this also results in electrostatic attraction between donor and acceptor (with different directionality characteristics). The typical partial charges involved are roughly 0 to +0.2 *e* units on H, and depend strongly on the particular system under study.

The bond energies of C–H··O interactions have been much debated. The energies are small and difficult to determine experimentally,[2] so that our knowledge is mainly based on computations. Earlier theoretical studies have been very inconsistent, but modern quantum chemical calculations seem to provide realistic energy estimations, at least for simple molecular systems *in vacuo* (*i.e.* isolated dimers or oligomers). Currently, there is consensus that C–H··O energies are typically $\leqslant 2$ kcal mol$^{-1}$ and gradually fade away with increasing H··O separation (compare 'normal' non-ionic O–H··O hydrogen bonds: *ca*. 3–8 kcal mol$^{-1}$).[6] Gavezotti called this a 'continuum from zero to a moderately strong interaction'.[15] Only for the most acidic C–H donors, and for interactions with partly or dominant ionic character, are energies > 2 kcal mol$^{-1}$ reported. As examples, bond energies for some C–H··O bonded dimers *in vacuo* as obtained by recent *ab initio* molecular orbital calculations[16,17] are given in Table 1 (for computational details, see Table legend). According to these computations, a C≡C–H··$OH_2$ interaction can be regarded as a 'proper' hydrogen bond with an energy of *ca*. 2.2 kcal mol$^{-1}$.[16] For the very weakly polarized donor $CH_4$, on the contrary, equilibrium bond energies are calculated to be 0.5–0.6 kcal mol$^{-1}$, which are dominated by a two-thirds van der Waals contribution.[17] It must be stressed that the above data are valid only for the particular situation they were calculated for: hydrogen bonds are strongly influenced by their surroundings, such as by the solvent and by other hydrogen bonds, so that interaction strengths in the liquid or solid state will in the general case deviate from the values in Table 1.

## Hydrogen bond distances

The shortest bonding C–H··O contacts observed in crystal structures have donor–acceptor separations for C··O of *ca*. 3.0 Å and for H··O of *ca*. 2.0 Å. Such short contacts occur only with acidic C–H donors such as those shown in Fig. 2; recent examples with $CH(NO_2)_3$ and Si–C≡C–H are shown in Fig. 3.[18] Even for acidic C–H, however, H··O contacts of *ca*. 2.0 Å are not the normal case; more typical are H··O distances in the range 2.1–2.3 Å.

If H··O separations in crystals are statistically characterized, different behaviour is observed for chemically different C–H types. For the strongest C–H donors, such as C≡C–H and $CHCl_3$, the frequency distributions of H··O interactions have a well defined maximum, probably corresponding to an optimal value, and fall off for longer distances (Fig. 4). This is a characteristic that is also observed for 'conventional' hydrogen bonds like O–H··O.[6] For weaker donors, the maximum is shifted to longer distances and becomes less pronounced, and for the weakest C–H donor species, there is no maximum and the number of contacts increases with increasing distance. Two realistic examples of such distributions are shown in Fig. 5 (the distance cutoff of these distributions will be discussed below). The observations for weak C–H donors are not straightforward to interpret, because one might expect to see a maximum (though a weak one) for these too. One of the probable determinants of the distributions is that, in competition with other intermolecular forces, hydrogen bonds from the less acidic C–H donors will more frequently be the loosers and be pushed out of optimal geometry than those from the more acidic ones.

Crystallographers are often tempted to associate hydrogen bond distances with hydrogen bond strengths. It is stressed that this is misleading, and that the shorter contact is not necessarily the stronger hydrogen bond, nor that a given contact is 'not a hydrogen bond' just because it is beyond a certain distance

**Table 1** Examples for calculated[a] hydrogen bond energies in C–H··O bonded dimers *in vacuo*. These values need *not* be valid for condensed state arrangements.

| System | Energy/ kcal mol$^{-1}$ | Reference |
|---|---|---|
| H–C≡C–H··O=$CH_2$ | −1.15 | 16 |
| H–C≡C–H··$OH_2$ | −2.19 | 16 |
| N≡C–H··$OH_2$ | −3.79 | 16 |
| $CH_4$··$OH_2$ | −0.59 | 17(*a*) |
| $CH_4$··$OH_2$ | −0.53 | 17(*b*) |
| $NH_2$–$CH_3$··$OH_2$ | −0.61 | 17(*b*) |
| $NH_3^+$–$CH_3$··$OH_2$ | −9.3 | 17(*b*) |

[a] *Ab initio* molecular orbital calculations *in vacuo*, optimised geometries, taking into account electron correlation and the basis set superposition error; ref. 16: DZP′ basis set at the MP2 level of theory; ref. 17(*a*) near HFL basis set at the MP2 level; ref. 17(*b*): D95++(d,p) basis set at the MP2 level.

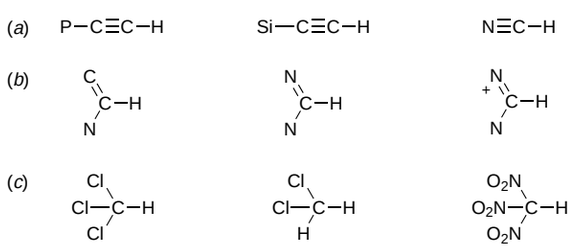



**Fig. 2** C–H groups that can donate short C–H··O hydrogen bonds with H··O around and below 2.1 Å. Examples are given for (*a*) C(sp$^1$)–H, (*b*) C(sp$^2$)–H and (*c*) C(sp$^3$)–H. The examples given for C(sp$^2$)–H are of particular importance for structural biology, because they occur in constituents of nucleic acids and of proteins.

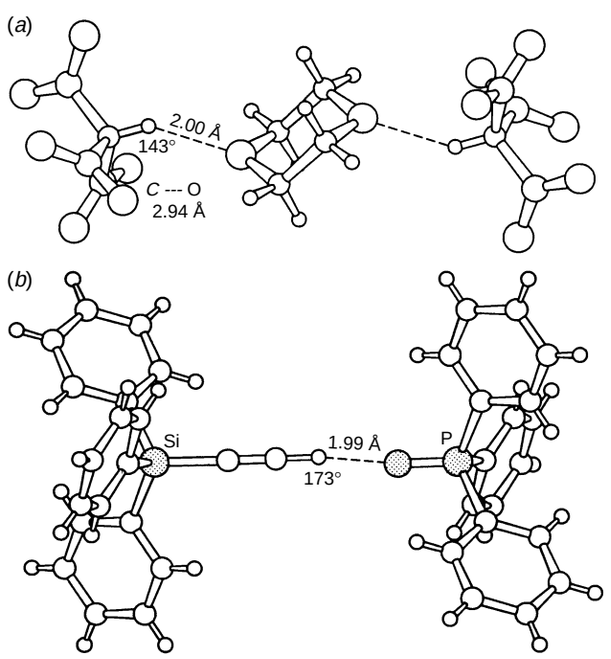



**Fig. 3** The short end of C–H··O hydrogen bonding: the crystalline adducts (*a*) trinitromethane–dioxane [ref. 18(*a*)] and (*b*) triphenylsilylacetylene–triphenylphosphine oxide [ref. 18(*b*)]. Numerical data is given for normalised hydrogen positions (C–H = 1.09 Å).

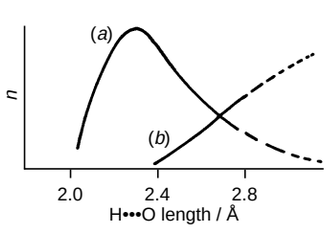



**Fig. 4** H··O Frequency distribution for (*a*) strong donors and (*b*) weak donors

limit. Attempts to obtain reliable bond length–bond energy correlations remained unsuccessful (the same is true for conventional hydrogen bonds). Still, it will be shown below that the *mean* H··O distances of large data samples of related hydrogen bonds carry relevant chemical information on donor and acceptor nature.

*Influence of donor acidity and acceptor basicity*

Certain 'strong' or 'activated' C–H donors form on average shorter contacts to oxygen than the less activated species. Quantification of this effect was achieved by Desiraju in a series of crystal correlation studies.[20–22] For chloroalkyl compounds, he demonstrated that the mean donor–acceptor separation of hydrogen bonds follows the sequence $Cl_3CH$ < $Cl_2CCH$ < $ClC_2CH$ < $C_3CH$, with mean C··O separations of 3.32, 3.40, 3.46 and 3.59 Å, respectively.[20] Similarly, alkynes form shorter contacts to oxygen than alkenes.[21] In an important generalisation, a direct correlation between average C··O separations and carbon acidity (in $Me_2SO$) could be shown (Fig. 6).[22] This correlation, however, is fairly sharp only for sterically unhindered donors, whereas for sterically hindered C–H groups, the average C··O separations are elongated compared to the values expected from Fig. 6. C–H acidity and therefore donor strengths can also be increased by steric strain on carbon, as was recently shown by Allen *et al.* for C–H in cyclopropane and related three-membered rings.[5d]

An effect of acceptor polarity on mean donor–acceptor separations was shown in a database analysis of small solvent molecules in varying crystal environments (Table 2).[19] In Table 2, the effect from donor polarisation shows up in the columns: with increasing C–H polarisation, the mean H··O separations reduce from 2.62 Å (for the Me groups of acetone) to 2.22 Å (for chloroform). This is a reduction of 0.4 Å. Note the fine gradation in the strengths of the weak methyl donors, which increase as N≡C–Me > O=S(Me)$_2$ > O=C(Me)$_2$, reflecting the different degrees of 'activation'. The effect from acceptor polarity (or basicity) is weaker, but can still be clearly seen in the rows: the variation in H··O separations between the strongest acceptor, C=O, and the weakest, C–O–C, is about 0.1 Å.

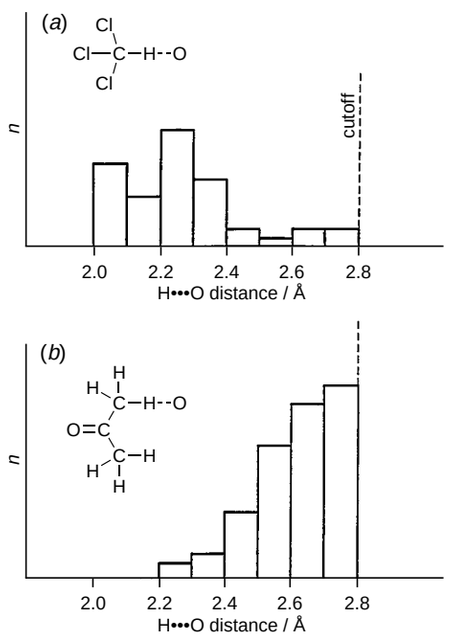



**Fig. 5** Two examples for realistic H··O frequency distributions in crystals for (*a*) chloroform donors, and (*b*) acetone donors; drawn using the data analysed in ref. 19

## Directionality

*Donor directionality of short C–H···O contacts*

Hydrogen bonds in general are directional interactions with a preference for linear geometry. For C–H··O interactions, this

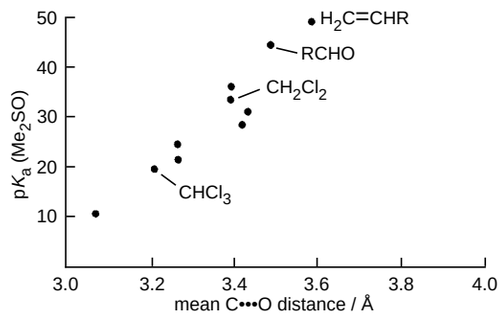



**Fig. 6** Correlation of mean C··O distance with the C–H acidity. Adapted from Pedireddi and Desiraju (ref. 22). Only data for sterically unhindered donors is shown. Each of the data points represents the mean value of broad distributions such as those in Fig. 5.

**Table 2** Mean C··O and H··O separations (Å) for C–H··O hydrogen bonds from small solvent molecules to various acceptor types (with H··O < 2.8 Å, for normalized H-positions)[a] (from ref. 19).

| | Acceptor | | | | | |
|---|---|---|---|---|---|---|
| Donor | C=O | $NO_2$ | S=O | C–OH | C–O–C | all O |
| **Mean C···O** | | | | | | |
| $CHCl_3$ | 3.16 (3) [13] | | | | 3.26 (4) [3] | 3.16 (2) [22] |
| $CH_2Cl_2$ | 3.21 (3) [13] | 3.32 (4) [7] | 3.3 (1) [3] | 3.51 (5) [3] | 3.43 (4) [17] | 3.33 (2) [54] |
| C($sp^3$)–C≡CH[b] | 3.28 (2) [15] | | | 3.37 (4) [22] | 3.38 (4) [8] | 3.35 (2) [49] |
| MeCN | 3.33 (6) [7] | 3.31 (6) [13] | | 3.42 (9) [4] | 3.37 (3) [18] | 3.35 (2) [47] |
| $Me_2SO$ | 3.41 (2) [25] | 3.45 (4) [18] | 3.51 (3) [26] | 3.44 (3) [11] | 3.59 (6) [3] | 3.46 (1) [85] |
| $Me_2CO$ | 3.49 (2) [32] | | | 3.55 (5) [8] | 3.61 (4) [8] | 3.52 (2) [54] |
| **Mean H···O** | | | | | | |
| $CHCl_3$ | 2.22 (5) [13] | | | | 2.31 (4) [3] | 2.22 (3) [22] |
| $CH_2Cl_2$ | 2.27 (4) [13] | 2.41 (5) [7] | 2.4 (1) [3] | 2.6 (1) [3] | 2.50 (4) [17] | 2.41 (2) [54] |
| C($sp^3$)–C≡CH[b] | 2.24 (3) [15] | | | 2.41 (5) [22] | 2.44 (6) [8] | 2.37 (4) [49] |
| MeCN | 2.44 (7) [7] | 2.55 (4) [13] | | 2.44 (7) [4] | 2.46 (4) [18] | 2.49 (2) [47] |
| $Me_2SO$ | 2.51 (2) [25] | 2.57 (3) [18] | 2.56 (2) [26] | 2.61 (4) [11] | 2.63 (6) [3] | 2.56 (1) [85] |
| $Me_2CO$ | 2.60 (2) [32] | | | 2.69 (2) [8] | 2.69 (3) [8] | 2.62 (2) [54] |

[a] Standard errors of the mean values given in parentheses, number of examples ($n_{CH}$) given in square brackets. Data for acceptors with $n_{CH}$ < 3 are not given individually, but included in the column for 'all O'. [b] Molecular residue.

property was first shown by Taylor and Kennard, who analysed the geometry of very short C–H··O contacts (H··O < 2.4 Å) in organic neutron crystal structures.[23] For these short contacts, the frequency distribution of C–H··O angles ψ is shown in Fig. 7(*a*): most frequent are slightly bent arrangements with angles in the interval ψ = 150–160°, whereas heavily bent contacts do not occur. To interpret this distribution properly, one must consider that the solid angle covered by an angular interval Δψ is smaller for linear than for bent angles (see inset of Fig. 7); if the distribution is weighted by 1/sin ψ, the more relevant figure to the right is obtained ('cone correction' as introduced by Kroon and Kanters[24]). This figure shows that linear contacts are preferred, as must be expected for electrostatic dipole interactions. For comparison, Fig. 7(*b*) also shows corresponding histograms for O–H··O hydrogen bonds in carbohydrates, which possess essentially the same characteristics, with an only slightly more pronounced preference for linearity.

*Donor directionality: the general case*

Fig. 7 demonstrates that C–H··O interactions are in principle directional. Due to the weakness of the interaction, however, the C–H··O hydrogen bond can be easily bent, so that directionality is blurred if steric hindrance or competition with other hydrogen bonding groups comes into play. This can be clearly observed for C–H··O contacts in carbohydrates, where O–H··O hydrogen bonds are the dominant intermolecular interaction forming a frame in which the weaker interactions have to adjust. Fig. 8 shows a scatterplot of ψ against H··O bond lengths for intermolecular C–H··O contacts in carbohydrate neutron crystal structures.[25] Most of the donors are of the type shown in Fig. 9, *i.e.* 'activated' C($sp^3$)–H groups. Despite the competitive situation, numerous C–H··O interactions with H··O separations down to about 2.25 Å are formed. The shortest of the contacts show the same preference for approximate linearity as those in Fig. 7, but with increasing distance the directionality rapidly becomes softer. From about H··O = 2.7 Å on, all angles ψ occur. The quasi-isotropic behaviour at longer distances should not be regarded as a sign of a lack of directionality; it is merely a consequence of competition with stronger forces.

Not every near-neighbour arrangement involving C–H and O is necessarily a hydrogen bond, and in a plot like Fig. 8 it is not generally possible to spot which of the data represent significant bonding interactions, which do not, and which are borderline cases. One of the circumstances causing this uncertainty is the occurrence of simultaneous contacts to atoms other than oxygen, in particular the ubiquitous repulsive H··H contacts. This problem can be illustrated[27] as shown for water acceptors in Fig. 10. A realistic example with a clearly repulsive and an 'uncertain' arrangement is shown in Fig. 11. The real problem is the uncertain cases, which are very difficult to interpret in individual crystal structures, and to filter them out from a given statistical data sample.

A problem that has as yet not been tackled seriously is the directionality behaviour of the weakest C–H donor types such as methyl groups. For these, contributions from dispersion forces are similar or even larger than the electrostatic contribution,[17] so that C–H··O interactions might become almost isotropic.

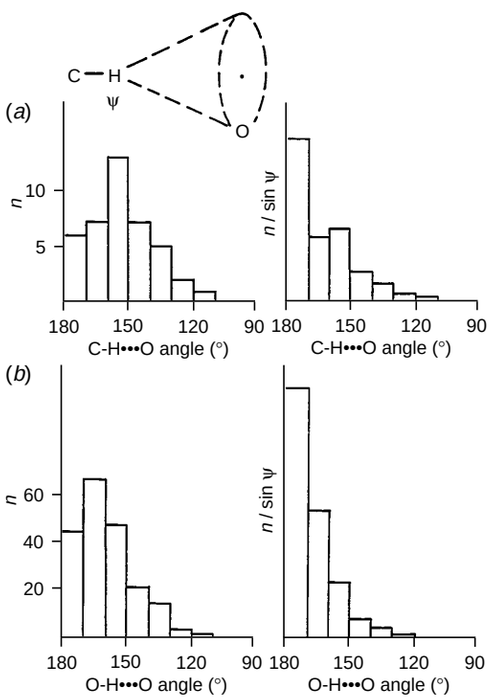



**Fig. 7** Frequency distribution of X–H··O angles (ψ) in crystal structures: (*a*) 41 intermolecular C–H··O contacts with H··O < 2.4 Å in organic neutron crystal structures (ref. 23); (*b*) 196 O–H··O hydrogen bonds in carbohydrate X-ray crystal structures (ref. 24). The inset illustrates the 'cone correction' (ref. 24) (weighting by 1/sin ψ) that relates the left and the right histograms. The idea to show C–H··O and O–H··O histograms in one figure was adapted from a lecture of J. Kroon (Utrecht, Sept. 5, 1995).

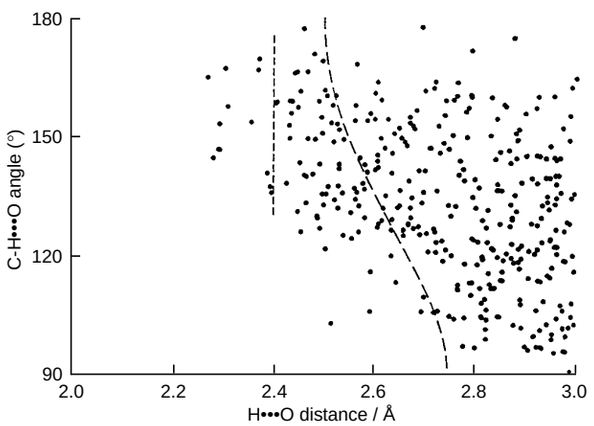



**Fig. 8** Scatterplot of the C–H··O angle against the H··O distance in intermolecular C–H··O contacts in carbohydrate neutron crystal structures. Drawn using data analysed in ref. 25. The straight dashed line at H··O = 2.4 Å shows the arbitrary distance cutoff used in ref. 23 (compare Fig. 7). The curved dashed line represents the H··O van der Waals separation based on a spherical oxygen atom and a non-spherical hydrogen atom (ref. 26). The conventional assumption of the van der Waals separation would be a vertical line at H··O = 2.6 or 2.7 Å.

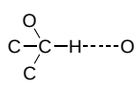



**Fig. 9** Typical C–H donor in carbohydrates

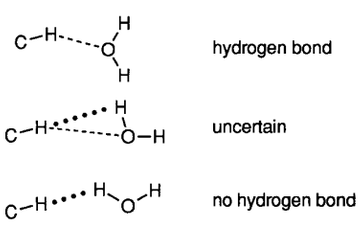



**Fig. 10** Possible geometries of C–H to water contacts

*Acceptor directionality*

The acceptors of hydrogen bonds exhibit complex but weak directionality behaviour that depends on their chemical nature. For carbonyl acceptors, X–H vectors tend to point at the oxygen 'lone-pair lobes' which are in the carbonyl plane, in theory forming angles of 120° with the C=O bond.[29] For ether, hydroxy and water acceptors, hydrogen bonds are weakly clustered in the bisecting plane of $R^1$–O–$R^2$.[30]

In the context of C–H··O hydrogen bonding, acceptor directionality has as yet only been discussed for C=O acceptors. Following initial indications,[23,31] the subject was studied in more detail in a crystal correlation study of acidic and sterically unhindered C–H donors which are not in competitive situations ($CHCl_3$, $CH_2Cl_2$, C≡C–H).[32] If the approach of C–H to O=C is characterized by the angle α (H··O=C) and the torsion angle ω (H··O=C–Y), the polar scatterplot shown in Fig. 12 is obtained. The histogram shows the distribution of angles ω and indicates a preference for in-plane contacts (ω ≈ 0). The acceptor directionality that becomes apparent from Fig. 12 is very soft, but significant.

## Notes on cutoff criteria

Formerly, it was common practice among crystallographers to define hydrogen bonds as X–H··Y contacts shorter than the H··Y or the X···Y van der Waals separation. It has been repeatedly pointed out that this concept is faulty:[6] there is no experimental or theoretical evidence that at a certain critical distance, the interaction is switched from 'hydrogen bond' to 'van der Waals' type. The electrostatic component of the hydrogen bond also operates beyond van der Waals separation. This is reflected in the appearance of Fig. 8, which lacks any discontinuities. The straight dashed line shows the conservative

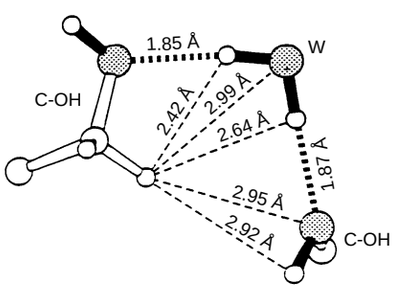



**Fig. 11** An example of long C–H··O contacts associated with repulsive H··H contacts. The C–H···water contact is presumably repulsive, and the net interaction of the C–H··OH contact is uncertain. In other geometries, such long C–H··O contacts can be assessed as weakly bonding in nature [adapted from ref. 25, using neutron diffraction data of β-cyclodextrin–11.6 $H_2O$ at 120 K (ref. 28)].

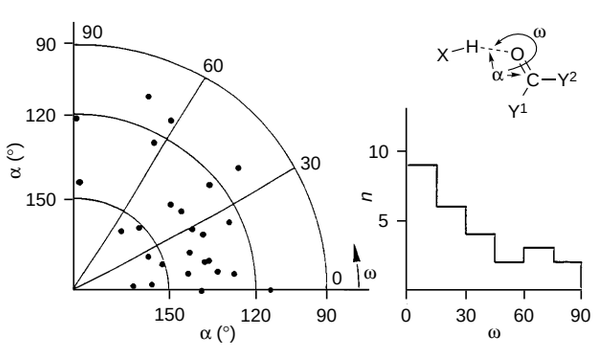



**Fig. 12** Approach of acidic and sterically unhindered C–H donors to C=O acceptors (26 data points) (ref. 32). Geometrical definitions are shown in the inset. The data are indicative of soft but significant acceptor directionality.

2.4 Å van der Waals cutoff used by Taylor and Kennard,[23] and the curved dashed line represents an alternative van der Waals cutoff[25] based on a possibly non-spherical H-atom.[27] Both divide the distribution as arbitrarily as any other cutoff would do.

In many instances, computational practice requires the use of cutoff definitions. A compromise must then be found between the desire not to omit too many attractive long-distance interactions, and not to include too many dubious (Fig. 10) or insignificant 'hydrogen bonds'. The first desire calls for a distance cutoff so long that maxima in distance distributions (if existing, Fig. 4) are included; this requires values > 2.6 Å. Since dubious arrangements, such as those shown in Fig. 10, occur mainly with long H··O separations > 2.8 Å,[27] the author has repeatedly used this value as a pragmatic cutoff distance in crystal correlation studies. In samples containing fewer dubious arrangements, longer cutoff values, such as 3.0 or 3.2 Å, can be justified. In any case, cutoff criteria are coarse instruments and should be avoided whenever possible.

## Effect on covalent geometries

Hydrogen bonding has consequences for the covalent bonding of the involved groups. In an interaction $R^1$–X–H··Y–$R^2$, the X–H and Y–$R^2$ bonds are weakened, resulting in bond lengthening and lowering of the stretching frequencies, and the $R^1$–X bond is strengthened and thereby shortened. These effects are very pronounced for O–H··O hydrogen bonds.[33] For the C–H··O interactions, analogous effects should be expected to occur on a smaller scale. In infrared absorption spectra, weakening of C–H and Y–R can in many instances be clearly observed,[2,34] but the extent to which the weakening reflects in the covalent geometry has been only poorly investigated. As a first such effect, slight lengthening of the C–H bond was shown from neutron diffraction data of amino acid $C_\alpha$–H bonds.[35*a*] The reported lengthening, of *ca*. 0.01 Å for contacts with H··O of *ca*. 2.3 Å, corresponds to a weakening of the C–H bond by roughly 0.03 valence units (for bond length–bond valence relations in general, see ref. 36).

In an individual neutron crystal structure, slight lengthening of an acetylenic C–H bond in a short C≡C–H··O interaction (H··O = 2.07 Å) was reported only recently.[35*b*]

## Cooperativity

Hydrogen bonds possess the important property of *cooperativity*; in arrays of *n* interconnected hydrogen bonds, the total bond energy is larger than the sum of *n* isolated hydrogen bonds ('*non-additivity*'). There are two different mechanisms that can produce this effect: functional groups which may act as hydrogen bond donor and acceptor simultaneously often form chains of the type $O^{\delta-}$–$H^{\delta+}$··$O^{\delta-}$–$H^{\delta+}$··$O^{\delta-}$. In these chains, due to mutual polarisation of the involved groups, the individual hydrogen bonds enhance each other's strengths by around 20%.[6] A different mechanism is charge flow in suitably polarizable π-bond systems ('*resonance assisted hydrogen bonds*'.[37])

Based on structural and electrostatic analogies, such effects can be postulated to occur also with weak hydrogen bond types. Of particular interest is the C≡C–H residue, which can donate C–H··Y and accept X–H··π hydrogen bonds simultaneously.[38–40] Three patterns that are topologically equivalent are shown in Fig. 13, and one may expect that they also have analogous cooperativity properties (of course, of different strengths).

(*a*) O–H------O–H------O

(*b*) C–H------O–H------O

(*c*) X–H----C≡C–H----O

**Fig. 13** Three topologically equivalent hydrogen bond patterns

Unfortunately, direct experimental evidence for energy enhancement is difficult to obtain. For arrangements like the one in Fig. 13(*c*), however, spectroscopic evidence for cooperativity has been supplied.[38a] The crystalline sex steroid mestranol contains cooperative and non-cooperative C≡C–H···O hydrogen bonds, which can be directly compared spectroscopically.[38b] More complex patterns have also been observed, such as the cycles shown in Fig. 14, for which non-additivity has been claimed.[40]

A well known example for conventional 'resonance assisted hydrogen bonding' is the carboxylic acid dimer shown in Fig. 15(*a*), and an analogous C–H··O pattern is shown in Fig. 15(*b*). It is supposed that this pattern is stronger than just the sum of two C–H··O=C hydrogen bonds. However, the mere structural analogy is not a proof for significant cooperativity effects in Fig. 15(*b*), so that further investigations are required.

A pattern with C–H··N bonding that is immediately suggestive of cooperativity is the infinite chains in crystalline HCN[41] (Fig. 16). Liquid HCN is composed of finite chains of this kind. In a recent *ab initio* quantum chemical study of $(HCN)_n$ chains, it was in fact calculated that the H··N distances and the C–H stretching frequencies reduce with increasing system size, whereas the C–H bond lengths increase. Even at the octamer stage, saturation of the effect had not yet completely been reached.[42]

Quantum chemical calculations have also been performed on the infinite molecular chains in crystalline *N*,*N*-dimethylnitroamine (Fig. 17). For these, using semiempirical molecular orbital calculations, Sharma and Desiraju estimated an energy enhancement of around 20%; the effect reaches saturation at about the pentamer stage.[43]

## Thermal vibrations

Hydrogen bonding reduces the thermal vibrations of the engaged residues. For C–H··O interactions, this effect was first shown for terminal alkynes.[44] The acetylenes are good probes in this context, because they are among the most acidic C–H donors and, at the same time, they enjoy pronounced vibrational freedom. The situation is sketched in Fig. 18.

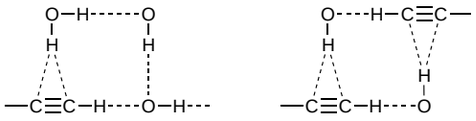


**Fig. 14** Two cooperative hydrogen bond cycles involving C–H···O interactions

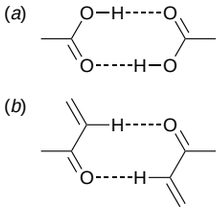


**Fig. 15** Resonance assisted hydrogen bonding

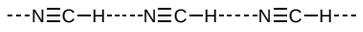


**Fig. 16** The infinite hydrogen bonded chains in crystalline HCN

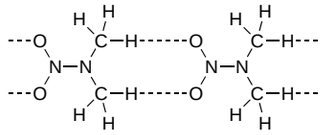


**Fig. 17** The infinite molecular chains of crystalline *N*,*N*-dimethylnitroamine

A free C≡C–H moiety can vibrate strongly, normally with the vibration amplitude largest for the terminal C-atom [Fig. 18(*a*)]. In a C≡C–H··X hydrogen bond, the alkynyl orientation is more restricted [Fig. 18(*b*)]. The vibration behaviour can be described semi-quantitatively by the ratio of isotropic displacement parameters $U(C2)/U(C1)$, which is significantly larger than 1 for the situation in Fig. 18(*a*), and close to 1.0 for that in Fig. 18(*b*). This ratio was correlated with the H··X separation for 51 C≡C–H groups in 42 crystal structures (X = O, N, π-acceptors), and the obtained correlation clearly shows the anticipated effect (Fig. 19):[44] on average, the *U* ratio continuously reduces with shortening H··X distance, indicating a reduction of the thermal vibration. It is of relevance that this effect is not only observed for the shortest hydrogen bonds, but also for relatively long contacts with H··X in the range 2.6–2.8 Å, reflecting the long-range nature of the interaction.

The complementary effect on the acceptor side was shown by Braga *et al.* for an organometallic compound[31] (Fig. 20). For metal-coordinated carbonyl groups, the ratio $U(O)/U(C)$ was reported to be larger for free M–CO [Fig. 20(*a*)] than for CO accepting M–CO··H–C interactions [Fig. 20(*b*)], indicating reduction of the acceptor vibration due to C–H··O hydrogen bonding.

## C–H···O replacing stronger hydrogen bonds

In many crystal structures, C–H··O interactions are observed as bystanders or subalterns to more dominant systems of stronger interactions. This can easily lead to the view that C–H··O interactions, although in principle of hydrogen bond type, are too weak to have similar functions in structure formation and

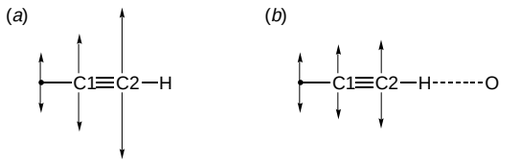


**Fig. 18** Thermal vibrations of the (*a*) unbonded and (*b*) C–H··O bonded C≡C–H moiety

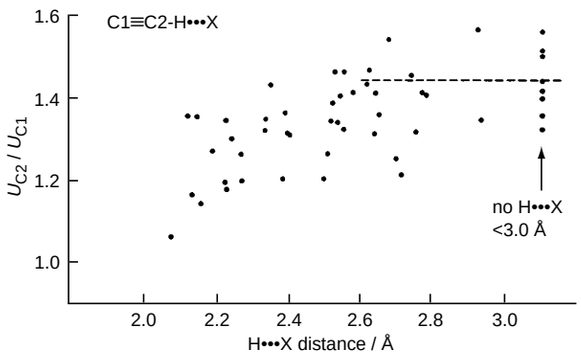



**Fig. 19** Correlation of the quantity $U(C2)/U(C1)$ with the H··X distance in C1≡C2–H··X hydrogen bonds (X = O, N, π-bonds), for normalized hydrogen positions. The horizontal line shows the mean value for C≡C–H groups with no H··X contact shorter than 2.8 Å (adapted from ref. 44).

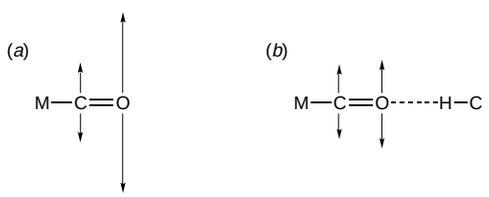


**Fig. 20** Thermal vibrations for the (*a*) unbonded and (*b*) M–C=O··H bonded M–CO moiety

stabilisation as the stronger O/N–H··O hydrogen bonds. However, this is not true in all cases (in many, though, it is), and opposite observations have also been made. The author first encountered this problem when studying the coordination of water molecules in various environments,[27,45,46] mainly from highly accurate neutron diffraction data. It became apparent that water molecules frequently accept C–H··$O_W$ interaction, which have the major function of 'filling up' the preferred two-fold acceptor functionality, if stronger O–H or N–H donors are not suitably available (Fig. 21). The coordination geometries of the arrangements shown are completely analogous. There is no doubt that these C–H··$O_W$ interactions are formed only as a last resort if stronger hydrogen bonds are lacking, but if they form, C–H donors actually take the role and function of O–H or N–H.

Several examples have been published where, in isomorphous crystal structures, an N/O–H··O hydrogen bond in one structure is isofunctionally replaced by a C–H··O interaction in the other. The classical examples are the isomorphous complexes urea–barbital and acetamide–barbital[47] (Fig. 22). Other examples are the isomorphous inclusion complexes of β-cyclodextrin with diethanolamine and with pentane-1,5-diol, where a clearly structure-stabilizing N–H··O bond is substituted by a C–H··O interaction of the same function,[48] and the replacement of an N–H··$Cl^-$ by a C–H··$Cl^-$ interaction in isomorphous adenosine derivatives.[49] In all these cases, both interactions have the same function in structure stabilisation, *i.e.* in these instances, the C–H··O interactions do in fact play the role of a stronger hydrogen bond.

## Outlook

The process of characterizing the hydrogen bond properties of C–H··O interactions is slow and troublesome, and far from being finished. Some of these properties are already well documented, whereas others appear vague and indistinct (making parts of the review unsatisfactory to write). Important points that are as yet only poorly understood are the long-distance properties of weak hydrogen bonds, cooperativity effects, non-additivity properties in general, the competition properties with other intermolecular forces, the roles of very weakly polarized groups like Me, the C–H groups of organic ions ($N^+$–C–H of various types, $P^+Ph_4$ *etc.*), the behaviour upon compression by other crystal forces or by intramolecular strain ('*forced contacts*') and the gradual transition from directional to isotropic interactions.

Relevant effects that cannot be studied by crystallographic methods are (for example) bond energies, thermodynamic properties in general and the influence of solvent. A large volume of quantum chemical calculations is required to obtain a broad picture of interaction energies under various conditions. This should include studies on non-additivity phenomena.

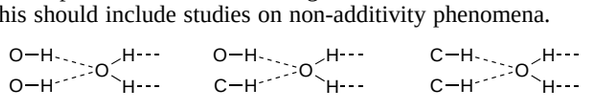


**Fig. 21** Analogous coordination geometries for two different forms of hydrogen bond

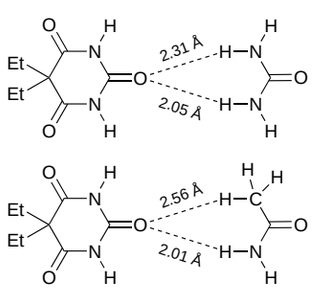



**Fig. 22** Isomorphous complexes of (*a*) urea–barbital and (*b*) acetamide–barbital

This review has concentrated on the special case of the weak hydrogen bonds formed between C–H donors and oxygen acceptors. Related directional interactions between other weak donor–acceptor combinations are also studied extensively, in particular with the important π-acceptors (see ref. 50 and literature cited therein). Also these interactions play important roles in structural chemistry and biology, and deserve further investigation.


## Acknowledgements

This study was supported by the Deutsche Forschungsgemeinschaft (Sa 196/25-1). The author thanks Professor W. Saenger for giving him the opportunity to carry out this work in his laboratory.


## Footnote

† This ChemComm is also available *via* the World Wide Web: http://chemistry.rsc.org/rsc/cccenha.htm

**Thomas Steiner was born in 1961 near Reutte (Tirol), Austria. He studied physics at the Technische Universität Graz, Austria, and obtained his PhD at the Freie Universität Berlin, Germany, in the field of neutron scattering (1990). Currently, he is a research scientist at the crystallography institute of the Freie Universität, Berlin. His active interests cover conventional and weak hydrogen bonding, isotropic intermolecular interactions, disorder phenomena, structure correlation, organic and bio-organic X-ray and neutron crystallography (acetylenes, peptides, carbohydrates, inclusion compounds, hydrates) and IR-spectroscopy.**

## References


1 S. Glasstone, *Trans. Faraday Soc.*, 1937, 200.
2 R. D. Green, *Hydrogen Bonding by C–H Groups*, Macmillan, London, 1974.
3 D. J. Sutor, *J. Chem. Soc.*, 1963, 1105.
4 J. Donohue, in *Structural Chemistry and Molecular Biology*, ed. A. Rich and N. Davidson, Freeman, San Francisco, 1968, p. 443.
5 (*a*) G. R. Desiraju, *Acc. Chem. Res.*, 1991, **24**, 290; 1996, **29**, 441; (*b*) J. Bernstein, M. C. Etter and L. Leiserowitz, in *Structure Correlation*, ed. H.-B. Bürgi and J. D. Dunitz, VCH, Weinheim, 1994, vol. 2, p. 431; (*c*) T. Steiner, *Crystallogr. Rev.*, 1996, **6**, 1; (*d*) F. Allen, J. P. M. Lommerse, V. J. Hoy, J. A. K. Howard and G. R. Desiraju, *Acta Crystallogr., Sect. B*, 1996, **52**, 734.
6 G. A. Jeffrey and W. Saenger, *Hydrogen Bonding in Biological Structures*, Springer, Berlin, 1991.
7 Z. Berkovitch-Yellin and L. Leiserowitz, *Acta Crystallogr., Sect. B*, 1984, **40**, 159.
8 (*a*) H. Satonaka, K. Abe and M. Hirota, *Bull. Chem. Soc. Jpn.*, 1988, **61**, 2031; (*b*) P. Seiler and J. D. Dunitz, *Helv. Chim. Acta*, 1989, **72**, 1125; (*c*) I. Chao and J.-C. Chen, *Angew. Chem.*, 1996, **108**, 200; (*d*) G. Müller, M. Lutz and S. Harder, *Acta Crystallogr., Sect. B*, 1996, **52**, 1014.
9 (*a*) L. J. W. Shimon, M. Vaida, L. Addadi, M. Lahav and L. Leiserowitz, *J. Am. Chem. Soc.*, 1990, **112**, 6215; (*b*) E. M. D. Keegstra, A. L. Spek, J. W. Zwikker and L. W. Jenneskens, *J. Chem. Soc., Chem. Commun.*, 1994, 1633; (*c*) G. R. Desiraju, *Angew. Chem., Int. Ed. Engl.*, 1995, **34**, 2311.
10 (*a*) I. Goldberg, *Acta Crystallogr., Sect. B*, 1975, **31**, 754; (*b*) P. D. J. Grootenhuis, J. van Eerden, P. J. Dijkstra, S. Harkema and D. N. Reinhoudt, *J. Am. Chem. Soc.*, 1987, **109**, 8044; (*c*) M. R. Caira and R. Mohamed, *Acta Crystallogr., Sect. B*, 1993, **49**, 760; (*d*) T. Steiner and K. Gessler, *Carbohydr. Res.*, 1994, **260**, 27; (*e*) T. Steiner and W. Saenger, *J. Chem. Soc., Chem. Commun.*, 1995, 2087; (*f*) D. Braga, F. Grepioni, J. J. Byrne and A. Wolf, *J. Chem. Soc., Chem. Commun.*, 1995, 125; (*g*) P. Behrens, G. van de Goor and C. C. Freyhardt, *Angew. Chem., Int. Ed. Engl.*, 1995, **34**, 2895.
11 (*a*) Z. S. Derewenda, U. Derewenda and P. M. Kobos, *J. Mol. Biol.*, 1994, **241**, 83; (*b*) Z. S. Derewenda, L. Lee and U. Derewenda, *J. Mol. Biol.*, 1995, **252**; 248; (*c*) M. Egli and R. V. Gessner, *Proc. Natl. Acad. Sci. USA*, 1995, **92**, 189; (*d*) G. A. Leonard, K. McAuley-Hecht, T. Brown and W. N. Hunter, *Acta Crystallogr., Sect. D*, 1995, **51**, 136;

(*e*) M. C. Wahl, S. T. Rao and M. Sundaralingam, M., *Nature Struct. Biol.*, 1996, **3**, 24.
12 F. H. Allen, O. Kennard and D. G. Watson, in *Structure Correlation*, ed. H.-B. Bürgi and J. D. Dunitz, VCH, Weinheim, 1994, vol. 1, p. 71.
13 F. H. Allen, J. E. Davies, J. E. Galloy, J. J. Johnson, O. Kennard, C. F. Macrae, E. M. Mitchell, G. F. Mitchell, J. M. Smith and D. G. Watson, *J. Chem. Inf. Comput. Sci.*, 1991, **31**, 187.
14 A. Allerhand and P. v. R. Schleyer, *J. Am. Chem. Soc.*, 1963, 1715.
15 A. Gavezzotti, *J. Phys. Chem.*, 1991, **95**, 8948.
16 L. Turi and J. J. Dannenberg, *J. Phys. Chem.*, 1993, **97**, 7899.
17 (*a*) J. J. Novoa, B. Tarron, M.-H. Whangbo and J. M. Williams, *J. Chem. Phys.*, 1991, **95**, 5179; (*b*) T. van Mourik and F. B. van Duijneveldt, *J. Mol. Struct.* (*Theochem.*), 1995, **341**, 63.
18 (*a*) H. Bock, R. Dienelt, H. Schödel and Z. Havlas, *J. Chem. Soc., Chem. Commun.*, 1993, 1793; (*b*) T. Steiner, J. van der Maas and B. Lutz, *J. Chem. Soc., Perkin Trans. 2*, (MS7/0072C/P2P).
19 T. Steiner, *J. Chem. Soc., Chem. Commun.*, 1994, 2341.
20 G. R. Desiraju, *J. Chem. Soc., Chem. Commun.*, 1989, 179.
21 G. R. Desiraju, *J. Chem. Soc., Chem. Commun.*, 1990, 454.
22 V. R. Pedireddi and G. R. Desiraju, *J. Chem. Soc., Chem. Commun.*, 1992, 988.
23 R. Taylor and O. Kennard, *J. Am. Chem. Soc.*, 1982, **104**, 5063.
24 J. Kroon and J. A. Kanters, *Nature* (*London*), 1974, **248**, 667.
25 T. Steiner and W. Saenger, *J. Am. Chem. Soc.*, 1992, **114**, 10146.
26 S. C. Nyburg, C. H. Faerman and L. Prasad, *Acta Crystallogr., Sect. B*, 1987, **43**, 106.
27 T. Steiner and W. Saenger, *J. Am. Chem. Soc.*, 1993, **115**, 4540.
28 V. Zabel, W. Saenger and S. A. Mason, *J. Am. Chem. Soc.*, 1986, **108**, 3664.
29 (*a*) R. Taylor, O. Kennard and W. Versichel, *J. Am. Chem. Soc.*, 1983, **105**, 5761; (*b*) P. Murray-Rust and J. P. Glusker, *J. Am. Chem. Soc.*, 1984, **106**, 1018.
30 J. Kroon, J. A. Kanters, J. G. C. M. van Duijneveldt-van de Rijdt, F. B. van Duijneveldt and J. A. Vliegenthart, *J. Mol. Struct.*, 1975, **24**, 109.
31 D. Braga, F. Grepioni, K. Biradha, V. R. Pedireddi and G. R. Desiraju, *J. Am. Chem. Soc.*, 1995, **117**, 3156.
32 T. Steiner, J. A. Kanters and J. Kroon, *Chem. Commun.*, 1996, 1277.
33 P. Gilli, V. Bertolasi, V. Ferreti and G. Gilli, *J. Am. Chem. Soc.*, 1994, **116**, 909.
34 B. Lutz, J. van der Maas and J. A. Kanters, *J. Mol. Struct.*, 1994, **325**, 203.
35 (*a*) T. Steiner, *J. Chem. Soc., Perkin Trans. 2*, 1995, 1315; (*b*) F. H. Allen, J. A. K. Howard, V. J. Hoy, G. R. Desiraju, D. S. Reddy and C. C. Wilson, *J. Am. Chem. Soc.*, 1996, **118**, 4081.
36 I. D. Brown, *Acta Crystallogr., Sect. B*, 1992, **48**, 553.
37 G. Gilli, F. Bellucci, V. Ferreti and V. Bertolasi, *J. Am. Chem. Soc.*, 1989, **111**, 1023.
38 (*a*) E. Steinwender, E. T. G. Lutz, J. H. van der Maas and J. A. Kanters, *Vib. Spectrosc.*, 1993, **4**, 217; (*b*) T. Steiner, B. Lutz, J. van der Maas, N. Veldman, A. M. M. Schreurs, J. Kroon and J. Kanters, *Chem. Commun.*, 1997, 191.
39 (*a*) M. A. Viswamitra, R. Radhakrishnan, J. Bandekar and G. R. Desiraju, *J. Am. Chem. Soc.*, 1993, **115**, 4868; (*b*) H. S. Rzepa, M. H. Smith and M. L. Webb, *J. Chem. Soc., Perkin Trans. 2*, 1994, 703.
40 K. Subramanian, S. Lakshmi, K. Rajagopalan, G. Koellner and T. Steiner, *J. Mol. Struct.*, 1996, **384**, 121.
41 W. J. Dulmage and W. N. Lipscomb, *Acta Crystallogr.*, 1951, **4**, 330.
42 K. Hermansson, personal communication.
43 C. V. Sharma and G. R. Desiraju, *J. Chem. Soc., Perkin Trans. 2*, 1994, 2345.
44 T. Steiner, *J. Chem. Soc., Chem. Commun.*, 1994, 101.
45 T. Steiner and W. Saenger, *Acta Crystallogr., Sect. D*, 1993, **49**, 592.
46 T. Steiner, *Acta Crystallogr., Sect. D*, 1995, **51**, 93.
47 Z. Berkovitch-Yellin and L. Leiserowitz, *J. Am. Chem. Soc.*, 1980, **102**, 7677.
48 T. Steiner, G. Koellner, K. Gessler and W. Saenger, *J. Chem. Soc., Chem. Commun.*, 1995, 511.
49 M. Jaskólski, *J. Cryst. Spect. Res.*, 1984, **14**, 45.
50 (*a*) T. Steiner, E. B. Starikov, A. M. Amado and J. J. C. Teixeira-Dias, *J. Chem. Soc., Perkin Trans. 2*, 1995, 1321; (*b*) T. Steiner, E. B. Starikov and M. Tamm, *J. Chem. Soc., Perkin Trans. 2*, 1996, 67; (*c*) T. Steiner, M. Tamm, A. Grzegorzewski, N. Schulte, N. Veldman, A. M. M. Schreurs, J. A. Kanters, J. Kroon, J. van der Maas and B. Lutz, *J. Chem. Soc., Perkin Trans. 2*, 1996, 2441; (*e*) P. K. Bakshi, A. Linden, B. R. Vincent, S. P. Roe, D. Adhikesavalu, T. S. Cameron and O. Knop, *Can. J. Chem.*, 1994, **72**, 1273; (*f*) T. Fujimoto, R. Yanagihara, K. Kobayashi and Y. Aoyama, *Bull. Chem. Soc. Jpn.*, 1995, **68**, 2113; (*g*) M.-F. Fan, Z. Lin, J. E. McGrady and D. M. P. Mingos, *J. Chem. Soc., Perkin Trans. 2*, 1996, 563.

*6/03049A*

# Tagging in combinatorial chemistry: the use of coloured and fluorescent beads

**Bryan J. Egner,[a] Sunil Rana,[a] Helen Smith,[a] Nathalie Bouloc,[a] Jeremy G. Frey,[a] William S. Brocklesby[b] and Mark Bradley*[a]**

[a] *Department of Chemistry, University of Southampton, Southampton, UK SO17 1BJ*
[b] *Department of Physics and Optoelectronics Research Centre, University of Southampton, Southampton, UK SO17 1BJ*

**Fluorescent confocal microscopy is a practical and very sensitive (fmol bead$^{-1}$) and non-destructive tagging technique for use in combinatorial chemistry.**

The power of solid phase and combinatorial chemistry is now being widely utilised by the major pharmaceutical players in the generation or optimisation of lead compounds in the drug discovery process.[1] Library generation can take place in a number of ways, perhaps the most powerful being the solid phase split and mix strategy such that each distinct 'bead' of the support contains only a single compound.[2] Screening from single beads requires means of compound identification and has led to the use of tagging, perhaps the most elegant approach being the arylcarbene system of Still.[3]

An addition to the area of tagging/decoding would be the use of the absorption or fluorescence spectrum of the resin bead. The simplest approach would be to covalently dye the beads and inspect under a microscope. The use of confocal fluorescence microscopy and complete spectrum analysis would enhance the sensitivity and potential of the system and enable the use of a number of fluorescent dyes which together with spectrum deconvolution would provide a very sensitive dye coding system.

In the first study a number of commercially available dyes† were covalently coupled by amide bond formation to TentaGel-S-$NH_2$ beads (130 μm) and a small peptide library (448 compounds $X_3X_2X_1$-linker-β-Ala-β-Ala-resin was prepared.[2] A selection of beads from the library were Edman sequenced and confirmed that the first residue ($X_1$) of the library was consistent with the colour of the single bead. The fluorescent microscope allowed ambiguities to be resolved, *e.g.* between pyrene and unlabelled TentaGel beads which were very similar by transmittance [Figs. 1(*a*)–(*c*)].

The fluorescence technique was extended by the use of a confocal microscope laser system.‡ The use of a single excitation line restricted the range of fluorescent dyes that could conveniently be used in these initial studies, however it was sufficient for initial proof of principle studies.

*Single dyes*–TentaGel beads (130 μm) were labelled with fluoroscein (0.01%) and erythrosin (0.02%).§ The beads were swollen in water, placed on a microscope slide with a cover slip and analysed under a confocal microscope‡ to give the spectra shown in Fig. 2. The spectra were clearly defined, relatively sharp and with distinguishable maxima. The degree of dye loading was varied by several orders of magnitude to give the spectra shown in Fig. 3. This showed the expected decrease in intensity with decreasing nominal bead loading and that as calculated increasing the bead loading above 0.1% did not give a uniform increase in relative fluorescence due to dye saturation. Fig. 3 shows loadings at 1 in $10^5$ and demonstrates that even at this level of tagging the fluorescent signals are clearly observable, corresponding to approximately 3–4 femtomoles bead$^{-1}$. Labelling down to 1 in $10^6$ (300–400 attomoles bead$^{-1}$) has also been demonstrated to be possible, although in this case the limits were determined by the amount of background fluorescence and Raman scattering from the bead

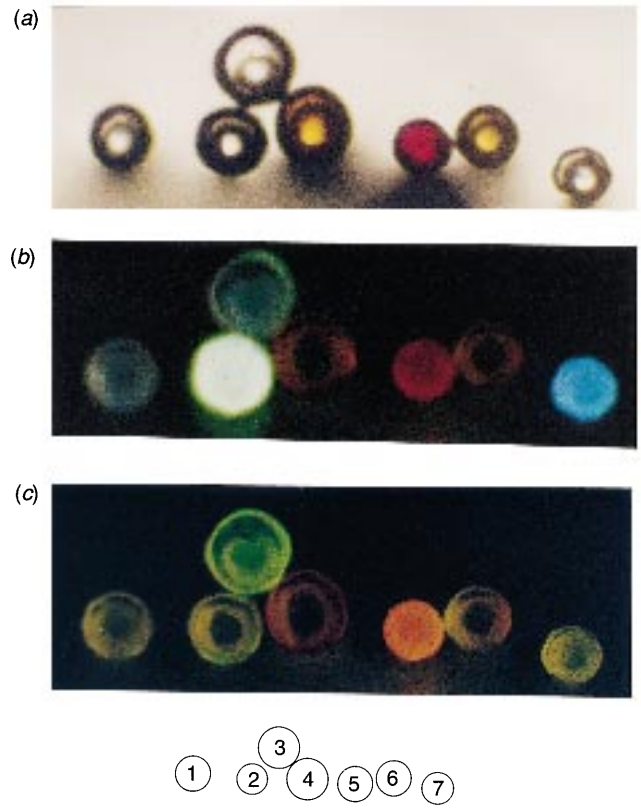



**Fig. 1** Tagged beads under differing observation conditions 1 = unlabelled bead, 2 = dansyl, 3 = fluorescein, 4 = methyl red, 5 = erythrosin, 6 = mordant orange, 7 = pyrene. (*a*) Transmittance. (*b*) Fluorescence (excitation 340–380 nm, suppression filter 425 nm). (*c*) Fluorescence (excitation 420–490 nm, suppression filter 515 nm).

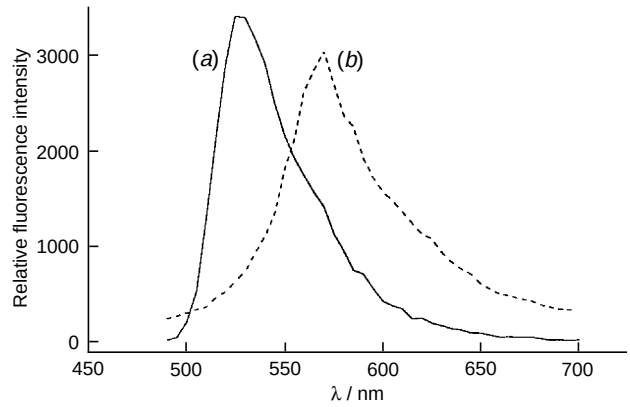



**Fig. 2** Fluorescence spectra obtained from single tagged TentaGel beads. (*a*) 0.01% Fluorescein. (*b*) 0.02% Erythrosin.

itself. The number of molecules excited in this case is approximately 20 000. The intensity of fluorescence between beads of the same loading was also relatively uniform.¶

*Multiple dyes*–The potential problems associated with using several dyes in a tagging system is one of internal quenching by either energy transfer or reabsorption by the dyes. However, we reasoned that, due to the unusual environment created within a bead such quenching phenomena might be reduced in nature due to site isolation, especially at low substitution levels. Initial studies using beads with approximately equimolar numbers of dye labelled sites (0.01%) gave spectra which showed quenching was taking place but that it was not complete. The experiments were repeated keeping one dye at a fixed level within the beads and varying the ratio of the other. The spectra are shown in Fig. 4.

We have in this initial study used two very similar dyes with strongly overlapping absorbance and emission spectra and clearly this is a worse-case scenario. It does however suggest that, by using several different dyes with varying absorbance/emission spectra and by varying the dye loadings (by orders of magnitude), a viable tagging method can be produced.

The simplicity of using dyed beads to allow initial position identification has been demonstrated. If spectra are known for the various starting beads then the initial reaction component of the library when added to the bead is therefore known. The technique is non-destructive, thus allowing full subsequent analysis by other techniques, very sensitive, with detection levels easily down to femtomoles of material/bead and with a linear response to tagging levels. Although limited in this report, it will be simple to expand these studies by the use of a greater range of dyes with reduced reactivity. The use of coloured and fluorescent beads has the potential, we believe, to simplify the identification of library members for single bead screening applications.

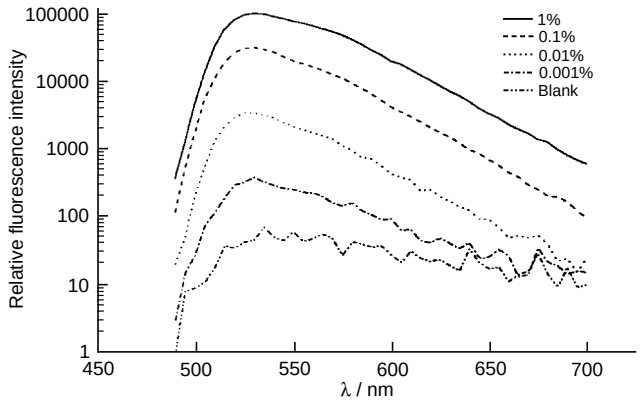



**Fig. 3** Fluorescence linearity with loading. Relative fluorescence intensity against wavelength at varying tagging levels.

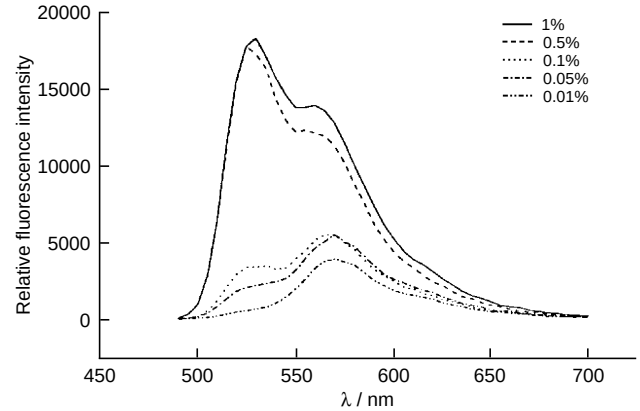



**Fig. 4** Dye combinations. Fixed erythrosin level (0.02%) with varying levels of fluorescein (1, 0.5, 0.1, 0.05 and 0.01%).

We thank the Royal Society for a University Research Fellowship (M. B.), the EPSRC for quota awards (B. J. E., H. S.) and the BBSRC/EPSRC (BMS) for grant B04846.

## Footnotes

† The dyes utilised in this study and the corresponding first amino acid in the library were pyrene butanoic acid (Val), methyl red (Ala), erythrosin B (Gln), dansyl chloride (Ser), fluorescein isothiocyanate, mordant orange (Asp) and succinylated disperse red (Leu), unlabelled beads (Lys). The following Fmoc amino acids were used in library generation: [$X_1$ = Ala, Asp(Bu$^t$), Gln, Leu, Lys(Boc), Ser(Bu$^t$), Val], [$X_2$ = Ala, Gly, Leu, Lys(Boc), Ser(Bu$^t$), Phe, Pro, Val], [$X_3$ = Asp(Bu$^t$), Gly, Leu, Lys(Boc), His(Trt), Ser(Bu$^t$), Phe, Val]. Four erythrosin labelled beads gave the amino acid sequences LAQ, HPQ(2) and GKQ, two pyrene labelled beads gave the sequences GPV and GFV, two methyl red labelled beads gave the sequences LPA and VQA and a mordant orange labelled bead gave the sequence GFD. TentaGel beads had a loading of *ca.* 300–400 pmoles bead$^{-1}$ as determined by Edman sequencing.

‡ Fluorescence was excited using a focused $Ar^+$ ion laser beam with a wavelength of 476 nm and a power of approximately 4 μW. The approximate spot radius was 0.5 μm, giving a laser intensity of *ca.* $5 \times 10^6$ W m$^{-2}$. This was well below the saturation intensity of the dye (approximately $10^9$ W m$^{-2}$) so all fluorescence should be linear in laser intensity. The area of the laser spot on the bead was *ca.* $8 \times 10^{-13}$ m$^2$. The illuminated region of the bead can be approximated as a cylinder with a cross-section equal to the laser spot size and a length equal to the bead diameter. The illuminated volume, $1 \times 10^{-16}$ m$^3$, is thus only 1 part in 11 000 of the total bead volume. Assuming the available binding sites ($400 \times 10^{-12}$ moles bead$^{-1}$) are evenly distributed throughout the bead, then there will be $2 \times 10^{10}$ binding sites within the illuminated volume and an effective concentration of 0.33 M if all the sites are filled. Taking into account the dye absorption coefficient, the path length through the bead and the effective concentration, the Beer–Lambert Law absorption by the bead will be $I = I_0e^{-a}$, with $a = 370$. If only a fraction, $f$ (filling factor), of the sites are loaded the absorption produced by the dyed bead is $I = I_0e^{-af}$. For occupancies above $f = 10^{-2}$ (*i.e.* > 1%) the bead will be optically thick and the exponential will depart significantly from a linear relationship between dye loading and fluorescent intensity—the addition of more dye will not significantly increase the fluorescence observed because all the available light is already being absorbed by the dye and so the addition of more dye produces no more fluorescence. The light was dispersed with a scanning triple monochromator and detected with a photomultiplier.

§ The beads were labelled by treatment with varying equivalents of FITC. The nominal % bead loading is the maximum number of sites which could be labelled under the reaction conditions. Beads were labelled with erythrosin using DIC and HOBt in DMF. Relative loadings for erythrosin were derived by comparison of the relative fluorescent intensities with FITC labelled beads and the extinction coefficients of the two dyes.

¶ The average fluorescent intensity of 12 beads (± S.D) at the nominal bead loading 1%, 123 000 ± 15 000; 0.1%, 27 400 ± 8000; 0.01%, 2950 ± 610; 0.001%, 271 ± 70.

## References

1 M. A. Gallop, R. W. Barrett, W. J. Dower, S. P. A. Fodor and E. M. Gordon, *J. Med. Chem*., 1994, **37**, 1233; N. K. Territ, M. Gardner, D. W. Gordon, R. J. Kobylecki and J. Steele, *Tetrahedron*, 1995, **51**, 8135; M. Rinnova and M. Lebl, *Collect. Czech. Chem. Commun*., 1996, **61**, 171.

2 A. Furka, F. Sebestyen, M. Asgedom and G. Dibo, *Int. J. Pept. Protein Res*., 1991, **36**, 487; R. A. Houghten, C. Pinilla, S. E. Blondelle, J. R. Appel, C. T. Dooley and J. H. Cuervo, *Nature*, 1991, **354**, 84; K. S. Lam, S. E. Salmon, E. M. Hersh, V. J. Hruby, W. M. Kazmierski and R. J. Knapp, *Nature*, 1991, **354**, 82.

3 H. P. Nestler, P. A. Bartlett and W. C. Still, *J. Org. Chem*., 1994, **59**, 4723; M. H. Ohlmeyer, R. N. Swanson, L. W. Dillard, J. C. Reader, G. Asouline, R. Kobayashi, M. Wigler and W. C. Still, *Proc. Natl. Acad. Sci*., USA, 1993, **90**, 10 922.

*Received, 23rd December 1996; Com. 6/08521K*

# Enantioselective [2,3] sigmatropic rearrangement mediated by a butyllithium–chiral ligand complex

**Shino Manabe*†**

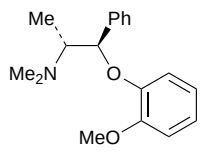
*Faculty of Pharmaceutical Sciences, University of Tokyo, Hongo, Bunkyo-ku, Tokyo 113, Japan*

**The first enantioselective [2,3] sigmatropic rearrangement of acyclic diprop-2-ynyl ethers and alkenyl benzyl ethers is achieved by a BuLi–chiral ligand complex.**

The [2,3] sigmatropic rearrangement has been studied with regard to its stereochemical course in view of its synthetic application to the preparation of highly functionalized derivatives.[1] Asymmetric [2,3] sigmatropic rearrangement involving chiral auxiliaries has been investigated by Nakai and co-workers and Enders and co-workers in order to achieve high diasteroselectivity.[2] However, the enantioselective version of this reaction has remained one of the unsolved problems in the field of synthetic organic chemistry. Marshall and Lebreton reported the first example of this reaction, in which a 13-membered cyclic ether afforded the prop-2-ynylic alcohol in 70% ee by the use of a chiral lithium amide.[3] But it has also been reported that the same lithium amide was not effective for acyclic substrates.[3,4] Fujimoto and Nakai demonstrated an enantioselective reaction for acyclic substrates *via* a boron ester enolate.[5] Gladysz and co-workers reported the enantioselective [2,3] sigmatropic rearrangement of sulfur ylides using a chiral rhenium complex.[6] However, no examples of an enantioselective reaction of acyclic substrates involving an $sp^3$ carbanion, which are the most typical substrates in this rearrangement, have been demonstrated so far. We report herein the first example of an enantioselective [2,3] sigmatropic rearrangement of acyclic ethers involving an $sp^3$ carbanion.[7]

Recently, this reaction was reported to proceed with complete inversion of configuration at the carbanion carbon centre to give the newly generated chiral centre.[8] On the other hand, Hoppe *et al.* and Beak and co-workers have shown that asymmetric deprotonations can be effected with $Bu^sLi$–(−)-sparteine complex to give a chiral dipole-stabilized carbanion which reacts with electrofiles to give enantiomerically enriched products.[9] So it is expected that an enantioselective [2,3] sigmatropic rearrangement could be possible if a chiral carbanion can be generated by use of a BuLi–chiral ligand complex. We have found that a complex of butyllithium with a chiral ligand **1**[10]‡§ exerts a pronounced effect on this rearrangement.

Initially acyclic diprop-2-ynyl ethers **2** were studied as they have simple and symmetrical structures. The first attempt at enantioselective [2,3] sigmatropic rearrangement of **2a** mediated by a complex of BuLi–(−)-sparteine was unsuccessful. Although (−)-sparteine is known as a good chiral ligand in many reactions, **3a** was obtained in only 23% yield and 9% ee. As a result the chiral amino ether **1** was designed, and was found to work as a good chiral ligand for BuLi in this reaction.¶ Some representative results are summarized in Table 1.‖




**1**

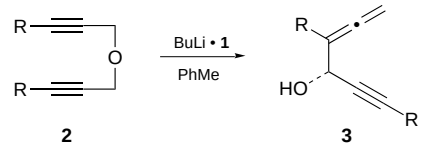
This chiral amino ether **1**–BuLi complex is effective not only for diprop-2-ynyl ether **2** but also for *cis*-but-2-enyl benzyl ether **4** (Scheme 1). The reaction gives *syn* alcohol **5** and *anti* alcohol **6** in a ratio of 9 : 1 in 50% yield.[11] The ee of *syn* alcohol **5** was 64% and the ee of *anti* alcohol **6** was 80%. Relative stereochemistries were determined by $^1H$ NMR coupling constants,[12] and the ee and absolute configuration of the *syn* alcohol were determined by $^1H$ NMR after conversion to the corresponding (*R*)-MTPA ester.[13]** The ee of *anti* alcohol **6** was determined directly by chiral HPLC [DAICEL CHIRALCEL OJ, hexanes–$Pr^iOH$ (50 : 1), 0.75 $cm^3$ $min^{-1}$, λ = 254 nm].

Interestingly, the ee was sensitive to the substitution pattern of the alkene. For instance, when *trans*-but-2-enyl benzyl ether is used, the reaction gives **5** and **6** in the ratio 65 : 35 in 48% yield. The ee of the *syn* alcohol **5** decreased to 16%, and the ee of the *anti* alcohol **6** also decreased to 12%. In the case of 3-methylbut-2-enyl benzyl ether **7** (Scheme 2), the desired product **8** was obtained in 68% yield and in 40% ee.††

In summary, the chiral ligand **1**–BuLi complex is effective for the enantioselective [2,3] sigmatropic rearrangement of acyclic ethers involving an $sp^3$ carbanion.

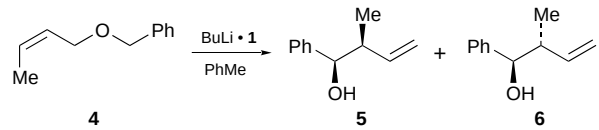
The author would like to thank Professor Kenji Koga for helpful discussions.

**Table 1** Rearrangement of **2** to give **3**



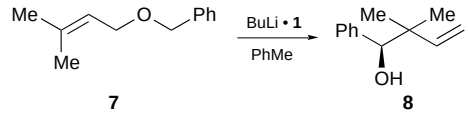

**2** **3**

| | R | Yield (%) of **3** | Ee (%) |
|---|---|---|---|
| **2a** | $C_7H_{15}$ | 50 | 61 |
| **2b** | c-Hex | 51 | 62 |
| **2c** | $Bu^t$ | 29 | 59 |
| **2d** | Ph | 57 | 48 |
| **2e** | $Me_3Si$ | 37 | 46 |




**4** **5** **6**

**Scheme 1**

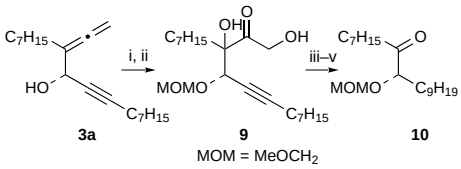



**7** **8**

**Scheme 2**

## Footnotes

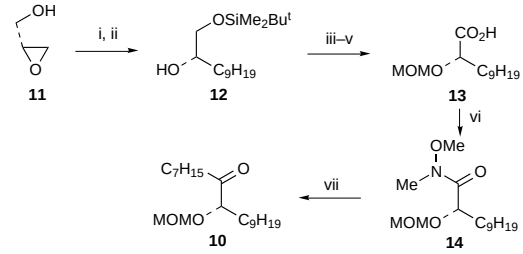
* E-mail: smanabe@postman.riken.go.jp
† Present address: The Institute of Physical and Chemical Research (RIKEN), Hirosawa, Wako-shi, Saitama 351-01 Japan.
‡ All new compounds gave satisfactory spectroscopic data.
§ Compound **1** was prepared from (1*R*, 2*R*)-(−)-norpseudoephedrine in two steps: (i) HCHO, $HCO_2H$ (100%); (ii) guaiacol, DEAD, $PPh_3$, THF (25%). $^1$H NMR (270 MHz, [$^2H_6$]benzene): δ 7.4–6.6 (9 H, m), 5.15 (1 H, d, *J* = 6.6 Hz), 3.43 (3 H, s), 3.13 (1 H, dd, *J* = 6.6, 6.9 Hz), 2.40 (6 H, s); mp 57 °C; $[\alpha]_D^{24}$ −79 (*c* 2.3, $CHCl_3$). Mitsunobu reaction proceeded, with net retention of configuration, *via* the azirizinium ion. The relative configuration was determined by X-ray analysis. The kind assistance of Dr Makoto Nakajima (Pharmaceutical Sciences, Hokkaido University) with the X-ray analysis is gratefully acknowledged.
¶ Typical procedure: To a solution of chiral ligand **1** (315 mg, 1.10 mmol) in toluene (16 cm$^3$), BuLi (0.63 cm$^3$, 1.67 M hexane solution, 1.05 mmol) was added dropwise at −78 °C under Ar atmosphere. After 5 min diprop-2-ynyl ether **2a** (290 mg, 1.0 mmol) in toluene (1 cm$^3$) was added dropwise to the resulting pale yellow solution *via* a cannula. The flask was rinsed with toluene (1 cm$^3$). The whole mixture was stirred at −78 °C for 5 h. The reaction was quenched with 1 M HCl (20 cm$^3$), and the aqueous layer was extracted with ethyl acetate (30 cm$^3$ × 3). The organic layer was washed with 1 M HCl (20 cm$^3$), saturated aqueous $NaHCO_3$ (20 cm$^3$) and brine (20 cm$^{-3}$). After drying the mixture over $Na_2SO_4$, the mixture was concentrated. The residue was then purified by silica gel column chromatography, and hydroxy allene **3a** (145 mg, 50%) was obtained as a colourless oil.
‖ *Spectroscopic data* for **3a**: $^1$H NMR: δ 4.95 (1 H, d, *J* = 3.0 Hz), 4.93 (1 H, d, *J* = 3.0 Hz), 4.82 (1 H, dd, *J* = 1.9, 1.9 Hz), 2.23 (1 H, dt, *J* = 1.9, 7.0 Hz), 2.22 (1 H, dt, *J* = 1.9, 7.0 Hz), 2.1–2.0 (2 H, m), 1.68 (1 H, brs), 1.6–1.1 (20 H, m), 0.89 (6 H, t, *J* = 6.3 Hz); $^{13}$C NMR: δ 204.37, 106.33, 86.38, 79.43, 79.03, 63.25, 31.81, 31.72, 29.27, 29.11, 28.77, 28.54, 27.68, 27.53, 22.59, 18.71, 14.04; $\nu_{max}$/cm$^{-1}$ 3400, 3000–2850, 2210, 1950, 850; *m/z* 290 ($M^+$), 289 ($M^+ - 1$); $[\alpha]_D^{24}$ + 18 (*c* 0.95, $CHCl_3$). For **3a**, **3b** and **3c**, ees were determined by HPLC analysis [DAICEL CHIRALCEL OD-H, hexanes–Pr$^i$OH (300 : 1), λ = 254 nm] of the corresponding *p*-nitrobenzoates. For **3c**, the ee was determined by chiral HPLC analysis [DAICEL CHIRALCEL OD-H, hexanes–Pr$^i$OH (300 : 1), λ = 254 nm] of the corresponding 3,5-dinitrobenzoates. For **3d**, the ee was determined by HPLC analysis [DAICEL CHIRALCEL OD-H, hexanes–Pr$^i$OH (300 : 1), λ = 254 nm]. Compound **3a** could be converted to ketone **10** in four steps, as shown in Scheme 3.



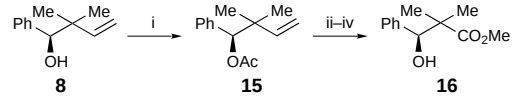

**Scheme 3** *Reagents and conditions*: i, $MeOCH_2Cl$, Pr$^i_2$NEt, $CH_2Cl_2$, 70%; ii, $OsO_4$, pyridine, PhH, 50%; iii, $H_2$, $Pd(OH)_2$–C, MeOH; iv, $NaBH_4$, MeOH; v, $NaIO_4$, acetone, water, 30% (3 steps)

The absolute configuration of **3a** was determined by comparison of the optical rotation of **10**, which was derived from commercially available (*R*)-glycidol **11**, as shown in Scheme 4.

For **3b**–**d**, the absolute stereochemistries were assumed to be of the same orientation as for **3a** according to the $^1$H NMR spectra of the corresponding (*R*)-*O*-methylmandelates. See J. A. Marshall and X. Xang, *J. Org. Chem.*, 1990, **55**, 2995.
** The absolute stereochemistry of the minor compound **12** was not determined.
†† Compound **8** was converted to **16** in four steps as shown in Scheme 5. The ee and the absolute configuration of compound **8** [$[\alpha]_D^{24}$ +22 (c = 0.84, $CHCl_3$)] were determined by optical rotation of compound **16**. The ee and absolute configuration of **16** are known: M. Gette, J. Capillon and J. P. Gette, *Tetrahedron*, 1973, **29**, 3659.




**Scheme 4** *Reagents and conditions*: i, Bu$^t$Me$_2$SiCl, Et$_3$N, DMAP, $CH_2Cl_2$, quant.; ii, octylmagnesium bromide, CuI, THF, 66%; iii, $MeOCH_2Cl$, Pr$^i_2$NEt, $CH_2Cl_2$, quant.; iv, $Bu_4NF$, THF, 82%; v, Jones' reagent, acetone; vi, MeNH(OMe)·HCl, Diethyl cyanophosphonate, Et$_3$N, DMF, 76% (2 steps); vii, heptylmagnesium bromide, THF, 97%




**Scheme 5** *Reagents and conditions*: i, $Ac_2O$, Et$_3$N, DMAP, $CH_2Cl_2$, 91%, ii, $O_3$, MeOH; iii, $H_2O_2$, aq. NaOH; iv, $CH_2N_2$, Et$_2$O, 30% (3 steps)

## References

1 For recent reviews see: T. Nakai and K. Mikami, *Org. React.*, 1994, **46**, 105; J. A. Marshall, in *Comprehensive Organic Synthesis*, ed. B. M. Trost and I. Fleming, Pergamon, London, 1991, vol. 3, pp. 975–1014; R. Brückner, in *Comprehensive Organic Synthesis*, ed. B. M. Trost and I. Fleming, Pergamon, London, 1991, vol. 6, pp. 873–908.
2 K. Mikami, O. Takahashi, T. Kasuga and T. Nakai, *Chem. Lett.*, 1985, 1729; K. Mikami, K. Fujimoto, T. Kasuga and T. Nakai, *Tetrahedron Lett.*, 1984, **25**, 6011; O. Takahashi, K. Mikami and T. Nakai, *Chem. Lett.*, 1987, 69; D. Enders, D. Backhaus and J. Runsink, *Angew. Chem., Int. Ed. Engl.*, 1994, **33**, 2098; D. Enders and D. Backhaus, *Synlett*, 1995, 631.
3 J. A. Marshall and J. Lebreton, *J. Am. Chem. Soc.*, 1988, **110**, 2925.
4 J. A. Marshall and X. Wang, *J. Org. Chem.*, 1992, **57**, 2747.
5 K. Fujimoto and T. Nakai, *Tetrahedron Lett.*, 1994, **35**, 5019.
6 P. C. Cagle, A. M. Arif and J. A. Gladysz, *J. Am. Chem. Soc.*, 1994, **116**, 3655; P. C. Cagle, O. Meyer, K. Weickhardt, A. M. Arif and J. A. Gladysz, *J. Am. Chem. Soc.*, 1995, **117**, 11 730.
7 S. Matsui (Manabe), M. Nakajima and K. Koga, *7th IUPAC Symposium on Organometallic Chemistry directed towards Organic Synthesis* (*OMCOS 7*), abstract 2B, Kobe, September, 1993; Nakai's group has also shown that this type of reaction proceeds in 70% ee: K. Tomooka, N. Komine and T. Nakai, *The Japan Chemical Society annual meeting*, abstract II 1208, Tokyo, March, 1996.
8 R. Hoffman and R. Brückner, *Angew. Chem., Int. Ed. Engl.*, 1992, **31**, 647; E. J. Verner and T. Cohen, *J. Am. Chem. Soc.*, 1992, **114**, 375; K. Tomooka, T. Igarachi, M. Watanabe and T. Nakai, *Tetrahedron Lett.*, 1992, **33**, 5795.
9 S. T. Kerrick and P. Beak, *J. Am. Chem. Soc.*, 1991, **113**, 9718; D. Hoppe, F.Hinze and P. Tebben, *Angew. Chem., Int. Ed. Engl.*, 1990, **29**, 1422; P. Beak and H. Du, *J. Am. Chem. Soc.*, 1992, **115**, 2516.
10 M. Okuda and K. Tomioka, *Tetrahedron Lett.*, 1994, **35**, 4585.
11 For transition state structure, see: K. Mikami, T. Uchida, T. Hirano, Y.-D. Wu and K. N. Houk, *Tetrahedron*, 1994, **50**, 5917 and references cited therein.
12 K. Mikami, Y. Kimura, N. Kishi and T. Nakai, *J. Org. Chem.*, 1983, **48**, 279.
13 J. A. Dale, D. L. Dull, and H. S. Mosher, *J. Org. Chem.*, 1969, **34**, 2543.

*Received in Cambridge, UK, 10th February 1997; Com. 7/00906B*

# Asymmetric epoxidation of enones employing polymeric α-amino acids in non-aqueous media

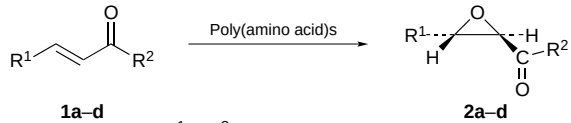
**Paul A. Bentley,[a] Sophie Bergeron,[a] Michael W. Cappi,[a] David E. Hibbs,[b] Michael B. Hursthouse,[b] Thomas C. Nugent,[a] Rosalino Pulido,[a] Stanley M. Roberts*[a] and L. Eduardo Wu[a]**

[a] *Department of Chemistry, University of Liverpool, Liverpool, UK L69 3BX*
[b] *School of Chemistry and Applied Chemistry, University of Wales, Cardiff, PO Box 912, Cardiff, UK CF1 3TB*

**Urea–hydrogen peroxide complex in an organic solvent and in the presence of DBU and poly-(L)-leucine causes rapid asymmetric epoxidation of the enones 1a, b and d.**

Poly(amino acid)s are cheap surrogates of enzymes for promoting some stereoselective organic reactions.[1] For example, Banfi *et al.* have described a method for the asymmetric epoxidation of chalcones using these polymeric catalysts; thus the enone **1a** was transformed into the chiral epoxy ketone **2a** (Scheme 1 and Table 1, entry 1).[2] The reaction involved a triphasic system comprising alkaline aqueous hydrogen peroxide, an organic solvent and the insoluble polymer. Subsequently the asymmetric epoxidation has been shown to be a reliable, robust reaction and the range of enones undergoing oxidation has been extended considerably; for example the dienone **1b** affords the unsaturated epoxy ketone **2b** in good yield and excellent enantiomeric excess (Table 1, entry 2).[3]

Nevertheless, several limitations to the protocol became evident. First, reaction times were often unacceptably long (≥3 days; Table 1, entry 2) and all of these reactions required continuous addition of oxidant and base. The use of aqueous sodium hydroxide caused slow degradation of the poly(amino acid) and precluded the epoxidation of compounds possessing alkali-sensitive functionality. Secondly, the polymer, prepared as an amorphous solid, required swelling (to form a gel) through contact with aqueous organic solvent for a period of 6 h. Thirdly, compounds of the type $R^1CH{=}CHCOC\mathit{H}R^2R^3$ or $R^1COCH{=}CHC\mathit{H}R^2R^3$, *i.e.* with 'active' hydrogen atoms, were oxidized slowly [often with poor selectivity (Table 1, entry 3)], or not at all (Table 1, entry 4).[4]




**1a–d** **2a–d**

**a** $R^1 = R^2$ = Ph
**b** $R^1$ = CH=CHPh, $R^2$ = 2-naphthyl
**c** $R^1$ = Ph, $R^2 = Pr^i$
**d** $R^1$ = Ph, $R^2$ = Me

**Scheme 1**

We have now found a satisfactory solution to many of these problems by conducting the asymmetric epoxidation in a two-phase non-aqueous system made up of oxidant, a non-nucelophilic base, immobilised poly(amino acid)[5] and an organic solvent.

Thus chalcone **1** (0.24 mmol) was added to dry THF (0.8 $cm^3$), immobilised poly-(L)-leucine[5] (PLL) (100 mg), urea–hydrogen peroxide complex (UHP)[6] (1.2 equiv.) and 1,8-diazabicyclo[5.4.0]undec-7-ene (DBU) (1.2 equiv.). The ensuing reaction was complete in 30 min and provided the epoxyketone **2a** in high yield and excellent optical purity after column chromatography (Table 1, entry 5). Use of immobilised poly-(D)-leucine (PDL) gave rise to the enantiomeric epoxy ketone *ent*-**2a** (Table 1, entry 6). The use of more solvent (2.0 $cm^3$) resulted in a slower reaction (96% conversion after 1 h) but no diminution in the optical purity of the product (96% ee). For these reactions the work-up procedure is very straightforward; the insoluble polymer is simply filtered off and, indeed, may be recycled (at least six times) without reduction in the rate of the epoxidation, the yield or the optical purity of the product.

Preliminary investigations also showed that changes could be made to the nature of the solvent, the base and the oxidant. Thus, repeating the non-aqueous Juliá oxidation of chalcone **1a** in 1,2-dimethoxyethane, *tert*-butyl methyl ether and ethyl acetate

**Table 1** Asymmetric epoxidation of some α,β-unsaturated ketones using oxidant and poly(amino acid) catalyst

| Entry | Enone | Epoxy ketone | Poly(amino acid)[a] | Solvent | Oxidant | Base | *t*/h | % Conversion (% yield) | Enantiomeric excess |
|---|---|---|---|---|---|---|---|---|---|
| 1 | **1a** | **2a** | PLL or PLA | $CH_2Cl_2$ or hexane | 30% $H_2O_2$ | NaOH–$H_2O$ | 18 | (87) | 88 |
| 2 | **1b** | **2b** | PLL | hexane | 30% $H_2O_2$ | NaOH–$H_2O$ | 72 | (78) | > 95 |
| 3 | **1c** | **2c** | PLL | $CH_2Cl_2$ | 30% $H_2O_2$ | NaOH–$H_2O$ | 168 | (60) | 62 |
| 4 | **1d** | **2d** | PLL | $CH_2Cl_2$ | 30% $H_2O_2$ | NaOH–$H_2O$ | 168 | (0) | — |
| 5 | **1a** | **2a** | PLL | THF | $NH_2CONH_2$–$H_2O_2$ | DBU | 0.5 | 100 (85) | > 95 |
| 6 | **1a** | *ent*-**2a** | PDL | THF | $NH_2CONH_2$–$H_2O_2$ | DBU | 0.5 | > 90 (85) | 94 |
| 7 | **1a** | **2a** | PLL | THF | $NH_2CONH_2$–$H_2O_2$ | DBN | 0.5 | > 95 | > 90 |
| 8 | **1a** | **2a** | PLL | THF | $NH_2CONH_2$–$H_2O_2$ | Hunig's base | 0.5 | 37 | 50 |
| 9 | **1a** | **2a** | PLL | THF | DABCO–1.5$H_2O_2$ | DBU | 0.5 | 95 | 95 |
| 10 | **1a** | **2a** | PLL | THF | 90% $H_2O_2$ | DBU | 0.5 | 77 | 65 |
| 11 | **1b** | **2b** | PLL | THF | $NH_2CONH_2$–$H_2O_2$ | DBU | 3 | 85 | > 95 |
| 12 | **1d** | **2d** | PLL | THF | $NH_2CONH_2$–$H_2O_2$ | DBU | 4 | (70) | 83 |

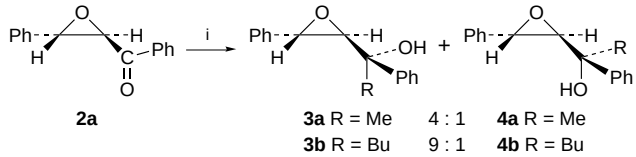
[a] PLL: poly-(L)-leucine; PLA: poly-(L)-alanine; PDL = poly-(D)-leucine.

gave results which were almost identical to those obtained using THF. Polar aprotic solvents such as dimethyl sulfoxide and dimethylformamide gave equally good results but dichloromethane, acetonitrile and toluene were less satisfactory, giving rise to longer reaction times and/or less enantioselective reactions.

While DBU can be replaced with 1,5-diazabicyclo-[4.3.0]non-5-ene (DBN), Hunig's base (*N*,*N*-diisopropylethylamine) is much less effective (Table 1, entries 7 and 8); triethylamine gave no reaction. 1,4-Diazabicyclo[2.2.2]octane–peroxide complex (DABCO–$1.5H_2O_2$)[7] may be used as the oxidant (Table 1, entry 9) but, in contrast, 90% hydrogen peroxide gave rise to a slower reaction and a product that was less optically pure (Table 1, entry 10).

It is very significant that α,β-unsaturated ketones, which required long reaction times when employing the Juliá triphasic conditions, were transformed quickly, with great selectivity, in the new biphasic system (Table 1, entry 11). Furthermore, styryl methyl ketone **1d** was oxidized to the epoxy ketone **2d** over 4 h in moderate yield and optical purity (Table 1, entry 12; *cf*. entry 4). Hence it seems that the new reaction conditions will broaden the range of epoxy ketones that can be prepared using this methodology.

In a parallel research programme we are investigating the further reactions of the chiral epoxy ketones available from the Juliá methodology. For example, we have shown that the epoxy ketone **2a** is alkylated diastereoselectively using methyllithium or butyllithium and $CeI_3$,[8] giving rise to compounds **3a** and **3b** as the major products which were separated from the minor isomers **4a** and **4b** by chromatography (Scheme 2). The structural identity of compound **3b** was elucidated by X-ray crystallography (Fig. 1).† This methodology gives rise to epoxides formally derived from allylic tertiary alcohols, compounds not readily obtainable in optically active form using the Sharpless technology.[9]




**Scheme 2** *Reagents and conditions*: i, MeLi or BuLi, $CeI_3$, THF, −70 °C

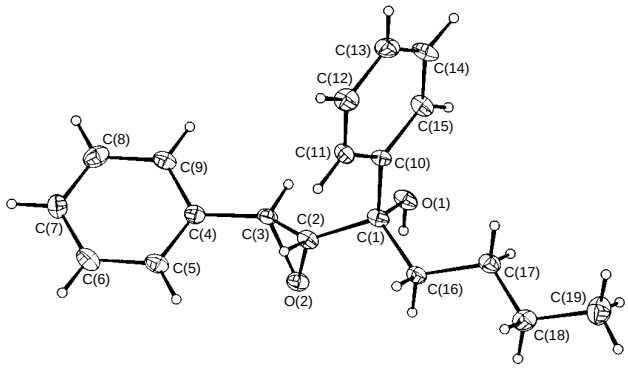



**Fig. 1** X-Ray crystal structure of compound **3b**

## Footnotes

* E-mail: sj11@liverpool.ac.uk

† *Crystal data* for $C_{19}H_{22}O_2$, $M$ = 282.37, monoclinic, space group $P2_1$, $a$ = 10.753(2), $b$ = 5.6320(10), $c$ = 13.403(2) Å, β = 104.930(4)° (by least-squares refinement of the setting angles for 250 reflections within θ = 1.96–24.98°), $V$ = 784.3(2) Å$^3$, $Z$ = 2, $D_c$ = 1.196 g cm$^{-3}$, $T$ = 150 K, μ(Mo-Kα) = 0.76 cm$^{-1}$, $F$(000) = 304, crystal size = 0.5 × 0.6 × 0.5 mm.

Data were collected on a FAST TV Area detector diffractometer following previously described methods (ref. 10). From the ranges scanned, 3383 data were recorded ($1.96 < \theta < 24.98°$; index ranges: $-11 < h <$, $-4 < k < 6$, $-14 < l < 14$) and merged to give 2170 unique [$R$(int) = 0.0653].

The structure was solved *via* direct methods (ref. 11) and refined on $F_o^2$ by full-matrix least-squares (ref. 12) using all unique data corrected for Lorentz and polarisation factors. All non-hydrogen atoms were anisotropic. The hydrogen atoms were inserted in idealised positions with $U_{iso}$ set at 1.5 times the $U_{eq}$ of the parent. The weighting scheme used was $w = 1/[\sigma^2(F_o)^2 + (0.0137P)^2]$, where $P = [\max(F_o)^2 + 2(F_c)^2]/3$; this gave satisfactory agreement analyses. Final $R_1$ (on $F$) and $wR_2$ (on $F_o^2$) values were 0.0544 and 0.0647 for all 2170 data and 192 parameters. The corresponding $R$ values were 0.0355 and 0.0615 for 1498 data with $I > 2\sigma(I)$. Sources of scattering factors as in ref. 12. The numbering of the atoms is shown in Fig. 1.

Atomic coordinates, bond lengths and angles, and thermal parameters have been deposited at the Cambridge Crystallographic Data Centre (CCDC). See Information for Authors, Issue No. 1. Any request to the CCDC for this material should quote the full literature citation and the reference number 182/394.

## References

1 S. Colonna, A. Manfredi and M. Spadoni, in *Modern Trends for Organic Synthesis*, ed. O. Chizhov, Blackwell, 1987, pp. 275–84.
2 S. Banfi, S. Colonna, H. Molinari, S. Juliá and J. Guixer, *Tetrahedron*, 1984, **40**, 5207.
3 M. E. Lasterra-Sánchez, U. Felfer, P. Mayon, S. M. Roberts, S. R. Thornton and C. J. Todd, *J. Chem. Soc., Perkin Trans. 1*, 1996, 343.
4 W. Kroutil, P. Mayon, M. E. Lasterra-Sánchez, S. J. Madrell, S. M. Roberts, S. R. Thornton, C. J. Todd and M. Tüter, *Chem. Commun.*, 1996, 845.
5 S. Itsuno, M. Sakakura and K. Ito, *J. Org. Chem.*, 1990, **55**, 6047.
6 H. Heaney, *Aldrichim. Acta*, 1993, **26**, 35; *Top. Curr. Chem.*, 1993, **164**, 1; M. S. Cooper, H. Heaney, A. J. Newbold and W. R. Sanderson, *Synlett*, 1990, 533.
7 Prepared from commercially available 30% $H_2O_2$ using a procedure based on that reported by A. A. Oswald and D. L. Guertin, *J. Org. Chem.*, 1963, **28**, 651; the procedure described by C. Lion, M. Hedayatullah, C. Charry, S. Vincent, S. Briand, J. Boileau, G. Delmas, G. Magnand, M. Desgranges and H. Sentenac-Roumanou, *Bull. Soc. Chim. Belg.*, 1994, **103**, 115 was unreliable in our hands.
8 *cf.* Y. Aoyama, H. Urabe and F. Sato, *Tetrahedron Lett.*, 1991, **32**, 6371; see also T. Imamoto, N. Takiyama, K. Nakamura, T. Hatajima and Y. Kajima, *J. Am. Chem. Soc.*, 1989, **111**, 4392.
9 R. A. Johnson and K. B. Sharpless, *Comprehensive Organic Synthesis*, ed. B. M. Trost, Pergamon, Oxford, 1991, 7, ch. 3.2; T. Yoshimitsu and K. Ogasawara, *J. Chem. Soc., Chem. Commun.*, 1994, 2197.
10 J. A. Darr, S. R. Drake, M. B. Hursthouse and K. M. A. Malik, *Inorg. Chem.*, 1993, **32**, 5704.
11 G. M. Sheldrick, *Acta Crystallogr., Sect. A*, 1990, **46**, 467.
12 G. M. Sheldrick, SHELXL93 Program for Crystal Structure Refinement, University of Göttingen, Germany, 1993.

*Received in Cambridge, UK, 23rd January 1997; Com. 7/00550D*

# Crystal and molecular structure of a ketocarboxylatocopper(II) intermediate in the oxygenation of a copper(I) flavonolate complex

**István Lippai,[a] Gábor Speier,*[a] Gottfried Huttner[b] and László Zsolnai[b]**

[a] *Department of Organic Chemistry, University of Veszprém, 8201 Veszprém, Hungary*
[b] *Ruprecht-Karls Universität, Anorganisch-Chemisches Institut, 69120 Heidelberg, Germany*

**Flavonol reacts with metallic copper in the presence of 2,2′-bipyridine to give dihydrogen and a mixture of compounds with the stoichiometric composition [$Cu^{I}$(bpy)(fla)] from which on standing only [$Cu^{I}(bpy)_2]_2[Cu^{I}(fla)_3$] can be isolated; oxygenation of the solution of the mixture results in the ketocarboxylatocopper(II) complex [$Cu^{II}$(bpy)(fla)(2-$HOC_6H_4COCO_2$)], which hints at a copper-mediated oxidative cleavage of the pyranone ring in the flavonolate ligand *via* a 1,2-dioxethane intermediate by $^3O_2$.**

Quercetin **1a** (3′,4′,5,7-tetrahydroxyflavonol) is metabolized in fungi to a depside (phenolic carboxylic acid ester) and carbon monoxide by quercetin 2,3-dioxygenase.[1] It is a Cu-containing dioxygenase and the coordination of **1a** to copper(II) at its active site was assumed as the key intermediate.[2] Flavonol **1b** forms stable complexes with copper(I)[3] and copper(II),[4] and simple copper complexes have been used in model reactions.[5] For the oxidative cleavage reaction of the heterocycle pathways *via* an endoperoxide (route a) and 1,2-dioxethane (route b) have been proposed (Scheme 1).[6]

Our aim was to prepare neutral mixed-ligand copper(I) flavonolate complexes and to investigate their oxygenation reaction in order to find possible chemical pathways of the enzymatic reaction. Equimolar amounts of flavonol **1b** (flaH) react with 2,2′-bipyridine (bpy) and metallic copper in acetonitrile at room temperature to yield a mixture of compounds with the stoichiometric composition of [$Cu^{I}$(fla)(bpy)] **6** according to Scheme 2. The compounds in the mixture are believed to be [$Cu^{I}$(fla)(bpy)] and anionic copper(I) species such as [$Cu^{I}(fla)_2]^-$, and [$Cu^{I}(fla)_3]_2^-$ with [$Cu^{I}(bpy)_2]^+$ counter cations from which on standing of the solution at room temperature only [$Cu^{I}(bpy)_2]_2[Cu^{I}(fla)_3$] **7** as red crystals are obtained. **7** consists of two cationic tetrahedral copper(I) ions each with two bpy ligands and a counter anion containing octahedral copper(I) with three flavonolate ligands. The structure of **7** was based on an X-ray structure determination, however the one N atom of bpy and one of the flavonolate ligands are heavily disordered, and thus full details are not provided. In this unique six-coordinated copper(I) species the average Cu–O distances are 2.069 Å (3 O–H) and 2.151 Å (4 C=O) and the average Cu–N bond length is 2.029 Å.

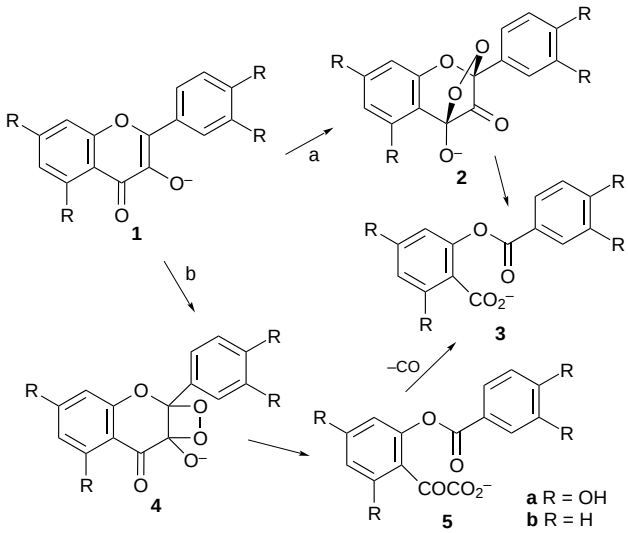
The oxygenation of the acetonitrile solution of the mixture **6** at room temperature and atmospheric dioxygen pressure proceeds very rapidly (few minutes) and green crystals of **8** are obtained in 11% yield (Scheme 2). Complex **8** shows bands in the UV–VIS region at 421 nm (log (ε/dm$^3$ mol$^{-1}$ cm$^{-1}$) 4.15), 311 (4.26), 258 (4.39) and 615 (1.73) nm and IR absorptions at 1605 cm$^{-1}$ [ν(CO)] and 3005 cm$^{-1}$ [ν(OH)]. It is paramagnetic with $\mu_{eff}$ = 1.83 $\mu_B$ and EPR parameters in acetonitrile are $g$ = 2.123 and $A_{Cu}$ = 77.18 G.

The crystal structure of [$Cu^{II}$(bpy)(fla)(2-$HOC_6H_4COCO_2$)]† is shown in Fig. 1.

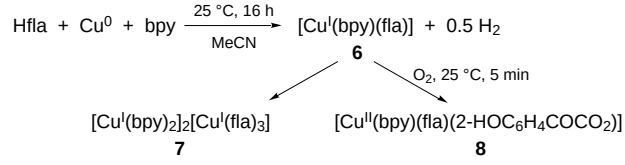
The complex has a square pyramidal geometry. Two oxygen atoms of the chelating flavonolate ligand and two nitrogen atoms of bpy occupy basal positions while the carboxylate oxygen atom of the ketocarboxylato ligand occupies the apical position. The copper–nitrogen bond distances [Cu–N(1) 1.982(7), Cu–N(2) 1.968(6) Å] do not differ much from those in [$Cu^{II}$(fla)(bpy)]$ClO_4$ [1.961(4), 1.978(4) Å] but are much shorter than those in [$Cu^{II}$(fla)(tmeda)(MeCN)]$ClO_4$ [2.023 (6), 2.024(7) Å].[7] The ketocarboxylate ligand is monodentate with a C–O bond distance of 2.231(5) Å. The plane of the keto group is perpendicular to the carboxylato group and lies in the plane of the 2-hydroxyphenyl moiety and forms through hydrogen-bonding with the OH group a stable six-membered ring. This may also contribute to the stability of its structure compared to that in bis(thienyl-2)-2-glyoxylatocopper(II), and its dihydrated complex, where both the keto and carboxylato groups are bonded to the copper with average Cu–O distances of 2.077 Å.[8]

The copper–oxygen bond distances [Cu–O(5) 2.190(9), Cu–O(6) 1.760(11) Å] with the flavonolate ligand involving the 4-CO and 3-OH groups are very different from those found for [Cu(fla)$(PPh_3)_2$][3] [Cu–O(2) 2.051(4); Cu–O(3) 2.167(5) Å] and for [Cu$(fla)_2$][4] [Cu–O(2) 1.901(2); Cu–O(3) 1.944(3) Å].

Complex [$Cu^{II}$(bpy)(fla)(2-$HOC_6H_4COCO_2$)] is probably formed according to Scheme 3. The coordinated flavonolate ligand **1b** in **6** rapidly takes up triplet dioxygen to yield a 1,2-dioxethane species **9**, which breaks down to the *O*-benzoyl-2-hydroxyphenylglyoxylatocopper species **10**. This reacts then




**Scheme 1**




**Scheme 2**

probably with further flavonol, and hydrolysis of the ester group leads to 2-hydroxyphenylglyoxylato copper(II) complex **8**. The ketocarboxylato copper(II) complex **8** is surprisingly stable towards decarbonylation. At 80 °C in acetonitrile no decarbonylation occurs over 7 h. At 150 °C in dmf carbon monoxide and salicylic acid are formed due to decarbonylation as established by GCMS.

The formation of a ketocarboxylatocopper complex **8** in the oxygenation of a copper flavonolate may suggest that the oxidative cleavage reaction of the coordinated flavonolate ligand could proceed *via* a 1,2-dioxethane intermediate **9** which upon the usual decomposition and hydrolysis of the ester linkage leads to the ketocarboxylato complex **8**. The easiness of the oxygenation allows the reasoning that this route (route b) for the scission reaction may be favoured over the route a as shown in Scheme 1. Singlet oxygen in its [2 + 2] reaction with flavonol

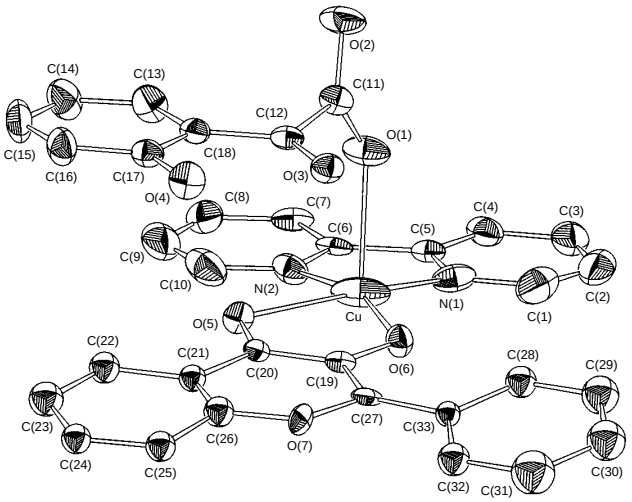
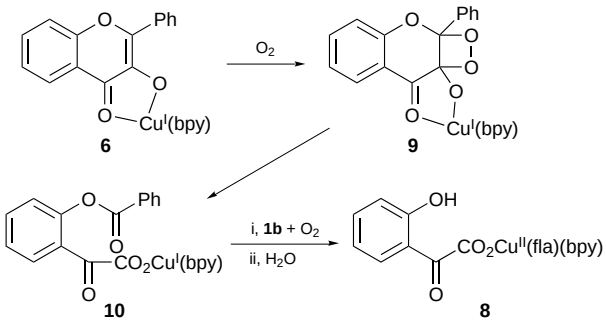



**Fig. 1** The structure of [Cu$^{II}$(bpy)(fla)(2-HOC$_6$H$_4$COCO$_2$)]. Relevant bond distances (Å) and bond angles (°): Cu–N(1) 1.982(7), Cu–N(2) 1.969(6), Cu–O(1) 2.231(5), Cu–O(5) 2.190(9), Cu–O(6) 1.760(11), C(19)–O(6) 1.350(11), C(20)–O(5) 1.286(2), C(19)–C(20) 1.369(14), C(19)–C(27) 1.437(2); O(5)–Cu–O(6) 81.4(4), O(6)–Cu–N(1) 110.5(4), N(1)–Cu–N(2) 81.5(2), N(2)–Cu–O(5) 84.4(3), Cu–O(5)–C(20) 105.8(9), Cu–O(6)–C(19) 116.8(7), O(5)–C(20)–C(19) 117.1(12), O(6)–C(19)–C(20) 118.7(9), O(6)–C(19)–C(27) 120.5(9).




**Scheme 3**

was found to proceed according to this reaction pathway. $^3O_2$ in the presence of copper ions seems to afford similar reactions and is unique in this type of reactions. Kinetic, photochemical (testing of chemiluminescence), and decarbonylation reactions are being carried out to shed light on the mechanism of this reaction route of quercetinase mimicking C–C bond cleavage.

We thank the Hungarian Research Fund (OTKA T-016285) and COST (ERBCIPECT926093, 12160) for financial support.

## Footnotes

* E-mail: speier@almos.vein.hu

† *Crystal data*: Cu(fla)(2-HOC$_6$H$_4$COCO$_2$)(bpy), $M$ = 621.06, monoclinic, space group $P2_1/c$, $a$ = 10.285(5), $b$ = 11.850(7), $c$ = 21.892(9) Å, $\alpha$ = 90.00(0), $\beta$ = 98.98(4), $\gamma$ = 90.00(0)°, $U$ = 2635(2) Å$^3$ (by least-squares refinement on diffractometer angles for 21 automatically centred reflections), $\lambda$ = 0.71073 Å, $Z$ = 4, $D_c$ = 1.565 g cm$^{-3}$, $F(000)$ = 1272. Dark green prism. Crystal dimensions 0.20 × 0.20 × 0.30 mm.

Data were collected at 200 K using graphite-monochromated Mo-K$\alpha$ radiation and $\omega$ scans on a Siemens R3m/V diffractometer in the 2$\theta$ range 5.1–47.1°, 3767 reflections measured with $I > 2\sigma(I)$.

The structure was solved by direct methods and refined by full-matrix least squares using SHELXS-86,[9] SHELXL-93.[9] All non-hydrogen atoms were refined using anisotropic thermal parameters; hydrogen atoms were included by use of a riding model and fixed isotropic thermal parameters. The final residual were $R$ = 0.0765, $R_w$ = 0.1812 and for 3524 reflections $R_{tot}$ = 0.0707, $w^{-1} = [\sigma^2(F_o) + F_o^2]$, 402 parameters, maximum residual electron density = 0.636 e Å$^{-3}$. Atomic coordinates, bond lengths and angles, and thermal parameters have been deposited at the Cambridge Crystallographic Data Centre (CCDC). See Information for Authors, Issue No. 1. Any request to the CCDC for this material should quote the full literature citation and the reference number 182/369.

## References

1 D. W. Westlake, G. Talbot, E. R. Blakely and F. J. Simpson, *Can. J. Microbiol.*, 1959, **5**, 62; F. J. Simpson, G. Talbot and D. W. S. Westlake, *Biochem. Biophys. Res. Commun.*, 1959, **2**, 621; S. Hattori and I. Noguchi, *Nature*, 1959, **184**, 1145; H. Sahamoto, *Seikagu* (*J. Jpn. Biochem. Soc.*), 1963, **35**, 633; T. Oka, F. J. Simpson and N. G. Krishnamurthy, *Can. J. Microbiol.*, 1977, **16**, 493.
2 E. Makasheva and N. T. Golovkina, *Zh. Obshch. Khim.*, 1973, **43**, 1640; M. Thomson and C. R. Williams, *Anal. Chim. Acta*, 1976, **85**, 375; K. Takamura and M. Ito, *Chem. Pharm. Bull.*, 1977, **25**, 3218.
3 G. Speier, V. Fülöp and L. Párkányi, *J. Chem. Soc., Chem. Commun.*, 1990, 512.
4 É. Balogh-Hergovich, G. Speier and G. Argay, *J. Chem. Soc., Chem. Commun.*, 1991, 551.
5 M. Utaka, M. Hojo, Y. Fujii and A. Takeda, *Chem. Lett.*, 1984, 635; M. Utaka and A. Takeda, *J. Chem. Soc., Chem. Commun.*, 1985, 1824.
6 T. Matsuura, *Tetrahedron*, 1977, **33**, 2869.
7 I. Lippai, G. Speier, G. Huttner and L. Zsolnai, *J. Chem. Soc., Dalton Trans.*, submitted.
8 P. C. Arnaud, R. Faure and H. Loiseleur, *Acta Crystallogr., Sect. C*, 1986, **42**, 814.
9 G. M. Sheldrick, SHELXS-86, A Program for Crystal Structure Refinement, University of Göttingen, 1990; G. M. Sheldrick, SHELXL-93, A Program for Crystal Structure Refinement, University of Göttingen, 1993.

*Received, 17th September 1996; Com. 6/06417E*

# Allylgallation reaction of carbon–carbon triple bonds with allylsilanes and $GaCl_3$

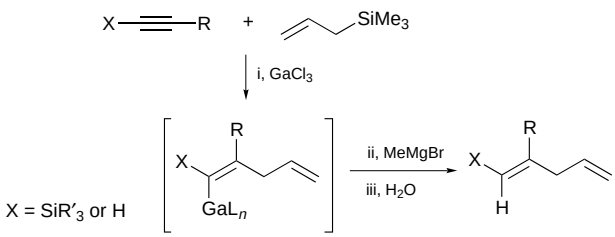
**Masahiko Yamaguchi,*† Takayuki Sotokawa and Masahiro Hirama**

*Department of Chemistry, Graduate School of Science, Tohoku University, Aoba, Sendai 980-77, Japan*

**Treatment of alkynes with allyltrimethylsilanes in the presence of $GaCl_3$ gives 1,4-dienes *via* allylgallation.**

Allylmetallation reactions of carbon–carbon triple bonds are known for organometallic compounds of magnesium, boron, aluminium, indium, zinc, titanium, zirconium and tantalum.[1] Metal-induced allylation reactions with allyltrimethylsilanes were also recently reported.[2] During our studies on the chemistry of novel organogallium compounds.[3,4] allylgallation reaction of silylalkynes or alk-1-ynes was found to take place upon treatment with allylsilanes and $GaCl_3$.

A mixture of an alkynyltrimethylsilane and allyltrimethylsilane in methylcyclohexane was treated with $GaCl_3$ at room temp. for 30 min. Then methylmagnesium bromide was added at −78 °C and 1-trimethylsilyl-2-substituted-1,4-diene was obtained after aqueous workup (Scheme 1 and Table 1). Although silylalkynes undergo self-dimerization in the presence of $GaCl_3$,[3] the cross-coupling reaction with allysilane is more rapid. C–C bond formation occurs regioselectively at the β-carbon atom of silylalkynes, and the (*E*)-relation between the silyl and allyl groups was determined by NOE. Primary and secondary aliphatic alkynes, and aromatic alkynes reacted smoothly. A tertiary aliphatic alkyne, however, was inert to the reaction. Triethylsilylethyne also reacted at the β-carbon atom giving a 1-silylpenta-1,4-diene with (*E*)-configuration (*J* 18.6 Hz). Since reaction of triethylsilylalkynes and allyltrimethylsilane gave 1-triethylsilylpenta-1,4-dienes and not trimethylsilyl derivatives, the silyl groups in the products are derived from silylalkynes. The allylation took place with alk-1-ynes as well as silylalkynes giving 2-substituted-1,4-dienes. Aliphatic and aromatic alk-1-ynes including a tertiary alkyl derivative could be allylated. The reaction was also carried out in other non-coordinating solvents such as benzene, chlorobenzene and dichloromethane. Some examples are shown in Table 1 in which chlorobenzene gave better results than methylcyclohexane because of the higher solubility of the substrates. Disubstituted alkynes, diphenylacetylenes and oct-4-yne, gave rise to oligomerization, and allylation products could not be detected.




**Scheme 1**

**Table 1** Allylgallation reactions of silylacetylenes and alk-1-ynes

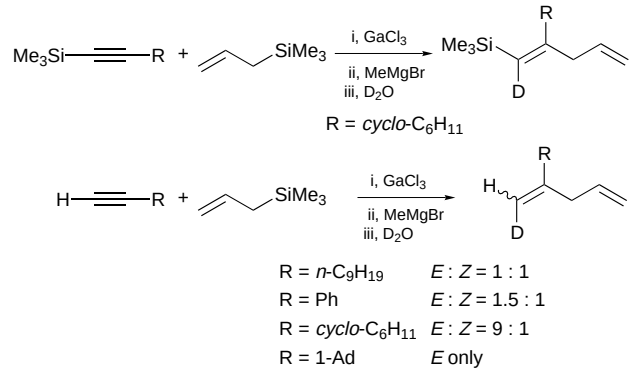
| X | R | Yield (%) |
|---|---|---|
| $SiMe_3$ | *n*-$C_5H_{11}$ | 81[a] |
| | *n*-$C_9H_{19}$ | 79[a] |
| | $Bu^tMe_2SiO(CH_2)_2$ | 68 |
| | –$(CH_2)_{10}$– | 55[b] |
| | *cyclo*-$C_6H_{11}$ | 77[a] |
| | Ph | 86[a] |
| | *p*-$BrC_6H_4$ | 76[a] |
| | *p*-$MeOC_6H_4$ | 63 |
| $SiEt_3$ | H | 75 |
| | *cyclo*-$C_6H_{11}$ | 30 |
| H | *n*-$C_9H_{19}$ | 74 |
| | $Bu^tMe_2SiO(CH_2)_2$ | 47[c] |
| | *n*-$C_9H_{19}CHMe$ | 52 |
| | *cyclo*-$C_6H_{11}$ | 56 |
| | 1-Adamantyl (1-Ad) | 56 |
| | Ph | 56 |
| | *p*-$MeOC_6H_4$ | 45[c] |

[a] (*E*)-Configuration was determined by NOE. [b] 4 mol equiv. of allylsilane was used, and yield of diallylated product is shown. [c] Reaction was conducted in chlorobenzene.

Deuteriation experiments indicated the formation of vinylgallium intermediates (Scheme 2). Thus, the present allylation takes place *via* allylgallation with carbon–carbon triple bonds. The organometal treatment before the aqueous workup is essential to attain satisfactory yields, which probably is required for the effective protonation of the vinylgallium intermediates.[4] While the allylgallation of silylalkynes gave *cis*-addition products, mixtures of isomers were obtained from alk-1-ynes depending on the substituents. *cis*-Addition took place predominantly with secondary and a tertiary alk-1-ynes, while comparable amounts of *trans* isomers formed for primary and aryl derivatives. The stereochemistries appear to reflect the relative thermodynamic stability of *E*- and *Z*-vinylgallium intermediates.

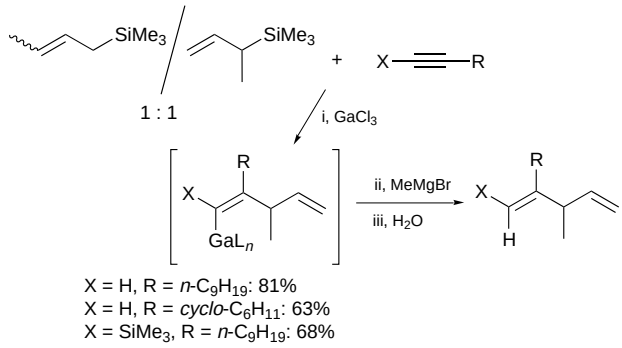
Substituted allylsilanes added to alkynes at the more hindered site irrespective of the structure of the starting organosilicon compounds. A 1 : 1 mixture of but-2-enylsilane and but-3-en-2-ylsilane[5] gave 3-methyl-1,4-diene exclusively (Scheme 3). Both oct-1-en-3-ylsilane **1** and oct-2-ene-1-ylsilane **2**[6] reacted similarly (Scheme 4).

Two mechanisms (I or II) are conceivable for the allylgallation reaction: (I) formation of an allylgallium intermediate by the transmetallation of allylsilane with $GaCl_3$ followed by the

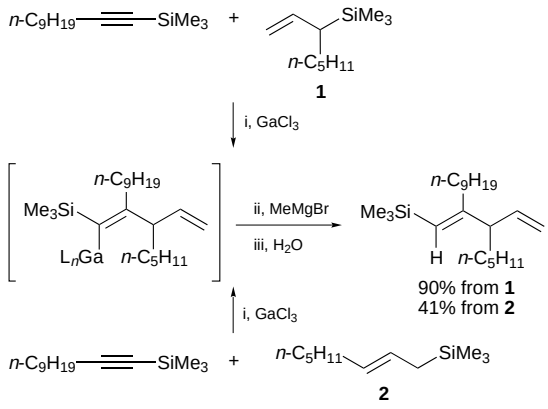



**Scheme 2**

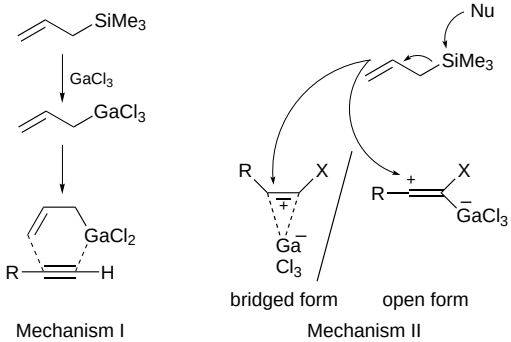
addition to a carbon–carbon triple bond or (II) attack of allylsilane to alkyne activated by $GaCl_3$, the structure of which can be either open or bridged (Scheme 5). Our recent studies showed both examples of the carbogallation reaction. The dimerization reaction of silylalkynes with $GaCl_3$ may involve an alkynylgallium intermediate formed by the transmetallation reaction (mechanism I).[3] In the aromatic β-silylvinylation reaction, attack of aromatic hydrocarbons to $GaCl_3$-activated silylethyne is a probable pathway (mechanism II).[4] The regioselectivity of substituted allylsilanes can be a probe to discriminate between the two mechanisms in the present system. Isomeric allylsilanes would give the same products *via* mechanism I provided that the allyl transposition of the allylgallium intermediate is rapid enough. Mechanism II would involve an $S_E2'$ pathway *via* allyl transposition of allylsilanes; C–C bond formation taking place at the γ-carbon atom of the silicon group. The reactions of substituted allylsilanes are consistent with mechanism I (Scheme 4). The lower yield in the reaction of **2** compared to **1** may be due to the inefficiency of such




**Scheme 3**




**Scheme 4**




**Scheme 5** Possible mechanisms of the allylgallation reaction

allylmetallations,[1,2] however, was not observed in some reactions of alk-1-ynes; primary and aromatic alk-1-ynes gave mixtures of *cis*- and *trans*-addition products (Scheme 2). We tentatively ascribed this to the isomerization of the initially formed *cis*-adducts to the thermodynamic equilibrium.

Allylmetallation reactions of other group 13 elements except for gallium are known. It is now known that allylgallation takes place with both silylalkynes and alk-1-ynes. Treatment of alk-1-ynes with allylsilane and a catalytic amount of $AlCl_3$ or $EtAlCl_2$ was recently reported to give the allylsilylation product. Jung proposed a mechanism involving allylation of silicon-stabilized vinyl cations,[2a] while Yamamoto proposed allylalumination related to our mechanism II (Scheme 5).[2b] In spite of the use of a similar allylating reagent system, allylsilane and a Lewis acid of the group 13 element, different mechanisms are proposed in these reactions and for our reaction. Determination of the precise mechanisms will be subject of future work.

This work was supported by a Grant-in-Aid for Scientific Research from the Ministry of Education, Science, and Culture, Japan (No. 07554065 and 08404050). Generous gifts of silicon reagents from Shin-Etsu Chemicals Co., LTD. are also gratefully acknowledged.

## Footnotes

* E-mail: yama@mail.pharm.tohoku.ac.jp
† Present address: Pharmaceutical Institute, Tohoku University, Aoba, Sendai 980-77, Japan.

‡ *Typical experimental procedure*: under an argon atmosphere, a 1.0 M solution of $GaCl_3$ in methylcyclohexane (1 ml, 1.0 mmol) was added dropwise over 10 min to a mixture of 1-trimethylsilyl-2-cyclohexylacetylene (0.18 g, 1.0 mmol) and allyltrimethylsilane (0.23 g, 2.0 mmol) in methylcyclohexane (10 ml) at room temp. After stirring for 30 min, the mixture was cooled to −78 °C, and 0.92 M methylmagnesium bromide in thf (6.4 ml, 6.0 mmol) was added dropwise. The cooling bath was removed, and stirring was continued for 1 h at room temp. Water was then added, and organic materials were extracted twice with hexane. The combined extracts were washed with saturated aqueous $NH_4Cl$ and brine, dried over $Na_2SO_4$, and concentrated. Flash column chromatography on silica gel (hexane) gave (*E*)-1-trimethylsilyl-2-cyclohexylpenta-1,4-diene (0.17 g, 77%).

## References

1 (*a*) Reviews: J. F. Normant and A. Alexakis, *Synthesis*, 1981, 841; P. Knochel, *Carbometallation of Alkenes and Alkynes*, in *Comprehensive Organic Synthesis*, ed. B. M. Trost, 1991, vol. 4, ch. 4.4, p. 865; (*b*) Mg. K. Okada, K. Oshima and K. Utimoto, *J. Am. Chem. Soc*., 1996, **118**, 6076; (*c*) Zn. E. Negishi and J. A. Miller, *J. Am. Chem. Soc*., 1983, **105**, 6761; G. A. Molander, *J. Org. Chem*., 1983, **48**, 5409; (*d*) Y. N. Bubnov, M. S. Grigorian, A. V. Tsyban' and B. M. Mikhailov, *Synthesis*, 1980, 902; Y. N. Bubnov, A. V. Tsyban' and B. M. Mikhailov, *Synthesis*, 1980, 904; D. A. Singleton, S. C. Waller, Z. Zhang, D. F. Frantz and S.-W. Leung, *J. Am. Chem. Soc*., 1996, **118**, 9986; (*e*) Al. J. A. Miller and E. Negishi, *Tetrahedron Lett*., 1984, **25**, 5863; (*f*) In. S. Araki, A. Imai, K. Shimizu, M. Yamada, A. Mori and Y. Butsugan, *J. Org. Chem*., 1995, **60**, 1841; (*g*) Ti. J. J. Eisch and M. P. Boleslawski, *J. Organomet. Chem*., 1987, **334**, Cl; (*h*) Zr. T. Takahashi, N. Suzuki, M. Kageyama, D. Y. Kondakov and R. Hara, *Tetrahedron Lett*., 1993, **34**, 4811; (*i*) Ta. K. Takai, M. Yamada, H. Odaka, K. Utimoto, T. Fujii and I. Furukawa, *Chem. Lett*., 1995, 315.
2 (*a*) S. H. Yeon, J. S. Han, E. Hong, Y. Do and I. N. Jung, *J. Organomet. Chem*., 1995, **499**, 159; (*b*) N. Asao, E. Yoshikawa and Y. Yamamoto, *J. Org. Chem*., 1996, **61**, 4874.
3 M. Yamaguchi, A. Hayashi and M. Hirama, *Chem. Lett*., 1995, 1093.
4 M. Yamaguchi, Y. Kido, A. Hayashil and M. Hirama, *Angew. Chem*., in the press.
5 H. Sakurai, Y. Kudo and H. Miyoshi, *Bull. Chem. Soc., Jpn*., 1976, **49**, 1433; A. Hosomi, A. Shirahata and H. Sakurai, *Chem. Lett*., 1978, 901.
6 J. G. Smith, S. E. Drozda, S. P. Petraglia, N. R. Quinn, E. M. Rice, B. S. Taylor and M. Viswanathan, *J. Org. Chem*., 1984, **49**, 4112.

*Received in Cambridge, UK, 23rd January 1997; Com. 7/00552K*

# Large negative cubic hyperpolarizability for the spin-crossover compound *cis*-bis(thiocyanato)bis[*N*-(2-pyridylmethylene)aminobiphenyl]iron(II)

**Jean-François Létard,[a] Sébastien Montant,[b,c] Philippe Guionneau,[c,d] Partick Martin,[b,c] Annie Le Calvez,[b,c] Eric Freysz,[b,c] Daniel Chasseau,[c,d] René Lapouyade[a] and Olivier Kahn[a]**

[a] *Laboratoire des Sciences Moléculaires, Institut de Chimie de la Matière Condensée de Bordeaux, UPR CNRS no. 9048, 33608 Pessac Cedex, France*
[b] *Centre de Physique Moléculaire Optique et Hertzienne, URA CNRS no. 283, France*
[c] *Université Bordeaux I, 351 Cours de la Libération, 33405 Talence, France*
[d] *Laboratoire de Cristallographie et Physique Cristalline, ERS, CNRS no. 133, France*

**The first example of a spin-crossover iron(II) compound with a large negative third-order polarizability, associated with an instantaneous electronic response, is reported; magnetic measurements show that this compound, *cis*-bis(thiocyanato)bis[*N*-(2-pyridylmethylene)aminobiphenyl]iron(II), characterized by X-ray structural data is in the high-spin form at room temperature.**

As future generations of optoelectronic devices for telecommunications and information storage, optical switching and signal processing will rely upon the development of materials with large non-linear optical (NLO) responses,[1] many studies have been carried out in this field over the last two decades.[1–9] Organic derivatives received much attention in view of their efficiency and fast NLO response times and their tailorability towards the chemical structure for a given NLO process.[1–5] Nevertheless, in the last years, investigations of metallo-organic compounds brought in many new variables and gave a new dimension to the area.[2,6–9] For instance, compared to organic molecules, metal complexes offer a larger variety of structures, such as diversity of metals, oxidation states and various arrangements of the ligands around the metal. Furthermore, some of these complexes may behave as molecular bistables between low-spin (LS) and high-spin (HS) states.[11–13] The vast majority of studies involving coordination compounds have been dedicated to quadratic optical non-linearities, while third-order responses have scarcely been investigated.[6–9] Here, we present the first example of an iron(II) derivative presenting a large negative third-order polarizability together with a cross-over between LS and HS states. Negative third-order non-linearities are uncommon, and have the property to induce a self-defocusing effect, which can be applied to eliminate the non-linear optical auto-optical annihilation of a potential all-optical device.[3] Additionally, the few negative third-order polarizabilities that have been measured[3,7–9] are relatively large in absolute magnitude compared to molecules with positive $\gamma$.[4,5] We report here a new iron(II) spin-crossover compound with a large negative polarizability at room temperature, where it is in its high-spin state.

*cis*-Bis(thiocyanato)bis[*N*-(2-pyridylmethylene)aminobiphenyl]iron(II), $[FeL_2(NCS)_2]$,† was prepared in anhydrous methanol by mixing *N*-(2-pyridylmethylene)aminobiphenyl‡ and $Fe(NCS)_2$. The ligand was synthesized from 2-pyridinecarbaldehyde and 4-aminobiphenyl. Single crystals of $[FeL_2(NCS)_2]$ were obtained by slow diffusion in methanol, using a H double-tube glass.

Fig. 1 shows the magnetic susceptibility measurements, performed first from 280 K by decreasing and then by increasing temperatures. The $\chi_M T$ ($\chi_M$ = molar magnetic susceptibility, $T$ = temperature) product decreases slightly from 3.68 $cm^3$ K $mol^{-1}$ at 280 K to 2.89 at 222 K, then drops suddenly around $T_c$ *ca.* 202 K down to 0.46 at 177 K, and reaches the lower limit of 0.02 in the vicinity of 120 K. The curve $\chi_m T$ *vs.* $T$, obtained in the warming up mode, is similar, with a thermal hysteresis of *ca.* 4 K. The magnetic measurements demonstrate that the iron compound exhibits a complete spin transition between high-spin ($S$ = 2) and low-spin ($S$ = 0) states.

The molecular structure§ of this compound in the high-spin state is shown in Fig. 2. The iron atom is located on a twofold axis and the two NCS groups have a *cis* conformation. The Fe–N($CS^-$) distances [Fe–N(2) 2.041(8) Å] are shorter than the Fe–

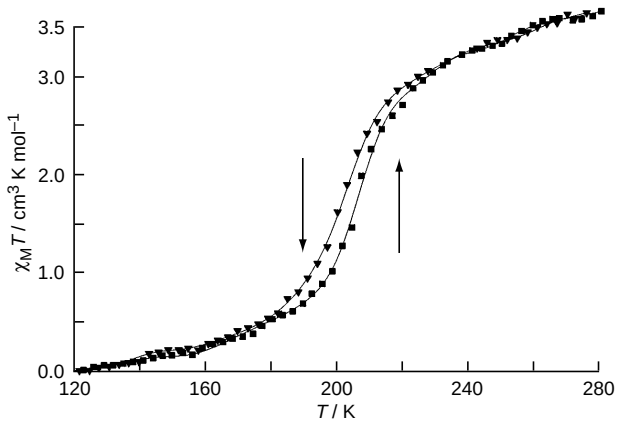



**Fig. 1** Magnetic properties of $[FeL_2(NCS)_2]$ at decreasing (▼▼▼) and increasing (■■■) temperatures

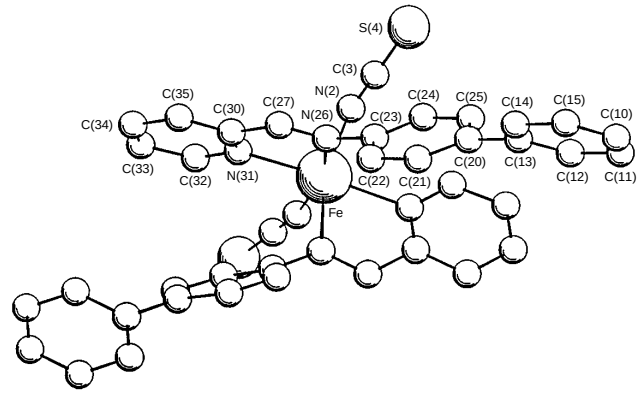



**Fig. 2** Perspective view of $[FeL_2(NCS)_2]$ including the numbering of non-hydrogen atoms. Hydrogen atoms were omitted for clarity. Fe–N bond lengths are consistent with high-spin $Fe^{II}$ and close to those reported for $[Fe(phen)_2(NCS)_2]$.[11] It can also be noticed that the $NCS^-$ groups are linear [N(2)–C(3)–S(4) 179.7°], whereas the Fe–N–C(S) linkages are bent (167.0°), as previously reported for $[Fe(phen)_2(NCS)_2]$ (179.4, 167.0°).[11]

N (organic ligand) distances [Fe–N(26) 2.250(8) Å, Fe–N(31) 2.228(8) Å], which leads to a pronounced distorsion of the $FeN_6$ octahedron. This is also illustrated by the N–Fe–N angles: N(26)–Fe–N(31) 74.4(3)°, N(31)–Fe–N(2) 90.3(3)° and N(26)–Fe–N(2) 96.0°.

The third-order non-linear optical susceptibility ($\gamma$) recorded by optical Kerr effect¶ at room temperature for $[FeL_2(NCS)_2]$ dissolved in acetonitrile is presented in Fig. 3 and compared to the response for pure acetonitrile. From this figure we can clearly conclude that (*i*) the $\gamma$ susceptibility of $[FeL_2(NCS)_2]$ is negative. This has been also observed for (cyclopentadienyl)-bis(phosphine)ruthenium σ-nitroarylacetylides ($\gamma = -210$ to $450 \times 10^{-36}$ esu),[7] metallotriazolohemiporphyrazines (with $Fe^{2+}$, $\gamma = -3100 \times 10^{-36}$ esu)[8] and metallophthalocyanines (with $Co^{2+}$, $\gamma = -32\,800 \times 10^{-36}$ esu);[9] (*ii*) the magnitude of the signal, recorded for the weak concentration of molecules largely overcomes the Kerr signal due to the acetonitrile solvent. Taking into account the molecular concentration, we obtain $\gamma = -130\,000 \times 10^{-36}$ esu (*vs.* $1 \times 10^{-36}$ esu for acetonitrile); (*iii*) the time response allows us to assign the Kerr signal to the electronic contribution exclusively. It is important to notice that no slower processes, such as reorientation mechanisms (picosecond timescale), are observed for $[FeL_2(NCS)_2]$, where the $\gamma$ signal at longer times is maily due to acetonitrile. It can be also noticed that the comparison between the signal recorded for $[FeL_2(NCS)_2]$ ($\gamma = -130\,000 \times 10^{-36}$ esu) and the ligand (L, $\gamma = 1500 \times 10^{-36}$ esu) in acetonitrile shows clearly that the negative magnitude is induced by the metal ion.

We noticed a very weak absorption of the sample around 800 nm, which may bring about a resonant contribution to the $\gamma$ susceptibility. In order to address this problem, we have recorded $\gamma$ as a function of the laser wavelengths. The data recorded for $[FeL_2(NCS)_2]$, dissolved in butyronitrile are presented in Fig. 4. The decrease of the negative signal intensity at shorter wavelength can be attributed to an increase of a positive component, due to the resonant contribution. This is further confirmed, if we compare the signal recorded for $[FeL_2(NCS)_2]$ in acetonitrile ($-130\,000 \times 10^{-36}$ esu at $\lambda = 800$ nm) and in butyronitrile ($-49\,000 \times 10^{-36}$ esu at $\lambda = 804$ nm), where the maxima of the UV–VIS spectra is bathochromically shifted; *i.e.* $\lambda$(acetonitrile) = 577 nm and $\lambda$(butyronitrile) = 620 nm, respectively.

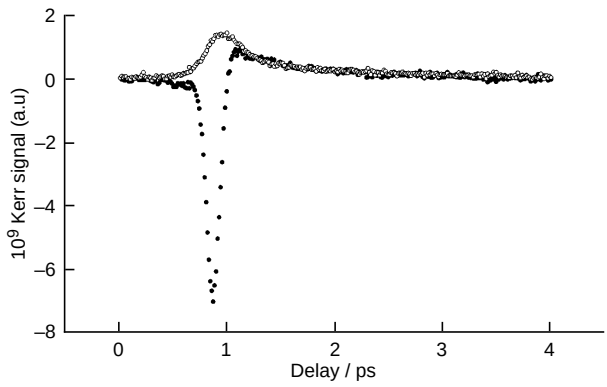



**Fig. 3** Third-order molecular optical non-linearities for acetonitrile (○○○) and $[FeL_2(NCS)_2]$ (●●●) in the HS state dissolved in acetonitrile ($c = 7.85 \times 10^{-4}$ mol dm$^{-3}$)

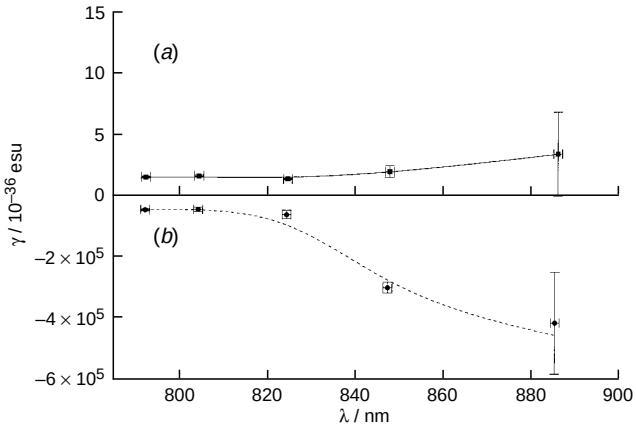



**Fig. 4** Third-order molecular optical non-linearities as a function of wavelength for (*a*) butyronitrile (—) and (*b*) $[FeL_2(NCS)_2]$ (---) dissolved in butyronitrile ($c = 10^{-4}$ mol dm$^{-3}$)

NLO measurements of this compound, with a low-spin state configuration, are in progress to further probe the role of the metal centre.

## Footnotes

† Anal. Calc. for $[FeL_2(NCS)_2]$, $C_{38}H_{28}FeN_6S_2$: C, 66.28; H, 4.07; N, 12.21; S, 9.30; Fe, 8.14. Found: C, 66.26; H, 4.09; N, 12.03; S, 8.90; Fe, 8.32%. IR (KBr) 3027, 2060, 1594, 1484, 1441, 1008, 850, 773, 700 cm$^{-1}$. λ/nm (KBr, nm) 400, 620.

‡ $^1$H NMR ($CDCl_3$, 200 MHz) 7.30–7.49 (6 H, m), 7.62–7.66 (4 H, t), 7.83–7.84 (1 H, t), 8.22–8.25 (1 H, d), 8.68 (s, 1 H), 8.71–8.75 (d, 1 H). MS: *m/z* 258 ($M^+$, 100), 231 (31), 152 (36), 79 (20).

§ *Crystal data* for $C_{38}H_{28}FeN_6S_2$: $M$ = 688, orthorhombic, space group *Pccn* ($Z$ = 4), $a$ = 12.949(7), $b$ = 15.183(2), $c$ = 17.609(5) Å; $U$ = 3462(2) Å$^3$; $D_c$ = 1.33; μ = 4.921 mm$^{-1}$. Measurements were made with a Nonius CAD-4 diffractometer; Cu-Kα radiation (1.5418 Å); crystal shape: black plate, 0.125 × 0.35 × 0.50 mm; the unit-cell parameters came from 25 reflections; Bragg angle $\theta < 65°$; empirical absorption correction $0.822 < T < 1.000$; scan type ω–θ; 3331 measured reflections, 1109 observed [$I > 3\sigma(I)$]; structural determination with MITHRIL and structural refinement with SHELX76; 215 parameters; $R$ = 0.045; $R_w$ = 0.035; $w = 1.985/[\sigma^2(F)]$; $(\Delta/\sigma)_{max}$ = 0.2; $\Delta\rho_{max,min}$: 0.20, −0.15 e Å$^{-3}$. Atomic coordinates, bond lengths and angles, and thermal parameters have been deposited at the Cambridge Crystallographic Data Centre (CCDC). See Information for Authors, Issue No. 1. Any request to the CCDC for this material should quote the full literature citation and the reference number 182/374.

¶ Third-order optical non-linearities $\chi^3$ ($-3\omega;\omega,\omega,\omega$) were performed at 800 nm using a CW mode-locked Ti : sapphire laser working at 76 MHz. The molecular $\gamma$ (esu unit) has been deduced from $\chi^3$ ($-3\omega;\omega,\omega,\omega$) by $\gamma = \chi^3/(LN\eta_a)$, where $\eta_a$ is the Avogadro number, $L$ the local field correction and $N$ is the concentration. All results are referenced to $\chi^3$ ($-3\omega;\omega,\omega,\omega$) of SF59 ($6.5 \times 10^{-21}$ m$^2$ V$^2$ = $4.6 \times 10^{-13}$ esu), which leads to $\gamma_{CS_2} = 4.32 \times 10^{-34}$ esu.

## References


1 D. S. Chemla and J. Zyss, *Nonlinear Optical Properties of Organic Molecules and Crystals*, Academic, Orlando, FL, 1987, vol. 1 and 2.
2 D. R. Kanis, M. A. Ratner and T. J. Marks, *Chem. Rev.*, 1994, **94**, 195.
3 C. W. Dirk, W. C. Herndon, F. Cervantes-Lee, H. Selnau, S. Martinez, P. Kalamegham, A. Tan, G. Campos, M. Velez, J. Zyss, I. Ledoux and L.-T. Cheng, *J. Am. Chem. Soc.*, 1995, **117**, 2214.
4 D. W. Samuel, I. Ledoux, C. Dhenaut, J. Zyss, H. H. Fox, R. R. Schrock and R. J. Silbey, *Science*, 1994, **265**, 1070.
5 H. S. Nalwa, *Adv. Mater.*, 1993, **5**, 341.
6 For recent general reviews of NLO materials involving organometallic and coordination complexes, see: H. S. Nalwa, *Appl. Organomet. Chem.*, 1991, **5**, 349; N. J. Long, *Angew. Chem., Int. Ed. Engl.*, 1995, **34**, 21.
7 I. R. Whittall and M. G. Humphrey, M. Samoc, J. Swiatkiewicz and B. Luther-Davies, *Organometallics*, 1995, **14**, 5493.
8 M. A. Díaz-García, I. Ledoux, F. Fernández-Lázaro, A. Sastre, T. Torres, F. Agulló-López and J. Zyss, *J. Phys. Chem.*, 1994, **98**, 4495; M. A. Díaz-García, I. Ledoux, F. Fernández-Lázaro, A. Sastre, T. Torres, F. Agulló-Lopez and J. Zyss, *Nonlinear Opt.*, 1995, **10**, 101.
9 M. A. Díaz-García, I. Ledoux, J. A. Duro, T. Torres, F. Agulló-López and J. Zyss, *J. Phys. Chem.*, 1994, **98**, 8761.
10 P. Gütlich, A. Hauser and H. Spiering, *Angew. Chem., Int. Ed. Engl.*, 1994, **33**, 2024; O. Kahn, J. Kröber and C. Jay, *Adv. Mater.*, 1992, **4**, 718.
11 B. Gallois, J.-A. Real, C. Hauw and J. Zarembowitch, *Inorg. Chem.*, 1990, **29**, 1152.


*Received, 2nd January 1997; Com. 7/00019G*

# Synthesis and isolation of an all-carbon tetraanion; a discrete $C_{60}^{4-}$ fulleride salt

**Yongping Sun and Christopher A. Reed***

*Department of Chemistry, University of Southern California, Los Angeles, CA 90089-0744, USA*

**The highly reduced, all-carbon tetraanion, $C_{60}^{4-}$, earlier identified as a discrete ion in solution by electrochemical and spectroscopic methods, can be synthesized and isolated as an analytically pure, sodium cryptand salt.**

There is considerable current experimental and theoretical interest in the high negative charge states attainable in small aromatic molecules.[1] The first isolable tetraanion of a π hydrocarbon (rubrene, $C_{42}H_{28}$) has recently been reported[2] and the all-carbon π frameworks of fullerenes present further interesting targets for the study of anionic charge buildup.

The electron accepting ability of $C_{60}$ is its most characteristic chemical property and the maximal extent of charge buildup is an intriguing phase-dependent question. In the gas phase, two electrons can bind to give the rare example of a stable dianion.[3] In the solid state, the heavier alkali- or alkaline-earth cations can interstitially stabilize negative valencies at least as large as 8 in the so-called superfullerides.[4] Intercalated lithium stabilizes the $C_{60}^{12-}$ state, presumably with some degree of covalency.[5] In solution, the highest $C_{60}^{n-}$ fullerides known are $n = 6$ on the electrochemical timescale[6] and $n = 5$ for low-temperature spectroscopic identification.[7] In synthetic chemistry, discrete fulleride salts have only been isolated up to $n = 3$.[8,9] We now report the successful synthesis and isolation of a discrete salt of the highly reduced tetraanion, $C_{60}^{4-}$ ion.

The nature of the $C_{60}^{4-}$ ion is of interest for a number of reasons. For alkali-metal intercalated $C_{60}$, it is not well understood why $A_4C_{60}$ salts are insulating while $A_3C_{60}$ salts are metallic and superconducting.[10] A detailed knowledge of the electronic structure of the discrete repeating units, namely $C_{60}^{4-}$ and $C_{60}^{3-}$, may be instructive. With its $t_{1u}^4$ configuration, $C_{60}^{4-}$ is the electron–hole equivalent of the $C_{60}^{2-}$ ion, whose electronic structure is controversial.[11,12] Mirrored properties would be interesting. The question of a singlet *vs*. a triplet ground state for $C_{60}^{4-}$ is particularly intriguing because unexpectedly, neither $C_{60}^{2-}$ nor $C_{60}^{3-}$ obeys Hund's rule.[9,11] For $C_{60}^{3-}$, it is presently unknown whether there is a relationship between Cooper pairs of superconducting electrons and the unanticipated tendency of localized spins on $C_{60}^{n-}$ fullerides to attain minimum multiplicity.

The synthesis of an analytically pure salt of $C_{60}^{4-}$ was achieved in an inert-atmosphere glovebox by stirring a suspension of $C_{60}$ (20.0 mg, 0.0278 mmol) in tetrahydrofuran (thf) (35 ml) with a piece of freshly cut sodium in the presence of 4.2 equiv. of cryptand 222 (44.0 mg, 0.117 mmol).† The reaction proceeds *via* successive reductions with $[Na(crypt)^+]_4[C_{60}^{4-}]$ precipitating as a dark brown, microcrystalline solid. The product was filtered off, the ball of excess sodium removed as completely as possible with tongs, and the product washed with thf and dried under vacuum (90%). Anal. calc. for $C_{132}H_{144}N_8Na_4O_{24}$: C, 68.38; H, 6.26; N, 4.83; Na, 3.97. Found: C, 67.69, 66.80; H, 6.16, 6.17; N, 4.88, 5.25; Na, 5.25%. Integration of the NOE-suppressed $^{13}C$ NMR signals (15 s pulse delay) of the cryptand (δ 67.9, 66.9, 52.1) *vs*. fulleride (see below) gives the expected 4 : 1 ratio of cation to anion. The product is exceedingly air sensitive, oxidizing initially to $C_{60}^{3-}$ as the major product. It dissolves without immediate decomposition in scrupulously dried, deoxygenated dimethyl sulfoxide. Electrochemical estimates[13] of the $pK_a$ of the conjugate acid, $C_{60}H^{3-}$ ($pK_a = 37$), suggest that $C_{60}^{4-}$ is a sufficiently powerful base to remove a proton from $Me_2SO$ ($pK_a = 31$). That this does not occur within a day or so indicates either that this reaction is very slow or that the $pK_a$ estimate is incorrect for electrolyte-free solvent. Traces of protonic solvents (*e.g.*, water) in the $Me_2SO$ cause immediate oxidation to $C_{60}^{3-}$, presumably *via* fullerene hydrocarbon formation. Attempted cation metathesis reactions with $NBu_4Cl$ and with $[N(PPh_3)_2]Cl$ both led to oxidation to $C_{60}^{3-}$, presumably due to acidity of the α-methylene protons in $NBu_4^+$ and redox instability[14] of $[N(PPh_3)_2]^+$, respectively.

The fingerprint region for the absorption spectrum of fullerides is in the near-IR region and corresponds to $t_{1u}$–$t_{1g}$ transitions of *ca*. 1 eV.[7,15] The VIS–NIR spectrum of $[Na(crypt)^+]_4[C_{60}^{4-}]$ in $Me_2SO$ is shown in Fig. 1. The absence of a band at 780 nm indicates the absence of $C_{60}^{3-}$. Maxima at 730 and 1195 nm are consistent with those reported for electrochemically generated $C_{60}^{4-}$ in benzonitrile (728, 1209 nm)[15] and rubidium-reduced $C_{60}^{4-}$ in liquid ammonia (715, 1175 nm).[7]‡

We have recently shown that for $n = 1$, 2 and 3, the $C_{60}^{n-}$ fullerides have broad, downfield-shifted resonances in their solution $^{13}C$ NMR spectra, the result of paramagnetism.[11,17] The same is true for $C_{60}^{4-}$, indicating that it too has significant paramagnetism at room temperature. The spectrum in $(CD_3)_2SO$ is shown in Fig. 2. The chemical shift of δ 185 is essentially the same as that of $C_{60}^-$ (δ 186) and $C_{60}^{2-}$ (δ 184) but different from that of $C_{60}^{3-}$ (δ 197). An integrity check on the NMR sample was run after measurement and, within the limits of VIS–NIR detection (*ca*. 5%), it indicated no decay to $C_{60}^{3-}$ ($\lambda_{max} = 780$ nm). Interestingly, the chemical shift of the discrete $C_{60}^{4-}$ ion (δ 185) is not very different from that in solid-state $K_4C_{60}$ (δ 180) and $Rb_4C_{60}$ (δ 182).[18] The interpretation of $^{13}C$ chemical shifts in fullerides is complex, but to a first approximation, the *ca*. 40 ppm downfield shift can be equated with an average spin density of about one unpaired electron per buckyball. This suggests that like $C_{60}^{2-}$, the singlet ($S = 0$) and triplet ($S = 1$) states are close in energy. Fast intersystem crossing and/or electron transfer would average the signal to that approximating an $S = 1/2$ system. Efforts to quantify the singlet–triplet splitting for $C_{60}^{4-}$ and $C_{60}^{2-}$ by NMR methods

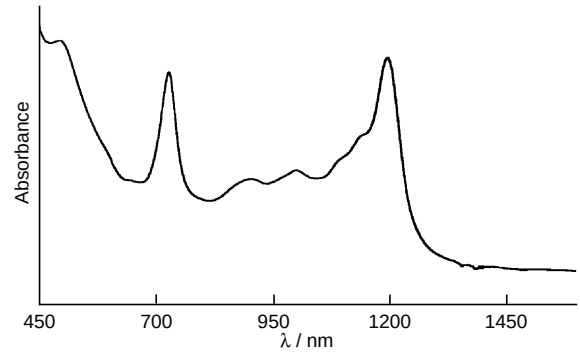



**Fig. 1** VIS–NIR spectrum of $C_{60}^{4-}$ in $Me_2SO$

are ongoing. The present results are in qualitative agreement with those on $Rb_4C_{60}$ where a localized singlet ground state is proposed with a close-lying triplet a few hundred $cm^{-1}$ higher in energy.[19]

EPR spectroscopy has been widely used to investigate the spin states of fullerides but interpretations have been bedeviled by problems of sensitivity to impurities, the difficulty of quantifying overlapping signals with widely differing line-widths, aggregation uncertainties in frozen solution, *etc.*[11,12] Preliminary results on $C_{60}^{4-}$ salts fare no better. Fig. 3 shows the low-temperature EPR spectrum of $C_{60}^{4-}$ in frozen $Me_2SO$ solution. Comparison to the spectrum of $C_{60}^{3-}$ under identical conditions of cation and solvent (also shown in Fig. 3) indicates the presence of $C_{60}^{3-}$ in the $C_{60}^{4-}$ sample even though this is undetectable by NIR. The additional, sharper signals are potentially ascribable to $C_{60}^{4-}$, but it would be premature to make such an assignment in view of the difficulties[11,12] associated with assigning the spectrum of $C_{60}^{2-}$, of which $C_{60}^{4-}$ is the electron–hole equivalent. Since these signals appear to have integrated intensities that are less than the trace $C_{60}^{3-}$ signal, the simplest interpretation is that $C_{60}^{4-}$ is EPR silent at 4 K because of a singlet ground state.§ However, a close-lying, thermally accessible triplet state is indicated by the paramagnetically shifted $^{13}C$ NMR signal seen at room temperature.

In summary, despite its exceedingly strong reducing nature (−2.35 V *vs*. ferrocene),[6] the discrete $C_{60}^{4-}$ ion can be isolated with an 'innocent' cation. This opens the way to deeper studies of its electronic and molecular structure and to studies of its chemical reactivity, particularly with electrophiles.[20]

We are grateful to Robert D. Bolskar for assistance and to the National Institutes of Health (USA) for support (GM 23851).

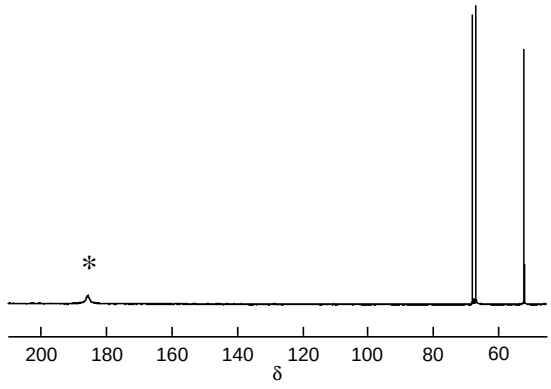



**Fig. 2** $^{13}C$ NMR spectrum of $C_{60}^{4-}$ in $(CD_3)_2SO$ (34196 scans, 125.8 MHz) Peak marked * at δ 185 is from $C_{60}^{4-}$; the others are from Na(cryptand 222)$^+$

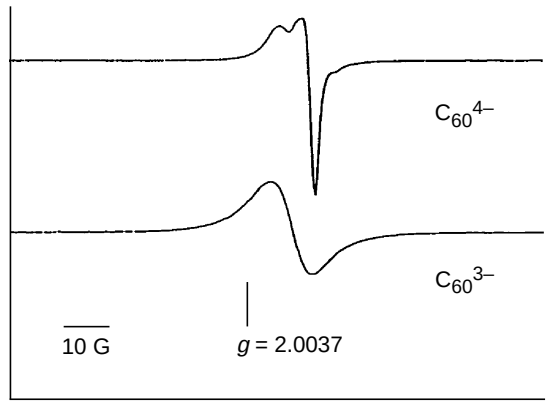



**Fig. 3** EPR spectra of $C_{60}^{4-}$ and $C_{60}^{3-}$ in frozen $Me_2SO$ solution at 5 K

## Footnotes

* E-mail: careed@chem1.usc.edu

† Cryptand 222 is a commercially available alternative to a crown ether for chelation of sodium ions (Aldrich 29, 111-0).

‡ A third report on the NIR of $C_{60}^{4-}$ with a single $\lambda_{max}$ at 934 nm is inconsistent with the present work and with refs. 7 and 15.[16]

§ $C_{60}^{4-}$ has been reported by Baumgarten *et al.*[16] to be diamagnetic because no EPR signal was found. However, since their NIR spectrum[16] is inconsistent with literature reports[7,15] and the present work, it is possible that their $C_{60}^{4-}$ product, if formed, was completely insoluble under the conditions used.

## References

1 M. Baumgarten, L. Gherghel, M. Wagner, A. Weitz, M. Rabinovitz, P.-C. Cheng and L. T. Scott, *J. Am. Chem. Soc.*, 1995, **117**, 6254.
2 H. Bock, K. Gharagozloo-Hubmannm, C. Nather, N. Nagel and Z. Havlas, *Angew. Chem., Int. Ed. Engl.*, 1996, **35**, 631.
3 M. K. Scheller, R. N. Compton and L. S. Cederbaum, *Science*, 1995, **270**, 1160.
4 A. J. Maxwell, P. A. Brühwiler, S. Andersson, N. Martensson and P. Rudolf, *Chem. Phys. Lett.*, 1995, **247**, 257; W. Andreoni, P. Giannozzi, J. F. Armbruster, M. Knupfer and J. Fink, *Europhys. Lett.*, 1996, **34**, 699 and references therein.
5 Y. Chabre, D. Djurado, M. Armand, W. R. Romanow, N. Coustel, J. P. McCauley, Jr., J. E. Fischer and A. B. Smith III, *J. Am. Chem. Soc.*, 1995, **114**, 764; J. Kohanoff, W. Andreoni and M. Parrinello, *Chem. Phys. Lett.*, 1992, **198**, 472.
6 Q. Xie, E. Perez-Cordero and L. Echegoyen, *J. Am. Chem. Soc.*, 1992, **114**, 3978.
7 W. K. Fullagar, I. R. Gentle, G. A. Heath and J. W. White, *J. Chem. Soc., Chem. Commun.*, 1993, 525.
8 C. Bossard, S. Rigaut, D. Astruc, M.-H. Delville, G. Félix, A. Février-Bouvier, J. Amiell, S. Flandrois and P. Delhaès, *J. Chem. Soc., Chem. Commun.*, 1993, 333.
9 P. Bhyrappa, P. Paul, J. Stinchcombe, P. D. W. Boyd and C. A. Reed, *J. Am. Chem. Soc.*, 1993, **115**, 11004.
10 M. J. Rosseinsky, *J. Mater. Chem.*, 1995, **5**, 1497; J. E. Fischer, in *The Chemical Physics of Fullerenes: 10* (*and 5*) *Years Later*, ed. W. Andreoni, NATO ARW Series E316, Kluwer, Dordrect, 1996, p. 359; R. Kerkoud, P. Auban-Senzier, D. Jerome, S. Brazovskii, I. Luk'yanchuk, N. Kirova, F. Rachdi and C. Goze, *J. Phys. Chem. Solids*, 1996, **57**, 143 and references therein.
11 P. D. W. Boyd, P. Bhyrappa, P. Paul, J. Stinchcombe, R. D. Bolskar, Y. Sun and C. A. Reed, *J. Am. Chem. Soc.*, 1995, **117**, 2907.
12 P. C. Trulove, R. T. Carlin, G. R. Eaton and S. S. Eaton, *J. Am. Chem. Soc.*, 1995, **117**, 6265.
13 M. E. Niyazymbetov, D. H. Evans, S. A. Lerke, P. A. Cahill and C. C. Henderson, *J. Phys. Chem.*, 1994, **98**, 13093.
14 M. Tilset, A. A. Zlota, K. Folting and K. G. Caulton, *J. Am. Chem. Soc.*, 1993, **115**, 4113.
15 D. R. Lawson, D. L. Feldheim, C. A. Foss, P. K. Dorhout, C. M. Elliott, C. R. Martin and B. Parkinson, *J. Electrochem. Soc.*, 1992, **139**, L68.
16 M. Baumgarten, A. Gügel and L. Gherghel, *Adv. Mater.*, 1993, **5**, 458.
17 Confirmation has been recently provided by J. Chen, F.-Y. Cai., Q.-F. Shao, Z.-E. Huang and S.-M. Chen, *Chem. Commun.*, 1996, 1111.
18 J. Reichenbach, F. Rachdi, I. Luk'yanchuk, M. Ribet, G. Zimmer and M. Mehring, *J. Chem. Phys.*, 1994, **101**, 4585.
19 G. Ruani, P. Guptasarma, C. Taliani and J. Fischer, *Physica C*, 1994, **235**, 2477; I. Lukyanchuk, N. Kirova, F. Rachdi, C. Goze, P. Molinie and M. Mehring, *Phys. Rev. B*, 1995, **51**, 3978.
20 Alkylation of $C_{60}$ has been reported *via* the reaction of alkyl halides with fullerides: J. W. Bausch, G. K. S. Prakash and G. A. Olah, *J. Am. Chem. Soc.*, 1991, **113**, 3205; C. Caron, R. Subramanian, F. D'Souza, J. Kim, W. Kutner, M. T. Jones and K. M. Kadish, *J. Am. Chem. Soc.*, 1993, **115**, 8505; J. Chen, R.-F. Cai, Q.-F. Shao, Z.-E. Huang, H.-M. Wu, S.-K. Jiang and Q.-F. Shao, *J. Chem. Soc., Chem. Commun.*, 1995, 1553; P. L. Boulas, Y. Zuo and L. Echegoyen, *Chem. Commun.*, 1996, 1547; K.-M. Mangold, W. Kutner, L. Dunsch and J. Fröhner, *Synth. Met.*, 1996, **77**, 73.

*Received in Bloomington, IN, USA, 2nd October 1996. Revised manuscript received 14th February 1997; Com. 7/01106G*

# ITQ-4: a new large pore microporous polymorph of silica

**Miguel A. Camblor,* Avelino Corma and Luis A. Villaescusa**

*Instituto de Tecnología Química, UPV-CSIC, Avda. Los Naranjos s/n, 46071 Valencia, Spain*

**A new silica polymorph of zeolitic nature with large pores, a large void volume and essentially no connectivity defects, is prepared by direct hydrothermal synthesis in a fluoride medium.**

An infinity of different hypothetical topologies can be built based on $TO_4$ tetrahedra sharing all their vertices to yield (4;2) three-dimensional nets,[1] and more than a hundred are actually known to occur as silica, aluminosilicate and aluminophosphate materials.[2] Among the pure silica materials the number of actual topologies is relatively small: several dense phases and clathrasils and only a limited number of microporous phases are known. It is notable that, until very recently, only two pure silica polymorphs having 12 membered ring (12MR) large pore structures, ZSM-12[3] and SSZ-24,[4] have been obtained by direct synthesis. This is despite recent calorimetric measurements[5] and theoretical calculations[6] which showed that the enthalpy of formation of microporous or dense pure silica phases relative to that of quartz is very small (below 15 kJ per mol of $SiO_2$). This result suggests there should be little energetic limitation to the synthesis of pure silica phases of ever decreasing framework density and thus is in contrast with the seeming difficulty to synthesize such phases. Obviously, it is not possible to directly extend these results to the template-mediated synthesis of pure silica phases, since what is actually synthesized is the composite silica framework/templating species. However, it has been suggested that the formation of pure silica phases is geometrically and kinetically, rather than energetically, controlled,[5] implying it is a matter of finding the right templating effect and the right chemical path. We reported recently the first synthesis of a true pure silica polymorph† with a three-dimensional zeolitic channel system of large pores (12MR), which beautifully exemplifies the above statement. In this case, the long-sought pure silica zeolite β spontaneously nucleates and grows free of connectivity defects under hydrothermal conditions, in the presence of both tetraethylammonium cations and $F^-$ anions.[7] Pure silica β is the $SiO_2$ polymorph with the lowest framework density ever reported by direct synthesis. Rather than on the templating ability of tetraethylammonium, the success of this synthesis relied on the use of fluoride anions at near neutral pH in a dense system ($H_2O/SiO_2$ *ca.* 7).[8] The use of $F^-$ anions for the synthesis of defect-free pure silica phases was first established by Flanigen and Patton[9] and subsequently developed by others.[10] The results we present here show how this methodology may be extended, revealing its successful application to the synthesis of another new, large pore microporous pure $SiO_2$ phase containing a large void volume. The synthesis of an increasing number of new microporous pure silica phases using this strategy can be anticipated, with the limits of the method with respect to pore size and void volume still to be established.

The synthesis of the new phase (denoted as ITQ-4, for Instituto de Tecnología Química-4)[11] in its pure $SiO_2$ form free of connectivity defects was achieved by using *N*-benzylquinuclidinium employing conditions similar to those previously described for pure silica zeolite β.[7] In a typical synthesis 24.59 g of tetraethylorthosilicate were added to 42.46 g of a $1.4 \times 10^{-3}$ mol $g^{-1}$ solution of *N*-benzylquinuclidinium hydroxide, and the mixture was stirred for 8 h at room temp. allowing evaporation of the ethanol produced. Then, after adding 10.12 g of water lost during the evaporation and 2.46 g of 48 mass% HF and stirring, the mixture was transferred to PTFE lined stainless steel 60 ml autoclaves, which were heated at 150 °C under tumbling (60 rpm) for 12.5 days. The resulting mixture (pH = 8.2) was then filtered and washed with deionized water. A white highly crystalline solid was obtained (15 g solid/100 g of initial reaction mixture, *i.e. ca.* 90% of the silica was recovered in the solid) having a characteristic powder X-ray diffraction (XRD) pattern shown in Fig. 1(*a*). This pattern was indexed as monoclinic with unit-cell dimensions of $a$ = 18.599(1), $b$ = 13.401(9), $c$ = 7.701(2) Å and β = 101.39(1)°. Chemical analysis reveals, within experimental error, that the sample contains no Al, and further suggests the organic cation to still be intact within the zeolitic channels [Anal. Found: C, 14.83; H, 1.91; N, 1.25. $(C_{14}H_{20}NF)_{2.16}Si_{32}O_{64}$ requires C, 15.12; H, 1.81; N, 1.26%]. Thermogravimetric and difference thermal analyses show no mass loss below 100 °C, indicating the presence of very little or no occluded water, while in the temperature range 200–750 °C there are two overlapping mass loss steps of roughly equal size which amount to about 20% mass, attributable to the oxidation of the template. The experimental chemical composition of $(C_{14}H_{20}NF)_{2.16}Si_{32}O_{64}$ has been calculated for a unit cell containing 32 $SiO_2$ units (the number of Si atoms per unit cell was derived from the measured void volume fraction and the unit-cell volume). The volume of two template molecules {*ca.* 310 $Å^3$ per molecule, assuming free rotation of both the quinuclidinium and benzene moieties around the N–$C^9$ and $C^9$–$C^{10}$ bonds, respectively, of the *N*-benzyl-1-azoniumbicyclo[2,2,2]octane} per unit cell is in very good agreement with the void volume derived by $N_2$ adsorption [670 $Å^3$ (u.c.)$^{-1}$, see below], suggesting that there is a close packing of the organics within the silica framework and that essentially all the void volume accessible to $N_2$ in the calcined sample is occupied by the *N*-benzylquinuclidinium in the as-made sample. This

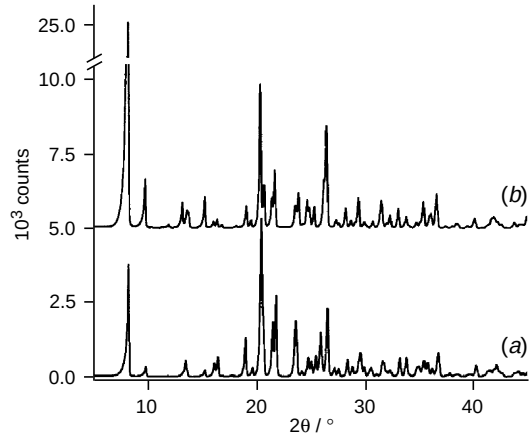



**Fig. 1** Powder X-ray diffractograms of (*a*) as prepared ITQ-4 and (*b*) ITQ-4 after calcination at 580 °C for 3 h. The changes to the pattern after calcination are related to a change in the unit-cell dimensions of the de-templated solid. Philips PW1820 diffractometer, Cu-Kα radiation, 0.020° 2θ step size and 0.500 s count time.

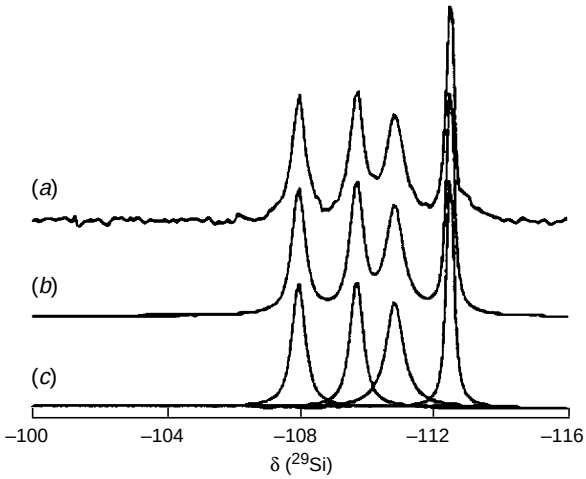



**Fig. 2** $^{29}$Si MAS NMR spectra of calcined ITQ-4, distinctly showing four resolved Si(4Si) crystallographic sites in the structure of the new pure $SiO_2$ polymorph: experimental (*a*), simulated (*b*) and deconvoluted components (*c*). Spectrum recorded on a Varian VXR400 SWB at 5 kHz spinning rate, 60 s recycle delay, 79.4586 MHz, 3π/8 rad, 3 μs pulse length, 264 scans.

implies that the void volume accessible to $N_2$ consists only of rather large cages or channels.

After calcination at 580 °C for 3 h the solid is freed of the organic material with retention of its crystallinity [Fig. 1(*b*)] and symmetry (as deduced from the laboratory XRD data, which were fully indexed with the same symmetry for the as-made and calcined materials). There are however significant changes in peak positions due to changes in the unit-cell parameters [*a* = 18.619(20), *b* = 13.478(9), *c* = 7.625(16) Å, β = 101.947(16)°]. Upon calcination, the unit cell shrinks in the *c* crystallographic direction, while it expands in the *a* and *b* directions, the overall result being a contraction of its volume by a factor of 0.5% (1880.66 and 1871.88 Å$^3$ for the as-made and calcined samples, respectively). Typically, zeolite frameworks expand upon removal of the organic molecules by calcination, while the effect observed here suggests a tight fit of the template within the zeolitic void volume, with the framework relaxing in the calcined form. No loss of crystallinity was observed after heating ITQ-4 to at least 1273 K. The high thermal stability of this phase is attributed to its pure silica nature and to the absence of Si–O–Si connectivity defects (see below). After calcination, the microporous nature of ITQ-4 was probed by its $N_2$ adsorption isotherm at 77 K, from which the following adsorption values were derived: microporous volume 0.21 cm$^3$ g$^{-1}$, micropore area 415 m$^2$ g$^{-1}$, BET surface area 433 m$^2$ g$^{-1}$. By adsorption of Ar at 87.3 K and using the Horvath–Kawazoe formalism a pore size of 6.2 Å was calculated suggesting ITQ-4 is a large 12MR pore material.

The true $SiO_2$ nature of ITQ-4 (*i.e.* a 4-connected three-dimensional net of $SiO_4$ tetrahedra with no Si–O–Si connectivity defects and no Al) is evidenced by $^{29}$Si MAS NMR spectroscopy of calcined pure silica ITQ-4 (Fig. 2). First, and within the limits of detection of this technique, no signals are detected in the region below δ 105, showing the absence of Si(3Si, 1OH) or Si(3Si, 1Al) species. Secondly, the spectrum shows a very high resolution of tetrahedral Si(4Si) sites, directly attributable to the crystallographically distinct Si environments in the structure. Such a high resolution is generally only observed in cases where there is essentially complete absence of Si–OH and Si–O–Al species. In Table 1 a list of the intensities and positions of the four deconvoluted components of the spectrum is given, together with the average Si–O–Si angles calculated using the relationship of Thomas *et al.*[12] for every resolved Si site. The rather small Si–O–Si average angle for

**Table 1** Results of the deconvolution of the $^{29}$Si MAS NMR spectrum of pure $SiO_2$ ITQ-4

| Signal (δ) | Relative intensity | Average Si–O–Si angle[12] |
|---|---|---|
| −107.97 | 23.8 | 142.5 |
| −109.71 | 23.9 | 145.5 |
| −110.86 | 27.6 | 147.5 |
| −112.52 | 24.8 | 150.3 |

every Si site in ITQ-4 (142–150°) is remarkable, the average value (146.5°) being *ca.* 5–10° smaller than the usual T–O–T angles typically found in pure silica zeolites (around 150–155°).

Finally, we note that in view of its characteristic XRD pattern, ITQ-4 appears to be related, being probably isomorphous, to a recently described zeolite of unknown structure, SSZ-42,[13] for which no report exists in the literature. The information contained in its original patent suggests this material is a large pore one. Very interestingly, SSZ-42, for which the template employed here can also be used, can not be synthesized in the absence of B atoms in the conditions reported in the patent ($OH^-$ media). Thus, the synthesis reported here, when viewed together with that already reported for pure $SiO_2$ β,[7] exemplifies how the appropriate synthesis method can help circumvent the apparent difficulty of synthesizing very open pure silica polymorphs, and corroborates the conclusion drawn by other authors concerning the small energetic limitations to the synthesis of large pore pure silica phases.[5]

The authors acknowledge the Spanish DGICYT (MAT 94-0359-C02-01) for financial support and Dr P. Barrett for helpful comments and discussions.

## Footnotes

* E-mail: macamblo@itq.upv.es

† Phases containing extensive Si–O–Si connectivity defects, frequently encountered in zeolite synthesis, are better formulated as $SiO_{2-x}(OH)_{2x}$, rather than as true pure $SiO_2$ polymorphs.

## References

1 J. V. Smith, *Chem. Rev.*, 1988, **88**, 149.
2 W. M. Meier, D. H. Olson and Ch. Baerlocher, *Atlas of Zeolite Structure Types*, Elsevier, London, 4th edn., 1996.
3 R. B. LaPierre, A. C. Rohrman, J. L. Schlenker, J. D. Wood, M. K. Rubin and W. J. Rohrbaugh, *Zeolites*, 1985, **5**, 346.
4 R. A. Van Nordstrand, D. S. Santilli and S. I. Zones, *ACS Symp. Ser.*, 1988, **368**, 236.
5 Y. Petrovic, A. Navrotsky, M. E. Davis and S. I. Zones, *Chem. Mater.*, 1993, **5**, 1805.
6 N. J. Henson, A. K. Cheetham and J. D. Gale, *Chem. Mater.*, 1994, **6**, 1647.
7 M. A. Camblor, A. Corma and S. Valencia, *Chem. Commun.*, 1996, 2365.
8 M. A. Camblor, A. Corma, S. Valencia and L. A. Villaescusa, manuscript in preparation.
9 E. M. Flanigen and R. L. Patton, *US Pat.*, 4073865, 1978.
10 J. L. Guth, H. Kessler, P. Caullet, J. Hazm, A. Merrouche and J. Patarin, *Proc. Ninth Int. Zeolite Conf.*, ed. R. von Ballmoos, J. B. Higgins and M. M. J. Treacy, Butterworth, Heinemann, 1993, p. 215.
11 L. A. Villaescusa, M. A. Camblor and A. Corma, *Sp. Pat.*, P9602685, 1996.
12 J. M. Thomas, J. Klinowski, S. Ramdas, B. K. Hunter and D. T. B. Tennakoon, *Chem. Phys. Lett.*, 1983, **102**, 158.
13 S. I. Zones, *WO Pat.*, 95/22507, 1995.

*Received in Cambridge, UK, 29th January 1997; Com. 7/00672A*

# Asymmetric synthesis of a rigid diphosphine ligand containing two phosphorus and four carbon stereogenic centres by means of a chiral palladium complex promoted Diels–Alder reaction

**Pak-Hing Leung,*[a] S. Selvaratnam,[a] C. R. Cheng,[a] K. F. Mok,[a] Nicholas H. Rees[b] and William McFarlane[b]**

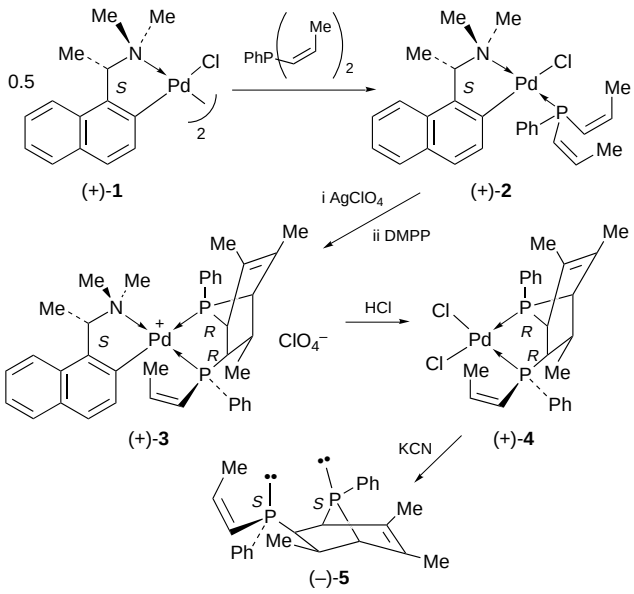
[a] *Department of Chemistry, National University of Singapore, Kent Ridge, Singapore 0511*
[b] *Department of Chemistry, University of Newcastle Upon Tyne, Newcastle Upon Tyne, UK NE1 7RU*

**An optically pure diphosphine ligand containing two phosphorus and four carbon stereogenic centres is prepared efficiently by a chiral organopalladium complex promoted asymmetric Diels–Alder reaction between phenyldi[(*Z*)-prop-1-enyl]phosphine and 1-phenyl-3,4-dimethylphosphole.**

Despite the critical importance of chiral phosphines in asymmetric catalysis,[1] only a few P-chiral phosphines have been obtained by means of asymmetric synthesis.[2] The majority of this class of chiral auxiliaries were prepared by optical resolutions which involved the somewhat technically tedious separation of diastereomers. Here we present a simple and highly stereoselective synthesis of a rigid diphosphine that contains two phosphorus and four carbon stereogenic centres.

As illustrated in Scheme 1, the monodentate phenyldi[(*Z*)-prop-1-enyl]phosphine was coordinated regiospecifically[3] to the chloro-bridged dimer (+)-**1** to give the monomeric compound (+)-**2** as pale yellow prisms, $[\alpha]_D$ +99.1 (*c* 1.1, $CH_2Cl_2$).† Upon coordination, the prochiral dienophile is activated and is capable of reacting with an adjacent coordinated cyclic diene, 1-phenyl-3,4-dimethylphosphole (DMPP).[4] Thus, chloro abstraction from (+)-**2** in $CH_2Cl_2$ using silver perchlorate followed by treatment with DMPP at room temp. for 6 h gave the corresponding [4 + 2] cycloaddition product (+)-**3** as colourless prisms in 70% isolated yield, mp 151–153°C (decomp.), $[\alpha]_D$ +10.9 (*c* 2.0, $CH_2Cl_2$). X-Ray analysis of (+)-**3** confirmed that the desired diphosphine coordination complex had formed (Fig. 1) and established the absolute stereochemistries of the six chiral centres created: *R* at P(13), P(20), C(14), C(17) and *S* at C(18), C(19).‡ In $CDCl_3$, the two-dimensional ROESY NMR spectrum[5] of the complex indicated that the new bidentate and the (*S*)-naphthylamine auxiliary interact stereochemically (Fig. 2). For example, Me(23) at the P–vinylic function shows an NOE contact with the protruding aromatic proton at C(2) (signal G). Similarly, the phenyl group at the bridgehead phosphorus shows proximity to both neighbouring N–Me groups (signals H and I). More dramatically, long-range interactions such as Me(24)···Me(27) (signal J) and Me(24)···Me(29) (signal K) are clearly seen in the spectrum. In the solid state, the C(24)···C(27) and C(24···C(29) distances are 4.54 and 4.73 Å, respectively. These interchelate NOE interactions confirm that the new chiral diphosphine is sensitive to the stereochemical environment of the palladium coordination sphere.

The (*S*)-naphthylamine auxiliary can be chemoselectively removed from (+)-**3** by treatment with conc. HCl to give the dichlor species (+)-**4** as stable pale yellow prisms in 85% isolated yield, mp 249–250°C (decomp.), $[\alpha]_D$ +44.5 (*c* 1.1, $Me_2SO$). The free diphosphine can be liberated quantitively from (+)-**4** by treating a dichloromethane solution of the dichloro complex with aqueous cyanide for 10 min. The




**Scheme 1**

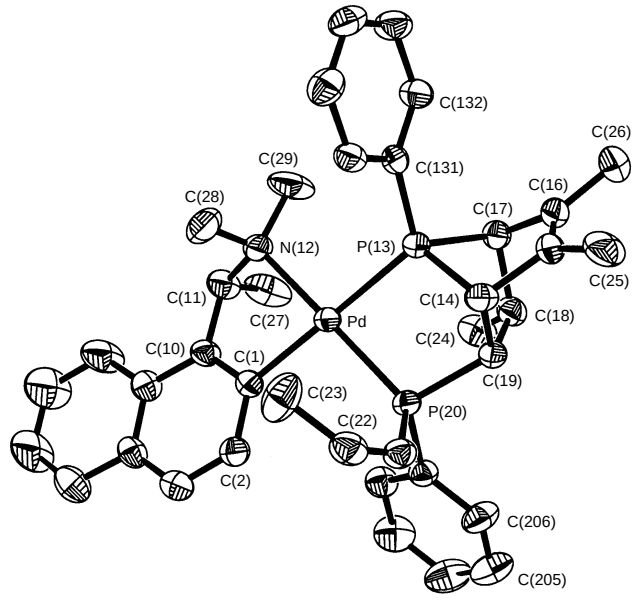



**Fig. 1** ORTEP drawing of the cation in (+)-**3** showing the six new chiral centres formed in the Diels–Alder reaction. Selected bond lengths (Å) and angles (°): Pd–C(1) 2.051(5), Pd–N(12) 2.129(4), Pd–P(13) 2.351(1), Pd–P(20) 2.256(2), P(13)–C(14) 1.853(5), P(13)–C(17) 1.843(5), C(15)–C(16) 1.323(7), P(20)–C(19) 1.852(5), P(20)–C(21) 1.806(5), C(21)–C(22) 1.312(7), C(14)–P(13)–C(17) 81.2(2), C(14)–C(19)–P(20) 105.0(3), C(19)–C(18)–C(24) 118.1(5), C(18)–C(19)–P(20) 115.3(3).

optically active diphosphine was obtained as a highly air-sensitive viscous colourless oil with $[\alpha]_D$ −53.9 (*c* 1.3, $CH_2Cl_2$). The $^{31}P$ NMR spectrum of free (−)-**5** in $CDCl_3$ exhibited a pair of doublets at δ 85.7 and 39.6 ($J_{PP}$ 51.3 Hz). The low-field signal confirms that the *exo–syn* stereochemistry is retained.[4] It is noteworthy that the apparent inversion of configuration that takes place at both phosphorus stereogenic centres when the diphosphine is liberated from the metal is merely a consequence of the Cahn–Ingold–Prelog (CIP) sequence rules.[6]

Investigations on the catalytic properties of transition-metal complexes containing this rigid optically active diphosphine are currently in progress.

We acknowledge the financial support for this project from the National University of Singapore (Grant RP 920606), research scholarships to S. S. and C. R. C. and UK EPSRC for NMR equipment.

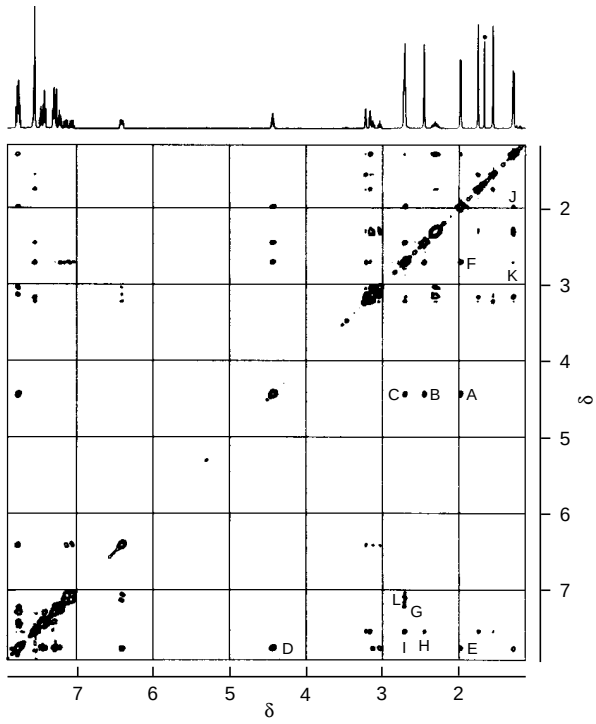



**Fig. 2** Two-dimensional $^1H$ ROESY NMR spectrum at 500 MHz of (+)-**3** in $CDCl_3$ at 296 K. Selected NOE contacts: A, H(11)–Me(27); B, H(11)–Me(28); C, H(11)–Me(29); D, H(11)–H(8); E, Me(27)–H(8); F, Me(27)–Me(29); G, H(2)–Me(23); H, Me(28)–Ph(13); I, M(29)–Ph(13); J, Me(24)–Me(27); K, Me(24)–Me(29); L, H(22)–Me(23). ●, $H_2O$ signal.

## Footnotes

* E-mail: chmlph@nus.sg

† All the new isolated complexes analysed satisfactorily. $^{31}P$ NMR (202 MHz, $CDCl_3$: (+)-**2**, δ −6.33; (+)-**3**, δ 13.50 [d, P(20) *J* 40.4 Hz], 112.78 [d, P(13), *J* 40.4 Hz]. Selected $^1H$ NMR for (+)-**3** (500 MHz, $CDCl_3$,) δ 1.29 [d, Me(24), *J* 7.3 Hz], 1.56 [s, Me(25)]. 1.75 [d, Me(26), *J* 1.2 Hz], 1.98 [d, Me(27), *J* 6.3 Hz], 2.31 [m, H(18)], 2.45 [d, Me(28), *J* 1.8 Hz], 2.70 [s, Me(29)], 2.71 [m, Me(23)], 3.08 [m, H(19)], 3.16 [m, H(17)], 3.22 [m, H(14)], 4.44 [m, H(11)], 6.41 [m, H(21)], 7.09 [m, H(22)], 7.21 [m, H(2)], 7.54 [m, Ph(13)], 7.70 [m, *o*-Ph(20)]. $^{31}P$ NMR for (+)-**4**: [202 MHz, $(CD_3)_2SO$], δ 5.54 (d, *J* 9.6 Hz), 121.90 (d, *J* 9.6 Hz).

‡ *Crystal data* for (+)-**3**: $C_{38}H_{45}ClNO_4P_2Pd$, *M* = 783. 54, monoclinic, space group $P2_12_12_1$; *a* = 8.931(3), *b* = 19.337(6), *c* = 21.428(8) Å, *U* = 3701(2) Å$^3$, *Z* = 4, $D_c$ = 1.406 g cm$^{-3}$, μ = 7.00 cm$^{-1}$. A clear prism of dimensions 0.10 × 0.25 × 0.30 mm was used. A total of 4779 independent reflections [$F > 3\sigma(F)$] were measured on a Siemens R3m/V four-circle diffractometer using graphite-monochromated Mo-Kα radiation (λ = 0.710 73 Å). Semiempirical absorption corrections were applied. The structure was solved by direct methods. All non-hydrogen atoms were refined anisotropically using full-matrix least squares based on $F^2$ to give $R$ = 0.036, $R_w$ = 0.071 and $S$ = 0.86. The absolute configuration was determined unambiguously by use of the Flack parameter [$x^+$ = 0.01]. Atomic coordinates, bond lengths and angles, and thermal parameters have been deposited at the Cambridge Crystallographic Data Centre (CCDC). See Information for Authors, Issue No. 1. Any request to the CCDC for this material should quote the full literature citation and the reference number 182/397.

## References

1 B. Bosnich, *Asymmetric Catalysis*, Martinus, Dordrecht, 1986; H. B. Kagan and M. Sasaki, in *The Chemistry of Organophosphorus Compounds*, ed. F. R. Hartley, Wiley, New York, 1990, vol. I, ch. 3; A. F. Noels, M. Graziani and A. J. Hubert, *Metal Promoted Selectivity in Organic Synthesis*, Kluwer, Dordrecht, 1991; K. M. Pietrusiewicz and M. Zablocka, *Chem. Rev*., 1994, **94**, 1375.

2 S. Juge, M. Stephan, J. A. Laffitte and J. P. Genet, *Tetrahedron Lett*., 1990, **31**, 6357; T. Imamoto, T. Oshiki, T. Onozawa and K. Sato, *J. Am. Chem. Soc*., 1990, **112**, 5244; E. J. Corey, Z. Chen and G. J. Tanoury, *J. Am. Chem. Soc*., 1993, **115**, 11000; A. R. Mcui, K. R. Campos and D. A. Evans, *J. Am. Chem. Soc*., 1995, **117**, 9075. B. H. Aw and P. H. Leung, *Tetrahedron: Asymmetry*, 1994, **5**, 1167; P. H. Leung, S. K. Loh, K. F. Mok, A. J. P. White and D. J. Williams, *Chem. Commun*., 1996, 591; S. Selvaratnam, K. F. Mok, P. H. Leung, A. J. P. White and D. J. Williams, *Inorg. Chem*., 1996, **35**, 4798.

3 S. Y. M. Chooi, T. S. A. Hor, P. H. Leung and K. F. Mok, *Inorg. Chem*., 1992, **31**, 1494.

4 J. A. Rahn, M. S. Holt, M. O'Neil-Johnson and J. H. Nelson, *Inorg. Chem*., 1988, **27**, 1316; R. Vac, J. H. Nelson, E. B. Milosavljevic, L. Solujic and J. Fischer, *Inorg. Chem*., 1989, **28**, 4132.

5 B. H. Aw, S. Selvaratnam, P. H. Leung, N. H. Rees and W. McFarlane, *Tetrahedron: Asymmetry*, 1996, **7**, 1753.

6 R. S. Cahn, C. K. Ingold and V. Prelog, *Angew Chem., Int. Ed. Engl*., 1966, **5**, 385.

*Received in Cambridge, UK, 14th January 1997; Com. 7/00314E*

# Unusual redox properties of a sterically hindered water-soluble chromium porphyrin. Electrochemical and spectral speciation

**Yu-Hui Lu and Y. Oliver Su***

*Department of Chemistry, National Taiwan University, Taipei, Taiwan 10764, Republic of China*

***meso*-Tetrakis(3-sulfonatomesityl)porphyrinato]chromium(III) [$Cr^{III}$(tsmp)] in aqueous solution can undergo electrochemical reduction to form a stable radical anion and oxidation to generate very stable radical cations $Cr^{III}$(tsmp$^{\cdot+}$) and O=$Cr^{IV}$(tsmp$^{\cdot+}$), which reacts with alkenes to produce enones at room temperature.**

Cytochrome P-450 is a monooxygenase which acts as a mediator for oxygen transfer reactions in biological systems. Metalloporphyrins have been intensively used as catalysts in mimicking cytochrome P-450.[1–3] Formation of a high-valent oxo–metal complex is essential for such catalytic reactions, and can be generated by reacting metalloporphyrins with chemical oxidants such as $ClO^-$,[4] $H_2O_2$,[5] alkyl peroxides,[6] percarboxylic acid,[7] iodosylbenzene,[8] $KHSO_5$,[9] or nitrogen oxides.[10] Also, electrochemical methods have been developed in aqueous[11] and non-aqueous[12] solutions.

We have synthesized water-soluble [*meso*-tetrakis(3-sulfonatomesityl)porphyrinato]chromium(III) [$Cr^{III}$(tsmp)] and found that the *ortho*-methyl groups in the tetramesitylporphyrin provided good steric protection for the *meso*-carbons upon radical cation or anion formation. The steric hindrance also prevents the formation of the μ-oxo dimer[13] in aqueous solutions. $Cr^{III}$(tsmp) exhibits two p$K_a$ values at 8.5 and 11.6, respectively, according to spectrophotometric titration and can be compared with the p$K_{a1}$ and p$K_{a2}$ values for [*meso*-tetrakis(4-sulfonatophenyl)porphyrinato]chromium(III) [$Cr^{III}$(tspp)] of 7.63 and 11.45, respectively.[14]

In pH 0.0–3.0 buffer solutions, $Cr^{III}$(tsmp)$(H_2O)_2$ undergoes a one-electron oxidation at a formal potential of 0.875 V (*vs.* Ag/AgCl), which is invariant in this pH range. $\lambda_{max}$ of the Soret band shifts from 448 to 424 nm and the molar absorption decreases dramatically. A broad band in the region 600–800 nm indicates cation radical formation in the porphine ring. An isosbestic point is observed clearly at 434 nm which shows only two components are present in equilibrium. The number of electrons transferred ($n$) and formal potential were determined from the literature procedure[15] to be 1.0 and +0.875 V, respectively. On the other hand, oxidation of $Cr^{III}$(tspp) leads to decomposition and the absorption spectrum becomes featureless. The instability of $Cr^{III}$(tspp) to oxidation is consistent with ring oxidation.[16]

In pH 3.2 buffer solution, two distinct one-electron transfer steps could be observed spectroelectrochemically and both oxidation products are very stable. The first oxidation follows the same pattern as that at pH 0.0–pH 3.0 and thus is ring-centred [Fig. 1(*a*)]. In the second step, $\lambda_{max}$ of the Soret band shifts from 424 to 406 nm with similar absorbance [Fig. 1(*b*)].

In pH 3.5–5.5 buffer solutions, the first oxidation potential is invariant while the second one shifts cathodically with increase in pH. The two oxidation potentials become closer and finally merge. In pH 6.0–8.0 buffer solutions, the two one-electron oxidations merge into a two-electron step (Fig. 2). The final absorption spectra are identical for both pH ranges. The number of electrons transferred ($n$) and the slope of formal potential were determined to be 2.0 and −56 mV/pH, respectively. Hence, according to the Nernst equation,[17] the oxidation step involves transfer of two protons upon two-electron oxidation.

Spectroelectrochemical studies show that O=Cr-$(H_2O)$(tsmp$^{\cdot+}$) is also very stable and can be reversibly reduced in 6.0 ⩽ pH ⩽ 8.0 buffer solution. This oxochromium(IV) porphyrin radical cation is apparently more stable than its iron counterpart.[11b]

Fig. 3 shows thin-layer spectra of $5 \times 10^{-5}$ M $Cr^{III}$-$(H_2O)_2$(tsmp) and 0.05 M cyclopent-2-en-1-acetic acid in pH 7.0 buffer solution at $E_{appl}$ = 0.73 V, which should correspond to a

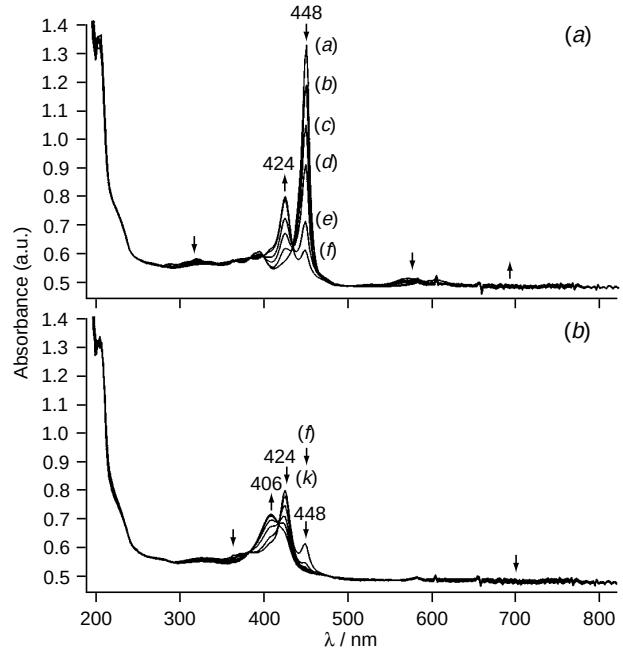



**Fig. 1** Thin-layer spectra of $5 \times 10^{-5}$ M Cr(tsmp) at different oxidation potentials in pH 3.2 buffer solution. $E_{appl}$ = (*a*) 0.50 (*b*) 0.83 (*c*) 0.85 (*d*) 0.87 (*e*) 0.91 (*f*) 0.95 (*g*) 1.01 (*h*) 1.07 (*i*) 1.09 (*j*) 1.11 (*k*) 1.15 V.

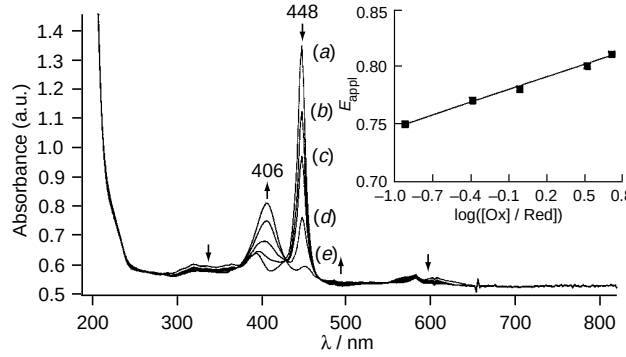



**Fig. 2** Thin-layer spectra of $5 \times 10^{-5}$ M Cr(tsmp) at different oxidation potentials in pH 6.0 buffer solution. $E_{appl}$ = (*a*) 0.50 (*b*) 0.77 (*c*) 0.78 (*d*) 0.80 (*e*) 0.89 V. Inset: plot of $E_{appl}$ *vs.* log ([Ox]/[Red]) for Cr(tsmp).

1 : 1 mixture of $Cr^{III}(H_2O)_2$(tsmp) and O=$Cr^{IV}$(tsmp$^{\cdot+}$). However, the absorption band of the latter at 406 nm is not seen. Rather, the absorption band of $Cr^{III}(H_2O)_2$(tsmp) decreases slightly. In the 240 nm region, an absorbance corresponding to enone formation[11] increases gradually. Bulk electrolysis of $5 \times 10^{-5}$ M $Cr^{III}(H_2O)_2$(tsmp) and 0.05 M cyclopent-2-en-1-acetic acid was conducted at $E_{appl}$ = 0.73 V in pH 7.0 buffer solution. Ion chromatography of the reaction mixture showed that the peak of cyclopent-2-en-1-acetic acid was reduced and a peak corresponding to cyclopent-2-en-4-one-1-acetic acid was observed (Fig. 3). The turnover rate is *ca*. 0.5 turnovers min$^{-1}$ based on the spectroelectrochemical results. Purging the solution with $N_2$ during electrolysis led to significantly less enone.

Electrocatalysis at $E_{appl}$ = 0.99 V in pH 3.6 buffer solution can also produce cyclopent-2-en-4-one-1-acetic acid but the turnover rate is slower, *ca*. 1/4 that at pH 7.0. To the best of our knowledge, this is the first reported oxochromium(IV) porphyrin radical cation reaction with alkenes in aqueous solutions at room temp.† The 424 nm band of $Cr^{III}(H_2O)_2$(tsmp$^{\cdot+}$) is still observed in the pH 3.6 solution while at pH 7.0 O=$Cr^{IV}(H_2O)$(tsmp$^{\cdot+}$) is reduced to $Cr^{III}(H_2O)_2$(tsmp). Reaction pathways are thus proposed in Scheme 1.[11]

We also observed spectroelectrochemically[15] that $Cr^{III}(H_2O)_2$(tsmp) can undergo stable and reversible one-electron reduction in pH 9.0 buffer solution. The Soret band shifts from 440 to 420 nm and the intensity drops to about 1/3. A broad band is observed in 600–800 nm region. The absorption spectrum indicates the formation of a radical anion, which is consistent with reported results by radiolysis.[20] It suggests that $Cr^{III}$, which has the surplus of an extra positive charge by subtracting the dianion of the porphyrin coordination, stabilizes the extra electron on the porphine ring. The stabilization effect does not occur with $Zn^{II}$(tsmp).[11*b*]

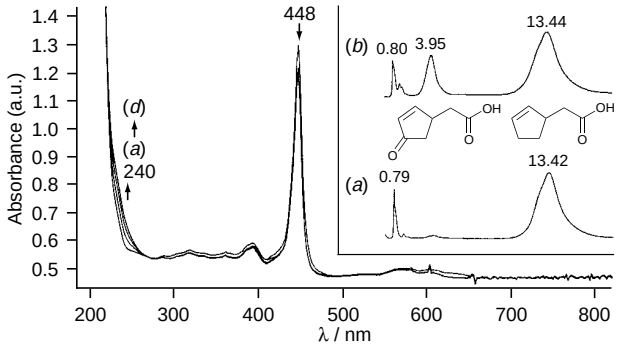
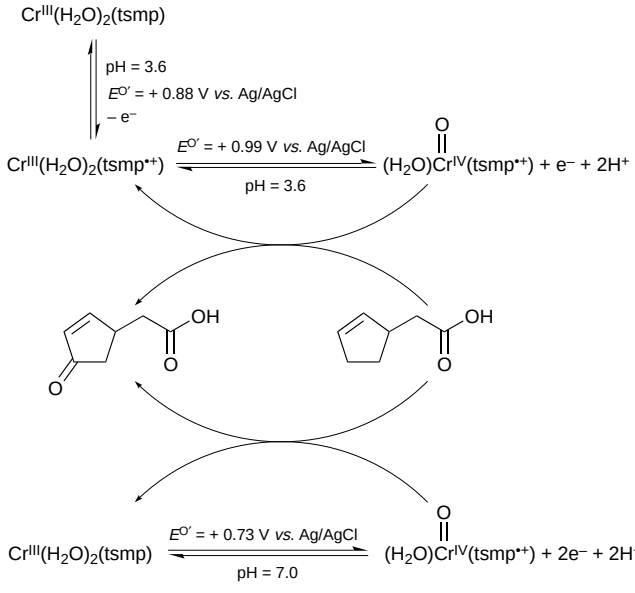



**Fig. 3** Thin-layer spectra of $5 \times 10^{-5}$ M Cr(tsmp) at different oxidation potentials in pH 7.0 buffer solution containing 0.05 M cyclopent-2-en-1-acetic acid. $E_{appl}$ = (*a*) 0.19 V (*b*) 0.73 V for 20 min. (*c*) 0.73 V for 30 min. (*d*) 0.73 V for 40 min. Inset: ion chromatograph of the mixture. (*a*) before electrolysis (*b*) after electrolysis at $E_{appl}$ = 0.73 V for 80 min.




**Scheme 1**

This work was supported by the National Science Council of the Republic of China under Grant No. NSC 85-2113-M-002-021.

## Footnotes

* E-mail: yosu@cc.ntu.edu.tw

† The reported catalytic oxidations of alkenes by chromium porphyrins have relied on the activity of the oxochromium(V) porphyrin. See refs. 18 and 19.

## References


1 *Catalytic Activation of Dioxygen by Metal Complexes*, ed. L. I. Simandi, Kluwer, Dordrecht, 1992.
2 *Metalloporphyrins in Catalytic Oxidations*, ed. R. A. Sheldon, Marcel Dekker, New York, 1994.
3 B. Meunier, *Chem. Rev.*, 1992, **92**, 1411; J. Muzart, *Chem. Rev.*, 1992, **92**, 113.
4 O. Bortolini and B. Meunier, *J. Chem. Soc., Chem. Commun.*, 1983, 1364.
5 P. Battioni, J.-P. Renaud, J. F. Bartoli and D. Mansuy, *J. Chem. Soc., Chem. Commun.*, 1986, 341; P. L. Anelli, S. Banfi, F. Legramandi, F. Montanari, G. Pozzi and S. Quici, *J. Chem. Soc., Perkin Trans. 1*, 1993, 1345.
6 L.-C. Yuan and T. C. Bruice, *J. Am. Chem. Soc.*, 1986, **108**, 1643; R. D. Arasasingham, S. Jeon and T. T. Bruice, *J. Am. Chem. Soc.*, 1992, **114**, 2536.
7 J. T. Groves and M. Stern, *J. Am. Chem. Soc.*, 1988, **110**, 8628.
8 J. T. Groves and Y. Watanabe, *J. Am. Chem. Soc.*, 1988, **110**, 8443.
9 J. Bernadou, A.-S. Fabiano, A. Robert and B. Meunier, *J. Am. Chem. Soc.*, 1994, **116**, 9375.
10 W.-H. Wong, D. Ostovic and T. C. Bruice, *J. Am. Chem. Soc.*, 1987, **109**, 3428.
11 (*a*) M. H. Liu and Y. O. Su, *J. Chem. Soc., Chem. Commun.*, 1994, 971; (*b*) M. H. Liu, C. Y. Yeh and Y. O. Su, *Chem. Commun.*, 1996, 1437; (*c*) T.-S. Lee and Y. O. Su, *J. Electroanal. Chem.*, 1996, **414**, 69; (*d*) M. H. Liu and Y. O. Su, *J. Electroanal. Chem.*, 1997, in the press.
12 S. E. Creager and R. W. Murray, *Inorg. Chem.*, 1985, **24**, 3824; S. E. Creager, S. A. Rayback and R. W. Murray, *J. Am. Chem. Soc.*, 1986, **108**, 4225; J. T. Groves, Z. Gross and M. Stern, *Inorg. Chem.*, 1994, **33**, 5065.
13 D. J. Liston, B. J. Kennedy, K. S. Murray and B. O. West, *Inorg. Chem.*, 1985, **24**, 1561; D. J. Liston and B. O. West, *Inorg. Chem.*, 1985, **24**, 1568.
14 K. R. Ashley, J. G. Leipoldt and V. K. Joshi, *Inorg. Chem.*, 1980, **19**, 1608; J. G. Leipoldt, S. S. Basson and D. R. Rabie, *J. Inorg. Nucl. Chem.*, 1981, **43**, 3239; K. R. Ashley and J. Kuo, *Inorg. Chem.*, 1988, **27**, 3556.
15 S.-M. Chen and Y. O. Su, *J. Chem. Soc., Chem. Commun.*, 1990, 491.
16 Y. O. Su, D. Kim and T. G. Spiro, *J. Electroanal. Chem.*, 1988, **246**, 363.
17 *Electrochemical Methods. Fundamentals and Applications*, ed. A. J. Bard and L. R. Faulkner, Wiley, New York, 1980.
18 W. A. Lee, L.-C. Yuan and T. C. Bruice, *J. Am. Chem. Soc.*, 1988, **110**, 4277; J. M. Garrison and T. C. Bruice, *J. Am. Chem. Soc.*, 1989, **111**, 191; S. Jeon and T. C. Bruice, *Inorg. Chem.*, 1991, **30**, 4311; 1992, **31**, 4843.
19 J. W. Buchler, K. L. Lay, L. Castle and V. Ullrich, *Inorg. Chem.*, 1982, **21**, 842.
20 D. M. Guldi, P. Hambright, D. Lexa, P. Neta and J.-M. Savéant, *J. Phys. Chem.*, 1992, **96**, 4459; D. M. Guldi and P. Neta, *J. Chem. Soc., Faraday Trans.*, 1992, **88**, 2013; 2337.


*Received in Cambridge, UK, 5th December 1996; Com. 6/08211D*

# Stable boat and chair isomers of dimetal complexes containing the $[M_2(\mu\text{-dppm})_2]$ unit (M = Re; dppm = $Ph_2PCH_2PPh_2$)

**Wengan Wu, Phillip E. Fanwick and Richard A. Walton***

*Department of Chemistry, Purdue University, West Lafayette, IN 47907-1393, USA*

**Reactions of the triply bonded complexes $[Re_2Br_3(\mu\text{-dppm})_2(CO)(CNR)]Y$ (dppm = $Ph_2PCH_2PPh_2$; R = 2,6-dimethylphenyl; Y = $O_3SCF_3$, $PF_6$) with RNC afford edge-sharing bioctahedral complexes of the type $[Re_2(\mu\text{-Br})_2(\mu\text{-dppm})_2Br(CO)(CNR)_2]Y$, which are shown to contain Re–Re single bonds and exist in novel isomeric forms with boat and chair conformations for the $Re_2(\mu\text{-dppm})_2$ unit.**

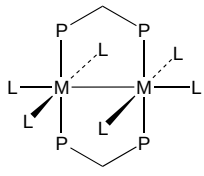
In the course of studies aimed at delineating the factors which determine the stabilities of various structural isomers of dimetal complexes of types **A** and **B** (P–P represents a bridging bidentate phosphine), and the mechanisms of the isomer conversions, we have encountered a new class of isomers which have relevance to the structural chemistry of open bioctahedra (**A**) and edge-sharing bioctahedra (**B**), as well as other classes of complexes which contain a $M_2(\mu\text{-dppm})_2$ unit (dppm = $Ph_2PCH_2PPh_2$).[1–3]

The mixed carbonyl–isocyanide complexes of the type $[Re_2X_3(\mu\text{-dppm})_2(CO)(CNR)_2]Y$ (X = Cl, Br; R = 2,6-dimethylphenyl; Y = $O_3SCF_3$, $PF_6$) have been identified in at least five different structural forms, with metal–metal bond orders ranging from 3 to 0 (Scheme 1).[4–10] In some instances, isomerizations have been observed to occur at elevated temperatures (*i.e.* **1** → **2** and **3** → **4**).[4–6,9] Previously, the X-ray structural characterizations of salts of **1**–**5** have shown that the $Re_2(\mu\text{-dppm})_2$ unit (two fused five-membered rings in the cases of **1**, **2**, **3** and **5** and an eight-membered ring for **4**) exists in a stable boat conformation. Further characterizations of the bromo complex **5** have now established that preparative samples of the $O_3SCF_3$ and $PF_6$ salts consist of a mixture of two isomers with the same basic structure as that depicted in Scheme 1, but which differ in possessing either a boat (**5a**) or chair (**5b**) conformation for the $Re_2(\mu\text{-dppm})_2$ unit.

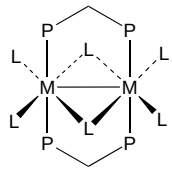
The reactions of the unsymmetrical, coordinatively unsaturated dirhenium(II) complexes $[Re_2Br_3(\mu\text{-dppm})_2(CO)(CNR)]Y$ (Y = $O_3SCF_3$, $PF_6$)[8,10] with 1 equiv. of RNC in $CH_2Cl_2$ or acetone afford mixtures which contain the salts of the isomeric pair (**5a**)Y and (**5b**)Y as the major product [yield 40–70%, product ratio (**5a**)Y : (**5b**)Y *ca.* 5 : 95).† The spectroscopic and electrochemical properties of diamagnetic (**5a**)Y and (**5b**)Y are very similar,[8] and do not readily permit a distinction to be made between the structures of the components of the mixture. However, an X-ray structure determination on a crystal of (**5a**)$PF_6$ has shown[8] the structure to be that of the isomer with the boat conformation [the Re–Re distance is 3.0456(8) Å]. Although we have been unable to obtain single crystals of the major isomers (**5b**)$O_3SCF_3$ and (**5b**)$PF_6$ directly from the preparative reaction mixtures which are of a quality suitable for an X-ray structure determination, we have done so by an alternative procedure.

Treatment of (**5b**)$O_3SCF_3$ with $[Co(\eta^5\text{-}C_5H_5)_2]$ in $CH_2Cl_2$ affords the paramagnetic, one-electron reduced product $[Re_2Br_3(\mu\text{-dppm})_2(CO)(CNR)_2]$ **6** in high yield. The addition of $[Fe(\eta^5\text{-}C_5H_5)_2]PF_6$ to a $CH_2Cl_2$ solution of **6** re-oxidizes it quantitatively to (**5b**)$PF_6$.‡ The structural identities of **6** and (**5b**)$PF_6$ have been established by X-ray crystallography which shows that both possess a chair conformation for the $Re_2(\mu\text{-dppm})_2$ unit.§ An ORTEP representation of the structure of **6** is shown in Fig. 1; the structure of the dirhenium cation present in (**5b**)$PF_6$ is essentially the same, with the exception of the parameters associated with the $Re_2(\mu\text{-Br})_2$ unit (see caption for Fig. 1). The Re–Re bond distances in the structures of (**5b**)$PF_6$ and **6** are 3.028(2) and 3.8023(10) Å, respectively; the former is essentially identical to the Re–Re distance in (**5a**)$PF_6$.[8] These distances, along with the magnetic properties of (**5b**)$PF_6$ and **6**, are consistent with the presence of Re–Re bonds of order one and zero, respectively. Accordingly, the one-electron reduction of (**5b**)$O_3SCF_3$ leads to a species $[(RNC)_2Re(\mu\text{-Br})_2(\mu\text{-dppm})_2ReBr(CO)]$ **6** which can best be considered formally as a charge separated $Re^{I}$–$Re^{II}$ species (18e–17e) rather than one containing a Re–Re bond of order 0.5.

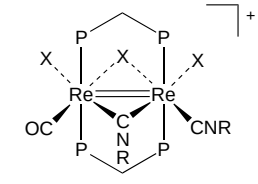
The properties of (**5b**)$PF_6$ as prepared by the ferrocenium oxidation of **6** are identical to samples which are present in previously reported[8] mixtures of (**5a**)$PF_6$ and (**5b**)$PF_6$. Accordingly, the reduction of (**5b**)$O_3SCF_3$ to **6**, and the oxidation of **6** to (**5b**)$PF_6$ occur with preservation of a chair conformation. The



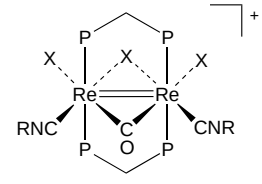
**A**



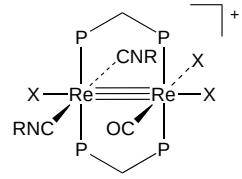
**B**



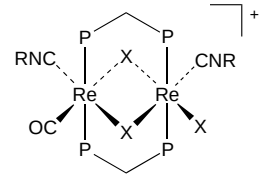
**1** (X = Cl, ref. 4)



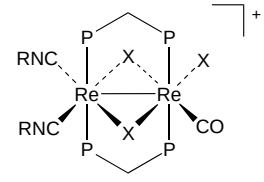
**2** (X = Cl, refs. 5,6)



**3** (X = Cl or Br, refs. 7,8)



**4** (X = Cl or Br, ref. 9)



**5** (X = Br, ref. 8)

**Scheme 1** Isomers of $[Re_2X_3(\mu\text{-dppm})_2(CO)(CNR)_2]^+$ **1**–**5**

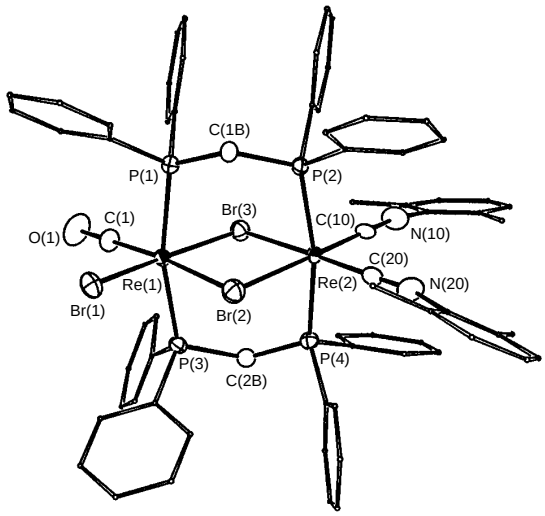



**Fig. 1** ORTEP representation of the structure of the dirhenium complex $[Re_2Br_3(\mu\text{-dppm})_2(CO)(CNR)_2]$ in crystals of **6**·$CH_2Cl_2$, showing the chair conformation for the $Re_2(\mu\text{-dppm})_2$ unit. Thermal ellipsoids are drawn at the 50% probability level except for the phenyl group atoms of the dppm ligands and the xylyl groups of the RNC ligands which are circles of arbitrary radius. Selected bond distances (Å) and bond angles (°): Re(1)···Re(2) 3.8023(10), Re(1)–C(1) 1.838(14), Re(1)–Br(1) 2.509(2), Re(1)–Br(2) 2.6184(11), Re(1)–Br(3) 2.5813(9), Re(1)–P(1) 2.444(2), Re(1)–P(3) 2.451(2), Re(2)–C(10) 1.929(7), Re(2)–C(20) 1.931(7), Re(2)–Br(2) 2.6289(9), Re(2)–Br(3) 2.6560(11), Re(2)–P(2) 2.407(2), Re(2)–P(4) 2.387(2); P(1)–Re(1)–P(3) 166.02(5), C(1)–Re(1)–Br(1) 91.9(4), C(1)–Re(1)–Br(3) 97.7(4), Br(1)–Re(1)–Br(2) 82.81(4), Br(3)–Re(1)–Br(2) 87.75(3), P(4)–Re(2)–P(2) 168.58(5), C(10)–Re(2)–C(20) 90.1(3), C(20)–Re(2)–Br(2) 94.7(2), C(10)–Re(2)–Br(3) 89.1(2), Br(2)–Re(2)–Br(3) 85.99(3), Re(1)–Br(2)– Re(2) 92.87(3), Re(1)–Br(3)–Re(2) 93.09(3). Note: the structure of the dirhenium cation present in the structure of (**5b**)$PF_6$·$2CH_2Cl_2$ is very similar to that of **6**, with the exception of the presence of a Re–Re single bond [3.028(2) Å]. This leads primarily to differences in the parameters for the $Re_2(\mu\text{-Br})_2$ unit between these two structures. The bond distances in the structure of the cation **5b** which correspond to Re(1)–Br(2), Re(1)–Br(3), Re(2)–Br(2), Re(2)–Br(3) in the structure of **6** are 2.556(2), 2.553(2), 2.599(3), and 2.604(3) Å, respectively, while the angles (°) which correspond to Re(1)–Br(2)–Re(2) and Br(2)–Re(1)–Br(3) are 71.95(9) and 109.50(9)°, respectively.

large increase in Re–Re distance which accompanies the reduction of the salts (**5b**)Y to **6** (*ca*. 0.78 Å), would be expected to reduce the ring strain in the $Re_2(\mu\text{-dppm})_2$ unit and allow conversion to the most stable ring conformation. Since no conformation change occurs, we can conclude that the chair conformation, as is already present in (**5b**)Y, is more stable than the boat conformation in (**5a**)Y. This is supported by the observation that solutions of (**5a**)$PF_6$ in dichloromethane convert slowly to the more thermodynamically stable isomer (**5b**)$PF_6$ (96 h at 25 °C, 24 h at reflux) in essentially quantitative yield.

Further studies are underway to examine the scope of this chemistry as it relates to other $M_2(\mu\text{-dppm})_2$ complexes, and the redox behaviour of the less stable boat conformer **5a**, which is typically obtained in much lower yield than **5b**.

Support from the National Science Foundation (Grant CHE94-09932 to R. A. W.) is gratefully acknowledged.

## Footnotes

* E-mail: walton@chem.purdue.edu

† An alternative method for the synthesis of mixtures of (**5a**)Y and (**5b**)Y is the reaction of the triply bonded, neutral complex $[Re_2Br_4(\mu\text{-dppm})_2(CO)(CNR)]$ with a mixture of TlY (1 equiv.) and RNC (2 equiv.).

‡ *Synthesis*: **6**: a sample of (**5b**)$O_3SCF_3$ (120 mg, 0.0659 mmol) was mixed with $[Co(\eta^5\text{-}C_5H_5)_2]$ (12.5 mg, 0.0661 mmol) in $CH_2Cl_2$ (15 ml) at 25 °C. The reaction mixture, which changed from red–brown to green within 5 min, was stirred for 30 min, filtered, and the volume of the filtrate reduced to 2 ml. An equal volume of $Et_2O$ was added to induce precipitation of yellow $[Co(\eta^5\text{-}C_5H_5)_2]O_3SCF_3$, which was filtered off and the filtrate stripped to dryness. The green residue (**6**) was washed with $Et_2O$ (3×5 ml) and dried; yield 94 mg (85%). Anal. Calc. for $C_{69}H_{62}Br_3N_2OP_4Re_2$: C, 49.59; H, 3.73; N, 1.68. Found: C, 49.21; H, 3.65; N, 1.48%. Recrystallization from $CH_2Cl_2$–$C_2H_5CO_2Me$ afforded X-ray quality crystals. IR spectrum (Nujol mull): ν(CN) 2050(sh), 2012s and 1919s, (br) $cm^{-1}$; ν(CO) 1858vs $cm^{-1}$. Cyclic voltammogram (0.1 M $Bu^n_4NPF_6$–$CH_2Cl_2$, Pt-bead electrode, ν = 200 mV $s^{-1}$, potentials *vs*. Ag/AgCl): $E_{\frac{1}{2}}^{ox3}$ = +1.43 V, $E_{\frac{1}{2}}^{ox2}$ = +0.65 V, $E_{\frac{1}{2}}^{ox1}$ = +0.10 V, $E_{\frac{1}{2}}^{red}$ = −0.83 V. Magnetic moment: $\mu_{eff}$ ≈ 1.4 $\mu_B$ (Evans method, $CDCl_3$).

(**5b**)$PF_6$: a mixture of **6** (42.0 mg, 0.0251 mmol) and $[Fe(\eta^5\text{-}C_5H_5)_2]PF_6$ (9.0 mg, 0.027 mmol) in 10 ml of $CH_2Cl_2$ was stirred at 25 °C. A change from green to red–brown occurred within a few min. After a period of 1 h the reaction solution was reduced in volume to *ca*. 1 ml, and 15 ml of $Et_2O$ added to induce precipitation of (**5b**)$PF_6$, which was filtered off and washed with $Et_2O$ (3 × 5 ml); yield 41.5 mg (91%). Recrystallization from $CH_2Cl_2$–$Pr^i_2O$ afforded X-ray quality crystals. The properties of (**5b**)$PF_6$ were identical to those of samples obtained previously[8] as mixtures with (**5a**)$PF_6$.

§ *Crystal data*: **6**·$CH_2Cl_2$ at 203 K: space group $P\bar{1}$ with $a$ = 13.330(4), $b$ = 16.226(3), $c$ = 16.327(6) Å, α = 99.29(2), β = 90.66(3), γ = 91.59(2)°, $Z$ = 2, $D_c$ = 1.674 g $cm^{-3}$. An empirical absorption correction was applied (μ = 5.434 $mm^{-1}$). Structure solved using the Enraf-Nonius structure determination package (MolEN) and refined through the use of SHELXL-93. Hydrogen atoms included but not refined. A cut-off $F_o^2 > 2\sigma(F_o)^2$ used for *R*-factor calculations to give $R(F_o)$ = 0.040, $R_w(F_o^2)$ = 0.112, and GOF = 1.099. Disorder between the terminal CO and Br ligands associated with Re(1); a disorder model involving fractional CO and Br occupancies for each site was refined satisfactorily to 0.707(6) CO/0.293(6) Br for one site and 0.293(6)CO/ 0.707(6)Br for the other.

(**5b**)$PF_6$·$2CH_2Cl_2$ at 203 K: space group $P\bar{1}$ with $a$ = 13.800(5), $b$ = 16.927(8), $c$ = 17.556(5) Å, α = 87.05(7), β = 77.56(6), γ = 69.67(7)°, $Z$ = 2, $D_c$ = 1.757 g $cm^{-3}$. An empirical absorption correction was applied (μ = 5.153 $mm^{-1}$). All other procedures as for the structure of **6**·$CH_2Cl_2$; the final residuals were $R(F_o)$ = 0.065, $R_w(F_o^2)$ = 0.185, and GOF = 1.021. Disorder between the terminal CO and Br ligands modeled satisfactorily as 0.50/0.50 for both sites. Full structural details for **6**·$CH_2Cl_2$ and (**5b**)$PF_6$·$2CH_2Cl_2$ will be published later.

Atomic coordinates, bond lengths and angles, and thermal parameters have been deposited at the Cambridge Crystallographic Data Centre (CCDC). See Information for Authors, Issue No. 1. Any request to the CCDC for this material should quote the full literature citation and the reference number 182/393.

## References

1 R. J. Puddephatt, *Chem. Soc. Rev*., 1983, 99.
2 B. Chaudret, B. Delavaux and R. Poilblanc, *Coord. Chem. Rev*., 1988, **86**, 191.
3 F. A. Cotton and R. A. Walton, *Multiple Bonds Between Metal Atoms*, 2nd edn., Oxford University Press, Oxford, UK, 1993.
4 W. Wu, P. E. Fanwick and R. A. Walton, *Organometallics*, 1997, **16**, in the press.
5 L. B. Anderson, F. A. Cotton, K. R. Dunbar, L. R. Falvello, A. C. Price, A. H. Reid and R. A. Walton, *Inorg. Chem*., 1987, **26**, 2717.
6 W. Wu, P. E. Fanwick and R. A. Walton, *Inorg. Chim. Acta*, 1996, **242**, 81.
7 W. Wu, P. E. Fanwick and R. A. Walton, *J. Cluster Sci*., 1996, **7**, 155.
8 W. Wu, P. E. Fanwick and R. A. Walton, *Inorg. Chem*., 1996, **35**, 5484.
9 W. Wu, P. E. Fanwick and R. A. Walton, *J. Am. Chem. Soc*., 1996, **118**, 13 091.
10 W. Wu, P. E. Fanwick and R. A. Walton, *Inorg. Chem*., 1995, **34**, 5810.

*Received in Bloomington, IN, USA, 21st January 1997; Com. 7/00555E*

# Unusual conversions of a zwitterionic polyfused triazine with electron-deficient dienophiles

**Zsuzsanna Riedl,[a] György Hajós,*[a] András Messmer,[a] Antal Rockenbauer,[a] László Korecz,[a] Gert Kollenz,[b] Walter M. F. Fabian,[b] Karl Peters[c] and Eva-Maria Peters[c]**

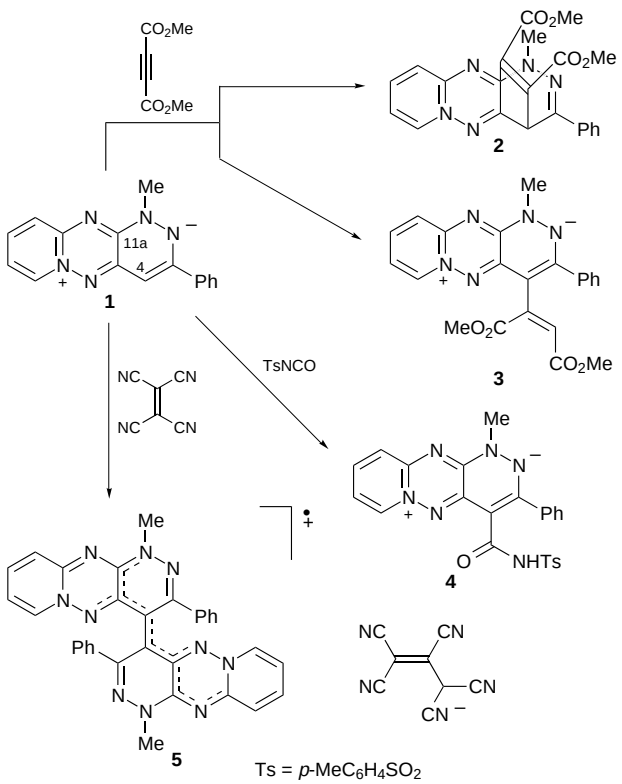
[a] *Central Research Institute for Chemistry, Hungarian Academy of Sciences, PO Box 17, H-1525, Budapest, Hungary*
[b] *Karl Franzens University, Department of Organic Chemistry, Heinrichstr. 28, A-8010 Graz, Austria*
[c] *Max-Planck-Institut for Solid Material Research, D-70569, Germany*

**Investigation of reactions of the zwitterionic polycycle 1 with electron-deficient dienophiles revealed that Michael addition products 3** and **4, selective cycloadducts 2 and, in a special case, a stable dimeric radical cation 5 are formed.**

As a result of our investigations on ring transformation reactions[1] with furo[2,3-*e*]pyrido[1,2-*b*][1,2,4]triazinium salts[2] we synthesized some new zwitterionic polyazaheterocycles (*e.g.* the 1,3-disubstituted pyrido[1,2-*b*]pyridazino[3,4-*e*]-[1,2,4]triazine derivative **1**), the reactivity of which towards dienophiles, because of their highly dipolar character seemed of particular interest. We decided to investigate the reactivity of the new derivative **1** with three different dienophiles (*i.e.* dimethyl acetylenedicarboxylate, toluene-*p*-sulfonyl isocyanate and tetracyanoethylene) (Scheme 1).

We found that zwitterion **1**, when treated with dimethyl acetylenedicarboxylate at room temperature in $CH_2Cl_2$ for 24 h, afforded a mixture of two components (1 : 1), which were separated by chromatography (silica, chloroform–methanol, 25 : 1). Structure elucidation of the more polar component (a pale yellow spot by TLC) by $^1$H NMR spectroscopy revealed the formation of the bridged [3 + 2]-cycloadduct **2**,†‡ whereas the less polar product (a brown–red spot) was proved *via* an X-ray analysis (Fig. 1) to be the Michael adduct **3**.†§ The X-ray data confirmed the *Z* configuration at the exocyclic double bond, as well as a strong predominance of the mesomeric form outlined on Scheme 1. The selective formation of cycloadduct **2** seemed to be in agreement with the results of the FMO analysis of this compound: positions 4 and 11a had the highest $c_{LUMO}$ values (0.6 and 0.54, respectively). Formation of Michael addition products was again experienced when **1** was reacted with toluene-*p*-sulfonyl isocyanate, thus exclusively affording compound **4**.¶

An unexpected result was obtained from the reaction of tricycle **1** with tetracyanoethylene. A blue crystalline compound was obtained, which could not be analysed by NMR spectroscopy. An X-ray investigation (Fig. 2) revealed the structure of compound **5** containing a highly delocalized radical cation, as established by EPR spectroscopy.‖ The central 'formal' C=C bond is the longest [C(1)–C(21) = 145.9 pm] of all the C–C bonds present in **5**.** The two tricyclic fused triazine units are highly twisted [torsion angle C(2)–C(1)–




**Scheme 1**

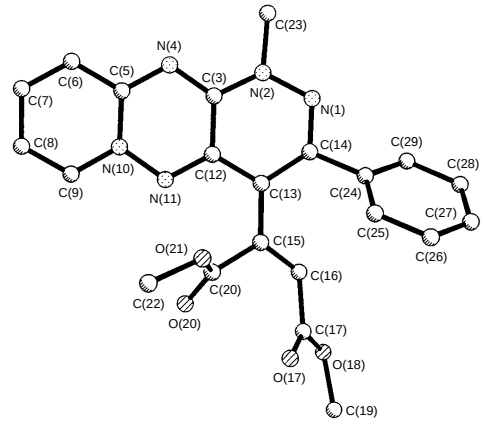



**Fig. 1** Stereoview of **3**

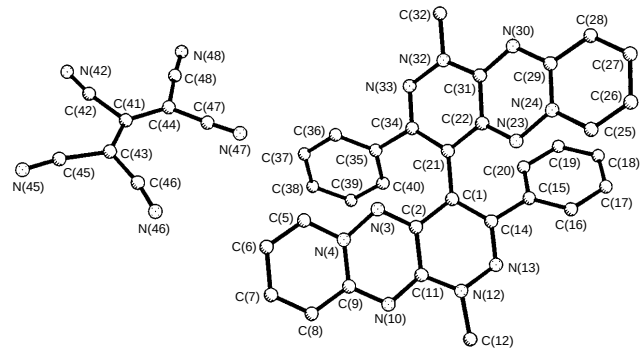



**Fig. 2** Stereoview of **5**

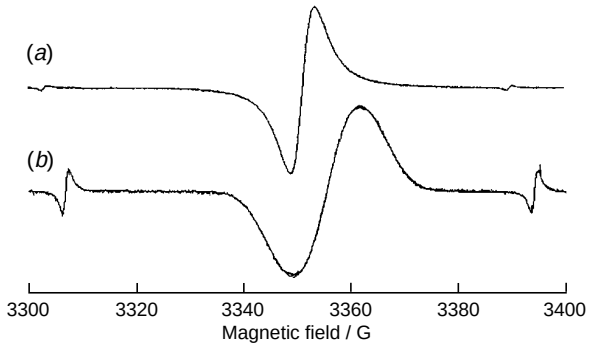



**Fig. 3** Calculated and experimentally found EPR spectra of **5** in (*a*) the solid and (*b*) the solution states

C(21)–C(22) = 131.3°] and arranged in an *anti* conformation. Formation of this unusual product can be rationalized by the primary attack of the reagent at position 4, followed by an oxidative coupling to the dimer radical cation which is stabilized by the pentacyanopropenide anion.[3,4] These anions are usually obtained either from dimerization of tetracyanoethylene under basic conditions[5] or through base-catalysed addition of malononitrile to tetracyanoethylene.[6]

The EPR spectrum of **5** (Fig. 3) showed one broad singlet, and dilution and degassing did not produce any hyperfine structure. Computer fitting of the line profile (Fig. 3) gave a perfect fit if proton splittings are removed from the AM1 calculations,[7] while the *K* proportionality constant for nitrogen is adjusted ($K_N$ = 2340) in the hyperfine coupling *versus* spin density relation $A_N = K_\rho$). The largest nitrogen coupling (2.6 G) is reasonable for the dimer cation radical when compared to the largest nitrogen coupling (7.1 G) in the monomeric cation radical of isoalloxanine,[8] and the observed *g* factor (2.0037) is also typical for cation radicals.[9] No EPR signal for an anion radical (*g* = 2.0026, well resolved hyperfine structure[10]) was detected.

Financial support from the Foundation 'Action Austria Hungary 23u17', as well as from OTKA 0167520, is gratefully acknowledged.

## Footnotes

† All new compounds gave spectroscopic and analytical data in accordance with their assigned structures.

‡ *Selected spectroscopic data* for **2**: Pale Yellow Crystals, mp 218–20 °C; $^1$H NMR (400 MHz, $CDCl_3$): δ 7.62 (1 H, d, H-7), 7.75, 7.35–7.30 (5 H, m, Ph), 7.25 (1 H, t, H-9), 7.06 (1 H, d, H-10), 6.52 (1 H, t, H-8), 4.84 (1 H, s, H-4), 3.83, 3.80 (6 H, s, $CO_2$Me), 3.27 (3 H, s, Me).

§ *Selected spectroscopic data* for **3**: Brown–red crystals, mp 198–202 °C; $^1$H NMR (400 MHz, $CDCl_3$— δ 7.32 (1 H, d, H-7), 7.30 (5 H, m, Ph), 7.05 (1 H, t, H-9), 7.02 (1 H, t, H-8), 6.30 (1 H, d, H-10), 5.83 (1 H, s, H-2′), 3.58, 3.42 (6 H, s, COMe), 3.13 (3 H, s, Me).

*X-Ray crystallographic analysis* of **3**. The brown–red crystal was grown by slow evaporation of an acetonitrile solution of **3**. The crystal was monoclinic, space group *C*2/*c*, with cell dimensions *a* = 1917.5(7), *b* = 838.6(3), *c* = 2561.1(9) pm and *V* = 4051(2) × $10^6$ pm$^3$. *Z* = 8 molecules ($C_{22}H_{18}N_5O_4$, $M_w$ = 417.43) in the unit cell ($D_c$ = 1.369 g cm$^{-3}$). Intensity data were measured for 6448 reflections (4651 unique) on a Siemens R3m/V diffractometer using a crystal with dimensions 0.4 × 1.3 × 0.25 mm (Mo-Kα radiation, graphite monochromator, Wyckoff-scan, θ range = 1.75–27.5°, linear absorbtion coefficient = 0.09 mm$^{-1}$, absorbtion correction: Ψ-scan). The structure was solved by direct phase determination and refined by full-matrix-least square analysis using Siemens SHELXTL PLUS (Micro VAX II); all hydrogen positions of riding model had fixed isotropic *U*. The data-to-parameter ratio was 12.83, *R*, $R_w$ = 0.054, 0.049; weighting scheme $w = 1/\sigma^2(F)$. The largest difference peak and hole in the last map were 0.32 and 0.21 e Å 4$^{-3}$, respectively.

¶ *Selected spectroscopic data* for **4**: Brown–red crystals, mp 228–230 °C (DMF); IR (KBr) ν/cm$^{-1}$ 3180, 3040, 2920, 1660, 1620, 1590, 1560, 1530.

‖ *Selected spectroscopic data* for **5**: Blue crystals, mp 240–42 °C; IR ν(KBr)/cm$^{-1}$ 2196, 1627, 1561, 1508.

** *X-Ray crystallographic analysis* of **5**: The dark blue crystal was triclinic, space group $P\bar{1}$, with cell dimensions *a* = 1299.7(2), *b* = 1349.7(2), *c* = 1078.0(2) pm, α = 92.31(1), β = 95.88(1), γ = 99.70(1)° and *V* = 1850.9(5) × $10^6$ pm$^3$. *Z* = 2 molecules ($C_{32}H_{24}N_{10}$ + $C_8N_5$, $M_w$ = 376.38) in the unit cell ($D_c$ = 1.282 g/cm$^{-3}$). Intensity data were measured for 8485 reflections (8485 unique) on a Siemens R3m/V diffractometer using a crystal with dimensions 0.5 × 0.7 × 0.15 mm (Mo-Kα radiation, graphite moinochromator, Wyckoff-scan, θ range 1.75–27.5°, linear absorbtion coefficient = 0.08 mm$^{-1}$, absorbtion correction: Ψ-scan). The structure was solved by direct phase determination and refined by full-matrix least-squares analysis using Siemens SHELXTL PLUS (MicroVAX II); all hydrogen positions of riding model had fixed isotropic *U*. The data-to-parameter ratio was 12.14, *R*, $R_w$ = 0.076, 0.069, respectively; weighting scheme $w = 1/\sigma^2(F)$. The largest difference peak and hole in the last map were 1.01 and 0.46 e Å$^{-3}$, respectively. Atomic coordinates, bond lengths and angles, and thermal parameters have been deposited at the Cambridge Crystallographic Data Centre (CCDC). See Information for Authors, Issue No. 1. Any request to the CCDC for this material should quote the full literature citation and the reference number 182/410.

## References

1 Z. Juhász-Riedl, G. Hajós, G. Kollenz and A. Messmer, *Chem. Ber*., 1989, **122**, 1935.
2 Z. Juhász-Riedl, G. Hajós, E. Gács-Baitz, G. Kollenz and A. Messmer, *Chem. Ber*., 1990, **123**, 1415.
3 K. Wallenfels, *Angew. Chem*., 1964, **76**, 275.
4 A. J. Fatiadi, *Synthesis*, 1986, 249; J. S. Miller, J. C. Calabrese, H. Rommelmann, S. R. Chittipeddi, J. H. Zhang, W. M. Reiff and A. J. Epstein, *J. Am. Chem. Soc*., 1987, **109**, 769; T. J. Johnson, K. W. Hipps and R. D. Willet, *J. Phys. Chem*., 1988, **92**, 6892.
5 W. J. Middleton, E. L. Little, D. D. Coffman and V. A. Engelhardt, *J. Am. Chem. Soc*., 1958, **80**, 2795.
6 C. L. Dickinson, D. W. Wiley and B. C. McKusick, *J. Am. Chem. Soc*., 1960, **82**, 6132.
7 M. J. S. Dewar, E. G. Zoebisch, E. F. Healy and J. J. P. Stewart, *J. Am. Chem. Soc*., 1985, **107**, 3902; T. Clark, VAMP, Erlangen Vectorized Molecular Orbital Package, Ver. 4.40, Computer-Chemie-Centrum, University of Erlangen-Nürnberg, Germany; S. F. Nelsen, *J. Chem. Soc., Perkin Trans. 2*, 1988, 1005.
8 J. Westerling, H. I. X. Mager and W. Berends, *Tetrahedron*, 1975, **31**, 437.
9 A. J. Dobbs, '*g*-Factors of Free Radicals in Fluid Solution', in *Electron Spin Resonance, Vol. 2, Specialist Periodical Reports*, ed. R. O. C. Norman, The Chemical Society, London, 1974, pp. 281–294.
10 W. D. Philipps, J. C. Rowell and S. I. Weissmann, *J. Chem. Phys*., 1960, **33**, 626.

*Received in Cambridge, UK, 12th December 1996; Com. 6/08344G*

# Poly(ethylene glycol) (PEG) as a reagent support: the preparation and utility of a PEG–triarylphosphine conjugate in liquid-phase organic synthesis (LPOS)

**Paul Wentworth Jr., Anthony M. Vandersteen and Kim D. Janda***

*Department of Chemistry, The Scripps Research Institute and the Skaggs Institute for Chemical Biology, 10550 N. Torrey Pines Rd., La Jolla CA92037, USA*

**The preparation and application in the Staudinger and Mitsunobu reactions of a liquid-phase, poly(ethylene glycol)-arylphosphine conjugate 1 is described.**

The development of both soluble and insoluble functionalized polymers is currently of tremendous interest in the fields of combinatorial chemistry, peptide synthesis and nucleic acid synthesis.[1] The conversion of reactions in solution to either soluble or insoluble polymer-supported chemical methodologies, with the benefits of ease of product isolation, minimization of side-reactions and the ability to use an excess of reagents to drive a reaction to completion, is an on-going challenge.

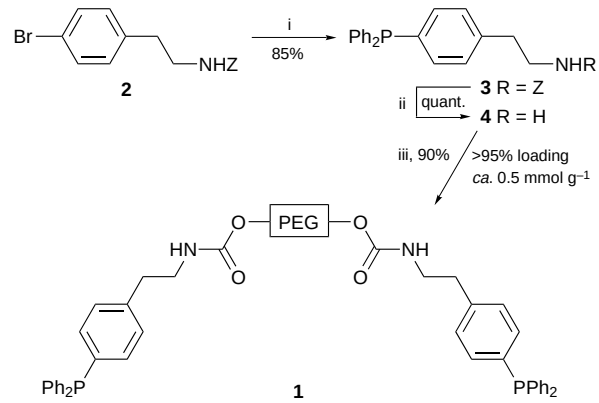
Because of problems associated with the use of insoluble polymeric reagents and substrates under heterogeneous conditions, such as lowered reactivities, extended reaction times, diffusion-limited reactivity and reagent leaching,[2] soluble-matrices such as poly(ethylene glycol) (PEG),[3] fluorous supports,[4] linear polystyrenes[5] and polyethylene[6] are receiving increasing attention for combinatorial synthesis[7] and as supports for heterogeneous catalysts.[8] Previous work from our group has demonstrated the preparation and utility of PEG derivatives for liquid-phase combinatorial synthesis (LPCS),[7] peptidomimetic synthesis[9] and as ligand supports for the Sharpless dihydroxylation reaction.[10]

We now report an extension of liquid-phase synthesis into the field of reagent supports.[11] In our latest effort, we have conjugated $PPh_3$ to $PEG_{3400}$ and studied its utility in the Staudinger and Mitsunobu reactions. There are a number of reports highlighting the utility of $PPh_3$ bound to solid polymeric supports, such as polystyrene and copolymers of styrene and divinylbenzene, in the Wittig reaction[12] and for azide reduction.[13] An important component of this work is a comparison between the liquid- and solid-phase reagent approaches.

For any successful polymer-supported strategy optimal loading is essential, therefore two important considerations biased our choice of a suitable matrix. First, the PEG polymer was chosen to have two free hydroxy groups per polymer strand. Second, we chose the PEG polymer with the lowest molecular weight possible which did not suffer from changes in its physical properties after attachment of the triphenylphosphine moiety. $PEG_{3400}$ was found to satisfy both of these requirements. Two synthetic strategies were developed for the preparation of the PEG-triarylphosphine conjugates. In the first, $PEG_{3400}$ was reacted with an excess of *p*-bromophenyl isocyanate in dichloromethane, to generate a carbamate linked *p*-bromophenyl PEG derivative in greater than 95% yield. The loading was almost quantitative as judged by the $^1H$ NMR resonance of the PEG methylene protons $\alpha$ to the carbamate linkage. The diphenylphosphine group was incorporated by a modification of the method of Relles and Schluentz.[14] A stirred suspension of the carbamate PEG derivative in THF was reacted with lithium diphenylphosphide under reflux for 16 h. $^1H$ NMR Spectral analysis showed that this reaction was accompanied by significant decomposition of the PEG support, determined by the appearance of multiple methylene signals outside the methylene envelope ($\delta_H$ 3.2–3.8) of the PEG polymer, reducing the yield of reagent to < 70%. No attempt was made to further characterize the PEG decomposition products, rather in a second approach, the substituted triarylphosphine derivative was synthesized separately from the polymer and incorporated in the final step (Scheme 1). Benzyloxycarbonyl (Z) protected *p*-bromophenethylamine **2** was reacted with potassium diphenylphosphide in degassed THF under reflux for 8 h. After silica gel chromatography, the triarylphosphine derivative **3** was obtained in 85% yield. Following a quantitative deprotection of the Z group of **3** by catalytic hydrogenation (Pd–C), amine **4** reacted smoothly with the bis-*p*-nitrophenyl carbonate of $PEG_{3400}$ (Shearwater Polymers Inc.) in degassed $CH_2Cl_2$ at room temp. for 2 h. Repeated precipitation of the reaction mixture from diethyl ether gave the PEG–phosphine reagent **1** in 90% yield, with no accompanying decomposition of the polymer. The oxidation state and purity of the phosphine reagent were confirmed by $^{31}P$ NMR spectroscopy ($\delta_P$ $CDCl_3$ −5.8) with no detectable arylphosphine oxide ($\delta_P$ $CDCl_3$ 28.4) being formed during the conjugation reaction. Polymer loading, measured by both $^1H$ NMR spectroscopy and by following the formation of *p*-nitrophenol during the course of reaction, was excellent (> 95%, 0.5 mmol of phosphine per gram of polymer).

One of the many chemoselective procedures available for the reduction of azides is the Staudinger reaction.[15] A recent report has shown that $PPh_3$ linked to polystyrene beads can perform the Staudinger reaction for a number of azides.[13] However, no precedence exists for a soluble polymer supported approach for this reaction. By using the soluble support **1** a range of alkyl and aryl azides were smoothly converted into their respective amines at room temperature. The reaction times were all faster than with an insoluble $PPh_3$ reagent and in one case no reduction was observed with the polystyrene-supported phosphine highlighting the improved utility of this liquid-phase methodology (Table 1).

The Mitsunobu[16] reaction is a commonly used procedure, with wide-ranging application throughout organic chemistry. It




**Scheme 1** *Reagents and conditions*: i, $KPPh_2$ (6.0 equiv.), THF, reflux, 24 h; ii, 10% Pd–C, $H_2$ (30 psi), $CH_2Cl_2$, room temp. 2 h; iii, $PEG_{3400}$–$PNP_2$, 2 h $CH_2Cl_2$, room temp.

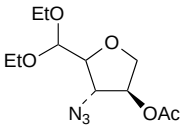
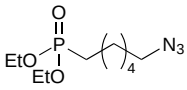
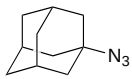
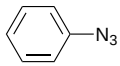
can be complicated by side-product formation with the result that isolation of the products is usually accompanied by chromatography. In an attempt to address such problems for combinatorial library synthesis, an insoluble polymer-supported approach to Mitsunobu ether formation has been reported.[17] However, in this example, the alcohol substrate was linked to the support and the reagent, $PPh_3$, was in solution, so the reaction was still heterogeneous in nature.

By utilising our liquid-phase approach, reaction of PEG–phosphine **1** with phenol and each of the alcohols outlined in Table 2, in the presence of diethylazodicarboxylate (DEAD), gave etherification under ambient conditions. Precipitation of the oxidized PEG–phosphine conjugate **1** from diethyl ether allowed isolation of the product, aryl alkyl ethers, in analytically pure form, without the need for silica gel chromatography. As found for the preceding Staudinger reduction, reaction times were shorter with the soluble reagent than for the heterogeneous reaction. In addition benzyl alcohol gave no ether product when treated with the solid phase reagent.

In summary, we have shown that a soluble PEG–phosphine reagent can be readily prepared and utilised in the liquid-phase Staudinger and Mitsunobu reactions. Product isolation is routine and the reactions are high yielding. The use of this novel liquid-phase reagent in LPOS offers considerable advantages over solution-based methodologies because the side-product is removed by simple filtration after precipitation of the spent reagent, so no chromatography is necessary. Furthermore, an excess of the reagent can be used without subsequent problems during purification. By comparison with the heterogeneous reaction, product yields are equivalent but reaction times are shorter and the reagent proved much more versatile, reacting with all the substrates tested. This work has highlighted a novel soluble polymer-supported reagent approach to LPOS and offers a new addition to polymer-bound phosphorane chemistries. Perhaps one of the most exciting features of this reagent is its generality, with potential application to many other phosphine-based methodologies such as the Wittig olefination and bromination of alcohols. More generally, for most reactions that are accompanied by unwanted side-products, this procedure may offer a routine solution to the problems encountered during product purifications. Finally this soluble polymer-supported reagent methodology should be compatible with high-throughput organic synthesis and automation technology.

This work supported in part by the R. W. Johnson Pharmaceutical Research Institute and the Skaggs Institute for Chemical Biology.

**Table 1** Comparative Staudinger reactions using **1** and polystyrene–$PPh_3$ with azides

| | **1** | | Polystyrene–$PPh_3$ | |
|---|---|---|---|---|
| Azide | Yield (%) | *t*/h[a,b] | Yield (%) | *t*/h[b,c] |
|  | 95 | 2 | – | No reaction |
|  | 98 | 1.5 | 82 | 8 |
|  | 91 | 4.5 | 95 | 11 |
|  | 90 | 3 | 94 | 3.5 |

[a] In a typical reaction the azide (1 mmol) and $PEG_{3400}$–$PPh_3$ conjugate (1.1 mmol) were dissolved in $CH_2Cl_2$ (5 ml), water was then added (1.1 equiv.) and the reaction mixture was stirred at room temp. On completion, the reaction mixture was concentrated to half its volume and poured onto cold diethyl ether. The spent PEG reagent was filtered under aspirator pressure using a frit and the mother liquor was evaporated to dryness to give the amines in analytically pure form. [b] The reaction was considered complete when no starting azide was detected by TLC. [c] In a typical reaction the conditions were the same as above with the exception that **1** was replaced by a polystyrene–$PPh_3$ resin (1.1 mmol) (Aldrich Chem. Co.). The work-up involved filtration of the resin followed by evaporation of the filtrate.

**Table 2** Alkyl aryl ethers prepared[a] with either **1** or polystyrene–$PPh_3$

| | **1** | | Polystyrene–$PPh_3$ | |
|---|---|---|---|---|
| Alcohol | Yield (%) | *t*/h[b] | Yield (%) | *t*/h[c] |
| Butan-1-ol | 85 | 3 | 87 | 8 |
| Isopropanol | 88 | 5 | 94 | 7 |
| Allyl alcohol | 87 | 2 | 82 | 5 |
| Benzyl alcohol | 75 | 10 | — | No reaction |

[a] In a typical reaction, phenol (1 mmol) was added to **1** or polystyrene–$PPh_3$ (1.5 mmol) in $CH_2Cl_2$ (3 ml) and stirred for 20 min. Then the listed alcohol (1 mmol) and DEAD (1.1 mmol) were added and the reaction stirred at room temp. [b] On completion, the reaction mixture was concentrated to half volume and the urea side-product filtered. The reaction mixture was then poured onto diethyl ether. The used PEG reagent was filtered and the mother liquor concentrated to give the pure ether products. [c] The workup procedure involved filtration of the resin and concentration to allow removal of the hydrazine side-product. The pure ether products were isolated by evaporation of the $CH_2Cl_2$.

## References


1 D. J. Gravert and K. D. Janda, in *Molecular Diversity and Combinatorial Chemistry: Libraries and Drugs*, ed. I. M. Chaiken and K. D. Janda, ACS Symposium Series, 1996, pp. 118; E. Bayer, *Angew. Chem., Int. Ed. Engl*., 1991, **30**, 113; J. S. Fruchtel and G. Jung, *Angew. Chem., Int. Ed. Engl*., 1996, **35**, 17; B. J. Backes and J. A. Ellmann, *Chem. Rev*., 1996, **96**, 550.

2 R. H. Andreatta and H. Rink, *Helv. Chim. Acta*., 1973, **56**, 1205; M. Mutter and E. Bayer, in *The Peptides*, ed. J. Mieinhofer and E. Gross, Academic, New York, 1978, vol. 3.

3 M. Mutter, *Tetrahedron Lett*., 1978, **31**, 2839; V. N. R. Pillai and M. Mutter, 1980, **45**, 5364.

4 D. P. Curran, *J. Org. Chem*., 1996, **61**, 6480; D. P. Curran, *Chemtracts: Org. Chem*., 1996, **9**, 75.

5 M. M. Shemyakin, Yu. A. Ovchinnikov, A. A. Kiryushkin and I. V. Kozhevnikova, *Tetrahedron Lett*., 1965, **27**, 2323; Yu. A. Ovchinnikov, A. A. Kiryushkin and I. V. Kozhevnikova *J. Gen. Chem. USSR*, 1968, **38**, 2551.

6 D. E. Bergbreiter, *CHEMTECH*, 1987, 686.

7 H. Han, M. M. Wolfe, S. Brenner and K. D. Janda, *Proc. Natl. Acad. Sci. USA*, 1995, **92**, 6419; K. D. Janda and H. Han, in *Methods in Enzymology*, ed. J. A. Abelson, Academic, New York, vol. 267, pp. 234.

8 J. C. Phelps and D. E. Bergbreiter, *Tetrahedron Lett*., 1989, **30**, 3915; D. E. Bergbreiter and R. Chandran, *J. Am. Chem. Soc*., 1987, **109**, 174; D. E. Bergbreiter and D. A. Weatherford, *J. Org. Chem*., 1989, **54**, 2726.

9 H. Han and K. D. Janda, *J. Am. Chem. Soc*., 1996, **118**, 2539.

10 H. Han and K. D. Janda, *J. Am. Chem. Soc*., 1996, **118**, 7632.

11 P. Wipf and S. Venkatraman, *Tetrahedron Lett*., 1996, **37**, 4659.

12 S. V. Mckinley and J. W. Rakshys, *J. Chem. Soc., Chem. Commun*., 1972, 134; M. Bernard and W. T. Ford, *J. Org. Chem*., 1983, **48**, 326.

13 T. Holletz and D. Cech, *Synthesis*, 1994, 789.

14 H. M. Relles and R. W. Schluenz, *J. Am. Chem. Soc*., 1974, **96**, 6469.

15 H. Staudinger, *Helv. Chim. Acta*., 1919, **2**, 635; R. D. G. Cooper, *Pure Appl. Chem*., 1987, **59**, 485.

16 O. Mitsunobu, *Synthesis*, 1980, 1.

17 V. Krchnak, Z. Flegelova, A. S. Weichsel and M. Lebl, *Tetrahedron Lett*., 1995, **36**, 6193.


*Received, 12th December 1996; Com. 6/08388I*

# Bifunctional molecular accelerator for catalytic asymmetric allylation: $R_2MSR'$ (M = B, Al) as a useful synergetic reagent

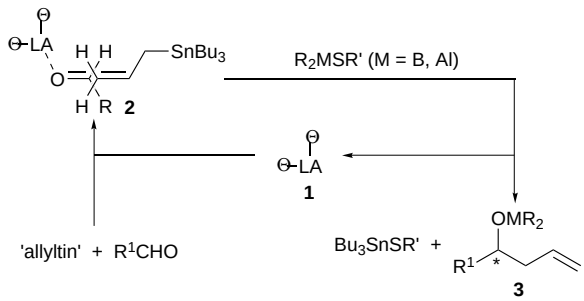
**Chan-Mo Yu,* Ha-Soon Choi, Won-Hyuk Jung, Hyuk-Jun Kim and Jaewook Shin**

*Department of Chemistry, Sung Kyun Kwan University, Suwon 440-746, Korea*

**Dramatic acceleration of the catalytic process of asymmetric allylation of achiral aldehydes is observed by the utilization of the bifunctional synergetic reagents $R_2MSR'$ (M = B, Al).**

Chiral homoallyl alcohols are very useful intermediates for the enantioselective synthesis of complex chiral substances.[1] The exceptional power of the allyl transfer reaction to aldehydes in forming optically active homoallylic alcohols has been enhanced by newly developed enantioselective versions, especially chiral Lewis acid-catalysed addition of the allyl transfer reagent to a carbonyl functionality.[2] The development of synthetic methods for achieving absolute stereoselection by the utilization of chiral catalysts increasingly requires precise control of the reaction pathway based on mechanistic behaviour and the rational design of new reagents and processes.[3] The geometrical possibilities offered by chemical transformation together with the predictable power of mechanistic behaviour can allow the design of new catalytic systems. Recently, we demonstrated the utilization of the molecular accelerator $Me_3SiSPr^i$, designed on the basis of mechanistic speculation, for catalytic asymmetric allylation that resulted in not only a significant increase in the reaction rate but also a reduced dosage of chiral catalyst.[4] Described herein is an extension of the molecular accelerating strategy aimed at finding new reagents and realizing useful and practical asymmetric syntheses. This research led to the discovery of the remarkable synergetic reagent $R_2M–SR'$ (M = B, Al), which expedites the catalytic process of asymmetric allylation with high levels of enantioselectivity. In the present research, two major advances have been made in the enantioselective synthesis of homoallylic alcohols: (i) this system exhibited a dramatic increase in catalytic ability; (ii) alkylthioborane has advantages over alkylthiosilane in terms of efficacy, stereoselectivity and applicability to other systems.

Our rationale for the introduction of a molecular accelerator into the catalytic system was based on speculation illustrated in Scheme 1. In order to increase catalytic ability, regeneration of chiral catalyst **1** as a consequence of dissociation of product **3** from the reaction complex must be achieved. We reasoned that if a bifunctional synergetic reagent, *i.e.* $R_2MSR'$(M = B, Al), could control the catalytic allylation process *via* the Sn–S (enhancement of Sn–C bond breaking) and M–O (dissociation of product **3**) bond forming steps to reinforce regeneration of catalyst **1**, practical and efficient catalytic asymmetric allylation might be realized in a predictable fashion. The key to this prediction is the strong Sn–S and M–O bonds relative to the weaker M–S bond.

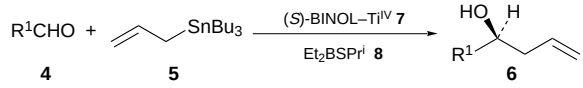



**Scheme 1**

The starting point of this present research was the availability of $R_2BSR'$; alkylthioboranes are readily prepared in quantity, easily purified by distillation and stable to storage.[5] Several alkylthioboranes ($R_2BSR'$: R = Et, Bu; R′ = Et, $Pr^i$, Bu, $Bu^t$, Ph) were prepared and examined for their abilities as synergetic reagents in the allylation of hydrocinnamaldehyde with allyltributylstannane in the presence of (*S*)-BINOL–$Ti^{IV}$ complex **7** (10 mol%).† Preliminary investigations indicated that efficient allylation was realized with $Et_2BSPr^i$ at −20 °C for 5 h (93% isolated yield; 97% ee); this result is superior to the control system (−20 °C for 70 h, 78% isolated yield with 94% ee). Upon optimisation, the catalytic allyl transfer reaction was conducted by dropwise addition of $Et_2BSPr^i$ (**8**, 1.2 equiv.) in $CH_2Cl_2$ at −20 °C to the mixture of **4** ($R^1$ = $CH_2CH_2Ph$, 1.0 equiv.) and **5** (1.3 equiv.) in the presence of chiral catalyst **7** (10 mol%) and 4 Å molecular sieves. After 5 h at −20 °C, the resulting reaction mixture was treated with aqueous $NaHCO_3$. After work up, the final purification of the homoallyl alcohol can be effected by silica gel chromatography.

This discovery prompted us to carry out more experiments with reduced amounts of chiral catalyst. Indeed, we were delighted to find that the same reaction proceeds with 1 mol%

**Table 1** Enantioselective allylation accelerated by $Et_2BSPr^i$ [a,b]




| Entry | $R^1$ | Catalyst **7** (mol%)[c] | Yield (%)[d] | Ee (%)[e] |
|---|---|---|---|---|
| 1 | $PhCh_2CH_2$ | 10 | 93 | 97 |
| 2 | $PhCH_2CH_2$ | 5 | 89 | 95 |
| 3 | $PhCH_2CH_2$ | 2 | 81 | 93 |
| 4 | $PhCH_2CH_2$ | 1 | 77 | 93 |
| 5 | $C_6H_{11}$ | 10 | 87 | 97 |
| 6 | $C_6H_{11}$ | 5 | 82 | 95 |
| 7 | $C_6H_{11}$ | 2 | 75 | 91 |
| 8 | $C_6H_{11}$ | 1 | 61 | 88 |
| 9 | c-$C_6H_{11}$ | 10 | 77 | 93 |
| 10 | c-$C_6H_{11}$ | 5 | 67 | 88 |
| 11 | c-$C_6H_{11}$ | 2 | 53 | 85 |
| 12 | c-$C_6H_{11}$ | 1 | 44 | 75 |
| 13 | Ph | 10 | 89 | 96 |
| 14 | Ph | 5 | 84 | 93 |
| 15 | Ph | 2 | 71 | 91 |
| 16 | Ph | 1 | 57 | 77 |

[a] All reactions were run at −20 °C in $CH_2Cl_2$. [b] Absolute configurations were determined by direct comparison with specific rotations of known alcohols. [c] BINOL–$Ti(OPr^i)_4$ = 2:1 ratio. [d] Chromatographed yields. [e] Enantiomeric exess was determined using chiral shift reagent [Eu(hfc)$_3$] and by preparation of (+)-MTPA ester derivatives, analysis by $^1$H NMR spectroscopy and comparison with authentic samples.

(*S*)-BINOL–$Ti^{IV}$ complex to give a 77% isolated yield with 93% ee. Additional experiments with various aldehydes were carried out and representative results are summarized in Table 1. The reactions are generally complete after 5–8 h at −20 °C. We observed that better enantioselectivities and chemical yields were obtained with less hindered aldehydes compared to the more substituted cyclohexanecarbaldehyde.

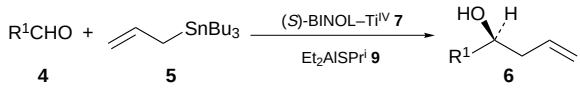
Although the role of $Et_2BSPr^i$ in accelerating the allyl transfer reaction must be a consequence of the dissociation of the product from reaction complex with regeneration of chiral catalyst, the exact mechanism has not been rigorously elucidated, and may involve concerted or stepwise participation.[6]

We next turned our attention to examining the feasibility of this system using a alkylthioalane.[7] Several catalytic allylations of aldehydes employing $R_2AlSR'$ were conducted under identical conditions to those described above, and the use of $Et_2AlSPr^i$ **9** proved to be most effective. Representative results are listed in Table 2. It is worthy of note that the catalyst–$Et_2AlSPr^i$ system affords high enantioselectivities and chemical yields with 10 mol% of catalyst after 5 h, while with reduced amount of catalyst, especially less than 5 mol%, sharply reduced levels of asymmetric induction are observed.‡

In conclusion, an efficient method for the catalytic enantioselective addition of allyltributylstannane to aldehyde is described which employs a molecular accelerator, $R_2MSR'$, and 1–2 mol% of BINOL–$Ti^{IV}$, furnishing homoallylic alcohol in good yield with useful levels of enantioselectivity. We believe that this approach to increasing catalytic ability by the use of synergetic reagents could be widely applicable, not only in the field of asymmetric carbonyl addition, but also in other related reactions.

Generous financial support of this work by grants from the Ministry of Education (BSRI 96-3420) and the Korea Science and Engineering Foundation (KOSEF 94-0501-08-01-03) is gratefully acknowledged.

**Table 2** Enantioselective allylation accelerated by $Et_2AlSpr^i$ [a]




**4** **5** **6**

| Entry | $R^1$ | Catalyst **7** (mol%) | Yield (%) | Ee (%) |
|---|---|---|---|---|
| 1 | $PhCh_2CH_2$ | 10 | 97 | 92 |
| 2 | $PhCH_2CH_2$ | 5 | 91 | 63 |
| 3 | $C_6H_{11}$ | 10 | 96 | 95 |
| 4 | $C_6H_{11}$ | 5 | 83 | 85 |
| 5 | c-$C_6H_{11}$ | 10 | 50 | 77 |
| 6 | c-$C_6H_{11}$ | 5 | 45 | 57 |
| 7 | Ph | 10 | 92 | 93 |
| 8 | Ph | 5 | 81 | 79 |

[a] All conditions are the same as in Table 1.

## Footnotes

† For the allylation reaction described herein, optimal enantioselectivity are observed with 2 : 1 BINOL–$Ti(OPr^i)_4$ in the presence of activated 4 Å molecular sieves.

‡ According to the results of control experiments under identical condition except for the use of catalyst, $Et_2BSPr^i$ did not catalyse allyl transfer, while $Et_2AlSPr^i$ turned out to be a very weak promoter. We did not observe any transmetallation reactions between Sn and B or Al.

## References

1 For a recent example, see T. Q. Dinh, X. Du and R. W. Armstrong, *J. Org. Chem.*, 1996, **61**, 6606.

2 K. Ishihara, M. Mouri, Q. Gao, T. Maruyama, K. Furuta and H. Yamamoto, *J. Am. Chem. Soc.*, 1993, **115**, 11 490; J. A. Marshall and Y. Tang, *Synlett*, 1992, 653; G. E. Keck, K. H. Tarbet and L. S. Geraci, *J. Am. Chem. Soc.*, 1993, **115**, 8467; G. E. Keck and L. S. Geraci, *Tetrahedron Lett.*, 1993, **34**, 7287; G. E. Keck, D. Krishnamurthy and M. C. Grier, *J. Org. Chem.*, 1993, **58**, 6543; A. L. Costa, M. G. Piazza, E. Tagliavini, C. Trombini and A. Umani- Ronchi, *J. Am. Chem. Soc.*, 1993, **115**, 7001; P. Bedeshi, S. Casolari, A. L. Costa, E. Tagliavini and A. Umani-Ronchi, *Tetrahedron Lett.*, 1995, **36**, 7897; J. W. Faller, D. W. Sams and X. Liu, *J. Am. Chem. Soc.*, 1996, **118**, 1217; A. Yanagisawa, H. Nakashima, A. Ishiba and H. Yamamoto, *J. Am. Chem. Soc.*, 1996, **118**, 4723; P. G. Cozzi, P. Orioli, E. Tagliavini and A. Umani- Ronchi, *Tetrahedron Lett.*, 1997, **38**, 145.

3 R. Noyori, *Asymmetric Catalysis in Organic Synthesis*, Wiley, New York, 1994; *Catalytic Asymmetric Synthesis*, ed. I. Ojima, VCH, New York, 1993.

4 C.-M. Yu, H.-S. Choi, W.-H. Jung and S.-S. Lee, *Tetrahedron Lett.*, 1996, **37**, 7095.

5 A. Pelter, K. Smith and H. C. Brown, *Borane Reagents*, Academic Press, New York, 1988, p. 436; A. Pelter, K. Rowe, D. N. Sharrocks, K. Smith and C. J. Subramanyam, *J. Chem. Soc., Dalton Trans.*, 1976, 2087.

6 The formation of $Bu_3SnSPr^i$ was confirmed by direct comparison with an authentic sample prepared from a literature procedure, see D. N. Harpp, T. Aida and T. H. Chan, *Tetrahedron Lett.*, 1979, **20**, 2853.

7 Diethyl(isopropylthio)alane **9** was prepared *in situ* from $Et_3Al$ and $Pr^iSH$, see E. J. Corey and D. J. Beames, *J. Am. Chem. Soc.*, 1973, **95**, 5829.

*Received in Cambridge, UK, 23rd January 1997; Com. 7/00543A*

# Catalytic asymmetric prop-2-ynylation involving the use of the bifunctional synergetic reagent $Et_2BSPr^i$

**Chan-Mo Yu,* Sook-Kyung Yoon, Ha-Soon Choi and Kwangwoo Baek**

*Department of Chemistry, Sung Kyun Kwan University, Suwon 440-746, Korea*

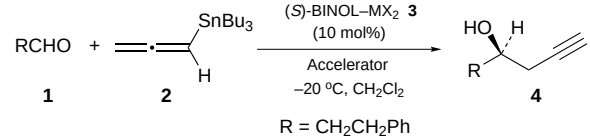
**Efficient catalytic asymmetric prop-2-ynylation of achiral aldehydes with allenyltributylstannane promoted by a BINOL–$Ti^{IV}$ complex (10 mol%) is achieved with high enantioselectivity by the use of $Et_2BSPr^i$.**

We report here a useful catalytic method for the enantioselective synthesis of but-3-yn-1-ols from the reaction of an allenyltin reagent with achiral aldehydes promoted by a chiral Lewis acid together with a synergetic reagent. Among the fundamental asymmetric reactions, allylic transfer from chiral reagents to a carbonyl functionality, forming enantiomeric rich homoallylic alcohols, attracts considerable attention from the synthetic community since the resulting products serve as chiral building blocks for multi-step syntheses.[1] In spite of the structural versatility of the prop-2-ynylic system, there have been few reports in this area compared with the allylic system, mainly due to a lack of reactivity and regiochemical problems.[2] While a couple of chiral allenyl reagents employing chiral auxiliaries have been developed to realize a highly enantio- and regio-selective synthesis of but-3-yn-1-ols,[3] catalytic chiral Lewis acids have been introduced in the reaction of aldehydes with allenylstannane.[4] Nonethless, the method for catalytic asymmetric prop-2-ynylation employing chiral Lewis acids is not ideal, mainly due to poor catalytic ability (50–100 mol%) and long reaction times (72–100 h). The method described herein is successful with a variety of aldehydes in the presence of a catalyst employing a bifunctional synergetic reagent and affords products of high enantiomeric purity. The process utilizes a readily available alkylthioborane as a synergetic reagent.

Our initial studies began with hydrocinnamaldehyde **1** and allenyltributylstannane **2**.[5] Treatment of **1** with **2** in the presence of (*S*)-BINOL–$Ti^{IV}$ (10 mol%) in $CH_2Cl_2$ at −20 °C for 24 h afforded only a barely detectable amount of adduct **4**. We subsequently observed that synergetic reagents, which were previously utilized for catalytic asymmetric allylation,[6] can also be employed for catalytic asymmetric prop-2-ynylation. After surveying series of alkylthioboranes and alkylthiosilanes, several key points emerged: (i) $Et_2BSPr^i$ was generally superior to other reagents, including $Me_3SiSPr^i$; (ii) a 1 : 1 mixture of the BINOL–$Ti(OPr^i)_4$† or BINOL–$Zr(OPr^i)_4$‡ complexes proved to be the most effective catalyst; (iii) the new systems exhibited a dramatic acceleration of the reaction rate as well as significantly increasing catalytic ability in comparison with the non-accelerator system;[4] (iv) optimal chemical yields and enantioselectivities were observed with the use of $CH_2Cl_2$ as a solvent compared to other solvents such as toluene, diethyl ether or propionitrile. Selected results for the preliminary studies are summarised in Table 1. Especial encouraging were entries 2 and 5; therefore, chiral catalysts BINOL–$Ti^{IV}$ and –$Zr^{IV}$ with $Et_2BSPr^i$ were chosen for systematic studies because they exhibited high level of enanatioselectivity with reasonable chemical yields.

The prop-2-ynylation reaction was performed according to the following procedure: all reactions were carried out in the presence of 4 Å molecular sieves to remove any trace of water. To a solution of **1** (R = $CH_2CH_2Ph$, 1 equiv.) and **2** (1.3 equiv. in the presence of (*S*)-BINOL–$Ti^{IV}$ **5** (10 mol%) at −20 °C was added dropwise $Et_2BSPr^i$ (1.2 equiv.) in $CH_2Cl_2$. After 9 h at −20 °C, the reaction mixture was quenched by the addition of saturated aqueous $NaHCO_3$. Work up and silica gel chromatography ($SiO_2$, deactivated with 1% of $Et_3N$ in hexane; eluent, hexane–EtOAc) afforded the alcohol **4** (R = $CH_2CH_2Ph$) in 86% isolated yield and 94% ee. Using these optimal conditions, a range of experiments on the catalytic asymmetric prop-2-ynylation of aldehydes was carried out. From Table 2 it can be seen that asymmetric prop-2-ynylations were conducted on a variety of aldehydes under identical conditions to furnish alcohols **4** with excellent enantioselectivities. Reaction times and chemical yields, as indicated in Table 2, were dependent on the steric environment of the substrates. It is worthy of note that the reaction also produced trace amounts of isomeric allenyl alcohol ( < 2%) according to analysis of the $^1H$ NMR spectra of the crude products. A reduced dosage of chiral catalyst **5**

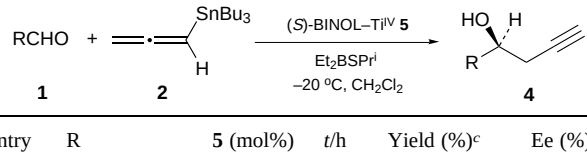
**Table 1** Selected data for preliminary investigations




| Entry | $MX_2$ | Accelerator | *t*/h | Yield (%) | Ee (%) |
|---|---|---|---|---|---|
| 1 | $Ti(OPr^i)_2$[a] | Control | 20 | Trace | — |
| 2 | $Ti(OPr^i)_2$[a] | $Et_2BSPr^i$ | 9 | 86 | 94 |
| 3 | $Ti(OPr^i)_2$[b] | $Et_2BSPr^i$ | 9 | 84 | 93 |
| 4 | $Ti(OPr^i)_2$[a] | $Me_3SiSPr^i$ | 9 | 57[c] | — |
| 5 | $Zr(OPr^i)_2$[d] | $Et_2BSPr^i$ | 8 | 72 | 92 |

[a] BINOL–$Ti(OPr^i)_4$ = 1 : 1. [b] BINOL–$Ti(OPr^i)_4$ = 2 : 1. [c] Isolated yield after desilylation ($Bu_4NF$). [d] BINOL + $Zr(OPr^i)_4$.

**Table 2** Catalytic prop-2-ynylation promoted by the BINOL–$Ti^{IV}$ complex[a,b]




| Entry | R | **5** (mol%) | *t*/h | Yield (%)[c] | Ee (%)[d] |
|---|---|---|---|---|---|
| 1 | $PhCH_2CH_2$ | 10 | 9 | 86 | 94 |
| 2 | $PhCH_2CH_2$ | 5 | 18 | 65 | 91 |
| 3 | $C_6H_{11}$ | 10 | 9 | 75 | 92 |
| 4 | $C_6H_{11}$ | 5 | 18 | 51 | 88 |
| 5 | c-$C_6H_{11}$ | 10 | 15 | 73 | 91 |
| 6 | $Me_2CHCH_2$ | 10 | 15 | 61 | 95 |
| 7 | Ph | 10 | 15 | 52 | 92 |

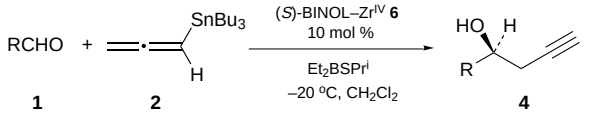
[a] All reactions were run at −20 °C. [b] Absolute configurations were verified by comparison of specific rotation sign with authentic and/or literature values. [c] Yields refer to isolated and purified products. [d] Enantiomeric excess values were determined by preparation of (+)-MTPA ester derivatives, analysis by $^1H$ NMR spectroscopy (C*H*OR) and comparison with authentic and racemic samples.

resulted in diminished chemical yields, longer reaction times and poorer stereoselectivites.

Catalytic asymmetric prop-2-ynylation promoted by the (*S*)-BINOL– $Zr^{IV}$ ‡ complex was also investigated under similar conditions to those described above. Most of the isolated major alcohols were contaminated with a trace of the isomeric allenyl alcohol ( < 3%), but in the case of cyclohexanecarbaldehyde the product ratio proved to be 93 : 7 as judged by $^1$H NMR spectroscopic analysis of the crude products. The data summarised in Table 3 allow the following points to be stated: (i) as expected, the process using the molecular accelerator is effective in terms of reaction time as well as chemical yield; (ii) in general, the $Zr^{IV}$ complex provides modest to excellent enantioselectivities, which are somewhat lower than those of the $Ti^{IV}$ complex; (iii) the enantioselectivities correlate with the degree of steric hindrance in the substrates.

The work disclosed here is innovative mainly because of the reinforcement of catalytic ability outlined, especially with the less reactive allenylstannane.[8] However, further extension of the understanding of this chemistry is required in the following areas: (i) the exact mechanism by which $Et_2BSPr^i$ accelerates the catalytic process,which involves dissociation of the product from the reaction complex and regeneration of the chiral catalyst; (ii) the origin of isomeric allenyl alcohols is also unclear, and may involve equilibration between allenyl- and prop-2-ynyl-tin reagents or α- and γ-orientation to tin in the transition state.

**Table 3** Catalytic prop-2-ynylation promoted by the BINOL-$Zr^{IV}$ complex




**1** **2** **4**

| Entry | R | *t*/h | Yield (%) | Ee (%) |
|---|---|---|---|---|
| 1 | $PhCH_2CH_2$ | 9 | 72 | 92 |
| 2 | $C_6H_{11}$ | 9 | 71 | 87 |
| 3 | c-$C_6H_{11}$ | 15 | 67 | 68 |
| 4 | $Me_2CHCH_2$ | 15 | 65 | 91 |
| 5 | Ph | 15 | 44 | 71 |

[a] All conditions were identical with those of Table 2.

In conclusion, the enantioselective prop-2-ynylation of achiral aldehydes, a process of clear synthetic potential, has been advanced to a new level of practicality and stereoselectivity as a result of the utilization of a molecular accelerator to increase catalytic ability and reactivity. Studies are in progress to extend this chemistry to more highly functionalised tin reagents, including racemic allenylstannanes for kinetic resolutions. We believe that further studies will provide a better understanding of this chemical phenomenon.

Generous financial support of this work by grants from the Ministry of Education (BSRI 96-3420) and the Korea Science and Engineering Foundation (KOSEF 94-0501-08-01-03) is gratefully acknowledged.

## Footnotes

† The (*S*)-BINOL–$Ti^{IV}$ complex was prepared from the reaction of (*S*)-BINOL with $Ti(OPr^i)_4$ in the presence of activated powdered 4 Å molecular sieves at 20 °C for 3 h (ref. 4).

‡ The (*S*)-BINOL–$Zr^{IV}$ complex was prepared from the reaction of (*S*)-BINOL with $Zr(OPr^i)_4$ in the presence of activated powdered 4 Å molecular sieves at 20 °C for 2 h (ref. 7).

## References

1 For comprehensive reviews, see Y. Yamamoto and N. Asao, *Chem. Rev*., 1993, **93**, 2207; J. A. Marshall, *Chem. Rev*., 1996, **96**, 31; M. Santell and J.-M. Pons, *Lewis Acids and Selectivity in Organic Chemistry*, CRC Press, New York, 1996, pp. 91–184.

2 H. Yamamoto, in *Comprehensive Organic Synthesis: Propargyl and Allenyl Organometallics*, ed. C. H. Heathcock, Pergamon, Oxford, 1991, vol. 2, pp. 81–98.

3 N. Ikeda, I. Arai and H. Yamamoto, *J. Am. Chem. Soc*., 1986, **108**, 483; E. J. Corey, C.-M. Yu and D.-H. Lee, *J. Am. Chem. Soc*., 1990, **112**, 878.

4 G. E. Keck, D. Krishnamurthy and X. Chen, *Tetrahedron Lett*., 1994, **35**, 8323.

5 H. Tanaka, A. K. M. Abdul Hai, H. Ogawa and S. Torri, *Synlett*, 1993, 835.

6 C.-M. Yu, H.-S. Choi, W.-H. Jung and S.-S. Lee, *Tetrahedron Lett*., 1996, **37**, 7095; C.-M. Yu, H.-S. Choi, W.-H. Jung, H.-J. Kim and J. Shin, *Chem. Commun*., 1997, preceding communication.

7 P. Bedeshi, S. Casolari, A. L. Costa, E. Tagliavini and A. Umani-Ronchi, *Tetrahedron Lett*., 1995, **36**, 7897.

8 J. A. Marshall, J. A. Jablonowski and G. S. Welmaker, *J. Org. Chem*., 1996, **61**, 2904 and references cited therein.

*Received in Cambridge, UK, 23rd January 1997; Com. 7/00540G*

# First enantiocontrolled syntheses of (+)-uleine and (+)-dasycarpidone

**Masanori Saito, Mitsuhiro Kawamura, Kou Hiroya and Kunio Ogasawara***

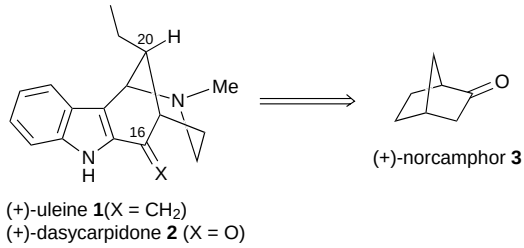
*Pharmaceutical Institute, Tohoku University, Aobayama, Sendai 980-77, Japan*

**Stereocontrolled syntheses of (+)-uleine and (+)-dasycarpidone are achieved for the first time in an enantiocontrolled way starting from (+)-norcamphor.**

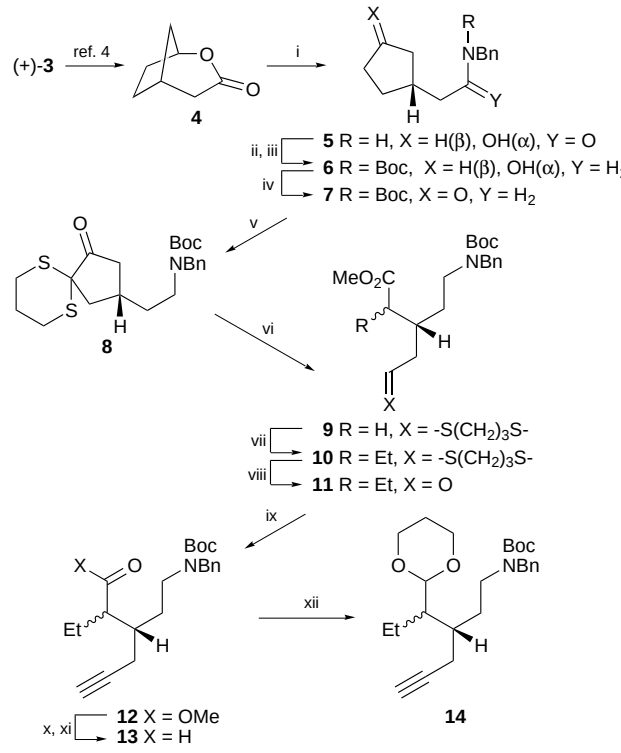
Although a number of racemic syntheses of the uleine type indole alkaloids have been reported,[1] no enantiocontrolled synthesis has been disclosed to date. We report here the first stereo- and enantio-controlled construction of the representatives of this group, (+)-uleine **1** and (+)-dasycarpidone **2**, using (+)-norcamphor **3** as starting material (Scheme 1).[2]

(+)-Norcamphor **3**† was first transformed into the δ-lactone **4**[3a] which was then condensed with benzylamine to give the amide alcohol **5**,‡ mp 94–95 °C, $[\alpha]_D^{33}$ −1.95 (*c* 0.55, $CHCl_3$), in 75% yield. Hydride reduction of **5** followed by *N*-carbamoylation of the resulting amine yielded the carbamate **6**, $[\alpha]_D^{27}$ −0.76 (*c* 1.0, $CHCl_3$), which was oxidized to give the cyclopentanone **7**, $[\alpha]_D^{30}$ +58.0 (*c* 0.9, $CHCl_3$), in 90% overall yield. Transformation of **7** into the α-diketone monothioketal[3,4] **8**, mp 72–74 °C, $[\alpha]_D^{29}$ −43.5 (*c* 0.742, $CHCl_3$), followed by alkaline cleavage[3–5] yielded the acyclic methyl ester **9**, $[\alpha]_D^{31}$ +43.1 (*c* 0.3, $CHCl_3$), in 59% overall yield after treatment of the resulting acid with diazomethane. Exposure of **9** to iodoethane in the presence of sodium hexamethyldisilazide in THF containing HMPA at −78 °C afforded the α-ethyl ester **10** in 73% yield as an inseparable epimeric mixture with recovery of 14% of the starting material. The dithiane group of **10** was hydrolysed to give the aldehyde **11** in 92% yield which was treated with dimethyl 1-diazo-2-oxopropylphosphonate[6] in the presence of potassium carbonate to furnish the terminal acetylene **12** in 90% yield. Compound **12** was then converted into the 1,3-dioxane **14** in 72% overall yield *via* the aldehyde **13** by sequential reduction, oxidation and acetalization[7] (Scheme 2).

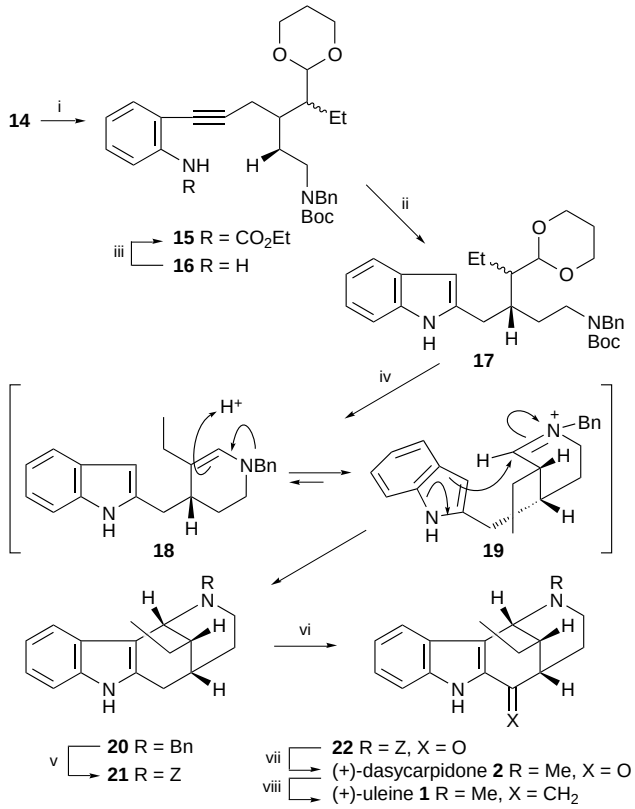
To construct the indole framework,[8,9] the acetylene **14** was first coupled with ethyl (2-iodophenyl)carbamate in the presence of dichlorobis(triphenylphosphine)palladium(II) [$PdCl_2(PPh_3)_2$] and copper(I) iodide in triethylamine[10] to give the arylacetylene **15** in 86% yield. Cyclization was then carried out by treating **15** with sodium ethoxide in ethanol[8,9] at reflux to furnish the indole **17** in 64% yield accompanied by 31% of the de-*N*-acylated product **16** which, after separation, was treated with ethyl chlorocarbonate in pyridine to recover the carbamate **15** in 81% yield. The indole **17**, on reflux with TFA, afforded stereoselectively the tetracyclic amine **20**, $[\alpha]_D^{29}$ −155.3 (*c* 0.7, $CHCl_3$), in 54% yield accompanied by the readily separable 20-epimer (4%) by spontaneous deacetalization, decarbamoylation and stereoselective cyclization. The observed stereoselectivity may be rationalised by intervention of the enamine intermediate **18** which allowed epimerization of the C-20 stereogenic centre and stereoselective generation of the iminium intermediate **19** followed by its stereoselective cyclization[2a,b,d] under the conditions. Since the amine **20** was found to be unstable under the oxidation conditions, it was first transformed into the carbamate **21**, $[\alpha]_D^{28}$ +89.4 (*c* 0.4, $CHCl_3$), in 74% overall yield by sequential catalytic debenzylation and carbamoylation.[2d] The resulting carbamate **21** was then treated with pyridinium dichromate (PDC) on Celite in the presence of *tert*-butyl hydroperoxide (TBHP)[11] in benzene to afford the 16-ketone **22**, $[\alpha]_D^{28}$ +231.8 (*c* 0.2, $CHCl_3$), in 54% yield. Concurrent *N*-deprotection and *N*-methylation of **22** under the reductive conditions[2d] in the presence of 37% formalin afforded (+)-dasycarpidone **2**, $[\alpha]_D^{30}$ +63.1 (*c* 0.7, $CHCl_3$) [natural: $[\alpha]_D^{26}$ +64.7 (*c* 1.02, $CHCl_3$)],[12] in 83% yield. By following the established procedure,[2a,b] (+)-dasycarpidone **2** obtained was transformed into (+)-uleine **1**, $[\alpha]_D^{27}$ +18.2 (*c* 0.3, $CHCl_3$) [natural: $[\alpha]_D^{25}$ +16.5 (*c* 0.91, $CHCl_3$);[12] $[\alpha]_D^{27}$ +20 (*c* 0.94, $CHCl_3$)[13]], in 71% overall yield on treatment with methyl-




**Scheme 1**




**Scheme 2** *Reagents and conditions*: i, $BnNH_2$, 180 °C (75%); ii, LAH, THF, reflux; iii, $Bo_2O$, aq. NaOH room temp. (95%); iv, pyridinium chlorochromate (PCC), NaOAc, $CH_2Cl_2$ (95%); v, pyrrolidine, benzene, reflux, then $TsS(CH_2)_3STs$, $Et_3N$, MeCN (59%); vi, KOH, Bu$^t$OH, 60 °C, acid workup, then $CH_2N_2$ (99%); vii, $NaN(SiMe_3)_2$, EtI, THF, HMPA, −78 °C (73%, recovery of 14% of **9**); viii, $Hg(ClO_4)_2$, $CaCO_3$, 20% aq. THF (92%); ix, $AcC(=N_2)P(O)(OMe)_2$, $K_2CO_3$, MeOH, room temp. (90%); x, LAH, THF; xi, Swern oxidation (87%); xii, $Me_3SiO(CH_2)_3OSiMe_3$, $Me_3SiOTf$ (cat.), THF, −78 °C (83%)




**Scheme 3** *Reagents and conditions*: i, $PdCl_2(PPh_3)_2$ (10 mol%), CuI (10 mol%), 2-$IC_6H_4NHCO_2Et$, $Et_3N$, reflux (86%); ii, NaOEt, EtOH, reflux (**16**: 31% and **17**: 64%); iii, $ClCO_2Et$, pyridine (81%); iv, TFA, reflux (54%; 20-epimer 4%); v, 10% Pd–C, $HCO_2NH_4$, MeOH, reflux, then $ClCO_2Bn$, $K_2CO_3$, $CH_2Cl_2$ (74%); vi, PDC–Celite, TBHP, benzene, room temp. (54%); vii, $H_2$, 10% Pd–C, 37% formalin, MeOH (83%); viii, MeLi, THF, then neutral $Al_2O_3$ (activity I), 120 °C (71% overall)

lithium followed by dehydration of the resulting tertiary alcohol with neutral alumina.

## Footnotes

* E-mail: konol@mail.cc.tohoku.ac.jp

† Prepared from (+)-*endo*-norborneol (*ca.* 95% ee) kindly provided by Chisso Corporation, Japan.

‡ Satisfactory analytical (combustion and/or high resolution mass) and spectral (IR, $^1H$ NMR, and MS) data were obtained for all new isolable compounds.

## References

1 J. E. Saxton, *Nat. Prod. Rep.*, 1995, **12**, 385 and the former reports; *The Chemistry of Heterocyclic Compounds*, ed. J. E. Saxton, Wiley-Interscience, New York, 1983, vol. 25, part 4, ch. 4; supplement to part 4, 1994.
2 Racemic syntheses: (*a*) A.Jackson, N. D. V. Wilson, A. J. Gaskell and J. A. Joule, *J. Chem. Soc. C*, 1969, 2738; (*b*) L. J. Dolby and H. Biere, *J. Org. Chem.*, 1970, **35**, 3843; (*c*) T. Kametani and T. Suzuki, *J. Org. Chem.*, 1971, **36**, 1291; (*d*) J. Gracia, N. Casamitjana, J. Bonjoch and J. Bosch, *J. Org. Chem.*, 1994, **59**, 3939; (*e*) G. Büchi, S. J. Gould and F. Näf, *J. Am. Chem. Soc.*, 1971, **93**, 2492.
3 Utilization of (+)-norcamphor as a starting material for enantio-controlled syntheses of natural products: (*a*) M. Kawamura and K. Ogasawara, *Tetrahedron Lett.*, 1995, **36**, 3369; (*b*) M. Saito, M. Kawamura and K. Ogasawara, *Tetrahedron Lett.*, 1995, **36**, 9003; (*c*) M. Kawamura and K. Ogasawara, *J. Chem. Soc., Chem. Commun.*, 1995, 2403; (*d*) M. Kawamura and K. Ogasawara, *Heterocycles*, 1997, **44**, 129.
4 *Cf.* S. Takano and K. Ogasawara, *J. Synth. Org. Chem. Jpn.*, 1977, **35**, 795; S. Takano, K. Hiroya and K. Ogasawara, *Chem. Lett.*, 1983, 255.
5 J. A. Marshall and D. E. Seitz, *J. Org. Chem.*, 1974, **39**, 1814.
6 R. Bernardi and D. Ghiringhelli, *J. Org. Chem.*, 1987, **52**, 5021; S. Müller, B. Liepold, G. J. Roth and H. J. Bestmann, *Synlett*, 1996, 521.
7 T. Tsunoda, M. Suzuki and R. Noyori, *Tetrahedron Lett.*, 1980, **21**, 1357.
8 T. Sakamoto, Y. Kondo and H. Yamanaka, *Heterocycles*, 1986, **24**, 31.
9 Utilization of this procedure for the natural product synthesis: S. Takano, T. Sato, K. Inomata and K. Ogasawara, *J. Chem. Soc., Chem. Commun.*, 1991, 402; K. Shin and K. Ogasawara, *Chem. Lett.*, 1995, 289; K. Shin and K. Ogasawara, *Synlett*, 1995, 859; K. Shin and K. Ogasawara, *Synlett*, 1996, 922.
10 K. Sonogashira, Y. Tohda and N. Hagiwara, *Tetrahedron Lett.*, 1975, 4467.
11 N. Chidambaram and S. Chandrasekaran, *J. Org. Chem.*, 1987, **52**, 5048.
12 J. A. Joule, M. Ohashi, B. Gilbert and C. Djerassi, *Tetrahedron*, 1965, **21**, 1717.
13 R. F. Garcia and K. S. Brown, Jr., *Phytochemistry*, 1976, **15**, 1093.

*Received in Cambridge, UK, 6th February 1997; Com. 7/00856B*

# Enantiocontrolled construction of sistodiolynne, an unusual polyketide from the wood-decay fungus *Sistrema raduloides*

**Tsutomu Sugahara and Kunio Ogasawara***

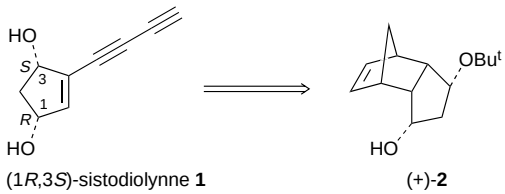
*Pharmaceutical Institute, Tohoku University, Aobayama, Sendai 980-77, Japan*

**Sistodiolynne, an unusual polyketide isolated from the wood decay fungus *Sistorema raduloides*, has been constructed stereoselectively from a chiral cyclopentenol building block to verify the proposed structure.**

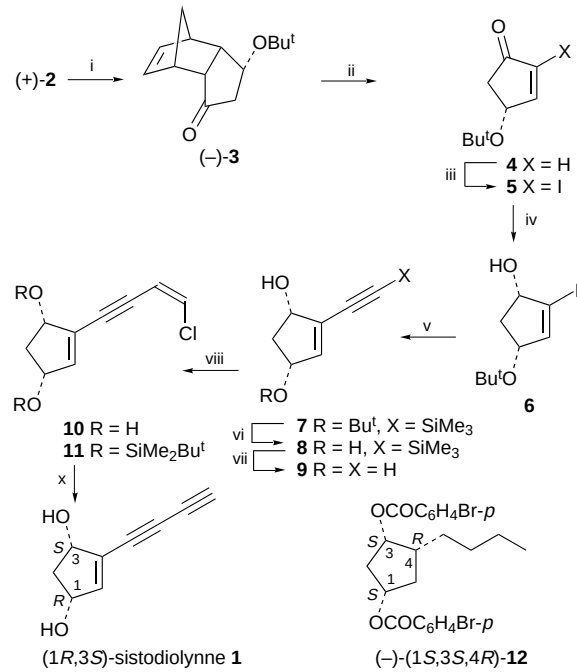
Sistodiolynne [(1*R*,3*S*)-4-butadiynylcyclopent-4-ene-1,3-diol] **1** is a metabolite of the wood rot decay fungus *Sistorema raduloides* (P. Karst) Donk which was recovered from indoor air of a museum in San Juan, Puerto Rico.[1] The compound **1** proved to be extremely air-sensitive and only stable in solution. It has been shown by labelling experiments that it arises from five acetate units with loss of a methyl carbon from one of the acetate units during the biosynthesis. Its structure was determined by spectroscopic methods, mainly, NMR, and the absolute configuration was proposed by circular dichroism of the di(4-bromobenzoate) of the perhydro derivative of the natural product. In relation to our recent synthesis of chiral cyclopentenone building blocks,[2,3] we were interested in converting our chiral cyclopentenol block **2** into sistodiolynne **1** so as to establish an enantiocontrolled synthesis and to confirm the proposed structure. Here we report the first construction of sistodiolynne **1** and the all-*cis* di(4-bromobenzoate) (−)-**12** of the perhydro derivative of **1**, which verified the proposed structure for the natural product (Scheme 1).

The optically pure tricyclic alcohol[2] (+)-**2**, $[\alpha]_D^{28}$ +75.4 (*c* 1.2, $CHCl_3$), mp 95 °C, obtained by lipase-mediated kinetic resolution,[2] was first transformed into the (*R*)-cyclopentenone[2,4] **4**, $[\alpha]_D^{28}$ +53.2 (*c* 0.9, MeOH), in 72% overall yield *via* the tricyclic ketone (−)-**3**, $[\alpha]_D^{26}$ −186.6 (*c* 1.0, $CHCl_3$), by sequential oxidation and thermolysis (Scheme 2). Although optically active **4** may be obtained more directly from the cyclopentenol precursor by a similar lipase-mediated resolution[2] or from racemic **4** by chemical resolution,[4] the present procedure seemed more appropriate with respect to the optical purity of the product. Exposure of **4** to iodine in the presence of pyridine[5] gave the air sensitive α-iodo enone **5**, which was immediately reduced with sodium borohydride–cerium(III) chloride[6] to give stereoselectively *cis*-4-*tert*-butoxy-2-iodocyclopent-2-enol†‡ **6**, $[\alpha]_D^{28}$ +41.0 (*c* 0.9, $CHCl_3$), mp 90–92.5 °C, as a single product in 92% overall yield from **4**. The stereochemistry of **6** was determined by a NOE experiment on the benzoate of **6**, which exhibited significant interaction between the C(1) ($\delta_H$ 5.70) and C(4) ($\delta_H$ 4.54) protons. Moreover, the stereochemistry of **6** was confirmed unambiguously by converting it into *cis*-4-*tert*-butoxycyclopent-2-enol[2] in 80% yield on exposure to *tert*-butyllithium followed by acetic acid in tetrahydrofuran (THF) at −78 °C. A cross-coupling reaction[7,8] between **6** and trimethylsilylacetylene proceeded without difficulty using dichlorobis(triphenylphosphine)palladium(II) $[PdCl_2(PPh_3)_2]$[9] as catalyst in the presence of copper(I) iodide in triethylamine to give the enyne **7**, $[\alpha]_D^{28}$ +70.2 (*c* 1.4, $CHCl_3$), in 96% yield. To remove the two different protecting groups, **7** was sequentially exposed to titanium(IV) chloride[2,10] and tetrabutylammonium fluoride to give *cis*-1-ethynylcyclopent-1-ene-3,5-diol **9**, $[\alpha]_D^{25}$ −40.8 (*c* 0.5, $CHCl_3$), in 70% overall yield *via* **8**.

Very fortunately, a mild two-step construction of a 1,3-diyne functionality from a terminal acetylene exists.[11] To apply this procedure, **9** was first coupled with *cis*-1,2-dichloroethylene in the presence of tetrakis(triphenylphosphine)palladium(0)[12] in butylamine to give the dienynediol **10**, accompanied by a trace of inseparable phenylphosphine impurities, which was isolated in the pure state as the di(*tert*-butyldimethylsilyl) ether **11**, $[\alpha]_D^{27}$ −43.8 (*c* 0.3, $CHCl_3$), by treating the mixture with *tert*-butyldimethylsilyl chloride in the presence of imidazole. The overall yield of **11** from **9** was 71%. Exposure of **11** to tetrabutylammonium fluoride (5 equiv.) in THF at room temperature[11] for 10 h furnished sistodiolynne **1** as a highly unstable oil by concurrent desilylation and dehydrochlorination. Although the product generated could not be isolated in a pure




**Scheme 1**




**Scheme 2** *Reagents and conditions*: i, $SO_3$·pyridine, $Me_2SO$, $Et_3N$, room temp. (94%); ii, *o*-dichlorobenzene, 180 °C, 2.5 h (77%); iii, $I_2$, pyridine, $CH_2Cl_2$; iv, $NaBH_4$–$CeCl_3$, MeOH, −78 °C (92% from **5**); v, CH≡CSiMe$_3$, $PdCl_2(PPh_3)_2$ (6 mol%), CuI (8 mol%), $Et_3N$, 4 h (96%); vi, $TiCl_4$, $CH_2Cl_2$, 0 °C, 2 min; vii, $Bu_4NF$, THF, room temp. (70% from **8**); viii, (*Z*)-ClHC=CHCl, $Pd(PPh_3)_4$ (5 mol%), CuI (15 mol%), $BuNH_2$, benzene, 0.5 h; ix, Bu$^t$Me$_2$SiCl, imidazole, DMF (71% from **9**); x, $Bu_4NF$ (5 equiv.), THF, room temp., 10 h

state as it polymerised even in a solution during purification as described,[1] its $^1$H NMR spectrum measured directly [in $(CD_3)_2CO$] was identical to that of the natural product.[1]

On the other hand, **11** was hydrogenated under medium-pressure conditions in the presence of palladized carbon to convert it into the mixture containing the stable perhydro derivative of the natural product **1** as the major product. The major product isolates as the di(4-bromobenzoate) **12**, after desilylation and 4-bromobenzoylation, had a circular dichroism (CD) spectrum, showing the first Cotton effect (negative) at 251 nm and the second (positive) at 234 nm, which was identical to that reported for **12** having the 1*S*,3*S*,4*R* configuration (negative at 251 nm and positive at 231 nm) originated from the natural product **1**. This indicated the stereochemistry of sistodiolynne **1** to be 1*R*,3*S* as proposed.

In summary, we could not isolate sistodiolynne **1** in a pure form owing to its intrinsic instability, however, the present synthesis verified the correctness of the proposed structure of the natural product made by spectroscopic methods.

## Footnotes

* E-mail: konol@mail.cc.tohoku.ac.jp

† Spectral (IR, $^1$H NMR, mass and analytical (combustion and/or high resolution mass) data were obtained for all isolable compounds.

‡ *Selected data* for representative compounds. For **6**: $\delta_H$ (300 MHz, $CDCl_3$) 6.23 (1 H br s), 4.41 (2 H, m), 2.73 (1 H, dt, *J* 14, 7 Hz), 1.71 (1 H, dt, *J* 14, 5 Hz), 1.10 (9 H, s). For **11**: $\delta_H$ (300 MHz, $CDCl_3$) 6.36 (1 H, d, *J* 7.3 Hz), 6.12 (1 H, d, *J* 1.8 Hz), 5.98 (1 H, d, *J* 7.3 Hz), 5.05 (1 H, br s), 4.98 (1 H, br s), 2.03 (2 H, m), 0.89 (9 H, s), 0.87 (9 H, s), 0.1 (6 H, s), 0.06 (6 H, s). $M^+$, 412.2017; $C_{21}H_{37}O_2Si_2{}^{35}Cl$ requires $M^+$, 412.2022. For **1**: $\delta_H$ [300 MHz, $(CD_3)_2CO$] 6.32 (1 H, s), 4.65 (2 H, m), 4.46 (1 H, d, *J* 6.5 Hz), 4.17 (1 H, d, *J* 6.5 Hz), 3.27 (1 H, s), 2.70 (1 H, ddd, *J* 13.2, 7.3, 7.3 Hz), 1.45 (1 H, *J* 13.2, 6.0, 6.0 Hz). $M^+$, 148.0494; $C_9H_8O_2$ requires $M^+$, 412.2022. For **12**: $\delta_H$ (300 MHz, $CDCl_3$) 7.90 (2 H, d, *J* 8.5 Hz), 7.74 (2 H, d, *J* 8.5 Hz), 7.58 (2 H, d, *J* 8.5 Hz), 7.46 (2 H, d, *J* 8.5 Hz), 5.42 (1 H, m), 5.38 (1 H, m), 2.60 (1 H, dt, *J* 13.5, 7.5 Hz), 2.42 (1 H, ddd, *J* 16, 8.0, 5.0 Hz), 2.19 (1 H, br d, *J* 16 Hz), 2.0 (1 H, m), 1.3–1.8 (7 H, m), 0.92 (3 H, br t, *J* 7.0). $M^+$, 522.0048; $C_{23}H_{24}O_4{}^{79}Br_2$ requires $M^+$, 522.0041.

## References

1 A. K. Amegadzie, W. A. Ayer and L. Sigler, *Can. J. Chem*., 1995, **73**, 2119.
2 T. Sugahara, Y. Kuroyanagi and K. Ogasawara, *Synthesis*, 1996, 1101.
3 A recent review for the chiral cyclopentenoid derivatives, see K. Ogasawara, *J. Synth. Org. Chem. Jpn*., 1996, **54**, 15.
4 B. M. Eschler, R. K. Haynes, M. D. Ironside, S. Kremmydas, D. D. Riley and T. W. Hambley, *J. Org. Chem*., 1991, **56**, 4760.
5 C. R. Johnson, P. A. Adams, M. P. Braun, C. B. W. Senanayake, P. M. Wovkulich and M. R. Uskokovic, *Tetrahedron Lett*., 1992, **33**, 1917.
6 A. L. Gemal and T. L. Luche, *J. Am. Chem. Soc*., 1981, **103**, 5454.
7 K. Sonogashira, Y. Toda and N. Hagiwara, *Tetrahedron Lett*., 1975, 4467.
8 A more related example, see T. Kamikubo and K. Ogasawara, *Chem. Commun*., 1996, 1679.
9 W. J. Scott, M. R. Pena, K. Sward, S. J. Stoessel and J. K. Stille, *J. Org. Chem*., 1985, **50**, 2302; E. J. Corey, M.-C. Kang, M. C. Desai, A. K. Ghosh and I. N. Houpis, *J. Am. Chem. Soc*., 1988, **110**, 649.
10 R. H. Schlessinger and R. A. Nugent, *J. Am. Chem. Soc*., 1982, **104**, 1116.
11 A. S. Kende and C. A. Smith, *J. Org. Chem*., 1988, **53**, 2655.
12 V. Ratovelomanana and G. Linstrumelle, *Tetrahedron Lett*., 1981, **22**, 315.

*Received in Cambridge, 8th January 1997; Com. 7/00186J*

# Characterisation of two different mixed-valence states in a strongly interacting dimolybdenum complex

**Andrzej Wlodarczyk,* Garry A. Doyle, John P. Maher, Jon A. McCleverty* and Michael D. Ward**

*School of Chemistry, University of Bristol, Cantock's Close, Bristol, UK BS8 1TS*

**The pyrazine-bridged bimetallic complex [{Mo(NO)[HB(dmpz)$_3$]Br}$_2$(μ-pz)]$^z$ [HB(dmpz)$_3$ = tris(3,5-dimethylpyrazolyl)borate] exists within a five-membered electron-transfer chain where $z$ = −2, −1, 0, +1 and +2; the mixed-valence species with $z$ = −1 is delocalised on the EPR and IR spectroscopic timescales whereas that with $z$ = +1 is valence-trapped.**

The most celebrated dimetallic mixed-valence compound is the so-called Creutz–Taube ion, [{Ru(NH$_3$)$_5$}$_2$(μ-pz)]$^{5+}$, derived by coupling two Ru$^{II}$ pentammine fragments by pyrazine followed by one-electron oxidation of the product.[1] It is now generally accepted that this ion exhibits class III mixed-valence behaviour, namely that the unpaired electron is delocalised over the metal ions and the bridging ligand.[2] Many other examples of such mixed-valence species have been described, showing a wide range of behaviour from fully delocalised to valence-trapped.[2] The majority of these species are usually assembled by coupling diamagnetic monometallic fragments using bridging ligands of varying lengths, geometries and delocalisation. In all but a few cases, these precursors are oxidised in a one-electron process to generate the mixed-valence ion, although two types of molybdenum complex, [{Mo(CO)$_3$(PR$_3$)}$_2$(1,4-pz)]$^-$ (ref. 3) and [{Mo(NO)[HB(dmpz)$_3$]X}$_2${C$_6$H$_4$(NH)$_2$-1,4}]$^-$ (X = Cl, Br, I),[4] are generated by reduction of the diamagnetic precursors, the former being described as a radical anionic ligand stabilised by metal carbonyl fragments,† whereas the latter is fully delocalised on the EPR timescale.

For a number of years we have been studying a series of binuclear molybdenum nitrosyls containing bridging dipyridine ligands. These complexes contain two metal-based redox centres whose interaction, determined electrochemically, is mediated significantly by the bridging ligand.[5] Furthermore, these compounds are paramagnetic (one unpaired electron on each metal atom), the unpaired spins being coupled either ferro- or antiferro-magnetically depending on bridging ligand geometry, and their EPR spectra reveal spin–spin correlation over remarkably long distances.[6] Our preceding work on molybdenum nitrosyl complexes of 4,4′-dipyridyl and its analogues, [{Mo(NO)[HB(dmpz)$_3$]Cl}$_2$(NC$_5$H$_4$EC$_5$H$_4$N)] [E = nothing, (CH=CH)$_n$, (C$_6$H$_4$)$_n$] has shown that the metal–metal interactions gradually diminish with increasing length of E. Conversely we expected that a dimetallic species containing 1,4-pyrazine as bridge should reveal very substantial electrochemical and magnetic interactions, at least twice as large as those in the Creutz–Taube ion ($\Delta E_p$, the separation between the redox potentials, is *ca*. 390 mV).

Our early attempts to make species of the type [{Mo(NO)[HB(dmpz)$_3$]X}$_2$(1,4-pz)] (X = Cl or I) were partially successful, revealing unexpectedly rich electrochemical behaviour,[7] although the species were difficult to purify and also appeared to decompose readily. However, we have now obtained pure samples of the bromo complex, [{Mo(NO)[HB(dmpz)$_3$]Br}$_2$(1,4-pz)].‡ In contrast to the behaviour of [{Ru(NH$_3$)$_5$}$_2$(1,4-pz)]$^{5+}$ in aqueous media, this species exhibits two reversible one-electron reductions (established coulometrically) as well as two reversible one-electron oxidations. The former occur at −0.95 and −2.39 V in dichloromethane *vs*. the ferrocene–ferrocenium couple, and the latter at +1.08 and +1.18 V, respectively. The separation between the reduction potentials, a measure of the coulombic interaction between the two redox centres, is 1440 mV, the largest we have so far detected and amongst the largest known, equivalent to a comproportionation constant $K_c = 2.2 \times 10^{24}$. For the first time we have also detected a separation between the oxidation processes in this class of dimetallic, *viz*. 100 mV ($K_c$ = 49). That interaction between the reduction processes is so much larger than that between the oxidations implies that the added electrons in the reduced form are substantially delocalised over the bridge whereas the unpaired electron in the oxidised form is not. Thus [{Mo(NO)[HB(dmpz)$_3$]Br}$_2$(1,4-pz)]$^z$ exists within a five-membered electron-transfer chain ($z$ = −2, −1, 0 +1 and +2), reminiscent of dithiolene complexes,[8] in which the formal valence-electron configuration of the two metals may be represented as {18 : 18}$^{2-}$, {18 : 17}$^-$, {17 : 17}, {17 : 16}$^+$ and {16 : 16}$^{2+}$.

The green isovalent parent species ($z$ = 0; {17 : 17}) is EPR 'silent' in contrast to related bipyridyl species [{Mo(NO)-[HB{dmpz)$_3$]Cl}$_2$(NC$_5$H$_4$EC$_5$H$_4$N)].[5,6] We expect that the unpaired spins in this species will be quite strongly coupled antiferromagnetically, as we have observed in analogues,[6] and in such circumstances EPR signals are not observed.§ The deep blue reduced monoanion ({18 : 17}$^-$), generated by cobaltocene reduction, exhibits an EPR spectrum composed of the superimposition of one, six and eleven line multiplets derived by a single electron coupling equally to both metal nuclei ($^{95}$Mo, $^{97}$Mo $I$ = 5/2; *ca*. 25% abundance in total),¶ with $g$ = 1.979, $A_{Mo}$ = 2.9 mT. The IR spectrum of the neutral precursor exhibits a single NO stretching frequency at 1626 cm$^{-1}$ (in $CH_2Cl_2$) which, on reduction, moves to 1585 cm$^{-1}$, but remains a single peak. Our spectral data are consistent with class III, fully delocalised mixed-valence behaviour for the {18 : 17}$^-$ monoanion on both the EPR and the IR timescale, implying that the electron exchange rate is $10^{13}$ s$^{-1}$ or faster. Our previously reported mixed-valence molybdenum complexes [{Mo(NO)[HB(dmpz)$_3$]X}$_2${C$_6$H$_4$(NH)$_2$-1,4}]$^-$ are delocalised on the EPR timescale,[4] but localised according to their IR spectra (two $\nu_{NO}$) indicating that the electron exchange rate lies between $10^8$ and $10^{13}$ s$^{-1}$. Such behaviour is very rare although it has been detected in binuclear iron carbonyls and rhenium nitrosyls.[9]

Further electrochemical reduction to generate the dianion, {18 : 18}$^{2-}$, which we predict should be diamagnetic, is difficult because of the proximity of the reduction process to the decomposition of the electrolysis medium, but by monitoring the EPR spectrum of the monoanion while reduction was occurring, we observed that the intensity of the signal decreased significantly without qualitative change in its appearance, *i.e*. consistent with the formation of diamagnetic material.

Oxidation of the neutral precursor by controlled potential electrolysis in dichloromethane at +1.05 V, afforded a brown solution of [{Mo(NO)[HB(dmpz)$_3$]Br}$_2$(1,4-pz)]$^+$ ({17 : 16}$^+$), the EPR spectrum of which was difficult to obtain due to decomposition but appeared unlike that of the monoanion described above and contained sextet signals with $A_{Mo}$ *ca*. 5.0 mT. However, the isoelectronic chloride,

$[\{Mo(NO)[HB(dmpz)_3]Cl\}_2(1,4\text{-pz})]^+$ (generated similarly), was more stable, exhibiting an EPR spectrum with $g$ = 1,979 and $A_{Mo}$ = 4.8 mT, having a one and six line superimposed pattern,¶ which shows that the unpaired electron is coupled with only one Mo atom. The IR spectrum of the bromo monocation exhibited two NO stretching frequencies, at 1720 and 1606 $cm^{-1}$ (the chloro species was similar, $\nu_{NO}$ = 1717, 1608 $cm^{-1}$). The fully oxidised brown dication $[\{Mo(NO)[HB(dmpz)_3]Br\}_2(1,4\text{-pz})]^{2+}$ ($\{16:16\}^{2+}$) was prepared by oxidation of the neutral parent by acetylferrocenium ion. It was EPR 'silent' and therefore probably diamagnetic, and exhibited only one $\nu_{NO}$ (1703 $cm^{-1}$). On the basis of these spectral data we conclude that the partially oxidised monocations $[\{Mo(NO)[HB(dmpz)_3]X\}_2(1,4\text{-pz})]^+$ (X = Cl, Br) are valence-trapped.

While the isovalent $[\{Mo(NO)[HB(dmpz)_3]Br\}_2(1,4\text{-pz})]$ ($\{17:17\}$) behaves in a way reminiscent of its ruthenium analogue, it exhibits more extensive electron-transfer capability. This is partly a function of solvent, base electrolyte, *etc.*, and the original Creutz–Taube ion was characterised electrochemically in aqueous media which has a more limited voltage window. Nevertheless, the dinuclear molybdenbum nitrosyl described here is one of the very few compounds in which mixed-valence behaviour is generated by oxidation and reduction and it is unique in giving rise, reversibly, to two different classes of mixed-valence states without significant structural modification. The electrochemical data nicely complement the EPR spectral results, since the character of the mixed-valence states is related to the comproportionation constants for the mixed-valence species, a large value of $K_c$ implying substantial delocalisation while a small $K_c$ implies significantly less interaction.

We are grateful to the EPSRC for the support of this work, and to the Politechnika Krakowska for leave of absence for A. W.

## Footnotes

* E-mail: jon.mccleverty@bris.ac.uk

† This system cannot be defined as a genuine mixed-valence species, since the metal-based orbitals are formally occupied (each metal centre has 18 valence electrons prior to reduction) and the LUMO must be predominantly bridging ligand based.

‡ Both $[\{Mo(NO)[HB(dmpz)_3]Br\}_2(1,4\text{-pz})]$ and $[Mo(NO)\{HB(dmpz)_3\}Br(1,4\text{-pz})]$ are prepared by refluxing $[Mo(NO)\{HB(dmpz)_3\}Br_2]$ with pyrazine in toluene containing triethylamine and are separated chromatographically on silica gel using dichloromethane–thf as eluent. FABMS: 1087 ($M^+$). (Found C, 38.1; H, 4.4; N, 20.4. $C_{22}H_{52}B_2Br_2Mo_2N_{16}O_2$ requires C, 37.6; H, 4.5; N, 20.6%). Cyclic voltammetry in $CH_2Cl_2$, using Pt bead electrode, ferrocene as reference, $[NBu^n_4]PF_6$ as base electrolyte, scan rate 50 and 100 mV $s^{-1}$.

§ Preliminary magnetic susceptibility measurements in the range 80–300 K show that $[\{Mo(NO)[HB(dmpz)_3]Cl\}_2(1,4\text{-pz})]$ exhibits antiferromagnetic behaviour ($J$ *ca.* −180 $cm^{-1}$) consistent with our recently reported findings regarding the sign and magnitude of $J$ (ref. 6).

¶ $^{95}Mo$ and $^{97}Mo$ have $I$ = 5/2, a relative overall abundance of *ca.* 25% and similar nuclear magnetic moments. For an electron coupled to one Mo atom, the signal consists of a singlet (*ca.* 75% of Mo nuclei, $I$ = 0) and a sextet (*ca.* 25% of Mo nuclei, $I$ = 5/2). For an electron coupled to two Mo atoms, the signal appears as a singlet ($I$ = 0, $I$ = 0), 1 : 1 : 1 : 1 : 1 : 1 sextet ($I$ = 5/2, $I$ = 0), and 1 : 2 : 3 : 4 : 5 : 6 : 5 : 4 : 3 : 2 : 1 11-fold multiplet ($I$ = 5/2, $I$ = 5/2) nuclear spin combinations. From previous data, we expect $A_{Mo}$ to be 4.5–5.0 mT for one electron coupled to one Mo centre and 2.4–2.5 mT for one coupled to two Mo centres (refs. 4, 5).

## References

1 C. Creutz and H. Taube, *J. Am. Chem. Soc.*, 1973, **95**, 1086; K. Kalyanasundaram and M. K. Nazeeruddin, *Inorg. Chim. Acta*, 1994, **226**, 213 and references therein.
2 M. D. Ward, *Chem. Soc. Rev.*, 1995, **34**, 121.
3 W. Bruins, W. Kaim, E. Waldhör and M. Krejcik, *Inorg. Chem.*, 1995, **34**, 663 and references therein.
4 A. Wlodarczyk, J. P. Maher, J. A. McCleverty and M. D. Ward, *J. Chem. Soc., Chem. Commun.*, 1995, 2397.
5 S. L. W. McWhinnie, C. J. Jones, J. A. McCleverty, D. Collison and F. E. Mabbs, *J. Chem. Soc., Chem. Commun.*, 1990, 940; J. A. Thomas, C. Jones, J. A. McCleverty, D. Collison, F. E. Mabbs, C. J. Harding and M. G. Hutchings, *J. Chem. Soc., Chem. Commun.*, 1992, 1796; A. Das, J. P. Maher, J. A. McCleverty, J. A. Navas and M. D. Ward, *J. Chem. Soc., Dalton Trans.*, 1993, 681.
6 A. M. W. Cargill Thompson, D. Gatteschi, J. A. McCleverty, J. A. Navas, E. Rentschler and M. D. Ward, *Inorg. Chem.*, 1996, **35**, 2701.
7 J. A. Thomas, Ph.D. Thesis, University of Birmingham, 1992.
8 U. T. Müller-Westerhoff, *Comprehensive Inorganic Chemistry*, ed. G. Wilkinson, R. D. Gillard and J. A. McCleverty, 1983; U. T. Müller-Westerhoff, B. Vance and D. I. Yoon, *Tetrahedron*, 1991, **47**, 909.
9 B. A. Eltzenhouser, M. D. Cavanaugh, H. N. Spurgeon and M. B. Sponsler, *J. Am. Chem. Soc.*, 1994, **116**, 2221; Y. Zhou, J. W. Seyler, W. Weng, A. M. Aric and J. A. Galdysz, *J. Am. Chem. Soc.*, 1993, **115**, 8509.

*Received in Basel, Switzerland, 3rd December 1996; Com. 6/08157F*

# Oxidation of monomeric *N*,*N*′-dilithium *N*,*N*′-bis(di-*tert*-butylmethylsilyl)hydrazide to the diazene

**Henning Witte-Abel, Uwe Klingebiel* and Mathias Noltemeyer**

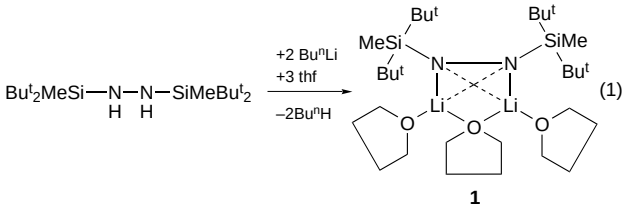
*Institut für Anorganische Chemie der Universität, Tammannstr. 4, D-37077 Göttingen, Germany*

**The reaction between the bis(silyl)hydrazine RNHNHR and butyllithium in thf affords the first monomeric dilithium bis(silyl)hydrazide RNLiNLiR·3thf 1 (R = SiBu$^t_2$Me) and the crystal structure of 1 is presented; the thermally stable bis(silyl)diazene RN=NR 2 (R = SiBu$^t_2$Me) is formed in the reaction between 1 and $Br_2$.**

The syntheses of the first silyl hydrazines were described by Aylett[1] and Wannagat and Liehr[2] in the 1950s. They developed essentially two methods of preparation;[3] the reaction of halogenosilanes (X = Cl, Br, I) with (*a*) hydrazines and (*b*) lithium hydrazides. Especially lithium derivatives of silyl hydrazines showed a large variety in substitution and oxidation reactions. In 1964 Bailey and West discovered the migration of silyl groups from one nitrogen atom to the other and opened up a new era in organometallic chemistry.[4,5] In 1968 Wiberg *et al*. prepared the first bis(silyl)diazene, $Me_3SiN{=}NSiMe_3$ in the reaction of lithium tris(trimethylsilyl)hydrazide with tosylazide, a very reactive, thermally unstable compound.[6,7]

In spite of the successful use of the lithium hydrazides in preparative chemistry, the first crystal structure analyses were carried out only about 30 years later.[3,8] Since then, the crystal structures of seven hydrazides, all of which are only silyl substituted, have been published. The results were often unexpected. Hexameric, tetrameric and dimeric hydrazides have been described.[3,8–12] The lithium ions in these oligomers are differently 'side-on' and 'end-on' coordinated to the N–N unit. The degree of oligomerisation decreases with increasing bulkiness of the silyl substituents. We present the first crystal structure analysis of a monomeric dilithium derivative of an *N*,*N*′-bis(silyl)hydrazine and its oxidation to the bis(silyl)-diazene.

Dilithiated *N*,*N*′-bis(di-*tert*-butylmethylsilyl)hydrazine **1** is formed in the reaction of the bis(silyl)hydrazine with 2 equiv. of *n*-butyllithium in thf [eqn. (1)].†‡




The crystal structure of **1**§ which is depicted in Fig. 1 consists of well separated monomers. The lithium ions are 'side-on' coordinated to the N–N bond. They are *cis*-positioned to the hydrazine unit. The coordination sphere of the lithium ions is saturated with three thf molecules. One thf molecule bridges two lithium cations. In this case, Li–O contacts [Li(1)–O(2) 219.3 pm] are longer (19 pm) than the other [Li(1)–O(1) 200.0 pm]. The Li–N distances differ by about 10 pm [Li(1)–N(1a) 196.1; Li(1)– N(1) 185.7 pm]. The structural analysis confirms the *ab initio* calculations,[13] according to which lithium cations in hydrazides can be coordinated equally by both N atoms of the hydrazine.

Silyl derivatives of diazenes can be prepared with different oxidation methods of lithium hydrazides.[7] We used as oxidation

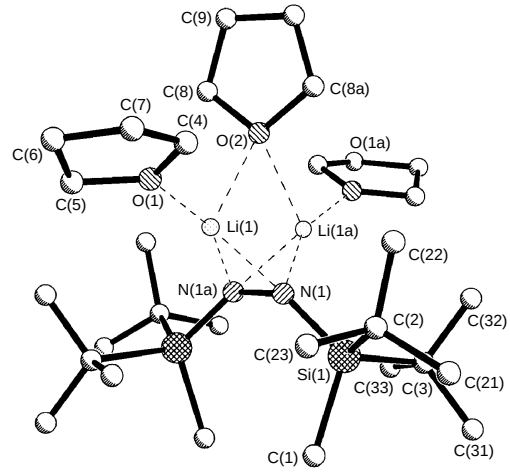
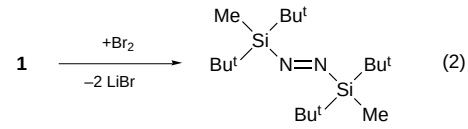



**Fig. 1** Molecular structure of **1**; selected bond lengths (pm) and angles (°): Si(1)–N(1) 168.2(4), Si(1)–C(1) 189.4(6), Si(1)–C(2) 192.6(5), Si(1)–C(3) 194.1(5), N(1)–N(1a) 153.1(6), N(1)–Li(1) 185.7(8), N(1)–Li(1a) 196.1(9), Li(1)–N(1a) 196.1(9), Li(1)–O(1) 200.0(9), Li(1)–O(2) 219.3(9); N(1a)–N(1)–Si(1) 131.7(2), N(1a)–N(1)–Li(1) 70.0(3), N(1a)–N(1)–Li(1a) 62.8(3), Si(1)–N(1)–Li(1a) 121.6(3), Li(1)–N(1)–Li(1a) 80.8(5), N(1)–Li(1)–N(1a) 47.2(3), N(1)–Li(1)–O(1) 139.2(5), N(1a)–Li(1)–O(1) 158.2(5), N(1)–Li(1)–O(2) 101.4(4), N(1a)–Li(1)–O(2) 98.1(4), O(1)–Li(1)–O(2) 99.7(4), Li(1)–O(2)–Li(1a) 68.7(4); atoms labelled a are related to unlabelled equivalents by the symmetry operation $-x + 1, y, -z + \frac{1}{2}$

reagent of **1** elemental bromine in thf and isolated the diazene **2** in about 50% yield [eqn. (2)].




Compound **2** is light green and thermostable in contrast to other known bis(silyl)diazenes,[7] which are thermally unstable, slowly decomposing above −35 °C and extremely air sensitive (inflammable in oxygen). **2** can be distilled at 90 °C (0.01 mbar) without decomposition and handled in the presence of air. Only one X-ray structural determination has been carried out of a bis(silyl)diazene, the bis(trimethylsilyl)diazene by Veith and Bärnighausen,[14] which shows that the diazene is *trans*-configurated with a planar SiNNSi framework. NMR measurements of **2** prove that it is only obtained as one stereoisomer.

This work was supported by the Deutsche Forschungsgemeinschaft and the Fonds der Chemischen Industrie.

## Footnotes

* E-mail: uklinge@gwdg.de

† *Preparative details*: **1**: *N*,*N*′-bis(di-*tert*-butylmethylsilyl)hydrazine (0.01 mol, 3.4 g) in *n*-hexane (20 ml) and thf (10 ml) was metallated with 2 equiv.

of *n*-butyllithium (23% in *n*-hexane). The mixture was heated to reflux for 4 h and **1** was obtained in crystalline form by slow cooling to −100 °C. Yield 95%.

**2**: **1** (0.03 mol, 10.3 g) was dissolved in 300 ml of thf. After cooling to −70 °C, a solution of bromine (0.025 mol, 4.00 g) in 100 ml thf was added slowly. The mixture was warmed to room temp. within 6 h and heated to reflux for 1 h. The crude product was purified by distillation. Yield 50%, bp 90 °C (0.01 mbar); FIMS: *m/z* (%) = 342 (100) $[M]^+$.

‡ *NMR data:* **1**: $^1$H NMR ($C_6D_6$, 250 MHz, $SiMe_4$), δ 0.28 (SiMe, 6 H), 1.15 ($SiCMe_3$, 36 H); $^{13}$C NMR ($C_6D_6$, 250 MHz, $SiMe_4$), δ −6.8 (SiC), 21.6 ($SiCC_3$), 29.9 ($SiCC_3$); $^7$Li NMR ($C_6D_6$, 250 MHz, LiCl), δ 0.67. **2**: $^1$H NMR ($C_6D_6$, 250 MHz, $SiMe_4$), δ −0.23 (SiMe, 6 H), 1.11 ($SiCMe_3$, 36 H); $^{13}$C NMR ($C_6D_6$, 250 MHz, $SiMe_4$), δ −11.89 (SiC), 20.29 ($SiCC_3$), 28.90 ($SiCC_3$); $^{29}$Si NMR ($C_6D_6$, 250 MHz, $SiMe_4$), δ 2.14.

§ *Crystal data for* **1**: a crystal of size 0.60 × 0.40 × 0.40 mm placed on a STOE/Siemens AED 2 four-circle diffractometer equipped with Mo-Kα radiation at 153 K. The space group is monoclinic, *C*2/*c*, with unit-cell dimensions $a$ = 18.840(6), $b$ = 12.104(7), $c$ = 18.170(7) Å, β = 117.48(2)°, $U$ = 3676.3 Å$^3$, $Z$ = 4; μ = 0.125 mm$^{-1}$, $F$(000) = 1272. 2548 Reflections up to 2θ = 45° were collected, of which 2396 were independent ($R_{int}$ = 0.05222). The structure was solved using direct methods (SHELXS) and refined on $F^2$ (SHELX-93) with no disorder indicated: $R_1[I > 2\sigma(I)]$ = 0.0767, $wR_2$ = 0.1878; for all 2548 data $R_1$ = 0.1104, $wR_2$ = 0.2203, GOF = 1.024. Atomic coordinates, bond lengths and angles and thermal parameters have been deposited at the Cambridge Crystallographic Data Centre (CCDC). See Information for Authors, Issue No. 1. Any request to the CCDC for this material should quote the full literature citation and the reference number 182/402.

## References


1 B. J. Aylett, *J. Inorg. Nucl. Chem*., 1956, **2**, 325.
2 U. Wannagat and W. Liehr, *Angew. Chem*., 1957, **69**, 783.
3 K. Bode and U. Klingebiel, *Adv. Organomet. Chem*., 1996, **40**, 1.
4 R. E. Bailey and R. West, *J. Am. Chem. Soc*., 1964, **86**, 5369.
5 R. West, *Adv. Organomet. Chem*., 1977, **16**, 1.
6 N. Wiberg, W.-Ch. Joo and W. Uhlenbrock, *Angew. Chem., Int. Ed. Engl*., 1968, **7**, 640.
7 N. Wiberg, *Adv. Organomet. Chem*., 1984, **23**, 131.
8 S. Dielkus, C. Drost, R. Herbst-Irmer and U. Klingebiel, *Angew. Chem*., 1993, **105**, 1689; *Angew. Chem., Int. Ed. Engl*., 1993, **32**, 1625.
9 N. Metzler, H. Nöth and H. Sachdev, *Angew. Chem*., 1994, **106**, 1837; *Angew. Chem., Int. Ed. Engl*., 1994, **33**, 1746.
10 H. Nöth, H. Sachdev, M. Schmidt and H. Schwenk, *Chem. Ber*., 1995, **128**, 105.
11 K. Bode, U. Klingebiel, H. Witte-Abel, M. Gluth, M. Noltemeyer, R. Herbst-Irmer, M. Schäfer and W. Shomaly, *Phosphorus, Sulfur, Silicon*, 1996, **108**, 121.
12 K. Bode, C. Drost, C. Jäger, U. Klingebiel, M. Noltemeyer and Z. Zak, *J. Organomet. Chem*., 1994, **482**, 285.
13 J. R. Dilworth, A. Rodriguez, G. R. Leigh and J. R. Murrell, *J. Chem. Soc., Dalton Trans*., 1983, **2**, 455.
14 M. Veith and H. Bärnighausen, *Acta Crystallogr., Sect. B*, 1974, **30**, 1806.



*Received in Cambridge, UK, 10th February 1997; Com. 7/00926G*

# $Fe(\eta^5\text{-}C_5H_5)^+$ initiated construction of hexaruthenium–polypyridine complexes

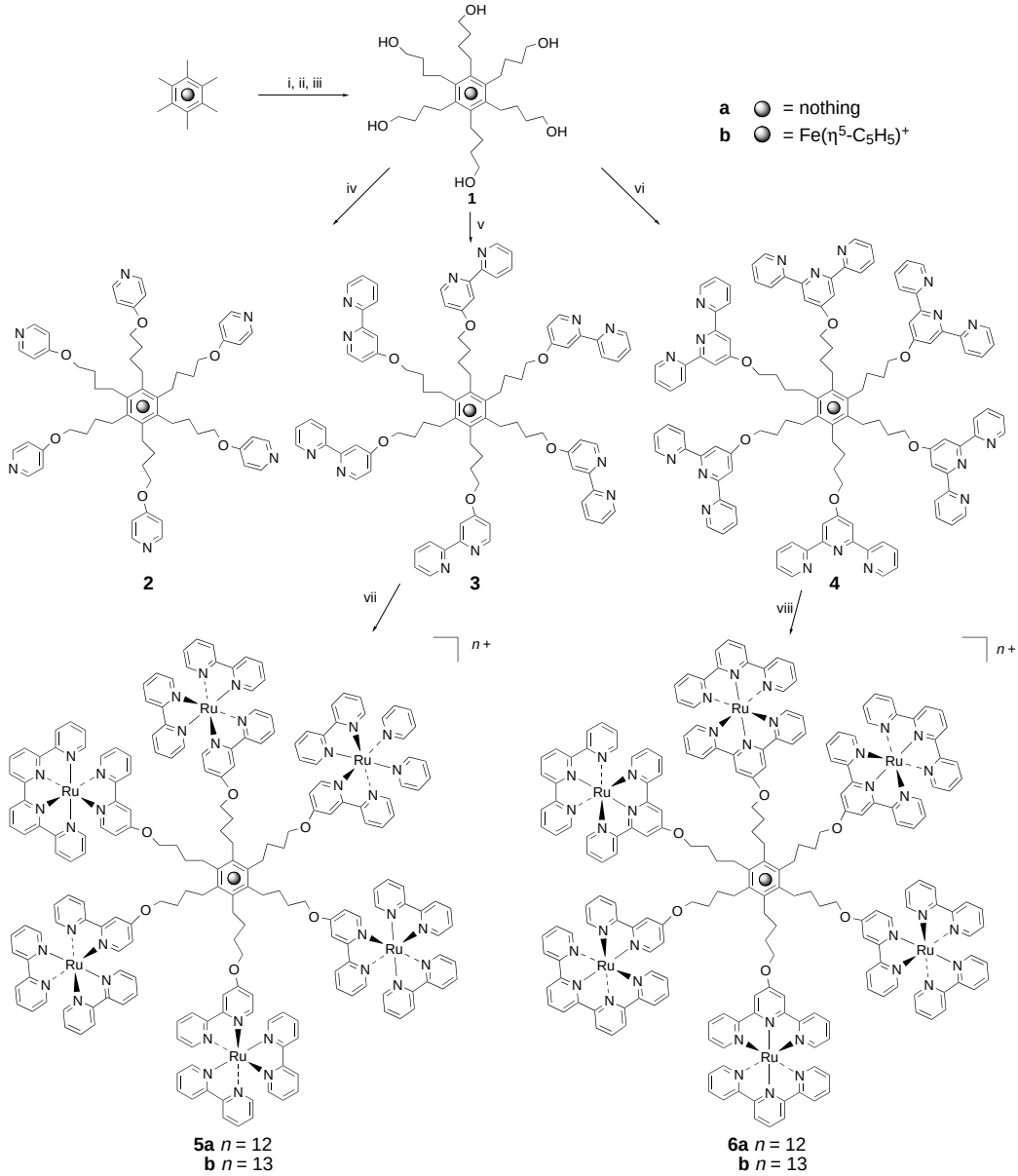
**Valérie Marvaud and Didier Astruc**

*Laboratoire de Chimie Organique et Organométallique, URA CNRS No 35, Université Bordeaux I, 33405 Talence Cédex, France*

**Aromatic stars containing hexa-pyridine, -bipyridine and -terpyridine branches are synthesised with or without the central $Fe(\eta^5\text{-}C_5H_5)^+$ group and coordinated to ruthenium(II) polypyridine moities to construct hexa- and hepta-nuclear hexa-bipyridine and -terpyridine complexes.**

Oligopyridines have recently fascinated the supramolecular chemistry community[1] as powerful building blocks for the construction of inorganic helicates,[2,3] antennas,[4] metallo-stars[5] and metallo-dendrimers[6] containing photoactive redox sites.[1,4,7] In this context, and given our interest in redox-active metallodendrimers for molecular recognition and electronics and polyelectronic redox catalysis,[8] we have synthesized 'inorganometallic' hexaruthenium(II) bipyridine and terpyridine complexes which we are now reporting for the first time.

Our standard route which involves the hexa-alkylation of $[Fe^{II}(\eta^5\text{-}C_5H_5)(\eta^6\text{-}C_6Me_6)]PF_6$ using iodoalkyl derivatives under basic conditions is very successful, for instance to




**Scheme 1** Synthesis of the hexaruthenium and heptametallic complexes; *Reagents and conditions*: i, Bu$^t$OK, allylbromide, thf; ii, if decomplexation is required: $h\nu_{vis}$, $PPh_3$, MeCN; iii, $BH_3$·thf, methylbut-2-ene, thf; then $H_2O_2$, $OH^-$; iv, KOH, $Me_2SO$, 4-bromopyridine, 30 °C; v, KOH, $Me_2SO$, 4-chloro-2,2′-bipyridine, 30 °C; vi, KOH, $Me_2SO$, 4′-chloro-2,2′:6′2″-terpyridine, 30 °C; vii, $[Ru(bipy)_2Cl_2]$, ethanol, 80 °C, $NH_4PF_6$; viii, $[Ru(terpy)Cl_3]$, *N*-ethylmorpholine, methanol, 80 °C, $NH_4PF_6$

synthesize hexaferrocene stars.[9] However, all attempts to obtain the hexapyridine compound by direct alkylation of $[Fe^{II}(\eta^5\text{-}C_5H_5)_2(\eta^6\text{-}C_6Me_6)]PF_6$ with 4-iodoalkyl-4′-methyl-2,2′-bipyridine in the presence of KOH and dimethoxyethane (dme) failed, apparently due to dehydrohalogenation or/and partial decomplexation of the $[Fe(\eta^5\text{-}C_5H_5)(\eta^6\text{-}C_6Me_6)]^+$ complex in the presence of 2,2′-bipyridine. A new synthetic strategy was therefore required, the principle of which consisted of synthesizing the hexol before coupling the 4-chloro-2,2′-bipyridine derivative by alkoxy dehalogenation.[10] Using this approach, we also synthesized the hexapyridine and hexaterpyridine compounds which were successfully hexaruthenated.

Perallylation of $[Fe^{II}(\eta^5\text{-}C_5H_5)(\eta^6\text{-}C_6Me_6)]PF_6$ eventually followed by visible photolysis, regiospecific hydroboration and oxidation using $H_2O_2$ under basic conditions yields the hexol **1a** and the corresponding iron complex **1b**, as already known,[9b] Scheme 1. The reaction of these two products, **1a** and **1b**, with bromo- or chloro-pyridyl compounds (4-bromopyridine, 4-chloro-2,2′-bipyridine and 4′-chloro-2,2′:6′,2″-terpyridine) in $Me_2SO$ in the presence of KOH gave the associated hexasubstituted products, soluble in organic solvents and fully characterised by NMR ($^1H$, $^{13}C$, COSY spectroscopy) and mass spectra ($FAB^+$). The analytical and spectroscopic data for hexapyridine **2a**, hexabipyridine **3a**, hexaterpyridine **5a**, $[Fe(\eta^5\text{-}C_5H_5)(\text{hexapyridine})]PF_6$ **2b** and $[Fe(\eta^5\text{-}C_5H_5)(\text{hexaterpyridine})]PF_6$ **5b**† show the expected structures. The reaction of **1b** with 4-chloro-2,2′-bipyridine was disappointing, the expected $Fe(\eta^5\text{-}C_5H_5)$ complex of the hexabipyridine **3b** was never cleanly obtained. This is probably due to a partial decomplexation of the $[Fe(\eta^5\text{-}C_5H_5)(\eta^6\text{-}C_6Me_6)]^+$ complex, as mentioned above. Interestingly, this decomplexation is limited with the terpyridine derivatives, the difference with the bipyridine case being explained by steric effects. The ruthenation of **3a**, **4a** and **4b** was carried out using standard procedures with $[Ru(bipy)_2Cl_2]$ and $[Ru(terpy)Cl_3]$ as starting materials. The products **5a** and **6a** were then obtained and fully characterized by NMR ($^1H$, $^{13}C$, COSY spectroscopy) and mass spectra (MALDI-TOF and electrospray, ES).

The MALDI-TOF spectra show peaks at *m/z* 5510.7 and 5499.1 which are assigned to (**5a** − $PF_6$) and (**6a** − $PF_6$); these results were confirmed by the ES spectra. Further evidence for the presence of the terminal $[Ru(bipy)_3]^{2+}$ moieties is given by electrochemical measurements where the set of $Ru^{II}$–$Ru^{III}$ redox systems gives a single and reversible anodic wave at +0.82 and +0.79 V (*vs.* Fc–$Fc^+$) respectively. For compound **6b**, partial decomplexation of the iron core is indicated by the ES data.

We have shown that a new synthetic route for metallo-stars is open *via* a combination of organometallic, organic and inorganic chemistry. We are currently carrying out further studies on the construction of higher generations of functionalised dendrimers containing ruthenium polypyridine complexes at the periphery.

We thank J. Guittard, J.-C. Blais, E. Leize and A. Van Dorsselaer for the mass spectroscopic studies.

## Footnotes

† Preparations of 4-chloro-2,2′-bipyridine[11a] and $[Ru(terpy)Cl_3]$[11b] were performed by the literature method.

**5a** (89% yield): $^1H$ NMR [250 MHz, $(CD_3)_2CO$], δ 8.73 (d, 5 H, CHbipy 3′), 8.20 (s 1 H, $CHbipy_{int}$ 3), 8.13 (d, 5 H, CHbipy 4′), 7.99 (d, 5 H, CHbipy 6′), 7.66 (d, 1 H, $CHbipy_{int}$ 6), 7.52 (m, 5 H, CHbipy 5′), 7.03 (m, 1 H, $CHbipy_{int}$ 5), 4.28 (br. s, 2 H, $CH_2O$), 2.67 (br. s, 2 H, C*H*$_2$Ar), 1.89 (br. s, 2 H, C*H*$_2$$CH_2O$), 1.65 (br. s, 2 H, C*H*$_2$$CH_2$Ar); $^{13}C$ NMR [250 MHz, $(CD_3)_2CO$], δ 167.64 ($C_q$O), 158.92 and 158.08 ($C_q$ bipy), 152.96 and 152.56 (CHbipy 6 and 6′), 138.72 (CHbipy 4′), 137.40 ($C_q$ Ar), 128.72 (CHbipy 5′), 125.22 (CHbipy 3′), 115.57 (CHbipy 5), 111.71 (CHbipy 3), 66.14 ($CH_2O$), 29.35, 29.05 and 25.82 ($CH_2$); MS (MALDI-TOF): *m/z* 5510.7 (M − $PF_6$), $C_{210}H_{186}F_{72}N_{36}O_6P_{12}Ru_6$ requires *m/z* 5655.97, −$PF_6$ *m/z* −5510.9.

**6a** (88% yield): $^1H$ NMR [250 MHz, $(CD_3)_2CO$], δ 8.97 (d, 2 H, $CHterpy_{ext}$ 3′), 8.71 (m, 4 H, CHterpy 3), 8.61 (s, 2 H $CHterpy_{int}$ 3′), 8.47 (t, 1 H, $CHterpy_{ext}$ 4′), 7.86 (m, 4 H, CHterpy 4), 7.73 and 7.60 (d, 4 H, CHterpy 6), 7.18 (br. s, 4 H, CHterpy 5), 4.85 (br. t, 2 H, $CH_2O$), 3.18 (br. s, 2 H, C*H*$_2$Ar), 2.44 (br. s, 2 H, C*H*$_2$$CH_2O$), 2.16 (br s, 2 H, C*H*$CH_2$Ar); $^{13}C$ NMR [250 MHz, $(CD_3)_2CO$], δ 167.00 ($C_q$terpyO), 159.34 and 156.84 ($C_q$ terpy 2 and 2′), 153.57 and 153.26 (CHterpy 6), 138.77 and 137.71 (CHterpy 4 and 4′), 137.71 ($C_q$ Ar), 128.55 (CHterpy 5), 125.5 and 125.24 (CHterpy 3), 124.72 ($CHterpy_{ext}$ 3′), 112.18 ($CHterpy_{int}$ 3′), 71.36 ($CH_2O$), 30.68, 30.25, 29.01 ($CH_2$); MS (MALDI-TOF): *m/z* 5499.1 (M − $PF_6$), $C_{210}H_{174}F_{72}N_{36}O_6P_{12}Ru_6$ requires *m/z* 5643.92, (−$PF_6$) *m/z* 5498.9.

**6b**: $^1H$ NMR [250 MHz, $(CD_3)_2CO$], δ 8.95 (br. d, 12 H, $CHterpy_{ext}$ 3′), 8.68 (br m, 24 H, CHterpy 3), 8.61 (br s, 12 H, $CHterpy_{int}$ 3′), 8.47 (br t, 6 H, $CHterpy_{ext}$ 4′), 7.88 (br m, 24 H, CHterpy 4), 7.72 and 7.58 (d, 24 H, CHterpy 6) 7.17 (br s, 24 H, CHterpy 5), 4.93 (br s, 5 H, $C_5H_5$), 4.82 (br. t, 12 H, $CH_2O$), 3.43 (br s, 12 H, C*H*$_2$Ar), 2.37 (br s, 12 H, C*H*$_2$$CH_2O$), 2.07 (br s, 12 H, C*H*$_2$$CH_2$Ar); $^{13}C$ NMR [250 MHz, $(CD_3)_2CO$], δ 166.98 ($C_q$terpyO), 158.32 and 155.63 ($C_q$terpy 2 and 2′), 152.56 and 152.07 (CHterpy 6), 138.68 and 137.75 ($CHterpy_{ext}$ 4 and 4′), 127.56 (CHterpy 5), 124.48 and 124.18 (CHterpy 3), 123.71 ($CHterpy_{ext}$ 3′), 111.21 ($CHterpy_{int}$ 3′), 102.55 ($C_q$ Ar), 78.32 ($C_5H_5$), 69.38 ($CH_2O$), 29.57, 28.86, 26.48 ($CH_2$). MS (ES): *m/z* 1333.8 ($M^{4+}$), 1037.6 ($M^{5+}$), 840.2 ($M^{6+}$), corresponding to a measured mass of 5911.92 ($M^+$), $C_{215}H_{179}FeF_{78}N_{36}O_6P_{13}Ru_6$ requires *m/z* 5912.37.

## References


1 J.-M. Lehn, *Supramolecular Chemistry*, VCH, Weinheim, 1995; V. Balzani and F. Scandola, *Supramolecular Photochemistry*, Ellis Horwood, New York, 1991. V. Balzani, *Supramolecular Photochemistry*, Reidel, Dordrecht, 1987, p. 35; F. Vögtle, *Supramolecular Chemistry*, 2nd edn., Wiley, Chichester.

2 K. Wärnmark, O. Heyke, J. A. Thomas and J.-M. Lehn, *Chem. Commun*., 1996, 2603; C. Fouquey, J.-M. Lehn and A.-M. Levelut, *Adv. Mater*., 1990, **2**, 254; T. Gulik-Krzywicki, C. Fouquey and J.-M. Lehn, *Proc. Natl. Acad. Sci. USA*, 1993, **90**, 163; R. Krämer, J.-M. Lehn and A. Marquis-Rigault, *Proc. Natl. Acad. Sci. USA*, 1993, **90**, 53934.

3 E. C. Constable, in *Comprehensive Supramolecular Chemistry*, ed. J.-P. Sauvage and M.-W. Hosseini, Pergamon, Oxford, 1996, vol. 9, ch. 6, pp. 213–252; C. Piguet, G. Hopfgartner, B. Bocquet, O. Schaad and A. F. Williams, *J. Am. Chem. Soc*., 1994, **116**, 9092; C. Piguet, J. C. G. Bunzli, G. Bernardinelli, G. Hopfgartner and A. F. Williams, *J. Chem. Soc., Chem. Commun*., 1995, 491; U. Velten and M. Rehahn, *Chem. Commun*., 1996, 2639.

4 S. Serroni, G. Denti, S. Campagna, A. Juris, M. Ciano and V. Balzani, *Angew. Chem*., 1992, **104**, 1540; *Angew. Chem., Int. Ed. Engl*., 1992, **31**, 1493; S. Denti, S. Campagna, S. Serroni, M. Ciano and V. Balzani, *J. Am. Chem. Soc*., 1992, **114**, 2944; S. Campagna, G. Denti, S. Serroni, M. Ciano, A. Juris and V. Balzani, *Inorg. Chem*., 1992, **31**, 2982; V. Balzani, A. Credi and F. Scandola, in *Transition Metals in Supramolecular Chemistry*, ed. L. Fabbrizzi and A. Poggi, Kluwer, Dordrecht, 1994, p. 1.

5 G. R. Newkome, F. Cardullo, E. C. Constable, C. N. Moorefield and A. M. W. Cargill Thomson, *J. Chem. Soc., Chem. Commun*., 1993, 925; E. C. Constable and P. Harverson, *Chem. Commun*., 1996, 33; E. C. Constable, P. Harverson and M. Oberholzer, *Chem. Commun*., 1996, 1821.

6 C. Moucheron, A. Kirsch-De Mesmaeker, A. Dupont-Gervais, E. Leize and A. Van Dorsselaer, *J. Am. Chem. Soc*., 1996, **118**, 12834.

7 V. Balzani, A. Juris, M. Venturi, S. Campagna and S. Serroni, *Chem. Rev*., 1996, **96**, 759; J.-P. Sauvage, S. Guillerez, C. Coudret, V. Balzani, F. Barigeletti, L. De Cola and L. Flamigni, *Chem. Rev*., 1994, **94**, 993; A. Juris, V. Balzani, F. Barigeletti, S. Campagna, P. Belser and A. Von Zelewski, *Coord. Chem. Rev*., 1988, **84**, 85; P. J. Steel, *Coord. Chem. Rev*., 1990, **106**, 227.

8 D. Astruc, *Electron Transfer and Radical Processes in Transition-Metal Chemistry*, VCH, New York, 1995, ch. 2; D. Astruc, in *Mechanisms and Processes in Molecular Chemistry*, ed. D. Astruc, Gauthier-Villard, Paris; *New J. Chem*., 1992, **16**, 305.

9 (*a*) J.-L. Fillaut, J. Linares and D. Astruc, *Angew. Chem*., 1994, **106**, 2540; *Angew. Chem., Int. Ed. Engl*., 1994, **33**, 2460; (*b*) F. Moulines and D. Astruc, *Angew. Chem*., 1988, **100**, 1394; *Angew. Chem., Int. Ed. Engl*., 1988, **27**, 1347.

10 C. A. Fyfe, in *The Chemistry of the Hydroxyl group*, Part 1, ed. S. Patai, Wiley, New York, 1971, pp. 83–124.

11 (*a*) R. A. Jones, B. d. Roney, W. H. F. Sasse and K. O. Wade, *J. Chem. Soc. B*, 1967, 106; (*b*) B. P. Sullivan, J. M. Calvert and T. Meter, *Inorg. Chem*., 1980, **19**, 1404.


*Received, 16th January 1997; Com. 7/00386B*

# A cyclometallated ruthenium(II) complex with a sterically hindered ligand displaying a long-lived MLCT excited state

**Jean-Paul Collin,[a] Robert Kayhanian,[a] Jean-Pierre Sauvage,[a]* Giuseppe Calogero,[b] Francesco Barigelletti,[b] André De Cian[c] and Jean Fischer[c]**

[a] *Laboratoire de Chimie Organo-Minérale, UA 422 au CNRS, Institut de Chimie, Université Louis Pasteur, 4 rue Blaise Pascal, F-67070 Strasbourg, France*
[b] *Istituto FRAE-CNR, via P. Gobetti 101, 40129 Bologna, Italy*
[c] *Laboratoire de Cristallochimie et de Chimie Structurale, UA 424 au CNRS, Institut de Chimie, Université Louis Pasteur, 4 rue Blaise Pascal, F-67070 Strasbourg, France*

**Two cyclometallated ruthenium(II) complexes incorporating mono- or di-substituted phenanthroline moieties are synthesized and characterized by single-crystal X-ray diffraction; the complex with a sterically hindered ligand displays a long-lived MLCT excited state.**

Transition-metal complexes exhibiting luminescence from metal-to-ligand charge transfer (MLCT) excited states have been the subject of numerous studies.[1] In this field, the $d^6$ polypyridyl complexes of $Ru^{II}$,[2] $Os^{II}$[3,4] and $Re^{I}$[5] form the major class of such compounds. Recently, cyclometallated complexes[6,7] of $d^6$ and $d^8$ transition-metal ions have also shown interesting photophysical properties. Since ruthenium terpyridine type complexes are particularly suitable to build up multicomponent systems,[8] the search for compounds of this type displaying long-lived MLCT excited states at room temperature remains a stimulating challenge. Here, we describe the synthesis, crystal structures and photophysical properties of two luminescent cyclometallated ruthenium complexes. Interestingly, the photophysical properties of the compounds can be strongly modified by introducing small structural changes in the cyclometallating ligand.

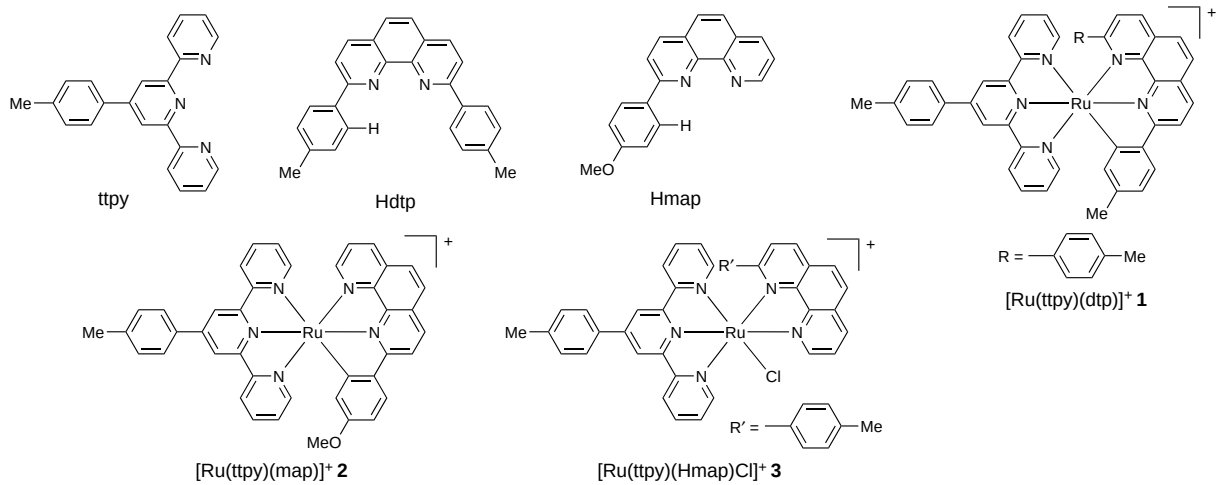
In the presently reported complexes, 4′-tolyl-2,2′:6′,6″-terpyridine (ttpy) affords NNN coordination. It is associated with the 1,10-phenanthroline ligand bearing different aromatic substituents in the 2 and 9 positions and leading to NNC coordination. The aromatic sustituents are two tolyl groups for Hdtp[9] and a *p*-anisyl group for Hmap[10] (Scheme 1).

The deep purple complexes $[Ru(ttpy)(dtp)]^+$ **1** and $[Ru(ttpy)(map)]^+$ **2** were prepared by the reaction of $[Ru(ttpy)Cl_3]$ with the phenanthroline ligand Hdtp or Hmap in refluxing acetic acid in the presence of one drop of *N*-ethylmorpholine. Considering that both cyclometallated (NNC) and the non-cyclometallated (NN) products could be obtained with Hmap, it is not surprising, in view of previous results[11] that Hdtp leads exclusively to the formation of the cyclometallated (NNC) compound. Satisfactory analytical data have been obtained for these complexes. Single crystals of **1** and **2** were obtained by slow diffusion of benzene into an acetonitrile solution of each compound. The structures of **1** and **2** were determined by single-crystal X-ray diffraction† and the ORTEP diagrams are shown in Fig. 1 and 2.

By comparing the X-ray structures of **1** and **2**, it is clear that the ruthenium(II) coordination polyhedra are very similar, except for one particular Ru–N distance. In fact, the bond between the metal and the nitrogen atom *ortho* to the linkage point of the tolyl group borne by the phenanthroline nucleus is *ca*. 0.06 Å longer in **1** than in the unsubstituted compound **2**. This difference probably reflects the steric effect of the aromatic group in the vicinity of the Ru coordination sphere, which is also in agreement with the close proximity between the tolyl group and the central pyridine ring of the ttpy chelate. This stacking situation is likely to result in donor–acceptor interactions involving the tolyl group (donor) and the Ru-bonded central pyridine (acceptor). This would explain the very different photophysical behaviour of **1** as compared to **2**.

The electrochemical and spectroscopic data for **1** and **2** are collected in Table 1.

It is of note that whereas **2** is practically not luminescent in acetonitrile at room temperature, **1** luminesces and displays a




**Scheme 1**

relatively long-lived excited state ($\tau$ = 95 ns). In fact, **1** seems to be one of the longest-lived[12] terpy-type ruthenium(II) complexes.

Clearly, the electronic properties of both compounds **1** and **2** seem to be almost identical (Table 1). The remarkable effect of the tolyl group onto the MLCT excited state lifetime of **1** could be related to the steric protection of the metal and strong rigidifying of the molecular edifice *via* $\pi$–$\pi$ interaction with the ttpy ligand of the complex.

This work has been supported by the CNRS (France) and by CNR (Italy). We thank Patrice Staub for his technical assistance.

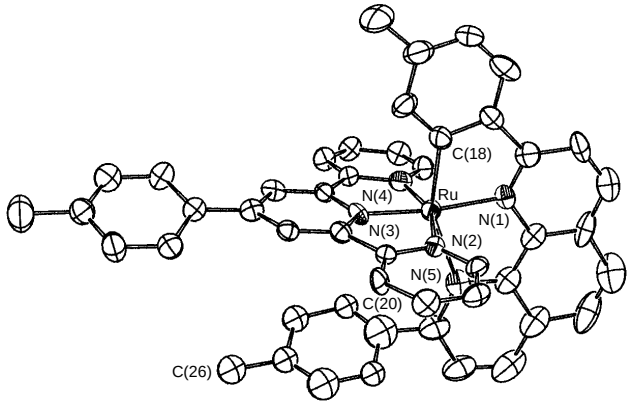



**Fig. 1** ORTEP view of the cationic part of **1** with partial labelling scheme. Ellipsoïds are scaled to enclose 30% of the electronic density. One orientation of the C(20)–C(26) tolyl moiety is shown. Hydrogen atoms are omitted. Selected distances (Å) and angles (°): Ru–N(1) 2.010(2), Ru–N(2) 2.256(3), Ru–N(3) 2.031(3), Ru–N(4) 1.942(3), Ru–N(5) 2.052(2), Ru–C(18) 2.037(4); N(1)–Ru–N(2) 76.6(1), N(1)–Ru–C(18) 78.3(1), N(1)–Ru–N(2) 100.6(1), N(3)–Ru–N(4) 79.8(1), N(4)–Ru–C(18) 93.5(1), N(2)–Ru–N(4) 111.5(1).

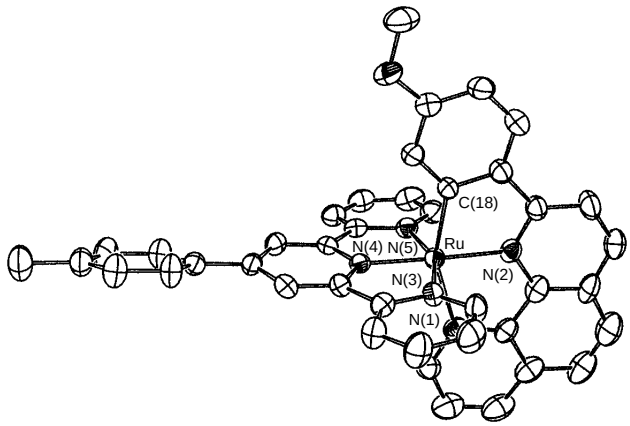



**Fig. 2** ORTEP view of the cationic part of **2** with partial labelling scheme. Ellipsoïds are scaled to enclose 30% of the electronic density. Selected distances (Å) and angles (°): Ru–N(1) 2.198(6), Ru–N(2) 2.009(6), Ru–C(18) 2.030(8), Ru–N(3) 2.050(5), Ru–N(4) 1.961(6), Ru–N(5) 2.062; N(1)–Ru–N(2) 76.9(2), N(1)–Ru–N(3) 93.7(2), N(1)–Ru–N(4) 105.4(2), N(2)–Ru–C(18) 79.1(3), N(3)–Ru–N(4) 78.8(2), N(4)–Ru–C(18) 98.6(3).

**Table 1** Electrochemical[a] and spectroscopic data[b]

| | Redox potential; V *vs.* SCE | | | | | |
|---|---|---|---|---|---|---|
| | $Ru^{3+/2+}$ | $L^{0/1-}$ | $\lambda_{abs}$/nm | $\lambda_{em}$/nm | $\tau$/ns | $\Phi$ |
| **1** | 0.54 | −1.57 | 527 | 802 | 95 | 0.02 |
| **2** | 0.54 | −1.54 | 518 | [c] | [c] | [c] |
| **3** | 0.77 | −1.50 | 508 | 820 | 6.6 | $\leqslant 1 \times 10^{-5}$ |

[a] Cyclic voltammetry in MeCN solution (0.1 M $NBu^n_4BF_4$); Pt working electrode. [b] MeCN solutions; room temperature; uncorrected luminescence band maxima. Luminescence quantum yields and lifetimes were determined as in F. Barigelletti, L. Flamigni, M. Guardigli, A. Juris, M. Beley, S. Chodorowski-Kimmes, J.-P. Collin and J.-P. Sauvage, *Inorg. Chem.*, 1996, **35**, 136. [c] Too weak to detect.

## Footnotes

* E-mail: sauvage@chimie.u-strasbg.fr

† *Crystal data*: **1**, purple crystals from benzene–acetonitrile. $2(C_{48}H_{36}F_6N_5PRu)\cdot CH_3CN$, $M$ = 1898.8, monoclinic, space group $P2_1/n$; $a$ = 21.196(6), $b$ = 17.212(5), $c$ = 11.312(3) Å, $\beta$ = 95.40(2), $U$ = 4103(3) Å$^3$, $Z$ = 2, $D_c$ = 1.537 g cm$^{-3}$, $\mu$ = 41.337 cm$^{-1}$. Measurements: Philips PW1100/16, $\theta$–2$\theta$ flying step-scans, Cu-K$\alpha$ graphite-monochromated radiation ($\lambda$ = 1.5418 Å), $T$ = 173 K. 5396 reflections ($\theta$ = 3–54°), of which 4334 unique with $I > 3\sigma(I)$ were used for structure solution (direct methods) and refinement (full-matrix least squares); $R$ = 0.081, $R_w$ = 0.143. The C(20)–C(26) tolyl moiety adopts two orientations (50/50); for one of them a MeCN solvent molecule is present. Atoms C(25)–C(26) in both orientations were introduced as fixed contributors with isotropic temperature factors allowed to vary during refinement. All other non-hydrogen atoms were refined anisotropically. The hydrogen atoms were calculated and fixed in idealized positions [$d$(C–H) = 0.95 Å, $B$(H) = 1.3 $B_{equiv}$ for the carbon to which it was attached] with the exception of C(20)–C(26) tolyl and $CH_3CN$ protons not introduced. **2**, dark blue crystals from benzene–acetonitrile. $C_{41}H_{30}F_6N_5OPRu$, $M$ = 854.8; monoclinic, space group $P2_1/n$; $a$ = 12.535(3), $b$ = 16.512(4), $c$ = 18.334(5) Å, $\beta$ = 107.86(2), $U$ = 3611(3) Å$^3$, $Z$ = 4, $D_c$ = 1.572 g cm$^{-3}$, $\mu$ = 5.387 cm$^{-1}$. Measurements: Nonius MACH3, $\theta$–2$\theta$ scans, Mo-K$\alpha$ graphite-monochromated radiation ($\lambda$ = 0.7107 Å), $T$ = 283 K. 8376 reflections ($\theta$ = 2–26°), of which 3664 unique with $I > 3\sigma(I)$ were used for structure solution (direct methods) and refinement (full-matrix least squares); $R$ = 0.056, $R_w$ = 0.076. The fluorine atoms of the $PF_6^-$ anion are disordered over two positions (50/50) and where assigned isotropic temperature factors. All other non-hydrogen atoms were refined anisotropically and treated as above. For all computations, the Nonius MolEN/Vax package was used.[13]

Atomic coordinates, bond lengths and angles, and thermal parameters have been deposited at the Cambridge Crystallographic Data Centre (CCDC). See Information for Authors, Issue No. 1. Any request to the CCDC for this material should quote the full literature citation and the reference number 182/389.

## References

1 V. Balzani and F. Scandola, *Supramolecular Photochemistry*, Ellis Horwood, Chichester, 1991.
2 A. Juris, V. Balzani, F. Barigelletti, S. Campagna, P. Belser and A. Von Zelewsky, *Coord. Chem. Rev.*, 1988, **84**, 85.
3 C. Creutz, M. Chou, T. L. Netzel, M. Okamura and N. Sutin, *J. Am. Chem. Soc.*, 1980, **102**, 1309.
4 E. M. Kober, J. L. Marshall, W. J. Dressick, B. P. Sullivan, J. V. Caspar and T. J. Meyer, *Inorg. Chem.*, 1985, **24**, 2755.
5 A. J. Lees, *Chem. Rev.*, 1987, **87**, 711.
6 F. Barigelletti, D. Sandrini, M. Maestri, V. Balzani, A. Von Zelewsky, L. Chassot, P. Jolliot and U. Maeder, *Inorg. Chem.*, 1988, **27**, 3644; J. P. Collin, M. Beley and J. P. Sauvage, *Inorg. Chim. Acta*, 1991, **186**, 91.
7 P. Spellane and R. J. Watts, *Inorg. Chem.*, 1993, **32**, 5633.
8 J.-P. Sauvage, J.-P. Collin, J.-C. Chambron, S. Guillerez, C. Coudret, V. Balzani, F. Barigelletti, L. De Cola and L. Flamigni, *Chem. Rev.*, 1994, **94**, 993.
9 C. O. Dietrich-Buchecker, J. F. Nierengarten, J. P. Sauvage, N. Armaroli, V. Balzani and L. De Cola, *J. Am. Chem. Soc.*, 1993, **115**, 11 237.
10 S. Chardon-Noblat and J.-P. Sauvage, *Tetrahedron*, 1991, **47**, 5123.
11 E. C. Constable and M. J. Hannon, *Inorg. Chim. Acta*, 1993, **211**, 101.
12 M. Maestri, N. Armaroli, V. Balzani, E. C. Constable and A. M. W. Cargill Thompson, *Inorg. Chem.*, 1995, **34**, 2759.
13 C. K. Fair, in MolEN, *An Interactive Intelligent System for Crystal Structure Analysis*, Nonius, Delft, The Netherlands, 1990.

*Received in Basel, Switzerland, 4th December 1996; Com. 6/08175D*

# Activation of $CO_2$ by laser-ablated group 6 metal atoms

**Philip F. Souter and Lester Andrews***

*Department of Chemistry, University of Virginia, Charlottesville, Virginia 22901, USA*

**The primary reaction products of laser-ablated group 6 atoms with $CO_2$ prove to be the insertion products OMCO and $O_2M(CO)_2$ (M = Cr, Mo, W) which are isolated in argon matrices and identified by the effects of isotopic substitution on their IR spectra.**

Carbon dioxide is a naturally abundant carbon source that has been implicated as a contributor to the predicted global warming often referred to as the 'greenhouse effect'. The interaction between $CO_2$ and transition-metal centres is receiving increased attention[1–4] as the possibilities of recycling $CO_2$ generated in industrial emissions[5] and also of replacing petroleum with $CO_2$ as the starting material for the synthesis of fine chemicals[6] both represent exciting and important goals. Previous studies of the interaction of metal atoms with $CO_2$ in low-temperature matrices focussed on the interaction of Li,[7] Cs[8] and Al[9] with $CO_2$. Additionally the interaction of several of the first-row transition metals, including Cr, with $CO_2$ has been investigated both experimentally in solid $CO_2$[10] and theoretically.[11] In this laboratory, the reactions of B, U, Ti and Be with $CO_2$ have been investigated and all four were found to insert into $CO_2$ to give OMCO (M = B, U, Ti, Be) as the primary reaction product.[12–15] Much attention has been devoted to the organometallic chemistry of $CO_2$ and a comprehensive review has recently been published.[4] The main problem with the chemistry of $CO_2$ lies in its inherent thermodynamic stability and methods of 'activating' $CO_2$ are consequently actively being sought. We have studied the reactions between laser-ablated group 6 metal atoms and $CO_2$–Ar mixtures and have trapped the reaction products, including OMCO and $O_2M(CO)_2$, in argon matrices and identified them by the effects of isotopic substitution.

The technique used for matrix investigation of the reactions of pulsed laser-ablated metal atoms has been detailed previously.[12–16] FTIR spectra were recorded on a Nicolet 550 at 0.5 $cm^{-1}$ resolution. Typically mixtures of between 0.5 and 2%

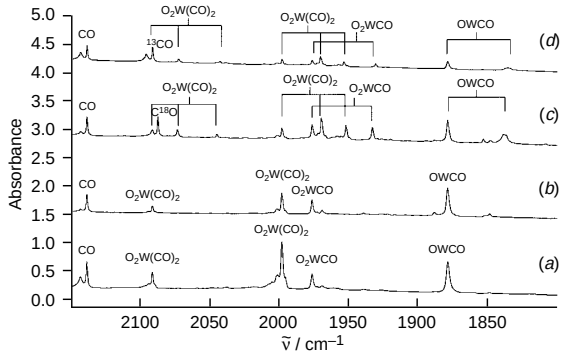



**Fig. 1** IR spectra in the region 2150–1800 $cm^{-1}$ for samples from the reactions of W atoms with $CO_2$ mixtures in argon during condensation at 6–7 K; (*a*) 2% $CO_2$, (*b*) 0.5% $CO_2$, (*c*) 0.5% $C^{16}O_2$–$C^{16}O^{18}O$–$C^{18}O_2$ and (*d*) 0.5% $^{12}CO_2$–$^{13}CO_2$ after annealing to 20 K followed by broad-band UV photolysis and further annealing to 30 K

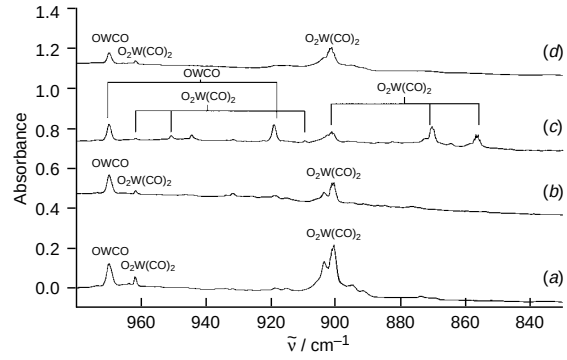



**Fig. 2** IR spectra in the region 980–830 $cm^{-1}$ for samples from the reactions of W atoms with $CO_2$ mixtures in argon during condensation at 6–7 K; (*a*) 2% $CO_2$, (*b*) 0.5% $CO_2$, (*c*) 0.5% $C^{16}O_2$–$C^{16}O^{18}O$–$C^{18}O_2$ and (*d*) 0.5% $^{12}CO_2$–$^{13}CO_2$ after annealing to 20 K followed by broad-band UV photolysis and further annealing to 30 K

**Table 1** Observed IR absorptions ($cm^{-1}$) of the dominant products in the reaction of laser-ablated group 6 atoms with $CO_2$ trapped in an Ar matrix at *ca.* 6–7 K

| Molecule | $CO_2$ | $^{13}CO_2$ | $^{12}CO_2$–$^{13}CO_2$ | $C^{18}O_2$ | $C^{16}O_2$–$C^{16}OC^{18}O$–$C^{18}O_2$ | Assignment |
|---|---|---|---|---|---|---|
| OCrCO[a] | 2014.4 | 1969.7 | 2014.4, 1969.7 | 1967.3 | 2014.4, 1967.3 | ν(C–O) |
| | 866.3 | 866.3 | 866.3 | 829.5 | 866.3, 829.5 | ν(Cr–O) |
| OMoCO[b] | 1847.0 | 1804.3 | 1847.0, 1804.3 | 1806.1 | 1847.0, 1806.1 | ν(C–O) |
| | 951.8 | 952.4 | 951.8, 952.4 | 905.3 | 951.8, 905.3 | ν(Mo–O) |
| OWCO | 1879.0 | 1837.0 | 1879.0, 1837.0 | 1838.8 | 1879.0, 1838.8 | ν(C–O) |
| | 969.6 | 969.6 | 969.6 | 918.9 | 969.6, 918.9 | ν(C–O) |
| $O_2Cr(CO)_2$[a] | 2123.2 | 2074.8 | 2123.2, 2074.8 | 2075.3 | 2123.2, 2107.2, 2075.3 | ν(C–O) |
| | 2059.7 | 2013.8 | 2059.7, 2013.8 | 2011.6 | 2058.7, 2027.6, 2011.6 | ν(C–O) |
| | 981.4 | 981.4 | 981.4 | 945.1 | 981.4, 975.4, 945.1 | ν(Cr–O)[c] |
| | 941.6 | 941.6 | 941.6 | 892.2 | 941.6, 903.0, 842.2 | ν(Cr–O)[d] |
| $O_2Mo(CO)_2$[b] | 2101.9 | 2053.9 | 2101.9, 2084.0, 2053.8 | 2054.7 | 2101.9, 2084.6, 2054.7 | ν(C–O) |
| | 2020.1 | 1975.4 | 2020.1, 1991.4, 1975.4 | 1972.7 | 2020.1, 1990.0, 1972.7 | ν(C–O) |
| | 885.6 | 885.6 | 885.6 | 846.1 | 885.6, 856.7, 846.1 | ν(Mo–O)[c] |
| $O_2W(CO)_2$ | 2091.1 | 2042.9 | 2091.1, 2072.7, 2042.9 | 2045.1 | 2091.1, 2073.4, 2045.1 | ν(C–O) |
| | 1998.2 | 1953.6 | 1998.2, 1970.4, 1953.6 | 1952.1 | 1998.2, 1969.7, 1952.1 | ν(C–O) |
| | 961.6 | 961.6 | 961.6 | 909.4 | 961.6, 944.3, 909.4 | ν(W–O)[d] |
| | 901.1 | 901.1 | 901.1 | 856.1 | 901.1, 870.4, 856.1 | ν(W–O)[c] |

[a] Refers to $^{52}$Cr. [b] Refers to $^{98}$Mo. [c] Antisymmetric M–O stretch. [d] Symmetric stretch.

$CO_2$ in Ar were deposited at a rate of *ca.* 3 mmol $h^{-1}$ for 1–2 h onto a CsI window held at 6–7 K while the metals were ablated using 35–50 mJ $pulse^{-1}$ of the YAG 1064 nm fundamental.

Figs. 1 and 2 show the effects of isotopic substitution upon the IR spectra of matrix-isolated deposits containing the products from the reaction of W with $CO_2$ in Ar. The frequencies of the observed bands from the reactions of $CO_2$ with Cr, Mo and W and their proposed assignments are presented in Table 1.

OMCO: the dominant product from the reactions of group 6 metal atoms with 0.5% $CO_2$–Ar mixtures is the direct insertion product OMCO. Full details are given in Table 1 for all three metals which behave in an analogous fashion. In the case of tungsten, absorptions at 1879.0 and 969.6 $cm^{-1}$ correspond to the CO and WO stretching fundamentals of the OWCO molecule. In experiments run with $^{13}CO_2$ and $C^{18}O_2$, these bands shift to 1837.0 and 969.6 $cm^{-1}$ and 1838.8 and 918.9 $cm^{-1}$, respectively, confirming that this molecule contains a CO and a WO group, based upon comparison of observed isotopic frequency ratios with calculated harmonic diatomic ratios. Experiments run with $^{12}CO_2$–$^{13}CO_2$, $C^{16}O_2$–$C^{18}O_2$ and $C^{16}O_2$–$C^{16}O^{18}O$–$C^{18}O_2$ all revealed isotopic doublets in the CO stretching region and the latter two revealed doublets in the WO stretching region. This isotopic pattern confirms the presence of exactly one CO group and exactly one WO group allowing definitive spectral assignment of these bands to the OWCO molecule. For both Cr and Mo isotopic splittings due to the natural abundances of the metal isotopes were observed for the MO stretching fundamental and the observed statistical distribution confirmed the presence of exactly one metal atom. These findings are in contrast to a previous study of the reaction of thermally generated chromium atoms with neat $CO_2$ in which there was no evidence for the insertion reaction.[10]†

$O_2M(CO)_2$: the other main product from these reactions proved to arise from the insertion of the metal atoms into two $CO_2$ molecules. As might be anticipated, by raising the concentration of $CO_2$ from 0.5 to 2% the relative yield of $O_2M(CO)_2$ to OMCO increases. In the CO stretching region for all three metals, the symmetric and antisymmetric CO stretching fundamentals were both observed. In the case of the reaction of W with $CO_2$, the bands at 2091.1 and 1998.2 $cm^{-1}$ can be assigned to the symmetric and antisymmetric CO stretching modes of $O_2W(CO)_2$ while the bands at 961.6 and 901.1 $cm^{-1}$ can be assigned to the symmetric and antisymmetric WO stretching modes of the $O_2W(CO)_2$ molecule. Reaction with $^{13}CO_2$ gave bands at 2042.9, 1953.6, 961.6 and 901.1 $cm^{-1}$, whereas reaction with $C^{18}O_2$ gave bands at 2045.1, 1952.1, 909.4 and 856.1 $cm^{-1}$. Reaction with either $C^{16}O_2$–$C^{18}O_2$ or $C^{16}O_2$–$C^{16}O^{18}O$–$C^{18}O_2$ gave rise to 1 : 2 : 1 triplets for all four bands. This is indicative of the presence of precisely two equivalent CO groups and two equivalent oxygen atoms and confirms that the two oxygens and CO groups bound to the tungsten must come from two different $CO_2$ molecules. Reaction with a $^{12}CO_2$–$^{13}CO_2$ mixture revealed a 1 : 2 : 1 isotopic triplet for both CO stretching fundamentals further confirming the presence of two equivalent CO groups. In the cases of both Cr and Mo, the presence of exactly one metal atom is clearly demonstrated by the statistical distribution of the metal isotopic pattern for the M–O antisymmetric stretching fundamental. There have been numerous previous studies involving the photolysis of $M(CO)_6$ with $O_2$[18–21] and bands in these spectra were assigned to the $O_2M(CO)_2$ molecules. The CO stretching region in these experiments was extremely congested but the bands that are observed here for $O_2Mo(CO)_2$ and $O_2W(CO)_2$ are essentially the same as those observed by Almond *et al.* for their species 'C' which was assigned to $O_2M(CO)_x$, not those observed for their species 'D' which was assigned to $O_2M(CO)_2$.[20] Our results for $O_2Cr(CO)_2$ do however confirm the previous correct identification of this molecule.[18,20]

Other bands: the previously characterised metal monoxides, MO,[21–23] were observed although this represents the first reported isolation of CrO (846.5 $cm^{-1}$) in a matrix. In the case of the reaction with tungsten, a bridged species $OW(\mu\text{-}CO)_2WO$, the dimer of OWCO, is formed. Only the antisymmetric CO stretching mode is observed in a region typical for bridging CO groups. The observed band at 1713.4 $cm^{-1}$ from the reaction of W with $CO_2$ shifts to 1674.5 $cm^{-1}$ on reaction of W with $^{13}CO_2$ and 1675.9 $cm^{-1}$ on reaction of W with $C^{18}O_2$. It shows a 1 : 2 : 1 triplet at 1713.4, 1692.8 and 1675.9 $cm^{-1}$ upon reaction with either $C^{16}O_2$–$C^{18}O_2$ or $C^{16}O_2$– $C^{16}O^{18}O$–$C^{18}O_2$, and a 1 : 2 : 1 triplet at 1713.4, 1691.9 and 1674.5 $cm^{-1}$ upon reaction with a $^{12}CO_2$–$^{13}CO_2$ mixture, indicating two equivalent CO groups. The product is not observed in reactions involving CO and its yield is suppressed by using higher concentrations (2%) of $CO_2$, presumably due to further reaction of OWCO with $CO_2$. The lack of an analagous product for Cr or Mo probably reflects the greater strength of the metal–metal bonding, present in such a complex, of tungsten. DFT calculations confirm the presence of metal–metal bonding in this molecule. Other products observed include the molecules $O_2MCO$, $OCr(CO)_2$ and the $CO_2$ complex $Cr(\eta^1\text{-}OCO)$ and these results will be discussed in a full paper.

## Footnotes

* E-mail: lsa@virginia.edu

† The band observed in ref. 10 at 960 $cm^{-1}$, tentatively assigned to a $CO_2$ reaction product, occurs at almost the same energy as the antisymmetric stretch of $CrO_2$, an almost inevitable impurity in a reaction involving thermally generated Cr atoms. With no isotopic data and no associated carbonyl stretches this band is most likely due to $CrO_2$ in a $CO_2$ matrix.

## References

1 J. A. Ibers, *Chem. Soc. Rev.*, 1982, **11**, 57.
2 C. Creutz, in *Electrochemical and Electrocatalytic Reactions of Carbon Dioxide*, ed. B. P. Sullivan, K. Krist and H. E. Guard, Elsevier, Amsterdam, 1993, ch. 2.
3 M. Arreseta, E. Quarntana and I. Tommasi, *New J. Chem.*, 1994, **18**, 133.
4 D. H. Gibson, *Chem. Rev.*, 1996, **96**, 2063.
5 M. M. Halmann, *Chemical Fixation of Carbon Dioxide. Methods for Recycling $CO_2$ into Useful Products*, CRC Press, Boca Raton, FL, 1993.
6 See for example, A. R. Cutler, P. K. Hanna and J. C. Vites, *Chem. Rev.*, 1988, **88**, 1363.
7 Z. H. Kafafi, R. H. Hauge, W. E. Billups and J. L. Margrave, *J. Am. Chem. Soc.*, 1983, **105**, 3886.
8 Z. H. Kafafi, R. H. Hauge, W. E. Billups and J. L. Margrave, *Inorg. Chem.*, 1984, **23**, 177.
9 A. M. LeQuere, C. Xu and L. Manceron, *J. Phys. Chem.*, 1991, **95**, 3031.
10 J. Mascetti and M. Tranquille, *J. Phys. Chem.*, 1988, **92**, 2177.
11 G. H. Yeung, *Mol. Phys.*, 1988, **65**, 669.
12 T. R. Burkholder and L. Andrews, *J. Phys. Chem.*, 1993, **97**, 3500.
13 T. J. Tague, Jr., L. Andrews and R. D. Hunt, *J. Phys. Chem.*, 1993, **97**, 10 920.
14 G. V. Chertihin and L. Andrews, *J. Am. Chem. Soc.*, 1995, **117**, 1595.
15 L. Andrews and T. J. Tague, Jr., *J. Am. Chem. Soc.*, 1994, **116**, 6856.
16 T. R. Burkholder and L. Andrews, *J. Chem. Phys.*, 1991, **95**, 8697.
17 G. V. Chertihin, W. D. Bare and L. Andrews, unpublished work.
18 M. Poliakoff, K. P. Smith, J. J. Turner and A. J. Wilkinson, *J. Chem. Soc. Dalton Trans.*, 1982, 651.
19 J. A. Crayston, M. J. Almond, A. J. Downs, M. Poliakoff and J. J. Turner, *Inorg. Chem.*, 1984, **23**, 3051.
20 M. J. Almond, J. A. Crayston, A. J. Downs, M. Poliakoff and J. J. Turner, *Inorg. Chem.*, 1986, **25**, 19.
21 M. J. Almond and A. J. Downs, *J. Chem. Soc., Dalton Trans.*, 1988, 809.
22 T. C. Devor and J. L. Gole, *Chem. Phys.*, 1989, **133**, 95.
23 J. K. Bates and D. M. Gruen, *J. Mol. Spectrosc.*, 1979, **78**, 284.
24 D. W. Green and K. M. Ervin, *J. Mol. Spectrosc.*, 1981, **89**, 145.

*Received in Columbia, MO, USA, 15th January 1997; Com. 7/00360I*

# *In situ* EPR studies of electron transfer across a polarised liquid/liquid interface

**Robert A. W. Dryfe, Richard D. Webster, Barry A. Coles and Richard G. Compton***

*Physical and Theoretical Chemistry Laboratory, Oxford University, South Parks Road, Oxford, UK OX1 3QZ*

**The design and operation of the first ever *in situ* EPR cell for studying charge-transfer processes accompanying polarisation of the liquid/liquid interface is presented as well as EPR absorption data obtained from the reduction of TCNQ (to $TCNQ^{\cdot -}$) and the oxidation of TTF (to $TTF^{\cdot +}$) by the ferro–ferri-cyanide redox couple at the water/1,2-dichloroethane interface.**

The liquid/liquid interface has attracted increasing attention, both from a theoretical and experimental standpoint, due to its potential relevance to fields as diverse as analytical chemistry, hydrometallurgy and membrane science.[1] Imposition of an external potential difference across this interface has allowed charge-transfer processes to be studied voltammetrically, but interpretations are frequently plagued by controversy because of the difficulty in conclusively identifying the participating species and, crucially, resolving ion- and electron-transfer processes from one another.[2] The latter is of particular interest as it involves bimolecular electron exchange which can be controlled through the potential difference imposed on the water/organic interface. Spectroscopic experiments, including EPR spectroscopy,[3,4] have been used successfully to clarify processes at the metal/electrolyte and semiconductor/electrolyte interfaces. To date spectroscopic reports of liquid/liquid processes have been confined to UV–VIS absorption and emission spectroscopy,[5,6] whereas *in situ* EPR spectroscopy is an ideal way to detect and identify paramagnetic participants, which has not been hitherto applied.

The cell used to perform the interfacial polarisation-EPR experiments is shown in Fig. 1 and is essentially a conventional silica flat cell[7] modified so that a counter and reference electrode can be inserted into either end. The cell was assembled by first filling the higher density solvent through the capillary at the base of the cell [Fig. 1(*f*)] using silicone tubing and a syringe, so that the solvent reached the midpoint of the flat portion of the cell [Fig. 1(*a*)], and then sealing the silicone tubing with a Hoffman clamp. The upper, less dense phase, was then introduced into the cell from the top using a Pasteur pipette. Using this filling method a liquid/liquid interface could be generated and maintained in the mid-portion of the flat part of the cell.

The EPR cell has two counter electrodes of coiled 0.5 mm diameter platinum wire located outside the thin layer section [Fig. 1(*b*) and (*d*)]. The two reference electrodes are 0.5 mm diameter silver wires, flattened at one end to a thickness which enabled their insertion into the flat part of the cell [Fig. 1(*c*) and (*e*)]. Both silver pseudo-reference electrodes were positioned to within 5 mm of the liquid/liquid interface. To obtain optimal control of the potential difference applied between the liquid phases, the portions of the reference electrodes outside the flat part of the cell were jacketed in Teflon tubing [Fig. 1(*h*)] and sealed with silicone rubber so that they were only in contact with the solutions inside the flat part of the cell. The inherent high resistivity of a flat cell combined with low relative permittivity solvents (*e.g.* 1,2-dichloroethane, DCE) can be partially overcome using this arrangement, and reasonable linear sweep voltammetry can be obtained using a four-electrode (two counter and two reference electrodes) potentiostat.

The use of the cell shown in Fig. 1 enabled EPR spectra to be obtained for both the interfacial reduction of TCNQ and

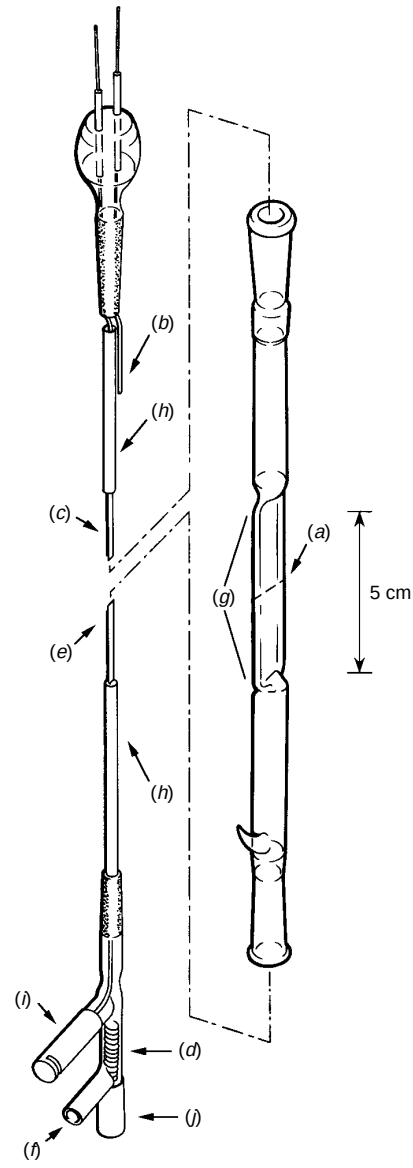



**Fig. 1** Silica cell for performing liquid/liquid electrochemical-EPR experiments: (*a*) interface between two immiscible liquids, (*b*) platinum wire counter electrode 1, (*c*) silver wire reference electrode 1, (*d*) platinum wire counter electrode 2, (*e*) silver wire reference electrode 2, (*f*) capillary to fill lower portion of cell, (*g*) thin layer portion of cell, (*h*) Teflon/silicone rubber sleeves surrounding lower portions of reference electrodes, (*i*) electrical contact to reference electrode 2 and (*j*) electrical contact to counter electrode 2

oxidation of TTF (dissolved in DCE) by the aqueous phase ferri–ferro-cyanide couple, following application of a potential difference directly to the liquid/liquid interface. The TCNQ–ferrocyanide system has been previously investigated using both external polarisation with a four-electrode potentiostat and the scanning electrochemical microscope, both techniques indicating that the charge-transfer process observed at the liquid/liquid interface is due to heterogeneous reduction of TCNQ by the aqueous couple[8,9] [eqn. (1)].

$$\mathrm{TCNQ(DCE) + Fe(CN)_6^{4-}(aq) \rightleftharpoons TCNQ^{\cdot-}(DCE) + Fe(CN)_6^{3-}(aq)} \quad (1)$$

A similar mechanism can be written for the oxidation of TTF [eqn. (2)], where in each case an appropriate potential difference (oxidising or reducing), relative to the two reference electrodes used, can be imposed across the water/DCE interface to drive the reaction in either the forward or reverse direction.

$$\mathrm{TTF(DCE) + Fe(CN)_6^{3-}(aq) \rightleftharpoons TTF^{\cdot+}(DCE) + Fe(CN)_6^{4-}(aq)} \quad (2)$$

The presence of the organic radicals, and hence the occurrence of an electron-transfer process, was verified using EPR spectroscopy. The EPR spectra obtained for $TCNQ^{\cdot-}$ and $TTF^{\cdot+}$ in DCE at room temperature consisted of single broad lines with peak-to-peak line widths of 5.2 and 3.0 G, respectively. It is unlikely that the line broadening observed is due to the $TCNQ^{\cdot-}$ and $TTF^{\cdot+}$ radicals interacting with the iron complexes in the aqueous phase as broad EPR spectra were also obtained from $TCNQ^{\cdot-}$ and $TTF^{\cdot+}$ radicals which had been generated electrochemically in the appropriate single-phase three-electrode cell[7] using DCE and the same supporting electrolyte, bis(triphenylphosphoranylidene)ammonium tetrakis(4-chlorophenyl)borate ($BTPPA^+TCPB^-$). The broadening of the EPR spectra is probably caused by the strong ion pairs formed between the product radicals and the organic phase electrolyte cation ($BTPPA^+$) or anion ($TCPB^-$) respectively, undergoing fast electron exchange with neutral TCNQ or TTF.[10]

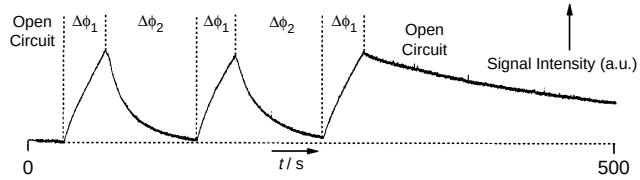



**Fig. 2** Time-sweep first derivative EPR spectrum of $TTF^{\cdot+}$ recorded at constant magnetic field using a liquid/liquid electrochemical-EPR cell. The organic phase (DCE) contained 5 mM TTF and 36 mM $BTPPA^+$ $TCPB^-$. The aqueous phase contained 25 mM $K_4[Fe(CN)_6]$, 25 mM $K_3[Fe(CN)_6]$ and 0.1 M $Li_2SO_4$. EPR sweep time = 500 s, sweep width = 0 G, modulation amplitude = 2.0 G and time constant = $10 \times 10^{-2}$ ms. $\Delta\phi_1$ = oxidising potential, $\Delta\phi_2$ = reducing potential. The potential difference imposed to induce oxidation of the TTF was +0.7 V, whilst this process was reversed using a potential difference of −0.1 V (*vs.* the Ag pseudo-reference electrodes used). See text for further details.

An EPR time-sweep experiment for the oxidation of TTF, where the magnetic field was held at a constant value corresponding to the maximum absorption, is shown in Fig. 2. The time-sweep EPR experiments were performed by applying a potential difference, between the silver pseudo-reference electrodes located in each liquid phase, which was sufficient to cause an electron to be transferred across the water/DCE interface from TTF to $[Fe(CN)_6]^{3-}$. The resulting increase in $TTF^{\cdot+}$ in the organic phase caused an increase in signal intensity of the absorption spectrum (Fig. 2), which displayed a square-root temporal dependence as expected for a potential-step occurring under conditions of one-dimensional diffusion.[11] Jumping to a potential difference sufficiently negative to drive the back reaction immediately caused a decrease in the intensity of the absorption signal (also Fig. 2) due to $TTF^{\cdot+}$ being reduced back to neutral TTF. The time-sweep EPR data obtained for the reduction of TCNQ was very similar to that reported for the oxidation of TTF. The spectrum in Fig. 2 also shows that when the potentiostat is open-circuited after generating $TTF^{\cdot+}$ the signal intensity decreases with time. $TTF^{\cdot+}$ is stable in DCE, therefore, the decay in signal intensity can be attributed to the radical diffusing away from the most sensitive part of the EPR cavity since the sensitivity shows a cosine squared dependence on distance, its maximum lying at the cavity centre.[3] Steps are currently in progress to enable accurate kinetic measurements to be made using this cell.

R. A. W. D. and R. D. W. gratefully acknowledge the Royal Commission for the Exhibition of 1851 and the Ramsay Memorial Fellowships Trust respectively for post-doctoral fellowships. We thank Mr J. Freeman for assistance with figures.

## References

1 H. H. Girault and D. J. Schiffrin, in *Electroanalytical Chemistry*, ed. A. J. Bard, Marcel Dekker, New York, 1989, vol. 15, p. 1.
2 V. J. Cunnane, G. Geblewicz and D. J. Schiffrin, *Electrochim. Acta*, 1995, **40**, 3005.
3 R. G. Compton and A. M. Waller, in *Spectroelectrochemistry: Theory and Practice*, ed. R. J. Gale, Plenum, New York, 1988, ch. 7.
4 R. D. Webster, A. M. Bond, B. A. Coles and R. G. Compton, *J. Electroanal. Chem.*, 1996, **404**, 303.
5 T. Kakiuchi and Y. Takasu, *Anal. Chem.*, 1994, **66**, 1853.
6 Z. Ding, R. G. Wellington, P. F. Brevet and H. H. Girault, *J. Phys. Chem.*, 1996, **100**, 10 658.
7 L. H. Piette, P. Ludwig and R. N. Adams, *Anal. Chem.*, 1962, **34**, 916.
8 Y. Cheng and D. J. Schiffrin, *J. Chem. Soc., Faraday Trans.*, 1994, **90**, 2517.
9 T. Solomon and A. J. Bard, *J. Phys. Chem.*, 1995, **99**, 17487.
10 N. Haren, Z. Luz and M. Shporer, *J. Am. Chem. Soc.*, 1974, **96**, 4788.
11 F. G. Cottrell, *Z. Phys. Chem.*, 1902, **42**, 385.

*Received in Exeter, UK, 19th February 1997; Com. 7/00640C*

# Synthesis and structural characterisation of two- and three-dimensional fluorinated indium phosphates

**Hongbin Du,[a] Jiesheng Chen,[a] Wenqin Pang,*[a] Jihong Yu[a,b] and Ian D. Williams*[b]**

[a] *Key Laboratory of Inorganic Hydrothermal Synthesis, Department of Chemistry, Jilin University, Changchun, China*
[b] *Department of Chemistry, Hong Kong University of Science and Technology, Clear Water Bay, Kowloon, Hong Kong*

**Hydrothermal synthesis of two new fluorinated indium phosphates [$InPO_4F$(Hen)] and [$In_5P_4F_3O_{16}(en)_3(OH_2)_2$] is carried out in the system $In_2O_3$–$P_2O_5$–en–HF–$H_2O$ (en = ethylenediamine); these have two- and three-dimensional inorganic frameworks respectively, with the latter having ten-membered ring channels spanned by coordinated en; the fluorides bridge exclusively between indium ions and may be linear or bent.**

The synthesis of new classes of inorganic microporous solids, with different architectures and pore chemistry to classical zeolite-related materials, remains an active area.[1–3] Extensive use of organic amines as structure directing agents promotes microporous solid formation, with frequent inclusion of the amine in the microporous channel. Using this approach, a rich chemistry has already been established for group 13 phosphates of Al[4–6] and Ga[7–10] and work is now emerging on the indium phosphate family. Previously three indium phosphates templated by organic amines have been reported, [$H_2$en]-[$In(HPO_4)_2$][11] [$In_8(HPO_4)_{14}(H_2O)_6](H_2O)_5(H_3O)(N_2C_3H_5)_3$[12] and [$C_5H_5NH$][$In(HPO_4)(H_2PO_4)_2$].[13]

The presence of fluoride as a mineraliser in hydrothermal synthesis frequently has a pronounced effect on the microporous phases produced[14] and may even result in the incorporation of fluoride into the inorganic framework, as observed for certain alumino-[15] and gallo-phosphates.[16] We report herein the synthesis and structure of two fluorinated indium phosphates, [$InPO_4F$(Hen)] **1** and [$In_5P_4F_3O_{16}(H_2O)_2(en)_3$] **2**, using ethylenediamine (en) as the organic structure directing agent in a fluoride-containing system.

Compounds **1** and **2** were synthesized hydrothermally. An aqueous mixture of indium hydroxide, 85% (m/m) phosphoric acid, ethylenediamine and 40% (m/m) hydrofluoric acid with the gel molar composition 1.0 $In(OH)_3$ : 1.0 $H_3PO_4$ : 1.0 en : 2.0 HF : 80 $H_2O$ was heated at 180 °C for 20 days under autogeneous pressure in a Teflon-lined stainless-steel autoclave. The resulting crystalline products were filtered off, washed thoroughly with water and dried at room temp. Microscopic examination revealed two phases, predominantly compound **1** which formed tablets of maximum dimension 150 μm, together with a small amount (*ca*. 10%) of a second phase, compound **2**, as small rectangular blocks of maximum dimension 60 μm. X-Ray photoelectron spectroscopy on the product mixture indicated the presence of In, P and stoichiometric amounts of fluorine. Energy dispersive X-ray analysis on selected single crystals of the two compounds confirmed the presence of these elements in both phases. Their structures were then determined by single-crystal X-ray diffraction.†

[$InPO_4F$(Hen)] **1** is a two-dimensional network with monoprotonated ethylenediamine groups $(Hen)^+$ pendant to $InPO_4F$ layers through coordination of one amino group to the indium. A view perpendicular to the layer is shown in Fig. 1. The two-dimensional sheet has chains of corner-shared indium octahedra which are linked to other chains by phosphate bridges forming $In_4P_2$ six-membered rings. The corner-sharing of the In octahedra is due to fluoride ions which bridge symmetrically in a bent manner between the In atoms [In–F 2.121, 2.129(5) Å, In–F–In 133.2(2)°]. Although crystallographically it is difficult to distinguish μ-F from μ-OH, this bridging position is the only chemically reasonable location for the fluorine which must be present in this compound. The phosphate groups point alternately above and below the layer and have three oxygen atoms forming In–O–P bridges and one terminal P–$O^-$ functionality. This is hydrogen bonded to three pendant ammonium $NH_3R^+$ chains of the adjacent layer, which serves to organise the overall packing of the structure.

Compound **2**, has a three-dimensional open framework with a 5 : 4 In : P ratio. Its structure is complex featuring ten-membered rings ($In_6P_4$) which are spanned by en bridges between opposite indium atoms (Fig. 2). In addition en acts as a simple chelate to one indium centre. Once more, the fluorides are assigned to bridging environments between In atoms but may be linear or bent. The bent bridges have similar geometry to those found for **1** [bent In–F 2.136, 2.135(5) Å, In–F–In 125.9(2)°]. The linear bridges are also assigned to be fluoride, rather than oxide, on the basis of charge balance. Linear In–F–In linkages are well established, and occur in several condensed phases including [InOF].[17] The shorter In–F bond [linear In–F 2.068(1) Å] found for the linear case, is expected due to involvement of the fluoride lone pairs in π bonding and the smaller radius of sp hybridised fluorine. All phosphate oxygen atoms form In–O–P bridges and the coordination environments of the indium atoms are completed by aqua ligands [In–O 2.295(9) Å].†

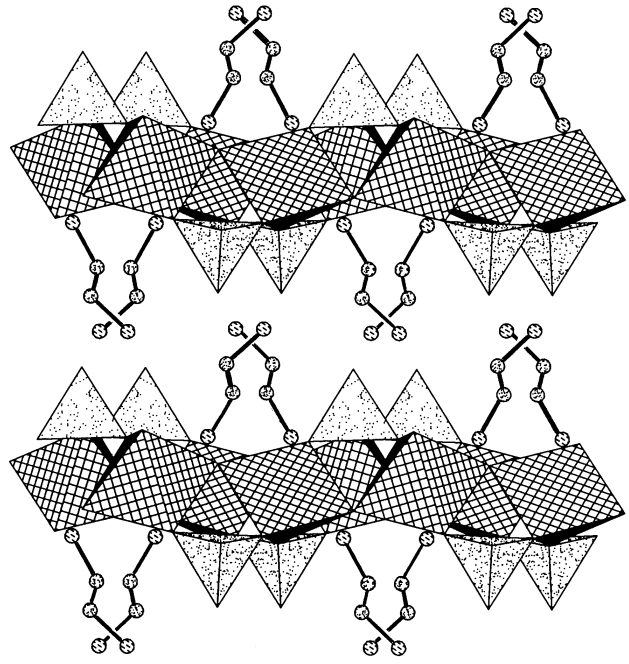


**Fig. 1** Projection of **1** along the *c*-axis showing a side view of the sheets with pendant [Hen] groups

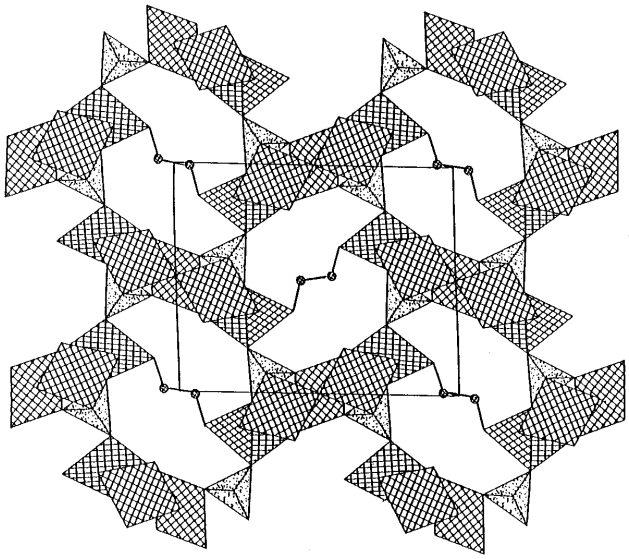


**Fig. 2** Polyhedral representation of **2** projected down [001]

Whilst use of stoichiometric levels of fluoride in these syntheses can result in $F^-$ incorporation, the use of lesser amounts can still promote crystallisation of indium phosphate phases not containing fluoride itself.[18] For example, in the same system for the synthesis of **1** and **2**, the use of 0.2 mol equiv. HF results in two other phases:[19] a two-dimensional layer compound $0.5[H_2en][InPO_4(OH)]$ (*ca.* 80%) and a chiral three-dimensional phase $[H_3O][InPO_4(OH)]$ (3%), which is isostructural with $Rb[InPO_4(OH)]$.[20]

The In/P ratios in **1** and **2** are unity or indium rich, in contrast to the previously reported indium phosphates containing template counterions, which are phosphorus rich.[11–13] Fluoride bridges and coordinated ethylenediamine groups exclusively occupy the surplus coordination sites of the octahedral indium atoms. This means that fewer phosphate groups are required than for constructing solely In–O–P linked systems, or that fewer oxygens need be in relatively unfavourable three-coordinate environments compared to $InPO_4$ itself. In conclusion, we believe more diverse stuctural types will continue to be found for mixed octahedral–tetrahedral framework materials and that use of fluoride may be a useful synthetic strategy to assist in their formation.

The authors acknowledge the support of the Research Grants Council of Hong Kong and the National Natural Science Foundation of China.

## Footnotes

* E-mail: CHWILL@USTHK.UST.HK

† *Crystal data*: **1**: $C_2H_9FInN_2O_4P$, *M*r = 289.9, monoclinic, space group $P2_1/c$ (no. 14), $a$ = 9.214(2), $b$ = 7.781(2), $c$ = 10.049(2) Å, β = 101.68(2)°, $U$ = 706.1(3) Å$^3$, $Z$ = 4, $D_c$ = 2.73 Mg m$^{-3}$, μ(Mo-Kα) = 3.6 mm$^{-1}$, $R$ = 0.043, $R_w$ = 0.040, for 1434 data with $F \geqslant 4\sigma(F)$.

**2**: $C_6H_{28}F_3In_5N_6O_{18}P_4$, $M_r$ = 1227.3, orthorhombic, space group *Pbam* (no. 55), $a$ = 10.562(2), $b$ = 13.406(4), $c$ = 9.827(4) Å, $U$ = 1391.7(8) Å$^3$, $Z$ = 2, $D_c$ = 2.93 Mg m$^{-3}$, μ(Mo-Kα) = 4.4 mm$^{-1}$, $R$ = 0.033, $R_w$ = 0.036, for 1369 data with $F \geqslant 4\ \sigma(F)$.

Atomic coordinates, bond lengths and angles, and thermal parameters have been deposited at the Cambridge Crystallographic Data Centre (CCDC). See Information for Authors, Issue No. 1. Any request to the CCDC for this material should quote the full literature citation and the reference number 182/403.

## References

1 R. M. Barrer, *Hydrothermal Chemistry of Zeolites*, Academic Press, London, 1982, p. 44.
2 M. E. Davis, *Acc. Chem. Res.*, 1993, **26**, 111.
3 J. L. Casci, *Stud. Surf. Sci. Catal.*, 1994, **85**, 329.
4 S. T. Wilson, B. M. Lok and E. M. Flanigen, *US Pat.*, 4310440, 1982.
5 Q. Huo and R. Xu, *J. Chem. Soc., Chem. Commun.*, 1992, 168.
6 Q. Huo, R. Xu, S. Li, Z. Ma, J. M. Thomas, R. H. Jones and A. M. Chippindale, *J. Chem. Soc., Chem. Commun.*, 1992, 875.
7 J. B. Parise, *J. Chem. Soc., Chem. Commun.*, 1985, 606.
8 G. Yang, S. Feng and R. Xu, *J. Chem. Soc., Chem. Commun.*, 1987, 1254.
9 M. Esterman, L. B. McCusker, C. Baerlocher, A. Merrouche and H. Kessler, *Nature*, 1991, **352**, 320.
10 R. Xu, J. Chen and S. Feng, *Stud. Surf. Sci. Catal.*, 1991, **60**, 63.
11 S. S. Dhingra and R. C. Haushalter, *J. Chem. Soc., Chem. Commun.*, 1993, 1665.
12 A. M. Chippindale, S. J. Brech, A. R. Cowley and W. M. Simpson, *Chem. Mater.*, 1996, **8**, 2259.
13 A. M. Chippindale and S. J. Brech, *Chem. Commun.*, 1996, 2781.
14 H. Kessler, J. Patarin and C. Schott-Darie, *Stud. Surf. Sci. Catal.*, 1994, **85**, 75.
15 J. L. Paillaud, B. Marler and H. Kessler, *Chem. Commun.*, 1996, 1293.
16 T. Loiseau and G. Ferey, *J. Chem. Soc., Chem. Commun.*, 1992, 1197.
17 M. Vlasse, J. C. Massies and B. L. Chamberland, *Acta Crystallogr., Sect. B*, 1973, **29**, 627.
18 H. Du, J. Chen and W. Pang, *Stud. Surf. Sci. Catal.*, 1997, **105**, 397.
19 H. Du, J. Chen, W. Pang, J. Yu and I. D. Williams, in preparation.
20 K. H. Lii, *J. Chem. Soc., Dalton Trans.*, 1996, 815.

*Received in Cambridge, UK, 3rd February 1997; Com. 7/00775B*

# First X-ray crystal structure of a lanthanide(III) monoporphyrinic complex using non-planar porphyrin rings

**Georgios A. Spyroulias,[a] Alexis Despotopoulos,[a] Catherine P. Raptopoulou,[b] Aris Terzis[b] and Athanassios G. Coutsolelos*[a]**

[a] *Laboratory of Bioinorganic Coordination Chemistry, Department of Chemistry, School of Science, University of Crete, PO Box 1470, 714 09-Heraklion, Crete, Greece*

[b] *Institute of Materials Science, N.C.S.R. 'Demokritos', 15310-Aghia Paraskevi, Athens, Greece*

**Twenty-three years after the first synthesis of lanthanide(III) porphyrins the X-ray crystal structure of [$Tb^{III}$(β-$Cl_8$tpp)($O_2$CMe)($Me_2SO_2$] is reported; the synthetic route to four halogenated porphyrins $H_2$(β-$X_n$tpp) (X = Cl or Br, *n* = 4 or 8) is described and compared with the corresponding [$Tb^{III}$(β-$X_n$tpp)($O_2$CMe)]; the highly distorted structure of the $Tb^{III}$ complex is compared with similar perhalogenated porphyrinic complexes; the X-ray structure of the brominated free base is also reported.**

Since the first reported synthesis of lanthanide monoporphyrinates in 1974,[1a] several studies on these systems have appeared in the literature.[1,2] Here, we report on the first X-ray structure of a lanthanide monoporphyrinate, [$Tb^{III}$(β-$Cl_8$tpp)($O_2$CMe)-($Me_2SO$)$_2$], and the structure of the inherently non-planar free base $H_2$(β-$Br_8$tpp). The synthesis of the [$Tb^{III}$(β-$X_n$tpp)($O_2$CMe)] and $H_2$(β-$X_n$tpp) derivatives, is also described (X = Cl or Br, *n* = 4 or 8). This new family of lanthanide(III) monoporphyrinates is promising both for the synthesis of novel homo- and hetero-leptic bisporphyrinates, formally analogous to the photosynthetic reaction centre special pair,[3] and for their photochemical[1b] and magnetic properties.[1d]

According to a previously reported chlorination procedure,[4] stirring an *o*-dichlorobenzene solution of [$Ni^{II}$(tpp)] (1 equiv.) at 150 °C for 2–3 h with 4.2 or 12 equiv. of bromo (or chloro) succinimide affords [2,7,12,17-*tetra*- or 2,3,7,8,12,13,17,18-octahalogeno-5,10,15,20-tetraphenylporphyrinato]nickel(II) respectively.†‡ The chromatographically pure ($Al_2O_3$/$CH_2Cl_2$) nickel(II) derivatives were then demetallated in concentrated $H_2SO_4$ (95%). The analytically pure free bases were obtained after extraction with $CH_2Cl_2$–$H_2O$, drying over $MgSO_4$, and chromatography (once or twice) on $Al_2O_3$/$CH_2Cl_2$.§ Reaction of tris(pentane-2,4-dionato)terbium(III) (15 equiv.) with $H_2$(β-$X_n$tpp) (1 equiv.) in refluxing 1,2,4-trichlorobenzene (tcb),[5] for 3 h affords the corresponding terbium monoporphyrinate complexes.¶‖ The terbium(III) complexes were purified by column chromatography on $Al_2O_3$ using, in order, toluene (elimination of tcb), $CH_2Cl_2$ (the unreacted free base is separated), MeOH–dmf (3 : 1 v/v) (part of the desired derivative) and $Me_2SO$ (the major quantity of the desired complex) as eluents. The last two fractions were collected, evaporated to dryness, and the solid residue was recrystallized by slow evaporation in a saturated toluene solution.

The ORTEP diagram of the complex [$Tb^{III}$(β-$Cl_8$tpp)($O_2$C-Me)($Me_2SO$)$_2$] shown in Fig. 1,** sheds light on the molecular structure of lanthanide monoporphyrinates. The coordination sphere of terbium consists of the four nitrogen atoms of the substituted porphyrin, the oxygen atoms of a bidentate acetate and the oxygen atoms of two $Me_2SO$ solvent molecules. The coordination geometry of the terbium(III) ion is square antiprismatic, the average dihedral angle between a pair of N–Tb–N and O–Tb–O planes being 46.74°. The mean Tb–N and Tb–O bond distances are 2.427 and 2.445 Å, respectively. The terbium(III) ion lies 1.282 and 1.469 Å out of the mean $N_4$ and mean $O_4$ plane, respectively, while the $N_4$ and $O_4$ mean planes manifest a dihedral tilt angle of 1.71°. Scheidt and Lee[6] have shown that the mean absolute perpendicular displacements of the β-carbons from the porphyrin mean plane ($C_\beta$) increase with decreasing dihedral angles between the phenyl rings and porphyrin core in saddled [M(tpp)]$^{n+}$ derivatives. The porphyrin ring of the $Tb^{III}$ complex also manifests a marked saddle distortion with a mean absolute perpendicular displacement for the β-carbons from the $N_4$ mean plane of 0.89 Å. Relative to [$Fe^{III}$(β-$Cl_8$tmp)Cl] ($C_\beta$ = 0.87 Å),[7] [Zn(β-$Cl_8$tfp)] ($C_\beta$ = 0.79 Å),[8a] and [Ru(β-$Cl_8$tfp)] ($C_\beta$ = 0.48 Å),[8b] this magnitude of distortion is the largest yet observed for a β-halogeno metalloporphyrin. The displacement of the individual chlorine atoms from the $N_4$ mean plane is in the range 1.03–2.18 Å, which is considerably larger than that found in [Zn(β-$Cl_8$tfp)] (1.17–1.48 Å)[8a] and [Ru(β-$Cl_8$tfp)] (0.68–1.11 Å).[8b] Finally, as in the following structure of the free base, rotation of the phenyl rings with respect to the porphyrin mean plane minimizes unfavourable steric interactions with the flanking chloride substituents. The dihedral angles formed between the phenyl rings and the $N_4$ mean plane are: 49.03° [C(21)–C(26)], 49.36° [C(27)–C(32)], 49.38° [C(33)–C(38)] and 49.74° [C(39)–C(44)].

The saddle distortion of $H_2$(β-$Br_8$tpp) is particularly severe (Fig. 2). Thus, the $C_\beta$ are canted well above the $N_4$ mean plane ($C_\beta$ = 1.263 Å) relative to that observed in the related species

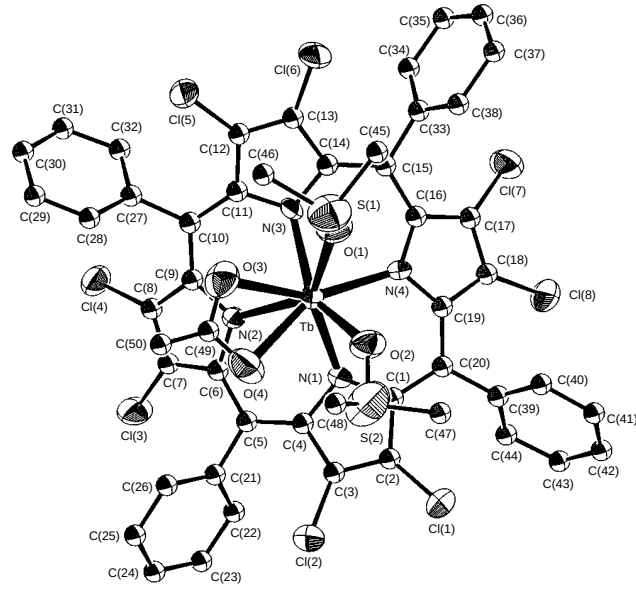



**Fig. 1** ORTEP diagram of [$Tb^{III}$(β-$Cl_8$tpp)($O_2$CMe)($Me_2SO$)$_2$]. All carbon atoms are shown isotropic for clarity, and heteroatoms are anisotropic with 30% probability thermal ellipsoids.

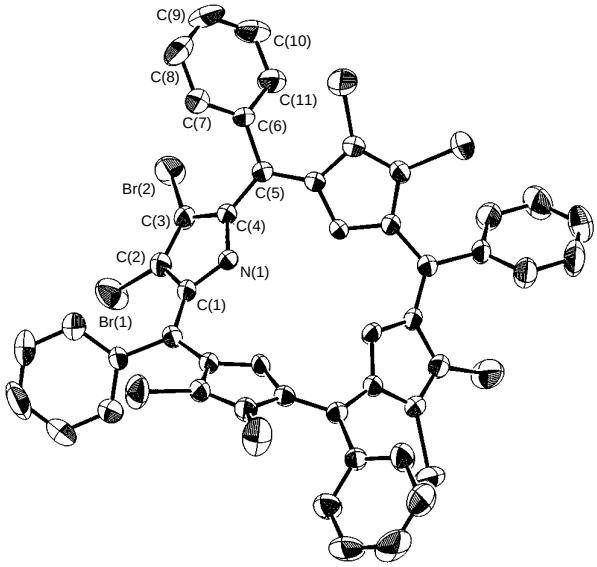



**Fig. 2** ORTEP diagram of $H_2$(β-$Br_8$tpp)·2dmf labelling the crystallographically independent atoms with 50% probability thermal elliposids

$H_2$(β-$Br_8$tfpp) ($C_\beta$ = 0.903 Å)[7] and $H_2$(β-$Br_8$tmp) ($C_\beta$ = 0.95 Å).[7,8b] The pronounced non-planarity of $H_2$(β-$Br_8$tpp) is also reflected by the large average perpendicular displacement of the *meso* carbons ($C_m$ = 0.317 Å) from the $N_4$ mean plane relative to that observed for $H_2$(β-$Br_8$tmp) ($C_m$ = 0.30 Å),[7,8b] and $H_2$(β-$Br_8$tfpp)[8a] ($C_m$ = 0.091 Å). The marked saddle distortion of $H_2$(β-$Br_8$tpp), and hence tipping of the pyrrole rings, results in particularly acute dihedral angles for the phenyl rings relative to the $N_4$ mean plane (29.7°). The pyrrole rings themselves are alternately canted above and below the $N_4$ mean plane with an average value of 44.6°.

The role played by non-planar porphyrin ligands in the coordination chemistry of rare-earth elements, and the unusual spectroscopic properties (UV–VIS, NMR data and electrochemical potentials) of their mono- or bis-porphyrinate complexes are two intriguing questions currently under investigation in our laboratory.

This research was supported by the Greek General Secretariat of Research and Technology through Grant A/A No. 1946 (1995) and by the General Secretariat of Athletic (OPAP). We are grateful to Dr O. Q. Munro for helpful discussions during the preparation of the manuscript. Mrs A. Athanassion is gratefully acknowledged for financial support to C. P. R.

## Footnotes

* E-mail: coutsole@pasifae.edu.uch.gr

† This lack of regiospecificity is justified by the predominant absence of localized double-bond character in the metalloporphyrin (see also ref. 4) which results in the introduction of one halogen atom in each pyrrolic/pyrrolenic ring; H. J. Callot, *Tetrahedron Lett.*, 1973, **50**, 4987.

‡ A detailed description of the synthesis, purification and the complete spectroscopic data of the nickel(II) β-tetra- and β-octa-halogenated tpp complexes as well as the X-ray study of [Ni(β-$Br_8$tpp)] will be published elsewhere, work in progress.

§ UV–VIS data in $CH_2Cl_2$, 20 °C, $\lambda_{max}$/nm, [log(ε/dm$^3$ mol$^{-1}$ cm$^{-1}$) in parentheses]: $H_2$(β-$Cl_4$tpp), 426 (5.44), 523 (4.35), 599 (3.56), 667 (3.54); $H_2$(β-$Cl_8$tpp), 453 (5.38), 551 (4.04), 601 (4.03), 719 (3.85); $H_2$(β-$Br_4$tpp), 430 (5.40), 527 (4.29), 598 (3.51), 673 (3.49); $H_2$(β-$Br_8$tpp), 469 (5.31), 569 (4.02), 625 (4.14), 745 (3.88). All complexes gave satisfactory elemental analysis data.

¶ The pyrolysis of $Tb^{III}(acac)_3$ during the course of this high temperature synthesis provides a reasonable explanation for the unexpected presence of the acetate ligand on the coordination sphere of terbium. For all the investigated complexes characteristic IR bands were observed at the regions 1440–1446 and 1490–1496 cm$^{-1}$, representative of the bidentate coordination of the $O_2$CMe ligand (see also: K. Nakamoto, in *Infrared and Raman Spectra of Inorganic and Coordination Compounds*, Wiley, 3rd edn., 1978).

‖ UV–VIS data in $CH_2Cl_2$, 20 °C, $\lambda_{max}$/nm, [log(ε/dm$^3$ mol$^{-1}$ cm$^{-1}$) in parentheses]: [$Tb^{III}$(β-$Cl_4$tpp)($O_2$CMe)], 432 (5.25), 563 (4.20), 596 (3.76); [$Tb^{III}$(β-$Cl_8$tpp)($O_2$CMe)], 460 (4.77), 553 (3.69), 598 (3.85), 652 (3.89); [$Tb^{III}$(β-$Br_4$tpp)($O_2$CMe)], 432 (5.20), 569 (4.15), 596 (3.64); [$Tb^{III}$(β-$Br_8$tpp)($O_2$CMe)], 474 (4.65), 552 (3.48), 612 (3.42), 669 (3.50). All complexes gave satisfactory elemental analysis data.

** *Crystal data*: [$Tb^{III}$(β-$Cl_8$tpp)($MeCO_2$)($Me_2SO$)$_2$], $C_{72}H_{63}Cl_8N_4O_5S_2Tb$, $M$ = 1570.91; monoclinic, space group $P2_1/c$; $a$ = 19.775(5), $b$ = 13.516(3), $c$ = 30.015(6) Å, β = 108.409(7)°, $U$ = 7612(3) Å$^3$, $Z$ = 4, $D_c$ ($D_m$) = 1.371 (1.36) g cm$^{-3}$, $T$ = 298 K. Atomic coordinates, bond lengths and angles, and thermal parameters have been deposited at the Cambridge Crystallographic Data Centre (CCDC). See Information for Authors, Issue No. 1. Any request to the CCDC for this material should quote the full literature citation and the reference number 182/407.

## References

1 (*a*) C.-P. Wong, R. F. Venteicher and W. Horrocks Dew, Jr., *J. Am. Chem. Soc.*, 1974, **96**, 7149; (*b*) W. Horrocks Dew, Jr., R. F. Venteicher, C. A. Spilburg and B. L. Vallee, *Biochem. Biophys. Res. Commun.*, 1975, **64**, 317; (*c*) W. Horrocks Dew, Jr. and C. P. Wong, *J. Am. Chem. Soc.*, 1976, **98**, 7157; (*f*) W. Horrocks Dew, Jr. and E. G. Hove, *J. Am. Chem. Soc.*, 1978, **100**, 4386; (*d*) J. W. Buchler, G. Eickelmann, L. Puppe, K. Rohbock, H. H. Schneehage and D. Weck, *Liebigs Ann. Chem.*, 1971, **745**, 135; (*e*) C.-P. Wong and W. Horrocks Dew, Jr., *Tetrahedron Lett.*, 1975, 2637.

2 M. Gouterman, C. D. Schumaker, T. S. Srivastava and T. Yotenani, *Chem. Phys. Lett.*, 1976, **40**, 456; L. A. Martarano, C.-P. Wong, W. Horrocks Dew, Jr. and A. M. P. Goncalves, *J. Phys. Chem.*, 1976, **80**, 2389; W. Horrocks Dew, Jr. and C.-P. Wong, *J. Am. Chem. Soc.*, 1976, **98**, 7157; W. Horrocks Dew, Jr. and E. G. Hove, *J. Am. Chem. Soc.*, 1978, **100**, 4386.

3 J. Deisenhofer, O. Epp, K. Miki, R. Huber and H. Michael, *Nature*, 1985, **318**, 618; C. Kirmaier and D. Holten, *Photosynth. Res.*, 1987, **13**, 225; D. Budil, P. Gast, C. H. Chang, M. Schifer and J. R. Norris, *Annu. Rev. Phys. Chem.*, 1987, **38**, 561.

4 T. Wijesekara, A. Matsumato, D. Dolphin and D. Lexa, *Angew. Chem., Int. Ed. Engl.*, 1990, **29**, 1028; M. J. Crossley, P. L. Burn, S. S. Chew, F. B. Cuttance and I. A. Newson, *J. Chem. Soc., Chem. Commun.*, 1991, 1564; M. J. Crossley, M. M. Harding and S. Sternhell, *J. Org. Chem.*, 1988, **53**, 1132.

5 W. Buchler, K, Elsasser, M. Kihn-Botulinski and B. Scharbert, *Angew. Chem., Int. Ed. Engl.*, 1986, **25**, 286 and references therein.

6 W. R. Scheidt and Y. J. Lee, in *Metal Complexes with Tetrapyrrole Ligands I*, ed. J. W. Buchler, Springer-Verlag, New York, 1987, vol. 64, pp. 2–70.

7 P. Ochsenbein, K. Ayougou, D. Mandon, J. Fisher, R. Weiss, R. N. Austin, K. Jayaraj, A. Gold, J. Terner and J. Fajer, *Angew. Chem., Int. Ed. Engl.*, 1994, **33**, 348.

8 (*a*) E. R. Birnbaum, J. A. Hodge, M. W. Grinstaff, W. P. Schaefer, L. Henling, J. A. Labinger, J. E. Bercaw and H. B. Gray, *Inorg. Chem.*, 1995, **34**, 3625; (*b*) E. R. Birnbaum, W. P. Schaefer, J. A. Labinger, J. E. Bercaw and H. B. Gray, *Inorg. Chem.*, 1995, **34**, 1751; (*c*) T. Takeuchi, H. B. Gray and W. A. Goddard, III, *J. Am. Chem. Soc.*, 1994, **116**, 973; (*d*) P. Ochsenbein, D. Mandon, J. Fisher, R. Weiss, R. N. Austin, K. Jayaraj, A. Gold, J. Terner, E. Bill, M. Müther and A. X. Trautwein, *Angew. Chem., Int. Ed. Engl.*, 1993, **32**, 1437.

*Received in Basel, Switzerland, 26th November 1996; Com. 6/08013H*

# Resin type can have important effects on solid phase asymmetric alkylation reactions

**Kevin Burgess* and Dongyeol Lim**

*Department of Chemistry, Texas A & M University, College Station, TX 77843-3255, USA*

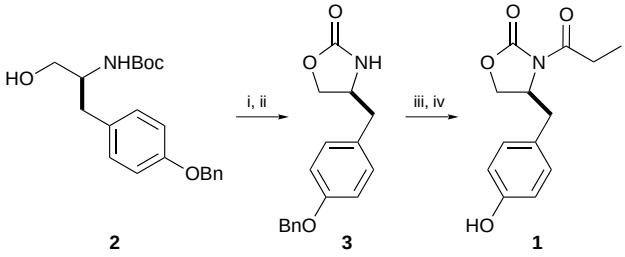
**A new *N*-propionylated oxazolidinone 1 is prepared; asymmetric alkylations of this auxiliary proceed with varying yields and enantioselectivities when supported on Merrifield, Wang and TentaGel R PHB resins.**

Techniques for solid phase organic syntheses[1] are pivotal for the development of combinatorial methods and other approaches to high throughput syntheses.[2–4] Asymmetric reactions on a solid phase have not been widely explored so far, yet they have potential advantages for some applications.[5] Supported chiral auxiliaries, for instance, can be recovered by filtration, and could potentially be recycled.

Two issues that need to be addressed for syntheses and applications of supported chiral auxiliaries are, first, how the auxiliary will be linked to the solid phase and, second, which solid phase will be used. At least two approaches to these problems have been reported. Leznoff initiated this area of research in studies wherein chiral amines were *O*-linked to Merrifield resin; condensations of these supported amines with cyclohexanone gave imines which were then deprotonated and *C*-methylated with high stereoselectivities.[6] More recently, Kurth and co-workers have attached pyrrolidine-based auxiliaries to Merrifield resin and used them in allylation/iodolactonization sequences.[7–9] Neither of these studies, however, embraced auxiliaries that are widely used in contemporary organic syntheses, and some of the supports that are now favoured for solid phase reactions. Here we describe an oxazolidinone **1** that can be conveniently linked to polymeric materials, and demonstrate that the choice of resin is important with respect to applications of the supported-auxiliary.

Synthesis of the oxazolidinone **1** began with commercially available Boc-Tyr(Bn) which was easily reduced to the corresponding alcohol **2** ($Pr^iOCOCl$, $NEt_3$, THF, then $NaBH_4$, $H_2O$). Removal of the *N*-protecting group and reaction with phosgene gave oxazolidinone **3** (Scheme 1). This material was then *N*-propionylated and subjected to hydrogenolysis to give the desired auxiliary **1**.

One of the attractive features of oxazolidinone **1** is that the phenolic hydroxy group is available for attachment to polymers. For Merrifield's resin this was accomplished *via* nucleophilic displacement of the benzylic chloride (3 equiv. of **1**, $Bu^tOK$, catalytic 18-crown-6/$Bu_4NI$, DMF, 75 °C, 3.5 d).[9] However, for the Wang and TentaGel resins Mitsunobu couplings[10] were used (3 equiv. of **1**, $EtO_2CNNCO_2Et$, $PPh_3$, 20 h).[11–13] Loadings of the auxiliary on the resins were difficult to determine accurately; after some experimentation, the following method was developed. The functionalized resins were reacted with lithium benzyloxide, and the benzyl propionate produced was quantified using HPLC and NMR. On the basis of these measurements it was calculated that approximately 30% of the available reactive sites on the Merrifield resin were coupled with the auxiliary under the conditions described above. For the Wang and TentaGel resins the corresponding loadings were 56 and 60% respectively.

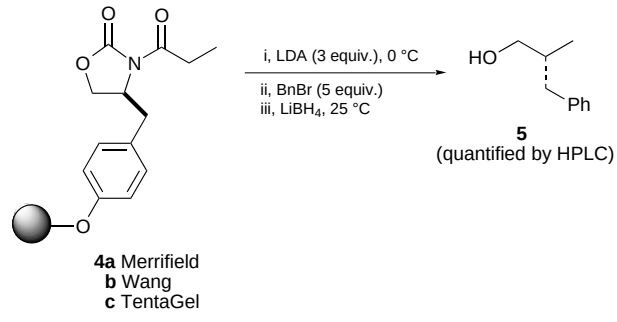



**Scheme 1** *Reagents and conditions*: i, HCl, $Et_2O$–EtOAc, 25 °C, 15 h (93%); ii, $COCl_2$, KOH–$K_2CO_3$ (aq), MePh, 0–25 °C, 12 h (98%); iii, $(EtCO)_2O$, LiCl, $NEt_3$, THF, −78–25 °C, 18 h (93%); iv, $H_2$, cat. Pd–C, MeOH–EtOAc, 25 °C, 12 h (96%)

Deprotonation of the supported oxazolidinones **4** with LDA in THF then reaction with benzyl bromide was chosen as a model transformation. These reactions were followed by IR (KBr disc). With Wang resin for instance, the supported oxazolidinones **4** had carbonyl stretches at 1704 and 1785 $cm^{-1}$. Benzylation of this material shifted the IR bands to 1701 and 1778 $cm^{-1}$. Hydrolytic cleavage of the benzylated propionate produced resin with a single carbonyl stretch at 1743 $cm^{-1}$, corresponding to the supported auxiliary. IR spectra of similar, but unsupported, auxiliaries have carbonyl stretches at *ca*. 1752 $cm^{-1}$.

A series of preliminary reactions showed the number of equivalents of base and the reaction times had a significant effect on the enantiomeric excess. It was also observed that reactions on the TentaGel resin were faster than on the Merrifield and Wang supports. Consequently, a series of experiments were performed in which 3 equiv. of LDA were added to the heterogeneous auxiliary at 0 °C. For the Merrifield and Wang resins, benzyl bromide was added after 30 min, allowed to react at 0 °C for 30 min, then for a systematically varied time at 25 °C. For the TentaGel based system, benzyl bromide was added after 20 min, and allowed to react for various times at 0 °C. The results of these studies are summarized in Fig. 1.

Fig. 1 shows that the yield of alcohol **5** reaches a maximum in the initial stages of the reaction, then decreases. For the TentaGel resin, the maximum yield is observed at short reaction times and decreases more precipitously as the reaction time is extended than for either the Merrifield or the Wang resins. Throughout, the HPLC traces of the material cleaved from the support show only one UV active product, hence the reduction in the yield is not due to formation of supported impurities with UV chromophores. Decreased yields could, however, be due to



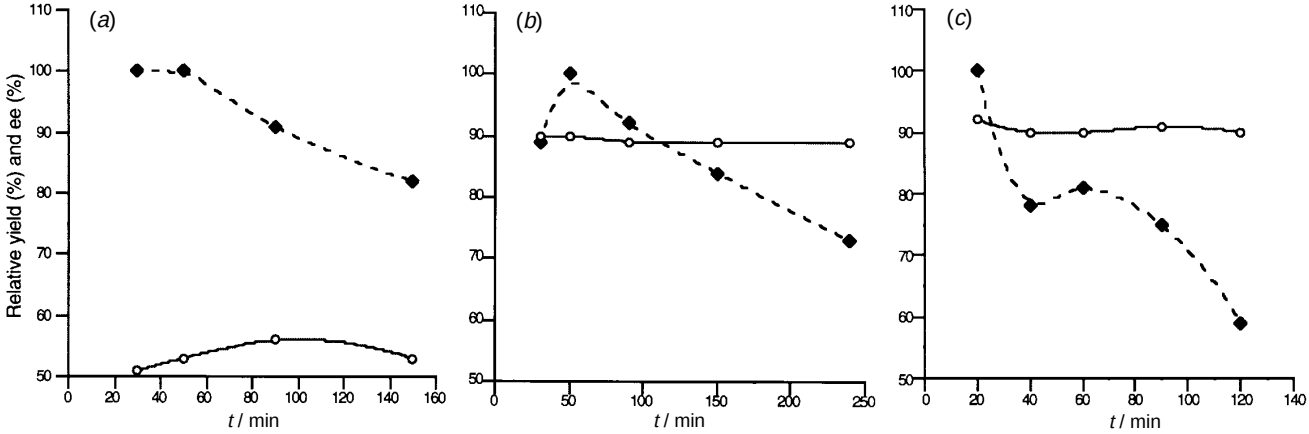
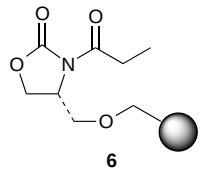



**Fig. 1** Percent yield (relative to the maximum for that reaction (◆) and enantiomeric excess (○) profiles for benzylation of the supported auxiliary **4** on (*a*) Merrifield, (*b*) Wang and (*c*) Tentagel R PHB resins. For conditions, see text.

**Table 1** Asymmetric alkylation reactions of the Wang-supported oxazolidinone **4b**

| | Reaction conditions | | | | |
|---|---|---|---|---|---|
| Alkylating agent | Equiv. LDA | Time/h at 0 °C | Time/h at 25 °C | Yield[a] (%) | Ee[b] (%) |
| BnBr | 3 | 0.5 | 0.33 | 66 | 90 |
| BnBr | 2 | 1.0 | 12 | 39 | 86 |
| $CH_2CHCH_2Br$ | 3 | 0.5 | 0.33 | 25 | 81[c] |
| $CH_2CHCH_2Br$ | 2 | 2.0 | 15 | — | 88 |
| $BnOCH_2Cl$ | 3 | 0.5 | 0.33 | 12 | 71[d] |
| $BnOCH_2Cl$ | 2 | 2.5 | 14 | 20 | 76[d] |

[a] For the alkylation and cleavage steps combined, determined by analytical HPLC using phenylpropanol as an internal standard. Authentic racemic products were prepared by solution phase syntheses and identified by $^1H$ and $^{13}C$ NMR spectroscopy. [b] Determined by analytical HPLC using a ChiralCel OD column. [c] Yields and ees were determined by using a chiral GC column prepared 'in house'. [d] Errors were relatively high because HPLC resolution of the enantiomers on a ChiralCel OD did not give baseline separation.



**6**

loss of the propionyl group from the oxazolidinone prior to cleavage.[14] Consistent with this, the IR stretch for the supported amide at 1701 $cm^{-1}$ diminishes with reaction time. Throughout, the measured enantiomeric excesses of the product **5** vary by ±3%; this fluctuation is probably within experimental error. However, in other experiments it was observed that after longer reaction times the enantiomeric excess of the product decreases measurably.

Overall, the data in Fig. 1 indicate that in terms of yield, enantiomeric excess and preservation of yield after extended reaction times, Wang resin is the preferred support. It is also cheaper than TentaGel resin, and has a higher loading capacity. Several more reactions were therefore performed using Wang resin and the results are summarized in Table 1. Yields and enantiomeric excesses obtained for benzyl bromide were superior to those obtained with other electrophiles. However, the results for these other electrophiles probably could be improved *via* optimization studies of the type carried out for the benzylation reactions.

After this work was complete, but before these studies were submitted for publication, other researchers reported the preparation of an oxazolidinone **6**, supported on Merrifield resin.[15] One alkylation reaction of this material was described (2 equiv. LDA, THF, 0 °C, then 2 equiv. BnBr; deprotonation and alkylation time unspecified), and that benzylation product (isolated as the acid) had an enantiomeric excess of 96%. We would have anticipated that the structural differences between auxiliaries **6** and **4** would be such that the tyrosine derivative **4** would give higher diastereoselectivities. In fact, **4** on Merrifield resin in our study gave stereoselectivities that are markedly inferior to those reported for **6** on the same resin, a result that we find surprising.

Overall, we conclude that optimization of these solid phase alkylation reactions is more difficult than for the corresponding solution phase reactions; the support has a marked effect and different resins may be most suitable for different oxazolidinones and electrophiles. Generally, solid phase reactions are more difficult to study than transformations in solution because they are more difficult to monitor. In addition, this work shows that resin type can be a significant variable that can further complicate the process of optimization.

We thank Dr Aroonsiri Shitangkoon for help with the chiral chromatography. Financial support for this research was obtained from The National Institutes of Health and The Robert A. Welch Foundation, and K. B. thanks the NIH for a Research Career Development Award and the Alfred P. Sloan Foundation for a fellowship. NMR facilities were provided by the NSF *via* the chemical instrumentation programme.

## References

1 L. A. Thompson and J. A. Ellman, *Chem. Rev.*, 1996, **96**, 555.
2 M. A. Gallop, R. W. Barrett, W. J. Dower, S. P. A. Fodor and E. M. Gordon, *J. Med. Chem.*, 1994, **37**, 1233.
3 E. M. Gordon, R. W. Barrett, W. J. Dower, S. P. A. Fodor and M. A. Gallop, *J. Med. Chem.*, 1994, **37**, 1385.
4 N. K. Terrett, M. Gardner, D. W. Gordon, R. J. Kobylecki and J. Steele, *Tetrahedron*, 1995, **51**, 8135.
5 M. Reggelin and V. Brenig, *Tetrahedron Lett.*, 1996, **37**, 6851.
6 C. R. McArthur, P. M. Worster, J.-L. Jiang and C. C. Leznoff, *Can. J. Chem.*, 1982, **60**, 1836.
7 X. Beebe, N. E. Schore and M. J. Kurth, *J. Am. Chem. Soc.*, 1992, **114**, 10061.
8 H.-S. Moon, N. E. Schore and M. J. Kurth, *Tetrahedron Lett.*, 1994, **35**, 8915.
9 H.-S. Moon, N. E. Schore and M. J. Kurth, *J. Org. Chem.*, 1992, **57**, 6088.
10 D. L. Hughes, *Org. React.*, 1992, **42**, 335.
11 L. S. Richter and T. R. Gadek, *Tetrahedron Lett.*, 1994, **35**, 4705.
12 T. A. Rano and K. T. Chapman, *Tetrahedron Lett.*, 1995, **36**, 3789.
13 V. Krchnak, Z. Flegelova, A. S. Weichsel and M. Lebl, *Tetrahedron Lett.*, 1995, **36**, 6193.
14 D. A. Evans, M. D. Ennis and D. J. Mathre, *J. Am. Chem. Soc.*, 1982, **104**, 1737.
15 S. M. Allin and S. J. Shuttleworth, *Tetrahedron Lett.*, 1996, **37**, 8023.

*Received, 19th December 1996; Com. 6/08524E*

# New vinylogous tetrathiafulvalene π-electron donors with lower oxidation potentials

**Lianhe Yu* and Daoben Zhu**

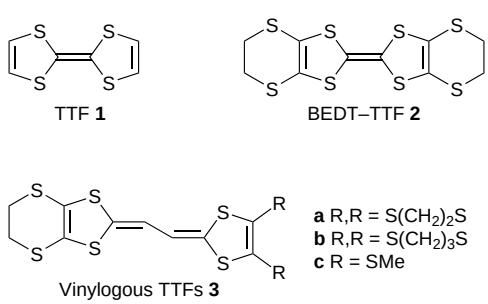
*Laboratory of Organic Solids, Institute of Chemistry, Chinese Academy of Sciences, Beijing 100080, PR China*

**The efficient synthesis of three new vinylogous TTF and three new 1,3-dithiole-2-thione derivatives is described; cyclic voltammetry establishes that the new donors have significantly lower solution oxidation potentials than BEDT–TTF.**

Among the organic donors, much work has been done on the tetrathiafulvalenes (TTF) **1** in the race for new organic conductors and/or superconductors.[1] Modification of the basic TTF framework leading to new functionalized π-donors has been intensively studied,[2] notably, bis(ethylenedithiol)tetrathiafulvalene (BEDT–TTF) **2** has produced organic superconductors with $T_c$ values as high as 12.8 K.[3] The synthesis of new π-donors related to TTF is central to the understanding of the solid-state properties of this fascinating class of materials. In particular, derivatives with lower oxidation potentials than the parent compounds TTF and BEDT–TTF are prime targets, an interesting type of such derivatives involves insertion of a conjugated spacer between two 1,3-dithiole rings, *i.e.* the so-called vinylogous TTF **3**.[4] The synthesis of such extended TTFs reported in the literature is mainly based on the Wittig–Horner reaction of a (1,3-dithiol-2-yl)phosphonium salt with an appropriate aldehyde.[4] Herein we report an alternative route to the new vinylogous **7** as well as new 1,3-dithiole-2-thiones **8** *via* base catalysed ring opening of 4-(1,4-dithiafulven-6-yl)-1,2,3-thiadiazole; this route seems to have been overlooked as an entry into the preparation of such vinylogous derivatives.[5]

The synthesis of the new donors is outlined in Scheme 1. The key starting material, 4-formyl-1,2,3-thiadiazole **4**, was prepared by the Hurd–Mori reaction,[6] while the (1,3-dithiol-2-yl)phosphonium salts **5** were synthesized by a well-established four-step reaction[7] from the corresponding readily available 1,3-dithiole-2-thiones.[8]

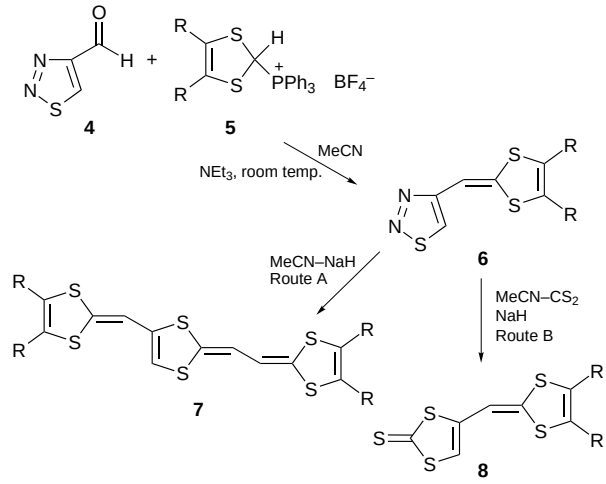
Equimolar amounts of **4** and **5** were condensed in dry acetonitrile in the presence of triethylamine at room temperature under nitrogen, which afforded **6** in 80–85% yield. Treatment of **6** with base (NaH 80% mineral dispersion) in neat acetonitrile at ambient temperature under nitrogen gave the corresponding novel vinylogous TTF derivatives **7a**–**c** in 40–70% yield after purification (route A).† However, when carbon disulfide was added, the NaH catalysed ring opening of **6** afforded new 1,3-dithiole-2-thione **8** in 70–85% yield (route B).‡ Compounds **8** are important synthetic building blocks for the construction of new types of (1,4-dithiafulven-6-yl)-substituted TTF derivatives. The target molecules **7a** and **7b** are very insoluble in organic solvents, nevertheless, the solubility of **7** can be improved by changing the R group, and indeed, **7c** (R = SMe) is very soluble in organic solvents such as $CH_2Cl_2$, $CHCl_3$, THF, MeCN. Molecular ion peaks of all new donors could not be obtained using EI, CI or FAB mass spectra, however, the field desorption mass spectra of **7** were successfully recorded.



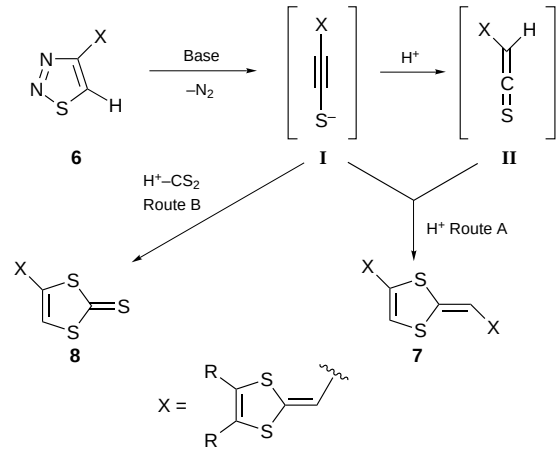

The mechanism of the base catalysed ring opening of 4-substituted 1,2,3-thiadiazole is briefly outlined in Scheme 2.[9]

Base catalysed decomposition of **6** afforded alkyne **I** and subsequently **II**. It is proposed that 1,3-addition of **I** to the thioketene **II** affords **7**,[9a] however, when $CS_2$ is added, 1,3-addition of **I** to $CS_2$ affords **8** in a similar manner.

The electrochemical properties of **7** were investigated by cyclic voltammetry. All new vinylogous derivatives **7a**–**c**




**Scheme 1** Synthesis of novel vinylogous TTF and 1,3-dithiole-2-thione derivatives




**Scheme 2** Mechanism for the formation of **7** and **8**

undergo two reversible, single-electron oxidations, *e.g*. Fig. 1 shows the cyclic voltammogram of compound **7b** recorded at 50 mV $s^{-1}$. Very similar results were obtained for the other donors. In order to compare the $E_1^{1/2}$ and $E_2^{1/2}$ values of **7** with those of the related vinylogous **3**, we have also synthesized the known donors **3a**–**c** according to the method described in the literature.[4] Table 1 shows the redox potentials of **7** along with TTF **1**, BEDT–TTF **2** and **3**.

From Table 1, two important consequences of enlarging the conjugated π-system are observed: (i), both the first and second oxidation potentials of **7** are lower in comparison with **1**, **2** and **3**, obviously demonstrating that **7** is a more efficient electron donor than BEDT–TTF as expected from the calculated ionization potentials, and (ii) the difference between the two redox waves $\Delta E^{1/2}$ is reduced in the vinylogues derivatives, evidence of reduced intramolecular Coulombic repulsion in the dication state, suggesting that there is scope for obtaining molecular conductors or magnets based upon entirely new π-electron donors.

As expected from these results, all new donors **7** behave as good precursors for organic metals, and thus further experiments are underway to prepare charge transfer complexes based on the novel donors.

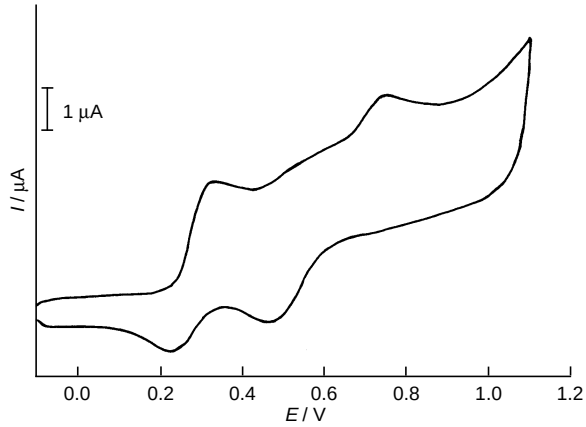



**Fig. 1** Cyclic voltammogram of **7b** range from 0.0 to 1.2 V

**Table 1** Cyclic voltammetric data for donors **1**, **2**, **3** and **7**[a]

| Compound | $E_1^{1/2}$/V | $E_2^{1/2}$/V | $\Delta E^{1/2}$/V |
|---|---|---|---|
| **1** | 0.36 | 0.80 | 0.44 |
| **2** | 0.46 | 0.96 | 0.50 |
| **3a** | 0.42 | 0.77 | 0.35 |
| **3b** | 0.49 | 0.71 | 0.22 |
| **3c** | 0.45 | 0.72 | 0.27 |
| **7a** | 0.41 | 0.62 | 0.21 |
| **7b** | 0.29 | 0.60 | 0.31 |
| **7c** | 0.30 | 0.61 | 0.31 |

[a] Experimental conditions: donors (*ca*. $1.0 \times 10^{-4}$ mol $dm^{-3}$), supporting electrolyte $Et_4N^+ClO4^-$ (*ca*. $1.0 \times 10^{-1}$ mol $dm^{-3}$) in dry dichloromethane, indicating electrode Pt, reference electrode SCE, scan rate 50 mV $s^{-1}$ using EG & G Parc Model 175 electrochemical analythesis meter.

We thank the China Postdoctoral Foundation and Chinese Academy of Sciences for funding this work. The authors thank Dr Louzhen Fan for her assistance in the determination of cyclic voltammetric data.

## Footnotes

† New compounds **7a**–**c** have been characterized and presented satisfactory spectra data. *Selected data* for **7a**: yellow solid (yield 40% after purified by chromatography through a short column of silica gel using carbon disulfide as eluent); mp > 270 °C; $^1$H NMR (200 MHz, $CS_2$–$CDCl_3$, $Me_4Si$) $\delta_H$: 3.12–3.30 (m, 8 H, $SCH_2$), 5.80–6.80 (m, 4 H, alkenyl hydrogens); $\nu_{max}$ (KBr)/$cm^{-1}$ 2920($CH_2$), 1642, 1528, 1505 (C=C); MS (FD) 524.1 ($M^+$); $\lambda_{max}$($CH_2Cl_2$) 404 nm ($\varepsilon = 4.3 \times 10^4$). For **7b**: Orange microcrystals (yield 72% after recrystallization from $CS_2$–$CHCl_3$); mp 218–220 °C; $^1$H NMR (200 MHz, $CDCl_3$, $Me_4Si$) $\delta_H$: 2.40 (m, 4 H, $CH_2$), 2.65 (m, 8 H, $SCH_2$), 5.64–5.90 (m, 4 H, CH); $\nu_{max}$ (KBr)/$cm^{-1}$ 2908 ($CH_2$), 1493 (C=C); MS(FD) 552 ($M^+$); $\lambda_{max}$($CH_2Cl_2$) 410 nm ($\varepsilon = 5.4 \times 10^4$). For **7c**: (yield 70% after recrystallization from dichloromethane–light petroleum (30–60 °C); mp 46–48 °C; $^1$H NMR (200 MHz, $CDCl_3$, $Me_4Si$) $\delta_H$: 2.41 (s, 12 H, $SCH_3$), 5.74–6.01 (m, 4 H, CH); $\nu_{max}$(KBr)/$cm^{-1}$ 2916 ($CH_2$), 1490, 1425 (C=C), 1022 (C–S); MS (FD) 528 ($M^+$); $\lambda_{max}$($CH_2Cl_2$) 412 nm ($\varepsilon = 4.9 \times 10^4$).

‡ *Selected data* for **8a**: red plates (yield 83% after recrystallization from chloroform–hexane), mp 190 °C; $^1$H NMR (200 MHz, $CDCl_3$, $Me_4Si$) $\delta_H$: 3.36 (s, 4 H, $SCH_2$), 6.26 (s, 1 H, CH), 6.39 (s, 1 H, CH); MS (EI) 338 ($M^+$, 100%), 310 ($M^+ - 28$, 20.3%), 262 ($M^+ - 76$, 25.6%), 234 ($M^+ - 104$, 43.2%). For **8b**: yellow needles (yield 80% after recrystallization from chloroform–light petroleum (60–90 °C); mp 184–186 °C; $^1$H NMR (200 MHz, $CDCl_3$, $Me_4Si$) $\delta_H$: 2.41 (m, 2 H, $CH_2$), 2.72 (m, 4 H, $SCH_2$), 6.16 (s, 1 H, CH), 6.58 (s, 1 H, CH); MS (EI) 352 ($M^+$, 100%), 276 ($M^+ - 76$, 24.5%), 244 ($M^+ - 108$, 9.3%), 229 ($M^+ - 123$, 15.4%). For **8c**: slightly oily crystals [yield 70% after chromatography on silica gel GF254 with $CH_2Cl_2$–light petroleum (30–60 °C) (1 : 1) as eluent]; $^1$H NMR (200 MHz, $CDCl_3$, $Me_4Si$) $\delta_H$: 2.43 (s, 6 H, $SCH_3$), 6.22 (s, 1 H, CH), 6.80 (s, 1 H, CH); MS (EI) 340 ($M^+$, 100%), 246 ($M^+ - 94$, 40.7%).

## References

1 For recent reviews see: G. Schukat, A. M. Richter and E. Fanghanel, *Sulfur Rep.*, 1993, **14**, 245; D. Schukat and E. Fanghanel, *Sulfur Rep.*, 1996, **18**, 1; M. R. Bryce, *J. Mater. Chem*., 1995, **5**, 1481; M. R. Bryce, *Chem. Soc. Rev*., 1991, **20**, 355.
2 T. K. Hansen and J. Becher, *Adv. Mater*., 1993, **5**, 288.
3 J. M. Williams, A. M. Kini, H. H. Wang, K. D. Carlson, U. Geiser, L. K. Montgomery, G. J. Pyrka, D. M. Watkins, J. M. Kommers, S. J. Boryschuk, A. V. Strieby, W. K. Kwok, J. E. Schiber, D. L. Overmyer, D. Jung and M.-H. Whangbo, *Inorg. Chem*., 1990, **29**, 3262.
4 A. J. Moore, M. R. Bryce, D. J. Ando and M. B. Hursthouse, *J. Chem. Soc., Chem. Commun*., 1991, 320.
5 R. P. Clausen and J. Becher, *Tetrahedron*, 1996, **52**, 3171.
6 C. D. Hurd and R. I. Mori, *J. Am. Chem. Soc*., 1955, **77**, 5359; T. Kobori, M. Fujita, T. Hiyama and K. Kondo, *Synlett*, 1992, 95.
7 A. J. Moore and M. R. Bryce, *Synthesis*, 1991, 26.
8 N. Sevenstrup and J. Becher, *Synthesis*, 1995, 215.
9 (*a*) A. Shafiee and I. Lalezari, *J. Heter. Chem*., 1973, **10**, 11; (*b*) I. Lalezari, A. Shafiee and M. Yalpani, *J. Org. Chem*., 1973, **38**, 338.

*Received in Cambridge, UK, 3rd December 1996; Com. 6/08146K*

# The first isolation of a π-complex precursor in Meisenheimer complex formation

**Patricia Sepulcri, Régis Goumont, Jean-Claude Hallé, Erwin Buncel*† and François Terrier***

*Laboratoire SIRCOB, EP CNRS 102, Bâtiment Lavoisier, Université de Versailles, 45, Avenue des Etats-Unis, 78035 Versailles Cedex 05, France*

**Treatment of 1,3,5-trinitrobenzene with indole-3-carboxylate ion in methanol affords an isolable π-complex which is the precursor of the N- and C-adducts expected from the interaction.**

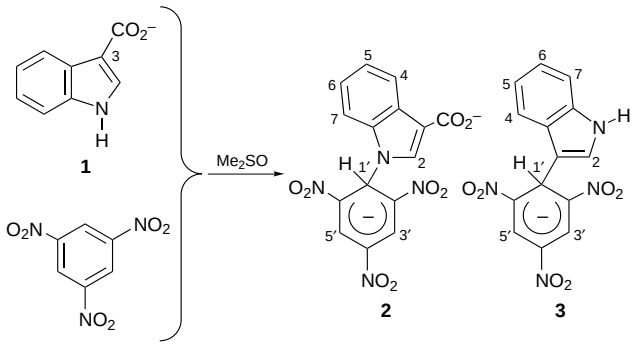
While the intermediacy of anionic σ-complexes in nucleophilic aromatic substitution is now well established,[1–5] the role of charge-transfer (CT) or π-complexes in such processes remains controversial.[6–10] A variety of experimental methods have provided evidence for the formation of CT or π-complexes in the interaction of electron-deficient aromatics (acceptors) and bases/nucleophiles (donors), but it is uncertain whether these species are formed in competing processes, concurrently, or whether they are present as intermediates on the $S_NAr$ reaction pathways. In a series of papers by Bunton and co-workers evidence has shown that π-complexes *and* charge-transfer (electron-transfer) complexes are formed prior to the anionic covalent σ-complex adducts, enroute to $S_NAr$ displacement, and are also intermediates in H/D exchange.[11–15] However, to our knowledge there has been no report so far of the actual isolation of CT or π-complexes in $S_NAr$ or σ-complex formation processes with a simple (classical) nitroaromatic compound such as 1,3,5-trinitrobenzene.[16] In this report we present evidence for the first instance of this kind.

The reaction of 1,3,5-trinitrobenzene (TNB) with indole-3-carboxylate (**1** as $Na^+$ salt) in $Me_2SO$, as followed by NMR spectroscopy, gives rise to the TNB N-adduct **2** concurrently with the TNB C-adduct **3** formed through decarboxylation (Scheme 1). These adducts could readily be characterized by $^1H$ and $^{13}C$ NMR spectroscopy (Table 1).[2,3]

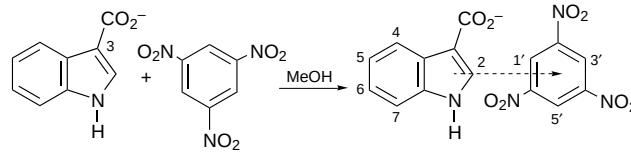
However, when carried out in methanol the reaction takes a different course. This reaction gives rise to an adduct which can be isolated from the solution as the sodium salt and which we formulate as the π-complex **4** (Scheme 2). The adduct can be simply prepared by mixing 0.2 M methanolic solutions of TNB and indole 3-carboxylate ($Na^+$ salt) and evaporating to dryness.

This brown solid has been characterized as follows. The UV–VIS spectrum contains new bands (not present in TNB or **1**) of low intensity characteristic of π- or CT complexes[17] at 385, 413, 474 and 500 nm. Especially noteworthy in the $^1H$ NMR spectrum (Table 1) is the substantial shift to high field of the protons relative to the parent nitro-aromatic ($\Delta\delta$ = 0.50 ppm).[18] ESI mass spectroscopy experiments show the expected peak corresponding to the molecular ion of **4** (*m/z* 373). Also, CAD (collision activated dissociation) of this molecular ion shows the required daughter peaks, *i.e.* the indolecarboxylate (*m/z* 160) and TNB, actually (TNB − H)$^-$, (*m/z* 212) portions.

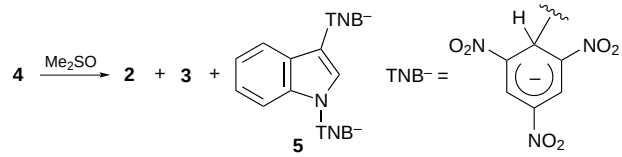
Interestingly, when **4** is placed in $Me_2SO$, it rapidly gives rise to the TNB N-adduct **2**, the TNB C-adduct **3** formed upon




**Scheme 1**




**Scheme 2**




**Scheme 3**

**Table 1** NMR parameters for the π-complex **4** and the σ-adducts **2** and **3**[a,b]

| Compound | $H_{1'}$ | $H_{3',5'}$ | $H_2$ | $H_4$ | $H_5$ | $H_6$ | $H_7$ | NH | Coupling constants/Hz |
|---|---|---|---|---|---|---|---|---|---|
| **2**[c] | 7.36 | 8.59 | 7.56 | 8.09 | 7.10 | 7.15 | 7.33 | — | $H_4$–$H_5$ = 8.07; $H_6H_7$ = 8.46; $H_5$–$H_7$ = 1.11 |
| **3**[c] | 5.98 | 8.36 | 7.16 | 7.49 | 6.95 | 7.03 | 7.30 | 11.01 | $H_4$–$H_5$ = 7.71; $H_4$–$H_6$ = 1.47; $H_6$–$H_7$ = 7.71; $H_5$–$H_7$ = 1.11; $H_2$–NH = 2.22 |
| **4**[d] | 8.83 | 8.83 | 7.68 | 8.02 | 6.95 | 6.95 | 7.20 | [e] | — |

[a] For comparison: TNB ($CD_3OD$) δ: 9.33; TNB [$(CD_3)_2SO$] δ: 9.19. [b] $^{13}C$ NMR of **4** (0.45 M) in $CD_3OD$: CO, δ: 174.83; $C_{2'6'4'}$, 149.09; $C_{3'5'1'}$, 123.99; $C_2$, 130.69; $C_3$, 115.47; $C_4$, 122.37; $C_5$, 120.96; $C_6$, 122.45; $C_7$, 112.18; $C_8$, 137.73; $C_9$, 128.00. [c] Solvent: $(CD_3)_2SO$; internal reference $Me_4Si$. [d] Solvent: $CD_3OD$; internal reference $Me_4Si$. [e] Exchangeable proton in $CD_3OD$.

decarboxylation, and the N–C diadduct **5** (Scheme 3). The mono-adduct **3** and the diadduct **5** were obtained previously from the direct reaction of TNB with indolide ion under more basic experimental conditions.[19]

While indole itself has been known to form a molecular complex with TNB,[20] the use in the present work of the indole-3-carboxylate ion (**1**) has allowed solubilization in methanol and, equally importantly, has increased charge density of the indole nucleus, thus stabilizing the π-complex.

Further work towards definitive characterization of π-complexes in these systems will be concerned with X-ray structure determination, kinetic studies, and structural variation of the indole moiety with the view of modulating the stability of these complexes.

Grants in aid of this research from CNRS (France) and NSERCC (Canada) are gratefully acknowledged.

## Footnotes

* E-mail: terrier@chimie.uvsq.fr
† Visiting Professor from Queen's University, Kingston, K7L 3N6, Canada.

## References

1 F. Terrier, in *Nucleophilic Aromatic Displacement; The influence of the nitro group, Organic Nitro Chem. Ser*., ed. H. Feuer, VCH, New York, 1991.
2 E. Buncel, M. R. Crampton, M. J. Strauss and F. Terrier, in *Electon deficient aromatic- and heteroaromatic-base interactions*, Elsevier, Amsterdam, 1984.
3 G. A. Artamkina, M. P. Egorov and I. P. Beletskaya, *Chem. Rev*., 1982, **82**, 427.
4 F. Terrier, *Chem. Rev*., 1982, **82**, 77.
5 E. Buncel, in *The chemistry of functional groups. Supplement F. The chemistry of amino, nitro and nitroso compounds*, ed. S. Patai, Wiley, London, 1982.
6 M. R. Crampton, A. B. Davis, C. Greenhalgh and J. A. Stevens, *J. Chem. Soc., Perkin Trans. 2*, 1989, 675.
7 L. Forlani, G. Guastadisegni and L. Raffellini, *J. Chem. Res. (S)*, 1989, 392; L. Forlani and C. Cimarelli, *J. Phys. Org. Chem*., 1989, **2**, 653; L. Forlani and E. Mezzina, *J. Chem. Soc., Perkin Trans. 2*, 1995, 2019.
8 R. I. Cattana, J. O. Singh, J. D. Anunziata and J. J. Silber, *J. Chem. Soc., Perkin Trans. 2*, 1987, 79.
9 J. Hajami, S. Otani, F. Yamaguchi and Y. Nishigawa, *Chem. Lett*., 1981, 739.
10 S. K. Dotterer and R. L. Harris, *J. Org. Chem*., 1988, **53**, 777.
11 R. Bacaloglu, C. A. Bunton and G. Cerichelli, *J. Am. Chem. Soc*., 1987, **109**, 621.
12 R. Bacaloglu, A. Blasko, C. A. Bunton, E. Dorwin, F. Ortega and C. Zucco, *J. Am. Chem. Soc*., 1991, **113**, 238.
13 R. Bacaloglu, A. Blasko, C. A. Bunton, F. Ortega and C. Zucco, *J. Am. Chem. Soc*., 1992, **114**, 7708.
14 R. Bacaloglu, C. A. Bunton and F. Ortega, *Int. J. Chem. Kinet*., 1988, **20**, 195.
15 R. Bacaloglu, C. A. Bunton, G. Cerichelli and F. Ortega, *J. Am. Chem. Soc*., 1988, **110**, 3495.
16 R. W. Read, R. J. Spear and W. P. Norris, *Austr. J. Chem*., 1984, **37**, 985.
17 R. Foster, in *Organic Charge-transfer Complexes*, Academic, London, 1969.
18 J. A. Chudek, R. Foster and D. R. Twiselton, *J. Chem. Soc., Perkin Trans. 2*, 1983, 1385.
19 J. C. Hallé, F. Terrier, M. J. Pouet and M. P. Simonnin, *J. Chem. Res. (S)*, 1980, 360.
20 B. Sabourault and J. Bourdais, *C. R. Acad. Sci*., 1972, **274 C**, 813.

*Received in Cambridge, UK, 10th January 1997. Com. 7/00231I*

# Unusual alkylidene ligands: synthesis and structure of the cyclopentadienylidene complex $[(\eta^5\text{-}C_5H_5)Ta(NEt_2)_2(=C_5H_4)]$

**Paula M. Briggs,[a] Victor G. Young, Jr.[b] and David E. Wigley*[a]**

[a] *Carl S. Marvel Laboratories of Chemistry, Department of Chemistry, University of Arizona, Tucson, Arizona 85721, USA*
[b] *X-Ray Crystallographic Laboratory, Department of Chemistry, University of Minnesota, Minneapolis, Minnesota 55455, USA*

**The unique alkylidene complex $[(\eta^5\text{-}C_5H_5)Ta(NEt_2)_2(=C_5H_4)]$ 2 is prepared in low yield from the reaction of $[(\eta^5\text{-}C_5H_5)Ta(NEt_2)_2Cl_2]$ 1 with 2 equiv. of MeLi and is fully characterised including an X-ray structural determination.**

Transition-metal cyclopentadienyl complexes are situated at the heart of modern organometallic chemistry.[1] Of the known bonding modes of $C_5H_5$ and its analogues, the $\eta^5:\eta^1\text{-}C_5H_4$ structure that bridges two metal centres is well established and has played a role in the development of transition-metal metallocene chemistry.[2] We wish to report a new bonding mode of the $C_5H_4$ ligand that is ostensibly formed upon decomplexing the $\eta^5$ portion of a bridging $\eta^5:\eta^1\text{-}C_5H_4$ moiety, *viz.* the $\eta^1\text{-}C_5H_4$ alkylidene, or cyclopentadienylidene, ligand in the mononuclear complex $[(\eta^5\text{-}C_5H_5)Ta(NEt_2)_2(=C_5H_4)]$.

Upon reacting a thf solution of $[Ta(NEt_2)_2Cl_3(OEt_2)]$[3] with 1 equiv. of $NaC_5H_5$, a red solution is obtained from which yellow–orange crystals of $[(\eta^5\text{-}C_5H_5)Ta(NEt_2)_2Cl_2]$ **1** can be isolated in high yield (Scheme 1).† When $[(\eta^5\text{-}C_5H_5)Ta(NEt_2)_2Cl_2]$ **1** is reacted with 2 equiv. of MeLi (−35 °C, toluene–$Et_2O$), the reaction quickly develops an orange colour and is accompanied by the evolution of a gas that is shown to be $CH_4$ by GCMS analysis (Scheme 1). After work-up of the oil obtained from this reaction, orange crystals of compound **2** may be obtained in low yield. In addition to resonances assigned to the $C_5H_5$ and $NEt_2$ ligands, the $^1$H NMR data for **2** {[$^2H_8$]thf} reveal two multiplets at δ 6.68 ($CH^\alpha$) and 5.49 ($CH^\beta$) that integrate to two protons each and its $^{13}$C NMR spectrum ($C_6D_6$) reveals three $^{13}$C resonances at δ 235.7, 124.5 and 113.6. On the basis of these NMR data, including HETCOR and NOE spectra, and an X-ray crystallographic study (*vide infra*), **2** is formulated as the terminal alkylidene, or cyclopentadienylidene, complex $[(\eta^5\text{-}C_5H_5)Ta(NEt_2)_2(=C_5H_4)]$ (Scheme 1).

Although the orange–brown oil obtained from the $[(\eta^5\text{-}C_5H_5)Ta(NEt_2)_2Cl_2]$ + 2MeLi reaction contains multiple products (including paramagnetic species), $[(\eta^5\text{-}C_5H_5)Ta(NEt_2)_2(=C_5H_4)]$ **2** is the only product that we could isolate from the reaction mixture and then in only *ca.* 15% yield based on $C_5H_5$ (7.5% based upon tantalum). This low yield is not improved by changes in the reaction time, temperature, solvent, or the work-up procedure, nor can $[(\eta^5\text{-}C_5H_5)Ta(NEt_2)_2(=C_5H_4)]$ **2** be prepared in greater yield by other synthetic methods.

$$[Ta(NEt_2)_2Cl_3(OEt_2)] + NaC_5H_5 \xrightarrow{thf} [(\eta^5\text{-}C_5H_5)Ta(NEt_2)_2Cl_2] + NaCl$$

$$[(\eta^5\text{-}C_5H_5)Ta(NEt_2)_2Cl_2] + 2MeLi \xrightarrow[-35\ °C,\ -CH_4]{toluene\text{–}Et_2O} [(\eta^5\text{-}C_5H_5)Ta(NEt_2)_2(=C_5H_4)] + \text{other products}$$

15%

**Scheme 1**

The molecular structure of $[(\eta^5\text{-}C_5H_5)Ta(NEt_2)_2(=C_5H_4)]$ **2** was determined by X-ray crystallography and is presented in Fig. 1.‡ The overall geometry can be described as a three-legged piano stool containing a terminal alkylidene ligand, as indicated by the short Ta–C(1) distance of 2.037(4) Å, which is well within the range expected for $d^0$ Ta=C double bonds.[4] The $C_5H_4$ ligand is planar and is clearly π localised as the diene, as indicated by the alternating C–C bond lengths around the ring. The plane of the $C_5H_4$ alkylidene ligand is slightly tilted from perpendicular with respect to the $\eta^5\text{-}C_5H_5$ plane (dihedral angle 74.8°) and the $NEt_2$ ligands are considerably tilted such that the Ta–N(3)–C(31)–C(33) plane is 54.9° and Ta–N(4)–C(41)–C(43) is 142.2° from the $\eta^5\text{-}C_5H_5$ plane. Such an arrangement places the two $TaNC_2$ planes nearly perpendicular (92.9°) to each other. Finally, the short Ta–N bonds of *ca.* 1.97 Å indicate significant $N(p_\pi)$–$Ta(d_\pi)$ electron donation from the amido ligand.[5]

Related structures containing $C_5H_4$ ligands have been described, for example the $\eta^5:\eta^1\text{-}C_5H_4$ ligand is well established in complexes such as $[(\eta^5\text{-}C_5H_5)(\eta^5:\eta^1\text{-}C_5H_4)NbH]_2$,[6] $[(\eta^5\text{-}C_5H_5)(\eta^5:\eta^1\text{-}C_5H_4)WH]_2$,[7] $[(\eta^5\text{-}C_5H_5)(\eta^5:\eta^1\text{-}C_5H_4)Mo]_2$[8] and $[(\eta^5\text{-}C_5H_5)(\eta^5:\eta^1\text{-}C_5H_4)Ti(PMe_3)]_2$.[9] If the *ipso* carbon (only) of the $\eta^5$ portion of an $\eta^5:\eta^1\text{-}C_5H_4$ ligand is decomplexed, an $\eta^4:\eta^1\text{-}C_5H_4$ ligand is generated, an example of which is seen in $[(\eta^5\text{-}C_5H_5)Co(\eta^4:\eta^1\text{-}C_5H_4)Co(\eta^5\text{-}C_5H_5)(PMe_3)]$,[10] and if the *ipso* carbon of an $\eta^1\text{-}C_5H_4$ ligand bridges two metals, a $\mu(\eta^1)\text{-}C_5H_4$ complex results as in Wilkinson's $[\{Re(=NBu^t)_2(\eta^1\text{-}C_5H_5)\}_2\{\mu(\eta^1)\text{-}C_5H_4\}(\mu\text{-}O)]$.[11] Finally, we note that Herrmann and coworkers have generated transient $[(\eta^5\text{-}C_5H_5)Mn(CO)_2(=C_5H_5)]$ from the reaction of

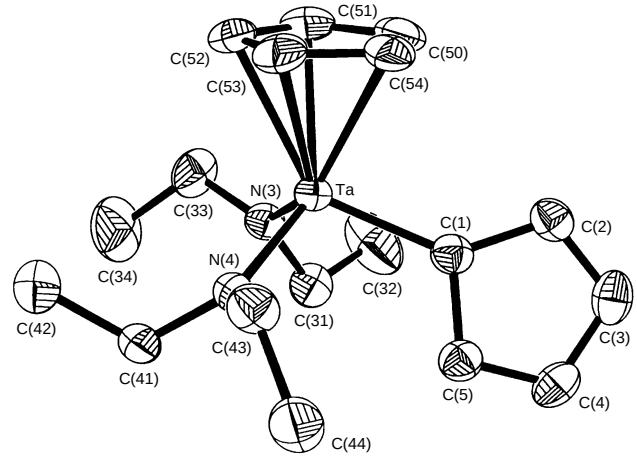



**Fig. 1** Molecular structure of $[(\eta^5\text{-}C_5H_5)Ta(NEt_2)_2(=C_5H_4)]$ **2** with atoms drawn as 50% ellipsoids. Selected bond distances (Å) and angles (°): Ta–C(1) 2.037(4), Ta–N(3) 1.969(3), Ta–N(4) 1.966(3), C(1)–C(5) 1.455(5), C(1)–C(2) 1.451(5), C(2)–C(3) 1.367(5), C(3)–C(4) 1.426(6), C(4)–C(5) 1.369(5); N(3)–Ta–N(4) 100.59(12), N(3)–Ta–C(1) 105.47(13), N(4)–Ta–C(1) 101.30(13), Ta–C(1)–C(2) 136.1(3), Ta–C(1)–C(5) 118.4(3), C(1)–C(2)–C(3) 109.4(3), C(2)–C(3)–C(4) 108.8(3), C(3)–C(4)–C(5) 108.1(3), C(4)–C(5)–C(1) 109.5(3).

$[(\eta^5\text{-}C_5H_5)Mn(CO)_2(thf)]$ with $N_2C_5H_4$,[12] but this complex rapidly dimerises by a [2 + 2] cycloaddition of the cyclopentadienylidene ligands to afford $[(\eta^5\text{-}C_5H_5)(CO)_2\text{-}Mn(=C_5H_4C_5H_4=)Mn(CO)_2(\eta^5\text{-}C_5H_5)]$.

The formation of $[(\eta^5\text{-}C_5H_5)Ta(NEt_2)_2(=C_5H_4)]$ **2** appears to involve both an intermolecular cyclopentadienyl transfer reaction and a C–H activation process of some type. Initial experiments have shown that $[(\eta^5\text{-}C_5H_5)Ta(NEt_2)_2Cl_2]$ **1** reacts with 2 equiv. of $CD_3Li$ to afford $CD_3H$ gas, but no $CH_4$. Further mechanistic experiments are in progress.

Acknowledgement is made to the Division of Chemical Sciences, Office of Basic Energy Sciences, Office of Energy Research, US Department of Energy (DE-FG03-93ER14349) for support of this research. We also thank Messrs. Mark Malcomson and Igor Filippov for their experimental assistance.

## Footnotes

* E-mail: dwigley@ccit.arizona.edu

† New compounds gave analytical and $^1H$ and $^{13}C$ NMR spectroscopic data in accord with their formulation.

‡ Crystal parameters for $C_{18}H_{29}N_2Ta$ **2**: space group *Pbca* (no. 61), $a$ = 15.1346(9), $b$ = 15.5030(9), $c$ = 15.6133(9) Å. Refinement: $R$ = 0.0231 and $R_w$ = 0.0495. Atomic coordinates, bond lengths and angles, and thermal parameters have been deposited at the Cambridge Crystallographic Data Centre (CCDC). See Information for Authors, Issue No. 1. Any request to the CCDC for this material should quote the full literature citation and the reference number 182/404.

## References

1 G. Wilkinson, *J. Organomet. Chem.*, 1975, **100**, 273.
2 W. A. Herrmann, G. Kriechbaum, C. Bauer, E. Guggolz and M. L. Ziegler, *Angew. Chem., Int. Ed. Engl.*, 1981, **20**, 815 and references therein.
3 Y.-W. Chao, S. Polson and D. E. Wigley, *Polyhedron*, 1990, **9**, 2709.
4 W. A. Nugent and J. M. Mayer, *Metal–Ligand Multiple Bonds*, Wiley, New York, 1988.
5 M. F. Lappert, P. P. Power, A. R. Sanger and R. C. Srivastava, *Metal and Metalloid Amides: Syntheses, Structures, and Physical and Chemical Properties*, Halsted Press, New York, 1980.
6 L. J. Guggenberger, *Inorg. Chem.*, 1973, **12**, 294.
7 C. Couldwell and K. Prout, *Acta Crystallogr., Sect. B*, 1979, **35**, 335.
8 B. Meunier and K. Prout, *Acta Crystallogr., Sect. B*, 1979, **35**, 2558.
9 L. B. Kool, M. D. Rausch, H. G. Alt, M. Herberhold, U. Thewalt and B. Honold, *J. Organomet. Chem.*, 1986, **310**, 27.
10 H. Wadepohl and H. Pritzkow, *Angew. Chem., Int. Ed. Engl.*, 1987, **26**, 127.
11 A. A. Danopoulos, G. Wilkinson and D. J. Williams, *J. Chem. Soc., Chem. Commun.*, 1991, 181.
12 W. A. Herrmann, J. Plank, M. L. Ziegler and K. Weidenhammer, *Angew. Chem.*, 1978, **90**, 817.

*Received in Cambridge, UK, 16th December 1996; Com. 6/08402H*

# Fluxional processes in organotransition-metal $C_{60}$ complexes

**Malcolm L. H. Green* and Adam H. H. Stephens**

*Inorganic Chemistry Laboratory, South Parks Road, Oxford, UK OX1 3QR*

**Variable-temperature and EXSY $^{13}$C NMR studies on [M(NO)(PPh$_3$)$_2$($\eta^2$-C$_{60}$)] (M = Co, Rh), [Ru(NO)(PPh$_3$)$_2$($\eta^2$-C$_{60}$)H] and [Rh(CO)(PPh$_3$)$_2$($\eta^2$-C$_{60}$)H] show the presence of C$_{60}$–metal moiety rotation and migration processes and the data allow extensive assignment of δ(C$_{60}$) $^{13}$C NMR resonances.**

The dynamical behaviour of organotransition-metal fullerene complexes has been little investigated. The only reported examples are fullerene–metal bond axis rotation for [M(CO)$_4$($\eta^2$-C$_{60}$)] (M = Fe, Ru) and [Fe(CO)$_4$($\eta^2$-C$_{70}$)][1,2] and metal moiety migration for [Pd(PR$_3$)$_2$($\eta^2$-C$_{60}$)] [R$_3$ = Me$_2$Ph, MePh$_2$, (OMe)$_3$] from preliminary variable-temperature $^{13}$C NMR studies.[3,4] Similar behaviour has been implicated for [C$_{60}${Ir(CO)(PEt$_3$)$_2$Cl}$_2$],[5] [C$_{60}${Pt(PEt$_3$)$_2$}$_6$],[6] [{Ru(η-C$_5$Me$_5$)(MeCN)$_2$}$_3$(C$_{60}$)]$^{3+}$[O$_3$SCF$_3^-$]$_3$[7] and [C$_{70}${Ir(CO)(PPh$_3$)$_2$Cl}$_2$.[8]

Here we report variable-temperature and two-dimensional EXSY $^{13}$C NMR spectroscopic studies of [M(NO)(PPh$_3$)$_2$(η$^2$-C$_{60}$)] (M = Co **1**, Rh **2**), [Ru(NO)(PPh$_3$)$_2$($\eta^2$-C$_{60}$)H] **3** and [Rh(CO)(PPh$_3$)$_2$(η$^2$-C$_{60}$)H] **4** which have allowed us to identify for the first time several fluxional processes. The $^1$H and $^{31}$P{$^1$H} NMR spectra remained unchanged between −90 and 50 °C, as expected. The new complexes were prepared by substitution of PPh$_3$ by C$_{60}$ from the relevant precursor.

At low temperatures the $^{13}$C NMR spectra of **1**–**4**, allowing for the commonly occurring accidental degeneracy of resonances, were consistent with a complex possessing $C_s$ symmetry (Table 1). Thus the structures are very similar to those previously determined for **4**[9] and the related complex of **3**, [Ru(NO)(PPh$_3$)$_2$($\eta^2$-C$_{60}$)Cl].[2]

On warming **2**, as illustrated in Fig. 1, the number and intensity of δ(C$_{60}$) $^{13}$C NMR signals changed to a 17 line $C_{2v}$ symmetry pattern (allowance again being made for isochronous resonances). Such changes are indicative of the onset of free rotation about the metal–fullerene bond. Observation of coupling for the C(1) (δ 83) carbon atoms and partially resolved coupling for C(2) (δ 160; see Fig. 2 for numbering scheme) carbon atoms to the $^{103}$Rh and $^{31}$P nuclei shows that the rotation is non-dissociative. The $^{13}$C{$^1$H} NMR spectra of **1** and **3** showed broadly similar features although signal coalescence occurred at different temperatures consistent with changes in the extent of π-back donation [$\Delta G^{\ddagger}$ *ca*. 9, 10 and 14 kcal mol$^{-1}$ for **1** at −60 °C, **2** at −50 °C and **3** at 0 °C, respectively (1 cal = 4.184 J)].

Further warming of samples of **1**, **2** and **4** resulted in all δ(C$_{60}$) resonances collapsing to a single broad peak at δ *ca*. 145 indicating that the metal moiety is migrating over the whole fullerene surface as all the carbon atoms have become chemically equivalent ($I_h$ symmetry). This migration was investigated using two-dimensional $^{13}$C EXSY NMR and, for the first time for a fullerene compound, it was possible to unambiguously assign it as a [1,3]-shift mechanism.

The two-dimensional $^{13}$C EXSY NMR ($\tau_{mix}$ = 0.5) spectrum of **1** (Fig. 2) reveals the expected number and nature of correlations for a [1,3] shift. For example, most signals, including C(2) and C(3), have four correlations (corresponding

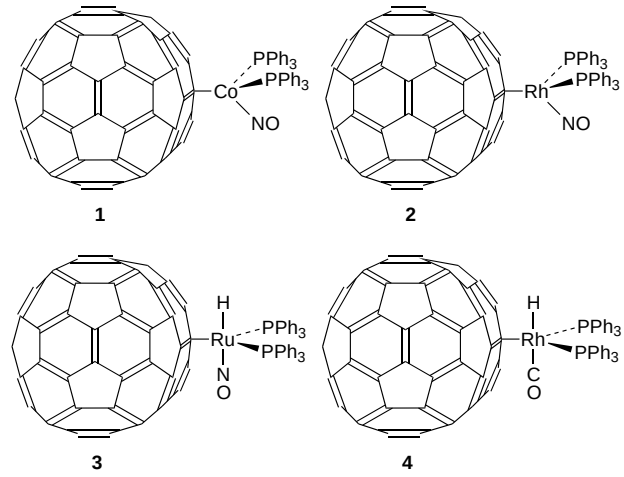



**Table 1** Summary of the δ(C$_{60}$) $^{13}$C NMR (125 MHz) intensity information for **1, 2, 3** and **4** and for model monoadducts with $C_s$, $C_{2v}$ and $I_h$ symmetry[a]

| Complex | *T*/°C | No. of peaks (intensity) | *T*/°C | No. of peaks (intensity) | *T*/°C | No. of peaks |
|---|---|---|---|---|---|---|
| **1** | −90 | 11(br)[b] | −10 | 4(2) + 11(4)<br>1(8) | 50 | 1(v br)[b,c] |
| **2** | −90 | 4(1) + 15(2)<br>1(4) + 1(6)<br>2(8) | −40 | 3(2) + 10(4)<br>1(6) + 1(8) | 25 | 1(v br)[b] |
| **3** | −90 | 2(1) + 13(2)<br>2(4) + 2(5)<br>1(6) + 1(8) | 50 | 4(2) + 11(4)<br>1(8) | | |
| **4** | −90 | 2(1) + 19(2)<br>2(3) + 2(4)<br>1(6) | | | 25 | 1(v br)[b,c] |
| $C_s$ | | 4(1) + 28(2) | | | | |
| $C_{2v}$ | | | | 4(2) + 13(4) | | |
| $I_h$ | | | | | | 1(60) |

[a] It is assumed that fullerene $T_1$ relaxation times do not vary significantly within a molecule. [b] Signals too weak and broad to be accurately integrated. [c] Recorded at 75 MHz.

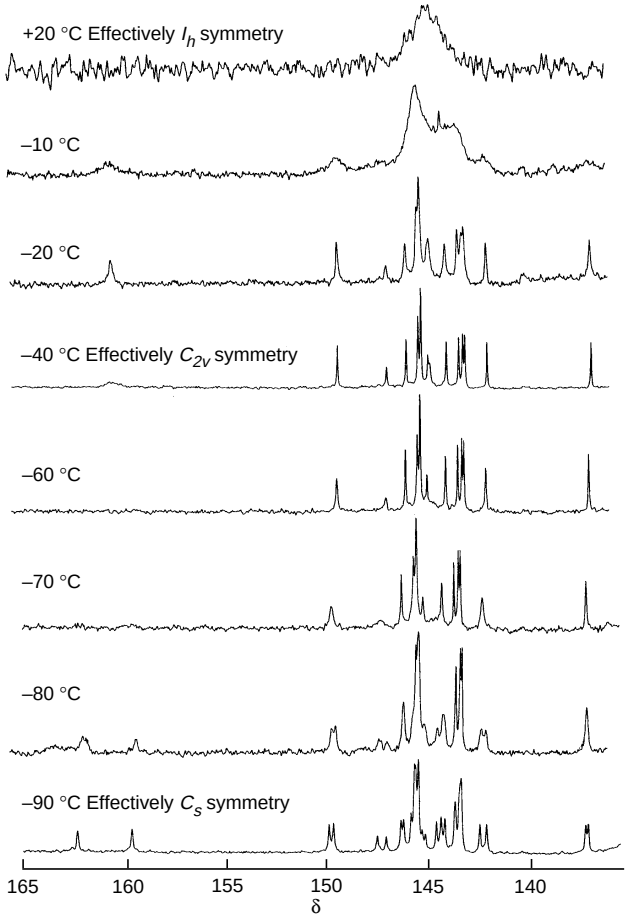



**Fig. 1** The $^{13}C\{^1H\}$ NMR (125 MHz, −90 to 25 °C, $C_4D_8O$) spectrum of **2** in the fullerene $sp^2$ region

to metal migration to the four adjacent C=C bonds). Also, C(1) showed only two correlations [to C(2) and C(3)] again indicating that only one type of migration, namely a [1,3] shift, is occurring. Owing to resonance overlap only 16 lines are clearly observable, although the total intensity is consistent with the presence of 60 fullerene carbon atoms. Tracing the unique set of correlations additionally allows assignment of most of the $\delta(C_{60})$ resonances† and out of approximately 400 fullerene compounds characterised by $^{13}C$ NMR spectroscopy this is only the second example. Interestingly, the assignment order has many similarities with that previously determined for $[(C_{60})OsO_4(4\text{-}Bu^tC_5H_4N)_2]$ using two-dimensional NMR INADEQUATE spectroscopy on an expensive isotopically enriched sample.[10] In consonance with both these studies and by observation of scalar couplings, a useful generality for fullerene assignments becomes apparent: For all 6,6-closed fullerene organic or organometallic adducts the lowest field signal(s) ($\delta > ca.$ 150) are due to the C(2) atoms and one, two or four resonances are present for a $C_{2v}$, $C_s$ or $C_1$ symmetry complex.

So far, we have not been able to unambiguously assign the mechanism to a dissociative (more likely) or an intramolecular $\eta^4$-$C_{60}$ process.

In summary, we have described the dynamical $^{13}C$ NMR properties of the compounds **1**–**4**. These studies have shown that the compounds collectively undergo rotation about the metal–fullerene bond axis and migration of the metal fragment over the surface of $C_{60}$. In each case the symmetry of the complexes is different and results in a significantly different $^{13}C$ NMR spectrum.

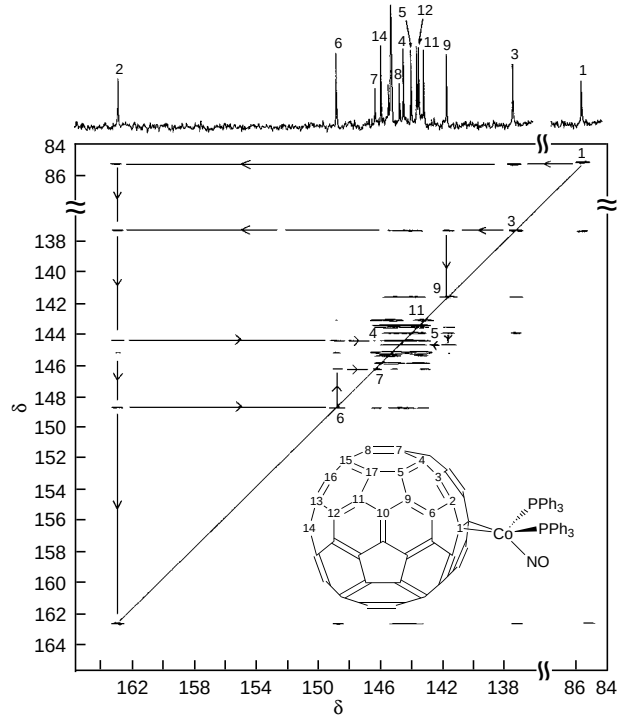



**Fig. 2** $^{13}C$–$^{13}C$ NMR (125 MHz, 5 °C, $C_4D_8O$) EXSY spectrum of **1** ($\tau_{mix}$ = 0.5 s)

We would like to thank Drs Mark Wormwald and Tim Claridge for help with the variable-temperature studies, Richard Douthwaite for supplying samples of $[Rh(CO)(PPh_3)_2(\eta^2\text{-}C_{60})H]$, and Lincoln College, Oxford for a JRF to A. H. H. S.

## Footnotes

* E-mail: malcolm.green@icl.ox.ac.uk

† *Selected $^{13}C$ NMR spectroscopic data for* **1**: (125 MHz, $C_4D_8O$, 5 °C) δ 162.6 [s, 4C, C(2)], 148.6 [s, 4C, C(6)], 146.1 [s, 2C, C(7)], 145.8 (s, 4C, $C_{60}$), 145.3 [s, 2C, C(14)], 145.1 (s, 4C, $C_{60}$), 145.0 (s, 8C, $C_{60}$), 144.6 [s, 2C, C(8)], 144.3 [s, 4C, C(4)], 143.8 [s, 4C, C(5)], 143.5 (s, 4C, $C_{60}$), 143.3 (s, 4C, $C_{60}$), 143.0 [s, 4C, C(11)], 141.5 [s, 4C, C(9)], 137.2 [s, 4C, C(3)], 135.2 (d, $^1J_{PC}$ 35 Hz, $PPh_3$, $C_{ipso}$), 135.1 (d, $^2J_{PC}$ 12 Hz, $PPh_3$ $C_{ortho}$), 130.8 (s, $PPh_3$, $C_{para}$), 129.3 (d, $^3J_{PC}$ 10 Hz, $PPh_3$, $C_{meta}$), 85.3 [s, 2C, C(1)]. See Fig. 2 for fullerene numbering scheme. $C_{60}$ refers to fullerene carbon resonances that could not be unambiguously assigned.

## References

1 R. E. Douthwaite, M. L. H. Green, A. H. H. Stephens and J. F. C. Turner, *J. Chem. Soc., Chem. Commun.*, 1993, 1522.
2 A. H. H. Stephens and M. L. H. Green, unpublished work.
3 H. Nagashima, H. Yamaguchi, Y. Kato, Y. Saito, M. Haga and K. Itoh, *Chem. Lett.*, 1993, 2153.
4 H. Nagashima, Y. Kato, H. Yamaguchi, E. Kimura, T. Kawanishi, M. Kato, Y. Saito, M. Haga and K. Itoh, *Chem. Lett.*, **1994**, 1207.
5 A. L. Balch, J. W. Lee, B. C. Noll and M. M. Olmstead, *Inorg. Chem.*, 1994, **33**, 5238.
6 P. J. Fagan, J. C. Calabrese and B. Malone, *Acc. Chem. Res.*, 1992, **25**, 134.
7 P. J. Fagan, J. C. Calabrese and B. Malone, *Science*, 1991, **252**, 1160.
8 A. L. Balch, J. W. Lee and M .M. Olmstead, *Angew. Chem., Int. Ed. Engl.*, 1992, **31**, 1356.
9 A. L. Balch, J. W. Lee, B. C. Noll and M. M. Olmstead, *Inorg. Chem.*, 1993, **32**, 3577.
10 J. M. Hawkins, S. Loren, A. Meyer and R. Nunlist, *J. Am. Chem. Soc.*, 1991, **113**, 7770.

*Received in Cambridge, UK, 16th January 1997; Com. 7/00385D*

# Epoxidation of unsaturated fatty esters over large-pore Ti-containing molecular sieves as catalysts: important role of the hydrophobic–hydrophilic properties of the molecular sieve

**M. A. Camblor, A. Corma,* P. Esteve, A. Martínez and S. Valencia**

*Instituto de Tecnología Química, CSIC-UPV, Avda de los Naranjos s/n, 46071 Valencia, Spain*

**Ti-β and Ti-MCM-41 catalysts are able to epoxidize methyl oleate using hydrogen peroxide or *tert*-butyl hydroperoxide as oxygen donors with high conversions and epoxide selectivities.**

Epoxidized fatty acids and their derivatives are useful commercial chemicals used, *e.g.* as stabilizers in halogen-containing polymers, as additives in lubricants, in the manufacture of cosmetics and pharmaceuticals, fungicidal and algicidal solutions, and in wood treatment.[1–5] In existing industrial processes the epoxide is produced by reacting the unsaturated compound with a peracid either preformed[6] or synthesized *in situ*[7] with an organic acid, usually acetic or formic acid, and hydrogen peroxide. Using this procedure, the yields to epoxide are relativelly low as a consequence of the low $H_2O_2$ selectivities. Thus, it would be interesting to replace the processes based on peracids by a more desirable catalytic one.[8–12]

Recently, it has been shown that the incorporation of Ti into the framework of zeolites produce oxidation catalysts with unique shape-selective properties.[13] Large-pore Ti-β zeolite[14] and the mesoporous material Ti-MCM-41,[15] when properly prepared, are active for the selective oxidation of bulky substrates that can not diffuse inside the Ti-silicalite channels.[16–17] Because of their oxidation properties and the advantages related to the use of solid catalysts in industrial processes, Ti-β and Ti-MCM-41 could open new possibilities in the field of fatty acids and esters if they could selectively epoxidize the double bound, forming stable epoxides.

Here we report a new and interesting application of large-pore zeolites containing Ti in the framework such as the selective epoxidation of unsaturated fatty acids using organic and inorganic peroxides. We will show that the hydrophobic–hydrophilic properties of the zeolite play an important role when, as in this case, the organic reactant has two moieties with different polarities and an aqueous solution of $H_2O_2$ is used as oxidant.

Hydrophilic Ti-β samples were prepared as follows: samples 1 and 2 were synthesized by diluting tetraethylammonium hydroxide (TEAOH) (35%, Aldrich, Na < 1 ppm, K < 47 ppm) with the required amount of water to which tetraethylorthotitanate (TEOTi, Alfa) and tetraethylorthosilicate (TEOS, Merck) were added at room temperature with stirring. Finally, a solution of aluminium nitrate (Merck) was also added. Sample 4 was prepared by the hydrolysis of TEOS in an aqueous solution of TEAOH and $H_2O_2$ (35%, Fluka) under stirring. TEOTi was added and the mixture was left under stirring to allow the evaporation of the ethanol produced. Finally, dealuminated zeolite-β seeds were added under stirring (4 g of solid per 100 g of total $SiO_2$ in the reaction mixture). Sample 3 was synthesized in the same way but using non-dealuminated zeolite-β seeds which determined the total Al content of the reaction mixture.

A hydrophobic Ti-β sample (sample 5) was prepared as follows: TEOS was hydrolysed in an aqueous solution containing TEAOH and $H_2O_2$ followed by the hydrolysis of TEOTi and allowing evaporation of ethanol and water to the resultant clear solution, water lost in the evaporation and the appropriate amount of HF (48%) were added.

The chemical composition of the gels are listed in Table 1. After crystallization at 413 K and rotation at 60 rpm, the solids were separated, washed until pH = 9, dried at 353 K and calcined at 853 K.

A Ti-MCM-41 sample was synthesised as follows: an aqueous solution of tetramethylammonium silicate (25% TMAOH, 10% $SiO_2$, Aldrich) was added to an aqueous solution containing 29.0% hexadecyltrimethylammonium bromide (CTAB, Merck). When the solution was homogenized, amorphous silica (Aerosil 200, Degussa) and titanium isopropoxide (Alfa) were added. The molar chemical composition of the synthesis mixture was: $SiO_2$ : 0.15 CTAB : 24.3 $H_2O$ : 0.26 TMAOH : 0.016 $TiO_2$. The gel was heated at 413 K under static conditions. After filtering, the solid was washed, dried and calcined at 813 K for 1 h in a flow of $N_2$, followed by 6 h in air. The Ti content of the final solid was 2.5 mass% expressed as $TiO_2$.

Reactions were carried out batchwise in a 5 ml round-bottomed flask with continuous stirring. The flask contained the catalyst (30 mg), the substrate (1 mmol of methyl oleate), the solvent, when used (2 ml), and the peroxide (0.25 mmol). Products were analysed by capillary gas chromatography (25 m, 5% methylphenylsilicone) and their identification was established by GCMS. Unreacted peroxide was determined by iodometric titration.

Table 2 shows the results obtained in the epoxidation of methyl oleate with hydrogen peroxide on Ti-β and Ti-MCM-41 catalysts. As can be seen, higher conversions and $H_2O_2$

**Table 1** Chemical composition of Ti-β samples

| | Gel synthesis | | | | | | Solid | |
|---|---|---|---|---|---|---|---|---|
| Sample | $SiO_2/TiO_2$ | $SiO_2/Al_2O_3$ | $TEAOH/SiO_2$ | $H_2O_2/SiO_2$ | $H_2O_2/SiO_2$ | $HF/SiO_2$ | Si/Al | $\%TiO_2$ |
| 1[a] | 60 | 769 | 0.54 | 10.0 | — | — | 112 | 3.92 |
| 2 | 60 | 400 | 0.55 | 12.0 | — | — | 138 | 4.04 |
| 3 | 60 | 1660 | 0.55 | 6.3 | 0.34 | — | 590 | 2.96 |
| 4 | 60 | — | 0.55 | 6.8 | 0.34 | — | ∞ | 2.36 |
| 5 | 25 | — | 0.56 | 7.5 | 0.34 | 0.62 | ∞ | 2.10 |

[a] Aerosil (Degussa) used as silica source.

**Table 2** Epoxidation of methyl oleate with $H_2O_2$ over Ti-β and Ti-MCM-41 catalysts[a]

| Catalyst | Solvent | Oleate Conv. (% of max.) | Epoxide selectivity (%) | $H_2O_2$ conv. (%) | $H_2O_2$ selectivity (%) |
|---|---|---|---|---|---|
| Ti-β[b] | MeCN | 45.3 | 97.2 | 89.6 | 50.6 |
| | MeOH | 40.1 | 31.8 | 62.0 | 64.6 |
| Ti-MCM-41 | MeCN | 26.7 | 88.3 | 86.7 | 30.8 |
| | MeOH | 21.9 | 42.9 | 81.8 | 26.7 |

[a] *Reaction conditions*: 296 mg methyl oleate, 2 ml solvent, 24 mg $H_2O_2$ (35 mass%), 30 mg catalyst. 50 °C, 8 h. [b] Sample 1.

**Table 3** Effect of Al content on Ti-β catalysts for the epoxidation of methyl oleate with $H_2O_2$[a]

| Sample | Chemical composition | | Oleate conv. (% of max.) | Epoxide selectivity (%) | $H_2O_2$ conv. (%) | $H_2O_2$ selectivity (%) |
|---|---|---|---|---|---|---|
| | Si/Al | %$TiO_2$ | | | | |
| 2 | 138 | 4.04 | 65.4 | 10.8 | 87.7 | 74.6 |
| 3 | 590 | 2.96 | 64.2 | 20.4 | 80.3 | 79.9 |
| 4 | ∞ | 2.36 | 78.6 | 34.9 | 90.2 | 87.2 |
| 5 | ∞ | 2.10 | 56.6 | 64.6 | 63.1 | 90.4 |
| Na-Ti-β (4) | ∞ | 2.36 | 59.1 | 90.1 | 85.2 | 69.4 |

[a] Reaction conditions as in Table 2. Methanol used as solvent.

selectivities were obtained on Ti-β. It has been reported[18] that polar solvents, such as methanol or acetonitrile, enhance the activity of hydrophilic materials as epoxidation catalysts. However, the higher hydrophility of Ti-MCM-41, as compared to Ti-β, has a detrimental effect because it decreases the adsorption of the organic substrate and, consequently, it favours $H_2O_2$ decomposition.[17]

The epoxide is practically the only product obtained in acetonitrile with both catalysts while the epoxide selectivities are lower in methanol. In the case of Ti-β, the Al atoms present in the zeolite framework generate surface acid groups which catalyse the ring opening of the epoxide by addition of a protic molecule. When decreasing the zeolite acidity, *i.e.* decreasing the Al content in the catalyst, the epoxide selectivity increases (Table 3). This increase is even larger when the hydrophobic Ti-β, sample 5, is used. When there are no Al atoms in the catalyst framework (Al-free Ti-β and Ti-MCM-41), opening of the oxirane ring still occurs. This means that there are sites other than those associated with the Al framework which are able to catalyse the side reaction. These acid sites have been assigned to peroxo or hydroperoxo species formed by the interaction of hydrogen peroxide with Ti atoms in the zeolite.[19,20] The selectivity to the epoxide is significantly improved (*ca.* 90%) when the Al-free Ti-β sample is washed with an aqueous solution containing $Na^+$ cations (Table 3), although the activity of the catalyst slightly decreased.

As the presence of water inhibits the catalytic activity of Ti-MCM-41, the epoxidation of methyl oleate was also carried out using *tert*-butyl hydroperoxide (TBHP) as oxygen donor (Table 4). In this case, no solvent is needed to perform the epoxidation, with corresponding savings in reactor volume and separation costs. Under such reactions conditions Ti-MCM-41 was a highly effective catalyst with high conversions and selectivities to the epoxide and TBHP (*ca.* 91 and 99%, respectively). Ti-β is also able to epoxidize methyl oleate using TBHP as oxidant. Although the reaction rate is slower with respect to $H_2O_2$ due to steric restrictions to the formation of the transition state, the epoxide and TBHP selectivities are > 80%.

**Table 4** Epoxidation of methyl oleate with TBHP over Ti-β and Ti-MCM-41 catalysts[a]

| Catalyst | Oleate conv. (% of max.) | Epoxide selectivity (%) | TBHP conv. (%) | TBHP selectivity (%) |
|---|---|---|---|---|
| Ti-β[b] | 49.3 | 97.4 | 51.9 | 95.0 |
| Ti-MCM-41 | 64.6 | 91.1 | 65.3 | 98.9 |

[a] *Reaction conditions*: 296 mg methyl oleate, 112 mg TBHP (80% in *tert*-butyl peroxide), 30 mg catalyst. 70 °C, 8 h. [b] Sample 5.

In conclusion, hydrophobic Ti-β/$H_2O_2$ and Ti-MCM-41/TBHP have been demonstrated to be effective catalytic systems to prepare epoxidized fatty esters with high conversions and selectivities to epoxide.

The authors thank CICYT, project MAT 94-0359-C02-01 and project PL-921686 for financial support. P. E. thanks the Generalidad Valenciana for a scholarship.

## References

1 H. Endres, H. Fischer, F. Loeffelholz, P. Wedl, K. Worchech, A. Hansen and G. Geismar, *DE Pat.*, 4,117,034, 1991.
2 V. Shaefer, R. Kohler, A. Pauli and A. Fessenbecker, *EP Pat.*, 557,839, 1992.
3 I. Scheuffsen and A. Meffert, *DE Pat.*, 3,326,455, 1983.
4 J. Yanagida, T. Matsumoto and M. Nakayama, *JP Pat.*, 04,134,001, 1990.
5 M. Niki and K. Otani, *JP Pat.*, 02,206,613, 1989.
6 T. Kato, *JP Pat.*, 62,99,348, 1985.
7 G. Diekelmann, K. Eckwert, L. Jeromin, E. Peukert and U. Steinberner, *DE Pat.*, 3,320,219, 1983.
8 P. E. Sonnet, M. E. Laukin and G. P. McNeill, *J. Am. Oil Chem. Soc.*, 1995, **72**, 199.
9 M. Quaglino, N. Bottazzini, C. Querci, M. Ricci and S. Cavalli, *J. Am. Oil Chem. Soc.*, 1992, **69**, 1248.
10 E. Ucciani, A. Borfand, G. Rafaralahitsimba and G. Cecchi, *Rev. Fr. Corps Gras*, 1992, **39**, 279.
11 M. C. Kuo and T. C. Chou, *Can. J. Chem. Eng.*, 1990, **68**, 831.
12 A. Debal, G. Rafaralahitsimba and E. Ucciani, *Fat Sci. Technol.*, 1995, **95**, 236.
13 U. Romano, A. Esposito, F. Maspero, C. Neri and C. Clerici, *Stud. Surf. Sci. Catal.*, 1990, **55**, 33.
14 M. A. Camblor, A. Corma, A. Martínez and J. Pérez-Pariente, *J. Chem. Soc., Chem. Commun.*, 1992, 589.
15 A. Corma, M. T. Navarro and J. Pérez-Pariente, *J. Chem. Soc., Chem. Commun.*, 1994, 147.
16 A. Corma, M. A. Camblor, P. Esteve, A. Martínez and J. Pérez-Pariente, *J. Catal.*, 1994, **145**, 151.
17 T. Blasco, A. Corma, M. T. Navarro and J. Pérez-Pariente, *J. Catal.*, 1995, **156**, 65.
18 A. Corma, P. Esteve and A. Martínez, *J. Catal.*, 1996, **161**, 11.
19 G. Bellussi, A. Carati, M. G. Clerici, G. Maddinelli and R. Millini, *J. Catal.*, 1992, **133**, 220.
20 M. A. Camblor, M. Costantini, A. Corma, L. Gilbert, P. Esteve, A. Martínez and S. Valencia, *Chem. Commun.*, 1996, 1339.

*Received in Cambridge, UK, 20th January 1997; Com. 7/00448F*

# Biosynthesis of fluoroacetate and 4-fluorothreonine by *Streptomyces cattleya*. Glycine and pyruvate as precursors

**John T. G. Hamilton,[a] Muhammad R. Amin,[b] David B. Harper*[a] and David O'Hagan*[b]†**

[a] *Microbial Biochemistry Section, Department of Food Science, The Queen's University of Belfast, Newforge Lane, Belfast, UK BT9 SPX*

[b] *University of Durham, Department of Chemistry, Science Laboratories, South Road, Durham, UK DH1 3LE*

**Using $^{19}F$ NMR spectroscopy, $^{13}C$-labelled glycines and pyruvates are shown to be incorporated at high levels into fluoroacetate and 4-fluorothreonine by resting cells of *Streptomyces cattleya*; the labelling patterns illustrate a conversion of glycine *via* serine to pyruvate, where the C-2 and C-3 carbon atoms of pyruvate contribute both carbon atoms of fluoroacetate and C-3 and C-4 of 4-fluorothreonine respectively.**

Fluorinated natural products are rare in nature.[1,2] The most ubiquitous of this class of natural product is fluoroacetate **1**, which is found in a wide variety of plant species in both arid and tropical regions around the world.[1,3] Only two bacterial strains, both actinomycetes, have been identified with the ability to biosynthesise organofluorine compounds. Fluoroacetate **1** and 4-fluorothreonine **2** are coproduced by *Streptomyces cattleya*[4] when grown in the presence of a source of fluoride and suspensions of resting cells of the organism provide an attractive system in which to explore the biosynthesis of these fluorinated metabolites.[5,6] Nucleocidin **3** was isolated[7] from *Streptomyces calvus* in 1957, although a correct structure for the molecule was not advanced until 1969.[8] Unfortunately more recent attempts to produce the antibiotic in culture have failed.[9] Here we report a study using $^{19}F$ NMR spectroscopy of the incorporation of [1-$^{13}C$]-, [2-$^{13}C$]-, [1,2-$^{13}C_2$]-glycine and [1-$^{13}C$]-, [2-$^{13}C$]-, [3-$^{13}C$]-pyruvate into both fluoroacetate **1** and 4-fluorothreonine **3** by *S. cattleya*. In each case the labelled precursors were incubated at a final concentration of 10 mM with resting cell suspensions and incorporation of $^{13}C$ label into the fluorometabolites was examined using GC–MS and $^{19}F$ NMR spectroscopy after 48 h.

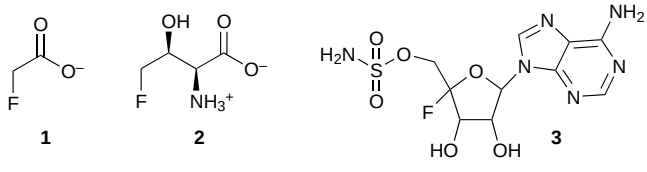
The results of the GC–MS study, which are reported elsewhere,[10] revealed several striking features. A low level of incorporation of $^{13}C$ label (< 4%) from [1-$^{13}C$]glycine into fluoroacetate **1** contrasted with a very high level of incorporation (40%) from [2-$^{13}C$]glycine. Furthermore the labelling patterns in fluoroacetate from [2-$^{13}C$]- and [1,2-$^{13}C_2$]-glycine were practically identical, indicating that the high proportion (80% of total $^{13}C$ incorporation) of double incorporation observed in the [1,2-$^{13}C_2$]glycine experiment is not due to the incorporation of glycine as an intact two carbon unit but rather that the C-2 of glycine is recombined during the biosynthesis of fluoroacetate.

It was not possible to assess from the GC–MS data the precise extent of recombination of C-2 of glycine into C-3 and C-4 of 4-fluorothreonine and so the degree of analogy between the labelling pattern in C-3 and C-4 of 4-fluorothreonine and the C-1 and C-2 of fluoroacetate could not be ascertained. The uncertainty was resolved by $^{19}F\{^1H\}$ NMR spectroscopy. A direct comparison of the incorporation of isotope into C-1 and C-2 of fluoroacetate with that into C-3 and C-4 of 4-fluorothreonine was made by $^{19}F\{^1H\}$ NMR spectroscopy after concentration of the supernatant at the end of each experiment. Proton decoupling was advantageous in simplifying the complexity of the $^{19}F$ NMR signals at −214.6 ppm for fluoroacetate and −229.15 ppm for 4-fluorothreonine, revealing coupling patterns which indicate intact $^{19}F$-$^{13}C$-$^{13}C$, $^{19}F$-$^{13}C$-$^{12}C$ and $^{19}F$-$^{12}C$-$^{13}C$ combinations ($^1J_{^{19}F\text{-}^{13}C}$ = 165 Hz, $^2J_{^{19}F\text{-}^{13}C}$ = 18 Hz) in the resultant metabolites. The signals for each of the two fluorinated metabolites obtained by $^{19}F\{^1H\}$ NMR spectroscopy always possessed a similar multiplicity indicating that $^{13}C$ incorporations in terms of magnitude and regiochemistry into C-1 and C-2 of fluoroacetate mirror those into C-3 and C-4 of 4-fluorothreonine. The most obvious interpretation of this observation is that both sets of carbons have an identical biosynthetic origin and that there is a single fluorinating enzyme operating in *S. cattleya*. Our previous studies[5,6] have ruled out a direct interconversion of one of the metabolites to the other, so we are forced to the conclusion that each fluorometabolite arises by metabolism of a (presently unknown) common fluorinated intermediate.

The $^{19}F\{^1H\}$ NMR spectrum resulting from incubation of [2-$^{13}C$]glycine with resting cells is shown in Fig. 1. This spectrum has identical features to that obtained after incubation with [1,2-$^{13}C_2$]glycine which is entirely consistent with the GC–MS data and confirms that only C-2 of glycine is contributing $^{13}C$ label to the fluorinated metabolites. The similarity in the patterns of the $^{19}F$ NMR signals of the resultant fluoroacetate and 4-fluorothreonine is striking. In each case the parent (unlabelled) signal (singlet) has a predominant doublet of doublets ($^1J_{^{19}F\text{-}^{13}C}$ = 160 Hz, $^2J_{^{19}F\text{-}^{13}C}$ = 18 Hz, α + β-shift = 0.09 ppm) associated with it due to populations of **1** and **2** (*ca*. 40%) with an intact $^{19}F$-$^{13}C$-$^{13}C$ combination. There is also a doublet ($^1J_{^{19}F\text{-}^{13}C}$ = 165 Hz, α-shift = 0.07 ppm) due to populations (*ca*. 5%) with an intact $^{19}F$-$^{13}C$-$^{12}C$ combination. This is apparent as a small increase in the intensity of the left hand arms of the predominant doublet of doublets. Finally the right hand arm of a doublet (18 Hz, β-shift = 0.02) can be seen at the base of the unlabelled peaks for **1** and **3** due to populations (*ca*. 7%) with an intact $^{19}F$-$^{12}C$-$^{13}C$ combination.

The high level of recombination of C-2 of glycine in both fluorometabolites and very low incorporation of C-1 is most readily explained if glycine is converted to serine or a metabolite of serine such as pyruvate (Scheme 1). In bacteria[11] glycine is cleaved and C-2 is processed *via* $N^5$, $N^{10}$-methylene-tetrahydrofolate by serine hydroxymethyltransferase and condensed with another molecule of glycine to generate serine. Further metabolism of serine by serine dehydratase generates pyruvate.

In order to explore this putative relationship further the incorporation of $^{13}C$-labelled pyruvates into fluorometabolites by resting cell suspensions of *S. cattleya* was examined by GC–MS and $^{19}F\{^1H\}$ NMR spectroscopy. The results of the GC–MS study are reported elsewhere and indicate that C-2 and C-3 of




**1** **2** **3**

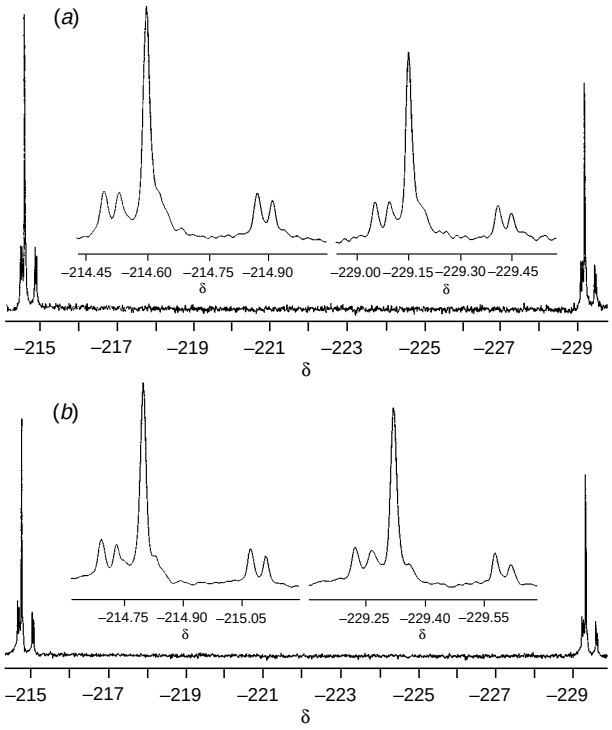
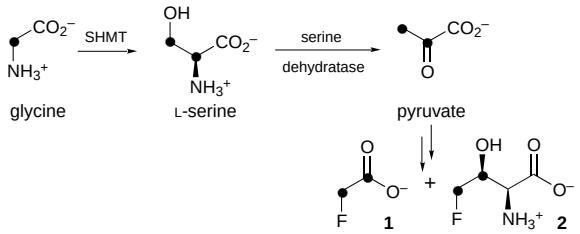



**Fig. 1** $^{19}F\{^{1}H\}$ NMR spectrum of fluoroacetate **1** (−214.60 ppm) and 4-fluorothreonine **2** (−229.15 ppm) in the supernatant after incubation of resting cells of *S. cattleya* for 48 h with (*a*) [2-$^{13}$C]-glycine and (*b*) [1,2-$^{13}C_2$]glycine. The insets show expansions of each signal.




**Scheme 1** Proposed pathway accounting for the labelling of the fluorometabolites by [2-$^{13}$C]glycine and $^{13}$C-labelled pyruvates

pyruvate are probably incorporated as a unit into fluoroacetate.[10] The supernatants from these experiments were analysed by $^{19}F\{^{1}H\}$ NMR spectroscopy to assess the extent of the similarity in the pattern of incorporation into the two metabolites. As with the experiments conducted with labelled glycines, the signals obtained from each of the fluorometabolites by $^{19}F\{^{1}H\}$ NMR spectroscopy always possessed a similar multiplicity indicating that $^{13}$C incorporation into C-1 and C-2 of fluoroacetate paralleled exactly that into C-3 and C-4 of 4-fluorothreonine.

Fig. 2 shows the $^{19}F\{^{1}H\}$ NMR spectrum obtained following incubation of [3-$^{13}$C]pyruvate with resting cell suspensions. It is clear that each of the signals assigned to fluorometabolites **1** (−214.8 ppm) and **2** (−229.3 ppm) has satellites ($^{1}J_{^{13}C\text{-}^{19}F}$ = 165 Hz) associated with it. These correspond to a population (*ca*. 30%) of molecules in each case which possess an intact $^{19}$F-$^{13}$C-$^{12}$C combination. No other labelled populations are apparent. Therefore we can conclude that C-3 of pyruvate has regiospecifically labelled the fluoromethyl groups of **1** and **2**. Similarly the resultant spectrum (not shown) from the [2-$^{13}$C]pyruvate feeding experiment had satellites associated with each fluorometabolite resonance, indicative of a two bond coupling between F and $^{13}$C ($^{1}J_{^{13}C\text{-}^{19}F}$ = 18 Hz). Thus C-2 of pyruvate has regiospecifically labelled C-1 of fluoroacetate and C-3 of 4-fluorothreonine (*ca*. 40%). Thus C-2 and C-3 of pyruvate contribute C-1 and C-2 of fluoroacetate and C-3 and C-4 of fluorothreonine as summarized in Scheme 1.

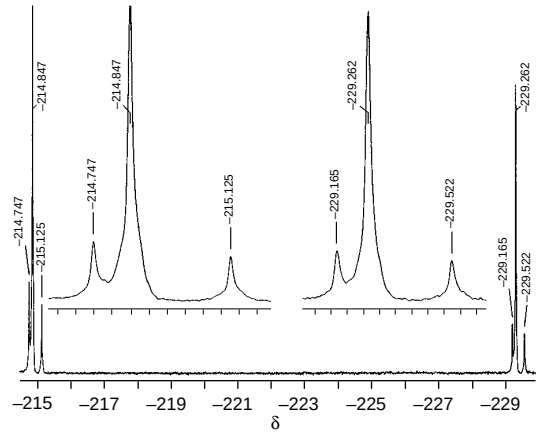



**Fig. 2** $^{19}F\{^{1}H\}$ NMR spectrum of fluoroacetate **1** (−214.8 ppm) and 4-fluorothreonine **2** (−229.3 ppm) in the supernatant after incubation of resting cells of *S. cattleya* for 48 h with [3-$^{13}$C]pyruvate. The insets show expansions of each signal

Although these results show clearly that pyruvate is a highly effective precursor of the fluorometabolites in resting cells of *S. cattleya*, it cannot be concluded that pyruvate, or a closely related metabolite such as β-hydroxypyruvate,[12] is the substrate for fluorination. Studies using stable and radiolabelled precursors[6,12] have shown that glycerol is a good precursor in fluoroacetate biosynthesis. The fluorination substrate must therefore be situated between pyruvate and glycerol on the glycolytic pathway. The very high incorporations observed into the fluorometabolites from labelled pyruvate may owe more to the tight channelling of intermediates in this pathway than the proximity of pyruvate to the carbon substrate for fluorination. The stereochemical processing of glycerol prior its incorporation into the fluorometabolites **1** and **2** is consistent with this hypothesis.[13]

We thank BNFL, Company Research Laboratory (CRL), Springfields, for financial support, Mr Ian H. MacKeag of the University of Durham for recording $^{19}F\{^{1}H\}$ NMR spectra and Dr Roy Bowden, BNFL Fluorochemicals and Dr Harry Eccles, BNFL CRL, for their close interest in this project.

## Footnote

† E-mail: david.o'hagan@durham.ac.uk

## References

1 D. B. Harper and D. O'Hagan, *Nat. Prod. Rep*., 1994, **11**, 123.
2 J. J. M. Meyer and D. O'Hagan, *Chem. Br*., 1992, 785.
3 D. O'Hagan, R. Perry, J. M. Lock, J. J. M. Meyer, L. Dasaradhi, J. T. G. Hamilton and D. B. Harper, *Phytochemistry*, 1993, **33**, 1043.
4 M. Sanada, T. Miyano, S. Iwadare, J. M. Williamson, B. H. Arison, J. L. Smith, A. W. Douglas, J. M. Liesch and E. Inamine, *J. Antibiot*., 1986, **39**, 259.
5 K. A. Reid, R. D. Bowden and D. B. Harper, in *Naturally Produced Organohalogens*, ed. A. Grimvall and E. W. B. de Leer, Kluwer Acadamic Publishers, Dordrecht, 1995, pp. 269–279.
6 K. A. Reid, J. T. G. Hamilton, R. D. Bowden, D. O'Hagan, L. Dasaradhi, M. R. Amin and D. B. Harper, *Microbiol*., 1995, **141**, 1385.
7 S. O. Thomas, V. L. Singleton, J. A. Lowery, R. W. Sharpe, L. M. Preuss, J. N. Porter, J. H. Mowat and N. Bohonos, *Antibiotics Ann*., 1957, **1956–7**, 716.
8 G. O. Morton, J. E. Lancaster, G. E. Van Lear, W. Fulmor and W. E. Meyer, *J. Am. Chem. Soc*., 1969, **91**, 1535.
9 A. R. McGuire, W-d. Meng, S. M. Roberts and A. J. Willetts, *J. Chem. Soc., Perkin Trans. 1*, 1993, 1795.
10 J. T. G. Hamilton, C. D. Murphy, M. R. Amin, D. O'Hagan and D. B. Harper, unpublished work.
11 S. M. Klein and R. D. Sagers, *J. Bacteriol*., 1962, **83**, 121.
12 T. Tamura, M. Wada, N. Esaki and K. Sato, *J. Bacteriol*., 1995, **177**, 2265.
13 J. Nieschalk, J. T. G. Hamilton, C. D. Murphy, D. B. Harper and D. O'Hagan, *Chem. Commun*., 1997, following paper.

*Received, 21st January 1997; Com. 7/00495H*

# Biosynthesis of fluoroacetate and 4-fluorothreonine by *Streptomyces cattleya*. The stereochemical processing of glycerol

**Jens Nieschalk,[a] John T. G. Hamilton,[b] Cormac D. Murphy,[b] David B. Harper*[b] and David O'Hagan*[a]†**

[a] *University of Durham, Department of Chemistry, Science Laboratories, South Road, Durham, UK DH1 3LE*
[b] *Microbial Biochemistry Section, Department of Food Science, The Queen's University of Belfast, Newforge Lane, Belfast, UK BT9 5PX*

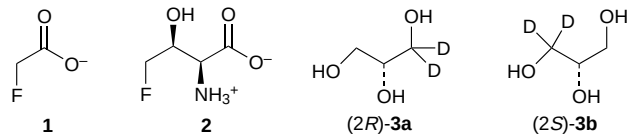
**When both (2*R*)-[1-$^2H_2$]- and (2*S*)-[1-$^2H_2$]-glycerol are incubated with resting cell suspensions of *S. cattleya*, only the 2*R*-enantiomer labels the fluoromethyl groups of fluoroacetate and 4-fluorothreonine, with retention of both deuterium atoms, placing metabolic and mechanistic limitations on the process of biological fluorination.**

*Streptomyces cattleya* is one of very few biological systems which have been identified with the capability of biosynthesising organofluorine natural products.[1] We are currently investigating[2–5] the pathways by which fluorometabolite biosynthesis is achieved in *S. cattleya* and have shown[4] the efficient incorporations of glycine and pyruvate into fluoroacetate **1** and 4-fluorothreonine **2** by resting cell suspensions of *S. cattleya*.

The incorporations are consistent with the conversion of glycine to serine and then serine to pyruvate,[4,5] and the labelling patterns indicate that C-2 and C-3 of pyruvate contribute C-1 and C-2 of fluoroacetate **1** and C-3 and C-4 of 4-fluorothreonine **2** respectively. Tamura *et al*.[6] have shown that [2-$^{13}$C]glycerol is efficiently incorporated into fluoroacetate **1** by cell suspensions of *S. cattleya*, the isotope becoming regiochemically located at C-1 of fluoroacetate. Together these findings suggest that, prior to incorporation into the fluorometabolites, pyruvate and glycerol enter a common pathway and the glycolytic pathway emerges as the most obvious candidate.

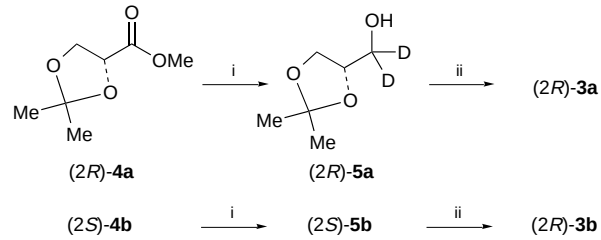
To shed further light on the role of glycerol we have investigated the stereochemical processing of glycerol during fluorometabolite biosynthesis in *S. cattleya*. Only two of the three carbon atoms of glycerol can contribute the carbons of fluoroacetate **1** and C-3 and C-4 of 4-fluorothreonine **2**, thus one of the prochiral hydroxymethyl groups of glycerol is cleaved during the biosynthetic process. In order to probe the cryptic stereochemistry of glycerol metabolism in *S. cattleya*, both (2*R*)-[1-$^2H_2$]- **3a** and (2*S*)-[1-$^2H_2$]-glycerol **3b** were prepared such that the prochiral hydroxymethyl groups of glycerol were independently labelled.

Isotopically enriched [1-$^2H_2$]glycerols **3a** and **3b** were synthesised as shown in Scheme 1 following a previously reported[7] protocol. This involved $LiAlD_4$ reduction of either (*R*)- or (*S*)-methyl 2,2-dimethyl-1,3-dioxolane-4-carboxylate, **4a** or **4b** {$[\alpha]_D$ −9.9 (neat) lit.,[8] −10.1 (neat)} respectively, to generate the corresponding alcohols **5a** and **5b** {$[\alpha]_D$ −12.2 (neat), lit.,[7] −14.9 (neat)}. Deprotection using aqueous mineral acid generated the desired glycerols **3a** and **3b**‡ in good overall yield as summarised in Scheme 1. The enantiomeric glycerols **3a** and **3b** were administered in separate experiments to resting cell suspension cultures[5] of *S. cattleya* at a final concentration of 7.5 mM. The level of isotope incorporation into the resultant fluoroacetate **1** was determined by GC–MS analysis[5] after 48 h in each case. The data indicated that deuterium had only become incorporated into fluoroacetate **1** from (2*R*)-[1-$^2H_2$]glycerol **3a** ($M$ + 2 = 28%, $M$ + 1 = 5%). No significant incorporation of isotope from (2*S*)-[1-$^2H_2$]glycerol **3b** was apparent.




This conclusion was confirmed by $^{19}F\{^1H\}$ NMR analysis of the supernatants from each experiment. The presence of a deuterium atom geminal to fluorine is readily diagnosed by an induced shift to lower frequency in the $^{19}F$ NMR spectrum.[9] The effect is additive and each deuterium atom induces a shift of *ca*. 0.6 ppm in magnitude. The resultant $^{19}F\{^1H\}$ NMR spectrum from the (2*R*)-[1-$^2H_2$]glycerol **3a** feeding experiment is shown in Fig. 1.

Proton decoupling simplifies the $^{19}F$ NMR signals of the two fluorometabolites and allows a more accurate assessment of the level of incorporation. The signals of both fluoroacetate **1** (−214.6 ppm) and 4-fluorothreonine **2** (−229.2 ppm) have an associated signal shifted to higher frequency, by 1.2 ppm. This




**Scheme 1** *Reagents and conditions*: i, $LiAlH_4$, $Et_2O$, 30 min., 77%; ii, HCl (2%), 2 h, room temp., 100%

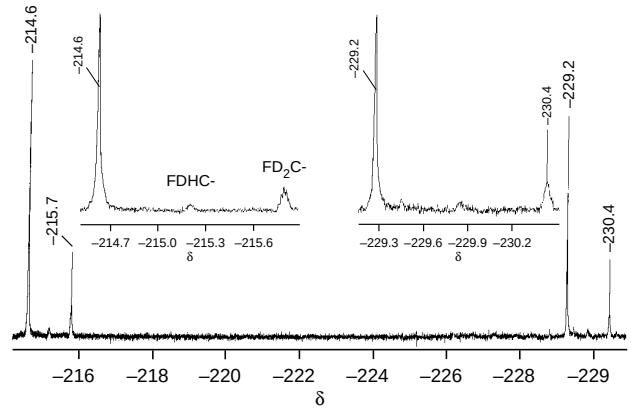


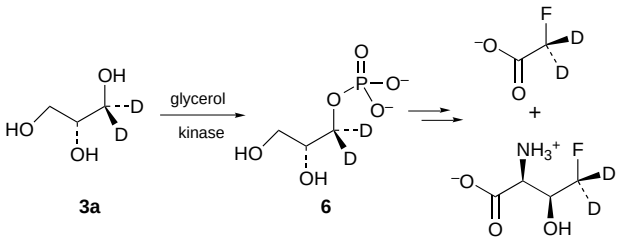

**Fig. 1** $^{19}F\{^1H\}$ NMR spectrum of fluoroacetate **1** (−214.6 ppm) and 4-fluorothreonine **2** (−229.2 ppm) formed on incubation of resting cell suspensions of *S. cattleya* with (2*R*)-[1-$^2H_2$]glycerol **3a**. Insets show expansions of the relevant regions of the spectrum. Both signals have deuterium-induced upfield shifted (1.2 ppm) signals associated with the incorporation of geminal di-deuterium labelled fluoromethyl groups ($FD_2C$). A shifted (0.6 ppm) signal of lower intensity indicates a population of molecules containing a single deuterium atom on the fluoromethyl groups (FDHC).

is assigned in each case to that population (*ca*. 28%) of molecules containing two deuterium atoms on the fluoromethyl group ($FD_2C$). There is also a minor signal in each case shifted to higher frequency by 0.6 ppm which corresponds to a smaller population (< 5%) of molecules carrying a single deuterium atom on the fluoromethyl group (FDHC). It should be noted that the levels and patterns of deuterium incorporation into fluoroacetate **1** and 4-fluorothreonine **2** are very similar, reinforcing the conclusion[4,5] that the fluoromethyl groups in the metabolites have a common origin and that there is consequently a single fluorinating enzyme in *S. cattleya*.

Only (2*R*)-[1-$^2H_2$]glycerol **3a** was incorporated into the fluorinated metabolites and therefore only the *pro-R* hydroxymethyl carbon of glycerol contributes C-2 of fluoroacetate **1** and C-4 of 4-fluorothreonine **2**. The *pro-S* hydroxymethyl group of glycerol must be cleaved and lost during fluorometabolite biosynthesis. The nature of this stereochemical processing allows certain conclusions to be drawn about the pathway leading to the substrate for fluorination. Glycerol is phosphorylated by glycerol kinase at its *pro-R* hydroxymethyl group to generate *sn*-glycerol-3-phosphate **6**, prior to its entry into the glycolytic pathway, as illustrated in Scheme 2.

Whilst these experiments do not reveal the substrate for the fluorination enzyme they do indicate that the carbon atom of glycerol which becomes activated by phosphorylation *in vivo* is also that one which is fluorinated downstream. Also the predominantly labelled populations in each of the fluorinated metabolites retained both deuterium atoms from (2*R*)-[1-$^2H_2$]glycerol **3a**, thus we can conclude that no obligatory oxidation is required at this carbon centre prior to fluorination.

The retention of both deuteriums is consistent with two minimal mechanistic hypotheses. The fluorination event may involve nucleophilic substitution by fluoride at the original phosphorylated (or enzymatically activated) carbon atom of *sn*-glycerol-3-phosphate **6** or of a metabolite derived from **6** on the glycolytic pathway to pyruvate. Alternatively fluoride may be introduced by an elimination–addition process on a glycolytic intermediate. This latter hypothesis intuitively appears less likely; however it is not ruled out by the labelling pattern observed. These results provide the first, albeit tentative, mechanistic insight into the process of biological fluorination based on empirical observation.




**Scheme 2** Observed incorporation (28%) of **3a** into fluoroacetate and 4-fluorothreonine in *S. cattleya*

We acknowledge BNFL Company Research Laboratory (CRL), Springfields, and the EC for financial support. We also thank Mr Ian H. McKeag of the University of Durham for recording $^{19}F\{^1H\}$ NMR spectra and Dr Roy Bowden, BNFL Fluorochemicals and Dr Harry Eccles, BNFL CRL for their close interest in this project.

## Footnotes

† E-mail: david.o'hagan@durham.ac.uk

‡ The glycerols **3a** and **3b** were purified over silica gel and showed identical $^1H$ NMR spectra to those previously reported.[7] The isotope content determined by FAB mass spectrometry was 99.4 atom% (double label) for each sample.

## References

1 M. Sanada, T. Miyano, S. Iwadare, J. M. Williamson, B. H. Arison, J. L. Smith, A. W. Douglas, J. M. Liesch and E. Inamine, *J. Antibiot*., 1986, **39**, 259.
2 K. A. Reid, R. D. Bowden and D. B. Harper, in *Naturally-produced Organohalogens*. ed. A. Grimwall and E. W. B. de Leer, Kluwer Academic Publishers, Dordrecht, 1995, pp. 269–279.
3 K. A. Reid, J. T. G. Hamilton, R. D. Bowden, D. O'Hagan, L. Dasaradhi, M. R. Amin and D. B. Harper, *Appl. Environ. Microbiol*., 1995, **141**, 1385.
4 J. T. G. Hamilton, M. R. Amin, D. B. Harper, and D. O'Hagan, *Chem. Commun*., 1997, preceding paper.
5 J. T. G. Hamilton, C. D. Murphy, M. R. Amin, D. O'Hagan and D. B. Harper, unpublished work.
6 T. Tamura, M. Wada, N. Esaki and K. Soda, *J. Bacteriol*., 1995, **177**, 2265.
7 R. E. Hill, A. Iwanow, B. G. Sayer, W. Wysocka and I. D. Spencer, *J. Biol. Chem*., 1987, **262**, 7463.
8 C. M. Lok, J. P. Ward and D. A. van Dorp, *Chem. Phys. Lipids*, 1976, **16**, 115.
9 See, for example: R. Keck, H. Haas and J. Rétey, *FEBS Lett*., 1980, **114**, 287.

*Received, 21st January 1997; Com. 7/00498B*

# Synthesis of a new solid acid: silica pillared lanthanum niobate with a supergallery

**Can-xiong Guo, Wen-hua Hou, Ming Guo, Qi-jie Yan* and Yi Chen**

*Department of Chemistry, Nanjing University, Nanjing 210093, China*

**Stepwise intercalations of *n*-decylamine and oligosiloxanes followed by calcination at 823 K in air results in a thermostable supergallery layered lanthanum niobate; the new material shows an interlayer free spacing of 17.4 Å along with a high Brunauer–Emmett–Teller surface area of 251 $m^2\ g^{-1}$; the acidity of the new pillared material is markedly enhanced with respect to the original lanthanum niobate.**

As an approach to obtain thermally stable porous materials, various inorganic oxo-cations have been intercalated into layered solids such as smectite clays and phosphates.[1,2] Calcination of these cation-intercalated materials formed inorganic pillared solids with different characteristics.[3] Metal oxides based on octahedral framework structures but possessing lamellar structures showed unusual properties in applications for separations, sorption and conduction[4] as well as photocatalysis.[5] However, the non-swelling nature of these layered metal oxides prevents the facile ion exchange of large oxo-cations so that only a few papers concerning pillared metal oxides have been published so far.[6] Among these lamellar oxides, lanthanum niobate (lanthanum niobium oxide, $HLaNb_2O_7$) whose layers are only built of corner-sharing octahedra to form thick perovskite slabs is found to show stronger Brønsted acidity than $HTiNbO_5$ and similar layered oxides.[7] Its photocatalytic activity is also notable.[5] Unfortunately, it loses almost all of its acidity upon heat treatment at 773 K due to the removal of interlayer water.[8]

In most of the reported lamellar solids pillared by inorganic pillars such as aluminium Keggin ions and tetrameric zirconium cations, the gallery heights are comparable to the van der Waals thickness of the host layers.[3,9] Pillared materials in which the gallery height is substantially larger than (twice or more) the thickness of the host layer have scarcely been obtained by pillaring with inorganic pillars to date.[10,11] Silica also is one of the most commonly used pillars. The lateral spacing of silica pillared materials may easily be varied based upon the preparation conditions.[11–13] The use of organosiloxanes as the source of silica enables facile intercalation of the pillar precursur and pore formation upon calcination of the organic groups.[11,12]

On the basis of progress concerning the pillared layered oxides materials made in the laboratory,[6,15,16] we report here the first synthesis of a new type of solid acid material: a silica pillared lanthanum niobate with a supergallery. The new material showed a supergallery of 17.4 Å accompanied by a Brunauer–Emmett–Teller (BET) surface area as high as 251 $m^2\ g^{-1}$. Additionally, the acidity of the new pillared material was markedly enhanced with respect to the original lanthanum niobate and hence its activity might be expected to be comparable to that of strong solid acid hydrated niobium oxide, $Nb_2O_5{\cdot}nH_2O$ for the dehydration of $Pr^iOH$.

The starting material, $KLaNb_2O_7$, was prepared by a solid-state reaction of a mixture of $K_2CO_3$, $La_2O_3$ and $Nb_2O_5$ in molar ratios of 1.25 : 1.0 : 2.0 at 1373 K overnight. The proton exchange reaction was carried out at 333 K in a solution of $HNO_3$ (6 mol $dm^{-3}$) for 3 d (solution changed daily). *n*-Hexylamine was intercalated by stirring lanthanum niobate powder with a *n*-hexylamine solution (50% v/v, EtOH) at 333 K for 36 h. After the separation of *n*-hexylamine-intercalated $HLaNb_2O_7$ by centrifugation, the solid (2 g, dried at 333 K) was treated with *n*-decylamine (100 $cm^3$, 50% v/v, EtOH) at 348 K for 2 weeks. Oligosiloxane-intercalated $HLaNb_2O_7$ was prepared by refluxing the *n*-decylammonium-intercalated lanthanum niobate with an aqueous solution of $H_2NC_3H_6Si(OEt)_3$ (20% v/v, 200 $cm^3$) for 4 days with stirring. The solid was then separated by centrifugation followed by drying at 363 K. The calcination of the above solid in air at 823 K resulted in the novel silica-pillared material with a supergallery.

The obtained $HLaNb_2O_7$ showed an X-ray diffraction (XRD) pattern [Fig. 1(*a*)] coincident with that reported in the literature.[7] The intercalation of *n*-hexylamine gave rise to a material with an expanded interlayer distance of *ca*. 26 Å shown by the (001) reflection at $2\theta = 3.4°$ where the peak positions other than (00*l*) reflections remain unchanged. Further substitution by *n*-decylammonium led to a layered material with (001) reflection at $2\theta = 2.45°$, which indicates the formation of an even larger basal spacing of *ca*. 36 Å. The interlayer gallery height occupied by *n*-decylammonium ions is *ca*. 28.4 Å by subtraction of the host layer thickness of 7.6 Å.[7] The oligosiloxane cation-intercalated $HLaNb_2O_7$ showed a (001) reflection at an even lower $2\theta$ value of 1.9°, corresponding to an interlayer distance of *ca*. 46 Å. After calcination at 823 K, the inorganic silica pillared material showed an interlayer distance of *ca*. 25.0 Å as suggested by the (001) reflection at $2\theta = 3.5°$ [Fig. 1(*b*)]. This indicates a 'supergallery' of *ca*. 17.4 Å which is substantially larger than the host layer thickness. A significant increase in gallery height is achieved compared to that of non-pillared $HLaNb_2O_7$ where the basal spacing is only *ca*. 10.8 Å. The layered structure of the new supergallery pillared material is thermally very stable and its structure was retained upon heat treatment at 973 K with only a slightly decreased interlayer distance of *ca*. 24.2 Å as shown by its (001) reflection at $2\theta = 3.6°$.

The porosity of $HLaNb_2O_7$ is greatly increased by pillaring with silica. The BET surface area of the new pillared material reaches 251 $m^2\ g^{-1}$ most of which arises from micropores (micropore area = 197 $m^2\ g^{-1}$). The original $HLaNb_2O_7$ is

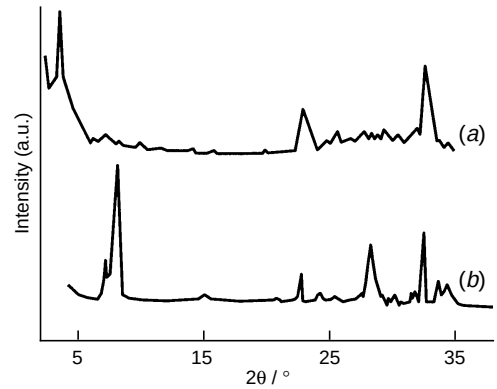



**Fig. 1** X-Ray diffraction (XRD) patterns of (*a*) $HLaNb_2O_7$ (dried at 333 K) and (*b*) silica-pillared $HLaNb_2O_7$

actually a non-porous solid with a surface area of only *ca*. 5 $m^2\ g^{-1}$. Considering the fact that the gallery height resulting from pillaring reaches 17.4 Å, a new type of nanoporous material[9] is thought to be formed by pillaring with silica. The new material shows an adsorption–desorption isotherm with a hysteresis loop (Fig. 2) upon $N_2$ adsorption at 77 K. The obtained hysteresis loop may be classified as type H4 or H3 (by IUPAC classification) suggesting the existence of narrow slit-like pores associated with aggregates of plate-like particles where the type I character of the adsorption isotherm indicates the microporosity predominated in the new material.[18] It is also in good agreement with the micropore area measurement.

The possibility of using this material for acid catalysed reactions was investigated by the probe reaction of $Pr^iOH$ decomposition at 573 K which showed complete conversion of the reactant to dehydration products, illustrating the strong acidic property of the new material. In comparison, non-pillared $HLaNb_2O_7$ pretreated at 573 K showed only 32% conversion under the same reaction conditions. A significant enhancement of acidity is achieved by pillaring the lanthanum niobium oxide with silica. The new pillared material showed catalytic activities as high as that of the strong solid acid niobic acid under the same conditions.

To conclude, silica pillared $HLaNb_2O_7$ is a thermostable porous layered solid acid material containing a supergallery. The new material is expected to show shape selective effects for catalytic reactions in which larger molecules can be used. The high thermal stability of the new pillared material also enables its application at some critical conditions either as an acid catalyst or as a catalyst support. Further systematic characterization of this new material and investigations on its shape selectivity in catalysis as well as other fields are actively being undertaken.

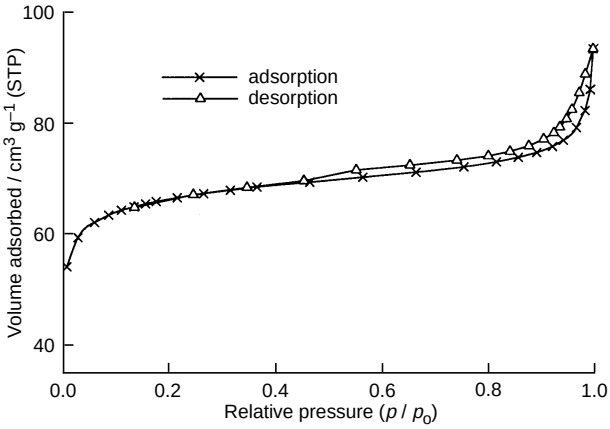



**Fig. 2** Adsorption–desorption isotherm of $N_2$ at 77 K on silica-pillared $HLaNb_2O_7$

Financial support of National Natural Science Foundation of China (NNSFC No. 29573108) and Natural Science Foundation of Jiansu Province are gratefully acknowledged.

## Footnote

* E-mail: physchem@netra.nju.edu.cn

## References

1 T. J. Pinnavaia, *Science*, 1983, **220**, 365.
2 *Pillared Layered Structures: Current Trends and Applications*, ed. I. V. Mitchell, Elsevier Applied Science, London, 1990, ch. 3.
3 F. Figueras, *Catal. Rev. Sci. Eng*., 1988, **30**, 741.
4 A. Clearfield, *Chem. Rev*., 1988, **88**, 125.
5 K. Domen, J. Yoshimura, T. Sekine, A. Tanaka and T. Onishi, *Catal. Lett*., 1990, **4**, 339.
6 Y.-S. Chen, W.-H. Hou, C.-X. Guo, Q.-J. Yan and Y. Chen, *J. Chem. Soc., Dalton Trans*., 1997, 359.
7 J. Gopalakrishan, V. Bhat and B. Raveau, *Mater. Res. Bull*., 1987, **22**, 413.
8 T. Matsuda, T. Fujita, N. Miyamae, M. Takeuchi and K. Kanda, *Bull. Chem. Soc. Jpn*., 1993, **66**, 1548; T. Matsuda, T. Fujita and N. Miyamae, *Catal. Today*, 1993, **16**, 455.
9 T. J. Pinnavaia, in *Materials Chemistry: An Emerging Discipline*, ed. L. V. Interrante, L. A. Casper and A. B. Ellis, American Chemical Society, Washington, DC, 1994, p. 283.
10 A. Moini and T. J. Pinavaia, *Solid State Ionics*, 1988, **26**, 119.
11 P. Sylvester, R. Cahill and A. Cleerfield, *Chem. Mater*., 1994, **6**, 1890.
12 J. Roziere, D. J. Jones and T. Cassagneau, *J. Mater. Chem*., 1991, **1**, 1081.
13 M. E. Landis, B. A. Aufdembrink, P. Chu, I. D. Johnson, G. W. Kirker and M. K. Rubin, *J. Am. Chem. Soc*., 1991, **113**, 3189.
14 A. G. Voronkov, *Topics in Current Chemistry*, Springer-Verlag, Berlin, 1982, p. 199.
15 W.-H. Hou, J. Ma, Q.-J. Yan and X.-C. Fu, *J. Chem. Soc., Chem. Commun*., 1993, 1141.
16 W.-H. Hou, Q.-J. Yan, B.-C. Peng and X.-C. Fu, *J. Mater. Chem*., 1995, **5**, 109.
17 K. Tanabe, *Mater. Chem. Phys*., 1987, **17**, 217; *Catal. Today*, 1990, **8**, 1; *CHEMTECH*, 1991, **21**, 628.
18 S. W. Sing, D. H. Everett, R. A. W. Haul, L. Moscou, R. A. Pierotti, J. Rouqerol and T. Siemieniewska, *Pure Appl. Chem*., 1985, **57**, 603.

*Received in Cambridge, UK, 24th January 1997; Com. 7/00567I*

# $[Li(dime)_2][W(CO)_5I]$ as a novel synthon for the preparation of silyl, amino and organyl derivatives of pentacarbonyl tungsten (dime = diethylene glycol dimethyl ether)

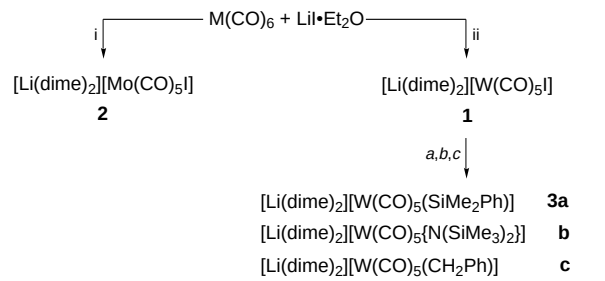
**W. Palitzsch, U. Böhme* and G. Roewer**

*Institut für Anorganische Chemie der TU Bergakademie Freiberg, Leipziger Str. 29, D-09596 Freiberg, Germany*

**The one-pot reactions of $M(CO)_6$ with dime in the presence of $LiI{\cdot}Et_2O$ give $[Li(dime)_2][M(CO)_5I]$ (M = W 1, Mo 2); the reaction of 1 with $LiSiMe_2Ph$, $LiN(SiMe_3)_2$ and $PhCH_2MgCl$ affords the novel complexes $[Li(dime)_2][W(CO)_5R]$ [R = $SiMe_2Ph$ 3a, $N(SiMe_3)_2$ 3b, $CH_2Ph$ 3c].**

Pentacarbonyl (alkyl- and aryl-alkoxycarbene) group 6 metal complexes have attracted much interest as useful reagents for organic synthesis.[1,2] The production of water-soluble catalysts is an area of considerable current interest.[3] The role of ionic metal complexes as active species in homogeneous catalysed reactions is well documented.[4,5] A simple chemical procedure for the synthesis of anionic monosubstituted derivatives of transition-metal carbonyls should be highly interesting, especially to generate coordinatively unsaturated species with potential applications in catalysis. The design of simple synthetic routes for these compounds is therefore very important.

Compounds containing the $[M(CO)_5X]^-$ ion (M = Mo,W; X = Br) have been synthesized *via* difficult routes.[6] We found a very simple way to generate such complexes. The one-pot reaction of $W(CO)_6$ with dime in presence of $LiI{\cdot}Et_2O$ leads to the hitherto unknown $[Li(dime)_2][W(CO)_5I]$ **1** (Scheme 1).




**Scheme 1** *Reagents and conditions*: i, M = Mo, dime, 80 °C, −CO, $-Et_2O$, 70%; ii, M = W, dime, 80 °C, −CO, $-Et_2O$, 80%; *a*, $LiSiMe_2Ph$, dme, 0 °C, −LiI, 64%; *b*, $LiN(SiMe_3)_2$, THF, 0 °C, −LiI, 84%; *c*, $CH_2PhMgCl$, $Et_2O$, 0 °C, −MgClI, 77%

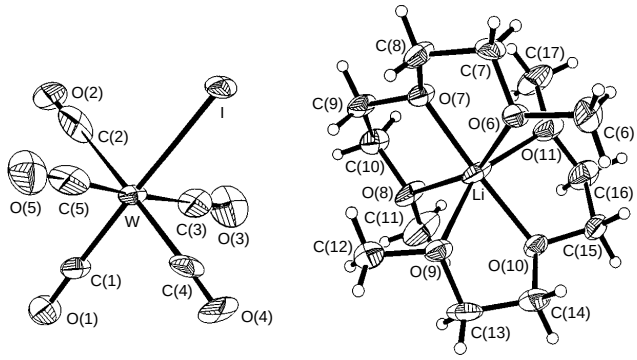



**Fig. 1** Crystal structure of **1**. Selected bond distances (Å) and angles (°): W–I 2.871(2), W–C(1) 1.97(2), W–C(2),C(3),C(4),C(5) 2.04(2)–2.10(2); I–W–C(1) 178.7(3), I–W–C(2),C(3),C(4),C(5) 86.7(4)–91.2(4); Li–O 2.00(2)–2.22(2).

The X-ray crystal structure analysis of **1** reveals the molecular structure shown in Fig. 1.‡ The structure was solved and refined in space group $P2_1/c$. The lithium atom is coordinated by two molecules of dime with a distorted octahedral coordination geometry. The $[W(CO)_5I]^-$ anion has nearly $C_{4v}$ symmetry with a W–I bond length of 2.871 Å.

First experimental studies showed a surprising stability of **1** during dissolving tests in protic solvents. We could observe only very slow decomposition in the air. The same synthetic route was applied to the synthesis of $[Li(dime)_2][Mo(CO)_5I]$ **2**.†

The $[W(CO)_5I]^-$ anion represents an interesting building block. It is very easy to substitute the iodine retaining the $d^6$ character of tungsten. We used the $[W(CO)_5I]^-$ anion as a starting tungsten complex for reactions with different nucleophilic reagents to substitute the iodine. For example, complex **1** reacts with $LiSiMe_2Ph$ to give compound **3a**, and with a lithium amide (*b*) to give compound **3b**.§ Treatment of **1** with a Grignard reagent (*c*) produces complex **3c** (Scheme 1).§ All new compounds were isolated and purified by extraction with pentane and subsequent recrystallization with dichloromethane.

Further studies to extend the scope of these reactions to molybdenum carbonylates and to other nucleophilic reagents, as well as studies on the reactivity of the obtained products are under way.

## Footnotes

* E-mail: boehme@silicium.aoch.tu-freiberg-de

† All new compounds gave satisfactory analytical data.

‡ *Crystal data* for $[Li(dime)_2][W(CO)_5I]$ **1** (yellow crystal from $CH_2Cl_2$–pentane): $C_{17}H_{28}ILiO_{11}W$, monoclinic, space group $P2_1/c$, $a$ = 14,610(3), $b$ = 13.232(1), $c$ = 14.658(2) Å, β = 113.01(2)°, $U$ = 2608.3(6) Å$^3$, $Z$ = 4, $D_c$ = 1.849 g cm$^{-3}$, μ = 17.927 mm$^{-1}$, $F(000)$ = 1392. A single crystal of approximate dimensions 0.15 × 0.2 × 0.2 mm was mounted on a glass fibre under paraffin oil and transfered to the diffractometer. Data were collected at −83 °C on an Enraf-Nonius CAD-4 diffractometer using graphite-monochromated Cu-Kα radiation (λ = 1.5418 Å) with ω–2θ scans. The structure was solved by direct methods and refined by full-matrix least squares on $F^2$ with anisotropic thermal parameters. Hydrogen atoms were calculated and allowed to ride on their corresponding carbon atoms. $R$ = 0.0772 for 4111 reflections ($F_o > 2\sigma F_o$) and 0.0970 for all 5352 reflections, GOF = 1.005. Atomic coordinates, bond lengths and angles, and thermal parameters have been deposited at the Cambridge Crystallographic Data Centre (CCDC). See Information for Authors, Issue No. 1. Any request to the CCDC for this material should quote the full literature citation and the reference number 182/411.

§ *Experimental details and selected spectroscopic data*: **1**: $^1$H NMR ($CDCl_3$, $SiMe_4$) δ 3.68, 3.57, 3.37 (dime); $^{13}$C NMR ($CDCl_3$, $SiMe_4$) δ 202.4, 196.97 (CO), 70.20, 68.99, 59.40 (dime); IR ($CDCl_3$, $\nu_{CO}$/cm$^{-1}$) 1975, 1915, 1850. **2**: $^1$H NMR ($CDCl_3$, $SiMe_4$) δ 3.71, 3.59, 3.41 (dime); $^{13}$C NMR ($CDCl_3$, $SiMe_4$) δ 219.59, 204.56 (CO); 70.49, 69.25, 59.44 (dime); IR ($CDCl_3$, $\nu_{CO}$/cm$^{-1}$) 1982, 1933, 1859. **3a**: $^1$H NMR ($CDCl_3$, $SiMe_4$) δ 7.54 (SiPh); 3.68, 3.59, 3.43 (dime); 0.58 ($SiMe_2$); $^{29}$Si NMR ($CH_2Cl_2$-$D_2O$) δ −6.13; IR ($CHCl_3$, $\nu_{CO}$/cm$^{-1}$) 1925, 1887, 1815. **3b**: $^1$H NMR ($CDCl_3$) δ 3.71, 3.60, 3.40 (dime); 0.00 ($SiMe_3$); $^{13}$C NMR ($CDCl_3$)

δ 205.67, 197.04 (CO); 70.43, 69.19, 59.45 (dime); 2.39 ($SiMe_3$); IR ($CDCl_3$, $\nu_{CO}/cm^{-1}$) 1928, 1874, 1855. **3c**: $^1H$ NMR ($CDCl_3$ $SiMe_4$) δ 7.26 (Ph); 3.74, 3.64, 3.44 (dime); 1.25 ($CH_2$); $^{13}C$ NMR ($CDCl_3$, $SiMe_4$) δ 138.78, 130.68, 128.73, 126.48 (Ph); 70.85, 69.58, 59.49 (dime); 45.58 ($CH_2$); IR ($CDCl_3$, $\nu_{CO}/ cm^{-1}$) 1934, 1916, 1885.

## References


1 K. H. Dötz, *Angew. Chem., Int. Ed. Engl*., 1984, **23**, 586; R. Aumann and P. Hinterding, *Chem. Ber*., 1990, **123**, 611.
2 L. S. Hegedus, M. A. McGuire, L. M. Schultze, Chen Yijun and O. P. Anderson, *J. Am. Chem. Soc*., 1984, **106**, 2680 and references therein.
3 W. A. Herrmann and C. W. Kohlpaintner, *Angew. Chem.*, 1993, **105**, 1588; *Angew. Chem., Int. Ed. Engl*., 1993, **32**, 1524.
4 H. H. Brintzinger, D. Fischer, R. Mülhaupt, B. Rieger and R. Waymouth, *Angew. Chem*., 1995, **107**, 1255; *Angew. Chem., Int. Ed. Engl*., 1995, **34**, 1143.
5 D. Forster, *Adv. Organomet. Chem*., 1979, **17**, 255.
6 R. M. Dahlgren and J. I. Zink, *J. Chem. Soc., Chem. Commun.*, 1978, 863.



*Received in Cambridge, UK, 9th January 1997; Com. 7/00215G*

ChemComm
FEATURE ARTICLE

# Synthesis of acyclic and heterocyclic natural products utilizing cyclitols as novel chiral building blocks

**Noritaka Chida† and Seiichiro Ogawa**

*Department of Applied Chemistry, Faculty of Science and Technology, Keio University, Hiyoshi, Kohoku-ku, Yokohama 223, Japan*

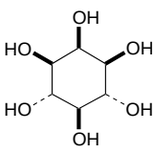
**The synthesis of biologically important natural products which contain acyclic or heterocyclic structures, starting from cyclitols, is described. Stereoselective functionalization and subsequent regioselective ring cleavage of cyclitol derivatives provides precursors for the synthesis of a wide variety of natural products. The successful synthesis of acyclic and heterocyclic natural products reveals the usefulness and importance of cyclitols as novel chiral building blocks.**

## Introduction

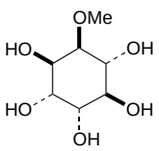
The synthesis of natural products possessing biological activity and interesting structures in an enantiomerically pure form is a highly important area of modern organic and medicinal chemistry. To construct the asymmetric centres in the target molecule, compounds with established asymmetric centres, such as naturally occurring amino acids,[1] terpenes[2] and carbohydrates, are frequently employed as the starting material (chiral building block).[3] Among them, carbohydrates, especially aldohexoses such as D-glucose, have been widely used due to their ready availability and versatility.[4] Cyclitols (polyhydroxycycloalkanes), which are classified as a type of carbohydrate, occur widely in nature.[5] *myo*-Inositol **1**, known as a constituent of a secondary messenger in cells which stimulates the release of calcium from storage sites, is easily obtained from corn-steep liquors and commercially available at relatively low price.‡ While *myo*-inositol is a meso compound, L-quebrachitol [1L-(−)-2-*O*-methyl-*chiro*-inositol] **2**, isolated in large quantities from the serum of the rubber tree,[6]§ is an optically active cyclitol possessing a methyl ether function. In spite of their abundance in nature and ready availability, cyclitols have not been utilized widely as starting materials for the synthesis of natural products other than cyclitol derivatives. Given that regioselective cleavage of their cyclohexane ring is possible, cyclitols are expected to be versatile starting materials for the synthesis of acyclic or heterocyclic natural products. In this article, the synthesis of several acyclic and heterocyclic natural products starting from cyclitols (*myo*-inositol and L-quebrachitol), based on tactics involving stereoselective functionalization followed by regioselective ring cleavage of the cyclitol ring, are described.

## Regioselective ring cleavage of the cyclohexane ring in cyclitols

A major advantage in using cyclitol as a starting material compared with aldohexoses is that there are no synthetic limitations imposed by the presence of a hemiacetal functionality. The cyclic structure as well as the established protection-deprotection methods of polyhydroxy groups[5] in cyclitols allowed us to introduce many kinds of functional groups stereoselectively on the cyclohexane ring. If one could cleave the cyclohexane ring in functionalized cyclitol derivatives at any chosen position, the array of chiral centres from the cyclitol derivatives, which are sometimes difficult to obtain from convensional sugars such as D-glucose, D-galactose, D-mannitol and so on, could be transferred to the target molecule. To cleave the cyclohexane ring in cyclitols, oxidative glycol cleavage would be anticipated to be an effective and reliable method. However, difficulty is sometimes encountered in distinguishing between the two newly formed formyl carbons. On the other hand, Baeyer–Villiger reaction of polyhydroxycyclohexanone derivatives possessing oxygen and other functionalities at the α-carbons is an attractive method to cleave the cyclohexane ring, since the terminal carbons of the product usually have different oxidative states. Early studies on the Baeyer–Villiger reaction of polyhydroxycyclohexanones derived from *myo*-inositol by Fukami *et al.*[7] revealed that the reaction proceeded in a highly regioselective manner, and suggested that the substituent on the α-carbon should be an important factor for influencing the regioselectivity. To clarify the governing factor controlling the regioselectivity, a series of unsymmetrical polyhydroxycyclohexanone derivatives were synthesized from *myo*-inositol and L-quebrachitol, and subjected to Baeyer–Villiger reaction.[8] Some results are shown in Scheme 1. This study showed that the migratory ability of substituted carbons adjacent to the carbonyl in the polyhydroxycyclohexanone system are strongly affected by the nature of substituents on the α-carbon; the migratory aptitudes are: a carbon possessing benzyloxy > methoxy > cyclic ketaloxy ≫ acyloxy ≈ methyl > hydrogen. These results suggested that n-electron density on the oxygen atom attached to the adjacent carbon to the carbonyl is of significance, implying that an n–σ*≠ interaction (Cieplak postulate[9]) might account for the observed regioselectivity. Thus it should now be possible to design polyhydroxycyclohexanone derivatives which undergo regioselective Baeyer–Villiger reaction.




*myo*-inositol **1**




L-quebrachitol **2**

## Synthesis of natural products starting from *myo*-inositol

### *Iduronic acid derivative and nojirimycin*

Since *myo*-inositol **1** is a *meso* compound, chemical transformation usually provides *meso* or racemic products. Therefore it is necessary to perform an asymmetric reaction[10] or optical resolution[11] to prepare optically pure *myo*-inositol derivatives. Cyclic ketal formation of **1** gave racemic **3**[12] in high yield (Scheme 2). After *O*-benzylation, diol **4** was obtained by acidic hydrolysis. When diol **4** was reacted with an equimolar amount of (*S*)-(+)-α-(acetoxy)phenylacetic acid in the presence of 1,3-dicyclohexylcarbodiimide (DCC) and 4-dimethylaminopyridine (DMAP) at −15 °C, formation of a pair of diastereoisomers (**5D** and **5L**) was observed. These compounds are easily separated by silica gel chromatography or recrystallization to

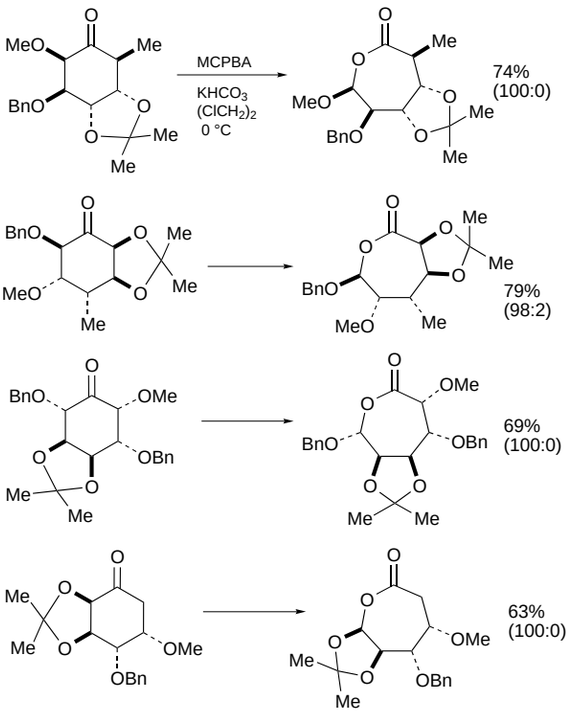
provide **5D** and **5L** in 36 and 35% isolated yields, respectively. Removal of the (*S*)-(+)-α-(acetoxy)phenylacetyl group from **5D** afforded **4D**, and from **5L** gave **4L**, both in quantitative yield. The absolute configurations of **4D** and **4L** were confirmed by comparison of their $[\alpha]_D$ values with literature ones,[11a] and the optical purities of **4D** and **4L** were estimated to be > 98% ee, respectively, by HPLC analyses using a chiral column (chiralcel OD).

Oxidation of **5L** afforded ketone **6**, whose Baeyer–Villiger reaction with MCPBA proceeded in a highly regioselective manner and provided the 7-membered acetal lactone **7**. Treatment of **7** with MeOH and $HC(OMe)_3$ in the presence of toluene-*p*-sulfonic acid (TsOH) caused the lactone ring to open, providing acyclic product **8** after methyl ester formation. This compound was transformed into L-iduronic acid derivative **9L**.[13] Similar treatment of **5D** provided the enantiomer **9D**.[13]

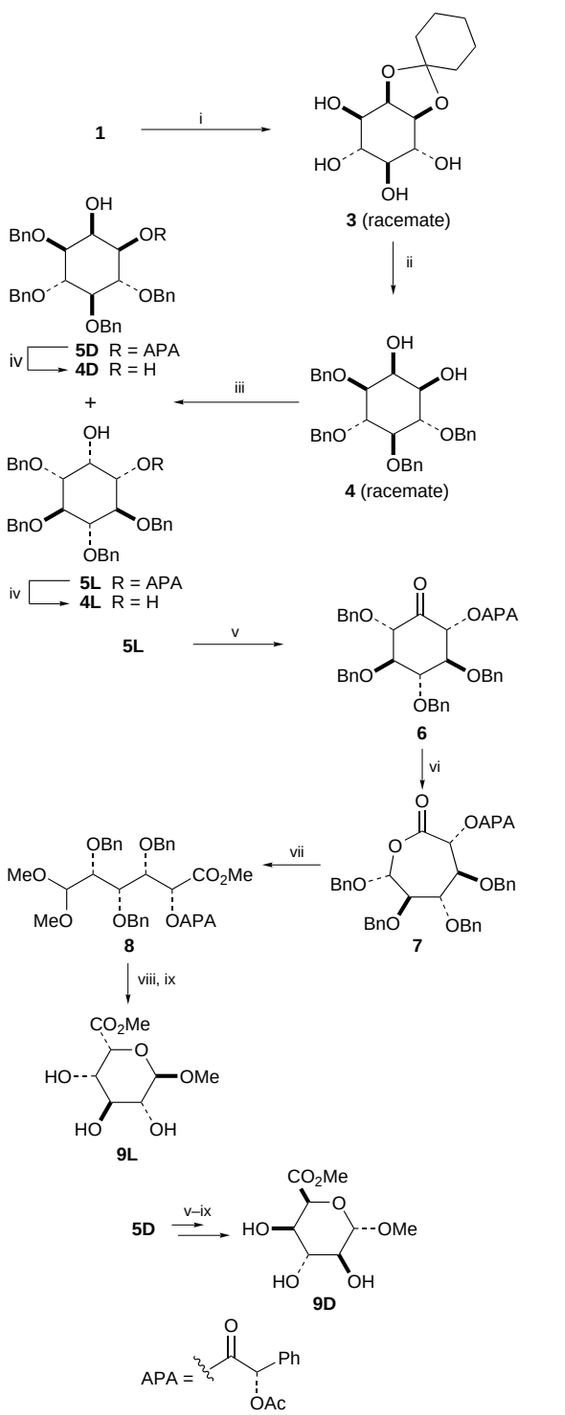
The acyclic sugar derivative **8** is a versatile intermediate for the synthesis of natural products possessing polyhydroxy functionality. DIBAL-H reduction of **8** gave diol **10** (Scheme 3), whose primary hydroxy group was selectively protected to afford **11**. Introduction of an amino functionality by Mitsunobu reaction provided **12**. Compound **12** was effectively converted into (+)-nojirimycin bisulfite adduct **13**.[14] (+)-Nojirimycin **14**[14] and (+)-1-deoxynojirimycin **15**[14b] were easily obtained from the adduct **13**.

*Sphingofungin D*

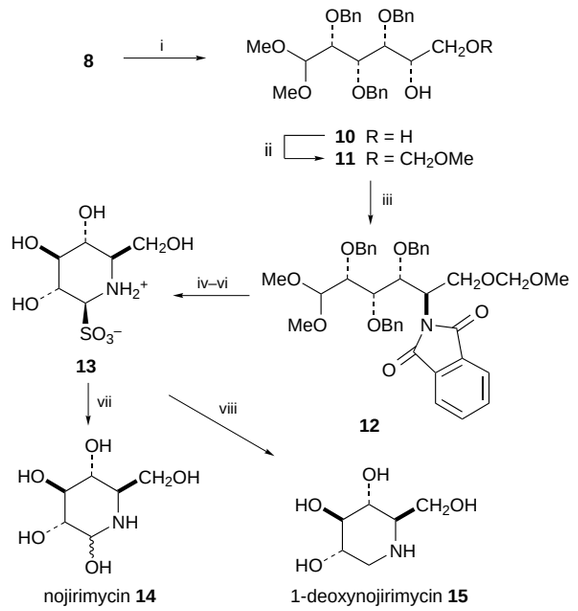
Compound **8** was also employed for the total synthesis of the novel antifungal agent sphingofungin D (*N*-acetyl asperfungin) (Scheme 4).[15] Acidic hydrolysis of the dimethyl acetal group in **8** afforded the corresponding acyclic *aldehydo*-sugar, whose Wittig reaction with $Ph_3P{=}CHCO_2Et$ provided *E*-alkene **16**. This was transformed into allyl bromide **18** in three steps. Reaction of **18** with sulfone **19**, which was synthesized from the coupling product of commercially available (*R*)-epoxyoctane and 4-[(tetrahydropyran-2-yl)oxy]butylmagnesium chloride in four steps, followed by desulfonization afforded the $C_{20}$ backbone **21** of sphingofungins. Removal of the acetonide group provided diol **22**. Although introduction of an amino functionality at the C-2 position in **22** by intermolecular $S_N2$ reaction was difficult, it was found that intramolecular nitrogen delivery worked well for this substrate. Thus, Mitsunobu reaction of **22** afforded epoxide **23**, which was transformed into primary azide **24**. Treatment of **24** with $Ph_3P$ followed by reaction with ZCl generated inverted aziridine **26**, whose




**Scheme 1** Partial decomposition of the products during silica gel chromatography was observed. The ratios of the major product and its regioisomer were determined by 270 MHz $^1$H NMR analysis of the products before isolation.




**Scheme 2** *Reagents and conditions*: i, cyclohexanone, TsOH, $C_6H_6$; ii, NaH, BnCl, DMF; iii, (*S*)-(+)-(AcO)CHPh$CO_2$H, DCC, DMAP, $CH_2Cl_2$, −15 °C; iv, MeONa, MeOH; v, $CrO_3$ in dil. $H_2SO_4$, $Me_2CO$, 0 °C; vi, MCPBA, $KHCO_3$, $(ClCH_2)_2$, 0 °C; vii, TsOH, $HC(OMe)_3$, MeOH, 80 °C, then $CH_2N_2$, $CH_2Cl_2$; viii, 3% methanolic HCl, reflux; ix, $H_2$, 20% $Pd(OH)_2$ on carbon, EtOH.

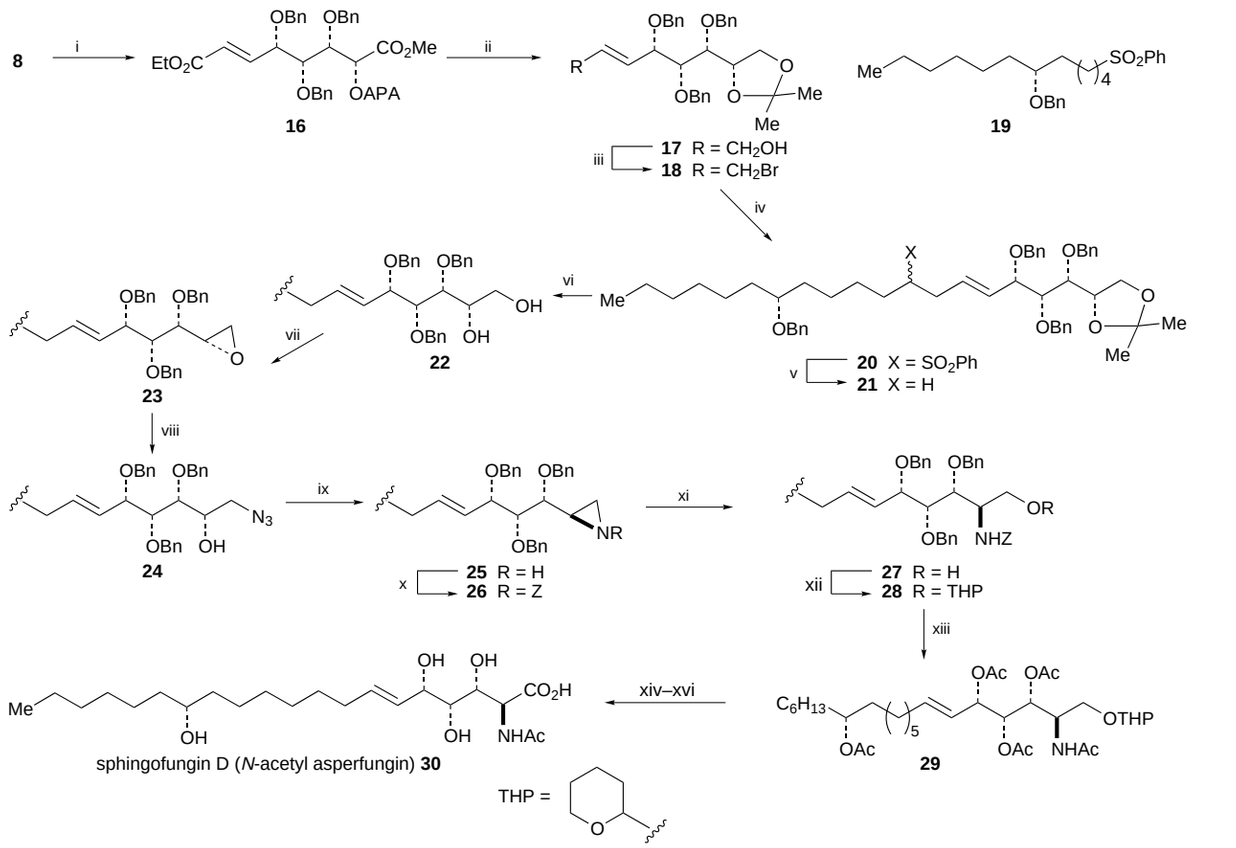



**Scheme 3** *Reagents and conditions*: i, $LiAlH_4$, THF, 0 °C; ii, $MeOCH_2Cl$, $Pr^i_2NEt$, $CH_2Cl_2$, 0 °C; iii, phthalimide, $Ph_3P$, diethyl azodicarboxylate (DEAD), THF, room temp.; iv, $H_2NNH_2{\cdot}H_2O$, MeOH, reflux, then $Boc_2O$, $Et_3N$, $CH_2Cl_2$; v, $H_2$, 20% $Pd(OH)_2$ on carbon, EtOH; vi, $SO_2$(gas), $H_2O$, 40 °C; vii, Dowex 1 X2 resin ($OH^-$ form), $H_2O$; viii, $H_2$, Raney-Ni (W-4), $Ba(OH)_2$, $H_2O$.

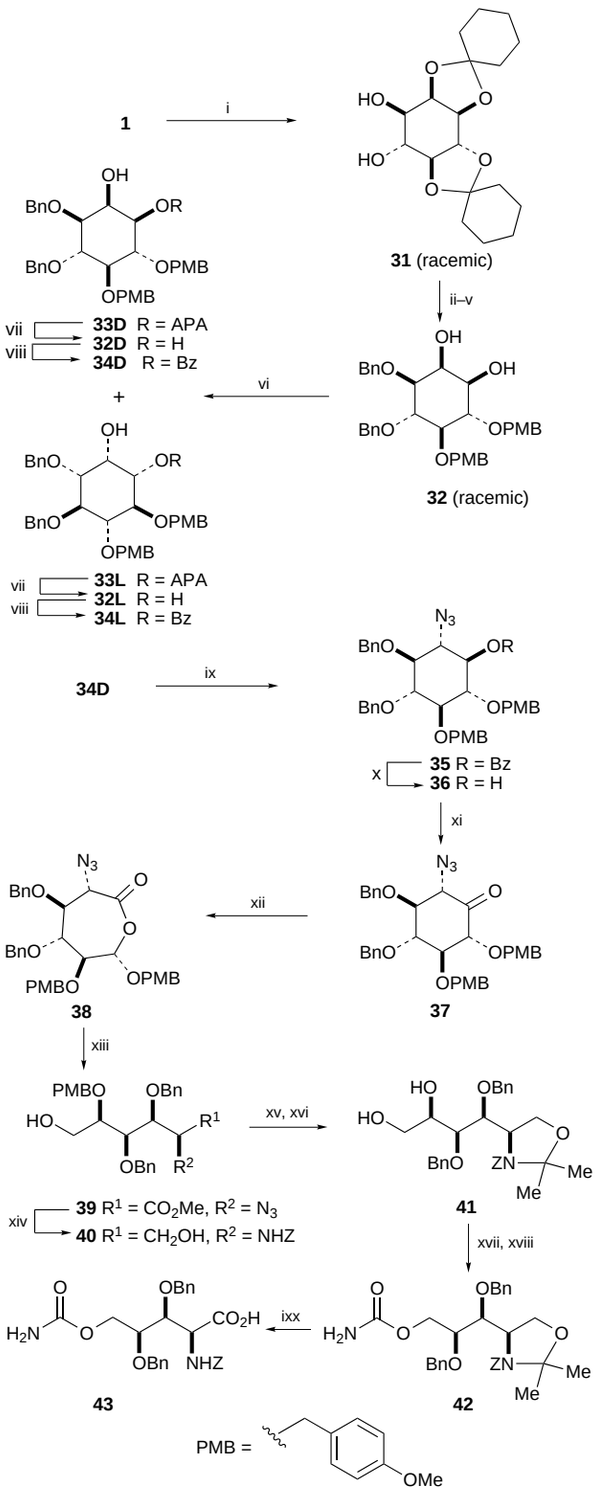
aziridine ring was cleaved with KOAc to provide **27** after hydrolysis of the *O*-acetyl function. The primary hydroxy group was protected as a tetrahydropyran-2-yl (THP) ether to afford **28**. Treatment of **28** with Li–$NH_3$ gave **29** after *N*,*O*-acetylation. Removal of the *O*-THP group and subsequent oxidation, followed by de-*O*-acetylation afforded sphingofungin D **30**. This total synthesis confirmed the proposed C-2–C-5 stereochemistry, and assigned the undetermined absolute configuration at C-14 in sphigofungins to be *R*.[15]

*Polyoxin J*

The antifungal antibiotic polyoxin J **55** consists of two fragments, amino acid portion **43** and nucleic acid portion **53**. These two key fragments were synthesized from a pair of optically resolved *myo*-inositol derivatives (**32D** and **32L**), respectively.[16] The known racemic diol **31**,[12] prepared from **1** in one step was converted into another racemic diol **32** (Scheme 5). Optical resolution of **32** using (*S*)-(+)-α-(acetoxy)phenylacetic acid afforded **33D** and **33L**, which are easily separated by silica gel chromatography. Basic methanolysis of **33D** and **33L** provided optically active diols **32D** and **32L**, respectively. Synthesis of the amino acid moiety in polyoxin J employed **32D**, which was converted into **34D**. After introduction of an azide group in an $S_N2$ fashion, ketone **37** was subjected to Baeyer–Villiger reaction to provide lactone **38** as the sole product. Basic opening of the lactone ring followed by reduction gave acyclic product **39**. Further reduction of the ester and azide functions and subsequent protection of the amino group afforded diol **40**. *N*,*O*-Acetalization and removal of the *para*-methoxybenzyl (PMB) group gave **41**, and subsequent



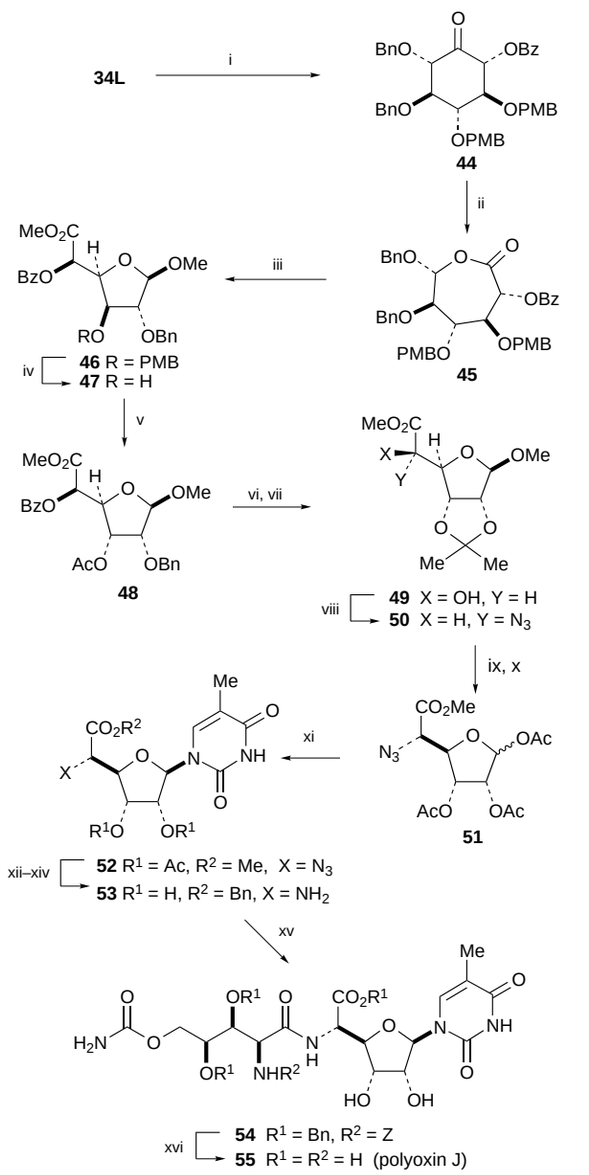

**Scheme 4** *Reagents and conditions*: i, AcOH–$H_2O$ (4:1), 80 °C, then $Ph_3P{=}CHCO_2Et$, $CH_2Cl_2$, room temp.; ii, DIBAL-H, $CH_2Cl_2$, 0 °C, then $Me_2CO$, camphorsulfonic acid (CSA), 0 °C; iii, $Ph_3P$, $CBr_4$, $CH_2Cl_2$, room temp.; iv, BuLi, **19**, THF–HMPA (10 : 1), −78 °C; v, Na–Hg (6%), $Na_2HPO_4$, THF–MeOH (1 : 1), room temp.; vi, CSA, MeOH, room temp.; vii, $Ph_3P$, DEAD, PhMe, reflux; viii, $NaN_3$, DMF–$H_2O$ (9 : 1), 100 °C; ix, $Ph_3P$, toluene, 50 °C, 30 min, then reflux; x, ZCl, $Et_3N$, $CH_2Cl_2$; xi, AcONa, 15-crown-5, DMF, 100 °C, then $K_2CO_3$, MeOH, room temp.; xii, 3,4-dihydro-2*H*-pyran, pyridinium toluene-*p*-sulfonate (PPTS), $CH_2Cl_2$, room temp.; xiii, Na, THF–liq. $NH_3$ (1 : 1), −78 °C, then $Ac_2O$, pyridine, room temp.; xiv, PPTS, EtOH, 50 °C; xv, $CrO_3$ in dil. $H_2SO_4$, acetone, 0 °C; xvi, LiOH, THF–$H_2O$ (2 : 1), room temp.



**Scheme 5** *Reagents and conditions*: i, 1,1-dimethoxycyclohexane, TsOH, DMF; ii, NaH, BnBr, DMF; iii, TsOH, EtOH, room temp.; iv, NaH, 4-$MeOC_6H_4CH_2Cl$, DMF; v, AcOH–$H_2O$ (4 : 1), 80 °C; vi, (*S*)-(+)-(AcO)CHPh$CO_2H$, DCC, DMAP, $CH_2Cl_2$, −15 °C; vii, MeONa, MeOH, 0 °C; viii, BzCl, DMAP, pyridine, room temp.; ix, $MeSO_2Cl$, pyridine, 50 °C, then $NaN_3$, DMF, 80 °C; x, MeONa, MeOH; xi, dimethyl sulfoxide, DCC, $CF_3CO_2H$, pyridine, $C_6H_6$, room temp.; xii, MCPBA, $KHCO_3$, $(ClCH_2)_2$, 0 °C; xiii, $NaBH_4$, MeONa, MeOH, 0 °C; xiv, $LiAlH_4$, $Et_2O$, then ZCl, $NaHCO_3$, THF–$H_2O$; xv, 2,2-dimethoxypropane, TsOH, DMF, then $Ac_2O$, pyridine; xvi, 2,3-dichloro-5,6-dicyano-1,4-benzoquinone (DDQ), $CH_2Cl_2$–$H_2O$, then MeONa, MeOH; xvii, $Pb(OAc)_4$, $C_6H_6$, room temp., then $NaBH_4$, MeOH; xviii, 4-nitrophenyl chloroformate, then $NH_3$–MeOH, $CH_2Cl_2$; ixx, TsOH, MeOH, room temp., then $CrO_3$ in dil. $H_2SO_4$, $Me_2CO$, 0 °C.

glycol cleavage followed by carbamoylation gave **42**. This was transformed into amino acid moiety **43**.

On the other hand, preparation of the nucleoside portion started from the enantiomeric diol **32L** (Scheme 6). Baeyer–Villiger reaction of the ketone **44** derived from **32L** in two steps afforded the acetal lactone **45** as the sole product. Acidic methanolysis of **45** followed by methyl ester formation provided furanoside **46** as the major product. Interestingly, the PMB group at C-3 in **45** was removed under the acidic reaction conditions. Inversion of the C-3 hydroxy group in **46** and subsequent exchange of the protecting groups gave **49**, into



**Scheme 6** *Reagents and conditions*: i, pyridinium dichromate, molecular sieves 4A, $CH_2Cl_2$; ii, MCPBA, $KHCO_3$, $(ClCH_2)_2$, 0 °C; iii, TsOH, $HC(OMe)_3$, MeOH, room temp., then MeI, $NaHCO_3$, DMF; iv, DDQ, $CH_2Cl_2$–$H_2O$; v, $(CF_3SO_2)_2O$, pyridine, $CH_2Cl_2$, 0 °C, then AcOK, DMF, 5 °C; vi, MeONa, MeOH then $H_2$, $Pd(OH)_2$, EtOH; vii, 2,2-dimethoxypropane, TsOH, DMF, room temp.; viii, $(CF_3SO_2)_2O$, pyridine, $CH_2Cl_2$ then $NaN_3$, DMF, room temp.; ix, Dowex 50W X8 ($H^+$ form), MeOH, room temp., then $Ac_2O$, pyridine; x, $Ac_2O$, $H_2SO_4$, $CH_2Cl_2$–AcOH; xi, 5-methyl-2,4-bis(trimethylsilyloxy)pyrimidine, $Me_3SiOSO_2CF_3$, $CH_2Cl_2$, room temp.; xii, $H_2$, 5% Pd–$BaSO_4$, dioxane–$H_2O$, then $Ba(OH)_2$, dioxane–$H_2O$, room temp.; xiii, $Boc_2O$, $K_2CO_3$, dioxane–$H_2O$, then BnBr, $NaHCO_3$, DMF, room temp.; xiv, $CF_3CO_2H$, EtOAc, 0 °C; xv, **43**, $(EtO)_2P(O)CN$, $Et_3N$, DMF, room temp.; xvi, $H_2$, 10% Pd–C, MeOH–$H_2O$.

which was introduced an azide function with inversion of configuration to provide **50**. Acetolysis of **50** gave **51**, which was condensed with 5-methyl-2,4-bis(trimethylsilyloxy)pyrimidine under Vorbruggen conditions to afford **52**. This was transformed into the benzyl ester of the nucleoside portion **53** of polyoxin J in four steps. Coupling of **43** with **53** using the Shioiri procedure gave **54**, deprotection of which provided polyoxin J **55**.[16]

## Synthesis of natural products starting from L-quebrachitol

### *Bengamide A, B and E*

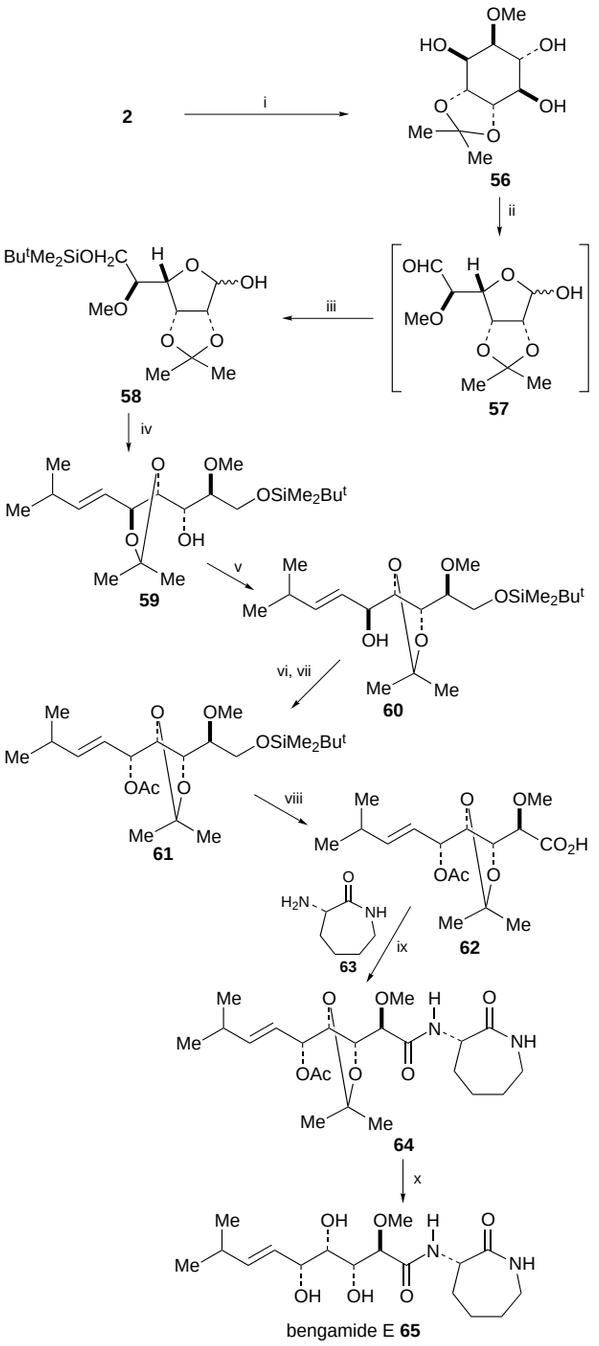
L-Quebrachitol **2** is optically active and has a convenient configuration for the selective protection of hydroxy groups. Compounds derived from **2** by cleavage of the cyclohexane ring are expected to be versatile and useful chiral building blocks for the synthesis of a variety of natural products. A short synthesis of L-mannitol from **2** reported by Angyal and Hoskinson[17] in 1963 revealed the effectiveness of this approach. We applied this approach to the total synthesis of the bengamides,[18,19] which are novel amino acid derivatives with anti-infectious disease activity isolated from marine organisms.

Periodate oxidation of mono-*O*-isopropylidene derivative **56**[20] of L-quebrachitol gave dialdofuranose derivative **57** (Scheme 7). Spontaneous furanose ring formation allowed us to distinguish the two formyl carbons generated by the oxidation. Treatment of **57** with $NaBH_4$ followed by silyl ether formation provided furanose **58**, which was subjected to Wittig olefination to give *E*-alkene **59** as the major product. In this reaction, the combination of base (BuLi) and solvent (benzene) was found to be essential for the selective formation of the *E*-alkene. Mild acid treatment of **59** caused the migration of acetonide group and the partial removal of the $SiMe_2Bu^t$ group. After resilylation, the C-5 hydroxy group in **60** was inverted by an oxidation-reduction procedure followed by *O*-acetylation to give **61**. Oxidation of the primary hydroxy group gave carboxylic acid **62**, which was condensed with cyclo-L-lysine **63** under the conditions of Shioiri to afford **64**. Deprotection of **64** provided bengamide E **65**. This first total synthesis fully confirmed the proposed structure of bengamide E.[18]

The novel hydroxylated caprolactams **68** and **69** found in bengamide A and B, respectively, were initially synthesized from L-glutamic acid[19*a*] in non-stereoselective manner, and later from L-quebrachitol stereoselectively using Pd-catalysed regio- and stereo-selective azidation of conduritol derivative **66** as the key reaction[19*b*] (Scheme 8). Similar condensation of the caprolactams **68** and **69** with **62** gave **70** and **71**, respectively. Selective acylation of **70** and **71** with myristic acid, (tetradecanoic acid), followed by deprotection, furnished the total synthesis of bengamide A **72**[19*a*] and B **73**.[19*b*]

### *Oudemansin X*

If one can introduce carbon substituents into cyclitol rings stereoselectively, the usefulness of cyclitols as chiral building blocks would be further extended. We pursued this idea, which culminated in the total synthesis of the novel antifungal antibiotic oudemansin X **86** (Scheme 9).[21] Peterson olefination of ketone **74**[20] derived from **2** in two steps, gave *exo*-alkene **75**. Removal of the *trans*-*O*-isopropylidene group gave **76**, whose hydrogenation afforded **77** exclusively. The bicyclic structure in **76** completely controlled the reaction face. Periodate oxidation of **77**, followed by reduction and benzoylation, provided **78**, which was converted into another diol **79**. Glycol cleavage of **79** followed by $NaBH_4$ treatment gave four-carbon unit **80**. After one-carbon homologation by introduction of a cyano group, the benzoyl group was deprotected and the resulting alcohol was oxidized to give aldehyde **83**. Wittig olefination and subsequent isomerization of the double bond, or Takai reaction (formation of *E*-vinyl iodide) followed by Pd-catalysed cross-coupling reaction of **83**, provided the β-styryl compound **84**. The nitrile group in **84** was converted into a methoxycarbonyl group to give **85**, whose lithium ester enolate was trapped with methyl formate; *O*-methylation with dimethyl sulfate completed the first total synthesis of oudemansin X **85**.[21]




**Scheme 7** *Reagents and conditions*: i, 2,2-dimethoxypropane, TsOH, DMF; ii, $NaIO_4$, $Me_2CO$–$H_2O$ (5:1), 0 °C; iii, $NaBH_4$, MeOH, 0 °C, then $Bu^tMe_2SiCl$, $Et_3N$, DMAP, $CH_2Cl_2$, room temp.; iv, $Me_2CHCH_2P^+Ph_3Br^-$, BuLi, $C_6H_6$, room temp.; v, TsOH (5 mol%), MeCN, 0 °C then $Bu^tMe_2SiCl$, $Et_3N$, DMAP, $CH_2Cl_2$; vi, $MnO_2$, $CH_2Cl_2$, room temp., then $Zn(BH)_4$, $Et_2O$–PhMe, −78–0 °C; vii, $Ac_2O$, pyridine, room temp.; viii, $Bu_4NF$, AcOH, THF, then $CrO_3$ in dil. $H_2SO_4$, $Me_2CO$, 0 °C; ix, **63**, $(EtO)_2P(O)CN$, $Et_3N$, DMF; x, MeONa, MeOH, then $CF_3CO_2H$–THF–$H_2O$.

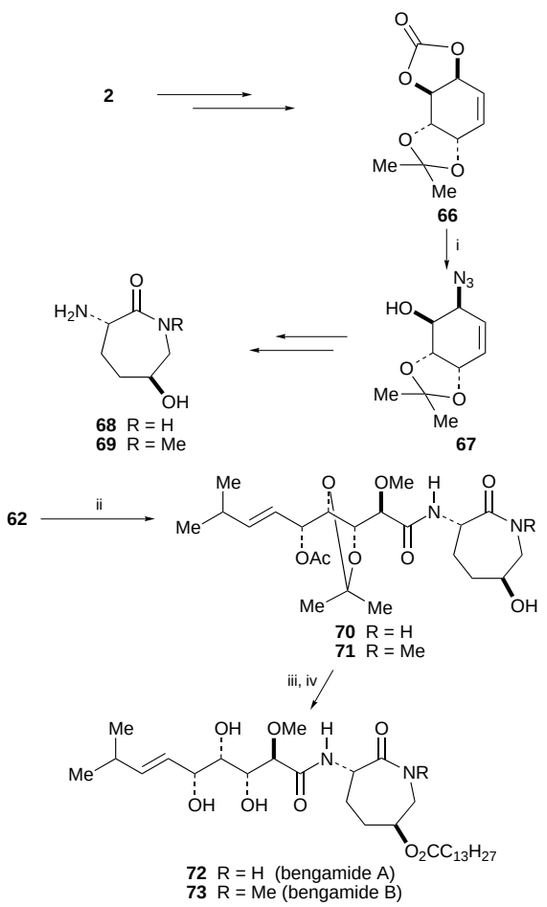
## Other related work

As discussed above, cyclitols, by their regioselective ring cleavage, have now become useful chiral building blocks for the preparation of acyclic and heterocyclic natural products. Successful implementation of this strategy by our group has given: D- and L-galactose derivatives,[6b] L-mannose, L-talo and L-guluronate derivatives,[22] (−)-isoavenaciolide,[23] (−)-ethisolide,[23b] (+)-galactostatin,[24] (+)-1-deoxygalactostatin,[24] restricticin[25] (from L-quebrachitol) and lincosamine[26] (from *myo*-inositol).

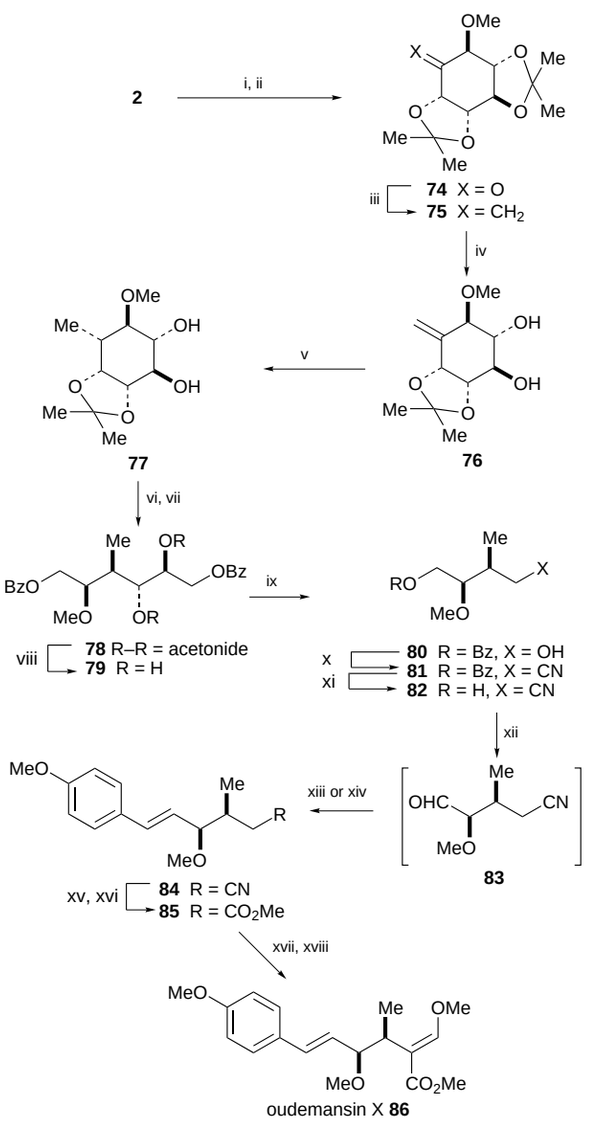
Since L-quebrachitol is an optically active polyhydroxy cyclohexane derivative, transformation of L-quebrachitol into natural or unnatural products having polyfunctional cyclohexane structures is also important work. Such approaches include syntheses of: aminocyclitols by Ogawa and co-workers,[27] carba-sugar derivatives by Paulsen *et al.*[28] (−)-ovalicine by Bath *et al.*[29] cyclophellitol by Akiyama and co-workers,[30] inositol phosphate derivatives by Kozikowski and co-workers,[31] Akiyama and co-workers[32] and Potter and co-workers,[33] and simmondsin by Chida and co-workers.[34] Utilization of L-quebrachitol as a chiral auxiliary in asymmetric synthesis is reported by Akiyama and co-workers.[35] Other applications of L-quebrachitol in the preparation of bioactive compounds are found in the recent excellent review by Kiddle.[36]

## Conclusions

We have shown that cyclitols are versatile chiral building blocks in natural product synthesis. The cyclic structure of cyclitols allowed us to introduce a variety of functionalities regio- and stereo-selectively on the cyclohexane ring. By subsequent cleavage of the cyclohexane ring at a chosen position, cyclitols serve as useful precursors for acyclic and heterocyclic natural products. The regioselective Baeyer–Villiger reaction can be used for the successful implementation of such approaches. As *myo*-inositol and L-quebrachitol are readily available in large quantities from plants, they are expected to be used widely as a chiral building block for the synthesis of structurally complex natural or non-natural products, and are also expected to be employed as raw materials for the preparation of non-carbohydrate products in the chemical industry.




**Scheme 8** *Reagents and conditions*: i, $NaN_3$, $Pd(PPh_3)_4$ (3 mol%), THF–$H_2O$ (5 : 1), room temp.; ii, **68** or **69**, $(EtO)_2P(O)CN$, $Et_3N$, DMF; iii, MeONa, MeOH, then $C_{13}H_{27}CO_2H$, 1-(3-dimethylaminopropyl)-3-ethylcarbodiimide hydrochloride, DMAP, $CH_2Cl_2$–THF, −50 to −15 °C; iv, MeONa, MeOH, then $CF_3CO_2H$–THF–$H_2O$.




**Scheme 9** *Reagents and conditions*: i, 2,2-dimethoxypropane, TsOH, DMF; ii, $RuO_2$, $NaIO_4$, $CHCl_3$, room temp.; iii, $Me_3SiCH_2MgCl$, THF, then KH, THF, room temp.; iv, TsOH, MeOH, 0 °C; v, $H_2$, Raney-Ni (W-4), EtOH, room temp.; vi, $NaIO_4$, $NaHCO_3$, $Me_2CO$–$H_2O$, 0 °C, then $NaBH_4$, MeOH, 0 °C; vii, BzCl, pyridine, viii, AcOH–$H_2O$ (4 : 1), 70 °C; ix, $NaIO_4$, $NaHCO_3$, $Me_2CO$–$H_2O$, 0 °C then $NaBH_4$, MeOH, 0 °C; x, $MeSO_2Cl$, pyridine, then NaCN, DMF, 50 °C; xi, MeONa, MeOH, 0 °C; xii, pyridinium chlorochromate, $CH_2Cl_2$; xiii, $Ph_3P^+CH_2C_6H_4(p\text{-OMe})Cl^-$, BuLi, THF, 0 °C then PhSH, AlBN, $C_6H_6$, reflux; xiv, $CHI_3$, $CrCl_2$, DMF–THF, room temp., then $(p\text{-OMe})C_6H_4MgBr$, $Pd(PPh_3)_4$ (5 mol%), $C_6H_6$, room temp.; xv, DIBAL-H, $CH_2Cl_2$, acidic (aq. $H_2SO_4$) work up; xvi, $NaClO_2$, $NH_2SO_3H$, $NaH_2PO_4$, Bu$^t$OH–$H_2O$, room temp., then $CH_2N_2$, $Et_2O$–$CH_2Cl_2$; xvii, $(Me_3Si)_2NLi$, THF, −78 to −40 °C, then $HCO_2Me$; xviii, $(MeO)_2SO_2$, $K_2CO_3$, $Me_2CO$, room temp.

**Acknowledgement**

We thank Yokohama Rubber Co. Ltd. (Tokyo, Japan), for a generous gift of L-quebrachitol. We also thank Yamakawa Chemical Industry Co. Ltd. (Tokyo), for donation of (*S*)-(+)-α-(acetoxy)phenylacetic acid. Financial support from the Japan Science Society, Ministry of Education, Science and Culture of Japan, and the Moritani Scholarship Foundation is gratefully acknowledged.

**Noritaka Chida was born in Sendai, Japan, in 1956. He received his PhD in 1983 from Tohoku University under the supervision of Professor Akira Yoshikoshi. From 1983 to 1986 he worked for Mercian Co. Ltd. as a researcher in the chemistry division. In 1986, he joined the Department of Applied Chemistry, Keio University, where he is now Associate Professor. In 1987–1988 he held a postdoctoral position with Professor Amos B. Smith, III, at the University of Pennsylvania. His research interests include the total synthesis of biologically important and structurally interesting natural products, and the development of novel and efficient chemical reactions.**

**Seiichiro Ogawa is now working on the synthesis of biologically active sugar mimics composed by cyclitols and carba-sugars. After obtaining his PhD in 1967 from Keio University, he joined the Faculty of Engineering, Keio University, and is currently Professor of Chemistry. He attended the University of Illinois as a postdoctoral researcher in 1967, and, seven years later he received the Alexander von Humboldt Fellowship and worked at Technische Hochschule, Darmstadt.**

## Footnotes

† E-mail: chida@applc.keio.ac.jp

‡ *myo*-Inositol is produced in large quantities as a food ingredient and can be purchased (*ca*. $100 per 1 kg) from most reagent suppliers.

§ L-Quebrachitol is now commercially available from MYFEC SDN, BHD, 76100 Durian Tunggal, Melaka, Malaysia.

## References

1 A. Fischli, in *Modern Synthetic Methods*, ed. R. Scheffold, Verlag Sauerländer, Frankfurt, 1980. p. 269; K. Drauz, A. Kleeman and J. Martens, *Angew. Chem., Int. Ed. Engl.*, 1982, **21**, 584.
2 K. Mori, in *The Total Synthesis of Natural Products*, ed. J. ApSimon, Wiley, New York, 1981, p. 1; T.-L. Ho, *Enantioselective Synthesis*, Wiley, New York, 1992.
3 J. W. Scott, in *Asymmetric Synthesis*, ed. J. D. Morrison and J. W. Scott, Academic Press, Florida, 1984, vol. 4, p. 1.
4 S. Hanessian, *Total Synthesis of Natural Products: The 'Chiron' Approach*, Pergamon Press, Oxford, 1983; B. Fraser-Reid and R. Tsang, in *Strategies and Tactics in Organic Synthesis*, ed. T. Lindberg and D. Barton, Academic Press, San Diego, 1989, vol. 2, p. 123.
5 L. Anderson, in *The Carbohydrates; Chemistry and Biochemistry*, ed. W. Pigman and D. Horton, Academic Press, New York, 1972, vol. 1a, p. 519.
6 (*a*) J. van Alphen, *Ind. Eng. Chem.*, 1951, **43**, 141; (*b*) N. Chida, M. Suzuki, M. Suwama and S. Ogawa, *J. Carbohydr. Chem.*, 1989, **8**, 319.
7 H. Fukami, H.-S. Koh, T. Sakata and M. Nakajima, *Tetrahedron Lett.*, 1967, 4771; 1968, 1701.
8 N. Chida, T. Tobe and S. Ogawa, *Tetrahedron Lett.*, 1994, **35**, 7249.
9 A. S. Cieplak, *J. Am. Chem. Soc.*, 1981, **103**, 4540; A. S. Cieplak, B. D. Tait and C. R. Johnson, *J. Am. Chem. Soc.*, 1989, **111**, 8447.
10 Y. Watanabe, A. Oka, Y. Shimizu and S. Ozaki, *Tetrahedron Lett.*, 1990, **31**, 2613; S. Ozaki, L. Ling, T. Ogasawara, Y. Watanabe and M. Hirata, *Carbohydr. Res.*, 1994, **259**, 307; G. M. Salamonczyk and M. Pietrusiewicz, *Tetrahedron Lett.*, 1994, **35**, 4233.
11 (*a*) V. I. Shvets, B. A. Klyashchitskii, A. E. Stepanov and R. P. Evstigneeva, *Tetrahedron*, 1973, **29**, 331; (*b*) P. J. Garegg, B. Lindberg, I. Kvarnstrom and S. C. T. Svensson, *Carbohydr. Res.*, 1985, **139**, 209; S. Ozaki, Y. Watanabe, T. Ogasawara, Y. Kondo, N. Shiotani, H. Nishii and T. Matsuki, *Tetrahedron Lett.*, 1986, **27**, 3157.
12 S. J. Angyal, M. E. Tate and S. D. Gero, *J. Chem. Soc.*, 1961, 4116; C. Jiang and D. C. Baker, *J. Carbohydr. Chem.*, 1986, **5**, 615.
13 N. Chida, E. Yamada and S. Ogawa, *J. Carbohydr. Chem.*, 1988, **7**, 555.
14 (*a*) N. Chida, Y. Furuno and S. Ogawa, *J. Chem. Soc., Chem. Commun.*, 1989, 1230; (*b*) N. Chida, Y. Furuno, H. Ikemoto and S. Ogawa, *Carbohydr. Res.*, 1992, **237**, 185.
15 N. Chida, H. Ikemoto, A. Noguchi, S. Amano and S. Ogawa, *Nat. Prod. Lett.*, 1995, **6**, 295.
16 N. Chida, K. Koizumi, Y. Kitada, C. Yokoyama and S. Ogawa, *J. Chem. Soc., Chem. Commun.*, 1994, 111.
17 S. J. Angyal and R. M. Hoskinson, *Methods Carbohydr. Chem.*, 1963, **2**, 87.
18 N. Chida, T. Tobe and S. Ogawa, *Tetrahedron Lett.*, 1991, **32**, 1063.
19 (*a*) N. Chida, T. Tobe, S. Okada and S. Ogawa, *J. Chem. Soc., Chem. Commun.*, 1992, 1064; (*b*) N. Chida, T. Tobe, K. Murai, K. Yamazaki and S. Ogawa, *Heterocycles*, 1994, **38**, 2383.
20 H. Paulsen and F. R. Heiker, *Liebigs Ann. Chem.*, 1981, 2180.
21 N. Chida, K. Yamada and S. Ogawa, *Chem. Lett.*, 1992, 687; *J. Chem. Soc., Perkin Trans. 1*, 1993, 1957.
22 N. Chida, K. Yamada, M. Suzuki and S. Ogawa, *J. Carbohydr. Chem.*, 1992, **11**, 137.
23 (*a*) N. Chida, T. Tobe, M. Suwama, M. Ohtsuka and S. Ogawa, *J. Chem. Soc., Chem. Commun*., 1990, 994; (*b*) *J. Chem. Soc. Perkin Trans. 1*, 1992, 2667.
24 N. Chida, T. Tanikawa, T. Tobe and S. Ogawa, *J. Chem. Soc., Chem. Commun.*, 1994, 1247.
25 N. Chida, T. Tobe, M. Yoshinaga, K. Osaka and S. Ogawa, *Carbohydr. Lett.*, 1996, **2**, 47.
26 N. Chida, K. Nakazawa, S. Ninomiya, S. Amano, K. Koizumi, J. Inaba and S. Ogawa, *Carbohydr. Lett.*, 1995, **1**, 335.
27 S. Ogawa and A. Isaka, *Carbohydr. Res.*, 1991, **210**, 105; S. Ogawa, A. Ohdate, K. Ohnishi, T. Tanikawa, H. Kimura and N. Chida, *Carbohydr. Lett.*, 1995, **1**, 255.
28 H. Paulsen, W. van Deyn and W. Röben, *Liebigs Ann. Chem.*, 1984, 433.
29 S. Bath, D. C. Billington, S. D. Gero, B. Quiclet-Sire and M. Samadi, *J. Chem. Soc., Chem. Commun.*, 1994, 1495.
30 T. Akiyama, H. Shima and S. Ozaki, *Synlett*, 1991, 831; T. Akiyama, H. Shima, M. Ohnari, T. Okazaki and S. Ozaki, *Bull. Chem. Soc. Jpn.*, 1993, **66**, 3760.
31 A. P. Kozikowski, J. J. Kiddle, T. Frew, M. Berggren and G. Powis, *J. Med. Chem.*, 1995, **38**, 1053; A. P. Kozikowski, V. I. Ognyanov, A. H. Fauq. S. R. Nahhorski and R. A. Wilcox, *J. Am. Chem. Soc.*, 1993, **115**, 4429 and references cited therein.
32 T. Akiyama, N. Takechi and S. Ozaki, *Tetrahedron Lett.*, 1990, **31**, 1433; T. Akiyama, N. Takechi, S. Ozaki and K. Shiota, *Bull. Chem. Soc. Jpn.*, 1992, **65**, 366.
33 C. Liu, S. R. Nahorski and B. V. L. Potter, *J. Chem. Soc., Chem. Commun.*, 1991, 1014; *Carbohydr. Res.*, 1992, **234**, 107; D. Lampe, C. Liu and B. V. L. Potter, *J. Med. Chem.*, 1994, **37**, 907; C. Liu, J. Al-Hafidh, J. Westwick and B. V. L. Potter, *Bioorg. Med. Chem.*, 1994, **2**, 253.
34 N. Chida, K. Yamada and S. Ogawa, *J. Chem. Soc., Chem. Commun.*, 1991, 588; *J. Chem. Soc., Perkin Trans. 1*, 1992, 1131.
35 T. Akiyama, H. Nishimoto, T. Kuwata and S. Ozaki, *Bull. Chem. Soc. Jpn.*, 1994, **67**, 180; T. Akiyama, K. Ishikawa and S. Ozaki, *Chem. Lett.*, 1994, 627; T. Aakiyama, K. Okada and S. Ozaki, *Tetrahedron Lett.*, 1992, **33**, 5763; T. Akiyama, H. Horiguchi, T. Ida and S. Ozaki, *Chem. Lett.*, 1995, 975 and references cited therein.
36 J. J. Kiddle, *Chem. Rev.*, 1995, **95**, 2189.

*6/03301F*

# Organic electroluminescent devices with Langmuir–Blodgett films of an amphiphilic complex with an 8-hydroxyquinoline as an emitter

**Jianming Ouyang,*[a] Ling Li,[b] Zihou Tai,[b] Zuhong Lu[c] and Guangming Wang[c]**

[a] *Department of Chemistry, Jinan University, Guangzhou, 510632, P.R. China*
[b] *State Key Laboratory of Coordination Chemistry, Coordination Chemistry Institute, Nanjing University, Nanjing, 210093, P.R. China*
[c] *National Laboratory of Molecular and Bioelectronics, Southeast University, Nanjing, 210096, P.R. China*

**Electroluminescent (EL) devices with a single layer structure [indium-tin-oxide/emitting layer (Langmuir–Blodgett films)/Al] are synthesised using an intensely fluorescent amphiphilic complex, bis(*N*-hexadecyl-8-hydroxyquinoline-2-carboxamide)lanthanum [La(HQ)$_2$(H$_2$O)$_4$Cl] as the emitter material; green–yellow electroluminescence is observed with a low drive voltage (9 V).**

Organic electroluminescent (EL) devices have recently received much attention because they can potentially produce emissions of all colours from blue to red in accordance with the wide selection of organic emitting materials, and because of their possible applications as large-area light-emitting displays,[1–7] which are difficult to achieve using inorganic light-emitting cells.

Thin aromatic hydrocarbon films that fluoresce could have practical significance as large area electroluminescent panels if ultra-thin high quality aromatic hydrocarbons films can be constructed.[8,9] Tang *et al.*[1,2] found that the 8-hydroxyquinoline-aluminium (Alq$_3$) complex can be used as an emitting element in EL devices. As an emitting material, Alq$_3$ has excellent properties such as highly stable film formation, high carrier transport and good heat resistance. In the EL diode Tang *et al.* designed, high external quantum efficiency, luminous efficiency and brightness are achievable at a driving voltage below 10 V. Hamada *et al.*[6] have developed other organic EL devices with 8-hydroxyquinoline–metal complexes, such as Znq$_2$, Beq$_2$, Mgq$_2$, Zn(mq)$_2$, Be(mq)$_2$ and Al(prq)$_3$ (mq and prq are 2-methyl-8-hydroxyquinoline and 7-propyl-8-hydroxyquinoline, respectively), as the emitter. The emissions of these devices are green or blue and they have a luminance of more than 3000 cd m$^{-2}$. For example, the EL device with Znq$_2$ has a luminance of 16 200 cd m$^{-2}$, higher than the luminance of Alq$_3$ (15 800 cd m$^{-2}$). There is no report of Langmuir–Blodgett (LB) films of 8-hydroxyquinoline complexes being used as an emitting layer. LB film techniques make it possible to prepare organic functional ultra-thin films with a controlled thickness at a molecular size and well-defined molecular orientation,[10,11] and the long chain 8-hydroxyquinoline complexes have strong fluorescence at room temperature.[12,13] Therefore, if these amphiphilic 8-hydroxyquinoline derivatives complexes can be incorporated in LB films, these films will be of higher quality than the general vacuum deposited films and may have potential applications in molecular electronic devices.[12]

The synthesis of the amphiphilic ligand, *N*-hexadecyl-8-hydroxyquinoline-2-carboxamide (HHQ) and its lanthanum complex, La(HQ)$_2$(H$_2$O)$_4$Cl, which has high fluorescence efficiency,[12] were carried out by a previously reported method.[12,14] The molecular structure of La(HQ)$_2$(H$_2$O)$_4$Cl is shown in Fig. 1. The EL device has a single layer structure: ITO/emitting layer (9- or 19-layer LB films)/Al, as shown in Fig. 1. The substrate is an indium-tin-oxide (ITO) coated glass with a sheet resistance of about 20 Ω/□, and it was cleaned by the known standard procedure.[15] The LB films of the La(HQ)$_2$(H$_2$O)$_4$Cl amphiphilic complex (the emitting layer) were prepared by a conventional LB technique. The amphiphilic complex was spread from a chloroform solution on a subphase of Millipore-filtered water. The transfer was performed at 0.025 N m$^{-1}$ with a dipping speed of 3 mm min$^{-1}$. After the various LB films were made aluminium to a thickness of 300 nm was deposited at 10$^{-5}$ Torr onto the LB film surface as the top electrode with a deposition rate of 1.0 nm s$^{-1}$. The emitting area was 2 × 3 mm$^2$. The luminance of the EL devices was measured with a luminance meter. All measurements were carried out at room temperature in air under DC bias conditions.

Fig. 2 shows the relationship of current density and voltage of the EL devices with 9- and 19-layer LB films. The shapes of the curves are strongly dependent on the thickness of the LB films of La(HQ)$_2$(H$_2$O)$_4$Cl (luminance layer). The driving voltage increases with increasing LB film layer. The driving voltage for

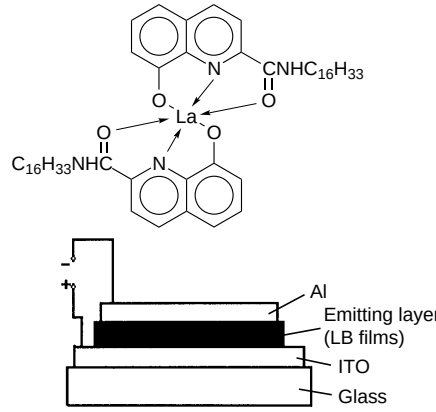



**Fig. 1** Configuration of the EL cells and the molecular structure of the material used in this study

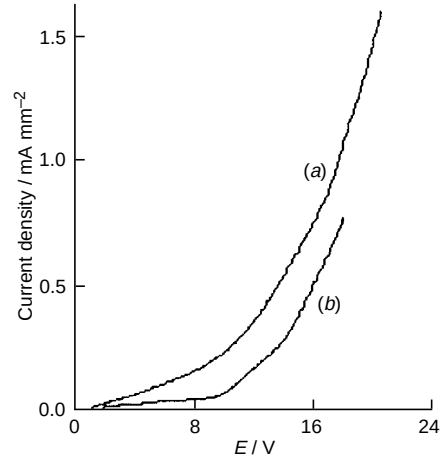



**Fig. 2** The relationship of current density and voltage of the EL cell with the emitter of the La(HQ)$_2$(H$_2$O)$_4$Cl LB films: (*a*) 9-layer, (*b*) 19-layer

the cell with 19-layer LB films was 9 V. At a given voltage, the current density for the EL cell with a thinner LB film emitter is higher than that for the thicker one. The curves can be fitted to an injection-limited model where the electron current is limited by electron emission from the cathode into the $La(HQ)_2(H_2O)_4Cl$ LB film layer.

The luminance–current density characteristics of the EL cell with the emitter of the 19-layer $La(HQ)_2(H_2O)_4Cl$ LB films are shown in Fig. 3. Green–yellow emission with a luminance of about 330 pw was achieved which was enhanced with the injection current elevation in the region of 0.1–1.00 mA $mm^{-2}$.

Comparison of the EL emission spectrum of the cell with the PL spectrum of 19-layer $La(HQ)_2(H_2O)_4Cl$ LB films[12] showed that the spectrum does not change greatly. The PL and EL peak wavelengths and the half values of these two spectra are 520, 515 and 170, 200 nm, respectively. The EL emission spectrum is independent of the driving voltage and current. This result indicated that the radiative recombination of injected electrons and holes takes place in the $La(HQ)_2(H_2O)_4Cl$ LB films.[1]

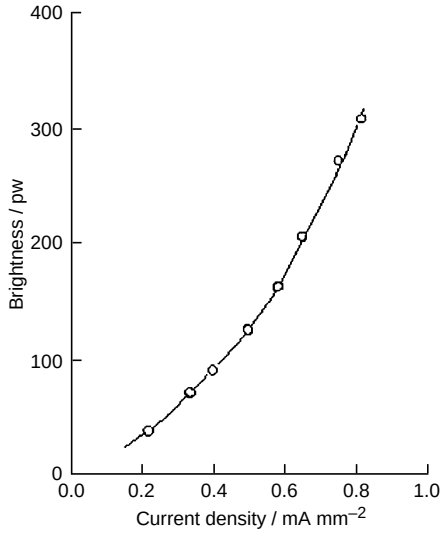



**Fig. 3** The relationship of brightness and current density of the EL cell with the emitter of the 19-layer $La(HQ)_2(H_2O)_4Cl$ LB film

This research was supported by a grant from the National Natural Science Foundation of China.

## References

1 C. W. Tang and S. A. Van Slyke, *Appl. Phys. Lett.*, 1987, **51**, 913.
2 C. W. Tang, S. A. Van Slyke and C. H. Chen, *J. Appl. Phys.*, 1989, **65**, 3610.
3 J. Kido, K. Nagai, Y. Okamoto and T. Skotheim, *Appl. Phys. Lett.*, 1991, **59**, 2760.
4 C. Adachi, S. Tokito, T. Tsutsui and S. Saito, *Jpn. J. Appl. Phys.*, 1988, **27**, L713.
5 J. H. Burroughes, D. D. C. Bradley and A. R. Brown, *Nature*, 1990, **347**, 539.
6 Y. Hamada, T. Sano, M. Fujita, T. Fujii, Y. Nishio and K. Shibata, *Jpn. J. Appl. Phys.*, 1993, **32**, L514.
7 P. L. Burn, A. B. Holmes and A. Kraft, *Nature* (*London*), 1992, **356**, 47.
8 J. Dresner, *RCA Review*, 1969, **30**, 322.
9 J. Dresner and A. M. Goodman, *Proc. IEEE*, 1970, **58**, 1868.
10 F. L. Carter, *Molecular Electronic Devices I*, Dekker, New York, 1982.
11 M. Schmelzer, S. Roth and C. P. Niesert, *Thin Solid Films*, 1993, **235**, 210.
12 J. Ouyang, Z. Tai and W. Tang, *J. Mater. Chem.*, 1996, **6**, 963.
13 Details in fluorescence of the complexes of HHQ will be reported elsewhere.
14 J. Ouyang, Z. Tai, C. Jiang and W. Tang, *Spectroscopy Lett.*, 1996, **29**, 763.
15 G. Wang, C. Yuan, H. Wu and Y. Wei, *Jpn. J. Appl. Phys.*, 1995, **34**, L182.

*Received, 31st January 1997; Com. 7/00742F*

# Fully selective intramolecular *ortho* photocycloaddition of 4-(4-methoxyphenoxy)-3-($N^3$-benzoylthymin-1-yl)but-1-ene: an unprecedented benzene–thymine photocycloaddition

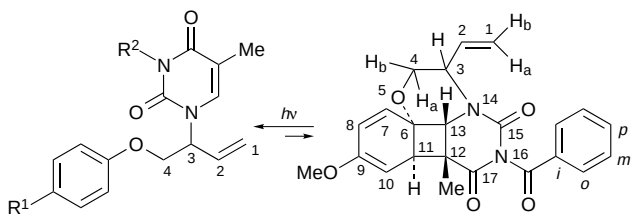
**Wim Saeyens,[a] Roger Busson,[b] Johan Van der Eycken,[c] Piet Herdewijn[a] and Denis De Keukeleire*[a]†**

[a] *Universiteit Gent, Faculty of Pharmaceutical Sciences, Harelbekestraat 72, B-9000 Gent, Belgium*
[b] *Katholieke Universiteit Leuven, Rega Institute, Minderbroedersstraat 10, B-3000 Leuven, Belgium*
[c] *Universiteit Gent, Department of Organic Chemistry, Krijgslaan 281 S4, B-9000 Gent, Belgium*

**On irradiation of 4-(4-methoxyphenoxy)-3-($N^3$-benzoylthymin-1-yl)but-1-ene 1 at 254 nm in THF a single photoadduct 2 is formed as a result of chemo-, regio- and stereo-selective intramolecular *ortho* photocycloaddition of the thymine double bond to the 1,2-positions of the phenyl ring.**

Covalent modification of DNA may occur by photochemical activation of complexes between intercalating drugs and DNA, and between proteins and DNA. 4-(4-Methoxyphenoxy)-3-($N^3$-benzoylthymin-1-yl)but-1-ene **1** can be considered as a model structure to study this cross-linking reaction. Compound **1** represents an arene–alkene bichromophore separated by a tether of three atoms. Intra- as well as inter-molecular photocycloadditions in such compounds are well documented.[1] Both *ortho* and *meta* photocycloadditions of the alkene to the arene have been observed, while the preferred reaction mode depends on subtle stereoelectronic effects. It was shown that the presence of a methoxy group in an *ortho* position favours attack of the alkene at the 1,2-positions.[2] On the other hand, 4-phenoxybut-1-enes undergo mainly 2,6-*meta* photocycloaddition.[2] Furthermore, introduction of a group allylic to the alkene has a major influence on the reaction outcome.[3] We were interested in examining the photocycloaddition of 4-(4-methoxyphenoxy)-3-($N^3$-benzoylthymin-1-yl)but-1-ene **1**, in which these features are combined. Moreover, this compound allowed us to study the competition between the alkene and the 5,6-double bond of the thymine ring in the photocycloaddition reaction. Additionally, we investigated the photoreactivity of compounds **3**–**5** as analogues of **1**.

Trichromophore **1**‡ was synthesized by reaction of 4-methoxyphenol with butadiene monoxide in $Me_2SO$ in the presence of KOH,§ followed by coupling of the resulting 3-hydroxy-4-(4-methoxyphenoxy)but-1-ene (57%) with $N^3$-benzoylthymine under Mitsunobu conditions (40%).[4] Irradiation of **1** in THF (50 mg in 20 ml, 254 nm, 20 min) yielded a single photoproduct **2** (23%) in addition to unchanged starting material. Increasing the reaction time (up to 90 min) did not appreciably change the ratio of **1** to **2** before formation of degradation products started. Photoadduct **2** was isolated by preparative HPLC on silica using ethyl acetate–hexane (3:7) as eluent. Irradiation (1 h) of **2** under conditions identical to those used for **1** afforded a mixture of **1** and **2** in approximately the same ratio as observed for the forward reaction.




**1** $R^1$ = OMe; $R^2$ = Bz
**3** $R^1$ = H; $R^2$ = Bz
**4** $R^1$ = OMe, $R^2$ = H
**5** $R^1$ = H; $R^2$ = H

**2**

The structure of **2**‡ (arbitrary numbering) was fully elucidated by $^1$H and $^{13}$C NMR. Analysis of the $^{13}$C NMR data clearly revealed eight instead of four signals for aliphatic carbons, in addition to the five benzoyl peaks and eight other $sp^2$-carbon signals. From a DEPT spectrum the presence of an intact vinyl group was inferred (a methylene $sp^2$-carbon at δ 118.71 and a methine $sp^2$-carbon at δ 131.64), together with two carbonyls (δ 169.38 and 150.51), an oxygenated non-protonated carbon (δ 155.48) and three methine $sp^2$-carbons at δ 129.35, 124.90 and 87.81. The two typical C-5 and C-6 thymine $sp^2$-resonances were absent. Apparently, chemoselective *ortho*-photocycloaddition of the thymine double bond at the 1,2-positions of the phenyl group had taken place leaving the vinyl group unaltered. Although [2 + 2] photocycloadducts of thymine and its derivatives are well known,[5] the type of arene–alkene photocycloaddition observed in this study is to our knowledge unprecedented.

The structure‡ of this photocycloadduct was further confirmed by a complete analysis of the $^1$H NMR spectrum *via* COSY and HETCOR experiments. The stereochemical relationships were derived from NOE experiments. The *cis* configuration of the methyl group and the methine proton (H-13), originally being H-6 of thymine, was established, as well as the *trans* relationship between the methyl group and the methine proton (H-11) originally at the *ortho* position of the alkoxy chain. Obviously, the rings annelated to the cyclobutane moiety are in the *cis–anti–cis* configuration. The [2 + 2] photocycloaddition is indeed expected to occur in the *cis* mode,[6] while the steric requirements are accomodated by the less constrained *anti* configuration. The stereochemistry at the remaining chiral centre (C-3) can be deduced on account of the conformational features of the 1-aza-4-oxacyclohexane ring. The proton is in a pseudo-axial position (*S*-configuration in structure **2**) as ascertained by the magnitude of the coupling constants with the vicinal H-4 protons (9.4 and 8.0 Hz) and by the observation of a NOE enhancement between H-3 and H-4b and not with H-4a. The existence of a NOE between the *ortho* hydrogen of the benzoyl group and H-11, and between the methyl group and H-8 and H-10, supports the stereochemical assignment.

The exclusive formation of photocycloadduct **2** can be rationalized in terms of the control elements present in **1**. The *ortho* photocycloaddition is accounted for by the presence of the *para*-methoxy group, which should exhibit similar electronic behaviour to an *ortho*-methoxy group.[2] A similar preference for the *ortho* reaction was also noted for 3-acetoxy-4-(4-methylphenoxy)but-1-ene.[7] On the other hand, the more pronounced polarization of the thymine double bond in comparison with the vinyl group would preferably lead to *ortho* addition, as this reaction mode predominates when the ionization potentials of the reacting entities differ to a certain extent.[8] Dimerization

usually encountered in thymine derivatives is prevented by carrying out the reaction in dilute medium and also by the efficiency of the intramolecular photocycloaddition.

Interestingly, independent irradiation of $N^3$-benzoylthymine and 4-phenoxy-3-($N^3$-benzoylthymin-1-yl)but-1-ene **3**, under the same conditions as described, resulted in complete substrate consumption yielding mainly polar constituents, in which loss of the benzoyl group was evident from the NMR data. Analogous thymine-unprotected compounds, such as 4-(4-methoxyphenoxy)-3-(thymin-1-yl)but-1-ene **4** and 4-phenoxy-3-(thymin-1-yl)but-1-ene **5**, proved to be light-stable, even after prolonged irradiation (24 h). It is, therefore, deduced that the presence of both the *para*-methoxy and the $N^3$-benzoyl groups is required in order to direct the intramolecular arene–alkene photocycloaddition thereby showing the sensitivity of this reaction to subtle and unexpected substituent effects. The *para*-methoxy group apparently creates suitable electronic conditions for *ortho* addition, while it remains to be clarified whether the benzoyl group activates or the secondary amide inhibits photocycloaddition.

In most instances, the *ortho* adducts, resulting from intramolecular arene–alkene photocycloaddition, suffer from further reactions depending on the varying stabilities of the particular compounds formed in the cascade. The bicyclo[4.2.0]octa-2,4-diene unit, present in such *ortho* photoadducts, normally rearranges on heating into a cyclooctatriene, which subsequently gives a mixture of [2 + 2] photocycloadducts. Only occasionally have primary *ortho* photoadducts been isolated as stable compounds, as was found on irradiation of pentafluorophenylprop-2-enyl ether,[9] 2-methyl-6-(4-fluorophenyl)-hex-2-ene[10] and 1-(2-methoxybenzyloxy)-3-methylbut-2-ene.[11] In the present case, after heating **2** in refluxing THF for several hours we were not able to detect cyclooctatriene-like structures, nor was there any evidence for a Diels–Alder-type reaction between the alkene and the cyclohexa-1,3-diene units present in **2**.

In conclusion, we have observed the intriguing photoreactivity of trichromophore **1** since a single, stable *ortho* photoadduct **2** arose under full chemo-, regio- and stereo-selective control. This unprecedented reaction may imply potential cross coupling of pyrimidine bases in nucleic acids with aromatic amino acids in proteins or with intercalating drugs by virtue of a [2 + 2] photocycloaddition, thereby inducing DNA alterations which may interfere with biological function. Hitherto, it was known that amino acids could photochemically add across the double bond of pyrimidine bases,[12] but results obtained for the present model system may shed light on yet different photochemical nucleic acids–protein and/or nucleic acids–drug interactions.

Financial support by the Special Research Fund of the University of Gent (project number 01109394) to D. D. K is gratefully acknowledged.

## Footnotes

† E-mail: Denis.DeKeukeleire@rug.ac.be

‡ Satisfactory spectral data for compounds **1** and **2** were obtained that were consistent with the assigned structures and satisfactory elemental analyses or high-resolution mass spectra were obtained. Data for **1**: mp 121.5–122 °C. $R_f$ (hexane–ethyl acetate, 7 : 3): 0.24. ν (KBr)/cm$^{-1}$ 1753, 1702, 1656, 1509, 1231. $\lambda_{max}$/nm (MeOH) (ε): 206 (26 500), 226 (16 000), 254 (18 600), 274 (11 100). $\delta_H$ (360 MHz, $CDCl_3$) 1.96 (3 H, s, T-Me) 3.78 (3 H, s, OMe), 4.24 (1 H, dd, 10.3 and 4.1 Hz, H-4a), 4.30 (1 H, dd, 10.3 and 5.6 Hz, H- 4b), 5.42 (1 H, m, H-3), 5.47 (1 H, dd app. d, 17.4 Hz, H-1a), 5.52 (1 H, dd app. d, 10.8 Hz, H-1b), 6.07 (1 H, ddd, 17.3, 10.7 and 5.7 Hz, H-2), 6.85 (4 H, s, Ar), 7.35 (1 H, s, T-6), 7.47 (2 H, t, 7.8 Hz, Bz), 7.64 (1 H, t, 7.4 Hz, Bz), 7.90 (2 H, dd app. d, 7.8 Hz, Bz). $\delta_C$ (360 MHz, $CDCl_3$): 12.46 (T-Me), 55.62 (OMe), 55.83 (C-3), 68.48 (C-4), 110.34 (T-5), 114.74 (Ar-*o*), 115.70 (Ar-*m*), 120.89 (C-1), 128.98 (Bz-*m*), 130.31 (Bz-*o*), 131.56 (C-2), 131.63 (Bz-*i*), 134.78 (Bz-*p*), 138.19 (T-6), 149.96, 152.00 (Ar-*i* and -*p*), 154.51 (T-2), 162.60 (T-4), 168.80 (Bz-CO). MS: 407 ($M^{+\cdot}$ + $H^+$; 10), 105 (100). For **2**: mp 173.7 °C. $R_f$ (pentane–ethyl acetate, 6 : 4): 0.53. ν (KBr)/cm$^{-1}$ 1743, 1700, 1673, 1437, 1232, 897, 796, 730. $\lambda_{max}$/nm (MeOH) (ε): 206 (21 500), 250 (16 800), 284 (3900). $\delta_H$ (Gemini 200 MHz, $CDCl_3$) 1.39 (3 H, s, $Me^{12}$), 3.53 (1 H, dd, −12.3 and 9.4 Hz, H-4a), 3.60 (3 H, s, OMe), 3.65 (1 H, d, 1.2 Hz, H-13), 4.01 (1 H, br d, *J* 6.9 Hz, H-11), 4.03 (1 H, dd, −12.2 and 8.0 Hz, H-4b), 4.58 (1 H, br d, 6.8 Hz, H-10), 5.03 [1 H, qt, 8 Hz (3 ×), H-3], 5.32 (1 H, dt, 10.3 and −1.3 Hz, H-1a), 5.34 (1 H, dt, 17.3 and −1.3 Hz, H-1b), 5.75 (1 H, ddd, 17.3, 10.3 and 5.6 Hz, H-2), 6.07 (1 H, dt, 10.3 and 1.3 Hz, H-7); 6.15 (1 H, dd, 10.1 and 1.9 Hz, H-8), 7.50 (2 H, tm, 7.4 Hz, Bz-*o*), 7.64 (1 H, tt, 7.3 and 1.4 Hz, Bz-*p*), 7.94 (2 H, dm, 7.1 Hz, Bz-*m*). $\delta_C$ (Gemini 200 MHz, $CDCl_3$) 16.84 ($Me^{12}$), 40.24 (C-12), 47.72 (C-11), 51.58 (C-3), 54.84 (OMe), 56.56 (C-13), 62.41 (C-4), 70.00 (C-6), 87.81 (C-10), 118.71 (C-1), 124.90 (C-7), 129.04 (Bz-*m*), 129.35 (C-8), 130.12 (Bz-*o*), 131.64 (C-2), 132.59 (Bz-*i*), 134.62 (Bz-*p*), 150.51 (C-15), 155.48 (C-9), 169.38 (C-17), 170.57 (Bz-CO). MS: 407 ($M^{+\cdot}$ + $H^+$; 5); 105 (100).

§ Cleavage of epoxides usually requires attack by reactive nucleophiles as described by Posner and Rogers (*J. Am. Chem. Soc.*, 1977, **99**, 8208). We were able to effect the reaction using 4-methoxyphenolate in $Me_2SO$ (57%). In the absence of the activating *para*-methoxy group the yield is significantly decreased (20%).

## References

1 J. Cornelisse, *Chem. Rev.*, 1993, **93**, 615.
2 D. De Keukeleire, S.-L. He, D. Blakemore and A. Gilbert, *J. Photochem. Photobiol. A: Chem.*, 1994, **80**, 233.
3 D. De Keukeleire, S.-L. He and C.-Y. Wang, University of Gent, Faculty of Pharmaceutical Sciences, unpublished results.
4 O. Mitsunobu, *Synthesis*, 1981, 1.
5 A. A. Lamola, *Photochem. Photobiol.*, 1968, **7**, 619; *Pure Appl. Chem.*, 1970, **24**, 599; G. J. Fisher and H. E. Johns, *Photochemistry and Photobiology of Nucleic Acids*, ed. S. Y. Wang, Academic Press, New York, 1976, vol. 1, p. 226.
6 W. Oppolzer and T. Godel, *J. Am. Chem. Soc.*, 1978, **100**, 2583; *Helv. Chim. Acta*, 1984, **67**, 1154; T. Umehara, Y. Inouye and H. Kakisawa, *Bull. Chem. Soc. Jpn.*, 1981, **54**, 3492; H. Seto, S. Tsunoda, H. Ikeda, Y. Fujimoto, T. Tatsuno and H. Yoshioka, *Chem. Pharm. Bull.*, 1985, **33**, 2594; J. D. Winkler, J. P. Hey and F. J. Hannon, *Heterocycles*, 1986, **25**, 55.
7 W. Saeyens, P. Herdewijn and D. De Keukeleire, University of Gent, Faculty of Pharmaceutical Sciences, unpublished results.
8 D. Bryce-Smith, A. Gilbert, B. Orger and H. M. Tyrrell, *J. Chem. Soc., Chem. Commun.*, 1974, 334.
9 B. Sket, N. Zupancic and M. Zupan, *Tetrahedron*, 1986, **42**, 753.
10 H. A. Neijenesch, R. J. P. J. de Ruiter, E. J. Ridderikhoff, J. O. van den Ende, L. J. Laarhoven, L. J. W. van Putten and J. Cornelisse, *J. Photochem. Photobiol. A: Chem.*, 1991, **60**, 325.
11 D. C. Blakemore and A. Gilbert, *J. Chem. Soc., Perkin Trans. 1*, 1992, **18**, 2265.
12 M. D. Shetlar, J. Christensen and K. Hom, *Photochem. Photobiol.*, 1984, **39**, 125.

*Received, 23rd January 1997; Com. 7/00554G*

# New chemistry of porphyrin β-ketoesters: synthesis of a novel covalently-linked dimer

**Robert T. Holmes, Jack J. Lin, Richard G. Khoury, Colin P. Jones and Kevin M. Smith*†**

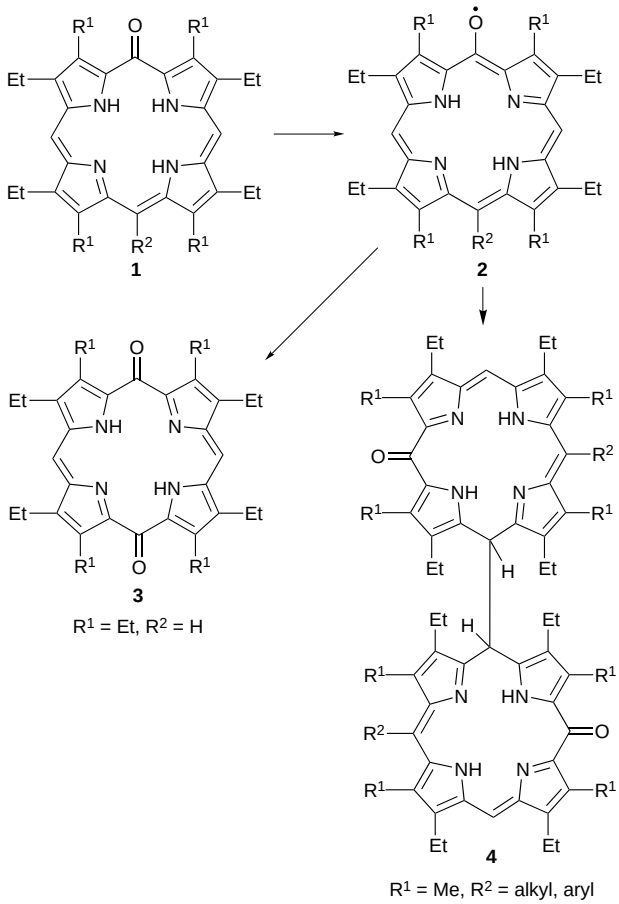
*Department of Chemistry, University of California, Davis, CA 95616, USA*

**Porphyrinyl β-ketoesters dimerize to afford novel bistetrapyrrole systems by way of a radical process; the X-ray structure of one such bistetrapyrrole 14 is reported.**

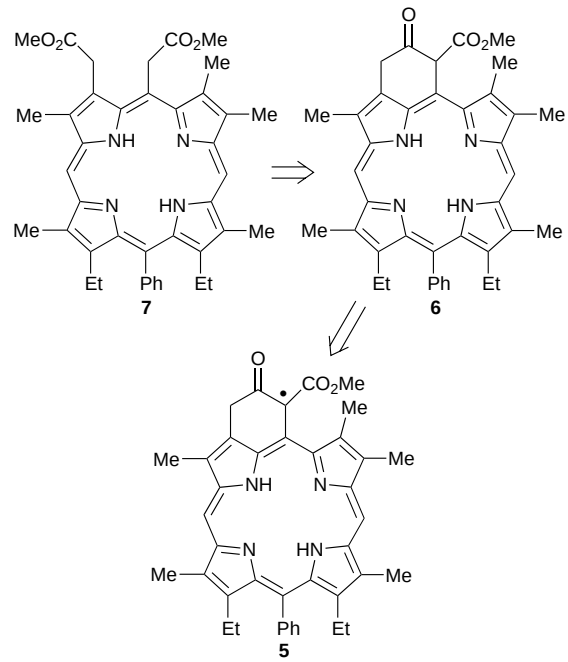
Oxophlorins **1** can be readily oxidized by dioxygen to form π-stabilized radicals **2**,[1] oxo derivatives **3**,[2] or covalently linked dimers **4**,[3] by mechanisms similar to those established in phenolic chemistry (Scheme 1).[4] An example of a very stable (sterically encumbered) oxophlorin π-radical was recently reported,[5] and although porphyrins can readily undergo one-electron oxidation (to give π-cation radicals) these transient species usually decompose to the parent porphyrin.[6] Based on knowledge of phenolic chemistry and its analogies with oxophlorin chemistry,[7] one might anticipate that any porphyrin system which could efficiently form a radical at a *meso*-benzylic atom (*e.g*. the carbonyl oxygen in oxophlorins, or a *meso*-benzylic methylene carbon) should undergo chemistry similar to that of oxophlorins (*e.g*. carbon–carbon dimerization, reaction with dioxygen). Literature precedent suggests[8] that benzylic porphyrin radicals (*e.g*. **5**) should, in principle, be accessible through porphyrins (*e.g*. **6**) suitably substituted with β-ketoester substituents (Scheme 2).

The precursor **7** of **6** was synthesized using established pyrrole chemistry; it was initially anticipated that Dieckmann cyclization of **7** would give **6**. The Michael acceptor pyrrole **8** was obtained from the formylpyrrole **9** by way of a Horner–Wadsworth–Emmons reaction (Scheme 3). Treatment of **8** with the 2-unsubstituted pyrrole **10** in refluxing acetic acid containing TFA gave the unsymmetrical dihydrodipyrrin **11**,[9] which upon catalytic bisdebenzylation gave **12**. MacDonald ('2 + 2') condensation between **13**[10] and the unsymmetrical dihydrodipyrrin dicarboxylic acid **12** in the presence of acid and zinc acetate, followed by removal of zinc with acid and then a basic work-up, did not yield the expected porphyrin **7**. Instead, a green compound was isolated ($\lambda_{max}$ 424, 606 nm). $^1$H NMR spectroscopy indicated a non-conjugated macrocycle had been formed [δ 12.67, 11.51 (each s, 1 H, NH)]. X-Ray crystallographic analysis‡ (Fig. 1) confirmed the structure of the compound to be the novel 10, 10′-bismacrocycle **14**. The linking 10,10′ carbon–carbon bond length is 1.58 Å. Along with dimer **14**, porphyrins **15** and **16** and the hydroxy-substituted chlorin **17** [$\lambda_{max}$ 424, 606 nm; δ 11.50, 8.93 (each br s, 1 H, OH)] were isolated. The structural assignment of **17** is based on spectroscopic similarities between **17** and the analogue in the 15-unsubstituted series, for which an X-ray crystal structure (not shown) has been obtained.

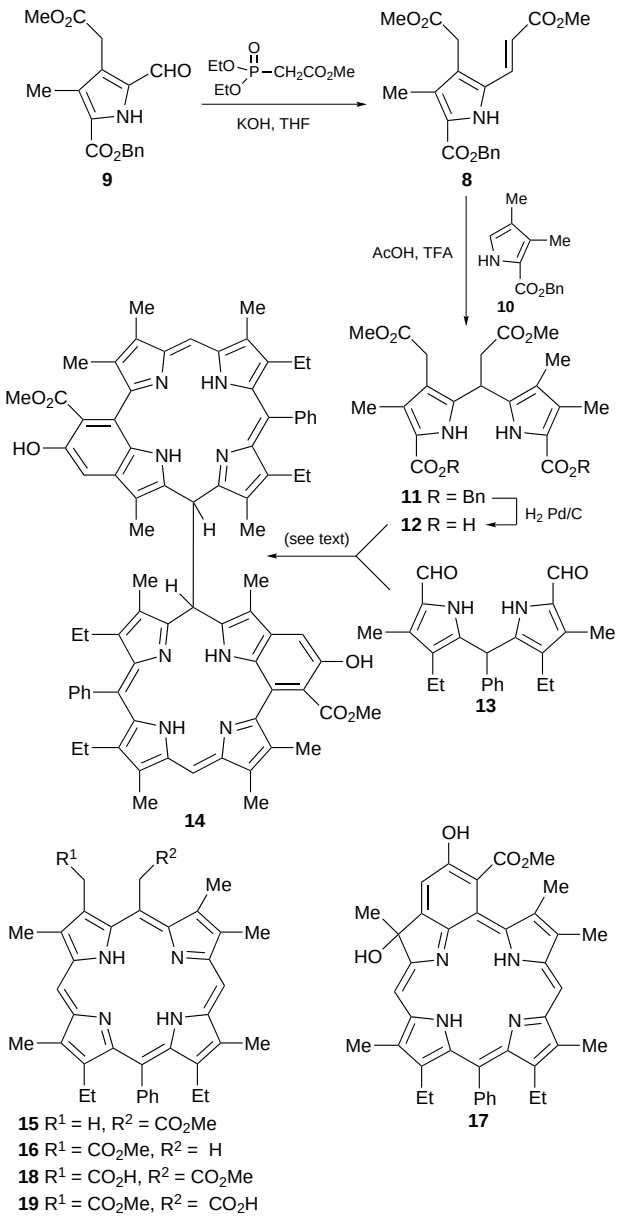
It was possible to isolate the target dimethyl ester porphyrin **7** in good yield by purifying the crude reaction mixture on neutral alumina instead of silica gel. Based on observations of the reactivity of **7** it became clear that the β-ketoester function




**Scheme 1**




**Scheme 2**




**Scheme 3**

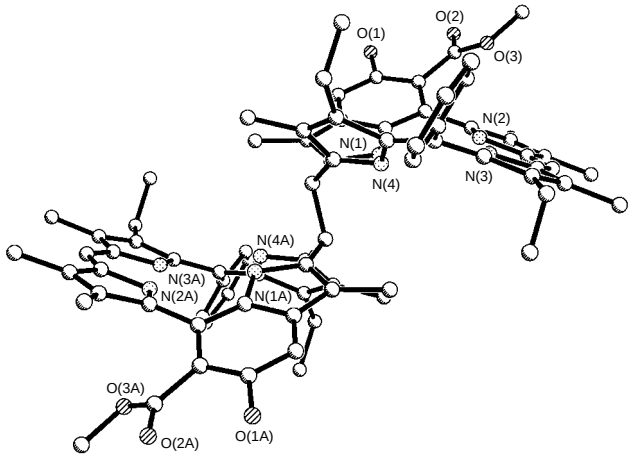



**Fig. 1** Molecular structure of dimer **14**

was not being formed by way of a base-catalysed Dieckmann process upon **7**. Subsequently, non-basic methods were developed to permit the controlled synthesis of covalent dimer **14** (by way of **6**), and the side products, simply by adsorbing porphyrin **7** on silica gel under $CH_2Cl_2$ for 14 h. Presumably, water present on the silica gel makes it possible for small amounts of the bis(methoxycarbonylmethyl)porphyrin **7** to hydrolyse and form monocarboxylic acid by-products such as **18** and **19**. At this point, decarboxylation would form porphyrin **15** (or **16**, depending upon which ester has been hydrolysed) or it could follow a mechanism to form the corresponding 'anhydro' derivative. The so-called anhydro-reaction[12,13] proceeds reversibly by way of an acid catalysed equilibrium which, in this case, would be driven by formation of the β-ketoester moiety on the periphery of the porphyrin **6** *via* attack by the methylene adjacent to the remaining ester in **18** upon a putative acylium species formed from its acetic acid substituent.

This work was supported by grants from the National Science Foundation (CHE-96-23117) and the National Institutes of Health (HL-22252).

## Footnotes

† E-mail: smith@chem.ucdavis.edu

‡ *Crystal data* for **14**. Crystals were grown from $CH_2Cl_2$–cyclohexane. A parallelepiped single crystal was selected with dimensions 0.18 × 0.13 × 0.05 mm. The unit cell was triclinic $P\bar{1}$ with cell dimensions $a$ = 11.208(2), $b$ = 12.474(3), $c$ = 14.368(3) Å, $\alpha$ = 78.35(3), $\beta$ = 76.86(3), $\gamma$ = 83.98(3)°, $V$ = 1912.2(7) Å$^3$, and $Z$ = 2 (FW = 748.7). X-ray diffraction data were collected on a Siemens $P2_1$ diffractometer with a fine-focus sealed tube [$\lambda$(Cu-K$\alpha$) = 1.54178 Å] at 130(2) K in $\theta$–2$\theta$ scan mode to $2\theta_{max}$ = 112°. Of 5278 reflections measured ($\pm h,\pm k,\pm l$) 3283 were independent and 1932 had $I > 2\sigma$ ($R_{int}$ = 0.039). The structure was solved by direct methods and refined (based on $F^2$ using all independent data) by full-matrix least-squares methods (Siemens SHELXTL V. 5.02); number of parameters = 441. Hydrogen atom positions were located by their idealized geometry and refined using a riding model. An absorption correction was applied using XABS2.[11] Final $R$ factors were $R1$ = 0.083 (based on observed data) and $wR2$ = 0.1998 (based on all data). Atomic coordinates, bond lengths and angles, and thermal parameters have been deposited at the Cambridge Crystallographic Data Center (CCDC). See Information for Authors, Issue No. 1. Any request to the CCDC for this material should quote the full literature citation and the reference number 182/406.

## References

1 J.-H. Fuhrhop, S. Besecke and J. Subramanian, *J. Chem. Soc., Chem. Commun*., 1973, 1.
2 J.-H. Fuhrhop, S. Besecke, J. Subramanian, Chr. Mengersen and D. Riesner, *J. Am. Chem. Soc*., 1975, **97**, 7141.
3 R. G. Khoury, L. Jaquinod, D. J. Nurco, R. K. Pandey and K. M. Smith, *Angew. Chem., Int. Ed. Engl*., 1996, **35**, 2496.
4 See for example: M. L. Mihailovic and Z. Cekovic, in *The Chemistry of the Hydroxyl Group*, part 1, ed. S. Patai, Wiley, New York, 1971, pp. 505–592.
5 R. G. Khoury, L. Jaquinod, A. M. Shachter, N. Y. Nelson and K. M. Smith, *Chem. Commun*., 1997, 215.
6 J.-H. Fuhrhop, in *Porphyrins and Metalloporphyrins*, ed. K. M. Smith, Elsevier, Amsterdam, 1975, pp. 612–614.
7 A. H. Jackson, G. W. Kenner and K. M. Smith, *J. Chem. Soc. (C)*, 1968, 302.
8 G. W. Kenner, S. W. McCombie and K. M. Smith, *J. Chem. Soc., Perkin Trans. 1*, 1974, 527.
9 D. H. Burns and K. M. Smith, *J. Chem. Res. (S)*, 1990, 178; (*M*), 1990, 1349.
10 D. A. Lee, J. M. Brisson and K. M. Smith, *Heterocycles*, 1995, **40**, 131; D. A. Lee and K. M. Smith, *J. Chem. Soc., Perkin Trans. 1*, 1997, 1215.
11 S. R. Parkin, B. Moezzi and H. Hope, *J. Appl. Crystallogr*., 1995, **28**, 53.
12 H. Fischer and H. Orth, *Die Chemie des Pyrrols*, Akademische Verlag, Leipzig, 1940, vol. 2, part 2, p. 84, 136. J.-H. Fuhrhop, in *The Porphyrins*, ed. D. Dolphin, Academic Press, New York, 1978, vol. 2, p. 137.
13 K. M. Smith and D. J. Simpson, *J. Am. Chem. Soc*., 1987, **109**, 6326.

*Received, 14th January 1997; Com. 7/00384F*

# Isonitrile–nitrile rearrangement promoted by samarium(II) iodide

**Han-Young Kang,*[a] Ae Nim Pae,[b] Yong Seo Cho,[b] Hun Yeong Koh*[b] and Bong Young Chung*[c]**

[a] *Department of Chemistry, Chungbuk National University, Cheongju 361-763, Korea*
[b] *Department of Applied Science, Korea Institute of Science and Technology, PO Box 131, Cheongryang, Seoul 130-650, Korea*
[c] *Department of Chemistry, Korea University, Seoul 136-701, Korea*

**A samarium(II) iodide-promoted rearrangement of isonitriles to nitriles, which requires an α-alkoxycarbonyl group at the carbon atom bearing the isonitrile group, occurs under very mild conditions and contrasts with the thermal version of the rearrangement, which usually requires high temperature.**

The isonitrile–nitrile rearrangement, which has been known for about ninety years, proceeds thermally with retention of stereochemistry at the migrating carbon [eqn. (1)].[1–3] This

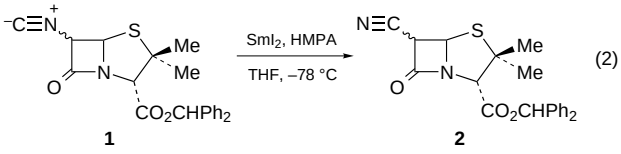


(1)

implies that the bond-forming and -breaking steps occur simultaneously and that there is little development of charge in the transition state. This rearrangement occurs at high temperature (250–280 °C) and is believed to take place *via* a radical intermediate. When the migrating carbon atom contains delocalizing groups such as alkoxycarbonyl or phenyl, then rearrangement also takes place but with low retention of configuration.[4] This reaction has also been the focus of theoretical investigation.[5]

Samarium(II) iodide is a useful tool for synthetic organic chemists since it is known for promoting various organic transformations.[6] Among the useful reactions of this reagent, reductive cleavage of α-heteroatom-substituted carbonyl substrates, involving deoxygenation of the functionality containing heteroatoms such as oxygen, sulfur and halogen, has been one of the most utilized.[7] However, in the case of functional groups containing a nitrogen atom, reductive cleavage has rarely been studied despite the importance of the transformation. The first systematic study of the reductive cleavage of aziridines adjacent to a carbonyl group has recently been reported.[8]

During the course of investigations on reactions promoted by samarium(II) iodide we had an opportunity to study the reaction of penicillanate **1** in the presence of this powerful single electron-transferring agent [eqn. (2)].



(2)

We anticipated a reduced product. However, to our surprise, a nitrile **2** was obtained in 70% yield (contained 5% of the reduced product). The diastereoisomers of **1** were separated,† and each was treated under the same reaction conditions. Both diastereoisomers (α-NC and β-NC) provided approximately the same ratio of **2** (α-CN : β-CN = 1 : 1.5), which indicated that the stereoselection induced by the migrating NC group and/or the β-lactam nucleus is low.

In order to investigate the generality and limitations of this isonitrile–nitrile rearrangement, various carboxylic acid derivatives with an α-isonitrile group were prepared. Synthesis of the substrates was easily achieved in a straightforward manner starting from the corresponding α-amino acids.‡

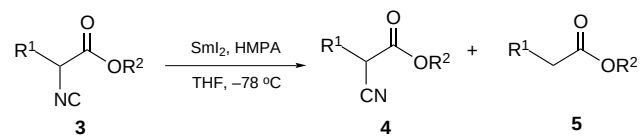
The results of the isonitrile–nitrile rearrangement promoted by samarium(II) iodide are summarized in Table 1. The rearrangement proceeds under very mild conditions in contrast to the thermal version, in which a temperature of up to 300 °C is required. The samarium(II) iodide-promoted isonitrile–nitrile rearrangement tolerates various types of functionality as shown in Table 1. Yields are variable, and usually formation of the corresponding reduced products **5** is also observed.

Decyanation of α-cyanocarboxylic esters promoted by samarium(II) iodide was reported by us.[9] Conversion of nitriles **4** to the reduced products **5** is precluded since this process in the presence of samarium(II) iodide requires higher temperature (room temperature). Therefore, the reduced products **5** are believed to be formed directly from the isonitrile substrate and not *via* the rearranged compounds, nitriles **4**. Under our conditions ($SmI_2$, THF–HMPA, −78 °C) the rearranged products **4** are usually formed predominantly. The substrate **3d**, having an isocyano group at the benzylic position, produced only the corresponding reduced product **5d**. Importantly, the isonitrile substrate has to be activated by an alkoxycarbonyl group for successful rearrangement. In the case of **3e** only the isonitrile group attached to the carbon α to the carbonyl group was isomerized, as expected.

Generally, 1.2–1.5 equiv. of samarium(II) iodide are sufficient for the rearrangement. However, in some cases, 2.5 equiv. were employed to complete the reaction. It is also appropriate to note that this process, which provides α-cyanocarboxylates and the corresponding reduced (deaminated) products, can be understood as an efficient method for deamination of α-amino acid derivatives, since the isonitriles prepared were made from the corresponding α-amino acids and at higher temperature α-cyanocarboxylates are known to undergo decyanation in the presence of samarium(II) iodide.[9]

From the view-point of the synthetic potential of this rearrangement, we investigated the possibility of utilization of the reaction for asymmetric synthesis (Table 2). We prepared

**Table 1** Isonitrile–nitrile rearrangement promoted by samarium(II) iodide




| Isonitrile | $R^1$ | $R^2$ | $SmI_2$ (equiv.) | Product (% yield) 4 | 5 |
|---|---|---|---|---|---|
| **3a** | H | PMB[a] | 1.2 | **4a** (50) | **5a** (11) |
| **3b** | $(CH_3)_2CHCH_2$ | PMB[a] | 1.2 | **4b** (50) | **5b** (10) |
| **3c** | Bn | Me | 1.0 | **4c** (57) | **5c** (12) |
| **3d** | Ph | Me | 2.5 | **4d** (0) | **5d** (46) |
| **3e** | $CN(CH_2)_4$ | PMB[a] | 2.5 | **4e** (50) | **5e** (20) |
| **3f** | $PMBO_2CCH_2$ | PMB[a] | 1.8 | **4f** (40) | **5f** (11) |

[a] PMB = *p*-methoxybenzyl.

the substrates shown in Table 2 having chiral oxazolidinone auxiliaries.§

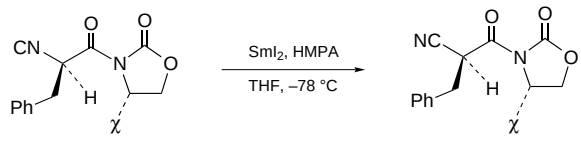
The efficiency of the differentiation of the diastereotopic faces by Evans' chiral auxiliaries (**3g** and **3h**) was first tested. Both cases show reasonable diastereoselectivities. Hoping to enhance the effectiveness of shielding to achieve a better de, a recently reported chiral auxilary (χ = $CHPh_2$; **3i** in Table 2) was also introduced.[10] However, in this case, no further increase in de was observed. Although only limited cases were tested, the results from Table 2 indicate that diastereoselectivity might be achieved if an appropriate chiral environment can be maintained. However, the systems considered here are not effective enough to obtain the desired level of diastereoselectivity. The reason could be either that the stereocentres responsible for the stereoselection are located far away from the carbon bearing the isocyano group or that the isocyano and cyano groups are linear, and thus are unable to provide efficient shielding of one diastereotopic face compared with the other.¶

Ito and co-workers have reported their investigation of the reaction of samarium(II) iodide with an isonitrile group.[11] In their cases, samarium(II) iodide promotes α-addition reactions of isonitriles. In our cases it is, however, probably reasonable to conclude that the reaction starts with an electron-transfer to the carbonyl group since no reaction was observed with a substrate without an α-alkoxycarbonyl group. The next step would involve breaking the bond between the migrating carbon atom and the nitrogen atom of the isocyano group, although the exact nature of the intermediate is not clear at the moment. At this stage, when benzylic stabilization is possible, return of the removed isonitrile moiety is not allowed and this results in exclusive formation of the reduced product. Otherwise the removed isonitrile moiety returns, with rearrangement, to the migrating carbon atom or, if this process cannot compete, the carbon atom previously bearing the isocyano group is captured by a hydrogen atom.

In conclusion, the samarium(II) iodide-promoted rearrangement of isonitriles to nitriles has been discovered and investigated. This rearrangement occurs under very mild conditions, in contrast to the thermal version of this rearrangement, which usually requires high temperature. This rearrangement should be included in the list of useful organic transformations promoted by samarium(II) iodide.

We are grateful to the Korea Ministry of Science and Technology and the Organic Chemistry Research Center (sponsored by the Korea Science and Engineering Foundation) for generous financial support.

**Table 2** Rearrangement of substrates with chiral auxiliaries




**3** **4**

| Isonitrile | χ | $SmI_2$ (equiv.) | Product (% yield) | De (%) |
|---|---|---|---|---|
| **3g** | $CH(CH_3)_2$ | 1.2 | **4g** (60) | 65 |
| **3h** | $CH_2Ph$ | 1.2 | **4h** (55) | 68 |
| **3i** | $CHPh_2$ | 1.2 | **4i** (48) | 68 |

## Footnotes

† Lichrosorb Si60 Semi-prep column, hexane–ethyl acetate = 3 : 1.

‡ The required isonitrile substrates were prepared by one of the following routes from the corresponding α-amino acids. Method A: i, $SOCl_2$, MeOH; ii, $HCO_2H$, $Ac_2O$, pyridine; iii, triphosgene, $Et_3N$, $CH_2Cl_2$, −78 °C. Method B: i, $HCO_2H$, $Ac_2O$; ii, *p*-Methoxybenzyl chloride, $K_2CO_3$, DMF; iii, triphosgene, $Et_3N$, $CH_2Cl_2$, −78 °C.

§ The purity of the substrates in Table 2 was checked by NMR spectroscopy. The isonitriles **3g**–**i** were all pure single diastereoisomers. For compounds **3g**–**i** the absolute stereochemistry of the carbon atom bearing the isonitrile group is, however, not clear at this point since epimerization could take place during the synthesis from the corresponding amino acids under the reaction conditions described in ref. 10. In all cases in Table 2, formation of the reduced products (corresponding to **5**) was not observed.

¶ The de values could be affected by epimerization during purification.

## References

1 J. Casanova, Jr., N. D. Werner and R. E. Schuster, *J. Org. Chem*., 1966, **31**, 3473.
2 M. Meier and R. Ruchardt, *Chem. Ber*., 1987, **120**, 1.
3 D. I. John and N. D. Tyrrell, *Tetrahedron*, 1983, **39**, 2477.
4 H. M. Walborsky and M. P. Periasamy, in *The Chemistry of Triple Bonded Functional Groups*, ed. S. Patai and Z. Rappoport, Wiley-Interscience, New York, 1983, Part 2, Suppl. C, ch. 20.
5 K. M. Maloney and B. S. Rabinvich, in *Isonitrile Chemistry*, ed. I. Ugi, Academic Press, New York, 1971, ch. 3.
6 For reviews, see N. R. Natale, *Org. Prep. Proceed Int*., 1983, **15**, 387; H. B. Kagan, M. Sasaki and J. Collin, *Tetrahedron*, 1986, **42**, 6573; H. B. Kagan, M. Sasaki and J. Collin, *Pure Appl. Chem*., 1988, **60**, 1725; G. A. Molander, in *The Chemistry of the Metal-Carbon Bond*, ed. F. R. Hartley, Wiley, Chichester, 1989, vol. 5, ch. 8; J. Inanaga and M. Yamaguchi, in *New Aspects of Organic Chemistry I*, ed. Z. Yoshida, T. Shiba and Y. Oshiro, VCH, New York, 1989, ch. 4; J. A. Soderquist, *Aldrichim. Acta*, 1991, **24**, 15; G. A. Molander, *Chem. Rev*., 1992, **92**, 29; D. P. Curran, T. L. Fevig, C. P. Jasperse and M. J. Totleben, *Synlett*, 1992, 943; G. A. Molander, in *Comprehensive Organic Synthesis*, ed. B. M. Trost and I. Fleming, Pergamon, Oxford, UK., 1991, vol. 1, ch. 1.9; T. Imamoto, *Lanthanides in Organic Synthesis*, Academic Press, London, 1994, ch. 4; G. A. Molander and C. R. Harris, *Chem. Rev*., 1996, **96**, 307.
7 G. A. Molander, *Org. React*., 1994, **46**, 211.
8 G. A. Molander and P. J. Stengtel, *J. Org. Chem*., 1995, **60**, 6660.
9 H.-Y. Kang, W. S. Hong, Y. S. Cho and H. Y. Koh, *Tetrahedron Lett*., 1995, **36**, 7661.
10 M. P. Sibi, P. K. Deshpande, A. J. La Loggia and J. W. Christensen, *Tetrahedron Lett*., 1995, **36**, 8961 and 8965.
11 M. Murakami, T. Kawano and Y. Ito, *J. Am. Chem. Soc*., 1990, **112**, 2437; M. Murakami, M. Hayashi and Y. Ito, *J. Org. Chem*., 1992, **57**, 793.

*Received in Cambridge, UK, 24th January 1997; Com. 7/00570I*

# Ruthenium-catalysed cross metathesis binding of functionalized olefins to polystyrene resin *via* a novel allylsilyl linker suitable for electrophilic cleavage

**Matthias Schuster, Norbert Lucas and S. Blechert*†**

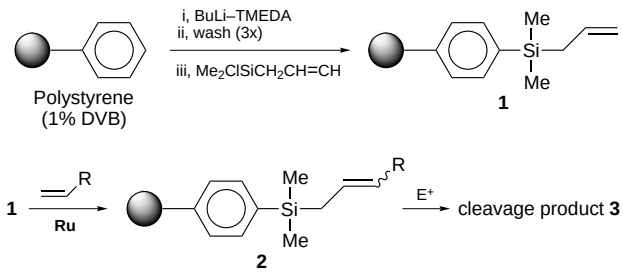
*Institut für Organische Chemie, Sekr. C3, Technische Universität Berlin, Straße des 17. Juni 135, D-10623, Germany*

**1% Divinylbenzene-crosslinked allyldimethylsilyl polystyrene 1 undergoes highly efficient ruthenium-catalysed cross-metathesis with functionalized terminal olefins and allows electrophilic cleavage of the resulting functionalized allylsilane.**

During the last decade, olefin metathesis has emerged as a powerful synthetic tool for the formation of C=C double bonds.[1] Most recently, it has been demonstrated that highly selective cross-coupling[2] between functionalized terminal olefins can be performed under catalysis of well defined metathesis catalysts.[3] In the advent of combinatorial chemistry there is an increasing demand for innovative chemistry on solid supports including novel linker concepts. Cross metathesis involving polymer-supported olefins should enable the binding of target molecules *via* the highly stable C=C double bond in a catalytic manner. In an initial report[4] we described the catalytic immobilisation of several small nonpolar molecules to a modified trityl polystyrene resin using Grubbs' ruthenium initiator[3] $Cl_2(PCy_3)_2$-Ru=CHPh **Ru** (Cy = cyclohexyl). Cross metathesis products were characterized after cleavage from the acid-labile trityl linker.

Here we present allyldimethylsilyl polystyrene **1**, which upon ruthenium-catalysed cross metathesis with terminal olefins yields immobilized products **2** (Scheme 1). Products **2** can be subject to electrophilic attack[5] resulting in C–Si cleavage and, thus, the formation of soluble products **3**. Cleavage can be performed either as protodesilylation or in combination with an additional synthetic step, when electrophiles other than $H^+$ are employed.

Polystyrene **1** closely resembles soluble allyltrimethylsilane, which was found to be an excellent cross metathesis partner by us and others.[2] The synthesis of **1** by treatment of polystyrene (1% DVB-crosslinked) (DVB = divinylbenzene) with BuLi–TMEDA and subsequently with allyldimethylsilyl chloride is based on the observation[6] that under these conditions metallation occurs in the *para*-position of the phenyl ring, exclusively.‡ The silicon content of **1** was determined by Inductive Coupled Plasma-Optical Emission Spectroscopy (ICP-OES) of sodium tertaborate melt samples. We found that removal of excess BuLi–TMEDA by repeated washing of the lithiated polymer ensures high loading capacities and significantly decreases the amount of the electrophile required. The resin employed throughout this study had a silicon content of 1.3 mmol $g^{-1}$. Cross metathesis was performed in refluxing dichloromethane using 0.05 mmol of **Ru** and 1.0–2.0 mmol of terminal olefin per gram of resin.§ Loadings of cross metathesis

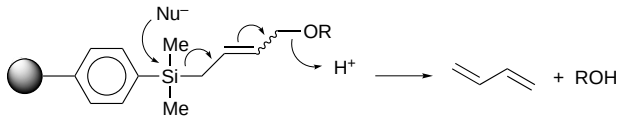



**Scheme 1** Synthesis of, **Ru**-catalysed cross-metathesis with, and electrophilic cleavage from polystyrene-supported allylsilane **1**

**Table 1** Results of the electrophilic cleavage of metathetically obtained polystyrene-supported allylsilanes **2**

| Metathesis product **2** | Cleavage product **3**[2] |
|---|---|
| R = | |
| **2a**[b] | **3a**[d] (0.5 mmol $g^{-1}$) |
| **2b**[b] | **3b**[d] (0.43 mmol $g^{-1}$) |
| **2c**[c] | **3c**[d] (0.34 mmol $g^{-1}$) |
| **2d**[c] | **3d**[d] (0.41 mmol $g^{-1}$) |
| **2e**[c] | **3e**[d] (0.59 mmol $g^{-1}$) |
| **2f**[c] | **3f**[e] (0.38 mmol $g^{-1}$) |
| **2g**[c] | **3g**[d] (<0.1 mmol $g^{-1}$) |
| **2a**[b] | **3h**[f] (0.50 mmol $g^{-1}$) |

[a] Isolated yield of cleavage product **3** per gram of **2** given in parentheses. [b] Methathesis conditions: 300 mg **1**; 0.6 mmol terminal olefin; 0.015 mmol **Ru**; 5 ml $CH_2Cl_2$ (reflux); 18 h. [c] Metathesis conditions: 300 mg **1**; 0.3 mmol terminal olefin; 0.015 mmol **Ru**; 5 ml $CH_2Cl_2$ (reflux); 18 h. [d] Cleavage conditions: 3% TFA in $CH_2Cl_2$, 18 h. [e] Cleavage conditions: 1.5% TFA in $CH_2Cl_2$, 24 h. [f] To 500 mg of **2a** in 20 ml $CH_2Cl_2$ was added 1.3 mmol 1,1-diethoxypropane and 1.3 mmol $TiCl_4$ at −78 °C. After 22 h aqueous work-up ($NaHCO_3$) and flash chromatography of the $CH_2Cl_2$ phase gave the product.




**Scheme 2** Proposed mechanism for the protodesilylation of allysilanes **2** with oxygen in the allyl position

immobilisation products **2** were calculated from the amount of soluble cleavage products **3**, liberated from **2** by protodesilylation with TFA (3% in $CH_2Cl_2$).

As shown in Table 1, protodesilylation of **2a** furnished the homologized product **3a**;¶ 0.5 mmol was released per gram of **2a**. This modification level indicates a highly effective metathesis reaction. A diester function does not affect the immobilisation reaction as demonstrated by the synthesis of **2b** with 0.43 mmol $g^{-1}$. Protodesilylation yields the expected product **3b**. A major goal of this study was to demonstrate that polyfunctional molecules of biological interest such as glycosides and amino acid derivatives can also be effectively coupled to **1**. Indeed **2c** was formed with a capacity of 0.34 mmol $g^{-1}$. Protodesilylation to **3c** proceeded with complete retention of the acetal, thus underlining the exceptionally mild cleavage conditions. However, cleavage of **2d** under identical conditions furnished tetra-*O*-acetyl glucose **3d** instead of the expected homoallyl glycoside. Possibly, deglycosylation of **2b** proceeds through a modified protodesilylation mechanism as shown in Scheme 2.

The same cleavage pattern should be obsered when allyl esters are used in the metathesis reaction. Indeed, cleavage of **2e** and **2f** furnished the respective free carboxylic acids **3e** and **3f**. This special type of allyl ester is even more acid sensitive than the Boc group, which remains intact when the cleavage reaction is performed using 1.5% TFA for 24 h. The scope of this unexpected cleavage reaction remains to be investigated. In contrast to isoleucin allyl ester derivatives the metathetical immobilisation of the protected *C*-allylglycinol was less successful, as demonstrated by the amount of **3g** that could be released from **2g**. Eventually, we wished to demonstrate the utility of solid phase-bound allylsilanes **2** as starting materials for C–C bond formation. To give a first example of the addition of a carbon electrophile to a polymer-supported allylsilane, a mixture of **2a** and 1,1-diethoxyethane was treated with $TiCl_4$. The yield of product **3h** proved comparable to the yield of the corresponding protodesilylation product **3a**.

In conclusion, we have presented a novel polystyrene resin containing an allylsilyl linker moiety. The linker enables both binding of functionalized olefins by catalytic cross metathesis and cleavage under exceptionally mild acidic conditions. The linker allows the cleavage to be performed under formation of an additional C–C bond. A cyclisation–cleavage strategy employing intramolecular electrophilic attack is currently being developed.

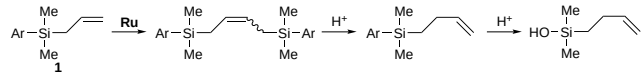
## Footnotes

† E-mail: sibl@wap0105.chem.tu-berlin.de

‡ Synthesis of **1**: 8 g of polystyrene (1% DVB) was suspended in 12 ml of cyclohexane, 12 ml (80 mmol) TMEDA and 48 ml (1.6 M in hexane, 77 mmol) BuLi were added and the suspension was gently shaken for 3 d at ambient temperature under exclusion of moisture and air. The supernatant was removed through a septum and replaced by 30 ml cyclohexane. This procedure was repeated twice, before 12 ml (80 mmol) allyldimethylsilyl chloride was added under shaking. After 1 h the reaction was quenched with 40 ml methanol, the resin was quickly filtered off, washed repeatedly with methanol, dichloromethane and MeOBu$^t$ and dried under vacuum.

§ Synthesis of **2b**: to 300 mg of **1** in 5 ml absolute dichloromethane was added 120 mg (0.6 mmol) of **2a** and 12 mg (0.015 mmol) of **Ru**. The resulting suspension was refluxed under argon atmosphere (glove box) for 18 h. The resin was filtered off and washed with 20 volumes each of DMF, chloromethane, methanol and diethyl ether. Residual diethyl ether was removed under high vacuum.

¶ After acidic cleavage homoallyldimethylsilanol was isolated as a minor byproduct. Its formation can be rationalized by the following reaction sequence:




## References

1 Reviewed in: H.-G. Schmalz, *Angew. Chem*., 1995, **107**, 1981; *Angew. Chem., Int. Ed. Engl*., 1995, **34**, 1833; U. Koert, *Nachr. Chem. Tech. Lab*., 1995, **43**, 809; R. H. Grubbs, *Acc. Chem. Res*., 1995, **28**, 446.

2 W. E. Crowe and D. R. Goldberg, *J. Am. Chem. Soc*., 1995, **117**, 5162; W. E. Crowe, D. R. Goldberg and Z. J. Zhang, *Tetrahedron Lett*., 1996, **37**, 2117; O. Brümmer, A. Rückert and S. Blechert, *Chem. Eur. J*., 1997, **3**, 207; J. Feng, M. Schuster and S. Blechert, *Synlett*, 1997, 129; E. Sh. Finkelshtein, N. V. Ushakov and E. B. Portnykh, *J. Mol. Catal*., 1992, **76**, 133; A. G. M. Barrett, J. C. Beall, V. C. Gibson, M. R. Giles and G. L. P. Walker, *Chem. Commun*., 1996, 2229; A. G. M. Barrett, S. P. D. Baugh, V. C. Gibson, M. R. Giles, E. L. Marshall and P. A. Procopiou, *Chem. Commun*., 1997, 155.

3 For ruthenium carbene initiators see: P. Schwab, M. B. France, J. W. Ziller and R. H. Grubbs, *Angew. Chem*., 1995, **107**, 2179; *Angew. Chem., Int. Ed. Engl*., 1995, **34**, 2039. For molybdenum carbene initiators see: K. B. Yap, J. Robbins, S. Cai and R. R. Schrock, *Inorg. Chem*., 1992, **31**, 2287.

4 M. Schuster, J. Pernerstorfer and S. Blechert, *Angew. Chem*., 1996, **108**, 2111; *Angew. Chem., Int. Ed. Engl*., 1995, **35**, 1979.

5 For a comprehensive review see: I. Fleming, J. Dunogues and R. Smithers, *Org. React*., 1989, **37**, 57.

6 E. J. Chalk, *Polym. Lett*., 1968, **6**, 649.

*Received in Cambridge, UK, 18th February 1997; Com. 7/01122I*

# A novel class of conformationally restricted oligonucleotide analogues: synthesis of 2′,3′-bridged monomers and RNA-selective hybridisation

**Poul Nielsen,[a] Henrik M. Pfundheller[a] and Jesper Wengel[b]*†**

[a] *Department of Chemistry, Odense University, 5230 Odense M, Denmark*
[b] *Department of Chemistry, University of Copenhagen, Universitetsparken 5, 2100 Copenhagen, Denmark*

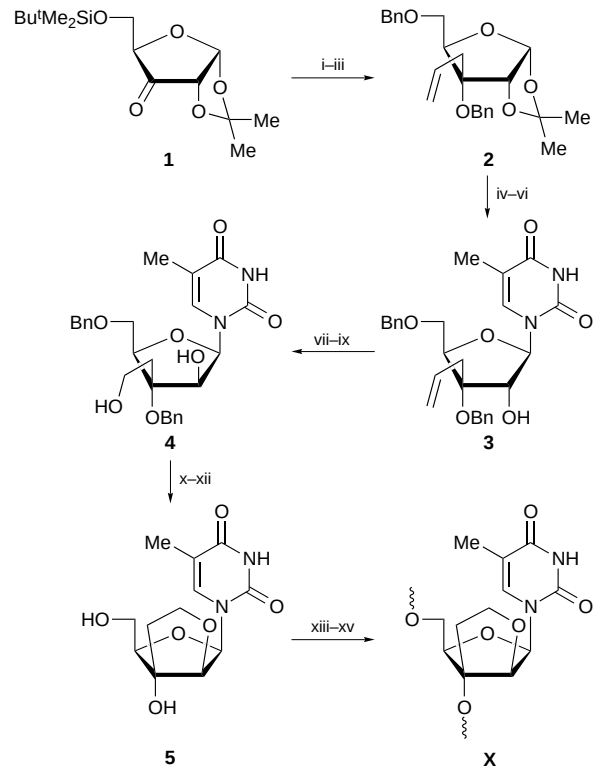
**A novel 2′,3′-bicyclic nucleoside 5 has been synthesised and incorporated into oligonucleotide analogues resulting in strong and selective binding to an RNA complement.**

Research towards modified oligonucleotides able to hybridise with ssRNA (antisense or ribozyme approach) as a novel class of therapeutic agents currently attracts much attention.[1] The potential of enhancing duplex stability using conformationally restricted oligonucleotide analogues has been investigated, as recently described in a review by Herdewijn.[2] Bicyclo nucleosides with an additional 3′,5′-ethylene bridge,[3] bicyclic carbocyclic nucleosides with a 1′,6′- or 4′,6′-methano bridge,[4] 2′,3′-riboacetal dimers,[5] 3′,6′-anhydrogluco-2′,5′-formacetal trimers[6] and conformationally restricted 1,5-anhydro-2,3-dideoxy-D-*arabino*-hexitol nucleosides[7] have been synthesised and incorporated into oligodeoxynucleotides in order to obtain an entropic advantage through the rigidity of the structures, thereby increasing duplex stability. Here we report on the synthesis and the promising melting results for 2′,3′-bridged bicyclic pentofuranose oligonucleotides. This work was stimulated by molecular modelling studies indicating the possibility of a preferential 3′-*endo* conformation of the monomers as required for RNA-selective binding.

The bicyclic nucleoside **5** was synthesised in twelve steps from the known ulose **1**[8] in an overall yield of 10% using a strategy (see Scheme 1) where the additional alkyl chain was introduced before, and the cyclisation accomplished after, the nucleoside coupling step.‡ Whereas Grignard additions on 3′-keto nucleosides afforded *xylo*-configured isomers as major products,[9] the presence of the 1,2-*O*-isopropylidene group in ulose **1** directs the addition of Grignard reagents to proceed from the β-face of the furanose. Thus, the first step was a stereoselective Grignard addition of an allyl group at the 3-*C*-position generating, after desilylation and concomitant benzylation, the furanoside **2** with the preferred *ribo* configuration in 59% yield. An allyl group was preferred to a vinyl group as this Grignard addition was more successful in our hands. The required inversion of the configuration at the 2-carbon could most conveniently be performed, using an anhydro-approach,[10] after the nucleoside coupling step. Using standard methods, furanose **2** was deprotected and acetylated, whereafter the 2′-*O*-unprotected nucleoside **3** was obtained in 79% yield (from **2**) using the silyl Hilbert–Johnson/Birkofer method as modified by Vorbrüggen and co-workers[11] followed by deacetylation. Mesylation and treatment with aqueous base gave a 2-*O*,2′-*O*-anhydro intermediate which was directly hydrolysed affording an *arabino*-configured nucleoside. The double bond was oxidatively cleaved and 3′-*C*-hydroxyethyl nucleoside **4** was obtained in 32% yield (from **3**) after reduction. Selective tosylation of the primary hydroxy group, cyclisation using strong base and debenzylation afforded the nucleoside **5** in 68% yield (from **4**).§ The new bicyclic nucleoside **5** was incorporated into oligonucleotides as monomer **X** (see Scheme 1) after 4,4′-dimethoxytrityl(DMT)-protection of the 5′-hydroxy group and conversion to the corresponding phosphoramidite building block.

Six modified oligonucleotides were synthesised[12] and evaluated towards both complementary single-stranded DNA and RNA.¶ As seen from Table 1, incorporation of one to four modified bicyclic nucleotides **X** into a 14-mer destabilises duplexes with the DNA complement $dA_{14}$ by 2–3 °C per modification, irrespective of **X** being incorporated in a row or alternating with unmodified nucleotides. Analogously, a lowering of the melting temperature by approximately 3 °C per modification was observed for duplexes with the RNA complement $rA_{14}$ when incorporating monomer **X** once or several times alternating with unmodified nucleotides.

More encouraging results were obtained towards the RNA complement when incorporating the bicyclic nucleoside **X** in a row of four (5′-$T_5\mathbf{X}_4T_5$-3′), as a minor increase in melting temperature compared to the unmodified control was observed. Following this trend, an increase in the melting temperature of




**Scheme 1** *Reagents and conditions*: i, allylMgBr, $Et_2O$, THF; ii, $Bu_4NF$, THF, 69% for two steps; iii, BnBr, NaH, DMF, 86%; iv, 80% AcOH, then $Ac_2O$, pyridine, 97%; v, thymine, *N*,*O*-bis(trimethylsilyl)acetamide, MeCN, $Me_3SiOSO_2CF_3$, 86%; vi, MeONa, MeOH, 95%; vii, $MeSO_2Cl$, pyridine, 89%; viii, NaOH, EtOH, $H_2O$, 74%; ix, $NaIO_4$, cat. $OsO_4$, THF, $H_2O$, then $NaBH_4$, THF, $H_2O$, 49%; x, *p*-$MeC_6H_4SO_2Cl$, pyridine; xi, NaH, DMF, 83% for two steps; xii, $H_2$, $Pd(OH)_2$–C, EtOH, 82%; xiii, DMTCl, pyridine, 97%; xiv, $NC(CH_2)_2OP(Cl)N(Pr^i)_2$, $EtN(Pr^i)_2$, $CH_2Cl_2$, 88%; xv, DNA synthesiser

12.5 °C was observed for the duplex between the (almost) fully modified oligonucleotide 5′-$\mathbf{X}_{13}$T-3′ and complementary RNA. These results indicate that these new 2′,3′-bicyclo oligonucleotides ('2′,3′-BcNAs') form a duplex structure with complementary RNA which is thermally significantly more stable than the corresponding unmodified DNA–RNA duplex. The structure of the duplex 2′,3′-BcNA–RNA is probably different from that of wild type DNA–RNA as indicated by the destabilising effect of one or two bicyclic nucleosides in an otherwise unmodified DNA strand. The shapes of the circular dichroism spectra, known to be diagnostic of a particular duplex structure, recorded for $T_{14}$ : $rA_{14}$ and $\mathbf{X}_{13}$T : $rA_{14}$ are, however, similar. It is thus clear that conclusions about the structural basis for the observed increase in thermal stability must await results from other sequences and from extensive molecular modelling and NMR studies.

Degradation by nucleases signifies a serious limitation to *in vivo* application of both natural and many modified oligonucleotides. We have therefore evaluated the novel 2′,3′-BcNA ($\mathbf{X}_{13}$T) against snake venom phosphodiesterase (a 3′-exonuclease) using a method described earlier.[13] Whereas the unmodified control ($T_{14}$) is fully degraded within 10 min, $\mathbf{X}_{13}$T (or $\mathbf{X}_{13}$) remains intact for the 60 min monitored. Thus, although other nucleases need to be evaluated, this result suggests that 2′,3′-BcNAs may be effectively protected against nucleolytic degradation.

In conclusion, a new bicyclic thymidine analogue **5** has been synthesised and used as a monomer to construct a novel class of conformationally restricted 2′,3′-bicyclo oligonucleotides ('2′,3′-BcNAs'). Melting experiments revealed excellent thermal stability of a 2′,3′-BcNA–RNA duplex, which, together with the observed stability towards 3′-*exo* nucleolytic degradation, suggests 2′,3′-BcNAs to be interesting candidates as antisense molecules.

**Table 1** Melting experiments of modified oligonucleotides[a]

| | Complimentary ssDNA ($dA_{14}$) | | Complimentary ssRNA ($rA_{14}$) | |
|---|---|---|---|---|
| Oligonucleotide | $T_m$/°C | $\Delta T_m$/°C | $T_m$/°C | $\Delta T_m$/°C |
| 5′-$T_{14}$-3′ | 34.5 | | 29.5 | |
| 5′-$T_7\mathbf{X}T_6$-3′ | 32.0 | −2.5 | 26.5 | −3.0 |
| 5′-$T_6\mathbf{X}_2T_6$-3′ | 30.0 | −4.5 | 28.0 | −1.5 |
| 5′-$T_6\mathbf{X}T\mathbf{X}T_5$-3′ | 29.5 | −5.0 | 23.0 | −6.5 |
| 5′-$T_5\mathbf{X}_4T_5$-3′ | 23.0 | −11.5 | 30.5 | +1.0 |
| 5′-$T_3(T\mathbf{X})_4T_3$-3′ | 23.0 | −11.5 | 16.5 | −13.0 |
| 5′-$\mathbf{X}_{13}$T-3′ | < 10 | < −24 | 42.0 | +12.5 |

[a] Measured at 260 nm in medium salt buffer: 1 mM EDTA, 10 mM $Na_3PO_4$, 140 mM NaCl, pH 7.2; concentration of each strand: 1.0 μM; T = thymidine monomer; dA = 2′-deoxyadenosine monomer; rA = adenosine monomer; **X** = monomer derived from nucleoside **5**; $T_m$ = melting temperature determined as the local maximum of the first derivative of the absorbance *vs*. temperature curve; $\Delta T_m$ = change in $T_m$ compared to unmodified controls.

We thank The Danish Natural Science Research Council for financial support. Dr Carl Erik Olsen is thanked for recording MALDI-MS.

## Footnotes

† E-mail: wengel@kiku.dk

‡ Full characterisation of all intermediates will be published as part of a forthcoming publication.

§ The structure of nucleoside **5** was verified from MS, $^1$H NMR, $^{13}$C NMR, $^1$H–$^1$H COSY and NOE experiments. *Selected data* for **5**: $^1$H NMR (250 MHz; [$^2H_6$]DMSO): δ 11.3 (1 H, br s, NH), 7.36 (1 H, d, *J* 1.1, 6-H), 5.80 (1 H, d, *J* 4.3, 1′-H), 5.61 (1 H, s, OH), 4.86 (1 H, m, 5′-Ha), 3.89 (1 H, d, *J* 4.2, 2′-H), 3.85 (1 H, m, 2″-H), 3.83–3.64 (3 H, m, 4′-H, 5′-Hb, 2″-H), 2.14 (1 H, m, 1″-H), 1.81 (1 H, m, 1″-H), 1.78 (3 H, d, *J* 1.0, Me); $^{13}$C NMR (62.9 MHz; $CD_3OD$): δ 166.7 (C-4), 152.2 (C-2), 139.7 (C-6), 110.1 (C-5), 89.4, 89.1, 85.5, 85.2 (C-1′, C-2′, C-3′, C-4′), 71.4 (C-2″), 61.6 (C-5′), 37.0 (C-1″), 12.7 (Me) (Found: C, 47.4; H, 5.7; N, 9.0; $C_{12}H_{16}N_2O_6\cdot H_2O$ requires C, 47.7; H, 6.0; N, 9.3%). Mutual NOE contacts between H-1′ and H-2′ and between H-1′ and H-4′, as well as the lack of contacts between H-5′ and H-1′ or H-2′ and between H-2′ and H-6, confirm the assigned β-*arabino* configuration.

¶ The oligonucleotides were synthesised on a Pharmacia Gene Assembler in 0.2 μmol scale using commercial 2-cyanoethyl phosphoramidites (2 min coupling time, *ca*. 99% stepwise yield) and the amidite derived from nucleoside **5** (2 × 12 min coupling time, *ca*. 95% stepwise yield). Purification of 5′-*O*-DMT-ON oligonucleotides was accomplished using disposable reversed-phase chromatography cartridges (Cruachem Inc.), which includes 5′-*O*-detritylation. The composition of the oligonucleotides were verified by MALDI-MS and the purity by capillary gel electrophoresis. Minor peaks (< 5%) originating from $\mathbf{X}_{10}$T, $\mathbf{X}_{11}$T and $\mathbf{X}_{12}$T were detected when running $\mathbf{X}_{13}$T.

## References

1 R. W. Wagner, *Nature*, 1994, **372**, 333; A. De Mesmaeker, R. Häner, P. Martin and H. E. Moser, *Acc. Chem. Res.*, 1995, **28**, 366.
2 P. Herdewijn, *Liebigs Ann. Chem.*, 1996, 1337.
3 M. Tarköy, M. Bolli, B. Schweizer and C. Leumann, *Helv. Chim. Acta*, 1993, **76**, 481; M. Tarköy and C. Leumann, *Angew. Chem., Int. Ed. Engl.*, 1993, **32**, 1432; M. Tarköy, M. Bolli and C. Leumann, *Helv. Chim. Acta*, 1994, **77**, 716; J. C. Litten and C. Leumann, *Helv. Chim. Acta*, 1996, **79**, 1129; M. Egli, P. Lubini, M. Dobler and C. Leumann, *J. Am. Chem. Soc.*, 1993, **115**, 5855.
4 K.-H. Altmann, R. Kesselring, E. Francotte and G. Rihs, *Tetrahedron Lett.*, 1994, **35**, 2331; K.-H. Altmann, R. Imwinkelried, R. Kesselring and G. Rihs, *Tetrahedron Lett.*, 1994, **35**, 7625.
5 R. Zou and M. Matteucci, *Tetrahedron Lett.*, 1996, **37**, 941.
6 R. J. Jones, S. Swaminathan, J. F. Millagan, S. Wadwani, B. S. Froehler and M. Matteucci, *J. Am. Chem. Soc.*, 1993, **115**, 9816.
7 A. van Aerschot, I. Verheggen, C. Hendrix and P. Herdewijn, *Angew. Chem., Int. Ed. Engl.*, 1995, **34**, 1338.
8 Y. Yoshimura, T. Sano, A. Matsuda and T. Ueda, *Chem. Pharm. Bull.*, 1988, **36**, 162.
9 P. Nielsen, K. Larsen and J. Wengel, *Acta. Chem. Scand.*, 1996, **50**, 1030.
10 J. J. Fox and N. C. Miller, *J. Org. Chem.*, 1963, **28**, 936.
11 H. Vorbrüggen, K. Krolikiewicz and B. Bennua, *Chem. Ber.*, 1981, **114**, 1234; H. Vorbrüggen and G. Höfle, *Chem. Ber.*, 1981, **114**, 1256.
12 M. H. Caruthers, *Acc. Chem. Res.*, 1991, **24**, 278.
13 P. Nielsen, F. Kirpekar and J. Wengel, *Nucleic Acids Res.*, 1994, **22**, 703.

*Received in Glasgow, UK, 5th December 1996; Com. 6/08231I*

# Five-component assembly of molecular loops†

**Edwin C. Constable*[a] and David Phillips[b]**

[a] *Institut für Anorganische Chemie, Spitalstrasse 51, CH-4056 Basel, Switzerland*
[b] *University Chemical Laboratory, Lensfield Road, Cambridge, UK CB2 1EW*

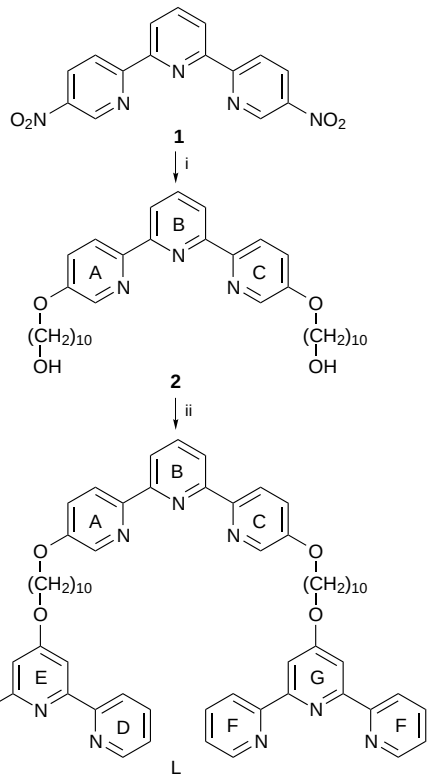
**The new tritopic ligand L contains three 2,2′:6′,2″-terpyridine (tpy) metal-binding domains and reacts with iron(II) salts to form a species of stoichiometry $[Fe_3L_2]^{6+}$ which adopts a doubly looped (bow tie) structure.**

Ligands containing multiple oligopyridine or 1,10-phenanthroline metal-binding domains are widely used in the metal-directed assembly of topologically and structurally novel supramolecules such as multiple helices, knots, boxes, grids and catenanes.[1] The majority of systems investigated to date have rigid or short flexible spacers between the metal-binding domains in order to limit the possibilities in conformational space. Here, we discuss the effect of introducing long flexible spacers.

Our target was molecule L which contains three 2,2′:6′,2″-terpyridine (tpy) metal-binding domains separated by a $O(CH_2)_{10}O$ spacer. This was prepared in two steps from 5,5″-dinitro-2,2′:6′,2″-terpyridine **1**[2] in 38% overall yield (Scheme 1). The reaction of **1** with an excess of decane-1,10-diol in $Me_2SO$ in the presence of KOH gave **2** as a white solid in 50% yield.‡ Subsequent reaction of **1** with 2 equiv. of 4′-chloro-2,2′:6′,2″-terpyridine[3] under the same reaction conditions gave L as a white crystalline solid‡ in 75% isolated yield. The free ligand L is highly symmetrical and the $^1H$ NMR spectrum clearly shows that rings A and C are equivalent, as are rings D and F, and rings E and G.

Ligand L contains three terdentate metal-binding domains and is expected to interact with six-coordinate metal centres. Whilst polymeric structures might be expected from an uncontrolled assembly process, the coding within the metal and ligand might be sufficient to lead to $M_3L_2$ species in which the 18 donors of two ligands are satisfied by three six-coordinate centres. A number of discrete $M_3L_2$ molecular species might be expected, including non-cyclic helical, catenated or looped structures (Fig. 1). Surprisingly, the reaction of L with 3 equiv. of $FeCl_2·4H_2O$ in $MeOH–CHCl_3$ gave a single purple product which was obtained as the $PF_6^-$ salt in 77% yield after recrystallisation from $MeCN–thf–H_2O$.

The stoichiometry $[Fe_3L_2][PF_6]_6$ was confirmed by microanalysis and the FAB mass spectrum exhibited peaks at *m/z* 2972 $\{Fe_3–L_2(PF_6)_5\}$ and 2827 $\{Fe_3L_2(PF_6)_4\}$. The doubly looped structure is easily distinguished from double helical and




**Scheme 1** *Reagents*: i, KOH, $HO(CH_2)_{10}OH$, $Me_2SO$; ii, 4′-chloro-2,2′;6′,2″-terpyridine, KOH, $Me_2SO$

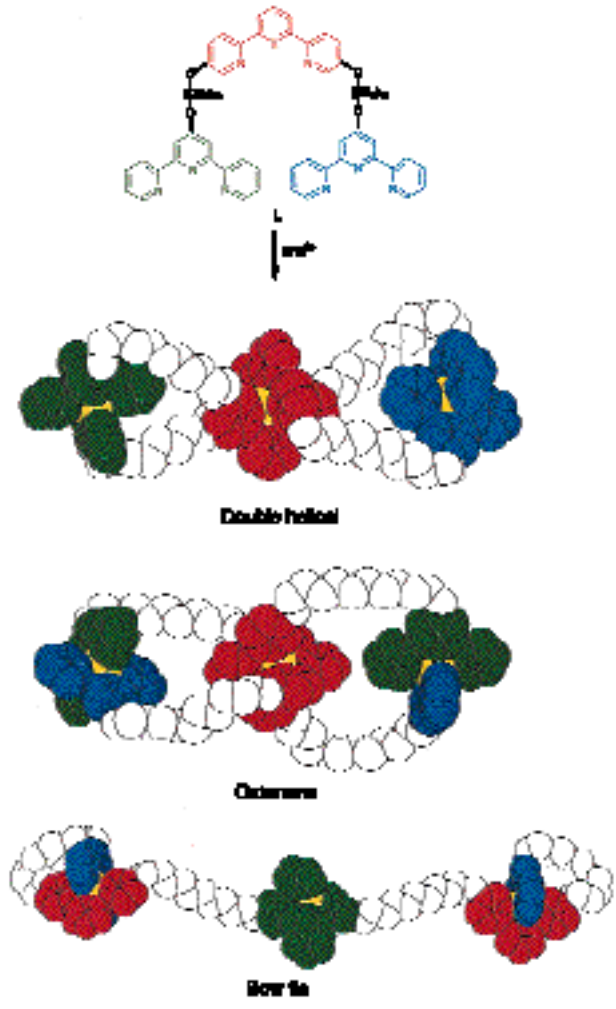



**Fig. 1** Possible consequences of the formation of 3:2 complexes with L

catenated structures on the basis of molecular symmetry. In the catenane and the double helix the two 4′-substituted tpy rings (green and blue) of each ligand are equivalent. This means that rings D and F are equivalent, as are rings E and G. Furthermore, the central (red) 5,5″-disubstituted tpy unit is symmetrical with rings A and C being equivalent. In contrast, the bow tie (double looped) structure is unique with the green and blue ligands being non-equivalent and rings A and C of the central red tpy unit also being non-equivalent. The 500 MHz $^1$H NMR spectrum of a $CD_3CN$ solution of $[Fe_3L_2][PF_6]_6$ is shown in Fig. 2 together with the assignments that follow from a COSY experiment and from comparison with model compounds. The simplest feature of note is the observation of two equal intensity signals for $H^{6A}$ and $H^{6C}$. This asymmetry of the central tpy unit is only possible in the doubly looped structure. The remaining assignments fully confirm the asymmetry that is only compatible with the looped structure.

The non-equivalence of the iron(II) centres is also seen in the differential pulse voltammogram of an acetonitrile solution of $[Fe_3L_2][PF_6]_6$ which exhibits a two-electron iron(II)/(III) process at +0.64 V (terminal metal centres) and a single electron process at +0.75 V corresponding to the central iron centre (all potentials quoted against internal ferrocene–ferrocenium couple). These potentials correspond well to the model compounds $[FeL^1{}_2][PF_6]_2$ ($L^1$ = 4′-ethoxy-2,2′:6′,2″-terpyridine, +0.60 V) and $[FeL^2{}_2][PF_6]_2$ [$L^2$ = 5,5″-bis(*n*-$C_{10}H_{21}O$)-2,2′:6′,2″-terpyridine, +0.73 V].

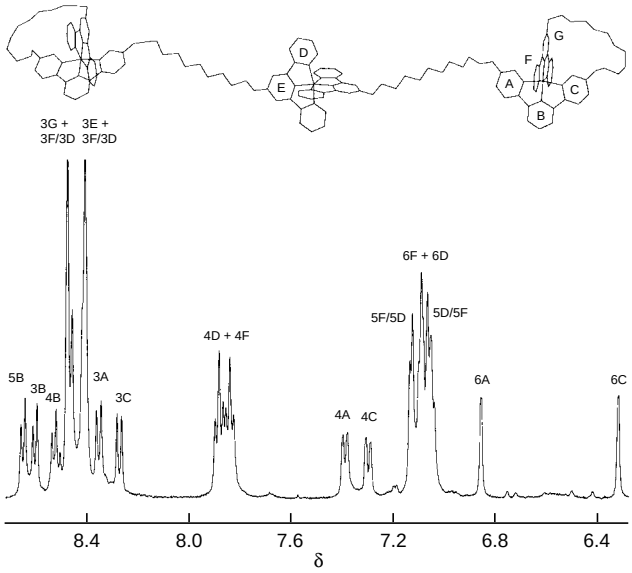



**Fig. 2** The aromatic region of the 500 MHz $^1$H NMR spectrum of a $CD_3CN$ solution of the looped complex $[Fe_3L_2][PF_6]_6$ showing the assignments

In conclusion, we have shown that the tritopic ligand L forms a doubly looped structure upon coordination to iron(II). Although singly looped structures have been described previously[4] we believe this to be the first example of such a five-component assembly of a doubly looped system. We are currently investigating the effects of varying the chain length and the metal centres.

We should like to thank the Schweizerischer Nationalfonds zur Förderung der wissenschaftlichen Forschung (Grant numbers: 21-37325.93 and 20-043359.95), the University of Basel and Ciba-Geigy for support.

## Footnotes

* E-mail: constable@ubaclu.unibas.ch

† This ChemComm is also available in enhanced multi-media format *via* the World Wide Web: http://chemistry.rsc.org/rsc/cccenha.htm

‡ All new compounds were fully characterised. Some pertinent details are presented below. L: mp 205 °C. MS: *m/z* 1040 ($M^+$). $^1$H NMR ($CDCl_3$): δ 8.70 (411, dd, $H^{6D}$), 8.53 (2 H, d, $H^{3A}$), 8.41 (4 H, d, $H^{3D}$), 8.35 (2 H, d, $H^{6A}$), 8.26 (2 H, d, $H^{3B}$, 8.00 (4 H, s, $H^{3E}$), 7.88 (1 H, t, $11^{4B}$), 7.85 (4 H, dd, $11^{4D}$), 7.32 (6 H, dd + dd, $H^{4A}$ + $H^{5D}$), 4.22 (4 H, t, 4′-tpyO$CH_2$), 4.06 (4 H, t, 5-tpyO$CH_2$), 1.2–1.7 (32 H, m).

**2**: mp 125–132 °C. MS: *m/z* 578 ($M^+$). $^1$H NMR ($CDCl_3$): δ 8.52 (2 H, d, $H^{3A}$), 8.35 (2 H, d, $H^{6A}$), 8.27 (2 H, d, $H^{3B}$), 7.87 (1 H, t, $H^{4B}$), 7.32 (2 H, dd, $H^{4A}$), 4.07 (4H, t, tpyO$CH_2$), 3.63 (4 H, t, $CH_2$OH), 1.83 (4 H, qnt, tpyO$CH_2CH_2$), 1.2–1.6 (28 H, m).

## References

1 *Comprehensive Coordination Chemistry*, ed. J.-M. Lehn, vol. 9, volume eds. J.-P. Sauvage and M. W. Hosseini, Pergamon, Oxford, 1996.

2 E. Matsumura, M. Ariga and Y. Tohda, *Bull. Chem. Soc. Jpn*., 1979, **52**, 2413; Y. Tahda, M. Eiraku, T. Nakagawa, Y. Usami, M. Ariga, T. Kawashima, K. Tani, H. Watanabe and Y. Mori, *Bull. Chem. Soc. Jpn*., 1990, **63**, 2820.

3 E. C. Constable and M. D. Ward, *J. Chem. Soc., Dalton Trans*., 1990, 1405.

4 J. C. Chambron, C. O. Dietrich-Buchecker, J. F. Nierengarten and J.-P. Sauvage, *J. Chem. Soc., Chem. Commun*., 1993, 801.

*Received in Cambridge, UK, 26th February 1997; Com. 7/01366C*

# Synthesis and structural characterization of a remarkably stable, anionic, incompletely condensed silsesquioxane framework

**Frank J. Feher,* Shawn H. Phillips and Joseph W. Ziller**

*Department of Chemistry, University of California, Irvine, CA 92697-2025, USA*

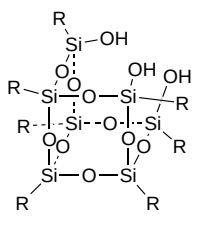
**The reaction of $[(C_6H_{11})_7Si_7O_9(OH)_3]$ 1 (2 equiv.) with $[(C_6H_{11})_7Si_7O_9(OTl)_3]$ 3 affords a conproportionation product that reacts with $[PPh_4]Cl$, $[PBu^n_4]Cl$ and $[NBu^n_4]Br$ to produce the corresponding salts of $[(C_6H_{11})_7Si_7O_{10}(OH)_2]^-$ 5 (*i.e.* the monoanion derived from deprotonation of 1); a single-crystal X-ray diffraction study of the $[(NBu^n_4)]^+$ salt of 5 indicates that the molecules exist as isolated ion pairs with strong intramolecular hydrogen bonding; implications of this result for the chemistry of silica are discussed.**

Silicates hold a unique place among major industrial raw materials because their constituent elements, mainly silicon and oxygen, together comprise nearly 80% of the atoms available on the earth's surface.[1] The inexhaustible supply of silicates, coupled with their impressive versatility, has led to thousands of applications and stimulated an intense interest in both the chemistry and physical properties of silicates.[2]

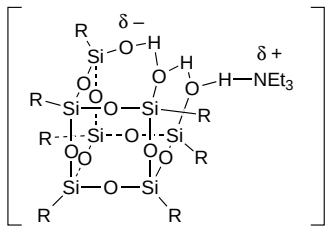
Numerous approaches have been explored for gaining molecular-level insights into the complex surface chemistry of siliceous materials, but detailed structural characterization and mechanistic studies on surface complexes are still inherently difficult. In order to assist and guide the study of silica and silica-supported catalysts, we[3] and others[4] have been exploring the chemistry of soluble siloxanes and silsesquioxanes,[5] as well as their metal-containing derivatives.[6] A large fraction of our work has focused on silsesquioxanes and metallasilsesquioxanes derived from trisilanol **1**, which can be conveniently prepared from $(C_6H_{11})SiCl_3$.[3a,7]

The chemistry of **1** is similar in many respects to the chemistry of other silanols,[6b] but there are a number of notable differences. For example, **1** is monosilylated with remarkable selectivity upon reaction with $Me_3SiCl$ in $NEt_3$–thf.[3b] Similarly, the reaction of **1** with an excess of $SbMe_5$ quickly produces a monofunctionalized product which only slowly reacts further with additional $SbMe_5$.[3e] Mechanistic studies relating to these and other observations strongly suggested that the unique reactivity of **1** was a consequence of increased acidity caused by hydrogen bonding between the three siloxy groups. In the case of silylation reactions, the intermediacy of ion pairs (*e.g.* **2**) was strongly implicated.[3b]

Here, we report the synthesis, spectroscopic characterization, and X-ray crystal structure of a remarkably stable anion that is formally derived from the deprotonation of **1**. In stark contrast to anions derived from simple alcohols and silanols, the monoanion of **1** does not react with phosphonium ions;[3d] it is also stable with respect to cyclocondensation. The implications of this result for the chemistry of silica surfaces will be discussed.



**1** R = $C_6H_{11}$

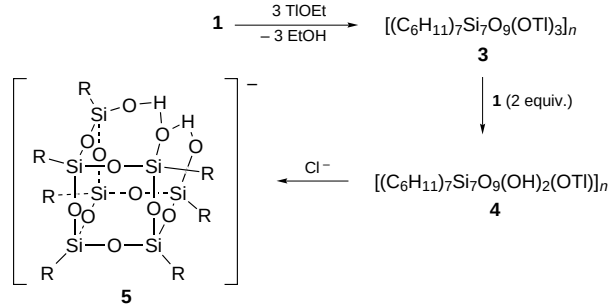


**2**

The reaction of **1** with thallium(I) ethoxide (Tl/SiOH = 1) affords an excellent yield of $[(C_6H_{11})_7Si_7O_9(OTl)_3]_n$ **3**,[8] which upon addition to a solution of **1** (2 equiv.) in $C_6D_6$ immediately produces a new complex which exhibits three methine (SiCH) resonances (3 : 3 : 1) in the room-temperature $^{13}C$ NMR spectrum; the most downfield resonance is exchange-broadened. On the basis of our previous work with Tl-substituted silsesquioxanes,[8] this data is most consistent with a $C_s$-symmetric conproportionation product (*e.g.* **4**) which undergoes facile exchange of one $Tl^I$ and two protons H between three siloxy groups on a $C_3$-symmetric $[R_7Si_7O_{12}]^{3-}$ framework.†

The addition of $[PPh_4]Cl$, $[PBu^n_4]Cl$ or $[NBu^n_4]Br$ to a solution of **4** in toluene immediately precipitates thallium halide to afford a quantitative NMR yield of a single silsesquioxane framework, which is spectroscopically indistinguishable from the product formed upon reaction of **1** with $Ph_3PCH_2$.[3d] $^1H$, $^{13}C$, $^{29}Si$ and $^{31}P$ NMR spectra of the products obtained from the reaction of **4** with $[PPh_4]Cl$ and $[PBu^n_4]Cl$ indicate the formation of a common silsesquioxane framework with free $[PPh_4]^+$ and $[PBu^n_4]^+$ as the only P-containing species in solution.‡ The NMR data provide no basis for distinguishing between a monomeric anionic silsesquioxane framework (*e.g.* **5**) and more complex oligomeric structures that are often adopted by silanols and incompletely condensed silsesquioxanes,[9] so a single-crystal X-ray diffraction study was performed to examine the nuclearity and extent of hydrogen bonding.§

Well formed crystals of the $[NBu^n_4]^+$ salt of **5** were obtained from toluene–hexane (2 : 1) at −35 °C. As illustrated in Fig. 1, the molecule crystallizes as isolated ion-pairs with strong intramolecular hydrogen bonding. The Si/O framework is remarkably symmetric and is nearly superimposable with a fully condensed $R_8Si_8O_{12}$ framework.[5,10] The O(1)···O(3) and O(2)···O(3) distances (2.576 and 2.569 Å) are shorter than O···O separations observed for most neutral, hydrogen-bonded silanols,[9] but they are well within the range observed for other hydrogen-bonded oxygen atoms.[11] Hydrogen atoms from the two siloxy groups, H(1) and H(2), were located and refined. In both cases, the atoms are involved in grossly unsymmetrical, nearly linear, hydrogen-bonding interactions with one short (0.88–0.89 Å) O–H bond and one long (1.68–1.70 Å) O···H bond. Similarly unsymmetrical hydrogen bonds are not uncommon when short O–H–O bonds do not straddle a symmetry element.[11] The structure represented by **5** nicely describes the overall hydrogen-bonding arrangement.



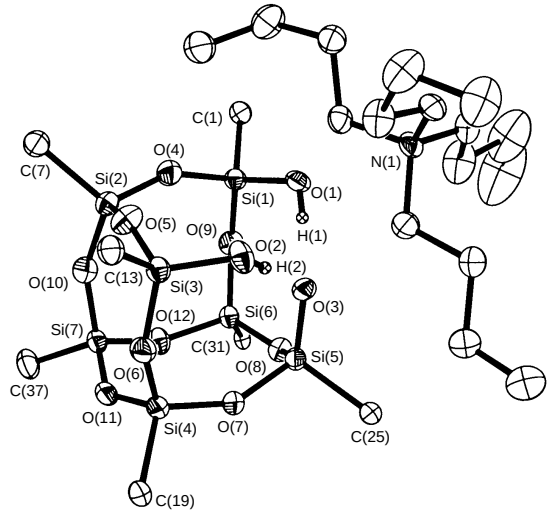



**Fig. 1** ORTEP plot of $[NBu^n_4]$ **5**. For clarity, thermal ellipsoids have been plotted at 50% probability and only C attached to Si are shown for cyclohexyl groups. Selected distances (Å) and angles (°): Si(1)–O(1) 1.618(3), Si(1)–O(4) 1.630(3), Si(3)–O(2) 1.606(4), Si(3)–O(5) 1.627(3), Si(5)–O(3) 1.588(3), Si(5)–O(7) 1.645(3), Si(1)–O(9) 1.637(3), Si(2)–O(4) 1.616(3), Si(3)–O(6) 1.624(3), Si(4)–O(7) 1.614(3), Si(5)–O(8) 1.651(3), Si(6)–O(9) 1.608(3), Si–C (av.) 1.862(5), N–C (av.) 1.521(6), Si(1)–O(1)–H(1) 113.8, Si(3)–O(2)–H(2) 114.2, O(1)–Si(1)–O(4) 110.9(2), O(1)–Si(1)O(9) 110.7(2), O(2)–Si(3)–O(5) 111.0(2), O(2)–Si(3)–O(6) 110.4(2), O(3)–Si(5)–O(7) 112.3(2), O(3)–Si(5)–O(8) 111.7(2), Si(2)–O(4)–Si(1) 152.5(2), Si(2)–O(5)–Si(3) 153.6(2), Si(4)–O(6)–Si(3) 146.7(2), Si(4)–O(7)–Si(5) 149.8(2), Si(6)–O(8)–Si(5) 138.7(2), Si(6)–O(9)–Si(1) 147.5(2), Si(7)–O(10)–Si(2) 153.4(2), Si(7)–O(11)–Si(4) 138.6(2), Si(7)–O(12)–Si(6) 149.7(2), O–Si–C (av.) 109.1(2), C–N–C (av.) 109.5(4), C–C–N (av.) 115.2(5).

The unexpected stability of **5** has a number of important implications for the chemistry of silica surfaces. Our results demonstrate that extensive hydrogen bonding can stabilize anions derived from multiply hydrogen-bonded silanols. In the case of **5**, the anion is so stable that it does not coordinate to a phosphonium ion, even in a hydrocarbon solvent. Because conjugate acids of stable anions are generally more acidic that conjugate acids of less stable anions, the acidity of silica surfaces sites possessing multiply hydrogen-bonded siloxy groups must be greater than the acidity of isolated SiOH groups. Although somewhat controversial, this conclusion is completely consistent with recent work by Drago[12] and Morrow,[13] which implicates the existence of a significant subset of hydrogen-bonded siloxy groups which is both more acidic and more reactive toward $SbMe_5$ than isolated siloxyl groups.

It is interesting to consider whether surfaces sites analogous to **5** could be detected on silica because similar arrangements should be both accessible and stable. Detailed examination of IR spectra might provide an answer, but the OH stretching frequency for the $[NBu^n_4]^+$ salt of **5** (3563 $cm^{-1}$ in thf) appears within the range assigned to vicinally hydrogen-bonded disilanols. It might, however, be possible to detect the hydrogen-bonded protons (δ *ca*. 11–12) by using solid-state NMR techniques.[14] We are currently exploring this possibility, as well as the rich reaction chemistry of **5**.

This work was supported by the National Science Foundation (USA).

## Footnotes

* E-mail: fjfeher@uci.edu

† $[(C_6H_{11})_7Si_7O_9(OH)_2(OTl)]$ **4**: $(C_6H_{11})_7Si_7O_9(OH)_3$ **1**[3a] (30 mg, 0.031 mmol) and $(C_6H_{11})_7Si_7O_9(OTl)_3$ **3**[8] (24 mg, 0.015 mmol) were dissolved in $C_6D_6$ (*ca*. 0.5 ml). Examination of the NMR spectra ($^1H$ and $^{13}C$) revealed the formation of a single silsesquioxane product. Although this product cannot be isolated in pure form, it reacts with a variety of halide salts to afford stable salts of **5**.

‡ $[NBu^n_4]^+$, $[PBu^n_4]^+$, and $[PPh_4]^+$ salts of $[(C_6H_{11})_7Si_7O_{10}(OH)_2]^-$ **5**: in a typical reaction, 1 mol. equiv. of $[NBu^n_4]Br$, $[PBu^n_4]Cl$ or $[PPh_4]Cl$ was added to a solution of **4** prepared from **1** (339 mg, 0.348 mmol) and **3** (276 mg, 0.174 mmol) in toluene (10 ml); in all cases, a white precipitate formed immediately. The solution was stirred for 8 h and then filtered to remove Tl halide. The $[NBu^n_4]^+$ salt of **5** was obtained in 83% yield as large rectangular crystals from hexane–toluene (−35 °C). The $[PBu^n_4]^+$ and $[PPh_4]^+$ salts were obtained as white microcrystalline precipitates in 71 and 59% yields by crystallization (−35 °C) from toluene–hexane and toluene–acetonitrile, respectively.

§ *Crystallographic data*: for $[NBu^n_4]$**5**: $C_{58}H_{115}NO_{12}Si_7$, $M$ = 1215.14, monoclinic, space group $P2_1/c$, $a$ = 15.329(4), $b$ = 18.943(6), $c$ = 24.109(7) Å, $U$ = 6838.6(35) Å$^3$, Z = 4. Intensities were measured at 158 K with Mo-Kα radiation (λ = 0.71073 Å) and corrected for Lorentz and polarization effects. The mean intensity of three standard reflections decreased by < 1% during the experiment. The structure was solved by direct methods; final refinements were carried out with anisotropic thermal parameters for all non-H atoms: 9506 unique reflections collected; 711 parameters refined; $R_1$ = 0.0548, $wR_2$ = 0.1165 for 9502 reflections with I > 2σ($I$). Atomic coordinates, bond lengths and angles, and thermal parameters have been deposited at the Cambridge Crystallographic Data Centre (CCDC). See Information for Authors, Issue No. 1. Any request to the CCDC for this material should quote the full literature citation and the reference number 182/412.

## References

1 N. N. Greenwood and A. Earnshaw, *Chemistry of The Elements*, Pergamon, New York, 1984.
2 (*a*) I. Fanderlik, *Silica glass and its application*, Elsevier, New York, 1991; (*b*) P. J. Heaney, C. T. Prewitt and G. V. Gibbs, *Silica: physical behavior, geochemistry and materials applications*, Mineralogical Society of America, Washington, D.C., 1994; (*c*) R. K. Iler, *The chemistry of silica: solubility, polymerization, colloid and surface properties, and biochemistry*, Wiley, New York, 1979; (*d*) R. P. W. Scott, *Silica gel and bonded phases: their production, properties, and use in LC*, Wiley, New York, 1993; (*e*) R. B. Sosman, *The Phases of Silica*, Rutgers University Press, New Brunswick, NJ, 1965; (*f*) K. K. Unger, *Porous silica, its properties and use as support in column liquid chromatography*, Elsevier Scientific Pub. Co., New York, 1979; (*g*) E. F. Vansant, P. v. d. Voort and K. C. Vrancken, *Characterization and chemical modification of the silica surface*, Elsevier, New York, 1995.
3 (*a*) F. J. Feher, D. A. Newman and J. F. Walzer, *J. Am. Chem. Soc.*, 1989, **111**, 1741; (*b*) F. J. Feher and D. A. Newman, *J. Am. Chem. Soc.*, 1990, **112**, 1931; (*c*) F. J. Feher, T. A. Budzichowski, K. Rahimian and J. W. Ziller, *J. Am. Chem. Soc.*, 1992, **114**, 3859; (*d*) F. J. Feher and S. H. Phillips, *J. Organomet. Chem.*, 1996, **521**, 391.
4 (*a*) N. Winkhofer, H. W. Roesky, M. Noltemeyer and W. T. Robinson, *Angew. Chem., Int. Ed. Engl.*, 1992, **31**, 599; (*b*) H.-J. Gosink, H. W. Roesky, M. Noltemeyer, H.-G. Schmidt, C. Freire-Erdbrügger and G. M. Sheldrick, *Chem. Ber.*, 1993, **33**, 279.
5 M. G. Voronkov and V. Lavrent'ev, *Top. Curr. Chem.*, 1982, **102**, 199.
6 (*a*) F. J. Feher and T. A. Budzichowski, *Polyhedron*, 1995, **14**, 3239; (*b*) R. Murugavel, A. Voigt, M. G. Walawalkar and H. W. Roesky, *Chem. Rev.*, 1996, **96**, 2205; (*c*) R. Murugavel, V. Chandrasekhar and H. W. Roesky, *Acc. Chem. Res.*, 1996, **29**, 183; (*d*) H. Bürgy, G. Calzaferri, D. Herren and A. Zhdanov, *Chimia*, 1991, **45**, 3.
7 J. F. Brown and L. H. Vogt, *J. Am. Chem. Soc.*, 1965, **87**, 4313.
8 F. J. Feher, K. Rahimian, T. A. Budzichowski and J. W. Ziller, *Organometallics*, 1995, **14**, 3920.
9 P. D. Lickiss, *Adv. Inorg. Chem.*, 1995, **42**, 147.
10 (*a*) U. Dittmar, B. J. Hendan, U. Flörke and H. C. Marsmann, *J. Organomet. Chem.*, 1995, **489**, 185; (*b*) F. J. Feher and T. A. Budzichowski, *J. Organomet. Chem.*, 1989, **373**, 153; (*c*) V. W. Day, W. G. Klemperer, V. V. Mainz and D. M. Millar, *J. Am. Chem. Soc.*, 1985, **107**, 8262; (*d*) G. Calzaferri, R. Imhof and K. Törnroos, *J. Chem. Soc., Dalton Trans.*, 1994, 3123; (*e*) G. Calzaferri, R. Imhof and K. W. Törnroos, *J. Chem. Soc., Dalton Trans.*, 1993, 3741.
11 A. F. Wells, *Structural Inorganic Chemistry*, Clarendon Press, Oxford, 1984.
12 C. W. Chronister and R. S. Drago, *J. Am. Chem. Soc.*, 1993, **115**, 4793.
13 Y. Wang and B. A. Morrow, *Langmuir*, 1996, **12**, 4153.
14 (*a*) G. E. Maciel, *Adv. Chem. Ser.*, 1994, **234**, 269; (*b*) G. E. Maciel, *NATO ASI Ser., Ser. C*, 1994, **447**, 401: (*c*) C. E. Bronnimann, R. C. Ziegler and G. E. Maciel, *J. Am. Chem. Soc.*, 1988, **110**, 2023.

*Received in Bloomington, IN, USA, 12th February 1997; Com. 7/01005B*

# Solution structures and exchange phenomena of the new alkene polymerization initiators (η-$C_5Me_5$)TiMe(E)(μ-Me)B($C_6F_5$)$_3$ (E = $C_6F_5$, $OC_6F_5$) and [(η-$C_5Me_5$)Ti($OC_6F_5$)$_2$][BMe($C_6F_5$)$_3$]

**Tracey L. Tremblay, Sean W. Ewart, Mark J. Sarsfield and Michael C. Baird***

*Department of Chemistry, Queen's University, Kingston, Ontario, Canada K7L 3N6*

**The solution structures and dynamics of the new alkene polymerization initiators (η-$C_5Me_5$)TiMe($C_6F_5$)(μ-Me)B($C_5F_5$)$_3$ 2, (η-$C_5Me_5$)TiMe($OC_6F_5$)(μ-Me)B($C_6F_5$)$_3$ 3 and [(η-$C_5Me_5$)Ti($OC_6F_5$)$_2$][BMe($C_5F_5$)$_3$] 4 are compared and contrasted with those of the known initiator (η-$C_5Me_5$)-TiMe$_2$(μ-Me)B($C_6F_5$)$_3$ 1; compound 2 undergoes neither spontaneous ion-pair dissociation to the solvent separated [(η-$C_5Me_5$)TiMe($C_6F_5$)]$^+$ and [BMe($C_6F_5$)$_3$]$^-$ nor borane dissociation to its precursors (η-$C_5Me_5$)TiMe$_2$($C_6F_5$) and B($C_6F_5$)$_3$; in contrast, 3 is more labile and does undergo ion-pair dissociation, while 4 exists in solution as the separated ion species in equilibrium with its precursors, (η-$C_5Me_5$)TiMe($OC_6F_5$)$_2$ and B($C_6F_5$)$_3$.**

There is currently considerable interest in the utilization of group 4 metal complexes of the types [(Cp′)$_2$MMe]$^+$X$^-$ and [(Cp′)MMe$_2$]$^+$X$^-$ (Cp′ = substituted cyclopentadienyl; M = Ti, Zr, Hf; X$^-$ = poorly coordinating anion) as initiators for alkene polymerization.[1–3] Since most of the more active molecular alkene polymerization initiators are cationic rather than neutral,[1–3] one might anticipate that increasing the Lewis acidity of the metal atoms by incorporation of more electron-withdrawing ligands would result in even hgher activities. However, binding of X$^-$ to the cationic species [(Cp′)$_2$MMe]$^+$ and [(Cp′)MMe$_2$]$^+$ may also be enhanced by increasing the Lewis acidity,[4] resulting in inhibition of monomer coordination, while the relative rates of initiation, propagation, termination and chain transfer are affected unpredictably by ligand substitution.[1,5] The result is that electron-withdrawing ligands sometimes result in both decreased catalytic activity and reduced polymer molecular masses.[5]

Although detailed studies of ion-pairing phenomena and their effects on catalytic activities of some metallocene systems [(Cp′)$_2$MMe]$^+$X$^-$ are available,[4] relatively little is known as yet of the behaviour of monocyclopentadienyl systems [(Cp′)MMe$_2$]$^+$X$^-$. Interestingly, it has been shown that the zwitterionic compound (η-$C_5Me_5$)TiMe$_2$(μ-Me)B($C_6F_5$)$_3$ **1** (Fig. 1, E = Me), formed by treating (η-$C_5Me_5$)TiMe$_3$ with B($C_6F_5$)$_3$ [eqn. (1)],[3] undergoes facile displacement of borate anion,

(η-$C_5Me_5$)TiMe$_2$E + B($C_6F_5$)$_3$ ⇌ (η-$C_5Me_5$)TiMeE(μ-Me)B($C_6F_5$)$_3$ (1)

E = Me **1**, $C_6F_5$ **2**, $OC_6F_5$ **3**

[BMe($C_6F_5$)$_3$]$^-$, on reaction with other ligands.[3] Furthermore, magnetization transfer experiments have demonstrated a low degree of reversible borate dissociation from **1** at 223 K [eqn. (2); E = Me][3] but no exchange between terminal and bridging methyl groups was detected, *i.e.* the borane in **1** does not 'hop' from one methyl to another [reverse of eqn. (2)],

(η-$C_5Me_5$)TiMeE(μ-Me)B($C_6F_5$)$_3$ ⇌ [(η-$C_5Me_5$)TiMeE]$^+$[BMe($C_6F_5$)$_3$]$^-$ (2)

as occurs in some metallocene systems.[4a–d]

In order to better understand the effects of ligand electronic properties on catalytic activities of this class of compounds, we have extended our investigation to the methyl-bridged chiral compounds (η-$C_5Me_5$)TiMe($C_6F_5$)(μ-Me)B($C_6F_5$)$_3$ **2** and (η-$C_5Me_5$)TiMe($OC_6F_5$)(μ-Me)B($C_6F_5$)$_3$ **3**, and to the achiral, apparently ionic compound [(η-$C_5Me_5$)Ti($OC_6F_5$)$_2$][BMe($C_6F_5$)$_3$] **4**. The new zwitterionic complexes **2** and **3**, in which one of the methyl ligands of **1** has been replaced by the more electronegative ligands $C_6F_5$ and $OC_6F_5$, formed cleanly on treatment of solutions of (η-$C_5Me_5$)TiMe$_2$($C_6F_5$)† and (η-$C_5Me_5$)TiMe$_2$($OC_6F_5$)† with 1 equiv. each of the borane B($C_6F_5$)$_3$ in $CD_2Cl_2$ at 195 K [eqn. (1)]. These complexes decompose above 283 K and could not be isolated, but have been fully characterized by $^1$H, $^{13}$C and $^{19}$F NMR spectroscopic studies ($CD_2Cl_2$, 223–283 K).†

The $^1$H, $^{19}$F and $^{13}$C{$^1$H} NMR spectra† of **2** and **3** are all consistent with structures as in Fig. 1, sharp terminal Ti–Me and broadened μ-MeB resonances being especially characteristic of the zwitterionic structures proposed.[3] Interestingly, however, the $^1$H NMR spectrum of **2** at 223 K exhibits a doublet Ti–Me resonance because of long-range coupling with one of the *o*-fluorine atoms of the Ti–$C_6F_5$ ligand ($J_{HF}$ 3.1 Hz), while the $^{19}$F spectrum of **2** at 223 K exhibits five equal intensity resonances attributable to the Ti–$C_6F_5$ group, On warming, the pairs of *o*- and *m*-$^{19}$F resonances broaden and coalesce at *ca.* 293 and 273 K, respectively, although the *p*-fluorine resonance and all of the borate fluorine resonances remain well resolved in the temperature range 223–283 K. These observations require that both rotation about the Ti–$C_6F_5$ bond and inversion at the chiral metal (involving ion-pair dissociation–recombination[4a–d]) be slow on the NMR timescale at 223 K, while consideration of the coalescence temperatures suggests an approximate $\Delta G^{\ddagger}$ of 50.6 ± 2.1 kJ mol$^{-1}$ for the exchange process(es).[7] This would represent a lower limit for both processes, and is to be compared with *ca.* 58 ± 19 kJ mol$^{-1}$ for ion-pair dissociation–reorganization processes of similar zirconocene and hafnocene complexes.[4a–d]

Consistent with this interpretation and in contrast to **1**,[3] attempted magnetization transfer experiments provided no evidence in the $^1$H NMR spectrum of **2** for dissociation of the borate anion [BMe($C_6F_5$)$_3$]$^-$; thus the (μ-Me)B($C_6F_5$) moiety is relatively strongly bound to the titanium centre in **2**. In contrast, irradiation of the μ-Me resonance of **3** did result in magnetization transfer and appearance of a weak free borate resonance, indicating an equilibrium between solvent separated ion pairs and the methyl bridged species, as with **1**.[3] With neither **2** nor **3**

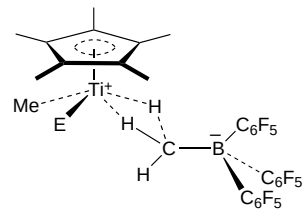



**Fig. 1** Proposed structure for **1** (E = Me), **2** (E = $C_6F_5$) and **3** (E = $OC_6F_5$)

was there evidence from spin-transfer experiments for Ti–Me/B–Me exchange, as occurs in zirconocene systems.[4a–d]

Compounds **1**,[3] **2** and **3** all behave as ethene and propene polymerization catalysts under strictly anhydrous conditions in toluene. While the polyethylene formed is generally too insoluble for even high-temperature GPC measurements, the molecular masses of the polypropylene formed at 195 K decrease in the order **2** ($M_w = 2.3 \times 10^6$, $M_w/M_n = 1.7$) > **3** ($M_w = 2.0 \times 10^6$, $M_w/M_n = 1.7$) > **1** ($M_w = 0.3 \times 10^6$, $M_w/M_n = 1.3$). The low dispersities observed are consistent with single site catalysts in all cases,[1] but the most Lewis acidic catalyst gives the highest molecular mass polymer, just the opposite to apparent trends in metallocene systems.[5] On the other hand, the yields of polymers obtained with **2** and **3** are about 30% lower than those obtained with **1**, consistent with stronger borate coordination to the more Lewis acidic catalytic sites. Thus combination of the types of Lewis acidic complexes described here with counter anions which, perhaps for steric reasons,[8] coordinate less weakly than $[BMe(C_6F_5)_3]^-$, may well lead to alkene polymerization catalysts of high activity.

The solution behaviour observed for **4** was most unexpected. The methyl abstraction reaction of (η-$C_5Me_5$)$TiMe(OC_6F_5)_2$ with 1 equiv. of $B(C_6F_5)_3$ in $CD_2Cl_2$ was monitored by $^1H$ and $^{19}F$ NMR spectroscopy in the temperature range 223–298 K, and it was found that the $^1H$ and $^{19}F$ spectra at 223 K exhibited resonances attributable only to the solvent separated species of **4**, $[(\eta\text{-}C_5Me_5)Ti(OC_6F_5)_2]^+$ and $[BMe(C_6F_5)_3]^-$; none were attributable to coordinated borate as in **1**–**3**. Remarkably, warming the NMR solution of **4** resulted in the reversible reappearance of the resonances of the neutral precursor (η-$C_5Me_5$)$TiMe(OC_6F_5)_2$, and at 263 K there was a substantial amount of both species present. Spin saturation transfer and variable-temperature experiments showed them to be in equilibrium, with $\Delta H = -1.25 \pm 0.1$ kJ mol$^{-1}$, $\Delta S = -46 \pm 4$ J K$^{-1}$ mol$^{-1}$ for conversion to the non-ionic species. The ability of **4** to engage in Ti–Me/B–Me exchange stands in contrast to **1**–**3** and even to methylzirconocene systems,[4a–d] for which variable-temperature NMR studies imply similar exchange but not the major shift in equilibrium noted here. Since $[(\eta\text{-}C_5Me_5)Ti(OC_6F_5)_2]^+$ is expected to be a relatively strong Lewis acid, its unusual disinclination to bind the borate anion must be attributed to steric hindrance by the three bulky ligands on the titanium hindering close approach of the borate anion. In **4**, moreover, it appears that the strong but sterically hindered Lewis acid $[(\eta\text{-}C_5Me_5)Ti(OC_6F_5)_2]^+$ effectively competes with $B(C_6F_5)_3$ for possession of the methyl group, presumably *via* a transient methyl bridged species although none was detected in the spin saturation experiments. An alternative structure for **4** such as $\{[(\eta\text{-}C_5H_5)Ti(OC_6F_5)(\mu\text{-}OC_6F_5)]_2\}^{2+}$ seems unlikely since (*a*) the pentafluorophenoxy groups are equivalent in the $^{19}F$ NMR spectrum and (*b*) **3** clearly does not contain such a μ-$OC_6F_5$ group.

We thank the Natural Sciences and Engineering Research Council of Canada (Research and Strategic Grants to M. C. B. and Graduate Scholarship to S. W. E.) and Alcan (Graduate Scholarship to S. W. E.) for financial support.

## Footnotes

* E-mail: bairdmc@qucdn.queensu.ca

† Reactions of the compounds (η-$C_5Me_5$)$TiCl_2Me$[6] and (η-$C_5Me_5$)-$TiMe_2Cl$[6] with appropriate amounts of $LiC_6F_5$ or $LiOC_6F_5$ in hexanes yielded the thermally robust, yellow compounds (η-$C_5Me_5$)$TiMe_2(C_6F_5)$, (η-$C_5Me_5$)$TiMe_2(OC_6F_5)$ and (η-$C_5Me_5$)$TiMe(OC_6F_5)_2$, all of which have been fully and satisfactorily characterized by elemental analyses and spectroscopic methods.

(η-$C_5Me_5$)$TiMe_2(C_6F_5)$. $^1H$ NMR ($CDCl_3$, 298 K), δ 1.98 (s, 15 H, $C_5Me_5$), 1.41 (t, 6 H, Ti–Me, $J_{HF}$ 2.0); $^{13}C\{^1H\}$ NMR ($CDCl_3$, 298 K); δ 127.0 ($C_5Me_5$), 80.0 (t, Ti–Me, $J_{CF}$ 3.3 Hz), 12.4 ($C_5Me_5$); $^{19}F$ NMR ($C_6D_6$, 298 K, ref. $CFCl_3$), δ −121.4 (m, 2 F, *o*-F), −155.6 (t, 1 F, *p*-F), −163.0 (m, 2 F, *m*-F).

(η-$C_5Me_5$)$TiMe_2(OC_6F_5)$. $^1H$ NMR ($CD_2Cl_2$, 223 K), δ 1.86 (s, 15 H, $C_5Me_5$), 0.55 (s, 3 H, Ti–Me); $^{13}C\{^1H\}$ NMR ($CD_2Cl_2$, 223 K), δ 141.1 (d, *o*-CF, $J_{CF}$ 231.5 Hz), 138.7 (d, *m*-CF, $J_{CF}$ 241.5 Hz), 135.5 (d, *p*-CF, $J_{CF}$ 241.5 Hz), 124.2 ($C_5Me_5$), 59.0 (Ti–Me), 12.1 ($C_5Me_5$); $^{19}F$ NMR ($CD_2Cl_2$, 298 K, ref. $CFCl_3$), δ −160.1 (m, 2 F, *o*-F), −167.0 (m, 2 F, *m*-F), −171.3 (t, 1 F, *p*-F).

(η-$C_5Me_5$)$TiMe(OC_6F_5)_2$. $^1H$ NMR ($CD_2Cl_2$, 223 K), δ 1.89 (s, 15 H, $C_5Me_5$), 1.09 (s, 3 H, Ti–Me); $^{13}C\{^1H\}$ NMR ($CD_2Cl_2$, 223 K), δ 139.9 (d, *o*-CF, $J_{CF}$ 251.5 Hz), 138.1 (d, *m*-CF, $J_{CF}$ 241.5 Hz), 135.2 (d, *p*-CF, $J_{CF}$ 251.5 Hz), 127.0 ($C_5Me_5$), 61.5 (Ti–Me), 10.9 ($C_5Me_5$); $^{19}F$ NMR ($CD_2Cl_2$, 223 K), δ −161.4 (m, 2 F, *o*-F), −167.0 (m, 2 F, *m*-F), −171.3 (t, 1 F, *p*-F).

(η-$C_5Me_5$)$TiMe(C_6F_5)$(μ-Me)$B(C_6F_5)_3$ **2**. $^1H$ NMR ($CD_2Cl_2$, 223 K), δ 2.61 (d, 3 H, Ti–Me, $J_{HF}$ 3.1), 2.10 (s, 15 H, $C_5Me_5$), 1.36 (br s, 3 H, μ-Me); $^{13}C\{^1H\}$ ($CD_2Cl_2$, 223 K), δ 138.2 ($C_5Me_5$), 109.9 (Ti–Me), 13.6 ($C_5Me_5$); $^{19}F$ ($CD_2Cl_2$, 223 K), δ −118.6 (m, 1 F, *o*-F of Ti–$C_6F_5$), −124.3 (m, 1 F, *o*-F of Ti–$C_6F_5$), −135.1 (m, 6 F, *o*-F of B–$C_6F_5$), −150.1 (t, 1 F, *p*-F of Ti–$C_6F_5$), −160.3 (m, 1 F, *m*-F of Ti–$C_6F_5$), −160.8 (t, 3 F, *p*-F of B–$C_6F_5$), −161.7 (m, 1 F, *m*-F of Ti–$C_6F_5$), −166.0 (m, 6 F *m*-F of B–$C_6F_5$).

(η-$C_5Me_5$)$TiMe(OC_6F_5)$(μ-Me)$B(C_6F_5)_3$ **3**. $^1H$ NMR ($CD_2Cl_2$, 223 K), δ 2.04 (s, 15 H, $C_5Me_5$), 1.89 (s, 3 H, Ti–Me), 0.62 (br s, 3 H, μ-Me); $^{13}C\{^1H\}$ ($CD_2Cl_2$, 223 K), δ 134.3 ($C_5Me_5$), 82.2 (Ti–Me), 12.2 ($C_5Me_5$); $^{19}F$ ($CD_2Cl_2$, 223 K), δ −135.4 (m, 6 F, *o*-F of B–$C_6F_5$), −159.7 (m, 2 F, *o*-F of Ti–$OC_6F_5$), −160.9 (t, 3 F, *p*-F of B–$C_6F_5$), −164.5 (m, 2 F, *m*-F of Ti–$OC_6F_5$), −165.0 (m, 2 F, *m*-F of Ti–$OC_6F_5$), −166.0 (m, 6 F, *m*-F of B–$C_6F_5$).

$[(\eta\text{-}C_5Me_5)Ti(OC_6F_5)_2][BMe(C_6F_5)_3]$ **4**. $^1H$ NMR ($CD_2Cl_2$, 223 K), δ 2.17 (s, 15 H, $C_5Me_5$), 0.37 (br s, 3 H, B–Me); $^{13}C\{^1H\}$ NMR ($CD_2Cl_2$, 223 K), δ 139.3 ($C_5Me_5$), 12.3 ($C_5Me_5$), $^{19}F$ NMR ($CD_2Cl_2$, 223 K), δ −133.7 (m, 6 F, *o*-F of B–$C_6F_5$), −159.2 (m, 4 F, *o*-F of O–$C_6F_5$), −165.1 (t, 3 F, *p*-F of B–$C_6F_5$), −163.5 (m, 4 F, *m*-F of O–$C_6F_5$), −162.4 (t, 2 F, *p*-F of O–$C_6F_5$), −168.4 (m, 6 F, *m*-F of B–$C_6F_5$).

## References

1 P. C. Möhring and N. J. Coville, *J. Organomet. Chem.*, 1994, **479**, 1; V. K. Gupta, S. Satish and I. S. Bhardwaj, *J. Macromol. Sci.*, 1994, **C34**, 439; H. H. Brintzinger, D. Fischer, R. Mülhaupt, B. Rieger and R. M. Waymouth, *Angew. Chem., Int. Ed. Engl.*, 1995, **34**, 1143; M. Bochmann, *J. Chem. Soc., Dalton Trans.*, 1996, 255. For recent theoretical considerations at the density functional level, see T. K. Woo, L. Fan and T. Ziegler, *Organometallics*, 1994, **13**, 2252.

2 For recent references, see: C. Pellecchia, D. Pappalardo, L. Oliva and A. Zambelli, *J. Am. Chem. Soc.*, 1995, **117**, 6593; A. Grassi, C. Pellecchia, L. Oliva and F. Laschi, *Macromol. Chem. Phys.*, 1995, **196**, 1093; A. Grassi, A. Zambelli and L. Oliva, *Organometallics*, 1996, **15**, 480; P. Foster, J. C. W. Chien and M. D. Rausch, *Organometallics*, 1996, **15**, 2404; J. C. Flores, J. S. Wood, J. C. W. Chien and M. D. Rausch, *Organometallics*, 1996, **15**, 4944; J. C. Flores, J. C. W. Chien and M. D. Rausch, *Macromolecules*, 1996, **29**, 8030.

3 (*a*) Q. Wang, R. Quyoum, D. J. Gillis, M.-J. Tudoret, D. Jeremic, B. K. Hunter and M. C. Baird, *Organometallics*, 1996, **15**, 693 and references therein; (*b*) Q. Wang, R. Quyoum, D. J. Gillis, D. Jeremic and M. C. Baird, *J. Organomet. Chem.*, 1997, **527**, 7.

4 (*a*) X. Yang, C. L. Stern and T. J. Marks, *J. Am. Chem. Soc.*, 1991, **113**, 3623; (*b*) X. Yang, C. L. Stern and T. J. Marks, *J. Am. Chem. Soc.*, 1994, **116**, 10015; (*c*) P. A. Deck and T. J. Marks, *J. Am. Chem. Soc.*, 1995, **117**, 6128; (*d*) M. A. Giardello, M. S. Eisen, C. L. Stern and T. J. Marks, *J. Am. Chem. Soc.*, 1995, **117**, 12114; (*e*) A. R. Siedle and R. A. Newmark, *J. Organomet. Chem.*, 1995, **497**, 119; (*f*) D. E. Richardson, N. G. Alameddin, M. F. Ryan, T. Hayes, J. R. Eyler and A. R. Siedle, *J. Am. Chem. Soc.*, 1996, **118**, 11244.

5 N. Piccolrovazzi, P. Pino, G. Consiglio, A. Sironi and M. Moret, *Organometallics*, 1990, **9**, 3098; I.-M, Lee, W. J. Gauthier, J. M. Ball, I. Bhagavathi and S. Collins, *Organometallics*, 1992, **11**, 2115.

6 M. Mena, P. Royo, R. Serrano, M. A. Pellinghelli and A. Tiripicchio, *Organometallics*, 1989, **8**, 476; A. Martín, M. Mena, M. A. Pellinghelli, P. Royo, R. Serrano and A. Tiripicchio, *J. Chem. Soc., Dalton Trans.*, 1993, 2117.

7 J. Sandstrom, *Dynamic NMR Spectroscopy*, Academic Press, New York, 1982, pp. 77–92.

8 See for example, Y.-X. Chen, C. L. Stern, S. Yang and T. J. Marks, *J. Am. Chem. Soc.*, 1996, **118**, 12451.

*Received in Bloomington, IN, USA, 10th January 1997; Com. 7/00232G*

# A PEO salt complex exhibiting photoresponsive ionic conductivity

**Isabelle Decker, Jean-Pierre Petit and Didier Delabouglise***

*Laboratoire d'Electrochimie et de Physicochimie des Matériaux et des Interfaces UMR CNRS-INPG 5631, ENSEEG, BP 75, 38402 St Martin d'Hères, France*

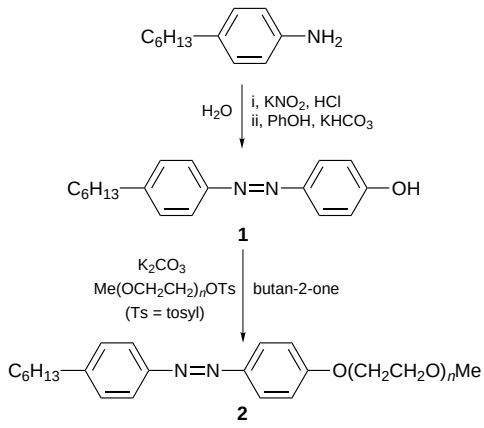
**A polymer electrolyte film made of lithium perchlorate dissolved in a mix of high molecular mass poly(ethylene oxide) (PEO) and shorter PEO–azobenzene diblocks, shows a reversible 70% conductivity increase under UV light irradiation at room temperature.**

Only few published works have dealt with light-induced reversible ionic conductivity changes in polymer films.[1–3] In most cases the studied effect arises from a single molecular mechanism. For instance, photoactivated reversible cation complexation is obtained for some spiropyrans[1] or crowned malachite greens.[2] Indeed a 5% reversible increase from $5.3 \times 10^{-6}$ S cm$^{-1}$ at 30 °C, was observed when a polymethacrylate bearing both methoxylated benzospiropyrans and short polyether chains and dissolving zinc chloride, was irradiated by UV light.[1] Fluctuations of very low ionic conductivity, about $10^{-10}$ S cm$^{-1}$, were also described for a crowned malachite green dissolved in a PEO matrix containing a sodium salt and submitted to pulsed UV light.[2] A similar effect for conductivities lying around $10^{-8}$ S cm$^{-1}$ at 80 °C, was also obtained with polyester composite films containing crowned azobenzenes and a lithium salt.[3] In this latter case however the azobenzene based molecules exhibited liquid-crystalline behaviour and the conductivity increase was related to a transition from the nematic phase to the isotropic liquid one.[3] Indeed *cis–trans* photoisomerism of azobenzenes is well known and the birefringent nematic phase of some linear *trans*-azobenzenes can be erased by UV light when the bent *cis* form thus produced disrupts the liquid-crystal order. This effect has been used for image storage in either nematic polymer films[4] or ferroelectric smectic layers.[5] For the present work, we used the azobenzene photoisomerism in a different way allowing efficient light monitoring of ionic conductivity of polymer electrolyte films at levels as high as about $10^{-4}$ S cm$^{-1}$.

The chemical method for coupling short monomethylated PEO chains ($M_w$ = 750) with alkylated azobenzene (Scheme 1)† was adapted from literature data.[6] 1-(4-Hydroxyphenyl) 2-(4-hexylphenyl)diazene **1** (AZOH),[6] exhibited several endothermic transitions at 33, 40, 53 and 77 °C on differential scanning calorimetry (DSC) recordings, the intensity of which increased in the same order as the transition temperatures. Several liquid-crystal phases appeared up to the isotropic liquid. For AZOH–PEO **2**, the DSC trace showed a unique melting point at 25 °C near that of the starting methylated PEO (30 °C). When lithium perchlorate was added, the endothermic melting peak became very weak at 36 °C and a glass transition became clearer at −33 °C. Self-supporting polymer electrolyte films were thus prepared by dissolving AZOH–PEO **2** and lithium perchlorate in commercial PEO ($M_w = 5 \times 10^6$) at an O/Li ratio of 12. The glass transition of this polymer electrolyte was at *ca.* −33 °C and the melting point at 36 °C suggesting that both crystalline and amorphous phases were present in the material. This point is of importance since ionic conduction of polymer films is restricted to their amorphous phase.[7]

The effect of UV-light laser irradiation (363 nm) in the conductivity of the films is clearly observable in the impedance spectra showed in Fig. 1. A *ca.* 70% increase of the conductivity arose under UV light. No detectable effect was obtained in identical conditions but for an electrolyte film which did not contain compound **2**. Increasing the light intensity from 0 up to 50 mW cm$^{-2}$ enhanced the conductivity growth according to a logarithmic law. A saturation effect was then observed for light power values above 70 mW cm$^{-2}$, as expected for an absorption phenomenon. Switching off the UV-light source restored reversibly the initial conducting state within a few minutes (Figs. 1 and 2). As shown in Fig. 3, the magnitude of the light-induced conductivity increase was roughly the same throughout the explored temperature range up to 50 °C. At higher temperatures the light effect tended to disappear.

The photoactivation mechanism of the ionic conductivity in our polymer films appears to be complex. The disorder resulting from the light-induced *trans–cis* structural change of the azobenzene moieties and also possibly from erasing long-range ordering of interacting *trans* azobenzene groups, obviously increased the free volume in the material. However the linear




**Scheme 1** Synthesis of compounds **1** and **2**

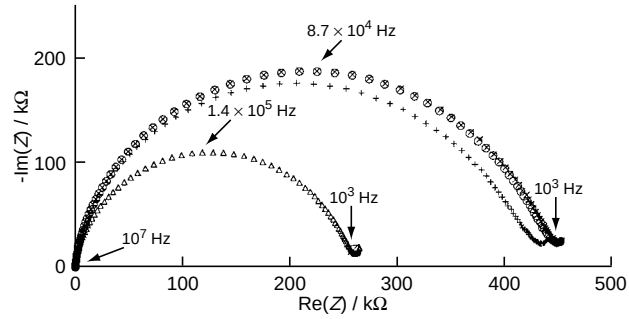



**Fig. 1** Nyquist plots of the complex impedances obtained at 20 °C for a polymer film made of PEO ($M_w$ 5 × 10$^6$) 50%, AZOH–PEO **2** 50% and $LiClO_4$ (O/Li = 12): (*a*) before UV irradiation (○), (*b*) under UV irradiation (363 nm, 75 mW cm$^{-2}$ (△), (*c*) 5 min after switching off the UV light (+), (*d*) 10 min after switching off the UV light (×). The conductivity cells were made of 410 μm thick polymer films sandwiched between two ITO-covered glass pieces.

part of the Arrhenius plots in Fig. 3 suggests an activated mechanism for the ionic conduction. Therefore an increase of the number of mobile charges in the photoactivated state, arising from a disorder induced ion-pair separation, could be put forward. Closer scrutiny of the 'semi-circles' in Fig. 1, reveals that they in fact include two dielectric relaxations with a different sensitivity to the UV irradiation. The latter could correspond either to a two-phase system or to different conduction mechanisms. One should also take into account that the *cis–trans* thermal back isomerism was probably not a time-limiting step for our system, as suggested by the symmetrical time variation of the conductivity after switching off or on the light irradiation (Fig. 2).

In conclusion, the possibility of efficient optical control of quite good conductivities for polymer electrolytes is demonstrated. Various technical applications could be envisioned, especially for systems using polymer electrolyte films. Further experiments are presently under way to investigate the mechanism of the optical transition and to obtain even larger effects.

We are indebted to Michel Armand (presently at the University of Montreal, Canada) for having favoured this work.

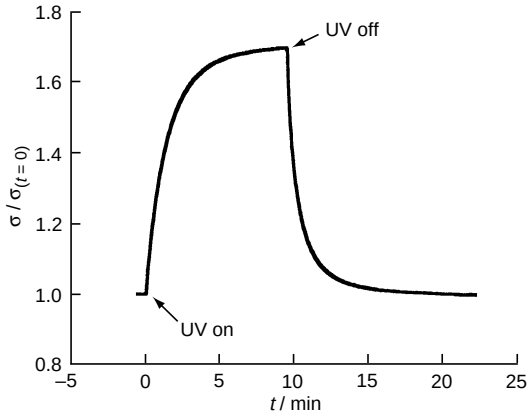



**Fig. 2** Time dependence of the conductivity after switching on and off the UV light. Experimental conditions as for Fig. 1 except for the temperature (15 °C) and the laser light power (65 mW cm$^{-2}$).

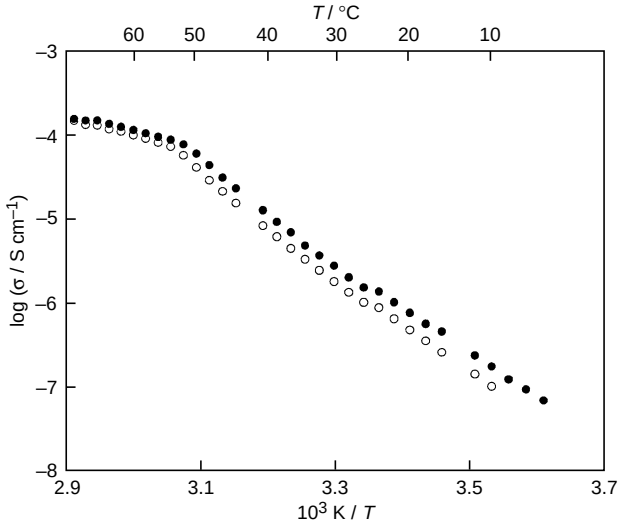



**Fig. 3** Conductivity–temperature plots in Arrhenius coordinates. Experimental conditions as for Fig. 1 except for the film thickness (730 μm) (*a*) in the dark (○) and (*b*) under UV light (●).

## Footnotes

* E-mail: didier.delabouglise@lepmi.inpg.fr

† Compounds **1** and **2** were characterized using chromatography and NMR. **2**: $^1$H NMR ($CDCl_3$, 250 MHz) δ 7.87 (d, 2 H), 7.78 (d, 2 H), 7.00 (d, 2 H), 4.2 (t, 2 H), 3.85 (t, 2 H), 3.6 (62 H), 3.3 (s, 3 H), 2.6 (t, 2 H), 1.6 (t, 2 H), 1.3 (6 H), 0.9 (t, 3 H).

## References

1 N. Kobayashi, S. Sato, K. Takazawa, K. Ikeda and R. Hirohashi, *Electrochimica Acta*, 1995, **13**–**14**, 2309.
2 K. Kimura, M. Kaneshige and M. Yokoyama, *Chem. Mater.*, 1995, **7**, 945.
3 H. Tokuhisa, M. Yokoyama and K. Kimura, *Chem. Mater.*, 1993, **5**, 989.
4 T. Ikeda and O. Tsutsumi, *Science*, 1995, **268**, 1873.
5 T. Ikeda, T. Sasaki and K. Ichimura, *Nature*, 1993, **361**, 428.
6 T. Saji, K. Ebata, K. Sugawara, S. Liu and K. Kobayashi, *J. Am. Chem. Soc.*, 1994, **116**, 6053.
7 M. Armand, *Annu. Rev. Mater. Sci.*, 1986, **16**, 245; *Adv. Mater.*, 1990, **2**, 279.

*Received in Bath, UK, 13th January 1997; Com. 7/00415J*

# A highly reactive functional model for catechol 1,2-dioxygenase: reactivity studies of iron(III) catecholate complexes of bis[(2-pyridyl)methyl][(1-methylimidazol-2-yl)methyl]amine

**Mark Duda, Matthias Pascaly and Bernt Krebs***

*Anorganisch-Chemisches Institut der Westfälischen Wilhelms-Universität, Wilhelm-Klemm-Str. 8, D-48149 Münster, Germany*

**The system consisting of an iron(III) salt and bis[(2-pyridyl)-methyl][(1-methylimidazol-2-yl)methyl]amine (bpia) in methanol reacts with various catechols with insertion of dioxygen; in the case of 3,5-di-*tert*-butylcatechol the efficient catalytic activity of the system is shown.**

Intradiol dioxygenases are non-haem iron enzymes and take part in biological mechanisms for metabolising aromatic compounds.[1] The enzymes catalyse the intradiol cleavage of catechols to *cis,cis*-muconic acids. Spectroscopic investigations indicate that the active site iron remains in the iron(III) oxidation state during the whole catalytic cycle. A variety of studies have tried to understand the mechanism in its enzymatic and model chemistry aspects and a number of functional models have been synthesised with various ligand systems.[2–4] Especially tetradentate ligands (L) have shown a great ability to influence the physical properties of the metal complexes and therefore the dioxygenase activity as the ligand sets are varied. Que and coworkers have found a correlation between the Lewis acidity of the iron centre in a series of iron(III) complexes of tripodal ligands, the product yield, and the reactivity.[2] According to these investigations a substrate activation rather than oxygen activation mechanism has been proposed. In this mechanism the substrate loses both of its protons upon coordination to the iron centre followed by partial oxidation of the catecholate due to ligand-to-metal charge transfer, resulting in a substrate with semiquinone character. The attack of $O_2$ on the activated substrate yields a transient alkylperoxy radical which combines with the equally short-lived iron(II) centre to generate an alkylperoxoiron(III) species. The peroxy adduct decomposes by a Criegee-type rearrangement to muconic anhydride. In most cases 3,5-di-*tert*-butylcatechol (dbc) has been used as a substrate in functional investigations, but little work has been devoted to the oxygenation of other catechols.[3]

We have prepared iron(III) catecholate complexes *in situ* under an argon atmosphere with bis[(2-pyridyl)methyl][(1-methylimidazol-2-yl)methyl]amine (bpia)[5] as a tetradentate ligand and a series of catechols (dbc, 4-mc, 4-bc, cat, tcc).† Their UV–VIS spectra in methanol solution are dominated by two moderately intense absorption bands. These bands are assigned as catcholate-to-$Fe^{III}$ charge-transfer transitions similar to those observed in the spectra of other iron catecholate complexes with tripodal ligands,[6] suggesting that a complex of the form [Fe(bpia)(catecholate)]$^+$ has been prepared. The positions of the lower energy band are dependent on the nature of the catecholate, with the LMCT bands observed to shift to lower energies by varying the substituents on the catecholate from electron-withdrawing to -donating (Table 1). The complexes have been isolated, and with tetrachlorocatecholate (tcc) as substrate we have obtained crystals to solve the structure of [Fe(bpia)(tcc)]$ClO_4$.[7] The crystal structure exhibits an asymmetrical chelated tetrachlorocatecholate ligand (Fig. 1). The Fe–O bond *trans* to the aliphatic N [Fe–O(1) 1.919(3) Å] is about 0.03 Å shorter than the corresponding bond *trans* to the heterocyclic N [Fe–O(2) 1.948(3) Å]. The difference in bond lengths is due to a *trans* effect where the catecholate oxygen with the shorter bond is in the *trans* position to the much weaker amine ligand.

All catecholate complexes of Table 1 react with dioxygen to yield products due to the oxidative cleavage of the catechol ring.‡ The immediate product appears to be the *cis,cis*-muconic anhydride, although only in the case of 3,5-di-*tert*-butylcatechol was this cleavage product isolated as 3,5-di-*tert*-butyl-1-oxacyclohepta-3,5-diene-2,7-dione. With 4-bc, 4-mc, and cat furanones derived from nucleophilic attack on one carbonyl of the anhydride, followed by cyclisation, were identified.

The kinetics of the reaction with dioxygen was followed by monitoring the disappearance of the lower energy charge-transfer band (Fig. 2). The reactions all exhibit pseudo-first-order kinetics under conditions where dioxygen is in excess after complex formation. The pseudo-first-order rate constants show a dependence on the nature of the substrate. The rates of the reactions increase in the order tcc $\ll$ cat < 4-bc $\approx$ 4-mc < dbc (Table 1). While [Fe(bpia)(tcc)]$^+$ is rather stable against dioxygen attack, the reaction rate of the [Fe(bpia)(dbc)]$^+$ complex with $O_2$ is rather high. This order of activity correlates with the energy of the lower energy LMCT band of the complexes: electron-donating substituents on the catechol result in a higher dioxygenase reactivity.

Accordingly the reactivity grows with increasing Lewis acidity of the iron centre within the series of [Fe(bpia)(catechol-

**Table 1** Properties of the [Fe(bpia)(catecholate)]$^+$ complexes

| Catechol | $\lambda_{max}$/nm | $k^a$/dm$^3$ mol$^{-1}$ s$^{-1}$ |
|---|---|---|
| dbc | 558, 865 | 4.3 |
| 4-mc | 515, 842 | 2.6 |
| 4-bc | 519, 836 | 2.3 |
| cat | 510, 800 | 0.083 |
| tcc | 528, 729 | $> 10^{-5}$ |

[a] Reactions run in methanol under air, 25 °C, $c = 5 \times 10^{-4}$ mol dm$^{-3}$, 2 equiv. of piperidine as base, $k = k_{obs}/[O_2]$.

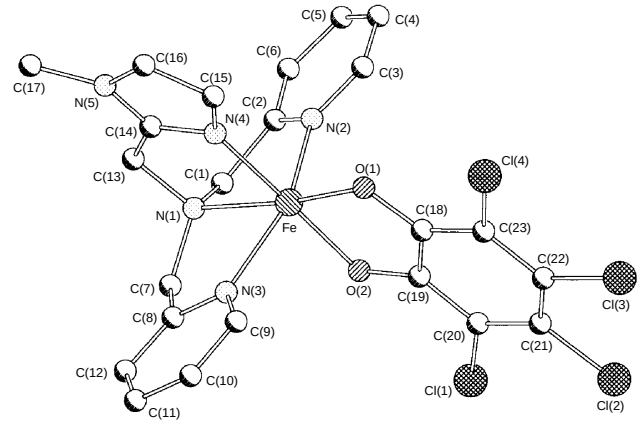



**Fig. 1** Structure of [Fe(bpia(tcc)]$^+$

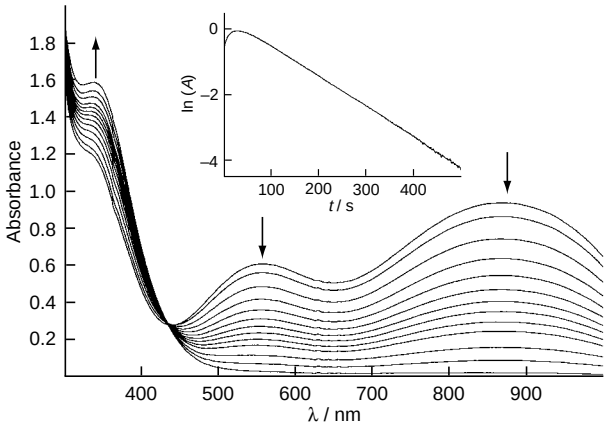



**Fig. 2** Progress of the reaction of $[Fe(bpia)(dbc)]^+$ with air in methanol. Inset: plot of ln (*A*) *vs.* *t* at 25 °C.

ate)]$^+$ complexes. Our observation supports the substrate activation mechanism proposed by Que.[2]

The system consisting of $Fe(ClO_4)_3 \cdot 9H_2O$ and bpia in acetonitrile catalyses the oxidation of dbc to *cis,cis*-muconic anhydride rapidly and efficiently. In the presence of 10% of the catalyst 90% of the desired cleavage product is obtained. We have isolated 3,5-di-*tert*-butyl-*o*-benzoquinone (dbq) as a by-product in small amounts. By reducing the amount of the iron catalyst the yield of dbq increases, but even with 1% $[Fe(bpia)(MeCN)_2]^{3+}$ nearly 80% of the catechol reacts with dioxygen in 12 h to 3,5-di-*tert*-butyl-1-oxacyclohepta-3,5-diene-2,7-dione. With turnover numbers up to 80 this iron(III) complex is the most effective catalyst for the oxidative cleavage of catechols reported yet.

Progress of the reaction can be followed by $^1$H NMR spectroscopy (Fig. 3). The signals of the free substrate (δ 6.82, 1.36, 1.24) disappear along with the appearance of signals of the muconic anhydride (δ 6.57, 6.16, 1.25, 1.14) and of the by-product, 3,5-di-*tert*-butyl-*o*-benzoquinone (δ 7.01, 6.14, 1.23, 1.19). The width of the signals is due to the formation of the paramagnetic $[Fe(bpia)(dbc)]^+$ complex in solution during the reaction. At the end of the reaction the signals become sharp indicating a μ-oxo-bridged dinuclear iron(III) complex with antiferromagnetic coupling in solution.

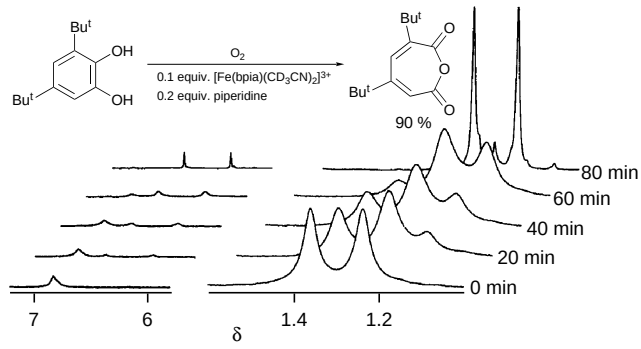



**Fig. 3** Catalytic oxidation of 3,5-di-*tert*-butylcatechol monitored by $^1$H NMR spectroscopy

We thank the Deutsche Forschungsgemeinschaft for financial support.

## Footnotes

* E-mail: KREBS@NWZ.UNI-MEUNSTER.DE

† Abbreviations used: bpia = bis[(2-pyridyl)methyl][(1-methylimidazol-2-yl)methyl]amine, dbc = 3,5-di-*tert*-butylcatechol, 4-bc = 4-*tert*-butylcatechol, 4-mc = 4-methylcatechol, cat = catechol, tcc = tetrachlorocatechol; dbq = 3,5-di-*tert*-butyl-*o*-benzoquinone.

‡ The oxidation product of tetrachlorocatechol has not been isolated, due to the high stability of the $[Fe(bpia)(tcc)]^+$ complex.

## References

1 L. Que, Jr. and R. Y. N. Ho, *Chem. Rev.*, 1996, **96**, 2607.
2 H. G. Jang, D. D. Cox and L. Que, Jr., *J. Am. Chem. Soc.*, 1991, **113**, 9200.
3 W. O. Koch and H. J. Krüger, *Angew. Chem.*, 1995, **107**, 2928, *Angew. Chem., Int. Ed. Engl.*, 1995, **34**, 2671.
4 R. Viswanathan and M. Palaniandavar, *J. Chem. Soc., Dalton Trans.*, 1995, 1259.
5 N. Wei, N. N. Murthy, Z. Tyeklár and K. D. Karlin, *Inorg. Chem.*, 1994, **33**, 1177.
6 D. D. Cox, S. J. Benkovic, L. M. Bloom, F. C. Bradley, M. J. Nelson, L. Que, Jr. and D. E. Wallick, *J. Am. Chem. Soc.*, 1988, **110**, 2026.
7 M. Duda, M. Pascaly and B. Krebs, manuscript in preparation.

*Received in Basel, Switzerland, 28th January 1997; Com. 7/00614D*

# Synthesis, structure and physical properties of the new selenium containing metal complex $NBu_4[Ni(ddds)_2]$ (ddds = 5,6-dihydro-1,4-dithiin-2,3-diselenolate)

**Hideki Fujiwara,* Emiko Arai and Hayao Kobayashi***

*Institute for Molecular Science, Myodaiji, Okazaki 444, Japan*

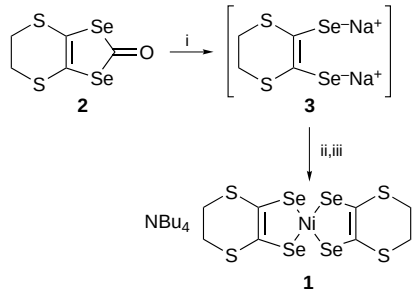
**The synthesis, structure and physical properties of the new selenium containing metal complex $NBu_4[Ni(ddds)_2]$ (ddds = 5,6-dihydro-1,4-dithiin-2,3-diselenolate) are described.**

In the past two decades development of new organic conductors has undergone rapid progress. Among them, conductors based on bis(ethylenedithio)tetrathiafulvalene (BEDT-TTF) have played a key and major role in the search for new organic superconductors.[1] On the other hand bis(dithiolene) metal complexes are also of great interest because they show a variety of crystal structures and conducting properties upon variation of central metal atoms and counter ions. However conducting salts of bis(dithiolene) metal complexes show a tendency to form one-dimensional structures and become insulating at low temperatures although some superconductors have been discovered from $[M(dmit)_2]$ complexes (dmit = 4,5-disulfanyl-1,3-dithiole-2-thione).[2] Recently, it has been reported that the radical cation salts of $[M(dddt)_2]$ complexes (M = Ni, Pd; dddt = 5,6-dihydro-1,4-dithiin-2,3-dithiolate) produce various highly conducting salts metallic down to low temperatures.[3] $[M(dddt)_2]$ complexes were first synthesized about ten years ago[4] and have structures remarkably similar to that of the BEDT-TTF molecule. In this context, development of selenium analogues of $[M(dddt)_2]$ has attracted our interest because the selenium substitution of inner sulfur atoms is expected to increase the transverse interaction and to stabilize the metallic state at low temperature. This strong stabilization of the metallic state has been shown in BETS [bis(ethylenedithio)tetraselenafulvalene], the selenium analogue of BEDT-TTF, from which new organic superconductors have been recently discovered.[5] Here, we report on the synthesis, structure and physical properties of the new selenium containing metal complex $NBu_4[Ni(ddds)_2]$ **1**.

$NBu_4[Ni(ddds)_2]$ was synthesized as shown in Scheme 1. Ketone **2**[6] was hydrolysed with 20% sodium ethoxide in dry thf at 0 °C to generate the corresponding diselenolate **3**, which was treated successively with an ethanol solution of nickel dichloride hexahydrate and tetrabutylammonium bromide to crystallize the tetrabutylammonium nickel complex. The resultant precipitate was collected and washed with methanol and recrystallized from acetone–isopropyl alcohol to afford dark green and air-stable platelike crystals in 84% yield.†

The crystal structure‡ of the present complex is different from each of reported structures of $NBu_4[Ni(dddt)_2]$.[4c,d] In the unit cell there is one crystallographically independent tetrabutylammonium cation and a $[Ni(ddds)_2]$ anion. The molecular structure of the $[Ni(ddds)_2]$ anion is shown in Fig. 1. The nickel is coordinated by the four selenium atoms of the ligands in a slightly distorted square planar geometry with a dihedral angle of 15.7° between two five-membered rings. Each of the two chelating ligands is almost planar except for the ethylene bridge. The mean Ni–Se distance in the present anion [2.267(3) Å] is longer than that of the corresponding $[Ni(dddt)_2]$ anion [2.132(9) Å][4c] and the difference between these values (*ca*. 0.14 Å) is almost equal to that between the atomic covalent radii of sulfur and selenium. The intramolecular Se···Se lengths [Se(1)···Se(2) 3.268(3), Se(3)···Se(4) 3.267(3) Å] are longer than that of inner sulfur atoms of $[Ni(dddt)_2]^-$ [3.068(3) Å][4a] and are closer to the S···S lengths [S(1)···S(2) 3.451(8), S(3)···S(4) 3.461(7) Å]. This result suggests that the expanse of electron clouds of chalcogen atoms is nearly uniform in the transverse direction over the whole anion, in contrast to the case of $[Ni(dddt)_2]^-$, and therefore more effective two-dimensional intermolecular interaction is expected in its conducting solids. Fig. 2 shows the *bc*-projection for $NBu_4[Ni(ddds)_2]$ from which it is seen that there is no stacking or columnar structure of the anions and each anion is surrounded by counter tetrabutylammonium cations.

Electrochemical properties were investigated by cyclic voltammetry. $NBu_4[Ni(ddds)_2]$ shows two pairs of reversible




**Scheme 1** *Reagents and conditions*: i, 20% NaOEt (4 equiv.), thf, 0 °C, 2 h; ii, $NiCl_2 \cdot 6H_2O$ (0.5 equiv.) in EtOH, 0 °C, 2 h; iii, $NBu_4Br$ (0.5 equiv.) in EtOH, 0 °C, 1 h

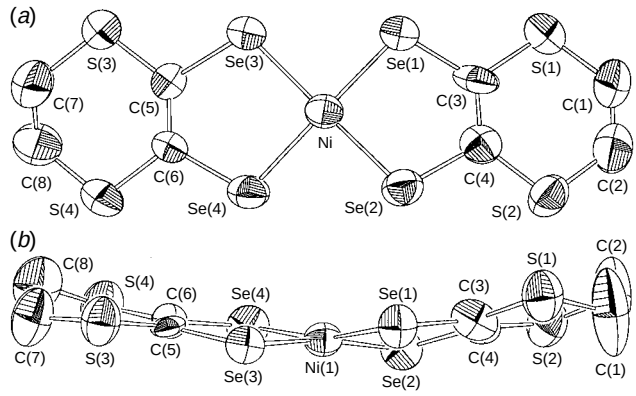
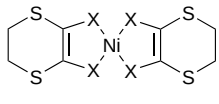



**Fig. 1** Structure of the anion moiety of $NBu_4[Ni(ddds)_2]$: (*a*) projection to the molecular plane and (*b*) side view




X = S; $[Ni(dddt)_2]^-$

X=Se; $[Ni(ddds)_2]^-$ **1**

redox waves, which correspond to the two redox processes leading the dianion to the neutral state, and one irreversible redox wave. The redox potentials of **1** and its related nickel dithiolene complexes are listed in Table 1. The first and second redox potentials are at −0.60 and +0.16 V, respectively, and are about 0.1 V higher than those of the sulfur derivative $NBu_4[Ni(dddt)_2]$ (−0.71 and +0.03 V) under identical conditions, suggesting that selenium lowers the electron-donating ability of **1**. On the other hand **1** shows an oxidation wave corresponding to the neutral to cationic state, although it is irreversible, suggesting the possibility of formation of radical cation salts of $[Ni(ddds)_2]$ similar to the case found for $[Ni(dddt)_2]$.

The room-temperature magnetic susceptibility of **1** was measured using a SQUID magnetometer at 1 T. Complex **1** is paramagnetic with $\mu_{eff}$ = 1.77 $\mu_B$ corresponding to one unpaired electron per molecular formula (calculated $\mu_{eff}$ = 1.73 $\mu_B$ for a one unpaired electron system) as a consequence of the crystal structure in which each anion is efficiently separated from others by bulky tetrabutylammonium cations, so preventing interaction.

Synthesis of $[M(ddds)_2]^-$ complexes with other central metal atoms and preparation of their neutral species and conducting salts are now in progress.

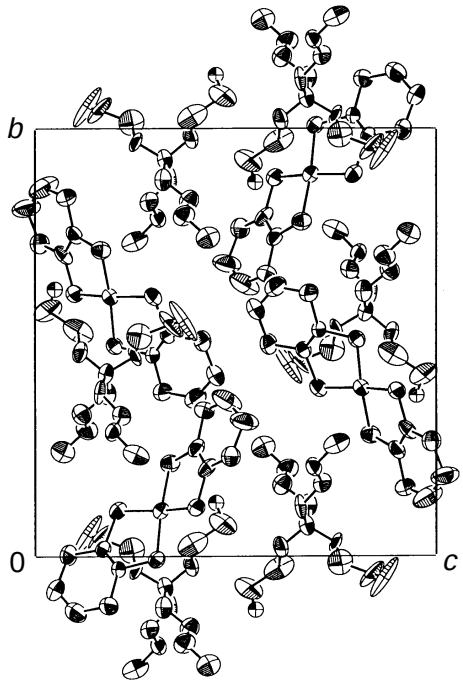



**Fig. 2** Crystal structure of $NBu_4[Ni(ddds)_2]$ viewed along the *bc*-plane

**Table 1** Redox potentials of **1** and related nickel dithiolene complexes[a]

| $[ML_2]^b$ | $[ML_2]^{2-}$–$[ML_2]^-$ | $[ML_2]^-$–$[ML_2]^0$ | $[ML_2]^0$–$[ML_2]^{xc}$ |
|---|---|---|---|
| $[Ni(ddds)_2]$ | −0.60 | +0.16 | +0.71[d] |
| $[Ni(dddt)_2]$ | −0.71 | +0.03 | +0.99[d] |
| $[Ni(dmit)_2]$ | −0.18 | +0.38 | |
| $[Ni(mnt)_2]$[e] | +0.21 | +1.19[d] | |

[a] $NBu_4PF_6$ 0.1 M in PhCN, Pt electrode, 20 °C, scan rate 200 mV $s^{-1}$, V *vs.* Ag/AgCl. [b] Tetrabutylammonium salt. [c] Oxidation state not clear. [d] Irreversible process with anodic peak potential quoted. [e] mnt = maleonitriledithiolate.

## Footnotes

* E-mail: fuji@ims.ac.jp

† $^1$H NMR (270 MHz, [$^2H_6$]acetone) δ 3.31 (8 H, m), 1.90 (8 H, m), 1.56 (8 H, m), 1.30 (8 H, m) and 1.07 (12 H, m); IR (KBr) ν/$cm^{-1}$ 2954m, 2866m, 1408s, 1282m, 1166w and 918w.

‡ *Crystal data* for $NBu_4[Ni(ddds)_2]$: $C_{24}H_{44}NNiS_4Se_4$, $M$ = 849.40, monoclinic, space group $P2_1/c$, $a$ = 9.668(5), $b$ = 19.260(3), $c$ = 18.099(2) Å, β = 97.87(2)°, $U$ = 3338(1) $Å^3$, $Z$ = 4, $D_c$ = 1.69 g $cm^{-3}$. Data collection was performed on a Rigaku AFC-5R diffractometer at 293 K equipped with graphite-monochromated Mo-Kα radiation (λ = 0.710 69 Å) and rotating anode generator. Intensities were collected to a maximum 2θ value of 55.0° by the ω–2θ scan technique. The total number of independent reflections measured was 7698, of which 2359 were considered to be observed [$I > 3.00\sigma(I)$]. The structure was solved by direct methods (SHELXS-86). The non-hydrogen atoms were refined anisotropically. Hydrogen atoms were included but not refined. The structure was refined by full-matrix least squares to $R$ = 0.065, $R_w$ = 0.054. Atomic coordinates, bond lengths and angles, and thermal parameters have been deposited at the Cambridge Crystallographic Data Centre (CCDC). See Information for Authors, Issue No. 1. Any request to the CCDC for this material should quote the full literature citation and the reference number 182/408.

## References

1 J. M. Williams, J. R. Ferraro, R. J. Thorn, K. D. Carlson, U. Geiser, H. H. Wang, A. M. Kini and M.-H. Whangbo, *Organic Superconductors*, Prentice Hall, New Jersey, 1992.

2 P. Cassoux, L. Valade, H. Kobayashi, A. Kobayashi, R. A. Clark and A. E. Underhill, *Coord. Chem. Rev.*, 1991, **110**, 115.

3 E. B. Yagubskii, A. I. Kotov, A. G. Khomenko, L. I. Buravov, A. I. Schegolev and R. P. Shibaeva, *Synth. Met.*, 1992, **46**, 255; E. B. Yagubskii, L. A. Kushch, V. V. Gritsenko, O. A. Dyachenko, L. I. Buravov and A. G. Khomenko, *Synth. Met.*, 1995, **70**, 1039; L. A. Kushch, V. V. Gritsenko, L. I. Buravov, A. G. Khomenko, G. V. Shilov, O. A. Dyachenko, V. A. Merzhanov, E. B. Yagubskii, R. Rousseau and E. Canadell, *J. Mater. Chem.*, 1995, **5**, 1633.

4 (*a*) C. T. Vance, R. D. Bereman, J. Bordner, W. E. Hatfield and J. H. Helms, *Inorg. Chem.*, 1985, **24**, 2905; (*b*) R. Kato, H. Kobayashi, A. Kobayashi and Y. Sasaki, *Bull. Chem. Soc. Jpn.*, 1986, **59**, 627; (*c*) A. J. Schultz, H. H. Wang, L. C. Soderholm, T. L. Sifter, J. M. Williams, K. Bechgaard and M.-H. Whangbo, *Inorg. Chem.*, 1987, **26**, 3757; (*d*) J. H. Welch, R. D. Bereman and P. Singh, *Inorg. Chem.*, 1988, **27**, 3680; (*e*) H. Kim, A. Kobayashi, Y. Sasaki, R. Kato and H. Kobayashi, *Bull. Chem. Soc. Jpn.*, 1988, **61**, 579.

5 H. Kobayashi, T. Udagawa, H. Tomita, K. Bun, T. Naito and A. Kobayashi, *Chem. Lett.*, 1993, 1559; H. Kobayashi, H. Tomita, T. Naito, H. Tanaka, A. Kobayashi and T. Saito, *J. Chem. Soc., Chem. Commun.*, 1995, 1225; L. K. Montgomery, T. Burgin, T. Miebach, D. Dunham, J. C. Huffman and J. E. Schirber, *Mol. Cryst. Liq. Cryst.*, 1996, **284**, 73; H. Tanaka, A. Kobayashi, T. Saito, K. Kawano, T. Naito and H. Kobayashi, *Adv. Mater.*, 1996, **8**, 812.

6 R. Kato, H. Kobayashi and A. Kobayashi, *Synth. Met.*, 1991, **41**–**43**, 2093.

*Received in Cambridge, UK, 17th February 1997; Com. 7/01113J*

# Large tunnels in the hydrothermally synthesized open-framework iron phosphate $[H_3N(CH_2)_3NH_3]_2[Fe_4(OH)_3(HPO_4)_2(PO_4)_3]\cdot xH_2O$

**Kwang-Hwa Lii* and Yuh-Feng Huang**

*Institute of Chemistry, Academia Sinica, Taipei, Taiwan*

**The synthesis and characterization of a microporous iron phosphate is described; the structure consists of infinite chains of iron–oxygen octahedra linked by phosphate groups to generate large tunnels containing 20-ring windows in which water molecules and the charge-compensating organic cations reside.**

A large number of molybdenum and vanadium phosphates with open-framework structures have been synthesized under mild hydrothermal conditions using organic amines as structure-directing agents.[1,2] These microporous materials are of interest because of their rich structural chemistry and potential applications as molecular sieves, ion-exchange materials and catalysts. Since we had synthesized a large number of ternary iron phosphates and arsenates with a variety of complex crystal structures by a high-temperature, high-pressure hydrothermal method,[3] the possibility of preparing three-dimensional frameworks containing large voids filled with cationic organic templates seemed reasonable. Recently, an organically templated iron phosphate $[H_3NCH_2CH_2NH_3]_{0.5}[Fe(OH)PO_4]$ was reported.[4,5] It is isotypic with the layered gallophosphate $[H_3NCH_2CH_2NH_3]_{0.5}[Ga(OH)PO_4]$ obtained in ethylene glycol.[6] We have also synthesized a 1,4-diazabicyclo[2.2.2]octane encapsulating iron phosphate, $[HN(CH_2CH_2)_3NH][Fe_8(HPO_4)_{12}(PO_4)_2(H_2O)_6]$.[7] It adopts a pillared layer structure and its framework is closely related to that of an imidazole encapsulating indium phosphate.[8] To our knowledge, these are the only two examples of organically templated iron phosphates in the literature. Here we describe the synthesis and structural characterization of a 1,3-diaminopropane encapsulating iron phosphate, $[H_3N(CH_2)_3NH_3]_2[Fe_4(OH)_3(HPO_4)_2(PO_4)_3]\cdot xH_2O$ **1**. Its framework structure is unique and contains two-dimensional arrays of large tunnels in which water molecules and the charge-compensating organic cations are located.

Hydrothermal treatment of $FeCl_3\cdot 6H_2O$ (1.5 mmol), $H_3PO_4$ (7.5 mmol), $H_2N(CH_2)_3NH_2$ (7.5 mmol), and water (10 ml) for 3 days at 180 °C yielded a yellow crystalline product. A yellow crystal was used to determine its structure by single-crystal X-ray diffraction.† The material is single phase as judged by comparison of the powder X-ray diffraction of the bulk product to the pattern simulated from the coordinates derived from the single-crystal study. Thermal gravimetric analysis showed mass loss in multiple steps over the temperature range 25–800 °C of 36.73%. Based on powder X-ray diffraction, the final decomposition product at 800 °C is a mixture of $FePO_4$ and $Fe_4(P_2O_7)_3$.[9] The observed total mass loss reflects the presence of lattice water molecules and agrees well with that calculated for the loss of 2 $H_2N(CH_2)_3NH_2$, 9 $H_2O$ of crystallization and 4.5 $H_2O$ from the decomposition of framework (36.7%), as indicated by eqn. (1).

$$[H_3N(CH_2)_3NH_3]_2[Fe_4(OH)_3(HPO_4)_2(PO_4)_3]\cdot 9H_2O \rightarrow 2\ FePO_4 + 0.5\ Fe_4(P_2O_7)_3 + 13.5\ H_2O \quad (1)$$

Samples of **1** appeared to lose water over time if stored in a desiccator. Only four lattice water oxygen sites could be located from the single-crystal X-ray diffraction study. The room-temperature Mössbauer spectrum is a doublet and does not show different Fe components as indicated from the crystal structure. The spectral parameters are δ (isomer shift) = 0.393 mm $s^{-1}$ (relative to iron foil at 300 K), $\Delta E_Q$ (quadrupole splitting) = 0.604 mm $s^{-1}$, and Γ (full width at half-height) = 0.36, 0.35 mm $s^{-1}$. The isomer shift is consistent with those for iron(III) phosphates.[10]

The structure of **1** consists of a three-dimensional covalently bonded framework built up from $FeO_6$ octahedra and phosphate tetrahedra. The fundamental building unit is an octahedral tetramer, which is shown in Fig. 1. The unit involves an edge-sharing $Fe(2)_2O_{10}$ dimer which further links at the shared corners to two $Fe(1)O_6$ octahedra forming a $Fe_4O_{20}$ tetramer. A topologically identical cluster exists in the iron phosphate mineral leucophosphite, $K_2[Fe_4(OH)_2(H_2O)_2(PO_4)_4]\cdot 2H_2O$.[11] The tetramer in **1** possesses $\bar{1}$ symmetry located at the midpoint of the shared edge. $Fe(2)O_6$ is more distorted than $Fe(1)O_6$ because of edge-sharing. The $\mu_3$- and μ-oxo atoms, O(11) and O(12), which coordinate to Fe atoms only, are the hydroxo oxygens. The H atoms are not involved in hydrogen bonding. Each tetramer is joined by corner-sharing, *via* –O(12)–Fe(1)–O(12)– bonds, to two other tetramers forming orthogonal, but non-intersecting infinite chains parallel to the <100> directions. One may regard the infinite chain as a column. In a unit cell, there are four layers of columns with *z* values equal to 0, 1/4, 1/2 and 3/4, respectively. Each column lies in an *a*-glide plane and columns in adjacent layers are $4_1$-screw axis related. The columns are interlinked by phosphate tetrahedra generating large tunnels running parallel to <100>, in which the diprotonated 1,3-diaminopropane and water molecules reside (Fig. 2). The amine molecules are well ordered, which can be attributed to the formation of extensive hydrogen bonds. Within tunnels are 20-ring windows formed by the edges of ten iron-oxygen octahedra and ten phosphate tetrahedra in an alternating manner. The P(1)–O(4)H groups project into the tunnels at a nearest O(4)···O(4) distance of 7.35 Å. The long side of the ring has a free dimension (minimum O···O distance less one O diameter of 2.6 Å) of 10.4 Å. The framework also contains open

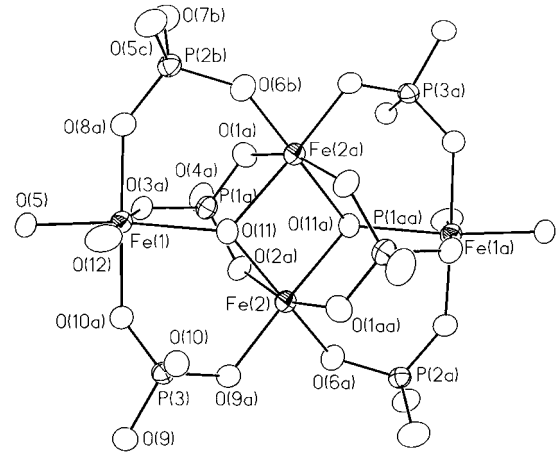



**Fig. 1** The tetranuclear iron cluster in compound **1**: thermal ellipsoids are shown at 60% probability

windows delimited by four infinite chains, through which they connect orthogonal, non-intersecting tunnels. The presence of large open windows is also reflected in the very low framework metal atom density. For **1**, there are 10.5 M atoms (M = Fe, P) per 1000 Å$^3$ compared with the value of 12.7 atoms per 1000 Å$^3$ for the very open faujasite (M = Si),[12] 12.1 atoms per 1000 Å$^3$ (M = Fe, P) for the phosphate mineral cacoxenite which contains enormous channels,[13] and 9.3 atoms per 1000 Å$^3$ for $[HN(CH_2CH_2)_3NH]K_{1.35}[V_5O_9(PO_4)_2]\cdot xH_2O$ (M = V, P) which is among the lowest framework density materials known.[2]

In summary, the synthesis and structure of an iron phosphate, $[H_3N(CH_2)_3NH_3]_2[Fe_4(OH)_3(HPO_4)_2(PO_4)_3]\cdot xH_2O$ is reported. The incorporation of $H_3N(CH_2)_3NH_3$ cations extends the iron phosphate framework into a large pore size range. The structures are very sensitive not only to the nature of the templates incorporated but also to reaction conditions. When 1,4-diazabicyclo[2.2.2]octane is used instead of diaminopropane, a different compound with a composition of $[HN(CH_2CH_2)_3NH]_3[Fe_8(HPO_4)_{12}(PO_4)_2(H_2O)_6]$ with a pillared layer structure is formed.[7] Other hydrothermally prepared iron phosphates with microporous structures have been prepared and will be reported elsewhere.

We thank the Institute of Chemistry, Academia Sinica and the National Science Council of the Republic of China (NSC 86-2113-M-001-014) for support, Professor S.-L. Wang and Ms F.-L. Liao at National Tsing Hua University for X-ray intensity data collection, and Professor T.-Y. Dong at National Sun Yat-Sen University for Mössbauer spectroscopy measurements.

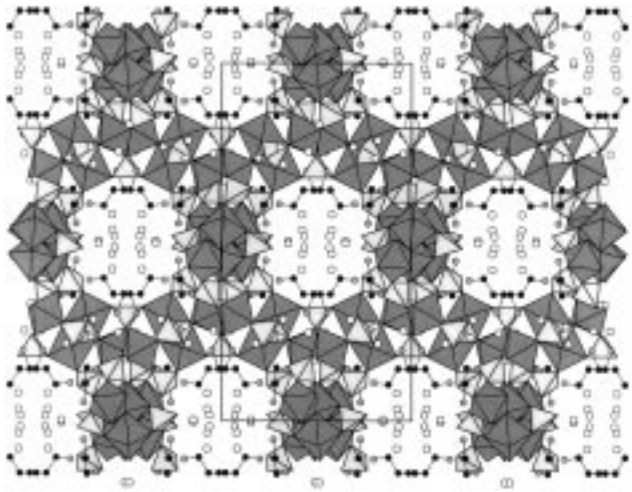


**Fig. 2** Polyhedral view of the structure of **1** along the *b* axis. Solid circles, C atoms; stippled circles, N atoms; open circles, water oxygen sites.

## Footnotes

* E-mail: lii@chem.sinica.edu.tw

† *Crystal data* for $[H_3N(CH_2)_3NH_3]_2[Fe_4(OH)_3(HPO_4)_2(PO_4)_3]\cdot xH_2O$: tetragonal, space group $I4_1/a$; $a$ = 15.4017(3), $c$ = 28.9421(4) Å, $U$ = 6840.1(8) Å$^3$, $Z$ = 8, $M_r$ = 903.58, $D_c$ = 1.755 g cm$^{-3}$, μ(Mo-Kα) = 19.8 cm$^{-1}$, λ = 0.710 73 Å, graphite monochromator, crystal dimensions: 0.18 × 0.12 × 0.12 mm. The crystal was mounted on a Siemens Smart-CCD diffractometer equipped with a normal focus, 3 kW sealed tube X-ray source. Intensity data were collected in 1200 frames with increasing ω (width of 0.30° per frame). Of the 4115 unique reflections collected ($2\theta_{max}$ = 57.5°), 2939 reflections were considered observed [$I > 3.0\sigma(I)$] after Lorentz polarization and semiempirical absorption corrections using the SHELXTL-PC program package ($T_{min,max}$ = 0.725, 0.761).[14] The structure was solved by direct methods: the Fe and P atoms were first located and the C, N, and O atoms were found in the final difference Fourier map. The H atoms were not located. Bond-valence calculations[15] indicated that both Fe atoms were trivalent, O(4), O(7), O(11) and O(12) had valence sums of 1.26, 1.15, 1.02 and 1.11, respectively, and all other oxygen atoms had values between 1.71 and 1.92. O(4), O(11) and O(12) are hydroxo oxygens. The valence sum of O(7) is satisfied by forming hydrogen bonds [O(7)···N(1) = 3.06, O(7)···O(4) 2.58 Å]. Four lattice water sites were located in the structural tunnels. Each site is partially occupied. Refinement (212 variables) was performed by full-matrix least-squares analysis, with isotropic thermal parameters for water oxygens and anisotropic thermal parameters for all other atoms. $(\Delta\rho)_{max,min}$ = 1.17, −0.80 e Å$^{-3}$. The reliability factors converged to $R(F)$ = 0.052, $R_w(F)$ = 0.058 and GOF = 1.78. Atomic coordinates, bond lengths and angles, and thermal parameters have been deposited at the Cambridge Crystallographic Data Centre (CCDC). See Information for Authors, Issue No. 1. Any request to the CCDC for this material should quote the full literature citation and the reference number 182/424.

## References

1 R. C. Haushalter and L. A. Mundi, *Chem. Mater.*, 1992, **4**, 31 and references therein.
2 M. I. Khan, L. M. Meyer, R. C. Haushalter, A. L. Schweitzer, J. Zubieta and J. L. Dye, *Chem. Mater.*, 1996, **8**, 43 and references therein.
3 B. Wang, S.-L. Wang and K.-H. Lii, *Chem. Commun.*, 1996, 1061 and references therein.
4 M. Cavellec, D. Riou and G. Ferey, *Acta Crystallogr., Sect. C*, 1995, **51**, 2242.
5 J. R. D. DeBord, W. M. Reiff, R. C. Haushalter and J. Zubieta, *J. Solid State Chem.*, 1996, **125**, 185.
6 R. H. Jones, J. M. Thomas, H. Qisheng, R. Xu, M. B. Hursthouse and J. Chen, *J. Chem. Soc., Chem. Commun.*, 1991, 150.
7 K.-H. Lii and Y.-F. Huang, *J. Chem. Soc., Dalton Trans.*, in press.
8 A. M. Chippindale, S. J. Brech, A. R. Cowley and W. M. Simpson, *Chem. Mater.*, 1996, **8**, 2259.
9 $FePO_4$, JCPDS file number 29-715; $Fe_4(P_2O_7)_3$, JCPDS file number 36-318.
10 C. Gleitzer, *Eur. J. Solid State Inorg. Chem.*, 1991, **28**, 77.
11 P. B. Moore, *Am. Mineral.*, 1972, **57**, 397.
12 W. M. Meier and D. H. Olson, *Atlas of Zeolite Structure Types*, Butterworth-Heinemann, Stoneham, MA, 1992.
13 P. B. Moore and J. Shen, *Nature*, 1983, **306**, 356.
14 G. M. Sheldrick, SHELXTL PC, Version 5, Siemens Analytical X-Ray Instruments, Inc., Madison, WI, USA, 1995.
15 I. D. Brown and D. Altermatt, *Acta Crystallogr., Sect. B*, 1985, **41**, 244.

*Received in Cambridge, UK, 17th February 1997; Com. 7/01109A*

# Photoreduction of carbon dioxide with hydrogen over $ZrO_2$

**Yoshiumi Kohno,* Tsunehiro Tanaka, Takuzo Funabiki and Satohiro Yoshida**

*Department of Molecular Engineering, Graduate School of Engineering, Kyoto University, Sakyo-ku, Kyoto 606-01, Japan*

**Among many transition-metal oxides, zirconium oxide is found to be active for photocatalytic reduction of carbon dioxide to carbon monoxide with hydrogen in the gas phase.**

From the viewpoint of environmental problems, catalytic reduction of carbon dioxide to more valuable compounds has been investigated extensively.[1–3] However, this reaction often requires severe conditions of high pressure and/or high temperature. In contrast, by photoirradiation, photocatalytic reduction of carbon dioxide with hydrogen may occur even under mild conditions.

As a photocatalyst for such types of reactions, noble metal/titanium oxide systems are the most well known and have been extensively investigated so far.[4–6] Zirconium oxide has rarely been reported to be active; however, Sayama *et al*. recently reported that zirconium oxide showed excellent photocatalytic activity for the decomposition of liquid water and photoreduction of aqueous carbonate.[7,8] They also reported that metal loading inactivated zirconium oxide, in contrast to the case of titanium oxide. In the present study, we report that zirconium oxide without metal loading is active for photocatalytic reduction of gaseous carbon dioxide with hydrogen under mild conditions of low pressure and room temperature. The wide band-gap of $ZrO_2$ (5.0 eV) permits the photoreduction of carbon dioxide with hydrogen.

Zirconium oxide used in this study was prepared from an aqueous solution of zirconium oxychloride by precipitation with 25 mass% $NH_3$(aq). The precipitate obtained was washed with distilled water followed by filtration until the filtrate was negative towards $AgNO_3$. The sample was dried at 373 K overnight, grounded to powder, and calcined at 773 K for 5 h in a dry air stream. The XRD pattern indicated that the resulting powder was zirconium oxide in a mixture of monoclinic and tetragonal phases. Other metal oxides were commercially available ones and they were calcined at 773 K for 5 h prior to use. Before reactions, the oxides were heated at 673 K for 30 min in the air and evacuated for 30 min at the same temperature, followed by treatment with 8 kPa $O_2$ for 75 min and evacuation for 30 min at 673 K.

The photocatalytic reaction was carried out in a closed static system connected to a vacuum line. A 500 W ultrahigh-pressure mercury lamp (Ushio Denki USH-500) was used as the light source. A metal oxide sample (0.3 g) was spread on the flat bottom of a quartz reactor and subjected to illumination from the bottom. A mixture of $CO_2$ (150 μmol) and $H_2$ (50 μmol) was admitted to the reactor, and the total pressure in the reactor was *ca*. 25 kPa. After the irradiation, the gases were analysed by an on-line TCD gas chromatograph (Shimadzu GC-8A) using argon as a carrier gas, which can detect $H_2$, $CH_4$ and CO. Temperature programmed desorption (TPD) experiments were carried out for zirconium oxide, and the desorbed gases were detected by a quadrupole-type mass spectrometer (ULVAC Massmate-100). To avoid the interference of nitrogen at the signal $m/z$ = 28, $^{13}C$ labelled CO or $CO_2$ was used.

Activity for photoreduction of $CO_2$ was investigated using $TiO_2$, $ZrO_2$, $V_2O_5$, $Nb_2O_5$, $Ta_2O_5$, $WO_3$ and ZnO. Among these, only $ZrO_2$ was found to be active, and other metal oxides showed no activity for this reaction at all. With $ZrO_2$, 1.0 μmol of CO was detected after 6 h photoirradiation, and no other reduced product was detected by an FID gas chromatograph (which can detect gaseous hydrocarbons and oxygenates) and a mass spectrometer, as well as the on-line TCD gas chromatograph. $ZrO_2$ is stable under photoirradiation and no appreciable difference was found in Zr $L_{III}$ edge XANES spectra of $ZrO_2$ before and after photoreaction. When the reaction was carried out in the dark, no CO was detected, although $CO_2$ is known to be adsorbed on the surface of $ZrO_2$. This indicates that photoirradiation is essential for this reaction. When the short wavelength region of the irradiated light was cut off by a series of filters which permits light with wavelength $\lambda > 370$, 330, 310 and 290 nm, the amount of evolved CO after 6 h photoirradiation changed from 1.0 μmol to 0, 0, 0.1 and 0.4 μmol, respectively. From these results, it can be concluded that the light with wavelength < 300 nm was required to enable this reaction to proceed.

Without introduction of $CO_2$ no trace of CO was detected after UV irradiation. When $^{13}CO_2$ was used instead of $^{12}CO_2$, only $^{13}CO$ was detected. These results show that CO was produced from the $CO_2$ admitted to the system.

Fig. 1 shows the time dependence of the amount of CO formed and $H_2$ consumed. The rate of CO formation mildly decreased from 8 to *ca*. 40 h irradiation. On the other hand, the consumption rate of $H_2$ was very fast at the beginning, and then slowed. The amount of consumed $H_2$ was larger than the amount of evolved CO at all times. This suggests that $H_2$ may be adsorbed onto the catalyst surface in a dissociated form[9] or incorporated into other compounds containing carbon atom(s). We then tried to decompose any adsorbed species by heating the catalyst sample after photoirradiation. More CO evolution was observed, while the amount of desorbed $H_2$ was small. After 6 h of photoirradiation, 1.0 μmol of CO was detected (as mentioned above), and when the catalyst sample was heated at 673 K for 20 min after 2 min evacuation, 3.3 μmol of CO was evolved. When the photoirradiation time was extended to 40.5 h, 3.2 μmol of CO was formed, and by heating the catalyst, 5.8 μmol of CO was evolved. This observation shows that

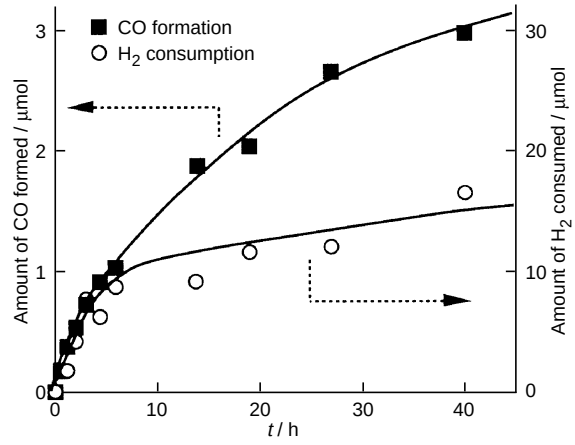



**Fig. 1** Time dependence of CO formation and $H_2$ consumption over $ZrO_2$ under irradiation; initial amounts of $CO_2$ and $H_2$ were 150 μmol and 50 μmol, respectively

photoirradiation of the catalyst surface produces some material decomposed into CO by heat. The most intriguing question at this stage is whether this CO source is photoadsorbed CO or arising from surface intermediates.

To elucidate this, TPD experiments were carried out. Samples of CO adsorbed $ZrO_2$ under photoirradiation and $ZrO_2$ used as the photocatalyst for $CO_2$ reduction were investigated. The CO TPD profiles are shown in Fig. 2. A single peak was observed for both samples in the range from 500–700 K, but the temperatures of the maxima are different. Photoadsorbed CO was desorbed at *ca*. 630 K, while the CO desorption maximum from the surface of the catalyst after photoreaction was observed at *ca*. 610 K. This result firmly suggests that the surface species differ for the two samples. In other words, surface intermediates may exist on the catalyst surface under irradiation, and the reaction is expected to proceed *via* intermediates to yield CO. Future studies will clarify the reaction mechanism through detection and identification of these intermediates.

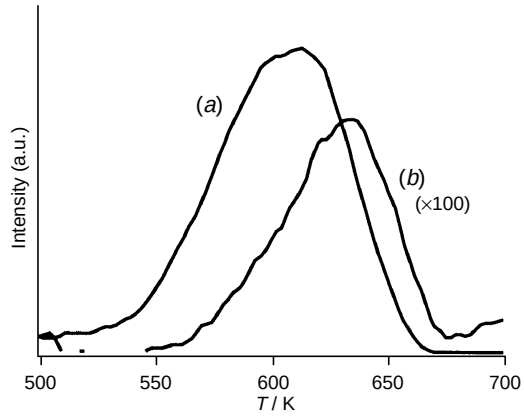



**Fig. 2** TPD profiles for (*a*) CO desorbed from the catalyst surface after photoreaction and (*b*) CO simply photoadsorbed on $ZrO_2$; the intensity of profile (*b*) is multiplied by 100

## Footnote

* E-mail: kohno@dcc.moleng.kyoto-u.ac.jp

## References

1 G. D. Weatherbee and C. H. Bartholomew, *J. Catal.*, 1981, **68**, 67.
2 F. Solymosi, A. Erdöhelyi and T. Bánsági, *J. Catal.*, 1981, **68**, 371.
3 D. E. Peebles, D. W. Goodman and J. M. White, *J. Phys. Chem.*, 1983, **87**, 4378.
4 K. Tennakone, *Sol. Energy Mater.*, 1984, **10**, 235.
5 K. R. Thampi, J. Kiwi and M. Grätzel, *Nature*, 1987, **327**, 506.
6 O. Ishitani, C. Inoue, Y. Suzuki and T. Ibusuki, *J. Photochem. Photobiol. A: Chem.*, 1993, **72**, 269.
7 K. Sayama and H. Arakawa, *J. Phys. Chem.*, 1993, **97**, 531.
8 K. Sayama and H. Arakawa, *J. Photochem. Photobiol. A: Chem.*, 1996, **94**, 67.
9 T. Onishi, H. Abe, K. Maruya and K. Domen, *J. Chem. Soc., Chem. Commun.*, 1985, 617.

*Received in Cambridge, UK, 8th January 1997; Com. 7/00185A*

# Synthesis and structures of platina-β-diketonato complexes of platina-β-diketones; organometallic analogues of platinum blue complexes

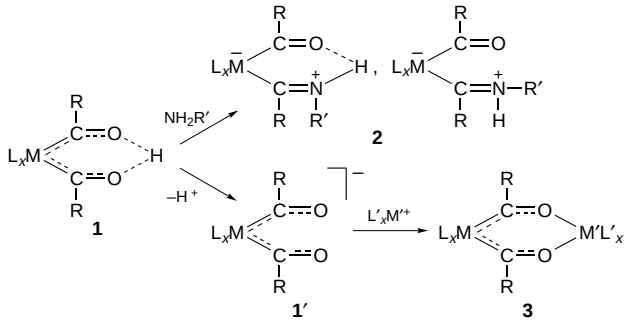
**Dirk Steinborn,* Michael Gerisch, Frank W. Heinemann and Clemens Bruhn**

*Institut für Anorganische Chemie, Martin-Luther-Universität Halle-Wittenberg, Kurt-Mothes-Str. 2, D-06120 Halle, Germany*

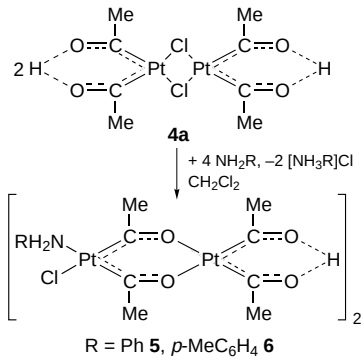
**The platina-β-diketone $[Pt_2(\mu\text{-}Cl)_2\{(COMe)_2H\}_2]$ 4a reacts with aniline or *p*-toluidine to give the first platina-β-diketonato complexes of platina-β-diketones $[\{(NH_2R)ClPt(\mu\text{-}COMe)_2Pt[(COMe)_2H]\}_2]$ (R = Ph 5, *p*-$MeC_6H_4$ 6), whose X-ray crystal structures reveal the formation of head-to-head dimers with zigzag $Pt_4$ chains analogous to platinum blue complexes.**

Metalla-β-diketones **1** are organometallic analogues of the enol tautomers of 1,3-diketones where the methine group is replaced formally by the $L_xM$ moiety.[1] It is known that complexes **1** react with primary amines $NH_2R'$ to give the corresponding metalla-β-ketoimines **2**.[1,2] The deprotonated complexes **1′** are capable of forming metal complexes of metalla-β-diketonates **3** with two bridging acyl ligands,[1,3] Scheme 1. Previously we described the synthesis of $[Pt_2(\mu\text{-}Cl)_2\{(COR)_2H\}_2]$ (R = Me **4a**, Et **4b**) being the first platina-β-diketones and, indeed, the first dinuclear metalla-β-diketones.[4] Here, we report the reactions of **4a** with aromatic amines to give, unexpectedly, platina-β-diketonato complexes of platina-β-diketones which were revealed to be of the platinum blue structural type.

The platina-β-diketone **4a** reacts with aniline and *p*-toluidine in a molar ratio 1 : 2.1 in dichloromethane as solvent to give the dimeric bis(acyl)-bridged platinum complexes **5** and **6** in high yield (73 and 68%, respectively), Scheme 2.† Intermediates in these reactions might include the monomeric complexes $[PtCl\{(COMe)_2H\}(NH_2R)]$ (R = Ph, *p*-$MeC_6H_4$), of which half is deprotonated with substitution of the chloro ligand to give **5** and **6**, respectively. An indication of this is the formation of $[NMe_4][Cl_2Pt(\mu\text{-}COMe)_2Pt\{(COMe)_2H\}]$[5] in the reaction of **4a** with $[NMe_4]OH$.



**Scheme 1**



**Scheme 2**

Compounds **5** and **6** crystallize from dichloromethane as well shaped, yellow and red, air-sensitive crystals of $[\{(NH_2R)ClPt(\mu\text{-}COMe)_2Pt[(COMe)_2H]\}_2]\cdot x CH_2Cl_2$ (R = Ph, *p*-$MeC_6H_4$; $x$ = 2), respectively, which lose 1 mol of $CH_2Cl_2$ upon drying *in vacuo* ($x$ = 1).‡ They melt with decomposition at 90–91 °C (**5**·$CH_2Cl_2$) and 92–93 °C (**6**·$CH_2Cl_2$). Solutions of **5** and **6** are quite unstable at room temperature. Complex **6** is monomeric in chloroform solution (found: 692.1 g $mol^{-1}$; calc. for $[\{NH_2(p\text{-}MeC_6H_4)\}ClPt(\mu\text{-}COMe)_2Pt\{(COMe)_2H\}]$ 706.0 g $mol^{-1}$). The C–O stretching vibrations for the bridging acyl ligands appear at lower wavenumbers (1514s, 1535vs $cm^{-1}$) than those in **4a** (1548 $cm^{-1}$) which is in agreement with the series: acyl {*e.g.* ν(C–O) 1639 $cm^{-1}$ in *trans*-[PtCl(COMe)$(PPh_3)_2$][6]} > β-diketone (**4a**) > μ-COMe (**5**, **6**). As expected, all four methyl groups of the organo ligands in **6** are chemically inequivalent in the $^1H$ NMR spectrum. In **5** two methyl groups are isochronous by chance.

The identities of **5** and **6** were confirmed by X-ray structure determinations.§ The molecular structures are shown in Figs. 1 and 2, with selected bond lengths and angles. They reveal the presence of head-to-head dimers in the solid state with a crystallographically imposed inversion centre ($C_i$). Both structures are very similar apart from the orientations of the amine ligands {torsion angle C(5)–N–Pt(1)–Pt(2) 105.9° [18.0°]}.¶

The coordination of Pt(1) [Cl, N, C(1), C(2)] and Pt(2) [C(3), C(4), O(1), O(2)] is square planar. These coordination planes are inclined at an angle of 95.7(6) [103.6(4)°]. Thus, the six-membered rings [Pt(1), C(1), O(1), Pt(2), C(2), O(2)] exhibit boat conformations with Pt(1)···Pt(2) distances of 3.284(1) [3.160(1) Å]. There are no significant differences between the four Pt–C {$d$(Pt–C) = 1.89(3)–1.98(2) [1.93(2)–2.00(2) Å]}

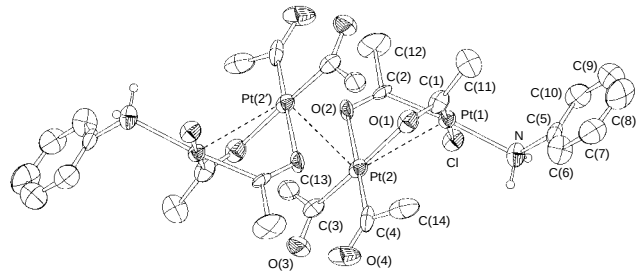



**Fig. 1** Molecular structure in the solid state with atomic labelling scheme for **5**; thermal ellipsoids are drawn at the 30% probability level, H-atoms are omitted for clarity. Selected distances (Å) and angles (°): Pt(1)–Pt(2) 3.284(1), Pt(2)–Pt(2′) 3.186(2), Pt(1)–C(1) 1.95(2), Pt(1)–C(2) 1.98(2), Pt(1)–Cl 2.409(6), Pt(1)–N 2.18(2), Pt(2)–O(1) 2.15(2), Pt(2)–O(2) 2.18(2), Pt(2)–C(3) 1.89(3), Pt(2)–C(4) 1.97(3), C(1)–O(1) 1.25(3), C(2)–O(2) 1.21(3), C(3)–O(3) 1.24(3), C(4)–O(4) 1.22(4), O(3)–O(4) 2.28(4); Cl–Pt(1)–N 84.0(5), Cl–Pt(1)–C(2) 93.6(7), N–Pt(1)–C(1) 98.5(9), C(1)–Pt(1)–C(2) 84(1), O(1)–Pt(2)–O(2) 85.0(7), C(3)–Pt(2)–C(4) 89(1), O(1)–Pt(2)–C(4) 94(1), O(2)–Pt(2)–C(3) 92(1), Pt(1)–Pt(2)–Pt(2′) 119.80(5).

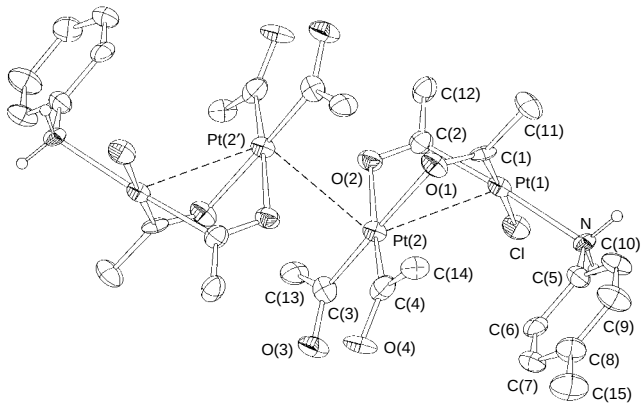



**Fig. 2** Molecular structure in the solid state with atomic labelling scheme for **6** with details as in Fig. 1. Selected distances (Å) and angles (°): Pt(1)–Pt(2) 3.160(1), Pt(2)–Pt(2′) 3.152(2), Pt(1)–C(1) 1.95(2), Pt(1)–C(2) 2.00(2), Pt(1)–Cl 2.390(4), Pt(1)–N 2.23(1), Pt(2)–O(1) 2.15(1), Pt(2)–O(2) 2.18(1), Pt(2)–C(3) 1.93(2), Pt(2)–C(4) 1.95(2), C(1)–O(1) 1.24(2), C(2)–O(2) 1.24(2), C(3)–O(3) 1.30(2), C(4)–O(4) 1.29(2), O(3)–O(4) 2.37(2); Cl–Pt(1)–N 86.0(3), Cl–Pt(1)–C(2) 91.9(5), N–Pt(1)–C(1) 95.8(6), C(1)–Pt(1)–C(2) 86.2(7), O(1)–Pt(2)–O(2) 84.6(4), C(3)–Pt(2)–C(4) 93.8(8), O(1)–Pt(2)–C(4) 89.5(7), O(2)–Pt(2)–C(3) 92.2(6), Pt(1)–Pt(2)–Pt(2′) 127.52(3)°.

and C–O bonds {*d*(C–O) = 1.21(3)–1.25(3) [1.24(2)–1.30(2) Å]} nor significant differences to those in **4a** [*d*(Pt–C) = 1.95(1) Å, *d*(C–O) = 1.23(1), 1.26(1) Å]. The O–H–O bridge in the remaining platina-β-diketone unit {*d*[O(3)···O(4)] = 2.28(4) [2.38(2) Å]} is comparable to that in **4a** [*d*(O···O) = 2.37(1) Å].

The most noticable structure feature of **5** and **6** is the zigzag chain of the $Pt_4$ unit with an angle between the Pt(1)–Pt(2) and Pt(2)–Pt(2′) vectors of 119.80(5) [127.52(3)°]. As expected for a $Pt^{II}$–$Pt^{II}$ ($d^8$–$d^8$) interaction,[7] the distance Pt(2)–Pt(2′) {3.186(2) [3.152(2) Å]} is rather long but comparable with those in $Pt^{II}$ complexes with columnar structures (3.09–3.60 Å)[8] and with those of amidate-bridged tetranuclear platinum complexes (platinum blue complexes[9]) with platinum in the +2.0 average oxidation state (3.13–3.24 Å).[10]

Besides **5** and **6**, the platinum blue complexes are the only ones with chain-like $Pt_4$ units. But there are important differences in the structures: in **5** and **6**, the Pt–Pt distances in the ligand bridging units {*d*[Pt(1)–Pt(2)] = 3.284(1) [3.160(1) Å]} are longer than those between the dinuclear units {*d*[Pt(2)–Pt(2′)] = 3.186(2) [3.152(2) Å]}. In the platinum blue complexes, the amidate-bridged Pt–Pt distances are the shortest ones (2.88–3.03 Å). Furthermore, the tilt angles between the platinum coordination planes in the ligand bridging units are between 30 and 40° in platinum blue complexes but 95.7(6)° in **5** and 103.6(4)° in **6**. Correspondingly, the Pt–Pt–Pt zigzag angles are greater by *ca*. 35–40° in platinum blue complexes than in **5** and **6**. Summarizing, the platina-β-diketonate complexes of platina-β-diketones **5** and **6** can be regarded as organometallic analogues of platinum blue complexes.

We thank the Deutsche Forschungsgemeinschaft and the Fonds der Chemischen Industrie for financial support and the companies Merck (Darmstadt) and Degussa (Hanau) for loans of chemicals.

## Footnotes

* E-mail: steinborn@chemie.uni-halle.de

† *Syntheses*: To a stirred solution of $[Pt_2(\mu\text{-}Cl)_2\{(COMe)_2H\}_2]$ (200 mg, 0.32 mmol) in $CH_2Cl_2$ (5 cm³), aniline (61 mg, 0.66 mmol) or *p*-toluidine (71 mg, 0.66 mmol) was added at 20 °C. The pale yellow solution turned deep yellow immediately. After stirring for 2 h at room temp., a precipitate of **5**/**6** and $[NH_3R]Cl$ was filtered off and extracted with $CH_2Cl_2$ (10 cm³). At −30 °C, **5** and **6** crystallized within 2 days as yellow and red crystals, respectively, which were filtered off and dried *in vacuo*.

**5**·$CH_2Cl_2$: yield 159 mg (73%). **6**·$CH_2Cl_2$: yield 155 mg (68%).

‡ *Selected spectroscopic data*: **5**·$CH_2Cl_2$: IR (CsBr): ν(C–O) 1545sh, 1535vs, 1514s; ν(Pt–Cl) 275m cm$^{-1}$. $^1$H NMR (200 MHz, 298 K, $CD_2Cl_2$): δ 2.39 (s, 3 H, $CH_3$), 2.44 (s, 6 H, 2 × $CH_3$), 2.49 (s, 3 H, $CH_3$), 4.92 (s, 2 H, $NH_2$), 6.75 (m, 3 H, *m*-, *p*-CH), 7.15 (m, 2 H, *o*-CH). $^{195}$Pt NMR {86 MHz, 293 K, $CD_2Cl_2$; relative to δ($^{195}$Pt) = 4521 for $Na_2[PtCl_6]$}: δ 1639 [s + d, $^3J$(PtPt) 372 Hz, Pt(2)], 1479 [br, Pt(1)].

**6**·$CH_2Cl_2$: IR (CsBr): ν(C–O) 1553sh, 1535vs, 1514s; ν(Pt–N) 450w; ν(Pt–Cl) 273m cm$^{-1}$. $^1$H NMR (500 MHz, 298 K, $CD_2Cl_2$): δ 2.07 (s, 3 H, $COCH_3$), 2.14 (s, 3 H, $COCH_3$), 2.26 (s, 3 H, $C_6H_4CH_3$), 2.38 (s, 3 H, $COCH_3$), 2.47 (s, 3 H, $COCH_3$), 5.00 (s, 2 H, $NH_2$), 6.89 (d, 2 H, *J* 7.9 Hz, CH), 7.01 (d, 2 H, *J* 7.9 Hz, CH). $^{195}$Pt NMR (86 MHz, 293 K, $CD_2Cl_2$): δ 1640 [s + d, $^3J$ (PtPt) 326 Hz, Pt(2)], 1481 [br, Pt(1)].

§ *Crystal data*: **5**·$2CH_2Cl_2$, $C_{15}H_{22}Cl_3NO_4Pt_2$, *M* = 776.87, monoclinic, space group $P2_1/n$, *a* = 9.964(2), *b* = 21.219(3), *c* = 10.633(2) Å, β = 98.61(2)°, *U* = 2222.8(6) Å$^3$, *T* = 297 K, $D_c$ = 2.321 g cm$^{-3}$, *Z* = 4, Stoe IPDS diffractometer, Mo-Kα radiation, λ = 0.71073 Å, μ = 12.951 mm$^{-1}$, numerical absorption correction ($T_{min}$ = 0.75, $T_{max}$ = 1.00), 10112 reflections measured ($\theta_{min}$ = 2.16, $\theta_{max}$ = 22.50°) of which 2911 independent ($R_{int}$ = 0.172), 2050 observed [$I > 2\sigma(I)$], 226 parameters, *R* = 0.0763, *wR*2 = 0.2028, GOF = 1.045, the residual electron density lies near the Pt atoms; 2.67, −2.68 e Å$^{-3}$.

**6**·$2CH_2Cl_2$, $C_{16}H_{24}Cl_3NO_4Pt_2$, *M* = 790.89, triclinic, space group $P\bar{1}$, *a* = 9.563(3), *b* = 10.317(3), *c* = 11.665(3) Å, α = 78.75(2), β = 87.59(2), γ = 83.80(2)°, *U* = 1121.9(6) Å$^3$, *T* = 200 K, $D_c$ = 2.341 g cm$^{-3}$, *Z* = 2, Stoe Stadi4 diffractometers, Mo-Kα radiation, λ = 0.71073 Å, μ = 12.832 mm$^{-1}$, empirical absorption correction *via* ψ-scans ($T_{min}$ = 0.29, $T_{max}$ = 1.00), 4136 reflections measured ($\theta_{min}$ = 1.78, $\theta_{max}$ = 22.50°) of which 2942 independent ($R_{int}$ = 0.0741), 2293 observed [$I > 2\sigma(I)$], 240 parameters, *R* = 0.0494, $wR_2$ = 0.1388, GOF = 1.008, the residual electron density lies near the Pt atoms; 2.62, −2.43 e Å$^{-3}$.

Atomic coordinates, bond lengths and angles, and thermal parameters have been deposited at the Cambridge Crystallographic Data Centre (CCDC). See Information for Authors, Issue No. 1. Any request to the CCDC for this material should quote the full literature citation and the reference number 182/417.

¶ Data relating to **6** given in square brackets.

## References

1 C. M. Lukehart, *Acc. Chem. Res.*, 1981, **14**, 109; *Adv. Organomet. Chem.*, 1986, **25**, 45.
2 C. M. Lukehart and J. V. Zeile, *J. Am. Chem. Soc.*, 1978, **100**, 2774; *Inorg. Chem.*, 1978, **17**, 2369; K. P. Darst and C. M. Lukehart, *Inorg. Chim. Acta*, 1980, **41**, 239; C. M. Lukehart and M. Raja, *Inorg. Chem.*, 1982, **21**, 1278; D. Afzal and C. M. Lukehart, *Inorg. Chem.*, 1983, **22**, 3954.
3 C. M. Lukehart and G. P. Torrence, *Inorg. Chem.*, 1979, **18**, 3150; C. M. Jensen, Y. J. Chen and H. D. Kaesz, *J. Am. Chem. Soc.*, 1984, **106**, 4046; D. Xu, H. D. Kaesz and S. I. Khan, *Inorg. Chem.*, 1991, **30**, 1341; E. Lippmann, C. Robl, H. Berke, H. D. Kaesz and W. Beck, *Chem. Ber.*, 1993, **126**, 933.
4 D. Steinborn, M. Gerisch, K. Merzweiler, K. Schenzel, K. Pelz, H. Bögel and J. Magull, *Organometallics*, 1996, **15**, 2454.
5 M. Gerisch, C. Bruhn and D. Steinborn, to be published.
6 M. Kubota, S. C. Boegeman, R. N. Keil and C. G. Webb, *Organometallics*, 1989, **8**, 1616.
7 K. Krogmann, *Angew. Chem.*, 1969, **81**, 10; *Angew. Chem., Int. Ed. Engl.*, 1969, **8**, 35.
8 J. S. Miller and A. J. Epstein, *Prog. Inorg. Chem.*, 1976, **20**, 1; J. M. Williams, *Adv. Inorg. Chem. Radiochem.*, 1983, **26**, 235.
9 K. A. Hofmann and G. Bugge, *Ber. Dtsch. Chem. Ges.*, 1908, **41**, 312; J. K. Barton and S. J. Lippard, *Ann. N. Y. Acad. Sci.*, 1978, **313**, 686 and references therein; S. J. Lippard, *Science* (*Washington, DC*), 1982, **218**, 1075; G. Bernardinelli, P. Castan and R. Soules, *Inorg. Chim. Acta*, 1986, **120**, 205; T. V. O'Halloran, P. K. Mascharak, I. D. Williams, M. M. Roberts and S. J. Lippard, *Inorg. Chem.*, 1987, **26**, 1261.
10 L. S. Hollis and S. J. Lippard, *J. Am. Chem. Soc.*, 1981, **103**, 1230; *Inorg. Chem.*, 1983, **22**, 2600; J.-P. Laurent, P. Lepage and F. Dahan, *J. Am. Chem. Soc.*, 1982, **104**, 7335.

*Received in Basel, Switzerland, 20th January 1997; Com. 7/00427C*

# Discrimination between magnesium(II) and calcium(II) by 1,4,7-tris(2-hydroxyalkyl)-1,4,7-triazacyclononane ligands

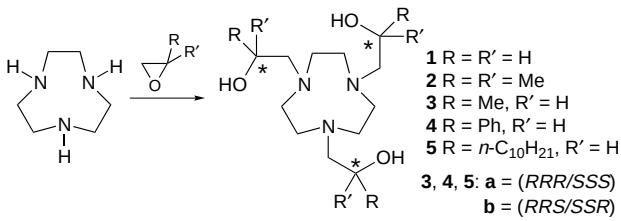
**Jurriaan Huskens[a] and A. Dean Sherry*[a,b]**

[a] *University of Texas at Dallas, Department of Chemistry, PO Box 830688, Richardson, Texas 75083-0688, USA*
[b] *University of Texas Southwestern Medical Center, Department of Radiology, the Rogers Magnetic Resonance Center, 5801 Forest Park Road, Dallas, Texas 75235-9085, USA*

**The title ligands and their possible diastereomeric forms show large selectivity differences for complexation of $Mg^{II}$ and $Ca^{II}$ which are related to the twist angle of the plane of coordinating hydroxy groups relative to the plane of macrocyclic ring nitrogens.**

Although calcium(II) and magnesium(II) both play vital roles in many biological processes, it is quite problematic to differentiate 'ionic' or weakly bound *vs*. tightly bound $Mg^{II}$ in a biological sample due to interference from ubiquitous $Ca^{II}$. Very few ligands have been reported that show a high enough selectivity for $Mg^{II}$ over $Ca^{II}$ to overcome this problem. This is especially evident in the development of ion-specific electrode methods for $Mg^{II}$ where the current technology requires a substantial correction for both $Ca^{II}$ and pH.[1] We recently described several 1,4,7-triazacyclononane derivatives containing methylene phosphinate ester, methylene phosphinate, or mixed acetate side-arms that showed a selectivity for $Mg^{II}$ over $Ca^{II}$ of, in some cases, more than two orders of magnitude.[2,3] Although the small cyclononane ring usually guarantees a higher Mg/Ca selectivity ($K_{sel} = K_{MgL}/K_{CaL}$) over most other ligand systems,[4] there are significant selectivity differences between known 1,4,7-triazacyclononane derivatives with different side-arm coordinating groups. For example, nota [1,4,7-triazacyclononane-1,4,7-tris(acetic acid)] has a $K_{sel}$ of 5.9[5] while notmp [1,4,7-triazacyclononane-1,4,7-tris(methylene methylphosphinate)] has a $K_{sel}$ of 170.[3] While investigating these selectivity differences in more detail, we discovered that the Mg/Ca binding selectivity of several trisubstituted 2-hydroxyalkyl derivatives of 1,4,7-triazacyclononane varied by three orders of magnitude and learned that stereochemistry of neighbouring side-chain groups defined the metal-ion selectivity. Although the ligands reported here did not bind significant amounts of $Mg^{II}$ or $Ca^{II}$ in aqueous solution, the dramatic selectivity of these systems for binding of $Mg^{II}$ in acetonitrile may serve as guide to developing better ion-specific membrane electrode systems.

All ligands were prepared by the reaction of 1,4,7-triazacyclononane with an excess of the corresponding epoxide (Scheme 1), as described before for **1**.[6] If R ≠ R′, two diastereomers of each derivative were formed when racemic epoxide was used. The ratio between the (*RRR*/*SSS*) (**a**) and the (*RRS*/*SSR*) (**b**) forms of **3**, **4** and **5** was in all cases 1 : 3, as statistically expected. Optically pure **3a** and **4a** were prepared from the corresponding chiral (*S*)-epoxides.




**Scheme 1**

The magnesium(II) and calcium(II) complexes of these ligands were studied by $^{13}C$ NMR spectroscopy (125 MHz) at room temp. using $CD_3CN$ as the solvent. The metal-to-ligand ratios were varied from 0–1.5 by the addition of magnesium(II) or calcium(II) perchlorate. In all cases, a 1 : 1 complex, in slow exchange with the free ligand, was formed completely upon addition of a stoichiometric amount of metal perchlorate. For **1** and **2**, single resonances were observed for all ring carbons and for all equivalent nuclei from the side-chains, while for **3a** and **4a** the ring carbons showed two resonances upon metal complexation. In the diastereomeric mixtures of **3**, **4** and **5**, eight equally intense ring carbon resonances could be detected for both MgL and CaL: two arise from the symmetrical (*RRR*/*SSS*)-isomer, while six belong to the unsymmetrical (*RRS*/*SSR*)-isomer. Analogously, the resonances of the side-chain nuclei appear as four equally intense lines.† Identification of the diastereomers of **3** and **4** was accomplished by comparison with the spectra of optically pure **3a** and **4a**, while for **5** the spectra were compared to the data obtained for **3**.

The Mg/Ca selectivities of the ligands were determined by $^{13}C$ NMR on samples with both $Mg^{II}$ and $Ca^{II}$ in excess. For a sample containing **3a** : **3b** : Mg : Ca = 1 : 3 : 6 : 6, the $^{13}C$ NMR spectrum (Fig. 1) showed that both $Mg^{II}$ and $Ca^{II}$ formed complexes with **3b** ($K_{sel}$ = 0.25), while **3a** only bound $Mg^{II}$. Selectivity experiments with pure **3a** indicated that $K_{sel}$ = 590 for this ligand. This led to the conclusion that the orientation of a single methyl group in these ligands results in a Mg/Ca selectivity difference of more than three orders of magnitude. Only **3a**, **4a** and **5a** exhibit good to excellent Mg/Ca selectivities (Table 1), while **1**, **2**, **3b**, **4b** and **5b** barely discriminate between $Mg^{II}$ and $Ca^{II}$.

To further investigate these large selectivity differences, we used molecular-mechanics calculations‡ to find the optimal

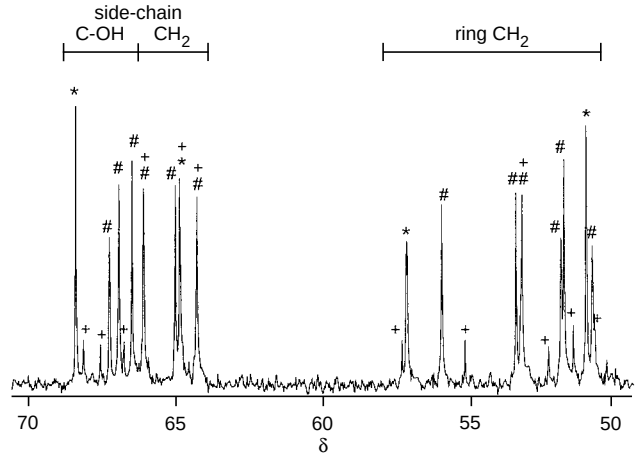



**Fig. 1** $^{13}C$ NMR spectrum of a sample with **3a** : **3b** : Mg : Ca = 1 : 3 : 6 : 6; * Mg(**3a**); + Mg(**3b**); # Ca(**3b**) (methyl resonances not shown)

structures of the magnesium(II) and calcium(II) complexes of **1**, **2**, **3a** and **3b**. Local energy minima were observed for structures in which the side-chains adopted one of three possible coordination modes (Fig. 2). The methyl groups in all optimized structures of **3a** and **3b** were pointing out from the centre, causing all side-chains to be in the same orientation for **3a**, while for **3b** two different side-chain orientations were present in each optimized structure. Table 1 shows the coordination mode of the lowest energy state of all magnesium(II) and calcium(II) complexes of **1**, **2** and **3**. Only for **3a**, the magnesium(II) complex had a different structure (AAA) than the calcium(II) complex (BBB).

The coordination modes AAA, BBB and CCC give rise to different 'twist angles', α, *i.e.* the rotation of the plane of coordinating oxygen atoms compared to the plane of ring nitrogens (Fig. 2). Since the carbon atoms of the macrocyclic ring are positioned alternately above and below the plane of ring nitrogens, these compounds contain an inherent twist of the plane of the side-chain carbon atoms directly connected to the ring nitrogens. Here, we define a positive α as a twist of the plane of coordinating oxygens in the same direction as the plane of side-chain carbons relative to the ring nitrogens. The twist α was large and positive for the AAA configuration, smaller (but positive) for BBB, and negative for CCC.§ Molecular mechanics showed that, for the magnesium(II) complexes, the large α (AAA) is only favoured when there is a driving force on the side-chains to put a residual R-group away from the centre and if any resulting steric hindrance between two side-chains is absent. As a result, Mg(**1**) adopted the BBB conformation because there is no driving force, while Mg(**2**) and Mg(**3b**) did not adopt AAA or AAB due to resulting steric hindrance between methyl groups of neighbouring side-chains. Only for Mg(**3a**) [and for Mg(**4a**) and Mg(**5a**)] were all factors optimal for adopting the AAA conformation. The large twist (AAA) makes the cavity for the metal ion quite small, so that this conformation is not optimal for the larger $Ca^{II}$ ion, which always preferred the BBB (or ABB) structure.

In conclusion, we have found that triazacyclononane derivatives that are able to accommodate $Mg^{II}$ in a small, tight cavity (large α) form complexes with structures (AAA), different from those of $Ca^{II}$ (BBB). This appears to be the origin of the large Mg/Ca selectivity seen for these ligands. Similar conformational changes that depend on the size of the metal ion have been observed in crystal structures of a few transition-metal complexes, *e.g.* the zinc(II) complex of **3a** adopted the BBB conformation,[7] while the smaller cations $Co^{III}$ and $Cr^{III}$ preferred the AAA structure.[8] For nota, the nickel(II) and nickel(III) and chromium(III) complexes adopted the BBB conformation, while the larger $Cu^{II}$ and $Fe^{III}$ preferred CCC.[9] The present study is the first, however, to relate this phenomenon to a (large) difference in metal ion selectivity. A more elaborate study involving acetate, phosphonate ester, and phosphinate side-chains will be published elsewhere.

This research was supported in part by grants from the Robert A. Welch Foundation (AT-584) and the NIH Biotechnology Research Program (P41-RR02584).

**Table 1** Selectivities, $K_{sel}$ (= $K_{MgL}/K_{CaL}$),[a] of the macrocyclic ligands (Scheme 1) as obtained from $^{13}C$ NMR competition experiments, and the preferred side-chain coordination modes (Fig. 2) as obtained from MMX calculations

| | | Mode | |
|---|---|---|---|
| Ligand L | $K_{sel}$ | MgL | CaL |
| **1** | 0.18 | BBB | BBB |
| **2** | 3.0 | BBB[b] | BBB |
| **3a** | 590 | AAA | BBB |
| **3b** | 0.25 | ABB | ABB |
| **4a** | 16 | | |
| **4b** | 0.06 | | |
| **5a** | 60[c] | | |
| **5b** | 0.28 | | |

[a] ±5%. [b] CCC has only slightly higher energy. [c] Lower limit; observed only for a mixture of **5a** and **b**.

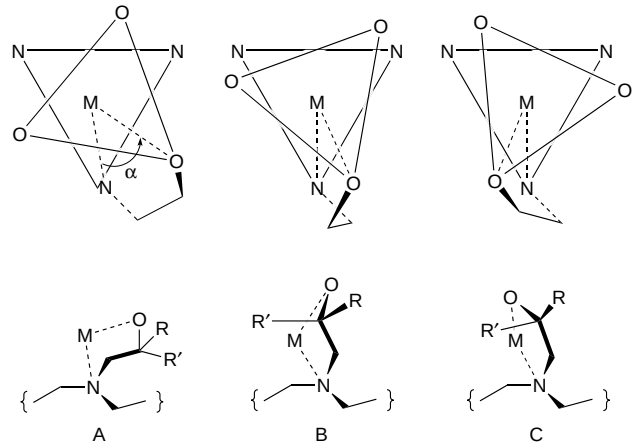



**Fig. 2** Schematic front and top views of the possible coordination modes of the side-chains of the metal complexes of **1**, **2** and **3** for which energy minima were observed by molecular-mechanics calculations, and the resulting twist angles, α, of the plane of coordinating oxygens relative to the plane of macrocyclic ring nitrogens

## Footnotes

* E-mail: sherry@utdallas.edu

† In **5**, only the first two carbon nuclei of R (= $n$-$C_{10}H_{21}$) were thus resolved.

‡ The geometries of the magnesium(II) and calcium(II) complexes of **1**, **2** and **3** were optimized using the built-in MMX forcefield of Hyperchem 4.5 on a 486DX, 66 MHz PC. Side-chains were positioned roughly into modes A, B or C (Fig. 2) before optimization, and the position of the OH protons in **1**, **2** and **3**, and of the methyl groups in **3** was varied systematically for observation of the local minima.

§ Trigonal prism: α = 0; octahedron: α = 60°. Twist angles observed for the magnesium(II) complexes were approximately +40, +10 and −30° for AAA, BBB, and CCC, respectively, while for the calcium(II) complexes these were +25, +5 and −20°.

## References

1 Z. Hu, T. Bührer, M. Müller, B. Rusterholz, M. Rouilly and W. Simon, *Anal. Chem.*, 1989, **61**, 574; W. Zhang, A. C. Truttmann, D. Lüthi and J. A. S. McGuigan, *Magnesium Bull.*, 1995, **17**, 4; N. N. Rehak, S. A. Cecco, J. E. Niemela, E. N. Hristova and R. J. Elin, *Clin. Chem.*, 1996, **42**, 880.
2 R. Ramasamy, I. Lazar, E. Brücher, A. D. Sherry and C. R. Malloy, *FEBS Lett.*, 1991, **280**, 121; J. Haveren, L. DeLeon, R. Ramasamy, J. van Westrenen and A. D. Sherry, *NMR Biomed.*, 1995, **8**, 197.
3 J. Huskens and A. D. Sherry, *J. Am. Chem. Soc.*, 1996, **118**, 4396.
4 M. J. van der Merwe, J. C. A. Boeyens and R. D. Hancock, *Inorg. Chem.*, 1985, **24**, 1208.
5 A. Bevilacqua, R. I. Gelb, W. B. Hebard and L. J. Zompa, *Inorg. Chem.*, 1987, **26**, 2699.
6 B. A. Sayer, J. P. Michael and R. D. Hancock, *Inorg. Chim. Acta*, 1983, **77**, L63.
7 I. Fallis, L. J. Farrugia, N. M. Macdonald and R. D. Peacock, *Inorg. Chem.*, 1993, **32**, 779.
8 A. A. Belal, L. J. Farrugia, R. D. Peacock and J. Robb, *J. Chem. Soc., Dalton Trans.*, 1989, 931; L. J. Farrugia, N. M. Macdonald, R. D. Peacock and J. Robb, *Polyhedron*, 1995, **4**, 541.
9 K. Wieghardt, U. Bossek, P. Chaudhuri, W. Herrmann, B. C. Menke and J. Weiss, *Inorg. Chem.*, 1982, **21**, 4308; M. J. van der Merwe, J. C. A. Boeyens and R. D. Hancock, *Inorg. Chem.*, 1983, **22**, 3490.

*Received in Cambridge, UK, 17th February 1997; Com. 7/01107C*

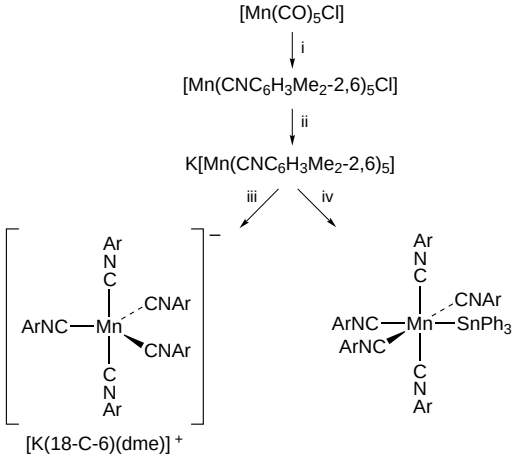
# Synthesis, derivatization, and structural characterization of $[Mn(CNC_6H_3Me_2\text{-}2,6)_5]^-$, a five-coordinate isonitrilate complex containing $Mn^{-I}$

**Tracy L. Utz, Patricia A. Leach, Steven J. Geib and N. John Cooper***

*Department of Chemistry and Materials Research Center, University of Pittsburgh, Pittsburgh, Pennsylvania 15260, USA*

**Naphthalenide reduction of $[Mn(CNC_6H_3Me_2\text{-}2,6)_5Cl]$ forms solutions of trigonal-bipyramidal $[Mn(CNC_6H_3Me_2\text{-}2,6)_5]^-$, as established by an X-ray diffraction study of a $[K(18\text{-}C\text{-}6)(dme)]^+$ salt and derivatization with $SnClPh_3$ to give $[Mn(CNC_6H_3Me_2\text{-}2,6)_5(SnPh_3)]$.**

Our recent syntheses of the first isonitrilates (homoleptic isonitrile complexes of metals in negative oxidation states) generated complexes of $Co^{-I}$ $\{[Co(CNC_6H_3Me_2\text{-}2,6)_4]^-\}$[1] and of $Ru^{-II}$ $\{[Ru(CNC_6H_3Me_2\text{-}2,6)_4]^{2-}$ and $[Ru(CNBu^t)_4]^{2-}\}$.[2] The existence of these complexes established that isonitrilates could be prepared with several different metals, with metals in oxidation states as low as −II, and with both alkyl and aryl substituents on the ligands. It remained unclear, however, whether isonitrilates could be prepared in geometries other than tetrahedral; the cobalt(−I) and ruthenium(−II) complexes are all four coordinate, and a tetrahedral geometry has been established crystallographically[1] for $[Co(CNC_6H_3Me_2\text{-}2,6)_4]^-$ and is consistent with IR data in the ruthenium(−II) case,[2] as would be anticipated on the basis of the $d^{10}$ configurations of the metals and by analogy with the isoelectronic carbonylmetalates $[Co(CO)_4]^-$[3] and $[Fe(CO)_4]^{2-}$.[4] Structurally characterized homoleptic carbonylmetalates are known in five[5,6] and six coordinate[7,8] geometries, but the established propensity of isonitrile ligands to couple in higher coordinate environments[9] left open whether isonitrilates would be accessible in similar geometries despite the close analogies between isonitriles and CO.[10] We have now examined the synthesis of five coordinate manganese(−I) isonitrilates, and we wish to report the synthesis of the trigonal-bipyramidal isonitrilate $[Mn(CNC_6H_3Me_2\text{-}2,6)_5]^-$ **1**$^-$ and its structural characterization as a $[K(18\text{-crown-}6)(dme)]^+$ salt (dme = dimethoxyethane), together with evidence that **1**$^-$ can react as a metal centred nucleophile with simple electrophiles (Scheme 1).




**Scheme 1** *Reagents and conditions*: i, $CNC_6H_3Me_2$-2,6; ii, 2 K(Naph); iii, 18-C-6, dme; iv, $SnClPh_3$

We recently reported that cobalt(−I) isonitrilates can be prepared by naphthalenide reduction of any of a range of cobalt(0), cobalt(I) and cobalt(II) precursors which contain an adequate number of isonitrile ligands,[1] and this led us to approach the synthesis of $[Mn(CNC_6H_3Me_2\text{-}2,6)_5]^-$ by reduction of $[Mn(CNC_6H_3Me\text{-}2,6)_5Cl]$ **2**.[11] Dropwise addition of 2 equiv. of a 0.4 M potassium naphthalenide [K(Naph)] solution[12] to an orange thf solution of **2** at −78 °C gave a blood-red solution. The sharp $\nu_{CN}$ bands of **2** at 2062s and 2008(sh) $cm^{-1}$ were replaced by two broad $\nu_{CN}$ absorptions at 1920s and 1710m $cm^{-1}$ indicating complete consumption of **2** and formation of a more reduced isonitrile complex. These solutions are extremely air sensitive, changing from blood red to cherry red in seconds, and are also thermally unstable, undergoing a similar colour change in a few days at room temperature.

Initial attempts to isolate the reduction product were unsuccessful, but it was readily established that this solution is an effective source of $[Mn(CNC_6H_3Me_2\text{-}2,6)_5]^-$ by addition of $SnClPh_3$ (1 equiv. in thf) at −78 °C. The solution became clear and yellow in colour, and IR spectra indicated complete consumption of the anion and formation of a new species with higher energy $\nu_{CN}$ bands at 2135m, 2064(sh) and 1998s $cm^{-1}$. The solvent was removed under reduced pressure and the product was purified by slow diffusive mixing of a pentane layer into a concentrated toluene solution to give crystals of $[Mn(CNC_6H_3Me_2\text{-}2,6)_5(SnPh_3)]$ **3**† in 88% yield.

Isolation of a crystalline salt of $[Mn(CNC_6H_3Me_2\text{-}2,6)_5]^-$ from the reduction of $[Mn(CNC_6H_3Me_2\text{-}2,6)_5Cl]$ required that samples be maintained at or below −30 °C, and began with filtration of a freshly prepared solution through a bed of Celite 545 into a flask containing 1 equiv. of neat 18-crown-6 (18-C-6). After 1 h the solvent was removed under reduced pressure and the mixture was washed with pentane to give a red–brown solid from which red–black crystals of [K(18-C-6]**1**† could be obtained in 53% yield by crystallization from a saturated dme solution following addition of a layer of pentane. This material does not entirely redissolve in dme; this behaviour is reminiscent of that of alkali-metal salts of $[M(CO)_5]^{2-}$ (M = Cr, Mo, W) in the solid state at room temperature.[6]

Crystals suitable for X-ray diffraction studies were grown from a freshly prepared sample of [K(18-C-6)]**1** by dissolving it in a minimal volume of dme and cooling the unfiltered solution to −30 °C overnight. A low-temperature diffraction study‡ established that these crystals contain [K(18-C-6)(dme)]**1**, a dme solvate of [K(18-C-6)]**1**, but this material is not stable in the solid state at room temperature and crystals do not diffract well if stored for more than few days.

In this salt of **1**$^-$ the bis-chelate dme and the 18-C-6 ligand are both coordinated to the $K^+$ counter ion, effectively blocking $K^+$– Mn$^-$ contact ion pairing in the solid state, and allowing the $[Mn(CNC_6H_3Me_2\text{-}2,6)_5]^-$ anion (Fig. 1) to adopt a geometry close to the trigonal bipyramid anticipated by analogy with the established structures of five coordinate carbonylmetalates[5,6] and of the isoelectronic $d^8$ homoleptic isonitrile complex $[Fe(CNBu^t)_5]$.[13] The C(1) and C(5) isonitriles are in the axial positions, but there are some irregularities in the coordination

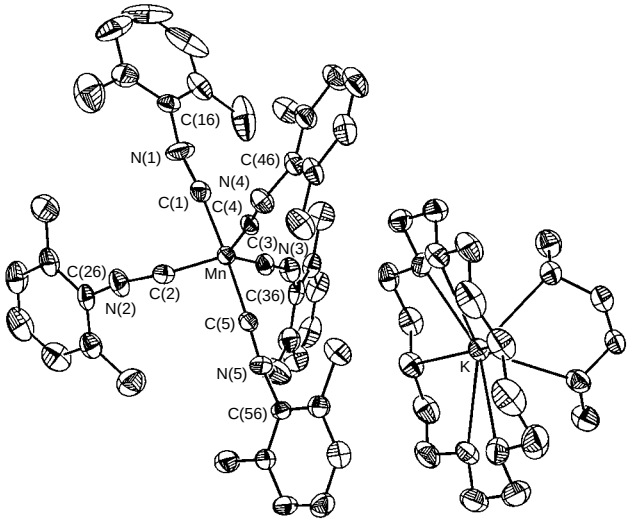



**Fig. 1** Molecular structure of [K(18-C-6)(dme)][Mn($CNC_6H_3Me_2$-2,6)$_5$] ([K(18-C-6)(dme)]**1**; 35% probability ellipsoids; hydrogen atoms omitted for clarity). Selected bond lengths (Å) and angles (°): Mn–C(1) 1.847(6), Mn–C(2) 1.724(6), Mn–C(3) 1.837(6), Mn–C(4) 1.806(6), Mn–C(5) 1.869(6), C(1)–N(1) 1.195(7), C(2)–N(2) 1.185(7), C(3)–N(3) 1.225(7), C(4)–N(4) 1.219(7), C(5)–N(5) 1.184(6) Å; C(1)–Mn–C(5) 174.4(3), C(2)–Mn–C(4) 123.7(3), C(2)–Mn–C(3) 111.9(3), C(3)–Mn–C(4) 124.3(2), C(1)–Mn–C(2) 82.9(3), C(1)–Mn–C(3) 98.1(3), C(1)–Mn–C(4) 85.3(2), C(2)–Mn–C(5) 94.2(2), C(3)–Mn–C(5) 87.4(2), C(4)–Mn–C(5) 92.4(2), C(1)–N(1)–C(16) 163.2(7), C(2)–N(2)–C(26) 143.3(6), C(3)–N(3)–C(36) 149.2(6), C(4)–N(4)–C(46) 149.2(5), C(5)–N(5)–C(56) 163.4(6)°.

sphere. The C(2) isonitrile in particular has Mn–C and C≡N bonds which are 0.097 Å ($>15\sigma$) and 0.04 Å ($>5\sigma$) shorter, respectively, than the average C≡N bonds in the other two equatorial isonitriles; we ascribe this shortening to distortions induced by van der Waals interactions between neighbouring [Mn($CNC_6H_3Me_2$-2,6)$_5$]$^-$ ions, consistent with the 2.95 and 2.72 Å distances between the hydrogen atoms on the *para* carbon and one *meta* carbon of the C(2) isonitrile and the aryl plane of the C(3) isonitrile ligand. It is interesting that the axial isonitriles are less bent at nitrogen (both 163°) than the equatorial isonitriles (av. 147°, range 143–149°); a similar pattern in metric parameters for [Fe($CNBu^t$)$_5$] was ascribed to more effective back bonding from the low-valent Fe(0) metal centre to the equatorial isonitrile ligands.[13]

Our results establish that isonitrilates can be prepared in five coordinate environments, and that a $d^8$ example adopts a trigonal bipyramidal geometry. The successful synthesis of [Mn($CNC_6H_3Me_2$-2,6)$_5$]$^-$ represents a significant addition to the small number of complexes accepted to contain manganese in the −I oxidation state,[14] and its derivatization with $SnClPh_3$ also suggests that **1**$^-$ may prove a valuable intermediate which will allow access to an isonitrile chemistry of Mn comparable to the carbonyl chemistry of Mn accessible from the isoelectronic carbonylmetalate [Mn(CO)$_5$]$^-$.[15]

We thank the National Science Foundation for financial support through grant CHE-9632202.

## Footnotes

* E-mail: cooperj+@pitt.edu

† **3**: IR $\nu_{CN}$; 2135m, 2064(sh). 1998s cm$^{-1}$. $^1$H NMR ($CD_2Cl_2$, 300 MHz): δ 7.60–7.57 (m, 5 H, *p*-H of $C_6H_3$), 6.99–6.87 (m, 25 H, *m*-H of $CNC_6H_3Me_2$ and $SnPh_3$), 2.42 (s, 6 H, $CH_3$ of $CNC_6H_3Me_2$ *trans* to $SnPh_3$), 2.16 (s, 24 H, $CH_3$ of $CNC_6H_3Me_2$ *cis* to $SnPh_3$).

[K(18-C-6)]**1**: IR $\nu_{CN}$: 1920s, 1710m cm$^{-1}$. $^1$H NMR ($CD_3CN$, 300 MHz): δ 6.92 (d, 7.2 Hz, 10 H, *m*-H of $CNC_6H_3Me_2$), 6.73 (t, 7.2 Hz, 1 H, *p*-H of $CNC_6H_3Me_2$), 3.53 (s, 24 H, $C_{12}H_{24}O_6$), 2.37 (s, 30 H, $CH_3$ of $CNC_6H_3Me_2$). The instability of the compound has precluded satisfactory combustion analysis, but the 18-C-6 : isonitrile ratio is confirmed by $^1$H NMR spectra. These spectra also establish that there is negligible dme in crystals prepared in this manner.

‡ *Crystal data*: [K(18-C-6)(dme)]**1**: triclinic, space group $P\bar{1}$, $Z$ = 2, $a$ = 11.825(5), $b$ = 12.623(6), $c$ = 22.663(2) Å, α = 99.12(4), β = 101.17(4), γ = 112.47(4)°, $U$ = 2964(2) Å$^3$, $T$ = 213(2) K. Of the 9842 reflections measured in the range $3.62 < 2\theta < 50.56°$ range, 9376 unique reflections were used in the structure solution by direct methods. Refinement on $F^2$ converged at $R$ = 0.0705 $R_w$ = 0.1958 (all data), with GOF = 1.037.

Atomic coordinates, bond lengths and angles, and thermal parameters have been deposited at the Cambridge Crystallographic Data Centre (CCDC). See Information for Authors, Issue No. 1. Any request to the CCDC for this material should quote the full literature citation and the reference number 182/392.

## References

1 P. A. Leach, S. J. Geib, J. A. Corella, G. F. Warnock and N. J. Cooper, *J. Am. Chem. Soc*., 1994, **116**, 8566.
2 J. A. Corella, R. L. Thompson and N. J. Cooper, *Angew. Chem., Int. Ed. Engl*., 1992, **31**, 83.
3 P. Z. Klüfers, *Z. Kristallogr*., 1984, **167**, 253; D. P. Schussler, W. R. Robinson and W. F. Edgell, *Inorg. Chem*., 1974, **13**, 153.
4 H. B. Chin and R. Bau, *J. Am. Chem. Soc*., 1976, **98**, 2434; R. G. Teller, R. G. Finke, J. P. Collman, H. B. Chin and R. Bau, *J. Am. Chem. Soc*., 1977, **99**, 1104.
5 [Mn(CO)$_5$]$^-$: B. A. Frenz and J. A. Ibers, *Inorg. Chem*., 1972, **11**, 1109; M. Heberhold, F. Wehrmann, D. Neugebauer and G. Huttner, *J. Organomet. Chem*., 1978, **152**, 329; B. Balbach, S. Baral, H. Biersack, W. A. Herrmann, J. A. Labinger, W. R. Scheidt, F. J. Timmers and M. L. Ziegler, *Organometallics*, 1992, **11**, 35; H. Ben Laarab, B. Chaudret, F. Dahan, J. Devillers, R. Poilblanc and S. Sabo-Etienne, *New J. Chem*., 1990, **14**, 321; W. Petz and F. Weller, *Z. Naturforsch., Teil B*, 1991, **46**, 297.
6 [W(CO)$_5$]$^{2-}$: J. M. Maher, R. P. Beatty and N. J. Cooper, *Organometallics*, 1985, **4**, 1354.
7 [M(CO)$_6$]$^-$ (M = V, Nb or Ta): R. D. Wilson and R. Bau, *J. Am. Chem. Soc*., 1974, **96**, 7601; L. D. Silverman, P. W. R. Corfield and S. J. Lippard, *Inorg. Chem*., 1981, **20**, 3106; F. Calderazzo, U. Englert, G. Pampaloni, G. Prelizzi and R. Zamboni, *Inorg. Chem*., 1983, **22**, 1865; F. Calderazzo, G. Pampaloni, D. Vitali and R. Zanazzi, *J. Chem. Soc., Dalton Trans*., 1982, 1993.
8 [M(CO)$_6$]$^{2-}$ (M = Ti, Zr or Hf): J. E. Ellis and K.-M. Chi, *J. Am. Chem. Soc*., 1990, **112**, 6022.
9 E. M. Carnahan, J. D. Protasiewicz and S. J. Lippard, *Acc. Chem. Res*., 1993, **26**, 90.
10 L. Malatesta, *Prog. Inorg. Chem*., 1959, **1**, 283; L. Malatesta and F. Bonati, *Isocyanide Complexes of Transition Metals*, Wiley, New York, 1969; P. M. Treichel, *Adv. Organomet. Chem*., 1973, **11**, 21; Y. Yamamoto, *Coord. Chem. Rev*., 1980, **32**, 193; E. Singleton and M. E. Oosthuizen, *Adv. Organomet. Chem*., 1983, **22**, 209.
11 Prepared by a procedure analogous to that used to prepare the corresponding CNPh complex: K. K. Joshi, P. L. Pauson and W. H. Stubbs, *J. Organomet. Chem*., 1963, **1**, 51; P. M. Treichel, G. E. Dirreen and H. J. Mueh, *J. Organomet. Chem*., 1972, **44**, 339.
12 J. M. Maher, R. P. Beatty, G. R. Lee and N. J. Cooper, *Organometallic Syntheses*; ed. R. B. King and J. J. Eisch, Elsevier, Amsterdam, 1986, vol. 3, p. 35.
13 J. M. Bassett, M. Green, J. A. K. Howard and F. G. A. Stone, *J. Chem. Soc., Chem. Commun*., 1977, 853; J. M. Bassett, D. E. Berry, G. K. Barker, M. Green and J. A. K. Howard, *J. Chem. Soc., Dalton Trans*., 1979, 1003.
14 There are few accepted examples other than [Mn(CO)$_5$]$^-$ and [Mn(NO)$_2$(CN)$_2$]$^{3-}$ (H. von Behrens, E. Linder and H. Schindler, *Z. Anorg. Allg. Chem*., 1969, **365**, 119): B. Chiswell, E. D. McKenzie and L. F. Lindoy, in *Comprehensive Coordination Chemistry*, ed. G. Wilkinson, R. D. Gillard and J. A. McCleverty, Pergamon, Oxford, 1987, vol. 4, ch. 41.
15 P. M. Treichel, in *Comprehensive Organometallic Chemistry II*, ed. E. W. Abel, F. G. A. Stone and G. Wilkinson, Pergamon, Oxford, 1995, vol. 6, section 1.3; P. M. Treichel, in *Comprehensive Organometallic Chemistry*, ed. G. Wilkinson, F. G. A. Stone and E. W. Abel, Pergamon, Oxford, 1982, vol. 4, section 29.2.

*Received in Bloomington, IN, USA, 3rd January 1997; Com. 7/00089H*

# New methoxy-substituted 9-phenylxanthen-9-ylamine linkers for the solid phase synthesis of protected peptide amides

**Mark Meisenbach,† Hartmut Echner and Wolfgang Voelter***

*Physiologisch-chemisches Institut, Abteilung für Physikalische Biochemie, Universität Tübingen, Hoppe-Seyler-Str. 4, D-72076 Tübingen, Germany*

**New methoxy-substituted 9-phenylxanthen-9-ylamine linkers are described for the solid phase synthesis of peptide amides *via* the Fmoc strategy; depending on the cleavage conditions, the peptide amides can be cleaved rapidly and in high purity in their protected or deprotected forms.**

Efficient stepwise solid-phase syntheses of C-terminal peptide amides yielding products of high purity are of interest for several reasons: (i) a considerable number of hormones, including secretin, calcitonin, oxytocin, thyroliberin and luliberin, bear a C-terminal acid amide function, (ii) several peptidyl amides, such as indolicin or protegrins, have potent antimicrobial activities, (iii) changing the C-terminal carboxy function of a biologically active peptide into a peptidyl or peptidyl N-alkyl amide often leads to analogues with more favourable or prolonged activity, and (iv) fully protected, but N-terminally free, peptide amides are needed for the assembly of longer chains.[1]

Highly acid-labile linkers are desirable, especially for the synthesis of peptide fragments in the protected form *via* the efficient Fmoc–Bu$^t$ SPPS strategy, as they allow the cleavage of peptide amides under very mild conditions. The xanthenylamine linker (XAL) system has been described as a useful handle for the synthesis of peptide amides,[2,3] but the conditions (30 min with 1% TFA–$CH_2Cl_2$ v/v)[1] used for their cleavage from the resin also cause, for example, loss of the trityl protection group from His, and it is therefore not suitable for the preparation of side chain-protected peptide segments with *e.g.* His(Trt)-containing peptide amides.[4] The rapid acidolysis (50% TFA, < 5 min) of the 9-phenylxanthen-9-yl (Pixyl) protection group for the carboxy amide function of asparagine and glutamine recently developed in our laboratory[5] prompted us to increase the acid lability of XAL by introducing methoxy-substituted phenyl residues in position 9.

The starting material, 3-hydroxyxanthen-9-one **1**, was synthesized in good yield *via* a three-step procedure from *o*-chlorobenzoic acid and *m*-methoxyphenol.[6,7] Treatment of **1** with sodium methoxide and chloromethylated polystyrene in *N*,*N*-dimethylacetamide (DMA) yielded resin **2**, free of chloride. The resulting xanthenol resins **3a** and **3b** were prepared from **2** *via* a Grignard reaction using the corresponding bromo reagents in THF. The disappearance of the CO band in the IR spectrum at 1645 cm$^{-1}$ indicated that the reaction had gone to completion. Both resins, **3a** and **3b**, were converted with AcCl in toluene into the chloro forms, and then by treatment with ammonia in $CH_2Cl_2$ into the amino compounds **4a** and **4b** (Scheme 1).‡

As a test case, Fmoc-Gly-OH was coupled to the resin using DCC (3 equiv., 2 h) and the remaining amino groups were capped with $Ac_2O$–Pr$^i_2$EtN (1 : 1) in $CH_2Cl_2$ for 20 min. To determine the extent of functionalization of the resin, the Fmoc-group was cleaved with 25% piperidine–DMF and the solution of the 9-fluorenylmethyl piperidine adduct was measured by UV spectroscopy at $\lambda$ = 290 nm. The loading determined was 0.52 and 0.58 mmol Fmoc-Gly g$^{-1}$ resin for **5a** and **5b**, respectively. Other Fmoc amino acids were attached to the resins and the degree of resin loading was found to be satisfactory, even with highly sterically hindered amino acids such as Fmoc-Val-OH ( > 0.43 mmol g$^{-1}$) and Fmoc-Asn(Trt)-OH ( > 0.35 mmol g$^{-1}$).

Kinetic studies were performed to compare the cleavage times of Fmoc amino acids from the resins **5a** and **5b** with those

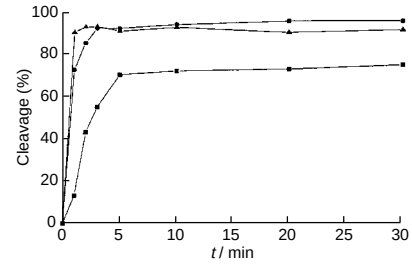
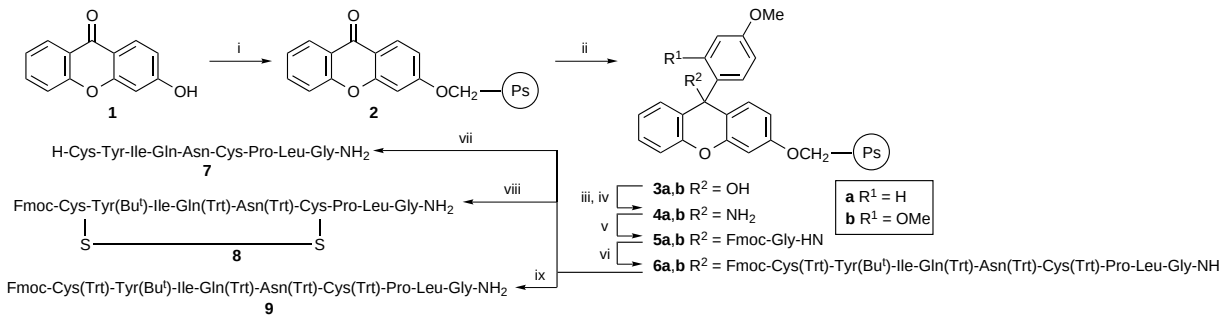



**Fig. 1** Cleavage kinetics of Fmoc-Gly-$NH_2$ from ( ▲ ) **5b**, (●) **5a** and (■) 9-aminoxanthen-3-yloxymethyl polystyrene resin (XAL)




**Scheme 1** *Reagents and conditions*: i, chloromethylated polystyrene (1.7 mmol g$^{-1}$, 2.5 equiv.) DMA, 65 °C, 15 h; ii, Mg (10 equiv.) and 4-bromoanisole (10 equiv.) (for **a**) or 1-bromo-2,4-dimethoxybenzene (10 equiv.) (for **b**), THF, 12 h, reflux; iii, AcCl (20 equiv.) PhMe, 40 °C, 1 h; iv, 50% $NH_3$ in $CH_2Cl_2$, −45 °C to room temp., 1 h; v, Fmoc-Gly-OH, DCC, $CH_2Cl_2$; vi, standard Fmoc–Bu$^t$ solid phase procedures (see footnote ‖); vii, 10% TFA–$CH_2Cl_2$, 15 min, TFA–thioanisole–ethanedithiol–$H_2O$–PhOH (10 : 0.5 : 0.5 : 0.5 : 0.5, v/v/v/v/w), TFA, 2 h, room temp.; viii, $I_2$ (10 equiv.) in 0.5% TFA–$CH_2Cl_2$ (v/v), 3–5 min; ix, 1% TFA–$CH_2Cl_2$ (v/v), 3–10 min

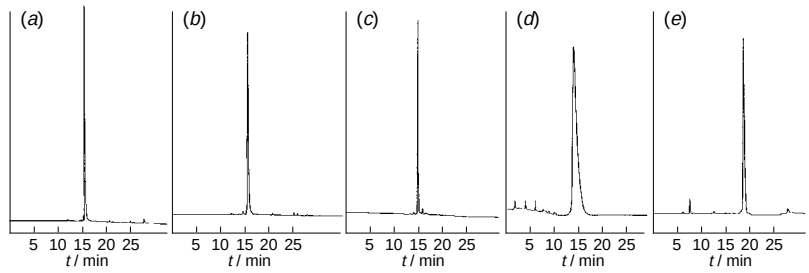



**Fig. 2** Reversed-phase high performance liquid chromatograms of synthetic oxytocin: (*a*) deprotected crude product **7** cleaved from **6a**; (*b*) deprotected crude product **7** cleaved from **6b**; (*c*) oxidized unprotected crude product cleaved from **6b**; (*d*) protected crude product **9** cleaved from **6b**; (*e*) protected oxidized crude product **8** cleaved from **6b**. Column: Nucleosil 5 μm $C_{18}$ 4.6 × 250 mm. Eluents: [for (*a*)–(*c*)] A = $H_2O$–TFA (1000 : 0.25), B = MeCN–$H_2O$–TFA (600 : 400 : 0.2); [for (*d*) and (*e*)] A = $H_2O$–TFA (1000 : 0.25), B = MeCN–TFA (1000 : 0.2). Gradients (A : B): [for (*a*)–(*c*)] 0–1 min (95 : 5), 1–31 min (95 : 5 to 5 : 95); [for (*d*)] 0–1 min (20 : 80), 1–11 min (20 : 80 to 0 : 100), 11–30 min (0 : 100); [for (*e*)] 0–1 min (40 : 60), 1–16 min (40 : 60 to 0 : 100), 16–30 min (0 : 100). Flow rate: 1 ml $min^{-1}$. Detection: λ = 214 nm. Concentration: 1 mg $ml^{-1}$.

from the 9-aminoxanthen-3-yloxymethyl polystyrene support (Novabiochem). The Fmoc-Gly-resins were treated with 1% TFA in $CH_2Cl_2$ and aliquots (*ca*. 5 mg) were periodically withdrawn from the reaction vessel to determine the degree of cleavage *via* UV spectroscopy,§ demonstrating the expected much higher acid lability of the new linkers compared to the commercially available XAL (Fig. 1).

The practicability of the new linker system is illustrated by the efficient synthesis of our model peptide oxytocin [Fmoc-Cys(Trt)-Tyr(Bu$^t$)-Ile-Gln(Trt)-Asn(Trt)-Cys(Trt)-Pro-Leu-Gly-$NH_2$], chosen as a test sequence for the synthesis of a disulfide-bridged protected peptide amide. The linear sequence **7** was smoothly synthesized batchwise using the Fmoc–Bu$^t$ strategy.¶ After incorporation of the last amino acid and removal of the N-terminal Fmoc group, the peptide was cleaved with 10% TFA–$CH_2Cl_2$ over 15 min. To remove the side chain protecting groups, the product was treated with TFA–ethanedithiol(EDT)–thioanisole(TA)–$H_2O$–PhOH (10 : 0.5 : 0.5 : 0.5 : 0.5, v/v/v/v/w), followed by diethyl ether precipitation and lyophilisation. The linear product **7** was obtained in 83 and 90% yield from **6a** and **6b**, respectively, demonstrating the stability of the peptidyl linker bond under the standard basic Fmoc–Bu$^t$ synthetic conditions. The crude reduced oxytocin showed excellent purity (Fig. 2) and was oxidized by air in $NH_4Ac$ buffer.‖

To yield the protected linear oxytocin **9** the cleavage was performed with 1% TFA–$CH_2Cl_2$ for 10 min from **6a** (80% yield) and 5 min from **6b** (93% yield).** The versatility of the linker is further illustrated by the simple and efficient method of oxidation with iodine during the cleavage. To obtain the cyclic protected oxytocin **8**, the product was cleaved with 0.5% TFA–$CH_2Cl_2$ (v/v) and the intramolecular disulfide bridge was simultaneous formed by oxidation with $I_2$ (10 equiv.) over 5 min for **6a** and 3 min for **6b** in 81 and 89% yield, respectively.††

Our results show that the introduction of the methoxy-substituted phenyl residue in position 9 of the xanthenyl system increased the acid lability as expected. The high yields and the excellent purity of the synthetic peptides produced on the resins show that the peptidyl linker bond is stable under the basic Fmoc–Bu$^t$ synthetic conditions and that these new linkers allow a far faster cleavage of peptide amides compared to the commercially available XAL. The linker is also suitable for the convenient preparation of cystine-containing protected peptide amides by simultaneous iodine oxidation and cleavage of the products. Therefore, our new linker can be recommended for the synthesis of peptide amides in both unprotected and protected form, and is almost free of side products.

## Footnotes

† E-mail: mark.meisenbach@uni-tuebingen.de

‡ The chloromethylated polystyrene (1.7 mmol $g^{-1}$) was treated with 2.5 equiv. of 3–hydroxyxanthen-9-one **1** and 2.5 equiv. of MeONa in DMA at 65 °C for 15 h. The Beilstein test and microanalysis for chloride were negative. The Grignard reactions of the 9-oxoxanthen-3-yloxymethyl polystyrene resin **2** were performed in THF refluxing for 12 h with the Mg adducts 4-bromoanisole and 1-bromo-2,4-dimethoxybenzene, respectively. The resins **3a** and **3b** were transformed into the dark red halide forms over 1 h with AcCl in toluene at 70 °C. To yield the orange 9-amino-9-(4-methoxyphenyl)xanthen-3-yloxymethyl and 9-amino-9-(2,4-dimethoxyphenyl)xanthen-3-yloxymethyl polystyrene resins **4a** and **4b**, respectively, the resins were treated with a cold (−45 °C) solution of ammonia in $CH_2Cl_2$ (50%) and allowed to warm to room temperature (1 h).

§ A 100 mg batch of each Fmoc-Gly-resin (**5a**, **5b** and XAL) was placed in a reaction vessel and allowed to swell in $CH_2Cl_2$ for 10 min, then treated with 20 ml of 1% TFA–$CH_2Cl_2$ (v/v); periodically, *ca*. 5 mg samples were taken out and washed immediately (3 × $CH_2Cl_2$, 3 × DMF 3 × MeOH, 2 × $CH_2Cl_2$ and $Et_2O$). To control the release of the amino acid, the remaining Fmoc groups were cleaved with 25% piperidine–DMF for determination by UV spectroscopy at λ = 290 nm, using the rule of Lambert–Beer.

¶ The solid phase syntheses of oxytocin were accomplished by Fmoc batchwise procedures using an ECOSYN P peptide synthesizer (Eppendorf-Biotronik). Carboxy activation was achieved by 2-(1*H*-benzotriazol-1-yl)-1,1,3,3-tetramethyluronium tetrafluoroborate (TBTU) and Pr$^i_2$EtN in DMF except for the Fmoc-Cys(Trt)OH residues, which were activated with diisopropylcarbodiimide and hydroxybenzotriazole (HOBt) in $CH_2Cl_2$ to prevent epimerization during the activation.[8] The Fmoc group was cleaved with 25% piperidine in DMF.

‖ The air oxidation of the synthetic oxitocin was performed in a $10^{-4}$ M solution in 0.1 M $NH_4Ac$ buffer at pH 7.5 in 2 h.

** The peptidyl resins were treated repeatedly with 1% TFA in $CH_2Cl_2$ and the solutions were filtered off after a short period of time (*ca*. 1 min) into a vessel containing 3% pyridine in $CH_2Cl_2$ to neutralize the TFA. The resulting mixture was extracted three times with $H_2O$, evaporated to remove the $CH_2Cl_2$ and Bu$^t$OH–$H_2O$ (4 : 1) was added before the product **9** was lyophilised.

†† For the cleavage and simultaneous oxidation, the peptidyl resins (**6a** and **6b**) were treated with a solution of 0.5% TFA and 10 equiv. of $I_2$ in $CH_2Cl_2$. The same procedure was then used as described in footnote ††, except that the excess of iodine was removed by an additional washing step with a 0.05 M $Na_2S_2O_3$ solution. The synthetic peptides gave the expected FAB, IS or MALDI-MS data.

## References

1 B. Riniker, A. Flörsheimer, H. Fretz, P. Sieber and B. Kamber, *Tetrahedron*, 1993, **49**, 9307.
2 Y. Han, S. L. Bontems, P. Hegyes, M. C. Munson, C. A. Minor, S. A. Kates, F. Albericio and G. Barany, *J. Org. Chem.*, 1996, **61**, 6326.
3 P. Sieber, *Tetrahedron Lett.*, 1987, **28**, 2107.
4 M. Meisenbach, G. Grübler, G. Paulus and W. Voelter, in *Peptides*, ed. H. L. S. Maia, 1994, ESCOM, 1995, p. 265.
5 H. Echner and W. Voelter, in *Peptides*, ed. C. H. Schneider and A. N. Eberle, 1992, ESCOM, 1993, p. 285.
6 C. Somlai, L.Nyereges, B. Penke, P. Hegyes and W. Voelter, *J. Prakt. Chem.*, 1994, **336**, 429.
7 H. Echner and W. Voelter, in *Peptide Chemistry*, ed. N. Yanaihara, 1992, ESCOM, 1993, p. 113.
8 T. Kaiser, G. J. Nicholson, H. J. Kohlbau and W. Voelter, *Tetrahedron Lett.*, 1996, **37**, 1187.

*Received in Cambridge, UK, 7th February 1997; Com. 7/00895C*

# Hydrothermal synthesis and structural determinations of some new polyoxofluorovanadates $[V_{14}O_{36}F_4]^{8-}$ interleaved by water molecules and organic cations $NH_3(CH_2)_nNH_3$ ($n$ = 4–6)

**Cyril Ninclaus, Didier Riou*† and Gérard Férey**

*Institut Lavoisier, UMR-CNRS C 173, Université de Versailles-St Quentin en Yvelines, 45 Avenue des Etats-Unis, 78035 Versailles Cedex, France*

**$[V_{14}O_{36}F_4]^{8-}$ polyanions are built up from two trimers of three edge-sharing $VO_5F$ octahedra, two dimers of two square pyramids related by their basal plane, two $VO_4$ tetrahedra and two $VO_4F$ trigonal bipyramids; between them are intercalated water molecules and diprotonated amines which stabilize the structures by hydrogen bonds.**

In the course of investigations on microporous materials, we first focused our attention on the hydrothermal behaviour of the quinary systems $M_2O_3$ (M = Al, Ga)–$P_2O_5$–HF–organic template–$H_2O$. This led to a new series, denoted ULM-*n*, of fluorinated alumino- and gallo-phosphates of which ULM-5[1] and ULM-16[2] are the more remarkable members. The free apertures of their 16-ring tunnels are 12.2 × 8.3 Å in ULM-5 and 10.4 × 10.4 Å in ULM-16. Recently, we proposed a mechanism for the formation of these phases[3] in which the chemical nature of the metallic element does not play a predominant role. The possibility to substitute completely aluminium or gallium by a 3d transition metal was thus explored and led to the synthesis and characterization of some microporous $Fe^{III}$ compounds with interesting magnetic properties[4–5] and vanadophosphates templated by organic cations.[6,7] We also synthesized the fresnoïte related $(NH_4)_2VO(V_{2-x}P_xO_7)$ (*x ca.* 1), which shows that $V^V$ and P atoms are statistically distributed on the same tetrahedral sites.[8] If such a substitution is possible in the ULM series containing vanadium, then the existence of vanadium oxides with microporous frameworks could become a reality. The only results reported up to now concern vanadium oxides with lamellar structures $V_2O_5$·0.5diamine,[9–11] $NMe_4V_4O_{10}$[12] and $(C_6H_{14}N_2)V_6O_{14}·H_2O$.[13]

The title compounds were synthesized hydrothermally using 1,4-diaminobutane (1,4-DAB), 1,5-diaminopentane (1,5-DAP) and 1,6-diaminohexane (1,6-DAH) as organic templates. The aqueous mixture with molar ratio 1 $V_2O_5$ : 2 HF : 0.8 diamine (1.4 in the case of 1,6-DAH) : 80 $H_2O$ was placed in a stainless-steel autoclave lined with Teflon and heated under autogenous pressure at 180 °C for 24 h. The pH of the liquid phase was constant at *ca*. 4–5 during the reaction. The solid phase was filtered off, washed with deionized water and dried in air at room temperature. The prepared products were pure with yields of around 70%. The crystals appear black but are blue after grinding. The crystal morphology of the compound prepared with 1,5-DAP is very striking. A scanning electron micrograph (Fig. 1), performed on a Hitachi S2300, shows that they grow as big hollow needles. Suitable single crystals of both phases intercalating 1,5-DAP and 1,6-DAH were isolated for structural determination‡ by X-ray diffraction. The quality of the crystals prepared with 1,4-DAB was not sufficient to perform the same study. Nevertheless, the IR spectra of the compounds (Fig. 2), recorded on a Nicolet Magna-IR 550 in the range 2000–300 $cm^{-1}$, show unambiguously that the three polyanions are similar. $\nu(V{=}O_{terminal})$ and $\nu(V{-}O_{bridging})$ are observed at 970 and 750 $cm^{-1}$ respectively, the bands observed around 1500–1600 $cm^{-1}$ are characteristic of $-NH_3^+$. Chemically, we measured for each compound (*i*) the fluorine content by potentiometric titration with a specific electrode, (*ii*) the vanadium content by redox titration using $MnO_4^-$ and $Fe^{2+}$ for $V^{4+}$ and $V^{5+}$ respectively, (*iii*) the amount of organic template and water by thermogravimetry performed on a SETARAM apparatus operating under air. These measurements give with a very good accuracy the general formula $[V^{4+}{}_2V^{5+}{}_{12}O_{36}F_4]$·4diamine·$n$$H_2O$ ($n$ = 6 for 1,4-DAB, 8 for 1,5-DAP and 4 for 1,6-DAH). In addition, some density measurements were realized on a Micromeritic multipycnometer under He flow for the two compounds whose structures have been solved by single-crystal X-ray diffraction [$D_m$ = 2.01(3) g $cm^{-3}$, $D_c$ = 2.016 for 1,5-DAP; $D_m$ = 2.01(4), $D_c$ = 1.982 for 1,6-DAH].

$V_{14}O_{36}F_4·4N_2C_6H_{18}·4H_2O$ **1** is triclinic and can be described as primitive pseudo-cubic stacking of $[V_{14}O_{36}F_4]^{8-}$ polyanions between which are intercalated the organic cations and the water molecules (Fig. 3). $V_{14}O_{36}F_4·4N_2C_5H_{16}·8H_2O$ **2** presents a similar organization but its symmetry is monoclinic and the polyanions are oriented in two different ways. Consequently, two parameters are doubled and $V$(**2**) = 4 $V$(**1**). The decrease of steric hindrance from 1,6-DAH to 1,5-DAP due to the shortening of the aliphatic chain ($C_5$ *vs*. $C_6$) is compensated by the presence of four additional water molecules in **2**.

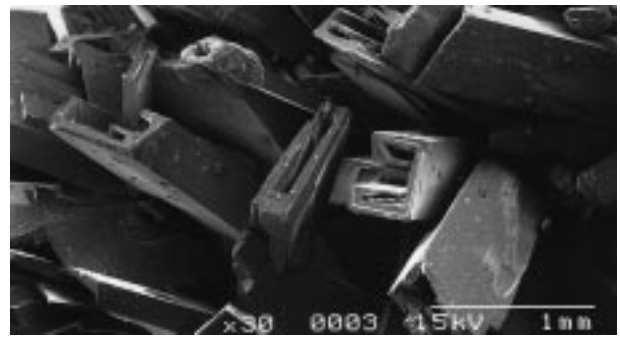



**Fig. 1** SE micrograph of $V_{14}O_{36}F_4·4N_2C_5H_{16}·8H_2O$ crystals

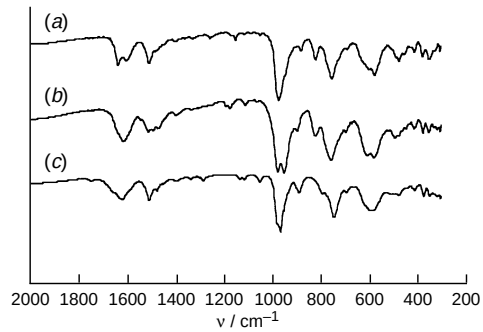



**Fig. 2** IR spectra of the polyanionic phases interleaving organic cations $NH_3(CH_2)_nNH_3$ with $n$ = 6 (*a*), 5 (*b*) and 4 (*c*)

The $[V_{14}O_{36}F_4]^{8-}$ anion contains four types of vanadium polyhedra. Two trimers of edge-sharing $VO_5F$ octahedra form the heart of the polyanion. In each trimer, the vertex shared by the three octahedra is fluorine, $F^-$ being characterized by bond valence analysis[14] and thermal parameters in agreement with the previous chemical analysis. Within each trimer, $V^{4+}$ occupies the octahedron which is not linked by edges to one of the four $V^VO_5$ square pyramids relating the two trimers. The connection exists in such a way that each square pyramid shares an edge with one octahedron of one trimer and the two other O atoms of its basal plane with two octahedra of the opposite trimer (Fig. 4). On the external side of each trimer are grafted a $V^VO_4$ tetrahedron and a $V^VO_4F$ trigonal bipyramid. Each trigonal bipyramid has three free apices, one of them is occupied by a F atom which gives rise to strong interactions with the H atoms of the amino groups. In **1** and **2**, the polyanions realize the same connectivities between the polyhedra. Nevertheless, in **1** the polyanions are built up around an inversion centre and possess $2 \times 7$ independent vanadium atoms whereas in **2**, each polyanion is built up from 14 vanadium atoms resulting from 14 independent crystallographic sites. The attribution of the $V^{4+}$ on one particular site was possible on the basis of the bond valence analysis[14] and on the detailed examination of the distribution of V–O bond lengths in the octahedra (supplementary material available from authors).

The presence of fluorine in a polyanionic phase is generally as encapsulating inside the polyanion where $F^-$ plays the role of template. Recently, we have shown in the $[V_4(HPO_4)(PO_4)_3O_6F]^{8-}$ polyanions[7] a fluorine atom linked to the vanadium atoms and divided between four $VO_5F$ octahedra building the core of the polyanion. This situation is almost comparable to the octahedral trimers described here and also encountered by Müller *et al.*[15] in $Na_6[H_6V_{12}O_{30}F_2]\cdot 22H_2O$. The originality of **1** and **2** is the presence of a third type of fluorine, located at the outer shell of the polyanion and which stabilizes the whole structure by strong hydrogen bonds.

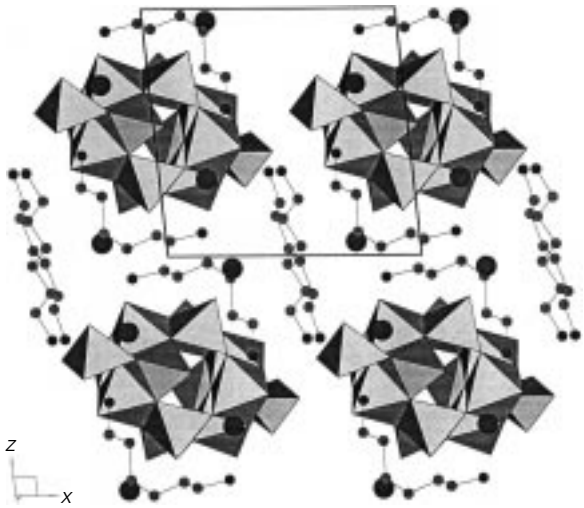



**Fig. 3** Projection along [010] of the structure of $V_{14}O_{36}F_4\cdot 4N_2C_6H_{18}\cdot 4H_2O$ with a polyhedral model for the $[V_{14}O_{36}F_4]^{8-}$ polyanions and a 'ball and stick' model for the diamines and the water molecules. Large circles refer to water and small circles to 1,6-DAH.

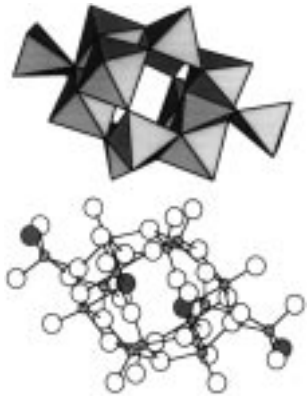


**Fig. 4** Polyhedral and 'ball and stick' representations of the $[V_{14}O_{36}F_4]^{8-}$ polyanion. Vanadium atoms are indicated by small circles, oxygen and fluorine atoms with open and large grey circles, respectively.

## Footnotes

† E-mail: riou@chimie.uvsq.fr

‡ *Crystal data*: $V_{14}O_{36}F_4\cdot 4N_2C_5H_{16}\cdot 8H_2O$: $M$ = 1296, monoclinic, space group $P2_1/n$ (no. 14); $a$ = 11.296(4), $b$ = 24.53(2), $c$ = 23.22(1) Å, $\beta$ = 99.34(7)°, $U$ = 6349(6) Å$^3$, $Z$ = 4, $D_c$ = 2.016, $D_m$ = 2.01(3) g cm$^{-3}$, $\mu$(Mo-K$\alpha$) = 20.73 cm$^{-1}$, $\lambda$ = 0.710 73 Å, graphite monochromator, crystal dimensions: 0.200 × 0.082 × 0.536 mm. The data were collected on an Enraf-Nonius CAD4 diffractometer up to $2\theta$ = 60°. A total of 19702 reflections was measured of which 6742 unique reflections ($R_{int}$ = 0.046) with $I \geqslant 2\sigma(I)$ were considered. The data were corrected for Lorentz-polarization effects, an absorption correction based on the crystal morphology did not improve the refinement. The structure was solved by direct methods analysis of SHELXS-86 (option TREF): the vanadium atoms were first located and the all remaining atoms including those of the amine skeleton were revealed from difference Fourier maps. Refinement (812 parameters) was performed by full-matrix least-squares analysis (SHELXL-93). The reliability factors converged to $R_1$ ($F_o$) = 0.052 and $wR_2$ ($F_o^2$) = 0.148. $V_{14}O_{36}F_4\cdot 4N_2C_6H_{18}\cdot 4H_2O$: $M$ = 1910, triclinic, space group $P\bar{1}$ (no. 2); $a$ = 11.746(1), $b$ = 11.960(2), $c$ = 12.717(1) Å, $\alpha$ = 115.547(7), $\beta$ = 93.261(6), $\gamma$ = 94.055(9)°, $U$ = 1600.2(3) Å$^3$, $Z$ = 1, $D_c$ = 1.982, $D_m$ = 2.01(4) g cm$^{-3}$, $\mu$(Mo-K$\alpha$) = 21.70 cm$^{-1}$, $\lambda$ = 0.710 73 Å, graphite monochromator, crystal dimensions: 0.057 × 0.179 × 0.270 mm. The data were collected on a Siemens AED2 four-circle diffractometer up to $2\theta$ = 60°. A total of 9316 reflections was measured of which 5707 with $I \geqslant 2\sigma(I)$ were considered. The data were corrected for Lorentz-polarization and absorption effects. The structure was solved by direct methods analysis of SHELXS-86 (option TREF): the vanadium atoms were first located then all the remaining atoms were deduced from difference Fourier maps. Refinement (400 variables) as above. Two carbon atoms whose thermal motion was rather high, were split over two crystallographic sites. The reliability factors converged to $R_1$ ($F_o$) = 0.046 and $wR_2$ ($F_o^2$) = 0.126. Atomic coordinates, bond lengths and angles, and thermal parameters have been deposited at the Cambridge Crystallographic Data Centre (CCDC). See Information for Authors, Issue No. 1. Any request to the CCDC for this material should quote the full literature citation and the reference number 182/388.

## References

1 Th. Loiseau, D. Riou, F. Taulelle and G. Férey, *Zeolites and Related Microporous Materials: State of the Art 1994, Stud. Surf. Sci. Catal.*, 1994, **84**, 395.
2 Th. Loiseau and G. Férey, *J. Mater. Chem.*, 1996, **6**, 1073.
3 G. Férey, *J. Fluorine Chem.*, 1995, **72**, 187.
4 M. Cavellec, C. Ninclaus, D. Riou, J. M. Grenèche and G. Férey, *Zeolites*, 1996, **17**, 250.
5 M. Cavellec, J. M. Grenèche, D. Riou and G. Férey, *Microporous Mater.*, 1997, **8**, 3.
6 D. Riou and G. Férey, *J. Solid State Chem.*, 1994, **111**, 422.
7 D. Riou, F. Taulelle and G. Férey, *Inorg. Chem.*, 1996, **35**, 6392.
8 C. Ninclaus, R. Retoux, D. Riou and G. Férey, *J. Solid State Chem.*, 1996, **112**, 139.
9 D. Riou and G. Férey, *J. Solid State Chem.*, 1995, **120**, 137.
10 D. Riou and G. Férey, *Inorg. Chem.*, 1995, **34**, 6520.
11 Y. Zhang, R. C. Haushalter and A. Clearfield, *Inorg. Chem.*, 1996, **35**, 4950.
12 P. Y. Zavalij, M. S. Whittingham, E. A. Boylan, V. K. Pecharsky and R. A. Jacobson, *Z. Kristallogr.*, 1996, **211**, 464.
13 L. F. Nazar, B. E. Koene and J. F. Britten, *Chem. Mater.*, 1996, **8**, 327.
14 N. E. Brese and M. O'Keeffe, *Acta Crystallogr., Sect. B*, 1991, **29**, 269.
15 A. Müller, R. Rohlfing, A. L. Barra and D. Gatteschi, *Adv. Mater.*, 1993, **5**, 915.

*Received, in Basel, Switzerland, 20th November 1996; Com. 6/07863J*

# Solubility control by UV irradiation of a copolymer having both photobase generating groups and photoacid generating groups

**Kanji Suyama*[a]† and Masahiro Tsunooka[b]‡**

[a] *Nissha Printing Co. Ltd., 3 Mibu-Hanai-Cho, Nakagyo, Kyoto 604, Japan*
[b] *Department of Applied Chemistry, College of Engineering, Osaka Prefecture University, 1-1 Gakuen-cho, Sakai, Osaka 593, Japan*

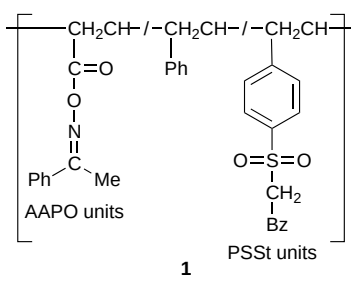
**An insoluble–soluble–insoluble contrast curve is obtained for a polymer film having both photobase and photoacid generating groups when it is developed using a polar solvent; the base groups are introduced before the acid groups.**

The solubility change of polymeric material upon irradiation is a key factor in their application to photoresists because photopatterning utilizes the solubility differences between irradiated and non-irradiated polymers. Many methods have been tried to improve the solubility change upon irradiation to obtain higher sensitivity and resolution. Photoacid generators have attracted increasing attention as a catalyst for high-sensitivity photoresist systems, the 'chemically amplification' type, where generated acids catalyse the thermolyses of carbonate groups into hydroxy groups.[1] Photobase generators have also been studied, including Co-amine salt,[2] polymers bearing *o*-acyloxyimino (AOI) groups,[3] *o*-nitrobenzyloxycarbonyl derivatives,[4,5] benzoyloxycarbonyl derivatives[6,7] and formamides.[8]

We have studied the photochemical behaviour of copolymers of acryloyl acetophenone oxime (AAPO), and found that AOI groups in AAPO units transformed into pendant amino groups upon irradiation, followed by hydrolysis.[3,9,10] On the other hand, we have also found that β-keto sulfone (β-KS) groups in phenacylsulfonyl styrene (PSSt) copolymers were transformed into pendant sulfinic or sulfonic acid groups upon irradiation.[11,12] From these results we expected that polymers bearing both acid and base units in the same polymer-chain would be obtained when a copolymer of AAPO and PSSt is irradiated.

On investigation of the photochemical behaviour of a polymer bearing both units, p(AAPO-St-PSSt) **1**, we found that **1** became soluble upon irradiation and then became insoluble on further irradiation when developed with a polar solvent. When developed with a non-polar solvent, **1** became insoluble. Here we report the dual-photoresist behaviour of **1**, Fig. 1.

Monomers were prepared as described in a previous paper,[9] and polymerized in degassed benzene at 60 °C using 0.2 mass% of AIBN as an initiator. The resulting polymeric material was reprecipitated three times from THF–MeOH to give **1** in 39.9% yield with *M*n = 75 000 (*M*w/*M*n = 1.66) determined by GPC analysis using THF as eluent and polystyrene as standard. The molar ratios of the monomers in **1** were AAPO : PSSt : St = 32.5 : 4.2 : 63.3, obtained from the $^1$H NMR integrated area ratio. The films were prepared by spin-coating a 7.5 mass% diglyme solution on a quartz or borosilicate glass plate, followed by drying in an oven at 85 °C for 20 min. The absorbance at 254 nm was *ca.* 1.5, and the film thickness was 0.35–0.5μm, measured by a Kosaka surface roughness meter ET-10. All irradiations were performed in air at room temperature using a Ushio UV-102 mercury lamp (100 W) without wavelength selection. The intensity of light was 3.01 mW cm$^{-2}$ at 254 nm and 4.62 mW cm$^{-2}$ at 366 nm, measured by an Orcs' UV-Light measure model UV-M02. After irradiation, the films were immersed into a 0.12 M HCl solution for 3 min and then in MeOH or THF for 10 min. All solutions were kept at 23 °C. UV spectra were measured by a Shimadzu UV-3100. The samples for IR spectral measurement were scratched away from the plate and measured on a Perkin-Elmer 1620.




**1**

(AAPO : St : PSSt = 33 : 63 : 4)

**Fig. 1**

Fig. 2 shows the relationship between the irradiation time and the normalized film thickness of **1** developed with MeOH. The dotted line shows the change of normalized film thickness, which were irradiated for a given time, HCl treated and developed with MeOH. As the irradiation time increased, the developed films became thin and dissolved completely after 2–4 min irradiation time. However, gelatinous material was obtained on the glass plate for longer irradiation times such as 10, 15 or 20 min, and it was impossible to measure the film thickness. When the films were cured at 100 °C before MeOH development, the films became hard enough to measure the thickness. In this case, the films dissolved only after 2–4 min irradiation time and became insoluble after further irradiation as indicated by the solid line in Fig. 2.

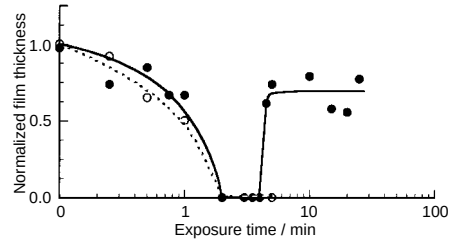



**Fig. 2** Contrast curves of films of **1** developed with MeOH after HCl treatment (- - ○ - -) and MeOH after HCl treatment and curing at 100 °C (—●—)

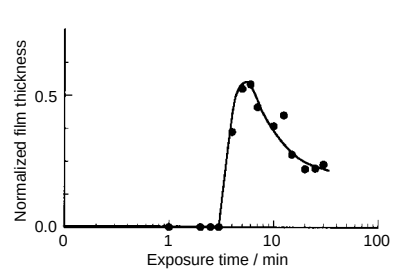
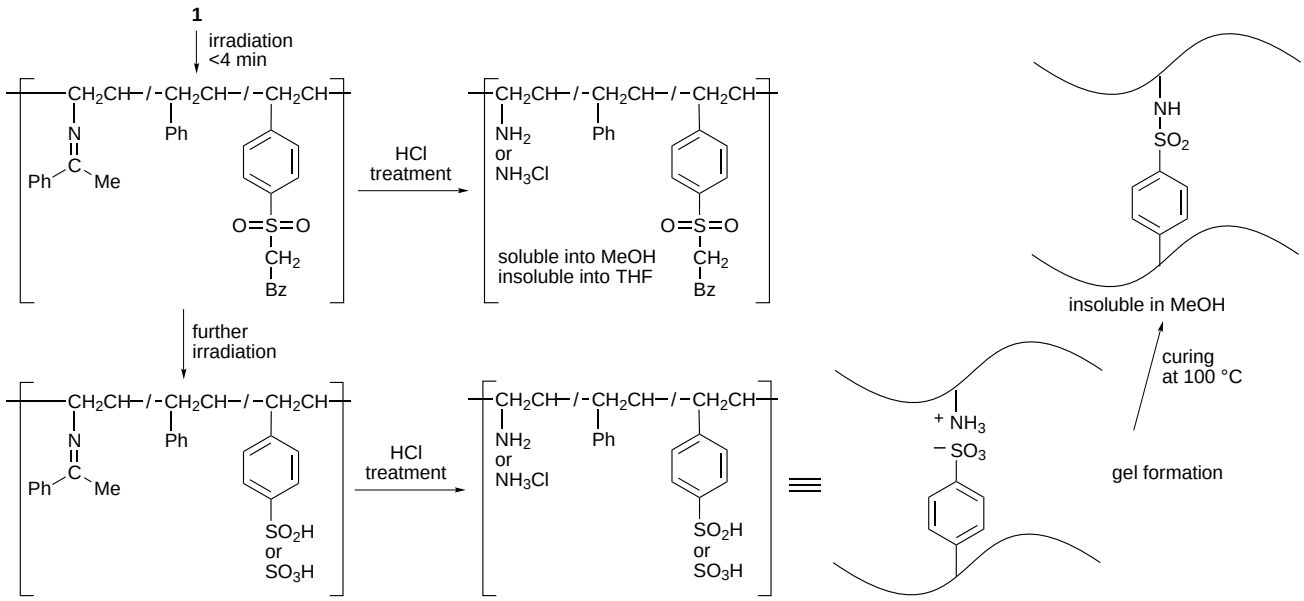



**Fig. 3** Contrast curve of films of **1** developed with THF




**Scheme 1** Photoreaction of **1**

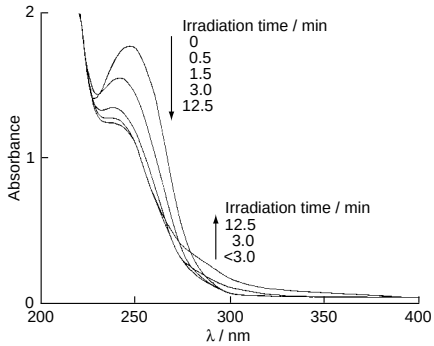



**Fig. 4** UV spectral changes of film of **1** upon irradiation

This film showed a different solubility behaviour when developed with THF. As shown in Fig. 3, the film irradiated for 4 min became insoluble in THF. With longer irradiation time, the thickness of the resulting films gradually decreased. This tendency in the later stage was similar to the phenomenon found in copolymers of PSSt and styrene or MMA.[12]

Fig. 4 shows the changes of the UV absorption spectra of the irradiated films. The peak at *ca.* 250 nm decreased after less than 3 min of irradiation. Upon further irradiation, however, the decrease almost stopped, and a new band appeared in the 260–380 nm region. The latter seems to relate to the β-KS groups because this band appeared in the PSSt and styrene or MMA copolymers upon irradiation[13] and not in those having AAPO units. The changes in the β-KS groups are thus deduced to occur after 3 min irradiation.

The structural change of this copolymer might be explained as shown in Scheme 1. Upon irradiation for less than 3 min, the AOI groups in the AAPO units decompose. The recombination of iminyl radicals and radicals on the main chain results in imino groups which are converted to amino groups by HCl treatment. At this stage the conversion of the β-KS groups appears to be very low. Upon further irradiation most of the AAPO units give imino (or amino) groups, and also β-KS groups are photo-transformed into sulfinic or sulfonic acid groups. The resulting acid groups form interaction points with amino groups, which afford intra- and inter-molecular cross-links. At this stage the film swelled in the developer. It is thus deduced that when cured at 100 °C the cross-links are transformed into sulfonamides.

The photo-decomposition of AOI groups can be explained by an effective energy transfer from β-KS groups to AOI groups, which restricts the photochemical change of β-KS groups until the AOI groups have decomposed almost completely. In fact, the sensitization of the decomposition of the AOI groups by β-KS groups was confirmed by photolysis at 366 nm. Although we used a mercury lamp without a wavelength selector as the light source for our experiments, we assumed that the energy transfer from the β-KS groups to the AOI groups is still important because the direct photolysis of AOI groups is slow compared to **1**.

We thank Mr T. Takemoto, Department of Applied Chemistry, Osaka Prefecture University, for measuring the NMR spectra.

## Footnotes

† E-mail: BXE05610@niftyserve.or.jp.
‡ E-mail: tsunooka@chem.osakafu-u.ac.jp

## References

1 *Microelectronics Technology, ACS Symposium Series 614*, ed. E. Reichmanis, C. K. Ober, S. A. MacDonald, T. Iwayanagi and T. Nishikubo, ACS, Washington, DC, 1995.
2 C. Kutal and C. G. Willson, *J. Electrochem. Soc.*, 1987, **134**, 2280.
3 K.-H. Song, A. Urano, M. Tsunooka and M. Tanaka, *J. Polym. Sci., Part C, Polym. Lett.*, 1987, **25**, 417.
4 J. F. Cameron and J. M. J. Fréchet, *J. Am. Chem. Soc.*,1991, **113**, 4303.
5 J. M. J. Fréchet, *Pure Appl. Chem.*, 1992, **64**, 1239.
6 J. F. Cameron and J. M. J. Fréchet, *J. Org. Chem.*, 1990, **55**, 5919.
7 J. M. J. Fréchet and J. F. Cameron, *Polym. Mater. Sci. Eng.*, 1991, **64**, 55.
8 T. Nishikubo, E. Takehara and A. Kameyama, *Polym. J.*, 1993, **25**, 421.
9 K.-H. Song, M. Tsunooka and M. Tanaka, *J. Photochem. Photobiol. A: Chem.*, 1988, **44**, 197.
10 K. Suyama and M. Tsunooka, *J. Polym. Sci., Polym. Chem. Ed.*, 1996, **34**, 2181.
11 M. Tsunooka, H. Yanagi, M. Kitayama and M. Shirai, *J. Photopolym. Sci. Technol*., 1991, **4**, 239.
12 M. Tsunooka, T. Ikehara, T. Takemoto and M. Shirai, *J. Photopolym. Sci. Technol.*, 1996, **9**, 17.
13 T. Takemoto and M. Tsunooka, unpublished results.

*Received, 1st November 1996; Com. 6/07434K*

# Novel 1,2-thiaphosphetanes from diferrocenyldithiadiphosphetane disulfide

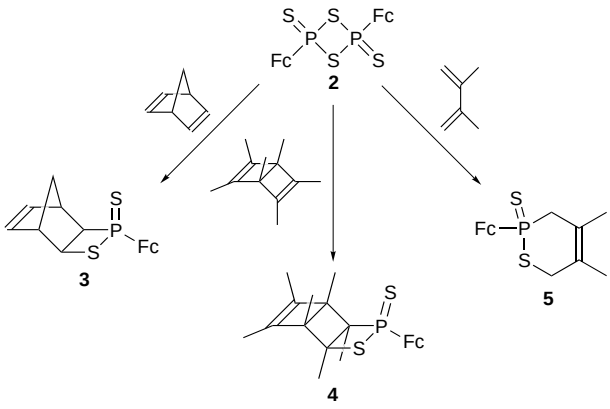
**Mark R. StJ. Foreman, Alexandra M. Z. Slawin and J. Derek Woollins*†**

*Department of Chemistry, Loughborough University, Loughborough, UK LE11 3TU*

**Diferrocenyldithiadiphosphetane disulfide reacts with bicyclic dienes to form four- and six-membered PS containing rings which are crystallographically characterised.**

We have recently reported on the synthesis[1] of a ferrocene analogue of Lawesson's reagent [*p*-(MeO)$C_6H_4P(S)S_2P(S)$-$C_6H_4$(OMe)] **1**. These types of system are used as reagents in thionation reactions but their potential in the formation of new heterocycles is less well developed although some reactions of **1** with 1,3-dienes to give Diels–Alder adducts at moderate temperatures have been described.[2] Lawesson's reagent has been reported to react with alkenes at high temperature to give anti-sludge additives for engine oils[3] and ferrocene derivatives have been studied as additives for fuels.[4] There have only been a few reports on the isolation of $RPS_2$ systems (R = 'supermesityl')[5] but from NMR studies[1] we have speculated on the transitory existence of $RPS_2$ in **1** and **2**. This observation has led us to investigate the cycloaddition chemistry of **2** and here we describe preliminary investigations into the low temperature reactions of alkenes with **2** together with the X-ray crystal structures of three new organophosphorus–sulfur heterocycles, which are the first examples of these ring types to be characterised crystallographically.[6]

The reactions are shown in Scheme 1. Treatment of **2** with norbornadiene at 80 °C leads to 4-ferrocenyl-3-thia-4λ$^5$-phosphatricyclo[4.2.1.0$^{2,5}$]non-7-ene 4-sulfide **3** in high yield (69%).‡ The X-ray structure§ of **3** reveals (Fig. 1) it to be the *exo*-isomer. The $C_2PS$ (thiaphosphorane) ring is close to planar [max. deviation from the $PSC_2$ mean plane 0.043(6) and −0.050(6) Å for C(16) and C(11) respectively]. The P=S and P–S bond lengths are similar to those in **2** whilst P(1)–C(16)




**Scheme 1**

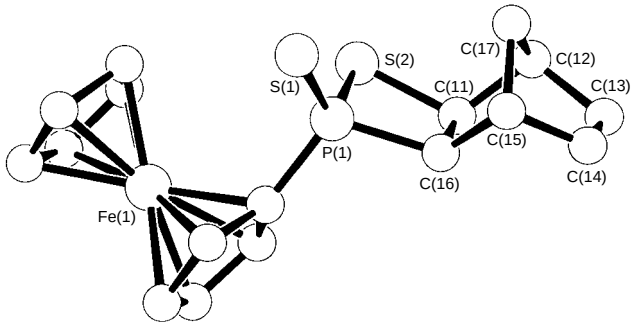



**Fig. 1** The X-ray structure of **3**. Selected bond lengths (Å) and angles (°): P(1)–S(1) 1.940(2), P(1)–S(2) 2.102(2), P(1)–C(16) 1.847(6), P(1)–C(1) 1.800(6), S(2)–C(11) 1.850(6), C(11)–C(16) 1.585(7), C(11)–C(12) 1.535(8), C(12)–C(13) 1.520(8), C(13)–C(14) 1.321(8), C(14)–C(15) 1.487(9), C(15)–C(16) 1.523(8), C(12)–C(17) 1.564(9), C(15)–C(17) 1.548(8), S(1)–P(1)–S(2) 122.0(1), S(1)–P(1)–C(1) 114.1(2), S(1)–P(1)–C(16) 118.9(2), S(2)–P(1)–C(1) 104.9(2), S(2)–P(1)–C(16) 83.8(2), C(1)–P(1)–C(16) 109.0(3), P(1)–S(2)–C(11) 80.1(2), S(2)–C(11)–C(16) 100.3(4), P(1)–C(16)–C(11) 95.7(4).

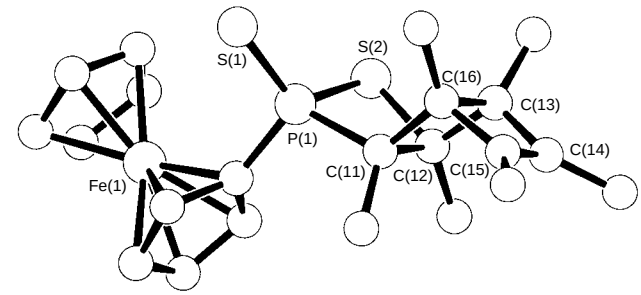



**Fig. 2** The X-ray structure of **4**. Selected bond lengths (Å) and angles (°): P(1)–S(1) 1.931(1), P(1)–S(2) 2.095(1), S(2)–C(12) 1.880(5), C(11)–C(12) 1.588(4), P(1)–C(11) 1.844(4), C(12)–C(13) 1.538(5), C(13)–C(14) 1.520(5), C(14)–C(15) 1.322(5), C(15)–C(16) 1.520(5), C(16)–C(11) 1.578(5), C(13)–C(16) 1.584(5), S(1)–P(1)–S(2) 122.9(1), S(1)–P(1)–C(1) 112.3(1), S(1)–P(1)–C(11) 122.4(1), S(2)–P(1)–C(1) 104.7(1), S(2)–P(1)–C(11) 83.7(1) C(1)–P(1)–C(11) 106.6(2), P(1)–S(2)–C(12) 79.9(1), S(2)–C(12)–C(11) 98.5(2).

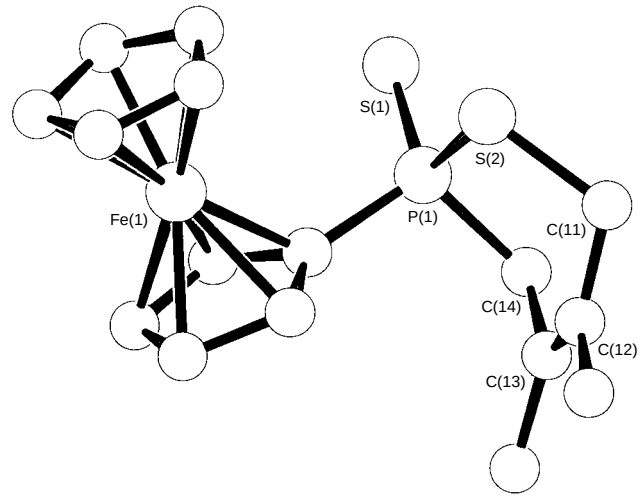



**Fig. 3** The X-ray structure of **5**. Selected bond lengths (Å) and angles (°): P(1)–S(1) 1.944(3), P(1)–S(2) 2.086(4), S(2)–C(11) 1.840(9), C(11)–C(12) 1.50(1), C(12)–C(13) 1.31(1), C(13)–C(14) 1.52(1), P(1)–C(14) 1.816(8), S(1)–P(1)–S(2) 1147.7(2), S(1)–P(1)–C(1) 112.5(3), S(1)–P(1)–C(14) 114.5(3), S(2)–P(1)–C(14) 101.6(3), S(2)–P(1)–C(1) 106.5(3), C(1)–P(1)–C(14) 106.0(4), P(1)–S(2)–C(11) 100.4(4), S(2)–C(11)–C(12) 112.4(6), C(11)–C(12)–C(14) 120.6(8), P(1)–C(14)–C(13) 111.4(6), C(12)–C(13)–C(14) 118.1(8).

[1.847(6) Å] and S(2)–C(11) [1.850(6) Å] are relatively long single bonds. The phosphorus centre is somewhat distorted from tetrahedral, in part because of the reduced angles within the $PSC_2$ ring. The exocyclic sulfur is pointing up (in the same direction as the $CH_2$ of the tricyclic system). No trace could be found of any homo-Diels–Alder adduct in the reaction products.

Reaction of **2** and hexamethyl Dewar benzene in toluene at 80 °C gives 4-ferrocenyl-1,2,5,6,7,8-hexamethyl-3-thia-4λ$^5$-phosphatricyclo[4.2.0.0$^{2,5}$]oct-7-ene 4-sulfide **4** after chromatography and recrystallisation.‡ The X-ray structure§ of **4** reveals (Fig. 2) it to be the *exo*-isomer. The bond lengths and angles in **4** display similar trends to those in **3** although the $PSC_2$ ring is less planar than that in **3** [maximum deviation from the $PSC_2$ mean plane 0.14(1) and −0.14(1) Å for C(12) and C(11) respectively]. The difference may be a consequence of the steric repulsion between the exocyclic methyl groups and the P=S in **4**. Like **3** the phosphorus centre is distorted with reduced angles within the $PSC_2$ ring.

Treatment of **2** with 2,3-dimethylbutadiene at *ca*. 80 °C gave 2-ferrocenyl-4,5-dimethyl-1-thia-2λ$^5$-phosphacyclohex-4-ene 2-sulfide **5** in high yield (86%). The thiaphosphorinine ring in **5** has a pseudo boat conformation (Fig. 3) with the P(1)–S(2)–C(11)–C(14) and C(11)–C(12)–C(13)–C(14) mean planes are inclined by 123° to each other. The bond lengths at phosphorus and sulfur are similar to those in **3** and **4** with, as expected, significantly less angular deviations about the phosphorus centres.

The new compounds described here illustrate the ability of **1** to behave as a source of $PS_2$ in ring forming reactions as well as providing the first structure determinations on two heterocyclic systems. Reactions with other multiple bonds are in progress.

## Footnotes

† E-mail: J.D.Woollins@lboro.ac.uk

‡ Satisfactory C, H microanalyses/accurate mass spectral data were obtained for all new compounds. *Selected spectroscopic data* for **3**: mp 120–121.5 °C; $\delta_P$ 64.0; $\delta_C$ 136.5 (d, $J$[$^{31}$P–$^{13}$C] 15 Hz), 135.9, 73.5 (d, $J$[$^{31}$P–$^{13}$C] 16 Hz), 72.4 (m), 70.0, 57.3 (d, $J$[$^{31}$P–$^{13}$C] 53 Hz), 47.2, 43.3, 42.7, 36.4 (d, $J$[$^{31}$P–$^{13}$C] 7 Hz). $\delta_H$ 6.3 (m, 2 H), 4.7 (d, $J$ 9.5 Hz, 2 H), 4.6 (m, 2 H), 4.2 (s, 4 H), 3.0 (m, 5 H), 1.6 (d, $J$ 9.8 Hz); MS(EI$^+$) *m/z* 372 (M$^+$), 280 ($FcPS_2$), 248, 217, 184, 155, 121.

For **4**: $\delta_P$ 68.4; $\delta_C$ 146.4, 140.1, 81 (d, $^1J$[$^{31}$P–$^{13}$C] 75 Hz), 76.0 (d, $^2J$[$^{31}$P–$^{13}$C] 15 Hz), 72.4 (d, $^3J$[$^{31}$P–$^{13}$C] 11 Hz), 72 (m), 70.2, 65 (d, $^1J$[$^{31}$P–$^{13}$C] 50 Hz), 57.2, 56.4, 55.0, 20.8, 16.3, 12.3 (d, $^3J$[$^{31}$P–$^{13}$C] 7 Hz), 11.7, 11.2 and 10.7; $\delta_H$ poorly resolved multiplets at 4.74, 4.64, 4.54 and 4.49 (1 H in each case), 4.33 (s, 5 H), 1.73 (s, 3 H), 1.58 (s, 3 H), 1.44 (s, 3 H), 1.35 (s, 3 H), 1.16 (s, 3 H), 0.97 (d, $^2J$[$^1$H–$^{31}$P] 24 Hz, 3 H); MS(EI$^+$) *m/z* 442 (M$^+$), 280 ($FcPS_2$), 248 (FcPS), 217 (FcS), 162, 147. Found 442.0641, calc. 442.0641. For **5**: $\delta_P$ 69.2; $\delta_C$ 130.6, 127.4, 73.6, 72.5, 72.2, 71.7, 70.0, 46.7 (d, $^2J$[$^{31}$P–$^{13}$C] 46 Hz, $CH_2$), 34.9 ($CH_2$), 21.0, 19.2; $\delta_H$ 4.63 (1 H), 4.37 (poorly resolved multiplet, 2 H), 4.28 (5 H) 4.17 (1 H), 3.57 (poorly resolved triplet, 1 H), 3.12 (dd, $^2J$[$^1$H–$^{31}$P] 21.5, $^2J$[$^1$H–$^1$H] 14.1 Hz, 1 H), 2.82 (complex multiplet, 2 H), 1.82 (d, $^4J$[$^{31}$P–$^1$H] 5.4 Hz, 4 H) and 1.56 (5 H). MS(EI$^+$) *m/z* 362(M$^+$), 280($FcPS_2$), 248(FcPS), 217(FcS), 184, 155, 121.

§ *Crystal data*. All measurements were performed at room temperature using a Rigaku AFC7S diffractometer, Cu-Kα radiation, λ = 1.54178 Å, ω-scans (2θ max = 120°). For **3**: $C_{17}H_{17}FePS_2$, $M$ = 372.3 monoclinic, space group $P2_1/c$, $a$ = 11.688(2), $b$ = 9.508(2), $c$ = 14.706(2) Å, β = 104.11(1)°. $U$ = 1585 Å$^3$, $Z$ = 4, $D_c$ = 1.56 g cm$^{-3}$, $F$(000) = 768, μ(Cu-Kα) = 11.0 mm$^{-1}$. Crystal dimensions 0.10 × 0.21 × 0.30 mm. Of 2670 measured data 2559 were unique and 1996 were observed [$I > 3.0\sigma(I)$]. The structure was solved by the heavy atom method and refined using absorption corrected data (Difabs) with the H-atoms in idealised positions to give $R$ = 0.049 and $R_w$ = 0.046. For **4**: $C_{22}H_{27}FePS_2$, $M$ = 442.4, monoclinic, space group $P2_1/n$, $a$ = 10.616(2), $b$ = 9.604(1), $c$ = 21.033(2) Å, β = 101.26(1)°. $U$ = 2103 Å$^3$, $Z$ = 4, $D_c$ = 1.40 g cm$^{-3}$, $F$(000) = 928, μ(Cu-Kα) = 8.33 mm$^{-1}$. Crystal dimensions 0.08 × 0.12 × 0.21 mm. Of 3540 measured data 3339 were unique and 2473 were observed [$I > 2.0\sigma(I)$]. The structure was solved by direct methods and refined using absorption corrected data (Difabs) with the H-atoms in idealised positions to give $R$ = 0.038 and $R_w$ = 0.031. For **5**: $C_{16}H_{19}FePS_2$, $M$ = 362.3 monoclinic, space group $P2_1/n$, $a$ = 6.875(3), $b$ = 12.459(4), $c$ = 19.496(6) Å, β = 96.91(3)°. $U$ = 1658 Å$^3$, $Z$ = 4, $D_c$ = 1.45 g cm$^{-3}$, $F$(000) = 752, μ(Cu-Kα) = 10.5 mm$^{-1}$. Crystal dimensions 0.10 × 0.10 × 0.18 mm. Of 2833 measured data 2708 were unique and 1665 were observed [$I > 3.0\sigma(I)$]. The structure was solved by the heavy atom method and refined to give $R$ = 0.070 and $R_w$ = 0.071. Atomic coordinates, bond lengths and angles, and thermal parameters have been deposited at the Cambridge Crystallographic Data Centre (CCDC). See Information to authors, Issue No. 1. Any request to the CCDC for this material should quote the full literature citation and the reference number 182/410.

## References

1 M. R. StJ. Foreman, A. M. Z. Slawin and J. D. Woollins, *J. Chem. Soc., Dalton Trans.*, 1996, 3653.
2 A. Ecker, I. Boie and U. Schmidt, *Monatsch. Chem.*, 1973, **104**, 503.
3 S. J. Brois, *US Pat.*, 1977, 4 042 523 (*Chem. Abstr.*, 1977, **87**, 204150e).
4 D. H. Farrar, *US Pat.*, 1990, 4 908 045 (*Chem. Abstr.*, 1990, **112**, 201939t).
5 M. Yoshifugi, A. Otoguro and K. Toyota, *Bull. Chem. Soc. Jpn.*, 1994, **67**, 1503.
6 For a review of four-membered organo P–E containing rings (E = O, S, NR, P) see: K. Afarinkia, *Heterocycles*, 1992, **34**, 369.

*Received, 21st November 1996; Com. 6/07889C*

# Photoresponsive dendrimers

**Denise M. Junge and Dominic V. McGrath*†**

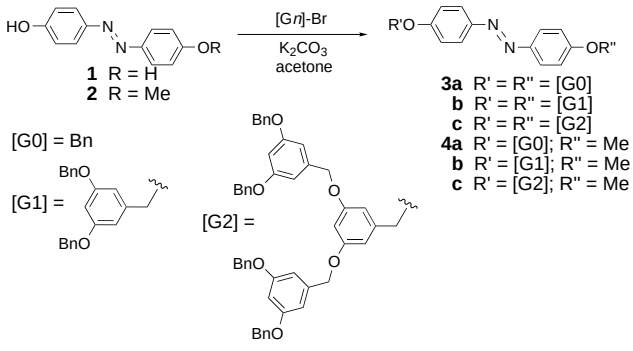
*Department of Chemistry, University of Connecticut, 215 Glenbrook Rd., Storrs, CT 06269-4060, USA*

**Benzyl aryl ether dendrimers with azobenzene central linkers undergo reversible *cis*/*trans* isomerization of the azobenzene moiety upon exposure to ultraviolet light.**

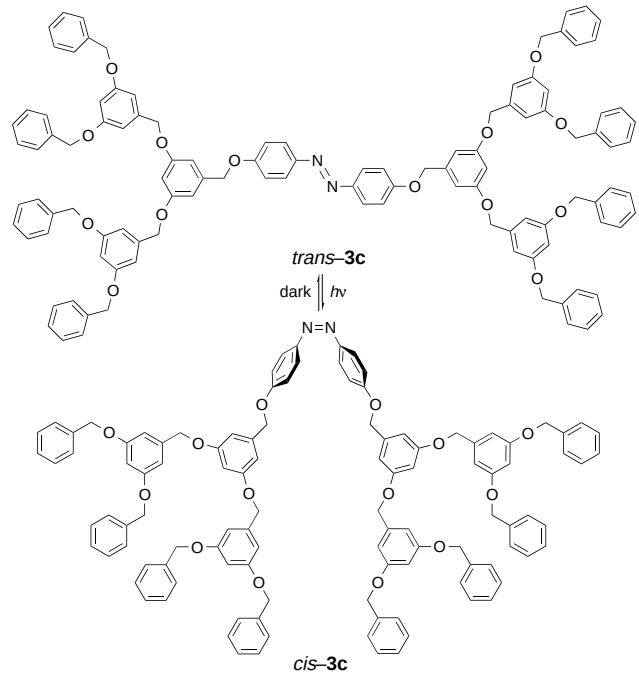
The elegance with which nature uses light energy to alter function in photoresponsive systems has led chemists to engage in much mimicry.[1] Progress has been made in designing systems containing photoresponsive moieties in small molecules,[2–4] polymers[5–8] and peptides[9–11] for the photocontrol of ion recognition and transport,[12] membrane permeability[13] and structure,[14] enzyme activity[2] and materials properties.[5,8,15] Typically, small molecule systems are well-understood. Their responsiveness is predictable and easily controlled. Macromolecular systems, however, while abundant and widely studied, are typically ill-defined and the photoresponsive effect is difficult to predict *a priori* or to control in a precise manner. Dendrimers, a new class of macromolecule in which the structure of the material is well-defined, are prepared in a way which would allow precise placement of a photoactive moiety within the dendrimer interior. More predictable control of photoinduced configurational changes should be possible, allowing potential reversible alteration of function. By placing a single photoactive moiety in the centre, rather than on the exterior,[16] of a dendrimer a small configurational change will effect a large conformational change throughout the dendrimer structure. Here we report the synthesis of dendrimers with azobenzene central linkers which undergo reversible configurational changes in response to light energy. This represents the first reversible topological change induced in a dendrimer through configurational change of the central linker.

Photoresponsive dendrimers of the zeroth, first and second generations were prepared by reaction of azobenzene-derivative central linkers **1**[17] and **2**‡ with the appropriate dendritic bromides[18] in the presence of $K_2CO_3$ in acetone (Scheme 1).§ Zeroth and first generation materials **3a** and **b** and **4a** and **b** are pale orange crystalline solids, while second generation materials **3c** and **4c** are orange glasses.¶

Dendrimers **3a–c** and **4a–c** all exhibited the expected photoresponsive behaviour. For example, dark incubation of a dichloromethane solution (40 μM) of second generation dendrimer **3c** served to maximize the absorbtion at 360 nm ($\varepsilon_{max}$ = 32 500) corresponding to the *trans*-azobenzene chromophore. Irradiation of this solution with 350 nm light resulted in clean photoisomerization to *cis*-**3c** (Scheme 2), as evidenced by a decrease in the absorbance at 360 nm and an increase in absorbances 314 and 450 nm (Fig. 1). A photostationary state was reached within approximately 60 s. Thermal reversion to the original dark-incubated spectrum was observed over the




**Scheme 1**




**Scheme 2**

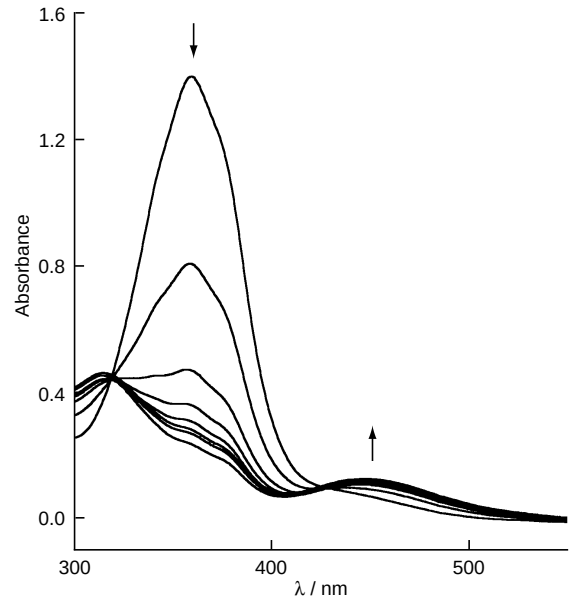



**Fig. 1** UV Absorption spectra of second generation photoresponsive dendrimer **4c** (40 μM in $CH_2Cl_2$) under irradiation conditions (350 nm; 0, 5, 10, 15, 20, 25, 30 and 60 s)

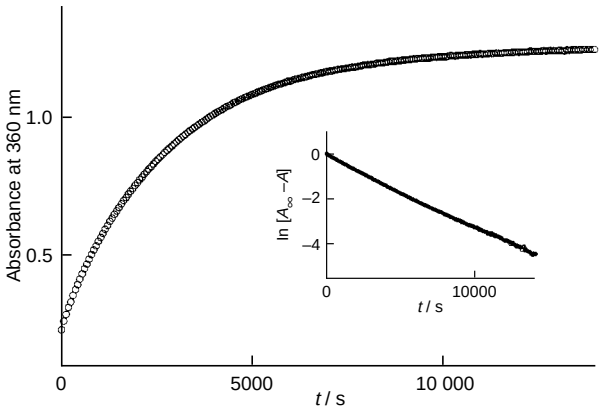



**Fig. 2** Plot of absorbance at 360 nm of a sample of **4c** kept in the dark at 293 K after irradiation (10 min at 350 nm). Inset: first order rate constant plot of $\ln[A_\infty - A]$ *vs.* time.

course of approximately 3 h at 293 K in the dark (Fig. 2). The first-order rate constant for this process ($k = 3 \times 10^{-4}$ s$^{-1}$; $t_{1/2} = 40$ min) is similar in magnitude to that of other azobenzenes.[19] Exposure to bright sunlight for a period of only several seconds also effected almost complete reversion to the *trans* isomer. Second generation compound **4c** serves as a steric control for **3c**. After isomerization to *cis*-**4c** (350 nm, 10 min), thermal isomerization to *trans*-**4c** occurs with an identical first-order rate constant ($k = 3 \times 10^{-4}$ s$^{-1}$; $t_{1/2} = 40$ min). This indicates that there is no strong steric influence on the thermal isomerization of *cis*- to *trans*-**3c**.

The photoinduced conversion of *trans*- to *cis*-dendrimer was also observed by $^1$H NMR spectroscopy. For example, the methoxy groups in *trans*- and *cis*-**4c** appear as singlets at δ 3.87 and 3.74, respectively, in $CDCl_3$. Irradiation of an NMR sample ($CDCl_3$) of **4c** resulted in a dramatic change in the ratio of these peaks, from 87 : 13 to 8 : 92. Similar changes were observed in the aromatic and benzylic regions of the spectrum.‖

We have demonstrated the photoresponsive properties of a series of simple dendrimers with azobenzene central linkers. We anticipate that switchable dendrimers of this type will have applications in transport systems based on the reversible perturbation of their ability to encapsulate small molecules. We hope to demonstrate these applications in our future studies.

The present work was supported by the donors of The Petroleum Research Fund, administered by the American Chemical Society, and the University of Connecticut Research Foundation. We thank B. Smith, J. Bocarsly, C. Kumar and G. Epling for suggestions and assistance.

## Footnotes

† E-mail: dmcgrath@nucleus.chem.uconn.edu

‡ Preparation of **2**: a solution of $NaNO_2$ (0.52 g, 7.5 mmol) in $H_2O$ (minimum to dissolve) was added dropwise to a cold (5 °C) solution of 4-methoxyaniline (0.89 g, 7.2 mmol) and 9 M $H_2SO_4$ (4 ml). The resulting solution was added dropwise to a cold (5 °C) solution of phenol (0.70 g, 7.4 mmol) and 2 M NaOH (10 ml). After stirring for an additional 1.5 h, the solution was neutralized (2 M NaOH), extracted with $CH_2Cl_2$ (3 × 50 ml) and the combined organic extracts were dried ($Na_2SO_4$) and concentrated. Chromatography ($SiO_2$, 1 : 3 ethyl acetate–light petroleum) gave **2** (1.06 g, 65%) as a yellow crystalline solid, mp 141.5–142.5 °C (lit.,[20] 142 °C); $^1$H NMR [400 MHz, $(CD_3)_2CO$]: δ 8.98 (s, 1 H), 7.85 (d, *J* 9.0 Hz, 2 H), 7.80 (d, *J* 8.9 Hz, 2 H), 7.07 (d, *J* 9.0 Hz, 2 H), 6.99 (d, *J* 8.9 Hz, 2 H), 3.88 (s, 3 H).

§ Representative dendrimer preparation (**3c**): a solution of **1** (54 mg, 0.25 mmol), [G2]-Br (ref. 18) (0.45 g, 0.55 mmol), $K_2CO_3$ (89 mg, 0.65 mmol) and dry acetone (10 ml) was kept at reflux for 24 h. After removal of the solvent by rotary evaporation, the resulting solid residue was partitioned between $H_2O$ (20 ml) and $CH_2Cl_2$ (20 ml). The organic layer was separated, the aqueous layer was further extracted with $CH_2Cl_2$ (3 × 20 ml) and the combined organic layers were dried ($Na_2SO_4$) and concentrated. Flash chromatography of the residue ($SiO_2$, 1 : 1 $CH_2Cl_2$–light petroleum gradient to $CH_2Cl_2$) gave dendrimer **3c** (0.34 g, 80%) as an orange glassy solid.

¶ Satisfactory elemental analyses and spectroscopic data were obtained for all new compounds reported. *Selected data* for **3c**: glassy solid; $^1$H NMR [400 MHz, $(CD_3)_2CO$]: δ 7.83 (d, *J* 9.1 Hz, 4 H), 7.46–7.30 (m, 40 H), 7.13 (d, *J* 9.1 Hz, 4 H), 6.76 (d, *J* 2.3 Hz, 4 H), 6.74 (d, *J* 2.3 Hz, 8 H), 6.61 (t, *J* 2.3 Hz, 6 H), 5.17 (s, 4 H), 5.09 (s, 16 H), 5.07 (s, 8 H); $^{13}$C NMR [100 MHz, $(CD_3)_2CO$]: δ 160.6, 160.2, 160.1, 147.2, 139.2, 139.1, 139.0, 136.8, 128.6, 128.0, 127.5, 124.4, 115.1, 106.4, 101.6, 70.13, 70.11, 70.0 (Calc. for $C_{110}H_{94}N_2O_{14}$: C, 79.20; H, 5.68; N, 1.68. Found: C, 78.83; H, 5.78; N, 1.54%). For **4c**: glassy solid; $^1$H NMR [400 MHz, $(CD_3)_2CO$]: δ 7.87 (d, *J* 9.1 Hz, 2 H), 7.84 (d, *J* 9.1 Hz, 2 H), 7.46–7.30 (m, 20 H), 7.14 (d, *J* 9.0 Hz, 2 H), 7.08 (d, *J* 9.0 Hz, 2 H) 6.80 (d, *J* 2.3 Hz, 2 H), 6.76 (d, *J* 2.3 Hz, 4 H), 6.62 (t, *J* 2.4 Hz, 3 H), 5.17 (s, 2 H), 5.09 (s, 8 H), 5.07 (s, 4 H), 3.89 (s, 3 H); $^{13}$C NMR [100 MHz, $(CD_3)_2CO$]: 161.6, 160.6, 160.2, 160.1, 147.2, 147.1, 139.2, 139.0, 136.8, 128.6, 128.0, 127.6, 124.4, 124.3, 115.1, 114.2, 106.4, 106.3, 101.7, 101.6, 70.1, 70.084, 70.0, 55.5 (Calc. for $C_{62}H_{54}N_2O_8$: C, 77.96; H, 5.70; N, 2.93. Found: C, 78.01; H, 5.89; N, 2.92%).

‖ *Selected data* for *cis*-**3c**: $^1$H NMR (400 MHz, $CDCl_3$): δ 7.40–7.29 (m, 20 H), 6.78–6.74 (m, 8 H), 6.64 (d, *J* 2.3 Hz, 4 H), 6.60 (d, *J* 2.0 Hz, 2 H), 6.55 (t, *J* 2.8 Hz, 2 H), 6.52 (t, *J* 2.4 Hz, 1 H), 5.01 (s, 8 H), 4.945 (s, 4 H), 4.938 (s, 2 H), 3.74 (s, 3 H).

## References

1 I. Willner and S. Rubin, *Angew. Chem., Int. Ed. Engl*., 1996, **35**, 367.
2 P. R. Westmark, J. P. Kelly and B. D. Smith, *J. Am. Chem. Soc*., 1993, **115**, 3416.
3 K. Murata, M. Aoki, T. Nishi, A. Ikeda and S. Shinkai, *J. Chem. Soc., Chem. Commun*., 1991, 1715.
4 For leading references, see S. Shinkai, A. Yoshioka, H. Nakayama and O. Manabe, *J. Chem. Soc., Perkin Trans. 2*, 1990, 1905.
5 M. Irie, *Pure Appl. Chem*., 1990, **62**, 1495.
6 For a review, see F. Ciardelli, O. Pieroni, A. Fissi, C. Carlini and A. Altomare, *Br. Polym. J*., 1989, **21**, 97.
7 F. Ciardelli, C. Carlini, R. Solaro, A. Altomare, O. Pieroni, J. L. Houben and A. Fissi, *Pure Appl. Chem*., 1984, **56**, 329.
8 M. Müller and R. Zentel, *Macromolecules*, 1996, **29**, 1609.
9 For leading references, see A. Fissi, O. Pieroni, G. Ruggeri and F. Ciardelli, *Macromolecules*, 1995, **28**, 302.
10 F. Ciardelli, D. Fabbri, O. Pieroni and A. Fissi, *J. Am. Chem. Soc*., 1989, **111**, 3470.
11 O. Pieroni, A. Fissi, J. L. Houben and F. Ciardelli, *J. Am. Chem. Soc*., 1985, **107**, 2990.
12 S. Shinkai, T. Nakaji, T. Ogawa, K. Shigematsu and O. Manabe, *J. Am. Chem. Soc*., 1981, **103**, 111.
13 T. Kinoshita, M. Sato, A. Takizawa and Y. Tsujita, *Macromolecules*, 1986, **19**, 51.
14 J. J. Effing and J. C. T. Kwak, *Angew. Chem., Int. Ed. Eng*., 1995, **34**, 88.
15 T. Öge and R. Zentel, *Macromol. Chem. Phys*., 1996, **197**, 1805.
16 For a dendrimer with azobenzene moieties on the exterior which undergoes a photoinduced size change, see H.-B. Mekelburger, K. Rissanen and F. Vögtle, *Chem. Ber*., 1993, **126**, 1161.
17 E. R. Atkinson, H. J. Lawler, J. C. Heath, E. H. Kimball and E. R. Read, *J. Am. Chem. Soc*., 1941, **63**, 730.
18 C. J. Hawker and J. M. J. Fréchet, *J. Am. Chem. Soc*., 1990, **112**, 7638.
19 S. Shinkai, T. Nakaji, Y. Nishida, T. Ogawa and O. Manabe, *J. Am. Chem. Soc*., 1980, **102**, 5860.
20 M. Krause, *Ber. Dtsch. Chem. Ges*., 1899, **32**, 124.

*Received in Cambridge, UK, 13th January 1997; Com. 7/00292K*

# Allylation of arenes catalysed by thiolate-bridged diruthenium complexes

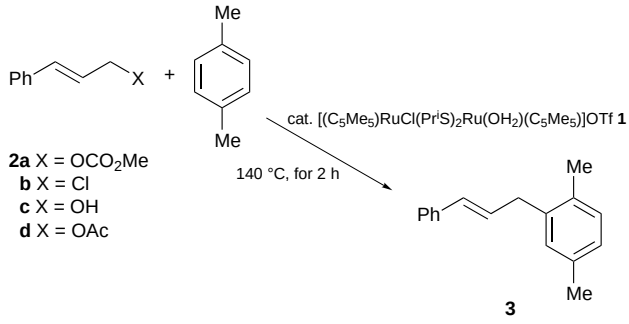
**Yoshiaki Nishibayashi, Masashi Yamanashi, Yukihiro Takagi and Masanobu Hidai***

*Department of Chemistry and Biotechnology, Graduate School of Engineering, The University of Tokyo, Hongo, Tokyo 113, Japan*

**In the presence of catalytic amounts of cationic thiolate-bridged diruthenium complexes, arenes react with allylic alcohols to afford the corresponding allylated aromatic products in high yields.**

Novel functions of multinuclear complexes in homogeneous catalysis are of current interest because such complexes can be expected to provide new types of reactive sites.[1] We have investigated the synthesis and reactivities of thiolate- or sulfur-bridged multinuclear complexes,[2–7] and have disclosed that a series of thiolate-bridged diruthenium complexes promote unique transformations of various substrates including acetylenes,[3] alkyl halides,[4] hydrazines,[5] aromatic aldehydes[6] and alkenes.[7] Attention has now been focused on the reactivity of allylic compounds at the diruthenium core. Although allylation of nucleophiles or electrophiles with allylic compounds has been extensively studied using various mononuclear transition metal complexes,[8] reactions of allylic compounds with arenes are still limited to the nickel- and palladium-catalysed allylation with arylmagnesium halides.[9] We envisaged the allylation of arenes with allylic compounds catalysed by thiolate-bridged diruthenium complexes, and preliminary results are reported herein.

Treatment of cinnamyl methyl carbonate **2a** with *p*-xylene in the presence of a catalytic amount of the cationic thiolate-bridged diruthenium complex $[(C_5Me_5)RuCl(SPr^i)_2Ru(OH_2)(C_5Me_5)]$ **1** at 140 °C for 2 h under nitrogen afforded




**Scheme 1**

**Table 1** Ruthenium-catalysed allylation of *p*-xylene with cinnamyl compounds[a]

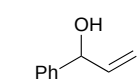
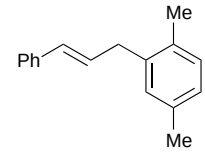
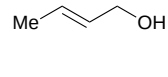
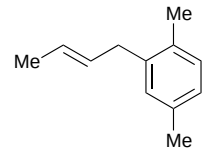
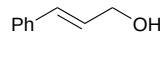
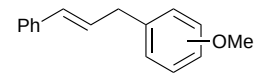
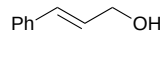
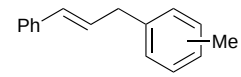
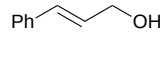
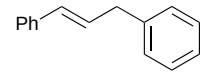
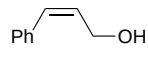
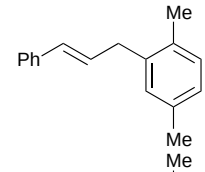
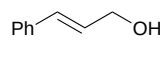
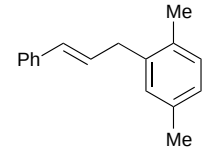
| Run | **1**/mol% | Substrate | Yield of **3** (%)[b] |
|---|---|---|---|
| 1 | 5 | **2a** | 75 |
| 2[c] | 5 | **2a** | > 99 |
| 3 | 5 | **2b** | > 99 |
| 4 | 1 | **2b** | > 99 |
| 5 | 0.2 | **2b** | 60 |
| 6 | 5 | **2c** | > 99 |
| 7 | 1 | **2c** | 30 |
| 8 | 5 | **2d** | 17 |

[a] All the reactions were carried out with a cinnamyl compound (0.25 mmol) and *p*-xylene (10 ml) at 140 °C for 2 h. [b] GLC yield. [c] For 6 h.

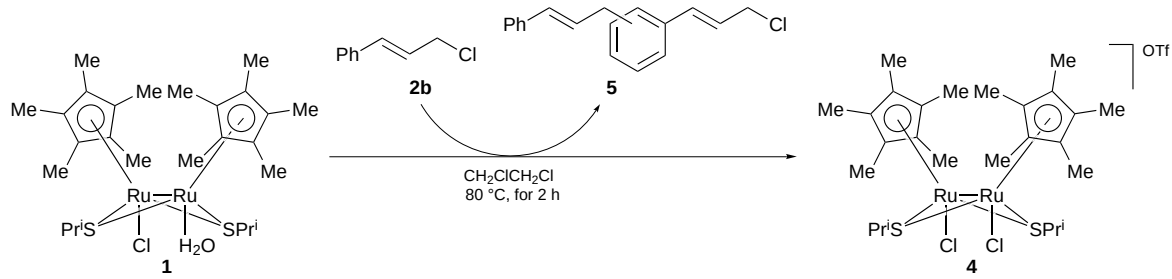
(*E*)-2-cinnamyl-1,4-dimethylbenzene **3** in 75% GLC yield (Scheme 1; Table 1, run 1). A longer reaction time (6 h) improved the yield of **3** (run 2). However, no reaction occurred using other thiolate-bridged diruthenium complexes such as $[(C_5Me_5)RuCl(SPr^i)]_2$, $[(C_5Me_5)Ru(SPr^i)_2Ru(C_5Me_5)]$ and $[(C_5Me_5)Ru(SPr^i)_3Ru(C_5Me_5)]$. Furthermore, $[(C_5Me_5)RuCl_2]_2$, which reacts smoothly with **2a** to afford a mononuclear ($\eta^3$-allyl)ruthenium complex,[10] showed only low catalytic activity. When cinnamyl chloride **2b** or *trans*-cinnamyl alcohol **2c** was used instead of **2a**, **3** was obtained in almost quantitative yield (runs 3, 4 and 6). On the other hand, cinnamyl acetate **2d** was less reactive than cinnamyl alcohol **2c** (run 8).

Recently, catalytic reactions that do not use organic halides have been receiving much attention because the production of unnecessary halogen-containing byproducts is avoided. Thus

**Table 2** Ruthenium-catalysed allylation of aromatic compounds[a]

| Run | Allylic compound | Aromatic compound | Product | Yield (%)[b] |
|---|---|---|---|---|
| 1 |  | *p*-Xylene |  | > 99[c] |
| 2[d] |  | *p*-Xylene |  | 64 |
| 3 |  | Anisole |  | 59[e] |
| 4[f] |  | Toluene |  | 52[g] |
| 5[h] |  | Benzene |  | 27 |
| 6 |  | *p*-Xylene |  | 11[c] |
| 7[i] |  | *p*-Xylene |  | > 99[c] |

[a] All the reactions were carried out in the presence of **1** (5 mol%) with an allylic compound (0.50 mmol) and an aromatic compound (20 ml) at 140 °C for 2 h. [b] Isolated yield. [c] GLC yield. [d] For 5 h. [e] Isomer ratio was $o:m:p$ = 12 : 0 : 88. [f] At 110 °C. [g] Isomer ratio was $o:m:p$ = 0 : 65 : 35. [h] At 80 °C. [i] **4** was used instead of **1**.




**Scheme 2**

the reactivities of allylic alcohols have been investigated in detail. The allylation of *p*-xylene, anisole, toluene and benzene with allylic alcohols afforded the corresponding allylic aromatic compounds in good yields. Typical results are given in Table 2. It is noteworthy that both 1-phenylprop-2-en-1-ol and **2c** react with *p*-xylene to give the same product, **3**. This suggests that a common (π-allyl)diruthenium complex is formed as an intermediate. The reactions of anisole and toluene with cinnamyl alcohol produced a 12 : 0 : 88 (*o* : *m* : *p*) mixture of (*E*)-cinnamylmethoxylbenzenes in 59% total yield (run 3) and a 0 : 65 : 35 (*o* : *m* : *p*) mixture of (*E*)-cinnamylmethyl benzenes in 52% total yield (run 4). Interestingly, the reaction between *cis*-cinnamyl alcohol and *p*-xylene proceeded very slowly at 140 °C resulting in the formation of **3** in poor yield. This is in sharp contrast to the reaction of *trans*-cinnamyl alcohol **2c** (*vide supra*).

Treatment of **1** with 5 equiv. of cinnamyl chloride **2b** in 1,2-dichloroethane at 80 °C for 2 h gave the cationic dinuclear ruthenium complex $[(C_5Me_5)Ru(SPr^i)Cl]_2[OTf]$ **4** in 29% yield, together with an allylated cinnamyl chloride **5** (Scheme 2). The structure of the paramagnetic complex **4** has been fully characterized by X-ray crystallography.† Complex **4** can also be used as a catalyst for the allylation of arenes with allylic alcohols (Table 2, run 7).

As described above, toluene was mainly allylated at the 3- and 4-positions (Table 2, run 4). This suggests that the reaction does not proceed *via* classical electrophilic aromatic substitution. Although the reaction mechanism is not yet clear, we assume that the first step involves the formation of a (π-allyl)diruthenium complex, which is followed by attack of arenes on the π-allyl moiety. In connection with this, the stereochemistry of the allyl moiety in allylated products was completely controlled, in contrast to the Lewis acid-catalysed allylation reactions of aromatic compounds.[11] This allylation of arenes with allylic alcohols using diruthenium complexes provides a new methodology for carbon–carbon bond formation. Molybdenum- and tungsten-catalysed allylation of aromatic compounds has very recently been reported, however, the catalytic activities of thiolate-bridged diruthenium complexes are much better than those of molybdenum and tungsten complexes.[12] Further studies on the detailed reaction mechanism and the application to organic synthesis are now in progress.

## Footnote

† Detailed experimental results will be reported in due course.

## References


1 G. Süss-Fink and G. Meister, *Adv. Organomet. Chem*., 1993, **35**, 41; in *Metal Clusters in Catalysis*, ed. B. C. Gates, L. Guzci and V. H. Knözinger, Elsevier, Amsterdam, 1986.

2 M. Hidai, Y. Mizobe and H. Matsuzaka, *J. Organomet. Chem*., 1994, **473**, 1 and references cited therein; Z. Tang, Y. Nomura, Y. Ishii, Y. Mizobe and M. Hidai, *Organometallics*, 1997, **16**, 151; K. Hashizume, Y. Mizobe and M. Hidai, *Organometallics*, 1996, **15**, 3303; M. Nishio, H. Matsuzaka, Y. Mizobe and M. Hidai, *Angew. Chem., Int. Ed. Engl*., 1996, **35**, 872; K. Hashizume, Y. Mizobe and M. Hidai, *Organometallics*, 1995, **14**, 5367; H. Matsuzaka, T. Ogino, M. Nishio, M. Hidai, Y. Nishibayashi and S. Uemura, *J. Chem. Soc., Chem. Commun*., 1994, 223; T. Murata, Y. Mizobe, H. Gato, Y. Ishii, T. Wakabayashi, F. Nakano, T. Tanase, S. Yano, M. Hidai, I. Echizen, H. Nanikawa and S.Motomura, *J. Am. Chem. Soc*., 1994, **116**, 3389.

3 M. Nishio, H. Matsuzaka, Y. Mizobe and M. Hidai, *Organometallics*, 1996, **15**, 965; H. Matsuzaka, Y. Takagi, Y. Ishii, M. Nishio and M. Hidai, *Organometallics*, 1995, **14**, 2153; M. Nishio, H. Matsuzaka, Y. Mizobe, T. Tanase and M. Hidai, *Organometallics*, 1994, **13**, 4214; H. Matsuzaka, Y. Takagai and M. Hidai, *Organometallics*, 1994, **13**, 13.

4 A. Takahashi, Y. Mizobe and M. Matsuzaka, S. Dev and M. Hidai, *J. Organomet. Chem*., 1993, **456**, 243.

5 S. Kuwata, Y. Mizobe and M. Hidai, *Inorg. Chem*., 1994, **33**, 3619.

6 H. Shimada, J.-P. Qü, H. Matsuzaka, Y. Ishii and M. Hidai, *Chem. Lett*., 1995, 671.

7 J.-P, Qü, H. Matsuzaka, Y. Ishii and M. Hidai, *Chem. Lett*., 1996, 767.

8 For an example, see *Comprehensive Organometallic Chemistry II*, ed. E. W. Abel, G. A. Stone and G. Wilkinson, Pergamon, Oxford, vol. 12, 1995.

9 T. Hayashi, M. Konishi, K. Yokota and M. Kumada, *J. Organomet. Chem*., 1985, **285**, 359.

10 T. Kondo, H. Ono, N. Satake, T. Mitsudo and Y. Watanabe, *Organometallics*, 1995, **14**, 1945.

11 T. Tsuchimoto, K. Tobita, T. Hiyama and S. Fukuzawa, *Synlett*, 1996, 557 and references cited therein.

12 I. Shimizu, T. Sakamoto, S. Kawaragi, Y. Maruyama and A. Yamamoto, *Chem. Lett*., 1997, 137.



*Received in Cambridge, UK, 17th February 1997; Com. 7/01115F*

# Regio- and stereo-selective oxidation of steroids using 2,6-dichloropyridine *N*-oxide catalysed by ruthenium porphyrins

**Tomoteru Shingaki,[a] Keiko Miura,[b] Tsunehiko Higuchi,[a] Masaaki Hirobe[a] and Tetsuo Nagano*[a]†**

[a] *Faculty of Pharmaceutical Sciences, University of Tokyo, 7-3-1 Hongo, Bunkyo-ku, Tokyo 113, Japan*
[b] *Tsukuba Res. Inst., Banyu Pharm. Co. Ltd., Okubo 3, Tsukuba 300-26, Japan*

**Ruthenium porphyrins catalyse oxygen transfer from 2,6-dichloropyridine *N*-oxide to steroids with retention of configuration at the asymmetric centre, giving novel steroids.**

Various oxidation systems for steroids have been developed,[1] and recently there has been increasing interest in metalloporphyrin-catalysed oxidation systems as a model of cytochrome P450 for alkanes[2] and steroids.[3] We have already shown that ruthenium porphyrins effectively catalyse the oxidation of alkenes, sulfides and alcohols in the presence of heteroaromatic *N*-oxides.[4] In particular, this catalytic system efficiently oxidizes unactivated aliphatic or aromatic hydrocarbons in high yield with an extremely high turnover number (up to $10^5$ times) in the presence of HCl or HBr. Here we report the regio- and stereo-selectivity of oxidation in steroids using this system.[5]

We investigated the oxidation of 5α-cholestan-3-one **1** with 2,6-dichloropyridine *N*-oxide catalysed by Ru(TPP)CO, Ru(TMP)CO and Ru(TDClPP)CO (Fig. 1) in the presence of HBr (runs 1–3). In the reaction catalysed by Ru(TPP)CO, **1** was oxidized to afford the 25-hydroxy derivative **2** in 11% yield (run 1). When the reaction was catalysed by Ru(TMP)CO or Ru(TDClPP)CO, **1** was oxidized to afford (20*S*)-20,25-dihydroxycholestan-3-one **3**, (20*S*)-20-hydroxycholestan-3-one **4** and 25-hydroxycholestane-3,15-dione **5** in addition to **2** (runs 2 and 3). The structures of these novel steroids **3**–**5** were identified by mass spectroscopy, $^1$H and $^{13}$C NMR analysis and IR analysis. The mass number of **3** was larger than that of the starting material **1** by 32 *m/z*. In the $^{13}$C NMR spectrum, methine carbon signals (δ 36, 28) were replaced by quaternary carbons (δ 74, 71, respectively), and in the $^1$H NMR spectrum, the signals of the methyl protons at the 21-, 25- and 26-positions each appeared as a singlet. The configuration of **3** at the 20-position was determined by an X-ray crystal structure analysis (Fig. 2).‡ Thus, hydroxylation with our catalytic system proceeds with retention of the configuration of the asymmetric centres. It is noteworthy that in the biosynthesis of progesterone, cholesterol is hydroxylated with retention of configuration at the 20-position *in vivo* by P450.[6] At least in this respect, our system can be regarded as a model of P450.

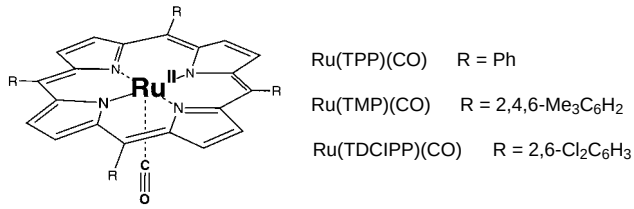



**Fig. 1** Structure of ruthenium porphyrins

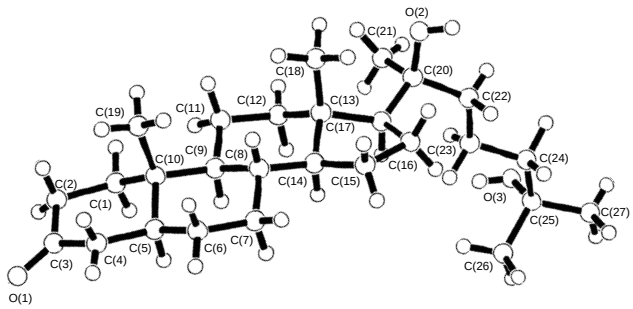
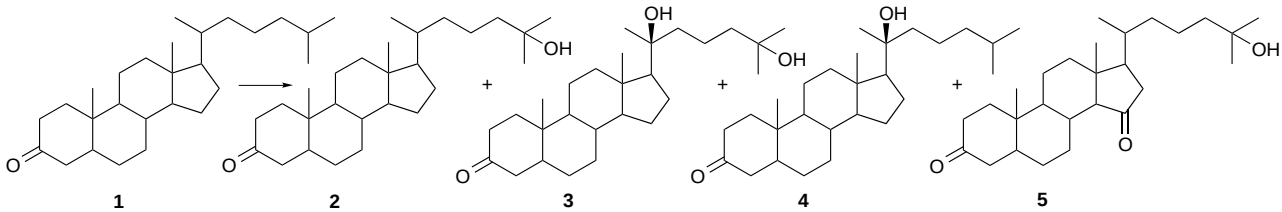


**Fig. 2** Molecular structure of (20*S*)-20,25-dihydroxycholestan-3-one **3**

The position of the hydroxy function of **4** and **5** was similarly identified. The location of the carbonyl function of **5** was supported by 2D NMR experiments ($^1$H-$^1$H and $^{13}$C-$^1$H shift correlation). From the results shown in Table 1 it can be suggested that the regioselectivity in the oxidation of **1** depends markedly upon the structure of the porphyrin. Because ruthenium porphyrins which have *o*-substituents on the aromatic ring at the *meso*-position showed higher reactivity than those which had no substituent (runs 2 and 3 *vs*. run 1), the regioselectivity may be influenced by changes in reactivity caused by steric hindrance arising from the *o*-substituents on the aromatic ring at the *meso*-position. Furthermore, Ru(TMP)CO has a different regioselectivity from Ru(TDClPP)CO, although the methyl group is as bulky as the chloride group (runs 2 and 3). This implies that variation of electron density caused by electron-donating or -withdrawing substituents on the aromatic ring at the *meso*-position is also important. Therefore, it can be assumed that the regioselectivity depends upon both the steric and electronic effects of the substituents.

Several other 5α-steroids were treated with this system (Scheme 2). As shown in Table 1, 5α-androstan-3,17-dione **6a** was not oxidized under these conditions and was recovered in 91% yield (run 4). 5α-Pregnan-3,20-dione **6b** was oxidized to afford the 5α- and 14α-hydroxy derivatives, **7b** and **8b**, respectively, in 18 and 6% yields, respectively (run 5). 5α-Cholestane **6c** was also oxidized in 73% yield and the 5α-hydroxy derivative **7c** was isolated in 28% yield (run 6). It

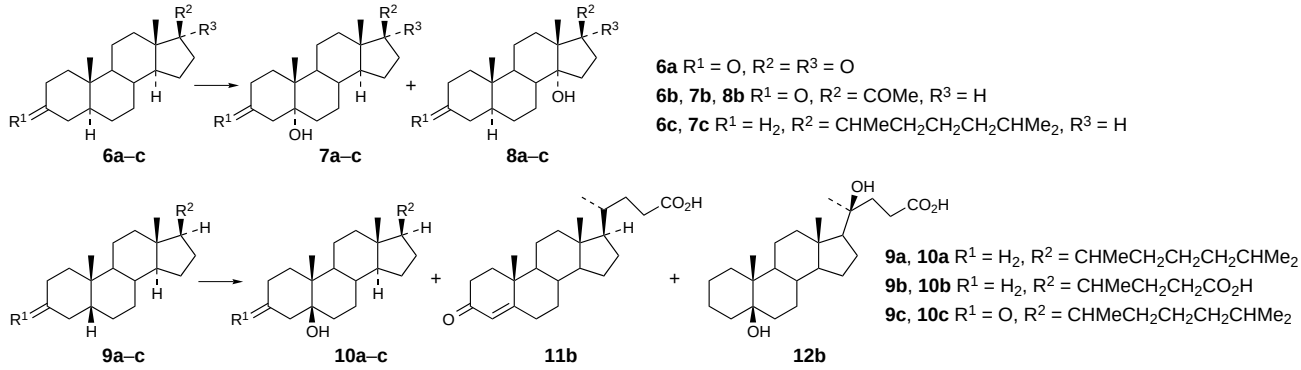



**Scheme 1** Oxidation of 5α-cholestan-3-one **1** with the ruthenium porphyrin-2,6-dichloropyridine *N*-oxide system

**Table 1** Oxidation of steroids with the ruthenium porphyrin-2,6-dichloropyridine *N*-oxide system[a]

| Run | Substrate | Catalyst | Products (yield %) | | | |
|---|---|---|---|---|---|---|
| 1[b] | **1** | Ru(TPP)CO | **2** (11%) | | | |
| 2 | **1** | Ru(TDClPP)CO | **2** (25%) | **3** (19%) | **4** (6%) | |
| 3[c] | **1** | Ru(TMP)CO | **2** (26%) | | **4** (7%) | **5** (12%) |
| 4 | **6a** | Ru(TMP)CO | None | | | |
| 5 | **6b** | Ru(TMP)CO | **7b** (18%) | **8b** (4%) | | |
| 6 | **6c** | Ru(TMP)CO | **7c** (28%) | | | |
| 7 | **6c** | Ru(TMP)CO | **7c** (14%)[d] | | | |
| 8 | **9a** | Ru(TMP)CO | **10c** (64%)[d] | | | |
| 9 | **9b** | Ru(TMP)CO | **10b** (70%) | **11b** (8%) | **12b** (4%) | |
| 10 | **9c** | Ru(TMP)CO | **10c** (42%) | | | |

[a] Reaction conditions: substrate (1 mmol), Ru(porphyrin) (2 μmol), 2,6-dichloropyridine *N*-oxide (3 mmol), 47% HBr (10 μl); molecular sieves 4 Å (150 mg) and benzene (6 ml) at 40 °C under an Ar atmosphere overnight. Yields are based on the substrate used. [b] 0.5 μmol of Ru(TPP)CO was used. [c] 4.5 mmol of 2,6-dichloropyridine *N*-oxide was used. [d] 1.2 mmol of 2,6-dichloropyridine *N*-oxide was used. The yields of **7c** and **10a** were determined by GLC.




**Scheme 2** Oxidation of 5α- and 5β-steroids with the ruthenium porphyrin-2,6-dichloropyridine *N*-oxide system

appears that substrates are oxidized at tertiary carbons in this system.

On the other hand, 5β-steroids were oxidized to the corresponding 5β-hydroxy derivatives in a good yield (Scheme 2). 5β-Cholestane **9a** afforded **10a** in 64% yield (run 8). In contrast, 5α-cholestane **6c** under the same conditions afforded **7c** in 14% yield (run 7). Both **6c** and **9a** were hydroxylated with retention of configuration. It is assumed that this difference in reactivity at the 5-position is due to the difference in steric hindrance of hydrogen at the 5-position. 5β-Cholan-24-oic acid **9b** afforded **10b**, **11b** and **12b**, and **10b** was obtained with the best yield in this report (70%). Since **10b** was oxidized to **11b** with this system, it is assumed that **10b** was an intermediate in the formation of **11b**. The identification of **12b** as a novel steroid was based on $^1$H and $^{13}$C NMR spectra, mass spectra and IR analysis. Compared with **9a** and **9b**, 5β-cholestan-3-one **9c** was less reactive (run 10), so the carbonyl function appears to reduce the reactivity in its vicinity in this oxidation system.

Oxidation of estrogens was also examined. 3-Hydroxyestra-1,3,5(10)-trien-17-one (estrone: **13**) was converted to a mixture of oxidized products which could not be separated. However, estrone methyl ether **14** afforded the 6-keto derivative **15** in 21% yield.

We have shown that the ruthenium porphyrin–2,6-dichloropyridine *N*-oxide system oxidizes steroids with retention of the configuration of the asymmetric centres. This is a critical feature for the synthesis of optically active compounds, so this system could have synthetic applications. It showed moderate regioselectivity in the oxidation of steroids. Since hydroxylation at the 20 and 25 positions is observed when cholesterol and vitamin $D_3$ are metabolized to progesterone[6] and 25-hydroxy vitamin $D_3$[7] *in vivo* by P450, respectively, our system could be useful for research on steroid metabolites. Moreover, four novel steroids were obtained with our oxidizing system. Because the regioselectivity depended markedly upon the structure of the porphyrin, further modification of the porphyrin may afford new oxidized steroids, which could provide clues to novel metabolic pathways *in vivo*.

This work was supported by a Grant-in-Aid for Scientific research from the Ministry of Education, Science, Sports and Culture, Japan.

## Footnotes

† E-mail: tlong@mol.f.u-tokyo.ac.jp

‡ *Crystal data* for (20*S*)-20,25-dihydroxycholestan-3-one **3**. $C_{27}H_{46}O_3$, $M$ = 418.66, crystal dimensions (mm) 0.5 × 0.3 × 0.03, monoclinic, space group $P2_1$ (no. 4), $a$ = 9.889(1), $b$ = 7.5383(6), $c$ = 16.7188(9) Å, β = 101.749(6)°, $Z$ = 2, $U$ = 1220.2(2) Å, $D_c$ = 1.139 g cm$^{-3}$, μ = 5.53 cm$^{-1}$, Cu-Kα radiation, λ = 1.54178 Å, $F$(000) = 446.00, $T$ = 293 K, $R$ = 0.042, $Rw$ = 0.035 [$w = 1/\sigma^2(F_o)$] for 1654 independent reflections [$I > 3\sigma(I)$] with 442 variables. The structure was solved by direct methods using MITHRIL90 and refined by full-matrix least-squares techniques using the TEXSAN program package of Molecular Structure Corporation. Atomic coordinates, bond lengths and angles, and thermal parameters have been deposited at the Cambridge Crystallographic Data Centre (CCDC). See Information for Authors, Issue No. 1. Any request to the CCDC for this material should quote the full literature citation and reference number 182/405.

## References

1 D. H. R. Barton, J. Boivin and P. Lelandais, *J. Chem. Soc., Perkin Trans. 1*, 1986, 1797; Y. Mazur, *Pure Appl. Chem.*, 1975, **41**, 145; Z. Cohen and Y. Mazur, *J. Org. Chem.*, 1979, **44**, 2318.
2 In *Cytochrome P450: Structure, Mechanism and Biochemistry*, ed. P. R. Oritz de Montellano, Plenum Press, New York, 1986; B. Meunier, *Chem. Rev.*, 1992, **92**, 1411.
3 J. T. Groves and R. Neumann, *J. Org. Chem.*, 1987, **53**, 3891; P. A. Grieco and T. L. Stuk, *J. Am. Chem. Soc.*, 1990, **112**, 7799.
4 T. Higuchi, H. Ohtake and M. Hirobe, *Tetrahedron Lett.*, 1989, **30**, 6545; 1991, **32**, 7435.
5 H. Ohtake, T. Higuchi and M. Hirobe, *J. Am. Chem. Soc.*, 1992, **114**, 10 660; T. Higuchi, C. Satake and M. Hirobe, 1995, **117**, 8879; H. Ohtake, T. Higuchi and M. Hirobe, *Heterocycles*, 1995, **40**, 867; T. Higuchi, *J. Synth. Org. Chem. Jpn.*, 1995, **53**, 644.
6 M. Morisaki, S. Sato and N. Ikekawa, *FEBS Lett.*, 1976, **72**, 337.
7 J. W. Blunt, H. F. DeLuca and H. K. Schonoes, *Biochemistry*, 1968, **7**, 3317.

*Received, 6th January 1997; Com. 7/00096K*

# Synthesis of prenylated cysteines from serine derivatives

**William W. Epstein*† and Zhaolin Wang**

*Department of Chemistry, University of Utah, Salt Lake City, Utah 84112, USA*

**Prenylated cysteines are prepared by the reaction of serine β-lactone with prenyl thiolate.**

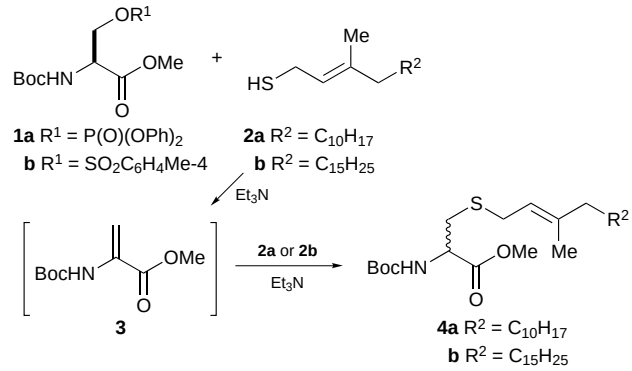
Prenylation, a recently discovered post-translational modification of proteins, has become a topic of substantial interest.[1–5] Prenylation involves covalent attachment of either farnesyl ($C_{15}$) or geranylgeranyl ($C_{20}$) isoprenoids to conserved carboxy-terminal cysteine residues by a family of prenyltransferase enzymes. Three types of carboxy-terminal cysteine sequences are substrates for this modification. The major class of these proteins has a CAAX motif (where C is a cysteine, A is usually an aliphatic amino acid and X is an amino acid that determines whether a protein is farnesylated or geranylgeranylated). The second and third types of proteins have CXC or CC motifs, respectively, in which both cysteines are geranylgeranylated. Subsequent to prenylation, proteins containing the CAAX motif are further processed by proteolytic removal of the three terminal amino acids (AAX) followed by methylation of the prenylcysteine carboxy group. Prenylation is common for many physiologically important proteins. Since oncogenic forms of Ras proteins require farnesylation for their ability to transform cells, inhibition of farnesylation has become a very attractive target for anti-cancer drug design.

Since Kamiya *et al.*[6] first synthesized farnesylcysteine, several methods for the preparation of prenylated cysteines and peptides have been reported.[7–9] These methods are based on alkylation of the sulfhydryl group of cysteine with prenyl halides. Despite the success achieved, there are two potential problems for prenylation of cysteine by this alkylation approach. Since basic conditions are generally required, free amino, hydroxy and carboxylate moieties, and especially other sulfide anions, are potential competing nucleophiles which can lead to major side reactions. The second and less important problem is that the required allylic prenyl halides are hard to purify. These potential difficulties led us to explore a new route to prenylated cysteines. Here we report a method for the synthesis of prenylated cysteines from a suitable serine precursor.

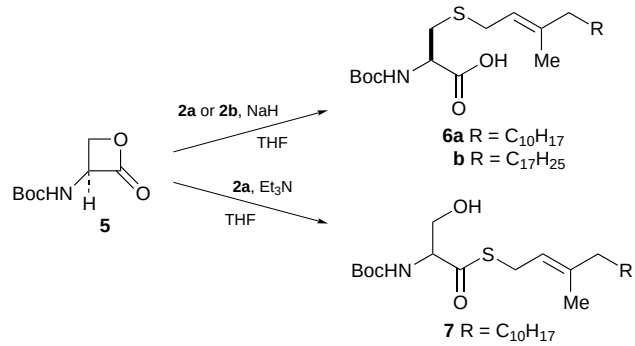
Our initial synthetic plan was based on activation of the serine hydroxy group and subsequent displacement with a prenyl thiol. *N*-Boc-*O*-diphenylphosphoryl-L-serine methyl ester **1a** and *N*- Boc-*O*-tosyl-L-serine methyl ester **1b** were prepared from Boc-L-serine methyl ester. The required prenyl thiols **2a** and **2b** were prepared from the $C_{15}$ and $C_{20}$ prenyl chlorides.[10] The low yields and lack of regiospecificity in the preparation of $C_{15}$ and $C_{20}$ prenyl halides were circumvented by using the method of Collington and Meyers.[11] Treatment of serine derivatives **1a** and **1b** with prenyl thiol **2a‡ or** 2b in the presence of triethylamine yielded racemic prenylated cysteine **4§** (Scheme 1). The isolation of **3** suggested to us that β-elimination may be the initial step of the reaction followed by Michael addition of the anion of **2a** or **2b** to the α,β-unsaturated substrate **3** to give the observed racemic mixture.

In order to avoid the above stereochemical problems, we turned to an alternative sequence. The synthetic methodology developed by Arnold *et al.*[12] for the preparation of β-substituted alanines and their derivatives seemed applicable to our problem. Thus we undertook the synthesis of prenylated cysteines by the stereospecific opening of serine β-lactone with prenyl thiols. The serine β-lactone **5** was prepared by reaction of Boc-serine with triphenylphosphine and diethyl azodicarboxylate (DEAD).[12]

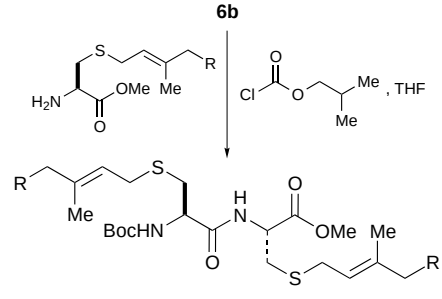
Although there are two possible ways of opening the β-lactone as shown in Scheme 2,[13] alkyl–oxygen cleavage occurred when farnesyl thiolate, prepared by the reaction of farnesyl thiol with sodium hydride, was used to give the desired stereochemically pure prenylated cysteines **6a¶** and **6b** in 52–60% yield. It should be noted that acyl–oxygen fission occurred when triethylamine was used as the base to give thioester **7** as the major product (61%). With **6b** in hand, the dipeptide **9‖** with two geranylgeranylated cysteines was pre-




**Scheme 1**




**Scheme 2**




**Scheme 3**

pared by coupling of **5b** with geranylgeranylated cysteine methyl ester **8** *via* the mixed anhydrides method.[14] Dipeptide **9** may serve as an important model compound to study geranylgeranylated Rab proteins.[2]

In summary we have described a practical and novel route to stereospecifically synthesize prenylated cysteines from serine β-lactone. The optical purity and simplicity of this approach to prenylated cysteines are attractive features compared with previous methods.[8]

## Footnotes

† E-mail: Epstein@chemistry.utah.edu

‡ All new compounds described herein have been fully characterized by $^1$H and $^{13}$C NMR spectral, HRMS and elemental analyses. *Selected data* for **2a**: $^1$H NMR (300 MHz, $CDCl_3$): δ 5.35 (m, 1 H), 5.10 (m, 2 H), 3.16 (dd, *J* 7.5, 0.6 Hz, 2 H), 2.11–1.97 (m, 8 H), 1.68 (d, *J* 0.9 Hz, 3 H), 1.66 (d, *J* 0.9 Hz, 3 H), 1.60 (s, 6 H), 1.40 (t, *J* 7.2 Hz, 1 H); $^{13}$C NMR (75 MHz, $CDCl_3$): δ 137.50, 135.30, 131.29, 124.31, 123.72, 123.28, 39.68, 39.38, 26.70, 26.27, 25.69, 22.11, 17.68, 16.02, 15.77; $\nu_{max}$(neat)/cm$^{-1}$ 2966.7, 2926.2, 1446.7, 1381.1 (Calc. for $C_{15}H_{26}S$: C, 75.56; H, 10.99. Found: C, 75.43; H, 11.03%).

§ *Selected data* for **4a**: $^1$H NMR (300 MHz, $CDCl_3$): δ 5.31 (d, *J* 6.6 Hz, 1 H), 5.21 (t, *J* 7.8 Hz, 1 H), 5.11–5.06 (m, 2 H), 3.76 (s, 3 H), 3.18 (t, *J* 8.1 Hz, 2 H), 2.95–2.81 (m, 2 H), 2.07–2.00 (m, 8 H), 1.68 (d, *J* 1.2 Hz, 3 H), 1.67 (d, *J* 1.2 Hz, 3 H), 1.60 (s, 6 H), 1.45 (s, 9 H); $^{13}$C NMR (75 MHz, $CDCl_3$): δ 171.94, 155.39, 140.16, 135.57, 131.51, 124.52, 123.93, 119.87, 80.27, 53.45, 52.67, 39.90, 39.83, 33.86, 30.23, 28.51, 26.92, 26.62, 25.91, 17.89, 16.34, 16.22. (Calc. for $C_{24}H_{41}NO_4S$: C, 65.57; H, 9.40; N, 3.19. Found: C, 65.63; H, 9.47; N, 3.15%).

¶ *Selected data* for **6a**: $^1$H NMR (300 MHz, $CDCl_3$): δ 5.35 (m, 1 H), 5.23 (t, *J* 7.8 Hz, 1 H), 5.09 (t, *J* = 6.9 Hz, 2 H), 4.48 (brs, 1 H), 3.21 (m, 2 H), 2.93 (m, 1 H), 2.09–2.00 (m, 8 H), 1.68 (d, *J* 0.9 Hz, 3 H), 1.67 (d, *J* 1.2 Hz, 3 H), 1.60 (s, 6 H),1.46 (s, 9 H); $^{13}$C NMR (75 MHz, $CDCl_3$): δ 170.00, 155.74, 140.11, 135.44, 131.46, 124.52, 124.01, 119.73, 80.03, 54.17, 39.90, 39.83, 29.90, 28.62, 28.54, 26.92, 26.70, 25.91, 17.89, 16.37, 16.21 (HRMS FAB): calc. for $C_{23}H_{39}NO_4S$, 424.2522. Found, 424.2503).

‖ *Selected data* for **9**: $^1$H NMR (300 MHz, $CDCl_3$): δ 7.13 (d, *J* 6.9 Hz, 1 H), 5.36 (brs, 1 H), 5.28–5.17 (m, 2 H), 5.11–5.07 (m, 6 H), 4.80–4.67 (m, 1 H), 4.30 (brs, 1 H), 3.23–3.07 (m, 4 H), 3.00–2.80 (m, 2 H), 2.10–1.98 (m, 24 H), 1.68 (s, 6 H), 1.60 (s, 18 H), 1.47 (s, 9 H); (HRMS CI): calc. for $C_{52}H_{86}N_2O_5S_2$ 882.5978. Found 882.5811).

## References


1 C. Marshall, *Science*, 1993, **259**, 1865; M. S. Brown and J. L. Goldstein, *Nature*, 1993, **366**, 14.
2 S. Clarke, *Annu. Rev. Biochem.*, 1992, **61**, 355.
3 P. J. Casey, *J. Lipid. Res.*, 1992, **33**, 1731.
4 W. R. Schafer and J. Rine, *Annu. Rev. Genet.*, 1992, **30**, 209.
5 H. C. Rilling, E. Breunger, W. W. Epstein and P. F. Crain, *Science*, 1990, **247**, 318; C. C. Farnsworth, M. H. Gelb and J. A. Glomset, *Science*, 1990, **247**, 320.
6 Y. Kamiya, A. Sakurai, S. Tamura, N. Takahashi, E. Tsuchiya, K. Abe and S. Fukui, *Agric. Biol. Chem.*, 1979, **43**, 363.
7 M. J. Brown, P. D. Milano, D. C. Lever, W. W. Epstein and C. D. Poulter, *J. Am. Chem. Soc.*, 1991, **113**, 3176.
8 C. C. Yang, C. K. Marlowe and R. Kania, *J. Am. Chem. Soc.*, 1991, **113**, 3177.
9 C. B. Xue, J. M. Becker and F. Naider, *Tetrahedron Lett.*, 1992, **33**, 1435.
10 E. C. Horning, *Org. Synth.*, 1955, **Coll. Vol. 2**, 363.
11 E. W. Collington and A. I. Meyers, *J. Org. Chem.*, 1971, **36**, 3044.
12 L. D. Arnold, T. H. Kalantar and J. C. Vederas, *J. Am. Chem. Soc.*, 1985, **107**, 7105.
13 H. Shao, S. H. Wang, C. W. Lee, G. Osapay and M. Goodman, *J. Org. Chem.*, 1995, **60**, 2956.
14 J. R. Vaughan, Jr. and R. L. Osato, *J. Am. Chem. Soc.*, 1952, **73**, 3547.



*Received in Corvallis, OR, USA, 20th January 1997; Com. 7/00428A*

# Synthesis of tricarbonylchromium(0) complexes of benzylic halides

**Susan E. Gibson (née Thomas)* and Gavin A. Schmid†**

*Department of Chemistry, Imperial College of Science, Technology and Medicine, South Kensington, London, UK SW7 2AY*

**Addition of $BX_3$ (X = Br, I, Cl) to tricarbonylchromium(0) complexes of benzylic alcohols and ethers provides tricarbonylchromium(0) complexes of benzylic halides in excellent yield (90–99%).**

(Arene)tricarbonylchromium(0) complexes have been widely applied in organic, organometallic and materials synthesis over the last thirty years and as a result complexes containing most organic functional groups have been synthesised and characterised.[1] Against this background it is perhaps surprising to find that tricarbonylchromium(0) complexes of benzylic halides are rarely mentioned in the literature. For example, the tricarbonylchromium(0) complex of benzyl bromide is to date unreported, the benzyl iodide complex is mentioned in just one study,‡ and the benzyl chloride complex is found in a mere handful of papers.[3]

The under-representation of benzylic halides in (arene)tricarbonylchromium(0) chemistry may be attributed to difficulties with their preparation. Reacting benzylic bromides, iodides and chlorides with even a labile source of tricarbonylchromium(0) such as $[(CO)_3(NH_3)_3Cr^0]$ under relatively mild conditions leads to insertion of the chromium(0) into the benzylic halide bonds, reductive coupling and the production of 1,2-diarylethanes rather than formation of $\eta^6$-arene complexes.[4] And whilst addition of HCl to (benzyl alcohol)tricarbonylchromium(0) gives (benzyl chloride)tricarbonylchromium(0) in acceptable yield (31–74%)[3] and has thus enabled this complex to be used in both mechanistic studies[3a] and in the synthesis of several heterobimetallic species,[3b–d] the corresponding reactions with HBr and HI are unreported.§

In view of the under-utilisation to date of tricarbonylchromium(0) complexes of benzylic bromides and iodides due to the perceived difficulties associated with their preparation, we report herein our recent discovery that tricarbonylchromium(0) complexes of benzylic halides are readily prepared in excellent yield by treatment of readily available tricarbonylchromium(0) complexes of either benzylic alcohols or benzylic ethers with the appropriate boron trihalide.

(Benzyl alcohol)tricarbonylchromium(0) **1a**[5] was prepared from benzyl alcohol and hexacarbonylchromium(0) (69%). Addition of two equivalents of $BBr_3$ to a suspension of **1a** in $CH_2Cl_2$ at −78 °C gave a brown–yellow solution which was stirred for 1 h at −78 °C and then quenched with aqueous $NaHCO_3$ [eqn. (1)]. Subsequent work-up gave a yellow solid




**1a–d** **2–5** (1)

which was identified as the novel tricarbonylchromium(0) complex of benzyl bromide **2** on the basis of its spectroscopic and microanalytical data (Table 1, entry 1).¶ Encouraged by the excellent yield obtained for this reaction (99%), the reaction of the benzyl alcohol complex **1a** was performed under identical conditions with $BI_3$ and $BCl_3$. These gave, respectively, the novel benzyl iodide complex **3**¶ in 99% yield and the previously reported[3] but as yet not fully characterised benzyl chloride complex **4**¶ also in 99% yield (Table 1, entries 2 and 3).

Tricarbonylchromium(0) complexes of benzylic ethers are easily synthesised and commonly used as intermediates in (arene)tricarbonylchromium(0) chemistry.[6] In order to ascertain whether or not these complexes may be regarded as precursors to benzylic halide complexes, the methyl and ethyl ether complexes **1b**[7] and **1c**[7] were synthesised by treatment of the alcohol complex **1a** with MeOH and EtOH, respectively, in the presence of $H_2SO_4$ (83 and 89% yield, respectively). Reaction of the methyl ether complex **1b** with $BBr_3$, $BI_3$ and $BCl_3$ and the ethyl ether complex **1c** with $BBr_3$ gave the corresponding benzyl halide complexes **2**–**4** in excellent yields (99–99%) (Table 1, entries 4–7). [It is worthy of comment at this point that reaction of the methyl ether complex **1b** with $BF_3$ failed to produce the corresponding benzyl fluoride complex. A related transformation has been reported recently, however, using cyclic benzylic alcohol complexes and the powerful fluoride source diethylaminosulfur trifluoride (DAST).[8]]

In order to test the effect of substitution at the benzylic centre, the secondary and tertiary benzylic ether complexes **1d** and **1e** were synthesised by Bu$^t$Li-promoted deprotonation of the methyl ether complex **1b** followed by quenching with iodomethane to give **1d**[9] (93%), and then Bu$^t$Li-promoted deprotonation of **1d** and quenching with iodoethane to give the novel complex **1e** (70%). Whilst treatment of **1d** with $BBr_3$ gave an excellent yield of the corresponding novel bromide **5** (99%) indicating that secondary benzylic halide complexes may be synthesised by this approach (Table 1, entry 8), reaction of **1e** with $BBr_3$ resulted in elimination and the production of an α,β-dimethylstyrene complex in significant yield (70%) (Table 1, entry 9).

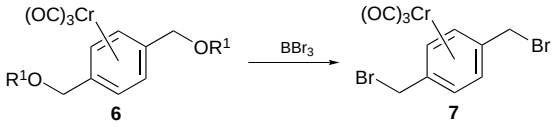
Finally, in order to test whether or not difunctionalised complexes may be accessed by boron trihalide treatment of alcohols and ethers, the novel dimethyl ether complex **6** was

**Table 1** Reaction of benzylic alcohol and ether complexes **1a**–**e** and **6** with boron trihalides to give benzylic halide complexes **2**–**5** and **7**[a]

| Entry | Substrate | $R^1$ | $R^2$ | $R^3$ | $BX_3$ | Product | $R^2$ | $R^3$ | X | Yield (%) |
|---|---|---|---|---|---|---|---|---|---|---|
| 1 | **1a** | H | H | H | $BBr_3$ | **2** | H | H | Br | 99 |
| 2 | **1a** | H | H | H | $BI_3$ | **3** | H | H | I | 99 |
| 3 | **1a** | H | H | H | $BCl_3$ | **4** | H | H | Cl | 99 |
| 4 | **1b** | Me | H | H | $BBr_3$ | **2** | H | H | Br | 95 |
| 5 | **1b** | Me | H | H | $BI_3$ | **3** | H | H | I | 99 |
| 6 | **1b** | Me | H | H | $BCl_3$ | **4** | H | H | Cl | 97 |
| 7 | **1c** | Et | H | H | $BBr_3$ | **2** | H | H | Br | 90 |
| 8 | **1d** | Me | Me | H | $BBr_3$ | **5** | Me | H | Br | 99 |
| 9 | **1e** | Me | Me | Et | $BBr_3$ | — | — | — | — | —[b] |
| 10 | **6** | Me | — | — | $BBr_3$ | **7** | — | — | Br | 95 |

[a] The experimental procedure for the synthesis of **2** from **1a** is typical: $BBr_3$ (1 M in $CH_2Cl_2$, 2 cm$^3$, 2 mmol) was added to a suspension of **1a** (0.244 g, 1.00 mmol) in $CH_2Cl_2$ (20 cm$^3$) at −78 °C. The resulting brown–yellow solution was stirred at −78 °C for 1 h and then quenched with sat. aq. $NaHCO_3$ (10 cm$^3$). The product mixture was allowed to warm to room temperature and then $H_2O$ (10 cm$^3$) was added before extracting the organic phase with diethyl ether (40 cm$^3$ and 20 cm$^3$). The organic phase was dried ($MgSO_4$), filtered through Celite and concentrated *in vacuo* to give complex **2** as a yellow solid (0.304 g, 99%). [b] Reaction of **1e** with $BBr_3$ resulted in elimination and the production of an α,β-dimethylstyrene complex (70%).

synthesised by methylation of 1,4-benzenedimethanol (NaH–MeI; 50%) and subsequent complexation [$(CO)_6Cr^0$; 85%]. Addition of $BBr_3$ to **6** [eqn. (2)] gave the novel dibromide




**6** **7** (2)

complex **7** in 95% yield (Table 1, entry 10).

## Footnotes

* E-mail: s.gibson@ic.ac.uk

† Undergraduate exchange student from ETH, Zürich.

‡ Reaction of $[(PhCH_2)(CO)_3Cr^0]_2Hg$, prepared in 65% yield from $(PhCH_2)_2Hg$ and $[(CO)_3(NH_3)_3Cr^0]$, with iodine gave (benzyl iodide)-tricarbonylchromium(0) in 79% yield.[2]

§ In our hands, addition of HBr to (benzyl alcohol)tricarbonylchromium(0) gave a moderate yield (*ca* 60%) of an inseparable 1 : 3 mixture of benzyl bromide and its tricarbonylchromium(0) complex, whilst the corresponding reaction with HI led to a product mixture from which only benzyl iodide containing a trace ( < 5%) of its tricarbonylchromium(0) complex could be extracted.

¶ *Selected data* for **2**: mp 73–5 °C; $\nu_{max}$(cyclohexane)/cm$^{-1}$ 1983vs and 1920vs (C≡O); $\delta_H(CDCl_3)$ 4.13 (2 H, s, $CH_2$) and 5.32–5.34 (5 H, m, ArH); $\delta_C(CDCl_3)$ 31.9 ($CH_2$), 91.6 ($C_{para}$), 92.3, 93.2 ($C_{ortho,meta}$), 105.5 ($C_{ipso}$) and 232.0 (C≡O); *m/z* (EI) 308/306 ($M^+$, 15%), 227 (M − Br, 10), 224/222 (M − 3CO, 20), 199 (M − Br − CO, 15), 143 (M − Br − 3CO, 30), 91 ($C_7H_7$, 100) and 52 (Cr, 100). For **3**: mp 85–88 °C (decomp.); $\nu_{max}$(cyclohexane)/cm$^{-1}$ 1982vs and 1920vs (C≡O); $\delta_H(CDCl_3)$ 4.08 (2 H, s, $CH_2$) and 5.26–5.37 (5 H, m, ArH); $\delta_C(CDCl_3)$ 3.6 ($CH_2$), 91.2 ($C_{para}$), 92.6, 92.9 ($C_{ortho,meta}$), 107.6 ($C_{ipso}$) and 232.3 (C≡O); *m/z* (EI) 354 ($M^+$, 50%), 298 (M − 2CO, 10), 270 (M − 3CO, 75), 227 (M − I, 25), 199 (M − I − CO, 50), 171 (M − I − 2CO, 15), 143 (M − I − 3CO, 65), 91 ($C_7H_7$, 100) and 52 (Cr, 70). For **4**: mp 59–61 °C; $\nu_{max}$(cyclohexane)/cm$^{-1}$ 1984vs and 1920vs (C≡O); $\delta_H(CDCl_3)$ 4.25 (2 H, s, $CH_2$) and 5.34–5.36 (5 H, m, ArH); $\delta_C(CDCl_3)$ 45.1 ($CH_2$), 91.6 ($C_{para}$), 92.3, 92.8 (C*ortho,meta*), 105.5 ($C_{ipso}$) and 231.9 (C≡O); *m/z* (EI) 262 ($M^+$, 15%), 178 (M − 3CO, 30), 143 (M − Cl − 3CO, 10), 91 ($C_7H_7$, 100) and 52 (Cr, 35).

## References

1 R. Davis and L. A. P. Kane-Maguire, in *Comprehensive Organometallic Chemistry*, ed. G. Wilkinson, F. G. A. Stone and E. W. Abel, Pergamon, Oxford, 1982, vol. 3, p. 1001–51; M. J. Morris, in *Comprehensive Organometallic Chemistry II*, ed. G. Wilkinson, F. G. A. Stone and E. W. Abel, Pergamon, Oxford, 1995, vol. 5, p. 480–491.

2 G. A. Razuvaev, A. N. Artemov, T. G. Kasatkina and E. N. Poselenova, *Izv. Akad. Nauk SSSR, Ser. Khim.*, 1982, 1131 (*Chem. Abstr.*, 1982, **97**, 182571v).

3 (*a*) J. D. Holmes, D. A. K. Jones and R. Pettit, *J. Organomet. Chem.*, 1965, **4**, 324; (*b*) V. Galamb, G. Palyi, F. Ungvary, L. Marko, R. Boese and G. Schmid, *J. Am. Chem. Soc.*, 1986, **108**, 3344; (*c*) M. G. McDougall, J. C. Gallucci and D. W. Meek, *Inorg. Chim. Acta*, 1991, **188**, 123; (*d*) M. R. Domingo, A. Irving, Y.-H. Liao, J. R. Moss and A. Nash, *J. Organomet. Chem.*, 1993, **443**, 233.

4 H. G. Wey and H. Butenschön, *Chem. Ber.*, 1990, **123**, 93.

5 B. Nicholls and M. C. Whiting, *J. Chem. Soc.*, 1959, 551.

6 S. G. Davies and T. D. McCarthy, in *Comprehensive Organometallic Chemistry II*, ed. G. Wilkinson, F. G. A. Stone and E. W. Abel, Pergamon, Oxford, 1995, vol. 12, p. 1039–1070.

7 J. Blagg, S. G. Davies, N. J. Holman, C. A. Laughton and B. E. Mobbs, *J. Chem. Soc., Perkin Trans. 1*, 1986, 1581.

8 C. Kermarrec, V. Madiot, D. Grée, A. Meyer and R. Grée, *Tetrahedron Lett.*, 1996, **37**, 5691.

9 J. Blagg, S. G. Davies, C. L. Goodfellow and K. H. Sutton, *J. Chem. Soc., Perkin Trans. 1*, 1987, 1805.

*Received in Liverpool, UK, 24th February 1997; Com. 7/01245D*

# Hydro(solvo)thermal synthesis and structure of a three-dimensional zinc fluorophosphate: $Zn_2(4,4'\text{-bipy})(PO_3F)_2$

**P. Shiv Halasyamani, Mark J. Drewitt and Dermot O'Hare*†**

*Inorganic Chemistry Laboratory, Oxford University, South Parks Road, Oxford, UK OX1 3QR*

**A new three-dimensional zinc fluorophosphate is prepared by using hydro(solvo)thermal conditions with ZnO, $(HF)_x$·py $H_3PO_4$ and 4,4′-bipyridyl; the single-crystal structure is determined.**

Meso- and micro-porous materials are of great industrial and academic interest due to their catalytic, adsorbent, and ion-exchange properties.[1–3] A three-dimensional open framework, with uniform pores, channels and active catalytic sites, facilitates and enhances these properties. One class of these open-framework materials are transition-metal phosphates.[3–5] Various examples with metals such as V,[6] Fe,[7] Co,[8] and Mo,[3] have recently been synthesised and characterised. In contrast to the closed-shell aluminosilicates, these new materials are potential candidates for atom abstraction and redox catalysis. Many of these metal phosphates were synthesised under hydro(solvo)thermal conditions with organic templating agents.

Recently, $(HF)_x$·py [pyridinium poly(hydrogen fluoride), 70% HF by mass] has been utilised to synthesise a variety of new mixed-metal materials.[9–11] The fluoride ion not only acts as a mineralizer, but also participates in the formation and structure of the final compound. Ferey[12] used fluoride in the synthesis of new fluorinated gallophosphates, and determined that temperature, pressure, time, pH, concentration of reactants, and the nature of the template all influence the existence and nature of the microporous phases. It is our aim to synthesise new microporous fluorinated phosphate materials, and in doing so synthesise open-framework compounds with fluoride channels. Here we report the hydro(solvo)thermal synthesis and crystal structure of a new zinc fluorophosphate.

Open-framework zinc phosphates have been prepared previously by mixing $Zn(NO_3)_2$, $H_3PO_4$ and alkaline base, which is then heated for several days at 70 °C. Using this method, analogues of sodalite, $Na_6(H_2O)_8(ZnPO_4)_6$ and zeolite Li–A(BW), $Li_4Zn_4P_4O_{16}$·$4H_2O$ have been synthesized.[5] Within the metal–$PO_3F^{2-}$ system compounds with Ni,[13] Sn,[14] Co,[15] Cu[16] and Zn,[17] have been reported. $Ni(H_2O)_6(NH_4)_2(PO_3F)_2$[13] and $SnPO_3F$[14] are molecular solids with isolated anions and cations, whereas $ZnPO_3F$·2.5 $H_2O$[17] contains both tetrahedrally and octahedrally coordinated $Zn^{2+}$, with the tetrahedral $Zn^{2+}$ coordinated to two oxygens and the fluorophosphate.

$Zn_2(4,4'\text{-bipy})(PO_3F)_2$ was synthesised by heating ZnO, $(HF)_x$·py, 85% $H_3PO_4$ and 4,4′-bipy in a 23 ml Teflon lined Parr autoclave at 180 °C.‡ It crystallises as clear colourless faceted crystals in 9% yield. The single-crystal X-ray structure determination indicates that it is a three-dimensional structure containing layers of zinc fluorophosphate moieties connected by 4,4′-bipy ligands (Fig. 1). Each zinc is tetrahedrally coordinated, bonded to three oxygens [Zn–O (av.) 1.927(3) Å] and one nitrogen [Zn–N 2.020(3) Å]. Each oxygen on the zinc is linked to a phosphorus, whereas the 4,4′-bipy ligands bridge the $Zn^{2+}$ cations in adjacent layers [$Zn^{2+}\cdots Zn^{2+}$ 11.100(1) Å]. The 4,4′-bipy ligand is not planar, rather the rings are twisted at an angle of 15.3(3)°. The fluorophosphate group, $PO_3F^{2-}$, contains tetrahedrally coordinated $P^{5+}$. Each phosphorus is linked to three oxygens [P–O(av.) 1.501(2) Å], that bridge to the $Zn^{2+}$, and a terminal fluoride [P–F(av.) 1.568(2) Å]. In terms of connectivity, the compound can be formulated as $PO_{3/2}F_{1/1}^{+}$ cations linked to $Zn(4,4'\text{-bipy})_{1/2}O_{3/2}^{-}$ anions. Similarly to $CoPO_3F$·$3H_2O$[15] and $CuPO_3F$·$2H_2O$[16] the fluorophosphate groups in $Zn_2(4,4'\text{-bipy})(PO_3F)_2$ bridge the metal exclusively through oxygen, whereas the fluorine atom is always monodentate. The bond distances and angles in $PO_3F^{2-}$ in the reported structure are in excellent agreement with those previously reported. An interesting feature of $Zn_2(4,4'\text{-bipy})(PO_3F)_2$ is the fluoride channel (Fig. 2). The size of this channel is a direct consequence of the Zn–(4,4′-bipy)–Zn linkage. The effect of the 4,4′-bipy ligand is twofold. First, it completes the $Zn^{2+}$ tetrahedra by inhibiting coordination to $F^-$, and second it increases the distance between the $Zn^{2+}$ and produces the observed channel. Experiments are currently in progress to

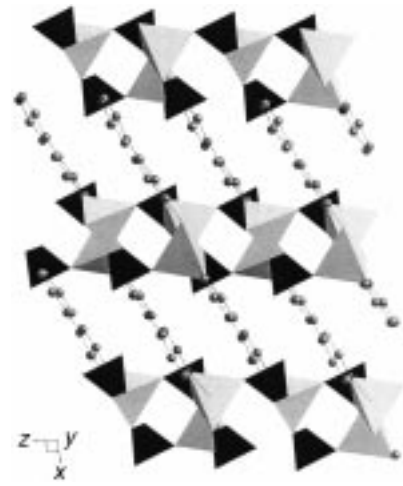



**Fig. 1** View of the single-crystal structure of $Zn_2(4,4'\text{-bipy})(PO_3F)_2$ along the crystallographic 010 direction

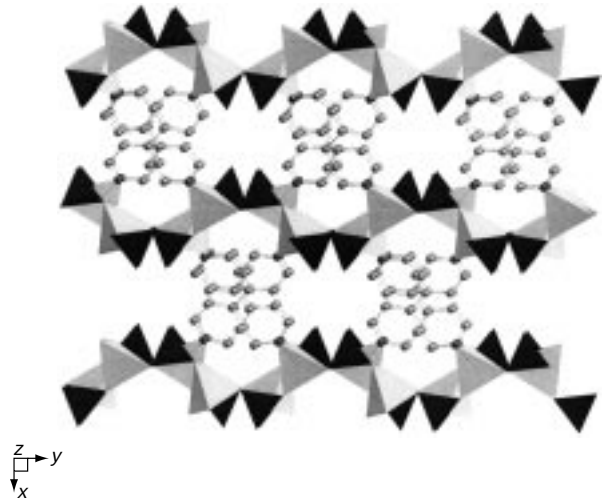



**Fig. 2** View of the single-crystal structure of $Zn_2(4,4'\text{-bipy})(PO_3F)_2$ along the crystallograpic 001 direction

increase this channel by using 1,4-bis(4-pyridyl)benzene and 1,4-bis(4-pyridylethenyl)benzene[18] as bridging ligands.

## Footnotes

* E-mail: dermot.ohare@icl.ox.ac.uk
† D. O'Hare is the Royal Society of Chemistry Sir Edward Frankland Fellow.
‡ *Synthesis*: $Zn_2(4,4'\text{-bipy})(PO_3F)_2$ was synthesised by adding 0.048 g ZnO, 0.51 g $(HF)_x{\cdot}py$, 0.40 g 85% $H_3PO_4$ and 0.5 g 4,4′-bipy to a 23 ml Teflon lined Parr autoclave. The autoclave was sealed and heated under static conditions for 12 h at 180 °C. To facilitate crystal growth, the reaction was cooled to room temp. over 2 h (starting $Zn : (HF)_x{\cdot}py : H_3PO_4 : 4,4'\text{-bipy}$ ratio 1 : 3.16 : 6.67 : 5.33). The product was filtered and thoroughly washed with acetone to remove recrystallised 4,4′-bipy. $Zn_2(4,4'\text{-bipy})(PO_3F)_2$ was recovered as clear colourless faceted crystals in 9% yield (0.025 g) based on ZnO. Elemental analysis, using the combustion method gave satisfactory C,H, and N values. The IR spectrum revealed P–F bands centred at 833 and 726 $cm^{-1}$ consistent with known phases.[16]

§ *Crystal data*: monoclinic, space group $P2_1/c$, $a$ = 17.996(9), $b$ = 9.813(2), $c$ = 8.229(4) Å, β = 99.727(2)°, $U$ = 1432.3(3) $Å^3$, $Z$ = 4, $D_c$ = 2.24 g $cm^{-3}$, μ = 37.1 $cm^{-1}$, crystal size *ca.* 0.40 × 0.21 × 0.19 mm, 15 188 total (2969 independent) reflections, $R$ = 0.031 and $R_w$ = 0.030 for 2112 reflections with $I > 5\sigma(I)$, max., min. peak in final Fourier difference map 0.54 and −0.68 e $Å^{-3}$ respectively. Data were collected on an image-plate Enraf-Nonius DIP 2000 diffractometer using graphite-monochromated Mo-Kα radiation at 150 K; 90 frames at a step of 2° yielded 15 188 reflections, $\theta_{max}$ = 26°. Corrections were made for Lorentz and polarisation effects.[19] The structure was solved by direct methods using SIR92[20] and refined using full-matrix least squares. Hydrogen atoms were fixed in geometrically idealised positions and allowed to ride on their attached carbon atoms with isotropic thermal parameters according to the atom to which they were connected (these were not refined). No correction was made for absorption. A Chebyshev weighting scheme[22] was applied in the refinement of the structure, the data corrected for the effects of anomalous dispersion and isotropic extinction (*via* an overall extinction parameter)[22] in the final stages of refinement. All crystallographic calculations were performed using the Oxford CRYSTALS system[23] running on a Silicon Graphics Indigo R4000 computer.

Atomic coordinates, bond lengths and angles, and thermal parameters have been deposited at the Cambridge Crystallographic Data Centre (CCDC). See Information for Authors, Issue No. 1. Any request to the CCDC for this material should quote the full literature citation and the reference number 182/418.

## References

1 M. E. Davis and R. F. Lobo, *Chem. Mater*., 1992, **4**, 756.
2 D. W. Breck, *Zeolite Molecule Sieves: Structure, Chemistry and Use*, Wiley, 1974.
3 P. B. Venuto, *Microporous Mater*., 1994, **2**, 297.
4 R. C. Haushalter and L. A. Mundi, *Chem. Mater*., 1992, **4**, 31.
5 T. E. Gier and G. D. Stucky, *Nature*, 1991, **349**, 508.
6 W. T. A. Harrison and M. L. F. Phillips, *Chem. Commun.*, 1996, 2771.
7 R. M. Barrier, *Hydrothermal Chemistry of Zeolites*, Academic Press, 1982.
8 R. Szostak, *Molecular Sieves: Principles of Synthesis and Identification*, Van Nostrand Reinhold, 1989.
9 P. Halasyamani, M. J. Willis, C. L. Stern, P. Lundquist, H. G. Wong and K. R. Poeppelmeier, *Inorg. Chem.*, 1996, **35**, 1367.
10 P. Halasyamani, K. R.Heier, M. J. Willis, C. L. Stern and K. R. Poeppelmeier, *Z. Anorg. Allg. Chem.*, 1996, **622**, 479.
11 P. Halasyamani, K. R. Heier, C. L. Stern and K. R. Poeppelmeier manuscript in preparation.
12 G. Ferey, *J. Fluorine Chem.*, 1995, **72**, 187 and references therein.
13 M. Berraho, C. R'Kha, A. Vegas and M. Rafiq, *Acta Crystallogr., Sect. C*, 1992, **48**, 1350.
14 A. F. Berndt, *Acta Crystallogr., Sect. B*, 1974, **30**, 529.
15 J. Durand, L. Cot, M. Berraho and M. Rafiq, *Acta Crystallogr., Sect. C*, 1987, **43**, 611.
16 M. Zeibig, B. Wallis, F. Mowius and M. Meisel, *Z. Anorg. Allg. Chem.*, 1991, **600**, 231.
17 P. J. Durand, A. Larbot, L. Cot, M. Duprat and F. Dabosi, *Z. Anorg. Allg. Chem.*, 1983, **504**, 163.
18 A. Das, J. P. Maher, J. A. McCleverty, J. A. N. Badiola and M. D. Ward, *J. Chem. Soc., Dalton Trans.*, 1993, 681.
19 A. C. T. North, D. C. Phillips and F. S. Matthews, *Acta Crystallogr., Sect. A*, 1968, **24**, 351.
20 A. Altomare, G. Cascarano, C. Giacovazzo, A. Guagliardi, G. Polidor, M. C. Burla and M. Camalli, *J. Appl. Crystallogr.*, 1994, **27**, 435.
21 J. R. Carruthers and D. W. Watkin, *Acta Crystallogr., Sect. A*, 1979, **35**, 698.
22 A. C. Larson, *Acta Crystallogr.*, 1967, **23**, 664.
23 J. R. Carruthers and D. J. Watkin, *CRYSTALS User Manual*, Oxford University Computing Centre, Oxford, 1975.

*Received in Cambridge, UK, 24th February 1997; Com. 7/01253E*

# Use of electrospray ionization mass spectrometry to characterize chiral reactive intermediates in a titanium alkoxide mediated sulfoxidation reaction

**Marcella Bonchio,[a] Giulia Licini,*[a] Giorgio Modena,[a] Stefano Moro,[a] Olga Bortolini,*[b] Piero Traldi[c] and William A. Nugent[d]**

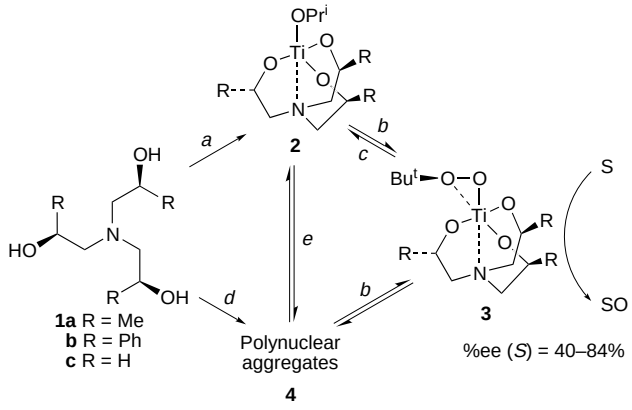
[a] *Università di Padova, Dip. di Chimica Organica, CMRO del CNR, via Marzolo 1, I-35131 Padova, Italy*
[b] *Università di Ferrara, Dip. di Chimica, via Borsari 46, 44100 Ferrara, Italy*
[c] *CSSRCC del CNR, via Marzolo 1, 35131, Padova, Italy*
[d] *The Du Pont Company, Central Research and Development, PO Box 80328, Wilmington, Delaware 19880-0328, USA*

**The ESIMS technique, combined with $^1$H NMR evidence, provides a precise inventory of the catalytic Ti$^{IV}$ precursors and the characterization of the reactive peroxometal complex involved in enantioselective sulfoxidation employing the Ti$^{IV}$–homochiral trialkanolamine–alkylhydroperoxide system.**

In the field of titanium(IV) alkoxide mediated homogeneous enantioselective oxidation using alkyl hydroperoxides as oxygen donors,[1] excellent results have been obtained in the asymmetric epoxidation of allylic alcohols[2] and in the sulfoxidation of sulfur containing compounds.[3] Characterization of the active catalysts in many of these reactions is complicated by the tendency of the alkoxides to form mixtures of polynuclear species equilibrating in solution.[4] In all cases a chiral titanium $\eta^2$-alkylperoxo species has been postulated as the reactive intermediate.[5] In this respect, the solid-state structure of the achiral $\eta^2$-*tert*-butylperoxo titanatrane dimer, in which the peroxide moiety has an $\eta^2$ arrangement, is so far the only characterized titanium(IV) peroxo complex.[6]

We recently developed a highly robust titanium alkoxide catalyst[7] for the enantioselective oxidation of organic sulfides to sulfoxides.[8] Catalyst **2** is generated *in situ* by addition of a stoichiometric amount of the homochiral trialkanolamine **1**, to a $CHCl_3$ solution of $Ti(OPr^i)_4$ (Scheme 1, pathway *a*).[7,8]

Described here is the novel observation that the catalytically active polynuclear titanium(IV)-based species **4** forms from the interaction of **2** and excess of ligand **1** (Scheme 1, pathway *e*). Our results include electrospray ionization mass spectrometric (ESIMS) studies[9]† which, together with $^1$H NMR evidence, allow (*i*) identification of the components in **4**, (*ii*) delineation of their reactivity with oxygen nucleophiles and (*iii*) characterization of the monomeric chiral titanium(IV) peroxo species **3** arising from the interaction of **2** and **4** with Bu$^t$OOH (Scheme 1, pathway *b*).




**Scheme 1** *Reagents and conditions*: *a*, stoichiometric $Ti(OPr^i)_4$, $CHCl_3$, 20 °C; *b*, Bu$^t$OOH; *c*, Pr$^i$OH; *d*, $Ti(OPr^i)_4$ (0.75 equiv.), $CH_2Cl_2$, 20 °C, followed by solvent removal; *e*, excess of **1**

$^1$H NMR studies in $CDCl_3$ indicate that when a precise 1 : 1 ligand : titanium ratio is employed the discrete monomeric complex **2** is formed.‡ Further addition of **1** causes the progressive disappearance of the resonances of the apical isopropoxy ligand in **2** and the synchronous appearance of two broader signals indicating the formation of a mixture of aggregates.§ The room-temperature $^1$H NMR spectrum of **4b** shows broad resonances and the absence of isopropoxy signals.¶ At lower temperature (−20 °C) the system freezes out and a complicated spectrum of sharper signals is obtained, consistent with the presence of a steady composition of aggregates. In contrast, at 60 °C only three broad singlets are observed, each corresponding to a different set of protons. However, regardless of the amount of **1** in excess, addition of Bu$^t$OOH to the system always restores a simple $^1$H NMR spectrum consistent with the mononuclear *tert*-butylperoxotitanium species **3**.[8]

ESIMS analysis, which has already been applied successfully to the characterization of various polynuclear complexes,[9,10] allowed us to identify the diverse species present in solution.

The positive ion ESI mass spectrum of preformed catalyst **4a** using methanol as the mobile phase is shown in Fig. 1.

The most significant ions, whose structures have been assigned on the basis of MS/MS analysis and comparison between the theoretical and experimental cluster ion peaks, are indicated. The overall ESIMS spectrum of Fig. 1 shows the molecular peaks of the species originated in the equilibrium reactions involving the titanium centre and the oxygen nucleophiles available in solution, *i.e.* trialkanolamine **1a**, methanol and water, present in traces in the mobile phase. Interaction of **4a** with water, gives rise to ions **I** (*m/z* 254), **IV** (*m/z* 489) and **VII** (*m/z* 724) which are mono-, di- and tri-nuclear titanium containing species, respectively. Those ions show incorporation of $^{18}$O ($\geqslant$65%) when $H_2{}^{18}O$ is added to the mobile phase. The reaction of **4a** with methanol is responsible for the appearance of ions **II** (*m/z* 268) and **V** (*m/z* 503), whose mass peaks show an increment of four and three mass units, respectively, when $CD_3OD$ is used as the mobile phase. Multiple interaction of **1a** with Ti$^{IV}$ [11] affords species **VIII** (*m/z* 897) and the lower homologue ions **VI** (*m/z* 662) and **III** (*m/z* 427).‖ These latter ions were also observed in the positive-ion ESI mass spectrum collected for an acidic chloroform solution of **4a** *i.e.* under conditions similar to those employed in catalytic sulfoxidation.[8] Complexes **4b** and **4c** give analogous ESI mass spectra where the same reactivity pattern can be recognized.**

Additional support for the NMR results comes from the characterization of the protonated titanium(IV) peroxo complex **3a** (*m/z* 326), achieved by ESIMS[13] when an excess of *tert*-butylhydroperoxide was added to the mobile phase containing **4a**. The structure of the cluster ion peaks and the MS/MS analysis of the 326 mass peak (Fig. 2) are consistent with the

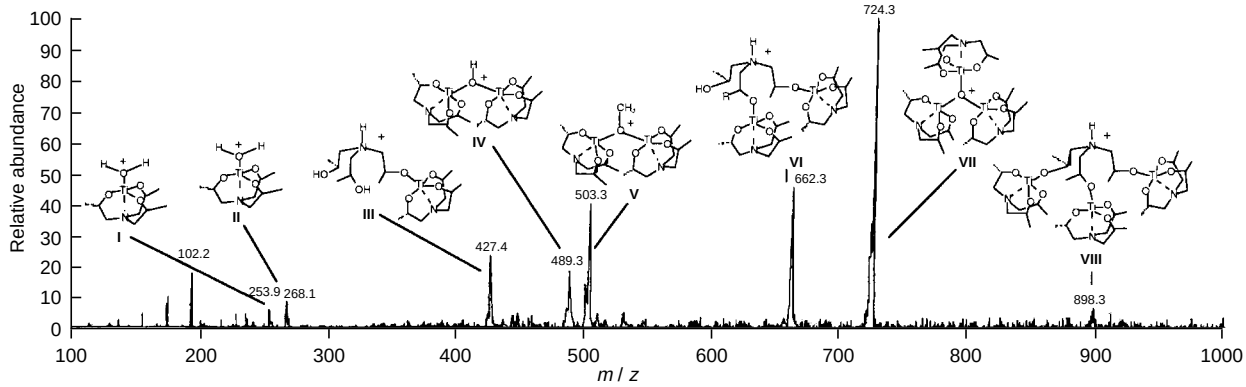



**Fig. 1** ESI mass spectrum of complex **2a** with peak assignments indicated

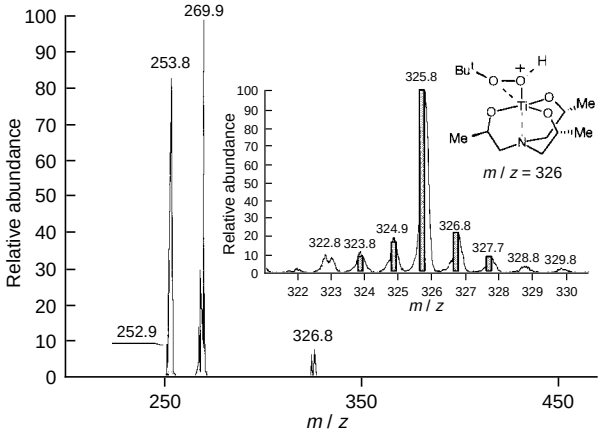



**Fig. 2** MS/MS fragment ions of the *m/z* 326 peak after collision induced dissociation. Calculated and observed isotope distribution patterns are shown in the inset.

monomeric character of the peroxometal complex **3a**.[8]†† Its fragmentation pattern (CID) occurs through the breaking of the O–Bu$^t$ bond (*m/z* 270, $M^+ - C_4H_8$) and of the peroxidic O–O bond yielding the water adduct, ion **I** (*m/z* 254, $M^+ - C_4H_8O$). The latter mode of decomposition is consistent with the proposed O–O bond scission during catalytic sulfoxidation.

ESIMS allowed also the characterization of the achiral peroxometal complex **3c** (*m/z* 284),‡‡ which, under the conditions employed, appears as a monomeric species.[6]

In conclusion, ESIMS allowed us to confirm the identity of the chiral peroxidic intermediate **3a** and that of the achiral analogue **3c**, both of which are monomeric complexes. Moreover, titanium(IV) aggregates with ligand-controlled architecture were identified, which react with *tert*-butylhydroperoxide yielding **3**. The fact that several highly labile and reactive metal complexes survive the conditions of the electrospray experiments bodes well for the extension of this approach to other early transition-metal alkoxide catalysts.

Grateful thanks are due to Dr Mahmoud Hamdan, Glaxo Wellcome, Verona, Italy, for useful discussions. Financial supports by 'Progetto Strategico: Tecnologie Chimiche Innovative' of CNR, MURST and INTAS Association (grant 94-1515) are gratefully acknowledged.

## Footnotes

* E-mail: Giulia@pdchor.unipd.it

† *Standard conditions*: Finnigan MAT LCQ ESI mass spectrometer with upper mass limit of *m/z ca*. 1850; direct infusion *via* a syringe pump; sample concentration = 0.5 μmol ml$^{-1}$; flow rate = 8 μl min$^{-1}$; nebulizing gas, $N_2$; spray voltage = 4 kV; capillary voltage = 25 V; capillary temperature = 80 °C.

‡ For complex (*S*,*S*,*S*)-**2a** see ref. 7; (*R*,*R*,*R*)-**2b**: $^1$H NMR ($CDCl_3$) δ 1.43 (6 H, dd, *J* 6.1, 1.7 Hz), 3.25 (3 H, dd, 12.4, 4.4 Hz), 3.32 (3 H, dd, 12.4, 10.5 Hz), 4.74 (1 H, spt, *J* 6.1 Hz), 5.87 (3 H, dd, *J* 10.5, 4.4 Hz), 7.24–7.39 (15 H, m).

§ For complex **2b** resonances appear at δ 3.54 (t, $CH_2$, *J* 11.3 Hz) and 6.02 (d, CH, *J* 11.3 Hz). A slight excess of ligand **1** strongly promotes the displacement of the isopropoxide group. When 2 equiv. of ligand **1a** are added to the *in situ* formed complex **2a**, 80% of the isopropoxide ligand is displaced.

¶ In the enantioselective sulfoxidation protocol, the active titanium(IV) peroxo complex **3** is normally generated from **4**, due to the higher reactivity (absence of Pr$^i$OH) and to the practical advantage in handling. **4b**: $^1$H NMR ($CDCl_3$) δ, 3.29 (6 H, br), 5.95 (3 H, br), 7.16–7.51 (15 H, m).

‖ Selected MS/MS spectra and isotopic distributions: **III**: *m/z* (%) 427 ($M^+$, 100), 409 ($M^+ - H_2O$, 10), 383 ($M^+$ − MeCHO, 22), 236 ($M^+$ − **1a**, 16), 174 (**1a** − $H_2O$, 80). Isotopic distribution (%) (exptl., theory), 425 (11, 11), 426 (12, 12), 427 (100, 100), 428 (23, 25), 429 (9, 14). **VI**: *m/z* (%) 662 ($M^+$, 29), 644 ($M^+ - H_2O$, 3), 489 (**IV**, 13), 409 [$M^+$ − Ti($CH_2CHMeO)_3$ − OH, 100]. Isotopic distribution (%) (exptl., theory): 660 (21, 17), 661 (24, 24), 662 (100, 100), 663 (45, 38), 664 (25, 21), 665 (6, 5). **VIII**: *m/z* (%): 897 ($M^+$, 8), 644 [$M^+$ − Ti($CH_2CHMeO)_3$ − OH, 18], 489 ($M^+$, **IV**, 4), 409 [$M^+$ − 2Ti($CH_2CHMeO)_3$ − O, 100]. Isotopic distribution (%) (exptl., theory): 895 (18, 16), 896 (29, 30), 897 (100, 100), 898 (64, 60), 899 (35, 33), 900 (13, 13).

** **4b**: 440 (**I′**), 454 (**II′**), 799 (**III′**), 861 (**IV′**), 875 (**V′**), 1220 (**VI′**), 1282 (**VII′**), 1641 (**VIII′**), **4c**: 212 (**I″**), 226 (**II″**), 343 (**III″**), 473 (**V″**), 536 (**VI″**), 729 (**VIII″**).

†† Isotopic distribution (%): 323 (11), 324 (12), 325 (19), 326 (100), 327 (22), 328 (9).

‡‡ CID for peak at *m/z* 284, 228 ($M^+ - C_4H_8$), 212 (**I″**).

## References

1 I. Ojima, *Catalytic Asymmetric Synthesis*, VCH, New York, 1993.
2 Y. Gao, R. M. Hanson, J. M. Klunder, S. Y. Ko, H. Masamune and K. B. Sharpless, *J. Am. Chem. Soc.*, 1987, **109**, 5765.
3 F. Di Furia, G. Modena and R. Seraglia, *Synthesis*, 1984, 325; P. Pitchen, E. Dunach, M. N. Deshmukh and H. B. Kagan, *J. Am. Chem. Soc.*, 1984, **106**, 8188; N. Komatsu, M. Hashizume, T. Sugita and S. Uemura, *J. Org. Chem.*, 1993, **58**, 4529.
4 D. C. Bradley, R. C. Mehrota and D. P. Gaur, *Metal Alkoxides*, Academic Press, London, 1978.
5 R. A. Johnson and K. B. Sharpless, in ref. 1, ch. 4.4.
6 G. Boche, K. Möbus, K. Harms and M. Marsh, *J. Am. Chem. Soc.*, 1996, **118**, 2770.
7 W. A. Nugent and R. L. Harlow, *J. Am. Chem. Soc.*, 1994, **116**, 6142 and references therein.
8 F. Di Furia, G. Licini, G. Modena, R. Motterle and W. A. Nugent, *J. Org. Chem.*, 1996, **61**, 5175.
9 R. Colton, A. D'Agostino and J. C. Traeger, *Mass Spectrom. Rev.*, 1995, **14**, 79 and references therein.
10 M. Romero, R. Ziessel, A. Dupont-Gervais and A. Van Dorsselaer, *Chem. Commun.*, 1996, 551 and references therein.
11 A. A. Naiini, S. L. Ringrose, R. A. Jacobson and J. G. Verkade, *Inorg. Chem.*, 1993, **32**, 1290.
12 For iron peroxo complexes see: M. Lubben, A. Meetsma, E. C. Wilkinson, B. Feringa and L. Que, Jr., *Angew. Chem., Int. Ed. Engl.*, 1995, **34**, 1512; J. W. Sam, X.-J. Tang and J. Peisach, *J. Am. Chem. Soc.*, 1996, **116**, 5250.

*Received in Cambridge, UK, 21st February 1997; Com. 7/01227F*

# Stepwise oxidation of a μ-alkylidene palladium–tungsten compound

**Philippus F. Engel,[a] Michel Pfeffer,*[a] André De Cian[b] and Jean Fischer[b]**

[a] *Laboratoire de Synthèses Métallo-induites, Université Louis Pasteur, 4, rue Blaise Pascal, F-67070 Strasbourg Cedex, France*
[b] *Laboratoire de Cristallochimie (URA 424 du CNRS), Université Louis Pasteur, 4, rue Blaise Pascal, F-67070 Strasbourg Cedex, France*

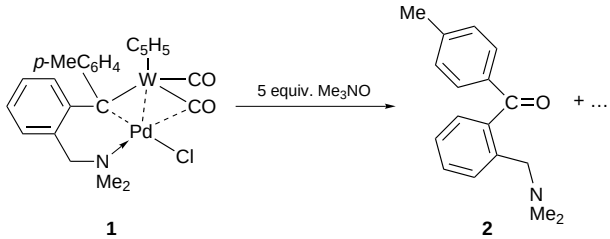
**The μ-alkylidene unit of a tungsten–palladium compound is oxidized to the corresponding ketone in the presence of an excess of $Me_3NO$, whereas with 2–4 equiv., mono- and di-oxotungsten derivatives, which are likely intermediates in the formation of the ketone, are instead obtained.**

We have recently established a novel synthetic route to μ-alkylidene complexes of palladium and tungsten of molybdenum, in which the carbon atom bridging the two metals has been synthesized through the formal insertion of tungsta- or molybda-alkylidyne units into the Pd–C bonds of cyclopalladated compounds.[1] The structural and spectral data of the complexes we have reported, make it difficult to rationalise the exact nature of the Pd(μ-C)W or Pd(μ-C)Mo bonds, or to assess the importance of the metal–metal interaction. We thus hoped that reactivity studies will allow us to gain a better understanding of the structure of these species. So far, despite the large number of related bimetallic compounds reported in the literature,[2] very few reactivity studies have been performed with them.[3] It is thus of real interest to evaluate their potential in synthetic chemistry.

We have shown recently that whereas the terminal carbonyl ligand can be readily displaced by *tert*-butyl isocyanide,[4] the other carbonyl group of these compounds, which is semibridging to the palladium atom, seemed to be much more strongly bonded to the tungsten or molybdenum atom. In order to labilize this CO ligand with the hope to obtain more reactive species, we treated the palladium–tungsten derivative with an excess of trimethylamine oxide (TAO). Thus, addition of TAO to a solution of complex **1** in dichloromethane induces $CO_2$ evolution and a change from orange to black–yellow. A mixture of several products can be obtained, depending on the quantity of TAO employed.

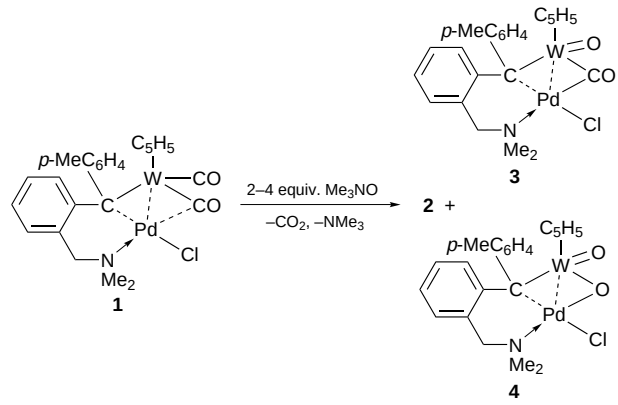
When ⩾5 equiv. of TAO was used, the reaction is most selective, and from the black residue obtained, the ketone O=C(4-$MeC_6H_4$)(2-$C_6H_4CH_2NMe_2$) **2** can be extracted as an orange–yellow oil in 77% yield (Scheme 1).†

Thus, the reaction between **1** and an excess of TAO leads to a breakdown of the μ-alkylidene geometry and the bridging carbene fragment is oxidized and liberated as a ketone. The remaining metal complexes have not yet been characterized. However further information on the reaction pathway that is followed by the reaction has been obtained by analysis of the reaction products of incomplete reactions. As noted above, the reaction between **1** and TAO usually leads to a mixture of products, in which the ketone **2** may be found. When < 5 equiv. of TAO is used in the reaction with **1** in dichloromethane, a similar gas evolution and colour change are observed, but novel metal complexes whose structures are related to that of **1** can be isolated.




**Scheme 1**

2–4 Equiv. of TAO react with **1** in dichloromethane to afford one major product, which has been identified as the novel oxo complex [{(η-$C_5H_5$)(O)(μ-CO)W}{μ-C(4-$MeC_6H_4$)(2-$C_6H_4CH_2NMe_2$)PdCl] **3** in low yield (21%, Scheme 2).† The structure of **3** has been established by an X-ray diffraction study,‡ and an ORTEP diagram is shown in Fig. 1. A complex similar to **3** which, however, was only obtained in trace amounts




**Scheme 2**

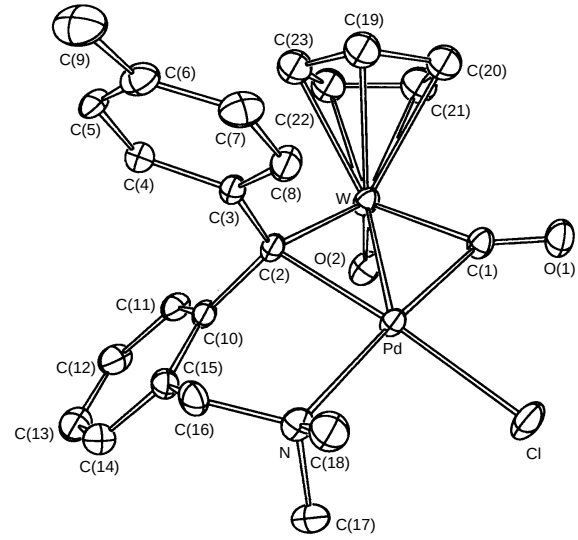



**Fig. 1** ORTEP diagram of **3** with atom labelling scheme (50% ellipsoids). Hydrogen atoms have been omitted for clarity. Bond distances (Å) and angles (°): Pd–Cl 2.409(2), Pd–C(2) 2.142(6), Pd–C(1) 2.009(7), Pd–N 2.268(6), Pd···W 2.6939(6), W–C(1) 2.075(7), W–O(2) 1.694(5), W–C(2) 2.074(6), Cl–Pd–C(2) 175.9(2), C(1)–Pd–C(2) 96.6(3), N–Pd–C(1) 174.2(2), C(2)–W–O(2) 107.2(2), C(1)–W–O(2) 101.2(3), W–C(1)–O(1) 146.6(6), Pd–C(1)–O(1) 130.8(5).

could be separated from **3** by column chromatography, and has also been characterized by an X-ray structure analysis, as the dioxo complex [{(η-$C_5H_5$)(O)(μ-O)W}{μ-C(4-$MeC_6H_4$)(2-$C_6H_4CH_2NMe_2$)}PdCl] **4** (Scheme 2). Attempts to obtain complex **4** in better yields have not been successful so far, and as a result, complex **4** has only been partially characterized.† An X-ray diffraction study‡ could however be carried out on a crystal of complex **4**, and the ORTEP diagram is shown in Fig. 2, together with selected interatomic distances and angles.

The most remarkable feature of the structures of compounds **3** and **4** is their similarity, as far as the interactions within the palladium–tungsten–alkylidene units are concerned, with those of compounds analogous to the starting material **1**, or of the related compound obtained with *tert*-butyl isocyanide[4] even though in these derivatives many fragments of the molecules are different. Thus, in both compounds **3** and **4**, the palladium atom is in close interaction with three atoms of the tungstaalkylidene unit, *i.e.* the tungsten atom, the alkylidene carbon and the C atom of the carbonyl C(1)O(1) or the O(1) atom in **3** and **4**, respectively. The W–C(2) and W–C(1) bond lengths in **3** and **4**, respectively, are close to that expected for tungsten–alkylidene units; in fact they are notably shorter than the corresponding distance in a compound analogous to **1** [2.158(4) Å],[1] in [$(OC)_5W{=}CPh_2$] [2.14(2) Å][5] or in a dimetallacyclopropene compound [$(CO)_5W$(μ-C(OMe)Ph}$Pt(PMe_3)_2$] [2.48(1) Å].[6] The tungsten–oxygen distances are in accord for W=O bonds.[7]

The behaviour of compound **1** towards a moderate oxidant such as $Me_3NO$ leading to a ketone is akin to that of 'classical' monometallic Fischer-type metallacarbenes.[8] It appears thus that compounds related to **1** are most likely to be the result of the interaction of an anionic tungsten–carbene unit with a cationic Pd centre. This would lead to a bonding mode involving a covalent bond between Pd and C(1) in **3** and between Pd and O(1) in **4** together with a $\eta^2$-interaction between the W=C unit and Pd in both compounds which accounts *inter alia* for the short distances found between Pd and W in both compounds. The formation of **3** and **4** establish that the tungsten atom has been oxidised in a stepwise manner by TAO concomitantly with the oxidation of the CO groups to $CO_2$, prior to the oxidation of the alkylidene unit. Somewhat related oxoalkylidene–tungsten complexes have been synthesised recently following completely different routes.[9] The major information that can be drawn from this study is that it demonstrates that not only Fischer-type metallaalkylidene complexes interact with $Pd^{II}$ as in compounds of type **1**, but this can also be encountered with molybda- or tungsta-alkylidenes in which the metal has a +VI oxidation state as in Schrock-type carbene complexes. Further work which makes use of this result is under way.[10]

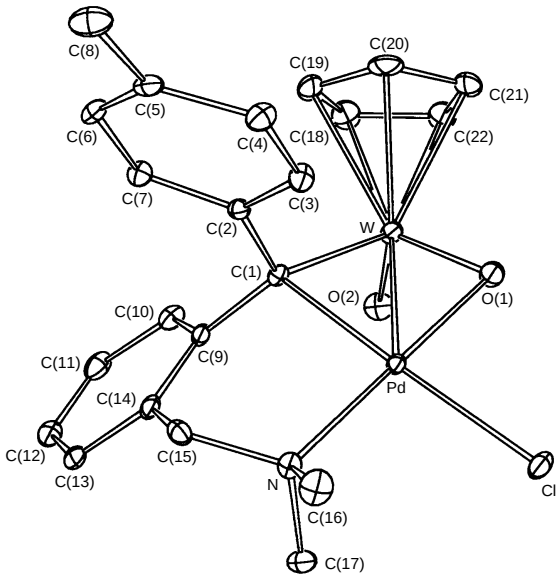



**Fig. 2** ORTEP diagram of **4** with atom labelling scheme (50% ellipsoids). Hydrogen atoms have been omitted for clarity. Bond distances (Å) and angles (°): Pd–Cl 2.395(1), Pd–N 2.121(4), Pd–C(1) 2.125(4), Pd···W 2.6753(4), Pd–O(1) 2.037(3), W–C(1) 2.100(4), W–O(1) 1.817(4), W–O(2) 1.712(4), N–Pd–O(1) 179.6(1), C(1)–Pd–O(1) 90.2(2), C(1)–W–O(1) 97.4(2), C(1)–W–O(2), O(1)–W–O(2) 107.9(2), W–O(1)–Pd 87.7(1).

## Footnotes

* E-mail: pfeffer@chimie.u-strasbg.fr

† *Selected analytical data*: **2**: $C_{17}H_{19}NO$. Mass spectrum: *m/z* 253 ($[M]^+$, 43%); $^1$H NMR ($CDCl_3$), δ 7.39–7.29 (m, 4 H, dmba), 7.64, 7.22 (AB pattern, 4 H, $^3J_{HH}$ 8.1 Hz, 4-tol), 3.39 (s, 2 H, $NCH_2$), 2.41 (s, 3 H, 4-Me), 1.94 (s, 6 H, $NMe_2$); $^{13}$C NMR (300 MHz, $CDCl_3$), δ 196.9 (C=O), 142.8, 139.7, 139.1, 135.6 ($C_{quat}$ arom.), 129.4, 129.2, 128.9, 128.8, 128.4, 126.9 (CH arom.), 61.1 ($CH_2$), 44.4 ($NMe_2$), 21.7 (Me); IR $\nu_{CO}$, 1652 $cm^{-1}$.

**3**: $^1$H NMR ($CDCl_3$): δ 8.27 (d, 1 H, $^2J_{HH}$ 7.5 Hz, dmba), 7.50–7.42 (m, 1 H, dmba), 7.34–7.19 (m, 2 H, dmba), 6.90 (br, 2 H, 4-tol), 6.57 (br, 2 H, 4-tol), 5.70 (s, 5 H, $C_5H_5$), 3.07, 2.79 (AB pattern, 2 H, $^2J_{HH}$ 12.4 Hz, $NCH_2$), 2.70, 2.36, 2.26 (3s, 9 H, $NMe_2$ and 4-Me); $^{13}$C NMR ($CDCl_3$), δ 204.8 (CO), 152.6, 152.3, 138.5, 137.1, 134.6, 130.6, 128.4, 127.9 (C arom.), 104.4 ($C_5H_5$), 64.5 (C arom. $CH_2$), 49.9, 47.0 ($NMe_2$), 20.7 (4-Me); IR (KBr), $\nu_{CO}$ 1830, $\nu_{W=O}$ 958 $cm^{-1}$.

**4**: $^1$H NMR ($CDCl_3$), δ 7.63 (d, 1 H arom., $^3J_{HH}$ 7.7 Hz), 7.55 (d, 1 H arom., $^3J_{HH}$ 8.0 Hz), 7.42–7.34 (m, 1 H arom.), 7.29–7.13 (m, 3 H arom.), 6.99, 6.54 (AB pattern, 2 H, $^3J_{HH}$ 8.0 Hz, 4-tol), 6.16 (s, 5 H, $C_5H_5$), 3.15, 2.68 (AB pattern, 2 H, $^2J_{HH}$ 12.2 Hz, $NCH_2$), 2.98, 2.56 (2 s, 6 H, $NMe_2$), 2.33 (s, 3 H, 4-Me).

‡ *Crystal data*: **3**: $C_{23}H_{24}ClNO_2PdW$, $M$ = 672.16, monoclinic, space group $P2_1/c$, $a$ = 12.579(4), $b$ = 10.994(4), $c$ = 16.165(5) Å, β = 97.47(2)°, $U$ = 2216 Å$^3$, $Z$ = 4, $D_c$ = 2.01 g $cm^{-3}$; $R(F)$ = 0.025, [$Rw(F)$ = 0.031] using 2561 reflections with $I > 3\sigma(I)$.

**4**: $C_2H_{24}ClNO_2PdW$, $M$ = 660.15, monoclinic, space group $P2_1/c$, $a$ = 11.663(4), $b$ = 10.958(4), $c$ = 16.661(3) Å, β = 94.37(2)°, $U$ = 2123 Å$^3$, $Z$ = 4, $D_c$ = 2.07 g $cm^{-3}$; $R(F)$ = 0.023, [$Rw(F)$ = 0.047] using 3359 reflections with $I > 3\sigma(I)$.

Atomic coordinates, bond lengths and angles, and thermal parameters have been deposited at the Cambridge Crystallograpic Data Centre (CCDC). See Information for Authors, Issue No. 1. Any request to the CCDC for this material should quote the full literature citation and the reference number 182/419.

## References

1 P. F. Engel, M. Pfeffer and J. Fischer, *Organometallics*, 1994, **13**, 4751.
2 W. A. Herrmann, *Adv. Organomet. Chem.*, 1982, **20**, 159; *Pure Appl. Chem.*, 1982, **54**, 65.
3 J. E. Hahn, *Prog. Inorg. Chem.*, 1984, **31**, 205; J. C. Jeffery and M. J. Went, *Polyhedron*, 1988, **7**, 775.
4 A. Macchioni, P. Pregosin, P. E. Engel, S. Mecking, M. Pfeffer, J. C. Daran and J. Wassermann, *Organometallics*, 1995, **14**, 1637.
5 C. P. Casey, T. J. Burkhardt, C. A. Bunnell and J. C. Calabrese, *J. Am. Chem. Soc.*, 1977, **99**, 2127.
6 T. V. Ashworth, J. A. K. Howard, M. Laguna and F. G. A. Stone, *J. Chem. Soc., Dalton Trans.*, 1980, 1593.
7 P. Legzdins, S. T. Rettig and L. Sanchez, *Organometallics*, 1985, **4**, 1470.
8 K. H. Dötz, *Angew. Chem., Int. Ed. Engl.*, 1984, **23**, 587.
9 P. Legzdins, E. C. Phillips and L. Sanchez, *Organometallics*, 1989, **8**, 940.
10 P. Lohner and M. Pfeffer, to be published.

*Received in Cambridge, UK, 31st January 1997; Com. 7/00741H*

# Molecular materials from 1,3,2-dithiazolyls. Solid-state structures and magnetic properties of 2,3-naphthalene and quinoxaline derivatives

**Tosha M. Barclay,[a] A. Wallace Cordes,[a] Noel A. George,[b] Robert C. Haddon,[c] Richard T. Oakley,*[b] Thomas T. M. Palstra,[b] Gregory W. Patenaude,[b] Robert W. Reed,[b] John F. Richardson[b] and Hongzhou Zhang[b]**

[a] *Department of Chemistry and Biochemistry, University of Arkansas, Fayetteville, Arkansas 72701, USA*
[b] *Department of Chemistry and Biochemistry, University of Guelph, Guelph, Canada, Ontario N1G 2W1*
[c] *Bell Laboratories, Lucent Technologies, Murray Hill, New Jersey 07974, USA*

**In the solid state, at room temperature, the radicals 2,3-naphthalene-1,3,2-dithiazolyl (NDTA) and quinoxaline-1,3,2-dithiazolyl (QDTA) are not dimerized; discrete molecules of NDTA are packed in a herringbone fashion, while those of QDTA adopt a slipped π-stack motif; NDTA is essentially paramagnetic at ambient temperatures, with weak antiferromagnetism developing below 190 K; QDTA is diamagnetic at low temperature, but limited paramagnetism sets in above 120 K.**

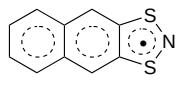
While derivatives of the 1,3,2-dithiazolyl ring (DTA) have been known for well over a decade,[1,2] relatively little is known of their structural and transport properties. In the solid state the 4,5-dicyano derivative forms the simple cofacial dimer.[3] The pyrazine-based compound (PDTA) also dimerizes cofacially,[4] but the dimers adopt a stacked dimer structure similar to that observed for many dithiadiazolyls.[5] Surprisingly, and despite its structural resemblance to PDTA, the benzo derivative (BDTA)[6] associates in a centrosymmetric manner and does not form π stacks. The trithiatriazapentalenyl radical (TTTA) represents a sharp contrast to the previous examples, in that dimerization is not observed.[7] Instead the crystal structure consists of evenly spaced slipped π stacks. Transport properties, however, have not been reported for this compound. In order to explore the architectural issues behind these diverse structural patterns we have examined the solid-state structures and transport properties of the 2,3-naphthalene- and quinoxaline-based 1,3,2-dithiazolyl radicals NDTA **1** and QDTA **2**.

The two radicals were prepared by standard methods. 2,3-Naphthalenedithiol[8] was oxidized with iodobenzene dichloride to give 2,3-naphthalene-bis(sulfenyl chloride), which was condensed with trimethylsilyl azide in $CH_2Cl_2$ solution to afford 2,3-naphthalene-1,3,2-dithiazolylium chloride. Reduction of this salt with triphenylantimony in acetonitrile afforded NDTA, which was separated by filtration and fractionally sublimed at 80–50 °C ($10^{-2}$ Torr) to give purple plates, mp 149–151 °C. QDTA was prepared by a modification of the literature procedure.[3] Black rod-like crystals of QDTA, mp 137–140 °C, were grown by fractional vacuum sublimation at 70–40 °C ($10^{-2}$ Torr).

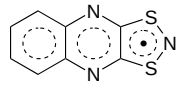
The crystal structure of NDTA† consists of discrete molecules of NDTA, with two molecules per asymmetric unit. The internal bond lengths of the two heterocyclic rings [mean *d*(S–N) = 1.645 Å, mean *d*(C–S) = 1.748 Å] are typical of those seen in dimeric derivatives[3,6] and indicative of the fact that dimerization effects minimal electronic reorganization. The crystal structure consists of antiparallel ribbons of radicals running in the *z* direction. Viewed down the *z* direction (Fig. 1) the packing pattern of the ribbons resembles the close-packed herringbone arrangement found many polycyclic aromatics,[9] *e.g.* naphthalene[10] and anthracene.[11] There is no dimerization of NDTA radicals, and the closest intermolecular S···S contacts ($d_1$–$d_5$) are well outside the van der Waals separation of 3.6 Å.[12]

The crystal structure of QDTA† also consists of undimerized radicals. Here too the internal bond lengths of the heterocyclic ring [mean *d*(S–N) = 1.649 Å, mean *d*(C–S) = 1.736 Å] are typical of those seen in simple dimers. As in the case of NDTA, the molecules lie in ribbon-like chains, but the packing of the ribbons (Fig. 2) takes on a slipped π-stack pattern similar to that observed for TTTA. Apart from intermolecular contacts associated with the cell repeat [3.7105(8) Å], there is only one S···S contact inside 4.0 Å ($d_1$) linking radicals in adjacent stacks.

The structural dichotomy observed between NDTA and QDTA is intriguing. The similarity of the NDTA structure to those of simple polycyclic aromatics suggests a similar cause.[9,13] Presumably, when the structure-making CH···ring interactions[14] which favour the herringbone arrangement are reduced by the replacement of peripheral CH groups by N atoms, as in QDTA, the preference for close-packing is diminished, and a slipped stack structure prevails. That dimerization does not occur, as it does in the smaller molecule PDTA, is probably a manifestation of a slightly weakened dimerization enthalpy coupled with the greater tendency for the




**1**




**2**

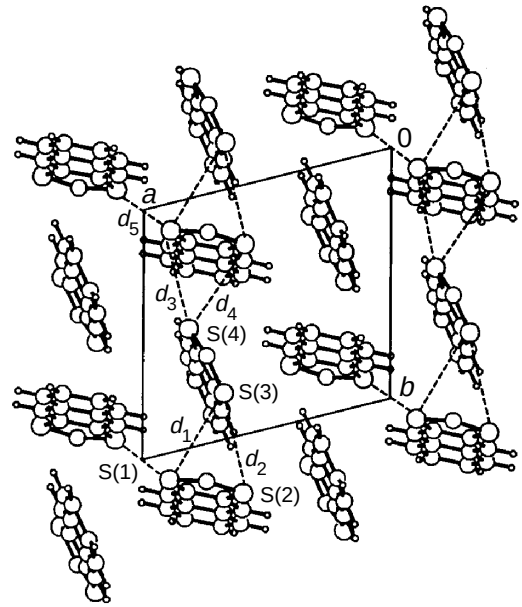



**Fig. 1** Herringbone packing of NDTA. Intermolecular S···S contacts are shown with dashed lines; $d_1$ = 3.869, $d_2$ = 3.868, $d_3$ = 3.821, $d_4$ = 3.863, $d_5$ = 3.602 Å.

crystal structure to be determined by general packing forces rather than local (intermolecular S···S) interactions.

The bulk magnetic susceptibilities of both NDTA and QDTA have been measured over the temperature range 5–400 K on a SQUID magnetometer; plots of $\chi$ *vs.* $T$ are shown in Fig. 3. Analysis of the susceptibility data for NDTA indicate that it is essentially paramagnetic above 200 K, with $\theta$ = 1.3 K and the fraction of the Curie spins per molecule, $f$ = 0.80 mol$^{-1}$. Below 200 K there is a phase transition to a more strongly antiferromagnetically coupled state with $\theta$ = 10.7 K and $f$ = 0.53 mol$^{-1}$. In QDTA the low-temperature susceptibility is consistent with a diamagnetic ground state, with $\chi_0 = -99 \times 10^{-6}$ emu mol$^{-1}$, $\theta = -0.1$ K and $f$ = 0.003 mol$^{-1}$. Above 120 K the susceptibility slowly rises and, at room temperature, $f$ is *ca.* 0.3 mol$^{-1}$. Pressed pellet measurements indicate room temperature conductivities of $< 10^{-6}$ S cm$^{-1}$ for both compounds.

The low conductivity of QDTA at room temperature is at first surprising, given the large fraction of unpaired spins and the fact that its evenly spaced π-stack structure nominally fulfils the prescription for a neutral π-radical conductor.[15] We conclude that, as in the case of stacked dithiadiazolyls,[5,16] the bandwidth associated with the half-filled energy band in QDTA is insufficient to overcome the large Coulombic barrier to charge transfer associated with the high electronegativity of the dithiazolyl ring. Accordingly the material is a Mott insulator.

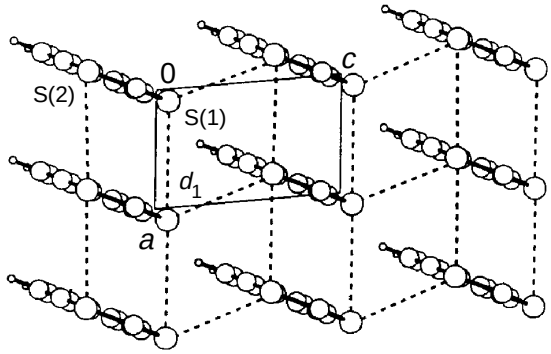



**Fig. 2** Slipped π-stack structure of QDTA. Intermolecular S···S contacts are shown with dashed lines; $d_1$ = 3.840 Å.

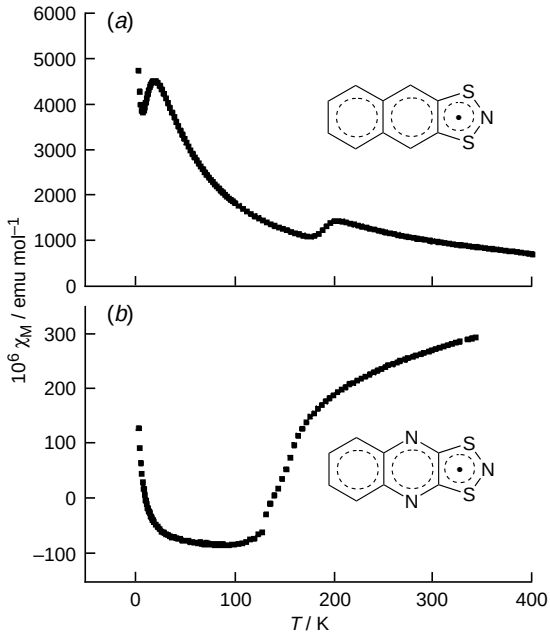



**Fig. 3** Magnetic susceptibility $\chi$ of NDTA (*a*) and QDTA (*b*), as a function of temperature

We thank the NSERC, the NSF/EPSCOR program and the State of Arkansas for financial support. T. M. B. acknowledges the Department of Education for a doctoral fellowship.

## Footnotes

* E-mail: oakley@chembio.uoguelph.ca

† *Crystal data* for NDTA and QDTA: data were collected (at 293 K) on an Enraf-Nonius CAD-4 automated diffractometer with graphite-monochromated Mo-K$\alpha$ radiation ($\lambda$ = 0.710 3 Å) using $\theta$–2$\theta$ scans to a $2\theta_{max}$ = 50°. The structures were solved by direct methods and refined by full-matrix least-squares analysis which minimized $\Sigma w(\Delta F)^2$.

NDTA: $C_{10}H_6NS_2$, $M$ = 204.28, triclinic, space group $P\bar{1}$, $a$ = 9.4516(18), $b$ = 9.5167(19), $c$ = 10.5397(13) Å, $\alpha$ = 76.911(13), $\beta$ = 86.139(12), $\gamma$ = 75.144(15)°, $U$ = 892.5(3) Å$^3$, $Z$ = 4, $D_c$ = 1.52 g cm$^{-3}$, $\mu$ = 0.52 mm$^{-1}$. 236 Parameters were refined using 1764 unique observed reflections [$I > 3\sigma(I)$] to give $R$ = 0.037 and $R_w$ = 0.058.

QDTA: $C_8H_4N_3S_2$, $M$ = 206.26, monoclinic, space group $P2_1$, $a$ = 3.7105(8), $b$ = 19.009(5), $c$ = 5.7864(9) Å, $\beta$ = 95.724(14)°, $U$ = 406.10(15) A$^3$, $Z$ = 2, $D_c$ = 1.69 g cm$^{-3}$, $\mu$ = 0.58 mm$^{-1}$. 117 Parameters were refined using 472 unique observed reflections [$I > 3\sigma(I)$] to give $R$ = 0.041 and $R_w$ = 0.056.

Atomic coordinates, bond lengths and angles, and thermal parameters have been deposited at the Cambridge Crystallographic Data Centre (CCDC). See Information for Authors, Issue No. 1. Any request to the CCDC for this material should quote the full literature citation and the reference number 182/415.

## References

1 K. F. Preston and L. H. Sutcliffe, *Magn. Reson. Chem.*, 1990, **28**, 189; Y.-L. Chung, S. A. Fairhurst, D. G. Gillies, K. F. Preston and L. H. Sutcliffe, *Magn. Reson. Chem.*, 1992, **30**, 666.
2 E. G. Awere, N. Burford, C. Mailer, J. Passmore, M. J. Schriver, P. S. White, A. J. Banister, H. Oberhammer and L. H. Sutcliffe, *J. Chem. Soc., Chem. Commun.*, 1987, 66; G. K. MacLean, J. Passmore, M. N. S. Rao, M. J. Schriver and P. S. White, *J. Chem. Soc., Dalton Trans.*, 1985, 1405; G. Wolmershäuser and G. Kraft, *Chem. Ber.*, 1989, **122**, 385; S. R. Harrison, R. S. Pilkington and L. H. Sutcliffe, *J. Chem. Soc., Faraday Trans. 1*, 1984, **80**, 669; S. A. Fairhurst, R. S. Pilkington and L. H. Sutcliffe, *J. Chem. Soc., Faraday Trans. 1*, 1983, **79**, 439; S. A. Fairhurst, R. S. Pilkington and L. H. Sutcliffe, *J. Chem. Soc., Faraday Trans. 1*, 1983, **79**, 925.
3 G. Wolmershäuser and G. Kraft, *Chem. Ber.*, 1990, **123**, 881.
4 G. Heckmann, R. Johann, G. Kraft and G. Wolmershäuser, *Synth. Met.*, 1991, **41**–**43**, 3287.
5 A. W. Cordes, R. C. Haddon and R. T. Oakley, in *The Chemistry of Inorganic Ring Systems*, ed. R. Steudel, Elsevier, Amsterdam, 1992, p. 295; A. W. Cordes, R. C. Haddon and R. T. Oakley, *Adv. Mater.*, 1994, **6**, 798.
6 E. G. Awere, N. Burford, R. C. Haddon, S. Parsons, J. Passmore, J. V. Waszczak and P. S. White, *Inorg. Chem.*, 1990, **29**, 4821; G. Wolmershäuser, M. Schnauber and T. Wilhelm, *J. Chem. Soc., Chem. Commun.*, 1984, 573.
7 G. Wolmershäuser and R. Johann, *Angew. Chem., Int. Ed. Engl.*, 1989, **28**, 920.
8 E. Block, V. Eswarakrishnan, M. Gernon, G. Ofori-Okai, C. Saha, K. Tang and J. Zunieta, *J. Am. Chem. Soc.*, 1989, **111**, 658.
9 A. Gavezzotti and G. R. Desiraju, *Acta Crystallogr., Sect. B*, 1988, **44**, 427.
10 J. D. Dunitz and C. P. Brock, *Acta Crystallogr., Sect. B*, 1982, **38**, 2218.
11 C. P. Brock and J. D. Dunitz, *Acta Crystallogr., Sect. B*, 1990, **46**, 795.
12 A. Bondi, *J. Phys. Chem.*, 1964, **68**, 441.
13 J. Bernstein, J. A. R. P. Sarma and A. Gavezzotti, *Chem. Phys. Lett.*, 1990, **174**, 361.
14 P. Hobza, H. L. Selzle and E. W. Schlag, *J. Am. Chem. Soc.*, 1994, **116**, 3500.
15 R. C. Haddon, *Nature*, 1975, **256**, 394; *Aust. J. Chem.*, 1975, **28**, 2343.
16 M. P. Andrews, A. W. Cordes, D. C. Douglass, R. M. Fleming, S. H. Glarum, R. C. Haddon, P. Marsh, R. T. Oakley, T. T. M. Palstra, L. F. Schneemeyer, G. W. Trucks, R. Tycko, J. V. Waszczak, K. M. Young and N. M. Zimmerman, *J. Am. Chem. Soc.*, 1991, **113**, 3559.

*Received in Columbia, MO, USA, 14th January 1997; Com. 7/00310B*

# Selective conversion of bromo oxirane into tetrahydropyranylacrylate by epoxide ring opening

**Munetaka Tokumasu, Asami Sasaoka, Ryukichi Takagi, Yoshikazu Hiraga and Katsuo Ohkata*†**

*Department of Chemistry, Faculty of Science, Hiroshima University, 1-3-1 Kagamiyama, Higashi-Hiroshima 739, Japan*

**In order to construct the tetrahydropyran ring of rhopaloic acid A and hippospongic acid A, the ring-expansion of methyl 2-bromomethyl-6,7-epoxyhept-2-enoate with various acids was studied; treatment of the bromo oxirane with Lewis acids ($TiBr_4$, $MgBr_2$ and $ZnBr_2$) afforded a tetrahydrofuran derivative as the major product, while reaction of the oxirane with silver salt ($AgNO_3$/$KPF_6$) gave a tetrahydropyran derivative as the major product.**

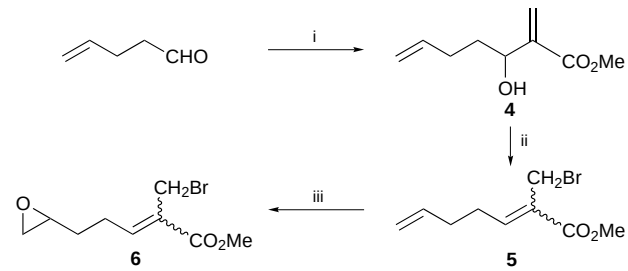
Marine sponges are known to produce structurally and bioactively interesting terpenoids such as rhopaloic acid A (**1**) and hippospongic acid A (**2**) which exhibit potent inhibition in gastrulation of starfish (*Asterina pectinifera*) embryos.[1,2] In particular, rhopaloic acid A, which was isolated from a marine sponge, *Rhopaloeides sp*., exhibited potent cytotoxicities *in vitro* against human myeloid cells, human leukemia cells, *etc*.[1] The interesting structure of these compounds consists of a hydrophilic pyranylacrylic acid moiety and a hydrophobic isoprenoid part. The interest in the structural features and potential of **1** and **2** and their analogues as probes of biological activities prompted us to undertake the selective synthesis of the pyranylacrylate moiety, 2-(1-methoxycarbonylvinyl)tetrahydropyran derivative **3**.

Our synthetic strategy consists of ring-expansion of oxiranes into tetrahydropyran rings followed by connection of various hydrophobic aliphatic chains (Scheme 1). The conversion of oxirane compounds to cyclic ethers is an interesting and useful synthetic methodology. Although extensive work has been reported on *endo*-cyclization of epoxy alcohols,[3] the ring expansion reaction of the epoxy group has hardly been investigated.[4] Recently, Murai and co-workers reported a method for the synthesis of the tetrahydropyran ring by the selective opening of the oxirane ring without directing groups by utilizing the epoxy group as a nucleophile.[4b] Here we describe the selective expansion of the oxirane ring into the tetrahydropyran ring along with simultaneous formation of an acrylate moiety.

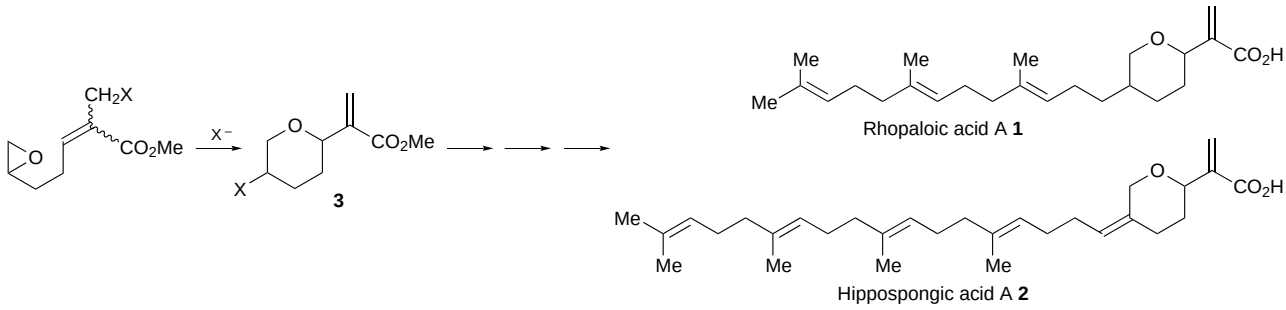
Baylis–Hillman reaction of pent-4-enal with methyl acrylate afforded the corresponding ester **4** in 79% yield. Bromination of **4** with $CBr_4$–$PPh_3$ gave bromo ester **5** as a 1 : 1 mixture of geometric isomers in 52% yield. Epoxidation of **5** with MCPBA furnished epoxy bromo ester **6** in 85% yield (Scheme 2).

Treatment of **6** with various acids afforded ring expansion products (tetrahydropyran and tetrahydrofuran derivatives **7a**–**c** and **8a**–**c**) and ring-opened products (**9a**,**b** and **10a**,**b**), Scheme 3 and Table 1. The product distribution was dependent upon the ring-opening reagents. Reaction of **6** (*E*/*Z*, 1 : 1 mixture) with 47% aqueous HBr in THF afforded a mixture of ring-opened products **9b** (11%) and **10b** (57%). Treatment of **6** with $TiCl_4$ gave the analogous chlorides **9a** (47%) and **10a** (44%), while reaction of **6** with $TiBr_4$ gave **8b** (46%), **9b** (14%) and **10b** (32%). Reactions of **6** with $MgBr_2$ and $ZnBr_2$ gave tetrahydrofuran derivative **8b** as a mixture of *cis*/*trans* isomers in 52 and 64% yields, respectively. The *cis*/*trans* ratio of the furan derivatives varied slightly depending on the Lewis acid used.

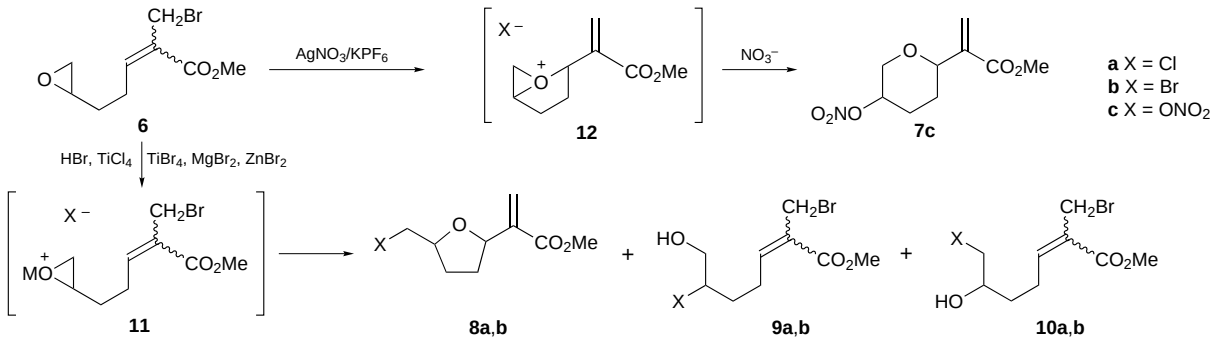
Since proton acid (HBr) and Lewis acids such as $TiCl_4$, $TiBr_4$, $MgBr_2$ and $ZnBr_2$ are considered to be oxophilic, it is reasonable to assume that the acids reacted with the epoxy group to give the intermediate **11**, followed by inter- or intramolecular nucleophilic attack to give **8a**,**b**, **9a**,**b** and **10a**,**b** (Scheme 3). On the other hand, the silver salt, which is known to have a high halide affinity, might be expected to eliminate bromide ion together with concomitant opening of the epoxy group in **6**. In fact, treatment of **6** with a mixed reagent ($AgNO_3$–$KPF_6$) in $Et_2O$–$H_2O$ (100 : 1) selectively gave tetrahydropyran derivative **7c** (11%; *cis*/*trans* = 0.4 : 1). The use of $CH_2Cl_2$ as solvent resulted in an increase in yield. The relative stereochemistry of the diastereoisomers was determined by the vicinal coupling patterns.‡§ In the silver-promoted reaction, the




**Scheme 2** *Reagents and conditions*: i, methyl acrylate, DABCO, room temp., 2 weeks, 79%; ii, $PPh_3$, $CBr_4$, $CH_2Cl_2$, room temp., 30 min, 52%; iii, MCPBA, $CH_2Cl_2$, room temp., 48 h, 85%




**Scheme 1**




**Scheme 3**

**Table 1** Reaction of bromo epoxide **6** with HBr and Lewis acids

| | | | | | Product yield (%) (*cis*/*trans* ratio)[a] | | | |
|---|---|---|---|---|---|---|---|---|
| Entry | Reagent | Solvent | Conditions | X | **7** | **8** | **9** | **10** |
| 1 | 47% aq HBr | THF | 25 °C, 6 h | Br | 0 | 0 | 11 | 57 |
| 2 | $TiCl_4$ | $CH_2Cl_2$ | −78 °C, 6 h/25 °C, 6 h | Cl | 0 | 0 | 47 | 44 |
| 3 | $TiBr_4$ | $CH_2Cl_2$ | −78 °C, 3 h/25 °C, 10 h | Br | 0 | 46 (5 : 1) | 14 | 32 |
| 4 | $MgBr_2$ | $Et_2O$ | −78 °C, 3 h/25 °C, 8 h | Br | 0 | 52 (1 : 1) | 12 | 15 |
| 5 | $ZnBr_2$ | $CH_2Cl_2$ | −78 °C, 6 h/25 °C, 6 h | Br | 0 | 64 (0.4 : 1) | 10 | 9 |
| 6 | $AgNO_3/KPF_6$ | $Et_2O$–$H_2O$ (100 : 1) | 25 °C, 18 h | $ONO_2$ | 11 (0.4 : 1) | 0 | 0 | 0 |
| 7 | $AgNO_3/KPF_6$ | $CH_2Cl_2$ | 25 °C, 6 h | $ONO_2$ | 56 (0.5 : 1) | 0 | 0 | 0 |

[a] The *cis*/*trans* ratio was determined by $^1$H NMR spectroscopy.

bridged oxonium ion **12** can be considered to form in the initial step by the intramolecular nucleophilic attack of the epoxy group. Then, the *endo*-attack to the intermediate **12** by nucleophile ($NO_3^-$) would produce 2-tetrahydropyranylacrylate derivative **7c**.[4–6]

The synthetic methodology shown above could be applied to synthesis of not only rhopaloic acid A (**1**), hippospongic acid A (**2**) and their analogues, but also to other natural products containing 5- and 6-membered oxygen heterocycles.[3]

NMR and MS measurements were made using JEOL GSX-270 and SX-102A spectrometers, respectively, at the Instrument Center for Chemical Analysis, Hiroshima University.

## Footnotes

† E-mail: ohkata@alpha01.sci.hiroshima-u.ac.jp

‡ Typical experimental procedure: to a suspension of $AgNO_3$ (70 mg, 0.4 mmol) and $KPF_6$ (80 mg, 0.4 mmol) in $CH_2Cl_2$ (10 ml) was added **6** (10 mg, 0.04 mmol). After stirring for 6 h at room temperature, the reaction mixture was filtered. The filtrate was poured into 5% aq. $NaHCO_3$ and extracted with $CH_2Cl_2$. The extracts were dried and evaporated and the residue was then purified by preparative TLC on silica gel (EtOAc–hexane, 3 : 7 v/v). Each geometric isomer, *trans*-**7c** and *cis*-**7c**, was obtained by recycle HPLC [Japan Analytical Industry Co., Ltd., JAIGEL-H ($CHCl_3$)].

All new compounds were fully characterized by $^1$H NMR spectroscopy and gave satisfactory high resolution mass spectra. Correct elemental analyses were also obtained for selected compounds. *Selected spectroscopic data* for *trans*-**7c**: ν(neat)/cm$^{-1}$ 1717 ($CO_2Me$), 1625, 1277 ($NO_2$); $\delta_H$(270 MHz, $CDCl_3$) 6.31 (dd, *J* 1.5, 1.0, 1 H), 5.98 (t, *J* 1.5, 1 H), 5.00 (m, 1 H), 4.29 (ddd, *J* 13.2, 2.5, 2.0, 1 H), 4.28 (dddd, *J* 9.3, 2.0, 1.5, 1.0, 1 H), 3.80 (dd, *J* 13.2, 1.5, 1 H), 3.77 (s, 3 H), 2.25-2.15 (m, 1 H), 2.09–1.85 (m, 2 H), 1.66–1.51 (m, 1 H); $\delta_C$(270 MHz, $CDCl_3$) 166.1, 140.9, 124.0, 78.0, 75.4, 74.3, 51.8, 31.8, 27.8 (HRMS: found, 185.0815 [M − $NO_2$]$^+$. Calc. for $C_9H_{13}O_4$, 185.0814). For *cis*-**7c**: ν(neat)/cm$^{-1}$ 1720 ($CO_2Me$), 1637, 1280 ($NO_2$); $\delta_H$(270 MHz, $CDCl_3$) 6.25 (t, *J* 1.5, 1 H), 5.94 (dd, *J* 1.5, 1.0, 1 H), 4.75 (tdd, *J* 6.8, 1.5, 1.0, 1 H), 4.61 (dd, *J* 11.7, 3.9, 1 H), 4.50 (dd, *J* 11.7, 5.9, 1 H), 4.29 (m, 1 H), 3.77 (s, 3 H), 2.41–2.31 (m, 1 H), 2.15–2.05 (m, 1 H), 1.81–1.67 (m, 2 H); $\delta_C$(270 MHz, $CDCl_3$) 166.0, 140.6, 125.3, 76.1, 74.9, 68.2, 51.8, 26.8, 26.3 (HRMS: found, 185.0820 [M − $NO_2$]$^+$. Calc. for $C_9H_{13}O_4$, 185.0814).

§ It is considered that the *cis* isomer exists as a nearly equimolar mixture of two indistinguishable conformers, whereas the *trans* isomer consists of two unequally populated conformers, the predominant e,e conformer and the much less abundant a,a conformer which has axial vinyl and nitro groups. The methine proton at C-2 of the tetrahydropyran ring shows a distinct difference in pattern between *cis*- and *trans*-**7c**. The axial disposition of a methine proton of *trans*-**7c** (δ 4.28) is clearly indicated by its coupling constants, which consist of an axial–axial (*J* 9.3), an axial–equatorial (*J* 2.0) and two allyl $^4J$ couplings (*J* 1.5 and 1.0). On the other hand, the coupling constants of the methine proton of *cis*-**7c** (δ 4.75) consist of an averaged vicinal (t, *J* 6.8) and two allyl $^4J$ couplings (*J* 1.5 and 1.0) since the tetrahydropyran ring of *cis*-**7c** is more flexible compared with that of *trans*-**7c**.

## References


1 S. Ohta, M. Uno, M. Yoshimura, Y. Hiraga and S. Ikegami, *Tetrahedron Lett.*, 1996, **37**, 2265.

2 S. Ohta, M. Uno, M. Tokumasu, Y. Hiraga and S. Ikegami, *Tetrahedron Lett.*, 1996, **37**, 7765.

3 W. C. Still and A. G. Romero, *J. Am. Chem. Soc.*, 1986, **108**, 2105; S. L. Schreiber, T. Sammakia, B. Hulin and G. Schulte, *J. Am. Chem. Soc.*, 1986, **108**, 2106; S. T. Russel, J. A. Robinson and D. J. Williams, *J. Chem. Soc., Chem. Commun.*, 1987, 351; K. C. Nicolaou, C. V. C. Prasad, P. K. Somers and C.-K. Hwang, *J. Am. Chem. Soc.*, 1989, **111**, 5330; K. C. Nicolaou, C. V. C. Prasad, P. K. Somers and C.-K. Hwang, *J. Am. Chem. Soc.*, 1989, **111**, 5335; T. Suzuki, O. Sato and M. Hirama, *Tetrahedron Lett.*, 1990, **31**, 4747; T. Hudlicky and G. Barbieri, *J. Org. Chem.*, 1991, **56**, 4598; I. Paterson, R. D. Tillyer and J. B. Smaill, *Tetrahedron Lett.*, 1993, **34**, 7137; C. Mukai, Y. Sugimoto, Y. Ikeda and M. Hanaoka, *Tetrahedron Lett.*, 1994, **35**, 2183.

4 (*a*) H. G. Richey, Jr. and D. V. Kinsman, *Tetrahedron Lett.*, 1969, 2505; (*b*) N. Hayashi, K. Fujiwara and A. Murai, *Chem. Lett.*, 1996, 341; N. Hayashi, K. Fujiwara and A. Murai, *Tetrahedron Lett.*, 1996, **37**, 6173.

5 L. A. Paquette and M. K. Scott, *J. Am. Chem. Soc.*, 1972, **94**, 6760.

6 T. Nakata, G. Schmid, B. Vranesic, M. Okigawa, T. Smith- Palmer and Y. Kishi, *J. Am. Chem. Soc.*, 1978, **100**, 2933; F. David, *J. Org. Chem.*, 1981, **46**, 3512; E. Alvarez, M. T. Díaz, R. Pérez, J. L. Ravelo, A. Regueiro, J. A. Vera, D. Zurita and J. D. Martín, *J. Org. Chem.*, 1994, **59**, 2848; T. Nakata, S. Nomura and H. Matsukura, *Tetrahedron Lett.*, 1996, **37**, 213; T. Nakata, S. Nomura, H. Matsukura and M. Morimoto, *Tetrahedron Lett.*, 1996, **37**, 217.



*Received in Cambridge, UK, 4th February 1997; Com. 7/00788D*

# Trimethylchlorosilane: a novel activating reagent in nucleotide synthesis *via* the phosphoramidite route

**Wojciech Dabkowski,[a] Izabela Tworowska,[a] Jan Michalski*[a] and Friedrich Cramer[b]**

[a] *Centre of Molecular and Macromolecular Studies, Polish Academy of Science, 90-363 Lódź, Sienkiewicza 112, Poland*
[b] *Max-Planck-Institut für experimentelle Medizin, 3400 Göttingen, Hermann-Rein Strasse 3, Germany*

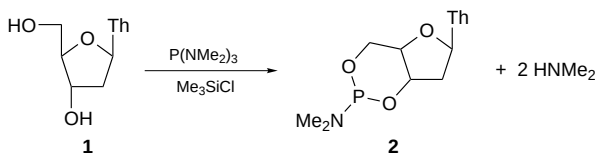
**Trimethylchlorosilane (TMSCl) is a remarkably efficient activator in the reaction of phosphorus(III) amides with nucleosides to give phosphorus(III) esters in excellent yield.**

Phosphoramidites are among the most important reagents in the synthesis of phosphates of biological interest by the 'phosphite approach'.[1] Tetrazole, tetrazole salts with amines and structural analogues of this heterocycle are generally used as activators of the reaction between alcohols and phosphoramidites.[2] Tetrazole, the most widely employed activator, must often be used in excess and be of high purity, which involves hazardous sublimation. Other activators like amine hydrochlorides[3] and acyl chlorides that act *via* intermediate formation of phosphorchloridites[4] have been used only occasionally.

In our recent studies on the synthesis of modified nuclotides we were confronted with the challenge of finding an alternative mode of activation without using tetrazole or similar compounds. Our earlier work on interaction of $P^{III}$ amides with halogenosilanes[5] suggested to us that phosphoramidites would react with alcohols in the presence of trimethylchlorosilane (TMSCl) as catalyst. This proved to be so, and was highly efficacious from a preparative point of view. The reaction of $P^{III}$ amidites with an equivalent amount of nucleoside proceeds in the presence of TMSCl in very high yield and at rates comparable or higher than those when tetrazole is used. Phosphitylations activated by TMSCl proceed at room temperature in solvents like THF, $CH_2Cl_2$ or MeCN. On average, the amount of activator required for an efficient coupling is *ca.* 30–60% of the stoichiometrical ratio. Most of our experiments were performed with $P^{III}$ amides derived from diisopropylamine in order to conform to the most popular phosphitylation procedures. Selected examples illustrating our metholology are chosen from nucleotide chemistry.†

A remarkable example of activation in the presence of a catalytic amount of TMSCl (0.6 equiv.) is the reaction of thymidine **1** with tris(dimethylamino)phosphine to give thymidine 3′,5′-cyclic dimethylphosphoramidite **2** in 95% yield. Activation by tetrazole is less effective in this case.The yield of cyclic amidite **2** is poor in the absence of TMSCl.[6]

Commercially available bis(diisopropylamino)-2-cyanoethoxyphosphine reacts in the presence of TMSCl (0.6 equiv.) with 5′-*O*-DMTr-nucleoside in a highly selective way to form 5′-*O*-DMTr-thymidine 3′-*O*-(2-cyano-*N*,*N*-diisopropyl)phosphoramidite **5a** and $N^6$-benzoyl-5′-*O*-DMTr-deoxyadenosine 3′-*O*-(2-cyanoethyl-*N*,*N*-diisopropyl)phosphoramidite **5b**‡ in over 97% yield. In this case the yield and purity of amidites **5a,b** are identical to those obtained by activation with tetrazole.[7]




**1** **2**

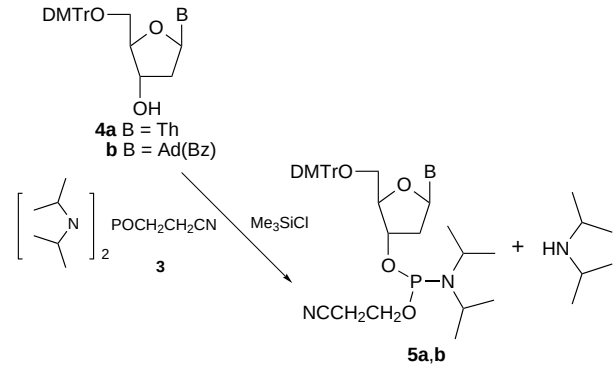
**Scheme 1** *Reagents and conditions*: **1** (1.0 equiv.), $P(NMe_2)_3$ (1.0 equiv.), TMSCl (0.6 equiv.), THF, room temp., 2 h

Excellent coupling procedures activated by TMSCl were noted for $P^{III}$ amides containing a fluorine ligand. For example, fluoro(diisopropylamino)-2-cyanoethoxyphosphine **6**§ reacts with 5′-*O*-DMTr-nucleoside **4a,b** in the presence of TMSCl (0.6 equiv.) to give 5′-*O*-DMTr-thymidine 3′-*O*-(2-cyanoethyl)-fluorophosphite **7a** and $N^6$-benzoyl-5′-*O*-DMTr-adenosine 3′-*O*-(2-cyanoethyl)fluorophosphite **7b**¶ in almost quantitative yield. The analogous reaction activated by tetrazole requires a 5-fold excess of activator and proceeds distinctly more slowly.

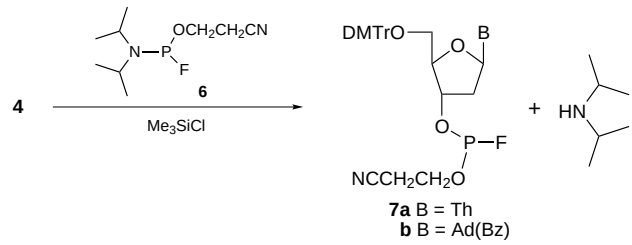
Efficient synthesis of 5′-*O*-DMTr-thymidine (3′-5′) 3′-*O*-DMT-thymidine phosphorfluoridite **10a** and $N^6$-benzoyl-5′-*O*-DMT-2′-deoxyadenosine (3′-5′)-3′-*O*-DMTr-thymidine phosphofluoridite **10b**‖ was achieved by coupling of 3′-*O*-nucleosidyl-phosphorfluoroamidites **8**[8] with a 3′-*O*-protected nucleoside in the presence of TMSCl (0.3 equiv.). The analogous reaction activated by tetrazole proceeds more slowly and requires a large excess of the activator.[9]

Synthesis of the 5′-*O*-DMTr-thymidine difluorophosphine **12**** was achieved by the coupling of diisopropylamino-difluorophosphine **11**[8] with 3′-*O*-protected nucleosides in the presence of TMSCl activator.

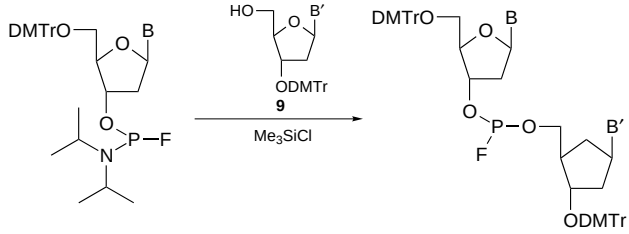
The mechanism of activation by TMSCl is presumed to involve its reaction with $P^{III}$ amide. This type of interaction has been discussed in our earlier paper[5] and more recently by Nifantyev.[10] The first step produces salt-like species $R_2P^+(SiMe_3)NR''_2Cl^-$ and $R_2PN^+R''_2(SiMe_3)Cl^-$ which react either



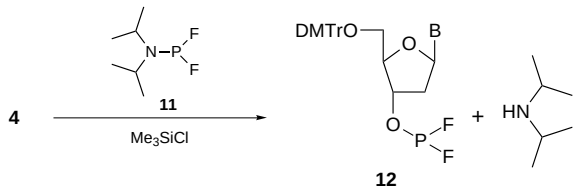

**Scheme 2** *Reagents and conditions*: **4** (1.0 equiv.), **3** (1.0 equiv.), TMSCl (0.6 equiv.), THF, room temp., 1 h




**Scheme 3** *Reagents and conditions*: **4** (1.0 equiv.), **6** (1.0 equiv.), TMSCl (0.6 equiv.), THF, room temp., 1 h




**Scheme 4** *Reagents and conditions*: **8** (1.0 equiv.), **9** (1.0 equiv.), TMSCl (0.30 equiv.), THF, room temp., 1 h




**Scheme 5** *Reagents and conditions*: **4** (1.0 equiv.), **11** (1.1 equiv.), TMSCl (0.6 equiv.), room temp., 1 h

directly with alcohol to give ester $R_2POR'$ or *via* intermediate formation of $R_2PCl$. In both cases TMSCl is regenerated. A mechanistic path may be considered in which TMSCl reacts with alcohol to form hydrogen chloride which then activates an $P^{III}$ amide *in situ*. But it is well known that TMSCl reacts very slowly with alcohols unless a catalyst is present.[11] Formation of hydrogen chloride would effect the removal of the acid labile DMTr group. This is actually observed when the commercial TMSCl contaminated with HCl is used. However when hydrogen chloride free TMSCl is utilized, this is not observed. Work is currently in progress aimed at utilizing the TMSCl activation for the synthesis of oligonucleotides on solids supports and better understanding its mechanistic features.

This work was supported by the State Committee for Scientific Research, Poland (No 3T09A 155 10), German–Polish project (X084-9) and Perstorp Pharma, Perstop, Sweden.

## Footnotes

* E-mail: wdabkow@free.polbox.pl

† All manipulations were performed under argon and all solvents dried prior to use. NMR spectra were recorded on a Bruker AC 200 spectrometer ($^{31}P$ 81.014 MHz, $H_3PO_4$ external standard; $^{19}F$ 188.15 MHz, $CFCl_3$ external standard). TMSCl was freshly distilled.

‡ *Selected data* for **5a**: yield 97%; $\delta_P$ ($CDCl_3$): 147.37, 147.93. For **5b** yield 98%; $\delta_P$ ($CDCl_3$): 147.49, 147.37.

§ Compound **6** was prepared in 90% yield from chloro(diisopropylamino)-2-cyanoethoxyphosphine *via* 2-cyanoethoxy(diisopropyl)amino-4-nitrophenoxyphospine by standard ligand exchange procedures (ref. 8). $\delta_P$ ($CDCl_3$): 162.8, 148.9 ($J_{P–F}$ 111.8.1 Hz); $\delta_F$ ($CDCl_3$): −75.1, −81.06 ($J_{P–F}$ 1118.4 Hz).

¶ *Selected data* for **7a**: yield 97%; $\delta_P$ ($C_6D_6$): 138.02, 123.03, 137.78, 122.78; $\delta_F$ ($C_6D_6$): −53.07, −59.51 ($J_{P–F}$ 1214.07 Hz), −53.44, −59.90 ($J_{P–F}$ 1216.05 Hz). For **7b**: yield 95%; $\delta_P$ ($C_6D_6$): 138.90 , 123.47; $\delta_F$ ($C_6D_6$): −52.99, −59.46 ($J_{P–F}$ 1216.9 Hz), −53.19, −59.58 ($J_{P–F}$ 1216.8 Hz).

‖ *Selected data* for **10a**: yield 98%; $\delta_P$ ($CDCl_3$): 138.42, 123.35, 139.72, 124.61; $\delta$ ($CDCl_3$): −53.91, −60.21 ($J_{P–F}$ 1220.63 Hz), −53.61, −60.07 ($J_{P–F}$ 1224.03 Hz). For **10b**: yield 98%, $\delta_P$ ($CDCl_3$): 138.50, 123.47, 140.04, 124.90; $\delta_P$ ($CDCl_3$): −52.18, −58.66 ($J_{P–F}$ 1221.24 Hz), −52.77, −59.29 ($J_{P–F}$ 1226.99 Hz).

** *Selected data* for **12**: yield 95%; $\delta_P$ ($CDCl_3$): 128.58, 111.77, 95.79 ($J_{P–F}$ 1295.4, $J_{P–F}$ 1294.9 Hz); $\delta_F$ ($CDCl_3$): −44.18, −51.06, −44.36, −51.63 ($J_{P–F}$ 1296.9, $J_{P–F}$ 1293.6 Hz).

## References

1 R. L. Letsinger and W. B. Lunsford, *J. Am. Chem. Soc*., 1976, **98**, 3655.
2 S. L. Beaucage and M. H. Caruthers, *Tetrahedron Lett*., 1981, **22**, 1859; E. Uhlman and A. Peyman, *Chem. Rev*., 1990, **90**, 543; S. L. Beaucage and R. P. Iyer, *Tetrahedron*, 1993, **48**, 2223.
3 S. M. Gryaznov and R. L. Letsinger, *Nucleic Acids Res*., 1992, **20**, 1879.
4 R. M. Karl, W. Richter, R. Klösel, M. Mayer and I. Ugi, *Nucleosides Nucleotides*, 1996, **15**, 379.
5 M. Cypryk, J. Chojnowski and J. Michalski, *Tetrahedron*, 1985, **41**, 2471.
6 G. Baschang and V. Kvita, *Angew. Chem*., 1973, 44; *Angew. Chem., Int. Ed. Engl*., 1973, **12**, 71; G. S. Bajwa and W. G. Bentrude, *Tetrahedron Lett*., 1978, **5**, 421.
7 A. Kraszewski and K. E. Norris, *Nucleic Acids Res. Symp. Ser*., 1987, **18**, 177.
8 W. Dabkowski and I. Tworowska, *Tetrahedron Lett*., 1995, **36**, 1095.
9 W. Dabkowski, I. Tworowska, J. Michalski and F. Cramer, *J. Chem. Soc., Chem. Commun*., 1995, 1435.
10 M. K. Gratchev, V. Yu. Mishina and E. E. Nifantyev, *Zh. Obshch. Khim*., 1993, **63**, 1671.
11 J. G. Lee and K. K. Kang, *J. Org. Chem*., 1988, **53**, 3634; D. C. Snyder, *J. Org. Chem*., 1995, **60**, 2638.

*Received in Glasgow, UK, 17th February 1997; Com. 7/01924F*

# One-pot synthesis and chemistry of bis[1,2]dithiolopyrroles

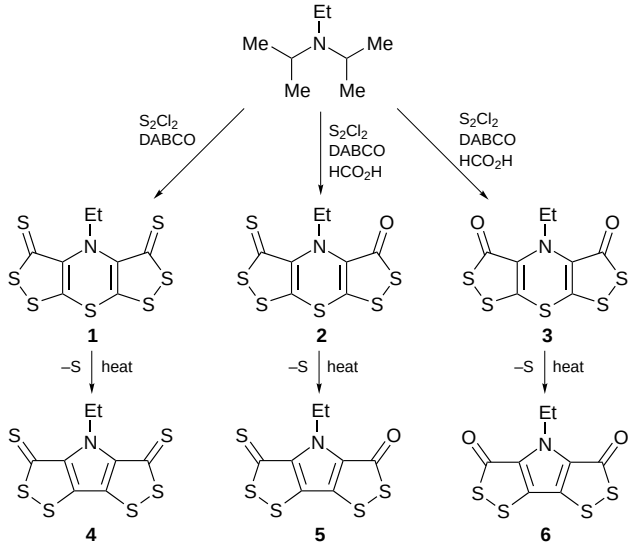
**Carlos F. Marcos,[a] Cecilia Polo,[a] Oleg A. Rakitin,[b] Charles W. Rees[c] and Tomás Torroba[a]**

[a] *Departamento de Química Orgánica, Facultad de Veterinaria, Universidad de Extremadura, 10071 Cáceres, Spain*
[b] *N. D. Zelinsky Institute of Organic Chemistry, Russian Academy of Sciences, Leninsky Prospekt 47, Moscow B-334, Russia*
[c] *Department of Chemistry, Imperial College of Science, Technology and Medicine, London, UK SW7 2AY*

**Hünig's base and $S_2Cl_2$ give the fused 1,4-thiazines 1 and (in the presence of formic acid) 2 and 3, each of which readily extrudes sulfur, selectively and quantitatively, to give the fused pyrroles 4, 5 and 6 respectively; at higher temperatures Hünig's base and $S_2Cl_2$ can be converted into the pyrroles in one pot, and the cycloadducts 8 and 10 are thus readily available in two steps.**

The formation of C–C bonds by thermal or catalytic sulfur extrusion reactions[1] has proved to be valuable in the synthesis of a wide range of organic structures, most notably that of Vitamin $B_{12}$ and the corrins.[2] We describe here the selective and quantitative desulfurisation of some polysulfur–nitrogen heterocyclic compounds which provides a new route to highly substituted fused pyrroles. Derivatives of sulfur heterocycles such as thiophene and 1,3-dithiole have been widely explored as new materials because of their superconducting[3] and optical and electronic switching properties.[4] We have synthesised sulfur–nitrogen systems with potentially similar properties, such as cyclopenta- and cyclohepta-dithiazoles[5] and liquid crystalline pseudoazulene 1,2-dithioles and 1,2-thiazines.[6]

During this work we discovered that ethyldiisopropylamine (Hünig's base), initially added as an inert base, reacted with disulfur dichloride in 1,2-dichloroethane or THF to give the first examples (**1**, **2** and **3**, Scheme 1) of the bis[1,2]dithiolo[5,4-*b*][5′,4′-*e*][1,4]thiazine ring system, in a one-pot process in which all 14 isopropyl C–H bonds of Hünig's base were replaced by C–S, C–O and C–C bonds.[7] The ready availability of these new 1,4-thiazines from commercial reagents, and their potential for sulfur extrusion[1,8] led us to study their thermal behaviour. We found that all three thiazines, **1**, **2** and **3**, underwent very clean and selective thermal extrusion of one sulfur atom only to give the first examples (**4**, **5** and **6**) of the bis[1,2]dithiolo[4,5-*b*][5′,4′-*d*]pyrroles. Furthermore the Hünig's base–$S_2Cl_2$ reaction and the sulfur extrusion could be combined to give immediate access to the new pyrrole ring system which, in turn, could be extended to polyheterocyclic pyrroles by cycloaddition reactions.




**Scheme 1**

Refluxing bisdithiolothiazine-3,5-dithione **1** in xylene for 0.5 h gave a deep purple solution from which **4** ($C_8H_5NS_6$, mp 242–243 °C) was obtained as black needles in quantitative yield.† All spectroscopic data agreed with the formation of a symmetrical structure, which requires the selective extrusion of the central ring sulfur atom to give the bisdithiolopyrrole-3,5-dithione **4**. The same product (42% after purification) was also obtained directly from Hünig's base when treated with an excess of $S_2Cl_2$ (10 equiv.) in chlorobenzene in the presence of 1,4-diazabicyclo[2.2.2]octane (DABCO, 10 equiv.) for 3 days at room temperature, followed by refluxing for 2 h. In these conditions none of the thiazine **1** survived. It is notable that in this overall reaction a carbon–carbon bond is formed between two (formally) unreactive methyl groups in Hünig's base, whilst the ethyl group is unchanged.

The mono-and bis-oxo thiazines **2** and **3** were equally good substrates for selective sulfur extrusion. Thus, when the 3-oxo 5-thione **2** or the 3,5-dione **3** were refluxed in xylene for 1 and 3 h, respectively, the 3-oxobisdithiolopyrrol-5-thione **5**,† light red crystals, mp 175–176 °C, and the bisdithiolopyrrole-3,5-dione **6**,† yellow crystals, mp 199–200 °C, respectively, were obtained in quantitative yield. All spectroscopic data, notably the $^{13}C$ NMR spectra, agreed with the unsymmetrical structure **5** and the symmetrical structure **6** for these products. Just as the fully sulfurated pyrrole **4** could be prepared directly from Hünig's base and $S_2Cl_2$ in chlorobenzene, so too could the mono- and bis-oxo pyrroles, **5** and **6**, in the presence of an oxygen donor. Thus, treating Hünig's base with $S_2Cl_2$ (10 equiv.) and DABCO (8 equiv.) in chlorobenzene for 3 days at room temperature, followed by addition of formic acid (20 equiv.) and refluxing for 7.5 h, gave the dione **6** (42%) as the only reaction product; TLC monitoring showed the intermediacy of the 1,4-thiazine **3**. If the period of refluxing were restricted to 2 h [with DABCO (10 equiv.) and formic acid (10 equiv.)] the oxo thione **5** (25%) was the main product, together with minor amounts of **4** and **6**.

Compounds **4**, **5** and **6** could be readily interconverted. Thiation of **5** or **6** with excess of $P_2S_5$ in refluxing xylene for 1 h gave the dithione **4** in almost quantitative yield. Similar thiation of the 1,4-thiazines **2** and **3**, under the same conditions, was accompanied by sulfur extrusion to give compound **4**, again in very high yield. Oxidation of **4** with mercuric acetate gave the dione **6** (35%). Nitrile oxides are known to convert 1,2-dithiolo 3-thiones into the 3-keto compounds;[9] treatment of dithione **4** or oxo thione **5** in THF at 0 °C for 15 min with an excess of ethoxycarbonyl nitrile oxide **7**, generated *in situ* from ethyl chlorooximidoacetate and triethylamine, gave the dione **6** (70–75%) (Scheme 2). Lowering the reaction temperature or reducing the amount of the reagent **7** led to mixtures of **5** and **6** with unchanged **4** and thus did not provide a satisfactory route to oxo thione **5**.

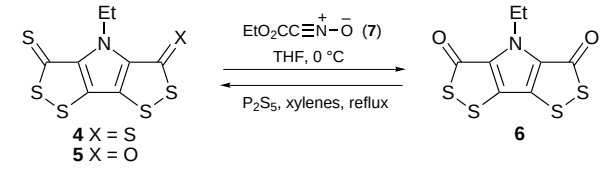
1,2-Dithiolo 3-thiones can also act as 1,3-dipoles.[10] Treatment of compound **5** with dimethyl acetylenedicarboxylate

(DMAD) (5 equiv.) in refluxing toluene for 2 h gave yellow crystals of the 1 : 2 adduct **8**,† mp 219–220 °C (65%), as the only recognisable product (Scheme 3). $^1$H NMR spectroscopy showed the presence of the *N*-ethyl group and four ester methyl groups, two of which were identical; $^{13}$C NMR showed four methoxycarbonyl groups (two identical), the carbonyl group, eight alkenyl carbons and one quaternary carbon corresponding to S–$CR_2$–S. Since the 1,2-dithiolo 3-one ring was still intact, both DMAD molecules had added to the 1,2-dithiolo 3-thione moiety to give the spiro[1,3-dithiolo-thiopyran] structure **8**, *via* the intermediate **9**.[11] In an exactly analogous manner dithiole **4** gave the 1 : 4 adduct ($C_{32}H_{29}NO_{16}S_6$), bis-spiro[1,3-dithiolo-thiopyran]pyrrole **10**† as yellow crystals, mp 224–225 °C, in 77% yield (Scheme 4). This symmetrical structure followed, as above, from spectroscopy, particularly $^1$H and $^{13}$C NMR and mass spectrometry; the fully substituted pentacyclic molecule was obtained from commercial Hünig's base in two steps in 32% overall yield.

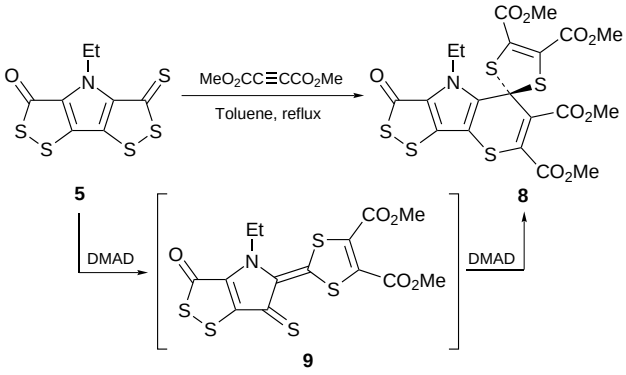
Thus new tricyclic (**4**, **5**, **6**), tetracyclic (**8**) and pentacyclic (**10**) systems, with pyrroles fused to 5- and 6-membered sulfur rings, are now readily available for assessment as new materials of the 1,2-dithiole type[12] and for biological screening.[13]

The quantitative, uncatalysed conversion of thiazines **1**, **2** and **3** into the respective pyrroles **4**, **5** and **6** occurs under much milder conditions than for other annelated 1,4-thiazines,[8] such as phenothiazines which require strong heating with copper to yield carbazoles.[14] This can be explained by stabilization of the key thiirane intermediates **11** (*cf*. refs. 8 and 14) by electron release from nitrogen and electron withdrawal by the carbonyl and thiocarbonyl groups, giving highly delocalised (**12**) intermediates on the way to the aromatic products (Scheme 5). The ene-thiolate contribution, for X = S, will be more stable than the enolate contribution, for X = O, in agreement with the observed rate of sulfur extrusion (**1** > **2** > **3**).

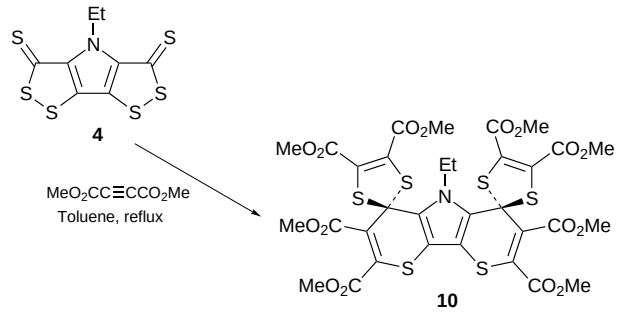
We gratefully acknowledge financial support from the Dirección General de Investigación Científica y Técnica of Spain (DGIGYT Project No. PB93-0414 and SAB94-0169), Consejería de Educación de la Junta de Extremadura y Fondo Social Europeo (EIA94-43), the Royal Society, MDL(UK) Ltd and INTAS (93-0624ext), and the Wolfson Foundation for establishing the Wolfson Centre for Organic Chemistry in Medical Science at Imperial College.



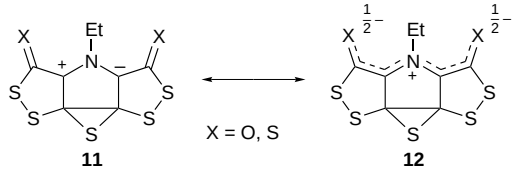

**Scheme 2**




**Scheme 3**




**Scheme 4**




**Scheme 5**

## Footnote

† All new compounds were fully characterized by spectroscopy and elemental analysis.

## References

1 C. R. Williams and D. N. Harpp, *Sulfur Rep*., 1990, **10**, 103.
2 A. Eschenmoser, *Quart. Rev*., 1970, **24**, 366.
3 M. R. Bryce, *Chem. Soc. Rev*., 1991, **20**, 355; J. Garín, *Adv. Heterocycl. Chem*., 1995, **62**, 249; Y. Misaki, N. Higuchi, H. Fujiwara, T. Yamabe, T. Mori, H. Mori and S. Tanaka, *Angew. Chem., Int. Ed. Engl*., 1995, **34**, 1222.
4 T. Jørgensen, T. K. Hansen and J. Becher, *Chem. Soc. Rev*., 1994, **23**, 41; W. F. Jager, J. C. De Jong, B. De Lange, N. P. M. Huck, A. Meetsma and B. L. Feringa, *Angew. Chem., Int. Ed. Engl*., 1995, **34**, 348; S. H. Kawai, S. L. Gilat, R. Ponsinet and J.-M. Lehn, *Chem. Eur. J*., 1995, **1**, 285; G. M. Tsivgoulis and J.-M. Lehn, *Chem. Eur. J*., 1996, **2**, 1399.
5 M. J. Plater, C. W. Rees, D. G. Roe and T. Torroba, *J. Chem. Soc., Perkin Trans. 1*, 1993, 769.
6 O. A. Rakitin, C. W. Rees, D. J. Williams and T. Torroba, *J. Org. Chem*., 1996, **61**, 9178.
7 C. F. Marcos, C. Polo, O. A. Rakitin, C. W. Rees and T. Torroba, *Angew. Chem., Int. Ed. Engl*., 1997, **36**, 281.
8 *cf*. M. Bohle and J. Liebscher, *Adv. Heterocycl. Chem*., 1996, **65**, 39.
9 F. Boberg and J. Knoop, *Liebigs Ann. Chem*., 1967, **708**, 148.
10 C. Th. Pedersen, *Adv. Heterocycl. Chem*., 1982, **31**, 63; D. M. McKinnon, in *Comprehensive Heterocyclic Chemistry*, ed. A. R. Katritzky and C. W. Rees, Pergamon, Oxford, 1984, vol. 6, ch. 4.31; and in *Comprehensive Heterocyclic Chemistry II*, ed. A. R. Katritzky, C. W. Rees and E. F. V. Scriven, Elsevier Science, Oxford, 1996, vol. 3, ch. 11.
11 For analogous dithiolethione ring-opened intermediates, see P. Leriche, A. Belyasmine, M. Sallé, P. Frère, A. Gorgues, A. Riou, M. Jubault, J. Orduna and J. Garín, *Tetrahedron Lett*., 1996, **37**, 8861; E. Fanghängel, T. Palmer, J. Kersten, R. Ludwigs, K. Peters and H. G. Von Schnering, *Synthesis*, 1994, 1067; D. D. Doxsee, C. P. Galloway, T. B. Rauchfuss, S. R. Wilson and X. Yang, *Inorg. Chem*., 1993, **32**, 5467.
12 A. Terzis, E. I. Kamitsos, V. Psycharis, J. S. Zambounis, J. Swiatek and G. C. Papavassiliou, *Synth. Met*., 1987, **19**, 481; E. Fanghängel, A. M. Richter, B. Kordts and N. Beye, *Phosphorus Sulfur*, 1989, **43**, 165.
13 M. L. Aimar and R. H. Rossi, *Tetrahedron Lett*., 1996, **37**, 2137 and references cited therein.
14 J. D. Loudon, in *Organic Sulfur Compounds*, ed. N. Kharash, Pergamon, Oxford, 1961, vol. 1, p. 299.

*Received in Liverpool, UK, 25th February 1997; Com. 7/01340J*

# New syntheses of aryl isothiocyanates from *N*-arylimino-1,2,3-dithiazoles

**Thierry Besson,[a] Jérôme Guillard,[a] Charles W. Rees[b] and Michel Thérisod[c]**

[a] *Laboratoire de Génie Protéique et Cellulaire, Pôle Sciences et Technologie, Université de La Rochelle, Avenue Marillac, F-17042 La Rochelle cedex 1, France*
[b] *Department of Chemistry, Imperial College of Science, Technology and Medicine, London, UK SW7 2AY*
[c] *S.E.S.N.AB., Pôle Sciences et Technologie, Université de La Rochelle, Avenue Marillac, F-17042 La Rochelle cedex 1, France*

**Treatment of *N*-arylimino-1,2,3-dithiazoles 2 with ethylmagnesium bromide (2 equiv.) gives the corresponding aryl isothiocyanates 13, providing a very mild two-step conversion of $ArNH_2$ into ArNCS avoiding hazardous reagents; alternatively the iminodithiazoles 2 can be converted into cyanothioformanilides 11 which rapidly give the same isothiocyanates with 1 equiv. of the Grignard reagent.**

4,5-Dichloro-1,2,3-dithiazolium choride **1**, which is readily prepared from chloroacetonitrile and disulfur dichloride, reacts rapidly with anilines in dichloromethane at room temperature to give the stable 5-(*N*-arylimino)-4-chloro-5*H*-1,2,3-dithiazoles **2** usually in very high yield.[1–3] These iminodithiazoles are susceptible to intramolecular (*e.g.* **3**) and intermolecular (*e.g.* **4**) nucleophilic substitution at both sulfur and both carbon atoms of the dithiazole ring and, in consequence, have proved to be very versatile synthetic intermediates. They can be converted in one step into the 2-cyano derivatives of benzoxazoles **5**,[2] benzothiazoles **6**,[2] benzimidazoles **7**,[4] benzoxazin-4-ones **8**,[3] benzothiazin-4-ones **9**[3] and 4-alkoxyquinazolines **10**,[5] and into the acyclic *N*-arylcyanothioformamides **11**.[3] Opening of the dithiazole ring by aliphatic amines (*e.g.* **4**) has also been shown by Kim and co-workers to be synthetically useful.[6] In all of these reactions the latent cyano group in the reagent **1** has been generated and retained in the products. We now find that with the more powerfully nucleophilic Grignard reagents, opening of the dithiazole ring is accompanied by elimination of the cyano group. A commercial solution of ethylmagnesium bromide (2 equiv.) in THF was added dropwise to a heated solution of the iminodithiazole **2** in THF under argon, and heated at reflux for 1 h. Hydrolysis followed by extraction of the product with dichloromethane and purification by column chromatography afforded the isothiocyanates **13** (45–60%) (Method A, Table 1). Similar yields were obtained from reactions run at room temperature overnight. Transposing this procedure to a open microwave oven specially designed for organic synthesis gave very similar results (reaction times, yields). An excess of ethylmagnesium bromide (5–6 equiv.) gave more complex reactions with lower yields of isothiocyanates.

The ready conversion of iminodithiazoles **2** into aryl isothiocyanates **13** is a new reaction of the heterocyclic ring, which provides a novel route to isothiocyanates. This mild two-step conversion of primary aromatic amines into isothiocyanates avoids the use of carbon disulfide and thiophosgene, and high temperature reactions.[7]

Opening of the dithiazole ring by the Grignard reagent is probably initiated by attack at S-2 and generation of the cyano group (Scheme 1), as with other nucleophiles.[6] Attack by a second molecule of the Grignard reagent on the same sulfur could result in formation of the isothiocyanate, dialkyl sulfide

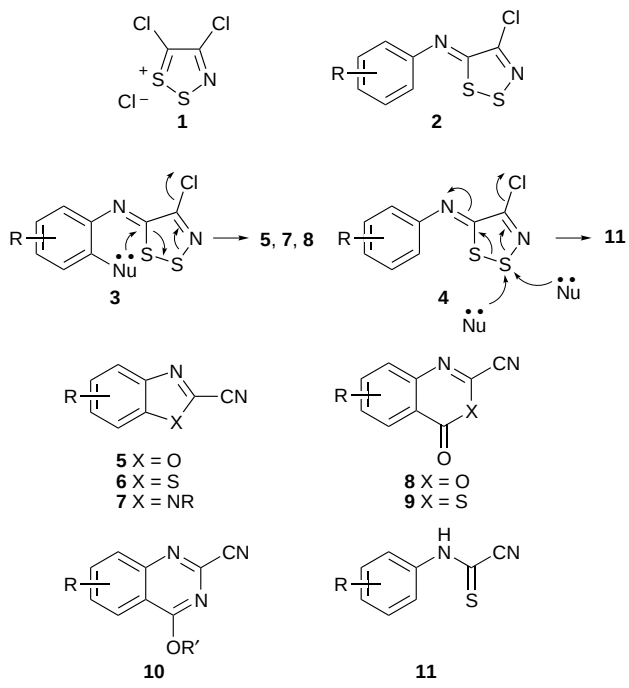
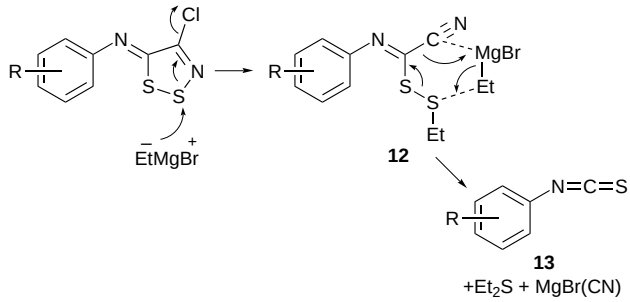



**Table 1** Synthesis of aryl isothiocyanates **13** from 5-(*N*-arylimino)-1,2,3-dithiazoles **2** and cyanothioformanilides **11**[a,b]

| Starting material | R | Product **13** | Yield (%) | Mp/°C |
|---|---|---|---|---|
| **2a** | H | **a** | 54 | oil[c] |
| **2b** | 2-F | **b** | 50 | oil[c] |
| **2c** | 2-CN | **c** | 55 (A); 76 (B)[d] | 64 |
| **2d** | 4-MeO | **d** | 44 (A); 75 (B) | oil[c] |
| **2e** | 4-CN | **e** | 60 | 123[c] |
| **2f** | 3,4-$(MeO)_2$ | **f** | 50 | oil |
| **2g** | 2-CN, 4,5-$(MeO)_2$[e] | **g** | 46 (A); 54 (B) | 134 |
| **2h** | 3,4-$(OCH_2CH_2O)$ | **h** | 47 (A); 73 (B) | 74 |
| **11d** | 4-MeO | **d** | 93[f] | oil |
| **11g** | 2-CN, 4,5-$(MeO)_2$ | **g** | 70[f] | 134 |
| **11h** | 3,4-$(OCH_2CH_2O)$ | **h** | 92[f] | 74 |

[a] All compounds were characterised by IR, NMR and HRMS. [b] Aryl isothiocyanates **13**: typical procedures from 5-(*N*-arylimino)-4-chloro-5*H*-1,2,3-dithiazoles **2**. *Method A*: Under an argon atmosphere, a solution of ethylmagnesium bromide (2 mmol, 1 M in THF) was added dropwise to a solution of the 5-imino-1,2,3-dithiazole **2** (1 mmol) in boiling THF (5 ml). The brown mixture obtained was heated for about 1 h, the reaction being followed by TLC. After addition of $CH_2Cl_2$ (20 ml) the solution was washed with water, the organic layer dried over sodium sulfate and the solvent evaporated. The crude product was then purified by column chromatography with light petroleum–$CH_2Cl_2$. The same procedure was transposed to a open microwave oven in a quartz reactor (Synthewave S402 Prolabo® microwave reactor monomode system which has variable speed rotation, visual control, irradiation monitor, infrared measurement and continuous feedback temperature controlled by PC computer). The products were purified as above. [c] Compound commercially available. [d] (A): method A; (B): method B (see above). [e] Treatment of the iminodithiazole **2g** with benzylmagnesium bromide gave the same yield of isothiocyanate **13g** as EtMgBr. [f] EtMgBr (1 equiv.), THF 50 °C, 30 min.




**Scheme 1**

and cyanide anion, possibly assisted by electrophilic catalysis in a cyclic transition state as shown in **12** (Scheme 1). It has been shown that treatment of some *N*-arylcyanothioformamides **11** with pyrrolidine gave minor amounts of thioureas, where the cyano group had been replaced by the amine, and the corresponding aryl isothiocyanate was proposed as a possible intermediate.[6a]

*N*-Aryliminodithiazoles **2** can be easily converted into cyanothioformanilides **11** in high yield by treatment with triphenylphosphine (2 equiv.) in undried $CH_2Cl_2$ at room temperature for 1–3 h.[3] We now find that HCN is also eliminated from these formanilides **11** by ethylmagnesium bromide (1 equiv.) in THF to give the isothiocyanates **13** in high yield. The two steps, **2** → **11** → **13**, can be readily combined (Method B, Table 1).

We thank the Comité de Charente-Maritime de la Ligue Nationale Contre le Cancer, Prolabo (Merck group) and MDL Information Systems (UK) Ltd for financial support, and the Wolfson Foundation for establishing the Wolfson Centre for Organic Chemistry in Medical Science at Imperial College.

## References

1 R. Appel, H. Janssen, M. Siray and F. Knoch, *Chem. Ber*., 1985, **118**, 1632.
2 R. F. English, PhD. Thesis, University of London, 1989; C. W. Rees, *J. Heterocycl. Chem*., 1992, **29**, 639; D. G. Roe, PhD Thesis, University of London, 1993.
3 T. Besson, K. Emayan and C. W. Rees, *J. Chem. Soc., Chem. Commun*., 1995, 1419; *J. Chem. Soc., Perkin Trans. 1*, 1995, 2097.
4 O. A. Rakitin, C. W. Rees and O. G. Vlasova, *Tetrahedron Lett*., 1996, **37**, 4589.
5 T. Besson and C. W. Rees, *J. Chem. Soc., Perkin Trans. 1*, 1996, 2857.
6 (*a*) H. Lee and K. Kim, *J. Org. Chem*., 1993, **58**, 7001; (*b*) H. Lee, K. Kim, D. Whang and K. Kim, *J. Org. Chem*., 1994, **59**, 6179.
7 J. Gilmore and P. T. Gallagher, in *Comprehensive Organic Functional Group Transformations*, ed. A. R. Katritzky, O. Meth-Cohn and C. W. Rees, Pergamon, Oxford, 1995, vol. 5, p. 1021.

*Received in Liverpool, UK, 23rd January 1997; Com. 7/00551B*

# The bis-*p*-nitrophenyl ester of iron(III) mesoporphyrin II acetate: preparation and incorporation into a model hemoprotein

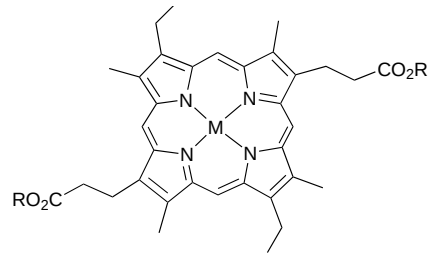
**Manxue Wang, Michelle L. Kennedy, Bradley R. Hart and David R. Benson***

*Department of Chemistry, University of Kansas, Lawrence, KS 66045-0046, USA*

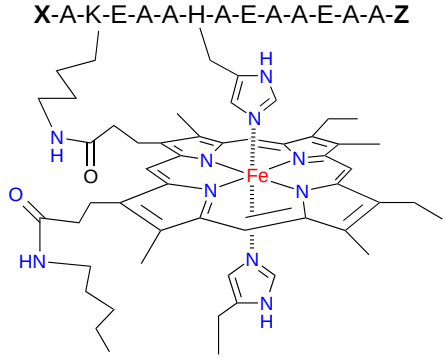
**A method for cleanly inserting iron into the bis-*p*-nitrophenyl ester of mesoporphyrin II, and use of the highly soluble product in the synthesis of a model hemoprotein, is reported.**

We have recently developed a new class of hemoprotein model compounds called peptide sandwiched mesohemes (PSMs; *e.g.* **1** and **2**), which consist of two peptides covalently attached to $Fe^{III}$ mesoporphyrin IX (MPIX).[1] Histidine (His) residues within each peptide coordinate to the mesohemin iron. In **1**[1] and **2**,[2] Fe–His coordination leads the initially random coil peptides to adopt conformations in which peptide helix content approaches 50 and 60%, respectively. A problem that arises with use of MPIX, a commercially available porphyrin, is that each resulting PSM exists as a pair of interconvertible diastereoisomers. Any physical studies done with PSMs assembled from MPIX will be complicated by this equilibrium. Our interest in developing a new generation of PSMs in which only a single stereoisomer is possible (*e.g.* **3**) prompted us to pursue the synthesis of mesoporphyrin II **4**,[3] a $C_{2h}$-symmetric isomer of MPIX. The symmetry properties of **4** have led to its incorporation in several designed receptors,[4–6] systems for the study of electron transfer,[7] and cofacial porphyrin dimers for catalysis of oxygen reduction.[8] The high symmetry of **4** leads to an unfortunate situation: the porphyrin is only soluble in a few, mostly uncommon, solvents including TFA and pyridine. Functionalization of the molecule is limited to reactions which are compatible with such solvents. One reaction which is complicated by lack of solubility is iron insertion. A literature search revealed no references for iron complexes of **4**, nor for any simple ester derivatives of an iron complex. Iron has been inserted into a cofacial porphyrin dimer constructed from **4**.[9] However, this approach may not work in all cases, for example in systems containing more than one metal binding site, or when iron insertion chemistry is not compatible. Because **4** is such an excellent scaffold upon which to build hemoprotein models, including PSMs, we felt it would be useful to explore ways of generating an activated ester derivative of an iron(III) complex of **4**. Our approach was to insert iron into the previously reported bis-*p*-nitrophenyl ester **5** to produce **6**.

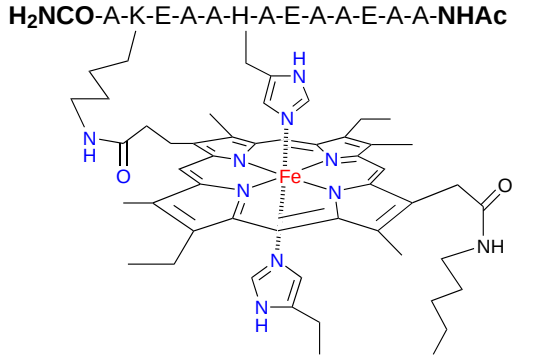
Synthesis of **4** followed Dolphin's method,[3] with subsequent conversion to **5** using the procedure of Collman *et al.*[8] Insertion of iron into porphyrins is commonly achieved using $Fe^{II}$ salts in acetic acid (AcOH) at 100 °C, conditions under which **4** and its bis-methyl ester are completely insoluble. Although solubility of **5** in AcOH is slightly higher, no evidence for iron insertion was observed even after refluxing for several days in the presence of $Fe(OAc)_2$. Halogenated solvents, including dichloromethane (DCM) and chloroform, increase the solubility of **5** in AcOH. However, the low boiling points of these solvents leads to unacceptably long reaction times for iron insertion. In contrast, 1,1,2,2-tetrachloroethane (TCE; bp 147 °C) as cosolvent dramatically improved both solubility and rate of metal insertion. Thus, porphyrin **5** (43 mg) was dissolved in 6 ml of a 1 : 1 mixture of dry TCE and glacial acetic acid at 100 °C under $N_2$. Acetic anhydride ($Ac_2O$; 5 vol%) was added to eliminate any adventitious water. A saturated solution of $Fe(OAc)_2$ in AcOH[10] (3 ml; also containing 5% $Ac_2O$) was added to the porphyrin solution *via* syringe and the mixture was stirred at 100 °C until iron insertion was complete as determined by UV–VIS spectroscopy (*ca.* 1 h). The cooled mixture was filtered to




**4** R = H; M = 2H
**5** R = $C_6H_4NO_2$-*p*; M = 2H
**6** R = $C_6H_4NO_2$-*p*; M = $Fe^{III}$-OAc




**1** X = NHAc; Y = $CONH_2$
**2** X = $CONH_2$; Y = NHAc




**3**

remove excess $Fe(OAc)_2$ and the solvent was evaporated *in vacuo*. The dark purple residue was taken up in dry TCE, refiltered, and the solvent was again evaporated. No hydrolysis products were observed by FAB mass spectrometry.† However, a signal corresponding to TCE was present even after the sample had been heated for 12 h at 100 °C *in vacuo*. Elemental analysis† of the recovered material (49 mg; 90%) is consistent with the presence of one equivalent of TCE and an acetate ligand to the iron. The product is highly soluble in AcOH, TCE, DCM, THF, DMF, $Me_2SO$, dioxane, ethyl acetate, acetonitrile and pyridine.

Conversion of **6** to PSM **3** was achieved using our previously reported method for PSMs constructed from $Fe^{III}$–MPIX.[1] The $Fe^{III}$ in **3** is low spin (Soret $\lambda_{max}$ = 403 nm; not shown), demonstrating that it is bis-His coordinated. Helix content of the new compound, as determined by circular dichroism[1] (Fig. 1), is similar to that measured for **2**[2] (*ca.* 60%) at 8 °C in 2 mM potassium phosphate (pH 7). A monopeptide analogue appended on the lysine ε-amine by indoleacetic acid (**7**) exhibits a

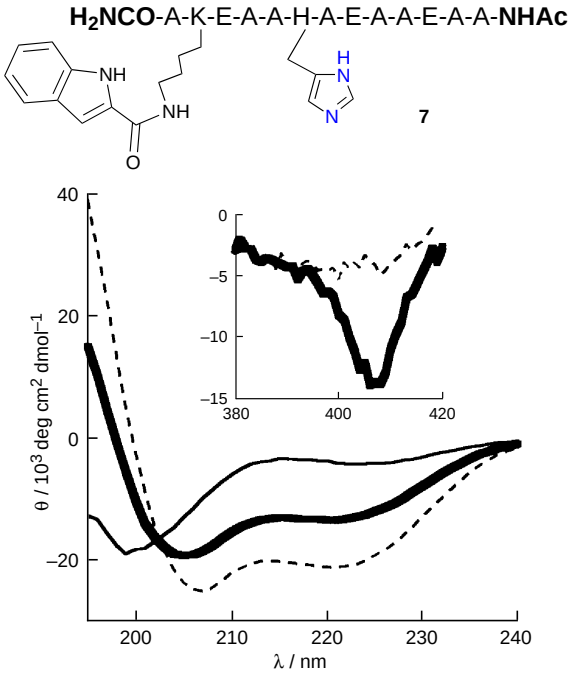



**Fig. 1** CD spectra at 8 °C: 21 μM **7** (thin line) and 8.1 μM **3** (bold line) in water; 8.1 μM **3** (dashed line) in 7 : 3 $H_2O$–PrOH. Each sample is buffered to pH 7 with 2 mM potassium phosphate.

random coil conformation under the same conditions (Fig. 1), confirming that Fe–His coordination in **3** is responsible for helix induction. A Soret induced CD (ICD) signal is recorded as well (Fig. 1), commensurate with the location of the porphyrin within an asymmetric environment. Interestingly, the intensity of this Soret ICD band is only about 25% that of the corresponding band for the two diastereoisomers of **2** (not shown) in aqueous solution. As helix content is increased by addition of propan-1-ol (PrOH), the Soret ICD signal intensity diminishes (Fig. 1) whereas in **2** it increases (not shown).[2] Maximal helix content (*ca.* 95%) is recorded for both **2** and **3** in the presence of 30% (v/v) PrOH (spectrum for **3** is shown in Fig. 1). Additional studies on this and related PSMs will be reported in due course.

This work was supported by National Institutes of Health grant R29-GM52431-01A1.

## Footnotes

* E-mail: benson@kuhub.cc.ukans.edu

† FAB MS *m/z* (relative intensity): 865 ($M^+$ + 3, 10%), 864 ($M^+$ + 2, 31), 863 ($M^+$ + 1, 83), 862 ($M^+$, 100), 860 ($M^+$ −2, 13). Anal. calc. for $C_{46}H_{42}N_6O_8Fe{\cdot}C_2H_3O_2{\cdot}C_2H_2Cl_4$: C, 55.12; H, 4.35; N, 7.71. Found: C, 55.28; H, 4.09; N, 8.04.

## References

1 D. R. Benson, B. R. Hart, X. Zhu and M. B. Doughty, *J. Am. Chem. Soc.*, 1995, **117**, 8502.
2 D. R. Benson, P. A. Arnold, M. Wang, M. L. Kennedy, D. J. Brink, G. S. Jas, D. T. Petasis and M. P. Hendrich, unpublished work.
3 J. B. Paine III, J. Hiom and D. Dolphin, *J. Org. Chem.*, 1988, **53**, 2796.
4 N. M. Richardson and I. O. Sutherland, *Tetrahedron Lett.*, 1985, **26**, 3739.
5 C. A. Hunter, M. N. Meah and J. K. M. Sanders, *J. Am. Chem. Soc.*, 1990, **112**, 5773.
6 A. Hamilton, J.-M. Lehn and J. L. Sessler, *J. Am. Chem. Soc.*, 1986, **108**, 5158.
7 P. Leighton and J. K. M. Sanders, *J. Chem. Soc., Perkin Trans. 1*, 1987, 2385.
8 J. P. Collman, P. Denisevich, Y. Konai, M. Marrocco, C. Koval, and F. C. Anson, *J. Am. Chem. Soc.*, 1980, **102**, 6027.
9 J. A. Cowan and J. K. M. Sanders, *J. Chem. Soc., Perkin Trans. 1*, 1987, 2395.
10 O. Warburg and E. Negelein, *Biochem. Z.* 1932, **244**, 9.

*Received in Bloomington, IN, USA, 12th February 1997; Com. 7/01007I*

# $^{13}C–^{15}N$ Coupling constants in a series of twisted amides: relationships with C(O)–N twist angles

**Shinji Yamada,*[a]† Maki Nakamura[b] and Ichiro Kawauchi[b]**

[a] *Department of Chemistry, Faculty of Science, Ochanomizu University, Otsuka, Bunkyo-ku, Tokyo 112, Japan*
[b] *Department of Materials Science, Faculty of Science, Kanagawa University, Hiratsuka, Kanagawa 259-12, Japan*

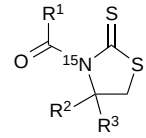
**For a series of $^{15}N$-labelled amides 1a–e with increasing C(O)–N twist angles, the one-bond $^{13}C–^{15}N$ coupling constants decrease, whereas the two-bond $^{13}C–^{15}N$ coupling constants increase.**

It is well-documented that amides have planar geometry due to the partial double bond character of the C(O)–N bond resulting from amide resonance.[1] However, a number of peptides, proteins and enzymes have been proved by X-ray analysis to contain non-planar deformation in the amide moiety.[2] Furthermore, Schreiber and his colleagues have recently suggested that the orthogonally orienting α-keto amide groups of the immunosuppressive agent FK506 and rapamycin may mimic the twisted amide transition-state of peptide substrates of FKBP rotamase.[3] Such twisted structures are of significant interest in relation to their biochemical functions. Synthetic twisted amides have also received considerable attention with regard to their structure and reactivity.[4,5]

The principal method for studying the non-planarity of amide bonds in solution is $^{13}C$, $^{15}N$ and $^{17}O$ NMR spectroscopy.[6,7] Although C–N coupling constants[8] seem to be another promising parameter for elucidation of amide deformation about the C(O)–N bond, no investigations have been reported. Here we describe the relationships between C(O)–N twist angles and $^1J_{C,N}$ and $^2J_{C,N}$ values in a series of twisted amides.

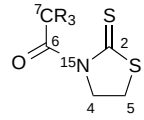
A series of twisted amides **1a–e**,[7]‡ enriched to 99% with $^{15}N$, was synthesized *via* several steps from commercially available [$^{15}N$] glycine and [$^{15}N$] leucine. The C–N coupling constants of **1a–e** were measured at 100.04 MHz using $^{13}C$ NMR spectroscopy. Table 1 shows the $^1J_{C,N}$ and $^2J_{C,N}$ values, and the previously reported C(O)–N twist angles τ and the $\chi_N$ values,[7,9] $^1J_{C(O),N}$ lies in the range of 2.5–7.8 Hz in $CDCl_3$, and 3.2–7.9 Hz in [$^2H_6$]DMSO. The plots of $^1J_{C(O),N}$ *versus* τ are a little scattered, but a rough correlation exists between them, as shown in Fig. 1(*a*). Thus, as the twist angle increases, the $^1J_{C(O),N}$ value decreases. By assuming the Fermi contact mechanism to be dominant, it has been reported that $^1J_{C,N}$ depends on the percentage s-character of the C and N atoms.[10] However, there are no clear-cut relationships between the $^1J_{C(S),N}$ and $^1J_{C4,N}$ values and the $\chi_N$ value, which represents the extent of pyramidalization of the N atom. These suggest that the contribution of the contact term to $^1J_{C(O),N}$ is not predominant in this case. Therefore, the orbital and dipolar terms,[11] which depend upon the p-electron distribution, may be the dominant factors governing $^1J_{C,N}$. The importance of the effect of the p-electron distribution on $^1J_{C,N}$ has been reported in substituted anilines: steric inhibition of nitrogen lone-pair delocalization in *N*,*N*-dimethylaniline derivatives reduces the $^1J_{C,N}$ value.[12] A similar explanation can be applied to the present case. Thus, rotation about the amide bond causes a decrease in the C–N double bond character resulting from amide resonance; consequently, the $J_{C,N}$ decreases. When [$^2H_6$]DMSO was used as the NMR solvent, the slope changed, becoming somewhat gentler compared to that in $CDCl_3$. This is because the polar solvent easily stabilizes the canonical form **II** (Scheme 1).

The $^2J_{C7,N}$ values are in the range 5.6–7.1 Hz, which is much narrower than that of $^1J_{C(O),N}$. On the other hand, $^2J_{C5,N}$ was not observed for any of the amides. In contrast to the relationship between $^1J_{C(O),N}$ and τ, the $^2J_{C7,N}$ value increases with increasing the twist angle, as shown in Fig. 1(*b*). It has been assumed that $^2J_{C,N}$ depends on the dihedral angle between the lone pair orbital and the Cα–Cβ bond. For example, $^2J_{C,N}$ of quinuclidine, whose dihedral angle is 180°, is only 0.2 Hz, whereas that of propylamine is 1.2 Hz.[13] Because the dihedral angle of the series of amides decreases with increasing C(O)–N twist angle, as shown in Fig. 2, the present results may also be




**1a** $R^1$ = Me, $R^2$ = $R^3$ = H
**b** $R^1$ = Bn, $R^2$ = $R^3$ = H
**c** $R^1$ = $R^2$ = $R^3$ = Me
**d** $R^1$ = $Bu^t$, $R^2$ = $R^3$ = H
**e** $R^1$ = $Bu^t$, $R^2$ = $Bu^i$, $R^3$ = H

**Table 1** $J_{C,N}$ values, $\chi_N$ and twist angle τ




| Compound | $^1J_{C(O),N}$[a] /Hz | $^1J_{C(O),N}$[b] /Hz | $^1J_{C(S),N}$[a] /Hz | $^1J_{C4,N}$[a] /Hz | $^2J_{C7,N}$[a] /Hz | $\chi_N$ (°) | τ (°) |
|---|---|---|---|---|---|---|---|
| **1a** | 7.8 | 7.9 | 8.9 | 10.2 | 5.8 | 11.9 | 20.1 |
| **1b** | 7.5 | 7.6 | 8.7 | 10.0 | 5.6 | 13.4 | 10.2 |
| **1c** | 7.0 | 7.1 | 8.7 | 6.9 | 6.0 | 12.2 | 36.5 |
| **1d** | 2.9 | 3.5 | 9.1 | 7.8 | 7.1 | 29.5 | 74.3 |
| **1e** | 2.5 | 3.2 | 9.1 | 6.8 | 6.7 | 31.4 | 65.5 |

[a] In $CDCl_3$. [b] In [$^2H_6$]DMSO.

ascribed to the directional effect of the nitrogen lone pair orbital.

Kainosho and Nagao reported[14] that the $^{13}C$–$^{15}N$ coupling constant between the Phe-97 carbonyl carbon and the ser-98 nitrogen in *Streptomyces* subtilisin inhibitor is unusually small, and they explained that it is a result of the non-planarity of peptide bonds in β-sheets and α-helices. The present result seems to support their hypothesis.

Financial support, in the form of Grants-in-Aid for Scientific Research from the Ministry of Education, Science, and Culture, Japan (No. 08640755 and 08554026), is acknowledged.

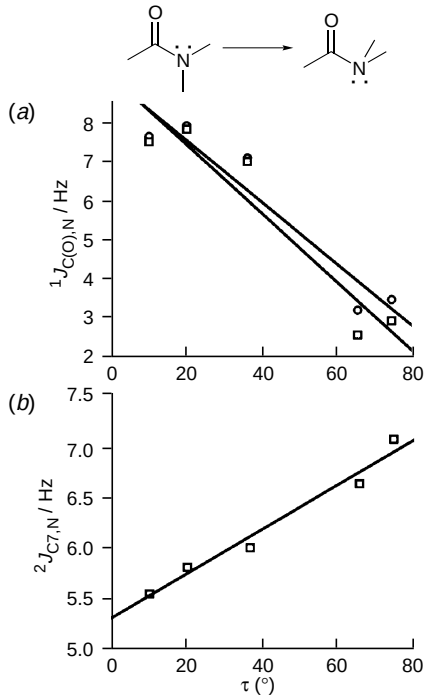
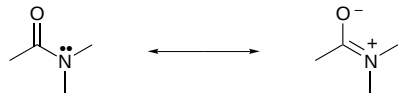



**Fig. 1** Plots of (*a*) $^1J_{C(O),N}$ (□ = in $CDCl_3$, ○ = in [$^2H_6$]DMSO) and (*b*) $^2J_{C7,N}$ *vs.* τ



**I** **II**

**Scheme 1**

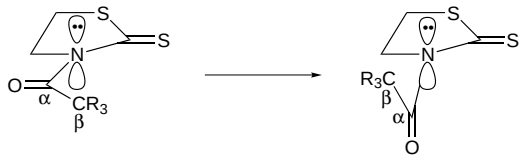


**Fig. 2**

## Footnotes

† E-mail: yamada@hososipc.chem.ocha.ac.jp

‡ EI-Mass spectral data for compounds **1a**–**e** at an ionizing voltage of 70 eV are as follows: **1a**, *m/z* (%) 162 (40, $M^+$), 120 (28), 60 (36), 43 (100); **1b**, *m/z* (%) 238 (12, $M^+$), 210 (5), 118 (69), 91 (100); **1c**, *m/z* (%) 190 (76, $M^+$), 148 (35), 101 (72), 43 (100); **1d**, *m/z* (%) 204 (39, $M^+$), 161 (3), 120 (38), 85 (34), 57 (100); **1e**, *m/z* (%) 260 (11, $M^+$), 203 (4), 175 (9), 57 (100).

## References

1 L. Pauling, *The Nature of the Chemical Bond*, Cornell University Press, Ithaca, NY, 1960; M. B. Robin, F. A. Bovey and H. Basch, *The Chemistry of Amides*, ed. J. Zabicky, Interscience, New York, 1970, ch. 1, p. 1.

2 G. N. Ramachandran and A. S. Kolaskar, *Biochim. Biophys. Acta*, 1973, **303**, 385; D. E. Stewart, A. Sarkar and J. E. Wampler, *J. Mol. Biol.*, 1990, **214**, 253; A. L. Morris, M. W. MacArthur, E. G. Hutchinson and J. M. Thornton, *Proteins: Struct. Funct. Genet.*, 1992, **12**, 345; M. W. MacArthur and J. M. Thornton, *J. Mol. Biol.*, 1996, **264**, 1180.

3 M. K. Rosen, R. F. Standaert, A. Galat, M. Nakatsuka and S. L. Schreiber, *Science*, 1990, **243**, 863; M. W. Albers, C. T. Walsh and S. L. Schreiber, *J. Org. Chem.*, 1990, **55**, 4984; M. K. Rosen and S. L. Schreiber, *Angew. Chem., Int. Ed. Engl.*, 1992, **31**, 384; S. T. Park, R. A. Aldape, O. Futer, M. T. DeCenzo and D. J. Livingston, *J. Biol. Chem.*, 1992, **267**, 3316.

4 For reviews, see A. Greenberg, *Structure and Reactivity*, ed. J. F. Liebman and A. Greenberg, VCH, Weinheim, 1988, ch. 4, p. 139; T. G. Lease and K. J. Shea, *Advances in Theoretically Interesting Molecules*, JAI Press, Greenwich, 1992, vol. 2, p. 79.

5 For recent reports on twisted amides, see S. Yamada, *Angew. Chem., Int. Ed. Engl.*, 1993, **32**, 1083; T. G. Lease and K. J. Shea, *J. Am. Chem. Soc.*, 1993, **115**, 2248; A. P. Evans, A. B. Holmes, I. Collins, P. R. Raithby and K. Russell, *J. Chem. Soc., Chem. Commun.*, 1995, 2325; S. Yamada, T. Sugaki and K. Matsuzaki, *J. Org. Chem.*, 1996, **61**, 5932.

6 A. J.Bennet, V. Somayaji, R. S. Brown and B. D. Santarsiero, *J. Am. Chem. Soc.*, 1991, **113**, 7563; I. P. Gerothanassis, A. Troganis and C. Vakka, *Tetrahedron*, 1995, **51**, 9493.

7 For non-labelled **1a**–**e**, see S. Yamada, *J. Org. Chem.*, 1996, **61**, 941.

8 For reviews, see G. C. Levy and R. L. Lichter, *Nitrogen-15N Nuclear Magnetic Resonance Spectroscopy*, Wiley, New York, 1979; M. Witanowski, L. Stefaniak and G. A. Webb, *Annual Reports on NMR Spectroscopy*, Academic Press, London, 1986, vol. 18.

9 For definitions of τ and $\chi_N$, see F. K. Winkler and J. D. Dunitz, *J. Mol. Biol.*, 1971, **59**, 169.

10 G. Binsch, J. B. Lambert, B. W. Roberts and J. D. Roberts, *J. Am. Chem. Soc.*, 1964, **86**, 5564; J. M. Schulman and T. Venanzi, *J. Am. Chem. Soc.*, 1976, **98**, 6739.

11 N. F. Ramsey and E. M. Purcell, *Phys. Rev.*, 1952, **85**, 143; N. F. Ramsey, *Phys. Rev.*, 1953, **91**, 303.

12 R. E. Wasylishen, *Can. J. Chem.*, 1976, **54**, 833; H. Martineau, M. Trierweiler and M. L. Martin, *Org. Magn. Reson.*, 1981, **17**, 182; T. Axenrod, C. M. Watnick, M. J. Wieder, S. Duangthai, G. A. Webb, H. J. C. Yeh, S. Bulusu and M. M. King, *Org. Magn. Reson.*, 1982, **20**, 11.

13 S. Berger and J. D. Roberts, *J. Am. Chem. Soc.*, 1974, **96**, 6757; R. L. Lichter, D. E. Dorman and R. Wasylishen, *J. Am. Chem. Soc.*, 1974, **96**, 930.

14 M. Kainosho and H. Nagao, *Biochemistry*, 1987, **26**, 1068.

*Received in Cambridge, UK, 10th February 1997; Com. 7/00931C*

# Quantitative determination of metal ions and anions in aqueous solution by using pH-responsive redox-active receptors

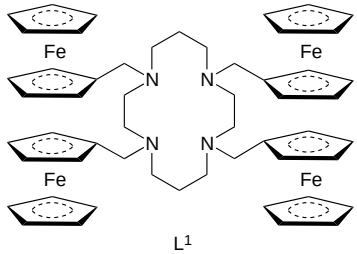
**Miguel E. Padilla-Tosta, Ramón Martínez-Máñez,* Teresa Pardo, Juan Soto and María José L. Tendero**

*Departamento de Química, Universidad Politécnica de Valencia, Camino de Vera s/n, 46071 Valencia, Spain*

**The redox-active polyazacycloalkane 1,4,8,11-ferrocenylmethyl-1,4,8,11-tetraazacyclotetradecane L$^1$ is a versatile receptor for the quantitative electrochemical determination of metal ions ($Cu^{2+}$, $Zn^{2+}$, $Cd^{2+}$) and ATP in aqueous solution.**

In recent years a number of work has been devoted to the development of new receptors containing binding sites and redox-active groups.[1] Two properties are common to those new molecules; their electroactive character and the ability to bind substrates. Some of those receptors bearing different redox-active groups (able to be reduced or oxidized), can electrochemically recognize alkali-metal and alkaline-earth-metal cations,[2] anions[3] and neutral species.[4] Additionally it has recently been reported that transition-metal ions can also adequately be recognised by using ferrocene-functionalised polyamines as receptors.[5,6] That approach leads to pH-responsive redox-active molecules where the shift of the oxidation potential in the presence of transition-metal ions is a function of the pH.[5] Additionally the functionalisation of polyaza molecules with redox groups are good candidates to electrochemically recognize anion coordination based on the property of those systems to act as polybases.[6] To further advance the use of redox-active receptors as practical electrochemical sensors we have performed electrochemical studies, using the redox-functionalised polyazacycloalkane 1,4,8,11-ferrocenylmethyl-1,4,8,11-tetraazacyclotetradecane L$^1$,[7] with the aim of quantitatively determining the concentration of cations and anions in solution.

Fig. 1 shows the variation of the oxidation potential ($E_{1/2}$, from rotating disk electrode techniques) *vs.* pH for the systems L$^1$–H$^+$–M$^{2+}$ (M = $Ni^{2+}$, $Cu^{2+}$, $Zn^{2+}$, $Cd^{2+}$, $Pb^{2+}$, ligand-to-metal ratio = 1:1) in thf–water (70:30 v/v) mixtures. The oxidation potential of L$^1$ shifts to more anodic potentials when the pH is reduced as a consequence of the successive protonation of the amino groups. In the presence of stoichimetric amounts ($M^{2+}/L^1$ = 1) of metal ions different curves are found. Some of them are quite different (for $Cu^{2+}$, $Zn^{2+}$, $Cd^{2+}$) and some quite similar (for $Pb^{2+}$ and $Ni^{2+}$) to that of the free receptor (see Fig. 1). We have also found that for ligand-to-metal ratios $<1$, curves between that of L$^1$ and that with $M^{2+}/L^1$ = 1 are obtained. At a fixed pH, $E_{1/2}$ for a determined $M^{2+}/L^1$ ratio is $E_{1/2} = x_L E_{1/2}{}^L + x_{ML} E_{1/2}{}^{ML}$ where $x_L$ and $x_{ML}$ are the molar fractions of the free receptor and the metal complex, respectively; whereas $E_{1/2}{}^L$ and $E_{1/2}{}^{ML}$ are the oxidation potential of L$^1$ and the oxidation potential of a 1:1 ligand-to-metal molar ratio. Knowing the amount of receptor used in the electrochemical experiments it is possible to determine the concentration of metal ions in solution. In a typical experiment we measured $E_{1/2}$ for an unknown $M^{2+}/L^1$ ratio at at least five different pH values and have determined an average concentration of the metal and the standard deviation. Working with L$^1$ concentrations in the range (4–5) $\times 10^{-4}$ mol dm$^{-3}$ we have been able to determine metal ion concentrations from $5 \times 10^{-5}$ to $4 \times 10^{-4}$ mol dm$^{-3}$. Probably lower limits of detection could be reached by using lower concentrations of receptor L$^1$. Table 1 shows the concentration of $Cu^{2+}$, $Zn^{2+}$ and $Cd^{2+}$ found and compared with the concentration by standard atomic absorption analysis. We have also developed studies on the quantitative determination of two metal ions showing different L$^1$–H$^+$–M$^{2+}$ curves to that of L$^1$ and have found that the simultaneous determination of $Cu^{2+}$, $Cd^{2+}$ and $Cu^{2+}$, $Zn^{2+}$ in mixtures containing both ions is possible if [L$^1$] = [$Cu^{2+}$] + [$Zn^{2+}$] or [L$^1$] = [$Cu^{2+}$] + [$Cd^{2+}$], whereas the method seems not to be accurate enough if the total concentration of the metals is unknown. Additionally the existence of some metal ions, as $Ni^{2+}$ and $Pb^{2+}$, with L$^1$–H$^+$–M$^{2+}$ curves close to that of L$^1$ suggests that the concentration of $Cu^{2+}$ (which probably has a higher stability constant with L$^1$ than $Ni^{2+}$ or $Pb^{2+}$) could be determined in the presence of those metal ions. Data in Table 1 confirm that [$Cu^{2+}$] can be selectively determined in the presence of $Ni^{2+}$ or $Pb^{2+}$. Even with large amounts of $Pb^{2+}$ copper(II) can be quite accurately determined {[$Cu^{2+}$] = $4.9 \times 10^{-5}$, $2.33 \times {}^1 10^{-4}$ and $3.32 \times 10^{-4}$ mol dm$^{-3}$ found in the presence of [$Pb^{2+}$] = $2.23 \times 10^{-3}$ for copper concentrations of $1.33 \times 10^{-4}$, $2.66 \times 10^{-4}$ and 3.33




L$^1$

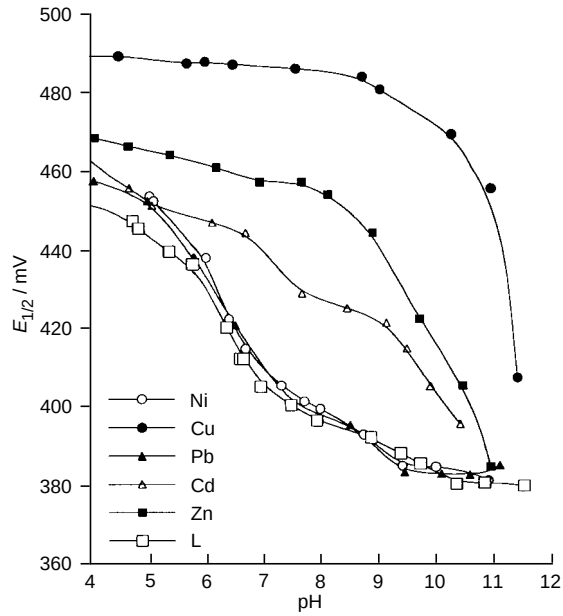



**Fig. 1** Plot of $E_{1/2}$ *vs.* pH for L$^1$–H$^+$ and L$^1$–H$^+$–M$^{2+}$ (M$^{2+}$ = $Ni^{2+}$, $Cu^{2+}$, $Zn^{2+}$, $Cd^{2+}$, $Pb^{2+}$)

**Table 1** Comparison between the determination of the concentration of metal ions by using electrochemical ($L^1$ as receptor) and standard atomic absorption methods

| $10^5$ [$Cu^{2+}$] | $10^5$ [$Zn^{2+}$] | $10^5$ [$Cd^{2+}$] | $10^5$ [$Cu^{2+}$] + [$Cd^{2+}$][a] | $10^5$ [$Cu^{2+}$] + [$Zn^{2+}$][d] | $10^5$ [$Cu^{2+}$][e] | $10^5$ [$Cu^{2+}$][f] |
|---|---|---|---|---|---|---|
| 8.8(6)[a] [9.1][b] | 5.2(9) [5.9] | 10.6(7) [11.1] | 13(2), 27(3) [12.9, 26.6] | 14(1), 26(1) [13.4, 26.1] | 11(4) [9.6] | 11(1) [9.7] |
| 17(1) [18.7] | 27(1) [28.4] | 19(1) [22.4] | 19(2), 20(3) [20.1, 19.5] | 20(1), 20(1) [20.1, 19.7] | 25(4) [19.3] | 20(1) [19.4] |
| 29(1) [28.0] | 18(1) [17.9] | 31(2) [33.6] | 28(1), 12(2) [26.9, 12.9] | 28(1), 12(1) [26.7, 13.2] | 30(3) [28.9] | 28(1) [28.9] |

[a] Concentration (mol $dm^{-3}$). Values in parentheses are the standard deviations in the last significant digit. [b] Metal concentration (mol $dm^{-3}$) found using standard atomic absorption methods. [c] Determination under the condition [$L^1$] = [$Cu^{2+}$] + [$Cd^{2+}$]. [d] Determination under the condition [$L^1$] = [$Cu^{2+}$] + [$Zn^{2+}$]. [e] [$Cu^{2+}$] determined in the presence of $Ni^{2+}$, [$Ni^{2+}$] = $20 \times 10^{-5}$ mol $dm^{-3}$. [f] [$Cu^{2+}$] determined in the presence of $Pb^{2+}$, [$Pb^{2+}$] = $20 \times 10^{-5}$ mol $dm^{-3}$.

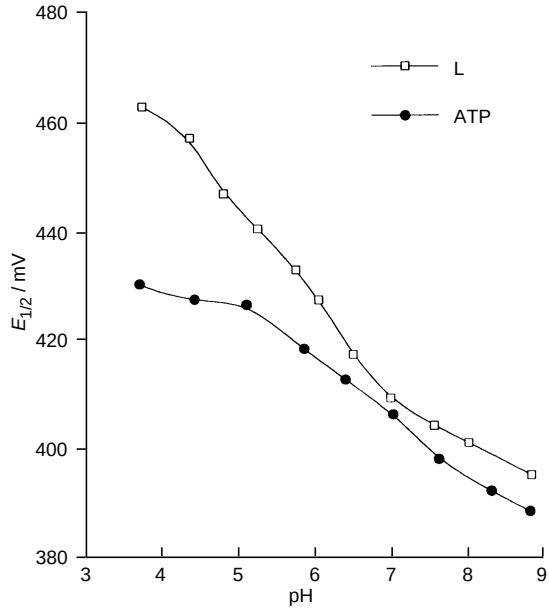



**Fig. 2** Plot of $E_{1/2}$ *vs.* pH for $L^1$–$H^+$ and $L^1$–$H^+$–ATP

$\times 10^{-4}$ mol $dm^{-3}$, respectively, from standard atomic absorption analysis}.

Finally Fig. 2 displays the $E_{1/2}$–pH curve obtained for receptor $L^1$ with ATP. The presence of the anion, as expected, does not change significantly the $E_{1/2}$–pH curve of $L^1$ when the pH is basic, but if the pH is reduced a steady shift to more cathodic potentials is observed. Based on that difference between the two $L^1$–$H^+$ and $L^1$–$H^+$–ATP systems and following a similar method to that used above we have determined ATP concentrations in aqueous solution (see Table 2). The results, which are as acurate as when metal ions are determined, although there is a small difference between $L^1$–$H^+$ and $L^1$–$H^+$–ATP curves, suggest that the method may prove useful in the determination of ATP or other anions using similar systems containing larger numbers of amino groups.

To our knowledge this is a new method for the quantitative determination of metal ions and anions in aqueous solution by using pH-responsive redox-active receptors. As an example molecule $L^1$ has proved to be a versatile receptor which can be used to quantitatively determine metal ions ($Cu^{2+}$, $Zn^{2+}$ or $Cd^{2+}$; mixtures of $Cu^{2+}$, $Cd^{2+}$ and $Cu^{2+}$, $Zn^{2+}$; $Cu^{2+}$ selectively in the presence of $Ni^{2+}$ or $Pb^{2+}$) and anions (ATP). The development of new sensors for quantitative recognition is now being carried out.

**Table 2** Determination of the concentration of ATP by using electrochemical methods and $L^1$ as receptor[a]

| $10^5$ [ATP] |
|---|
| 17(2)[b] [16.4] |
| 21(1) [18.9] |
| 40(2) [41.1] |

[a] Data for the ATP determination have been taken from pH 3.5 to 5. [b] Concentration (mol $dm^{-3}$). Values in parentheses are the standard deviations in the last significant digit.

We should like to thank the DGICYT (proyecto PB95-1121-C02-02) for support.

## Footnote

* E-mail: rmaez@qim.upr.es

## References

1 P. D. Beer, *Chem. Soc. Rev.*, 1989, **18**, 409.
2 P. D. Beer, J. P. Danks, D. Hesek and J. McAleer, *J. Chem. Soc., Chem. Commun.*, 1993, 1735; A. Kaifer, D. A. Gustowski, L. Echegoyen, V. J. Gatto, R. A. Goli, A. M. Rios and G. W. Gokel, *J. Am. Chem. Soc.*, 1995, **107**, 1958.
3 P. D. Beer, *Chem. Commun.*, 1996, 689; C. Dusemund, K. R. A. S. Sandanayake and S. Sinkai, *J. Chem. Soc., Chem. Commun.*, 1995, 333; P. D. Beer, M. G. B. Drew, D. Hesek and R. Jagessar, *J. Chem. Soc., Chem. Commun.*, 1995, 1187.
4 P. D. Beer, Z. Chen, M. G. B. Drew and P. A. Gale, *J. Chem. Soc., Chem. Commun.*, 1995, 1851; A. Ori and S. Sinkai, *J. Chem. Soc., Chem. Commun.*, 1995, 1771.
5 M. J. L. Tendero, A. Benito, R. Martínez-Máñez, J. Soto, J. Payá, A. J. Edwards and P. R. Raithby, *J. Chem. Soc., Dalton Trans.*, 1996, 343; M. J. L. Tendero, A. Benito, R. Martínez-Máñez, J. Soto, E. García-España, J. A. Ramirez, M. I. Burguete and S. V. Luis, *J. Chem. Soc., Dalton Trans.*, 1996, 2923.
6 P. D. Beer, Z. Chen, M. G. B. Drew, J. Kingston, M. Ogden and P. Spencer, *J. Chem. Soc., Chem. Commun.*, 1993, 1046; P. D. Beer, Z. Chen, M. G. B. Drew, A. O. M. Johnson, D. K. Smith and P. Spencer, *Inorg. Chim. Acta*, 1996, **246**, 143.
7 P. D. Beer, J. E. Nation, S. L. W. McWhinnie, M. E. Harman, M. B. Hursthouse, M. I. Ogden and A. H. White, *J. Chem. Soc., Dalton Trans.*, 1991, 2485.

*Received in Cambridge, UK, 29th January 1997; Com. 7/00674H*

# First mononuclear organometallics of $Mo^{II}$ and $Mo^{III}$ containing terminal hydroxide ligands. X-Ray structure of $[Mo(\eta^5\text{-}C_5H_5)(OH)(PMe_3)_3]BF_4$

**James C. Fettinger,[a] Heinz-Bernhard Kraatz,[b] Rinaldo Poli*[a,c] and E. Alessandra Quadrelli[a]**

[a] *Department of Chemistry and Biochemistry, University of Maryland, College Park, Maryland 20742, USA*
[b] *Steacie Institute for Molecular Science, National Research Council of Canada, 100 Sussex Drive, Ottawa, Canada, K1N 0R6*
[c] *Laboratoire de Synthèse et d'Electrosynthèse Organometallique, Faculté des Sciences "Gabriel", Université de Bourgogne, 6 Boulevard Gabriel, 21100 Dijon, France*

**The new complexes $[Mo(\eta^5\text{-}C_5H_5)(OH)(PMe_3)_2]$ and $[Mo(\eta^5\text{-}C_5H_5)(OH)(PMe_3)_3]^+$ are unique examples of electronically unsaturated organometallics of $Mo^{II}$ and $Mo^{III}$ containing terminal hydroxide ligands; they show no tendency to dimerize with formation of hydroxo-bridges.**

Hydroxide ligands are ubiquitous of Werner-type coordination chemistry, whereas they are less commonly found in organometallic compounds. The availability of lone pairs on the oxygen atom frequently leads a terminal hydroxide complex (**I**) to lose ligands and afford doubly or triply bridged oligomers, *e.g.* **II** and **III**.[1–4] Organometallic compounds with terminal hydroxide ligands have rarely been observed for early- and late-transition-metal systems,[5–10] and for low-oxidation state saturated (18-electron) systems with tightly bonded ancillary ligands, examples of which are $[Mo(OH)(NO)(dppe)_2]$[11] and $[W(CO)_5(OH)]^-$.[12] We consider it therefore quite surprising to find the existence and stability toward dimerization of a mononuclear and paramagnetic organometallic $Mo^{II}$ hydroxo complex with a 16-electron configuration. To the best of our knowledge, there are only two previous examples of formally 16-electron $Mo^{II}$ complexes with terminal OH ligands, *i.e.* [MoL(NO)(O)(OH)] (L = 1,4,7-triisopropyl-1,4,7-triazacyclononane), and its corresponding protonated form, $[MoL(NO)(OH)_2]^+$.[13] These, however, do not contain M–C bonds and are diamagnetic, probably because extra π donation from the oxo lone pair(s) renders the compounds effectively saturated.

The reaction of $[Mo(\eta^5\text{-}C_5H_5)Cl(PMe_3)_3]$[14] with dry KOH in thf leads to the exchange of the chloride ion and the formation of paramagnetic $[Mo(\eta^5\text{-}C_5H_5)(OH)(PMe_3)_2]$ **1** [eqn. (1)].† The

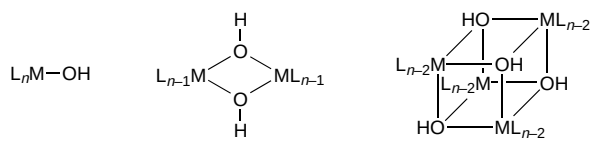
$$[Mo(\eta^5\text{-}C_5H_5)Cl(PMe_3)_3] + KOH \rightarrow \underset{\mathbf{1}}{[Mo(\eta^5\text{-}C_5H_5)(OH)(PMe_3)_2]} + KCl + PMe_3 \qquad (1)$$

same transformation occurs in $C_6D_6$, allowing the observation of 1 equiv. of free $PMe_3$ by a $^1H$ NMR monitoring experiment (Fig. 1). The $^1H$ NMR spectrum of **1** shows contact-shifted resonances at δ 21.8 and 20.3 in the correct ratio for the $PMe_3$ and $C_5H_5$ protons. The $^{31}P$ NMR spectrum shows only the resonance of free $PMe_3$. The compound is extremely soluble in saturated hydrocarbons, thus preventing its isolation in crystalline form. The formulation of the complex as mononuclear rather than dinuclear is based on a comparison with literature analogues: $[Mo(\eta^5\text{-}C_5Me_5)ClL_2]$ (L = $PMe_3$, $PMe_2Ph$ or $L_2$ = dppe) and $[Mo(\eta^5\text{-}C_5H_5)Cl(PMe_2Ph)_2]$ are also mononuclear paramagnetic ($S$ = 1) complexes,[15] and show contact-shifted $^1H$ NMR resonances similar to those of **1**. On the other hand, $[\{Mo(\eta^5\text{-}C_5H_5)(\mu\text{-}Br)(\eta^4\text{-}C_4H_6)\}_2]$ is dinuclear and diamagnetic.[16] Mononuclear 16-electron $[Mo(\eta^5\text{-}C_5H_5)XL_2]$ complexes also exist with a spin-singlet ground state,[17] whereas there are no paramagnetic 18-electron complexes in this class. A bis(μ-hydroxo) dimeric structure for **1** is therefore ruled out.

It is rather peculiar that **1** is stable not only toward dimerization, but also toward coordination of the $PMe_3$ ligand [eqn. (1)]. The corresponding chloro parent compound does not have any tendency to lose the third $PMe_3$. However, sterically more encumbered $[Mo(\eta^5\text{-}C_5Me_5)Cl(PMe_3)_3]$ and $[Mo(\eta^5\text{-}C_5H_5)Cl(PMe_2Ph)_3]$ exist in equilibrium with the corresponding 16-electron bis-phosphine complexes.[15] This behaviour is in line with the greater π-donating ability of OH *vs.* Cl. The paramagnetism of **1** parallels that of the chloro analogues, but is in contrast with the diamagnetism of the phosphido or arsenido derivatives $[Mo(\eta^5\text{-}C_5Me_5)(PPh_2)L_2]$[17] and $[Mo(\eta^5\text{-}C_5H_5)(AsBu^t_2)(CO)_2]$.[18] We have previously rationalized this phenomenon in terms of differences in MO interactions (single-sided *vs.* double-sided π donors) and pairing energy stabilization.[15,19] Elaborating on those arguments, the paramagnetism of **1** might suggest the involvement of both oxygen lone pairs in two orthogonal two-centre–three electron interactions.[20]

Further treatment of the **1**–$PMe_3$ solution in thf with $[Fe(\eta^5\text{-}C_5H_5)_2]BF_4$ leads to at least two products. Crystallization from acetone–heptane affords yellow needles of $[Mo(\eta^5\text{-}C_5H_5)(OH)(PMe_3)_3]BF_4$ **2** and red cubes of $[Mo(\eta^5\text{-}C_5H_5)O(PMe_3)_2]BF_4$ **3**. The structure of **2** (Fig. 2)‡ shows a terminal mode for the hydroxide ligand in the expected four-legged piano-stool geometry, as found[14] for the related $[Mo(\eta^5\text{-}C_5H_5)Cl(PMe_3)_3]^+$. The structural parameters are normal for this class of compounds,[21] with the Mo–O bond measuring 2.084(2) Å. To the best of our knowledge, **2** is the first reported organometallic hydroxide of $Mo^{III}$, and the first complex of $Mo^{III}$ (including Werner-type and clusters) with a terminally bonded hydroxide.[22–25] A deprotonated form of the $Mo^{III}$ aquo complex $[Mo(H_2O)_6]^{3+}$ is known, but this corresponds to a μ-hydroxo dimer, *i.e.* $[\{Mo(H_2O)_4(\mu\text{-}OH)\}_2]^{4+}$.[26] **3** has been previously reported.[27]§

The formation of **2** by oxidation of **1** occurs according to the stoichiometry of eqn. (2). Half-sandwich $Mo^{III}$ complexes are




**I** **II** **III**

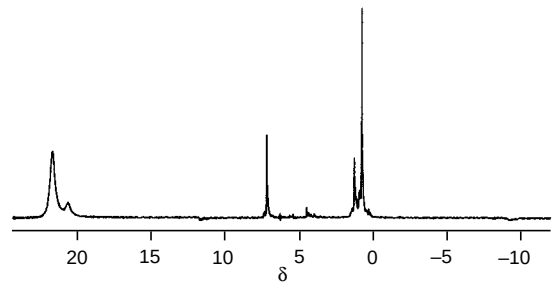



**Fig. 1** Room-temperature $^1H$ NMR spectrum of the products of reaction (1); solvent $C_6D_6$

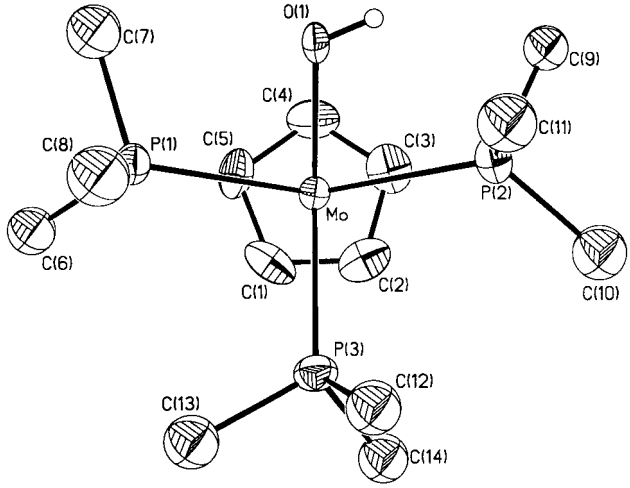



**Fig. 2** Top view of the cation in compound **2**. Ellipsoids drawn at 30% probability. Selected bond lengths (Å) and angles (°): Mo–P(1) 2.4530(12), Mo–P(2) 2.4984(12), Mo–P(3) 2.4741(11), Mo–O(1) 2.084(2), Mo–Cp 1.980(4); P(1)–Mo–P(2) 94.19(5), P(1)–Mo–P(3) 93.21(4), P(1)–Mo–O(1) 139.27(10), P(1)–Mo–Cp 108.5(1), P(2)–Mo–P(3) 132.81(4), P(2)–Mo–O(1) 71.53(8), P(2)–Mo–Cp 110.7(1), P(3)–Mo–O(1) 72.75(8), P(3)–Mo–Cp 110.8(1), O(1)–Mo–Cp 112.2(2). Cp is the $C_5H_5$ ring centroid.

known to prefer the 17-electron configuration.[21,28] The nature of the observed product **2** shows that a bis(μ-hydroxo)-bridged $[\mathbf{1}_2]^{2+}$ complex would be unstable relative to the mononuclear 17-electron $PMe_3$ adduct. The hydroxide proton in complex **2** can be reasonably expected to be acidic. Presumably, the presence of free $PMe_3$ or other adventitious proton acceptors during the formation of **2** induces a deprotonation equilibrium to afford a neutral $Mo^{III}$ oxo species which is then easily oxidized by $[Fe(\eta^5\text{-}C_5H_5)_2]^+$ to afford the observed product **3** [eqn. (3)].

$$[Mo(\eta^5\text{-}C_5H_5)(OH)(PMe_3)_2] + PMe_3 + [Fe(\eta^5\text{-}C_5H_5)_2]^+ \rightarrow [Mo(\eta^5\text{-}C_5H_5)(OH)(PMe_3)_3]^+ + [Fe(\eta^5\text{-}C_5H_5)_2] \quad (2)$$

$$[Mo(\eta^5\text{-}C_5H_5)(OH)(PMe_3)_3]^+ + [Fe(\eta^5\text{-}C_5H_5)_2]^+ \xrightarrow{-H^+\text{-}PMe_3} [Mo(\eta^5\text{-}C_5H_5O)(PMe_3)_2]^+ + [Fe(\eta^5\text{-}C_5H_5)_2] \quad (3)$$

In conclusion, we have reported here for the first time the existence and stability of terminal hydroxo complexes of paramagnetic organometallics of $Mo^{II}$ and $Mo^{III}$ in defiance of the possible dimerization with formation of hydroxo-bridges. For the dimerization process to occur, **2** would have to lose the stabilization of the $Mo^{III}$–$PMe_3$ bond, whereas compound **1** would have to pay the price of pairing the electrons. Terminal hydroxo complexes of $Mo^{IV}$, on the other hand, have been previously reported.[2,29–34]

This research was supported by the US Department of Energy Office of Energy Research (grant DEFG0295ER14550) and the National Science Foundation (grant CHE-9508521).

## Footnotes

* E-mail: poli@u-bourgogne.fr

† By carrying out all operations under a dinitrogen atmosphere, solid KOH (pre-dried at 110 °C and 6 mmHg for 48 h; *ca*. 300 mg, *ca*. 5.3 mmol) was added to a blue solution of $[Mo(\eta^5\text{-}C_5H_5)Cl(PMe_3)_3]$ (215 mg, 0.507 mmol) in 6 ml of thf. After stirring overnight at room temp., complete evaporation of the solvent from the yellow–brown solution yielded an oily residue, which was extracted into heptane (3 × 5 ml). An aliquot of this solution was dried under reduced pressure and the residue was investigated by $^1H$ NMR in $C_6D_6$: δ 21.8 (br, $w_{1/2}$ 90 Hz, 18 H, Me), 20.3 (br, $w_{1/2}$ 75 Hz, 5 H, $C_5H_5$). Concentration of the heptane solution and cooling to −80 °C did not separate any solid.

‡ *Crystal data* for **2**: $C_{14}H_{33}BF_4MoOP_3$, $M$ = 493.06, orthorhombic, space group $Pna2_1$, $a$ = 20.525(5), $b$ = 13.380(4), $c$ = 7.9740(7) Å, $U$ = 2189.9(9) Å$^3$, $Z$ = 4, $D_c$ = 1.496 Mg m$^{-3}$, μ(Mo-Kα) = 0.851 mm$^{-1}$, $2\theta_{max}$ = 49.96°, ω–2θ scan mode, λ = 0.710 73 Å, $T$ = 293(2) K, $R_1$ = 0.0353 ($wR_2$ = 0.0734) for all data, $R_1$ = 0.0267 ($wR_2$ = 0.0567) for 226 parameters and 3339 observed [$I > 2\sigma(I)$] data (3712 collected and independent reflections). Atomic coordinates, bond lengths and angles, and thermal parameters have been deposited at the Cambridge Crystallographic Data Centre (CCDC). See Information for Authors, Issue No. 1. Any request to the CCDC for this material should quote the full literature citation and the reference number 182/429.

§ The $^1H$ NMR properties match with those reported.[27] $^{31}P$ NMR ($CD_3COCD_3$): 13.8. The identity of this compound is also verified by an X-ray crystallographic study, which will be reported separately.

## References

1 M. E. Falkley and A. Pidcock, *J. Chem. Soc., Dalton Trans.*, 1977, 1444.
2 V. Albano, P. Bellon, G. Cini and M. Manassero, *Chem. Commun.*, 1969, 1242.
3 U. Sartorelli, L. Garlaschelli, G. Ciani and G. Bonora, *Inorg. Chim. Acta*, 1971, **5**, 191.
4 M. Herberhold, G. Süß, J. Ellermann and H. Gäbelein, *Chem. Ber.*, 1978, **111**, 2931.
5 G. L. Hillhouse and J. E. Bercaw, *J. Am. Chem. Soc.*, 1984, **106**, 5472.
6 S. A. Al-Jibori, *J. Organomet. Chem.*, 1996, **506**, 119.
7 V. V. Grushin and H. Alper, *Organometallics*, 1996, **15**, 5242.
8 T. G. Appleton and M. A. Bennett, *Inorg. Chem.*, 1978, **17**, 738.
9 D. P. Arnold and M. A. Bennett, *J. Organomet. Chem.*, 1980, **199**, 119.
10 D. P. Arnold and M. A. Bennett, *Inorg. Chem.*, 1984, **23**, 2110.
11 C. T. Kan, P. B. Hitchcock and R. L. Richards, *J. Chem. Soc., Dalton Trans.*, 1982, 79.
12 J. L. Cihonski and R. A. Levenson, *Inorg. Chem.*, 1975, **14**, 1717.
13 J. Böhmer, G. Haselhorst, K. Wieghardt and B. Nuber, *Angew. Chem., Int. Ed. Engl.*, 1994, **33**, 1473.
14 F. Abugideiri, M. A. Kelland, R. Poli and A. L. Rheingold, *Organometallics*, 1992, **11**, 1303.
15 F. Abugideiri, J. C. Fettinger, D. W. Keogh and R. Poli, *Organometallics*, 1996, **15**, 4407.
16 L.-S. Wang, J. C. Fettinger and R. Poli, *J. Am. Chem. Soc.*, in the press.
17 R. T. Baker, J. C. Calabrese, R. L. Harlow and I. D. Williams, *Organometallics*, 1993, **12**, 830.
18 M. Luksza, S. Kimmer and W. Malisch, *Angew. Chem., Int. Ed. Engl.*, 1983, **22**, 416.
19 F. Abugideiri, D. W. Keogh and R. Poli, *J. Chem. Soc., Chem. Commun.*, 1994, 2317.
20 R. Poli, *Chem. Rev.*, 1996, **96**, 2135.
21 R. Poli, *J. Coord. Chem. B*, 1993, **29**, 121.
22 K. Wieghardt, M. Hahn, W. Swiridoff and J. Weiss, *Inorg. Chem.*, 1984, **23**, 94.
23 K. Wieghardt, M. Guttmann, P. Chaudhuri, W. Gebert, M. Minelli, C. G. Young and J. H. Enemark, *Inorg. Chem.*, 1985, **24**, 3151.
24 A. G. Sykes, in *Comprehensive Coordination Chemistry*, ed. G. Wilkinson, R. D. Gillard and J. McCleverty, Pergamon, Oxford, 1987, ch. 36.1.
25 K. Wieghardt, U. Bossek, A. Neves, B. Nuber and J. Weiss, *Inorg. Chem.*, 1989, **28**, 432.
26 D. T. Richens and A. G. Sykes, *Inorg. Synth.*, 1985, **23**, 130.
27 M. Brookhart, K. Cox, F. G. N. Cloke, J. C. Green, M. L. H. Green, P. M. Hare, J. Bashkin, A. E. Derome and P. D. Grebenik, *J. Chem. Soc., Dalton Trans.*, 1985, 423.
28 I. Cacelli, D. W. Keogh, R. Poli and A. Rizzo, *New J. Chem.*, 1997, **21**, 133.
29 K. Prout, T. S. Cameron, R. A. Forder, S. R. Critchley, B. Denton and G. V. Rees, *Acta Crystallogr., Sect. B*, 1974, **30**, 2290.
30 P. R. Robinson, E. O. Schlemper and R. K. Murmann, *Inorg. Chem.*, 1975, **14**, 2035.
31 M. R. Churchill and F. J. Rotella, *Inorg. Chem.*, 1978, **17**, 668.
32 M. Berry, N. J. Cooper, M. L. H. Green and S. J. Simpson, *J. Chem. Soc., Dalton Trans.*, 1980, 29.
33 K. Wieghardt, G. Backes-Dahman, W. Holzbach, W. J. Swirdoff and J. Weiss, *Z. Anorg. Allg. Chem.*, 1983, **499**, 44.
34 T. Adachi, D. L. Hughes, S. K. Ibrahim, S. Okamoto, C. J. Pickett, N. Yabanouchi and T. Yoshida, *J. Chem. Soc., Chem. Commun.*, 1995, 1081.

*Received in Cambridge, UK, 7th March 1997; Com. 7/01616F*

# A novel organometallic oxide cluster with multi-valley sites: synthesis and structure of $[NBu^n_4]_2[\{(\eta^5\text{-}C_5Me_5)Rh\}_2Mo_6O_{20}(OMe)_2]$ and its framework transformations

**Satoshi Takara, Takanori Nishioka, Isamu Kinoshita and Kiyoshi Isobe***

*Department of Material Science, Faculty of Science, Osaka City University, Sugimoto, Sumiyoshi-ku, Osaka 558, Japan*

**A novel organometallic oxide cluster $[NBu^n_4]_2[\{(\eta^5\text{-}C_5Me_5)Rh\}_2Mo_6O_{20}(OMe)_2]$ 1 with multi-valley sites is synthesized by the reaction of $[NBu^n_4]_2[Mo_2O_7]$ and $\{(\eta^5\text{-}C_5Me_5)RhCl(\mu\text{-}Cl)\}_2$ in a molar ratio of 4:1 in methanol, and displays unique framework transformations upon treatment with organometallic and oxometalate compounds.**

Theoretical studies on catalytic hydrocarbon transformation on metal oxides showed that coordinatively unsaturated metal sites and valley sites in integrated cubic cluster models play an important role for activation of hydrocarbons.[1] Indeed, organometallic oxide clusters, such as the incomplete cubane-type cluster $[\{(\eta^5\text{-}C_5Me_5)Rh\}_2Mo_3O_9(OMe)_4]$ **2**,[2a] the face-shared triply fused cubane-type cluster $[\{(\eta^5\text{-}C_5Me_5)Rh\}_4Mo_4O_{16}]$ **3**,[2b] the valley-site structure $[\{(\eta^5\text{-}C_5Me_5)Rh\}_4V_6O_{19}]$[2c,d] and the planar cluster $[NBu^n_4]_2[\{(\eta^3\text{-}C_4H_7)_2Rh\}_2V_4O_{12}]$[2f] supported on silica, exhibit significant catalytic abilities and higher selectivities for oxidation and metathesis of propene.[3] Thus, our current efforts concentrate on the design and development of synthetic strategies for new organometallic oxide clusters with active sites owing to characteristic structures such as lacunary, incomplete cubic, or valley-site frameworks.[2a–e]

Here, we report on the structure and synthesis of the organometallic oxide cluster $[NBu^n_4]_2[\{(\eta\text{-}C_5Me_5)Rh\}_2Mo_6O_{20}(OMe)_2]$ **1** with multi-valley sites and its framework transformations.

A mixture of $[NBu^n_4]_2[Mo_2O_7]$[4] (2.55 g, 3.24 mmol) and $[\{(\eta^5\text{-}C_5Me_5)RhCl(\mu\text{-}Cl)\}_2]$[5] (0.50 g, 0.81 mmol) in 20 ml of methanol was allowed to stand for 4 h with stirring at room temp. and concentrated to 5 ml. Diethyl ether (80 ml) was then added slowly to give an orange precipitate of **1**. The crude product is recrystallized from methanol–diethyl ether (1.22 g, 79% yield based on Rh).† The formation of **1** may proceed according to eqn. (1).‡

$$[\{(\eta^5\text{-}C_5Me_5)RhCl(\mu\text{-}Cl)\}_2] + 3[NBu^n_4]_2[Mo_2O_7] + 2MeOH \rightarrow [NBu^n_4]_2[\{(\eta^5\text{-}C_5Me_5)Rh\}_2Mo_6O_{20}(OMe)_2] \quad \mathbf{1} \quad + 4[NBu^n_4]Cl + H_2O \qquad (1)$$

An X-ray analysis of **1** reveals that the anion of **1** has $C_i$ symmetry and is composed of four $MoO_6$ and two $MoO_5(\mu\text{-}OMe)$ octahedra interlinked along edges and two $(\eta^5\text{-}C_5Me_5)Rh$ groups each sharing two edges with the octahedra (Fig. 1).§ The framework of **1** is in some respects similar to that of the $\gamma\text{-}[Mo_8O_{26}]^{4-}$ isomer found in $[(Me_3N(CH_2)_6NMe_3]_2[Mo_8O_{26}]\cdot 2H_2O$, which also has $C_i$ symmetry and is composed of six $MoO_6$ octahedra interlinked along edges and two $MoO_5$ trigonal bipyramids each sharing two edges with the octahedra.[6] The structure of **1** can be regarded as a framework which contains two $(\eta^5\text{-}C_5Me_5)Rh(\mu\text{-}OMe)$ groups rather than two $MoO_5$ trigonal bipyramids. It is noteworthy that $(\eta^5\text{-}C_5Me_5)Rh$ moieties and methoxy groups in the framework of **1** form two unique large valley sites, constructed by Rh(1)Mo(3*)Mo(1)Mo(2*) and Rh(1*)Mo(3)Mo(1*)Mo(2), while two small ones are constructed by Mo(1)Mo(2)Mo(3) and Mo(1*)Mo(2*)Mo(3*). For these two kinds of valley sites, a space-filling model¶ suggests that the small sites are much more open with exposed highly basic oxygens [O(2), O(4), O(8)], whereas the larger ones are rimmed with bulky pentamethylcyclopentadienyl, methoxy and Mo=O groups so as to form shallow cavities.

Bearing in mind that **1** might show high reactivity due to the presence of valley sites, we have been prompted to investigate the reactivity of **1** towards organometallic (electrophile) and oxometalate (nucleophile) compounds. Consequently, cluster framework transformations of **1** occur in both, for example, by treatments with $\{(\eta^5\text{-}C_5Me_5)Rh\}^{2+}$ and with $[Mo_2O_7]^{2-}$ in methanol to produce the incomplete double cubane-type cluster of **2** and the triply fused cubane-type cluster of **3**, respectively (Scheme 1).‖ The basic bridging oxygens [O(2), O(4), O(8)] in the small valley sites can interact freely with metal cations, hence in the formation of **2**, landing of the added $\{(\eta^5\text{-}C_5Me_5)Rh\}^{2+}$ cations on the small valley sites probably triggers an initial step of the transformation. On the other hand for the formation of **3**, the added $[Mo_2O_7]^{2-}$ anions will approach the rhodium(III) centres in the shallow cavities by electrostatic force of attraction: the parts of $Rh^{III}$ centres in the shallow cavities are most exposed to attack by nucleophiles. By the action of an excess of $[Mo_2O_7]^{2-}$ some of the weak Rh–O

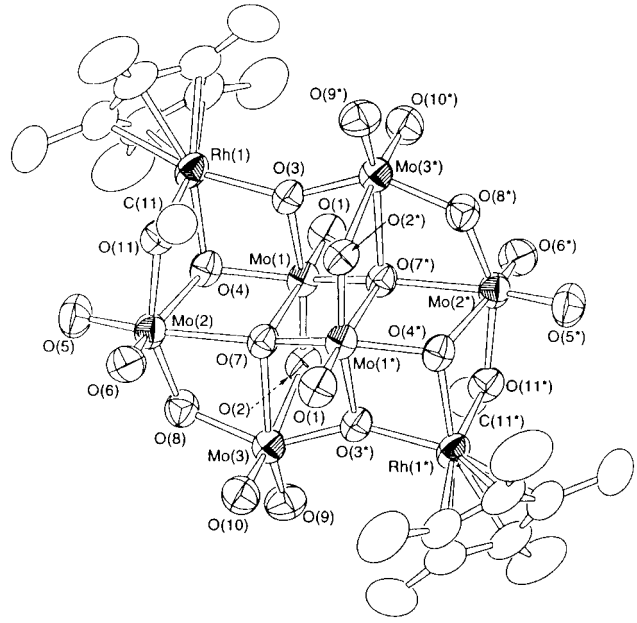
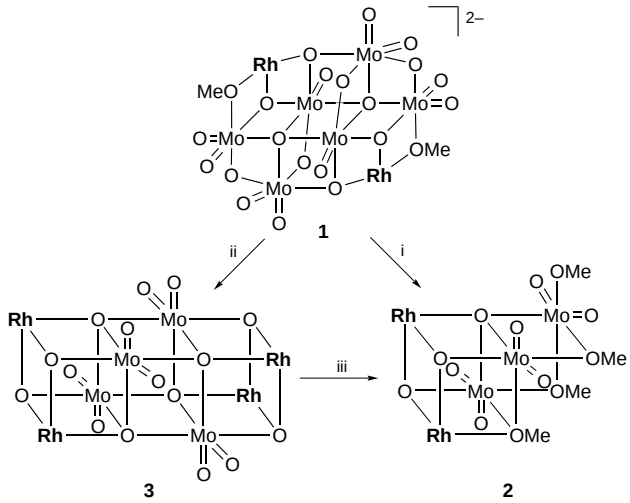



**Fig. 1** Structure of the anion in **1**. Selected bond lengths (Å): Mo(1)–O(1) 1.696(3), Mo(1)–O(2) 1.744(3), Mo(1)–O(3) 2.152(3), Mo(1)–O(4) 1.928(3), Mo(1)–O(7) 1.916(3), Mo(2)–O(4) 2.178(3), Mo(2)–O(5) 1.695(4), Mo(2)–O(6) 1.708(3), Mo(2)–O(7) 2.299(3), Mo(2)–O(8) 1.892(3), Mo(2)–O(11) 1.411(6), Mo(3)–O(2) 2.363(3), Mo(3)–O(3) 1.908(3), Mo(3)–O(7) 2.277(3), Mo(3)–O(8) 1.946(3), Mo(3)–O(9) 1.703(4), Mo(3)–O(10) 1.704(4), Rh(1)–O(3) 2.068(3), Rh(1)–O(4) 2.100(3), Rh(1)–O(11) 2.109(3).




**Scheme 1** **Rh** = Rh($\eta^5$-$C_5Me_5$). *Reagents and conditions:* i, [{($\eta^5$-$C_5Me_5$)RhCl($\mu$-Cl)}$_2$] 1 equiv., MeOH, 27 °C; ii, [$NBu^n_4$]$_2$[$Mo_2O_7$] 4 equiv., MeOH, 27 °C; iii, *p*-hydroquinone, MeOH, reflux; see ref. 2(*a*).

[*e.g.* Rh(1)–O(11) and Rh(1)–O(3)] bonds in the large valley sites may be cleaved to cause a new condensation of oxomolybdates on the vacant sites of the ($\eta$-$C_5Me_5$)Rh centres to afford the most stable species, the triply fused cubane-type cluster [{($\eta^5$-$C_5Me_5$)Rh}$_4$$Mo_4O_{16}$] **3**. Although the transformations mentioned above to form **2** and **3** might contain complicated steps to be elucidated, the unique valley sites of **1** can fulfil its function to initiate the framework transformations and cluster **1** may act as a convenient molecular platform towards other cationic and anionic transition-metal fragments. The transformations are also particularly important for constructing new oxide cluster architecture; the multi-valley sites cluster **1** is a prominent building block for preparation of larger clusters.

The authors gratefully acknowledge Professors Atsushi Yagasaki (Kwansei Gakuin University, Japan) and Vadim Yu. Kukushkin (St. Petersburg State University, Russian Federation) for invaluable discussions. This work was supported by a Grant-in-Aid Scientific Research (No. 07404038) from the Ministry of Education, Science and Culture, Japan and the Sasakawa Scientific Research Grant from The Japan Science Society.

## Footnotes

* E-mail: isobe@cubane.sci.osaka-cu.ac.jp

† The cluster was analysed satisfactorily (C, H, N) for **1**. Selected IR data (**1**, Nujol) $\nu$/cm$^{-1}$ 440w, 487w, 522m, 638m, 680s, 742m, 858s, 900s, 1040m, 1063m, 1162w, 1663m, 3500m (br).

‡ Excess dimolybdate acts as a base for deprotonation of methanol molecules coordinated to molybdenum atoms. 1 Equiv. of dimolybdate is insufficient to produce **3**, formation of **3** needing 4 equiv. of $[Mo_2O_7]^{2-}$ relative to **1**, as described in Scheme 1.

§ *Crystal data* for $C_{54}H_{108}Mo_6N_2O_{22}Rh_2$, **1**: single crystals of **1** suitable for X-ray crystallography were grown by slow diffusion of diethyl ether into a methanol solution. An orange crystal of dimensions 0.4 × 0.2 × 0.2 mm was mounted on a glass fibre. Cluster **1** crystallizes in the trigonal space group $R\bar{3}$ (no. 148) with $a$ = 41.954(3), $c$ = 12.925(3) Å, $U$ = 19701(4) Å$^3$, $Z$ = 9, and $D_c$ = 1.455 g cm$^{-3}$. A total of 10 722 reflections were collected on a Rigaku AFC-7 diffractometer with graphite-monochromated Mo-K$\alpha$ radiation *via* a $\omega$-scan technique in the limit of $2\theta \leqslant 55.0°$ at 296 K. The reflections with $I > 3\sigma(I)$ were corrected for Lorentz-polarization factors but not for extinction. An absorption correction was applied using an empirical $\psi$-scan method. All crystallographic calculations were carried out using teXsan programs. The positions of the rhodium and molybdenum atoms were obtained by SHELXS86 direct methods. The remaining atoms were located on difference Fourier maps. Hydrogen atoms were fixed at calculated positions and used for structure-factor calculations. 388 variables were refined by full-matrix least-squares techniques using 5960 independent reflections and converged to $R$ = 0.035, $R_w$ = 0.041 and GOF = 1.21. A final difference Fourier map yielded $\Delta\rho_{max}$ = +0.40 e Å$^{-3}$, $\Delta\rho_{min}$ = −0.38 e Å$^{-3}$. Atomic coordinates, bond lengths, angles and thermal parameters have been deposited at the Cambridge Crystallographic Data Centre (CCDC). See Information for Authors, Issue No. 1. Any request to the CCDC for this material should quote the full literature citation and the reference number 182/428.

¶ Available as supplementary data.

‖ Complexes **2** and **3** were identified by spectroscopic data; see ref. 2(*a*) and 2(*b*).

## References

1 K. Sawabe, N. Koga, K. Morokuma and Y. Iwasawa, *J. Chem. Phys*., 1992, **97**, 6871; R. Cain, L. J. Matienzo and F. Emmi, *J. Phys. Chem*., 1990, **29**, 228.

2 (*a*) Y. Do, X.-Z. You, C. Zhang, Y. Ozawa and K. Isobe, *J. Am. Chem. Soc*., 1991, **113**, 5892; (*b*) Y. Hayashi, K. Toriumi and K. Isobe, *J. Am. Chem. Soc*., 1988, **110**, 3666; (*c*) Y. Hayashi, Y. Ozawa and K. Isobe, *Inorg. Chem*., 1991, **30**, 1025; (*d*) *Chem. Lett*., 1989, 425; (*e*) K. Isobe and A. Yagasaki, *Acc. Chem. Res*., 1993, **26**, 524; (*f*) H. Akashi, K. Isobe, Y. Ozawa and A. Yagasaki, *J. Cluster. Sci*., 1991, **2**, 291.

3 M. Ichikawa, W. Pan, Y. Imada, M. Yamaguchi, K. Isobe and T. Shido, *J. Mol. Catal., A*, 1996, **107**, 23; Y. Imada, T. Shido, H. Ohtani, K. Isobe and M. Ichikawa, *Chem. Lett*., 1995, 717; K. Takahashi, M. Yamaguchi, T. Shido, H. Ohtani, K. Isobe and M. Ichikawa, *J. Chem. Soc., Chem. Commun*., 1995, 1301.

4 N. H. Hur, W. G. Klemperer and R.-C. Wang, *Inorg. Synth*., 1990, **27**, 79.

5 C. White, A. Yates and P. M. Maitlis, *Inorg. Synth*., 1992, **29**, 228.

6 M. L. Niven, J. J. Cruywagen and J. B. B. Heyns, *J. Chem. Soc., Dalton Trans*., 1991, 2007.

*Received in Cambridge, UK, 7th March 1997; Com. 7/01618B*

# Hydrothermal synthesis and X-ray structural characterisation of calcium benzene-1,3,5-tricarboxylate

**M. John Platers,* R. Alan Howie and Alexander J. Roberts**

*Department of Chemistry, Aberdeen University, Meston Walk, Aberdeen, UK AB24 3UE*

**Benzene-1,3,5-tricarboxylic acid ($H_3$btc) forms a calcium salt of stoichiometry Ca(hbtc)·2$H_2O$ which possesses an infinite layered structure.**

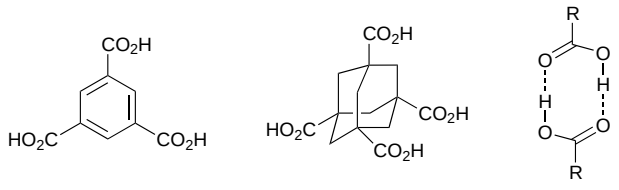
The synthesis of novel crystal structures from polar tectons by hydrogen-bond directed self-assembly and metal-ion or ligand-directed assembly has allowed the preparation of networked microporous materials with potential applications as absorbents,[1] ion exchangers,[2] protonic conductors[3] and catalysts. An inherent difficulty in the formation of microporous materials by the hydrogen-bond controlled self-assembly of tectons[4] such as benzene-1,3,5-tricarboxylic acid ($H_3$btc) **1** or adamantane-tetracarboxylic acid ($H_4$atc) **2** is the tendency for packing to minimise voids and maximise van der Waals contacts in the crystal lattice.[5] Infinite lattice networks of $H_3$btc[6] and $H_4$atc stabilised by the hydrogen-bond dimers **3** would possess large micropores but in practice the dimeric hydrogen bonding is too weak to stabilise these open frameworks and a different condensed crystal structure forms. Recently Yaghi *et al.* reported a solution to this problem by preparing divalent metal ion (Co, Ni, Zn) salts of $H_3$btc which possess a stable networked structure with hydrated divalent metal ions forming strong ionic bonds between the rigid btc tectons.[7] Heating dehydrates the metal ions leaving micropores in the crystal lattice with the metal ions lining the channels.

The work described here is part of an investigation into the hydrothermal synthesis and structural characterisation of the alkaline-earth metal (Ca, Sr, Ba) salts of benzene-1,3,5-tricarboxylic acid with the aim of producing stable microporous materials.† Heating $H_3$btc with calcium acetate in water in a sealed bomb to 180 °C followed by slow cooling gave colourless crystals whose structure was solved by X-ray analysis.‡ The compound did not have the expected 1 : 2 btc : Ca ratio but instead gave crystals of formula Ca(hbtc)·2$H_2O$.† The IR spectrum also showed a stretch at 1695 $cm^{-1}$ indicative of an aromatic carboxylic acid.

The structure consists of infinite two-dimensional layers of hbtc dianions alternating with layers of Ca and water molecules in the *c*-axis direction. The proton H(5) bonded to O(5) of one of the carboxylate groups forms a strong hydrogen bond O(5)–H(5)···O(35) linking the hbtc anions in chains perpendicular to (1,1,0) (Fig. 1). The layers of hbtc anions are composed of such chains packed side-by-side and related in pairs and therfore inverted in orientation by crystallographic centres of symmetry as are the layers themselves. As a result the O(1)–C(7)–O(2) carboxylate groups of the anions in a particular hydrogen-bonded chain lie on one side of the layer while the same carboxylate groups of the neighbouring chains lie on the other side of the layer.

In the layers of Ca and water molecules lying between the layers of hbtc anions the Ca cations occur in centrosymmetrically related pairs. Ca is irregularly coordinated by eight oxygens with Ca–O distances in the range 2.4121(18)–2.5701(16) Å (Fig. 2). Seven of these contacts arise from interaction of Ca with five distinct carboxylate anions. Three anions operate as monodentate ligands generating the Ca contacts with O(14), O(23) and O(62). The last two anions coordinate in a bidentate fashion to generate pairs of contacts with Ca [O(1) and O(2) and O(31) and O(41) respectively]. The coordination of Ca is completed by a contact with one of the water molecules [Ca–O(1w) 2.4199(20) Å]. A feature of the Ca coordination is the presence of the Ca–O(14) and Ca–O(23) contacts which involve distinct carboxylate anions which are in the same layer but related by a cell translation along the *a* axis. The contacts then produce linked pairs of chains interleaved with symmetry related and differently oriented linked chain pairs.

The molecular formula and the asymmetric unit both contain two water molecules. The presence of water was shown by the IR spectrum which showed OH stretches at 3542 and 3342 $cm^{-1}$. One of these [O(1w), H(11w), H(12w)] is not only involved in the coordination of Ca but also forms hydrogen bonds as O(1w)–H(11w)···O(46) to a carboxylate oxygen and



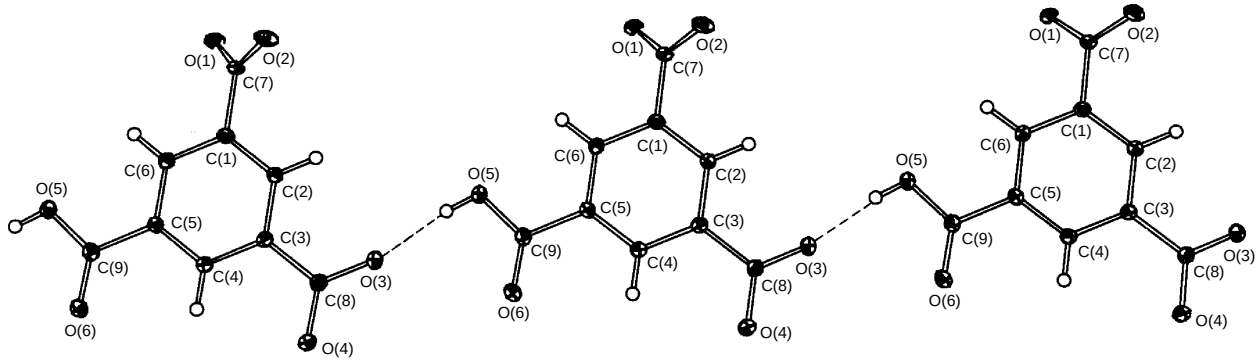




**Fig. 1** Array of hydrogen-bonded hbtc dianions occurring in Ca(hbtc)·2$H_2O$

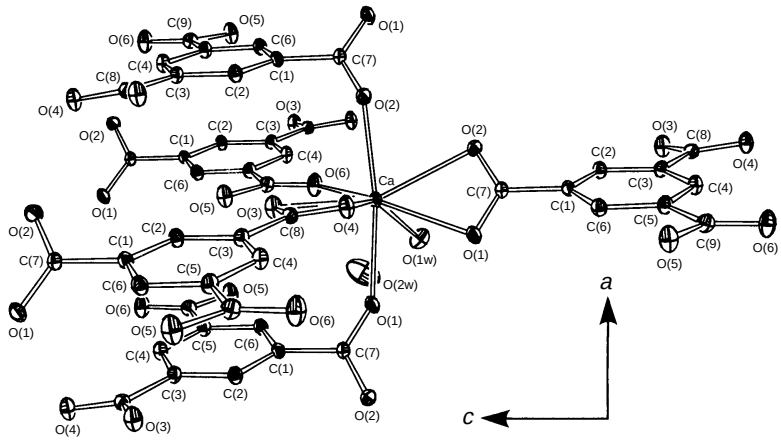



**Fig. 2** The coordination of $Ca^{2+}$ by two bidentate and three monodentate carboxylates and one water molecule

O(1w)–H(12w)···O(2w) to the second water molecule. The hydrogens of the second water molecule involving O(2w) are disordered and have been modelled in terms of three sites two of which, H(21w) and H(23w), have been assigned fixed site occupancy factors of 0.5 while the third, H(22w), is fully occupied. H(22w) participates in the formation of the hydrogen bond O(2w)–H(22w)···O(1w) complementing the O(1w)–H(12w)···O(2w) bond described. Whereas H(23w) is involved in the formation of the O(2w)–H(23w)···O(47) hydrogen bond H(21w) does not participate in hydrogen-bond formation.

Thermal gravimetric analysis from room temperature to 230 °C showed a gradual mass loss finally corresponding to the loss of two water molecules per formula unit showing that both the loosely bound and calcium coordinated water can be eliminated. Upon rehydration the X-ray powder diffraction pattern was virtually identical to that of the hydrated material suggesting that the polymeric anion layers and high Ca carboxylate coordination stabilises micropores after removal of water from the lattice. Further detailed studies on these and related materials will be reported shortly.

## Footnotes

* E-mail: m.j.plater@abdn.ac.uk

† Prior to the publication of ref. 7 our independent attempts to characterise a calcium salt of $H_3$btc by single-crystal X-ray crystallography were unsuccessful. We were naively following hydrothermal synthesis procedures without slow cooling of the sample which gave poor quality crystals.

*Typical procedure*: $H_3$btc (400 mg, 1.9 mmol) and $Ca(O_2CMe)_2$ (301 mg, 1.9 mmol) in water (25 ml) were sealed in a 45 ml Teflon-lined safety bomb[8] and placed in an oven at 180 °C. After about 10 h the oven temperature was slowly reduced over a 36 h period to 80 °C and then allowed to cool to room temp. Colourless crystals were collected and washed with distilled water (494 mg, 91%). The homogeneity of the sample was shown by satisfactory carbon and hydrogen microanalysis and by the X-ray powder diffraction pattern which was identical to the calculated pattern.

‡ *Crystal data*: **2**: $C_9H_8CaO_8$, triclinic, space group $P\bar{1}$ (no. 1), $a$ = 6.853(5), $b$ = 9.007(9), $c$ = 9.987(6) Å, $\alpha$ = 102.23(6), $\beta$ = 100.53(5), $\gamma$ = 110.21(7), $U$ = 543.2(8) Å$^3$, $Z$ = 2, $D_c$ = 1.737 g cm$^{-3}$, data collection and cell refinement: Nicolet P3 diffractometer using a graphite monochromator with $\mu$(Mo-K$\alpha$) = 0.063 mm$^{-1}$, $T$ = 293 K. Data collection used $\omega$ scan rates of 5.33 ($I_p$ < 150) to 58.6 ($I_p$ > 2500)° min$^{-1}$, where $I_p$ was the prescan intensity. Scan widths $\omega$ were 2.4–2.8°. Data reduction *via* RDNIC.[9] The structure was solved by direct methods to yield positions for all non-hydrogens except the oxygens of the water molecules which were obtained later from difference maps as were the positions of hydrogens attached to oxygens. The final $R$ value was 0.041 ($R_w$ = 0.048). Refinement was by full-matrix least squares. All non-hydrogen atoms were refined anisotropically. For the anion the acid hydrogen H(5) was refined isotropically in the usual manner but the hydrogen attached to carbons were placed in calculated positions with C–H = 0.95 Å and refined with a riding model and common group $U_{iso}$. Hydrogens of the water molecules were also refined with group $U_{iso}$ values, one for each molecule. The disorder of the hydrogen associated with O(2w) has already been described in the text. Atomic coordinates, bond lengths and angles, and thermal parameters have been deposited at the Cambridge Crystallographic Data Centre (CCDC). See Information for Authors, Issue No. 1. Any request to the CCDC for this material should quote the full literature citation and the reference number 182/421.

## References

1 O. M. Yaghi, G. Li and H. Li, *Nature*, 1995, **378**, 703.
2 O. M. Yaghi and H. Li, *J. Am. Chem. Soc.*, 1995, **117**, 10 401.
3 V. Soghomonian, Q. Chen, R. C. Haushalter and J. Zubieta, *Angew. Chem., Int. Ed. Engl.*, 1995, **34**, 223.
4 M. Simard, D. Su and J. Wuest, *J. Am. Chem. Soc.*, 1991, **113**, 4696.
5 O. Ermer, *J. Am. Chem. Soc.*, 1988, **110**, 3747; O. Ermer and A. Eling, *Angew. Chem., Int. Ed. Engl.*, 1988, **27**, 829.
6 J. E. D. Davies, P. Finocchiaro and F. H. Herbstein, *Inclusion Compounds*, vol. 2, ed. J. L. Atwood, J. E. D. Davies and D. D. MacNicol, Academic Press, London, 1984.
7 O. M. Yaghi, H. Li and T. L. Groy, *J. Am. Chem. Soc.*, 1996, **118**, 9096.
8 Scientific and Medical Products Ltd., Shirley Inst., 856 Wilmslow Road, Didsbury, Manchester, M20 2SA. Supplier for the Parr Instrument Company, Moline, IL, USA.
9 R. A. Howie, RDNIC: Data Reduction Program for Nicolet P3 Diffractometer, University of Aberdeen, Scotland, 1980.

*Received in Cambridge, UK, 29th January 1997; Com. 7/00675F*

# Double C–H activation in pentamethylcyclopentadienylruthenium complexes

**Shane R. O'Leary, Harry Adams and Peter M. Maitlis***

*Department of Chemistry, The University of Sheffield, Sheffield, UK S3 7HF*

**Two methyls in each $\eta^5$-$C_5Me_5$ are activated in [{($\eta^5$-$C_5Me_5$)$RuCl_2$}$_2$] 1 [by (*i*) air, (*ii*) *N*-chlorosuccinimide and (*iii*) air]; after carbonylation a mixture of the 1,3- and 1,2-isomers [{$\eta^5$-$C_5Me_3(CH_2Cl)_2$}$Ru(CO)_2Cl$] 4a,b is obtained; the X-ray structure of 4a is determined.**

There is considerable interest in the activation of methyls in pentamethylcyclopentadienyl complexes. This has been particularly so for ruthenium,[1] where the technique has allowed us to prepare new ranges of molecules that have the potential to act as catalysts, as well as for rhodium and iridium,[2] and for other metals.[3]

One C–H bond in pentamethylcyclopentadienylruthenium chloride **1** (or bromide) is easily cleaved under the influence of oxygen (1 atm, 20 °C, $CHCl_3$ solution). The reaction sequence has been shown to proceed *via* a μ-oxo dinuclear complex which effectively dehydrates to give the tetramethylfulvene complex **2**.[1] Carbonylation then gives the final product, the chloromethyl dicarbonyl complex **3**, obtained in 82% overall yield from **1** (Scheme 1).

We now report that the reactions can be repeated so that the C–H bonds on two different methyls (either 1,2- or 1,3-) of one ring are activated. To do this the above reaction sequence is carried out as far as the tetramethylfulvene complex **2**. This does not need to be isolated or purified but is treated directly with 2 equiv. of *N*-chlorosuccinimide (NCS) in $CH_2Cl_2$ (Scheme 2). A second aeration is then carried out, followed by a carbonylation (1 atm, 20 °C) to give a mixture of the red isomeric bis(chloromethyl)dicarbonyl chlorides, [{$\eta^5$-$C_5Me_3(CH_2Cl)_2$}-$Ru(CO)_2Cl$] shown by NMR to be composed of **4a**,**b** in a 1 : 1 ratio. The complexes were separated by chromatography on a silica column (3 × 40 cm) in diethyl ether–light petroleum (bp 40–60 °C). Two bands were eluted, the first was shown by NMR spectroscopy and crystallography to be [{$\eta^5$-$C_5Me_3(CH_2Cl)_2$-1,3}$Ru(CO)_2Cl$] **4a** (40% isolated yield),† while the second was shown by NMR to contain [{$\eta^5$-$C_5Me_3(CH_2Cl)_2$-1,2}$Ru(CO)_2Cl$] **4b** (32% isolated yield).†

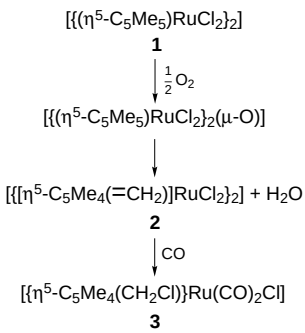
The isomers were initially identified by the relative positions of the ring methyls in the NMR spectra. As the $CH_2Cl$ substituents deshield it was assumed that the complex with a single methyl signal at higher frequency than the two equivalent methyls was the 1,3 isomer **4a**, since the unique methyl is affected by two neighbouring $CH_2Cl$ groups, while the 1,2 isomer **4b**, has the unique methyl at lower frequency since it lies between two methyls there. The assignments were confirmed by the crystal structure of the 1,3 isomer **4a**.

Similar reactions occurred when complex **1** was reacted with *N*-bromosuccimide but in this case mixtures of isomers were formed that could be separated only with great difficulty.

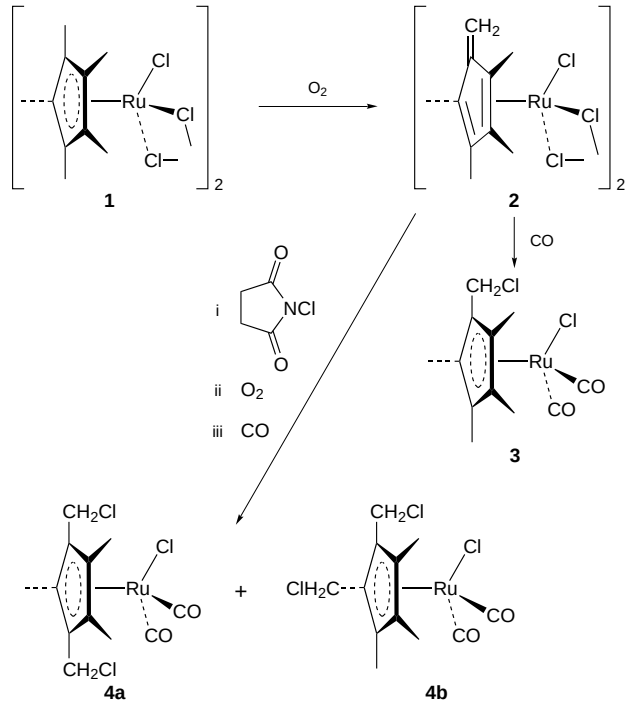
A crystal of complex **4a** for X-ray analysis was grown by slowly cooling a concentrated diethyl ether solution and leaving it at −23 °C for several days.‡ The structure is illustrated in Fig. 1 and clearly shows the 1,3-arrangement of the chloromethyl substituents. The bond lengths are very similar to those previously found for complex **3**: Ru–Cl 2.409(2), 2.412(2) Å for **4a**; 2.422(3) Å for **3**; C–Cl 1.815(8), 1.812(7), 1.794(8), 1.806(8) Å for **4a**; 1.787(12) Å for **3**. As found in complex **3**, the Ru–C bond lengths to the carbons bearing the $CH_2Cl$ substituents in **4a** are slightly shorter than the other Ru–ring C distances, but the differences are again only just significant.

Reaction of the isomeric mixture of **4a**,**b** dissolved in thf with a small amount of water and 2,4,6-trimethylpyridine gave a mixture of the two bishydroxymethyl complexes **5a**,**b**,[4] which were separated by chromatography on a silica column (eluent 7% MeOH in $CH_2Cl_2$), which gave two bands, the first contained [{$C_5Me_3(CH_2OH)_2$-1,2}$Ru(CO)_2Cl$] **5b**† (37% yield) while the second was found to be [{$C_5Me_3(CH_2OH)_2$-1,3}$Ru(CO)_2Cl$] **5a**† (28% yield).

Although several double activations of $\eta^5$-$C_5Me_5$ ligands in early transition metal complexes are known,[5] they are still rare for the late transition metals. However, we have previously noted sequential reactions[6] and very recently two double activations have been reported. The rhodium and iridium




**Scheme 1**




**Scheme 2**

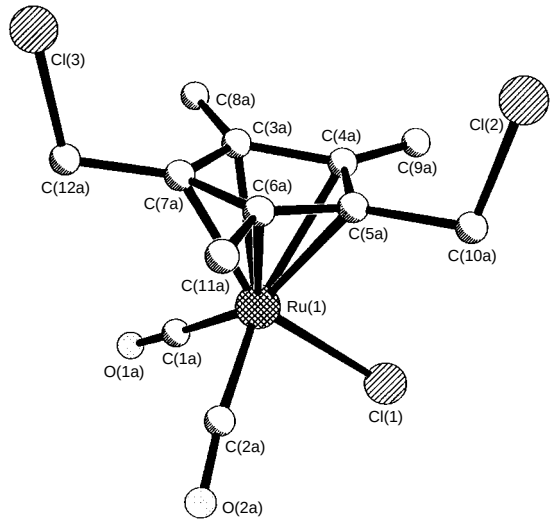



**Fig. 1** Molecular structure of [{$\eta^5$-$C_5Me_3(CH_2Cl)_2$-1,3}$Ru(CO)_2Cl$] **4a** (hydrogens omitted)

complexes [{($\eta^5$-$C_5Me_5$)$MCl_2$}$_2$] (M = Rh, Ir) react with the diphosphine chelate $(C_6F_5)_2PCH_2CH_2P(C_6F_5)_2$ to give [M{$\eta^5$-$C_5Me_3[CH_2C_6F_4P(C_6F_5)CH_2]_2$-1,3}Cl]$^+$ where a C–C bond has been formed by elimination of HF between two *ortho*-C–F groups of the ligand and 1,3-dimethyl groups of the $\eta^5$-$C_5Me_5$ ligand.[7] In the other reaction [{($\eta^5$-$C_5Me_5$)$RhCl_2$}$_2$] undergoes reaction with diphenylvinylphosphine in acetonitrile in the presence of potassium *tert*-butoxide to give a mixture of two complexes [M{$\eta^5$-$C_5Me_3[CH_2CH_2CH_2P(Ph)]_2$}Cl]$^+$ where the C–H groups of two methyl groups (1,2- and 1,3-) have added to the vinyl groups.[8] The mechanisms of neither of these reactions is clear, but ethanol solvent is required for the first, and base plays a significant role in the second. At present it looks as if the formation of **4** from **1** (or **2**) may involve radical intermediates of some type.

We thank the EPSRC for the award of a ROPA grant to support this work.

## Footnotes

* E-mail: P.Maitlis@Sheffield.ac.uk

† *Selected spectroscopic data*: **4a**: ν(CO) 2046, 1999 cm$^{-1}$ ($CH_2Cl_2$); $^1$H NMR ($CDCl_3$), δ 4.23 (m, 2 × $CH_2Cl$), 2.06 (s, Me), 2.04, (s, 2 × Me); $^{13}$C NMR, δ 196.0 (CO); 110.2, 104.9, 92.3 [$C_5Me_3(CH_2Cl)_2$]; 36.0 ($CH_2Cl$); 9.6, 9.5 (2 × $CH_3$). **4b**: ν(CO) 2046, 1999 cm$^{-1}$ ($CH_2Cl_2$); $^1$H NMR ($CDCl_3$), δ 4.28 (br, 2 × $CH_2Cl$); 2.11 (s, 2 × Me); 1.98 (s, Me); $^{13}$C NMR, δ 196.3 (CO); 110.4, 106.1, 96.0 [$C_5Me_3(CH_2Cl)_2$]; 35.2 ($CH_2Cl$); 9.9, 9.7 (2 × $CH_3$). **5a**: ν(CO) 2044, 1993 cm$^{-1}$ ($CH_2Cl_2$); $^1$H NMR ($CDCl_3$), δ 4.31 (br, 2 × C$H_2$OH); 2.55 (br, 2 × OH); 2.09 (s, 2 × Me); 2.03 (s, Me); $^{13}$C NMR, δ 197.3 (CO); 104.7, 101.2, 98.2, [$C_5Me_3(CH_2OH)_2$]; 55.0 ($CH_2OH$); 9.8, 9.7 ($CH_3$). **5b**: ν(CO) 2044, 1993 cm$^{-1}$ ($CH_2Cl_2$); $^1$H NMR ($CDCl_3$), δ 4.28 (m, 2 × C$H_2$OH); 3.56 (br, 2 × OH); 2.01 (s, 2 × Me); 1.90 (s, Me); $^{13}$C NMR, δ 197.1 (CO); 109.9, 103.8, 97.8, [$C_5Me_3(CH_2OH)_2$]; 54.7 ($CH_2OH$); 9.8 ($CH_3$).

‡ *Crystal data* for **4a**: $C_{24}H_{28}Cl_6O_5Ru_2$; $M$ = 811.30; crystal dimensions 0.88 × 0.42 × 0.40 mm. orthorhombic, space group $P2_12_12_1$ ($D_2^4$, no. 19), $a$ = 8.9670(10), $b$ = 13.971(3), $c$ = 24.503(3) Å, $U$ = 3069.7(8) Å$^3$, $Z$ = 4, $D_c$ = 1.755 g cm$^{-3}$, Mo-Kα radiation ($\bar{\lambda}$ = 0.710 73 Å), μ(Mo-Kα) = 1.538 mm$^{-1}$, $F$(000) = 1608. Three-dimensional, room-temperature X-ray data were collected in the range 3.5 < 2θ < 45° on a Siemens P4 diffractometer by the ω-scan method. Of the 2998 reflections measured, all of which were corrected for Lorentz and polarisation effects (but not for absorption), 2743 independent reflections exceeded the significance level $|F|/\sigma(|F|) > 4.0$. The structure was solved by direct methods and refined by full-matrix least squares on $F^2$. Hydrogen atoms were included in calculated positions and refined in riding mode. Refinement converged at a final $R$ = 0.0398 ($wR_2$ = 0.1033 for all 2811 unique data, 334 parameters, mean and maximum δ/σ 0.000, 0.000), with allowance for the thermal anisotropy of all non-hydrogen atoms. Minimum, maximum final electron density −1.362, 0.573 e Å$^{-3}$. A weighting scheme $w = 1/[\sigma^2(F_o^2) + (0.0799\,P)^2 + 1.2036\,P]$ where $P = (F_o^2 + 2F_c^2)/3$ was used in the latter stages of refinement. Complex scattering factors were taken from the program package SHELXL93[9] as implemented on the Viglen 486dx computer.

Atomic coordinates, bond lengths and angles, and thermal parameters have been deposited at the Cambridge Crystallographic Data Centre (CCDC). See Information for Authors, Issue No. 1. Any request to the CCDC for this material should quote the full literature citation and the reference number 182/420.

## References

1 L. Fan, M. L. Turner, M. B. Hursthouse, K. M. A. Malik, O. V. Gusev and P. M. Maitlis, *J. Am. Chem. Soc.*, 1994, **116**, 385; L. Fan, M. L. Turner, H. Adams, N. A. Bailey and P. M. Maitlis, *Organometallics*, 1995, **14**, 676; S. R. O'Leary, H. Adams, N. A. Bailey and P. M. Maitlis, *J. Chem. Soc., Chem. Commun.*, 1995, 2019; L. Fan, C. Wei, F. I. Aigbirhio, M. L. Turner, O. V. Gusev, L. N. Morozova, D. R. T. Knowles and P. M. Maitlis, *Organometallics*, 1996, **15**, 98; O. V. Gusev, L. N. Morozova, S. R. O'Leary, H. Adams, N. A. Bailey and P. M. Maitlis, *J. Chem. Soc., Dalton Trans.*, 1996, 2571.

2 J. A. Miguel-Garcia and P. M. Maitlis, *J. Chem. Soc., Chem. Commun.*, 1990, 1472; O. V. Gusev, A. Z. Rubezhov, J. A. Miguel-Garcia and P. M. Maitlis, *Mendeleev Commun.*, 1991, 21; J. A. Miguel-Garcia, H. Adams, N. A. Bailey and P. M. Maitlis, *J. Organomet. Chem.*, 1991, **413**, 427; J. A. Miguel-Garcia, H. Adams, N. A. Bailey and P. M. Maitlis, *J. Chem. Soc., Dalton Trans.*, 1992, 131.

3 H. Werner, G. T. Crisp, P. W. Jolly, H.-J. Kraus and C. Krueger, *Organometallics*, 1983, **2**, 1370; F. D. Miller and R. D. Sanner, *Organometallics*, 1988, **7**, 818; D. S. Glueck and R. G. Bergman, *Organometallics*, 1990, **9**, 2862; M. Booij, A. Meetsma and J. H. Teuben, *Organometallics*, 1991, **10**, 3246; G. A. Luinstra and J. H. Teuben, *J. Am. Chem. Soc.*, 1992, **114**, 3361; A. D. Horton, *Organometallics*, 1992, **11**, 3271; U. Koelle, B.-S. Kang and U. Thewalt, *J. Organomet Chem.*, 1990, **386**, 267; A. H. Klahn, M. H. Moore and R. N. Perutz, *J. Chem. Soc., Chem. Commun.*, 1992, 1699; M. Herberhold, G.-X. Jin and A. L. Rheingold, *J. Chem. Soc., Chem. Commun.*, 1996, 2645.

4 Method due to D. R. T. Knowles, H. Adams and P. M. Maitlis, unpublished work.

5 J. W. Pattiasina, C. E. Hissink, J. L. de Boer, A. Meetsma, J. H. Teuben and A. L. Spek, *J. Am. Chem. Soc.*, 1985, **107**, 7758; F. G. N. Cloke, J. C. Green, M. L. H. Green and C. P. Morley, *J. Chem. Soc., Chem. Commun.*, 1985, 945; S. T. Carter, W. Clegg, V. C. Gibson, T. P. Kee and R. D. Sanner, *Organometallics*, 1989, **8**, 253.

6 J. A. Miguel-Garcia, H. Adams, N. A. Bailey and P. M. Maitlis, *J. Organomet. Chem.*, 1991, **413**, 427.

7 M. J. Atherton, J. Fawcett, J. H. Holloway, E. G. Hope, A. Karacar, D. R. Russell and G. C. Saunders, *J. Chem. Soc., Chem. Commun.*, 1995, 191; *J. Chem. Soc., Dalton Trans.*, 1996, 3215.

8 L. P. Barthel-Rosa, V. J. Catalano and J. H. Nelson, *J. Chem. Soc., Chem. Commun.*, 1995, 1629; L. P. Barthel-Rosa, V. J. Catalano, K. Maitra and J. H. Nelson, *Organometallics*, 1996, **15**, 3924.

9 G. M. Sheldrick, SHELXL 93, An integrated system for solving and refining crystal structures from diffraction data, University of Göttingen, Germany 1993.

*Received in Cambridge, UK, 27th February 1997; Com. 7/01373F*

# Neutral [2]catenanes from oxidative coupling of π-stacked components

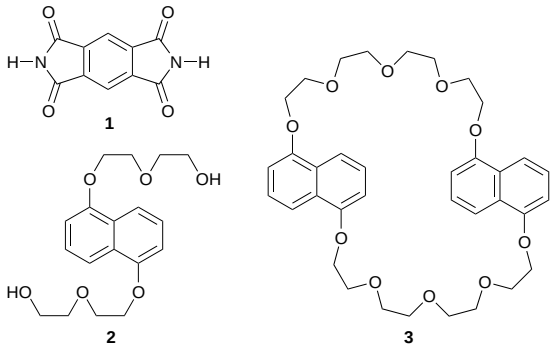
**Darren G. Hamilton,*[a] Jeremy K. M. Sanders,*[a]† John E. Davies,[a] William Clegg[b] and Simon J. Teat[b]**

[a] *Cambridge Centre for Molecular Recognition, University Chemical Laboratory, Lensfield Road, Cambridge, UK CB2 1EW*
[b] *Department of Chemistry, University of Newcastle, Newcastle-Upon-Tyne, UK NE1 7RU*

**Oxidative dimerisation of bis-acetylenic precursors in the presence of a dinaphtho-crown ether affords neutral [2]catenanes in good yields; the interaction of the complementary donor–acceptor π-systems ensures assembly in a geometry favouring catenane formation.**

Recent studies of mechanically interlocked molecules such as catenanes, rotaxanes and knots may be classified according to the nature of the intermolecular association employed in templating their formation. Contemporary organic synthesis has yielded three distinct approaches to such templating: (i) π-stacking of electron-deficient aromatic dications with electronically complementary aromatic molecules,[1] (ii) chelation of metal cations[2] and (iii) amide hydrogen-bonding interactions.[3] Stoddart's methodology for the synthesis of interlocked molecules based on the π-stacking of electron-rich aromatic ethers with electron-poor bipyridinium cations that are generated *in situ* is a landmark in the field.[4,5] Here we describe the synthesis of *neutral* π-stacked interlocked systems from building blocks with pre-programmed recognition characteristics. These systems are structurally and chemically robust, and yet, by virtue of their good solubility characteristics, also amenable to modification using traditional organic chemistry.

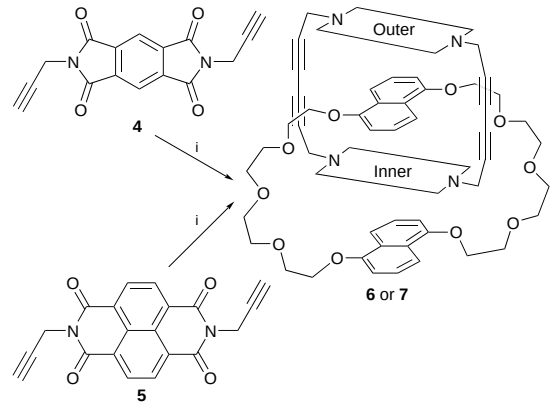
The conceptual background to the present work was provided by reports of the inclusion of π-electron-rich aromatic ethers and π-electron-deficient aromatic diimides in a series of donor–acceptor cyclophanes[6] and two self-assembling supramolecular systems.[7] These reports prompted an investigation of some simple co-crystals,[8] such as that formed between pyromellitic diimide **1** and the dialkoxynaphthalene derivative **2**. The solid-state structure of the **1.2** co-crystal reveals alternating stacks of donor (aromatic ether) and acceptor (diimide) molecules; the long axes of the sub-units are approximately perpendicular and a consistent interplanar separation of *ca.* 3.5 Å is maintained between adjacent stack members. These features appeared compatible with the development of a catenane synthesis based on the revealed superstructural design.



Oxidative coupling of terminal acetylenes has previously been applied to the synthesis of a variety of macrocyclic host systems,[9] including some phenanthroline-based catenates,[10] and the butadiyne linker so generated is ideally suited to bridge the *ca.* 7 Å span demanded by our target structure. A pyromellitimide derivative **4** bearing two terminal acetylenes was readily prepared from the condensation of prop-2-ynylamine with pyromellitic dianhydride. An analogous bis-acetylene **5**, derived from the closely related 1,4,5,8-naphthalenetetracarboxylic dianhydride system, was prepared in 67% yield using an identical procedure (Scheme 1). To link two 1,5-substituted naphthalene residues we selected **3**, available in two steps from 1,5-dihydroxynaphthalene by a modification of a literature route.[11] When a 1:2 molar ratio of **3** and **4** are mixed in dry DMF (50 °C, *ca.* 15 mM crown concentration) an immediate orange colour is established in solution, strongly indicative of charge transfer complex formation. Large excesses of anhydrous CuCl (100 equiv.) and $CuCl_2$ (20 equiv.) were added to effect the coupling process. After 2 days stirring in dry air, the [2]catenane **6** could be isolated from the reaction mixture as an orange–red solid by simple work-up and chromatography. Over several runs conducted on various scales the isolated yield of **6** was in the range 25–33%.‡ Under identical reaction conditions (DMF, 50 °C, 15 mM concentration) a 1 : 2 mixture of **3** and **5** gave the [2]catenane **7** as a purple solid in 29% yield. The increased solubility of this system allowed the reaction to be repeated at room temperature. The isolated yield of **7** rose to 52%, an efficiency comparable with those obtained in previous [2]catenane syntheses.

Fast-ion bombardment mass spectrometry of **6** and **7** reveals peaks at *m/z* 1239 and 1339 respectively, corresponding to the addition of a sodium ion to the catenane structures ($M_r$ = 1216 and 1316 respectively). In both spectra the only other significant peak at high mass occurs at *m/z* 769 ([**3** + Cs]$^+$). This behaviour is a spectral characteristic of catenated structures where the first bond scission leads to unravelling of the interlocked structure.[12] Such fragmentation is not observed under electrospray ionisation conditions where for each structure the only detected peak corresponds to the catenane ([*M* + Na]$^+$).

At ambient temperature, the $^1$H NMR spectrum of **6** reveals an AB quartet for the methylene protons of the pyromellitimide macrocycle and upfield shifts of all the aromatic protons relative to the precursors **3** and **4**, as a result of the ordered π-stacking in the molecule. The aromatic pyromellitimide protons appear as a sharp singlet, indicating fast exchange of the inner and outer pyromellitimide sub-units on the chemical shift




**Scheme 1** *Reagents and conditions*: i, CuCl, $CuCl_2$, $O_2$, DMF

time scale. In contrast, two clearly resolved sets of multiplets for the naphthalene sub-units of the crown macrocycle are readily identified revealing the comparatively slower rotation of this component. Catenane **7** exhibits a similar $^1$H NMR spectrum to **6**, indicating similar dynamic behaviour. Variable temperature $^1$H NMR analysis reveals site exchange processes for **6** that parallel those observed in previously reported systems.[4,5]

Very small single crystals of **6** of a quality apparently suitable for an X-ray structural analysis could be readily grown from deuterated dimethyl sulfoxide ([$^2H_6$]$Me_2SO$). However, no reflections could be measured for any of these samples when mounted on commercial diffractometers. The structure presented here was obtained by X-ray synchrotron diffraction.§ This radiation source is several orders of magnitude stronger than that employed in routine crystallographic analyses and allowed the structure to be solved with relative ease (Fig. 1).

The two interlocked neutral macrocycles that comprise the catenane adopt a structure where the respective π-rich and π-poor ring systems can align themselves in a similar manner to that observed in the **1.2** co-crystal. Indeed, the validity of the supramolecular design on which the catenane is based is truly revealed when a packing diagram is generated; individual catenane molecules pack one above another to continue the alternating donor–acceptor stack and the typical interplanar spacings of *ca*. 3.4 Å are observed throughout. Hydrogen bonding interactions between the pyromellitimide methylene protons and oxygen donor atoms in the crown polyether chain are also observed, these interactions may prove to play an important role in the templated synthesis. The unit cell contains two catenane molecules and four molecules of [$^2H_6$]$Me_2SO$ (each disordered over two occupancies). The pyromellitimide ring systems are rotated by 15° relative to each other, inducing a helical twist in this macrocycle, and the connecting butadiyne links are substantially bowed (∠ C–C≡C 169–174°).

[2]Catenanes **6** and **7** represent the first examples of a new class of neutral π-associated interlocked molecules. The electrochemical[13] and photochemical[14] properties of aromatic diimides, and the chemical functionality present in our systems, augur well for the future development of functional and structural derivatives. Indeed, the imide and acetylenic groups are independently reducible and the structural changes so conferred would be likely to alter or destroy the observed π-stacking interactions. Such removal of the templating interaction employed to assemble **6** and **7** would represent an irreversible counterpart to Sauvage's use of transition metal-ion coordination to assemble [*n*]catenates.

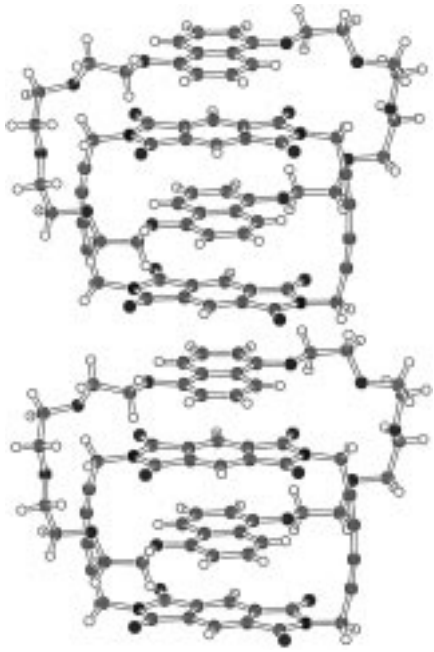


**Fig. 1** Ball and stick representation of the solid-state structure of 6

We gratefully acknowledge the financial support of the Ramsay Memorial Fellowships Trust (D. G. H.), the Engineering and Physical Sciences Research Council and the Daresbury Laboratory. We thank Dr Paul R. Raithby for his assistance during the X-ray synchrotron structural analysis and Dr Nick Bampos for recording the VT NMR spectra.

## Footnotes

† E-mail: jkms@cam.ac.uk

‡ *Selected spectroscopic data* for **6**: $^1$H NMR (400 MHz, $CDCl_3$, 20 °C) 7.13 (d, $^3J$ 8 Hz, 2 H), 6.90 (s, 4 H), 6.80 (d, $^3J$ 8 Hz, 2 H), 6.73 (t, $^3J$ 8 Hz, 2 H), 6.68 (t, $^3J$ 8 Hz, 2 H), 6.44 (d, $^3J$ 8 Hz, 2 H), 6.28 (d, $^3J$ 8 Hz, 2 H), 4.40 (d, AB system, $^2J$ 18 Hz, 4 H), 4.22 (d, AB system, $^2J$ 18 Hz, 4 H), 4.12 (m, 4 H), 4.00 (m, 8 H), 3.90–3.85 (m, 20 H); ES–MS (positive-ion) *m/z* 1241.1 ([*M* + Na]$^+$, 100%), 1256.6 ([*M* + K]$^+$, 12%).

§ *Crystal data* for **6**.[$^2H_6$]$Me_2SO$: $C_{68}H_{56}N_4O_{18}$, $M_r$ = 1217.2, triclinic, *a* = 13.409(3), *b* = 15.014 (7), *c* = 16.640(6) Å, α = 100.33(4), β = 90.16(6), γ = 98.76(8)°, *V* = 1628 Å$^3$, space group $P\bar{1}$, *Z* = 2, $\rho_{calcd}$ = 1.40 g cm$^{-3}$. Crystal of size 0.30 × 0.12 × 0.10 mm. Siemens SMART CCD diffractometer on the single-crystal diffraction station (No. 9.8) at the Daresbury Laboratory Synchrotron Radiation Source (UK): 160 K, λ = 0.6956 Å. Overnight, several series of narrow frames (0.2° in ω) provided coverage of a hemisphere of reciprocal space to $\theta_{max}$ 25.8° and corrections were applied for incident beam decay. The structure was solved by direct methods and refined by full-matrix least-squares on $F^2$; 23612 reflections measured of which 11683 were observed as unique. The structure was refined to $R$ = 0.093, $R_w$ = 0.243, including disordered solvent molecules. Atomic coordinates, bond lengths and angles, and thermal parameters have been deposited at the Cambridge Crystallograpic Data Centre (CCDC). See Information for Authors, Issue No. 1. Any request to the CCDC for this material should quote the full literature citation and the reference number 182/443. Structure ref. code TIDKEW.

## References

1 D. B. Amabilino and J. F. Stoddart, *Chem. Rev.*, 1995, **95**, 2725.
2 J. C. Chambron, C. O. Dietrich-Buchecker, J. F. Nierengarten and J.-P. Sauvage, *Pure Appl. Chem.*, 1994, **66**, 1543.
3 C. A. Hunter, *J. Am. Chem. Soc.*, 1992, **114**, 5303; F. Vögtle, T. Dunnwald and T. Schmidt, *Acc. Chem. Res.*, 1996, **29**, 451; A. G. Johnston, D. A. Leigh, R. J. Pritchard and M. D. Deegan, *Angew. Chem., Int. Ed. Engl.*, 1995, **34**, 1209.
4 P. R. Ashton, T. T. Goodnow, A. E. Kaifer, M. V. Reddington, A. M. Z. Slawin, N. Spencer, J. F. Stoddart, C. Vicent and D. J. Williams, *Angew. Chem., Int. Ed. Engl.*, 1989, **28**, 1396.
5 P. L. Anelli, P. R. Ashton, R. Ballardini, V. Balzani, M. Delgado, M. T. Gandolfi, T. T. Goodnow, A. E. Kaifer, D. Philp, M. Pietraszkiewicz, L. Prodi, M. V. Reddington, A. M. Z. Slawin, N. Spencer, J. F. Stoddart, C. Vicent and D. J. Williams, *J. Am. Chem. Soc.*, 1992, **114**, 193.
6 L. G. Schroff, R. L. J. Zsom, A. J. A. van der Weerdt, P. I. Schrier, J. P. Geerts, N. M. M. Nibbering, J. W. Verhoeven and T. J. de Boer, *Recl. Trav. Chim. Pays-Bas*, 1976, **95**, 89.
7 A. Bilyk and M. M. Harding, *J. Chem. Soc., Chem. Commun.*, 1995, 1697; R. S. Lokey and B. L. Iverson, *Nature*, 1995, **375**, 303.
8 D. G. Hamilton, D. E. Lynch, K. A. Byriel and C. H. L. Kennard, *Aust. J. Chem.*, in the press.
9 H. L. Anderson and J. K. M. Sanders, *J. Chem. Soc., Perkin Trans. 1*, 1995, 2223 and following five papers; D. O'Krongly, S. R. Denmeade, M. Y. Chiang and R. Breslow, *J. Am. Chem. Soc.*, 1985, **107**, 5544; A. J. Kennan and H. W. Whitlock, *J. Am. Chem. Soc.*, 1996, **118**, 3027; S. Anderson and H. L. Anderson, *Angew. Chem., Int. Ed. Engl.*, 1996, **35**, 1956.
10 C. O. Dietrich-Buchecker, C. Hemmert, A.-K. Khémiss and J.-P. Sauvage, *J. Am. Chem. Soc.*, 1990, **112**, 8002.
11 D. Marquis, H. Greiving, J.-P. Desvergne, N. Lahrahar, P. Marsau, H. Hopf and H. Bouas-Laurent, *Liebigs Ann. Rec.*, 1997, 97.
12 W. Vetter, E. Logemann and G. Schill, *Org. Mass Spectrom.*, 1977, **12**, 351.
13 A. Viehbeck, M. J. Goldberg and C. A. Kovac, *J. Electrochem. Soc.*, 1990, **137**, 1460.
14 M. P. Debreczeny, W. A. Svec, E. M. Marsh and M. R. Wasielewski, *J. Am. Chem. Soc.*, 1996, **118**, 8174; C. A. Hunter and R. K. Hyde, *Angew. Chem., Int. Ed. Engl.*, 1996, **35**, 1936.

*Received in Liverpool, UK, 14th February 1997; Com. 7/01048F*

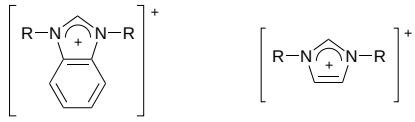
# First example of interdigitated U-shape benzimidazolium ionic liquid crystals

**Kwang Ming Lee, Ching Kuan Lee and Ivan J. B. Lin*†**

*Department of Chemistry, Fu-Jen catholic University, Hsinchuang, Taipei 242, Taiwan*

**Self-assembly of U-shaped 1,3-dialkylbenzimidazolium salts through hydrogen bonds and interdigitation of alkyl chains produces a bilayer structure with lamellar α and β mesophases.**

Self-assembly of molecules through hydrogen bonds and hydrophobic interactions to form supramolecular structures is currently an important chemical issue.[1,2] Hydrogen bonds are especially important in biological systems and in the design of new materials.[3] Specifically, hydrogen bonds have been used in the formation of liquid crystalline phases.[4] Here we report a new class of thermotropic ionic liquid crystals, 1,3-dialkyl-benzimidazolium [$(C_n)_2$-Bim] and -imidazolium [$(C_n)_2$-Im] salts. This model system is a good combination of liquid crystalline compounds having (1) extended C–H···X (X = halides) hydrogen bonds, (2) aromatic rigid cores and (3) hydrophobic interactions between alkyl chains.



$[(C_n)_2\text{-Bim}]^+$ (R = $C_nH_{2n+1}$) $[(C_n)_2\text{-Im}]^+$ (R = $C_nH_{2n+1}$)

$(C_n)_2$-Bim chlorides and bromides ($n$ = 12, 14, 16, 18) were obtained by the alkylation of 1-alkylbenzimidazoles as previously reported.[5,6] Crystals of $(C_{12})_2$-Bim chlorides and bromides suitable for X-ray single crystal diffraction were recrystallized from $CH_2Cl_2$.‡ $PF_6$ ($n$ = 6, 12, 14, 16, 18) and iodide salts ($n$ = 16) were prepared quantitatively *via* the simple displacement of anions. $R_2$-Im salts ($n$ = 16, X = Cl, Br and $PF_6$) were prepared in a similar fashion. The purity of all compounds was confirmed by elementary analysis and $^1$H NMR spectroscopy.

The molecular structure of $[(C_{12})_2$-Bim]Cl is shown in Fig. 1(*a*). Two *N*-alkyl chains are approximately orthogonal to the Bim-aromatic plane (5° off the plane normal). The geometry looks like a two-leg stool. Each plane of Bim connects side by side to the neighbouring molecules through C–H···Cl hydrogen bonds, such that the aromatic rings line up in a row with all the legs pointing in the same direction. Each row further connects with the other through hydrogen bonds to form a plane, like a tiled roof and again with all the legs pointing in the same direction. Interdigitation of two such planes with interpenetrating alkyl chains generates a bilayer of 17.7 Å thickness. Each bilayer is further linked with anions through C–H···Cl and C–H···$H_2$O···Cl hydrogen bonds to form a lamellar structure with a separation of 3.4 Å between the bilayers [Fig. 1(*b*)]. Hydrogen bonds play an important role in the formation of this structure and mesophase. Anions are not in the proximity of the positively charged N atoms, rather, each anion forms hydrogen bonds with four C–H groups [H(2), H″(5), H(10A) and H′(22A)] from three neighbouring Bim planes and two additional hydrogen bonds with $H_2O$ molecules which bridge two H(22A) atoms [Fig. 1(*c*)]. The formation of hydrogen bonds between anions and positively charged H(2), H(10A) and H(22A) are known.[7,8] However, such interactions between anions and H″(5) was until now unknown. If one considers each alkyl chain as a rod, the rods exhibit hexagonal close-packing and the distances between the neighbouring rods are 4.1–4.6 Å. $[(C_{12})_2$-Bim]Br has a similar structure except that (1) the separation between neighbouring bilayers is 3.6 Å and (2) the alkyl chains tilt 20° from the plane normal. Therefore the bromide salt has a smaller bilayer thickness (16.8 Å) than that of the chloride (17.7 Å). To the best of our knowledge, this is the first ionic liquid crystal with lamellar structure formed from interdigitated U-shape molecular ions. Recently, imidazolium salts with liquid crystal behaviour were reported.[9] A rod-like structure with alkyl chains parallel to aromatic rings and perpendicular to the layer normal was proposed to produce the mesophase.

For $(C_n)_2$-Bim and $(C_n)_2$-Im salts, formation of mesomorphism depends on the type of anions and the length of the alkyl chains. $(C_n)_2$-Bim salts of chloride ($n$ = 12, 14, 16, 18) and bromide ($n$ = 14, 16, 18), show liquid crystal behaviour but not the iodide and $PF_6$ salts from $n$ = 12 to 18. The ease of anions to form liquid crystals follows the order: Cl > Br > I, $PF_6$. This order is the same as the order of the strength of the C–H···X hydrogen bonds and is the reverse order of the anionic sizes and the separations between the bilayers. Table 1 gives the thermotropic properties of Bim and Im salts obtained from differential scanning calorimetry (DSC) spectra. Taking $[(C_{16})_2$-Bim]Cl as an example, three crystal phases and two mesophases were observed. $[(C_{16})_2$-Bim]Br, however, only

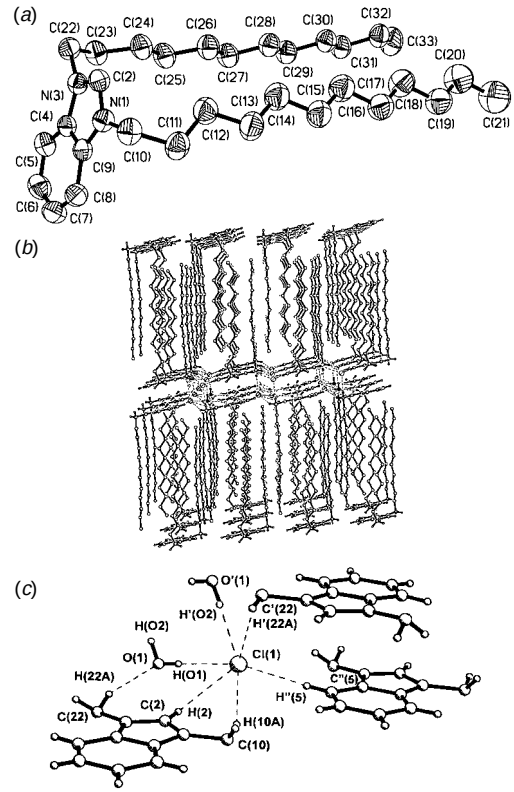



**Fig. 1** (*a*) ORTEP drawing of the cation of $[(C_{12})_2$-Bim]Cl (50% thermal ellipsolids) with atomic numbering, alkyl chain hydrogen atoms being omitted for clarity; (*b*) stacking of the bilayered structure *b*; (*c*) hydrogen bonds between the chloride anion and Bim cations, the tail end of alkyl chains being omitted for clarity

shows one crystal phase and one mesophase. Both chloride and bromide salts have similar K-S transition temperatures irrespective of their anion and carbon chain length differences. Chloride salts have a wider mesophase temperature range than that of the bromide salts of the same carbon chain lengths. The temperature range of mesophase increases upon increasing the carbon chain lengths. $(C_{16})_2$-Im salts have much lower melting points and wider mesophase temperature ranges than those of $(C_{16})_2$-Bim salts (Table 1).

The results of investigations of $[(C_{16})_2$-Bim]Cl using polarized optical microscopy (POM) and X-ray diffraction (XRD) are in close resemblance to those found for 1,2,ψ,ω-*n*-alkanetetraols, which form lamellar thermotropic liquid crystal phases.[10] The fan-like texture at 130 °C (Fig. 2) is characteristic for the lamellar α phase ($L_\alpha$) as it is for that of tetraols. The XRD spectrum [Fig. 3(*a*)] indicates that the mesomorphic structure has a layer period of 28.4 Å and has no order in the lamellar planes. On cooling to 110 °C, the texture has hyperbolic lines across the fans (not shown) and is characteristic for the lamellar β phase ($L_\beta$), as was proposed for that of tetraols. The corresponding XRD spectrum [Fig. 3(*b*)] shows that the $L_\beta$ has a layer period of 34.4 Å and has ordered layers. The layer period in $L_\beta$ is 6 Å longer than the one at 25 °C [Fig. 3(*c*)]. In brief, from crystal to $L_\beta$, there is a sudden elongation of the layer period and there is an order in the layers; from $L_\beta$ to $L_\alpha$ the layer period decreases and the order in the layers disappears. POM and XRD studies show that $[(C_{16})_2$-Bim]Br has a similar mesomorphism, although the DSC spectrum does not detect the $L_\beta$–$L_\alpha$ phase transition.

**Table 1** Transition temperatures (°C) of compounds $[(C_n)_2$-Bim]Cl (**A**-*n*), $[(C_n)_2$-Bim]Br (**B**-*n*) and $[(C_{16})_2$-Im]X (C-X, X = Cl, Br, $PF_6$) (Δ*H* in kJ mol$^{-1}$ in parentheses) determined by DSC at cooling rate of 10 °C min$^{-1}$

| Cpd | $K_1$ | $K_2$ | $L_\beta$ | $L_\alpha$ | I |
|---|---|---|---|---|---|
| **A**-18 | • 78.9 (34.5) | • 105.5 (69.7) | • 111.8 (20.9) | • 150.4 (4.9) | • |
| **A**-16 | • 76.1 (25.5) | • 102.1 (47.0) | • 110.9 (17.8) | • 147.8 (4.7) | • |
| **A**-14 | • 79.7 (38.2) | • 102.0 (56.7) | • 109.0 (25.6) | • 140.5 (7.2) | • |
| **A**-12 | • 79.9 (5.6) | • 98.1 (60.6) | • 112.7 (22.6) | • 127.1 (5.8) | • |
| **B**-18 | • 80.4 (8.8) | • 103.9 (72.7) | • 110.3[a] (n.d.) | • 145.3 (4.3) | • |
| **B**-16 | • | 101.1 (85.0) | • 109.5[a] (n.d.) | • 132.2 (3.6) | • |
| **B**-14 | • 76.7 (4.4) | • 103.6 (41.5) | | • 129.5 (2.7) | • |
| C-Cl | • 31.1 (25.9) | | | • 151.5 (2.7) | • |
| C-Br | • 45.7 (31.2) | | | • 142.6 (2.2) | • |
| C-$PF_6$ | • 61.3 (46.1) | | | • 103.3 (2.0) | • |

K = crystal; $L_\alpha$, $L_\beta$ = lamellar mesophases; I = isotropic liquid; n.d. = not determined. [a] Determined by polarized optical microscopy.



**Fig. 2** The fan-like texture of $[(C_{16})_2$-Bim]Cl at 130 °C

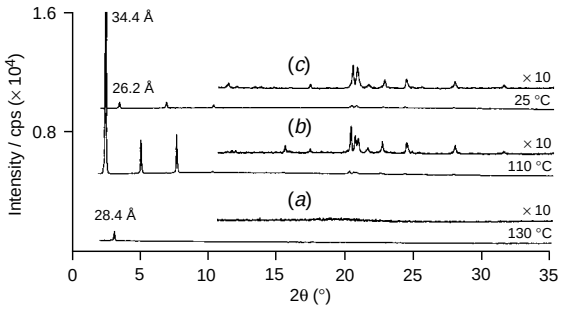



**Fig. 3** Temperature dependence of XRD for $[(C_{16})_2$-Bim]Cl at (*a*) 130 °C; (*b*) 110 °C; (*c*) 25 °C

In summary, the self assembly of 1,3-dialkyl substituted Bim and Im salts forms bilayered lamellar supramolecules through extended hydrogen bonds. These ionic salts show liquid crystal behaviour of unprecedented mesomorphism compared to other known ionic liquid crystals. An extended mesophase range can be adjusted by altering the aromatic core, alkyl chain length and anion. This system presents an unusual ionic liquid solvent with lamellar structure. Ionic liquid solvents can modify the course of chemical reactions.[11] Lamellar liquid crystal solvents may even have profound effects on chemical reactions, especially when they contain intercalating metal ions, such as $Pd^{2+}$. They are therefore potentially useful ionic solvents and catalysts. This bilayer structure also mimics biological membranes.

We thank Professor C. Y. Lii and Miss C. I. Hsu of the Institute of Chemistry of Academia Sinica of Taiwan for the XRD spectra. A research grant (NSC 86-2113-M-030-001) from National Science Council of Taiwan is greatly appreciated.

## Footnotes

† E-mail: chem.1001@fujens.fju.edu.tw

‡ *Crystal data* for $[(C_{12})_2$-Bim]Cl. $C_{31}H_{57}N_2OCl$, $M$ = 509.24, triclinic, space group $P\bar{1}$, $a$ = 8.7589(10), $b$ = 8.778(2), $c$ = 21.218(2) Å, α = 82.695(14), β = 88.744(8), γ = 79.19(2)°, $V$ = 1589.3(4) Å$^3$, $Z$ = 2, $F$(000) = 564, $D_c$ = 1.064 mg m$^{-3}$, $T$ = 296 K, crystal dimensions 0.6 × 0.5 × 0.5 mm; intensity data were collected on Siemens P4 diffractometer with graphite monochromatized MoKα radiation (λ = 0.71073 Å), 5606 non-zero (2σ) reflections out of 6012 collected with 2 < 2θ < 50°, solution SHELXS-86, refinement SHELXL-93 on $F^2$, $R$ = 0.0403, $wR_2$ = 0.0953, C, N, O, Cl anisotropic, H isotropic. The final fourier difference map showed residual electron density of 0.170 e Å$^{-3}$. For $[(C_{12})_2$-Bim]Br. $C_{31}H_{57}N_2OBr$, $M$ = 553.70, triclinic, space group $P\bar{1}$, $a$ = 9.143(2), $b$ = 9.1720(10), $c$ = 20.340(3) Å, α = 90.344(12), β = 101.47(2), γ = 100.724(14)°, $V$ = 1640.8(4) Å$^3$, $Z$ = 2, $F$(000) = 600, $D_c$ = 1.121 mg m$^{-3}$, $T$ = 296 K, Crystal dimensions 0.6 × 0.3 × 0.2 mm; 3997 non-zero (2σ) reflections out of 4302 collected with 3.5 < 2θ < 45°, solution SHELXS-86, refinement SHELXL-93 on $F^2$, $R$ = 0.0520, $wR_2$ = 0.0693, C, N, O, Cl anisotropic, H isotropic. The final fourier difference map showed residual electron density of 0.187 e Å$^{-3}$. Atomic coordinates, bond lengths and angles, and thermal parameters have been deposited at the Cambridge Crystallographic Data Centre (CCDC). See Information for Authors, Issue No. 1. Any request to the CCDC for this material should quote the full literature citation and the reference number 182/425.

## References

1 G. R. Desiraju, *Crystal Engineering. The Design of Organic Solids*, Elsevier, Amsterdam, 1989.
2 J.-M. Lenh, *Angew. Chem., Int. Ed. Engl.*, 1995, **34**, 58.
3 C. B. Aakeroy and K. R. Seddon, *Chem. Soc. Rev.*, 1993, 397.
4 C. M. Paleos and D. Tsiourvas, *Angew. Chem., Int. Ed. Engl.*, 1995, **34**, 1696.
5 A. K. Abdul-Sada, A. M. Greenway, P. B. Hitchcock, T. J. Mohammed, K. R. Seddon and J. A. Zora, *J. Chem. Soc., Chem. Commun.*, 1986, 1753.
6 K. J. Harlow, A. F. Hill and T. Welton, *Synthesis*, 1996, 697.
7 A. G. Avent, P. A. Chalonerm, M. P. Day, K. R. Seddon and T. Welton, *J. Chem. Soc., Dalton. Trans.*, 1994, 3405.
8 A. Elaiwi, P. B. Hitchcock, K. R. Seddon, N. Srinivasan, Y.-M. Tan, T. Welton and J. A. Zora, *J. Chem. Soc., Dalton Trans.*, 1995, 3467.
9 C. J. Bowlas, D. W. Bruce and K. R. Seddon, *Chem. Commun.*, 1996, 1625.
10 F. Hentrich, S. Diele and C. Tschierske, *Liq. Cryst.*, 1994, **17**, 827.
11 R. G. Weiss, *Tetrahedron*, 1988, **44**, 3413.

*Received, 23rd December 1996; Com. 6/08517B*

# Intrazeolite assembly of a chiral manganese salen epoxidation catalyst

**Steven B. Ogunwumi and Thomas Bein***

*Department of Chemistry, Purdue University, West Lafayette, IN 47907, USA*

**Asymmetric manganese salen epoxidation catalysts are assembled and trapped in a multistep synthesis in the cages of zeolite EMT; these heterogeneous catalysts produce high enantiomeric excess in the epoxidation of aromatic alkenes with NaOCl.**

Asymmetric epoxidation of alkenes is of great interest for the synthesis of chiral intermediates in the pharmaceutical and agrochemical fields.[1,2] Zeolite cage structures are attractive hosts for the design of hybrid systems.[3] Such an inclusion strategy is expected to result in easy recovery or continuous use of the catalyst, diffusional selectivity of the reaction, and potentially increased stability *via* site isolation. Very few asymmetric reactions have been performed on zeolites.[4] Here we present an active, asymmetric epoxidation catalyst that was assembled and trapped in the cages of crystalline zeolite EMT. This novel heterogeneous system produces high enantiomeric excess (ee) in the epoxidation of aromatic alkenes with NaOCl (aq).

Chiral manganese salen epoxidation catalysts[5] are particularly active for the epoxidation of *cis*-substituted aryl alkenes. This family of complexes can be assembled in a stepwise manner in the cages of the zeolite EMT. This zeolite is a hexagonal form of the well known faujasite structure.[6,7] The hypercages of EMT are accessible through three 12-ring windows with free dimensions of 0.69 × 0.74 nm and two 0.74 nm circular apertures, while the hypocages have only three windows. EMT was synthesized as previously reported,[7] followed by calcination at 450 °C, washing with water, and dehydration at 300 °C and $10^{-4}$ Torr before use.

One specific intrazeolite assembly sequence was found to result in active and enantioselective heterogeneous epoxidation catalysts. A mixture of 1.00 g (0.16 mmol) calcined and dehydrated zeolite EMT and 1 equiv. [0.16 mmol (18.4 mg)] of (*R*,*R*)- or (*S*,*S*)-1,2-*trans*-diaminocyclohexane per EMT unit cell were stirred and refluxed in 80 ml of dry thf for 15 h under $N_2$. The solvent was evaporated, and 2.00 equiv. of the required salicylaldehyde (2-hydroxybenzaldehyde or 3-*tert*-butyl-5-methylsalicylaldehyde) were added and stirred at 80 °C under $N_2$ for 1 h, followed by refluxing under stirring in thf for 12 h. The zeolite host turns yellow during this process. 1 Equiv. of $Mn(O_2CMe)_2{\cdot}4H_2O$ (39 mg) per unit cell of EMT was added to the slurry, which was exposed to air to oxidize the $Mn^{II}$. Another 15 h refluxing under air resulted in a brownish slurry, to which was added 1 equiv. of solid LiCl per hypercage, followed by 24 h under reflux in thf, filtration, drying at 80 °C under vacuum, and Soxhlet extraction in $CH_2Cl_2$ for 24 h to remove excess complex, salen ligand, and reactants from the zeolite exterior and interior. Intrazeolite chloro[*N*,*N*′-bis(3-*tert*-butyl-5-methylsalicylidene)cyclohexanediamine]manganese(III) (**1**) is denoted **1–**EMT, chloro[*N*,*N*′-bis(salicylidene)-cyclohexanediamine]manganese(III) (**2**) is denoted **2–**EMT, and chloro[*N*,*N*′-bis(3-*tert*-butyl-5-methylsalicylidene)cyclohexanediamine]manganese(II) **3** (obtained by reacting intrazeolite salen ligand with $Mn^{II}$ under inert conditions) is denoted **3–**EMT. Complexes **1** and **2** were also synthesized in the homogeneous phase according to ref. 5.

Before assembly of the intrazeolite guest, the micropore volume of degassed EMT is 0.325 ml $g^{-1}$.[6] The chiral manganese salen complexes have dimensions of *ca.* 1.5 (**1**) and 1.3 nm (**2**; with modifications from crystallographic data of **1**, kindly provided by E. N. Jacobsen), preventing escape of the assembled complex from within the zeolite (crystallographic data for EMT: see ref. 8; Fig. 1). This general approach has been termed 'ship-in-the-bottle synthesis'.[9] No close van der Waals contacts were observed when the complexes were positioned in the hypercages.

The Soxhlet-extracted samples contain 0.50 ± 0.09 Mn per unit cell of EMT in the case of **1**–EMT, and 0.65 ± 0.09 Mn per unit cell in the case of **2**–EMT (XRF data). The free intrazeolite pore volume remaining after encapsulation of the complexes was determined using *T*-plot analysis from $N_2$ sorption, after evacuating the Soxhlet extracted samples at 120 °C. The original void volume of calcined EMT was reduced to 0.18 ml $g^{-1}$ in both **1**–EMT and **2**–EMT, showing that a significant fraction of the pore volume remains accessible after assembly of the intrazeolite salen complexes in spite of some water remaining in the zeolite after degassing.

Electronic absorption spectra in Fig. 2 show ligand transitions of the brownish oxidized complex **1** (in solution) at 322 and 438 nm and a weak d–d transition at 500 nm [Fig. 2(*a*)].[10] Upon zeolite encapsulation, the former bands shift to 335 and 422 nm, while the weak d–d transition is still observed at about 500 nm [Fig. 2(*b*)]. Strikingly, the d–d transition at 500 nm characteristic for $Mn^{III}$ in these complexes is absent in the spectrum of **3**–EMT [Fig. 2(*c*)], with bands at 266, 333 and 438 nm. In the IR spectrum (not shown), we observe the imine band at 1638 $cm^{-1}$ and a mode at 1458 $cm^{-1}$ for the salen ligand of **1**, assembled in the zeolite and dehydrated at 110 °C ($10^{-5}$ Torr)



**Fig. 1** View of the molecular fit of **1** in EMT (Cerius[2] software)

*in situ* to minimize interference with the zeolite water band at 1635 $cm^{-1}$. In solution, the imine C=N stretch vibration of the free ligand at 1631 $cm^{-1}$ shifts to 1610 $cm^{-1}$ upon complexation with $Mn^{III}$.[10b,11] A striking shift of the imine band to 1583 $cm^{-1}$ occurs upon complexation with $Mn^{II}$ and oxidation to form **1** in the EMT host which shows that a large majority of the ligands is now coordinating the Mn ions.

The encapsulated Mn salen complexes were studied as asymmetric epoxidation catalysts using different substrates (Table 1). In a representative reaction, 1 ml of dichloromethane or acetonitrile, 1 ml NaOCl (5.25%, 0.70 mmol), 0.005 ml $Na_2HPO_4$ (0.05 M), 0.005 ml *n*-decane (GC standard) and 1 drop of 1 M NaOH were added to a solution containing 0.15 mmol of an alkene such as *cis*-β-methylstyrene, along with 100 mg of **1**–EMT catalyst. The slurry was stirred at 4 °C for 1 h, followed by stirring at room temp. for ⩾23 h. The ratio of Mn to alkene was typically adjusted to 5 mol% (commonly used in homogeneous reactions). No conversion was observed when using an $Mn^{II}$-exchanged, air-treated zeolite EMT without the chiral salen ligand. The X-ray crystallinity of the zeolite host is retained after assembly of the intrazeolite complexes, and only slightly reduced after completion of the catalytic experiments.

The following observations can be noted (see also Table 1). (*i*) **1**–EMT with the bulky ligand is more active than **2**–EMT (*e.g.* conversion of *cis*-β-methylstyrene with **1**–EMT was 15% (after 24 h), and with **2**–EMT it was only 1%. The catalytic activity increases significantly on addition of axial ligands such as pyridine *N*-oxide, with which conversion of *cis*-β-methylstyrene was 47%. Formally, 100% conversion corresponds to a lower limit of 20 turnovers, but only a small fraction of the intrazeolite salen complexes may be accessed by the substrate during reaction. (*ii*) With PhIO as oxidant, **2**–EMT showed conversion of styrene and was more active than the sterically more encumbered **1**–EMT, suggesting that the access of the bulky terminal oxidant was hindered in the zeolite–**1** assembly (not in Table 1). (*iii*) The highest ee in epoxide, 88% was achieved with *cis*-β-methylstyrene, **1**–EMT plus pyridine *N*-oxide as catalyst, and NaOCl as oxidant, in dichloroethane. (*iv*) *trans*-β-Methylstyrene gives relatively high yields of *trans*-epoxide but the ee is lower. (*v*) Smaller (non-prochiral) alkenes such as 2,3-dimethylbut-2-ene give higher conversions than the more bulky but more reactive aromatic alkenes, suggesting a strong influence of the zeolite pore structure on diffusional access to the active salen complex encapsulated in the zeolite host. Proof for intrazeolite reactions is obtained by reacting cholesterol with the encapsulated **1**–EMT catalyst. While no conversion was observed with the encapsulated catalyst after 18 h, in solution the epoxidation proceeded to 13% conversion during the same time. This behaviour shows that the catalysis of the smaller substrates truly proceeds in the zeolite pores.

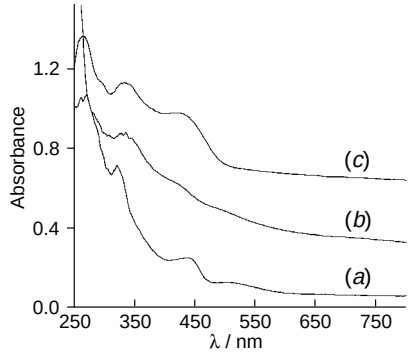



**Fig. 2** UV–VIS spectra (in diffuse reflectance mode) of oxidized **1** in solution (*a*), **1**–EMT (*b*) and **3**–EMT containing $Mn^{II}$ complexed by the salen ligand of **1** (*c*)

**Table 1** Heterogeneous and homogeneous catalysis reactions of [Mn(salen)Cl] in EMT[a]

| Substrate | Substrate conv.(%) | Epoxide selectivity (%) | ee (%) | Confign. |
|---|---|---|---|---|
| Heterogeneous | | | | |
| $Me_2C{=}CMe_2$[b] | 40 | 75 | NC[c] | NC |
| PhC(H)=$CH_2$ | 15 | 87 | 34 | *S*-(−) |
| (*E*)-PhC(H)=CH(Me) | 29 | 62 | 20 | 1*S*,2*S*-(−) |
| (*Z*)-PhC(H)=CH(Me)[d] | 15 | 67 | 80 | 1*S*,2*R*-(−) |
| (*Z*)-PhC(H)=CH(Me)[e] | 47 | 58 | 88 | 1*S*,2*R*-(−) |
| Cholesterol | None | — | — | — |
| Homogeneous | | | | |
| PhC(H)=$CH_2$ | 55 | 95 | 35 | *S*-(−) |
| (*Z*)-PhC(H)=CH(Me) | 85 | 97 | 80 | 1*S*,2*R*-(−) |
| Cholesterol[f] | 13 | 85 | — | — |

[a] Salen = (*S*,*S*)-*N*,*N*′-bis(3-*tert*-butyl-5-methylsalicylidene)-cyclohexanediamine. (Other products and distribution not given.) *Reagents and conditions:* 5 mol % catalyst, reaction maintained at 0 °C for 1 h then room temp. for 24 h; solvent, $CH_2Cl_2$; oxidant, NaOCl; Astec chiraldex B-TA column (decane: GC standard). [b] Reactivity of a non-prochiral alkene. [c] Not chiral. [d] Initial experiments addressing the recyclability of the catalyst after Soxhlet extraction with acetonitrile showed significantly lower ee; the origin of this reduced enantioselectivity is currently being studied. [e] Catalyst with pyridine *N*-oxide (5 mol%); solvent dichloroethane. [f] Isolated yield determined by $^1H$ NMR using $CH_2Br_2$ as internal standard (after 18 h).


The authors gratefully acknowledge funding from the U.S. Department of Energy for this work. We thank Professor Merritt B. Andrus for assistance with chromatographic separations.


## References


1 R. A. Sheldon and J. K. Kochi, *Metal-Catalysed Oxidation of Organic Compounds*, Academic Press, New York, 1981; J. Gorzynski Smith, *Synthesis*, 1984, 629.

2 Li. Deng and E. N. Jacobsen *J. Org. Chem*., 1992, **57**, 4320; D. M. Hodgson, P. J. Parsons and P. A. Stones, *J. Chem. Soc., Chem. Commun*., 1988, 217.

3 D. E. De Vos, J. L. Meinershagen and T. Bein, *Angew. Chem., Int. Ed. Engl.*, 1996, **35**, 2211; P. P. Knops Gerrits, D. E. De Vos, F. Thibault-Starzyk and P. A. Jacobs, *Nature*, 1994, **369**, 543.

4 (*a*) S. Feast, D. Bethell , P. C. B. Page, F. King, C. H. Rochester, M. R. H. Siddiqui, D. J. Willock and G. J. Hutchings, *J. Chem. Soc., Chem. Commun*., 1995, 2409; (*b*) A. Corma, M. Iglesias, C. del Pino and F. Sanchez, *J. Chem. Soc., Chem. Commun*., 1991, 1253; (*c*) A. Carmona, A. Corma, M. Iglesias, A. San Jose and F. Sanchez, *J. Organomet. Chem.*, 1995, **492**, 11; (*d*) A. Corma, M. Iglesias, V. M. Martin and F. Sanchez, *Tetrahedron Asymmetry*, 1992, **3**, 845; (*e*) U. Böhmer, K. Morgenschweis and W. Reschetilowski, *Catal. Today*, 1995, **24**, 195; (*f*) A. Corma, A. Fuerte, M. Iglesias and F. Sanchez, *J. Mol. Catal. A*, 1996, **107**, 225.

5 W. Zhang, J. L. Loebach, S. R. Wilson and E. N. Jacobsen, *J. Am. Chem. Soc*., 1990, **112**, 2801; T. Katsuki, *Coord. Chem. Rev*., 1995, **140**, 189 and references therein.

6 E. J. P. Feijen, K. De Vadder, M. H. Bosschaerts, J. L. Lievens, J. A. Martens, P. J. Grobet and P. A. Jacobs, *J. Am. Chem. Soc.*, 1994, **116**, 2950.

7 S. L. Burkett and M. E. Davis, *Microporous Mater*., 1993, **1**, 265.

8 J. L. Lievens, J. P. Verduijn, A.-J. Bons and W. J. Mortier, *Zeolites*, 1992, **12**, 698.

9 N. Herron, *Inorg. Chem.*, 1986, **25**, 4714.

10 (*a*) M. T. Rispens, A. Meetsma and B. L. Feringa, *Recl. Trav. Chim. Pays-Bas*, 1994, **113**, 413; (*b*) J. Skarzewski, A. Gupta and A. Vogt, *J. Mol. Catal. A.*, 1995, **103**, L63.

11 J. R. Dilworth, C. A. McAuliffe and B. J. Sayle, *J. Chem. Soc., Dalton Trans*., 1977, 849.



*Received in Bloomington, IN, USA, 20th November 1996; Com. 6/07879F*





Typeset and printed by Black Bear Press Limited, Cambridge, England

ChemComm
FEATURE ARTICLE

# Allenylidenes: their multifaceted chemistry at rhodium

**Helmut Werner**

*Institut für Anorganische Chemie der Universität Würzburg, D-97074 Würzburg, Germany*

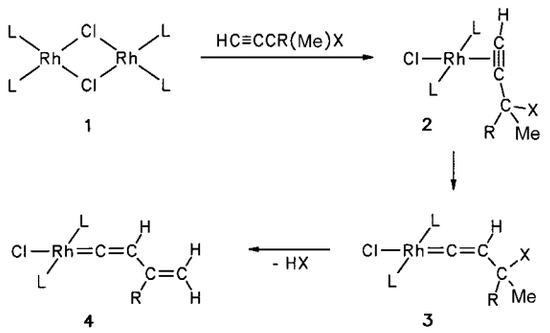
**Rhodium allenylidenes, which represent a class of 'flat' metallabutatrienes, are useful tools for the generation of metal-bound species that are hardly accessible (sometimes not accessible at all) by other synthetic routes. In contrast to various *octahedral* allenylidene metal complexes, *e.g.* of $Cr^0$, $Mn^I$ or $Ru^{II}$, the square-planar rhodium compounds *trans*-$[RhX(=C=C=CRR')(PPr^i_3)_2]$ are attacked by both nucleophiles and electrophiles. Moreover, non-polar substrates such as $H_2$ or $Cl_2$ react cleanly with the title complexes to give products in which the allenylidene unit is preserved as part of a newly formed ligand. Attempts to prepare a square-planar cationic metallaheptahexaene, *trans*-$[Rh(=C=C=CRR')_2(PPr^i_3)_2]^+$, unexpectedly led to the formation of two isomeric hexapentaenerhodium(I) complexes of which the isomer having the polyene coordinated in an unsymmetrical fashion is the thermodynamically more stable. C–C coupling reactions also occur on treatment of *trans*-$[RhCl(=C=C=CPh_2)(PPr^i_3)_2]$ with vinyl Grignard reagents or phenylacetylene leading to highly unsaturated $RhC_5$ and $RhC_5P$ frameworks from which vinylallenes and phosphacumuleneylides are obtained.**

## Introduction

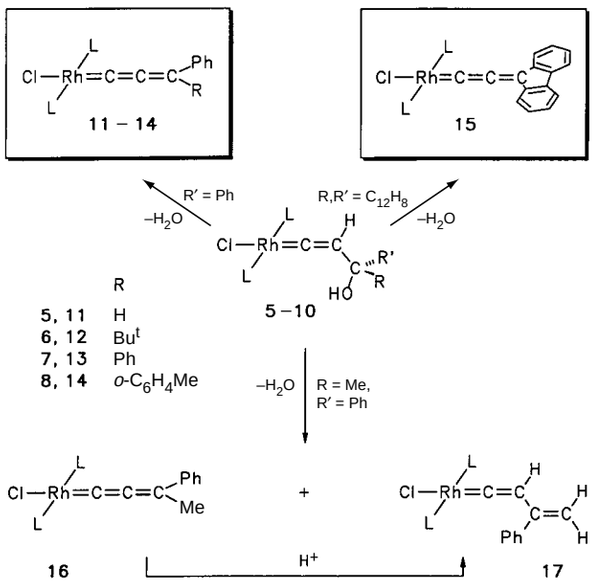
One of the most exciting areas in chemical research which emerged in the last decades undoubtedly is that of transition-metal carbene chemistry. Numerous compounds of general composition $[M(=CRR')L_n]$ (L = non-carbene ligands) have been prepared, structurally characterized and used particularly in organic synthesis and homogeneous catalysis.[1] Regarding the date of the landmark report on the isolation of the first carbenemetal complex (1964),[2] and the furious development which started almost immediately thereafter,[3] the chemistry of related metal compounds containing *unsaturated* carbenes as ligands has much more hesitantly explored. As far as *allenylidenes* are concerned, the breakthrough came in 1982 with the paper by Selegue which illustrated that propargylic alcohols HC≡CCRR′OH can be converted quite smoothly into a C=C=CRR′ unit in the coordination sphere of an electron-rich transition-metal centre by elimination of water.[4] Since this report, a variety of allenylidene–metal complexes have been prepared, the elements of the chromium, manganese and iron triads thereby playing a dominant role.[5]

As part of our work on *vinylidene* complexes $[M(=C=CRR')L_n]$ (M = Ru, Os, Rh, Ir),[6] we recently observed that γ-functionalized alkynes HC≡CCR(Me)X (R = H, Me; X = OH, $NH_2$) react with $[RhCl(PPr^i_3)_2]_2$ **1** to give, *via* the alkyne rhodium derivatives **2** as intermediates (Scheme 1), the square-planar compounds **3** which on treatment with $Al_2O_3$ or traces of acid undergo elimination of HX to afford the rhodium vinylvinylidenes **4** in excellent yield.[7] If, however, instead of HC≡CCH(Me)OH or HC≡CC(Me)$_2$OH the corresponding phenyl-substituted alkynols HC≡CCR(Ph)OH (R = H, $Bu^t$, Ph, *o*-$C_6H_4Me$) or the fluorenone-derived species HC≡CC($C_{12}H_8$)OH are used, the four-coordinate allenylidene complexes **11**–**15** (Scheme 2) are exclusively obtained.[8,9] They are formed from the initially generated rhodium vinylidenes **5**–**9** (**9**: R, R′ = $C_{12}H_8$) by abstraction of water. The reaction of **10** (R = Me, R′ = Ph) with neutral alumina gives a mixture of **16** and **17** (ratio *ca.* 1:9) which can be converted quantitatively into **17** by treatment with an excess of acidic $Al_2O_3$ in benzene at room temperature.[8] With regard to the studies described in this paper it should be mentioned that the allenylidene complexes **11**–**15** are crystalline, only moderately air-sensitive solids which are quite easy to handle and can be stored under argon for weeks.

The aim of the present article is to illustrate that compounds of composition *trans*-$[RhCl(=C=C=CRR')(PPr^i_3)_2]$ are not only interesting as far as their synthesis and molecular structure are concerned but that they also offer new insights into the reactivity of metal-containing cumulenes. It will be shown that the behaviour in some respects is different to that of the analogous metal vinylidenes *trans*-$[RhCl(=C=CRR')(PPr^i_3)_2]$ which is not unexpected insofar as the stereochemistry of the




**Scheme 1** L = $PPr^i_3$; R = H, Me; X = OH, $NH_2$




**Scheme 2** L = $PPr^i_3$

latter corresponds to that of *allenes* while the complexes **11**–**15** are relatives of *butatrienes* (Fig. 1).

### Ligand substitution reactions of the metallabutatrienes: Part I

Since allenylidenes like carbon monoxide, isocyanides and vinylidenes (*i.e.* strictly isoelectronic species CX if X is O, NH or $CH_2$) are good π-acceptor ligands,[10] we had anticipated that in square-planar complexes of general composition *trans*-[RhX(=C=C=CRR′)($PPr^i_3$)$_2$] the allenylidene unit would exert a strong influence on the ligand in the *trans* position. Substitution of the chloride in complexes **11**–**15** should therefore be favoured and this has been confirmed with various nucleophiles. While it is not surprising that on treatment of **12**, **13** or **14** with KI or $NaC_5H_5$ products such as **18**, **19** or **20**, **21** are formed, the preparation of the hydroxo derivatives **22**–**24** (Scheme 3) constitutes a more interesting example. This is due to the fact that hydroxo complexes of platinum group metals are not only quite rare,[11] but that compounds **22**–**24** open the gate to a variety of other square-planar rhodium allenylidenes *trans*-[RhX{=C=C=C(Ph)R}($PPr^i_3$)$_2$] (see Scheme 4) which are not accessible *via* any other route.

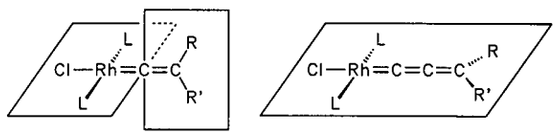
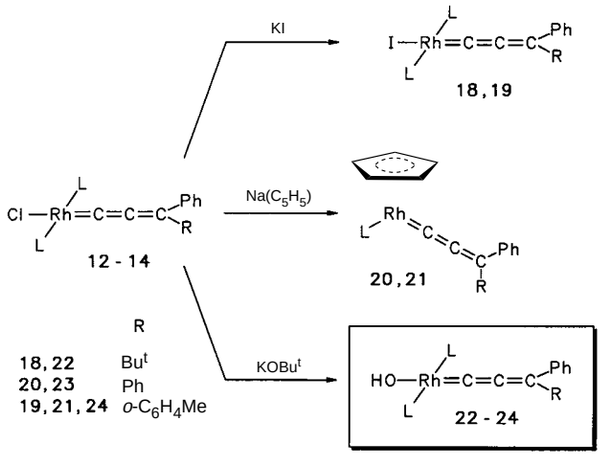


**Fig. 1** Different stereochemistry of rhodium vinylidenes ('metallaallenes') and rhodium allenylidenes ('metallabutatrienes'); L = $PPr^i_3$



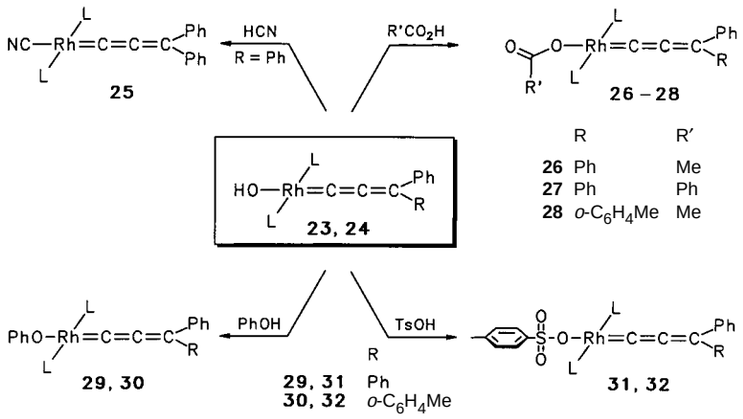

**Scheme 3** L = $PPr^i_3$

In contrast to the tosylato compounds **31** and **32**, which on treatment with carbon monoxide lose the allenylidene unit to give **33** (Scheme 5), the acetato and phenolato derivatives **26**, **28** and **29**, **30** react with CO to yield the 1 : 1 adducts **34**–**37** almost quantitatively.[12] As the X-ray crystal structure analysis of **36** reveals, a migration of the phenolato ligand to the γ-carbon atom of the allenylidene moiety has taken place and a new functionalized alkynyl unit is formed. The Rh–C$^1$ distance [2.037(4) Å] is significantly longer than in complex **14** [1.855(5) Å][8] and nearly identical to the Rh–C bond lengths in the five-coordinate bis(alkynyl)hydrido rhodium(III) compound [RhH(C≡CC$Pr^i_2$OH)$_2$($PPr^i_3$)$_2$] (**57**, see Scheme 13 later).[13] The Rh–C–C–C chain in **36** is almost linear while the two phenyl substituents at C$^3$ are orthogonal to each other, thus presumably minimizing the repulsion between the C–H units.

For the elucidation of the mechanism of the migratory insertion process leading to **34**–**37** some crossover experiments with **26** and **30** as starting materials were performed. Unfortunately, they did not give a conclusive answer. We found that the Rh–O bond in the acetato and phenolato allenylidene complexes is extremely labile and thus, before CO was passed through the solution of **26** and **30** in benzene, a random exchange took place and a mixture of **26**, **28**, **29** and **30** was formed. The observation, however, that the reaction of **29** with CO in the presence of acetate ions exclusively yields **36** (and not a mixture of **34** and **36**) indicates that the formation of the alkynyl complexes **34**–**37** occurs intramolecularly and does not involve a heterolytic cleavage of the Rh–OR bond. The formal 1,4-shift of the acetato or phenolato group may take place stepwise *via* an OR-substituted allenylmetal intermediate which rapidly rearranges to the final product. Since the reaction of *trans*-[Rh(OMe)(CO)($PPr^i_3$)$_2$] with CO yields *trans*-[Rh($CO_2$Me)(CO)($PPr^i_3$)$_2$],[14] it should be noted that on treatment of **29** and **30** with carbon monoxide no insertion into the Rh–OR bond takes place.

### Ligand substitution reactions of the metallabutatrienes: Part II

Attempts to replace the halide ligand in the diphenylallenylidene complex **13** by C-nucleophiles such as alkyls, aryls or vinyls led to a surprising result. While the reaction of **13** with MeMgI or PhMgBr gives a mixture of products among which the anticipated species *trans*-[Rh(R)(=C=C=$CPh_2$)($PPr^i_3$)$_2$] (R = Me, Ph) could not be unequivocally identified,[15] on treatment of **13** with $CH_2$=CHMgBr in toluene–thf both the substitution of chloride by vinyl *and* the coupling of the C-nucleophile and the allenylidene ligand occurs.[16] To explain the formation of the π-allylic complex **38** (Scheme 6), we assume that initially a four-coordinate intermediate **A** is generated which rearranges by migratory insertion of the allenylidene unit into the Rh–CH=$CH_2$ bond to give **38**. In this context, it is remarkable that the rhodium vinylidenes *trans*-




**Scheme 4** L = $PPr^i_3$

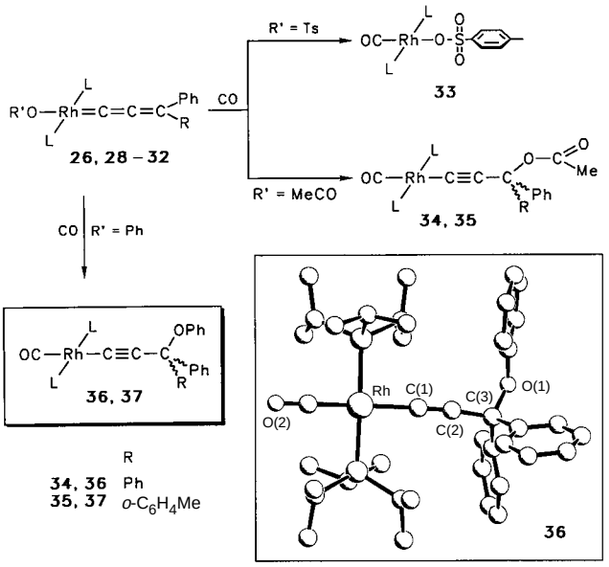
[RhCl(=C=CHR)($PPr^i_3$)$_2$] (R = H, Bu$^t$, Ph) react with $CH_2$=CHMgBr to give the *isolable* complexes *trans*-[Rh(CH=$CH_2$)(=C=CHR)($PPr^i_3$)$_2$] which upon heating to 45–50 °C in benzene slowly isomerize to give the allylic C–C coupling products [Rh($\eta^3$-$CH_2CHC$=CHR)($PPr^i_3$)$_2$].[17]

Compound **38** reacts with CO even below room temperature almost instantaneously to give the yellow crystalline 1 : 1 adduct **39** in excellent yield.[16] The addition of CO to the metal centre is accompanied by a π–σ conversion of the $C_5$ ligand, possibly *via* an 18-electron intermediate [Rh($\eta^3$-$CH_2CHC$=C=$CPh_2$)(CO)($PPr^i_3$)$_2$]. As shown in Scheme 6, the X-ray crystal structure analysis of **39** confirmed a square-planar coordination sphere around rhodium and a nearly linear $C^1$–$C^4$–$C^5$ chain with the vinyl carbon atoms $C^2$ and $C^3$ lying in the same plane as Rh, $C^1$, $C^4$ and $C^5$. The cleavage of the Rh–C σ bond in **39** by an equimolar amount of acetic acid proceeds smoothly and affords the new vinylallene **40** quantitatively.[16]

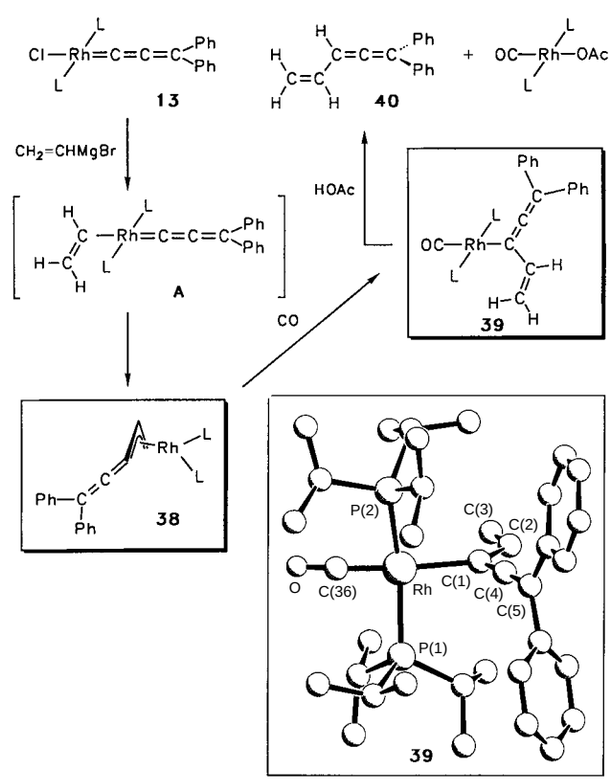
A second [$C_2$ + $C_3$] coupling reaction which involves one of the phosphine ligands of **13** is even more exceptional. Upon treatment of a solution of **13** in benzene with phenylacetylene at 10 °C, a gradual change of colour occurred and a light-red crystalline product **41**, formally corresponding to a 1 : 1 adduct of the allenylidene complex and the alkyne, was isolated in practically quantitative yield.[16] The $^{31}$P NMR spectrum of **41** already showed the presence of two distinctly different $PPr^i_3$ groups, and the X-ray structural analysis finally confirmed that only one of the phosphines is still coordinated to the metal centre. The other is part of a π-bonded ylide which is formed from the allenylidene, the alkyne and the second phosphine unit. While the $PC_5$ ligand in **41** is coordinated in a π-allylic fashion (see Scheme 7), the distances between the rhodium and the carbon atoms $C^1$, $C^2$ and $C^3$ differ by *ca.* 0.15 Å, probably due to the different hybridization at $C^3$ compared with $C^1$ and $C^2$ and to the different influence of the ligands $Cl^-$ and $PPr^i_3$ in *trans* positions. Although the carbon atoms of the =C=$CPh_2$ unit are not coplanar with the allylic fragment, the $C^3$–$C^4$–$C^5$ chain in **41** is almost linear with $C^3$–$C^4$ and $C^4$–$C^5$ distances that are comparable to those in the allenylidene complex **14** and in **39**. The free ylide **42**, formerly unknown, was generated from **41** on treatment with CO and characterized by $^1$H, $^{13}$C and $^{31}$P NMR spectroscopy.[16]

### Addition reactions of the metallabutatrienes: the unexpected products

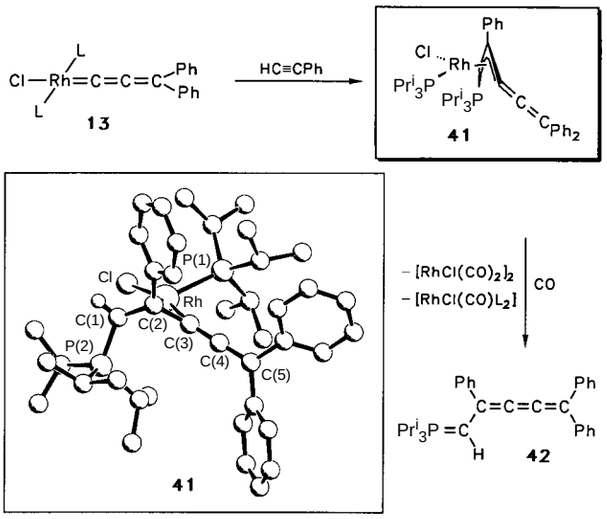
Following the idea that the bonding capabilities of CO and unsaturated carbenes are similar,[10,19] we had anticipated that in analogy to the carbonyl derivative *trans*-[RhCl(CO)($PPr^i_3$)$_2$][20] also the Rh-containing metallabutatrienes would react with substrates such as HCl, MeI and $H_2$ by oxidative addition and formation of octahedral rhodium(III) complexes. This, however, is not the case. Compound **13** (which was chosen for these studies as an easily accessible starting material) adds 1 equiv. of HCl quite rapidly but instead of the six-coordinate hydridorhodium complex [$RhHCl_2$(=C=C=$CPh_2$)($PPr^i_3$)$_2$] the five-coordinate allenyl compound **43** (Scheme 8) is quantitatively formed.[15] To explain the course of this unexpected reaction, we assume that initially the electrophile attacks the Lewis-basic metal centre to give the salt-like intermediate [RhHCl(=C=C=$CPh_2$)($PPr^i_3$)$_2$]$^+$Cl$^-$,[21] which by 1,2-H shift from rhodium to the α-carbon atom of the allenylidene unit, accom-




**Scheme 5** L = $PPr^i_3$




**Scheme 6** L = $PPr^i_3$




**Scheme 7** L = $PPr^i_3$

panied by nucleophilic addition of $Cl^-$ to the metal, yields the final product. We note that the *octahedral* metallabutatriene complex $[RuCl_2(=C=C=CPh_2)\{Pr^i_2PCH_2C(OMe)=O\text{-}\kappa P\}\{Pr^i_2PCH_2C(OMe)=O\text{-}\kappa^2P,O\}]$ reacts with HCl by attack of the electrophile to the $C_\alpha$–$C_\beta$ and not to the Ru–$C_\alpha$ double bond and attribute this difference to the 18-electron configuration of the metal centre.[22]

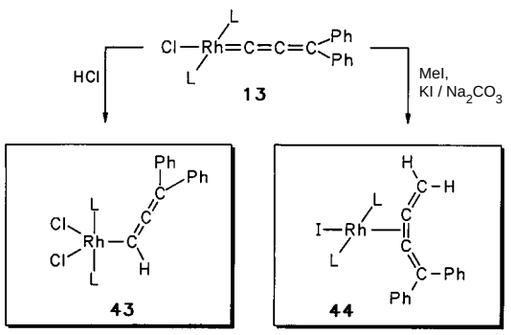
Methyl iodide, which we used as a counterpart to HCl in the course of the investigations into the reactivity of **13**, also reacts in an unexpected way with **13**. While in the absence of a basic substrate the reaction of **13** with MeI proceeds very slowly and gives a mixture of products, the novel 1,1-diphenylbutatriene complex **44** is formed as the major species besides **47** (see below) in the presence of $Na_2CO_3$. Subsequent treatment of the reaction mixture with KI yields **44** almost quantitatively.[23] As far as the mechanism of formation of **44** is concerned, we assume that in the initial step the expected oxidative addition of MeI at the rhodium centre takes place which is followed by an insertion of the allenylidene unit into the Rh–Me bond. The intermediate containing the allene-type $RhC(Me)=C=CPh_2$ moiety then reacts by a β-H shift to give a butatriene(hydrido)-diiodorhodium(III) compound that upon reductive elimination of HI (facilitated by $Na_2CO_3$) generates the final product. Analogous to the first two steps is the formation of $[IrCl(I)\{C(Me)=CH_2\}(PPr^i_3)_2]$ and $[IrI\{C(Me)=CH_2\}\{N(SiMe_2CH_2PPh_2\text{-}\kappa^3N,P,P)_2\}]$ from the corresponding vinylidene complexes and methyl iodide.[24] In this case, however, a subsequent β-H shift does not occur.

There is also a second route to convert a metal-bonded allenylidene unit into a butatriene ligand (Scheme 9). Both compounds **12** and **13** react with excess diazomethane at room temperature to afford the butatriene complexes **45** and **46** in excellent yield.[23] The coordination of the $C_4$ cumulenes *via* the $C=CH_2$ bond is not only supported by the $^1H$ and $^{13}C$ NMR spectra, but also confirmed by the X-ray structure analysis of **46**. This reveals a distorted square-planar geometry around the metal centre with the Cl, Rh and $C^1$–$C^4$ atoms lying in one plane. Although the $C=CH_2$ unit is bonded unsymmetrically to the metal (as is shown by the linearity of the Cl–Rh–$C^2$ axis), the distances Rh–$C^1$ and Rh–$C^2$ are nearly identical and quite similar to the Rh–C bond lengths in structurally related allene rhodium(I) compounds.[25] The P–Rh–P axis in **46** deviates somewhat from linearity which is probably due to the steric requirements of the bulky phosphine ligands.

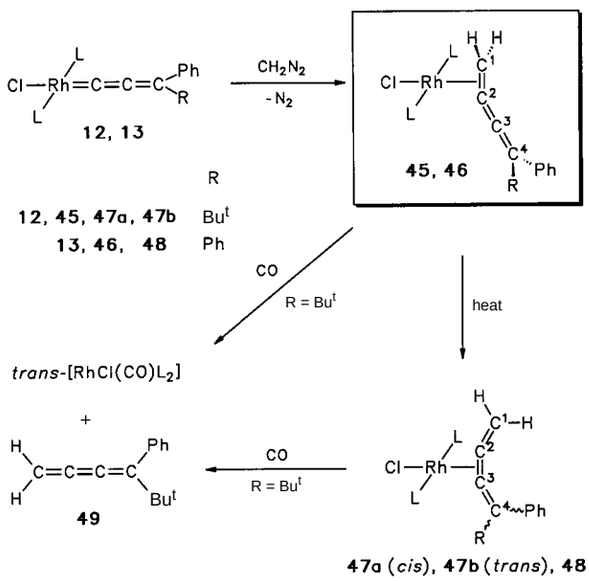
Both **45** and **46** are thermally labile and upon heating in toluene at 80–90 °C rearrange to the thermodynamically more stable complexes **47** and **48**. For **47**, a mixture of two isomers **47a,b** (see Scheme 9) is formed which differ in the relative positions of the phenyl and *tert*-butyl groups to the rhodium centre. Although isomer **47a** is the dominating and probably preferred species, even after heating the mixture of **47a,b** in toluene at 90 °C for 10 h a complete conversion of **47b** to **47a** does not occur. Nevertheless, complex **47a** could be isolated analytically pure upon fractional crystallization and, by comparison of the NMR data with those of **47b**, identified as the isomer in which the Bu$^t$ group at $C^4$ is directed towards the metal. In all of the previously described 1,1,4,4-tetrasubstituted butatrienerhodium(I) compounds *trans*-$[RhCl(\eta^2\text{-}R_2C=C=C=CR_2)(PPh_3)_2]$, which were prepared from $[RhCl(PPh_3)_3]$ and butatrienes,[26] the *central* C=C bond is linked to the metal. The coordination of a *terminal* $R_2C=C$ bond, as it has been observed for **45** and **46**, was only recently reported by White and Stang for platinum(0) as the central atom.[27] The two isomeric forms **45** and **47a,b** as well as **46** and **48** rapidly react with CO to yield *trans*-$[RhCl(CO)(PPr^i_3)_2]$ by ligand exchange. Of the butatrienes formed in these conversions, the one with $CPh_2$ as the terminal unit is quite labile undergoing secondary reactions whereas the hitherto unknown cumulene **49** has been characterized by GC–MS and spectroscopic techniques.[23]

The allenylidene ligand of **13** can be converted not only to a butatriene but also to an allene. The reaction of **13** with $H_2$ in benzene at room temperature is rather slow but after 40 h, by cleavage of the Rh=C double bond, the square-planar rhodium(I) complex **50** (Scheme 10) is quantitatively formed.[15,23] Remarkably, under the chosen conditions no hydrogenation of the allene ligand occurs. Since the $^1H$ NMR spectrum of **50** displays only one signal for the $CH_2$ protons, there is no doubt that it is the *unsubstituted* double bond of the allene which is bonded to the metal. On treatment of **50** with CO, the alkenic ligand is readily displaced and together with the allene **51** the carbonyl complex *trans*-$[RhCl(CO)(PPr^i_3)_2]$ is formed.

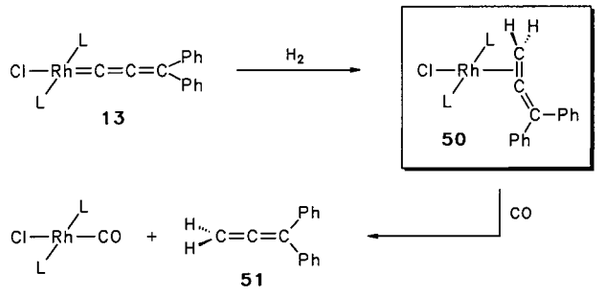
The reaction of **13** with a solution of chlorine in thf–hexane yields a 1 : 1 adduct **52** by oxidative addition which, however, does not have the expected octahedral geometry. The $^1H$, $^{13}C$ and $^{31}P$ NMR spectra display two completely different sets of signals for the hydrogen, carbon and phosphorus atoms of the $PPr^i_3$ groups and, since only one of the $^{31}P$ NMR resonances




**Scheme 8** L = $PPr^i_3$




**Scheme 9** L = $PPr^i_3$




**Scheme 10** L = $PPr^i_3$

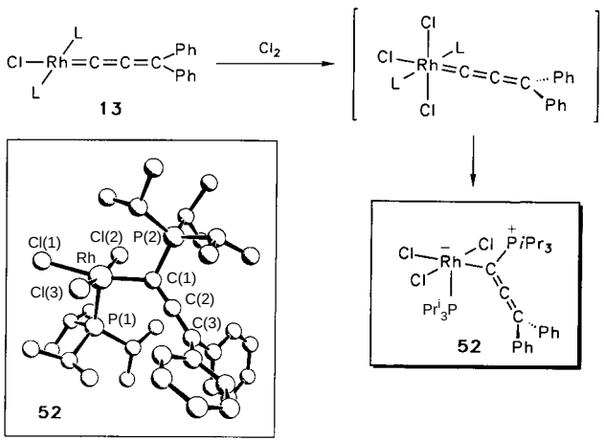
shows a strong Rh–P coupling, it is clear that one of the phosphines is not linked to rhodium. The X-ray crystal structure analysis of **52** (Scheme 11) indeed reveals that a five-coordinate rhodium(III) complex has been formed which contains in addition to one phosphine and three chlorides the phosphacumuleneylide $Pr^i_3P{=}C{=}C{=}CPh_2$ as an $\eta^1$-bonded ligand. The geometry around the metal centre is best described as square-pyramidal with the triisopropylphosphine in the apical position. The two planes containing the substituents at $C^1$ (Rh and $P^2$) and $C^3$ (*ipso*-carbons of $C_6H_5$) are orthogonal to each other, in agreement with the allene-type structure of the molecule.[28] Related phosphacumuleneylide ligands to that found in **52** are known from $[(C_5H_5)Mn\{C(PPh_3){=}C{=}CPh_2\}(CO)_2]$ and $[Cr\{C(PPh_3){=}C{=}CPr^i_2\}(CO)_5]$, but have been generated by attack of free triphenylphosphine on allenylidene complexes.[29]

### $[C_3 + C_3]$ coupling reactions: are metallabutatrienes involved?

When we considered proceeding one step further in the investigation of rhodium-containing metallacumulenes, the question arose whether it would be possible to generate a cation like **II** (Fig. 2) which would be structurally comparable to the dicarbonyl species **I** recently prepared in our laboratory.[30] For this purpose we attempted to apply a methodology which by using the $\eta^3$-benzyl complex **53** as starting material led to the formation of alkynyl rhodium vinylidenes **54** and, on further reaction with HCl and CO, finally to enynes and butatrienes (Scheme 12).[31]

With the reactivity of compound **53** towards terminal alkynes such as HC≡CPh or HC≡CBu$^t$ in mind, we were not surprised that on treatment of **53** with 2 equiv. of $HC{\equiv}CCR_2OH$ (R = Me, Ph, Pr$^i$) a rapid reaction occurred that led to the formation of crystalline, only slightly air-sensitive solids **55**–**57** in *ca.* 70% yield.[13] The IR and NMR spectra of the products illustrated quite clearly that instead of the expected alkynyl(vinylidene)-rhodium(I) complexes *trans*-$[Rh(C{\equiv}CCR_2OH)(=C{=}CHCR_2OH)(PPr^i_3)_2]$ the bis(alkynyl)hydridorhodium(III) isomers $[RhH(C{\equiv}CCR_2OH)_2(PPr^i_3)_2]$ were formed. These five-coordinate compounds possess a square- pyramidal and not trigonal-bipyramidal configuration, as was confirmed by the crystal structure analysis of **57**.[13] The SCHAKAL diagram, which is included in Scheme 13, shows that the basal plane of the pyramid consists of an exactly linear P–Rh–P and an almost linear C–C–Rh–C–C arrangement with Rh–C bond lengths that are nearly identical to those of the octahedral bis(alkynyl)-hydrido complex $[RhH(C{\equiv}CPh)_2(PMe_3)_3]$.[32] The structure of **57** found in the crystal is most probably also preserved in solution since the $^1$H NMR spectrum (like the spectra of **55** and **56**) displays a doublet of triplets at $\delta$ −30.5 which together with a Rh–H coupling constant of 50 Hz is most typical for five-coordinate hydridorhodium(III) species.[33]

Compound **55** is not completely inert in benzene solution and at room temperature reacts slowly to give the OH-functionalized alkynyl(vinylidene)rhodium(I) derivative **58** (Scheme 14) in good yield.[13] The formation of this complex (which is structurally related to the species **54** shown in Scheme 12) is




**Scheme 11** L = $PPr^i_3$

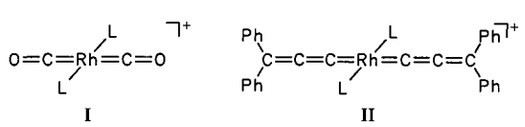
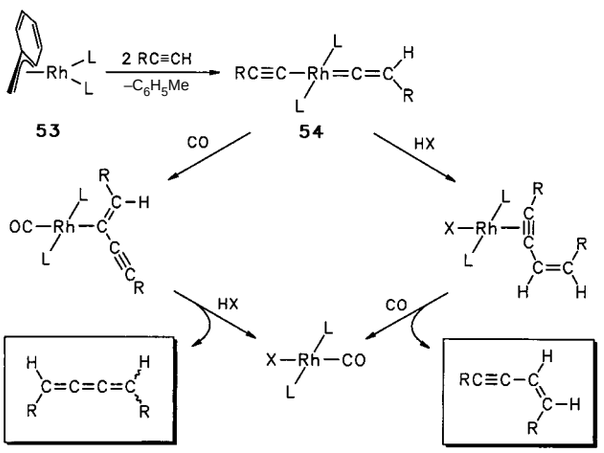
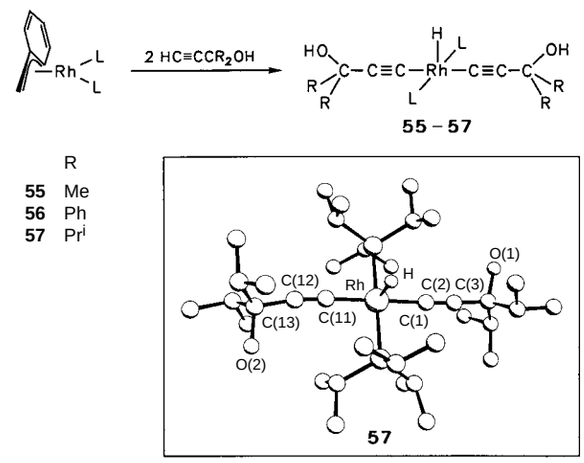


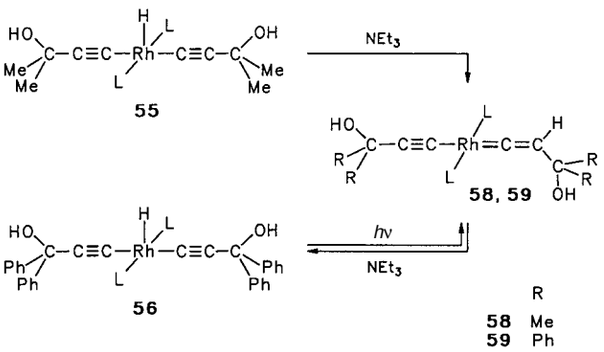

**Fig. 2** Formal relation between the cationic dicarbonylrhodium and bis(allenylidene)rhodium complexes **I** and **II**; L = $PPr^i_3$




**Scheme 12** L = $PPr^i_3$




**Scheme 13** L = $PPr^i_3$




**Scheme 14** L = $PPr^i_3$

significantly facilitated by addition of $NEt_3$, probably due to a weakening interaction of the amine with the Rh–H bond. A complete rearrangement of **56** to the isomer **59** does not proceed under thermal conditions but takes place on irradiation of the bis(alkynyl)hydrido compound in benzene. Unlike **58**, the analogous complex **59** is not stable in benzene or toluene solution and, particularly in the presence of $NEt_3$, partly rearranges to the isomer **56** until an equilibrium of **56**:**59** = 30:70 is reached. No isomerization of compound **57** occurs, neither thermally nor photochemically, which could be due to the efficient shielding of the β-carbon atom of the alkynyl ligands by the bulky isopropyl groups.[13]

While the reactions of **56** and **59** with CO followed established routes and gave by addition and (in the case of **59**) by migratory insertion the carbonyl complexes $[RhH(C{\equiv}CCPh_2OH)_2(CO)(PPr^i_3)_2]$ and *trans*-$[Rh\{\eta^1$-$(Z)$-$C(C{\equiv}CCPh_2OH){=}CHCPh_2OH\}CO)(PPr^i_3)_2]$, respectively, treatment of **56** and **59** with acidic $Al_2O_3$ in the presence of chloride ions led to a completely unexpected result. In analogy to the preparation of **13** from **7** (see Scheme 2) we anticipated the formation of *trans*-$[Rh(C{\equiv}CCPh_2OH)(=C=C=CPh_2)(PPr^i_3)_2]$ or, hopefully, of a salt of the bis(allenylidene)rhodium(I) cation *trans*-$[Rh(=C=C=CPh_2)_2(PPr^i_3)_2]^+$. However, we isolated (besides small amounts of **13**) the novel hexapentaene complex **60** (Scheme 15) in 70% yield.[13] If the time for the interaction of **56** or **59** with $Al_2O_3/H^+/Cl^-$ is not sufficient, an isomeric mixture of **60** and **61** is formed which, however, can be quantitatively converted to **60** by stirring a solution of **60**/**61** in benzene at room temperature. The assumption that **61** is the kinetically preferred and **60** the thermodynamically preferred isomer could be confirmed by stepwise synthesis of the two compounds from dimer **1**. The more symmetrical complex **61** was exclusively obtained from **1** and the hexapentaene $Ph_2C{=}C{=}C{=}C{=}CPh_2$ **62** in toluene at −30 °C, provided that the solution was worked up quickly at low temperature. The further rearrangement of **61** to **60** proceeded at 25 °C. Both compounds **60** and **61** smoothly react with carbon monoxide by ligand displacement to give *trans*-$[RhCl(CO)(PPr^i_3)_2]$ and the cumulene **62**. With regard to the structure of the more stable isomer **60**, the X-ray analysis showed that the $C_6$ chain is bent, possessing C–C–C angles which are similar to those found in related butatrienerhodium(I) complexes.[23,26] The plane of the carbon atoms $C^1$–$C^6$ is exactly perpendicular to the plane containing the metal, the chloride and the phosphorus atoms, the dihedral angle being 89.8(1)°.

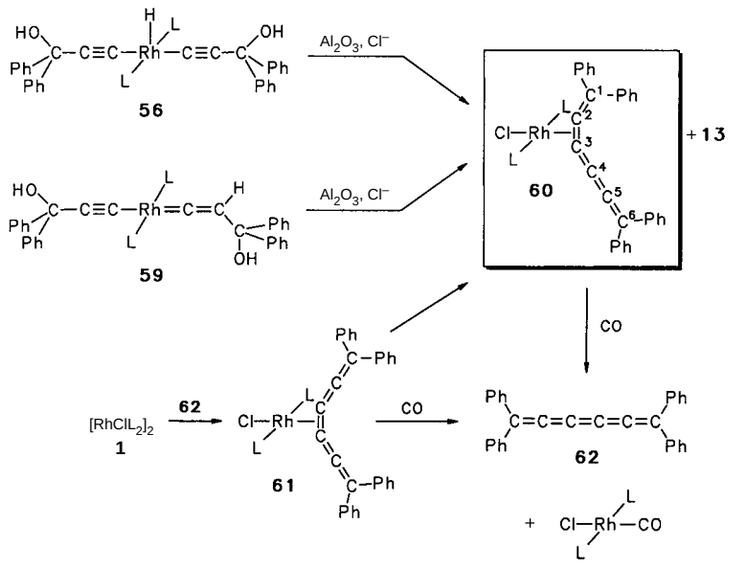
The proposed mechanism of formation of **60** and **61** is outlined in Scheme 16. We assume that in analogy with the preparation of **13** from **7** and $Al_2O_3$ an alkynyl(allenylidene)-rhodium(I) intermediate **B** is generated initially which can be converted either by proton attack (and elimination of water) to the bis(allenylidene)metal cation **C** or, alternatively, by solvent-assisted migration of the alkynyl ligand to the α-carbon atom of the allenylidene unit to give **D**. Coupling of the two $C_3$ fragments of **C** or acid-initiated abstraction of $OH^-$ from **D** could then generate the hexapentaene ligand and, on addition of $Cl^-$, afford complex **61**. There is precedent for the linkage of two allenylidene moieties to give a tetra-substituted hexapentaene insofar as on heating of $[(C_5H_5)Mn(CO)_2(=C=C=CBu^t_2)]$ small quantities of $Bu^t_2C{=}C{=}C{=}C{=}C{=}CBu^t_2$ are formed.[34]

## Why rhodium?

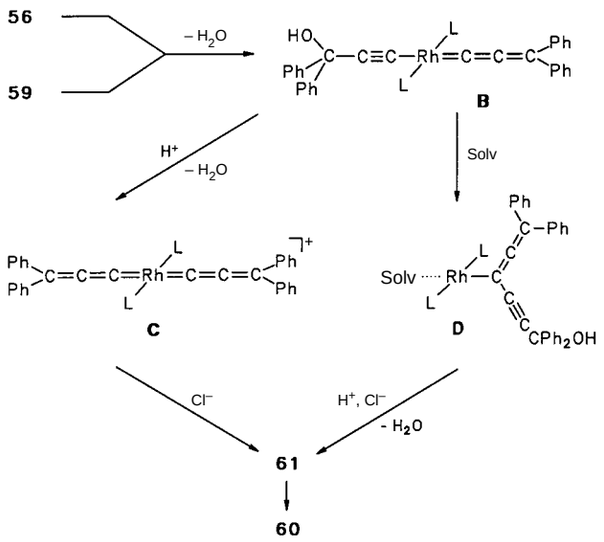
In summarizing the results shown in Schemes 3–16, the question certainly arises whether the square-planar rhodium allenylidenes are unique as far as their reactivity is concerned. Although a conclusive answer is as yet not possible, a few trends emerge which can be described as follows.

(*i*) The allenylideneiridium(I) compound **65** (Scheme 17), which is prepared from the dihydridoiridium(III) derivative **63** and $HC{\equiv}CCPh_2OH$ *via* **64** as intermediate, reacts rapidly with $H_2$ in dichloromethane at room temperature to give the allene complex **66** in excellent yield.[35] In this respect, compound **65** behaves in an exactly analogous manner to the rhodium counterpart **13** (see Scheme 10). However, in contrast to **13** the iridium allenylidene **65** is rather inert towards HCl and $CH_3I$ which is probably due to the increased kinetic stability of Ir=C compared with Rh=C double bond systems.

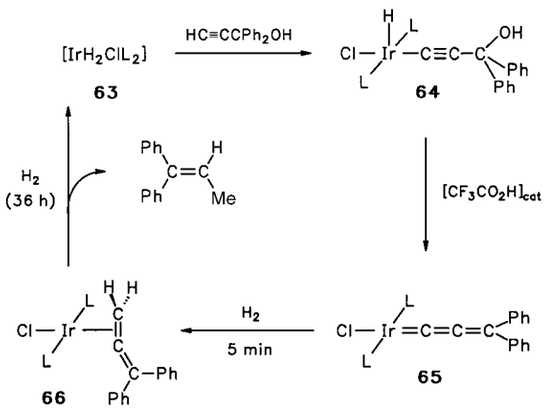
(*ii*) Allenylideneruthenium(II) complexes, which since the first studies in this field constitute the largest group of compounds containing an M=C=C=CRR′ unit,[5] are quite reactive towards *nucleophiles*. Work by Dixneuf and coworkers[36] and more recently by Gimeno and coworkers[37] has shown that in particular *cationic* compounds such as **67** and **69** (Scheme 18) are easily attacked by alcohols, alcoholates and also acetylides. The reaction of **69** with NaOMe affords a functionalized alkynyl ligand which is related to the rhodium-bound $C{\equiv}CCPh_2(OPh)$ unit generated on treatment of the neutral allenylidene rhodium complex **29** with CO (see Scheme 5).



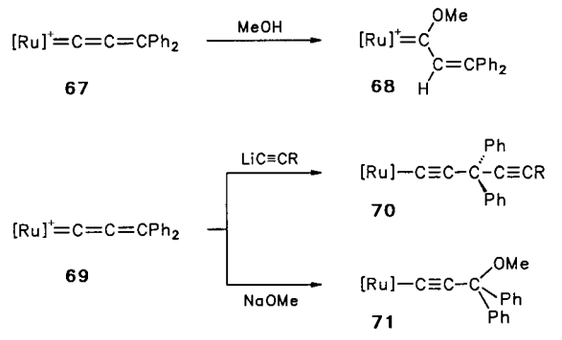

**Scheme 15** L = $PPr^i_3$



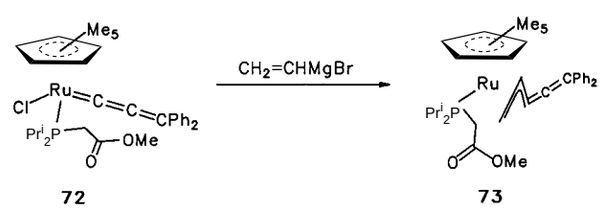
**Scheme 16** L = $PPr^i_3$



**Scheme 17** L = $PPr^i_3$



**Scheme 18** For **67**, **68**: [Ru] = $(C_6Me_6)RuCl(PMe_3)$; for **69**–**71**: [Ru] = $(C_9H_7)Ru(PPh_3)_2$



**Scheme 19**

Attempts to attack the allenylidene ligand in the *neutral* ruthenabutatrienes $[RuCl_2(=C=C=CPh_2)\{Pr^i_2PCH_2C(OMe)=O\text{-}\kappa P\}\{Pr^i_2PCH_2C(OMe)=O\text{-}\kappa^2P,O\}]$[22] and $[(C_5Me_5)RuCl(=C=C=CPh_2)\{Pr^i_2PCH_2C(OMe)=O\text{-}\kappa P\}]$ **72**[38] by methanol or dimethylamine failed. The half-sandwich type compound **72**, however, cleanly reacts with $CH_2$=CHMgBr in $C_6H_6$–thf to give the $\eta^3$-3,4,5-pentatrienyl complex **73** (Scheme 19) in good yield.[38] We were really surprised that this reaction occurred smoothly even at room temperature since compared with rhodium in the square-planar compound **13** (see Scheme 6) the ruthenium centre in **72** is more effectively shielded and thus a nucleophile attack of the Grignard reagent should be more hindered. For the success of the C–C coupling reaction leading to **73** it could be important that the two C-bonded ligands in the supposed intermediate $[(C_5Me_5)Ru(CH=CH_2)(=C=C=CPh_2)\{Pr^i_2PCH_2C(OMe)=O\text{-}\kappa P\}]$ are *cis* disposed since this should favour the migration of the vinyl group to the α-carbon atom of the allenylidene unit forming the pentatrienyl moiety.

## Conclusion

It is shown in this article that square-planar rhodium allenylidenes of general composition *trans*-$[RhX(=C=C=CRR')(PPr^i_3)_2]$, which are easily accessible from $[RhCl(PPr^i_3)_2]_2$ and propargylic alcohols, react with both nucleophiles and electrophiles. They are also attacked by phenylacetylene as well as by non-polar substrates such as $H_2$ or $Cl_2$ to give products in which the allenylidene unit is preserved as part of a newly formed ligand. In this respect, compounds having a metallabutatriene framework Rh=C=C=CRR′ behave quite differently to those containing a related metallaallene type unit Rh=C=CRR′.

Current work in our laboratory is aimed *inter alia* at the use of the rhodium allenylidenes also for catalytic purposes. The focus will be on reaction conditions which allow the conversion, *e.g.* of the butatriene complexes **45**–**48** upon treatment with $HC{\equiv}CCPh_2OH$ to the starting materials **12** and **13** and free butatrienes. Moreover, the exploration of new C–C coupling reactions using compounds such as **12**–**14** and **22**–**28** as starting materials will be on the agenda for further investigations.


## Acknowledgements

It is a pleasure to acknowledge the efforts and creativity of two coworkers, in particular, who did most of the experimental work discussed in this article: Dr Ralf Wiedemann and Matthias Laubender. I am also indebted to Dr Justin Wolf and Dr Thomas Rappert who laid the foundation of the chemistry of rhodium vinylidenes and allenylidenes, to Dr Oliver Nürnberg, Dr Norbert Mahr, Bettina Windmüller, Paul Steinert and Olaf Gevert who did all the crystallographic work, and to the Deutsche Forschungsgemeinschaft (SFB 347), the Volkswagen Stiftung and the Fonds der Chemischen Industrie for financial support.


---

**Helmut Werner's research interests are in the field of synthetic and mechanistic organometallic chemistry, ranging from triple-decker sandwich complexes to C–H activation and C–C coupling reactions. After obtaining his Diploma degree with Franz Hein at Jena, he escaped from East Germany and went to Munich to work for his PhD with Ernst Otto Fischer. Following postdoctoral work at Caltech (Pasadena) and finishing his Habilitation at the Technische Universität in Munich, he joined the Faculty at the University of Zurich, Switzerland, where he became Professor of Inorganic Chemistry in 1970. He returned to Germany at the end of 1975 to take up the chair of Inorganic Chemistry at the University of Würzburg. He has been honoured by the awards of the Pacific West Coast Inorganic Lectureship (1987) by the American Chemical Society, the Alfred-Stock-Gedächtnispreis by the German Chemical Society (1988), the Centenary Lectureship by the Royal Society of Chemistry (1993), the Max-Planck-Forschungspreis (1994), the**

**Paolo-Chini-Memorial Lectureship by the Italian Chemical Society (1995) and most recently by the Alexander-von-Humboldt/J. C. Mutis Award. Since 1988, he has been a fellow of the Deutsche Akademie der Naturforscher Leopoldina.**

## References


1 K. H. Dötz, H. Fischer, P. Hofmann, F. R. Kreissl, U. Schubert and K. Weiss, *Transition Metal Carbene Complexes*, Verlag Chemie, Weinheim, 1983; *Advances in Metal Carbene Chemistry*, ed. U. Schubert, Kluwer Academic, Dordrecht, 1989.
2 E. O. Fischer and A. Maasböl, *Angew. Chem.*, 1964, **76**, 645; *Angew. Chem., Int. Ed. Engl.*, 1964, **3**, 580.
3 E. O. Fischer, *Angew. Chem.*, 1974, **86**, 651; *Adv. Organomet. Chem.*, 1976, **14**, 1.
4 J. P. Selegue, *Organometallics*, 1982, **1**, 217; for an earlier variant of this preparative route see: H. Berke, *Chem. Ber.*, 1980, **113**, 1370.
5 M. I. Bruce, *Chem. Rev.*, 1991, **91**, 197.
6 H. Werner, *Nachr. Chem. Tech. Lab.*, 1992, **40**, 435; H. Werner, *J. Organomet. Chem.*, 1994, **475**, 45.
7 T. Rappert, O. Nürnberg, N. Mahr, J. Wolf and H. Werner, *Organometallics*, 1992, **11**, 4156; H. Werner and T. Rappert, *Chem. Ber.*, 1993, **126**, 669.
8 H. Werner, T. Rappert, R. Wiedemann, J. Wolf and N. Mahr, *Organometallics*, 1994, **13**, 2721.
9 For the preparation of **12** see: M. Laubender, Diploma Thesis, Universität Würzburg, 1995.
10 B. E. R. Schilling, R. Hoffmann and D. L. Lichtenberger, *J. Am. Chem. Soc.*, 1979, **101**, 585.
11 H. E. Bryndza and W. Tam, *Chem. Rev.*, 1988, **88**, 1163.
12 H. Werner, R. Wiedemann, M. Laubender, J. Wolf and B. Windmüller, *Chem. Commun.*, 1996, 1413.
13 H. Werner, R. Wiedemann, N. Mahr, P. Steinert and J. Wolf, *Chem. Eur. J.*, 1996, **2**, 561.
14 T. Yoshida, T. Okano, Y. Ueda and S. Otsuka, *J. Am. Chem. Soc.*, 1981, **103**, 3411.
15 R. Wiedemann, Dissertation, Universität Würzburg, 1995.
16 R. Wiedemann, P. Steinert, O. Gevert and H. Werner, *J. Am. Chem. Soc.*, 1996, **118**, 2495.
17 R. Wiedemann, P. Steinert, M. Schäfer and H. Werner, *J. Am. Chem. Soc.*, 1993, **115**, 9864; R. Wiedemann, J. Wolf and H. Werner, *Angew. Chem.*, 1995, **107**, 1359; *Angew. Chem., Int. Ed. Engl.*, 1995, **34**, 1244.
18 H. Werner, N. Mahr, G. Frenking and V. Jonas, *Organometallics*, 1995, **14**, 619.
19 N. M. Kostic and R. F. Fenske, *Organometallics*, 1982, **1**, 974.
20 C. Busetto, A. D'Alfonso, F. Maspero, G. Perego and A. Zazetta, *J. Chem. Soc., Dalton Trans.*, 1977, 1828; K. Wang, G. P. Rosini, S. P. Nolan and A. S. Goldman, *J. Am. Chem. Soc.*, 1995, **117**, 5082.
21 For a related, formally isoelectronic neutral ruthenium(II) species see: M. A. Esteruelas and H. Werner, *J. Organomet. Chem.*, 1986, **303**, 221.
22 H. Werner, A. Stark, P. Steinert, C. Grünwald and J. Wolf, *Chem. Ber.*, 1995, **128**, 49.
23 H. Werner, M. Laubender, R. Wiedemann and B. Windmüller, *Angew. Chem.*, 1996, **108**, 1330; *Angew. Chem., Int. Ed. Engl.*, 1996, **35**, 1237.
24 A. Höhn and H. Werner, *J. Organomet. Chem.*, 1990, **382**, 255; M. D. Fryzuk, L. Huang, N. T. McManus, P. Paglia, S. J. Rettig and G. S. White, *Organometallics*, 1992, **11**, 2979.
25 H. Werner, D. Schneider and M. Schulz, *J. Organomet. Chem.*, 1993, **451**, 175; H. Werner, P. Schwab, N. Mahr and J. Wolf, *Chem. Ber.*, 1992, **125**, 2641.
26 L. Hagelee, R. West, J. Calabrese and J. Norman, *J. Am. Chem. Soc.*, 1979, **101**, 4888; P. J. Stang, M. R. White and G. Maas, *Organometallics*, 1983, **2**, 720.
27 M. R. White and P. J. Stang, *Organometallics*, 1983, **2**, 1654.
28 M. Laubender, O. Gevert and H. Werner, unpublished work.
29 H. Berke, P. Härter, G. Huttner and L. Zsolnai, *Z. Naturforsch. B*, 1981, **36**, 929; N. E. Kolobova, L. L. Ivanov, O. S. Zhvanko, O. M. Khitrova, A. S. Batsanov and Yu. T. Struchkov, *J. Organomet. Chem.*, 1984, **265**, 271.
30 O. Nürnberg and H. Werner, *J. Organomet. Chem.*, 1993, **460**, 163.
31 M. Schäfer, N. Mahr, J. Wolf and H. Werner, *Angew. Chem.*, 1993, **105**, 1377; *Angew. Chem., Int. Ed. Engl.*, 1993, **32**, 1315.
32 P. Chow, D. Zargarian, N. J. Taylor and T. B. Marder, *J. Chem. Soc., Chem. Commun.*, 1989, 1545.
33 R. L. Harlow, D. L. Thorn, R. T. Baker and N. L. Jones, *Inorg. Chem.*, 1992, **31**, 993; B. Windmüller, J. Wolf and H. Werner, *J. Organomet. Chem.*, 1995, **502**, 147.
34 H. Berke, *Angew. Chem.*, 1976, **88**, 684; *Angew. Chem., Int. Ed. Engl.*, 1976, **15**, 624.
35 R. W. Lass, Dissertation, Universität Würzburg, 1996.
36 H. Le Bozec, K. Ouzzine and P. H. Dixneuf, *J. Chem. Soc., Chem. Commun.*, 1989, 219; D. Pilette, K. Ouzzine, H. Le Bozec, P. H. Dixneuf, C. E. F. Rickard and W. R. Roper, *Organometallics*, 1992, **11**, 809; N. Pirio, D. Touchard and P. H. Dixneuf, *J. Organomet. Chem.*, 1993, **462**, C18.
37 V. Cadierno, M. P. Gamasa, J. Gimeno and E. Lastra, *J. Organomet. Chem.*, 1994, **474**, C27.
38 T. Braun, P. Meuer and H. Werner, *Organometallics*, 1996, **15**, in the press.


*6/04362C*

# Synthesis and characterization of mesoporous SAPO

**Basab Chakraborty,[a] Alex C. Pulikottil,[a] Siddhartha Das[b] and Balasubramaniam Viswanathan*[a]**

[a] *Department of Chemistry, Indian Institute of Technology, Madras 600 036, India*
[b] *Department of Metallurgical Engineering, Indian Institute of Technology, Madras 600 036, India*

**Self-assembled ordered cetyltrimethylammonium bromide (CTAB) is used as a template for the synthesis of mesoporous silicoaluminophosphates with varying Si/Al ratio.**

Aluminophosphate-based molecular sieves are known to exist in a wide range of structural and compositional diversity. Substitution of Si in the framework of aluminophosphate molecular sieves imparts acidity to the material and makes it active for a variety of acid catalysed reactions. These materials exhibit characteristics of zeolites and of aluminophosphates and also unusual properties ascribable to its composition. The extent of Si substitution in the aluminophosphate is however limited and is determined by the topology of the structure. The synthesis of phosphate-based molecular sieves has resulted in the formation of large pore materials with ring systems greater than the conventional 12T atom rings present in large-pore zeolites.[1,2] In all these systems, in spite of their large pores, their pore openings do not exceed 10–12 Å.

Self-assembled ordered organic molecules can be used to direct the synthesis of molecular sieves by a cooperative assembly of inorganic matrix over organic arrays. This approach was first used by Kresge *et al*.[3] to synthesize a family of silica-based mesoporous molecular sieves designated as M41S. Sayari *et al*.[4] have adopted this approach to synthesize a lamellar aluminophosphate using long-chain alkyl- or dimethyl-alkyl-amine as structure directing agents. Here, we have extended the use of cetyltrimethylammonium bromide (CTAB) as a structure directing agent for the first time, for the synthesis of silicoaluminophosphates with the aim of obtaining large-pore mesoporous materials.

In a typical synthesis, 8 g of aluminium isopropoxide (Loba Chemie) was mixed with dilute phosphoric acid (6.2 ml $H_3PO_4$ in 60 ml $H_2O$) and stirred vigorously for 1 h at 333 K. This was followed by the addition of CTAB (8 g in 20 ml $H_2O$) with subsequent addition of the appropriate amount of tetraethyl-orthosilicate (Merck) dissolved in 4 ml of tetramethylammonium hydroxide and the gel was stirred for another hour. The pH of the resulting gel was around 2.5. The molar composition of the resulting gel thus obtained was 71.2 $P_2O_5$ : 26.8 $Al_2O_3$ : 1.0 $SiO_2$ : 31.5 CTAB : 6082 $H_2O$.

The gel was autoclaved for 48 h at 383 K without stirring. After crystallization the pH of the mother liquor increased to 7. The crystalline materials were washed several times with hot water and dried in an air oven at 383 K for 12 h. Samples were calcined initially in nitrogen atmosphere for 1 h at 873 K followed by heating in air for 12 h.

All samples were characterized using XRD, TEM, sorption studies and solid-state MAS NMR measurements. X-Ray diffractograms were recorded on a Rich Seifert XRD 3000P instrument using Cu-K$\alpha$ radiation (35 kV, 30 mA, 2° $min^{-1}$). TEM studies were carried out on a Philips CM12 scanning transmission electron microscope operating at 100 kV. Adsorption isotherms were determined at 77 K using a Carlo Erba sorptomatic series 1800 instrument using nitrogen as the adsorbent. MAS NMR spectra were recorded using a JEOL GSX400 instrument. The Larmor frequencies were 104.1, 161.8, 79.4 MHz for $^{27}Al$, $^{31}P$ and $^{29}Si$ respectively. Data were acquired at a MAS speed of 5.5 KHz.

X-Ray diffractograms of all the calcined samples of silicoaluminophosphates (SAPO) shown in Fig. 1 indicate the crystalline nature of all the samples. All the samples exhibit characteristic low-angle peaks typical of mesoporous materials. The low-angle peaks are indexed on the basis of hexagonal symmetry. The $d_{100}$ values for all the samples are given in Table 1. There are two peaks at 2θ 20.39 and 20.74° for sample S-III and in the same 2θ range for the other two samples in the X-ray diffractograms studied. The indexing of these planes from which these reflections arise could not be done immediately as the precise value of both the lattice parameters could not be obtained from indexing the low-angle reflections, namely 100, 110 and 200. Hence these peaks have been left unindexed. However a single-crystal X-ray study will be able to resolve this aspect. The crystal of the calcined SAPO materials as revealed from TEM studies have a faceted nature. From the two dimensional projected image, as obtained from TEM, it appears that the synthesised materials have hexagonal external morphology. The crystals are found to grow along the densely packed plane. The average size of the crystals is found to be 50–75 nm. It can be seen from the chemical analysis results of the synthesised materials given in Table 1 that not all of the silica in the original gel is incorporated in the synthesised materials. No change in phases is also observed in the XRD pattern with increase in silica content of the synthesised SAPO materials.

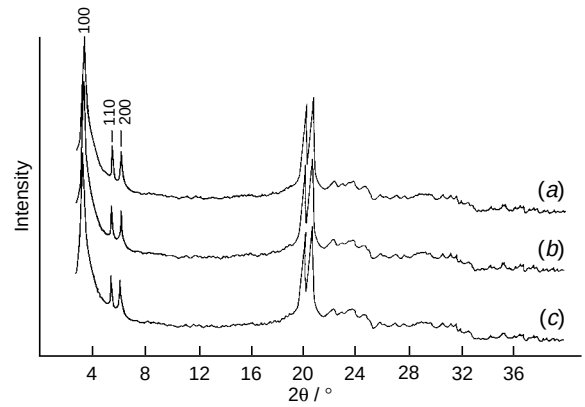



**Fig. 1** XRD patterns of the calcined mesoporous SAPO materials; (*a*) S-I, (*b*) S-II, (*c*) S-III

**Table 1** The molar ratios of the synthesis gel and that of the samples as obtained from elemental analysis along with the surface areas, pore diameters and $d_{100}$ line spacings of the samples

| | Al/P molar ratio | | Al/Si molar ratio | | | | |
|---|---|---|---|---|---|---|---|
| Sample | Gel | As synth. | Gel | As synth. | $d_{100}$/Å | Surface area/ $m^2\ g^{-1}$ | Pore diameter/ Å |
| S-I | 0.38 | 0.81 | 87.1 | 90.02 | 28.14 | 920 | 29 |
| S-II | 0.38 | 1.01 | 53.7 | 61.04 | 28.28 | 940 | 30 |
| S-III | 0.38 | 1.13 | 29.3 | 34.80 | 28.44 | 980 | 30 |

Nitrogen adsorption isotherms of all the samples show type IV isotherm behaviour with hysteresis in the mesopore filling region. The pore size distributions computed on the basis of BJH analysis indicate a narrow distribution with the maximum centred around 30 Å reflecting a uniform pore texture of the samples. All the samples exhibit surface areas around 900 $m^2$ $g^{-1}$. The average pore diameters and the BET surface areas of all the samples are given in Table 1.

Solid-state MAS NMR was carried out in order to understand the local structure and environments in these samples. The solid-state MAS NMR spectra of $^{29}Si$, $^{27}Al$ and $^{31}P$ nucleii of the calcined S-III are shown in Fig. 2. The $^{27}Al$ MAS NMR spectrum of the calcined S-III sample gives a single sharp resonance at δ 37.2 which is typical of Al in tetrahedral coordination.[5] The absence of other resonance lines implies the absence of amorphous or other phases in which aluminium has higher coordination in the synthesised samples. The $^{31}P$ MAS NMR spectrum of the calcined S-III samples [Fig. 2(*b*)] consists of a sharp peak centred at δ −30.9 indicating a uniform environment of the phosphorus atom. This is characteristic of tetrahedrally coordinated phosphorus in silicoaluminophosphates.[5] The single symmetric peak at δ −30.9 can be assigned to a single P(4Al) environment.[6] This resonance is observed for all the three SAPO samples irrespective of the amount of Si present. This is in agreement with the fact that P–O–Si linkages are absent in silicoaluminophosphates. The presence of such a sharp single signal for $^{31}P$ and $^{27}Al$ further confirms the phase homogeneity of the prepared samples. Although much information on the local environment of P and Al could not be directly deduced from the $^{31}P$ and $^{27}Al$ MAS NMR, $^{29}Si$ MAS NMR [Fig. 2(*a*)] provides a better insight into the local ordering of silicon in these mesoporous silicoaluminophosphates. Peaks centred around δ −90.1, −94.3, −98, −104 and −108.2 are observed indicating a multiple environment for Si in these samples. The resonances thus obtained were assigned as follows: δ −90.1 to Si(4Al), δ −94.3 to Si(3Al), δ −98 to Si(2Al), δ −104 to Si(1Al) and δ −108.2 to Si(0Al). Similar assignments are reported in literature for the various environments of Si in SAPOs.[7–9] The absence of any other peak in the range δ −86 to −111 excludes the possibility of P–O–Si linkages.[7] A detailed NMR studies on these materials will be reported soon.

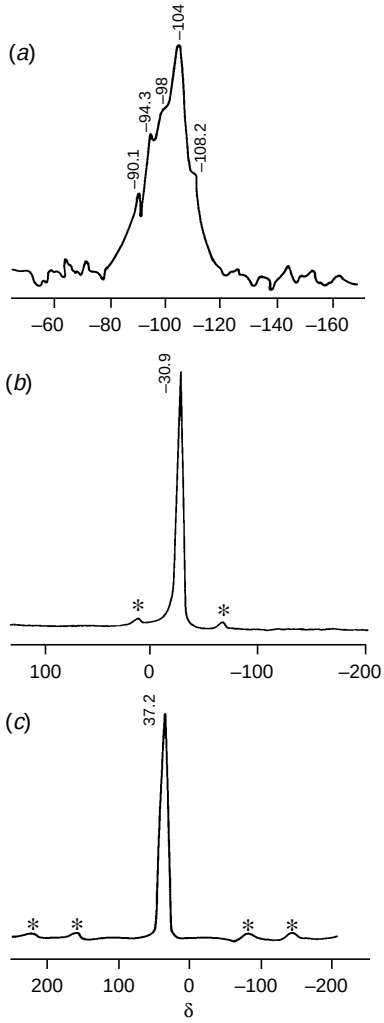



**Fig. 2** Solid-state MAS NMR of the calcined S-III sample, (*a*) $^{29}Si$, (*b*) $^{31}P$ and (*c*) $^{27}Al$; * indicates spinning side bands

Mesoporous silicoaluminophosphates with pore size of *ca*. 30 Å with varying amounts of Si content have been synthesised. The local environment around Si, Al and P is found to be similar in comparison to other SAPO materials.

Financial assistance received from the Council for Scientific and Industrial Research, India and the Department of Science and Technology, India is gratefully acknowledged.

## References

1 M. E. Davis, C. Saldarriaga, C. Montes, J. Garces and C. Crowder, *Nature*, 1988, **331**, 698.
2 Q. Huo, R. Xu, S. Li, Z. Ma, J. M. Thomas, R. H. Jones and A. M. Chippindale, *J. Chem. Soc., Chem. Commun.*, 1992, 875.
3 C. T. Kresge, M. E. Leonowicz, W. J. Roth, J. C. Vartuli and J. S. Beck, *Nature*, 1992, **359**, 710.
4 A. Sayari, V. R. Karra, J. S. Reddy and I. L. Moudrakovksi, *Chem. Commun.*, 1996, 411.
5 D. Muller, E. Jahn, B. Fahlke, G. Ladwig and U. Haubenreisser, *Zeolites*, 1985, **5**, 53.
6 C. S. Blackwell and R. L. Patton, *J. Phys. Chem.*, 1988, **92**, 3965.
7 J. A. Martens, C. Janssens, P. J. Grobet, H. K. Beyer, P. A. Jacobs, *Zeolites: Facts, Figures, Future*, ed. P. A. Jacobs and R. A. van Santen, Elsevier Scientific Publishers, Amsterdam, 1989, p. 215.
8 S. Ashtekar, Satyanarayana V. V. Chilukuri and D. K. Chakraborty, *J. Phys. Chem.*, 1994, **98**, 4878.
9 L. S. de Saldarriaga, C. Saldarriaga and M. E. Davis, *J. Am. Chem. Soc.*, 1987, **109**, 2686.

*Received in Cambridge, UK, 19th February 1997; Com. 7/01195D*

# Oxidative addition of a C–Se bond to a $Pt^{II}$ centre: contrasting reactions of $[MCl_2(PhCN)_2]$ (M = Pd, Pt) with cyclohepteno-1,4-diselenin

**C. Matthew Bates,[a] Pawan K. Khanna,[a] Christopher P. Morley*[a] and Massimo Di Vaira[b]**

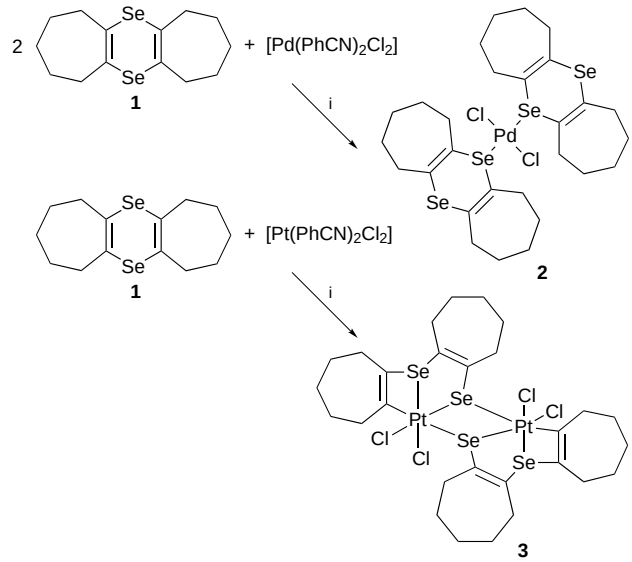
[a] *Department of Chemistry, University College of Swansea, Singleton Park, Swansea, UK SA2 8PP*
[b] *Dipartimento di Chimica, Universita degli Studi di Firenze, Via Maragliano 75/77, 50144 Firenze, Italy*

**The reaction of cyclohepteno-1,4-diselenin 1 with $[PtCl_2(PhCN)_2]$ proceeds *via* unprecedented oxidative addition of a C–Se bond to yield a platinum(IV) product, whose novel dimeric structure has been determined by X-ray crystallography; by contrast, 1 reacts with $[PdCl_2(PhCN)_2]$ to form *trans*-$[PdCl_2L_2]$ (L = 1).**

The chemistry of selenium-containing ligands is a subject of growing interest,[1] as a result of both their increasing accessibility, and the realisation that they may display significantly different properties from their sulfur-containing analogues. Despite their ready preparation from 1,2,3-selenadiazoles,[2] and the range of possible bonding modes (mono- or bi-dentate; terminal, bridging or chelating), the coordination chemistry of 1,4-diselenins has scarcely been investigated. Their use as precursors in the preparation of iron diselenolenes has been reported, but these reactions involved fragmentation of the ligand.[3] A number of complexes of the related selenanthrenes have also been prepared.[4,5] We have previously determined the structure of bis(cycloocteno)-1,4-diselenin,[6] and have now studied the reactions of cyclohepteno-1,4-diselenin **1** with the palladium(II) and platinum(II) complexes $[MCl_2(PhCN)_2]$.

Stirring 2 equiv. of **1** with $[PdCl_2(PhCN)_2]$ in dichloromethane solution at room temp. leads to rapid formation of an orange–red product **2**, with stoichiometry $[PdCl_2L_2]$ (L = **1**) (Scheme 1). Compound **2** exhibits a single band in the far IR at *ca*. 360 $cm^{-1}$, characteristic of dichloropalladium(II) complexes having *trans*-geometry.[7] The structure proposed for **2** is one in which each 1,4-diselenin is acting as a monodentate ligand. Analogous complexes of dialkylselenides have been known for a long time.[8]

The corresponding platinum chemistry, however, takes a different course (Scheme 1). The reaction between $[PtCl_2(PhCN)_2]$ and **1** is somewhat slower, and if 2 equiv. of 1,4-diselenin are used then one is recovered unchanged. The NMR spectroscopic data for the product **3** show that the symmetry of the coordinated 1,4-diselenin has been broken: for example, each carbon atom of the ligand gives a separate $^{13}C$ resonance.†




**Scheme 1** *Reagents and conditions*: i, $CH_2Cl_2$, room temp.

The molecular structure of **3** has been determined by X-ray crystallography‡ and is shown in Fig. 1. The platinum has inserted into a carbon–selenium bond of the 1,4-diselenin, so that it has become a tridentate (C, Se, Se) ligand. The typical octahedral coordination of $Pt^{IV}$ is achieved *via* dimerisation using bridging selenium atoms, although there is significant asymmetry in the $Pt_2Se_2$ unit: there are two long Pt–Se bonds of *ca*. 2.62 Å. This reflects the different *trans*-influence of the carbon and chlorine atoms bound to platinum (*vide infra*). There is no evidence that the steric effect of the alicyclic rings is preventing closer approach of the two platinum moieties: the carbon atoms in each half of the molecule are at least 3.3 Å apart. There are small differences between the distances from platinum to the two selenium atoms of a single ligand, the bonds to the disubstituted Se(2) and Se(4) being shorter by *ca*. 0.04 Å than those to Se(1) and Se(3). In fact both pairs of Pt–Se distances (av. 2.422, 2.386 Å) are considerably shorter than those previously reported for $Pt^{IV}$–Se bonds. For example in the complexes $[PtXMe_3(MeSeCH{=}CHSeMe)]$ average values for Pt–Se are 2.528 Å (X = Cl) and 2.533 Å (X = I):[9] this shows how sensitive the Pt–Se bond length is to the influence of the *trans*-ligand (which in these examples is a methyl group). The platinum–chlorine bonds differ in length in a similar fashion, with those to the chlorine atoms *trans* to Se(2) and Se(4) being *ca*. 0.03 Å shorter, so that overall the coordination polyhedra are

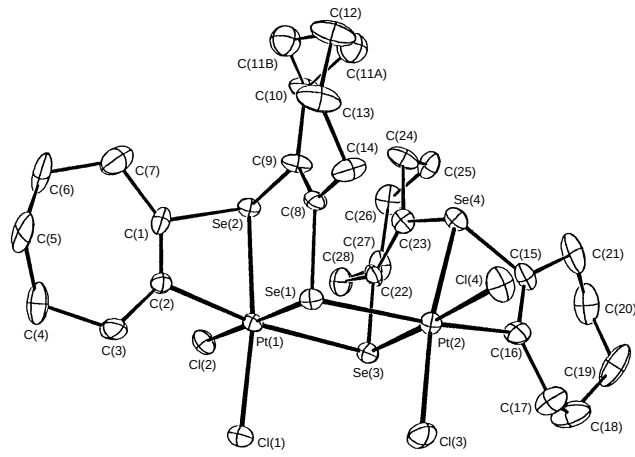



**Fig. 1** Structure of **3** with H atoms omitted for clarity. Selected bond lengths (Å) and angles (°): Pt(1)–Se(1) 2.421(2), Pt(2)–Se(3) 2.423(2), Pt(1)–Se(2) 2.384(2), Pt(2)–Se(4) 2.388(2), Pt(1)–Se(3) 2.620(2), Pt(2)–Se(1) 2.624(2), Pt(1)–Cl(1) 2.342(5), Pt(2)–Cl(3) 2.330(5), Pt(1)–Cl(2) 2.367(5), Pt(2)–Cl(4) 2.359(5), Pt(1)–C(2) 2.103(18), Pt(2)–C(16) 2.079(20); Se(2)–Pt(1)–Se(3) 100.9(1), Se(2)–Pt(1)–C(2) 70.9(5), Pt(1)–Se(2)–C(1) 77.8(6), Se(2)–C(1)–C(2) 103.7(1.4), Pt(1)–C(2)–C(1) 107.6(1.4).

somewhat compressed along one axis. This distortion is not chemically significant, but arises as a consequence of the geometric constraints imposed by the presence of the metal-containing four-membered ring.

The dimeric structure does not appear to be maintained in solution. The $^{77}$Se NMR spectrum of **3** in $CD_2Cl_2$ contains two resonances, each with only one set of $^{195}$Pt satellites: δ 315 [$^1J(^{77}Se^{195}Pt)$ 295 Hz], δ 278 [$^1J(^{77}Se^{195}Pt)$ 154 Hz]. There are few values in the literature for $^1J(^{77}Se^{195}Pt)$, but the coupling constants for **3** are similar in magnitude to those previously observed.[10]

Oxidative addition to platinum(II) centres is common for halogens, alkyl halides, *etc.*,[11] but the reaction reported here represents the first example involving cleavage of a C–Se bond. Indeed a wide range of diorganochalcogen complexes of platinum(II) has previously been prepared.[12] The insertion of a $d^8$ metal centre into a C–Se bond has only previously been observed in an iridium(I) complex of a coordinated selenophene.[13] Clearly the behaviour of the cycloalkeno-1,4-diselenins is unique, and further investigation of their coordination chemistry is in progress.

This work was supported by EPSRC and the Ministero dell' Università e della Ricerca Scientifica e Technologica. We thank Johnson Matthey plc for the loan of palladium and platinum salts, the University of Wales for the provision of a studentship (to C. M. B.), and Pangiotis Angaridis and Irene Geogakaki for experimental assistance.

## Footnotes

* E-mail: c.p.morley@swan.ac.uk

† *Synthesis of* **3**: A mixture of $[PtCl_2(PhCN)_2]$ (0.100 g, 0.21 mmol) and **1** (0.073 g, 0.21 mmol) in $CH_2Cl_2$ (10 cm$^3$) was stirred overnight. The solvent was removed by evaporation under reduced pressure and the residue washed with light petroleum, to leave the product as an orange–brown powder. This was purified by recrystallisation from dichloromethane–toluene. Yield: 0.080 g (62%); mp 205 °C (decomp.); $^1$H NMR (400 MHz, $CD_2Cl_2$, $SiMe_4$), δ 3.19 (m, 1 H), 2.85–2.65 (m, 3 H), 2.65–2.35 (m, 11 H), 1.45 (m, 1 H); $^{13}$C NMR (100 MHz, $CD_2Cl_2$, $SiMe_4$), δ 149.1, 133.5, 131.9, 126.1, 39.4, 37.0, 35.9, 34.5, 31.8, 29.2, 29.0, 28.1, 27.6, 25.2; $^{77}$Se NMR (47.7 MHz, $CD_2Cl_2$, external $SeMe_2$), δ 315 [$J(^{77}Se^{195}Pt)$ 295 Hz], 278 [$J(^{77}Se^{195}Pt)$ 154 Hz]; IR (KBr disk), 2921vs, 2849s, 1443s, 1385m, 1359m, 1267m, 1215m, 1071m, 967m cm$^{-1}$; Far IR (Nujol mull, CsI plates): 330m, 310m cm$^{-1}$; UV–VIS ($CH_2Cl_2$): $\lambda_{max}$/nm (ε/dm$^3$ mol$^{-1}$ cm$^{-1}$) = 490 (≈ 200, vbr), 330 (9000), 285 (15000), 260 (17000), 230 (22000); MS (FAB): *m/z* (%), 1187 (≈ 1) [$M^+$ − Cl], 348 (45) [$\mathbf{1}^+$], 267 (100) [$\mathbf{1}^+$ − SeH]; C, H analysis ($C_{28}H_{40}Cl_4Pt_2Se_4$, 1224.46): calc. C 27.45, H 3.27; found C 27.78, H 3.41 %.

‡ *Crystal data for* **3**: $C_{28}H_{40}Cl_4Pt_2Se_4$; $M_r$ = 1224.46; crystal size 0.07 × 0.13 × 0.27 mm; orthorhombic, space group *Pcab*; *a* = 15.203(2), *b* = 17.301(4), *c* = 25.935(4) Å, *U* = 6821(2) Å$^3$, *Z* = 8, *F*(000) = 4544, $D_c$ = 2.384 g cm$^{-3}$, μ(Cu-Kα) = 234.4 cm$^{-1}$. Data collection (Enraf-Nonius CAD4, graphite-monochromated Cu-Kα radiation, λ = 1.5418 Å, *T* = 295 K), ω—2θ scans, 3 < θ < 60°. 4831 measured reflections (+*h*, +*k*, +*l*), 3875 unique, 2887 with $l > 3\sigma_l$ used in final refinement. Structure solution and refinement: direct methods, with SIR,[14] and heavy-atom procedures with SHELX-76. A series of Fourier syntheses provided the positions of all non-hydrogen atoms. An empirical absorption correction (min., max. correction factors 0.92, 1.11) was applied at isotropic convergence.[15] In the final refinement cycles, performed against *F* by full-matrix least squares, all non-hydrogen atoms were assigned anisotropic temperature factors, except for a methylene carbon atom which was found to occupy two positions, in a disordered fashion. Its two fractions were assigned an overall isotropic temperature factor and the complementary occupancy factors of the two sites were refined. The four C–C bond distances formed by the two fractions of the disordered C atom with the other atoms of the ring were linked, allowing for a 0.01 Å σ, to a unique value, which was refined. The hydrogen atoms were introduced in calculated positions, with C–H = 0.96 Å and $U_H$ = 1.2 $U_C$, where $U_C$ is the equivalent isotropic temperature factor of the carrier C atom, and were not refined. With 343 parameters refined the data : parameter ratio was 8.4. Final *R* values: *R* = 0.045, $R_w$ = 0.053. Max., min. values of residual electron density: +0.82, −0.87 e Å$^{-3}$.

Atomic coordinates, bond lengths and angles, and thermal parameters have been deposited at the Cambridge Crystallographic Data Centre (CCDC). See Information for Authors, Issue No. 1. Any request to the CCDC for this material should quote the full literature citation and the reference number 182/422.

## References

1 E. G. Hope and W. Levason, *Coord. Chem. Rev.*, 1993, **122**, 109.
2 H. Meier and E. Voigt, *Tetrahedron*, 1972, **28**, 187.
3 A. J. Mayr, H.-S. Lien, K. H. Pannell and L. Parkanyi, *Organometallics*, 1985, **4**, 1580.
4 U. Behrens, P. Berges, R. Bieganowski, W. Hinrichs, C. Schiffling and G. Klar, *J. Chem. Res.* (*S*), 1986, 326; (*M*), 2801.
5 H. Kacholdt, P. Berges, G. Klar and W. Hinrichs, *Transition Met. Chem.*, 1987, **12**, 515.
6 M. R. J. Dorrity, A. Lavery, J. F. Malone, C. P. Morley and R. R. Vaughan, *Heteroatom Chem.*, 1992, **3**, 87.
7 G. E. Coates and C. Parkin, *J. Chem. Soc.*, 1963, 421.
8 E. Fritzmann, *Z. Anorg. Allg. Chem.*, 1924, **133**, 19.
9 E. W. Abel, S. K. Bhargava, K. G. Orrell, A. W. G. Platt, V. Sik and T. S. Cameron, *J. Chem. Soc., Dalton Trans.*, 1985, 345.
10 I. M. Blacklaws, E. A. V. Ebsworth, D. W. H. Rankin and H. E. Robertson, *J. Chem. Soc., Dalton Trans.*, 1978, 753; V. K. Jain, S. Kannan, R. J. Butcher and J. P. Jasinski, *J. Chem. Soc., Dalton Trans.*, 1993, 1509.
11 G. K. Anderson, *Platinum–Carbon σ-bonded Complexes*, in *Comprehensive Organometallic Chemistry II*, ed. E. W. Abel, F. G. A. Stone and G. Wilkinson, Pergamon, Oxford, 1995, vol. 9.
12 S. G. Murray and F. R. Hartley, *Chem. Rev.*, 1981, **81**, 365.
13 C. J. White, R. J. Angelici and M.-G. Choi, *Organometallics*, 1995, **14**, 332.
14 A. Altomare, M. C. Burla, M. Camalli, G. Cascarano, C. Giacovazzo, A. Guagliardi and G. Polidori, *J. Appl. Crystallogr.*, 1994, **27**, 435.
15 N. Walker and D. Stuart, *Acta Crystallogr., Sect. A*, 1983, **39**, 158.

*Received in Cambridge, UK, 21st November 1996; Com. 6/07904K*

# Crystal and molecular structure of an aluminium clathrate exhibiting an unusual tertiary arrangement and an extraordinary degree of solvation

**Jan Ondráček,[a] Alexandr Jegorov,*[b] Zdeňka Kovářová,[c] Michal Hušák[a] and František Jursík[c]**

[a] *Department of Solid State Chemistry, Prague Institute of Chemical Technology, 166 28 Praha 6, Czech Republic*
[b] *Galena Co., Research Unit, 370 05 České Budějovice, Czech Republic*
[c] *Department of Inorganic Chemistry, Prague Institute of Chemical Technology, 166 28 Praha 6, Czech Republic*

**In the course of our study of aluminium complexes, a new complex with *N*-salicylidene-*o*-aminophenol ($H_2L$) is isolated, which is unique because of its stereochemistry, degree of solvation, the manner of tertiary arrangement and by the crystal packing; the crystal and molecular structure of this complex is established by X-ray structure analysis.**

Adverse effects of elevated aluminium concentration in the environment[1] attract attention to its coordination chemistry in biological systems. Among others, the Schiff bases as typical 'hard donor ligands' exhibit some similarity with ligands present in biological systems. Thus they can serve as a suitable *in vitro* model mimicking the coordination chemistry of Al *in vivo*.

The source material was obtained from *N*-salicylidene-*o*-aminophenol (6 mmol), NaOH (6 mmol), $AlCl_3 \cdot 6H_2O$ (6 mmol) in methanol–water (55 ml, 10 : 1) precipitated with sodium acetate (5% m/v in water, 25 ml). The yellow needles of the complex were obtained in 30–40% yield by the slow diffusion of diethyl ether into the solution containing the crude precipitate (50 mg), acetone (2 ml) and water (50 μl). The fact that the crystals immediately decompose upon removing them from the mother-liquor indicated that appropriate guests are necessary to stabilize the three-dimensional framework structure. Hence, a single crystal was adjusted in a glass capillary filled with diethyl ether for the X-ray analysis.†

Since the discovery of crown ethers a considerable number of various classes of host–guest compounds have been described,[2] including clathrates, framework silicates, Zintl phases, polycations and others. The new aluminium clathrate exhibits a combination of several new structural features. The primary structure of the complex is composed of two independent polynuclear moieties A and B. Moiety A is the binuclear complex $[(H_2O)LAl(\mu\text{-}MeCO_2)(\mu\text{-}OH)AlL(H_2O)]$ (Fig. 1), while moiety B consists of the $[\{LAl(H_2O)(OH_2)\}_2Al(\mu\text{-}OH)_2Al\{LAl(H_2O)(OH)_2\}_2]$ hexanuclear unit which is symmetrical along the twofold crystallographic axis (Fig. 2). Thus, in contrast to many other clathrates of cadmium[3] or nickel[4] cyanides or framework silicates,[2] bridging anions do not create the infinite network, and the structure consists of independent neutral polynuclear coordination compounds. The repeating of hydrogen-bond networks including the $A_2B$ cyclic tertiary arrangement and four methanol molecules leads to infinite channels parallel to the *c* crystallographic axis (Fig. 3). The quite unusual cavity dimension (18 × 15 Å) and degree of solvation have some analogy with pore-forming proteins,[5] but

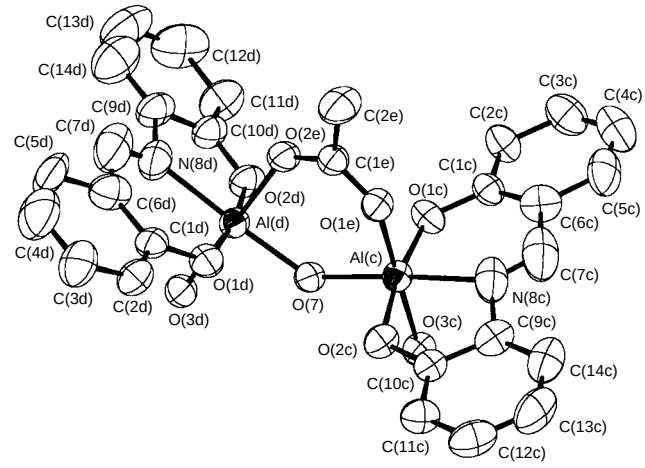



**Fig. 1** Structure of the binuclear $[(H_2O)LAl(\mu\text{-}MeCO_2)(\mu\text{-}OH)AlL(H_2O)]$ complex

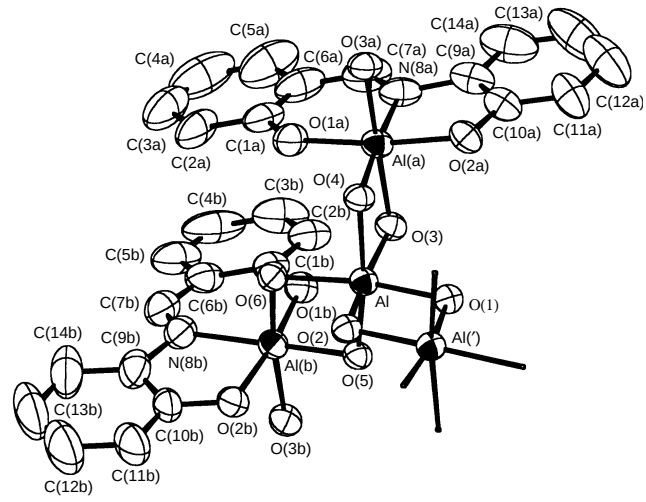



**Fig. 2** Structure of the hexanuclear $[\{LAl(H_2O)(OH)_2\}_2Al(\mu\text{-}OH)_2Al\{LAl(H_2O)(OH)_2\}_2]$ complex [half of the molecule with the bridging $Al(\mu\text{-}OH)_2Al'$ moiety]

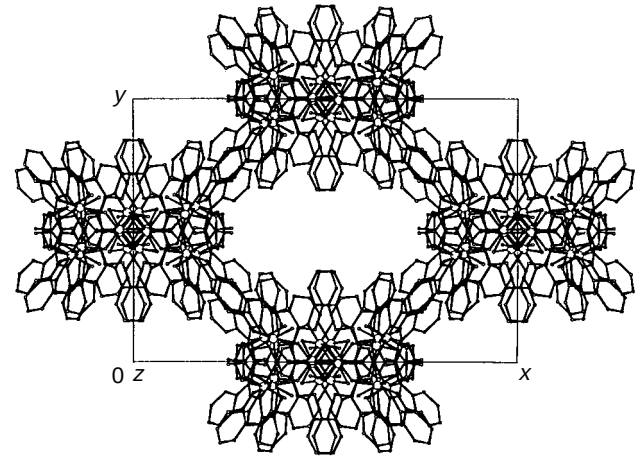



**Fig. 3** Crystal packing of $2[(H_2O)LAl(\mu\text{-}MeCO_2)(\mu\text{-}OH)AlL(H_2O)]\cdot[\{LAl(H_2O)(OH)_2\}_2Al(\mu\text{-}OH)_2Al\{LAl(H_2O)(OH)_2\}_2]\cdot 4MeOH\cdot n Et_2O$

on the other hand, is quite unexpected among coordination compounds. Another unusual feature of the present compound is the high degree of solvation. Since inclusion compounds of highly volatile guests are often unstable,[6] it is quite unexpected, that a compound containing approximately 45% of disordered diethyl ether molecules forms mechanically stable crystals at ambient temperature. In conclusion, the stereochemistry of this complex indicates that the ability of aluminium to create structures mimicking some structures typical of living systems should be considered for the evaluation of its *in vivo* toxicity.

## Footnotes

* E-mail: husakm@marvin.jcu.cz

† *Crystal data*: $C_{52}H_{54}Al_6N_4O_{22}\cdot 2C_{28}H_{26}Al_2N_2O_9\cdot 4CH_4O\cdot nC_2H_6O$, $M$ = 2554.038 (without diethyl ether), monoclinic, space group $C2/c$, $a$ = 29.143(7), $b$ = 18.302(4), $c$ = 32.631(8) Å, β = 115.19(2)°, $U$ = 15749.4(13) Å$^3$, $Z$ = 4, $D_c$ = 1.0771 g cm$^{-3}$, μ = 11.965 cm$^{-1}$. The intensity data were collected through a glass capillary containing diethyl ether on an Enraf-Nonius CAD4 diffractometer with graphite-monochromated Cu-Kα radiation (λ = 1.540 56 Å) with $R_{int}$ = 0.019, and the structure was solved by direct methods with SHELXS-86.[7] All the non-hydrogen atoms were refined anisotropically with the exception of methanol atoms using SHELXL-93.[8] The final cycle of full-matrix least-squares refinement was based on 6761 observed reflections [$I > 2\sigma(I)$] and 661 variable parameters with $R(wR_2)$ = 0.120 (0.394). Due to the high content of solvated molecules, the structure was refined by methods commonly used for proteins with SWAT parameter $g$ = 3.70(21) for $U$ = 4.00. Atomic coordinates, bond lengths and angles, and thermal parameters have been deposited at the Cambridge Crystallographic Data Centre (CCDC). See Information for Authors, Issue No. 1. Any request to the CCDC for this material should quote the full literature citation and the reference number 182/435.

## References

1 M. R. Wills and J. Savory, *Clin. Lab. Sci.*, 1989, **27**, 59.
2 A. Müller, H. Reuter and S. Dillinger, *Angew. Chem., Ind. Ed. Engl.*, 1995, **34**, 2328.
3 T. Kitazawa, T. Kikuyama, M. Takeda and T. Iwamoto, *J. Chem. Soc., Dalton Trans.*, 1995, 3715.
4 S. Nishikiori, C. I. Ratcliffe and J. A. Ripmeester, *Can. J. Chem.*, 1993, **71**, 1810.
5 R. Ghadiri, J. R. Granja, R. A. Milligan D. E. McRee and N. Khazanovich, *Nature*, 1993, **366**, 324.
6 J. Barbour, M. R. Caira and L. R. Nassimbeni, *J. Chem. Soc., Perkin Trans. 2*, 1993, 1413.
7 G. M. Sheldrick, SHELXS-86, University of Göttingen, 1986.
8 G. M. Sheldrick, SHELXL-93, University of Göttingen, 1994.

*Received in Cambridge, UK, 14th February 1997; Com. 7/01050H*

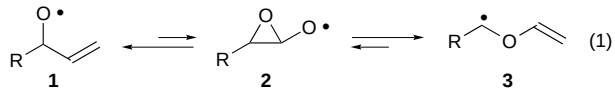
# Oxiranylmethyl radicals: EPR detection by spin trapping

**Loris Grossi* and Samantha Strazzari**

*Dipartimento di Chimica Organica 'A. Mangini', Università di Bologna, Viale Risorgimento, 4, I-40136 Bologna, Italy*

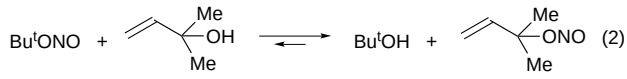
**The EPR detection of oxiranylmethyl radicals, formed *via* a 3-*exo-trig* process from the corresponding allyloxyl radical, is performed with Bu$^t$ONO as a spin trap.**

The 3-*exo-trig*[1] process involving allyloxyl radicals could be a useful method for synthesizing epoxides.[2] However, this reaction was usually reported to have failed because the intermediate oxiranylmethyl radical **2** can rapidly undergo either C–O bond fission (to give **1**) or C–C bond fission (to give **3**) [eqn. (1)].



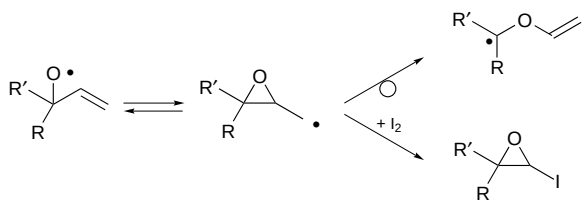

Nevertheless, Galatsis and Millan[2c] have recently reported the preparation of α-iodo epoxides by photolysing tertiary allylic alcohols in the presence of bis(acetoxy)iodobenzene and iodine. This process is based on competition between the two possible reaction pathways that the intermediate oxiranylmethyl radical can follow (Scheme 1), and relies on the more efficient trapping by iodine.

However, no direct EPR evidence for the detection of these radical species has been reported[3] and, to account for this, a fast decay process for **2** has always been claimed.[3,4] One possible method of investigation could be the spin-trap technique, *i.e.* conversion of the oxiranylmethyl radical into a more persistent radical species. Previous experiments conducted by our group had shown the ability of alkyl nitrites to act as a spin trap[5] for short-lived alkyl radicals and, in particular, *tert*-butyl nitrite seemed to be quite efficient. Moreover, since the oxiranylmethyl radicals derive from a rearrangement process involving allyloxyl radicals, it was considered convenient to generate the latter by photolysis of the corresponding nitrites. These can be prepared, in almost quantitative yield, *via* an easy exchange reaction[6] between the corresponding alcohols and *tert*-butyl nitrite, which is known to behave as a nitrosyl source [eqn. (2)].




This method could then be used also to supply the required spin trap directly into the medium. In fact, in performing the nitrosyl transfer to the alcohols with an excess of Bu$^t$ONO it was possible that a part of it could act as the trap.

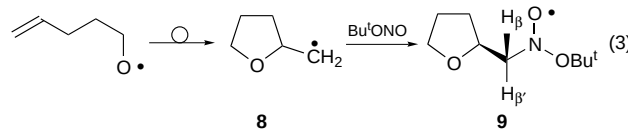
The experiments were conducted under continuous flow conditions on acetonitrile solutions of tertiary allylic alcohols in the presence of an excess of Bu$^t$ONO, which were photolysed in the EPR spectrometer cavity at different temperatures.




**Scheme 1**

When 2-methylbut-3-en-2-ol was investigated, two radical species were detected; the methyl *tert*-butoxy nitroxide **7** (Table 1), formed by trapping of the methyl radical which comes from the competitive β-process that the allyloxyl radical can undergo, and an alkyl alkoxy nitroxide, characterised by an alkyl group with two magnetically inequivalent β-hydrogens. The EPR spectroscopic parameters of this species suggested structure **4**, which is chiral[7] by virtue of the asymmetric oxiranyl group, and therefore justifies the detection of inequivalent β-$CH_2$ hydrogens even if there is rapid internal rotation about the N–$C_\beta$ bond. A possible reaction mechanism for the formation of both radical species could be that outlined in Scheme 2.

Since, to the best of our knowledge, this is the first spectroscopic evidence for the detection of the oxiranylmethyl radical, it was necessary to confirm the suggested structure of **4** with further experiments. The pent-4-en-1-ol–Bu$^t$ONO system was then studied using the same experimental conditions used for 2-methylbut-3-en-2-ol. It was hypothesized that the tetrahydrofurfuryl radical **8**, formed by the fast 1,5-*exo* ring closure[8] of the intermediate pent-4-enoxyl radical, would react with *tert*-butyl nitrite, leading to the formation of **9**, [eqn. (3)].



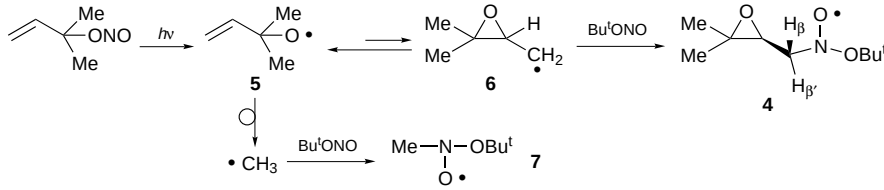

As this radical is chiral due to the presence of an asymmetric tetrahydrofuran-2-yl group, the corresponding EPR spectrum should show two magnetically inequivalent β-hydrogens; this proved to be the case. Further support came from experiments with a reduced amount of *tert*-butyl nitrite, which gave the bis(tetrahydrofurfuryl) nitroxide **10** and which confirmed the presence of the rearranged radical **8** in the medium.

Although these results strengthened our hypothesis, it was still necessary to obtain direct confirmation; for example, to

**Table 1** EPR results for **4**, **7** and **9**–**13**

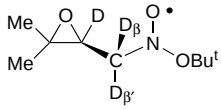
| | Hyperfine coupling constant/Gauss (no. nucleii) | | | | | |
|---|---|---|---|---|---|---|
| Radical | $a_\alpha$ | $^*a_\beta$ | $^*a_{\beta'}$ | $a_\gamma$ | $a_\delta$ | $g$ |
| **4** | 25.65 (1 N) | 5.60 (1 H) | 9.10 (1 H) | 0.22 (1 H) | — | 2.0053 |
| **7** | 25.75 (1 N) | $8.87_5$ (3 H) | — | — | — | 2.0054 |
| **9** | $25.37_5$ (1 N) | 4.00 (1 H) | 12.00 (1 H) | 0.35 (1 H) | $0.17_5$ (2 H) | 2.0053 |
| **10** | 14.25 (1 N) | 6.75 (2 H) | 11.25 (2 H) | — | — | 2.0058 |
| **11** | 25.65 (1 N) | 0.80 (1 D) | 1.35 (1 D) | — | — | 2.0053 |
| **12** | 25.70 (1 N) | $8.12_5$ (2 H) | — | 0.30 (3 H) | — | 2.0053 |
| **13** | 25.72 (1 N) | $5.62_5$ (1 H) | 9.25 (1 H) | 0.25 (1 H) | — | 2.0053 |

* The hfc of $H_\beta$ can be attributed to $H_{\beta'}$ and *vice versa*.



**Scheme 2**

prove that the two inequivalent hydrogens of the $CH_2$ group of radical **4** originate from the vinyl $CH_2$ group in radical **5**. For this purpose, 2-methyl[3,4,4-$^2H_3$]but-3-en-2-ol was synthesized.[9] Experiments conducted on this substrate, using the same experimental conditions used for the analogous hydrogenated compound, led to the detection not only of the methyl *tert*-butoxy nitroxide, but also of the alkoxy alkyl nitroxide **11**, whose EPR spectrum showed a nitrogen coupling constant exactly matching that of the corresponding atom in radical **4**, and two inequivalent deuterium atoms with coupling constants of *ca*. 1/6 of that of the corresponding hydrogen atoms.



**11**

Finally, support for our hypothesis was also obtained from experiments with 3-methylpent-1-en-3-ol, which gave adducts to the *tert*-butyl nitrite of all the radical species deriving from the intermediate allyloxyl radical, *i.e.* the oxiranylmethyl *tert*-butoxy nitroxide **13**, the methyl *tert*-butoxy nitroxide **7** and the ethyl *tert*-butoxy nitroxide **12**.

These results confirmed the involvement of a 3-*exo-trig* process in oxiranylmethyl radical formation from a tertiary allyloxyl radical and showed the utility of *tert*-butyl nitrite as a trap for these species. This work is currently being extended to other tertiary and secondary allylic alcohols.

## References


1 J. E. Baldwin, *J. Chem. Soc., Chem. Commun.*, 1976, 734.
2 (*a*) A. L. Nussbaum, S. D. Millan, E. Yuan, O. Zagneetko and E. P. J. Oliveto, *J. Am. Chem. Soc.*, 1962, **84**, 1070; (*b*) H. Suginome and J. B. Wang, *J. Chem. Soc., Chem. Commun.*, 1990, 1629; (*c*) P. Galatsis and S. D. Millan, *Tetrahedron Lett.*, 1991, **32**, 7493; (*d*) P. Galatsis, S. D. Millan and T. Faber, *J. Org. Chem.*, 1993, **58**, 1215.
3 D. Laurie, D. C. Nonhebel, C. J. Suckling and J. C. Walton, *Tetrahedron*, 1993, **49**, 5869; F. E. Zigler and A. K. Petersen, *J. Org. Chem.*, 1994, **59**, 2707; F. E. Ziegler and A. K. Petersen, *J. Org. Chem.*, 1995, **60**, 2666; A. G. Davies and B. Muggleton, *J. Chem. Soc., Perkin Trans. 2*, 1976, 502.
4 J. M. Dickinson, J. A. Murphy and N. F. Wuster, *J. Chem. Soc., Perkin Trans. 1*, 1990, 1179.
5 L. Grossi, *Tetrahedron*, 1997, **53**, 3205; 1997, in the press.
6 M. P. Doyle, J. W. Terpstra, R. A. Pickering and D. M. LePoire, *J. Org. Chem.*, 1983, **48**, 3379.
7 Y. Maeda and K. U. Ingold, *J. Am. Chem. Soc.*, 1979, **101**, 4975.
8 R. D. Rieke and N. A. Moore, *J. Org. Chem.*, 1972, **37**, 413.
9 Starting from 2-methyl[4-$^2$H]but-3-yn-2-ol, the trideuterio derivative was synthesized following Baldwin's method: J. E. Baldwin and K. A. Black, *J. Org. Chem.*, 1983, **48**, 2778.



*Received in Cambridge, UK, 31st January 1997; Com. 7/00715I*

# Enantioselective synthesis of homoallylic alcohols using (*E*)-but-2-enyltrichlorosilane and chiral diamines

**Richard M. Angell,[b] Anthony G. M. Barrett,*[a] D. Christopher Braddock,[a] Steven Swallow[c] and Benjamin D. Vickery[a]**

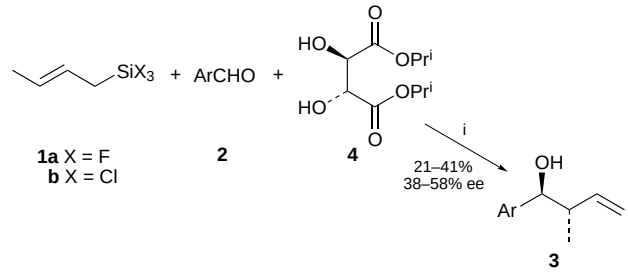
[a] *Department of Chemistry, Imperial College of Science, Technology and Medicine, London, UK SW7 2AY*
[b] *Department of Medicinal Chemistry, Glaxo Wellcome Research Ltd., Gunnels Wood Road, Stevenage, Hertfordshire, UK SG1 2NY*
[c] *Department of Chemistry, Roche Discovery Welwyn, 40 Broadwater Road, Welwyn Garden City, Hertforshire, UK AL7 3AY*

**Condensation of aromatic aldehydes and (*E*)-but-2-enyltrichlorosilane in the presence of (*S*)-(+)-4-(2-methylpropyl)-2-(2-pyridinyl)-2-oxazoline gives the corresponding homoallylic alcohols in excellent *anti*-diastereoselectivity ( > 99%) and good enantioselectivity (36–74%).**

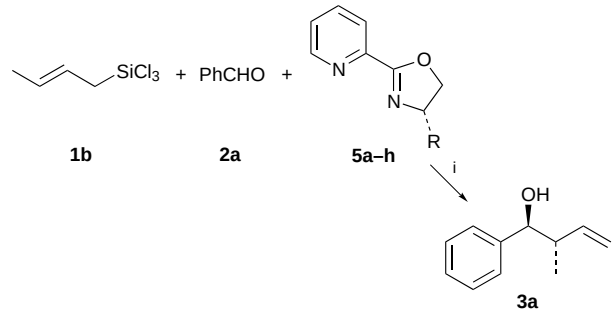
The nucleophilic addition of allylmetal moieties to carbonyl compounds is a powerful method for the construction of carbon–carbon bonds and represents an invaluable tool in organic synthesis.[1] The catalytic use of chiral Lewis acids derived from titanium(IV) complexes and (*R*)- or (*S*)-BINOL developed independently by the groups of Keck and of Tagliavini and Umani-Ronchi for the addition of allylstannane reagents to achiral aldehydes has been demonstrated to furnish homoallylic alcohols both in excellent yield and enantiomeric excess for aromatic and aliphatic aldehydes alike.[2,3] Similarly, modified titanium(IV)–BINOL systems have been found to catalyse the Sakurai–Hosomi allylation of aldehydes.[4–6] Here the advantage lies in the use of inexpensive, non-toxic silicon derivatives. A mechanistically distinct approach is the use of Lewis bases to mediate the addition of crotyltrifluorosilane **1a** to aldehydes. For instance, Sakurai has shown that the addition of stoichiometric amounts of lithium fluoride,[7] dilithium catecholate[8] or catechol[9] furnishes homoallylic alcohols in excellent yield and with relative stereochemical control. Kobayashi has pioneered the use of DMF and HMPA as the Lewis base for the addition of crotyltrichlorosilane **1b** to aldehydes[10] and some success has also been achieved by the replacement of these achiral additives with chiral phosphoramides providing homoallylic alcohols in high yield and variable enantiomeric excess (21–88% ee).[11] Very recently Wang *et al*[12] have shown that (2*R*,3*R*)-(+)-diisopropyl tartrate **4**, a bidentate *O*-donor, can be used as the asymmetric Lewis base additive giving the alcohol product **3** in 27–71% ee, and these results prompt us to disclose our own observations in this area. Herein, we now report the enantioselective crotylation of aldehydes using (*E*)-but-2-enyltrichlorosilane **1b** in the presence of chiral bidentate Lewis bases.

Our investigations commenced with the use of bidentate *O*-donors for the addition of crotyltrifluorosilane **1a** to aromatic aldehydes **2**. Whereas (±)-BINOL and (2*S*,3*S*)-butanediol were ineffective, we found that (2*R*,3*R*)-(+)-diisopropyl tartrate **4** promoted the condensation, but gave only racemic homoallylic alcohol adduct **3**. Employing crotyltrichlorosilane **1b** in place of fluorosilane **1a** resulted in the isolation of enantiomerically enriched products **3** (Scheme 1) and these results closely parallel those reported by Wang.[12]

After further screening of potential bidentate catalysts, we found that 2,2′-bipyridyl also promoted the reaction between crotyltrichlorosilane **1b** and benzaldehyde **2a** (−55 °C, 60 h, 87% yield). This promising result encouraged us to produce and test chiral pyridine derivatives in enantioselective crotylation reactions. To our great delight, use of (*S*)-(−)-4-isopropyl-2-(2-pyridinyl)-2-oxazoline **5d**[13]† provided product **3a** in 59% yield and 43% ee (−55 °C, 60 h). Consequently, a number of chiral pyridinyloxazolines **5a**–**h** were synthesised[14] and used as auxiliaries‡ with varying degrees of success (Scheme 2 and Table 1). Clearly, the leucine derived ligand **5c** gives the best results and we were able to obtain a reproducible 72% yield of exclusively the *anti*-diastereoisomeric adduct **3a** in 74% ee. A




**Scheme 1** *Reagents and conditions*: i, $NPr^i_2Et$, $CH_2Cl_2$, −55 °C, 2.5 d

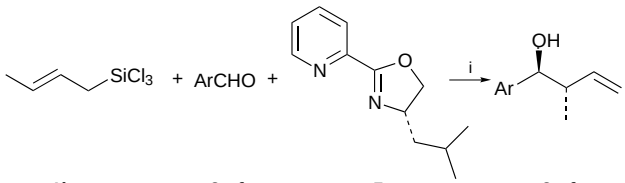



**Scheme 2** *Reagents and conditions*: i, $CH_2Cl_2$, −78 °C, 4 h

**Table 1** Preparation of homoallylic alcohol **3a** promoted by ligands **5a**–**h**

| Entry | R | Ligand | Yield (%) | Ee (%)[a] |
|---|---|---|---|---|
| 1 | Me[b] | **5a** | 42 | 22 |
| 2 | (*S*)-CH(Me)Et | **5b** | 18 | 42 |
| 3 | $CH_2CHMe_2$ | **5c** | 72 | 74 |
| 4 | $Pr^i$ | **5d** | 40 | 45 |
| 5 | *c*-$C_6H_{11}$ | **5e** | 23 | 55 |
| 6 | Ph | **5f** | 15 | 41 |
| 7 | $CH_2$-*c*-$C_6H_{11}$ | **5g** | 43 | 72 |
| 8 | Bn | **5h** | 41 | 53 |

[a] Determined by HPLC analysis (Chiracel OD). [b] Ligand **5a** was prepared from D-alaninol and gave (1*R*,2*R*)-2-methyl-1-phenylbut-3-en-1-ol as the major enantiomer.




**1b** **2a-f** **5c** **3a-f**

**Scheme 3** *Reagents and conditions*: i, $CH_2Cl_2$, −78 °C, 4 h

**Table 2** Preparation of homoallylic alcohols **3a–f** using ligand **5c**

| Entry | R | Product | Yield (%) | Ee (%)[a] |
|---|---|---|---|---|
| 1 | Ph | **3a** | 72 | 74 |
| 2 | 4-$MeC_6H_4$ | **3b** | 70 | 72 |
| 3 | 4-$MeOC_6H_4$ | **3c** | 79 | 46 |
| 4 | 4-$O_2NC_6H_4$ | **3d** | 66 | 36 |
| 5 | 4-$FC_6H_4$ | **3e** | 61 | 74 |
| 6 | PhCH=CH | **3f** | 91 | 60 |

[a] Determined by HPLC analysis (Chiracel OD, Chiracel OD-H or Chirapak AD).

number of aldehydes were examined to test the scope of the reaction (Scheme 3 and Table 2). In most cases alcohols **3a-f** were obtained in good yield and ee.

There has been much discussion about the transition state of the crotylation reaction. That products with *anti* stereochemistry are produced indicates a closed cyclic transition state, probably involving a penta- or hexa-coordinate silicon. However, the precise nature of the factors controlling the degree of asymmetric induction are as yet not clear. Work is currently underway for a clearer mechanistic understanding of this transformation and to apply our knowledge for the design of novel, second generation catalysts.

We thank Glaxo Wellcome Research Ltd. for the most generous endowment (to A.G.M.B.), the Wolfson Foundation for establishing the Wolfson Centre for Organic Chemistry in Medical Science at Imperial College, the EPSRC, the DTI, Glaxo Wellcome Research Ltd. and Roche Discovery Welwyn for a studentship under the Link Asymmetric Scheme (to B. D. V.), and Dr D. J. Berrisford (UMIST) for helpful discussions.

## Footnotes

† Pyridinyloxazolines **5a–f,h**[13] were prepared following literature procedures[14] from 2-cyanopyridine and the respective amino alcohol in good yield. Novel diamine **5g** was prepared according to an analogous procedure and was fully characterised.

‡ In a typical procedure, crotyltrichlorosilane **1b** (0.353 ml, 2.2 mmol) was added to a cold (−78 °C) solution of (*S*)-(+)-4-(2-methylpropyl)-2-(2-pyridinyl)-2-oxazoline **5c** (0.450 g, 2.2 mmol) in dry dichloromethane (3.6 ml). To the bright yellow solution, was added a mixture of benzaldehyde **2a** (0.204 ml, 2.0 mmol) in dichloromethane (0.4 ml) dropwise over a period of five min. After 4 h, the mixture was poured into a mixture of saturated aqueous $NaHCO_3$ (5 ml) and 1 M NaF (5 ml). The aqueous layer was extracted with diethyl ether (3 × 25 ml). The ethereal extracts were dried and concentrated to give a yellow residue, which was chromatographed (silica, hexanes–ethyl acetate 12 : 1) to provide 2-methyl-1-phenylbut-3-en-1-ol **3a** (0.235 g, 72%) as a colourless oil.

## References

1 W. R. Roush, in *Comprehensive Organic Synthesis*, ed. B. M. Trost, I. Fleming and C. H. Heathcock, Pergamon, Oxford, 1991, vol. 2, pp. 1–53.
2 A. L. Costa, M. G. Piazza, E. Tagliavini, C. Trombini and A. Umani-Ronchi, *J. Am. Chem. Soc*., 1993, **115**, 7001; G. E. Keck, K. H. Tarbet and L. S. Geraci, *J. Am. Chem. Soc*., 1993, **115**, 8467; G. E. Keck and L. S. Geraci, *Tetrahedron Lett*., 1993, **34**, 7827; G. E. Keck, D. Krishnamurthy and M. C. Grier, *J. Org. Chem*., 1993, **58**, 6543; J. W. Faller, D. W. I. Sams and X. Liu, *J. Am. Chem. Soc*., 1996, **118**, 1217; S. Weigard and R. Brükner, *Chem. Eur. J*., 1996, **2**, 1077.
3 For the use of boron derived chiral Lewis acid, see J. A. Marshall and Y. Tang, *Synlett*, 1992, 653.
4 For a review of the Sakurai–Hosomi allylation, see A. Hosomi, *Acc. Chem. Res*., 1988, **21**, 200.
5 Boron derived chiral Lewis acid: K. Furuta, Makoto Mouri and H. Yamamoto, *Synlett*, 1991, 561; Titanium derived Lewis acid: D. R. Gauuthier, Jr. and E. M. Carreira, *Angew. Chem., Int. Ed. Engl*., 1996, **35**, 2363.
6 For the use of a titanium–(*R*)-BINOL derived Lewis acid which generates ene adducts from the addition of allysilanes to aldehydes, see K. Mikami and S. Matsukawa, *Tetrahedron Lett*., 1994, **35**, 3133.
7 M. Kira, M. Kobayashi and H. Sakurai, *Tetrahedron Lett*., 1987, **28**, 4081.
8 M. Kira, K. Sato and H. Sakurai, *J. Am. Chem. Soc*., 1988, **110**, 4599.
9 M. Kira, K. Sato and H. Sakurai, *J. Am. Chem. Soc*., 1990, **112**, 257.
10 S. Kobayashi and K. Nishio, *Tetrahedron Lett*., 1993, **34**, 3453; S. Kobayashi and K. Nishio, *J. Org. Chem*., 1994, **59**, 6620; S. Kobayashi and K. Nishio, *Chem. Lett*., 1994, 1773.
11 S. E. Denmark, D. M. Coe, N. E. Pratt and B. D. Griedel, *J. Org. Chem*., 1994, **59**, 6161; K. Iseki, Y. Kuroki, M. Takahashi and Y. Kobayashi, *Tetrahedon Lett*., 1996, **37**, 5149.
12 Z. Wang, D. Wang and X. Sui, *Chem. Commun*., 1996, 2261.
13 C. Bolm, K. Weickhardt, M. Zehnder and T. Ranff, *Chem. Ber*., 1991, **124**, 1173.
14 H. Brunner and U. Obermann, *Chem. Ber*., 1989, **122**, 499.

*Received in Liverpool, UK, 24th February 1997; Com. 7/01244E*

# Cation encapsulation within a ten-oxygen spheroidal cavity of conformationally preorganized 1,5-3,7-calix[8]bis-crown-3 derivatives

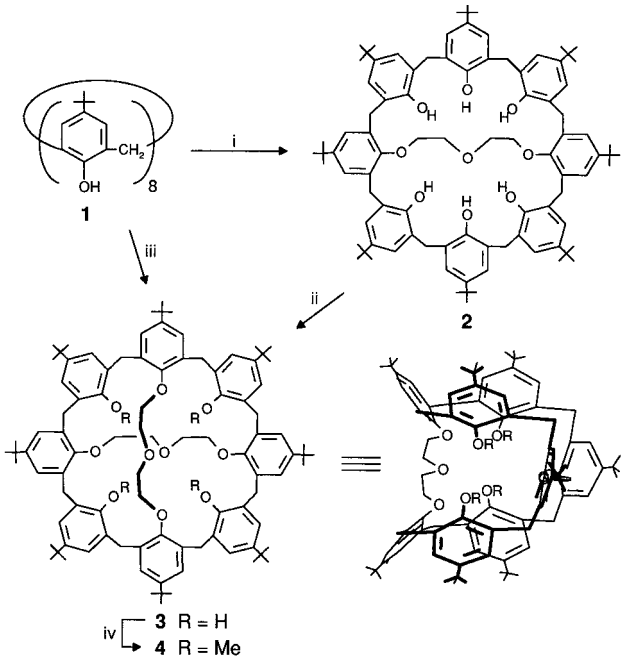
**Corrada Geraci, Gianni Chessari, Mario Piattelli and Placido Neri***

*Istituto per lo Studio delle Sostanze Naturali di Interesse Alimentare e Chimico-Farmaceutico, CNR, Via del Santuario 110, I-95028 Valverde (CT), Italy*

**Conformationally preorganized, $D_{2d}$-symmetrical 1,5-3,7-calix[8]bis-crown-3 derivatives have been synthesized which are able to encapsulate cations with a size dependent selectivity.**

In recent years remarkable host properties have been reported for functionalized calix[4]arenes.[1,2] In contrast, calix[8]arenes have shown no complexing abilities worthy of note,[1] apart from the remarkable case of buckminsterfullerene complexation.[3] This can be explained in terms of the preorganization principle[4] and by considering the floppy nature of the larger macrocycle.[5] In order to circumvent this problem, rigidification of calix[8]-arenes has been actively investigated by our[6] and other research groups,[7] giving particular attention to the preorganization by intramolecular bridging. However, notwithstanding the interesting results obtained in this direction,[6–7] to the best of our knowledge no complexing abilities have been registered so far. Here we report the first example of calix[8]arenes that by virtue of their conformational preorganization are able to encapsulate cations with a size-dependent selectivity.

As an extension of our previous studies on the synthesis of calix[8]crowns[6b,d,e] we envisaged that the use of one or more short polyether chains (diethylene glycol) could lead to a better preorganization of the macrocycle.[8] To achieve this aim, we reacted *p-tert*-butylcalix[8]arene **1** with diethylene glycol ditosylate in DMF in the presence of $Cs_2CO_3$ obtaining 1,5-crown-3 derivative **2** in 78% yield (Scheme 1), in accordance with the previously observed regioselectivity under analogous conditions.[6d] Further alkylation of **2** in the presence of NaH in THF–DMF (10 : 1, v/v) resulted in the introduction of another bridge with very high regioselectivity, thus affording 1,5-3,7-calix[8]bis-crown-3 **3** in 85% yield.† Interestingly, direct alkylation of *p-tert*-butylcalix[8]arene **1** in the presence of NaH, under conditions previously found to be well suited for 1,4-bridging with longer chains (tri- to penta-ethylene glycol),[6d] also gave **3** in 10% yield. This result is in line with the observations of Ikeda *et al*., who reported that intrabridging of **1** with bis(bromomomethyl)arenes under similar conditions results in 1,4-bridging with longer and 1,5-bridging with shorter reagents.[7c]




**Scheme 1** *Reagents and conditions*: i, $TsO(CH_2CH_2O)_2Ts$, $Cs_2CO_3$, DMF, 70 °C; ii, $TsO(CH_2CH_2O)_2Ts$, NaH, THF–DMF (10 : 1, v/v), reflux; iii, $TsO(CH_2CH_2O)_2Ts$, NaH, THF–DMF (10 : 1, v/v), reflux; iv, MeI, NaH, DMF, 70 °C

The presence of a single or double bridge in **2** and **3**, respectively, was deduced by FAB(+) mass spectra, while the bridging pattern was assigned on the basis of the molecular symmetry evidenced in NMR spectra. Thus, the presence of three *tert*-butyl signals in the $^1$H NMR spectrum ($CDCl_3$, 330 K) of **2** at δ 1.24, 1.28 and 1.31 (1 : 2 : 1) is clear evidence of a calix[8]arene molecule bisected by two orthogonal 2-fold symmetry elements and hence of the 1,5-bridging pattern. Similarly, the presence in the spectrum of **3** [Fig. 1(*a*)] of two equal intensity *tert*-butyl singlets at δ 1.20 and 1.21 coupled with a single AX system for $ArCH_2Ar$ (δ 3.45 and 4.26, $J$ = 14.6 Hz) is compatible, among the 22 possible isomers, only with the most symmetrical 1,5-3,7-bis-crown structure.

The presence of an AX system for the $ArCH_2Ar$ protons of **3** is clear proof of a strong reduction of the conformational mobility of the macrocycle. This was confirmed by dynamic NMR studies in $CDCl_2CDCl_2$, which showed no hint of coalescence for these signals when raising the temperature up to 380 K, indicating the absence of conformational interconver-

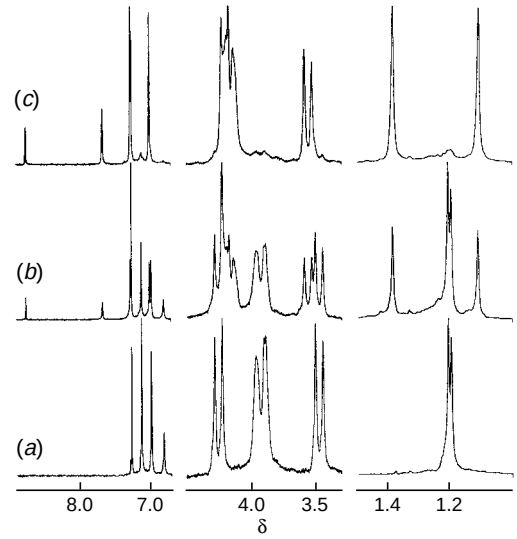



**Fig. 1** Caesium cation encapsulation by 1,5-3,7-bis-crown **3**. $^1$H NMR spectra (250 MHz, $CDCl_3$) of free ligand **3** (*a*), 24 h (*b*) and 48 h (*c*) after addition of solid caesium picrate

sion. The large chemical shift separation of the two doublets of the $ArCH_2Ar$ protons ($\Delta\delta$ = 0.81 ppm) indicates a *syn* orientation of each couple of vicinal aromatic rings with a geometry very similar to that of calix[4]arenes in the cone conformation. This was confirmed by the $^{13}C$ NMR chemical shift value of $\delta$ 32.1 for the $ArCH_2Ar$ groups.

In order to get an insight into the conformation adopted by **3** we undertook a Monte Carlo conformational search using the MacroModel ver.4.5 program[9] and imposed the symmetry equivalences evidenced by NMR. An idealized molecular model was thus obtained (Fig. 2) to be considered as the average structure in solution and possessing four different clefts, each with a structure closely reminiscent of a calix[4]arene cone depleted of an aryl ring ($\frac{3}{4}$ cone). This structure possesses a $D_{2d}$ symmetry and is very similar to that proposed by Ikeda *et al*. for a calix[8]arene 1,5-3,7-doubly-bridged with *ortho* xylene units.[7c] However, this idealized structure does not correspond to an energy minimum and, indeed, its unconstrained full-matrix minimization as well as an independent unconstrained Monte Carlo search originates unsymmetrical geometries with large distortions of the $\frac{3}{4}$ cone units. These deformations can be described as a combination of $C_{4v}$ to $C_{2v}$ transitions typical of calix[4]arene cone[8] for each subunit of the structure.

In the idealized structure the ten oxygens are symmetrically located delimitating a polyhedral, almost spheroidal cavity. The four hydroxylic oxygens describe a planar square with an average diagonal of 6.3 Å, while the central oxygens of the crowns are symmetrically situated at *ca*. 4.1 Å above and below this square. These geometrical features are reminescent of the structure of cryptands, compounds well known as strong complexing agents for alkali metal cations.[10] On the basis of this analogy, we tested the complexing abilities of compound **3**. Thus, preliminary $^1H$ NMR experiments showed that immediately after the addition of solid caesium picrate to a $CDCl_3$ solution of **3** no appreciable changes can be observed in the spectrum, but after standing for 24 h at room temp. a new set of signals appeared, due to the complex $Cs^+\subset$**3** formation [Fig. 1(*b*)]. A further 24 h standing led to complete complexation [Fig. 1(*c*)]. In the homogeneous phase ($CD_3CN$–$CDCl_3$, 9 : 1 v/v) completion of the reaction required only a few minutes. The 1 : 1 stoichiometry was confirmed by signal integration in the spectrum. In the complex $Cs^+\subset$**3** the cation appears to be encapsulated inside the ten-oxygen spheroidal cavity, as indicated by the substantial downfield shift experienced by the protons of the crown chains, the aromatic rings and the hydroxy groups. Downfield shifts were also observed in the $^{13}C$ NMR spectrum for the pertinent carbon signals.

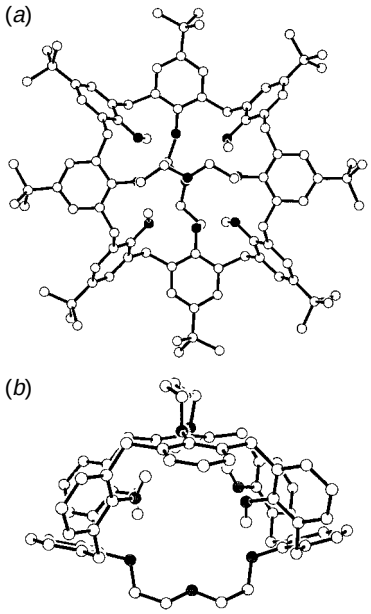



**Fig. 2** Computer model of idealized conformation of **3**: (*a*) top view (H atoms omitted); (*b*) side view (H atoms and *tert*-butyl groups omitted)

The selectivity of complexation was investigated by standard two-phase picrate extraction experiments.[11] Thus, it was shown that different cations can be encapsulated besides $Cs^+$ with the following equilibrium constants: $K_e$ ($dm^6\ mol^{-2}$) = $3.7 \times 10^4$ for $Na^+$, $11 \times 10^4$ for $K^+$, $10 \times 10^4$ $NH_4^+$, $640 \times 10^4$ for $Rb^+$ and $5200 \times 10^4$ for $Cs^+$. The $K_e(Cs^+)/K_e(Na^+)$ selectivity factor is therefore 1400, thus confirming the cation/cavity size complementarity expected for the encapsulation process.‡

It is to be expected that chemical modifications of **3** can have a profound influence on the complexing properties. We prepared the tetramethyl derivative **4** (MeI–NaH–DMF, 80% yield), whose complexing properties toward caesium cations do not differ substantially from that of **3**. Interestingly, an upfield shift from $\delta$ 3.44 to 2.84 is observed, upon $Cs^+$ complexation, for the OMe groups in the $^1H$ NMR spectrum of **4** ($CD_3CN$–$CDCl_3$, 9 : 1 v/v) indicating that they are forced to point inside the shielding $\frac{3}{4}$ cone aromatic cavities. However, the determination of picrate extraction equilibrium constants [$K_e$ ($dm^6\ mol^{-2}$) = $1.3 \times 10^4$ for $Na^+$, $3.9 \times 10^4$ for $K^+$, $4.0 \times 10^4$ for $NH_4^+$, $16 \times 10^4$ for $Rb^+$ and $87 \times 10^4$ for $Cs^+$] revealed a reduced $K_e(Cs^+)/K_e(Na^+)$ selectivity factor (67). A more detailed investigation of the complexation properties of **3**, **4** and other analogues is currently carried out in our laboratory.

Thanks are due to Mr R. Rapisardi (ICTMP, CNR, Catania) for FAB MS measurements and to Mrs C. Rocco (ISSN, CNR, Valverde) for NMR spectra acquisition.

## Footnotes

* E-mail: neri@issn.ct.cnr.it

† Satisfactory microanalytical and spectral data were obtained for all new compounds.

‡ This selectivity factor cannot be directly compared to the $Cs^+/Na^+$ selectivity [$S = \beta(Cs^+)/\beta(Na^+)$] calculated as the ratio of stability constants ($\beta$) and usually reported for caesium-selective 1,3-alternate calix[4]crowns [for which $S \geqslant 10^5$, refs. 2(*a*), (*b*)].

## References

1 V. Böhmer, *Angew. Chem., Int. Ed. Engl.*, 1995, **34**, 713 and references cited therein.
2 (*a*) A. Casnati, A. Pochini, R. Ungaro, F. Ugozzoli, F. Arnaud, S. Fanni, M.-J. Schwing, R. J. M. Egberink, F. de Jong and D. N. Reinhoudt, *J. Am. Chem. Soc.*, 1995, **117**, 2767; (*b*) Z. Asfari, J. M. Harrowfield, A. N. Sobolev and J. Vicens, *Aust. J. Chem.*, 1994, **47**, 757; (*c*) H. Yamamoto and S. Shinkai, *Chem. Lett.*, 1994, 1115; (*d*) Y. Kubo, S. Maeda, S. Tokita and M. Kubo, *Nature*, 1996, **382**, 522.
3 C. L. Raston, J. L. Atwood, P. J. Nichols and I. B. N. Sudria, *Chem. Commun.*, 1996, 2615.
4 D. J. Cram, *Angew. Chem., Int. Ed. Engl.*, 1988, **27**, 1009.
5 C. D. Gutsche and L. J. Bauer, *J. Am. Chem. Soc.*, 1985, **107**, 6059; G. M. L. Consoli, F. Cunsolo, M. Piattelli and P. Neri, *J. Org. Chem.*, 1996, **61**, 2195.
6 (*a*) F. Cunsolo, M. Piattelli and P. Neri, *J. Chem. Soc., Chem. Commun.*, 1994, 1917; (*b*) C. Geraci, M. Piattelli and P. Neri, *Tetrahedron Lett.*, 1995, **36**, 5429; (*c*) F. Cunsolo, G. M. L. Consoli, M. Piattelli and P. Neri, *Tetrahedron Lett.*, 1996, **37**, 715; (*d*) C. Geraci, M. Piattelli and P. Neri, *Tetrahedron Lett.*, 1996, **37**, 3899; (*e*) 7627.
7 (*a*) A. Arduini, A. Pochini, A. Secchi and R. Ungaro, *J. Chem. Soc., Chem. Commun.*, 1995, 879; (*b*) M. Mascal, R. T. Naven and R. Warmuth, *Tetrahedron Lett.*, 1995, **36**, 9361; (*c*) A. Ikeda, K. Akao, T. Harada and S. Shinkai, *Tetrahedron Lett.*, 1996, **37**, 1621.
8 A. Arduini, W. M. McGregor, D. Paganuzzi, A. Pochini, A. Secchi, F. Ugozzoli and R. Ungaro, *J. Chem. Soc., Perkin Trans. 2*, 1996, 839.
9 F. Mohamadi, N. G. J. Richards, W. C. Guida, R. Liskamp, M. Lipton, C. Caufield, G. Chang, T. Hendrickson and W. C. Still, *J. Comput. Chem.*, 1990, **11**, 440.
10 B. Dietrich, P. Viout and J.-M. Lehn, *Macrocyclic Chemistry*, VCH, Weinheim, 1993, pp. 241–356.
11 A. Arduini, A. Pochini, S. Reverberi, R. Ungaro, G. D. Andreetti and F. Ugozzoli, *Tetrahedron*, 1986, **42**, 2089.

*Received in Cambridge, UK, 17th February 1997; Com. 7/01114H*

# Two free radical routes for the preparation of novel difluoromethylene-linked serine-*O*-glycopeptide analogues

**Timothée F. Herpin, William B. Motherwell* and Jean-Marc Weibel**

*Christopher Ingold Laboratories, Department of Chemistry, University College London, 20 Gordon Street, London, UK WC1H 0AJ*

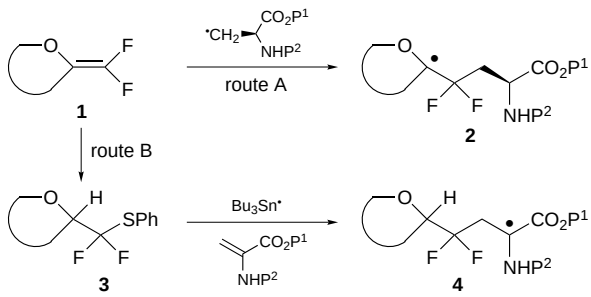
**The first examples of *gem*-difluoromethylene-linked analogues of serine-derived glycopeptides have been prepared in a highly stereoselective manner using two complementary free radical chain reactions.**

The importance of the carbohydrate moiety in molecular recognition processes involving glycoproteins[1,2] and the considerable potential of glycosylated peptide drugs[3] have stimulated intense current research interest in the synthesis of modified glycopeptides, where the customary *O*- or *N*-glycosidic bond linking the amino acid component to the sugar portion is replaced by a carbon-based unit of greater stability and resistance towards enzymatic deglycosylation. Thus, methods have been described, both for the synthesis of *C*-glycosyl amino acids in which the anomeric carbon is directly bound to the α-carbon of the amino acid[4–8] and for methylene-bridged glycopeptides[9–14] in which the additional methylene group can serve as a heteroatom mimic. Even the latter, however, lead to derivatives with a truncated chain when compared with the corresponding serine-*O*-glycopeptides.

Our objective in this area was to achieve site specific replacement of the exocyclic anomeric oxygen atom in a serine-derived glycopeptide fragment by a difluoromethylene group. This tetrahedral and electronegative unit has been shown to be of particular value as an oxygen atom replacement in several difluoromethylene phosphonate analogues of naturally occurring phosphates.[15]

As shown in Scheme 1, our intention was to capitalise on the chemical versatility of readily prepared carbohydrate *gem*-difluoro enol ethers[16] **1**, either as radicophiles[17] for the addition of an amino acid-derived radical to give the anomeric radical **2** (route A), or *via* their thiophenol adducts **3**,[18] as apposite precursors for difluoroalkyl radical trapping by a dehydroalanine derivative to give the carbon centred radical **4** around the amino acid unit (route B).

Thus, in a preliminary study, slow addition of tributylstannane and AIBN as initiator to a refluxing benzene solution of carbohydrate **5** and the iodoalanine reagent[19,20] **6** developed by Baldwin[21,22] afforded out first example of a difluoromethylene-linked serine analogue **7**, albeit in a disappointing 14% yield (Scheme 2). Efforts to optimise this reaction or to extend it to other *gem*-difluoro enol ether substrates were unsuccessful.



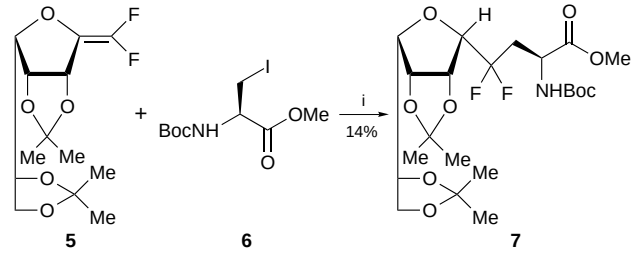

**Scheme 1**

We reasoned that a much more compact and conformationally restricted radical reagent was required, and elected to prepare the cyclic bis(trifluoromethyl)oxazolidinone derivative **10** which should find general use as a convenient bromoalanine reagent. Thus, as shown in Scheme 3, protection of aspartic acid **8** with gaseous hexafluoroacetone[23] was followed by conversion to the acid chloride[24] **9** which was transformed *via* the acylthiohydroxamate to the desired bromide **10** using the radical variant of the Hünsdieker reaction.[25]

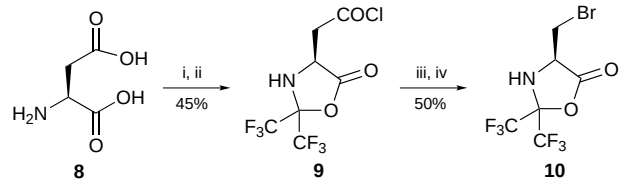
Addition of **10** to *gem*-difluoro enol ethers under tributylstannane-mediated conditions proceeded in acceptable yields with a range of substrates (Scheme 4), with abstraction of the hydrogen atom occurring exclusively from the less hindered convex face[14,26] in the case of the gulose **5** → **11** and erythrose **12** → **13** derivatives. Reaction of the ribose derivative **14** however produced an equimolar mixture of both anomers **15**, and on replacement of the methyl ether by the bulky *tert*-butyldimethylsilyl group, no addition products were observed.

The utility of the labile bis(trifluoromethyl)oxazolidinone protecting group was demonstrated by simple treatment of **11** with L-phenylalanine *tert*-butyl ester to afford the dipeptide **16** (Scheme 5).

Finally, we have also carried out a preliminary study of the alternative approach outlined in Scheme 1 route B, which effectively circumvents problems created by the steric bulk of the carbohydrate. The chiral dehydroalanine derivative (2*R*)-*N*-benzoyl-2-(*tert*-butyl)-4-methylidene-1,3-oxazolidin-5-one **17** prepared from (*S*)-alanine and used by Beckwith[13] as a radicophile, was accordingly selected to ensure diastereoselectivity at the α-carbon atom of the amino acid unit. In the final analysis, we also elected to use the phenylselanyl congeners of our previously described[18] thiophenol adducts in order to

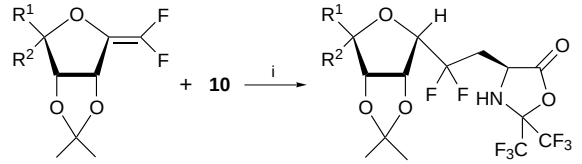



**Scheme 2** *Reagents and conditions*: i, AIBN, $Bu_3SnH$ (slow addition), benzene, reflux



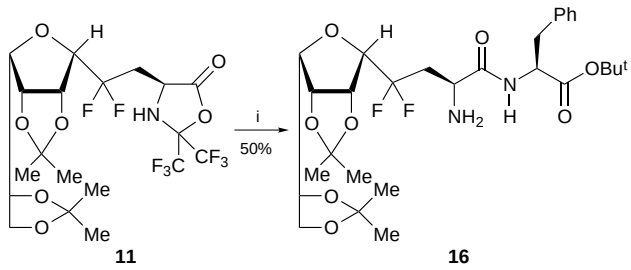

**Scheme 3** *Reagents and conditions*: i, $(CF_3)_2CO$, DMSO, 50 °C; ii, $SOCl_2$, reflux; iii, 2-sulfanylpyridine 1-oxide sodium salt, THF, −15 °C; iv, $BrCCl_3$, *h*ν (tungsten)

facilitate generation of the required difluoroalkyl radicals. The results for the three carbohydrates **18**–**20** in Scheme 6 indicate that this tributylstannane-mediated coupling gives consistently higher yields than those obtained by the previous method. The successful coupling of the hindered ribose derivative **20** is particularly noteworthy since the alternative coupling strategy had been unsuccessful. From a stereochemical standpoint, the ratio of the two diastereoisomers produced in each reaction is consistent with the results obtained by Beckwith[13] with the same chiral auxiliary.

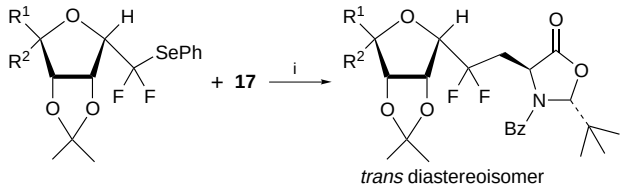



| Compound | $R^1$ | $R^2$ | Product | Yield(%) |
|---|---|---|---|---|
| **5** | H |  | **11** | 30 |
| **12** | H | H | **13** | 20 |
| **14** | $CH_2OMe$ | H | **15** | 41[a] |

**Scheme 4** *Reagents and conditions*: i, AIBN, $Bu_3SnH$ (slow addition), benzene, reflux. [a] Obtained as a 1 : 1 mixture of diastereoisomers at the anomeric centre.




**Scheme 5** *Reagents and conditions*: i, L-phenylalanine *tert*-butyl ester, $Et_2O$, room temp., 24 h




| Compound | $R^1$ | $R^2$ | Product | Ratio | Yield(%) |
|---|---|---|---|---|---|
| **18** | H |  | **21** | 80 : 20 | 91 |
| **19** | H | H | **22** | 85 : 15 | 86 |
| **20** | $CH_2OSiMe_2Bu^t$ | H | **23** | 86 : 14 | 71 |

**Scheme 6** *Reagents and conditions*: i, AIBN, $Bu_3SnH$ (slow addition), benzene, reflux

In summary, the two complementary free radical routes described herein provide a convenient approach for the synthesis of a wide range of *C*-glycosylated amino acid units in which the difluoromethylene group serves not only as a potential heteroatom mimic but also contributes to providing the correct number of atoms in the crucial linkage between the carbohydrate and amino acid components of the structures.

We acknowledge the support of the Ministere de l'Enseignement Supérieur et de la Recherche for the award of a studentship to T. F. H. J. M. W. is grateful to the European Community for the award of a Research Fellowship.

## References

1 H. Lis and N. Sharon, *Eur. J. Biochem*., 1993, **218**, 1.
2 J. Montreuil, in *Comprhensive Biochemistry*, ed. A. Neuberger and L. L. van Deene, Elsevier, Amsterdam, 1982, vol. 19 BII, 1.
3 J. F. Fisher, A. W. Harrison, G. L. Bundy, K. F. Wilkinson, B. D. Rush and M. J. Ruwart, *J. Med. Chem*., 1991, **34**, 3141.
4 G. Rassu, F. Zanardi, L. Battistini and G. Casiraghi, *Tetrahedron: Asymmetry*, 1995, **6**, 371.
5 L. Colombo, G. Casiraghi and A. Pattalis, *J. Org. Chem*., 1991, **56**, 3897.
6 G. Casiraghi, L. Colombo, G. Rassu and P. Spanu, *J. Org. Chem*., 1991, **56**, 6523.
7 P. Garner and J. M. Park, *J. Org. Chem*., 1990, **55**, 3772.
8 A. G. M. Barrett and S. A. Lebold, *J. Org. Chem*., 1990, **55**, 3853.
9 C. R. Bertozzi, P. D. Hoepricht and M. D. Berdnarski, *J. Org. Chem*., 1992, **57**, 6092.
10 M. K. Gurjar, A. S. Mainkar and M. Syamala, *Tetrahedron: Asymmetry*, 1993, **4**, 2343.
11 G. Simchen and E. Pürkner, *Synthesis*, 1990, 524.
12 H. Kessler, V. Wittmann, M. Köck and M. Kottenhahn, *Angew. Chem., Int. Ed. Engl*., 1992, **31**, 902.
13 J. R. Axon and A. L. J. Beckwith, *J. Chem. Soc., Chem. Commun*., 1995, 549.
14 B. Giese, *Angew. Chem., Int. Ed. Engl*., 1989, **28**, 969.
15 G. M. Blackburn, *Chem. Ind. (London)*, 1981, 134; G. M. Blackburn, D. E. Kent and F. Kolkmann, *J. Chem. Soc., Perkin Trans*., 1984, 1119; R. D. Chambers, R. Jaouhari and D. O'Hagen, *Tetrahedron*, 1989, **45**, 5101.
16 J. S. Houlton, W. B. Motherwell, B. C. Ross, M. J. Tozer, D. J. Williams and A. M. Z. Slawin, *Tetrahedron*, 1993, **49**, 8087.
17 T. F. Herpin, W. B. Motherwell and M. J. Tozer, *Tetrahedron: Asymmetry*, 1994, **5**, 2269.
18 W. B. Motherwell, B. C. Ross and M. J. Tozer, *Synlett*, 1989, 68.
19 J. A. Bajgrowicz, A. El Hallaoui, R. Jacquier, C. Pigierre and P. Viallefont, *Tetrahedron*, 1985, **41**, 1833.
20 R. F. W. Jackson, N. Wishart, A. Wood, K. James and M. J. Wythes, *J. Org. Chem*., 1992, **57**, 3397.
21 J. E. Baldwin, R. E. Adlington, D. J. Birch, J. A. Crawford and J. B. Sweeney, *J. Chem. Soc., Chem. Commun*., 1986, 1339.
22 J. E. Baldwin, R. Fieldhouse and A. T. Russel, *Tetrahedron Lett*., 1993, **34**, 5491.
23 K. Burger, H. Neuhauser and M. Rudolph, *Chem.-Ztg*., 1990, **114**, 249.
24 K. Burger, M. Gold, H. Neuhauser and M. Rudolph, *Chem.-Ztg*., 1991, **115**, 77.
25 D. H. R. Barton, Y. Hervé, P. Potier and J. Thierry, *Tetrahedron*, 1988, **44**, 5479; D. H. R. Barton, D. Crich and W. B. Motherwell, *Tetrahedron*, 1985, **41**, 3901.
26 D. H. R. Barton, S. D. Gero, Quiclet-Sire and M. Samadi, *Tetrahedron: Asymmetry*, 1994, **5**, 2123.
27 A. L. J. Beckwith, S. G. Pyne, B. Dikic, C. L. L. Chai, P. A. Gordon, B. W. Skelton, M. J. Tozer and A. H. White, *Aust J. Chem*., 1993, **46**, 1425.

*Received in Cambridge, UK, 10th February 1997; Com. 7/00928C*

# Photo- and electro-chromism of a 1,4-anthraquinone derivative. A multi-mode responsive molecule

**Sadao Miki,* Ryuki Noda and Koushi Fukunishi**

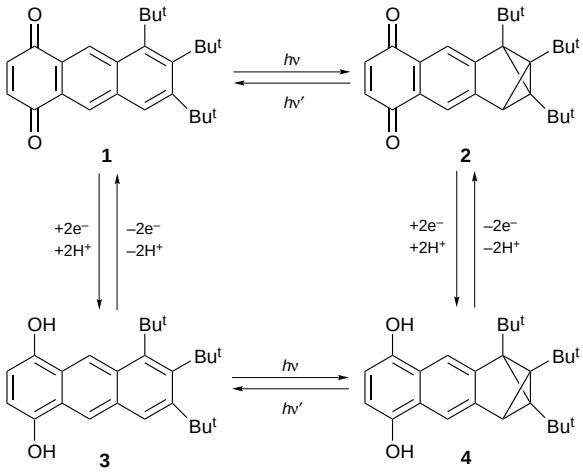
*Department of Chemistry and Materials Technology, Kyoto Institute of Technology, Matsugasaki, Sakyo-ku, Kyoto 606, Japan*

**5,6,7-Tri-*tert*-butyl-1,4-anthraquinone shows electro- and photo-chromism, independently based on the electrochemical redox reaction of the carbonyl groups and the χ[2 + 2]-type photo-valence isomerization of the aromatic ring.**

In the context of the importance of multi-mode responsive molecules in chemionics,[1] optical–electrical dual-mode responsive molecular devices have been the subject of much recent interest.[2–4] It is desirable that such a device can be reversibly converted between all of the four possible states,[2] and that the photo- and electro-chromic properties are completely integrated within a single structure.[4] However, among the examples reported so far, the number of molecular systems possessing these characteristics is very limited. Here, we report that 5,6,7-tri-*tert*-butyl-1,4-anthraquinone **1** shows electro- and photo-chromism independently and can be converted reversibly between all of the four possible states (Scheme 1). The 1,4-anthraquinone derivative **1** was synthesized by the thermal decarbonylation of 5,6,7-tri-*tert*-butyl-5,8-oxomethano-5,8-dihydro-1,4-anthraquinone prepared previously by us.[5]

Steady-state photolysis of **1** was performed with a degassed solution of **1** ($5.6 \times 10^{-4}$ M) in hexane at room temperature with 460 nm light from a xenon lamp using a monochromator. As shown in Fig. 1, the absorption spectral changes upon photolysis revealed isobestic points indicating that the photoreaction proceeded without forming by-products. Spectroscopic and analytical data for the product were compatible with the valene-type isomer **2**. The photo-valence isomerization of **1** was photochemically reversible. Upon irradiation of the solution of **2** with 402 nm light (one of the isobestic points), absorption bands for **1** were recovered, reaching a photostationary state with a composition of **1**:**2** = 7.2:1. Spectral changes for the reverse reaction were also accompanied by distinct isobestic points. Thus, the 1,4-anthraquinone derivative **1** shows photochromism based on χ[2 + 2]-type photo-valence isomerisation similar to other tri-*tert*-butyl-substituted polyacenequinones.[5,6]

It is well known that 9,10-anthraquinone undergoes a reversible two-step redox reaction to the hydroanthraquinone dianion *via* a semiquinone radical in aprotic solvents, and correspondingly its polarograph in DMF shows two reduction waves at $E_{1/2}$ = −0.98 and −1.74 V (*vs.* SCE).[7] 1,4-Anthraquinone derivative **1** showed electrochemical behaviour similar to that of 9,10-anthraquinone, and the cyclic voltammogram of **1** in dry DMF containing $Bu_4NClO_4$ revealed two reversible redox waves at $E_{1/2}$ = −0.71 V (*vs.* SCE), assignable to the redox between **1** and its semiquinone radical, and at −1.43 V, for the redox between the semiquinone radical and hydroanthraquinone dianion. Spectral changes upon electrolysis were measured using a thin-layer cell (*ca*. 0.3 mm thickness) made of transparent indium–tin oxide coated glass (ITO glass) and using the indium film on the glass as the working electrode. The spectral changes for the cathodic reduction of **1** in dry DMF (containing $Bu_4NClO_4$) were not simple because of the simultaneous formation of the semiquinone radical and the hydroanthraquinone dianion. Therefore, Fig. 2 shows the time scanning spectral changes for the reduction of **1** at −1.0 V (*vs.* SCE), where most of **1** could be reduced to semiquinone radical, in the presence of acetic acid (0.03 M) as a proton source. The spectral changes showed a simple decrement of the bands (474 and 333 nm) due to **1** and the appearance of a new band (400 nm) and its increment accompanied by distinct isobestic points. In the presence of the proton source, the semiquinone radical of **1** will be protonated rapidly to give monohydroanthraquinone radical, and successive disproportionation of the radical will form 5,6,7-tri-*tert*-butyl-1,4-hydroanthraquinone **3** and **1**. The product responsible for the new absorption was assigned to **3** based on the fact that the new absorption spectrum was in good agreement with that obtained for **3** chemically synthesized from **1** as follows. A diethyl ether solution of **1** and aq. $Na_2S_2O_4$ were mixed together in an optical cell, and after degassing by freeze-thaw cycles the contents were sonicated. In the absorption spectrum of the




**Scheme 1**

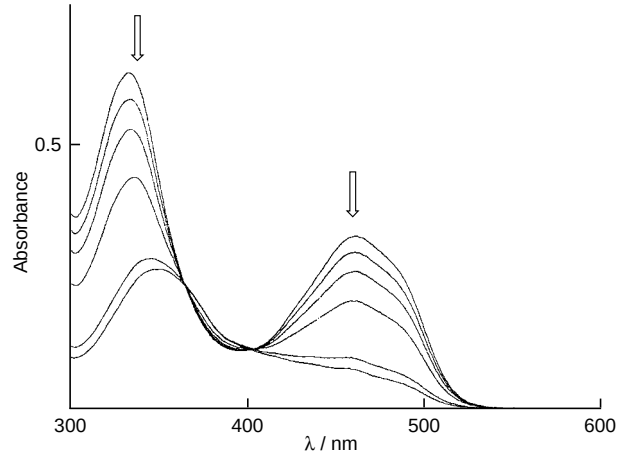



**Fig. 1** Spectral changes upon photolysis of **1** at 460 nm in hexane at room temperature. [**1**] = $5.6 \times 10^{-4}$ M

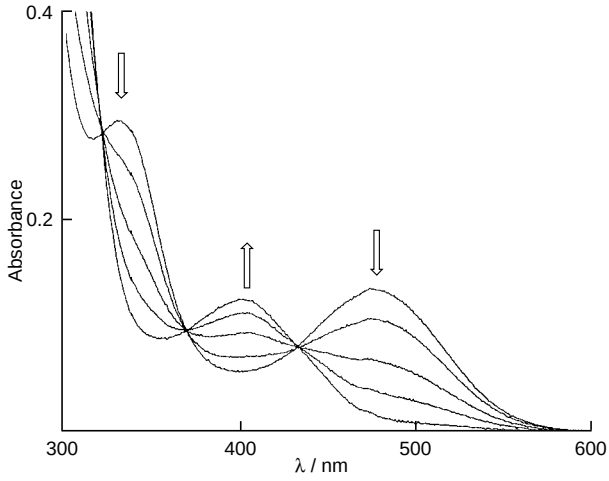



**Fig. 2** Spectral changes upon cathodic reduction of **1** at −1.0 V *vs.* SCE in DMF containing acetic acid (0.03 M) and $Bu_4NClO_4$ (0.1 M)

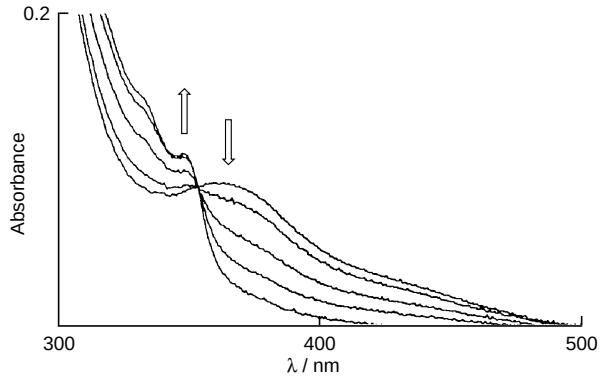



**Fig. 3** Spectral changes upon cathodic reduction of **2** at −1.0 V *vs.* SCE in DMF containing acetic acid (0.03 M) and $Bu_4NClO_4$ (0.1 M)

ethereal layer, the bands due to **1** were not observed and a band at 398 nm appeared. Upon exposure of the ethereal solution to air, the band at 398 nm disappeared and the bands for **1** were recovered completely. $^1$H NMR spectroscopy of the product obtained by $Na_2S_2O_4$ reduction of **1** was consistent with the structure of **3** (*vide infra*).

The electrochemical reaction of **1** was reversible. After cathodic reduction of **1** in the thin-layer cell, the polarity of the electrode was changed and the spectral changes were followed for anodic oxidation at +0.2 V (*vs.* SCE). The band at 400 nm due to **3** decreased with concomitant increases of the bands due to **1** finally giving the complete recovery of the latter.

The electrochemical behaviour of the valene isomer **2** was similar to that of **1**, and its cyclic voltammogram also revealed two reversible redox waves at −0.65 and −1.42 V (*vs.* SCE). Fig. 3 shows the spectral changes that occurred during the cathodic reduction (−1.0 V *vs.* SCE) of **2** in dry DMF containing acetic acid and $Bu_4NClO_4$. The new absorption spectrum was in good agreement with that of the hydronaphthoquinone derivative **4** obtained by $Na_2S_2O_4$ reduction of **2**. The electrochemical reaction was also reversible, and upon anodic oxidation at +0.5 V (*vs.* SCE), **4** disappeared and **2** was recovered completely.

A diethyl ether solution of **3** ($1.06 \times 10^{-4}$ M) was prepared by the method described above. In the spectral changes following the photolysis (436 nm) of the solution (Fig. 4), the band at 398 nm for **3** decreased and new bands at 347 nm and 330 nm appeared and increased. The new absorption spectrum was in good agreement with the spectrum of **4** obtained by $Na_2S_2O_4$ reduction or cathodic reduction of **2**. The reaction was photochemically reversible, and upon photolysis of the photo-

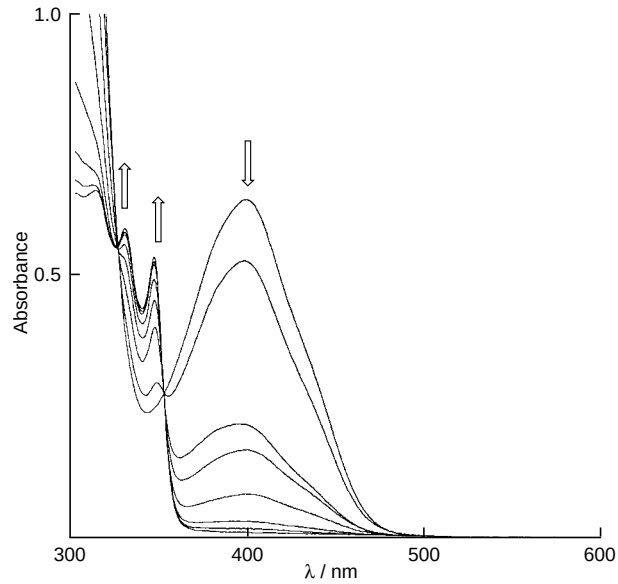



**Fig. 4** Spectral changes upon photolysis of **3** at 436 nm in diethyl ether at room temperature. [**3**] = $1.06 \times 10^{-4}$ M

lysate at 347 nm, the absorption bands for **4** decreased and the bands for **3** were recovered. Spectral changes for both of the forward and the reverse reactions revealed distinct isobestic points. The photochemical interconversion between **3** and **4** was followed also by $^1$H NMR spectroscopy as follows. A solution of **1** in $CDCl_3$ was put in an NMR sample tube and a solution of $Na_2S_2O_4$ in $D_2O$ was added. In the $^1$H NMR spectrum measured after sonication, signals due to **1** disappeared and a set of signals for **3** appeared [δ 8.99 (s, 1 H), 8.32 (s, 1 H), 7.51 (s, 1 H), 6.52 (s, 2 H), 1.76 (s, 9 H), 1.48 (s, 9 H) and 1.37 (s, 9 H)]. After irradiation at 436 nm, the signals for **3** disappeared and a new set of signals for **4** appeared [δ 7.90 (s, 1 H), 7.58 (s, 1 H), 6.50 (ABq, 2 H), 2.36 ( s, 1 H, benzylic H), 1.58 (s, 6 H, two methyl groups of the *tert*-butyl group on benzylic carbon) and 1.22 (s, 21 H, two *tert*-butyl groups and one methyl group); the *tert*-butyl group on the benzylic carbon gave split signals due to restricted rotation]. It was confirmed that the changes in the $^1$H NMR spectra were photochemically reversible.

The present system is considered to be an example of a multimode chemical transducer. All of the four states (**1**, **2**, **3** and **4**) have infinite thermal stability, while in the reported case of phenylazoquinones, the *cis*-phenylazo isomers are kinetically unstable.[2]

This work was supported by a Grant-in-Aid on Priority Area Research 'Photoreaction Dynamics' (06239106) and a Grant-in Aid for Scientific Research (08651009) from the Ministry of Education, Science and Culture, Japan.

## References

1 J.-M. Lehn, *Angew Chem., Int. Ed. Engl.*, 1990, **29**, 1304.
2 T. Saika, T. Iyoda, K. Honda and T. Shimidzu, *J. Chem. Soc., Perkin Trans. 2*, 1993, 1181.
3 J. Daub, J. Salbeck, T. Knochel, C. Fischer, H. Kunkely and K. M. Rapp, *Angew Chem., Int. Ed. Engl.*, 1989, **28**, 1494.
4 S. H. Kawai, S. L. Gilat and J.-M. Lehn, *J. Chem. Soc., Chem. Commun.*, 1994, 1011.
5 S. Miki, J. Ito, R. Noda, N. Nishijima and K. Fukunishi, *Tetrahedron*, 1996, **52**, 4269.
6 S. Miki, H. Kagawa, K. Matsuo, O. Kobayashi, M. Yoshida and Z. Yoshida, *Tetrahedron*, 1992, **48**, 1567.
7 M. E. Peover, *J. Chem Soc.*, 1962, 4540.

*Received in Cambridge, UK, 8th January 1997; Com. 7/00187H*

# Cyclopropanation of alkenes with ethyl diazoacetate catalysed by ruthenium porphyrin complexes

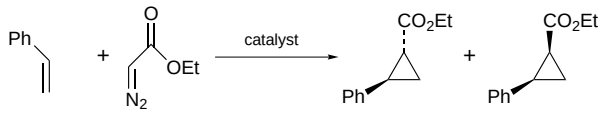
**Erwan Galardon, Paul Le Maux and Gérard Simonneaux***

*Laboratoire de Chimie Organométallique et Biologique, associé au CNRS, Université de Rennes 1, 35042 Rennes cedex, France*

**Ruthenium porphyrin complexes are active catalysts for the cyclopropanation of styrene derivatives by ethyl diazoacetate with good to very good diastereoselectivity; moderate enantiomeric excesses (34%) are observed using a chiral porphyrin as catalyst.**

The development of efficient and selective methods for the synthesis of cyclopropanes is of great interest in organic synthesis, in particular because of their role in biological processes.[1] Several years ago, Callot *et al*. reported that rhodium porphyrins catalysed the cyclopropanation of alkenes by ethyl diazoacetate (EDA).[2] Recently, efficient asymmetric cyclopropanation of alkenes with diazoacetates catalysed by bis(oxazolinyl)pyridine ruthenium complexes has been reported by Nishiyama and co-workers.[3,4] Very recently, osmium[5] and iron[6] porphyrins were also found to be active catalysts for the formation of cyclopropanes in good yield. Despite the periodic relationship of ruthenium to iron and osmium, and the syntheses of ethoxycarbonyl carbene complexes of ruthenium 5,10,15,20-tetratolylporphyrin[7] and ruthenium 5,10,15,20-tetramesitylporphyrin,[8] no cyclopropanation reactions were observed using ruthenium porphyrins as catalysts; only the coupling products diethyl maleate and fumarate were found.[8] We present herein the first ruthenium porphyrin-catalysed cyclopropanation of styrene derivatives by ethyl diazoacetate.

The complexes $Ru^{II}$(por)(CO) (por = TPP,† TMP†)[9,10] or $Ru^{VI}$(por)$(O)_2$[10] (por = TMP†), in catalytic amounts, quickly react with ethyl diazoacetate in the presence of an excess of styrene to give quantitatively‡ the corresponding cyclopropyl esters, with a large excess of the *anti* isomer (Scheme 1). The diastereoselectivity (Table 1) is reminiscent of that observed with osmium and iron catalysts and differs from the *syn* selectivity observed with rhodium porphyrins.[2,11] As shown in the data, the porphyrin structure is important since the use of the unencumbered TPP instead of the crowded TMP results in an increase in the *anti* : *syn* ratio of the cyclopropyl esters from 7.9 to 13.1. The cyclopropane formation also exhibits a substrate shape preference that may be useful for selective cyclopropanation of polyalkenes. Only alk-1-enes and 1,1-disubstituted alkenes react efficiently. Thus styrene and α-methylstyrene are cyclopropanated efficiently, whereas with β-methylstyrene and cyclohexene, diethyl maleate and fumarate are formed in very high yield in a ratio of up 30 : 1 under the same conditions.[8] These coupling products are typically produced when the carbene transfer to the alkene is not observed.[8] The catalyst is also sensitive to the electronic nature of the alkene since aromatic alkenes are better substrates, as previously observed with iron or osmium porphyrins.[5,6] For example, only traces of the cyclopropane products are detected when the reaction is carried out with 4-vinylcyclohex-1-ene.




**Scheme 1**

**Table 1** Cyclopropanation of styrene derivatives by ethyl diazoacetate using ruthenium porphyrin complexes as catalysts

| Substrate | Catalyst | Ratio of *anti* : *syn* products[a] | Alkene yield[b] (%) |
|---|---|---|---|
| Styrene | Ru(TPP)(CO) | 13.1 | 7 |
| Sytrene | Ru(TMP)(CO) | 7.9 | < 5 |
| Styrene | $Ru(TMP)(O)_2$ | 7.1 | < 5 |
| α-Methylstyrene | Ru(TPP)(CO) | 3.1 | 7 |
| α-Methylstyrene | Ru(TMP)(CO) | 1.6 | < 5 |
| α-Methylstyrene | $Ru(TMP)(O)_2$ | 1.5 | < 5 |
| *p*-Chlorostyrene | Ru(TPP)(CO) | 14.0 | 8 |
| *p*-Chlorostyrene | Ru(TMP)(CO) | 8.2 | < 5 |

[a] Determined by GC. [b] Diethyl maleate and fumarate.

The reaction of styrene with ethyl diazoacetate in the presence of the dioxoruthenium(VI) picket-fence complex bearing optically active α-methoxy-α-(trifluoromethyl)phenylacetyl residues on both sides of the porphyrin plane (α,β,α,β isomer)[12] (Fig. 1) gave a mixture (*anti* : *syn* = 9 : 1) of optically active cyclopropane derivatives, *e.g*. *anti* and *syn* ethyl 2-phenylcyclopropane-1-carboxylic esters with 14 and 34% enantiomeric excess, respectively.§

We presume that the active intermediate in the ruthenium porphyrin-catalysed reactions is a ruthenium carbene species formed by reaction of ruthenium(II) with ethyl diazoacetate, by analogy to previous work in which it was demonstrated that osmium(II) porphyrin carbenes are catalytically active.[5] Actually, when the reaction is monitored at room temperature, a $Ru^{II}$ carbene complex is detected by $^1$H NMR spectroscopy when Ru(TMP)(CO) is used as the catalyst. As expected,[8] the α-carbon proton appears in the proton spectrum at δ 13.23.¶ The presence of both the carbene ligand and the carbonyl group coordinated to the ruthenium has been confirmed, by IR ($\nu_{CO}$ = 1941 $cm^{-1}$) after isolation of the complex at the end of the reaction, when Ru(TMP)(CO) is used as catalyst. Such a

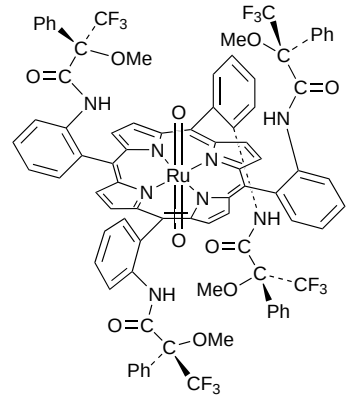



**Fig. 1**

carbene is also observed with ethyl diazoacetate in the presence of the optically active dioxoruthenium(VI) picket-fence complex and a large excess of the alkene, but is not detectable when the porphyrin is the TPP.

In conclusion, the ruthenium porphyrin compounds described here, which are more easily handed than their air-sensitive iron(II) porphyrin analogues, are promising catalysts for cyclopropanation reactions.

We gratefully acknowledge the financial support of the MESR for a grant to E. G.

## Footnotes

* E-mail: gerard.simonneaux@univ-rennes1.fr

† Abbreviations used: TPP = 5,10,15,20-tetraphenylporphyrin dianion; TMP = 5,10,15,20-tetramesitylporphyrin dianion.

‡ Based on ethyl diazoacetate conversion. In a typical experiment, ethyl diazoacetate (1.14 mmol) is slowly added over approximately 4 h to a vigorously stirred solution of the ruthenium catalyst (2.6 μmol) and alkene (1.71 mmol) at room temperature under inert atmosphere. The reaction mixture is then stirred for 1 h and the cyclopropyl ester formation is analysed by GC.

§ Enantiomeric excesses for cyclopropyl esters were determined using the chiral shift reagent tris[3-(heptafluoropropylhydroxymethylene)-(+)-camphorato]europium(III). For the *trans* product, measurement of the optical rotation allowed identification of the absolute configuration as (+)-(1*S*,2*S*).[13]

¶ *Selected spectral data*: $^1$H NMR ($CDCl_3$): δ 13.23 (carbene CH, s, 1 H), 8.28 (Hβ, s, 8 H), 7.25 ($H_m$ s, 4 H), 7.20 ($H_{m'}$, s, 4 H), 2.67 ($CH_2$, q, 2 H, *J* 7.3 Hz), 2.63 (*p*-Me, s, 12 H), 1.94 (*o*-Me, s, 12 H), 1.80 (*o*′-Me, s, 12 H), 0.30 ($CH_3$, t, 3 H, *J* 7.3 Hz)

## References

1 C. J. Suckling, *Angew. Chem., Int. Ed. Engl*., 1988, **27**, 537.
2 H. J. Callot, F. Metz and C. Piechocki, *Tetrahedron*, 1982, **38**, 2365.
3 H. Nishiyama, Y. Itoh, H. Matsumoto, S. B. Park and K. Itoh, *J. Am. Chem. Soc*., 1994, **116**, 2223.
4 S. B. Park, N. Sakata and H. Nishiyama, *Chem. Eur. J*., 1996, **2**, 303.
5 D. A. Smith, D. N. Reynolds and L. K. Woo, *J. Am. Chem. Soc*., 1993, **115**, 2511.
6 J. R. Wolf, C. G. Hamaker, J. P. Djukic, T. Kodadek and L. K. Woo, *J. Am. Chem. Soc*., 1995, **117**, 9194.
7 J. P. Collman, P. J. Brothers, L. McElwee-White, E. Rose and L. J. Wright, *J. Am. Chem. Soc*., 1985, **107**, 4570.
8 J. P. Collman, E. Rose and G. D. Venburg, *J. Chem. Soc., Chem. Commun*., 1993, 934.
9 J. J. Bonnet, S. S. Eaton, G. R. Eaton, R. H. Holm and J. A. Ibers, *J. Am. Chem. Soc*., 1973, **95**, 2141.
10 J. T. Groves and R. Quinn, *Inorg. Chem*., 1984, **23**, 3844.
11 J. L. Maxwell, S. O'Malley, K. C. Brown and T. Kodadek, *Organometallics*, 1992, **11**, 645; S. O'Malley and T. Kodadek, *Organometallics*, 1992, **11**, 2299.
12 P. Le Maux, H. Bahri and G. Simonneaux, *J. Chem. Soc., Chem. Commun*., 1994, 1287.
13 A. Nakamura, A. Konishi, Y. Tatsuno and S. Otsuka, *J. Am. Chem. Soc*., 1978, **100**, 3443.

*Received in Cambridge, UK, 6th January 1997; Com. 7/00098G*

# Mechanism of oxygenation of vitamin K hydroquinone

**Seung Wook Ham* and Ji Sang Yoo**

*Department of Chemistry, Chung-Ang University, Seoul 156-760, Korea*

**When the monoanion of vitamin K hydroquinone is treated with $^{18}O_2$ in THF, the product, vitamin K oxide, carries a full atom of $^{18}O$ at the epoxide oxygen and partial incorporation (34%) of a second atom of $^{18}O$ at the carbonyl oxygen, which is most reasonably ascribed to the dioxetane mechanism.**

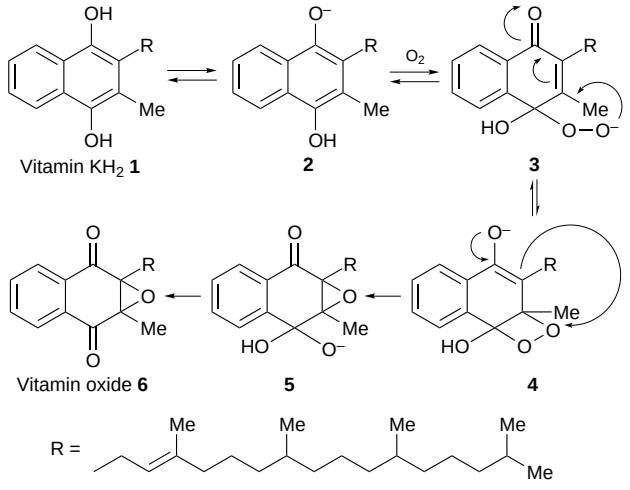
Vitamin K in its hydroquinone form, vitamin $KH_2$, is required as a cofactor for a microsomal enzyme that converts N-terminal glutamates in proteins of the blood clotting cascade to γ-carboxyglutamates.[1] Vitamin $KH_2$ is transformed into vitamin K oxide concurrent with the abstraction of the γ-hydrogen of glutamate, leading to γ-carboxyglutamate.[2] In studies of the mechanism of action of vitamin K, the role of molecular oxygen in the formation of vitamin K oxide was explored.[3,4] Key features of this mechanism are the rearrangement to a strong alkoxide base **5** *via* the dioxetane intermediate **4** (Scheme 1), proposed on the basis of results of a parallel oxygen-16 and oxygen-18 experiment,[3] and the corresponding oxidation of a model system.[4]

The nonenzymic model approach that supports the chemical principle used 2,4-dimethylnaphthol in place of vitamin $KH_2$.[4] However, the most important difference between the model and the vitamin K dependent carboxylase resides in the structure of vitamin K. Vitamin K is a 1,4-dioxygenated naphthalene, whereas the model carries only one oxygen. Since molecular oxygen can add to the 2-position of vitamin $KH_2$ **1** yielding a hydroperoxy anion **7** which might produce vitamin K oxide **6**,[5] it was interesting to compared the *in vivo* oxygenation reaction of vitamin K hydroquinone itself, in the absence of the enzyme.

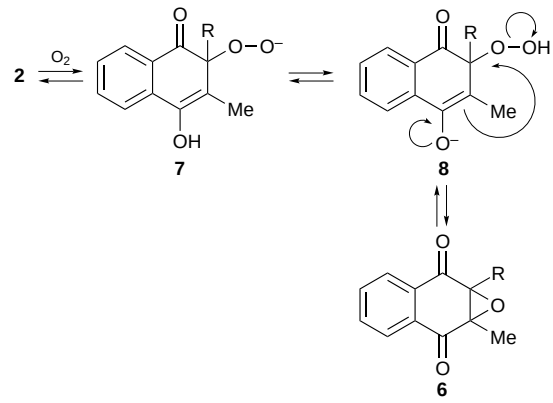
It is well-established that hydroquinones are unstable in air and rapidly oxidize to yield quinone. Indeed, when a chloroform solution of vitamin K hydroquinone **1** was stirred under an oxygen atmosphere, vitamin K was formed within 30 min. By contrast, when the monoanion of vitamin $KH_2$ **2** was stirred under an oxygen atmosphere, vitamin K oxide **6** was isolated in 88% yield (Scheme 2). These spontaneous oxidations in the chemical model system are clearly important for the mechanism of action of vitamin $KH_2$ in biological systems. Therefore, experiments employing oxygen-18 were next used to examine the involvement of the dioxetane intermediate, as shown in Scheme 1, because 2-hydroperoxide **8** could be differentiated from the dioxetane mechanism by $^{18}O$ labelling experiments.

Typical experimental conditions consisted of stirring a THF solution of a monoanion of vitamin $KH_2$ **2** at room temperature with 18-crown-6 and delivering $^{18}O_2$ from a sealed tube to yield vitamin K oxide **6**.† Examination of the mass spectrum reveals that an atom of $^{18}O$ has been incorporated into the vitamin K oxide **6**, since the molecular ion peak moves from *m/z* 466 to 468. The $^{18}O$ label could, in principle, be located at any of the three oxygen positions, but the mass spectrum is most consistent with location of the $^{18}O$ at the epoxide position. Thus, the *m/z* 423 peak is unchanged when comparing the unlabelled with the labelled spectrum; the $M^+ - 43$ peak at *m/z* 423 arises from cleavage of the epoxide and loss of a MeCO fragment.[3] Moreover, the intensity of the peak at *m/z* 470 was 41% of the parent peak at *m/z* 468, which is much larger than would be expected on the basis of natural abundance $^{13}C$.[6] After correcting for natural abundance $^{13}C$, the presence of 36% of a second atom of $^{18}O$ in the vitamin K oxide from the labelling experiment is indicated, and this is most reasonably ascribed to the dioxetane mechanism (Scheme 3).

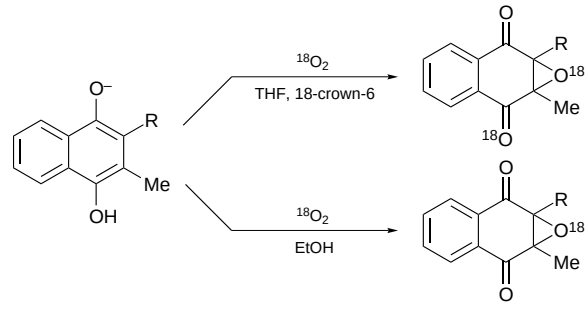
In EtOH, the product of oxygenation of vitamin $KH^-$ **2** under $^{18}O_2$ resulted in a shift of the *m/z* 466 peak to 468, with no increase in the intensity of the $M^+ + 4$ peak. The path leading to




**Scheme 1**




**Scheme 2**




**Scheme 3**

the formation of vitamin K oxide in an aprotic solvent could be different from that in protic solvent. In the oxygenation of the vitamin K anion **2** in EtOH, the 2-peroxy anion intermediate **7** might predominate and might be protonated by EtOH, yielding the hydroperoxide **8**. If the phenolic hydroxy group of peroxide **7** is deprotonated by the resulting ethoxide, and with the assistance of a hydrogen bonding of solvent, the hydroperoxide could yield vitamin K oxide.

This solvent-dependent regioselectivity observed in the oxygenation of the vitamin K anion **2** might be rationalized in terms of the stability of the peroxy anion intermediates **3** and **7**. Since it is known that the potassium ion associates with crown ether more strongly than with protic solvents,[7] the peroxy anion intermediate would be naked. The resulting free peroxy anion **7** at the 2-position might experience electronic repulsion by the carbonyl group, whereas the peroxy anion **3** at the 4-position is stabilized by hydrogen bonding with the *gem*-hydroxy group.[8] therefore, the addition of oxygen using THF with 18-crown-6 might be preferred in the 4-position (Fig. 1).

The peroxy anion intermediate in EtOH seems to undergo stabilization by association with the counter cation $K^+$ and partly also by solvation through hydrogen bonding.[7] In this case, the stabilization of the peroxy anion **7** at the 2-position appears to be due to chelation with the carbonyl group of the intermediate.

The biological transformation of vitamin K oxide **6** appears to be shielded from water by the enzyme or membrane environment.[9] Therefore the chemical formation of vitamin K oxide **6** has parallels in the biological formation. However, another possibility for incorporation of $^{18}O$ into vitamin K oxide **6** would involve label exchange between $^{18}O$ labelled hydroxide and the product in THF, even though formation of hydroxide anion might be unfavourable under aprotic conditions. This path cannot be ruled out at present, and the appropriate control reactions remain to be conducted.

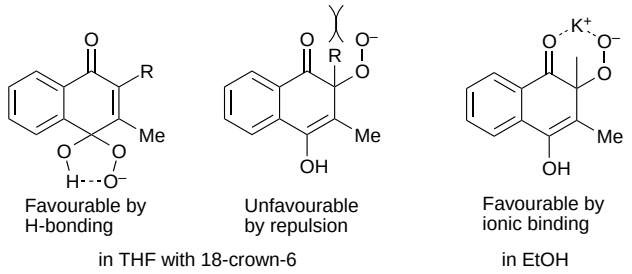



**Fig. 1** Proposed solvent-dependent regioselectivity of peroxide in the oxygenation of the vitamin K hydroquinone monoanion

This research was generously supported by a grant from the Ministry of Education (BSRI-96-3416). The authors also acknowledge partial support from Chung-Ang University.

## Footnotes

* E-mail: swham@cau.ac.kr

† Typical experiment: oxygenation of **2** with $^{18}O_2$. A solution of 142.8 mg (0.316 mmol) of vitamin K hydroquinone **1** in 4 ml of dry THF was added to a suspension of 12.6 mg (0.315 mmol) of potassium hydride and 1 ml of dry THF *via* a double tipped needle and stirred for 10 min under an atmosphere of argon at room temperature. 18-Crown-6 (60.0 mg, 0.227 mmol) was then added. $^{18}O_2$ [96% enriched in 18-oxygen (ICON), 100 ml] was added through a break seal. After stirring for 20 min at room temperature, the reaction mixture was quenched with 5 ml of water and extracted with diethyl ether (3 × 10 ml). The combined diethyl ether layers were washed with saturated aqueous potassium chloride, dried over $MgSO_4$ and concentrated to yield 101.8 mg of the crude product as a yellow oil, which was checked by GC–MS (Hewlett-Packard 5890 Series II gas chromatograph and a Hewlett-Packard 5970 mass selective detector).

## References

1 A. F. Wagner and K. Folkers, *Vitamins and Coenzymes*, Interscience, New York, 1964, pp. 407–434.
2 J. W. Suttie, *Biofactors*, 1988, **1**, 55; J. W. Suttie, *Annu. Rev. Biochem.*, 1985, **54**, 459; R. E. Olson, *Annu. Rev. Nutr.*, 1984, **4**, 281; P. Dowd, R. Hershline, S. W. Ham and S. Naganathan, *Science*, 1995, **269**, 1684.
3 P. Dowd, S. W. Ham and S. J. Geibs, *J. Am. Chem. Soc.*, 1991, **113**, 7734; P. Dowd, S. W. Ham and R. Hershline, *J. Am. Chem. Soc.*, 1992, **114**, 7613.
4 S. W. Ham and P. Dowd, *J. Am. Chem. Soc.*, 1990, **112**, 1660.
5 K. Alder, F. H. Flock and H. Baumling, *Chem. Ber.*, 1960, **93**, 1896. Compound **8** is also proposed as a vitamin K intermediate for the base-promoted pathway; J. W. Suttie, A. E. Larson, L. M. Canfield and T. L. Carlisle, *Fed. Proc. Am. Soc. Exp. Biol.*, 1978, **37**, 2605.
6 The calculated ratio of the *m/z* 468, 469, 470 peaks is 100: 34.4: 6.3: J. H. Beynon, *Mass Spectrometry and its Applications to Organic Chemistry*, Elsevier, Amsterdam, 1960, p. 524.
7 R. Alexander and A. J. Parker, *J. Am. Chem. Soc.*, 1967, **89**, 5549.
8 A. Nishinaga, T. Itahara, T. Shimizu and T. Matsuura, *J. Am. Chem. Soc.*, 1978, **100**, 1820.
9 J. J. Mctigue and J. W. Suttie, *J. Biol. Chem.*, 1983, **258**, 12 129; D. A. Anton and P. A. Friedman, *J. Biol. Chem.*, 1983, **258**, 14 084.

*Received in Cambridge, UK, 17th February 1997; Com. 7/01091E*

# Methanol dramatically enhances serine protease activity under anhydrous conditions

**Gillian A. Hutcheon,[a] Marie Claire Parker,[b] Allan James[a] and Barry D. Moore*[a]**

[a] *Department of Pure and Applied Chemistry, University of Strathclyde, Thomas Graham Building, 295 Cathedral Street, Glasgow, UK G1 1XL*

[b] *Edinburgh Centre for Protein Technology, University of Edinburgh, Kings Building, West Mains Road, Edinburgh, UK EH9 3JJ*

**The catalytic activity of rigorously dried lyophilised subtilisin Carlsberg and α-chymotrypsin in anhydrous solvents is enhanced dramatically on addition of dry methanol, while ethanol and propanol produce no effect.**

Enzymes are being increasingly used for catalysis of organic reactions in non-aqueous media. Hence, there is considerable interest in understanding the factors affecting their activity, selectivity, and stability under these conditions.[1] The catalytic activity of lyophilised enzyme powders suspended in organic solvents can often be increased substantially if the protein is hydrated above a critical level.[2] The precise reasons for this are not known but it has been proposed that water acts as a 'molecular lubricant' and enhances the conformational flexibility of the protein.[2] Certain solvents or 'additives' including dimethyl sulfoxide, formamide and ethylene glycol have been reported to increase enzyme activity when added into the organic media along with small amounts of water.[3,4] However, the effects of additives on rigorously dried enzyme preparations, where possible activation by water has been eliminated, have not been well explored. Here we show, for the first time, that methanol is a remarkably efficient promoter of both subtilisin Carlsberg and α-chymotrypsin activity under anhydrous conditions. This effect could be of considerable synthetic utility in enzyme catalysed reactions where the build up of hydrolytic side-products needs to be avoided.

The starting point for this work was a study of subtilisin Carlsberg activity at low hydration levels. Rate comparisons were made between the enzyme catalysed transesterification of acetylphenylalanine ethyl ester (APEE) by propanol or methanol, in hexane, at various known hydration levels.† Hydration was controlled by equilibrating the system with saturated salt solutions of known thermodynamic water activity, $a_w$.[5] Anhydrous conditions were obtained by lyophilisation of the protein followed by repeated dehydration with freshly activated molecular sieves and the use of completely dry solvents.‡ This treatment appears to leave only internally bound water molecules associated with the protein.[6]

As anticipated, under anhydrous conditions the transesterification rate with propanol was low but measurable (see Table 1). Initial hydration of the system to $a_w$ = 0.11 led to an unexpected small drop in catalytic activity but on further hydration to $a_w$ = 0.43 there was a slight increase in enzyme activity as reported previously.[2,7] In sharp contrast, using methanol as the nucleophile, even rigorously dried enzyme exhibited good catalytic activity and higher transesterification rates than with propanol were observed at all hydrations levels, with a 65-fold difference at $a_w$ = 0.43. These remarkable enhancements for methanol compared to propanol were also observed when the ester concentration was varied from 5–15 mM.

Since it was possible the differences arose simply because deacylation was the rate limiting step under these conditions§ a competitive nucleophile experiment was carried out under anhydrous conditions. Fig. 1(*a*) shows the time course of a reaction mixture which initially contained anhydrous subtilisin, APEE and propanol in dry hexane. For the first 50 min very little reaction was observed whereupon 5 μl of dry methanol was added. Immediately rapid formation of both the methyl and propyl esters commenced. A similar effect was seen with another serine protease, α-chymotrypsin, Fig. 1(*b*). The observation of a dramatic increase in the rate of formation of the

**Table 1** Effect of water activity on initial rates of transesterification

| | Initial rate[b]/nmol min$^{-1}$ mg$^{-1}$ | |
|---|---|---|
| Water activity | 0.5 M Methanol | 0.5 M Propanol |
| Anhydrous[a] | 24.5 | 1.5 |
| 0.11 | 47.8 | 1.4 |
| 0.22 | 64.4 | 1.1 |
| 0.43 | 102.2 | 1.6 |

[a] Enzyme dried over regenerated molecular seives.[6] [b] Reaction conditions: 10 mM APEE, 0.5 M alcohol and 1 mg ml$^{-1}$ enzyme in hexane.

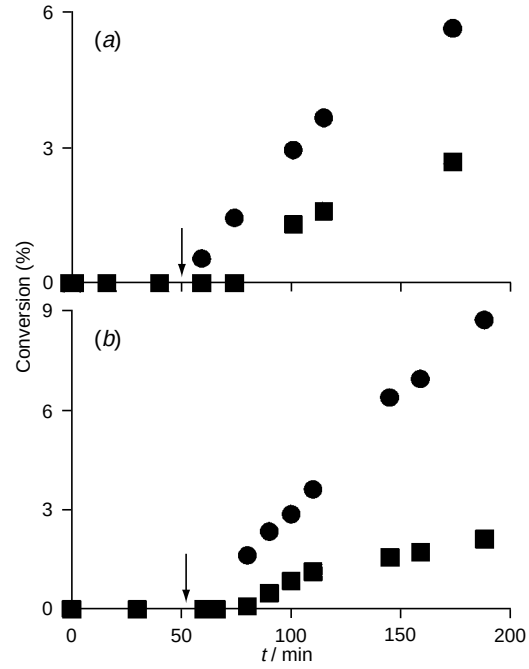



**Fig. 1** Reaction course for the enzyme catalysed transesterification of APEE to the propyl ester (■) and methyl ester (●). The reaction mixture contained 5 mM APEE, 268 mM propanol, 1 mg lyophilised anhydrous enzyme and 1 ml of dry hexane (< 0.005% water). After 50 min (↓) 5 μl of anhydrous methanol, (125 mM) was added. The reaction mixture was shaken at 200 rpm at 20 °C and analysis was by gas chromatography. HPLC analysis of the reaction mixture showed that none of the hydrolysis product, *N*-acetyl-L-phenylalanine, was formed under these conditions. (*a*) Catalysed by subtilisin Carlsberg, (*b*) catalysed by α-chymotrypsin.

propyl ester shows that methanol cannot just be a better nucleophile since then only the rate of methyl ester production would be affected.¶ Rather the results suggest that solvation of the protein by methanol stimulates an increase in the intrinsic catalytic activity of both subtilisin Carlsberg and α-chymotrypsin under anhydrous conditions.‖ Since these serine proteases have very different secondary and tertiary structures similar effects might be expected with other related enzymes.

To eliminate the possibility that trace impurities (*e.g.* drying agent) or changes in particle size were responsible for the activation, a lyophilised powder sample of subtilisin Carlsberg was equilibrated with methanol through the vapour phase in the presence of molecular sieves. Gravimetric measurements showed that this procedure resulted in adsorption of low levels of the solvent onto the protein. Following resuspension in hexane, enzyme activity was assayed using APEE and 0.5 M propanol. Again a transesterification rate enhancement was observed compared to an untreated sample and with no lag period.** However, here the main reaction product was found to be the propyl ester. This suggests that the low levels of methanol adsorbed onto the enzyme were sufficient to activate it but the resultant concentration of methanol in the reaction mixture was not high enough for it to compete as a nucleophile. Importantly equilibration of subtilisin with ethanol or propanol vapour under identical experimental conditions gave absolutely no rate enhancement nor did the addition of ethanol to the reaction mixture. Thus, the effect of methanol is very specific and the activation mechanism cannot be simply ascribed to a hydrogen bonding phenomena.

Further study of the rates in Table 1 reveal an interesting effect when methanol and water were added to the enzyme together. With dry subtilisin and 0.5 M methanol the transesterification rate is 24.5 nmol $min^{-1}$ $mg^{-1}$ while with enzyme equilibrated to $a_w$ = 0.43 and using 0.5 M propanol the rate is 1.6 nmol $min^{-1}$ $mg^{-1}$. If we now compare the rate obtained at $a_w$ = 0.43 and 0.5 M methanol, 102.2 nmol $min^{-1}$ $mg^{-1}$, we see that it is closer to the product than the sum of the individual rates. This observation is not consistent with a single activation mechanism since then the contributions would be expected to be approximately additive. Instead it points to a cooperative effect whereby methanol and water activate the enzyme *via* two or more different processes. As a consequence the ubiquitous 'molecular lubrication model' will need to be revised and we are currently working on this problem.

Finally we sought to show that methanol could activate a serine protease without simultaneously acting as a substrate. Hence, a series of active site titrations were carried out on subtilisin in hexane using the irreversible inhibitor PMSF. Anhydrous enzyme was equilibrated for 3 h in hexane in the presence or absence of either methanol or propanol and with and without PMSF.†† Since in the inhibition process, no deacylation occurs, methanol will not be directly involved in the reaction scheme. Following equilibration the enzyme samples were repeatedly resuspended in pure dry hexane (which removed the PMSF if present) and then dried. The resultant enzymic activities were measured by monitoring transesterification of APEE with methanol in hexane‡‡ and are shown in Table 2. It can be seen that enzyme equilibrated with PMSF in either hexane or hexane–propanol gave very similar activities to the control samples showing only a small percentage of active sites had been titrated. This is consistent with the low activity of the enzyme under these condition (see Table 1). In comparison the presence of methanol during the PMSF equilibration resulted in significant inhibition of the enzyme preparation.§§ This is exactly what would be expected from the transesterification measurements and provides conclusive evidence that methanol activates anhydrous serine proteases *via* a solvation process.

**Table 2** Effect of PMSF titration on subtilisin Carlsberg activity in hexane

| | Initial rate[a]/ nmol $min^{-1}$ $mg^{-1}$ | | |
|---|---|---|---|
| Alcohol | No PMSF[b] | PMSF[b] | Inhibition (%) |
| None | 22.5 | 21.3 | 5.4 |
| Propanol | 11.5 | 10.5 | 13 |
| Methanol | 42 | 4.5 | 89 |

[a] Reaction conditions: 10 mM APEE, 0.5 M methanol and 1 mg $ml^{-1}$ enzyme in hexane. [b] The enzyme was shaken with or without 10 mM PMSF and 0.5 M alcohol in hexane for 3 h, washed with hexane to remove unbound PMSF and dried over molecular sieves prior to rate analysis.

## Footnotes

* E-mail: b.d.moore@strath.ac.uk

† The variation in amount of enzyme bound water as a function of water activity in nonpolar solvents has been measured previously (ref. 8).

‡ Residual water levels in the dried solvents were measured *via* Karl–Fischer titration and found to be hexane < 0.005%, methanol 0.009%, propanol 0.01%.

§ The nucleophilic specificity of methanol relative to propanol has been shown to be 4.61 for this subtilisin catalysed reaction in hexane at $a_w$ = 0.59.[9]

¶ The argument that the methyl ester product may be more reactive is not valid as the acyl intermediate will be identical whichever ester reacts with the enzyme and hence back reaction of the methyl ester cannot lead to an overall increase in rate.

‖ $^2H$ NMR difference measurements in hexane showed 50 deuterated methanol molecules bound per subtilisin molecule at a methanol concentration of 3 mM.

** Transesterification rates were; untreated enzyme, 1 nmol $min^{-1}$ $mg^{-1}$, enzyme equilibrated with propanol, 1 nmol $min^{-1}$ $mg^{-1}$, enzyme equilibrated with methanol, 6.8 nmol $min^{-1}$ $mg^{-1}$.

†† PMSF is inert towards reaction with dry alcohols over the period employed (ref. 10).

‡‡ The exact conditions used for the assay will not affect the findings since it is the remaining activity following titration which is being measured. The assay used was convenient because of the known high activity of dry subtilisin in the presence of methanol.

§§ The increased activity of the control sample in the presence of methanol is reproducible and under study.

## References

1 *Enzymatic Reactions in Organic Media*, ed. A. P. M. Koskinen and A. M. Klibanov, Blackie Academic and Professional, Glasgow, 1996 and references cited therein.
2 A. Zaks and A. M. Klibanov, *J. Biol. Chem.*, 1988, **263**, 8017.
3 M. Reslow, P. Adlercreutz and B. Mattiasson, *Biocatalysis*, 1992, **6**, 307.
4 Ö. Almarsson and A. M. Klibanov, *Biotechnol. Bioeng.*, 1996, **49**, 87.
5 P. J. Halling, *Biochim. Biophys. Acta*, 1990, **1040**, 225.
6 M. Dolman, P. J. Halling, B. D. Moore and S. Waldron, *Biopolymers*, 1997, **41**, 313–321.
7 M. C. Parker, B. D. Moore and A. J. Blacker, *Biocatalysis*, 1994, **10**, 269.
8 M. C. Parker, B. D. Moore and A. J. Blacker, *Biotechnol. Bioeng.*, 1995, **46**, 452.
9 A. K. Chaudhary, S. V. Kamat, E. J. Beckman, D. Nurok, R. M. Kleyle, P. Hajdu and A. J. Russell, *J. Am. Chem. Soc.*, 1996, **118**, 12 891.
10 G. T. Jame, *Anal. Biochem.*, 1978, **86**, 574.

*Received in Liverpool, UK, 18th February 1997; Com. 7/01162H*

# Asymmetric Diels–Alder polymerization using a chirally modified Lewis acid catalyst

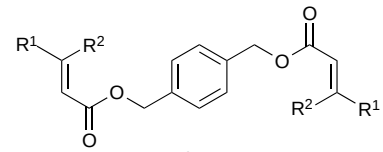
**Shinichi Itsuno,* Shoichi Tada and Koichi Ito**

*Department of Materials Science, Toyohashi University of Technology, Tempaku-cho, Toyohashi 441, Japan*

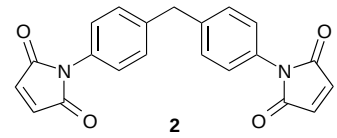
**The asymmetric Diels–Alder reaction between bisdiene and bisdienophile monomers occurs in the presence of a chirally modified Lewis acid catalyst to give optically active polymers.**

Synthesis of optically active polymers has attracted a great deal of interest and a large number of papers on asymmetric polymerization have been published.[1] An important contribution in this area is the preparation of such polymers having macromolecular asymmetry that originates from the helical structure; these include the polymerization of methacrylates,[2] chloral,[3] isocyanides[4–6] and isocyanates.[7] On the other hand, in the recent remarkable development of catalytic asymmetric synthesis, many useful reactions have been proposed for C–C bond formation with induction of chirality. However, there are only a few reports on asymmetric polymerization based on such enantioselective C–C bond formations using chiral catalysts. For example, some successful asymmetric alternating copolymerizations of α-olefins with carbon monoxide have been reported only recently.[8,9] Of the excellent asymmetric transformations developed, the enantioselective Diels–Alder reaction is one of the most important C–C bond formation reactions to create a unique chiral cyclic structure. Indeed, recent extensive studies on designing chiral Lewis acids based on boron, aluminium and titanium led to fruitful results in the control of the absolute stereochemistry of various pericyclic reactions, particularly Diels–Alder reactions producing various enantiopure cyclic adducts, key starting materials for synthesis of complex optically active compounds.[10] This impressive stereoselectivity of chiral Lewis acid catalysts in Diels–Alder reactions presents unprecedented opportunities for the molecular design of polymers that are difficult to prepare with other polymerization methods. Asymmetric, Lewis acid catalysed, Diels–Alder polymerization should provide a novel strategy for the synthesis of optically active polymers whose chirality derives from configurational main-chain stereochemistry. Although polymer synthesis *via* repetitive Diels–Alder reactions is well known for the preparation of thermostable polyimides and conjugated polymers with ladder structures,[11–15] to the best of our knowledge, a chiral polymer has not been synthesized by asymmetric Diels–Alder polymerization. Here we report the asymmetric Diels–Alder polymerization between bisdiene and bisdienophile monomers in the presence of a chirally modified Lewis acid catalyst.

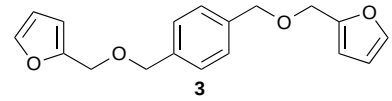
We designed several bifunctional monomers. α,β-Unsaturated esters are well known to be important dienophiles in Diels–Alder reactions. Bisdienophile monomers **1** were thus easily prepared from α,α′-dichloro-*p*-xylene and the appropriate carboxylic acids such as acrylic acid **1a**, monomethyl fumarate **1b** and monomethyl maleate **1c**. *N*-Phenylmaleimide is another reactive dienophile. Useful bisdienophile, 1,1′-(methylenedi-4,1-phenylene)bismaleimide **2** is commercially available, and has often been used as a Diels–Alder monomer.[16,17] Since furyl and butadienyl groups are well known in Diels–Alder chemistry, we designed bisdiene monomers having these structures. Bisdiene **3** and **4a** were prepared from α,α′-dichloro-*p*-xylene and furfuryl alcohol and 3-methylenepent-4-enol,† respectively. The monomer **4b** was also easily prepared by Ni- catalysed Grignard coupling[18] of the bis-Grignard reagent from 1,4-dibromobenzene with chloroprene. Monomer **4a** contains a flexible methylene chain, compared to the relatively rigid structure available in **4b**, in which the butadienyl group links directly to the benzene ring.



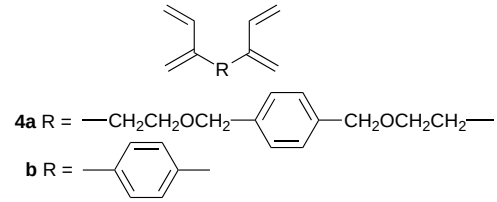
**1a** $R^1 = R^2 = H$
**b** $R^1 = CO_2Me$, $R^2 = H$
**c** $R^1 = H$, $R^2 = CO_2Me$



**2**



**3**



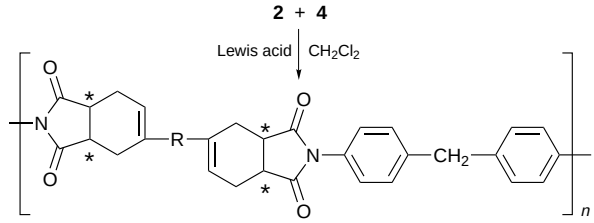
**4a** R = $-CH_2CH_2OCH_2-C_6H_4-CH_2OCH_2CH_2-$
**b** R = $-C_6H_4-$

First, we tried to polymerize the bisdienophile **1** with bisdiene monomers. However, we found that the reactivity of **1** is not sufficient to obtain chiral polymers in the presence of Lewis acid catalyst at room temperature. On the other hand, although no reaction between bismaleimide **2** and bisdiene **3** occurred at room temperature in the absence of catalyst, added diethylaluminium chloride ($Et_2AlCl$) as Lewis acid interacted with carbonyl oxygen of **2** and the rate of the reaction with **3** was enhanced considerably to give the Diels–Alder polymer smoothly with high molecular weight (Table 1, run 1). Since enantioselective Diels–Alder reactions have been extensively studied by using chiral metal complexes,[10,19,20] and high enantioselectivities were obtained by using chiral aluminium chloride generated *in situ* from $Me_3Al$ or $Et_2AlCl$ with chiral diols[21,22] and bis(sulfonamide),[23] we first chose chiral aluminum complex **6** as a catalyst for the asymmetric Diels–Alder polymerization of these monomers. The obtained polymer showed optical activity as shown in Table 1 (run 2). The butadienyl group of **4** also reacted with **2** in the presence of a chiral Lewis acid catalyst to afford optically active polymers in quantitative yield (Scheme 1). Asymmetric polymerization of **4a** and **2** with a chiral Lewis acid gave optically active polymer **5a** having somewhat lower molecular weight. The higher molar optical rotation ($[\Phi]_D$ +94) for the polymer from **4a** was

**Table 1** Asymmetric Diels–Alder polymerization between bisdienophile **2** and bisdiene monomers[a]

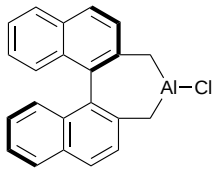
| Run | Lewis acid | Bisdiene monomer | Polymer | | | | |
|---|---|---|---|---|---|---|---|
| | | | Yield (%)[b] | $M_n$[c] | $M_w/M_n$[c] | $[\Phi]_D$[d] | $[\Phi]_{435}$[d] |
| 1 | $Et_2AlCl$ | **3** | 46 | 15 000 | 1.33 | — | — |
| 2 | **6** | **3** | 79 | 12 000 | 2.19 | −12[e] | |
| 3 | **6** | **4a** | 99 | 4 800 | 1.36 | 17 | |
| 4 | **6** | **4b**[f] | 99 | 9 800 | 1.51 | 243 | 578 |
| 5 | **6** | **4b**[g] | 99 | 10 800 | 1.90 | 114 | 281 |
| 6 | **7** | **4a** | 99 | 5 800 | 1.26 | −35 | |
| 7 | **7** | **4b**[h] | 99 | 12 100 | 1.85 | −14 | |
| 8 | **8** | **4a** | 99 | 4 500 | 1.28 | 94 | |
| 9 | **8** | **4b**[i] | 99 | 13 200 | 1.74 | 7.6 | |

[a] Reaction was carried out with bisdienophile **2** (1 equiv.) and bisdiene (1 equiv.) in the presence of 20 mol% of Lewis acid catalyst in $CH_2Cl_2$ at room temp. for 24 h, unless otherwise noted. [b] Isolated yield. [c] Determined by GPC measurement with polystyrene standard. [d] Measured in $CHCl_3$, *c* 1.0. [e] Measured in DMF, *c* 1.0. [f] At −30 °C, 6 h. [g] At room temp., 6 h. [h] At −78 °C, 6 h + room temp., 6 h. [i] At room temp., 6 h.

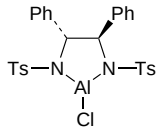



**Scheme 1**

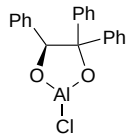
attained when the catalyst **8** was used (Table 1, run 8). Further, use of sterically more rigid bisdiene monomer **4b** having reactive phenylbutadiene units has proved to exhibit excellent polymerization behavior. The corresponding chiral polymers **5b** were obtained with relatively higher molar optical rotations up to $[\Phi]_{435}$ +578 (Table 1, run 4) by using (*R*)-1,1′-binaphth-2-ol derived Lewis acid catalyst **6**. This is the first example of synthesis of the chiral polymer having a high optical rotation value using asymmetric Diels–Alder polymerization.‡




**6**




**7**




**8**

Another feature of this polymerization is that optically active prepolymers with reactive end groups accessible for further reactions can be readily obtained. Nonstoichiometric Diels–Alder polymerization with a slight excess of one monomer should provide the possibility to synthesize such polymers. For example, when a small excess of monomer **2** was polymerized with **3**, a polymer having reactive maleic double bond end groups was obtained, which acts as a good Michael acceptor for further modification of the chiral polymer.

This research was supported by a Grant-in-Aid for Scientific Research in Priority Areas (No. 08246227) from the ministry of Education, Science, Sports and Culture, Japan, and The Tatematsu Foundation.

## Footnotes

* Email: itsuno@tutms.tut.ac.jp

† This compound was successfully prepared by a new method using the ene reaction of trioxane with isoprene in the presence of $Et_2AlCl$ in $CH_2Cl_2$.

‡ All polymerizations were performed in $CH_2Cl_2$; replacing the solvent with $CHCl_3$ or THF gave the polymers with only low optical rotations ($[\Phi]_D$ +30 and −5.4, respectively).

## References

1 Y. Okamoto and T. Nakano, *Chem. Rev.*, 1994, **94**, 349.
2 Y. Okamoto and E. Yashima, *Prog. Polym. Sci.*, 1990, 263.
3 O. Vogl and G. D. Jaycox, *Chemtech*, 1986, 698.
4 T. J. Deming and B. M. Novak, *J. Am. Chem. Soc.*, 1992, **114**, 7926.
5 F. Takei, K. Yanai, K. Onitsuka and S. Takahashi, *Angew. Chem., Int. Ed. Engl.*, 1996, **35**, 1554.
6 Y. Ito, T. Ohara, R. Shima and M. Suginome, *J. Am. Chem. Soc.*, 1996, **118**, 9188.
7 M. M. Green, M. P. Reidy, R. J. Johnson, G. Darling, D. J. O′Leary and G. Willson, *J. Am. Chem. Soc.*, 1989, **111**, 6452.
8 K. Nozaki, N. Sato and H. Takaya, *J. Am. Chem. Soc.*, 1995, **117**, 9911.
9 M. Brookhart, M. I. Wagner, G. G. A. Balavoine and H. A. Haddou, *J. Am. Chem. Soc.*, 1994, **116**, 3641.
10 K. Narasaka, *Synthesis*, 1991, 1.
11 P. E. Cassidy, *Thermally Stable Polymers*, Dekker, New York, 1980, p. 103.
12 P. R. Ashton, G. R. Brown, N. S. Isaacs, D. Giuffrida, F. H. Kohnke, J. P. Mathias, A. M. Z. Slawin, D. R. Smith, J. F. Stoddart and D. J. Williams, *J. Am. Chem. Soc.*, 1992, **114**, 6330.
13 J. K. Stille and L. Plummer, *J. Org. Chem.*, 1961, **26**, 4026.
14 A. -D. Schlüter, M. Löffler and V. Enkelmann, *Nature*, 1994, **368**, 831.
15 S. Wegner and K. Müllen, *Macromolecules*, 1993, **26**, 3037.
16 N. Kuramoto, K. Hayashi and K. Nagai, *J. Polym. Sci.: Part A, Polym. Chem.*, 1994, **32**, 2501.
17 G. Alhakimi, E. Klemm and H. Görls, *J. Polym. Sci.: Part A, Polym. Chem.*, 1995, **33**, 1133.
18 K. Tamao, K. Sumitani, Y. Kiso, M. Zembayashi, A. Fujioka, S. Kodama, I. Nakajima, A. Minato and M. Kumada, *Bull. Chem. Soc. Jpn.*, 1976, **49**, 1958.
19 Y. Motoyama, M. Terada and K. Mikami, *Synlett*, 1995, 967.
20 K. Maruoka, N. Murase and H. Yamamoto, *J. Org. Chem.*, 1993, **58**, 2983.
21 J. Bao and W. D. Wulff, *J. Am. Chem. Soc.*, 1993, **115**, 3814.
22 K. Maruoka, T. Itoh, T. Shirasaka and H. Yamamoto, *J. Am. Chem. Soc.*, 1988, **110**, 310.
23 E. J. Corey and M. A. Letaric, *J. Am. Chem. Soc.*, 1995, **117**, 9616.

*Received in Cambridge, UK, 7th March 1997; Com. 7/01613A*

# Solid-state and solution complexation of cobalt(III) sepulchrate by a water-soluble calix[6]arene host

**René Castro,*[a] Luis A. Godínez,[a] Cecil M. Criss,[a] Simon G. Bott[b] and Angel E. Kaifer[a]**

[a] *The Department of Chemistry, University of Miami, Coral Gables, FL 33124-0431, USA*
[b] *The Department of Chemistry, University of North Texas, Denton, TX 76203, USA*

**A calix[6]arene hexasulfonate host forms a stable 1:1 complex with cobalt(III) sepulchrate in aqueous media while a 2:1 guest:host stoichiometry is observed in the solid state.**

Calixarenes are versatile hosts for inclusion complexation due to their flexible cavities, availability in various sizes, and rugged skeletons amenable to diverse functionalization.[1] Various calixarene complexes involving metal ions[2] and organic molecules[3] have been reported. We have also recently reported on ferrocene and viologen complexes involving calixarene hosts.[4]

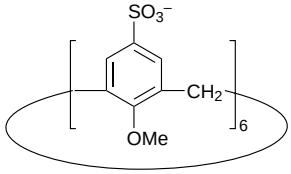
In 1977 Sargeson and coworkers reported the facile preparation of the caged metal-ion complex cobalt(III) sepulchrate ($\mathbf{2}^{3+}$).[5a] The unusual stabilization of certain metal-ion oxidation states as well as other structural and electronic properties exhibited by this and related complexes prompted numerous investigations.[5] Several prominent examples are the incorporation of sepulchrate complexes in photochemical water-splitting systems,[6a–c] the attachment of sepulchrates to protein backbones to study electron-transfer reactions,[6d] and the recent incorporation of sepulchrate in an electrochemical sensor for $H_2$ and $H_2S$.[6e] The literature also contains several reports of ion-pairing interactions involving sepulchrates and relatively simple anions, but the corresponding association constants are rather low (*e.g.* $K$ = 100 dm$^3$ mol$^{-1}$ for $SO_4^{2-}$ at $I$ = 0.01).[7] Here we report on the complexation of cobalt sepulchrate by sulfonated calix[6]arene host $\mathbf{1}^{6-}$.† While second-sphere coordination of metal-ion complexes is a well known phenomenon,[8] to the best of our knowledge, this is the first report on the complexation of metal-ion sepulchrates.

The strong interaction between $\mathbf{1}^{6-}$ and $\mathbf{2}^{3+}$ was immediately apparent upon preparing a dilute solution of the two compounds in $D_2O$ for NMR analysis. A precipitate appeared which was assumed to be a complex since both compounds are extremely water soluble. Elemental analysis of the dried precipitate revealed a 2:1 stoichiometry ($\mathbf{2}^{3+}:\mathbf{1}^{6-}$) with no counter ions. This ratio makes the complex electrically neutral, thus explaining its low solubility in water. Since the interaction seemed to be largely driven by electrostatics, further studies were conducted in aqueous 0.2 M NaCl in order to be able to use larger concentrations of the compounds without precipitation. A $^1$H NMR spectroscopic binding study performed in $D_2O$ (0.2 M NaCl) gave a binding constant of 1 600 dm$^3$ mol$^{-1}$. This is one of the stronger binding constants reported for a calixarene complex, the strongest ones being around $10^4$ dm$^3$ mol$^{-1}$,[3] and the value would surely be much higher in pure water where there is no electrolyte to shield the charges from each other. The NMR chemical shift data perfectly fit a 1:1 binding model and, therefore, the interaction in high ionic strength media seems to be bimolecular. The direction (to higher field) and magnitude of the complexation induced shifts on the sepulchrate proton resonances ($\Delta\delta_{comp}$ −0.45 ppm) both suggest that the sepulchrate is at least partially included by the anionic calixarene host.

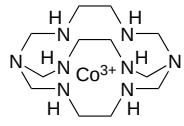
Solution flow calorimetry (in 0.2 M NaCl) was used to corroborate the NMR binding results and to gain insight into the thermodynamic parameters involved.‡ The resulting calorimetric data gave values of −1.0 kcal mol$^{-1}$ (1 cal = 4.184 J) for $\Delta H°$ and 3.4 kcal mol$^{-1}$ for $T\Delta S°$ at 298 K. This translates into a $\Delta G°$ of −4.4 kcal mol$^{-1}$ or $K$ = 1 770 dm$^3$ mol$^{-1}$ (again the data perfectly fit a 1:1 complex stoichiometry). Not only is this in excellent agreement with our NMR data, but it points to a large entropic driving force for complexation. Even though there is a large favourable enthalpic change in bringing two such highly charged species together, this is cancelled by the unfavourable enthalpy associated with unsheathing them from their solvation spheres. The return of these water molecules to the bulk, however, carried with it a substantially favourable and uncompensated entropic change which drives the complexation process.

Crystals suitable for X-ray crystallographic analysis grew from the flow calorimetry effluent solution that was left standing for a few weeks. The unit cell consists of four sepulchrate and two calixarene units along with several water molecules but no counter ions (see Fig. 1).§ This confirms the electroneutral termolecular stoichiometry of the complex in the solid state suggested by the elemental analysis. Interestingly, the calixarene molecules exhibit a configuration similar to that reported for the solid state structure of the pure unmethylated calixarene analogue even though the intramolecular hydrogen bonds involving the partially deprotonated phenolic groups, which are detected in the latter,[2b] are not possible in $\mathbf{1}^{6-}$. To our knowledge, this is the first reported crystal structure for calixarene $\mathbf{1}^{6-}$.

The crystal structure shows the calixarene to be in a rather disorganized conformation with four of the sulfonate groups pointing outwards from the central cavity, one pointing up and the other down. The closest atomic distances between the two ionic components are between the sepulchrate's secondary amine protons and the sulfonate oxygen atoms (dotted lines) on the calixarene. Since hydrogen bonding and electrostatic interactions would be much stronger with the sulfonate groups than with the methoxy groups, these, along with the lack of inclusion complexation, seem to be the main organizing features dominating the structural organization of the solid state lattice. Indeed, the lattice seems to be a net of these ionic/hydrogen bonds with each calixarene bonded to two in-plane sepulchrates through single hydrogen bonds and to one sepulchrate above or below through a bifurcated hydrogen bond. No inclusion complexation is apparent from the crystal structure suggesting the interaction to be mainly ionic in nature. While this does not rule out the possibility of inclusion complexation in solution, it poses interesting questions about




$\mathbf{1}^{6-}$




$\mathbf{2}^{3+}$

the nature of the stable 1 : 1 complex detected in 0.2 M NaCl. The 2 : 1 complex stoichiometry could become prevalent in low ionic strength media, at high concentration, or in a crystal lattice due to packing forces, thus explaining our solid-state data.

The role of the ionic strength of the solvent in mitigating complexation was explored by titrating a 2 : 1 mixture of $\mathbf{1}^{6-}$ and $\mathbf{2}^{3+}$ (0.33 mM $\mathbf{2}^{3+}$, 0.05 M NaCl) in an NMR tube with a 5 M NaCl solution containing the same 2 : 1 mixture of the two compounds. Fig. 2 shows the chemical shift response of the sepulchrate proton resonances as the ionic strength is changed. That the sepulchrate is totally shielded from the calixarene at high NaCl concentrations is shown by the fact that the sepulchrate's proton resonances reach the same chemical shift that they exhibit in the absence of calixarene, thus further proving that its interaction with $\mathbf{1}^{6-}$ is driven by electrostatic forces.

The authors gratefully acknowledge the support of this research by the NSF (to A. E. K., CHE-9633434). L. A. G. thanks the Universidad Nacional Autónoma de México for a graduate fellowship.

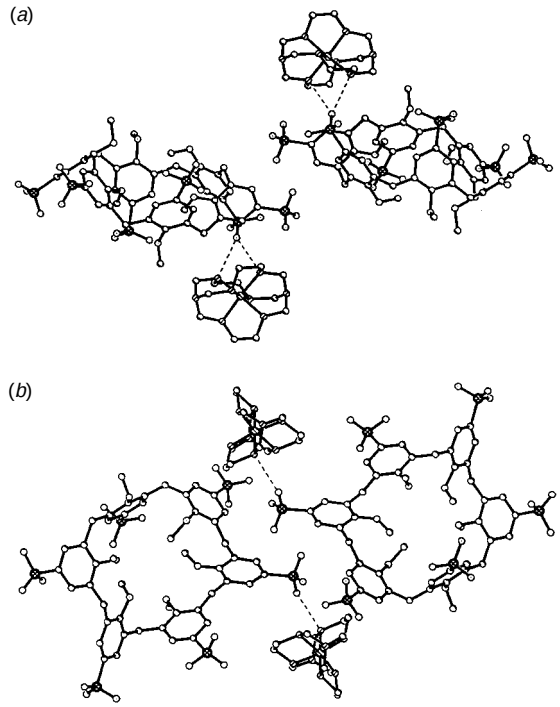



**Fig. 1** X-Ray crystal structure of the unit cell of the $\mathbf{1}^{6-}$–$\mathbf{2}^{3+}$ solid-state complex. (*a*) Edge-on view through the plane of the calix[6]arenes showing the two sepulchrate units above and below the plane, omitting the two in-plane sepulchrates. (*b*) View orthogonal to the plane of the calixarenes showing the two in-plane sepulchrate units, omitting the above and below sepulchrates for clarity. Water molecules were also omitted for clarity.

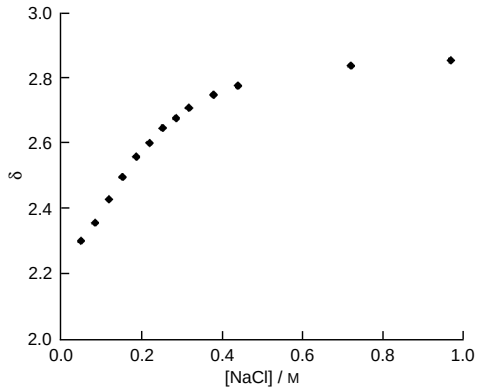



**Fig. 2** Observed $^1$H NMR ($D_2O$) chemical shift of the $-NCH_2CH_2N-$ sepulchrate proton resonance in a 2 : 1 solution of $\mathbf{1}^{6-}$ and $\mathbf{2}^{3+}$ as a function of NaCl concentration

## Footnotes

* E-mail: akaifer@umiami.ir.miami.edu

† $\mathbf{1}^{6-}$ was synthesized according to ref. 3(*d*) and used as its sodium salt; $\mathbf{2}^{3+}$ was synthesized according to ref. 5(*b*) and used as the chloride salt.

‡ Details of the calorimetric experiments were as previously described.[9]

§ *Crystal data*. Enraf-Nonius CAD-4 four-circle diffractometer, Mo-Kα radiation (λ = 0.710 73 Å), graphite monochromator, $T$ = 293 K, empirical absorption correction, direct methods, blocked least-squares refinement, Co and $SO_3$ group anisotropic, H at idealized positions riding on attached atom [$B$ = 1.3$B$(attached)], water molecules refined with partial occupancy based on initial common temperature factor refinement. $C_{72}H_{124.5}Co_2N_{16}O_{35.25}S_6$, $M$ = 2088.63, triclinic, space group $P\bar{1}$, $a$ = 18.182(2), $b$ = 20.730(3), $c$ = 28.982(6) Å, $\alpha$ = 107.45(1), $\beta$ = 105.48(1), $\gamma$ = 90.13(1)°, $U$ = 10002.6(28) Å$^3$, $Z$ = 4, $D_c$ = 1.387 g cm$^{-3}$, μ(Mo-Kα) = 5.33, $2\theta_{max}$ = 44°, ω scan, crystal dimensions *ca*. 0.24 × 0.28 × 0.32 mm, 23 250 unique reflections, $R(R_w)$ = 0.0673 (0.1707) for 8412 reflections with $I > 2\sigma(I)$ or 0.1421 (0.1857) for all data, 13337 variables. Atomic coordinates, bond lengths and angles, and thermal parameters have been deposited at the Cambridge Crystallographic Data Centre (CCDC). See Information for Authors, Issue No. 1. Any request to the CCDC for this material should quote the full literature citation and the reference number 182/427.

## References

1 C. D. Gutsche, in *Calixarenes*, in *Monographs in Supramolecular Chemistry*, ed. J. F. Stoddart, Royal Society of Chemistry, London, 1989; *Calixarenes: A Versatile Class of Macrocyclic Compounds*, ed. V. Böhmer and J. Vicens, Kluwer Academic, Dordrecht, 1991; C. D. Gutsche, *Aldrichim. Acta*, 1995, **28**, 3; V. Böhmer, *Angew. Chem., Int. Ed. Engl.*, 1995, **34**, 713.

2 (*a*) S. Shinkai, H. Koreishi, K. Ueda, T. Arimura and O. Manabe, *J. Am. Chem. Soc.*, 1987, **109**, 6371; (*b*) J. L. Atwood, D. L. Clark, R. K. Juneja, G. W. Orr, K. D. Robinson and R. L. Vincent, *J. Am. Chem. Soc.*, 1992, 7558; (*c*) A. Ikeda and S. Shinkai, *J. Am. Chem. Soc.*, 1994, **116**, 3102 and references cited in ref. 1.

3 (*a*) K. N. Koh, K. Araki, A. Ikeda, H. Otsuka and S. Shinkai, *J. Am. Chem. Soc.*, 1996, **118**, 755; (*b*) J. M. Lehn, R. Meric, J. P. Vigneron, M. Cesario, J. Guilhem, C. Pascard, Z. Asfari and J. Vicens, *Supramol. Chem.*, 1995, **5**, 97; (*c*) S. Shinkai, S. Mori, T. Arimura and O. Manabe, *J. Chem. Soc., Chem. Commun.*, 1987, 238; (*d*) S. Shinkai, S. Mori, H. Koreishi, T. Tsubaki and O. Manabe, *J. Am. Chem. Soc.*, 1986, **108**, 2409 and references cited in ref. 1.

4 L. Zhang, L. A. Godínez, T. Lu, G. W. Gokel and A. E. Kaifer, *Angew. Chem. Int. Ed. Engl.*, 1995, **34**, 235; A. R. Bernardo, T. Lu, E. Córdova, L. Zhang, G. W. Gokel and A. E. Kaifer, *J. Chem. Soc., Chem. Commun.*, 1994, 529; L. Zhang, A. Macías, T. Lu, J. I. Gordon, G. W. Gokel and A. E. Kaifer, *J. Chem. Soc., Chem. Commun.*, 1993, 1017.

5 (*a*) I. I. Creaser, R. J. Geue, J. M. Harrowfield, A. J. Herlt, A. M. Sargeson, M. R. Snow and J. Springborg, *J. Am. Chem. Soc.*, 1977, **99**, 3181; (*b*) I. I. Creaser, R. J. Geue, J. M. Harrowfield, A. J. Herlt, A. M. Sargeson, M. R. Snow and J. Springborg, *J. Am. Chem. Soc.*, 1982, **104**, 6016; (*c*) R. J. Geue, T. W. Hambley, J. M. Harrowfield, A. M. Sargeson and M. R. Snow, *J. Am. Chem. Soc.*, 1984, **106**, 5478; (*d*) A. M. Sargeson, *Pure Appl. Chem.*, 1986, **58**, 1511.

6 (*a*) I. I. Creaser, A. Hammershøi, A. Launikonis, A. W.-H. Mau, A. M. Sargeson and W. H. F. Sasse, *Photochem. Photobiol.*, 1989, **49**, 19; (*b*) M. A. R. Scandola, F. Scandola, A. Indelli and V. Balzani, *Inorg. Chim. Acta*, 1983, **76**, L67; (*c*) V. Houlding, T. Geiger, U. Kölle and M. Grätzel, *J. Chem. Soc., Chem. Commun.*, 1982, 681; (*d*) D. W. Conrad and R. A. Scott, *J. Am. Chem. Soc.*, 1989, **111**, 3461; (*e*) A. V. Kroll, V. I. Smorchkov and A. Y. Nazarenko, *Sens. Actuators B*, 1994, **21**, 97.

7 J. Sotomayor, H. Santos and F. Pina, *Can. J. Chem.*, 1991, **69**, 567; J. Sotomayor, J. C. Costa, Q. G. Mulazzani and F. Pina, *J. Photochem. Photobiol. A*, 1989, **49**, 195; U. Sakaguchi, S. Tamaki, K. Tomioka and H. Yoneda, *Inorg. Chem.*, 1985, **24**, 1624.

8 J. F. Stoddart and R. Zarzycki, *Recl. Trav. Chim. Pays-Bas*, 1988, **107**, 515.

9 L. A. Godínez, S. Patel, C. M. Criss and A. E. Kaifer, *J. Phys. Chem.*, 1995, **99**, 17449.

*Received in Columbia, MO, USA, 14th January 1997; Com. 7/00315C*

# X-Ray crystallographic structure of $Ga_8(pz)_{12}O_4Cl_4{\cdot}2thf$: a novel gallium pyrazololate complex with a $Ga_4O_4$ core

**Mario V. Capparelli,[a] Paul Hodge,[b] and Brian Piggott*[b]**

[a] *Centro De Quimica, Instituto Venezolano De Investigaciones Cientificas (IVIC), Apartado 21827, Caracas 1020.A, Venezuela*
[b] *Division of Chemistry, University of Hertfordshire, College Lane, Hatfield, Hertfordshire, UK AL10 9AB*

**The reaction of $Na[MeGa(pz)_3]$ with $GaCl_3$ leads to the formation of the novel cubane $Ga_8(pz)_{12}O_4Cl_4{\cdot}2thf$ 1, and not the expected product $[\{MeGa(pz)_3\}_2Ga][GaCl_4]$; the ease with which 1 forms is illustrated by its formation in a subsequent reaction of $Na[MeGa(pz)_3]$ with $GaCl_3$.**

There has been a resurgence of interest in compounds of main-group metals with a heterocubane core.[1–6] The recent work on gallium–group 16 cubanes describes the synthesis and structure of compounds with $Ga_4S_4$, $Ga_4Se_4$ and $Ga_4Te_4$ cores.[7]

However, prior to this communication there are no reported examples of compounds with a $Ga_4O_4$ cubane core. We herein describe the synthesis (albeit serendipitous) and X-ray crystallographic structure of such a compound, namely $Ga_8(pz)_{12}O_4Cl_4{\cdot}2thf$.

In previous publications we drew attention to two significant features of some trispyrazolyl derivatives of group 13 [specifically $HB(3\text{-}Bu^tPz)_3^-$ and $HB(3\text{-}PhPz)_3^-$], namely their stabilisation of low oxidation states and their redox properties with main-group metals.[8,9] We now identify a third significant feature of a member of this class of ligand [specifically $MeGa(pz)_3^-$], *viz*. heterocubane formation.

In an attempt to synthesise a gallium analogue of $[\{MeGa(pz)_3\}_2In][InI_4]$,[10] *i.e*. $[\{MeGa(pz)_3\}_2Ga][GaCl_4]$ **2**, we reacted $Na[MeGa(pz)_3]$ with $GaCl_3$ in dry thf under an atmosphere of argon, filtered the precipitated NaCl and left the filtrate to crystallise at −10 °C. After several months crystals of **1** formed which were subjected to elemental, mass spectral, $^{71}Ga$, $^1H$ and $^{13}C$ NMR analysis.† An X-ray crystal structure determination of **1** was also undertaken. The results are shown in Fig. 1(*a*) and (*b*) with selected bond lengths and angles given in Table 1.‡ The structure is based on a distorted $Ga_4O_4$ cube. Coordinated to and above each cube oxygen is a Ga atom, the centres of which define a tetrahedron. In addition, each of these Ga atoms is coordinated to three pyrazole rings and a chloride such that the five-coordinate Ga, $[OGa(pz)_3Cl]$, is trigonal bipyramidal *TBPY*. The three pyrazole rings of each *TBPY* Ga coordinate

**Table 1** Mean values[a] of selected bond lengths (Å) and angles (°)

| | | | |
|---|---|---|---|
| Ga(e)–Cl | 2.278(1)* | | |
| Ga(e)–O | 1.931(2)* | Ga(c)–O | 2.003(1) |
| Ga(e)–N | 1.976(2) | Ga(c)–N | 2.017(2) |
| Coordination about Ga(e) (*TBPY*) | | | Coordination about Ga(c) (*octahedral*) |
| Cl–Ca(e)–O | 179.35(6)* | *trans*-O–Ga(c)–N | 162.39(6) |
| N–Ga(e)–N | 119.63(9) | *cis*-O–Ga(c)–N | 83.44(6)[b] |
| Cl–Ga(e)–N | 93.53(6) | *cis*-O–Ga(c)–N | 104.78(6)[b] |
| O–Ga(e)–N | 86.49(6) | O–Ca(c)–O | 81.08(6) |
| | | N–Ga(c)–N | 92.52(8) |
| Coordination about O (*tetrahedral*) | | | |
| Ga(c)–O–Ga(c) | 98.26(6) | | |
| Ga(c)–O–Ga(e) | 119.16(6) | | |

[a] Bond lengths and angles are weighted averages, $x = \Sigma\ \sigma_i^{-2}x_i/\Sigma\sigma_i^{-2}$, where $\sigma_i$ are the e.s.ds from least-squares refinement; errors (within parentheses) are $s = (\Sigma\ \sigma_i^{-2})^{-1/2}$. Values marked with an asterisk are averages of four values; all other values are averages of 12 values. [b] There are two different types of *cis*-O–Ga(c)–N angles, depending if the O and N atoms belong to the same (83.44°) or to different (104.78°) five-membered chelate rings O–Ga(e)–N–N–Ga(c).

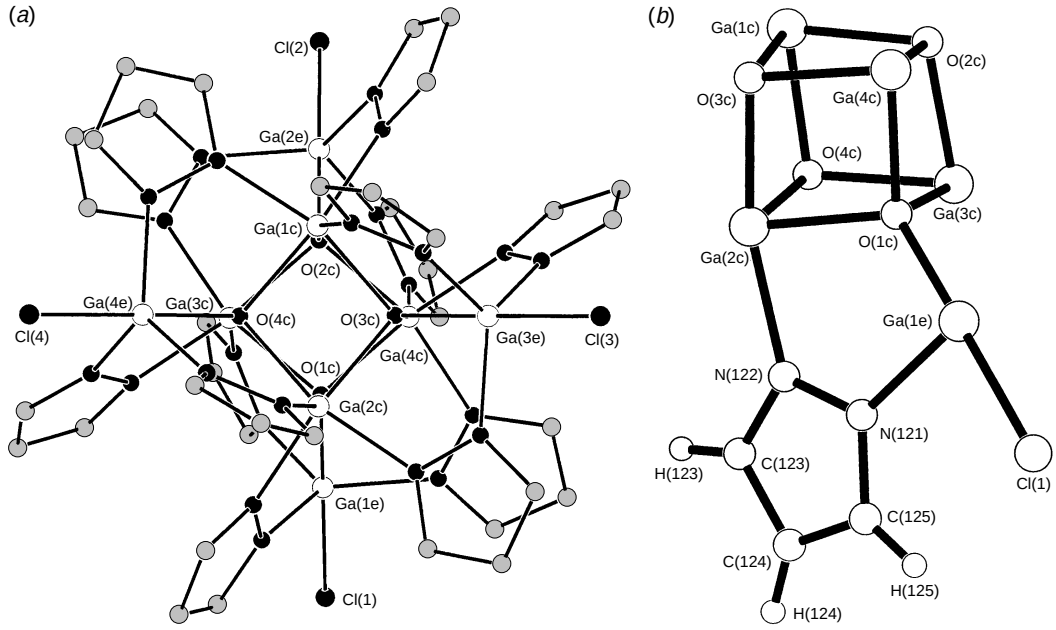



**Fig. 1** (*a*) Structure of compound **1** and (*b*) with some of the 'outer atoms' omitted to show the $Ga_4O_4$ core

through their second nitrogen to the three Ga atoms of the cube that are edge connected to the same oxygen, thus making each cube Ga six-coordinate (3N,3O).

The formation of this compound raises problems, *e.g*. what is the source of the oxygen atoms? A possible solution is that on prolonged standing at low temperature traces of air or water, or both, entered the system resulting in oxygen incorporation. Therefore, to investigate this problem, a second attempt was made to synthesise **2** (the assumption being that this, or a similar gallium complex, is the precursor of **1**) in order to study its controlled hydrolysis. Elemental, mass spectral, $^{71}$Ga, $^{1}$H and $^{13}$C NMR analyses of the small block-like single crystals that formed,† are very similar to those of **1**. These results indicated that this sample and **1** are very probably identical. This was confirmed by an X-ray crystallographic structure determination.

## Footnotes

† *Synthesis*: all manipulations were performed under argon using standard Schlenk techniques and all solvents dried prior to use.

**1** *method A*: to a Schlenk tube charged with $GaCl_3$ (0.04 g 2.27 mmol) in 20 cm$^3$ of thf was added a solution of Na[MeGa(pz)$_3$] (0.52 g 1.68 mmol) in 15 cm$^3$ of thf. An immediate turbidity occurred and the resulting solution stirred for 3 days. The solution was filtered and stored at −30 °C for one week. Attempts were made to filter the large crystals that formed but these redissolved on slight warming. A further 20 cm$^3$ of thf was added to the solution which was then stored at −30 °C for about six months. After this time the small block-like clear crystals that had formed were filtered. These crystals, although twinned, were used for the X-ray crystallographic structure determination. Yield 0.14 g (17%).

*Method B*: Na[MeGa(pz)$_3$] (2.28 g, 7.38 mmol) in 60 cm$^3$ thf was added to a Schlenk tube charged with freshly distilled $GaCl_3$ (1.30 g, 7.38 mmol). The resulting white slurry was stirred for three days after which time the thf was removed under vacuum. 60 cm$^3$ of dichloromethane was added to the resulting white mass, the slurry stirred and then filtered. The filtrate was evaporated to dryness. Dissolution of this in 60 cm$^3$ of MeCN, evaporation under vacuum to about 30 cm$^3$ and storing for one week at −30 °C produced small block-like single crystals of X-ray quality. Yield 1.92 g (61%). $^{1}$H NMR [250 MHz, $(CD_3)_2SO$] δ 8.29 (d, 12 H, Ar H), 6.21 (t, 12 H, Ar H), 5.72 (d, 12 H, Ar H), 3.40 (8 H, thf), 1.28 (8 H, thf). $^{71}$Ga NMR [250 MHz, $(CD_3)_2SO$] (dissolution only achieved with warming and sonication) δ 250.5 (ω 46 Hz), 10.7 (ω 912 Hz). IR (KBr) ν/cm$^{-1}$ 2094, 2871, 1499, 1425, 1381, 1295, 1186, 1163, 1059, 973, 769, 620, 535, 342, 308. MS (FAB) 1570 $(M + H)^+$ < 1%.

‡ *Crystal data* for **1**: $C_{44}H_{52}Cl_4Ga_8N_{24}O_6$, $M$ = 1712.62, triclinic, space group $P\bar{1}$ (no. 2), $a$ = 12.494(4), $b$ = 21.415(4), $c$ = 12.349(4) Å, α = 91.90(2), β = 108.74(3), γ = 90.21(2)°, $U$ = 3126(1) Å$^3$, $Z$ = 2, $D_c$ = 1.819 Mg m$^{-3}$, $F$(000) = 1696, λ = 0.710 69 Å, $T$ = 296 K, μ(Mo-Kα) = 36.23 cm$^{-1}$. Absorption correction with DIFABS. Data were collected on a Rigaku AF7TS diffractometer. Of a total of 6162 collected reflections 5802 were unique. The structure was solved by direct methods. After refining all atoms in the molecule, a difference Fourier synthesis showed a large number of peaks of residual electron density located in empty regions of the unit cell, out of the range of bonding distances of the molecule, which were attributed to disordered solvent (thf) molecules. Two $C_5$ rings could be modelled, each one disordered over two positions, with total occupancies of 0.87 and 0.82. These C atoms were assigned fixed occupancies, fixed coordinates and refined isotropic displacement parameters. In the final difference Fourier synthesis the ten largest peaks (0.34–0.96 e Å$^{-3}$) were located in the vicinity of the $C_5$ ring atoms. Refinement was by full-matrix least squares on $F$, final $R$ indices [$I > 2\sigma(I)$] $R$ = 0.0309, $R_w$ = 0.0381. Atomic coordinates, bond lengths and angles, and thermal parameters have been deposited at the Cambridge Crystallographic Data Centre (CCDC). See Information for Authors, Issue No. 1. Any request to the CCDC for this material should quote the full literature citation and the reference number 182/423.

## References


1 S. Schulz, H. W. Roesky, H. J. Koch, G. M. Sheldrick, D. Stalke and A. Kuhn, *Angew. Chem., Int. Ed. Engl*., 1993, **32**, 1729.
2 T. Belgardt, H. W. Roesky, M. Noltemeyer and H. G. Schmidt, *Angew. Chem., Int. Ed. Engl*., 1993, **32**, 1056.
3 M. Rhiel, F. Weller, J. Pebler and K. Dehnicke, *Angew. Chem., Int. Ed. Engl*., 1994, **33**, 569.
4 T. Belgardt, S. D. Waegada, H. W. Roesky, H. Gorntzka, L. Häming and D. Stalke, *Inorg. Chem*., 1994, **33**, 6247.
5 R. A. Alton, D. Barr, A. J. Edwards, M. A. Paver, P. R. Raithby, M.-A. Rennie, C. A. Russell and D. S. Wright, *J. Chem. Soc., Chem. Commun*., 1994, 1481.
6 C. Dohmeier, D. Loos and H. Schnöckel, *Angew. Chem., Int. Ed. Engl*., 1996, **35**, 129.
7 A. R. Barron, *Chem. Soc. Rev*., 1993, **22**, 93.
8 A. Frazer, B. Piggott, M. B., Hursthouse and H. Mazid, *J. Am. Chem. Soc*., 1994, **116**, 4127.
9 A. Frazer, P. Hodge and B. Piggott, *Chem. Commun*., 1996, 1727.
10 A. Frazer, B. Piggott, M. Harman and M. B. Hursthouse, *Polyhedron*, 1992, **23**, 3013.



*Received in Cambridge, UK, 13th February 1997; Com. 7/01044C*

# Solid-state NMR and diffraction studies of *p-tert*-butylcalix[4]arene·nitrobenzene·xenon†

**Eric B. Brouwer,[a,b] Gary D. Enright[a] and John A. Ripmeester*[a,b]**

[a] *Steacie Institute for Molecular Science, National Research Council of Canada, Ottawa, Ontario, Canada K1A 0R6*
[b] *Ottawa-Carleton Chemistry Institute, Department of Chemistry, Carleton University, 1125 Colonel By Drive, Ottawa, Ontario, Canada K1S 5B6*

**Xenon is enclathrated in the *p-tert*-butylcalix[4]arene cavity and behaves both as a guest and a cavity probe; $^{129}$Xe NMR and X-ray diffraction data show Xe to occupy two cavity sites defined by static disordered host *tert*-butyl groups.**

The *p-tert*-butylcalix[4]arene (*t*-BC) cavity (interatomic distance *d ca.* 10 Å at the upper rim, *d ca.* 3.8 Å at the lower rim: with a depth of *ca.* 4 Å) is a micropore‡ that to date, has not been examined by any of the common solid-state void space characterization techniques.[1] $^{129}$Xe NMR spectroscopy is one such technique that is particularly sensitive to micropore geometry and size.[2]

We have previously reported *t*-BC compounds with aliphatic guests prepared by vapour diffusion of the guest into a saturated solution of *t*-BC in nitrobenzene.[3] In a similar fashion (in which Xe replaces the aliphatic guest), *t*-BC·$C_6H_5NO_2$·Xe **1**, is prepared.§ This first example of a *t*-BC·gas clathrate[4] is characterized by both single-crystal X-ray crystallography (XRD) as well as $^{129}$Xe NMR spectroscopy using a complementary approach. Importantly, for the first time, $^{129}$Xe NMR spectral features are related to specific single-crystal XRD structural aspects.

The XRD structure of **1** (Fig. 1)¶ confirms that the host geometry is identical to that of *t*-BC·$C_6H_5NO_2$ **2**.[5] In **1**, 17% of the cavities are occupied by Xe, with the remainder occupied by nitrobenzene. The off-axis orientation of the nitrobenzene guest is similar in the two structures. Whereas substitution of nitrobenzene by Xe does not influence the position of the disordered host *tert*-butylphenol groups (two of the four groups disordered), it does change the ratio of disordering in *tert*-butylphenol group *C* to 0.66 : 0.34 from 0.79 : 0.21 (Fig. 1). If the relationship between nitrobenzene content and the ratio of group *C* *tert*-butylphenol disorder present in **2** is constant, the change in disordering in **1** is consistent with Xe solely occupying a cavity defined by the majority disordered position in group *C*.

Xe sits at the centre of the cavity, 4.33 Å from the basal plane defined by the four phenolic oxygens. Xe shows no protrusion from the cavity and is in fact, located deep in the cavity relative to other *t*-BC·guest species. The closest Xe···host contacts are to the lower three carbons of each *p-tert*-butylphenol unit [C(1),C(2),C(6)], with an average distance of 4.13 Å from these carbons to Xe; these distances are slightly greater than the sum of the van der Waals radii (4.0 Å). The closest approach of a *t*-BC carbon to the Xe along the direction perpendicular to the capping *t*-BC bilayer is 5.4 Å.

The two lines ($\delta_{iso}$ 59, $I$ = 0.6, site I; $\delta_{iso}$ 64, $I$ = 0.4, site II) in the $^{129}$Xe CP MAS NMR spectrum [Fig. 2(*a*)] indicate that Xe samples two inequivalent sites which possess slightly different Xe occupancies and void space volumes, as indicated by the intensity and $\Delta_{iso}$ values respectively.

The components of the chemical shift anisotropy (CSA) tensors are obtained for the two sites from the static $^{129}$Xe CP NMR spectrum [Fig. 2(*b*)], and reflect both the chemical environment and symmetry of the two cavity sites. The spectrum was fitted [Fig. 2(*c*)][6] using a two-site model employing the $^{129}$Xe NMR $\delta_{iso}$ values from the MAS spectrum (site I: $\delta_{iso}$ 59; $\Delta\delta$ = 27 ppm; $\delta_{11}$ 49; $\delta_{22}$ 54; $\delta_{33}$ 76; site II: $\delta_{iso}$ 64, $\Delta\delta$ = 19 ppm, $\delta_{11}$ 56, $\delta_{22}$ 60, $\delta_{33}$ 75).‖

Both Xe powder patterns are characterized by somewhat asymmetric CSA tensors ($\eta$ = 0.3), and accurately reflect the

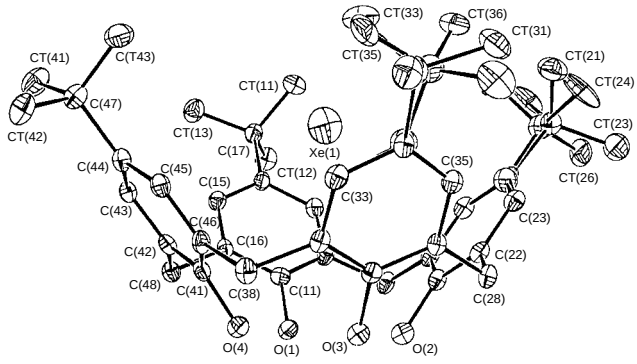



**Fig. 1** ORTEP of **1** showing only the Xe guest; atoms shown in 30% thermal ellipsoids. Hydrogen atoms removed for clarity.

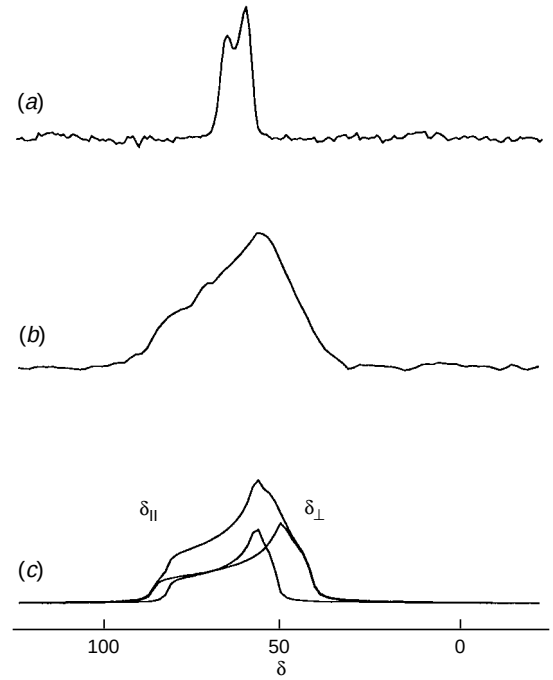



**Fig. 2** 49.8 MHz $^{129}$Xe CP NMR spectra of **1**: (*a*) with MAS, 1219 transients; recycle time: 2 s; TD = 512; 20 Hz line broadening; $\nu$ = 2.65 kHz; (*b*) static 2080 transients; recycle time: 3 s; TD = 256; (*c*) fitted spectra. Both experimental spectra were collected on a Bruker CXP-180 NMR spectrometer with a Doty 7 mm spinning probe: $\pi/2$ pulse = 3.5 μs; contact time = 3.5 ms; 16 K points; SW = 20 kHz.

small departures from axial symmetry of both calix cavities. The least shielded component of both patterns ($\delta_{33} = \delta_{\|}$ is along the *z* axis, and since $\delta_{\|}^{I} = \delta_{\|}^{II}$, the two cavities share similar dimensions along this axis. Since $\delta_{\|}$ is the least shielded CSA component, the CSA tensor has positive anisotropy indicative of a prolate spheroidal cavity.[7,8] The difference in the $\delta_{11}$ and $\delta_{22}$ values for the two patterns indicates that Xe samples different dimensions in the *xy* plane for each cavity.

Because Xe sits in a cavity defined by the majority disordered position in *tert*-butylphenol group *C*, only the positional disordering in *tert*-butylphenol group *B* (0.57 : 0.43) influences cavity size. Disordering in *B* gives two cavities of dimensions of 10.15 × 10.52 Å (majority site) and 10.15 × 10.65 Å (minority site) defined by the central carbon of the *tert*-butyl groups (Fig. 3). Two cavities differing in one dimension in the *xy* plane by 0.17 Å result from the disordering in *B*. The differences along the *z* axis arising from the *tert*-butylphenol disordering are insignificant ($\Delta d < 0.03$ Å).

Specific features of each technique can now be correlated. On the basis of the position and intensities of the two $^{129}$Xe NMR lines I and II are assigned to the majority of (10.15 × 10.52 Å) and minority (10.15 × 10.65 Å) cavities respectively. The intensities of the $^{129}$Xe NMR lines agree with the ratio of *tert*-butylphenol disordering in *B* determined by XRD. The presence of two Xe sites indicates that, in contrast to the dynamic *tert*-butylphenol disordering observed in *t*-BC·$C_6H_5Me$,[9] *tert*-butylphenol *B* disordering in **1** is static. Finally, the degree of $^{129}$Xe NMR δ shielding of the two sites is consistent with the cavity size/$\delta_{iso}$ relationship for void spaces,[7] and is to date the largest clathrate cavity defined by $^{129}$Xe NMR in such a fashion (although ring-current effects[10] from the aromatic host walls likely interfere with any quantitative determinations of the cavity size). For comparison, Xe in zeolite A (one Xe per α cage, *d ca*. 9.8 Å), gives $\delta_{iso}$ 75.[11]

In summary, the *t*-BC·$C_6H_5NO_2$·Xe compound illustrates three key features: (*i*) it is the first example of gas inclusion in the *t*-BC cavity, (*ii*) since Xe behaves both as a guest and a probe, specific XRD and NMR data may (for the first time) be correlated, and (*iii*) NMR data establishes that the host *tert*-butylphenol disordering is static.

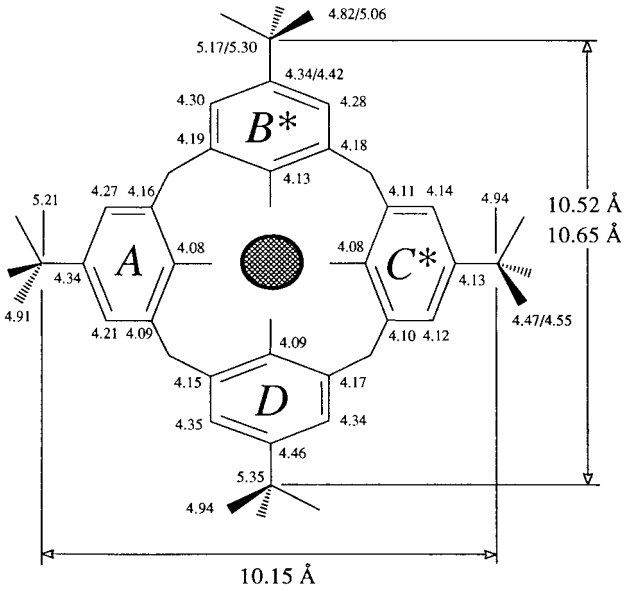



**Fig. 3** The Xe position in the *t*-BC cavity in **1**. The smaller numbers indicate the distance (in Å) to Xe, and the larger numbers indicate the cavity dimensions in the Xe *xy* plane; two values reflect disordering in carbon atoms. The starred letters indicate disordered *p-tert*-butylphenol units: *B* 57 : 43; *C* 66 : 34.

We thank the Natural Sciences and Engineering Research Council of Canada for support in the form of operating (J. A. R.) and post-graduate PGS-B (E. B. B.) awards.

## Footnotes

* E-mail: jar@ned1.sims.nrc.ca

† Issued as NRCC No. 40819.

‡ $^{13}$C CP MAS NMR evidence shows that solid empty *t*-BC takes up small hydrocarbons on contact with the liquid.

§ *Synthesis*: A saturated nitrobenzene solution of *p-tert*-butylcalix[4]arene (*T* = 80 °C) is cooled to room temp. in a closed vessel pressurized with Xe (2 atm).

¶ *Crystal data* for **1**: $C_{48.98}H_{60.15}O_{5.66}N_{0.83}Xe_{0.17}$, $M_w$ = 773.43, *T* = 150 K, orthorhombic, space group $Pc2_1n$, *a* = 12.4872(7), *b* = 12.8909(8), *c* = 26.6893(17) Å, *U* = 4296.2(5) Å$^3$, *Z* = 4, *F*(000) = 1666.76, $D_c$ = 1.199 g cm$^{-3}$, μ(Cu-Kα) = 1.63 mm$^{-1}$. Intensities of 5416 reflections were measured on an Enraf-Nonius CAD-4 diffractometer using Cu-Kα radiation (graphite monochromator, θ–2θ scan mode). Three standard reflections were measured to monitor crystal stability. Absorption corrections were not applied. The structure was solved by using NRCVAX suite of programs.[12] Refinement converged at $R = \Sigma\|F_o| - |F_c\|/\Sigma|F_o| = 0.048$, $R_w = [\Sigma w(|F_o| - |F_c|)^2/\Sigma w|F_o|^2]^{1/2} = 0.062$ and GOF = $[\Sigma w(|F_o| - |F_c|)^2/(m - n)]^{1/2} = 1.92$ for 4258 reflections with $I \geqslant 2.50(I)$. Two of the four *tert*-butylphenol groups were disordered in 0.57 : 0.43 and 0.66 : 0.34 ratios. The final Fourier difference map showed no residual density outside of −0.290 and 0.210 e Å$^{-3}$. Atomic coordinates, bond lengths and angles, and thermal parameters have been deposited at the Cambridge Crystallographic Data Centre (CCDC). See Information for Authors, Issue No. 1. Any request to the CCDC for this material should quote the full literature citation and the reference number 182/426.

‖ $|\delta_{33} - \delta_{iso}| > |\delta_{22} - \delta_{iso}|, |\delta_{11} - \delta_{iso}|$; $\Delta\delta = \delta_{33} - \delta_{iso}$; $\delta_{iso} = (\delta_{11} + \delta_{22} + \delta_{33})/3$; $\eta = |\delta_{22} - \delta_{11}|/|\delta_{33} - \delta_{iso}| = 0.3$; uncertainties: ±2 ppm.

## References

1 H. Lao and C. Detellier, *Comprehensive Supramolecular Chemistry*, ed. J. E. D. Davies and J. A. Ripmeester, Pergamon, Oxford, 1996, vol. 8, pp. 277–306.
2 J. A. Ripmeester and C. I. Ratcliffe, in *Comprehensive Supramolecular Chemistry*, ed. J. E. D. Davies and J. A. Ripmeester, Pergamon, Oxford, 1996, vol. 8, pp. 323–380.
3 E. B. Brouwer, G. D. Enright and J. A. Ripmeester, *Supramol. Chem*., 1996, **7**, 143.
4 C. D. Gutsche, *Calixarenes*, RSC, Cambridge and London, 1989; *Calixarenes*, ed. J. Vicens and V. Bohmer, Kluwer, Dordrecht, 1990, R. Ungaro, A. Arduini, A. Casnati, O. Ori, A. Pochini and F. Ugozzoli, in *Computational Approaches in Supramolecular Chemistry*, ed. G. Wipff, *NATO ASI Ser. C*, 1994, **426**, 277; V. Bohmer, *Angew. Chem., Int. Ed. Engl*., 1995, **34**, 713.
5 E. B. Brouwer, G. D. Enright and J. A. Ripmeester, *Supramol. Chem*., 1996, **7**, 7.
6 Program WINFIT: Bruker-Franzen Analytik GmbH, version 950425.
7 J. A. Ripmeester, C. I. Ratcliffe and J. S. Tse, *J. Chem. Soc., Faraday Trans. 1*, 1988, **84**, 3731.
8 F. Lee, E. Gabe, J. S. Tse and J. A. Ripmeester, *J. Am. Chem. Soc*., 1988, **110**, 6014.
9 E. B. Brouwer, G. D. Enright, C. I. Ratcliffe and J. A. Ripmeester, *Supramol. Chem*., 1996, **7**, 79.
10 T. Komoto, I. Ando, Y. Nakamoto and S. Ishida, *J. Chem. Soc., Chem. Commun*., 1988, 135.
11 J. A. Ripmeester and C. I. Ratcliffe, *J. Phys. Chem*., 1990, **94**, 7652; C. J. Jameson, A. K. Jameson, R. Gerald II and A. C. de Dios, *J. Chem. Phys*., 1992, **96**, 1676.
12 E. J. Gabe, Y. Le Page, J.-P. Charland, F. L. Lee and P. S. White, *J. Appl. Crystallogr*., 1989, **22**, 384.

*Received in Columbia, MO, USA, 28th October 1996; Com. 6/07352B*

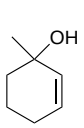
# A concise asymmetric synthesis of the pheromone 1-methylcyclohex-2-enol *via* a 'merged substitution-elimination reaction'

**David P. G. Hamon*† and Kellie L. Tuck**

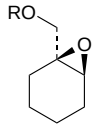
*Chemistry Department, University of Adelaide, S.A. 5005, Australia*

**The title compound is prepared (> 94% ee) by a three step synthesis from 1-methylcyclohexene *via* a 'merged substitution-elimination reaction' involving a phenylselenide ion.**

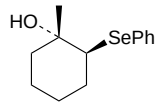
One of the constituents of the pheromone system of the beetle *Dendroctonus pseudotsugae Hopkins*, an economically important pest of the Douglas fir tree, is the aggregation pheromone 1-methylcyclohex-2-enol **1**. Previous syntheses of the optically active pheromone **1** have involved the conversion of optically active intermediates, prepared by classical resolution,[1] enzymically,[2,3] from the chiral pool,[4] or by multistep asymmetric syntheses.[5,6]




**1**




**2**



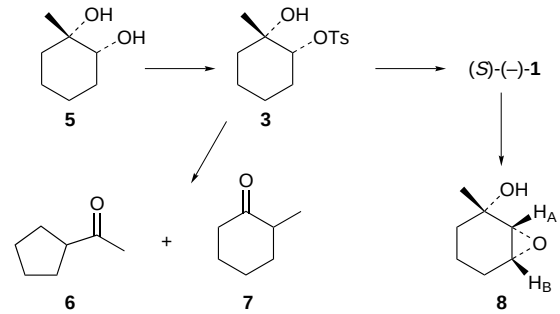

**4**

If asymmetric syntheses are to become important for industrial preparations it is necessary to illustrate that they can be made simple and short. However, this is not necessarily a trivial exercise. With this pedagogical principle in mind, we sought to modify our earlier route[5] in the hope that the separate enantiomers might be more readily prepared. Serendipity has played an important role in providing a simple solution to this problem and we disclose a three step asymmetric synthesis of this pheromone which is applicable to the synthesis of either enantiomer, and which gives the constituent in an enantiomeric purity exceeding 94% ee. Ironically the aggregation pheromone found naturally is only 10% ee[7] but the challenge of the asymmetric synthesis has been pedagogically both useful and exciting. A key step in our earlier synthesis[5] of this pheromone involved nucleophilic substitution of the epoxide **2**. Although both the leaving groups in the epoxide **2** and the tosylate **3** are in a *pseudo* neopentyl location, a study of models suggests that tosylate **3** is considerably more hindered to nucleophilic attack than the epoxide **2**. However, it was considered that with the powerful nucleophile NaSePh, tosylate **3** might also, like epoxide **2**, react to give in this case the selenide **4**. Thermal elimination of the selenoxides[5] derived from **4** would give the pheromone **1**. Asymmetric dihydroxylation of 1-methylcyclohexene should give the optically active diol **5** from which the tosylate **3** could be prepared.

After this work had commenced, Sharpless reported,[9] as a footnote, the ee (52%, by chiral HPLC) for the asymmetric dihydroxylation (AD β mix) of 1-methylcyclohexene to the diol **5**, but no experimental details for the preparation were provided. Owing to the water solubility and considerable volatility of the diol **5**, we have found it necessary to modify, somewhat, the standard work-up procedures for this reaction by removal of the KOH wash normally used to remove methanesulfonamide. The product is then isolated, in 85% yield, by fractional distillation of all solvents, chromatography and sublimation (50 °C/0.5 Torr). Conversion of the diol **5** to the mono secondary tosylate **3** (85% yield, 94% yield for the racemate on a larger scale) gives material which, although it is initially only 75% of the major enantiomer,‡ can nevertheless be fractionally recrystallised to high enantiomeric purity (94% ee after four recrystallisations from diethyl ether–hexane, 37% yield, the racemate is less soluble).

Treatment of the tosylate **3** with NaSePh (PhSeSePh, $NaBH_4$, EtOH[10]), in boiling EtOH, did not give the sought after substitution reaction. Rather surprisingly an elimination reaction occurred instead. The initial reaction gave a mixture of the alcohol **1** and the ketones **6** and **7**. It had been assumed from the outset that base treatment of the tosylate **3** would give the ketones **6** and **7**, by a negative-ion pinacol rearrangement,[11] and this was confirmed by treatment of the tosylate with $KOBu^t$ (in THF at room temperature, **6** : **7** = 8 : 1, 90%). Selenide ion is too weak a base to abstract a proton from an alcohol and it was likely that ketones **6** and **7** were artifacts formed from adventitious sources of base. A wash of the glassware with $NH_4Cl$ solution prior to the reaction of tosylate **3** with NaSePh, obviates the formation of these ketones and the volatile alcohol (*S*)-(−)-**1**§ is isolated, in 78% yield, by fractional distillation. The enantiomeric purity of the tertiary allylic alcohol **1** could not be obtained directly by chiral shift NMR experiments and we did not have access to complexation GC.[1] Conversion of the alcohol to the epoxide **8** (with slow addition of MCPBA to alcohol **1**, $NaHCO_3$, $Et_2O$, 0 °C, 70%, the diastereomer is not formed) and chiral shift NMR experiments‡ on this (94% ee) confirmed that the enantiomeric purity from the tosylate had been maintained.

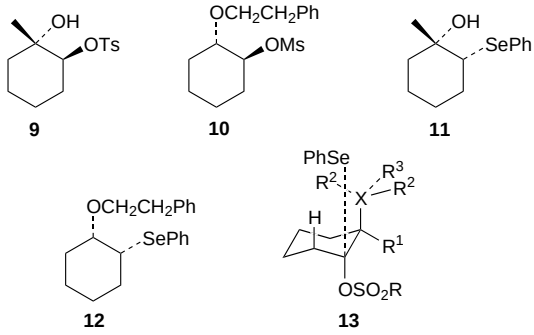
The mechanism for the elimination reaction observed is intriguing. The reaction of the tosylate **3** with NaSePh in EtOH is not an $E_1$ mechanism since the qualitative observation is that the half-life for the reaction is concentration dependent; because no products from pinacol rearrangement are observed when care is taken to remove adventitious base; and because the tosylate is recovered unchanged after reflux in EtOH. The question arises, therefore, as to why selenide anion, a powerful nucleophile to carbon but non-nucleophilic to hydrogen attached to the oxygen of an alcohol, should suddenly change allegiance and become a nucleophile to hydrogen attached to carbon. Winstein, in a paper published in 1956,[8] first drew attention to the dichotomy of weak bases but good nucleophiles which promote elimination reactions when he wrote about merged substitution-elimination reactions. Since then there has been considerable debate[12,13] as to the veracity of his suggestion but, in our opinion, no clear




**Scheme 1**

explanation has been given for what is actually occurring in these reactions. Since our example appears to be one of the more extreme examples of this phenomenon, we would like to present our observations in the hope that they will rekindle debate on this subject.

Under the same conditions, with NaSePh, as when the tosylate **3** gives only the elimination product **1**, both the racemic isomeric *trans*-tosylate **9** and the racemic mesylate **10** undergo clean substitution reactions to give the selenide derivatives **11**¶[14] and **12** respectively. It has been shown[15] that for the




4-*tert*-butylcyclohexyl derivatives the axial tosylate reacts faster than the equatorial tosylate in $S_N2$ reactions. Conformational mobility is clearly demonstrated for the tosylate **3**, even at room temperature, since it is likely that the compounds **6** and **7** come from two different chair conformers. From a study of models it is seen that when the leaving group is axial not only is the rear-side attack less hindered but, the nucleophile, the reaction centre and the leaving group can stay co-linear throughout the reaction.‖ Perhaps herein lies an explanation for our observations. It is likely that the selenide ion follows a trajectory co-incident with the dipole axis of the molecule and that in both the compounds **9** and **10** the propensity for carbon nucleophilicity is not thwarted by steric barriers since only lone pairs (see **13**) would hinder the approach. In the case of the tosylate **3**, however, the methyl group would clearly present an obstacle to rear-side attack and the deflected nucleophile might then encounter the hydrogen atom, held in an antiperiplanar relationship to the leaving group, with sufficient energy to overcome the barrier to elimination and this then becomes the lower energy process.

In conclusion, therefore, we have developed a three step asymmetric synthesis of the pheromone, from achiral starting materials. The route is probably far more efficient than any to date and will be extremely efficient if further developments to the Sharpless procedure allows a more enantioselective preparation of the diol **5**. Furthermore the synthesis has revealed an intriguing elimination reaction which may help to unravel the paradoxes arising in the mechanism of weak-base elimination reactions.

We thank Rebecca Kennedy for the experiments referred to in ref. 14.

## Footnotes

† E-mail: dhamon@chemistry.adelaide.edu.au

‡ All chiral shift NMR experiments were run in 15% $C_6D_6$ in $CCl_4$ with Eu(hfc)$_3$. Racemic tosylate **6**. $\delta_H$ (200 MHz, $CDCl_3$) 1.14 (s, 3 H, $CH_3$), 1.2–1.8 (complex, 8 H, methylene envelope), 1.59 (s, 1 H, OH), 2.45 (s, 1 H, Ar-$CH_3$), 4.36 (dd, 1 H, *J* 4.04, 9.94 Hz, H1), 7.34 (d, 2 H, *J* 8.22 Hz, Ar-H), 7.80 (d, 2 H, *J* 8.22 Hz, Ar-H). The doublet originally at δ 7.80 separates, to baseline, into two doublets with the shift reagent. Racemic epoxide **8**. $\delta_H$ (200 MHz, $CDCl_3$) 1.2–2.1 (complex, 6 H, methylene envelope), 1.33 (s, 3 H, $CH_3$), 2.40 (br s, 1 H, OH), 3.10 (d, 1 H, *J* 4.0 Hz, H2), 3.36 (m, 1 H, H3). The multiplet originally at δ 3.36 separates, to baseline, into two broadened singlets with the shift reagent.

§ Pheromone **1**. $\delta_H$ (200 MHz, $CDCl_3$) 1.29 (s, 3 H, $CH_3$), 1.5–1.8 (complex, 4 H, methylene envelope), 2.0 (m, 2 H, H4), 5.60 (br d, 1 H, *J* 10.0 Hz, H2), 5.75 (td, 1 H, *J* 4.0, 10.0 Hz, H3). $\delta_C$ (75.5 MHz, $CDCl_3$) 19.5, 25.0, 29.3, 37.8, 67.9, 128.9, 133.7.

¶ A referee has suggested that this compound might have the structure **4** if it arose through double inversion *via* the epoxide. However, optically active compound **4** is already known[5] and the spectral data are different.

‖ A study of a model (axial leaving group down) shows that the reacting centre can move up smoothly towards the nucleophile as overlap of the orbitals takes place. This would give the product in the boat conformation. No such smooth pathway exists for the equatorial leaving group. We believe that this requirement would also account for the known *trans*-diaxial opening of cyclic epoxides.

## References

1 K. Mori, B. G. Hazra, R. J. Pfeiffer and A. K. Gupta, *Tetrahedron*, 1987, **43**, 2249.
2 K. Mori and J. I. J. Ogoche, *Liebigs Ann. Chem.*, 1988, 903.
3 B. D. Johnston, B. Morgan, A. C. Oehlschlager and S. Ramaswamy, *Tetrahedron: Asymmetry*, 1991, **2**, 377.
4 P. Ceccherelli, M. Curini, F. Epifano, M. C. Marcotullio and O. Rosati, *J. Org. Chem.*, 1996, **61**, 2882.
5 D. P. G. Hamon, R. A. Massy-Westropp and J. L. Newton, *Tetrahedron: Asymmetry*, 1990, **1**, 771.
6 A. B. Bueno, M. C. Carreno, J. L. G. Ruano and C. Hamdouchi, *Tetrahedron: Asymmetry*, 1995, **6**, 1237.
7 B. S. Lindgren, G. Gries, H. D. Pierce and K. Mori, *J. Chem. Ecol.*, 1992, **18**, 1201.
8 S. Winstein, D. Darwish and N. J. Holness, *J. Am. Chem. Soc.*, 1956, **78**, 2915.
9 H. C. Kolb, M. S. VanNieuwenhze and K. B. Sharpless, *Chem. Rev.*, 1994, **94**, 2483 and footnote 53 therein.
10 K. B. Sharpless and R. F. Lauer, *J. Am. Chem. Soc.*, 1973, **95**, 2697.
11 P. D. Bartlett and R. H. Rosenwald, *J. Am. Chem. Soc.*, 1934, **56**, 1900.
12 D. J. McLennan, *Tetrahedron*, 1975, **31**, 2999.
13 H. Kwart, K. A. Wilk and D. Chatellier, *J. Org. Chem.*, 1983, **48**, 756.
14 D. P. G. Hamon and R. J. Kennedy, unpublished observations.
15 E. L. Eliel, S. H. Wilen and L. N. Mander, in *Stereochemistry of Organic Compounds*, Wiley, New York, 1994, p. 723.

*Received in Cambridge, UK, 13th March 1997; Com. 7/01756A*

# Iron(III) catalysis of the Michael reaction of 1,3-dicarbonyl compounds and enones

**Jens Christoffers**

*Technische Universität Berlin, Institut für Organische Chemie, Sekretariat TC 2, Straße des 17. Juni 124, D-10623 Berlin, Germany*

**Iron(III) chloride hexahydrate catalyses the Michael reaction of β-dicarbonyl compounds and enones under mild and neutral conditions with excellent yields and product selectivity.**

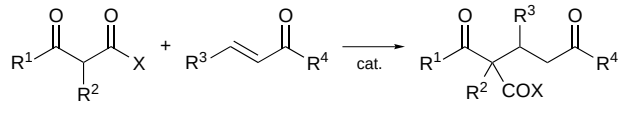
The reaction of enolates with α,β-unsaturated carbonyl compounds (Michael reaction) is a fundamental C–C bond forming methodology, which classically is a high yielding base catalysed process, and can even be performed with high stereoselection.[1] However, there are some disadvantages of base catalysis, *e.g.* incompatibility with base sensitive or acidic functionalities, ester solvolysis, reverse and other side reactions. In these terms it seems interesting that the Michael reaction is known to be catalysed under neutral conditions by transition metal compounds, in particular by Group VIII 1,3-dionato complexes.[2] Also, some lanthanide catalysts have been reported to be efficient under neutral and mild conditions.[3]

Although the strong tendency of $Fe^{III}$ to form 1,3-dionato complexes is well known,[4] catalysis of the Michael reaction by $FeCl_3·6H_2O$ has not yet been reported to the best of our knowledge,† despite the fact that in terms of economical and ecological considerations iron should be the transition metal of choice.

Iron(III) chloride hexahydrate is an extraordinarily efficient catalyst for the Michael reaction shown in Scheme 1. We have been investigating the catalytic activity of several transition metal halides on the reaction of **1a** with **2a**, and some did show activity, but only with $FeCl_3·6H_2O$ did we observe complete conversion at room temperature. For about the first 30% conversion the turn over number was *ca.* 2 $min^{-1}$, and using 1 mol% $Fe^{III}$ the reaction was quantitative within 3 h. It has to be pointed out that as the product and starting materials are liquid at room temp. and no solvents needed to be used, and since no side reactions have been observed, workup is very simple: filtration using a small column of silica gel removes all iron-containing materials.

The best results were obtained with cyclic ketoesters and methyl vinyl ketone (**2a**; products **3a**, **b**,‡ **d**, **e**§). With only 1 mol% $FeCl_3·6H_2O$ full conversion within a few hours is observed, even if bulkier ester functions are present (**3b**). Although starting from a methyl ester **1e**, some hydrolysis and subsequent decarboxylation reactions, presumably resulting from hydrate water, are noticed. This is negligible if 1 mol% $Fe^{III}$ is applied, but with 5 mol% yield drops significantly to 72%. Using β-diketones or other species other than cyclic ketoesters, conversion is a little slower, but with 5 mol% catalyst results are still satisfying (in Table 1 some optimized examples are listed).

While $Fe^{III}$ catalysis seems to be effective with **2a**, some restrictions have to be made in the use of other enones: although even bulkier *E*-enones like **2b** or **2c** form Michael products (the higher reaction temperature might be due to steric effects; solvent had to be applied in these cases), no reaction was observed with enones with a *Z*-substituent like cyclopentenone or mesityl oxide. This might give some insight into a possible mechanism of the $Fe^{III}$ catalysis (actually, chloride does not play a role, because the same results have been observed using



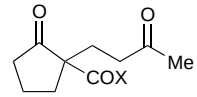
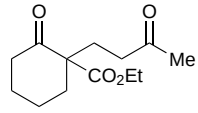
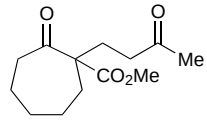
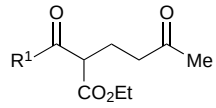
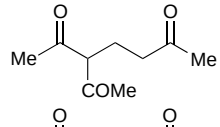
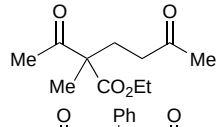
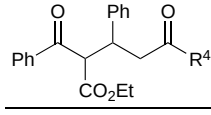

**1** **2** **3**

**1a** X = OEt, $R^1$, $R^2$ = –$(CH_2)_3$–
**b** X = $OBu^i$, $R^1$, $R^2$ = –$(CH_2)_3$–
**c** X = Me, $R^1$, $R^2$ = –$(CH_2)_3$–
**d** X = OEt, $R^1$, $R^2$ = –$(CH_2)_4$–
**e** X = OMe, $R^1$, $R^2$ = –$(CH_2)_5$–
**f** X = OEt, $R^1$ = Me, $R^2$ = H
**g** X = OEt, $R^1$ = Ph, $R^2$ = H
**h** X = Me, $R^1$ = Me, $R^2$ = H
**i** X = OEt, $R^1$ = $R^2$ = Me

**2a** $R^3$ = H, $R^4$ = Me
**b** $R^3$ = Ph, $R^4$ = Me
**c** $R^3$ = $R^4$ = Ph

**Scheme 1** Iron(III) catalysed Michael reactions, (cat. = $FeCl_3·6\ H_2O$).

**Table 1** Reaction of **1** and **2** to give **3**

| Product | | | Conditions[a] | Yield (%)[b] |
|---|---|---|---|---|
|  | X = OEt | **3a** | 1, room temp. | 97 |
| | X = $OBu^i$ | **3b** | 1, toom temp. | 95 |
| | X = Me | **3c** | 5, room temp. | 86 |
|  | **3d** | | 1, room temp. | 94 |
|  | **3e** | | 1, room temp. | 91[c] |
|  | $R^1$ = Me | **3f** | 5, room temp. | 90 |
| | $R^1$ = Ph | **3g** | 5, room temp. | 87 |
|  | **3h** | | 5, room temp. | 77[d] |
|  | **3i** | | 5, room temp. | 78 |
|  | $R^4$ = Me | **3j** | 5, 50[e] | 84[f] |
| | $R^4$ = Ph | **3k** | 5, 50[e] | 90[f] |

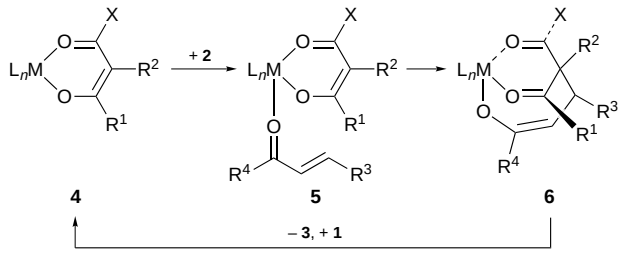
[a] Mol% $FeCl_3·6\ H_2O$, reaction temp./°C, no solvent. [b] Isolated yields. [c] Use of 5 mol% catalyst resulted in 72% yield. [d] Chromatographic separation from byproducts was necessary. [e] Solvent ($CHCl_3$) was used. [f] Isolated as a mixture of two diastereoisomers.

$Fe^{III}$ nitrate or sulfate). Starting from a diketonato complex **4**, in which the ligand is planar and particularly stabilized by π-delocalization, the enone **2** is proposed to coordinate in a vacant coordination site to form species **5** (Scheme 2). Subsequently, the central carbon centre of the dionato ligand is thought to be alkylated by the coordinated enone, but only if the enone is in the S-*cis* conformation, which is obviously impossible for cyclopentenone and strongly disfavoured in mesityl oxide. In complex **6**, the central carbon centre of the dione ligand is tetrahedral, thus π-delocalization is impossible, and the compound is destabilized. Product **3** is liberated and complex **4** reformed *via* ligand exchange. All together, $Fe^{III}$ catalysis of the Michael reaction seems to show a classic template effect,[6] where both reactants are coordinated at the same time and activated by a metal centre. And in fact $Fe(acac)_3$, which offers no vacant coordination site to an enone, does not catalyse the Michael reaction at all, that means a dionato ligand like acac can not be alkylated by non-coordinated **2a**, which was proved by a stoichiometric experiment. Also, it was impossible to achieve bis-substitution by converting, *e.g*. **3g** with **2a**, at even higher temperatures. This fits into the outlined picture of the mechanism, if we assume that the oxobutyl side chain of **3g** is donating itself to the centre metal and blocking a possibly vacant coordination site.

In summary, catalysis of the Michael reaction of β-dicarbonyl compounds and enone by $FeCl_3 \cdot 6H_2O$ is a very effective alternative to the classic base catalysis. The selectivity of this method is excellent in most cases, reaction conditions are mild and neutral, and performance is reasonably easy (no anhydrous or inert conditions, simple workup procedure), although it seems not to be appliable for enones bearing a *Z*-substituent.

Supplementary Information containing experimental details and characterization data for **3a**–**k** is available from the author on request.

Support from Professor S. Blechert and the Institut für Organische Chemie der TU Berlin is gratefully acknowledged.




**Scheme 2** Proposed mechanism for the iron(III) catalysed Michael reaction

The author also thanks the Fonds der Chemischen Industrie for a fellowship.

## Footnotes

† In one case the application of a combination of $Ni(acac)_2$ and $FeCl_3$ was reported, but the authors ascribe the role of $Fe^{III}$ to be a Lewis acid (activation of the enone).[5]

‡ *2-(3-Oxobutyl)cyclopentanone-2-carboxylic acid 2-methylpropyl ester* (**3b**): A mixture of oxo ester **1b** (1.03 g, 5.60 mmol), enone **2a** (0.500 ml, 6.00 mmol), and $FeCl_3 \cdot 6H_2O$ (15 mg, 0.055 mmol) was stirred overnight at room temp., then chromatographed on silica gel [hexane–methyl *tert*-butyl ether (MTB) 1 : 5, $R_f$ = 0.45] to afford 1.35 g (5.32 mmol, 95%) of **3b** as a colourless oil. $^1$H NMR (400 MHz, $CDCl_3$): δ 0.91 (d, *J* = 6.6 Hz, 6 H, 2 $CH_3$), 1.84–2.15 (m, 6 H, CH, $CH_2$), 2.13 (s, 3 H, $CH_3$), 2.25–2.52 (4 H, $CH_2$), 2.70 (ddd, *J* = 18, *J* = 9.1, *J* = 6.2 Hz, 1 H, CH*H*), 3.84–3.92 (m, 2 H, $OCH_2$). $^{13}$C NMR (50 MHz, $CDCl_3$): δ 18.72 (2 $CH_3$), 19.37 ($CH_2$), 26.79 ($CH_2$), 27.47 (CH), 29.62 ($CH_3$), 34.08 ($CH_2$), 38.62 ($CH_2$), 58.73 (C), 71.08 ($OCH_2$), 171.13 (C=O), 207.38 (C=O), 214.42 (C=O).

§ *2-(3-Oxobutyl)cycloheptanone-2-carboxylic acid methyl ester* (**3e**): A mixture of oxo ester **1e** (929 mg, 5.46 mmol), enone **2a** (0.500 ml, 6.00 mmol), and $FeCl_3 \cdot 6\ H_2O$ (15 mg, 0.055 mmol) was stirred overnight at room temp., then chromatographed on silica gel (hexane–MTB 1 : 5, $R_f$ = 0.45) to give 1.20 g (4.99 mmol, 91%) of **3e** as a colourless oil. $^1$H NMR (400 MHz, $CDCl_3$): δ 1.38–1.55 (m, 2 H, $CH_2$), 1.58–1.75 (m, 5 H, $CH_2$), 1.79–1.92 (m, 1 H, CH*H*), 1.88 (ddd, *J* = 14, *J* = 10, *J* = 5.6 Hz, 1 H, C*H*H), 2.10 (s, 3 H, $CH_3$), 2.15 (ddd, *J* = 14, *J* = 10, *J* = 5.6 Hz, 1 H, CH*H*), 2.39 (ddd, *J* = 18, *J* = 10, *J* = 5.6 Hz, 1 H; C*H*H), 2.45–2.65 (m, 3 H, $CH_2$), 3.70 (s, 3 H, $OCH_3$). $^{13}$C NMR (50 MHz, $CDCl_3$): δ 24.49 ($CH_2$), 24.99 ($CH_2$), 28.82 ($CH_2$), 29.34 ($CH_2$), 29.38 ($CH_3$), 33.48 ($CH_2$), 38.57 ($CH_2$), 41.68 ($CH_2$), 51.69 ($OCH_3$), 61.32 (C), 172.39 (C=O), 206.99 (C=O), 208.87 (C=O).

## References

1 H. Sasai, T. Arai, Y. Satow, K. N. Houk and M. Shibasaki, *J. Am. Chem. Soc*., 1995, **117**, 6194; H. Sasai, E. Emori, T. Arai and M. Shibasaki, *Tetrahedron Lett*., 1996, **37**, 5561; T. Arai, Y. M. A. Yamada, N. Yamamoto, H. Sasai and M. Shibasaki, *Chem. Eur. J*., 1996, **2**, 1368.

2 J. H. Nelson, P. N. Howells, G. C. DeLullo, G. L. Landen and R. A. Henry, *J. Org. Chem*., 1980, **45**, 1246; C. P. Fei and T. H. Chan, *Synthesis*, 1982, 467; H. Brunner and B. Hammer, *Angew. Chem*., 1984, **96**, 305; *Angew. Chem., Int. Ed. Engl*., 1984, **32**, 312; P. Kocovsky and D. Dvorak, *Tetrahedron Lett*., 1986, **27**, 5015.

3 F. Bonadies, A. Lattanzi, L. R. Orelli, S. Pesci and A. Scettri, *Tetrahedron Lett*., 1993, **34**, 7649; E. Keller and B. L. Feringa, *Tetrahedron Lett*., 1996, **37**, 1879; A. Soriente, A. Spinella, M. DeRosa, M. Giordano and A. Scettri, *Tetrahedron Lett*., 1997, **38**, 289.

4 Literature cited in *Gmelins Handbuch der Anorganischen Chemie*, Eisen, Verlag Chemie, Berlin, 1932, vol. 59 B, pp. 554.

5 P. Laszlo, M.-T. Montaufier and S. L. Randriamahefa, *Tetrahedron Lett*., 1990, **31**, 4867.

6 M. C. Thompson and D. H. Busch, *J. Am. Chem. Soc*., 1962, **84**, 1762.

*Received in Cambridge, UK, 5th February 1997; Com. 7/00838D*

# Hydrothermal synthesis and lanthanide doping of complex fluorides, $LiYF_4$, $KYF_4$ and $BaBeF_4$ under mild conditions

**Chunyan Zhao,[a] Shouhua Feng,*[a] Ruren Xu,[a] Chunsan Shi[b] and Jiazuan Ni[b]**

[a] *Key Laboratory of Inorganic Hydrothermal Synthesis and Department of Chemistry, Jilin University, Changchun 130023, P.R. China*

[b] *Laboratory of Rare Earth Chemistry and Physics, Changchun Institute of Applied Chemistry, Chinese Academy of Science, Changchun 130021, P.R. China*

**The complex fluorides $LiYF_4$, $KYF_4$, $BaBeF_4$ and $AYF_4Eu_x$ (A = Li, K) are hydrothermally synthesized at 140–240 °C and characterized by powder X-ray diffraction, thermogravimetric analysis, IR spectroscopy, scanning electron microscopy and luminescence measurements.**

Recently, we reported on a mild hydrothermal synthesis of the complex fluorides $LiBaF_3$ and $KMgF_3$ with perovskite structures at 120–240 °C,[1] which gives rise to the possibility of making new functional fluoride compounds with various structures and particular properties under mild conditions. It is well known that complex fluorides with strong potential application as luminescence materials can be prepared by solid-state reactions at high temperatures.[2,3] This solid-state synthetic apparatus however requires a complicated set-up due to the erosion of fluorides and thus has limited the study of fluoride chemistry.[4] Mild hydrothermal synthesis, as a low energy-costing and less-polluting method, can enhance the reactivity of reactants in solution and can be used to prepare important crystalline solids which are difficult to prepare or can not be prepared by solid-state reactions, such as in the case of microporous crystals. We have synthesized a number of novel oxides or complex oxides such as microporous solids and solid electrolytes by this moderate preparative technique.[5–10] As an extension of the study on hydrothermal synthesis of complex fluorides with perovskite structures ($ABF_3$), we have investigated the synthesis of $ABF_4$-type complex fluorides as well as hydrothermal doping of photo-sensitive lanthanide elements into the fluorides. The aim of our research is to search for a mild hydrothermal synthesis route to produce a variety of complex fluorides and to study the possibility for hydrothermal equilibrium doping of lanthanide ions into the fluorides.

The starting materials for the syntheses of $LiYF_4$ and $KYF_4$ were LiOH (A.R.), KF (A.R.), $Y_2O_3$ (99.99%) and $HN_4HF_2$ (A.R.). Under typical synthesis conditions the mole ratios of the starting materials were 2.0 LiOH : 1.0 $Y_2O_3$ : 10.0 $NH_4HF_2$ : 500 $H_2O$ and 3.0 KF : 1.0 $Y_2O_3$ : 4.0 $NH_4HF_2$ : 300 $H_2O$ for the syntheses of $LiYF_4$ and $KYF_4$, respectively. The typical synthetic procedure for crystalline $LiYF_4$ was as follows: 0.08 g LiOH, 0.23 g $Y_2O_3$ and 0.57 g $NH_4HF_2$ were added to 9 ml of deionized water (for the synthesis of $KYF_4$, 0.29 g KF, 0.38 g $Y_2O_3$ and 0.38 g $NH_4HF_2$ were used in this step), to form a reaction mixture with a pH of *ca.* 4. The reaction mixture was sealed in a Teflon-lined stainless-steel autoclave and heated at 240 °C under autogenous pressure for 7 days. After the autoclaves were cooled and depressurised, the final powder products were washed with deionized water and air-dried at room temperature. In the hydrothermal doping experiment, $Eu_2O_3$ (99.999%) was used as a reactant in the synthesis of $AYF_4Eu_x$ (A = Li, K), and the reactant mixtures had mole compositions: 2.0 LiOH : 1.0 $Y_2O_3$ : 10.0 $NH_4HF_2$ : 500 $H_2O$ : 0.09 $Eu_2O_3$ and 3.0 KF : 1.0 $Y_2O_3$ : 4.0 $NH_4HF_2$ : 300 $H_2O$ : 0.09 $Eu_2O_3$, for $LiYF_4Eu_x$ and $KYF_4Eu_x$ respectively; the reaction mixtures were heated in Teflon-lined stainless-steel autoclaves at 240 °C for 7 days.

$BaBeF_4$ was prepared by hydrothermal crystallization of a reaction mixture with a mole composition: 1.0 $Ba(OH)_2$ : 2.0 $BeF_2$ : 2.0 $NH_4HF_2$ : 200 $H_2O$ in Teflon-lined autoclaves at 140 °C for 4 days. The typical synthesis procedure was as follows: 0.79 g of barium hydroxide and 0.24 g of beryllium fluoride (A.R.) were dissolved in 9 ml of deionized water to form a solution, then 0.28 g of $NH_4HF_2$ (A.R.) was added dropwise to the solution under magnetic stirring. Hydrofluoric acid (40 mass%, A.R.) was used to adjust the pH to 2–4.

All products were characterized by X-ray diffraction (XRD) on a Rigaku D/max-γA diffractometer with a rotating target with Ni-filtered Cu-Kα radiation at room temperature. The XRD data for indexing and cell-parameter calculation were collected by a scanning mode with a step length of 0.02° and a scanning rate of 0.2° $min^{-1}$. Silicon was used as an internal standard. Observation of the crystallites was performed on a Hitachi X-650 scanning electron microscope (SEM). Thermogravimetric analysis (TGA) was conducted on a TGS-2 thermogravimetric system. IR spectra were obtained with a Nicolet 5DX spectrometer using the KBr pellet technique. Optical measurements were performed at room temperature using a Spex Fluorolog 2 spectrofluorometer.

Table 1 shows the hydrothermal synthesis conditions for $LiYF_4$, $KYF_4$ and $BaBeF_4$. In the syntheses, ratios of initial composition and the pH of the reaction system were found to be crucial to the formation, crystallization and purity of the products. In the synthesis of $BaBeF_4$, the ratio of Ba/Be is a

**Table 1** Hydrothermal synthesis conditions for $BaBeF_4$, $LiYF_4$ and $KYF_4$

| Starting materials | | a : b mole ratio | pH | *t*/day | *T*/°C | Phases in product |
|---|---|---|---|---|---|---|
| a | b | | | | | |
| $Ba(OH)_2$ | $BeF_2$ | 1 : 1 | 4 | 4 | 140 | $BaBeF_4$ |
| $Ba(OH)_2$ | $BeF_2$ | 1 : 1 | 4 | 4 | 180 | $BaBeF_4$ |
| $Ba(OH)_2$ | $BeF_2$ | 1 : 1 | 4 | 4 | 200 | $BaBeF_4$ |
| $Ba(OH)_2$ | $BeF_2$ | 1 : 1 | 4 | 4 | 240 | $BaBeF_4$ |
| $Ba(OH)_2$ | $BeF_2$ | 2 : 1 | 4 | 4 | 240 | $BaBeF_4$ + $BaF_2$ |
| $Ba(OH)_2$ | $BeF_2$ | 1 : 2 | 4 | 4 | 240 | $BaBeF_4$ |
| $Ba(OH)_2$ | $BeF_2$ | 1 : 1 | 4 | 2 | 240 | $BaBeF_4$ |
| $Ba(OH)_2$ | $BeF_2$ | 1 : 1 | 4 | 3 | 240 | $BaBeF_4$ |
| $Ba(OH)_2$ | $BeF_2$ | 1 : 1 | 4 | 4 | 240 | $BaBeF_4$ |
| $Ba(OH)_2$ | $BeF_2$ | 1 : 1 | 4 | 5 | 240 | $BaBeF_4$ |
| LiOH | $Y_2O_3$ | 1 : 1 | 4 | 7 | 240 | $LiYF_4$ + $Y_2O_3$ |
| LiOH | $Y_2O_3$ | 1 : 1 | 3 | 7 | 240 | $LiYF_4$ + $Y_2O_3$ |
| LiOH | $Y_2O_3$ | 2 : 1 | 4 | 7 | 240 | $LiYF_4$ |
| LiOH | $Y_2O_3$ | 2 : 1 | 3 | 7 | 240 | $LiYF_4$ |
| LiOH | $Y_2O_3$ | 3 : 1 | 13 | 5 | 240 | —[a] |
| LiF | $Y_2O_3$ | 1 : 1 | 2 | 5 | 240 | —[a] |
| KF | $Y_2O_3$ | 2 : 1 | 4 | 7 | 240 | $KYF_4$ + $Y_2O_3$ |
| KF | $Y_2O_3$ | 3 : 1 | 4 | 8 | 240 | $KYF_4$ |
| KF | $Y_2O_3$ | 3 : 1 | 4 | 7 | 240 | $KYF_4$ |
| KF | $Y_2O_3$ | 3 : 1 | 4 | 3 | 240 | —[a] |
| KF | $Y(NO_3)_3$ | 3 : 1 | 2 | 7 | 240 | $KYF_4$ |

[a] Unknown phases.

**Table 2** Lattice parameters of $BaBeF_4$, $LiYF_4$ and $KYF_4$

| | | Lattice parameters/Å | | | | | |
|---|---|---|---|---|---|---|---|
| | | Obs. | | | JCPDS[a] | | |
| Compound | Symmetry | *a* | *b* | *c* | *a* | *b* | *c* |
| $BaBeF_4$ | Orthorhombic | 8.828 | 5.324 | 7.043 | 8.83 | 5.34 | 7.03 |
| $LiYF_4$ | Tetragonal | 5.166 | | 10.744 | 5.168 | | 10.736 |
| $KYF_4$ | Hexagonal | 8.132 | | 10.043 | 8.131 | | 10.117 |

[a] JCPDS cards 20-118, 17-874 and 27-466, respectively.

dominating factor. When the Ba/Be ratio was 0.5, $BaBeF_4$ was formed but when Ba/Be = 2, impurity phases appeared. In the synthesis of $LiYF_4$, when LiOH and $Y_2O_3$ were employed and the ratio of Li/Y was unity, $NH_4HF_2$ must be added and a pH of 3–4 was required, addition of a small excess of $NH_4HF_2$ did not result in the formation of impurities. In the synthesis of the $KYF_4$, when KF and $Y_2O_3$ were utilized as starting materials, a ratio of K/Y of 3/2 was optimal. In this case, $NH_4HF_2$ was also used to supply $F^-$ and to adjust the pH to 2–4.

The pH of the reaction system considerably influences the crystallization of the complex fluorides. For example, using KF and $Y_2O_3$ as starting materials, $KYF_4$ can be synthesized at pH *ca.* 4, whereas when $Y(NO_3)_3$ and KF are used, $KYF_4$ can be prepared at pH *ca.* 2.

It is known that $F^-$ ion is an effective mineralizer in both aqueous and non-aqueous systems.[11–13] In the synthesis of $BaBeF_4$, $LiYF_4$ and $KYF_4$, $F^-$ ion was either a reactant or a mineralizer. Excess $F^-$ ions may lower remarkably the temperature of crystallization. Thus $KYF_4$ can be crystallized even at 180 °C, when excess $F^-$ ions are added. Crystallization temperature and time were also important factors for an effective synthesis. Although $BaBeF_4$ can be crystallized below 240 °C, prolonged reaction times are required. For instance, in the $BeF_2$–$BaF_2$–HF–$H_2O$ system, $BaBeF_4$ is formed after 2 days at 240 °C, but at 140 °C 4 days are required (Table 1).

The XRD patterns of the $BaBeF_4$, $LiYF_4$ and $KYF_4$ can be indexed in orthorhombic, tetragonal and hexagonal systems, respectively (Table 2; full XRD data available from the authors on request). The cell of hydrothermally prepared $KYF_4$ is smaller then that of $KYF_4$ prepared by solid-state reaction. For $BaBeF_4$ and $LiYF_4$, the two synthetic methods give almost the same cell sizes.

The thermal stability of the $BaBeF_4$, $LiYF_4$ and $KYF_4$ were studied by TG–DTA in air. There are no phase transformations up to 600 °C in all three systems and no mass losses were observed between 50 and 600 °C. This indicates that the samples are not hydrated and are stable in air, as confirmed by IR spectroscopy in this temperature range.

The morphology of the samples was examined by SEM at room temperature. The results show that the grain size of the product particles is related to the pH of reaction solutions and the nature of cations used in the synthesis. Uniform grain texture of $BaBeF_4$ can be observed with grain sizes ranging from 0.2 to 5 μm. The SEM morphologies of $LiYF_4$ and $KYF_4$ show regular shapes with grain sizes in the range 0.2–10 μm.

The optimum doping concentrations of $Eu^{3+}$ ions in $LiYF_4$ and $KYF_4$ were $x = 0.09$ mole in $AYF_4Eu_x$ (A = Li, K) and the highest doping concentration of $Eu^{3+}$ ions was $x = 0.2$. Both excitation and emission spectra show the d–f transition typical of $Eu^{3+}$ compounds. The room-temperature excitation spectrum shows a peak at 393 nm, while the emission spectrum shows $^5D_0$–$^7F_J$ ($J = 0, 1, 2, 3, 4$) five-line peaks and a maximum at 615 nm. All hydrothermally prepared samples showed significant luminescence properties. In the room-temperature excitation spectrum of samples obtained from hydrothermal systems, no charge transition states were observed. This indicates there is no oxygen insertion in the samples which usually occurs in solid-state reactions. A comparison of relative emission intensities for both hydrothermally and solid-state prepared samples is in progress to understand if the equilibrium doping concentration is suitable for optimizing luminescence properties.

In summary, the complex fluorides $BaBeF_4$, $LiYF_4$ and $KYF_4$ were hydrothermally prepared at 140–240 °C. The molar ratio and pH in the initial reaction mixture associated with the reaction temperature dominate the crystallization of the products. $BaBeF_4$, $LiYF_4$ and $KYF_4$ crystallize in orthorhombic, tetragonal and hexagonal systems, respectively, and all products have uniform grain sizes. The compounds are air stable and show no insertion of oxygen. Hydrothermal doping of $Eu^{3+}$ ions into $LiYF_4$ and $KYF_4$ is successful and measurements of the excitation and emission spectra of $AYF_4Eu_x$ (A = Li, K) reveal the same energy level schemes as those previously established based on samples prepared by solid-state reactions. In addition, luminescence studies demonstrate that crystallization of our samples in hydrothermal systems is complete. The hydrothermal synthesis and doping routes are apparently advantageous compared with traditional high-temperature solid-state methods.

This work was supported by the Chinese NSF through the National Outstanding Youth Science Fund, the State Education Commission through the Excellent Investigator Plan and the State Science and Technology Commission through a PANDENG Plan (S. F.).

## References

1 H. S. Kiliaan, A. Meijerink and G. Blasse, *J. Lumin.*, 1986, **35**, 155.
2 G. M. Renfor, J. C. Windscheif, *et al., J. Lumin.*, 1980, **22**, 51.
3 A. R. West, *Solid State Chemistry and its Applications*, Wiley, New York, 1984, p. 338.
4 L. N. Dermianets, *Prog. Cryst. Growth Charact.*, 1990, **21**, 299.
5 S. Feng and M. Greenblatt, *Chem. Mater.*, 1992, **4**, 462.
6 S. Feng and M. Greenblatt, *Chem. Mater.*, 1993, **5**, 1277.
7 Y. An, S. Feng, Y. Xu, R. Xu and Y. Yue, *J. Mater. Chem.*, 1994, **4**, 985.
8 X. Yu, S. Feng and W. Pang, *J. Solid State Chem.*, 1995, **119**, 197.
9 Y. An. S. Feng, Y. Xu and R. Xu, *Chem. Mater.*, 1996, **8**, 356.
10 Y. Xu, S. Feng and W. Pang, *Chem. Commun.*, 1996, 1305.
11 C. Zhao, S. Feng, Z. Chao, C.-S. Shi, R. Xu and J. Ni, *Chem. Commun.*, 1996, 1641.
12 J. L. Guth, H. Kessler and R. Wey, *Proc. 7th Int. Zeolite Conf.*, Tokyo, 1986, p. 121.
13 M. Estermann, L. B. Mccusker, C. Baerlocher, A. Merrouche and H. Kessler, *Nature*, 1991, **352**, 320.

*Received, 16th October 1996; Com. 6/07066C*

# A new ambient-pressure organic superconductor $(TMET\text{-}STF)_2BF_4$ [TMET-STF = trimethylene(ethylenedithio)diselenadithiafulvalene]

**Reizo Kato,*[a] Ken Yamamoto,[a] Yoshinori Okano,[a] Hiroyuki Tajima[a] and Hiroshi Sawa[b]**

[a] *The Institute for Solid State Physics, The University of Tokyo, Roppongi, Minato-ku, Tokyo 106, Japan*
[b] *Department of Physics, Faculty of Science, Chiba University, Yayoi-cho, Inage-ku, Chiba 263, Japan*

**Under ambient pressure, the cation radical salt $(TMET\text{-}STF)_2BF_4$, where the tight-binding band calculation suggests coexistence of one- and two-dimensional Fermi surfaces associated with two different conduction layers within the crystal, shows two types of resistivity anomalies around 115 and 13 K, followed by a superconducting transition at 4.1 K (onset).**

Extensive studies on organic superconductors have revealed that they display various electronic structures ranging from the quasi-one-dimensional type (*e.g.* TMTSF salts) to the two-dimensional type (*e.g.* BEDT-TTF salts) (TMTSF = tetramethyltetraselenafulvalene, BEDT-TTF = bis(ethylenedithio)tetrathiafulvalene].[1] The dimensionality of the electronic structure is one of the essential factors which determine the physical properties of the system. The organic donor TMET-STF [trimethylene(ethylenedithio)diselenadithiafulvalene] is a hybrid between BEDT-TTF and HMTSF (hexamethylenetetraselenafulvalene) and was first reported in 1986.[2] We found an improved synthetic route to this molecule *via* a titanocene complex and pointed out the possibility of coexistence of one- and two-dimensional Fermi surfaces in its $ClO_4$ salt, $(TMET\text{-}STF)_2ClO_4$.[3] We report here that the isostructural $BF_4$ salt is an ambient-pressure superconductor with $T_c$ (onset) = 4.1 K.

Plate-like single crystals used for the resistivity and magnetization measurements were grown by galvanostatic electrolysis (1 μA) of TMET-STF (9.8 mg) in the presence of $NBu^n_4BF_4$ (50.2 mg) in thf (20 ml) at 20 °C under Ar. An H-tube and platinum electrodes (1 mm diameter) were used. The electrical resistivity in the crystallographic *ac* plane was measured by the standard four-probe method. Gold leads (15 μm diameter) were attached to the sample with carbon paste. The contacts remained ohmic through the measurement. Resistivity measurements under pressure were performed in a clamp cell with a 1 : 1 mixture of Fluorinert No. FC70 and FC77 as the pressure transmitting medium. The pressure was calibrated with the superconducting transition temperature of Sn. The dc magnetization was measured with a Quantum Design MPMS SQUID magnetometer. Four crystals with a total mass of 0.06 mg were glued onto a sample holder (polypropylene, 1.17 mg) with a small amount of grease (Apiezon N).

Fig. 1 shows the temperature dependence of the resistivity under ambient pressure. The room-temperature resistivity was *ca.* $2 \times 10^{-2}$ Ω cm. With lowering temperature, the resistivity decreased monotonously and displayed a first upturn around 115 K. The resistivity, however, formed a small peak around 100 K and decreased again. The second upturn appeared around 13 K. The ratio of ρ(4.1 K)/ρ(13 K) was sample dependent and ranged between 2 and 9. We did not observe hysteresis at either resistivity anomaly. An abrupt drop of the resistivity occurred at 4.1 K (onset) and we observed this behaviour in all seven samples. An application of pressure effectively suppressed the first upturn of the resistivity, while the second one remained up to *ca.* 7 kbar. The pressure effect on the transition temperature for the abrupt resistivity drop was rather moderate ($dT_c/dP \approx -0.2$ K kbar$^{-1}$).

Fig. 2 shows the zero-field-cooled (ZFC) and field-cooled (FC) temperature dependence of the dc magnetization, uncorrected for demagnetization, at a fixed field of 10 Oe perpendicular (approximately) to the crystallographic *ac* plane. The protocol was as follows: after cooling to 1.8 K in zero field, a magnetic field of 10 Oe was applied and the dc magnetization was measured while warming to 6.0 K (ZFC). The sample was then cooled to 2.0 K under the same field, 10 Oe (FC). The onset of a diamagnetic transition was observed at 3.8 K. This value is consistent with the result of the resistivity measurement. From the ZFC curve, we can roughly estimate that a volume fraction is *ca.* 50% of perfect diamagnetism; accuracy, however, is not high as the amount of the sample was very small. Such a large diamagnetism and the abrupt resistivity drop can be explained only by the appearance of a superconducting phase. Hysteresis

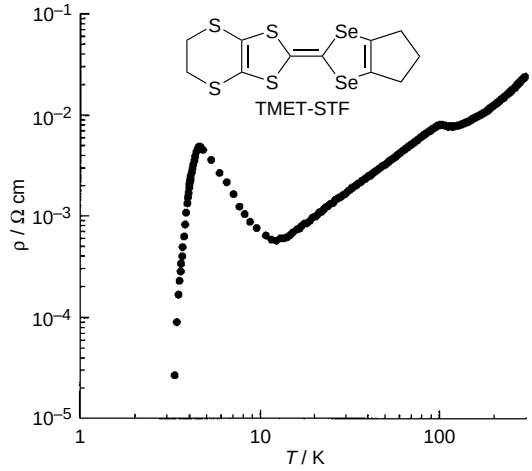



**Fig. 1** Temperature dependence of the resistivity at ambient pressure

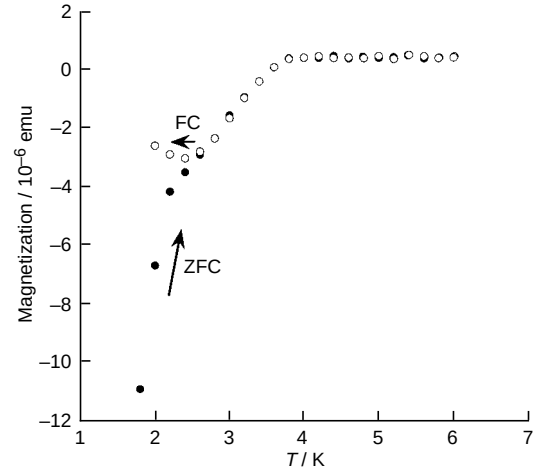



**Fig. 2** Temperature dependence of the zero-field-cooled (ZFC) and field-cooled (FC) dc magnetization with a fixed applied field of 10 Oe

between the FC and ZFC curves indicates that flux is trapped in the sample as it is cooled below the transition temperature.

This $BF_4$ salt is isostructural with the $ClO_4$ salt.[3]† The unit cell contains two crystallographically independent donor molecules (A, B) which are associated with conduction layers A and B, respectively (Fig. 3). In both layers, unsymmetrical donor molecules are stacked alternately in a slightly dimerized fashion. The molecular packing in layer B is very similar to that in TMTSF salts. On the other hand, in layer A, donor molecules are packed more loosely. This can be seen by enlarged interplanar distances and seems to be related to a positional disorder of the terminal ethylene group as reflected by the largely elongated thermal ellipsoids (Fig. 3). By comparison, it should be noted that the ethylene group is completely ordered in layer B. Comparison of the bond lengths in these two donor units (A, B) suggests that the difference in the formal charge is rather small and therefore the formal charge is close to +0.5 for each molecule. Layers A and B are separated from each other by an anion layer.

A very unique feature is that these two donor layers differ in anisotropy of the intermolecular interaction, which has been examined by overlap integrals among the HOMOs obtained by the extended Hückel method.[4] As is the case of the $ClO_4$ salt,[3] the intracolumn interactions in the layer A are largely reduced, which results in a reduction of the anisotropy. The interaction between layers A and B is very small. The conduction band (3/4 filled) is constructed by the HOMO and is composed of two branches associated with the layers A and B, respectively. The tight-binding band calculations, where the interlayer interaction is neglected, indicate that layer A provides a two-dimensional Fermi surface, while layer B provides a quasi-one-dimensional one (Fig. 3).‡ Therefore, the electronic structure of this compound can be described as a hybrid between the TMTSF and BEDT-TTF systems. Almost all superconducting cation radical salts have a single type of conducting layer (column) within the crystal and thus a single type of Fermi surface in the Brillouin zone. In $(TMET\text{-}STF)_2BF_4$, however, there exist two crystallographically independent conduction layers composed of the 'same' molecule, within the 'same' crystal providing different types of Fermi surfaces. Although we neglected the interlayer interaction in the band calculation, there should be small but significant interactions between layers A and B which would affect the physical properties.

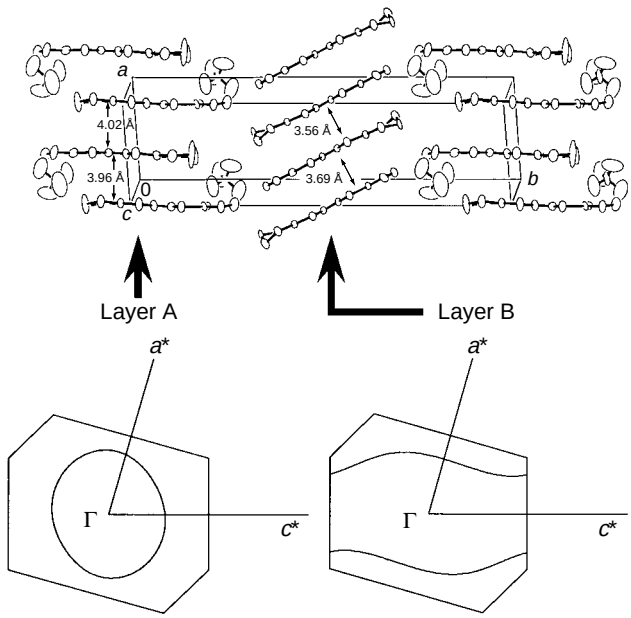



**Fig. 3** Crystal structure and calculated Fermi surfaces of $(TMET\text{-}STF)_2BF_4$

The resistivity measurement clearly suggests two types of anomalies in the metallic state which have never previously been observed in conventional organic superconductors. Although they are suggestive of a special electronic state mechanistic details await clarification.

The resistivity behaviour of the isostructural $ClO_4$ salt was similar to that of the $BF_4$ salt, except that a superconducting transition was not observed down to 1.5 K under pressures from 1 bar to 16.8 kbar.

In summary, the ambient-pressure superconductivity in the cation radical salt $(TMET\text{-}STF)_2BF_4$ has been established by resistivity and magnetization measurements. This system is a 'two-band' system associated with (quasi) one- and two-dimensional conduction layers within the crystal and is of special interest in view of an interplay among one-dimensional charge localization, higher dimensionality, and superconductivity. TMET-STF is known to provide a variety of cation radical salts.[5–7] Detailed studies on structural and physical properties of these salts are in progress.

This work was partially supported by Grants-in-Aid for Scientific Research on Priority Area 'Novel Electronic States in Molecular Conductors' (Area No. 253/06243105) from the Ministry of Education, Science and Culture, Japan.

## Footnotes

* E-mail: reizo@issp.u-tokyo.ac.jp

† *Crystal data* for $(TMET\text{-}STF)_2BF_4$: $C_{22}H_{20}BF_4S_8Se_4$, $M_w$ = 943.50, triclinic, space group $P\bar{1}$, $a$ = 8.030(1), $b$ = 29.646(5), $c$ = 6.546(1) Å, $\alpha$ = 92.48(1), $\beta$ = 105.65(1), $\gamma$ = 93.86(1)°, $U$ = 1494.1(4) Å$^3$, $Z$ = 2, $D_c$ = 2.10 g cm$^{-3}$, $F(000)$ = 914.00, $R$ = 0.079, $R_w$ = 0.077, GOF = 3.77. X-Ray diffraction data were collected on a MAC Science automatic four-circle diffractometer with monochromated Mo-K$\alpha$ ($\lambda$ = 0.710 69 Å; 50 kV, 300 mA) radiation up to $2\theta$ = 60°. The intensities were corrected for Lorentz and polarization effects. The analytical absorption correction was carried out. The structure was solved by the direct method and refined with full-matrix least-squares using 5022 reflections with $I \geqslant 3\sigma(I)$. Anisotropic thermal parameters were used for non-hydrogen atoms. Hydrogen atoms were included but not refined. All calculations were performed with use of the 'teXsan' crystallographic software package of Molecular Structure Corporation. Two carbon atoms of the ethylene group in molecule A exhibit very large thermal parameters due to positional disorder. It was impossible to refine this ethylene group as a superposition of two possible conformations. Atomic coordinates, bond lengths and angles, and thermal parameters have been deposited at the Cambridge Crystallographic Data Centre (CCDC). See Information for Authors, Issue No. 1. Any request to the CCDC for this material should quote the full literature citation and the reference number 186/439.

‡ It has been assumed that the transfer integral ($t$) is proportional to the overlap integral ($S$), $t = \varepsilon S$ ($\varepsilon$ is a constant of the same order as the orbital energies of the HOMO). Based on the filling of each band, we estimated the formal charge of the molecule A to be +0.4 and that of the molecule B to be +0.6. This is consistent with the result of the bond length analysis; each molecule has a formal charge close to +0.5.

## References

1 J. Wosnitza, *Fermi Surfaces of Low-Dimensional Organic Metals and Superconductors*, Springer Tracts in Modern Physics Vol. 134, Springer, Berlin, 1996.
2 K. Kikuchi, T. Namiki, I. Ikemoto and K. Kobayashi, *J. Chem. Soc., Chem. Commun.*, 1986, 1472.
3 Y. Okano, H. Sawa, S. Aonuma and R. Kato, *Chem. Lett.*, 1993, 1851.
4 Semiempirical parameters for Slater-type atomic orbitals used in the calculation were previously published: see R. Kato, S. Aonuma, Y. Okano, H. Sawa, M. Tamura, K. Oshima, A. Kobayashi, K. Bun and H. Kobayashi, *Synth. Met.*, 1993, **61**, 199.
5 Y. Okano, H. Sawa, S. Aonuma and R. Kato, *Synth. Met.*, 1995, **70**, 1161.
6 Y. Okano, K. Yamamoto, T. Imakubo, H. Sawa and R. Kato, *Synth. Met.*, in the press.
7 S. Uji, T. Terashima, H. Aoki, S. Valfells, J. S. Brooks, K. Yamamoto, Y. Okano, H. Sawa and R. Kato, *Synth. Met.*, in the press.

*Received in Cambridge, UK, 28th January 1997; Com. 7/00629B*

# Synthesis and characterization of mesostructured aluminophosphates using the fluoride route

**Pingyun Feng, Yin Xia, Jianglin Feng, Xianhui Bu and Galen D. Stucky***

*Department of Chemistry, University of California, Santa Barbara, California 93106, USA*

**The room-temperature synthesis of the hexagonal mesostructured aluminophosphate and its phase transition into the lamellar phase are reported.**

Since Mobil researchers first demonstrated in 1992 that through a micelle-assisted crystallization of the inorganic phase, the hexagonally packed mesoporous silicate and aluminosilicate materials (MCM-41) with uniformly sized pores could be synthesized,[1] there has been much interest in synthesizing mesoporous aluminophosphates owing to the previous success in the synthesis of microporous aluminophosphates[2] with framework topology identical or similar to aluminosilicate zeolites. However, so far attempts in synthesizing the mesostructured aluminophosphates have had very limited success.

It has been demonstrated that lamellar aluminophosphates can be made from non-aqueous or aqueous systems by using a liquid-crystal templating approach.[3–7] The presence of the hexagonal mesostructured aluminophosphate has been suggested in a brief description by Kimura *et al.*[8] Here, we demonstrate that in the presence of $F^-$ ions and using EtOH–$H_2O$ as a solvent, pure hexagonal mesostructured aluminophosphate of relatively high quality can be obtained. We have found that the formation of the hexagonal phase precedes the formation of the lamellar phase and that a phase transition from the hexagonal phase to the lamellar phase in the aluminophosphate system can be induced.

A typical sample preparation was: aluminium isopropoxide (4.01 g) was mixed with 7.28 g of ethanol. After stirring, 40.0 g of distilled water was added, followed by the addition of 2.79 g of 85% $H_3PO_4$ and 0.67 g of 49% HF. After further stirring, 1.86 g of $C_{16}H_{33}Me_3NBr$ (surfactant/Al ratio = 0.26) was added. Finally, 10.40 g of 25% $NMe_4OH$ was slowly added until the pH of the solution was *ca*. 8.3. The mixture was stirred at room temp. for 4 h. The pure hexagonal mesostructured phase was obtained after filtering and washing with distilled water. However, if after stirring for 4 h at room temp. the gel was placed in an oven at 70 °C for a few days, the hexagonal phase was converted partially into a mesostructured lamellar phase. At higher temperatures such as 100 °C, the transition to the lamellar phase proceeded at a faster rate and the complete conversion took only 2 days. The X-ray powder patterns with different reaction conditions are shown in Fig. 1.

Postsynthesis treatment was found to enhance the crystalline quality of the hexagonal mesostructured phase.[9] The above-room-temperature synthesized hexagonal sample was further treated by putting the sample into deionized water at 70 °C for about a week, then filtered and dried. The sample was subsequently stirred in ethanol overnight, filtered off and dried. The intensity of the XRD peaks was greatly enhanced by this treatment. The treated sample was used for the subsequent characterization including TEM and $^{27}Al$ MAS NMR.

The hexagonal phase obtained was further confirmed by the TEM image (Fig. 2) which was recorded on a 2000FX JEOL microscope operated at 200 keV. The TEM sample was prepared by collecting a large number of crystallites onto a holey carbon film on a Ni grid. $^{27}Al$ MAS NMR spectra were obtained on a General Electric GN-300 spectrometer system at a frequency of 78.30 MHz with a spinning speed of *ca*. 5 kHz, a delay time of 2 s. and a pulse width of 4.0 μs. A four-pulse composite 90° pulse was used for background suppression.[10] Aluminium nitrate solution was used as external reference. The $^{27}Al$ MAS NMR of the hexagonal mesostructured material gave two lines at δ 43.8 and −8.7 corresponding to tetrahedrally and octahedrally coordinated Al species, respectively. $^{27}Al$ NMR of

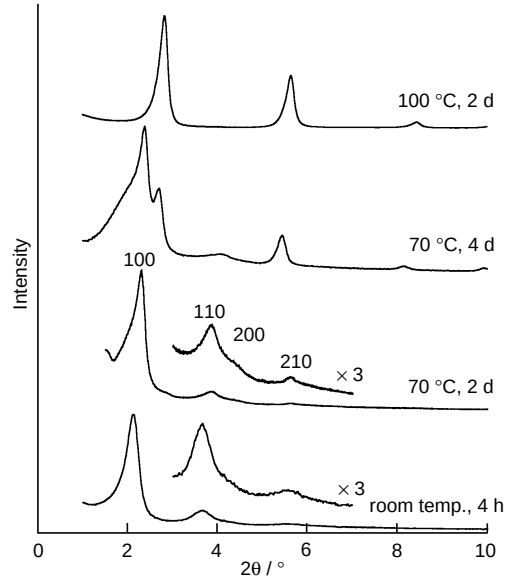



**Fig. 1** Powder diffraction patterns showing the phase transition from the hexagonal phase to the lamellar phase under different reaction conditions

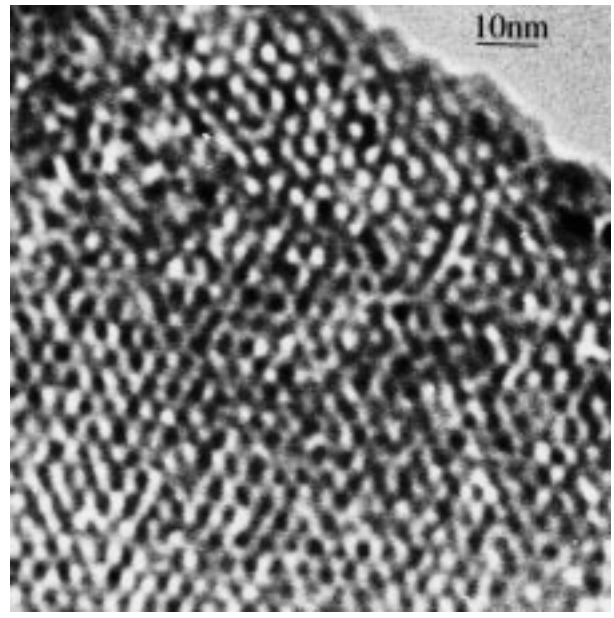



**Fig. 2** The TEM image of the hexagonal mesostructured aluminophosphate

the lamellar mesostructure showed one narrow line at δ 40.06 and a very small bump at δ −8.2 suggesting the tetrahedral coordination for the majority of the Al species in the lamellar phase (Fig. 3). The inclusion of $F^-$ anions into the hexagonal phase was verified by elemental analysis (results in mass%: 9.38 Al, 9.14 P, 3.56 F, 26.19 C, 1.55 N, 7.77 H, < 0.5 Br) which was performed by Galbraith Laboratories, Inc. The molar ratio between polyhedral centres (Al + P) and the surfactant is comparable to that found in the silica-based MCM-41 material.[11] Thermogravimetric analysis (TG) and differential thermal analysis (DTA) on the hexagonal phase showed that the mass loss occurred between 300 and 700 °C accompanied by endothermic events. The calcination of the as-synthesized hexagonal phase into a mesoporous structure has not yet been achieved and further investigation is in progress.

Compared to silica-based mesoporous materials, the formation of aluminophosphate mesostructured phases appears more sensitive to some of the starting materials. For example, both NaOH and $NMe_4OH$ have been successfully used in the synthesis of silica-based mesoporous materials. However, when NaOH, KOH or $NH_4OH$ were used as the base in place of $NMe_4OH$ in the phosphate system, only amorphous materials were obtained. The source of aluminium is another important factor. In our experiments, the use of either $Al(NO_3)_3$ or Catapal B alumina as the aluminium source also led to amorphous materials. However, the surfactant/Al ratio could be varied within a certain range since we found that the same hexagonal phase could be prepared with a surfactant/Al ratio of 0.90. The use of ethanol as the cosolvent together with the addition of HF is necessary in order to synthesize good quality materials.

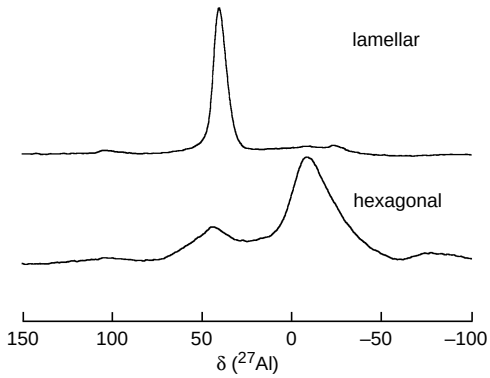



**Fig. 3** $^{27}$Al NMR spectra showing that the hexagonal–lamellar phase transition is accompanied by a change in the Al coordination polyhedra

It is of interest to compare the relative stability of hexagonal and lamellar phases in the aluminophosphate system with those in the silica-based phases. Both lamellar–hexagonal and hexagonal–lamellar phase transitions have been reported for the silica-based materials prepared using $NMe_3(C_{16}H_{33})^+$ and $NMe_3(C_{20}H_{41})^+$.[9,11,12] In the aluminophosphate system, we find that the hexagonally packed aluminophosphate undergoes a phase transition into the lamellar phase under hydrothermal treatment similar to that employed for the silica-based material.[9] Noteworthy in this regard is the tetrahedral coordination of the Al in the lamellar phase, suggesting that condensation of the octahedral aluminium species found in the hexagonal phase is an important factor in the phase transformation of this mesostructured aluminium phosphate.

We would like to thank Dr Qisheng Huo for helpful discussions. This research was supported in part by the National Science Foundation under Grant DMR 95-20971.

## Footnote

* E-mail: stucky@SBXRAY.UCSB.edu

## References

1 J. S. Beck, J. C. Vartuli, W. J. Roth, M. E. Leonowicz, C. T. Kresge, K. D. Schmitt, C. T. W. Chu, D. H. Olson, E. W. Sheppard, S. B. McCullen, J. B. Higgins and J. L. Schlenker, *J. Am. Chem. Soc.*, 1992, **114**, 10 834.
2 S. T. Wilson, B. M. Lok, C. A. Messina, T. R. Cannan and E. M. Flanigen, *J. Chem. Soc., Chem. Commun.*, 1982, 1146.
3 S. Oliver, A. Kuperman, N. Coombs, A. Lough and G. A. Ozin, *Nature*, 1995, **378**, 47.
4 S. Oliver, N. Coombs and G. A. Ozin, *Adv. Mater.*, 1995, **7**, 931.
5 G. A. Ozin and S. Oliver, *Adv. Mater.*, 1995, **7**, 943.
6 A. Chenite, Y. L. Page, V. R. Karra and A. Sayari, *Chem. Commun.*, 1996, 411.
7 A. Sayari, V. R. Karra, J. S. Reddy and I. L. Moudrakovski, *Chem. Commun.*, 1996, 413.
8 T. Kimura, Y. Sugahara and K. Kuroda, *Book of Abstracts, 11th International Zeolite Conference*, Seoul, Korea, 1996, RP45.
9 Q. S. Huo, D. I. Margolese and G. D. Stucky, *Chem. Mater.*, 1996, **8**, 1147.
10 J. L. White, L. W. Beck, D. B. Ferguson and J. F. Haw, *J. Magn. Reson.*, 1992, **100**, 336.
11 Q. S. Huo, D. I. Margolese, U. Ciesla, D. G. Demuth, P. Y. Feng, T. E. Gier, P. Sieger, A. Firouzi, B. F. Chmelka, F. Schuth and G. D. Stucky, *Chem. Mater.*, 1994, **6**, 1176.
12 A. Monnier, F. Schuth, Q. S. Huo, D. Kumar, D. Margolese, R. S. Maxwell, G. D.Stucky, M. Krishnamurty, P. Petroff, A. Firouzi, M. Janicke, and B. F. Chmelka, *Science*, 1993, **61**, 1299.

*Received in Bloomington, IN, USA, 10th January 1997, Com. 7/00233E*

# Aryl isonitrile binding to $[Fe_4S_4]$ clusters: formation of $[Fe_4S_4]^+$ and $[\{Fe_4S_4\}_2]^{2+}$ cores

**Michael Harmjanz, Wolfgang Saak,* Detlev Haase and Siegfried Pohl†**

*Fachbereich Chemie, Carl-von-Ossietzky Universität Oldenburg, Postfach 2503, D-26111 Oldenburg, Germany*

**Aryl isonitriles (ArNC; Ar = 2,4,6-$Me_3C_6H_2NC$ 1, 2,6-$Me_2C_6H_3NC$ 2) react with $[Fe_4S_4I_4]^{2-}$ 3 and $[Co(\eta\text{-}C_5H_5)_2]$ to afford $[Fe_4S_4I(ArNC)_9]$ 4a, b; substitution of iodide by $RS^-$ (R = 2,4,6-$Me_3C_6H_2$) yields $[Fe_4S_4(SR)(ArNC)_9]$ 5 and reaction of $[Fe_4S_4I(2,4,6\text{-}Me_3C_6H_2NC)_9]$ 4b with $KB(4\text{-}Cl\text{-}Ph)_4$ leads to $[\{Fe_4S_4(2,4,6\text{-}Me_3C_6H_2NC)_9\}_2][B(4\text{-}ClPh)_4]_2$ 6.**

Among the extended class of cuboidal $Fe_4S_4$ clusters, species with octahedrally coordinated iron atoms are rather uncommon. Typical examples with monodentate ligands are the well known $[Fe_4S_4(CO)_{12}]$[1] and the 2:2 site-differentiated clusters $[Fe_4S_4X_2(Bu^tNC)_6]$ (X = Cl, Br, RS).[2,3] Prior to the present work uncharged mixed-ligand clusters of the latter type with an $[Fe_4S_4]^+$ core were unknown. Even though the relevance of these clusters in biological systems is limited, especially 3:1 functionalized $Fe_4S_4$ clusters could serve as models for the examination of biological and non-biological catalytic processes. As demonstrated in this work these clusters also represent versatile starting materials for the formation of Fe–S clusters of higher nuclearity.

As shown elsewhere[2] alkyl isonitriles readily react with $[Fe_4S_4X_4]^{2-}$ clusters (X = Cl, Br) to yield the [2:2] site-differentiated clusters $[Fe_4S_4X_2(RNC)_6]$ containing an $[Fe_4S_4]^{2+}$ core. Aryl isonitriles (ArNC) which have slightly higher π-acceptor abilities than alkyl isonitriles[4] should stabilize lower $[Fe_4S_4]$ oxidation states. However, the complexation of $Fe_4S_4$ clusters by aryl isonitriles had only been realized in $[Fe_4S_4(LS_3)(ArNC)_3]^-$ ($LS_3$ = trithiolate ligand).[3]

When stoichiometric mixtures of the 2,6-dimethylphenylisonitrile **2** and the tetraiodo cluster anion **3** were combined in the presence of stoichiometric amounts of $[Co(\eta^5\text{-}C_5H_5)_2]$ [eqn. (1)] the novel uncharged cluster $[Fe_4S_4I(2,6\text{-}Me_2C_6H_3NC)_9]$ **4a** precipitated together with $[Co(\eta^5\text{-}C_5H_5)_2]I$ and some $N(CH_2Ph)Bu_3I$. The byproducts can easily be removed by washing the crude product with acetonitrile (yield 90%).‡

$$\underset{\mathbf{3}}{[Fe_4S_4I_4]^{2-}} + 9\ \underset{\mathbf{2}}{2,6\text{-}Me_2C_6H_3NC} + [Co(\eta\text{-}C_5H_5)] \rightarrow \underset{\mathbf{4a}}{[Fe_4S_4I(2,6\text{-}Me_2C_6H_3NC)_9]} + 2\ I^- + [Co(\eta\text{-}C_5H_5)_2]I \quad (1)$$

The formation of $[Fe_4S_4I(ArNC)_9]$ **4b** (Ar = 2,4,6-trimethylphenylisonitrile) can also be achieved as well as analogues with sterically less encumbering aryl isonitriles.

The redox behaviour of **4a** has been examined in thf by cyclic voltammetry. Chemically irreversible reduction takes place at −630 mV *vs.* SCE and a quasi-reversible oxidation wave is observed at −90 mV *vs.* SCE ($i_{pa}/i_{pc}$ = 0.95, $E_{pa} - E_{pc}$ = 100 mV). Chemical oxidation of **4a** involving the oxidation state change $[Fe_4S_4I(ArNC)_9]^{0/+}$ was not successful. Investigation of the chemical reduction of **4a** in the presence of excess isonitrile is currently being carried out in this laboratory. This reaction should lead to $[Fe_4S_4(ArNC)_{12}]$.

Substitution reaction at the iodide site can be accomplished by addition of 1 equiv. of mesitylenethiolate to a suspension of **4a** in thf. On filtration and addition of ether $[Fe_4S_4(2,4,6\text{-}Me_3C_6H_2S)(2,6\text{-}Me_2C_6H_3NC)_9]$ **5** precipitates as red needles (yield 68%).‡ The cyclic voltammogram of the thiolate derivative **5** in thf shows an irreversible reduction at −1040 mV, a quasi-reversible oxidation at −240 mV ($i_{pa}/i_{pc}$ = 0.96, $E_{pa} - E_{pc}$ = 70 mV) and a quasi-reversible oxidation at 420 mV *vs.* SCE ($i_{pa}/i_{pc}$ = 1.2, $E_{pa} - E_{pc}$ = 85 mV).

Single crystals of **5** can be obtained by addition of ether to concentrated solutions of **5** in thf. Compound **5** crystallizes as a thf solvate and its structure is shown in Fig. 1. The trigonal distortion of the $[Fe_4S_4]^+$ core originates from the different coordination environments around the iron atoms. One sulfur atom is surrounded by three octahedrally coordinated $Fe^{II}$ and three sulfur atoms by two octahedrally $Fe^{II}$ and one tetrahedrally coordinated $Fe^{III}$. The Fe–S distances form three sets, with three Fe–S bonds at the tetrahedral site Fe(1) (mean 2.247 Å), three at S(3) (mean 2.347 Å) and six at octahedrally coordinated sites Fe(2,3,4) (mean 2.379 Å). The distortion of the $[Fe_4S_4]^+$ core results in three short Fe···Fe distances (mean 3.014 Å) between the octahedrally and tetrahedrally coordinated iron sites and three long Fe···Fe distances between the octahedrally coordinated iron sites (mean 3.481 Å). The latter are comparable with those in $[Fe_4S_4(CO)_{12}]$ (mean 3.466 Å)[1] and imply no bonding interactions between those iron atoms. The iron–thiolate distance in **5** is comparable with those in $[Fe_4S_4(PhS)_2(Bu^tNC)_6]$ (mean 2.281 Å).[2]

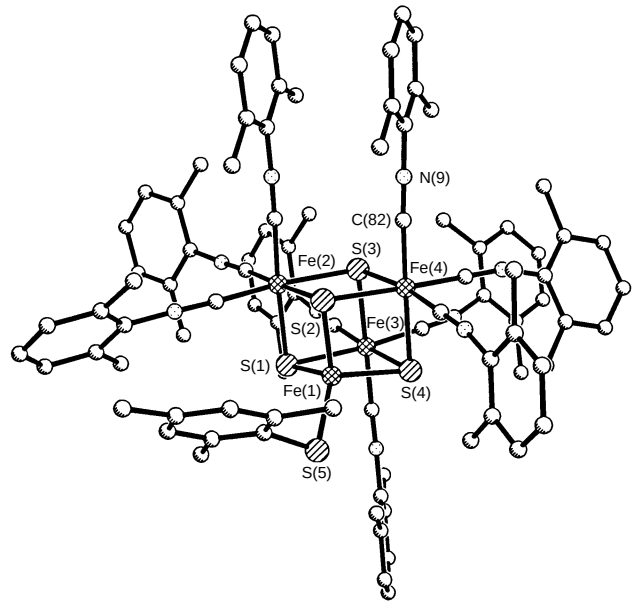



**Fig. 1** Molecular structure of **5** with atom numbering scheme. Selected bond lengths (Å) and angles (°): Fe(1)–S(1) 2.253(2), Fe(1)–S(2) 2.240(2), Fe(1)–S(4) 2.248(2), Fe(1)–S(5) 2.300(2), Fe(1)···Fe(2) 2.9610(10), Fe(1)···Fe(3) 3.078(2) Fe(1)···Fe(4) 3.002(2), Fe(2)–S(1) 2.377(2), Fe(2)–S(2) 2.385(2), Fe(2)–S(3) 2.3459(15), Fe(2)···Fe(3) 3.466(2), Fe(2)···Fe(4) 3.505(2), Fe(3)- S(1) 2.387(2), Fe(3)–S(3) 2.3420(14), Fe(3)–S(4) 2.364(2), Fe(3)···Fe(4) 3.473(2), Fe(4)–S(2) 2.377(2), Fe(4)–S(3) 2.3535(15), Fe(4)–S(4) 2.383(2), Fe–C 1.835 [range 1.820(6)–1.860(6)], C(1)–S(5)–Fe(1) 103.2(2).

A condensation of the 3:1 site-differentiated cluster can easily be achieved upon reaction of $[Fe_4S_4I(2,4,6\text{-}Me_3C_6H_2NC)_9]$ **4b** with stoichiometric amounts of $KB(4\text{-}ClPh)_4$ [eqn. (2); Ar = 2,4,6-$Me_3C_6H_2$].‡

$$\underset{\mathbf{4b}}{2\,[Fe_4S_4I(ArNC)_9]} + 2KB(4\text{-}ClPh)_4 \rightarrow \underset{\mathbf{6}}{[\{Fe_4S_4(ArNC)_9\}_2][B(4\text{-}ClPh)_4]_2} + 2KI \qquad (2)$$

**6** was characterized spectroscopically and the structure of **6** has been established by X-ray structure analysis.§ The differential pulse voltammogram of **6** shows two one-electron reduction steps at −760 and −935 mV *vs.* SCE and two one-electron oxidation steps at 200 and 460 mV *vs*. SCE, respectively.

Apart from the octahedrally ligated iron sites, the core structure of **6** is comparable with the previously synthesized neutral dicubane $[\{Fe_4S_4[P(C_6H_{11})_3]_3\}_2]$.[5] Fe–S dicubane clusters with non-phosphorus ligands are, as yet, not known. Furthermore, $[\{Fe_4S_4(2,4,6\text{-}Me_3C_6H_2NC)_9\}_2]^{2+}$ represents the first dicubane cluster including two charged $[Fe_4S_4]^+$ cores. As shown in Fig. 2 the two $[Fe_4S_4]^+$ cores are linked by two Fe–S bonds forming a central $Fe_2S_2$ rhombus. Compared with $[\{Fe_4S_4[P(C_6H_{11})_3]_3\}_2]$[5] the Fe···Fe distance in **6** [2.766(4) Å] within the central $Fe_2S_2$ unit is elongated [2.681(8) Å)] whereas the Fe–S distances are almost equal {2.285(3) Å, **6**; 2.309(7) Å, $[\{Fe_4S_4[P(C_6H_{11})_3]_3\}_2]$}. Although S(1) is additionally linked with an iron atom [Fe(1a)] of the second cuboidal fragment, the distortion of the $[Fe_4S_4]^+$ fragment from $T_d$ symmetry mainly originates from the two structurally and electronically distinct iron sites. As a consequence the twelve Fe–S distances divide into three sets (3 + 3 + 6) and the Fe···Fe distances into two sets (3 + 3). The mean values of the Fe–S and Fe···Fe distances as well as the Fe–C distances are comparable with those in **5**.

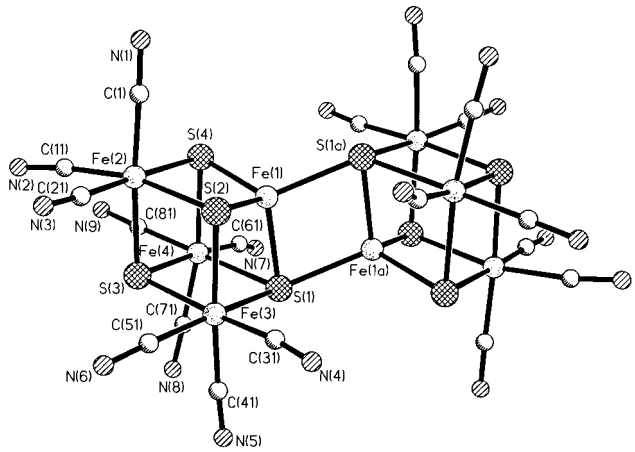



**Fig. 2** Core structure of **6** with atom numbering scheme (arene moiety omitted for clarity). Selected bond lengths (Å) and angles (°): Fe(1)-S(1) 2.253(4), Fe(1)–S(2) 2.219(4), Fe(1)–S(4) 2.215(4), Fe(1)–S(1a) 2.285(3), Fe(1)–Fe(1a) 2.766(4), Fe(1)···Fe(2) 2.934(3), Fe(1)···Fe(3) 2.969(3) Fe(1)···Fe(4) 2.982(3), Fe(2)–S(2) 2.377(4), Fe(2)–S(3) 2.334(4), Fe(2)–S(4) 2.392(4), Fe(2)···Fe(3) 3.470(3), Fe(2)···Fe(4) 3.469(3), Fe(3)–S(1) 2.433(4), Fe(3)–S(2) 2.359(4), Fe(3)–S(3) 2.335(4), Fe(3)···Fe(4) 3.520(3), Fe(4)–S(1) 2.417(4), Fe(4)–S(3) 2.325(4), Fe(4)–S(4) 2.379(4), Fe–C 1.83 [range 1.78(2)–1.88(2)], S(1)–Fe(1)–S(1a) 104.91(12).

Financial support from the Deutsche Forschungsgemeinschaft is gratefully acknowledged.

## Footnotes

† Deceased. Correspondence should be addressed to W. Saak.

‡ The used aryl isonitriles were prepared by puplished methods.[6] Cluster **3** was exclusively used as its benzyltri-*n*-butylammonium salt.[7] All reactions were carried out under a nitrogen atmosphere in dried and degassed solvents. Satisfactory elemental analyses were obtained for new compounds. **4a**: $\lambda_{max}$ (thf) 327 nm. IR (KBr): 2108vs, 2058vs $cm^{-1}$ ($\nu_{NC}$). **4b**·$Et_2O$: $\lambda_{max}$ (thf) 320 nm. IR (KBr): 2106vs, 2064vs $cm^{-1}$ ($\nu_{NC}$). **5**: $\lambda_{max}$ (thf) 313 nm. IR (KBr): 2104vs, 2054vs $cm^{-1}$ ($\nu_{NC}$). **6**: isolated in 65% yield. $\lambda_{max}$ (thf) 315 nm. IR (KBr): 2118vs, 2076vs $cm^{-1}$ ($\nu_{NC}$).

§ *Crystal data*: **5**·thf: $C_{94}H_{100}Fe_4N_9OS_5$, $M$ = 1755.53, monoclinic, space group $P2_1/c$, $a$ = 13.802(1), $b$ = 24.633(2), $c$ = 27.829(2) Å, β = 103.93(1)°, $U$ = 9183.2(12) Å$^3$, $T$ = 297(1) K, $Z$ = 4, $D_c$ = 1.270 g $cm^{-3}$, μ(Mo-Kα) = 0.783 $mm^{-1}$. A suitable crystal was mounted on a AED2 Siemens four-circle diffractometer. Data collection using Mo-Kα radiation (λ = 0.710 73 Å) and 2θ scans gave 12789 independent reflections ($\theta_{max}$ 23.01°), of which 9706 with $I > 2\sigma(I)$ were used in all calculations. The structure was solved by direct methods and the solution developed using full-matrix least-squares refinement on $F^2$ and difference Fourier synthesis. Displacement parameters were refined for non-H atoms, H-atoms were included in fixed calculated positions.[8] At convergence, $R$ = 0.0641, $wR_2$ = 0.1541, GOF = 1.182 for 885 parameters.

**6**·MeCN·thf: $C_{234}H_{241}B_2Cl_8Fe_8N_{19}OS_8$, $M$ = 4343.96, triclinic, space group $P\bar{1}$, $a$ = 19.444(8), $b$ = 19.566(6), $c$ = 19.752(7) Å, α = 60.66(4), β = 74.86(3), γ = 61.64(3)°, $U$ = 5760(4) Å$^3$, $T$ = 297(1) K , $Z$ = 1, $D_c$ = 1.252 g $cm^{-3}$, μ(Mo-Kα) = 0.709 $mm^{-1}$, data collection, refinement and solution as above, 10727 independent reflections ($\theta_{max}$ 20.01°), $R$ = 0.1093, $wR_2$ = 0.2419, GOF = 1.195 for 1071 parameters. Atomic coordinates, bond lengths and angles, and thermal parameters have been deposited at the Cambridge Crystallographic Data Centre (CCDC). See Information for Authors, Issue No. 1. Any request to the CCDC for this material should quote the full literature citation and the reference number 182/437.

## References

1 L. L. Nelson, F. Y. Lo, A. D. Rae and L. F. Dahl, *J. Organomet. Chem.*, 1982, **225**, 309.
2 C. Goh, J. A. Weigel and R. H. Holm, *Inorg. Chem.*, 1994, **33**, 4861.
3 J. A. Weigel, K. K. P. Srivastava, E. P. Day, E. Münck and R. H. Holm, *J. Am. Chem. Soc.*, 1990, **112**, 8015.
4 W. S. Mialki, D. E. Wigley, T. E. Wood and R. A. Walton, *Inorg. Chem.*, 1982, **21**, 480; A. Vogler, in *Isonitrile Chemistry*, ed. I. Ugi, Academic Press, New York and London, 1971.
5 L. Cai, B. M. Segal, J. R. Long, M. J. Scott and R. H. Holm, *J. Am. Chem. Soc.*, 1995, **117** 8863; C. Goh, B. M. Segal, J. Huang, J. R. Long and R. H. Holm, *J. Am. Chem. Soc.*, 1996, **118**, 11844.
6 R. Appel, R. Kleinstück and K.-D. Ziehn, *Angew. Chem.*, 1971, **83**, 143.
7 W. Saak and S. Pohl, *Z. Naturforsch. Teil B*, 1985, **40**, 1105 and unpublished work.
8 G. M. Sheldrick, *Acta Crystallogr., Sect. A*, 1990, **46**, 467; SHELXTLPC and SHELXL-93, G. M. Sheldrick, University of Göttingen.

*Received in Basel, Switzerland, 28th January 1997; Com. 7/00613F*

# New strongly coupled dinuclear metal centres in organometallic *s*-indacene complexes

**Douglas R. Cary, Catherine G. Webster, Mark J. Drewitt, Stephen Barlow, Jennifer C. Green and Dermot O'Hare*†**

*Inorganic Chemistry Laboratory, South Parks Road, Oxford, UK OX1 3QR*

**The complexes *cis*-[{Fe(CO)$_3$}$_2$L] and *cis*-[{Co(CO)$_2$}$_2$L] are prepared from 1,3,5,7-tetra-*tert*-butyl-*s*-indacene; in solution, the diiron complexes exhibit very strong electron–electron coupling between iron centres as evidenced by a 810 mV separation between the 0/+ and +/2+ redox waves.**

Oligomers or polymers based on metallocenes bridged by fused-ring ligands such as pentalene or *s*-indacene are anticipated to show interesting delocalised properties.[1,2] Indeed, EPR, Mössbauer, electrochemical and magnetic data show very strong metal–metal interactions in the bimetallic species {L$^1$[M(C$_5$Me$_5$)]$_2$}$^{n+}$ (L$^1$ = pentalene, *s*-indacene; M = Fe, Co, Ni; $n$ = 0, 1 2).[3] However, the stepwise construction of higher oligomers has been hampered by escalating insolubility with increasing oligomerisation.[4] Here we report the use of the stable 1,3,5,7-tetra-*tert*-butyl-*s*-indacene L in the synthesis of new binuclear organometallic derivatives.

According to Hückel's rule, fully conjugated planar polycyclic alkenes with 4$n$ + 2 π-electrons should display benzenoid properties; those with 4$n$ π-electrons are termed antiaromatic.[5] However, it has been shown that some 4$n$ π-systems display 'aromatic character'.[6] *s*-Indacene has an antiaromatic 12 π-electron system and the relationship between its reactivity, aromaticity and stability has been the subject of many studies by theoretical organic chemists. According to LCAO calculations, *s*-indacene should have an electron delocalisation energy similar to that of the tropylium cation, yet the system can be expected to exhibit high reactivity due to the low energy difference of its ground and excited state.[7]

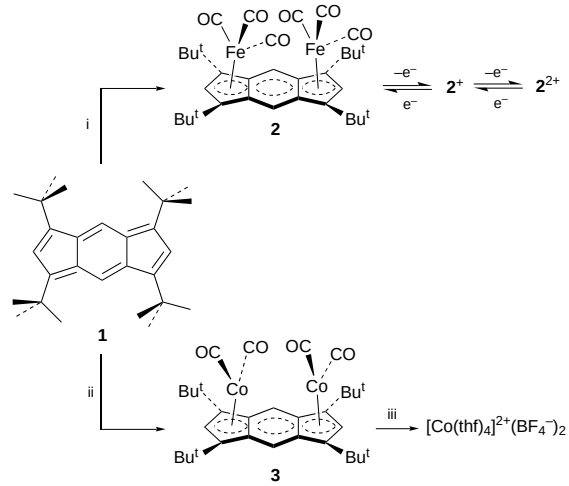
Due to the thermal instability of *s*-indacene, it has been necessary to synthesise more stable substituted derivatives. 1,3,5,7-Tetra-*tert*-butyl-*s*-indacene **1** is kinetically stabilised by the bulky alkyl groups, and has been studied intensively in this respect; its synthesis was briefly outlined by Hafner *et al*.[8]

Refluxing **1** with an excess of [Fe$_2$(CO)$_9$] for 2 h gave an emerald green solution from which dark-green crystals could be obtained by recrystallisation from toluene. Elemental microanalysis and mass spectral data were consistent with the formulation [{Fe(CO)$_3$}$_2$L] **2** (Scheme 1). The room temperature $^1$H and $^{13}$C NMR data indicated that the indacene ligand was complexed to two iron centres in such a way as to produce no change in the local symmetry of the ligand environment. However, the spectroscopic data did not allow us to determine unambiguously the bonding mode of the Fe centres.

The single-crystal X-ray structure determination of **2**‡ revealed that two iron tricarbonyl moieties have been coordinated to the indacene ligand (Fig. 1). This is a rare example of an indacene complex with two metal fragments coordinated to the same face of an indacene ligand. The distances Fe(1) to C(1), C(2), C(3), C(9) and C(10) and the distances Fe(2) to C(5), C(6), C(7), C(11) and C(12) suggest that each iron atom is coordinated to **1** in a very distorted manner. For example, the Fe(1)–C(10) and Fe(2)–C(12) bond lengths are *ca*. 0.11 Å longer than the Fe(1)–C(9) and Fe(2)–C(11) distances, respectively. The average Fe–CO distance is 1.793 Å and is very typical for iron carbonyl complexes. The indacene framework has been distorted in the following manner: the C(1), C(2) and C(3) plane twists [relative to the long $C_2$ axis that is present in the free ligand] so that C(3) becomes closer in space to C(9) than in the free indacene. The distortion also occurs for C(5), C(6) and C(7) plane with C(7) being closer to C(11).

Refluxing **1** with an excess of [Co$_2$(CO)$_8$] in light petroleum (bp 40–60 °C) for 2 h gave a dark-red powder from an orange solution. Dark-red crystals of [{Co(CO)$_2$}$_2$L] **3** could be obtained by recrystallisation of the powder from toluene–pentanes. The single-crystal X-ray structure determination of **3**‡ revealed that two cobalt dicarbonyl units have been coordinated to the same face of **1** (Fig. 2). The distances Co(1)–C(1), Co(1)–C(2), Co(1)–C(3), Co(2)–C(5), Co(2)–C(6) and Co(2)–C(7) are very similar with a mean value of 2.077(2) Å. The two cobalt centres also have longer contacts to the central carbons C(9), C(10), C(11) and C(12) with a mean value of 2.229(2) Å. The average Co–CO distance is 1.738(3) Å.

The solution electrochemistry of **2** and **3** has been investigated in order to gauge the degree of interaction between the two metal centres in these compounds. The cyclic voltammogram (CV) of **2** in dichloromethane clearly shows two reversible waves at $E_{1/2}$ = 0.26 and −0.55 V (*vs.* [Fe(η-C$_5$H$_5$)$_2$]–[Fe(η-C$_5$H$_5$)$_2$]$^+$, in CH$_2$Cl$_2$) corresponding to two successive one-electron transfers *i.e.* oxidation to the mono- and di-cations respectively. The redox waves are separated by 0.81 V, which indicates that the second electron is more difficult to remove than the first. The extremely large value for Δ$E$ is characteristic of strong electronic interactions between the metal centres and extensive delocalisation in the mixed-valence form of the complex. The CV of **3** in CH$_2$Cl$_2$ is much more complex and at moderate scan rates no reversible electrochemical events can be measured.




**Scheme 1** *Reagents and conditions*: i, [Fe$_2$(CO)$_9$] (1.2 mol equiv.), toluene, 2 h reflux, 67%; ii, [Co$_2$(CO)$_8$] (1.2 mol equiv.), light petroleum (bp 40–60 °C), 2 h reflux, 75%; iii, AgBF$_4$ (2 mol equiv.), thf, room temp.

Density functional theory (DFT) has been used to try and rationalise the bonding of the indacene moiety to the $Fe(CO)_3$ and $Co(CO)_2$ metal fragments. Indacene has six occupied π orbitals which bear a close resemblance to linear combinations of the occupied orbitals of two cyclopentadienyl anions, though they include contributions from the π-orbitals of the two central carbons where symmetry allows, *i.e.* for the $b_{1u}$ and $b_{2g}$ combinations. Normal electron counting procedures for **2** and **3**, including all π electrons of the indacene ligand, result in an electron count of 40 for **2** and 38 for **3** for these binuclear systems, four and two electrons in excess of that required for two 18 electron metal centres.

Density functional calculations, including geometry optimisations, have been carried out for both $[Fe_2(CO)_6(C_{12}H_8)]$ **4** and $[Co_2(CO)_4(C_{12}H_8)]$ **5** using a generalised gradient approximation as implemented in the Amsterdam density functional code.[9] Initially the symmetries of **4** and **5** were constrained to $C_{2v}$ symmetry, but subsequently the optimisation was carried out in each case with a constraint of $C_2$ symmetry. In the case of **4** relaxation of the symmetry constraint to $C_2$ led to an optimised geometry with a bond length pattern and buckling of the ring close to that found for **2**. For **5** there was little departure from $C_{2v}$ symmetry for the optimised structure as was found experimentally for **3**.

In the case of **4** both the HOMO ($a_1$ in $C_{2v}$) and the SOMO ($b_1$ in $C_{2v}$) are mainly localised on the metals and the two indacene central carbons, C(4) and C(8). The interaction between the metals and these carbons is antibonding. We suggest that it is the occupancy of these two orbitals by the four excess electrons that leads the metals to be closer to the outer carbons and drives the structural distortion with the consequent relief of the antibonding character of these interactions. Both the HOMO and SOMO are stabilised on distortion, the SOMO more than the HOMO. Lower energy orbitals conform to the expectations for three legged piano stools. In the case of **5** the HOMO is of $b_2$ symmetry, with a node at the central indacene carbons, and metal indacene antibonding though metal CO bonding. The antibonding interaction is evenly distributed along the indacene and leads to less displacement towards the outer carbons than found in **4** and no obvious distortion.

We believe that the indacene ligand will be able to form π complexes with a wide range of metal fragments. The extensive π-electron delocalisation of the ligand orbitals means that the metal centres will be able to interact strongly with each other.

We thank the EPSRC for support, studentships (M. J. D and S. B.) and Mass Spectrometry Services (University of Wales, Swansea). We would also like to thank Dr A. N. Chernega and Grant Taylor for their assistance with crystallography and NMR, respectively.

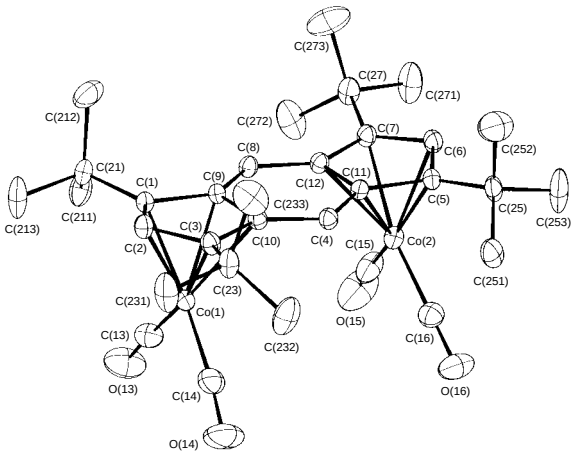



**Fig. 1** Molecular structure of **2**. Selected interatomic distances (Å): Fe(1)–Fe(2) 5.414(5), Fe(1)–C(1) 2.131(5), Fe(1)–C(2) 2.065(6), Fe(1)–C(3) 2.166(5), Fe(1)–C(9) 2.325(5), Fe(1)–C(10) 2.436(5), Fe(2)–C(5) 2.143(5), Fe(2)–C(6) 2.069(5), Fe(2)–C(7) 2.165(5), Fe(2)–C(1) 2.350(5), Fe(2)–C(12) 2.446(5), C(1)–C(2) 1.420(7), C(1)–C(9) 1.452(6), C(2)–C(3) 1.427(6), C(3)–C(10) 1.467(6), C(4)–C(10) 1.384(6), C(4)–C(11) 1.416(7), C(5)–C(11) 1.449(6), C(5)–C(6) 1.418(6), C(6)–C(7) 1.428(6), C(7)–C(12) 1.456(7), C(8)–C(12) 1.383(6), C(8)–C(9) 1.413(6), C(9)–C(10) 1.459(6), C(11)–C(12) 1.462(6).

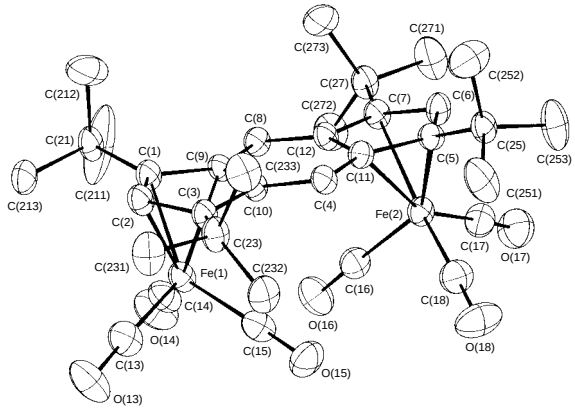



**Fig. 2** Molecular structure of **3**. Selected interatomic distances (Å): Co(1)–Co(2) 4.931(3), Co(1)–C(1) 2.087(2), Co(1)–C(2) 2.073(2), Co(1)–C(3) 2.079(2), Co(1)–C(9) 2.234(2), Co(1)–C(10) 2.227(2), Co(2)–C(5) 2.080(2), Co(2)–C(6) 2.070(2), Co(2)–C(7) 2.075(2), Co(2)–C(11) 2.233(2), Co(2)–C(12) 2.224(2), C(1)–C(2) 1.416(3), C(1)–C(9) 1.470(3), C(2)–C(3) 1.422(3), C(3)–C(10) 1.468(3), C(4)–C(10) 1.393(3), C(4)–C(11) 1.393(3), C(5)–C(11) 1.472(3), C(5)–C(6) 1.417(3), C(6)–C(7) 1.421(3), C(7)–C(12) 1.466(3), C(8)–C(12) 1.400(3), C(8)–C(9) 1.395(3), C(9)–C(10) 1.447(3), C(11)–C(12) 1.446(3).

## Footnotes

* E-mail: dermot.ohare@icl.ox.ac.uk
† D. O'Hare is the Royal Society of Chemistry Sir Edward Frankland Fellow.

‡ X-Ray crystal structure analyses: **2**: monoclinic, space group $P2_1/n$, $a$ = 10.4730(9), $b$ = 18.147(1), $c$ = 17.366(1) Å, β = 95.397(5), $U$ = 3285.8 Å$^3$, $Z$ = 4, $D_c$ = 1.23 g cm$^{-3}$, μ = 9.2 cm$^{-1}$, crystal size *ca.* 0.16 × 0.22 × 0.27 mm, $T$ = 170 K, 70 frames, 39 683 total (7195 independent) reflections, $R$ = 0.055 and $R_w$ = 0.058 for 4352 reflections with $I > 4\sigma(I)$, max., min. peak in final Fourier difference synthesis 0.45, −0.62 e Å$^{-3}$, respectively. **3**: triclinic, space group $P\bar{1}$, $a$ = 10.588(1), $b$ = 12.509(1), $c$ = 14.103(1) Å, α = 70.090(2), β = 80.401(2), γ = 67.942(2)°, $U$ = 1604.9 Å$^3$, $Z$ = 2, $D_c$ = 1.33 g cm$^{-3}$, μ = 10.5 cm$^{-1}$, crystal size *ca.* 0.50 × 0.60 × 0.70 mm, $T$ = 150 K, 90 frames, 22358 total (6967 independent) reflections, $R$ = 0.039 and $R_w$ = 0.044 for 5796 reflections with $I > 3\sigma(I)$, max., min. peak in final Fourier difference synthesis 0.68, −0.54 e Å$^{-3}$, respectively. Atomic coordinates, bond lengths and angles, and thermal parameters have been deposited at the Cambridge Crystallographic Data Centre (CCDC). See Information for Authors, Issue No. 1. Any request to the CCDC for this material should quote the full literature citation and the reference number 182/418.

## References

1 T. J. Katz and J. Schulman, *J. Am. Chem. Soc.*, 1964, **86**, 3169.
2 T. J. Katz, N. Acton and J. McGinnis, *J. Am. Chem. Soc.*, 1972, **94**, 6205.
3 J. M. Manriquez, M. D. Ward, W. M. Reiff, J. C. Calabrese, N. L. Jones, P. J. Carroll, E. E. Bunel and J. S. Miller, *J. Am. Chem. Soc.*, 1995, **117**, 6182.
4 B. Oelckers, I. Chávez, J. M. Manríquez and E. Román, *Organometallics*, 1993, **12**, 3396.
5 E. Hückel, *Z. Phys.*, 1931, **70**, 204.
6 K. Hafner, *Angew. Chem., Int. Ed. Engl.*, 1964, **3**, 165 and references therein.
7 R. D. Brown, *J. Chem. Soc.*, 1951, 2391.
8 K. Hafner, B. Stowasser, H. P. Krimmer, S. Fischer, M. C. Bohm and H. J. Lindner, *Angew. Chem., Int. Ed. Engl.*, 1986, **25**, 630.
9 ADF (2.0.1), Dept. of Theoretical Chemistry, Vrije Universiteit, Amsterdam, 1996.

*Received in Basel, Switzerland, 13th January 1997; Com. 7/00297A*

# Thioacyl complexes of molybdenum and tungsten

**Darren J. Cook and Anthony F. Hill***

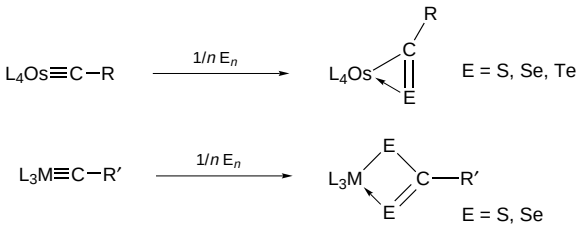
*Department of Chemistry, Imperial College of Science Technology and Medicine, South Kensington, London, UK SW7 2AY*

**The reactions of a range of alkylidyne complexes of molybdenum and tungsten [M(≡CR)$L_n$] with 2-methylthiirane provide the first thioacyl complexes [M(η²-SCR)$L_n$] of these elements, which serve as precursors for complexes bearing dithiocarboxylate, thioselenocarboxylate, thiolatocarbene and α-thioalkyl ligands and thioacyl-bridged binuclear complexes.**

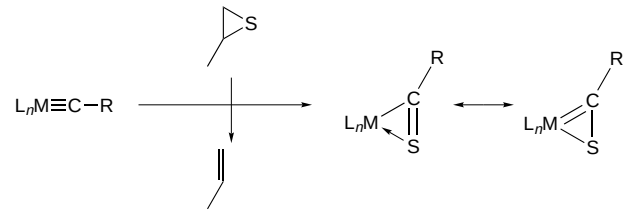
The addition of chalcogens to the metal–carbon multiple bonds of alkylidyne complexes takes one of two courses depending on the metal centre (Scheme 1):[1] Roper and coworkers originally showed that elemental chalcogens add once to group 8 toluidyne complexes to provide chalcotoluoyl ligands.[2] Alkylidyne complexes of molybdenum and tungsten, however, add sulfur or selenium twice to provide dichalcocarboxylate complexes,[3] which Kreißl subsequently obtained from the reaction of these precursors with cyclohexene sulfide.[4] Whilst no intermediate thio- or seleno-acyl complexes have been observed or isolated from these reactions, even for sterically congested systems,[5] Kreißl has shown that [W(η²-$S_2CC_6H_4$Me)-$(CO)_2$(η-$C_5H_5$)] reacts with $PMe_3$ to provide the adduct [W{η²-SC($PMe_3$)$C_6H_4$Me}$(CO)_2$(η-$C_5H_5$)].[6] We have recently shown that thiobenzoyl complexes of ruthenium are obtained from the reaction of [Ru(≡CPh)Cl$(CO)(PPh_3)_2$] with $CS_2$ or isothiocyanates,[7] a result which further prompted our curiosity as to why these ligands appear to be disfavoured for group 6 metals. We report herein that thioacyl complexes of molybdenum and tungsten are indeed accessible and that they are useful precursors to a wide range of mono- and di-nuclear complexes.

Under careful control of reagent stoichiometry and reaction conditions, we find that the alkylidyne complexes shown in Scheme 2 react cleanly with 2-methylthiirane to provide the corresponding thioacyl complexes. The formulation follows from spectroscopic data† and their subsequent reactions with sulfur or excess propylene sulfide to provide the appropriate dithiocarboxylate complex. Most notable amongst these data are the $^{13}C$ NMR chemical shifts for the thioacyl carbon which typically appear in the range δ 260–280, this being to slightly higher field of those previously observed for group 8 metals (δ *ca*. 310).[2,7] Scheme 2 also indicates some instances where this reaction fails: notably alkylidyne complexes of chromium, sterically congested benzylidyne complexes and aminomethylidyne complexes. This last result is perhaps surprising given that thiocarboxamide complexes have been prepared by alternative strategies and are stable and robust species.[8] The M–C multiple bond of aminomethylidyne complexes is, however, well known to be comparatively unreactive.[1] Finally for completeness, it should be noted that ruthenium benzylidynes also react with 2-methylthiirane to provide thiobenzoyl complexes, although this approach offers no advantage over the use of elemental sulfur.

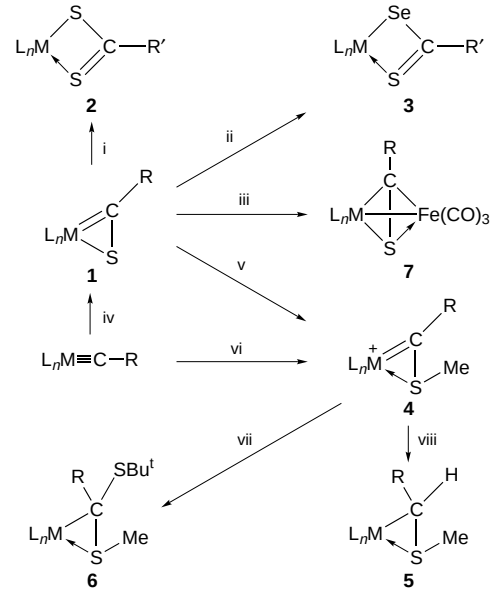
All of the thioacyl complexes obtained are somewhat thermally and photolytically sensitive both as solids and in solution. Nevertheless, these compounds serve as useful precursors for a number of transformations, some of which are summarised in Scheme 3. These include (*i*) the synthesis of mixed thioselenocarboxylate ligands (to our knowledge previously unknown), *e.g.* [Mo(η²-SSeC$C_6H_4$OMe-4)$(CO)_2$-{HB($pz)_3$}] **3** (pz = pyrazol-1-yl); (*ii*) alkylation at sulfur to provide bidentate thiolatocarbene complexes, *e.g.* [Mo(η²-MeSC$C_6H_4$OMe)$(CO)_2${HB($pz)_3$}]$BF_4$ **4**‡ which may be converted to bidentate α-thiolatoalkyl or α,α-bis(thiolato)alkyl




**Scheme 1** Chalcogen addition to alkylidynes of group 6 and 8 metals. R = $C_6H_4$Me-4; R′ = $C_6H_4$Me-4, $CH_2Bu^t$; $L_4Os$ = OsCl$(CO)(PPh_3)_2$;[2] $L_3M$ = Mo{$P(OMe)_3$}$_2$(η-$C_5H_5$), W$(CO)_2$(η-$C_5H_5$).[3]




**Scheme 2** R = Ph, $C_6H_4$Me-4, $C_6H_4$OMe-4, 2-$C_4H_3S$; $L_nM$ = MoBr-(bipy)$(CO)_2$, Mo$(CO)_2${HB($pz)_3$}, WBr(bipy)$(CO)_2$, W$(CO)_2${HB($pz)_3$}, RuCl$(CO)(PPh_3)_2$ (not all combinations). Reaction fails for: R = $C_6H_2Me_3$-2,4,6, $NPr^i_2$; $L_nM$ = CrBr(bipy)$(CO)_2$, MoBr$(CO)_2$(tmeda), MoBr(pico-line)$_2(CO)_2$].




**Scheme 3** R = $C_6H_4$OMe-4; $ML_n$ = Mo$(CO)_2${HB($pz)_3$}. *Reagents and conditions* (25 °C): i, $S_8$ or $C_3H_6S$, $CH_2Cl_2$; ii, Li[$Et_3BH$] : $Se_8$ = 8 : 1, thf; iii, [$Fe_2(CO)_9$] thf; iv, $SC_3H_6$, $CH_2Cl_2$; v, [$Me_3O$]$BF_4$ $CH_2Cl_2$; vi, [$MeSSMe_2$]$BF_4$, $CH_2Cl_2$; vii, $HSBu^t$, DBU, $CH_2Cl_2$; viii, Li[$BHEt_3$], thf.

complexes with Li[BHEt$_3$] or *tert*-butylthiolate, respectively,§ *e.g.* the complexes [Mo{η$^2$-MeSCHC$_6$H$_4$OMe-4}(CO)$_2$-{HB(pz)$_3$}] **5** and [Mo{η$^2$-MeSC(SBu$^t$)C$_6$H$_4$OMe-4}(CO)$_2$-{HB(pz)$_3$}] **6**; (*iii*) bridge-assisted metal–metal bond formation providing the bimetallic complex [MoFe(μ-SCC$_6$H$_4$OMe-4)(CO)$_5${HB(pz)$_3$}] **7**.[11]

The results above show that the previous unavailability of thioacyl complexes of group 6 metals has been due to a lack of suitable synthetic strategy rather than any intrinsic instability in the 'metallathiirene' unit. Furthermore, preliminary studies of the reactivity of these ligands, once constructed, clearly indicate considerable synthetic utility, a feature we are investigating further.

We wish to thank the Engineering and Physical Sciences Research Council (UK) for the award of a studentship (to D. J. C.) and Royal Society for financial support.

## Footnotes

* E-mail: a.hill@ic.ac.uk

† *Selected data* for representative new complexes {25 °C, IR [ν(CO), $CH_2Cl_2$], NMR ($CDCl_3$), satisfactory microanalytical and FABMS data}. **1**: [Mo(≡CC$_6$H$_4$OMe-4)(CO)$_2${HB(pz)$_3$}] (1.00 g, 1.90 mmol) and 2-methylthiirane sulfide (0.14 cm$^3$, 1.9 mmol) were stirred in $CH_2Cl_2$ (20 cm$^3$) in the dark for 12 h. The solvent was removed and the residue chromatographed (alumina, 10 °C, $Et_2O$). The blue–purple eluate was concentrated and then diluted with hexane and cooled (−20 °C). Yield 1.01 g (97%). IR: 1976, 1891 cm$^{-1}$. NMR: $^1$H, δ 3.94 ($CH_3$), 6.24, 7.39, 7.74 (pz); 7.08, 8.04 [$(AB)_2$, $C_6H_4$]. $^{13}$C{$^1$H}: 278.0 (CS), 233.6 (CO), 162.5–124.8 ($C_6H_4$ and pz), 55.6 ($CH_3$). **2**: yield 80%. IR: 1951, 1867 cm$^{-1}$. NMR: $^1$H, δ 3.88 ($CH_3$), 6.25 [t, 3 H, H$^4$(pz)], 6.91, 8.00 [$(AB)_2$, $C_6H_4$], 7.68, 8.16 [H$^{3,5}$(pz)]. $^{13}$C{$^1$H}: 250.4($S_2$C); 222.3 (CO), 163.6–105.9 ($C_6H_4$ and pz), 55.6 ($CH_3$). **3** Yield 87%. IR: 1943, 1861 cm$^{-1}$. NMR: $^1$H, δ 3.87 ($CH_3$), 6.25 [t, H$^4$(pz)], 6.89, 7.99 [$(AB)_2$, $C_6H_4$], 7.69, 8.20 [H$^{3,5}$(pz)]. $^{13}$C{$^1$H}: 249.7 [CSeS, *J*(SeC) 23 Hz], 223.5 (CO), 163.7–113.9 ($C_6H_4$ and pz) 55.5 ($CH_3$). **4** Yield 94%. IR: 2053, 1986 cm$^{-1}$. NMR: insufficiently soluble. FABMS: *m/z* 533 [M]$^+$, 505 [M − CO]$^+$, 477 [M − 2CO]$^+$, 343 [M − 2CO, Me, C*C*$_6$H$_4$OMe]$^+$. **5**: Yield 76%. IR: 1949, 1812 cm$^{-1}$. NMR: $^1$H, δ 2.10 ($SCH_3$), 3.86 ($OCH_3$), 5.79 (MoCH), 6.18 [br s, 3 H, H$^4$(pz)], 6.98, 7.47 [$(AB)_2$, $C_6H_4$, *J*(AB) 8.1 Hz], 7.59–8.10 [m, 6 H, H$^{3,5}$(pz)]. $^{13}$C{$^1$H}, δ 234.8, 229.7 (CO), 158.8–105.7 ($C_6H_4$ and pz), 72.4 (MoCS), 55.3 ($OCH_3$), 19.9 ($SCH_3$). **6** Yield 80%. IR: 1950, 1820 cm$^{-1}$. NMR: $^1$H, δ 1.11 [s, 9 H, C($CH_3$)$_3$]; 2.68 (s, 3 H, $SCH_3$); 3.70 (s, 3 H, $OCH_3$); 6.03–7.95 [13 H, H(pz), $C_6H_4$] $^{13}$C{$^1$H}, δ 237.9, 233.6 (CO), 157.9–104.9 (pz and $C_6H_4$), 55.2 ($OCH_3$), 51.1 ($SCMe_3$), 31.2 (C$CH_3$], 23.7 ($SCH_3$). **7** (R = $C_6H_4$Me-4). Yield 44%. IR: 2051, 1982, 1843 cm$^{-1}$ NMR: $^1$H, δ 2.41 ($CH_3$); 6.10, 6.25, 6.33 [H$^4$(pz)]; 7.19–7.86 [$C_6H_4$ and H$^{3,5}$(pz)]. $^{13}$C{$^1$H}, δ 231.8, 226.8, 209.9, 209.7, 208.0 (CO), 144.7–135.7 ($C_6H_4$ and pz), 21.3 ($CH_3$).

‡ The related salt [W(η$^2$-HCSMe)(CO)$_2${HB(pz)$_3$}]$BF_4$ has been described, and results from the protonation ($HBF_4$) of [W(≡CSMe)(CO)$_2${HB(pz)$_3$}] see ref. 9.

§ For related examples of the reactions of dihapto-thiocarbene complexes with nucleophiles see ref. 10.

## References

1 For a general review on alkylidyne complexes see: A. Mayr and H. Hofmeister, *Adv. Organomet. Chem.*, 1992, **32**, 227.
2 G. R. Clark, K. Marsden, W. R. Roper and L. J. Wright, *J. Am. Chem. Soc.*, 1980, **102**, 6570.
3 D. S. Gill, M. Green, K. Marsden, I. Moore, A. G. Orpen, F. G. A. Stone, I. D. Williams and P. Woodward, *J. Chem. Soc., Dalton Trans.*, 1984, 1343.
4 F. R. Kreißl and N. Ullrich, *J. Organomet. Chem.*, 1989, **361**, C30.
5 S. Anderson, A. F. Hill and B. A. Nasir, *Organometallics*, 1995, **14**, 2987.
6 F. R. Kreißl, N. Ullrich, A. Wirsing and U. Thewalt, *Organometallics*, 1991, **10**, 3275.
7 R. B. Bedford, A. F. Hill, A. J. P. White and D. J. Williams, *Angew. Chem., Int. Ed. Engl.*, 1996, **35**, 95.
8 R. J. Angelici, *Acc. Chem. Res.*, 1972, **18**, 335.
9 H. P. Kim, S. Kim, R. A. Jacobson and R. J. Angelici, *Organometallics*, 1984, **3**, 1124.
10 C. Ogric, W. Schutt, T. Lehotkay, E. Herdtweck and F. R. Kreißl, *Z. Naturforsch., Teil B*, 1995, **50**, 1839; H. P. Kim and R. J. Angelici, *Organometallics*, 1986, **5**, 2489.
11 For an alternative synthesis of related complexes see: A. F. Hill, B. A. Nasir and F. G. A. Stone, *Polyhedron*, 1989, **8**, 179.

*Received in Cambridge, UK, 24th February 1997; Com. 7/01270E*

# Synthesis and X-ray crystal structure of a novel neutral trinuclear copper(II) hydridotris(3,5-dimethylpyrazolyl)borate complex with 1,1-azido bridges

**Michael H. W. Lam,*[a] Yan-Yee Tang,[a] Ka-Man Fung,[a] Xiao-Zeng You[b] and Wing-Tak Wong[c]**

[a] *Department of Biology & Chemistry, City University of Hong Kong, Tat Chee Ave, Kowloon Tong, Hong Kong*
[b] *Coordination Chemistry Institute, Nanjing University, PR China*
[c] *Department of Chemistry, University of Hong Kong, Pokfulam Road, Hong Kong*

**The X-ray crystal structure and magnetic properties of a neutral trinuclear 1,1-azido bridged copper(II) complex [LCu(μ-$N_3$)$_2$Cu(μ-$N_3$)$_2$CuL] 2 [L = hydridotris(3,5-dimethylpyrazolyl)borate], produced from the reaction between [$Cu_3L_2$]Cl 1 and an excess of trimethylsilyl azide, are reported.**

Recent interest in copper hydridotris(pyrazolyl)borate complexes has been aroused by its resemblance to active sites in some copper-containing metalloproteins[1] and their catalytic properties towards cyclopropanation and aziridination.[2] In this work, we report the reaction between [$Cu_3L_2$]Cl **1**† and trimethylsilyl azide in polar solvents such as acetone and methanol which gives a neutral trinuclear copper(II) hydridotris(3,5-dimethylpyrazolyl)borate complex, [LCu(μ-$N_3$)$_2$Cu(μ-$N_3$)$_2$CuL] **2**,‡ containing four 1,1-azido bridges. To the best of our knowledge, with the exception of one structure containing an infinite chain of $Cu^{II}$–$N_3$ units[3] and a recently reported hexanuclear copper(II) complex with 1,3-azides,[4] all reported copper(II)–μ-azido systems were binuclear.[5]

Complex **1** is obtained by slow addition of 0.5 equiv. of ligand KL to a suspension of copper(I) chloride in acetone. Such an approach is adopted in order to prevent formation of a copper(I)–polypyrazolylborate dimer.[6] The pink–white solid **1** is air-stable but its dichloromethane solution is air-sensitive. FABMS of **1** (noba matrix) gives the highest mass ion at *m/z* 785. This suggests that **1** possesses an oligomeric structure of two L ligands and three Cu metal ions. A trinuclear structure (Fig. 1) is proposed in which each $Cu^{I}$ is coordinated to two 3,5-dimethylpyrazolyl units from two L ligands. $^1$H NMR (300 MHz, $CD_2Cl_2$) of **1** supports the proposed structure. Three sets of protons in 3 : 3 : 1 ratio are observed which can be assigned as follows: δ 1.65 (s, 18 H, pyrazolyl-$CH_3$), 2.42 (s, 18 H, pyrazolyl-$CH_3$) and 5.92 (s, 6 H, pyrazolyl-H). To the best of our knowledge, complex **1** represents a new mode of coordination for the well studied copper(II)–polypyrazolylborate system.

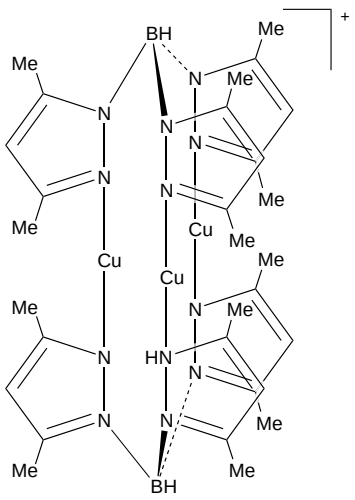



**Fig. 1** The proposed structure of **1**

Complex **2** is obtained by the addition of trimethylsilyl azide to a suspension of **1** in a polar solvent such as acetone or methanol. The ν(B–H) stretch of L in complexes **1** and **2** is observed at 2526 and 2528 $cm^{-1}$, respectively. The asymmetric ν($N_3$) stretch of **2** is found at 2075 $cm^{-1}$ which is consistent with the presence of 1,1-bridging azides. The structure of **2** is shown in Fig. 2.§ The structure contains a square-planar central $Cu^{II}$ and two distorted square-pyramidal terminal $Cu^{II}$ atoms. The molecule is centrosymmetric with only half of the molecule crystallographically independent. The hydridotris(3,5-dimethylpyrazol-1-yl)borate acts as a tripodal ligand coordinating to the terminal $Cu^{II}$ with bond distances and angles (1.96–2.18 Å, 86.9–92.0°) comparable to known copper(I) polypyrazolylborate complexes.[1f,g,6] The three $Cu^{II}$ atoms are bridged by four 1,1-azides with a $Cu^{II}$–N(azido) average distance of 1.99 Å. The average Cu–N(azido)–Cu angle is 101.4° and are typical for the 1,1-azido copper moiety.[5a,c] The μ-azides are considered symmetrical with N–N bond distances of 1.15(2)–1.20(2) Å. The N–N–N angles are all 179.0(3)°. The average Cu···Cu distance is 3.05 Å.

It is known that magnetic orbital interactions between the $Cu^{II}$ ions in many binuclear 1,1-azido systems result in ferromagnetic coupling.[5a,c] However, this is not observed in our trinuclear system (Fig. 3). The $\chi_M T$ is found to be independent of temperature throughout the temperature range of 75.5–300 K. The $\chi_M^{-1}$ *vs.* $T$ variation of **2** shows typical Curie–Weiss behaviour with a Curie constant of 1.34 $cm^3$ K $mol^{-1}$ and a Weiss temperature, θ, of −0.20 K. The $\mu_{eff}$ of **2** within the

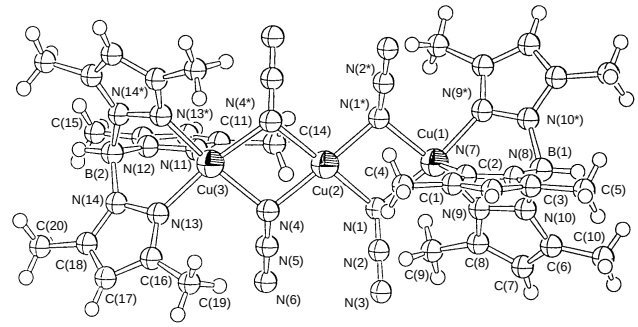



**Fig. 2** Perspective view of [LCu(μ-$N_3$)$_2$Cu(μ-$N_3$)$_2$CuL] **2**. Selected bond lengths (Å) and angles (°): Cu(1)–N(1) 2.03(1), Cu(1)–N(7) 2.15(2), Cu(1)–N(9) 1.96(1), Cu(2)–N(1) 1.95(1), Cu(2)–N(4) 1.96(1), Cu(3)–N(4) 2.00(1), Cu(3)–N(11) 2.18(2), Cu(3)–N(13) 1.96(1), N(1)–N(2) 1.20(2), N(2)–N(3) 1.15(2), N(4)–N(5) 1.18(2), N(5)–N(6) 1.17(2), Cu(1)···Cu(2) 3.082(3), Cu(2)···Cu(3) 3.63(3); N(1)–Cu(1)–N(1*) 76.2(8), N(7)–Cu(1)–N(9) 92.0(5), N(9)–Cu(1)–N(9*) 86.9(7), N(1)–Cu(2)–N(4) 101.0(5), N(1)–Cu(2)–N(4*) 177.5(7), N(4)–Cu(3)–N(4*) 76.2(7), N(11)–Cu(3)–N(13) 91.9(4), N(13)–Cu(3)–N(13*) 87.6(7), Cu(1)–N(1)–Cu(2) 101.5(6), Cu(2)–N(4)–Cu(3) 101.2(6), N(1)–N(2)–N(3) 179(3), N(4)–N(5)–N(6) 179(2).

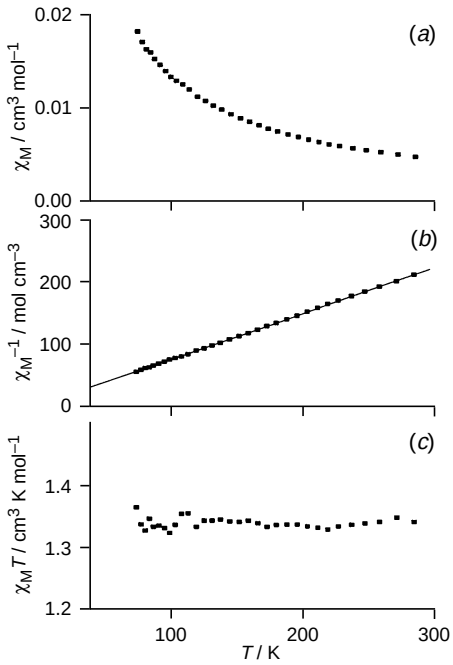



**Fig. 3** Magnetic properties of **2**: (*a*) temperature dependence of $\chi_M$; (*b*) $\chi_M^{-1}$ *vs. T*, the solid line is the best fit for the Curie–Weiss behaviour, $\chi = C/(T - \theta)$, with $C = 1.34$ cm$^3$ K mol$^{-1}$ and $\theta = -0.20$ K; (*c*) temperature dependence of the product $\chi_M T$

above temperature range is found to be fairly constant at *ca.* 3.3 $\mu_B$. These indicate a weak antiferromagnetic coupling[5e,7] among adjacent $Cu^{II}$ centres in **2**. The magnetic properties of this trinuclear 1,1-azido bridged copper(II) system will be further studied.

We would like to acknowledge the City University of Hong Kong for supporting this work.

## Footnotes

* E-mail: bhmhwlam@cityu.edu.hk

† **1** was synthesized by slow addition of an acetone solution of potassium tris(3,5-dimethylpyrazolyl)borohydride (0.5 equiv.) to a suspension of copper(I) chloride in acetone under a nitrogen atmosphere. The resultant pink–white suspension was allowed to stir at room temp. in darkness under a nitrogen atmosphere for 12 h. The crude product of **1** was collected by filtration and was washed with diethyl ether. Yield 60%. IR (cm$^{-1}$): 2526 ν(B–H). $^1$H NMR (300 MHz, $CD_2Cl_2$) and FABMS (NOBA matrix) data: see text. The crude product was used in subsequent synthesis without further purification.

‡ **2** was synthesized by addition of 0.45 g of trimethylsilyl azide to a suspension of 0.50 g of **1** in 20 ml methanol in open atmosphere. The suspension immediately turned yellow–green. Further stirring at room temp. (8 h) yielded a green–brown precipitation of crude **2** which was collected by filtration and washed with diethyl ether. Yield 35%. X-Ray quality crystals of **2** were obtained by slow diffusion of diethyl ether into a dichloromethane solution. IR (cm$^{-1}$): 2522 ν(B–H), 2075 ν($N_3$). Satisfactory elemental analysis.

§ *Crystal data*; $C_{30}H_{52}B_2Cu_3N_{24}$ **2**, $M = 961.16$, monoclinic, space group $P2_1/m$ (no. 11), $T = 296$ K, $a = 8.036(2)$, $b = 13.232(3)$, $c = 23.407$ Å, $\beta = 94.41(1)°$, $U = 2481.7(7)$ Å$^3$, crystal size 0.22 × 0.23 × 0.33 mm, $Z = 2$, $D_c = 1.286$ g cm$^{-3}$, $F(000) = 994.00$, graphite monochromated Mo-Kα radiation, $\lambda = 0.71069$ Å, $\mu = 13.22$ cm$^{-1}$, of 3711 reflections, 3428 were unique with $R_{int} = 0.058$; the structure was solved by Patterson methods (DIRDIF92 PATTY) and refined by full-matrix least squares, function minimized: $\Sigma w(|F_o| - |F_c|)^2$ where $w = [\delta_c^2(F_o) + (p^2/4)(F_o)^2]^{-1}$, residuals: $R = 0.054$, $R_w = 0.056$. Atomic coordinates, bond lengths and angles, and thermal parameters have been deposited at the Cambridge Crystallographic Data Centre (CCDC). See Information for Authors, Issue No. 1. Any request to the CCDC for this material should quote the full literature citation and the reference number 182/441.

## References

1 (*a*) R. Österberg, *Coord. Chem. Rev.*, 1974, **12**, 309; (*b*) *The Biochemistry of Copper*, ed. J. Peisach and P. Aisen, W. E. Blumberg, Academic Press, New York, 1966; (*c*) J. O. Allen, L. Yen and N. J. Farrier, *J. Am. Chem. Soc.*, 1970, **92**, 4475; (*d*) M. I. Bruce and A. P. P. Ostazewski, *J. Chem. Soc., Dalton Trans.*, 1973, 2433; (*e*) M. I. Bruce, *J. Organomet. Chem.*, 1972, **44**, 209; (*f*) C. S. Arcus, J. L. Wilkinson, C. Mealli, T. J. Marks and J. A. Ibers, *J. Am. Chem. Soc.*, 1974, **96**, 7564; (*g*) C. S. Arcus, J. L. Wilkinson, C. Mealli, T. J. Marks and J. A. Ibers, *J. Am. Chem. Soc.*, 1976, **98**, 711.

2 M. P. Doyle, *Chem. Rev.*, 1986, **86**, 919; G. Maas, *Top. Curr. Chem.*, 1987, **137**, 75; D. A. Evans, K. A. Woerpel, M. M. Hinman and M. M. Faul, *J. Am. Chem. Soc.*, 1911, **113**, 728; C. J. Tokar, P. B. Kettler and W. B. Tolmar, *Organometallics*, 1992, **11**, 2737; U. Leutenegger, G. Umbricht, C. Fahrni, P. V. Matt and A. Pfaltz, *Tetrahedron*, 1992, **48**, 2143; J. P. Pedro, M. Brookhart and J. L. Templeton, *Organometallics*, 1993, **12**, 261.

3 R. Söderquist, *Acta Crystallogr. Sect. B.*, 1968, **24**, 450.

4 R. Vicente, A. Escuer, X. Solans and M. Font-Bardia, *J. Chem. Soc., Dalton Trans.*, 1996, 1835.

5 (*a*) J. Comarmond, P. Plumere, J.-M. Lehn, Y. Angus, R. Louis, R. Weiss, O. Kahn and I. Morgenstern-Badarau, *J. Am. Chem. Soc.*, 1982, **104**, 6330; (*b*) K. D. Karlin, J. C. Hayes, J. P. Hutchinson and J. Zubieta, *J. Chem. Soc., Chem. Commun.*, 1983, 376; (*c*) O. Kahn, S. Sikorav, J. Gouterson, S. Jeannin and Y. Jeannin, *Inorg. Chem.*, 1983, **22**, 2877; (*d*) K. D. Karlin, A. Farooq, J. C. Hayes, B. I. Cohen, T. M. Rowe, E. Sinn and J. Zubieta, *Inorg. Chem.*, 1987, **26**, 1271; (*e*) R. Cortés, M. K. Urtiaga, L. Lezama, J. I. R. Larramendi, M. I. Arriortua and T. Rojo, *J. Chem. Soc., Dalton Trans.*, 1993, 3685.

6 J. S. Thompson, R. L. Harlow and J. F. Whitney, *J. Am. Chem. Soc.*, 1983, **105**, 3522.

7 C. J. O'Connor, *Prog. Inorg. Chem.*, 1982, **29**, 203.

*Received in Cambridge, UK, 29th January 1997; Com. 7/00666G*

# Room-temperature oxidation of 2-aminobenzoyl- to 2-aminobenzoato-palladium(II) complexes and of coordinated $PPh_3$ by atmospheric oxygen; X-ray crystal structure of $[(PPh_3)_2Pd(NH_2C_6H_4CO_2\text{-}2)Pd\{C(O)C_6H_4NH_2\text{-}2\}(PPh_3)]O_3SCF_3$

**José Vicente,*† José-Antonio Abad,*‡ Andrew D. Frankland and M.-Carmen Ramírez de Arellano**

*Grupo de Química Organometálica,§ Departamento de Química Inorgánica, Facultad de Química, Universidad de Murcia, Aptdo. 4021, E-30071 Murcia, Spain*

***trans*-$[Pd(C_6H_4NH_2\text{-}2)I(PPh_3)_2]$ reacts with CO to give the insertion product *trans*-$[Pd\{C(O)(C_6H_4NH_2\text{-}2)\}(PPh_3)_2]O_3SCF_3$ or, in the presence of atmospheric oxygen, $[(PPh_3)_2Pd(NH_2C_6H_4CO_2\text{-}2)Pd\{C(O)C_6H_4NH_2\text{-}2\}(PPh_3)]O_3SCF_3$, whose crystal structure is solved.**

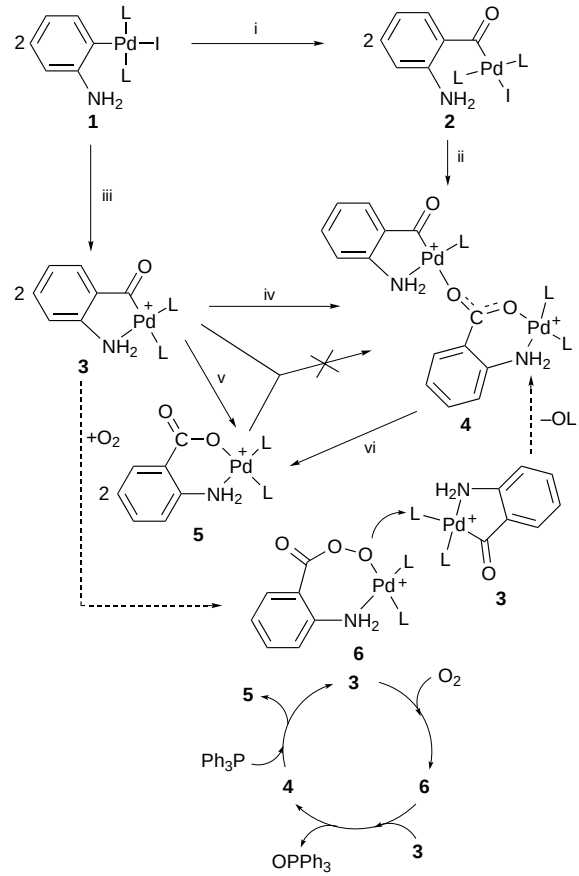
2-Aminophenylpalladium complexes appear to be intermediates in the palladium-catalysed formation of nitrogen-containing heterocycles from *o*-iodo- or *o*-bromo-anilines and, for example, alkynes,[1] dienes,[2] or vinyl cyclopropanes and cyclobutanes,[3] as well as in intramolecular cascade cyclisations.[4] Recently, a one-pot palladium catalysed synthesis of 2-aryl and 2-vinyl-4*H*-3,1-benzoxazin-4-ones from 2-iodoaniline, carbon monoxide and unsaturated halides or triflates has been reported.[5] These results have prompted us to try to isolate intermediates in such carbonylation reactions and to study their reactivity in order to gain more insight into the mechanism of the palladium-catalysed carbon–carbon bond formation.[6] Palladium-catalysed carbonylation of aryl halides and allylic compounds has been shown to occur through (acyl)palladium complexes.[7]

*o*-Iodoaniline reacts with $Pd(dba)_2$ in the presence of 2 equiv. of $PPh_3$ to give *trans*-$[Pd(C_6H_4NH_2\text{-}2)I(PPh_3)_2]$ **1**. When carbon monoxide is bubbled through dichloromethane solutions of **1**, the insertion product *trans*-$[Pd\{C(O)(C_6H_4NH_2\text{-}2)\}I(PPh_3)_2]$ **2** is formed and isolated as a moisture-stable solid (Scheme 1, step i). When complex **2** was reacted with $TlO_3SCF_3$, the dimer $[(PPh_3)_2Pd(NH_2C_6H_4CO_2\text{-}2)Pd\{C(O)C_6H_4NH_2\text{-}2\}(PPh_3)]O_3SCF_3$ **4** was isolated instead of the expected $[Pd\{C(O)C_6H_4NH_2\text{-}2\}(PPh_3)_2]O_3SCF_3$ **3** (Scheme 1, step ii). This product can be viewed as resulting from the replacement of the $PPh_3$ ligand *trans* to the carbonyl group in **3**, for the complex $[Pd\{OC(O)C_6H_4NH_2\text{-}2\}(PPh_3)_2]O_3SCF_3$ **5**. The displaced $PPh_3$ appears in solution as $OPPh_3$ ($^{31}P$ NMR).

Both **3** and **5** can be independently isolated. Thus, if **1** is reacted with $TlO_3SCF_3$ under an atmosphere of CO the expected complex **3** is isolated (Scheme 1, step iii). It is reasonable to assume that **3** is an intermediate in the formation of **4**. In fact, when a solution of **3** is stirred in the open air it transforms into **4** (Scheme 1, step iv).

Contrary to the above mentioned relationship between complexes **3**, **4** and **5**, complexes **3** and **5** do not react with each other. This observation, and the formation of $OPPh_3$, can be interpreted assuming that the oxidation occurs not only on the benzoyl group but also on $PPh_3$ while it is still coordinated. We assume that this process occurs by formation of a peroxobenzoyl complex **6** which interacts with the phosphine *trans* to the carbonyl group in **3**, as depicted in Scheme 1. By reacting **3** or **4** with $PPh_3$ in the presence of oxygen, complex **5** can be isolated. These results can be explained by the cyclic process shown in Scheme 1.

The formation of organoperoxometal, ROO[M], complexes by insertion of $O_2$ into a R–[M] bond has been described.[8] However, we are not aware of such a process with an acyl transition–metal complex such as **3**. Di(acyl)nickel(II) complexes are proposed to be intermediates in reactions of benzyne $Ni^0$ complexes with CO in the presence of traces of air giving phthalatonickel(II) complexes.[9] Photolysis of $Me_3SiC(O)R$ (R = H, Me, Ph) in $O_2$-doped argon matrices gives mainly $Me_3SiOOC(O)R$.[10] Both these results are in accordance with our proposal for the intermediate **6** in Scheme 1. With a less oxophilic metal ion like $Pd^{II}$, the insertion of oxygen into the metal–carbon bond requires stronger oxidizing agents.[11] In addition, peroxo-palladium(II) and platinum(II) complexes $[M(R)(OOR')L_2]$ (M = Pd, Pt; R = activated alkyl; R′ = H, Bu$^t$; L = phosphine),[12] or $[Pt\{OOC(O)Ph\}Cl(PPh_3)_2]$,[13] have




**Scheme 1** L = $PPh_3$. *Reagents and conditions:* i, + 2 CO (1 atm.); ii, + 2 $TlO_3SCF_3$ + $O_2$ − 2 TlI − $OPPh_3$; iii, + 2 $TlO_3SCF_3$ + 2 CO (1 atm.) − 2 TlI; iv, + $O_2$ − $OPPh_3$; v, + $O_2$ + $PPh_3$ − $OPPh_3$; vi + $O_2$ + 2 $PPh_3$ − $OPPh_3$

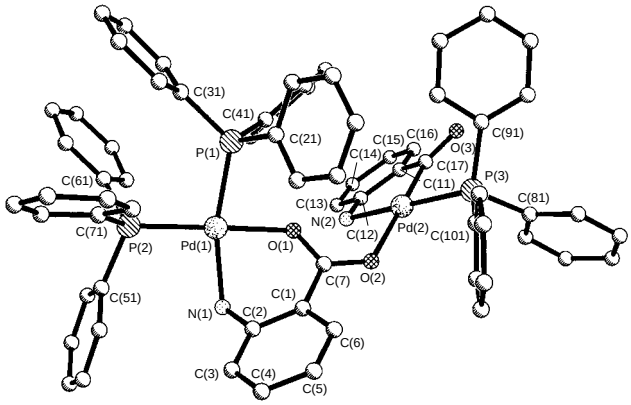



**Fig. 1** Structure of complex **3**. Hydrogen atoms have been omitted for clarity. Selected bond lengths (Å) and angles (°): Pd(1)–O(1) 2.074(2), Pd(1)–N(1) 2.116(3), Pd(2)–C(17) 1.959(3), Pd(2)–N(2) 2.129(3), Pd(2)–O(2) 2.165(2), O(1)–C(7) 1.284(4), O(2)–C(7) 1.247(4), O(3)–C(17) 1.209(4); O(1)–Pd(1)–N(1) 81.35(10), N(1)–Pd(1)–P(2) 96.96(8), O(1)–Pd(1)–P(1) 84.59(7), P(2)–Pd(1)–P(1) 97.45(3), C(17)–Pd(2)–N(2) 83.22(13), N(2)–Pd(2)–O(2) 93.14(10), C(17)–Pd(2)–P(3) 90.83(11), O(2)–Pd(2)–P(3) 92.71(7), O(2)–C(7)–O(1) 122.0(3).

been shown to react with free $PPh_3$ to give $OPPh_3$ but not with coordinated phosphines, as occurs in our case.

Acylpalladium(II) complexes are obtained by reacting CO with alkyl-,[7,14–16] π-allyl,[14] or arylpalladium(II)[17] complexes. There are few reported palladium complexes with a phosphine *trans* to an acyl group, however, they are too unstable to be isolated as pure compounds.[16,18] Therefore, as far as we are aware, complex **3** is the first isolated complex containing such ligands in *trans* positions. We believe that the mutual destabilizing effect of carbon and phosphorus ligands in *trans* positions is responsible for the instability of these complexes, the facile oxygen insertion in complex **3**, and the oxidation of the phosphine *trans* to the carbonyl group. We have found that such *trans*phobia[19] leads to C–P bond coupling processes,[20] and believe it is also responsible for other important C–C and C–N coupling reactions.

The isolated complexes **1**–**5** have been fully characterized by C, H, N analyses, IR spectroscopy and $^1$H, $^{31}$P and $^{13}$C NMR (Supplementary material). The X-ray crystal structure of complex **3** (the cation of which is shown in Fig. 1 and Scheme 1),¶ shows it to be dimeric with the *o*-aminobenzoato ligand bridging, *via* the O atoms of the carboxylate group, the two metal centres. The square-planar geometry of the palladium atoms is fulfilled, in the case of Pd(1), by two phosphine ligands and the N and O atoms of the *o*-aminobenzoato group, and for Pd(2) the other O atom of this ligand, one phosphine and the *o*-aminobenzoyl ligand. All bonding distances and angles are unremarkable.

We thank Dirección General de Investigación Científica y Técnica (PB92-0982-C) for financial support. A. D. F. and M. C. R. A. are grateful to Ministerio de Educación y Ciencia for a Grant and a Contract, respectively.

## Footnotes

† E-mail: jvs@fcu.um.es
‡ E-mail: jaab@fcu.um.es
§ WWW: http://www.scc.um.es/gi/gqo/

¶ *Crystal data*: **3**·4$CH_2Cl_2$, $C_{74}H_{65}Cl_8F_6N_2O_9P_3Pd_2S_2$, $M$ = 1893.71, yellow prism of dimensions 0.62 × 0.60 × 0.28 mm, triclinic, space group $P\bar{1}$, $a$ = 15.245(2), $b$ = 16.005(2), $c$ = 17.158(2) Å, α = 87.882(8), β = 71.080(10), γ = 86.266(8)°, $U$ = 3951.3(9) Å$^3$, $Z$ = 2, $D_c$ = 1.592 Mg m$^{-3}$, $2\theta_{max}$ = 50°, Siemens P4 diffractometer, Mo-Kα (λ = 0.710 73 Å), ω-scan, $T$ = 173 K, 18 038 reflections collected of which 13 857 were independent, ψ-scans absorption correction (max., min. transmission = 0.267, 0.208), direct primary solution and refinement on $F^2$ using Siemens-SHELXTL program,[21] 1009 refined parameters, riding hydrogens, $R1$ = 0.0354 [$I > 2\sigma(I)$], $wR2$ (all data) = 0.0955 [$R1 = \sigma||F_o| - |F_c||/\sigma|F_o|$, $wR2 = \{\sigma[w(F_o^2 - F_c^2)^2]/\sigma[w(F_o^2)^2]\}^{0.5}$, $w = 1/[\sigma^2(F^2) + (aP)^2 + bP]$, $P = (2F_c^2 + F_o^2)/3$]; residual electron density 1.660 (−0.901) e Å$^{-3}$, three of the dichloromethane molecules are disordered over two sites.

Atomic coordinates, bond lengths and angles, and thermal parameters have been deposited at the Cambridge Crystallographic Data Centre (CCDC). See Information for Authors, Issue No. 1. Any request to the CCDC for this material should quote the full literature citation and the reference number 182/430.

## References

1 R. C. Larock and E. K. Yum, *J. Am. Chem. Soc.*, 1991, **113**, 6689.
2 R. C. Larock and L. Q. Guo, *Synlett*, 1995, 465.
3 R. C. Larock and E. K. Yum, *Tetrahedron*, 1996, **52**, 2743.
4 R. Grigg, P. Fretwell, C. Meerholtz and V. Sridharan, *Tetrahedron*, 1994, **50**, 359; C. C. Yang, P. J. Sun and J. M. Fang, *J. Chem. Soc., Chem. Commun.*, 1994, 2629; S. Brown, S. Clarkson, R. Grigg and V. Sridharan, *J. Chem. Soc., Chem. Commun.*, 1995, 1135.
5 S. Cacchi, G. Fabrizi and F. Marinelli, *Synlett*, 1996, 997.
6 J. Tsuji, *Palladium Reagents and Catalysts*, Wiley, Chichester, 1995; R. F. Heck, *Palladium Reagents in Organic Synthesis*, Academic Press, New York, 1985.
7 Y. Yamamoto, *Bull. Chem. Soc. Jpn.*, 1995, **68**, 433.
8 M. J. Kendrick and W. Al-Akhdar, *Inorg. Chem.*, 1987, **26**, 3971; R. D. Arasasingham, A. L. Balch and L. Latos-Grazynski, *J. Am. Chem. Soc.*, 1987, **109**, 5846; R. D. Arasasingham, A. L. Balch, and C. R. Cornman, *J. Am. Chem. Soc.*, 1989, **111**, 4357; R. D. Arasasinghamn, A. L. Balch, R. L. Hart and L. Latos-Grazynski, *J. Am. Chem. Soc.*, 1990, **112**, 7566; G. Ferguson, P. K. Monagham, M. Parvez and R. J. Puddephatt, *Organometallics*, 1985, **4**, 1669.
9 M. A. Bennett, D. C. R. Hockless, M. G. Humphrey, M. Schultz and E. Wenger, *Organometallics*, 1996, **15**, 928.
10 M. Trommer and W. Sander, *Organometallics*, 1996, **15**, 189.
11 C. Sinha, *Transition Met. Chem.*, 1994, **19**, 41; S. Chattopadhyay, C. Sinha, S. B. Choudhury and A. Chakravorty, *J. Organomet. Chem.*, 1992, **427**, 111; P. K. Sinha, J. Chakravarty and S. Bhattacharya, *Polyhedron*, 1996, **15**, 2931; A. K. Mahapatra, D. Bandyopadhyay, P. Bandyopadhyay and A. Chakravorty, *Inorg. Chem.*, 1986, **25**, 2214; P. L. Alsters, H. T. Teunissen, J. Boersma, A. L. Spek and G. van Koten, *Organometallics*, 1993, **12**, 4691; P. L. Alsters, J. Boersma and G. van Koten, *Organometallics*, 1993, **12**, 1629; J. M. Valk, R. Vanbelzen, J. Boersma, A. L. Spek and G. van Koten, *J. Chem. Soc., Dalton Trans.*, 1994, 2293; R. Bhawmick, H. Biswas and P. Bandyopadhyay, *J. Organomet. Chem.*, 1995, **498**, 81.
12 G. Strukul, R. A. Michelin and R. Ros, *Inorg. Chem.*, 1982, **21**, 495.
13 M. J. Y. Chen and J. K. Kochi, *J. Chem. Soc., Chem. Commun.*, 1977, 204.
14 A. Yamamoto, *J. Organomet. Chem.*, 1995, **500**, 337.
15 M. J. Green, G. J. P. Britovsek, K. J. Cavell, B. W. Skelton and A. H. White, *Chem. Commun.*, 1966, 1563; G. Dekker, A. Buijs, C. J. Elsevier, K. Vrieze, P. Vanleeuwen, W. J. J. Smeets, A. L. Spek, Y. F. Wang and C. H. Stam, *Organometallics*, 1992, **11**, 1937; H. Jin, K. J. Cavell, B. W. Skelton and A. H. White, *J. Chem. Soc., Dalton Trans.*, 1995, 2159; D. L. Reger and D. G. Garza, *Organometallics*, 1993, **12**, 554; B. A. Markies, D. Kruis, M. H. P. Rietveld, K. A. N. Verkerk, J. Boersma, H. Kooijman, M. T. Larkin, A. L. Spek and G. Vankoten, *J. Am. Chem. Soc.*, 1995, **117**, 5263; P. Wehman, R. E. Rulke, V. E. Kaasjager, P. C. J. Kamer, H. Kooijman, A. L. Spek, C. J. Elsevier, K. Vrieze and P. Vanleeuwen, *J. Chem. Soc., Chem. Commun*., 1995, 331.
16 F. Ozawa, T. Hayashi, H. Koide and A. Yamamoto, *J. Chem. Soc., Chem. Commun.*, 1991, 1469.
17 G. K. Anderson and R. J. Cross, *Acc. Chem. Res.*, 1984, **17**, 67; V. V. Grushin and H. Alper, *Organometallics*, 1993, **12**, 1890; J. L. Hoare, K. J. Cavell, R. Hecker, B. W. Skelton and A. H. White, *J. Chem. Soc., Dalton Trans.*, 1996, 2197; P. E. Garrou and R. F. Heck, *J. Am. Chem. Soc.*, 1976, **98**, 4115.
18 P. W. N. M. van Leeuwen, C. F. Roobeek and H. van der Heijden, *J. Am. Chem. Soc.*, 1994, **116**, 12 117; C. G. Anklin and P. S. Pregosin, *J. Organomet. Chem.*, 1983, **243**, 101.
19 J. Vicente, A. Arcas, D. Bautista and P. G. Jones, *Organometallics*, in the press.
20 J. Vicente, A. Arcas, D. Bautista, A. Tiripicchio and M. Tiripicchio-Camellini, *New J. Chem.*, 1996, **20**, 345.
21 G. M. Sheldrick, SHELXL 93, University of Göttingen, 1993.

*Received in Cambridge, UK, 5th March 1997; Com. 7/01552F*

# Fluorocyclohexane ring inversion in a solid thiourea inclusion compound studied by fluorine-19 magic-angle spinning NMR with high-power proton decoupling

**Alison Nordon,[a] Robin K. Harris,*[a] Lily Yeo[b] and Kenneth D. M. Harris[b]**

[a] *Department of Chemistry, University of Durham, South Road, Durham, UK DH1 3LE*
[b] *School of Chemistry, University of Birmingham, Edgbaston, Birmingham, UK B15 2TT*

**Variable-temperature $^{19}F$ magic-angle spinning NMR experiments involving high-power proton decoupling are used to examine the conformational preference and ring-inversion kinetics in the fluorocyclohexane–thiourea inclusion compound.**

One of the most interesting and potentially important aspects of solid-state inclusion chemistry is the fact that the behaviour of molecules constrained as guests within a solid host structure is often very different from the behaviour of the same molecules in other environments (such as in their pure crystalline phase, in dispersed phases, or as guests in other host structures). In this regard, the conformational properties of substituted cyclohexane guest molecules can provide a sensitive probe of the structural constraints imposed by a solid host structure, and form a basis for comparison between different types of host structure. Thiourea forms solid inclusion compounds with cyclohexane and certain substituted cyclohexanes. In such compounds, the thiourea (host) structure contains tunnels in which the guest molecules reside.[1,2] Thiourea inclusion compounds containing mono- and di-substituted cyclohexane guests have been the subject of a number of studies. Much of the interest concerns the conformational dependence of the cyclohexane ring in the thiourea tunnels upon the substituent (X). For monosubstituted cyclohexanes with X = Me, $NH_2$ and OH, the equatorial conformer predominates. In comparison, when X = Cl, Br and I, the axial conformer predominates. Many of these results have been obtained using solid-state $^{13}C$ NMR spectroscopy.[3–5] In this study we have used $^{19}F$ NMR, with high-power proton decoupling, to examine the fluorocyclohexane–thiourea inclusion compound. Previous studies[4,5] indicate that in this system, both conformations of fluorocyclohexane are present in equal proportions. Fluorine-19 NMR has a considerable advantage over $^{13}C$ NMR, namely its greatly superior sensitivity. However, because of the close proximity of the $^{1}H$ and $^{19}F$ frequencies (within 6%) and the high powers required for decoupling in the solid state, a specially designed 'HF' probe[6,7] is needed, so that until very recently $^{19}F$ MAS NMR has been little used for systems containing both fluorine and hydrogen.[8]

Fluorine-19 MAS NMR spectra were recorded with a Chemagnetics CMX 200 NMR spectrometer operating at 200.13 MHz for $^{1}H$ and 188.28 MHz for $^{19}F$. A Chemagnetics HF double-resonance probe was used which accepts 4 mm o.d. zirconia rotors fitted with a Vespel end-cap, spacer and drive tip. Typical spectral conditions were: $\pi/2$ pulse duration, 3 μs; pulse delay, 60 s; $^{1}H$ decoupling power, 105 kHz; spin rate, 7.0 kHz. Variable-temperature operation involved passing cool nitrogen gas over the sample. Temperatures were calibrated using tetrakis(trimethylsilyl)silane soaked in liquid methanol.[9] Fluorine-19 chemical shifts were referenced externally, by rotor replacement, to hexafluorobenzene ($\delta$ −166.4 with respect to $CFCl_3$). The $^{19}F$ chemical shifts obtained from experiments involving $^{1}H$ decoupling have been corrected for the Bloch–Siegert effect.[10]

At room temperature, a single resonance was observed in the $^{19}F$ MAS NMR spectrum. However on lowering the temperature, this resonance broadened and then sharpened to give two peaks of approximately equal intensity at 177 K (Fig. 1). This can be attributed to the well documented ring-inversion process in cyclohexane type molecules. The resonances at $\delta$ −163.9 and −187.0 at 177 K can be assigned to the equatorial and axial conformers respectively using solution-state NMR data.[11] To investigate the kinetics of the ring-inversion process, bandshape analysis was carried out assuming a two-site exchange model. This involved comparing 'by eye' the simulated and experimental data. Bandshape analysis shows that upon increasing the temperature there is a very slight shift in the equilibrium position towards the axial conformer. To demonstrate that ring-inversion occurs on the NMR timescale at temperatures well below coalescence, a two-dimensional $^{19}F$ exchange[12] spectrum was recorded at 227 K. With a mixing time of 50 ms, all four peaks are of equal intensity, indicating that exchange is complete. Away from the coalescence temperature, bandshapes are insensitive to the ring-inversion rate constant, so $^{19}F$ selective polarisation inversion experiments[13] were carried out at 217, 197 and 177 K. The method for selectively inverting one of the resonances involved offsetting the transmitter from one peak by a frequency equal to the

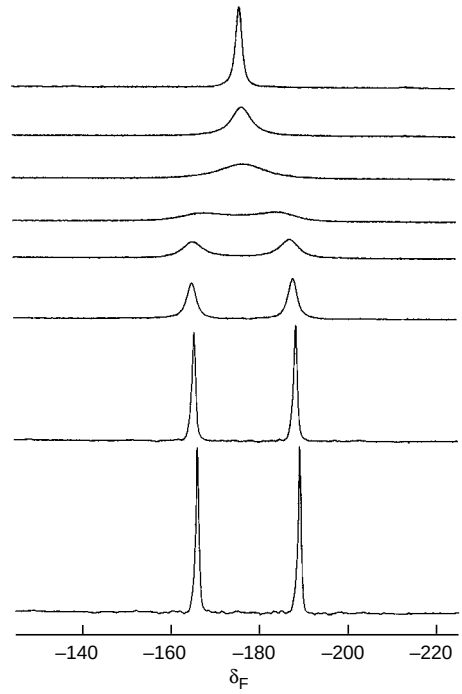



**Fig. 1** Variable-temperature $^{19}F$ MAS NMR spectra, acquired with $^{1}H$ decoupling, of the fluorocyclohexane–thiourea inclusion compound. From bottom to top: 177, 217, 237, 247, 258, 268, 278, 300 K.

separation between the two peaks.[14] Exchange between the two sites was monitored by varying the mixing time, and the results of the experiment performed at 197 K are shown in Fig. 2.

The rate constants determined by the two methods were used to study the thermodynamics of the ring-inversion process. The average activation parameters obtained from an Eyring plot are: $\Delta H^{\ddagger} = 39.4 \pm 2.6$ kJ mol$^{-1}$, $\Delta S^{\ddagger} = -11.9 \pm 11.0$ J mol$^{-1}$ K$^{-1}$ and $\Delta G^{\ddagger}$ (263 K) = 42.5 ± 5.5 kJ mol$^{-1}$. The values that we have obtained for $\Delta H^{\ddagger}$ and $\Delta S^{\ddagger}$ differ from those reported using $^{13}$C NMR in a previous study,[5] although data for $\Delta G^{\ddagger}$ (263 K) are comparable. However, we have studied the ring-inversion process over a wider temperature range (120 K) using the sensitivity advantage of $^{19}$F NMR, and have obtained, with selective polarisation inverson, rate constants in the slow-exchange regime where bandshape analysis lacks precision. For this reason we believe that the studies reported here have led to significantly improved values for the activation parameters.

We have demonstrated that $^{19}$F NMR can be used to probe the ring-inversion process in the fluorocyclohexane–thiourea inclusion compound in the same way that $^{13}$C NMR has been used to investigate other substituted cyclohexane–thiourea inclusion compounds. However, the greater sensitivity of $^{19}$F NMR in comparison to $^{13}$C NMR enables spectra to be obtained in shorter times and hence two-dimensional experiments are more feasible, particularly at low temperatures.

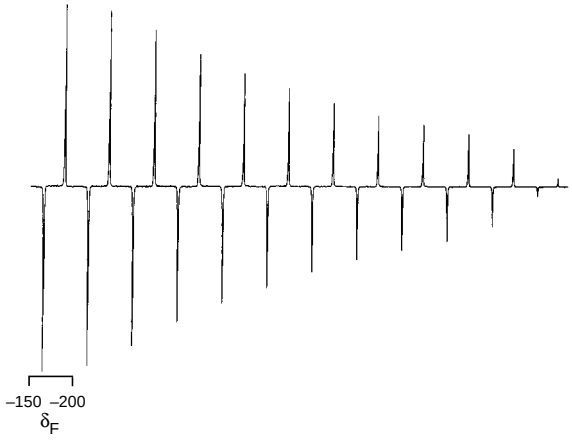



**Fig. 2** Fluorine-19 selective polarisation inversion experiment at 197 K, with mixing times of: 0.001, 1.0, 5.0, 10.0, 15.0, 20.0, 25.0, 30.0, 35.0, 40.0, 50.0 and 100.0 ms (from left to right). A spin rate of 8.6 kHz was used and a time of 116 μs was used to create a phase difference of 180° between the two magnetisation vectors for the axial and equatorial spins.[15]

The fluorocyclohexane–thiourea inclusion compound was prepared by slowly cooling a solution containing fluorocyclohexane and thiourea in methanol. The crystals were collected and washed with 2,2,4-trimethylpentane to remove any fluorocyclohexane molecules adhering to their external surfaces. Powder X-ray diffraction studies at ambient temperature indicated that these crystals have the rhombohedral thiourea tunnel structure,[1] as found for thiourea inclusion compounds containing other cyclohexane-based guest molecules.

We thank EPSRC for a studentship and ICI for a scholarship to one of us (A. N.). We also thank EPSRC for research grant L02906 and for access to the Durham-based research service in solid-state NMR.

## Footnote

* E-mail: r.k.harris@durham.ac.uk

## References

1 M. D. Hollingsworth and K. D. M. Harris, *Comprehensive Supramolecular Chemistry*, ed. D. D. MacNicol, F. Toda and R. Bishop, Pergamon, 1996, vol. 6, p. 177.
2 K. D. M. Harris, *J. Mol. Struct.*, 1996, **374**, 241.
3 A. E. Aliev and K. D. M. Harris, *J. Am. Chem. Soc.*, 1993, **115**, 6369.
4 M. S. McKinnon and R. E. Wasylishen, *Chem. Phys. Lett.*, 1986, **130**, 565.
5 K. Müller, *Magn. Reson. Chem.*, 1995, **33**, 113.
6 S. A. Carss, U. Scheler, R. K. Harris, P. Holstein and R. A. Fletton, *Magn. Reson. Chem.*, 1996, **34**, 63.
7 R. K. Harris, S. A. Carss, R. D. Chambers, P. Holstein, A. P. Minoja and U. Scheler, *Bull. Magn. Reson.*, 1996, **17**, 37.
8 J. M. Miller, *Prog. NMR Spectrosc.*, 1996, **28**, 255.
9 A. E. Aliev and K. D. M. Harris, *Magn. Reson. Chem.*, 1994, **32**, 366.
10 S. A. Vierkötter, *J. Magn. Reson. A*, 1996, **118**, 84.
11 F. A. Bovey, E. W. Anderson, F. P. Hood and R. L. Kornegay, *J. Chem. Phys.*, 1964, **40**, 3099.
12 J. Jeener, B. H. Meier, P. Bachmann and R. R. Ernst, *J. Chem. Phys.*, 1979, **71**, 4546.
13 P. Caravatti, G. Bodenhausen and R. R. Ernst, *J. Magn. Reson.*, 1983, **55**, 88.
14 C. Connor, A. Naito, K. Takegoshi and C. A. McDowell, *Chem. Phys. Lett.*, 1985, **113**, 123.
15 N. M. Szeverenyi, A. Bax and G. E. Maciel, *J. Am. Chem. Soc.*, 1983, **105**, 2579.

*Received in Cambridge, UK, 5th March 1997; Com. 7/01558E*

# Synthesis, photophysics and crystal structures of hexanuclear copper(I) and silver(I) acetylide complexes

**Vivian Wing-Wah Yam,* Wendy Kit-Mai Fung and Kung-Kai Cheung**

*Department of Chemistry, The University of Hong Kong, Pokfulam Road, Hong Kong*

**The luminescent complexes $[M_3(\mu\text{-}Ph_2PCH_2PPh_2)_3(\mu_3\text{-}\eta^1\text{-}C{\equiv}CC_6H_4C{\equiv}C\text{-}p)M_3(\mu\text{-}Ph_2PCH_2PPh_2)_3][BF_4]_4$ are synthesized by the reaction of $[M_2(\mu\text{-}Ph_2PCH_2PPh_2)_2(MeCN)_2]^{2+}$ and 1,4-diethynylbenzene in the presence of $Bu^nLi$ in thf (M = Cu 1, Ag 2); X-ray crystal structures of both are determined.**

The highly conjugated polyynes and their transition-metal complexes have attracted enormous attention as precursors for non-linear optical materials and rigid-rod molecular wires.[1] Recently, we synthesized the first luminescent binuclear $Re^I$ organometallics with a rigid-rod acetylide backbone.[2] With our recent interest in polynuclear $Cu^I$ and $Ag^I$ acetylide complexes,[3] we believe that these complexes would be ideal building blocks for the design of luminescent rigid-rod oligomers. Here, we report the first synthesis of two novel luminescent diyne-bridged hexanuclear copper(I) and silver(I) complexes $[Cu_3(\mu\text{-}Ph_2PCH_2PPh_2)_3(\mu_3\text{-}\eta^1\text{-}C{\equiv}CC_6H_4C{\equiv}C\text{-}p)Cu_3(\mu\text{-}Ph_2PCH_2PPh_2)_3][BF_4]_4$ **1** and $[Ag_3(\mu\text{-}Ph_2PCH_2PPh_2)_3(\mu_3\text{-}\eta^1\text{-}C{\equiv}CC_6H_4C{\equiv}C\text{-}p)Ag_3(\mu\text{-}Ph_2PCH_2PPh_2)_3][BF_4]_4$ **2**; both of which contain two triangular $M^I_3$ units linked *via* an extended conjugated diyne backbone.

$Bu^nLi$ was added at room temperature to a solution of 1,4-diethynylbenzene[4] in predried, degassed thf under an inert atmosphere of nitrogen; a solid sample of $[Cu_2(\mu\text{-}dppm)_2(MeCN)_2][BF_4]_2$[5] was then added and stirred at room temp. for 24 h. After evaporation to dryness, the resulting solution was extracted with $CH_2Cl_2$. Subsequent diffusion of diethyl ether into the concentrated solution gave **1** as air-stable yellow crystals. Complex **2** was obtained as air-stable pale yellow crystals by a similar method except that $[Ag_2(\mu\text{-}dppm)_2(MeCN)_2][BF_4]_2$[6] was used. Both **1** and **2** have been characterized by elemental analyses, $^1H$ NMR, IR and Raman spectroscopy.† The X-ray crystal structures of **1** and **2** have also been determined.‡

A perspective drawing of the complex cation of **1** with atomic numbering is shown in Fig. 1. The complex cation of **1** consists of two triangular arrays of copper atoms with a dppm ligand bridging each edge to form two roughly planar $Cu_3P_6$ cores bridged by a 1,4-diethynylbenzene unit to form a dumb-bell shaped structure. The Cu···Cu distances, which are comparable to those found in the related monocapped systems,[3a,c,7,8] are suggestive of at best only very weak Cu···Cu interactions. The bridging mode of the alkynyl group is asymmetric and the C≡C bond length is typical of metal–acetylide σ bonding. It is interesting that the phenyl ring of the acetylide unit which sits in the middle of the complex is almost parallel to the two phenyl rings [C(51)–(56), C(51*)–(56*)] of the dppm units, one on each of the triangular core, respectively, indicative of the presence of π-stacking interactions. The complex cation of **2** is isostructural to **1** and similar π-stacking interactions are observed.

The absorption spectra of **1** and **2** display strong absorptions in the UV region at *ca*. 258–324 nm, tentatively assigned as ligand-localized transitions. Longer wavelength absorptions appear as vibronically structured bands at *ca*. 370–416 nm for **1** and *ca*. 324–364 nm for **2** in $CH_2Cl_2$, with vibrational progressional spacings of *ca*. 1475–1500 $cm^{-1}$, typical of ν(C≒C) stretching modes of the aromatic ring in the excited state. Excitation of a solid sample of complex **1** at λ > 350 nm both at 77 K and room temp. produces intense yellow–orange luminescence. The room-temp. solid-state emission spectrum shows an intense band at *ca*. 583 nm, which is also vibronically structured with progressional spacings of *ca*. 1500–1520 $cm^{-1}$, characteristic of the aromatic ν(C≒C) stretch. Upon cooling to 77 K, the emission bands become better resolved. Similar emission bands are observed in fluid solution. Excitation of a solid sample of **2** at λ > 350 nm both at 77 K and room temp. give intense green–yellow luminescence. The solid-state emission spectrum also shows an intense vibronically structured band at *ca*. 513 nm at both room temp. and 77 K (Table 1). The excitation spectra of both **1** and **2** show vibronically structured bands at *ca*. 360–420 and 320–362 nm, respectively, which coincide with those of their respective absorption spectra. The excitation and emission spectra of **2** in degassed dichloromethane at 298 K are shown in Fig. 2.

It is interesting that both the absorption and emission bands of **1** occur at lower energy than those of **2**. A possible assignment for the origin of the emission involves emissive states derived from ligand-to-metal charge transfer (acetylide-to-metal

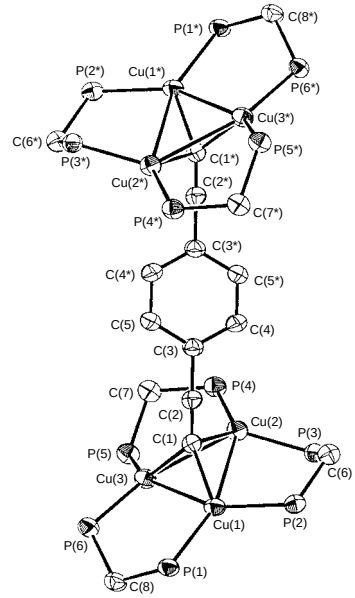



**Fig 1** Perspective drawing of the complex cation of **1** with atomic numbering scheme. Hydrogen atoms and phenyl rings have been omitted for clarity. Thermal ellipsoids are shown at the 40% probability level. Selected bond lengths (Å) and angles (°): **1** C(1)–C(2) 1.223(9), C(1)–Cu(1) 1.996(7), C(1)–Cu(2) 2.101(7), C(1)–Cu(3) 2.042(7), Cu(1)···Cu(2) 3.243(1), Cu(1)···Cu(3) 2.862(2), Cu(2)···Cu(3) 2.885(1); Cu(1)–C(1)–C(2) 143.3(7), Cu(2)–C(1)–C(2) 87.5(5), Cu(3)–C(1)–C(2) 125.1(6), Cu(1)–Cu(2)–Cu(3) 55.31(3), Cu(2)–Cu(1)–Cu(3) 55.98(3), Cu(1)–Cu(3)–Cu(2) 68.71(3). **2** C(1)–C(2) 1.24(2), C(1)–Ag(1) 2.28(1), C(1)–Ag(2), 2.29(1), C(1)–Ag(3) 2.23(1), Ag(1)···Ag(2) 3.338(1), Ag(1)···Ag(3) 3.163(1), Ag(2)···Ag(3) 3.079(1); Ag(1)–C(1)–C(2) 120.6(9), Ag(2)–C(1)–C(2) 114.9(9), Ag(3)–C(1)–C(2) 140.2(10), Ag(1)–Ag(2)–Ag(3) 58.89(3), Ag(2)–Ag(1)–Ag(3) 56.46(3), Ag(1)–Ag(3)–Ag(2) 64.65(3).

LMCT) transition mixed with d–s character. The red shift in the 77 K solid-state emission energy of *ca*. 0.28 eV from **2** to **1** is comparable to the value of 0.31 eV reported for the related hexanuclear $Ag^I$ and $Cu^I$ thiocarbamate clusters, $[Ag_6(mtc)_6]$ and $[Cu_6(mtc)_6]$ (mtc = di-*n*-propylmonothiocarbamate), where an origin of mixed d → s and LMCT character has been suggested.[9] Besides, a similar red shift in emission energy (*ca*. 0.27 eV) on going from $Ag^I$ to $Cu^I$ chalcogenido clusters has been reported,[10a–c] in which a mixed d → s/LMCT origin has also been suggested and is supported by molecular orbital calculations.[10d,e] Another possible origin for the observed red shift in energy from **2** *cf*. **1** involves states derived from metal-to-ligand charge transfer [MLCT d(M) → π*(acetylide)] transition. As $Cu^I$ is much more easily oxidized, given the higher energy of the $Cu^I$ 3d orbitals relative to those of the $Ag^I$ 4d orbitals,[11] the MLCT transition for $Cu^I$ should also occur at lower energy than that for $Ag^I$. In view of the fact that the ionization energy of $Ag^+(g)$ is nearly $10^4$ $cm^{-1}$ larger than that for $Cu^+(g)$,[11] an assignment of the emissive state as derived from a MLCT transition for the small energy shift observed from **2** to **1** is unlikely. The long lifetime of the emissive state in the μs range is probably suggestive of triplet origin. However, the possibility of an involvement of an intraligand excited state of 1,4-diethynylbenzene should not be overlooked given the unusually long lifetime of the emissive state and the low-lying π* orbital energy of the diynyl unit. Therefore, it is likely that the low-energy emission is derived from states of LMCT parentage mixed with a metal-centred $nd^9(n + 1)s^1$ state, with large intraligand ππ* character.

V. W. W. Y. acknowledges financial support from the Research Grants Council and The University of Hong Kong. W. K. M. F. acknowledges the receipt of a Postgraduate studentship and a Hung Hing Ying Scholarship, both of which are administered by The University of Hong Kong.

**Table 1** Photophysical data for complexes **1** and **2**

| Complex | Medium (*T*/K) | Absorption $\lambda_{max}$/nm ($10^{-4}$ $\varepsilon_{max}$/$dm^3$ $mol^{-1}$ $cm^{-1}$) | Emission $\lambda_{em}$/nm ($\tau_o$/μs) |
|---|---|---|---|
| **1** | $CH_2Cl_2$ (298) | 260(sh) (8.32), 294(sh) (4.41), 370(sh) (1.69), 390 (2.32), 416 (2.46) | 596 (40) |
| | Solid (298) | | 583 (222) |
| | Solid (77) | | 582 |
| | EtOH–MeOH (v/v 1 : 4) glass (77) | | 579 |
| **2** | $CH_2Cl_2$ (298) | 258(sh) (5.52), 324 (1.40), 340 (1.47), 364 (1.64) | 515 (426) |
| | Solid (298) | | 513 (351) |
| | Solid (77) | | 515 |
| | EtOH–MeOH (v/v 1 : 4) glass (77) | | 510 |

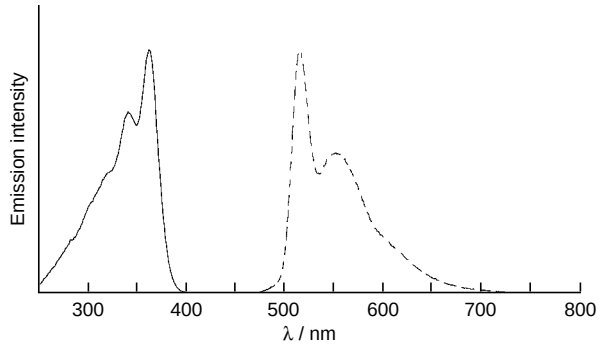



**Fig. 2** Excitation (—) and emission (---) spectra of **2** in degassed $CH_2Cl_2$ at 298 K

## Footnotes

* E-mail: wwyam@hkucc.hku.hk

† **1**: yield, 53%. $^1$H NMR ($CD_2Cl_2$), δ 3.4 (m, 6 H, $CH_2$), 3.6 (m, 6 H, $CH_2$), 6.8–7.4 (m, 120 H, $PPh_2$), 7.5 (s, 4 H, Ph). IR(Nujol) ν/$cm^{-1}$: 1062s [ν(B–F)]. Raman (solid sample) ν/$cm^{-1}$: 1955s [ν(C≡C)]. Satisfactory elemental analysis. **2**: yield, 46%. $^1$H NMR ([$^2H_6$]acetone), δ 3.8 (m, 6 H, $CH_2$), 3.9 (m, 6 H, $CH_2$), 7.0–7.6 (m, 120 H, $PPh_2$), 7.7 (s, 4 H, Ph). IR(Nujol) ν/$cm^{-1}$: 1054s [ν(B–F)]. Raman (solid sample) ν/$cm^{-1}$: 2015s [ν(C≡C)]. Satisfactory elemental analysis.

‡ *Crystal data*: for **1**: $C_{160}H_{136}B_4Cu_6F_{16}P_{12}\cdot 2CH_2Cl_2$; $M$ = 3328.88, triclinic, space group $P\bar{1}$ (no. 2), $a$ = 14.134(4), $b$ = 22.139(6), $c$ = 13.783(3) Å, α = 106.62(2), β = 99.28(3), γ = 102.78°, $U$ = 3912(2) $Å^3$, $Z$ = 1, $D_c$ = 1.413 g $cm^{-3}$, μ(Mo-Kα) = 10.61 $cm^{-1}$, $F$(000) = 1698, $T$ = 301 K. Convergence for 864 variable parameters by least-squares refinement on $F$ with $w = 4F_o^2/\sigma^2(F_o^2)$, where $\sigma^2(F_o^2) = [\sigma^2(I) + (0.030F_o^2)^2]$ for 6585 reflections with $I > 3\sigma(I)$ was reached at $R$ = 0.064 and $R_w$ = 0.087.

For **2**: $C_{160}H_{136}Ag_6B_4F_{16}P_{12}\cdot 4CH_2Cl_2$; $M$ = 3764.67, triclinic, space group $P\bar{1}$ (no. 2), $a$ = 14.393(3), $b$ = 22.346(5), $c$ = 14.323(5) Å, α = 95.38(2), β = 95.07(2), γ = 106.06(2)°, $U$ = 4375(2) $Å^3$, $Z$ = 1, $D_c$ = 1.429 g $cm^{-3}$, μ(Mo-Kα) = 9.52 $cm^{-1}$, $F$(000) = 1890, $T$ = 301 K. Convergence for 946 variable parameters by least-squares refinement on $F$ with $w = 4F_o^2/\sigma^2(F_o^2)$, where $\sigma^2(F_o^2) = [\sigma^2(I) + (0.016F_o^2)^2]$ for 9594 reflections with $I > 3\sigma(I)$ was reached at $R$ = 0.073 and $R_w$ = 0.102. Atomic coordinates, bond lengths and angles, and thermal parameters have been deposited at the Cambridge Crystallographic Data Centre (CCDC). See Information for Authors, Issue No. 1. Any request to the CCDC for this material should quote the full literature citation and the reference number 182/448.

## References

1 T. B. Marder, G. Lesley, Z. Yuan, I. R. Jobe, N. J. Taylor, I. D. Williams and S. K. Kurtz, *ACS Symp. Ser.*, 1991, **455**, 605; R. M. Laine, in *Inorganic and Organometallic Polymers with Special Properties*, ed. H. B. Fyfe, M. Mlekuz, G. Stringer, N. J. Taylor and T. B. Marder, Kluwer Academic, Elsevier, 1992, p. 331.
2 V. W. W. Yam, V. C. Y. Lau and K. K. Cheung, *Organometallics*, 1996, **15**, 1740.
3 (*a*) V. W. W. Yam, W. K. Lee and T. F. Lai, *Organometallics*, 1993, **12**, 2383; (*b*) V. W. W. Yam, W. K. Lee, P. K. Yeung and D. Phillips, *J. Phys. Chem.*, 1994, **98**, 7545; (*c*) V. W. W. Yam, W. K. Lee, K. K. Cheung, B. Crystall and D. Phillips, *J. Chem. Soc., Dalton Trans.*, 1996, 3283; (*d*) V. W. W. Yam, W. K. Lee and K. K. Cheung, *J. Chem. Soc., Dalton Trans.*, 1996, 2335; (*e*) V. W. W. Yam, W. K. M. Fung and K. K. Cheung, *Angew. Chem., Int. Ed. Engl.*, 1996, **35**, 1100; (*f*) V. W. W. Yam, W. K. Lee, K. K. Cheung, H. K. Lee and W. P. Leung, *J. Chem. Soc., Dalton Trans.*, 1996, 2889; (*g*) V. W. W. Yam, S. W. K. Choi, C. L. Chan and K. K. Cheung, *Chem. Commun.*, 1996, 2067.
4 S. Takahashi, Y. Kuroyama, K. Sonogshira and N. Hagihara, *Synthesis*, 1980, 627.
5 J. Diéz, M. P. Gamasa, J. Gimeno, A. Tiripicchio and M. T. Camellini, *J. Chem. Soc., Dalton Trans.*, 1987, 1275.
6 M. Lusser and P. Peringer, *Polyhedron*, 1985, **4**, 1997.
7 M. P. Gamasa, J. Gimeno, E. Lastra, A. Aguirre and S. J. García-Granda, *J. Organomet. Chem.*, 1989, **378**, C11.
8 J. Diéz, M. P. Gamasa, J. Gimeno, A. Aguirre and S. García-Granda, *Organometallics*, 1991, **10**, 380; J. Diéz, M. P. Gamasa, J. Gimeno, E. Lastra, A. Aguirre and S. García-Granda, *Organometallics*, 1993, **12**, 2213.
9 F. Sabin, C. K. Ryu, P. C. Ford and A. Vogler, *Inorg. Chem.*, 1992, **31**, 1941; P. C. Ford and A. Vogler, *Acc. Chem. Res.*, 1993, **26**, 220.
10 (*a*) V. W. W. Yam, W. K. Lee and T. F. Lai, *J. Chem. Soc., Chem. Commun.*, 1993, 1571; (*b*) V. W. W. Yam, K. W. W. Lo and K. K. Cheung, *Inorg. Chem.*, 1996, **35**, 3459; (*c*) V. W. W. Yam, K. W. W. Lo, C. R. Wang and K. K. Cheung, *Inorg. Chem.*, 1996, **35**, 5116; (*d*) C. R. Wang, K. W. W. Lo and V. W. W. Yam, *Chem. Phys. Lett.*, 1996, **262**, 91; (*e*) C. R. Wang, K. W. W. Lo and V. W. W. Yam, *J. Chem. Soc., Dalton Trans.*, 1997, 227.
11 C. E. Moore, *Natl. Stand. Ref. Data Ser.*, (*US Natl. Bur. Stand.*), 1971, NSRDS-NBS, **35**, 51; *Natl. Stand. Ref. Data Ser.*, (*US Natl. Bur. Stand.*), 1971, NSRDS-NBS, **35**, 116.
12 D. R. Lide, *CRC Handbook of Chemistry and Physics*, CRC Press, Boston, MA, 71st edn., 1990, pp. 10–210.

*Received in Cambridge, UK, 18th February 1997; Com. 7/01133D*

# Sensor molecules for silver(I)-selective membranes based on mono- to quadri-dentate podands

**Sarah Chung,[a] Wantae Kim,[a] Sung Bae Park,*[a] Il Yoon,[b] Shim Sung Lee[b] and Dae Dong Sung[c]**

[a] *Department of Chemistry, Inje University, Kimhae 621-749, Korea*
[b] *Department of Chemistry, Gyeongsang National University, Chinju 660-701, Korea*
[c] *Department of Chemistry, Dong-A University, Pusan 604-714, Korea*

**A series of podands containing nitrogen and sulfur atoms are utilized as sensing components to prepare $Ag^+$-selective polymeric membrane electrodes whose characteristics are dependent on the structure of each podand used.**

Crown ether type synthetic molecules have been employed in polymeric sensors as ionophores for the determination of metallic ions ($Li^+$, $Na^+$, $K^+$, $Ca^{2+}$).[1–3] Nitrogen- and oxygen-containing cryptands have also been used for the measurement of $Zn^{2+}$ and other heavy-metal ions.[4,5] A group of polythiacrown ethers and acyclic polythia compounds have been exploited for the measurement of $Ag^+$.[6,7] Recently podand structures, acyclic oligoethers, have also been shown to be valuable additions to the above chemical species for ionophores.[8,9] Obtained simply and cheaply, the podand structures containing oxygen and sulfur as the binding sites have been studied in conjunction with the extraction and detection of precious metal ions such as $Ag^+$.[9,10] Soft coordination sites like sulfur of the thia compounds seem to generate great affinity toward the $d^{10}$ transition-metal ions such as $Ag^+$ and $Hg^{2+}$.

It would be interesting to compare the relationship between molecular structure and electrochemical properties for ionophore-based membrane sensors. Employing similarly structured thioethers, Teixidor *et al*. have reported that any molecule with thioether group(s) could be highly selective towards silver(I).[6] The present report may provide an exception to this hypothesis.

Here we report on sensors based on a series of multiarmed podands that have essentially the same type but different numbers of arms (Fig. 1). All the podand structures were prepared as reported previously.[11] PVC-based ion-selective electrode (ISE) membranes were prepared by the method of Simon and coworkers.[12] The membrane compositions in the present work are listed in Table 1. Cell potentials were measured at ambient temperature (18 °C). The potentiometric cell used was as follows: Ag/AgCl(s)/4 M KCl saturated with AgCl/tris buffer/sample solution/ion-selective membrane/1 mM $AgNO_3$/AgCl(s)/Ag. A tris buffer solution consisting of 0.05 M tris(hydroxymethyl)aminomethane (Trizma Base) adjusted with $HNO_3$ solution to pH 9.0 was used as the working buffer for the potentiometric measurements. Selectivity coefficients, $k^{pot}_{Ag/X}$, were obtained by using the separate solution method.[13]

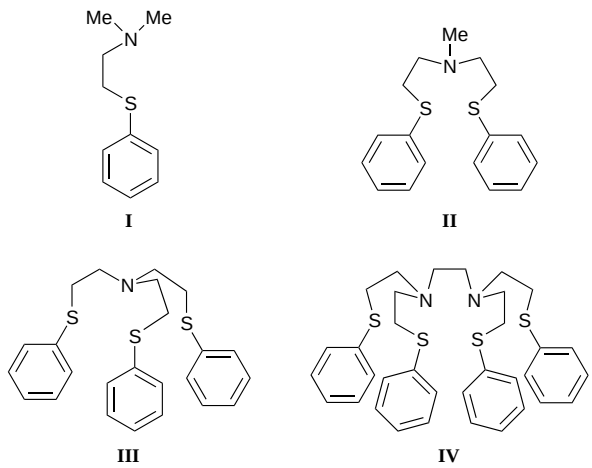



**Fig. 1** Structures of some podand-type ionophores used in the preparation of $Ag^+$-selective membrane electrodes

**Table 1** Formulation and electrochemical properties of podand-based $Ag^+$-selective membrane electrodes

| Electrode | Podand[a,b] | PVC[a] | DIDA[a] | Detection limit/M[c] | Slope/mV decade$^{-1}$[c,d] |
|---|---|---|---|---|---|
| E1 | 4.0, **I** | 32.0 | 64.0 | N/A | N/A |
| E2 | 4.0, **II** | 32.0 | 64.0 | $1.6 \times 10^{-5}$ | 45.5 |
| E3 | 6.0, **III** | 32.0 | 62.0 | $0.8 \times 10^{-6}$ | 58.0 |
| E4 | 4.0, **III** | 32.0 | 64.0 | $0.8 \times 10^{-6}$ | 58.5 |
| E5 | 2.0, **III** | 32.0 | 66.0 | $0.9 \times 10^{-6}$ | 57.0 |
| E6 | 1.0, **III** | 32.0 | 67.0 | $1.4 \times 10^{-6}$ | 47.2 |
| E7 | 4.0, **IV** | 32.0 | 64.0 | $1.0 \times 10^{-6}$ | 58.5 |
| E8 | $Ag_2S$ | | | $0.8 \times 10^{-6}$ | 59.1 |

[a] Numbers indicate mass%. [b] Bold roman characters indicate the podands in Fig. 1. [c] E1–E7, average of three membranes; E8 is a $Ag_2S$-based solid-state electrode. [d] Between detection limit and 1 mM.

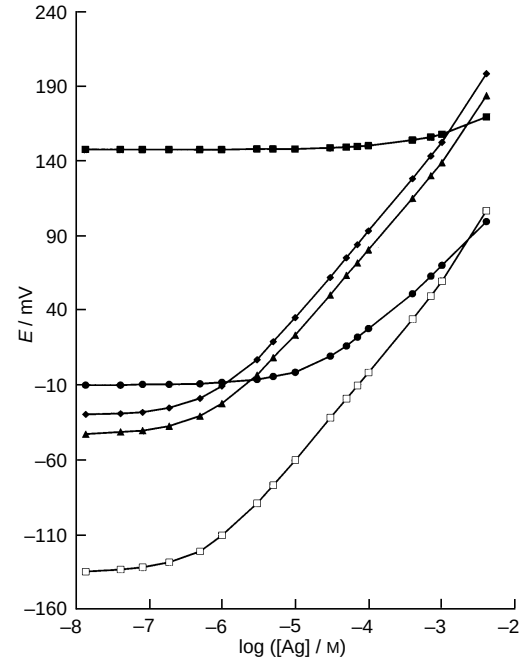



**Fig. 2** Typical potentiometric $Ag^+$ ion responses of the podand-based PVC membrane electrodes: (■) E1, (●) E2, (▲) E4, (◆) E7 and (□) E8 in Table 1. Measurements were made in 0.05 M tris buffer, pH 9.0.

The equilibrium potentiometric responses of the new podand-based PVC membrane electrodes in the concentration range of 0–10 mM are shown in Fig. 2. As summarized in Table 1, almost Nernstian slopes are observed in podand **III**- and **IV**-based membrane electrodes. On the other hand, podand **I**- and **II**-based electrodes give negligible and small response slopes, respectively. The response time of each electrode is short; the time required to reach 90% of the equilibrium mV values was < 2 s. In terms of the lifetime of the PVC membrane electrodes, response stability was observed for over a month.

Table 2 lists the potentiometric selectivity coefficient data of some podand-based PVC membrane electrodes for the interfering cations relative to $Ag^+$.

Among thiapodands, $NS_3$ and $N_2S_4$ donor set podands (**III** and **IV** in Fig. 1) seem to show the best response and selectivity to $Ag^+$. Values of log $k_{Ag/X}$ range from −3.5 for $K^+$ to −5.1 for $Ba^{2+}$, $Ca^{2+}$ and $Mg^{2+}$. The high selectivity toward $Ag^+$ is due to the high affinity of sulfur atoms in the ionophores. It is well known that $Ag^+(d^{10})$ exhibits a strong affinity towards sulfur-derived ligands and shows a remarkable preference for linear coordination.[7] For the $Hg^{2+}$ ion, the selectivity coefficient (log $k_{Ag/Hg}$) was −4.0. Compared to that of an $Ag_2S$-based electrode, the relative selectivity toward $Ag^+$ over $Hg^{2+}$ is much improved.

**Table 2** Static-mode potentiometric selectivity coefficients,[a] log $k^{pot}_{Ag/x}$, of the podand-based membrane electrodes[b]

| | Electrode[c] | | | |
|---|---|---|---|---|
| Cation | E2 (**II**) | E4 (**III**) | E7 (**IV**) | E8 ($Ag_2S$) |
| $Ag^+$ | 0 | 0 | 0 | 0 |
| $NH_4^+$ | −1.8 | −3.7 | −3.5 | −4.0 |
| $Na^+$ | −1.8 | −3.7 | −3.5 | −4.0 |
| $K^+$ | −1.8 | −3.7 | −3.5 | −4.0 |
| $Ba^{2+}$ | −3.1 | −5.1 | −4.9 | −5.2 |
| $Ca^{2+}$ | −3.1 | −5.1 | −4.9 | −5.2 |
| $Mg^{2+}$ | −3.2 | −5.1 | −4.9 | −5.2 |
| $Cu^{2+}$ | −3.2 | −5.0 | −4.8 | −4.7 |
| $Cd^{2+}$ | −2.6 | −4.9 | −4.7 | −5.1 |
| $Co^{2+}$ | −2.4 | −5.0 | −4.5 | −5.1 |
| $Pb^{2+}$ | −2.9 | −4.9 | −4.8 | −5.2 |
| $Ni^{2+}$ | −2.9 | −5.0 | −4.8 | −5.2 |
| $Hg^{2+}$ | −2.9 | −4.0 | −4.0 | −2.1 |

[a] Measured by the separate solution method at 1 mM cation concentrations in 0.05 M tris–nitric acid, pH 9.0. [b] Membrane compositions (E1–E8) listed in Table 1. [c] Bold roman characters in parentheses indicate the podands in Fig. 1.

In our previous study,[11] it was found that all of the podands tested in this study form 1 : 1 stoichiometric complexes with $Ag^+$ in methanol. The sequence of stability constants, log *K*, of complexes was found to be **IV** (12.43 ± 0.22) > **III** (9.29 ± 0.16) > **II** (7.02 ± 0.12) > **I** (3.4 ± 0.3) (assuming the stoichiometry for **I**–$Ag^+$ system is 1 : 1). In the same study, it was also revealed that the complex stability of the podands is mainly enthalpic in origin. From $Ag^+$-induced chemical shift measurements, it was also found that nitrogen atoms behave as strong donors for $Ag^+$ as do sulfur atoms.[11] Because of no or lower selective affinity of nitrogen for soft cations including $Ag^+$, both the total number of nitrogen/sulfur and the fraction of sulfur in a podand system seem to be related to the total response and selectivity of the membrane sensors toward $Ag^+$. The present study shows that the simple hypothesis of Teixidor *et al.*,[6] has exceptions for complex molecules including our nitrogen–sulfur containing podands.

S. B. P. and D. D. S. acknowledge financial support from Korean Ministry of Education (BSRI-96-3446). S. S. L. is grateful to the Korea Science and Engineering Foundation (94-1400-10-01-03).

## Footnote

* E-mail: chempsb@ijnc.inje.ac.kr

## References

1 S. R. Sheen and J. S. Shih, *Analyst*, 1992, **117**, 1691.
2 K. Suzuki, H. Yamada, K. Sato, K. Watanabe, H. Hisamato, Y. Tobe and K. Kobiro, *Anal. Chem*., 1993, **65**, 3404.
3 F. N. Assubaie, G. J. Moody and J. D. R. Thomas, *Analyst*, 1989, **114**, 1545.
4 S. K. Srivastava, V. K. Gupta and S. Jain, *Anal. Chem*., 1996, **68**, 1272.
5 G. G. Cross, T. M. Fyles and V. V. Suresh, *Talanta*, 1994, **41**, 1589.
6 F. Teixidor, M. Flores, L. Escriche, C. Viñas and J. Casabó, *J. Chem. Soc., Chem. Commun*., 1994, 963.
7 J. Casabó, T. Flor, M. I. Romero, F. Teixidor and C. Pérez-Jiménez, *Anal. Chim. Acta*, 1994, **294**, 207.
8 C. Seel and F. Voegtle, *Angew. Chem., Int. Ed. Engl*., 1992, **31**, 528.
9 A. Chowdhury and S. Kamada, *Chem. Lett*., 1994, 489.
10 S. Chung, W. Kim, S. B. Park, D. Y. Kim and S. S. Lee, *Talanta*, in the press.
11 S. S. Lee, J. M. Park, D. Y. Kim, J. H. Chung and M. H. Cho, *Chem. Lett*., 1995, 1009.
12 P. Schulthess, D. Ammann, W. Simon, C. Caderas, R. Stepanek and B. Krautler, *Helv. Chim. Acta*, 1984, **67**, 1026.
13 G. Moody and J. Thomas, *Selective Ion-Selective Electrodes*, Merrow, Watford, 1971.

*Received in Cambridge, UK, 24th February 1997; Com. 7/01259D*

# Stereochemical control of the intramolecular Diels–Alder reaction by remote allylic substituents on the diene

**Michael J. Lilly and Michael S. Sherburn***

*Department of Chemistry, Massey University, Private Bag 11222, Palmerston North, New Zealand*

**Intramolecular Diels–Alder reactions of substrates with stereocontrolling elements attached to the diene terminus provide *exo*-cycloadducts in good yields and high diastereofacial selectivity.**

The Diels–Alder reaction is one of the most powerful and most commonly used reactions in synthetic organic chemistry. The stereochemical consequences of employing chiral precursors or catalysts have been actively studied for several years,[1] with much recent interest directed towards the application of chiral, acyclic dienes in intermolecular reactions,[2] particularly when a stereocentre is present at the allylic position of the diene.[2a] Reported methods for the stereochemical control of intramolecular Diels–Alder (IMDA) reactions[3] involve the placement of suitable substituents on the linking chain (tether) between the diene and dienophile,[4] by attaching auxiliaries to the dienophile[5] and the application of enantioselective catalysis.[6] We were intrigued by the possibility of controlling the diastereofacial selectivity of the IMDA reaction by constructing chiral substrates with a stereocontrolling element at the terminus of an acyclic diene, *i.e.* remote to the linking chain (Fig. 1). This approach offers new insights into the stereochemical preferences of the Diels–Alder reaction, since previous reports in this area employ either stereochemically-biased semicyclic dienes, or are complicated by the presence of tether substituents and dienophile auxiliaries.[7]

We chose to investigate a series of ester-tethered intramolecular cycloadditions with *Z*-alkene dienophiles bearing both internal and terminal ester activating groups, since a previous report indicated reasonably facile thermal reaction and high *exo*-selectivity.[8] The series of enantiopure compounds (**7a**–**d**) was prepared from inexpensive and readily available L-ascorbic acid as shown in Scheme 1. Thus, the α-hydroxy ester **1**[9] was silylated and reduced to afford the α-silyloxy aldehyde **2**. Wittig reaction with stabilised phosphorane **3** gave a mixture of stereoisomers from which the *E*,*E*-diene ester **4** was obtained upon isomerisation. After reduction, esterification of dienol **5** with maleic anhydride gave acid **6**, which was used for the preparation of the four precursors for IMDA reaction. Thus, treatment of **6** with diazomethane furnished the *tert*-butyldimethylsilyloxy methyl ester **7c**. Desilylation of **6** followed by methylation gave hydroxy methyl ester **7a**. The trimethylsilyl and triisopropylsilyl derivatives **7b** and **7d** were prepared by reacting alcohol **7a** with the requisite trialkylsilyl triflate.

Thermolysis of the IMDA precursors under identical conditions (Table 1) produced mixtures containing only two of the four possible cycloadducts in each case.† These products were characterised following derivatisation and extensive NMR studies including HETCOR, COSY and NOESY experiments. Coupling constants pointed to a *trans*-ring junction geometry‡ in each case, indicating that all products isolated were the result of the expected *exo*-cycloaddition mode. The alcohol substrate (**7a**) exhibited only a modest diastereofacial preference between the two *exo*-cycloadducts, but this improved considerably on replacement with silyloxy protecting groups. Furthermore, a progressive improvement in selectivity was observed as the size of the silyl group was increased. The triisopropylsilyl derivative **7d**, the most sterically demanding protecting group examined, provided a remarkably high level of stereocontrol. Interestingly, the major product for the alcohol substrate corresponded to the major product for the silyl ethers.§

It is noteworthy that the π-facial selectivity of these IMDA reactions is of the opposite sense to that witnessed for intermolecular Diels–Alder reactions between simple chiral dienols (and ether derivatives) and maleic anhydride.[2a] The reasons for this difference are not known but the absence of a

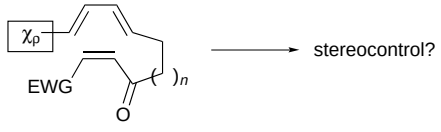
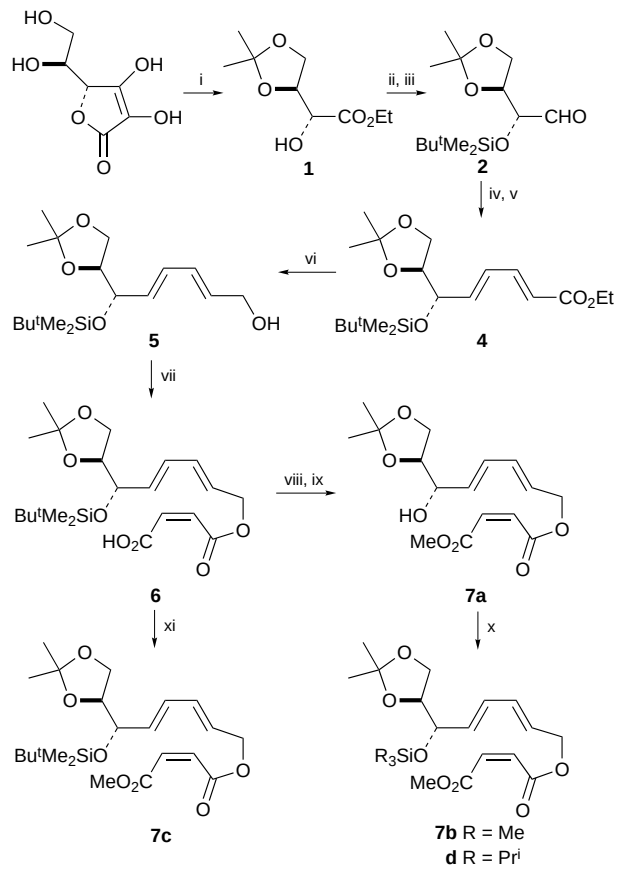
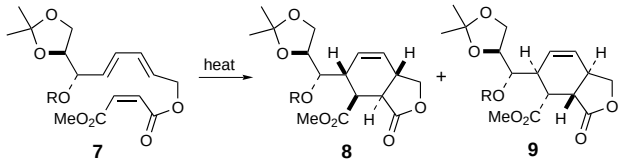



**Fig. 1**




**Scheme 1** *Reagents and conditions*: i, see ref. 9 (63% over 3 steps); ii, $Bu^tMe_2SiCl$, imidazole, DMF, 20 °C, 68%; iii, DIBAL-H, $CH_2Cl_2$, −90 °C, 89%; iv, $Ph_3P{=}CHCH{=}CHCO_2Et$ **3**, $CH_2Cl_2$, reflux; v, PhSH, AlBN, PhH, *hν*, reflux; vi, DIBAL-H, $CH_2Cl_2$, −78 to 0 °C, 53% for 3 steps; vii, maleic anhydride, $Et_3N$, DMAP, $CH_2Cl_2$, 20 °C, 100%; viii, $Bu_4NF$, THF, 20 °C, 85%; ix, $CH_2N_2$, $Et_2O$, 20 °C, 74%; x, $R_3SiOSO_2CF_3$, pyridine, $CH_2Cl_2$, 20 °C, 51% for R = Me, 58% for R = $Pr^i$; xi, $CH_2N_2$, $Et_2O$, 20 °C, 80%

**Table 1** Thermal IMDA reactions of **7**[a]




**7** **8** **9**

| Substrate **7** | R | *t*/h[b] | Yield (%)[c] | **8**:**9**[d] |
|---|---|---|---|---|
| **a** | H | 5 | 86 | 66:34 |
| **b** | $Me_3Si$ | 12 | 67 | 82:18 |
| **c** | $Bu^tMe_2Si$ | 15 | 80 | 91:9 |
| **d** | $Pr^i_3Si$ | 18 | 68 | 96:4 |

[a] Reactions were carried out in refluxing toluene at [**7**] = 0.05 M under Ar with BHT (0.20 equiv.); [b] Reactions were followed by TLC; [c] Isolated yield of **8** + **9**; [d] Ratio determined from $^1$H NMR spectra of crude reaction mixtures.

*cis*-substituent on the diene and the presence of the dioxolane moiety in the precursors may be contributing factors.[2a] Moreover, recent NMR studies have shown that subtle factors affect the conformational preferences of chiral allylic secondary alcohols and derivatives.[10] Clearly, a complicated situation exists and a detailed explanation of these results must await further studies. The stereochemical outcome of the present series of reactions does, however, follow the same trend as silyl acetal-tethered IMDA reactions[11] in which the stereocontrolling element is part of the tether.¶

In summary, this work demonstrates that the stereochemical outcome of the intramolecular Diels–Alder reaction can be controlled by the incorporation of stereochemical information on the diene remote to the diene–dienophile tether. Remarkably high levels of stereoselectivity can be obtained for thermal (uncatalysed) reactions by judicious selection of the alcohol protecting group in the precursor. The products obtained from these reactions are enantiomerically pure and rich in functionality, offering the prospect of further elaboration into a multitude of useful chiral building blocks.

The authors would like to thank Dr Pat Edwards for assistance with NMR, Massey University for a Graduate Assistant Scholarship (to M. J. L.) and The New Zealand Lotteries Board for funding.

## Footnotes

* E-mail: m.sherburn@massey.ac.nz

† In these experiments we observed small amounts of other compounds which may be the products of *endo*-mode cycloaddition. Thus far we have not been able to isolate sufficient quantities of pure compounds to allow characterisation of these very minor products.

‡ The coupling constants between protons at the ring junction (*J* 13.7 Hz) were consistent throughout this series and compared favourably with literature values for similar compounds (see ref. 8).

§ Silylation of a 1.9:1 mixture of **8a** and **9a** ($Me_3SiCl$, imidazole, DMF, 20 °C, 61%) furnished a 1.9:1 mixture of two compounds identical in all respects to **8b** and **9b**. The major isomer from this experiment corresponded with the major isomer from thermolysis of **7b**.

¶ We thank a referee for drawing our attention to this work.

## References

1 For reviews on asymmetric Diels–Alder reactions, see W. Oppolzer, *Angew. Chem., Int. Ed. Engl.*, 1984, **23**, 876; W. Oppolzer, in *Comprehensive Organic Synthesis*, ed. B. M. Trost, I. Fleming and L. A. Paquette, Pergamon, Oxford, 1991, vol. 5, p. 315; For reviews on enantioselective catalysis, see K. Narasaka, *Synthesis*, 1991, 1; H. B. Kagan and O. Riant, *Chem. Rev.*, 1992, **92**, 1007.

2 (*a*) Chiral 1-substituted 1,3-dienes: R. Tripathy, R. W. Franck and K. D. Onan, *J. Am. Chem. Soc.*, 1988, **110**, 3257; W. Adam, J. Glaser, K. Peters and M. Prein, *J. Am. Chem. Soc.*, 1995, **117**, 9190; G. T. Crisp and M. G. Gebauer, *J. Org. Chem.*, 1996, **61**, 8425; (*b*) Chiral 2-substituted 1,3-dienes: R. Bloch and N. Chaptal-Gradoz, *J. Org. Chem.*, 1994, **59**, 4162; J. Barluenga, M. Tomas, A. Suarez-Sobrino and L. A. Lopez, *J. Chem. Soc., Chem. Commun.*, 1995, 1785 and references cited therein.

3 For recent reviews, see D. Craig, *Chem. Soc. Rev.*, 1987, **16**, 187; W. R. Roush, in *Advances in Cyloaddition*, ed. D. P. Curran, JAI, Greenwich, CT, 1990, vol. 2, p. 91; W. R. Roush, in *Comprehensive Organic Synthesis*, ed. B. M. Trost, I. Fleming and L. A. Paquette, Pergamon, Oxford, 1991, vol. 5, p. 513.

4 For recent examples, see P. J. Ainsworth, D. Craig, A. J. P. White and D. J. Williams, *Tetrahedron*, 1996, **52**, 8937; W. R. Roush, J. A. Champoux and B. C. Peterson, *Tetrahedron Lett.*, 1996, **37**, 8989.

5 W. R. Roush, H. R. Gillis and A. I. Ko, *J. Am. Chem. Soc.*, 1982, **104**, 2269; D. A. Evans, K. T. Chapman and J. Bisaha, *Tetrahedron Lett.*, 1984, **25**, 4071; W. Oppolzer and D. Dupuis, *Tetrahedron Lett.*, 1985, **26**, 5437; D. A. Evans, K. T. Chapman and J. Bisaha, *J. Am. Chem. Soc.*, 1988, **110**, 1238.

6 K. Furuta, A. Kanematsu, H. Yamamoto and S. Takaoka, *Tetrahedron Lett.*, 1989, **30**, 7231; K. Narasaka, H. Kusama and Y. Hayashi, *Chem. Lett.*, 1991, 1413; K. Narasaka, M. Saitou and N. Iwasawa, *Tetrahedron: Asymmetry*, 1991, **2**, 1305; K. Ishihara, H. Kurihara and H. Yamamoto, *J. Am. Chem. Soc.*, 1996, **118**, 3049.

7 B. Fraser-Reid, Z. Benko, R. Guiliano, K. M. Sun and N. Taylor, *J. Chem. Soc., Chem. Commun.*, 1984, 1029; D. A. Evans and W. C. Black, *J. Am. Chem. Soc.*, 1993, **115**, 4497; D. J. Hart, W.-L. Wu and A. P. Kozikowski, *J. Am. Chem. Soc.*, 1996, **117**, 9369.

8 J. D. White and B. G. Sheldon, *J. Org. Chem.*, 1981, **46**, 2273.

9 E. Abushanab, P. Vemishetti, R. W. Leiby, H. K. Singh, A. B. Mikkilinelli, D. C.-J. Wu, R. Saibaba and R. P. Panzica, *J. Org. Chem.*, 1988, **53**, 2598.

10 B. W. Gung, J. P. Melnick, M. A. Wolf and A. King, *J. Org. Chem.*, 1995, **60**, 1947 and references cited therein.

11 D. Craig and J. C. Reader, *Tetrahedron Lett.*, 1992, **28**, 4073.

*Received in Cambridge, UK, 18th February 1997; Com. 7/01125C*

# Mass spectrometric determination of methyl group positions in long chain methyl ethers and alcohols *via* nitriles

**Stefan Schulz***

*Institut für Organische Chemie, Universität Hamburg, Martin-Luther-King-Platz 6, D-20146 Hamburg, Germany*

**Mass spectra of long chain branched nitriles are used to determine the position of the methyl groups along the chain in naturally occurring methyl ethers, alcohols and fatty acids.**

Recently we showed that lipids occur on the silk of spiders.[1,2] Extracts of this silk contain long chain, methyl branched 1-methoxy alkanes as their major component[2] which are not known from any other natural source. The silk of the golden orb weaver *Nephila clavipes* (Araneidae) is currently being intensively studied because of its high tensile strength and elasticity.[1,3] Investigations of web extracts by GC–MS showed the presence of alkanes, alcohols and 1-methoxy alkanes with multiple methyl branches. The 1-methoxy alkanes exhibit a more complex branching pattern than those previously known from the Linyphiidae.[2] For the determination of the position of the methyl groups in the chain we developed a new method applicable to microgram amounts of complex mixtures.

Methyl branches in long chain alkanes can be determined by their mass spectra and gas chromatographic retention indices.[4] This becomes more difficult with alcohols, aldehydes and 1-methoxy alkanes because they easily loose water or methanol under the mass spectrometric conditions. The localization of the methyl groups is thus only possible in special cases.[5] Methyl ester branches between C-2 and C-4 can be easily determined because of the high ion-density caused by carbonyl induced fragmentations, but methyl groups at other positions are much more difficult to identify due to low ion intensities.[6,7]

Derivatives of such compounds can be used in some cases to determine the branching positions. Fatty acids can be transformed into alkanes *via* reduction, chloride formation and reductive dehalogenation.[7] Free acids can also be converted *via* their acid chlorides into 3-pyridylmethyl esters or pyrrolidides, the mass spectra of which clearly show the branching positions.[8] Long chain branched alcohols have been converted into alkyl chlorides, deuterated alkanes and nicotinic acid derivatives.[8,9] All methods have drawbacks when used on the microgram scale, *i.e.* the low intensity of diagnostic ions and by-products introduced into the sample during derivatization or interference with other compounds present in the extract.

Investigations of branched alkyl nitriles showed that their mass spectra exhibit intense molecular ions and an ion series $C_nH_{2n-2}$ dominating in the region above 100 amu. Branching positions can be easily determined by the ions **A** and **A** + 1 which arise by cleavage besides the methyl group (see Fig. 1). In the higher mass region the ions **B** and **B** + 1 also become prominent. The respective ions **A** − 14 are of low abundance. Nitrogen containing ions dominate the spectrum above 100 amu. The cyano group obviously stabilizes the cations obtained by cleavage of σ-bonds, so that the information on the branching positions is preserved in the spectra (see Fig. 2). Below 100 amu this fragmentation pattern is overlayed with ions arising from other processes,[10] thus making the detection of the methyl groups at C-2, C-3 and C-4 difficult. While a methyl group at C-6 is clearly visible [see Fig. 2(*a*)], a methyl group near the cyano group can only be detected by the ion *m/z* 111, which intensity becomes comparable to the one of the ion *m/z* 97 [see Fig. 2(*b*)]. On the other hand, methyl ethers can be converted in methyl esters on a microscale using $RuO_4$,[2] thus enabling the location of the methyl groups between C-2 and C-4.

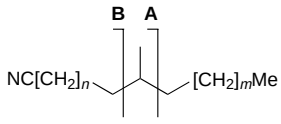



**Fig. 1** Mass spectrometric fragmentation pattern of long chain branched 1-methoxy alkanes

Methyl ethers or alcohols can be cleanly transformed in high yield into nitriles by a microprocedure.† They are first converted into the respective iodides using $Me_3SiI$,[2] followed by reaction with $Et_4NCN$ in dichloromethane. After completion, the solvent is substituted with pentane, leaving a clean derivatized extract, almost free of reagents and impurities. Extracts of silk from *Nephila clavipes* containing complex mixtures of alkanes, alcohols and methyl ethers in microgram amounts were successfully characterized by this method.[11] As an example, 1-methoxy-16,20,24,28-tetramethylhentriacontane

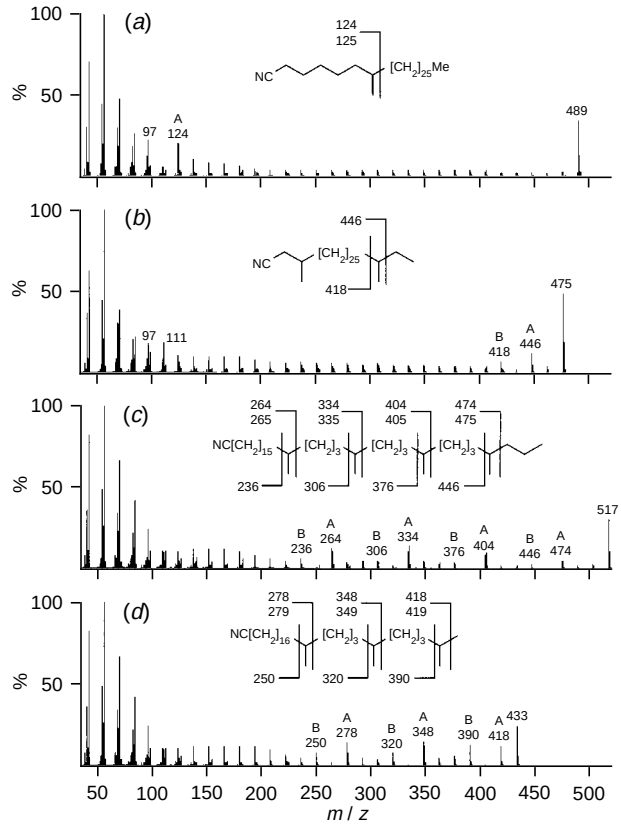



**Fig. 2** Mass spectra (70 eV, EI) of (*a*) 6-methyldotriacontyl cyanide (synthetic); (*b*) 2,28-dimethyltriacontyl cyanide (from *N. clavipes*); (*c*) 16,20,24,28-tetramethylhentriacontyl cyanide (from *N. clavipes*); (*d*) 17,21,25-trimethylhexacosyl cyanide (synthetic)

and 1-methoxy-2,28-dimethyltriacontane could be identified (the mass spectra of their nitriles are shown in Fig. 2). Advantages of the analysis of the methyl branching positions *via* nitriles are the very characteristic mass spectra carrying the information of the functional group position, mild reaction conditions and clean products. In addition, all compounds easily convertible by microprocedures into alcohols, like fatty acids or their esters, can also be analysed.[12]

## Footnotes

* E-mail: sschulz@chemie.uni-hamburg.de

† *Experimental procedure for the microderivatization of methyl ethers or alcohols.* The reactions were performed in 1 ml mini-vials (Chromatography Research Supplies). To 50 μl of a $CH_2Cl_2$ solution of the educts 20 μl $Me_3SiI$ was added under nitrogen. After 2 h at 60 °C in a dark place (oven) and cooling, 50 μl sat. aq. $NaHCO_3$ and 200 μl $CH_2Cl_2$ were added and the mixture thoroughly shaken. The aqueous phase was removed and NaCl added for drying. The organic phase was transferred into another vial and the NaCl residue was again washed with 200 μl $CH_2Cl_2$. After addition of $Et_4NCN$ (5 mg, washed with pentane prior to use) to the combined organic phases the mixture was stirred overnight, 50 μl $H_2O$ was added and the aqueous phase removed after vigorous stirring. The solvent was evaporated at 45 °C bath temperature, the residue twice taken up in 100 μl pentane, and the combined pentane extracts concentrated to a volume suitable for analysis.

## References

1 S. Schulz, *Angew. Chem.*, 1977, **109**, 324; *Angew. Chem., Int. Ed. Engl.*, 1997, **36**, 314.
2 S. Schulz and S. Toft, *Tetrahedron*, 1993, **49**, 6805.
3 R. V. Lewis, *Acc. Chem. Res.*, 1992, **25**, 392; M. A. Colgin and R. V. Lewis, *Chem. Ind. (London)*, 1995, 1009; J. Kuemmerlen, J. D. van Beek, F. Vollrath and B. H. Meier, *Macromolecules*, 1996, **29**, 2920; P. J. Willcox, S. P. Gido, W. Muller and D. L. Kaplan, *Macromolecules*, 1996, **29**, 5106; R. V. Lewis, M. Hinman, S. Kothakota and M. Fournier, *Protein Expression Purif.*, 1996, **7**, 400; P. J. Willcox, S. P. Gido, W. Muller and D. L. Kaplan, *Macromolecules*, 1996, **29**, 5106; P. A. Guerette, D. G. Ginzinger, B. H. F. Weber and J. M. Gosline, *Science*, 1996, **272**, 112; A. H. Simmons, C. A. Michal and L. W. Jelinski, *Science*, 1996, **271**, 84; C. A. Michal, A. H. Simmons, B. G. M. Chew, D. B. Zax and L. W. Jelinski, *Biophys. J.*, 1996, **70**, 489.
4 J. G. Pomonis, H. Hakk and C. L. Fatland, *J. Chem. Ecol.*, 1989, **15**, 2319; Y. V. Kissin, G. P. Feulmer and W. B. Payne, *J. Chromatogr. Sci.*, 1986, **24**, 164; K. H. Lockey, *Comp. Biochem. Physiol.*, 1988, **89B**, 595; G. J. Blomquist, D. R. Nelson and M. de Renobales, *Arch. Insect Biochem. Physiol.*, 1987, **6**, 227.
5 K.-A. Karlsson, B. E. Samuelsson and G. O. Steen, *Chem. Phys. Lipids*, 1973, **11**, 17.
6 R. Ryhage and E. Stenhagen, *Arkiv för Kemi*, 1961, **15**, 291.
7 E. Simon, W. Kern and G. Spiteller, *Biomed. Environ. Mass Spectrom.*, 1990, **19**, 129.
8 D. J. Harvey, in *Advances in Lipid Methodology*, ed. W. W. Christie, The Oily Press, Alloway, 1992, vol. 1, p. 19.
9 D. R. Nelson and C. L. Fatland, *Insect Biochem. Molec. Biol.*, 1992, **22**, 111.
10 F. W. McLafferty and F. Tureĉek, in *Interpretation of Mass Spectra*, University Science Books, Mill Valley, 1993.
11 S. Schulz, R. Ehn and H. Tichy, unpublished work.
12 A.-G. Bagnères, M. Trabalon, G. J. Blomquist and S. Schulz, unpublished work.

*Received in Glasgow, UK, 17th February 1997; Com. 7/01925D*

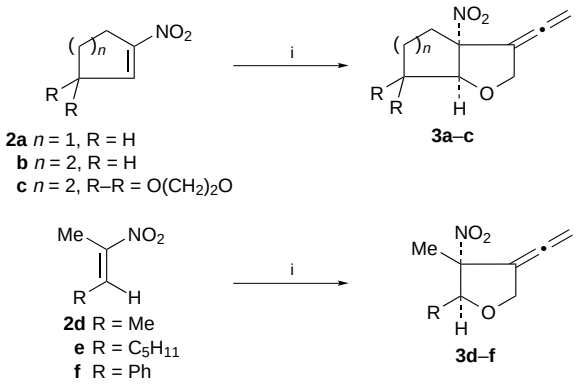
# Tandem oxa-Michael addition–$S_N2'$ substitution of 4-chlorobut-2-yn-1-ol with nitroalkenes: a total allylic 1,3-strain-controlled diastereoselective synthesis of 3-vinylidenetetrahydrofurans

**Jean-Pierre Dulcère* and Estelle Dumez**

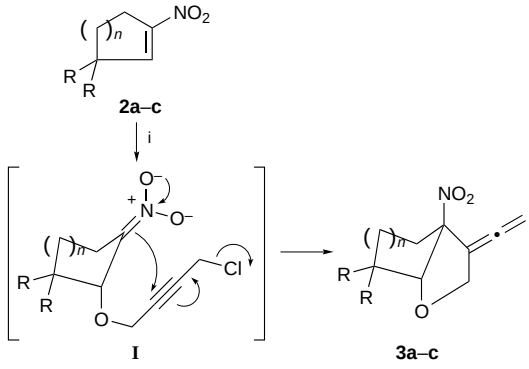
*RéSo, Réactivité en Synthèse organique, Faculté des Sciences et Techniques, Centre de St. Jérôme, UMR 6516, av. Esc. Normandie-Niemen, Boîte D 12, F-13397 Marseille Cedex 20, France*

**Bu$^t$OK-promoted reaction of 4-chlorobut-2-yn-1-ol 1 with nitroalkenes 2 affords 3-vinylidenetetrahydrofurans 3 in good yields with total diastereoselectivity.**

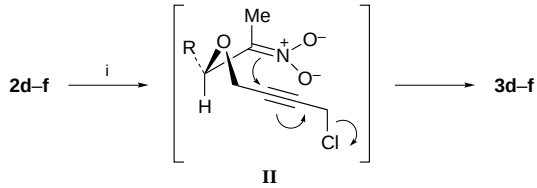
The tetrahydrofuran ring is present in a number of biologically significant natural products[1] and the synthesis of tetrahydrofurans bearing unsaturated substituents is of great interest for further transformations. Among these substituents, the allenyl functionality has received very little attention. In a recent report,[2] we disclosed a radical-mediated carbocyclisation of bromoalkynyloxiranes which gave vinylidenetetrahydrofurans. Very recently,[3] oxa-Michael initiated tandem conjugate reactions of 1-nitrocyclohexene with 4-hydroxybut-2-ynoates were shown to afford alkylidenetetrahydrofurans. Provided the oxa-Michael addition is followed by an $S_N2'$ substitution, this tandem reaction should constitute an alternative route to vinylidenetetrahydrofurans.




**Scheme 1** *Reagents and conditions*: i, **2** (1 equiv.), THF, Bu$^t$OK (1.5 equiv.), **1** ($ClCH_2C{\equiv}CCH_2OH$, 1.5 equiv.), 0 °C, 10 min, then room temp., 15–30 min, 70–78%




**Scheme 2** *Reagents and conditions*: i, see Scheme 1




**Scheme 3** *Reagents and conditions*: i, see Scheme 1

We present here our preliminary results on the oxa-Michael–$S_N2'$ substitution of 4-chlorobut-2-yn-1-ol **1** with nitroalkenes **2a**–**f**. Nitroalkenes **2a**–**f**† (Scheme 1) were reacted at 0 °C in THF with **1**, in the presence of Bu$^t$OK. After 10 min the mixture was warmed to room temperature, where it was maintained until completion of the reaction (10–30 min). Vinylidenetetrahydrofurans **3a**–**f** were isolated‡ as the sole products (70–78% yield) after flash chromatography on silica gel.

According to the known reactivity of nitroalkenes with oxygen nucleophiles,[4] the oxa-Michael addition first affords nitronate **I** which then undergoes $S_N2'$ substitution to provide the allenyl moiety[5] (Scheme 2). Bicyclic adducts **3a**–**c** are *cis* ring-fused.

Interestingly, acyclic (*E*)-nitro alkenes **2d**–**f**§ afford, under the same reaction conditions, vinylidenetetrahydrofurans **3d**–**f** in a totally diastereoselective way.¶ We assume that this is due to allylic 1,3-strain, which allows only one conformation **II** for the transition state and thereby leads to the *trans* stereoselectivity observed in the intramolecular cyclisation into vinylidenetetrahydrofurans **3d**–**f** (Scheme 3). Indeed, due to the allylic 1,3-strain effect,[4b,6] excellent diastereoselectivities have been reported for the kinetically controlled protonation of nitrones bearing substituents which differ in steric hindrance[7] and for intermolecular nitrone cycloadditions when a stereogenic centre is present at C-2.[8] However, allylic 1,3-strain does not play a significant role in Michael additions to nitroalkenes bearing a stereogenic centre at C-3, which proceed with remarkable 1,2-asymmetric induction due to steric and stereoelectronic control.[9]

In conclusion, the tandem oxa-Michael addition–intramolecular $S_N2'$ substitution of nitroalkenes constitutes an efficient and stereocontrolled procedure for the preparation of synthetically valuable and relatively unknown vinylidenetetrahydrofurans.

## Footnotes

* E-mail: Jean-pierre.dulcere@reso.u_3mrs.fr

† Prepared by literature procedures: **2a**–**c** (ref. 10); **2d**–**f** [refs. 11, 12(*b*)].

‡ Satisfactory analytical and spectral data were obtained for all compounds. *Selected data* for **3b**: $\nu_{max}/cm^{-1}$ 2950, 2870, 1985, 1965, 1550, 1365, 1080, 1040; $\delta_H$ (400 MHz, $CDCl_3$) 1.64–1.99 (m, 4 H), 2.12–2.40 (m, 4 H), 4.49 (dt, *J* 12, 4.2 Hz, (1 H), 4.58 (dt, *J* 12, 4.8 Hz, 1 H), 4.67 (dd, *J* 9, 6 Hz, 1 H), 5.18 and 5.22 (ddd, *J* 11.9, 4.8, 4.2 Hz, 2 H); $\delta_C$ (100.61 MHz, $CDCl_3$) 201.6, 100.6, 97.5, 82.8, 81.2, 66.2, 30.7, 27.7, 22.1, 21.6; *m/z* 196 (M + 1), 149 (6%), 99 (12), 87 (30), 81 (100), 69 (24).

§ (*E*)-Stereochemistry for **2d**–**f** was assigned by comparison of $^1H$ NMR spectra with previously reported data (ref. 12).

¶ *Selected data* for **3e**: $\delta_H$ (400 MHz, $CDCl_3$) 0.87 (t, *J* 6.9 Hz, 3 H), 1.28–1.32 (m, 6 H), 1.44–1.50 (m, 2 H), 1.62 (s, 3 H), 4.43 (m, 1 H), 4.45 (dt, *J* 11.8, 3.7 Hz, 1 H), 4.55 (dt, *J* 11.8, 4.9 Hz, 1 H), 5.15 (dd, *J* 4.9, 3.7 Hz, 2 H); $\delta_C$ (100.61 MHz, $CDCl_3$) 200.8, 104.6, 96.3, 86.1, 83.0, 67.3, 31.7, 29.7, 25.4, 22.5, 18.9, 14.0; by using a NOESY 2D correlation experiment, NOE interactions detected between the Me at C-4 and the $CH_2$ at C-5 allowed the assignment of *trans* stereochemistry to **3e**.

## References


1 M. H. D. Postema, *Tetrahedron*, 1992, **48**, 8545; W. Westle, *Polyether Antibiotics: Naturally Occuring Acid Ionophores*, Marcel Dekker, New York, 1982, vol. 1 and 2.
2 J. P. Dulcère, E. Dumez and R. Faure, *J. Chem. Soc., Chem. Commun.*, 1995, 897.
3 T. Yakura, T. Tsuda, Y. Matsumara, S. Yamada and M. Ikeda, *Synlett*, 1996, 985.
4 (*a*) V. V. Perekalin, E. S. Lipina, V. M. Berestovitskaya and D. A. Efremov, *Nitroalkenes*, Wiley, 1994, p. 67; (*b*) A. G. M. Barrett and G. G. Graboski, *Chem. Rev.*, 1986, **86**, 751.
5 G. M. Coppola and H. F. Schuster, *Allenes in Organic Chemistry*, Wiley, New York, 1984, p. 12.
6 F. Johnson, *Chem. Rev.*, 1968, **68**, 375; R. W. Hoffmann, *Chem. Rev.*, 1989, **89**, 1841.
7 D. Seebach, A. Beck, T. Mukhopadhyay and E. Thomas, *Helv. Chim. Acta*, 1982, **65**, 1101; M. Eyer and D. Seebach, *J. Am. Chem. Soc.*, 1985, **107**, 3601; N. Ono, A. Kamimura, H. Sasatani and A. Kaji, *J. Org. Chem.*, 1987, **52**, 4133; A. Kamimura and N. Ono, *Tetrahedron Lett.*, 1989, **30**, 731.
8 P. DeShong and J. M. Leginus, *J. Am. Chem. Soc.*, 1983, **105**, 1686.
9 A. G. M. Barrett and D. J. Rys, *J. Chem. Soc., Perkin Trans. 1*, 1995, 1009; A. G. M. Barrett and S. A. Lebold, *J. Org. Chem.*, 1990, **55**, 3853; A. G. M. Barrett, *Chem. Soc. Rev.*, 1991, **20**, 95.
10 E. J. Corey and H. Estreicher, *J. Am. Chem. Soc.*, 1978, **100**, 6294; Y. D. Vankar and N. C. Chaudhuri, *Synth. Commun.*, 1991, **21**, 885.
11 A. Sprang and E. F. Degering, *J. Am. Chem. Soc.*, 1942, **64**, 1063.
12 (*a*) A. K. Saikia, N. C. Barua, R. P. Sharma and A. C. Ghosh, *Synthesis*, 1994, 685; (*b*) R. Ballini, R. Castagnani and M. Petrini, *J. Org. Chem.*, 1992, **57**, 2160; (*c*) N. Ono, A. Kaminura, T. Kawai and A. Kaji, *J. Chem. Soc., Chem. Commun.*, 1987, 1550.



*Received in Liverpool, UK, 18th February 1997; Com. 7/01160A*

# Biosynthetic short activation of the 2,3,6-trideoxysugar L-rhodinose

**Jürgen Rohr,*[a] Sven-Eric Wohlert,[a] Carsten Oelkers,[a] Andreas Kirschning,*[b] and Monika Ries[b]**

[a] *Institut für Organische Chemie der Universität, Tammannstr. 2, D-37077 Göttingen, Germany*
[b] *Institut für Organische Chemie, TU Clausthal, Leibnizstr. 6, D-38678 Clausthal-Zellerfeld, Germany*

**The successful incorporation of non-activated [2,3-$^2H_2$]-L-rhodinose 4b into landomycin A 7 proves the existence of a short activation pathway for L-rhodinose 4; this result provides evidence of a general saving pathway for deoxysugar building blocks and their biosynthetic intermediates, respectively, which become accidentally deactivated during the biosynthetic deoxygenation cascades.**

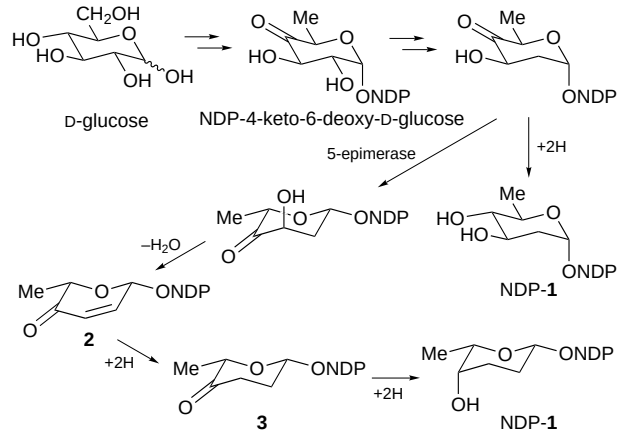
Deoxysugars, for example L-rhodinose **4** and D-olivose **1**, occur as structural moieties of many bioactive natural products and often play an important role in their mechanism of action, in particular for the DNA interaction of anti-cancer drugs.[1] For instance, the cytostatic activity of the different landomycins,[2] anti-tumour antibiotics of the angucycline group[3] which vary only in their oligosaccharide moieties, is directly dependent on the length of the phenolglycosidically-linked deoxyoligosaccharide chains.[2c] Landomycin A **7**, the most active anti-cancer compound of the landomycin family, exhibits the longest glycan moiety. While we have been investigating the biosynthesis of this hexadeoxysaccharide chain and the pathways leading to its two single deoxysugar building blocks,[2d–f] D-olivose (**1**, 2,6-dideoxy-D-*arabino*-hexopyranose) and L-rhodinose (**4**, 2,3,6-trideoxy-L-*threo*-hexopyranose), we have also been working on the development of synthetic methods in this context.

For the biosynthetic formation of deoxyhexoses it is generally accepted that the deoxygenation steps occur on nucleoside diphosphate (NDP) intermediates,[4] which are activated substrates for glycosyl transfer. The activation pathway always starts with a hexose-6-phosphate, which is transformed into the activated NDP-sugar by a pyrophosphorylase after its rearrangement into the corresponding hexose-1-phosphate. This activation mechanism occurs prior to all deoxygenation steps, and thus was assumed to exclude the activation of 6-deoxysugars.

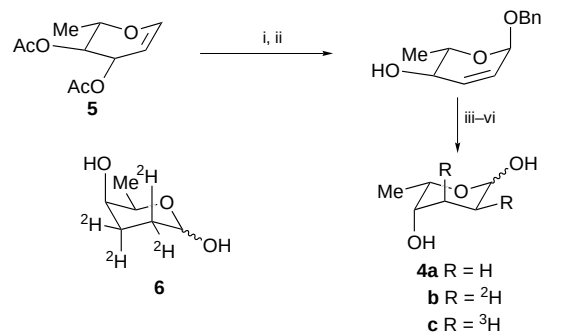
Since diphosphates, and in particular 2-deoxysugar derivatives, are chemically labile,[5] there is a considerably high chance that the activated (deoxy)sugar may be 'deactivated' through hydrolysis, *e.g.* to the trideoxysugar rhodinose (**4**, see Scheme 1). Thus these sugars would be unable to participate in the final biosynthetic glycosyl transfer reactions, if nature did not provide for the possibility of 'recycling', best achieved in a 'short activation pathway'. Such a second activation pathway was first recognized for L-fucose,[6] a 6-deoxysugar, which normally arises as an activated guanosyldiphosphate (GDP)-derivative from GDP-D-mannose.

Feeding experiments, in which synthetically prepared (Scheme 2)[7] unlabelled L-rhodinose **4a** was added to a growing culture of the landomycin A **7** producer *Streptomyces cyanogenus* (strain S-136, DSM 5087) showed that L-rhodinose **4a** was consumed within 12 h (HPLC, RI-detector control), and therefore seemed to be transported into the cells. Furthermore, experiments with radiolabelled [2,3-$^3H_2$]-L-rhodinose **4c** analogously synthesized[7] using $^3H_2$ (prepared[8] from $NaB^3H_4$ and $^3H_2O$) showed incorporation into **7**. However, quenching effects interfered with the scintillation counting and therefore only low specific incorporation was indicated. In addition, it remained unproven whether the radiolabel was exclusively located in the rhodinose moieties of **7**. Thus, the final proof of a successful incorporation of non-activated L-rhodinose into the L-rhodinose moeties of landomycin A (**7**, Scheme 3) was obtained from feeding [2*S*,3*R*-$^2H_2$]-L-rhodinose **4b** (synthesized[7] with $^2H_2$; Scheme 2). The $^2H$ NMR spectrum clearly showed $^2H$ enriched signals exclusively for 2C–$H_e$, 3C–$H_a$, 2F–$H_e$ and 3F–$H_a$ (Fig. 1). The assignment of all the protons of **7** and its octaacetate, respectively, was achieved *via* long range C,H couplings (COLOC, HMBC).[2a,b] Thus, the $^2H$-labelled L-rhodinose **4b** must have been activated through an alternative pathway to the standard deoxygenation pathway (see Scheme 1 for our current hypothesis). This 'short activation pathway' may play the role of a general saving mechanism. A control experiment, in which [2,2,3,3-$^2H_4$]-D-rhodinose **6**, prepared[7] from L-threonine, was fed to *S. cyanogenus*, showed—as expected—no incorporation.

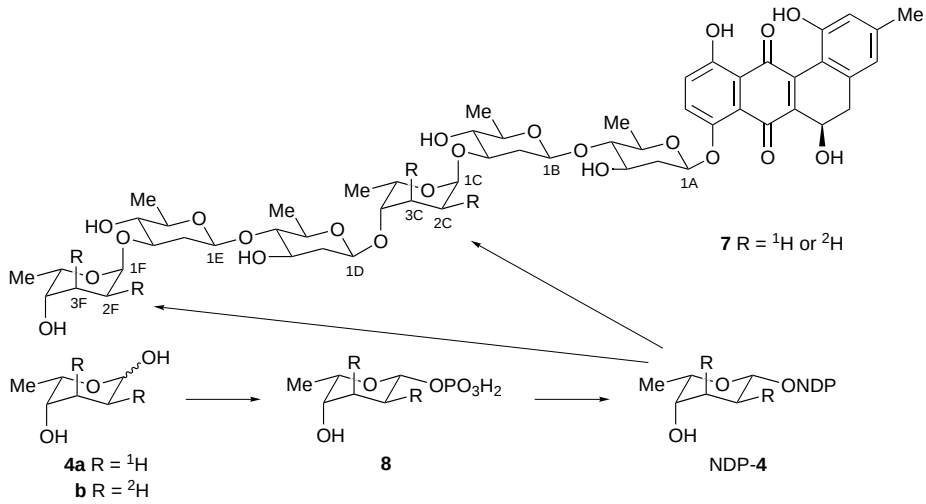
For the short activation it is assumed that L-rhodinose, as was demonstrated for L-fucose,[6] is first converted into the corresponding 1-phosphate **8** by a kinase and then activated into the NDP-derivative (NDP-**4**) through a pyrophosphorylase-mediated coupling reaction (see Scheme 3). That an activation of a 6-deoxyhexose is principally possible has also been indicated




**Scheme 1**




**Scheme 2** *Reagents and conditions*: i, BnOH, $BF_3{\cdot}OEt_2$; ii, MeOH, $NEt_3$, $H_2O$; iii, BzOH, DEAD, $PPh_3$, $OH^-$; iv, Pd–C, $H_2(^2H_2, ^3H_2)$; v, MeOH, NaOMe; vi, $H^+$




**Scheme 3**

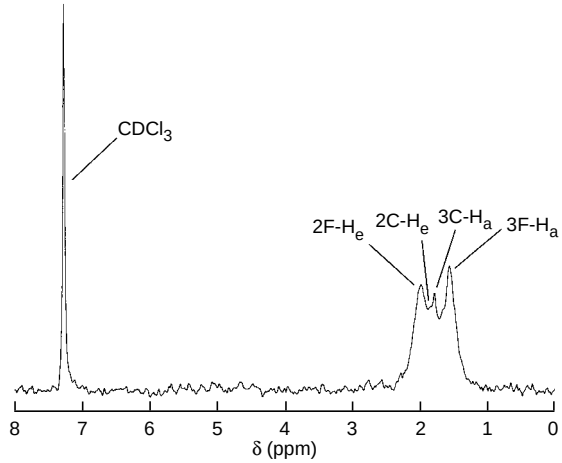



**Fig. 1** $^2$H NMR spectrum of the isolated landomycin A (**7**) after feeding of [2*S*,3*R*-$^2H_2$]-L-rhodinose (**4b**) to growing cultures of *Streptomyces cyanogenus* S-136. $^2$H signals were assigned based on the $^1$H signals [ref. 2(*a*), (*b*)].

from experiments in which 6-deoxy-D-glucose derivatives were successfully incorporated into neomycin.[9]

One can assume for organisms which produce deoxysugar-containing natural products that the short activation is feasible for all deactivated 'intermediates' of a certain biosynthetic deoxygenation cascade. Thus, the results described here open up attractive options in the context of chemical and biochemical aspects of deoxysugars. For instance, they pave the way for more convenient biosynthetic investigations on deoxysugar biosynthesis cascades, since it is obviously possible to feed and incorporate isotope labelled deoxysugars, *i.e.* non-activated analogues of the postulated intermediates of a certain deoxygenation pathway. For our investigations, labelled L-aculose or L-cinerulose, whose NDP-derivatives **2** and **3** respectively we assume to be intermediates of NDP-L-rhodinose (NDP-**4**, see Scheme 1), are important candidates to be fed to cultures of the landomycin producer *S. cyanogenus*. As another consequence of our findings, it will be profitable to look for genes of such short activation pathways, since the corresponding enzymes, preferably a kinase plus a pyrophosphorylase, should express a broad substrate flexibility and thus may be able to activate various deoxyhexoses, presumably at least all intermediates of a given deoxygenation cascade. Therefore, these enzymes may serve as powerful tools in enzymatic oligosaccharide syntheses.

The authors thank the European Community (BIO4-CT96-0068), the Fonds der Chemischen Industrie, and especially the Deutsche Forschungsgemeinschaft (grants Ro 676/5-1, 5-2 and Ki 397/2-1 to 2-3) for generous financial support. Dr David O'Hagan and Dr Ian McKeag, Department of Chemistry, University of Durham, UK, are gratefully acknowledged for excellent $^2$H NMR spectra.

## References

1 A. Kirschning, A. Bechthold and J. Rohr, *Top. Curr. Chem.*, 1997, **188**, 1; J. F. Kennedy and C. A. White, *Bioactive Carbohydrates in Chemistry, Biochemistry, and Biology*, Ellis Horwood, Chichester, 1983; S. J. Danishefsky and M. T. Bilodeau, *Angew. Chem.*, 1996, **108**, 1483.
2 (*a*) T. Henkel, J. Rohr, J. M. Beale and L. Schwenen, *J. Antibiot.*, 1990, **43**, 492; (*b*) S. Weber, C. Zolke,J. Rohr and J. M. Beale, *J. Org. Chem.*, 1994, **59**, 4211; (*c*) S.-E. Wohlert, E. Künzel, J. Rohr and J. Frevert, unpublished results; (*d*) S.-E. Wohlert, Diplomarbeit, Universität Göttingen, 1994; Beninga, Diplomarbeit, Universität Göttingen, 1994; U. Weissbach, Diplomarbeit, Universität Göttingen, 1996.
3 J. Rohr and R. Thiericke, *Nat. Prod. Rep.*, 1992, **9**, 103; K. Krohn and J. Rohr, *Top. Curr. Chem.*, 1997, **188**, 127.
4 O. Gabriel, *Adv. Chem. Ser.*, 1973, **117**, 387; H.-w. Liu and J. S. Thorson, *Annu. Rev. Microbiol.*, 1994, **48**, 223; J. S. Thorson, S. F. Fo, H.-w. Liu and C. R. Hutchinson, *J. Am. Chem. Soc.*, 1993, **115**, 6993; W. Piepersberg, *Crit. Rev. Biotechnol.*, 1994, **14**, 251.
5 G. Srivastava, O. Hindsgaul and M. M. Palcic, *Carbohydr. Res.*, 1993, **245**, 137.
6 J. G. Bekesi and R. J. Winzler, *J. Biol. Chem.*, 1967, **242**, 3873; M. L. Reitman, I. S. Trowbridge and S. Kornfeld, *J. Biol. Chem.*, 1980, **255**, 9900.
7 A. Kirschning, U. Hary and M. Ries, *Tetrahedron*, 1995, **51**, 2297.
8 A. Levy, J. B. Brown and C. J. Lyons, *Ind. Eng. Chem.*, 1960, **52**, 211.
9 S. K. Goda and M. Akhtar, *J. Antibiot.*, 1992, **45**, 984.

*Received in Cambridge, UK, 21st November 1996; Revised manuscript received, 27th March 1997; Com. 7/02125I*

# A modular approach to ligands for asymmetric π-allyl palladium catalysed additions

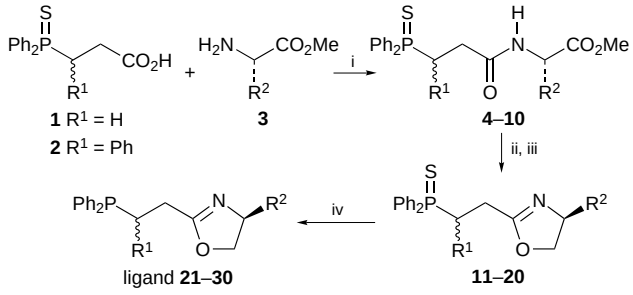
**Scott R. Gilbertson* and Cheng-Wei T. Chang**

*Department of Chemistry, Washington University, St. Louis, Missouri 63130, USA*

**A route to phosphinodihydrooxazoles is reported, which is used to synthesize ten new ligands whose ability to asymmetrically catalyse the addition of dimethyl malonate to 1,3-diphenylprop-2-enyl acetate is investigated; the best gave a palladium complex which catalyses the addition of dimethyl malonate to 1,3-diphenylprop-2-enyl acetate in 99% yield and 97% ee.**

The pace for the development of new asymmetric ligands is often determined by the availability of new ligand structures. Hence we have been interested in developing a building block based approach to the systematic synthesis of new, structurally varied ligands. Such an approach offers the potential for the discovery of new synthetically useful metal–ligand complexes, as well as the optimization of ligand systems that are known to work to a limited extent. To date, this work has focused on the synthesis and utility of amino acid based phosphine derivatives, for the construction of peptide based ligands.[1–4] We report here that the building blocks used in that approach can also be employed in the synthesis of a variety of phosphinodihydrooxazole ligands. This route allows access to new phosphine ligands without the difficulties often associated with C–P bond formation. We have used this chemistry to synthesize ten new phosphinodihydrooxazole ligands. These ligands have been screened for their ability to control the palladium catalysed asymmetric addition of malonate to 1,3-diphenylprop-2-enyl acetate.[5–7] A number of successful ligands were discovered with the best giving, at room temperature, the addition of malonate with 97% ee. This study also resulted in the observation of an interesting inverse temperature effect, in which the best ligand **28** gives higher ees at room temperature than at −30 °C.

As the starting point for our design we decided to use phosphine dihydrooxazole ligands that were structurally similar to those reported by Pfaltz, Helmchen and Williams.[8–12] This type of ligand has proven useful in asymmetric π-allyl additions[8–12] and asymmetric Heck reactions.[13] To date, the most successful ligands of this type have been six-member chelates with the phosphine attached to the dihydrooxazole through a phenyl ring. To the best of our knowledge only a single system with the phosphine attached to the nitrogen ligand by an alkyl bridge has been reported. That system, which forms a five-member chelate, gave poorer selectivity than the best systems.[10] Our approach makes ligands available that link the phosphine and dihydrooxazole groups with a two-carbon alkyl chain, thus forming a six-member chelate upon metal coordination and allowing a direct comparison to the six-member chelates studied previously by others.[8–12] The use of an alkyl chain to connect the chelating functionality allows the introduction of a second chiral centre, which is next to the phosphine. This results in diastereomeric ligands in which the two chiral centres can, potentially, act in concert or dissonance. Results with both diastereomeric possibilities are reported.




**Scheme 1** *Reagents and conditions:* i, EDC, HOBT, $CH_2Cl_2$, MeCN, room temp.; ii, $LiBH_4$, THF, 0 °C to room temp.; Burgess reagent, THF, reflux; iv, Raney Ni, MeCN, 60–80%

The synthesis of the library of ligands began with modular building blocks **1**, **2** and **3**. We chose to use amino acids **3** and phosphine containing acids (**1** and **2**) as our modules, allowing the synthesis of new ligands by amide bond formation. For the study reported here, we used two phosphine containing acids. One was a diphenylphosphine derivative of acrylate **1**, and the other a derivative of cinnamic acid **2**. The acrylate derivative **1** has been reported earlier as an intermediate in the synthesis of diphenylphosphinoserine.[1,2] The synthesis of the phenyl derivative **2** was performed in the same manner from cinnamic acid.

The synthesis of the ligands began with the coupling of phosphine acids **1** or **2** to a given amino acid yielding the phosphine sulfide amides **4–10** (Scheme 1). The desired ligands were then obtained by a simple three step procedure. Reduction of the methyl ester with $LiBH_4$ followed by cyclization with Burgess reagent[14] [$MeO_2CNSO_2NEt_3$] gave the dihydrooxazole phosphine sulfides **11–20**. Reaction with Raney nickel then removed the sulfur and gave the free phosphines. Reaction of **2** with an amino acid gave two diastereomeric products. These diastereomers were readily separated by chromatography, after $LiBH_4$ reduction, yielding both the (*SS*) and (*RS*) pair of diastereomers. The ligands are fully characterized as the phosphine sulfides. After reduction of the phosphine sulfides to the free phosphines the ligands were treated with palladium and used in catalysis without purification.†

The ligands were investigated in two groups; ligands with one chiral centre (Table 2) and ligands with two chiral centres (Table 3). Of the ligands with one chiral centre, the ligands derived from phenylalanine ($R^2$ = Bn) **22** and valine ($R^2$ = $Pr^i$) **23** gave the highest ees (87 and 86%) (Table 2, entries 2 and 3).

**Table 1** Synthesis of phospine dihydrooxazole ligands

| $R^1$ | $R^2$ | Compound | Yield (%) | Compound | Yield (%) | Ligand |
|---|---|---|---|---|---|---|
| H | Me (*S*) | **4** | 33 | **11** | 62 | **21** |
| H | Bn (*S*) | **5** | 31 | **12** | 66 | **22** |
| H | $Pr^i$ (*S*) | **6** | 64 | **13** | 72 | **23** |
| H | Ph (*S*) | **7** | 56 | **14** | 84 | **24** |
| Ph (*S*) | Bn (*S*) | **8** | 69[a] | **15** | 71 | **25** |
| Ph (*R*) | Bn (*S*) | **8** | 69[a] | **16** | 85 | **26** |
| Ph (*S*) | $Pr^i$ (*S*) | **9** | 62[a] | **17** | 45 | **27** |
| Ph (*R*) | $Pr^i$ (*S*) | **9** | 62[a] | **18** | 91 | **28** |
| Ph (*S*) | Ph (*S*) | **10** | 47[a] | **19** | 48 | **29** |
| Ph (*R*) | Ph (*S*) | **10** | 47[a] | **20** | 90 | **30** |

[a] Yields reported for **8**–**10** are for the mixture of the two diastereomers.

The effect of solvent on the reaction was probed using ligand **23** and the $Bu_4N^+$/BSA cation base combination (entries 3, 8, 9 and 10).[15] Of the solvents tested, $CH_2Cl_2$ was found to be the best solvent for this ligand (entry 3). The counter ion and base associated with the malonate anion have been shown to be important in these additions and so their effect was also investigated (entries 3, 5, 6 and 7). The optimal system for this class of ligand was found to be $(C_6H_{13})_4N^+$/BSA, as the counter ion and base, and $CH_2Cl_2$ as the solvent (entry 6), giving an ee of 90%.

Of the ligands with two chiral centres, the ligands derived from valine were again found to perform the best. Both combinations of the two chiral centres were looked at. It is interesting to note that the chirality at the carbon next to the phosphine had little effect on the selectivity of the catalysis, 90 *vs*. 93% ee for the (*SS*) *vs*. (*RS*) pair (Table 3, entries 3 and 4). Ligand **28** with a (*RS*) configuration, was found to be the most selective ligand (entry 4). The optimal reaction conditions for this ligand were then determined. The best solvent system for this ligand was found to be MeCN, and the best counter ion system was $(C_6H_{13})_4N^+$/BSA (entry 14).

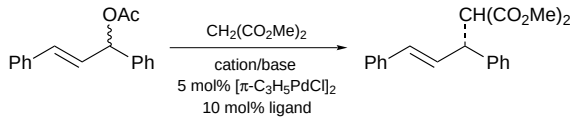



**Table 2** Results with ligand containing single chiral centre

| Entry | Ligand (config.) | Cation/base | Yield (%) | ee (%)[a] | Solvent |
|---|---|---|---|---|---|
| 1 | **21** (*S*) | $Bu_4N^+$/BSA | 67 | 82 | $CH_2Cl_2$ |
| 2 | **22** (*S*) | $Bu_4N^+$/BSA | 78 | 87 | $CH_2Cl_2$ |
| 3 | **23** (*S*) | $Bu_4N^+$/BSA | 94 | 86 | $CH_2Cl_2$ |
| 4 | **24** (*S*) | $Bu_4N^+$/BSA | 82 | 37 | $CH_2Cl_2$ |
| 5 | **23** (*S*) | $K^+$/BSA | 87 | 66 | $CH_2Cl_2$ |
| 6 | **23** (*S*) | $(C_6H_{13})_4N^+$/BSA | 62 | 90 | $CH_2Cl_2$ |
| 7 | **23** (*S*) | $(C_6H_{13})_4NBr$/Me/NaH | 22 | 81 | THF |
| 8 | **23** (*S*) | $Bu_4N^+$/BSA | 93 | 11 | CN |
| 9 | **23** (*S*) | $Bu_4N^+$/BSA | 14 | 64 | THF |
| 10 | **23** (*S*) | $Bu_4N^+$/BSA | 25 | 78 | $C_6H_6$ |

[a] The enantiomeric excesses were determined by chiral shift reagent [Eu(hfbc)$_3$] (ref. 11). BSA = bis(trimethylsilyl)acetamide.

**Table 3** Results with ligands containing two chiral centres[a]

| Entry | Ligand (config.) | Cation/base | Yield (%) | ee (%) | Solvent |
|---|---|---|---|---|---|
| 1 | **25** (*S*,*S*) | $Bu_4N^+$/BSA | 100 | 84 | MeCN |
| 2 | **26** (*R*,*S*) | $Bu_4N^+$/BSA | 53 | 93 | MeCN |
| 3 | **27** (*S*,*S*) | $Bu_4N^+$/BSA | 91 | 90 | MeCN |
| 4 | **28** (*R*,*S*) | $Bu_4N^+$/BSA | 80 | 93 | MeCN |
| 5 | **29** (*S*,*S*) | $Bu_4N^+$/BSA | 56 | 22 | MeCN |
| 6 | **30** (*R*,*S*) | $Bu_4N^+$/BSA | 37 | 54 | MeCN |
| 7 | **27** (*S*,*S*) | $Bu_4N^+$/BSA | 91 | 90 | MeCN |
| 8 | **27** (*S*,*S*) | $Bu_4N^+$/BSA | 43 | 65 | $CH_2Cl_2$ |
| 9 | **28** (*R*,*S*) | $Bu_4N^+$/BSA | 80 | 93 | MeCN |
| 10 | **28** (*R*,*S*) | $Bu_4N^+$/BSA | 33 | 85 | $CH_2Cl_2$ |
| 11 | **28** (*R*,*S*) | $Bu_4N^+$/BSA | 48 | 88 | THF |
| 12 | **28** (*R*,*S*) | $Bu_4N^+$/BSA | 49 | 79 | $C_6H_6$ |
| 13 | **28** (*R*,*S*) | TBAOAc/BSA | 93 | 82 | MeCN |
| 14 | **28** (*R*,*S*) | $(C_6H_{13})_4N^+$/BSA | 99 | 97 | MeCN |

[a] General procedure given in the footnote†.

In the case of the ligands reported by Pfaltz, where the phosphine is attached to the dihydrooxazole through a phenyl ring, a phenyl substituent next to the nitrogen gave the highest selectivities, with isopropyl only slightly poorer.[9] In the system reported here, the best substituent, in the position next to nitrogen, was isopropyl while phenyl was found to be the poorest (ligand **28** *vs*. **30**). The source of the difference between the two systems is unknown, but probably has its origins in different conformational preferences for the two complexes. The positioning of an $sp^3$ hybridized carbon, with a phenyl ring attached, changes the canting of the phenyl rings on the phosphine. This effect may be responsible for the difference between these two ligands.

Through the use of modular building blocks we have developed a new ligand for palladium catalysed π-allyl additions. We are currently studying the use of these ligands in other metal catalysed reactions. We are also using the phosphine acid building blocks discussed here in the synthesis of other collections of ligands for a variety of transition metal catalysed reactions.

We gratefully acknowledge the Washington University High-Resolution NMR Facility, partially supported by NIH 1S10R02004, and the Washington University Mass Spectrometry Resource Center, partially supported by NIHRR00954, for their assistance.

## Footnotes

* E-mail: srg@wuchem.wustl.edu

† *General procedure* for π-allyl addition: The phosphinooxazoline ligand was mixed with $[Pd(\eta^3\text{-}C_3H_5)Cl]_2$ in degassed MeCN. After 30 min, 1,3-diphenylprop-2-enyl acetate (10 equiv.) in MeCN was added. To this solution at the desired reaction temperature, a solution of dimethyl malonate (30 equiv.), $Bu_4NF$ (30 equiv.) and BSA (30 equiv.) in MeCN was added over 1 h. After complete reaction, as judged by TLC, the reaction mixture was worked up extractively.

## References

1 S. R. Gilbertson, G. Chen and M. McLoughlin, *J. Am. Chem. Soc*., 1994, **116**, 4481.
2 S. R. Gilbertson and X. Wang, *J. Org. Chem*., 1996, **61**, 434.
3 S. R. Gilbertson and R. V. Pawlick, *Angew. Chem., Int. Ed. Engl*., 1996, **35**, 902.
4 S. R. Gilbertson and G. W. Starkey, *J. Org. Chem*., 1996, **61**, 2922.
5 C. G. Frost, J. Howarth and J. M. J. Williams, *Tetrahedron: Asymmetry*, 1992, **3**, 1089.
6 O. Reiser, *Angew. Chem., Int. Ed. Engl*., 1993, **32**, 547.
7 B. M. Trost and D. L. Van Vranken, *Chem. Rev*., 1996, **96**, 395.
8 G. C. Lloyd-Jones and A. Pfaltz, *Angew. Chem., Int. Ed. Engl*., 1995, **34**, 462.
9 P. von Matt and A. Pfaltz, *Angew. Chem., Int. Ed. Engl*., 1993, **32**, 566.
10 J. Sprinz and G. Helmchen, *Tetrahedron Lett*., 1993, **34**, 1769.
11 J. V. Allen, S. J. Coote, G. J. Dawson, C. G. Frost, C. J. Martin and J. M. J. Williams, *J. Chem. Soc., Perkin Trans. 1*, 1994, 2065.
12 G. J. Dawson, C. G. Frost and J. M. J. Williams, *Tetrahedron Lett*., 1993, **34**, 3149.
13 O. Loiseleur, P. Meier and A. Pfaltz, *Angew. Chem., Int. Ed. Engl*., 1996, **35**, 200.
14 P. Wipf and S. Venkatraman, *Tetrahedron Lett*., 1996, **37**, 4659.
15 B. M. Trost and D. J. Murphy, *Organometallics*, 1985, **4**, 1143.

*Received in Corvallis, OR, USA, 21st October 1996; Com. 6/07200C*

# Synthesis and characterisation of the novel metallocenes $[Fe(\eta^5\text{-}C_5H_5EMe_2)_2]$ (E = Si, Sn) and $[Fe(\eta^5\text{-}C_5H_5SnMe_2)(\eta^6\text{-}C_6H_6)]_2[Fe_2Cl_6]$

**Brian F. G. Johnson,*[a] Caroline M. Martin,[a] Mathias Nowotny,[a] Warwick Palmer[a] and Simon Parsons[b]**

[a] *University Chemical Laboratories, Lensfield Road, Cambridge, UK CB2 1EW*
[b] *Department of Chemistry, University of Edinburgh, West Mains Road, Edinburgh, UK EH9 3JJ*

**The novel bis-heterocyclohexadienyl metallocene complexes $[Fe(\eta^5\text{-}C_5H_5EMe_2)_2]$ (E = Si, Sn) are prepared by reaction of anhydrous $FeCl_2$ with the appropriate lithium salt; $[Fe(\eta^5\text{-}C_5H_5SnMe_2)_2]$ undergoes a further unusual reaction with $CHCl_3$ to displace one $SnMe_2$ fragment and afford the mixed sandwich complex $[Fe(\eta^5\text{-}C_5H_5SnMe_2)(\eta^6\text{-}C_6H_6)]_2[Fe_2Cl_6]$.**

Despite the class of the open metallocenes having been long established by the pioneering work of Ernst,[1] there are few reported examples of systems employing ligands of the type $C_5H_5ER_2$ (E = C[2], P[3,4]), in which the open pentadienyl moiety is stabilised by linking the ends together in a non-conjugative mannar *via* a group 14 or 15 bridging unit $ER_2$.

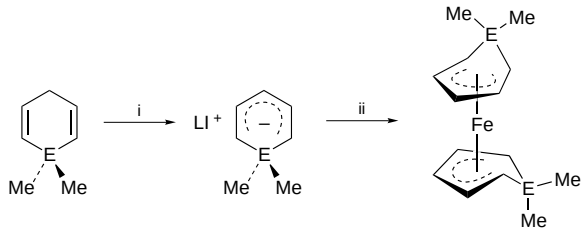
Such ligands are of interest since they provide both the possibility of introducing sterically controlling groups R, and an electropositive heteroatom E that may increase electron density at the transition-metal centre. The activity of group 4 metallocene Ziegler–Natta catalysts may benefit from the increased electron density on the metal centre imposed by these electropositive ligands.[5]

Here we report the formation of the bis-heterocyclohexadienyl metallocene complexes $[Fe(\eta^5\text{-}C_5H_5EMe_2)_2]$ (E = Si **1**, Sn **2**). The ligand precursors 1,1-dimethyl-1-stannacyclohexa-2,5-diene[6] and 1,1-dimethyl-1-silacyclohexa-2,5-diene[7,8] were prepared by literature methods. The heterocyclohexadienes were deprotonated with LDA and the resulting heterocyclohexadienyl anions were treated with anhydrous $FeCl_2$ to afford the metallocene complexes **1** and **2** (Scheme 1).

A formal displacement of $Me_2SnCl_2$ by $CHCl_3$ caused the precipitation of a few crystals of the mixed-sandwich complex $[Fe(\eta^5\text{-}C_5H_5SnMe_2)(\eta^6\text{-}C_6H_6)]_2[Fe_2Cl_6]$ **3** from a solution of complex **2** in this halogenated solvent within several days, while complex **1** is not noticeably affected by $CHCl_3$.

Complexes **1** and **2** have been fully characterised on the basis of their spectroscopic data.† Single-crystal X-ray structures of **1** and **3** are also presented. The molecular structures of complex **1** and of the mixed-sandwich cation in **3** are shown in Fig. 1 and 2, respectively.‡ The 1,1-dimethyl-1-stannacyclohexadienyl ring in the mixed-sandwich complex **3** is representative of the environment in **2**, and so may be usefully compared to the environment of the 1,1-dimethyl-1-silacyclohexadienyl rings in the symmetrical metallocene complex **1**. The heterocyclohexadienyl moiety in **1**, **2** and **3** bonds to Fe in an $\eta^5$ manner *via* the five essentially planar carbon atoms, the mean deviation from planarity being ±0.078 and ±0.0149 Å for complexes **1** and **3**, respectively. The heteroatom is pushed out of the plane away from the transition metal. The angle between the C(5)–Si(1)–C(1) plane and the C(1)···C(5) plane is 36.9° in **1**. The corresponding angle in complex **3** is of similar magnitude at 37.6°. The non-bonding FeSi(1) distance in **1** is 2.861 Å compared to a non-bonding Fe(2)···Sn(2) distance in **3** of 3.142 Å. These distances are remarkably short though the Fe···Si distance exceeds the shortest, to our knowledge, non-bonding Si···Fe contact at 2.636 Å in $Ph_2Si(C_5H_4)_2Fe$.[9]

The open and closed carbocyclic ligands in **1** and **3** adopt an essentially coplanar arrangement represented by interplanar angles of 3.7 and 3.8°, respectively. The conformational angle of 38.6° adopted by the ligands in **1** is significantly smaller than the value of 59.7° found in the open ferrocene bis(2,4-dimethylpentadienyl)iron **4**.[5] The distances from the heterocyclohexadienyl ring centroids to Fe remain comparable at 1.543 and 1.531 Å for complexes **1** and **3** respectively and are of the same order of magnitude as the distance of 1.50 Å in **4**, while the distance from the benzene ring centroid to Fe in **3** is slightly longer at 1.559 Å. This may be compared with the value




**Scheme 1** Synthesis of the novel metallocenes **1** and **2**. *Reagents and conditions*: i, LDA, thf, 0.5 h, 258 K; ii, $FeCl_2$, thf, 1 h 200 K, 12 h, 298 K, subsequent work-up by filtration through silica and crystallisation of **1** from hexane.

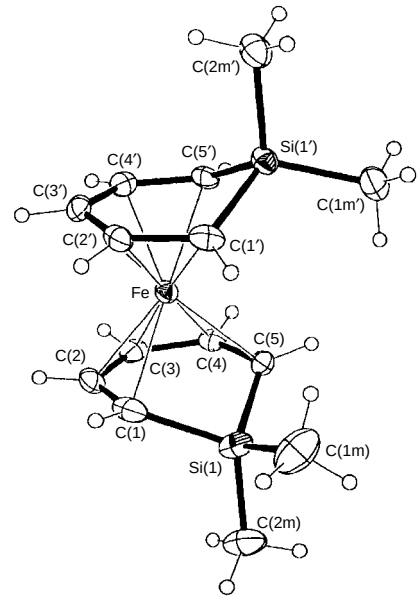



**Fig. 1** Molecular structure of **1**. Selected bond lengths (Å) and angles (°): Si(1)–C(1m) 1.865(5), Si(1)–C(2m) 1.874(5), Si(1)–C(1) 1.842(5), Si(1)–C(5) 1.832(5), C(1)–C(2) 1.395(7), C(2)–C(3) 1.420(6), C(3)–C(4) 1.410(6), C(4)–C(5) 1.398(6), Fe–Si(1) 2.861(2); C(4)–C(5)–Si(1) 120.3(4), C(2)–C(1)–Si(1) 120.2(4), C(1m)–Si(1)–C(2m) 107.7(2), C(1)–Si(1)–C(5) 93.4(2), C(2)–C(3)–C(4) 122.0(4), C(1)–C(2)–C(3) 122.9(4), C(3)–C(4)–C(5) 123.0(4). C(1)–Si(1)–C(1m) 113.2(2), C(5)–Si(1)–C(2m) 114.1(2).

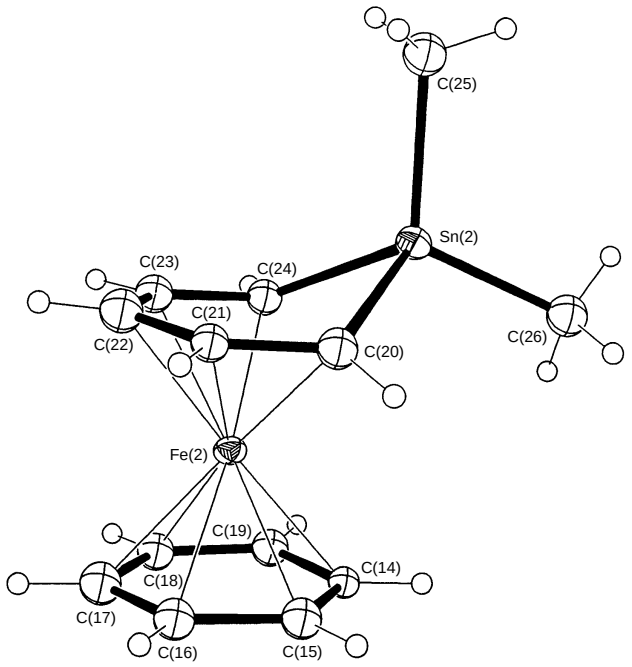



**Fig. 2** Molecular structure of the complex cation **3** with the $Fe_2Cl_6^{2-}$ counter ion omitted for clarity. Selected bond lengths (Å) and angles (°): Sn(2)–C(25) 2.11(2), Sn(2)–C(26) 2.09(2), Sn(2)–C(24) 2.14(2). Sn(2)–C(20) 2.11(2), C(24)–C(23) 1.40(2), C(23)–C(22) 1.41(2), C(22)–C(21) 1.39(2), C(21)–C(20) 1.38(2), Fe(2)–Sn(2) 3.142(1), C(14)–C(15) 1.37(2), C(15)–C(16) 1.41(2), C(16)–C(17) 1.42(2), C(17)–C(18) 1.40(2), C(18)–C(19) 1.38(2), C(19)–C(14) 1.39(2), C(25)–Sn(2)–C(26) 113.6(7), C(20)–Sn(2)–C(24) 82.2(7), C(20)–Sn(2)–C(25) 114.1(7), C(24)–Sn(2)–C(26) 116.4(7), C(21)–C(22)–C(23) 122(2), C(22)–C(23)–C(24) 126(2). C(22)–C(21)–C(20) 127(2), C(21)–C(20)–Sn(2) 122.0(13), C(23)–C(24)–Sn(2) 119.9(14).

of 1.55 Å found in the analogous complex $[Fe(\eta^5\text{-}C_5H_5)(\eta^6\text{-}C_6Et_6)]PF_6$.[10]

Spectroscopic data show that the heteroatom methyl substituents are non-equivalent and may be classified as *mexo* and *mendo*. The difference in chemical shift between the *mendo* and *mexo* methyl groups is a function of the ring carbon–heteroatom distance, since the ring current generated by the heterocyclohexadienyl system decreases in strength away from the ring centroid. The C(24)–Sn(2) distance in **3** is indeed longer, at 2.14(2) Å, than the C(5)–Si(1) distance in **1**, 1.832(5) Å, and the *mendo*–*mexo* methyl NMR signals have a greater difference in **2** than **1** as a result.

The electrochemical behaviour of **1** and **2** resemble that of the open ferrocene **4**[11] with the reversible one-electron oxidation occurring at a far lower potential for **1** than **2** reflecting the greater electron density at the Fe centre for the system with the more electropositive heteroatom.§ Likewise, an orthorhombic *g* tensor is observed in the EPR spectra of both **1** and **2** in frozen solution.

This new class of metallocene complexes employing heterocyclic ligands is being extended to include the early transition-metal elements, and further direct replacement of the $SnMe_2$ moiety by a variety of other heteroatoms is under examination.

We gratefully acknowledge Professor C. Elschenbroich and Drs B. Metz and O. Schiemann for the conduction of EPR and electrochemical measurements and Dr J. E. Davies for the collection of crystallographic data. The EPSRC (W. P., M. N.), Tioxide (W. P.) and Deutsche Forschungsgemeinschaft (M. N.) are acknowledged for financial support.

## Footnotes

* E-mail: bfgj1@cam.ac.uk

† *Selected spectroscopic data* for **1**: $^1$H NMR ($CDCl_3$, 250 MHz, 295 K) δ −0.65 [s, 3 H, C(2m)–H *mexo*-$CH_3$], 0.66 [s, 3 H, C(1m)–H, *mendo*-$CH_3$], 2.20 [d, 2 H, $^3J$(*o*,*m*) 10.2 Hz, C(1,5)–H, *o*-CH], 4.85 [dd, 2 H, $^3J$(*m*,*o*) 10.2 Hz, $^3J$(*m*,*p*) 5.8 Hz, C(2,4)H, *m*-CH], 4.97 [t, 1 H, $^3J$(*p*,*m*) 5.8 Hz, C(3)–H, *p*-CH]; $^{13}$C NMR ($CDCl_3$, 250 MHz, 295 K) δ −1.14 [C(2m), $CH_3$], 7.78 [C(1m), $CH_3$], 38.87 [C(1,5), *o*-CH], 78.54 [C(2,4), *m*-CH], 94.47 [C(3), *p*-CH]; EPR (**1**$^+$, $CHCl_3$, 77 K), $g_1$ = 2.033, $g_2$ = 2.090, $g_3$ = 2.165; EIMS (70 eV) 302 (61%, $[M]^+$), 287 (69%, $[M - CH_3]^+$), 244 (11%, $[M - SiMe_2]^+$), 229 (100%, $[M - SiMe_2 - CH_3]^+$), 179 (40%, $[M - C_7H_{11}Si]^+$, 164 (51%, $[M - C_7H_{11}Si - CH_3]^+$). HRMS: *m*/*z* 302.06014, mass deviation 7.62 ppm.

**2**: $^1$H NMR ($CDCl_3$, 250 MHz, 295 K) δ −0.29 (s, 3 H, *mexo*-$CH_3$), 0.63 (s, 3 H, *mendo* $CH_3$), 2.32 [d, 2 H, $^3J$(*o*,*m*) 9.17 Hz, *o*-CH], 4.83 (m, 1 H, *p*-CH), 4.85 (m, 2 H, *m*-CH); $^{13}$C NMR ($CDCl_3$, 250 MHz, 295 K) δ −8.79 (*mexo*-$CH_3$), 0.67 (*mendo*-$CH_3$), 39.62 (*o*-CH), 79.74 (*p*-CH), 97.55 (*m*-CH); EPR (**2**$^+$, $CHCl_3$, 77 K), $g_1$ = 2.011, $g_2$ = 2.052, $g_3$ = 2.127; EIMS (70 eV) 484 (6%, $[M]^+$), 336 (2%, $[M - SnMe_2]^+$), 321 (4%, $[M - SnMe_2 - CH_3]^+$), 186 (100%, $[M - 2SnMe_2]^+$). HRMS: *m*/*z* 485.9155, mass deviation 8.4 ppm.

‡ *Crystal data*: for **1**: $C_{14}H_{22}FeSi_2$, 0.27 × 0.19 × 0.16 mm, $T$ = 150(2) K, $M$ = 302.35, monoclinic, space group $P2_1/c$, $a$ = 13.209(7), $b$ = 9.516(7), $c$ = 11.997(7) Å, β = 100.06(5)°, $U$ = 1485(2) Å$^3$, $Z$ = 4, $D_c$ = 1.353 Mg m$^{-3}$, λ = 0.71073 Å, $F$(000) = 640, $R_1$ = 0.0407 [1914 reflections with $F_o > 4\sigma(F_o)$], $wR_2$ = 0.0902 for 1922 independent reflections corrected for adsorption [μ(Mo-Kα) = 1.154 mm$^{-1}$] and 189 parameters (all non-H atoms anisotropic).

For **3**: $C_{13}H_{17}Cl_3Fe_2Sn$, 0.12 × 0.10 × 0.10 mm, $T$ = 154(2) K, $M$ = 510.01, monoclinic, space group $P2_1/n$, $a$ = 14.843(5), $b$ = 14.209(5), $c$ = 17.098(6) Å, β = 106.97(2)°, $U$ = 3449(2) Å$^3$, $Z$ = 8, $D_c$ = 1.964 Mg m$^{-3}$, λ = 0.71073 Å, $F$(000) = 1984, $R_1$ = 0.0701 [2723 reflections with $F_0 > 4\sigma(F_o)$], $wR_2$ = 0.1844 for 4492 independent reflections and 295 parameters (Fe, Sn and Cl atoms anisotropic). Compound **3** crystallises with two half-dianions and two cations per asymmetric unit; each anion possessing a crystallographic centre of symmetry. The benzene ring of one cation is disordered over two sites with partial occupancies of 0.62 and 0.38.

The structures were solved by direct methods,[12] and a series of difference Fourier maps were used to locate all light atoms except the H atoms, these being added in calculated positions (C–H 0.96 Å) riding on the respective C atoms. All other calculations were performed using SHELXL-93.[13]

Atomic coordinates, bond lengths and angles, and thermal parameters have been deposited at the Cambridge Crystallographic Data Centre (CCDC). See Information for Authors, Issue No. 1. Any request to the CCDC for this material should quote the full literature citation and the reference number 182/436.

§ The cyclic voltammograms (CVs) of **1** and **2** were recorded using a glassy-carbon/platinum electrode system referenced to calomel in dme–0.1 M $NBu_4PF_6$, $v$ = 100 mV s$^{-1}$ at 298 K. A one-electron reversible oxidation with $E_{\frac{1}{2}}$(0/+1) {$\Delta E_p$} = 169 {67} and −200 {58} mV was observed for **1** and **2** respectively. Irreversible reduction waves were registered at $E_{pc}$ = −2.315 and −2.191 V for **1** and **2**, respectively.

## References

1 R. D. Ernst, *Acc. Chem. Res.*, 1985, **18**, 56 and references therein.
2 P. T. DiMauro and P. T. Wolczanski, *Organometallics*, 1987, **6**, 1947.
3 G. Märkl and C. Martin, *Angew. Chem., Int. Ed. Engl.*, 1974, **13**, 408.
4 T. Dave, S. Berger, E. Bilger, H. Kaletsch, J. Pebler, J. Knecht and K. Dimroth, *Organometallics*, 1985, **4**, 1565. G. Baum and W. Massa, *Organometallics*, 1985, **4**, 1572.
5 G. Henrici-olivé and S. Olivé, *Angew. Chem., Int. Ed. Engl.*, 1971, **10**, 105.
6 W. Fink, *Helv. Chim. Acta*, 1976, **59**, 276.
7 A. J. Ashe III, *J. Am. Chem. Soc.*, 1971, **93**, 1804.
8 P. Jutzi and J. Baumgärtner, *J. Am. Chem. Soc.*, 1978, **148**, 257.
9 H. Stoeckli, A. G. Osborne and R. H. Whitely, *Helv. Chim. Acta*, 1976, **59**, 2402.
10 J. Hamon, J. Saillard, A. LeBeuze, M. J. McGlinchey and D. Astruc, *J. Am. Chem. Soc.*, 1982, **104**, 7549.
11 E. Bilger, C. Elschenbroich, R. D. Ernst, M. S. Kralik and D. R. Wilson, *Organometallics*, 1985, **4**, 2068.
12 G. M. Sheldrick, SHELXS-86, Program for crystal structure solution, *Acta Crystallogr., Sect. A*, 1990, **46**, 467.
13 G. M. Sheldrick, SHELXL-93, University of Göttingen, Germany, 1993.

*Received in Cambridge, UK, 24th January 1997; Com. 7/00576H*

# Synthesis, X-ray structure and electrochemical characterisation of a binuclear thiolate bridged Ni–Fe–nitrosyl complex, related to the active site of NiFe hydrogenase

**Frank Osterloh,* Wolfgang Saak, Detlev Haase and Siegfried Pohl†**

*Fachbereich Chemie, Universität Oldenburg, Postfach 2503, D-26111 Oldenburg, Germany*

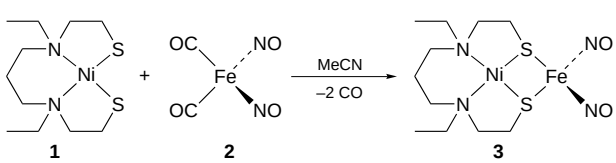
**[NiL] 1 (L = *N*,*N*′-diethyl-3,7-diazanonane-1,9-dithiolate) reacts with [Fe(CO)$_2$(NO)$_2$] 2 to afford [Ni(L)Fe(NO)$_2$] 3, in which a Ni$^{II}$ ion and a nitrosylated Fe$^{-II}$ centre are bridged *via* two μ-S atoms from the chelating ligand.**

The NiFe hydrogenase from *D. gigas* catalyses the reversible oxidation of molecular hydrogen. This enzyme utilises a binuclear complex as the active site, in which one Ni and one Fe atom are covalently linked by the S atoms of two cysteine residues and by one unidentified ligand.[1–3] Two additional cysteine S atoms complete the square-pyramidal coordination sphere of Ni, whereas the Fe atom binds to three unidentified diatomic ligands, possible candidates being CO, $CN^-$, NO and $C{\equiv}CH^-$. These non-protein ligands give rise to unusual absorption bands (1800–2100 cm$^{-1}$) in the IR spectra of many NiFe hydrogenases and appear to be a constant feature of these enzymes.[1,4] These observations prompted us to search for synthetic pathways to binuclear, μ-S thiolate bridged NiFe complexes in which NO binds to an Fe atom.

When a solution of the neutral complex [NiL] **1** in acetonitrile is combined with a stoichiometric amount of liquid [Fe(CO)$_2$(NO)$_2$] **2**, the colour changes immediately from purple to deep brown. CO is liberated from the solution, indicating rapid substitution of CO by the Ni complex, a reaction type that has been well established on **2** with other nucleophiles.[5] The mixture was refluxed for 15 min to complete the reaction and then kept at room temperature for 24 h (Scheme 1).

Black needles of [Ni(L)Fe(NO)$_2$] **3** formed, which were filtered off, washed with acetonitrile and dried *in vacuo*. When the volume of the mother-liquor was reduced *in vacuo*, a second crop of **3** could be obtained, which had to be recrystallized from hot acetonitrile; the total yield was 57%.‡

The result of an X-ray structure analysis§ of **3** is shown in Fig. 1 and bond lengths and angles are given in Table 1. The most striking structural feature is the short Ni–Fe distance of 279.7(1) pm, which remains lower than the value of 290 pm of the binuclear complex of the active centre of NiFe hydrogenase.[1] Other known μ-SR bridged NiFe compounds exhibit Ni–Fe distances between 280.6(5) and 376(1) pm.[6–8] The small Ni–Fe separation in **3** is, at least in part, due to the low coordination number of the nitrosylated iron atom which is in a distorted tetrahedral $N_2S_2$ environment. The two NO ligands are slightly bent towards each other resulting in Fe–N–O angles of 167.0(5) and 174.6(5)°. These values are unexceptional; similar Fe–N–O angles were found in other complexes with $S_2Fe(NO)_2$ fragments, *e.g.* [(PhS)$_2$Fe(NO)$_2$]$^-$ [168.5(2), 169.4(2)°].[9] As in the latter complex, the NO groups in **3** are linear and hence must be viewed as three-electron donors to the Fe atom, which is formally at the -II oxidation level and has 18 valence electrons. Judged from structural details no significant electron delocalization from the reduced Fe centre to Ni$^{II}$ takes place. Such a transfer of charge should influence the geometry of the Ni coordination environment, which apart from a decreased S–Ni–S angle (by 4°) and an increased N–Ni–N angle (by 3.7°) is almost identical to that of a similar mononuclear nickel(II) complex.[10]




**1** **2** **3**

**Scheme 1**

The IR spectrum of **3** shows two intense absorption bands at 1663 and 1624 cm$^{-1}$, which were assigned to the symmetrical and the asymmetrical stretching vibration of the nitrosyl ligands. The lowering of these values in comparison to **2** (1810 and 1766 cm$^{-1}$ in cyclohexane)[11] indicates an increased transfer of electron density from Fe into π* orbitals of the NO ligands (back bonding), which is accompanied by a weakening of the NO triple bonds.

Although the IR spectrum of **3** does not reproduce the characteristic absorption pattern of NiFe hydrogenases at 1800–2100 cm$^{-1}$, a nitrosyl ligand at the active centre of NiFe hydrogenase cannot be excluded on the basis of IR spectroscopy. Variations of the band positions could result from

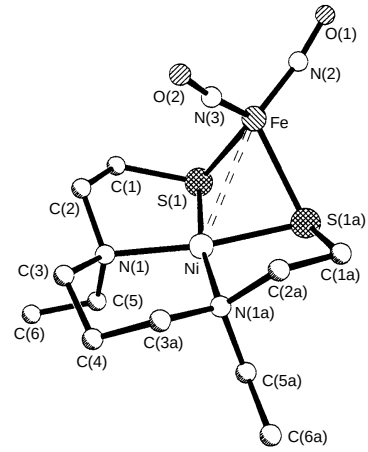



**Fig. 1** Molecular structure of **3** with atom labelling scheme; **3** exhibits crystallographic mirror symmetry; H atoms have been omitted

**Table 1** Selected interatomic distances (pm) and angles (°) for **3**

| | | | |
|---|---|---|---|
| Ni···Fe | 279.7(1) | S(1)–Ni–S(1a) | 81.46(6) |
| Ni–S(1) | 217.6(1) | S(1)–Ni–N(1) | 88.7(1) |
| Ni–N(1) | 198.5(3) | N(1)–Ni–N(1a) | 101.0(2) |
| Fe–S(1) | 235.6(1) | S(1)–Fe–S(1a) | 74.10(6) |
| Fe–N(2) | 165.8(5) | S(1)–Fe–N(2) | 113.6(2) |
| Fe–N(3) | 164.7(6) | S(1)–Fe–N(3) | 114.8(2) |
| N(2)–O(1) | 118.3(7) | N(2)–Fe–N(3) | 118.2(3) |
| N(3)–O(2) | 119.7(7) | Ni–S(1)–Fe | 76.11(4) |
| | | Fe–N(2)–O(1) | 167.0(5) |
| | | Fe–N(3)–O(2) | 174.6(5) |

different oxidation levels and from the different coordination environments of the Fe centres in both heterobimetallic complexes. However, it should be noted that other μ-SR bridged NiFe complexes, in which CO acts as a ligand to the Fe atom, mimic the IR properties of NiFe hydrogenases well.[8a]

In acetonitrile and dichloromethane solutions **3** can be quasi-reversibly oxidised at −120 mV (*vs*. SCE). Since the oxidation of $N_2S_2$ bound $Ni^{II}$, *e.g.* in $[Ni^{II}(NiL)_2]^{2+}$, cannot be achieved at potentials below +860 mV (*vs*. SCE in MeCN),[12] this process was tentatively assigned to the redox couple $Fe^{-II/-I}$. Interestingly, **2** in dmf solution can be consecutively reduced to the $[Fe(CO)_2(NO)_2]^{2-}$ dianion but has no tendency toward oxidation.[13] The differences in the redox properties of **2** and **3** have to be attributed to the better electron-donating capability of the μ-S thiolates in comparison to CO.

Attempts to oxidise **3** chemically have been unsuccessful. When treated with $[Fe(C_5H_5)_2]BF_4$ in dichloromethane or acetonitrile solution, **3** decomposes into various products, of which $[Ni^{II}(NiL)_2][BF_4]_2$ could be isolated as black or reddish needles, depending on the solvent. The formation of trinuclear cations, such as $[Ni^{II}(NiL)_2]^{2+}$ in which a central $Ni^{II}$ binds to four bridging thiolate S atoms of two [NiL] fragments, has been commonly observed when $Ni^{II}$ complexes like **1** are reacted with oxidising agents.[14]

We thank Dr H. Strasdeit for a critical review of the manuscript. Financial support from the Deutsche Forschungsgemeinschaft and the Fonds der Chemischen Industrie is gratefully acknowledged.

## Footnotes

* E-mail: osterloh@chemie.uni-oldenburg.de
† Deceased. Correspondence should be addressed to F. Osterloh.

‡ The nickel complex **1** can be obtained as purple crystals by reaction of nickel(II) acetylacetonate with $H_2L$ in thf solution. $H_2L$ is readily available by reaction of *N*,*N*′-diethyl-1,3-diaminopropane (Aldrich) with 2 equiv. of ethylenesulfide in toluene solution according to Karlin and Lippard.[15] **2** was synthesised from $Fe(CO)_5$ and $NaNO_2$–HOAc according to Hieber and Beutner.[16] *Analytical data* for **3**: IR (KBr): ν(NO) 1663vs, 1624vs $cm^{-1}$. UV–VIS spectrum (MeCN): $\lambda_{max}$/nm (ε/$dm^3$ $mol^{-1}$ $cm^{-1}$) = 570 (370), 410 (1620). Satisfactory elemental analysis. Electrochemistry of **3** (in MeCN with $NBu^n_4PF_6$ as electrolyte): $E_0$ = −120 mV (*vs*. SCE); $\Delta E_p$ = 67 mV; $i_c/i_a$ = 0.91; scan rate 100 mV $s^{-1}$. **3** is readily soluble in dmf, MeCN and $CH_2Cl_2$. Crystals isolated from the reaction mixture were sufficient for X-ray crystallography.

§ *Crystal data* for **3**: $C_{11}H_{24}FeN_4NiO_2S_2$, $M$ = 423.02, orthorhombic, space group *Pnma*, $a$ = 1177.0(1), $b$ = 1018.4(1), $c$ = 1471.2(1) pm, $U$ = 1.7635(3) $nm^3$, $T$ = 296 K, $Z$ = 4, $D_c$ = 1.593 Mg $m^{-3}$, μ(Mo-Kα) = 2.134 $mm^{-1}$. A black single crystal of **3** with dimensions 0.72 × 0.40 × 0.28 mm was sealed in a glass capillary and mounted on a Siemens-Stoe AED 2 four-circle diffractometer. Data collection using Mo-Kα radiation (λ = 71.073 pm) and ω–2θ scans gave 1641 independent reflections ($\theta_{max}$ = 25°), of which 1536 with $I > 2\sigma(I)$ were used in the final structure refinement. A semiempirical absorption correction using ψ-scans was applied. The structure was solved by direct methods and the solution developed using full-matrix least-squares refinements on $F^2$ and difference Fourier syntheses. Anisotropic displacement parameters were refined for all non-H atoms. H atoms were included on calculated positions with isotropic displacement parameters tied to those of the corresponding carbon atoms.[17] At convergence, $R_1$ = 0.0497, $wR_2$ = 0.1099, GOF = 1.295 for 106 parameters. Atomic coordinates, bond lengths and angles, and thermal parameters have been deposited at the Cambridge Crystallographic Data Centre (CCDC). See Information for Authors, Issue No. 1. Any request to the CCDC for this material should quote the full literature citation and the reference number 182/446.

## References

1 A. Volbeda, E. Garcin, C. Piras, A. L. de Lacey, V. M. Fernandez, E. C. Hatchikian, M. Frey and J. C. Fontecilla-Camps, *J. Am. Chem. Soc.*, 1996, **118**, 12989.
2 A. Volbeda, M.-H. Charon, C. Piras, E. C. Hatchikian, M. Frey and J. C. Fontecilla-Camps, *Nature*, 1995, **373**, 580; A. Volbeda, M.-H. Charon, C. Piras, E. C. Hatchikian, M. Frey and J. C. Fontecilla-Camps, *J. Inorg. Biochem.*, 1995, **59**, 637.
3 M. A. Halcrow, *Angew. Chem.*, 1995, **107**, 1307; *Angew. Chem., Int. Ed. Engl.*, 1995, **34**, 1193.
4 T. M. Van Der Spek, A. F. Arendsen, R. P. Happe, S. Yun, K. A. Bagley, D. J. Stufkens, W. R. Hagen and S. P. J. Albracht, *Eur. J. Biochem.*, 1996, **237**, 629.
5 J. P. Crow, W. R. Cullen, F. G. Herring, J. R. Sams and R. L. Tapping, *Inorg. Chem.*, 1971, **10**, 1616; W. Hieber and J. S. Anderson, *Z. Anorg. Allg. Chem.*, 1933, **211**, 132.
6 F. Osterloh, W. Saak, D. Haase and S. Pohl, *Chem. Commun.*, 1996, 777; F. Osterloh and S. Pohl, unpublished work.
7 G. J. Colpas, R. O. Day and M. J. Maroney, *Inorg. Chem.*, 1992, **31**, 5053.
8 (*a*) C.-H. Lai, J. H. Reibenspies and M. Y. Darensbourg, *Angew. Chem.*, 1996, **108**, 2551; *Angew. Chem., Int. Ed. Engl.*, 1996, **35**, 2390; (*b*) D. K. Mills, Y. M. Hsiao, P. J. Farmer, E. V. Atnip, J. H. Reibenspies and M. Y. Darensbourg, *J. Am. Chem. Soc.*, 1991, **113**, 1421.
9 H. Strasdeit, B. Krebs and G. Henkel, *Z. Naturforsch. B*, 1986, **41**, 1357 and references therein.
10 G. J. Colpas, M. Kumar, R. O. Day and M. J. Maloney, *Inorg. Chem.*, 1990, **29**, 4779.
11 C. G. Barraclough and J. Lewis, *J. Chem. Soc.*, 1960, 4842.
12 G. Musie, P. J. Farmer, T. Tuntulani, J. H. Reibenspies and M. Y. Darensbourg, *Inorg. Chem.*, 1996, **35**, 2176.
13 G. Piazza and G. Paliani, *Z. Phys. Chem.*, 1970, **71**, 91.
14 P. J. Farmer, T. Solouki, D. K. Mills, T. Soma, D. H. Russell, J. H. Reibenspies and M. Y. Darensbourg, *J. Am. Chem. Soc.*, 1992, **114**, 4601.
15 K. D. Karlin and S. J. Lippard, *J. Am. Chem. Soc.*, 1976, **98**, 6951.
16 W. Hieber and H. Beutner, *Z. Anorg. Allg. Chem.*, 1963, **320**, 101.
17 G. M. Sheldrick, *Acta Crystallogr., Sect. A*, 1990, **46**, 467; G. M. Sheldrick, SHELXTL-PC and SHELXL-93, University of Göttingen.

*Received in Basel, Switzerland, 7th February 1997; Com. 7/00884H*

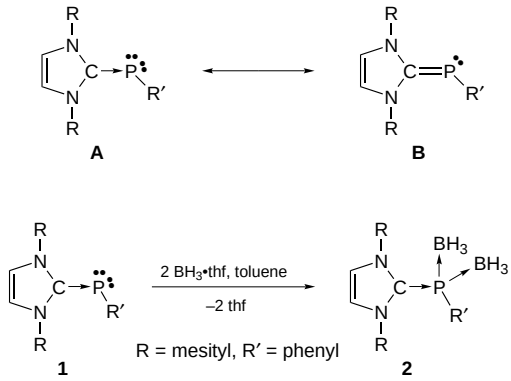
# Nature of the bonding in a carbene–phosphinidene: a main group analogue of a Fischer carbene complex? Isolation and characterisation of a bis(borane) adduct

**Anthony J. Arduengo, III,[a] Claire J. Carmalt,[b] Jason A. C. Clyburne,[b] Alan H. Cowley*[b] and Radha Pyati[b]**

[a] *DuPont Science and Engineering Laboratory, Experimental Station, Wilmington, Delaware, 19880, USA*
[b] *Department of Chemistry and Biochemistry, The University of Texas at Austin, Austin, Texas 78712, USA*

**The reaction of the carbene–phosphinidene (1,3-dimesityl-imidazolin-2-ylidene)PPh 1 with $BH_3$·thf affords the corresponding P-bonded bis(borane) adduct, thus demonstrating the availability of two lone pairs on the phosphorus centre; base competition studies reveal that 1 is a strong phosphorus base and, by means of cyclic voltammetry, it is established that 1 undergoes facile oxidation.**

It has been demonstrated recently[1,2] that stabilised carbenes are sufficiently nucleophilic to depolymerise cyclopolyphosphines such as $(PPh)_5$ and $(PCF_3)_4$ and produce compounds of the type (carbene)PR. Two extreme canonical forms, **A** and **B**, can be written for such species. Form **A** represents a phosphinidene adduct of a carbene and involves a carbon–phosphorus dative bond of order one whilst **B** corresponds to a conventional phosphaalkene and features a double bond between carbon and phosphorus. There is, in fact, an interesting parallel with transition metal carbene complexes, albeit with the roles of metal and carbene being played by carbene and phosphinidene respectively in the cases of forms **A** and **B**. Thus the low-valent form **A** resembles a Fischer-type complex and the high-valent form **B** is akin to a Schrock-type alkylidene complex. In terms of metrical parameters, it has been found[1,2] that the P–C(carbene) bond is only *ca*. 4% longer than the P–C(R) single bond and that the P–C(R) moiety is twisted out of the carbene plane by 18–20°. Taken in concert with the high-field $^{31}P$ chemical shifts, these data imply that the pπ–pπ bond between carbon and phosphorus is not well developed. It occurred to us that further important information regarding the electronic structures of these compounds might stem from Lewis-basicity and electrochemical studies. The Lewis-base behaviour was expected to be particularly revealing since a conspicuous difference between **A** and **B** concerns the fact that these forms feature two and one phosphorus lone pairs, respectively. Treatment of **1**[2] with $BH_3$·thf in toluene solution resulted in the exclusive formation of the bis(borane) adduct **2** (Scheme 1).†




**Scheme 1**

Interestingly, no evidence for a 1:1 $BH_3$ adduct could be found by NMR titration.‡ The X-ray crystal structure of **2** (Fig. 1)§ confirmed the attachment of two $BH_3$ groups to the phosphorus centre and, in addition, showed that the P–C(carbene) bond lengthened by 0.093 Å and the C–P–C angle increased by 4.9° in the conversion of **1** to **2**. An increase in bond length is anticipated if it is assumed that **1** features a modicum of back π-bonding from phosphorus to the carbene carbon atom which is lost upon borane attachment. Such a view finds a parallel in the molecular orbital theory of Fischer-type carbene complexes.[3] It should be noted, however, that some of the increase in the P–C(carbene) bond length could be accounted for by increased steric interactions. The increase in bond angle is consistent with the valence shell electron pair repulsion (VSEPR) model[4] in the sense that two lone pairs in **1** are replaced by two bond pairs in **2**. The P–B bond lengths [av. 1.946(2) Å] are normal and the geometry at phosphorus is approximately tetrahedral. The following additional points are also noteworthy: (*i*) the formation of **2** can be regarded as an example of base-induced coordination[5] of an electrophilic fragment (a phosphinidene in this case), and (*ii*) given that $BH_3$ and $M(CO)_5$ moieties (M = Cr, Mo, W) are isolobal, there is an interesting parallel between **2** and base·$E(R)[M(CO)_5]_2$ (E = P, As) complexes.[6]

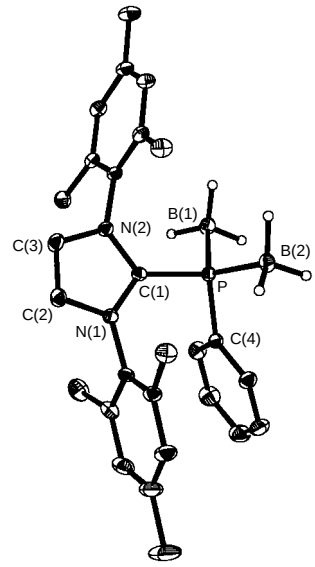



**Fig. 1** Molecular structure of **2** showing the atom numbering scheme. Selected distances (Å) and angles (°): P–C(1) 1.856(2), P–C(4) 1.828(2), P–B(1) 1.945(2), P–B(2) 1.948(2), C(1)–N(1) 1.355(2), N(1)–C(2) 1.377(2), C(2)–C(3) 1.337(2), N(2)–C(3) 1.374(2), C(1)–N(2) 1.358(2); C(1)-P–C(4) 104.78(7), C(1)–P–B(1) 109.33(8), C(1)–P–B(2) 109.20(8), B(1)–P–B(2) 117.46(10), C(4)–P–B(1) 106.60(9), C(4)–P–B(2) 108.71(9), N(1)–C(1)–N(2) 105.14(13), C(1)–N(1)–C(2) 110.33(14), N(1)–C(2)–C(3) 106.9(2), C(2)–C(3)–N(2) 107.6(2), C(3)–N(2)–C(1) 109.96(13).

An attempt at qualitative basicity assessment of **1** was made by treatment of **2** with 1,8-diazabicyclo[5.4.0]undec-7-ene (DBU), 1,5-diazabicyclo[4.3.0]non-5-ene (DBN), and $PAr_3$ **3** [Ar = $C_6H_2(OMe)_3$-2,4,6]. It was found that both DBU and DBN removed the $BH_3$ moieties from **2** quantitatively whilst **3**, the most basic tertiary phosphine known so far ($pK_a$ 11.2),[7] failed to react. The $pK_a$ of **1** is therefore likely to exceed 11.2.

Further support for the carbene–phosphinidene bonding description (form **A**) stemmed from cyclic voltammetry experiments.¶ Thus, acetonitrile solutions of **1** exhibit an irreversible one-electron oxidation at −0.08 V (*vs.* SCE). Such a low oxidation potential is consistent with an electron-rich phosphorus centre since the one-electron oxidation potentials of typical phosphaalkenes fall in the range 1.07–2.94 V (*vs.* SCE).[8]

Finally, an effort was made to prepare a 1 : 1 adduct of **1** by treatment with an equimolar quantity of the more sterically demanding Lewis acid, $BPh_3$. Interestingly, this reaction resulted in phenylphosphinidene extrusion and formation of the cyclopolyphosphines $(PPh)_3$, $(PPh)_4$, and $(PPh)_5$.[9] The facile oxidation of carbene–phosphinidenes, coupled with the high basicity at phosphorus, portends an interesting reaction chemistry for these species.

We thank the National Science Foundation and the Robert A. Welch Foundation for financial support.

## Footnotes

* E-mail: cowley@mail.utexas.edu

† *Experimental procedure*: $BH_3$·thf (3.3 $cm^3$, 1 M solution in thf) was added dropwise over a 5 min period to a stirred solution of the 1,3-dimesitylimidazolin-2-ylidenephenylphosphinidene complex (0.68 g, 1.65 mmol)[2] in 50 $cm^3$ of toluene. During the course of the addition, the solution turned from yellow to colourless. A large amount of white precipitate formed, and an NMR assay of the supernatant liquid indicated complete precipitation of all phosphorus-containing species. The supernatant liquid was removed, and the residual solid was pumped dry and recrystallised from $CH_2Cl_2$ (1 day, −20 °C) (yield 0.53 g, 1.2 mmol, 73%), mp 200–203 °C. Anal. Calc. for $C_{27}H_{35}B_2N_2P$; C, 73.67; H, 8.01; N, 6.36. Found: C, 73.60; H, 7.98; N, 6.21%.

‡ *Selected spectroscopic data* for **2**: $^1$H NMR ($CD_2Cl_2$, 300.10 MHz, 298 K) δ 7.59–7.52 (m, aryl, 2 H), 7.30–7.25 (m, aryl, 1 H), 7.12 (s, NCH, 2 H), 7.10–7.05 (m, aryl, 2 H), 6.92 (s, mes CH, 4 H), 2.34 (s, mes *p*-$CH_3$, 6 H), 2.05 (s, mes *o*-$CH_3$, 12 H), 0.25–1.0 (br, $BH_3$, 6 H). $^{13}$C{$^1$H} NMR ($CD_2Cl_2$, 75.48 MHz, 298 K) δ 152.3 (d, $^1J_{PC}$ 32 Hz, NCP), 141.2 (s, *ipso* $C_{mes}$), 135.9 (s, *o*-$C_{mes}$), 135.0 (d, $^2J_{PC}$ 8 Hz, *o*-$C_{aryl}$), 132.9 (s, *p*-$C_{mes}$), 130.1 (d, $^1J_{PC}$ 39 Hz, *ipso*-$C_{aryl}$), 130.0 (s, *p*-$C_{aryl}$), 129.5 (s, *m*-$C_{mes}$), 127.7 (d, $^3J_{PC}$ 8 Hz, *m*-$C_{aryl}$), 126.4 (s, CN*C*), 21.2 (s, *p*-$CH_3$), 18.4 (s, *o*-$CH_3$). $^{31}$P{$^1$H} NMR ($CD_2Cl_2$, 121.50 MHz, 298 K) δ 4 (br).

§ *Crystal data* for **2**: $C_{27}H_{35}B_2N_2P$, $M$ = 440.16, monoclinic, space group $P2_1/c$, $a$ = 19.957(1), $b$ = 8.462(1), $c$ = 15.163(1) Å, β = 94.551(4)°, $U$ = 2552.9(4) Å$^3$, $Z$ = 4, $D_c$ = 1.145 g cm$^{-3}$, $F$(000) = 944, $T$ = 153(2) K. 5851 independent reflections were collected on a Siemens P4 diffractometer using graphite-monochromated Mo-Kα radiation (λ = 0.710 73 Å), 2.05 < θ < 27.50°, μ = 1.25 cm$^{-1}$, an absorption correction was applied (face indexed): $wR_2 = \{\Sigma[w(F_o^2 - F_c^2)^2]/\Sigma[w(F_o^2)^2]\}^{\frac{1}{2}}$ = 0.10 and $R = \Sigma \mid F_o - F_c \mid /\Sigma F$ = 0.045 for reflections with $I/2\sigma(I) > 2.0$. Atomic coordinates, bond lengths and angles, and thermal parameters have been deposited at the Cambridge Crystallographic Data Centre (CCDC). See Information for Authors, Issue No. 1. Any request to the CCDC for this material should quote the full literature citation and the reference number 182/434.

¶ Cyclic voltammetry experiments were performed in a helium-filled drybox using a BAS100 electrochemical analyser and a platinum disk working electrode (area = 0.031 $cm^2$). The reference electrode, a silver wire immersed in 0.01 M $AgSO_3CF_3$–MeCN within a frit, was referenced to an SCE after experiments.

## References

1 A. J. Arduengo, III, H. V. Rasika Dias and J. C. Calabrese, *Chem. Lett.*, 1997, 143.
2 A. J. Arduengo, III, J. C. Calabrese, A. H. Cowley, H. V. Rasika Dias, J. R. Goerlich, W. J. Marshall and B. Riegel, *Inorg. Chem.*, in the press.
3 See, for example, T. E. Taylor and M. B. Hall, *J. Am. Chem. Soc.*, 1984, **106**, 1575.
4 R. J. Gillespie and E. A. Robinson, *Angew. Chem., Int. Ed. Engl.*, 1996, **35**, 495.
5 N. Burford, P. Losier, S. V. Sereda, T. S. Cameron and G. Wu, *J. Am. Chem. Soc.*, 1994, **116**, 6474.
6 G. Huttner and K. Evertz, *Acc. Chem. Res.*, 1986, **19**, 406.
7 M. Wada and S. Hagashizaki, *J. Chem. Soc., Chem. Commun.*, 1984, 482. Certain polycyclic phosphorus systems are more powerful bases, see J.-S. Tang and J. G. Verkade, *Angew. Chem., Int. Ed. Engl.*, 1993, **32**, 896.
8 W. W. Schoeller, J. Niemann, R. Thiele and W. Hang, *Chem. Ber.*, 1990, **124**, 417.
9 Identified by $^{31}$P NMR. See M. Baudler, B. Carlsohn, W. Bohm and G. Reuschenbach, *Z. Naturforsch., Teil B*, 1976, **31**, 558.

*Received in Bloomington, IN, USA, 13th January 1997; Com. 7/00296C*



Typeset and printed by Black Bear Press Limited, Cambridge, England

ChemComm
FEATURE ARTICLE

# Recent advances in stereoselective synthesis involving diazocarbonyl intermediates

**Michael P. Doyle[a] and M. Anthony McKervey[b]**

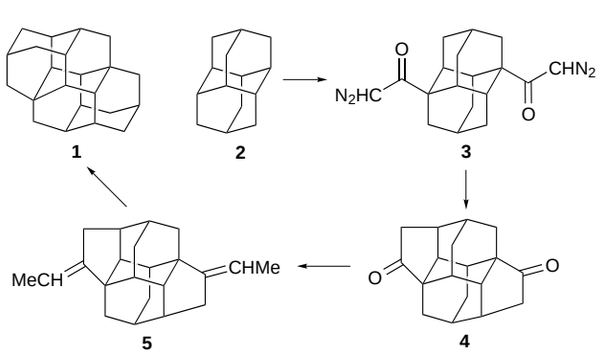
[a] *Department of Chemistry, Trinity University, San Antonio, Texas 78212, USA*
[b] *School of Chemistry, The Queen's University, Belfast, UK BT9 5AG*

**Two aspects of recent developments in enantioselective organic synthesis involving diazocarbonyl intermediates are highlighted: the introduction of chiral catalysts for asymmetric transformations and the use of enantiopure diazoketones derived from amino acids and peptides as chiral educts.**

## Introduction

Although much of our recent research in diazocarbonyl chemistry has been directed towards catalysed asymmetric synthesis and the use in synthesis of enantiopure diazoketones derived from natural amino acids and peptides, for one of us the first encounter with diazocarbonyl chemistry in the laboratory occurred in 1976 during the synthesis of the polycyclic hydrocarbon, *anti*-tetramantane **1**, a $C_{22}$ fragment of the diamond lattice.[1] The plan was to transform diamantane **2** into *anti*-tetramantane by establishing new bridgehead positions *via* C–H insertion reactions of α-ketocarbenoid intermediates (Scheme 1). This could be realised by treatment of the diamantane bisdiazoketone **3** with copper sulfate in benzene, whereupon the heptacyclic diketone **4** was produced, albeit in low yield. The carbonyl groups of **4** were then used to add four more carbon atoms to produce diene **5**, an isomer of *anti*-tetramantane; and to complete the synthesis, the rearrangement of one to the other was brought about in the gas phase in hydrogen at 300 °C on a platinum–silica catalyst. Twenty years on there are still few chemical ways of functionalising unactivated C–H bonds as useful and versatile as metal-catalysed decomposition of diazoketones or diazoesters. In fact, C–H insertion is but one of an entire cornucopia of diazocarbonyl reactions with numerous useful applications in organic synthesis. These reactions include cyclopropanation, X–H insertion (X = C, N, O, S, Si, Se, P), aromatic cycloaddition, ylide formation, dipolar cycloaddition, Wolff rearrangement, acid-catalysed cyclisation, α,α-substitution, addition to aldehydes and ketones, β-elimination and oxidation.[2]

Diazocarbonyl chemistry often gets a bad press. While it is unquestionably true that substances such as diazomethane and sulfonyl azides such as tosyl azide and mesyl azide, important reagents in diazocarbonyl synthesis, are hazardous,[3] when due care is taken they can be handled confidently even on a large scale. The Merck thienamycin synthesis,[4] for example, involving a rhodium-catalysed N–H insertion of a diazomalonate whose synthesis requires the use of an arylsulfonyl azide, is routinely conducted on a multikilogram scale.

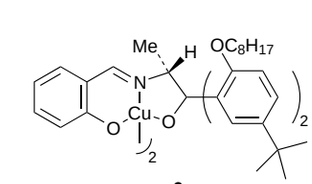



**Scheme 1**

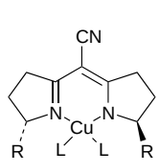
## Asymmetric synthesis of diazocarbonyl reactions: development of chiral catalysts

There are numerous opportunities for asymmetric synthesis employing diazocarbonyl substrates with the option of either covalently attaching a chiral auxiliary to one of the reactants or of using a chiral catalyst (or both). However, when one considers that the most synthetically useful diazocarbonyl reactions are in fact metal catalysed, the attractions of the latter option become very compelling.

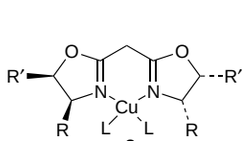
Up to the late 1970s,[5] the single most important metal in catalysed diazocarbonyl decomposition was copper and the most frequently used reaction was cyclopropanation. The first successful asymmetric combination was that devised by Aratani[6] who prepared a series of chiral copper(II) chelates **6** from salicylaldehyde and optically active amino alcohols with which to catalyse intermolecular cyclopropanation of alkenes and dienes with ethyl diazoacetate. Enantioselectivities exceeding 90% could be achieved in selected cases as, for example, in the synthesis of ethyl 2,2-dimethylcyclopropane carboxylate [eqn. (1)]. There are now several copper-based catalysts capable of producing ee values up to 99% over a range of alkenes. These include the catalysts of Pfaltz **7**,[7] Masamune **8**,[8] Evans **9**[9] and Ito and Katsuki **10**,[10] all containing heterocyclic $C_2$-symmetric auxiliaries. Eqns. (2–4) illustrate some representative examples of their successes in enantioselective cyclopropanation.



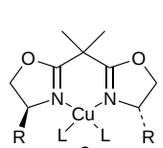

**6**



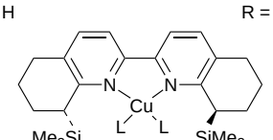

**7**
R = $CMe_2OH$



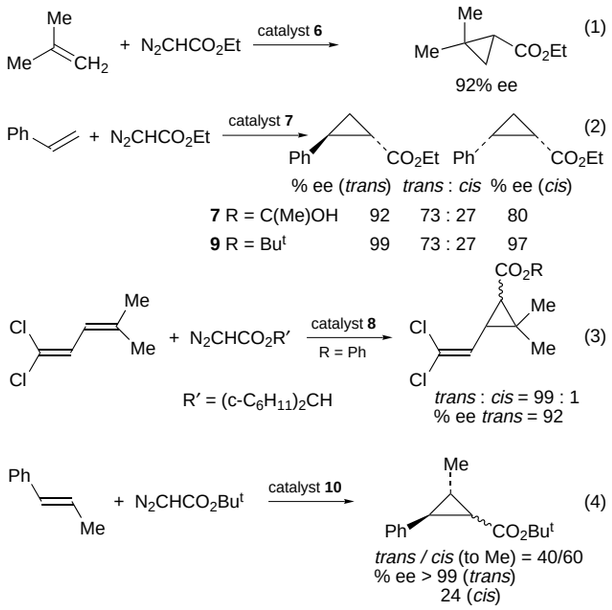

**8**
R = Me, R′ = Ph
R = $CH_2OH$, R′ = H
R = Et, R′ = H




**9**
R = $CHMe_2$
R = $Bu^t$



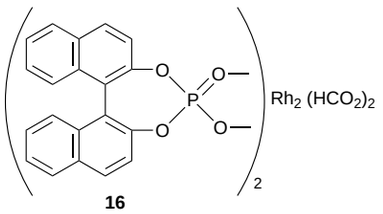

**10**




The introduction of rhodium(II) carboxylates for diazocarbonyl decomposition by Teyssie, Hubert and Noels[11] in 1973 opened the way to new initiatives in catalysed asymmetric synthesis. Unlike many of the copper catalysts whose catalytic activity was restricted largely to cyclopropanation, rhodium(II) carboxylates were to display a reactivity that, in addition to cyclopropanation, encompassed C–H, N–H, O–H, S–H, Si–H and Se–H insertion, aromatic and 1,3-dipolar cycloaddition, electrophilic substitution, and ylide formation with sigmatropic rearrangement. It was not surprising therefore that interest turned towards chiral rhodium(II) catalysts. Three groups, those of Brunner,[12] Ikegami[13] and McKervey,[14] independently introduced rhodium(II) salts with chiral carboxylates attached to the metal core. Enantiopure carboxylates of the type $R^1R^2R^3CCO_2$ **11**, whose substituents varied from H, Me and Ph to OH, NHAc and $CF_3$, were assessed by Brunner for enantioselective cyclopropanation of styrene with ethyl diazoacetate with disappointing results ( < 12% ee).

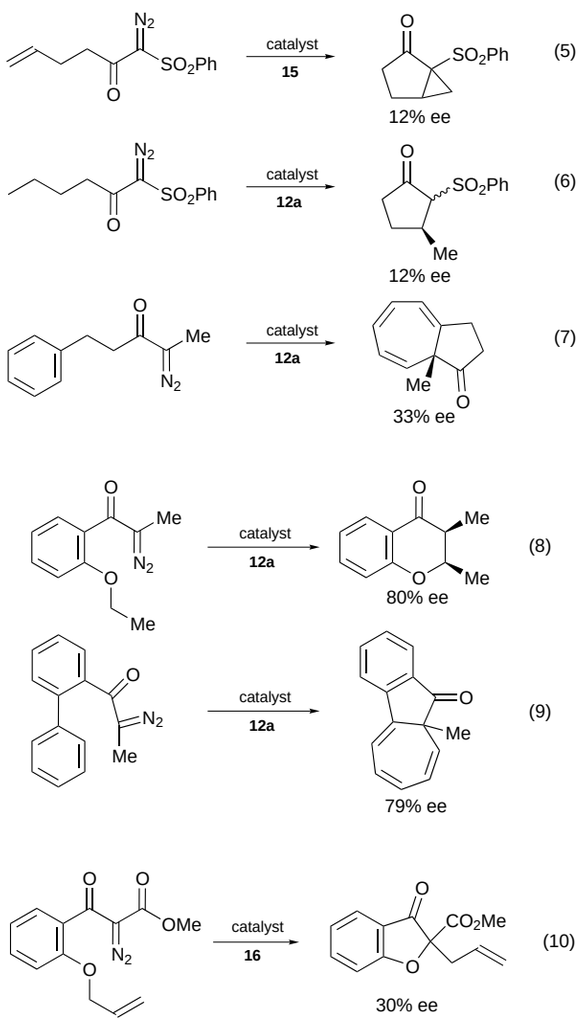
In our own work the availability of a range of enantiopure α-amino acids prompted a survey of their efficacy as rhodium(II) carboxylate catalysts **12**–**14**. Rhodium(II) (*S*)-mandelate **15**,[15] a known compound, was also included in the survey. While these catalysts proved to be very efficient chemically, in some cases at temperatures as low as −80 °C, early results suggested that the extent to which they are capable of exerting enantiocontrol in selected intramolecular reactions, *viz* cyclopropanation, 12% ee [eqn. (5)]; C–H insertion, 12% ee [eqn. (6)] and aromatic cycloaddition, 33% ee [eqn. (7)], was limited.[14] However, recent work with more rigid substrates has shown that significantly higher levels of enantiocontrol can be achieved in C–H insertion where ee values of up to 80% have been realised with the *N*-benzenesulfonyl (*L*)-prolinate catalyst **12a** [eqn. (8)]. Similarly, in the aromatic cycloaddition reaction shown in eqn. (9), use of the prolinate catalyst[16] produced an ee of 79%.[17]

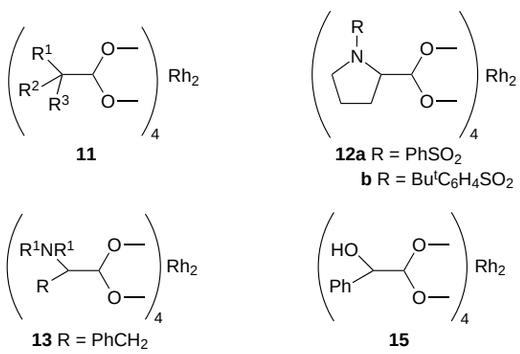
The rhodium(II)-(*S*)-(+)-1,1′-binaphthyl phosphate catalyst **16**[18] introduced in 1992 also shows promise in other diazocarbonyl reactions. For example, the tandem ylide formation–[2,3]sigmatropic rearrangement process in eqn. (10) can be catalysed by **16** to give the furanone product with an ee of 30%.



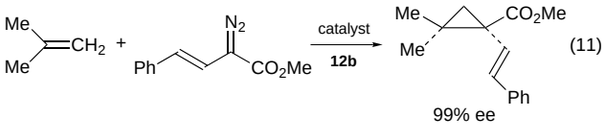

**16**

One feature of the performance of the amino acid based catalysts[19] which offered scope for optimisation was the dependence of the enantioselectivity on the nature of the protecting group on the nitrogen atom. This is nicely illustrated in the use of rhodium(II) prolinates as catalysts for intermolecular cyclopropanation, where enantioselectivities up to 97% have now been achieved. Whereas the benzenesulfonyl derivative **12a** exhibits limited enantiocontrol in cyclopropanation with ethyl diazoacetate, Davies has reported that



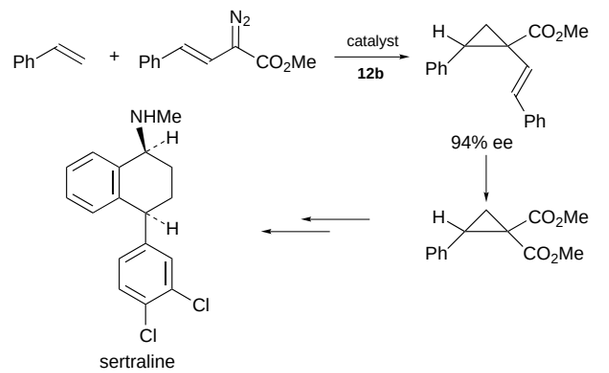



the *p-tert*-butylbenzenesulfonyl counterpart **12b** is especially active for highly enantioselective cyclopropanations with vinyl diazoesters, an illustration being that in eqn. (11). Enantiomeric excesses of 59% ($EtOCH{=}CH_2$) and higher, but generally at or greater than 90% were observed for monosubstituted alkenes.[20]



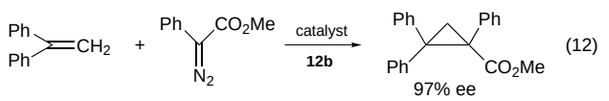

(11)

Higher ee values were reported for reactions in pentane as compared with benzene or dichloromethane. Corey and Grant[21] have used this methodology for cyclopropanation of styrene (94% ee) in an asymmetric synthesis of sertraline (Scheme 2). In a detailed study of the asymmetric synthesis of 2-phenylcyclopropane-1-amino acid, Davies *et al.*[22] concluded that the optimised catalyst for addition of vinyldiazoesters was rhodium *p*-dodecylbenzenesulfonyl prolinate.




**Scheme 2**

We have established that the *p-tert*-butylbenzenesulfonylprolinate catalyst **12b** gives the highest levels of enantiocontrol relative to either chiral rhodium(II) carboxamidates or bisoxazoline ligated copper(I) **9** for intermolecular cyclopropanation reactions of methyl phenyldiazoacetate, where 97% ee has been realized with 1,1-diphenylethene [eqn. (12)], and we have proposed that solvent enhancement of enantiocontrol is due to solvent-induced favourable orientation of the prolinate ligands.[23]



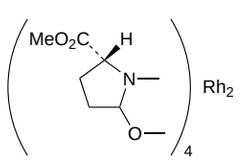

(12)

Efficient syntheses of carboxamidate-ligated dirhodium(II)[24] have made possible the construction of a set of chiral catalysts whose applications have already demonstrated exceptional enantiocontrol for intramolecular and certain intermolecular reactions of diazoacetates and diazoacetamides. Exemplified by $Rh_2$(5*S*-MEPY)$_4$ and its enantiomer $Rh_2$(5*R*-MEPY)$_4$ **17**, where MEPY = methyl 2-oxopyrrolidine-5-carboxylate, the dirhodium(II) core is surrounded by four bridging amide ligands with two oxygen and two nitrogen donor atoms bound to each rhodium in a *cis* configuration. Analogous chiral dirhodium(II) carboxamidates derived from oxazolidinones **18**[25] and imidazolidinones **19** and **20**[26] provide a set of catalysts that effectively control regioselectivity and diastereoselectivity, as well as enantioselectivity in reactions that involve metal carbene intermediates. In each of these catalysts the chiral centre of the ligand is the carbon atom directly bonded to nitrogen, so that the $CO_2Me$ functional attachment lies in a spatial region that influences both the orientation of the bound carbene and the approach of the substrate to the carbene centre.

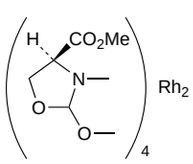
The exceptional ability of chiral dirhodium(II) carboxamidates to direct highly enantioselective intramolecular cyclopropanation reactions has been demonstrated with allylic and homoallylic diazoacetates and diazoacetamides [eqns. (13) and (14)], where with allylic substrates % ee values > 92% are, with few exceptions, obtained.[27,28] Applications of this catalytic methodology include Martin's synthesis of 1,2,3-trisubstituted cyclopropanes as conformationally restricted peptide isosteres for renin **21**[29] and collagenese[30] inhibitors and Poulter's synthesis of presqualene diphosphate **22** by intramolecular cyclopropanation of farnesyl diazoacetate [eqn. (15)].[31] With homoallylic systems there is a moderate reduction in enantiocontrol with the use of these catalysts (71–90% ee).[27] Other chiral catalysts have not proven to be similarly effective for intramolecular cyclopropanation reactions of this wide range of diazocarbonyl compounds.[32]

Dirhodium(II) catalysts are uniquely effective for intramolecular carbon–hydrogen insertion reactions and, as exemplified in eqn. (16),[25] chiral carboxamidate ligands provide high enantiocontrol for the synthesis of lactones and lactams. The exceptional regiocontrol of these reactions has been demonstrated in the construction of chiral lignan lactones such as (−)-hinokinin **23** in a synthetic process that begins with a cinnamic acid (Scheme 3).[33] The high level of diastereocontrol that can be achieved in these reactions is exemplified in the short synthesis of deoxyxylolactone **24** from 1,3-dichloropropan-2-ol (Scheme 4).[34] Even higher diastereoselectivities have been reported for the syntheses of **25** [eqn. (17)][35] and its fused carbocyclic analogues from cycloalkyl diazoacetates.[26,36] The construction of pyrrolizidine bases such as heliotridane **26**, whose pendant methyl group is *syn* is dependent on the use of chiral carboxamidate ligated dirhodium(II) (Scheme 5).[37] Individual enantiomers of substituted cyclohexyl diazoacetates or 2-octyl diazoacetates matched with a configurationally suitable chiral dirhodium(II) carboxamidate catalyst provide an effective methodology for the synthesis of lactones with exceptional diastereo- and regio-control,[38] forming only one isomer out of at least four that are possible.

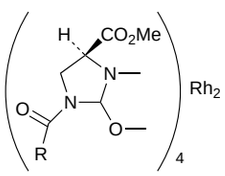
Applications to intermolecular cyclopropenation (carbene addition to alk-1-ynes[39] and β-lactam formation by intramolecular C–H insertion[40]) have also been reported. In general, Doyle's chiral carboxamide dirhodium(II) catalysts are recognized as providing the highest levels of stereocontrol in cyclopropanation and C–H insertion reactions of diazoacetates and diazoacetamides. There are other X–H insertion reactions of ketocarbenoids which have not yet reached stages of development comparable to these highly efficient asymmetric C–H insertions. Although several examples of inter- and intramolecular O–H insertions of water and alcohols are known,[2]




$Rh_2$ (5*R*-MEPY)$_4$
**17**

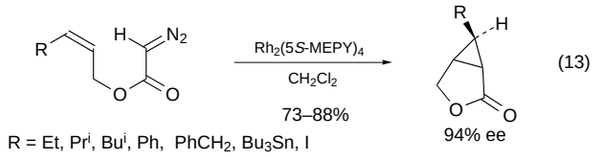



$Rh_2$ (4*S*-MEOX)$_4$
**18**



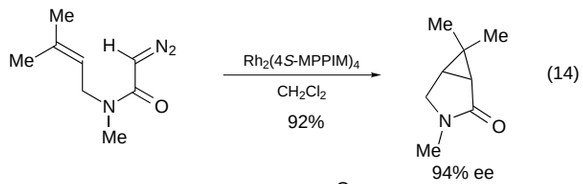

$Rh_2$ (4*S*-MACIM)$_4$
R = Me
**19**

$Rh_2$ (4*S*-MPPIM)$_4$
R = $PhCH_2CH_2$
**20**

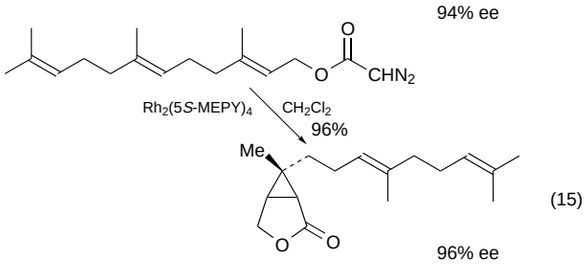



R = Et, Pr$^{i}$, Bu$^{i}$, Ph, $PhCH_2$, $Bu_3Sn$, I

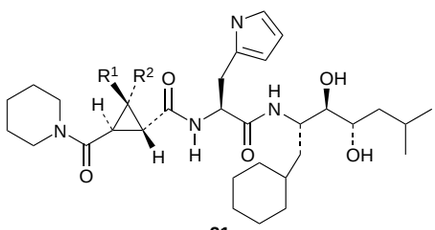
(13)



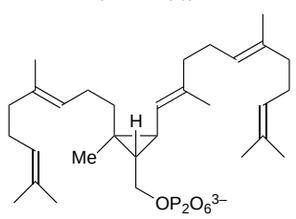

(14)



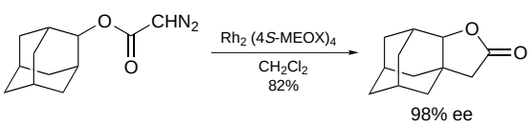

(15)



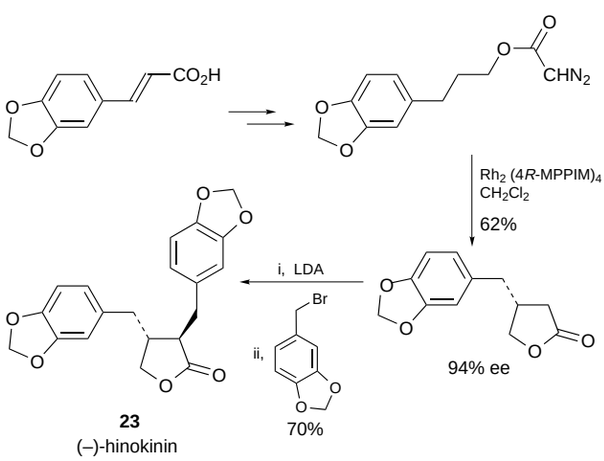

**21**
renin inhibitor




**22**
presqualene diphosphate



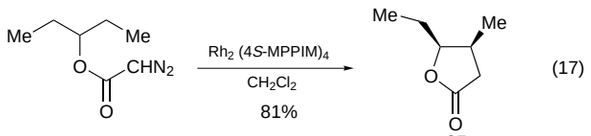

(16)




**23**
(–)-hinokinin

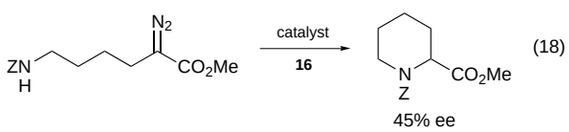
**Scheme 3**

high enantioselectivities through the use of chiral catalysts have yet to be realised.[41] There is now one example of the use of chiral catalysts in asymmetric N–H insertion where rhodium(II) (*S*)-mandelate was used to produce the pipecolic acid derivative in eqn. (18) with an ee of 45%.[42] Asymmetric Si–H insertion into $PhMe_2SiH$ with methyl phenydiazoacetate has been reported to occur in 46% ee with the use of $Rh_2(MEPY)_4$ catalysts.[43]




**25**
99% ee
94% de

(17)



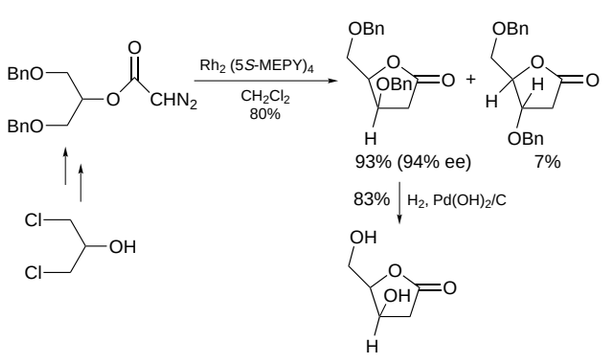

45% ee

(18)

## Transformations of enantiopure α-diazoketones derived from α-amino acids and peptides

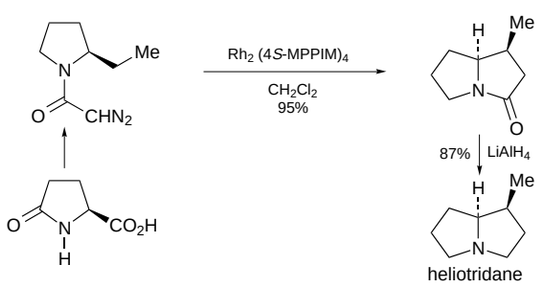
Whereas the primary objective of using chiral catalysts in diazocarbonyl reactions was to achieve high levels of enantiocontrol in selected reactions, that of using α-diazoketones derived from α-amino acids and peptides was to have enantiopure educts for chiral group transfer reactions. With appropriate *N*-protection α-amino acids and peptides can be easily transformed into diazoketones without racemization [eqn. (19)].[44]

A selection of the many racemization-free reactions which these diazoketones undergo are summarised in eqns. (20–25), the feature common to all being the transfer of an enantiopure α-amino ketone moiety to a new structural or functional group environment. It is possible, for example, to titrate *N*-protected




**24** (3*R*, 4*R*)-2-deoxyxylolactone

**Scheme 4**

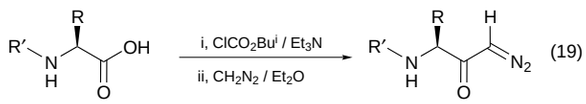



heliotridane
**26**

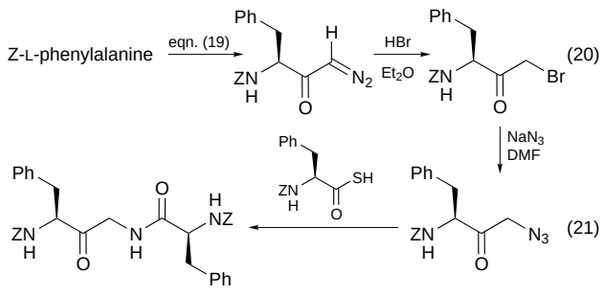
**Scheme 5**

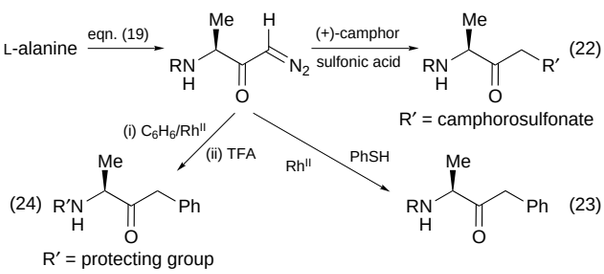
α-amino diazoketones with ethereal hydrogen chloride or bromide to form enantiopure α-halogenoketones[45] [eqn. (20)] which in turn provide access to α-keto azides of the type shown in eqn. (21). Reductive acylation of these α-keto azides using *N*-protected aminothiocarboxylic *S*-acids derived from *N*-protected amino acids produces homopeptides.[46] A typical example of this type of peptide modification is shown in eqn. (21). α-Keto sulfonates can be similarly prepared using sulfonic acids [eqn. (22)].[47] Insertion into S–H bonds under rhodium(II) catalysis provides access to α-sulfenyl ketones [eqn. (23)].[47] Aromatic cycloaddition, again with rhodium(II) assistance, can be used to prepare cycloheptatrienes which rearomatise in the presence of trifluoroacetic acid to yield enantiopure α-amino benzyl ketones [eqn. (24)] from benzene.[48] Rhodium catalysed ring unravelling reactions of furan yield polyfunctional aldehydes (eqn. (25)].[49] Yet another intermolecular process which provides access to enantiopure polyfunctional molecules is that involving the formation of lithium enolates from diazoketones without disturbing the diazofunction using suitable bases, *e.g.* LDA. These enolates can add to aldehydes or ketones to form diazoketols which on brief exposure to catalytic rhodium(II) acetate are smoothly transformed into β-diketones (Scheme 6).[44]

The Arndt–Eistert homologation of diazoketones has long been a popular way of converting α-amino acids into β-amino acids, although with early examples it is not always clear that retention of configuration has been adequately established. However, modern techniques do indicate that in the majority of cases retention is observed. In our own work, we have used the Arndt–Eistert reaction as one step in a process, the overall objective of which was to devise a synthesis of enantiopure α-keto-β-amino carboxylic acids and esters,[50] molecules already known in racemic form to possess significant inhibitory

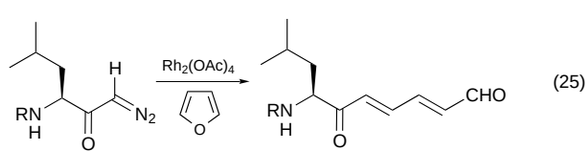


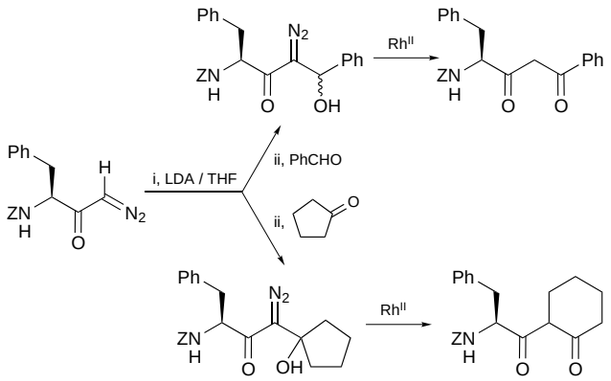

R′ = protecting group or amino acid residue (peptide)




R′ = protecting group

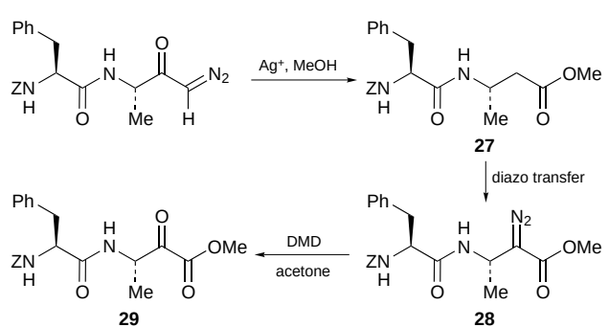


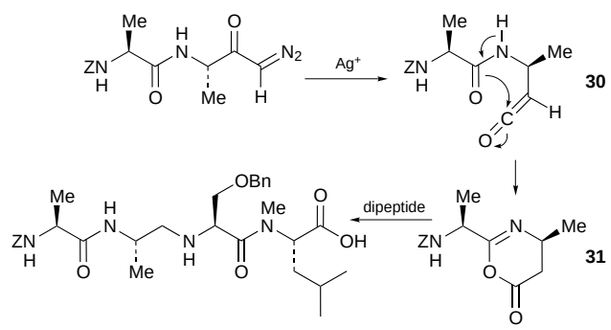

**Scheme 6**

activity towards members of the protease family of enzymes. The process, illustrated in Scheme 7, for the Phe-Ala derivative, commenced with Arndt–Eistert homologation using silver benzoate in methanol. Next, a diazo group was reintroduced alpha to the ester function of **27** to form **28** and in the final stage the diazo group was replaced by a carbonyl group as in **29** *via* oxidation with dimethyldioxirane in acetone. Retention of configuration was maintained throughout the sequence. Seebach and Podlech[51] have recently described a particularly useful application of the Arndt–Eistert process to the formation of homopeptides from diazoketones. The objective was to generate a peptidic ketene **30** from a diazoketone in an non-nucleophilic solvent and trap it intermolecularly with the free amino function of a second amino acid or peptide. An example of the process is shown in Scheme 8 where the ketene is derived from L-alanine and the amino function is that of a dipeptide. Although ketene **30** is undoubtedly an intermediate in the process, closer inspection revealed that it is not the immediate precursor of the homopeptide product. Rather, it was transformed, through involvement of the neighbouring amide bond, into dihydrooxazinone **31**, a reactive cyclic iminoanhydride which is readily attacked to form homopeptides.

Intramolecular insertion reactions of amino acid-derived diazoketones are also possible. We and others have found that



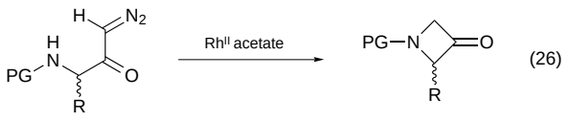

**Scheme 7**



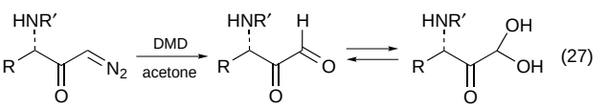

**Scheme 8**

rhodium(II) acetate-catalysed decomposition of the diazoketones in eqn. (26) furnish enantiopure 2-substituted azetidin-3-ones *via* N–H insertion.[52] The product from L-serine was subsequently tranformed by Hanessian[52b] *et al.* into *cis*- and *trans*-polyoximic acid.

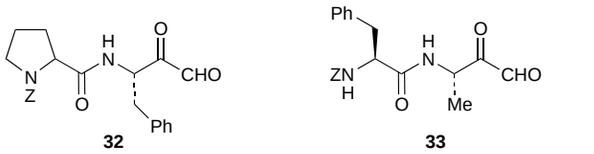
We have already touched briefly on the use of dimethyldioxirane in acetone as an oxidant in the synthesis of enantiopure β-amino-α-keto esters **26**. Distilled DMD in acetone offers particular advantages as an oxidant when one wishes to generate delicate intermediates in a clean environment free of extraneous nucleophiles or electrophiles. Terminal diazoketones derived from amino acids or peptides are also prone to DMD oxidation yielding glyoxals which have proved to be useful enantiopure educts.[53] Prior to this work, α-amino glyoxals were unknown; without *N*-protection they would be expected to undergo spontaneous polymerisation. We found that with suitable *N*-protection amino diazoketones can be oxidised to amino glyoxals in quantitative yield. Some representative examples are shown in eqn. (27). The glyoxals were obtained exclusively in the hydrated form. Interestingly, several of the dipeptide glyoxals were found to possess significant protease inhibitory properties.[54] For example, the sequences Z-Pro-Phe-CHO **32** and Z-Phe-Ala-CHO **33** inhibit chymotrypsin and cathepsin B, respectively, with $K_i$ values some 10-fold lower than those for the corresponding peptide aldehydes. These glyoxals could also be used directly as reaction intermediates, there being no by-products of oxidation other than acetone and nitrogen. Among the reactions that we have used to demonstrate the versatility of *N*-protected amino glyoxals as enantiopure educts in amino acid and peptide modification are alkenation with Wittig reagents, *e.g.* eqns. (28), (29) and (30), condensation with amines to form imines, *e.g.* eqn. (31), and with 1,2-diaminobenzene to form quinoxalines,[53] *e.g.* eqn. (32). These compounds are in turn potentially useful enantiopure educts for further amino acid and peptide modification. Their biological properties, particularly their efficacy as protease inhibitors, are under investigation in collaboration with Dr B. Walker, School of Biology and Biochemistry, Queen's University.



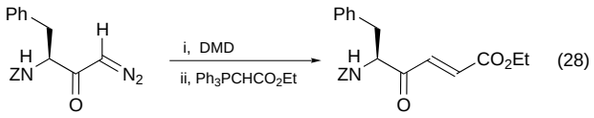

PG = Boc or Z; R = Me, Pr$^i$, $PhCH_2$, $PhCH_2OCOCH_2$

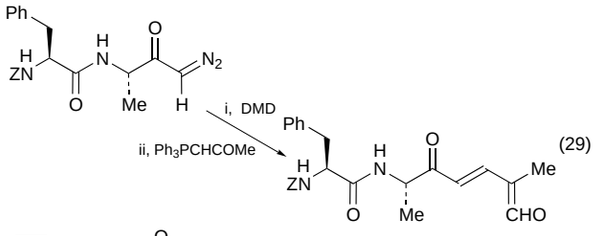


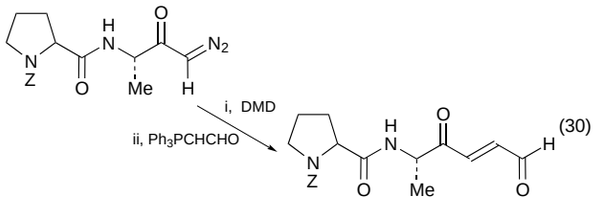

R = $PhCH_2$, Me, $Me_2CH$
R′ = protecting group or peptide residue

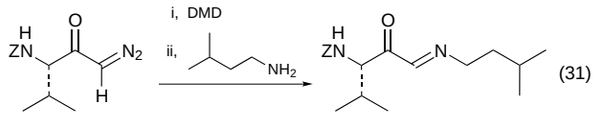


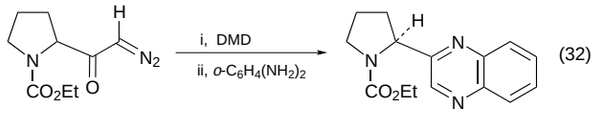
**32** **33**




## Conclusion

We hope that we have demonstrated that modern organic synthesis with ever increasing requirements for stereocontrol *via* catalysed or uncatalysed transformation continues to benefit from the outstanding versatility of diazocarbonyl compounds.


## Acknowledgements

We are indebted to our co-workers whose names appear in the references with whom it has been a great pleasure to work.


**Michael P. Doyle was raised in Minneapolis, Minnesota. He received his PhD degree with W. S. Trahanovsky from Iowa State University in 1968, where he was a U.S. Public Health Service Predoctoral Fellow. He was a postdoctoral associate with J. Rocek and Instructor at the University of Illinois at Chicago before he began his academic career at Hope College in 1968. In 1984 he moved to Trinity University as the first Dr D. R. Semmes Distinguished Professor of Chemistry. His research interests include the design of chiral catalysts for highly enantioselective chemical tranformations, the development of new synthetic methods involving metal carbenes, and macrocyclization reactions.**

**M. Anthony McKervey received his BSc, PhD and DSc degrees from Queen's University, Belfast and, following a period at M.I.T., joined the academic staff at Queen's in 1966. In 1976 he was appointed to the Chair of Organic Chemistry in University College Cork, Irish Republic. He returned to Belfast in 1990 as Professor of Organic Chemistry and Head of the Research Division of the School of Chemistry. Apart from diazocarbonyl chemistry, his research interests include calixarenes, the synthetic chemistry of furans, and clean synthesis for chemical development.**

## References


1 W. Burns, M. A. McKervey, T. R. B. Mitchell and J. J. Rooney, *J. Am. Chem. Soc.*, 1978, **100**, 906.
2 For a recent review of applications of diazocarbonyl intermediates in organic synthesis see Tao Ye and M. A. McKervey, *Chem. Rev.*, 1994, **94**, 1091.
3 For a recent quantitative assessment of the hazards associated with the use of diazotransfer reagents see F. W. Bollinger and L. D. Tuma, *Synlett*, 1996, 407.
4 L. D. Cama and B. G. Christensen, *Tetrahedron Lett.*, 1978, 4233; T. N. Salzmann, R. W. Ratcliffe, B. G. Christensen and F. A. Bouffard, *J. Am. Chem. Soc.*, 1980, **102**, 6161.
5 For a comprehensive account of catalysed asymmetric cyclopropanation up to 1985, see G. Maas, *Top Curr. Chem.*, 1987, **137**, 75.

6 T. Aratani, Y. Yoneyoshi and T. Nagase, *Tetrahedron Lett.*, 1975, 1707; T. Aratani, Y. Yoneyoshi and T. Nagase, *Tetrahedron Lett.*, 1982, **23**, 685.
7 D. Muller, G. Umbricht, B. Weber and A. Pfaltz, *Helv. Chim. Acta*, 1991, **74**, 232.
8 R. E. Lowenthal and S. Masamune, *Tetrahedron Lett.*, 1991, **32**, 7373.
9 D. A. Evans, K. A. Woerpel and M. M. Hinman, *J. Am. Chem. Soc.*, 1991, **113**, 726.
10 K. Ito and T. Katsuki, *Tetrahedron Lett.*, 1993, **34**, 2661.
11 R. Paulissen, H. Reimlinger, E. Hayez, A. J. Hubert and P. Teyssie, *Tetrahedron Lett.*, 1973, 2233; A. F. Noels, D. N. Petiniot, A. J. Hubert and Ph. Teyssie, *Tetrahedron Lett.*, 1982, **38**, 2733.
12 H. Brunner, H. Kluschanzoff and K. Wutz, *Bull. Soc. Chem. Belg.*, 1989, **98**, 63.
13 S. Hashimoto, N. Watanabe and D. Ikegami, *Tetrahedron Lett.*, 1990, **31**, 5173.
14 M. Kennedy and M. A. McKervey, *J. Chem. Soc., Chem. Commun.*, 1988, 1028; M. Kennedy, M. A. McKervey, A. R. Maguire and G. H. P. Roos, *J. Chem. Soc., Chem. Commun*., 1990, 361.
15 P. A. Agaskar, F. A. Cotton, L. R. Falvello and S. Han, *J. Am. Chem. Soc.*, 1986, **108**, 1214.
16 M. A. McKervey and Tao Ye, *J. Chem. Soc., Chem. Commun.*, 1992, 823; Tao Ye, C. Fernandez Garcia and M. A. McKervey, *J. Chem. Soc., Perkin Trans. 1*, 1995, 1373.
17 M. A. McKervey and N. McCarthy, unpublished results.
18 N. McCarthy, M. A. McKervey, T. Ye, M. McCann, E. Murphy and M. P. Doyle, *Tetrahedron Lett.*, 1992, **33**, 5983.
19 G. H. P. Roos and M. A. McKervey, *Synth. Commun.*, 1992, **22**, 1751.
20 H. M. L. Davies and D. K. Hutcheson, *Tetrahedron Lett.*, 1993, **34**, 7243.
21 E. J. Corey and T. G. Grant, *Tetrahedron Lett.*, 1994, **35**, 5373.
22 H. M. L. Davies, P. Bruzinski, D. H. Lake, N. Kong and M. J. Fall, *J. Am. Chem. Soc.*, 1996, **118**, 6897.
23 M. P. Doyle, Q.-L. Zhou, C. Charnsangavej, M. A. Longoria, M. A. McKervey and C. F. Garcia, *Tetrahedron Lett.*, 1996, **37**, 4129.
24 M. P. Doyle, W. R. Winchester, J. A. A. Hoorn, V. Lynch, S. H. Simonsen and R. Ghosh, *J. Am. Chem. Soc.*, 1993, **115**, 9968.
25 M. P. Doyle, A. B. Dyatkin, M. N. Protopopova, C. I. Yang, C. S. Miertschin and W. R. Winchester, *Rec. Trav. Chim. Pays-Bas* (Chirality Issue, Invited Contribution), 1995, **114**, 163.
26 M. P. Doyle, Q.-L. Zhou, C. E. Raab, G. H. P. Roos, S. H. Simonsen and V. Lynch, *Inorg. Chem.*, 1996, **35**, 6064.
27 M. P. Doyle, R. E. Austin, A. S. Bailey, M. P. Dwyer, A. B. Dyatkin, A. V. Kalinin, M. M. Y. Kwan, S. Liras, C. J. Oalmann, R. J. Pieters, M. N. Protopopova, C. E. Raab, G. H. P. Roos, Q.-L. Zhou and S. F. Martin, *J. Am. Chem. Soc.*, 1995, **117**, 5763.
28 M. P. Doyle and A. V. Kalinin, *J. Org. Chem.*, 1996, **61**, 2179.
29 S. F. Martin, R. E. Austin, C. J. Oalmann, W. R. Baker, S. L. Condon, E. DeLara, S. H. Rosenberg, K. P. Spina, H. H. Stein, J. Cohen and H. D. Kleinert, *J. Med. Chem.*, 1992, **35**, 1710.
30 S. F. Martin, C. J. Oalmann and S. Liras, *Tetrahedron*, 1993, **49**, 3521.
31 D. H. Rogers, E. C. Yi and C. D. Poulter, *J. Org. Chem.*, 1995, **60**, 941.
32 M. P. Doyle, C. S. Peterson, Q.-L. Zhou and H. Nishiyama, *Chem. Commun.*, 1997, 211.
33 J. W. Bode, M. P. Doyle, M. N. Protopopova and Q.-L. Zhou, *J. Org. Chem.*, 1996, **61**, 9146.
34 M. P. Doyle, A. B. Dyatkin and J. S. Tedrow, *Tetrahedron Lett.*, 1994, **35**, 3853.
35 M. P. Doyle, Q.-L. Zhou, A. B. Dyatkin and D. A. Ruppar, *Tetrahedron Lett.*, 1995, **36**, 7579.
36 M. P. Doyle, A. B. Dyatkin, G. H. P. Roos, F. Canas, D. A. Pierson, A. van Basten, P. Muller and P. Polleux, *J. Am. Chem. Soc.*, 1994, **116**, 4507.
37 M. P. Doyle and A. V. Kalinin, *Tetrahedron Lett.*, 1996, **37**, 1371.
38 M. P. Doyle, A. V. Kalinin and D. G. Ene, *J. Am. Chem. Soc.*, 1996, **118**, 8837.
39 M. P. Doyle, M. N. Protopopova, P. Muller, D. Ene and E. A. Shapiro, *J. Am. Chem. Soc.*, 1994, **116**, 8492.
40 M. P. Doyle and A. V. Kalinin, *Synlett*, 195, 1075.
41 E. Aller, D. S. Browne, G. G. Cox, D. J. Miller and C. J. Moody, *J. Org. Chem,.*, 1995, **60**, 4449.
42 C. F. Garcia, M. A. McKervey and Tao Ye, *Chem. Commun.*, 1966, 1465.
43 R. T. Buck, M. P. Doyle, M. J. Drysdale, L. Ferris, D. C. Forbes, D. Haigh, C. J. Moody, N. D. Pearson and Q.-L. Zhou, *Tetrahedron Lett.*, 1996, **37**, 7631.
44 Tao Ye and M. A. McKervey, *Tetrahedron*, 1992, **48**, 8007.
45 R. E. Shute, B. Dunlap and D. H. Rich, *J. Med. Chem.*, 1987, **30**, 71.
46 M. A. McKervey, M. B. O'Sullivan, P. L. Myers and R. H. Green, *J. Chem. Soc., Chem. Commun.*, 1993, 94.
47 J. C. Collins, B. M,. Dilworth, N. T. Garvey, M. Kennedy, M. A. McKervey and M. B. O'Sullivan, *J. Chem. Soc., Chem. Commun.*, 1990, 362.
48 M. A. McKervey, D. N. Russell and M. F. Twohig, *J. Chem. Soc., Chem. Commun.*, 1985, 491.
49 M. A. McKervey and M. B. O'Sullivan, unpublished observations.
50 P. Darkins, N. McCarthy, M. A. McKervey, K. O'Donnell, Tao Ye and B. Walker, *Tetrhaedron: Asymmetry*, 1994, **5**, 195.
51 J. Podlech and D. Seebach, *Angew. Chem., Int. Ed. Engl.*, 1995, **34**, 471.
52 (*a*) M. A. McKervey, B. Dilworth and J. C. Collins, unpublished work; (*b*) S. Hanessian, J.-M. Fu. J.-L. Chiara and R. Di Fabio, *Tetrahedron Lett.*, 1993, **34**, 4157; (*c*) J. Podlech and D. Seebach, *Helv. Chim. Acta*, 1995, **78**, 1238.
53 P. Darkins, N. McCarthy, M. A. McKervey and Tao Ye, *J. Chem. Soc., Chem. Commun.*, 1993, 1222.
54 B. Walker, N. McCarthy, A. Healy, Tao Ye and M. A. McKervey, *Biochem. J.*, 1993, **293**, 321.


*6/04972C*

# A new method for the formation of the P–F bond

**Martin Bollmark and Jacek Stawinski***

*Department of Organic Chemistry, Arrhenius Laboratory, Stockholm University, S-106 91 Stockholm, Sweden*

**Iodine-promoted desulfurization of phosphorothioate and phosphorodithioate diesters in the presence of triethylamine tris(hydrofluoride) (TAF) furnish a rapid and quantitative formation of the corresponding phosphorofluoridates and phosphorofluoridothioates; under the reaction conditions phosphoroselenoate and phosphoroselenothioate diesters undergo deselenization affording the phosphorofluoridate and phosphorofluoridothioate diesters, respectively.**

The reaction of phosphorochloridate diesters with alkali metal fluorides in aprotic solvents is the method of choice for the preparation of simple dialkyl phosphorofluoridates.[1] However, in the synthesis of natural product derivatives containing the P–F bond, this approach is of limited value owing to the scant availability of the corresponding phosphorochloridates and the often detrimental reaction conditions.

Recently, we have reported on a new, simple and efficient method for the preparation of nucleoside phosphorofluoridate and nucleoside phosphorofluoridothioate diesters[2] and monoesters[3] *via* the iodine promoted oxidation of the corresponding H-phosphonates and H-phosphonothioates in the presence of triethylamine tris(hydrofluoride) (TAF). These studies have been directed towards the development of a synthetic procedure enabling the introduction of fluorine at a preselected phosphorus centre in an oligonucleotide, in order to investigate this kind of DNA surrogates as, *inter alia*, potential antisense/antigene therapeutics.

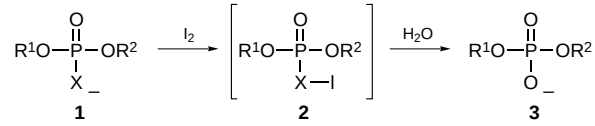
Although dinucleoside phosphorofluoridate and dinucleoside phosphorofluoridothioate diesters are stable solids, that can be purified by silica gel chromatography, the fluorine atom (particularly that in the phosphorofluoridate derivatives) may undergo nucleophilic substitution. This can happen, *e.g.* during the final deprotection of an oligonucleotide and thus would call for significant changes in a solid phase synthesis protocol (*e.g.* the use of more labile base protecting groups, a special procedure for the cleavage of a modified oligomer from the support). For these reasons we have been searching for a synthetic procedure allowing the introduction of fluorine into an unprotected oligonucleotide and in this way alleviating a potential problem of the degradation of a modified oligonucleotide (or the removal of fluorine) during the deprotection step or during its splitting from a support.

As a possible candidate for this purpose we considered phosphorothioate or phosphoroselenoate diesters bearing a sulfur or a selenium atom in the nonbridging position. Owing to the biochemical and medical importance of nucleoside phosphorothioates,[4] on the one hand, and the advances in the chemical synthesis of oligonucleotides, on the other, this class of compounds has recently emerged as most important oligonucleotide analogues.[5]

Since the reaction of iodine with sulfur is known to be a highly selective process[6–11] that can be carried out on unprotected oligonucleotides, we considered as a viable approach for the formation of the P–F bond an iodine-promoted desulfurization (or deselenization) of a suitable phosphorothioate (or phosphoroselenoate) diester in the presence of fluoride anions. The mechanism of this type of reactions (*e.g.* Scheme 1) is unknown but, most likely, it involves the initial formation of the corresponding oxaphosphoranesulfenyl (or oxaphosphoraneselenenyl) iodide (compounds of type **2**), which may undergo a subsequent nucleophilic substitution at the phosphorus centre.

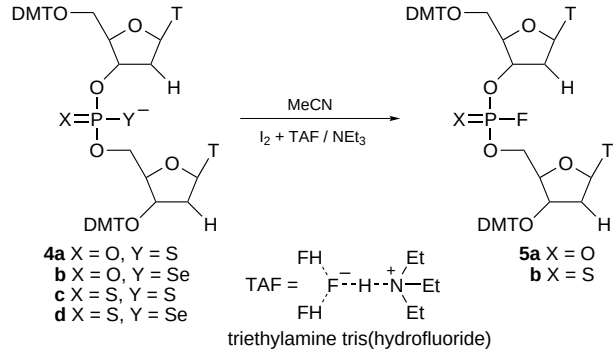
The efficacy of this approach to the formation of phosphorofluoridate diesters was evaluated by reacting the dinucleoside phosphorothioate **4a**[12] with iodine (2.5 equiv.) in acetonitrile in the presence of TAF (1 equiv.) and triethylamine (2 equiv.), Scheme 2. The reaction was fast and clean, as judged by $^{31}$P NMR spectroscopy. Within 5 min the resonances due to the starting material **4a** ($\delta_P$ 57.5)† completely disappeared and only signals assigned to the expected product, the dinucleoside phosphorofluoridate **5a**[2] [$\delta_P$ −9.8, $^1J_{PF}$ = 978 (d), $^3J_{PH}$ = 7.3 Hz, (q) and $\delta_P$ −10.2, $^1J_{PF}$ = 985 (d), $^3J_{PH}$ = 7.3 Hz, (q); ratio *ca.* 1 : 1], were detected. No changes were observed in the reaction mixture when it was left to stand for 2–3 h. The phosphorofluoridate **5a** was also formed as the sole phosphorus-containing product ($^{31}$P NMR spectroscopy) when the dinucleoside phosphoroselenoate **4b**[7] ($\delta_P$ = 52.1[13]) was subjected to the reaction with iodine under analogous reaction conditions.

We also checked the feasibility of using this approach for the synthesis of phosphorofluoridothioates. To this end, the dinucleoside phosphorodithioate **4c**[12] was treated with iodine (2.5 equiv.) in acetonitrile in the presence of TAF (1 equiv.) and triethylamine (2 equiv.). The reaction proceeded to completion within 5 min ($^{31}$P NMR) as was apparent from the disappearance of the starting material **4c** ($\delta_P$ 115.4) and a clean and quantitative formation of the phosphorofluoridothioate **5b**[2] [$\delta_P$ 62.0, $^1J_{PF}$ = 1076 (d), $^3J_{PH}$ = 8.6 Hz, (q) and $\delta_P$ 61.2, $^1J_{PF}$ = 1085 (d), $^3J_{PH}$ = 8.5 Hz, (q); ratio *ca.* 1 : 1]. We did not observe any desulfurization of **5b** under the reaction conditions. This was, in principle, expected in light of the known inertness of




X = S or Se
$R^1$ and $R^2$ = nucleoside moieties

**Scheme 1**




**Scheme 2**

phosphorothioate triesters (and probably other uncharged phosphorus compounds bearing the thiophosphoryl function) towards iodine.[6]

In dinucleoside phosphoroselenothioate diesters, there are two centres which may react with iodine, *i.e.* selenium and sulfur. Owing to differences in the standard reduction potentials of selenium and sulfur ($E°_{Se} = -0.924$ and $E°_{S} = -0.476$ V), it is the former which should undergo preferential oxidation with iodine. Indeed, the reaction of **4d**[7] ($\delta_P$ 104.2 and 103.7) with iodine in the presence of fluoride anion under the conditions as for **4c** afforded exclusively the phosphorofluoridothioate **5b**, as was apparent from the chemical shift value of the product and the absence of a characteristic $^1J_{PSe}$ coupling.

The above reactions were also run on a preparative scale. In a typical experiment, the dinucleoside phosphorothioate **4a** (triethylammonium salt, 0.05 mmol) was rendered anhydrous by repeated evaporation of the added acetonitrile and dissolution in the same solvent (3 ml) containing triethylamine (2 equiv.) and TAF (1 equiv.). A solution of iodine (2.5 equiv.) in acetonitrile (0.5 ml) was then added. After 10 min the reaction mixture was diluted with chloroform (10 ml) and extracted with aq. 10% $Na_2S_2O_3$ (1 × 10 ml). The organic phase was dried over $NaSO_4$, concentrated *in vacuo*, and the residue was chromatographed on a silica gel column using ethyl acetate–toluene (1 : 1, v/v) as eluent. Using this procedure the phosphorofluoridate **5a** was obtained in 70–85% yield‡ (starting from **4a** or **4b**) and the phosphorofluoridothioate **5b** in > 90% yield (starting from **4c** or **4d**). Compounds **5a** and **5b** prepared in this study were identical (TLC, $^1$H and $^{31}$P NMR and FABMS) with those synthesised *via* the iodine-promoted oxidation of the corresponding dinucleoside H-phosphonate and H-phosphonothioate in the presence of TAF.[2]

The relevance of the procedure to the preparation of oligonucleotide analogues was assessed by carrying out some preliminary $^{31}$P NMR experiments on unprotected dinucleoside phosphorothioates. To this end, dithymidine phosphorothioate (obtained by the detritylation of **4a**, followed by trituration with diethyl ether) was subjected to the reaction with iodine (5 equiv.) in pyridine in the presence of fluoride anion (1 equiv. TAF). A clean formation of the corresponding dithymidine phosphorofluoridate [$\delta_P$ −9.4, $^1J_{PF}$ = 977 Hz (d) and $\delta_P$ −9.8 ppm, $^1J_{PF}$ = 985 Hz (d); ratio *ca.* 1 : 1] was observed (5 min, $^{31}$P NMR). The detritylated dinucleoside phosphorodithioate derived from **4c** reacted similarly under the reaction conditions producing the corresponding phosphorofluoridothioate [$\delta_P$ 61.3, $^1J_{PF}$ = 1078 Hz (d) and $\delta_P$ 60.9, $^1J_{PF}$ = 1085 Hz (d); ratio *ca.* 1 : 1].

In conclusion, iodine promoted desulfurization or deselenization of the appropriate phosphorothioate and phosphoroselenoate diesters in the presence of fluoride anions offers a new means for the formation of the P–F bond under exceedingly mild reaction conditions and using easily accessible substrates. Since the method is based on a highly selective activation of sulfur or selenium centres by iodine, it is compatible with the presence of unprotected functional groups in a substrate molecule. This, and the possibility of replacing fluorine with other functionalities, makes the method of particular relevance to the synthesis of oligonucleotides and other analogues bearing labile modifications at the phosphorus centre.

We are indebted to Professor Per J. Garegg for his interest in this work and to the Swedish Research Council for Engineering Sciences and the Swedish Natural Science Research Council for financial support.

## Footnotes

* E-mail: js@lab12.organ.su.se

† Signals for the two phosphorus diastereomers were not resolved.

‡ Lower yields were probably due to partial decomposition during silica gel chromatography.

## References

1 *Methoden der organischen Chemie*, ed. E. Müller, George Thieme Verlag, Stuttgart, 1964, vol. X 11/2, p. 104.
2 M. Bollmark, R. Zain and J. Stawinski, *Tetrahedron Lett.*, 1996, **37**, 3537.
3 M. Bollmark and J. Stawinski, *Tetrahedron Lett.*, 1996, **37**, 5739.
4 F. Eckstein, *Ann. Rev. Biochem.*, 1985, **54**, 367.
5 U. Englisch and D. M. Gauss, *Angew. Chem., Int. Ed. Engl.*, 1991, **30**, 613.
6 B. A. Connolly, B. V. L. Potter, F. Eckstein, A. Pingoud and L. Grotjahn, *Biochemistry*, 1984, **23**, 3443.
7 J. Stawinski and M. Thelin, *J. Org. Chem.*, 1994, **59**, 130.
8 T. W. Wyrzykiewicz and D. L. Cole, *Nucleic Acids Res.*, 1994, **22**, 2667.
9 G. Lowe, G. Tansley and P. M. Cullis, *J. Chem. Soc., Chem. Commun.*, 1982, 595.
10 R. D. Sammons and P. A. Frey, *J. Biol. Chem.*, 1982, **257**, 1138.
11 J. H. Cummins and B. V. L. Potter, *J. Chem. Soc., Chem. Commun.*, 1985, 800.
12 J. Stawinski and M. Thelin, *J. Org. Chem.*, 1991, **56**, 5169.

*Received in Glasgow, UK, 12th March 1997; Com. 7/01728F*

# Tandem 1,3-dipolar cycloadditions of münchnones. Syntheses and molecular structures of 10-azatetracyclo[6.3.0.0$^{4,11}$.0$^{5,9}$]undecanes and azahomopentaprismane

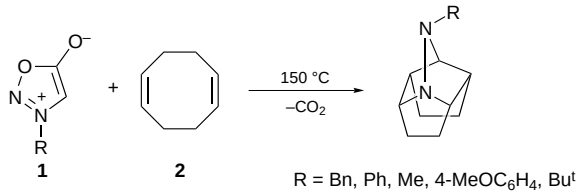
**Gordon W. Gribble,*[a] William R. Sponholtz III,[a] Frank L. Switzer,[a] Ferdinando J. D'Amato[a] and Marianne P. Byrn[b]**

[a] *Department of Chemistry, Dartmouth College, Hanover, NH 03755-3564, USA*
[b] *Department of Chemistry and Biochemistry, The J. D. McCullough X-ray Crystallography Laboratory, University of California, Los Angeles, CA 90095-1569, USA*

**Photocyclization of 10-benzyl-9,11-diphenyl-10-azatetracyclo[6.3.0.0$^{4,11}$.0$^{5,9}$]undeca-2,6-diene 11, prepared in one step from münchnone 7 and cycloocta-1,3,5,7-tetraene 10, gives azahomopentaprismane 12.**

Although the prismanes and other polycyclic cage compounds are well known and continue to be of great interest,[1] only a few examples of azapolycyclic cage hydrocarbons have been prepared.[2] In continuation of our interest in azapolycyclic compounds[3] we report the first synthesis of an azahomopentaprismane, namely 4-benzyl-3,5-diphenyl-4-azahexacyclo-[5.4.0.0$^{2,6}$.0$^{3,10}$.0$^{5,9}$.0$^{8,11}$]undecane **12**.

Our approach to this ring system for a projected conversion to pentaprismane[4] was inspired by the remarkable reaction that Weintraub reported in 1970.[5] Thus, mesoionic sydnones **1** undergo a tandem 1,3-dipolar cycloaddition reaction with cycloocta-1,5-diene **2** to give the novel 9,10-diazatetracyclo-[6.3.0.0$^{4,11}$.0$^{5,9}$]undecanes **3**.[5,6]

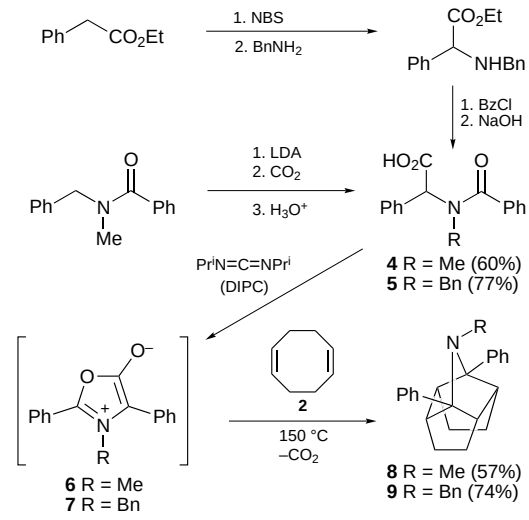



**1** **2**

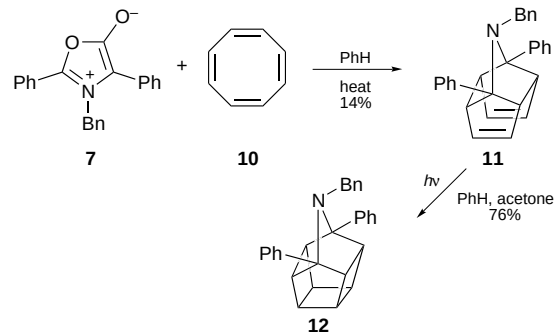
We have now found that the mesoionic münchnones (1,3-oxazolium-5-olates) react similarly with **2** to afford 9,11-diphenyl-10-azatetracyclo[6.3.0.0$^{4,11}$.0$^{5,9}$]undecanes **8**–**9** as shown in Scheme 1. The münchnone precursor amino acids **4** and **5** were synthesized according to classical methods[6,7] and the münchnones **6** and **7** (3-methyl- and 3-benzyl-2,4-diphenyl-oxazolium-5-olate, respectively) were generated using the original method of Huisgen[8] as modified by Anderson,[9] but using diisopropylcarbodiimide to effect cyclodehydration. Although münchnones **6** and **7** could be isolated as yellow solids, it was found that the yields of **8** and **9** were higher if **6** and **7** were generated and trapped with cycloocta-1,5-diene (COD) **2** *in situ*. The resulting azatetracycles **8**† (oil) and **9**† (mp 167–168 °C) have been fully characterized including an X-ray crystal structure for **9**.[10] As we have recently reported, **8** and **9** exhibit not only the expected restricted nitrogen inversion ($\Delta G^{\ddagger}$ = 12.2 and 10.6 kcal mol$^{-1}$, respectively, 1 cal = 4.184 J), but they also display remarkably slow bridgehead phenyl rotation ($\Delta G^{\ddagger}$ = 9.8 kcal mol$^{-1}$).[10]

In an obvious extension of this tandem 1,3-dipolar cycloaddition reaction, we now report that münchnone **7** reacts with cycloocta-1,3,5,7-tetraene (cot) **10** to afford cycloadduct **11** (10-benzyl-9,11-diphenyl-10-azatetracyclo[6.3.0.0$^{4,11}$.0$^{5,9}$]-undeca-2,6-diene) in low yield (Scheme 2). The X-ray crystallographic molecular structure of **11**‡ is shown in Fig. 1. This product represents one of the very few bis-cycloadducts of cot.[11]

Photolysis of **11** (350 W Hanovia medium pressure lamp, pyrex filter, benzene–acetone, 5 : 1, 4 h, room temperature) was followed by NMR spectroscopy and yielded the desired azahomopentaprismane **12**† (4-benzyl-3,5-diphenyl-4-aza-hexacyclo[5.4.0.0$^{2,6}$.0$^{3,10}$.0$^{5,9}$.0$^{8,11}$]undecane) in good yield. It is interesting to note that a similar photolysis of the oxygen analogue of **11** failed to yield oxahomopentaprismane.[12] The X-ray crystallographic molecular structure of **12** is shown in Fig. 2. This compound represents the first example of this ring system and attempts to convert **12** to the corresponding diphenylpentaprismane are in progress.




**Scheme 1**




**7** **10** **11** **12**

**Scheme 2**

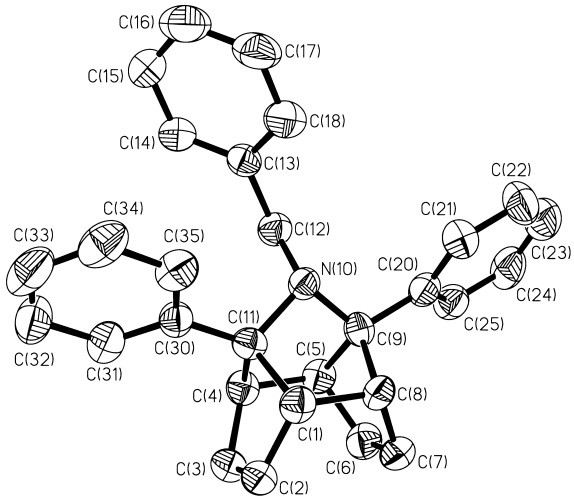



**Fig. 1** ORTEP view of the molecular structure of **11**. The hydrogens have been omitted for clarity. Thermal ellipsoids are drawn at the 50% probability level. Selected bond distances (Å) and angles (°) for **11**: C(1)–C(8) 1.607(7), C(4)–C(5) 1.595(7), C(1)–C(2) 1.505(7), C(3)–C(4) 1.520(7), C(1)–C(11) 1.564(6), C(4)–C(11) 1.578(7), C(2)–C(3) 1.323(8), C(6)–C(7) 1.320(8), C(9)–N(10) 1.459(6), C(12)–N(10) 1.464(6), C(9)–C(20) 1.507(6), C(9)–N(10)–C(11) 97.2(3).

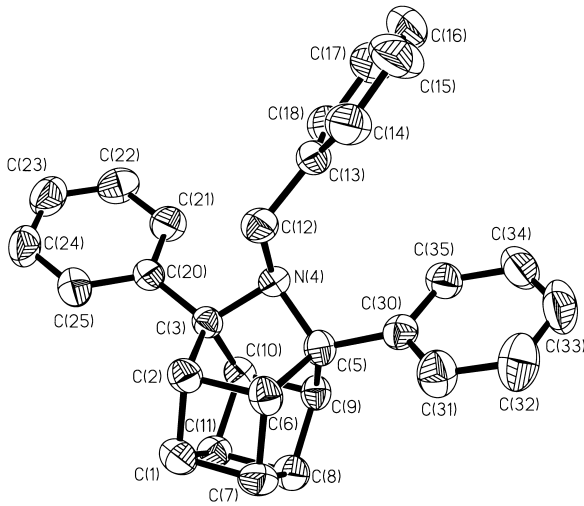



**Fig. 2** ORTEP view of the molecular structure of **12**. The hydrogens have been omitted for clarity. Thermal ellipsoids are drawn at the 50% probability level. Selected bond distances (Å) and angles (°) for **12**: C(2)–C(6) 1.547(7), C(9)–C(10) 1.555(7), C(6)–C(7) 1.555(7), C(8)–C(9) 1.550(7), C(6)–C(7) 1.567(8), C(5)–C(9) 1.550(7), C(7)–C(8) 1.562(9), C(1)–C(11) 1.560(9), C(1)–C(7) 1.560(8), C(8)–C(11) 1.568(7), C(3)–N(4) 1.485(6), C(12)–N(4) 1.470(7), C(3)–C(20) 1.512(7), C(3)–N(4)–C(5) 97.0(4).

We thank the donors of the Petroleum Research Fund administered by the American Chemical Society for support of this project and for a summer faculty fellowship to F. L. S., and the National Science Foundation Research Experiences for Undergraduates Program for a fellowship to F. J. D. We also thank Professors David Lemal and David Glueck of this department for their assistance with the photolysis experiments and useful discussions, and Professor Michael Walters for the use of his laboratory.

## Footnotes

* E-mail: grib@dartmouth.edu

† *Selected physical and spectroscopic data* for **8**: oil; $\delta_H$ (300 MHz, $CDCl_3$) 7.56 (m, 4 H), 7.38 (m, 4 H), 7.28 (m, 2 H), 2.71 (s, 4 H), 1.80 (m, 4 H), 1.69 (s, 3 H) and 1.62 (m, 4 H); $\delta_C$ ($CDCl_3$) 140.0, 128.1, 128.0, 126.9, 83.5, 33.3 and 23.0; *m/z* 315, 286, 246 and 172; HRMS calc. for $M^+$ 315.1987, found 315.1989. For **9**: mp 167–168 °C; $\delta_H$ (300 MHz, $CDCl_3$) 7.50 (m, 4 H), 7.15 (m, 7 H), 6.84 (m, 2 H), 6.57 (m, 2 H), 3.20 (s, 2 H), 2.74 (s, 4 H) and 1.64 (m, 4 H); $\delta_C$ ($CDCl_3$) 141.8, 139.9, 128.6, 128.2, 127.7, 126.9, 126.8, 125.0, 83.9, 50.5, 47.3 and 23.1; *m/z* 391, 301 and 91; anal. calc. for $C_{29}H_{29}N$: C, 88.96; H, 7.47; N, 3.58. Found: C, 88.84; H, 7.44; N, 3.54%. For **11**: mp 190 °C; $\delta_H$ (300 MHz, $CDCl_3$) 7.4 (dd, 4 H, *J* 6.6 and 1 Hz), 7.1 (m, 6 H), 6.9 (m, 3 H), 6.7 (m, 2 H), 5.9 (s, 4 H), 3.2 (s, 2 H) and 3.1 (s, 4 H); $\delta_C$ ($CDCl_3$) 141.2 (2), 134.6. 129.1, 128.7, 127.7, 127.2, 126.9, 125.6, 97.3, 54.7 and 49.7; HRMS calc. for $M^+$ 387.1987, found 387.1990. For **12**: mp 201 °C; $\delta_H$ (300 MHz, $CDCl_3$) 7.3 (dd, 4 H, *J* 7.0 and 1 Hz), 7.15 (m, 6 H), 6.95 (m, 3 H), 6.9 (m, 2 H), 3.55 (s, 4 H), 3.36 (s, 2 H) and 3.3 (s, 4 H); $\delta_C$ ($CDCl_3$) 141.7, 141.0, 128.9, 128.1, 128.0, 127.4, 126.6, 125.6, 90.8, 77.4, 53.3 and 41.7; *m/z* 388, 322, 309, 246, 233, 218 and 91; HRMS calc. for $M^+$ 387.1987, found 387.1992.

‡ *Crystal data* for **11**: The compound crystallized from acetone as colourless needles in the tetragonal system $P\bar{4}$. Unit cell dimensions are as follows: $a = b = 18.44(4)$, $c = 6.13(1)$ Å, $V = 2086(7)$ Å$^3$, $Z = 4$. The crystal was examined on a Syntex (Crystal Logic) diffractometer, Cu-Kα radiation, at 298 K. Total data collected = 1715 and 1326 with $I > 3\sigma(I)$. Full-matrix least-squares refinement based on *F* of 275 parameters has an agreement value, *R*, of 0.046 and a weighted *R* of 0.054. The error of fit is 1.715 and the maximum residual density is 0.69 e Å$^{-3}$. For **12**: The compound crystallized from acetone as colourless needles in the tetragonal system $P\bar{4}$. Unit cell dimensions are as follows: $a = b = 18.399(8)$, $c = 6.038(3)$ Å, $V = 2044(2)$ Å$^3$, $Z = 4$. The crystal was examined on a Syntex (Crystal Logic) diffractometer, Cu-Kα radiation, at 298 K. Total data collected = 1678 and 1104 with $I > 3\sigma(I)$. Full-matrix least-squares refinement based on *F* of 271 parameters has an agreement value, *R*, of 0.044 and a weighted *R* of 0.048. The error of fit is 1.405 and the maximum residual density is 0.32 e Å$^{-3}$. Atomic coordinates, bond lengths and angles, and thermal parameters have been deposited at the Cambridge Crystallographic Data Centre (CCDC). See Information for Authors, Issue No. 1. Any request to the CCDC for this material should quote the full literature citation and the reference number 182/444.

## References

1 A. P. Marchand, *Chem. Rev.*, 1989, **89**, 1011; T.-C. Chou, Y.-L. Yeh and G.-H. Lin, *Tetrahedron Lett.*, 1996, **37**, 8779; T. D. Golobish and W. P. Dailey, *Tetrahedron Lett.*, 1996, **37**, 3239.
2 S. L. Sacks, J. R. Scheffer, C.-Z. Teh and A. Tse, *J. Med. Chem.*, 1985, **28**, 819; D. P. Becker, R. Nosal, D. L. Zabrowski and D. L. Flynn, *Tetrahedron*, 1997, **53**, 1.
3 G. W. Gribble and B. H. Hirth, *J. Heterocycl. Chem.*, 1996, **33**, 719; G. W. Gribble, F. L. Switzer, J. H. Bushweller, J. G. Jewett, J. H. Brown, J. L. Dion, C. H. Bushweller, M. P. Byrn and C. E. Strouse, *J. Org. Chem.*, 1996, **61**, 4319; C. H. Bushweller, J. H. Brown, C. M. DiMeglio, G. W. Gribble, J. T. Eaton, C. S. LeHoullier and E. R. Olson, *J. Org. Chem.*, 1995, **60**, 268; G. W. Gribble, N. R. Easton, Jr. and J. T. Eaton, *Tetrahedron Lett.*, 1970, 1075.
4 For the synthesis of pentaprismane, see P. E. Eaton, Y. S. Or and S. J. Branca, *J. Am. Chem. Soc.*, 1981, **103**, 2134; P. E. Eaton, Y. S. Or, S. J. Branca and B. K. R. Shankar, *Tetrahedron*, 1986, **42**, 1621; W. G. Dauben and A. F. Cunningham, Jr., *J. Org. Chem.*, 1983, **48**, 2842.
5 P. M. Weintraub, *J. Chem. Soc., Chem. Commun.*, 1970, 760.
6 For a recent study of this reaction, see G. W. Gribble and B. H. Hirth, *J. Heterocycl. Chem.*, 1996, **33**, 719.
7 R. R. Fraser, G. Boussard, I. D. Postescu, J. J. Whiting and Y. Y. Wigfield, *Can. J. Chem.*, 1973, **51**, 1109.
8 R. Huisgen, H. Gotthardt, H. O. Bayer and F. C. Schaefer, *Chem. Ber.*, 1970, **103**, 2611.
9 W. K. Anderson and A. R. Heider, *Synth. Commun.*, 1986, **16**, 357.
10 G. W. Gribble, F. L. Switzer, J. H. Bushweller, J. G. Jewett, J. H. Brown, J. L. Dion, C. H. Bushweller, M. P. Byrn and C. E. Strouse, *J. Org. Chem.*, 1996, **61**, 4319.
11 K. Saito, Y. Omura, E. Maekawa and P. G. Gassman, *Bull. Chem. Soc. Jpn.*, 1990, **63**, 395.
12 A. P. Marchand, T.-C. Chou, J. D. Ekstrand and D. van der Helm, *J. Org. Chem.*, 1976, **41**, 1438.

*Received in Corvallis, OR, USA, 5th February 1997; Com. 7/00857K*

# Ultrasound-assisted electrochemical reduction of emulsions in aqueous media

**Frank Marken,[a] Richard G. Compton,*[a] Steven D. Bull[b] and Stephen G. Davies[b]**

[a] *Physical and Theoretical Chemistry Laboratory, Oxford University, South Parks Road, Oxford, UK OX1 3QZ*
[b] *Dyson Perrins Laboratory, Oxford University, South Parks Road, Oxford, UK OX1 3QY*

**The electrochemical reduction of diethylmaleate, diethylfumarate and diethylacetylene dicarboxylate in the form of microscopic droplets generated by applying power ultrasound to aqueous electrolyte media allows a clean hydrogenation of the carbon–carbon double/triple bond whilst providing a novel and versatile methodology for electrochemistry of insoluble materials in aqueous environments.**

In terms of practical applications water can be regarded as an ideal reaction environment for organic electrochemical processes with good conductivity and polarity, stabilizing effects on radical intermediates, and straightforward product isolation by extraction or filtration.[1] Further it is preferable to organic solvents on environmental grounds. Therefore the extension of the range of systems undergoing electrochemical transformations in water is of considerable interest and studies employing surfactant-stabilized emulsions and suspensions have been described.[2]

Ultrasound emitted by a horn source situated in a conventional electrochemical cell[3] allows the formation of emulsions without stabilizing agents simply by mechanical forces which arise at the liquid/liquid phase boundaries.[4] In this study it is demonstrated how this novel experimental approach allows direct voltammetry and electrolysis in aqueous media of materials hitherto thought to be essentially insoluble.

A thermostatted electrochemical cell equipped with an ultrasonic horn probe as shown in Fig. 1 can be used for the study of sonoelectrochemical processes.[3] The cell which has recently been used in the study of homogeneous systems[5] may be used without further modification for voltammetric and bulk electrolysis experiments with emulsions. In Fig. 2 voltammograms obtained for the reduction of emulsions† of diethylfumarate, diethylmaleate and cyclohex-2-en-1-one in aqueous 1.0 M $MgCl_2$ at a 3 mm diameter glassy carbon disc electrode are shown. For diethylfumarate a well defined response for the reduction process at $E_{\frac{1}{2}} = -1.16$ V *vs.* SCE can be observed.

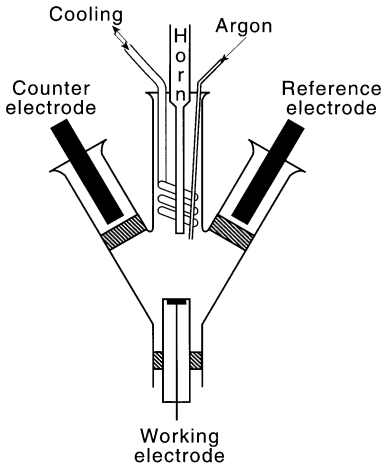



**Fig. 1** Schematic drawing of the thermostatted small volume (20 ml) sonoelectrochemical cell employed for sonovoltammetric and electrolysis experiments

The response is sigmoidally shaped and therefore well behaved even at the very high rates of mass transport applied in the presence of ultrasound. For homogeneous solutions the rate of mass transport[5] is related to the diffusion layer thickness, δ, and the diffusion cofficient, $D$ [eqn. (1)].

$$I_{\text{lim}} = \frac{n F D A C_{\text{total}}}{\delta} \quad (1)$$

In the following we use this equation to quantify the rates of mass transport and for two-phase systems we report 'apparent diffusion coefficients', $D_{\text{app}}$, which have no direct physical significance other than allowing comparison with homogeneous conditions. For the reduction process described here the additional parameters in eqn. (1) are the number of transferred electrons, $n = 2$ (*vide infra*), the Faraday constant, $F$, the electrode area, $A = 7.06 \times 10^{-6}$ m$^2$, the total concentration, $c_{\text{total}}$, and the observed limiting current, $I_{\text{lim}}$. The determined apparent diffusivity for diethylfumarate, $D_{\text{app}} = 0.58 \times 10^{-9}$ m$^2$ s$^{-1}$, is somewhat smaller than the one estimated[6] for the hypothetical case of diethylfumarate dissolved homogeneously in water (Table 1), but is still rather large and sufficient for bulk electrolysis purposes. The physicochemical meaning of the observed magnitude of the limiting currents is more complex and determined either by parameters such as the rate of dissolution, the size of the microdroplets, and the approach distance between microdroplets and the electrode surface or a 'wetting' process.[1] Nevertheless, the magnitude of the $D_{\text{app}}$ values suggests the ability of ultrasound to assist the electrolysis of insoluble materials at efficiencies approaching those that would be accomplished if the substrates were soluble.

For the reduction of diethylfumarate at a glassy carbon electrode the Toměs criterion, $E_{3/4} - E_{1/4} = 80$ mV, suggests an overall fast and in the electrochemical sense almost reversible

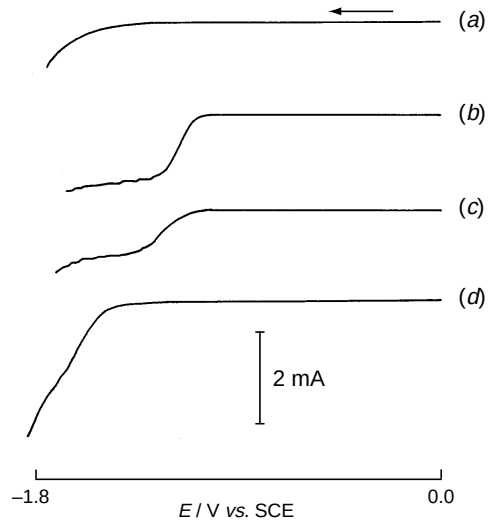



**Fig. 2** Voltammograms obtained for the reduction of 10 μl diethylfumarate (*b*), diethylmaleate (*c*), and cyclohex-2-en-1-one (*d*) emulsified in 20 ml 1.0 M aqueous $MgCl_2$ [(*a*) background] at a 3 mm diameter glassy carbon electrode (25 °C, 150 W cm$^{-2}$, scan rate 0.1 V s$^{-1}$)

**Table 1** Sonovoltammetric data[a] for the reduction of 10 μl insoluble organic compound emulsified in 20 ml aqueous 1.0 M $MgCl_2$ in the presence of 150 W $cm^{-2}$ ultrasound

| Compound | $E_{1/2}$/ V *vs.* SCE | *n* | $10^3$ $c_{total}$/ M | $I_{lim}$/ μA | $10^9$ $D_{sol}$[b]/ $m^2$ $s^{-1}$ | $10^9$ $D_{app}$[c]/ $m^2$ $s^{-1}$ |
|---|---|---|---|---|---|---|
| Diethylfumarate | −1.16 | 2 | 3.0 | 1500 | 0.61 | 0.58 |
| Dimethylmaleate | −1.34 | 2 | 4.0 | 2500 | 0.73 | 0.73 |
| Diethylmaleate | −1.23 | 2 | 3.1 | 1050 | 0.61 | 0.39 |
| Dibutylmaleate | −1.24 | 2 | 2.2 | 180 | 0.50 | 0.09 |
| Diethylacetylene dicarboxylate | −1.28 | 4 | 3.0 | *ca.* 500 | 0.60 | 0.20 |
| Cyclohex-2-en-1-one | −1.58 | 2 | 5.2 | *ca.* 1700 | 0.83 | 0.38 |

[a] Voltammograms obtained at 25 °C, scan rate 0.1 V $s^{-1}$, at a 3 mm diameter glassy carbon disc electrode. $E_{1/2}$ corresponds to the half wave potential for sigmoidal responses. [b] An empirical expression introduced by Wilke and Chang allows the diffusivity, $D_{sol}$, to be estimated to within ± 10% accuracy.[6] [c] The apparent diffusivity $D_{app}$ has been calculated assuming a homogeneous solution based on eqn. (1) and using the approximate diffusion layer thickness δ = 1.6 μm.[5]

electrode process. In the case of diethylmaleate at $E_{1/2}$ = −1.23 V *vs.* SCE also a well defined response can be observed, although now the voltammetric wave is more drawn out ($E_{3/4} - E_{1/4}$ = 100 mV). For comparison, the electrochemical reduction of diethylmaleate dissolved in *N,N*-dimethylformamide described by Bard *et al.*[7] involves the *cis–trans* isomerization of the radical anion formed as a short-lived intermediate in the vicinity of the electrode surface. It was also shown that in *N,N*-dimethylformamide solution the reduction of diethylmaleate occurs at potentials approximately 0.2 V more negative of those for the reduction of the fumarate. In regard of the contrasting voltammetric features in water and in organic media, for the reduction of diethylmaleate in aqueous media an extremely fast rate of the *cis–trans* isomerization possibly due to the solvent polarity may be predicted.

The comparison of the electrochemical reduction of dimethyl-, diethyl-, and dibutyl-maleate emulsions in aqueous 1.0 M $MgCl_2$ demonstrates the effect of the substrate solubility on the cathodic limiting currents (Table 1). The increase in the chain length of the carbon residue significantly alters the magnitude of the apparent diffusivity in agreement with the mechanism generally applied[1] for electrochemical processes in emulsion systems [eqn. (2)–(4)].

$$A_{oil} \rightleftharpoons A_{solution} \quad (2)$$

$$A_{solution} + 2\ e^- + 2\ H^+ \rightarrow B_{solution} \quad (3)$$

$$B_{solution} \rightleftharpoons B_{oil} \quad (4)$$

Under ultrasound condition the oil microdroplets penetrate into the Nernst diffusion layer at the electrode surface and act as a local source of the depolarizer [eqn. (2)]. After the product, $B_{solution}$, has been generated at the electrode surface the reaction step (4) is essential for maintaining an active electrode surface by re-absorbing the product. Depending on the kinetic regime of the process the equilibrium concentration of the depolarizer in the aqueous electrolyte or the rate of dissolution in step (2) govern the limiting current.

In order to analyse the nature of the observed reduction process bulk electrolyses‡ of diethylfumarate, diethylmaleate, and diethylacetylene dicarboxylate emulsified in aqueous 1.0 M $MgCl_2$ were performed. The reduction of emulsions of diethylfumarate and -maleate assisted by additives and special hydrophobic electrodes in the absence of ultrasound has been reported recently[8] by Nonaka and coworkers. Not surprisingly, the scale-up of the sonoelectrochemical process involves a non-simple dependence of the observed limiting current for the reduction reaction on the amount of reactant present. On glassy carbon electrodes a tenfold increase in the amount of organic phase resulted in sonovoltammetric responses with decaying limiting currents characteristic for electrode-blocking processes. However, a clean reduction process at a large surface area gold electrode following a two-electron–two-proton reaction pathway with reduction of the alkenic double bond was observed for diethyl-fumarate and -maleate. Due to the more negative reduction potential diethylacetylene dicarboxylate is reduced directly in a 4e$^-$ process to diethylsuccinate. After passing two- to three-fold excess charge the products were isolated by simple extraction with chloroform and analysed by NMR spectroscopy. Yields of the isolated compounds are typically 50–70% based on the starting material and increase with the amount of charge passed. Side-products due to processes such as hydrodimerization or polymerization have not been observed. The process responsible for the loss of faradaic efficiency appears to be hydrogen evolution.

Although details of the mechanism for sonoelectrochemical redox processes in emulsions remain to be studied, it is clear that the effect of ultrasound, to generate microscopically small droplets whilst ensuring extremely high rates of mass transport, considerably extends and facilitates the possibilities in emulsion electrochemistry.

## Footnotes

* E-mail: compton@ermine.ox.ac.uk

† The ultrasound generator employed was a VCX400 model sonic horn (Sonics and Materials, USA) equipped with a stepped titanium microtip (electrically insulated) of 3 mm diameter emitting 20 kHz sound with a power level set to 150 W $cm^{-2}$ (calorimetrically determined). For electrochemical experiments a thermostatted cell,[5] and a PAR 173 (EG&G) potentiostat controlled by an Oxford Electrodes programmer and connected to a Lloyd P3 plotter were used. Electrodes used were a 3 mm diameter glassy carbon disc (BAS), a graphite rod as a counter, and a saturated calomel reference electrode. Chemical reagents and electrolyte salt (Aldrich) were of highest commercially available quality.

‡ Bulk electrolysis experiments were performed typically with 200 mg substrate in a 20 ml electrolyte volume at a large surface area gold wire electrode and 150 W $cm^{-2}$ ultrasound intensity.

## References

1 H. Feess and H. Wendt, in *Technique of Electroorganic Synthesis*, ed. N. L. Weinberg and B. V. Tilak, Wiley, New York, 1982, Part III, p. 81f.
2 *Electrochemistry in Colloids and Dispersions*, ed. R. A. Mackay and J. Texter, VCH, Weinheim, 1992.
3 D. J. Walton and S. S. Phull, *Adv. Sonochem.*, 1996, **4**, 205.
4 T. J. Mason and J. P. Lorimer, *Sonochemistry: Theory, Applications and Uses of Ultrasound in Chemistry*, Ellis Horwood, Chichester, 1988.
5 H. A. O. Hill, Y. Nakagawa, F. Marken and R. G. Compton, *J. Phys. Chem.*, 1996, **100**, 17395.
6 C. R. Wilke, P. Chang, *AIChE J.*, 1955, 264.
7 A. J. Bard, V. J. Puglisi, J. V. Kenkel and A. Lomax, *Faraday Discuss.*, 1973, **56**, 353.
8 Y. Kunugi, P.-C. Chen, T. Nonaka, Y.-B. Chong and N. Watanabe, *J. Electrochem. Soc.*, 1993, **140**, 2833.

*Received in Exeter, UK, 5th March 1997; Com. 7/01642E*

# Trimanganese complexes with a linear $Mn^{II}Mn^{III}Mn^{II}$ assemblage bridged by carbohydrates

**Shigenobu Yano,*[a] Mayumi Doi,[a] Saori Tamakoshi,[a] Wasuke Mori,[b] Masahiro Mikuriya,[c] Akio Ichimura,[d] Isamu Kinoshita,[d] Yasuhiro Yamamoto[e] and Tomoaki Tanase*[a]**

[a] *Department of Chemistry, Faculty of Science, Nara Women's University, Nara-shi, Nara 630, Japan*
[b] *Department of Chemistry, Faculty of Science, Osaka University, Toyonaka-shi, Osaka 560, Japan*
[c] *Department of Chemistry, School of Science, Kwansei Gakuin University, Nishinomiya-shi, Hyougo 514, Japan*
[d] *Department of Chemistry, Faculty of Science, Osaka City University, Sumiyoshi-ku, Osaka 662, Japan*
[e] *Department of Chemistry, Faculty of Science, Toho University, Miyama, Funabashi, Chiba 274, Japan*

**Reaction of manganese(II) salts ($MnX_2 \cdot nH_2O$, X = Cl, Br, $NO_3$) with tris[(*N*-aldosyl)aminoethyl]amines $L^n$, prepared by the reaction between tris(aminoethyl)amine (tren) with aldose [D-mannose (D-man) ($L^1$)] or L-rhamnose [L-rha = 6-deoxy-L-man) ($L^2$)] *in situ*, affords red–orange crystals formulated as $[(MnL^n)_2Mn(H_2O)]X_3$ (*n* = 2, X = Cl 1; *n* = 2, X = Br 2; *n* = 2, X = $NO_3$ 3; *n* = 1, X = Cl 4), complexes 3 and 4 are characterized by X-ray crystallography.**

Carbohydrates are indispensable building blocks and energy sources to living organisms and play important roles in many biological functions.[1] Interactions of carbohydrates with metal ions have become a significant subject in the bioinorganic field, since many sugar-metabolizing enzymes have been revealed to function with metal ions such as $Mg^{2+}$, $Mn^{2+}$, $Co^{2+}$, and $Zn^{2+}$ in the active sites.[2–6] Xylose isomerases, which promote the aldose–ketose isomerization, involves carboxylate-bridged dinuclear $Mg^{2+}$, $Mn^{2+}$ and $Co^{2+}$ ions in the active site with a *ca*. 4.9 Å metal–metal separation.[4] The similar dinuclear centre of $Mg^{2+}$ or $Mn^{2+}$ with a *ca*. 3.7 Å separation also promotes the cleavage of phosphate esters in fructose 1,6-bisphosphatase.[5] We have studied the chemistry of transition-metal complexes with carbohydrates utilizing *N*-glycosidic bond formation,[7] and wish to report herein the synthesis and characterization of novel trimanganese complexes with a linear $Mn^{II}Mn^{III}Mn^{II}$ core bridged by carbohydrates.

The potentially heptadentate *N*-glycoside ligands, tris[(*N*-aldosyl)aminoethyl]amine $L^n$, prepared by the reaction between tris(aminoethyl)amine (tren) with aldose [D-mannose (D-man) ($L^1$) or L-rhamnose (L-rha = 6-deoxy-L-man) ($L^2$)] *in situ*, were treated with manganese(II) salts ($MnX_2 \cdot nH_2O$; X = Cl, Br, $NO_3$) in methanol. The work-up of the resultant solutions afforded red–orange crystals formulated as $[(MnL^n)_2Mn(H_2O)]X_3 \cdot nH_2O$ in 10–42% yield (**1**·$11H_2O$: *n* = 2, X = Cl; **2**·$10H_2O$: *n* = 2, X = Br; **3**·$8H_2O$: *n* = 2, X = $NO_3$; **4**·$2H_2O$: *n* = 1, X = Cl).† These trimanganese–sugar complexes were assumed to have an almost identical structure to each other on the basis of electronic absorption and circular dichroism spectra[8] and magnetic susceptibilities, $\mu_{eff}$ = 15.1–16.0 $\mu_B$ per $Mn_3$ unit (23 °C, solid state).‡

The structures of **3** and **4** were determined by X-ray crystallography to comprise a linearly ordered trimanganese core bridged by two carbohydrate residues with a Mn···Mn separation of 3.845(2) Å (**3**) and 3.911(5) (av.) Å (**4**) and a Mn–Mn–Mn angle of 180.0° (**3**) and 171.0(1)° (**4**), Fig. 1. The terminal Mn atoms are seven-coordinate with a distorted monoface-capped octahedral geometry ligated by $L^n$ through three oxygen atoms of C-2 hydroxy groups, three *N*-glycosidic nitrogen atoms, and a tertiary amino nitrogen atom, as observed in $[CoL^2]SO_4$ **6**.[7i] The $C_3$ helical configurations and the NO chelate conformations are denoted as Δ-*lel*($\lambda_3$) and Λ-*lel*($\delta_3$), respectively, for **3** and **4**.[7i] The central Mn atoms are five-coordinate ligated by four oxygen atoms of carbohydrate residues in the $L^n$ ligands and one water molecule, resulting in a square-pyramidal geometry. On the basis of the bond lengths, the oxidation states of the terminal and central manganese atoms are assumed to be $Mn^{II}$ and $Mn^{III}$, respectively. This formulation of Mn oxidation states is also consistent with the relatively nitrogen-rich coordination sphere on the terminal Mn atoms. The C-2 and C-3 hydroxy groups of the bridging sugar moieties are also estimated to be deprotonated from the short bond lengths to the central Mn atom (1.88–1.96 Å). Alternatively, the complex cations can be viewed as two seven-coordinate manganese(II) complexes, $[MnL^n]^{2+}$, trapping a $Mn^{III}$ ion through a sugar tentacle. To our knowledge, the present trimanganese complex is the first example of $Mn^{II}$-$Mn^{III}Mn^{II}$ linear assemblage, whereas many $Mn^{II}{}_3$[8] and $Mn^{III}$-$Mn^{II}Mn^{III}$[9] compounds have already been reported.

The structurally characterized examples of dimetal complexes with bridging carbohydrates are extremely rare. Only two structures have been reported, namely, $[Mo_2O_5$(D-lyx)] **7**[10] (lyx = lyxose) and $[Mn_2\{N,N'$-(D-man)$_2$-$N,N'$-$Me_2$en$\}\{N$-(D-man)-$N,N'$-$Me_2$en$\}(MeOH)]Cl_2$ **8**,[7a] both of which involve a

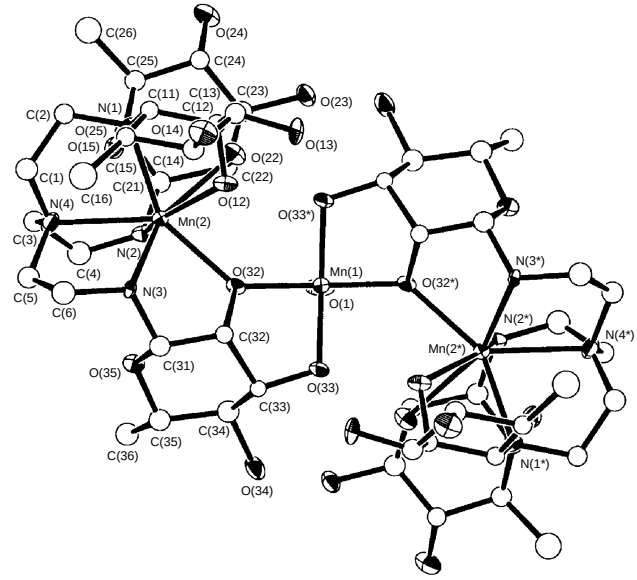



**Fig. 1** ORTEP diagram of the complex cation of $[(MnL^2)_2Mn(H_2O)]^{3+}$, viewed down vertical to the central square plane. Selected bond lengths (Å) and angles (°): Mn(1)–O(1) 2.16(1), Mn(1)–O(32) 1.891(7), Mn(1)–O(33) 1.921(8), Mn(2)–O(12) 2.299(9), Mn(2)–O(22) 2.579(9), Mn(2)–O(32) 2.250(8), Mn(2)–N(1) 2.25(1), Mn(2)–N(2) 2.24(1), Mn(2)–N(3) 2.23(1), Mn(2)–N(4) 2.43(1) Å; Mn(1)–O(32)–Mn(2) 136.3(4).

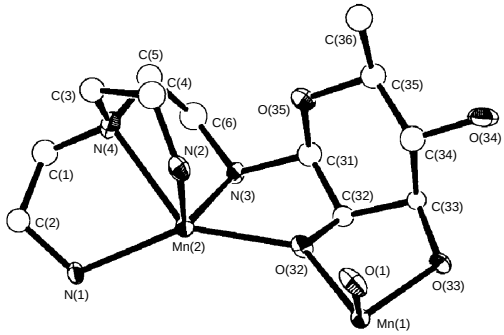



**Fig. 2** A perspective drawing of the sugar bridging part in **3**

β-furanose bridging system. In complexes **3** and **4**, a β-mannopyranosyl skeletal unit with a chair conformation bridges the two manganese ions with the C-2 μ-alkoxo group joining two metal ions and the C-1 *N*-glycosidic amino and the C-3 alkoxo groups coordinating to each metal centre (Fig. 2). These structural features could lead to a new general equatorial–axial–equatorial bridging system of sugars and suggested stronger affinity of the mannose-type aldoses, having 2,3-*cis* configuration, to dimetal centres than that of the glucose type aldoses which possess a 2,3-*trans* configuration.

The present study reports the unprecedented mixed-valence trimanganese(II,III,II) complexes with *N*-glycoside ligands, which could provide useful insight into the interaction of carbohydrates with dimetal ions and interesting physical properties in the multinuclear manganese chemistry.

We are grateful to Professor Kotaro Osakada of Tokyo Institute of Technology. This work was partially supported by a Grant-in-Aid for Scientific Research from the Ministry of Education of Japan and Grants from Iwatani, Nippon Itagarasu, Mitsubishi-Yuka, and Nagase Foundations, and the San-Ei Gen Foundation for Food Chemical Research.

## Footnotes

* E-mail: tanase@cc.nara-wu.ac.jp

† Detailed synthetic procedures and analytical, spectral, and magnetic data for **1**–**4** are available on request from the authors.

‡ The preliminary temperature dependent magnetic data showed a very weak antiferromagnetic interaction between the central and terminal metal centres, which could be tentatively ascribable to the relatively long metal–metal distances and the square-pyramidal geometry of the central metal ions (see X-ray structures). The detailed results will be reported in our subsequent full report. The crystals of **4** are very unstable in air and hygroscopic, and a crystal was sealed into a glass-tube capillary with a small amount of mother-liquor at low temperature. This sampling procedure may lead to the low quality of the X-ray structure.

§ *Crystal data*: for **3**·5$H_2O$: orthorhombic, space group $C222_1$ (no. 20), $a$ = 12.925(5), $b$ = 21.255(7), $c$ = 26.871(7) Å, $U$ = 7382 Å$^3$, $Z$ = 4, $D_c$ = 1.461 g cm$^{-3}$, $T$ = −147 °C, $R$ = 0.074, $R_w$ = 0.074 [$w = 1/\sigma^2(F_o)$] for 2319 refs. with $I > 3\sigma(I)$.

**4**·6$H_2O$: trigonal, space group $P3_1$ (no. 144), $a$ = 12.712(8), $c$ = 41.053(9) Å, $U$ = 5744 Å$^3$, $Z$ = 3, $D_c$ = 1.438 g cm$^{-3}$, $T$ = −147 °C, $R$ = 0.083, $R_2$ = 0.091 [$w = 1/\sigma^2(F_o)$] for 3108 refs. with $I > 3\sigma(I)$. The structures were solved and refined with teXsan program package.

Atomic coordinates, bond lengths and angles, and thermal parameters have been deposited at the Cambridge Crystallographic Data Centre (CCDC). See Information for Authors, Issue No. 1. Any request to the CCDC for this material should quote the full literature citation and the reference number 182/431.

¶ An ORTEP plot of the complex cation of **4** is available on request from the authors.

## References

1 J. F. Kennedy and C. A. White, *Bioactive Carbohydrates in Chemistry, Biochemistry and Biology*, Wiley, New York, 1983.
2 R. W. Gracy and E. A. Noltmann, *J. Biol. Chem.*, 1968, **243**, 4109; R. W. Gracy and E. A. Noltmann, *J. Biol. Chem.*, 1968, **243**, 5410.
3 R. L. Root, J. R. Durrwachter and C.-H. Wong, *J. Am. Chem. Soc.*, 1985, **107**, 2997.
4 J. Jenkins, J. Janin, F. Rey, M. Chiadmi, H. Tilbeurgh, I. Lasters, M. D. Maeyer, D. V. Belle, S. J. Wodak, M. Lauwereys, P. Stanssens, N. T. Mrabet, J. Snauwaert, G. Matthyssens and A.-M. Lambeir, *Biochemistry*, 1992, **31**, 5449; M. Whitlow, A. J. Howard, B. C. Finzel, T. L. Poulos, E. Winborne and G. L. Gilliland, *Proteins*, 1991, **9**, 153.
5 Y. Zhang, J.-Y. Liang, S. Huang, H. Ke and W. N. Lipscomb, *Biochemistry*, 1993, **32**, 17; Y. Xue, S. Huang, J.-Y. Liang, Y. Zhang and W. N. Lipscomb, *Proc. Natl. Acad. Sci. USA*, 1994, **91**, 12482.
6 K. D. Hardman, R. C. Agarwal and M. Freiser, *J. Mol. Biol.*, 1982, **157**, 69.
7 (*a*) S. Yano, *Coord. Chem. Rev.*, 1988, **92**, 113 and references therein; (*b*) S. Yano and M. Ohtsuka, *Metal Ions in Biological Systems*, ed. H. Sigel and A. Sigel, Marcel Dekker, New York, 1995, vol. 32, p. 27; (*c*) K. Ishida, S. Nonoyama, T. Hirano, S. Yano, M. Hidai and S. Yoshikawa, *J. Am. Chem. Soc.*, 1989, **111**, 1599; (*d*) K. Ishida, M. Yashiro, S. Yano, M. Hidai and S. Yoshikawa, *J. Chem. Soc., Dalton Trans.*, 1989, 1241; (*e*) T. Takei, T. Tanase, S. Yano and M. Hidai, *Chem. Lett.*, 1991, 1629; (*f*) T. Tanase, T. Takei, M. Hidai and S. Yano, *J. Chem. Res.*, 1992, (*S*) 252, (*M*) 1922; (*g*) T. Tanase, R. Nouchi, Y. Oka, M. Kato, N. Nakamura, T. Yamamura, Y. Yamamoto and S. Yano, *J. Chem. Soc., Dalton Trans.*, 1993, 2645; (*h*) S. Yano, M. Kato, H. Shioi, T. Takahashi, T. Tsubomura, K. Toriumi, T. Ito, M. Hidai and S. Yoshikawa, *J. Chem. Soc., Dalton Trans.*, 1993, 1699; (*i*) T. Tanase, M. Nakagoshi, A. Teratani, M. Kato, Y. Yamamoto and S. Yano, *Inorg. Chem.*, 1994, **33**, 6.
8 R. L. Rardin, P. Poganiuch, A. Bino, D. P. Goldberg, W. B. Tolman, S. Liu and S. J. Lippard, *J. Am. Chem. Soc.*, 1992, **114**, 5240; M. J. Baldwin, J. W. Kampf and V. L. Pecoraro, *J. Chem. Soc., Chem. Commun.*, 1993, 1741.
9 D. P. Kessissoglou, M. L. Kirk, M. S. Lah, X. Li, C. Raptopoulou, W. E. Hatfield and V. L. Pecoraro, *Inorg. Chem.*, 1992, **31**, 5424.
10 G. E. Taylor and J. M. Waters, *Tetrahedron Lett.*, 1981, **22**, 1277.

*Received in Cambridge, UK, 20th February 1997; Com. 7/01198I*

# Stable mixed phenanthroline copper(I) complexes. Key building blocks for supramolecular coordination chemistry†

**Michael Schmittel* and Andrea Ganz**

*Institut für Organische Chemie der Universität Würzburg, Am Hubland, D-97074 Würzburg, Germany*

**A simple procedure is presented that is used to synthesise, for the first time, pure mixed phenanthroline copper(I) complexes that do not exchange ligands.**

Our current interest in the coordination chemistry of phenanthroline ligands[1–7] stems from their fascinating potential to allow for the construction of the novel redox-active structures **A** as well as nanotubes **B** (Scheme 1) through the simple self-assembly of (*i*) $Cu^{I}$ as coordinating metal ion with a tetrahedral geometry, (*ii*) a macrocyclic bisphenanthroline with *exo*-coordination sites, and (*iii*) either a macrocyclic bisphenanthroline with *endo*-coordination sites (for **A**) or linear 3,8-linked oligophenanthrolines (for **B**).

As a prerequisite for the successful construction of such novel topologies a strategy is needed for the defined synthesis of mixed phenanthroline copper(I) complexes according to eqn. (1) while avoiding the formation of the two symmetrical complexes, eqn. (2).

$$L^1 + L^2 + Cu^+ \rightarrow [CuL^1L^2]^+ \quad (1)$$

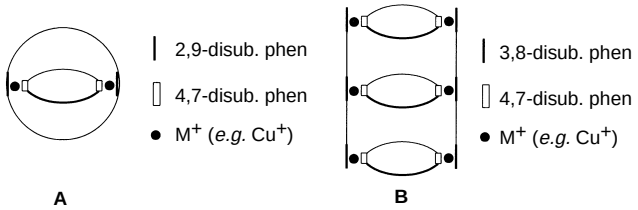
$$2\ L^1 + 2\ L^2 + Cu^+ \rightarrow [CuL^1{}_2]^+ + [CuL^2{}_2]^+ \quad (2)$$

Remarkably, there is no report so far on the clean formation of mixed-phenanthroline copper(I) species[8] except for oligomeric phenanthroline complexes[9] and in cases where the geometrical constraints of a phenanthroline with *endo*-coordination sites embedded in a cyclic ring system prevent formation of symmetrical complexes[3,10] according to eqn. (2).

Herein, we report, for the first time, on a general strategy to synthesise mixed phenanthroline copper(I) complexes using acyclic ligands and its use for the preparation of a model complex of **A** demonstrating the feasibility of our approach.

The synthesis of phenanthrolines **1**–**4** is straightforward,[11–14] or is described elsewhere.[15] As expected, the symmetrical copper(I) complexes $[Cu(\mathbf{1a})_2]BF_4$ and $[Cu(\mathbf{2a})_2]BF_4$ formed quantitatively within seconds by mixing 2 equiv. of the ligands with $[Cu(MeCN)_4]BF_4$ in MeCN.[16]

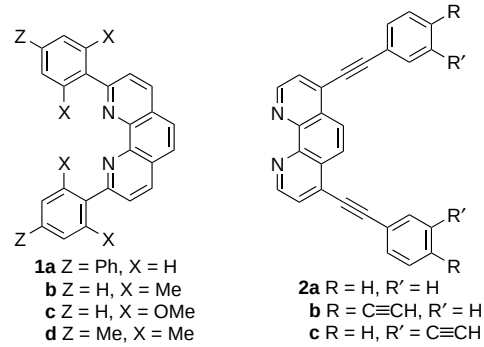
In order to synthesise mixed complexes of type $[CuL^1L^2]^+$ several mechanistic investigations using low-temperature NMR techniques on the influence of solvent, temperature and sequence of addition of the phenanthroline ligand were undertaken. The results proposed that the preparation of the mixed-ligand complex could possibly be achieved by adding 1 equiv. of the 4,7-disubstituted **2a** to $[Cu(MeCN)_4]^+$ followed by addition of **1a** at low temperature in dichloromethane as solvent.




**Scheme 1** Schematic representation of the ball-type structure **A** and nanotube **B** as examples of interesting topologies resulting from mixed phenanthroline copper(I) complexes with tetrahedral coordination

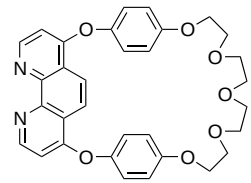
Indeed, after mixing 1 equiv. of **2a** with $[Cu(MeCN)_4]^+$ at −80 °C in $CD_2Cl_2$ and adding 1 equiv. of **1a** complex $[Cu(\mathbf{1a})(\mathbf{2a})]^+$ formed almost quantitatively. However, upon raising the temperature ($T > -50$ °C) increased formation of $[Cu(\mathbf{1a})_2]^+$ was observed. Mixing $[Cu(\mathbf{2a})_2]^+$ with 2 equiv. of ligand **1a** led to formation of the mixed complex $[Cu(\mathbf{1a})(\mathbf{2a})]^+$ besides the symmetrical complex $[Cu(\mathbf{1a})_2]^+$ in a ratio of 1 : 2 remaining constant at −20 °C over several days. Apparently, the thermodynamics of the copper(I) complex equilibria follows qualitatively the course depicted in Fig. 1, but isolation of $[Cu(\mathbf{1a})(\mathbf{2a})]^+$ is precluded because of the rather low barrier for $[Cu(\mathbf{1a})(\mathbf{2a})]^+ \rightarrow [Cu(\mathbf{1a})_2]^+$.

From the above results the use of 2,9-disubstituted phenanthrolines **1b**–**d** is proposed the steric congestion of which through larger groups (X = Me, OMe) precludes formation of symmetrical complexes $[Cu(\mathbf{1})_2]^+$. Indeed, when we reacted $[Cu(MeCN)_4]^+$ with 2 equiv. of sterically encumbered 2,9-disubstituted phenanthrolines **1b**–**d**, formation of $[Cu(\mathbf{1b}–\mathbf{d})_2]^+$ was not observed! Now the reaction of $[Cu(MeCN)_4]^+$ with 1 equiv. of each, **1b**–**d** and **2a**–**c**, resulted in the almost

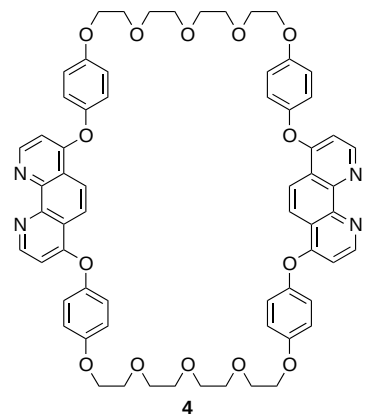



**1a** Z = Ph, X = H
**b** Z = H, X = Me
**c** Z = H, X = OMe
**d** Z = Me, X = Me

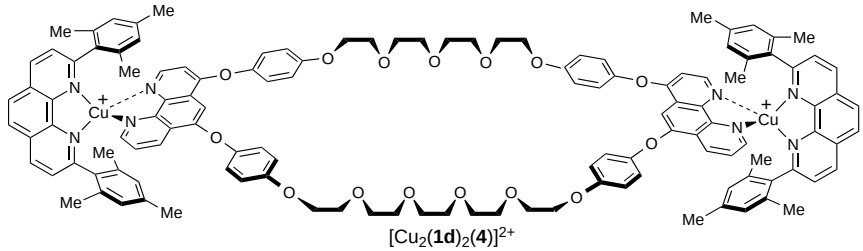
**2a** R = H, R′ = H
**b** R = C≡CH, R′ = H
**c** R = H, R′ = C≡CH



**3**



**4**



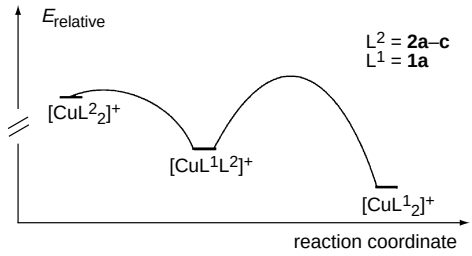




**Fig. 1** Energy diagram for the complexation equilibria of $[CuL^1L^2]^+$ complexes in solution

**Table 1** Half-wave potentials $E_{1/2}$ (V *vs.* Fc–Fc$^+$)‡ of mixed-ligand copper(I) complexes determined by cyclic voltammetry in dichloromethane at $v$ = 100 mV s$^{-1}$ (electrolyte: $NBu^n_4PF_6$) and yields after purification

| Copper(I) complex | Yield (%) | $E_{1/2}$ | $\Delta E_p$/mV |
|---|---|---|---|
| $[Cu(\mathbf{1a})_2]BF_4$ | 95 | +0.40 | 70 |
| $[Cu(\mathbf{2a})_2]BF_4$ | 83 | −0.05 | 150[a] |
| $[Cu(\mathbf{1b})(\mathbf{2a})]BF_4$ | 86 | +0.36 | 60 |
| $[Cu(\mathbf{1c})(\mathbf{2a})]BF_4$ | 97 | +0.04 | 70 |
| $[Cu(\mathbf{1d})(\mathbf{2a})]BF_4$ | 86 | +0.30 | 70 |
| $[Cu(\mathbf{1d})(\mathbf{3})]BF_4$ | 81 | +0.21 | 130[a] |
| $[Cu_2(\mathbf{1d})_2(\mathbf{4})][BF_4]_2$ | 92 | +0.20 | 220[a] |

[a] Large peak broadening because of slow heterogeneous electron transfer.

quantitative formation of the unsymmetrical complexes $[Cu(\mathbf{1b–d})(\mathbf{2a–c})]^+$ that could easily be isolated at room temperature. All compounds were characterised by NMR, elemental analysis and/or ESI mass spectra.

Cyclic voltammetry investigations on the novel mixed complexes revealed fully or quasi-reversible waves for $Cu^I \rightleftharpoons Cu^{II}$ indicating that the complexes remain intact despite the redox process.

The mixed-complex preparation technique was then used for the first time with macrocyclic phenanthroline ligands with *exo*-coordination sites in order to probe our concept for the preparation of precursors to the novel supramolecular systems **A** and **B**. Reaction of $[Cu(MeCN)_4]^+$ with 1 equiv. of **3** and **1c** or **1d** each provided $[Cu(\mathbf{1c})(\mathbf{3})]^+$ and $[Cu(\mathbf{1d})(\mathbf{3})]^+$, whereas with 1 equiv. of **4** and 2 equiv. of **1d** the complex $[Cu_2(\mathbf{1d})_2(\mathbf{4})]^{2+}$ was furnished.

Upon addition of phenanthroline **2a** to $[Cu(\mathbf{1d})(\mathbf{3})]^+$ the immediate formation of a mixture of $[Cu(\mathbf{1d})(\mathbf{2a})]^+$ and unreacted $[Cu(\mathbf{1d})(\mathbf{3})]^+$ was observed (ratio: 1 : 1). At the same time the $^1$H NMR peaks were broadened indicating a dynamic process on the NMR timescale. Conversely, addition of phenanthroline **1d** to the complex $[Cu(\mathbf{1c})(\mathbf{3})]^+$ also led to a mixture of $[Cu(\mathbf{1d})(\mathbf{3})]^+$ and unreacted $[Cu(\mathbf{1c})(\mathbf{3})]^+$ in a ratio of 1 : 3 that remained constant over several days at room temperature.

To accommodate this observation we have to assume that the mixed complexes $[Cu(\mathbf{1})(\mathbf{3})]^+$ are always in a rapid dissociation–association equilibrium with a small amount of $[Cu(\mathbf{1})]^+$ + **3** as well as $[Cu(\mathbf{3})]^+$ + **1** present. Using sterically hindered 2,9-disubstituted phenanthrolines with X = Me or OMe, however, we have prevented the formation of $[Cu(\mathbf{1b–d})_2]^+$ and forced the system to form the mixed-ligand complexes solely. As a consequence of such controlled ligand exchange processes the straightforward self-assembly of structures **A** and **B** should now be possible.

Financial support from the DFG and the Fonds der Chemischen Industrie is gratefully acknowledged. We are grateful to Professor Dr U. Lüning (Kiel) for the generous gift of phenanthrolines **1b**, **c** and to Dr M. Hederich and Professor Dr P. Schreier (Würzburg) for recording the ESIMS spectra.

## Footnotes

* E-mail: mjls@chemie.uni-wuerzburg.de

† New building blocks for sensors and supramolecular arrays, Part 4; for Part 3 see ref. 7(*a*).

‡ All potentials are referred to the ferrocene–ferrocenium redox couple. By addition of +0.39 V the values *vs.* SCE can be obtained.

## References

1 *Frontiers in Supramolecular Organic Chemistry and Photochemistry*, ed. H.-J. Schneider and H. Dürr, VCH, Weinheim, 1991; B. Dietrich, P. Viout and J.-M. Lehn, *Macrocyclic Chemistry*, VCH, Weinheim, 1993.
2 E. C. Constable, *Prog. Inorg. Chem.*, 1994, **42**, 67; D. S. Lawrence, T. Jiang and M. Levett, *Chem. Rev.*, 1995, **95**, 2229.
3 (*a*) C. O. Dietrich-Buchecker and J.-P. Sauvage, *Chem. Rev.*, 1987, **87**, 795; (*b*) J.-P. Sauvage, *Acc. Chem. Res.*, 1990, **23**, 319.
4 B. Hasenkopf, J.-M. Lehn, B. O. Kneisel, G. Baum and D. Fenske, *Angew. Chem., Int. Ed. Engl.*, 1996, **35**, 1838.
5 I. Lüer, K. Rissanen and F. Vögtle, *Chem. Ber.*, 1992, **125**, 1873.
6 O. Kocian, R. J. Mortimer and P. D. Beer, *J. Chem. Soc., Perkin Trans. 1*, 1990, 3203; E. C. Constable, *Angew. Chem., Int. Ed. Engl.*, 1991, **30**, 1450; F. Vögtle, I. Lüer, V. Balzani and N. Armaroli, *Angew. Chem., Int. Ed. Engl.*, 1991, **30**, 1333; P. D. Beer, O. Kocian, R. J. Mortimer and C. Ridgway, *J. Chem. Soc., Dalton Trans.*, 1993, 2629; P. Belser, A. von Zelewsky, M. Frank, C. Seel, F. Vögtle, L. De Cola, F. Barigelletti and V. Balzani, *J. Am. Chem. Soc.*, 1993, **115**, 4076; L. J. Charbonniere, G. Bernardinelli, C. Piguet, A. M. Sargeson and A. F. Williams, *J. Chem. Soc., Chem. Commun.*, 1994, 1419.
7 (*a*) M. Schmittel, H. Ammon and C. Wöhrle, *Chem. Ber.*, 1995, **128**, 845; (*b*) M. Schmittel and H. Ammon, *J. Chem. Soc., Chem. Commun.*, 1995, 687.
8 R. Colton, B. D. James, I. D. Potter and J. C. Traeger, *Inorg. Chem.*, 1993, **32**, 2626; Y. Lei and F. C. Anson, *Inorg. Chem.*, 1995, **34**, 1083.
9 U. Velten and M. Rehahn, *Chem. Commun.*, 1996, 2639.
10 S. S. Zhu, P. J. Caroll and T. M. Swager, *J. Am. Chem. Soc.*, 1996, **118**, 8713.
11 U. Lüning and M. Müller, *Chem. Ber.*, 1990, **123**, 643.
12 M. Sjögren, S. Hanson, P. Norrby, B. Akermark, M. Cucciolito and A. Vitagliano, *Organometallics*, 1992, **11**, 3954.
13 R. Ziessel, J. Suffert and M.-T. Youinou, *J. Org. Chem.*, 1996, **61**, 6535.
14 F. H. Case, *J. Org. Chem.*, 1951, **16**, 941.
15 M. Schmittel and A. Ganz, *Synlett*, 1997, in press.
16 M. A. Masood and P. S. Zacharias, *J. Chem. Soc., Dalton Trans.*, 1991, 111.

*Received in Cambridge, UK, 4th March 1997; Com. 7/01509G*

# Reaction of $R_3PI_2$ (R = Ph, $Pr^i$, $Pr^n$); structural characterisation of the novel 'subvalent' indium(II) complex $In_2I_4(PPr^n_3)_2$ which contains an In–In bond, the four- and five-coordinate indium(III) complex $InI_3(PPh_3)_2{\cdot}InI_3(PPh_3)$, and the tetrahedral indium(III) complex $InI_3(PPr^i_3)$

**Stephen M. Godfrey, Katharine J. Kelly, Peter Kramkowski, Charles A. McAuliffe and Robin G. Pritchard**

*Department of Chemistry, University of Manchester Institute of Science and Technology, Manchester, UK M60 1QD*

**Reaction of $R_3PI_2$ (R = Ph, $Pr^n$, $Pr^i$) with indium metal powder produces a variety of novel indium metal complexes: where R = Ph, the four- and five-coordinate metal(III) complex $InI_3(PPh_3)_2{\cdot}InI_3(PPh_3)$ results; where R = $Pr^n$, the 'subvalent' indium(II) complex $In_2I_4(PPr^n_3)_2$ is formed, the first example of an indium tertiary phosphine complex containing an indium–indium bond; whereas for R = $Pr^i$, the monomeric tetrahedral indium(III) complex $InI_3(PPr^i_3)$ results; these complexes illustrate the subtle effect of the organic substituents on the phosphorus atom for the reaction of $R_3PI_2$ with indium metal powder and the novel indium complexes which are available.**

Virtually nothing was known about the coordination chemistry of indium with tertiary phosphines until the pioneering work of Carty and Tuck,[1–4] who produced tetrahedral $InX_3(PR_3)$, trigonal-bipyramidal $InX_3(PR_3)_2$, and the molecular octahedral species $InX_3(PR_3)_3$, although for this last stoichiometry it was found that one mole of tertiary phosphine was easily removed by the application of a vacuum. No complex of stoichiometry $InX_3(PR_3)$ containing a tertiary phosphine ligand has been crystallographically characterised, but the analogous complexes $InI_3(PHR_2)$ (R = Ph, $Bu^t$) containing secondary phosphines have recently been structurally characterised.[5] The trigonal-bipyramidal molecules $InX_3(PR_3)_2$ have received a little more attention: the first structurally characterised complex of this stoichiometry, $InCl_3(PPh_3)_2$, was reported in 1969,[6] and has the expected trigonal-bipyramidal geometry exhibiting very long axial indium–phosphorus bonds, 2.71(1) Å. The trimethylphosphine derivative $InCl_3(PMe_3)_2$ has been structurally characterised[7] as have $InBr_3(PPhMe_2)_2$ and $InI_3(PPh_2Me)_2$;[8] all these complexes exhibit regular trigonal-bipyramidal geometry.

We are engaged in a study of the oxidising power of a variety of $R_3EX_2$ compounds (E = P, As, Sb; $X_2$ = $Br_2$, $I_2$, IBr) with unactivated metal powders in diethyl ether solution. The strong oxidising power of some of these reagents, *e.g.* $Me_3EI_2$ (E = P, As), is illustrated by their ability to oxidise crude nickel, cobalt[9–14] and even gold[15] metal powders directly to the tripositive oxidation state in a simple one-step reaction.

We have now turned out attention to the reaction of these agents with indium metal powder, principally for three reasons: firstly, little is known concerning the coordination chemistry of indium halides with tertiary phosphine donor ligands; secondly, as we have already seen, novel complexes unobtainable from established synthetic techniques are available from our synthetic route, so there is the possibility of synthesising previously unavailable indium halide tertiary phosphine complexes; if such compounds are available they may have applications in the microelectronics industry as precursors for MOCVD. Finally, indium chemistry has been hampered by the difficulty of synthetic entries, *i.e.* the relatively low activity of the metal and the insolubility of InX and of $InX_3$, and so the approach taken by us represents a significant advance.

$Ph_3PI_2$ reacts with indium metal powder in a 3:2 stoichiometric ratio, eqn. (1).

$$3Ph_3PI_2 + 2In \xrightarrow[N_2,\ \text{room temp.}]{ca.\ 7\text{d},\ Et_2O} \underset{\mathbf{1}}{InI_3(PPh_3)_2{\cdot}InI_3(PPh_3)} \quad (1)$$

Recrystallisation of the pale yellow powder from diethyl ether produced yellow crystals, one of which was selected for analysis by single-crystal X-ray diffraction. The structure of the indium(III) complex was revealed to be $InI_3(PPh_3)_2{\cdot}InI_3(PPh_3)$, **1**. Surprisingly, the structure contains both tetrahedral and trigonal-bipyramidal indium(III) centres within the unit cell. No complex of indium(III) of this stoichiometry has previously been identified.

$Pr^n_3PI_2$ reacts with indium metal powder according to eqn. (2).

$$2Pr^n_3PI_2 + 2In \xrightarrow[N_2,\ \text{room temp.}]{ca.\ 2\text{d},\ Et_2O} \underset{\mathbf{2}}{[InI_2(PPr^n_3)]_2} \quad (2)$$

Recrystallisation of the white powder from diethyl ether solution at 60 °C and subsequent cooling to room temp. produced a large quantity of colourless crystals, from which one was selected for analysis by single-crystal X-ray diffraction,† revealing the dinuclear indium(II) complex $[InI_2(PPr^n_3)]_2$, **2**‡ Fig. 1. This is an unusual result, since we had anticipated a monomeric tetrahedral or a trigonal-bipyramidal indium(III) complex, in agreement with all previous studies of the conventional reaction of indium(III) halides with tertiary phosphines; **2** therefore represents a new, previously unconsidered, indium(II) halide complex containing tertiary phosphine ligands, and the first example of such a complex containing an indium–indium bond; *d*(In–In) in **2** is 2.745(3) Å. Our new synthesis may offer a route to 'subvalent' group 13 metal complexes. Although there are no examples of tertiary phosphine complexes containing an indium–indium bond, the organometallic species $In_2[CH(SiMe_3)_2]_4$ has been characterised by Uhl *et al.*[16] and $In_2IBr_3(C_6H_{16}N_2)_2$ by Tuck and coworkers.[17] The In–In bond distances for these complexes are 2.828(5) and 2.775(2) Å, respectively; both complexes were prepared from the conventional reaction of an indium(II) halide with the appropriate ligand(s).

$Pr^i_3PI_2$ reacts with indium metal powder according to eqn. (3).

$$3Pr^i_3PI_2 + 2In \xrightarrow[N_2,\ \text{room temp.}]{ca.\ 7\text{d},\ Et_2O} \underset{\mathbf{3}}{2InI_3(PPr^i_3)} \quad (3)$$

Recrystallisation of the white powder from diethyl ether produced colourless crystals. One of these was selected for

analysis by single-crystal X-ray diffraction.† The structure of **3**,§ Fig. 2, was revealed to be the tetrahedral monomeric $InI_3(PPr^i_3)$. Although the existence of complexes of this stoichiometry has previously been postulated by Carty and Tuck,[4] this complex nevertheless represents the first indium(III) complex of this stoichiometry containing a tertiary phosphine ligand to be crystallographically characterised. The indium–iodine distances are 2.689(3), 2.701(3) and 2.705(3) Å and the indium–phosphorus distance is 2.569(7) Å.

In conclusion, these new results clearly indicate that subtle changes in the nature of our oxidising agents result in the production of different complexes of indium in different oxidation states, *viz*. reaction of $Ph_3PI_2$ with indium metal powder produces the indium(III) complex $InI_3(PPh_3)_2{\cdot}InI_3(PPh_3)$, containing the indium(III) centres in trigonal-bipyramidal and tetrahedral geometry, and the reaction of $Pr^n_3PI_2$ with indium metal powder produces the unique indium(II) tertiary phosphine complex, $In_2I_4(PPr^n_3)_2$, which contains an indium–indium bond. On the other hand, the reaction of $Pr^i_3PI_2$ with indium metal powder produces the monomeric tetrahedral indium(III) complex $InI_3(PPr^i_3)$. The compound $In_2I_4(PPr^n_3)_2$ represents the first example of a dimeric complex containing tertiary phosphine donor ligands, and since a complex of this type has never previously been observed, its synthesis may be attributed to our synthetic method and it may not be available from conventional techniques.

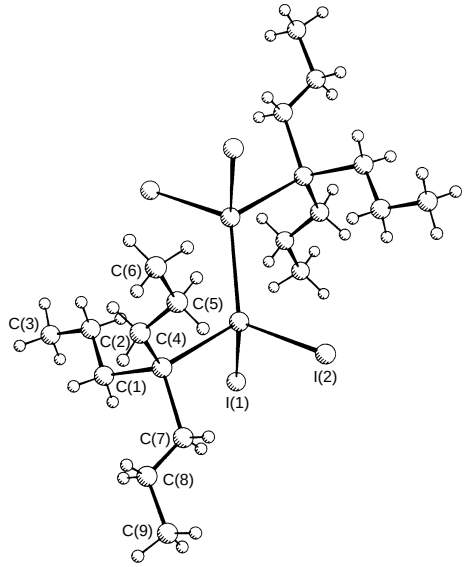



**Fig. 1** Perspective view of the molecular structure of $In_2I_4(PPr^n_3)_2$: selected bond lengths (Å) and angles (°): In(1)–I(1) 2.750(2), In(2)–I(1) 2.745(3), In(1)–P(1) 2.585(6), I(1)–In(1)–I(2) 107.75(7), I(1)–In(1)–In(1) 115.36(8), I(1)–In(1)–P(1) 97.1(1), I(2)–In(1)–In(1) 116.57(8), I(2)–In(1)–P(1) 99.8(1), In(1)–In(1)–P(1) 117.5(2)

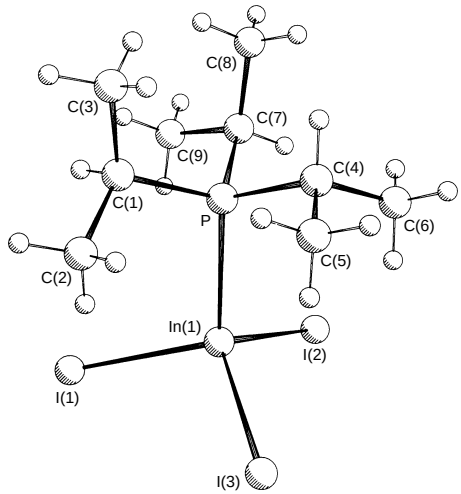



**Fig. 2** Perspective view of the molecular structure of $InI_3(PPr^i_3)$: selected bond lengths (Å) and angles (°): I(1)–In 2.705(3), I(2)–In 2.701(3), I(3)–In 2.689(3), In–P(1) 2.569(7), I(1)–In–I(2) 109.7(1), I(1)–In–I(3) 106.87(9), I(1)–In–P(1) 108.9(2); I(2)–In–I(3) 112.4(1); I(2)–In–P(1) 106.1(2), I(3)–In–P(1) 112.9(2)

## Footnotes

* E-mail: e.jenkins@umist.ac.uk

† *Crystal data*: $In_2I_4(PPr^n_3)_2$: monoclinic $P2_1/n$ (no. 14), $a$ = 9.166(4), $\beta$ = 97.41(4)°, $U$ = 1699(2) Å$^3$, $Z$ = 2, $D_c$ = 2.067 g cm$^{-3}$, $\mu$ = 50.32 cm$^{-1}$, $F(000)$ = 980. The structure analysis is based on 3319 reflections (Mo-K$\alpha$, $\theta_{max}$ = 50.0) 1189 observations [$I > 3.00(I)$], 118 parameters. Absorption correction (min/max transmission 0.77–1.10). The structure was solved by direct methods and refined by full-matrix least squares. Final residuals $R$ = 0.043, $R_w$ = 0.051.

$InI_3(PPr^i_3)$: monoclinic $Cc$ (no. 9), $a$ = 11.836(2), $b$ = 10.796(5), $c$ = 14.410(2) Å, $U$ = 1820(1) Å$^3$, $Z$ = 4, $D_c$ = 2.393 g cm$^{-3}$, $\mu$ = 63.81 cm$^{-1}$, $F(000)$ = 1191. The structure analysis is based on 1789 reflections (Mo-K$\alpha$, $\theta_{max}$ = 50.1°) 1209 observed [$I > 3.00\,\sigma(I)$], 125 parameters. The structure was solved by direct methods and refined by full-matrix least squares. Final residuals $R$ = 0.052, $R_w$ = 0.060.

Atomic coordinates, bond lengths and angles, and thermal parameters have been deposited at the Cambridge Crystallographic Data Centre (CCDC). See Information for Authors, Issue No. 1. Any request to the CCDC for this material should quote the full literature citation and the reference number 182/414.

‡ $In_2I_4(PPr^n_3)_2$ colourless crystals, correct elemental analysis (C, H, I), mp 56–57 °C. $^{31}P\{H\}$ NMR, $\delta$ 8.74 (s); $^1H$ NMR, $\delta$ 1.0 (t), 1.1 (t), 1.7 (m), 2.3 (m), intensities approximately 1 : 3 : 3 : 2. Low-frequency Raman spectrum (50–550 cm$^{-1}$): 136 cm$^{-1}$ (vs, sp), In–I; 186 cm$^{-1}$ (br), In–P; no band could be readily assigned to $\nu$(In–In).

§ $InI_3(PPr^i_3)$ colourless crystals, correct analysis (C, H, I), mp 110–111 °C. $^{31}P\{H\}$ NMR, $\delta$ 39.7 (s) $^1H$ NMR, $\delta$ 1.5 (spt), 2.8 (s), intensities *ca*. 9 : 1. Low-frequency Raman spectrum (50–550 cm$^{-1}$): 56 cm$^{-1}$ (vs, br); 137 cm$^{-1}$ (vs, sp), In–I; 156 cm$^{-1}$ (s, sp), In–P.

## References

1 A. J. Carty and D. G. Tuck, *J. Chem. Soc. A*, 1966, 1081.
2 A. J. Carty, *Can. J. Chem*., 1967, **45**, 345.
3 A. J. Carty, T. Hinsberger and P. M. Boorman, *Can. J. Chem*., 1970, **48**, 1959.
4 A. J. Carty and D. G. Tuck, *Prog. Inorg. Chem*., 1975, **19**, 243.
5 N. W. Alcock, I. A. Degnan, O. W. Howarth and M. G. H. Wallbridge, *J. Chem. Soc., Dalton Trans*, 1990, 2775.
6 M. V. Veidis and G. J. Palenik, *J. Chem. Soc., Chem. Commun*., 1969, 586.
7 N. W. Alcock, I. A. Degnan, S. M. Roe and M. G. H. Wallbridge, *Acta Crystallogr., Sect. C*, 1992, **48**, 995.
8 W. Clegg, N. C. Norman and N. L. Pickett, *Acta Crystallogr., Sect. C*, 1994, **50**, 36.
9 S. M. Godfrey, D. G. Kelly, A. G. Mackie, C. A. McAuliffe, R. G. Pritchard and S. M. Watson, *J. Chem. Soc., Chem. Commun*., 1991, 1447.
10 C. A. McAuliffe, S. M. Godfrey, A. G. Mackie and R. G. Pritchard, *Angew. Chem*., 1992, **104**, 932; *Angew. Chem., Int. Ed. Engl*., 1992, **31**, 919.
11 S. M. Godfrey, H. P. Lane, C. A. McAuliffe and R. G. Pritchard, *J. Chem. Soc., Dalton Trans*., 1993, 1599.
12 S. M. Godfrey, C. A. McAuliffe and R. G. Pritchard, *J. Chem. Soc., Chem. Commun*., 1994, 45.
13 S. M. Godfrey, C. A. McAuliffe and R. G. Pritchard, *J. Chem. Soc., Dalton Trans*., 1993, 2875.
14 N. Bricklebank, S. M. Godfrey, C. A. McAuliffe and R. G. Pritchard, *J. Chem. Soc., Dalton Trans*., 1996, 157.
15 S. M. Godfrey, N. Ho, C. A. McAuliffe and R. G. Prictchard, *Angew. Chem., Int. Ed. Engl*., 1996, **35**, 2343.
16 S. Uhl, M. Layh and W. Hiller, *J. Organomet. Chem*., 1989, **368**, 139.
17 M. A. Khan, C. Peppe and D. G. Tuck, *Can. J. Chem*., 1984, **62**, 601.

*Received in Basel, Switzerland, 5th December 1996; Com. 6/08230K*

# Identification of lead(II) sulfide and pararealgar on a 13th century manuscript by Raman microscopy

**Robin J. H. Clark* and Peter J. Gibbs**

*Christopher Ingold Laboratories, University College London, 20 Gordon Street, London, UK WC1H 0AJ*

**The *in situ* non-intrusive chemical analysis by Raman microscopy of a very rare, early 13th century, Byzantine/ Syriac Gospel lectionary implies that the serious pigment blackening of many hues and affecting most of the illuminations is caused by the degradation of lead white to lead(II) sulfide, and that pararealgar ($As_4S_4$) never previously identified on any manuscript was used throughout as a deep yellow pigment.**

Raman microscopy is now established as the analytical procedure which is the most specific, sensitive, spatially refined and immune to interference for the *in situ* analysis of inorganic pigments on manuscripts.[1] The use of Raman microscopy in the field of manuscript analysis has been dominated by the study of illuminated manuscripts in order to characterize the artist's palette,[1–10] but, as shown in this article, this technique can now be used to provide critical information for conservation of a manuscript.

The 13th century Byzantine/Syriac Gospel lectionary, from the British Library Oriental and India Office Collection, dates from 1216–1220 AD and is a heavy (10 kg), large (470 × 395 × 107 mm) volume. It consists of 264 folios with text and sixty illuminations and is valued at more than US$1 million. The large number of illuminations distributed throughout a manuscript of this type is very unusual; they are of high quality and have a rich palette which includes vermilion, lazurite, orpiment, lead white, realgar and pararealgar. Some of the illuminations have suffered serious deterioration of the white pigment, which has turned black in parts. The deterioration is mainly around the edges of the illuminations, and while there are often unaffected central areas for comparison, there are also places where the whole picture is affected. The phenomenon is most striking where the faces of the figures, apparently initially coloured with a mixture of white and red pigments, are affected, creating blackened areas devoid of features (Fig. 1).

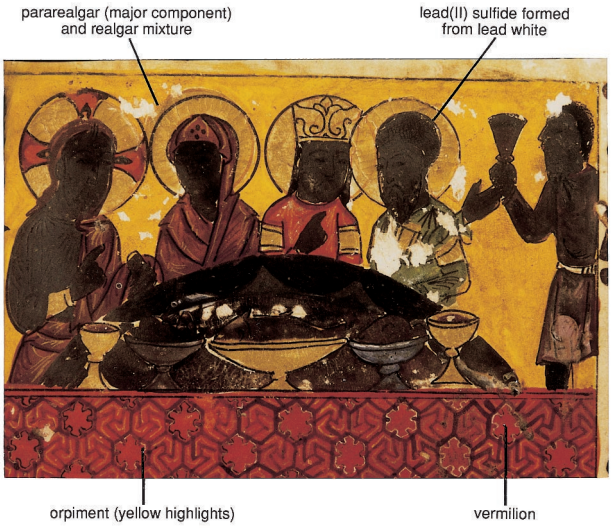



**Fig. 1** A detail of the illumination of *f*.67*r*

The size of the microscope constricted the study to some of the pages and to only a limited area of each page; nevertheless, it was still possible to analyse certain areas of fourteen of the sixty illuminations, sufficient to cover the full palette. Analysis of the inks and illuminations of the lectionary by Raman microscopy revealed unambiguously the presence of seven pigments.

The most important observation was that the black compound which appears to result from the deterioration of a white pigment, basic lead(II) carbonate $2PbCO_3 \cdot Pb(OH)_2$, commonly known as 'lead white' (Fig. 1), was identified unambiguously to be lead(II) sulfide by comparison of its Raman spectrum with that of a standard sample (Fig. 2). Lead white was identified both pure and mixed with red, blue, purple and brown pigments. All of these mixtures were prone to degradation, but it was invariably the lead white that had degraded whereas the intact blue and red pigments, for example, could sometimes still be detected in areas which were heavily discoloured.

The most likely source of sulfur (as $H_2S$) causing the deterioration was the polluted London atmosphere of the latter half of the 19th century and first half of this century.[11] The town-gas lighting in use in the British Museum until the 1880s may also have contributed to the problem.

The only recognized conservation treatment for 'reversing' the darkening of lead white on illuminated manuscripts and paintings involves treatment with hydrogen peroxide.[11] Although such a procedure leads to an aesthetic improvement, the white pigment so generated is lead(II) sulfate. The worry about this procedure is that, since two chemical transformations have been carried out *in situ* on the paper [basic lead(II) carbonate → lead(II) sulfide → lead(II) sulfate], the binding of the pigment (through volume expansion/ contraction) could deteriorate, and the lead(II) sulfate become friable and crumble from the paper.

The study of the palette of the lectionary also led to the identification of vermilion [mercury(II) sulfide] and lazurite $[Na_8(Al_6Si_6O_{24})]S_n$, a sulfur-containing sodium aluminium silicate extracted from the mineral lapis lazuli. The analysis of the yellow pigments was especially interesting. The well known

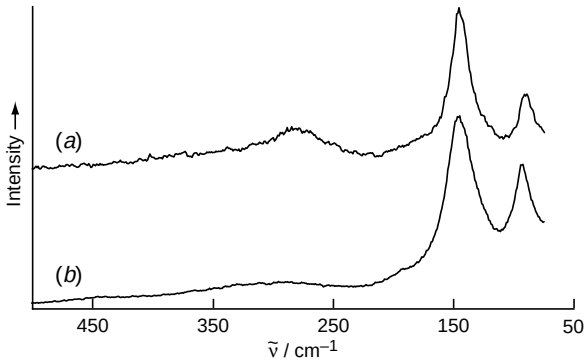



**Fig. 2** Raman spectra (by Raman microscopy, $\lambda_0$ = 514.5 nm) of (*a*) discoloured area of the illumination of *f*.67*r* and (*b*) a standard sample of lead(II) sulfide

throughout the manuscript, but it was not the only yellow pigment used. In thirty-two of the sixty illuminations there are examples of a very rich yellow colouration (see, for example, Fig. 1) which differs significantly in appearance from that of orpiment, which has a much lighter hue. Viewed through the microscope, the pigment appears to be dominated by yellow crystals with a significant number of orange ones. Analysis by Raman microscopy revealed that the orange crystals were realgar,[12] arsenic(II) sulfide ($As_4S_4$), and that the yellow crystals were pararealgar,[13,14] a light-induced transformation product of realgar first identified in 1980 (Fig. 3).[15] There are

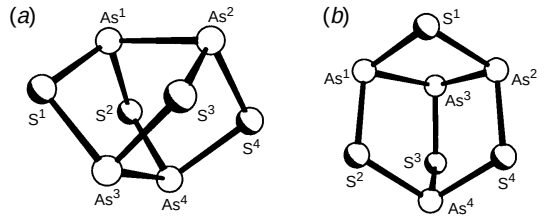



**Fig. 3** Structures of (*a*) realar (both α- and β-polymorphs)[12] and (*b*) pararealgar[13]

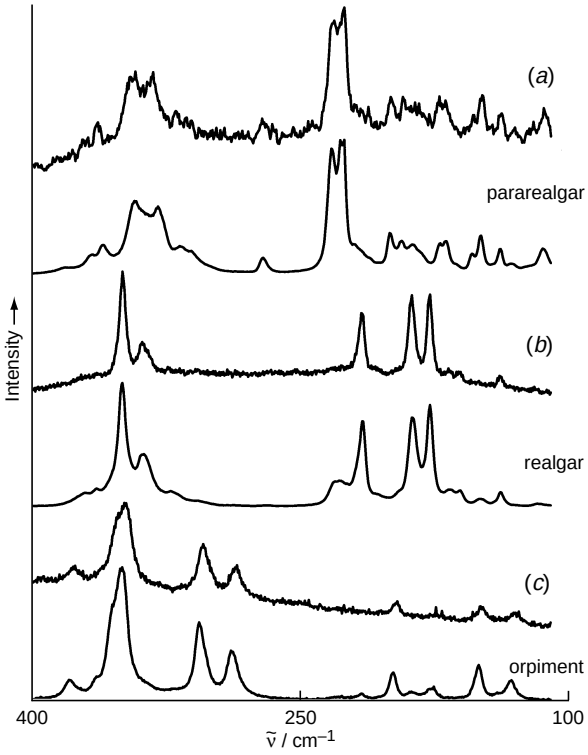



**Fig. 4** Raman spectra (by Raman microscopy, $\lambda_0$ = 647.1 nm) of (*a*) the major component of the yellow–orange pigment on *f*.67*r*, (*b*) the minor component of the yellow–orange pigment on *f*.67*r* and (*c*) the yellow pigment used for highlighting the base of the illumination on *f*.67*r*, and of pararealgar, realgar and orpiment

phase, α-$As_4S_4$, a metastable high-temperature phase, β-$As_4S_4$, and a light-induced form, χ-realgar. All transform to pararealgar on irradiation with light of wavelengths in the range 500–670 nm, most rapidly with those in the range 530–560 nm.[16] The mechanism of transformation is believed to involve photo-induced breakage and reformation of As–As bonds.[14–16] The rich yellow hue of the pigment always appears in the correct context, and the usage of this particular shade of yellow is widespread throughout the manuscript.

It is clear that the artist did not mistake pararealgar for the more common yellow pigment, orpiment: the artist often used both pigments on the same illumination, showing that he had access to and had used them both as distinct yellow pigments. This is the first time that pararealgar has been observed (*in situ* or otherwise) on any manuscript and it was identified unambiguously by comparison with a genuine sample. The Raman spectra of orpiment, realgar and pararealgar are illustrated in Fig. 4, together with spectra obtained from the yellow pigments used in the illumination on *f*.67*r* of the lectionary (Fig. 1).

This study has resulted in the first effective use of Raman microscopy to determine the nature of a serious conservation problem affecting a very valuable manuscript, and also in the first identification of pararealgar on an illuminated manuscript. These results confirm that Raman microscopy is one of the most useful analytical tools for *in situ* and non-intrusive archaeometric analysis, and one that can provide invaluable information for both scientists and conservators alike.

We thank the Leverhulme Trust for support and the British Library for the loan of the lectionary.

## References

1 S. P. Best, R. J. H. Clark and R. Withnall, *Endeavour*, 1992, **16**, 66.
2 R. J. H. Clark, *Chem. Soc. Rev*., 1995, **24**, 187.
3 S. P. Best, R. J. H. Clark, M. A. M. Daniels, C. A. Porter and R. Withnall, *Stud. Conserv*., 1995, **40**, 31.
4 S. P. Best, R. J. H. Clark, M. A. M. Daniels and R. Withnall, *Chem. Br*., 1993, **29**, 118.
5 C. Coupry, A. Lautie, M. Revault and J. Dufilho, *J. Raman Spectrosc*., 1994, **25**, 89.
6 M. Ley, M. D. Brisant and M. Rudler, *Analysis*, 1993, **21**, M47.
7 R. J. H. Clark, P. J. Gibbs, K. R. Seddon, N. M. Brovenko and Y. A. Petrosyan, *J. Raman Spectrosc*., 1997, **28**, 91.
8 R. J. H. Clark, L. Cridland, B. M. Kariuki, K. D. M. Harris and R. Withnall, *J. Chem. Soc., Dalton Trans*., 1995, 2577.
9 L. Burgio, D. A. Ciomartan and R. J. H. Clark, *J. Raman Spectrosc*., 1997, **28**, 79.
10 L. Burgio, D. A. Ciomartan and R. J. H. Clark, *J. Mol. Struct*., 1997, **405**, 1.
11 R. J. Gettens, H. Kuhn and W. T. Chase, in *Artists' Pigments*, ed. A. Roy, Oxford University Press, New York, vol. 2, 1993.
12 D. J. E. Mullen and W. Nowacki, *Z. Kristallogr*., 1972, **136**, 48.
13 P. Bonazzi, S. Menchetti and G. Pratesi, *Am. Mineral*., 1995, **80**, 400.
14 K. Trentelman, L. Stodulski and M. Pavlosky, *Anal. Chem*., 1996, **68**, 1755.
15 A. C. Roberts, H. G. Ansell and M. Bonardi, *Can. Mineral*., 1980, **18**, 525.
16 D. L. Douglas, C. Shing and G. Wang, *Am. Mineral*., 1992, **77**, 1266.

*Received in Cambridge, UK, 17th March 1997; Com. 7/01837A*

# Control of interpenetrating copper(I) adamantoid networks: synthesis and structure of $\{[Cu(bpe)_2]BF_4\}_n$

**Alexander J. Blake, Neil R. Champness,* Simon S. M. Chung, Wan-Sheung Li and Martin Schröder*†**

*Department of Chemistry, The University of Nottingham, Nottingham, UK NG7 2RD*

**Lengthening of linking bipyridyl ligands in interlocking copper(I)-heterocycle adamantoid arrays increases the volume of the adamantoid cages and consequently the number of observed interpenetrating networks: factors influencing the observed structures of these interpenetrating complexes are described in the context of the structure of $\{[Cu(bpe)_2]BF_4\}_n$ [bpe = 1,2-*trans*-(4-pyridyl)ethene].**

The construction of solid-state architectures and crystal engineering has become an area of increasing interest over recent years.[1–4] Much study has been centred upon the use of supramolecular contacts and in particular hydrogen-bonding between suitable organic molecules to generate multi-dimensional arrays and networks.[1–3] The design of inorganic networks is much less well developed[4–8] but recent examples have helped to extend the understanding of this developing area. The construction of adamantoid or super-diamondoid arrays is a common feature amongst some of these infinite three-dimensional networks[4–7] and are often based upon linear bridging ligands bound to tetrahedral metal ions such as $Cu^I$ or $Ag^I$.[5,6] Interpenetration of independent networks is often encountered in adamantoid networks as the crystal avoids the formation of large cavities within the crystalline lattice.[4–7,9,10] The number of independent interpenetrating networks can vary in these three-dimensional polymers[10] from two to as many as eight and nine.[11–13] However, the factors that control the observed degrees of interpenetration in these systems remain largely unknown and/or unproven, and to this end we have begun studies into how ligand functionality can be used to control overall structure of three-dimensional arrays.

Red kite-shaped crystals of a complex product were grown over a period of days at the interface of layered solutions of 1,2-*trans*-(4-pyridyl)ethene (bpe) in MeCN and $[Cu(MeCN)_4]BF_4$ in $CH_2Cl_2$. A single-crystal X-ray structure determination‡ confirmed the product to be a three-dimensional polymer, $\{[Cu(bpe)_2]BF_4\cdot 0.5CH_2Cl_2\}_n$, in which each $Cu^I$ centre is coordinated in a tetrahedral geometry to four bpe ligands [Cu–N 2.003(5)–2.084(6) Å] which are in turn bound to four other $Cu^I$ centres. The three-dimensional structure (Fig. 1) builds through the formation of edge-sharing adamantoid units. The Cu···Cu distances across the edge of each adamantoid unit ranges from 13.33 to 13.82 Å to create large cavities within this first three-dimensional lattice. These cavities are filled with four other $\{[Cu(bpe)_2]^+\}_n$ lattices which are positioned such that they interpenetrate each other to fill the spaces left by each other. All five independent lattices are polycatenated with channels throughout the structure parallel to the direction of translation for the five networks and within the adamantoid units (Fig. 2): these channels accommodate $BF_4^-$ counter ions and $CH_2Cl_2$ solvent molecules.

This structure is related to that observed for $\{[Cu(4,4'\text{-bipy})_2]PF_6\}_n$[5] and $\{[Ag(4,4'\text{-bipy})_2]CF_3SO_3\}_n$[6] in which four independent adamantoid networks are formed. Thus, by lengthening the linking bipyridyl ligand *via* insertion of a *trans* C=C double bond between the pyridyl units the length of the edges of the adamantoid units are extended from 11.16 Å for $\{[Cu(4,4'\text{-bipy})_2]PF_6\}_n$[5] to 13.55 Å (average) in the structure of $\{[Cu(bpe)_2]BF_4\}_n$ reported here. This increase in length of the adamantoid unit edge in $\{[Cu(bpe)_2]BF_4\}_n$ creates a larger cavity within the structure which is filled by the inclusion of one

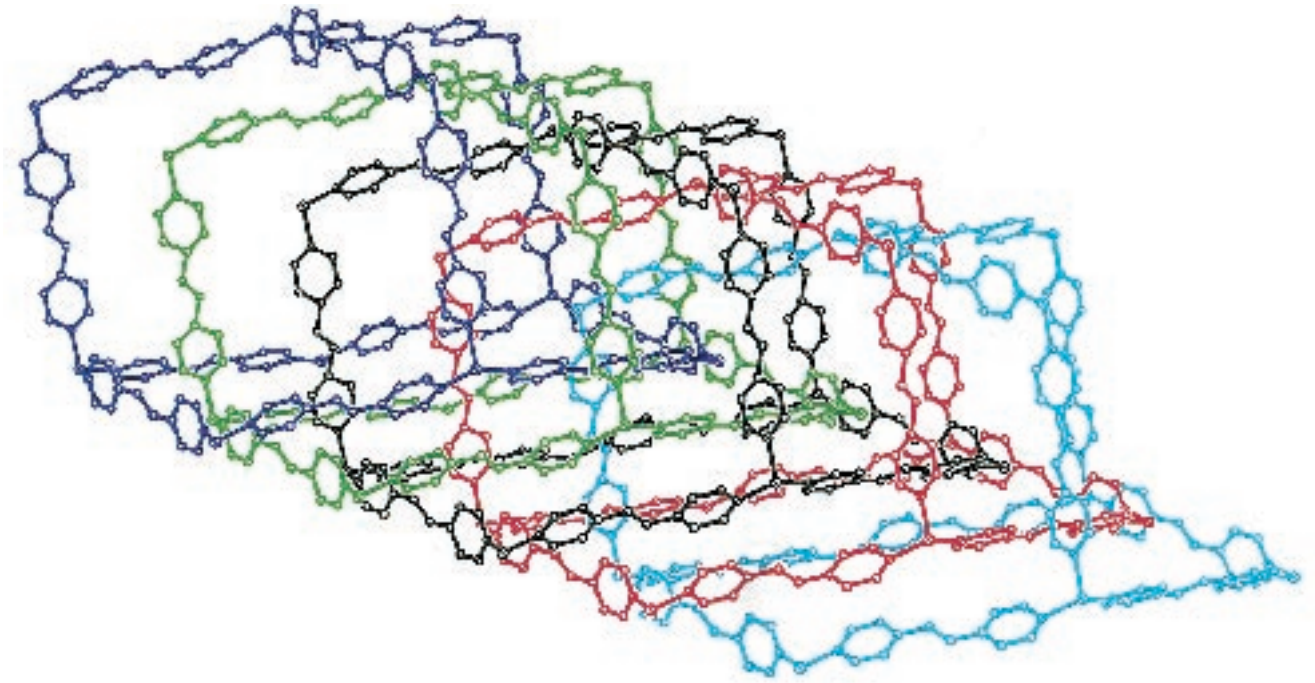


**Fig. 1** View of the structure of $\{[Cu(bpe)_2]BF_4\}_n$ showing five interlocking adamantoid cages

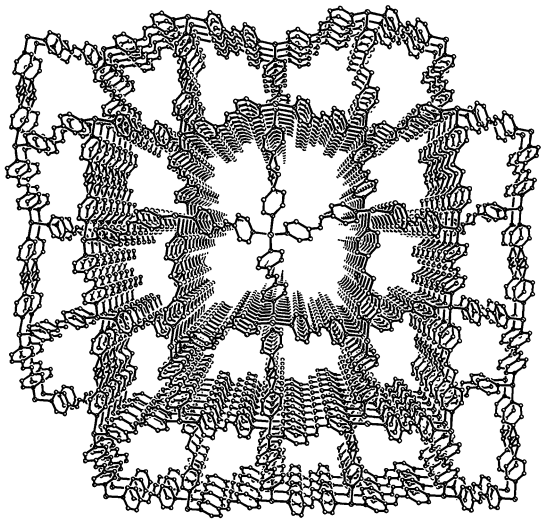


**Fig. 2** View of the structure of $\{[Cu(bpe)_2]BF_4\}_n$

extra independent $\{[Cu(bpe)_2]^+\}_n$ lattice. Also, $CH_2Cl_2$ fills the extra volume created within the counter anion channels. Thus, by altering the ligand length, the degree of interpenetration has been increased from four independent lattices for $\{[Cu(4,4'\text{-bipy})_2]PF_6\}_n$[5] and $\{[Ag(4,4'\text{-bipy})_2]CF_3SO_3\}_n$[6] to five independent arrays, representing control over the degree of interpenetration. There are only two previous examples of systems with five independent interpenetrating arrays, firstly the hydrogen-bonded array of adamantane-1,3,5,7-tetracarboxylic acid[9] and secondly the polymer involving $Cu^I$ and 1,4-dicyanobenzene for which the nature of interpenetration was not fully discussed.[4]

The separations between adjacent adamantoid cages in $\{[Cu(bpe)_2]BF_4\}_n$ is controlled further by face-to-face π–π stacking interactions of 3.659 and 3.855 Å between sets of bpe ligands marked *a* and *b*, respectively, in Fig. 1. Other seemingly adjacent bpe ligands have larger gaps between them along the other sides of the adamantoid cages [*c* in Fig. 1]. Nonetheless, π–π stacking is clearly important in the overall control of this extended structure and the presence of this interaction along the direction in which the adamantoid cages propagate may reveal how such long-range structure is formed during crystallisation. Interestingly, the related complex $\{[Ag\{NC(C_6H_4)_2CN\}_2]PF_6\}_n$ has nine independent adamantoid networks[13] despite only a relatively small increase in the M···M distance of 16.42 Å, compared with 13.55 Å (average) in the present study. This higher degree of interpenetration in $\{[Ag\{NC(C_6H_4)_2CN\}_2]PF_6\}_n$ is enabled by the closer approach of adjacent lattices in this complex: this is not allowed in $\{[Cu(bpe)_2]BF_4\}_n$ due to steric repulsion between pyridyl groups coordinated to Cu centres from adjacent cages.

The present study on $\{[Cu(bpe)_2]BF_4\cdot 0.5CH_2Cl_2\}_n$ reveals direct evidence of control over the fascinating phenomenon of interpenetration and highlights the factors (namely, ligand length, π–π and steric interactions) which will allow design of further supramolecular architectures *via* control of separations between adjacent interlocking cages.

We thank the Nuffield Foundation (to S. S. M. C.) and the EPSRC for support.

## Footnotes

† E-mail: m.schroder@nottingham.ac.uk

‡ *Crystal data* for $[Cu(bpe)_2]BF_4\cdot 0.5CH_2Cl_2$. $C_{24.5}H_{21}BClCuF_4N_4$, $M$ = 557.25, triclinic, space group $P\bar{1}$ (no. 2), $a$ = 7.310(3), $b$ = 13.144(5), $c$ = 13.800(4) Å, α = 83.46(3), β = 82.88(4), γ = 84.71(3)°, $U$ = 1303.0(8) Å$^3$, $Z$ = 2, $F(000)$ = 566, $D_c$ = 1.420 g cm$^{-3}$, μ(Mo-Kα) = 0.989 mm$^{-1}$. Red kite-shaped crystal (0.29 × 0.23 × 0.12 mm). Stoe Stadi-4 four-circle diffractometer, graphite monochromated Mo-Kα radiation, ω–2θ scans with ω-scan width of 1.1°. Numerical absorption corrections were applied to the data ($T_{min}$ = 0.828, $T_{max}$ = 0.900), 4593 unique reflections ($2\theta_{max}$ = 50°, $R_{int}$ = 0.0489), of which 3763 had $F_0 \geqslant 4\sigma(F_0)$, were used in all calculations. The position of the Cu atom was deduced by Patterson synthesis[14] and all the remaining non-H atoms were located from subsequent difference-Fourier methods.[15] Atom C(16), an ethylene carbon on one of the bipyridyl groups, and three of the F-atoms of the $BF_4^-$ anion are each disordered into two equal components. Full-matrix least-squares procedures were used for refinement and all non-F and C atoms [except for C(11), C(12), C(13), C(14), C(15), (one pyridyl unit), and C(1s) from the $CH_2Cl_2$ solvent molecule] were refined with anisotropic displacement parameters; hydrogen atoms were placed geometrically for all non-disordered carbon atoms and thereafter allowed to ride on their parent C-atoms with $U_{iso}(H) = 1.2\,U_{eq}(C)$. The weighting scheme $w^{-1} = [\sigma^2(F_o^2) + (0.1131P)^2 + 8.1717P]$, $P = \frac{1}{3}[\max(F_o^2,0) + 2F_c^2]$, gave satisfactory agreement analyses. Final $R_1$ [$F_o \geqslant 4\sigma(F_o)$] = 0.0892, $wR_2$ (all data) = 0.2553 for 234 refined parameters, $S$ = 1.095, $(\Delta/\sigma)_{max}$ = 0.03, $\Delta\rho_{max}$ = 1.50 e Å$^{-3}$ [in the proximity of the C(1s) and Cl atoms]. Atomic coordinates, bond lengths and angles, and thermal parameters have been deposited at the Cambridge Crystallographic Data Centre (CCDC). See Information for Authors, Issue No. 1. Any request to the CCDC for this material should quote the full literature citation and the reference number 182/432.

## References

1 G. R. Desiraju, in *Crystal Engineering: Design of Organic Solids*, Elsevier, Amsterdam, 1989.
2 *The Crystal as a Supramolecular Entity*, ed. G. R. Desiraju, Wiley, 1995.
3 G. R. Desiraju, *Angew. Chem., Int. Ed. Engl.*, 1995, **34**, 2311.
4 R. Robson, B. F. Abrahams, S. R. Batten, R. W. Gable, B. F. Hoskins and J. Liu, *Supramolecular Architecture*, ACS publications, 1992, ch. 19.
5 L. R. MacGillivary, S. Subramanian and M. J. Zaworotko, *J. Chem. Soc., Chem. Commun.*, 1994, 1325.
6 L. Carlucci, G. Ciani, D. M. Proserpio and A. Sironi, *J. Chem. Soc., Chem. Commun.*, 1994, 2755.
7 S. B. Copp, S. Subramanian and M. J. Zaworotko, *J. Am. Chem. Soc.*, 1992, **114**, 8719; S. B. Copp, S. Subramanian and M. J. Zaworotko, *J. Chem. Soc., Chem. Commun.*, 1993, 1078; S. B. Copp, K. T. Holman, J. O. S. Sangster, S. Subramanian and M. J. Zaworotko, *J. Chem. Soc., Dalton Trans.*, 1995, 2233.
8 D. Venkataraman, S. Lee, J. S. Moore, P. Zhang, K. A. Hirsch, G. B. Gardner, A. C. Covey and C. L. Prentice, *Chem. Mater.*, 1996, **8**, 2030; B. F. Abrahams, S. R. Batten, H. Hamit, B. F. Hoskins and R. Robson, *Angew. Chem., Int. Ed. Engl.*, 1966, **35**, 1690; J. Black, N. R. Champness, W. Levason and G. Reid, *Inorg. Chem.*, 1996, **35**, 4432; L. Carlucci, G. Ciani, D. M. Prosperio and A. Sironi, *J. Am. Chem.. Soc.*, 1995, **117**, 4562; B. F. Hoskins and R. Robson, *J. Am. Chem. Soc.*, 1990, **112**, 1546; O. M. Yaghi and H. Li, *J. Am. Chem. Soc.*, 1995, **117**, 10 401; D. M. L. Goodgame, S. Menzer, A. M. Smith and D. J. Williams, *Angew. Chem., Int. Ed. Engl.*, 1995, **34**, 574; P. C. M. Duncan, D. M. L. Goodgame, S. Menzer and D. J. Williams, *Chem. Commun.*, 1996, 2127.
9 O. Ermer, *J. Am. Chem. Soc.*, 1988, **110**, 3747.
10 D. B. Amabilino and J. F. Stoddart, *Chem. Rev.*, 1995, **95**, 2725.
11 B. F. Abrahams, S. R. Batten, H. Hamit, B. F. Hoskins and R. Robson, *Chem. Commun.*, 1996, 1313.
12 L. Carlucci, G. Ciani, D. M. Proserpio and A. Sironi, *Chem. Commun.*, 1996, 1393.
13 K. A. Hirsch, D. Venkataraman, S. R. Wilson, J. S. Moore and S. Lee, *J. Chem. Soc., Chem. Commun.*, 1995, 2199.
14 SHELXS-96: G. M. Sheldrick, Universität Göttingen, 1996.
15 SHELXL-96: G. M. Sheldrick, Universität Göttingen, 1996.

*Received, in Cambridge, UK, 6th February 1997; Com. 7/00866J*

# Nucleation and growth of nano-gold colloidal lattices

**Toshihiko Sato*[a] David Brown[b] and Brian F. G. Johnson[b]**

[a] *Hitachi Cambridge Laboratory, Hitachi Europe Ltd., Cavendish Laboratory, Madingley Road, Cambridge, UK CB3 0HE*
[b] *Department of Chemistry, University of Cambridge, Lensfield Road, Cambridge, UK CB2 1EW*

**A two-dimensional array of 10 nm gold colloidal particles is formed by a submonolayer deposition technique using a bifunctional aminosilane followed by a mobility-restoration treatment with alkanethiol, converting the disordered submonolayer deposition to a highly-ordered two-dimensional array.**

Driven by interest in the quantum-confined electronic properties of nanometer scale metal/semiconductor particles, the investigation of nanostructured materials is becoming an exciting area of interdisciplinary research. The device application[1,2] of these nanostructured particles requires techniques of ordering particles in one- , two- or three-dimensional structures; such requirements for nanoarchetecture provide challenges to sample preparation technology. Recently, a method for depositing nanometer-scale gold colloidal particles on $SiO_2$ surfaces was demonstrated using alkylsiloxane molecules as an adhesion agent.[3] The self-limiting nature of this method stopped the deposition at submonolayer coverage density. The compatibility of this method with conventional electron beam lithography was tested and the deposition was carried out only on prescribed positions on the substrate surface. Further, highly-ordered, hexagonally-packed two-dimensional (2D) lattice formation was observed by the electrophoretic deposition of a colloidal gold from the bulk solution onto a carbon-coated electron microscope grid.[4] It was also shown that metal particles including gold and other transition metal clusters can form densely packed monolayers on electron microscope grids when they are ligated by organic surfactant molecules.[5]

In this work, the method of forming a hexagonally-packed 2D lattice of nanoparticles on a $SiO_2$-grown Si substrate is described using a gold colloid solution in combination with organic surfactant treatments of both the substrate and colloid particles. We have been successful in performing surfactant ligation of the gold colloidal particles after they are immobilised on a substrate surface by a bifunctional aminosilane. By this reaction scheme, the switching between mobile/immobile conditions takes place in the gold colloid adsorption.

This method starts with the submonolayer coating of a $SiO_2$ surface with 10 nm gold colloidal particles (GCP) from solution (*viz.* a citrate sol with an average size of *ca.* 10 nm and a size variation of *ca.* 10% standard deviation prepared according to the recipe described in ref. 6) using the method described in ref. 3. A Si substrate covered with a thermally-grown $SiO_2$ (200 nm thick) was cleaned by brief (*ca.* 30 s) oxygen plasma ashing. Immediately afterwards, the sample was immersed in a 2.3 mM aqueous solution of a bifunctional aminosilane [*i.e.* 3-(2-aminoethlyamino)propyltrimethoxysilane, APTMS $[(MeO)_3Si(CH_2)_3NHCH_2CH_2NH_2]$ for 5 min. After the APTMS immersion, the sample was rinsed in two distilled water baths, dried with a nitrogen gun, and placed in a 120 °C oven for 30 min to complete Si–O bond formation. The APTMS treatment replaces the hydroxy groups (OH) adsorbed on the $SiO_2$ substrate with APTMS molecules forming a siloxane bond between the Si on one end of the APTMS molecules and an oxygen atom on the $SiO_2$ surface. As a consequence, the amino group attached on the other end of the APTMS molecule is oriented away from the substrate. These amino groups on the APTMS molecules immobilise gold particles onto the substrate because of the affinity of the amino group to the gold [see Fig. 1(*a*)].[3]

The APTMS treated sample was then immersed in the GCP for 8–12 h, rinsed with two distilled water baths, and dried with a nitrogen gun. This procedure gave a sub-monolayer coating of the GCPs. Since immobilised particles on the substrate are still covered with ionic adsorbates of citrate ions,[7] there is always an electrostatic repulsive force between the colloidal particles. Therefore, the GCP deposition automatically stops before it reaches a close-packing density.[3] Fig. 2(*a*) shows a scanning electron micrograph of the submonolayer coated sample (the observation was carried out using S-900, Hitachi, which has an in-lens type electron optics and a cold cathode electron gun). The micrograph demonstrates a disordered particle deposition with the inter-particle spacing of 10–50 nm.

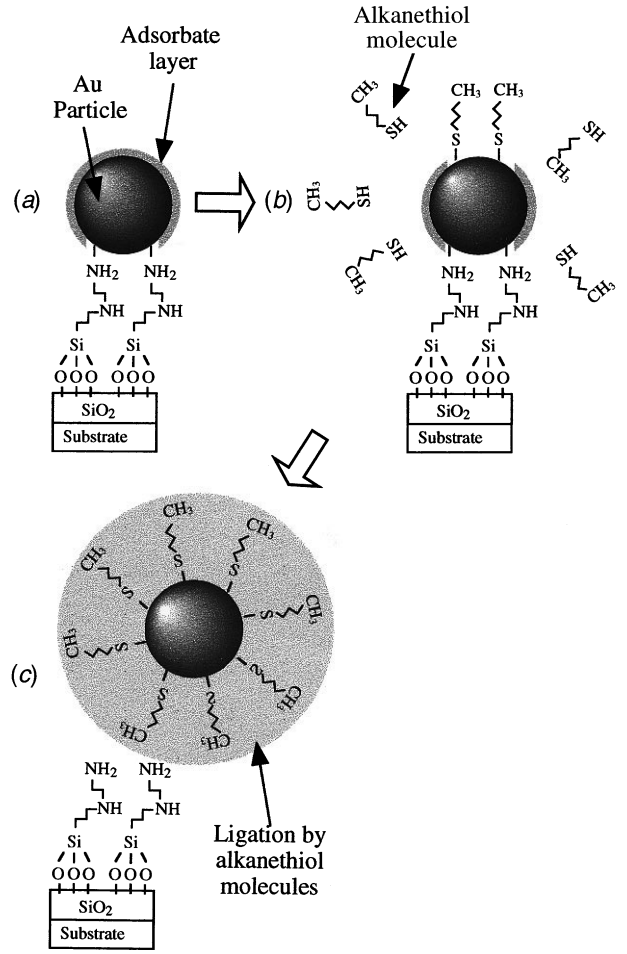



**Fig. 1** Mobility restoration mechanism by a displacement reaction. (*a*) Gold colloidal particle immobilised by a bifunctional aminosilane. (*b*) Ligation of gold particles by alkanethiol molecules displacing the adsorbates and Au–$NH_2$ bonds. (*c*) Mobility restoration by complete ligation of the gold particle.

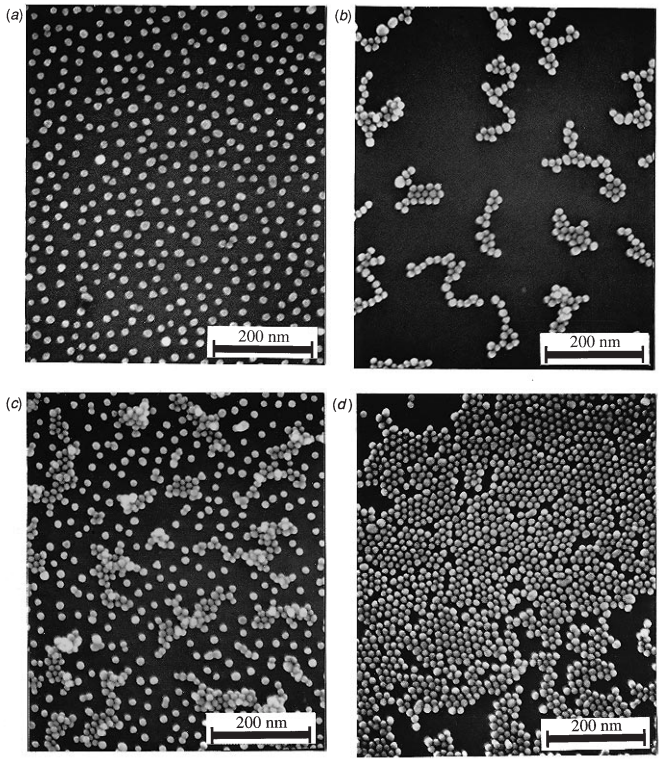



**Fig. 2** Scanning electron micrograph observation of the gold particle crystal nucleation and growth. (*a*) Disordered submonolayer deposition of gold particles from a gold colloid solution using a bifunctional amino silane. Nominal particle size is 10 nm (10% standard deviation). (*b*) Nucleation of gold colloidal crystal initiated by the mobility restoration reaction induced by alkanethiol treatment. (*c*) Additional particle supply from the gold colloid solution on the vacant sites between the nuclei formed in the previous process. (*d*) Highly-ordered two-dimensional gold particle lattice formed by the repetitive application of gold colloid immobilisation and disorder-to-order conversion.

After the sub-monolayer GCP coating, an alkanethiol treatment was carried out to initiate the nucleation of the 2D structure of GCPs. The sample was immersed in a 5 mM ethanolic solution of dodecane-1-thiol [$Me(CH_2)_{11}SH$] for *ca.* 24 h, and rinsed with an ethanol bath, and dried with a nitrogen gun. Because of the strong affinity of sulfur to gold, this treatment replaces citrate adsorbates with the alkanethiol molecules [Fig. 1(*b*)]. In addition to the adsorbate removal, the bonding between the sulfur and gold can even displace the bonding between the amino group and gold. This results in the complete ligation of the gold particle with alkanethiol molecules [Fig. 1(*c*)]; as a consequence, since the molecular binder of the bifunctional aminosilanes are detached from the gold particles, once immobilised particles are now released from the substrate and acquire some mobility on the substrate surface.

Because of the restored surface mobility, particles move and collide with each other on the substrate surface. However, because of the short-range steric repulsion due to the alkanethiol ligation, the particles will not undergo diffusion-limited aggregation which results in 'fractal' structures;[7] instead, they form hexagonally-packed ordered nuclei and grow two-dimensionally given the particle supplies from the migration of GCPs on the substrate surface. Fig. 2(*b*) shows a scanning electron micrograph of a sample after the alkanethiol treatment showing the initiation of ordered 2D nuclei.

Fig. 2(*b*) also shows that the nuclei are deposited with substantial spacing between them. These vacant areas are expected to be covered with the bifunctional aminosilanes. Therefore, when the sample is immersed in the GCP solution again, additional particles can land on those vacant spaces from the GCP solution and are immobilised on the substrate. Fig. 2(*c*) shows a scanning electron micrograph of the sample after the second GCP solution immersion. Individual GCPs are filling the vacant spaces with similar inter-particle distances to that of the first GCP solution immersion.

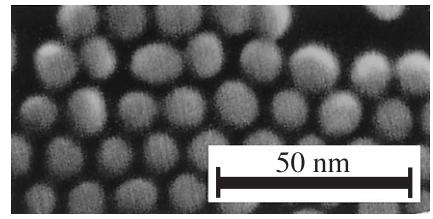



**Fig. 3** Scanning electron micrograph of a highly-ordered two-dimensional array of 10 nm gold particles

Then, the alkanethiol treatment are applied to the sample after the second GCP solution immersion in order to mobilise them and grow the nuclei larger. In this sense, the second GCP solution immersion is playing a role supplying additional materials for the growth of GCP grains. Repetitive application of the GCP immersion with the subsequent alkanethiol treatment enlarges the GCP grain size further. After four repetitions, the grains with different orientations are connected with each other and reach a continuous film of GCP with a densely packed two-dimensional order as is shown in Fig. 2(*d*). Further repetition of the GCP immersion and alkanethiol treatment, however, did not improve the monolayer coverage density; instead, multilayer growth becomes dominant.

From micrographs with a greater magnification as shown in Fig. 3, the average gap between the particles is estimated to be about 2 nm, which is about the twice the thickness of a self-assembled monolayer of dodecanethiol on Au(111) (*i.e.* 1.2 nm).[8] This confirms that the inter-particle distances are determined by the steric repulsion between the alkanethiols attached on the gold particle surfaces.

In conclusion, a highly-ordered two-dimensional array of 10 nm gold particles was formed by the surfactant treatment of both the substrate and gold particles. A bifunctional amino-silane treatment of the substrate immobilised the gold particles from a gold colloid solution with a coverage density of a submonolayer. Subsequent alkanethiol treatment converted the disordered deposition to an ordered one by giving surface mobility to the gold particles. Repetitive applications of immobilisation and disorder-to-order conversion grew the two-dimensionally ordered GCP grains until they were connected together.

The authors wish to acknowledge support given by Professor H. Ahmed (Microelectronics Research Centre, University of Cambridge). This work was performed under the management of FED as a part of the MITI R&D of Industrial Science and Technology Frontier Program (Quantum Functional Device project) supported by NEDO.

## References

1 V. L. Colvin, M. C. Schlamp and A. P. Alivisatos, *Nature*, 1994, **370**, 354.
2 T. Sato and H. Ahmed, unpublished work; D. L. Klein, P. L. McEuen, J. E. B. Katari, R. Roth and A. P. Alivisatos, *Appl. Phys. Lett.*, 1996, **68**, 2574.
3 T. Sato, D. G. Hasko and H. Ahmed, *J. Vac. Sci. Technol B*, in the press.
4 M. Giersig and P. Mulvaney, *J. Phys. Chem.*, 1993, **97**, 6334.
5 M. T. Reetz, M. Winter and B. Tesche, *Chem. Commun.*, 1997, 147; B. Dusemund, A. Hoffmann, T. Salzmann, U. Kreibig and G. Schmid, *Z. Phys. D*, 1991, **20**, 305.
6 D. A. Handley, in *Colloidal Gold—Principles, Methods, and Applications*, ed. M. A. Hayat, Academic Press, New York, 1989, vol. 1, p. 13.
7 D. A. Weitz and M. Y. Lin, *Surface Sci.*, 1985, **158**, 147.
8 P. E. Laibins, R. G. Nuzzo and G. M. Whitesides, *J. Phys. Chem.*, 1992, **96**, 5097.

*Received in Cambridge, UK, 7th March 1997; Com. 7/01627A*

# Synthesis of thermally stable mesoporous hexagonal aluminophosphate molecular sieves

**Dongyuan Zhao, Zhaohua Luan and Larry Kevan***

*Department of Chemistry, University of Houston, Houston, Texas 77204-5641, USA*

**Thermally stable mesoporous hexagonal aluminophosphates (UHM-1) and silicoaluminophosphates (UHM-3) are synthesized based on ion-pair interactions of aluminophosphate species in the presence of tetramethylammonium hydroxide with a cationic surfactant [$C_{16}H_{33}NMe_3Cl$].**

Aluminophosphate materials (AlPO-*n*) are recently developed crystalline microporous materials of potential use in catalysis.[1,2] For catalytic processing of larger micelles, mesoporous AlPO-*n* materials are desirable. Lamellar mesostructures of aluminophosphate have been synthesized by using an amphiphilic alkylamine ($C_{10}H_{21}NH_2$) in tetraethylene glycol[3] and by using dimethylalkylamines with $C_8$–$C_{16}$ alkyl groups in water,[4] but these materials are thermally unstable as are lamellar mesostructures of M41S silicates.[5]

The M41S family of silica-based mesoporous molecular sieves is formed by a self-assembly process involving electrostatic interactions between positively charged quaternary ammonium surfactants ($S^+$) and inorganic anions ($I^-$).[5] This process can form hexagonal MCM-41 silica tubes. The electrostatic assembly method has been generalized.[6] A neutral precursor assembly method involving hydrogen bonding between neutral amine surfactants ($S^0$) and neutral silica precursors ($I^0$) in alcohol–water solvent has also been demonstrated.[7]

Here we report the synthesis of thermally stable mesoporous hexagonal aluminophosphate and silicoaluminophosphate molecular sieves by a $S^+I^-$ route. Our approach is based on self-assembly between a cationic surfactant ($S^+$) and an aluminophosphate precursor ($I^-$) in the presence of alkylammonium hydroxide. This method produces stable hexagonal mesostructures of aluminophosphate (UHM-1) and silicoaluminophosphate (UHM-3).

Mesoporous aluminophosphate and silicoaluminophosphate were prepared using cetyltrimethylammonium chloride (CTAC, Aldrich, 25% in water) as a surfactant and the following gel composition: $Al_2O_3 : xP_2O_5 : ySiO_2 : \mu CTAC : \nu NR_4OH : \omega H_2O$, where R = Me, Et, $Bu^n$; $x$ = 0.6–3.4, $y$ = 0–0.6, $\mu$ = 0.24–0.50, $\nu$ = 8.5–47 and $\omega$ = 200–642. In a typical preparation of aluminophosphate, 3.53 g dried aluminium hydroxide (USP Pfaltz & Bauer Inc.) was slowly added to a solution of 4.2 g phosphoric acid (85 mass%, EM Industries) in 15 g water under vigorous stirring. The mixture was added to a solution of 11.6 g CTAC (25 mass%) in 100 g water with stirring. After 0.5 h, 17.3 g tetramethylammonium hydroxide (TMAOH, Aldrich, 25 mass% in water) was slowly added dropwise into the above mixture until pH 9.5 was achieved. In a typical silicoaluminophosphate preparation, an aluminophosphate gel prepared according to the above procedure and 0.79 g tetraethylorthosilicate (TEOS, Aldrich) was added to 11.6 g CTAC in 100 g water with stirring for 3 h. Then 19.0 g TMAOH was added dropwise to obtain pH 9.5. The gels obtained using these procedures were then stirred for 72 h at room temperature. The solid product was recovered, washed and air-dried at 70 °C. The template was removed by calcination at 500 °C for 1 h in flowing nitrogen, followed by 6 h in flowing oxygen.[5]

Powder X-ray diffraction (XRD) patterns of products were obtained on a Siemens D5000 diffractometer with a scan rate of 1° $min^{-1}$ and Cu-K$\alpha$ radiation ($\lambda$ = 0.154 18 nm). Transmission electron micrographs (TEM) were measured on a JEOL 2000 FX microscope with an accelerating voltage of 100 kV. Electron probe microanalysis was performed on a JEOL JXA-8600 spectrometer. Thermogravimetric analysis (TGA) was performed on a DuPont 2100 thermal analyser with a heating rate of 10 °C $min^{-1}$ in air. Surface areas of the samples were measured on a Monosorb (Quantachrome Corp.) surface area analyser by the single point method.

Powder X-ray diffraction patterns of as-synthesized and calcined UHM-1 and UHM-3 are shown in Fig. 1. The XRD patterns show a prominent peak corresponding to (100) reflections and much weaker but clearly present peaks corresponding to (110), (200) and (210) reflections in the as-synthesized material which can be indexed to a hexagonal lattice and which are similar to typical XRD patterns for siliceous hexagonal MCM-41 materials.[5,6] This shows that mesoporous hexagonal mesostructural aluminophosphate and

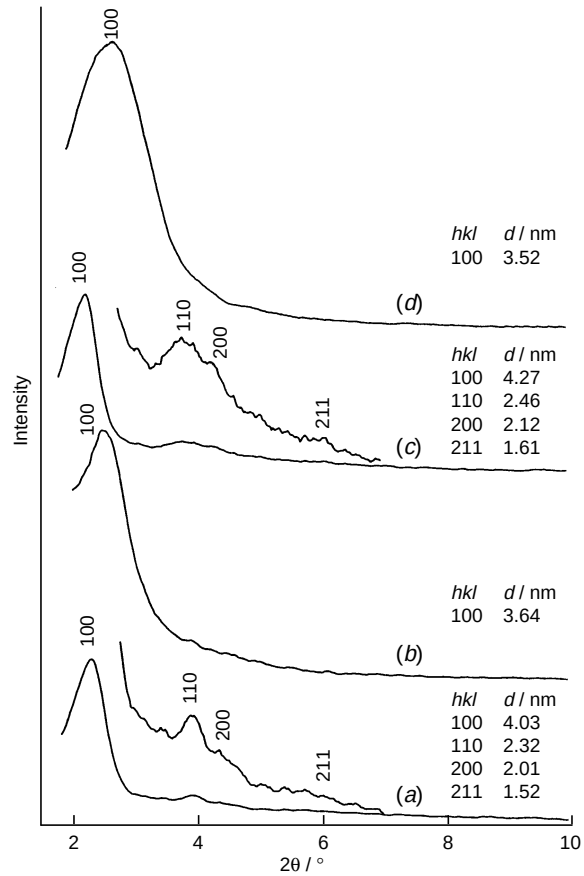



**Fig. 1** Powder XRD patterns of (*a*) as-synthesized UHM-1 (P/Al = 2.0), (*b*) calcined UHM-1 (P/Al = 2.0), (*c*) as-synthesized UHM-3 (P/Al = 0.8, Si/P = 0.2) and (*d*) calcined UHM-3 (P/Al = 0.8, Si/P = 0.2)

silicoaluminophosphate have been synthesized. As-synthesized UHM-1 and UHM-3 show a *d*(100) spacing of 4.1 nm. All XRD patterns of calcined UHM-1 and UHM-3 are similar and exhibit a single broad diffraction peak corresponding to a *d*(100) spacing of 3.6 nm.

The broadening of the (100) reflection on calcination arises from less long-range crystallographic order.[7,8] The intensity of the *d*(100) reflection of calcined UHM-1 and calcined UHM-3 decreases in comparison with that of as-synthesized UHM-1 or UHM-3 as has been observed for hexagonal MCM-41.[5,6,9]

Transmission electron micrographs of as-synthesized UHM-1 (Fig. 2) show hexagonal-shaped pores of about 4 nm diameter which is in agreement with the value (4.1 nm) measured from XRD. These results are similar to, but show more disorder, than those of siliceous MCM-41 materials,[5,6,9] supporting that as-synthesized UHM-1 and UHM-3 essentially have long-range hexagonal packing but with some disorder.

Synthesis of mesoporous aluminophosphate (UHM-1) is successful with aluminium hydroxide but replacement of aluminium hydroxide by Capatal alumina produces only amorphous or lamellar aluminophosphate (designated UHM-2). UHM-2 with *d*(100) of 2.97 nm is similar to the lamellar aluminophosphate previously reported.[4] For the formation of silicoaluminophosphate, TEOS is used as the silica source.

UHM-1 can be formed over a range of P/Al mole ratios (3.4–0.6) in the gel which is different from a fixed P/Al ratio (*ca.* 1.0) required for synthesis of microporous aluminophosphates.[10] However, the P/Al ratio in the product is always less than unity and decreases with decreasing P/Al in the gel. This is perhaps why the products show better resolved XRD with higher P/Al gel ratios. The product P/Al ratio of $< 1$ suggests that hydroxy aluminium species are involved in the mesoporous assembly process. Mesoporous aluminophosphate can be synthesized for a range of surfactant to alumina ratios of 0.24–0.50. At higher surfactant/$Al_2O_3$ ratios of 1–3 only amorphous material is formed.

Mesoporous hexagonal aluminophosphate can be synthesized at pH values from 7.5 to 9.5 at room temperature. At higher temperatures up to 100 °C formation of the hexagonal phase requires pH $> 8.5$. Mesoporous hexagonal aluminophosphate is formed with cationic surfactants only in the presence of alkylammonium hydroxide, $NR_4OH$ (R = Me, Et, $Bu^n$). Replacement of $NR_4OH$ with 0.1 M NaOH led to no mesostructural materials.

The BET surface areas of calcined UHM-1 average 772 $m^2\ g^{-1}$ and of UHM-3 average 928 $m^2\ g^{-1}$ and are independent of the P/Al or Si/P gel ratios. These values reflect the thermal stability of UHM-1 and UHM-3 to calcination at 500 °C as do the TEM results.

Thermogravimetric analysis of UHM-1 shows a large mass loss of *ca.* 70% on heating to 700 °C. Three endothermic losses near 80 °C (15 mass%), 240 °C (30 mass%) and 340 °C (25 mass%) are observed. The 80 °C loss is assigned to water desorption. The 240 and 340 °C losses are assigned to desorption and decomposition of TMAOH and CTAC in either order.

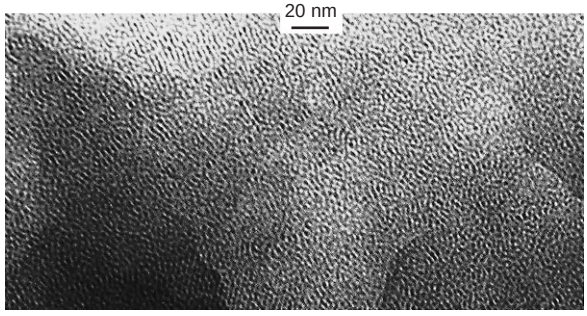



**Fig. 2** Transmission electron micrograph (TEM) of as-synthesized UHM-1. TEMs for calcined UHM-1 and for UHM-3 are similar.

We postulate that the formation of UHM-1 and UHM-3 materials occurs by a modified $S^+I^-$ ion-pair process. The inorganic precursors ($I^-$) are non-ideal aluminophosphate species of low polymerization degree with some hydroxy groups. When TMAOH is added, it reacts with the hydroxy group of these aluminophosphate species to produce a weak ion pair ($I^-\cdots TMA^+$) since the $TMA^+$ cation has a large ionic radius. These ion-pair species diffuse to the surfactant ($S^+$) assembly (micelle) interface and interact strongly with the cationic surfactant headgroups. The interaction of the aluminophosphate species with the cationic surfactant headgroups is stronger than that with $TMA^+$ cation. The micellar structure then organizes the condensation and polymerization of adjacent aluminophosphate species to form an ordered hexagonal mesostructure.[5,11]

The function of the organic ammonium cation from TMAOH seems to be to modify the strength of the electrostatic interaction between the aluminophosphate species and the cationic surfactant micelle assembly to form a $S^+I^-\cdots TMA^+$ ion pair. If NaOH is used the $Na^+$ cation with a smaller ionic radius than $TMA^+$ has a stronger ion-pair interaction with the aluminophosphate species and prevents sufficient interaction with the cationic surfactant assembly. Thus the assembly of mesostructural aluminophosphate fails. Aluminium hydroxide may form a less polymerized aluminophosphate with many hydroxy groups and favour the assembly of the mesostructure compared to Capatal alumina.

We conclude that mesoporous hexagonal aluminophosphate UHM-1 and silicoaluminophosphate UHM-3 molecular sieves can be synthesized *via* modified ion-pair interactions. The calcined materials are characterized by a hexagonal structure with *d*(100) *ca.* 4.0 nm and high surface area which reveals their thermal stability. These materials seem to have greater thermal stability than very large pore AlPO-*n* materials like VPI-5.

This research was supported by the R. A. Welch Foundation, the National Science Foundation and the University of Houston Energy Laboratory.

## Footnote

* E-mail: kevan@uh.edu

## References

1 S. T. Wilson, B. M. Lok, C. A. Messina, T. R. Connan and E. M. Flanigan, *J. Am. Chem. Soc.*, 1992, **104**, 1176.
2 M. E. Davis, C. Saldaraga, C. Montes, J. Garces and C. Crowder, *Nature*, 1988, **331**, 698.
3 S. Oliver, A. Kuperman, N. Coombs, A. Louth and G. A. Ozin, *Nature*, 1995, **378**, 47.
4 A. Sayari, V. R. Karra, J. S. Reddy and I. L. Moudrakovski, *Chem. Commun.*, 1996, 411; A. Chenite, Y. L. Page, V. R. Karra and A. Sayari, *Chem. Commun.*, 1996, 413.
5 C. T. Kresge, M. E. Leonowicz, W. J. Roth, J. C. Vartuli and J. S. Beck, *Nature*, 1992, **359**, 710; J. S. Beck, J. C. Vartuli, W. J. Roth, M. E. Leonowicz, C. T. Kresge, K. D. Schmitt, C. T.-W. Chu, D. H. Olson, E. W. Sheppard, S. B. McCullen, J. B. Higgins and J. L. Schlenker, *J. Am. Chem. Soc.*, 1992, **114**, 10834.
6 Q. Huo, D. I. Margolese, U. Cielsa, P. Feng, T. E. Gier, P. Sieger, R. Leon, P. M. Petroff, F. Schuth and G. D. Stucky, *Nature*, 1994, **368**, 317; Q. Huo, D. I. Margolese, U. Cielsa, D. G. Demuth, P. Feng, T. E. Gier, A. Firouzi, B. F. Chmelka, F. Schuth and G. D. Stucky, *Chem. Mater.*, 1994, **6**, 1176.
7 P. T. Tanev and T. J. Pinnavaia, *Science*, 1995, **267**, 865; S. A. Bagshaw, E. Prouzet and T. J. Pinnavaia, *Science*, 1995, **269**, 1242; P. T. Tanev, M. Chibwe and T. J. Pinnavaia, *Nature*, 1994, **368**, 321.
8 R. Schmidt, D. Akporiaye, M. Stöcker and O. H. Ellestad, *Stud. Surf. Sci. Catal.*, 1994, **84**, 61.
9 C.-Y. Chen, H.-Y. Li, S. L. Burkett and M. E. Davis, *Microporous Mater.*, 1993, **2**, 27.
10 R. Szostak, in *Molecular Sieves, Principles of Synthesis and Identification*, Van Nostrand Reinhold, New York, 1989, pp. 253–276.
11 M. E. Davis, C.-Y. Chen, S. L. Burkett and R. F. Lobo, *Mater. Res. Soc. Symp. Proc.*, 1994, **346**, 831.

*Received in Columbia, MO, USA, 11th February 1997; Com. 7/00965H*

# Sulfoxide induced sigmatropic rearrangement (SISR) of methyl 1-methylsulfanylvinyl sulfoxides

**Bianca F. Bonini,[a] Mauro Comes Franchini,[a] Germana Mazzanti,*[a] Jan-Willem Slief,[b] Margreth A. Wegman[b] and Binne Zwanenburg*[b]**

[a] *Dipartimento di Chimica Organica 'A. Mangini', Università di Bologna, Viale Risorgimento 4, I-40136 Bologna, Italy*
[b] *Department of Organic Chemistry, NSR Centre for Molecular Structure, Design and Synthesis, University of Nijmegen, Toernooiveld, 6525 ED Nijmegen, The Netherlands*

**Treatment of methyl 1-methylsulfanylvinyl sulfoxides with sodium thiophenolate in MeOH gives 1-methylsulfanylalk-1-en-3-ols.**

The sigmatropic rearrangement of allylic sulfoxides in the presence of a thiophilic reagent leads to allylic alcohols.[1] A special sequence which includes this reaction is the rearrangement of α-arylsulfinylacrylates to 4-hydroxyalk-2-enoate esters.[2] In this sequence a thiophilic base first gives an *in situ* isomerization of the vinyl sulfoxide moiety into an allylic sulfoxide, which then undergoes a 2,3-sigmatropic rearrangement and a subsequent thiophilic cleavage of the thus-formed intermediate sulfenic esters by the same base. A practical variant of this synthesis of γ-hydroxyalkenoic esters is the so-called SPAC (sulfoxide piperidine and carbonyl) reaction[3,4] in which the sulfinylacrylates are prepared by a Knoevenagel-type condensation of an appropriate aldehyde and arylsulfinyl acetates, and subsequently rearranged under the same conditions in a one-pot operation.

Here we report on a new related sulfoxide induced sigmatropic rearrangement (SISR) of methyl 1-methylsulfanylvinyl sulfoxides. The required starting materials were conveniently prepared from the corresponding dithiocarboxylic esters by deprotonation with LDA and subsequent *S*-methylation. The ketene dithioacetals thus prepared were oxidized to the *S*-monoxides with 1 equiv. of MCPBA. In all cases the *E*-isomers were formed preferentially. The dithioesters were prepared from Grignard reagents and carbon disulfide, followed by methylation with methyl iodide[5] (Scheme 1). The products **1**–**3** were characterized by IR, mass and NMR spectroscopy. The various compounds **3** prepared in this manner are listed in the Table 1.

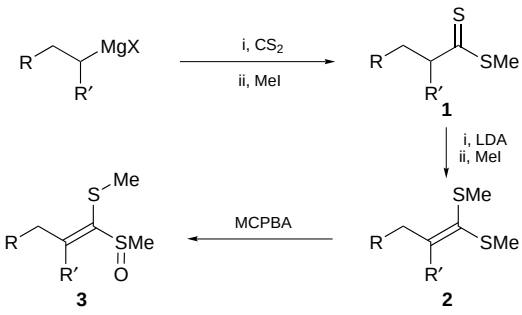
It is of interest to note that an alternative preparation of sulfoxides **3** from the *S*-oxides of dithioesters **1**, by deprotonation and subsequent *S*-alkylation of the intermediate vinylsulfenate anion,[6] was unsuccessful due to the limited stability[7] of the dithioesters of *S*-oxides and the formation of complex mixtures of products.

For the SISR reaction, first the recommended conditions for the SPAC reactions were tried for substrate **3a**. Prolonged treatment of **3a** with a large excess of piperidine in MeCN at room temperature did not give any reaction. Reaction at 85 °C for five days, adding 10 equiv. of piperidine every day, gave a 70% yield of 1-methylsulfanylpent-1-en-3-ol **6a** which had almost exclusively the *E* configuration (*E*:*Z* ratio greater than 95:5). More convenient conditions involved treatment with 5 equiv. of sodium thiophenolate in MeOH at room temperature for four days. In this manner **6a** was obtained in 75% yield almost exclusively in the *E* form. The formation of **6a** from **3a** can readily be explained by invoking an initial base-induced prototropic shift to give allylic sulfoxide **4a**, which then undergoes a 2,3-sigmatropic rearrangement to produce sulfenate ester **5a**. Subsequent thiophilic reaction of **5a** with thiophenolate then leads to product **6a**. It is quite surprising that thiophenoxide serves as thiophilic reagent[1] as well as base. These newly established conditions were also successful for the sequential prototropic shifts and sigmatropic rearrangement reactions of the substrates **3b**–**e**. The corresponding 1-methylsulfanylalk-1-en-3-ols **6b**–**e** were all obtained in yields ranging from 75–98%. The products **6a**–**e** have been characterized by IR, mass and NMR spectroscopic data.† The spectral characteristics revealed that all products **6** predominantly have the *E* configuration with *E*:*Z* ratio exceeding 90:10 (Scheme 2, Table 2).

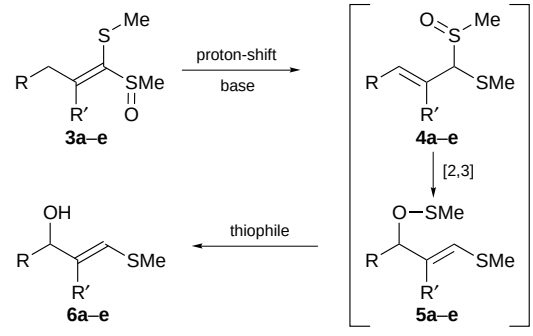
**Table 1** Synthesis of compounds **3**

| | Substituents | | Product yields (%)[a] | | | |
|---|---|---|---|---|---|---|
| | R | R′ | **1** | **2** | **3** | *E*:*Z* ratio[b] |
| **a** | Et | H | 95 | 95 | 72 | 95:5 |
| **b** | Pr | H | 98 | 98 | 82 | 92:8 |
| **c** | Bn | H | 85 | 83 | 78 | 92:8 |
| **d** | $PhO(CH_2)_2$ | H | 30 | 98 | 60 | 91:9 |
| **e** | $-(CH_2)_3-$ | — | 75 | 98 | 80 | — |

[a] Yields of pure isolated products. [b] Determined by NMR spectroscopy.




**Scheme 1**




**Scheme 2**

**Table 2** Synthesis of **6** using thiophenoxide as thiophile

| | Substituents | | Yield of **6** | |
|---|---|---|---|---|
| | R | R′ | (%)[a] | *E* : *Z* ratio[b] |
| **a** | Et | H | 75 | 95 : 5 |
| **b** | Pr | H | 75 | 92 : 8 |
| **c** | Bn | H | 89 | 95 : 5 |
| **d** | $PhO(CH_2)_2$ | H | 90 | 97 : 3 |
| **e** | $-(CH_2)_3-$ | | 90 | — |

[a] Yields of pure isolated products. [b] Determined by NMR spectroscopy.

It is worth noting that the yield is also high for the formation of **6e**, where the initial isomerization is accompanied by a considerable increase of torsional strain.

The SISR reaction of sulfoxides **3**, of which no precedent is known in the literature, leads to γ-hydroxyvinyl sulfides, which can serve as a synthetic equivalent for β-hydroxy aldehydes[8,9] The synthetic potential of this new SISR reaction is currently under investigation, including chirality transfer from sulfur to carbon when optically active sulfoxides are used as the substrates. Furthermore, the SISR reaction will be investigated for vinyl sulfoxides with other heteroatoms at the geminal position of the sulfoxide group.

Financial support of this work by the Ministero dell' Università e della Ricerca Scientifica e Tecnologica (MURST), Italy, is gratefully acknowledged. J. S. and M. A. W. are grateful for the support from the Erasmus programme (ICP-95-NL-1007/13).

## Footnote

† *Selected data* for *E*-**6a**: yellow oil; $\nu_{max}(CCl_4)/cm^{-1}$ 3620 (OH); $^1H$ NMR (200 MHz, $CDCl_3$): δ 0.90 (3 H, t, *J* 7.0 Hz), 1.50–1.65 (2 H, m), 1.70 (1 H, br s), 2.25 (3 H, s), 4.05 (1 H, q, *J* 7.0 Hz), 5.36 and 5.45 (1 H, dd, *J* 15.0 and 7.5 Hz), 6.30 (1 H, d, *J* 15.0 Hz); *m/z* 132 ($M^+$), 114 ($M^+-H_2O$).

For *E*-**6b**: yellow oil; $\nu_{max}(CCl_4)/cm^{-1}$ 3620 (OH); $^1H$ NMR (200 MHz, $CDCl_3$): δ 0.88 (3 H, t, J 7.5 Hz), 1.20–1.75 (5 H, m), 2.20 (3 H, s), 4.10 (1 H, br q, *J* 6.5 Hz), 5.33 and 5.40 (1 H, dd, *J* 14.5 and 7.3 Hz), 6.25 (1 H, d, *J* 14.5 Hz); $^{13}C$ NMR (50.3 MHz, $CDCl_3$): δ 13.78, 14.31, 18.53, 39.38, 72.64, 126.25, 128.00; *m/z* 146 ($M^+$), 129 ($M^+-H_2O$).

For *E*-**6c**: yellow oil; $\nu_{max}(CCl_4)/cm^{-1}$ 3610 (OH); $^1H$ NMR (200 MHz, $CDCl_3$): δ 2.00 (1 H, br s), 2.26 (3 H, s), 2.80 and 2.90 (2 H, ABq, *J* 13.6, 7.8 and 5.8 Hz), 4.40 (1 H, br q, *J* 4.4 Hz), 5.45 and 5.52 (1 H, dd, *J* 15.6 and 7.0 Hz), 6.33 (1 H, d, *J* 15.6 Hz), 7.40–7.60 (5 H, m); $^{13}C$ NMR (50.3 MHz, $CDCl_3$): δ 14.30, 44.02, 73.35, 126.32, 126.64, 128.25, 129.39, 137.40; *m/z* 194 ($M^+$), 176 ($M^+-H_2O$).

For *E*-**6d**: yellow oil; $\nu_{max}(CCl_4)/cm^{-1}$ 3620 (OH); $^1H$ NMR (200 MHz, $CDCl_3$): δ 1.99 (2 H, q, *J* 6.0 Hz), 2.15 (1 H, br s), 2.22 (3 H, s), 3.95–4.20 (2 H, m), 4.35–4.50 (1 H, m), 5.42 and 5.47 (1 H, dd, *J* 15.7 and 6.7 Hz), 6.35 (1 H, d, *J* 15.7 Hz), 6.85–6.95 (3 H, m), 7.20–7.35 (2 H, m); $^{13}C$ NMR (50.3 MHz, $CDCl_3$): δ 13.98, 36.33, 64.24, 69.62, 114.12, 120.37, 126.37, 126.82, 129.05, 158.31; *m/z* 224 ($M^+$).

For **6e**: yellow oil; $\nu_{max}(CCl_4)/cm^{-1}$ 3615 (OH); $^1H$ NMR (200 MHz, $CDCl_3$): δ 1.30–1.50 (2 H, m), 1.50–1.70 (2 H, m), 1.85–1.95 (1 H, br s), 2.05 (3 H, s), 3.70–3.95 (2 H, m), 4.10–4.20 (1 H, m), 5.70–5.80 (1 H, m); $^{13}C$ NMR (50.3 MHz, $CDCl_3$): δ 16.27, 21.25, 28.06, 35.14, 74.45, 119.78, 142.73; *m/z* 144 ($M^+$).

## References

1 D. A. Evans and G. C. Andrews, *Acc. Chem. Res*., 1974, **7**, 147.
2 S. Yamagiwa, H. Sato, N. Hoshi, H. Kosugi and H. Uda, *J. Chem. Soc., Perkin Trans. 1*, 1979, 570.
3 R. Tanikaga, Y. Nozaki, T. Tamura and A. Kaji, *Synthesis*, 1983, 134.
4 K. Burgess, I. Cassidy and I. Henderson, *J. Org. Chem*., 1991, **56**, 2050.
5 I. Meiser, P. Vermeer and L. Brandsma, *Recl. Trav. Chim. Pays-Bas*, 1973, **92**, 601.
6 G. E. Veenstra and B. Zwanenburg, *Recl. Trav. Chim. Pays-Bas*, 1976, **95**, 37.
7 P. Metzner and T. N. Pham, *J. Chem. Soc., Chem. Commun*., 1988, 390.
8 B. M. Trost and A. C. Lavoie, *J. Am. Chem. Soc*., 1983, **105**, 5075 and references cited therein.
9 B. T. Grobel and D. Seebach, *Synthesis*, 1977, 357.

*Received in Cambridge, UK, 19th March 1997; Com. 7/01942D*

# Diene-transmissive hetero-Diels–Alder reaction of cross-conjugated azatrienes: a novel and efficient method for the synthesis of ring-fused nitrogen heterocycles

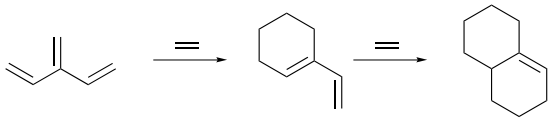
**Takao Saito,* Hiroaki Kimura, Tomomichi Chonan, Takayuki Soda and Takayuki Karakasa**

*Department of Chemistry, Faculty of Science, Science University of Tokyo, Kagurazaka, Shinjuku-ku, Tokyo 162, Japan*

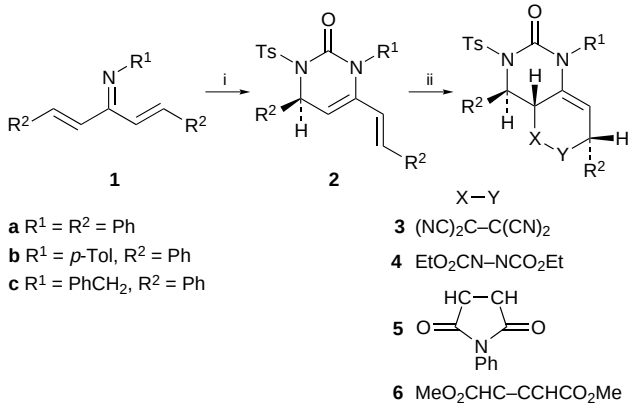
**A diene-transmissive hetero-Diels–Alder reaction of cross-conjugated azatrienes, which provides a novel and efficient synthetic method for ring-fused, nitrogen-heterocyclic frameworks such as quinazolin-2-ones and pyrimido[5,4-*c*]-pyridazin-6-ones, is described for the first time.**

The diene-transmissive Diels–Alder (DTDA) reaction is defined by two sequential (tandem) DA cycloadditions that involve an initial DA reaction of a cross-conjugated triene (or its equivalent) with a dienophile, followed by a second DA reaction of the mono-adduct on the newly-formed diene unit to give a bis-adduct (Scheme 1).[1] Tsuge *et al.* have developed the DTDA reactions.[2] However, the diene-transmissive hetero-Diels–Alder (DTHDA) reaction, in which one or more heteroatoms are contained within either a triene framework or a dienophile skeleton or both, has not been studied extensively, despite its high potential for construction of a wide range of ring-fused heterocycles; only a few reports have appeared so far.[3–6] In our previous reports, we disclosed the first examples of the DTHDA reactions in both inter- and intra-molecular modes of cycloadditions, in which divinyl thioketones were used as cross-conjugated heterotrienes.[3,4] Recently, Tsuge *et al.* reported the aza-DTHDA reaction of carbotrienes with strong diazo dienophiles such as azodicarboxylate and triazolinedione, and the oxa-DTHDA reaction of divinyl ketones with an enamine (initial cycloaddition) followed by tetracyanoethylene or triazolinedione (second cycloaddition).[5] Spino and Liu showed that cyclic 2-formyl 1,3-dienes also took part in the oxa-DTHDA reaction for the construction of a quassinoid framework.[6] Although azabutadienes constitute a class of widely investigated heterodienes in HDA cycloaddition reactions,[7] there are no reports on the aza-DTHDA cycloaddition of cross-conjugated azatrienes capable of 4π participation. We report here for the first time on the aza-DTHDA reaction of such azatrienes. The methodology constitutes a new facile access to a variety of functionalized, ring-fused nitrogen heterocycles with high efficiency and predictable stereoselectivity.

When the di-β-styrylmethanimine **1**† (16 mmol) was allowed to react with tosyl isocyanate (2–3 equiv.) at room temp. in xylene (15 $cm^3$) for 0.5–1 h, the 1 : 1 cycloadduct **2**‡ was obtained in good yield (Scheme 2, Table 1). Neither the regioisomer nor the bis-adduct were detected in the reaction mixture. A second DA cycloaddition of the diene **2** with tetracyanoethylene (TCNE) proceeded smoothly at room temp. to give a quantitative yield of the cycloadduct **3**‡ with complete stereoselectivity. The stereochemistry of the cycloadduct **3** was deduced from its $^1$H NMR spectrum based mainly on the coupling constants, for example for **3a** $^3J_{4,4a}$ 5.0, $^4J_{4a,7}$ 2.3, $^4J_{4a,8}$ 2.3 and $^3J_{7,8}$ 3.6 Hz, suggesting that, in the second cycloaddition, the dienophile cycloadds from the less hindered bottom side (*anti* to $R^2$) of **2** in which the substituent $R^2$ at C-4 occupies an axial arrangement in accord with the observed coupling constant $J_{4,5}$ (*e.g.* 6.9 Hz for **2a**). Dimethyl azodicarboxylate (DAD) also afforded highly stereoselectively the



**Scheme 1**




**Scheme 2** *Reagents and conditions*: i, TsNCO, xylene, room temp., 0.5–1 h; ii, X=Y, solvent, room temp. or heat

**Table 1** Initial cycloaddition of **1** to afford mono-cycloadducts **2**

| Azatriene | Reaction time/h | Cycloadduct (% yield)[a] |
|---|---|---|
| **1a** | 1 | **2a** (90) |
| **1b** | 0.5 | **2b** (91) |
| **1c** | 0.5 | **2c** (93) |

[a] Isolated yield in a one-pot reaction from the divinyl ketones *via* method A.†

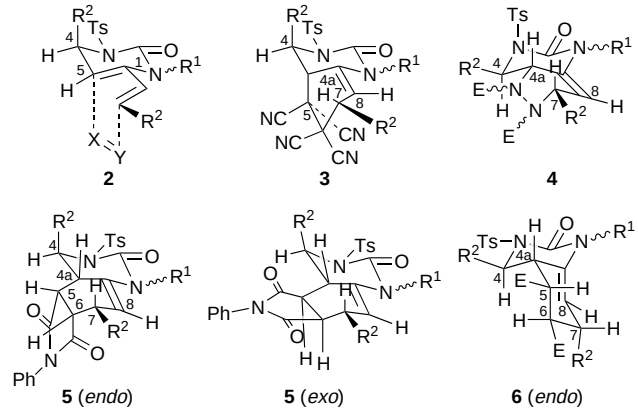



**Fig. 1**

**Table 2** Second cycloaddition of **2** to afford bis-cycloadducts **3**–**6**

| Run | Dienophile[a] | Diene | Reaction conditions | Cycloadduct (% yield)[b] | Ratio[c] |
|---|---|---|---|---|---|
| 1 | TCNE | **2a** | Benzene, room temp., 5 min | **3a** (99) | — |
| 2 | | **2b** | Benzene, room temp., 5 min | **3b** (97) | — |
| 3 | | **2c** | Benzene, room temp., 5 min | **3c** (99) | — |
| 4 | DAD | **2a** | Toluene, 110 °C, 10 min | **4a** (94) | — |
| 5 | | **2b** | Toluene, 110 °C, 10 min | **4b** (89) | — |
| 6 | | **2c** | Toluene, 110 °C, 10 min | **4c** (99) | — |
| 7 | NPMI | **2a** | Toluene, 110 °C, 7 h | **5a** (97) | 56 : 44 |
| 8 | | **2b** | Toluene, 110 °C, 17 h | **5b** (88) | 70 : 30 |
| 9 | | **2c** | Toluene, 110 °C, 4 h | **5c** (99) | 38 : 62 |
| 10 | DMF | **2a** | Toluene, 110 °C, 9 h | **6a** (99) | 57 : 43 |
| 11 | | **2b** | Toluene, 110 °C, 17 h | **6b** (91) | 59 : 41 |
| 12 | | **2c** | Toluene, 110 °C, 9 h | **6c** (99) | 53 : 47 |

[a] TCNE: tetracyanoethylene; DAD: diethyl azodicarboxylate; NPMI: *N*-phenylmaleimide; DMF: dimethyl fumarate. [b] Isolated yield. [c] Ratio (*endo* : *exo*) determined by $^1$H NMR spectroscopy. The term *endo* refers to a *cis*-relationship between $H_{4a}$ and $H_5$ and the term *exo* a *trans*-relationship.

cycloadduct **4**‡ in good yield. With *N*-phenylmaleimide (NPMI) and dimethyl fumarate (DMF) second cycloadditions were effected upon heating in toluene for 4–17 h to produce excellent yields of the cycloadducts **5** and **6** with complete diastereoisoface selectivity but with almost no *endo* : *exo*-selectivity. The results are summarised in Table 2. Fig. 1 shows the most probable stereochemical (conformational and configurational) structures of the mono- (**2**) and bis-cycloadducts (**3**–**6**) which were deduced from $^1$H NMR spectroscopic studies and computational calculations using MOPAC 93, CONFLEX, LAOCOON III and 3JHH2 programs.[4,10,11]

Thus, it has been shown that the DTHDA methodology of cross-conjugated azatrienes is successfully applied to a synthesis of ring-fused nitrogen heterocycles.

## Footnotes

† The imine **1** was prepared by Barluenga's method involving the reaction of iminophosphorane with prop-2-ynyltriphenylphosphonium salt, followed by successive treatment with an aldehyde, butyllithium and an aldehyde (Method B, 60–70% yield).[8] Otherwise, the imine **1** was more conveniently prepared by the condensation reaction of di-β-styryl ketone with an amine in the presence of $TiCl_4$ and triethylamine (method A, 90–95% yield).[9]

‡ *Selected data* for **2a**: mp 132–133 °C; *m/z* 506 ($M^+$, 0.5%) and 309 ($M^+$ − TsNCO, 100%); $\nu_{max}$ (KBr)/cm$^{-1}$ 1170, 1362 ($SO_2$) and 1698 (CO); $\delta_H$ (270 MHz, $CDCl_3$) 2.19 [s, 3 H, $CH_3$ (Ts)], 5.73 (d, 1 H, *J* 6.9 Hz, 5-H), 5.85 (d, 1 H, *J* 16.2 Hz, 7-H), 6.09 (d, 1 H, *J* 6.9 Hz, 4-H), 6.57 (d, 1 H, *J* 16.2 Hz, 8-H), 6.90 (d, 2 H, *J* 8.58 Hz, ArH), 6.97–7.02 (m, 2 H, ArH) and 7.08–7.31 (m, 15 H, ArH); $\delta_C$ (DEPT, $CDCl_3$) 21.5 ($CH_3$), 56.9 (CH), 103.8 (CH, C-5), 120.5 (CH), 125.6 (2CH), 125.8 (2CH), 127.0 (CH), 127.4 (CH), 127.5 (CH), 127.6 (2CH), 127.7 (2CH), 127.8 (2CH), 128.0 (2CH), 128.06 (2CH), 128.10 (2CH), 131.3 (CH), 135.8 (C), 136.0 (C), 137.1 (C), 137.5 (C), 140.3 (C), 140.0 (C) and 150.0 (CO). For **3a**: mp 160–163 °C; *m/z* (FAB) 635 ($M^+$ + 1, 2%), 309 ($M^+$ − TCNE − TsNCO, 98%) and 308 (100%); HRMS (FAB) found $M^+$ + 1 635.1860 $C_{37}H_{27}O_3N_6S$ requires M + 1, 635.1868; $\nu_{max}$ (KBr)/cm$^{-1}$ 1174, 1364, 1718 (CO) and 2256 (CN); $\delta_H$ (270 MHz, $CDCl_3$, [H,H]-COSY) 2.31 [s, 3 H, $CH_3$ (Ts)], 3.92 (dd, 1 H, *J* 5.0, 2.3 and 2.3 Hz, 4a-H), 4.32 (dd, 1 H, *J* 3.6 and 2.3 Hz, 7-H), 5.29 (dd, 1 H, *J* 3.6 and 2.3 Hz, 8-H), 6.14 (d, 1 H, *J* 5.0 Hz, 4-H), 6.99 (d, 2 H, *J* 8.6 Hz, ArH) and 7.29–7.48 (m, 17 H, ArH); $\delta_C$ (DEPT, $CDCl_3$) 21.5 ($CH_3$), 42.7 (C), 45.5 (C), 47.7 (CH), 49.1 (CH), 59.4 (CH), 108.0 (CN), 109.1 (CN), 110.3 (CN), 111.2 (CN), 111.7 (CH), 127.4 (2CH), 128.0 (2CH), 128.8 (2CH), 129.1 (CH), 129.3 (4CH), 129.76 (2CH), 129.81 (CH), 130.1 (2CH), 130.3 (2CH), 130.6 (CH), 131.0 (C), 135.0 (C), 135.4 (C), 137.1 (C), 137.2 (C), 144.9 (C) and 149.4 (CO). For **5a** (*exo*): mp 151–152 °C; *m/z* 679 ($M^+$ + 1, 24%), 525 ($M^+$ − TsH, 32%) and 481 (100%); $\nu_{max}$ (KBr)/cm$^{-1}$ 1170, 1386 and 1716 (CO); $\delta_H$ (270 MHz, $[^2H]_{10}$- *p*-xylene, [H,H]- and [C,H]-COSY in $CDCl_3$) 1.86 [s, 3 H, $CH_3$ (Ts)], 2.21 (dd, 1 H, *J* 10.6 and 10.6 Hz, 5-H), 2.66 (br d, 1 H, *J* 10.6 Hz, 4a-H), 3.13 (br d, 1 H, *J* 10.6 Hz, 7-H), 3.34 (dd, 1 H, *J* 10.6 and 10.6 Hz, 6-H), 4.83 (br s, 1 H, 8-H), 6.90 (br s, 1 H, 4-H) and 6.58–7.82 (m, 24 H, ArH); $\delta_C$ (DEPT, $CDCl_3$) 21.5 ($CH_3$), 43.2 (CH), 43.6 (CH), 46.1 (CH), 48.2 (CH), 58.7 (CH), 115.8 (CH), 126.1 (2CH), 126.3 (2CH), 127.4 (CH), 127.8 (CH), 128.3 (2CH), 128.5 (2CH), 128.68 (CH), 128.75 (2CH), 128.9 (3CH), 129.1 (6CH), 129.6 (CH), 131.3 (C), 135.4 (C), 137.0 (C), 139.3 (C), 139.4 (C), 141.5 (C), 144.4 (C), 150.7 (CO), 174.7 (CO) and 176.7 (CO).

## References


1 For excellent reviews and monographs on such sequential, multistep processes (the so-called domino, tandem or cascade strategy) involving a Diels–Alder reaction, see F. Fringuelli and A. Taticchi, *Dienes in the Diels–Alder Reaction*, Wiley, New York, 1990; T.-L. Ho, *Tandem Organic Reactions*, Wiley, New York, 1992; L. F. Tietze and U. Beifuss, *Angew. Chem., Int. Ed. Engl.*, 1993, **32**, 131; L. F. Tietze, *Chem. Rev.*, 1996, **96**, 115; S. E. Denmark and A. Thorarensen, *Chem. Rev.*, 1996, **96**, 137; J. D. Winkler, *Chem. Rev.*, 1996, **96**, 167. For recent publications, see 'Cascade Reactions', *Tetrahedron Symposia-in-Print*, 1996, **52**, 11 385; K. H. Ang, S. Brase, A. G. Steinig, F. E. Meyer, A. Llebaria, K. Voigt and A. de Meijere, *Tetrahedron*, 1996, **52**, 11 503; S. E. Denmark and C. B. W. Senanayake, *Tetrahedron*, 1996, **52**, 11 579; A. Franz, P.-Y. Eschler, M. Thrin and R. Neier, *Tetrahedron*, 1996, **52**, 11 643; A. Hosomi, T. Masunari, Y. Tominaga, T. Yanagi and M. Hojo, *Tetrahedron Lett.*, 1990, **31**, 6201.

2 O. Tsuge, S. Kanemasa, E. Wada and H. Sakoh, *Yuki Gosei Kagaku Kyokaishi*, 1986, **44**, 756; O. Tsuge, E. Wada and S. Kanemasa, *Chem. Lett.*, 1983, 239; O. Tsuge, E. Wada, S. Kanemasa and H. Sakoh, *Bull. Chem. Soc. Jpn.*, 1984, **57**, 3221; O. Tsuge, S. Kanemasa, H. Sakoh and E. Wada, *Bull. Chem. Soc. Jpn.*, 1984, **57**, 3234; S. Kanemasa, H. Sakoh, E. Wada and O. Tsuge, *Bull. Chem. Soc. Jpn.*, 1985, **58**, 3312; S. Kanemasa, H. Sakoh, E. Wada and O. Tsuge, *Bull. Chem. Soc. Jpn.*, 1986, **59**, 1869.

3 S. Motoki, Y. Matsuo and Y. Terauchi, *Bull. Chem. Soc. Jpn.*, 1990, **63**, 284.

4 T. Saito, H. Kimura, K. Sakamaki, T. Karakasa and S. Moriyama, *Chem. Commun.*, 1996, 811.

5 O. Tsuge, T. Hatta, K. Yakata and H. Maeda, *Chem. Lett.*, 1994, 1833; O. Tsuge, T. Hatta, H. Yoshitomi, K. Kurosaka, T. Fujiwara, H. Maeda and A. Kakehi, *Heterocycles*, 1995, **41**, 225.

6 G. Spino and G. Liu, *J. Org. Chem.*, 1993, **58**, 817.

7 D. L. Boger and S. M. Weinreb, *Hetero Diels–Alder Methodology in Organic Synthesis*, Academic, New York, 1987; D. L. Boger, in *Comprehensive Organic Synthesis*, ed. B. M. Trost, I. Fleming and L. A. Paquett, Pergamon, Oxford, 1991, vol. 5, p. 451; J. Barluenga, *Adv. Heterocycl. Chem.*, 1993, **57**, 1.

8 J. Barluenga, I. Merino and F. Palacios, *J. Chem. Soc., Perkin Trans.* 1, 1991, 341; K. Eiter and H. Oediger, *Justus Liebigs Ann. Chem.*, 1965, **682**, 62.

9 D. L. Boger, W. L. Cobett, T. T. Curran and A. M. Kasper, *J. Am. Chem. Soc.*, 1991, **113**, 1713.

10 S. Moriyama, T. Karakasa, T. Inoue, K. Kurashima, S. Satsumabayashi and T. Saito, *Synlett*, 1996, 72.

11 LAOCOON III, D. F. Detar, Computer Programs for Chemistry, W. A. Benjamin, Inc., New York 1968, vol. 1, p 10; Chemistry and Software No. 8007 program was used. The following JCPE (Japan Chemistry Program Exchange) programs were used: CONFLEX (program No. P040), MOPAC 93 (program No. P081), and 3JHH2 (program No. P012).



*Received in Cambridge, UK, 6th March 1997; Com. 7/01575E*

# Novel biocatalytic reduction of aryl azides: chemoenzymatic synthesis of pyrrolo[2,1-*c*][1,4]benzodiazepine antibiotics[1]

**Ahmed Kamal,* Y. Damayanthi, B. S. Narayan Reddy, B. Lakminarayana and B. S. Praveen Reddy**

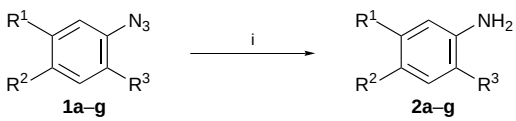
*Indian Institute of Chemical Technology, Hyderabad 500 007, India*

**The chemoselective reduction of aryl azides to aryl amines, and the synthesis of the imine-containing pyrrolo[2,1-*c*]-[1,4]benzodiazepine DNA-binding antitumour antibiotics by selective biocatalytic reductive cyclization of azido aldehydes, has been achieved by employing baker's yeast.**

In the recent years there has been a growing interest in biocatalysis and, in particular, transformations[2] mediated by baker's yeast (*Saccharomyces cerevisiae*). Reduction of carbonyl compounds by baker's yeast has become a valuable strategy in organic synthesis.[3] A variety of new and novel abilities of baker's yeast have been reported by us,[4,5] for example regeneration of carbonyl compounds and biooxidative conversion of thio to oxo functionality. In continuation of these efforts, we herein report a novel reduction of aryl azides to aryl amines in quantitative yield. This is an exceptionally mild, convenient and facile reduction employing baker's yeast. However, in the literature[6] alkyl keto azides have been reduced by baker's yeast to afford the corresponding alkyl azido alcohols. This is consistent with our finding that various alkyl azides, *e.g.* 1-azido-3-aryloxypropan-2-ols, are resistant to baker's yeast reduction. Further, this biocatalytic reductive methodology has been applied to the chemoenzymatic synthesis of the DNA-binding pyrrolo[2,1-*c*][1,4]benzodiazepine (PBD) system[7] *via* the reductive cyclization of aryl azido aldehydes. Interestingly, this investigation has revealed the unusual chemoselective reduction of the aryl azido group in the presence of an aldehyde group by baker's yeast.

Some representative aryl azides **1a**–**g** have been reduced by baker's yeast to afford the corresponding aryl amines **2a**–**g** (yields 83–92%), as illustrated in Scheme 1.†

This biocatalytic reduction employing baker's yeast has been extended to the chemoenzymatic synthesis of the PBD class of antitumour antibiotics. Although PBDs with either a secondary amine or amide functionalty at N(10)–C(11) are readily synthesised, the introduction of an imine or amino alcohol at this position is problematic due to the reactivity of these functional groups.[8] In the literature, various approaches to the synthesis of these antibiotics have been investigated.[9] Our interest in the design and synthesis of PBD analogues[10] has led us to develop a new chemoenzymatic methodology for the DNA-interactive PBDs. This approach is based on the formation of the seven-membered ring *via* an enzymatic azido reductive cyclization process. This enables cyclization of the diazepine ring to take place under extremely mild and ambient conditions, and involves a simple and rapid work-up procedure.



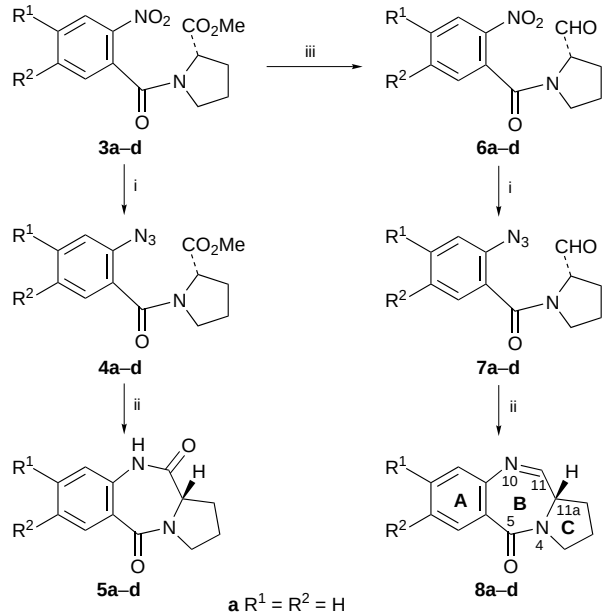

**a** $R^1 = R^2 = R^3 = H$
**b** $R^1 = R^3 = H$, $R^2 = Cl$
**c** $R^1 = R^3 = H$, $R^2 = F$
**d** $R^1 = R^3 = H$, $R^2 = Me$
**e** $R^1 = R^3 = H$, $R^2 = OMe$
**f** $R^1 = R^2 = H$, $R^3 = CO_2H$
**g** $R^1 = Me$, $R^2 = H$, $R^3 = OH$

**Scheme 1** *Reagents and conditions*: i, baker's yeast (phosphate buffer, pH 7.2), aq. EtOH, 6–8 h

The initial studies were carried out on the preparation of PBD dilactams by the azido bioreductive cyclization process to assess the scope of this reaction. The starting materials, methyl (2*S*)-*N*-(2-nitrobenzoyl)pyrrolidine-2-carboxylate esters **3**, were prepared[8] from 2-nitrobenzoic acids *via* their acid chlorides, which were coupled with (*S*)-proline methyl ester hydrochloride. The reaction of **3** with $NaN_3$ in HMPA‡ gave the azido derivatives **4** which, upon reduction with baker's yeast, gave the PBD dilactams **5a**–**d** in quantitative yield (Scheme 2).

The precursor for PBD imine **8** was prepared by the reduction of **3** with DIBAL-H to give the corresponding (2*S*)-*N*-(2-nitrobenzoyl)pyrrolidine-2-carboxaldehydes **6**. These, upon subsequent reaction with $NaN_3$ in HMPA followed by reduction with baker's yeast and chromatography of the crude product (silica, chloroform–methanol, 9.8 : 0.2), gave the PBD imines **8a**–**d**.§ This novel biocatalytic methodology has also been extended to the synthesis of the natural product DC-81 **8c**.

The results contained in this report demonstrate that it is not only possible to convert aryl azides to the amino arenes by employing baker's yeast, but also the usefuleness of baker's




**a** $R^1 = R^2 = H$
**b** $R^1 = H$, $R^2 = Me$
**c** $R^1 = OH$, $R^2 = OMe$
**d** $R^1 = OBn$, $R^2 = OMe$

**Scheme 2** *Reagents and conditions*: i, $NaN_3$, HMPA, 6–8 h; ii, baker's yeast (phosphate buffer, pH 7.2), aq. EtOH, 1–2 d; iii, DIBAL-H, $CH_2Cl_2$, −78 °C, 45 min

yeast in the chemoenzymatic synthesis of natural and synthetic analogues of PBDs. The present approach, which is performed under extremely mild conditions, should maintain the stereochemical integrity at C(11a) and may not effect the DNA binding potential of the PBD imines, unlike other chemical methods.[10d]

## Footnotes

* E-mail: root@csiict.ren.nic.in

† *General procedure*. To a solution of 2-azidobenzoic acid **1a** (0.31 mmol) in aq. EtOH (50%, 2 $cm^3$) was added to a preincubated suspension of baker's yeast (2 g) in phosphate buffer solution of pH 7.2 (20 $cm^3$) and shaken in an orbital shaker for 6 h. The reaction was monitored by TLC (EtOAc–hexane, 1 : 1). On completion of the reaction, EtOAc (20 $cm^3$) was added to the reaction mixture. The organic phase was separated, dried over anhydrous $Na_2SO_4$ and concentrated under reduced pressure. The residue obtained was subjected to column chromatography (silica gel, EtOAc–hexane, 1 : 1) to afford the reduced product, 2-aminobenzoic acid **2a** in 85% yield.

‡ *General procedure*. A solution of nitro esters **3** (514 mg, 1.85 mmol) or nitro aldehydes **6** (459 mg, 1.85 mmol) and sodium azide (247 mg, 3.80 mmol) in HMPA (15 $cm^3$) was stirred at room temperature for 6–8 h. The reaction mixture was poured onto water and then extracted several times with diethyl ether. Evaporation of the combined diethyl ether extract gave the crude azides in 90–95%, which was further purified by column chromatography on silica gel. *Selected spectra data* for **7a**: $^1$H NMR (200 MHz, $CDCl_3$): δ 1.90–2.39 (m, 4 H), 3.32 (t, 2 H, *J* 7.0 Hz), 4.74 (t, 1 H, *J* 7.2 Hz), 7.50–7.98 (m, 3 H), 8.29 (d, 1 H, *J* 6.2 Hz); 9.87 (d, 1 H, *J* 4.2 Hz); *m/z* 244 ($M^+$, 8%).

§ *Selected spectra data* for **8a**: $^1$H NMR (200 MHz, $CDCl_3$): δ 1.56–2.48 (m, 4 H), 3.20–3.89 (m, 3 H), 7.10–7.59 (m, 3 H), 7.66 (d, 1 H *J* 4.2 Hz), 8.02 (d, 1 H, *J* 5.8 Hz); *m/z* 200 ($M^+$ 100%).

## References


1 Part of the work presented in the Indo-German Symposium 'Organic Synthesis—Growing Interface with Adjacent Sciences' Sept. 1996, Hyderabad, India; Indian Patent applied for, Oct. 1996.
2 S. Servi, *Synthesis*, 1990, 1.
3 R. Czuk and B. I. Glanzer, *Chem. Rev*., 1991, **91**, 49.
4 A. Kamal, M. V. Rao and H. M. Meshram, *J. Chem. Soc., Perkin Trans. 1*, 1991, 2056.
5 A. Kamal and B. S. P. Reddy, *Bioorg. Med. Chem. Lett*., 1991, **1**, 159.
6 C. Fuganti and P. Grasseli, *Tetrahedron Lett*., 1985, **26**, 101.
7 D. E. Thurston, Advances in the Study of Pyrrolo[2,1-*c*][1,4]benzodazepine (PBD) Antitumour Antibiotics, in *Molecular Aspects of Anticancer Drug–DNA Interactions*, ed. S. Neidle and M. J. Waring, Macmillan Press, 1993, vol. 1, pp. 54–88.
8 D. E. Thurston and D. S. Bose, *Chem. Rev*., 1994, **94**, 433.
9 W. Leimgruber, A. B. Batcho and R. C. Crajkowski, *J. Am. Chem. Soc*., 1968, **90**, 5461; J. W. Lown and A. V. Joshua, *Biochem. Pharmacol*., 1979, **28**, 2017; T. Kaneko, H. Wong, T. W. Doyle, W. C. Rose and W. T. Bradner, *J. Med. Chem*., 1985, **28**, 388; D. R. Langley and D. E. Thurston, *J. Org. Chem*., 1987, **52**, 91; M. Mori, M. Kimura, Y. Uozumi and Y. Ban, *Tetrahedron Lett*., 1985, **26**, 5947; N. Langlois, F. Farve and A. Rojas, *Tetrahedron Lett*., 1993, **34**, 4635; S. M. Courtney and D. E. Thurston, *Tetrahedron Lett*., 1993, **34**, 5327; P. Molina, I. Diaz and A. Tarraga, *Tetrahedron*, 1995, **51**, 5617; S. Eguchi, K. Yamashita, Y. Matsushita and A. Kakchi, *J. Org. Chem*., 1995, **60**, 4006; S. C. Wilson, P. W. Howard and D. E. Thurston, *Tetrahedron Lett*., 1995, **36**, 6333.
10 (*a*) A. Kamal, B. S. P. Reddy and D. E. Thurston, *Bioorg. Med. Chem. Lett*., 1993, **3**, 743; (*b*) A. Kamal and N. V. Rao, *Tetrahedron Lett*., 1995, **36**, 4299; (*c*) A. Kamal and N. V. Rao, *Chem. Commun*., 1996, 385; (*d*) A. Kamal, B. S. P. Reddy and B. S. N. Reddy, *Tetrahedron Lett*., 1996, **37**, 2281; (*e*) A. Kamal, P. W. Howard, B. S. N. Reddy, B. S. P. Reddy and D. E. Thurston, *Tetrahedron*, 1997, **53**, 3223.


*Received in Cambridge, UK, 24th February 1997; Com. 7/01249G*

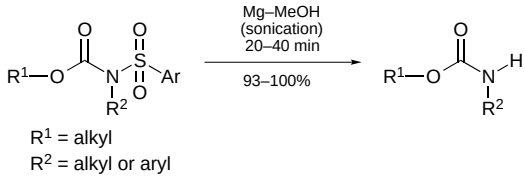
# Mild, efficient cleavage of arenesulfonamides by magnesium reduction

**Barthélémy Nyasse,[a] Leif Grehn[b] and Ulf Ragnarsson*[b]**

[a] *Department of Organic Chemistry, University of Yaoundé I, Box 812, Yaoundé, Cameroon*
[b] *Department of Biochemistry, University of Uppsala, Biomedical Center, Box 576, S-751 23 Uppsala, Sweden*

**The cleavage of arenesulfonamides *via* *N*-arenesulfonylcarbamates is achieved within a few minutes under ultrasonic conditions by reaction with magnesium in anhydrous methanol.**

For a long time, aromatic sulfonic acids have been used in the derivatization of amines and the protection of amino functions[1] and the resultant, generally crystalline sulfonamides are very resistant to nucleophilic attack. In addition, sulfonamides derived from primary amines can be readily deprotonated and the anions can serve as nucleophiles in reactions with alkylating reagents.[2] For the cleavage of the prototype *N*-tosyl group, reagents like sodium in liquid ammonia,[3] refluxing strong acid such as HBr in the presence of phenol[3] and sodium naphthalenide have been applied.[4] The need for such drastic conditions in the deprotection step restricted the use of tosyl and similar protecting groups to only very stable molecules and excluded the simultaneous application of many other protecting groups currently used. However, the scope widened with the development of new deprotection methods which included $SmI_2$,[5] $Bu_3SnH$–AIBN[6] and electrolysis.[7a] In the meantime, efforts were made to modify the tosyl group to make it more labile to acid. As a result, a new generation of arenesulfonyl protecting groups have emerged, *e.g.* 4-methoxybenzenesulfonyl (Mbs),[8] and the 2,2,5,7,8-pentamethylchromane-6-sulfonyl[9] and heteroarene-2-sulfonyl groups.[5b–d]




In continuation of our work dealing with the cathodic cleavage of substituted benzenesulfonamides and the corresponding *tert*-butyl sulfonylcarbamates,[7a] we now report a fast and simple method for the deprotection of substituted phenylsulfonylcarbamates using magnesium† in methanol as the cleaving agent under ultrasonic conditions. Although this system has been used previously for the cleavage of primary and secondary alkyl phenyl sulfones,[10,11] only one example dealing with the cleavage of a tosyl group attached to an indole nitrogen with magnesium turnings has been briefly reported.[12]

The *tert*-butyl *N*-arylsulfonylcarbamates and *N*-acylsulfonamides used as starting material in this work were prepared according to the procedures previously described.[7] In general primary amino functions of alkylamines and amino acids were first converted to the corresponding sulfonamides which in turn afforded alkyl arylsulfonylcarbamates almost quantitatively after treatment with $Boc_2O$ under DMAP catalysis.

Initial cleavage experiments were carried out using 20 equiv. of magnesium in methanol at room temperature with stirring. Long reaction times (6–24 h) were thereby required to attain the

**Table 1** Cleavage experiments with magnesium in methanol

| Entry | Substrate | Equiv. of Mg | *t*/min | Product[a] | Yield (%) |
|---|---|---|---|---|---|
| 1 | Boc-N(Ph)-Ts | 5 | 20 | Boc-NHPh | 99 |
| 2 | Boc-N(Bn)-$SO_2$Ph | 5 | 20 | Boc-NHBn | 99 |
| 3 | Boc-N(Bn)-Ts | 5 | 20 | Boc-NHBn | 99 |
| 4 | Boc-N(Bn)-$SO_2C_6H_4$Br-4 | 5 | 20 | Boc-NHBn | 98 |
| 5 | Boc-N(Bn)-Cbs[b] | 5 | 40 | Boc-NHBn | 100 |
| 6 | Boc-N(Bn)-$SO_2C_6H_4NO_2$-4 | 5 | 80 | not isolated | |
| 7 | Boc-N(Bn)-Mbs | 15 | 20 | Boc-NHBn | 100 |
| 8 | Boc-N(Bn)-$SO_2C_6H_2Me_3$-2,4,6 | 10 | 25 | Boc-NHBn | 95 |
| 9 | Boc-N(Bn)-$SO_2C_6H_2Pr^i_3$-2,4,6 | 10 | 25 | Boc-NHBn | 97 |
| 10 | Boc(Ts)-D-Ala-OEt | 5 | 60 | Boc-D-Ala-OMe | 97 |
| 11 | Z(Ts)-D-Ala-OEt | 5 | 40 | Z-D-Ala-OMe | 98 |
| 12 | Boc(Cbs)-L-Ala-OBn | 5 | 35 | Boc-L-Ala-OMe | 100 |
| 13 | Boc(Ts)N[$CH_2$]$_2$-NHZ[c] | 6 | 20 | Boc-NH[$CH_2$]$_2$-NHZ | 99 |
| 14 | Boc(Ts)N[$CH_2$]$_2$-NHTroc[c] | 5 | 40 | Boc-NH[$CH_2$]$_2$NHDoc | 87 |
| 15 | Boc(Ts)N-N(Bn)Z[c] | 10 | 35 | Boc-NH-N(Bn)Z | 100 |
| 16 | Boc(Cbs)N-N(Bn)Z | 10 | 35 | Boc-NH-N(Bn)Z | n.d.[d] |
| 17 | Ac-N(Bn)-Ts | 10 | 40 | Ac-NHBn | 81 |
| 18 | Bz-N(Bn)-Ts | 10 | 40 | mixture | — |
| 19 | Ts-Indole | 5 | 20 | indole | 100 |

[a] Products were identical with reference substances by TLC, $^1$H NMR and/or melting point. [b] Typical experimental procedure: to a solution of substrate (186 mg, 0.5 mmol) in MeOH (6 cm$^3$) was added Mg powder (61 mg, 2.5 mmol, 5 equiv.). The resulting suspension was sonicated for 20 min, when TLC on silica (diethyl ether–light petroleum, 1 : 2) indicated that all starting material had been consumed. The reaction was diluted with dichloromethane (15 cm$^3$) and poured into 0.5 M HCl. The organic phase was washed twice with 1 M $NaHCO_3$ and brine and then dried ($MgSO_4$). Filtering through a short silica column and crystallization gave 103 mg (100%) of white crystalline product, identical with Boc-NHBn. For substrates not readily soluble in MeOH, THF can be added. A mixture of MeOH–THF 3 : 1 worked as well as neat MeOH. [c] New compound (L. Grehn, B. Nyasse and U. Ragnarsson, manuscript in preparation). [d] n.d. = not determined.

complete deprotection of $PhSO_2$, 4-cyanophenylsulfonyl (Cbs), 4-$BrC_6H_4SO_2$ and Ts groups of the corresponding *tert*-butyl arylsulfonylcarbamates, but Mbs did not cleave completely even after 24 h. When the same amount of magnesium was used and the reactions were allowed to proceed under ultrasonic conditions‡ very fast and clean cleavage took place even with Mbs-protected and sterically hindered substrates. Reactions were subsequently optimised with the *tert*-butyl *N*-benzyl derivatives in each case under sonication with the results that (i) 5 equiv. of magnesium powder were sufficient for an efficient deprotection of the $PhSO_2$, 4-$BrC_6H_4SO_2$, Cbs and Ts groups and (ii) 10 equiv. for the 2,4,6-$Me_3C_6H_2SO_2$ and 2,4,6-$Pr^i_3C_6H_2SO_2$ groups, whereas (iii) at least 15 equiv. were required for the cleavage of the Mbs-carbamate. These findings were subsequently applied in the preparative cleavage experiments involving derivatives of alanine, ethylenediamine, hydrazine and *N*-acyl sulfonamides listed in Table 1.

It should be noted that during the experiment involving the 4-$NO_2C_6H_4SO_2$ group (entry 6), a yellow mixture was obtained, probably resulting from reduction of the nitro group. The Troc containing sulfonylcarbamate (entry 14), although cleaved completely, underwent a known alkyl halide reduction mediated by the reagent,[13] giving rise to the 2,2-dichloroethoxycarbonyl (Doc) derivative. Furthermore, transesterification took place (entries 10 and 11) as previously observed during the reduction of an α,β-unsaturated ethyl ester.[14] Concerning the *N*-Ac and *N*-Bz sulfonamides (entries 17 and 18), it is worth mentioning that the cleavage of the tosyl group proceeded more selectively in the former case.

In summary, since arenesulfonamides derived from primary amines are easily converted to *tert*-butyl and similar sulfonylcarbamates by DMAP-catalysed acylation,[7] this reductive cleavage completes a two-step procedure from sulfonamides to carbamates. Furthermore, since the required sulfonylcarbamates can also be directly obtained from alcohols by the Mitsunobu reaction,[2] such carbamates can now also be made more conveniently by the present procedure.

During the tenure of this work, B. N. was a recipient of a fellowship from the Swedish Institute which is gratefully acknowledged. This research is part of a programme supported by the Swedish Natural Science Research Council.

## Footnotes

* E-mail: urbki@bmc.uu.se

† Magnesium powder (Merck 105815, particle size 0.06–0.3 mm) was used. The quality of methanol is critical for these experiments: we found that after addition of 0.5% of water, no reaction took place. For other applications of Mg–MeOH, see *Encyclopedia of Reagents for Organic Synthesis*, ed. L. A. Paquette, Wiley, Chichester, 1995, vol. 5, pp. 3202–3204.

‡ 35 kHz, 120–240 W (Bandelin, Berlin, type RK106).

## References

1 (*a*) T. W. Greene and P. G. M. Wuts, *Protective Groups in Organic Chemistry*, Wiley-Interscience, New York, 2nd edn., 1991; (*b*) P. J. Kocienski, *Protecting Groups*, Thieme, New York, 1994.
2 J. R. Henry, L. R. Marcin, M. C. McIntosh, P. M. Scola, G. D. Harris and S. M. Weinreb, *Tetrahedron Lett*., 1989, **30**, 5709.
3 R. C. Roemmele and H. Rapaport, *J. Org. Chem*., 1988, **53**, 2367 and references cited therein.
4 S. Ji, L. B. Gortler, A. Waring, A. Battisti, S. Bank, W. D. Closson and P. Wriede, *J. Am. Chem. Soc*., 1967, **89**, 5311.
5 (*a*) E. Vedejs and S. Lin, *J. Org. Chem*., 1994, **59**, 1602; (*b*) C. Goulaouic-Dubois, A. Guggisberg and M. Hesse, *J. Org. Chem*., 1995, **60**, 5969; (*c*) C. Goulaouic-Dubois, A. Guggisberg and M. Hesse, *Tetrahedron*, 1995, **51**, 12 573; (*d*) E. Vedejs, S. Lin, A. Klapars and J. Wang, *J. Am. Chem. Soc*., 1996, **118**, 9796.
6 A. F. Parsons and R. M. Pettifer, *Tetrahedron Lett*., 1996, **37**, 1667.
7 (*a*) B. Nyasse, L. Grehn, U. Ragnarsson, H. L. S. Maia, L. S. Monteiro, I. Leito, I. Koppel and J. Koppel, *J. Chem. Soc., Perkin Trans. 1*, 1995, 2025 and references cited therein; (*b*) L. Grehn, K. Gunnarsson and U. Ragnarsson, *Acta Chem. Scand., Ser. B*, 1986, **40**, 745.
8 O. Nishimura and M. Fujino, *Chem. Pharm. Bull*., 1976, **24**, 1568.
9 R. Ramage, J. Green and A. J. Blake, *Tetrahedron*, 1991, **47**, 6353.
10 A. C. Brown and L. A. Carpino, *J. Org. Chem*., 1985, **50**, 1749.
11 G. H. Lee, E. B. Choi, E. Lee and C. S. Pak, *Tetrahedron Lett*., 1993, **34**, 4541.
12 Y. Yokoyama, T. Matsumoto and Y. Murakami, *J. Org. Chem*., 1995, **60**, 1486.
13 R. O. Hutchins, Suchismita, R. E. Zipkin and I. M. Taffer, *Synth. Commun*., 1989, **19**, 1519.
14 A. Zarecki and J. Wicha, *Synthesis*, 1996, 455.
15 L. Grehn, K. Gunnarsson and U. Ragnarsson, *Acta Chem. Scand., Ser. B*, 1987, **41**, 18.

*Received in Cambridge, UK, 28th February 1997; Com. 7/01408B*

# Time-resolved solid-state REDOR-edited NMR detection of a transient enzyme–intermediate

**Dan J. Mitchell, David L. Jakeman, Tatyana I. Igumenova, Wendy A. Shuttleworth, Keith D. Miller and Jeremy N. S. Evans***

*Department of Biochemistry and Biophysics, Washington State University, Pullman, WA 99164-4660, USA*

**Time-resolved solid-state rotational echo double resonance-edited NMR has been used to detect transient enzyme–intermediates containing two dipolar coupled spins that are unique to the intermediate, so that even resonances buried in the natural abundance background can be detected.**

The technique of time-resolved solid-state NMR spectroscopy was introduced by this laboratory for the direct detection of transient enzyme–intermediates, and first demonstrated for 5-enolpyruvylshikimate-3-phosphate (EPSP) synthase,[1–4] and uridine diphosphate *N*-acetylglucosamine (UDP-NAG) enolpyruvyl transferase.[5] The time-resolved method[6] involves rapid freeze-quench of enzyme–substrate mixtures at discrete time intervals, enabling the pre-steady-state kinetic trapping of transient species as a function of time, followed by low-temperature solid-state NMR analysis of the samples at each time point. Enzymatic reactions which have either single or multiple intermediates can in theory be stopped along the reaction coordinate. When coupled with rotational echo double resonance (REDOR) solid-state NMR, enzyme active site distance information for discrete ground state species can be obtained as a function of time. This laboratory first demonstrated the direct detection of the intermolecular dipolar coupling in the transient enzyme–intermediate complexes of the enzymes EPSP synthase[7] and UDP-NAG enolpyruvyl transferase.[8]

The REDOR technique was introduced by Schaefer and coworkers,[9] and relies on the fact that the effect of the dipolar interaction between two spins on the rotational echo can be manipulated by π-pulses. The dephasing of magnetization of one spin involved in dipolar coupling to another heteronucleus in the presence and absence of these π-pulses, and subsequent refocusing as a function of the magic angle spinning frequency, leads to a variation of resonance intensities. This intensity variation is related to the dipolar coupling constant. The first spectrum is obtained using a standard cross polarization pulse sequence with π-pulses on the observed nucleus (*e.g.* $^{13}$C) in the middle of the evolution period. During this period, the observable magnetization evolves under the influence of the chemical shifts and the heteronuclear dipolar interaction. The π-pulses refocus both interactions, leading to a signal $S_0$ during the acquisition period. The second spectrum is obtained with an additional train of π-pulses on the dipolar-coupled spin (*e.g.* $^{31}$P). These pulses affect the observed signal by preventing rotational refocusing of the dipolar interaction. The magnetization is therefore not completely refocused, and the signal intensity drops by an amount $\Delta S$. For weak dipolar coupling, the change in signal intensity is related to the distance between the coupled spins by[12] eqn. (1), where $N_c$ is the number of

$$\Delta S/S_0 = KD^2N^2_c\nu_r^{-2} \quad (1)$$

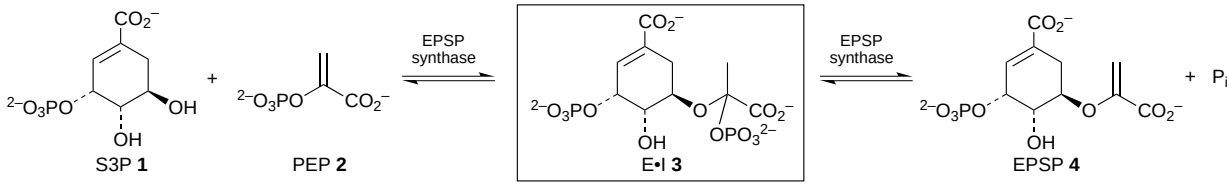
rotor cycles during the evolution period, $\nu_r$ is the spinning speed (in Hz), $D$ is the dipolar coupling (in Hz), and $K$ is a dimensionless constant (= 1.066). Measurement of $D$ can be used to calculate internuclear distance ($r$) according to eqn. (2), where $\gamma_I$ and $\gamma_S$ are the gyromagnetic ratios for the

$$D = \left(\frac{\mu_0}{4\pi}\right)\frac{\gamma_I\gamma_S\hbar}{2\pi r^3} \quad (2)$$

two heteronuclear spins involved, and $\hbar$ is Planck's constant divided by 2π. This experiment therefore yields the internuclear distance, which for an isolated spin pair (*e.g.* $^{13}$C–$^{15}$N or $^{31}$P–$^{13}$C) can be determined to an accuracy of around ±0.1 Å. In addition to making quantitative distance measurements, the technique can also be used for qualitative measurements between spins within the distance dictated by the limits of the two nuclei involved in dipolar coupling.[7,8]

Here we report the first application of time-resolved REDOR-edited solid-state NMR spectroscopy to the detection of a reactive intermediate species trapped at the active site of an enzyme containing a strongly dipolar coupled spin pair unique to the intermediate, thereby editing an otherwise crowded solid-state NMR spectrum. To test this approach, we have used a well-characterized enzyme,[10–13] EPSP synthase (EC 2.5.1.19), which catalyses the penultimate step in the aromatic amino acid biosynthetic pathway in higher plants and bacteria. EPSP **4** is formed from shikimate-3-phosphate (S3P) **1** and phosphoenolpyruvate (PEP) **2** (Scheme 1). The enzyme is a monomer with molecular weight $M_r$ = 46 kDa and the cloned *E.coli* gene has been used to generate a hyperexpressing strain,[14] so that the bacterial enzyme is available in gram quantities. Furthermore, EPSP synthase is the primary site of action of the herbicide glyphosate,[15] or *N*-phosphonomethylglycine. Schaefer and coworkers[16–19] have used solid-state REDOR NMR experiments to investigate the conformation of the bound inhibitor glyphosate in the ternary complex, and its relation to the enzyme active site. This is particularly significant, since all attempts to crystallize the ternary complex have failed thus far.

The rationale for selecting EPSP synthase for testing the time-resolved REDOR-edited NMR approach was as follows. Since the enzyme–intermediate has already been thoroughly characterized by our laboratory in solution[11,12] and in the solid-state,[1,2,4] and this enzyme–intermediate contains a unique dipolar coupled spin pair (*e.g* $^{31}$P–$^{13}$C), this then provides an




**Scheme 1**

unusual opportunity to test whether this approach is amenable for application to other enzymes. Fig. 1 shows {$^{31}$P}$^{13}$C CP-MAS REDOR difference ($\Delta S$) and full echo ($S_0$) time-resolved solid-state NMR spectra of EPSP synthase·S3P mixed with [2-$^{13}$C]PEP under pre-steady-state conditions, followed by lyophilisation at low temperature.† The substrates in these experiments were present in an 10-fold excess over the enzyme. At this stage lyophilised solids have been employed because of technical difficulties associated with performing REDOR measurements on frozen solutions. The enzyme–intermediate complex was trapped under time-resolved conditions (the time-resolution being 50 ms in this case), and the sample kept at low temperature ($< 263$ K) throughout the lyophilisation. The spectra were obtained using the REDOR pulse sequence with dephasing π-pulses applied to the $^{31}$P nuclei and detection on $^{13}$C. The rationale for this choice of spin pairs was guided by the fact that apart from enzyme-free or bound [2-$^{13}$C]PEP, none of the species present *except* the tetrahedral intermediate (**3**) contains strongly dipolar coupled $^{13}$C and $^{31}$P. Thus the spectrum is edited with respect to those $^{13}$C atoms which are dipolar coupled to $^{31}$P, and the conditions can be adjusted (determined by the number of dephasing π-pulses) so that *predominantly* C–O–P linkages are detected. In the P–C REDOR difference spectrum ($\Delta S$ in Fig. 1), in addition to the substrate [2-$^{13}$C]PEP and possibly product EPSP at δ 152.5 (both species have closely similar chemical shifts[4]), and their associated rotational sidebands (RSB), which of course also contains a C–O–P linkage, the enzyme–intermediate (E·I) complex is evident at δ 104. This is consistent with our previously published NMR data on the enzyme–intermediate of EPSP synthase both in solution[16,17] and in the solid-state.[1,2,4] With 32 $^{31}$P dephasing π-pulses, the predominant interaction arises from C–O–P linkages and other species experiencing dipolar interactions within a radius of 5 Å. Examples of the latter case are evident in Fig. 1, where resonances due to dipolar coupling between the phosphate of PEP/S3P or EPSP and the $^{13}$C natural abundance of tris buffer can be seen at δ 62.1, both of which were present in excess over the enzyme. Also evident are residual contacts to the enzyme backbone carbonyl resonances at δ 174.5.

These data establish the viability of this approach for picking out resonances due to enzyme–intermediates bearing C–O–P linkages, and indeed any linkage containing a pair of unique isotopic labels. It also provides further evidence that even the unstable transient intermediate of EPSP synthase, formed from the true substrate under pre-steady-state conditions, can survive in the lyophilised solid. Schaefer and co-workers[20,21] have recently reported using P–C REDOR to investigate species that form in very slow reactions catalysed by mutant forms of EPSP synthase in the solid-state, although it is unclear at this stage whether the species they are detecting have any relevance to the mechanistic course of the enzyme. These results therefore represent the first example of the application of time-resolved solid-state REDOR-edited NMR spectroscopy for the detection of transient enzyme–intermediate complexes. The stage is now set for the application of this approach to other enzymes in which a unique dipolar coupled spin pair occurs only in the putative intermediate, so that its mechanistic details may be delineated.

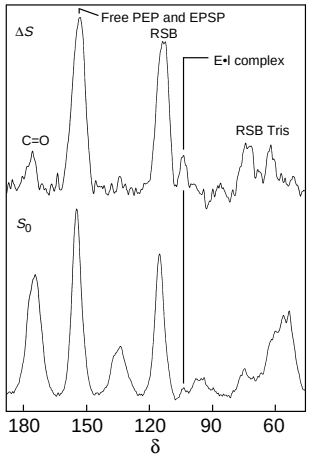



**Fig. 1** 9.4-T {$^{31}$P}$^{13}$C (P–C) CP-MAS REDOR difference NMR spectra of EPSP synthase plus shikimate-3-phosphate reacted with [2-$^{13}$C]PEP for 50 ms followed by lyophilisation at low temperature and obtained with and without $^{31}$P dephasing. The full echo $S_0$ spectrum is without $^{31}$P dephasing, and the $\Delta S$ spectrum is the difference spectrum of that obtained with and without $^{31}$P dephasing.

The technique development aspects of this work were supported by NSF grant MCB-9506117, and the specific application to EPSP synthase supported by NIH grant GM43215. The WSU NMR Center equipment was supported by NIH grant RR0631401 and NSF grants CHE-9115282 and DBI-9604689. We thank Greg Helms for managing our NMR Facility and maintaining the NMR spectrometers.

## Footnotes

* E-mail: evansj@wsu.edu

† The time-resolved REDOR difference NMR spectra were obtained by rapid mix and freeze-quench (in 50 ms) of EPSP synthase (12.2 Units mg$^{-1}$) S3P with a solution of [2-$^{13}$C]PEP in 50 mM tris·HCl (pH 7.8) buffer to final concentrations of 5.8, 58 and 58 mM, respectively. The rapidly frozen sample was then lyophilised at $< 263$ K for 72 h. Approximately 70 mg of protein was used and the spectra were acquired at 233 K. The freeze-quench apparatus used is described in detail elsewhere (refs. 3 and 4). The EPSP synthase was isolated by literature methods (ref. 14). NMR spectroscopy was carried out as previously described (ref. 8).

## References

1 J. N. S. Evans, R. J. Appleyard and W. A. Shuttleworth, *Bull. Magn. Reson.*, 1992, **14**, 81.
2 J. N. S. Evans, R. J. Appleyard and W. A. Shuttleworth, *J. Am. Chem. Soc.*, 1992, **115**, 1588.
3 R. J. Appleyard and J. N. S. Evans, *J. Magn. Reson., Ser. B*, 1993, **102**, 245.
4 R. J. Appleyard, W. A. Shuttleworth and J. N. S. Evans, *Biochemistry*, 1994, **33**, 6812.
5 C. A. Ramilo, R. J. Appleyard, F. Krekel, C. Wanke, N. Amrhein and J. N. S. Evans, *Biochemistry*, 1994, **33**, 15 071.
6 J. N. S. Evans, in *Encyclopedia of NMR*, Wiley, 1995, pp. 4757–4763.
7 Y. Li, R. J. Appleyard, W. A. Shuttleworth and J. N. S. Evans, *J. Am. Chem. Soc.*, 1994, **116**, 10 799.
8 Y. Li, F. Krekel, C. A. Ramilo, N. Amrhein and J. N. S. Evans, *FEBS Lett.*, 1995, **377**, 208.
9 T. Gullion and J. Schaefer, *Adv. Magn. Reson.*, 1989, **13**, 57.
10 K. S. Anderson, J. A. Sikorski and K. A. Johnson, *Biochemistry*, 1988, **27**, 7395.
11 P. N. Barlow, R. J. Appleyard, B. J. O. Wilson and J. N. S. Evans, *Biochemistry*, 1989, **28**, 7985; 10 093.
12 J. N. S. Evans, in *Pulsed Magnetic Resonance: NMR, ESR and Optics (A Recognition of E. L. Hahn)*, ed. D. Bagguley, Oxford University Press, 1992, pp.123–173.
13 K. S. Anderson, R. D. Sammons, G. C. Leo, J. A. Sikorski, A. J. Benesi and K. A. Johnson, *Biochemistry*, 1990, **29**, 1460.
14 W. A. Shuttleworth, C. D. Hough, K. P. Bertrand and J. N. S. Evans, *Protein Engineering*, 1992, **5**, 461.
15 H. C. Steinrucken and N. Amrhein, *Eur. J. Biochem.*, 1984, **143**, 351.
16 A. M. Christensen and J. Schaefer, *Biochemistry*, 1993, **32**, 2868.
17 L. M. McDowell, C. A. Klug, D. D. Beusen and J. Schaefer, *Biochemistry*, 1996, **35**, 5395.
18 L. M. McDowell, A. Schmidt, E. R. Cohen, D. R. Studelska and J. Schaefer, *J. Mol. Biol.*, 1996, **256**, 160.
19 D. R. Studelska, C. A. Klug, D. D. Beusen, L. M. McDowell and J. Schaefer, *J. Am. Chem. Soc.*, 1996, **118**, 5476.
20 D. R. Studelska, C. Klug and J. Schaefer, *36th Experimental NMR Conference Proceedings*, Boston, 1995, 285.
21 D. R. Studelska, M. P. Espe, L. M. McDowell and J. Schaefer, *XVIIth International Conference on Magnetic Resonance in Biological Systems Proceedings*, Keystone, 1996, 139.

*Received, in Glasgow, UK, 14th February 1997; Com. 7/01926B*

# Highly chemoselective synthesis of functionalized diselenides from alkyl halides using benzyltriethylammonium tetrathiomolybdate

**Kandikere R. Prabhu and Srinivasan Chandrasekaran***

*Department of Organic Chemistry, Indian Institute of Science, Bangalore 560012, India*

**A variety of functionalized selenocyanates generated *in situ* from the corresponding alkyl halides undergo a facile reductive coupling on treatment with benzyltriethylammonium tetrathiomolybdate 1 under very mild conditions to give the corresponding diselenides in very good yields.**

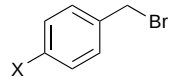
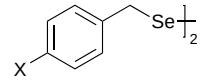
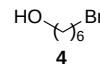
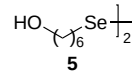
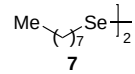
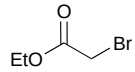
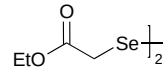
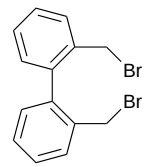
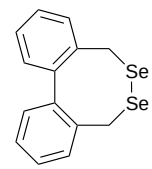
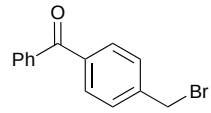
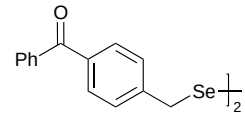
Organoselenium compounds have emerged as important reagents and intermediates in organic synthesis[1] and they also have biological importance as proteins containing selenium are essential components of certain bacterial and mammalian enzyme systems.[2] Hence a convenient synthesis of these selenium compounds in general and functionalised organic diselenides in particular continues to be a challenging task.

From the large number of methods available for the synthesis of diselenides, the most important routes involve either the reaction of metal diselenides on alkyl halides[3] or the preparation of selenols which can be subjected to further oxidation.[4] Recently Salama and Bernad[5] reported that organic selenocyanates, on treatment with $LiEt_3BH$ followed by air oxidation, give the corresponding diselenides in good yields. Most of the methods available are generally useful only for the synthesis of simple diselenides lacking reactive functional groups.

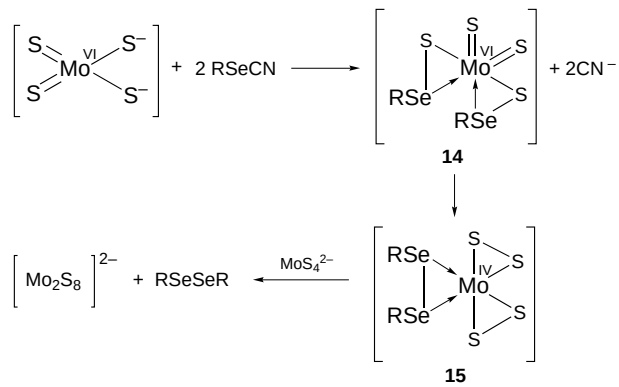
In our earlier work we have demonstrated that benzyltriethylammonium tetrathiomolybdate $[PhCH_2NEt_3]_2MoS_4$ **1** is a useful sulfur transfer reagent in organic synthesis[6] as well as a reagent that can mediate reductive dimerization of alkyl azides[7] and organic thiocyanates.[8] In exploring further the utility of induced internal redox reactions of tetrathiomolybdate **1** in organic synthesis it appeared quite attractive to study the reductive dimerization of organic selenocyanates with **1**. Here we present the results of such an investigation.

Treatment of a number of alkyl halides with KSeCN (1.1 equiv.) in MeCN (25 °C, 0.5 h) generated the corresponding alkyl selenocyanates *in situ* which, on further reaction with tetrathiomolybdate **1** (1.2 equiv., 25 °C, 0.5–24 h), led to the formation of the alkyl diselenides in high yields (85–96%).† The results are summarized in Table 1. As can be seen, except in the case of hydroxy bromide **4** (entry 5), all the substrates reacted with great facility in a short period of time (0.5–6.0 h). Particularly noteworthy are the successful reactions of the substrates **2b**,**c**,**d**, **8** and **12**, which contain easily reducible groups such as nitro, cyano, ester and keto functionalities. The methodology involving use of $LiEt_3BH$[5] or $NaBH_4$[9] for the synthesis of diselenides cannot be applied successfully in many of these cases. This kind of high chemoselectivity obtainable in a room temperature reaction is very unusual. The facile synthesis of a cyclic 8-membered diselenide **11** from dibromide **10** (entry 8) in high yield also demonstrates the high potential of the methodology. Unlike the earlier reported reactions of alkyl selenocyanates, which proceed *via* alkyl selenol intermediates,[5,9] we believe that the present methodology does not involve alkyl selenols as intermediates.‡ A tentative mechanism based on the reactivity of alkyl thiocyanates[8] with tetrathiomolybdate **1** is presented in the Scheme 1. It is likely that, in the reaction of organic selenocyanates, the attack of $MoS_4^{2-}$ on the selenium of selenocyanate leads to mononuclear molybdenum species of type **14**. The second stage of the reaction can be represented as an induced internal electron-transfer from a sulfur ligand to $Mo^{VI}$ to produce $Mo^{IV}$ species **15**.[10] Further reaction of **15** with **1** results in the formation of alkyl diselenides and $Mo_2S_8^{2-}$.§

**Table 1** Formation of diselenides

| Entry | Starting material | *t*/h[a] | Product | Yield (%)[b,c] |
|---|---|---|---|---|
| |  | |  | |
| 1 | **2a** X = H | 0.5 | **3a** | 89 |
| 2 | **2b** X = $NO_2$ | 2 | **3b** | 90 |
| 3 | **2c** X = CN | 1 | **3c** | 86 |
| 4 | **2d** X = $CO_2Et$ | 6 | **3d** | 95 |
| 5 |  **4** | 24 |  **5** | 96 |
| 6 |  **6** | 0.5 |  **7** | 85 |
| 7 |  **8** | 0.5 |  **9** | 90 |
| 8 |  **10** | 0.5 |  **11** | 88 |
| 9 |  **12** | 4 |  **13** | 87 |

[a] Time refers to conversion of selenocyanate to diselenide. [b] Refers to isolated yield. [c] All the products exhibited expected analytical and spectral data.



**Scheme 1**

In conclusion, we have demonstrated that a variety of functionalized alkyl diselenides can be synthesised in high yield from alkyl halides *via* alkyl selenocyanates under mild conditions. Further work is in progress to extend this methodology to unsymmetrical diselenides and seleno sulfides.

We thank the Department of Science and Technology, New Delhi, for financial support of this investigation.

## Footnotes

* E-mail: scn@orgchem.iisc.ernet.in

† No trace of selenol could be detected in the reaction mixture, and tetrathiomolybdate **1** does not convert selenols to diselenides.

‡ *Typical procedure*. To a solution of benzyl bromide **2a** (1 mmol) in MeCN (5 ml) was added KSeCN (1.1 mmol). The mixture was stirred at room temperature (25 °C) for 0.5 h (until the starting material had disappeared, as shown by TLC), and benzyltriethylammonium tetrathiomolybdate **1** (1.2 mmol) was added. The mixture stirred for 0.5 h, the solvent was evaporated *in vacuo* and the black residue thus formed was extracted with $CH_2Cl_2$–$Et_2O$ (1 : 9, 20 ml × 5) and filtered through a Celite pad. The filtrate was concentrated and the crude product was purified by column chromatography (silica gel, light petroleum (60–80 °C)–ethyl acetate, 9 : 1) to yield dibenzyl diselenide **3a** as a solid, mp 90–91 °C (lit.,[3] 90–91 °C) in 87% yield.

§ The IR spectrum (KBr) of the molybdenum byproduct shows a strong absorption at 515 $cm^{-1}$ assignable to a persulfido molybdenum species.

## References

1 D. Liotta and R. Monahan III, *Science*, 1986, **231**, 356 and references cited therein.
2 T. C. Stadman, *Science*, 1974, **183**, 915; D. Illman, *Chem. Eng*., 1994, 53; K. Schwarz and Fredga, *Bioinorg. Chem*., 1974, **3**, 153.
3 J. Y. Wang, W. Cui and Y. Hu, *J. Chem. Soc., Perkin. Trans. 1*, 1994, 2341 and references cited therein.
4 A. Krief, A. F. De Mahien, W. Dumont and M. Trabelsi, *Synthesis*, 1988, 131 and references cited therein.
5 P. Salama and C. Bernad, *Tetrahedron Lett*., 1995, **36**, 5711.
6 A. R. Ramesha and S. Chandrsekaran, *Synth. Commun*., 1992, **22**, 3277; A. R. Ramesha and S. Chandrasekaran, *J. Org. Chem*., 1994, **59**, 1354.
7 A. R. Ramesha, S. Bhat and S. Chandrasekaran, *J. Org. Chem*., 1995, **60**, 7682.
8 K. R. Prabhu, A. R. Ramesha and S. Chandrasekaran, *J. Org. Chem*., 1995, **60**, 7142.
9 Cordora-reys, E. VandenHoven, A. Mohammad and B. M. Pinto, *Can. J. Chem*., 1995, **73**, 113.
10 E. L. Coyle, M. H. Harmer, G. N. George, M. Daage and E. I. Steifel, *Inorg. Chem*., 1990, **29**, 14.

*Received in Cambridge, UK, 4th March 1997; Com. 7/01512G*

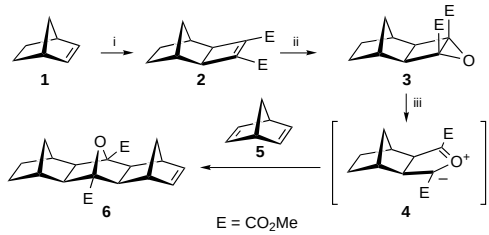
# A new building BLOCK technique based on cycloaddition chemistry for the regiospecific linking of alicyclic sub-units as a route to large, custom-functionalised structures

**Ronald N. Warrener,*[a]† Austin C. Schultz,[a] Douglas N. Butler,[a] Shudong Wang,[a] Indu B. Mahadevan[b] and Richard A. Russell*[b]**

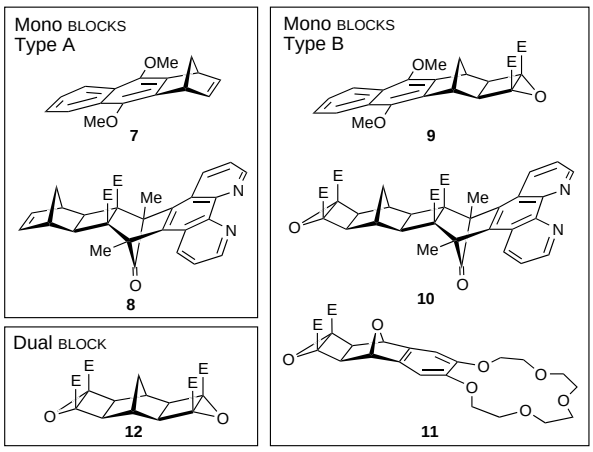
[a] *Centre for Molecular Architecture, Central Queensland University, Rockhampton, Queensland, 4702, Australia*
[b] *School of Biological and Chemical Sciences, Deakin University, Geelong, Victoria, 3217, Australia*

**A new building BLOCK approach to synthesis has been developed where functionalised norbornenes (BLOCK A) are coupled with functionalised cyclobutene epoxides (BLOCK B) to produce A + B structures of defined geometry; use of a dual (spacer) BLOCK allows the formation of large structures where crown ether, ligand and redox centres are incorporated in similar or mixed pairings.**

It is well established that there is a continuing need for the development of new substrates for supramolecular applications[1] which, in turn, requires the development of new synthetic methodology. We have recently reported the synthesis of rigid alicyclic molecules where separate donor and quencher chromophores are fused to the carbocyclic framework[2] using a serial cycloaddition technique, and this has been extended to the production of cavity-shaped crown ethers.[3] We now report a convergent method which uses preformed building BLOCKS with the particular chromophore inbuilt, and joins them thermally in a stereospecific process. The new construction technique lends itself to the production of large structures having inbuilt functional units of different types.




**Scheme 1** *Reagents and conditions*: i, DMAD, $RuH_2CO(PPh_3)_3$ (*cf.* ref. 7); ii, Bu$^t$OOH, MeLi, −78 °C, 75%; iii, 110 °C, 3 h, 64%




This A + B building BLOCK method developed from our discovery that fused, ester-activated cyclobutene epoxides ring-open to 1,3-dipolar species such as **4** which can be trapped stereospecifically by ring-strained alicyclic dipolarophiles.‡ We envisaged that fused norbornenes could act as one building BLOCK and fused cyclobutene epoxides could act as the other. This was confirmed by heating norbornadiene **5** (prototype building BLOCK A) with epoxide **3**§ (prototype building BLOCK B) to produce the *exo,exo*-coupled product **6**§ (Scheme 1).¶ A + B products formed by this coupling process retain their rigid alicyclic character as the newly formed 7-oxanorbornane unit seamlessly joins the two reactants.

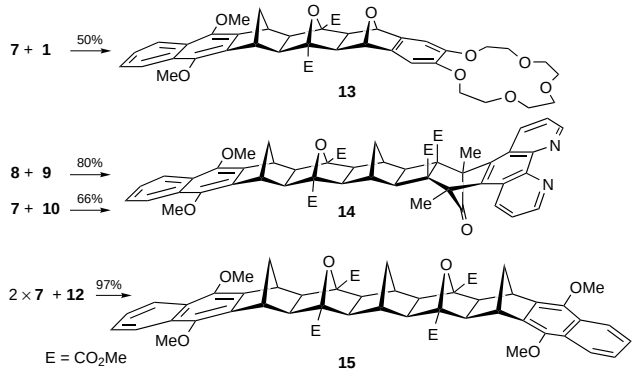
To illustrate this building block strategy further, we have assembled a small selection of functionalised molecules which form a pool of A and B reagent BLOCKS **7**–**11**. In the longer term, this pool would grow to cover other functional units and these basic A and B BLOCKS, together with the dual (spacer) BLOCK **12**, would be available in a selection of geometrical configurations (shapes). The building BLOCKS can be drawn upon in A + B pairs, depending on the type of functionality required, and heated together to form the final product. Preparation of the building BLOCKS, which are of two basic types, is made simpler as the fused norbornenes, available as the type A building BLOCK, can be converted to fused cyclobutene epoxides (type B building BLOCKS) in a two-step process involving Ru-catalysed [2 + 2] cycloaddition of dimethyl acetylenedicarboxylate (DMAD),[7] followed by epoxidation (MeLi, Bu$^t$OOH),‖ as illustrated by the conversion of **1** to **3** (Scheme 1). Simply heating BLOCK A with BLOCK B yields the coupled product in good yield and with high stereospecificity.**

While all combinations of type A plus type B BLOCKS are feasible, especially as a combinatorial exercise, only a representative set **13**–**15** (Scheme 2) is reported here. Heating the dipolarophilic norbornene **7**[8] as the type A building BLOCK containing a dimethoxynaphthalene with the cyclobutene epoxide **11** with crown ether functionality as the incipient 1,3-dipole, yielded the specifically *exo,exo*-coupled product **13** (Scheme 2). Similar A + B coupling between dipolarophile **8**[2] as the ligand carrier and epoxide **9** as the transporter for the dimethoxynaphthalene gave coupled product **14**.§ The same product **14** could be formed by the alternative A + B assembly process in which the epoxide **10** provided the ligand and norbornene **7** furnished the dimethoxynaphthalene. These routes to **14** represent new approaches to rigid polyalicyclic structures containing metal chelating centres linked with redox-active components, the first members of which were only recently reported as model systems for the study of electron and energy transfer.[2,9]

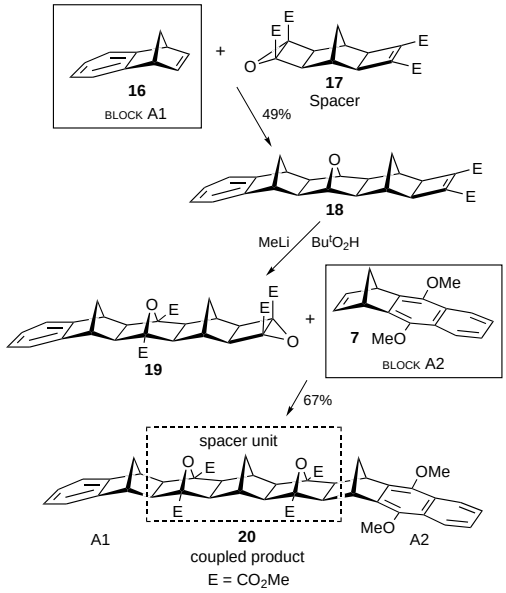
Large functionalised polynorbornanes containing two sets of the same functionality can be produced using the combination of the type A BLOCK with a dual epoxide BLOCK (Scheme 2). This approach was used to prepare the polynorbornane **15** by reaction of 2 equiv. of **7** with bis-epoxide **12**. This example illustrates special features of the methodology: (i) it provides a

mechanism for coupling reagents with functional units unstable to the epoxidation conditions, and therefore unsuitable for conversion to type B BLOCKS, by employing epoxide co-reagents; (ii) the polynorbornane framework significantly affects the geometry of the final product, especially the relative orientation of the functional unit; this can be varied by choice of the dual BLOCK.

The final example illustrates the most versatile route to large differentially functionalised structures. Treatment of spacer molecule **17**, where there is one cyclobutane epoxide (the second is latently positioned as the cyclobutene-1,2-diester), with benzonorbornadiene **16** (BLOCK Al, boxed in Scheme 3) provided the coupled product **18**, which was converted to the extended epoxide **19** by epoxidation under the usual conditions. Subsequent reaction of **19** (a standard BLOCK B) with the naphthonorbornadiene **7** (BLOCK A2, boxed in Scheme 3) furnished the large product **20** (the spacer component is designated by a dashed box in Scheme 3). Future work will involve dual BLOCKS as a carrier of separate functionality, thereby opening the way for triad formation.




**Scheme 2**




**Scheme 3**

These results establish the potential of this reaction to act as a coupling method for the construction of large polyalicyclic structures. We are developing fused norbornenes containing other important functionality, so the opportunity for building an array of bioactive products by this or related coupling methods[10,11] is well-advanced and such results will be published in due course.

## Footnotes

† E-mail: r.warrener@cqu.edu.au

‡ Huisgen has reported many examples of epoxide ring-opening to 1,3-dipolar species (ref. 4), and there is one example of the thermal ring-opening of an cyclobutene epoxide with phenyl substituents on the epoxide (ref. 5), but application in the alicyclic field is new. We refer to this type of coupling as the ACE reaction, where the acronym is derived from **a**lkene plus **c**yclobutene **e**poxide coupling.

§ All new compounds gave satisfactory analytical and spectral data.

¶ Norbornene **1** reacts with **3** to produce the dihydro derivative of **6**, which is identical with that formed by an alternative route (ref. 6).

‖ Use of BuLi leads to mixtures where ester exchange products interfere.

** The success of this technique was assured when separate reaction of A or B provided no evidence for self-assembly under the coupling conditions.

## References

1 J. M. Lehn, *Supramolecular Chemistry—Concepts and Perspectives*, VCH, Weinheim, 1995.
2 R. N. Warrener, M. A. Houghton, A. C. Schultz, F. R. Keene, L. S. Kelso, R. Dash and D. N. Butler, *Chem. Commun*., 1996, 1151; R. N. Warrener, A. B. B. Ferreira, A. C. Schultz, D. N. Butler, F. R. Keene and L. S. Kelso, *Angew. Chem., Int. Ed. Engl*., 1996, **108**, 2651.
3 R. N. Warrener, S. Wang, R. A. Russell and M. J. Gunter, *Synlett*, 1997, 47.
4 R. Huisgen, *Angew. Chem., Int. Ed. Engl*., 1977, **16**, 572.
5 E. F. Ulmann and W. A. Henderson, *J. Am. Chem. Soc*., 1966, **88**, 4942.
6 V. G. Seitz and H. Wassmuth, *Chem. -Z*., 1988, **112**, 80; F. Thalhammer, U. Wallfahrer and J. Sauer, *Tetrahedron Lett*., 1988, **29**, 3231; G. Seitz and C. H. Gerninghaus, *Pharmazie*, 1994, **49**, 102.
7 T. Mitsudo, H. Naruse, T. Kondo, Y. Ozaki and Y. Watanabe, *Angew. Chem., Int. Ed. Engl*., 1994, **33**, 580; T. Mitsudo, K. Kokuryo, T. Shinsugi, Y. Nakagawa, Y. Watanabe and Y. Takegami, *J. Org. Chem*., 1979, **44**, 4492.
8 L. A. Paquette, F. Bellamy, M. C. Bohm and R. J. Gleiter, *J. Org. Chem*., 1980, **45**, 4913.
9 J. M. Lawson, A. M. Oliver, D. F. Rothenfluh, Y.-Z. An, G. A. Ellis, M. G. Ranasinghe, S. A. Khan, A. G. Franz, P. S. Ganapathi, M. J. Shephard, M. N. Paddon-Row and Y. Rubin, *J. Org. Chem*., 1996, **61**, 5032.
10 R. N. Warrener, D. Margetic, E. R. T. Tiekink and R. A. Russell, *Synlett*, 1997, 196.
11 R. N. Warrener, D. Margetic, A. C. Schultz and R. A. Russell, unpublished results.

*Received, 2nd January 1997; Com. 7/00010C*

# The origin of the β-lactam carbons of clavulanic acid

**Jan E. Thirkettle,[a] Jack E. Baldwin,[a] Jeff Edwards,[b] John P. Griffin[b] and Christopher J. Schofield*[a]**

[a] *Dyson Perrins Laboratory, South Parks Road, Oxford, UK OX1 3QY*
[b] *SmithKline Beecham Pharmaceuticals, Clarendon Road, Worthing, West Sussex, UK BN14 8QH*

**Pyruvate is the most likely primary metabolic source of the three β-lactam carbons of clavulanic acid.**

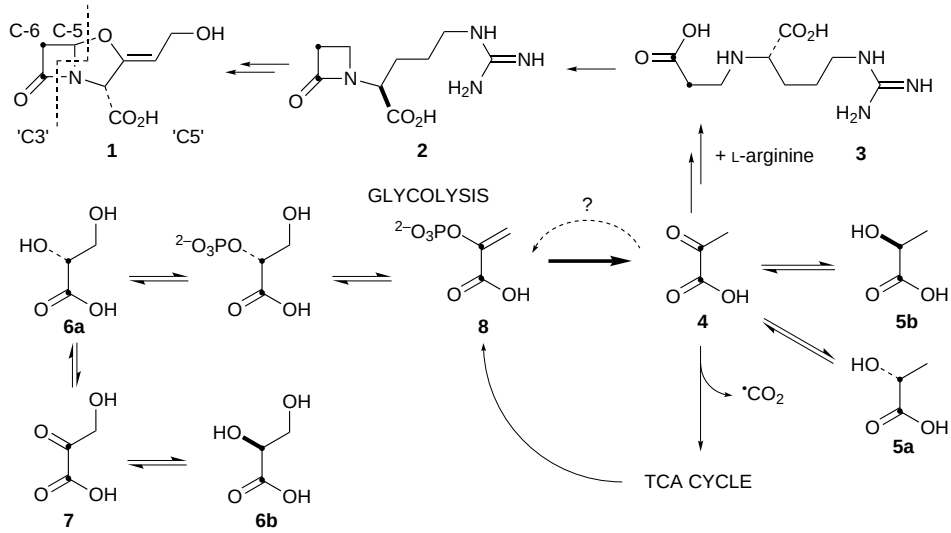
Clavulanic acid **1** is a commercially important inhibitor of β-lactamases, and is produced *via* fermentation of *Streptomyces clavuligerus*. It is known that the primary metabolic precursor of the five-carbon unit (Scheme 1) of clavulanic acid is arginine,[1] Pioneering studies by Elson *et al.*[2] and Townsend *et al.*[3] have demonstrated that the precursor of the three-carbon unit is a three-carbon primary metabolite (both pyruvate[2] and glycerate[3] have been proposed) although no conclusive evidence has yet been presented. Monocyclic β-lactam **2** has been identified as an intermediate in clavulanic acid **1** biosynthesis (Scheme 1) and there is evidence[4] that it is precursed by the acyclic compound **3**, but the pathway from primary metabolism to these putative intermediates is unknown.

Feeding experiments using labelled precursors have apparently demonstrated that glycerol,[3,5] propionate,[5] β-hydroxypropionate,[6] pyruvate,[3] and D- and L-glycerates[3] are specifically incorporated into the β-lactam ring of **1**. It has been reported that both L- and D-[2-$^{3}$H, 1-$^{14}$C]glycerate are specifically incorporated into **1** to similar levels, but that only in the case of the D-isomer is any $^{3}$H incorporated at C-6 of **1**. A recent study[3b] using racemic [1,2-$^{13}C_2$, 2,3,3,-$^{2}H_3$]glycerate, however, reported that no incorporation of the C-2 label into C-6 of **1** was observed. Other possible 3-carbon precursors such as malonic acid semi-aldehyde, β-hydroxypropionate or acrylate cannot be ruled out by these previous studies.

Herein we report studies using optically active $^{13}$C and $^{2}$H labelled lactates and glycerates which imply that pyruvate **4** and not glycerate is the primary metabolic precursor of the three β-lactam carbons of **1**.† 1,2-$^{13}$C labelled species were used in order to generate doublets in the $^{13}$C NMR spectra separating the signals arising from labelled material from the relatively intense singlet of the unlabelled material, allowing accurate incorporation levels to be determined. Retention levels of $^{2}$H were analysed by the observation of splitting or isotopic shifts of the doublets.

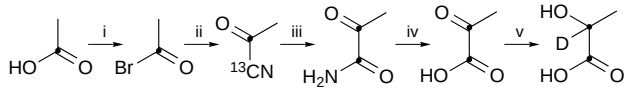
The L- and D-[1,2-$^{13}C_2$, 2-$^{2}$H]lactates **5a**,**b** were synthesised[7,8] in 23% yield (and > 98% isotopic purity) from [1-$^{13}$C]acetic acid (Scheme 2). Notably Tris-HCl buffer was used for the enzyme catalysed reductions of pyruvate to L- and D-lactates rather than phosphate buffer[9] which resulted in a mixture of lactates with $^{1}$H and $^{2}$H at C-2. Synthesis of DL-[1,2-$^{13}C_2$, 2,3,3-$^{2}H_3$]glycerate[10]‡ was achieved from [$^{2}H_2$]formaldehyde (Scheme 3) in an overall yield of 80% and > 98% isotopic purity. DL-[1,2-$^{13}C_2$, 1,1-$^{18}O_2$]glycerate was synthesised in a similar fashion. Resolution of the racemic labelled glycerate was achieved by HPLC on a preparative C-18 column using the method of Horikawa *et al.*[11] In the lactate and glycerate syntheses, hydrolysis of the intermediate nitriles to the acids by literature conditions[12,13] was low yielding. Use of strong acid ion exchange resin however resulted in good yields and trivial product purification.

The labelled precursors were fed to shake flask cultures of a *Streptomyces clavuligerus* wild-type re-isolate (SC2) in a minimal medium.[5] Clavulanic acid **1** was isolated as its benzyl ester after gel and silica chromatography and analysed by $^{13}$C NMR spectroscopy acquired under fully quantitative conditions. It was found that optimisation of the aquisition parameters was required in order to obtain spectra which were suitable for integration due to the large pertubations in signal intensity caused by the $^{13}$C and $^{2}$H isotope effect on spin relaxation rates. Samples were also examined by $^{2}$H NMR spectroscopy to corroborate results. The spectra recorded for **1** derived from the labelled lactates indicated that whilst both D- and L-lactate **5a**,**b** were specifically incorporated into **1** to similar levels (1.2 and 1.9% respectively), in neither case had any retention of $^{2}$H at C-6 of **1** occurred. This implies that lactate **5a**,**b** must pass *via* pyruvate **4** before incorporation into **3**. The spectra recorded for

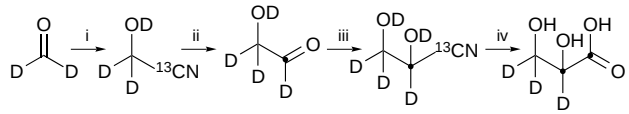



**Scheme 1** Proposed biosynthesis of clavulanic acid **1** ($^{2}$H labels not shown)

the L- and D-glycerates **6a**,**b** similarly showed no evidence for retention of $^2H$ at C-6 of **1**. In contrast, 80% of the clavulanic acid **1** derived from either D- or L-labelled glycerate was labelled with $^2H$ at C-5. These results are consistent with results reported by Pitlik and Townsend using racemic material.[3b] The total carbon incorporation for D-glycerate **6a** was 1.9% whilst that for L-glycerate **6b** was only 0.3%. The $^2H$ labelling of C-5 of **1** is in good agreement with previous results.[3,14,15] The intact incorporation of the 1,2-$^{13}C$ labels from lactate and glycerate together with the lack of incorporation of the C-2 $^2H$ label from either substrate indicate that neither is the primary metabolic precursor for the β-lactam carbons of **1**. Instead the results imply that pyruvate is the precursor. Oxidation of lactate **5a**,**b** to pyruvate **4** will result in the loss of the 2-$^2H$ label whilst retaining the carbon skeleton. Glycolysis of glycerate **6a**,**b** to pyruvate **4** will similarly remove the 2-$^2H$ label and result in some loss of the 3-$^2H$ label through enolisation. The low level of incorporation of L-glycerate **6b** probably reflects the differences between metabolism of L- and D-glycerate in *S. clavuligerus*. In mammalian systems it is known that L-glycerate may be epimerised to D-glycerate *via* oxidation to hydroxypyruvate[16] **7**. The low incorporation of $^{18}O$ (19%) into the C-7 carbonyl of **1** from DL-[1,2-$^{13}C_2$, 1,1-$^{18}O_2$]glycerate is




**Scheme 2** Synthesis of L- and D-[1,2-$^{13}C_2$, 2-$^2H$]lactates **5a**,**b**. *Reagents and conditions*: i, $PBr_3$; ii, $Cu^{13}CN$; iii, HCl, $Et_2O$ then $H_2O$; iv, DOWEX-50 ($H^+$), $H_2O$, 80 °C; v, D- or L-lactate dehydrogenase, $NAD^+$, yeast alcohol dehydrogenase, Tris-HCl, $CD_3CD_2OD$, pH 8.5, 25 °C.




**Scheme 3** Synthesis of DL-[1,2-$^{13}C_2$, 2,3,3-$^2H_3$]glycerate **6a/b**. *Reagents and conditions*: i, $K^{13}CN$, pH 8.5, 25 °C, $D_2O$; ii, Pd–$BaSO_4$, $D_2$, pH 1.7, $D_2O$; iii, $K^{13}CN$, pH 8.5, 25 °C, $D_2O$; iv, AMBERLITE IR-120 ($H^+$), $D_2O$, 95 °C.

**Table 1** Incorporation data for labelled lactate and glycerate

| Precursor | Carbon[e] incorporation (%) | Retention at C-6[d] (%) | Retention at C-5[d] (%) |
|---|---|---|---|
| L-[1,2-$^{13}C_2$, 2-$^2H$]lactate[a] **5b** | 1.9 | < 2 | n/a |
| D-[1,2-$^{13}C_2$, 2-$^2H$]lactate[a] **5a** | 1.2 | < 2 | n/a |
| DL-[1,2-$^{13}C_2$, 2,3,3-$^2H_3$]glycerate **6a**/**b** | 1.6 | < 1 | 80 |
| L-[1,2-$^{13}C_2$, 2,3,3-$^2H_3$]glycerate[b] **6b** | 0.3 | < 5 | 80 |
| D-[1,2-$^{13}C_2$, 2,3,3-$^2H_3$]glycerate[c] **6a** | 1.9 | < 2 | 80 |
| DL-[1,2-$^{13}C_2$, 1,1-$^{18}O_2$]glycerate[c] | 1.8 | (C-7 retn: 19% $^{18}O$) | |

[a] > 98% ee. [b] > 90% ee. [c] > 95% ee. [d] As a proportion of carbon incorporation; levels measured by $^2H$ NMR were within 5%. [e] Adjusted to allow for the amount of **1** present before addition of labelled species, in order to allow for more reliable comparison of labelling results between different fermentation batches.

an additional indication of the metabolic conversions that this species must undergo before incorporation into **2**. Cell extracts from fermentations of labelled lactate, analysed by $^{13}C$-INADEQUATE NMR, showed that an accumulation of [1,2-$^{13}C_2$]alanine could be detected indicating conversion of lactate **5a**,**b** to pyruvate **4**. It is conceivable that lactate is converted to glycerate before assimilation into **3**, however, metabolism *via* the TCA cycle will break the 1-2 $^{13}C$–$^{13}C$ bond and is thus ruled out. Additionally the direct conversion of pyruvate **4** to phosphoenol pyruvate **8** has not been reported for *Streptomyces* ssp. and would not explain the loss of all the 2-$^2H$ label (and 20% of the 3-$^2H$ labels) in the labelled glycerate fermentions which imply oxidation of C-2 to the ketone. We conclude that the most likely primary metabolic source of the β-lactam carbons of clavulanic acid **1** is pyruvate **4** not glycerate **6a**,**b** or lactate **5a**,**b**.

We thank T. Claridge for advice on NMR, B. Barton, S. W. Elson and H. Holms for helpful discussions and encouragement, and the BBSRC/SmithKline Beecham Pharmaceuticals for a CASE award to J. E. T.

## Footnotes

* E-mail: christopher.schofield@dpl.ox.ac.uk
† This work was first presented at the Royal Australian Chemical Institute 15th national conference (2nd July 1996).
‡ The same material was prepared using an alternative route by Pitlik and Townsend [ref. 3(*b*)].

## References

1 B. P. Valentine, C. R. Bailey, A. Doherty, J. Morris, S. W. Elson, K. H. Baggaley and N. H. Nicholson, *J. Chem. Soc., Chem. Commun.*, 1993, 1210.
2 S. W. Elson, in *Recent Advances in the Chemistry of* β*-Lactam Antibiotics*, ed. G. I. Gregory, Royal Society of Chemistry, London, 1981, p. 142.
3 (*a*) C. A. Townsend and M. Ho, *J. Am. Chem. Soc.*, 1985, **107**, 1066; (*b*) J. Pitlik and C. A. Townsend, *Chem. Commun.*, 1997, 225.
4 S. W. Elson, K. H. Baggaley, M. Fulston, N. H. Nicholson, J. W. Tyler, J. Edwards, H. Holms, I. Hamilton and D. Mosdale, *J. Chem. Soc., Chem. Commun.*, 1993, 1211.
5 S. W. Elson and R. S. Oliver, *J. Antibiot.*, 1978, **31**, 586.
6 A. L. Gutman, V. Ribon and A. Boltanski, *J. Chem. Soc., Chem. Commun.*, 1985, 1627.
7 H. S. Anker, *J. Biol. Chem.*, 1948, **176**, 133.
8 R. C. Thomas, C. H. Wang and B. E. Christensen, *J. Am. Chem. Soc.*, 1951, **73**, 5914.
9 S. S. Shapiro and D. Denis, *Biochemistry USA*, 1965, **4**, 2283.
10 A. S. Serianni, H. N. Nunez and R. Barker, *Carbohydr. Res.*, 1979, **72**, 71.
11 R. Horikawa, H. Sakamoto and T. Tanimura, *J. Liq. Chromatogr.*, 1986, **9**, 537.
12 A. P. Doerschuk, *J. Am. Chem. Soc.*, 1951, **73**, 821.
13 H. J. Sallach, *J. Am. Chem. Soc.*, 1952, **74**, 2415.
14 A. Basak, S. P. Salowe and C. A. Townsend, *J. Am. Chem. Soc.*, 1990, **112**, 1654.
15 C. A. Townsend and S. Mao, *J. Chem. Soc., Chem. Commun.*, 1987, 86.
16 F. Dickens and D. H. Williamson, *Biochem. J.*, 1959, **72**, 496.

*Received in Glasgow, UK, 19th February 1997; Com. 7/01934C*

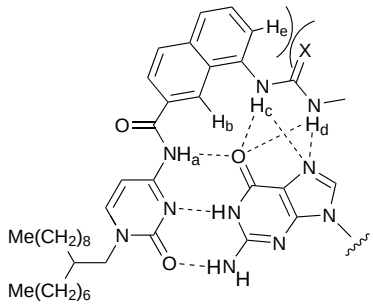
# Fluorescence-mediated sensing of guanosine derivatives based on multitopic hydrogen bonding

**Shigeru Amemiya, Philippe Bühlmann and Yoshio Umezawa***

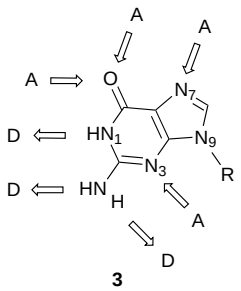
*Department of Chemistry, School of Science, The University of Tokyo, Hongo, Bunkyo-ku, Tokyo 113, Japan*

**The fluorescence emission of receptor 1 is selectively quenched upon binding of a guanosine derivative by five hydrogen bonds.**

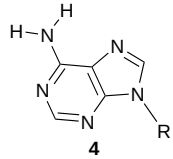
Because of their critical role in nearly all biological processes, molecular recognition of nucleotides has attracted much attention. By analogy with the formation of double-stranded DNA or RNA, many artificial receptors have been designed and synthesized to recognize nucleobases by complementary hydrogen bonding.[1] While a few of them have chromogenic or fluorogenic groups for optical signalling,[2–4] the moderate strengths of their complexes, which are stabilized by only three hydrogen bonds, are still unsatisfactory in view of optical sensor applications. Here we demonstrate very selective quenching of the fluorescence emission of receptors **1** and **2** upon binding of a guanosine derivative by five hydrogen bonds in a binary solvent mixture of chloroform and DMSO, and report on an application of receptor **1** in a fluorescence-based optical sensor[5] for guanosine 5′-triphosphate.



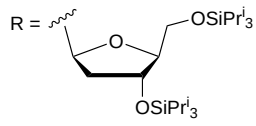

**1** X = O
**2** X = S




**3**




**4**




In addition to the Watson–Crick type hydrogen bonding site on the N-1 side (two hydrogen bond donor atoms and an acceptor in a DDA array), natural guanosine derivatives have an acceptor–donor (AD) and an acceptor–acceptor (AA) hydrogen bonding site on the side of N-3 and N-7, respectively (for instance, see **3**). On the basis of the secondary interaction model,[6] hydrogen bonded complexes with the AA·DD motif are expected to be more stable than those with the AD·DA motif. We therefore linked a urea or thiourea group as DD hydrogen bonding site to the cytosine group by using 8-amino-naphthalene-2-carboxylic acid as rigid spacer, giving receptors† **1** and **2** with a fairly high level of preorganization.

Complexation of receptor **1** or **2** (1.0 mM) with the lipophilic guanosine derivative **3** (0–25 mM) in the binary solvent mixture of $CDCl_3$ and [$^2H_6$]DMSO (4 : 1, v/v) was confirmed by $^1H$ NMR spectroscopy. In this concentration range, neither the receptors nor guest were observed to self-associate. For receptor **1**, complexation-induced downfield shifts for all NH hydrogens of both **1** and **3** were found, confirming the formation of hydrogen bonds. A $^1H$ NMR titration experiment showed the association constant ($K_{ass}$) to be $1.7 \times 10^2$ dm$^3$ mol$^{-1}$.

The occurrence of a downfield shift for all NHs of **1** and **3**, and the similarity of the association constants as determined for $H_a$, $H_b$, $H_c$ and $H_d$, suggest the formation of a 1 : 1 complex based on five hydrogen bonds.‡ To the best of our knowledge this is only the second receptor that forms more than three hydrogen bonds with the guanine base.[7] While improving its preorganization might further increase its binding strength [for a guanine receptor with very high preorganization, $K_{ass} > 1.9 \times 10^5$ dm$^3$ mol$^{-1}$ in $CDCl_3$–[$^2H_6$]DMSO (4 : 1, v/v)],[7] the most interesting aspect of receptor **1** is its fluorescent property (*vide infra*).

Similar results were obtained with thiourea **2**.‡ Upon complexation, downfield shifts were observed for all NH hydrogens of both **2** and **3**. Only the $H_c$ hydrogen of **2** underwent an opposite (upfield) shift. Because the NH hydrogens of thioureas are more acidic than those of ureas, stronger binding was expected for **2** than for **1**.[8] However, the association constant for the complex of **2** and **3** was found to be only $1.2 \times 10^2$ dm$^3$ mol$^{-1}$, which is slightly smaller than for the complex of receptor **1**. A possible explanation for the unexpectedly weak stability of the complex of **2** may be that steric hindrance between the sulfur and the aromatic hydrogen $H_e$ of **2** leads to a loss of coplanarity between the thiourea group and the naphthyl ring, which is unfavorable for the recognition of the planar guanine base. Indeed, crystal structures as found in the Cambridge Structural Database show that arylthioureas are in general less planar than arylureas.§

With a view to applying these receptors in optical sensors, their UV–VIS and fluorescent spectra were investigated in the binary mixture of $CHCl_3$ and DMSO (4 : 1, v/v). While the UV–VIS spectra of **1** or **2** did not change significantly in the presence and absence of **3**, complexation-induced quenching of their fluorescence emission was observed. Solutions of receptor **1** exhibit strong fluorescence emission in the range 420–530 nm. Upon addition of **3**, the fluorescence emission is strongly quenched. A plot of the ratio of the fluorescence intensity in the absence ($I_0$) and in the presence ($I$) of **3** *versus* the concentration of **3** is linear (Fig.1) and allows the determination of the association constant, $K_{ass}$, of the 1 : 1 complex of **1** and **3** according to eqn. (1),

$$I_0/I = 1 + K_{ass}[C] \quad (1)$$

where [C] is the concentration of **3**. The resulting $K_{ass}$ is $1.8 \times 10^2$ dm$^3$ mol$^{-1}$, which is in excellent agreement with $K_{ass}$ as obtained by $^1H$ NMR spectroscopy. This shows that the decrease in fluorescence emission is not due to dynamic quenching based on collision of the receptor and the guest in its

excited state, but to static quenching based on complexation. On the other hand, the fluorescence spectrum of receptor **1** was not perturbed at all by addition of the lipophilic adenosine derivative **4** (Fig.1). Increasing the number of hydrogen bonding sites gives a very selective fluorogenic receptor with a significantly larger binding strength than previously reported for chromogenic or fluorogenic nucleobase receptors with only three hydrogen bonding sites ($K_{ass} = 2.8 \times 10^2$ or $9 \times 10^2$ $dm^3\ mol^{-1}$ in $CDCl_3$ or $CD_2Cl_2$, respectively[2,3]). A highly selective quenching by **3** but not by **4** was also observed for receptor **2** (data not shown). However, the fluorescence intensity of receptor **2** was twenty times smaller than that of **1**, and receptor **2** does not appear to be photostable because the fluorescence intensity increased monotonously in repetitive emission scans of a dilute solution.

The fluorescent responses of an optical sensor based on a plasticized poly(vinyl chloride) membrane containing receptor **1** is shown in Fig. 2.¶ The response mechanism of this sensor (a bulk optode) is based on an anion-exchange equilibrium between the sample solution and the optode membrane.[9] An increase in the nucleotide concentration in the sample solution leads to receptor-assisted uptake of the nucleotide into the membrane in exchange for $Cl^-$, thereby changing the intensity of the receptor fluorescence. As expected, stronger quenching of the emission was observed for 5′-GTP than for 5′-ATP, which is due to preferential complexation of **1** with the guanine moiety of 5′-GTP. This is the first example of an optode based on multitopic hydrogen-bond mediated complexation of an analyte and a synthetic receptor. While this optode is very sensitive for 5′-GTP (detection limit < 10 μM), high background concentrations of $Cl^-$ as occurring in biological samples may make a higher discrimination of $Cl^-$ desirable. To improve the selectivity over $Cl^-$, nucleotide-selective optodes containing two receptor types[10] (receptor **1** and bis-thiourea receptors[8] for binding the nucleobase and phosphate groups, respectively) are conceivable.

This work was supported by grants from the Ministry of Education, Science and Culture, Japan.

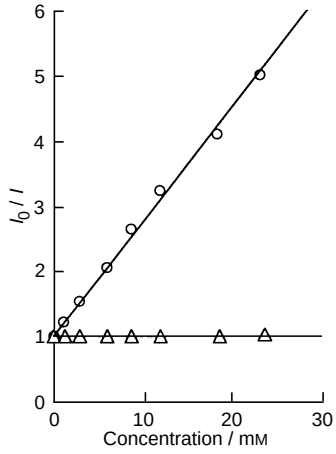



**Fig. 1** Plot of the ratios of fluorescence intensities of solutions of receptor **1** (0.11 mM) in $CHCl_3$–DMSO (4 : 1, v/v) in absence ($I_0$) and in presence ($I$) of guest **3** (○) or **4** (△). Excitation at 373 nm, emission at 488 nm.

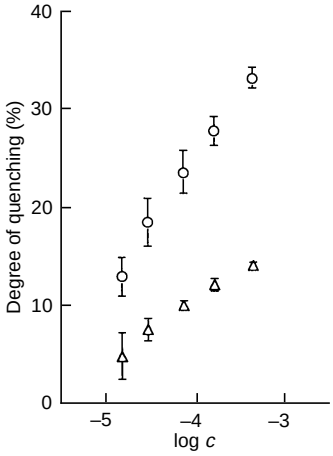



**Fig. 2** Fluorescence responses of a membrane¶ based on receptor **1** as a function of the concentration of 5′-GTP (○) and 5′-ATP (△) in an aqueous buffer solution (10 mM tris/HCl at pH 7.4). Excitation at 375 nm, emission at 470 nm.

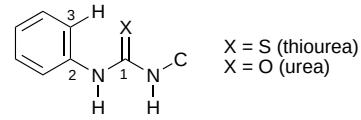
## Footnotes

* E-mail: umezawa@utsc.s.u-tokyo.ac.jp

† Both receptors gave satisfactory $^1H$ NMR, IR and mass spectra and elemental analyses.

‡ Non-linear regression analysis of the $^1H$ NMR titration data gave the association constants ($K_{ass}$) and the differences in chemical shifts ($\Delta\delta_{max}$) of complexed and uncomplexed receptor using the residual solvent signal (δ 2.55) for [$^2H_6$]DMSO as reference: receptor **1**, $K_{ass}$ = 173, 171, 153 and 174 $dm^3\ mol^{-1}$ and $\Delta\delta_{max}$ = 0.80, 0.39, 0.09 and 1.45 ppm, respectively, for $H_{a–d}$ (δ 10.38, 8.86, 8.60 and 6.09, respectively, in its uncomplexed form); receptor **2**, $K_{ass}$ = 127, 127, 120 and 122 $dm^3\ mol^{-1}$ and $\Delta\delta_{max}$ = 0.56, 0.39, −0.12 and 1.70 ppm, respectively, for $H_{a–d}$ (δ 10.70, 8.87, 9.50 and 7.43, respectively, in its uncomplexed form).

§ The torsional angle C(1)–N–C(2)–C(3) in *N*-phenyl and *N*,*N*′- diphenyl derivatives of urea and thiourea is a good measure of the coplanarity between the aryl ring and urea or thiourea plane. For arylthioureas, the average of the torsional angles in eight cases was found to be 57°, seven of them being in the range from 42 to 87°. For arylureas, the average of the torsional angles in 61 cases was found to be 20°, 50 of them being smaller than 34°.




¶ The membrane was prepared by pouring 200 μl of a THF solution of the membrane components [0.50 mg receptor **1**, 1.94 mg tridodecylmethylammonium chloride (400 mol% relative to receptor **1**), 7.61 mg bis(ethylhexyl) sebacate and 4.95 mg PVC in 5 ml THF] on a glass plate (12 × 25 × 2.5 mm) and letting the solvent evaporate overnight.

## References

1 J. Rebek, Jr., *Acc. Chem. Res.*, 1990, **23**, 399; A. D. Hamilton, E. Fan, S. V. Arman, S. J. Geib and J. Yang, *Philos. Trans. R. Soc. Lond. A*, 1993, **345**, 57.
2 M. Inouye, K. Kim and T. Kitao, *J. Am. Chem. Soc*., 1992, **114**, 778.
3 M. Abe, J. Otsuki and K. Araki, *Chem. Lett*., 1993, 1541.
4 M. M. H. Khalil, F. C. De Schryver, H. Keller and J.-M. Lehn, *Supramol. Sci*., 1995, **2**, 175–182.
5 O. S. Wolfbeis, *Fiber Optic Chemical Sensors and Biosensors*, CRC Press, Boca Raton, FL, 1991.
6 J. Pranata, S. G. Wierschke and W. L. Jorgensen, *J. Am. Chem. Soc*., 1991, **113**, 2810.
7 T. W. Bell, Z. Hou, S. C. Zimmerman and P. A. Thiessen, *Angew. Chem., Int. Ed. Engl*., 1995, **34**, 2163. For guanine receptors with three hydrogen bonding sites (see also ref. 2): A. D. Hamilton and N. Pant, *J. Chem. Soc., Chem. Commun*., 1988, 765; T. Ishida, H. Iyo, H. Ueda, M. Doi and M. Inoue, *J. Chem. Soc., Chem. Commun*., 1990, 217; H. Furuta, K. Kuruta and J. L. Sessler, *J. Am. Chem. Soc*., 1991, **113**, 4706; T. K. Park, J. Schroeder and J. Rebek, Jr., *Tetrahedron*, 1991, **47**, 2507; S. Metzger and B. Lippert, *Angew. Chem., Int. Ed. Engl*., 1996, **35**, 1228; S. Amemiya, P. Bühlmann, K. Tohda and Y. Umezawa, *Anal. Chim. Acta*, in the press; K. Tohda, S. Amemiya, S. Nagahora, S. Tanaka, T. Ohki, P. Bühlmann and Y. Umezawa, unpublished results.
8 S. Nishizawa, P. Bühlmann, M. Iwao and Y. Umezawa, *Tetrahedron Lett*., 1995, **36**, 6483; P. Bühlmann, S. Nishizawa, K. P. Xiao and Y. Umezawa, *Tetrahedron*, 1997, **53**, 1647.
9 W. E. Morf, K. Seiler, B. Lehmann, C. Behringer, K. Hartman and W. Simon, *Pure Appl. Chem*., 1989, **61**, 1613.
10 K. Tohda, R. Naganawa, X. M. Lin, M. Tange, K. Umezawa, K. Odashima, Y. Umezawa, H. Furuta and J. L. Sessler, *Sens. Actuators B*, 1993, **13/14**, 669.

*Received in Columbia, MO, USA, 14th January 1997; Com. 7/00316A*

# Multiple nitrene insertions into the copper–sulfur bonds of dithiocarbamate ligands: synthesis and molecular structure of the tetraamido complex [Cu{η²-RNSC(NMe₂)SNR}₂] (R = SO₂C₆H₄Me-*p*)

**Graeme Hogarth,* Andrew Pateman and Andrea Sella**

*Chemistry Department, University College London, 20 Gordon Street, London, UK WC1H 0AJ*

**During the aziridination of styrene with PhI=NR (R = $SO_2C_6H_4Me$-*p*) the copper(III) catalyst [Cu(η²-$S_2CNMe_2$)$_2$][$FeCl_4$] is converted into the crystallographically characterised tetraamido complex [Cu{η²-RNSC($NMe_2$)SNR}$_2$], a result of nitrene insertion into all four copper–sulfur bonds.**

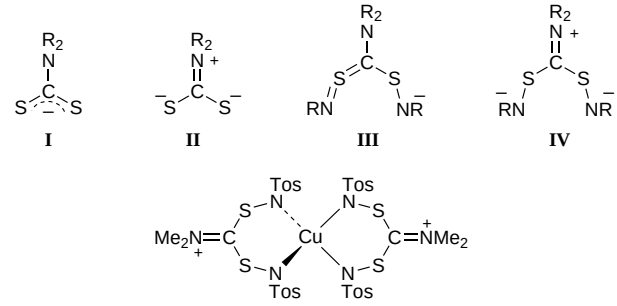
Recent work, primarily by the groups of Evans[1] and Jacobsen,[2] has revealed that a wide range of copper complexes can act as homogeneous catalysts towards the aziridination of alkenes. Although the nature of this catalytic process is not well understood, preliminary results from the Jacobsen group are strongly suggestive of the formation of a copper–nitrene complex.[3] While this would appear to be a sensible proposal, the nitrene (imido) ligand is a strong π donor and is generally associated with high-valent metal centres, that is those with low d electron counts.[4] Thus, while complexes with $d^0$–$d^2$ centres are abundant, those with electron counts of $d^3$–$d^6$ are extremely rare and there are no well authenticated examples of mononuclear complexes of this type with higher electron counts.[4]

Our work in this area has been concerned with gaining a better understanding of the catalytic process with a view to developing new, more efficient and selective, aziridination catalysts.[5] As part of this effort, and in an attempt to elucidate the oxidation state of the active catalyst, we have shown that, under the correct reaction conditions, copper(I)–(III) dithiocarbamate complexes are all highly active catalysts. After a number of these catalytic runs we noted the formation of a small amount of a new green solid which we sought to characterise in order to gain insight into the catalytic process. Herein we report details of the structure of the novel tetraamido complex [Cu{η²-RNSC($NMe_2$)SNR}$_2$] **1**, formally resulting from the insertion of nitrene groups into all four sulfur–copper bonds of the catalyst.

While carrying out the aziridination of styrene using PhI=NR as a nitrene source and the copper(III) dithiocarbamate complex [Cu(η²-$S_2CNMe_2$)$_2$][$FeCl_4$] as catalyst, after the reaction was complete, extraction into dichloromethane and layering with toluene resulted in the deposition of green paramagnetic crystals characterised by X-ray crystallography as the tetraamido copper(II) complex [Cu{η²-RNSC($NMe_2$)SNR}$_2$] **1** as shown in Fig. 1.†

The molecule consists of a four-coordinate copper(II) centre bound by two new chelating ligands, formed as a result of nitrene insertion into the copper–sulfur bonds of the dithiocarbamate ligand. It has overall $D_{2d}$ symmetry, the copper centre being a compressed tetrahedron, with a dihedral angle of 35.4° between $CuN_2$ planes. The ligand has a bite angle of 87.4(2)° and an angle of 97.7(2)° separates the two. The six-membered ring is puckered with the tosyl (Tos) groups on nitrogen adopting an alternating up–down configuration, and copper–nitrogen distances of 2.016(4) and 2.005(4) Å are similar to those found in related copper(II) complexes.[6]

Resonance forms **I** and **II** are commonly used to explain the ability of the dithiocarbamate ligand to stabilise both low- and high-valent metal centres, respectively,[7] and similar structures




**III** and **IV** can be considered for the new ligand in **1**. Close inspection of the structural parameters of the ring reveal that only the diamido form **IV** contributes to any extent. Thus, while the ring itself is severely puckered, the dithiocarbamate unit is quite flat [max. deviation 0.008 Å by C(30)] and planar about N(3). Further, the backbone carbon–nitrogen bond, C(30)–N(3), at 1.330(6) Å is short and similar to those found in related dithiocarbamate complexes.[7,8] That resonance form **III** does not contribute significantly is also shown by the relatively long sulfur–carbon [S(3)–C(30) 1.579(5), S(4)–C(30) 1.781(5)

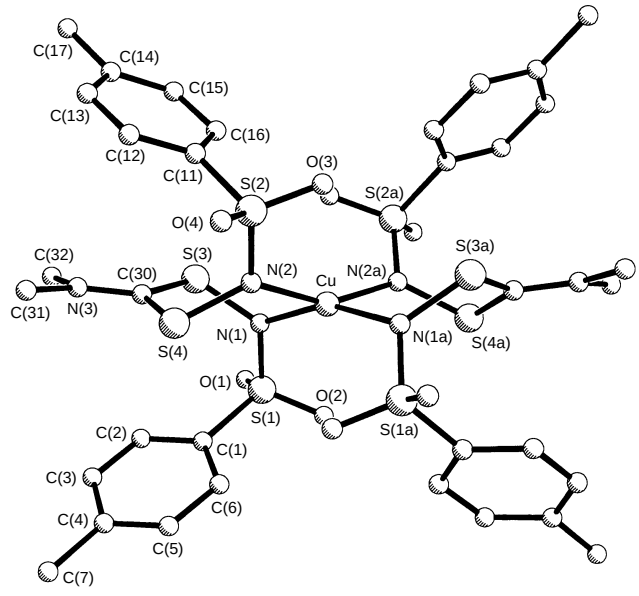



**Fig. 1** Molecular structure of **1** with selected bond lengths (Å) and angles (°): Cu–N(1) 2.005(4), Cu–N(2) 2.016(4), S(1)–N(1) 1.642(4), S(2)–N(2) 1.649(4), S(3)–N(1) 1.687(4), S(4)–N(2) 1.694(4), S(3)–C(30) 1.759(5), S(4)–C(30) 1.781(5), N(3)–C(30) 1.330(6); N(1)–Cu–N(2) 87.4(2), N(1)–Cu–N(2A) 97.7(2), N(1)–Cu–N(1A) 157.0(2), N(2)–Cu–N(2A) 154.5(2), Cu–N(1)–S(3) 124.3(2), N(1)–S(3)–C(30) 103.5(2), S(3)–C(30)–S(4) 119.3(3), C(30)–S(4)–N(2) 103.5(2), S(4)–N(2)–Cu 124.1(2)

Å] and sulfur–nitrogen [N(1)–S(3) 1.687(4), N(2)–S(4) 1.694(4) Å] bonds within the ring, the former being considerably longer than those in related copper(II) dithiocarbamate complexes,[8] while the latter are longer than the sulfur–nitrogen bonds to the tosyl groups [N(1)–S(1) 1.642(4), N(2)–S(2) 1.649(4) Å]. Thus, the zwitterionic diamido formulation **IV** is the most apt ligand description. Further, the ring nitrogens N(1) and N(2) are essentially planar as shown by the sum of the bond angles at each of 359.3 and 358.9°, respectively.

As far as we are aware, the chelating ligand found in **1** has not previously been characterised although it appears to be quite stable. The mode of formation of **1** is also unknown. While a number of novel rearrangements[9] and insertions into the dithiocarbamate backbone[9,10] have been reported, we are unaware of examples of nitrene or related insertions into the metal–sulfur bonds. What is clear, however, from the isolation of **1** is that nitrene coordination to the copper centre must be facile and this supports Jacobsen's recent observations.[3] We have previously reacted known copper aziridination catalysts with the nitrene source and, while in all cases a rapid reaction takes place (as evidenced by the dissolution of the nitrene source), we have previously been unable to characterise the product(s).[5] Copper-catalysed aziridination reactions are generally carried out in the presence of an excess of the alkene, which is known to bind to the copper centre.[11] We speculate, then, that during the normal course of catalysis, nitrene transfer to the precoordinated alkene from the highly reactive copper–nitrene species is facile, giving rise to aziridines. However, in the absence of the alkene, the copper-bound nitrene moiety may react with other metal-bound ligands as is found in **1**.

Since formation of **1** involves the multiple insertion of nitrene fragments we are currently trying to determine whether this is a stepwise process and we are also assessing the ability of **1** to act as an aziridination catalyst. Direct addition of an excess of the nitrene source to $[Cu(\eta^2\text{-}S_2CNMe_2)_2][FeCl_4]$ initially affords a red solution and later a green precipitate. While neither contains **1**, the latter appears to combine nitrene, copper and dithiocarbamate fragments and its identity and relationship to **1** are under investigation.

We thank the EPSRC for the provision of a research studentship to A. P.

## Footnotes

* E-mail: g.hogarth@ucl.ac.uk

† *Crystal data* for **1**·$2CH_2Cl_2$: crystal dimensions 0.36 × 0.26 × 0.24 mm, $C_{36}H_{44}Cl_4CuN_6O_8S_8$, monoclinic, space group *C*2/*c* (no. 15), *M* = 1150.59, *a* = 12.457(2), *b* = 22.648(5), *c* = 19.224(4) Å, β = 106.59(3)°, *U* = 5198(2) Å$^3$, *Z* = 4, $D_c$ = 1.470 g cm$^{-3}$, μ(Mo-Kα) = 9.98 cm$^{-1}$, *F*(000) = 2364. Data were obtained at 25 ± 1 °C on a Nicolet R3mV diffractometer using graphite-monochromated Mo-Kα radiation. A total of 4469 reflections (4274 unique) were collected using the ω scan method within a 2θ range 5–50°. The structure was solved by direct methods and refined by full-matrix least-squares methods using 3086 reflections [$I_o > 2\sigma(I)$]. The final refinement converged to $R$ = 0.0624 and $R_w$ = 0.1462. Atomic coordinates, bond lengths and angles, and thermal parameters have been deposited at the Cambridge Crystallographic Data Centre (CCDC). See Information for Authors, Issue No. 1. Any request to the CCDC for this mnaterial should quote the full literature citation and the reference number 182/450.

## References

1 D. A. Evans, M. M. Faul and M. T. Bilodeau, *J. Am. Chem. Soc*., 1994, **116**, 2742; D. A. Evans, M. M. Faul, M. T. Bilodeau, B. A. Anderson and D. M. Barnes, *J. Am. Chem. Soc*., 1993, **115**, 5328.
2 Z. Li, K. R. Conser and E. N. Jacobsen, *J. Am. Chem. Soc*., 1993, **115**, 5326.
3 Z. Li, R. W. Quan and E. N. Jacobsen, *J. Am. Chem. Soc*., 1995, **117**, 5889.
4 D. E. Wigley, *Prog. Inorg. Chem*., 1994, **42**, 239.
5 G. Hogarth, A. Pateman and A. Sella, unpublished work.
6 C. H. Wei, *Inorg. Chem*., 1972, **11**, 2315; H. Hope and P. P. Power, *Inorg. Chem*., 1984, **23**, 936.
7 A. M. Bond and R. L. Martin, *Coord. Chem. Rev*., 1984, **54**, 23.
8 B. H. O'Conner and E. N. Maslen, *Acta Crystallogr*., 1966, **21**, 828; F. W. B. Einstein and J. S. Field, *Acta Crystallogr., Sect. B*, 1974, **30**, 2928.
9 T. A. Coffey, G. D. Forster and G. Hogarth, *J. Chem. Soc., Dalton Trans*., 1996, 183 and references therein.
10 C. G. Young, X. F. Yan, B. L. Fox and E. R. T. Tiekink, *J. Chem. Soc., Chem. Commun*., 1994, 2579.
11 P. J. Perez, M. Brookhart and J. L. Templeton, *Organometallics*, 1993, **12**, 261; R. W. Quan, Z. Li and E.N. Jacobsen, *J. Am. Chem. Soc*., 1996, **118**, 8156.

*Received in Basel, Switzerland, 3rd March, 1997; Com. 7/01483J*

# Formation and transformation of mesoporous and layered manganese oxides in the presence of long-chain ammonium hydroxides

**Jian Luo[a] and Steven L. Suib*[a,b]**

[a] *U-60, Department of Chemistry, University of Connecticut, Storrs, CT 06269-4060, USA*
[b] *Department of Chemical Engineering and Institute of Materials Science, University of Connecticut, Storrs, CT 06269-4060, USA*

**Mesoporous manganese oxides are prepared by reduction and oxidation mechanisms and by interconversions of layered materials.**

Two methods (oxidation and reduction) have been developed to synthesize mesoporous manganese oxides ($MnO_x$). Organic ammonium cations are introduced into layered birnessite-type $MnO_x$. Transformations from a mesoporous $MnO_x$ to a layered material and from a layered $MnO_x$ to a mesoporous structure have been observed.

The synthesis of molecular sieves of large micropores (VPI-5[1]) and mesopores (MCM-41[2,3]) has long been a focus of many researchers. Since the development of the Mobil MCM series of mesoporous silicates and aluminosilicates using templates such as long-chain ammonium-type surfactants, several studies[4–7] have been published on the synthesis, characterization, and applications of these mesoporous materials. Some transition metals,[8,9] such as Ti, have also been successfully incorporated into mesoporous structures. In those studies, silica or metallosilicate gel (usually from the hydrolysis of metal ethoxides) is precipitated around the hexagonally packed micelles of surfactant molecules to form a mesoporous inorganic framework. Neither reduction nor oxidation is generally used in the syntheses of these materials.

However, few studies, to our knowledge, have yet been published of the synthesis and related research on manganese containing mesoporous materials. The conversion from a mesoporous structure to a layered structure, and observations that a typical layered $MnO_x$ can be converted into a mesoporous structure have not been reported.

The oxidation of $Mn^{II}$ and reduction of $Mn^{VII}$ are employed herein to prepare mesoporous $MnO_x$ in the presence of long-chain organic ammonium hydroxides. The two methods are thus referred to as oxidation and reduction syntheses, respectively. A method to incorporate organic ammonium cations into a birnessite-type layered manganese oxide to prepare large *d*-spacing layered materials is also presented. The conversions from a mesoporous $MnO_x$ to a layered material and that from a birnessite to a mesoporous structure have been investigated.

For a typical oxidation synthesis, 8.0 g of $MnCl_2{\cdot}4H_2O$ in 50 ml deionized distilled water (DDW) was slowly added to a 1 l beaker containing a 200 ml solution of $(C_{12}H_{25})NMe_3OH$ (*ca.* 30 mass%) with a glass rod, with vigorous stirring with a stirring bar. A gel of $Mn(OH)_2$ having pyrochroite structure was formed and was stirred for 30 min. Oxygen gas from a cylinder was then bubbled in to the solution with a gas flow rate of *ca.* 100 ml $min^{-1}$ *via* a glass frit, without stirring. In order to prevent formation of a foam, a few drops of ethanol are added to the beaker every 10 min. Bubbling was continued for *ca.* 8 h after which the resultant black precipitate was transferred to a 500 ml glass bottle, which was aged in a water-bath at 40 °C.

In the oxidation synthesis, $Mn(OH)_2$ having pyrochroite structure (JCPDS card 18-787) was formed when $MnCl_2$ was added to the $(C_{12}H_{25})NME_3OH$ solution. When oxygen was bubbled for 30 min, $Mn(OH)_2$ was converted to hydrohausmannite [a mixture of β-MnO(OH) and γ-$Mn_3O_4$, JCPDS 18-804 and 24-734, respectively]. Further bubbling of oxygen into the system led to oxidation of hydrohausmannite to a substance having only one broad XRD peak at 2θ *ca.* 18–20°. This broad peak did not change even when oxygen bubbling was continued for a day. The XRD pattern also remained the same when the system was aged at 40 °C for 4 h. However, at $t$ = 10 h, an XRD peak at *ca.* 30 Å *d*-spacing appears, indicating the evolution of mesoporous $MnO_x$ in the system [Fig. 1(*a*)]. Both the *d*-spacing and the intensity of the peak increase with increasing ageing time until at $t$ = 20 h the intensity reaches a maximum for the peak at a *d*-spacing of 46 Å [Fig. 1(*b*)]. During this period mesoporous $MnO_x$ is formed and its amount is increased with increasing ageing time. The time before formation of mesoporous $MnO_x$ is referred to as the induction period. From $t$ = 20 h to $t$ = 36 h both the intensity and *d*-spacing value remain almost constant and this is denoted the steady-state period.

Beyond an ageing time of 48 h, the XRD peak at 45 Å *d*-spacing was found to decrease and continued to decrease with increasing time. The *d*-spacing value also decreased to some extent. Meanwhile, a new set of XRD peaks characteristic of a layered structure appears. The peaks occur at 25.4 Å (001), 12.7 Å (002), 8.6 Å (003), 6.4 Å (004) and 5.1 Å (005) [Fig. 1(*c*)] where the numbers in parentheses are the reflection indices. The 46 Å peak corresponding to a mesoporous structure is shifted to 39 Å at $t$ = 48 h and finally disappears at $t$ = 4 d, with the presence of only peaks for the layered structure, whose

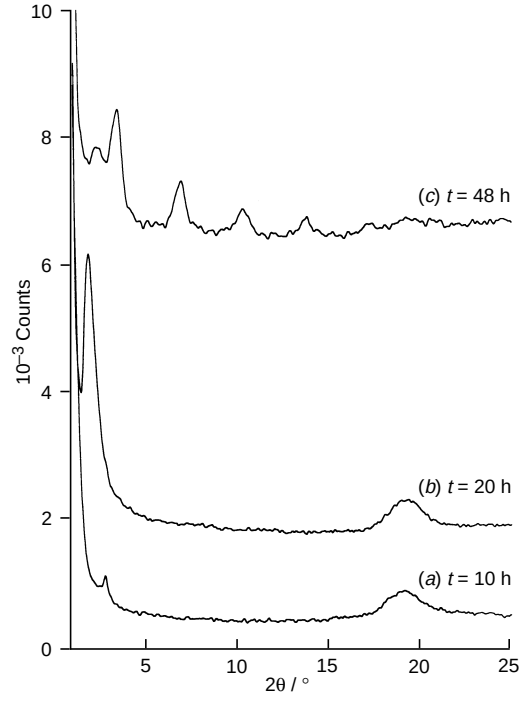



**Fig. 1** XRD patterns showing the formation and transformation of mesoporous $MnO_x$ during the oxidation synthesis at different ageing times

*d*-spacings are also decreased slightly to 23.9 (001), 11.9 (002), 7.9 (003), 6.0 (004) and 4.8 Å (005), respectively. This indicates that the mesoporous $MnO_x$ has completely converted to a layered structure.

The reduction synthesis employs alcohols such as ethanol as reductants to reduce $(C_{12}H_{25})NMe_3MnO_4$ in the presence of $(C_{12}H_{25})NMe_3OH$. Typically a slurry containing 20 g of freshly prepared $(C_{12}H_{25})NMe_3MnO_4$‡ was added to a 100 ml solution of $C_{12}H_{25}NMe_3OH$ (*ca*. 30 mass%) with stirring, forming a uniform slurry. Absolute ethanol (100 ml) was then poured into the slurry. The resultant gel was stirred for *ca*. 30 min and aged at 65–85 °C in an oven.

In the reduction synthesis, the product before ageing was an amorphous $MnO_x$ material. When it was aged at 65 °C for 2 days, the amorphous material became mesoporous, with only one XRD peak at 57 Å. Unlike the mesoporous material produced during the oxidation synthesis, it exhibited no peaks in the range 2θ 18–20. In addition, this material showed no conversion to any layered structure even after ageing at 65 °C for 5 days.

The synthesis of birnessite and subsequent conversion of the layered $MnO_x$ into a mesoporous structure was performed by adding, with stirring, 10 g of $KMnO_4$ dissolved in 150 ml DDW to a mixture of 100 ml absolute ethanol and 50 ml DDW containing 30 g KOH. A brownish gel was formed, which (after 30 min stirring) was kept in an oven at 85 °C for 2 days. After being filtered, the gel was washed with DDW until the pH of the filtrate was < 10. The product was potassium birnessite. While still wet, it was transferred to a beaker containing 200 ml of 1 M $HNO_3$ and stirred at room temp. for 3 h to allow $H^+$ exchange. The exchange was repeated, giving H-birnessite, which was washed, filtered and transferred to a beaker containing 200 ml of DDW while stirring. A solution of 10 ml of 20–40 mass% of different organic ammonium hydroxides was added to introduce different types of ammonium ions into the birnessite.

The XRD pattern of the prepared H-birnessite is shown in Fig. 2(*a*). Only two main peaks with *d*-spacings of 7.3 and 3.6 Å were present in this preferentially oriented XRD pattern.

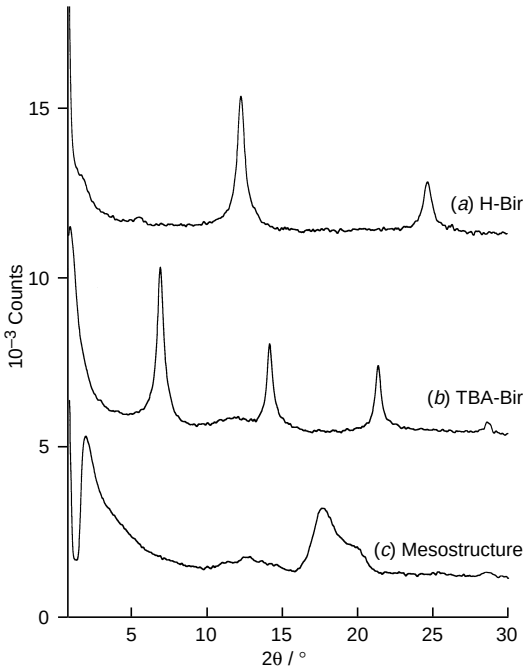



**Fig. 2** XRD patterns showing the conversion of a layered $MnO_x$ birnessite into a mesoporous material

When an organic ammonium species is introduced, the interlayer spacing is increased to an extent which depends on the dimension of the individual organic ammonium ion. For a $(C_{12}H_{25})NME_3$-birnessite, the preferentially oriented XRD reflections were at 24.1 (001), 12.0 (002), 8.0 (003), 6.0 (004), 4.8 (005) and 4.0 Å (006). This is almost identical to that of a layered $MnO_x$ converted from a mesoporous $MnO_x$ which was prepared from the oxidation of $Mn^{II}$ with oxygen in the presence of $(C_{12}H_{25})NMe_3OH$. When a smaller organic ammonium ion, *e.g*. tetrabutylammonium hydroxide (TBAOH), is used the XRD reflections of the layered $MnO_x$ are at 12.8 (001), 6.4 (002), 4.2 (003) and 3.2 Å (004) [Fig. 2(*b*)], *i.e*. at substantially lower values than for $(C_{12}H_{25})NMe_3$-birnessite.

When $Mg(MeCO_2)_2{\cdot}6H_2O$ (20 g) in 50 ml DDW was added to H-birnessite prior to the addition of the organic ammonium hydroxide, no exchange of $Mg^{2+}$ for $H^+$ was observed even if the system was stirred for more than a week. However, when TBAOH was added to H-birnessite containing $Mg^{2+}$ ions and the system was stirred for two days, the layered material was converted to a mesoporous $MnO_x$ structure [Fig. 2(*c*)]. The layered mesoporous $MnO_x$ material exhibits a basal XRD reflection at 42.3 Å, with several broad small peaks at 2θ 15–20°. This XRD pattern is quite similar to that of the mesoporous $MnO_x$ produced in the oxidation syntheses.

IR studies show that the mesoporous materials all have a strong absorption around 700 $cm^{-1}$, arising from Mn–O bond vibrations. The layered materials, including both those converted from mesoporous $MnO_x$ formed during oxidation syntheses and those containing organic ammonium introduced into birnessites, all have framework vibrations similar to those of birnessite. Detailed characterization of the materials, including TEM, thermal properties, sorptive properties, Mn oxidation state, acid–base properties and catalytic properties are under way. The mechanisms of formation and transformations associated with the mesoporous $MnO_x$ are also being studied.

## Footnotes

* E-mail: suib@uconnvm.uconn.edu

† $(C_{12}H_{25})NME_3OH$ was prepared by adding a slurry of an excess of AgOH (freshly prepared from the reaction of $AgNO_3$ and NaOH and washed to neutral pH) to a solution of $(C_{12}H_{25})NMe_3Br$. The system was stirred overnight and was then filtered to give a solution of $(C_{12}H_{25})NMe_3OH$.

‡ $(C_{12}H_{25})NMe_3MnO_4$ was prepared by addition of a solution of $Ba(MnO_4)_2$ to a slight excess of $H_2SO_4$, with the $BaSO_4$ solid filtered off to give a solution of $HMnO_4$. An excess of $(C_{12}H_{25})NME_3OH$ was then added to the $HMnO_4$ solution to produce $(C_{12}H_{25})NMe_3MnO_4$.

## References

1 M. E. Davis, C. Saldarriaga, C. Montes, J. Graces and C. Crowder, *Nature*, 1988, **331**, 698.
2 C. T. Kresge, M. E. Leonowicz, W. J. Roth, J. C. Vartuli and J. S. Beck, *Nature*, 1992, **359**, 710.
3 J. S. Beck, J. C. Vartuli, W. J. Roth, M. E. Leonowicz, C. T. Cresge, K. D. Schmitt, C. T-W. Chu, D. H. Olson, E. W. Sheppard, S. B. McCullen, J. B. Higgins and J. L. Schlenker, *J. Am. Chem. Soc*., 1992, **114**, 10 834.
4 C. F. Cheng, Z. Luan and J. Klinowski, *Langmuir*, 1995, **11**, 2815.
5 C. Chen, H. Li and M. E. Davis, *Microporous Mater*., 1993, **2**, 17.
6 A. Monnier, F. Schuth, Q. Huo, D. Kumar, D. Margolese, R. S. Maxwell, G. D. Stucky, M. Krishnamurty, P. Petroff, A. Firouzi, M. Janicke and B. G. Chmelka, *Science*, 1993, **261**, 1299.
7 N. Coustel, F. D. Renzo and F. Fajula, *J. Chem. Soc., Chem. Commun*., 1994, 967.
8 A. Corma, M. T. Navarro and J. Perez-Pariente, *J. Chem. Soc., Chem. Commun*., 1994, 147.
9 D. M. Antonelli and J. Y. Ying, *Angew. Chem., Int. Ed. Engl*., 1995, **34**, 2014.

*Received in Cambridge, UK, 11th March 1997; Com. 7/01690E*

# 1*H*-Phosphiranes and -enes invert at phosphorus *via* a turnstile rotation†

**Andreas Göller and Timothy Clark***

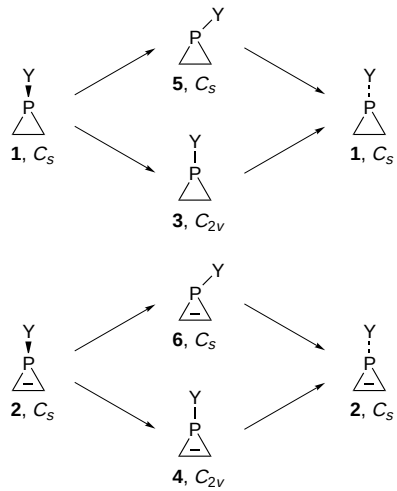
*Computer-Chemie-Centrum, Institut für Organische Chemie, Friedrich-Alexander-Universität Erlangen-Nürnberg, Nägelsbachstraße 25, D-91052 Erlangen, Germany*

***Ab initio* (CCSD(T)/6-31+G*) calculations suggest that 1*H*-phosphiranes and 1*H*-phosphirenes invert their configuration at phosphorus by a rotation of the PX group (X = H, F, Cl, Br) above the $C_2$ moiety, rather than the more usual planar trigonal inversion pathway *via* a $C_{2v}$ transition state.**

Because of the high inherent barrier to inversion at three-coordinate phosphorus, phosphanes can be isolated as pure enantiomers.[1] The additional effect of inclusion in a three-membered ring increases inversion barriers further,[2] so that 1*H*-phosphiranes and, even more so, 1*H*-phosphirenes should have particularly high inversion barriers. However, our recent studies on σ*-aromatic 1*H*-phosphirenium ions[3] have revealed unusual bonding effects and so we have investigated the inversion process in 1*H*-phosphiranes[4] and 1*H*-phosphirenes.[5] Our studies reveal an unusual inversion mechanism caused by the avoidance of large bond angles at phosphorus and, in the unsaturated systems, by the potential antiaromaticity of the trigonal inversion transition states.[2,6] This mechanism is analogous to that for $PF_3$ inversion *via* a T-shaped transition state,[7] but is favoured by additional ring strain and conjugation effects.

1*H*-phosphiranes **1** and 1*H*-phosphirenes **2** can undergo inversion at phosphorus by two distinct mechanisms (absolute energies and geometries are given in Tables 1 and 2 of the Supplementary material,‡ respectively). The first is *via* the $C_{2v}$ structures **3** and **4** for the saturated and unsaturated systems, respectively, as described by Bachrach.[2,8] The structures **3** are found to be real transition states (one calculated imaginary frequency), but **4** is found to be a second-order saddle point (hilltop) for all ligands X except hydrogen, for which **4** is also a transition state. *Ab initio*[9a] [CCSD(T)[10]/6-31+G*[11]//(MP2[12]/6-31+G*)] calculations performed with GAUSSIAN 94[9b] give energy differences between **1** and **3** at 0 K of 66.5 kcal mol$^{-1}$ (1 cal = 4.184 J) (X = H), 99.9 kcal mol$^{-1}$ (X = F), 86.0 kcal mol$^{-1}$ (X = Cl), and 82.3 kcal mol$^{-1}$ (X = Br) and those between **2** and **4** of 85.4 kcal mol$^{-1}$ (X = H), 45.5 kcal mol$^{-1}$ (X = F), 55.4 kcal mol$^{-1}$ (X = Cl), and 50.9 kcal mol$^{-1}$ (X = Br) (see Table 3 of Supplementary material). For the π-donor halogen ligands, the barrier to trigonal inversion is unexpectedly lower for the 1*H*-phosphirenes **2** than for the 1*H*-phosphiranes **1**. This is the result of the partial dissociation of **4** into an aromatic phosphirenylium cation–halide ion pair. This dissociation is analogous to that found for the fluoromethyl anion,[13] which can be regarded as a carbene–fluoride complex. Note that all the above barriers are considerably lower than the 120–130 kcal mol$^{-1}$ found[7] for the 8π-electron $PF_3$.

The second route is the simple rotation of the PX group roughly around an axis through the phosphorus atom and the centre of the C–C bond. This process occurs for the phosphiranes **1** *via* transition state **5** and is found to be more favourable than trigonal inversion for all ligands except hydrogen. The calculated barriers at 0 K are 77.1 kcal mol$^{-1}$ (X = F), 70.6 kcal mol$^{-1}$ (X = Cl) and 65.2 kcal mol$^{-1}$ (X = Br). For X = H, **5** collapses to **3** on geometry optimisation, so that in this




**Scheme 1**

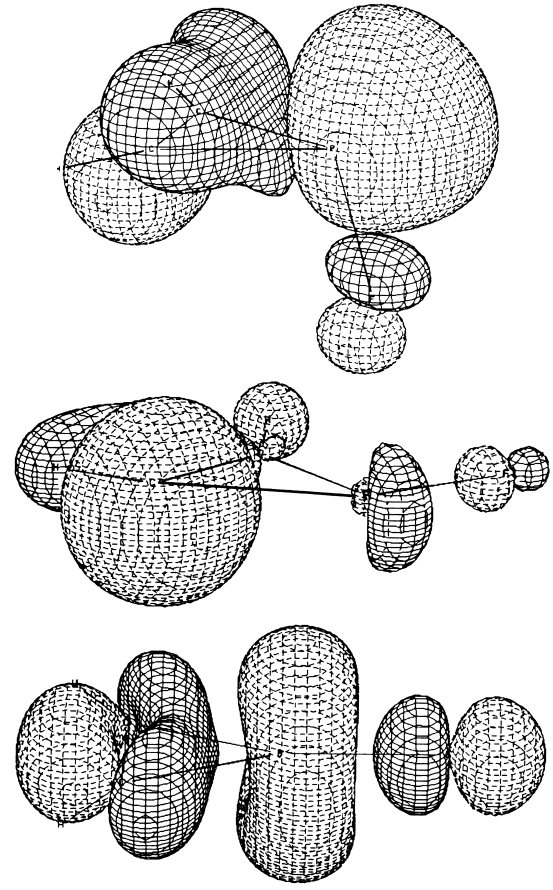


**Fig. 1** MO plots of the 'phosphorus lone pair' for the 1-fluoro-1*H*-phosphirene ground state (top), turnstile transition state (middle) and trigonal inversion transition state (bottom)

case the trigonal inversion mechanism applies. The $C_s$ structures **5** are found to be transition states for the halogen ligands. Thus, for electronegative ligands on phosphorus, the 1*H*-phosphiranes **1** show a 10–20 kcal mol$^{-1}$ preference for the 'turnstile' inversion process *via* transition states **5**.

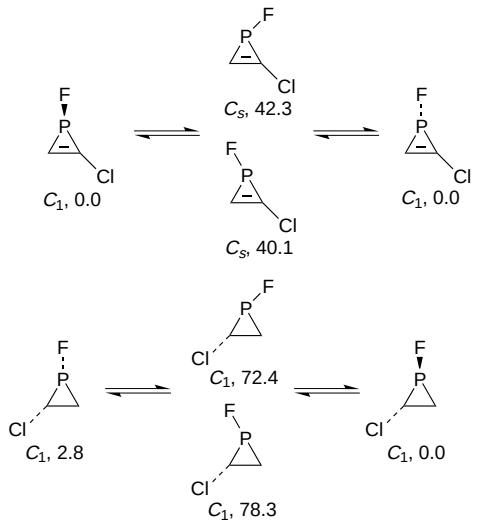
The situation is, however, made even clearer in the 1*H*-phosphirenes **2** by the potential antiaromaticity of **2** and **3**. Because of the unfavourable 4π interaction in these species, **2** strongly prefers the turnstile inversion. By rotating, rather than inverting, the PX group, the 4π-antiaromatic interaction can be avoided completely in the transition state. Furthermore, the antiaromatic destabilisation decreases on going from **2** to **6**, thus favouring the turnstile mechanism. The C–P bond *trans* to the ligand X is lengthened by negative hyperconjugation[14] with the phosphorus lone pair in the transition states **6**, even to the extent that for X = H the transition state is essentially ring-opened. The calculated barrier at 0 K are 52.2 kcal mol$^{-1}$ (X = H), 38.4 kcal mol$^{-1}$ (X = F), 43.4 kcal mol$^{-1}$ (X = Cl) and 40.2 kcal mol$^{-1}$ (X = Br).

Fig. 1 shows the HOMOs of **2**, **4** and **6** (X = F) and illustrates the partial dissociation of the P–F bond in **4**. The turnstile rotation (**2** to **6**) involves a simple rotation of the PF-group orbitals with strong negative hyperconjugation into the *anti* C–P bond. **4** avoids antiaromaticity by rotating the F lone-pair component into a σ* orientation relative to phosphorus, rather than forming an extra occupied π orbital. The plots were generated with PSI 88.[15]

The turnstile mechanism of inversion at phosphorus also means that there are two non-equivalent transition states to inversion of 2-substituted phosphirenes and phosphiranes.

This is shown for chlorine-substituted **1** and **2**. As expected, the transition state in which the lone pair can conjugate with the chlorine-substituted P–C bond (F and Cl *anti*) is favoured. Donor substituents should show the opposite trend.

Thus, our results indicate that inversion of configuration at phosphorus in **1** and **2** is an easier process than might have been expected and that it occurs *via* an unusual turnstile mechanism. A strong experimental indication of the proposed mechanism would be the cumulative effect of ring substituents on inversion barriers.




**Scheme 2**

This work was supported by the Deutsche Forschungsgemeinschaft as part of the Graduiertenkolleg 'Phosphorchemie als Bindeglied verschiedener chemischer Disziplinen' and by the Fonds der Chemischen Industrie. We thank Manfred Regitz and Heinrich Heydt for helpful discussions.

## Footnotes

* E-mail: clark@organik.uni-erlangen.de

† This ChemComm (and Supplementary material) is also available in enhanced multi-media format *via* the World Wide Web: http://chemistry.rsc.org/rsc/cccenha.htm

‡ Available on request from the authors.

## References

1 A. Rouk, J. D. Androse, W. G. Frick, R. Tang and K. Mislow, *J. Am. Chem. Soc*., 1971, **93**, 6507; W. Egan, R. Tang, G. Zon and K. Mislow, *J. Am. Chem. Soc*., 1971, **93**, 6205; K. Mislow, *Trans. N. Y. Acad. Sci*., 1973, **35**, 237; P. Schwerdtfeger, L. Laakkonen and P. Pyykkö, *J. Chem. Phys*., 1992, **96**, 6807.

2 S. M. Bachrach, *J. Phys. Chem*., 1989, **93**, 7780.

3 A. Göller, H. Heydt and T. Clark, *J. Org. Chem*., 1996, **61**, 5840.

4 R. I. Wagner, *US Pat*., 3086053 and 3086056, 1963, *Chem. Abstr*., 1963, **59**, 10124, *Chem. Abstr*., 1964, **60**, 559; R. I. Wagner, L. V. D. Freeman, H. Goldwhite and D. G. Roswell, *J. Am. Chem. Soc*., 1967, **89**, 1102.

5 F. Mathey, *Chem. Rev*., 1990, **90**, 997; B. Deschaumps and F. Mathey, *New J. Chem*., 1988, **12**, 755; F. Mathey, *Angew. Chem., Int. Ed. Engl*., 1987, **26**, 275; F. Mathey and M. Regitz, in *Comprehensive Heterocyclic Chemistry II*, Band 1, ed. A. R. Katritzky, C. W. Rees, E. F. V. Scriven and A. Padwa, Pergamon-Elsevier, Oxford, 1996, ch. 6; M. Regitz, *Chem. Rev*., 1990, **90**, 191; M. Regitz and P. Binger, in *Multiple Bonds and Low Coordination in Phosphorus Chemistry*, ed. M. Regitz and O. Scherer, Thieme, Stuttgart, 1990; M. Regitz, *J. Heterocycl. Chem*., 1994, **31**, 663.

6 O. Wagner, M. Ehle and M. Regitz, *Angew. Chem., Int. Ed. Engl*., 1989, **28**, 225.

7 D. A. Dixon and A. J. Arduengo, III, *J. Chem. Soc., Chem. Commun*., 1987, 498.

8 S. M. Bachrach, *J. Org. Chem*., 1991, **56**, 2205; *THEOCHEM* (*J. Mol. Struct*.), 1992, **87**, 207.

9 (*a*) W. J. Hehre, L. Radom, P. v. R. Schleyer and J. A. Pople, *Ab Initio Molecular Orbital Theory*, Wiley, New York, 1986; (*b*) M. J. Frisch, G. W. Trucks, H. B. Schlegel, P. M. W. Gill, B. G. Johnson, M. A. Robb, J. R. Cheeseman, T. Keith, G. A. Petersson, J. A. Montgomery, K. Raghavachan, M. A. Al-Laham, V. G. Zakrzewski, J. V. Ortiz, J. B. Foresman, J. Cioslowski, B. B. Stefanov, A. Nanayakkara, M. Challacombe, C. Y. Peng, P. Y. Ayala, W. Chen, M. W. Wong, J. L. Andres, E. S. Replogle, R. Gomperts, R. L. Martin, D. J. Fox, J. S. Binkley, D. J. Defrees, J. Baker, J. P. Stewart, M. Head-Gordon, C. Gonzales and J. A. Pople, Gaussian, Inc., Pittsburgh, PA, 1995.

10 J. A. Pople, M. Head-Gordon and K. Raghavachari, *J. Chem. Phys*., 197, **87**, 5968.

11 R. Krishnan and J. A. Pople, *Int. J. Quantum Chem*., 1978, **14**, 91; R. Krishnan, M. Frisch and J. A. Pople, *J. Chem. Phys*., 1980, **72**, 4244.

12 C. Møller and M. S. Plesset, *Phys. Rev*., 1934, **46**, 618; J. A. Pople, R. Krishnan, H. B. Schlegel and J. S. Brinkley, *Int. J. Quantum Chem. XIV*, 1978, 545.

13 C. Lambert and P. v. R. Schleyer, in *Carbanionen*, ed. M. Hanack, Houben-Weyl, Band E 19 d, Georg Thieme Verlag, Stuttgart, 1993, pp. 1–9; A. M. El-Nahas and P. v. R. Schleyer, *J. Comput. Chem*., 1994, **15**, 596.

14 P. v. R. Schleyer and Alexander J. Kos, *Tetrahedron*, 1983, **39**, 1141.

15 D. L. Severance and W. L. Jorgensen, Dept. of Chemistry, Yale University, New Haven, CT, 1988.

*Received in Cambridge, UK, 14th March 1997; Com. 7/01788J*

# Synthesis and aqueous solution properties of novel zwitterionic block copolymers

**A. B. Lowe, N. C. Billingham and S. P. Armes***

*School of Chemistry, Physics and Environmental Science, University of Sussex, Falmer, Brighton, UK BN1 9QJ*

**A series of near-monodisperse poly[2-(dimethylamino)ethyl methacrylate-*block*-2-tetrahydropyranyl methacrylate] precursors is synthesised using group-transfer polymerisation chemistry; the 2-tetrahydropyranyl methacrylate protecting group is quantitatively removed under mild conditions and the resulting zwitterionic block copolymers undergo reversible temperature-induced micellisation in aqueous media.**

Over the last decade or so group-transfer polymerisation[1,2] has become recognised as an excellent method for the synthesis of methacrylate (co)polymers of controlled structure and narrow molecular mass distribution. Recently we have used this technique to prepare well defined homopolymers and block copolymers based on 2-(dimethylamino)ethyl methacrylate (DMAEMA).[3,4] DMAEMA homopolymer is a weak polybase which is soluble at neutral pH or in acidic media due to protonation of the tertiary amine groups. Over the last few years we have explored several synthetic routes to zwitterionic DMAEMA-based block copolymers using *tert*-butyl methacrylate and benzyl methacrylate as protected monomers for methacrylic acid residues. GPC analysis of a DMAEMA homopolymer treated under conditions required for quantitative removal of the *tert*-butyl group in poly(*tert*-butyl methacrylate) [toluene-*p*-sulfonic acid, 80 °C for 7 h in toluene–methanol (5 : 1)] indicated some degree of intermolecular cross-linking between the DMAEMA residues, showing this protecting group to be unsuitable.[5] The alternative benzyl protecting group is normally readily removed by catalytic hydrogenolysis[6,7] but we found only minimal deprotection of DMAEMA–benzyl methacrylate block copolymers; this is believed to be due to catalyst poisoning by the tertiary amine groups. Prompted by a recent disclosure by Teyssie and coworkers[8] we now describe a facile route to well defined zwitterionic block copolymers using 2-tetrahydropyranyl methacrylate (THPMA) as the protected monomer.† This protecting group is easily removed by acid hydrolysis at room temp. to yield near-monodisperse zwitterionic DMAEMA–methacrylic acid block copolymers (Fig. 1). In contrast, we found that the deprotection route favoured by Patrickios *et al.*[9]‡ for DMAEMA–methyl methacrylate–THPMA triblocks was unsatisfactory: the appearance of a band at *ca.* 1806 $cm^{-1}$ in the IR spectrum of the deprotected polymer indicated significant anhydride formation had occurred after thermolysis for 48 h at 140 °C. Furthermore, our control experiments with DMAEMA homopolymer suggested that intermolecular cross-linking of the DMAEMA residues occurs under these thermolysis conditions.[5]

A series of DMAEMA–THPMA block copolymers was prepared using group-transfer polymerisation under conditions similar to those previously described.[4] All copolymerisations were carried out using 1-methoxy-1-trimethylsiloxy-2-methylprop-1-ene (MTS) as initiator and tetrabutylammonium dibenzoate (TBADB) as catalyst at 25 °C in dry THF using Schlenk techniques. The DMAEMA monomer was polymerised first and near-quantitative copolymer yields were obtained in all syntheses. The relative proportions of the two comonomers were varied at a fixed monomer/initiator ratio in order to control the copolymer composition. Comonomer/initiator ratios were varied in order to control the copolymer molecular mass. The molecular masses, polydispersities and compositions of the resulting block copolymers are summarised in Table 1. Narrow molecular mass distributions were obtained in all cases ($M_w/M_n \leqslant 1.22$) as judged by gel permeation chromatography (THF eluent, PMMA standards, RI detector). The actual copolymer compositions as determined by $^1$H NMR spectroscopy corresponded within experimental error to those expected from the comonomer feeds. The DMAEMA–THPMA copolymers were either dissolved or dispersed (depending on the DMAEMA content) in 0.1 M HCl at 25 °C. Complete

**Table 1** A summary of the molecular masses, polydispersities, copolymer compositions and isoelectric points of the DMAEMA–THPMA block copolymers determined using gel permeation chromatography, $^1$H NMR spectroscopy and acid titration, respectively

| Sample | Observed $M_n$[a] | DMAEMA–THPMA copolymer composition[b] | $M_w/M_n$[a] | Observed isoelectric point[c] |
|---|---|---|---|---|
| AB1 | 8500 | 77 : 23 | 1.08 | — |
| AB2 | 24700 | 82 : 18 | 1.16 | 8.56 |
| AB3 | 35700 | 64 : 36 | 1.15 | 7.40 |
| AB4 | 34000 | 51 : 49 | 1.22 | 6.74 |
| AB5 | 42400 | 43 : 57 | 1.19 | 5.62 |

[a] As determined by GPC (THF), calibrated with PMMA standards. [b] As determined by $^1$H NMR spectroscopy. [c] As determined by acid titration.

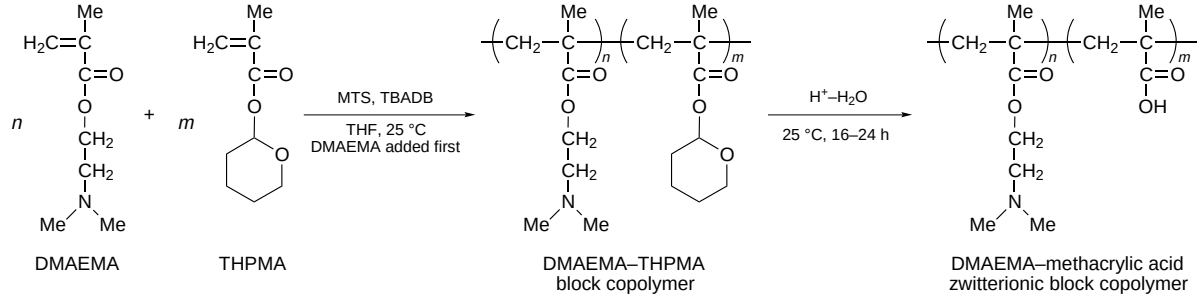



**Fig. 1** Reaction scheme for the synthesis of the DMAEMA–methacrylic acid zwitterionic block copolymers *via* group-transfer polymerisation

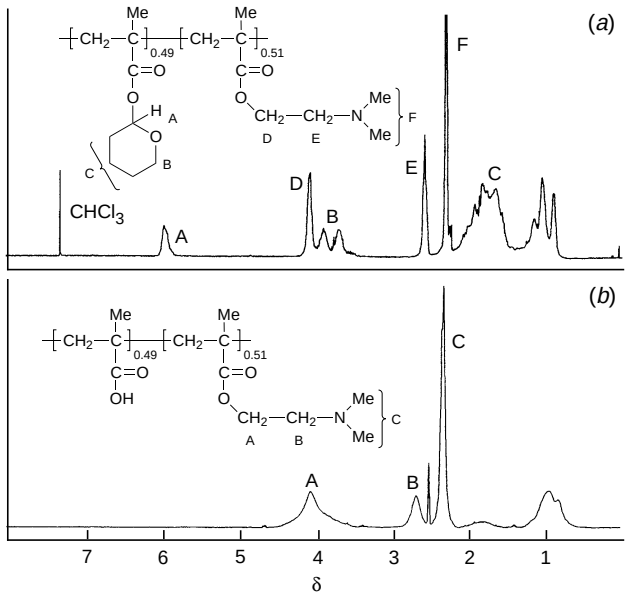



**Fig. 2** Proton NMR spectra of (*a*) a 51 : 49 DMAEMA–THPMA block copolymer dissolved in $CDCl_3$; (*b*) the same block copolymer after acid hydrolysis under mild conditions dissolved in $(CD_3)_2SO$. Note the complete disappearance of the signals due to the THP group.

deprotection was achieved simply by stirring these aqueous solutions for 16–24 h at 25 °C.

Proton NMR spectra of a 51 : 49 DMAEMA–THPMA block copolymer before and after deprotection are shown in Fig. 2. The signals at δ 5.8–6.0 and 3.7–3.8 assigned to the THP protecting group disappear completely after acid hydrolysis. Despite the very mild deprotection conditions, it was considered prudent to verify that no side-reactions (*e.g.* chain scission or cross-linking) had occurred. This was confirmed by analysing the deprotected DMAEMA–methacrylic acid block copolymers using aqueous gel permeation chromatography (Pharmacia Superdex column; RI detector; PEG/PEO standards; TRIZMA pH 8.5 buffer in 1.0 M NaCl eluent at a flow rate of 1.5 ml $min^{-1}$). In all cases narrow, unimodal molecular mass distributions were obtained, with polydispersities comparable to those of the protected precursor blocks ($M_w/M_n$ 1.18–1.24).

The isoelectric points (i.e.p.s) for the DMAEMA–methacrylic acid block copolymers were determined by acid titration and are summarised in Table 1. As expected, the i.e.p.s vary with block copolymer composition, with higher i.e.p.s being obtained for the more DMAEMA-rich copolymers. Precipitation of the copolymers occurred at their respective i.e.p.s: above and below the i.e.p.s the zwitterionic copolymers were soluble in aqueous media.

Examination of a 1.0% m/v solution of the 43 : 57 DMAEMA–methacrylic acid block copolymer in 0.01 M NaCl at pH 9.5 by dynamic light scattering (Malvern 4700 instrument, 80 mW argon ion laser, 90° scattering angle) confirmed very weak light scattering and unimer sizes at 25 °C. Heating this aqueous solution to 50 °C produced much more intense light scattering and visual inspection confirmed that the solution was slightly turbid. CONTIN analysis indicated the formation of near-monodisperse micellar aggregates with an intensity average diameter of 376 nm (see Fig. 3). This aggregation was completely reversible: the copolymer solution became optically transparent again on cooling. In the absence of 0.01 M NaCl, micellar aggregates of *ca*. 700 nm were obtained. At pH 9.5 the methacrylic acid residues should be fully ionised, whereas the DMAEMA residues are almost completely deprotonated.[10] The cloud-point temperature for a 1.0% m/v aqueous solution of

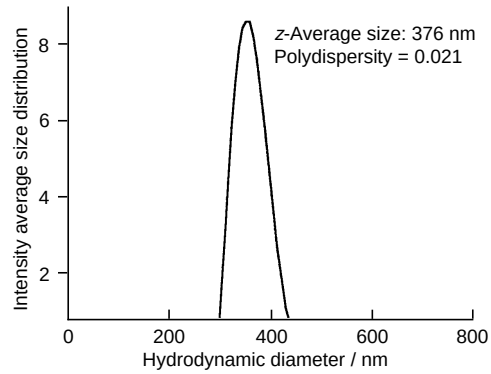



**Fig. 3** Intensity average size distribution of the micellar aggregates formed at 50 °C in a 1.0% m/v aqueous solution of a 43 : 57 DMAEMA–methacrylic acid zwitterionic block copolymer in the presence of 0.01 M NaCl at pH 9.5

DMAEMA homopolymer is in the range 32–46 °C depending on its molecular mass.[11] Thus, at 50 °C the interior of the micellar aggregates most likely contains the now hydrophobic DMAEMA block, with the ionised methacrylic acid block forming the solvated micellar corona.

According to Teyssie and coworkers[8] and Patrickios *et al.*,[9] potential applications for these new zwitterionic copolymers include pigment dispersion and protein separation, respectively. The reversible micellisation behaviour observed in aqueous media also suggests potential drug delivery applications.

The EPSRC and ICI Paints are thanked for a CASE D.Phil. studentship for A. B. L. An EPSRC ROPA grant (GR/K86855) was used to purchase the argon-ion laser for the dynamic light scattering studies.

## Footnotes

* E-mail: S.P.Armes@sussex.ac.uk

† The 2-tetrahydropyranyl methacrylate monomer is not commercially available: it was synthesised by reacting methacrylic acid with 3,4-dihydro-2*H*-pyran at 55 °C using 50% sulfuric acid as catalyst. The crude monomer was dried and distilled under vacuum prior to passage through a basic alumina column to remove residual methacrylic acid.

‡ These workers also used trimethylsilyl methacrylate as a protecting group for triblock copolymers containing methacrylic acid residues. There are no deprotection problems associated with this monomer but it is well known that, under GTP conditions, its polymerisation is slow and incomplete (see ref. 7).

## References

1 O. W. Webster, W. R. Hertler, D. Y. Sogah, W. B. Farnham and T. V. RanjanBabu, *J. Am. Chem. Soc.*, 1983, **105**, 5706.
2 I. B. Dicker, G. M. Cohen, W. B. Farnham, W. R. Hertler, E. D. Langanis and D. Y. Sogah, *Macromolecules*, 1990, **23**, 4034.
3 F. L. Baines, S. P. Armes and N. C. Billingham, *Macromolecules*, 1996, **29**, 3416.
4 F. L. Baines, S. P. Armes, N. C. Billingham and Z. Tuzar, *Macromolecules*, 1996, **29**, 8151.
5 A. B. Lowe, D. Phil. Thesis, University of Sussex, 1997; A. B. Lowe, N. C. Billingham and S. P. Armes, manuscript in preparation.
6 J. Mykytiuk, N. C. Billingham and S. P. Armes, *Polym. Bull.*, 1992, **29**, 139.
7 S. P. Rannard, J. Mykytiuk, S. P. Armes and N. C. Billingham, *Eur. Polym. J.*, 1993, **29**, 407.
8 S. Creutz, P. Teyssie and R. Jerome, *Macromolecules*, 1997, **30**, 6.
9 C. S. Patrickios, W. R. Hertler, N. L. Abbott and T. A. Hatton, *Macromolecules*, 1994, **27**, 930.
10 N. G. Hoogeveen, M. A. Cohen-Stuart, G. J. Fleer, W. Frank and M. Arnold, *Macromol. Chem. Phys.*, 1996, **197**, 2553.
11 V. Butun, N. C. Billingham and S. P. Armes, unpublished work.

*Received in Bath, UK, 14th March 1997; Com. 7/02116J*

# Modulation of metal–fluorophore communication to develop structurally simple fluorescent sensors for transition metal ions

**B. Ramachandram and A. Samanta***

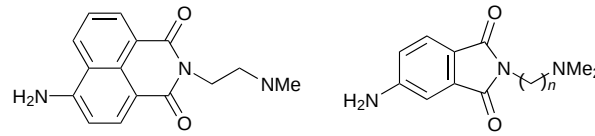
*School of Chemistry, University of Hyderabad, Hyderabad 500 046, India*

**Fluorophores 2a and 2b show significant fluorescence enhancement in the presence of transition metal ions.**

Molecular systems that contain a guest binding site (receptor) and a photon interaction site (fluorophore) as components with a mechanism of communication between the two are considered useful as chemosensors or molecular switching devices.[1–6] A variety of photoinduced electron transfer (PET) chemosensors in 'Fluorophore–Spacer–Receptor' format have been developed in recent years[1–5] which perform light-induced simple YES or NO logic operations and hence may find application as photonic molecular devices in molecular information processing. While the majority of these chemosensors possess one input and one output functionality, logic systems with two input devices which act as AND gates are also reported.[3]

While molecular signalling systems for several ions have been available for some time, only very recently an anthracene derivative with a cryptand receptor has been developed by Ghosh *et al*. that is described as the first sensor for transition metal ions such as $Ni^{II}$ and $Cu^{II}$.[4] In the PET sensing mechanism, the receptor–fluorophore interaction 'switches off' the fluorescence and the 'switching on' takes place in the presence of a guest (usually protons or metal ions) when the fluorophore is released as a result of guest binding with the receptor. Therefore, the fluorescence sensing mechanism requires the metal ion (M)–fluorophore (F) communication to be less than the M–receptor (R) interaction. Obviously, for transition metal ions, which are efficient quenchers for organic fluorophores, the M–F communication is too strong compared with the other interaction for commonly used receptors. The recent success of Ghosh *et al.* has been ascribed to the special topology of the cryptand receptor that binds M more strongly within the cavity making it unavailable for fluorescence quenching.[4] In other words, the M–R interaction has been increased to reduce indirectly the communication between M and F. We find that no attempt has been made to find out whether direct manipulation of the M–F communication can be made to develop fluorescent sensors or switches for the transition metal ions. Since redox interaction between F and M is one of the important quenching mechanisms,[7] it should be possible to reduce this communication simply by making the fluorophore more electron deficient either by suitable substitution or simple structural modifications. Such modification not only minimises the redox activity between M and F in the metal-bound state but also enhances PET in the unbound state, both favouring an increase in the efficiency of the system. Since no studies based on this approach have been reported, the following work was undertaken.

The proton sensory behaviour of some compounds related to **1** is reported in the literature with low fluorescence enhancement (FE) values.[8] The fluorescence outputs of **1**† in the presence of some transition metal ions are collected in Table 1. These values are too low to consider this system as a possible fluorescent switch for d-block transition metal ions. We ascribe this failure partly to inefficient PET[9] and partly to the quenching interaction between M and F. Since, according to our rationale, both these drawbacks can be rectified by choosing a structurally similar but relatively electronically deficient fluorophore, 4-aminophthalimide (AP),‡ much improved switching functions are expected from **2a** and **2b**. Further, it may be noted that the higher singlet energy of these derivatives is also expected to enhance PET and hence their performance.




**1** **2a** $n = 2$ **b** $n = 3$

The fluorescence spectra of **2a** and **2b**† are characterised by broad bands typical of an intramolecular charge transfer transition within the fluorophore.[10] Attachment of the spacer and receptor results in a reduction of the fluorescence quantum yield of the original fluorophore, AP by a factor of *ca*. 50 in **2a** and 27 in **2b** in acetonitrile§ which is a clear indication of PET in both cases. The driving force ($\Delta G^*$) for the PET process, estimated from the measured redox potentials of the couples

**Table 1** Fluorescence output of **1**, **2a** and **2b** as a function of different metal ion input[a]

| | **1** | | **2a** | | **2b** | |
|---|---|---|---|---|---|---|
| Input metal ion[b] | [M]/ mol dm$^{-3}$[c] | Output[d] FE | [M]/ mol dm$^{-3}$[c] | Output[d] FE | [M]/ mol dm$^{-3}$[c] | Output[d] FE |
| $Cr^{III}$ | $4.3 \times 10^{-5}$ | 1.1 | $1.2 \times 10^{-4}$ | 39 | $1.1 \times 10^{-4}$ | 25 |
| $Fe^{III}$ | $2.6 \times 10^{-5}$ | 1.1 | $1.0 \times 10^{-4}$ | 34 | $1.0 \times 10^{-4}$ | 27 |
| $Co^{II}$ | $1.1 \times 10^{-5}$ | 1.1 | $1.9 \times 10^{-4}$ | 38 | $9.2 \times 10^{-4}$ | 12 |
| $Ni^{II}$ | $1.7 \times 10^{-5}$ | 1.1 | $3.0 \times 10^{-4}$ | 37 | $1.8 \times 10^{-2}$ | 22 |
| $Cu^{II}$ | $2.6 \times 10^{-5}$ | 1.2 | $2.7 \times 10^{-4}$ | 41 | $4.0 \times 10^{-4}$ | 27 |
| $Zn^{II}$ | $2.2 \times 10^{-4}$ | 1.3 | $3.9 \times 10^{-4}$ | 55 | $6.8 \times 10^{-4}$ | 30 |

[a] Experimental conditions: *ca.* $5 \times 10^{-5}$ mol dm$^{-3}$ acetonitrile solution of the compounds was used, at 298 K, $\lambda_{exc}$ = 425 nm for **1** and 400 nm for **2a** and **2b**, excitation and emission band widths were 3 nm. [b] The salts used for the experiments were $CrCl_3 \cdot 6H_2O$, $FeCl_3$, $Co(NO_3)_2 \cdot 6H_2O$, $Ni(ClO_4)_2 \cdot 6H_2O$, $Cu(NO_3)_2 \cdot 3H_2O$ and $Zn(ClO_4)_2 \cdot 6H_2O$. [c] Represents the concentration of the metal ion for which FE was maximum, any further increase in concentration beyond this led to fluorescence quenching. [d] With reference to the fluorescence intensity of the respective compound in the absence of metal ion.

using the Weller equation [$\Delta G^* = E_{ox}$ (R) $- E_{red}$ (F) $- E_{0,0}$] is more negative for **2** [−6.6 kcal mol$^{-1}$ for **1** and −12.7 kcal mol$^{-1}$ for **2** in acetonitrile (1 cal = 4.184 J)].¶ Since the fluorescence decay curves of **2a** and **2b** are biexponential‖ with one short component representing the lifetime of the PET quenched state and a long-lived component whose lifetime is very similar in magnitude to that of the methylated AP, a through-space quenching mechanism with two dominant configurations of the fluorophore is suggested; one in which proximity of the fluorophore and receptor results in quenching and the other in which spatial distribution of the two is unfavourable for PET.

Fig. 1 illustrates the effect of the addition of metal ions on the fluorescence intensity of the compounds. As can be seen, beyond a certain concentration of the metal ion (values of which are indicated in Table 1 for each metal ion) the quenching influence starts becoming visible. The metal ion induced FE is associated with a shift of the fluorescence maximum. Similar shifts with these metal ions are also observed in the case of **1** and **2b**. Since metal ion addition to solutions of AP or 1,8-naphthalimide (ANP) did not produce any shift, the shift does not originate from a change in the polarity of the environment. Further, it also clearly indicates that the M–F interaction alone is not responsible for the shift. Therefore, we conclude that the shift arises from an interaction of the metal ion involving both the receptor and the fluorophore.

The FE values of **2a** and **2b** with the metal ions, collected in Table 1, are large enough to consider these simple systems as efficient fluorosensors for transition metal ions. A comparatively larger FE value for **2a** (for any given metal ion) is due to enhanced PET in the unbound state because of a favourable conformation. The maximum FE value is observed with $Zn^{II}$ due to its non-quenching nature. The fluorescence recovery in this case is nearly 100%. It is gratifying to note a 35-fold enhancement even in the case of $Fe^{III}$, reported to be the most quenching transition metal ion[7] and for which no reported FE data has come to our notice. Further, it can be seen that the quenching influence of the metal ions is more visible at a lower concentration in the case of electron rich **1** than with electron deficient **2a** or **2b**. This is a reflection of the modification of redox activity between M and R.

In summary, we have shown for the first time that metal–fluorophore communication can be directly modulated to develop structurally much simpler PET fluorosensors (OR gate) for the d-block metal ions and as such there is no need to design a receptor with any special topology that involves more synthesis. Further, for the first time, fluorescence enhancement in the presence of metal ions such as $Fe^{III}$ and $Cr^{III}$, known for their high quenching abilities, has been observed.

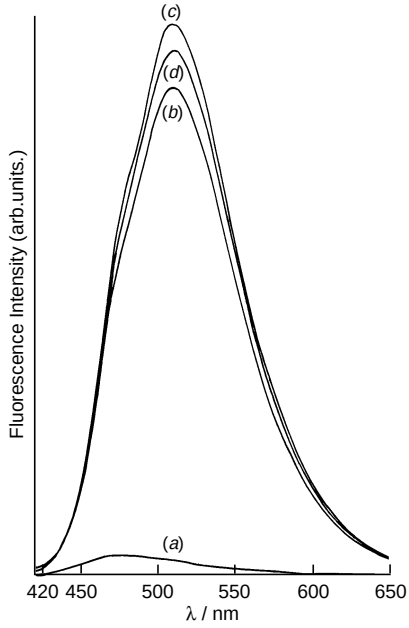



**Fig. 1** Fluorescence spectra of **2a** in acetonitrile for different concentrations of $Fe^{III}$: (*a*) 0, (*b*) 5.3 × 10$^{-5}$, (*c*) 1.0 × 10$^{-4}$ and (*d*) 1.6 × 10$^{-4}$ mol dm$^{-3}$

This research was supported by the Department of Science and Technology, Government of India. B. R. thanks Council of Scientific and Industrial Research for a fellowship.

## Footnotes

* E-mail: assc@uohyd.ernet.in

† **1** was prepared by reacting 4-amino-1,8-naphthalic anhydride with *N*,*N*-dimethylaminoethylamine. **2a** and **2b** were prepared by condensation of 4-aminophthalimide with corresponding dialkylaminoamines.

‡ The measured $E_{ox}$ of AP and 4-amino-1,8-naphthalimide are 1.50 V and 1.27 V (Ag–AgCl reference electrode), respectively.

§ The fluorescence quantum yield of 4-aminophthalimide in acetonitrile, as reported in ref. 10(*a*), is 0.63.

¶ The $E_{ox}$ for triethylamine used for calculation is 0.49 V, ref. 11. The SCE value was corrected for Ag–AgCl electrode by subtracting 0.27 V. The $E_{red}$ values of AP and 4-amino-1,8-naphthalimide (ANP) used for the calculations are −1.66 and −1.61, respectively. $E_{0,0}$ values, estimated from the fluorescence maxima of AP and ANP, are 62.2 and 55.04 kcal mol$^{-1}$.

‖ The lifetimes of the PET quenched state of **2a** and **2b** in acetonitrile are *ca.* 0.5 and 0.8 ns, respectively, with 98 and 64% contribution to the total decay at time $t = 0$. The unquenched component has lifetime in the range 17–18 ns. The measured lifetime of methylated AP in acetonitrile is 18.5 ns.

## References

1 M. E. Huston, K. W. Haider and A. W. Czarnik, *J. Am. Chem. Soc.*, 1988, **110**, 4460.
2 A. P. de Silva, H. Q. N. Gunaratne and G. E. M. Maguire, *J. Chem. Soc., Chem. Commun.*, 1994, 1213; A. P. de Silva, H. Q. N. Gunaratne, T. Gunnlaugsson and M. Nieuwenhuizen, *Chem. Commun.*, 1996, 1967; A. P. de Silva, H. Q. N. Gunaratne, C. McVeigh, G. E. M. Maguire, P. R. S. Maxwell and E. Hanlon, *Chem. Commun.*, 1996, 2191.
3 A. P. de Silva, H. Q. N. Gunaratne and C. P. McCoy, *Nature*, 1993, **364**, 42; A. P. de Silva, H. Q. N. Gunaratne and C. P. McCoy, *Chem. Commun.*, 1996, 2399.
4 P. Ghosh, P. K. Bharadwaj, S. Mandal and S. Ghosh, *J. Am. Chem. Soc.*, 1996, **118**, 1553.
5 R. A. Bissel, A. P. de Silva, H. Q. N. Gunaratne, P. L. M. Lynch, G. E. M. Maguire and K. R. A. S. Sandanayake, *Chem. Soc. Rev.*, 1992, **21**, 187; *Fluorescent Chemosensors for Ion and Molecule Recognition*, ed. A. W. Czarnik, American Chemical Society, Washington, DC, 1993; R. A. Bissel, A. P. de Silva, H. Q. N. Gunaratne, P. L. M. Lynch, G. E. M. Maguire, C. P. McCoy and K. R. A. S. Sandanayake, *Top. Curr. Chem.*, 1993, **168**, 223; A. W. Czarnik, *Acc. Chem. Res.*, 1994, **27**, 302; A. W. Czarnik, in *Topics in Fluorescence Spectroscopy*, ed. J. R. Lakowicz, Plenum, New York, 1994, vol. IV, p. 49; B. Valeur, in *Topics in Fluorescence Spectroscopy*, ed. J. R. Lakowicz, Plenum, New York, 1994, vol. IV, p. 21; T. D. James, P. Linnane and S. Shinkai, *Chem. Commun.*, 1996, 281.
6 *Molecular Electronic Devices*, ed. F. L. Carter, R. E. Siatkowski and H. Wohltjen, Elsevier, Amsterdam, 1988; J. M. Lehn, *Angew Chem., Int. Ed. Engl.*, 1988, **27**, 89; J. M. Lehn, *Angew. Chem., Int. Ed. Engl.*, 1990, **29**, 1304.
7 A. W. Varnes, R. B. Dodson and E. L. Wehry, *J. Am. Chem. Soc.*, 1972, **94**, 946; J. A. Kemlo and T. M. Shepherd, *Chem. Phys. Lett.*, 1977, **47**, 158.
8 A. Pardo, J. M. L. Poyato, E. Martin, J. J. Camacho and D. Reyman, *J. Lumin.*, 1990, **46**, 381; D. Yuan and R. G. Brown, *J. Chem. Res.* (*S*), 1994, 418.
9 Inefficient PET in a structurally similar molecule is recently reported. A. P. de Silva, H. Q. N. Gunaratne, J. L. Habib-Jawan, C. P. McCoy, T. E. Rice and J. P. Soumillion, *Angew. Chem., Int. Ed. Engl.*, 1995, **34**, 1728.
10 (*a*) T. Soujanya, R. W. Fessenden and A. Samanta, *J. Phys. Chem.*, 1996, **100**, 3507; (*b*) T. Soujanya, T. S. R. Krishna and A. Samanta, *J. Phys. Chem.*, 1992, **96**, 8544.
11 H. Siegerman, in *Techniques of Chemistry*, ed. N. L. Weinberg, Wiley, New York, 1975, vol. V, part II, p. 803.

*Received in Cambridge, UK, 13th February 1997; Com. 7/01030C*

# Copper(I) salt promoted homo-coupling reaction of organosilanes†

**Kazutaka Ikegashira, Yasushi Nishihara, Kazunori Hirabayashi, Atsunori Mori* and Tamejiro Hiyama**

*Research Laboratory of Resources Utilization, Tokyo Institute of Technology, 4259 Nagatsuta, Midori-ku, Yokohama, Kanagawa 226, Japan*

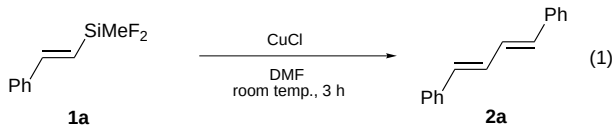
**Alkenylfluorosilanes, phenylfluorosilanes or alkynylsilanes smoothly dimerize in the presence of a copper(I) salt in a polar solvent such as *N*,*N*-dimethylformamide (DMF) or dimethyl sulfoxide (DMSO) to give the 1,3-conjugated dienes, biphenyl or 1,3-conjugated diynes, respectively.**

We have been studying the Pd-catalysed cross-coupling reaction of organosilanes in the presence of fluoride ion. The reaction has been found to proceed *via* the formation of a pentacoordinate organosilicate, which allows transmetalation of the organic group from Si to Pd *via* activation with the fluoride ion[1] or a corresponding promoter.[2]

A part of our interest has thus been centred on the possibility of transmetalation by other metallic species. Kumada and co-workers documented the fact that treatment of alkenylpentafluorosilicates with a $Cu^{I}$ salt[3] in the solid state at 250 °C resulted in the formation of homo-coupling products (1,3-conjugated dienes). As observed in these reactions, activation by converting tetrahedral organofluorosilanes into organopentafluorosilicates is necessary to attain transmetalation from silicon to copper, although no example of the transmetalation of organosilanes to copper has been reported, to the best of our knowledge.[4]

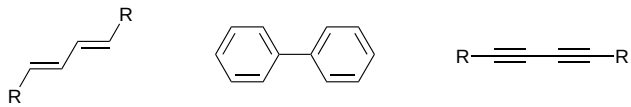
Herein, we report our preliminary results on the transmetalation of organosilane compounds **1** to copper(I) salts, and subsequent homo-coupling reactions under extremely mild and neutral conditions. The reactions proceeded without an activator such as fluoride ion.

We first investigated the reaction of **1a** with an equimolar amount of KF in the presence of CuCl in *N*,*N*-dimethylformamide (DMF),[5] and found homo-coupling product **2a** was produced in 98% yield. This observation encouraged us to study the reaction in more detail and found that it took place without KF [eqn. (1)].




**1a** **2a** (1)

DMSO, a polar solvent, also promoted the reaction, whereas none of the desired product was obtained in THF or diethyl ether. Copper cyanide (CuCN), although effective for transmetalation of organotin reagents,[6] required a longer reaction time (72 h) and gave **2a** in 75% yield. In contrast, CuI[7] and $CuCl_2$[8] were much less reactive.




**2a** R = Ph
**b** R = $C_6H_{13}$

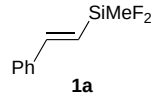
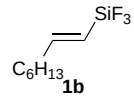
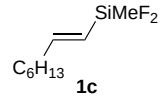
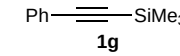
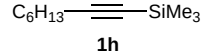
**3**

**4a** R = Ph
**b** R = $C_6H_{13}$

A typical procedure for the homo-coupling reaction of **1a** to **2a** is as follows. DMF (0.5 ml) and **1a** (37 mg, 0.2 mmol) were successively added to CuCl (20 mg, 0.2 mmol) placed in a reaction tube equipped with a magnetic stirrer. The reaction mixture was stirred for 3 h at room temperature and quenched with 1 M hydrochloric acid. The aqueous layer was extracted with diethyl ether, and the organic layer was separated. The combined ethereal layer was washed with water and brine, and dried over $Na_2SO_4$. The homo-coupling product, (*E*,*E*)-1,4-diphenylbuta-2,3-diene **2a**, was obtained in 98% yield.

Results using various organosilicon compounds are summarized in Table 1. It is noteworthy that the reactivity of the silicon substrate is strongly dependent upon the number of fluorine atoms attached to silicon. Thus, the yield of **2b** from trifluoro(oct-1-enyl)silane **1b** is higher than that from difluoro(methyl)(oct-1-enyl)silane **1c** (run 2 *vs*. 3). In all cases the isomeric purity of hexadeca-7,9-diene **2b** was more than 99%, as confirmed by $^1H$ NMR spectroscopy. Thus, these reactions occurred with retention of configuration. The treatment of trifluorophenylsilane **1d** or ethyl(difluoro)phenylsilane **1e** with an equimolar amount of CuCl afforded biphenyl **3** (runs 4 and 5), whereas **1f** gave only a trace amount of **3**. Indeed, it has been reported that phenylcopper decomposes to produce biphenyl and copper metal.[9] The biphenyl formation from fluoro(phenyl)silane **1d** or **1e** is ascribed to transmetalation from Si to

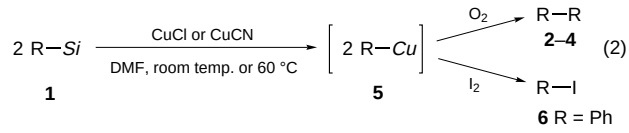
**Table 1** CuCl promoted homo-coupling reactions of organosilanes **1**[a]

| Run | Organosilane | *T*/°C | *t*/h | Product | Yield (%)[b] |
|---|---|---|---|---|---|
| 1 |  **1a** | rt | 3 | **2a** | 98 |
| 2 |  **1b** | 60 | 24 | **2b** | 50 |
| 3[c] |  **1c** | 60 | 3 | **2b** | 38 |
| 4 | $PhSiF_3$ **1d** | 60 | 12 | **3** | 79 |
| 5 | $PhSiEtF_2$ **1e** | 60 | 12 | **3** | 75 |
| 6 | $PhSiMe_2F$ **1f** | 60 | 12 | **3** | trace |
| 7 |  **1g** | 60 | 6 | **4a** | 100 |
| 8 |  **1h** | 60 | 3 | **4b** | 80 |

[a] Conditions: **1** (0.2 mmol), CuCl (0.2 mmol), DMF (0.5 ml). [b] GC yield. [c] CuCl (0.4 mmol) was used.

$Cu^I$ to give a phenylcopper intermediate. Alkynyltrimethylsilanes **1g** and **1h** also underwent the homo-coupling reaction to give the corresponding 1,3-diynes[10] in excellent yields. The results are consistent with the fact that the cross-coupling reaction of alkynylsilanes is accomplished by the use of the trimethylsilyl group.[11]

Although the reaction mechanism of the homo-coupling remains unclear, the following results are helpful for understanding of the mechanism of the transmetalation from silicon to copper. The reaction of **1d** with CuCl in DMF under an argon atmosphere at room temperature over 3 h did not give any trace of biphenyl **3**, despite complete consumption of **1d**. However, consequent exposure to the air or treatment with iodine gave **3** in 40% yield or iodobenzene **6** in 68% yield, respectively. These results suggest that the initial step of the homo-coupling reaction promoted by a $Cu^I$ salt is the transmetalation of organosilanes (R*Si*) with $Cu^I$ salt, and that the corresponding organocopper species (R*Cu*) **5** is actually involved as an intermediate [eqn. (2)]. The presence of air or oxygen is crucial for the formation of R–R.



(2)

In summary, the organic group of organosilanes **1** is found to transmetalate to $Cu^I$, and the resulting organocopper species undergo the homo-coupling reaction to give 1,3-dienes, biphenyl or 1,3-diynes. This is the first example of transmetalation of organosilanes to copper without activation of organosilanes with fluoride ion and provides the most practical and convenient method for the preparation of homo-coupling products. Details of the reaction mechanism and further synthetic applications are now under investigation.

The present work was partially supported by a Grant-in-aid for General Scientific Research (No. 0705042) and one for Scientific Research in the Priority Area of Constraction of Organic Molecules (No. 08245218), both from the Ministry of Education, Science, Sports, and Culture, Japan.

## Footnotes

* E-mail: amori@res.titech.ac.jp

† *Note added in proof.* Since submission of this manuscript a related study has appeared in which several organosilanes induce homo-coupling catalysed by CuI but a stoichiometric amount of TBAF is required: S.-K. Kong, T.-H. Kim and S. J. Pyun, *J. Chem. Soc., Perkin Trans. 1*, 1997, 797.

## References

1 T. Hiyama and Y. Hatanaka, *Pure Appl. Chem.*, 1994, **66**, 1471; H. Matsuhashi, M. Kuroboshi, Y. Hatanaka and T. Hiyama, *Tetrahedron Lett.*, 1994, **35**, 6507; H. Matsuhashi, Y. Hatanaka, M. Kuroboshi and T. Hiyama, *Heterocycles*, 1996, **42**, 375; H. Matsuhashi, S. Asai, K. Hirabayashi, Y. Hatanaka, A. Mori and T. Hiyama, *Bull. Chem. Soc. Jpn.*, 1997, **70**, 445; C. Chuit, R. J. P. Corriu, C. Reye and J. C. Young, *Chem. Rev.*, 1993, **93**, 1371; K. A. Horn, *Chem. Rev.*, 1995, **95**, 1371.

2 H. Matsuhashi, Y. Hatanaka, M. Kuroboshi and T. Hiyama, *Tetrahedron Lett.*, 1995, **36**, 1539; E. Hagiwara, K.-i. Gouda, Y. Hatanaka and T. Hiyama, *Tetrahedron Lett.*, 1996, **38**, 439.

3 J.-i. Yoshida, K. Tamao, T. Kakui and M. Kumada, *Tetrahedron Lett.*, 1979, **13**, 1141.

4 For reviews on transmetalation in organocopper chemistry, see P. Wipf, *Synthesis*, 1993, 537 and references cited therein.

5 It has been reported that the allylation of aldehydes with allyltrichlorosilanes could be promoted by DMF or HMPA: S. Kobayashi and K. Nishio, *Tetrahedron Lett.*, 1993, **34**, 3453; *J. Org. Chem.*, 1994, **59**, 6620; S. E. Denmark, D. M. Coe, N. E., Pratt and B. D. Griedel, *J. Org. Chem.*, 1994, **59**, 6161.

6 J. R. Falck, R. K. Bhatt and J. Ye, *J. Am. Chem. Soc.*, 1995, **117**, 5973.

7 T. Takeda, K.-i. Matsunaga, Y. Kabasawa and T. Fujiwara, *Chem. Lett.*, 1995, 771; S.-K. Kang, T. Yamaguchi, T.-H. Kim and P.- S. Ho, *J. Org. Chem.*, 1996, **61**, 9082.

8 J.-i. Yoshida, K. Tamao, A. Kurita and M. Kumada, *Tetrahedron Lett.*, 1978, 1809.

9 J. F. Normant, *Synthesis*, 1972, 63.

10 For the preparation of 1,3-conjugated diynes, see A. S. Hay, *J. Org. Chem.*, 1962, **27**, 3320; G. E. Jones, D. A. Kendrick and A. B. Holmes, *Org. Synth.*, 1987, **65**, 52.

11 Y. Hatanaka, K. Matsui and T. Hiyama, *Tetrahedron Lett.*, 1989, **30**, 2403.

*Received in Cambridge, UK, 18th March 1997; Com. 7/01898C*

# Rationalisation of the regioselective hydrolysis of aliphatic dinitriles with *Rhodococcus rhodochrous* AJ270

**Otto Meth-Cohn* and Mei-Xiang Wang**

*Chemistry Department, Sunderland University, Sunderland, UK SR1 3SD*

**Aliphatic dinitriles undergo regioselective hydrolysis with the title organism to give monoacids with up to four methylenes between the nitrile functions (optimally 2–3) or when either an oxygen is placed β, γ or δ to the nitrile (δ-placement being optimal) or β or γ (optimally γ) but not δ sulfur substituents are present; nitrogen substituents appear to behave as for oxygen but suffer a steric limitation of the size of the nitrogen substituent.**

We have demonstrated[1] that the title organism is a powerful, general nitrile hydrolysing organism, involving two enzymes effecting nitrile-to-amide and amide-to-acid conversions respectively. As a prelude to studying the hydrolysis of prochiral dinitriles we have made a broad study of the effect of structure on the regioselectivity of hydrolysis of aliphatic dinitriles. The literature contains a number of papers on this topic but the overall background picture is decidedly unclear.

In 1980 Yamada showed that a *Fusarium* strain transformed glutaronitrile to 4-cyanobutyric acid[2] and 1,3,6-tricyanohexane to a mixture of diacids,[3] the former transformation also being accomplished by a *Pseudomonas* organism. Gutman[4] observed that the series $NC[CH_2]_nCN$ with $n$ = 3–5 hydrolysed with no selectivity to the diacids with *Rhodococcus rhodochrous* NCIB 11 216 grown on propionitrile while Yamada[5] observed selective monohydrolysis of glutaronitrile ($n$ = 3) using *R. rhodochrous* K22 in quantitative yield. Schneider[6] made similar observations to Yamada with another *R. rhodochrous* strain while Turner[7] showed that succinonitrile gave solely 3-cyanopropionic acid while glutaronitrile gave both mono- and diacids, ratios depending upon time of reaction. Prochiral glutaronitriles were hydrolysed by Kakeya[8] and by Turner[9] to give enantio-efficient monohydrolysis in some cases, although not in others. A chiral malononitrile has been converted[10] into its monoacid monoamide derivative utilising an *R. rhodochrous* strain. Other organisms have been used for the efficient monohydrolysis of 1,4-cycohexanedicarbonitrile,[11] while the conversion of adiponitrile to adipic acid has been closely studied by Moreau[12] utilising a *Brevibacterium*.

We first examined the selectivity of hydrolysis in a series of α,ω-dinitriles, monitoring the reaction against time (Table 1). As we noted in earlier work,[1] the low molecular weight nitriles tended to be metabolised by other enzymes in the organism, limiting overall yields. However, a clear pattern emerged: dinitriles with more than four methylenes separating the functions gave solely diacids irrespective of reaction time. With less than four methylenes, regioselective monohydrolysis occurred.

We next examined a series of α,ω-dinitriles $NC[CH_2]_nX[CH_2]_nCN$ **4** containing a heteroatom X in the chain (Table 2). With the oxygen or sulfur series, reactions were rapid and generally efficient, whereas with NH or NMe the nitriles proved unstable. We therefore included the NAr series which, probably for steric reasons, reacted slowly and with $n$ > 2, not at all, even with added co-solvents such as acetone or methanol. A remarkable feature emerges: regioselectivity is principally dependent upon the placement of the heteroatom, not the overall chain length. Thus a δ-oxygen is optimally efficient, with regiocontrol being effective with a β- or γ-oxygen also. However a γ-sulfur allows optimal regiocontrol, the β-analogue showing selectivity but not the δ-analogue. In the nitrogen series we cannot yet define the limits of regiocontrol with chainlength but good selectivity is shown with a β-nitrogen. Interestingly, in this slowly hydrolysed series, a much greater sensitivity to *p*-substituents is evident than in the hydrolysis of mononitriles.

We explain the regioselectivity on the basis of chelation-deactivation of the enzyme. We believe that hydrolysis occurs by complexation of the nitrile nitrogen to a metal (iron or cobalt) followed by hydration of the nitrile function by the presumed

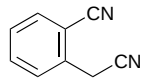
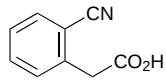
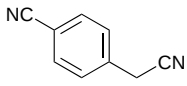
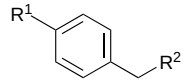
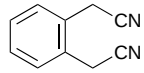
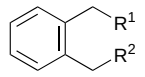
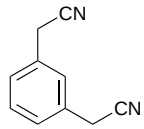
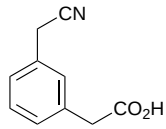
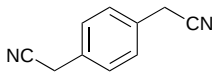
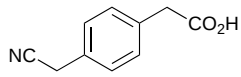
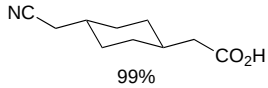
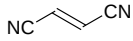
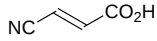
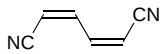
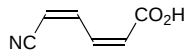
**Table 1** Conversion of $NC[CH_2]_nCN$ **1** into $NC[CH_2]_nCO_2H$ **2** and/or $HO_2C[CH_2]_nCO_2H$ **3**

| | Substrate **1** | Conditions | | Product yields | |
|---|---|---|---|---|---|
| Entry | $n$ | Conc./mmol | $t$/h | **2** (%) | **3** (%) |
| 1 | 2 | 5 | 3 | 30 | |
| 2 | 2 | 5 | 24 | 17 | |
| 3 | 3 | 5 | 3 | 41 | |
| 4 | 3 | 5 | 16 | 35 | |
| 5 | 4 | 5 | 3 | 41 | 4 |
| 6 | 4 | 5 | 24 | 28 | 23 |
| 7 | 4 | 5 | 48 | — | 26 |
| 8 | 5 | 3 | 3 | — | 46 |
| 9 | 5 | 3 | 48 | — | 74 |
| 10 | 6 | 3 | 48 | — | 78 |
| 11 | 7 | 3 | 48 | — | 88 |
| 12 | 8 | 3 | 48 | — | 89 |

**Table 2** Conversion of $NC[CH_2]_nX[CH_2]_nCN$ **4** into $NC[CH_2]_nX[CH_2]_nCO_2H$ **5** and/or $HO_2C[CH_2]_nX[CH_2]_nCO_2H$ **6**

| | Substrate **4** | | Conditions | | Yield (%) | | |
|---|---|---|---|---|---|---|---|
| Entry | $n$ | X | Conc./mmol | $t$/h | **5** | **6** | **4** |
| 1 | 2 | O | 3 | 48 | 61 | — | — |
| 2 | 3 | O | 5 | 1 | 35 | tr | 35 |
| 3 | 3 | O | 3 | 72 | — | 70 | — |
| 4 | 4 | O | 3 | 2 | 73 | — | — |
| 5 | 4 | O | 3 | 120 | 75 | 5 | — |
| 6 | 5 | O | 3 | 2 | — | 25 | 60 |
| 7 | 5 | O | 3 | 48 | — | 97.5 | — |
| 8 | 2 | S | 5 | 1 | 45 | — | 10 |
| 9 | 2 | S | 3 | 48 | — | 60 | — |
| 10 | 3 | S | 3 | 2 | 52 | — | 29 |
| 11 | 3 | S | 3 | 2 | 83 | — | — |
| 12 | 4 | S | 3 | 2 | — | 83 | tr |
| 13 | 4 | S | 3 | 96 | — | 86 | — |
| 14 | 2 | NPh | 2 | 64 | 93 | — | — |
| 15 | 2 | $NC_6H_4Cl$-*p* | 2 | 168 | 71 | — | 26 |
| 16 | 2 | $NC_6H_4OMe$-*p* | 2 | 72 | 91 | — | — |
| 17 | 3 | NPh | 1.5 | 168 | — | — | 95 |
| 18 | 3 | $NC_6H_4OMe$-*p* | 1.5 | 168 | — | — | 92 |
| 19 | 4 | NPh | 1.5 | 168 | — | — | 94 |
| 20 | 5 | NPh | 1.5 | 168 | — | — | 99 |

**Table 3** Conversion of miscellaneous dinitriles into acids

| Entry | Substrate | Conditions: Conc./mmol | Conditions: *t*/h | Product(s) and yields |
|---|---|---|---|---|
| 1 |  | 2 | 24 |  80% |
| 2 |  | 2 | 24 |  $R^1$ = CN, $R^2$ = $CO_2H$ 65%<br>$R^1$ = $CO_2H$, $R^2$ = CN 16% |
| 3 |  | 3 | 24 |  $R^1$ = $R^2$ = CN 13%<br>$R^1$ = CN, $R^2$ = $CO_2H$ 11%<br>$R^1$ = $R^2$ = $CONH_2$ 65% |
| 4 |  | 3 | 30 |  67% |
| 5 |  | 3 | 30 |  69% |
| 6 |  | 1.5 | 39 |  99% |
| 7 |  | 5 | 14 |  67% |
| 8 |  | 5 | 14 |  86% |

cofactor present in such nitrile hydratases, pyrroloquinoline quinone, as documented elsewhere.[13] When a suitably placed ligand atom is also present in the nitrile a bidentate complexation to the metal occurs, which interferes with the hydration of the nitrile function. This ligand may be a suitably placed $CO_2H$ function or a heteroatom. The glutaronitrile **1** ($n$ = 3) bears a δ-oxygen ligand as does the ether **4** ($n$ = 4, X = O). The C–S bond is considerably longer than the C–O bond (1.81 and 1.43 Å respectively) and not surprisingly therefore a γ placement lends optimal regioselectivity. If this mechanism is correct, the above ligands should behave as competitive inhibitors in the hydrolysis of other easily hydrolysed nitriles.† This is indeed found to be the case. Thus when the hydrolysis of benzonitrile is followed (by HPLC) in the presence or absence of $NCCH_2CH_2CH_2SCH_2CH_2CH_2CO_2H$, we find that the rate of benzonitrile disappearance is dramatically slower in the former case. Thus after 5 min reaction, about 20% of unreacted benzonitrile remained with no added cyano acid. In the presence of the inhibitor almost 40% remained. After 10 min the figures were *ca*. 2 and 25%. Furthermore the rate of decrease of amide and rate of formation of acid are both significantly slower in the presence of the cyano acid.

When the aliphatic α,ω-dinitrile chain is interrupted by vinyl or aryl substituents, regiocontrol is efficiently observed in almost all cases that we have examined except for *o*-phenylenediacetonitrile (Table 2, entry 3). Although the regiocontrol here (and in the case of aromatic dinitriles[14]) may derive from a different basis, it is tempting to suggest that the π-systems can also act as effective ligands for the iron when chelation allows (Table 3). Also included in Table 3 is *trans*-cyclohexane-1,4-diacetonitrile (entry 6) which shows total regioselective hydrolysis, presumably by way of chelation of its axial or twist–boat conformer.

In conclusion, we have defined the extent to which regiocontrol can be expected in the hydrolysis of dinitriles bearing O, S and to a limited extent N substituents, and considered the control with π-functionalised dinitriles. The application of these ideas to prochiral and chiral systems is now being actively examined.

We thank the BBSRC for a generous research grant that made this work possible.

## Footnotes

* E-mail: otto.meth-cohn@sunderland.ac.uk

† We thank a referee for this suggestion.

## References

1 O. Meth-Cohn and M.-X. Wang, *Tetrahedron Lett*., 1995, **36**, 9561; *J. Chem. Soc., Perkin 1*, in the press.
2 Y. Asano, S. Ando, Y. Tani and H. Yamada, *Agric. Biol. Chem*., 1980, **44**, 2497; H. Yamada, Y. Asano and Y. Tani, *J. Ferment. Technol*., 1980, **58**, 495.
3 H. Yamada, Y. Asano and Y. Tani, Y. Asano, S. Ando, Y. Tani, H. Yamada and T. Ueno, *Agric. Biol. Chem*., 1981, **45**, 57.
4 C. Bengis-Garber and A. L. Gutman, *Tetrahedron Lett*., 1988, **29**, 2589; *Appl. Microbiol. Biotechnol*., 1989, **32**, 11.
5 M. Kobayashi, N. Yanaka, T. Nagasawa and H. Yamada, *Tetrahedron* 1990, **46**, 5587.
6 P. Hönicke-Schmidt and M. P. Schneider, *J. Chem. Soc., Chem. Commun*., 1990, 648.
7 M. A. Cohen, J. Sawden and N. J. Turner, *Tetrahedron Lett*., 1990, **31**, 7223.
8 H. Kakaye, N. Sakai, A. Sano, M. Yokoyama, T. Sugai and H. Ohta, *Chem. Lett*., 1991, 1823.
9 J. A. Crosby, J. S. Parratt and N. J. Turner, *Tetrahedron: Asymmetry*, 1992, **3**, 1547; A. Kerridge, J. S. Parratt, S. M. Roberts, F. Theil, N. J. Turner and A. J. Willetts, *Bioorg. Med. Chem. Lett*., 1994, **2**, 447; S. Maddrell, N. J. Turner, A. Kerridge, A. J. Willetts and J. A. Crosby, *Tetrahedron Lett*., 1996, **37**, 6001.
10 M. Yokoyama, T. Sugai and H. Ohta, *Tetrahedron: Asymmetry*, 1993, **4**, 1081.
11 H. Nishise, M. Kurihara and Y. Tani, *Agric. Biol. Chem*., 1987, **51**, 2613; Y. Tani, M. Kurihara, H. Nishise and K. Yamamoto, *Agric. Biol. Chem*., 1989, **53**, 3143; Y. Tani, M. Kurihara and H. Nishise, *Agric. Biol. Chem*., 1989, **53**, 3151; K. Yamamoto, Y. Ueno, K. Otsubo, H. Yamane, K.-I. Komatsu and Y. Tani, *J. Ferment. Bioeng*., 1992, **73**, 125.
12 J. L. Moreau, F. Bigey, S. Azza, A. Arnaud and P. Galzy, *Biocatalysis*, 1994, **10**, 325 and references cited therein.
13 T. Nagasawa, H. Namba, K. Ryuno, K. Takeuchi and H. Yamada, *Eur. J. Biochem*., 1987, **162**, 691.
14 J. Crosby, J. Moilliet, J. S. Parratt and N. J. Turner, *J. Chem. Soc., Perkin Trans. 1*, 1994, 1679 and references cited therein; L. Martínková, P. Olšovský, I. Prepechalová and V. Kren, *Biotechnol. Lett*., 1995, **17**, 1219.

*Received in Cambridge, UK, 6th February 1997; Com. 7/00859G*

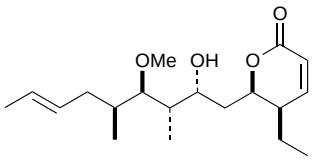
# Total synthesis of (−)-PA-48153C (pironetin) utilising L-quebrachitol as a chiral building block

**Noritaka Chida,* Mitsukane Yoshinaga, Takahiko Tobe and Seiichiro Ogawa**

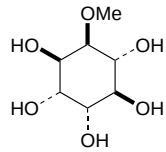
*Department of Applied Chemistry, Faculty of Science and Technology, Keio University, Hiyoshi, Kohoku-ku, Yokohama 223, Japan*

**The chiral and stereoselective synthesis of (−)-PA-48153C (pironetin) 1, a novel immunosuppressant, is described; the acyclic portion possessing four contiguous chiral centres in 1 was constructed stereoselectively from L-quebrachitol and the 2-pyranone moiety was prepared from L-malic acid.**

PA-48153C (pironetin) **1** is a novel 2-pyranone derivative isolated from the culture broth of *Streptomyces*[1,2] and is reported to show a potent immunosuppressive,[1] cytotoxic[1] and plant growth regulator activities.[2a] Its interesting mode of action, its suppressive effect on the responses of both T and B lymphocytes to mitogens[1] as well as its unique structure[1,2b] has attracted much synthetic interest and three total syntheses of **1** have been reported to date.[3] Recently, reports on the synthesis and the structure–activity relationship study of the analogues of **1** have appeared.[4] Here we report an alternative approach to **1**, which utilises L-quebrachitol **2**, an optically active cyclitol obtained in a large quantity from the serum of the rubber tree[5,6] as a chiral building block.



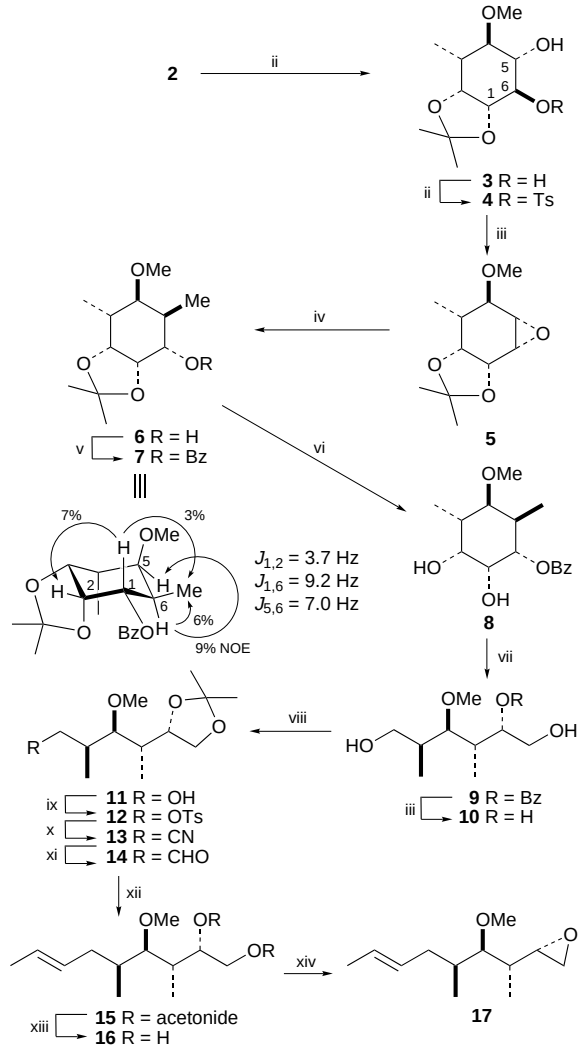

PA-48153C (pironetin) **1**




L-quebrachitol **2**

The known 1D-(1,2,3,5/4,6)-1,2-*O*-isopropylidene-3-methyl-4-*O*-methylcyclohexane-1,2,4,5,6-pentol **3**,[6a] prepared stereoselectively from **2** in five steps, was chosen as the starting material for the preparation of the acyclic moiety in **1**. Reaction of **3** with dibutyltin oxide[7] followed by treatment with *p*-toluenesulfonyl chloride (TsCl) afforded **4** in 82% yield.† Base treatment of **4** provided α-epoxide **5** in 93% yield. Reaction of **5** with trimethylaluminium in $CH_2Cl_2$–hexane at room temp. caused the *trans*-diaxial opening of the epoxide ring with the methyl group to afford **6**, which was isolated after *O*-benzoylation to provide **7** in 56% yield from **5**. The observed coupling constants and NOE of **7** clearly supported the assigned structure. The *O*-isopropylidene group in **7** was removed to give **8** (96%). The cyclohexane ring in **8** was cleaved by periodate oxidation to provide acyclic diformyl derivative, which, without isolation, was reduced with $NaBH_4$ to afford diol **9** in 90% yield. Removal of the *O*-benzoyl group in **9** and protection of the resulting 1,2-diol moiety gave **11** (89% yield from **9**), which was converted into the nitrile derivative **13** *via* *O*-tosylate **12** (97% for two steps). Reduction of the nitrile function in **13** with DIBAL-H, followed by acidic work-up provide **14**. Wittig olefination of **14** with $Ph_3P{=}CHMe$, followed by photo-induced isomerization, showed low *E*-selectivity and gave an inseparable mixture of **15** and its *Z*-isomer in a ratio of 3 : 1 (61% yield from **13**). Fortunately, better results were obtained when **14** was reacted with $MeCHI_2$ in the presence of $CrCl_2$ (Takai reaction)[8] to provide **15** as the major product (*E* : *Z* = 11 : 1, 74% yield from **13**).‡ Acid hydrolysis of the mixture, followed by chromatographic separation afforded geometrically pure **16** in 89% isolated yield. Treatment of **16** under the conditions of Mitsunobu[9] furnished the acyclic moiety, epoxide **17** in 71% yield.

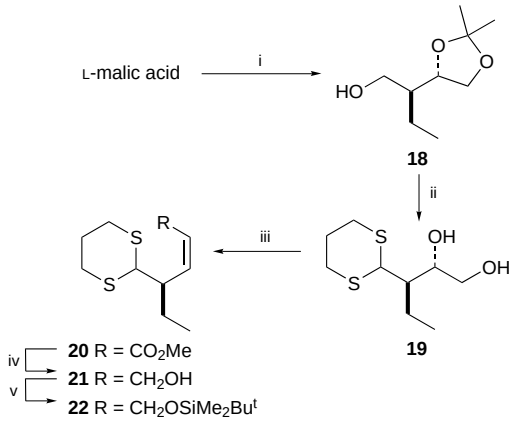
The synthesis of the precursor of the 2-pyranone portion in **1** commenced with known (2*S*,3*S*)-2-ethyl-3,4-isopropylidenedioxypropan-1-ol **18**, obtained from L-malic acid in 6



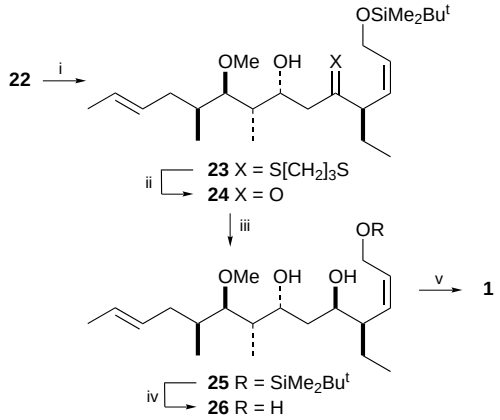

**Scheme 1** Ts = $SO_2C_6H_4$(*p*-Me) *Reagents and conditions*: i, see ref. 6(*a*); ii, $Bu_2SnO$, MeOH, reflux, then TsCl, DMAP, 1,4-dioxane, room temp.; iii, MeONa, MeOH; iv, $Me_3Al$ (10 equiv.), $CH_2Cl_2$–hexanes (1 : 1), room temp.; v, BzCl, pyridine, DMAP, room temp.; vi, 10-camphorsulfonic acid (CSA, 0.2 equiv.), MeOH, room temp.; vii, $NaIO_4$, acetone–$H_2O$ (1 : 1), 0 °C, then $NaBH_4$, MeOH, 0 °C; viii, acetone, CSA, 0 °C; ix, TsCl, pyridine; x, NaCN, 15-crown-5, DMF 60 °C; xi, DIBAL-H, $CH_2Cl_2$, −78°C, then 5% aqueous $H_2SO_4$–$CH_2Cl_2$, 0 °C, 40 min.; xii, $MeCHI_2$ (2 equiv.), $CrCl_2$ (8 equiv.), THF, room temp., 3 h; xiii, CSA, MeOH, 60 °C; xiv, $Ph_3P$, diethyl azodicarboxylate, toluene, reflux, 36 h

steps.[10] Oxidation of **18** with pyridinium chlorochromate (PCC) on alumina,[11] followed by treatment with propane-1,3-dithiol in the presence of $BF_3{\cdot}OEt_2$ gave diol **19** in 63% yield. Glycol cleavage and subsequent modified Wittig–Horner reaction[12] gave desired *Z*-alkene **20** (63% yield) along with its *E*-isomer (14%). DIBAL-H reduction of **20** followed by protection of the resulting alcohol function provided 2-pyranone precursor **22** in 68% yield from **20**.

Deprotonation of **22** with *tert*-butyllithium in the presence of hexamethylphosphoramide (HMPA),[13] followed by addition of epoxide **17** afforded the coupling product **23** in 56% yield. Deprotection of the dithioacetal function in **23** was achieved by treatment with *N*-chlorosuccinimide (NCS) and $AgNO_3$[14*a*] in the presence of 2,4,6-collidine[14*b*]§ to give **24** quantitatively. Reduction of the ketone carbonyl in **24** with $NaBH(OAc)_3$[15] in MeCN–AcOH afforded *anti*-diol **25** as the major product in 65% isolated yield (*syn* isomer 25% yield). Removal of the *O*-silyl protecting group in **25** afforded triol **26** in 82% yield. The final step was successfully achieved by $MnO_2$ oxidation of




**Scheme 2** *Reagents and conditions*: i, see ref. 10(*a*); ii, PCC, $Al_2O_3$, $CH_2Cl_2$, room temp., then 1,3-propanedithiol (1.5 equiv.), $BF_3{\cdot}OEt_2$ (0.3 equiv.), $CH_2Cl_2$, room temp.; iii, $Pb(OAc)_4$, $K_2CO_3$, benzene, room temp., then $(CF_3CH_2O)_2P(O)CH_2CO_2Me$, $KN(SiMe_3)_2$, 18-crown-6, THF, −78 °C; iv, DIBAL-H $CH_2Cl_2$, −78 °C; v, *tert*-butyldimethylsilyl trifluoromethanesulfonate, 2,6-lutidine, $CH_2Cl_2$, 0 °C




**Scheme 3** *Reagents and conditions*: i, ButLi, HMPA, THF, −78 °C, 10 min, then THF solution of **17**, −78 °C, 30 min; ii, NCS (4 equiv.), $AgNO_3$ (4.5 equiv.), 2,4,6-collidine (8 equiv.), MeCN–$H_2O$ (4 : 1), 0 °C, 1 min; iii, $NaBH(OAc)_3$, MeCN–AcOH (2 : 1), 0 °C, 5 h; iv, tetrabutylammonium fluoride, THF, room temp.; v, $MnO_2$, $CH_2Cl_2$, room temp., 3 h

**26** to furnish **1** in 87% yield. The spectroscopic ($^1H$ and $^{13}C$ NMR) data for synthetic **1** were identical with those of natural PA-48153C, and the physical properties of **1** [mp, 74–76 °C; $[\alpha]_D^{21}$ − 141 (*c* 0.18, $CHCl_3$); lit.[1,2*b*] mp, 78–79 °C; $[\alpha]_D^{27}$, −143.7[1] (*c* 0.5, $CHCl_3$); −136.6[2*b*] (*c* 1, $CHCl_3$)] showed a good accord with those reported for the natural product.

We thank Dr Kenji Kawada (Shionogi & Co., Ltd., Osaka, Japan) for providing us with natural PA-48153C. We also thank Yokohama Rubber Co. Ltd., (Tokyo, Japan) for the gift of L-quebrachitol. Financial support of the Moritani Scholarship Foundation is gratefully acknowledged.

## Footnotes

* E-mail: chida@applc.keio.ac.jp

† When this reaction was carried out with TsCl and DMAP in pyridine at 50 °C, compound **4** and its positional isomer (5-*O*-tosylate) were obtained in 37 and 22 isolated yield, respectively.

‡ Reaction of **12** (or its corresponding *O*-triflate derivative) with prop-1-enyllithium in the presence of $Cu^I$ salts directly afforded **15**, however, the yield of **15** was low (less than 10%).

§ In the absence of collidine, the formation of cyclic hemi-ketal derivative, which arose from undesired deprotection of *O*-silyl group, was observed.

## References

1 T. Yoshida, K. Koizumi, Y. Kawamura, K. Matsumoto and H. Itazaki, *Jpn. Pat. Kokai*, 1993, 5-310 726; *Eur. Pat.*, 1993, 560 389 A1.

2 (*a*) S.Kobayashi, K. Tsuchiya, T. Harada, M. Nishide, T. Kurokawa, T. Nakagawa, N. Shimada and K. Kobayashi, *J. Antibiot.*, 1994, **47**, 697; (*b*) S. Kobayashi, K. Tsuchiya, T. Kurokawa, T. Nakagawa, N. Shimada and Y. Iitaka, *J. Antibiot.*, 1994, **47**, 703.

3 K. Yasui, Y. Tamura, T. Nakatani, K. Kawada and M. Ohtani, *J. Org. Chem.*, 1995, **60**, 7567; M. K. Gurjar, J. T. Henri Jr, D. S. Bose and A. V. Rama Rao, *Tetrahedron Lett.*, 1996, **37**, 6615; M. K. Gurjar, A. Chakrabarti and A. V. Rama Rao, *Heterocycles*, 1997, **45**, 7.

4 K. Yasui, Y. Tamura, T. Nakatani, I. Horibe, K. Kawada, K. Koizumi, R. Suzuki and M. Ohtani, *J. Antibiot.*, 1996, **49**, 173.

5 Isolation of L-quebrachitol, see; J. van Alphen, *Ind. Eng. Chem.*, 1951, **43**, 141; N. Chida, M. Suzuki, M. Suwama and S. Ogawa, *J. Carbohydr. Chem.*, 1989, **8**, 319.

6 Utilisation of L-quebrachitol in organic synthesis, see; (*a*) N. Chida, K. Yamada and S. Ogawa, *J. Chem. Soc., Perkin Trans. 1*, 1993, 1957; (*b*) N. Chida and S. Ogawa, *Chem. Commun*., 1997, 807; J. J. Kiddle, *Chem. Rev.*, 1995, **95**, 2189.

7 Y. Tsuda, M. Nishimura, T. Kobayashi, Y. Sato and K. Kanemitsu, *Chem. Pharm. Bull.*, 1991, **39**, 2883; S. David and S. Hanessian, *Tetrahedron*, 1985, **41**, 643.

8 K. Takai, K. Nitta and K. Utimoto, *J. Am. Chem. Soc.*, 1986, **108**, 7408; T. Okazoe, K. Takai and K. Utimoto, *J. Am. Chem. Soc.*, 1987, **109**, 951.

9 L. Hughes, *Org. React.*, 1993, **42**, 656.

10 (*a*) M. Nakata, T. Ishiyama, S. Akamatsu, Y. Hirose, H. Maruoka, R. Suzuki and K. Tatsuta, *Bull. Chem. Soc. Jpn.*, 1995, **68**, 967; (*b*) D. Wasmuth, D. Arigoni and D. Seebach, *Helv. Chim. Acta*, 1982, **65**, 344.

11 Y.-S. Cheng, W.-L. Liu and S. Chen, *Synthesis*, 1980, 223.

12 W. C. Still and C. Gennari, *Tetrahedron Lett.*, 1983, **24**, 4405.

13 K. C. Nicolaou, K. Ajito, A. P. Patron, H. Khatuya, P. K. Richter and P. Bertinato, *J. Am. Chem. Soc.*, 1996, **118**, 3059.

14 (*a*) E. J. Corey and B. W. Erickson, *J. Org. Chem.*, 1971, **36**, 3553; (*b*) S. Shimizu, S. Nakamura, M. Nakada and M. Shibasaki, *Tetrahedron*, 1996, **52**, 13363.

15 D. A. Evans, K. T. Chapman and E. M. Carreira, *J. Am. Chem. Soc.*, 1988, **110**, 3560; A. K. Saksena and P. Magiaracina, *Tetrahedron Lett.*, 1983, **24**, 273.

*Received in Cambridge, UK, 28th February 1997; Com. 7/01404J*

# Tandem prop-2-ynyl carbenoid–aldehyde insertion into zirconacycles

**George J. Gordon and Richard J. Whitby***

*Department of Chemistry, Southampton University, Southampton, Hampshire, UK SO17 1BJ*

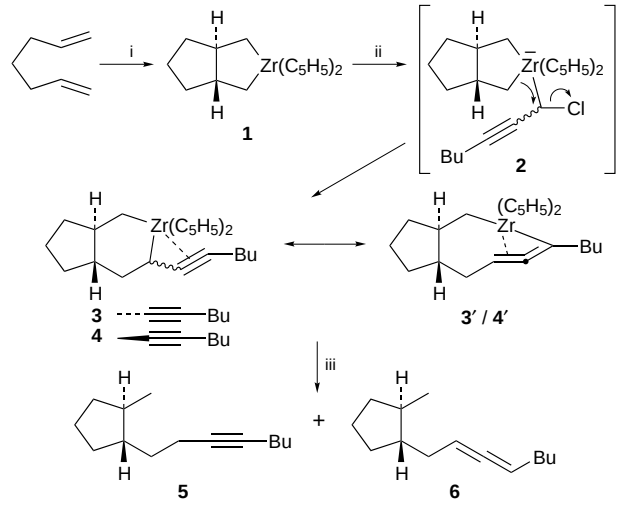
**Insertion of 1-lithio-1-chloroalk-2-ynes into zirconacycles gives cyclic zirconocene η³-prop-2-ynyl/allenyl complexes which afford useful organic products on protonation or Lewis acid induced addition of aldehydes.**

The co-cyclisation of alkenes and alkynes induced by the zirconocene equivalent, zirconocenebut-1-ene (generated *in situ* from dibutylzirconocene—the 'Negishi reagent'[1]) is a useful method for carbon–carbon bond formation.[2] Efficient use of the transition metal requires productive methods for elaboration of the intermediate zirconacycles. Although conventional electrophiles such as alkyl halides are unreactive, reagents with carbenic reactivity such as carbon monoxide and isocyanides insert into the carbon–zirconium bonds very rapidly.[3] We recently reported[4] the insertion of lithium chloroallylides into zirconacycles to afford η³-allylzirconium species which could be further elaborated by the addition of a variety of electrophiles. We now describe the extension of this insertion reaction to 1-chloro-1-lithioalk-2-ynes (prop-2-ynyl carbenoids) to give novel η³-prop-2-ynyl/allenyl zirconium species, and their further elaboration.

Co-cyclisation of hepta-1,6-diene using zirconocenebut-1-ene gave the zirconacyclopentane **1**. Addition of 1-chlorohept-2-yne followed by a solution of lithium 2,2,6,6-tetramethylpiperidide (LiTMP) at −78 °C gave clean conversion into a 1 : 1 mixture of the diastereoisomeric zirconacyclohexanes **3** and **4**, presumably *via* the 'ate' complex **2**. Since both the carbenoid and the zirconacycle are chiral, but racemic, the 1 : 1 ratio of **3** : **4** suggests that there is little 'chiral recognition' between the carbenoid and zirconacycle, and little equilibration of the 'ate' complex **2** which could favour one of the two diastereoisomers on rearrangement. Heating the mixture of **3** and **4** did not cause any change in the isomer ratio. The complexes **3** and **4** were remarkably resistant to protonolysis showing no change after eight days dissolved in $CD_3OD$–$C_6D_6$ (1 : 2) (*cf.* **1** which protonates in < 2 min). Acetic acid caused rapid protonation of **4** (< 5 min at room temp.) to give **5**† and **6** (2 : 1) but left **3** untouched. Aqueous work-up followed by recrystallisaton of the crude product from hexane gave **3** as fine white crystals in an overall yield of 27%. The crystallisation liquor was purified by column chromatography to yield 1-methyl-2-(oct-3-ynyl)cyclopentane **5** (31%) and 1-methyl-2-(octa-2,3-dienyl)cyclopentane **6** (14%). Protonation of **3** with acetic acid took 24 h to reach completion and gave a 1 : 1.5 mixture of **5** and **6**.

The NMR shifts of the prop-2-ynyl unit in both **3** ($\delta_C$ 73.6, 115.1, 122.3) and **4** ($\delta_C$ 76.7, 121.1, 123.2) are consistent with η³-bonding (*i.e.* with a substantial contribution from the η³-allenyl representation **3′**/**4′**), and are comparable to those in $(C_5H_5)_2Zr(Me)(\eta^3\text{-}CH_2C{\equiv}CPh)$ ($\delta_C$ 55.5, 114.2, 120.5) reported by Wojecicki.[5] The small number of known η³-prop-2-ynyl complexes of transition metals have recently been reviewed.[6] The relative stereochemistries of **3** and **4** were tentatively assigned as shown based on the marked difference in stability towards hydrolysis. In **3** (chair zirconacyclohexane) the alkyne moiety is ideally positioned for donation of electron density into the empty orbital on zirconium[7] whereas in **4** the zirconacyclohexane ring must adopt a higher energy twisted boat conformation (Fig. 1).‡ We have previously noted a correlation between an 18 electron configuration at a zirconocene centre, and stability of carbon–zirconium bonds towards hydrolysis[8] and believe that hydrolysis occurs *via* the 16 electron η¹-prop-2-ynyl forms of **3** and **4**, more readily attained by the later. By analogy with our successful elaboration of cyclic zirconocene allyl complexes with aldehydes activated with $BF_3{\cdot}Et_2O$[4] we exposed the mixture of **3** and **4** to these conditions, but no reaction occurred. The products isolated after aqueous work-up comprised **5**, **6** and **3**.

We next examined the insertion of prop-2-ynyl carbenoids into unsaturated zirconacycles. Treatment of the bicyclic zirconacyclopentenes **7a** and **7b**, derived from the intramolecular co-cyclisation of enynes, with 1-chloro-3-phenylprop-2-yne or 1-chlorohept-2-yne and LiTMP at −78 °C gave clean conversion to the ring expanded zirconacycles **8a**–**c**, each as a 1 : 1 mixture of diastereoisomers (Scheme 2). Protonolysis of **8a** with methanol was selective for one diastereoisomer (< 5 min for complete protonation of one isomer, half life of around 4 h at room temp. for the other). Unfortunately, we could not cleanly isolate a single isomer which made assignment of NMR data difficult. To avoid the problem we synthesised the monocyclic zirconium species **7c**[9] and treated it with various prop-2-ynyl carbenoids to give the single isomer ring expanded products **8d**–**g** in quantitative yield by NMR spectroscopy. Protonation of the zirconacycles **8a**–**f** gave alkyne **9** and/or allene products **10** in good yields (Table 1), the ratio of products




**Scheme 1** *Reagents and conditions*: i, $(C_5H_5)_2ZrCl_2$ + 2 BuLi, THF, −78 °C to room temp; ii, $BuC{\equiv}CCH_2Cl$, THF, LiTMP, −78 °C to room temp; iii, AcOH

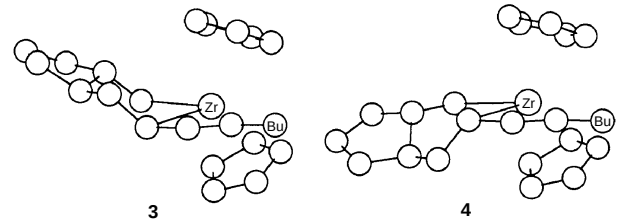
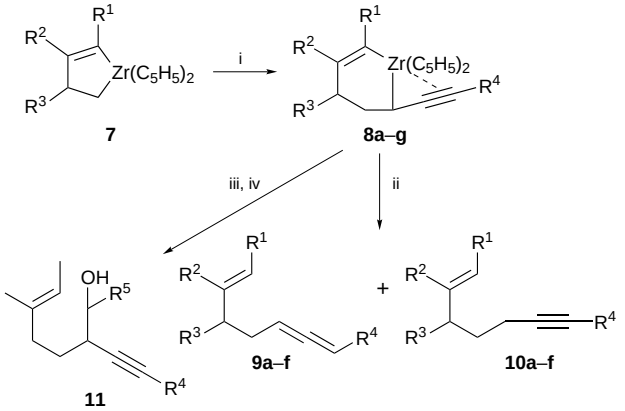



**Fig. 1** Minimum energy conformations of **3** and **4** from ZINDO calculations




**Scheme 2** *Reagents and conditions*: i, $R^4C{\equiv}CCH_2Cl$ or $MeC{\equiv}CCH_2O$-$CO(NPr^i_2)$, LiTMP, THF, −78 °C; ii, $NaHCO_3$ aq. or HCl aq. or MeOH or AcOH; iii, $R^5CHO$, $BF_3{\cdot}Et_2O$ or $TiCl_4$, 10 h, room temp; iv, $NaHCO_3$ aq.

**Table 1** Definition of **7**–**10** and protonation results

| $R^1$ | $R^2$ | $R^3$ | **7** | $R^4$ | **8** | Quench | Yield (%)[a] **9** + **10** | Ratio[b] **9**:**10** |
|---|---|---|---|---|---|---|---|---|
| Bu | | –$(CH_2)_3$– | **7a** | Bu | **8a** | $NaHCO_3$aq. | 76 | 21:79 |
| Bu | | –$(CH_2)_3$– | **7a** | Bu | **8a** | AcOH | — | 0:100 |
| Bu | | –$(CH_2)_3$– | **7a** | Bu | **8a** | MeOH | — | 63:37 |
| Bu | | –$(CH_2)_3$– | **7a** | Ph | **8b** | $NaHCO_3$aq. | 86 | 52:48 |
| Bu | | –$(CH_2)_3$– | **7a** | Ph | **8b** | HCl aq. | — | 48:52 |
| Bu | | –$(CH_2)_3$– | **7a** | Ph | **8b** | AcOH | — | 15:85 |
| Bu | | –$(CH_2)_3$– | **7a** | Ph | **8b** | MeOH | — | 83:17 |
| Ph | | –$(CH_2)_3$– | **7b** | Ph | **8c** | AcOH | 90 | 13:87 |
| Ph | | –$(CH_2)_3$– | **7b** | Ph | **8c** | MeOH | 86 | 79:21 |
| Me | Me | H | **7c** | Ph | **8d** | AcOH | 79 | 14:86 |
| Me | Me | H | **7c** | Ph | **8d** | MeOH | 71 | 93:7 |
| Me | Me | H | **7c** | $SiMe_3$ | **8e** | AcOH | 81 | 0:100 |
| Me | Me | H | **7c** | $SiMe_3$ | **8e** | MeOH | 75 | 0:100 |
| Me | Me | H | **7c** | Me | **8f** | AcOH | 68 | 0:100 |
| Me | Me | H | **7c** | Me | **8f** | MeOH | 74 | 70:30 |
| Me | Me | H | **7c** | Bu | **8g** | —[c] | | |

[a] Yield of pure mixture of **9** and **10** before separation. [b] From $^1$H NMR spectra of the crude product. [c] Protonation not attempted.

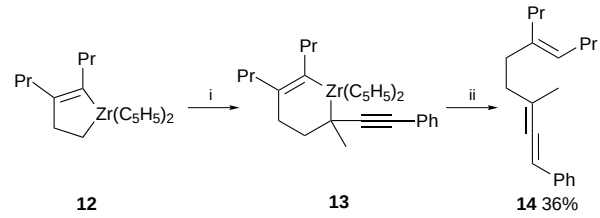
**Table 2** Reaction of **8d**–**g** with $R^5CHO$ to give **11**

| $R^4$ | $R^5$ | Lewis acid | Yield of **11** (%) | Dr[a] |
|---|---|---|---|---|
| Bu | Ph | $TiCl_4$ | 86 | 1:2.9 |
| Bu | Ph | $BF_3{\cdot}Et_2O$ | 77 | 1:1.2 |
| Ph | Ph | $TiCl_4$ | 76 | 1:4.2 |
| Ph | $C{\equiv}CC_5H_{11}$ | $BF_3{\cdot}Et_2O$ | 88 | 1:2.3 |
| $SiMe_3$ | Ph | $BF_3{\cdot}Et_2O$ | 36 | 1:1.4 |
| Me | Ph | $BF_3{\cdot}Et_2O$ | 61 | 1:1.1 |

[a] Diastereoisomer ratio, measured by NMR.

proving to be dependent on the reagent. Quenching with acetic acid favoured formation of the alkyne (exclusive for $R^4$ = alkyl or $SiMe_3$), whereas MeOH favoured the allene, except for the trimethylsilyl substituted case when only the alkyne was obtained.

Reaction of the η$^3$-prop-2-ynyl complexes **8e**–**g** with aldehydes in the presence of $BF_3{\cdot}Et_2O$ or $TiCl_4$ gave adducts **11** in good yield (Table 2), as a mixture of diastereoisomers. Somewhat better diastereocontrol was found using $TiCl_4$ as the Lewis acid. The regiochemistry of insertion into the η$^3$-prop-2-ynyl system is opposite to that previously observed with the analogous η$^3$-allyl complexes.[4] The zirconabicycle **8a** also




**Scheme 3** *Reagents and conditions*: i, PhC≡CCHMeCl, THF, LiTMP, −78 °C; ii, MeOH, −78 °C to room temp.

reacted with aldehydes, but the increased number of diastereoisomeric products formed prevented proper characterisation.

Finally we examined the insertion of a secondary prop-2-ynyl carbenoid, derived by deprotonation of 1-phenyl-3-chlorobut-1-yne, into the zirconacycle **12**. Insertion occurred readily, but the intermediate zirconacycle **13** was too unstable for NMR characterisation, probably due to β-hydride elimination from the methyl group. Protonation with methanol gave exclusively the allene **14**, confirming that insertion had occurred and illustrating that steric hinderence in the carbenoid is well tolerated (Scheme 3).

We have demonstrated a new method for the elaboration of zirconacycles to provide organic products in good yields. We have also synthesised and characterised a range of novel η$^3$-prop-2-ynyl/allenyl zirconacycles, some of which are remarkably unreactive towards air and water.

We thank the EPSRC for a quota award. R. J. W. thanks Pfizer UK and Zeneca for generous uncommitted financial support.

## Footnotes

* E-mail: rjw1@soton.ac.uk

† All organic compounds were fully characterised (high field $^1$H and $^{13}$C NMR, IR, MS, and HRMS) as pure compounds, with the exception of the diastereoisomers of **11** which were not separated.

‡ Structures based on ZINDO (INDO/1)[10] calculations carried out using CACHE software (Oxford Molecular). The calculations indicate that **4** is 6.4 kJ mol$^{-1}$ higher in energy than **3**, and that the chair form of **4** with the alkyne axial, and not coordinated to the metal, is 23 kJ mol$^{-1}$ higher in energy than the η$^3$-prop-2-ynyl boat form.

## References

1 E. Negishi, F. E. Cederbaum and T. Takahashi, *Tetrahedron Lett.*, 1986, **27**, 2829.
2 M. Mori, N. Uesaka, F. Saitoh and M. Shibasaki, *J. Org. Chem.*, 1994, **59**, 5643; E. Negishi and T. Takahashi, *Acc. Chem. Res.*, 1994, **27**, 124; M. I. Kemp, R. J. Whitby and S. J. Coote, *Synlett*, 1994, 451.
3 D. Swanson, C. Rousset, E. Negishi, T. Takahashi, T. Seki, M. Saburi and Y. Uchida, *J. Org. Chem.*, 1989, **54**, 3521; E. Negishi, S. J. Holmes, J. M. Tour, J. A. Miller, F. E. Cederbaum, D. R. Swanson and T. Takahashi, *J. Am. Chem. Soc.*, 1989, **111**, 3336; J. M. Davis, R. J. Whitby and A. Jaxa-Chamiec, *Tetrahedron Lett.*, 1992, **33**, 5655; G. D.Probert, R. J. Whitby and S. J. Coote, *Tetrahedron Lett.*, 1995, **36**, 4113; K. Aoyagi, K. Kasai, D. Y. Kondakov, R. Hara, N. Suzuki and T. Takahashi, *Inorg. Chim. Acta*, 1994, **220**, 319.
4 T. Luker and R. J. Whitby, *Tetrahedron Lett.*, 1994, **35**, 785, 9465; 1995, **36**, 4109; G. J. Gordon and R. J. Whitby, *Synlett*, 1995, 77.
5 P. W. Blosser, J. C. Gallucci and A. Wojcicki, *J. Am. Chem. Soc.*, 1993, **115**, 2994.
6 A. Wojcicki, *New J. Chem.*, 1994, **18**, 61; G. Rodriguez and G. C. Bazan, *J. Am. Chem. Soc.*, 1997, **119**, 343.
7 J. W. Lauher and R. Hoffmann, *J. Am. Chem. Soc.*, 1976, **98**, 1729.
8 T. Luker, R. J. Whitby and M. Webster, *J. Organomet. Chem.*, 1995, **492**, 53.
9 T. Takahashi, M. Kageyama, V. Denisov, R. Hara and E. Negishi, *Tetrahedron Lett.*, 1993, **34**, 687.
10 W. P. Anderson, T. R. Cundarai, R. S. Drago and M. C. Zerner, *Inorg. Chem.*, 1990, **29**, 1; D. F. Taber, J. P. Louey, Y. Wang, W. A. Nugent, D. A. Dixon and R. L. Harlow, *J. Am. Chem. Soc.*, 1994, **116**, 9457.

*Received in Liverpool, UK, 6th March 1997; Com. 7/01592E*

# Crystallization and X-ray structures of $[NaYb(C_5H_5)_3]$ and $Yb(C_5H_5)_2$

**Christos Apostolidis,[a] Glen B. Deacon,[b] Ernst Dornberger,[c] Frank T. Edelmann,[d] Basil Kanellakopulos,[c] Peter MacKinnon[b] and Dietmar Stalke[e]**

[a] *European Commission, Joint Research Centre, Institute for Transuranium Elements, Postfach 2340, D-76125 Karlsruhe, Germany*
[b] *Chemistry Department, Monash University, Clayton, Victoria 3168, Australia*
[c] *Forschungszentrum Karlsruhe, Institut für Technische Chemie, Postfach 3640, D-76021 Karlsruhe, Germany*
[d] *Chemisches Institut der Otto-von-Guericke-Universität, Universitätsplatz 2, D-39106 Magdeburg, Germany*
[e] *Institut für Anorganische Chemie der Universität Würzburg, Am Hubland, D-97074 Würzburg, Germany*

**The complex $[NaYb(C_5H_5)_3]$ ($C_5H_5$ = cyclopentadienyl), prepared from $Yb(C_5H_5)_3$ and sodium naphthalenide in tetrahydrofuran (thf) or from $Yb(C_5H_5)_2$ and $Na(C_5H_5)$ in tetrahydrofuran and crystallized at *ca.* 400 °C ($< 10^{-4}$ mm Hg), is a three-dimensional polymer in which $\mu$-$\eta^5$:$\eta^5$-$C_5H_5$ groups link sodium and ytterbium (each metal having a pseudo-triangular arrangement of $C_5H_5$ ligands); $Yb(C_5H_5)_2$, similarly crystallized, has a polymeric chain structure with one terminal and two bridging $C_5H_5$ ligands per ytterbium, and there is $\eta^1$-bonding between adjacent chains.**

No X-ray structure of an unsolvated $[MLn^{II}Cp'_3]$ (M = alkali metal, Cp′ = cyclopentadienyl or substituted cyclopentadienyl) complex has been reported,[1] and only one of a solvated analogue, *viz.* $[NaSm(thf)(\mu\text{-}\eta^5:\eta^2\text{-}C_5H_4Bu^t)_3]$ (thf = tetrahydrofuran).[2] Ions of the type $Ln(C_5H_5)_3^-$ (Ln = Eu, Sm, Yb) have been detected electrochemically,[3a] but only $[KSm(C_5H_5)_3]$ has been isolated and in a form unsuitable for X-ray crystallography.[3b] Similarly, X-ray characterized unsolvated bis(cyclopentadienyl)lanthanide(II) complexes are limited to the substituted cyclopentadienyls $[Ln(C_5Me_5)_2]$ (Ln = Sm, Eu, Yb)[4] and $[Ln\{C_5H_3(SiMe_3)_2\text{-}1,3\}_2]$ (Ln = Eu, Yb).[5] Structures of $Ln(C_5H_5)_2$ and $[MLn(C_5H_5)_3]$ would be of great interest, especially as there is disagreement over the colour (red or green) of $Yb(C_5H_5)_2$,[6] but crystallization of these compounds presents difficulties. They are perceived either as involatile or volatile with extreme difficulty [green $Yb(C_5H_5)_2$ is stated to sublime with decomposition at 400 °C ($< 10^{-4}$ mmHg)],[6b] they are insoluble in non-polar solvents, and are complexed by polar solvents. We now report that use of high-temperature sublimation has enabled the preparation of crystallographically characterizable green $[NaYb(C_5H_5)_3]$ [perhaps accounting for green $Yb(C_5H_5)_2$] and red $Yb(C_5H_5)_2$.

Green $[NaYb(C_5H_5)_3]$ has been obtained from the $Yb(C_5H_5)_3$/Na route previously reported to give green $Yb(C_5H_5)_2$.[6b] After reaction of sodium naphthalenide, $Na(C_{10}H_8)$, with $Yb(C_5H_5)_3$ in thf under argon, removal of naphthalene by sublimation (100 °C, $10^{-2}$ mmHg), extraction with thf, followed by elimination of the solvent in vacuo (150 °C, $10^{-2}$ mmHg) gave crystalline $[NaYb(C_5H_5)_3]$ in high yield [eqn. (1)].

$$Yb(C_5H_5)_3 + Na(C_{10}H_8) \rightarrow [NaYb(C_5H_5)_3] + C_{10}H_8 \quad (1)$$

Single crystals of the bimetallic were obtained by sublimation (*ca.* 400 °C, $< 40^{-4}$ mmHg). The compound was also prepared straightforwardly in high yield by reaction of $Yb(C_5H_5)_2$ with sodium cyclopentadienide in thf, and purified by sublimation under vacuum [eqn. (2)].

$$Na(C_5H_5) + Yb(C_5H_5)_2 \rightarrow [NaYb(C_5H_5)_3] \quad (2)$$

The identical nature of the two sublimed products and the unsublimed material was established by near and far† IR spectra. The latter was highly characteristic and remarkably similar to that of $Yb(C_5H_5)_3$ suggesting that $[NaYb(C_5H_5)_3]$ has a triangular arrangement of $C_5H_5$ ring centroids similar to that of $Yb(C_5H_5)_3$.[7]

The X-ray crystal structure of $[NaYb(C_5H_5)_3]$. (Fig. 1)‡ shows a highly symmetrical three-dimensional array of alternating sodium and ytterbium atoms bridged by $\mu$-$\eta^5$:$\eta^5$-cyclopentadienyl groups with a near linear Na–Cp–Yb arrangement. There is a pseudo-triangular arrangement of three $C_5H_5$ ligands around both sodium and ytterbium. The Yb–C distances (av. 2.73 Å) are longer than those in $Yb(C_5Me_5)_2$ (av. 2.67 Å)[4b] but shorter than in $Yb(C_5H_5)_2$, which is considered ten coordinate. Subtraction of an ionic radius for nine-coordinate $Yb^{2+}$, extrapolated from Shannon's values,[8] from Yb–C gives 1.53 Å (av.), rather shorter than the usual value, 1.64 ± 0.4 Å, for the cyclopentadienide ionic radius.[9] The Na–Cp distance (2.58 Å) falls in the range typical for other crystallographically characterised cyclopentadienylsodium derivatives[10] {*e.g.* 2.40 Å in $Na(C_5Me_5)(py)_3$ (py = pyridine)[11] and 2.65 Å in $[Na(C_5H_5)(tmeda)]_n$ (tmeda = *N,N,N′,N′*-tetramethylethylenediamine)[12]}.

Brick-red $Yb(C_5H_5)_2$ from desolvation of $Yb(C_5H_5)_2(dme)$[6d] (dme = 1,2-dimethoxyethane) at 100 °C ($10^{-3}$ to $4 \times 10^{-5}$ mmHg) for 12 h and crystallized in low yield as red crystals by sublimation at 420 °C ($4 \times 10^{-5}$ mmHg) in a sealed tube, has a polymeric, $C_5H_5$-bridged, zigzag chain structure (Fig. 2)‡ within the metal centres related by $C_2$ and $C_i$ symmetry, and there are weak interchain C–Yb interactions. The X-ray data

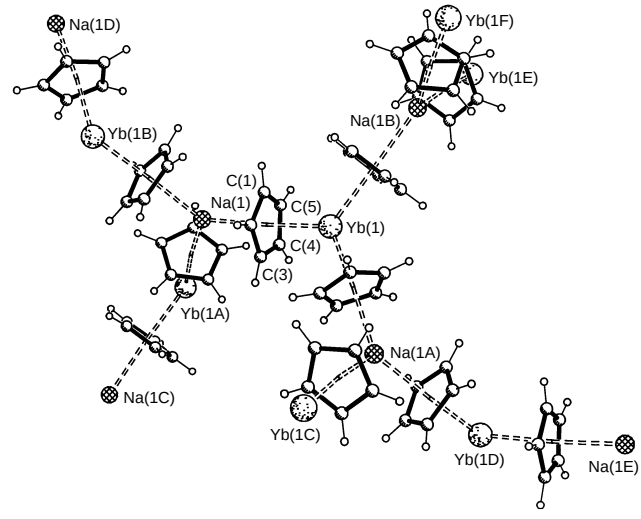



**Fig. 1** Section from the packing diagram of $[NaYb(C_5H_5)_3]$. Selected bond lengths (Å) and angles (°): Yb(1)–C 2.73 (av.), Na–C 2.83 (av.), Yb–Cp 2.46, Na–Cp 2.58; Yb–Cp–Na 176. Cp represents the centroid of the $C_5H_5$ rings.

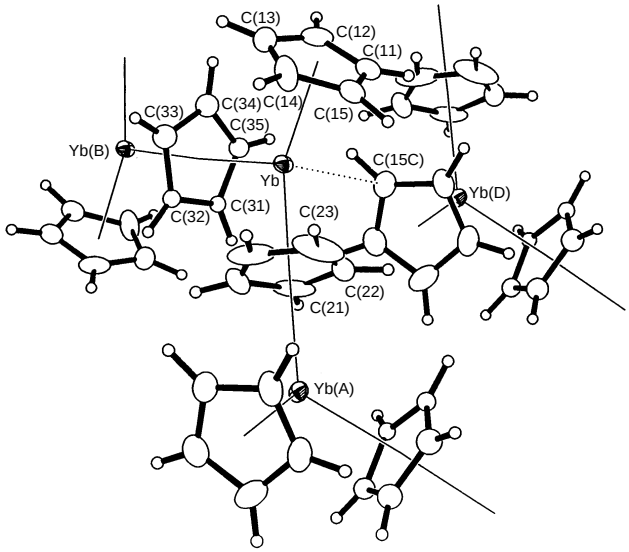



**Fig. 2** Part of the polymeric structure of $Yb(C_5H_5)_2$ [C(31a)–C(35a) of the disordered ring omitted for clarity]. Selected bond lengths (Å) and angles (°): $C_5H_5(1)$ [C(11)–C(15)], Yb–C 2.769 (av.); $C_5H_5(2)$ [C(21), C(22), C(23), C(23b), C(22b)], C(21)–Yb 2.692(4), C(22)–Yb 2.784(10), C(23)–Yb 2.967(12), C(23b)–Yb 2.957(12), C(22b)–Yb 2.821(10); $C_5H_5(3)$ [C(31)–C(35)], Yb–C 2.858 (av.); $C_5H_5(3')$, Yb–C 2.852 (av.); Cp–Yb–Cp 117.6 (av.), Yb–Cp(2)–Yb 164.3, Yb–Cp(3)–Yb 177.6 Interchain Yb–C(15c) 2.996.

show the complex to be isostructural with $Ca(C_5H_5)_2$.[13] Each ytterbium has three $C_5H_5$ ligands, (1)–(3), with $C_5H_5(1)$ essentially terminal (but $\eta^1$-bound to the next chain), $C_5H_5(2)$ bridging on the two-fold axis, and $\mu$-$\eta^5$:$\eta^5$-$C_5H_5(3)$ disordered about the inversion centre. $C_5H_5(2)$, reported as $\mu$-$\eta^3$:$\eta^3$ for $Ca(C_5H_5)_2$,[13] has three shorter Yb–C distances [av. 2.77 Å, comparable with Yb–C of $C_5H_5(1)$] and two longer (av. 2.96 Å). Thus strong $\mu$-$\eta^3$:$\eta^3$ bonding of an allylic four-electron donor unit [C(21), C(22), C(22b)] is indicated, but the more distant C(23), C(23b) are sufficiently close to be $\mu$-$\eta^2$:$\eta^2$ bonded. The distances are comparable with those of formally seven-coordinate $[Yb(C_5Me_5)_2(\eta^2\text{-MeC}{\equiv}\text{CMe})]$ [Yb–C > 2.85(1) Å],[14] and Eu–C (av. 3.00 Å) of nine-coordinate $[Eu(\eta^6\text{-}C_6Me_6)(AlCl_4)_2]_4$,[15] when the potential formal ten coordination of $Yb(C_5H_5)_2$ is considered. They are marginally shorter than the interchain Yb–$\eta^1$-$C_5H_5$ distance (2.996 Å), which is notably ( > 0.1 Å) shorter than the interchain Ca–$\eta^1$-$C_5H_5$ interaction of $Ca(C_5H_5)_2$ ($Ca^{2+}$ and $Yb^{2+}$ have similar ionic radii[8]). Interestingly, there is a close topological relationship between the structures of $Yb(C_5H_5)$ and $Yb(C_5H_4Me)_2(thf)$[16] with the interchain Yb–$\eta^1$-$C_5H_5$ linkage of $Yb(C_5H_5)_2$ replacing Yb–O of the latter.

We are grateful to the Australian Research Council and the Otto-von-Guericke-Universität for financial support and to Monash University for a Postdoctoral Fellowship (to P. McK.).

## Footnotes

* E-mail: frank.edelmann@chemie.uni-magdeburg.de

† *FIR data*: $[NaYb(C_5H_5)_3]$; 260(sh) (Al), 240m (Al), 180vs (br) (e), 164(sh) (Al), 146(sh) (e), 109s (e) $cm^{-1}$. $Yb(C_5H_5)_2$: 252s(sh) (Al), 244vs, 230vs, 217vs (e), 168sh (Al), 150m (e), 109m (e) $cm^{-1}$.

‡ *Crystal data*: $[NaYb(C_5H_5)_3]$: $C_5H_5Na_{0.33}Yb_{0.33}$, cubic, space group $Pa\bar{3}$, $a$ = 14.238(2) Å, $U$ = 2886.2(6) Å$^3$, $Z$ = 24, $D_c$ = 1.801 g cm$^{-3}$, $\mu$ = 6.485 mm$^{-1}$, $F(000)$ = 1488, crystal dimensions 0.4 × 0.4 × 0.05 mm, 4117 reflections measured in the range of $5 < 2\theta < 45°$, all 638 unique reflections and 40 restraints were used to refine 52 parameters; $g^1$ = 0.0, $g^2$ = 42.95. The refinement converged to $wR_2$ = 0.170 (all data) and $R_1$ = 0.069 [$F > 4\sigma(F)$] and a final residual electron density of 0.545/ −0.914 e Å$^{-3}$.

$Yb(C_5H_5)_2$: $C_{10}H_{10}Yb$, $M$ = 303.22, monoclinic, space group $C2/c$, $a$ = 13.908(5), $b$ = 8.571(3), $c$ = 15.325(8) Å, $\beta$ = 111.95(3)°, $U$ = 1694.3(12) Å$^3$, $Z$ = 8, $D_c$ = 2.38 g cm$^{-3}$, $\mu$ = 10.50 mm$^{-1}$, $F(000)$ = 1120, $T$ = 293 K. 1509 unique reflections were collected ($4 < 2\theta < 50°$) with 1272 [$F_o \geqslant 4\sigma(F_o)$]; $R$ = 0.036; $R_w$ = 0.037, weighting scheme $[\sigma^2(F_o) + 0.0008\ 14(F_c)^2]^{-1}$. Atomic coordinates, bond lengths and angles, and thermal parameters have been deposited at the Cambridge Crystallographic Data Centre (CCDC). See Information for Authors, Issue No. 1. Any request to the CCDC for this material should quote the full literature citation and the reference number 182/413.

## References

1 F. T. Edelmann, in *Comprehensive Organometallic Chemistry II*, ed. E. W. Abel, F. G. A. Stone and G. Wilkinson, Pergamon, New York, 1995, vol. 4, p. 11.
2 V. K. Bel'skii, Y. K. Gun'ko, B. M. Bulychev, A. I. Sizov and G. L. Soloveichik, *J. Organomet. Chem.*, 1990, **390**, 35.
3 (*a*) A. M. Bond, G. B. Deacon and R. H. Newnham, *Organometallics*, 1986, **5**, 2312; (*b*) G. B. Deacon, G. N. Pain and T. D. Tuong, *Polyhedron*, 1985, **4**, 1149.
4 (*a*) W. J. Evans, L. A. Hughes and T. P. Hanusa, *J. Am. Chem. Soc.*, 1984, **106**, 4270; *Organometallics*, 1986, **5**, 1285; (*b*) C. J. Burns, Ph.D. Thesis, University of California, 1987.
5 P. B. Hitchcock, J. A. K. Howard, M. F. Lappert and S. Prashar, *J. Organomet. Chem.*, 1992, **437**, 177.
6 (*a*) E. O. Fischer and H. Fischer, *Angew. Chem.*, 1964, **76**, 52; *Angew. Chem., Int. Ed. Engl.*, 1964, **3**, 132; (*b*) F. Calderazzo, R. Pappalardo and S. Losi, *J. Inorg. Nucl. Chem.*, 1966, **28**, 987; (*c*) R. G. Hayes and J. L. Thomas, *Inorg. Chem.*, 1969, **8**, 2521; (*d*) G. B. Deacon, A. J. Koplick and T. D. Tuong, *Aust. J. Chem.*, 1984, **37**, 517.
7 M. Adam, U. Behrens and R. D. Fischer, *Acta Crystallogr., Sect. C*, 1991, **47**, 968.
8 R. D. Shannon, *Acta Crystallogr., Sect. A*, 1976, **22**, 751.
9 K. N. Raymond and C. W. Eigenbrot, Jr., *Acc. Chem. Res.*, 1980, **13**, 276.
10 D. Stalke, *Angew. Chem., Int. Ed. Engl.*, 1994, **33**, 2168.
11 G. Rabe, H. W. Roesky, D. Stalke, F. Pauer and G. M. Sheldrick, *J. Organomet. Chem.*, 1991, **403**, 11.
12 T. Aoyagi, H. M. M. Shearer, K. Wade and G. Whitehead, *J. Organomet. Chem.*, 1979, **175**, 21.
13 R. Zerger and G. Stucky, *J. Organomet. Chem.*, 1974, **80**, 7.
14 C. J. Burns and R. A. Andersen, *J. Am. Chem. Soc.*, 1987, **109**, 941.
15 H. Liang, Q. Shen, S. Jin and Y. Lin, *J. Chem. Soc., Chem. Commun.*, 1992, 480.
16 H. A. Zinnen, J. J. Pluth and W. J. Evans, *J. Chem. Soc., Chem. Commun.*, 1980, 810.

*Received in Basel, Switzerland, 23rd January 1997; Com. 7/00531H*

# Measurement of the different affinities of the two halves of glycopeptide dimers for acetate

**Ben Bardsley and Dudley H. Williams***

*Cambridge Centre for Molecular Recognition, Department of Chemistry, Lensfield Road, Cambridge, UK CB2 1EW*

**The titration of sodium acetate into solutions of the vancomycin group antibiotics eremomycin and chloroeremomycin has been studied by observing the downfield movement of the $^1$H NMR signals due to amide protons in the antibiotic binding pocket; this change in chemical shift has been used to determine the different affinities of the two halves of the dimers for acetate ligand.**

The vancomycin antibiotics are clinically important in the treatment of infections by Gram-positive bacteria and are currently the last line of defence against methicillin-resistant *Staphylococcus aureus* (MRSA).[1,2] They act by binding to the terminal -Lys-D-Ala-D-Ala sequence of bacterial cell wall precursors, inhibiting transglycosylation and ultimately causing cell death.[3,4] In recent work, we have shown that these glycopeptide antibiotics form asymmetric homodimers in solution and that dimerisation is, in all but one case, cooperative with binding to bacterial cell wall precursor analogues.[5] The asymmetry arises from a head-to-head orientation of the saccharide portions attached to residue 4 of the antibiotics, disrupting the $C_2$-symmetry of the head-to-tail peptide backbones.[6–9] A consequence of this asymmetry for the antibiotic ristocetin A is that the two halves of its dimer bind ligands with different affinities.[10,11] However, eremomycin, which also forms an asymmetric dimer, was shown to bind this ligand with approximately equal affinities into each side of such a dimer. Thus, although the asymmetric eremomycin dimer might be expected in principle to bind ligands in each half of the dimer with different affinities, the observation of similar or identical affinities suggested a smaller interaction of the ligand with the disaccharide of eremomycin compared to the tetrasaccharide of ristocetin A.

Previously, it has not been possible to directly measure binding affinities of ligands to antibiotic dimers. This is because binding affinities have been measured at low antibiotic concentrations (typically $\leqslant$50 μm) by UV difference spectrophotometry,[4] capillary zone electrophoresis[12] or isothermal calorimetry.[13] At such concentrations, weakly dimerising antibiotics, such as vancomycin and ristocetin A, are present at $>$90% monomer, and strongly dimerising antibiotics, such as eremomycin and chloroeremomycin, are present at $>$50% monomer.

We now describe a method, analogous to the UV difference spectrophotometric method, for the determination of binding constants of acetate to antibiotic at a concentration of 5 mM ($>$95% dimer). The binding of bacterial cell-wall precursors is crucially dependent on the recognition of their terminal carboxy groups and acetate thus provides the simplest model for the study of this interaction.

UV difference spectrophotometry plots the change in absorbance of the antibiotic as a function of ligand concentration. The method described here plots the change in $^1$H NMR chemical shift of the amide protons $w_2$, $w_3$ and $w_4$ (Fig. 1) as a function of ligand concentration, at pH 4.5 and 300 K. These three protons, and in particular $w_2$, have been extensively studied previously and a strong correlation has been observed between their limiting downfield chemical shift (shift when $>$95% antibiotic is bound) and the free energy of association for a variety of ligands.[14,15] Table 1 lists the chemical shifts of $w_2$, $w_3$ and $w_4$ of eremomycin and chloroeremomycin when free and when fully bound to acetate. For both antibiotics, two signals are observed for each of these protons: one signal for each half of the asymmetric dimer. Each of these signals is time-averaged between the bound and free state, as acetate binding is in fast exchange on the NMR time scale. As a result, they move gradually downfield during titration of acetate into the antibiotic, reflecting the proportion of the antibiotic bound by acetate at a particular ligand concentration. Thus, the chemical shift of each of these protons is analogous to the change in absorbance measured by UV difference spectrophotometry, and a binding

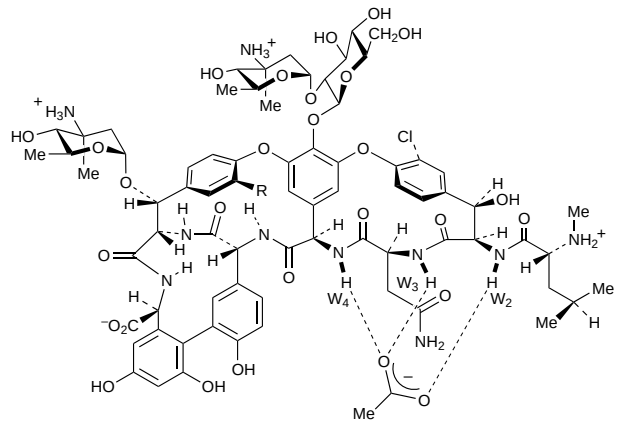



**Fig. 1** Structures of the antibiotics eremomycin (R = H) and chloroeremomycin (R = Cl) binding to acetate. The three amide protons mentioned in the text, $w_2$, $w_3$ and $w_4$, are labelled. Hydrogen bonds to acetate are shown by dashed lines.

**Table 1** Chemical shifts of amide protons in the antibiotic binding pocket when free and when fully bound to acetate. The protons from each half of the dimer are distinguished by the presence or absence of an asterisk (*). All values are in ppm relative to internal trimethylsilyl propionate (TSP, δ = 0)

| | | δ | | | | | |
|---|---|---|---|---|---|---|---|
| Antibiotic | State | $w_2$* | $w_2$ | $w_3$* | $w_3$ | $w_4$* | $w_4$ |
| Eremomycin | Free | 8.50 | 8.45 | 8.23 | 8.23 | 7.91 | 7.84 |
| Eremomycin | Bound | 10.46 | 10.16 | 9.29 | 9.19 | 8.61 | 8.37 |
| Chloroeremomycin | Free | 8.84 | 8.69 | 8.39 | 8.29 | 7.78 | 7.78 |
| Chloroeremomycin | Bound | 10.52 | 10.37 | 9.27 | 9.25 | 8.75 | 8.70 |

**Table 2** Binding constants of acetate to eremomycin and chloroeremomycin measured by following the chemical shifts of individual amide protons at varying concentrations of acetate. The presence or absence of an asterisk (*) distinguishes protons in each half of the dimer. $w_2$* of chloroeremomycin was not visible above the baseline at enough concentrations of acetate for a meaningful binding constant to be determined

| | $K_b$/dm$^3$ mol$^{-1}$ | | | | | |
|---|---|---|---|---|---|---|
| Antibiotic | $w_2$* | $w_2$ | $w_3$* | $w_3$ | $w_4$* | $w_4$ |
| Eremomycin | 19.5 ± 0.4 | 8.8 ± 0.6 | 14.8 ± 1.0 | 8.6 ± 0.5 | 17.4 ± 0.8 | 6.3 ± 0.6 |
| Chloroeremomycin | | 13.5 ± 5.2 | 24.4 ± 0.7 | 12.9 ± 0.6 | 21.0 ± 1.6 | 17.5 ± 1.5 |

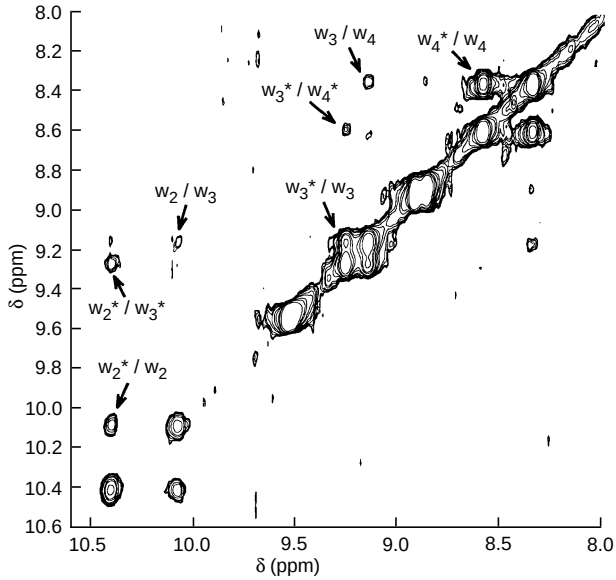



**Fig. 2** Portion of the 50 ms NOESY spectrum of eremomycin fully bound to acetate. Labelled are NOE cross peaks between adjacent protons in the same binding pocket and chemical exchange cross peaks between equivalent protons in each half of the dimer. These confirm the assignments of the separate peaks to a particular half of the dimer.

constant can be calculated from the titration curves using a least-squares curve fitting procedure.[16]

Table 2 shows the binding constants measured from these curves. A two-dimensional NOESY spectrum with a mixing time of 50 ms was used to confirm the assignments of the protons in each of the binding pockets. Due to the short mixing time, the extent of chemical exchange was low and thus strong NOE cross peaks were only observed between signals from protons within the same binding pocket (Fig. 2).

There are two points of note. Firstly, the binding affinities of acetate to chloroeremomycin are greater than those to eremomycin. This is similar to previously measured binding constants which also show ligand affinities for chloroeremomycin which are greater than those for eremomycin.[5] Secondly, for both antibiotics the binding constant for one half of the dimer is greater than that to the other half; by a factor in the region of 1.7–2.8 in the case of eremomycin, and by a factor in the region of 1.2–1.9 in the case of chloroeremomycin.

The resonance of $w_2$ can also be used to demonstrate the very useful correlation between limiting chemical shift and free energy of binding mentioned previously.[14,15] If points for $w_2$ and $w_2$* are added to such a curve for eremomycin, using the binding free energies measured in this study, it can be seen that both lie almost exactly on this curve (Fig. 3), *i.e.* the protons from the half of the dimer with the greater affinity for acetate are also further downfield. This emphasises the sensitivity of the correlation between binding affinity and limiting chemical shift of $w_2$ and how it may potentially be used to extract binding affinities from chemical shift data.

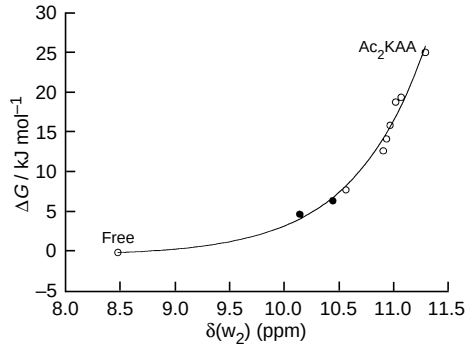



**Fig. 3** Plot of free energy of association against limiting chemical shift of $w_2$ for a variety of bacterial cell-wall precursor analogues binding to eremomycin. The two solid black points are those for $w_2$ and $w_2$* in the eremomycin/acetate complex, as determined in the present study.

We are grateful to SmithKline Beecham (UK) for donations of eremomycin and Eli Lilly (USA) for chloroeremomycin. B. B. thanks the EPSRC and Roussell for financial support.

## Footnote

* E-mail: dhw1@cam.ac.uk

## References

1 M. Foldes, R. Munro, T. C. Sorrell, S. Shankar and M. Toohey, *J. Antimicrob. Chemother.*, 1983, **11**, 21.
2 H. C. Neu, *Science*, 1992, **257**, 1064.
3 D. C. Jordan and P. E. Reynolds, in *Antibiotics*, ed. J. W. Corcoran and F. E. Hahn, Springer-Verlag, Berlin, 1974, vol. III.
4 M. Nieto and H. R. Perkins, *Biochem. J.*, 1971, **123**, 780.
5 J. P. Mackay, U. Gerhard, D. A. Beauregard, R. A. Maplestone and D. H. Williams, *J. Am. Chem. Soc.*, 1994, **116**, 4573.
6 M. Schäfer, T. R. Schneider and G. M. Sheldrick, *Structure*, 1996, **4**, 1509.
7 P. Groves, M. S. Searle, J. P. Mackay and D. H. Williams, *Structure*, 1994, **2**, 747.
8 P. Groves, M. S. Searle, J. P. Waltho and D. H. Williams, *J. Am. Chem. Soc.*, 1995, **117**, 7958.
9 P. J. Loll, A. E. Bevivino, B. D. Korty and P. H. Axelsen, *J. Am. Chem. Soc.*, 1997, **119**, 1516.
10 Y. R. Cho, A. J. Maguire, A. C. Try, M. S. Westwell, P. Groves and D. H. Williams, *Chem. Biol.*, 1996, **3**, 207.
11 G. Batta, M. F. Cristofaro, G. J. Sharman and D. H. Williams, *Chem. Commun.*, 1996, 101.
12 N. E. Allen, D. L. LeTourneau and J. N. Hobbs, *Antimicrob. Agents Chemother.*, 1997, **41**, 66.
13 A. Rodriguez-Tebar, D. Vázquez, J. L. P. Velázquez, J. Laynez and I. Wadsö, *J. Antibiot.*, 1986, **39**, 1578.
14 P. Groves, M. S. Searle, M. S. Westwell and D. H. Williams, *J. Chem. Soc., Chem. Commun.*, 1994, 1519.
15 M. S. Searle, G. J. Sharman, P. Groves, B. Benhamu, D. A. Beauregard, M. S. Westwell, R. J. Dancer, A. J. Maguire, A. C. Try and D. H. Williams, *J. Chem. Soc., Perkin Trans. 1*, 1996, 2781.
16 W. H. Press, B. P. Flannery, S. A. Tenkolsky and W. T. Vetterling, *Numerical recipes in Pascal*, Cambridge University Press, Cambridge, 1989.

*Received in Glasgow, UK, 27th March 1997; Com. 7/02128C*

# Gas permselectivity of carbonized polypyrrolone membrane

**Hidetoshi Kita,* Makoto Yoshino, Kazuhiro Tanaka and Ken-ichi Okamoto**

*Department of Advanced Materials Science and Engineering, Faculty of Engineering, Yamaguchi University, Tokiwadai, Ube 755, Japan*

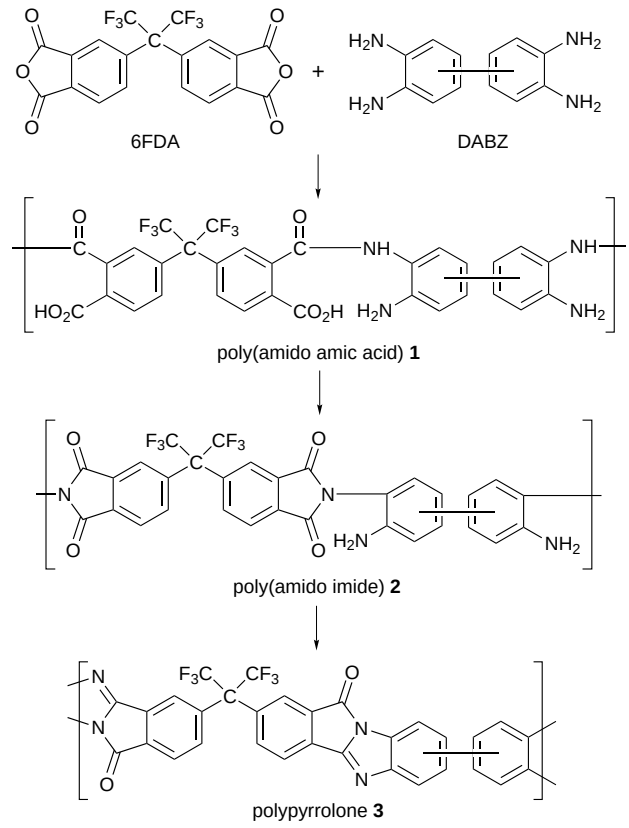
**Gas permeability and permselectivity through a polypyrrolone membrane is increased by heat treatment; the selectivity of the membrane carbonized at 700 °C was one or two orders of magnitude higher than that of presently available polymers.**

The development of membrane processes for the separation of gas mixtures has made remarkable progress during the last two decades and strong interest exists in the synthesis of membranes that exhibit both higher gas permeabilities and selectivities than presently available polymers.[1] The objective of recent works is therefore to create, in effect, a 'molecular sieve membrane'. Although carbon molecular sieves produced from the pyrolysis of polymeric materials have been studied extensively in adsorption applications, membrane application of carbon molecular sieves does not satisfactorily exhibit a 'molecular sieve effect' because the measured gas selectivities are very low, sometimes lower than those of the original polymer membranes, due to the presence of cracks or large pores causing gas leaks.[2,3] Here, we report gas permeability and permselectivity through a carbonized polypyrrolone membrane. Recently there have been several reports[4–7] that carbon molecular sieve membranes produced from polyimide precursors have higher separation performance than those of conventional polymer membranes. Polypyrrolone is a step-ladder polymer with high thermal and chemical stability. Because of the rigidity of the main chain of polypyrrolone, intersegmental packing and segmental mobility should be inhibited, providing a precursor for a carbon membrane with higher gas permeability and permselectivity than polyimides.

Polypyrrolone was prepared by a two step synthesis (Scheme 1) as described previously.[8] First, poly(amidoamic acid) **1** was prepared from 3,3′,4,4′-diphenylhexafluoroisopropylidene tetracarboxylic dianhydride (6FDA) and 3,3′-diaminobenzidine (DABZ) in *N*,*N*-dimethylacetamide (DMAc) under nitrogen atmosphere at 0 °C. This prepolymer was cast from DMAc solution at a polymer concentration of 10wt% onto a glass plate. The orange-coloured film was taken off and thermally imidized at 150 °C for 12 h *in vacuo* to give the poly(amino imide) **2**. The intermediate poly(amino imide) was subjected to thermal cyclodehydration at 300 °C for 2 h or at 400 °C for 10 h *in vacuo* to give the polypyrrolone **3**. Polypyrrolone prepared in this way was insoluble and characterized by FTIR spectroscopy and elemental analysis.

Polypyrrolone membranes were heated up to 800 °C at a heating rate of 5–8 °C $min^{-1}$ under nitrogen atmosphere to give carbon membranes which were *ca*. 40–50 μm in thickness. Under nitrogen atmosphere, polypyrrolone exhibited excellent stability up to 500 °C, without weight loss from the membrane. Thermogravimetry was carried out in flowing He at a heating rate of 5 °C $min^{-1}$ up to 1000 °C and the evolved gases were simultaneously determined by mass spectroscopy. The gaseous products evolved include carbon monoxide, carbon dioxide, hydrogen fluoride and carbon tetrafluoride, with traces of ammonia and hydrogen cyanide. The total weight loss up to 800 °C was *ca*. 40%. The membrane rapidly degraded at about 650 °C when heated in air.

Permeability coefficients were measured by the vacuum time-lag method at 35 °C and 1 atm. Two different membranes prepared at each temperature were evaluated. For each membrane, measurements were made three times. The precision in permeability was estimated to be within ±10%. Table 1 shows typical examples of the gas permeability and permselectivity of carbonized polypyrrolone **3** together with the corresponding polyimide **2** and polypyrrolone precursors and the membranes from polyimide precursors.[4–7] The gas permeability and permselectivity of polypyrrolone were larger than those of corresponding polyimide. Introduction of a ladder structure in the backbone chains of polyimide enhanced the gas permeability and maintained the permselectivity of gases, due to simultaneous inhibition of chain packing and intramolecular motion.[8] Furthermore, the permeability of polypyrrolone membranes carbonized at 500–700 °C was enhanced by two orders magnitude compared with the polypyrrolone precursor. The permeability decreased in proportion to the increasing kinetic molecular diameter of the penetrant gas and the permselectivity of the membranes was much higher than those reported in conventional polymeric materials,[1] indicating that the membrane behaves more like a 'molecular sieves'. On the other hand, raising the carbonizing temperature to 800 °C brought about a decrease of permeability and permselectivity. Heating time also affected the membrane performance. Increasing the heating time to 2 h brought about a slight increase of permeability and a sharp decrease of permselectivity. Thus,




**Scheme 1**

**Table 1** Permeability and permselectivity of poly(amino imide) **2** and polypyrrolone **3** at 35 °C

| Polymer | Heating conditions | Permeability/$10^{-10}$ cm$^3$ (STP) cm cm$^{-2}$ s$^{-1}$ cmHg$^{-1}$ | | | | | Permselectivity | | | |
|---|---|---|---|---|---|---|---|---|---|---|
| | | $H_2$ | $CO_2$ | $O_2$ | $N_2$ | $CH_4$ | $H_2/CH_4$ | $CO_2/CH_4$ | $CO_2/N_2$ | $O_2/N_2$ |
| **2** | 150 °C, 12 h | 14.6 | 3.48 | 1.04 | 0.171 | 0.0712 | 210 | 49 | 20 | 6.1 |
| **3** | 300 °C, 2 h | 87.4 | 33.0 | 6.92 | 1.11 | 0.507 | 170 | 65 | 30 | 6.2 |
| | 400 °C, 10 h | 176 | 73.5 | 19.2 | 3.15 | 1.81 | 97 | 41 | 23 | 6.1 |
| | 500 °C, 1 h | 6580 | 2970 | 674 | 74.3 | 24.7 | 270 | 120 | 40 | 9.1 |
| | 500 °C, 2 h | 6410 | 3520 | 815 | 100 | 41.1 | 160 | 86 | 35 | 8.2 |
| | 550 °C, 2 h | 5860 | 2660 | 669 | 88.3 | 51.3 | 110 | 52 | 30 | 7.6 |
| | 700 °C, 1 h | 1720 | 250 | 68.1 | 6.43 | 1.43 | 1200 | 180 | 39 | 11 |
| | 500 °C, 1 h → 700 °C, 1 h | 1340 | 125 | 35.8 | 2.18 | 1.50 | 890 | 83 | 57 | 16 |
| | 700 °C, 5 h | 2180 | 712 | 145 | 16.8 | 8.44 | 260 | 84 | 42 | 8.6 |
| | 800 °C, 1 h | 25.4 | 0.178 | 0.183 | 0.0235 | 0.0251 | 1000 | 7.1 | 7.6 | 7.8 |
| Kapton[a] | 800 °C | — | 13 | 1.2 | 0.26 | — | — | — | 50 | 4.6 |
| 6FDA/BPDA–polyimide[b] | 500 °C, 2 h | — | — | 20–50[c] | — | — | — | — | — | 8.5–11.5 |
| | 550 °C, 2 h | — | — | 15–40[c] | — | — | — | — | — | 11–14 |
| Kapton[d] | 600 °C, 2 h | 1500 | 1200 | 300 | 100 | — | — | — | 12 | 3 |
| | 800 °C, 2 h | 790 | 200 | 60 | 10 | — | — | — | 20 | 6 |
| BPDA–ODA–polyimide[e] | 600 °C | — | 330 | — | 11 | 4.1 | — | 80 | 30 | — |
| | 700 °C | — | 160 | — | 2.9 | 2.7 | — | 60 | 55 | — |
| | 800 °C | — | 7.8 | — | 0.26 | 0.078 | — | 100 | 30 | — |

[a] Measured at 20 °C (ref. 4). [b] Measured by mixed gas at ambient temperature (ref. 5). [c] Permeance [$10^{-6}$ cm$^3$ (STP) cm$^{-2}$ s$^{-1}$ cmHg$^{-1}$]. [d] Measured at 100 °C (ref. 6). [e] Measured at 25–30 °C (ref. 7).

polypyrrolone carbonized at 700 °C for 1 h showed the highest membrane performance compared with the carbonized polyimides.[4–7] This is a promising membrane for gas separation because of its high permeability and permselectivity.

## Footnote

* E-mail: kita@po.cc.yamaguchi.u.ac.jp

## References

1 S. A. Stern, *J. Membr. Sci.*, 1994, **94**, 1.
2 J. E. Koresh and A. Sofer, *Sep. Sci. Technol.*, 1983, **18**, 723.
3 A. S. Damle, S. K. Gangwal and V. K. Venkataraman, *Gas Sep. Purification*, 1994, **8**, 137.
4 H. Hatori, Y. Yamada, M. Shiraishi, H. Hakata and S. Yoshitomi, *Carbon*, 1992, **30**, 305.
5 C. W. Jones and W. J. Koros, *Carbon*, 1994, **32**, 1419.
6 H. Suda and K. Haraya, *J. Chem. Soc., Chem. Commun.*, 1995, 1179.
7 J. Hayashi, M. Yamamoto, K. Kusakabe and S. Morooka, *Ind. Eng. Chem. Res.*, 1995, **34**, 4364.
8 H. Kita, Y. Yashiki, K. Tanaka and K. Okamoto, *Polym. Prepr. Jpn.*, 1992, **41**, 644.

*Received in Cambridge, UK, 2nd January 1997; Com. 7/00048K*

# Synthesis and applications of a new class of phosphorus donor ligands for asymmetric catalysis

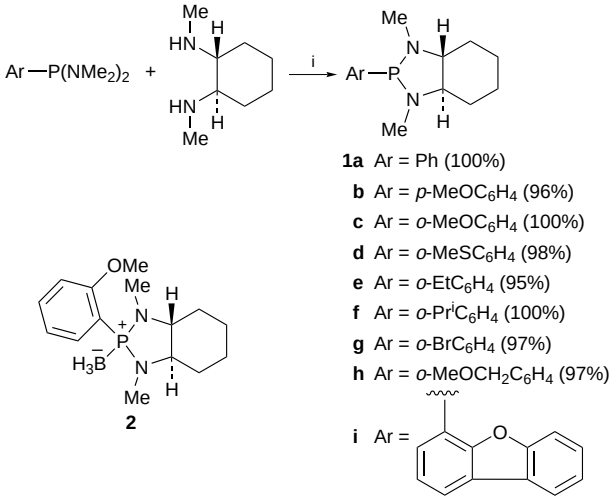
**Heather Tye,[a] Donald Smyth,[a] Colin Eldred[b] and Martin Wills*[a]**

[a] *Department of Chemistry, University of Warwick, Coventry, UK CV4 7AL*
[b] *Glaxo-Wellcome Research and Development Ltd, Glaxo-Wellcome Medicines Research Centre, Gunnels Wood Road, Stevenage, Hertfordshire, UK SG1 2NY*

**The synthesis and applications to allylic substitutions of a range of novel ligands based on diazaphospholidines is described; enantiomeric excesses of up to 89% were achieved in an allylic substitution reaction.**

Recent years have seen dramatic developments in asymmetric catalysis.[1] Allylic substitution reactions in particular have been the subject of attention from a number of research groups and several excellent ligands have been developed for this particular application.[2] Of these, diphosphines and combined phosphine–amine donors have proven to be especially well suited to the required role.[2] As part of an ongoing programme[3] directed at the development of a range of phosphorus donor ligands with a wide range of applications to asymmetric synthesis, we wished to investigate diazaphospholidines **1** in this capacity. We anticipated that such ligands would benefit from a high level of conformational rigidity and would project a suitable chiral environment within organometallic complexes of which they may form a part. Furthermore we were aware of the facile synthesis of such materials from the corresponding $C_2$ symmetric chiral diamines.[4] Although similar compounds have been reported to act as effective chiral shift reagents, we were unaware of any catalytic asymmetric transformations to which they had been applied.[5]

The preparation of a series of ligands was achieved following literature precedents (Scheme 1).[4] The bis(dimethylamino)phosphine precursors to **1a**, **1b**, **1c**, **1e**, **1h** and **1i** were formed by the reaction of the corresponding lithiated aromatic compound with preformed $(Me_2N)_2PCl$. The corresponding precursors for **1d** and **1f** could not be prepared by this method. However lithiation and transmetallation with zinc dichloride, followed by reaction with phosphorus tirchloride and subsequently treatment with an excess of dimethylamine furnished the required intermediates. The precursor to compound **1g** was synthesised following the published procedure of Drewelies and Latscha.[6] Each intermediate bis(dimethylamino)phosphine was heated under reflux with (*R*,*R*)-*N*,*N*′-dimethyl-1,2-diaminocyclohexane until no further dimethylamine could be detected in the nitrogen stream from the reaction. At this point solvent removal provided the pure ligands **1**. Although always handled under an inert atmosphere when in solution, each of the ligands proved to be resistant to atmospheric oxidation when in solid form. Treatment of **1c** with $BH_3{\cdot}SMe_2$ complex resulted in formation of a highly stable borane complex **2** which could be purified by chromatography. We have in previous work demonstrated that related borane complexes could be used as a source of protected ligand[3] (borane may be removed by an amine), however in the case of **2** all attempts to remove the borane resulted in decomposition.

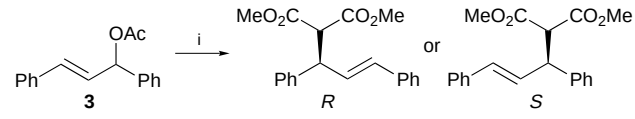



**Scheme 1** *Reagents and conditions*: i, PhMe, heat, 8–24 h

We have applied the series of ligands thus produced to a number of asymmetric transformations. In particular the ligands appear to be particularly well disposed to the nucleophilic allylic substitution reaction of 1,3-diphenyl-3-acetoxyprop-1-ene **3**. In most cases the substitution reaction with dimethyl malonate (Scheme 2) gave good yields and, in the best cases, excellent asymmetric inductions (Table 1). A number of interesting trends become apparent upon analysis of the results. In particular a general improvement and reversal of selectivity is observed upon introduction of an *ortho* substituent. The level of electron density in the aromatic ring does not appear to influence the selectivity to any great extent (compare ligands **1a** and **1b**). Although the best results, 89 and 78% ee in favour of the *R* enantiomer, were achieved using the ligands **1c** and **1d**, the same product enantiomer was obtained using ligands which do not contain coordinating groups (*i.e.* **1e** and **1f**). This suggests that all may share a common mode for directing the asymmetric transformation. The importance of the size of the *ortho* substituent is also difficult to gauge since the ethyl and isopropyl substituted ligands **1e** and **1f** gave similar selectivities. We were unable to prepare the corresponding *tert*-butyl-substituted reagent.

At present there is insufficient evidence to determine the exact means by which asymmetric induction by the ligand is achieved. It would appear that whilst the introduction of an *ortho* substituent in the ligand is crucial to their success, the observation of similar results from coordinating and non-coordinating groups suggests that the ligand is probably only appended to the palladium through the phosphorus atom. If this is the case then their mechanism of action may have a parallel with the phosphine ligand MOP, which has been demonstrated to be effective for this application through the formation of a 1 : 1 phosphine–metal complex.[7]

Of significance is the *pseudo*-$C_2$ symmetry of the ligand and potential participation of a conformational rigidity conferred to




**Scheme 2** *Reagents and conditions*: i, **1a–i**, $[Pd(\eta\text{-}C_3H_5)Cl]_2$, dimethyl malonate, $(Me_3Si)N{:}CMe(OSiMe_3)$, NaOAc, $CH_2Cl_2$

**Table 1** Asymmetric addition of dimethyl malonate to **3** catalysed by **1a–i**

| Ligand | Pd (mol%) | Ligand (mol%) | *t*/h | Yield (%) | ee (%)[a] (config.) |
|---|---|---|---|---|---|
| **1a** | 10 | 20 | 16 | 97 | 28 (*S*) |
| **1b** | 10 | 20 | 16 | 71 | 23 (*S*) |
| **1c** | 10 | 20 | 16 | 97 | 89 (*R*) |
| **1c** | 10 | 10 | 20 | 89 | 83 (*R*) |
| **1c** | 5 | 10 | 12 | 85 | 85 (*R*) |
| **1c** | 2 | 4 | 20 | 94 | 82 (*R*) |
| **1d** | 10 | 20 | 24 | 90 | 78 (*R*) |
| **1e** | 10 | 20 | 16 | 84 | 59 (*R*) |
| **1f** | 10 | 20 | 16 | 91 | 56 (*R*) |
| **1g** | 10 | 20 | 24 | 85 | 66 (*R*) |
| **1h** | 10 | 20 | 24 | 84 | 51 (*R*) |
| **1i** | 10 | 20 | 20 | 92 | 35 (*R*) |

[a] Enantiomeric excess determined by $^1$H NMR spectroscopy using (+)-Eu(hfc)$_3$ as a chiral shift reagent.

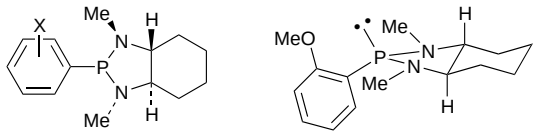
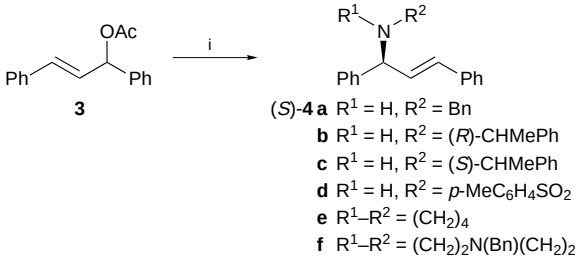


**Fig. 1**




**Scheme 3** *Reagents and conditions*: i, **1c**, [Pd(η-$C_3H_5$)Cl]$_2$, R$^1$R$^2$NH, NaOAc, THF or $CH_2Cl_2$

the nitrogen methyl groups by the adjacent chiral centre. Studies by others,[4,8] and our own X-ray crystal structure of the borane complex **2**[9] indicate that the nitrogen atoms are partially tetrahedral, the result of the methyl groups avoiding eclipsing interactions with the adjacent C–C bonds (Fig. 1). The X-ray crystal structure also reveals that the *ortho* substituent favours a position away from the heterocyclic ring (Fig. 1). This suggests that steric interactions may prevent a 180° rotation about the P–C(aryl) bond. This proposition is supported by our observation that 2,6-disubstituted aromatic ring diazaphospholidines failed to be formed using our general method (Scheme 1). If this conformational preference is maintained in the palladium complex then clearly this *ortho* group may be projected into the region of the appended allylic group, and thus provide a means to influence the reaction selectivity. Precisely how this effect is transferred to the asymmetric reaction, however, is at present unclear.

In an attempt to increase the observed selectivity we attempted some studies of diazaphospholidines bearing larger groups on the nitrogen atoms. The dibenzyl derivative of **1c** gave a product of 64% ee in 78% yield for the reaction depicted in Scheme 2. The diisopropyl ligand failed to form using our standard procedure, possibly due to steric hindrance.

Having identified **1c** as the best of the series of ligands, we have examined the use of nitrogen nucleophiles in the substitution reaction (Scheme 3, Table 2). The results obtained using benzylamine and sodium toluene-*p*-sulfonamide compared favourably to those previously reported using other ligands,[2,10] but were significantly lower (although in the same sense) than the selectivity achieved using dimethyl malonate as nucleophile. The presence of a chiral centre in the nucleophile

**Table 2** Asymmetric addition of nitrogen nucleophiles catalysed by **1c**

| Product | Solvent | *t*/h | Yield (%) | ee[a] (%) (config.) |
|---|---|---|---|---|
| **4a** | $CH_2Cl_2$ | 42 | 68 | 78 (*S*) |
| **4a** | THF | 20 | 49 | 73 (*S*) |
| **4a** | THF | 5 | 77 | 68 (*S*) |
| **4b** | $CH_2Cl_2$ | 168 | 67 | 78 (*S*) |
| **4b** | THF | 8 | 51 | 61 (*S*) |
| **4c** | THF | 8 | 67 | 61 (*S*) |
| **4d** | $CH_2Cl_2$ | 64 | 45 | 76 (*S*) |
| **4e** | $CH_2Cl_2$ | 41 | 48 | 68 (*S*) |
| **4f** | $CH_2Cl_2$ | 16 | 63 | 58 (*S*) |

[a] Enantiomeric excess determined by chiral HPLC using a chiralcel OD column.

(α-methylbenzylamine of either configuration) appeared to have no effect on the enantioselectivity of the reaction or the sense of induction. Use of the cyclic amines pyrrolidine and *N*-benzylpiperazine as nucleophiles resulted in the formation of novel allylic amines **4e** and **4f** respectively, in excellent yields but reduced enantioselectivities.

In conclusion a novel class of diazaphospholidine ligands has been synthesised and their application to palladium-catalysed allylic substitution has been demonstrated. Ongoing work is directed towards the synthesis of improved ligands based on this class for a variety of transition metal-catalysed asymmetric transformations.

We thank the EPSRC and Glaxo-Wellcome Research and Development for support of an Industrial CASE studentship (to H. T.) and Dr J. Ballantine of the EPSRC National Mass Spectroscopic service (Swansea) for HRMS analysis of certain compounds.

## Footnote

* E-mail: m.wills@warwick.ac.uk

## References

1 R. Noyori, *Asymmetric Catalysis in Organic Synthesis*, Wiley, NY, 1994; I. Ojima, *Catalytic Asymmetric Synthesis*, VCH, Berlin, 1993.
2 B. M. Trost and D. L. Van Vranken, *Chem. Rev.*, 1996, **96**, 395; J. M. J. Williams, C. G. Frost and J. Howarth, *Tetrahedron: Assymmetry*, 1992, **3**, 1089.
3 G. Brenchley, E. Merifield, M. Wills and M. Fedouloff, *Tetrahedron Lett.*, 1994, **35**, 2791; G. Brenchley, M. Fedouloff, M. F. Mahon, K. C. Molloy and M. Wills, *Tetrahedron*, 1995, **51**, 10 581; G. Brenchley, M. Fedouloff, E. Merifield and M. Wills, *Tetrahedron: Asymmetry*, 1996, **7**, 2809.
4 A. Alexakis, S. Mutti and P. Mangeney, *J. Org. Chem.*, 1992, **57**, 1224; R. Hulst, N. Keon de Vries and B. L. Feringa, *Tetrahedron: Asymmetry*, 1994, **5**, 699; R. Hulst, R. M. Kellogg and B. L. Feringo, *Recl. Trav. Chim. Pays-Bas*, 1995, **114**, 115; P. G. Devitt, M. C. Mitchell, J. M. Weetman, R. J. Taylor and T. Kee, *Tetrahedron: Asymmetry*, 1995, **6**, 2039.
5 G. Buono and P. Cros, *Nouv. J. Chim.*, 1987, **11**, 573; W. J. Richter, *Chem. Ber.*, 1984, **117**, 2328.
6 K. Drewelies and H. P. Latscha, *Angew. Chem., Int. Ed. Engl.*, 1982, **21**, 638.
7 T. Hayashi, H. Iwamura, Y. Uozumi, Y. Matsumoto and F. Ozawa, *Synthesis*, 1994, 526; T. Hayashi, H. Iwamura, M. Naito, Y. Matsumoto, Y. Uomuzi, M. Miki and K. Yanagi, *J. Am. Chem. Soc.*, 1994, **116**, 775.
8 A. Alexakis, N. Lensen, J.-P. Tranchier, P. Mangeney, J. Feneau-Dupont and J. P. Declercq, *Synthesis*, 1995, 1038; S. E. Denmark and R. L. Dorow, *J. Am. Chem. Soc.*, 1990, **112**, 864; S. E. Denmark, P. C. Miller and S. R. Wilson, *J. Am. Chem. Soc.*, 1991, **113**, 1468; C. J. Cramer, S. E. Denmark, P. C. Miller, R. L. Dorow, K. A. Swiss and S. R. Wilson, *J. Am. Chem. Soc.*, 1994, **116**, 2437; S. Hanessian and S. Beaudoin, *Tetrahedron Lett.*, 1992, **33**, 7655.
9 N. Alcock, H. Tye and M. Wills, unpublished result.
10 P. Von Matt, O. Lieseleur, G. Koch, A. Pfaltz, C. Lefeber, T. Feucht and G. Helmchen, *Tetrahedron: Asymmetry*, 1995, **5**, 573; R. Jumnah, A. C. Williams and J. M. J. Williams, *Synlett*, 1995, 821.

*Received in Cambridge, UK, 19th March 1997; Com. 7/01922J*

# Titanocene(II)-promoted reaction of thioacetals with alkynes: highly stereoselective preparation of conjugated dienes

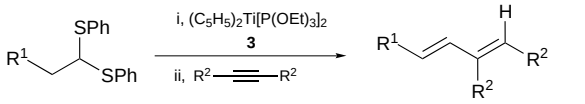
**Takeshi Takeda,* Hirohisa Shimokawa, Yoshinaga Miyachi and Tooru Fujiwara**

*Department of Applied Chemistry, Tokyo University of Agriculture and Technology, Koganei, Tokyo 184, Japan*

**The reaction of organotitanium species, prepared by the desulfurizative titanation of thioacetals using $(C_5H_5)_2Ti[P(OEt)_3]_2$, with alkynes gives conjugated dienes in good yields with high stereoselectivity.**

Titanacyclobutene **1** is a useful intermediate for the synthesis of homoallyl alcohols,[1] β,γ-unsaturated ketones,[1,2] conjugated dienes[3] and substituted pyridines.[2] The titanium species **1** is generally prepared by the reaction of Tebbe reagent $[(C_5H_5)_2Ti\text{-}CH_2\cdot AlMe_2Cl]$ or dimethyltitanocene with an alkyne,[4,5] which is believed to proceed *via* methylidenetitanocene. Recently we have shown that the treatment of β,γ-unsaturated thioacetals or their analogues with titanocene(II)–alkene complexes produces vinylcyclopropanes.[6] Olefination of a variety of carbonyl compounds also proceeds using the organotitanium species formed from thioacetals **2** and the alkene-free titanocene(II), $(C_5H_5)_2Ti[P(OEt)_3]_2$ **3**.[7] Since we assumed that the intermediate of these reactions was alkylidenetitanocene **4**, we have also studied the formation of titanacyclobutene **1** by the treatment of the organotitanium intermediate **4** with an alkyne **5**.

It was found that the reaction of hydrocinnamaldehyde diphenyl thioacetal **2a** with **3** at room temperature for 3 h followed by treatment with oct-4-yne **5c** for 20 h gave 1-phenyl-4-propylocta-2,4-diene **6c** in 72% yield. The reaction proceeded with high stereoselectivity and the 2*E*,4*E* isomer was produced with 99% selectivity (Scheme 1).† The use of higher reaction temperature reduced the reaction time (Table 1, entry 3).‡ Similar reactions of several thioacetals **2** with alkynes **5** afforded the corresponding conjugated dienes **6** in good yields.




**2a** $R^1$ = Bn
**b** $R^1$ = $C_6H_{13}$
**c** $R^1$ = $Pr^i$

**5a** $R^2$ = Me
**b** $R^2$ = Et
**c** $R^2$ = Pr
**d** $R^2$ = Ph

**6a** $R^1$ = Bn, $R^2$ = Me
**b** $R^1$ = Bn, $R^2$ = Et
**c** $R^1$ = Bn, $R^2$ = Pr
**d** $R^1$ = $C_6H_{13}$, $R^2$ = Pr
**e** $R^1$ = $Pr^i$, $R^2$ = Pr
**f** $R^1$ = $Pr^i$, $R^2$ = Ph

**Scheme 1**

**Table 1** The reaction of thioacetals **2** with alkynes **5**

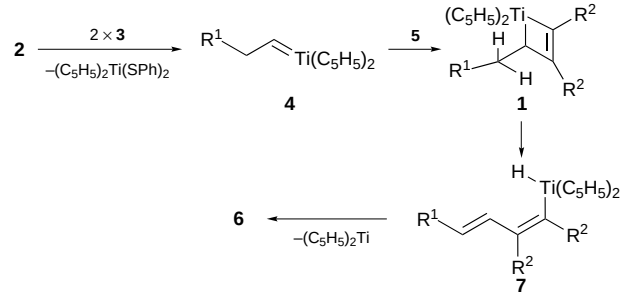
| Entry | 2 | 5 | 6 (% yield)[a] | E : Z[b] |
|---|---|---|---|---|
| 1[c] | **2a** | **5a** | **6a** (72[d]) | 98 : 2 |
| 2 | **2a** | **5b** | **6b** (71) | 99 : 1 |
| 3 | **2a** | **5c** | **6c** (80) | 99 : 1 |
| 4 | **2b** | **5c** | **6d** (72) | 99 : 1 |
| 5 | **2c** | **5c** | **6e** (76) | 100 : 0 |
| 6 | **2c** | **5d** | **6f** (50) | 2 : 98 |

[a] Isolated yields based on quantity of **5** used. [b] The configuration of trisubstituted double bond. As for the disubstituted double bond, only the *E* isomers were produced. [c] The reaction was carried out using 1.2 equiv. of **5a**. [d] Isolated yield based on quantity of **2a** used.

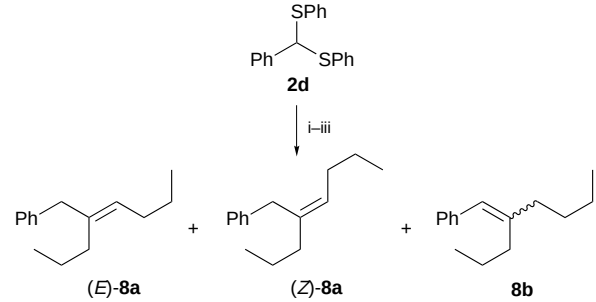
When an unsymmetrical alkyne was employed, the reaction proceeded with mixed regioselectivity. For example, 3-pentylundeca-2,4-diene and 7-methylpentadeca-6,8-diene were formed in 69% total yield by the reaction of oct-2-yne with **2b** carried out at room temperature for 20 h. The ratio of the two regioisomers was found to be 57 : 43, respectively.

The stereoselective formation of conjugated dienes **6** is explained by the reaction pathway depicted in Scheme 2. As would be expected, the reaction of alkylidenetitanocene **4**, formed by the desulfurizative titanation of thioacetal **2**, with an alkyne **5** produces the titanacyclobutene intermediate **1**. Then β-hydride elimination proceeds to afford the vinyltitanium species **7**. Subsequent reductive elimination gives the diene **6** with retention of configuration of the trisubstituted double bond. This reaction pathway was substantiated by the fact that the reaction of benzaldehyde diphenyl thioacetal **2d** with **5c** gave the structurally isomeric alkenes **8a** and **8b** [(*E*)-**8a**: (*Z*)-**8a**: **8b** = 81 : 1 : 18] in 58% yield (Scheme 3). It is reasonable to assume that these alkenes are formed by protonation of the intermediate titanacyclobutene **1**.

Preparation of higher homologues of methylidenetitanocene *via* titanium–aluminium metallacycles was not successful, owing to decomposition by β-hydride elimination.[8] Although it has been suggested that the alkylidenetitanocenes are produced by thermolysis of dibenzyl-,[9] bis[(trimethylsilyl)methyl]-,[10] dicyclopropyl-,[11] dialkenyl-[5b,d] and alkylalkenyl-titanocene,[5d,12] the formation of simple alkylidene complexes from dialkyltitanocene is improbable because of the preferential formation of titanocene(II)–alkene complexes.[13] The present




**Scheme 2**




**Scheme 3** *Reagents and conditions*: i, **3**, room temp., 10 min; ii, **5c**, room temp., 20 h; iii, 1 M NaOH

work is the first example of formation of titanacyclobutene **1** from an alkylidenetitanocene possessing a β-hydrogen bonded to an $sp^3$ carbon atom and shows that **1** thus formed easily decomposes by β-hydride elimination. In conclusion, the titanocene-promoted reaction of thioacetals with alkynes is an excellent method for the stereoselective preparation of conjugated dienes. Further aspects of this reaction will be reported in due course.

## Footnotes

* E-mail: takeda-t@cc.tuat.ac.jp

† The configuration of **6** was determined by a NOE experiment.

‡ *Typical experimental procedure*: to a flask charged with finely powdered molecular sieves 4 Å (150 mg), magnesium turnings (1.8 mmol) and titanocene dichloride (1.5 mmol) were added THF (4 ml) and triethyl phosphite (3 mmol) successively with stirring. After 3 h, a THF (2 ml) solution of **2** (0.6 mmol) was added and stirring was continued for 10 min. Then **5** (0.5 mmol) in THF (1 ml) was added dropwise over 15 min. After being refluxed for 3 h, the reaction was quenched with 1 M NaOH, and the insoluble materials were filtered off through Celite. The organic materials were extracted with diethyl ether, dried ($Na_2SO_4$) and concentrated. Purification was accomplished by PTLC providing **6** as a clear, colourless oil.

## References

1 J. D. Meinhart and R. H. Grubbs, *Bull. Chem. Soc. Jpn*., 1988, **61**, 171.
2 K. M. Doxsee and J. K. M. Mouser, *Organometallics*, 1990, **9**, 3012.
3 K. M. Doxsee and J. K. M. Mouser, *Tetrahedron Lett*., 1991, **32**, 1687.
4 N. A. Petasis and D.-K. Fu, *Organometallics*, 1993, **12**, 3776 and references cited therein; K. M. Doxsee, J. J. J. Juliette, J. K. M. Mouser and K. Zientara, *Organometallics*, 1993, **12**, 4682.
5 For the preparation of trimethylsilyl- and methylene-titanacyclobutenes, see (*a*) N. A. Petasis, J. P. Staszewski and D.-K. Fu, *Tetrahedron Lett*., 1995, **36**, 3619; (*b*) R. Beckhaus, K.-H. Thiele and D. Ströhl, *J. Organomet. Chem*., 1989, **369**, 43; (*c*) R. Beckhaus, J. Sang, T. Wagner and U. Englert, *Organometallics*, 1996, **15**, 1176; (*d*) N. A. Petasis and Y.-H. Hu, *J. Org. Chem*., 1997, **62**, 782.
6 Y. Horikawa, T. Nomura, M. Watanabe, I. Miura, T. Fujiwara and T. Takeda, *Tetrahedron Lett*., 1995, **36**, 8835.
7 Y. Horikawa, M. Watanabe, T. Fujiwara and T. Takeda, *J. Am. Chem. Soc*., 1997, **119**, 1127.
8 F. N. Tebbe and L. J. Guggenberger, *J. Chem. Soc., Chem. Commun*., 1973, 227; F. W. Hartner, Jr. and J. Schwartz, *J. Am. Chem. Soc*., 1981, **103**, 4979.
9 N. A. Petasis and E. I. Bzowej, *J. Org. Chem*., 1992, **57**, 1327.
10 N. A. Petasis and I. Akritopoulou, *Synlett*, 1992, 665.
11 N. A. Petasis and E. I. Bzowej, *Tetrahedron Lett*., 1993, **34**, 943.
12 R. Beckhaus, J. Oster and T. Wagner, *Chem. Ber*., 1994, **127**, 1003.
13 J. X. McDermott, M. E. Wilson and G. M. Whitesides, *J. Am. Chem. Soc*., 1976, **98**, 6529.

*Received in Cambridge, UK, 20th March 1997; Com. 7/01952A*

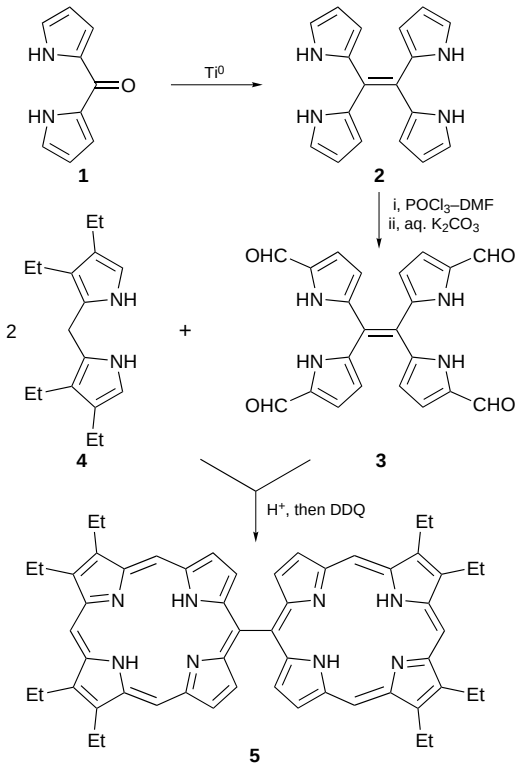
# Rational approach to the synthesis of meso–meso (5,5′) linked bis-porphyrins

**Richard G. Khoury, Laurent Jaquinod and Kevin M. Smith***

*Department of Chemistry, University of California, Davis, CA 95616, USA*

**A novel approach for the synthesis of 5,5′-directly linked metal-free bis-porphyrins is reported; McMurry type coupling of dipyrroketones (*e.g.* 1) leads to 1,1,2,2-tetra(2-pyrrolyl)ethene 2, which after tetra-formylation (to give 3) and MacDonald macrocyclization with a 1,9-di-unsubstituted dihydrodipyrrin 4, affords the 5,5′-bis-porphyrin 5.**

Publications of structural data on bacterial photosynethetic reaction centres[1] have encouraged interest in the synthesis of oligoporphyrin systems which can act as mimics of reaction centres and antenna systems in photosynthetic bacteria and plants.[2,3] Many porphyrin arrays, including dimers and trimers, have been synthesized for this purpose, and for use in supramolecular photonics.[4] Distance, geometry and orientation have been recognized as important factors for control of the efficiency of energy and electron transfer processes.[5,6] Electronic interaction between porphyrin rings is essential and for this reason we set out to design a number of porphyrin oligomers in which the individual π-systems can interact. A number of dimeric porphyrin arrays, with various spacers, have been synthesized.[7] We surmised that a bis-porphyrin system possessing a direct meso–meso (5,5′) link would be potentially interesting. In the recent publication of Segawa and coworkers[8a] an attempt to prepare a trimeric porphyrin system resulted in serendipitous formation of a bis-porphyrin linked by a single bond between meso positions; this report has caused us to report our rational synthetic approach to this type of bis-porphyrin. After submission of the present paper an additional report of the synthesis of meso–meso bisporphyrins, *via* oxidative coupling of a zinc(II) porphyrin, appeared.[8b]




**Scheme 1**

2,2′-Dipyrroketone[9] **1** was coupled under McMurry conditions[10,11] in the presence of pyridine at room temperature to afford a 56% yield of the 1,1,2,2-tetra(2-pyrrolyl)ethene **2** (Scheme 1).[12]† As observed with simpler 1,2-di(2-pyrrolyl)-ethenes,[13,14] compound **2** was highly fluorescent. In the solid state the 1,1,2,2-tetra(2-pyrrolyl)ethene was stable, but in solution slow decomposition was observed. The molecular structure of **2**‡ was confirmed by X-ray crystallography (Fig. 1).

Attempted MacDonald-type ('2 + 2') macrocyclization of the tetrapyrrolylethene **2** with 1,9-diformyl-2,3,7,8-tetraethyldihydrodipyrrin led to a mixture of products. But tetraformylation of **2** using excess $POCl_3$–DMF, followed by treatment with $K_2CO_3$, afforded the tetra[5-formyl-2-pyrrolyl]ethene **3**§ in 92% yield. Condensation of **3** with 2 equiv. of 2,3,7,8-tetraethyldihydrodipyrrin **4**, followed by oxidation with DDQ and filtration through a plug of silica gel, led to the symmetrical 5,5′-bis-porphyrin **5**¶ in 7% yield. The molecular structure of **5**‡ was confirmed by X-ray crystallography [Fig. 2(*a*)]. Each porphyrin subunit is fairly planar, exhibiting a mean plane

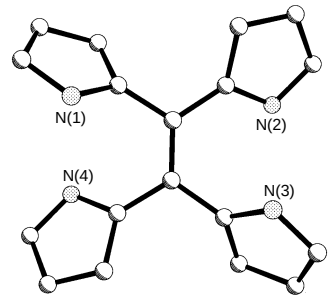



**Fig. 1** Molecular structure of the 1,1,2,2-tetra(2-pyrrolyl)ethene **2**. Hydrogen atoms have been omitted for clarity.

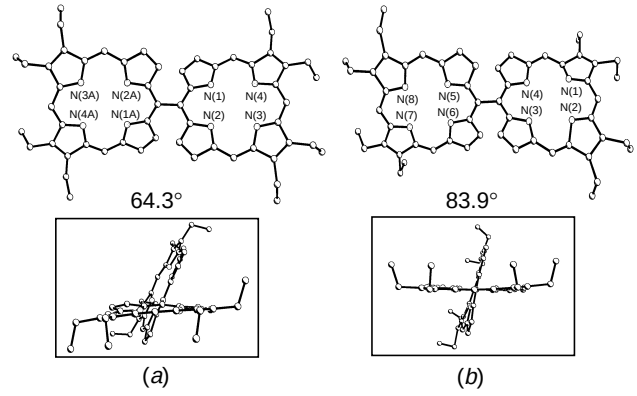



**Fig. 2** Molecular structure of the 5,5′-bis-porphyrin **5**. (*a*) The form crystallized from THF–hexane. (*b*) The form crystallized from dichloromethane–methanol. The boxes beneath each structure show side views along the 5,5′-bond. Hydrogen atoms have been omitted for clarity.

deviation of 0.10 Å from the 24 core atoms. A covalent single bond (1.51 Å) links both porphyrin subunits at the meso position. The angle between both porphyrin planes is 65°, and this is almost certainly a feature of lattice packing. When **5** was crystallized from a different solvent system, a second crystal structure‡ was obtained [Fig. 2(*b*)]; this showed the angle between both macrocyclic planes to be 83.9°.

Further work is aimed at synthesis of unsymmetrically substituted 5,5′-bis-porphyrin systems, and higher oligomers.

This work was supported by grants from the National Science Foundation (CHE-96-23117) and the National Institutes of Health (HL-22252). Mass spectrometric analyses were performed by the University of California, San Francisco, Mass Spectrometry Facility (A. L. Burlingame, Director) supported by the Biomedical Research Technology Program of the National Center of Research Resources, NIH NCRR BRTP 01614.

## Footnotes

* E-mail: smith@chem.ucdavis.edu

† *Selected data* for **2**: Mp 180–182 °C UV–VIS $\lambda_{max}$ ($CH_2Cl_2$) 302 nm (ε 9200), 364 (15 800); $\delta_H$ (300 MHz, $CDCl_3$) 6.07 (m, 4 H, β-H), 6.18 (d, 4 H, β-H), 6.69 (d, 4 H, β-H), 7.93 (s, 4 H, NH). HRMS $C_{18}H_{16}N_4$ requires: *m/z* 288.1374, found: 288.1378.

‡ *Crystal data*: The structures were solved by direct methods and refined (based on $F^2$ using all independent data) by full matrix least-squares methods (Siemens SHELXTL V. 5.02). Hydrogen atom positions were located by their idealized geometry and refined using a riding model. For each structure an absorption correction was applied using XABS2.[15] For **2** ($C_{18}H_{16}N_4$): X-ray diffraction data were collected on a Siemens $P2_1$ diffractometer with a fine-focus sealed tube [λ(Cu Kα) = 1.54178 Å] at 130(2) K in θ/2θ scan mode to $2\theta_{max}$ = 112°. Crystals were grown from a mixture of dichloromethane and cyclohexane. A single parallelipeped crystal was selected with dimensions 0.40 × 0.12 × 0.10 mm. The unit cell was triclinic and space group $P\bar{1}$ with cell dimensions: $a$ = 8.231(2), $b$ = 9.335(2), $c$ = 9.671(2) Å, α = 98.64(3), β = 103.22(3), γ = 93.22(3)°, $V$ = 712.0(2) Å$^3$ and $Z$ = 2 (FW = 288.35, $\rho_{calc}$ = 1.345 g cm$^{-3}$, μ = 0.652 mm$^{-1}$). Of 1948 reflections measured (±*h*, ±*k*, +*l*) 1923 were independent and 1431 had $I > 2\sigma$ ($R_{int}$ = 0.012); number of parameters = 199. Final $R$ factors were $R1$ = 0.0524 (based on observed data) and $wR2$ = 0.1304 (based on all data). For **5**: X-ray diffraction data were collected on a Siemens P4 rotating anode diffractometer with a fine-focus sealed tube [λ(Cu Kα) = 1.54178 Å] at 130(2) K in θ/2θ scan mode to $2\theta_{max}$ = 113°. First structure [Fig. 2(*a*)]; single crystals of **5** ($C_{56}H_{58}N_8{\cdot}C_4H_8O{\cdot}1.5H_2O$) were grown from a mixture of THF and hexane. A single pyramidal crystal was selected with dimensions 0.18 × 0.12 × 0.10 mm. The unit cell was monoclinic $C2/c$ with cell dimensions: $a$ = 26.068(6), $b$ = 17.644(3), $c$ = 13.842(3) Å, β = 115.99(2)°, $V$ = 5723(2) Å$^3$, and $Z$ = 4 (FW = 987.25, $\rho_{calc}$ = 0.587 g cm$^{-3}$, μ = 0.555 mm$^{-1}$). Of 4086 reflections measured (±*h*, +*k*, +*l*) 3783 were independent and 2594 had $I > 2\sigma$ ($R_{int}$ = 0.117); number of parameters = 343. Final $R$ factors were $R1$ = 0.0921 (based on observed data) and $wR2$ = 0.3064 (based on all data). Second structure [Fig. 2(*b*)]: Crystals of **5** ($C_{56}H_{58}N_8$) were grown from a mixture of dichloromethane and methanol. A single parallelipeped crystal was selected with dimensions 0.34 × 0.14 × 0.06 mm. The unit cell was triclinic and space group $P\bar{1}$ with cell dimensions $a$ = 8.4926(14), $b$ = 12.859(2), $c$ = 21.648(3) Å, α = 96.469(11), β = 97.470(12), γ = 101.096(12)°, $V$ = 2277(6) Å$^3$ and $Z$ = 2 (FW = 843.10, $\rho_{calc}$ = 1.230 g cm$^{-3}$, μ = 0.567 mm$^{-1}$). Of 6700 reflections measured (±*h*, ±*k*, +*l*) 6006 were independent and 4430 had $I > 2\sigma$ ($R_{int}$ = 0.034); number of parameters = 199. Final $R$ factors were $R1$ = 0.0601 (based on observed data) and $wR2$ = 0.1745 (based on all data). Atomic coordinates, bond lengths and angles, and thermal parameters have been deposited at the Cambridge Crystallographic Data Centre (CCDC). See Information for Authors, Issue No. 1. Any request to the CCDC for this material should quote the full literature citation and the reference number 183/433.

§ *Selected data* for **3**: Mp 190–193 °C; UV–VIS **3**: $\lambda_{max}$ ($CH_2Cl_2$) 438 nm (ε 29 900); $\delta_H$ (300 MHz, $CDCl_3$): 5.21 (d, 4 H, β-H), 6.11 (d, 4 H, β-H), 8.58 (s, 4 H, CHO), 10.20 (br s, 4 H, NH); MS $C_{22}H_{16}N_4O_4$ requires: *m/z* 400.6, found: 400.11.

¶ *Selected data* for **5**: Mp > 300 °C; UV–VIS $\lambda_{max}$ ($CH_2Cl_2$) 400 nm (ε 141 000), 436 (155 000), 508 (41 700), 574 (19 600), 626 (8100); $\delta_H$ (300 MHz, $CDCl_3$): −2.95 (br s, 4 H, NH) 2.01 (m, 24 H, $CH_2CH_3$), 4.18 (m, 16 H, $CH_2CH_3$), 8.19 (s, 4 H, β-H), 9.06 (s, 4 H, β-H), 10.22 (s, 2 H, meso-H), 10.26 (s, 4 H, meso-H); MS $C_{56}H_{58}N_8$ requires: *m/z* 843.14, Found: 843.38.

## References

1 J. Deisenhofer, O. Epp, K. Miki, R. Huber and H. Michel, *J. Mol. Biol.*, 1984, **180**, 385; J. P. Allen and G. Feher, *Proc. Natl. Acad. Sci. USA*, 1984, **81**, 4795; J. P. Allen, G. Feher, T. O. Yeates, D. C. Rees, J. Deisenhofer, H. Michel and R. Huber, *Proc. Natl. Acad. Sci. USA*, 1986, **83**, 8589; G. McDermott, S. M. Prince, A. A. Freer, A. M. Hawthorne-Lawless, M. Z. Papíz, R. J. Cogdell and N. W. Isaacs, *Nature* (*London*), 1995, **374**, 517.

2 C. K. Chang and I. Abdalmuhdi, *J. Org. Chem.*, 1983, **48**, 5388; *Angew Chem., Int. Ed. Engl.*, 1984, **23**, 164; *J. Org. Chem.*, 1985, **50**, 411; J. L. Sessler, M. R. Johnson, T. Y. Lin and S. E. Creager, *J. Am. Chem. Soc.*, 1988, **110**, 3659; J. L. Sessler, J. Hugdahl and M. R. Johnson, *J. Org. Chem.*, 1986, **51**, 2838.

3 For reviews see: M. R. Wasielewski, *Photochem. Photobiol.*, 1988, **47**, 923; D. Gust and T. A. Moore, *Science*, 1989, **244**, 35; 'Symposium in Print' on Covalently Linked Donor acceptor Photosynthetic Model Systems, ed. D. Gust and T. A. Moore, *Tetrahedron*, 1989, **45** and refs. cited therein; M. R. Wasielewski, D. G. Johnson, W. A. Svec, K. M. Kersey and D. W. Minsek, *J. Am. Chem. Soc.*, 1988, **110**, 7219; G. McClendon and D. W. Heiler, *J. Am. Chem. Soc.*, 1987, **109**, 604; H. Kurreck and M. Huber, *Angew. Chem., Int. Ed. Engl.*, 1995, **34**, 849.

4 M. P. O'Neil, M. P. Niemczyk, W. A. Svec, D. Gosztola, G. L. Gaines III and M. R. Wasielewski, *Science*, 1992, **257**, 63; M. R. Wasielewski, *Chem. Rev.*, 1992, **92**, 435; R. W. Wagner and J. S. Lindsey, *J. Am. Chem. Soc.*, 1994, **116**, 9759.

5 D. Gust, T. A. Moore, A. L. Moore, L. R. Makings, G. R. Seely, X. Ma, T. T. Trier and F. Gao, *J. Am. Chem. Soc.*, 1988, **110**, 3659; T. A. Moore, D. Gust, P. Mathis, J. C. Mialocq, C. Chachaty, R. V. Bensasson, E. J. Land, D. Doizi, P. A. Liddell, W. R. Lehman, G. A. Nemeth and A. L. Moore, *Nature* (*London*), 1984, **307**, 630.

6 A. Osuka, Y. Hiroko and K. Maruyama, *Chem. Lett.*, 1990, 1905; A. Osuka and K. Maruyama, *J. Chem. Soc., Chem. Commun.*, 1988, 1243.

7 S. Prathapan, T. E. Johnson and J. S. Lindsey, *J. Am. Chem. Soc.*, 1993, **115**, 7519; V. S.-Y. Lin and M. J. Therien, *Chem. Eur. J.*, 1995, **1**, 645.

8 (*a*) K. Susumu, T. Shimidzu, D. Tanaka and H. Segawa, *Tetrahedron Lett.*, 1996, **37**, 8399; (*b*) A. Osuka and H. Shimidzu, *Angew. Chem., Int. Ed. Engl.*, 1997, **36**, 135.

9 P. S. Clezy and G. A. Smythe, *Aust. J. Chem.*, 1969, **22**, 239.

10 J. E. McMurry, T. Leckta and J. G. Rico, *J. Org. Chem.*, 1989, **54**, 3748; J. E. McMurry, *Chem. Rev.*, 1989, **89**, 1513.

11 R. Paolesse, R. K. Pandey, T. P. Forsyth, L. Jaquinod, K. R. Gerzeveske, D. J. Nurco, M. O. Senge, S. Licoccia, T. Boschi and K. M. Smith, *J. Am. Chem. Soc.*, 1996, **118**, 3869; M. G. H. Vicente and K. M. Smith, *J. Org. Chem.*, 1991, **56**, 4407; L. Jaquinod, M. O. Senge, R. K. Pandey, T. P. Forsyth and K. M. Smith, *Angew. Chem., Int. Ed. Engl.*, 1996, **35**, 1840.

12 H. Fischer and H. Orth, *Die Chemie des Pyrrols*, Akademische, Leipzig, 1934, vol. 1, p. 390.

13 A. Hayes, A. H. Jackson, J. M. Judge and G. W. Kenner, *J. Chem. Soc.*, 1965, 4385.

14 H. Xie, D. A. Lee, D. M. Wallace, M. O. Senge and K. M. Smith, *J. Org. Chem.*, 1996, **61**, 8508.

15 S. R. Parkin, B. Moezzi and H. Hope, *J. Appl. Cryst.*, 1995, **28**, 53.

*Received in Corvallis, OR, USA, 20th February 1997; Com. 7/01218G*

# Use of the *p*-nitrobenzyloxycarbonyl group as an orthogonal amine protecting group in the synthesis of β-GlcNAc terminating glycosides

**Xiangping Qian and Ole Hindsgaul***

*Department of Chemistry, University of Alberta, Edmonton, Alberta, Canada T6G 2G2*

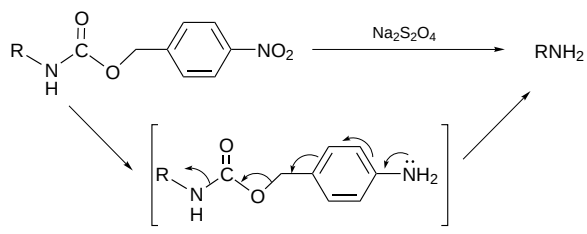
**The *p*-nitrobenzyloxycarbonyl group serves as a participating group in the stereoselective formation of 2-amino-β-glucosides and as an N-protecting group which can be readily removed either by hydrogenolysis or by reaction with sodium dithionite under neutral conditions.**

β-D-Glycosides of *N*-acetyl-2-amino-2-deoxy sugars are widely distributed in living organisms where they constitute building blocks of glycoconjugates.[1] The synthesis of such glycosides requires glycosyl donors where the amino group is protected. The phthalimido (Phth) and azido groups have been the most widely used.[2,3]

More recently, the carbamate functionality has been used for protection of the amino group in peptide, protein and carbohydrate synthesis.[4–7] Boullanger *et al*. conducted a systematic study on the glycosylation of simple acceptor alcohols with various *N*-alkoxycarbonyl derivatives of glucosamine, including the *p*-nitrobenzyloxycarbonyl (PNZ) group.[8] It was found that β-glycosides were obtained stereoselectively in good yield without the formation of an oxazolidinone when the β-acetate of these carbamate derivatives was used as glycosyl donor in the presence of a Lewis acid. The 2,2,2-trichloroethyl and allyl carbamates have since been effectively applied in the synthesis of glycoconjugates containing 2-acetamido glycosides.[7,9] These can be deprotected with zinc dust in acetic acid[7] and with $Pd^0$ complexes,[9] respectively.

We chose to investigate the potential of the *p*-nitrobenzyl carbamates of 2-amino sugars since this group should be selectively cleavable by the reduction of the electron-withdrawing nitro group to the electron-donating amine substituent followed by 1,6-elimination[4] (Scheme 1). As there are many methods for reducing the aromatic nitro group, mild and chemoselective deprotection methods should be readily available. Furthermore, unlike the 2,2,2-trichloroethyl or allyl carbamates, the *p*-nitrobenzyl carbamate can be removed by hydrogenolysis at the end of a synthesis along with the standard *O*-benzyl protecting groups.

As shown in Scheme 2, treatment of glucosamine hydrochloride **1** with 1 equiv. of NaOMe in MeOH, followed by *p*-nitrobenzyl chloroformate–$Et_3N$ and *O*-acetylation gave **2**. The trichloroacetimidate **3**† was formed by regioselective deacetylation at O-1 with benzylamine followed by treatment of the reducing sugar with $CCl_3CN$ in the presence of $K_2CO_3$.[10] Imidate **3** was evaluated as a glycosyl donor in $CH_2Cl_2$ using $BF_3{\cdot}Et_2O$ as a promoter.‡§ The octyl β-glycoside **4** was formed in 82% yield.¶ Glycosylation of **5** gave the β-(1 → 6) linked disaccharide **6** in 91% yield (Scheme 3).†,¶ The reaction of **3** with the less reactive 4-OH groups of **10** and **11** also gave β-(1 → 4) linked disaccharides **12**† and **13** in good yields (79 and 75%,¶ respectively) (Scheme 4). These results indicate that the combination of the PNZ moiety with anomeric trichloroacetimidate activation can afford β-glycosides in high yield with high stereoselectivity.

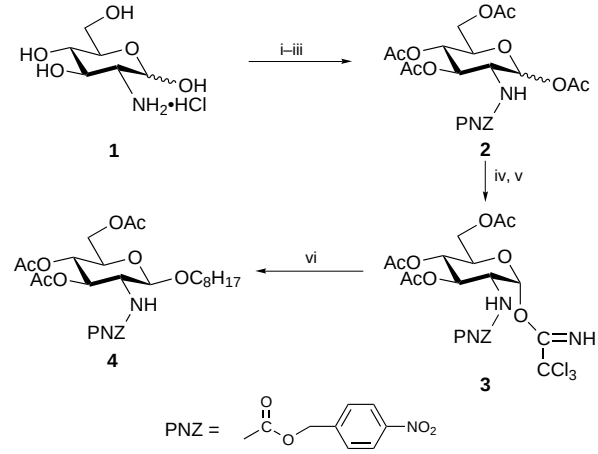



**Scheme 1**

A major disadvantage of using the *N*-phthalimido group in oligosaccharide synthesis is that its deprotection requires vigorous conditions, and esters usually do not survive.[11] Recently, the more reactive tetrachlorophthaloyl (TCP) group was applied as an amine protecting group.[12,13] The TCP group can be removed under milder conditions than the Phth group, either by a slight excess of ethylenediamine at 60 °C or by $NaBH_4$ reduction. Although the extent of cleavage of carboxylate ester groups is significantly reduced under these conditions, yields are still moderate especially in the presence of 3-OAc and 6-OAc groups when using ethylenediamine.[12*b*] Ketone or aldehyde functionalities may also be reduced by $NaBH_4$ during the removal of the TCP group. Clearly, chemoselective removal of the PNZ group under conditions where esters are inert would enhance its utility.

Methods for the removal of the PNZ group were examined using the simple glycoside **4** as a model compound. Removal of the PNZ group and acetylation of the resulting amine can be directly achieved in one step by hydrogenolysis using 10% Pd–C under $H_2$ flow in the presence of $Ac_2O$, yielding **9** in 83% yield.¶ As shown in Scheme 3, the free amine **8** could also be isolated (76%¶) when the hydrogenolysis was performed in the absence of $Ac_2O$.

Attempted reduction with stannous chloride[14] in non-acidic and non-aqueous media (EtOH or EtOAc) was ineffective. *p*-Nitrobenzyl esters can, however, be reductively cleaved by sodium dithionite ($Na_2S_2O_4$) under neutral or slightly alkaline conditions.[15] We found that sodium dithionite was a very

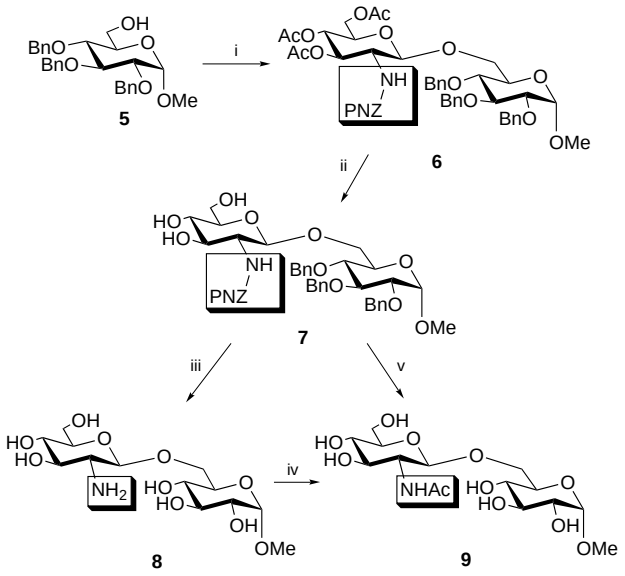



**Scheme 2** *Reagents and conditions*: i, NaOMe (1 equiv.), MeOH, 10 min; ii, *p*-nitrobenzyl chloroformate (1 equiv.), $Et_3N$ (1 equiv.), 0 °C to room temp; iii, $Ac_2O$, pyridine, 16 h, 78% (3 steps); iv, $BnNH_2$ (1.1 equiv.), THF, 16 h; v, $CCl_3CN$ (10 equiv.), $K_2CO_3$, $CH_2Cl_2$, 7 h, 75% (2 steps); vi, $BF_3{\cdot}Et_2O$ (0.5 equiv.), octanol (0.7 equiv.), 4 Å molecular sieves, $CH_2Cl_2$, −30 to 0 °C, 2 h, 82% (based on octanol)

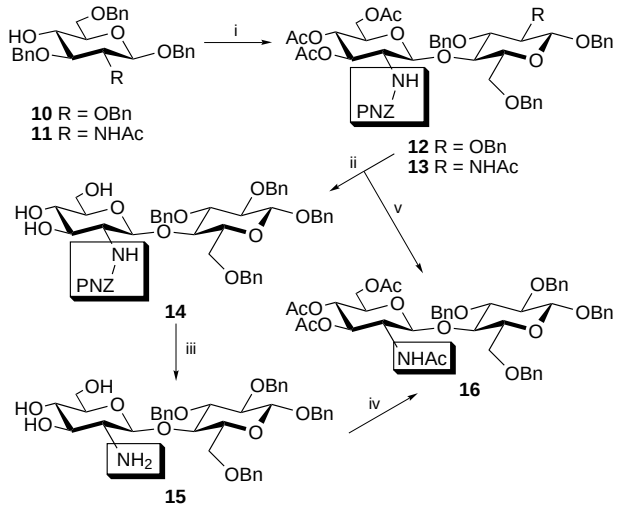
effective reducing agent even in the absence of base. The PNZ group can be readily removed quickly in quantitative yield. As shown in Scheme 4, deacetylation of **12** using NaOMe in MeOH followed by cleavage of PNZ and re-acetylation with $Ac_2O$–pyridine gave **16**.† When disaccharide **12** was treated directly with sodium dithionite in MeCN–EtOH–$H_2O$ solution, followed by *N*-acetylation using $Ac_2O$ in MeOH, disaccharide **16** was obtained, demonstrating the stability of the three *O*-acetate groups to the reduction conditions. The free amine group can also be transformed into the acetamido group in 'one pot' by simply adding $Ac_2O$ directly to the reaction mixture. Disaccharide **16** was thus formed in a 'one pot' reaction in 86% yield.¶

In summary, we have demonstrated that the PNZ group functions as a good participating group for the formation of 2-amino-β-glucosides. This N-protecting group can be conveniently removed either by hydrogenolysis along with *O*-benzyl ethers or selectively by sodium dithionite under neutral conditions where carboxylate esters remain stable. Since *O*-acetyl groups can be removed by treatment with NaOMe–MeOH in the presence of the PNZ group, this group is effectively an orthogonal protecting group and should thus find unique application in oligosaccharide synthesis.

We gratefully acknowledge the Natural Sciences and Engineering Research Council of Canada for financial support and Drs J. C. McAuliffe and Z. G. Wang for helpful suggestions.




**Scheme 3** *Reagents and conditions*: i, $BF_3{\cdot}Et_2O$ (0.5 equiv.), **3** (1.5 equiv.), 4 Å molecular sieves, $CH_2Cl_2$, −30 to 0 °C, 2 h, 91%; ii, NaOMe, MeOH, 2.5 h, 93%; iii, $H_2$, 10% Pd–C, MeOH, 76%; iv, $Ac_2O$, EtOH, 1 h, 87%; v, $H_2$, 10% Pd–C, MeOH, $Ac_2O$, 83%




**Scheme 4** *Reagents and conditions*: i, $BF_3{\cdot}Et_2O$ (0.5 equiv.), **3** (1.5 equiv.), 4 Å molecular sieves, $CH_2Cl_2$, −30 to 0 °C, 2 h, 79% for **12**, 75% for **13**; ii, NaOMe, MeOH, 3.5 h, quant.; iii, $Na_2S_2O_4$ (8 equiv.), EtOH–$H_2O$, 10 min, quant.; iv, $Ac_2O$, pyridine, 16 h, 93%; v, $Na_2S_2O_4$ (8 equiv.), MeCN–EtOH–$H_2O$, 1 h; then $Ac_2O$, 10 min, 86%

## Footnotes

* E-mail: ole.hindsgaul@ualberta.ca

† *Selected data* for **3**: $^1$H NMR ($CDCl_3$) δ 8.75 (s, 1 H, C=NH), 6.39 (d, 1 H, $J_{1,2}$ 3.6 Hz, H-1). For **6**: $J_{C1H1}$ 168.5 Hz, $J_{C1'H1'}$ 160.4 Hz; HR-ESMS for $C_{48}H_{54}N_2O_{17}Na$ (M + $Na^+$): calc. 953.3320, found 953.3348. For **12**: $J_{C1H1}$ 160.0 Hz, $J_{C1'H1'}$ 158.1 Hz; HR-ESMS for $C_{54}H_{58}N_2O_{17}Na$ (M + $Na^+$): calc. 1029.3633, found 1029.3634. For **15**: HR-ESMS for $C_{40}H_{47}NO_{10}Na$ (M + $Na^+$): calc. 724.3098, found 724.3119. For **16**: $^1$H NMR ($CDCl_3$) δ 4.55 (d, 1 H, $J_{1,2}$ 8.4 Hz, H-1), 4.45 (d, 1 H, $J_{1',2'}$ 7.6 Hz, H-1′); $J_{C1H1}$ 161.8 Hz, $J_{C1'H'}$ 159.2 Hz.

‡ Typical procedure of glycosylation: compound **3** (236 mg, 0.375 mmol), **5** (116 mg, 0.25 mmol) and powdered 4 Å molecular sieves (250 mg) in dry $CH_2Cl_2$ (5 ml) were stirred for 10 min at −30 °C under nitrogen. Then $BF_3{\cdot}Et_2O$ (15 μl, 0.125 mmol) in dry $CH_2Cl_2$ (0.75 ml) was added, and the reaction mixture was stirred for a further 2 h below 0 °C. After neutralization with $Et_3N$, the reaction mixture was filtered through Celite, washed with $CH_2Cl_2$ and concentrated. Column chromatography (3 : 2, hexane–EtOAc) gave disaccharide **6** (211 mg, 91%).

§ The $^1$H NMR spectra of most disaccharides containing the PNZ moiety gave broad peaks which make assignments difficult. The β-linkage of the disaccharides was confirmed by $^{13}$C–$^1$H HMQC experiments and NMR data for the *N*-acetyl disaccharide obtained by N-acetylation after the reductive cleavage step.

¶ Yields were calculated based on the weight of pure compounds isolated by column chromatography.

## References

1 A. Varki, *Glycobiology*, 1993, **3**, 97; R. A. Dwek, *Chem. Rev.*, 1996, **96**, 683.
2 J. Banoub, P. Boullanger and D. Lafont, *Chem. Rev.*, 1992, **92**, 1167; S. H. Kahn and O. Hindsgaul, in *Molecular Glycobiology*, ed. M. Fukuda and O. Hindsgaul, IRL, Oxford, 1994, ch. 5.
3 F. Barresi and O. Hindsgaul, *J. Carbohydr. Chem.*, 1995, **14**, 1043; T. B. Grindley, in *Modern Methods in Carbohydrate Synthesis*, ed. S. H. Khan and R. A. O'Neill, Harwood Academic, Amsterdam, 1995, p. 241.
4 T. W. Greene and P. G. M. Wuts, *Protective Groups in Organic Synthesis*, Wiley, NY, 1991, p. 339.
5 L. Zervas and S. Konstas, *Chem. Ber.*, 1960, **93**, 435.
6 K. Heyns, R. Harrison and H. Paulsen, *Chem. Ber.*, 1967, **100**, 271; J. Lessard, H. Driguez and J. P. Vermes, *Tetrahedron Lett.*, 1970, 4887.
7 M. Imoto, H. Yoshimura, T. Shimamoto, N. Sakaguchi, S. Kusumoto and T. Shiba, *Bull. Chem. Soc. Jpn.*, 1987, **60**, 2205; V. Pozsgay, in *Carbohydrates-Synthetic Methods and Applications in Medicinal Chemistry*, ed. H. Ogura, A.Hasagawa and T. Suami, Kodansha, Tokyo, 1992, p. 199.
8 P. Boullanger, M. Jouineau, B. Bouammali, D. Lafont and G. Descotes, *Carbohydr. Res.*, 1990, **202**, 151.
9 D. Lafont, P. Boullanger, J. Banoub and G. Descotes, *Can. J. Chem.*, 1990, **68**, 828; D. Lafont, P. Boullanger and B. Fenet, *J. Carbohydr. Chem.*, 1994, **13**, 565.
10 R. R. Schmidt and W. Kinzy, *Adv. Carbohydr. Chem. Biochem.*, 1994, **50**, 21.
11 F. A. W. Koeman, J. W. G. Meissner, H. R. P. van Ritter, J. P. Kamerling and J. F. G. Vliegenthart, *J. Carbohydr. Chem.*, 1994, **13**, 1; P. Stangier and O. Hindsgaul, *Synlett*, 1996, 179.
12 (*a*) J. S. Debenham, R. Madsen, C. Roberts and B. Fraser-Reid, *J. Am. Chem. Soc.*, 1995, **117**, 3302; (*b*) J. S. Debenham and B. Fraser-Reid, *J. Org. Chem.*, 1996, **61**, 432.
13 J. C. Castro-Palomino and R. R. Schmidt, *Tetrahedron Lett.*, 1995, **36**, 5343.
14 F. D. Bellamy and K. Ou, *Tetrahedron Lett.*, 1984, **25**, 839.
15 E. Guibe-Jampel and M. Wakselman, *Synth. Commun.*, 1982, **12**, 219.

*Received in Corvallis, OR, USA, 23rd January 1997; Com. 7/00549K*

# Improved transport of nucleotide monophosphates by lipophilic phosphonium–nucleobase conjugates

**Yong-Gyu Jung, Woon-Seok Yeo, Sang Bok Lee and Jong-In Hong***

*Department of Chemistry, Seoul National University, Seoul 151-742, Korea*

**Lipophilic phosphonium–nucleobase conjugates 3 and 5 showed improved transport of AMP and GMP in comparison with lipophilic phosphonium salts, lipophilic complementary nucleobases, or a joint co-carrier system consisting of a lipophilic phosphonium salt and a nucleobase.**

Nucleotide analogues which have potential antiviral activity *in vitro* cannot penetrate across lipophilic cell membranes due to their highly charged and hydrophilic nature.[1] Therefore, there has been increasing effort towards developing phosphate-binding receptors.[2] However, there are a few artificial carrier systems known which are capable of transporting phosphate-bearing nucleotides through organic liquid membranes.[3] Recently, lipophilic phosphonium salts were developed as carriers for 5′-AMP (AMP) and 5′-GMP (GMP) in our laboratory.[4] They showed better transport rates for AMP and GMP compared with transport by the structurally similar, lipophilic trioctylmethylammonium chloride.[3c,5] In addition, moderate rate enhancements were observed when a phosphonium salt and a lipophilic nucleoside were used together as joint co-carriers. We expected that lipophilic phosphonium salts connected covalently to a complementary nucleobase would display better transport rates for AMP and GMP in comparison with a joint co-carrier system. Here we report improved extraction and transport of AMP and GMP by lipophilic phosphonium–nucleobase conjugates **3** and **5**.†

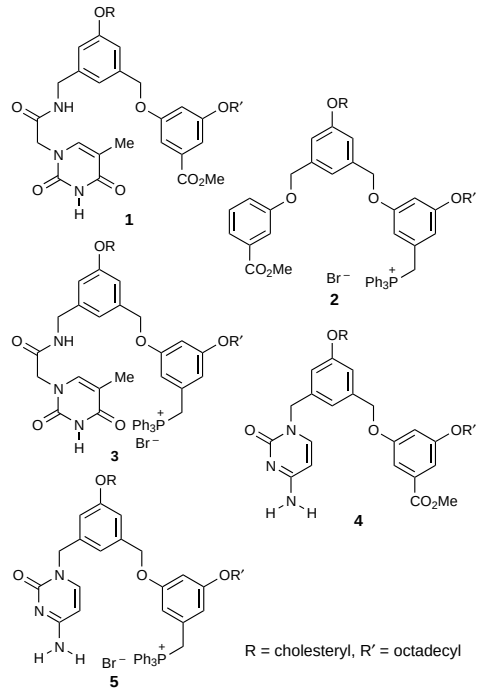


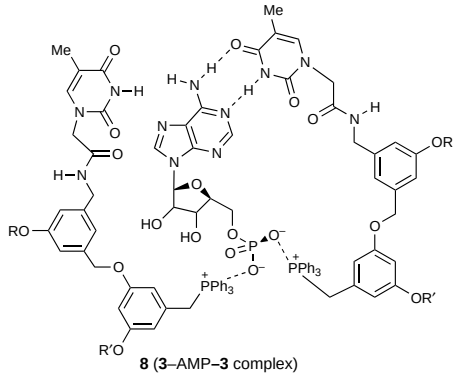

Table 1 shows extraction and transport data for AMP or GMP by lipophilic complementary nucleobases (**1** and **4**), a phosphonium salt (**2**) and phosphonium–nucleobase conjugates (**3** and **5**). There exist qualitative correlations between the extraction and the transport data. AMP (or GMP) is dissociated mostly into its monoanion ($AMP^-$ or $GMP^-$) at pH 5, while only one third of AMP (or GMP) exists as $AMP^-$ or $GMP^-$ at pH 7. As shown in Table 1, the phosphonium carrier (**2**) exhibits a better transport rate for AMP and GMP at pH 5 than at pH 7 for entropic reasons.[4]

The phosphonium carrier is expected to mediate more efficient through-membrane transport of AMP or GMP with the aid of base-pairing in either an inter- or intra-molecular fashion.[3e,h,i,6] Previously we used an organic-soluble nucleobase as a co-carrier to improve through-membrane transport of nucleotide monophosphates by a phosphonium cation.[4]‡ Either at pH 5 or 7, in the presence of lipophilic uridine or cytidine as a co-carrier, moderate rate enhancements were observed in the case of AMP or GMP transport, respectively. To make more effective and selective carriers for AMP or GMP compared to the joint co-carrier system would require the construction of phosphonium–nucleobase conjugates, in which an adenine or guanine recognition unit is appended directly onto the phosphate-binding phosphonium centre. Compounds **3** and **5** extract and transport AMP or GMP, respectively, more efficiently than **2**, presumably because of base-pairing of the complementary nucleobase moiety of **3** or **5** with the nucleobase of AMP or GMP. In fact, the thymine (or cytosine)-bearing phosphonium carrier **3** (or **5**) was found to be much more effective for AMP (or GMP) transport, either at pH 5 or 7. As shown in Table 1, the receptor **3** displayed a higher transport rate for AMP (by a factor of 39 at pH 5 and 157 at pH 7) than the thymine-free phosphonium salt **2**. In the case of GMP transport, the cytosine-substituted phosphonium receptor **5** showed a similar rate enhancement (by a factor of 66 at pH 5 and 103 at pH 7) in comparison with the cytosine-free phosphonium salt **2**. However, control experiments (**5**/AMP and **3**/GMP) employing noncomplementary nucleobase–phosphonium conjugates led to decreased transport of AMP and GMP, respectively, compared to the complementary nucleobase–phosphonium carrier systems (**3**/AMP and **5**/GMP). This clearly shows that selective

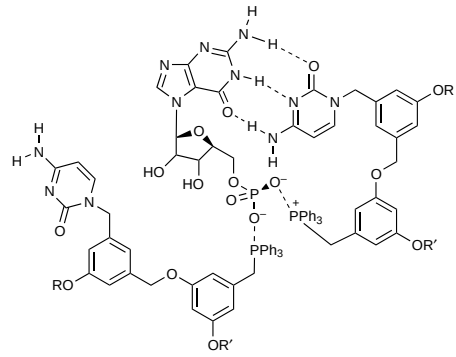
**Table 1** Extraction and transport of AMP and GMP by **1**–**5**

| | | Extraction (%)[a] | | Transport rate/ $10^{-9}$ mol $h^{-1}$ $cm^{-2}$[b] | |
|---|---|---|---|---|---|
| Carrier | Guest | pH 5.0 | pH 7.0 | pH 5.0 | pH 7.0 |
| **1** | AMP | [c] | [c] | [c] | [c] |
| **2** | AMP | 7.4 | 6.3 | 0.14 | 0.03 |
| **3** | AMP | 10 | 9 | 5.4 | 4.7 |
| **5** | AMP | 12 | 7 | 0.5[d] | 0.2 |
| **4** | GMP | 6 | 2 | [c] | [c] |
| **2** | GMP | 13 | 8 | 0.08 | 0.04 |
| **5** | GMP | 33 | 33 | 5.3 | 4.1 |
| **3** | GMP | 13 | 15 | [c] | 0.06 |

[a] [Carrier] = $1 \times 10^{-2}$ M in $CHCl_3$, [Guest] = $1 \times 10^{-4}$ M in deionized water. [b] Source phase: [AMP] (or [GMP]) = 0.05 M in $H_2O$. Receiving phase: [NaBr] = 0.025 M in $H_2O$. Organic phase: [carrier] = 0.001 M in $CHCl_3$. [c] Not detected. [d] No transport observed after 24 h.



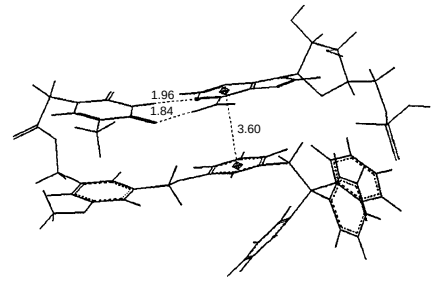
**8** (**3**–AMP–**3** complex)



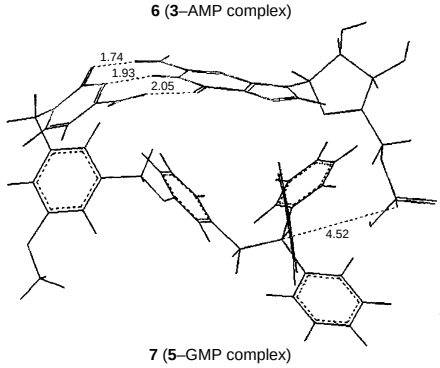
**9** (**5**–GMP–**5** complex)

R = cholesteryl, R′ = octadecyl

**Fig. 1** Possible structures for the transport complexes **8** and **9** at pH 7




**6** (**3**–AMP complex)




**7** (**5**–GMP complex)

**Fig. 2** Energy-minimized structures of the possible transport complexes **6** and **7** at pH 5 (DISCOVER 95.0 with CVFF force field)

base pairing contributes to increased transport. The fact that a phosphonium-free nucleobase **1** or **4** doesn't transport AMP or GMP at all indicates the importance of the phosphate group solubilization in $CHCl_3$ for transport of nucleotide monophosphates.

A concentration-dependent extraction study supports possible structures for the neutral supramolecular transport complexes between the phosphonium–nucleobase conjugate carriers (**3** or **5**) and nucleotide monophosphates, as depicted in Figs. 1 and 2. When aqueous solutions containing varying amounts of AMP (or GMP) were shaken with a chloroform solution of **3** or **5** ($1.0 \times 10^{-5}$ M), the maximum extractability of AMP (or GMP) was 105% (or 119%) at pH 5 and 54% (or 49%) at pH 7, respectively. This result supports the suggestion that **3** (or **5**) undergoes formation of a 1 : 1 complex (**3**–AMP or **5**–GMP) at pH 5 (Fig. 2) and a 2 : 1 complex (**3**–AMP–**3** or **5**–GMP–**5**) at pH 7 in the organic phase (Fig. 1). Since formation of the bimolecular complex **6** (or **7**) between **3** (or **5**) and the monobasic forms of AMP (or GMP) is entropically more favourable than that of the termolecular complex **8** (or **9**) between two molecules of **3** (or **5**) and the dibasic form of AMP (or GMP), **3** (or **5**) transports either AMP or GMP slightly more efficiently at pH 5 than at pH 7.

Computer-generated structures§ of the possible transport complexes **6** and **7** at pH 5 are shown in Fig. 2. While in the case of **6** hydrogen-bonding (base-pairing), electrostatic interactions, and aromatic stacking interactions are clearly visible, hydrogen-bonding and electrostatic interactions are shown to be operative in the case of **7**.

In summary, we have showed that the transport of normally organic-insoluble AMP or GMP can be improved by using appropriately designed lipophilic nucleobase-substituted phosphonium carriers.

We thank Ministry of Education (BSRI-96-3416), OCRC, and KOSEF (Grant No. 961-0302-008-2) for financial support.

## Footnotes

* E-mail: jihong@plaza.snu.ac.kr

† All new compounds gave satisfactory spectroscopic and analytical data.

‡ A joint co-carrier system showed a better transport rate than the phosphonium carrier, by a factor of 2–3, when an equimolar amount of the phosphonium salt and the nucleobase was used. Increasing the concentration of the co-carrier (nucleobase) led to better transport of the corresponding nucleotide monophosphate (ref. 4).

§ The energy-minimization (CVFF force field) with conjugate gradient algorithm was performed with DISCOVER 95.0 of MSI (1995) on a Silicon Graphics INDY workstation.

## References

1 *Nucleotide Analogues as Antiviral Agents*, ed. J. C. Martin, American Chemical Society, Washington, D.C., 1989.

2 D. M. Rudkevich, Z. Brzozka, M. Palys, H. C. Visser, W. Verboom and D. N. Reinhoudt, *Angew. Chem., Int. Ed. Engl.*, 1994, **33**, 467; M. W.Hosseini, A. J. Blacker and J.-M. Lehn, *J. Am. Chem. Soc.*, 1990, **112**, 3896; V. Jubian, R. P. Dixon and A. D. Hamilton, *J. Am. Chem. Soc.*, 1992, **114**, 1120; G. Deslongchamps, J. Rebek, A. Galan and J. de Mendoza, *Angew. Chem., Int. Ed. Engl.*, 1994, **33**, 467; B. L. Iverson, K. Shreder, V. Kral and J. L. Sessler, *J. Am. Chem. Soc.*, 1993, **115**, 11 022; F. P. Schmidtchen, *Tetrahedron Lett.*, 1989, **30**, 4493; S. Nishizawa, P. Buhlmann, M. Iwao and Y. Umezawa, *Tetrahedron Lett.*, 1995, **36**, 6483.

3 (*a*) I. Tabushi, Y. Kobuke and J.-i. Imuta, *J. Am. Chem. Soc.*, 1980, **102**, 1744; (*b*) I. Tabushi, Y. Kobuke and J.-i. Imuta, *J. Am. Chem. Soc.*, 1981, **103**, 6152; (*c*) K. Maruyama, H. Tsukube and T. Araki, *J. Am. Chem. Soc.*, 1982, **104**, 3197; (*d*) H. Furuta, M. J. Cyr and J. L. Sessler, *J. Am. Chem. Soc.*, 1991, **113**, 6677; (*e*) V. Kral, J. L. Sessler and H. Furuta, *J. Am. Chem. Soc.*, 1992, **114**, 8704; (*f*) F. Diederich and T. Li, *J. Org. Chem.*, 1992, **57**, 3449; (*g*) T. Li, S. J. Krasne, B. Persson, H. R. Kaback and F. Diederich, *J. Org. Chem.*, 1993, **58**, 380; (*h*) J. L. Sessler, H. Furuta and V. Kral, *Supramol. Chem.*, 1993, **1**, 209 and references cited therein; (*i*) V. Kral and J. L. Sessler, *Tetrahedron*, 1995, **51**, 539; (*j*) C. Andreu, A. Galan, K. Kobiro, J. de Mendoza, T. K. Park, J. Rebek, A. Salmeron and N. Usman, *J. Am. Chem. Soc.*, 1994, **116**, 5501; (*k*) K. Yasuhisa, H. Hatekayama, H. Seshimo and H. Ogoshi, *Supramol. Chem.*, 1994, **3**, 267.

4 S. B. Lee, H. Choo and J.-I. Hong, details will be published elsewhere.

5 J.-P. Behr and J.-M. Lehn, *J. Am. Chem. Soc.*, 1973, **95**, 6108; H. Tsukube, *J. Chem. Soc., Perkin Trans. 1*, 1983, 29.

6 H. Furuta, T. Morishima, V. Kral and J. L. Sessler, *Supramol. Chem.*, 1993, **3**, 5.

*Received in Cambridge, UK, 23rd January 1997; Com. 7/00527J*

# Regioselective oxyfunctionalization of peptides by dimethyldioxirane: tertiary C–H σ-bond oxygen atom insertion into leucine derivatives and leucine-containing dipeptides

**Maurizio Mezzetti, Enrico Mincione* and Raffaele Saladino*†**

*Dipartimento Agrochimico Agrobiologico, Università degli studi di Viterbo 'La Tuscia', via San Camillo de Lellis, 01100 Viterbo, Italy*

**A simple and straightforward approach to selective C–H σ-bond oxygen atom insertion into Leu residues on peptides using dimethyldioxirane is described; this procedure is compatible with Gly, Ala, Val, Ile and Phe residues.**

Proteins with altered functions can be prepared from existing molecules by genetic manipulations[1] or, particularly in the case of small peptides, by chemical methods, *via* side-chain alteration and backbone modifications. Several chemical methods for performing side-chain alterations have been reported. The tryptophan side-chain is efficiently transformed by $Ru^{VIII}$, generated *in situ* from $RuCl_3$ and $NaIO_4$, to that of aspartic acid.[2] A $Ru^{VIII}$ reagent has subsequently been used to oxidize 13 to the 20 coded α-amino acids[3] and for a novel protein backbone modification by C(α)–C side-chain scission.[4] Moreover, selective modification of serine- and threonine-containing peptides has been accomplished with lead tetraacetate to give α-acyloxyglycine derivatives, which can be easily transformed into α-alkylthio- and α-halogeno-glycines.[5] Recently, a simple approach to selective iodination of tyrosine residues on peptides using $IPy_2BF_4$ (Py = pyridine) has been described,[6] and preliminary studies revealed that the method might be also suitable for iodination of phenylalanine derivatives.

In spite of extensive work on side-chain transformations of aromatic, heterocyclic and heteroatom moieties in peptides, no general methods have been described for oxygen atom insertion into the C–H σ-bond present in the side-chain of α-amino acids, with the exception of the glycine-selective chemical modification by Nickel peroxide,[7] in which case a concomitant backbone modification was observed, probably because of the low reactivity generally shown by this bond.

A powerful and selective oxidant for this purpose,[8] which performs under strictly neutral conditions, is dimethyldioxirane (DMD). The advantages of dioxiranes, especially DMD, in synthetic chemistry have been well documented in alkene epoxidations, heteroatom oxidations and C–H σ-bond insertions. To the best of our knowledge, DMD has been used in the chemistry of α-amino acids and peptides to perform the oxidation of α-diazo ketones derived from α-amino acids,[9] and in the synthesis of enantiomerically pure N-protected β-amino-α-keto esters from α-amino acids and dipeptides.[10] In each case, the possible oxygen atom insertion into the side-chain was not observed. We report here a simple, selective and straightforward approach to the C–H σ-bond oxygen atom insertion into Leucine (Leu) and Leu-containing dipeptides.

The oxidation of Boc-Leu-OMe **1** (1 mmol) performed with a freshly prepared solution of DMD (0.09 mol $dm^{-3}$ acetone solution, 6.0 equiv.)[11] in $CH_2Cl_2$ (5 $cm^3$) at 25 °C for 3 days afforded the 4,4-dimethyl-4-butanolide derivative **2** as the only recovered product in 42% isolated yield (Scheme 1),‡ with some unreacted substrate. Compound **2** is probably formed by selective oxygen atom insertion into the tertiary C–H σ-bond of Leu followed by cyclization.

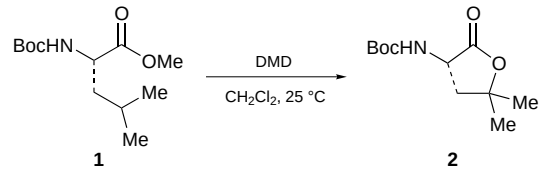
Some other protected α-amino acids bearing an alkyl side-chain (Boc-Gly-OMe, Boc-Ala-OMe, Boc-Val-OMe, Boc-Ile-OMe and Boc-Phe-OMe) were then studied. The reactions performed with DMD (0.09 mol $dm^{-3}$ acetone solution) in $CH_2Cl_2$ (5 $cm^3$) at 25 °C for 3 days did not give products in appreciable amounts, even in the presence of a large excess of DMD and after longer reaction times.

It is known that the DMD oxygen atom insertion into the C–H σ-bond shows a pronounced tertiary–secondary–primary selectivity.[8] Furthermore, this transformation is extremely sensitive to solvent[12] and stereoelectronic effects. In particular, a dipolar group close to the reactive centre may influence the reaction, favouring a chemo- and stereo-specific attack,[13] or preventing the oxidation.[14]

We can put forward only hypotheses to explain the unexpected stability of the valine substrate in the DMD oxidation. A rationalization based on simple electronic deactivation by the amino functionality on the more proximate tertiary C–H σ-bond with respect to leucine seems reasonable. This hypothesis is in accord with the recently reported procedure[15] for the selective oxyfunctionalization of unactivated C–H σ-bonds of alkylamines in acid medium by methyl(trifluoromethyl)dioxirane, in which the strong electron-withdrawing nature of the ammonium group deactivates the oxidation of even tertiary C–H σ-bonds at the α and β positions. In our case, the reaction appears to be operative only when a tertiary C–H σ-bond is in the remote C(γ) position with respect to the amino acid functionality.

The feasibility of transformation of **1** by DMD with respect to the other α-amino acids bearing an alkyl side-chain promped us to evaluate the possibility to obtain a chemo- and regio-selective modification of Leu-containing dipeptides. The oxidation of Boc-Ala-Leu-OMe **3** and Boc-Leu-Ala-OEt **5** with an excess of DMD in $CH_2Cl_2$ (5 $cm^3$) at 25 °C for 3 days afforded the butanolide derivate **4**§ and the peptide derivative 6¶ in 35 and 38% isolated yield, respectively, plus some unreacted substrates (Scheme 2). Compound **4**, which is obtained by selective modification of the Leu residue, may be formed by selective oxygen atom insertion into the tertiary bond present in the side-chain of Leu, followed by cyclization. On the other hand, the presence of a free alcoholic moiety in **6** (as shown by the OH group absorption at 3390 $cm^{-1}$ in the IR spectrum) suggests that, in this case, a spontaneous cyclization process is not operative. This hypothesis was further confirmed by the absence of a detectable amount of the butanolide derivative **2** in the reaction mixture.

Finally, we studied the oxidation of the dipeptide Boc-Leu-Leu-OMe **7** by DMD under similar experimental conditions.[16]




**1** **2**

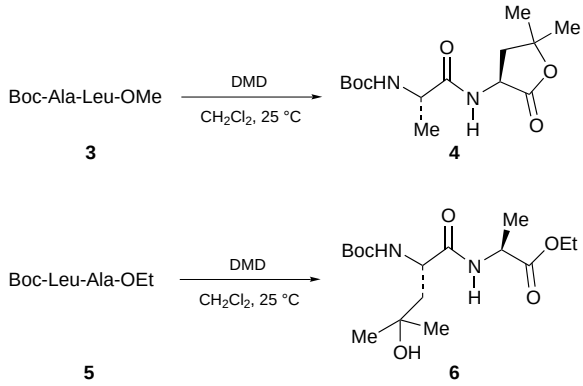
**Scheme 1**

The oxidation of **7** with DMD (0.09 mol $dm^{-3}$ acetone solution, 6.0 equiv.) in $CH_2Cl_2$ (5 $cm^3$) at 25 °C for 3 days afforded the butanolide derivative **8** in 33% isolated yield (Scheme 3).‖ Minor amounts of **9** were also formed, as shown by $^1H$ and $^{13}C$ NMR spectral analyses of the crude reaction mixture prior to purification.

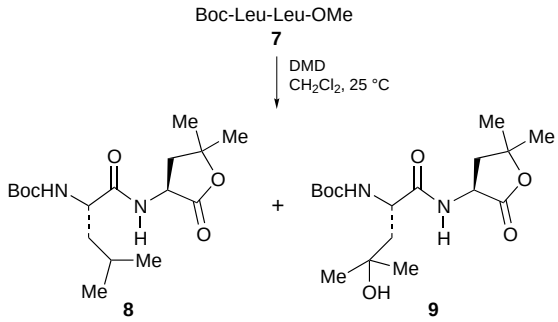
These data show that the reactivity of the Leu residue towards DMD is extremely sensitive to the position (C/N-terminal position) of the residue into the peptide. In particular, C-terminal Leu appears to be more reactive than the N-terminal residue towards DMD. In this case, steric factors may operate, since dioxiranes are generally sensitive to steric hinderance,[8] even if electronic deactivation by the two amino acid functionalities of the Leu N-terminal residue cannot be ruled out.

The high selectivity observed for the Cγ–H σ-bond of Leu towards DMD offers a novel synthetic route to modified peptides without backbone modifications. Work is in progress in our laboratories to study the reactivity pattern of the other coded α-amino acids towards DMD oxidation, as well as to transform the newly introduced hydroxy moieties into other useful functionalities.

Financial support from Italian MURST is acknowledged.




**Scheme 2**




**Scheme 3**

## Footnotes

† E-mail: saladino@unitus.it

‡ Compound **2** was purified by flash-chromatography. MS analysis for **2** (ESI-MS) shows *m/z* 229 $[M]^+$, in agreement with the proposed structure.

§ Compound **4** was purified by flash-chromatography. MS analysis for **4** (ESI-MS) shows *m/z* 299 $[M + H]^+$, in agreement with the proposed structure.

¶ Compound **6** was purified by flash-chromatography. MS analysis for **6** (ESI-MS) shows *m/z* 334 $[M]^+$, in agreement with the proposed structure.

‖ Compound **8** was purified by flash-chromatography. MS analysis for **8** (ESI-MS) shows *m/z* 330 $[M]^+$, in agreement with the proposed structure.

## References

1 M. Mutter, *Angew. Chem., Int. Ed. Engl.*, 1985, **24**, 639; M. Mutter and S. Vuilleumier, *Angew. Chem., Int. Ed. Engl.*, 1989, **28**, 535.
2 S. Ranganathan, D. Ranganathan and D. Bhattacharyya, *J. Chem. Soc., Chem. Commun.*, 1987, 1085.
3 S. Ranganathan, D. Ranganathan, D. Bhattacharyya, S. Bamezai, W. P. Singh, G. P. Battacharyya, G. P. Singh, R. K. Rathi, S. Saini, N. Jayaraman and B. K. Patel, *Pure Appl. Chem.*, 1990, **62**, 1433; S. Ranganathan, D. Ranganathan and D. Bhattacharyya, *Tetrahedron Lett.*, 1991, **32**, 5616.
4 D. Ranganathan, N. K. Vaish and K. J. Shah, *J. Am. Chem. Soc.*, 1994, **116**, 6545.
5 G. Apitz and W. Steglich, *Tetrahedron Lett.*, 1991, **27**, 3163.
6 J. Barlunga, M. A. Garcìa-Martin, J. M. Gonzàles, P. Clapés and G. Valencia, *Chem. Commun.*, 1996, 1505.
7 C. J. Easton, S. K. Eichinger and M. J. Pitt, *J. Chem. Soc., Chem. Commun.*, 1992, 1295.
8 W. Adam, R. Curci and J. O. Edwards, *Acc. Chem. Res.*, 1989, **22**, 205; R. Curci, in *Advances in Oxygenated Processes*, ed. A. L. Baumstark, JAI Press, Grenwhich, CT, 1990, vol. 2.
9 W. Adam and L. P. Hadjiarapoglou, *Top. Curr. Chem.*, 1993, **164**, 45.
10 P. Darkins, N. McCarthy, T. McKervey and T. Ye, *J. Chem. Soc., Chem. Commun.*, 1993, 1222.
11 W. Adam, J. Bialas and L. P. Hadjiarapoglou, *Chem. Ber.*, 1991, **124**, 2377.
12 R. W. Murray and D. Gu, *J. Chem. Soc., Perkin Trans. 2*, 1994, 451.
13 R. Ballini, F. Papa and P. Bovicelli, *Tetrahedron Lett.*, 1996, **37**, 3507 and references cited therein.
14 P. Bovicelli, P. Lupattelli, E. Mincione and V. Fiorini, *Tetrahedron Lett.*, 1993, **34**, 6103.
15 G. Asensio, M. E., Gonzales-Nùnez, C. B. Bernardini, R. Mello and W. Adam, *J. Am. Chem. Soc.*, 1993, **115**, 7250.
16 Recently, Rosner and co-workers reported the importance of the dileucine motifs in biological systems. In particular, dileucine motifs have been implicated in the internalization of degradation of many membrane proteins: P. Morrison, K. C. Chung and M. R. Rosner, *Biochemistry*, 1996, **35**, 14 618.

*Received in Liverpool, UK, 10th March 1997; Com. 7/01650F*

# New pyridine dithiols: synthesis and structures of complexes with acids

**Bartjan Koning,[a]† Ron Hulst,[a] Arjan Bouter,[a] Jan Buter,[a] Auke Meetsma[b] and Richard M. Kellogg*[a]**

[a] *Department of Organic and Molecular Inorganic Chemistry, University of Groningen, Nijenborgh 4, Groningen 9747 AG, The Netherlands*

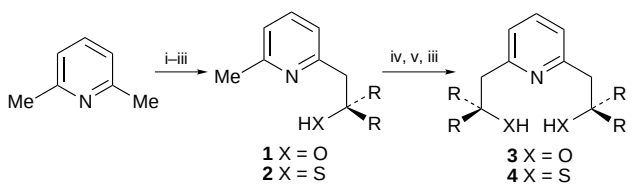
[b] *Crystal Structure Centre, University of Groningen, Nijenborgh 4, Groningen 9747 AG, The Netherlands*

**Pyridine dithiols have been synthesized by base-induced addition of 2,6-lutidine to (non-enolisable) thioketones, and have been found to encapsulate various acids.**

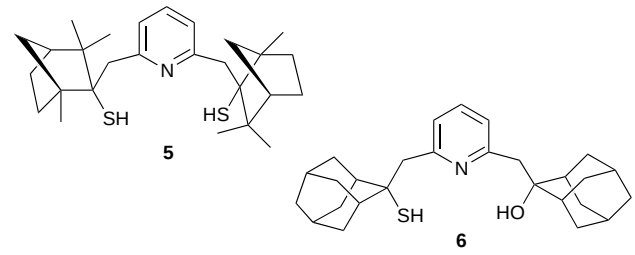
The addition products ('pyridine diols' **3**, Scheme 1) of 2 equiv. of ketone with 2,6-dimethylpyridine (2,6-lutidine) are tridentate ligands capable of encapsulating metal ions or acids.[1] Extensive structural variation is possible: benzophenone, fluorenone, acetone, acetophenone, adamantanone, fenchone and camphor are examples of ketones that have been used.[1d,2] Replacement of 2,6-lutidine by 2,9-dimethylphenanthroline leads to tetradentate ligands.[3] As an example of the opportunities for encapsulation of acids, we have described the crystal structure of the HCl complex of **3** whereby adamantanone was used as ketone.[3] The host organizes itself so that the acid is perfectly enclosed in a cavity wherein Cl is hydrogen bonded to the two hydroxy groups and the proton of HCl is directed towards the pyridine nitrogen.

We find that the approach of Scheme 1 can be extended to the preparation of certain 'pyridine dithiols' **4**. This method is more straightforward and efficient (overall yields 65–70%) than the multi-step synthesis of pyridine dithiols that has been reported previously and which is limited to thiols with relatively acidic α-protons.[1a–d] No products derived from addition of the carbanion to the sulfur of the thioketone have been isolated.[4] The two step addition shown leads to far better yields than either a single step approach involving direct deprotonation of 2,6-lutidine with 2 equiv. $Bu^nLi$ followed by addition of 2 equiv. thioketone or a two step, one pot approach in which the mono-adduct is not isolated. An additional advantage of this approach is that the 'single-armed' derivative **2** (or **1**) can be obtained and studied separately. The bis-lithium salt of **4a** ($–CR_2–$ = adamantane-2,2-diyl) is remarkably stable, as was confirmed by means of $^7Li$ NMR spectroscopy, and is completely converted to the dithiol only after stirring for several hours with 5 M HCl. The pyridine dithiols can be handled without special precautions except that exposure to air should be limited to prevent oxidation.

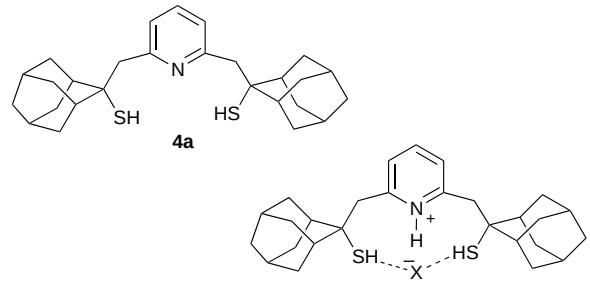
The $C_2$ symmetrical double condensation product **5** obtained from optically pure (*R*)-thiofenchone can also be prepared; the crystal structure (not shown) confirms addition from the *exo* side of thiofenchone. Thiocamphor fails to undergo addition owing to formation of the thioenolate; competitive enolate formation appears to be a limitation to the direct approach of Scheme 1 when thioketones are used. The mixed adduct **6** can be prepared by lithiation of the 'single-armed' derivative **1** followed by a quench with 1 equiv. of thioadamantanone.




**Scheme 1** *Reagents and conditions*: i, $Bu^nLi$ (1.1 equiv.), THF, −80°C; ii, −80 °C → −40 °C; iii, $R_2C{=}X$; iv, $Bu^nLi$ (1.2 equiv.), THF, −80 °C; v, −80 °C → −50 °C




The complexation behaviour of **4a** has been studied extensively; other pyridine dithiols appear to behave in a related fashion. Treatment of **4a** with 1 equiv. HCl or HBr (titrated saturated $CH_2Cl_2$ solutions) leads to the air- and moisture-stable complexes **4a**·HCl and **4a**·HBr in quantitative yields. On addition of 1 equiv. of aqueous $HNO_3$ to **4a** in $CHCl_3$ at 0 °C, **4a**·$HNO_3$ is obtained; on complexation at ambient temperature, however, the thiol groups are partly oxidized. Attempted encapsulation of phosphonic acids failed.




Complexation with $ZnCl_2$ in MeOH provides the dimer [**4a**·$ZnCl_2$·MeOH]$_2$, whereas complexation of $Zn(NO_3)_2·4H_2O$ affords a monomeric and unstable **4a**·$Zn(NO_3)_2$ complex

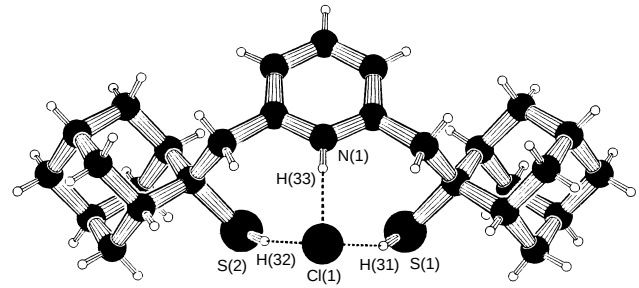



**Fig. 1** The molecular structure of **4a**·HCl. Selected distances (Å) and angles (°): H(31)–Cl 2.58(3), H(32)–Cl 2.45(5), H(33)–Cl 2.19(3), N–H(33) 0.86(3), N–Cl 3.056(2), S(1)–H(31)–Cl 162(3), S(2)–H(32)–Cl 168(3), N–H(33)–Cl 178(3).

(characterized spectroscopically), which in MeOH or MeCN is slowly converted to the **4a**·$HNO_3$ complex.‡ These structures are not shown for reasons of space.

Crystal structures of all complexes except those with HBr and $Zn(NO_3)_2$ have been determined. Those of **4a**·HCl§ (Fig. 1) and **4a**·$HNO_3$ (Fig. 2)§ are shown, and for purposes of illustration some salient features of the former are briefly mentioned.

Monomeric HCl is firmly embedded in a cavity and held in place by bonding to pyridine nitrogen and the two thiols. The free pyridine dithiol **4a** (structure not illustrated) is not preorganized in this arrangement. In the complex the thiol groups are clearly hydrogen bonded to the chloride, although the bonds are of unequal length [H(31)··Cl(1) 2.58(3), H(32)··Cl(1) 2.45(5) Å], probably as a result of crystal packing effects. The thiol groups bond from the same face (roughly a plane of symmetry in the complex) whereas in the corresponding pyridine diol complex, the hydroxy groups hydrogen bond to chloride from opposite faces (approximate $C_2$ molecular symmetry, an analogous arrangement is seen in the structure of **4a**·$HNO_3$ shown in Fig. 2).[3a] The H··Cl bond distance in **4a**·HCl is 2.19 Å, which is 0.92 Å longer than the covalent HCl bond length in the gas phase (1.27 Å).[5] A search of the Cambridge Database for pyridine··HCl complexes revealed an average bond length for the H··Cl bond distance of 2.20 Å with a deviation of 0.17 Å for 39 hits. For this screening a minimum N··H··Cl bond angle of 120° was included.

In the $^1$H NMR spectrum of **4a**·HCl (in $CDCl_3$) downfield shifts are seen at the 3- and 4-positions of the pyridine ring comparable in magnitude to those observed for the complex of 2,6-lutidine with HCl. We concluded that the NMR and bond length data are consistent with the tight ion pair (formulation **A**) rather than the covalent formulation **B**.¶

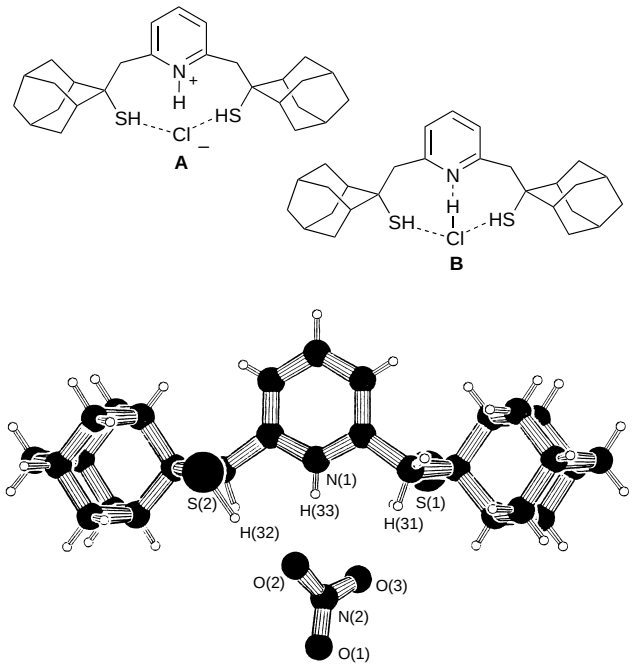



**Fig. 2** The molecular structure of **4a**·$HNO_3$. Selected distances (Å) and angles (°): H(31)–O(3) 2.21(5), H(32)–O(2) 2.26(5), H(33)–O(2) 1.92(5), H(33)–O(3) 2.58(5), H(33)–N(1) 0.87(5), N(1)–O(2) 2.762(6), S(1)–H(31)–O(3) 160(3), S(2)–H(32)–O(2) 156(3), N(1)–H(33)–O(2) 162(5), N(1)–H(33)–O(3) 143(4).

In summary, pyridine dithiols can be obtained from direct addition of 2,6-lutidine to (non-enolisable) thioketones in the presence of a strong base. These pyridine dithiols provide a well-defined cavity, perhaps even better than the pyridine diols, in which various acids are encapsulated by three point bonding. We are examining methods to transfer these complexed acids from chiral nonracemic pyridine dithiols such as **5** to suitable acceptors such as prochiral epoxides.

## Footnotes

* E-mail: r.m.kellogg@chem.rug.nl

† B. Koning is partially supported by a grant from the Dutch National Science Foundation (NWO) administered through the Office for Chemical Research (SON).

‡ Unless otherwise mentioned, satisfactory elemental analyses and/or X-ray structure analyses were obtained for all new compounds. $^1$H NMR and infrared (IR) spectra were in accord with expectations for all compounds.

§ Atomic coordinates, bond lengths and angles, and thermal parameters have been deposited at the Cambridge Crystallographic Data Centre (CCDC). See Information for Authors, Issue No. 1. Any request to the CCDC for this material should quote the full literature citation and the reference number 182/449.

¶ Formulation **B** is mentioned because of puzzling physical properties and observations in the infrared (IR) spectra. Upon exposure of the solid to low pressure we observed that the HCl evaporates. This is not observed for other complexes, for example 2,6-lutidine·HCl. IR spectra of **4a**·HCl in KBr are complicated by the fact that the HCl absorptions are hidden under the strong adamantyl C–H bands. This led us to the study of the DCl complex. In some cases the **4a**·DCl complex shows a sharp absorption at 2211 $cm^{-1}$, which is partially masked by a broad pyridine–$D^+$ absorption in the region 2212–1850 $cm^{-1}$. The 2211 $cm^{-1}$ absorption is close to that expected for *covalent* D–Cl. For example, values of 2091 and 2090 $cm^{-1}$ for monomeric DCl in, respectively, the gas phase[6a] and in an Ar matrix[6b] are given in the recent literature. The $^1$H NMR spectra as well as the IR spectra indicate clearly that D–Cl has not exchanged with S–H (attempts to prepare the S–D derivative of **4a** have been unsuccessful owing to the failure of the S–H groups to exchange with D at a measurable rate either in free **4a** or in the D–Cl complex). The 2211 $cm^{-1}$ absorption is not observed in the D–Cl complex with 2,6-lutidine.

## References

1 (*a*) J. M. Berg and R. H. Holm, *J. Am. Chem. Soc.*, 1985, **107**, 917; (*b*) R. H. Holm and J. M. Berg, *Acc. Chem. Res.*, 1986, **19**, 363; (*c*) B. Kaptein, L. Wang-Griffin, G. Barf and R. M. Kellogg, *J. Chem. Soc., Chem. Commun.*, 1987, 1458; (*d*) B. Kaptein, G. Barf, R. M. Kellogg and F. Van Bolhuis, *J. Org. Chem.*, 1990, **55**, 1890.

2 J. Buter and R. M. Kellogg, unpublished work.

3 (*a*) J. J. H. Edema, R. Libbers, A. M. Ridder, R. M. Kellogg, F. Van Bolhuis, H. Kooijman and A. L. Spek, *J. Chem. Soc., Chem. Commun.*, 1993, 625; see also (*b*) R. Hof and R. M. Kellogg, *J. Chem. Soc., Perkin Trans 1*, 1996, 1651.

4 P. Beak and J. W. Worley, *J. Am. Chem. Soc.*, 1972, **94**, 5970; 1970, **92**, 4142.

5 N. N. Greenwood and A. Earnshaw, *Chemistry of the Elements*, Pergamon Press, New York, 1984, p. 949.

6 (*a*) Y. P. Zeng, S. W. Sharpe, D. Reifschneider, C. Wittig and R. A. Beandet, *J. Chem. Phys.*, 1990, **93**, 183; (*b*) C. E. Truscott and B. S. Ault, *J. Phys. Chem.*, 1984, **88**, 2323.

*Received in Liverpool, UK, 13th March 1997; Com. 7/01774J*

# Introduction of bromine and chlorine substituents in medium ring ethers and lactones

**Justin G. Bendall, Andrew N. Payne, Thomas E. O. Screen and Andrew B. Holmes***

*University Chemical Laboratory, Lensfield Road, Cambridge, UK CB2 1EW*

**A convenient preparation of α-halo enamines using oxalyl halides is described together with applications of these reagents in the halogenation of β-hydroxy cyclic ethers and lactones.**

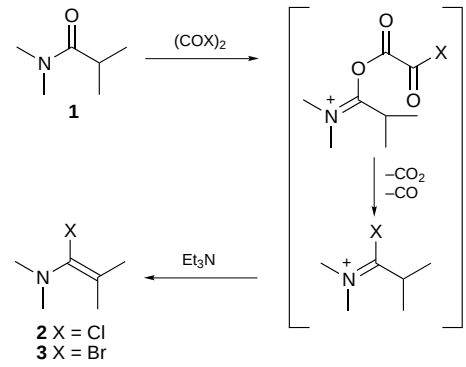
There has recently been considerable interest in the synthesis of medium ring ether marine natural prducts, and significant progress has been achieved both in ring expansion reactions and in the controlled cyclisation of acyclic precursors.[1] Of all the features present in the various *Laurencia* and related cyclic ether metabolites which have been isolated from red algae the β-halo ether substituent is probably the most challenging. In connection with our own studies towards the synthesis of medium ring marine natural products[2–4] we required a method for the stereospecific introduction of chlorine and bromine β to the ring oxygen. The most common way to achieve this so far has been displacement of hydroxy group using a phosphorus activating reagent,[5] a xanthate,[6] or a metal-mediated epoxide opening.[7] Alternatively, the halogen can be present before ring closure as in the radical cyclisations employed by Lee.[8] The β-ring oxygen can suppress nucleophilic displacement of a leaving group substantially,[9] and can potentially promote oxonium ion formation and rearrangement.[10] Here we report the use of α-halo enamine reagents to effect halide introduction by substitution reactions.

An α-halo enamine reagent was initially introduced by Speziale,[11] who prepared *N*,*N*-diethyltrichlorovinylamine and showed subsequently that it could be used to transform alcohols into alkyl chlorides with stereochemical inversion.[12] The more reactive 1-chloro-*N*,*N*,2-trimethylpropenamine **2** was later developed by Ghosez[13,14] who demonstrated conversion of carboxylic acids into acid halides.[15] We subsequently used this reagent for the first time with allylic alcohols and showed that it could be used to introduce an allylic chloro substituent into the side chain of the *cis*-maneonenes isolated from *Laurencia nidifica*.[16] Further examples have subsequently been reported by Ghosez to prepare simple alkyl halides,[17] and there are examples of steroid halogenation in the patent literature.[18] Despite having the advantage that they can be used under essentially neutral conditions these reagents have received little attention from organic chemists, possibly owing to the need to use liquid phosgene to prepare the α-chloro enamine **2**, and a subsequent bromide displacement reaction to convert **2** into the α-bromo enamine **3**.[14] In the present work, it has been found that the amide **1** reacts with oxalyl chloride or oxalyl bromide followed by treatment with triethylamine to furnish the respective α-halo enamines **2** and **3**† (Scheme 1).

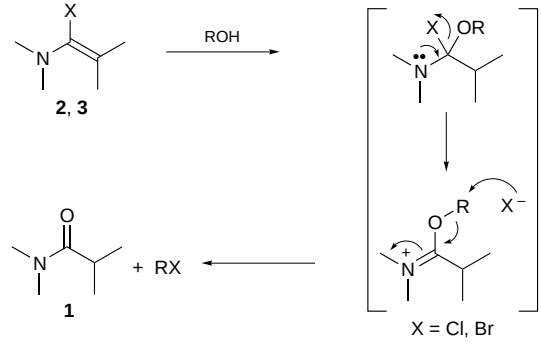
The reagents **2** and **3** smoothly converted alcohols into alkyl halides in $CH_2Cl_2$ at room temperature (Scheme 2). The displacement was shown to take place with inversion of configuration as illustrated (Table 1, entry 1) for the conversion of (−)-menthol into (+)-neomenthyl halides.[17] A trace of alkene elimination product (*ca.* 5%) was also detected. This could be suppressed by performing the reactions at −78 °C.

The successful halogenation of β-hydroxy cyclic ethers was initially demonstrated (Table 1, entry 2) using 3-hydroxytetrahydrofuran. β-Hydroxy 9- and 10-membered lactones[19] were halogenated readily, and the stereochemical inversion was confirmed by comparison of the $^1$H NMR difference NOE spectra of **13** and **15**.‡ In the chloro compound **15** a large (11%) NOE was observed between the signals due to H-8 (δ 4.46, dt, *J* 9, 4, 4 Hz) and H-9 (δ 4.95–5.05, m), but no NOE was observed between the signals due to H-8 and H-9 in the alcohol **13**. The hydroxy-substituted 8-membered lactones **19**[20] and 9-membered cyclic ethers **21**[4] proved more problematical, and underwent either isobutyryl esterification or decomposition, resulting in low yields of halides. By changing the solvent to a mixture (1 : 1) of propylene oxide and $CH_2Cl_2$ the decomposition was suppressed, although the reaction rate was much slower, and the reaction was generally conducted at room temperature. Incorporation of dried 4 Å molecular sieves prevented esterification.§ The reaction was also used to prepare the (*E*)-pentenynyl bromide **25** from the alcohol **24**, which gave poor yields of bromide using other methods (Table 1, entry 8).

In summary, an exceptionally mild method of preparing the α-halo enamine reagents **2** and **3** has been described. These versatile reagents are effective in converting hydroxy compounds into the corresponding halo compounds under mild conditions, even under circumstances where rate suppression occurs due to the β-oxygen effect. Applications in the synthesis of halogenated medium ring ether natural products can be expected to follow.

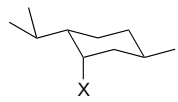
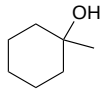
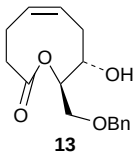
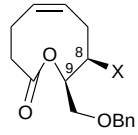
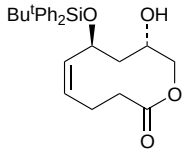
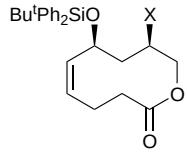
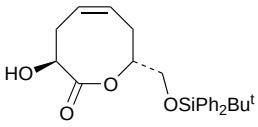
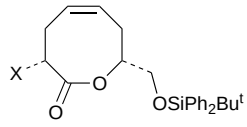
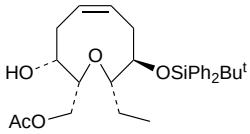
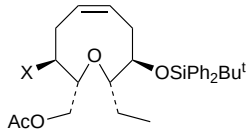
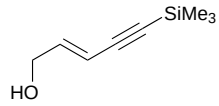
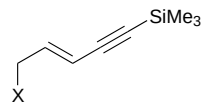



**Scheme 1**




**Scheme 2**

**Table 1** Halogenation of alcohols using α-halo enamines

| Entry | Alcohol | Alkyl halide |
|---|---|---|
| 1 |  **4** |  **5** X = Br 97%[a]<br>**6** X = Cl 84% |
| 2 |  **7** |  **8** X = Br 70%<br>**9** X = Cl 56% |
| 3 |  **10** |  **11** X = Br 67%<br>**12** X = Cl 0% |
| 4 |  **13** |  **14** X = Br 78%<br>**15** X = Cl 81% |
| 5 |  **16** |  **17** X = Br 72%<br>**18** X = Cl 86% |
| 6 |  **19** |  **20** X = Br 42%[b] |
| 7 |  **21** |  **22** X = Br 45%[c]<br>**23** X = Cl 71% |
| 8 |  **24** |  **25** X = Br 72% |

[a] See footnote ¶. [b] 38% starting material recovered; [c] 54% starting material recovered.

We thank the EPSRC for financial support and provision of the Swansea Mass Spectrometry Service and we thank Mr K. N. Keavey for preparing the 8-membered lactone.

## Footnotes

† Preparation of α-bromo enamine **3** from oxalyl bromide. A solution of freshly distilled *N*,*N*,2-trimethylpropionamide **1** (5.0 g, 43 mmol) in dry $CH_2Cl_2$ (10 cm³) was added dropwise over 20 min to a cooled (0 °C), mechanically stirred solution of oxalyl bromide (10.0 g, 46 mmol) in dry $CH_2Cl_2$ (10 cm³), producing mild effervescence. The mixture was stirred for 2 h and was then cooled further (−78 °C). Freshly distilled dry $Et_3N$ (7.0 cm³, 50 mmol) was added dropwise to the white paste over 10 min. The mixture was warmed to room temperature, stirred for 2 h, and then filtered and distilled under vacuum to give 1-bromo-*N*,*N*,2-trimethylpropenamine **3** as a clear, moisture-sensitive liquid (4.3 g, 55%), bp 44 °C at 10 mmHg, $\rho^{20}$ 1.20 (Found: C, 40.1; H, 7.1; N, 7.9. $C_6H_{12}BrN$ requires C, 40.5; H, 6.8; N, 7.9%); $\nu_{max}$(neat)/cm$^{-1}$ 1654, 1450, 1298, 1124, 1011, 803; $\delta_H$(400 MHz, $CDCl_3$) 1.77 (6H, s, $CMe_2$), 2.28 (6H, s, $NMe_2$); $\delta_C$(100 MHz, $CDCl_3$) 21.6 ($CMe_2$), 43.7 ($NMe_2$), 126.0 (C-2), 140.4 (C-1).

‡ All new compounds provided satisfactory spectroscopic ($^1$H and $^{13}$C NMR, IR, MS) and microanalytical or high resolution MS data.

§ Representative procedure for the preparation of the bromo compound **22**. Dried 4 Å molecular sieves (100 mg) were added to a stirred solution of the alcohol **21**[4] (17 mg, 34 μmol) in $CH_2Cl_2$ (0.3 cm³) and propylene oxide (0.3 cm³) under nitrogen, which after 10 min was cooled (−78 °C). α-Bromo enamine **3** (0.05 cm³) was added and the mixture was warmed to ambient temperature and left overnight. MeOH (0.05 cm³) was added and the mixture was chromatographed on silica gel (hexanes–diethyl ether) to give the bromide **22** (8 mg, 45%) and starting material **21** (9 mg, 54%).

¶ $[\alpha]_D$ + 73 (*c* 0.83, EtOH) [lit.,[21] +59 and +58 (*c* 1.38 and 1.44 in EtOH)]. NMR data were identical to those reported.[22]

## References

1 C. J. Moody and M. J. Davies, in *Studies in Natural Product Chemistry*, ed. Atta-ur-Rahman, Elsevier, 1992, vol. 10, pp. 201–239; M. C. Elliott, *Contemp. Org. Synth*., 1994, **1**, 457; G. Rousseau, *Tetrahedron*, 1995, **51**, 2777; K. C. Nicolaou, *Angew. Chem., Int. Ed. Engl*., 1996, **35**, 589.
2 R. W. Carling, J. S. Clark and A. B. Holmes, *J. Chem. Soc., Perkin Trans. 1*, 1992, 83; R. W. Carling, J. S. Clark, A. B. Holmes and D. Sartor, *J. Chem. Soc., Perkin Trans. 1*, 1992, 95.
3 J. S. Clark and A. B. Holmes, *Tetrahedron Lett*., 1988, **29**, 4333.
4 N. R. Curtis, A. B. Holmes and M. G. Looney, *Tetrahedron Lett*., 1992, **33**, 671.
5 T. Masamune, H. Murase, H. Matsue and A. Murai, *Bull. Chem. Soc. Jpn*., 1979, **52**, 135; K. Tsushima and A. Murai, *Tetrahedron Lett*., 1992, **33**, 4345. M. Bratz, W. H. Bullock, L. E. Overman and T. Takemoto, *J. Am. Chem. Soc*., 1995, **117**, 5958.
6 A. P. Kozikowski and J. M. Lee, *Tetrahedron Lett*., 1988, **29**, 3053; *J. Org. Chem*., 1990, **55**, 863.
7 L.-X. Gao and A. Murai, *Tetrahedron Lett*., 1992, **33**, 4349.
8 E. Lee, C. M. Park and J. S. Yun, *J. Am. Chem. Soc*., 1995, **117**, 8017.
9 A. Streitwieser, *Solvolytic Displacement Reactions*, McGraw-Hill, New York, 1962, p. 113.
10 K. Fujiwara, M. Tsunashima, D. Awakura and A. Murai, *Tetrahedron Lett*., 1995, **36**, 8263.
11 A. J. Speziale and R. C. Freeman, *J. Am. Chem. Soc*., 1959, **81**, 903.
12 A. J. Speziale and R. C. Freeman, *J. Am. Chem. Soc*., 1960, **82**, 909.
13 A. Colens, M. Demuylder, B. Techy and L. Ghosez, *Nouv. J. Chem*., 1977, **1**, 369.
14 B. Haveaux, A. Dekoker, M. Rens, A. R. Sidani, J. Toye and L. Ghosez, *Org. Synth*., 1980, **59**, 26.
15 A. Devos, J. Remoin, A. M. Fisque-Hesbian, A. Colens and L. Ghosez, *J. Chem. Soc., Chem. Commun*., 1979, 1180.
16 A. B. Holmes, C. L. D. Jennings-White and D. A. Kendrick, *J. Chem. Soc., Chem. Commun*., 1983, 415.
17 F. Munyemana, A.-M. Frisque-Hesbain, A. Devos and L. Ghosez, *Tetrahedron Lett*., 1989, **30**, 3077.
18 N. P. van Vliet (N. V. Organon), ZA 7 200 618 (*Chem. Abstr*., 1973, **78**, 136532).
19 M. S. Congreve, A. B. Holmes, A. B. Hughes and M. G. Looney, *J. Am. Chem. Soc*., 1993, **115**, 5815.
20 J. W. Burton, J. S. Clark, S. Derrer, T. C. Stork, J. G. Bendall and A. B. Holmes, submitted for publication (*cf. J. Am. Chem. Soc*., 1996, **118**, 6806).
21 A. Wagner, M.-P. Heitz and C. Miokowski, *Tetrahedron Lett*., 1989, **30**, 557.
22 G. Lange and C. Gottardo, *Magn. Res. Chem*., 1990, **28**, 659.

*Received, in Cambridge, UK, 24th March 1997; Com. 7/01999H*

# Mechanistic study on *meso*-hydroxyoctaethylporphyrin formation from an $Fe^{III}(oep)–H_2O_2$ complex

**Kunihiko Tajima,*[a] Kohji Tada,[b] Masato Shigematsu,[b] Kenji Kanaori,[a] Nagao Azuma[b] and Keisuke Makino[a]**

[a] *Department of Polymer Science and Engineering, Kyoto Institute of Technology, Matsugasaki, Sakyo-ku, Kyoto 606, Japan*
[b] *Department of Chemistry, Faculty of Science, Ehime University, Matsuyama 790, Japan*

**The benzoyl ester of an iron(III) *meso*-hydroxyoctaethylporphyrin complex, containing $^{18}O$ derived from molecular oxygen, is isolated from the reaction solution of the complex $[Fe^{III}(oep)(OOH)(OH)]^-$ which is prepared by reduction of $[Fe^{II}(oep)(py)(^{18}O_2)]$ with sodium ascorbate.**

Haem enzyme–hydrogen peroxide complexes have been thought to be produced by the following two reactions: (*i*) coordination of hydrogen peroxide to the haem chromophore of enzymes, such as peroxides[1] and catalases,[2] (*ii*) one-electron reduction of the iron(II) oxygen complex of haem oxygenase[3] and P450.[4] We have reported the formation of the six coordinate $[Fe^{III}(oep)(OOH)(OH)]^-$ complex by reaction between hydrogen peroxide and $[Fe^{III}(oep)Cl]$.[5] In addition, the complex was similarly produced by reduction of the $Fe^{II}(oep)–O_2$ adduct with sodium ascorbate.[5] In the latter reaction system, the hydrogen peroxide complex was readily converted to octaethylverdohaem[6] at −30 °C. However, the possible transient intermediate species involved in the reaction pathway was still uncertain.[7] Here, the chemical reactivity of the hydrogen peroxide complex was studied by focusing upon formation of *meso*-hydroxy-oep derivatives, by means of EPR, optical absorption and product analysis using $^{18}O_2$.

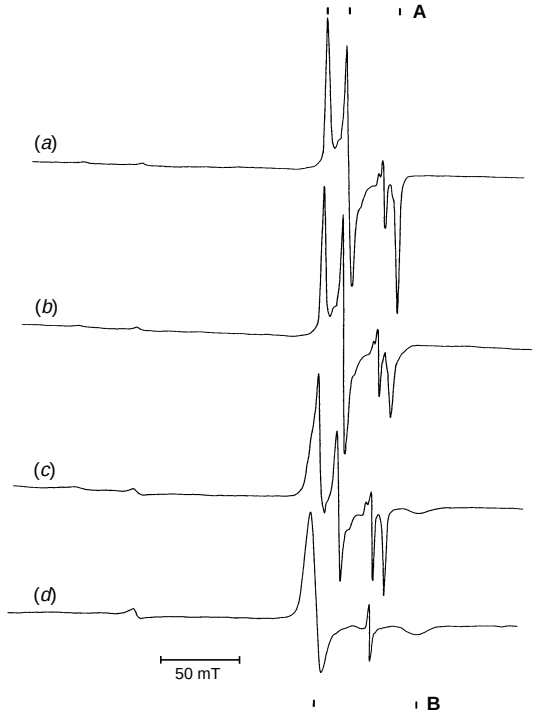



**Fig. 1** (*a*) EPR spectrum observed at 77 K for the reaction solution containing $[Fe^{III}(oep)(OH)(OOH)]^-$; (*b*) with $^{17}O_2$ (39% enrichment); (*c*) after standing a solution of (*a*) for 30 min at −50 °C, and (*d*) after 60 min at −50 °C. The signal detected in the free-spin region is ascribed to the ascorbic acid radical.

A reaction solution containing $[Fe^{III}(oep)(OOH)(OH)]^-$ was prepared in a quartz EPR tube (5.0 mm diameter), by addition of aqueous sodium ascorbate (0.5 M, 0.016 ml) to a pre-cooled (−40 °C) dmf–pyridine (py) (9 : 1) solution of $[Fe^{III}(oep)Cl]$ (1.0 mM, 0.4 ml). After 3 min of continuous oxygen bubbling in the reaction mixture, the solution was frozen at −78 °C, and the atmosphere of the sample tube was changed to nitrogen. Then the sample was immediately frozen to 77 K. EPR signals [Fig. 1(*a*)] due to an iron(III) low-spin species (**A**; $g_1$ = 2.287, $g_2$ = 2.176, $g_3$ = 1.956) were clearly recorded, and the *g*-values agreed well with previous results[5] (Table 1). Fig. 1(*b*) show that a similar EPR spectrum was successfully detected using $^{17}O_2$ (39% enrichment), with the linewidth of the $g_3$ component broadened by unresolved splitting due to $^{17}O$ ($I$ = 5/2).[8] This demonstrates the fact that the peroxide anion, ligated axially in **A**, was derived from atmospheric oxygen.

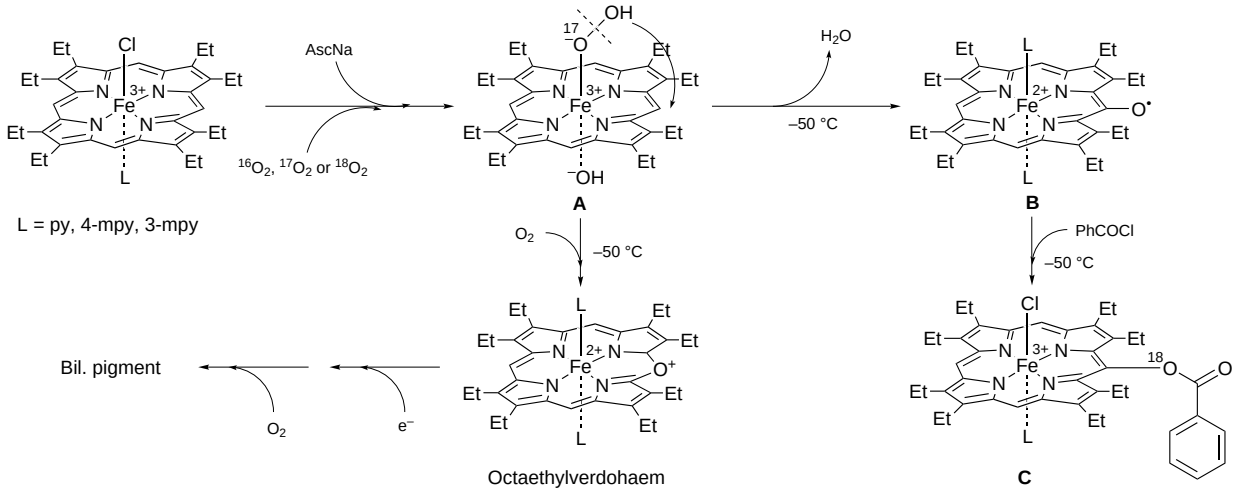
Quantitative EPR analysis was performed by means of graphic integration, using an ESPRIT ESR data analyser (JEOL). In the present case, the EPR spectrum recorded for a dmf solution of $[Cu^{II}(tpp)]$ ($S$ = 1/2) was employed as a standard to calibrate the integrated EPR signal intensity of **A**. The concentration of **A** was evaluated to be *ca*. 0.8 mM. By using the dmf solution of $[Fe^{III}(oep)Cl]$ as the standard, the total concentration of observed iron(III) high-spin species ($g$ = 6, 4.3) arising from remaining $[Fe^{III}(oep)Cl]$ and a decomposed tetrapyrrole iron complex,[8] was also estimated to be *ca*. 0.1–0.15 mM. Therefore the maximum percentage of **A** in the fresh frozen mixture was confirmed to be *ca*. 80% of the initial concentration of $[Fe^{III}(oep)Cl]$.

On standing the reaction solution at −50 °C for 30 min, new EPR signals ($g_\perp$ = 2.3, $g_\parallel$ = 1.8) began to merge with that of complex **A**, as shown in Fig. 1(*c*). After 60 min, signals due to

**Table 1** EPR parameters at 77 K of $Fe^{III}(oep)–H_2O_2$ and *meso*-hydroxy complexes[a]

| Complex | Ligand | EPR parameters | | |
|---|---|---|---|---|
| | | $g_1$ | $g_2$ | $g_3$ |
| **A** | py | 2.287 | 2.176 | 1.956 |
| | py[b] | 2.269 | 2.162 | 1.961 |
| | py[c] | 2.269 | 2.162 | 1.961 |
| | OH[c,d,e] | 2.286 | 2.171 | 1.953 |
| | 4-mpy | 2.291 | 2.174 | 1.957 |
| | 3-mpy | 2.29 | 2.17 | 1.95 |
| | 2-mpy | Not detected | | |
| | 2,6-dmpy | Not detected | | |
| **B** | py | 2.290 | 1.805[f] | |
| | py[g] | 2.31 | 1.87[f] | |
| | 4-mpy | 2.310 | 1.768[f] | |
| | 3-mpy | 2.310 | 1.778[f] | |
| | 2-mpy | Not detected | | |
| | 2,6-dmpy | Not detected | | |

[a] Reductant is sodium ascorbate unless indicated otherwise. [b] Prepared under $^{17}O_2$ (39% enrichment). [c] Ref. 5. [d] No reductant. [e] $H_2O_2$ added. [f] Axial symmetry $g_1 = g_\perp$, $g_2 = g_\parallel$. [g] Ref. 6.




**Scheme 1** Possible reaction mechanisms for the formation of *meso*-hydroxy-oep *via* $[Fe^{III}(oep)(OH)(OOH)]^-$

the new species (denoted **B**; $g_\perp$ = 2.290, $g_\parallel$ = 1.805) was exclusively observed [Fig. 1(*d*)], while those of **A** completely disappeared. **A** was unstable under oxygen, and immediately changed to a green diamagnetic species (388, 493, 527 and 650 nm), after oxygen gas bubbling into the solution at −50 °C. The resulting species was isolated and identified as bis(pyridine)(octaethylverdohaem) iron(II),[9] from its NMR, and optical absorption parameters. This observation indicates that **B** is one of the intermediate species in the process of verdohaem derivative formation from **A**.

Similar EPR measurements were performed using methylated pyridine derivatives, 2-, 3-, 4-mpy, and 2,6-dmpy, in order to clarify the role of **A** in the process of verdohaem formation. Similar EPR spectra to **A** were recorded for the reaction systems composed of 3- and 4-mpy, and the observed EPR parameters agreed well to those of **A** (Table 1). Furthermore, the EPR signal of **B** was clearly detected with 3- and 4-mpy instead of py, and the observed *g*-values agreed with each other, although formation of **A** and **B** was not detected using 2-mpy or 2,6-dmpy. EPR signals of $[Fe^{III}(oep)Cl]$ completely disappeared, suggesting that the complex is reduced to the iron(II) form Fe(oep) and the formation of the oxygen complex $[Fe^{II}(oep)(O_2)]$ could be markedly suppressed. Accordingly, this provided experimental evidence that the $Fe^{II}(oep)$–$O_2$ complex is converted to **B** *via* **A** (Scheme 1).

In terms of the observed *g*-parameters, **B** is assigned as the porphyrinoxyl radical form of iron(II) *meso*-hydroxyoctaethylporphyrin (Table 1);[10] however, the origin of the oxygen atom of the hydroxy group was still debatable. MS measurements were thus performed for **B** isolated from $^{18}O_2$ (96% enrichment) as its benzoyl ester by addition of a dmf solution of benzoyl chloride (0.1 M, 0.4 ml) to a solution of **B** at −50 °C. The brownish yellow species obtained, **C** [$\lambda_{max}$ = 379, 508, 535, 636 nm ($CHCl_3$) $g$ = 6, 2 at 77 K] gave an IR band at 1740 $cm^{-1}$ due to ν(CO) of the benzoyl ester moiety. NMR was consistent for a *meso*-benzoyloxyoctaethylporphyrin iron(II) bispyridine complex.[11] MS for **C**, isolated from $^{16}O_2$ and $^{18}O_2$ atmosphere, revealed weak parent ion peaks (*m/z* 743, 745), and major fragment peaks ($M^+ - Cl^-$ at *m/z* 708, 710), respectively. In addition, a common fragment peak was detected for both samples at *m/z* 588, which corresponds to Fe(oep) after fragmentation of the chlorine and benzoyl moieties from **C**. Based on the observed *m/z* value **C** was formulated as $C_{43}H_{48}N_4{}^-(^{16}O)_2Cl$ and $C_{43}H_{48}N_4{}^-(^{16}O)(^{18}O)Cl$, respectively, indicative that the oxygen atom attached at the *meso* carbon was derived from molecular oxygen. Detectable fragment peaks due to the $^{16}O$ structure were scarcely detected in the mass spectrum of the $^{18}O$ analogue, indicating that the oxygen atoms of $H_2O$ and $OH^-$, derived from aqueous sodium ascorbate, are not the oxygen source in **C**.

Noting that **B** was produced *via* **A**, the axially ligating $OOH^-$ is regarded as the most probable oxygen source. These results are reasonably interpreted by assuming an intramolecular electrophilic addition of $OOH^-$ to the porphyrin ring resulting in the formation of the cationic form of *meso*-hydroxyporphyrin,[12] which was readily converted to **B** by loss of two protons,[10] under alkaline conditions (Scheme 1). In the process of O–O bond cleavage in **A** the formation of high-valent iron species are also postulated, however, these species are expected to be shortlived in the presence of ascorbate, and readily reduced to **B** with loss of water. Consequently, the haem $H_2O_2$ complex is the most important intermediate in the process of *meso*-oxygenation. The results described here demonstrate the role of the haem–$OOH^-$ complex in the process of haem metabolism catalysed not only by the coupled oxidation of haem,[7] but also by naturally occurring haem-oxygenases.[12]

## References


1 H. B. Dunfold and J. S. Stillman, *Coord. Chem. Rev.*, 1976, **19**, 187; T. Ogura, K. Takahashi, K. Shinzawa-Itoh, S. Yoshikjawa and T. Kitagawa, *Bull. Chem. Soc. Jpn.*, 1991, **64**, 2901.
2 L. P. Hager, D. L. Doubeck, R. M. Silverstein, J. H. Hargis and J. V. Martin, *J. Am. Chem. Soc.*, 1972, **94**, 4364.
3 R. Tenhunen, S. H. Marver and R. Schmid, *Proc. Natl. Acad. Sci., USA*, 1968, **61**, 748.
4 R. E. White and M. J. Coon, *Annu. Rev. Biochem.*, 1980, **49**, 315.
5 K. Tajima, M. Shigematsu, J. Jinno, K. Ishizu and H. Ohya-Nishiguchi, *J. Chem. Soc., Chem. Commun.*, 1990, 144.
6 K. Tajima, K. Tada, A. Yasui, H. Ohya-Nishiguchi and K. Ishizu, *J. Chem. Soc., Chem. Commun.*, 1993, 282.
7 R. Lemberg, *Biochem. J.*, 1935, **29**, 1322; P. O'Carra, in *Porphyrin and Metalloporphyrins*, ed. K. M. Smith, Elsevier, Amsterdam, Oxford, New York, 1975, ch. 4, p. 123.
8 K. Tajima, M. Shigematsu, J. Jinno, Y. Kawano, K. Mikami, K. Ishizu and H. Ohya-Nishiguchi, *Biochem. Biophys. Res. Commun.*, 1990, **166**, 924.
9 T. Hirota and H. A. Itano, *Tetrahedron Lett.*, 1983, **24**, 995.
10 S. Sano, T. Sano, I. Morishima, Y. Shiro and Y. Maeda, *Proc. Natl. Acad. Sci., USA*, 1986, **83**, 531; I. Morishima, H. Fujii and Y. Shiro, *J. Am. Chem. Soc.*, 1986, **108**, 3858.
11 R. Bonnett and M. J. Dimsdale, *J. Chem. Soc., Perkin Trans. 1*, 1972, 2540.
12 C. K. Chang, G. Aviles and N. Bag, *J. Am. Chem. Soc.*, 1994, **116**, 12 127; J. Torpey, D. A. Lee, K. M. Smith and P. R. de Montellano, *J. Am. Chem. Soc.*, 1996, **118**, 9172.



*Received in Cambridge, UK, 2nd December 1996; Com. 6/08115K*

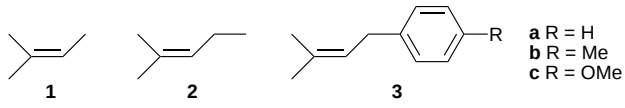
# Generation and reactivity of singlet oxygen within zeolites: remarkable control of hydroperoxidation of alkenes

**Rebecca J. Robbins and V. Ramamurthy***

*Department of Chemistry, Tulane University, New Orleans, LA 70118, USA*

**A highly selective oxidation of alkenes included within a Y zeolite is achieved by generating singlet oxygen *via* excitation of a monomeric dye exchanged within a zeolite; conformational control brought forth by the medium is suggested to be responsible for the observed remarkable selectivity.**

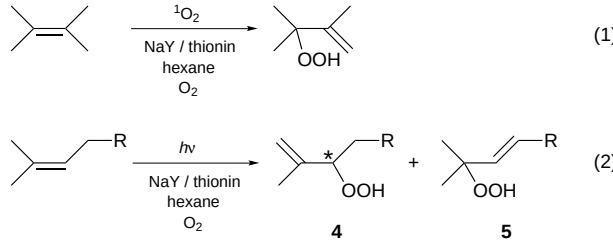
One well known reaction of singlet oxygen is the hydroperoxidation of alkenes containing allylic hydrogens, often referred to as the 'ene' reaction or Schenk reaction.[1] Reaction with substrates containing several distinct allylic hydrogens produces several distinct products. Although the peroxidation *via* singlet oxygen has found much synthetic application, regio- and stereo-control are still difficult issues.[2] We show here that the interior of a zeolite offers one possible solution to this important problem. When the oxidation of alkenes **1**–**3** is conducted within the supercages of faujasite Y type zeolite a remarkable selectivity of the hydroperoxidation is observed.




Although the mechanistic details of the ene reaction are still being debated, certain trends have been identified.[3] Experiments by several groups have brought out the importance of the geometrical arrangement of the allylic hydrogens with respect to the attacking singlet oxygen during the hydroperoxide formation.[4] This suggested to us that if one succeeds in controlling the conformation of the alkene and thus the accessibility of the allylic hydrogen(s) to the reagent, singlet oxygen, one might be able to achieve selectivity in the oxidation process. We have already established that one can use zeolite as a medium to achieve conformational control on ketones that undergo Norrish type reactions.[5] With this in mind, we set out to use a similar strategy to demonstrate that zeolite can play a vital role in oxidation processes initiated by singlet oxygen. Indeed, this strategy has yielded remarkable results in terms of obtaining predominantly a single hydroperoxide from the alkenes **1**–**3** within the supramolecular assembly of alkene, thiazine dye, oxygen and zeolite.

In our system, generation of singlet oxygen entails irradiation of a thiazine dye located within the supercages of the zeolite lattice. These dyes (thionin, methylene blue and methylene green) are placed within the zeolite *via* a cation-exchange process.[6] The exchange involves dropping the zeolite (*e.g.* 600 mg unactivated NaY) in a prestirred aqueous solution of thionin (2 mg in 250 ml of water). Continuous stirring for 3 h followed by filtration and aqueous washes (or Soxhlet extraction) yields a pink zeolite. The presence of water in the zeolite has a dramatic effect on the state of aggregation of the organic dye within the zeolite cage. With coadsorbed water or in 'wet' zeolite, thionin exists as a dimer, whereas in 'dry' zeolite the organic dye exists as a monomer and as a result the zeolite turns blue.[6] It is only the monomeric form of the dye which functions as a sensitizer and generates singlet oxygen. Initial experimentation showed that in the absence of alkene, irradiation of 'dry' Na Y/thionin/oxygen generated an emission at 1268 nm corresponding to $^1O_2$. Irradiation of the dye-exchanged zeolite in the presence of 2,3-dimethylbut-2-ene, a standard alkene known to react with singlet oxygen, gave the same hydroperoxide as in the isotropic solution medium [Scheme 1, eqn. (1)].[7] This demonstrated that not only was $^1O_2$ generated in the zeolites, but that it was reactive as well.

Having established that generation of singlet oxygen within a zeolite is feasible, we tested our conformational control proposition with the alkenes **1**–**3a**–**c**. Irradiation took place in a Kimax tube containing a zeolite and alkene as a slurry in hexane. Product hydroperoxide(s) were extracted from the zeolite with tetrahydrofuran and were analysed by GC and NMR after reduction with $PPh_3$. The only products obtained are those reported. The isolated yield ranged between 65 and 75%. Products were compared and found consistent with literature reports.[8] Table 1 compares the ratio of secondary (**4**) to tertiary




**Scheme 1**

**Table 1** A comparison of the ratio of secondary to tertiary hydroperoxides in various media

| Alkene | Conditions | Secondary hydroperoxide **4** | Tertiary hydroperoxide **5** |
|---|---|---|---|
| **1** | Thionin/MeCN | 51 | 49 |
| | Rose Bengal/MeCN | 50 | 50 |
| | NaY/thionin | 72 | 28 |
| **2** | Thionin/MeCN | 40 | 60 |
| | NaY/thionin | 100 | — |
| **3a** | Thionin/MeCN | 50 | 50 |
| | Rose Bengal/MeCN | 54 | 46 |
| | LiY/thionin | 100 | — |
| | NaY/thionin | 85 | 15 |
| | RbY/thionin | 80 | 20 |
| | CsY/thionin | 66 | 34 |
| **3b** | Rose Bengal/MeCN | 56 | 44 |
| | LiY/thionin | 100 | — |
| | NaY/thionin | 100 | — |
| | RbY/thionin | 94 | 6 |
| | CsY/thionin | 92 | 8 |
| **3c** | Rose Bengal/MeCN | 52 | 48 |
| | LiY/thionin | 100 | — |
| | NaY/thionin | 100 | — |
| | RbY/thionin | 100 | — |
| | CsY/thionin | 100 | — |

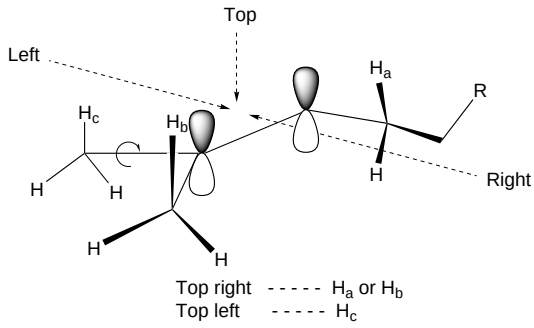



**Fig. 1**

(**5**) hydroperoxides obtained in an acetonitrile solution to that obtained in the zeolite oxidation reaction. For additional confirmation, the tertiary alcohol product of **3a** was independently synthesized as an authentic sample. Retention times and NMR of the authentic samples are consistent with the observed products. Also, the hydroperoxides generated from Rose Bengal sensitized oxidation were stirred overnight in a slurry of hexane and NaY/thionin. Both products were recovered in the same ratio as prior to zeolite treatment. These control experiments confirmed that the observed unprecedented selectivity is not an experimental artifact.

Formation of both hydroperoxides **4** and **5** in solution has been rationalized on the basis that singlet oxygen attacks the alkene from the top-right side (Fig. 1).[4] In such an approach, the transition state is stabilized by secondary interactions between the oxygen and the allylic hydrogens which are situated parallel to the π–p orbitals. As per this accepted model the methyl group on the top-left side (Fig. 1) does not participate in the oxidation process. Results within the zeolites clearly suggest that the methylene hydrogens $H_a$ of **2** and **3** (Fig. 1) are not abstracted by the singlet oxygen. While the lack of formation of **5** within zeolites is an indication that the methylene hydrogens are excluded from the reaction, selective formation of **4** does not indicate which of the two (or both) methyl groups participates in the oxidation process. Without further experiments that would distinguish between the *gem* dimethyl groups, we can only provide a tentative model for the observed selectivity.

We suggest that the R group in the alkene (Fig. 1) plays a crucial role in the type of product(s) formed. While in solution, the most favoured conformation places both the methyl and methylene hydrogens in an appropriate geometry for abstraction (Fig. 1), it is quite likely that such a conformation may not be favoured within a zeolite. In a supramolecular assembly one will have to consider the interactions that arise between the adsorbent/guest and the environment. We speculate that within a zeolite, the alkene will be adsorbed to the surface *via* cation–π interactions.[9] A rotation of the $C^3$–$C^4$ bond might result under such conditions to relieve the steric strain that develops between the bulky R group and the surface. Such a rotation will place the methylene hydrogens away from the incoming singlet oxygen (Fig. 2) and therefore no tertiary hydroperoxide would be formed. The extent of steric repulsion between the surface and the R group may depend on the distance between the group and the surface. Larger cations such as Cs ion may place the alkene slightly further from the surface and thus reduce the steric strain between the surface and the R group. Formation of small amounts of tertiary hydroperoxide **5** in the case of **3a** and **3b** is

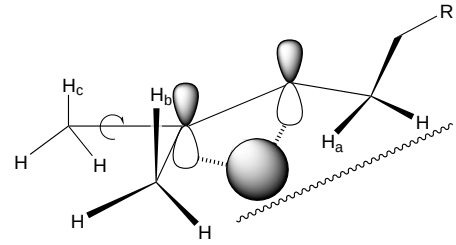



**Fig. 2**

consistent with this speculation. A comparison of the product distribution from **1** and **2** (and **3**) makes it clear that in order to achieve selectivity it is necessary to replace at least one hydrogen of the methyl group (in **1**) by a larger group such as methyl or phenyl. We recognize that the above model is only a working hypothesis and further experiments are needed to understand this unusual selectivity. The use of zeolite as a medium to achieve selective oxidation has been established and we are in the process of exploring this strategy with other alkenes. The ability to generate singlet oxygen and to achieve regioselective hydroperoxidation of alkenes within a zeolite has prompted us to consider stereoselective hydroperoxidation of alkenes with zeolite as the medium.[10]

The authors thank ACS-PRF and the Division of Chemical Sciences, Office of Basic Energy Sciences, Office of Energy Research, US Department of Energy for support of this program.

## Footnote

* E-mail: Murthy@mailhost.tcs.tulane.edu

## References

1 *Singlet Oxygen*, ed. H. H. Wasserman and R. W. Murray, Academic Press, New York, 1979; *Singlet Oxygen*, ed. A. A. Frimer, CRC Press, Boca Raton, FL, 1985, vol. 1–4.
2 M. Prein and W. Adam, *Angew. Chem.*, 1996, **35**, 477.
3 A. A. Frimer and L. M. Stephenson, in *Singlet Oxygen*, ed. A. A. Frimer, CRC Press, Boca Raton, FL, 1985, pp. 67–92; K. Gollnick and H. J. Kuhn, in *Singlet Oxygen*, ed. H. H. Wasserman and R. W. Murray, Academic Press, New York, 1979, pp. 287–429.
4 L. M. Stephenson, M. J. Grdina and M. Orfanopoulos, *Acc. Chem. Res.*, 1980, **13**, 419; J. R. Hurst and G. B. Schuster, *J. Am. Chem. Soc.*, 1982, **104**, 6854; A. A. Gorman, H. Hartman and H. Paur, *J. Am. Chem. Soc.*, 1982, **104**, 7098.
5 D. R. Corbin, D. F. Eaton and V. Ramamurthy, *J. Am. Chem. Soc.*, 1988, **110**, 4848; V. Ramamurthy, D. R. Corbin and L. J. Johnston, *J. Am. Chem. Soc.*, 1992, **114**, 3870.
6 V. Ramamurthy, D. F. Eaton and D. R. Sanderson, *J. Am. Chem. Soc.*, 1993, **115**, 10438.
7 C. S. Foote and G. Uhde, in *Organic Photochemical Synthesis*, ed. R. Srinivasan, Wiley-Interscience, New York, 1971, vol. 1, pp. 60–61.
8 T. T. Fujimoto, Dissertation, University of California, Los Angeles, 1972, Univ. Microfilm, 72-18125; *Diss. Abstr. B.*, 1972, **32**, 6910.
9 M. A. Hepp, V. Ramamurthy, C. R. Corbin and C. Dybowski, *J. Phys. Chem.*, 1992, **96**, 2629; R. H. Staley and J. L. Beauchamp, *J. Am. Chem. Soc.*, 1975, **97**, 5920.
10 M. Leibovitch, G. Olovsson, G. Sundarababu, V. Ramamurthy, J. R. Scheffer and J. Trotter, *J. Am. Chem. Soc.*, 1996, **118**, 1219; G. Sundarababu, M. Leibovitch, D. R. Corbin, J. R. Scheffer and V. Ramamurthy, *Chem. Commun.*, 1996, 2049.

*Received in Columbia, MO, USA, 11th February 1997; Com. 7/00977A*



Typeset and printed by Black Bear Press Limited, Cambridge, England

ChemComm
FEATURE ARTICLE

# Metallodendrimers: metal ions as supramolecular glue†

**Edwin C. Constable‡**

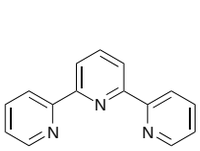
*Institut für Anorganische Chemie, Spitalstrasse 51, CH-4056 Basel, Switzerland*

**The coordination of appropriate organic molecules containing multiple metal-binding domains to metal ions provides a versatile alternative to carbon–carbon or carbon–heteroatom bond formation for the assembly of dendrimers.**

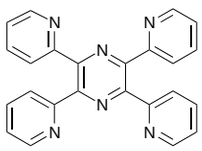
## Introduction: metallosupramolecular chemistry

In the past two decades, dendritic molecules have developed from laboratory curiosities to components of burgeoning new technologies.[1] The majority of dendrimers are purely 'organic', with the descriptor 'organic' referring both to the chemical character of the molecular components used in the assembly and to the type of chemical reaction used in their combination. Conventionally, dendrimers are prepared with key assembly steps which involve the formation of carbon–carbon or carbon–heteroatom bonds. Although this methodology is well developed, it has a number of inherent disadvantages; whilst such bonds tend to be kinetically stable once formed, there may be significant energy barriers to their formation.

We have developed metallosupramolecular chemistry, in which the characteristic and preferred coordination numbers and geometries of metal ions are matched with the inherent bonding characteristics of polydentate ligands to control the assembly of novel supramolecular architectures.[2] A basic concept is that of a ligand domain as a metal-binding motif which may be introduced into multifunctional ligands. In our studies, we have adopted oligopyridine metal-binding domains as our favoured motif and, for reasons documented elsewhere, we have concentrated upon 2,2′:6′,2″-terpyridine **1** (tpy) domains.[3]



**1**

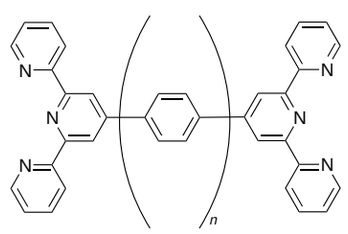


**2**

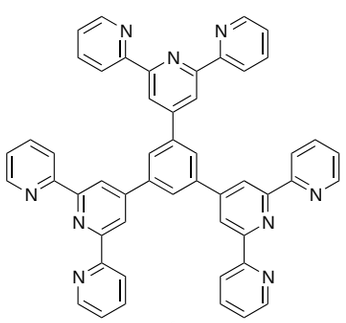
We and others[4,5] have developed metallosupramolecular approaches to dendrimers in which the key growth steps involve metal-donor atom interactions as opposed to carbon–carbon or carbon–heteroatom bond formation. This methodology is predicated on the thermodynamic and kinetic features of coordinate bond formation as opposed to conventional covalent bond formation. We describe such systems as metallodendrimers, and they may bear multiple functionality at inner generations or at the surface generation. Dendritic systems incorporating metal centres are of current interest as novel magnetic, electronic or photo-optical materials.

## Building metallodendrimers: prototype systems

The simplest methodology relies upon the synthesis of organic molecules bearing two or more metal-binding domains, which are subsequently combined with the complementary metal components to give the desired metallodendrimers. When the tpy-based ligands are used, a six-coordinate metal centre is the appropriate complement to two tpy domains. In general, this approach leads to divergent or near-divergent syntheses. Our initial studies involved the prior synthesis of ligands containing two or more tpy metal-binding domains. Although we did not initially consider the simplest condensed bis(tpy) system, 2,3,4,5-tetra(2-pyridyl)pyrazine **2** (tppz), this, together with related pyrazine derivatives, has proved to be a useful bridging ligand[6] and we have recently embarked upon its incorporation into metallosupramolecules.[7] The first generation of ligands consisted of covalently linked tpy domains with variable length spacers **3** and the study of these compounds led to a continuing collaboration with the group of Jean-Pierre Sauvage in Strasbourg. We utilised the 'complexes as metals, complexes as ligands'[4] approach and the new ligands behaved very much as expected and gave us valuable experience in the assembly of low-nuclearity metallodendrimers.[8–11] This approach allowed the synthesis of multinuclear systems designed to give directional and spatial control over electron and/or energy transfer in components of photoconversion systems. Simple developments of the ligand syntheses lead to **4**, the progenitor of a metallosupramolecular starburst system.[11]

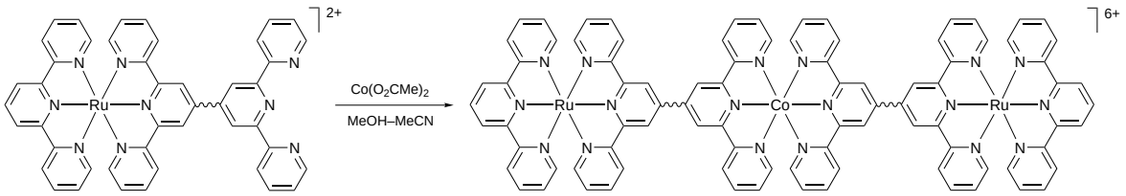


**3** $n = 0–4$



**4**

However, there were a number of inherent disadvantages with the methodology we had developed. Firstly, we were spending ever more time in ligand design and synthesis, and secondly, the routes tended to be divergent. In addressing the latter problem, we became concerned with the genesis of a convergent approach utilising labile first-row transition-metal centres in combination with kinetically inert ruthenium(II) centres (Scheme 1).[10] In the example shown, the reaction is essentially quantitative and is complete in minutes, in contrast to the formation of the corresponding triruthenium complex in lower yield after several hours at reflux. Subsequent oxidation gives a kinetically inert cobalt(III)diruthenium(II) complex. This approach partially overcame the problems associated with the

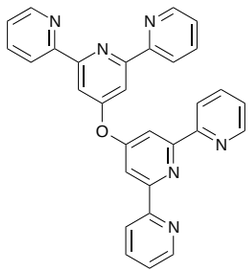



**Scheme 1**

divergent synthesis, but we were aware that many of the advantages of the metallodendritic approach would be lost if time-consuming ligand synthesis was an essential prerequisite.

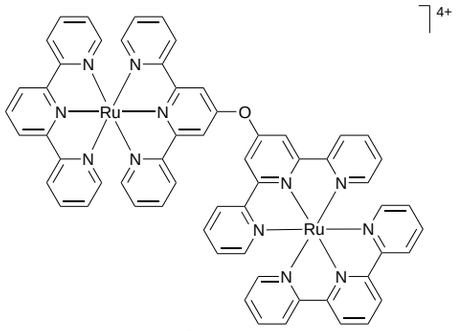
### Metal-directed reactions: *in situ* ligand synthesis

In the next phase of our work, we decided to develop *in situ* ligand assembly reactions to avoid the prior synthesis of bridging ligands. We had previously shown that the electrophilic character of 4-halopyridines was dramatically enhanced upon coordination to a transition metal[8,12] and we now extended this methodology to the *in situ* synthesis of the ether-bridged ligand **5**. The key components are the nucleophilic organic compound **6** and the electrophilic 4′-chloro-2,2′:6′,2″-terpyridine (Cltpy) complex **7** and reaction proceeds smoothly in the presence of base to give **8** in excellent yield (Scheme 2). The formation of **5** was established unambiguously by an X-ray structural determination of ligand prepared in a metal-free synthesis.[13]



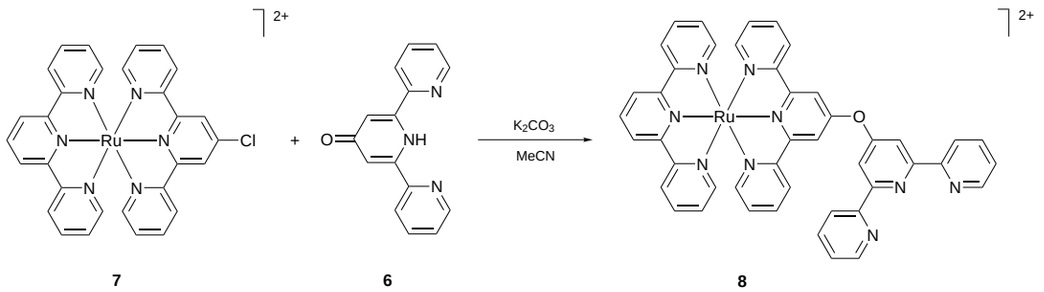
**5**

We had hoped to extend the methodology to the direct formation of multinuclear complexes by the reactions of complexes of **6** with **7**; however, coordination of **6** to a metal sufficiently reduces its nucleophilicity that it does not react with **7**. However, **8** contains a non-coordinated tpy domain and so may be further reacted with appropriate metal species. Typical reactions have involved termination to yield dinuclear species **9** or the convergent assembly of trinuclear species with central iron, cobalt or ruthenium centres using the route shown in Scheme 1. It also proved to be possible to prepare **10** from the reaction of $[Ru(Cltpy)_2]^{2+}$ with **6**; this is a complex which can act as a bridging ligand.



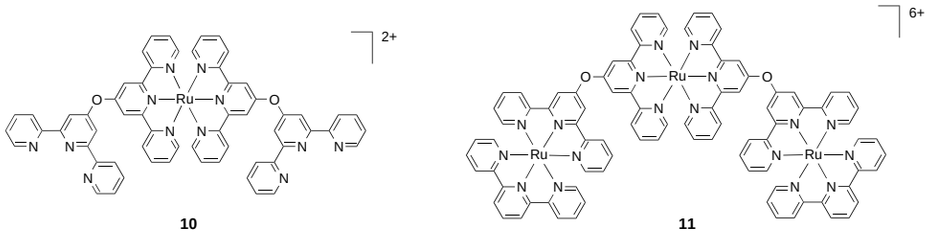

**9**

The next question related to the formation of higher generations using this methodology. The key compound **11** could be prepared in good yield from the divergent reaction of **10** with $[Ru(Cltpy)Cl_3]$ or the convergent reaction of $[(Cltpy)Ru(\mathbf{5})]^{2+}$ with ruthenium trichloride. Analogues could be prepared using extensions of Scheme 1 with $[(Cltyp)Ru(\mathbf{5})]^{2+}$. We had hoped to react the surface Cltpy ligands with




**7** **6** **8**

**Scheme 2**




**10** **11**

additional **6** to create new surface tpy metal-binding sites. However, it turned out that further homologation is not possible and that attack of **6** at a surface generation Cltpy is disfavoured compared to attack at inner generation ether links to give mononuclear complexes of **5** and **6** as the major products.

At this stage, we had shown that metal-directed reactions of a coordinated electrophile could be used for the formation of ether linkages within a given generation, but those new bonds were not stable under the reaction conditions required for the use of analogous reactions at later generations. Furthermore, the only control over topology and morphology came from the design of the ligand containing the multiple tpy domains.

### A second *in situ* synthesis

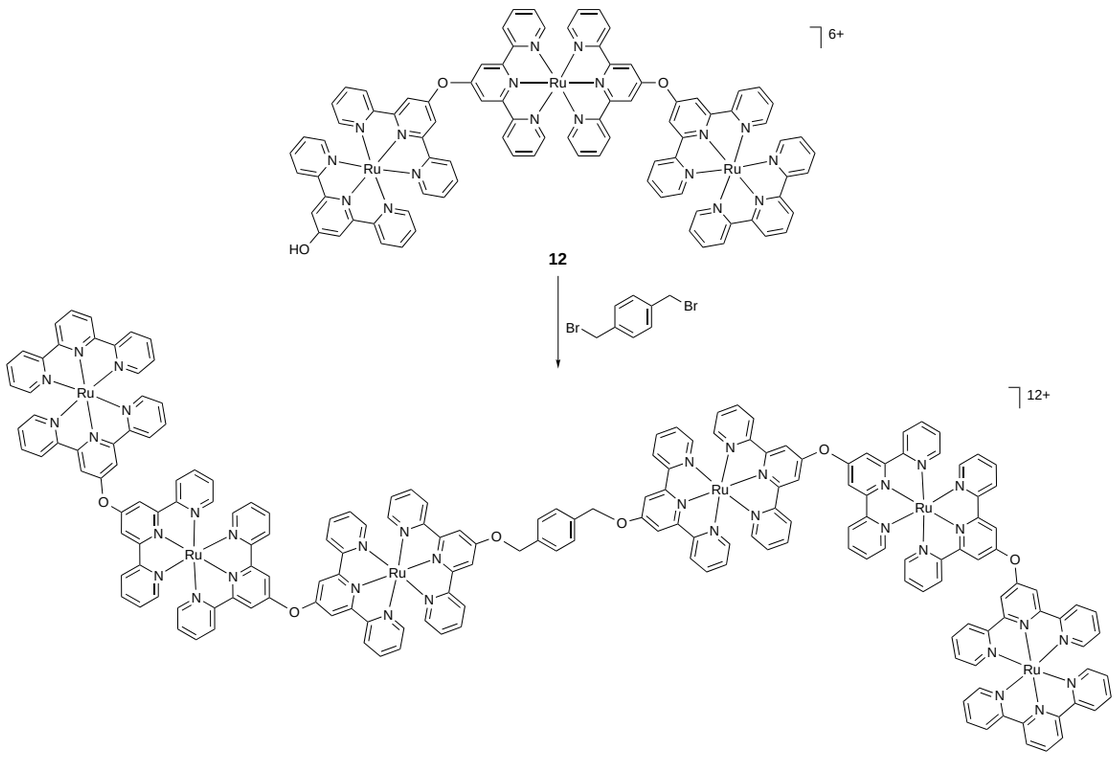
We noted above that complexes of **6** would not react with coordinated Cltpy electrophiles. We wondered if the use of a better electrophile might be successful and investigated the reactions of coordinated **6** with benzyl halides. In particular, we felt that the use of bis(bromomethyl)benzenes would lead to linear growth reactions. Furthermore, it was not necessary to use mononuclear complexes containing **6**, the ready accessibility of multinuclear complexes using the routes described above meant that it would be possible to incorporate building containing variable numbers and types of metal centres. This approach proved successful and a typical reaction leading to a hexanuclear species is shown in Scheme 3.[14] It is also interesting to note that this change in methodology also leads to a convergent synthesis; the hexanuclear species is formed from two trinuclear intermediates. The reaction with the electrophile occurred without any consequence for inner generation ether linkages and we could use the reaction of a coordinated electrophile with a nucleophile for the formation of one generation and the reaction of a coordinated nucleophile with an electrophile to prepare the subsequent generation.

We also noted that the convergent approach would permit us to bring more than two subunits together, and this led us to investigate the use of a 1,3,5-tris(bromomethyl)benzene centre for the assembly of three subunits. This approach was also successful and allowed the synthesis of a range of high-nuclearity species including a nonanuclear complex.[14] Finally, we considered the reaction with hexakis(bromomethyl)benzene—when the trinuclear complex **12** was used, a convergent synthesis of an octadecanuclear complex should result. Although we worried that steric interactions might prevent the reaction from proceeding to completion, we were very pleasantly surprised to find that **12** reacted smoothly with hexakis-(bromomethyl)benzene to give the desired octadecanuclear species **13**.[15]

### A return to classical strategies

At this point, the use of the benzene central growth point led us to reconsider some aspects of our strategy. Although we had adopted the metallodendritic approach to circumvent kinetic barriers experienced in 'pure' organic chemistry, it now seemed that we could use high-yielding 'organic' reactions for the preparation of the central site of the dendrimer, with subsequent generations being built using the metallodendritic methodology. Preliminary experiments in collaboration with George Newkome established the viability of this hybrid approach, although we found the complexity of the organic components involved to be discouraging.[16]

We decided to adopt pentaerythrytol as a cheap and readily available starting point. The reaction of pentaerythrytol with an excess of Cltpy gave **14** with four tpy domains in excellent yield;[17] in contrast, when the pentaerythrytol was in excess, the monofunctionalised compound **15** could be isolated.[18] A related ligand **16** incorporating six tpy domains is readily prepared from dipentaerythrytol. The growth of metallodendrimers from **14** and **16** is facile; reaction with [Ru(Xtpy)$Cl_3$] gives the expected first generation tetranuclear or hexanuclear complexes in excellent yields. One of current interests lies in the incorporation of pendant functionality at the surface generation in high-nuclearity metallodendrimers and the a 40-boron first-generation *ortho*-carbaboranyl-functionalised metallodendrimer **17** is a typical example of such compounds.[17]




**Scheme 3**

The new building block **15** now allows us to use a genuinely dendritic approach for the synthesis of metallodendrimers. The key species is **18**, which is a surface generation Xtpy functionalised species. However, in this case, the X-functionality incorporates three nucleophilic hydroxy groups. Subsequent reaction with the electrophilic complex **7** yields the expected hexadecanuclear complex.[18]

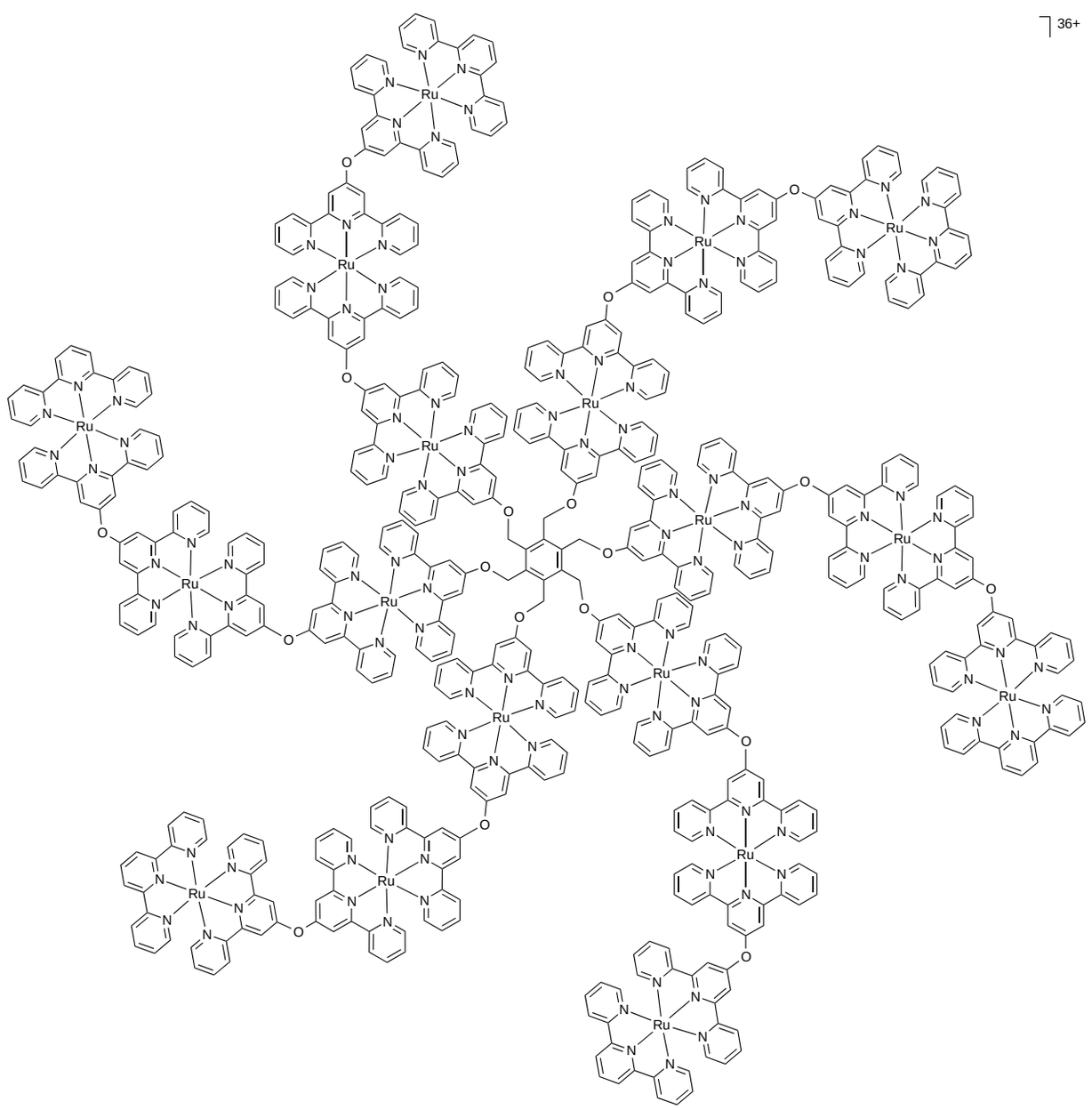
## Metallocentric dendrimers

The strategies discussed above proved effective, but there were still a number of problems associated with the use of carbon-based central units. Firstly, the connectivity will be related to the three common geometries observed at carbon : linear, trigonal planar or tetrahedral and increases in connectivity can only be associated with an increase in the complexity of the central unit. Secondly, a central tetrahedral carbon centre with four identical (non-chiral) groups attached cannot function as a site for chiral initiation. In chiral dendrimers, the chirality cannot commence at a central carbon bearing four identical groups. These considerations led us to our final development to using a metal centre for dendrimer initiation.

Our rationale was quite simple and based upon a number of established features from coordination chemistry. The connectivity (coordination number) at a metal may vary from two to twelve with a wide range of coordination geometries possible. For example, four-coordinate metal centres may be square-planar or tetrahedral, in contrast, four-coordinate carbon is almost invariably tetrahedral. In addition, six-coordinate metal bonded to three didentate chelating metal-binding domains are inherently chiral, with Δ and Λ enantiomers. This point must be stressed, a metal centre bearing three identical didentate chelating ligands is inherently chiral.

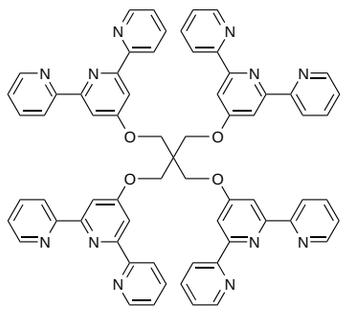
## Divergent metallocentric metallodendrimers

We initially considered a divergent approach to metallocentric systems based upon a central {M(bpy)$_3$} (bpy = 2,2′-bipyridine) unit based upon our earlier metal-directed

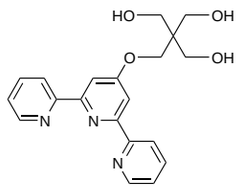



13

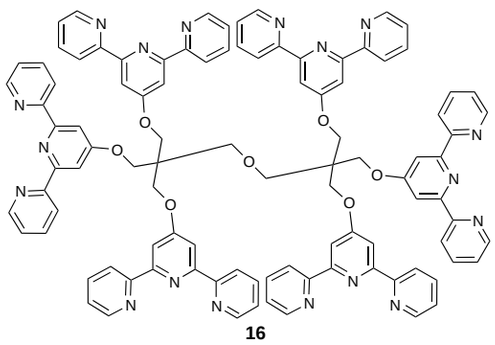
methodology. To establish the principle, we prepared $[Ru(Cl_2bpy)]^{2+}$ ($Cl_2bpy$ = 4,4′-dichloro-2,2′-bipyridine) which can, in principle, be resolved into Δ and Λ enantiomers. The coordinated halopyridine is activated towards attack by nucleophiles and the complex reacts smoothly with **6** to give a complex bearing six non-coordinated tpy domains distributed about a central, chiral, metal site. We planned the incorporation of the next generation by reaction of this species with $[Ru(tpy)Cl_3]$ (Scheme 4). This combination of chiral $\{M(bpy)_3\}$ and achiral $\{M(tpy)_2\}$ domains should avoid problems of diastereoselectivity associated with metallodendrimers based upon $\{M(bpy)_3\}$ domains alone. Unfortunately, this resulted in an inseparable mixture of compounds in which five or six sites had reacted. Clearly, steric constraints are becoming paramount in this divergent approach and we are currently designing suitable spacer groups for incorporation between the bpy and tpy domains. However, in addition to this longer term strategy, we also wondered if the steric problems might be relieved by the adoption of an alternative convergent metallocentric strategy.



**14**



**15**

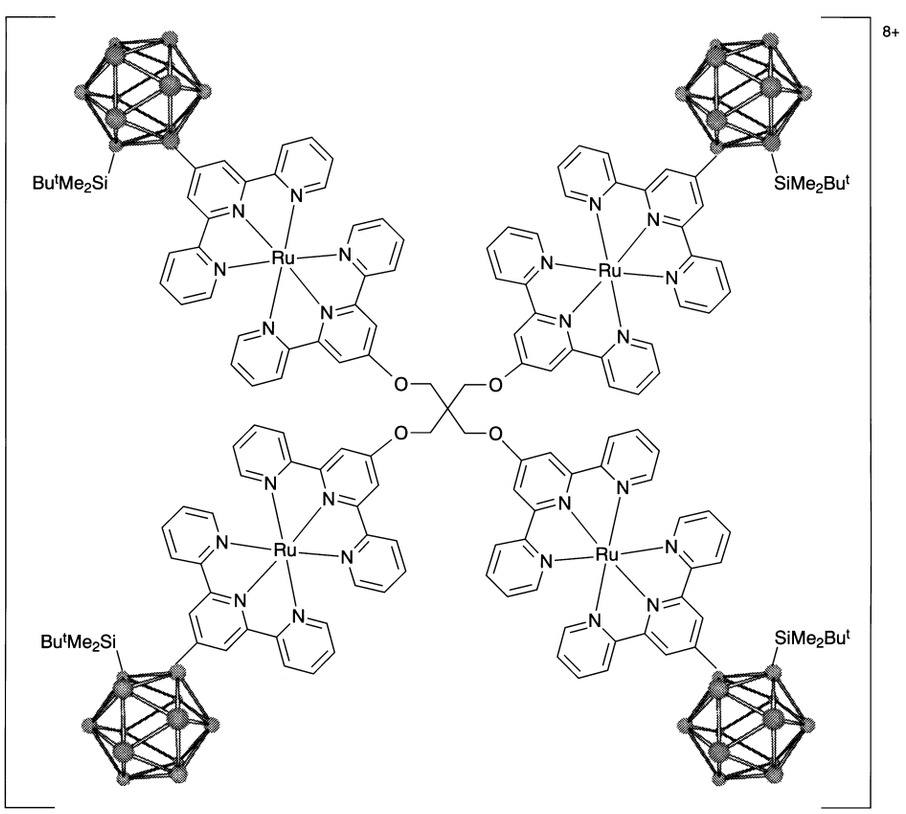


**16**

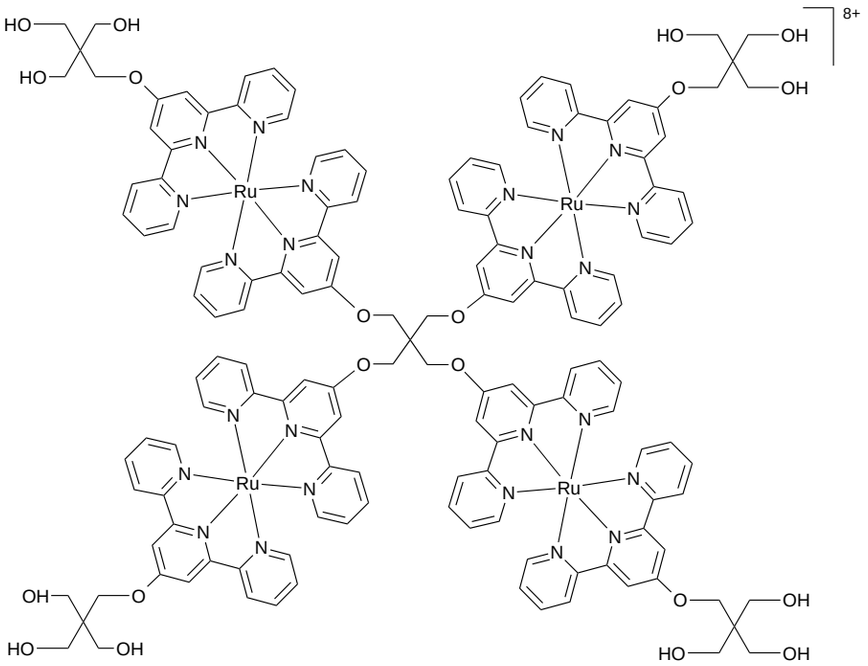
### Convergent metallocentric metallodendrimers

In our latest development, we combine many of the strategies discussed earlier. We commence by reacting a coordinated **6** ligand with an excess of a good electrophile to give a new complex **19** with an electrophilic site remote from the metal which can subsequently be reacted with a nucleophile (Scheme 5). We have selected 4,4′-dihydroxy-2,2′-bipyridine as a nucleophile which contains a didentate metal-binding domain that will eventually be used to generate a potentially chiral $\{M(bpy)_3\}$ domain. The product **20** is a dinuclear complex in which two $\{Ru(tpy)_2\}$ domains are linked by a non-coordinated bpy domain; in essence, this complex is simply a disubstituted 2,2′-bipyridine, which is expected to coordinate rapidly to labile first-row transition-metal ions such as iron(II) or cobalt(II). The reaction of the dinuclear complex **20** with either iron(II) or cobalt(II) is indeed rapid and leads to the convergent assembly of the desired heptanuclear metallocentric metallodendrimer **21** in near quantitative yield.

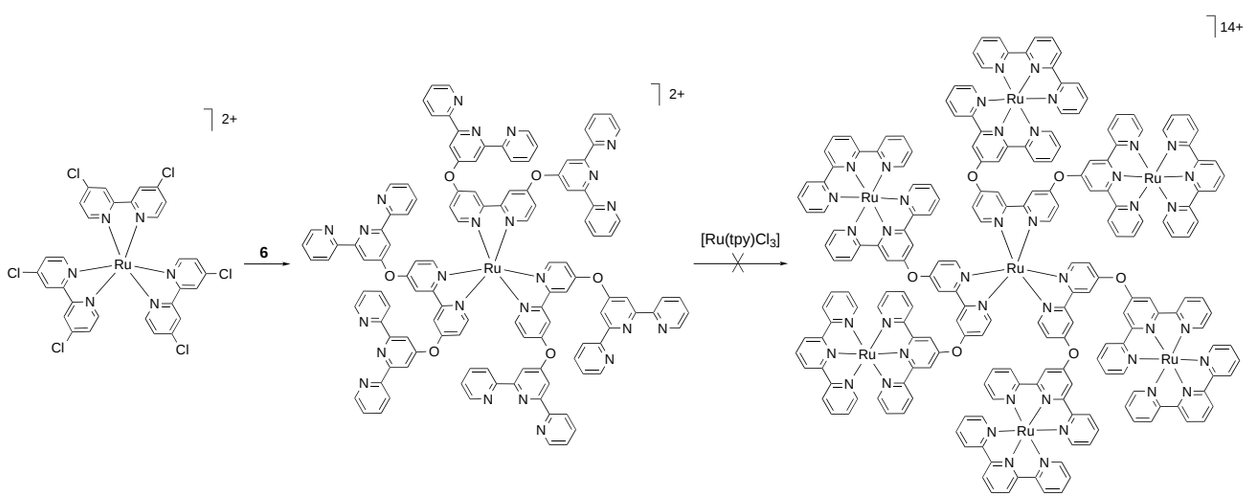
These convergent and divergent metallocentric methodologies are in many senses complementary. The divergent methodology allows the stereoretentive incorporation of predefined chirality (Δ or Λ) at the central metal site, whilst the convergent synthesis leads to a racemic mixture of the two enantiomers in the absence of chiral auxiliaries. We are presently designed a series of surface generation chiral tpy



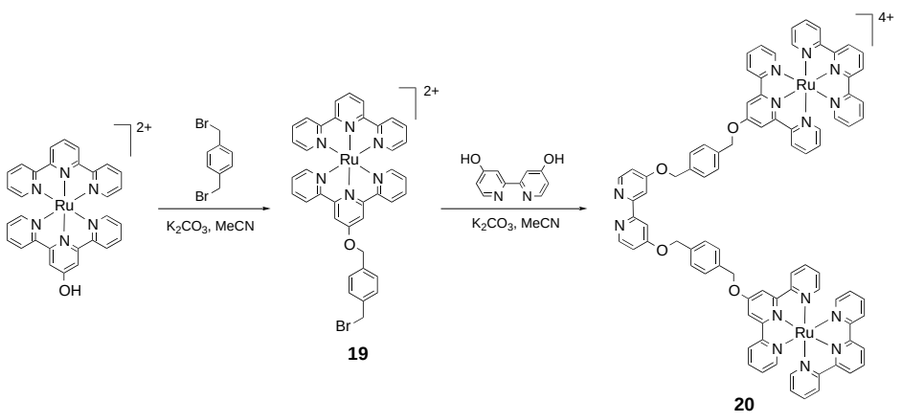

**17**



**18**

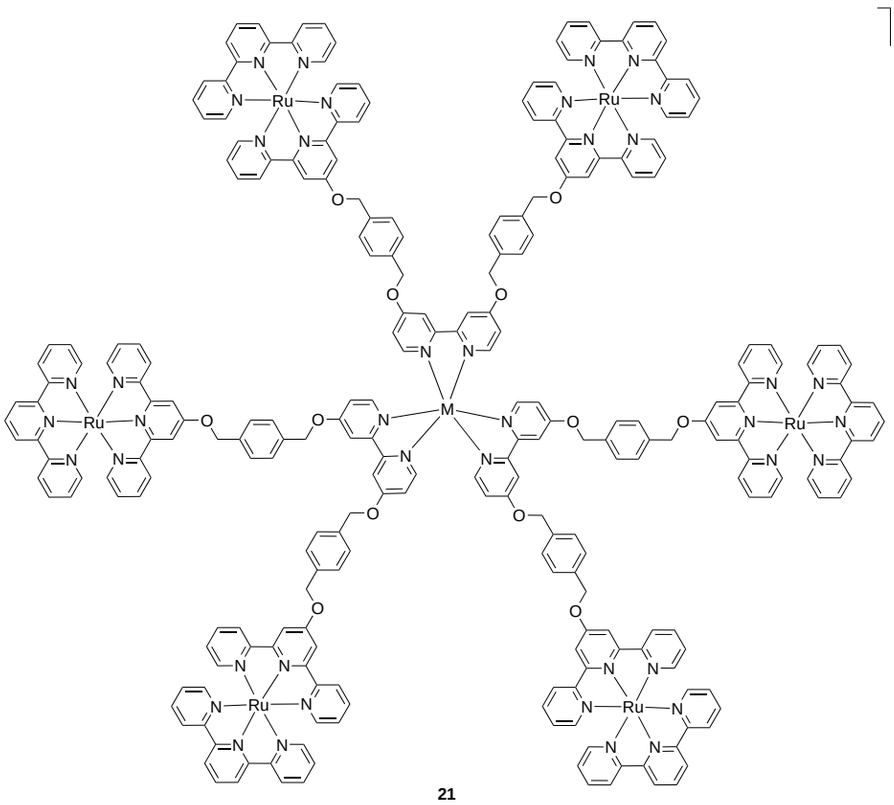


**Scheme 4**



**19** **20**

**Scheme 5**




**21**

ligands to impose diastereoselectivity in the convergent synthesis. However, the two strategies are also fundamentally different. In the divergent case, the chiral information is propagated outwards as the dendrimer grows. In contrast, the use of chiral auxiliaries in the surface generation may allow the resolution to occur at the final stage through information transfer in an 'inwards' sense.

## Some concluding remarks

I hope that this brief overview of metallodendritic chemistry serves to emphasise some of the advantages of the methodology. The structures are attractive and the molecules themselves are tractable and may be fully characterised by the conventional techniques of the molecular chemist. Solubility is controlled by the counterions; the chloride salts are water and methanol soluble, the hexafluorophosphate salts dissolve in acetonitrile or acetone, and the tetraphenylborate salts may be dissolved in dichloromethane.

## Acknowledgements

It remains to thank the talented and hard-working coworkers who have been and are involved in this work: the initial studies of metallodendrimers were made by Dr Alex Cargill Thompson in his doctoral and post-doctoral studies and continued by Peter Harverson, who has developed the complementary electrophile–nucleophile sequences in his doctoral studies. The pentaerythrytol systems are part of the doctoral work of Dave Phillips and Marco Cattalini, with the cluster-functionalised surface generations being studied by Marco and Dr Dominique Armspach. The metallocentric systems have been studied by Pete Harverson and Dr Martin Oberholzer. The cluster-functionalisation is part of a wider collaborative project with Dr Catherine Housecroft. I should also like to thank the EPSRC, the Schweizerischer Nationalfonds zur Förderung der wissenschaftlichen Forschung, the University of Basel and Ciba-Geigy plc for support. This work is part of a continuing collaborative effort involving groups in Basel, Bologna and Strasbourg.

## Footnotes

† This ChemComm is also available in enhanced multi-media format *via* the World Wide Web: http://chemistry.rsc.org/rsc/cccenha.htm

‡ E-mail: constable@ubaclu.unibas.ch

---

**Edwin Constable was born in Edinburgh, Scotland. In 1978 he obtained a first class honours degree in chemistry from St Catherine's College, Oxford; he remained in Oxford to undertake research in the design of photocatalysts under the supervision of Dr K. R. Seddon. In 1980 he received a DPhil and a SERC post-doctoral fellowship enabled him to conduct research in macrocyclic chemistry with Professor J. Lewis, University of Cambridge. After a research fellowship from the Commissioners for the Exhibition of 1851 he held a demonstratorship and lectureship at the University of Cambridge. In 1993 he moved to a chair of Inorganic Chemistry at the Institute for Inorganic Chemistry, University of Basel. He has held visiting professorships at the Université Louis Pasteur, Strasbourg, the University of Capetown and the University of Pavia. His research interests cover many aspects of supramolecular and coordination chemistry.**

---

## References

1 *Advances in Dendritic Macromolecules*, ed. G. R. Newkome, JAI Press, Greenwich, 1995, vol. 2 and references therein.
2 E. C. Constable, *Chem. Ind.*, 1994, 56; *Prog. Inorg. Chem.*, 1994, **42**, 67; E. C. Constable and D. Smith, *Chem. Br.*, 1995, **31**; in *The Polymeric Materials Encyclopedia*, ed. J. Solomon, CRC Press, Boca Raton, FL, 1996.
3 E. C. Constable, A. M. W. Cargill Thompson and D. A. Tocher, in *Supramolecular Chemistry*, ed. V. Balzani and L. De Cola, Kluwer Academic Press, Dordrecht, 1992, p. 219; E. C. Constable, in *Transition*

*Metals in Supramolecular Chemistry*, ed. L. Fabbrizzi and A. Poggi, Kluwer, Dordrecht, 1994, p. 81.
4 See for example: G. Denti, S. Serroni, S. Campagna, A. Juris, M. Ciano and V. Balzani, in *Perspectives in Coordination Chemistry*, ed. A. F. Williams, C. Floriani and A. E. Merbach, VHCA, Basel, 1992, p. 153; S. Campagna, G. Denti, S. Serroni, A. Juris, M. Venturi, V. Ricevuto and V. Balzani, *Chem. Eur. J*, 1995, **1**, 211.
5 See for example: S. Achar and R. J. Puddephatt, *J. Chem. Soc., Chem. Commun.*, 1994, 1895; *Angew. Chem., Int. Ed. Engl.*, 1994, **33**, 847; Y. H. Liao and J. R. Moss, *Chem. Commun.*, 1993, 1774; G. R. Newkome, R. Guther, C. N. Moorefield, F. Cardullo, L. Echegoyen, E. Perez-Cordero and H. Luftmann, *Angew. Chem., Int. Ed. Engl*., 1995, **34**, 2023.
6 See for example: L. M. Vogler, C. Franco, S. W. Jones and K. J. Brewer, *Inorg. Chim. Acta*, 1994, **221**, 55; J. B. Cooper, D. B. MacQueen, J. D. Petersen and D. W. Wertz, *Inorg. Chem.*, 1990, **29**, 3701; R. R. Ruminski and C. Letner, *Inorg. Chim. Acta*, 1989, **162**, 175; M. Graf, B. Greaves and H. Stoeckli-Evans, *Inorg. Chim. Acta*, 1993, **204**, 239; R. G. Brewer, G. E. Jensen and K. J. Brewer, *Inorg. Chem.*, 1994, **33**, 124; C. R. Arana and H. D. Abruña, *Inorg. Chem.*, 1993, **32**, 194; R. Ruminski, J. Kiplinger, T. Cockroft and C. Case, *Inorg. Chem.*, 1989, **28**, 370; R. P. Thummel and S. Chirayil, *Inorg. Chim. Acta*, 1988, **154**, 77.
7 E. C. Constable, A. J. Edwards, D. Phillips and P. R. Raithby, *Supramol. Chem.*, 1995, **5**, 93.
8 E. C. Constable, A. M. W. Cargill Thompson and D. A. Tocher, *New J. Chem.*, 1992, **16**, 855.
9 E. C. Constable and A. M. W. Cargill Thompson, *J. Chem. Soc., Dalton Trans.*, 1992, 3467; F. Barigelletti, L. Flamigni, V. Balzani, J.-P. Collin, J.-P. Sauvage, A. Sour, E. C. Constable and A. M. W. Cargill Thompson, *J. Chem. Soc., Chem. Commun.*, 1993, 942; *Coord. Chem. Rev.*, 1994, 132, 209; *J. Am. Chem. Soc.*, 1994, **116**, 7692; E. C. Constable, A. M. W. Cargill Thompson and D. A. Tocher, *Polymer Prepr.*, 1993, **34**, 110.
10 E. C. Constable, A. M. W. Cargill Thompson and D. A. Tocher, *Supramol. Chem.*, 1993, **3**, 9; *Makromol. Symp.*, 1994, **77**, 219; E. C. Constable and A. M. W. Cargill Thompson, *J. Chem. Soc., Dalton Trans.*, 1995, 1615.
11 E. C. Constable and A. M. W. Cargill Thompson, *J. Chem. Soc., Chem. Commun.*, 1992, 617.
12 E. C. Constable, *Inorg. Chim. Acta*, 1984, **82**, 53; *Metals and Ligand Reactivity—An Introduction to the Organic Chemistry of Metal Complexes*, VCH, Weinheim, 1995; E. C. Constable and T. A. Leese, *Inorg. Chim. Acta*, 1988, **146**, 55.
13 E. C. Constable, A. M. W. Cargill Thompson, P. Harveson, L. Macko, M. Neuberger and M. Zehnder, *Chem. Eur. J.*, 1995, **1**, 360.
14 E. C. Constable and P. Harverson, *Chem. Commun.*, 1996, 33.
15 E. C. Constable and P. Harverson, *Inorg. Chim. Acta*, 1996, **252**, 281.
16 G. R. Newkome, F. Cardullo, E. C. Constable, C. N. Moorefield and A. M. W. Cargill Thompson, *J. Chem. Soc., Chem. Commun.*, 1993, 925.
17 D. Armspach, M. Catallini, E. C. Constable, C. E. Housecroft and D. Phillips, *Chem. Commun.*, in the press.
18 D. Armspach, M. Catallini, E. C. Constable, C. E. Housecroft and D. Phillips, unpublished results.
19 E. C. Constable, P. Harverson and M. Oberholzer, *Chem. Commun.*, 1996, 1821.

*6/05102B*

# γ-Radiation synthesis and characterization of polyacrylamide–silver nanocomposites

**Yingjie Zhu,[a,b] Yitai Qian,*[a,b] Xiaojun Li[c] and Manwei Zhang[c]**

[a] *Structure Research Laboratory, University of Science and Technology of China, Hefei, Anhui 230026, P. R. China*
[b] *Department of Chemistry, University of Science and Technology of China, Hefei, Anhui 230026, P. R. China*
[c] *Department of Applied Chemistry, University of Science and Technology of China, Hefei, Anhui 230026, P. R. China*

**Polyacrylamide–silver nanocomposites with a silver particle size distribution ranging from 2 to 20 nm in a polyacrylamide matrix are synthesized by γ-irradiation at room temperature.**

Most research has concentrated on the preparation and characterization of single phase materials. More recently the field of interest has broadened to include nanocomposite materials, because of their interesting electrical and optical properties,[1] their possible commercial exploitation and their importance in providing models for understanding the physics of ultrafine particles. Among these materials, organic–inorganic nanocomposites have recently aroused much interest and attention.[2,3] This class of totally innovative materials synergize properties of both components, leading to many applications.[4]

Only a few methods have been used to prepare polymer–metal nanocomposites. Watkins and McCarthy[5] prepared nanocomposites of platinum and poly(4-methylpent-1-ene) **I** by exposing **I** to a solution of dimethyl(cyclooctadiene)platinum in supercritical fluid $CO_2$ for 4 h and subsequent reduction of platinum. Bronstein *et al*.[6] reported a method for the preparation of polymer–cobalt nanocomposites by mixing $Co_2(CO)_8$ with a polyacrylonitrile copolymer or an aromatic polyamide in dimethylformamide (dmf). $Co_2(CO)_8$ interacts with dmf giving the complex $[Co(dmf)_6]^{2+}[Co(CO)_4]_2^-$, which is converted to nanodispersed Co particles by thermolysis.

In these methods, polymerization of organic monomer and formation of nanocrystalline metal particles are performed separately, and the polymer matrix and metal nanoparticles are hybridized physically to form polymer–metal nanocomposites. Thus, metal nanoparticles are not well dispersed homogeneously in the polymer matrix. Furthermore, thermal treatment or pressure is necessary in these methods. To date, little work has been published regarding the room-temperature preparation of polymer–metal nanocomposites. Recently, we have developed the γ-radiation method to prepare ceramic–metal nanocomposites at room temperature.[7,8] Here, we report a new method for the preparation of polymer–metal nanocomposites by γ-irradiation at room temperature and atmospheric pressure. In this method, the metal salt and organic monomer are mixed homogeneously at the molecular level in the solution, and the formation of nanocrystalline metal particles and polymerization of monomer are simultaneous in solution, leading to a homogeneous dispersion of nanocrystalline metal particles in the polymer matrix.

Solutions were prepared by dissolving analytically pure $AgNO_3$ in distilled water and adding acrylamide as the monomer. Solutions were irradiated in the field of a $2.59 \times 10^{15}$ Bq $^{60}Co$ γ-ray source. After γ-irradiation, brown–red, transparent, gelatinous products were obtained. The product was dried in air, and ground to powder which was washed with distilled water and then dried. The concentration of metallic silver in the polyacrylamide matrix was determined by precipitation titration. The sample was dissolved in acetic acid–ethylene glycol (3 : 1, v/v) and nitric acid, adding $NH_4Fe(SO_4)_2$ as a precipitimetric indicator, then titrated using KSCN as a precipitant.

X-Ray powder diffraction (XRD) patterns were recorded using a $D_{max}$ $\gamma_A$ X-ray diffractometer (Japan) with graphite-monochromated Cu-Kα radiation (λ = 0.541 78 nm). TEM images were taken with a Hitachi Model H-800 transmission electron microscope.

The radiation reduction of $Ag^+$ ions by hydrated electrons produced during γ-irradiation in solution leads to the formation of metallic silver nanoparticles.[9] This process can be written in terms of eqns. (1) and (2).

$$Ag^+ + e_{eq}^- \rightarrow Ag^0 \text{ (reduction)} \quad (1)$$

$$nAg^0 \rightarrow Ag_n \text{ (aggregation)} \quad (2)$$

At the same time, polymerization of acrylamide monomer occurs in solution upon γ-irradiation.[10] Because reduction and polymerization occur simultaneously in the solution, the silver nanoparticles are dispersed homogeneously within the polyacrylamide network, which effectively prevents further growth of silver nanoparticles.

Fig. 1 shows the XRD pattern of a typical sample of a polyacrylamide–silver nanocomposite prepared by γ-irradiation of a solution containing 0.05 M $AgNO_3$ and 3.52 M acrylamide with a radiation dose of $2.7 \times 10^4$ Gy. This shows that the sample consisted of two phases, *i.e*. metallic silver, as indicated by diffraction peaks (111), (200), (220), (311), and non-crystalline polyacrylamide. The average particle size of silver is 11 nm, as estimated by the Scherrer formula. The amount of silver present as metallic species in the nanocomposite is 2.09%, as measured by precipitation titration.

A TEM micrograph of the sample prepared under the same experimental conditions as in Fig. 1 is shown in Fig. 2, from which one can see that the nanocomposite contained fine quasi-spherical metallic silver particles homogeneously dispersed and well separated in the polyacrylamide matrix. A histogram of the silver nanoparticles (Fig. 3) shows a distribution of particle sizes ranging from 2 to 20 nm. The average particle size calculated by the reported method[11] was 10.8 nm, with a standard deviation of 2.3.

In summary, γ-irradiation has been used for the first time to prepare, at room temperature, polyacrylamide–silver nanocomposites with a homogeneous dispersion of silver nanopar-

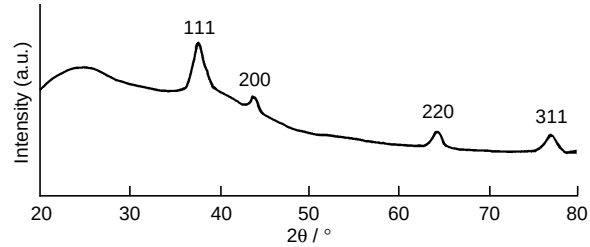



**Fig. 1** XRD pattern of the sample prepared by γ-radiation. Solution: 0.05 M $AgNO_3$–3.52 M acrylamide; radiation dose: $2.7 \times 10^4$ Gy.

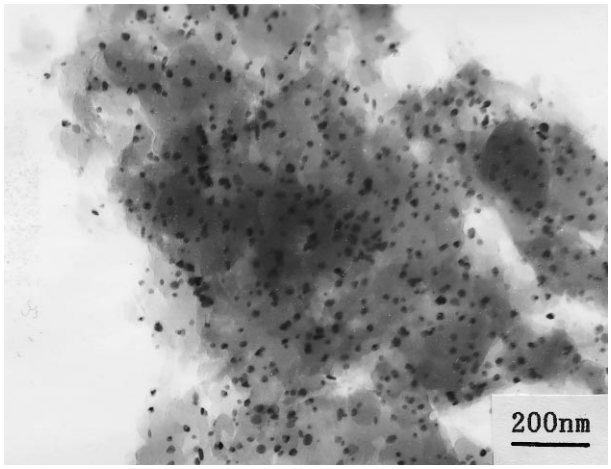



**Fig. 2** TEM micrograph of the same sample as in Fig. 1

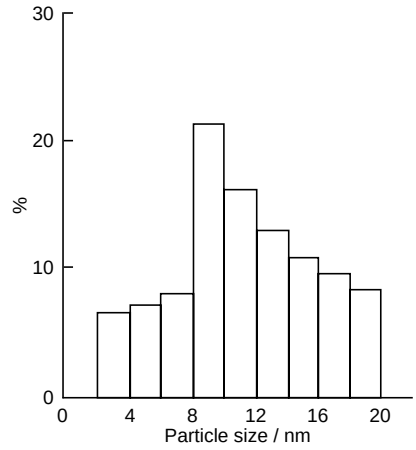



**Fig. 3** Histogram of silver particle size in the sample of Fig. 1

ticles in the polyacrylamide matrix. The radiation induced reduction of metal ions and polymerization of organic monomer occurs simultaneously in solution during γ-irradiation, leading to the formation of polymer–metal nanocomposites in a single step. By appropriate control of the experimental parameters, we predict that the γ-radiation method may be extended to the preparation of a variety of polymer–metal nanocomposites as well as polymer–inorganic compound (*e.g*. polymer–metal oxide, polymer–metal sulfide, *etc*.) nanocomposites.

Financial support from a grant for a key research project in the Climbing Programme from the State Science and Technology Commission of China is gratefully acknowledged.

## Footnote

* Present address: Department of Chemistry, University of Science and Technology of China, Hefei, Anhui 230026, P. R. China, Fax: (0086) 0551 3631760, E-mail: yqian@mail.ach.ustc.edu.cn

## References

1 D. Chakravorty, *Bull. Mater. Sci*., 1984, **6**, 193.
2 P. Judeinstein, P. W. Oliveira, H. Krug and H. Schmidt, *Chem. Phys. Lett*., 1994, **220**, 35.
3 R. Flitton, J. Johal, S. Maeda and S. P. Armes, *J. Colloid Interface Sci*., 1995, **173**, 135.
4 H. Krug and H. Schmidt, *New J. Chem*., 1994, **18**, 1125.
5 J. J. Watkins and T. J. McCarthy, *Polym. Mater. Sci. Eng*., 1995, **73**, 158.
6 L. M. Bronstein, E. Sh. Mirzoeva, M. V. Seregina, P. M. Valetsky, S. P. Solodovnikov and R. A. Register, *ACS Symp. Ser*., 1996, **622**, 102.
7 Y. Zhu, Y. Qian, M. Zhang, Z. Chen and G. Zhou, *J. Mater. Chem*., 1994, **4**, 1619.
8 Y. Zhu, Y. Qian, H. Huang, M. Zhang and S. Liu, *Mater. Lett*., 1996, **28**, 259.
9 Y. Zhu, Y. Qian, M. Zhang, Z. Chen, B. Lu and C. Wang, *Mater. Lett*., 1993, **17**, 314.
10 J. W. T. Spinks and R. J. Woods, *An Introduction to Radiation Chemistry*, 2nd edn. Wiley-Interscience, 1976.
11 B. Champagnon, B. Andrianasolo, A. Ramos, M. Gandais, M. Allais and J. P. Benoit, *J. Appl. Phys*., 1993, **73**, 2775.

*Received in Cambridge, UK, 3rd February 1997, Com. 7/02946B*

# A new and efficient synthesis of rosefuran. A general synthesis of furans by palladium-catalysed cycloisomerization of (*Z*)-2-en-4-yn-1-ols

**Bartolo Gabriele and Giuseppe Salerno***

*Dipartimento di Chimica, Università della Calabria, 87030 Arcavacata di Rende, Cosenza, Italy*

**(*Z*)-3,7-Dimethylocta-2,6-dien-4-yn-1-ol, readily available from (*Z*)-3-methylpent-2-en-4-yn-1-ol, undergoes cycloisomerization in the presence of catalytic amounts of $K_2PdI_4$ to give rosefuran in high yield.**

We report a new, efficient and selective synthesis of rosefuran **3**, a natural product present in the highly prized oil of rose[1] and many other natural sources.[2] The synthesis is realized in two steps with a 60% overall isolated yield, according to Scheme 1.

The key step consists of a Pd-catalysed cycloisomerization of (*Z*)-3,7-dimethylocta-2,6-dien-4-yn-1-ol **2**, readily obtainable in 78% yield from the commercially available (*Z*)-3-methylpent-2-en-4-yn-1-ol **1** *via* Pd/Cu-catalysed coupling with 1-bromo-2-methylpropene.[3] Thus, by reacting **2** (1.88 g, 12.5 mmol) under nitrogen in 5 ml of dry *N*,*N*-dimethylacetamide (DMA) at 100 °C for 24 h in the presence of $PdI_2$ (45 mg, 0.125 mmol) and KI (41.5 mg, 0.25 mmol), rosefuran **3** was obtained in 85% GLC yield. After the usual work-up, **3** was isolated by transfer distillation (1.44 g, 77%).

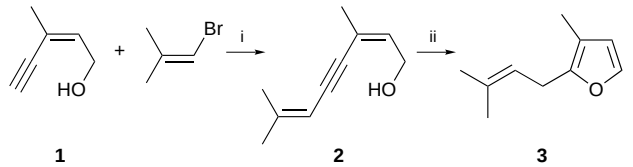
The Pd-based catalytic system here reported also works very well with substrates bearing a terminal triple bond, thus providing a general method for the synthesis of furans by cycloisomerization of (*Z*)-2-en-4-yn-1-ols (Scheme 2).

Terminal enynols are indeed much more reactive than internal ones, and were easily converted to the corresponding furans in excellent yields and with high catalytic efficiencies at 20–45 °C. For example, **1** (3.0 g, 31.2 mmol) was allowed to react under nitrogen at 20 °C† for 18 h without solvent in the presence of $PdI_2$ (22.5 mg, 0.062 mmol) and KI (20.7 mg, 0.125 mmol) to give, after transfer distillation, 2.6 g of 2,3-dimethylfuran (87%). GLC yield was higher than 92%.

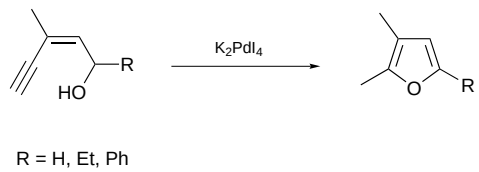
The cycloisomerization process may involve an *anti-exo-dig* intramolecular nucleophilic attack of the hydroxy group to the triple bond coordinated to palladium(II)[4] with formation of a vinylpalladium intermediate **I** and HI (Scheme 3; anionic iodide ligands are omitted for simplicity). Protonolysis of **I** followed by acid-catalysed aromatization leads to the final product with regeneration of the catalytically active species (path *a*). Aromatization of **I** followed by protonolysis is another possibility, however (path *b*).

There are few other methods for synthesis of rosefuran starting from nonfuranoid substrates.[5,6] Very recently, **3** was obtained in 11% overall yield by a four-step synthesis involving a [3 + 2] nitrile oxide cycloaddition as the key step.[6g] Another approach utilized the acid-catalysed cyclization into furans of aliphatic β,γ-dihydroxy ketones, obtained by Ru-catalysed addition of allyl alcohols and alkynes followed by dihydroxylation with $OsO_4$, and afforded **3** in 23% overall yield; isorosefuran (which contains a terminal double bond) was also formed (rosefuran : isorosefuran ratio = 4).[6f] It is noteworthy that a previously reported synthesis of rosefuran starting from enynol **1** required a sequence of five steps and afforded a *ca.* 3 : 1 mixture of **3** and a β-lactone derivative; the latter had to be separated and recycled.[6e]

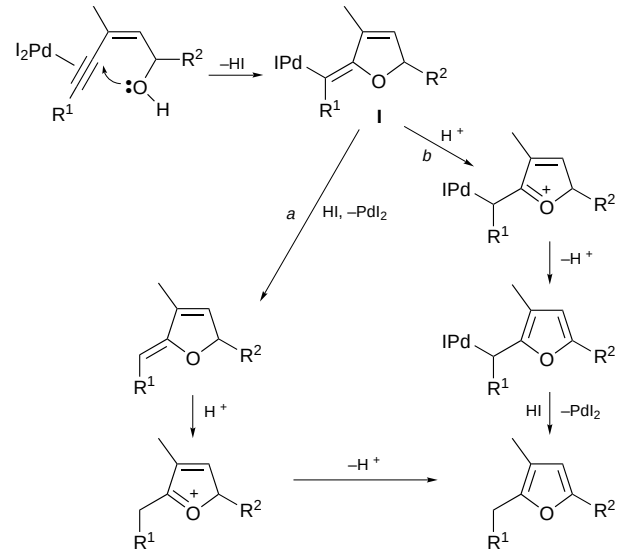
The Ru-catalysed cycloisomerization of (*Z*)-2-en-4-yn-1-ols has been reported, but it could only be applied to terminal enynols.[7] On the other hand, a recently proposed Pd-based catalytic system suitable for internal enynols did not work with substrates bearing a triple bond conjugated with a double bond such as **2**.[7b] The catalytic system here described, in spite of its simplicity, allows the conversion of (*Z*)-2-en-4-yn-1-ols with either internal and terminal triple bonds into the corresponding furans in high yields and with high catalytic efficiencies, and can also be applied to the synthesis of fragile biologically active furan derivatives, such as rosefuran.




**Scheme 1** *Reagents and conditions*: i, $Pd(PPh_3)_2Cl_2$, CuI, $Et_2NH$, 78%; ii, $K_2PdI_4$, DMA, 77%




**Scheme 2**




**Scheme 3**

## Footnotes

* E-mail: g.salerno@unical.it

† The reaction temperature must be controlled with the aid of a water bath owing to the exothermicity of the reaction.

## References

1 K. Bauer, D. Garbe and H. Surburg, *Common Fragrance and Flavour Materials*, VCH, Weinheim, 1990.

2 For recent examples, see: A. O. Tucker and M. J. Maciarello, *J. Essent. Oil Res.*, 1995, **7**, 653; O. Nishimura, *J. Agric. Food Chem.*, 1995, **43**, 2941; D. Karasawa, S. Shatar, A. Erdenechimeg, Y. Okamoto, H. Tateba and S. Shimizu, *J. Essent. Oil Res.*, 1995, **7**, 255.

3 K. Sonogashira, Y. Tohda and N. Hagihara, *Tetrahedron Lett.*, 1975, 4467.

4 C. Lambert, K. Utimoto and H. Nozaki, *Tetrahedron Lett.*, 1984, **25**, 5323.

5 Reported syntheses of rosefuran from furan derivatives: G. Buchi, E. Sz. Kovats, P. Enggist and G. Uhde, *J. Org. Chem.*, 1968, **33**, 1227; O. P. Vig, A. K. Vig, V. K. Handa and S. D. Sharma, *J. Indian Chem. Soc.*, 1974, **51**, 900; A. J. Birch, J. Slobbe, *Tetrahedron Lett.*, 1976, 2079; A. Takeda, K. Shinhama and S. Tsuboi, *Bull. Chem. Soc. Jpn.*, 1977, **50**, 1903; N. D. Ly and M. Schlosser, *Helv. Chim. Acta*, 1977, **60**, 2085; D. R. Gedge and G. Pattenden, *Tetrahedron Lett.*, 1977, 4443; Z. M. Ismail and H. M. R. Hoffmann, *Angew. Chem.*, 1983, **95**, 737; S. Araki and Y. Butsugan, *Bull. Chem. Soc. Jpn.*, 1983, **56**, 1446; L. Meier and H. D. Scharf, *Liebigs Ann. Chem.*, 1986, 731; W. S. Leal, Y. Kuwahara, T. Suzuki and H. Nakao, *Agric. Biol. Chem.*, 1989, **53**, 3279; S. Araki, S.-J. Jin and Y. Butsugan, *J. Chem. Soc., Perkin Trans. 1*, 1995, 549; P. Weyerstahl, A. Schenk and H. Marschall, *Liebigs Ann. Chem.*, 1995, 1849.

6 Reported syntheses of rosefuran from nonfuranoid substrates: (*a*) R. Okazaki, Y. Negishi and N. Inamoto, *J. Org. Chem.*, 1984, **49**, 3819; (*b*) S. Takano, M. Morimoto, S. Satoh and K. Ogasawara, *Chem. Lett.*, 1984, 1261; (*c*) H. Tsukasa, *Agric. Biol. Chem.*, 1989, **53**, 3091; (*d*) R. Iriye, T. Uno, I. Ohwa and A. Konishi, *Agric. Biol. Chem.*, 1990, **54**, 1841; (*e*) J. A. Marshall and W. J. DuBay, *J. Org. Chem.*, 1993, **58**, 3602; (*f*) B. M. Trost and J. A. Flygare, *J. Org. Chem.*, 1994, **59**, 1078; (*g*) A. Barco, S. Benetti, C. De Risi, G. P. Pollini and V. Zanirato, *Tetrahedron*, 1995, **51**, 7721.

7 (*a*) B. Seiller, C. Bruneau and P. H. Dixneuf, *J. Chem. Soc., Chem. Commun.*, 1994, 493; (*b*) B. Seiller, C. Bruneau and P. H. Dixneuf, *Tetrahedron*, 1995, **51**, 13089; (*c*) H. Kucukbay, B. Cetinkaya, S. Guesmi and P. H. Dixneuf, *Organometallics*, 1996, **15**, 2434.

*Received in Liverpool, UK, 21st March 1997; Com. 7/01988B*

# Novel methodology for stereocontrolled synthesis of *cis*-decalins

**Puo-Yi Hsiu and Chun-Chen Liao***

*Department of Chemistry, National Tsing Hua University, Hsinchu, Taiwan 30043*

**Highly functionalized *cis*-decalins are stereoselectively prepared from commercially available catechol derivatives.**

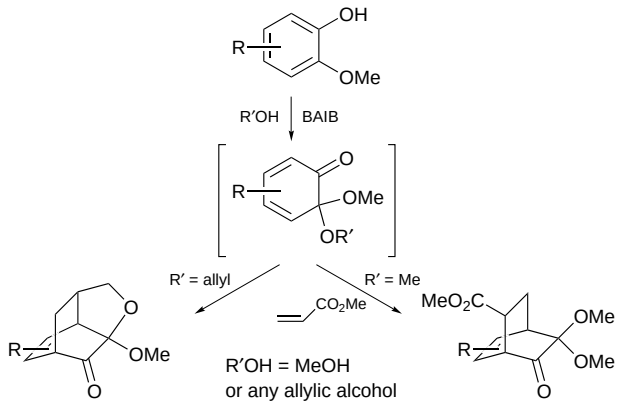
A large variety of natural products of biological importance contain the decalin skeleton as an integral part of their structures.[1–3] Owing to the importance of this structural type in nature, a large number of methodologies have been developed. The Robinson annulation has been the most popular among these strategies. The requirements of modern day stereocontrolled synthesis have been the root cause of the sustained interest in this area, as reflected by the flurry of recent reports by various groups including ours.[4–11]

In our laboratory, a research programme towards the development of a general strategy for the synthesis of clerodane and labdane diterpenoids[2] is underway. The basic skeleton of these terpenoids is a decalin moiety with a considerable number of chiral centres. Towards this end we have recently developed a four-step methodology for the stereocontrolled synthesis of *cis*-decalins starting from commercially available catechol derivatives (Scheme 1).[11] We have already made use of this methodology in the synthesis of an alleged *cis*-clerodane diterpenoic acid.[12] We now report a more simple and efficient methodology starting from commercially available catechol derivatives and 2,4-dienols.

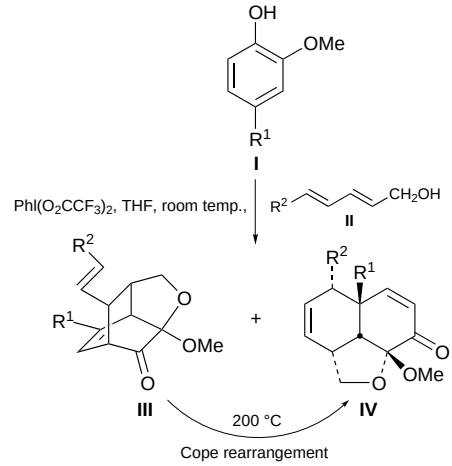
We have been quite successful in using masked *o*-benzoquinones, generated *in situ* from 2-methoxyphenols *via* oxidation by bis(acetoxy)iodobenzene (BAIB) or bis(trifluoroacetoxy)iodobenzene (BTIB), as dienes in inter- and intra-molecular Diels–Alder reactions.[13] The use of this type of cyclohexadienone as a dienophile has not been investigated much.[14] Since the cyclohexadienone moiety can act either as a diene or dienophile, it occurred to us that, if the allylic alcohol is replaced with a 2,4-dienol, it might give rise to *cis*-decalins **IV** and/or tricyclic compounds of the type **III** (Scheme 2).

Accordingly, we first carried out the reaction of *trans*-penta-2,4-dienol and methyl vanillate, which gave both the expected products **IIIe** and **IVe** in 1 : 1 ratio. The tricyclic compound **IIIe**, when heated to 200 °C in mesitylene, underwent Cope rearrangement smoothly. The total yield of decalin is about 60% (procedure A†). Then we extended this methodology to a variety of catechol derivatives and dienols. The ratio of **III** to **IV** depends on the substituents. The reaction conditions and results are shown in Table 1. To make the whole transformation simple, the crude Diels–Alder reaction mixtures were concentrated using a kugelrohr apparatus after the usual work-up and the residues were dissolved in mesitylene and heated to 200 °C to obtain decalins as the sole products in good yields (Table 1, procedure B‡).

As shown in Scheme 3, the intramolecular Diels–Alder reaction can afford three products. However, we could isolate only two products **III** and **IV**. Therefore, in both modes, the cycloaddition seems to be *endo*-selective.

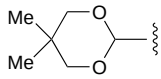



**Scheme 1**




**Scheme 2**

**Table 1** Preparation of *cis*-decalins

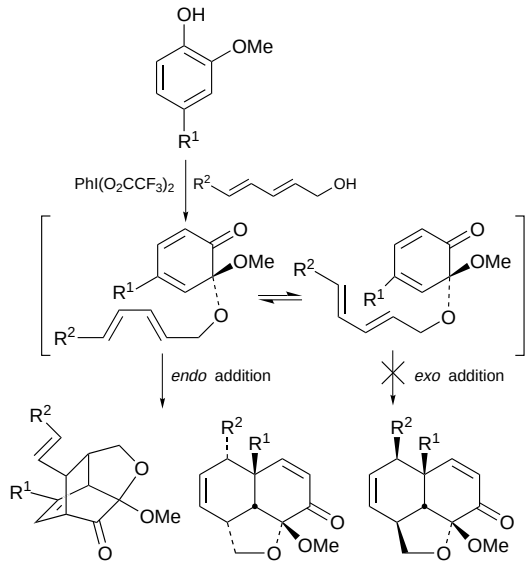
| | | Yield (%) | | Ratio | Yield of **IV** (%) | | |
|---|---|---|---|---|---|---|---|
| $R^1$ | $R^2$ | **III** | **IV** | **III : IV** | From **III** | Procedure A | Procedure B |
| Me | Me | 46 | 16 | 3 : 1 | 95 | 60 | 72 |
| | H | 40 | 20 | 2 : 1 | 93 | 57 | 62 |
| $CO_2Me$ | Me | 16 | 46 | 1 : 3 | 93 | 61 | 55 |
| | H | 31 | 31 | 1 : 1 | 92 | 60 | 50 |
|  | Me | 60 | 10 | 6 : 1 | 93 | 66 | 73 |
| | H | 57 | 19 | 3 : 1 | 100 | 76 | 60 |

When *cis*-penta-2,4-dienol **V** was employed as a dienol, only tricyclic compounds **VI** were obtained (Table 2). This may be due to the fact that the *o*-benzoquinone moiety acts more efficiently as a diene than a dienophile (Table 1). In addition to this, the equilibrium between s-*trans* and s-*cis* forms of the acyclic diene moiety should favour the s-*trans* form as a consequence of steric requirements. Predictably, these compounds did not undergo Cope rearrangement.

All the new compounds were characterized by IR, $^1$H and $^{13}$C NMR and mass spectral analysis. The stereochemistry of **IVa** was established by NOE studies, and those of other compounds **IV** were assigned by analogy with **IVa**.

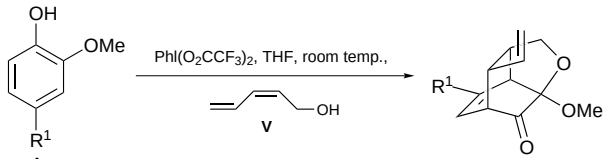
In conclusion, our methodology should be among the simplest for the preparation of such highly functionalized decalins with total stereocontrol. The utilization of this methodology in the synthesis of decalin-based natural products is under active investigation in our laboratory.

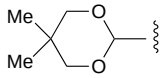
We thank National Science Council (NSC) of Taiwan, R.O.C., for financial support, and Dr P. Dharma Rao for helpful discussions.




**Scheme 3**

**Table 2** Diels–Alder reaction of *cis*-penta-2,4-dienol




| $R^1$ | Yield (%) |
|---|---|
| Me | 52 |
| $CO_2Me$ | 47 |
|  | 36 |

## Footnotes

† *Procedure A: Diels–Alder reaction:* To a stirred mixture of catechol derivative (10 mmol) and dienol (100 mmol) in dry THF (25 ml), a solution of bis(trifluoroacetoxy)iodobenzene (BTIB) (15 mmol) in dry THF (25 ml) was added dropwise during 10 min using a syringe pump at room temperature under nitrogen atmosphere. After 6 h stirring, solid $NaHCO_3$ (30 mmol) was added. After 10 min stirring, water (25 ml) was added and the layers were separated. The aqueous layer was extracted with ethyl acetate (3 × 25 ml). The combined organic layer was dried over anhydrous $MgSO_4$. The solvent was removed under reduced pressure on a rotavapor, followed by removal of the excess dienol using a kugelrohr apparatus. The two products **III** and **IV** were separated by column chromatography on silica gel using 15% ethyl acetate in hexane as eluent.

*Cope rearrangement*: To a solution of compound **III** (5 mmol) in mesitylene was added trimethyl orthoformate (5 mmol) and the resulting mixture was degassed with argon for 30 min. The reaction mixture was then heated for 8 h at 200 °C, cooled and the mesitylene was removed using a kugelrohr apparatus under reduced pressure to give pure product **IV** in excellent yield.

‡ *Procedure B:* The Diels–Alder reaction mixture after work-up (see Procedure A) was concentrated using a kugelrohr apparatus and the crude product mixture thus obtained was dissolved in mesitylene. To this was added 1 equiv. of trimethyl orthoformate and the resulting mixture was degassed and subjected to heating at 200 °C for 8 h. Then mesitylene was removed using a kugelrohr apparatus and the residue thus obtained was purified by column chromatography on silica gel using 15% ethyl acetate in hexane as eluent to give compound **IV** as the sole product.

## References

1 The Chemistry of Natural Products, ed. R. H. Thomson, Blackie Academic and Professional, London, 1993.
2 J. R. Hanson, *Nat. Prod. Rep.*, 1995, **12**, 207 and references cited therein.
3 S. V. Ley and A. T. Merritt, *Nat. Prod. Rep.*, 1992, **9**, 243.
4 W. P. Jackson and S. V. Ley, *J. Chem. Soc., Perkin Trans. 1*, 1981, 1516.
5 J. F. Lavallee and P. Deslongchamps, *Tetrahedron Lett.*, 1988, **29**, 6033.
6 H.-J. Liu and Y. Hen, *Tetrahedron Lett.*, 1993, **34**, 423.
7 G. Muller and G. Jas, *Tetrahedron Lett.*, 1992, **33**, 4417.
8 Y. Sato, S. Watanabe and M. Shibasaki, *Tetrahedron Lett.*, 1992, **33**, 2589.
9 H. Bouchard and J. Y. Lallemand, *Tetrahedron Lett.*, 1990, **31**, 5151.
10 T.-H. Chan and O. Z. Pereira, *J. Org. Chem.*, 1994, **59**, 6710.
11 T. H. Lee, C.-C. Liao and W.-C. Liu, *Tetrahedron Lett.*, 1996, **37**, 5897.
12 T.-H. Lee and C.-C. Liao, *Tetrahedron Lett.*, 1996, **37**, 6869.
13 C.-S. Chu, T.-H. Lee and C.-C. Liao, *Synlett*, 1994, 635.
14 R. S. Coleman and E. B. Grant, *J. Am. Chem. Soc.*, 1995, **117**, 10 889.

*Received in Cambridge, UK, 7th April 1997; Com. 7/02363D*

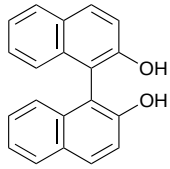
# New chiral ammonium salt hosts derived from amino acids: very efficient optical resolution of 2,2′-dihydroxy-1,1′-binaphthyl by complexation with these host compounds

**Fumio Toda* and Kenya Tanaka**

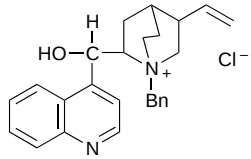
*Department of Applied Chemistry, Faculty of Engineering, Ehime University, Matsuyama, Ehime 790, Japan*

**Chiral ammonium salt hosts are prepared from amino acids by transformation of their $NH_2$ and $CO_2H$ groups into $Me_3N^+Br^-$ and $CH_2OH$ groups, respectively, *via* three simple reaction steps; by complexation with these hosts, 2,2′-dihydroxy-1,1′-binaphthyl is resolved very efficiently.**

It has been reported that ′onium salts such as ammonium[1–5] and phosphonium salts[6] form inclusion complexes with alcohol and phenol derivatives *via* hydrogen bond formation between the counter anion of the ′onium salt host and the hydroxy group of the alcohol or phenol guest. In these inclusion complexes, molecular recognition between the host and guest occurred and separation of isomers of the guest was accomplished. When a chiral ′onium salt host is used, *rac*-guest compounds were resolved. For example, *rac*-2,2′-dihydroxy-1,1′-binaphthyl **1**

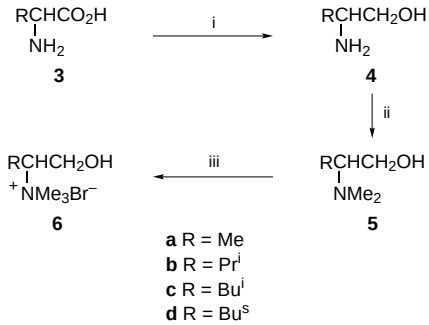



**1**




(–)-**2**

was easily resolved by complexation with *N*-benzylcinchonidinium chloride **2**, because **2** forms a 1 : 1 inclusion complex with (*R*)-(+)-**1** selectively.[4] X-Ray crystal structure analysis of the complex showed that the complex is mainly constructed *via* formation of an intermolecular hydrogen bond between $Cl^-$ of **2** and the OH group of **1**. It was also found that an intramolecular hydrogen bond between the OH group of **2** and $Cl^-$ plays an important role in forming the complex.[5] This finding suggests that a chiral compound which has $Me_3N^+X^-$ and OH groups would be a good host for resolution of *rac*-**1**. According to this idea, chiral β-hydroxy trimethylammonium bromide hosts **6a–d** were prepared from the corresponding β-amino acids **3a–d** by transformation of their $NH_2$ and $CO_2H$ groups into $Me_3N^+Br^-$ and $CH_2OH$ groups, respectively, *via* the three step reaction shown in Scheme 1.




**Scheme 1** *Reagents*: i, $LiAlH_4$; ii, $HCO_2H$, HCHO; iii, MeBr

For example, treatment of L-leucinol **4c**, prepared by $LiAlH_4$ reduction of L-leucine **3c** in 99% yield,[7] with formaldehyde and formic acid according to the reported procedure[8] gave *N*,*N*-dimethyl-L-leucinol **5c** in 98% yield. Treatment of **5c** with MeBr gave the quaternary ammonium salt host, (+)-1-hydroxymethyl-3-methylbutyl(trimethyl)ammonium bromide **6c** in 77% yield as colourless prisms.† By the same procedure, (−)-**6a**, (+)-**6b** and (+)-**6d** were prepared from L-alanine (**3a**), L-valine (**3b**) and L-isoleucine (**3d**), respectively.

When a solution of (+)-**6c** (0.5 g, 2.08 mmol) and *rac*-**1** (1.19 g, 4.16 mmol) in EtOH (6 ml) was kept at room temperature for 24 h, a 1 : 1 inclusion complex of (+)-**6c** and (+)-**1** was obtained as colourless prisms. The crude complex was recrystallised from diethyl ether to give pure complex crystals‡ and then the pure complex crystals were dissolved in a mixture of diethyl ether and water. From the diethyl ether solution, (+)-**1** (100% ee)§ was obtained (0.42 g, 70% yield). From aqueous solution, **6c** was recovered (0.43 g, 86% yield). By the same complexation experiments of *rac*-**1** with (−)-**6a**, (+)-**6b** and (+)-**6d**, (−)-**1** (100% ee, 68% yield), (+)-**1** (100% ee, 36% yield) and (−)-**1** (100% ee, 48% yield) were obtained, respectively. In all cases, host compounds were recovered in almost quantitative yield and could be reused.

In comparison to the resolution of *rac*-**1** by complexation with **2**, the present resolution with **6** of about half mole of **2** has many advantages. Since **6** can easily be prepared in large quantities from cheap L-amino acid *via* a simple three step reaction, the present resolution method is more economical than that *via* the relatively expensive **2**. Furthermore, either (+)-**1** or (−)-**1** can be obtained according to demand, as (−)-**6a** and (+)-**6d** include (−)-**1** and (+)-**6b** and (+)-**6c** include (+)-**1**.

By using the precise chiral recognition between **1** and **6** in the inclusion complex, *rac*-**6** can also be resolved by optically active **1**. For example, when a solution of *rac*-**6d** (0.34 g, 1.40 mmol), prepared from *rac*-isoleucine (*rac*-**3d**) and (−)-**1** (0.2 g, 0.69 mmol) in EtOH (3.5 ml) was kept at room temperature for 24 h, a 1 : 1 complex of (−)-**1** and (+)-**6d** was obtained, after recrystallisation from EtOH, as colourless prisms (0.28 g, 76% yield). The pure complex crystals were dissolved in a mixture of diethyl ether and water. From aqueous solution, (+)-**6d** (100% ee) was obtained (0.13 g, 76% yield). From diethyl ether solution, (−)-**1** was recovered (0.15 g, 76% yield).

We thank the Ministry of Education, Science and Culture, Japan, for a grant-in-aid for Scientific Research on Priority Areas, No. 0642105.

## Footnotes

* E-mail: toda@en3.ehime-u.ac.jp

† *Selected data* for (−)-**6a**: no clear mp; $[\alpha]_D$ −4.6 (*c* 0.5, MeOH); $\nu_{max}$ (Nujol)/cm$^{-1}$ 3292 (OH); Calc. for $C_6H_{16}ONBr$: C, 36.38; H, 8.14; N, 7.07. Found: C, 36.35; H, 8.12; N, 7.10%. For (+)-**6b**: mp 153–160 °C; $[\alpha]_D$ +6.9 (*c* 0.5, MeOH); $\nu_{max}$(Nujol)/cm$^{-1}$ 3275 (OH); Calc. for $C_8H_{20}ONBr$: C, 42.49; H, 8.91; N, 6.19. Found: C, 42.19; H, 8.91; N, 6.33%. For **6c**: mp 153–156 °C; $[\alpha]_D$ +18.0 (*c* 0.5, MeOH); $\nu_{max}$(Nujol)/cm$^{-1}$ 3290 (OH); Calc. for $C_9H_{22}ONBr$: C, 52.56; H, 7.35; N, 5.11. Found: C, 52.49; H, 7.09;

N, 5.03%. For (+)-**6d**: mp 156–157 °C; $[\alpha]_D$ + 8.9 (*c* 0.5, MeOH); $\nu_{max}$(Nujol)/cm$^{-1}$ 3275 (OH); Calc. for $C_9H_{22}ONBr$: C, 52.56; H, 7.85; N, 5.11. Found: C, 52.30; H, 7.10; N, 5.30%.

‡ *Selected data* for complex of (+)-**6c** and (+)-**1**: 0.96 g, 88% yield; no clear mp; $[\alpha]_D$ +33.2 (*c* 0.5, THF), $\nu_{max}$(Nujol)/cm$^{-1}$ 3200 (OH); Calc. for $C_{12}H_{20}ONBr$: C, 65.91; H, 6.98; N, 2.63. Found: C, 65.80; H, 6.90; N, 2.90%.

§ All optical purities of (+)- and (−)-**1** were determined by HPLC using a column containing an optically active solid phase (Chiralpak AS) and hexane–EtOH (95 : 5) as eluent. The Chiralpak AS is available from Daicel Chemical Industries Ltd., Himeji, Japan.

## References


1 F. Vogtle, H.-G. Lohr, J. Franke and D. Worsch, *Angew. Chem., Int. Ed. Engl*., 1985, **24**, 727.

2 F. Toda, K. Tanaka, T. Okada, S. A. Bourne and L. R. Nassimbeni, *Supramol Chem*., 1994, **3**, 291.

3 K. Tanaka, K. Tamura and F. Toda, *J. Chem. Soc., Perkin Trans. 2*, 1995, 1571.

4 K. Tanaka, T. Okada and F. Toda, *Angew. Chem., Int. Ed. Engl*., 1993, **32**, 1147.

5 F. Toda, K. Tanaka, Z. Stein and I. Goldberg, *J. Org. Chem*., 1994, **59**, 5748.

6 F. Toda, K. Tanaka and H. Sawada, *J. Chem. Soc., Perkin Trans. 1*, 1995, 3065.

7 A. W. Rastou and D. N. Eggenberger, *J. Am. Chem. Soc*., 1947, **69**, 2095.

8 C. C. Tseng, S. Terashima and S. Yamada, *Chem. Pharm. Bull*., 1977, **25**, 29.



*Received, in Cambridge, UK, 11th March 1997; Com. 7/01682D*

# Synthesis and structure of an open-framework tin phosphate, $[H_3N(CH_2)_4NH_3]_{0.5}^{2+}[Sn_4P_3O_{12}]^-$, containing intersecting channels

**Srinivasan Natarajan and Anthony K. Cheetham***

*Materials Research Laboratory, University of California, Santa Barbara, CA 93106, USA*

**A novel open-framework tin phosphate made of strictly alternating $SnO_3$ and $PO_4$ moieties contains two intersecting channels; the protonated 1,4-diaminobutane molecules are situated in one of the channels and the lone pairs of $Sn^{II}$ extend into the other, preventing access to the channel.**

The use of structure-directing agents (templates) in the synthesis of new solids exhibiting open-framework structures has gained prominence, following the seminal work at Mobil in the late 1960s and early 1970s.[1] It is now well established that for the synthesis of new micro- and meso-porous materials, an organic structure-directing agent can be used to steer the process of crystallization to form open architectures.[2–5] Not only is it possible to synthesize materials resembling naturally occurring zeolites,[6–8] but new aluminosilicate and phosphate materials with interesting structures have been synthesized and studied in great detail.[9–11] The organic moiety is normally accommodated within the cavities and channels of these open structures and, in many cases, can be removed by post-synthesis treatments such as calcination or chemical extraction (leaching). In the course of a programme[12–15] aimed at producing new open-framework structures, we have recently shown that open-framework tin phosphate compounds can be synthesized with the aid of organic structure-directing molecules.[16] We now report the synthesis and structure of a new tin phosphate with the same composition as that reported previously,[16] but synthesized in the presence of a different organic molecule: 1,4-diaminobutane rather than ethylenediamine. A new open-framework architecture is thereby created.

The title compound was synthesised from a starting tin phosphate gel containing 1,4-diaminobutane as the structure directing agent. Tin(II) oxalate (Aldrich), phosphoric acid (85 mass%, Aldrich), 1,4-diaminobutane [$H_2N(CH_2)_4NH_2$, Aldrich] and water in the ratio $SnC_2O_4 : 0.5P_2O_5 : 1.0H_2N(CH_2)_4NH_2 : 55H_2O$ were mixed and stirred until homogeneous. The mixture was sealed in a Teflon lined stainless steel autoclave (Parr, USA) and heated at 170 °C for 2 days under autogeneous pressure. The resulting product, containing a mixture of powder and colourless single crystals, was filtered and washed thoroughly with deionised water. The single crystals were separated easily by ultrasonication. The powder X-ray diffraction indicated that the product was a new material; the pattern is entirely consistent with the structure determined by single-crystal X-ray diffraction. Thermogravimetric analysis (TGA) under an oxygen atmosphere in the range from room temperature to 700 °C show only one mass loss in the region 400–475 °C. The mass loss corresponds to about 4.97% of the total mass of the sample and can be directly correlated to the decomposition of the occluded organic cation, diprotonated diaminobutane (calc. 5.3%). The powder X-ray diffraction pattern of the decomposed sample indicated the presence of another new phase.

The structure, which was solved by single-crystal X-ray diffraction,† is based on a network of strictly alternating $SnO_3$ and $PO_4$ units in which all the vertices are shared. The $SnO_3$ and $PO_4$ units form a framework with the formula $[Sn_4P_3O_{12}]^-$. Charge neutrality is achieved by the incorporation of the template in its diprotonated form; there are $0.5[H_3N(CH_2)_4NH_3]^{2+}$ ions per framework formula unit. The asymmetric unit contains 22 independent non-hydrogen atoms [Fig. 1(*a*)]: three phosphate goups are linked *via* oxygens to four tin atoms to form the building block of the framework. All the P–O distances are in the range 1.495–1.544 Å (av. 1.526 Å) and the bond angles are in the range 105.5–113.5° (av. 109.5°), which is in good agreement with those previously observed.[12–15] All the Sn atoms are three-coordinated with respect to oxygen with Sn–O distances in the range 2.075–2.206 Å (av. 2.118 Å) and the Sn–O bond angles are in the range 81.5–93.59° (av. 86.87°). These values are typical of three-coordinated Sn in the 2+ oxidation state and are in excellent agreement with other previously known tin phosphates in the literature.[16–20] The three oxygen atoms form a trigonal pyramid around the Sn with the lone pair of electrons on the Sn atoms presumably occuping the base vertex of a tetrahedron. The lone pair of electrons associated with $Sn^{II}$ opens up the possibility of using this material, or others like it, in base-catalysed reactions; zeolites and aluminophosphates are normally used for acid-catalysed processes.

The entire framework structure can be considered to be built from the networking of four-, six-, eight- and twelve-membered rings. The four- and six- (slightly distorted) membered rings are so connected as to form a one-dimensional eight-membered

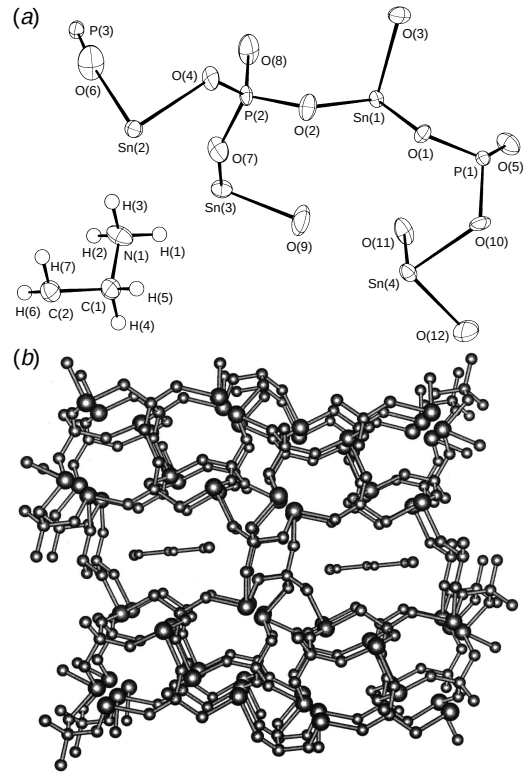



**Fig. 1** (*a*) The asymmetric unit of $[H_3N(CH_2)_4NH_3]_{0.5}^{2+}[Sn_4P_3O_{12}]^-$ and (*b*) the structure showing the uniform eight-membered channel along the *b* axis. The hydrogens on the amine molecule are not shown for clarity.

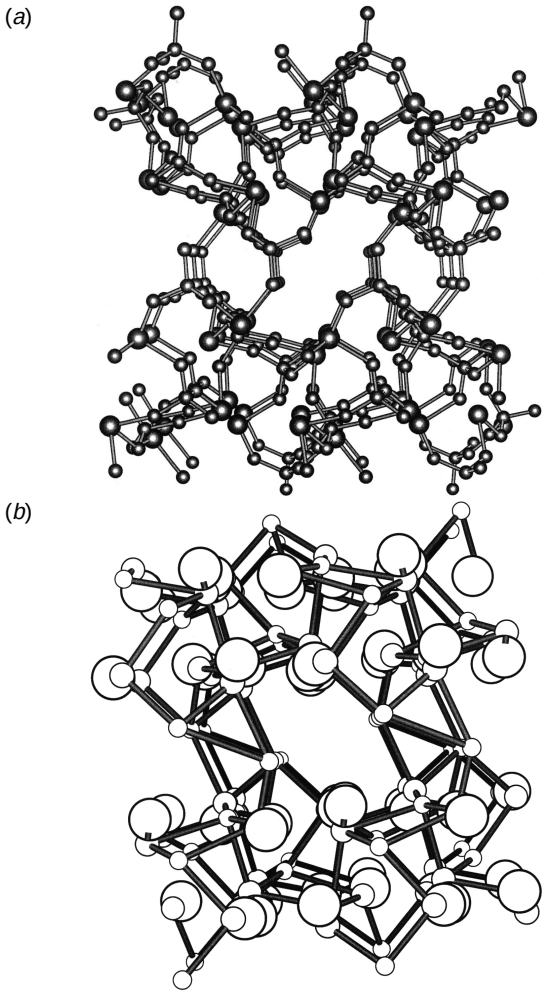



**Fig. 2** (*a*) View showing the staggered twelve-membered ring channel along the *c* axis. The amine molecule is not shown for clarity. (*b*) View showing the staggered twelve-membered ring channel along with the lone pair of electrons on the Sn atoms. The amine molecule and the oxygens are not shown.

channel along the *b* axis. The width of this channel is 9.4 × 6.2 Å. The template molecule sits in the middle of this channel [Fig. 1(*b*)]. Along the *c* direction, there is another channel delineated by twelve-membered rings. However, the twelve-membered rings are staggered and, in projection, create the appearance of a compressed eight-membered ring channel of width 9.6 × 5.1 Å [Fig. 2(*a*)]. The lone pair of electrons of the $Sn^{II}$ atoms extend into this channel and prevent access completely for any guest molecules [Fig. 2(*b*)]. The intersection of these two channels forms a cage which can be considered to be a pseudo-cube. The organic template is located at this intersection.

Presently, our efforts to remove the organic molecule by thermal methods to render the material microporous were not successful and we are pursuing softer chemical techniques (*e.g.* Soxhlet extraction) for this step. Our continuing research on tin phosphates indicates that further open-framework structures are formed under hydrothermal conditions using other structure directing agents.

The work was funded by the MRSEC program of the National Science Foundation under the award DMR 9632716.

## Footnotes

† A suitable single crystal (0.04 × 0.04 × 0.10 mm) was carefully selected under a polarizing microscope. *Crystal data* for $[H_3N(CH_2)_4NH_3]_{0.5}^{2+}[Sn_4P_3O_{12}]^-$: $M$ = 804.75(3), monoclinic, space group $P2_1/c$ (no. 14), $a$ = 10.0163(14), $b$ = 7.8878(4), $c$ = 20.1187(33) Å, β = 101.24(2)°, $U$ = 1558.84(1), $Z$ = 4, graphite-monochromated Cu-Kα radiation, λ = 1.5418 Å, $T$ = 293 K, $D_c$ = 3.428(1) g cm$^{-3}$. Data collection was performed on an Enraf-Nonius CAD4-MACH four-circle diffractometer equipped with a Rigaku rotating anode using ω–2θ scans with the width of Δω = (1.0 + 0.15tanθ)° extending 25% on each side for background measurement. The unit-cell constants were determined from 25 well centred reflections within the 2θ range 29.3–64.9°. A total of 4154 reflections were collected. These were merged to give 2955 unique data ($R_{merg}$ = 5.27) of which 2569 were considered to be observed with $I > 3\sigma(I)$. The structure was solved by direct methods using SHELX-86[21] and difference Fourier syntheses. The absorption correction was carried out using DIFABS calculation routine. Hydrogen atoms on the amine molecules were placed geometrically and held in the 'riding' mode. Final $R_F$ = 0.0414 and $R_w$ = 0.0485 (unit weights), $S$ = 1.04, were obtained for a total of 200 parameters. The final Fourier map had a minimum and maximum of −1.36 and 1.55 e Å$^{-3}$ respectively. Full-matrix least-squares structure refinement was carried out using the CRYSTALS[22] package of programs. Atomic coordinates, bond lengths and angles, and thermal parameters have been deposited at the Cambridge Crystallographic Data Centre (CCDC). See Information for Authors, Issue No. 1. Any request to the CCDC for this material should quote the full literature citation and the reference number 182/440.

## References

1 R. J. Argauer and G. R. Landolt, *US Pat*. 3 702 886, 1972.
2 J. M. Thomas, *Philos. Trans. R. Soc. London A*, 1990, **333**, 173.
3 Q. Huo, D. I. Margolese, U. Ciesla, P. Feng, T. E. Gier, P. Sieger, R. Leon, P. M. Petroff, F. Schuth and G. D. Stucky, *Nature*, 1994, **368**, 317.
4 J. V. Smith, *Chem. Rev.*, 1988, **88**, 149.
5 M. E. Davis, *Acc. Chem. Res.*, 1993, **26**, 111.
6 J. J. Pluth, J. V. Smith and J. M. Bennett, *Acta Crystallogr., Sect. C*, 1986, **42**, 283.
7 W. H. Baur, *Am. Mineral.*, 1964, **49**, 697.
8 W. H. Mortier, J. J. Pluth and J. V. Smith, *Mater. Res. Bull.*, 1977, **12**, 241.
9 P. A. Wright, R. H. Jones, S. Natarajan, R. G. Bell, J. Chen, M. B. Hursthouse and J. M. Thomas, *J. Chem. Soc., Chem. Commun.*, 1993, 633.
10 G. T. Kokotailo, S. L. Lawton, D. H. Olson and W. M. Meier, *Nature*, 1978, **272**, 437.
11 C. C. Freyhardt, M. Tsapatsis, R. F. Lobo, K. J. Balkus Jr. and M. E. Davis, *Nature*, 1996, **381**, 295.
12 A. M. Chippindale, A. V. Powell, R. H. Jones, J. M. Thomas, A. K. Cheetham, Q. Huo and R. Xu, *Acta Crystallogr., Sect. C*, 1994, **50**, 1537.
13 M. P. Attfield, R. E. Morris, E. Gutierrez-Puebla, A. Monge-Bravo and A. K. Cheetham, *J. Chem. Soc., Chem. Commun.*, 1995, 843.
14 S. Natarajan, J.-C. Gabriel and A. K. Cheetham, *Chem. Commun.*, 1996, 1415.
15 S. J. Weigel, S. C. Weston, A. K. Cheetham and G. D. Stucky, *Chem. Mater.*, 1997, in the press.
16 S. Natarajan, M. P. Attfield and A. K. Cheetham, *Angew. Chem.*, 1997, in the press.
17 M. Mathew, L. W. Schroeder and T. H. Jordan, *Acta Crystallogr., Sect. B*, 1977, **33**, 1812; T. H. Jordan, B. Dickens, L. W. Schroeder and W. E. Brown, *Inorg. Chem.*, 1980, **19**, 2251.
18 L. W. Schroeder and E. Prince, *Acta Crystallogr., Sect. B*, 1976, **32**, 3309; T. H. Jordan, L. W. Schroeder, B. Dickens and W. E. Brown, *Inorg. Chem.*, 1976, **15**, 1810.
19 A. F. Brendt, *Acta Crystallogr., Sect. B*, 1974, **30**, 529.
20 R. C. McDonald and K. Eriks, *Inorg. Chem.*, 1980, **19**, 1237.
21 G. M. Sheldrick, SHELXS-86, Program for Crystal Structure Determination, University of Gottingen, 1986, *Acta. Crystallogr., Sect. A*, 1990, **46**, 467.
22 D. J. Watkin, J. R. Carruthers and P. W. Betterridge, CRYSTALS User Guide, Chemical Crystallography Laboratory, University of Oxford, 1985.

*Received in Bloomington, IN, USA, 18th February 1997; Com. 7/01141E*

# Synthesis and structure of a dinuclear zinc(II) triple helix of an *N,N*-bis-bidentate Schiff base: new building blocks for the construction of helical structures

**Noboru Yoshida* and Kazuhiko Ichikawa**

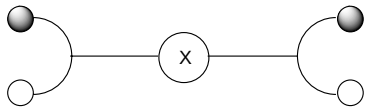
*Laboratory of Molecular Functional Chemistry, Division of Material Science, Graduate School of Environmental Earth Science, Hokkaido University, Sapporo 060, Japan*

**The formation of a novel helical zinc(II) complex of an *N,N*-bis-bidentate Schiff base is reported; the edge-to-face and face-to-face π···π interactions play an important role in the metal-assisted self-assembling process in solution.**

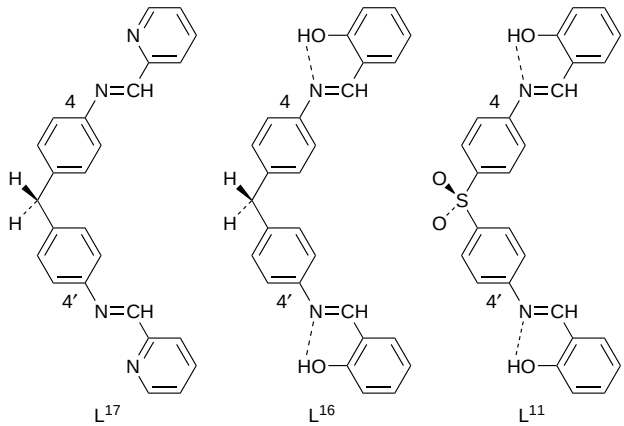
Weak non-covalent interactions play an important role in the kinetics of the molecular recognition by α-cyclodextrin in aqueous solution.[1] Contrary to our expectation, enthalpic rather than entropic factors are the principal driving force to form a regioselective host–guest complex[1c–e] in which weak interactions such as London dispersion forces, dipole–dipole and CH··π interactions[2] operate. Recently, great interest has been focused on metal-assisted self-assembly of helical[3] and box-like[4] supramolecular complexes in which the stereochemical preference of a labile metal centre is exploited.[3]

Another very important aspect of self-assembly investigations has been the development of the design at ligands which induces cooperative behaviour *via* the weak interactions. From this point of view, a new type of bis-bidentate ligand has been developed (Scheme 1).[5,6]

Recently, we have focused on some semi-*N,O*-bidentate and bis-*N,O*-bidentate Schiff-base ligands which can be electronically and configurationally controlled, leading to a systematic study of the self-assembly process in solution.[7] Thus, bis-*N,N*- and bis-*N,O*-bidentate Schiff-base ligands, $L^{11}$, $L^{16}$ and $L^{17}$, have been designed (Scheme 2) to bind two separate metal ions owing to the fact that the bridging group (X = $–C_6H_4CH_2C_6H_4–$ or $–C_6H_4SO_2C_6H_4–$) prevents the metal ions from forming 1 : 1 four coordinate complexes.




**Scheme 1** X = –CONHC*H(R)$CH_2$C*H(R)NHCO– (ref. 5) or $–(CH_2)_n–$ (ref. 6*a*); ⊘ = strong donor atom, ○ = weak donor atom




**Scheme 2**

Here we report the facile synthesis of helical zinc(II) complexes utilizing weak interactions in which CH··π and π··π interactions of aromatic rings between two or three bridging groups (X = $–C_6H_4CH_2C_6H_4–$ or $–C_6H_4SO_2C_6H_4–$) having high conformational freedom may be involved in the self-assembling process.

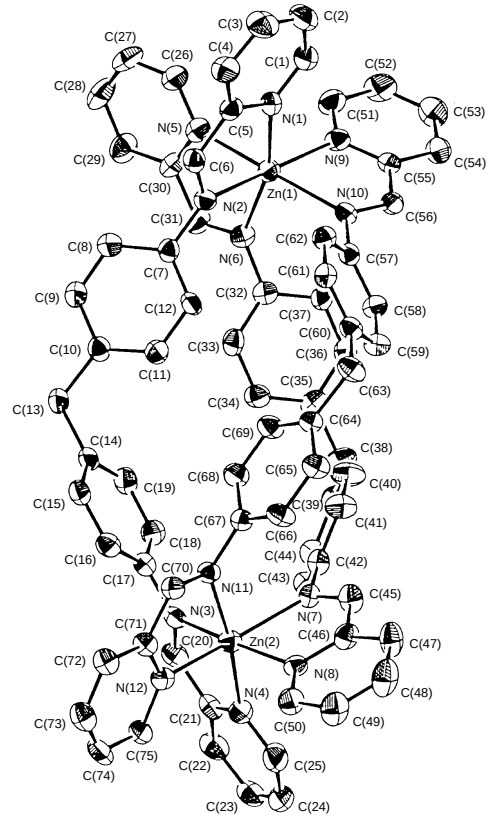



**Fig. 1** Molecular structure of the complex cation of **1**. Hydrogen atoms have been omitted for clarity. Selected bond lengths (Å) and angles (°): Zn(1)–N(1) 2.158(6), Zn(1)–N(2) 2.195(5), Zn(1)–N(5) 2.186(7), Zn(1)–N(6) 2.193(6), Zn(1)–N(9) 2.154(6), Zn(1)–N(10) 2.176(6), Zn(2)–N(3) 2.174(6), Zn(2)–N(4) 2.132(7), Zn(2)–N(7) 2.247(6), Zn(2)–N(8) 2.167(6), Zn(2)–N(11) 2.200(6), Zn(2)–N(12) 2.187(6); N(1)–Zn(1)–N(2) 76.7(2), N(1)–Zn(1)–N(5) 91.3(3), N(1)–Zn(1)–N(6) 164.7(2), N(1)–Zn(1)–N(9) 98.4(2), N(1)–Zn(1)–N(10) 94.5(2), N(2)–Zn(1)–N(5) 87.6(2), N(2)–Zn(1)–N(6) 93.5(2), N(2)–Zn(1)–N(9) 173.6(2), N(2)–Zn(1)–N(10) 99.9(2), N(5)–Zn(1)–N(6) 76.5(2), N(5)–Zn(1)–N(9) 96.7(2), N(5)–Zn(1)–N(10) 171.4(2), N(6)–Zn(1)–N(9) 92.1(2), N(6)–Zn(1)–N(10) 98.7(2), N(9)–Zn(1)–N(10) 76.2(2), N(3)–Zn(2)–N(4) 77.3(3), N(3)–Zn(2)–N(7) 96.0(2), N(3)–Zn(2)–N(8) 170.1(2), N(3)–Zn(2)–N(11) 100.6(2), N(3)–Zn(2)–N(12) 97.9(2), N(4)–Zn(2)–N(7) 93.2(2), N(4)–Zn(2)–N(8) 97.1(3), N(4)–Zn(2)–N(11) 173.3(2), N(4)–Zn(2)–N(12) 98.4(2), N(7)–Zn(2)–N(8) 76.1(2), N(7)–Zn(2)–N(11) 93.4(2), N(7)–Zn(2)–N(12) 163.6(2), N(8)–Zn(2)–N(11) 85.8(2), N(8)–Zn(2)–N(12) 90.9(2), N(11)–Zn(2)–N(12) 75.4(2).

Reactions of $L^{16}$ and $L^{11}$ with $Zn(MeCO_2)_2\cdot 2H_2O$ in 1 : 1 molar ratio in hot ethanol afforded a strongly fluorescent yellow powder with many long fibres at the wall of the reaction vessel. The melting point of the formed zinc(II) complexes were > 300 °C. They were insoluble in all organic solvents. Elemental analysis indicated formation of 1 : 1 polymeric complexes. Ligand $L^{17}$ was synthesized by Schiff-base condensation[8] of bis(4-aminophenyl)methane and pyridine-2-aldehyde and reaction with $Zn(ClO_4)_2\cdot 6H_2O$ in methanol at room temp. gave a pale yellow crystalline powder (yield *ca.* 60%).† This was recrystallized from dmf–MeCN (1 : 2)–diethyl ether to give crystals of **1**·2MeCN·dmf; MeCN was indispensable for crystallization. Elemental analysis and FAB mass spectroscopy were consistent with the empirical formula of a 2 : 3 complex $[Zn_2L^{17}{}_3][ClO_4]_4\cdot$dmf·2MeCN.

The structure of **1** shown in Fig. 1‡ confirms the existence of a dinuclear triple helix. The complex contains two $Zn^{II}$ ions and three $L^{17}$ ligands. The building units, particularly the bridging groups ($-C_6H_4CH_2C_6H_4-$), are stacked face-to-face ($\pi\cdot\cdot\pi$) and edge-to-face ($CH\cdot\cdot\pi$) to each other. Formation of a helix arises from a twisting of these bridging groups. Each $Zn^{II}$ ion is six-coordinate with Zn–N(pyridyl) distances in the range 2.132(7)–2.187(6) Å and Zn–N(–CH=N) 2.174(6)–2.247(6) Å. There are three sets of bond angles N–Zn–N in the range 75.4(2)–77.3(3)°, 85.8(2)–100.6(2), and 163.6(2)–173.6(2)°, respectively. A pseudo-octahedral array of nitrogen atoms provided by three pyridylazomethine ($C_5H_4NCH=N-$) moieties are in *fac* configuration. The pyridyl nitrogen atom as a stronger donor of one ligand is situated *trans* to the weaker azomethine (–CH=N–) nitrogen atom of another ligand (Fig. 1 and Scheme 1).[8]

The new ligand system in this study is notable with regard to the synthetic advantage that the use of the C=N bond[9] allows a wide range of different supramolecular structures. This provides a basis for modelling many structural aspects and the utilization of the weak interactions in metallosupramolecular chemistry.

## Footnotes

* E-mail: nyoshida@high.hokudai.ac.jp

† **CAUTION**. Perchlorate salts of metal complexes with organic ligands are potentially explosive. Only small amounts of material should be prepared, and handled with care.

‡ Since the crystals were sensitive to moisture in the air, all measurements were conducted with the sample sealed in a glass capilliary using a Rigaku RAXIS IV imaging plate area detector with graphite monochromated Mo-K$\alpha$ radiation.

*Crystal data*: **1**·dmf·2MeCN: $C_{82}H_{73}Cl_4N_{15}O_{17}Zn_2$; approximate dimensions 0.30 × 0.10 × 0.05 mm, $M$ = 1813.14, pale yellow crystal, monoclinic, space group $C2/c$ (no. 15), $a$ = 54.89(2), $b$ = 13.822(2), $c$ = 22.01(1) Å, β = 95.40(3)°, $U$ = 16639.9004 Å$^3$, $Z$ = 8, $D_c$ = 1.447 g cm$^{-3}$, μ(Cu-K$\alpha$) = 7.82 cm$^{-1}$, $F$(000) = 7472.00. Data were collected on a Rigaku RAXISII diffractometer, 10268 reflections, 6756 observed [$I > 3\sigma(I)$]. The structure was solved by direct methods, and expanded using Fourier techniques. The final cycle of full-matrix least-squares refinements was based on 65756 observed reflections [$I > 3\sigma(I)$] and 1081 variable parameters and converged at $R$ = 0.061, $R_w$ = 0.084, Maximum, minimum residual electron density: +0.80, −0.61 e Å$^{-3}$. All calculations were performed using the teXsan crystallographic software package of the Molecular Structure coorporation. Atomic coordinates, bond lengths and angles, and thermal parameters have been deposited at the Cambridge Crystallograpic Data Centre (CCDC). See Information for Authors, Issue No. 1. Any request to the CCDC for this material should quote the full literature citation and the reference number 182/452.

## References

1 (*a*) A. Hersey and B. H. Robinson, *J. Chem. Soc., Faraday Trans. 1*, 1984, **80**, 2039; (*b*) A. Seiyama, N. Yoshida and M. Fujimoto, *Chem. Lett.*, 1985, 1013; (*c*) N. Yoshida, A. Seiyama and M. Fujimoto, *J. Phys. Chem.*, 1990, **94**, 4246; (*d*) N. Yoshida, *J. Chem. Soc., Perkin Trans. 2*, 1995, 2249; (*e*) P. Bugnon, P. G. Lye, A. A. Hamdan and A. E. Merbach, *Chem. Commun.*, 1996, 2787.

2 M. Nishio, Y. Umezawa, M. Hirota and Y. Takeuchi, *Tetrahedron*, 1995, **51**, 8665.

3 D. Philp and J. F. Stoddart, *Angew. Chem., Int. Ed. Engl.*, 1996, **35**, 1154 and references therein. Recent papers: E. C. Constable, M. Neuburger, D. R. Smith and M. Zender, *Chem. Commun.*, 1996, 1917; V. C. M. Smith and J.-M. Lehn, *Chem. Commun.*, 1996, 2733.

4 C. A. Hunter, *Angew. Chem., Int. Ed. Engl.*, 1995, **34**, 582; J. C. Jeffery, P. L. Jones, K. L. N. Mann, E. P. Psillakis, J. A. McCleverty, M. D. Ward and C. M. White, *Chem. Commun.*, 1997, 175.

5 E. J. Enemark and T. D. P. Stack, *Angew. Chem., Int. Ed. Engl.*, 1995, **34**, 996.

6 (*a*) M. Albrecht, H. Roettele and P. Burger, *Chem. Eur. J.*, 1996, **2**, 1264; (*b*) M. Albrecht and S. Kotila, *Chem. Commun.*, 1996, 2309.

7 N. Yoshida, N. Ito and K. Ichikawa, 1996 Annual Meeting on the Coordination Chemistry, Osaka, Japan.

8 N. Yoshida and M. Fujimoto, *Bull. Chem. Soc. Jpn.*, 1976, **49**, 1557.

9 R. H. Holm and G. W. Everett, *Prog. Inorg. Chem.*, 1966, **7**, 83.

*Received in Cambridge, UK, 10th March 1997; Com. 7/01669G*

# Preparation and crystal structure of a new gallium phosphate $[H_3N(CH_2)_3NH_3]^{2+}[GaH(PO_4)_2]^{2-}$ from water–$Me_2SO$

**Thierry Loiseau, Fabien Serpaggi and Gérard Férey***

*Institut Lavoisier, I.R.E.M., UMR CNRS 173, Université de Versailles-Saint Quentin en Yvelines, 45, Avenue des Etats-Unis, 78035 Versailles Cedex, France*

**A novel gallium phosphate is synthesized in the presence of 1,3-diaminopropane from water–dimethyl sulfoxide ($Me_2SO$); its structure consists of twisted chains of $GaO_4$ and $PO_4$ tetrahedra separated by diprotonated 1,3-diaminopropane.**

Zeolite like materials are generally synthesized from an aqueous system under hydrothermal conditions. During the last decade, some reports[1–3] have mentioned the influence of the organic or mixed organic–water solvents on the preparation of the microporous compounds. A wide variety of alcohols (mainly glycols) has been tested for the synthesis of zeolites and also phosphate-based compounds.[4] The use of organic solvents has resulted in the discovery of new open-framework structures such as the aluminophosphates JDF-20[5] and DAF-1[6] for example, and therefore has opened the field for the investigation of new microporous compounds. Nevertheless, although some work has reported that the use of apolar organic solvents may induce the growth of large single crystals with dimensions in the size range 0.4–5.0 mm,[7] the influence of such solvents has been less studied.

We report here on the synthesis of a new gallium phosphate from organic–water mixtures in the presence of 1,3-diaminopropane as a structurant agent. With this organic template, in the purely aqueous system and depending on the pH of the reaction, the fluorinated gallium phosphates[8] ULM-3, ULM-4 and ULM-6 have been obtained. Some attempts have been performed by using mixed alcohol–water solvents (butan-1-ol, ethylene glycol) but no effect has been observed for the formation of these phases in these conditions. However, the utilization of less polar molecules like dimethyl sulfoxide ($Me_2SO$) shows significant changes for the crystallization of such compounds. This paper deals with the preparation and the crystal structure of $[H_3N(CH_2)_3NH_3]^{2+}[GaH(PO_4)_2]^{2-}$, a new gallium phosphate hydrothermally synthesized from a non-purely aqueous system in which $Me_2SO$ was used as the co-solvent.

The reagents were gallium oxyhydroxide [GaO(OH)], phosphoric acid ($H_3PO_4$, Fluka 99%), hydrofluoric acid (HF, RP Normapur 40%), dimethyl sulfoxide ($Me_2SO$, Aldrich 99.9%) and 1,3-diaminopropane (DAP, Aldrich, 99%). The starting mixture, with molar ratio 1 GaO(OH) : 1 $H_3PO_4$ : 1 HF : 1.2 DAP : 10 $Me_2SO$ : 13 $H_2O$, was placed in a Teflon-lined stainless-steel autoclave and heated at 150 °C for 24 h. The as-synthesised crystalline product was filtered off, washed with distilled water and dried at room temperature. Examination under an optical microscope indicated a powder corresponding to GaO(OH) and colourless large faceted prismatic-shaped crystals of the title compound. A suitable single crystal was easily isolated for the structure determination by X-ray diffraction.†

The structure consists of infinite macroanionic chains of empirical formula $[GaH(PO_4)_2]^{2-}$ separated by $[H_3N(CH_2)_3NH_3]^{2+}$ cations. The basic structural unit of the inorganic chain contains one Ga and two P centred tetrahedra. All of the vertices of the $GaO_4$ tetrahedron are shared with the $PO_4$ units, with Ga–O distances in the range 1.810–1.831 Å. The two inequivalent crystallographic $PO_4$ tetrahedra share two vertices with the $GaO_4$ unit (P–O 1.553–1.565 Å) and each $PO_4$ group has two terminal oxygen atoms (P–O 1.503–1.531 Å). The $GaO_4$ and $PO_4$ tetrahedra are linked in a strictly alternating manner giving rise to an infinite square-twisted chain running along [001]. This type of ribbon has previously been reported as

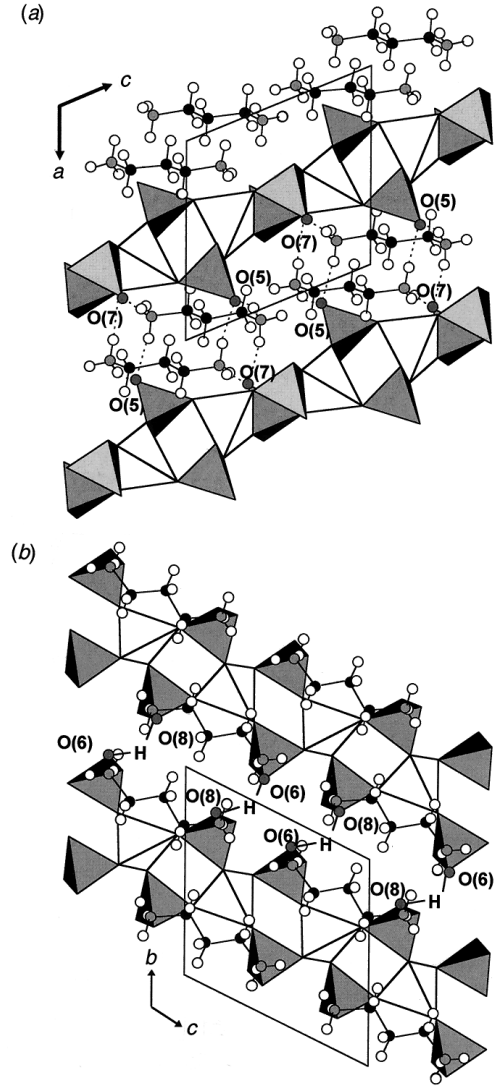



**Fig. 1** (*a*) View of the structure of $[H_3N(CH_2)_3NH_3][GaH(PO_4)_2]$ along [010] showing the hydrogen bonds (dotted lines) between the inorganic chain and the diprotonated 1,3-diaminopropane. (*b*) View of the structure along [100] showing the connection of two adjacent chains *via* hydrogen atoms between the $PO_4$ groups. For both figures, $GaO_4$ and $PO_4$ tetrahedra are indicated by white and grey shaded polyhedra, respectively. Nitrogen atoms are represented by grey circles, carbon atoms by black circles and hydrogen atoms by open circles. The terminal oxygens (with corresponding labels) of the $PO_4$ tetrahedra are indicated by grey circles at the vertices of the polyhedra.

*ts* in Smith's nomenclature.[9] Along [100], the cohesion of the structure [Fig. 1(*a*)] is ensured by strong hydrogen bonds between the hydrogen atoms of the ammonium groups of the organic molecule and one terminal oxygen atom of each $PO_4$ tetrahedron [labelled O(5) and O(7) on the figure] with the distance range $d_{N–H\cdots O}$1.868–1.923 Å. Indeed, the valence units for the corresponding oxygen atoms O(5) and O(7) are 1.45 and 1.47, respectively, instead of 2 expected for an oxygen atom. To satisfy the electroneutrality of the structure, one hydrogen atom must be added. The valence-bond analysis indicates that this hydrogen may be shared between O(6) (valence unit = 1.23) and O(8) (valence unit = 1.22) oxygen atoms from two distinct $PO_4$ tetrahedra [Fig 1(*b*)]. Moreover, the short O(6)···O(8) distance (2.444 Å) suggests the presence of positive charge between these two anions. Along [010], the cohesion of the structure is completed by hydrogen bonds between this hydrogen atom and the terminal oxygen atoms O(6) and O(8) of the $PO_4$ groups.

The authors are grateful to Professor M. Leblanc (Université du Maine) for the X-ray data collection and Rhône-Poulenc for financial support.

## Footnotes

* E-mail: ferey@chimie.uvsq.fr; loiseau@chimie.uvsq.fr

† *Crystal data* for $[H_3N(CH_2)_3NH_3][GaH(PO_4)_2]$: triclinic space group $P\bar{1}$ (no. 2); $a$ = 8.325(1), $b$ = 8.633(1), $c$ = 8.903(1) Å, $\alpha$ = 111.725(5), $\beta$ = 107.559(6), $\gamma$ = 98.394(6)°, $U$ = 542.2(1) Å$^3$, $Z$ = 2, $M_r$ = 336.82, $D_c$ = 2.06 g cm$^{-3}$, crystal dimensions: 0.152 × 0.0684 × 0.912 mm, $\mu$(Mo-K$\alpha$) = 28.63 cm$^{-1}$, $\lambda$ = 0.710 69 Å, X-rays monochromatised by graphite. The data were collected on a Siemens AED-2 four-circle diffractometer in the range $2\theta \leqslant 80°$. A total of 5255 reflections with $I \geqslant 2\sigma(I)$ was considered for the refinement. The data were corrected for Lorentz-polarisation and absorption effects. The structure was solved by direct methods analysis (SHELXS-86): one gallium and two phosphorus atoms were first located and all the remaining atoms except the isolated hydrogen atoms between the $PO_4$ groups were revealed from the difference Fourier map. The Fourier map analysis indicated three electron density residues around the two nitrogen atoms corresponding to the ammonium groups. Refinement (147 variables) was performed by full-matrix least-squares analysis (SHELXL-93): the reliability factors converged to $R$ = 0.032, $wR_2$ = 0.091. Atomic coordinates, bond lengths and angles, and thermal parameters have been deposited at the Cambridge Crystallographic Data Centre (CCDC). See Information for Authors, Issue No. 1. Any request to the CCDC for this material should quote the full literature citation and the reference number 182/445.

## References

1 D. M. Bibby and M. P. Dale, *Nature*, 1985, **317**, 157.
2 W. A. van Erp, H. W. Kouwenhoven and J. M. Nanne, *Zeolites*, 1987, **7**, 286.
3 Q. Huo, S. Feng and R. Xu, *J. Chem. Soc., Chem. Commun.*, 1988, 1486.
4 Q. Huo and R. Xu, *J. Chem. Soc., Chem. Commun.*, 1990, 783.
5 Q. Huo, R. Xu, S. Li, Z. Ma, J. M. Thomas, R. H. Jones and A. M. Chippindale, *J. Chem. Soc., Chem. Commun.*, 1992, 875.
6 P. A. Wright, R. H. Jones, S. Natarajan, R. G. Bell, J. Chen, M. B. Hursthouse and J. M. Thomas, *J. Chem. Soc., Chem. Commun.*, 1993, 633.
7 A. Kuperman, S. Nadimi, S. Oliver, G. A. Ozin, J. M. Garcés and M. M. Olken, *Nature*, 1993, **365**, 239.
8 G. Ferey, *J. Fluorine Chem.*, 1995, **72**, 187.
9 J. V. Smith, *Chem. Rev.*, 1988, **88**, 149.

*Received in Basel, Switzerland, 3rd February, 1997; Com. 7/00745K*

# Thymine functionalised polymers *via* living ring-opening metathesis polymerisation

**Vernon C. Gibson,*[a]† Edward L. Marshall,[a] Michael North,*[b] David A. Robson[a] and Paul J. Williams[b]**

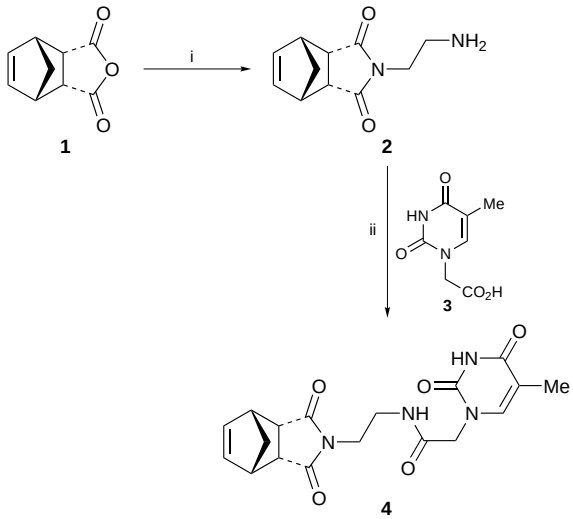
[a] *Department of Chemistry, Imperial College, Exhibition Road, South Kensington, London, UK SW7 2AY*
[b] *Department of Chemistry, University of Wales, Bangor, Gwynedd, UK LL57 2UW*

**Thymine functionalised poly(norbornene)s are synthesised *via* living ring-opening metathesis polymerisation using the ruthenium initiator {$RuCl_2(CHPh)[P(C_6H_{11})_3]_2$}.**

In recent years there has been rapid progress in the controlled assembly of polymers *via* living chain-growth polymerisation. Some of the most dramatic advances have occurred in ring-opening metathesis polymerisation (ROMP),[1] where well-defined transition metal initiators allow control over many aspects of the polymer assembly, including its molecular weight and molecular weight distribution,[2] alkene backbone configuration[3] and tacticity.[4] An important recent addition to the armoury of initiators is the ruthenium system introduced by Grubbs,[5] which has been shown to give the widest tolerance yet of key functionalities, including aldehydes, primary amines and most significantly the Brønsted acid groups OH and $CO_2H$. Thus, it is now possible to address the controlled synthesis of highly functionalised polymers incorporating features of complex biological macromolecules. In a previous report[6] we described the synthesis of polymers derived from amino ester-containing monomers, and the synthesis of polymers from carbohydrate derived monomers has also been disclosed.[7–9] Here, we report the application of ring-opening metathesis polymerisation to the synthesis of nucleotide base functionalised poly(norbornene)s, synthetic macromolecules that may be viewed as a first step *en route* to all-carbon backbone analogues of deoxyribonucleic acid (DNA).

The nucleotide base-substituted monomer **4** was prepared according to Scheme 1. Treatment of himic anhydride **1** with excess ethylenediamine in refluxing toluene gave monoamine **2**‡ in 30% yield. Coupling of amine **2** with thymineacetic acid[10] **3** was achieved using 1-(3-dimethylaminopropyl)-3-ethylcarbodiimide hydrochloride (EDC, water-soluble carbodiimide) as the coupling agent in DMF and gave monomer **4** as a white solid in 74% yield. The *exo*-isomer of **4** can be obtained by a closely related series of transformations with the exception that it is necessary to protect one end of the ethylenediamine with a triphenylmethyl group prior to its reaction with *exo*-norborn-5-ene-2,3-dicarboxylic anhydride and subsequently to remove the protecting group with trifluoroacetic acid.

Direct evidence that ring-opening occurs in a controlled manner is provided by $^1$H NMR spectroscopy and MALDI-TOF mass spectrometry. Fig. 1 shows the crude $^1$H NMR spectrum obtained after treatment of {$RuCl_2(CHPh)[P(C_6H_{11})_3]_2$} with 3 equiv. of **4** in [$^2H_8$)]THF in a sealed NMR tube for 90 min. The resonance at δ 20.35 corresponds to the carbene hydrogen of the initiator, while the nearby doublet of doublets resonance at δ 19.09 may be attributed to the carbene hydrogen arising from ring-opening of the first monomer unit, with couplings to the β-hydrogen and the remaining ruthenium-bound tricyclohexylphosphine ligand. Upon standing for several hours this resonance broadens as more monomer is incorporated. In a separate experiment, 3 equiv. of *exo*-**4** were added to the initiator, the mixture stirred for 24 h, and then terminated by addition of ethyl vinyl ether. The MALDI-TOF spectrum of the resultant product [Fig. 2(*a*)] confirms that multiple insertions have occurred to give a narrow molecular weight distribution product ($M_n$ 2340, $M_w$ 2500, $M_w/M_n$ = 1.07).§ The most intense signals are due to protonated oligomers {$[M + H]^+$} with observable minor signals due to sodium {$[M + Na]^+$} and potassium {$[M + K]^+$} salts. The mass of each oligomer confirms the repeat unit (372.38 amu) and the presence of benzylidene and methylidene end-groups arising from the ruthenium initiator and the ethyl vinyl ether terminating agent respectively. The observed $M_n$ is higher than $M_n$(calc) (1221)




**Scheme 1** *Reagents and conditions*: i, $H_2NCH_2CH_2NH_2$ (6 equiv.), toluene, heat; ii, EDC, DMF

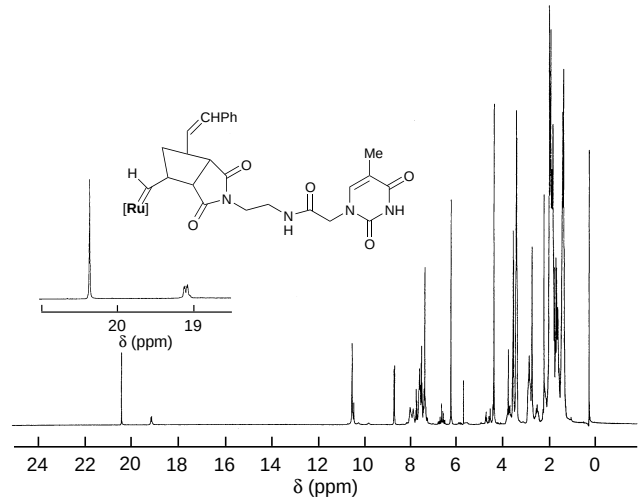



**Fig. 1** 250 MHz $^1$H NMR spectrum ([$^2H_8$]THF) of the products arising from treatment of {$RuCl_2(CHPh)[P(C_6H_{11})_3]_2$} with **4** (2 equiv.); [Ru] = [$RuCl_2(PCy_3)$]

due to the faster rate of propagation *versus* initiation for this monomer–initiator combination.

The MALDI-TOF spectrum of the product mixture prior to the addition of terminating agent is shown in Fig. 2(*b*). In this experiment, which employed indoleacetic acid as the matrix, the oligomers were detected as their sodium salts. The most intense signals are attributable to chains bearing benzylidene and oxo (aldehyde) end-groups, the latter arising from a termination reaction with molecular oxygen.¶ This reaction bears close similarity to that established for well-defined molybdenum initiators.[11] However, unlike the molybdenum system, in which the resultant aldehyde end-capped polymer reacts further with the propagating molybdenum alkylidene species to give a product of twice the anticipated molecular weight, in the case of ruthenium the aldehyde end-groups are tolerated by the ruthenium carbene and thus no further reaction occurs. Interestingly, in the ruthenium-initiated system, signals are also present (indicated by arrows) that correspond to ($n$ − 1) protonated chains that remain attached to the propagating ruthenium centres, *i.e.* $[RuCl_2(PCy_3)]$. The presence of $[M + Na]^+$ and $[M + K]^+$ signals for these species explains the greater multiplicity of signals in Fig. 2(*b*).

Overall, these observations provide direct evidence for a controlled polymerisation of nucleotide base-substituted monomers, and afford insight into a key termination reaction in the ruthenium system. In future publications, extensions of this work to other nucleotide base polymers and copolymers will be described.

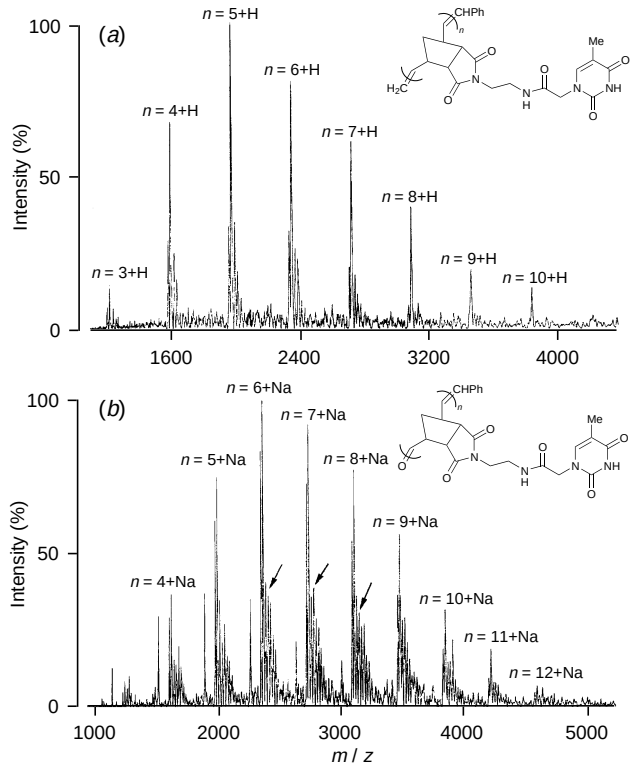



**Fig. 2** The MALDI-TOF mass spectrum of poly-*exo*-**4**: (*a*) after termination by ethyl vinyl ether (dihydroxybenzoic acid matrix); (*b*) prior to termination by ethyl vinyl ether but after exposure to atmospheric oxygen (indoleacetic acid matrix)

The authors thank the EPSRC Innovative Polymer Synthesis Initiative for a postdoctoral fellowship to E. L. M., the BBSRC for a postdoctoral fellowship to P. J. W., and Miss Amelia Jackson and Dr Paul Humphrey (Kratos Analytical) for measuring the MALDI-TOF spectra.

## Footnotes

† E-mail: v.gibson@ic.ac.uk

‡ All new compounds gave satisfactory analytical and spectroscopic data.

§ Measured on a Kratos Analytical Kompact MALDI IV spectrometer in linear positive ion mode, accelerating voltage 20 kV, electron multiplier detector. The data presented are a running average of 250 laser shots over the sample position. It should be noted that MALDI-MS has been shown in certain cases to observe components of lower mass preferentially (ref. 12). This results in *M*w being lowered to a greater extent than *M*n, consequently affording a lower molecular weight distribution than the true value. The detector response is also known to affect the measured polymer weight distribution (ref. 13).

¶ Solutions of the ruthenium initiator are known to be sensitive to dioxygen. The reaction observed here occurs upon preparation of the sample slides under non-anaerobic conditions.

## References

1 K. J. Ivin and J. C. Mol, *Olefin Metathesis and Metathesis Polymerization*, Academic Press, London, 1997; R. H. Grubbs and W. Tumas, *Science*, 1989, **243**, 907; R. R. Schrock, *Acc. Chem. Res.*, 1990, **23**, 158; W. J. Feast and V. C. Gibson, 'Olefin Metathesis', in *Chemistry of the Metal-Carbon Bond*, ed. F. R. Hartley, Wiley, New York, 1989, vol. 5.

2 See, for example: G. C. Bazan, R. R. Schrock, E. Khosravi, W. J. Feast, V. C. Gibson, M. B. O'Regan, J. K. Thomas and W. M. Davis, *J. Am. Chem. Soc.*, 1990, **112**, 8378; G. C. Bazan, R. R. Schrock, H.-N. Cho and V. C. Gibson, *Macromolecules*, 1991, **24**, 4495.

3 W. J. Feast, V. C. Gibson and E. L. Marshall, *J. Chem. Soc., Chem. Commun.*, 1992, 1157.

4 D. H. McConville, J. R. Wolf and R. R. Schrock, *J. Am. Chem. Soc.*, 1993, **115**, 4413; J. H. Oskam and R. R. Schrock, *J. Am. Chem. Soc.*, 1993, **115**, 11 831.

5 P. Schwab, M. B. France, J. W. Ziller and R. H. Grubbs, *Angew. Chem., Int. Ed. Engl.*, 1995, **34**, 2039; P. Schwab, R. H. Grubbs and J. W. Ziller, *J. Am. Chem. Soc.*, 1996, **118**, 100.

6 M. P. Coles, V. C. Gibson, L. Mazzariol, M. North, W. G. Teasdale, C. M. Williams and D. Zamuner, *J. Chem. Soc., Chem. Commun.*, 1994, 2505.

7 K. H. Mortell, M. Gingras and L. L. Kiessling, *J. Am. Chem. Soc.*, 1994, **116**, 12 053; K. H. Mortell, R. V. Weatherman and L. L. Kiessling, *J. Am. Chem. Soc.*, 1996, **118**, 2297.

8 C. Fraser and R. H. Grubbs, *Macromolecules*, 1995, **28**, 7248.

9 K. Nomura and R. R. Schrock, *Macromolecules*, 1996, **29**, 540.

10 L. Kosynkina, W. Wang and T. C. Liang, *Tetrahedron Lett.*, 1994, **35**, 5173.

11 W. J. Feast, V. C. Gibson, E. Khosravi, E. L. Marshall and J. P. Mitchell, *Polymer*, 1992, **33**, 872.

12 P. M. Lloyd, K. G. Suddaby, J. E. Varney, E. Scrivener, P. J. Derrick and D. M. Haddleton, *Eur. Mass Spectrom.*, 1995, **1**, 293.

13 J. Axelsson, E. Scrivener, D. M. Haddleton and P. J. Derrick, *Macromolecules*, 1996, **29**, 8875.

*Received in Liverpool, UK, 26th February 1997; Com. 7/01363I*

# Synthesis of penicillin derived polymers utilising ring-opening metathesis polymerisation methodology

**Stefano C. G. Biagini,[a] Vernon C. Gibson,*[b]† Matthew R. Giles,[b] Edward L. Marshall[b] and Michael North*[a]**

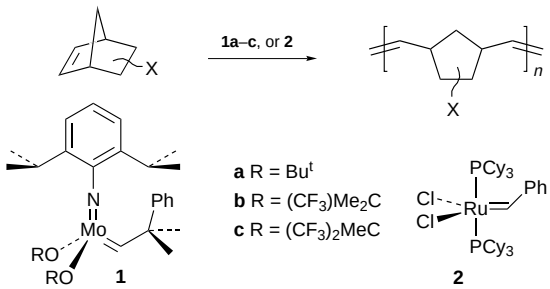
[a] *Department of Chemistry, University of Wales, Bangor, Gwynedd, UK LL57 2UW*
[b] *Department of Chemistry, Imperial College of Science, Technology and Medicine, Exhibition Road, South Kensington, London, UK SW7 2AY*

**Penicillin functionalised poly(norbornene)s are synthesised *via* living ring-opening metathesis polymerisation using the ruthenium initiator {$RuCl_2(CHPh)[P(C_6H_{11})_3]_2$}.**

There is currently much interest in the synthesis of new polymeric structures possessing unusual functionalities and/or molecular architectures. One of the most versatile approaches to the preparation of such polymers is the ring-opening metathesis polymerisation (ROMP) of strained ring systems, especially norbornenes, using well defined polymerisation initiators based upon molybdenum,[1] *e.g.* **1a**–**c**, or ruthenium,[2] *e.g.* **2**, as illustrated in Scheme 1. This process allows the preparation of polymers *via* a living polymerisation which gives excellent control of the molecular weight and polydispersity, and facilitates the synthesis of more complex polymer architectures such as block copolymers. The molybdenum based initiators **1a**–**c** also allow the alkene geometry within the polymer to be controlled, whilst ruthenium based initiator **2** is tolerant of a wide range of functional groups.

In recent reports, we have described the use of ROMP initiators **1a**–**c** and **2** to prepare polymers derived from amino acids[3] and from nucleic acid bases,[4] respectively. The synthesis of carbohydrate derived polymers has also been reported.[5]

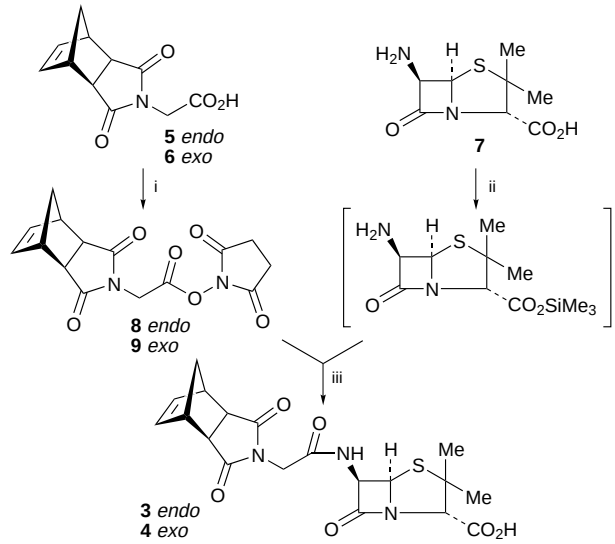
Here, we show how this methodology may be used to prepare polymers incorporating penicillin units. Penicillin was chosen as an archetypal, biologically active peptide, which is also susceptible to decomposition under a wide range of reaction conditions.[6] Thus the preparation of polymers incorporating this group would demonstrate both the ability to prepare polymers with potential biological activity, and illustrate the compatibility of the methodology with even the most sensitive of functional groups. Polymers derived from penicillin or other biologically active peptides have a number of potential applications: high molecular weight polymers may be suitable for the preparation of slow release capsules or bandages for the treatment of surface wounds, whilst low molecular weight oligomers may be able to deliver multiple copies of a drug to its site of action simultaneously, thus helping to circumvent problems of drug resistance. It should also be possible to prepare chromatography columns from polymers of this type, and to utilise these in isolating the biological receptors.




**Scheme 1**

The synthesis of the desired monomers **3** and **4**‡ was achieved as shown in Scheme 2, the preparation of *endo* and *exo* glycine derivatives **5** and **6** having been previously reported.[7] All attempts to couple activated derivatives (preformed acid chloride or *N*-hydroxysuccinimide ester) of acids **5** and **6** directly to (+)-6-aminopenicillanic acid (6-APA) **7** were unsuccessful, resulting in extensive decomposition of the penicillin ring. Eventually, we found that monomers **3** and **4** could be prepared by treatment of 6-APA first with bis-(trimethylsilyl)acetamide to protect the acid functionality,[8] followed, without isolation of the ester, by coupling with the *N*-hydroxysuccinimide esters **8** and **9**, and aqueous workup. Samples of monomers **3** and **4** prepared in this way contained silyl alcohol and/or silyl ether by-products which could not be removed without extensive decomposition, but were suitable for use in subsequent polymerisation reactions. So far, our polymerisation studies have focused on the *exo* derivative **4** which we have found to polymerise in a more controlled fashion than its *endo* isomer **3**.

Addition of initiator **2** to a stirred solution of **4** (10 equiv.) in acetone afforded a magenta solution which within a few minutes turned light brown and precipitated a beige solid. This suspension was stirred at room temperature for 22 h. The polymerisation was then terminated by addition of ethyl vinyl ether (50 μl) and the resultant solid collected and dried *in vacuo* for 2 h. It proved possible to follow the reaction of the closely related but more soluble silyl ester derivative of **4** by NMR spectroscopy in $CDCl_3$. The 270 MHz $^1H$ NMR spectrum of a sample containing the ruthenium initiator and 10 equiv. of $Me_3Si$-**4**, recorded a few minutes after mixing, is shown in Fig. 1. The sharp singlet resonance at δ 19.9 is attributable to the carbene hydrogen of unconsumed initiator, while the broadened resonance closeby is due to the carbene hydrogens of the [Ru]




**Scheme 2** *Reagents and conditions*: i, DCC, *N*-hydroxysuccinimide; ii, $MeC(OSiMe_3)=NSiMe_3$; iii, $H_2O$

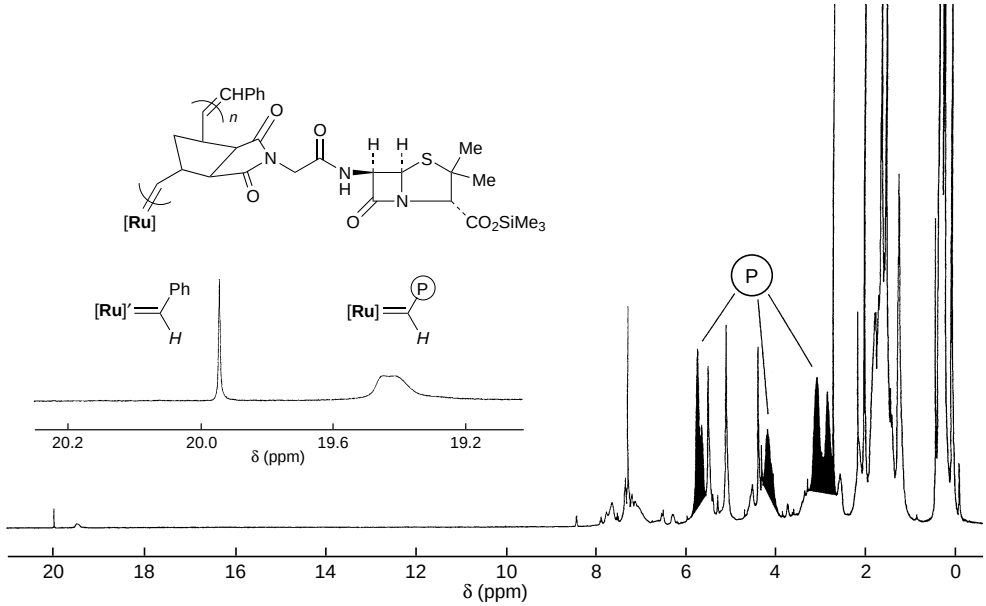



**Fig. 1** 270 MHz $^1$H NMR spectrum ([$^2$H]chloroform) of the products arising from treatment of $\{RuCl_2(CHPh)[P(C_6H_{11})_3]_2\}$ with ($Me_3Si$-**4**) (10 equiv.); [Ru] = $[RuCl_2(PCy_3)]$, [Ru]′ = $[RuCl_2(PCy_3)_2]$

end-groups of the propagating polymer chains. The shaded resonances in the region δ 2–6 are attributable to protons attached to the hydrocarbon backbone of the ring-opened products. In the olefinic region (*ca.* δ 5.5–6.0) there are two principal resonances (shaded); the more intense signal is tentatively assigned to the vinylene hydrogens of the *trans* polymer, consistent with the predominantly *trans* products arising from polymerisations of other closely related glycine-functionalised monomers with this ruthenium initiator (typically 80–90% *trans*[9]).

An infrared spectrum on the isolated polymer shows that the penicillin ring system survives intact during the polymerisations; a characteristic high frequency absorption at 1770 $cm^{-1}$ is observed for the β-lactam carbonyl. Attempts to further characterise the polymers by GPC were frustrated due to their insolubility in standard GPC solvents, and abnormal elution from the column when DMF was used as the GPC solvent. An approximate value for the number average molecular weight ($M_n$) could, however, be obtained from the $^1$H NMR spectrum of living poly($Me_3Si$-**4**); integration of the chain-end ruthenium carbene hydrogen resonance *versus* the olefinic hydrogens of the polymer backbone gave an approximate value for $M_n$ of 11800, corresponding to *ca.* 24 repeat units.§ To date, unlike for thymine-functionalised poly(norbornene)s,[4] it has not proved possible to obtain good quality MALDI-TOF mass spectra on these polymers. Electrospray mass spectrometry on the other hand does give some, if limited, information on the molecular weight distributions of the resultant polymers. The negative ion electrospray mass spectrum in DMF–MeCN–$H_2O$ of a polymer prepared from 10 equiv. of *exo*-monomer **4** and ruthenium initiator **2** shows molecular ion or fragment (loss of $CO_2$) peaks attributable to polymer chains containing 8–17 monomer units. The corresponding positive ion spectrum shows a series of fragment peaks attributable to consecutive loss of penicillin residues from the polymer chains. Thus, in addition to providing information on the molecular weights of the polymer chains, the mass spectra also provide corroborative evidence that the β-lactam ring survives intact.

In conclusion, we have shown that ROMP methodology using well-defined ruthenium initiators is compatible with the penicillin ring system. Our work on the synthesis of biomimetic polymers using ROMP methodology is continuing, and further results will be presented in due course.

The authors thank the EPSRC (Innovative Polymer Synthesis Initiative) for financial support, and Novartis Pharmaceuticals and the EPSRC for a studentship to M. R. G. Mass spectra were acquired by the EPSRC mass spectrometry service at the University of Wales, Swansea, and GPC analyses in DMF were carried out by the EPSRC service at RAPRA. The staff of these services are thanked for their efforts.

## Footnotes

† E-mail: v.gibson@ic.ac.uk

‡ All new compounds were characterised by $^1$H NMR, IR, specific rotation and mass spectrometry. *Selected data* for **3**: mp 64 °C, with decomposition; $[\alpha]_D^{21}$ + 103.6 (*c* 1, MeOH). For **4**: mp 75 °C, with decomposition; $[\alpha]_D^{21}$ + 163.8 (*c* 1, MeOH).

§ It is not possible to perform a similar end-group analysis on the isolated polymer due to overlap of the end-group resonances with the signals of other groups within the polymer.

## References

1 See, for example: R. R. Schrock, J. S. Murdzek, G. C. Bazan, J. Robbins, M. DiMare and M. O'Regan, *J. Am. Chem. Soc.*, 1990, **112**, 3875; G. C. Bazan, R. R. Schrock, H.-N. Cho and V. C. Gibson, *Macromolecules*, 1991, **24**, 4495; G. C. Bazan, E. Khosravi, R. R. Schrock, W. J. Feast, V. C. Gibson, M. B. O'Regan, J. K. Thomas and W. M. Davis, *J. Am. Chem. Soc.*, 1990, **112**, 8378.

2 For leading references, see: D. M. Lynn, S. Kanaoka and R. H. Grubbs, *J. Am. Chem. Soc.*, 1966, **118**, 784; P. Schwab, M. B. France, J. W. Ziller and R. H. Grubbs, *Angew. Chem., Int. Ed. Engl.*, 1995, **34**, 2039; Z. Wu, S. T. Nguyen, R. H. Grubbs and J. W. Ziller, *J. Am. Chem. Soc.*, 1995, **117**, 5503.

3 M. P. Coles, V. C. Gibson, L. Mazzariol, M. North, W. G. Teasdale, C. M. Williams and D. Zamuner, *J. Chem. Soc., Chem. Commun.*, 1994, 2505.

4 V. C. Gibson, E. L. Marshall, M. North, D. A. Robson and P. J. Williams, *Chem. Commun.*, in the press.

5 K. H. Mortell, R. V. Weatherman and L. L. Kiessling, *J. Am. Chem. Soc.*, 1996, **118**, 2297; C. Fraser and R. H. Grubbs, *Macromolecules*, 1995, **28**, 7248; K. H. Mortell, M. Gingras and L. L. Kiessling, *J. Am. Chem. Soc.*, 1994, **116**, 12053; K. Nomura and R. R. Schrock, *Macromolecules*, 1996, **29**, 540.

6 R. J. Simmonds, *Chemistry of Biomolecules; An Introduction*, The Royal Society of Chemistry, Cambridge, 1992, ch. 8.

7 S. C. G. Biagini, S. M. Bush, V. C. Gibson, L. Mazzariol, M. North, W. G. Teasdale, C. M. Williams, G. Zagotto and D. Zamuner, *Tetrahedron*, 1995, **51**, 7247.

8 P. D. Berry, A. C. Brown, J. C. Hanson, A. C. Kaura, P. H. Milner, C. J. Moores, J. K. Quick, R. N. Saunders, R. Southgate and N. Whittall, *Tetrahedron Lett.*, 1991, **32**, 2683.

9 M. R. Giles and V. C. Gibson, unpublished observations.

*Received in Liverpool, UK, 3rd March 1997; Com. 7/01494E*

# Polyaminoquinone self-assembled films on electrodes: synthesis of all-organic molecular wires by solution phase epitaxy

**Jukka Lukkari,* Kari Kleemola, Minna Meretoja and Jouko Kankare**

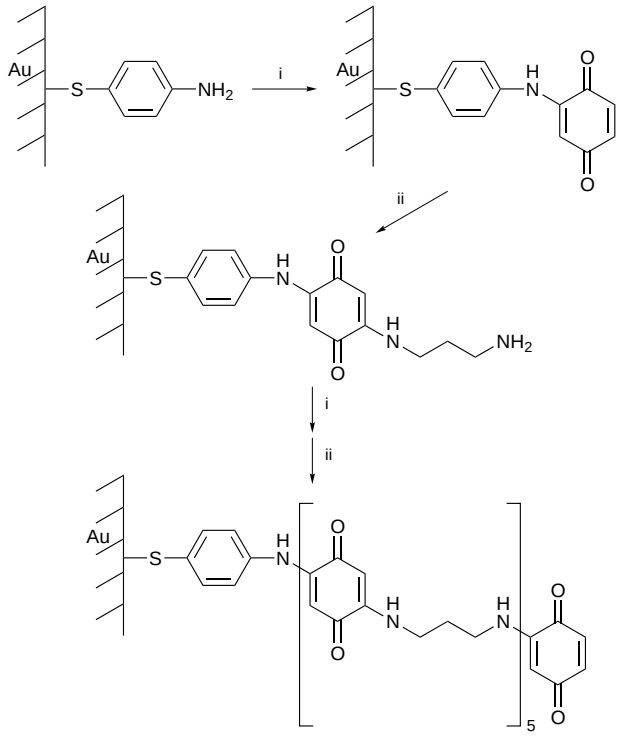
*Department of Chemistry, University of Turku, FIN-20014 Turku, Finland*

**Redox active molecular wires consisting of successive benzoquinone and diamino moieties are formed on a gold surface using repetitive self-assembly and solution epitaxy.**

Quinones constitute an interesting group of electroactive compounds which take part in several biologically important oxidation–reduction processes. The electrochemistry of quinones has been extensively studied and their complex redox mechanisms considered in detail.[1a,2] The reactivity of quinones towards nitrogen addition is also well known.[1b] The reaction of 1,4-benzoquinone with an amine is kinetically facile and proceeds, in the presence of an oxidant, *via* successive addition of amines predominantly at the 2,5-positions. Nitrogen addition lowers the redox potential of quinone and, therefore, unreacted benzoquinone can serve as an oxidant in the process. Several aliphatic diaminoquinones have been prepared and their spectral and electrochemical properties studied.[3,4]

Berlin and co-workers have employed 1,4-amino addition, using aromatic diamines, to prepare aminoquinone polymers.[1c] These polymers are obtained as dark powders, which are insoluble in most solvents, rendering their purification and study difficult. They were, however, found to possess semiconducting properties, which makes them interesting candidates for molecular wires and other devices in molecular electronics.[5] In order to avoid problems in the synthesis and purification of aminoquinone oligomers we have utilised repetitive self-assembly onto a solid substrate in order to grow aminoquinone molecular wires by solution epitaxy. The process involves successive immobilisation of quinones and diamines on a suitable primed electrode surface (Scheme 1), as originally suggested by Katz and Schmidt.[6] We have chosen *p*-mercaptoaniline for surface priming because it has been shown to form well ordered monolayers on Au(111).[7]

The sequential formation of polyaminoquinone on the surface of a polycrystalline gold electrode was followed by cyclic voltammetry (Fig. 1).† The gold electrode primed with the monolayer of *p*-mercaptoaniline exhibits no electroactivity in the potential range studied. After the immobilisation of the




**Scheme 1** *Reagents and conditions*: i, benzoquinone (0.5 M), MeCN–phosphate buffer (pH 7.2) (1 : 1), 3 h; ii, 1,3-diaminopropane in EtOH (30% v/v), 40 min

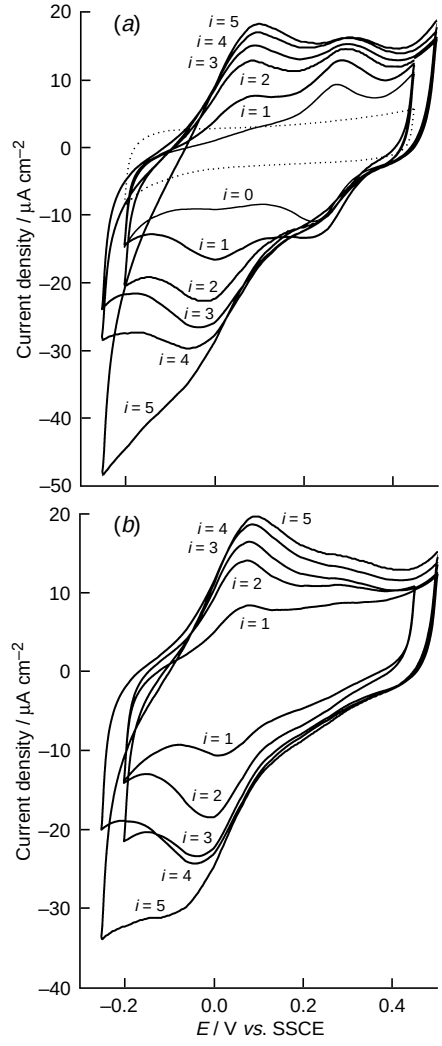



**Fig. 1** Cyclic voltammograms of (*a*) quinone terminated Au–SPhNH–$(Q–A)_i$–Q, and (*b*) amino terminated Au–SPhNH–$(Q–A)_i$ electrodes in 0.5 M $HClO_4$ at 100 mV $s^{-1}$. Dotted curve is Au–$SPhNH_2$ electrode.

first quinone the peaks due to the oxidation and reduction of amino substituted quinone appear at +0.26 V *vs.* sodium saturated calomel electrode (SSCE). The redox potential shifts 58 mV decade$^{-1}$ to the cathodic direction in the pH range from 0 to 8, showing the ($2H^+$, $2e^-$) nature of the reaction. The surface density of aminoquinone was calculated from the charge under the oxidation wave. Using the real surface area of the electrode, determined by oxidation of the bare gold electrode in 0.5 M $H_2SO_4$ up to the Burshtein minimum, a surface density of $1.75 \times 10^{-11}$ mol cm$^{-2}$ was obtained.[8] This is somewhat lower than reported for naphthoquinone or benzoquinone monolayer electrodes with aliphatic amino thiol primer.[6,9] The width of the voltammetric peak is 86 mV, which is much larger than the theoretically expected value of 90.6/*n* mV.

Fig. 1(*a*) and (*b*) shows the voltammograms of the successively formed quinone and amino terminated surfaces, respectively. Qualitatively the trend is very clear. The peaks due to monoaminoquinone in the Au–SPhNH–Q electrode (Q = benzoquinone) disappear after treating the electrode with 1,3-diaminopropane (A). Instead, a pair of peaks appears at 0.045 V *vs*. SSCE indicating the formation of a Au–SPhNH–Q–A electrode. A small residual peak can be seen at +0.26 V, which shows that the conversion is not complete, and the charge under this peak corresponds to *ca.* 12% of the total charge. After further reaction with benzoquinone the peak originating from monoaminoquinone reappears. It disappears after treatment with 1,3-diaminopropane with a concomitant increase in the peak attributable to diaminoquinone. These observations indicate the formation of Au–SPhNH–Q–A–Q and Au–SPhNH–Q–A–Q–A surfaces, respectively. It is noteworthy that the amount of the residual monoaminoquinone does not increase in the last step. The same process can be repeated with the same observed voltammetric behaviour, so that the final curves in Fig. 1(*a*) and (*b*) correspond to Au–SPhNH–(Q–A)$_5$–Q and Au–SPhNH–(Q–A)$_5$ electrode surfaces, respectively.

The quantitative determination of the charges under the waves in the cyclic voltammograms is complicated due to the large width of the waves. We chose to fit the data to the sum of two reversible surface waves, with separate linear baselines.[10]

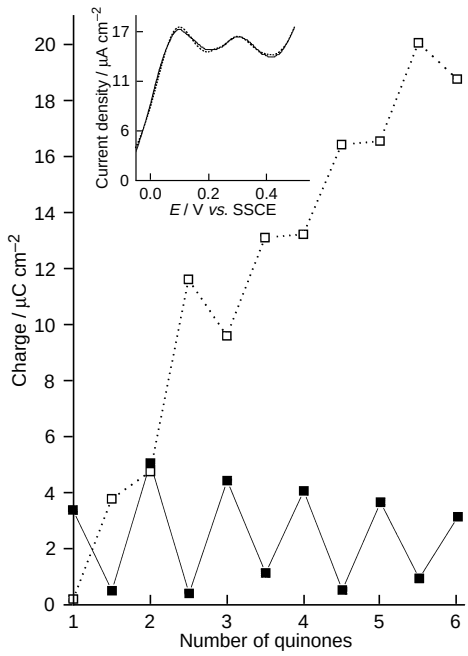



**Fig. 2** Charges calculated from oxidation peaks in Fig. 1; monoaminoquinone (■) and diaminoquinone (□). Inset shows the fit (dashed line) to the curve with $i = 4$ in Fig. 1(*a*) (solid line).

The results of such analysis are shown in Fig. 2, where the half-integer values on the *x*-axis refer to amino terminated surfaces. The inset shows an example of fitting results and demonstrates the reasonably good success of the simple model used. The charge due to the monoaminoquinone oscillates between *ca*. zero and 4 μC cm$^{-2}$, with very little damping. On the other hand, the charge due to diaminoquinones increases upon amine addition but stays more or less constant during the addition of quinone to the chain. This kind of behaviour is exactly what is expected for the sequential formation of polyaminoquinone chains on the electrode surface. Other charge integration procedures used all produced qualitatively the same result, *i.e*. a saw-tooth curve for the monoaminoquinone and a staircase curve for the diaminoquinone.

We have demonstrated the feasibility of building long aminoquinone chains on a solid substrate by repetitive self-assembly. The approach is very flexible and using only commercially available quinones and diamines it is possible to create, with minimal synthetic work, a large variety of structures with different properties. Preliminary results show that Au–SPhNH–(Q–A)$_5$–Q electrode retains *ca*. 70% of its total electroactivity after 40 days when stored in water under ambient atmosphere. The data in Fig. 2 show that the conversion efficiency is not markedly decreased with increasing number of quinone units. This implies that the reactivity of the chains, as a function of length, is not a limiting factor for attainable aminoquinone chain lengths. On the other hand, peak separations and widths increase with increasing chain length. These effects can be attributed to non-equal positions of the quinones within the chain and to the intra-chain interactions between the quinone redox centres. A detailed study of the structure, electrochemical and spectroelectrochemical properties of mono- and poly-aminoquinone modified electrodes, with aliphatic and aromatic diamines, is underway in our laboratory and will be reported in forthcoming papers.

## Footnotes

* E-mail: jukka.lukkari@utu.fi

† The Au rod was cleaned in hot piranha solution for 2 min (**WARNING!** Piranha solution reacts violently with organic material and should be treated with extreme care), rinsed with water (18 MΩ, Millipore) and immersed in 20 mM ethanol solution of bis(4-aminophenyl) disulfide (Aldrich) overnight.

## References

1 (*a*) J. Q. Chambers, in *The chemistry of the quinonoid compounds*, ed. S. Patai, Wiley, New York, 1974, pp. 737–792; (*b*) K. T. Finley, in *The chemistry of the quinonoid compounds*, ed. S. Patai, Wiley, New York, 1974, pp. 877–1144; (*c*) A. S. Lindsey, in *The chemistry of the quinonoid compounds*, ed. S. Patai, Wiley, New York, 1974, pp. 793–855.
2 E. Laviron, *J. Electroanal. Chem.*, 1984, **164**, 213.
3 J. L. Huntington and D. G. Davies, *J. Electrochem. Soc.*, 1971, **118**, 57.
4 J. L. Huntington and D. G. Davies, *J. Magn. Reson.*, 1970, **3**, 456.
5 J.-M. Lehn, *Supramolecular Chemistry. Concepts and Perspectives*, VCH, Weinheim, Germany, 1995, ch. 8.
6 E. Katz and H.-L. Schmidt, *J. Electroanal. Chem.*, 1993, **360**, 337.
7 Y.-T. Kim, R. L. McCarley and A. J. Bard, *J. Phys. Chem.*, 1992, **96**, 7416.
8 H. Angerstein-Kozlowska, in *Comprehensive Treatise of Electrochemistry*, ed. E. Yeager, J. O'M. Bockris, B. E. Conway and S. Sarangaponi, Plenum, New York, 1984, Vol. 9, p. 24.
9 F. Mukae, H. Takemura and K. Takehara, *Bull. Chem. Soc. Jpn.*, 1996, **69**, 2461.
10 A. J. Bard and L. R. Faulkner, *Electrochemical Methods. Principles and Applications*, Wiley, New York, 1980, p. 522.

*Received in Cambridge, UK, 18th March 1997; Com. 7/01895I*

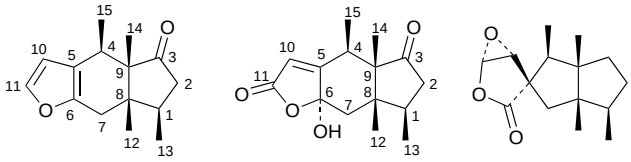
# Stable isotope labelling studies on the biosynthesis of pinguisane-type sesquiterpenes in axenic cultures of *Aneura pinguis*

**Hiroyuki Tazaki,*[a] Hiroshi Soutome,[a] Takeshi Iwasaki,[a] Kensuke Nabeta[a] and Duilio Arigoni[b]**

[a] *Department of Bioresource Chemistry, Obihiro University of Agriculture and Veterinary Medicine, Obihiro, 080 Japan*
[b] *Laboratorium fur Organische Chemie, ETH-Z, 8092 Zurich, Switzerland*

**$^2$H and $^{13}$C NMR analyses of 6α-hydroxy-3-oxopinguis-5(10)-ene-11,6-olide produced by axcenic cultures of the liverwort *Aneura pinguis* in the presence of $^2$H- and $^{13}$C-labelled mevalonates clarify the biosynthesis of pinguisane-type sesquiterpenes from FPP *via* a 1,2-hydride shift, two 1,2-methyl shifts, a cleavage of the main FPP chain and then recyclization.**

Pinguisone **1**[1] and its biosynthetically related compounds have been isolated from many Metzgeriales and Jungermanniale liverworts.[2] They are biosynthetically interesting since the biogenesis of their structures is difficult to explain simply in terms of the isoprene rule. This led us to investigate the structures and biosynthesis of pinguisane-type sesquiterpenes. In previous work, we isolated three new pinguisane-type sesquiterpenes as co-occurring compounds[3] and proposed a biosynthetic pathway to **1** in an axenic culture of gametophytes of *Aneura pinguis* by feeding [2-$^{13}$C]acetate.[4] As a probe of the biosynthetic pathway of pinguisane-type sesquiterpenes, we administered labelled mevalonates ([4,5-$^{13}C_2$]-, [5-$^{13}$C]-, [2-$^2H_2$]- and [6-$^2H_3$]-MVA) to the cultured gametophyte of *A. pinguis*. The results revised the previous route.[4] Here we propose the most plausible biosynthetic pathway to form the pinguisane skeleton.



**1** **2** **12**

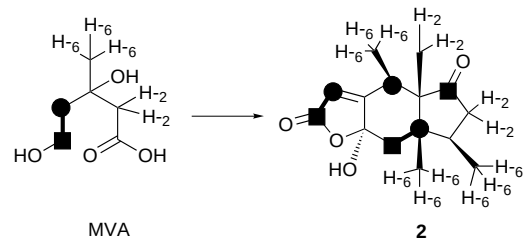
[4,5-$^{13}C_2$]-, [5-$^{13}$C]-, [2-$^2H_2$]- and [6-$^2H_3$]-MVA were prepared by procedures reported previously.[5] Axenic cultures of gametophyte of *A. pinguis* were grown in Gamborg B5 medium,[6] to which were fed 10.0 mmol of potassium MVA, under continuous light at 20 °C. 6α-Hydroxy-3-oxopinguis-5(10)-ene-11,6-olide **2** was the main sesquiterpene isolated from axenic cultures of *A. pinguis*. Compound **2** was biosynthesized from [4,5-$^{13}C_2$]-, [5-$^{13}$C]-, [2-$^2H_2$]- and [6-$^2H_3$]-MVA and isolated by HPLC as described previously.[3] Deviations in the levels of $^2$H and $^{13}$C enrichment (1.50–9.45 atom% excess) were observed among the differently labelled MVAs but may have been caused by variations in the incubation periods. Analysis of the resulting $^2$H and $^{13}$C labelled **2** (and its methyl ester) clearly showed the incorporation patterns illustrated in Fig. 1.

The presumed locations of $^2$H at the C-12, C-13 and C-15 positions in **2**, originating from C-6 of MVA, and at the C-2 and C-14 positions in **2**, originating from C-2 of MVA, were confirmed by feeding [2-$^2H_2$]- and [6-$^2H_3$]-MVA. Deuterium incorporation in the methyl groups at the C-12 and C-15 positions shows that these originate from the C-6 of MVA and provided evidence for 1,2-methyl migrations from C-9 to C-8 and C-5 to C-4 in the formation of the pinguisane skeleton. On the other hand, feeding [2-$^2H_2$]-MVA revealed that, in contrast to previous route,[4] the methyl group at the C-14 originates from the C-2 of MVA.

In the $^{13}$C NMR spectrum of **2** incorporating [4,5-$^{13}C_2$]-MVA, $^{13}$C–$^{13}$C coupling was observed between C-7 and C-8 ($J_{C\text{-}7,C\text{-}8}$ = 35.4 Hz), and between C-10 and C-11 ($J_{C\text{-}10,C\text{-}11}$ = 64.7 Hz). The enhanced singlets at C-3 ($\delta_C$ 217.3, 1.47 atom% excess) and C-4 ($\delta_C$ 32.2, 2.27 atom% excess) originate from C-5 and C-4 of MVA, respectively. The presumed location of $^{13}$C at the C-3 position in **2**, originating from C-5 of MVA, was confirmed by feeding [5-$^{13}$C]-MVA. These results indicated that a cleavage of the C-9–C-10 bond of FPP took place in the formation of pinguisane skeleton.

On the basis of these data, the biosynthetic pathway shown in Fig. 2 is proposed for the pinguisane-type sesquiterpenes of axenic cultures of *A. pinguis.* A postulated cyclized cation (**3**) may be formed *via* the formation of a C-6–C-11 bond from FPP without elimination of diphosphate. Cation **3** is converted to diphosphate **4** with the migration of a 1,2-methyl and a 1,2-hydride shift. Formation of the C-3–C-10 bond in **4** with the elimination of diphosphate gives the bicyclic cation **5**. Rupture of the C-9–C-10 bond of **4** and recyclization to form a cyclopentane ring in **5** gives the indane cation **6** which is further converted to the pinguisane skeleton by a 1,2-methyl shift. An alternative sequence, *i.e.* FPP → cation **13** → **5**, is excluded by the following reasons. The formation of **13** implies an unprecedented *cis*-addition to the isopropylidene double bond. The migration of the H-ligand in **13** would leave the positive charge on a forbidden bridgehead position. Furthermore, the migration of a 1,2-hydride shift from C-9 to C-8 in **13** would be predicted to result in the wrong stereochemistry for the secondary methyl group in the cyclopentane ring.

Recently, compound **11** has been isolated from the liverwort *Dicranolejeunea yoshinagana* (Hatt.) Mizut.[7] Compound **11** is most probably a biogenetic byproduct of a pinguisane-type sesquiterpene formed from cation **6** by a 1,2-vinyl shift. On the other hand, β-monocyclonerolidol **7** isolated from *Ptychanthus striatus* (Lehm. st Lindenb) Nees[8] which co-occurrs with striatene **8** and ptychanolide **12**, and the oxygenated sesquiterpene ricinocarpin A **9** from *Ricinocarpus natans*[9] is postulated to be derived from cation **3**. Similarly, striatene **8** may be also derived from the cyclohexene diphosphate **4**. In addition,



MVA **2**

**Fig.1** $^2$H and $^{13}$C labelling of **2**

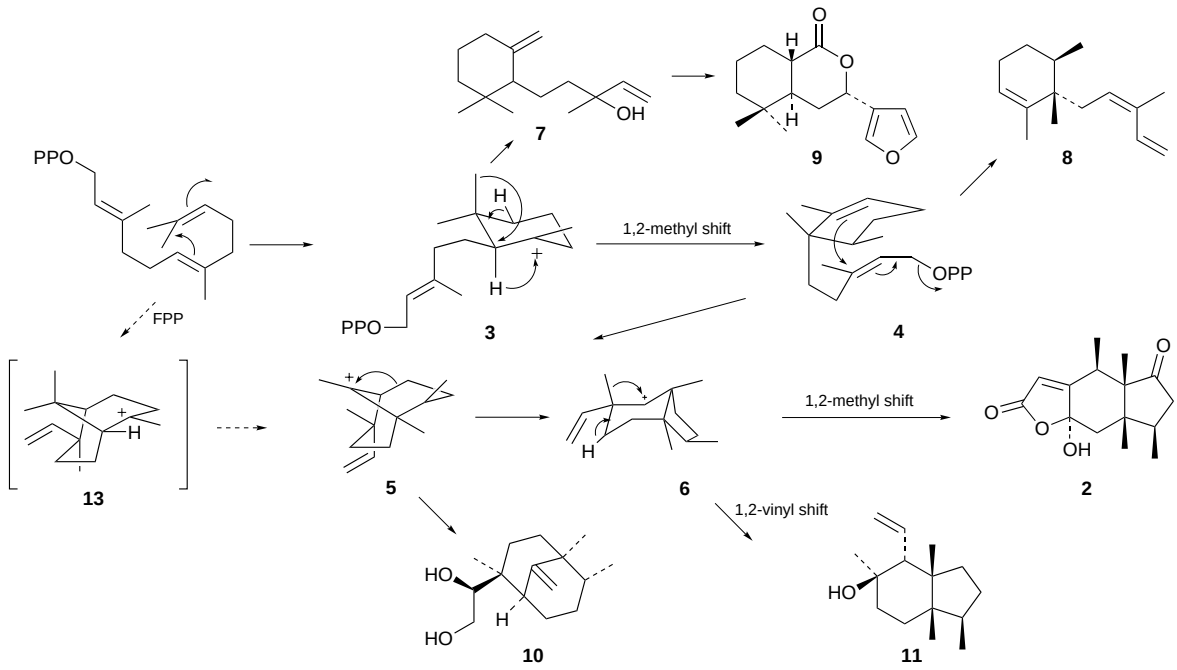



**Fig. 2** Proposed biosynthetic pathway of pinguisane type and related sesquiterpenes

trifarienol A **10** isolated from *Cheilolejeanea trifaria* is postulated to be formed from cation **5**. Thus, the biosynthetic pathway illustrated in Fig. 2 seems to be widely occurring in liverworts which produce not only pinguisane-type sesquiterpene but also three other skeletal sesquiterpenes represented by **7**, **8** and **10**.

While the pathway shown in Fig. 2 satisfies the results of labelling studies, the sequence of steps involved need to be proven by enzymatic studies.

This research was supported financially by the Agricultural Chemical Research Foundation of the Japan Society for Bioscience, Biotechnology and Agrochemistry, the Suhara Memorial Foundation, and a Grand-in-aid for Scientific Research from the Ministry of Education, Science and Culture, Japan.

## References

1 V. Benesova, Z. Samek, V. Herout and F. Sorm, *Collect. Czech. Chem. Commun.*, 1969, **34**, 1810.

2 Y. Asakawa, in *Progress in the Chemistry of Organic Natural Products*, ed. W. Hers, H. Griesbach, G. W. Kirby, R. E. Moore, W. Steglich and C. Tamm, Springer, Wein, 1995, vol. 65, pp. 1–618.

3 H. Tazaki, H. Soutome, K. Nabeta, H. Okuyama and H. Becker, *Phytochemistry*, 1996, **42**, 465.

4 H. Tazaki, K. Nabeta, H. Okuyama and H. Becker, *Biosci. Biotechnol. Biochem.*,1995, **59**, 158.

5 K. Nabeta, T. Ishikawa, T. Kawae and H. Okuyama, *J. Chem. Soc., Chem. Commun.*, 1995, 681; (*b*) K. Nabeta, T. Ishikawa and H. Okuyama, *J. Chem. Soc., Perkin Trans. 1*, 1995, 3111.

6 O. L. Gamborg, R. A. Miller and K. Ojima, *Exp. Cell. Res.*, 1968, **50**, 151.

7 M. Toyota, H. Koyama, T. Hashimoto and Y. Asakawa, *Chem. Pharm. Bull.*, 1995, **43**, 714.

8 R. Takeda, H. Naoki, T. Iwashita, K. Mizukawa, Y. Hirose, T. Isida and M. Inoue, *Bull. Chem. Soc. Jpn.*, 1983, **56**, 1125.

9 G. Wurzel and H. Becker, *Phytochemistry*, 1990, **29**, 2565.

10 T. Hashimoto, H. Koyama, S. Takaoka, M. Tori and Y. Asakawa, *Tetrahedron Lett.*, 1994, **35**, 4787.

*Received, in Cambridge, UK, 14th March 1997; Com. 7/01784G*

# Crystal structure of an imine–$SnCl_4$ complex. The intermediate in catalytic aziridination reactions

**Kaare G. Rasmussen, Rita G. Hazell and Karl Anker Jørgensen***

*Department of Chemistry, Aarhus University, DK-8000 Aarhus C, Denmark*

**An imine–$SnCl_4$ complex, which is an intermediate in Lewis acid catalysed aziridination reactions, is isolated and characterised by X-ray diffraction; the structure and catalytic properties of the complex are discussed.**

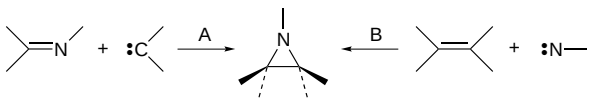
The metal-catalysed aziridination reaction is a new area of organic transformation. Two new catalytic aziridination reactions have been presented within the last few years; one is the metal-catalysed addition of a carbene fragment to an imine (Scheme 1, route A),[1] the other is the addition of a nitrene fragment to an alkene (Scheme 1, route B).[2]

The formation of aziridines from imines and ethyl diazoacetate (EDA) as the carbene-donor fragment (Scheme 1, route A) can take place by two different reaction paths, either by the formation of a metal–carbene, formed by reaction of the metal with EDA with elimination of $N_2$, then reaction with the imine giving an ylide as the intermediate,[1a,c] or by activation of the imine by the metal—a Lewis acid—followed by a nucleophilic attack by EDA followed by elimination of $N_2$.[1d,f,h,i]

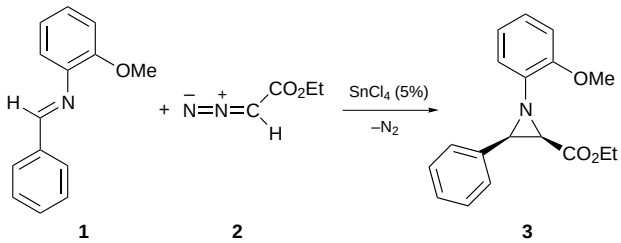
In an attempt to develop a selective aziridination of imines we have turned our attention to potentially bidentate substrates. Here we present the isolation and characterisation of the intermediate in the Lewis acid catalysed aziridination using $SnCl_4$ as the catalyst. This imine–$SnCl_4$ intermediate gives important information about the reaction course for the Lewis acid catalysed aziridination of imines using EDA as the carbene fragment donor.

Reaction of *N*-benzylidine-*o*-anisidine **1** with EDA **2** in the presence of $SnCl_4$ as the catalyst (5 mol%) gives the *cis*-aziridine **3** selectively in reasonable yields (Scheme 2).† In the absence of $SnCl_4$ no reaction takes place.

Choosing imine **1** as the substrate was an attempt to utilise the nitrogen and oxygen lone-pair electrons to give bidentate coordination to the metal. $^{13}C$ NMR spectroscopic investigations of **1** and $SnCl_4$ in $CDCl_3$ shows a 1:1 complex **4** in solution. The major changes in the $^{13}C$ NMR chemical shifts of **4**, relative to **1**, are (data in brackets are for **1**): δ 168.6 (161.3), 135.2 (131.2), 131.9 (126.6), 131.2 (128.8), 129.5 (128.6), 113.1 (111.4), 58.1 (55.8). It appears from the $^{13}C$ NMR data that some of the major changes are in the shifts of the imine and methoxy carbon atoms, from δ 161.3 to 168.6 and from δ 55.8 to 58.1, respectively, by coordination to $SnCl_4$.




**Scheme 1**




**1** **2** **3**

**Scheme 2**

Complex **4** was prepared by the addition of $SnCl_4$ (23.4 mg, 0.20 mmol) to a solution of imine **1** (35.7 mg, 0.20 mmol) in 0.7 ml $CDCl_3$ under Ar. When pale yellow crystals formed the solvent was decanted off to give **4** (50.5 mg, 54%) [mp = 166–72 °C (decomp.)]. The structure of **4**, determined by X-ray diffraction, is depicted in Fig. 1.‡

The structure of **4** consists of the imine **1** coordinated to $SnCl_4$ by the nitrogen and oxygen atoms giving a nearly octahedral geometry at the metal. The X-ray structure shows several interesting structural features, the most remarkable being is the change of geometry of **1**, which in **4** has a *cis*-geometry. The structure of **1** in solution ($CDCl_3$) has been studied by $^1H$ NMR spectroscopy. A NOEDIF spectrum gives a coupling between the hydrogen atom of the imine and the *ortho*-hydrogen atom in the *o*-anisidine substituent of −3%, showing that **1** is *trans* in solution. The imine **1** isomerises thus by coordination to $SnCl_4$.[3] A mechanism for the *trans* to *cis* isomerisation of **1** by reaction with $SnCl_4$ is proposed in Scheme 3. The first step is a nucleophilic attack of the imine at $SnCl_4$, giving a zwitterion intermediate **I**. The imine part in the zwitterion now has a C–N bond with single bond character which allows rotation, resulting in the *cis* isomer found in **4**. The reason for this isomerisation is probably steric repulsion between the *C*-phenyl substituent and one of the equatorial chlorides. This steric repulsion has been confirmed by modelling of the *trans* isomer of **1** coordinated to $SnCl_4$.

The structural data for **4** presented in Fig. 1 show that the Sn–N and Sn–O bond lengths are 2.222(5) and 2.370(4) Å, respectively, of which the former is similar to the same bond length in the only complex characterised having tin bound to four chlorides and a nitrogen and an oxygen atom.[4] The imine C(1)=N bond in **4** [1.285(8) Å] is not affected by the coordination to $SnCl_4$ and is similar to other imines charac-

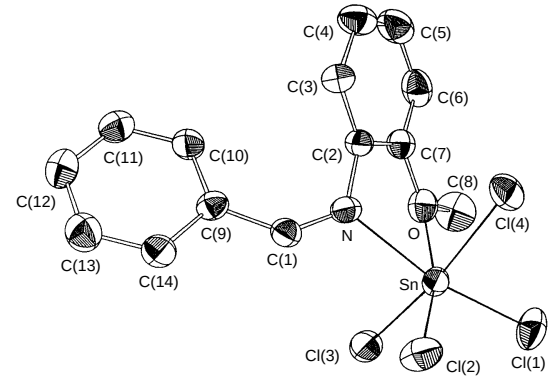
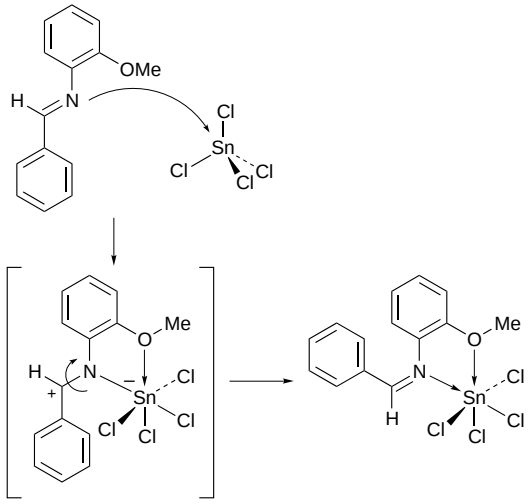



**Fig. 1** Molecular structure of **4**. C–H hydrogen atoms are not shown. Selected distances (Å) and angles (°) for **4**: Sn–N 2.222(5), Sn–O 2.370(4), Sn–Cl(1) 2.356(2), Sn–Cl(2) 2.351(2), Sn–Cl(3) 2.372(2), Sn–Cl(4) 2.385(2), N–C(1) 1.285(8), N–C(2) 1.439(7), C(7)–O 1.389(7), O–C(8) 1.439(7), N–Sn–O 68.3(2), Sn–N–C(1) 119.9(4), Sn–N–C(2) 112.8(4), N–C(1)–C(9) 136.0(6), N–C(1)–C(9)–C(10) 8(1), C(1)–N–C(2)–C(3) 47.3(9).




**I** **4**

**Scheme 3**

terised.§ The angle between the C(1)–C(9)–C(10)–C(14) and N–C(2)–C(3)–C(7) planes is 48°, which is due to steric repulsion between the two aromatic substituents at the imine.

The 1 : 1.2 reaction between complex **4** and EDA gives the aziridine **3**. However, the isolated yield of **3** is relatively low, caused by the decomposition of the aziridine by $SnCl_4$. Furthermore, we have tried to perform the catalytic reaction of the imine **1** with EDA in the presence of chiral ligands, especially chiral diamines, under various reaction conditions, but racemic **3** was formed. Based on the X-ray structure of **4** and the assumption that the chiral ligand replaces the two equatorial chlorides in **4** modelling studies account for the missing enantioselectivity in aziridination reactions by suggesting that the chiral ligand does not discriminate between the two faces of the imine.

Further work is in progress to understand the catalytic properties of **4** and to develop selective reactions based on this approach.

## Footnotes

† *Reaction conditions:* imine 1 (1.0 mmol) was added to a 5 ml Schlenk flask which was evacuated and filled twice with Ar. $CH_2Cl_2$ (4 ml) was added, followed by $SnCl_4$ or **4** (0.05 mmol). The solution was cooled to −15 °C before the addition of EDA **2** (1.3 mmol). When the evolution of $N_2$ ceased the reaction mixture was poured onto ice and the resulting aqueous phase was extracted with $CH_2Cl_2$ (3 ml). The organic phase was washed with 5% aq. $NaHCO_3$ and brine and dried with $Na_2SO_4$. The crude product was then purified by flash chromatography on silica gel using 5% EtOAc–light petroleum as eluent to give the pure aziridine **3**; $\delta_H$ 0.95 (t, *J* 7.2, 3H), 3.09 (d, *J* 6.5, 1H), 3.59 (d, *J* 6.5, 1H), 3.82 (s, 3H), 3.93–4.12 (m, 2H), 6.85–6.89 (m, 2H), 6.94–7.03 (m, 2H), 7.28–7.36 (m, 3H) and 7.54–7.57 (m 2H); $\delta_C$ 13.9, 45.9, 47.6, 55.4, 60.8, 111.0, 119.8, 120.6, 123.9, 127.6, 127.8, 127.9, 134.8, 140.8, 152.1 and 168.1; *m/z* 297.133 ($C_{18}H_{19}NO_3$ requires 297.133, 19%), 252 (13) and 224 (100).

‡ *Crystallographic data* for **4**: $C_{14}H_{13}NOCl_4Sn$, monoclinic, space group *C*2/*c*, *a* = 30.9076(1), *b* = 7.6820(1), *c* = 16.3239(1) Å, β = 119.773(1)°, *V* = 3443.07(7) Å$^3$, *Z* = 8; 4361 independent reflections measured at 298 K on a Siemens SMART CCD diffractometer; Mo-Kα; 2750 reflections with $I > 3\sigma(I)$ and 191 variables yields $R = 0.038$, $R_w = 0.052$. Atomic coordinates, bond lengths and angles, and thermal parameters have been deposited at the Cambridge Crystallographic Data Centre (CCDC). See Information for Authors, Issue No. 1. Any request to the CCDC for this material should quote the full literature citation and the reference number 182/457.

§ A search in the CCDA data file gave for a series of very similar imines an average C=N bond length of 1.28 Å.

## References

1 (*a*) K. B. Hansen, N. S. Finney and E. N. Jacobsen, *Angew. Chem., Int. Ed. Engl.*, 1995, **34**, 676; (*b*) K. G. Rasmussen and K. A. Jørgensen, *J. Chem. Soc., Chem. Commun.*, 1995, 1401; (*c*) M. Moran, G. Bernardinelli and P. Müller, *Helv. Chem. Acta*, 1996, **78**, 2048; (*d*) H.-J. Ha, K.-H. Kang, J.-M. Suh and Y.-G. Ahn, *Tetrahedron Lett.*, 1996, **37**, 7069; (*e*) Z. Zhu and J. H. Esperson, *J. Am. Chem. Soc.*, 1996, **118**, 9901; *J. Org. Chem.* 1995, **60**, 7090; (*f*) L. Casarrubios, J. A. Pérez, M. Brookhart and J. L. Tempelton, *J. Org. Chem.*, 1996, **61**, 8358; (*g*) V. K. Aggerwal, A. Thompson, R. V. H. Jones and M. C. H. Standen, *J. Org. Chem.*, 1996, **61**, 8368; (*h*) R. Bartnik and G. Mloston, *Synthesis*, 1983, 924; (*i*) K. G. Rasmussen and K. A. Jørgensen, *J. Chem. Soc., Perkin Trans. 1*, 1997, 1287.

2 D. A. Evans, M. M. Faul and M. T. Bilodeau, *J. Am. Chem. Soc.*, 1994, **116**, 2742; *J. Org. Chem.*, 1991, **56**, 6744; D. A. Evans, M. M. Faul, M. T. Bilodeau, B. A. Anderson and D. M. Barnes, *J. Am. Chem. Soc.*, 1993, **115**, 5328; D. A. Evans, K. A. Woerpel, M. M. Hinman and M. M. Faul, *J. Am. Chem. Soc.*, 1991, **113**, 726; A. M. Harm, J. G. Knight and G. Stemp, *Tetrahedron Lett.*, 1996, **37**, 6189; Z. Li, K. R. Conser and E. N. Jacobsen, *J. Am. Chem. Soc.*, 1993, **115**, 5326; Z. Li, R. W. Quan and E. N. Jacobsen, *J. Am. Chem. Soc.*, 1995, **117**, 5889; J.-P. Mahy, G. Bedi, P. Battioni and D. Mansuy, *J. Chem. Soc., Perkin Trans.* 2, 1988, 1517; K. J. O'Conner, S.-J. Wey and C. J. Burrows, *Tetrahedron Lett.*, 1992, **33,** 1001; K. Noda, N. Hosoya, R. Irie and T. Katsuki, *Synlett*, 1993, 469; P. Müller, C. Baud and Y. Jacueier, *Tetrahedron*, 1996, **52**, 1543.

3 Acid-catalysed isomerisation of imines has been observed before: D. Y. Curtin and J. W. Hausser, *J. Am. Chem. Soc.*, 1961, **83**, 3474; G. A. Olah and D. J. Donovan, *J. Org. Chem.*, 1978, **43**, 860.

4 A search in the CCDA data file gave only one complex with $SnCl_4$ coordinated to a nitrogen and an oxygen atom of an organic ligand(s): P. Domiano, A. Musatti, N. Nardelli, C. Pelizzi and G. Predieri, *Inorg. Chem. Acta*, 1980, **9**, 38.

*Received in Cambridge, UK, 12th March 1997; Com. 7/01734K*

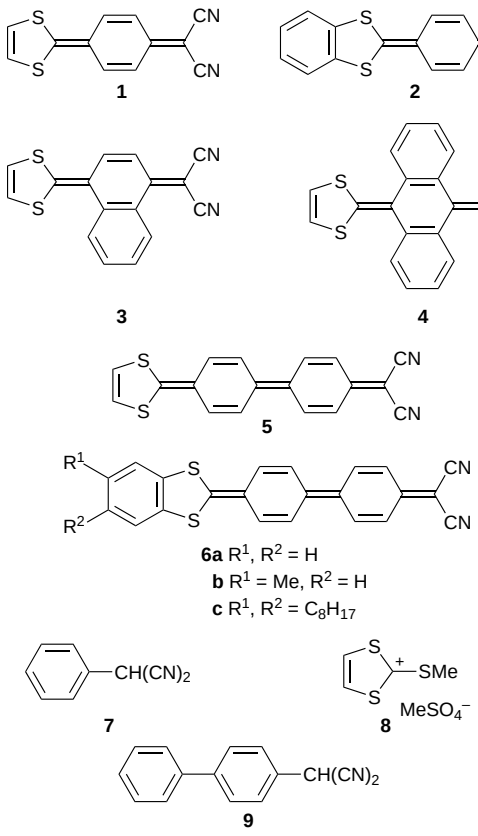
# Push-pull type of diphenoquinoid chromophores as novel near-infrared dyes

**Shinobu Inoue, Yoshio Aso and Tetsuo Otsubo***

*Department of Applied Chemistry, Faculty of Engineering, Hiroshima University, Kagamiyama 1-4-1, Higashi-Hiroshima 739, Japan*

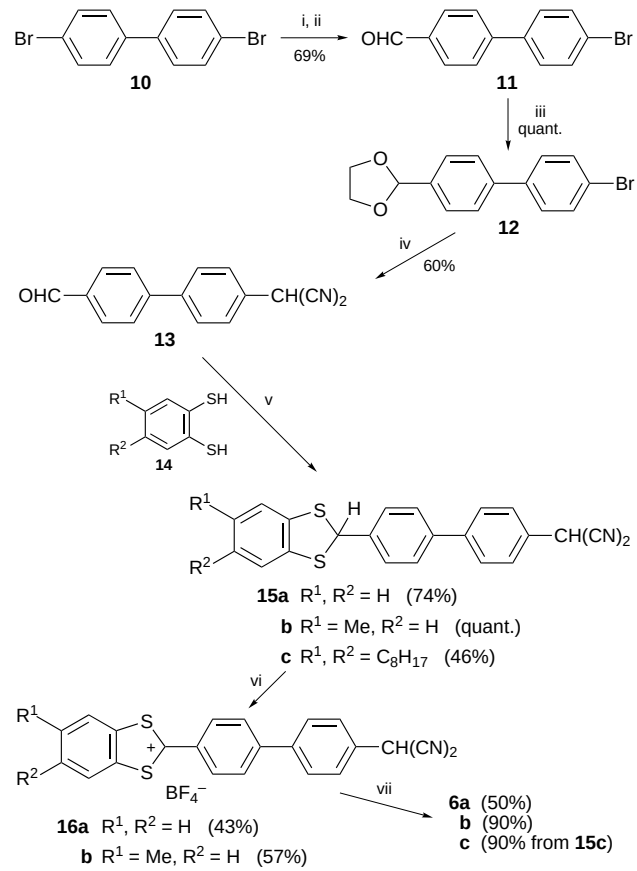
**Novel push-pull diphenoquinoid chromophores, in which one of the terminal positions carries a strong donor group, benzo-1,3-dithiol-2-ylidene, and the other a strong acceptor group, dicyanomethylene, are synthesized and show a strong absorption in the near-infrared region.**

The search for highly-coloured organic compounds has attracted current attention in terms of advanced optoelectronic materials, such as near-infrared dyes and nonlinear optics.[1,2] Push-pull types of conjugated π-electronic systems provide an entry to highly-coloured chromophores.[3] Such compounds containing a quinoid ring are especially interesting, because the push-pull stabilization can be promoted by the aromatization of the ring. Some time ago, Gompper *et al.* reported the quinoid compound **1** and benzo-fused derivative **2**, in which one of the terminal positions carries a strong donor group, 1,3-dithiol-2-ylidene, and the other a strong acceptor group, dicyanomethylene.[4] These compounds showed a strong intramolecular charge-transfer absorption band in the visible region (*vide infra*). The 1,4-naphthoquinoid analogue **3** and the 9,10-anthraquinoid one **4** were also prepared, but their absorption bands showed rather hypsochromic shifts.[4,5] The extensively conjugated diphenoquinoid systems **5** and **6**, so far unknown, are expected to show a bathochromic shift of the absorption band and serve as a receptor for near-infrared light. Here we report the synthesis and spectroscopic properties of the benzo derivatives **6a**–**c**.




Although the Gompper method, involving reaction of dicyanomethylbenzene **7** with 2-methylthio-1,3-dithiolium methanesulfonate **8**, is very convenient and useful for the preparation of the benzoquinoid system,[4] attempted syntheses of the diphenoquinoid compounds **5** and **6** by the same method using 4-dicyanomethylbiphenyl **9** were unsuccessful. Alternatively, we synthesized **6a**–**c** by another route starting with 4,4′-dibromobiphenyl **10** as shown in Scheme 1: one of the functional groups of **10** was converted *via* lithiation to a formyl group, and then the other one to a dicyanomethyl group by the Takahashi reaction.[6] The intermediate **13** thus obtained was reacted with benzenedithiol **14** in the presence of a catalytic amount of toluene-*p*-sulfonic acid to give the dithioacetal **15**, which was then dehydrogenated *via* the carbonium salt **16** to the desired compound **6**.[7] All the reactions proceeded in reasonable to excellent yields.†

The benzoquinoid compounds **1** and **2** are blue in $CH_2Cl_2$ solution, and their electronic absorption spectra show a strong




**Scheme 1** *Reagents and conditions*: i, Bu$^n$Li, $Et_2O$, −15 °C, 0.5 h; ii, DMF, −78 °C to room temp., 1 h; iii, $HOCH_2CH_2OH$, TsOH, benzene, reflux, 1 h; iv, $NaCH(CN)_2$, $Pd(PPh_3)_4$, THF, reflux, 4 h; v, TsOH, benzene, reflux, 1 h; vi, $Ph_3CBF_4$, $CH_2Cl_2$–MeCN, 60 °C, 3 h; vii, $Et_3N$, MeCN, room temp., 2 h

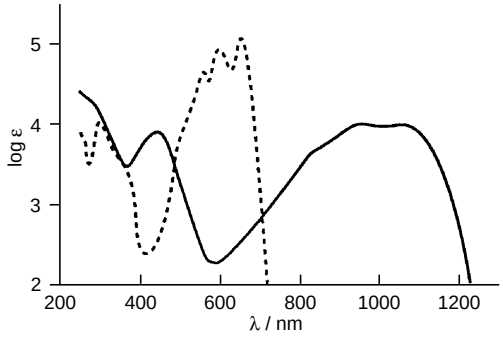
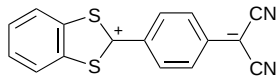


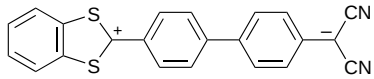

**Fig. 1** Electronic spectra of **2** (- - -) and **6a** (——) in $CH_2Cl_2$

colour-determining band with fine structure in the region of 550–650 nm. The band shows very little solvent shift. On the other hand, the diphenoquinoids **6a–c** look green–black in the solid state but are faint yellow in solution, and their electronic spectra have a characteristic broad band in the near-infrared region as well as a second band at around 450 nm. Fig. 1 demonstrates the specific spectral features of **2** and **6a**, and Table 1 summarizes the electronic absorption maxima and nitrile vibrational absorptions of **1**, **2** and **6a–c**. Interestingly, the absorption bands of **6**, unlike those of **1** and **2**, show large negative solvatochromism with increasing solvent polarity: for example, $\lambda_{max}$ of **6a** is 957 and 1045 nm in $CH_2Cl_2$, 934 nm in PhCN, and 790 nm in $Me_2SO$.

It is reasonable to assume that the push-pull quinoid systems **2** and **6** exist as a resonance hybrid with the zwitterionic forms **17** and **18**, respectively. Infrared spectra provide definite




**17**




**18**

information on these resonance structures: the nitrile vibrational absorption of **2** appears at a much lower frequency (2195 $cm^{-1}$) than that of TCNQ (2226 $cm^{-1}$). This indicates a considerable contribution by the ionic form **17**. The absorptions of **6a–c** are further shifted (2174–2180 $cm^{-1}$) and comparable to those of lithium phenyldicyanomethanide (2178 $cm^{-1}$) and sodium phenyldicyanomethanide (2188 $cm^{-1}$). This indicates that the diphenoquinoid system **6** predominantly exists as the ionic form **18**, consistent compatible with the large negative solvatochromism. The predominance of the ionic form **18** must presumably be promoted by the benefit of gaining double aromaticity.

The present results clearly demonstrate that the diphenoquinoid compounds **6a–c** are an interesting push-pull system with highly polar character and a new type of dyes strongly absorbing near-infrared light.

**Table 1** $\lambda_{max}$ and $\nu_{CN}$ of quinoid compounds **1**, **2** and **6**

| Compound | $\lambda_{max}$/nm[a] | $\nu_{CN}$/$cm^{-1}$ [b] |
|---|---|---|
| **1** | 551(4.46), 592(4.78), 644(4.89) | 2191 |
| **2** | 548(4.68), 589(4.93), 641(4.97) | 2195 |
| **6a** | 957(3.71), 1045(3.91) | 2174 |
| **6b** | 962(4.41), 1042(4.42) | 2180 |
| **6c** | 963(4.46), 1031(sh, 4.25) | 2180 |

[a] Measured in $CH_2Cl_2$. [b] Measured on a KBr disk.

## Footnotes

* E-mail: otsubo@ipc.hiroshima-u.ac.jp

† All the new compounds were characterized by spectroscopic measurements and elemental analyses.

## References

1 J. Fabian and R. Zahradnik, *Angew. Chem., Int. Ed. Engl.*, 1989, **28**, 677.
2 J. Fabian, H. Nakazumi and M. Matsuoka, *Chem. Rev.*, 1992, **92**, 1197.
3 R. Gompper and H.-U. Wagner, *Angew. Chem., Int. Ed. Engl.*, 1988, **27**, 1437.
4 R. Gompper, H.-U. Wagner and E. Kutter, *Chem. Ber.*, 1968, **101**, 4123.
5 R. Gompper and H.-U. Wagner, *Tetrahedron Lett.*, 1968, 165.
6 M. Uno, K. Seto and S. Takahashi, *J. Chem. Soc., Chem. Commun.*, 1984, 932.
7 R. Neidlein and H. Zeiner, *Angew. Chem., Int. Ed. Engl.*, 1980, **19**, 204.

*Received in Cambridge, UK, 7th March 1997; Com. 7/01626C*

# Cross metathesis of the amino acid homoallylglycine

**Susan E. Gibson (née Thomas),* Vernon C. Gibson and Stephen P. Keen**

*Department of Chemistry, Imperial College of Science, Technology and Medicine, South Kensington, London, UK SW7 2AY*

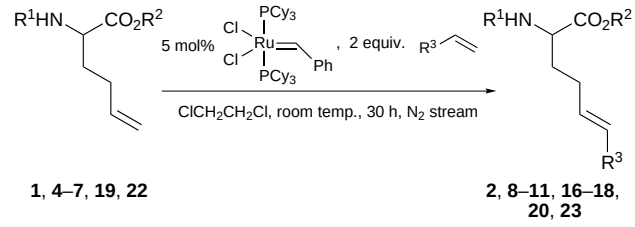
**Reaction of various protected forms of the amino acid homoallylglycine with aryl- and alkyl-substituted alkenes in the presence of 5 mol% $Cl_2(PCy_3)_2Ru$=CHPh gives cross metathesis products in acceptable synthetic yield (43–66%).**

The development of olefin metathesis, until recently a reaction applied mainly in bulk chemical production and polymer synthesis, into a reaction of general use in fine organic chemical synthesis continues to gain momentum. Seminal studies earlier this decade[1] led to the ring closing metathesis reaction (RCM) being used in several successful pioneering organic syntheses,[2] and the number of applications of this reaction in the past year suggests that it is now accepted as a useful synthetic tool.[3] The entropically more challenging but equally promising cross metathesis reaction has received much less attention from synthetic chemists and has been the subject of a mere handful of reports to date: early studies involved styrenes[4] and acrylonitrile[5] and very recently successful reactions using allylsilanes,[6] polymer-bound amino alcohols[7] and allyl stannanes[8] have been reported. Styrene cross metathesis has been applied recently to the elaboration of allylboration products[9] and β-lactams.[10]

In view of their biological role and myriad applications, it is not surprising that amino acids and their protected derivatives are attracting considerable attention as metathesis substrates. Initially they were ROMPed into polymers[11] and there now appears to be phrenetic interest in the use of amino acid derived substrates in RCM reactions.[12] In view of the level of activity in this area and the increasing interest in cross metathesis, we report here the first examples of cross metathesis reactions involving (protected) amino acids.

Homoallylglycine (Hag) was prepared by alkylation of diethyl acetamidomalonate with 4-bromobut-1-ene, ester loss and hydrolysis,[13] and subsequent amide hydrolysis. Standard protection procedures were then employed to generate the various protected forms of Hag discussed below.

Initially BocHagOMe **1**[14] was reacted with 2 equiv. of styrene in the presence of the ruthenium metathesis catalyst $Cl_2(PCy_3)_2Ru$=CHPh[15] using a variety of solvents, temperatures, reaction times, catalyst loadings and BocHagOMe concentrations. The yields of the cross metathesis product **2** were also measured from a reaction performed in a glove box under nitrogen, and from reactions carried out using Schlenk line techniques under both a static pressure and a steady stream of both nitrogen and argon. Interestingly there was no advantage to working in the glove box or under argon and, more significantly, changing the nitrogen atmosphere from a static pressure (*ca*. 1 atm) to a steady stream across the reaction mixture led to a 30% yield enhancement. The optimum conditions for the cross metathesis reaction between **1** and styrene were found to involve stirring a 0.25 M solution of BocHagOMe **1** in dichloroethane with 2 equiv. of styrene and 5 mol% of $Cl_2(PCy_3)_2Ru$=CHPh at room temperature with a steady stream of nitrogen blowing across the top of the reaction mixture for 30 h. These conditions gave a 52% isolated yield of the novel amino acid **2**† (based on BocHagOMe **1**) and a 40% yield of the BocHagOMe self metathesis product **3** (also based on **1**) (Table 1, entry 1).




In order to assess the merits of various protecting groups in the cross metathesis reaction, PhthHagOMe **4**, AcHagOMe **5**, BocHagOBn **6**[14] and BocHagOBu$^t$ **7**[16] were synthesised and reacted with styrene under the conditions described above. The

**Table 1** Cross metathesis of homoallylglycine derivatives with styrene, hex-1-ene and oct-1-ene[a]

| Entry | Substrate | Alkene R1 | Alkene R2 | Alkene R3 | Cross metathesis product[b] | Isolated yield (%)[c] | Self metathesis product[d] | Isolated yield (%)[e] |
|---|---|---|---|---|---|---|---|---|
| 1 | **1** | Boc | Me | Ph | **2** | 52 | **3** | 40 |
| 2 | **4** | Phth | Me | Ph | **8** | 55 | **12** | 35 |
| 3 | **5** | Ac | Me | Ph | **9** | 43 | **13** | 48 |
| 4 | **6** | Boc | Bn | Ph | **10** | 53 | **14** | 44 |
| 5 | **7** | Boc | Bu$^t$ | Ph | **11** | 55 | **15** | 45 |
| 6 | **1** | Boc | Me | Bu | **16** | 55 | **3** | 43 |
| 7 | **1** | Boc | Me | Hex | **17** | 66 | **3** | 28 |
| 8 | **7** | Boc | Bu$^t$ | Hex | **18** | 63 | **15** | 28 |
| 9 | **19** | Fmoc | Me | Hex | **20** | 58 | **21** | 25 |
| 10 | **22** | Fmoc | H | Hex | **23** | 58[d] | **24** | 18 |

[a] The experimental procedure for the conversion of **1** to **17** (entry 7) is typical: A nitrogen-saturated solution of **1** (0.121 g, 0.50 mmol) and oct-1-ene (0.156 cm$^3$, 1.00 mmol) in dichloroethane (2 cm$^3$) was added *via* a cannula to solid $Cl_2(PCy_3)_2Ru$=CHPh (0.021 g, 0.0235 mmol). The resulting purple solution was stirred under a steady stream of nitrogen for 30 h at room temperature. The dichloroethane was subsequently replaced with diethyl ether (*ca*. 50 cm$^3$) and the mixture stirred for 16 h under air to effect decomposition of the catalyst. Removal of the diethyl ether *in vacuo* and flash chromatography [$SiO_2$; light petroleum (40–60 °C)–diethyl ether, 1 : 0–5 : 1–1 : 2 gradient elution] gave the cross metathesis product **17** (0.108 g, 66%) and the self metathesis product **3** (0.032 g, 28%) as microanalytically pure colourless oils. [b] $R^3$ = Ph, *trans* : *cis* ≥ 10 : 1; $R^3$ = alkyl, *trans* : *cis ca.* 4 : 1. [c] Based on amino acid substrate. [d] Amino acid self metathesis product; alkene self metathesis products were also observed. [e] Product contaminated with 6% starting material.

yields of the cross metathesis products **2**, **8**–**11** and the self metathesis products **3**, **12**–**15** indicated that, with the exception of AcHagOMe **5**, the course of the reaction is independent of the nature of the protecting groups (Table 1, entries 1–5).

In order to determine whether the cross metathesis of Hag may be used to introduce alkyl groups into the amino acid side chain, BocHagOMe **1** and BocHagOBu$^t$ **7** were reacted with hex-1-ene and oct-1-ene (Table 1, entries 6–8). Comparison of the yields of the cross metathesis products **16**–**18** with entries 1 and 5 reveals that whilst the yields obtained for styrene and the relatively volatile hex-1-ene are essentially equivalent, use of the less volatile oct-1-ene gives significantly higher yields of cross metathesis product than styrene. Reaction of FmocHagOMe **19** with oct-1-ene also gave an acceptable yield of the cross metathesis product **20** together with some self metathesis product **21** (Table 1, entry 9) indicating that the commonly used Fmoc protecting group is compatible with these cross metathesis conditions.

Finally, in view of the importance of FmocXaaOH components in solid phase peptide synthesis, a cross metathesis reaction between FmocHagOH **22** and oct-1-ene was examined. This gave the cross metathesis product **23** (and the self-metathesis product **24**) in good yield (Table 1, entry 10) thus demonstrating that an unprotected carboxylic acid may be used in cross metathesis reactions.

We gratefully acknowledge the EPSRC for a studentship (S. P. K.).

## Footnotes

* E-mail: s.gibson@ic.ac.uk

† The novel substrates **4**, **5**, **19**, **22** and the novel cross metathesis products **2**, **8**–**11**, **16**–**18**, **20**, **23** all gave satisfactory microanalytical and spectroscopic (IR, $^1$H and $^{13}$C NMR, MS) data.

## References

1 G. C. Fu and R. H. Grubbs, *J. Am. Chem. Soc.*, 1992, **114**, 5426; G. C. Fu, S. T. Nguyen and R. H. Grubbs, *J. Am. Chem. Soc.*, 1993, **115**, 9856.

2 See, for example: S. F. Martin, Y. Liao, Y. Wong and T. Rein, *Tetrahedron Lett.*, 1994, **35**, 691; B. C. Borer, S. Deerenberg, H. Bierräugel and U. K. Pandit, *Tetrahedron Lett.*, 1994, **35**, 3191; A. F. Houri, Z. M. Xu, D. A. Cogan and A. H. Hoveyda, *J. Am. Chem. Soc.*, 1995, **117**, 2943.

3 See, for example: J. S. Clark and J. G. Kettle, *Tetrahedron Lett.*, 1997, **38**, 123 and 127; A. Furstner and K. Langemann, *J. Org. Chem.*, 1996, **61**, 8746; A. Kinoshita and M. Mori, *J. Org. Chem.*, 1996, **61**, 8356; P. Bertinato, E. J. Sorensen, D. F. Meng and S. J. Danishefsky, *J. Org. Chem.*, 1996, **61**, 8000; K. C. Nicolaou, Y. He, D. Vourloumis, H. Vallberg and Z. Yang, *Angew. Chem., Int. Ed. Engl.*, 1996, **35**, 2399; Z. M. Xu, C. W. Johannes, S. S. Salman and A. H. Hoveyda, *J. Am. Chem. Soc.*, 1996, **118**, 10 926; K. G. Nicolaou, M. H. D. Postema, E. W. Yue and A. Nadin, *J. Am. Chem. Soc.*, 1996, **118**, 10 335; B. Konig and C. Horn, *Synlett*, 1996, 1013; A. Furstner and N. Kindler, *Tetrahedron Lett.*, 1996, **37**, 7005; H. J. Lim and G. A. Sulikowski, *Tetrahedron Lett.*, 1996, **37**, 5243; M. A. McKervey and M. Pitarch, *Chem. Commun.*, 1996, 1689; S. Holder and S. Blechert, *Synlett*, 1996, 505; H. S. Overkleeft and U. K. Pandit, *Tetrahedron Lett.*, 1996, **37**, 547.

4 W. E. Crowe and Z. J. Zhang, *J. Am. Chem. Soc.*, 1993, **115**, 10 998.

5 W. E. Crowe and D. R. Goldberg, *J. Am. Chem. Soc.*, 1995, **117**, 5162.

6 W. E. Crowe, D. R. Goldberg and Z. J. Zhang, *Tetrahedron Lett.*, 1996, **37**, 2117.

7 M. Schuster, J. Pernerstorfer and S. Blechert, *Angew. Chem., Int. Ed. Engl.*, 1996, **35**, 1979.

8 J. Feng, M. Schuster and S. Blechert, *Synlett*, 1997, 129.

9 A. G. M. Barrett, J. C. Beall, V. C. Gibson, M. R. Giles and G. L. P. Walker, *Chem. Commun.*, 1996, 2229.

10 A. G. M. Barrett, S. P. D. Baugh, V. C. Gibson, M. R. Giles, E. L. Marshall and P. A. Procopiou, *Chem. Commun.*, 1996, 2231.

11 M. P. Coles, V. C. Gibson, L. Mazzariol, M. North, W. G. Teasdale, C. M. Williams and D. Zamuner, *J. Chem. Soc., Chem. Commun.*, 1994, 2505.

12 S. J. Miller and R. H. Grubbs, *J. Am. Chem. Soc.*, 1995, **117**, 5855; T. D. Clark and M. R. Ghadiri, *J. Am. Chem. Soc.*, 1995, **117**, 12 364; F. Garro-Hélion and F. Guibé, *Chem. Commun.*, 1996, 641; S. J. Miller, H. E. Blackwell and R. H. Grubbs, *J. Am. Chem. Soc.*, 1996, **118**, 9606; J. H. van Maarseveen, J. A. J. den Hartog, V. Engelen, E. Finner, G. Visser and C. G. Kruse, *Tetrahedron Lett.*, 1996, **37**, 8249; F. P. J. T. Rutjes and H. E. Schoemaker, *Tetrahedron Lett.*, 1997, **38**, 677.

13 J. E. Baldwin, C. Hulme and C. J. Schofield, *J. Chem. Res.* (*S*), 1992, 173.

14 M. J. Dunn, R. F. W. Jackson, J. Pietruszka and D. Turner, *J. Org. Chem.*, 1995, **60**, 2210.

15 P. Schwab, R. H. Grubbs and J. W. Ziller, *J. Am. Chem. Soc.*, 1996, **118**, 100.

16 J. R. Hauska, P. Dorff, S. Julin, J. DiBrino, R. Spencer and R. Williams, *J. Med. Chem.*, 1992, **35**, 4284.

*Received in Liverpool, UK, 24th March 1997; Com. 7/02027I*

# Alkyl and alkylidene derivatives of titanium supported by carbazole ligation

**Patrick N. Riley, Phillip E. Fanwick and Ian P. Rothwell***

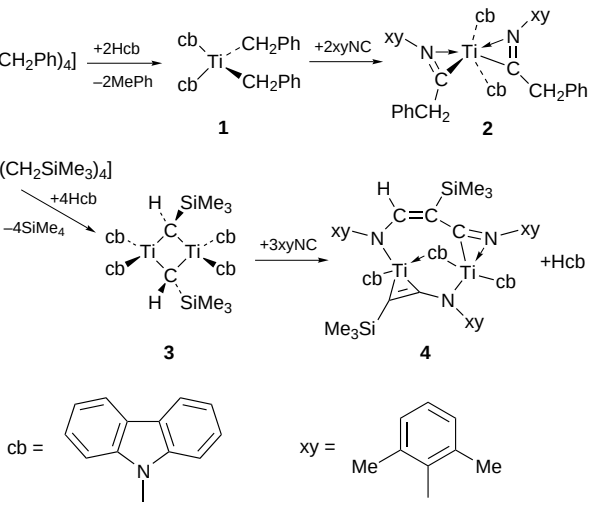
*1393 Brown Building, Department of Chemistry, Purdue University, West Lafayette, IN 47907-1393, USA*

**The bis(benzyl) $[(cb)_2Ti(CH_2Ph)_2]$ 1 and alkylidene bridged dimer $[(cb)_2Ti(\mu\text{-}CHSiMe_3)_2Ti(cb)_2]$ 3 are formed by adding carbazole (Hcb) to the tetraalkyls $[TiR_4]$ (R = $CH_2Ph$, $CH_2SiMe_3$); the reaction of 1 and 3 with 2,6-dimethylphenyl isocyanide leads to organometallic products containing new carbon–carbon bonds.**

There has recently been considerable research interest in the organometallic chemistry of the group 4 metals associated with amido ligation.[1–3] In this context we communicate here our studies of some organotitanium chemistry of the carbazole ligand, an amido group predicted to be a weaker π donor than dialkylamido ligands.[4]

The addition of carbazole (2 equiv.) to hydrocarbon solutions of $[Ti(CH_2Ph)_4]$[5] lead to the bis(benzyl) compound **1** in moderate yield (Scheme 1). The spectroscopic data† on **1** indicate that the benzyl ligands are $\eta^1$-bound.[6] Solutions of **1** react with 2 equiv. of 2,6-dimethylphenyl isocyanide (xyNC) to produce the bis($\eta^2$-iminoacyl) complex **2**. The iminoacyl carbon chemical shift of δ 246.9 in the $^{13}C$ NMR spectrum indicates $\eta^2$-C,N binding and this is confirmed by the solid-state molecular structure of **2** (Fig. 1).[7] The coordination geometry and iminoacyl parameters in **2** are similar to those found in other group 4 metal bis($\eta^2$-iminoacyl) compounds,[7,8] the only significant difference being the non-parallel orientation of the iminoacyl units in **2**.

The reaction of the more bulky alkyl substrate $[Ti(CH_2SiMe_3)_4]$[9] with carbazole is slow (as monitored by $^1H$ NMR) at ambient temperatures. At 100 °C the reaction produces a sparingly soluble product identified (Fig. 2) as the alkylidene bridged dimer $[(cb)_2Ti(\mu\text{-}CHSiMe_3)_2Ti(cb)_2]$ **3**. In the $^1H$ NMR spectrum of **3** a singlet at δ 14.75 can be assigned to the alkylidene proton. The structural parameters for the 1,3-dimetallacyclobutane unit in **3** are similar to those found in related molecules and in particular the methylidene bridged $[\{(C_6H_{11})_2N\}_2Ti(\mu\text{-}CH_2)_2Ti\{N(C_6H_{11})_2\}_2]$.[2] Treatment of **3** with xyNC (> 3 equiv.) slowly ($^1H$ NMR) produces a single organometallic species **4** and 1 equiv. of free carbazole. The molecular structure of **4** (Fig. 3) shows it to be dinuclear, containing a total of three isocyanides within two distinct bridging units. Two terminal and one non-symmetrically bridged carbazole ligand are also present. The structural parameters lead us to propose the structure for **4** shown in Scheme 1. Although the exact sequence of events leading to **4** is presently unknown, reasonable elementary steps for its formation can be proposed. One of the bridging units in **4** [N(6)–C(7)–C(8)] is best described as an amidoalkyne ligand. Identical




**Scheme 1**

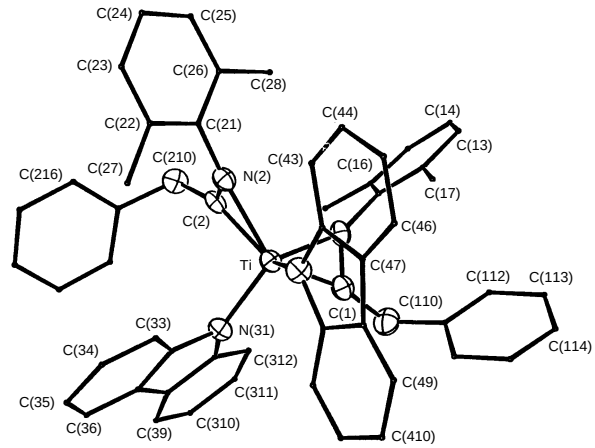



**Fig. 1** Molecular structure of **2** showing the atomic numbering scheme. Selected interatomic distances (Å) and angles (°): Ti–N(1) 2.017(2), Ti–N(2) 2.150(2), Ti–N(31) 2.008(2), Ti–N(41) 2.030(2), Ti–C(1) 2.067(3), Ti–C(2) 2.065(3), C(1)–N(1) 1.268(4), C(2)–N(2) 1.281(4); N(1)–Ti–N(2) 100.54(9), N(31)–Ti–N(41) 108.5(1), C(1)–Ti–C(2) 119.0(1).

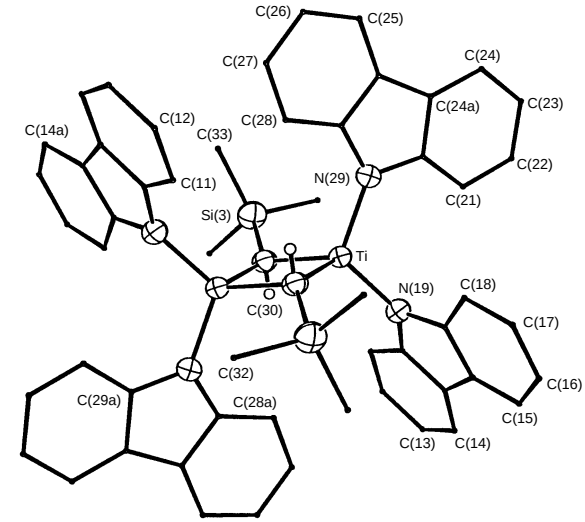



**Fig. 2** Molecular structure of **3** showing the atomic numbering scheme. Selected interatomic distances (Å) and angles (°): Ti···Tiʹ 2.9504(8), Ti–N(19) 1.950(2), Ti–N(29) 1.969(2), Ti–C(30) 2.026(2), Tiʹ–C(30) 2.035(2); N(19)–Ti–N(29) 113.29(7), C(30)–Ti–C(30)ʹ 86.83(9), Ti–C(30)–Tiʹ 93.17(9).

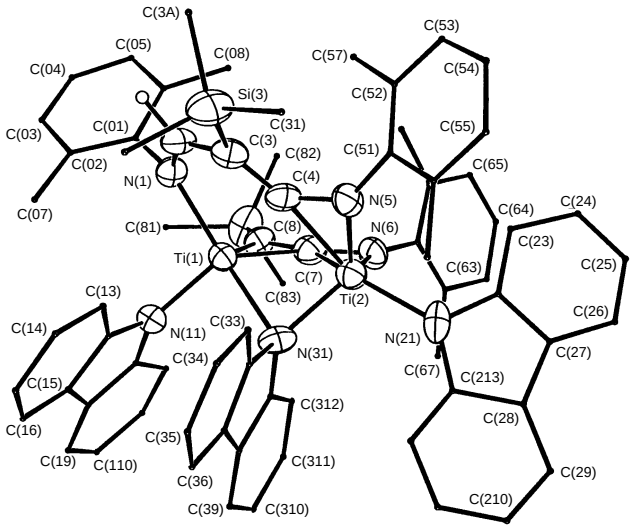



**Fig. 3** Molecular structure of **4** showing the atomic numbering scheme. Selected interatomic distances (Å): Ti(1)···Ti(2) 2.804(2), Ti(1)–N(1) 2.064(7), Ti(1)–N(11) 2.006(7), Ti(1)–N(31) 2.321(7), Ti(1)–C(8) 1.970(8), Ti(1)–C(7) 2.097(9), Ti(2)–C(7) 2.16(1), Ti(2)–N(21) 2.013(8), Ti(2)–N(31) 2.018(7), Ti(2)–N(6) 1.936(7), Ti(2)–N(5) 1.950(8), Ti(2)–C(4) 2.250(9), Ti(2)–C(7) 2.163(10), C(7)–C(8) 1.34(1), C(7)–N(6) 1.34(1), C(4)–N(5) 1.31(1), C(3)–C(4) 1.44(1), C(2)–C(3) 1.38(1), N(1)–C(2) 1.37(1).

ligands have been formed by addition of xyNC to trimethylsilylmethylidyne bridges in 1,3-dimetallacyclobutadiene derivatives of Nb or Ta.[4] The unit may have originated *via* initial α-hydrogen abstraction to produce an alkylidyne intermediate or by hydrogen abstraction from an initially formed iminoacyl. In both cases the hydrogen abstraction takes place by a carbazole ligand. The other bridging unit corresponds to the insertion of 2 equiv. of isocyanide into an alkylidene bridge combined with a 1,2-hydrogen shift. The transfer of adjacent hydrogen to iminoacyl carbon atoms has precedence.[7]

An interesting feature of the molecular structure of **4** concerns the distances within the iminoacyl component. Specifically the Ti–N(5) and Ti–C(4) distances lead to a value of −0.3 Å for the parameter [*d*(Ti–N)−*d*(Ti–C)].[7] This value combined with the long C(4)–N(5) distance are consistent with the much debated amido-carbene resonance picture.[10]

We thank the National Science Foundation (Grant CHE-9321906) for financial support of this research.

## Footnotes

† *Selected spectroscopic data*: $^1$H NMR ($C_6D_6$, 500 MHz, 30 °C): **1**, δ 6.58–7.91 (m, 18 H, aromatics), 3.24 (s, 4 H, Ti*CH*$_2$Ph); **2**, δ 6.39–8.02 (m, 32 H, aromatics), 3.69 (s, 4 H, C*H*$_2$Ph), 1.46 (s, 12 H, *Me*$_2$C$_6$H$_3$); **3**, δ 14.75 (s, 2 H, μ-C*H*SiMe$_3$), −0.50 (s, 18H, μ-CHSi*Me*$_3$); **4**, δ 2.55 (s, 3 H), 2.47 (s, 3 H), 2.45 (s, 3 H), 1.66 (s, 3 H), 1.64 (s, 3 H), 1.17 (s, 3 H, *Me*C$_6$H$_3$). $^{13}$C NMR ($C_6D_6$, 30 °C): **1**, δ 98.3 (*C*H$_2$Ph); **2**, δ 246.9 (xyN*C*), 43.5 (*C*H$_2$Ph), 18.5 (xy*Me*).

‡ *Crystal data*: for **2** at 203 K: $C_{59}H_{51}N_4Ti$, $M$ = 863.99, monoclinic, space group $C2/c$ (no. 15), $a$ = 37.22(1), $b$ = 12.153(3), $c$ = 21.069(9) Å, β = 104.23(3)°, $U$ = 9237(10) Å$^3$, $D_c$ = 1.242 g cm$^{-3}$, $Z$ = 8. Of the 6154 unique reflections collected (5.36 ⩽ 2θ ⩽ 45.34°) with Mo-Kα radiation (λ = 0.710 73 Å), the 6154 with $F_o^2 > 2\sigma(F_o^2)$ were used in the final least-squares refinement to yield $R(F_o)$ = 0.045 and $R_W(F_o^2)$ = 0.112.

For **3** at 296 K: $C_{56}H_{52}N_4Si_2Ti_2$, $M$ = 933.04, triclinic, space group $P\bar{1}$ (no. 2), $a$ = 10.066(2), $b$ = 10.481(2), $c$ = 13.170(3) Å, α = 109.17(2), β = 104.98(2), γ = 93.62(2)°, $U$ = 1251(1) Å$^3$, $D_c$ = 1.238 g cm$^{-3}$, $Z$ = 1. Of the 5056 unique reflections collected (5.32 ⩽ 2θ ⩽ 52.64°) with Mo-Kα radiation (λ = 0.710 73 Å), the 5056 with $I > 3\sigma(I)$ were used in the final least-squares refinement to yield $R$ = 0.036 and $R_W$ = 0.041.

For **4** at 233 K: $C_{71}H_{68}N_6Si_2Ti_2$, $M$ = 1157.35, monoclinic, space group $P2_1/n$ (no. 14), $a$ = 12.788(2), $b$ = 33.329(5), $c$ = 14.616(3) Å, β = 96.76(2)°, $U$ = 6186(3) Å$^3$, $D_c$ = 1.242 g cm$^{-3}$, $Z$ = 4. Of the 8122 unique reflections collected (5.26 ⩽ 2θ ⩽ 113.70°) with Cu-Kα radiation (λ = 1.541 84 Å), the 8122 with $F_o^2 > 2\sigma(F_o^2)$ were used in the final least-squares refinement to yield $R(F_o)$ = 0.074 and $R_W(F_o^2)$ = 0.184. Atomic coordinates, bond lengths and angles, and thermal parameters have been deposited at the Cambridge Crystallographic Data Centre (CCDC). See Information for Authors, Issue No. 1. Any request to the CCDC for this material should quote the full literature citation and the reference number 182/447.

## References

1 R. R. Schrock, *Acc. Chem. Res*., 1997, **30**, 9; P. W. Wanandi, W. D. Davis and C. C. Cummins, *J. Am. Chem. Soc*., 1995, **117**, 2110; R. K. Minhas, L. Scoles, S. Wong and S. Gambarotta, *Organometallics*, 1996, **15**, 1113; J. D. Scollard and D. H. McConville, *Organometallics*, 1995, **14**, 5478; K. Aoyagi, P. K. Gantzel, K. Kalai and T. D. Tilley, *Organometallics*, 1996, **15**, 923; A. D. Horton, J. de With, A. J. van der Linden and H. van de Weg, *Organometallics*, 1996, **15**, 2672.
2 L. Scoles, R. Minhas, R. Duchateau, J. Jubb and S. Gambarotta, *Organometallics*, 1994, **13**, 4978.
3 R. P. Planalp, R. A. Andersen and A. Zalkin, *Organometallics*, 1983, **2**, 16.
4 P. N. Riley, R. D. Profilet, P. E. Fanwick and I. P. Rothwell, *Organometallics*, 1996, **15**, 5502.
5 G. R. Davies, J. A. J. Jarvis and B. T. Kilbourn, *Chem. Commun*., 1971, 1511.
6 S. L. Latesky, A. K. McMullen, I. P. Rothwell and J. C. Huffman, *Organometallics*, 1985, **4**, 902.
7 I. P. Rothwell and L. D. Durfee, *Chem. Rev*., 1988, **88**, 1059.
8 L. R. Chamberlain, L. D. Durfee, P. E. Fanwick, L. H. Kobriger, S. L. Latesky, A. K. McMullen, I. P. Rothwell, K. Folting, J. C. Huffman, W. E. Streib and R. Wang, *J. Am. Chem. Soc*., 1987, **109**, 390.
9 M. R. Collier, M. F. Lappert and R. Pearce, *J. Chem. Soc., Dalton Trans*., 1973, 445.
10 K. Tatsumi, A. Nakamura, P. Hofmann, P. Stauffert and R. Hoffmann, *J. Am. Chem. Soc*., 1985, **107**, 4440.

*Received in Bloomington, IN, USA, 3rd March 1997; Com. 7/01493G*

# An *ab initio* study of the aggregation of LAuX molecules and $[LAuL]^+[XAuX]^-$ ions

**Pekka Pyykkö,*[a] Wolfgang Schneider,[b] Andreas Bauer,[b] Angela Bayler[b] and Hubert Schmidbaur*[b]**

[a] *Department of Chemistry, University of Helsinki, P.O.B. 55 (A. I. Virtasen aukio 1), FIN-00014 Helsinki, Finland*
[b] *Anorganisch-chemisches Institut der Technischen Universität München, Lichtenbergstrasse 4, D-85747 Garching, Germany*

**Pseudopotential *ab initio* calculations on dimers and tetramers of formula $\{[(H_3P)_2Au]^+[AuCl_2]^-\}_n$ ($n$ = 1, 2) which are the products of a ligand distribution of systems $(H_3PAuCl)_{2n}$, show that the different experimentally observed structures are actually energetically quite comparable.**

Many neutral gold(I) complexes of the type LAuX (L = neutral donor, X = anionic ligand) undergo facile ligand scrambling: NMR data on solution equilibria,[1,2] and solid-state structural data (*e.g.* L = $C_5H_5N$, X = halide;[3] L = $C_4H_8Se$, X = I;[4] L = $PMe_2Ph$, X = $GeCl_3$;[5] L = $Ph_2C{=}NH$, X = Cl, Br[6]), suggest that the energy differences associated with the ligand exchange according to eqn. (1) are very small, but there are no calculations to support this assumption.

$$2\ LAuX \rightleftharpoons (L_2Au)^+ + (AuX_2)^- \qquad (1)$$

It appears that solvation of the species in solution and aggregation of the components in the crystal play an important role in determining the equilibria.

When examining the details of the supramolecular chemistry of representative examples in the solid state, very unexpected modes of aggregation have been discovered[5] including non-standard ion sequences following the pattern [−++−] or [+−−+], instead of [+−+−], for tetramers of the formula $[LAuX]_4 = \{[L_2Au]^+[AuX_2]^-\}_2$.

In order to analyse the effects governing the aggregation modes, both Hartree–Fock (HF) and second-order Møller–Plesset (MP2) calculations (Table 1) were performed for di- and tetra-nuclear species of this type, and the previous $(H_3P)AuCl$ model, using GAUSSIAN 94 and either 11 or 19 valence-electron (11- or 19-VE) pseudopotentials.[7] We have pointed out earlier the importance of correlation and relativistic effects[8–10] for the underlying $Au^I\cdots Au^I$ interactions.[11] The use of a $PH_3$ group to model the structures with higher $PR_3$ groups was found to be acceptable,[12] although this approach at the semiempirical level has been criticised.[13] At *ab initio* MP2 level, $PMe_3$ gives the same interaction depth, but larger $R_e$,[14] as $PH_3$.

The dihedral angles (P–Au–Au–Cl, Cl–Au–Au–Cl or P–Au–Au–P) were fixed at 90° in the dimers $(\mathbf{1})_2$, **2** and linear tetramers **3**, **4**, **6** (Fig. 1 and Table 2). The $Au_4$ geometry in cyclic tetramers **5** $[(\mathbf{5a})_2]$, was assumed to be rectangular with a parallel arrangement of all PAuP and ClAuCl axes. The Au···Au distance, $R_{intra}$, established for the dimers was kept constant in the tetramers. The 19-VE geometries of the monomers **1**, **2a** and **2b** (Table 1) were adopted for the 11-VE calculations.

**Table 1** Optimized monomer properties at the 19-VE MP2 level. Distances in pm, energies in $E_h$ ($E_h$ = 4.35975 × $10^{-18}$ J)

| System | Au–P/pm | Au–Cl/pm | P–H/pm | Au–P–H/° | $-E$ |
|---|---|---|---|---|---|
| $(H_3P)AuCl$ **1** | 224.3 | 226.3 | 141.3 | 117.42 | 158.47013 |
| | | | | | 56.69561[a] |
| $Au(Ph_3)_2^+$ **2a** | 233.0 | — | 141.1 | 115.39 | 151.58419 |
| | | | | | 49.81742[a] |
| $AuCl_2^-$ **2b** | — | 228.8 | — | — | 165.21778 |
| | | | | | 63.45385[a] |

[a] 11-VE energies with the optimized 19-VE geometry.

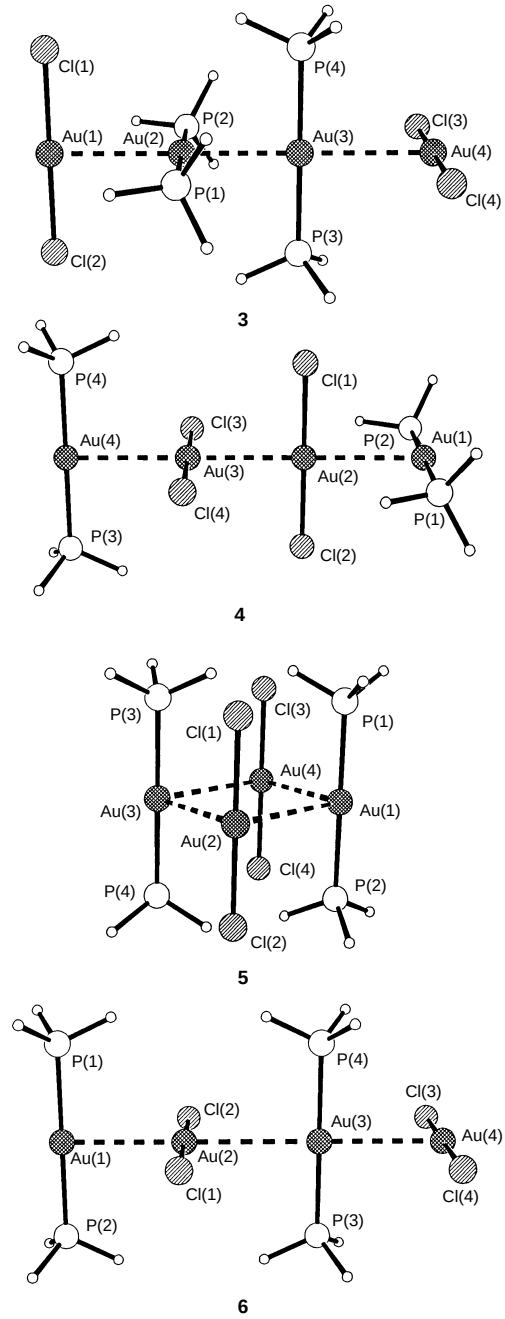



**Fig. 1** The different linear-chain and cyclic tetramers on which the calculations were performed

**Table 2** Calculated 'intramolecular' Au···Au distances, $R_{intra}$, of the ion pair $[Au(PH_3)_2^+AuCl_2^-]$ **2**, 'intermolecular' distances, $R_{inter}$, of the tetranuclear species, and the corresponding energy changes relative to molecular $[(H_3P)AuCl]_2$ dimers. A counterpoise correction is included ($E_h$ = 627.5095 kcal mol$^{-1}$)[a]

| System | $R_{intra}$ | $R_{inter}$ | $\Delta E$/ kcal mol$^{-1}$ | Pseudopotential |
|---|---|---|---|---|
| $[(H_3P)AuCl]_2$ (**1**)$_2$ | 320.9 | — | 0 | 19 VE |
| | 321.7 | — | 0 | 11 VE |
| [+−], **2** | 289.5 | — | +9.5 | 19 VE |
| | 294.2 | — | −0.9 | 11 VE |
| [−++−], **3** | 294.2 | 313.1 | −6.6 | 11 VE |
| [+−−+], **4** | 294.2 | 306.7 | −5.4 | 11 VE |
| [+−], **5a** | 324.1 | — | −3.4 | 11 VE |
| $\begin{bmatrix}+ & - \\ - & +\end{bmatrix}$, **5** | 324.1 | 366.8 | −32.3 | 11 VE |
| [+−+−], **6** | 294.2 | 313.7 | −11.4 | 11 VE |

[a] 1 cal = 4.184 J.

The energies and gold··gold distances obtained for the di- and tetra-meric systems are summarized in Table 2. The former were calculated starting from the monomeric units (**1**, **2a**, **2b**), complemented by their interaction energies as obtained by subtracting the value for monomers (dimers) from those of the dimer (tetramer), including a counterpoise correction.

In all three linear tetramers a short $R_{inter}$ Au···Au contact is observed. The shortest distance is found for the [+−−+] system followed by [−++−] and finally [+−+−]. A similar result is observed experimentally for the compound $[(Me_2PhP)_2Au^+$-$Au(GeCl_3)_2^-]$ {sequence [+−−+]} which indeed shows the shortest Au···Au contact between the two anions. This result is clearly at variance with Coulomb's law. However, focussing on the natural bond orbital (NBO) populations of the Au atoms, it is easier to understand the insensitivity of the total energy to the ionic arrangement. All gold atoms of $AuCl_2^-$ have charges between 0.53320 and 0.57567 (0.60541 in the monomeric $AuCl_2^-$, **2b**, and 0.56730 in the dimer [+−], **2**), and those in cations between 0.473 59 and 0.494 71 {0.442 63 in the monomeric $Au(PH_3)^+$, **1a**, and 0.47359 in the dimer [+−], **2**}. The Mulliken Au populations vary more and are in the ranges 0.26500–0.39708 and −0.02241–0.13594 for anions and cations, respectively.

It should be mentioned that the $R_{intra}$ values of the dimers were kept constant in every tetramer, and therefore the geometries obtained may not be the absolute minima on the energy surfaces. We have also not attempted a full-crystal simulation, and it should finally be noted that a short Au···Au contact does not necessarily correlate with the lowest energy. The main point is that all curves in Fig. 2 are evidence for attractive interactions and that the distances in Tables 2 and 3 are comparable.

The cyclic tetramer shows a larger $R_{inter}$ distance probably due to the steric repulsion between the hydrogen and the chlorine atoms, which come very close together in the parallel arrangement of the individual units. Nevertheless this oligomer has the lowest energy as compared to the linear-chain tetramers. The optimum arrangement for two dipoles [+−] and the occurrence of one additional Au···Au interaction between dimers may be the reasons for this preference.

In conclusion, we have found that the molecular and ionic dimers of the type $[(H_3P)AuCl]_2$ and $[(H_3P)_2Au^+AuCl_2^-]$ are closely comparable in energy. This is made plausible by the close similarity of the gold atom NBO charges in the anion, cation and neutral monomer.

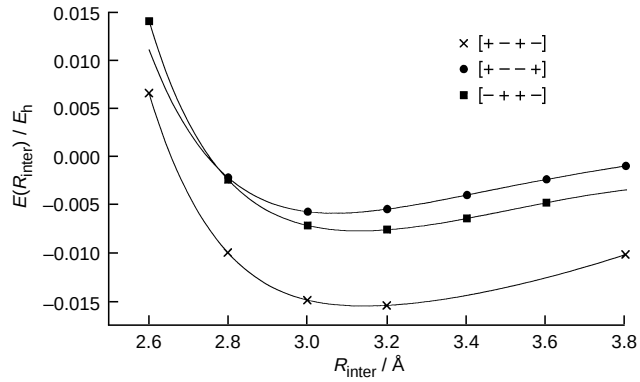



**Fig. 2** Calculated bond energies for the intermolecular gold···gold contacts in the linear-chain tetramers using the 11 VE pseudopotential at MP2 level

**Table 3** $R_{intra}$ and $R_{inter}$ distances of some experimentally known compounds

| Compound | $R_{intra}$/pm | $R_{inter}$/pm |
|---|---|---|
| (py)AuCl, type **3** and **5**[3b] | 324.9(3) | 341.6(4) |
| (py)AuBr, type **6**, infinite chain[3a] | 330.2(2) | 356.3(2) |
| (py)AuBr, type **3**[3a] | 324.6(1) | 349.6(2) |
| (py)AuI, type **3**[3b] | 299.0(1) | 329.1(1) |
| $[(Me_2PhP)_2Au]^+[Au(GeCl_3)_2]^-$, type **4**[5] | 297.9 av. | 288.1(1) |
| $[(Ph_2CNH)_2Au]^+[AuCl_2]^-$, type **5**, Z-shaped[6] | 319.44(5) | 360.4(1) |

The calculations were carried out on DEC Alpha stations at Helsinki. We thank DAAD for travel scholarships and Dr Fernando Mendizabal for discussions. P. Pyykkö is Research Professor of The Academy of Finland.

## References

1 A. L. Hormann-Arendt and C. F. Shaw III, *Inorg. Chem.*, 1990, **29**, 4683.
2 M. N. Akhtar, I. H. Gazi, A. A. Isab, A. R. Al-Arfaj, M. I. M. Wazeer and M. S. Hussain, *J. Coord. Chem.*, 1995, **36**, 149.
3 (*a*) W. Conzelman, W. Hiller and J. Strähle, *Z. Anorg. Allg. Chem.*, 1984, **512**, 169; (*b*) H.-N. Adams, W. Hiller and J. Strähle, *Z. Anorg. Allg. Chem.*, 1982, **485**, 81.
4 S. Ahrland, K. Dreisch, B. Norén and A. Oskarsson, *Mater. Chem. Phys.*, 1993, **35**, 281.
5 A. Bauer, H. Schmidbaur, *J. Am. Chem. Soc.*, 1996, **118**, 5324.
6 W. Schneider, A. Bauer and H. Schmidbaur, *J. Chem. Soc., Dalton Trans.*, in press.
7 Au (11-VE): P. J. Hay and W. R. Wadt, *J. Chem. Phys.*, 1985, **82**, 270, (3s3p3d1f)/[2s2p2d1f], $\alpha_f$ = 0.20. Au (19-VE): D. Andrae, U. Häussermann, M. Dolg, H. Stoll and H. Preuss, *Theor. Chim. Acta*, 1990, **77**, 123, (8s7p6d2f)/[6s5p3d2f], $\alpha_f$ = 0.20 and 1.19. P (5-VE): A. Bergner, M. Dolg, W. Küchle, H. Stoll and H. Preuss, *Mol. Phys.*, 1993, **80**, 1431, (4s4p1d)/[2s2p1d], $\alpha_d$ = 0.34. Cl (7-VE): (4s5p1d)/[2s3p1d], $\alpha_f$ = 0.514; H: T. H. Dunning Jr. and P. J. Hay, in *Modern Theoretical Chemistry*, ed. H. F. Schaefer III, Plenum, New York 1977, vol. 3, pp. 1–28, (4s1p)/[2s1p], $\alpha_p$ = 0.800.
8 P. Pyykkö and Y.-F. Zhao, *Angew. Chem.*, 1991, **103**, 622; *Angew. Chem., Int. Ed. Engl.*, 1991, **30**, 604.
9 J. Li and P. Pyykkö, *Chem. Phys. Lett.*, 1992, **197**, 586.
10 P. Pyykkö, J. Li and N. Runeberg, *Chem. Phys. Lett.*, 1994, **218**, 133.
11 H. Schmidbaur, *Gold Bull.*, 1990, **23**, 11.
12 O. D. Häberlen and N. Rösch, *J. Phys. Chem.*, 1993, **97**, 4970.
13 R. Boca, *J. Chem. Soc., Dalton Trans.*, 1994, 2061.
14 P. Pyykkö, N. Runeberg and F. Mendizabal, *Chem. Eur. J.*, in press.

*Received in Basel, Switzerland, 16th December 1996; Com. 6/08428A*

# Novel (silylimino)diarylphosphoranyl(trimethylsilyl)methyl-*C*,*N* ligands $[CH(SiMe_3)PPh_2{=}NSiMe_3]^-$ ($[LL']^-$) and $[CH(SiMe_3)\{Ph(1,2\text{-}C_6H_4)P{=}NSiMe_2\}]^-$ ($[LL'']^-$) and the structures of $[Li(LL'')]_2$ and $[Pb(LL')_2]$†

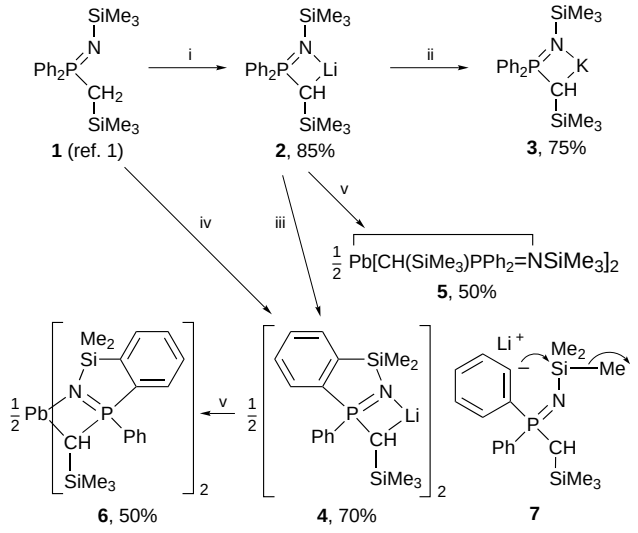
**Peter B. Hitchcock, Michael F. Lappert* and Zhong-Xia Wang**

*The Chemistry Laboratory, University of Sussex, Brighton, UK BN1 9QJ*

**Metal complexes containing the ligands $[CH(SiMe_3)PPh_2{=}NSiMe_3]^-$ {≡$[LL']^-$} and $[CH(SiMe_3)\{Ph(1,2\text{-}C_6H_4)P{=}NSiMe_2\}]^-$ {≡$[LL'']^-$} are reported [from, as initial precursor, $CH_2(SiMe_3)PPh_2{=}NSiMe_3$]: Li(LL′), K(LL′), $[Li(LL'')]_2$ 4, Pb(LL′)$_2$ 5 and Pb(LL″)$_2$; mass and multinuclear NMR spectra and single-crystal X-ray diffraction data for 4 (a fused tricyclic complex having a central LiNLiN ring) and 5 are presented.**

We report the synthesis and characterisation of five lithium, potassium and lead(II) homoleptic derivatives of two novel *C*,*N*-centred (iminophosphoranyl)methyl ligands, including the X-ray structures of two of them.

Treatment of the phosphinimine $CH_2(SiMe_3)PPh_2{=}NSiMe_3$ **1**[1] with LiBu$^n$ yielded (Scheme 1, step i) colourless $[Li\{CH(SiMe_3)PPh_2{=}NSiMe_3\}]_2$ {≡$[Li(LL')]_2$} **2**, which with KOBu$^t$ in hexane afforded (Scheme 1, step ii) the insoluble, pale yellow K(LL′) **3**, which was soluble in thf or pyridine. Reacting **2** with LiBu$^n$ gave (Scheme 1, step iii) the colourless *ortho*-silylated product $[Li(CH(SiMe_3)\{Ph(1,2\text{-}C_6H_4)P{=}NSiMe_2\})]_2$ {=$[Li(LL'')]_2$} **4**, which was also accessible (Scheme 1, step iv) from **1** and 1.2 equiv. of LiBu$^n$. The product obtained (Scheme 1, step v) from $PbCl_2$ and either **2** or **4** was the yellow Pb(LL′)$_2$ **5** or the colourless Pb(LL″)$_2$ **6**. The yields shown in Scheme 1 refer to isolated, pure, crystalline (or for **3**, powder) **2**–**6**.




**Scheme 1** Synthesis of (silylimino)diarylphosphoranyl(trimethylsilyl)methyl-*C*,*N*]metal complexes **2**–**6**. *Reagents and conditions*: i, LiBu$^n$, hexane, −20 °C to room temp., 3 h; ii, KOBu$^t$, hexane, room temp., 3 h; iii, LiBu$^n$, hexane, reflux, 4 h; iv, 1.2 equiv. LiBu$^n$, hexane, −20 °C to room temp., 5 d; v, 1/2 $PbCl_2$, $Et_2O$, −45 to *ca*. 20 °C.

The conversion of **2** to **4** (Scheme 1, step iii) probably proceeded *via* an *ortho*-lithiated intermediate, followed by an intramolecular displacement of Me$^-$ at silicon by the aromatic anion, as shown in **7**. In a separate experiment (Scheme 1, step iv) it was shown that the transformation **2** to **4** was effected catalytically using 0.2 mol excess of LiBu$^n$.

Each of the compounds **2**–**6** (except **3**), were hydrocarbon-soluble, gave satisfactory microanalytical, as well as $^1$H, $^{13}$C{$^1$H}, $^{31}$P{$^1$H}, $^7$Li{$^1$H} (**2** and **4**) and $^{207}$Pb{$^1$H} (**5** and **6**) NMR‡ and EI mass spectra {which showed as the highest ion $[M - Li \text{ (or K)} + 1]^+$ (*ca*. 30% for **2** or **3**), $[M - Li]^+$ (58% for **4**) and $M^+$ (1% for **5** and 5% for **6**)} (thf = $OC_4H_8$, M = the mononuclear molecular ion). Single-crystal X-ray diffraction data§ established the molecular structures of **4** (Fig. 1), **5** (Fig. 2) and **6**; the structure of **6** will be presented in the full paper.

Noteworthy features of the NMR spectra‡ include the demonstration of (*i*) long-range phosphorus–silylmethyl coupling in the $^{13}$C{$^1$H} NMR spectrum of **2**, $^3J(^{13}C–^{31}P)$ 3.5, 4.6

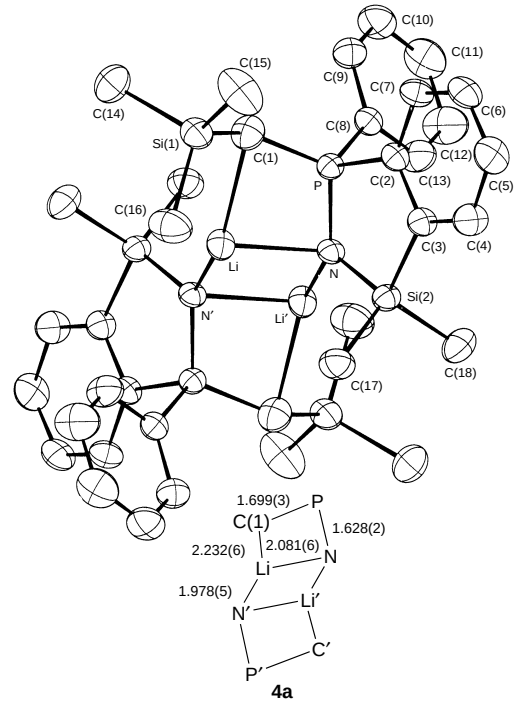
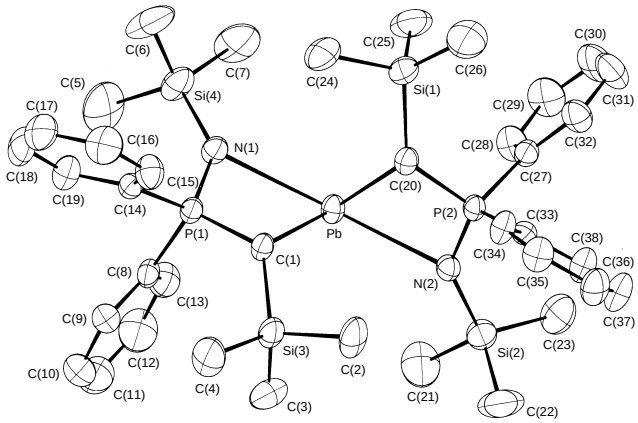


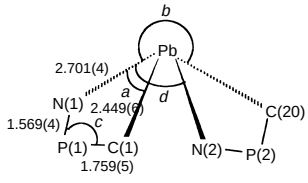

**Fig. 1** The molecular structure of crystalline complex **4**. Selected bond lengths (Å) (see also **4a**) and angles (°): N–Li–C(1) 80.1(2), N–Li–N′ 103.8(2), N′–Li–C(1) 135.0(3), N–P–C(1) 113.18(14), P–N–Li 86.2(2), P–N–Li′ 126.4(2), P–C(1)–Li 79.9(2), Li–N-Li′ 76.2(2).

Hz for the two $SiMe_3$ groups; (*ii*) separate (axial and equatorial) Si–Me $^1$H signals due to the endocyclic $SiMe_2$ group in **4** and **6**; and (*iii*) $^2J(^{31}P–^{207}Pb)$ and $^2J(^{207}Pb–^{31}P)$ in **5** and **6**.

The structures of crystalline $[Li\{CH_2PMe_2{=}NSiMe_3\}]_4$ **8** and $[Li\{CMe_2PPr^i_2{=}NSiMe_3\}]_2$ **9** have the lithium atoms bridged by carbon.[2] It is surprising, therefore, that the dinuclear crystalline **4** (Fig. 1) has the imido nitrogen atoms bridging the lithium atoms, the skeletal structure being ladder-shaped, **4a**. The central LiNLi′N′ ring is planar, with the angle at N narrower [76.2(2)°] than that at Li, 103.8(2)°. The terminal LiNPC rings are puckered, Li lying 0.26 Å out of the NPC plane. The bond angles at the three-coordinate Li range from 80.1(2) [N–Li–C(1)] to 135.0(3)° [N′–Li–C(1)], the sum of the angles at Li being *ca*. 319°. The six bond angles at N (av. 108°) vary from 76.2(2) to 129.6(2)° [Si(2)–N–Li]. The Li–N and Li–C bond lengths are unexceptional,[3] while the Li···P contact of 2.556(5) Å is similar to the 2.56 (av.), 2.58 (av.) or 2.520(9) Å found in $[\{Li(thf)_2\}_2\{PhPCH_2CH_2PPh\}]$,[4] $[\{Li(tmen)\}_2$-$C_6H_4(PPh)_2$-1,2$\}]$,[5] or $Li(thf)_2[\{N(SiMe_3)\}_2PPh_2]$,[6] respectively [tmen = $(Me_2NCH_2)_2$]. The average Li–N and Li–C distances are 2.03 (**8**) and 1.928 (**9**), and 2.39 (**8**) and 2.27 (**9**), respectively.[2] The X-ray structure of $[Li\{2\text{-}C_6H_4PPh_2{=}NSi$-$Me_3\}_2Li(OEt)_2]$ is available.[7]

Crystalline **5** is mononuclear, Fig. 2. The four-coordinate lead has a stereochemically active lone pair of electrons. The phosphorus approximates to its having tetrahedral geometry. A simplified bonding pattern is shown in **5a**. The P–N bond length of 1.569(4) Å indicates a double bond, while the mean endocyclic P–C distance of 1.757(6) Å is slightly shorter than usual for a $P^V$–C single bond. The average Pb–N distance of 2.678 Å is much longer than in anionic nitrogen-centred lead(II) compounds, *e.g.*, 2.24(2) Å in $Pb[N(SiMe_3)_2]_2$,[8] or 2.465 Å (av.) in $Pb[\{N(SiMe_3)\}_2PPh_2]_2$,[9] while the mean Pb–C($sp^3$) bond length of 2.448 Å in **5** may be compared with the Pb–C($sp^2$) distance of 2.336 Å in $Pb[C_6H_2(CF_3)_3$-2,4,6$]_2$.[10]




**5a** [*a*, 62.52(14); *b*, 107.6(2); *c*, 107.2(2); *d*, 167.27(11)°]

**Fig. 2** The molecular structure of crystalline complex **5**. Selected bond lengths (Å) and angles (°) (see also **5a**): Pb–C(20) 2.447(5), Pb–N(2) 2.654(4), P(2)–C(20) 1.756(5), P(2)–N(2) 1.569(4); C(20)–Pb–C(1) 88.2(2), C(20)–Pb–N(2) 63.6(2), C(1)–Pb–N(2) 106.69(14), C(20)–Pb–N(1) 107.6(2), N(2)–Pb–N(1) 167.27(11), N(2)–P(2)–C(20) 108.1(2).

The new ligands $[LL']^-$ and $[LL'']^-$ should have an extensive coordination chemistry. Using Li(LL′) **2** or Li(LL″) **4**, we have made *inter alia* $Sn(LL')_2$, $Sn(LL'')_2$, $[Sn(LL')]_2$, $Pb(LL'')_2$ and $[Fe(LL')_3]$, as well as some analogues of Li, K, $Sn^{II}$, $Fe^{II}$ and $Co^{II}$.

We thank the Chinese Government and the British Council for the award of a studentship to Z.-X. W. and the EPSRC for other support.

## Footnotes

* E-mail: M.F.Lappert@sussex.ac.uk

† No reprints available.

‡ *Selected NMR data* [$^1$H 360.1, $^7$Li{$^1$H} 97.3, $^{31}$P{$^1$H} 101.3, $^{207}$Pb{$^1$H} 52.1 MHz; 298 K; $C_5D_5N$ for **3**, $C_6D_6$ for **2** and **4**–**6**; *J*, Hz]. **2**: $^1$H δ 0.10 (s, 9 H, $SiMe_3$), 0.13 (s, 9 H, $SiMe_3$), 0.17 (d, 1 H, CH, *J* 13.8), 7.19 (s, Ph), 7.21 (s, Ph), 7.84–7.89 (m, Ph); $^7$Li{$^1$H} δ 2.23; $^{31}$P{$^1$H} δ 33.32. **3**: $^1$H δ 0.26 (s, 9 H, $SiMe_3$), 0.29 (s, 9 H, $SiMe_3$), 7.20–7.58 (m, Ph), 8.18–8.22 (m, Ph); $^{31}$P{$^1$H} δ 20.23. **4**: $^1$H δ −0.02 (s, 9 H, $SiMe_3$), 0.32 (s, 3 H, SiMe), 0.59 (s, 3 H, SiMe), 0.92 (d, 1 H, CH, *J* 4.9), 7.03–7.15 (m, 5 H, Ph), 7.44–7.56 (m, 2 H, $C_6H_4$), 7.77–7.83 (m, 2 H, $C_6H_4$); $^7$Li{$^1$H} δ 2.05; $^{31}$P{$^1$H} δ 48.70. **5**: $^1$H δ −0.01 (s, 18 H, $SiMe_3$), 0.20 (s, 18 H, $SiMe_3$), 1.37 (d, 2 H, CH, *J* 15.8), 7.00–7.05 (m, Ph), 7.15–7.22 (m, Ph), 7.64–7.69 (m, Ph), 7.79–7.85 (m, Ph); $^{31}$P{$^1$H} δ 19.52 (s, with satellite peaks, *J* 308); $^{207}$Pb{$^1$H} δ 2787.63 (t, *J* 306). **6**: $^1$H δ 0.31 (s, 18 H, $SiMe_3$), 0.53 (s, 6 H, SiMe), 0.69 (s, 6 H, SiMe), 1.43 (d, 2 H, CH, *J* 9.5), 7.06–7.25 (m, Ph + $C_6H_4$), 7.54–7.65 (m, Ph + $C_6H_4$); $^{31}$P{$^1$H} δ 40.27 (s, with satellite peaks, *J* 311.8); $^{207}$Pb{$^1$H} δ 1998.26 (t, *J* 313.3).

§ *Crystal data*: **4**, $C_{36}H_{50}Li_2N_2P_2Si_4$: *M* = 699.0, triclinic, space group $P\bar{1}$ (no. 2), *a* = 9.904(1), *b* = 10.259(3), *c* = 11.175(1) Å, α = 109.10(2), β = 95.79(1), γ = 104.44(2)°, *U* = 1018.2(2) Å$^3$, *F*(000) = 372; *Z* = 1, $D_c$ = 1.14 g cm$^{-3}$, specimen 0.3 × 0.3 × 0.3 mm, 3578 independent reflections, 2706 reflections with $[|F^2| > 2\sigma(F^2)]$; $R_1$ = 0.054, $wR_2$ = 0.152 (for all data). **5**, $C_{38}H_{58}N_2P_2PbSi_4$: *M* = 924.4, triclinic, space group $P\bar{1}$ (no. 2), *a* = 10.767(2), *b* = 14.091(2), *c* = 16.775(2) Å, α = 87.07(1), β = 72.01(1), γ = 69.77(1)°, *U* = 2266.9(6) Å$^3$, *F*(000) = 936; *Z* = 2, $D_c$ = 1.35 g cm$^{-3}$, specimen 0.3 × 0.3 × 0.1 mm, 13179 independent reflections, 7752 reflections with $[|F^2| > 2\sigma(F^2)]$; $R_1$ = 0.056, $wR_2$ = 0.102 (for all data).

Intensities were measured to $\theta_{max}$ 25° (for **4**) or 30° (for **5**) on an Enraf-Nonius CAD4 diffractometer using monochromated Mo-Kα (μ = 0.25 mm **4**, 3.92 mm **5**) radiation (λ = 0.71073 Å); absorption correction from ψ scan for **5**. Structure refinements were by SHELXL-93, with H atoms in riding mode. Atomic coordinates, bond lengths and angles, and thermal parameters have been deposited at the Cambridge Crystallographic Data Centre (CCDC). See Information for Authors, Issue No. 1. Any request to the CCDC for this material should quote the full literature citation and the reference number 182/455.

## References

1 J. C. Wilburn and R. H. Neilson, *Inorg. Chem.*, 1979, **18**, 347.
2 A. Müller, B. Neumüller and K. Dehnicke, *Chem. Ber.*, 1996, **129**, 253.
3 *cf.* K. Gregory, P. v. R. Schleyer and R. Snaith, *Adv. Inorg. Chem.*, 1991, **37**, 47; W. N. Setzer and P. v. R. Schleyer, *Adv. Organomet. Chem.*, 1985, **24**, 353.
4 D. M. Anderson, P. B. Hitchcock, M. F. Lappert and I. Moss, *Inorg. Chim. Acta*, 1988, **141**, 157.
5 D.M. Anderson, P. B. Hitchcock, M. F. Lappert, W.-P. Leung and J. A. Zora, *J. Organomet. Chem.*, 1987, **333**, C13.
6 A. Steiner and D. Stalke, *Inorg. Chem.*, 1993, **32**, 1977.
7 A. Steiner and D. Stalke, *Angew. Chem., Int. Ed. Engl.*, 1995, **34**, 1752.
8 T. Fjeldberg, H. Hope, M. F. Lappert, P. P. Power and A. J. Thorne, *J. Chem. Soc., Chem. Commun.*, 1983, 639.
9 U. Kilimann, M. Noltemeyer and F. T. Edelmann, *J. Organomet. Chem.*, 1993, **443**, 35.
10 S. Brooker, J.-K. Buijink and F. T. Edelmann, *Organometallics*, 1991, **10**, 25.

*Received in Basel, Switzerland, 27th January 1997; Com. 7/00609H*

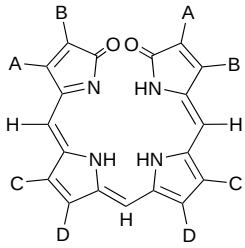
# Axial ligation modulates the electron distribution in helical cobalt complexes derived from octaethylbilindione

**Saeed Attar, Andrew Ozarowski, Pamela M. Van Calcar, Krzysztof Winkler† and Alan L. Balch***

*Department of Chemistry, University of California, Davis, California 95616, USA*

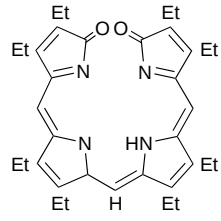
**Addition of pyridine to the four-coordinate cobalt(II) complex, $[Co^{II}(oebOx)]I_3$, which shows an EPR spectrum with well resolved Co hyperfine coupling, converts the complex into one with $Co^{III}$/ligand radical structure and an EPR spectrum with $g_z$ = 1.98, and $g_{xy}$ = 2.02 and no cobalt hyperfine coupling.**

Biliverdin 1Xa, **1a**, a product of haem catabolism, has been recently reported to have two interesting physiological activities: antioxidant activity and anti-HIV activity.[1] In order to understand the molecular bases for these activities, we have undertaken the study of redox behaviour of biliverdin analogues and their metal complexes. Octaethylbilindione, **1b**, a symmetrically substituted version of biliverdin 1Xa, forms a series of helical metal complexes with cobalt, nickel and copper in which the electronic structure indicates a significant contribution from a ligand-based free radical.[2–7] Upon treatment with an oxidant (*e.g.* diiodine) **1b** undergoes a facile two-electron oxidation to form **2** which has been isolated in a protonated form.[8] Recently we have shown that the cobalt complex of **1b**, Co(**1b**), undergoes a series of reversible, one-electron redox reactions as shown in eqn. (1).[9] Two members of this series, [Co(**1b**)] **3** and $[Co(C_{35}H_{43}N_4O_2)]^+$ **4**$^+$, have been isolated and thoroughly characterized. The electronic structure of four-coordinate **3** has been described in terms of contributions from both the $Co^{III}$/$oeb^{3-}$ and $Co^{II}$/$oeb^{\cdot 2-}$ forms, where $oeb^{\cdot 2-}$ is the radical obtained by one-electron oxidation of $oeb^{3-}$.[4] Complex **4**$^+$ has been isolated as the triiodide salt. In the solid state the Co–$I_3$ distance is long (2.818 Å) and has been interpreted in terms of an ion-paired structure.[9] The structural and magnetic properties of [**4**$^+$]$I_3$ indicate that it is a cobalt(II) complex of the two-electron oxidized ligand **2**, *i.e.* it is $[Co^{II}(oebOx)]I_3$.[9] Here we demonstrate that the electronic structure of [**4**$^+$] is altered by the addition of axial pyridine ligands.




**1a** A = C = methyl
B = vinyl
D = propionate

**1b** A = B = C = D = ethyl
($H_3$oeb)




**2** (HoebOx)

$$[Co(\mathbf{1b})]^{2-} \underset{+e^-}{\overset{-e^-}{\rightleftharpoons}} [Co(\mathbf{1b})]^{-} \underset{+e^-}{\overset{-e^-}{\rightleftharpoons}} [Co(\mathbf{1b})]\ \mathbf{3} \underset{+e^-}{\overset{-e^-}{\rightleftharpoons}} [Co(\mathbf{1b})]^{+}\ \mathbf{4} \quad (1)$$

The EPR spectrum of [**4**$^+$]$I_3$, like other cobalt(II) complexes, is sensitive to its environment. At 77 K it shows a rhombic pattern that can be fit with $g_1$ = 2.42, $g_2$ = 2.23 and $g_3$ = 2.01 but hyperfine coupling from cobalt was not resolved.[9] However, in dichloromethane–methanol at 77 K the spectrum shown in Fig. 1(*a*) is obtained. The parallel portion of the spectrum is clearly resolved with $g_z$ = 2.013 and $A_z$ = 89.3 × $10^{-4}$ $cm^{-1}$. The perpendicular region is more difficult to interpret because of the dependence of linewidth on both orientation and the quantum number $M_I$. However, $g_x$ and $g_y$ are estimated at 2.29 with $A_x$ *ca.* 16 × $10^{-4}$ $cm^{-1}$ and $A_y$ *ca.* 35 × $10^{-4}$ $cm^{-1}$. This spectrum is indicative of the formulation of the complex as $[Co^{II}(oebOx)]I_3$. Addition of pyridine to a sample of [**4**$^+$]$I_3$ in MeOH–$CH_2Cl_2$ results in the formation of $[(py)_2Co^{III}(oeb\cdot)]I_3$, [**5**$^+$]$I_3$, as shown by a marked alteration in the EPR spectrum. The resulting spectrum for a solution frozen at 77 K is shown in Fig. 1(*b*). The new spectrum shows a sharp, slightly anisotropic signal ($g_{x,y}$ = 1.996, $g_z$ = 2.018) near the free electron *g* value. The cobalt hyperfine interaction is also lost. These alterations in the EPR spectrum suggest that a significant rearrangement of the electronic structure of the complex [**4**$^+$]$I_3$ occurs when axial pyridine ligands are present and that the pyridine adduct behaves as if it contains a ligand-based free radical.

Deep purple prisms of [**5**$^+$]$I_3$ may be isolated by dissolving a sample of [**4**$^+$]$I_3$ in pyridine and allowing the solution to stand. The structure of [**5**$^+$]$I_3$ has been determined by X-ray crystallography.‡ A view of the cation, which has crystallographic $C_2$ symmetry with the rotation axis passing through the cobalt ion and the unique methine carbon atom, is shown in Fig. 2. The cobalt ion is six-coordinate with bonds to the nitrogen atoms of two axial pyridine ligands and the four nitrogen atoms of the helical tetrapyrrole ligand. The Co–N bond distances [Co–N(1) 1.950(5), Co–N(2) 1.956(4) and Co–N(3) 1.997(5) Å] are indicative of the presence of a $Co^{III}$ centre in the complex.[10] The Co–N distances [1.916(7), 1.910(7), 1.926(7) and 1.898(7) Å] in [**4**$^+$]$I_3$ are slightly shorter than the equatorial Co–N distances in [**5**$^+$]$I_3$.[9] However, the pattern of Co–N distances seen for [**5**$^+$]$I_3$ is similar to those of low-spin cobalt(III) porphyrin complexes such as $[Co^{III}(ttp)(Him)_2]^+$ (where Him is imidazole

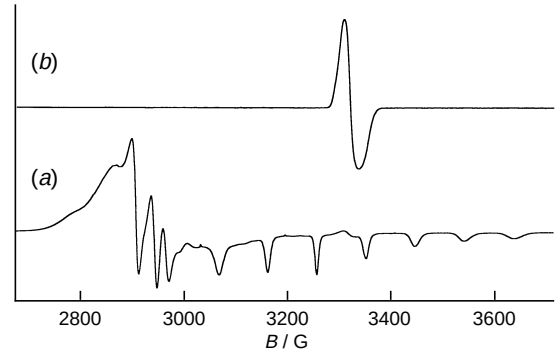



**Fig. 1** EPR spectra of frozen solutions at 77 K of (*a*) $[Co^{II}(oebOx)]I_3$ in $CH_2Cl_2$–MeOH and (*b*) $[Co^{III}(oebO\cdot)(py)_2]I_3$ {obtained by adding py to a $CH_2Cl_2$–MeOH solution of $[Co^{II}(oebOx)]I_3$}

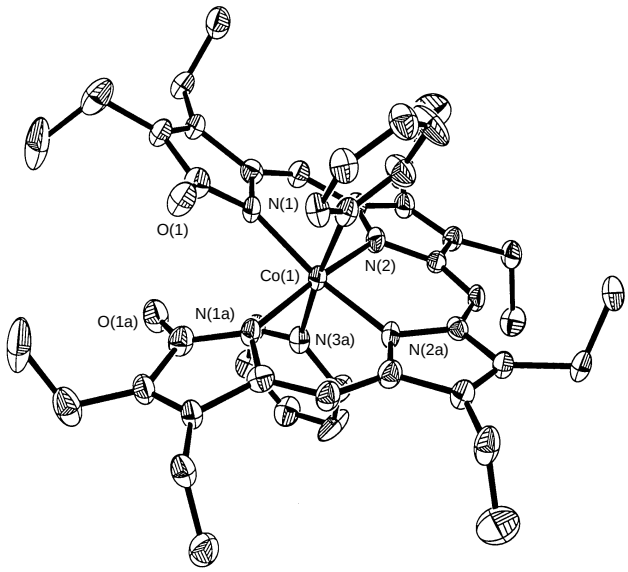



**Fig. 2** A perspective view of $[Co(oebO\cdot)py)_2]^+$ with 50% thermal contours for all atoms. Selected bond lengths (Å) and angles (°): Co–N(1) 1.950(5), Co–N(2) 1.956(4), Co–N(3) 1.997(5), C(1)–O 1.216(7); N(1)–Co–N(2) 89.8(2), N(1)–Co–N(3) 85.6(2), N(1)–Co–N(1a) 91.3(3), N(2)–Co–N(3) 94.6(2), N(2)–Co–N(2a) 92.0(3), N(2)–Co–N(1a) 167.2(2), N(3)–Co–N(3a), 174.5(3).

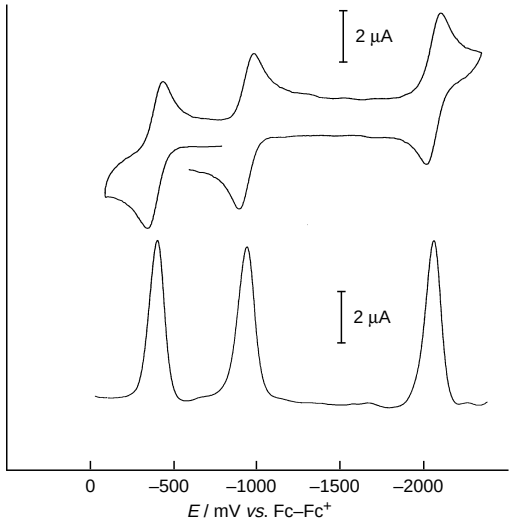



**Fig. 3** Cyclic voltammogram and differential pulse voltammogram of Co(oeb) (1.6 mM) in pyridine solution with 0.1 M $NBu^n_4ClO_4$ as supporting electrolyte

and ttp is the dianion of tetraphenylporphyrin) which has a Co–$N_{(axial)}$ distance of 1.93(2) Å and an average Co–$N_{eq}$ distance of 1.98(2) Å.[11] In marked contrast, the axial Co–N distances are longer than the in-plane Co–N distances for cobalt(II) porphyrins. For example in $[Co^{II}(oep)(3Me\text{-}py)_2]$ the axial Co–N distance is 2.386(2) Å while the in-plane Co–N distances average 1.992 Å.[12]

$[\mathbf{5}^+]I_3$ dissolves readily in dichloromethane solution to produce a purple solution with $\lambda_{max}$/nm ($\varepsilon$/dm$^3$ mol$^{-1}$ cm$^{-1}$): 290 (46 900), 360 (32 400), 628 (9900). The magnetic moment of a dichloromethane solution of the complex $[\mathbf{5}^+]I_3$ is 2.0(2) $\mu_B$.

Electrochemical studies show that in pyridine solution a four-membered electron transfer series exists for this family of cobalt complexes. Fig. 3 shows cyclic voltammetric and Osteryoung square-wave voltammetric data for Co(oeb) in pyridine solution. One reversible oxidation [at −388 mV with $\Delta E_p$ = 64(2) mV and $w_{1/2}$ = 112(2) mV] and two reversible reductions [at −924 mV with $\Delta E_p$ = 66(2) mV and $w_{1/2}$ = 118(2) mV and at −2046 mV with $\Delta E_p$ = 66(2) mV and $w_{1/2}$ = 112(2) mV] are observed. The reversible nature of these processes suggests that the axial ligation of cobalt does not change during the redox process and previous work has demonstrated spectral changes for Co(oeb) in pyridine as compared to dichloromethane solution that are indicative of axial ligation by pyridine.

The alteration in internal oxidation states in $[Co^{II}(oebOx)]I_3$, $[\mathbf{4}^+]I_3$, and $[Co^{III}(oeb\cdot)(py)_2]I_3$, $[\mathbf{5}^+]I_3$, has some parallels in the valence tautomerization observed for other transition-metal complexes. For example the oxidation of $Ni^{II}$(porphyrin) is known to yield either $[Ni^{III}(porphyrin)]^+$ or $[Ni^{II}(porphyrin\ radical)]^+$.[13] Cobalt complexes of dioxolene ligands also experience valence tautomerization, $Co^{III}$(bipy)(semiquinone)(catecholate)/$Co^{II}$(bipy)(semiquinone).[14] In all these complexes the redox potentials of the ligands and the metal centres are close in energy so that the electron distribution between these components is markedly effected by environmental effects, which in the present case involve the availability of axial ligands.

We thank the National Institutes of Health (Grant GM26226) for financial support.

## Footnotes

* E-mail: albalch@ucdavis.edu
† On leave from the Institute of Chemistry, University of Warsaw, Bialystôk Branch, Poland.

‡ *Crystal data*: purple prisms of $C_{45}H_{53}CoI_3N_6O_2$ obtained by addition of pyridine to a $CH_2Cl_2$ solution of $[Co^{II}(oepOx)]I_3$ form in the monoclinic space group *C*2/*c* with *a* = 14.471(3), *b* = 17.436(3), *c* = 19.048(4) Å, β = 107.50(2)° at 130(2) K with *Z* = 4 with the use of nickel filtered Cu-Kα (λ = 1.541 78 Å) radiation. A correction was applied for the 3% decay in two standard reflections that was observed over the course of the data collection. Refinement of 2892 reflections and 259 parameters yielded $wR_2$ = 0.093 for all data and a conventional $R_1$ = 0.045 based on 2499 reflections with $I > 2\sigma(I)$. The largest peak and hole in the final difference map are 0.98 and −1.07 e Å$^{-3}$. Atomic coordinates, bond lengths and angles, and thermal parameters have been deposited at the Cambridge Crystallographic Data Centre (CCDC). See Information for Authors, Issue No. 1. Any request to the CCDC for this material should quote the full literature citation and the reference number 182/456.

## References

1 R. Stocker, Y. Yamamoto, A. F. McDonagh, A. N. Glazer and B. N. Ames, *Science*, 1987, **235**, 1043; T. Nakagami, S. Taji, M. Takahashi and K. Yamanishi, *Microbiol. Immunol.*, 1992, **36**, 381.
2 R. Bonnett, D. G. Buckley and D. Hamzetash, *J. Chem. Soc., Perkin Trans. 1*, 1981, 322.
3 J. V. Bonfiglio, R. Bonnett, D. G. Buckley, D. Hamzetash, M. B. Hursthouse, K. M. Abdul Malik, A. F. McDonagh and J. Trotter, *Tetrahedron*, 1983, **39**, 1865.
4 A. L. Balch, M. Mazzanti, B. C. Noll and M. M. Olmstead, *J. Am. Chem. Soc.*, 1994, **116**, 9114.
5 A. L. Balch, M. Mazzanti, B. C. Noll and M. M. Olmstead, *J. Am. Chem. Soc.*, 1993, **115**, 12 206.
6 A. L. Balch, M. Mazzanti, T. M. St. Claire and M. M. Olmstead, *Inorg. Chem.*, 1995, **34**, 2194.
7 A. L. Balch, L. Latos-Grażyński, B. C. Noll, M. M. Olmstead and N. Safari, *J. Am. Chem. Soc.*, 1993, **115**, 9056.
8 A. L. Balch, R. Koerner, M. M. Olmstead, M. Mazzanti, N. Safari and T. St. Claire, *J. Chem. Soc., Chem. Commun.*, 1995, 643.
9 S. Attar, A. L. Balch, P. M. Van Calcar and K. Winkler, *J. Am. Chem. Soc.*, 1997, **119**, 3317.
10 W. R. Scheidt, *The Porphyrins*, 1978, **3**, 463.
11 J. W. Lauher and J. A. Ibers, *J. Am. Chem. Soc.*, 1974, **96**, 4447.
12 R. G. Little and J. A. Ibers, *J. Am. Chem. Soc.*, 1974, **96**, 4440.
13 G. S. Nahor, P.Neta, P. Hambright and L. R. Robinson, *J. Phys. Chem.*, 1991, **95**, 5515; D. Kim, L. A. Miller and T. G. Spiro, *Inorg. Chem.*, 1986, **25**, 2468; E. C. Johnson, T. Niem and D. Dolphin, *Can. J. Chem.*, 1978, **56**, 1381; A. Wolberg and J. Manassen, *Inorg. Chem.*, 1970, **10**, 2365.
14 O.-S. Jung, D. H. Jo, Y. A. Lee, Y. S. Sohn and C. G. Pierpont, *Angew. Chem., Int. Ed. Engl.*, 1996, **35**, 1694; O.-K. Jung and C. G. Pierpont, *Inorg. Chem.*, 1994, **33**, 2227.

*Received in Bloomington, IN, USA, 18th February 1997; Com. 7/01139C*

# Enantiomeric separation of [60]fullerene derivatives with an inherent chiral addition pattern

**Birgit Gross,[a] Volker Schurig,*[a] Iris Lamparth,[b] Andrea Herzog,[b] Francis Djojo[b] and Andreas Hirsch*[b]**

[a] *Institut für Organische Chemie, Auf der Morgenstelle 18, 72076 Tübingen, Germany*
[b] *Institut für Organische Chemie, Henkestr. 42, 91054 Erlangen, Germany*

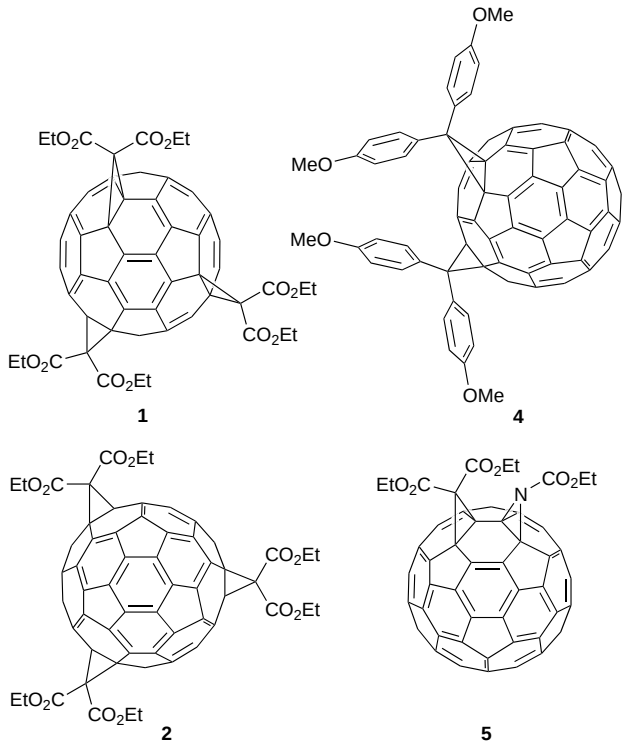
**Enantiomeric separation of bis-, tris- and hexakis-adducts of [60]fullerene with achiral addends and an inherent chiral addition pattern is achieved by HPLC using a chiral Whelk-O1 phase.**

Investigations on chiral fullerene derivatives is a topic attracting increasing interest.[1] Recently there has been a lot of effort directed towards the synthesis and characterization of various chiral [60]fullerene adducts. If the addends themselves are achiral, chirality is still possible due to the nature of the addition pattern. In these cases the fullerene based π-systems themselves are chiral, and the chiroptical properties are due to an asymmetric fullerene chromophore.

We recently reported the synthesis and characterization of several regioisomeric bis- and tris-adducts of [60]fullerene with both identical and different addends, *e.g.* diethoxycarbonylmethylene $C(CO_2Et)_2$, dianisylmethylene $C(anisyl)_2$ and ethoxycarbonylnitrene $NCO_2Et$.[2,3] Some of these isomers are chiral due to their addition pattern and they were isolated and characterised as racemates. In order to isolate single enantiomers[4,5,6] of chiral fullerene derivatives two different approaches can be considered: (1) enantioselective synthesis of enantiomerically enriched or pure products, which has been demonstrated, *e.g.* with asymmetric bisosmylation[4] and enantioselective addition of malonates[5] and (2) enantiomeric separation by means of preparative chromatography (HPLC) on a chiral stationary phase.

Chiral Whelk-O1 HPLC columns are well suited to the separation of enantiomers with either π-acidic or π-basic groups. Welch *et al.* were the first to resolve enantiomeric monoadducts of [60]fullerene on a Whelk-O1 column.[7] [76]Fullerene monoadducts[8] as well as a [70]fullerene monoadduct[9] were also successfully separated using this chiral stationary phase. Recently, a malonate bisadduct of [60]fullerene was resolved into its enantiomers.[5]

Here we report the enantiomeric separation of several racemic bis-, tris- and hexakis-adducts of [60]fullerene by chiral HPLC using a (*R*,*R*)-Whelk-O1 column† and we show the circular dichroism spectra of the single enantiomers. The HPLC separation of the enantiomers of the $C_3$-symmetric trisadduct **1** (*f*C)-I,eI,eII[11,12] and (*f*A)-I,eI,eII with an *e*,*e*,*e*-addition pattern and of the $D_3$-symmetric trisadduct **2** (*f*C)-I,III*,III* and (*f*A)-I,III*,III* with a *trans*-3, *trans*-3, *trans*-3 addition pattern represents the first resolution of racemic fullerene trisadducts. A chiral $C_1$-symmetrical hexakisadduct $C_{66}(CO_2Et)_{12}$ **3** of unknown structure, which is a side product in the synthesis of the corresponding $T_h$-symmetrical hexakisadduct,[13] is the first example of the separation of a racemic hexakisadduct of [60]fullerene. Successful chromatographic resolution was also achieved with the enantiomers of bisadduct **4** (*f*C)-I,III and (*f*A)-I,III as well as **5** (*f*C)-I,II and (*f*A)-I,II. The chromatogram of the enantiomeric separation of **3** is shown in Fig. 1. Several solvent compositions were tested for the five racemic derivatives. Usually fullerene adducts are only sparingly soluble in solvents like MeCN, MeOH or water. Therefore all the fullerene separations described in the literature so far are carried out in the normal phase mode, using toluene or solvent mixtures with *e.g.* either hexane or $CH_2Cl_2$. The bisadducts **4** and **5** are very soluble in toluene and hexane or heptane mixtures. Trisadducts **1** and **2** as well as the hexakisadduct **3** were separated using a reversed phase mode. Whereas with MeOH only broad peaks leading to poor resolution were observed, the use of MeCN–



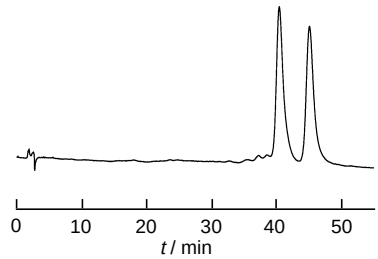




**Fig. 1** Chromatogram of the enantiomer separation of **3** on Whelk-O1 Eluent: MeCN–$H_2O$, 75:25; flow rate: 0.8 ml $min^{-1}$; UV detection: 254 nm.

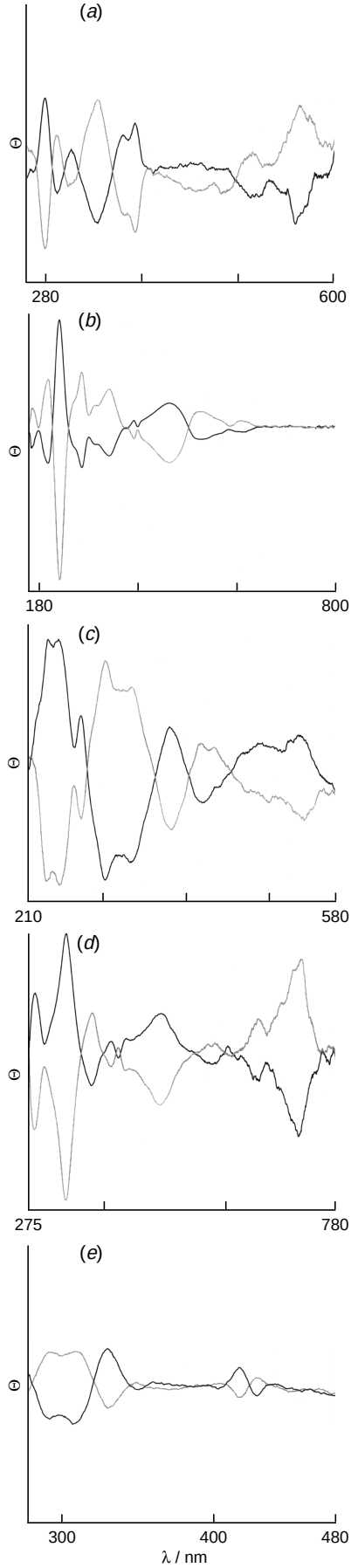



**Fig. 2** Circular dichroism spectra of the enantiomers **1**–**5**: (*a*) **1**, (*b*) **2**, (*c*) **3**, (*d*) **4** and (*e*) **5**. — First eluted enantiomer. **—** Second eluted enantiomer.

water mixtures guaranteed a good separation into the corresponding enantiomers **1**–**3** with chiral separation factors α in the range 1.04–1.12. The best separation was achieved with the hexakisadduct **3** showing a resolution $R_s$ = 2.37. In pure toluene the resolution for the bisadducts **4** and **5** was very poor. Increasing percentages of hexane or heptane lead to an improvement of the α- and $R_s$-values. As these adducts are less soluble in hexane or heptane, a higher percentage of these solvents in toluene leads to bad peak shapes and no further improvement in separation.

After separation of the enantiomers of **1**–**5** on a semipreparative scale CD spectra were recorded (Fig. 2),‡ which are comparable to those reported for other fullerene adducts.[4–10] Since in our case chirality arises exclusively from the addition pattern on the carbon cluster itself, the CD originates from the chiral functionalized fullerene chromophore. Each derivative gives rise to mirror image CD curves for the enantiomers (Fig. 2).

We thank the BMBF, the Fonds der Chemischen Industrie and the Hoechst AG for financial support. We thank R. Süssmuth for recording the CD spectra and C. Welch for a gift of a Whelk-O1 column.

## Footnotes

* E-mail: volker.schurig@uni-tuebingen.de

† Chromatographic analysis was performed using a GRAS (CPISOS/LC) pump (Chrompack, Frankfurt, Germany) and a Chrompack UV-variable wavelength UV detector. Injections were performed using a Rheodyne model 7125 injector with a 20 μl sample loop. An analytical 250 mm × 4.6 mm i.d. (*R*,*R*)-Whelk-O1 column was a gift from Regis Chemical Company (Morton Grove, IL, USA). Conditions: MeCN–$H_2O$ mixtures for **1**–**3**, 85:15 (**1**), 90:10 (**2**), 75:25 (**3**); toluene–hexane mixtures for **4** and **5**, 65:35 (**4**), 80:20 (**5**).

‡ CD spectra were obtained on a J720 spectrometer from Asco (Tokyo, Japan) using a 0.02 cm pathlength quartz cell with a resolution of 0.5 nm. **1**–**3** were recorded in acetonitrile, **4**–**5** in toluene.

## References

1 F. Diederich, C. Thilgen and A. Herrmann, *Nachr. Chem. Tech. Lab.*, 1996, **44**, 9.
2 A. Hirsch, I. Lamparth and H. R. Karfunkel, *Angew. Chem., Int. Ed. Engl.*, 1994, **33**, 437.
3 F. Djojo, A. Herzog, I. Lamparth, F. Hampel and A. Hirsch, *Chem. Eur. J.*, 1996, **2**, 1537.
4 J. M. Hawkins, A. Meyer and M. Nambu, *J. Am. Chem. Soc.*, 1993, **115**, 9844.
5 J.-F. Nierengarten, V. Gramlich, F. Cardullo and F. Diederich, *Angew. Chem., Int. Ed. Engl.*, 1996, **35**, 2101.
6 E. Nakamura, H. Isobe, H. Tokuyama and M. Sawamura, *Chem. Commun.*, 1996, 1747.
7 S. R. Wilson, Y. Wu, N. A. Kaprinidis, D. I. Schuster and C. J. Welch, *J. Org. Chem.*, 1993, **58**, 6548.
8 A. Herrmann and F. Diederich, *Helv. Chim. Acta*, 1996, **79**, 1741.
9 Y. Wang, D. I. Schuster, S. R. Wilson and C. J. Welch, *J. Org. Chem.*, 1996, **61**, 5198.
10 A. Herrmann, M. Rüttimann, C. Thilgen and F. Diederich, *Helv. Chim. Acta*, 1995, **78**, 1673.
11 For the nomenclature of bond labelling in fullerene adducts see: A. Hirsch, I. Lamparth and G. Schick, *Liebigs Ann. Chem.*, 1996, 1725.
12 C. Thilgen, A. Herrmann and F. Diederich, *Helv. Chim. Acta*, 1997, **80**, 183.
13 I. Lamparth, C. Maichle-Mössmer and A. Hirsch, *Angew. Chem.*, 1995, **107**, 1755; *Angew. Chem., Int. Ed. Engl.*, 1995, **34**, 1607.

*Received in Cambridge, UK, 24th February 1997; Com. 7/01241A*

# Chemoselective transfer hydrogenation of nitroarenes, aldehydes and ketones with propan-2-ol catalysed by Ni-stabilized zirconia

**T. T. Upadhya, S. P. Katdare, D. P. Sabde, Veda Ramaswamy and A. Sudalai***

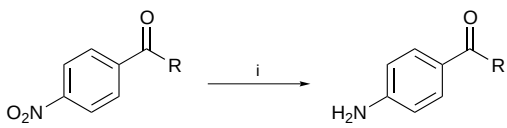
*National Chemical Laboratory, Pune-411 008, India*

**Nickel-stabilized zirconia ($Zr_{0.8}Ni_{0.2}O_2$), a reusable, solid catalyst, efficiently catalyses the chemoselective reduction of nitroarenes, aldehydes and ketones using propan-2-ol and KOH, in the liquid phase, exhibiting the reactivity order $NO_2 \gg C{=}O > C{-}X \gg C{=}C$.**

The chemoselective reduction of organic compounds is synthetically important, both in the laboratory and in industry. In comparison with catalytic reduction using molecular hydrogen,[1] transfer reduction using hydrogen donors, *viz.* propan-2-ol, has real and potential advantages because neither hydrogen containment nor a pressure vessel is required. Moreover, the transfer hydrogenation method could offer enhanced selectivity in the reduction process. A wide variety of homogeneous and heterogeneous catalytic systems in combination with different hydrogen donors have been employed to selectively reduce most major functional groups attached to aliphatic and aromatic structures.[2] Chemoselective reduction of the functional groups can be achieved by classical Meerwein–Ponndorf–Verley reductions. However, the use of aluminium isopropoxide in stoichiometric amounts and under drastic reaction conditions often leads to undesired side reactions.[3] Recently, transfer hydrogenation of ketones using homogeneous complexes of Cu, Fe, Rh, Ru, Ir, Pd and Ni with propan-2-ol has been reported.[4] However, it has been observed that controlling the reduction rates is difficult with these active catalysts.[5] On the other hand, the use of heterogeneous catalysts offers several advantages over the homogeneous systems such as ease of recovery, recycling and enhanced stability. Raney Ni catalyst has also been extensively used in combination with hydrazine hydrate or propan-2-ol as a hydrogen source for reductions. However, Raney Ni is pyrophoric and does not show any selectivity towards functional groups such as C–X, C=O and $NO_2$, reducing all of them simultaneously. Further it has been observed that the use of Raney Ni for the reduction of aromatic ketones leads to hydrogenolysis of alcohols quite easily at the benzylic position.[6]

Considerable efforts have been devoted in use of zirconium oxide, which is known to be a bifunctional catalyst, either as a single oxide or in a mixed metal oxide, for application in organic synthesis as is evident from the literature.[7] Here, we report the potential application of nickel-stabilized zirconia as an active, heterogeneous catalyst for chemoselective reduction of nitro and carbonyl functions under transfer hydrogenation conditions in the liquid phase using propan-2-ol (Scheme 1).

Zirconia samples stabilized by Cr, Mn, Fe, Co or Ni were prepared by the procedure reported from our laboratory.[8] In particular, $Zr_{0.8}Ni_{0.2}O_2$ was prepared by treating an aqueous solution of zirconyl nitrate and nickel nitrate (molar ratio 80 : 20) with tetramethylammonium hydroxide (25% aqueous solution) as a precipitating agent under vigorous stirring until a pH of 8.0 was achieved. The resultant hydroxide precipitate was washed with deionised water, acetone and dried at 110 °C for 24 h and was subsequently heated to 500 °C under a programmed heating rate of 2 °C $min^{-1}$ and then calcined for 8 h. It was then characterized by powder X-ray diffraction, FTIR, surface area determination by the BET method, X-ray fluorescence (XRF), temperature programmed reduction (TPR) and cyclic voltammetry (CV) techniques.




**Scheme 1** *Reagents and conditions:* i, $Zr_{0.8}Ni_{0.2}O_2$ (cat.), $Pr^iOH$, KOH, reflux, 3 h

The XRD profiles of nickel-stabilized zirconia shows the formation of a cubic (fluorite) phase The FTIR spectrum in the framework region shows a broad band at *ca.* 480 $cm^{-1}$ characteristic of the cubic phase of $ZrO_2$.[9] Scanning electron microscopy indicates the presence of uniform particles with sizes ranging between 0.5 and 1.0 μm. The surface area of the sample as determined by the BET method† was 96 $m^2\ g^{-1}$. The chemical composition determined by XRF[10] was 79.97 mol% Zr and 20.03 mol% Ni. TPR[11] shows a single peak at *ca.* 417 °C which can be attributed to a single step reduction of $Ni^{2+}$ to $Ni^0$. The cyclic voltammogram of nickel-stabilized zirconia shows a reversible system ($E_{pa}$ + 0.32 V, $E_{pc}$ = 0.40 V *vs.* SCE with $E_{1/2}$ = 0.04 V). This electrochemical behaviour is attributed to the $Ni^{2+}$–$Ni^0$ redox cycle indicating that Ni in the solid matrix of zirconia undergoes a facile two-electron transfer process.[12]

The selective and rapid reduction of nitro compounds is an interesting area of research, particularly when other potentially reducible moieties are present in the molecule.[13] The results of the reduction of nitrobenzene to aniline over various catalysts are presented in Table 1 which shows that nickel-stabilized zirconia exhibits significantly higher activity and selectivity than pure $ZrO_2$, $Ni(O_2CMe)_2$ or Raney Ni. In the absence of either catalyst or KOH, no reaction took place. In a typical reaction procedure, a mixture of nitrobenzene (1 g, 0.0081 mol), KOH pellets (0.045 g, 0.0008 mol) and $Zr_{0.8}Ni_{0.2}O_2$ (10% *m/m*)

**Table 1** Transfer hydrogenation of nitrobenzene to aniline with propan-2-ol over different catalysts[a]

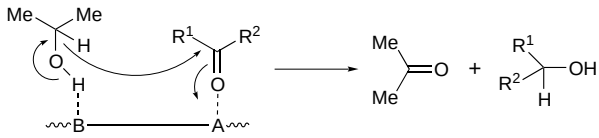
| | | | Yield[b] | |
|---|---|---|---|---|
| Entry | Catalyst | Surface area/ $m^2\ g^{-1}$ | Aniline (mass%) | Unreacted nitrobenzene (mass%) |
| 1 | No catalyst/No KOH | — | 0 | 100 |
| 2 | $ZrO_2$ | 56 | 14.5 | 85.5 |
| 3 | $Ni(O_2CMe)_2$ | — | 10.0 | 90.0 |
| 4 | Raney Ni | — | 21.2 | 78.8 |
| 5 | $Zr_{0.8}Cr_{0.2}O_2$ | 118 | 28.1 | 71.9 |
| 6 | $Zr_{0.8}Mn_{0.2}O_2$ | 105 | 39.0 | 61.0 |
| 7 | $Zr_{0.8}Fe_{0.2}O_2$ | 102 | 38.4 | 61.6 |
| 8 | $Zr_{0.8}Co_{0.2}O_2$ | 98 | 50.0 | 50.0 |
| 9 | $Zr_{0.8}Cu_{0.2}O_2$ | 94 | 70.8 | 29.2 |
| 10 | $Zr_{0.8}Ni_{0.2}O_2$ | 96 | 96.0 | 4.0 |

[a] *Reaction conditions*: nitrobenzene (8 mmol), KOH pellets (8 mmol) and catalyst (10% *m/m*) in propan-2-ol (15 ml), refluxing for 3 h. [b] Determined by capillary gas chromatography.

**Table 2** Transfer hydrogenation of nitroarenes and carbonyl compounds with propan-2-ol catalysed by Ni-stabilized zirconia ($Zr_{0.8}Ni_{0.2}O_2$)[a]

| Entry | Substrate | *t*/h | Product[b] | Yield[c] (mass%) |
|---|---|---|---|---|
| 1 | Nitrobenzene | 3 | Aniline | 96 |
| 2 | 4-Chloronitrobenzene | 3 | 4-Chloroaniline | 85 |
| 3 | 4-Nitroacetophenone | 3 | 4-Aminoacetophenone | 88 |
| 4 | 2-Nitroanisole | 2 | *o*-Anisidine | 86 |
| 5 | Benzaldehyde | 6 | Benzyl alcohol | 87 |
| 6 | 4-Methoxybenzaldehyde | 5 | 4-Methoxybenzyl alcohol | 86 |
| 7 | 4-Chlorobenzaldehyde | 6 | 4-Chlorobenzyl alcohol | 90 |
| 8 | 4-Hydroxybenzaldehyde | 5 | 4-Hydroxybenzyl alcohol | 88 |
| 9 | Furan-2-carbaldehyde | 4 | 2-Furfuryl alcohol | 81 |
| 10 | Acetophenone | 4 | 1-Phenethyl alcohol | 90 |
| 11 | Benzophenone | 5 | Benzhydrol | 91[d] |
| 12 | 4-Methoxybenzophenone | 5 | 4-Methoxybenzhydrol | 70 |
| 13 | 4-Bromobenzophenone | 5 | 4-Bromobenzhydrol | 90 |
| 14 | 3,4-Dichlorobenzophenone | 4 | 3,4-Dichlorobenzhydrol | 95 |
| 15 | Octan-2-one | 4 | Octan-2-ol | 68 (25[e]) |
| 16 | 2-Methylcyclohexanone | 6 | 2-Methylcyclohexanol | 58 |
| 17 | 4-Nitrobenzophenone | 3 | 4-Aminobenzophenone | 90 |
| 18 | 2-Nitrobenzaldehyde | 3 | 2-Aminobenzyl alcohol | 80 |
| 19 | Cinnamaldehyde | 3 | Cinnamyl alcohol | 72 |

[a] *Reaction conditions:* substrate (8 mmol), KOH pellets (8 mmol) and $Zr_{0.8}Ni_{0.2}O_2$ catalyst (10% *m/m*) in propan-2-ol (15 ml); reflux for 3–6 h. [b] Products were characterized by IR, $^1$H, $^{13}$C NMR and MS. [c] Isolated yield after chromatographic purification, the remainder is essentially unreacted starting material. [d] Diphenylmethane is obtained with Raney Ni.[6] [e] Yield with Raney Ni.[6]




**Scheme 2**

in propan-2-ol (15 ml) was refluxed for 3–5 h. The progress of the reaction was monitored by TLC, the catalyst was then filtered off and the product purified by flash chromatography to afford aniline (96% yield).

As summarized in Table 2, in refluxing propan-2-ol (82 °C), the present catalytic system efficiently reduces both nitroarenes and carbonyl compounds in excellent yields. Both aromatic and aliphatic aldehydes and ketones are reduced to the corresponding alcohols. It is remarkable that both C–Br and C–Cl bonds are not reduced and are stable under the reaction conditions (Table 2: entries 2, 7, 13 and 14). Another notable feature of this catalytic system is that both 4-nitroacetophenone and 4-nitrobenzophenone undergo chemoselective reduction to 4-aminoacetophenone and 4-aminobenzophenone, respectively, in high yields without reduction of the carbonyl function. Further, cinnamaldehyde is reduced chemoselectively to cinnamyl alcohol without reducing C=C. The present catalytic system did not reduce functional groups such as $CO_2H$, CN, $CO_2R$, *etc.*, under the present experimental conditions. The catalyst was easily recovered by filtration, and could be reused three times for the reduction of nitrobenzene without affecting the activity or selectivity of the process. The XRD pattern of the used catalyst shows no structural deterioration.

Mechanically, stabilization of zirconia by nickel does not alter its bifunctional behaviour.[7] Propan-2-ol is adsorbed on the basic site (B) and the ketone on the adjacent acidic site (A); the $Ni^{2+}$ on the surface promotes dehydrogenation of propan-2-ol by KOH, and is reduced to the active $Ni^0$ species as evident from CV measurements and finally the hydrogen is transferred as hydride as shown in Scheme 2. It appears that the active $Ni^0$ species, formed instantaneously during the reaction, is responsible for the catalytic reduction.

In conclusion, incorporation of Ni into the bulk structure of $ZrO_2$, not only stabilizes $ZrO_2$ in its cubic (fluorite) form but also moderates the reactivity of Ni in the stabilized zirconia enabling chemoselective functional group reduction.

S. P. K. thanks CSIR (New Delhi) for the award of Senior Research Fellowship and T. T. U. and D. P. S. are grateful to the Director, NCL for providing facilities. Special thanks are given to Dr S. G. Hegde and Dr A. V. Ramaswamy for fruitful discussions.

## Footnotes

* E-mail: otech@ems.ncl.res.in

† Determination of specific surface area by BET (Brunner, Emmett, Teller), using $N_2$ adsorption on a Omnisorp 100CX apparatus.

## References

1 P. N. Rylander, *Hydrogenation Methods*, Academic Press, London, 1985.
2 R. A. W. Johnstone, A. H. Wilby and I. D. Entwistle, *Chem. Rev.*, 1985, **85**, 129.
3 A. L. Wilds, *Org. React.*, 1944, **2**, 178.
4 R. Spogliarich, G. Zassinovich, G. Mestroni and M. Graziani, *J. Organomet. Chem.*, 1979, **179**, C45; R. L. Chowdhary and J. E. Backvall, *J. Chem. Soc., Chem. Commun.*, 1991, 1063; G. Z. Wang and J. E. Backvall, *J. Chem. Soc., Chem. Commun.*, 1992, 980; S. Iyer and J. O. Varghese, *J. Chem. Soc., Chem. Commun.*, 1995, 465; A. Nose and T. Kudo, *Chem. Pharmacol. Bull.*, 1988, **36**, 1529.
5 D. J. Pasto, *J. Am. Chem. Soc.*, 1979, **101**, 6852.
6 M. J. Andrews and C. N. Pillai, *Ind. J. Chem., Sect. B*, 1978, **16**, 465.
7 K. Tanabe and T. Yamaguchi, *Catal. Today*, 1994, **20**, 185; T. Yamaguchi, *Catal. Today*, 1994, **20**, 199; M. Shibagaki, K. Takahashi and S. Matsushita, *Bull. Chem. Soc. Jpn.*, 1988, **61**, 3283.
8 A. Keshavaraja and A. V. Ramaswamy, *Chem. Commun.*, 1996, 397; V. R. Chowdhary, B. S. Uphade, S. G. Pataskar and A. Keshavaraja, *Angew. Chem., Int. Ed. Engl.*, 1996, **35**, 2393.
9 C. M. Phillippi and K. S. Mazdayami, *J. Am. Ceram. Soc.*, 1971, **54**, 254; A. Keshavaraja and A. V. Ramaswamy, *J. Mater. Res.*, 1994, **9**, 837.
10 *Instrumental Methods Of Chemical Analysis*, ed. G. Ewing, McGraw-Hill, Kogakusha Ltd, Tokyo, 1975.
11 A. Jones and B. McNicol, *Temperature Programmed Reduction for Solid Materials Characterization*, Marcel Dekker, New York, 1986.
12 A. J. Bard and L. R. Faulkner, *Electrochemical Methods*, Wiley, New York, 1980, ch. 6.
13 G. W. Kabalka and R. S. Varma, in *Comprehensive Organic Synthesis*, ed. B. M. Trost and I. Fleming, Pergamon, Oxford, 1991, vol. 8, p. 363.

*Received in Cambridge, UK, 4th March 1997; Com. 7/01518F*

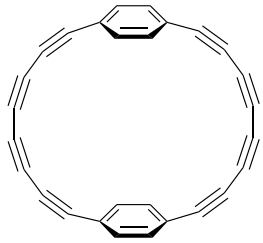
# Cyclophyne chemistry: synthesis and study of an octacobalt complex of [8.8]paracyclophaneoctayne

**Michael M. Haley* and Brandi L. Langsdorf**

*Department of Chemistry, University of Oregon, Eugene, Oregon 97403, USA*

**Use of a palladium/cobalt/copper alkyne reaction strategy provides the cobalt-stabilized complex of a highly strained cyclophane.**

The recent discovery of the fullerenes[1] and related carbon nanotubes[2] has prompted a flurry of activity directed toward the synthesis and study of curved, fully conjugated π-systems.[3] In a similar regard, there have been numerous attempts to prepare related belt-shaped molecules possessing conjugated π-electron circuits; the various belt- and hoop-shaped compounds studied include cyclacenes,[4] [*n*]cyclocarbons,[5] cyclic paraphenylenes[6] and others.[7] Recently, two groups reported the successful preparation of fully conjugated, belt-shaped compounds. Oda and co-workers produced cyclic paraphenylacetylenes containing six and eight subunits.[8] Herges and co-workers isolated a 'picotube' based on four anthracene units.[9] Our recent work on polyacetylenic macrocycles[10] spurred an interest in systems possessing the cyclic π-orbital motif. We report herein our work toward the synthesis of [8.8]paracyclophaneoctayne **1**, a cyclophane-cyclocarbon hybrid nicknamed a cyclophyne.[11]

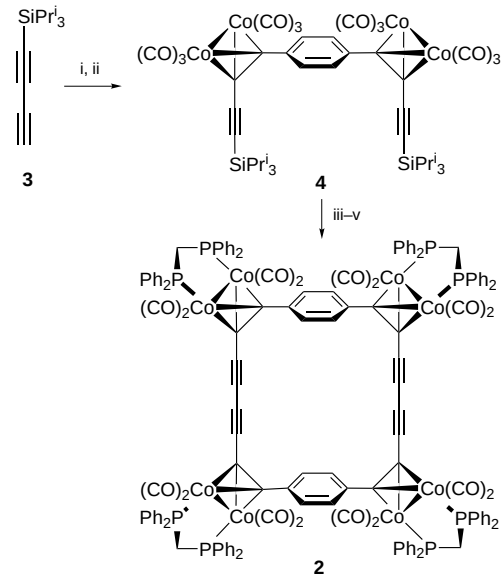


**1**

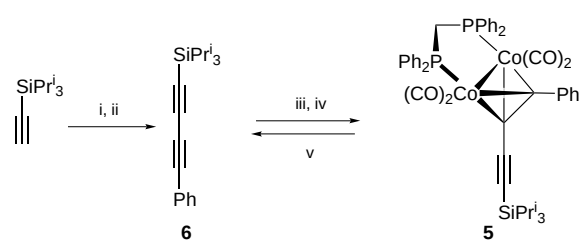
An octacobalt complex such as **2** was envisioned for the immediate precursor to the target macrocycle as: (*i*) the carbon skeleton could be assembled quickly and efficiently using known methodology, and (*ii*) the alkyne C≡C–C angles in this type of (μ-acetylene)dicobalt hexacarbonyl complex are reduced to *ca.* 140°, thus allowing the complex to participate in reactions that might be difficult or otherwise impossible for the rigid, unbound molecule to undergo. The synthesis of **2** is depicted in Scheme 1. Palladium-catalysed alkynylation of 1,4-diiodobenzene with excess triisopropylsilylbutadiyne **3**[12] furnished a pale yellow tetrayne, which in turn reacted with 2 equiv. of octacarbonyldicobalt to provide the sterically favoured tetracobalt complex **4**.† Attempted desilylation with tetrabutylammonium fluoride led to complete decomposition of **4**. Ligand exchange[5a] with bis(diphenylphosphino)methane (dppm) afforded a bridged complex (85% yield) stable to fluoride ion; desilylation now proceeded in high yield ( > 95%). Eglinton coupling[13] of the terminal acetylenes provided fine, deep maroon crystals of **2**† in 47% yield. Spectroscopic data supported formation of the strain-free dimeric structure.

In their work with the hexacobalt complex of [18]cyclocarbon, Diederich *et al.* were unable to free $C_{18}$ of the protecting groups by mild oxidation.[5a,14] With this problem in mind, we prepared model complex **5**† (Scheme 2) in order to investigate various methods to remove the cobalts. Of the numerous reagents and conditions explored, only oxidation by molecular iodine was found to regenerate butadiyne **6** cleanly and in excellent yield.

Application of the iodine-promoted decomplexation method to **2** provided dppm as the sole organic-soluble component along with a copious amount of insoluble material. Analysis of an aliquot of the crude reaction mixture by $^1$H NMR showed a broad signal at δ 7.6 attributable to the phosphine ligand; no other aromatic peaks were observed. Although disappointing, this result is not wholly unexpected. A survey of the current literature reveals that, despite significant efforts on the part of several research groups, systems containing contiguous, bent triynes and higher polyynes have proven elusive.[5] Only strained monoyne[8,15] and diyne[16] derivatives are known. The cyclocarbons represent the ultimate bent polyyne macrocycles; $C_{18}$ is predicted to exhibit C≡C–C bond angles near 160°, leading to a strain energy of around 72 kcal mol$^{-1}$.[5b] Cyclophyne **1** should be similarly strained as the triple bond angles are calculated to




**Scheme 1** *Reagents and conditions*: i, 1,4-diiodobenzene, $Pd(PPh_3)_2Cl_2$, CuI, $Et_3N$, 73%; ii, $Co_2(CO)_8$, $Et_2O$, 66%; iii, dppm, toluene, 85%; iv, $Bu_4NF$, THF, > 95%; v, $Cu(OAc)_2{\cdot}H_2O$, py, 47%




**Scheme 2** *Reagents and conditions*: i, $CBr_4$, $PPh_3$, $CH_2Cl_2$, 85%; ii, phenylacetylene, CuCl, $NH_2OH{\cdot}HCl$, $PrNH_2$, MeOH, $H_2O$, 82%; iii, $Co_2(CO)_8$, $Et_2O$, 76%; iv, dppm, toluene, 87%; v, $I_2$, THF, 85%

be between 161.7 and 163.6°.[17] Whether the failure to prepare these two classes of macrocycles is due to the extreme reactivity of the distorted polyyne moiety or to the lack of a viable synthetic route is not certain. Thus isolation and characterization of smaller bent hexatriyne- and octatetrayne-containing systems should help answer these questions. To this end, we are currently studying dehydrobenzoannulenes possessing higher polyynes distorted on one or more edge.[18] These results will be reported in due course.

We acknowledge the donors of The Petroleum Research Fund, administered by the American Chemical Society, and the University of Oregon for generous support of this research.

## Footnotes

* E-mail: haley@oregon.voregon.edu

† *Selected spectral data* ($^1$H NMR: 300.13 MHz, $^{13}$C NMR: 75.5 MHz). For **2** $\delta_H$ ($CD_2Cl_2$) 7.93 (8 H, s), 7.53 (16 H, m), 7.45–7.12 (64 H, m), 3.72 (4 H, dt), 3.39 (4 H, dt); $\delta_C$ ($CD_2Cl_2$) 206.61, 201.59, 142.67, 137.32, 135.03, 132.85, 131.78, 130.45, 130.03, 129.56, 128.89, 128.72, 100.11, 87.19, 83.50, 65.60, 37.73; $\nu_{max}$ (KBr)/cm$^{-1}$ 3033, 2154, 2089, 2055, 2023 For **4** $\delta_H$ ($CDCl_3$) 7.65 (4 H, s), 1.14 (42 H, s); $\delta_C$ ($CDCl_3$) 138.36, 129.77, 105.30, 104.03, 88.93, 69.59, 18.65, 11.37; $\nu_{max}$ (KBr)/cm$^{-1}$ 3069, 3056, 2130, 2092, 2038, 2006, 1976. For **5** $\delta_H$ ($CD_2Cl_2$) 7.87 (2 H, d), 7.51 (4 H, m), 7.42–7.16 (19 H, m), 3.66 (1 H, dt), 3.36 (1 H, dt), 1.12 (21 H, s); $\delta_C$ ($CD_2Cl_2$) 207.25, 201.38, 143.91, 139.00, 133.44, 131.37, 130.64, 129.87, 129.39, 128.97 (2), 128.94, 128.64, 127.11, 110.33, 99.04, 96.89, 65.36, 34.80, 19.21, 12.16; $\nu_{max}$ (KBr)/cm$^{-1}$ 3056, 2102, 2062, 2027, 2004, 1975.

## References

1 H. W. Kroto, J. R. Heath, S. C. O'Brien, R. F. Curl and R. E. Smalley, *Nature*, 1985, **318**, 162; W. Krätschmer, L. D. Lamb, K. Fostiropoulos and D. R. Huffman, *Nature*, 1990, **347**, 354; H. W. Kroto, *Angew. Chem., Int. Ed. Engl.*, 1992, **31**, 111.

2 S. Iijima, *Nature*, 1991, **354**, 56; S. Iijima, T. Ichihashi and Y. Ando, *Nature*, 1992, **356**, 776.

3 R. Faust, *Angew. Chem., Int. Ed. Engl.*, 1995, **34**, 1429; L. T. Scott, *Pure Appl. Chem.*, 1996, **68**, 291.

4 P. R. Ashton, G. R. Brown, N. S. Isaacs, D. Giuffrida, F. H. Kohnke, J. P. Mathias, A. M. Z. Slawin, D. R. Smith, J. F. Stoddart and D. J. Williams, *J. Am. Chem. Soc.*, 1992, **114**, 6330 and references cited therein; R. J. Graham and L. A. Paquette, *J. Org. Chem.*, 1995, **60**, 5770; R. M. Cory, C. L. McPhail, A. J. Dikmans and J. J. Vittal, *Tetrahedron Lett.*, 1996, **37**, 1983; R. M. Cory and C. L. McPhail, *Tetrahedron Lett.*, 1996, **37**, 1987.

5 (*a*) Y. Rubin, C. B. Knobler and F. Diederich, *J. Am. Chem. Soc.*, 1990, **112**, 4966; (*b*) F. Diederich and Y. Rubin, *Angew. Chem., Int. Ed. Engl.*, 1992, **31**, 1101 and references cited therein; (*c*) Y. Tobe, T. Fulii, H. Matsumoto, K. Naemura, Y. Achiba and T. Wakabayashi, *J. Am. Chem. Soc.*, 1996, **118**, 2758; (*d*) Y. Tobe, H. Matsumoto, K. Naemura, Y. Achiba and T. Wakabayashi, *Angew. Chem., Int., Ed. Engl.*, 1996, **35**, 1800.

6 R. Fiederich, M. Nieger and F. Vögtle, *Chem. Ber.*, 1993, **126**, 1723.

7 F. Vögtle, A. Schröder and D. Karbach, *Angew. Chem., Int. Ed. Engl.*, 1991, **30**, 575; A. Schröder, D. Karbach, R. Günther and F. Vögtle, *Chem. Ber.*, 1992, **125**, 1881; W. Josten, D. Karbach, M. Nieger, F. Vögtle, K. Hägele, M. Svoboda and M. Przybylski, *Chem. Ber.*, 1994, **127**, 767; W. Josten, S. Neumann, F. Vögtle, M. Nieger, K. Hägele, M. Przybylski, F. Beer and K. Müllen, *Chem. Ber.*, 1994, **127**, 2089; Y. Rubin, T. C. Parker, S. I. Khan, C. L. Holliman and S. W. McElvany, *J. Am. Chem. Soc.*, 1996, **118**, 5308.

8 T. Kawase, H. R. Darabi and M. Oda, *Angew. Chem., Int. Ed. Engl.*, 1996, **35**, 2664.

9 S. Kammermeier, P. G. Jones and R. Herges, *Angew. Chem., Int. Ed. Engl.*, 1996, **35**, 2669.

10 M. M. Haley, M. L. Bell, J. J. English, C. A. Johnson and T. J. R. Weakley, *J. Am. Chem. Soc.*, 1997, **119**, 2956; M. M. Haley, S. C. Brand and J. J. Pak, *Angew. Chem., Int. Ed. Engl.*, 1997, **36**, 836.

11 This work was presented in part at the 8th International Symposium on Novel Aromatics in Braunschweig, Germany on 30.07.95, poster 35.

12 L. Blanco, H. E. Helson, M. Hirthammer, H. Mestdagh, S. Spyroudis and K. P. C. Vollhardt, *Angew. Chem., Int. Ed. Engl.*, 1987, **26**, 1246.

13 G. Eglinton and W. McRae, *Adv. Org. Chem.*, 1963, **4**, 225.

14 Y. Rubin, Ph.D. Thesis, University of California, Los Angeles, 1991. The thesis states that only three different methods were tried in the attempts to free $C_{18}$ from the cobalt atoms; apparently, no model systems were investigated.

15 Recent examples of strained monoynes: X. M. Wang, R. J. Wang, T. C. W. Mak and H. N. C. Wong, *J. Am. Chem. Soc.*, 1990, **112**, 7790; T. Kawase, N. Ueda, H. R. Darabi and M. Oda, *Angew. Chem., Int. Ed. Engl.*, 1996, **35**, 1556.

16 Recent examples of strained diynes: Q. Zhou, P. J. Carroll and T. M. Swager, *J. Org. Chem.*, 1994, **59**, 1294; K. P. Baldwin, A. J. Matzger, D. A. Scheiman, C. A. Tessier, K. P. C. Vollhardt and W. J. Youngs, *Synlett*, 1995, 1215; Y. Tobe, N. Utsumi, K. Kawabata and K. Naemura, *Tetrahedron Lett.*, 1996, **52**, 9325.

17 Calculations performed at the *ab initio* HF/6-31G(d) level using GAUSSIAN 92. We thank Dr Andreas Maulitz, University of Essen, for obtaining these data.

18 We have recently prepared the first examples of triyne- and tetrayne-linked dehydrobenzoannulenes. These systems, however, are relatively strain-free: M. M. Haley, M. L. Bell and D. B. Kimball, unpublished work.

*Received in Corvallis, OR, USA, 10th March 1997; Com. 7/01712J*

# Enhanced polar ordering in ferroelectric liquid crystals induced by atropisomeric dopants

**Despina Vizitiu, Brian J. Halden and Robert P. Lemieux***

*Department of Chemistry, Queen's University, Kingston, Ontario, Canada K7L 3N6*

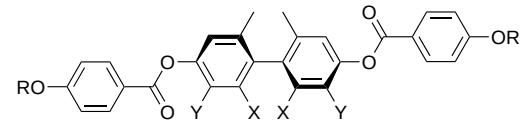
**The spontaneous polarization of a $S_C$* liquid crystal phase induced by atropisomeric dopants with large transverse molecular dipoles exhibits a very strong dependence on the nature of the $S_C$ liquid crystal host.**

A ferroelectric smectic C* liquid crystal phase possesses a permanent dipole moment, the spontaneous polarization ($P_S$), which is a macroscopic manifestation of molecular chirality.[1] The dependence of $P_S$ on the molecular structure of the chiral component(s) of a $S_C$* phase has received considerable attention over the past 15 years as it relates directly to the performance optimization of FLC light valves and displays.[2–4] In general, ferroelectric liquid crystals suitable for display applications are induced $S_C$* phases obtained by mixing a chiral dopant with high polarization power ($\delta_P$) in a $S_C$ liquid crystal host mixture with low viscosity and broad temperature range. The polarization power is a measure of the propensity of a chiral dopant to induce a spontaneous polarization in a $S_C$ host as expressed by eqn. (1), in which $P_o$ is the reduced polarization of the FLC and $x_d$ is the dopant mole fraction.[5]† In most cases, the polarization power of a chiral dopant is independent of the nature of the $S_C$ host. However, Stegemeyer has reported several examples of chiral dopants with rigid chiral cores that exhibit a dependence of $\delta_P$ on the nature of the $S_C$ host; these compounds are referred to as Type II dopants.[6]

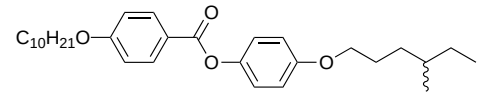
$$\delta_p = \left(\frac{dP_o(x_d)}{dx_d}\right)_{x_d \to 0} \quad (1)$$

Recently, we reported the induction of a $S_C$* phase by the atropisomeric dopant (−)-**1**, which exhibited a pronounced Type II host dependence in the $S_C$ liquid crystal hosts PhBz and NCB76 (Fig. 1).[7] We proposed that polar ordering of (−)-**1** in the $S_C$ lattice originates from a small asymmetric bias in the rotation of the biphenyl core about the ester C–O bonds, which we estimated by AM1 calculations on the model compound 3-methyl-5-nitrophenyl benzoate at 0.4 kcal mol$^{-1}$ (1 cal = 4.184 J). We have extended this conformational analysis to other phenyl benzoate derivatives as model compounds, and found that shifting the symmetry-breaking $NO_2$ group to the *ortho*-position with respect to the ester group raises the rotational bias about the ester C–O bond to 1.1 kcal mol$^{-1}$. In order to test the validity of this conformational analysis in predicting the relative polar ordering of atropisomeric dopants, and to further investigate the generality of Type II behaviour in these systems, we have synthesized the dopant (−)-**2** in optically pure form and measured its polarization power in the $S_C$ hosts PhBz,[8] NCB76 (E. Merck) and DFT.[9]

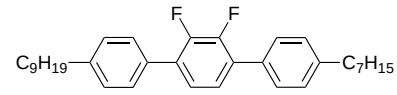
The precursor **5** was synthesized in racemic form starting with the known benzidine **3**,[10] as shown in Scheme 1, and resolved by chiral stationary phase HPLC using a Daicel Chiralcel OJ column to give the (−) enantiomer in optically pure form.‡ The latter was esterified under mild conditions using DCC/DMAP to give the diester (−)-**2**, which showed no liquid crystalline behaviour by differential scanning calorimetry. Compound (−)-**2** was doped in the $S_C$ hosts PhBz, DFT and NCB76 at four different concentrations in the range $0.01 < x_d < 0.05$. Each mixture was introduced into polyimide-coated ITO glass cells with a 4 μm gap, and aligned by slow cooling from isotropic liquid to the $S_C$* phase at $T–T_{AC} = -5$ °C. Spontaneous polarization and tilt angle (θ) values were measured as a function of $x_d$ by the triangular wave method using a Displaytech APT II polarization testbed (100 Hz, 6 V μm$^{-1}$).[11] At $x_d = 0.03$, the dopant (−)-**2** gave a $P_S$ value of −2.5 nC cm$^{-2}$ (θ = 9.5°) in NCB76, and a $P_S$ value of −1.7 nC cm$^{-2}$ (θ = 10.5°) in DFT. In these two hosts, a plot of $P_o$ *vs.* $x_d$ gave a good linear fit, from which $\delta_P$ values were



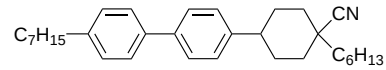

(–)-**1** X = $NO_2$, Y = H, R = $C_8H_{17}$
(–)-**2** X = Me, Y = $NO_2$, R = $C_9H_{19}$




PhBz; phase sequence: Cr 35 $S_C$ 70 $S_A$ 72 N 75 I

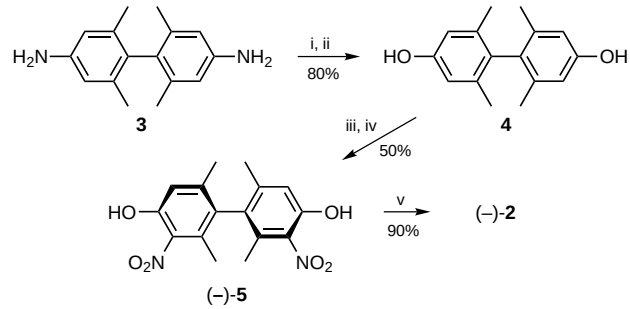



DFT; phase sequence: Cr 49 $S_C$ 77 $S_A$ 93 N 108 I




NCB76; phase sequence:
Cr 66 ($S_G$ 55) $S_C$ 73 $S_A$ 117 N 125 I

**Fig. 1**




**Scheme 1** *Reagents and conditions*: i, $NaNO_2$, HCl, 5 °C; ii, 10% $H_2SO_4$, reflux; iii, $Fe(NO_3)_3 \cdot 9H_2O$, EtOH, reflux; iv, chiral stationary phase HPLC resolution, semiprep Daicel Chiralcel OJ column, hexanes–EtOH 9 : 1, 3 ml min$^{-1}$; v, 4-nonyloxybenzoic acid, DCC, DMAP, $CH_2Cl_2$, 25 °C

obtained (Fig. 2).† In the host PhBz, $P_S$ was too low to be measured at $x_d$ = 0.05; an upper limit value for $\delta_P$ was estimated based on the instrument detection limit (0.3 nC cm$^{-2}$) and an observed tilt angle of 10° at $T$–$T_{AC}$ = −5 °C. These results are presented in Table 1, including previously unreported data for dopant (−)-**1** in DFT, and correlated with dielectric anisotropy values ($\Delta\varepsilon = \varepsilon_{\parallel} - \varepsilon_{\perp}$) measured in the nematic phase for structurally analogous mesogens.§ The $\Delta\varepsilon$ values are consistent with the increase in transverse dipole moment of the mesogens in the order PhBz < DFT < NCB76.

In NCB76 and DFT, the dopant (−)-**2** shows a much higher polarization power than (−)-**1**, which is consistent with the increase in rotational bias about the ester C–O bond predicted by the AM1 calculations. Furthermore, (−)-**2** exhibits a very strong dependence of $\delta_P$ on the nature of the $S_C$ host. To the best of our knowledge, the > 15-fold enhancement in polarization power shown by (−)-**2** as a function of the $S_C$ host is the largest thus far reported for a Type II dopant. For each dopant, a correlation exists between the polarization power and the dielectric anisotropy of the $S_C$ host, which suggests that the Type II dependence observed in this case arises from enhanced coupling of the dopant with the $S_C$ lattice *via* transverse dipole–dipole interactions. This coupling mechanism is likely to induce polar ordering of the $S_C$ host and cause an asymmetric distortion of the achiral $S_C$ lattice that further enhances rotational ordering of the atropisomeric core. We plan to continue testing the validity of this model through the design and characterization of new series of atropisomeric dopants analogous to **1** and **2**.

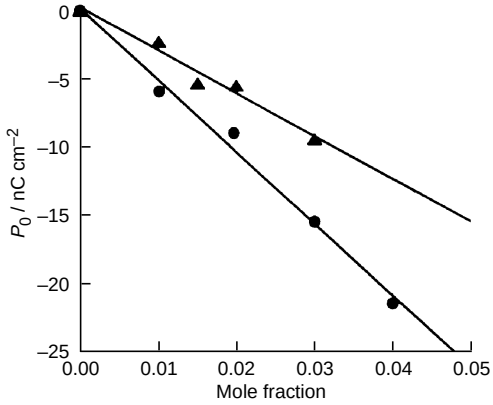



**Fig. 2** Reduced polarization $P_o$ as a function of mole fraction for the dopant (−)-**2** in the $S_C$ hosts NCB76 (circles) and DFT (triangles) at $T$–$T_{AC}$ = −5 °C

**Table 1** Polarization power values for dopants (−)-**1** and (−)-**2** in the $S_C$ hosts NCB76, DFT and PhBz

| | | $\delta_P$/nC cm$^{-2}$ [a] | | | |
|---|---|---|---|---|---|
| Host | $\Delta\varepsilon$ [b] | (−)-**1** | sign | (−)-**2** | sign |
| NCB76 | −4.7 | 170 [c] | + | 523 | − |
| DFT | −1.7 | 63 [d] | + | 312 | − |
| PhBz | −0.35 | < 20 | − | < 34 | − |

[a] Measured at $T$–$T_{AC}$ = −5 °C. [b] Dielectric anisotropy values measured in the nematic phase for the structural analogues 4-(4′-pentylbiphenyl-4-yl)-1-propylcyclohexanecarbonitrile, 2′,3′-difluoro-4,4″-dipropyl-*p*-terphenyl,[12] and 4-hexyloxyphenyl 4-decyloxybenzoate.[13] [c] From ref. 7. [d] This value was extrapolated from a single $P_o$ measurement at $x_d$ = 0.04.

We are grateful to the Natural Sciences and Engineering Research Council of Canada for financial support of this work, and to Professor H. Stegemeyer for a generous gift of NCB76.

## Footnotes

* E-mail: lemieux@chem.queensu.ca

† The reduced polarization is intrinsic to the chiral component(s) of the $S_C$* phase at a fixed temperature difference below the $S_C$*–$S_A$* phase transition ($T$–$T_{AC}$), and is related to the spontaneous polarization ($P_S$) and tilt angle ($\theta$) of the $S_C$* phase by the equation:

$$P_o = P_S/\sin\theta$$

‡ All new compounds gave satisfactory spectral data ($^1$H, $^{13}$C NMR and mass spectra) and combustion analyses.

§ Dielectric anisotropy values for PhBz, DFT, NCB76 are currently unavailable.

## References

1 D. M. Walba, in *Advances in the Synthesis and Reactivity of Solids*, ed. T. E. Mallouck, JAI Press, Greenwich, CT, 1991, vol. 1, pp 173–235.
2 D. M. Walba, *Science*, 1995, **270**, 250.
3 J. W. Goodby, R. Blinc, N. A. Clark, S. T. Lagerwall, M. A. Osipov, S. A. Pikin, T. Sakurai, K. Yoshino and B. Zeks, *Ferroelectric Liquid Crystals: Principles, Properties and Applications*, Gordon and Breach, Philadelphia, 1991.
4 J. Dijon, in *Liquid Crystals: Applications and Uses*, ed. B. Bahadur, World Scientific, Singapore, 1990, vol. 1, ch. 13.
5 K. Siemensmeyer and H. Stegemeyer, *Chem. Phys. Lett.*, 1988, **148**, 409.
6 H. Stegemeyer, R. Meister, U. Hoffmann, A. Sprick and A. Becker, *J. Mater. Chem.*, 1995, **5**, 2183.
7 K. Yang, B. Campbell, G. Birch, V. E. Williams and R. P. Lemieux, *J. Am. Chem. Soc.*, 1996, **118**, 9557.
8 P. Keller, *Ferroelectrics*, 1984, **58**, 3.
9 G. W. Gray, M. Hird, D. Lacey and K. J. Toyne, *J. Chem. Soc., Perkin Trans. 2*, 1989, 2041.
10 R. B. Carlin, *J. Am. Chem. Soc.*, 1945, **67**, 928.
11 K. Miyasato, S. Abe, H. Takezoe, A. Fukuda and E. Kuze, *Jpn. J. Appl. Phys.*, 1983, **22**, L661.
12 V. Reiffenrath, J. Krause, H. J. Plach and G. Weber, *Liq. Cryst.*, 1989, **5**, 159.
13 L. Bata, A. Buka and J. Szabon, *Wiss. Beitr.-Martin-Luther- Univ. Halle-Wittenberg*, 1983, **41**, 7.

*Received in Corvallis, OR, USA, 10th March 1997; Com. 7/01713H*

# Triruthenium cluster complexes of $C_{70}$. Synthesis and structural characterization of $\{Ru_3(CO)_9\}_x(\mu_3\text{-}\eta^2,\eta^2,\eta^2\text{-}C_{70})]$ ($x$ = 1, 2)

**Hsiu-Fu Hsu, Scott R. Wilson and John R. Shapley***

*School of Chemical Sciences, University of Illinois at Urbana-Champaign, Urbana, IL 61801, USA*

**The interaction of $C_{70}$ and $[Ru_3(CO)_{12}]$ provides $[Ru_3(CO)_9(\mu_3\text{-}\eta^2,\eta^2,\eta^2\text{-}C_{70})]$, in which the $Ru_3$ triangle is coordinated to only one of the three possible six-membered ring types; analogous double-addition products are isolated and one structurally characterized.**

The prolate ellipsoidal fullerene $D_{5h}$-$C_{70}$ displays a striking variety of structural features, with five types of carbon atoms, eight types of C–C bonds, two types of five-membered rings, and three types of six-membered rings (Scheme 1). Theoretical as well as structural studies of $C_{70}$ are in agreement that bond types 2 and 4 near the poles are the shortest in the molecule, whereas the equatorial belt bonds of type 8 are the longest.[1] Within the six-membered rings, bond distance alternation is marked in type I rings, moderate in type II rings, and non-existent in type III rings; the equatorial type III rings have been characterized as 'aromatic'.[2]

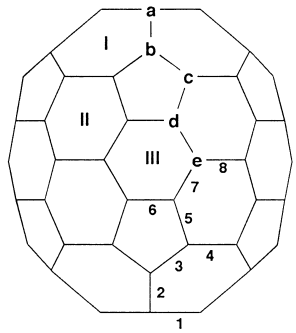
Additions to $C_{70}$ occur primarily at the 'double' bonds of types 2 and 4, with addition at the more pyramidalized bond 2 generally favoured.[3–7] We were interested in the possible ligating characteristics of six-membered ring types I–III toward an arene-complexing fragment, in particular, $Ru_3(CO)_9$.[8] Recently, the coordination of this group to $C_{60}$ has been described.[9] Here we report the preparation and structure of the first hexahapto complex of $C_{70}$, $[Ru_3(CO)_9(\mu_3\text{-}\eta^2,\eta^2,\eta^2\text{-}C_{70})]$ **1**, in which the $Ru_3$ triangle is bonded to a six-membered ring of type I. In addition, we have prepared and separated the expected three isomers of the double substitution product, $[\{Ru_3(CO)_9\}_2C_{70}]$ **2** and have determined the structure of one isomer.

Heating a mixture of $C_{70}$ and $[Ru_3(CO)_{12}]$ in *n*-hexane for several days produces little visible change, since the fullerene is poorly soluble and a precipitate is present throughout. However, extraction of the precipitate with carbon disulfide followed by preparative thin-layer chromatography on silica provides a new compound in addition to recovered $C_{70}$. Compound **1** was crystallized from carbon disulfide by slow infusion of benzene. The results of a single-crystal X-ray diffraction study of **1**·$CS_2$ revealed two inequivalent molecules (A and B) in the unit cell; the structure of molecule A is illustrated in Fig. 1.†

The triruthenium unit is coordinated to one of the type I rings, with one Ru bonded to a type 4 C–C bond and the other two Ru atoms bonded to type 2 C–C bonds. However, each Ru–$C_2$ interaction shows one longer and one shorter Ru–C distance, which alternate around the ring, consistent with a slight twist of the $Ru_3$ triangle with respect to the $C_6$ ring. The Ru–C distances average 2.24, 2.27 Å in A and 2.23, 2.32 Å in B, and the twist angles are 2 and 4° in A and B, respectively. Accompanying the twist between the two attached rings is a threefold twist of each $Ru(CO)_3$ moiety that positions each axial carbonyl at an angle to the axis perpendicular to the $Ru_3$ plane; these angles average 10° in A and 12° in B. These structural features were also seen in $[Ru_3(CO)_9(\mu_3\text{-}\eta^2,\eta^2,\eta^2\text{-}C_{60})]$ **3**[9] as well as in $[Ru_3(CO)_9(\mu_3\text{-}\eta^2,\eta^2,\eta^2\text{-}C_6H_6)]$ **4**,[8] and they were attributed to packing forces acting on a relatively flat potential for small angles of rotation around the $Ru_3$–$C_6$ axis. The two different sets of structural parameters observed for molecules A and B of **1** provide direct support for this idea. Overall, the local structures for **1** and **3** are closely comparable.

The Ru–Ru bond distances in **1** [2.894(5), 2.918(3), 2.836(3) Å in A and 2.861(4), 2.875(4), 2.869(3) Å in B] are on average slightly longer than those in $[Ru_3(CO)_{12}]$ [2.855(1) Å].[10] Although the e.s.d.s are large, the C–C bond distances of the coordinated six-membered ring seem to show short–long alternation, with averages 1.39, 1.49 Å for A and 1.40, 1.48 Å for B. The average C–C bond lengths for the different types of bond in the unsubstituted halves of the $C_{70}$ ligands in molecules A and B of **1** show the same patterns seen in previous $C_{70}$ structure analyses.[1,6,7]

The coordination of the $Ru_3$ triangle to a six-membered ring of type I is in conformity with the positions of other single-metal addends as mentioned above. This result suggests that the formation of **1** may be a kinetically controlled reaction, in which coordination of the first metal atom at a type 2 bond determines




**Scheme 1**

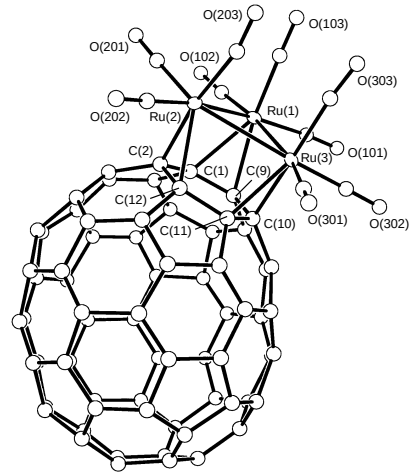
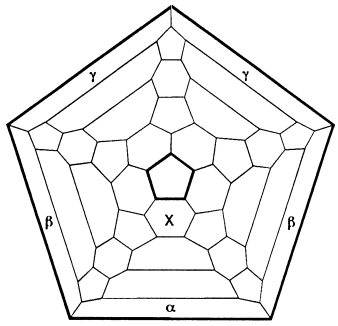



**Fig. 1** A perspective view of **1** (molecule A), showing part of the atom labelling scheme. Selected bond lengths (Å): Ru(1)–Ru(2) 2.894(5), Ru(2)–Ru(3) 2.918(3), Ru(1)–Ru(3) 2.836(3), Ru(1)–C(1) 2.33(2), Ru(1)–C(9) 2.25(2), Ru(2)–C(2) 2.21(2), Ru(2)–C(12) 2.26(2), Ru(3)–C(10) 2.24(2), Ru(3)–C(11) 2.27(2), C(1)–C(2) 1.48(3), C(1)–C(9) 1.37(3), C(2)–C(12) 1.45(3), C(9)–C(10) 1.51(3), C(10)–C(11) 1.36(3), C(11)–C(12) 1.48(3).

the coordination sites of the remaining two metal atoms. On the other hand, these sites are already the most pyramidal in the molecule, and they require relatively little further distortion to coordinate favourably to the $Ru_3$ framework, by comparison of bond angles at coordinated *vs.* uncoordinated carbons. In contrast the type III rings, which have been characterized as aromatic on the basis of their essentially equivalent C–C distances, are actually slightly concave (carbons e,e are *ca.* 0.1 Å below the plane of the four d carbons[7]), so that coordination of one of these rings to a metal triangle would involve considerable distortion of the $C_{70}$ framework. However, since good evidence for the addition of radical moieties in the equatorial region has been presented,[11] the possible coordination of ring types II and III with more reactive reagents or in the formation of higher addition products remains to be explored.




**Scheme 2**

The addition of a second $Ru_3$ unit to the $C_{70}$ ligand in **1** could result in three disubstituted isomers, as shown in Scheme 2, assuming the second unit is added to the same type of six-membered ring in the opposite polar region. Indeed, increasing the ratio of $[Ru_3(CO)_{12}]$ to $C_{70}$ under the same reaction conditions produces three new products, **2α**, **2β**, and **2γ**, which can be separated by preparative thin-layer chromatography ($CS_2/SiO_2$). The new compounds **2α**, **2β**, and **2γ** (isolated ratio 2 : 3 : 1) are formulated as disubstituted derivatives $C_{70}[Ru_3(CO)_9]_2$ on the basis of molecular ion multiplets seen by FABMS spectroscopy. All three isomers have two IR ($\nu_{CO}$) bands at 2074 and 2046 $cm^{-1}$, and the only difference among them is the position of the third peak at 2010, 2013 and 2012 $cm^{-1}$ for **2α**, **2β**, and **2γ**, respectively. These IR spectra are almost identical to that of **1**, which suggests the same bonding mode is adopted for both $Ru_3$ units as in **1**. Single crystals of isomer **2β** suitable for X-ray diffraction study were obtained from carbon disulfide by slow diffusion of methanol; a structural diagram of **2β** is shown in Fig. 2.‡ The two $Ru_3$ units are each bonded to type I six-membered rings in a fashion analogous to **1**, and their relative positions conform to the idealized $C_2$ symmetry of isomer **2β**. Attempts to characterize the structures of the other two double addition products, presumably $C_{2v}$-**2α** and $C_2$-**2γ**, are underway.

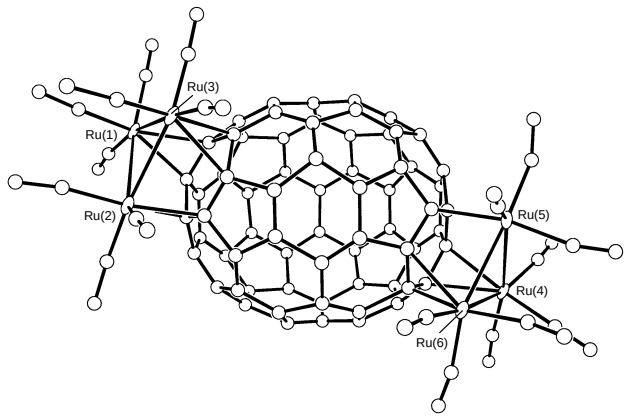



**Fig. 2** A perspective view of **2β**, showing part of the atom labelling scheme. Selected bond lengths (Å): Ru(1)–Ru(2) 2.911(3), Ru(2)–Ru(3) 2.889(3), Ru(1)–Ru(3) 2.855(3), Ru(4)–Ru(5) 2.877(3), Ru(5)–Ru(6) 2.878(3), Ru(6)–Ru(4) 2.866(3).

This work was supported by a grant from the National Science Foundation (CHE 9414217). Purchase of the Siemens Platform/CCD diffractometer by the School of Chemical Sciences was supported by NSF grant CHE 9503145.

## Footnotes

* E-mail: shapley@aries.scs.uiuc.edu

† *Crystallographic data*: for **1**·$CS_2$: orthorhombic, space group $Pna2_1$, $a$ = 18.9367(8), $b$ = 49.491(2), $c$ = 10.0460(4), $U$ = 9415.1(6) Å$^3$, $Z$ = 8; crystal size 0.05 × 0.09 × 0.46 mm. Diffraction data were collected at 198 K on a Siemens Platform/ CCD automated diffractometer. A total of 33 910 reflections were corrected for absorption [empirical; μ(Mo-Kα) = 1.122 $mm^{-1}$; max., min. transmission factor = 0.922, 0.824] and used for structure solution and refinement (SHELXTL, Siemens). The ruthenium triangles in both molecules (A and B) were disordered. Primary site occupancy for Ru(1,2,3) converged at 0.878(5) and for Ru(4,5,6) at 0.883(2). Anisotropic displacement parameters for disordered pairs of ruthenium atoms were constrained to equivalent values. Full-matrix least-squares refinement on $F^2$ of 892 parameters against 8383 independent reflections gave final agreement factors of $R_1$ = 0.0858 (against $|F|$) and $wR_2$ = 0.1650 [against $|F^2|$ for 6041 data with $I > 2\sigma(I)$].

For **2β**·1.5$CS_2$: triclinic, space group $P\bar{1}$, $a$ = 10.2197(4), $b$ = 17.0637(5), $c$ = 19.3880(8) Å, α = 99.2130(10)°, β = 98.6960(10)°, γ = 105.9410(10)°, $U$ = 3140.5(2) Å$^3$, $Z$ = 2; crystal size 0.26 × 0.11 × 0.04 mm. Diffraction data were collected at 198 K on a Siemens Platform/ CCD automated diffractometer. Intensities from the major component (75%) of this twinned crystal that suffered from overlap with intensities from the minor component were omitted. A total of 6468 reflections were corrected for absorption [empirical; μ(Mo-Kα) = 1.595 $mm^{-1}$; max., min. transmission factor = 0.985, 0.749] and used for structure solution and refinement (SHELXTL, Siemens). Full-matrix least-squares refinement on $F^2$ of 511 parameters against 4374 independent reflections gave final agreement factors of $R_1$ = 0.0850 (against $|F|$) and $wR_2$ = 0.1746 [against $|F^2|$, for 2985 data with $I > 2\sigma(I)$]. Atomic coordinates, bond lengths and angles, and thermal parameters have been deposited at the Cambridge Crystallographic Data Centre (CCDC). See Information for Authors, Issue No. 1. Any request to the CCDC for this material should quote the full literature citation and the reference number 182/470.

## References

1 J. Mestres, M. Duran and M. Sola, *J. Phys. Chem.*, 1996, **100**, 7449.
2 G. E. Scuseria, *Chem. Phys. Lett.*, 1991, **180**, 451; J. Baker, P. W. Fowler, P. Lazzeretti, M. Malagoli and R. Zanasi, *Chem. Phys. Lett.*, 1991, **184**, 182.
3 J. M. Hawkins, A. Meyer and M. A. Solow, *J. Am. Chem. Soc.*, 1993, **115**, 7499.
4 A. B. Smith, III, R. M. Strongin, L. Brard, G. T. Furst, J. H. Atkins, W. J. Romanow, M. Saunders, H. A. Jimenez-Vazquez, K. G. Owens and R. J. Goldschmidt, *J. Org. Chem.*, 1996, **61**, 1904; A. L. Balch, D. A. Costa and M. M. Olmstead, *Chem. Commun.*, 1996, 2449.
5 C. Bingel and H. Schiffer, *Liebigs Ann.*, 1995, 1551.
6 A. L. Balch, V. J. Catalano, J. W. Lee, M. M. Olmstead and S. R. Parkin, *J. Am. Chem. Soc.*, 1991, **113**, 8953; A. L. Balch, J. W. Lee and M. M. Olmstead, *Angew. Chem., Int. Ed. Engl.*, 1992, **31**, 1356; A. L. Balch, L. Hao and M. M. Olmstead, *Angew. Chem., Int. Ed. Engl.*, 1996, 35**, 188.**
7 A. Herrmann, F. Diederich, C. Thilgen, H.-U. ter Meer and W. H. Müller, *Helv. Chim. Acta*, 1994, **77**, 1689; P. Seiler, A. Herrmann and F. Diederich, *Helv. Chim. Acta*, 1995, **78**, 344.
8 D. Braga, P. J. Dyson, F. Grepioni and B. F. G. Johnson, *Chem. Rev.*, 1994, **94**, 1585.
9 H.-F. Hsu and J. R. Shapley, *J. Am. Chem. Soc.* 1996, **118**, 9192.
10 M. R. Churchill, F. J. Hollander and J. P. Hutchinson, *Inorg. Chem.*, 1977, **16**, 2655.
11 R. Borghi, L. Lunazzi, G. Placucci, P. J. Krusic, D. A. Dixon, N. Matsuzawa and M. Ata, *J. Am. Chem. Soc.*, 1996, **118**, 7608; P. R. Birkett, A. G. Avent, A. D. Darwish, H. W. Kroto, R. Taylor and D. R. M. Walton, *J. Chem. Soc., Chem. Commun.*, 1995, 683; T. Akasaka, E. Mitsuhida and W. Ando, *J. Am. Chem. Soc.*, 1994, **116**, 2627.

*Received in Bloomington, IN, USA, 12th March 1997; Com. 7/01753G*

# Fluorous-phase soluble rhodium complexes: X-ray structure of [RhCl(CO)(P($C_2H_4C_6F_{13}$)$_3$)$_2$]

**John Fawcett,[a] Eric G. Hope,*[a] Raymond D. W. Kemmitt,[a] Danny R. Paige,[a] David R. Russell,[a] Alison M. Stuart,[a] David J. Cole-Hamilton[b] and Marc J. Payne[b]**

[a] *Department of Chemistry, University of Leicester, Leicester, UK LE1 7RH*
[b] *School of Chemistry, University of St. Andrews, St. Andrews, Fife, UK KY16 9ST*

**Rhodium(I) complexes of the ligands P($CH_2CH_2C_6F_{13}$)$_3$ and P($C_6H_4C_6F_{13}$-4)$_3$, which can be compared to their perprotio analogues, maintain their structures in fluorous solvents.**

Following the first report of the alternative approach to two-phase catalysis called the 'fluorous biphase system' (FBS)[1] this methodology has been employed in a number of organic reactions,[2] and catalytically in the epoxidation of alkenes.[3] In short, the FBS approach involves derivatising inorganic or organic reagents with long perfluorinated aliphatic 'ponytails' which renders these reagents soluble in a perfluorocarbon phase allowing the facile separation of these reagents, after catalysis, from the substrate/product dissolved in an organic solvent. The approach is attracting significant interest since it should allow the facile separation of catalyst from reactants and products using simple liquid/liquid separation techniques and benign, non-toxic, reusable perfluorocarbon solvents for industrial scale homogeneous catalysis. However, although it has been shown that catalyst separation is readily achieved under FBS regimes,[1–3] the exact nature and the influence of the highly electron-withdrawing fluorous ponytails on these fluorous-soluble catalysts has not been established. Since (*i*) phosphorus(III) ligands have found wide application in homogeneous catalysis, (*ii*) the first FBS report outlined the use of an uncharacterised rhodium–phosphine catalyst[1] and (*iii*) we have a long-standing interest in fluorinated phosphorus(III) ligands,[4] we have been investigating the coordination chemistry of a series of derivatised phosphine ligands and here report the synthesis and characterisation of some rhodium(I) complexes and the first structural characterisation of a fluorous-phase soluble metal complex.

The reaction of either of the tris-derivatised fluorous-phase soluble ligands P($CH_2CH_2C_6F_{13}$)$_3$ or P($C_6H_4C_6F_{13}$-4)$_3$[5] with [{RhCl(CO)$_2$}$_2$] yields the complexes [RhCl(CO)$L_2$], in high yields, as slightly air-sensitive yellow solids. Despite the unusually high molecular masses of these complexes, they have been characterised by standard techniques.† The influence of the $C_6F_{13}$ units can be probed by a comparison of the $\nu$(CO) and $^1J$(RhP) data with that for the analogous triethyl- and triphenylphosphine complexes {$\nu$(CO): [RhCl(CO)(P$Et_3$)$_2$] 1953 cm$^{-1}$, [RhCl(CO)(P$Ph_3$)$_2$] 1961 cm$^{-1}$; $^1J$(RhP): [RhCl(CO)(P$Et_3$)$_2$] 116 Hz, [RhCl(CO)(P$Ph_3$)$_2$] 124 Hz}.[6] In both cases, although the $^1J$(RhP) values are very similar, $\nu$(CO) is significantly higher as a result of introducing the fluorous ponytails, suggesting that the electron-withdrawing capacity of the ponytails is removing electron density from the metal centres.

Crystals of [RhCl(CO){P($CH_2CH_2C_6F_{13}$)$_3$}$_2$], suitable for crystallographic characterisation, have been obtained by slow evaporation from perfluoro-1,3-dimethylcyclohexane solution (Fig. 1).‡ The $^1$H, $^{19}$F and $^{31}$P{$^1$H} NMR, IR and mass spectra of **1a** and **1b** are entirely consistent with this structure.† The metal coordination geometry is very similar to that obtained for a range of *trans*-square-planar complexes, [RhCl(CO)$L_2$] (L = monodentate phosphine) Rh–$P_{mean}$ 2.328 Å, Rh–$Cl_{mean}$ 2.386 Å, Rh–$C_{mean}$ 1.803 Å.[7] For **1a**, the Rh–P and Rh–Cl bond distances are shorter than these calculated mean values, but are not the shortest metal–ligand distances seen for this class of complex and are very similar to those reported for trisalkyl phosphine ligands, *e.g.* [RhCl(CO)(P$Me_3$)$_2$] (Rh–P 2.307, 2.310 Å; Rh–Cl 2.354 Å).[8] Although there are no unusual angles at phosphorus, there are two types of fluorinated tails. Two pairs on each phosphorus spiral, in a similar fashion to that observed for fully fluorinated hydrocarbons, above and below the Cl–Rh–CO axis in nearly planar 'rugby-post' arrangements. These sets of rugby-posts stack on top of each other in adjacent unit cells. The third, unique, ponytail on each phosphorus does not spiral but kinks, in the same direction, either above or below the Cl–Rh–CO axis into the space in the unit cell between adjacent sets of rugby-posts pointing, generally, away from any other fluorous part of the molecule.

We were interested to establish whether these complexes dissolve, without reaction, in fluorous solvents and have investigated the first coordination sphere at the metal centre in the solid-state and in fluorous solution by rhodium K-edge

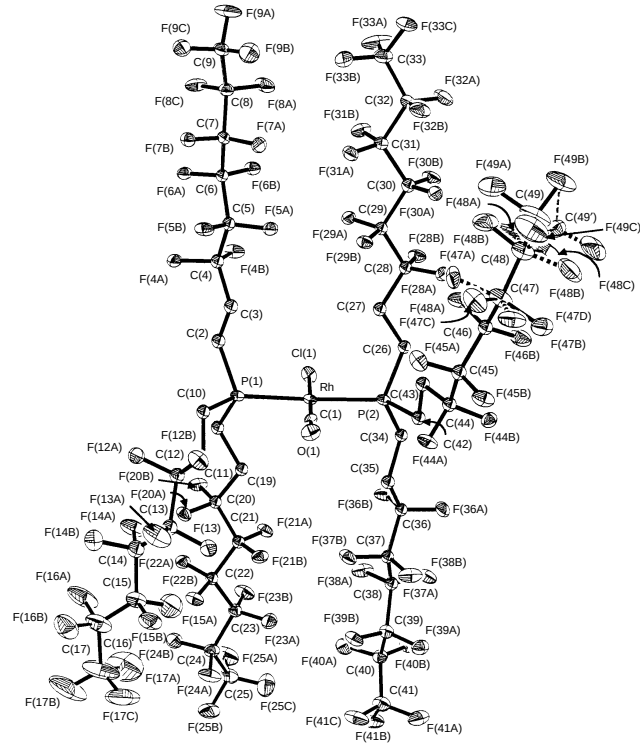



**Fig. 1** Molecular structure of **1a**. Selected interatomic distances (Å) and angles (°): Rh–P(1) 2.300(2), Rh–P(2) 2.304(2), Rh–Cl 2.356(2), Rh–C(1) 1.807(5), C(1)–O(1) 1.152(6), P(1)–C(2) 1.835(6), P(1)–C(10) 1.833(5), P(1)–C(18) 1.830(5), P(2)–C(26) 1.829(5), P(2)–C(34) 1.834(6), P(2)–C(42) 1.844(5), av. C–C 1.523(8), av. C–F 1.341(6), P(2)–Rh–P(1) 172.12(10), C(1)–Rh–Cl 179.4(5), av. C–P–Rh 115.3(2).

**Table 1** Metal-centred interatomic distances for **1a**[a]

| | X-Ray | Solid-state EXAFS[b] | | Solution EXAFS[c] | |
|---|---|---|---|---|---|
| | *d*/Å | *d*/Å | $2\sigma^2$/Å[d] | *d*/Å | $2\sigma^2$/Å[d] |
| Rh–P | 2.300(2), 2.304(2) | 2.300(1) | 0.005(1) | 2.301(2) | 0.010(1) |
| Rh–Cl | 2.356(2) | 2.360(9) | 0.016(1) | — | — |
| Rh–C | 1.807(5) | 1.787(4) | 0.004(1) | 1.792(6) | 0.008(1) |
| Rh···O | 2.959 | 2.929(6) | 0.016(1) | 2.912(5) | 0.013(1) |
| C–O | 1.152(6) | 1.142 | — | 1.120 | — |

[a] Standard deviation in parentheses. [b] Transmission EXAFS data collected on station 9 : 2 using a Si(220) monochromator for **1a** diluted with boron nitride and held between Sellotape strips. Note that the systematic errors in bond distances arising from the data collection and analysis procedures are *ca*. ±0.02 Å for the first coordination shells and *ca*. ±0.04 Å for subsequent shells. Fit index = $\Sigma_i[\chi^T \circledcirc \chi^E)k_i^3]^2$ = 0.380. $R$ = $[\int(\chi^T \circledcirc \chi^E)k^3 dk / \int\chi^E k^3 dk]$ = 23.0% [c] Transmission EXAFS data for a *ca*. 0.013 mol dm$^{\circledcirc 3}$ solution of **1a** in perfluoro-1,3-dimethylcyclohexane in a flattened FEP (perfluoroethylene–propylene copolymer) tube.[10] The poorer data quality did not allow for the distinction between the Rh–P and Rh–Cl shells. The fit given here is for a single shell of 3 P atoms. Fit index = $\Sigma_i[(\chi^T \circledcirc \chi^E)k_i^3]^2$ = 0.580. $R$ = $[\int(\chi^T \circledcirc \chi^E)k^3 dk / \int\chi^E k^3 dk]$ = 22.6%. [d] Debye–Waller factor.

EXAFS (Table 1). The data, analysed by standard procedures,[9,10] clearly indicate that these complexes dissolve without reaction in fluorous solvents and that the active sites of fluorous soluble metal catalysts could be probed in this way; the active sites of hydrocarbon soluble metal catalysts have been probed, under catalytic conditions, by EXAFS.[9] Further work on the coordination chemistry of these, and related, ligands and the catalytic activity of these metal complexes under the FBS regime is underway.

We would like to thank the EPSRC (D. R. P., A. M. S. and M. J. P.), the Royal Society (E. G. H.) and BP Chemicals Ltd (D. R. P. and M. J. P.) for financial support. We would also like to thank Dr M. Jones (BP Chemicals Ltd.) for helpful discussions, Dr I. Horváth for the gift of some $P(C_2H_4C_6F_{13})_3$ (D. J. C. H. and M. J. P.), the Director of the Daresbury laboratory for the provision of facilities and the EPSRC for the provision of low-temperature crystallographic facilities.

## Footnotes

* E-mail: egh1@le.ac.uk

† *Data* for **1a**, Anal. Calc. for $C_{49}H_{24}ClF_{78}OP_2Rh$: C 25.5, H 1.0, F 64.1. Found: C 25.4, H 1.0, F 63.1%. MS(FAB): *m/z* 2311($M^+$). IR 1990 cm$^{\circledcirc 1}$ [$\nu$(CO)]. NMR: $\delta_H$ [250.13 MHz, $(CD_3)_2CO$], 2.62 (2 H, m, $CH_2$) 3.22 (2 H, t, *J* 12 Hz, $CH_2$): $\delta_P$ [101.26 MHz, $(CD_3)_2CO$] 22.9 [d, $^1J$(RhP) 121 Hz]: $\delta_F$ [235.34 MHz, $(CD_3)_2CO$] $\circledcirc$ 80.36 (3F, t, *J* 11 Hz, $CF_3$), $\circledcirc$ 114.39 (2F, m), $\circledcirc$ 121.69 (2F, m) $\circledcirc$ 122.70 (2F, m), $\circledcirc$ 122.96 (2F, m), $\circledcirc$ 126.07 (2F, m).

For **1b**, Anal. Calc. for $C_{73}H_{24}ClF_{78}OP_2Rh$: C, 33.7, H, 0.9, P, 2.4; Found: C, 33.5, H, 0.9, P, 2.5%. MS(FAB): *m/z* 2535 ([M $\circledcirc$ Cl $\circledcirc$ CO]$^+$). IR 1992 [$\nu$(CO)]. NMR: $\nu_H$ (250.13 MHz, $CDCl_3$) 7.65 (2 H, m), 7.80 (2 H, m): $\delta_P$ (101.26 MHz, $CDCl_3$) 30.0 [d, $^1J$(RhP) 131 Hz]; $\delta_F$ (235.34, $CDCl_3$) $\circledcirc$ 81.40 (3F, t, *J* 11.5 Hz, $CF_3$), $\circledcirc$ 111.73 (2F, m), $\circledcirc$ 121.89 (2F, m), $\circledcirc$ 122.05 (2F, m), $\circledcirc$ 123.29 (2F, m), $\circledcirc$ 126.69 (2F, m).

‡ *Crystal data* for **1a**: $C_{49}H_{24}ClF_{78}OP_2Rh$, *M* = 2310.98, triclinic, space group $P\bar{1}$, *a* = 11.205(9), *b* = 15.062(4), *c* = 22.506(5) Å, $\alpha$ = 84.70(2), $\beta$ = 86.23(4), $\gamma$ = 79.93(2)°, *U* = 3719(3) Å$^3$, *Z* = 2, $D_c$ = 2.064 Mg m$^{\circledcirc 3}$, *F*(000) = 2240, $\mu$(Mo-K$\alpha$) = 0.815 mm$^{\circledcirc 1}$, crystal dimensions 0.71 $\circledcirc$ 0.40 $\circledcirc$ 0.12 mm. Accurate unit-cell dimensions were determined by least-squares refinement of 37 centred reflections with 2.53 < $\theta$ < 12.5°. Data were measured on a Siemens P4 diffractometer at 150 K with Mo-K$\alpha$ radiation using $\omega$-scans. 15 371 reflections were measured with $\theta$ < 25° and $\circledcirc$ 1 ◀ *h* ◀ 12, $\circledcirc$ 17 ◀ *k* ◀ 17, $\circledcirc$ 26 ◀ *l* ◀ 26. The reflections were corrected for Lorentz and polarisation effects and merged to give 11 855 independent reflections ($R_{int}$ = 0.0188). An analytical absorption correction was applied to the data ($T_{max}$, $T_{min}$ = 0.88, 0.65, respectively). The structure was solved by direct methods using the program SHELXTL-PC. The terminal atoms of one of the chains were found to be disordered with the atoms having 60 : 40 occupancy over two sites. All hydrogen atoms were included in calculated positions (C–H 0.96 Å) with isotropic displacement parameters set to 1.2 $U_{eq}$ of the bonded C atom. The first six carbon atoms of each chain were refined with isotropic displacement parameters and all other atoms were refined with anisotropic thermal parameters. Final cycles of refinement with full-matrix least squares on $F^2$ gave $R_1$ = 0.0560, $wR_2$ = 0.1287. The maximum and minimum residual electron densities in the final $\Delta F$ map were 1.686 and $\circledcirc$ 0.571 e Å$^{\circledcirc 3}$. Atomic coordinates, bond lengths and angles, and thermal parameters have been deposited at the Cambridge Crystallograpic Data Centre (CCDC). See Information for Authors, Issue No. 1. Any request to the CCDC for this material should quote the full literature citation and the reference number 182/459.

## References

1 I. T. Horváth and J. Rábai, *Science*, 1994, **266**, 72; *US Pat.*, 5,463,082, 1995.
2 D. P. Curran and S. Hadida, *J. Am. Chem. Soc.*, 1996, **118**, 2531; D. P. Curran and M. Hoshino, *J. Org. Chem.*, 1996, **61**, 6480.
3 G. Pozzi, S. Banfi, A. Manfredi, F. Montanari and S. Quici, *Tetrahedron*, 1996, **52**, 11 879.
4 M. J. Atherton, K. S. Coleman, J. Fawcett, J. H. Holloway, E. G. Hope, A. Karaçar, L. A. Peck and G. C. Saunders, *J. Chem. Soc., Dalton Trans.*, 1995, 4029; J. H. Holloway, E. G. Hope, D. R. Russell, G. C. Saunders and M. J. Atherton, *Polyhedron*, 1996, **15**, 173; M. J. Atherton, J. Fawcett, J. H. Holloway, E. G. Hope, A. Karaçar, D. R. Russell and G. C. Saunders, *J. Chem. Soc., Dalton Trans.*, 1996, 3215.
5 P. Bhattacharya, D. Gudmunsen, E. G. Hope, R. D. W. Kemmitt, D. R. Paige and A. M. Stuart, in preparation.
6 J. Chatt and B. L. Shaw, *J. Chem. Soc., A*, 1966, 1437; B. E. Mann, C. Masters and J. Chatt, *J. Chem. Soc., A*, 1971, 1104.
7 See for example: A. Monae, E. Gutierrez-Puebla, J. V. Heras and E. Pinilla, *Acta Crystallogr. Sect. C*, 1983, **39**, 446; A. Ceriotti, G. Ciani and A. Sironi, *J. Organomet. Chem.*, 1983, **247**, 345; R. L. Harlow, S. A. Westcott, D. L. Thorn and R. T. Baker, *Inorg. Chem.*, 1992, **31**, 323.
8 S. E. Boyd, L. D. Field, T. W. Hambley and M. G. Partridge, *Organometallics*, 1993, **12**, 1720.
9 N. A. Cruise and J. Evans, *J. Chem. Soc., Dalton Trans.*, 1995, 3089; D. Bogg, M. Conyngham, J. M. Corker, A. J. Dent, J. Evans, R. C. Farrow, V. L. Kambhampati, A. F. Masters, D. N. McLeod, C. A. Ramsdale and G. Salvini, *Chem. Commun.*, 1996, 647.
10 S. A. Brewer, A. K. Brisdon, J. H. Holloway, E. G. Hope, L. A. Peck and P. G. Watson, *J. Chem. Soc., Dalton Trans.*, 1995, 2945.

*Received in Cambridge, UK, 15th April 1997; Com. 7/02560B*

# Magnesium oxide-catalysed reaction of carbon dioxide with an epoxide with retention of stereochemistry

**Takashi Yano,[a] Hideo Matsui,[a] Takahiro Koike,[a] Hiroyasu Ishiguro,[a] Hisashi Fujihara,[b] Masakuni Yoshihara*[a] and Toshihisa Maeshima[a]**

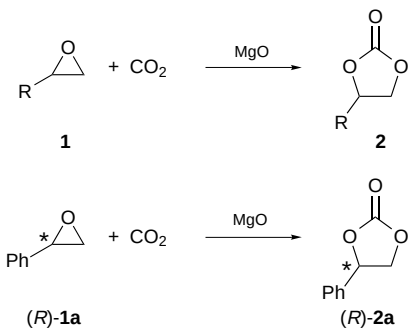
[a] *Department of Applied Chemistry, Faculty of Science and Engineering, Kinki University, Kowakae, Higashi-Osaka 577, Japan*
[b] *Environmental Science Research Institute, Kinki University, Kowakae, Higashi-Osaka 577, Japan*

**Magnesium oxide is an efficient catalyst for the cycloaddition of carbon dioxide to epoxides under mild conditions; the reaction of carbon dioxide with (*R*)-styrene oxide in the presence of magnesium oxide gives (*R*)-phenyl carbonate in 97% ee with retention of stereochemistry.**

Carbon dioxide fixation has recently received much attention owing to environmental concerns and the reaction of carbon dioxide with epoxides has been of interest as a useful catalytic fixation method.[1]

The synthesis of organic compounds using metal oxides as catalysts is also of considerable current interest. For example, magnesium oxide possesses both acid and base surface sites, and many of the catalytic applications of magnesium oxide are based on the principle of acid–base catalysis. Several reports on the adsorption of carbon dioxide on the surface of magnesium oxide prompted us to develop a new method for its fixation using the metal oxide,[2] although magnesium oxide has not been used as a catalyst for the conversion of carbon dioxide. We have now found that the reaction of carbon dioxide with epoxide is promoted by the addition of magnesium oxide as a catalyst under atmospheric pressure. Here we present a novel method for the fixation of carbon dioxide by metal oxide together with the stereochemistry of the carboxylation of epoxide with carbon dioxide in the presence of magnesium oxide.

Preliminary carboxylation studies were carried out using styrene oxide **1a** as a model compound (Scheme 1). A typical experimental procedure for the carboxylation of epoxide with carbon dioxide is as follows. Magnesium oxide (0.4 g) was added to a solution of epoxide **1a** (10 mmol) in *N*,*N*-dimethylformamide (DMF, 3 ml) in a pressure bottle under a $CO_2$ atmosphere.† The mixture was heated at 135 °C for 12 h and then filtered. The magnesium oxide was washed with acetone and the filtrates were combined. The solvents were removed under reduced pressure and the crude product was chromatographed on silica gel to give the corresponding cyclic carbonate **2a**. The product was analysed by NMR, IR and MS spectroscopy and microanalysis and the results are shown in Table 1.




**Scheme 1**

The reaction of **1a** with carbon dioxide in the presence of uncalcined magnesium oxide led to the formation of phenyl carbonate **2a** in 47% yield (Table 1, entry 1). Magnesium oxide was found to be effective in the carboxylation of epoxide with carbon dioxide. An analogous result was obtained by using the calcined magnesium oxide at 300 °C (entry 2). When calcined magnesium oxide at 400 °C was used for the reaction, the yield of the carbonate **2a** was somewhat increased (entry 3). The carbon dioxide incorporation into the epoxide ring was further examined for a few epoxides (Table 1, entries 4 and 5). The aliphatic terminal epoxides afforded the corresponding cyclic carbonates in good yields. This is, to the best of our knowledge, the first example of the activation of carbon dioxide using magnesium oxide.

The yield of the carbonate **2a** in the reaction of **1a** with carbon dioxide was increased by increasing amount of magnesium oxide (Fig. 1).‡ On the other hand, the carbon dioxide pressure had no effect on the yield of the carbonate **2a**, as shown in Fig. 2, although it has been reported that the epoxide–$CO_2$ reaction required a high pressure of carbon dioxide.[1]

**Table 1** MgO catalysed carboxylation of epoxides **1** with $CO_2$[a]

| Entry | Epoxide **1** | R | Calcination temp./°C[b] | Yield of **2** (%) |
|---|---|---|---|---|
| 1 | **a** | Ph | —[c] | 47 |
| 2 | **a** | Ph | 300 | 49 |
| 3 | **a** | Ph | 400 | 60 |
| 4 | **b** | Me | 400 | 41 |
| 5 | **c** | Et | 400 | 72 |

[a] Reaction conditions: MgO (0.4 g), $CO_2$ pressure 20 kg cm$^{-2}$, epoxide (10 mmol), DMF (3 ml), 135 °C, 12 h. [b] MgO was calcined for 3 h. [c] Uncalcined MgO.

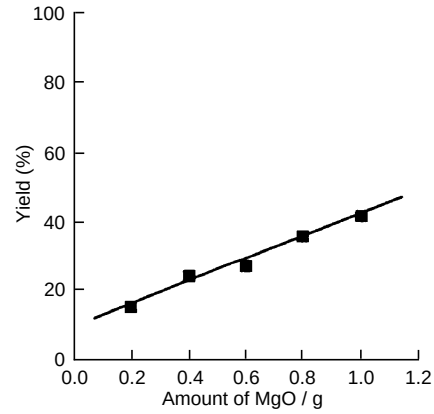



**Fig. 1** Relationship between the yield of phenyl carbonate **2a** and the amount of MgO. The reaction was carried out with epoxide **1a** (5 mmol) in the presence of MgO in DMF (2 ml) under $CO_2$ (20 kg cm$^{-2}$) at 135 °C for 4 h.

Interestingly, magnesium oxide controlled the stereochemistry of the epoxide, *i.e*. treatment of a chiral epoxide, (*R*)-**1a**, with carbon dioxide in the presence of magnesium oxide gave (*R*)-(⍯)-phenyl carbonate, (*R*)-**2a**, in 63% chemical yield with 99% ee (Scheme 1).§ The absolute configuration of this compound was *R*, as deduced from (*R*)-(⍯)-1-phenylethane-1,2-diol which was obtained from the hydrolysis of (*R*)-**2a** with 1 M NaOH.¶ Thus the carboxylation proceeded with retention of the epoxide configuration. We thus propose the following mechanism (Scheme 2). Carbon dioxide and the epoxide are adsorbed on MgO to form the complex **3** and then the carboxylate anion of **3** attacks the *β*-carbon atom of the epoxide to generate the oxy anion of **4**, which subsequently attacks the carbonyl group of **4** to afford the cyclic carbonate **2**.

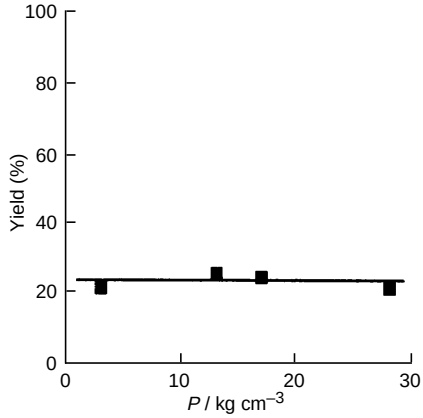
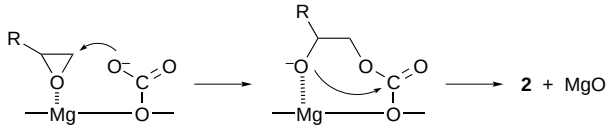



**Fig. 2** Relationship between the yield of phenyl carbonate **2a** and the pressure of $CO_2$. The reaction was carried out with epoxide **1a** (5 mmol) in the presence of MgO (0.4 g) in DMF (2 ml) under $CO_2$ at 135 °C for 4 h.




**Scheme 2**

This work was supported in part by a Grant-in-Aid for Science Research from the Japan Private School Promotion Foundation and also the Environmental Science Institute of Kinki University. We also thank the Osaka Organic Chemical Industry Ltd. for the donation of a chiral column.

## Footnotes

† MgO was obtained from Wako Pure Chemical Industries Ltd. The surface area of MgO was 47.2 $m^2$ $g^{⍯1}$.
‡ The yield of carbonate **2a** in the absence of MgO was 8%.
§ The enantiomeric excess of (*R*)-(⍯)-phenyl carbonate was determined by HPLC using Daicel Chiralcel (eluent, hexane–propan-2-ol, 9 : 1) at 40 °C.
¶ Hydrolysis of (*R*)-**2a**, led to (*R*)-(⍯)-1-phenyl ethane-1,2-diol, $[\alpha]_D^{25}$ ⍯ 38.6 (*c* 2.4, EtOH) [lit., [3] $[\alpha]_D^{25}$ ⍯ 39.7 (*c* 4.33, EtOH].

## References

1 N. Kihara, N. Hara and T. Endo, *J. Org. Chem*., 1993, **58**, 6198 and references cited therein.
2 Y. Fukuda and K. Tanabe, *Bull. Chem. Soc. Jpn*., 1973, **46**, 1616.
3 J. A. Dale and H. S. Mosher, *J. Org. Chem*., 1970, **35**, 4002.

*Received, in Cambridge, UK, 2nd December 1996; Com. 6/08102I*

# Second-order non-linear optical response of a novel type of charge-transfer complex, $[4\text{-DMSP}]_4[NH_2Me_2]_2HSiFeMo_{11}O_{40}\cdot 3H_2O$

**Xiao-Min Zhang, Bao-Zhen Shan, Cun-Ying Duan and Xiao-Zeng You***

*Coordination Chemistry Institute, State Key Laboratory of Coordination Chemistry, Nanjing University, Nanjing 210093, P.R. China*

**A novel charge-transfer complex, $[4\text{-DMSP}]_4[NH_2Me_2]_2HSiFeMo_{11}O_{40}\cdot 3H_2O$ 1 {4-[DMSP]I = 4[*p*-(dimethylamino)styryl]pyridine methiodide} prepared and crystallized in a non-centrosymmetric (space group *P*1) structure, exhibits second harmonic generation (SHG) of 1064 nm radiation with an efficiency 1.2 times that of $KH_2PO_4$ under the same conditions.**

Non-linear optical (NLO) materials have attracted great interest in recent years, for their wide range of applications in laser technology, telecommunications, data storage and optical switches.[1–6] Most investigations, so far, have concentrated on inorganic crystals, organometallic compounds, organic molecules and polymers with delocalized $\pi$-electron systems.[7–15] It is known that there are three main factors influencing the magnitude of second harmonic generation, namely, (*a*) the presence of electron donor and acceptor groups in the molecule, (*b*) the nature and relative position of the groups and their ability to promote charge-transfer transitions between them and (*c*) extension of the conjugated path through which electrons are transferred under the influence of electric fields.

According to the concepts of 'molecular self-organization' and 'molecular engineering', we have designed and synthesized a new type of charge-transfer compound. We chose a hemicyanine dye as the organic cation, which contains electron donor and acceptor groups and possesses large SHG efficiency.[16,17] Since SHG is only observed in acentric materials, a simple way to meet this condition is to use molecules that can crystallize in accentric space groups. We selected Keggin structure heteropolyanions $XM_{12}O_{40}$ (X = P, Si; M = Mo, W) as electron acceptors, as $XO_4$ in the polyanions has $T_d$ symmetry and readily accepts electrons.[18] By using this method, a non-centrosymmetric molecular material is obtained when [4-DMSP]I and $[NBu_4]_4KH_2SiFeMo_{11}O_{40}$ are reacted. The procedure of design of such NLO molecular materials can be expressed by eqn. (1).

$$[\text{donor}\text{–}\pi\text{–acceptor}]^{+}{}_n[\text{polyanion}]^{n\ominus} \underset{h\nu_2}{\overset{h\nu_1}{\rightleftharpoons}} [\text{donor}\text{–}\pi\text{–acceptor}]^{1+\delta}{}_n[\text{polyanion}]^{n(1+\delta)\ominus} \quad (1)$$

In this work, we synthesized the charge-transfer salt $[4\text{-DMSP}]_4[NH_2Me_2]_2HSiFeMo_{11}\cdot 3H_2O$ **1**, and determined its SHG and crystal structure.

The determination of the second harmonic intensity of powdered samples (Kurtz powder test) was made relative to that of powdered $KH_2PO_4$. A pulse Q-switched Nd : YAG laser with a pulse (width 60 ps, repetition 1 Hz) of energy 1 mJ at a wavelength of 1064 nm was used to generate an SHG signal from the sample. The backward scattered SHG light was collected using a spherical concave mirror and passed through a filter which transmits only 532 nm radiation. Boxcar gate sampling was used to provide data points averaged over ten pulses and the mean of ten of these points provided the quoted values of relative harmonic intensity for second harmonic generation.

The electronic spectra of **1** [4-DMSP]I and $[NBu_4]_4KH_2SiFeMo_{11}O_{40}$ (*ca.* $1 \times 10^{-3}$ M) are shown in Fig. 1. Neither the cation $4\text{-DMSP}^+$ nor $[NBu_4]_4KH_2SiFeMo_{11}O_{40}$ show any absorption in the range 600–1100 nm. However, **1** shows a broad absorption in this range, and a weak absorption at *ca.* 1000 nm, which suggests the presence of a strong charge-transfer interaction between the polyanion and the organic cation and explains the source of second harmonic generation.

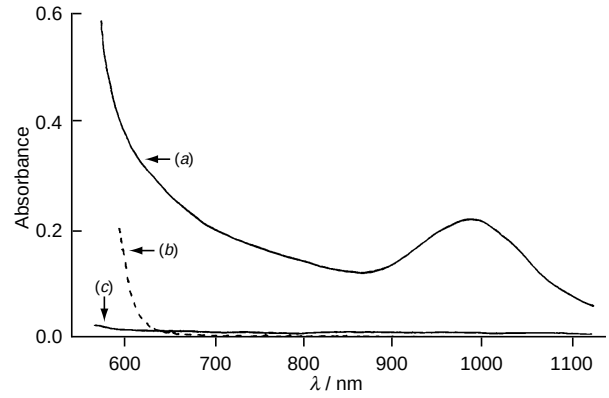



**Fig. 1** Comparison of the electronic spectra of [4-DMSP]I, $[NBu_4]_4KH_2SiFeMo_{11}O_{40}$ and **1** in dmf; (*a*) **1**, (*b*) [4-DMSP]I, (*c*) $[NBu_4]_4KH_2SiFeMo_{11}O_{40}$. All spectra were obtained for $1 \times 10^{-3}$ M solutions at 15 °C.

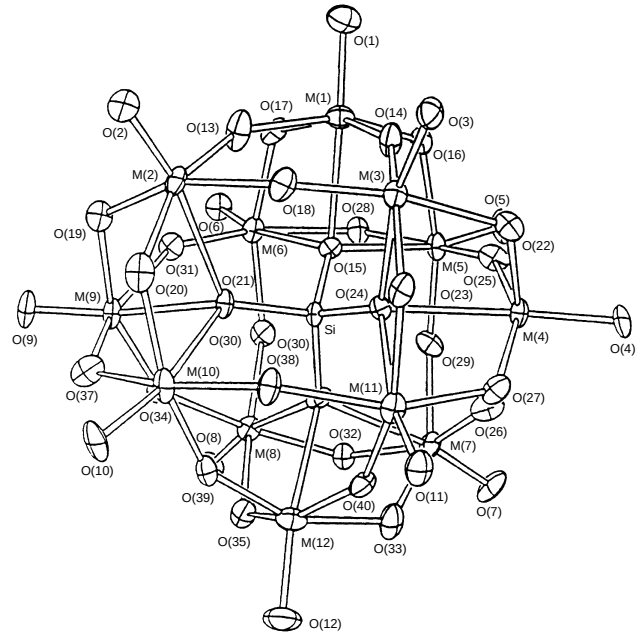



**Fig. 2** ORTEP of the polyoxoanion $[SiFeMo_{11}O_{40}]^{7-}$, showing 30% thermal elipsoids; M represents Fe or Mo (SOF = 11/12 for Mo and 1/12 for Fe at each M atom). Average bond distances (Å) for the polyoxoanion: Si–$O_a$ (central) 1.612(3), M–$O_a$ 2.357(3), M–$O_t$ (terminal) 1.673(3), M–$O_b$ (bridging) 1.871(3).

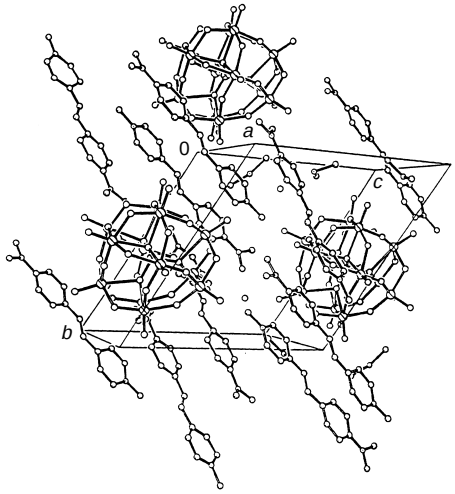



**Fig. 3** Crystal packing of **1** viewed down the *a* axis

The X-ray crystal structure analysis indicates that **1** crystallizes in the space group $P\bar{1}$, and the molecular structure is shown in Fig. 2, with the molecule packing diagram shown in Fig. 3. The shortest contacts between the polyanion and organic cation are C(16)···O(4) 3.056(3) Å and C(49)···O(5) 2.963(3) Å, respectively, indicating the presence of strong hydrogen bonding. This means that there is an interaction between the polyanion and the organic substrate, leading to partial charge transfer.

A significant new result from the work is that the design and synthesis of a new type of charge-transfer salt from the view point of molecular engineering has led to a material which possesses a larger SHG than $KH_2PO_4$ and is the most efficient than that we have ever reported.[19] However, the SHG is lower than that reported for some transition-metal complexes.[20] The above result shows that a new system showing non-linear optical properties is found and we expect enhanced properties if the polyoxometalates are mixed valence species.[21]

We thank Associate Professor Z.-G. Cai for the SHG measurement. Our thanks are also given to the State Science and Technology Commision and the National Nature Science Foundation of China.

## Footnotes

* E-mail: cciuu@netra.nju.edu.cn

† Complex **1** was prepared by reacting 139.4 mg (0.5 mmol) of $[NBu_4]_4KH_2SiFeMo_{11}O_{40}$[22] dissolved in 20 ml of acetonitrile with 915.6 mg (2.5 mmol) of [4-DMSP]I. A suitable red prism crystal obtained from dmf was investigated by single-crystal X-ray diffraction.

‡ *Crystal data* for $C_{68}H_{97}FeMo_{11}N_{10}O_{43}Si$, triclinic, space group $P\bar{1}$, $a$ = 13.647(3), $b$ = 14.877(2), $c$ = 15.279(2) Å, $\alpha$ = 105.53(1), $\beta$ = 108.71(2), $\gamma$ = 111.35(2)°, $U$ = 2462.7(6) Å$^3$, $Z$ = 1. A red prismatic crystal with dimensions of 0.32 × 0.28 × 0.22 mm was mounted on a glass fibre. The intensities were collected at 291 K on a Siemens P4 four-circle diffractometer with monochromated Mo-K$\alpha$ ($\lambda$ = 0.710 73 Å) radiation using the $\theta$–2$\theta$ scan mode with a variable scan speed 5.0–50.0° min$^{-1}$ in $\omega$. The data were corrected for Lorentz and polarization effects during data reduction using XSCANS. The structure was solved by direct methods and refined on $F^2$ by full-matrix least-squares methods using SHELXTL (version 5.0). The two $NH_2Me_2^+$ ions are disordered [site occupancy factor (SOF) is 1/2 for N(10), C(68) and N(11), C(69), C(70), respectively]. In the polyanion structure, the positions of Fe and Mo atom can not be indentified; M represents Fe or Mo (SOF = 11/12 for Mo, and 1/12 for Fe at each M atom). All the non-hydrogen atoms were refined anisotropically. All the hydrogen atoms were placed in caculated positions (C–H 0.96 Å) assigned fixed isotropic thermal parameters at 1.2 times the equivalent isotropic $U$ of the atoms to which they are attached (1.5 times for the methyl groups) and allowed to ride on their respective parent atoms. The contributions of these hydrogen atoms were included in the structure-factor calculations. Structure solution and refinement based on 12 255 reflections and 1234 parameters gave $R_1$ = 0.0667. Atomic coordinates, bond lengths and angles, and thermal parameters have been deposited at the Cambridge Crystallographic Data Centre (CCDC). See Information for Authors, Issue No. 1. Any request to the CCDC for this material should quote the full literature citation and the reference number 182/465.

## References

1 *Molecular Nonlinear Optics: Materials, Physical and Devices*, ed. J. Zyss, Academic Press, Boston, MA, 1993.
2 *Introductive to Nonlinear Optical Effects in Molecular and Polymers*, ed. P. N. Prasad and D. J. Williams, Wiley, New York, 1991.
3 *Nonlinear Optical Materials*, ed. H. Kuhn and J. Robillard, CRC Press, Boca Raton, FL, 1992.
4 G. J. Ashwell, R. C. Hargreaves, C. E. Baldwin, G. S. Bahra and C. R. Brown, *Nature*, 1992, **357**, 393.
5 R. G. Denning, *J. Mater. Chem.*, 1995, **5**, 365.
6 D. F. Eaton, *Science*, 1991, **253**, 281.
7 P. A. Franken, A. E. Hill and C. W. Peters, *Phys. Rev. Lett.*, 1961, **7**, 118.
8 G. D. Boyd, R. C. Miller, K. Nassau, W. L. Bond and A. Savage, *Appl. Phys. Lett.*, 1964, **5**, 234.
9 N. S. P. Bhuvanesh, B. Ragharendra Prasad, C. K. Subramanian and J. Gopalakrishnan, *Chem. Commun.*, 1996, 289.
10 D. J. Williams, *Angew. Chem., Int. Ed. Engl.*, 1984, **23**, 690.
11 *Nonlinear Optical Properties of Organic Molecules*, ed. G. Khanarian, SPIE, Bellingham, WA, 1988, p. 971.
12 *Nonlinear Optical and Electroactive Polymers*, ed. P. N. Prasad and D. R. Ulrich, Plenum, New York, 1988.
13 C. Dehu, F. Meyers and J. L. Bredas, *J. Am. Chem. Soc.*, 1993, **115**, 6198.
14 W. E. Moerner and S. M. Silence, *Chem. Rev.*, 1994, **94**, 127.
15 L. Daqi, C. Guanhua, W. P. Joseph and A. G. William, *J. Am. Chem. Soc.*, 1994, **116**, 10 697.
16 T. Yoshimura, *J. Appl. Phys.*, 1987, **62**, 2028.
17 R. S. Marder, J. W. Perry and W. P. Schaefer, *Science*, 1989, **245**, 626.
18 M. T. Pope, *Heteropoly and Isopoly Oxometalates*, Springer, Berlin, 1983.
19 J.-Y. Niu, X.-Z. You, C.-Y. Duan, H.-K. Fun and Z.-Y. Zhou, *Inorg. Chem.*, 1996, **35**, 4211.
20 B. J. Coe, J.-D. Foulon, T. A. Hamor, C. J. Jones, J. A. McCleverty, D. Bloor, G. H. Cross and T. L. Axon, *J. Chem. Soc., Dalton Trans.*, 1994, 3427.
21 W. M. Laidlaw, R. G. Denning, T. Verbiest, E. Chauchard and A. Persoons, *Nature*, 1993, **362**, 58.
22 K. Nomiya, M. Sugaya and M. Miwa, *Bull. Chem. Soc. Jpn.*, 1979, **52**, 3107.

*Received in Cambridge, UK, 2nd January 1997; Com. 7/00025A*

# Conversion of alkenes and alcohols to azides over zeolite-supported sodium azide

**R. Sreekumar,*[a] R. Padmakumar[b] and P. Rugmini[b]**

[a] *Department of Physiology, University of Wisconsin, Madison, USA*
[b] *Department of Chemistry and Biochemistry, University of Nebraska, Lincoln, USA*

**Zeolite-supported sodium azide reagents are versatile catalysts for the conversion of various alkenes and alcohols to the corresponding azides in good yield under mild conditions.**

Azides are important precursors of nitrenes or amino compounds and belong to a large family of 1,3-dipoles which undergo cycloaddition to alkenes.[1] While aromatic azides can be obtained by a variety of methods, aliphatic azides are mainly prepared by substitution of alkyl halides, diazo transfer to aliphatic amines or additions to alkenes.[2] In recent years there have been several reports on the use of zeolites for selective organic transformations leading to the synthesis of various fine chemicals.[3–5] Here we report a convenient heterogeneous catalytic methodology for the conversion of alkenes and alcohols to the corresponding azides over zeolite-supported sodium azide reagents (Table 1).

The alkenes and alcohols were purchased from Aldrich and Fluka Chemical Co. and the zeolites (Y-Zeolite, EMT, ZSM-5 and Zeolite beta) were synthesized according to the reported procedure.[6] The Na-zeolites thus obtained were converted to H-zeolites by treatment with aqueous $NH_4Cl$ followed by filtration and activation at 450 °C for 12 h.

Zeolite-supported sodium azide reagents were prepared by dissolving $NaN_3$ (1 mmol) in 5 ml of deionized water in a 15 ml flask. About 0.75 g of Zeolite were then added and the mixture was stirred for 3 h at room temperature. The mixture was then filtered and washed several times with deionized water. Prior to use the zeolite supported reagents were further dried at 65 °C (5 Torr) for 2 h in a current of air.

The loading amount of $NaN_3$ (*A* wt%) and the amount of residual water (*B* wt%) on a zeolite supported reagent were defined as shown in eqns. (1) and (2), where *z* is the weight

$$A = 100\ \{z / [z+(1-\alpha/100)y]\} \quad (1)$$

$$B = 100\{[W - W_o - z(1 - \alpha/100)y]/(W - W_o)\} \quad (2)$$

of $NaN_3$ supported, *y* is the weight of zeolite used, $\alpha$ is the wt% of physisorbed water in the zeolite, $W_o$ is the mass of the flask used for the preparation of the zeolite supported reagent and *W* is the mass of the flask containing the zeolite supported reagent after drying at 65 °C (5 Torr) for 2 h. The value of $\alpha$ was determined by thermogravimetric analysis of the zeolite-supported reagent in the temperature range of 30–250 °C. The zeolite supported reagent used for the present study contained 8 wt% loading of $NaN_3$ and 15 wt% of residual water. Zeolites consist of small uniform pores or channels and the exterior surface area of zeolite is only 0.5–2.0% of the total surface area.[7] Hence most of the supported $NaN_3$ seems to be finely dispersed inside the pores or channels of zeolite and interacts with water molecules or hydroxy groups on the surface of the zeolite. The role of the small amount of water associated with supported reagents and its reactivity has been discussed by Ando *et al.*[7] Probably the water molecules, as well as the hydroxy groups on the zeolite surface, coordinate to the dispersed $NaN_3$ to loosen the ion-pairing of $[Na^+\cdots N_3^-]$, leading to the enhancement in nucleophilicity of the azide anion.

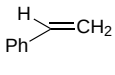
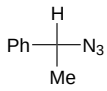
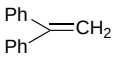
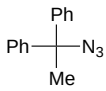
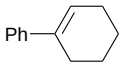
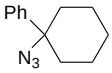
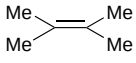
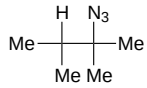
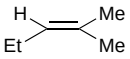
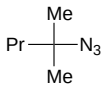
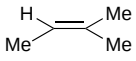
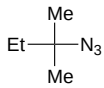
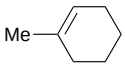
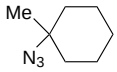
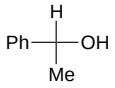
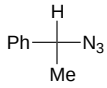
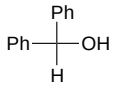
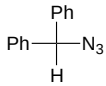
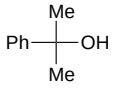
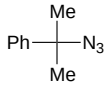
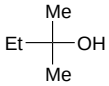
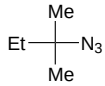
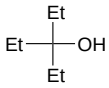
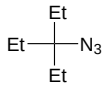
Azide ions ($N_3^-$) have strong and characteristic IR bands in the region of 2100 $cm^{-1}$ arising from the asymmetric stretching mode while the solid $NaN_3$ has a diagnostic absorption at 2130 $cm^{-1}$.[8] A 25 wt% $NaN_3$ supported zeolite reagent shows a new peak at 2065 $cm^{-1}$ in addition to the parent peak at 2130 $cm^{-1}$, whereas 8 wt% loaded samples have an absorption peak at only 2065 $cm^{-1}$ (Nujol mull). After zeolite-supported reagents (1 g) were treated with styrene (1 mmol) in the different solvents listed in Table 2 (10 ml) at 70 °C for 2 h, the supported reagents were analysed immediately by IR spectroscopy. It was found that the intensity of the peak at 2065 $cm^{-1}$ decreased dramatically compared with the peak at 2130 $cm^{-1}$ in 25 wt% $NaN_3$ supported zeolite reagents. In the case of 8 wt% loaded samples, the intensity of 2065 $cm^{-1}$ peak was very low. These results indicate that the azide ions showing the lower frequency peak of 2065 $cm^{-1}$ are much more reactive for the conversion of alkenes and alcohols to the corresponding azides than the azide ions which appeared at 2130 $cm^{-1}$. Hence, we speculate that the finely dispersed form of $NaN_3$ shows absorption at 2065 $cm^{-1}$ and the coagulated $NaN_3$ crystals exhibit absorption at 2130 $cm^{-1}$. Under the same reaction conditions, the low loading (8 wt%) samples show higher reactivity for the conversion of styrene to 1-azido-1-phenylethane (84%) compared to a 25 wt% loaded samples (42%). Hence in further studies 8 wt% $NaN_3$ supported zeolite reagents were used.

Initially the reactions were carried out in a flow reactor as reported elsewhere.[5] The styrene (1 mmol) dissolved in dry cyclohexane (20 ml) was introduced at the top of the reactor by means of an infusion pump (flow rate 20 ml $h^{-1}$). The liquid products were collected in a water-cooled receiver and the removal of cyclohexane did not furnish any product. The zeolite was removed from the reactor and extracted with 50 ml of methanol. Analysis of the methanol extract by GC (Hewlett Packard, 5890 Series II, gas chromatograph with a flame ionization detector, capillary column : OV-1, 25 m) showed only 29% conversion of styrene to 1-azido-1-phenylethane.

The experiments were then carried out in a magnetically stirred Teflon-lined autoclave equipped with a temperature controller. Styrene (1 mmol) dissolved in 10 ml of dry cyclohexane was added to a suspended mixture of HY-zeolite-supported $NaN_3$ (1 g) in cyclohexane (15 ml) and the mixture was stirred at 70 °C for 2 h under nitrogen atmosphere, after which it was filtered. The cyclohexane filtrate did not contain any dissolved matter. The product was extracted from the pores of the zeolite by washing with methanol (3 × 50 ml). Removal of methanol and further purification of the crude material by flash chromatography using an alumina column and $CH_2Cl_2$ as eluent furnished 84% of the corresponding azide. The recovered zeolite could be reused after $NaN_3$ treatment and activation.

Even in a heterogeneous reaction system where the zeolite supported $NaN_3$, a reactant and a solvent were mixed, the polarity of the solvent influenced the reaction rate to a significant extent. The extent of conversion of styrene and 1-phenylethanol to the corresponding azide in different solvents over HY-zeolite and HEMT supported reagents at 70 °C for 2 h was found to be in the order of cyclohexane > $C_6H_6$ > $CHCl_3$ > MeCN, and the results are summarized in Table 2. This could

**Table 1** Comparison of the yields of various azides over different zeolite-supported $NaN_3$[a]

| Substrate | Product[b] | Yield (%)[c] HY-Zeolite | HEMT | HZSM-5 | H-Zeolite beta |
|---|---|---|---|---|---|
|  |  | 84 | 82 | 76 | 79 |
|  |  | 72 | 69 | 56 | 64 |
|  |  | 89 | 73 | 70 | 80 |
|  |  | 93 | 87 | 85 | 91 |
|  |  | 76 | 68 | 71 | 75 |
|  |  | 91 | 86 | 82 | 78 |
|  |  | 90 | 92 | 80 | 76 |
| $PhCH_2OH$ | $PhCH_2N_3$ | 82 | 69 | 76 | 74 |
|  |  | 90 | 94 | 70 | 86 |
|  |  | 77 | 82 | 61 | 73 |
|  |  | 86 | 72 | 65 | 78 |
| $Bu^tOH$ | $Bu^tN_3$ | 93 | 89 | 91 | 88 |
|  |  | 90 | 81 | 74 | 79 |
|  |  | 84 | 76 | 71 | 80 |

[a] $T$ = 70 °C, $t$ = 2 h. [b] All products were characterized by IR, $^1H$ NMR and mass spectral data. [c] Yield of isolated pure compounds.

be attributed to the stronger adsorbtion of solvent on the zeolite surface affecting (weakening) its acidic properties.

In order to compare homogeneous reagent systems with the zeolite-supported reagent system, styrene dissolved in aqueous methanol was treated with $NaN_3$ and unsupported HY-zeolite at 70 °C for 2 h and furnished 1-azido-1-phenylethane in low yield (14%); in the case of 1-phenylethanol the yield of the corresponding azide was only 12%. In a control experiment, triphenylmethanol (1 mmol), a molecule which cannot enter the pores of HZSM-5 due to its large size, was dissolved in 10 ml of dry cyclohexane and added to a suspention of zeolite-supported $NaN_3$ (1 g) in dry cyclohexane (15 ml). The reaction

**Table 2** Effect of solvent in the conversion of styrene and 1-phenylethanol to the corresponding azide over HEMT and HY-zeolite[a]

| Solvents | Yield[b,c] HY-Zeolite | HEMT |
|---|---|---|
| Cyclohexane | 84 (90) | 82 (94) |
| $C_6H_6$ | 69 (73) | 76 (67) |
| $CHCl_3$ | 42 (34) | 39 (30) |
| MeCN | 9 (5) | 11 (7) |

[a] $T$ = 70 °C, $t$ = 2h. [b] Yield of isolated pure product. [c] Yield of azide from 1-phenylethanol in parentheses.

mixture was stirred for 2 h at 70 °C and afforded the corresponding azide in 5% yield, while over HY-zeolite (a large pore zeolite)-supported reagent the yield of the azide was 68%. This result indicates that in zeolite-supported $NaN_3$ reagents most of the $NaN_3$ is located inside the pores, not on the outside surface of the zeolites. Silica gel and alumina mediated addition of $HN_3$ to alkenes has been studied in the past and attempts to add $HN_3$ to diphenylethene in the presence of a strong acid, such as sulfuric acid, led to considerable decomposition due to the susceptability of the resulting azide to protonation and Schmidt rearrangement.[9] The observed efficient performance of HY-zeolite may be attributed to its large pore openings (0.74 nm) and three dimensional channel system and the comparitively low yields of the desired products over HZSM-5 may be due to its small pore opening (0.56 nm).[7] Zeolite-supported sodium azide, when mediating the conversion of alkenes to the corresponding azides, furnished only the Markovnikoff product.

In summary, we have established a facile heterogeneous catalytic method for the conversion of alkenes and alcohols to the corresponding azides. The positive features of these inexpensive zeolites include stability, ease of handling, lack of corrosiveness and other environmental hazards and ease of separation of the product and regeneration of the catalyst.

R. S. thanks Professor C. N. Pillai, IIT, Madras and Professor J. Weitkamp, University of Stuttgart, Germany, for providing the facilities for the synthesis of zeolites.

## References

1 R. S. Atkinson, in *Comprehesive Organic Chemistry*, Pergamon Press, Oxford, 1987, vol. **2**, p. 256; *Chemistry of the Azido Groups*, ed. S. Patai, Interscience, New York, 1971.
2 P. A. S. Smith, *Open-Chain Nitrogen Compounds*, Benjamin, New York, 1966, vol. II, pp. 211–256.
3 W. Holderich, Hesse and F. Naumann, *Angew. Chem., Int. Ed. Engl*., 1988, **27**, 226; V. Ramamurthy, D. R. Corbin and L. J. Johnston, *J. Am. Chem. Soc*., 1992, **114**, 3870.
4 S. L. Suib, *Chem. Rev*., 1993, **93**, 803; V. Ramamurthy, D. R. Corbin and D. F. Eaton, *J. Org. Chem*., 1990, **55**, 5269.
5 R. Sreekumar, Y. V. S. N. Murthy and C. N. Pillai, *J. Chem. Soc*., *Chem. Commun*., 1992, 1624; R. Sreekumar and C. N. Pillai, *Catal. Lett*., 1993, **19**, 281; R. Sreekumar and R. Padmakumar, *Tetrahedron Lett*., 1996, **30**, 5281.
6 F. Dougnier, J. Patarin, J. L. Guth and D. Anglerot, *Zeolites*, 1992, **12**, 160; P. Caullet, J. Hazm, J. L. Guth, J. F. Joly, J. Lynch and F. Raatz, *Zeolites*, 1992, **12**, 240; R. L. Argauer and G. R. Landolf, *US Pat*., 3 702 886, 1972.
7 T. Ando, T. Kawate, J. Yamawaki and T. Hanafusa, *Chem. Lett*., 1982, 935 and references cited therein; P. B. Venuto and P. S. Landis, in *Advances in Catalysis*, ed. D. D. Eley and H. Pines, Academic Press, New York, 1968, vol. 18, p. 259.
8 L. J. Bellamy, *The Infra-red Spectra of Complex Molecules*, 2nd edn., Chapman and Hall, London, 1980, vol. 2, p. 65.
9 G. W. Breton, K. A. Daus and P. J. Kropp, *J. Org. Chem*., 1992, **57**, 6646; S. N. Ege and K. W. Sherk, *J. Am. Chem. Soc*., 1953, **75**, 354.

*Received in Corvallis, OR, USA, 27th January 1997; Com. 7/00627F*

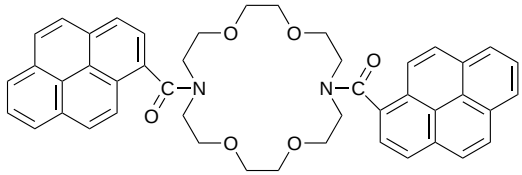
# Fluorescent diaza crown ether sensitive to complexation, conformation and microenvironment

**Greg E. Collins* and Ling-Siu Choi**

*Naval Research Laboratory Chemistry Division, Code 6116 Washington DC 20375-5342, USA*

**A newly synthesized diaza crown ether, BPDC, demonstrates sensitivity to solvent polarity, microviscosity and metal complexation with spectroscopic changes in monomer and excimer fluorescence.**

In order to address the sensing challenges presented by complex, real-world matrices, we are designing new molecules tailored with fluorescent sidearms sensitive to the complexation, molecular conformation and microenvironment of the sensing molecule. Specifically, our interest is in the development of a metal sensing probe operable in ship bilge water, a matrix that contains heavy-metal ions in a complex and variable environment of surfactants, oils, and other contaminants. To study the nature of metal complexation in these environments, we synthesized a new, sensor molecule, *N*,*N*-bis(1-pyrenecarbonyl)-7,16-diaza 18-crown-6 (BPDC), designed to signal the sensitive complexation of heavy-metal ions, as well as respond spectroscopically to changes in its microenvironment. While bis-pyrene linked probes have been previously used for monitoring microviscosity,[1] metal ion concentration,[2] and organics,[3] this communication describes the response to all three of these variables together in a single probe.



BPDC

The vibronic fine structure of pyrene fluorescence is very sensitive to solvent polarity changes with changes in the ratio of $I_1/I_3$.[4] According to their protic or aprotic nature, solvents were classified into two, linear polarity scales by BPDC. Comparison of the $I_1/I_3$ ratios and Dimroth's $E_T$ values are shown in Fig. 1. The $E_T$ scale is an excellent measure of solvent polarity generated from the intramolecular charge-transfer band of Reichardt's dye.[5]

The ability of BPDC to form an intramolecular excimer provides additional insight into the conformation and microviscosity experienced by this sensor molecule. The intensity of excimer fluorescence, $I_e$, is correlated with the probability that an excited pyrene moiety can rotate to a position of close, parallel molecular contact with an unexcited pyrene neighbour prior to its own electronic, excited singlet state decay (as monomer fluorescence, $I_{monomer}$).[6] This probability is dependent on both (*i*) the conformation of the molecule in the solvent, a feature that is strongly linked to the solvent's relative permittivity $\varepsilon$, and (*ii*) the viscosity, $\gamma$, of the medium. A plot of the relative monomer emission, $I_m$ [$I_m = I_{monomer}/(I_{monomer}{}^{+}I_e)$], from BPDC *vs*. the product $\varepsilon\gamma$ for various protic and aprotic solvents is shown in Fig. 2. With the exception of *n*-hexane and *n*-heptane, the possibility of intermolecular excimer formation was precluded by sequential dilution of BPDC until no changes were evident in $I_m$.

Examining the aprotic solvents in Fig. 2, as the solvent changes from *n*-heptane to $CHCl_3$ [(*a*)–(*f*)] there is only a minor change in the viscosity. This indicates that it is the increase in relative permittivity which is primarily responsible for the increase in monomer emission. BPDC has very low solubility in solvents of low relative permittivity, *n*-hexane and *n*-heptane, owing to poor solvation of the crown ether backbone. Aggregation of BPDC could explain the smaller $I_m$ values apparent in these solvents. As the relative permittivity of the solvent increases, the solvent sheath formed about the crown ether backbone forces apart the two pyrene moieties. For solvents with $\varepsilon > 7$, both the crown ether backbone and pyrene linkages are effectively solvated and BPDC adopts a similar conformation with $I_m$ *ca.* 0.7.

For protic solvents, as the solvents progress from methanol to pentanol [Fig. 2(*i*)–(*m*)], the increase in viscosity causes the

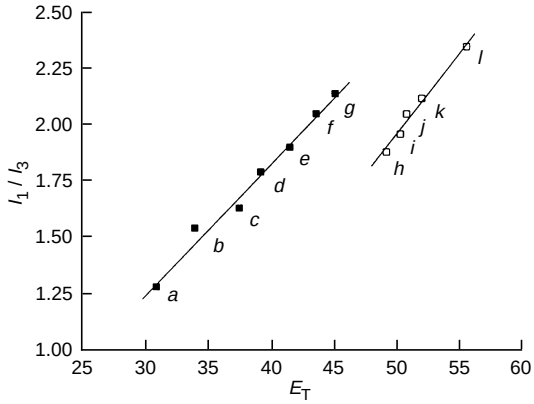



**Fig. 1** Plot of the intensity ratio $I_1/I_3$ from the emission of BPDC *vs*. Dimroth's $E_T$ values in various aprotic (■) and protic (□) solvents. Solvent: (*a*) *n*-hexane, (*b*) toluene, (*c*) THF, (*d*) $CHCl_3$, (*e*) $CH_2Cl_2$, (*f*) DMF, (*g*) $Me_2SO$, (*h*) *n*-pentanol, (*i*) *n*-butanol, (*j*) *n*-propanol, (*k*) ethanol, (*l*) methanol; [BPDC] = 2.9 μM.

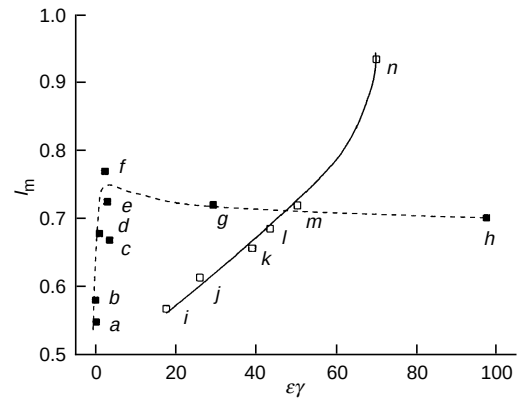



**Fig. 2** Plot of the relative monomer emission, $I_m$, from BPDC *vs*. the product of the relative permittivity ($\varepsilon$) and the viscosity ($\gamma$). Aprotic solvents (■): (*a*) *n*-heptane (*b*) *n*-hexane, (*c*) $CH_2Cl_2$, (*d*) toluene, (*e*) THF, (*f*) $CHCl_3$, (*g*) DMF, (*h*) $Me_2SO$; protic solvents (□): (*i*) methanol, (*j*) ethanol, (*k*) *n*-propanol, (*l*) *n*-butanol, (*m*) *n*-pentanol, (*n*) water; [BPDC] = 2.9 μM.

monomer emission to increase owing to a reduction in mobility of the pyrene appendages as well as an improvement in solvation of the pyrene groups. Water, because of its extremely high relative permittivity and hydrogen-bonding ability, leads to the highest monomer emission for BPDC. This result is in contrast to the majority of bis-pyrene molecules studied previously, which exhibit significant intramolecular excimer formation in water due to the hydrophobic interaction of the two pyrene appendages.[7,8] For BPDC, water is apparently so effective at stabilizing the crown ether backbone that the pyrene moieties are effectively isolated from one another due to hydrophobic repulsion.

In order to monitor the influence of metal complexation on the conformation of BPDC the $I_1/I_3$ ratio and $I_m$ parameters were additionally studied. From Fig. 3 it is evident that as [$Cu^{II}$] increases, there is a strong quenching of the emission due to a paramagnetic effect of the complexed metal ion.[9] It is interesting to note from the inset chart that both $I_1/I_3$ and $I_m$ decrease linearly with the increase in [$Cu^{II}$]. Fig. 2 indicates that

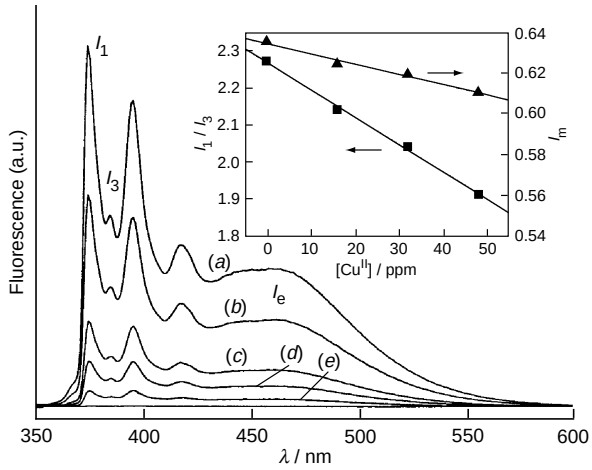



**Fig. 3** Fluorescence spectra recorded for BPDC in ethanol at different $CuCl_2$ concentrations. The inset chart graphs the change in $I_1/I_3$ and $I_m$ with the addition of $Cu^{II}$ metal ions in solution. [$CuCl_2$] in ppm = (*a*) 0, (*b*) 16, (*c*) 32, (*d*) 48, (*e*) 64, (*f*) 128; [BPDC] = 2.9 $\mu$M.

the two pyrene moieties of BPDC are preferentially oriented to one side of the crown ether backbone when dissolved in ethanol. As expected, complexation of a $Cu^{II}$ metal ion does not compete for binding on this side of the compound, but, instead, binds to the exposed, crown ether side. Distortion of the diaza crown ether binding sites for binding of the metal ion results in the two pyrene moieties being brought in closer proximity to each other, increasing intramolecular excimer formation. Similarly, the decrease seen in $I_1/I_3$ is indicative of the more non-polar environment encountered by the molecule due to the enhanced association of the two pyrene appendages on one side of the diaza crown ether.

In conclusion, the present study demonstrates that the introduction of bis-pyrene appendages to a metal complexing agent can be an important tool for understanding the complexation, conformation and microenvironment of the sensing molecule.

The authors gratefully acknowledge John H. Callahan and Mona Shahgholi for the mass spectroscopic identification of compound BPDC, and the Office of Naval Research for partial funding support of this study.

## Footnotes

* E-mail: gcollins@ccf.nrl.navy.mil

## References

1 K. A. Zachariasse, *Chem. Phys. Lett.*, 1978, **5**7, 429.
2 I. Aoki, H. Kawabata, K. Nakashima and S. Shinkai, *J. Chem. Soc., Chem. Commun.*, 1991, 1771.
3 I. Suzuki, M. Ohkubo, A. Ueno and T. Osa, *Chem. Lett.*, 1992, 269.
4 D. C. Dong and M. A. Winnik, *Photochem. Photobiol*, 1982, **35**, 17.
5 C. Reichardt, *Chem. Rev.*, 1994, **94**, 2319.
6 Y.-C. Wang and H. Morawetz, *J. Am. Chem. Soc.*, 1976, **98**, 3611.
7 K. Char, C. W. Frank and A. P. Gast, *Langmuir*, 1989, **5**, 1335.
8 J. H. Krech and S. L. Rose-Pehrsson, *Appl. Spectrosc.*, 1996, **50**, 1528.
9 B. L. Bales and M. Almgren, *J. Phys. Chem.*, 1995, **99**, 15 153.

*Received in Columbia, MO, USA; 24th February 1997; Com. 7/01240C*

# A superoctahedral complex derived from a polyoxometalate: the hexakis(arylimido)hexamolybdate anion $[Mo_6(NAr)_6O_{13}H]^{2\ominus}$

**Joseph B. Strong,[a] Brian S. Haggerty,[b] Arnold L. Rheingold[b] and Eric A. Maatta*[a]**

[a] *Department of Chemistry, Kansas State University, Manhattan, Kansas 66506, USA*
[b] *Department of Chemistry, University of Delaware, Newark, Delaware 19716, USA*

**Reaction of $[Mo_6O_{19}]^{2\ominus}$ with an excess of 2,6-diisopropylphenyl isocyanate (ArNCO) affords the title anion in which the hexamolybdate framework serves as an octahedral nexus for six terminal arylimido ligands.**

The rich diversity of structure and function afforded by various polyoxometalate clusters[1] is evidenced by their relevance in areas ranging from catalysis to chemotherapy to molecular magnetism.[2] In many instances, the global symmetry of a polyoxometalate ion conforms to that present within its core: for example, the idealized $T_d$ symmetry of the Keggin phosphomolybdate $[Mo_{12}O_{40}P]^{3\ominus}$ mirrors that of its encapsulated tetrahedral $[PO_4]^{3\ominus}$ unit, while the idealized $O_h$ symmetry of the Lindquist hexamolybdate $[Mo_6O_{19}]^{2\ominus}$ reflects the octahedral environment surrounding its central $[O]^{2\ominus}$ core. We were intrigued by the prospect of exploiting the radiating $O_h$ symmetry of the hexamolybdate by using this anion as a nexus for the construction of a superoctahedral derivative. Although multiple functionalization of polyoxometalates has been achieved in the preparations of various organoimido derivatives of $[Mo_6O_{19}]^{2\ominus}$,[3] and in the highly functionalized *p*-tolylimido complex $[Mo_{10}(NC_6H_4Me\text{-}p)_{12}O_{18}(py)_2]$,[4] a complete derivatization which maintained the global symmetry of the polyoxometalate parent had not been realized. Here we establish that the hexamolybdate ion can serve as an octahedrally directing template for the incorporation of six terminal arylimido ligands along the Cartesian axes of its framework.

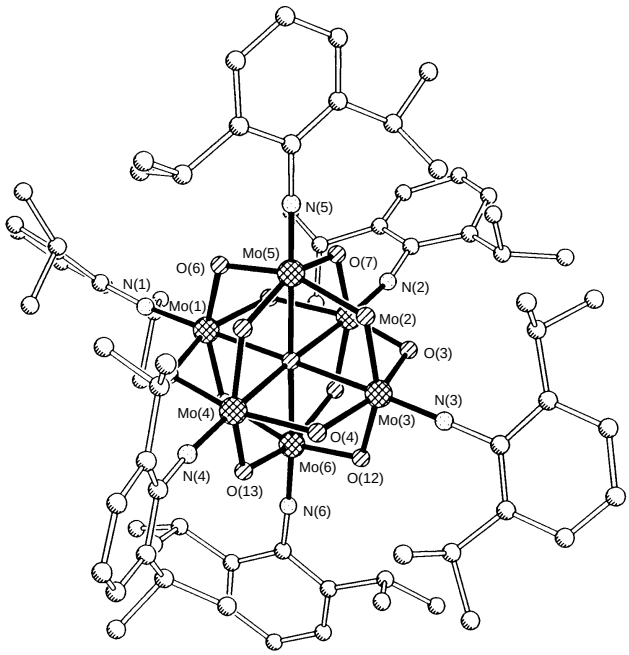



**Fig. 1** Structure of the $[Mo_6(NAr)_6O_{13}H]^{2\ominus}$ anion of **1**. Selected bond lengths (Å) and angles (°): Mo(1)–N(1) 1.725(10), Mo(2)–N(2) 1.737(14), Mo(3)–N(3) 1.742(11), Mo(4)–N(4) 1.727(14), Mo(5)–N(5) 1.755(10), Mo(6)–N(6) 1.734(10), Mo(1)–N(1)–C(6) 172.7(9), Mo(2)–N(2)–C(18) 170.5(9), Mo(3)–N(3)–C(30) 176.6(10), Mo(4)–N(4)–C(42) 171.0(10), Mo(5)–N(5)–C(54) 175.0(12), Mo(6)–N(6)–C(66) 176.4(12).

Reaction of $[NBu_4]_2[Mo_6O_{19}]$ with a twenty-fold molar excess of 2,6-diisopropylphenyl isocyanate (ArNCO) in refluxing pyridine for three weeks occurs with the evolution of $CO_2$ and the development of a dark orange–red solution. After removal of volatiles under vacuum and washing the residue with ether (in which some of the product dissolves), a red solid was obtained. Fractional crystallization ($CH_2Cl_2$–$Et_2O$) led to the initial separation of crystalline $[NBu_4]_2[Mo_6O_{14}(NAr)_5]$;[3a] the remaining mother-liquor was concentrated and additional ether vapour was admitted causing the growth of dark red crystals of $[NBu_4][Mo_6(NAr)_6O_{13}H]$ **1**, as the monoetherate in *ca.* 20% yield.† At room temperature, a single arylimido environment is seen in the $^1$H NMR spectrum of the complex. The incorporation of a proton into the hexamolybdate framework of **1** is without precedent among complexes derived from the $[Mo_6O_{19}]^{2\ominus}$ system and testifies to the greatly enhanced electron donation provided by the arylimido ligand set. Although no $^1$H NMR resonance for the bound proton was observed in either $CD_3CN$ or $CDCl_3$ solution, a band at 3550 $cm^{\ominus 1}$ in the IR spectrum of **1** corroborates its presence; the most likely source of the proton is through reaction with adventitious water. The IR spectrum is devoid of bands assignable as $\nu$(Mo≡O) in the 900–1000 $cm^{\ominus 1}$ region, containing only a single medium intensity absorption at 995 $cm^{\ominus 1}$, which may be associated with the Mo≡NAr units.

The molecular structure of the $[Mo_6(NAr)_6O_{13}H]^{2\ominus}$ anion as determined by single-crystal X-ray diffraction is shown in Fig. 1.‡ Six terminal arylimido ligands radiate from the octahedral $Mo_6$ core; the distance between opposed *para*-aryl carbon atoms averages 1.634 nm. The six Mo–N bond lengths span the range 1.725(10)–1.755(10) Å, and the associated Mo–N–C angles are all essentially linear [170.5(9)–176.6(10)°]. Comparison of the metrical data for the $\{Mo_6O_{13}\}$ core within **1** to that within the $[Mo_6O_{19}]^{2\ominus}$ parent reveals little perturbation as a result of the introduction of the six arylimido ligands: in **1**, the distances from the central O(1) atom to the surrounding set of six Mo atoms average 2.313(9) Å, while in the hexamolybdate the corresponding average is 2.319(4) Å.[5] Similarly, the Mo–O distances involving the $\mu$-O atoms of **1** span the range 1.903(7)–2.019(8) Å, while in $[Mo_6O_{19}]^{2\ominus}$ analogous bond lengths range from 1.855(4) to 2.005(4) Å. Scrutiny of the metrical parameters of **1** reveals no evidence for the localization of the proton; most likely, it is disordered over the twelve $\mu$-O atoms in the solid state.

We propose that in solution the proton undergoes rapid exchange throughout the set of $\mu$-O atoms, thus accounting for both its non-observance and the equivalence of the six arylimido ligand environments in the $^1$H NMR spectrum of **1**. A possible low-energy pathway for such a proton exchange can be visualized in the alternate view of the anion structure provided in Fig. 2, in which the isopropyl methyl groups have been omitted for clarity. Each particular $\mu$-O atom can be seen to be have four nearest-neighbour oxygen atoms which, in combination, define two trigonal faces of the superoctahedron. These $O_b\cdots O_b$ separations within the anion average 2.70 Å, a value

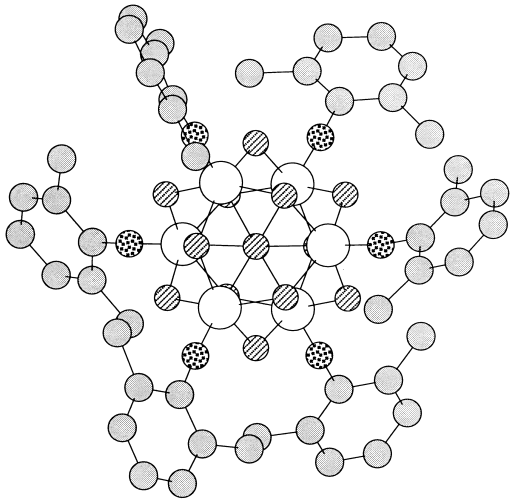


**Fig. 2** Alternate view of the $[Mo_6(NAr)_6O_{13}H]^{\ominus}$ anion emphasizing the $\{Mo_6O_{13}\}$ core

which is reminiscent of the corresponding 2.76 Å separation within ice[6] and which can enable facile proton migration *via* O–H···O interchanges.

If the superoctahedral derivatization of the hexamolybdate described herein can be replicated with organoimido ligands whose substituents bear appropriate remote functionality,[3c,7] then we can anticipate the designed construction of extended three-dimensional networks of tunable porosity; such systems are currently being explored.

We thank the Office of Basic Energy Sciences, Department of Energy (USA) for support of this work.

## Footnotes

* E-mail: eam@ksu.edu

† *Selected data* for **1**·$Et_2O$: $C_{92}H_{149}Mo_6N_7O_{14}$ requires (found) C, 51.33 (51.47); H, 6.98 (7.13); N, 4.55 (4.43%). $^1$H NMR (400 MHz, $CD_3CN$, 298 K): $\delta$ 7.12 (d, 12 H, *m*-Ar), 6.99 (t, 6 H, *p*-Ar), 4.03 (spt, 12 H, CH), 3.21 (q, 4 H, $OCH_2$), 3.06 (m, 8 H, $NCH_2$), 1.58 (m, 8 H, $CH_2$), 1.30 (m, 8 H, $CH_2$), 1.29 (d, 72 H, $CHMe_2$), 1.14 (q, 6 H, ether $CH_3$), 0.96 (t, 12 H, $CH_3$). Selected IR bands (thin film/ KBr plate): 3550, 995, 765, 751, 722 $cm^{\ominus 1}$. UV–VIS (MeCN): $\lambda_{max}$(log $\varepsilon$/$dm^3$ $mol^{\ominus 1}$ $cm^{\ominus 1}$) = 364(5.0), 271(5.1), 244(5.1), 208(5.2).

‡ *Crystal data* for **1**·$Et_2O$: Siemens R3m/V diffractometer, Mo-K$\alpha$ radiation, 249 K; dark red plate, monoclinic, space group $P2_1/c$, $a$ = 27.196(8), $b$ = 14.874(2), $c$ = 27.431(8) Å, $\beta$ = 116.45(2)°, $U$ = 9935(4) $Å^3$, $Z$ = 4, $M$ = 2152.9, $\mu$ = 0.795 $mm^{\ominus 1}$; 14087 independent reflections collected ($2\theta_{max}$ = 48°), 8291 observed [$F_o > 4\sigma(F_o)$] extinction correction, structure solved by direct methods and refined by full-matrix least squares (972 parameters), riding model (fixed isotropic $U$) for hydrogen atoms, $R(F)$ = 0.0684, $R(wF)$ = 0.0907. One of the butyl groups in the counter ion is severely disordered; the $\gamma$-carbon atom is disordered over two positions and the $\delta$-carbon atom could not be located. Atomic coordinates, bond lengths and angles, and thermal parameters have been deposited at the Cambridge Crystallographic Data Centre (CCDC). See Information for Authors, Issue No. 1. Any request to the CCDC for this material should quote the full literature citation and the reference number 182/458.

## References

1 M. T. Pope, *Heteropoly and Isopolyoxometalates*, Springer-Verlag, New York, 1983; M. T. Pope and A. Müller, *Angew. Chem., Int. Ed. Engl.*, 1991, **30**, 34.

2 *Polyoxometalates: From Platonic Solids to Anti-Retroviral Activity*, ed. M. T. Pope and A. Müller, Kluwer, Dordrecht, 1994.

3 (*a*) J. B. Strong, R. Ostrander, A. L. Rheingold and E. A. Maatta, *J. Am. Chem. Soc.*, 1994, **116**, 3601; (*b*) A. Proust, R. Thouvenot, M. Chaussade, F. Robert and P. Gouzerh, *Inorg. Chim. Acta*, 1994, **224**, 81; (*c*) W. Clegg, R. J. Errington, K. A. Fraser, S. A. Holmes and A. Schäfer, *J. Chem. Soc., Chem. Commun.*, 1995, 455.

4 A. Proust, S. Taunier, V. Artero, F. Robert, R. Thouvenot and P. Gouzerh, *Chem. Commun.*, 1996, 2195.

5 H. R. Allcock, E. C. Bissell and E. T. Shawl, *Inorg. Chem.*, 1973, **12**, 2963.

6 L. Pauling, *The Nature of the Chemical Bond*, Cornell University, Ithaca, 3rd edn., 1960, pp. 464 ff.

7 P. L. Hill, G. P. A. Yap, A. L. Rheingold and E. A. Maatta, *J. Chem. Soc., Chem. Commun.*, 1995, 737; J. B. Arterburn, I. M. Fogarty, K. A. Hall, K. C. Ott and J. C. Bryan, *Angew. Chem., Int. Ed. Engl.*, 1996, **35**, 2877.

*Received in Bloomington, IN, USA, 13th March 1997; Com. 7/01782K*

# Synthesis of manoalide using a 1,2-metallate rearrangement

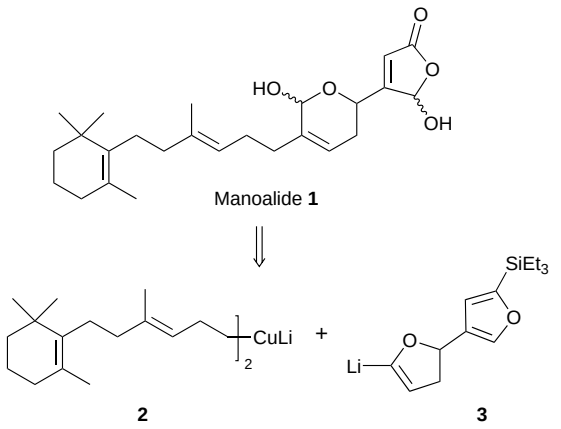
**Agnès Pommier and Philip J. Kocieński***

*Department of Chemistry, University of Glasgow, Glasgow, UK G12 8QQ*

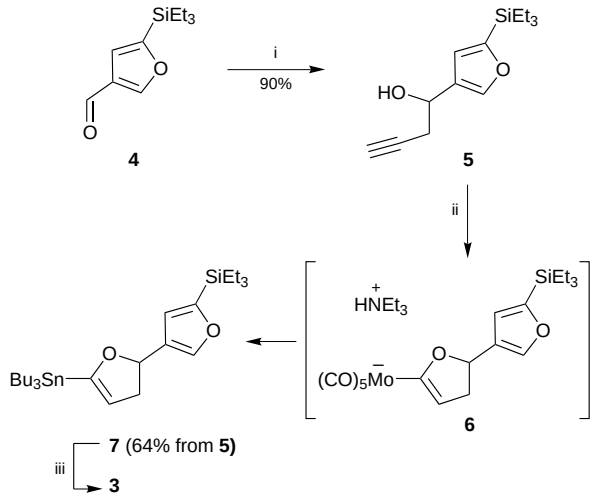
**Manoalide, a marine antiinflammatory sesterterpenoid, has been synthesised using a 1,2-metallate rearrangement of a higher order cuprate and a $Pd^0$-catalysed carbonylation of an iodo alkene to generate the central dihydropyranone ring.**

Manoalide **1** is a sesterterpenoid metabolite isolated from the Pacific sponge *Luffariella variablis*.[1] As a potent inhibitor of phospholipase $A_2$, it has been evaluated in phase II clinical trials for the treatment of psoriasis.[2] We now report a short synthesis of racemic manoalide from the homocuprate **2** and lithiated dihydrofuran **3** (Scheme 1) which features the use of a 1,2-metallate rearrangement of a higher order cuprate and a $Pd^0$-catalysed carbonylation of an iodo alkene to generate the central dihydropyranone ring.

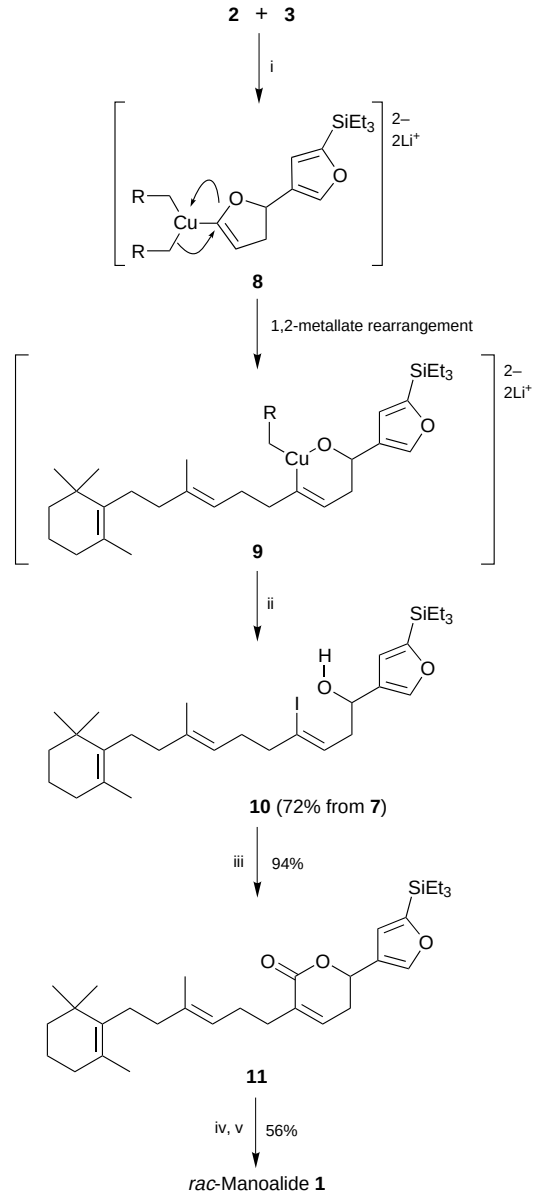
The lithiated dihydrofuran **3** was prepared as shown in Scheme 2. Addition of prop-2-ynylmagnesium bromide to 5-triethylsilyl-3-furaldehyde **4**† gave the homoprop-2-ynylic alcohol **5** in 90% yield. The Fischer carbene complex generated by electrophilic cyclisation of **5** with $(CO)_5Mo{\cdot}NEt_3$‡ was converted *in situ* to the alkenylstannane **7** in the presence of $Bu_3SnOTf$ according to the procedure of McDonald *et al.*[3] (64% overall from **5**). Transmetallation of the alkenylstannane to the desired alkenyllithium **3** was plagued by competing metallation at the 2-position of the furan ring and success was only achieved after a protracted study of the reaction conditions. Clean transmetallation was eventually accomplished with $Bu^sLi$




**Scheme 1**




**Scheme 2** *Reagents and conditions*: i, prop-2-ynylmagnesium bromide, $Et_2O$, ② 40 °C → room temp.; ii, $(CO)_5Mo{\cdot}NEt_3$, $Bu_3SnOTf$, $Et_2O$–$Et_3N$, room temp., 48 h; iii, $Bu^sLi$, $Et_2O$–pentane, ② 60 °C, 20 min




**Scheme 3** *Reagents and conditions*: i, add a solution of **3** in $Et_2O$–pentane to a solution of **2** in $Et_2O$–$Me_2S$ (1 : 1) at ② 40 °C; ii, $I_2$ (4 equiv.), ② 30 °C; iii, $Pd(PPh_3)_4$, $Pr^i_2NEt$, THF–MeOH, CO (2 atm), 60 °C, 24 h; iv, DIBAL-H, $CH_2Cl_2$, ② 80 °C; v, $O_2$, h$\nu$, rose bengal, MeOH, ② 80 °C

in a diethyl ether–pentane mixture at ② 60 °C for 20 min and the lithium reagent **3** used immediately in the next step.

The key step in our synthesis involved a 1,2-metallate rearrangement[4] of the higher order cuprate **8** derived from addition of alkenyllithium **3** to the lower order homocuprate **2**§ which occurred with clean inversion of configuration to give the alkenylcuprate **9** (Scheme 3). Attempts to carboxylate **9** with $CO_2$ in the presence of triethyl phosphite[5]—a ploy which had been successful in our synthesis of the related terpenoid luffariolide E[6,7]—failed to give any of the desired lactone **11**. We therefore quenched the alkenylcuprate **9** with iodine at ② 30 °C to give iodo alkene **10** in 72% overall yield from **7**, and then introduced the remaining carbon (94% yield) by $Pd^0$-catalysed carbonylation using a modification of conditions previously described by Heck.[8] Finally, reduction of the lactone to the lactol with DIBAL-H (94%) and photooxidation of the silylfuran (60%)[9] gave manoalide, identical by high field NMR spectroscopy ($^1H$ and $^{13}C$) and mass spectrometry with a sample prepared previously and correlated with the natural product.[10]

The synthesis of racemic manoalide reported herein was accomplished in a total of 12 steps (4% overall) from commercially available *β*-ionone and 3-furaldehyde. The discovery of conditions for transmetallating stannyldihydrofuran **6** without competing metallation of the furan was a crucial advance. Another tactical advance was the iodination of the metallate rearrangement product **10** which provided a clean, efficient and highly stereoselective route to the (*Z*)-iodo alkene **11**, itself a useful precursor to a wide range of trisubstitued alkenes. The overall yield of our synthesis compares favourably with previous syntheses.[10–14]

We thank the EPSRC for financial support, Dr Michael Garst for NMR spectra of authentic manoalide and Rhonan Ford for technical advice.

## Footnotes

* E-mail: p.kocienski@chem.gla.ac.uk

† 5-Triethylsilyl-3-furaldehyde was prepared in one pot from commercial 3-furaldehyde in 73% yield by (i) addition of lithium morpholide to the aldehyde; (ii) metallation of the resultant adduct with $Bu^sLi$, and (iii) addition of chlorotriethylsilane (ref. 15).

‡ The yellow complex $(CO)_5Mo{\cdot}NEt_3$ is formed by irradiation of hexacarbonylmolybdenum with intense visible light (Hg lamp) in diethyl ether containing triethylamine at 0 °C.

§ For details of the preparation of cuprate **2** see ref. 6. The homoallylic iodo alkane precursor to cuprate **2** was prepared in four steps (25% overall) from *β*-ionone by analogy to the procedure described for the corresponding homoallylic bromo alkane (ref. 10).

## References

1 E. D. de Silva and P. J. Scheuer, *Tetrahedron Lett.*, 1980, **21**, 1611.
2 G. W. De Vries, G. Lee, L. Amdahl, M. Wenzel, D. Harcourt, J. Holmes, E. Syage, M. Garst and L. A. Wheeler, *Drugs Future*, 1990, **15**, 460.
3 F. E. McDonald, C. C. Schultz and A. K. Chatterjee, *Organometallics*, 1995, **14**, 3628.
4 P. Kocieński, S. Wadman and K. Cooper, *J. Am. Chem. Soc.*, 1989, **111**, 2363.
5 J.-F. Normant, G. Cahiez, C. Chuit and J. Villieras, *J. Organomet. Chem.*, 1974, **77**, 281.
6 G. Hareau-Vittini, P. Kocieński and G. Reid, *Synthesis*, 1995, 1007.
7 G. Hareau-Vittini and P. Kocieński, *Synlett*, 1995, 893.
8 A. Schoenberg, I. Bartoletti and R. F. Heck, *J. Org. Chem.*, 1974, **39**, 3318.
9 G. C. M. Lee, E. T. Syage, D. A. Harcourt, J. M. Holmes and M. E. Garst, *J. Org. Chem.*, 1991, **56**, 7007.
10 P. Bury, G. Hareau-Vittini, P. Kocieński and D. Dhanak, *Tetrahedron*, 1994, **50**, 8793.
11 S. Katsumura, S. Fujiwara and S. Isoe, *Tetrahedron Lett.*, 1985, **26**, 5827.
12 S. Katsumura, S. Fujiwara and S. Isoe, *Tetrahedron Lett.*, 1988, **29**, 1173.
13 M. E. Garst, E. A. Tallman, J. N. Bonfiglio, D. Harcourt, E. B. Ljungwe and A. Tran, *Tetrahedron Lett.*, 1986, **27**, 4533.
14 V. E. Amoo, S. De Bernardo and M. Weigele, *Tetrahedron Lett.*, 1988, **29**, 2401.
15 G. C. M. Lee, J. M. Holmes, D. A. Harcourt, and M. E. Garst, *J. Org. Chem.*, 1992, **57**, 3126.

*Received in Liverpool, UK, 21st March 1997; Com. 7/01936J*

# The novel, chelating C, N-bidentate 2,6-bis(dimethylamino)phenyl ligand ($R^{②}$), showing ambidentate N,N′-character in $M(R)_2$ (M = Ge, Sn, Pb) and Sn(R)X [X = $N(SiMe_3)_2$, $CH(SiMe_3)_2$, Cl]†

**Christian Drost, Peter B. Hitchcock, Michael F. Lappert* and Luc J.-M. Pierssens**

*The Chemistry Laboratory, University of Sussex, Brighton, UK BN1 9QJ*

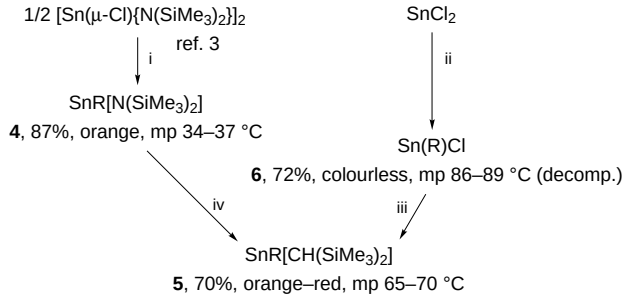
**Treatment of $MCl_2$ or $[Sn(\mu\text{-}Cl)\{N(SiMe_3)_2\}]_2$ with $[Li(\mu\text{-}R)]_3$ [R = $C_6H_3(NMe_2)_2$-2,6] under mild conditions and in appropriate stoichiometry affords $MR_2$ (M = Ge 1, Sn 2, Pb 3) or Sn(R)X [X = $N(SiMe_3)_2$ 4, Cl 6], while 4 or 6 with $LiCH(SiMe_3)_2$ give $SnR[CH(SiMe_3)_2]$ 5; compounds 1–6 are characterised by their multinuclear NMR and MS spectra and 1–3 by X-ray crystal structures.**

We draw attention to the chelating, C,N-bidentate, monoanionic terminal ligand $^{②}C_6H_3(NMe_2)_2$-2,6 ($R^{②}$) having ambidentate N,N′-character which promises to find a useful role in organometallic chemistry. It was previously known only as the lithium complex $[Li(\mu\text{-}R)]_3$ in which $R^{②}$ was C,N-chelating and N′-bridging.[1] The ligand $R^{②}$ differs from the well established $^{②}C_6H_3(CH_2NMe_2)_2$-2,6, which is tripodal, as in $Sn[C_6H_3(CH_2NMe_2)_2$-2,6]X (X = Cl, $C_6H_4Me$-4).[2]

At this time, we report the synthesis and characterisation of (*i*) the monomeric homoleptic 2,6-bis(dimethylamino)phenylmetal(II) heavy group 14 metal carbene analogues $MR_2$ (M = Ge **1**, Sn **2**, Pb **3**), (*ii*) the first monomeric heteroleptic aryltin(II) amide and alkyl $SnR[N(SiMe_3)_2]$ **4** and $SnR[CH(SiMe_3)_2]$ **5** and (*iii*) Sn(R)Cl **6**.

The yellow, crystalline complexes **1** (65%, mp 142–145 °C), **2** (90%, mp 85–90 °C) and **3** (70%, mp 126–130 °C [decomp.]) were prepared from $[Li(\mu\text{-}R)]_3$[1] and $MCl_2$ in appropriate stoichiometry at *ca*. 25 °C in diethyl ether for **2** and **3**, but preferably in tetrahydrofuran (thf) for **1**. An alternative procedure, from 2 RH + $Sn[N(SiMe_3)_2]$, proved unsuccessful; despite the fact that aromatic stannation using this tin(II) amide and $C_6H_4[N(SiMe_3)H]_2$-2,6 had readily yielded $Sn_3[\{1,3\text{-}(Me_3Si)N\}_2C_6H_3$-2]$_2$.[3]

The syntheses, in good yields and under mild conditions, of compounds **4**–**6** are illustrated in Scheme 1. Treatment of 1/3$[Li(\mu\text{-}R)]_3$ and 1/2$[Sn(\mu\text{-}Cl)\{N(SiMe_3)_2\}]_2$[4] or $SnCl_2$ afforded the colourless, crystalline **6** or the orange **4**, (Scheme 1, steps i or ii). From either **4** or **6** and 1/3 $[Li(\mu\text{-}R)]_3$, the orange–red **5** was obtained, (Scheme 1, steps iii or iv). Pure, crystalline compounds **4** and **5** were isolated after vacuum distillation.




**Scheme 1** Synthesis of the heteroleptic aryltin(II) complexes **4**–**6** [R = $C_6H_3(NMe_2)_2$-2,6]. *Reagents and conditions*: i, LiR, hexane, 0 °C, 12 h; ii, LiR, $Et_2O$, 0 °C, crystallisation from $Et_2O$–hexane; iii, LiR + $SnCl_2$, $Et_2O$, 25 °C, 12 h, (*in situ*) $LiCH(SiMe_3)_2$, hexane; iv, $LiCH(SiMe_3)_2$, hexane, 0 °C, 12 h, $Et_2O$.

Each of the hydrocarbon-soluble compounds **1**–**6** gave satisfactory microanalytical, as well as $^1H$, $^{13}C\{^1H\}$, $^{29}Si\{^1H\}$ (**4**, **5**), $^{119}Sn\{^1H\}$ (**2**, **4**–**6**) and $^{207}Pb\{^1H\}$ (**3**) NMR‡ and EI (70 eV) mass spectra (each giving, as the highest *m/z* peak,the parent monomeric molecular ion in significant intensity: from 8% for **4** to 35% for **2**). Additionally, single-crystal X-ray diffraction data established the molecular structures of the isomorphous, isostructural complexes **1**, **2** (Fig. 1) and **3**;§ the structures of **1** and **3** will be discussed in the full paper.

The $^1H$ NMR spectra of each of the homoleptic complexes $MR_2$ **1**–**3** in $C_6D_6$ (**1**, **3**) or [$^2H_8$]toluene (**2**)‡ showed singlets for both the $NMe_2$ and the 3,5-aromatic protons at 298 K, but for **2** each split into two separate signals at 178 K. This indicates that at the higher temperature there is a rapid exchange process involving 2-$Me_2N\cdots M \rightleftharpoons$ 6-$Me_2N\cdots M$ exchange; while at the lower temperature, the spectra are consistent with the solid-state structures,§ having each ligand $R^{②}$ bonded in a bidentate chelating fashion, with one of the $NMe_2$ groups being non-bonding. This analysis is supported by the $^{119}Sn$ NMR spectra for **2**.‡ Thus, the magnitude of the $^{119}Sn\{^1H\}$ chemical shift in PhMe–$C_6D_6$, $\delta$ 442.2 at 298 K (similarly, $\delta$ $^{207}Pb\{^1H\}$ 3919 in **3**) reflects a higher than two-coordinate metal(II) environment,[5] and moreover was similar to the CP MAS value of $\delta$ 492. The $^{119}Sn\{^1H\}$ NMR spectral chemical shifts in the heteroleptic complexes Sn(R)X **4**–**6** ($\delta$ 422 **4**, 758 **5** and 380 **6**) are consistent with their having three-coordinate tin(II), being intermediate between the values for the homoleptic $SnR_2$ **2** and $SnX_2$ [X = $N(SiMe_3)_2$, $\delta$ 776; X = $CH(SiMe_3)_2$, $\delta$ 2310 at 373 K[6*a*] (or 2315 at 375 K[6*b*]) for $Sn[CH(SiMe_3)_2]_2$ in [$^2H_8$]toluene and $\delta$ 725, 745 by CP MAS for the dimer[6*b*]]. The $^1H$ NMR solution spectra of **4**–**6**‡ also showed single $NMe_2$ and identical 3- and 5-aromatic proton environments at 298 K; low-temperature data are not yet to hand for **1** or **3**–**6**. The low-temperature $^1H$ NMR solution spectra of both **2** (containing the C,N-chelating $R^{②}$) and $Sn[C_6H_3(CH_2NMe_2)_2$-2,6]Cl[2] (having the C,N,N′-tripodal ligand) were consistent with their solid-state structures, but at higher temperatures each showed fluxional behaviour.

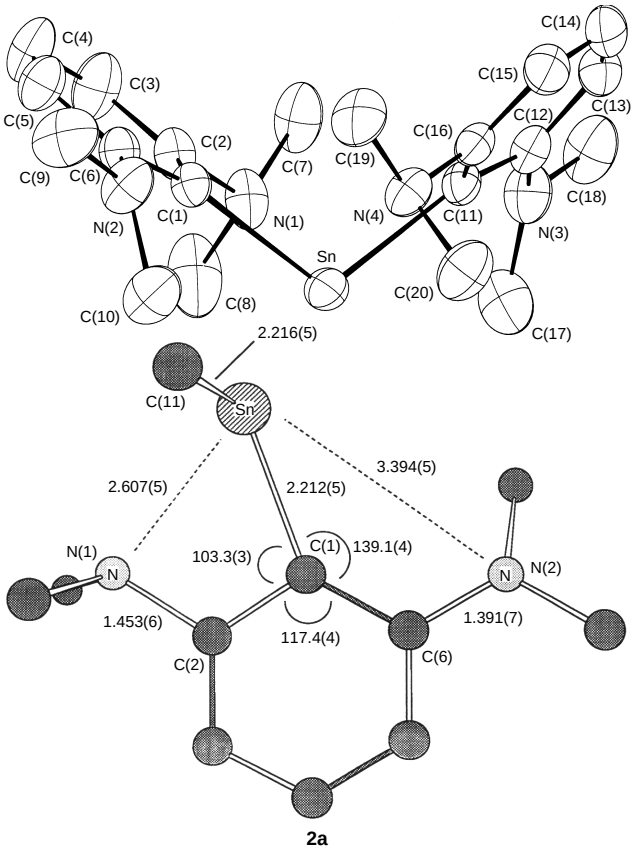
Complex $SnR[N(SiMe_3)_2]$ **4** is similar to the three-coordinate tin(II) compound $Sn[C(SiMe_3)_2C_5H_4N$-2][$N(SiMe_3)_2$],[5] both with respect to its yellow colour and $^{119}Sn\{^1H\}$ chemical shift, $\delta$ 319; while $\delta$ [$^{119}Sn\{^1H\}$] for the four-coordinate $SnR_2$ **2** is at a higher frequency than for the similarly coordinated tin(II) complexes $Sn[C(SiMe_3)_2C_5H_4N$-2]$_2$ ($\delta$ 139),[5] $Sn[C_6H_3(CH_2NMe_2)_2$-2,6]X (X = Cl, $\delta$ 155.6; X = $C_6H_4Me$-4, $\delta$ 209.5),[2] or $Sn(C_{10}H_6NMe_2$-8)$_2$ ($\delta$ 150.9 at ② 80 °C).[7]

The aryltin(II) chloride **6** was reasonably thermally stable, but in solution it slowly deposited metallic tin. Its stability is attributed to its three-coordinate nature, as in $Sn[C(SiMe_3)_2C_5H_4N$-2]Cl;[5] attempts to make $Sn[CH(SiMe_3)_2]Cl$ from $Sn[CH(SiMe_3)_2]_2$ + $SnCl_2$ afforded $Sn[CH(SiMe_3)_2]_2Cl_2$ + Sn.[8] However, **6** was clearly less robust than the four-coordinate tin(II) complex $Sn[C_6H_3(CH_2NMe_2)_2$-2,6]Cl.[2]

Crystalline $SnR_2$ **2**, illustrated in Fig. 1 and **2a**, is a mononuclear, four-coordinate tin(II) complex, the shortest Sn···Sn separation being 6.7 Å.§ The C(1)–Sn–C(11) angle of 105.6(2)° is typical of two-coordinate $SnX_2$ complexes, *e.g.* 103.6(1)° in $Sn(C_6H_2Bu^t_3\text{-}2,4,6)_2$,[9] but significantly different from those in the four-coordinate tin(II) complexes $Sn[C(SiMe_3)_2C_5H_4N\text{-}2]_2$ [125.0(2)°][5] or $Sn(C_{10}H_6NMe_2\text{-}8)_2$ [93.8(5)°];[7] the nature of the chelate bite-angle is clearly a major factor. The coordinating $NMe_2$ groups, one from each ligand, are arranged in a transoid fashion around the distorted trigonal-pyramidal tin centre, assuming that a lone pair of electrons occupies an equatorial site. The three CNC angles at each of the coordinating N atoms [N(1), N(4)] range from 108.9(5) to 114.1(5)° (av. 111.1°), while those at the more remote N atoms [N(2), N(3)] vary from 115.5(5) to 120.1(6)° (av. 117.7°), thus approximating to $sp^3$ and $sp^2$ N environments, respectively. The Sn···N(1) and Sn···N(4) distances (av. 2.64 Å) may be compared with an average of 2.42 Å in $Sn[C(SiMe_3)_2C_5H_4N\text{-}2]_2$[5] or 2.56 Å in $Sn[C_6H_3(CH_2NMe_2)(CH_2NMe_2)\text{-}2,6]_2Cl$.[2] To ensure optimal Sn···N(1) [or N(4)] donation, the Sn–C(1) and Sn–C(11) bonds are strongly tilted towards N(1) and N(4); hence, the C(2)–C(1)–Sn and C(16)–C(11)–Sn angles (av. 104.0°) and C(6)–C(1)–Sn and C(12)–C(11)–Sn (av. 138.2°) are severely distorted from $sp^2$ values.

The Sn–C(1) and Sn–C(11) bond lengths (av. 2.214 Å) are similar to the Sn–$C_{aryl}$ bond lengths in $Sn(C_6H_2Bu^t_3\text{-}2,4,6)_2$ [av. 2.261(4) Å][9] and $Sn[C_6H_2(CF_3)_3\text{-}2,4,6]_2$ [av. 2.281(5) Å],[10] the latter having significant Sn···F contacts with each of the 2- and 6-$CF_3$ groups.

The average Li–C and Li–N(N′) bond distances in $[Li(\mu\text{-}R)]_3$ are rather similar, 2.17 and 2.12 Å, respectively,[1] whereas in **2** the Sn–C bonds are considerably (*ca*. 20%) shorter than the chelating Sn–N distances.




**2a**

**Fig. 1** CAMERON representation of the molecular structure of $Sn[C_6H_3(NMe_2)_2\text{-}2,6]_2$ **2**. Selected bond lengths (Å) and angles (°) (see also **2a**): Sn···N(1) 2.607(5), Sn···N(4) 2.669(5); C(1)–Sn–C(11) 105.6(2), Sn–C(11)–C(16) 104.7(3), Sn–C(11)–C(12) 137.4(4).

The data here presented, together with experiments in progress, including the formation of a thermally stable tin-centred radical and cation $^{\cdot}SnR_3$ and $[SnR_2\{CH(SiMe_3)_2\}]BPh_4$, respectively, and the borane adduct $SnR_2(BH_3)$, encourage us to regard this ligand as having considerable potential.

We thank the European Commission for fellowships for C. D. (category 30) and L. J.-M. P. (cat. 20), Mr J. Keates and Dr G. A. Lawless for the CP MAS spectra and Dr A. Abdul-Sada for the MS spectral data and the EPSRC for other support.

## Footnotes

* E-mail: M.F.Lappert@sussex.ac.uk

† No reprints available.

‡ *NMR spectroscopic data* [$^1$H NMR at 250.0 MHz in $C_6D_6$ or (for **2**) [$^2H_8$]toluene; $^{13}C\{^1H\}$ NMR at 62.9 MHz, $^{29}Si\{^1H\}$ at 49.7 MHz and $^{119}Sn\{^1H\}$ at 93.2 MHz, all in PhMe with $C_6D_6$; $^{119}$Sn CPMAS NMR at 11.5 kHz]. **1**: $^1$H $\delta$ 2.62 (s, 12 H, $NMe_2$), 6.61 (d, 2 H, 3-CH) ($^3J$ 8 Hz), 7.14 (t, 1 H, 4-CH) ($^3J$ 8 Hz). **2**: $^1$H $\delta$ 2.70 (s, 12 H, $NMe_2$), 6.63 (d, 2 H, 3-CH) ($^3J$ 8 Hz), 7.22 (t, 1 H, 4-CH) ($^3J$ 8 Hz);$^{119}Sn\{^1H\}$ $\delta$ 442 [$^1J(^{119}Sn^{13}C)$ 432 Hz], $^{119}Sn\{^1H\}$ CP MAS $\delta$ 492. **3**: $^1$H $\delta$ 2.71 (s, 12 H, $NMe_2$), 7.00 (d, 2 H, 3-CH) ($^3J$ 7 Hz), 7.27 (t, 1 H, 4-CH) ($^3J$ 7 Hz); $^{207}Pb\{^1H\}$ $\delta$ 3919. **4**: $^1$H $\delta$ 0.27 (s, 18 H, $SiMe_3$), 2.52 (s, 12 H, $NMe_2$), 6.38 (d, 2 H, 3-CH) ($^3J$ 8 Hz), 7.12 (t, 1 H, 4-CH) ($^3J$ 8 Hz); $^{29}Si\{^1H\}$ $\delta$ ② 1.0; $^{119}Sn\{^1H\}$ $\delta$ 422. **5**: $^1$H $\delta$ 0.09 (s, 1 H, CH), 0.29 (s, 18 H, $SiMe_3$), 2.51 (s, 12 H, $NMe_2$), 6.38 (d, 2 H, 3-CH) ($^3J$ 8 Hz), 7.14 (t, 1 H, 4-CH) ($^3J$ 8 Hz); $^{29}Si\{^1H\}$ $\delta$ ② 2.37; $^{119}Sn\{^1H\}$ $\delta$ 758. **6**: $^1$H $\delta$ 2.45 (s, 12 H, $NMe_2$), 6.28 (d, 2 H, 3-CH) ($^3J$ 8 Hz), 7.09 (t, 1 H, 4-CH) ($^3J$ 8 Hz); $^{119}Sn\{^1H\}$ $\delta$ 380.

§ *Crystal data*: **2**, $C_{20}H_{30}N_4Sn$; $M$ = 445.2, monoclinic, space group $P2_1/c$ (no. 14), $a$ = 11.608(2), $b$ = 10.569(3), $c$ = 17.393(3) Å, $\beta$ = 98.85(1)°, $Z$ = 4, $U$ = 2108.5(8) Å$^3$, $F$(000) = 912, $D_c$ = 1.40 g cm$^{-3}$, $\mu$(Mo-K$\alpha$) = 12.2 cm$^{-1}$, specimen 0.6 ③ 0.2 ③ 0.1 mm, 6386 reflections collected for $2 < \theta < 30°$, 3507 reflections with $I > 2\sigma(I)$, $R_1$ = 0.060, $wR_2$ = 0.161 (for all data) ($T$ = 293K). Enraf-Nonius CAD4 diffractometer ($\lambda$ = 0.710 73 Å). Full-matrix least-squares refinement with SHELXL-93, H atoms in riding mode and all non-H atoms anisotropic. Atomic coordinates, bond lengths and angles, and thermal parameters have been deposited at the Cambridge Crystallograpic Data Centre (CCDC). See Information for Authors, Issue No. 1. Any request to the CCDC for this material should quote the full literature citation and the reference number 182/438.

## References

1 S. Harder, J. Boersma, L. Brandsma, J. A. Kanters, W. Bauer and P. v. R. Schleyer, *Organometallics*, 1989, **8**, 1696.
2 J. T. B. H. Jastrzebski, P. A. van der Schaaf, J. Boersma, G. van Koten, M. C. Zoutberg and D. Heijdenrijk, *Organometallics*, 1989, **8**, 1373.
3 H. Braunschweig, C. Drost, P. B. Hitchcock, M. F. Lappert and L. J.-M. Pierssens, *Angew. Chem., Int. Ed. Engl.*, 1997, **36**, 261.
4 R. W. Chorley, P. B. Hitchcock, B. S. Jolly, M. F. Lappert and G. A. Lawless, *J. Chem. Soc., Chem. Commun.*, 1991, 1302.
5 B. S. Jolly, M. F. Lappert, L. M. Engelhardt, A. H. White and C. L. Raston, *J. Chem. Soc., Dalton Trans.*, 1993, 2653.
6 (*a*) S. J. Smith, D. Phil. thesis, University of Sussex, 1986; (*b*) K. W. Zilm, G. A. Lawless, R. M. Merrill, J. M. Millar and G. G. Webb, *J. Am. Chem. Soc.*, 1987, **109**, 7236.
7 J. T. B. H. Jastrzebski, P. A. van der Schaaf, J. Boersma, G. van Koten, D. Heijdenrijk, K. Goubitz and D. J. A. de Ridder, *J. Organomet. Chem.*, 1989, **367**, 55.
8 D. E. Goldberg, P. B. Hitchcock, M. F. Lappert, K. M. Thomas, A. J. Thorne, T. Fjeldberg, A. Haaland and B. E. R. Schilling, *J. Chem. Soc., Dalton Trans.*, 1986, 2387.
9 M. Weidenbruch, J. Schlaefke, A. Schäfer, K. Peters, H. G. von Schnering and H. Marsmann, *Angew. Chem., Int. Ed. Engl.*, 1994, **33**, 1846.
10 H. Grützmacher, H. Pritzkow and F. T. Edelmann, *Organometallics*, 1991, **10**, 23.

*Received in Basel, Switzerland, 23rd January 1997; Com. 7/00528H*

# Insertion of arylsulfonylnitrene fragments into Pd–Pd bonds. Crystallographic characterization of the novel $[Pd_2Cl_2(\mu\text{-dppm})_2(\mu\text{-}NSO_2C_6H_4NO_2\text{-}2)]$ A-frame adduct

**Gábor Besenyei,* László Párkányi, Isabella Foch, László I. Simándi† and Alajos Kálmán**

*Central Research Institute for Chemistry, Hungarian Academy of Sciences, H-1525 Budapest, P.O. Box 17, Hungary*

**The dimeric palladium complex $[Pd_2Cl_2(\mu\text{-dppm})_2]$ reacts with arylsulfonyl azides affording novel arylsulfonylnitrene-bridged dinuclear A-frame complexes, $[Pd_2Cl_2(\mu\text{-dppm})_2(\mu\text{-}NSO_2Ar)]$.**

We have reported earlier that palladium complexes catalyse the carbonylation of sulfonamide derivatives such as salts of *N*-chloroarylsulfonamides, arylsulfonyliodoimines and arylsulfonylselenylimines with CO to the corresponding arylsulfonyl isocyanates.[1] These reactions are of potential interest in the phosgene-free synthesis of arylsulfonylurea type herbicides. Although the mechanisms of these reactions are not known, it is reasonable to assume that arylsulfonylnitrene intermediates may be involved as isocyanate precursors reacting with CO in the coordination sphere of the palladium catalyst. Mononuclear arylsulfonylnitrene complexes have been isolated from reactions of complexes of Mo and W with various sources of the $ArSO_2N$ fragment and obtained *via* oxidation of the coordinated $ArSO_2NH$ moiety.[2,3] The arylsulfonamide ligand has also been observed in complexes of Pt, Ru and Os.[4–6]

To our knowledge no palladium complexes containing the arylsulfonylnitrene ligand have thus far been synthesised and characterised although Lee and Trogler have reported on a palladium complex bearing phenylnitrene ligands that span over two palladium centres.[7] We now report the first examples of dimeric palladium complexes in which the arysulfonylnitrene ligand occupies a bridging position.

We have observed that the dimeric palladium complex $[Pd_2Cl_2(\mu\text{-dppm})_2]$ [**1**, dppm = bis(diphenylphosphino)methane] reacts readily with arylsulfonyl azides **2** at room temp. in $CH_2Cl_2$ [eqn. (1)], affording the novel A-frame type palladium

$$[Pd_2Cl_2(\mu\text{-dppm})_2] + ArSO_2N_3 \longrightarrow [Pd_2Cl_2(\mu\text{-dppm})_2(\mu\text{-}NSO_2Ar)] + N_2 \quad (1)$$

**1** **2** **3**

**a** Ar = 4-$MeC_6H_4$
**b** Ar = Ph
**c** Ar = 2-$NO_2C_6H_4$
**d** Ar = 2-Naphthyl

complexes **3** with the $ArSO_2N$ ligand in an apical position. The reaction is accompanied with characteristic changes in the UV–VIS spectrum and the evolution of *ca*. 0.95 mol $N_2$ per mol Pd complex, as demonstrated by gas volumetric measurements. In a typical experiment the reacting solution contained 0.2 mmol of **1** and 0.3 mmol of **2**, and the expected volume of $N_2$ was released in *ca*. 2 h. Evaporation and precipitation with MeOH afforded the products in better than 90% yield.

According to X-ray structure analysis, **3c** has an extended boat conformation of the eight-membered Pd–P–C ring (Fig. 1),‡ which is typical for A-frame adducts.[8–11] Remarkably, the coordination geometry of the bridging nitrogen is almost planar [$\Sigma\phi(N)$ = 356.2°; the N atom is located only 0.204 Å above the Pd(1)Pd(2)S plane]. An analogous feature has been observed for the complex $[Ir_2(CO)_2(dppm)_2(\mu\text{-NPh})]$.[12] The short S–N(1) bond distance (1.544 Å) is indicative of $d_\pi$–$p_\pi$ interaction, shifting electron density from the bridging nitrogen to the sulfonyl group. The contribution of resonance structures with negatively charged sulfonyl oxygen atoms is in line with the low values recorded for the $\nu_{as}(SO_2)$ bands (1240–1252 $cm^{-1}$). Although the S–N(1) bond has a pronounced double bond character, rotation around this axis should be considered feasible.

$^1H$ and $^{31}P$ NMR chemical shifts and coupling constants of **3a–d**, diagnostic for the dppm ligand in A-frame complexes, fall within a very narrow interval, supporting the close structural similarity of these complexes (Table 1). The observed splitting patterns in the $^1H$ NMR spectra and the singlets observed for the P nuclei show the equivalence of the diphosphine ligands.[8,9] The nature of the Ar group exerts only a negligible influence on the NMR parameters. We have found that complexes **3** are inert

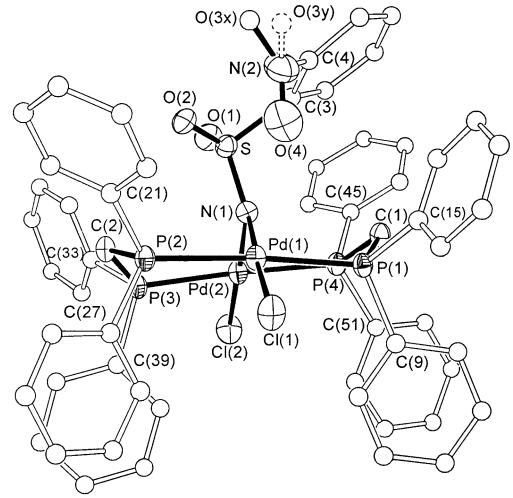



**Fig. 1** The molecular structure of $[Pd_2Cl_2(\mu\text{-dppm})_2(\mu\text{-}NSO_2C_6H_4NO_2\text{-}2)]$, **3c**. Selected bond distances (Å) and angles (°): Pd(1)–Pd(2) 3.282(1), Pd(1)–N(1) 2.016(4), Pd(2)–N(1) 2.029(4), Pd(1)–Cl(1) 2.316(1), Pd(2)–Cl(2) 2.306(2), S–N(1) 1.544(4), S–O(1) 1.444(4), S–O(2) 1.445(4), O(3x)–N(2) 1.204(3), O(4)–N(2) 1.226(7), Pd(1)–O(4) 3.099(7), S–O(4) 3.324(5); Pd(1)–N(1)–Pd(2) 108.4(2), S–N(1)–Pd(1) 125.7(2), S–N(1)–Pd(2) 122.1(2), N(1)–Pd(1)–Cl(1) 177.1(1), N(1)–Pd(2)–Cl(2) 175.2(1).

**Table 1** NMR data of complexes **3a–d**[a]

| Complex | $\delta_H$ | $J_{HH}$/Hz | $J_{HP}$/Hz | $\delta_P$[b] |
|---|---|---|---|---|
| **3a** | 4.10 (2 H, dq) | 12.8 | 5.9 | 7.2(s) |
| | 2.57 (2 H, dq) | | 3.4 | |
| **3b** | 4.01 (2 H, dq) | 12.8 | 5.8 | 7.1(s) |
| | 2.59 (2 H, dq) | | 3.4 | |
| **3c** | 4.17 (2 H, dq) | 12.9 | 5.8 | 6.0(s) |
| | 2.65 (2 H, dq) | | 3.4 | |
| **3d** | 4.13 (2 H, dq) | 12.7 | 5.9 | 7.1(s) |
| | 2.53 (2 H, dq) | | 3.3 | |

[a] s = Singlet, d = doublet, q = quintet. [b] Relative to 85% $H_3PO_4$.

toward CO. Exposure of **3a** and **3c** in $CH_2Cl_2$ to 30 bar CO at 20 °C for 18 h did not afford any products derived from the sulfonylnitrene moieties. This is in agreement with the observation of Ge and Sharp,[13] who demonstrated that CO is inserted into the Rh–N bond of $[Rh_2(CO)_2(dppm)_2(\mu\text{-NR})]$ only if R is not a strongly electron-withdrawing group. Similar factors may be responsible for the lack of reactivity of compounds **3**.

Although arylsulfonylnitrene complexes are probably involved in the carbonylation of sulfonamide derivatives, complexes **3** as model intermediates are too stable for reaction with CO, but very convenient for structural characterisation.

Work is in progress to further explore synthetic routes leading to palladium sulfonylnitrene complexes and their role in catalytic N-carbonylations.

We thank the Hungarian Research Fund (OTKA) for financial support (Grants T-16213 and B-033).

## Footnotes

† E-mail: simandi@cric.chemres.hu

‡ *Crystal data* for **3c**: $C_{56}H_{48}Cl_2N_2O_4P_4Pd_2S{\cdot}CHCl_3$, orange plate, 0.45 × 0.30 × 0.08 mm, monoclinic, space group $P2_1/n$, $a$ = 12.827(1), $b$ = 19.622(1), $c$ = 23.149(6) Å, β = 98.74(2)°, $U$ = 5758.7(16) Å$^3$, $Z$ = 4, $D_c$ = 1.582 Mg m$^{-3}$, μ = 1.051 mm$^{-1}$. Data were collected at 293 K on an Enraf-Nonius CAD4 four-circle diffractometer using graphite-monochromated Mo-Kα radiation. Reflections were collected in the range 2.44 ⩽ θ ⩽ 29.46° and 15935 independent reflections were used in the structure analysis. A semi-empirical (ψ-scan) absorption correction has been applied to the data. The structure was solved by the heavy-atom method and refined against all $F^2$ data (SHELXL-93)[14] to $R_1$ = 0.0490 [for 12251 $F^2 > 2\sigma(F^2)$]; $wR_2$ = 0.1555 and goodness of fit = 0.978 for all 15935 $F^2$, 731 parameters; all non-hydrogen atoms anisotropic except the minor disorder component of O(3) and three Cl atoms of out of nine disordered positions of the solvent. The highest peak of 1.254 e Å$^{-3}$ in the final difference map is located in the vicinity of the Pd(1) atom. Atomic coordinates, bond lengths and angles, and thermal parameters have been deposited at the Cambridge Crystallographic Data Centre (CCDC). See Information for Authors, Issue No. 1. Any request to the CCDC for this material should quote the full literature citation and the reference number 182/462.

## References

1 G. Besenyei, S. Németh and L. I. Simándi, *Angew. Chem., Int. Ed. Engl.*, 1990, **29**, 1147; G. Besenyei and L. I. Simándi, *Tetrahedron Lett.*, 1993, **34**, 2839; G. Besenyei, S. Németh and L. I. Simándi, *Tetrahedron Lett.*, 1994, **35**, 9609.
2 E. W. Harlan and R. H. J. Holm, *J. Am. Chem. Soc.*, 1990, **112**, 186.
3 P. J. Pérez, P. S. White, M. Brookhart and J. L. Templeton, *Inorg. Chem.*, 1994, **33**, 6050.
4 W. Beck, M. Bauder, G. La Monica, S. Cenini and R. Ugo, *J. Chem. Soc. A*, 1971, 113.
5 W.-H. Leung, M.-C. Wu, J. L. C. Chim and W.-T. Wong, *Inorg. Chem.*, 1996, **35**, 4801.
6 M. R. Churchill, F. J. Hollander, J. R. Shapley and J. B. Keister, *Inorg. Chem.*, 1980, **19**, 1272.
7 S. W. Lee and W. C. Trogler, *Inorg. Chem.*, 1990, **29**, 1099.
8 B. Chaudret, B. Delavaux and R. Poilblanc, *Coord. Chem. Rev.*, 1988, **86**, 191.
9 G. Besenyei, L. Párkányi, L. I. Simándi and B. R. James, *Inorg. Chem.*, 1995, **34**, 6118, and references therein.
10 F. Neve, M. Longeri, M. Ghedini and A. Crispini, *Inorg. Chim. Acta*, 1993, **205**, 15.
11 F. Neve and M. Ghedini, *Organometallics*, 1992, **11**, 795.
12 Ch. Ye and P. R. Sharp, *Inorg. Chem.*, 1995, **34**, 55.
13 Y.-W. Ge and P. R. Sharp, *Inorg. Chem.*, 1992, **31**, 379.
14 G. M. Sheldrick, SHELXL-93, University of Göttingen, 1993.

*Received in Basel, Switzerland, 10th February, 1997; Com. 7/00942I*

# Unusually long open times, determined by planar bilayer conductances studies, for a synthetic tris(macrocycle) that functions as a transmembrane channel in a phospholipid bilayer

**Ernesto Abel, Eric S. Meadows, Iwao Suzuki, Takashi Jin and George W. Gokel***

*Bioorganic Chemistry Program and Department of Molecular Biology and Pharmacology, Washington University School of Medicine, 660 South Euclid Avenue, Campus Box 8103, St. Louis, MO 63110 USA*

**Two tris(macrocycle)s are shown by bilayer clamp studies to function as cation channels in a phospholipid bilayer; one of the pair of closely related compounds shows unusually long open times compared either to the other tris(macrocycle) or to natural channel-forming proteins.**

The transport of sodium, potassium, and calcium cations *in vivo* is accomplished almost exclusively with the aid of proteins believed to have multiple transmembrane spans. Many of the structural features of natural cation-conducting channels have been inferred from biophysical and molecular biological studies.[1] The critical importance to biology of protein channel compounds and the fact that the chemical details of channel function remain obscure has fostered the design, synthesis, and study of several model channel systems. We have recently reviewed this area.[2] Our own cation channel model system was designed to possess macrocyclic polyethers that function both as head groups and as entry portals for cations. The original design used flexible *n*-dodecyl chains to connect the head-groups to a third macrocycle that was intended to function as a 'relay' unit, midway between the two.[3] The headgroups were attached on each distal side to a second 12-carbon chain that was expected to interact with the phospholipid bilayer in which it was embedded and to stabilize the extended conformation. The fact that alkyl-substituted crowns can serve as head groups for the formation of micelles[4] and stable vesicles[5] comports with our design. Based on the accumulated experimental evidence,[3] we believe that the benzyl channel (**1**, shown) adopts the conformation illustrated in Fig. 1.

We have prepared several channel model compounds in this class in which the distal macrocycles are substituted by aralkyl residues. Such residues include benzyl (**1**), methoxybenzyl[6] (**2**) and indolylmethyl.[7] We have previously shown that these structures conduct $Na^+$ through a phospholipid bilayer using a dynamic NMR method previously described.[8] We now show that these compounds exhibit cation transport behaviour typical of, if somewhat less effective than, that of transmembrane protein channels. These results were obtained by using a patch clamp amplifier and a bilayer headstage (planar bilayer conductance or pbc method). The black lipid bilayer membrane† is formed over a pinhole in a Teflon disk separating two compartments containing salt solutions. Bilayer formation is detected by a sudden drop in conductance. A continuous series of 10 mV, square-wave pulses (train pulse) is applied to the membrane to monitor its capacitance. A $10^{-6}$ M channel solution (in $CF_3CH_2OH$) was added and the solution was stirred for 1–10 min. A holding potential (see Figs. 2 and 3)was then applied and the channel responses were recorded.‡ The data shown in Fig. 2 (applied potential +100 mV) are typical for compound **2** but they represent only a small fraction of the data collected.

The recordings show the ion flux, usually for a single channel. The baseline corresponds to periods in which there is no observed cation flux. When a flat-topped peak is observed, it indicates that ions (presumably $Na^+$) are flowing. If each channel passes ions by the same mechanism, then a fixed peak height will be observed corresponding to whether the system is open or closed. When more than one channel is open simultaneously, similar flat-topped peaks will be observed but these will have an amplitude multiplied by an integer corresponding to the number of channels open. Well behaved, one- and two-channel opening behaviour is apparent in the traces shown in Fig. 2.

Similar, albeit somewhat noisier, data were obtained for **1** and are shown in Fig. 3(*a*). The traces shown are selected from and typical of approximately 100× the amount of data shown for **1**. Plotting current amplitude of single transitions *vs*. holding voltage for this system gives a straight line with $R > 0.98$ for 11

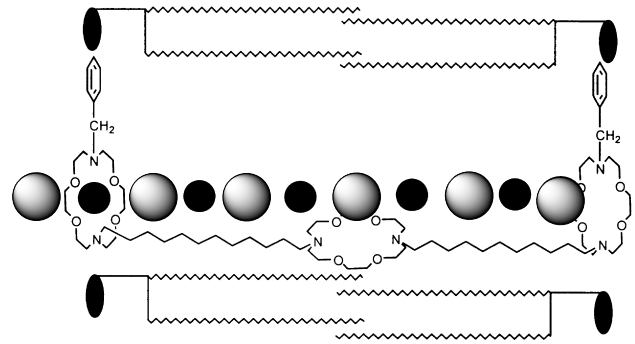
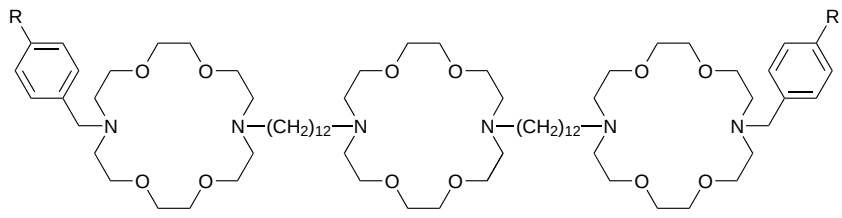


**Fig. 1** Conformation of **1** in a phospholipid bilayer inferred from experimental evidence. Sodium (larger spheres) and water are shown schematically only to indicate their presumed presence.



**1** R = H, **2** R = OMe

points. The linear relationship between current amplitude and applied voltage for benzyl channel **1** shows that it obeys Ohm's law and that there are no voltage-gated phenomena. The slope of the curve gives the channel's conductance. For **1**, it was determined to be 12.8 pS for a 0.1 M NaCl solution. We note that although the overall behaviour of **1** and **2** are similar to that observed for a typical, natural sodium channel, the magnitude of ion flux [12.8 pS for **2** (100 mM $Na^+$)] is less than the *ca*. 18 pS typically observed for the transmembrane proteins.[9] This channel is thus remarkably active for such a low molecular mass system. The methoxybenzyl channel (**2**) appears by $^{23}Na$ NMR studies to be about half as effective as the gramicidin channel,[10] a dimeric peptide, which also exhibits a lower flux than do proteins.

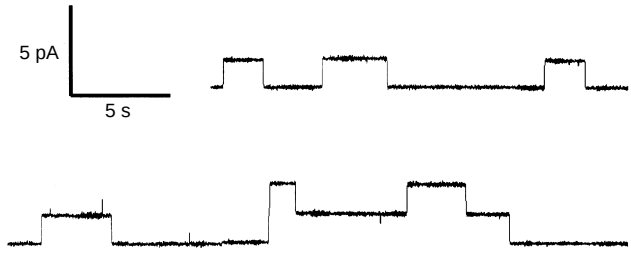



**Fig. 2** Bilayer clamp traces for methoxybenzyl channel (**2**) recorded at +100 mV

Traces are shown in Fig. 3 for **1** and **2** (additional data) on the same scale as each other and as in Fig. 2. Data were recorded at 120 mV for **1** and at 80 mV for **2**. These differences in holding voltage are expected to change the amplitude but not to have a significant effect on channel open times. Benzyl channel, **1**, opens and closes on a timescale of a few seconds typical of many proteins [Fig. 3(*a*)]. As in the methoxybenzyl case, integral amplitudes are observed for the square peaks. Compound **1** shows peaks indicating both longer and shorter opening times but none of the traces thus far obtained indicate that any channel remains open for more than *ca*. 5 s. As apparent in Fig. 2, **2** also shows 'typical' opening and closing behaviour much of the time. During the course of recording, however, several of the data segments showed behaviour that stood in striking contrast to this 'typical' behaviour. Specifically, **2** showed peaks indicating that single channels remained open for more than 30 s [Fig. 3(*b*)]. These remarkably long open times for **2** have been observed at several different applied potentials

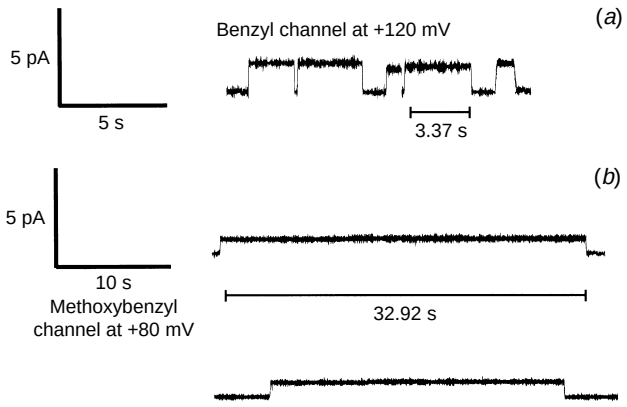



**Fig. 3** Comparison of observed open times for the benzyl channel (**1**) and methoxybenzyl channel (**2**)

in the range ±80–120 mV. Thus, this unusual behaviour does not appear to correlate with potential differences or polarity.

Channel structures **1** and **2** have a molecular mass of *ca*. 1300 and an extended length of > 30 Å. It seems remarkable that changing a hydrogen to a methoxy group at the distal ends of this system could so dramatically alter the cation transport behaviour. We are currently attempting to clarify the cause of this behaviour and to determine if other terminal groups can lifewise affect cation transport so dramatically.

We thank the NIH for a grant (GM 36262) that supported this work.

## Footnotes

* E-mail: ggokel@pharmdec.wustl.edu

† Bilayers were prepared by the 'painting method' using L-α-lecithin (a soybean lipid mixture containing 20% phosphatidylcholine, remainder unspecified). The bilayers (capacitance ≥100 pF) were allowed to stabilize for ≥1 h prior to adding the transporter (2–40 pmol). After addition of the ionophore, the mixture was stirred for *ca*. 10 min and then the membrane was allowed to equilibrate for *ca*. 5 min. Recordings were obtained during *ca*. 9 h for the benzyl channel (membrane stable) and *ca*. 3 h for the methoxybenzyl channel ( > 100-fold the amount shown). Each experiment was repeated a minimum of three times.

‡ Single channel signals were detected and recorded using a Warner Instruments PC-505 Patch Clamp Amplifier equipped with a bilayer headstage (50 GΩ), a Digidata 1200A A/D converter, and the computer based data acquisition software Axoscope (v. 1.1.1). The holding voltage was changed manually to obtain channel responses at different voltages. Single-channel current amplitude and standard deviations were determined using Axoscope and/or pCLAMP6.

§ 'Unmodified $Na^+$ channels activated by batrachotoxin have a dominant conductance of 18 ± 2 pS in 100 mM $Na^+$.[9]

## References

1 D. G. Nicholls, *Proteins, Transmitters and Synapses*, Blackwell Science, Oxford, 1994; B. Hille, *Ionic Channels of Excitable Membranes*, Sinauer Press, Sunderland, MA, 1992; W. D.Stein, *Channels, Carriers and Pumps*, Academic Press, New York, 1990.

2 G. W. Gokel and O. Murillo, *Acc. Chem. Res.*, 1996, **29**, 425.

3 A. Nakano, Q. Xie, J. Mallen, L. Echegoyen and G. W. Gokel, *J. Am. Chem. Soc.*, 1990, **112**, 1287; O. Murillo, S. Watanabe, A. Nakano and G. W. Gokel, *J. Am. Chem. Soc.*, 1995, **117**, 7665.

4 M. Okahara, P. L.Kuo, S. Yamamura and I. Ikeda, *J. Chem. Soc., Chem. Commun.*, 1980, 586; I. Ikeda, K. Iwaisako, Y. Nakatsuji, and M. Okahara, *Yukagaku*, 1986, **35**, 1001 (*Chem. Abstr.*, 106:86714, 1986); T.Kuwamura and T. Kawachi, *Yukagaku*, 1979, **28**, 195 (*Chem. Abstr.*, 90:206248, 1979); T. Kuwmura, M. Akimaru, H. L. Takahashi and M. Arai, *Kenkyu Hokoku-Asahi Garasu Kogyo Gijutsu Shorekai*, 1979, **35**, 45 (*Chem. Abstr.*, 95:61394q, 1979); T. Kuwamura and S. Yoshida, *Nippon Kagaku Kaishi*, 1980, 427 (*Chem. Abstr.*, 93:28168e, 1980).

5 S. Muñoz, J. V. Mallén, A. Nakano, Z. Chen, L. Echegoyen, I. Gay and G. W. Gokel, *J. Chem. Soc., Chem. Commun.*, 1992, 520; S. Muñoz, J. Mallén, A. Nakano, Z. Chen, I. Gay, L. Echegoyen and G. W. Gokel, *J. Am. Chem. Soc.*, 1993, **115**, 1705.

6 O. Murillo, I. Suzuki, E. Abel and G. W. Gokel, *J. Am. Chem. Soc.*, 1996, **118**, 7628.

7 O. Murillo, E. Abel, G. E. M. Maguire and G. W. Gokel, *Chem. Commun.*, 1996, 2147.

8 F. Riddell and M. Hayer, *Biochim. Biophys. Acta*, 1985, **817**, 313; D. Buster, J. Hinton, F. Milltee and D. Shungu, *Biophys. J.*, 1988, **53**, 145.

9 W. A. Catterall, *Science*, 1988, **242**, 50.

10 S. B. Hlodky and D. A. Haydon, *Biochim. Biophys. Acta*, 1972, **274**, 294; *Nature* (*London*), 1970, **225**, 451.

*Received in Columbia, MO, USA, 19th February, 1997; Com. 7/01188A*

# Reichardt's dye as a probe for surface polarity of chemically and thermally treated silicas

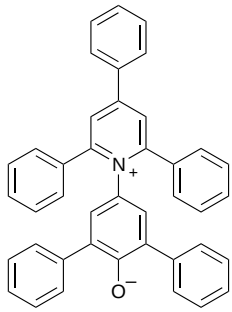
**Stewart J. Tavener, James H. Clark,* Gary W. Gray, Paul A. Heath and Duncan J. Macquarrie**

*Department of Chemistry, University of York, Heslington, York, UK YO1 5DD*

**The polarity of surfaces may be conveniently estimated by measuring the energy of the π → π* transition of adsorbed Reichardt's dye.**

Surface polarity strongly affects the ability of material surfaces to adsorb compounds, which may in turn affect many useful properties of solids including catalytic activity. In heterogeneous catalysis, the reaction occurs either at the catalyst surface, inside pores, or in the slow moving liquid film at the surface (Nernst layer). The adsorption of substrates and the desorption of products are important steps in heterogeneous catalytic processes and are often rate limiting.[1] In certain cases, such as supported phase-transfer catalysts, the compatability of the surface with the reactant phases is critical.[2] However, measuremants of surface polarity are not easy and are rarely used in practice.

Reichardt's dye (**I**) is a useful indicator of solvent polarity.[3]



**I**

It is strongly solvatochromic, and shows a range of energies for its π → π* absorption band from 147 kJ mol$^{-1}$ (810 nm) in diphenyl ether to 264 kJ mol$^{-1}$ (453 nm) in water. Solvent polarity is measured simply by recording the energy of the π → π* transition in kJ mol$^{-1}$. This may be normalised to avoid non-SI units [eqn. (1)].

$$E_T^N = \frac{E_{T(solvent)} - E_{T(TMS)}}{E_{T(water)} - E_{T(TMS)}} \quad (1)$$

Reichardt's dye immobilised on silica gel has recently been reported as being a sensitive optical chemical sensor, giving significant shifts in $\lambda_{max}$ when the liquid environment of the sensor was changed, although these shifts were smaller than those seen for the free dye in solution.[4] Reichardt's dye doped organic polymers have been used as optical sensors for humidity, gaseous ammonia, and for polar additives in hydrocarbon blends.[5]

Some attempts have been made to measure solvatochromic parameters for the surfaces of inorganic oxides, but these investigations have usually involved the study of the solid in contact with a mobile liquid phase.[6] Silica samples studied as a suspension in 1,2-dichloroethane were found to have an $E_T^N$ value of 0.798 to 0.842,[7] and were also found to have extremely high polarities as measured by the UV adsorption maximum of adsorbed 4-nitroanisole.[8] Reichardt's dye has been used to demonstrate that dry alumina surfaces have a greater polarity than bulk water.[9]

We now wish to report that Reichardt's dye will also act as a convenient probe for the polarity of surfaces of chemically and thermally treated silica surfaces. A solution of the dye (in dichloromethane) is simply added to the the material under study, the solvent removed on a rotory evaporator and the material dried on a vacuum line for 10 min, after which no residual dichloromethane could be detected on the material by DRIFTS. Care must be taken to avoid overloading the surface with dye, as dimerisation is known to occur in solution at higher concentrations: the amount of dye added was therefore restricted to 1 μmol g$^{-1}$ (*ca.* 2 nmol m$^{-2}$).[9] The choice of solvent used to download the dye is critical: alcohols and ketones will react with or bind strongly to surface hydroxy groups on silica surfaces,[10] and the dye is insufficiently soluble in apolar solvents such as aliphatic hydrocarbons. THF also proved troublesome as high peroxide concentrations caused bleaching of the dye. Dichloromethane was found to be the most suitable solvent by virtue of its high volatility and chemical stability. The π → π* transition energy of the adsorbed dye is measured by diffuse reflectance UV–VIS spectrophotometry, although the polarity may be estimated by eye: very polar surfaces such as untreated silicas are red, ranging through purple and blue for organosilicas, to green for non-polar surfaces such as macroporous polystyrene. The values for $E_T^N$ presented here are calculated using a modified version of eqn. (1), using $E_{T(surface)}$ instead of $E_{T(solvent)}$.

The dye may not be used in strongly acidic environments as the oxygen centre becomes protonated, preventing the solvatochromic transition.[11] Residual adsorded HCl prevents sensible values from being obtained for the surface polarities of silicas treated with chlorosilanes.

A range of thermally treated silicas were prepared by heating commercial mesoporous silicas (Kieselgel 60 and Kieselgel 100, *ex Merck*) for 20 h at the desired temperature under a flowing nitrogen atmosphere before being treated with the dye solution. Thermal dehydration of silica gel is known to have a

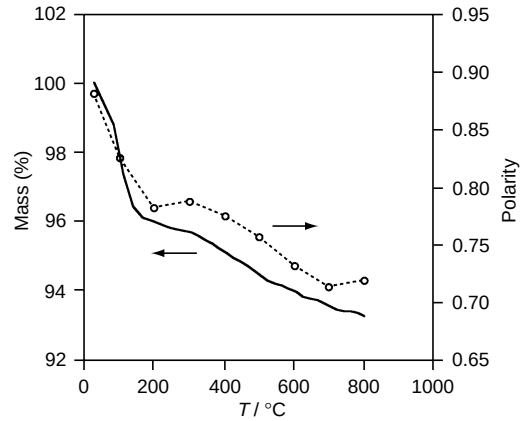



**Fig. 1** Thermogravimetric analysis and the effect of thermal treatment on the polarity ($E_T^N$) of Kieselgel 60 silica

large effect on surface chemistry of the silica, but comparatively little effect on its surface area: heating silica to 810 °C will decrease the surface area by only 25%, but will decrease the concentration of surface hydroxy groups by 80%.[12] Thermal treatment of both silicas was found to have a marked effect on its polarity, with the $E_T^N$ value reflecting thermogravimetric analysis data (Fig. 1). Initial heating causes a rapid loss of mass as loose, physisorbed water is removed from the surface, and a decrease in polarity as the adsorbed dye is no longer in a wet 'supported water' environment, but now sees a hydrogen-bonded network of surface silanols.[10] Further heating will remove some of these silanols, producing isolated polar groups whose polarity is not mediated by hydrogen bonding, this is reflected in the slight increase in polarity observed in the 300–400 °C region for both silicas. As the temperature is raised to 700 °C, more surface hydroxy groups react, eliminating water and producing more and more siloxane bridges (Fig. 2). Both

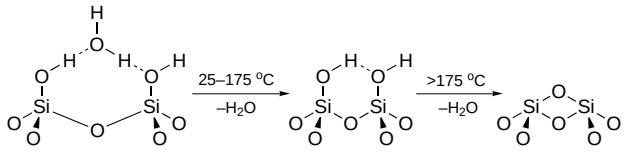



**Fig. 2** Thermal dehydration of a silica surface

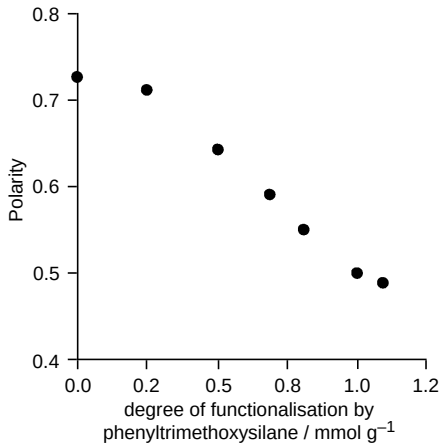



**Fig. 3** Effect of the degree of functionalisation on the polarity ($E_T^N$) of silicas treated with phenyltrimethoxysilane

**Table 1** Polarities of a range of organically modified silicas

| Material[a] | Degree of functionalisation[b]/ mmol g$^{-1}$ | $\lambda_{max}$/nm | $E_T^N$ | $\Delta E_T^N$/ mmol$^{-1}$ g |
|---|---|---|---|---|
| Silica–OH[c] | — | 477 | 0.967 | — |
| Silica–OSiMe$_3$ | 0.53 | 560 | 0.630 | −0.634 |
| Silica–Ph | 1.00 | 610 | 0.500 | −0.467 |
| Silica–(CH$_2$)$_3$Cl | 0.64 | 554 | 0.645 | −0.503 |
| Silica–(CH$_2$)$_3$NH$_2$ | 0.99 | 590 | 0.546 | −0.425 |
| Silica–(CH$_2$)$_2$CN | 0.99 | 557 | 0.636 | −0.334 |
| Silica–(CH$_2$)$_3$N[d] | 0.97 | 611 | 0.497 | −0.485 |
| Polystyrene[e] | — | 752 | 0.225 | — |

[a] Prepared by reaction with the appropriate organosilane, unless otherwise stated. [b] Measured by C, N elemental microanalysis. [c] Kieselgel 100, untreated. [d] Imidazole functionalised silica; for preparation method see ref. 14. [e] Amberlite XAD4 macroporous polystyrene.

silicas show an increase in polarity on heating beyond 700 °C. The cause of this is not clear but may be due to a low energy restructuring of the gel matrix, although no energy changes could be detected by differential scanning calorimetry. The temperature is lower than the quartz–tridymite phase change for crystalline silicas, which occurs at 870 °C.[10]

Silicas chemically modified by reaction with organosilane reagents such as phenyltrimethoxysilane show a reverse linear correlation between degree of functionalisation and polarity as measured by the $E_T^N$ values (Fig. 3). For these materials the dye is exposed to greasy non-polar organic functions as well as fewer polar surface hydroxy groups, compared with the unmodified silica. The measured polarities of a range of organically modified silicas at specific degrees of functionalisation are given in Table 1. There was no observable change in the IR spectra of the various materials after absorption of the dye, although it should be noted that the dye is present in quantities approximately 1000 times smaller than those of the surface bound organic groups, and is below the limits of detectability by IR.

Although all of the organic groups studied reduce the polarity of silica, they do so by different degrees. The decrease in polarity per mmol of organic groups per gram of silica ($\Delta E_T^N$) increases in the order: cyanoethyl < aminopropyl < imidazole < phenyl < chloropropyl < trimethylsiloxyl which is broadly in agreement with the $E_T^N$ values found for comparable compounds in the liquid phase: TMS = 0.000, benzene = 0.111, 1-chlorobutane = 0.191, *n*-butylamine = 0.213, propionitrile = 0.401, water = 1.00.[13]

Adsorption of Reichardt's dye on chemically and thermally treated silicas is an easy and rapid method for reliably determining the polarity of surfaces. This method should prove to be a valuble technique in the study of adsoption and desorption in liquid/solid catalytic systems.

We thank the EPSRC clean technology unit for a ROPA award (to S. J. T.), the Royal Academy of Engineering/EPSRC for a Fellowship (to J. H. C.) and the Royal Society for a fellowship (to D. J. M.).

## Footnote

* E-mail: jhcl@york.ac.uk

## References

1 M. Tomoi and W. T. Ford, *J. Am. Chem. Soc.*, 1981, **103**, 3821.
2 S. L. Regen, D. Bolikal and C. Barcelon, *J. Org. Chem.*, 1981, **103**, 3828; P. Tundo and P. Venturello, *J. Am. Chem. Soc.*, 1979, **101**, 6606.
3 K. Dimroth , C. Reichardt, T. Siepmann and F. Bohlmann, *Liebigs Ann. Chem.*, 1963, **661**, 1; C. Reichardt, *Solvents and Solvent Effects in Organic Chemistry*, VCH Publishers, 2nd edn., 1988.
4 D. Crowther and X. Liu, *J. Chem. Soc., Chem. Commun.*, 1995, 2445.
5 Y. Sadaoka, M. Matsguchi, Y. Sakai and Y.-U. Murata, *Chem. Lett.*, 1992, 53; C. Hubert, D. Fichou, P. Valat and F. Garner, *Polymer*, 1995, **36**, 2663.
6 J. L. Jones and S. C. Rutan, *Anal. Chem.*, 1991, **63**, 1318; Z. Li and S. C. Rutan, *Anal. Chim. Acta*, 1995, **312**, 127; M. Kosmulski, *J.Colloid Interface Sci.*, 1996, **179**, 128.
7 S. Spange, A. Reuter and E. Vilsmeier, *Colloid Polym. Sci.*, 1996, **274**, 59.
8 C. G. Flowers, S. Lindley and J. E. Leffler, *Tetrahedron Lett.*, 1984, **25**, 4997.
9 J. J. Michels and J. G. Dorsey, *Langmuir*, 1990, **6**, 414.
10 R. K. Iler, *The Chemistry of Silica*, Wiley, 1979.
11 C. Reichardt, *Chem. Soc. Rev.*, 1992, 147.
12 W. K Lowen and E. C. Broge, *J. Phys. Chem.*, 1961, **65**, 16.
13 Y. Marcus, *Chem. Soc. Rev.*, 1993, 409.
14 O. Leal, D. L. Anderson, R. G. Bowman, F. Basolo and R. L. Burwell Jr., *J. Am. Chem. Soc.*, 1975, **97**, 5125.

*Received in Cambridge, UK, 11th March 1997; Com. 7/01681F*

# Isolation and structural characterisation of $[\{(Me_3Si)_2NMg[\mu\text{-}OC(H)Ph_2]\cdot(O{=}CPh_2)\}_2]$, an intermediate in the β-hydride transfer reaction between an alkyl(amido)magnesium and benzophenone

**Kenneth W. Henderson,* John F. Allan and Alan R. Kennedy**

*Department of Pure and Applied Chemistry, University of Strathclyde, Glasgow, UK G1 1XL*

**The *in situ* reaction of $Bu_2Mg$ with 2 mol. equiv. of $(Me_3Si)_2NH$ followed by addition of $Ph_2CO$ yields the heteroleptic amide/alkoxide complex $[\{(Me_3Si)_2NMg[\mu\text{-}OC(H)Ph_2]\cdot(O{=}CPh_2)\}_2]$ 1, whereas reaction of purified $[\{(Me_3Si)_2N\}_2Mg]$ 2 with $Ph_2CO$ results in formation of the solvate $[\{(Me_3Si)_2N\}_2Mg\cdot(O{=}CPh_2)_2]$ 3, the difference being due to incomplete amination of the bis(alkyl)magnesium compound resulting in β-hydride transfer to the ketone, which is the first example of this type of transformation using an alkyl(amido)magnesium reagent.**

While Hauser bases[1] ($R_2NMgX$) and bis(amido)magnesium compounds[2] $[(R_2N)_2Mg]$ have been in the literature for some time, very little is known regarding their use as reagents to perform organic transformations. Magnesium amides are more thermally stable and less reactive than the widely used lithium amides ($R_2NLi$), leading to selectivity variations between these reagents.[3]

We are interested in studying selective deprotonation reactions between magnesium amide bases and ketones carrying an α-hydrogen, to yield magnesium enolates.[3b,4] With this in mind we decided to prepare a pre-enolisation complex[5] of a magnesium amide, for use as a model intermediate in the enolisation reaction. This involved reacting $Bu_2Mg$† (5 mmol) with hexamethyldisilazane, hmds, (10 mmol) in 10 ml of hexane for 3 h at 25 °C, followed by the addition of the non-enolisable ketone benzophenone (5 mmol).[6] It was expected that a simple ketone solvated bis(amido)magnesium complex would be produced, which could then be used for further analysis. To our surprise the only isolable product from the reaction was the crystalline compound $[\{(Me_3Si)_2NMg[\mu\text{-}OC(H)Ph_2]\cdot(O{=}CPh_2)\}_2]$ **1**.

The identity of **1** was confirmed by $^1H$ NMR analysis,‡ and its crystal structure was determined by an X-ray study (Fig. 1).§ Clearly, benzophenone had been reduced and the solvated, secondary alkoxide was obtained. The origin of the hydride was then investigated. A reaction was carried out in $C_6D_6$ to determine if the hydride was derived from the solvent; however, **1** was produced without deuterium incorporation. To exclude the possibility of moisture contamination as the hydride source, a reaction was conducted under strictly hydrophobic conditions, using triply distilled amine and sublimed $Ph_2CO$, again **1** was obtained. Our next avenue of inquiry proved to be more successful. Pure, crystalline $[\{(Me_3Si)_2N\}_2Mg]$ **2** was prepared by refluxing $Bu_2Mg$ (20 mmol) and hmds (40 mmol) in 20 ml of heptane for 3 h and on cooling to approximately 40 °C, large, colourless, crystalline blocks of **2** were deposited from solution.¶ The solid was isolated by filtration and stored in an argon-filled glove box. This procedure is high yielding and much simpler than the recently reported electrochemical synthesis.[3b] Reaction of the pure bis(amide) (5 mmol) with benzophenone (10 mmol) in 5 ml of hexane gave a clear yellow solution, which yielded needle crystals of the solvated bis(amide) $[\{(Me_3Si)_2N\}_2Mg\cdot(O{=}CPh_2)_2]$ **3**, on standing at room temperature. Hence, the explanation for the preparation of **1** must lie in performing the amination reaction followed by solvation *in situ*.

To investigate the amination process, a reaction between $Bu_2Mg$ and hmds was performed in $C_6D_6$ at 25 °C. A $^1H$ NMR spectrum of the solution after 3 h showed that alkyl peaks were still evident. This indicates that amination ceases or at least slows, at the alkyl(amido) state $[(Me_3Si)_2NMgBu]$[7] at this temperature. Using this information it is possible to propose a pathway for reduction of the ketone *via* β-hydride transfer from the alkyl(amido)magnesium intermediate (Scheme 1).[8]

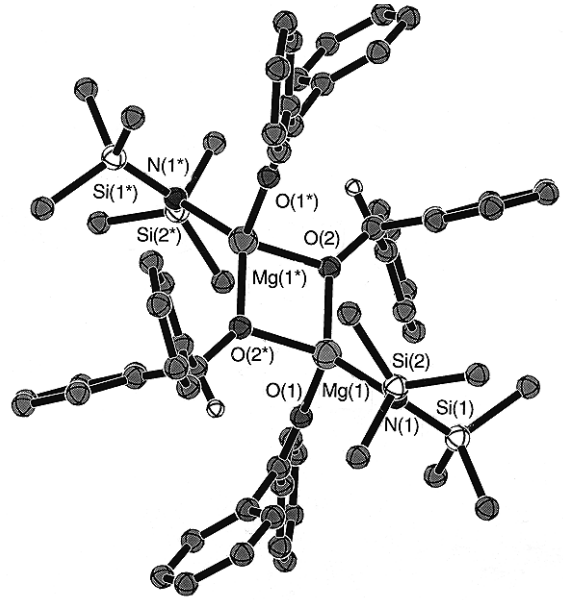
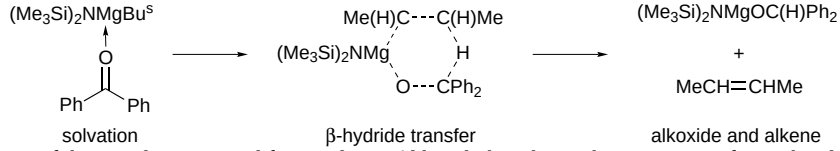



**Fig. 1** Crystal structure of **1** with hydrogen atoms (except the alkoxide H) omitted for clarity. Starred atoms are related by the symmetry operation 1-*x*, -*y*, -*z*. Key bond lengths (Å) and angles (°): Mg(1)–N(1) 2.019(3), Mg(1)–O(1) 2.046(3), Mg(1)–O(2) 1.967(2), Mg(1)–O(2*) 1,991(2); O(2)–Mg(1)–O(2*) 82.9(1), O(2)–Mg(1)–N(1) 127.0(1), O(1)–Mg(1)–O(2) 109.1(1), O(1)–Mg(1)–O(2*) 98.1(1), O(2*)–Mg(1)–N(1) 129.5(1).




**Scheme 1**. The aggregation state of the complex is ignored for simplicity. Although the scheme shows reaction of a *sec*-butyl function, a similar reaction will occur with an *n*-butyl producing but-1-ene.

To test the feasibility of this route [$(Me_3Si)_2NMgBu^S$] was prepared and isolated as a pure compound[9] and reacted with benzophenone. The solid produced from this reaction was identified as **1**. It therefore appears that the origin of the hydride is indeed from the alkyl group attached to magnesium and that this is still present due to incomplete amination of the bis(alkyl)magnesium.

Complex **1** may be regarded as an intermediate in the reduction reaction of a ketone to an alcohol, *i.e.* prior to hydrolysis. To our knowledge, this is the only example of a magnesium alkoxide prepared *via* reduction to be structurally characterised. Although a wealth of information is available on the preparation of alcohols using metal reagents, the exact nature of the reacting species is still unclear. We also believe that this is the first report of the use of an alkyl(amido)magnesium compound as a hydride transfer reagent.[10] An alternative reaction possible between the alkyl(amido)magnesium and the ketone is alkylation, to give a tertiary alcohol (after hydrolysis). This is the preferred reaction mode between [$MeMgNR_2$] ($NR_2$ = $NPr^i_2$, $NPh_2$ or $NC_5H_8Me_2$) and the cyclic ketones 4-*tert*-butylcyclohexanone and 2,2,6,6-tetramethyl-4-*tert*-butylcyclohexanone.[11] The combined steric bulk of the alkyl anion and the phenyl groups of the ketone appear to negate this possibility in our system.

Turning to the structure of **1** a dimeric arrangement utilising bridging alkoxide anions is found. Each metal bonds terminally to one amide anion and tetracoordination is completed by carbonyl solvation from a benzophenone unit. Each magnesium adopts a distorted tetrahedral environment, with angles ranging from 82.9(1)° for O(2)–Mg(1)–O(2*) to 129.5(1)° for O(2*)–Mg(1)–N(1). Although the structural motif of a dimer is not unusual for magnesium,[12] the constitution of **1** is novel. Heteroleptic magnesium compounds where the metal is attached to two different anions are rare,[13] and surprisingly **1** is the first homometallic amide/alkoxide magnesium compound to be structurally characterised.[14]

Also noteworthy in **1** is the bis solvation by benzophenone. In this system **1** is prepared preferentially over further reduction by [$(Me_3Si)_2NMgBu$]. A maximum conversion of ketone to alcohol is therefore 50% due to deactivation of the coordinated $Ph_2CO$. Strong solvation of the highly Lewis-acidic magnesium centre by the carbonyl may disfavour the dissociation necessary for further reduction to take place.

The work reported herein illustrates the merit in isolating pure organometallic reagents before further reaction, as opposed to performing *in situ* transformations. We are currently studying the chemoselective properties of alkyl(amido)magnesium compounds and their use as asymmetric induction reagents.

## Footnotes

* E-mail: k.w.henderson@strath.ac.uk

† $Bu_2Mg$ is commercially available from Aldrich as a statistical 1 : 1 mixture of *n*- and *sec*-butylmagnesium.

‡ $^1$H NMR (400 MHz, $C_6D_6$, 298 K) for **1**: δ 0.26 (s, 18 H, $Me_3Si$), 6.27 (s, 1 H, CH), 6.91 (t, 2 H, *p*-H), 7.00–7.14 (m, 10 H, *p*-, *m*-H ×2), 7.51 (d, 4 H, *o*-H), 7.61 (d, 4 H, *o*-H). Yield of first batch of crystals = 32% based on consumption of $Ph_2CO$, mp 128–131 °C.

§ *Crystal data* for **1**: $C_{64}H_{78}Mg_2N_2O_4Si_4$, $M$ = 1100.28, $T$ = 20 °C, monoclinic, space group $P2_1/n$, $a$ = 12.837(1), $b$ = 13.537(3), $c$ = 18.049(2) Å, β = 93.741(9)°, $U$ = 3129.8(8) Å$^3$, $Z$ = 2, $D_c$ = 1.167 Mg m$^{-3}$, $2\theta_{max}$ = 52°, 6719 reflections collected, 6429 unique reflections, $R_{int}$ = 0.036, observed limit, $I > 2\sigma(I)$, observed reflections = 2771, number of variables = 382, full-matrix least-squares refinement on $F$ converged to $R$ = 0.044, $R_w$ = 0.048 and $S$ = 1.43. Structure solution using SAPI91 (F. Hai-Fu, 1991, structure analysis program with intelligent control, Rigaku Corporation, Tokyo, Japan). Calculation and graphics using TEXSAN (crystal structure analysis package, version 1.6, 1993, Molecular Structure Corporation, The Woodlands, Texas 77381). Atomic coordinates, bond lengths and angles, and thermal parameters have been deposited at the Cambridge Crystallographic Data Centre (CCDC). See Information for Authors, Issue No. 1. Any request to the CCDC for this material should quote the full literature citation and the reference number 182/461.

¶ $^1$H NMR (250 MHz, $C_6D_6$, 298 K) for **2**: δ 0.17 (s, $Me_3Si$), 0.39 (s, $Me_3Si$), 0.46 (s, $Me_3Si$). The two highest frequency singlets represent bridging and terminal anions in a dimer, and the low-frequency singlet is derived from monomeric amide. A concentration study showed increasing monomer present with increasing dilution. Yield = 70%, mp 122 °C.

‖ $^1$H NMR (250 MHz, $C_6D_6$, 298 K) for **3**: δ 0.39 (s, 36 H, $Me_3Si$), 6.96–7.12 (m, 12 H, *m*-, *p*-H), 7.74 (d, 8 H, *o*-H). Yield = 78% based on consumption of $Ph_2CO$, mp 118–119 °C.

## References


1 C. R. Hauser and H. G. Walker, *J. Am. Chem. Soc.*, 1947, **69**, 295.

2 E. C. Ashby, J. J. Lin and A. B. Goel, *J. Org. Chem.*, 1978, **43**, 1564; W. Clegg, K. W. Henderson, R. E. Mulvey and P. A. O'Neil, *J. Organomet. Chem.*, 1992, **439**, 237.

3 (*a*) P. E. Eaton, C. H. Lee and Y. Xiong, *J. Am. Chem. Soc.*, 1989, **111**, 8016; (*b*) D. Bonafoux, M. Bordeau, C. Biran, P. Cazeau and J. Dunogues, *J. Org. Chem.*, 1996, **61**, 5532.

4 For examples of the uses of Hauser bases see: bromomagnesium 2,2,6,6-tetramethylpiperidine (mtmp) reacts with β-silyl ether ketones to give the *E*-enolates: N. A. Van Draanen, S. Arseniyadis, M. T. Crimmins and C. H. Heathcock, *J. Org. Chem.*, 1991, **56**, 2499; sulfoxides with α-hydrogens react with mtmp to give dithioacetals: K. Kobaiyashi, M. Kawakita, T. Mannami, O. Morikawa and H. Konishi, *Chem. Lett.*, 1994, 1551.

5 Carbonyl adducts of lithium and magnesium compounds have been characterised: P. G. Williard, Q. Y. Liu and L. Lochmann, *J. Am. Chem. Soc.*, 1992, **113**, 348; L. Lochmann and M. Sorm, *Collect. Czech. Chem. Commun.*, 1973, **38**, 3449. Similarly a nitrile complex of lithium hexamethyldisilazide has been characterised: G. Boche, I. Langlotz, M. Marsch, K. Harms and G. Frenking, *Angew. Chem., Int. Ed. Engl.*, 1993, **32**, 1171.

6 For a report of the deprotonating ability of the reagent $Bu_2Mg$ see: A. W. Duff, P. B. Hitchcock, M. F. Lappert, R. G. Taylor and J. A. Segal, *J. Organomet. Chem.*, 1985, **293**, 271.

7 The constitution of the butyl function will be predominately *sec*-butyl due to kinetic considerations, see: K. W. Henderson, A. E. Dorigo and R. E. Mulvey, *J. Organomet. Chem.*, 1996, **518**, 139.

8 N. Greaves, *Comprehensive Organic Synthesis*, ed. B. M. Trost and I. Fleming, Pergamon, New York, 1991, vol. 8, ch. 1.

9 L. M. Engelhardt, B. S. Jolly, P. C. Junk, C. L. Raston, B. W. Skelton and A. H. White, *Aust. J. Chem.*, 1986, **39**, 1337.

10 For a list of reduction reagents see: R. C. Larock, *Comprehensive Organic Transformations*, VCH, New York, 1989, 527.

11 E. C. Ashby and G. F. Williard, *J. Org. Chem.*, 1978, **43**, 4094.

12 P. R. Markies, O. S. Akkerman, F. Bickelhaupt, W. J. J. Smeets and A. L. Spek, *Adv. Organomet. Chem.*, 1991, **32**, 147.

13 K. W. Henderson, R. E. Mulvey, W. Clegg and P. A. O'Neil, *Polyhedron*, 1993, 2535.

14 For the first structural characterisation of a mixed lithium amide/alkoxide complex see: K. W. Henderson, D. S. Walther and P. G. Williard, *J. Am. Chem. Soc.*, 1995, **117**, 8680.


*Received in Basel, Switzerland, 17th March 1997; Com. 7/01875D*

ChemComm
FEATURE ARTICLE

# Pheromones: synthesis and bioactivity†

**Kenji Mori**

*Department of Chemistry, Science University of Tokyo, Kagurazaka 1-3, Shinjuku-ku, Tokyo 162, Japan*

**Pheromones play an important role in chemical communication among organisms. Various chiral and non-racemic pheromones have been identified since the late 1960s. Their enantioselective syntheses were achieved so as to establish the absolute configuration of the naturally occurring pheromones and also to clarify the relationship between absolute configuration and the bioactivity of the chiral pheromones.**

**Four recent examples of pheromone synthesis are given. The enantiomers of sordidin 14, the banana weevil pheromone, have been synthesized starting from (*S*)-propylene oxide. (−)-*exo*-Isobrevicomin 17 and its (−)-*endo*-isomer 21, the components of the volatiles of the mountain pine beetle, have been synthesized by employing the Sharpless asymmetric dihydroxylation and lipase-catalysed acetylation as the key reactions. The enantiomers of (*Z*)-hexadeca-7,15-dien-4-olide 24, the sex pheromone of the yellowish elongate chafer, have been synthesized *via* lipase-catalysed resolution. Lurlene 27, the pheromone of the green flagellate *Chlamydomonas allensworthii*, has been synthesized by employing a phenyl sulfone coupling reaction as the key reaction.**

**The relationships between absolute configuration and bioactivity are diverse. For example, neither the (*R*)- nor the (*S*)-enantiomer of sulcatol 10, the aggregation pheromone of the ambrosia beetle *Gnathotrichus sulcatus*, is bioactive, but when combined to give an enantiomeric mixture they become active. In the case of olean 46, the olive fruit fly pheromone, (*R*)-46 is active for the males, while (*S*)-46 is active for the females.**

## Introduction

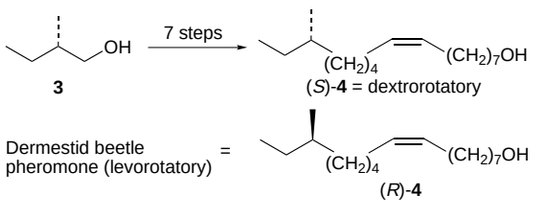
Pheromone chemistry began in 1959 when Butenandt established the structure **1** of bombykol, the sex pheromone of the silkworm moth (*Bombyx mori*). Subsequently in late 1960s a number of chiral pheromones were identified, as exemplified by *exo*-brevicomin **2**, the aggregation pheromone of the western pine beetle (*Dendroctonus brevicomis*). The absolute configuration of a chiral and non-racemic pheromone must be studied to elucidate the stereostructure of the naturally occurring material and also to clarify the relationship between stereochemistry and pheromone activity.

Mori demonstrated in 1973 that the naturally occurring and levorotatory dermestid beetle pheromone was (*R*)-**4** by converting the commercially available (*S*)-**3** to the dextrorotatory (*S*)-**4** (Scheme 1).[1,2] This work was the first successful identification of the absolute configuration of an insect pheromone by its enantioselective synthesis.

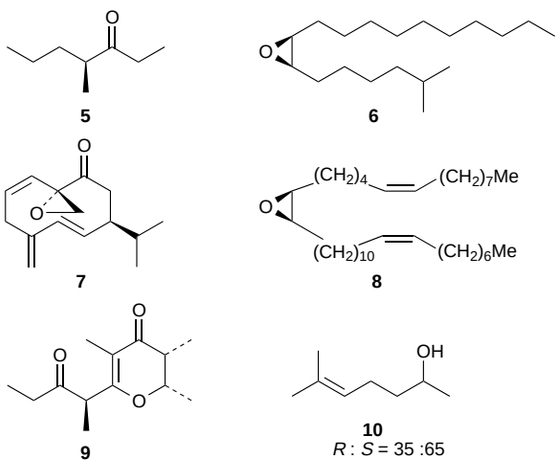
In 1974 three independent groups synthesized both the enantiomers of three different insect pheromones. Riley *et al*. synthesized the enantiomers of the alarm pheromone of the leaf-cutting ant (*Atta texana*), and found the (*S*)-isomer **5** to be about 400 times more active than the (*R*)-isomer.[3] The enantiomers of disparlure, the gypsy moth (*Lymantria dispar*) pheromone, were synthesized by Marumo's group, and they examined the electroantennographical (EAG) and behavioural responses of the male gypsy moth to the enantiomers.[4] (7*R*,8*S*)-(+)-Disparlure **6** was the most effective, (±)-**6** came second, while the (7*S*,8*R*)-(−)-isomer inhibited the activity of (+)-**6**.[4] Mori synthesized both the enantiomers of *exo*-brevicomin by starting from the enantiomers of tartaric acid.[5] Only (+)-*exo*-brevicomin **2** was bioactive against the western pine beetle.[6] The discovery that the absolute configuration of pheromones was of the utmost importance to the expression of their bioactivities accelerated stereochemical studies on insect pheromones.

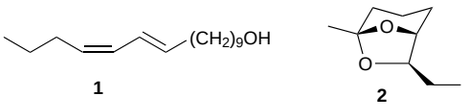
Synthesis of pheromone enantiomers can solve the stereochemical problems in pheromone chemistry, if proper methods are available for the discrimination of the enantiomers. Limited availability of the naturally occurring chiral pheromones makes it difficult to determine their absolute configuration by conventional means, especially because most of the pheromones are volatile liquids. A synthetic sample of a pheromone with known absolute configuration is useful as a reference material to assign the absolute configuration of the naturally occurring one. Accordingly, one must compare the synthetic sample with the natural pheromone by physical and/or biological methods.

The classical and accepted method for the assignment of absolute configuration is the comparison of the specific rotation of an unknown sample with that of the reference. The magnitude of the specific rotation, however, varies very much according to




**Scheme 1**



the structure of the pheromone. The largest $[\alpha]_D$ value observed among insect pheromones was $[\alpha]_D^{24}$ −547 (hexane) in the case of periplanone A **7**, the American cockroach pheromone,[7] and the smallest was $[\alpha]_D$ 0 in the case of the nymph recognition pheromone **8** of the cockroach, *Nauphoeta cinerea*.[8] Therefore, in the case of the latter, an attempt to measure the specific rotation of the natural product does not provide useful information as to its absolute configuration. If a chiral pheromone has carbonyl chromophores such as in the case of stegobinone **9**, the drugstore beetle pheromone, its CD spectrum provides useful information.[9]

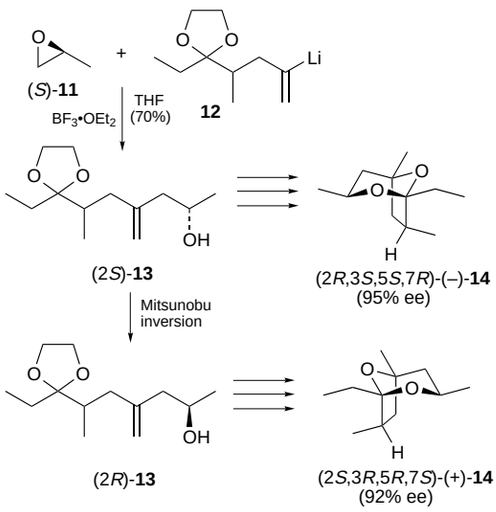
Determination of the absolute configuration and estimation of the enantiomeric composition of a chiral pheromone are possible by NMR spectroscopic methods, if a sufficient amount of the sample is available to measure the spectrum in the presence of a chiral shift reagent and/or after derivatization with a chiral derivatizing reagent. The enantiomeric purity of sulcatol **10**, the male-produced aggregation pheromone of the ambrosia beetle *Gnathotrichus sulcatus*, was determined as 30% ee [(*S*)-(+) > (*R*)-(−)] by the NMR method.[10]

HPLC with cellulose-based chiral stationary phases or GC with cyclodextrin-based chiral stationary phases are two popular methods for determination of the absolute configuration of pheromones.[11] Even with achiral stationary phases, HPLC and GC are useful for analysing chiral pheromones after derivatization with a chiral derivatizing reagent. Cyclodextrin-based GC columns are particularly useful, and almost all of the recent results on stereochemical studies of pheromones have been obtained using them.[11,12]

## Synthesis of the enantiomers of sordidin

Aspects of pheromone synthesis have been reviewed.[13–16] In particular two of them deal with enantioselective synthesis of pheromones.[15,16] Enantioselective synthesis of a chiral and non-racemic pheromone can be executed by one of the following three methods: (i) derivation from a known chiral and non-racemic building block, (ii) use of chemical or enzymatic asymmetric reactions, and (iii) use of chemical or enzymatic enantiomer separation (*i.e.* resolution) at a certain stage of the synthesis. Four recent examples from our group will be given here.

The enantiomers of sordidin **14**, the male-produced aggregation pheromone of the banana weevil (*Cosmopolites sordidus*),[17] were synthesized as summarized in Scheme 2.[18] (*S*)-Propylene oxide **11** was employed as the chiral building block. Cleavage of **11** with the alkenyllithium **12** in the presence of boron trifluoride–diethyl ether yielded the homoallylic alcohol (2*S*)-**13**. This was converted to (−)-sordidin **14**. Mitsunobu inversion of (2*S*)-**13** afforded (2*R*)-**13**, which furnished (+)-sordidin **14**. The enantiomers of **14** were compared with the natural pheromone by GC analysis (Cyclodex B® column), and (+)-**14** coincided with the natural product. The absolute configuration of natural sordidin was therefore determined as 1*S*,3*R*,5*R*,7*S*.[18]

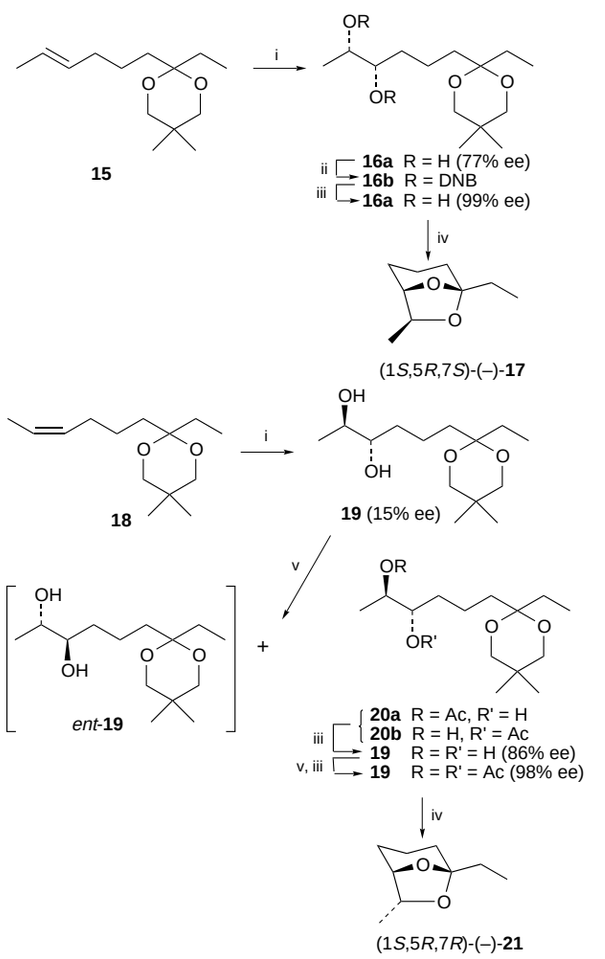



**Scheme 2**

## Synthesis of (−)-*exo*- and (−)-*endo*-isobrevicomins

Both the *exo*- and *endo*-isomers of isobrevicomin **17** and **21** were isolated in 1996 by Francke *et al*. as the components of the volatiles obtained from male mountain pine beetles (*Dendroctonus ponderosae*).[19] They synthesized (1*S*,5*R*,7*S*)-(−)-**17** by starting from (+)-tartaric acid, and the natural **17** was found to be (1*S*,5*R*,7*S*)-**17** of at least 90% ee by GC analysis.[19]

The naturally occurring *endo*-isobrevicomin may share the same (1*S*,5*R*)-6,8-dioxabicyclo[3.2.1]octane skeleton as depicted for **21**, but it needed to be proved. We therefore synthesized both (1*S*,5*R*,7*S*)-**17** and (1*S*,5*R*,7*R*)-**21** as summarized in Scheme 3.[20] Sharpless asymmetric dihydroxylation of **15** with AD-mix-α® gave the diol **16a** (77% ee). This was purified *via* the crystalline *bis*- 3,5-dinitrobenzoate **16b** to give pure **16a** (99% ee), which furnished (1*S*,5*R*,7*S*)-**17** by acid treatment. Similar dihydroxylation of **18** with AD-mix-α® afforded the diol **19** of 15% ee. The diol **19** was then purified by lipase-catalysed asymmetric acetylation. Treatment of **19** (15%




**Scheme 3** *Reagents*: i, AD-mix-α®, $MeSO_2NH_2$, $Bu^tOH$, $H_2O$ (94% for both **16a** and **19**); ii, 3,5-dinitrobenzoyl chloride (DNBCl), $C_5H_5N$, $CH_2Cl_2$, then recrystallization (59%); iii, $K_2CO_3$, MeOH [92% for **16a** (99% ee); 53% for **19** (86% ee) based on **19** (15% ee); 77% for **19** (98% ee) based on **19** (86% ee); iv, dil. HCl (64%); v, $CH_2$=CHOAc, immobilized lipase PS (Amano), $Bu^tOMe$, then chromatographic separation of *ent*-**19** and **20a**,**b**

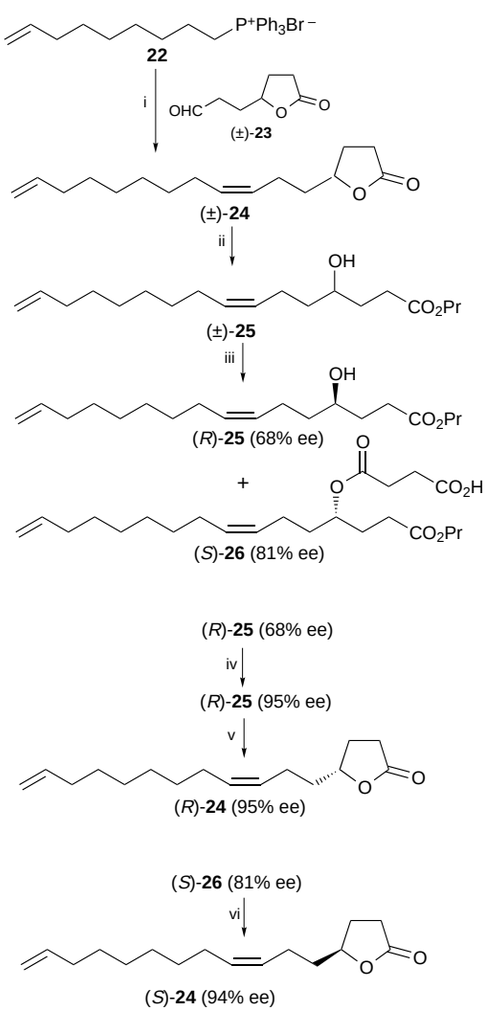
ee) with vinyl acetate and immobilized lipase PS (Amano) gave a mixture of *ent*-**19** and **20a**,**b** which could be separated by chromatography. Deacetylation of **20a**,**b** to give **19** (86% ee) was followed by the second enzymatic enrichment of the enantiomeric purity to give **19** of 98% ee. Acid treatment of **19** (98% ee) furnished (−)-*endo*-isobrevicomin **21**. Gas chromatographic comparison of (−)-**21** with the naturally occurring *endo*-isobrevicomin established its absolute configuration.

### Synthesis of the enantiomers of (*Z*)-hexadeca-7,15-dien-4-olide

(*R*,*Z*)-Hexadeca-7,15-dien-4-olide **24** is the female-produced sex pheromone of the yellowish elongate chafer (*Heptophylla picea*).[21] The absolute configuration of the natural pheromone was assigned as *R* by the conversion of (*S*)-malic acid to (*R*)-**24**, which was identical with the natural product.[21]

We became interested in synthesizing both the enantiomers and the racemate of **24** so as to clarify the stereochemistry–bioactivity relationship. Because (±)-**24** had to be prepared for its biological evaluation, its optical resolution was considered to be the most convenient way to prepare both the enantiomers of **24**. The synthesis is summarized in Scheme 4.[22] The Wittig reagent prepared from **22** reacted with the aldehyde (±)-**23** under the Bestmann conditions to give (±)-lactone **24**, ($Z:E$ = 96.5 : 3.5). Enzymatic methods were employed for the optical resolution of (±)-**24**. The lactone (±)-**24** was first converted to the hydroxy ester (±)-**25**, which was treated with succinic anhydride in the presence of lipase PS (Amano) to give (*R*)-**25** (68% ee) and (*S*)-**26** (81% ee). The mixture was readily separable by chromatography. Treatment of (*R*)-**25** (68% ee) with pig pancreatic lipase (PPL) in diethyl ether converted (*R*)-**25** (68% ee) to a mixture of (*R*)-**25** (95% ee) and (*S*)-**24** (30% ee), which was separated by chromatography. Subsequent treatment of the hydroxy ester (*R*)-**25** (95% ee) with Amberlyst-15 yielded the (*R*)-lactone **24**, (95% ee). For the preparation of the non-natural (*S*)-lactone (**24**), the (*S*)-succinoyl ester **26**, (81% ee) was submitted to enzymatic lactonization catalysed by lipase OF-360 (Meito) to give the enantiomerically enriched (*S*)-**24** (94% ee). In the present case, asymmetric catalysis of lipases was useful for the preparation of both the enantiomers of **24**. Biotransformations catalysed by enzymes and microorganisms are frequently employed in pheromone synthesis.[15,23]

Bioassay of our synthetic samples revealed both (*R*)-**24** and (±)-**24** to be bioactive. This means that (*S*)-**24** is not inhibitory.




**Scheme 4** *Reagents*: i, $NaN(SiMe_3)_2$, THF (66%); ii, KOH, $H_2O$, then PrBr, DMF(91%); iii, succinic anhydride, lipase PS (Amano), $Pr^i{}_2O$ [56% of (*R*)-**25** and 41% of (*S*)-**26**]; iv, PPL, $Et_2O$ (74%); v, Amberlyst-15, hexane (89%); vi, lipase OF-360 (Meito), 0.3 M phosphate buffer (pH = 7) (52%)

### Synthesis of lurlene

The sex pheromone produced by the female gametes of *Chlamydomonas allensworthii* was isolated, named as lurlene, and identified as **27** by Starr, Jaenicke and Marner in 1995.[24,25] Lurlene **27** attracts the male gametes at a concentration as low as $10^{-12}$ M.[24] Our first synthesis of **27** was achieved by employing the palladium-catalysed Stille coupling between the stannane **28** and the allylic acetate **29** as the key step (Scheme 5).[26] The coupling reaction, however, brought about the partial isomerization of the (*E*) double bond at C-12 to give a mixture of **30** and its (12*Z*)-isomer in a ratio of 2 : 1.[26] This mixture could not be separated, and therefore was processed to give the final product as a bioactive mixture of lurlene **27** and its (12*Z*)-isomer.

Our second synthesis of lurlene **27** utilized the sulfone coupling reaction, and afforded the final product as pure (12*E*)-lurlene **27**.[27] The crucial steps of the second synthesis are also shown in Scheme 5. The isoprenoidal side-chain part **31** was synthesized from (*E*,*E*)-farnesol, converted to the corresponding dianion, and alkylated with the aromatic part **32** to give the phenyl sulfone **33**. Palladium-catalysed reductive desulfonylation[28] of **33** gave the pure aglycone part **34**, which was converted to lurlene **27** *via* **30**.

The pheromones of organisms other than insects are now under active investigation.

### Stereochemistry–bioactivity relationships among insect pheromones

The most notable advance in pheromone science in the last two decades is the recognition of the importance of chirality in pheromone perception. Fig. 1 summarizes the stereochemistry–pheromone activity relationships. The relationships are divided into ten categories as detailed below.

#### (*a*) *Only a single enantiomer is bioactive, and its opposite enantiomer does not inhibit the action of the pheromone*

This is the most common relationship, and the majority (about 60%) of the chiral pheromones belong to this category. Other bioregulators such as hormones generally belong to this category. Many people therefore believed that this relationship must be the only reasonable one. As we shall see later, there are many other cases.

Only the (1*R*,5*S*,7*R*)-isomer of *exo*-brevicomin (**2**) is bioactive.[6] (3*S*,4*R*)-Faranal **35** is the bioactive enantiomer of the trail following pheromone of the pharaoh's ant.[29]

(*b*) *Only one enantiomer is bioactive, and its opposite enantiomer inhibits the action of the pheromone*

Disparlure (7*R*,8*S*)-**6** is the first studied pheromone which belongs to this group.[4] Under field conditions, males of the gypsy moth (*Lymantria dispar*) and males of the nun moth (*Lymantria monacha*) responded to (7*R*,8*S*)-**6**. However, the addition of (7*S*,8*R*)-**6** significantly suppressed response by *L. dispar*, while (7*S*,8*R*)-**6** did not show such an effect on the response of *L. monacha*.[30]

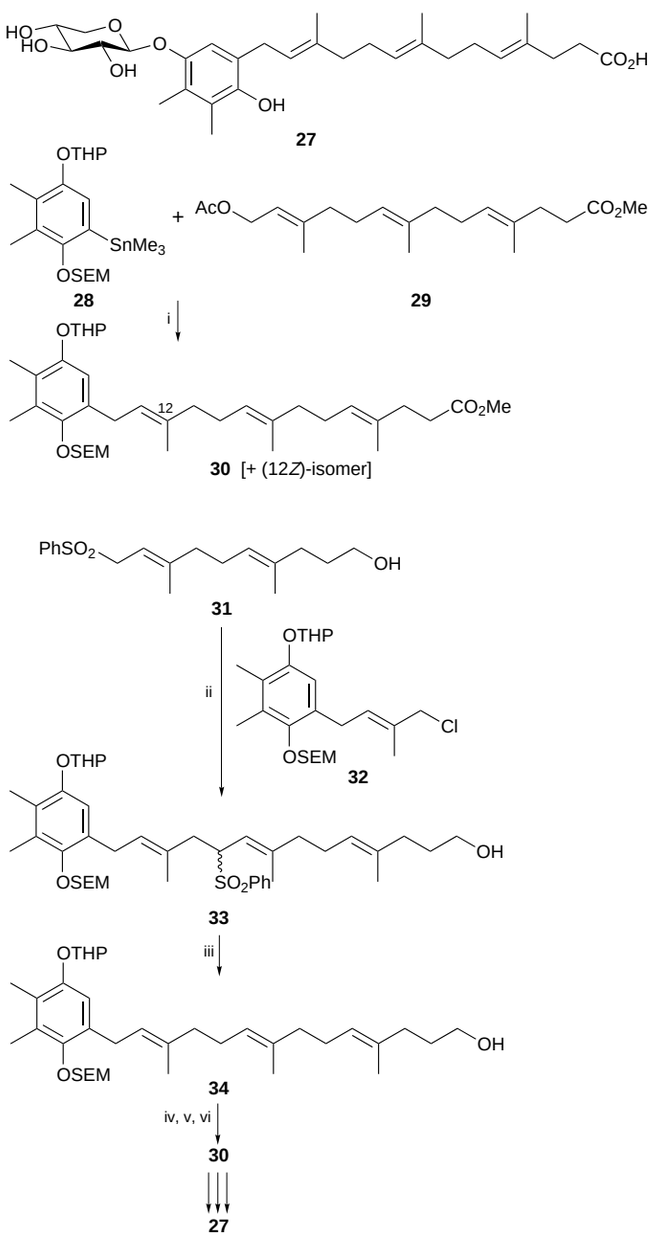
Japonilure (*R*)-**36** is the female-produced sex pheromone of the Japanese beetle.[31] The bioactive enantiomer is (*R*)-(+)-**36**, while (*S*)-**36** strongly inhibits the action of (*R*)-**36**. Accordingly, (+)-**36** of 99% ee was about 2/3 as active as the pure (*R*)-**36**, that of 90% ee was about 1/3 as active as (*R*)-**36**, that of 80% ee was about 1/5 as active as (*R*)-**36**, and both (+)-**36** of 60% ee and (±)-**36** were inactive.[31]

For the practical use of pheromones belonging to this category, one must synthesize highly pure enantiomers in order to ensure trap capture of the insects. Enantiomerically pure commercial products are now available in the cases of disparlure **6** and japonilure **36**.

(*c*) *Only one enantiomer is bioactive, and its diastereomer inhibits the action of the pheromone*

Sericornin (4*S*,6*S*,7*S*)-**37** is the female-produced sex pheromone of the cigarette beetle. Bioactivity of the stereoisomers of **37** was studied by Mori *et al.* in the course of developing practical pheromone traps.[32] Only (4*S*,6*S*,7*S*)-**37** was bioactive, and its (4*S*,6*S*,7*R*)-isomer was inhibitory against the action of (4*S*,6*S*,7*S*)-**37**. Accordingly, the commercial pheromone lure must be manufactured without contamination with the (4*S*,6*S*,7*R*)-isomer.

Stegobinone (2*S*,3*R*,1′*R*)-**9** is one of the two components of the female-produced sex pheromone of the drugstore beetle. It has been shown that the addition of (2*S*,3*R*,1′*S*)-epistegobinone




**Scheme 5** *Reagents*: i, 0.05 equiv. bis(dibenzylideneacetone)palladium(0) [$Pd(dba)_2$], 3 equiv. LiCl, DMF (98%, $E : Z = 2 : 1$); ii, 2 equiv. BuLi, THF, HMPA (62%); iii, 0.1 equiv. $PdCl_2$[1,3-bis(diphenylphosphino)propane] [$PdCl_2(dppp)$], 3 equiv. $LiBEt_3H$, THF (93%); iv, Dess–Martin periodinane; v, $NaClO_2$, $NaH_2PO_4$, DMSO, MeCN, $H_2O$; vi, $CH_2N_2$, $Et_2O$ (73% based on **34**)

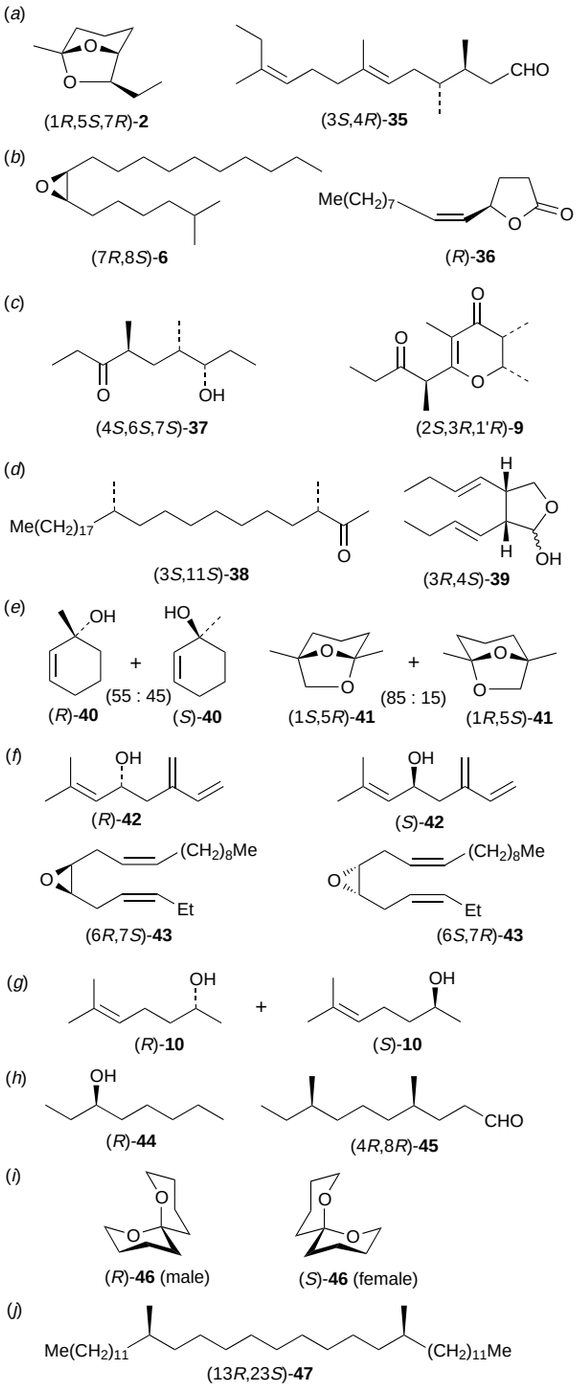



**Fig. 1** Relationships between stereochemistry and bioactivity of insect pheromones. The names of the insects which release the pheromones **2**, **6**, **9** and **35**–**47** are listed below: (*a*) **2** (*exo*-brevicomin), western pine beetle *Dendroctonus brevicomis*; **35** (faranal), pharaoh's ant *Monomorium pharaonis*; (*b*) **6** (disparlure), gypsy moth *Lymantria dispar*; **36** (japonilure), Japanese beetle *Popillia japonica*; (*c*) **37** (serricornin), cigarette beetle *Lasioderma serricorne*; **9** (stegobinone), drugstore beetle *Stegobium paniceum*; (*d*) **38**, German cockroach *Blattella germanica*; **39**, spined citrus bug *Biprorulus bibax*; (*e*) **40**, Douglas-fir beetle *Dendroctonus pseudotsugae*; **41** (frontalin), southern pine beetle *Dendroctonus frontalis*; (*f*) **42** (ipsdienol), (*R*)-isomer: bark beetles *Ips calligraphus* and *I. avulsus*; (*S*)-isomer: California five spined ips *I. paraconfusus*; (*R*) and (*S*)-isomers: pine engraver *Ips pini*; **43**, (6*R*,7*S*)-isomer; geometrid moth *Colotois pennaria*; (6*S*,7*R*)-isomer: geometrid moth *Erannis defoliaria*; (*g*) **10** (sulcatol), ambrosia beetle *Gnathotrichus sulcatus*; (*h*) **44**, ant *Myrmica scabrinodis*; **45** (tribolure), red-flour beetle *Tribolium castaneum*; (*i*) **46** (olean), olive fruit fly *Bactrocera oleae*; (*j*) **47**, tsetse fly *Glossina pallidipes*.

to **9** significantly reduces the response of the male drugstore beetles to the pheromone.[33]

*(d) The natural pheromone is a single enantiomer, while its antipode or diastereomer is also active*

Male German cockroaches do not discriminate among the four stereoisomers of the female-produced sex pheromone, although the natural product is (3*S*,11*S*)-**38**.[34]

The male spined citrus bug produces (3*R*,4*S*)-**39** as an aggregation pheromone. The opposite (3*S*,4*R*)-enantiomer of the pheromone is also bioactive, indicating that the insect does not discriminate between the enantiomers.[35]

*(e) The natural pheromone is an enantiomeric mixture, and both the enantiomers are separately active*

Female Douglas-fir beetles produce a 55 : 45 mixture of (*R*)- and (*S*)-**40** as a component of their aggregation pheromone. The combined effect of the enantiomers of **40** was additive, rather than synergistic, and both the enantiomers are required for maximum response.[36]

Male southern pine beetles produce an 85 : 15 mixture of (1*S*,5*R*)-frontalin **41** and its (1*R*,5*S*)-isomer.[37] In laboratory and field bioassays, the response of the beetles was significantly greater to the mixture of (1*S*,5*R*)-**41** and α-pinene than to (1*R*,5*S*)-**41** and α-pinene, although both were active. Both the enantiomers of **41** stimulated the same olfactory cells, suggesting that each cell has at least two types of enantioselective receptors.[37]

*(f) The different enantiomers or diastereomers are used by different species*

(*S*)-Ipsdienol **42** is the pheromone component of the California five spined ips (*Ips paraconfusus*), while other bark beetles *I. calligraphus* and *I. avulsus* respond to (*R*)-**42**.[38] Further detailed study was reported on variation of the enantiomeric purity of **42** in the bark beetle *I. pini*.[39]

Chirality of pheromones is important for discrimination between two species of the winter-flying geometrid moths in Middle Europe. Thus (6*R*,7*S*)-**43** is the pheromone of *Colotois pennaria*, while *Erannis defoliaria* uses (6*S*,7*R*)-**43** as its pheromone.[40]

*(g) Both the enantiomers are required for bioactivity*

Sulcatol **10** is the male-produced aggregation pheromone of the ambrosia beetle *Gnathotrichus sulcatus*. Neither (*R*)-**10** nor (*S*)-**10** was bioactive. But when combined to give a racemic mixture, the synthetic **10** was more active than the natural pheromone, which was a mixture of (*R*)-**10** and (*S*)-**10** in a ratio of 35 : 65.[41]

*(h) One enantiomer is more active than the other stereoisomer(s), but an enantiomeric or a diastereomeric mixture is more active than the most active enantiomer alone*

In the case of the trail following pheromone **44** of the ant *Myrmica scabrinodis*, the naturally occurring mixture of (*R*)-**44** and (*S*)-**44** (*R* : *S* = 9 : 1) was more attractive than pure (*R*)-**44** or (±)-**44**, while (*S*)-**44** was inactive.[42]

Tribolure (4*R*,8*R*)-**45** is the male-produced aggregation pheromone of the red-flour beetle *Tribolium castaneum*. Suzuki *et al*. found (4*R*,8*R*)-**45** to be as active as the natural pheromone, while a mixture of (4*R*,8*R*)-**45** and its (4*R*,8*S*)-isomer in a ratio of 8 : 2 was about ten times more active than (4*R*,8*R*)-**45** alone.[43]

*(i) One enantiomer is active on male insects, while the other is active on females*

Olean **46** is the female-produced sex pheromone of the olive fruit fly. Its (*R*)-isomer was active on the males, while the

(*S*)-isomer was active on the females.[44] The natural olean was racemic.[44]

### (*j*) *Only the* meso-*isomer is active*

In the case of the tsetse fly sex pheromones, *meso*-alkanes seem to be bioactive. Thus (13*R*,23*S*)-**47** was active as the sex-stimulant pheromone of the female tsetse fly, *Glossina pallidipes*, while neither (13*R*,23*R*)-**47** nor (13*S*,23*S*)-**47** was bioactive.[45]

## Conclusion

The progress of synthetic organic chemistry in this last quarter of the 20th century is manifested by the fact that we can now synthesize the pure enantiomers of a pheromone with even higher enantiomeric purity than that of the naturally occurring one. This has been made possible by the development of various methods of both asymmetric synthesis and stereochemical analysis. We can now determine the absolute configuration of a natural pheromone and investigate the stereochemistry–bio-activity relationships on the basis of highly enantioselective synthesis of the pheromones.

Chemists and biologists are able to unveil the remarkable biodiversity in the stereochemical aspects of pheromone perception. Insects use chirality to enrich their communication systems. The next task for biochemists and molecular biologists is to clarify the biochemical mechanisms which make the diversity possible.

Finally, from the standpoint of practical applications, one must not forget that the stereoisomers of pheromones can be inhibitors of the pheromone action.

I thank my co-workers, whose names appear in the references cited. I also thank Dr H. Takikawa for his help in preparing the manuscript. My thanks are due to the Kumagai Foundation for Science and Technology for financial support.

## Footnote

† This ChemComm is also available *via* the World Wide Web: http://chemistry.rsc.org/rsc/ccenha.htm

---

**Kenji Mori obtained his BSc (1957, agricultural chemistry), MSc (1959, biochemistry) and PhD (1962, organic chemistry) degrees from the University of Tokyo. He remained there until March 1995 (1962–1968, assistant; 1968–1978, associate professor; 1978–1995, professor) and then moved to Science University of Tokyo. His research interests are in enantioselective synthesis of bioactive natural products, biotransformations and chemical ecology. He has been honoured by awards of the Japan Academy (in 1981 in the presence of the late Emperor Hirohito) and the International Society of Chemical Ecology (Silver Medal in 1996 in Prague).**

---

## References


1 K. Mori, *Tetrahedron Lett.*, 1973, 3869.
2 K. Mori, *Tetrahedron*, 1974, **30**, 3817.
3 R. G. Riley, R. M. Silverstein and J. C. Moser, *Science*, 1974, **183**, 760.
4 S. Iwaki, S. Marumo, T. Saito, M. Yamada and K. Katagiri, *J. Am. Chem. Soc.*, 1974, **96**, 7842.
5 K. Mori, *Tetrahedron*, 1974, **30**, 4223.
6 D. L. Wood, L. E. Browne, B. Ewing, K. Lindahl, W. D. Bedard. P. E. Tilden, K. Mori, G. B. Pitman and P. R. Hughes, *Science*, 1976, **192**, 896.
7 S. Kuwahara and K Mori, *Tetrahedron*, 1990, **46**, 8083.
8 K. Mori and N. P. Argade, *Liebigs Ann. Chem.*, 1994, 695.
9 K. Mori and T. Ebata, *Tetrahedron*, 1986, **42**, 4413.
10 E. L. Plummer, T. E. Stewart, K. Byrne, G. T. Pearce and R. M. Silverstein, *J. Chem. Ecol.*, 1976, **2**, 307.
11 K. Mori, in *Methods in Chemical Ecology*, ed. J. Millar and K. Haynes, Chapman and Hall, New York, 1996, in the press.
12 W. A. König, *Gas Chromatographic Enantiomer Separation with Modified Cyclodextrins*, Hüthig, Heidelberg, 1992.
13 K. Mori, in *The Total Synthesis of Natural Products*, ed. J. W. ApSimon, John Wiley, New York, 1981, vol. 4, pp. 1–183.
14 K. Mori, in *The Total Synthesis of Natural Products*, ed. J. W. ApSimon, John Wiley, New York, 1992, vol. 9, pp. 1–534.
15 K. Mori, *Tetrahedron*, 1989, **45**, 3233.
16 K. Mori, in *Advances in Asymmetric Synthesis*, ed. A. Hassner, JAI Press, Greenwich, 1995, vol. 1, pp. 211–269.
17 J. Beauharire, P.-H. Ducrot, C. Malosse, D. Rochat, J. O. Ndiege and D. O. Otiens, *Tetrahedron Lett.*, 1995, **36**, 1043.
18 K. Mori, T. Nakayama and H. Takikawa, *Tetrahedron Lett.*, 1996, **37**, 3741.
19 W. Francke, F. Schröder, P. Philipp, H. Meyer, V. Sinnwell and G. Gries, *Bioorg. Med. Chem.*, 1996, **4**, 363.
20 K. Mori, H. Takikawa, Y. Nishimura and H. Horikiri, *Liebigs Ann.*, 1997, 327.
21 W. S. Leal, S. Kuwahara, M. Ono and S. Kubota, *Bioorg. Med. Chem.*, 1996, **4**, 315.
22 T. Nakayama and K. Mori, *Liebigs Ann.*, in the press.
23 K. Mori, *Synlett*, 1995, 1097.
24 R. C. Starr, F.-J. Marner and L. Jaenicke, *Proc. Natl. Acad. Sci. USA*, 1995, **92**, 641.
25 L. Jaenicke and F.-J. Marner, *Liebigs Ann.*, 1995, 1343.
26 K. Mori and S. Takanashi, *Tetrahedron Lett.*, 1996, **37**, 1821.
27 K. Mori and S. Takanashi, *Proc. Jpn. Acad. Ser. B.*, 1996, **72**, 174.
28 M. Mohri, H. Kinoshita, K. Inomata and H. Kotake, *Chem. Lett.*, 1985, 451.
29 M. Kobayashi, T. Koyama, K. Ogura, S. Seto, F. J. Ritter and J. E. M. Brüggemann-Rotgans, *J. Am. Chem. Soc.*, 1980, **102**, 6602.
30 J. P. Vité, D. Klimetzek, G. Loskant, R. Hedden and K. Mori, *Naturwissenschaften*, 1976, **63**, 582.
31 J. H. Tumlinson, M. G. Klein, R. E. Doolittle, T. L. Ladd and A. T. Proveaux, *Science*, 1977, **197**, 789.
32 M. Mori, K. Mochizuki, M. Kohno, T. Chuman, A. Ohnishi, H. Watanabe and K. Mori, *J. Chem. Ecol.*, 1986, **12**, 83.
33 H. Kodama, K. Mochizuki, M. Kohno, A. Ohnishi and Y. Kuwahara, *J. Chem. Ecol.*, 1987, **13**, 1859.
34 R. Nishida and H. Fukami, *Mem. Coll. Agric. Kyoto Univ.*, 1983, **122**, 1.
35 D. G. James and K. Mori, *J. Chem. Ecol.*, 1995, **21**, 403.
36 B. S. Lindgren, G. Gries, H. D. Pierce, Jr. and K. Mori, *J. Chem. Ecol.*, 1992, **18**, 1201.
37 T. L. Payne, J. V. Richerson, J. C. Dickens, J. R. West, K. Mori, C. W. Berisford, R. L. Hedden, J. P. Vité and M. S. Blum, *J. Chem. Ecol.*, 1982, **8**, 873.
38 J. P. Vité, G. Ohloff and R. F. Billings, *Nature*, 1978, **272**, 817.
39 S. J. Seybold, T. Ohtsuka, D. L. Wood and I. Kubo, *J. Chem. Ecol.*, 1995, **21**, 995.
40 G. Szöcs, M. Tóth, W. Francke, F. Schmidt, P. Philipp, W. A. König, K. Mori, B. S. Hansson and C. Löfstedt, *J. Chem. Ecol.*, 1993, **19**, 2721.
41 J. H. Borden, L. Chong, J. A. McLean, K. N. Slessor and K. Mori, *Science*, 1976, **192**, 894.
42 M.-C. Cammaerts and K. Mori, *Physiol. Entomol.*, 1987, **12**, 381.
43 T. Suzuki, J. Kozaki, R. Sugawara and K. Mori, *Appl. Entomol. Zool.*, 1984, **19**, 15.
44 G. Haniotakis, W. Francke, K. Mori, H. Redlich and V. Schurig, *J. Chem. Ecol.*, 1986, **12**, 1559.
45 P. G. McDowell, A. Hassanali and R. Dransfield, *Physiol. Entomol.*, 1985, **10**, 183.


*6/06625I*

# Non-resonant third-order optical non-linearity of porphyrin derivatives

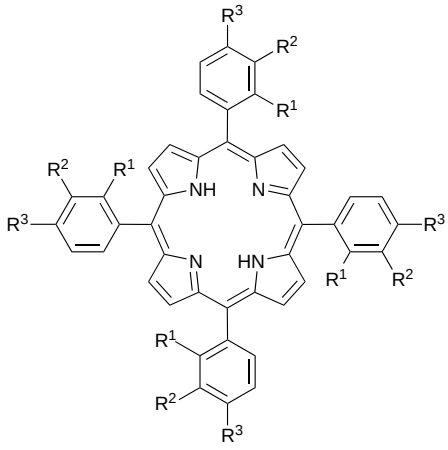
**K. Kandasamy,[a] Shankar J. Shetty,[b] P. N. Puntambekar,[a] T. S. Srivastava,[b] T. Kundu[a] and Bhanu P. Singh*[a]**

[a] *Department of Physics, Indian Institute of Technology, Bombay-400 076, India*
[b] *Department of Chemistry, Indian Institute of Technology, Bombay-400 076, India*

**Non-resonant second molecular hyperpolarisabilities ($\gamma$) of tetraphenylporphyrin ($H_2$tpp) and five substituted derivatives are measured by the *Z*-scan technique at 784 nm; the relationship between the various structures and their corresponding molecular hyperpolarisabilities is explained on the basis of electronic interaction between the external substituents and the porphyrin core.**

The non-linear optical properties of π-conjugated organic molecules[1,2] have been the subject of intense scientific research owing to their potential applications in photonic technology. Porphyrin derivatives are attractive owing to their large polarisable π-electron system. Further, these hold the promise of vast improvement in their optical non-linearities by way of molecular engineering. This requires an understanding of the structure–non-linearity relationship. Such an understanding is still in its infancy and more systematic studies are needed. With this motivation, we have undertaken the investigation of the effect of external substituents in porphyrin structures on their second molecular hyperpolarisabilities using the *Z*-scan technique.

Six porphyrin structures (Fig. 1) having external substitution of ester and methoxy groups at systematically varying positions of the phenyl ring have been synthesised using standard procedures.[3–5] Substituents were chosen such that their electron donating/accepting capacity varies. The third-order non-linear optical susceptibilities of $10^{-4}$ M solutions of these compounds in toluene were measured using the *Z*-scan[6] technique. A self-mode-locked Ti : sapphire laser, generating 60 fs transform limited pulses at 784 nm, was employed for these experiments. The laser beam was focused to a spot size of 25 μm using an 8 cm focal length lens and the 1 mm sample cell was scanned through its focal region. The experimental set-up was standardised by toluene. Its measured $\chi^{(3)}(-\omega,\omega,-\omega,\omega)$ value ($4.55 \times 10^{-13}$ esu) is in excellent agreement with the earlier reported value of $4.76 \times 10^{-13}$ esu obtained by the optical Kerr effect.[7] The intensity levels in *Z*-scans of various samples varied in the range of 0.8–33.0 kW to contain the phase variation below π radians. For the measurement of non-resonant non-linearities, an excitation wavelength of 784 nm is chosen far away from the B (*ca*. 419 nm) and Q (*ca*. 615 nm) absorption bands of the porphyrins.




**1** $R^1$ = H, $R^2$ = H, $R^3$ = H
**2** $R^1$ = $OCH_2CO_2Et$, $R^2$ = H, $R^3$ = H
**3** $R^1$ = H, $R^2$ = $OCH_2CO_2Et$, $R^3$ = H
**4** $R^1$ = H, $R^2$ = H, $R^3$ = $OCH_2CO_2Et$
**5** $R^1$ = H, $R^2$ = $OCH_2CO_2Et$, $R^3$ = $OCH_2CO_2Et$
**6** $R^1$ = H, $R^2$ = OMe, $R^3$ = $OCH_2CO_2Et$

**Fig. 1** Structures of porphyrins used in this study. 5,10,15,20-Tetraphenylporphyrin **1**, 5,10,15,20-tetrakis[2-(carboethoxymethyleneoxy)phenyl]porphyrin **2**, 5,10,15,20-tetrakis[3-(carboethoxymethyleneoxy)phenyl]porphyrin **3**, 5,10,15,20-tetrakis[4-(carboethoxymethyleneoxy)phenyl]porphyrin **4**, 5,10,15,20-tetrakis[3,4-bis(carboethoxymethyleneoxy)-phenyl]porphyrin **5**, 5,10,15,20-tetrakis[2-(carboethoxymethyleneoxy)-phenyl]porphyrin **6**.

A typical closed-aperture *Z*-scan for **2** is shown in Fig. 2. In all samples, it exhibits a pre-focal maximum followed by a post-focal minimum. This indicates a negative non-linear index of refraction. No transmittance variations in any of the open-aperture *Z*-scans are observed. This suggests that the measured non-linearities are predominantly refractive and non-resonant. Third-order non-linear susceptibilities $\chi^{(3)}$ for the solutions and the solvent were obtained by fitting the experimental *Z*-scan data to the expressions for the closed-aperture transmittance given in ref. 6. For a dilute solution of non-interacting particles, the second hyperpolarisability ($\gamma$) of the solute in a pairwise additive model,[8] is given by eqn. (1).

$$\gamma = \frac{\chi^{(3)}_{\text{soln}} - \chi^{(3)}_{\text{solvent}}}{L^4 N_{\text{solute}}} \quad (1)$$

where $N_{\text{solute}}$ is the number density of solute, $L = (n^2 + 2)/3$ is the local-field factor[9] and $n$ is the refractive index of the medium. The $\chi^{(3)}_{\text{soln}}$ was found to vary linearly with concentration

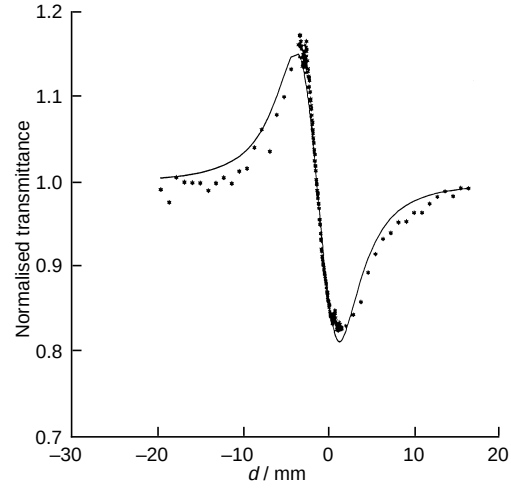



**Fig. 2** Closed-aperture *Z*-scan trace of **2** in neutral conditions at 784 nm. The solid line represents the theoretical fit to eqn. (1).

for all the porphyrin derivatives. This justifies the applicability of pairwise additive model.

Table 1 shows the measured second molecular hyperpolarisabilities for six porphyrin derivatives. The influence of external substitution on the γ values is clearly evident. A very large enhancement of γ (nearly six times that of $H_2$tpp) is seen for **2** having ester groups at *ortho* positions. The external substituents can influence the γ values by perturbing the charge density in the porphyrin core. As a preliminary attempt to explain the systematics of the observed variation of γ with structural modification, the correlation was sought with the Hammett constant σ, a measure of substituents electron-donating/accepting capacity. The net Hammett constant[10] is given by

$$\sigma = Ca_r\sigma_r + a_i\sigma_i \quad (2)$$

where $a_r$ and $a_i$ represent the relative contributions of resonant and inductive effects, and $C = 0.075$ for the *meta* position and unity otherwise. The values of the resonant ($\sigma_r$) and inductive ($\sigma_i$) parts of the Hammett constant for ester and methoxy groups are $\sigma_r = -0.4$, $\sigma_i = 0.33$ and $\sigma_r = -0.45$, $\sigma_i = 0.34$, respectively.

A linear relation between γ and σ is observed considering a 70% inductive and 30% resonant contribution. The inductive effect is expected to dominate as all these molecules in their free-base form have $D_{2h}$ symmetry, since the porphine core and the phenyl ring are perpendicular to each other. Compound **2** has not been included in this correlation as the Hammett constant cannot be defined for substituents at the *ortho* positions. It is seen from Table 1 that a more positive value of σ results in reduced hyperpolarisability. The positive sign of σ indicates electron withdrawal from the core to the substituents. This leads to a decrease of the core electron density and hence a reduction of the hyperpolarisability.

To substantiate the above, the pH environment of porphyrin molecules was changed by adding a drop of trifluoroacetic acid to the samples. In the acidic environment, the symmetry changes from $D_{2h}$ to $D_{4h}$ owing to the formation of the dication[11] and a dramatic increase of the second hyperpolarisability was observed. A linear relation between γ and σ was observed when assuming a 70% resonant and 30% inductive effect. The resonant contribution is expected to dominate the interaction between the porphyrin core and the substituent, as for the $D_{4h}$ symmetry, the core and the phenyl ring are almost parallel.[12] The calculated Hammett constants along with the observed hyperpolarisabilities are listed in Table 1. The negative sign of the Hammett constant implies an increase of the electron density in the core owing to electron donation by the substituents. It can be seen from Table 1 that the second molecular hyperpolarisability increases with increasing negative value of the Hammett constant. Thus, the observed trend of γ with the variation of substituent site is again consistent with our argument. The enhancement in the γ value of $H_2$tpp in an acidic environment over a neutral one may be attributed to increased π-electron delocalisation in the planar molecule, which is reflected in the red shift (*ca*. 20 nm) of the HOMO–LUMO gap in the absorption spectrum.

**Table 1** Values of γ for six porphyrin derivatives in neutral and acidic environments. From repeated measurements and stability of the laser, the measurement tolerance is estimated to be ±2%

| | Neutral | | Acidic | |
|---|---|---|---|---|
| | $10^{30}$ γ/esu | σ | $10^{30}$ γ/esu | σ |
| **2** | −48.2 | — | −273.5 | — |
| **1** | −8.5 | 0.0 | −20.7 | 0.0 |
| **4** | −6.7 | 0.11 | −31.0 | −0.18 |
| **3** | −6.5 | 0.22 | −17.1 | 0.08 |
| **5** | −6.3 | 0.33 | −25.7 | −0.10 |
| **6** | −6.2 | 0.34 | −25.4 | −0.10 |

The important finding of this study is the massive enhancement of the non-linearity (*ca*. six times that of neutral $H_2$tpp) in **2** having substituents at *ortho* positions. An even larger non-linearity of this molecule (*ca*. 36 times that of neutral $H_2$tpp) is observed in an acidic environment. This high non-resonant non-linearity is large enough for practical non-linear optical devices.

In view of the arguments presented above, large enhancement of γ in **2** should arise due to (*i*) enhanced charge density in the core and (*ii*) increased π-electron delocalization.

Both of these effects will operate when the phenyl ring is not perpendicular to the core. The strong interaction between the β-pyrrole hydrogen and oxygen of the ester substituents at *ortho* positions may lead to increased planarity between the core and the phenyl ring.[13] The degree of planarity will depend upon the relative strength of the interaction between the β-pyrrole hydrogen and oxygen and steric hindrance due to the substituents. Substitution at *ortho* positions is expected to lead to more effective electron donation owing to its shear proximity to the core. In acidic conditions, further increased planarity in **2** will lead to still larger enhancement of the non-linearity for the above reasons.

In conclusion, non-linear properties of porphyrins can be vastly improved by external substitution of strong electron-donor groups at *ortho* positions of the planar porphyrin molecule. Further work to understand the origin of this enhancement at the microscopic level is in progress. However, this preliminary study provides some guidelines for molecular engineering.

We thank the Department of Science and Technology for financial support. Professor T. S. Srivastava would like to thank the All India Council of Technical Education for financial support.

## Footnote

* E-mail: bhanups@niharika.phy.iitb.ernet.in

## References

1 J. L. Bredas, C. Adant, P. Tackx and A. Persoons, *Chem. Rev.*, 1994, **94**, 243.
2 D. V. G. L. N. Rao, F. J. Aranda, J. F. Roach and David E. Remy, *Appl. Phys. Lett.*, 1991, **58**, 1241.
3 S. A. Syrbu, A. S. Semeikin, B. D. Berezin and O. I. Koifman, *Khim. Geterotsikl. Soedin*, 1989, **10**, 1373.
4 S. J. Shetty, S. Murugashan, S. R. Chatterjee, S. Banerjee, T. S. Srivastava, O. P. D. Noronha and A. M. Samuel, *J. Labelled Compd. Radiopharm.*, 1996, **38**, 411.
5 A. M. D'A Rocha Gonsalves, T. B. Varjao Jorge and M. M. Pereira, *J. Heterocycl. Chem.*, 1991, **28**, 635.
6 A. Sheik Bahae, A. A. Said, T. Wei, D. J. Hagan and E. W. Vanstryland, *IEEE J. Quantum Electron.*, 1990, **26**, 760.
7 P. P. Ho and R. R. Alfano, *Phys. Rev. A*, 1979, **20**, 2170.
8 Ming-Tang, B. P. Singh and P. N. Prasad, *J. Chem. Phys.*, 1988, **89**, 5535.
9 C. Sauturet, J. P. Hermann, R. Frey, F. Pradere, J. Ducuing, R. M. Baughman and R. R. Chance, *Phys. Rev. Lett.*, 1976, **36**, 956.
10 M. Meot-Ner and A. D. Adler, *J. Am. Chem. Soc.*, 1975, **97**, 5107.
11 M. Gouterman, in *The Porphyrins*, ed. D. Dolphin, Academic Press, New York, 1978, vol III.
12 E. B. Fleischer, *Acc. Chem. Res.*, 1970, **3**, 105.
13 F. R. Longo, M. G. Finarelli and J. B. Kim, *J. Heterocycl. Chem.*, 1969, **6**, 927.

*Received in Cambridge, UK, 26th March 1997; Com. 7/02098H*

# Synthesis and structure of [Sb{(Pr$^i$N)$_2$CNHPr$^i$}{(Pr$^i$N)$_2$CNPr$^i$}]; a distorted trigonal-bipyramidal antimony(III) complex with a helical hydrogen-bond network

**Philip J. Bailey,*[a] Robert O. Gould,[a] Christopher N. Harmer,[b] Stuart Pace,[a] Alexander Steiner[b] and Dominic S. Wright*[b]**

[a] *Department of Chemistry, University of Edinburgh, West Mains Road, Edinburgh, UK EH9 3JJ*
[b] *Department of Chemistry, University of Cambridge, Lensfield Road, Cambridge, UK CB2 1EW*

**1,2,3-Triisopropylguanidine [(Pr$^i$NH)$_2$C=NPr$^i$], reacts with antimony tris(dimethylamide) [Sb(NMe$_2$)$_3$] to provide [Sb{(Pr$^i$N)$_2$CNHPr$^i$}{(Pr$^i$N)$_2$CNPr$^i$}] 1, a heavily distorted trigonal-bipyramidal complex in which the Sb is chelated by a [C(NPr$^i$)$_3$]$^{2-}$ dianion and a [(Pr$^i$N)$_2$CNHPr$^i$]$^-$ monoanion; in the solid state the complexes form helices by N–H···N hydrogen bonding of the single proton.**

Our recent interest in trisubstituted guanidines and their anions as ligands has led to the characterisation of a number of new complexes which have demonstrated the flexibility of this new ligand system in both chelating and bridging coordination modes.[1–4] The ligands also exhibit a marked ability to stabilise higher oxidation states in transition-metal complexes.[4] The ability of the system to coordinate as a neutral ($H_2L$), monoanionic ($HL^-$) or dianionic ($L^{2-}$) ligand, and the presence of ionisable protons on the former two, adds to its flexibility. Hydrogen bonding plays an important role in much of the chemistry of guanidines and molecules containing the guanidine unit such as the nucleic acid base guanine, and we have thus become interested in the hydrogen-bonding properties of metal coordinated guanidines containing residual protons. Here we report a complex containing a single hydrogen which is formed by chelation of a trivalent metal by two trisubstituted guanidines, one a monoanion and the other a dianion, thus providing an N–H hydrogen-bond donor on one ligand and a imine nitrogen hydrogen-bond acceptor on the other.

Treatment of 1,2,3-triisopropylguanidine with 1 mol. equiv. of [Sb(NMe$_2$)$_3$][5] in toluene solution provides a yellow solution. Reduction of this solution to dryness in vacuum and dissolution of the residue in warm hexane followed by filtration, concentration and cooling provided highly air-sensitive crystals of [Sb{(Pr$^i$N)$_2$CNHPr$^i$}{(Pr$^i$N)$_2$CNPr$^i$}] **1** in 10% yield.† The presence of both the anion $HL^-$ and dianion $L^{2-}$ is confirmed by the $^1$H NMR spectrum of **1** which shows that there are five independent isopropyl groups in the ratio 1 : 1 : 1 : 1 : 2, consistent with free rotation only about the uncoordinated C–NHPr$^i$ bond of the $HL^-$ ligand whilst the C=NPr$^i$ bond of the $L^{2-}$ remains static. The formation of **1**, which retains an N–H hydrogen despite the presence of sufficient metallating agent in the reaction mixture to remove all such hydrogens, is worthy of note and may be a result of preferential crystallisation of the hydrogen-bonded partially metallated species, *vide infra*, and explain its low yield. Unfortunately, the extreme air sensitivity of **1** prevented the recording of any IR spectra.

Crystals of **1** are chiral with space group $P3_121$ or $P3_221$ and a low-temperature X-ray crystallographic study‡ shows that there are two independent, but chemically equivalent, molecules in the unit cell which differ only marginally in the conformations of their isopropyl groups and in their bond lengths and angles. One molecule lies on a twofold rotational axis relating the two ligands (Fig. 1), whilst the other (molecule 2, not shown) lacks this axis. The complex consists of [Sb{(Pr$^i$N)$_2$CNHPr$^i$}{(Pr$^i$N)$_2$CNPr$^i$}] molecules in which each Sb$^{III}$ centre is formally chelated by a monoanion $HL^-$ and a dianion $L^{2-}$ ligand. The molecular structure of **1** is consistent with the ten-electron count of the Sb centre and can best be described as a heavily distorted trigonal-bipyramidal $N_4Sb$ molecule with the fifth coordination site being occupied by the lone pair. In both independent molecules the Sb$^{III}$ centres are asymmetrically coordinated by the two guanidine ligands [*e.g.* Sb(1)–N(11) 2.227(6) Å, Sb(1)–N(13) 2.069(6) Å]. This pattern of bond lengths is consistent with the description of the structure as distorted trigonal bipyramidal since in this geometry each ligand would be coordinated to an axial and an equatorial position. The nature of the distortion can be appreciated if it is considered that in this structure trigonal-bipyramidal geometry requires the chelating angle at the metal (N–Sb–N) to be 90°, whilst in **1** far more acute angles at Sb are found as a consequence of the geometric constraints arising from the chelation by the rigid guanidine ligands [*e.g.* N(11)–Sb(1)–N(13) 62.0(2)°]. The result of this is that the N–Sb–N angle between the axial N centres is distorted from the 180° [to

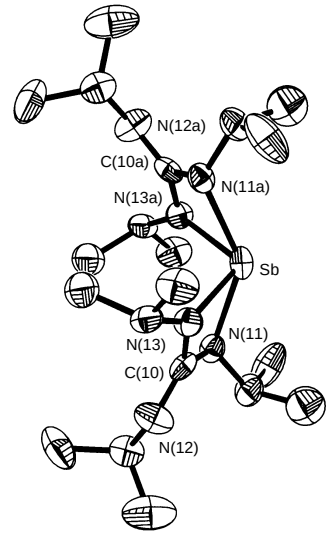



**Fig. 1** Molecular structure of **1**. Hydrogen atoms have been omitted for clarity. Selected bond lengths (Å) and angles (°): molecule 1: Sb(1)–N(11) 2.227(6), Sb(1)–N(13) 2.069(6), C(10)–N(11) 1.372(10), C(10)–N(12) 1.311(11), C(10)–N(13) 1.342(10); N(11)–Sb(1)–N(13) 62.0(2), N(11)–Sb(1)–N(11a) 140.3(3), N(13)–Sb(1)–N(13a) 104.5(3), N(13)–Sb(1)–N(11a) 93.1(2); N(12)···N(12a) 3.148(12), N(12)–H(12)–N(12) 160; molecule 2: N(31)–Sb(2) 2.320(6), N(33)–Sb(2) 2.098(6), N(41)–Sb(2) 2.133(6), N(43)–Sb(2) 2.050(5), C(30)–N(31) 1.325(9), C(30)–N(32) 1.353(9), C(30)–N(33) 1.341(9), C(40)–N(41) 1.402(9), C(40)–N(42) 1.273(9), C(40)–N(43) 1.381(9); N(31)–Sb(2)–N(33) 59.9(2), N(41)–Sb(2)–N(43) 63.9(2), N(41)–Sb(2)–N(31) 140.2(2), N(33)–Sb(2)–N(43) 104.2(2), N(33)–Sb(2)–N(41) 92.7(2), N(31)–Sb(2)–N(43) 93.4(2); N(32)···N(42) 3.125(12), N(32)–H(32)–N(42) 172, N(42)–H(42)–N(32) 144.

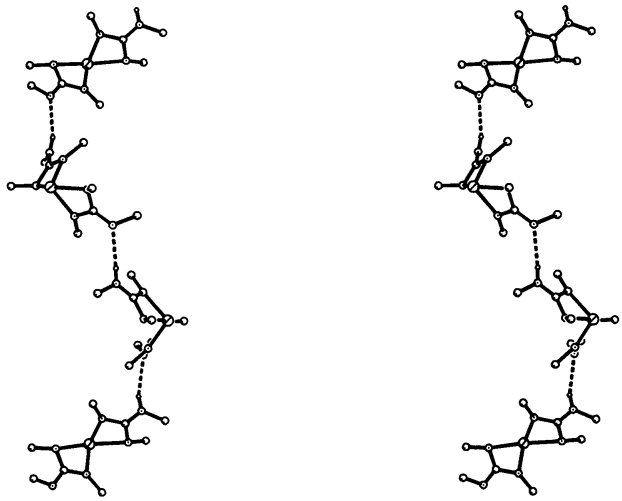


**Fig. 2** Stereoview showing the association of molecules of **1** *via* N–H···N hydrogen bonds into helices. Symmetry transformations used to generate equivalent atoms a, *x–y*, *–y*, *–z* + 1/3.

140.3(3)° for N(11)–Sb(1)–N(11a)] and that for the equatorial N centres is distorted from the 120° [to 104.5(3)° for N(13)–Sb(1)–N(13a)] required for ideal trigonal-bipyramidal geometry. The distorted trigonal-bipyramidal geometries of the $Sb^{III}$ centres of **1** are very similar to those observed for the central metal atom in the $[\{(Me_2N)_2Sb(NC_6H_{11})_2\}_2Sb]^-$ monoanion,[6] which is the only other structurally characterised unit containing an $Sb^{III}$ centre four-coordinated by nitrogen ligands.

Although the ligands in each molecule of **1** must formally be a monoanion and a dianion to provide the necessary trianionic ligand set for the $Sb^{III}$ centre, in the crystal they cannot be distinguished in this way since each of the uncoordinated $NPr^i$ groups is involved in hydrogen bonding to an adjacent molecule with an N···N distance of 3.184(12) Å and N–H···N angle of 160°. As a consequence of the alignment of these groups, which is dictated directly by the distorted trigonal-bipyramidal geometry present in the molecular units of **1**, the resulting hydrogen-bonded H···L–Sb–L–H···L–Sb–L–H··· chains form left-handed helices through the crystal studied with three molecules of **1** per 360° turn (Fig. 2). It is probable that other crystals have the opposite chirality and hence right-handed chirality. Helical association of monomer units has been identified in a few polymeric phosphido and amido lithium complexes[7] and packing of molecules of $[Ru_3(CO)_9\{\mu\text{-}NCH(SiMe_3)_2\}(\mu\text{-}N(C_6H_2Pr^i_3\text{-}2,4,6)_2]$ exclusively into β helices occurs in the solid state.[8] However, helical packing or association of molecules is extremely rare in transition and main group metal compounds and, to our knowledge, the helical hydrogen-bonded association found in **1** is unprecedented for any metallo-organic complex.

We gratefully acknowledge the EPSRC (studentships for C. N. H. and S. P.), The Leverhulme Trust (P. J. B.), The Royal Society (P. J. B., D. S. W.) and The European Community (Fellowship for A. S.) for financial support.

## Footnotes

* E-mail: philip.bailey@ed.ac.uk

† 1,2,3-Triisopropylguanidine (0.928 g, 5.0 mmol) was dissolved in toluene (10 $cm^3$) and 2.6 $cm^3$ of a 1.93 M solution of $[Sb(NMe_2)_3]$ in toluene (1.275 g, 5.02 mmol) was added by syringe under argon. Over a period of 2 h the solution became yellow and the solvent was then removed *in vacuo*. The residue was dissolved in warm hexane (25 $cm^3$) and filtered through Celite to give a clear yellow solution. The volume was reduced to *ca*. 5 $cm^3$ and the resulting microcrystalline precipitate redissolved by warming. Gradual cooling in a water bath over two days provided X-ray quality crystals of **1** (*ca*. 10%). (Found: C, 48.2; H, 8.81; N, 16.4. $C_{20}H_{43}N_6Sb$ requires C, 49.1; H, 8.80; N, 17.1%). $^1$H NMR (250 MHz) in [$^2H_6$]benzene: δ 0.7–1.6 [m, 36 H, $CH(CH_3)_2$], 3.34 [br, 2 H, $CH(CH_3)_2$/NH], 3.72 [spt, 2 H, $CH(CH_3)_2$], 4.12 [spt, 1 H, $CH(CH_3)_2$], 4.35 [spt, 1 H, $CH(CH_3)_2$], 4.83 [spt, 1 H, $CH(CH_3)_2$].

‡ *Crystal data* for **1**: $C_{20}H_{43}N_6Sb$, $M_w$ = 489.35, trigonal, space group $P3_221$, $a$ = 17.356(2), $b$ = 17.356(2), $c$ = 21.919(4) Å, $U$ = 5718(2) $Å^3$, $Z$ = 9, λ = 0.710 73 Å, $D_c$ = 1.279 Mg $m^{-3}$, μ(Mo-Kα) = 1.101 $mm^{-1}$. Data were collected on a Siemens-Stoe AED diffractometer using an oil-coated crystal[8] of dimensions 0.2 × 0.2 × 0.2 mm using the θ–ω method ($4.04 \leqslant \theta \leqslant 22.73°$). Of a total of 6438 reflections collected, 4985 ($R_{int}$ 0.026) were independent. The crystal studied was intimately twinned, giving a diffraction pattern approximating to 6/*mmm* ($D_{6h}$) symmetry. Twin refinement in space group $P3_221$ with [1$\bar{1}$0] as the twin axis gave 56.46(9)% as the contribution of the major component and 0.03(3) as the Flack *x*-parameter, indicating that both twins have the same correct absolute structure. No conclusons may be drawn about the chirality of the other crystals in the batch. The structure was solved by Patterson methods, and refined by full-matrix least squares on $F^2$ to final values of $R_1$ = 0.027 [for 4985 data with $F > 4\sigma(F)$] and $wR_2$ = 0.070 (all data) [$R_1 = \Sigma||F_o| - |F_c||/\Sigma|F_o|$, $wR_2 = \{[\Sigma w(F_o^2 - F_c^2)]^2/\Sigma wF_o^4\}^{0.5}$, $w = 1/[\sigma^2(F_o^2) + (0.040P)^2 + 4.26P]$, $P = (F_o^2 + 2F_c^2)/3$].[10] Largest difference between peak and hole in the final difference map, 0.42, −0.38 e $Å^{-3}$. The hydrogen-bonded N–H hydrogens were placed in calculated positions and allowed to ride between their respective nitrogen atoms with a site occupancy of 0.5. Atomic coordinates, bond lengths and angles, and thermal parameters have been deposited at the Cambridge Crystallographic Data Centre (CCDC). See Information for Authors, Issue No. 1. Any request to the CCDC for this material should quote the full literature citation and the reference number 182/460.

## References

1 P. J. Bailey, A. J. Blake, M. Kryszczuk, S. Parsons and D. Reed, *J. Chem. Soc., Chem. Commun.*, 1995, 1647.
2 P. J. Bailey, L. A. Mitchell, P. R. Raithby, M.-A. Rennie, K. Verhorevoort and D. S. Wright, *Chem. Commun.*, 1996, 1359.
3 P. J. Bailey, L. A. Mitchell and S. Parsons, *J. Chem. Soc., Dalton Trans.*, 1996, 2839.
4 P. J. Bailey, S. F. Bone, L. A. Mitchell, S. Parsons, K. J. Taylor and L. J. Yellowlees, *Inorg. Chem.*, 1997, **36**, 867.
5 For synthetic applications of $[SbNMe_2)_3]$ see, M. A. Paver, C. A. Russell and D. S. Wright, *Angew. Chem.*, 1995, **107**, 1677; *Angew. Chem., Int. Ed. Engl.*, 1995, **34**, 1545.
6 A. J. Edwards, M. A. Paver, M.-A. Rennie, C. A. Russell, P. R. Raithby and D. S. Wright, *Angew. Chem.*, 1994, **106**, 1334; *Angew. Chem., Int. Ed. Engl.*, 1994, **33**, 1277; M. A. Beswick, C. A. Harmer, M. A. Paver, P. R. Raithby, A. Steiner and D. S. Wright, *Inorg. Chem.*, 1997, in the press.
7 R. S. Bartlett, M. M. Olmstead and P. P. Power, *Inorg. Chem.*, 1986, **25**, 1243; E. Hey and F. Weller, *J. Chem. Soc., Chem. Commun.*, 1988, 782; N. D. R. Barnett, R. E. Mulvey, W. Clegg and P. A. O'Neil, *J. Am. Chem. Soc.*, 1991, **113**, 8187.
8 C. J. Cardin, D. J. Cardin, M. A. Convery, Z. Danter, D. Fenske, M. Devereux and M. B. Power, *J. Chem. Soc., Dalton Trans.*, 1996, 1133.
9 T. Kottke and D. Stalke, *J. Appl. Crystallogr.*, 1993, **26**, 615.
10 G. M. Sheldrick, SHELXL-96, structure refinement package, University of Göttingen, 1996.

*Received in Basel, Switzerland, 10th March 1997; Com. 7/01675A*

# Dehalogenation of organic halides by flash vacuum pyrolysis over magnesium: a versatile synthetic method

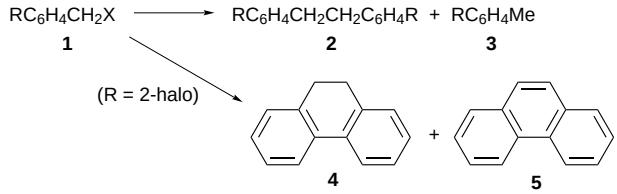
**R. Alan Aitken,*[a] Philip K. G. Hodgson,[b] Adebayo O. Oyewale[a] and (in part) John J. Morrison[a]**

[a] *School of Chemistry, University of St. Andrews, North Haugh, St. Andrews, Fife, UK KY16 9ST*
[b] *B. P. Research Centre, Chertsey Road, Sunbury-on-Thames, Middlesex, UK TW16 7LN*

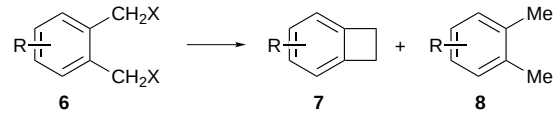
**Flash vacuum pyrolysis over magnesium at 600 °C results in efficient dehalogenation of a variety of organic halides and provides a preparatively useful method for C–C bond formation and other reactions.**

Pyrolytic processes in organic chemistry normally involve either fragmentation or rearrangement. The thermal generation of species such as radicals or carbenes may be followed by dimerisation but their high reactivity frequently leads to other competing processes. In order to develop a general method for C–C bond formation in the gas phase we decided to examine the pyrolysis of organic halides over solid magnesium. There has been little previous work on gas phase pyrolysis over solid reagents but pyrolysis over solid bases has been used effectively by Denis and co-workers.[1] Dehydrofluorination of alicyclic precursors over iron or nickel has been used to obtain fluorinated aromatics,[2] and pyrolysis of hexachlorocyclopentadiene over iron results in C–C bond formation to give perchlorofulvalene.[3] The few studies using other metals have all involved the generation of highly reactive species for spectroscopic detection. Thus, benzocyclobutadiene was first generated by flash vacuum pyrolysis (FVP) of diiodobenzocyclobutene over zinc at 230 °C[4] and can alternatively be formed by FVP of α,α,α′α′-tetrabromo-*o*-xylene over magnesium at 440–470 °C,[5] while FVP of $PXCl_3$ (X = O, S) over silver at 880 °C leads to generation of the reactive $P^{III}$ species, Cl–P=X[6] and FVP of trichloroacetyl chloride over zinc at 420 °C gives dichloroketene.[7] We report here that FVP of organic halides over freshly resublimed magnesium at 600 °C provides a versatile and preparatively useful method for C–C bond formation.

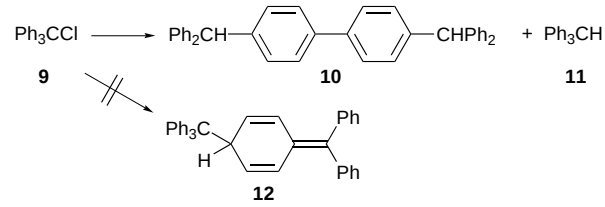
Initial experiments using benzyl chloride established that for maximum activity the magnesium had to be used in the range 500–700 °C and was best prepared by freshly subliming the metal over the surface of glass wool.† FVP of benzyl chloride through the system at 600 °C gave a liquid in the cold-trap which proved to be toluene (16%) and a solid at the furance exit which was essentially pure bibenzyl (58%). By using excess benzyl chloride it was established that approximately 20% of the magnesium used was available for reaction assuming conversion to $MgCl_2$. The method was equally effective for a range of substituted benzyl chlorides and bromides (Table 1)




giving the bibenzyls **2** and toluenes **3** in good to excellent combined yield. The bibenzyls were readily obtained in pure form by a single recrystallisation of the solids from the furnace exit and this represents a gas-phase alternative to the Wurtz coupling. The somewhat unexpected formation of the reduction products was a general observation in these studies and presumably results from sacrificial carbonisation of the substrate. For 2-halobenzyl halides, further dehalogenation to give dihydrophenanthrene **4** and phenanthrene **5** was observed as a minor process. The result for 2-methylbenzyl bromide shows a clear distinction from pyrolysis without magnesium which results in 1,4-loss of HBr and cyclisation of the resulting *o*-xylylene to give benzocyclobutene as the major product.[9] Reaction of 1,2-bis(halomethyl)benzene derivatives results in efficient formation of the benzocyclobutenes and this was used to obtain the 3- and 4-fluoro compounds **7** directly from **6** as

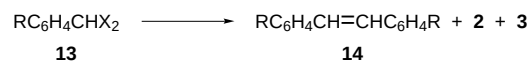



compared to the literature method which takes three steps for this transformation.[10] Bromo- and chloro-diphenylmethane behaved similarly giving tetraphenylethane (60–70%) and diphenylmethane (20%), apparently derived respectively from dimerisation and reduction of the corresponding radical. It was therefore of great interest to investigate trityl chloride **9** in view




of the long-standing controversy over the structure of the trityl radical dimer.[11] The products were **10** (46%) and triphenylmethane **11** (39%) with none of the non-benzenoid dimer **12** formed from dimerisation of $Ph_3C^{\cdot}$ in solution. The conditions used have obviously favoured *p–p* dimerisation of the reactive intermediate involved followed by two 1,5-hydrogen shifts to give the stable aromatic product. It is interesting to note that this is also the product formed from photochemical dimerisation of the trityl cation in solution.[12]

The method it also effective in coupling benzylidene chlorides **13** to give the corresponding stilbenes **14** in moderate




yield (Table 1), together with the reduction products **2** and **3**. Convenient direct access to polycyclic aromatic systems is also possible as illustrated by conversion of 2-chlorobenzylidene dichloride into phenanthrene (47%) and 1,3-bis(dibromomethyl)benzene into pyrene (54%) and this method should be amenable to formation of specifically substituted products. An unexpected result was obtained for the 2-methoxy compounds **15a, b** where the main products **16**, formed in 60 and 51% yields, respectively, seem likely to result from the sequence shown in Scheme 1 involving two intramolecular hydrogen atom transfers between the adjacent groups and decarbonyla-

tion. This is in contrast to the pyrolysis of these substrates without magnesium which gives benzofurans by a carbene route.[13]

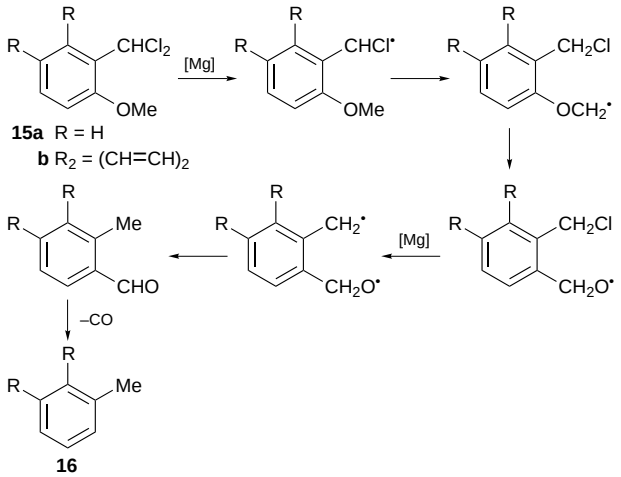
In order to gain further insight into the nature of the intermediates involved, we examined the reactivity of some aliphatic halides. Neopentyl bromide was of particular interest since the products formed from generation of both neopentyl radical and the carbene, neopentylidene, under very similar conditions have been described.[14] The products obtained over magnesium, 2-methylbut-2-ene (43%) and 2-methylbut-1-ene (33%) together with a trace of 2-methylpropene, indicate that neither the free gas-phase radical (2-methylpropene : 2-methylbut-1-ene, 1.2 : 1) nor the carbene (1,1-dimethylcyclopropane as main product) are involved. Where dehydrohalogenation is possible it usually occurs, as shown by the high yielding synthesis of 2,3-dimethylbuta-1,3-diene (84%) from the inexpensive precursor 2,3-dichloro-2,3-dimethylbutane, but C–C bond formation is also possible as shown by formation of cyclopropane (60%) from 1,3-dibromopropane. For longer α,ω-dihalides an intramolecular hydrogen transfer occurs and this is optimal for 1,6-dibromohexane resulting in the remarkably efficient formation of hex-1-ene (72%) by loss of $Br_2$. Further evidence against the involvement of free gas-phase radicals was provided by reaction of 6-bromohex-1-ene which gave mainly cyclohexene (50%) and isomeric hexadienes (23%) with no major products derived from cyclopentylmethyl radical.[15] It appears that the reactions may proceed by way of surface-adsorbed organomagnesium species.‡

Whatever the nature of the intermediates involved, this method appears to allow a range of synthetically useful transformations and further applications to organic halides and halides of other main group elements will be reported shortly.

We thank British Petroleum Research International Limited for a Research Studentship (A. O. O.) and The Royal Society for a Warren Research Fellowship (R. A. A.).

**Table 1** FVP of organic halides over magnesium

| Starting material | R | X | Products (% yield) |
|---|---|---|---|
| **1** | H | Cl | **2**(58) **3**(16) |
| **1** | H | Br | **2**(69) **3**(20) |
| **1** | 2-Me | Br | **2**(70) **3**(20) |
| **1** | 4-Me | Cl | **2**(60) **3**(23) |
| **1** | 2-F | Cl | **2**(73) **3**(7) **4**(5) |
| **1** | 2-F | Br | **2**(80) **3**(11) **4**(3) |
| **1** | 3-F | Br | **2**(67) **3**(12) |
| **1** | 4-F | Br | **2**(73) **3**(12) |
| **1** | 4-Cl | Cl | **2**(37) **3**(6) |
| **1** | 2-Br | Br | **2**(51) **3**(24) **4**(2) **5**(6) |
| **1** | 4-Br | Br | **2**(43) **3**(28) |
| **1** | 2-I | Cl | **2**(40) **3**(1) **4**(31) **5**(12) |
| **6** | H | Cl | **7**(73) **8**(15) |
| **6** | 3-F | Br | **7**(77) **8**(8) |
| **6** | 4-F | Br | **7**(80) **8**(8) |
| **13** | H | Cl | **14**(49) **2**(20) **3**(12) |
| **13** | 2-Me | Cl | **14**(36) **2**(10) **3**(13) |
| **13** | 3-Me | Cl | **14**(48) **2**(12) **3**(11) |
| **13** | 4-Me | Cl | **14**(63) **2**(21) **3**(6) |
| **13** | 2-Cl-6-F | Cl | **14**(58) **3**(2) |




**Scheme 1**

## Footnotes

* E-mail: raa@st-and.ac.uk

† *Pyrolysis procedure.* Using the normal apparatus for FVP described previously (ref. 8), magnesium turnings (1–2 g) were placed between two plugs of glass wool in the centre of the pyrolysis tube. The system was connected up as normal except that a stopper was used in place of the inlet tube, and the evacuated pyrolysis tube was briefly heated to 650–700 °C until the magnesium melted and sublimed evenly over the surface of the glass wool. Careful observation at this stage revealed an initial vigorous reaction on the wool, interpreted as the formation of magnesium silicide, but this was subsequently covered by magnesium and does not play a significant part in the reactions. The furnace was then cooled to the pyrolysis temperature, usually 600 °C, the pump was isolated and the system cautiously refilled with dry nitrogen to atmospheric pressure. The stopper was then removed, the inlet tube containing the substrate (5–10 mmol) attached (*CAUTION*: admission of air at this stage may lead to an explosion), and the pyrolysis continued as normal. After the pyrolysis was complete, the products were removed from the cold trap and analysed using the normal methods. The used pyrolysis tube was disposed of by cautiously placing it in a bath of 2 M HCl behind a safety shield (*CAUTION*: this results in a vigorous reaction accompanied by explosive ignition of the pyrophoric gases evolved. This is thought to be due to low molecular weight silanes formed by hydrolysis of the magnesium silicide).

‡ For comparison, FVP of each substrate was examined without magnesium at 600 °C and this led to formation of the previously reported (refs. 9, 13) dehydrohalogenation products for **1** (R = 2-Me), **6**, **13** (R = 2-Me) and **15** and to recovery of unchanged starting material in all other cases.

## References

1 J.-C. Guillemin and J.-M. Denis, *Tetrahedron*, 1988, **44**, 4431; J.-C. Guillemin, J.-M. Denis, M.-C. Lasne and J.-L. Ripoll, *Tetrahedron*, 1988, **44**, 4447.
2 P. L. Coe, C. R. Patrick and J. C . Tatlow, *Tetrahedron*, 1960, **9**, 240.
3 A. E. Ginsberg, R. Paatz and F. Korte, *Tetrahedron Lett.*, 1962, 779.
4 O. L. Chapman, C. C. Chang and N. R. Rosenquist, *J. Am. Chem. Soc.*, 1976, **98**, 261.
5 T. Koenig, D. Imre and J. A. Hoobler, *J. Am. Chem. Soc.*, 1979, **101**, 6446.
6 M. Binnewies, B. Solouki, H. Bock, R. Becherer and P. Ahlrichs, *Angew. Chem., Int. Ed. Engl.*, 1984, **23**, 731.
7 B. Rozsondai, J. Tremmel, I. Hargittai, V. N. Khabashesku, N. D. Kagramanov and O. M. Nefedov, *J. Am. Chem. Soc.*, 1989, **111**, 2845.
8 R. A. Aitken and J. I. Atherton, *J. Chem. Soc., Perkin Trans. 1*, 1994, 1281.
9 A. G. Loudon, A. MacColl and S. K. Wong, *J. Am. Chem. Soc.*, 1969, **91**, 7577; M. J. Morello and W. S. Trahanovsky, *Tetrahedron Lett.*, 1979, 4435; P. Schiess, S. Rutschmann and V. V. Toan, *Tetrahedron Lett.*, 1982, 3665, 3669.
10 W. Adcock, B. D. Gupta and T.-C. Khor, *Aust. J. Chem.*, 1976, **29**, 2571.
11 J. M. McBride, *Tetrahedron*, 1974, **30**, 2009.
12 E. E. Van Tamelen and T. M. Cole, Jr., *J. Am. Chem. Soc.*, 1971, **93**, 6158.
13 A. Hussain and J. Parrick, *Tetrahedron Lett.*, 1983, **24**, 609.
14 M. R. Banks, J. I. G. Cadogan, I. Gosney, P. K. G. Hodgson, A. G. C. Jack and D. R. Rodger, *J. Chem. Soc., Chem. Commun.*, 1989, 1033.
15 C. Walling and M. S. Pearson, *J. Am. Chem. Soc.*, 1964, **86**, 2262.

*Received in Liverpool, UK, 24th February 1997; Revised manuscript received 25th April 1997; Com. 7/02652H*

# A novel crown ether–cryptand photoswitch

**James H. R. Tucker,*[a†] Henri Bouas-Laurent,[b] Pierre Marsau,[c] Stuart W. Riley[a] and Jean-Pierre Desvergne*[b]**

[a] *Department of Chemistry, University of Exeter, Stocker Road, Exeter, UK EX4 4QD*
[b] *Photochimie Organique, CNRS URA 348, Université Bordeaux 1, F-33405 Talence, France*
[c] *Laboratoire de Cristallographie et Physique Cristalline, CNRS URA 144, Université Bordeaux 1, F-33405 Talence, France*

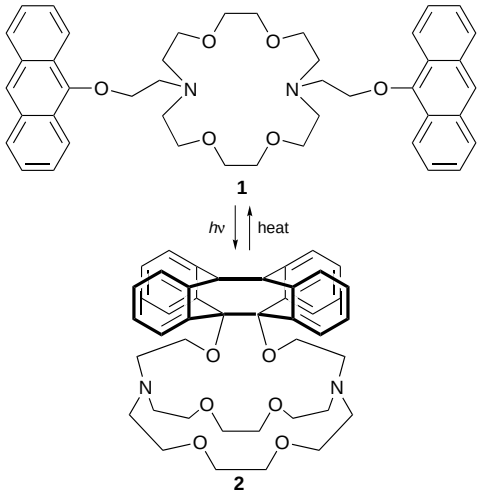
**A new photoactive bis-anthracenyl crown undergoes a reversible photocyclisation to form a cryptand, with the efficiency of the forward reaction and the rate of the thermal reverse reaction strongly affected by the presence of cation substrates.**

Photoresponsive molecular devices are of current interest due to their relevance to semiochemistry, substrate transport and sensor technology.[1] A number of supramolecular systems incorporating the photoactive anthracene moiety have previously been studied,[1f,2] including iono-photoswitches, where light is used to affect the ion binding properties of a system.[3] Here we report a new bis-9-anthracenyl crown ether **1** (Scheme 1) and give preliminary results on its unusual spectroscopic properties and photoreactivity in the absence and presence of guest substrates.

Compound **1** can be synthesised from diaza-18-crown-6 *via* two different routes; either directly from the reaction with 9-bromoethyloxyanthracene[4] or with 9-anthracenyloxyacetyl chloride,‡ followed by reduction using a method described previously.[5] An X-ray crystallographic study fully confirms the structure of **1** with the two pendant arms *trans* to one another.[6]

Complex formation with $H^+$, $Na^+$, $K^+$, $Cs^+$ and $Rb^+$ is evidenced by changes to the $^1H$ NMR spectrum of **1** (300 MHz) in $CDCl_3$–$CD_3OD$ (1 : 1; 0.04 M). Addition of aliquots of Group 1 cations to **1** confirms the 1 : 1 stoichiometry of each complex, which can, in principle, adopt either a *cis* or *trans* geometry (Fig. 1). The observation of only one set of signals throughout each titration indicates that cation exchange between free ligand and complex, as well as any interconversion between the two isomers, is fast on the NMR timescale.

Previous crystallographic studies on Group 1 complexes of a closely related diaza-crown ether derivative[7] suggest that a *cis* orientation is favoured for larger ions, with the cation situated




**Scheme 1**

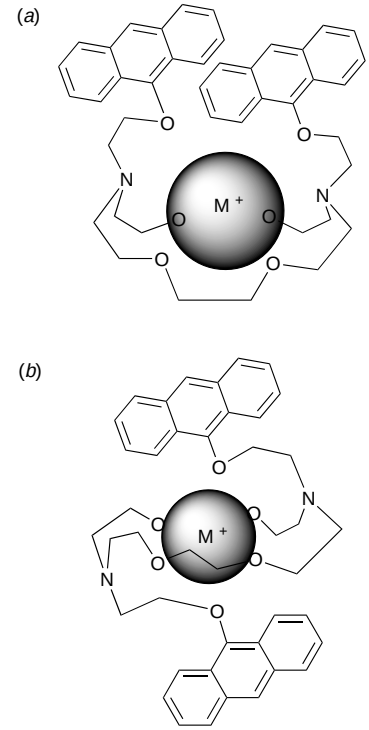



**Fig. 1** The complex **1** : $M^+$ with the anthracenyl groups depicted (*a*) *cis* and (*b*) *trans* to one another

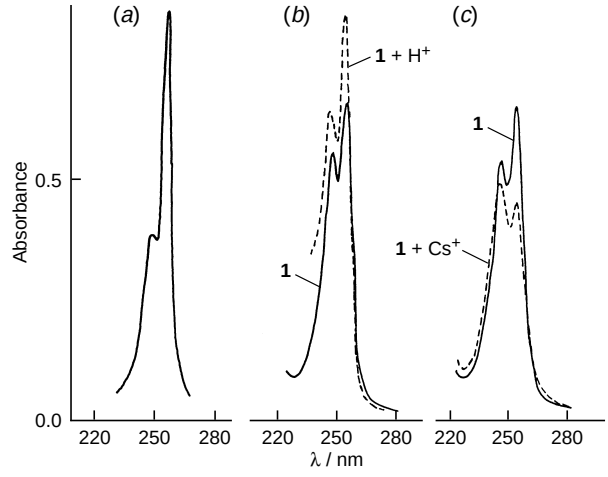



**Fig. 2** UV spectra in $CH_3OH$ (conc *ca.* $5 \times 10^{-5}$ M, room temp.) of (*a*) 1-(9-anthryloxy)-3,6,9-trioxadecane, as the monochromophoric reference compound; (*b*) compound **1** (—); **1** + $CF_3COOH$ (*ca.* $10^{-2}$ M) (----); (*c*) compound **1** (—); **1** + $CsClO_4$ (*ca.* $10^{-2}$ M) (----)

above the plane or the ring [Fig. 1(*a*)], whereas a *trans* orientation is prefered for complexes of smaller ions, with the cation symmetrically located in the plane of the macrocycle [Fig. 1(*b*)]. For this system, the addition of either $Rb^+$ or $Cs^+$ to **1** produce NMR spectra markedly different from those found with other guests. In particular, large upfield shifts for all five anthracene signals are observed upon the addition of $Rb^+$ and $Cs^+$ (and to a lesser extent with $K^+$) which is indicative of a strong π-π interaction.[8] Such an interaction is consistent with the *cis* conformation being favoured as the size of the guest increases.

Previous UV studies on bis-anthracenes have shown that the shape of the second electronic transition band ($^1$Bb) is characteristic of the mutual interaction between the two aromatic (A) rings: For an isolated A ring [Fig. 2(*a*)], the 256 nm component largely predominates; conversely the 248 nm component intensity increases as a function of the degree of interring interaction.[3b] The UV spectrum of **1** [Fig. 2(*b*) and (*c*), solid line] in MeOH is thus indicative of a mixture of *cis* and *trans* isomers. Addition of excess $CF_3CO_2H$ [Fig. 2(*b*), dotted line] induces a slight increase of the 256 nm component intensity, in keeping with an increase of the *trans*/*cis* ratio. With $Cs^+$ in excess, however, the intensity of the 248 nm band increases [Fig. 2(*c*), dotted line] which points to an increase of the *cis*/*trans* ratio. Similar results were obtained with $K^+$ and $Rb^+$ but no significant spectral modifications were displayed with $Na^+$.

The fluorescence emission spectrum of **1** is complex; it consists of a structured part (monomer emission) and a non-structured red-shifted band originating in exciplex (amine–anthracene) and excimer (anthracene–anthracene) species (Fig. 3). In the presence of a large excess of $CF_3CO_2H$, a strong increase of the fluorescence intensity and a clear decrease of the long wavelength contribution are observed. Among the metal cations investigated, $Cs^+$ gives the highest excimer/monomer ratio (Fig. 3), presumably because the 1:1 complex *cis* conformation, favoured in the ground state, displays the best geometry for excimer formation.

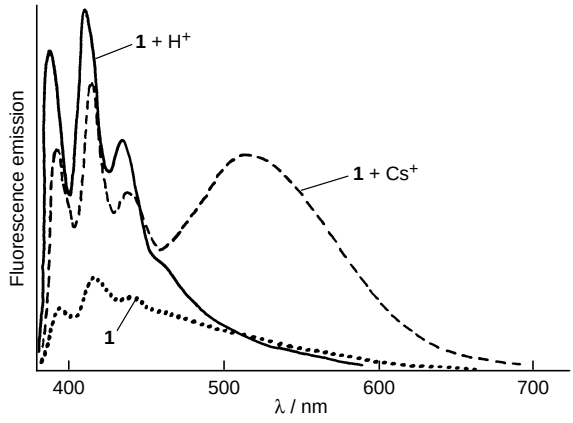



**Fig. 3** Corrected fluorescence spectra (conc. *ca.* $5 \times 10^{-5}$ M, $\lambda_{exc}$ = 380 nm, room temp.) in degassed MeOH and fluorescence quantum yield ($\phi_F$) of: **1** free ligand (●●●●) $\phi_F$: 0.04; **1** + $CF_3COOH$ (*ca.* $10^{-2}$ M) (—) $\phi_F$: 0.16; **1** + $CsClO_4$ (*ca.* $10^{-2}$ M) (----) $\phi_F$: 0.145. For comparison, 1-(9-anthryloxy)-3,6,9-trioxadecane has $\phi_F$: 0.29.

**Table 1** Intramolecular photocylcoaddition quantum yields ($\phi_R$) for the formation of **2** from **1** (*ca.* $5 \times 10^{-5}$ M) in the absence and in the presence of an excess of cations (*ca.* $10^{-2}$ M) in degassed MeOH (366 nm) and thermal dissociation rate constants for the reverse process at 25 °C

| System | $\Phi_R$ (366 nm) | $k_{diss}/10^{-6}$ s$^{-1}$ | $t_{1/2}$/h |
|---|---|---|---|
| **1** | 0.10 | 5 | 38 |
| **1** + $CF_3CO_2H$ | 0.03 | 1.2 | 160 |
| **1** + $CsClO_4$ | 0.04 | 0.3 | 638 |

On irradiation of a methanol solution of **1** (*ca.* $5 \times 10^{-5}$ M) at 366 nm, the photocycloadduct **2** is formed as evidenced by the disappearance of the $^1$La UV absorption (300–400 nm) and the emergence of a new absorption (270–290 nm) characteristic of an *o*-xylene system. The reaction efficiency for this process ($\Phi_R$ = 0.10) is much greater than those found for analogous processes with more sterically hindered systems.[3b] Cryptand **2** reverts back to the crown **1** in the dark with a half life of 38 h. Preliminary photocyclisation studies have been carried out in the presence of $H^+$ and $Cs^+$ (*ca.* 1000-fold excess) with the relevant data displayed in Table 1. The closing and opening rates clearly depend upon the type of guest present; significantly, $Cs^+$ retards the rate of both the forward and reverse processes. It is likely that this substrate dependency is a result of increased steric hindrance for the forward process and an increased stabilisation of the cryptand geometry for the reverse process, as a consequence of the cation being enclosed within the cryptand cavity.

This is the first example of a molecular system that, upon the action of an external trigger, can switch *reversibly* between a crown and cryptand.[9] Preliminary studies indicate that the photocyclisation quantum yields and the rates of the thermal reverse reactions are clearly influenced by the nature of the bound substrate. Detailed studies of the cation binding ability of both **1** and **2** and also the transient kinetic analysis and electrochemical properties of **1** are currently underway.

We thank the CNRS, la Région Aquitaine and the University of Exeter for financial support and J. Lauret, M. Gotta and Tran Thanh Hung Linh for technical assistance.

## Footnotes

† E-mail: j.h.r.tucker@exeter.ac.uk

‡ 9-Anthracenyloxyacetyl chloride is readily prepared from the acid, which is obtained by reacting anthrone with ethyl bromoacetate in the presence of base.

## References

1 (*a*) J. M. Lehn, *Supramolecular Chemistry—Concepts and Perspectives*, VCH, Weinheim, 1995; (*b*) B. L. Feringa, W. F. Jager and B. de Lange, *Tetrahedron*, 1993, **49**, 8267; (*c*) *Chemosensors of Ion and Molecule Recognition*, ed. J.-P. Desvergne and A. W. Czarnik, NATO ASI Series C, vol. 492, Kluwer Academic Publishers, Dordrecht, 1997; (*d*) P. Tundo and J. H. Fendler, *J. Am. Chem. Soc.*, 1980, **102**, 4553; (*e*) A. Beeby, D. Parker and J. A. G. Williams, *J. Chem. Soc., Perkin Trans. 2*, 1996, 1565; (*f*) L. Fabbrizzi and A. Poggi, *Chem. Soc. Rev.*, 1995, **24**, 197.

2 H. Bouas-Laurent, A. Castellan, M. Daney, J.-P. Desvergne, G. Guinand, P. Marsau and M.-H. Riffaud, *J. Am. Chem. Soc.*, 1986, **108**, 315; R. A. Bissell, A. P. de Silva, H. Q. N. Gunaratne, P. L. M. Lynch, G. E. M. Maquire and K. R. A. S. Sandanayake, *Chem. Soc. Rev.*, 1992, 187.

3 (*a*) J.-P. Desvergne and H. Bouas-Laurent, *J. Chem. Soc., Chem. Commun.*, 1978, 403; (*b*) D. Marquis, J.-P. Desvergne and H. Bouas-Laurent, *J. Org. Chem.*, 1995, **60**, 7984; (*c*) G. Deng, T. Sakaki, K. Nakashima and S. Shinkai, *Chem. Lett.*, 1992, 1287.

4 W. H. Pirkle and J. M. Finn, *J. Org. Chem.*, 1983, **48**, 2779.

5 J.-P. Desvergne, J. Rau, O. Cherkaoui, R. Zniber, H. Bouas-Laurent, N. Lahrahar, U. Meyer and P. Marsau, *New J. Chem.*, 1996, **20**, 881.

6 P. Marsau and N. Lahrahar, unpublished work.

7 D. Wang, Y. Ge, H. Hu, K. Yu and Z. Zhou, *J. Chem. Soc., Chem. Commun.*, 1991, 685.

8 C. A. Hunter, *J. Chem. Soc., Chem. Commun.*, 1991, 749; M. Shionoya, T. Ikeda, E. Kimura and M. Shiro, *J. Am. Chem. Soc.*, 1994, **116**, 3848.

9 For an irreversible example, see R. Warmuth, E. Grell, J. M. Lehn, J. W. Bats and G. Quinkert, *Helv. Chim. Acta*, 1991, **74**, 671.

*Received in Liverpool, UK, 21st March 1997; Com. 7/01989K*

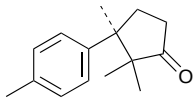
# New asymmetric construction of the benzylic quaternary stereogenic centre: an enantiocontrolled access to (−)-α-cuparenone

**Takamitsu Kosaka, Toshikazu Bando and Kozo Shishido***

*Institute for Medicinal Resources, University of Tokushima, Sho-machi 1, Tokushima 770, Japan*

**An efficient and enantiocontrolled formal total synthesis of (−)-α-cuparenone has been accomplished by employing a new asymmetric construction methodology for formation of the benzylic quaternary stereogenic centre.**

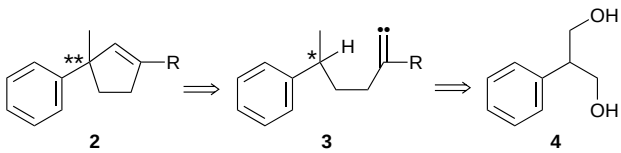
Development of the methodology for assembling an asymmetric quaternary stereogenic centre has been a challenging and important target in organic synthesis.[1] Particularly, construction of benzylic quaternary centres has become of special interest[2] since it is involved in many biologically significant molecules. Here we present a new and efficient strategy for the asymmetric construction of the benzylic quaternary carbon centre by illustrating an enantiocontrolled formal total synthesis of (−)-α-cuparenone **1**.[3] Our basic strategy is shown in Scheme 1.



**1**

We envisaged that a pivotal construction of the benzylic quaternary carbon in **2** might be realized by employing the diastereoselective [1,5] C–H insertion reaction of alkylidene carbene **3**,[4] in which the benzylic tertiary asymmetric centre should be generated *via* a lipase-mediated asymmetric acetylation[5] of the prochiral diol **4**. It is well known that the C–H insertion reaction proceeds with complete retention of configuration.[4b,c]

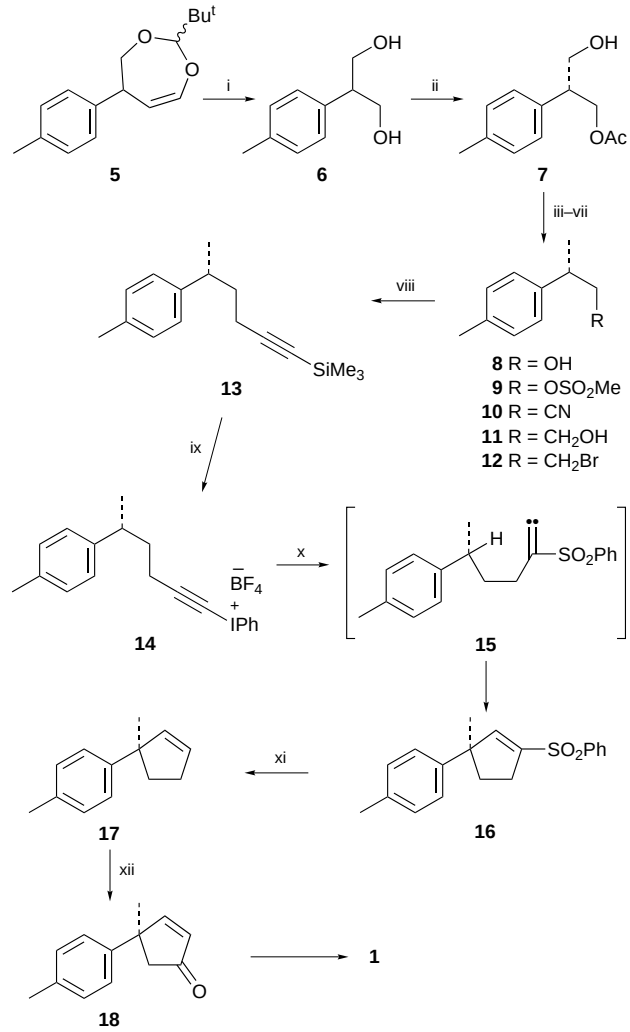
Treatment of 2-*tert*-butyl-4,5-dihydro-5-(4-methylphenyl)-1,3-dioxepine **5**,[6a] prepared by the Heck reaction[6] between 4-methyliodobenzene and 2-*tert*-butyl-4,7-dihydro-1,3-dioxepine,[7] under ozonolytic cleavage conditions followed by reductive workup with $NaBH_4$ provided the prochiral 1,3-diol **6** in 84% yield (Scheme 2). It should be noted that the procedure is efficient and superior to the conventional method.[8] With the prochiral diol in hand, we examined the optimum conditions for asymmetric acetylation using some lipases.[9] Of these, porcine pancreatic lipase (PPL)-catalysed transesterification in diethyl ether using vinyl acetate as an acetyl donor at room temperature proved to be the best choice and (*R*)-monoacetate **7**, $[\alpha]_D$ + 15.6 (*c* 1.28, $CHCl_3$) {lit.,[9] for the (*S*)-isomer; $[\alpha]_D$ − 16.2 (*c* 1.20, $CHCl_3$)}, was obtained in 84% yield. The enantiomeric excess was 99% as determined by $^1H$ NMR analysis of its MTPA ester derivative. Removal of the hydroxy moiety in **7** by tosylation and subsequent reduction with $NaBH_4$ in $Me_2SO$[9] furnished the alcohol **8**, which was mesylated to give **9** in 88% yield from **7**. Sequential cyanation, DIBAL-H reduction–acidic workup, and further reduction with $NaBH_4$ gave one-carbon elongated alcohol **11** in 75% overall yield. Reaction of the bromide **12**, prepared from **11** by a standard method, with lithium trimethylsilylacetylide produced the alkynylsilane **13** in 69% yield.



**2** **3** **4**

**Scheme 1**

The stage was now set to explore the crucial construction of the quaternary stereogenic centre *via* the [1,5] C–H insertion reaction of the alklidene carbene. For this purpose, we intended to use the procedure developed by Ochiai,[4d,e,g] since the product obtained by this method is vinyl sulfone, which would be



**5** **6** **7** **8** R = OH, **9** R = $OSO_2Me$, **10** R = CN, **11** R = $CH_2OH$, **12** R = $CH_2Br$, **13** **14** **15** **16** **17** **18** **1**

**Scheme 2** *Reagents and conditions*: i, $O_3$ then $NaBH_4$, $CH_2Cl_2$, −78 to 0 °C, 84%; ii, vinyl acetate, PPL, $Et_2O$, room temp., 84%; iii, TsCl, $Et_3N$, DMAP, $CH_2Cl_2$, room temp., then $NaBH_4$, $Me_2SO$, 60 °C, 73%; iv, MsCl, $Pr^i_2NEt$, $CH_2Cl_2$, room temp., 88%; v, KCN, 18-crown-6, $Me_2SO$, 60 °C, 90%; vi, DIBAL-H, hexane–$CH_2Cl_2$ (1 : 1), −78 °C then 1 M HCl, $NaBH_4$, MeOH, 75%; vii, $Ph_3P$, $CBr_4$, $CH_2Cl_2$, −40 °C, 94%; viii, $Bu^nLi$, HC≡$CSiMe_3$, THF, HMPA, −78–0 °C, 69%; ix, $(PhIO)_n$, $BF_3$·$OEt_2$, $CH_2Cl_2$, 0 °C; x, $PhSO_2Na$, $H_2O$, 0 °C, 83% for 2 steps; xi, Na–Hg (5%), MeOH, sonication, room temp., 70%; xii, PDC, $Bu^tOOH$, Celite, benzene, 10 °C–room temp., 72%

convenient for further transformations. Thus, treatment of **13** with iodosylbenzene in the presence of boron trifluoride–diethyl ether in $CH_2Cl_2$ at 0 °C followed by treatment with aqueous sodium tetrafluoroborate provided the iodonium tetrafluoroborate **14**, which was immediately exposed to aqueous sodium benzenesulfinate at 0 °C to give the cyclized vinyl sulfone **16**,† *via* the alkylidene carbene intermediate **15**, in 83% overall yield from **13** as the sole product. The absolute configuration at the newly-generated quaternary centre was deduced to be *R*, which was confirmed by the following conversion. Removal of the benzenesulfonyl moiety in **16** using Na–Hg under sonication[10] afforded **17** in 70% yield. Finally, oxidation of the allylic methylene in **17** with pyridinium dichromate (PDC) in the presence of *tert*-butylhydroperoxide and Celite[11] produced the enone **18**, whose $^1$H NMR data and optical rotation, $[\alpha]_D$ + 101 (*c* 1.28, EtOH) {lit.[3a] $[\alpha]_D$ + 114 (*c* 1.36, EtOH)}, were identical with those reported. Since the compound **18** has already been converted into (−)-α-cuparenone **1** by a two-step sequence,[3a] the present synthesis constitutes a formal total synthesis of **1**.

In summary, we have developed an efficient and unprecedented methodology for assembling benzylic quaternary stereogenic centres and demonstrated the formal total synthesis of (−)-α-cuparenone as an application of the procedure.

We are grateful to Professor Masahito Ochiai and Mr Takuya Sueda, University of Tokushima, for valuable discussions.

## Footnotes

* E-mail: shishido@ph.tokushima-u.ac.jp

† *Selected spectroscopic data* for **16**; pale yellow oil; $[\alpha]_D$ +34.6 (*c* 0.38, $CHCl_3$); $\delta_H$(200 MHz, $CDCl_3$) 1.45 (3 H, s), 2.14–2.21 (2 H, m), 2.31 (3 H, s), 2.54–2.73 (2 H, m), 6.82 (1 H, s), 7.09 (4 H, s), 7.55–7.61 (3 H, m), 7.91–8.43 (2 H, m); $\delta_C$(100 MHz, $CDCl_3$) 20.9 ($CH_3$), 26.6 ($CH_3$), 30.0 ($CH_2$), 41.0 ($CH_2$), 52.9 (C), 124.5 (CH × 2), 128.0 (CH × 2), 129.2 (CH × 2), 129.3 (CH × 2), 133.5 (CH), 136.2 (C), 139.5 (C), 143.2 (C), 143.8 (C), 149.5 (CH); *m*/*z* (EI) 312 ($M^+$); HRMS (EI) calc. for $C_{19}H_{20}O_2S$, 312.1184. Found: 312.1169. Anal. calc. for $C_{19}H_{20}O_2S$: C, 73.04; H, 6.45. Found: C, 72.89; H, 6.49%.

## References

1 K. Fuji, *Chem. Rev.*, 1993, **93**, 2037.
2 T. Takemoto, M. Sodeoka, H. Sasai and M. Shibasaki, *J. Am. Chem. Soc.*, 1993, **115**, 8477.
3 For recent representative chiral syntheses of (−)-α-cuparenone; (*a*) A. I. Meyers and B. A. Lefker, *J. Org. Chem.*, 1986, **51**, 1541; (*b*) M. M. Gharpure and A. S. Rao, *Synth. Commun.*, 1989, **19**, 1813; (*c*) H. Nemoto, H. Ishibashi, M. Nagamochi and K. Fukumoto, *J. Org. Chem*., 1992, **57**, 1707; (*d*) J. L. Canet, A. Fadel and J. Salaün, *J. Org. Chem.*, 1992, **57**, 3463, and references are cited therein. For (+)-α-cuparenone, (*e*) T. Honda, N. Kimura and M. Tsubuki, *Tetrahedron Asymmetry*, 1993, **4**, 21; (*f*) J. B. Schwarz and A. I. Meyers, *J. Org. Chem.*, 1995, **60**, 6511; (*g*) K. Maruoka, M. Oishi and H. Yamamoto, *J. Am. Chem. Soc.*, 1996, **118**, 2289.
4 For cyclopentene annulation *via* [1,5] C–H insertion of alkylidene carbene; (*a*) J. Wolinsky, G. W. Clark and P. C. Thorstenson, *J. Org. Chem.*, 1976, **41**, 745; (*b*) J. C. Gilbert, D. H. Giamalva and U. Weerasooriya, *J. Org. Chem.*, 1983, **48**, 5251; (*c*) J. C. Gilbert, D. H. Giamalva and M. E. Baze, *J. Org. Chem.*, 1985, **50**, 2557; (*d*) M. Ochiai, M. Kunishima, Y. Nagao, K. Fuji, M. Shiro and E. Fujita, *J. Am. Chem. Soc.*, 1986, **108**, 8281; (*e*) M. Ochiai, M. Kunishima, S. Tani and Y. Nagao, *J. Am. Chem. Soc.*, 1991, **113**, 3135; (*f*) S. Ohira, K. Okai and T. Moritani, *J. Chem. Soc., Chem. Commun.*, 1992, 721; (*g*) M. Ochiai, K. Uemura and Y. Masaki, *J. Am. Chem. Soc.*, 1993, **115**, 2528; (*h*) S. Ohira, T. Moritani, T. Ida and M. Yamato, *J. Chem. Soc., Chem. Commun.*, 1993, 1299; (*i*) R. R. Tykwinski, P. J. Stang and N. E. Persky, *Tetrahedron Lett.*, 1994, **35**, 23; (*j*) M. Kunishima, K. Hioki, S. Tani and A. Kato, *Tetrahedron Lett.*, 1994, **35**, 7253; (*k*) D. F. Taber and R. P. Meagley, *Tetrahedron Lett.*, 1994, **35**, 7909; (*l*) S. Kim and C. M. Cho, *Tetrahedron Lett.*, 1994, **35**, 8405; (*m*) D. F. Taber, A. Sahli, H. Yu and R. P. Meagley, *J. Org. Chem.*, 1995, **60**, 6571; (*n*) D. F. Taber, R. P. Meagley and D. J. Doren, *J. Org. Chem.*, 1996, **61**, 5723.
5 H. M. Sweers and C.-H. Wong, *J. Am. Chem. Soc.*, 1986, **108**, 6421; Y.-F. Wang and C.-H. Wong, *J. Org. Chem.*, 1988, **53**, 3127; Y.-F. Wang, J. J. Lalonde, M. Momongan, D. E. Bergbreiter and C.-H. Wong, *J. Am. Chem. Soc.*, 1988, **110**, 7200.
6 (*a*) S. Takano, K. Samizu and K. Ogasawara, *Synlett*, 1993, 393; (*b*) T. Sakamoto, Y. Kondo and H. Yamanaka, *Heterocycles*, 1993, **36**, 2437; (*c*) Y. Koga, M. Sodeoka and M. Shibasaki, *Tetrahedron Lett.*, 1994, **35**, 1227.
7 H. Frauenrath, *Synthesis*, 1989, 721.
8 P. A. Levene and G. M. Meyer, *Org. Synth.*, 1943, Coll. Vol. II, 288.
9 G. Guanti, E. Narisano, T. Podgorski, S. Thea and A. Williams, *Tetrahedron*, 1990, **46**, 7081.
10 R. E. Dabby, J. Kenyon and R. F. Mason, *J. Chem. Soc.*, 1952, 4881.
11 N. Chidambaram and S. Chandrasekaran, *J. Org. Chem.*, 1987, **52**, 5048.

*Received in Cambridge, UK, 18th April 1997; Com. 7/02667F*

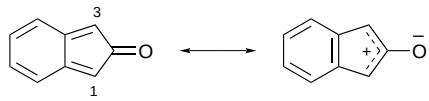
# Generation and inter- and intra-molecular trapping of isoindenones (inden-2-ones)

**David W. Jones* and Tracie C. L. M. Ryder**

*School of Chemistry, The University, Leeds, UK LS2 9JT*

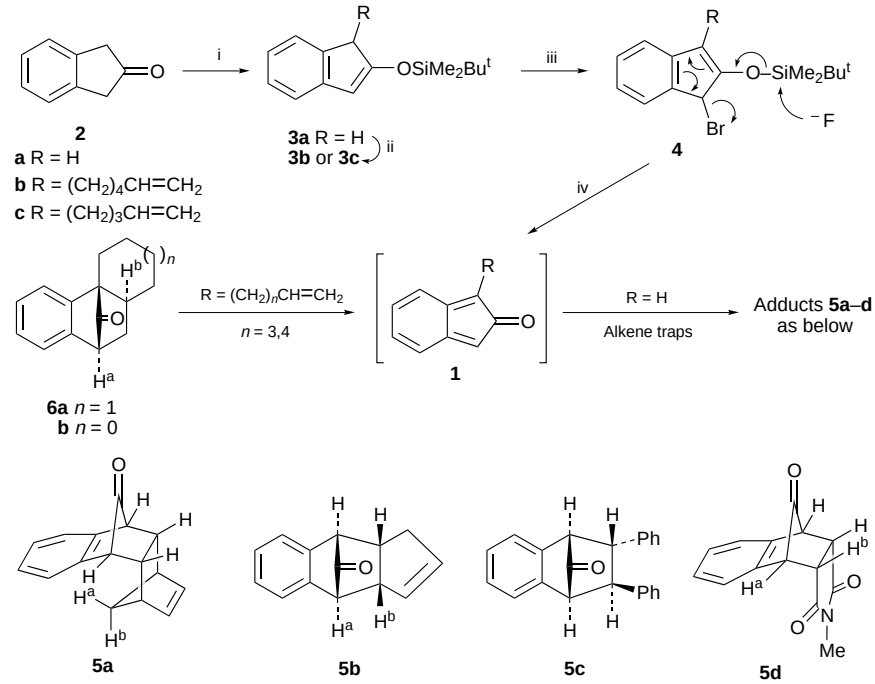
**Inden-2-one and some simple derivatives are smoothly generated by reaction of caesium fluoride with 1-bromo-2-*tert*-butyldimethylsilyloxyindenes and they can be efficiently trapped in both intra- and inter-molecular additions; the intramolecular additions proceed with *exo*-addition of the tether, in contrast to the intermolecular additions and intramolecular additions to 2-benzopyran-3-ones.**

Isoindenones (inden-2-ones) are of interest as derivatives of two very reactive dienes, *o*-quinodimethane and cyclopentadienone; resonance involving the oxyallyl structure is also a possibility (Scheme 1).

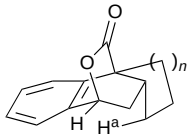


**Scheme 1**

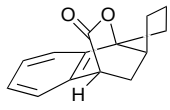
From the MO point of view the HOMO–LUMO energy gap is expected to be particularly small for isoindenones as it is for cyclobutadienes and other antiaromatic species.[1] We have shown that 1,3-diphenylinden-2-one is readily generated by dissociation of its dimer,[2] and that it is efficiently trapped by a range of alkenes in Diels–Alder reactions.[2,3] We further showed that the potentially more synthetically useful parent system (Scheme 1) could be generated from 1,3-dibromoindan-2-one by reaction with copper powder or sodium iodide, but generation/trapping was inefficient (8% yield of adduct with cyclopentadiene using copper powder in boiling benzene).[4] We now describe an efficient method of generating and trapping simple inden-2-ones **1** (Scheme 2). Commercially available indan-2-one **2** was converted into enol silyl ether **3a** (64%). This could be alkylated to give either **3b** or **3c** in 61 and 75% yield, respectively. With *N*-bromosuccinimide in refluxing $CCl_4$ and irradiation with a sun lamp (500 W), **3b** and **3c** gave **4b** (75%) and **4c** (71%) respectively. Slow addition of **4b** (syringe pump) to a refluxing mixture of MeCN and CsF gave the adduct **6a** in good yield (66%).† The adduct showed a characteristic high frequency carbonyl stretch at 1778 $cm^{-1}$. In the $^1H$ NMR spectrum a shielded resonance such as that found for related *endo*-2-benzopyran-3-one adducts like **7** (*n* = 1 or 2) was absent.[5] A similar adduct **6b** was obtained in 73% yield† from **4c** but again the NMR spectrum showed the absence of a shielded proton. Since modelling[6] suggested a very similar location of the proton $H^a$ with respect to the aromatic ring in the (hypothetical) *endo*-chain adducts from the isoindenones and the known *endo*-chain adducts of the 2-benzopyran-3-ones,[5] an *exo*-chain addition to the isoindenones seemed likely. The assignment was reinforced by Baeyer–Villiger oxidation of **6b** to **8** (79% yield) which also failed to show a shielded proton, although if **8** were an *endo*-chain adduct the location of $H^a$ with respect to the aromatic ring would be very similar to that in **7** (*n* = 1). Finally the stereochemistry of **6a** was confirmed by



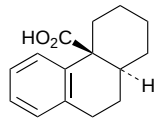

**Scheme 2** *Reagents and conditions*: i, LDA (1.4 equiv.), THF, −78 °C, 10 min; then $Bu^tMe_2SiCl$ (1 equiv.), −78 °C, 10 min, then HMPA, −78 °C, 15 min, allowed to warm to 20 °C; ii, BuLi (1 equiv.), THF, 0 °C, 10 min, then iodo-alkene (1.7 equiv.), HMPA (1 ml $g^{-1}$ of base) added, allowed to warm to 20 °C and stirred for 10 min; iii, NBS, $CCl_4$, AIBN, reflux, sun lamp (500 W), 2 h; iv, CsF (2 equiv.), MeCN, reflux, bromo compound added in MeCN (10 ml mg) *via* syringe pump, 4 h



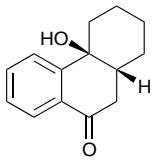
*n* = 2, $\delta H^a$ = 0.68
*n* = 1, $\delta H^a$ = 0.74
**7**



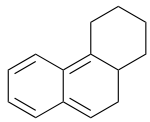
**8**



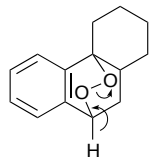
**9**



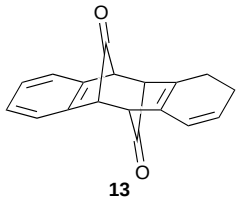
**10**



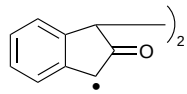
**11**



**12**



**13**



**14**

modified Haller–Bauer cleavage[7] to give the *trans* acid **9** (62%), mp 164.5–167 °C (lit.,[8] mp 162 °C: the *cis* acid has mp 143 °C). Accordingly, and in contrast to the IMDA additions to 2-benzopyran-3-ones, the inden-2-one additions proceed with clean *exo*-selectivity.

The synthetic utility of products of type **6a** is illustrated by the foregoing cleavage of **6a** to **9** and photodecarbonylation of **6a** in the presence of oxygen; **6a** in benzene saturated with oxygen was irradiated through silica with a MP 125 W mercury lamp with slow passage of oxygen through the solution to give the hydroxy ketone **10** (70% yield). This probably arises *via* the expected *o*-quinodimethane **11** and the *endo* peroxide **12** in the manner indicated by the arrows in **12**. An alternative mechanism for the decomposition of related peroxides involves homolytic cleavage of the O–O bond.[9] Such a route is also possible for our example.

This route to inden-2-ones appears general as it can be applied to the parent compound **1a** (Scheme 2). Allylic bromination of **3a** gave **4a** (62%) which, upon reaction with CsF in the presence of norbornadiene (10 equiv.), gave the *endo* norbornadiene adduct **5a** (68% yield). The related norbornene adduct was obtained in a similar way (43% yield), as was the cyclopentadiene adduct **5b** (49% yield). Trapping with *trans*-stilbene was less satisfactory, giving **5c** in 8% yield. Trapping with *N*-methylmaleimide gave only 22% yield of **5d**, although here there is a problem isolating the adduct from a considerable amount of polymeric material derived from the dienophile, which streaked extensively upon chromatography.

In view of the *exo*-chain addition observed for the intramolecular reactions, the exclusive *endo*-addition† in the intermolecular reactions is noteworthy. Evidence for the *endo* configuration of the intermolecular adducts includes the value of the vicinal coupling constant $J_{HaHb}$ (see structures **5b** and **5d**, Scheme 2). This is *ca*. 4 Hz, as expected for an *endo*-adduct ($\phi_{ab}$ *ca*. 40°) rather than < 0.5 Hz expected for an *exo*-adduct ($\phi_{ab}$ *ca*. 80°). Additional evidence is provided by the strong shielding of *endo*-disposed groups, *e.g.* $H^a$ in the norbornadiene adduct **5a** resonates at δ −0.64 and $H^b$ at δ +0.47. In the corresponding norbornene adduct, $H^a$ and $H^b$ appear at δ −0.72 and +0.34, respectively. In the *N*-methylmaleimide adduct **5d** the NMe resonance is shielded (δ 2.2) in comparison with the methyl in *N*-methylmaleimide (δ 3.07). The contrasting stereochemistry of the intra- and inter-molecular additions is presumably due to conformational factors in the connecting chain. Work on this question is continuing.

In the absence of a trap, **1** (R = H) gives the dimer **13**† of a formal $\pi^4s^+\pi^4s$ addition. The parent isoindenone therefore dimerises in the same way as its diphenyl derivative. As in that case[2] a biradical intermediate like **14** is likely to be involved in forming this orbital symmetry forbidden product.

In summary, we have provided an efficient way of generating simple inden-2-ones and trapping them both intra- and intermolecularly. In addition to their theoretical interest, these molecules are useful intermediates in making benzonorbornenones and hence products like **9** and **10**. Regioselective Haller–Bauer-like cleavage,[7] in combination with the clean *exo*-selective addition of the tether observed in the IMDA additions, is clearly of potential use in the synthesis of diterpenoids like pisiferic acid which have the *trans*-BC ring junction.[10]

## Footnotes

* E-mail: d.w.jones@chem.leeds.ac.uk

† For the intramolecular additions the TLC and 300 MHz $^1$H NMR spectra of the crude reaction products failed to reveal any *endo* addition product. Similarly, the adduct fraction obtained by chromatography indicated a single adduct in both cases. The intermolecular additions proceeded somewhat less cleanly and the presence of some 5–10% of *exo*-adduct cannot be excluded. In the preparation of **5a** without the use of slow addition (syringe pump), the spectra of the crude product clearly showed the presence of the dimer **13**.

## References

1 C. W. G. Fishwick and D. W. Jones, ortho-*Quinonoid Compounds*, in *The Chemistry of Quinonoid Compounds*, ed. S. Patai and Z. Rappoport, 1988, Wiley, vol. II, pp. 403–453.
2 J. M. Holland and D. W. Jones, *J. Chem. Soc., Chem. Commun.*, 1969, 587.
3 D. W. Jones and R. L. Wife, *J. Chem. Soc., Perkin Trans. 1*, 1976, 1654.
4 J. M. Holland, PhD Thesis, University of Leeds, 1969.
5 D. W. Jones and F. M. Nongrum, *J. Chem. Soc., Perkin Trans. 1*, 1995, 705.
6 Using CHEM 3D Pro, ver. 3.5, Cambridge Soft Corporation, Cambridge, Mass.
7 P. G. Gassman and F. V. Zalar, *Tetrahedron Lett.*, 1964, 3031.
8 G. Sinha, S. K. Maji, V. R. Ghatak, M. Mukherjee, A. K. Mukerjee and A. K. Chakravarty, *J. Chem. Soc., Perkin Trans. 1*, 1983, 2519.
9 M. Kamata, Y. Nishikata and M. Kato, *Chem. Commun.*, 1996, 2407.
10 T. Kametani, H. Kondon, M. Tsubuki and T. Honda, *J. Chem. Soc., Perkin Trans. 1*, 1990, 5; J. Geiwis and E. Haslinger, *Helv. Chim. Acta*, 1995, **78**, 818.

*Received in Liverpool, UK, 11th April 1997; Com. 7/02505J*

# Exclusive production of a cycloadduct from selective excitation of the charge-transfer complex between acenaphthylene and tetracyanoethylene in the crystalline state in contrast to failure of reaction in solution

**Naoki Haga,*[a] Hiroyuki Nakajima,[a] Hiroaki Takayanagi[a] and Katsumi Tokumaru[b]**

[a] *School of Pharmaceutical Sciences, Kitasato University, Minato-ku, Tokyo 108, Japan*
[b] *University of Tsukuba, Tsukuba, Ibaraki 305, Japan*

**Selective excitation of the charge-transfer complex between acenaphthylene and tetracyanoethylene in the crystalline state exclusively affords a 1:1 [2 + 2] cycloadduct, in contrast to the excitation in solution, which gives no product.**

Many electron donors and acceptors give charge-transfer (CT) complexes in solution and in the solid state, and their behaviour on photochemical irradiation has been investigated.[1,2] We now report that irradiation with light of wavelength longer than 500 nm of the crystalline CT complex between acenaphthylene **1** and tetracyanoethylene **2** affords a 1 : 1 [2 + 2] cycloadduct **3** of **1** and **2** as the sole product, whereas excitation in solution does not induce any reaction. To the best of our knowledge, this is the first observation of excitation of a CT complex leading to reaction in the crystal but not in solution.

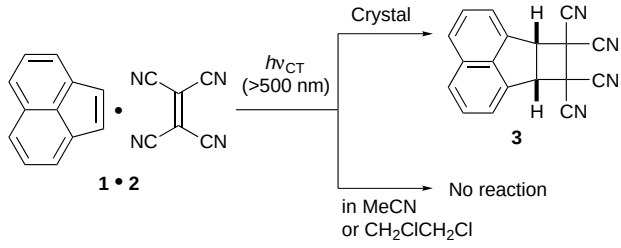
Mixing **1** and **2** in organic solvents immediately produces a tan–brown colour due to formation of their CT complex (with an absorption extending to 700 nm) in equilibrium with **1** and **2**. Evaporation of the solvent from an equimolar mixture of **1** and **2** in ethyl acetate affords crystals of a 1 : 1 CT complex **1·2** as tan–brown cubes (satisfactory elemental analysis, mp 103.0–105.0 °C, orthorhombic, space group $P2_1/n$).

X-Ray crystallographic diffraction of **1·2** indicates that molecules of **1** and **2** are stacked alternately with a distance of 4.0 Å between the **1** and **2** planes, with a dihedral angle of 0.8°. The alkenic parts of **1** and **2** are aligned with interatomic distances of 3.3–3.9 Å and a torsion angle of 62.2°.

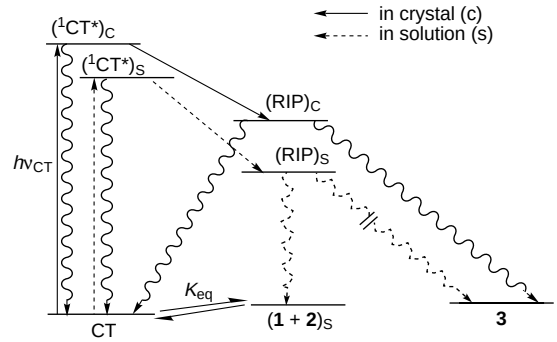
On irradiation of crystalline **1·2** with light of wavelength longer than 500 nm at 20 °C, where neither **1** nor **2** was excited, **3** was isolated in a 80% yield (based on consumed **1**) as the sole product (Scheme 1).† The quantum yield for formation of **3** was *ca.* 4 (±1) × $10^{-3}$ under irradiation with 546.1 nm monochromatic light.[3]‡

In contrast, irradiation of an equimolar (0.1 M) mixture of **1** and **2** in MeCN or dichloroethane with light of > 500 nm did not result in any reaction; however, irradiation with light of > 400 nm to excite **1** led to formation of **3** in low yield accompanied by larger amounts of the dimer of **1**.

A tan–brown fine powder prepared by pulverizing an equimolar mixture of **1** and **2** was irradiated with light of > 500 nm to give *ca.* 5% of **3** with larger amounts of the dimer of **1**. Formation of the dimer of **1** reflects the presence of two molecules of **1** in close proximity in the fine powder, whereas in the crystal the nearest two molecules of **1** are separated by more than 6 Å.




**Scheme 1**




**Scheme 2**

Excitation of the CT complex can induce electron-transfer from **1** to **2**. The standard free energy change for this process,[4] $\Delta G^0$, is estimated to be −132 kJ $mol^{-1}$ in MeCN.§

On excitation of the CT complex, the initially produced Frank–Condon excited CT state will rapidly change to a relaxed state or radical ion pair (RIP). In solution, the RIP is solvated and, therefore, much more stabilized than in the absence of solvents. The lack of reaction resulting from the CT excitation in solution indicates that the excited CT state and/or the RIP undergo facile deactivation and/or backward electron-transfer preceeding to charge separation in solution.[5] On the other hand, production of the cycloadduct from excitation of the CT complex crystal suggests that the fixed positions of **1** and **2**, separated by 3–4 Å in both the excited CT state and the resultant RIP in the crystal, might retard the deactivation and backward electron-transfer and enable them to undergo cycloaddition. Moreover, the absence of solvent molecules precludes stabilization of the RIP; therefore, this will also retard backward electron-transfer and enable the RIP to undergo cycloaddition (Scheme 2).

Finally it should be noted that the present results provide for the possibility of exclusive production of a cycloadduct *via* selective excitation of a crystalline CT complex when the proper conditions are met. Furthermore, the remarkable contrast in reactivity between the crystalline state and solution on CT excitation seems to indicate the important role of solvents for stabilization of the RIP. Full details of this present result will be published elsewhere.

This work was partly supported by a Grant-in Aid for Scientific Research (No. 08640696, N. H.) from the Ministry of Education, Science, and Culture, Japan.

## Footnotes

† A 40 mg sample of **1·2** placed between two disk glass filters was irradiated using a 400 W high pressure Hg lamp in a thermostat. The products (**3** and dimers of **1**) and unreacted **1** were isolated by column chromatography.

Compound **3** (ref. 6) and the dimers of **1** (ref. 7) were identified by comparison with authentic samples prepared by alternative methods.

‡ The quantum yield for the reaction was determined according to the method of Ito *et al.* (ref. 8).

§ The $\Delta G^0$ was obtained based on the oxidation potential for **1** [1.58 V *vs.* SCE in MeCN (ref. 9)], the reduction potential of **2** [−0.2 V *vs.* Ag electrode in MeCN (ref. 10)] and the singlet excitation energy of **1** [257 kJ $mol^{-1}$ (ref. 11)].

## References


1 R. F. Foster, *Charge-Transfer Complexes in Organic Chemistry*, Academic Press, New York, 1963; M. Oh-hashi, *Kagaku Sosetsu*, No. 33, Gakkai Shuppan Center, Tokyo, 1982, pp. 61.

2 T. Suzuki, T. Fukushima, Y. Yamashita and T. Miyashi, *J. Am. Chem. Soc.*, 1994, **116**, 2793; H. Koshima, K. Ding, Y. Chisaka, T. Matsuura, Y. Ohashi and M. Mukasa, *J. Org. Chem.*, 1996, **61**, 2352.

3 J. G. Calvert and J. N. Pitts Jr., *Photochemistry*, Wiley, Inc., New York, 1966, pp. 739.

4 D. Rehm and A. Weller, *Isr. J. Chem.*, 1970, **8**, 259.

5 H. Miyasaka, S. Ojima and N. Mataga, *J. Phys. Chem.*, 1989, **93**, 3380; S. Ojima, H. Miyasaka and N. Mataga, *J. Phys. Chem.*, 1990, **94**, 5834; T. Asahi, M. Ohkohchi and N. Mataga, *J. Phys. Chem.*, 1993, **97**, 13 132.

6 Y. Shirota, J. Nagata, Y. Nakano, T. Nogami and H. Mikawa, *J. Chem. Soc., Perkin Trans. 2*, 1977, 14.

7 D. O. Cowan and R. L. Drisco, *J. Am. Chem. Soc.*, 1970, **92**, 6286.

8 Y. Ito, T. Matsuura and K. Fukuyama, *Tetrahedron Lett.*, 1988, **29**, 3097.

9 I. Tanimoto, K. Kushioka and K. Maruyama, *Bull. Chem. Soc. Jpn.*, 1979, **52**, 3586.

10 J. E. Mulvaney, R. J. Cramer and H. K. Hall, *J. Polym. Sci. Polym. Chem. Ed.*, 1983, **21**, 309.

11 H. Levanon, P. Neta and A. M. Trozzolo, *Chem. Phys. Lett.*, 1978, **54**, 181.



*Received in Cambridge, UK, 15th April 1997; Com. 7/02564E*

# Atom transfer radical polymerisation (ATRP) of methyl methacrylate in the presence of radical inhibitors

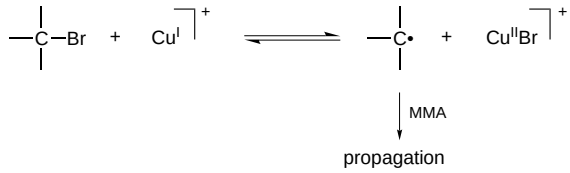
**D. M. Haddleton,* A. J. Clark, M. C. Crossman, D. J. Duncalf, A. M. Heming, S. R. Morsley and A. J. Shooter**

*Department of Chemistry, University of Warwick, Coventry, UK CV4 7AL*

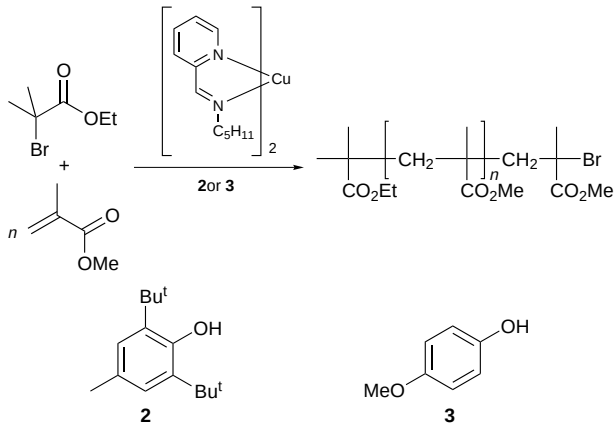
**Atom transfer radical polymerisation of methyl methacrylate mediated by copper(I) bromide, alkyl bromides and *N*-pentyl-2-pyridylmethanimine has been shown to be enhanced by the addition of substituted phenols, traditionally used as radical inhibitors.**

Atom transfer radical polymerisation has emerged as an efficacious method for the living polymerisation of vinyl monomers.[1–8] The ATRP process involves the combination of an alkyl halide and a low valent metal complex, *e.g.* $Cu^{I}Br$–bipyridine,[1–3] $Ru^{II}Cl_2(PPh_3)_2$,[4] $Ni^{II}[C_6H_3(CH_2NMe_2)_2$-2,6]Br,[7] which is capable of being oxidised to the $n + 1$ state by addition of a halogen atom. The mechanism proposed by both Matyjaszewski *et al.*[1] and ourselves[9] involves abstraction of the halogen atom from the propagating polymer to give a carbon-based radical and a new metal halide with the metal in the $n$ +1 oxidation state, *e.g.* $Cu^{II}$. Propagation is then proposed to be *via* free radical attack of the polymer radical on a monomer as in normal free radical polymerisation. Termination is prevented by the reverse abstraction of halogen atom from the metal halide to give a new polymeric alkyl halide (Scheme 1).

Polymerisation of methyl methacrylate in the presence of copper(I), ruthenium(II) and nickel(II) salts gives polymers with stereochemistry similar to that from normal free radical polymerisation.[2,4,7] All three metal-based catalysts have also been reported to lead to polymerisation which is completely inhibited by free radical inhibitor, *e.g.* galvinoxyl. The reactivity ratios for the copolymerisation of butyl and methyl methacrylate have also been shown to be entirely consistent with free radical propagation.[10] Thus all evidence presented to date is consistent with free radical propagation where the halogen atom is abstracted from the growing polymer chain. The objective of the present work was to investigate how robust ATRP is towards various functional groups. Surprisingly, we have found that phenolic free radical inhibitors enhance ATRP as opposed to suppressing polymerisation, as would have been expected for a free radical polymerisation or indeed an anionic polymerisation.

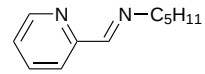



**Scheme 1**




**Scheme 2**

Atom transfer radical polymerisation of methyl methacrylate (MMA) was carried out with ethyl 2-methyl-2-bromopropionate as initiator in conjunction with *N*-pentyl-2-pyridylmethanimine **1** and copper(I) bromide in xylene solution at




**1**

90 °C (Scheme 2) in the presence of 2,6-di-*tert*-butyl-4-methylphenol **2** or 4-methoxyphenol **3**, or in the absence of phenol, as a control reaction. Both **2** and **3** are commonly added to commercial monomers to prevent polymerisation on transport and storage. Although phenolic inhibitors are more effective in the presence of oxygen they still inhibit radical reactions *via* transfer of a phenolic hydrogen atom in the absence of oxygen.[11] Polymerisation of methyl methacrylate in the presence of an equimolar amount of **2** with respect to initiator leads to poly(methyl methacrylate) with a polydispersity index (PDI) of 1.21 after 240 min (Table 1). Increasing the amount of **2** ([**2**] : [initiator] = 10 : 1) again leads to polymer with narrow PDI with *M*n increasing linearly with converstion (Fig. 1), as would be expected for a living polymerisation. Indeed this increase in the amount of **2** results in an acceleration in the rate of polymerisation so that 74.6% conversion is achieved in 240 min as opposed to 56.8% with stochiometric equivalents of initiator and **2**. The same is observed when **2** is replaced with **3**. Fig. 2 shows the increase in

**Table 1** Polymerisation of methyl methacrylate *via* ATRP

| Phenol[a] | [Phenol] : [initiator] | *t*/min | Conversion (%)[b] | *M*n (SEC) | PDI (SEC) |
|---|---|---|---|---|---|
| **2** | 1 | 240 | 56.8 | 7460 | 1.21 |
| **2** | 10 | 30 | 25.1 | 3700 | 1.18 |
| **2** | 10 | 60 | 34.8 | 4320 | 1.21 |
| **2** | 10 | 120 | 52.4 | 5710 | 1.22 |
| **2** | 10 | 180 | 61.2 | 6560 | 1.23 |
| **2** | 10 | 240 | 74.6 | 7970 | 1.21 |
| **3** | 1 | 240 | 54.4 | 7010 | 1.23 |
| **3** | 10 | 30 | 31.0 | 4120 | 1.18 |
| **3** | 10 | 60 | 35.7 | 4690 | 1.25 |
| **3** | 10 | 120 | 51.5 | 6460 | 1.22 |
| **3** | 10 | 180 | 61.3 | 7240 | 1.25 |
| **3** | 10 | 240 | 74.0 | 8970 | 1.25 |
| None | — | 240 | 54.0 | 6790 | 1.21 |

[a] All reactions carried out with [MMA] : [initiator] : [**1**] : [CuBr] = 100 : 1 : 3 : 1, under nitrogen at 90 °C at 37 mass% in degassed xylene solution. [b] From gravimetry.

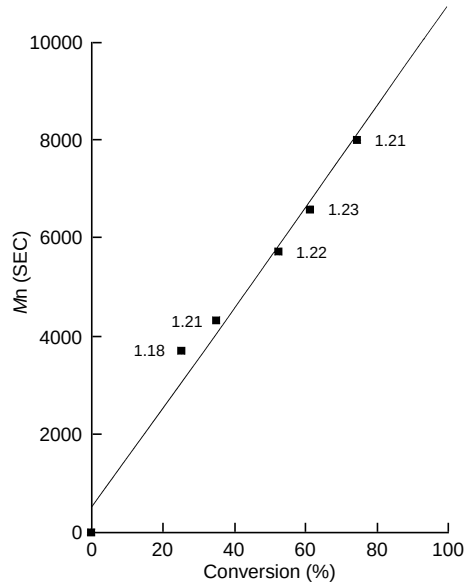



**Fig. 1** Plot showing how *M*n from SEC increases with conversion for ATRP of MMA in the presence of **2** in a ten-fold excess with respect to initiator. SEC carried out in THF at 1 ml min$^{-1}$ with calibration against poly(methyl methacrylate) narrow molecular weight standards. Polydispersity index (PDI) is given for each point.

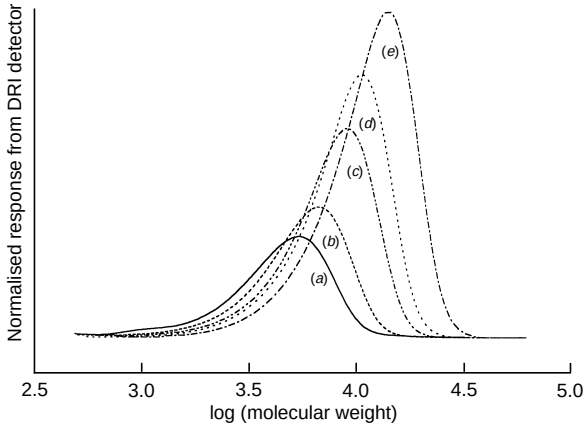



**Fig. 2** SEC traces for ATRP of MMA in the presence of **3** in a ten-fold excess with respect to initiator. The area beneath each trace has been normalised for conversion where conversion at 240 min is 74%: (*a*) 30 min, PDI = 1.18; (*b*) 60 min, PDI = 1.25, (*c*) 120 min, PDI = 1.22; (*d*) 180 min, PDI = 1.25; (*e*) 240 min, PDI = 1.25.

molecular weight with conversion (time) with a ten-fold excess of **3** with respect to initiator, as observed by size exclusion chromatography (SEC).

Fig. 3 shows the results of following the polymerisation by automated dilatometry, collecting one data point every 20 s over 8 h, in the presence and absence of a stochiometric equivalent of **3** with respect to initiator. The final rate of polymerisation is similar in both the presence and absence of **3**. Both are fairly constant between 60 and 180 min prior to showing a decrease in $k_p$[Pol*], the gradient of the graph (where Pol* is the active polymerisation centre). However, in the absence of **3** an induction period is present of *ca.* 60 min as observed by an increase in $k_p$[Pol*]; an induction period has previously been observed in ATRP of MMA using Ni$^{II}$ catalyst.[7] The induction period is removed by **3**, accounting for the increase in yield in the presence of substituted phenols.

Atom transfer radical polymerisation of MMA with bis(*N*-pentyl-2-pyridylmethanimine)copper(I) is enhanced by

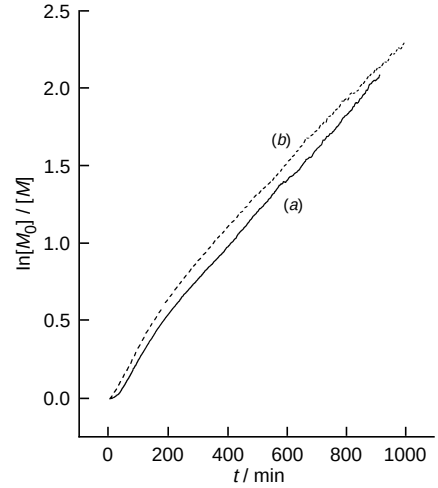



**Fig. 3** First order plots from automated dilatometry for the ATRP of MMA (*a*) in the absence of added phenol, and (*b*) with an equimolar amount of **3** with respect to initiator

substituted phenolic radical inhibitors. This indicates that propagation does not take place *via* a carbon-centred free radical. It is more likely that the copper(I) coordinates to the bromide, weakening the carbon–bromine bond and allowing single electron nucleophilic attack on monomer resulting in the transfer of a bromine atom in a concerted fashion. The active copper(I) species is not a simple four coordinate *pseudo*-tetrahedral compound as might have been expected. It appears that the active catalyst is formed during the initial stages of the reaction. Formation of the active species is accelerated by phenolic compounds. The role of the phenol is currently under investigation in our laboratory. In summary, ATRP does not take place *via* a normal free radical mechanism and the living polymerisation is enhanced by the addition of certain substituted phenols in excess relative to the amount of initiator.

We thank the EPSRC (D. J. D. and M. C. C., GR/K90364, GR/L10314; A. M. H., studentship; A. J. S., CASE award) and Courtaulds for funding.

## Footnote

* E-mail: msrgs@csv.warwick.ac.uk

## References

1 K. Matyjaszewski, T. E. Patten and J. Xia, *J. Am. Chem. Soc.*, 1997, **119**, 674.
2 K. Matyjaszewski and J.-S. Wang, *Macromolecules*, 1995, **28**, 7901.
3 J.-S. Wang and K. Matyjaszewski, *J. Am. Chem. Soc.*, 1995, **117**, 5614.
4 M. Kato, M. Kamigaito, M. Sawamoto and T. Higashimura, *Macromolecules*, 1995, **28**, 1721.
5 V. Percec, B. Barboiu, A. Neumann, J. C. Ronda and M. Zhao, *Macromolecules*, 1966, **29**, 3665.
6 V. Percec and B. Barboiu, *Macromolecules*, 1995, **28**, 7970.
7 C. Granel, P. Teyssie, P. DuBois and P. Jerome, *Macromolecules*, 1996, **29**, 8576.
8 D. M. Haddleton, C. Waterson, P. J. Derrick, C. B. Jasieczek and A. J. Shooter, *Chem. Commun.*, 1997, 683.
9 D. M. Haddleton, C. B. Jasieczek, M. J. Hannon and A. J. Shooter, *Macromolecules*, 1997, in the press.
10 D. M. Haddleton, M. C. Crossman, K. H. Hunt, C. Topping, C. Waterson and K. G. Suddaby, *Macromolecules*, in the press.
11 G. Moad and D. H. Solomon, *The chemistry of free radical polymerisation*, Pergamon, Oxford, 1995, p. 263.

*Received in Cambridge, UK, 1st April 1997; Com. 7/02166F*

# Homo- and hetero-dimetallic ethynyl- and butadiynyl-bridged bisphthalocyaninato complexes

**Eva María Maya, Purificación Vázquez and Tomás Torres***

*Departamento de Química Orgánica (C-I), Facultad de Ciencias, Universidad Autónoma de Madrid, 28049-Madrid, Spain*

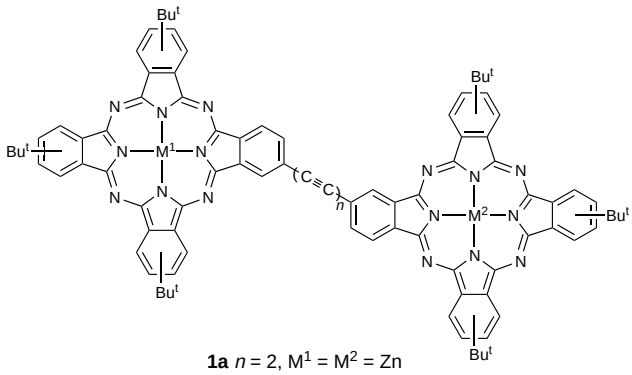
**A new type of phthalocyanine-based chromophore system having two metallophthalocyanine rings bound together through ethynyl linkages has been synthesized.**

Much effort has been expended in recent years to exploit electronic- and photonic-based cooperation between individual subunits of porphyrins.[1] However, despite the great interest of the related phthalocyanine (Pc) chromophore,[2] for example as a building block for the construction of new molecular materials, the effort devoted to preparing multiphthalocyanine arrays has not been as large. The main reason could be the difficulty of preparing unsymmetric Pcs,[3] necessary for a stepwise approach to building more complex Pc systems,[4] and in the purification of Pcs[2] in comparison with porphyrins. Non-conjugated binuclear Pcs, in which the two Pc nuclei are covalently bound *via* various kinds of linkage, have been reported.[5] However, to date very few examples of systems having phthalocyanine-to-phthalocyanine conjugated connections, namely planar binuclear phthalocyanines, have been described.[6]

Ethyne and oligoethyne bridges between chromophores have been recognized as ideal linkages, enabling unusually high excitonic and electron coupling between chromophore centres.[7] Recently, symmetric[8] and unsymmetric[9] Pcs having ethynyl functions have been described, but to the best of our knowledge the ethynyl linkage has not been used hitherto to assemble phthalocyanine systems with extended conjugation.

We are presently concentrating on the synthesis of Pcs and related compounds for nonlinear optics (NLO).[10] In this regard, the preparation of multiphthalocyanine arrays with extended conjugation represents an important goal.[10b]

Here the well-known metal-mediated cross- and homo-coupling methodology is applied for the first time to the preparation of homo- and hetero-dimetallic ethynyl- and butadiynyl-bridged bis(phthalocyaninato)zinc and nickel complexes **1a**,**b** and **2a**,**b**.



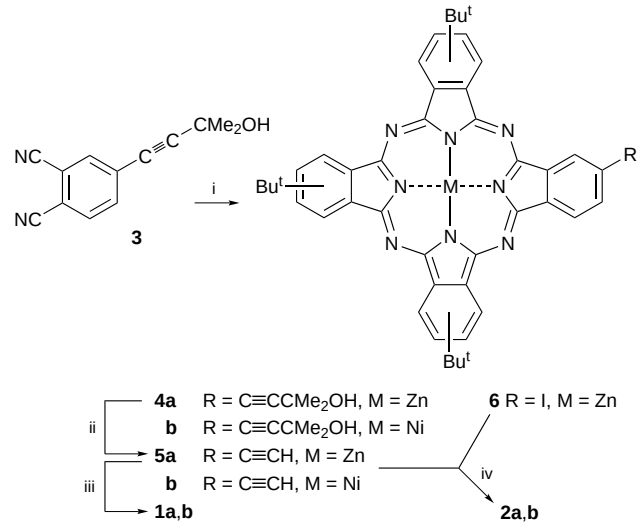

**1a** $n$ = 2, M$^1$ = M$^2$ = Zn
**b** $n$ = 2, M$^1$ = M$^2$ = Ni
**2a** $n$ = 1, M$^1$ = M$^2$ = Zn
**b** $n$ = 1, M$^1$ = Zn, M$^2$ = Ni

4-Iodophthalonitrile[11] was reacted with commercially available 2-methylbut-3-yn-2-ol in the presence of bis[triphenylphosphine]palladium(II) dichloride and copper(I) iodide[11,12] to yield aryl alcohol **3**. The mixed condensation of this phthalonitrile with an excess of 4-*tert*-butylphthalonitrile in the presence of the corresponding metal(II) chloride afforded the corresponding zinc and nickel complexes **4a**,**b**† in moderate yield, as a statistical mixture of isomers in each case (Scheme 1). The protecting group was then removed by treatment with sodium hydroxide in toluene[12] to give ethynyl derivatives **5a**,**b**†‡ in good yields. Similarly, compound **6**†‡ was obtained by statistical mixed condensation of 4-iodophthalonitrile with 4-*tert*-butylphthalonitrile and zinc chloride, in low yield (*ca*. 20%) after chromatographic purification.

Oxidative homocoupling[11] of terminal alkynes **5a**,**b** in the presence of copper(II) acetate monohydrate in a mixture of dry pyridine and dry methanol led, after purification by chromatography on silica gel, to the homonuclear dimetallic complexes **1a**,**b**† in *ca*. 50% yield.

Cross-coupling of alkynes **5a**,**b** with monoiodophthalocyanine **6** in freshly distilled and deaerated piperidine, in the presence of a catalyst formed *in situ* by the addition of tris(dibenzylideneacetone)dipalladium(0) [$Pd_2(dba)_3$] and triphenylarsine[1a,13] afforded the corresponding homonuclear and heterodimetallic butadiynyl-bridged bis(phthalocyaninato) complexes **2a**,**b**† in *ca*. 40% yield, after chromatographic purification. The same cross-coupling was accomplished in lower yield and with longer reaction times (12 h) by using the catalytic system $Pd(PPh_3)_2Cl_2$ and CuI[8] in freshly distilled and deaerated $NEt_3$ as solvent.

Fig. 1 shows the electronic absorption spectrum of butadiynyl-bridged bis(phthalocyaninato)zinc complex **1a**. The optical features of this new chromophoric system differ remarkably from that of the unsymmetric parent compound **5a**. The Soret (B) transition of **1a** occurring in the blue region of the spectra span wavelength ranges of 300–450 nm, similar to that




**Scheme 1** *Reagents and conditions*: i, 4-*tert*-butylphthalonitrile (3 equiv.), dimethylaminoethanol, reflux, $MCl_2$ (M = Zn, Ni); ii, toluene, NaOH; iii, $CuOAc{\cdot}H_2O$, 5% MeOH–pyridine, 55–60 °C, 90 min; iv, $Pd_2(dba)_3$, $As(Ph_3)_3$, piperidine, 35 °C, 4 h

of compound **5a** (maximum at 350 nm). However, while ethynyl compound **5a** exhibits only one Q-band at 684 nm, typical of metalated Pcs, dimer **1a** shows a splitting of this Q-band as well as a remarkable broadening and redshift of this transition, most probably resulting from the extended π-conjugation.§ Thus in compound **1a** two intense bands appear at 675 and 709 nm, respectively. In addition, at higher concentrations, a shoulder centred at *ca*. 770 nm is observed which extends to *ca*. 820 nm.¶

Fig. 2 shows the UV–VIS spectra of ethynylbis(phthalocyaninato)-zinc and -nickel complexes **2a**,**b**. The spectrum of **2a** is quite similar to that of **1a**, with the absorption maximum of the B-band slightly shifted to the blue (maximum at 344 nm), whereas the absorption maxima of the Q-bands appear slightly redshifted at 678 and 710 nm. In this case a broad band centred at 770 nm is also observed. The heterodimetallic compound **2b** shows only one intense absorption of the Q-band zone at 678 nm, with a shoulder at 713 nm.

The absorption coefficients of the Q-bands in **1** and **2** decrease, with regard to the mononuclear species **5**, due to increasing conjugation. The spectra are essentially unchanged down to $5 \times 10^{-7}$ M. Compounds **1a**,**b** and **2a**,**b** show no sign of intermolecular aggregation in $CHCl_3$ at concentrations below $5 \times 10^{-5}$ M. At higher concentrations, however, intermolecular aggregation takes place in some cases.

The degree of intramolecular aggregation in solution and the extent of electronic coupling between the two halves of the binuclear molecules in unsymmetrically substituted derivatives are under investigation.[15]

This series of alkynyl-bridged bis(phthalocyaninato)metal compounds **1** and **2** represent a basis set of supramolecular chromophore systems for studying electron and excitation transfer processes. On the other hand, the stepwise synthetic procedure described will allow the preparation of systems with distinct central metals and different kinds of substituents, for example donor and acceptor, in each one of the Pc subunits for NLO purposes.[10*b*]

This work was supported by CICYT and Comunidad de Madrid (Spain) through grants MAT 96-0654 and 06T/017/96, respectively, and by the EC, grant ERBCHRX-CT94-0558.

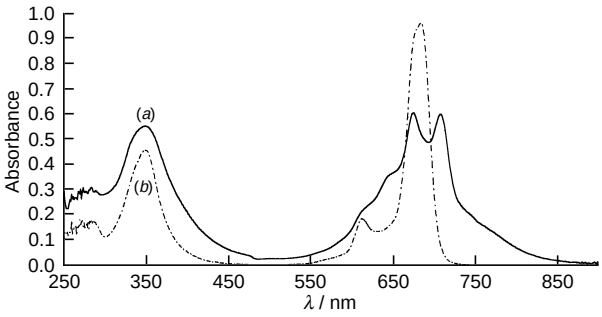



**Fig. 1** Electronic spectra of (*a*) **1a** ($1.1 \times 10^{-5}$ mol dm$^{-3}$) and (*b*) **5a** ($3.3 \times 10^{-6}$ mol dm$^{-3}$) in $CHCl_3$

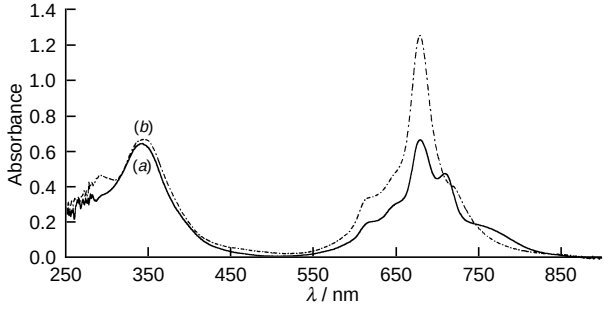



**Fig. 2** Electronic spectra of (*a*) **2a** ($3.6 \times 10^{-5}$ mol dm$^{-3}$) and (*b*) **2b** ($1.3 \times 10^{-5}$ mol dm$^{-3}$) in $CHCl_3$

## Footnotes

* E-mail: tomas.torres@uam.es

† Elemental analysis and spectral data [FAB-MS, $^1$H NMR ($CDCl_3$), IR (KBr) and UV–VIS ($CHCl_3$)] for compounds **1**–**6** were consistent with assigned structures.

*Selected data* (for UV–VIS see Figs. 1 and 2) for **1a**: *m/z* 1539 (M + H$^+$); $\delta_H$ 9.5–7.2 (br signals, arom-H), 1.6 [br signals, C(CH$_3$)$_3$]. For **1b**: *m/z* 1525 (M + H$^+$); $\delta_H$ 9.4–7.1 (br signals, arom-H), 1.6 [br signals, C(CH$_3$)$_3$]. For **2a**: *m/z* 1514 (M + H$^+$); $\delta_H$ 9.4–7.0 (br signals, arom-H), 1.6 [br signals, C(CH$_3$)$_3$]. For **2b**: *m/z* 1507 (M + H$^+$); $\delta_H$ 9.5–7.2 (br signals, arom-H), 1.6 [br signals, C(CH$_3$)$_3$]. For **3**: *m/z* 211 (M + H$^+$); $\delta_H$ 4.0 (OH), 1.4 (CH$_3$); $\delta_C$ 115.2 (CN), 101.4 (C≡C), 30.0 (CH$_3$). For **4a**: *m/z* 826 (M + H$^+$); $\delta_H$ 8.4–7.2 (br signals, arom-H), 4.0 (OH), 1.6 [br signals, C(CH$_3$)$_3$], 1.4 (CH$_3$). For **4b**: *m/z* 820 (M + H$^+$); $\delta_H$ 8.2–7.3 (br signals, arom-H), 4.0 (OH), 1.6 [br signals, C(CH$_3$)$_3$], 1.4 (CH$_3$). For **5a**: *m/z* 768 (M + H$^+$); $\delta_H$ 9.0–7.5 (br signals, arom-H), 3.4 (C≡CH), 1.6 [br signals, C(CH$_3$)$_3$]; $\nu_{max}$/cm$^{-1}$ 3295, 2103 (C≡C–H). For **5b**: *m/z* 762 (M + H$^+$); $\delta_H$ 9.0–7.6 (br signals, arom-H), 3.4 (C≡CH), 1.6 [br signals, C(CH$_3$)$_3$]; $\nu_{max}$/cm$^{-1}$ 3295, 2103 (C≡C–H). For **6**: *m/z* 870 (M + H$^+$).

‡ Tri-*tert*-butylethynyl- (**5a**) and tri-*tert*-butyliodo-phthalocyanine (**6**) have been recently prepared following a different procedure (ref. 9).

§ Taking into account that compounds **1** and **2** are definitely a mixture of structural isomers, it could be considered that a higher ratio of one or more of these isomers might be the reason of the splitting of the Q-bands observed in the UV–VIS spectra (ref. 14). However, the magnitude of the splitting, the kind of substituents involved, the lack of splitting in the starting materials **5** and **6** (which are also mixtures of isomers) and preliminary results obtained for other symmetrically substituted dimers (ref. 15), suggest that the observed splitting is due, to a major degree, to the extended π-conjugation of the system.

¶ Similarly to **1a**, compound **1b** shows a broad absorption between 550 and 850 nm, with the only clear maximum at 670 nm. The Q-band of the parent compound **5b** appears at 673 nm.

## References

1 (*a*) R. W. Wagner, T. E. Johnson, F. Li and J. S. Lindsey, *J. Org. Chem.*, 1995, **60**, 5266; (*b*) V. S.-Y. Lin and M. J. Therien, *Chem. Eur. J.*, 1995, 645; (*c*) N. Nishino, R. W. Wagner and J. S. Lindsey, *J. Org. Chem.*, 1996, **61**, 7534.
2 *Phthalocyanines: Properties and Applications*; ed. C. C. Leznoff and A. B. P. Lever, VCH, Weinheim, 1989, 1993, 1996, vols. 1–4.
3 A. Weitemeyer, H. Kiesch and D. J. Wöhrle, *J. Org. Chem.*, 1995, **60**, 4900; S. V. Kudrevich, S. Gilbert and J. E. van Lier, *J. Org. Chem.*, 1996, **61**, 5706; A. Sastre, B. del Rey and T. Torres, *J. Org. Chem.*, 1996, **61**, 8591.
4 B. Hauschel, P. Stihler and M. Hanack, *Trends Polym. Sci.*, 1996, **4**, 348.
5 See citations in ref. 6(*a*) and 6(*d*).
6 See for example (*a*) C. C. Leznoff, H. Lam, S. M. Marcuccio, W. A. Nevin, P. Janda, N. Kobayashi and A. B. P. Lever, *J. Chem. Soc., Chem. Commun.*, 1987, 699; (*b*) D. Lelievre, L. Bosio, J. Simon, J.-J. André and F. Bensebaa, *J. Am. Chem. Soc.*, 1992, **114**, 4475; (*c*) D. Lelievre, O. Damette and J. Simon, *J. Chem. Soc., Chem. Commun.*, 1993, 939; (*d*) J. Yang and M. R. Van De Mark, *Tetrahedron Lett.*, 1993, **33**, 5223; (*e*) N. Kobayashi, H. Lam, W. A. Nevin, P. Janda, C. C. Leznoff, T. Koyama, A. Monden and H. Shirai, *J. Am. Chem. Soc.*, 1994, **116**, 879.
7 V. S.-Y. Lin, S. G. DiMagno and M. J. Therien, *Science*, 1994, **264**, 1105; V. Grosshenny, A. Harriman and R. Ziessel, *Angew. Chem., Int. Ed. Engl.*, 1995, **34**, 2705.
8 D. S. Terekhov, K. J. M. Nolan, C. R. McArthur and C. C. Leznoff, *J. Org. Chem.*, 1996, **61**, 3034.
9 H. Ali and J. E. van Lier, *Tetrahedron Lett.*, 1997, **38**, 1157.
10 (*a*) A. Sastre, T. Torres, M. A. Diaz-García, F. Agulló-López, C. Dhenaut, S. Brasselet, I. Ledoux and J. Zyss, *J. Am. Chem. Soc.*, 1996, **118**, 2746; (*b*) G. de la Torre, T. Torres and F. Agulló-López, *Adv. Mater.*, 1997, **9**, 265.
11 S. M. Marcuccio, P. I. Svirskaya, S. Greenberg, A. B. P. Lever and C. C. Leznoff, *Can. J. Chem.*, 1985, **63**, 3057.
12 D. E. Ames, D. Bull and C. Takundwa, *Synthesis*, 1981, 364.
13 T. Ukai, H. Kawazura, Y. Ishii, J. J. Bonnet and J. A. Ibers, *J. Organomet. Chem.*, 1974, **65**, 253.
14 T. G. Linssen and M. Hanack, *Chem. Ber.*, 1994, **127**, 205.
15 E. M. Maya, P. Vázquez and T. Torres, unpublished work.

*Received in Liverpool, UK, 21st March 1997; Com. 7/01991B*

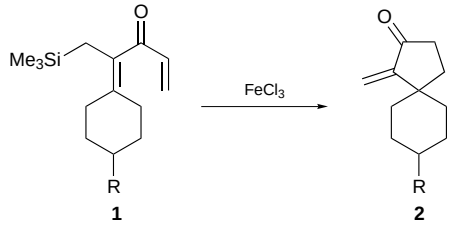
# Iron(III)-induced tandem Nazarov cyclization–rearrangement of α-(trimethylsilylmethyl)divinyl ketone. Synthesis of the bicyclo[4.3.0]nonane ring system *via* spiro[4.4]nonane

**Chiaki Kuroda,* Hiroshi Sumiya, Atsushi Murase and Akira Koito**

*Department of Chemistry, Rikkyo University, Nishi-Ikebukuro, Toshima-ku, Tokyo 171, Japan*

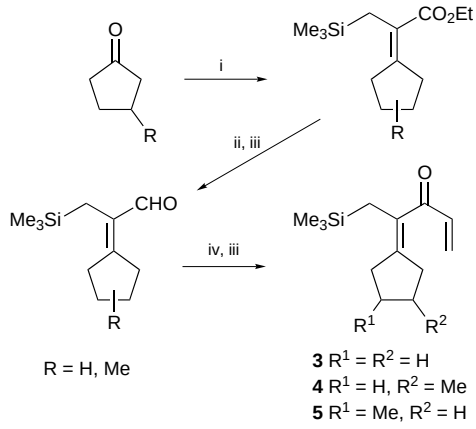
**6-Methylbicyclo[4.3.0]non-8-en-7-one was synthesized by $FeCl_3$-induced tandem Nazarov cyclization–rearrangement of 4-cyclopentylidene-5-trimethylsilylpent-1-en-3-one, *via* 7-methyl-1-methylenespiro[4.4]nonan-2-one as intermediate.**

Construction of various carbocyclic ring systems is fundamental chemistry in the synthesis of terpenoids and related compounds.[1] Allylsilanes have been developed as useful intermediates for this purpose.[2] We are studying the synthesis of carbocycles[3] and lactones,[4] basic structures of terpenoids,[5] utilizing intramolecular cyclization of β-(ethoxycarbonyl)-allylsilane. Recently we reported that Nazarov cyclization of α-(trimethylsilylmethyl)divinyl ketone derivatives **1**, derived from β-(ethoxycarbonyl)allylsilane attached to a six-membered ring, gives spiro[4.5]decanes **2** (Scheme 1).[6,7] Here we report that the α-(trimethylsilylmethyl)divinyl ketone attached to a five-membered ring undergoes tandem Nazarov cyclization–skeletal rearrangement to yield the bicyclo[4.3.0]nonane ring.[8]




**Scheme 1**

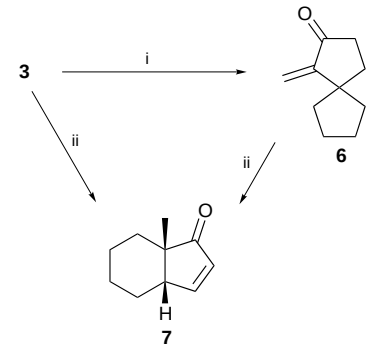
Synthesis of the cyclization precursors, α-(trimethylsilylmethyl)divinyl ketone **3**, was executed from cyclopentanone in five steps according to Scheme 2.[6] Similarly, **4** and **5** were prepared from 3-methylcyclopentanone and were separated by column chromatography.




**Scheme 2** *Reagents and conditions*: i, $(EtO)_2POCH(CO_2Et)CH_2SiMe_3$, NaH, DME, room temp.; ii, $LiAlH_4$, $Et_2O$, 0 °C; iii, $MnO_2$, $CH_2Cl_2$, room temp.; iv, $CH_2$=CHMgBr, THF, 0 °C

The Nazarov cyclization of **3** was carried out by treatment with $FeCl_3$ (2.5 equiv.) in $CH_2Cl_2$ at 0 °C† for 4 h, giving spiro[4.4]nonane **6**‡ in 56% yield. However, when **3** was subjected to the same treatment at room temperature§ for 24 h, compound **7** [9]¶ was obtained as the sole product in 62% yield. Treatment of **6** under the same reaction conditions (room temp., 24 h)§ gave **7** in 60% yield. From this result, along with the observation of behaviour on TLC, it was suggested that **7** was formed from **3** *via* **6** as intermediate (Scheme 3).

A further study of the stereochemistry of this Nazarov cyclization and subsequent skeletal rearrangement was made using methyl derivatives **4** and **5** as substrates. First, **4** and **5** were treated with $FeCl_3$ at 0 °C,† giving two isomers of spiro[4.4]nonanes¶ **8** and **9** as inseparable mixtures. The ratios of the two isomers were **8** : **9** = 4 : 1 from **4**, and 1 : 1 from **5**. The tandem Nazarov cyclization–rearrangement reaction was next examined and the results are summarized in Table 1. The rearranged product **10** consisted of five isomers **10a–e** as inseparable mixtures. Although the exact structures of each isomer could not be determined, the major isomer **10a** was shown to have the illustrated structure by $^1$H NMR spectroscopy. It was confirmed here again that the bicyclo-[4.3.0]nonene is formed *via* spiro[4.4]nonane. Thus both direct treatment of **4** (entry 1) and treatment of spiro compounds obtained from **4** (entry 3) afforded **10** in similar ratios. Compound **5** showed parallel results (entries 2 and 4). Different ratios of the isomers were obtained when the reaction




**Scheme 3** *Reagents and conditions*: i, $FeCl_3$, $CH_2Cl_2$, −30 to 0 °C, 4 h; ii, $FeCl_3$, $CH_2Cl_2$, −30 °C to room temp., 24 h

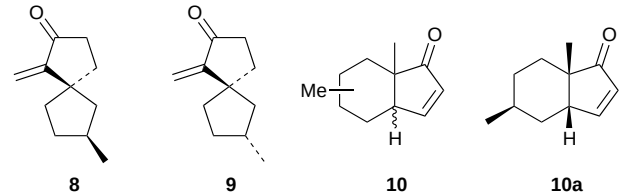
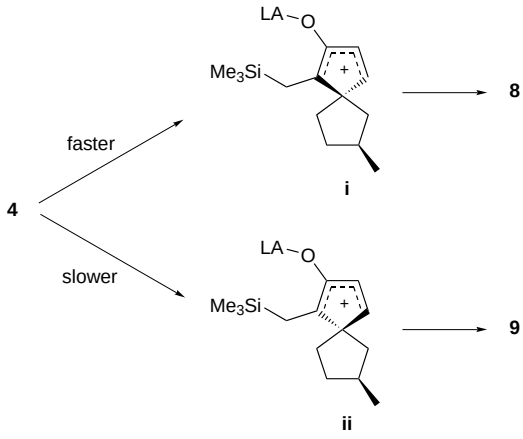


**Table 1** Nazarov cyclization–rearrangement of **4** and **5**[a]

| Entry | Substrate | Temp. | *t*/h | Yield (%) | Ratio of isomers[b] **10a : 10b : 10c : 10d : 10e** |
|---|---|---|---|---|---|
| 1 | **4** | room temp.[e] | 25 | 64 | 72 : 12 : 5 : 3 : 8 |
| 2 | **5** | room temp.[e] | 26 | 65 | 46 : 32 : 10 : 6 : 6 |
| 3 | **8** + **9** (4 : 1)[c] | room temp.[e] | 49 | 67 | 69 : 13 : 5 : 4 : 9 |
| 4 | **8** + **9** (1 : 1)[d] | room temp.[e] | 53 | 63 | 42 : 25 : 10 : 11 : 12 |
| 5 | **5** | room temp.[f] | 25 | 67 | 13 : 13 : 9 : 26 : 39 |

[a] The reactions were carried out in $CH_2Cl_2$ with $FeCl_3$ (2.5 equiv.). [b] **10a**: δ 5.90 (dd, *J* 2.5, 6 Hz) and 6.70 (dd, *J* 2, 6 Hz); **10b**: δ 5.88 (dd, *J* 2.5, 6 Hz) and 6.65 (dd, *J* 2, 6 Hz); **10c**: δ 5.84 (dd, *J* 1.5, 6 Hz) and 6.85 (dd, *J* 3, 6 Hz); **10d**: δ 5.81 (br d, *J* 5.5 Hz) and 6.96 (br d, *J* 5.5 Hz); **10e**: δ 5.80 (br d, *J* 5.5 Hz) and 6.95 (br d, *J* 5.5 Hz) (in $C_6D_6$). [c] Obtained from **4**; see text. [d] Obtained from **5**; see text. [e] The reagents were added at −30 °C and then the mixture was slowly warmed to room temp. over period of 7 h, which is included in the reaction time. [f] The reagents were added at −30 °C and the cooling bath was immediately removed.




**Scheme 4**

temperature was raised immediately after addition of the reagent (entry 5).

In contrast, this type of skeletal rearrangement did not proceed when analogous spiro[4.5]decanes **2** (R = H, Me, and Bu$^t$)[6] were subjected to the same treatment. Accordingly, the rearrangement is considered to be limited to the strained spiro five-five membered ring system.

The stereochemistry of the Nazarov cyclization of **4** and **5** can be explained by steric interaction between the methyl group and the vinyl group, but not the trimethylsilylmethyl group (Scheme 4). Thus intermediate **i** derived from **4** is favoured over **ii**, in which the methyl group and the vinyl group are on the same side of the cyclopentane ring, while the distance between these two groups gives non-stereoselectivity for **5**.

Although the reaction mechanism of the rearrangement (*e.g.* **6** to **7**) is not clear, it can be deduced that **10a** is produced from **8** with *ca.* 90% selectivity. Similarly, **10b** must be the major product from **9**.

In conclusion, a new entry to bicyclo[4.3.0]nonane carbon framework was established *via* a tandem Nazarov cyclization–skeletal rearrangement of α-(trimethylsilylmethyl)divinyl ketone. Synthesis of the bicyclo[4.3.0]nonane ring system from a compound having a five-membered ring is one of the classical methods.[1] However, this new entry from cyclopentanone is different, since (i) the newly-formed ring is still five-membered, and (ii) the original five-membered ring becomes a six-membered ring.[10] We have previously reported a synthesis of the bicyclo[4.3.0]nonane ring system using β-(ethoxycarbonyl)allylsilane.[3] Thus the same carbon framework can be synthesized from β-(ethoxycarbonyl)allylsilane by two independent strategies.

We thank Dr M. M. Ito and Dr T. Niitsu, Soka University, for the measurements of mass spectra.

## Footnotes

† The reagents were added at −30 °C and the reaction mixture was slowly warmed to 0 °C.

‡ Compound **6**: UV (pentane) 223 nm; IR (neat) 1730, 1645 cm$^{-1}$; $^1$H NMR ($C_6D_6$) δ 1.31 (2 H, t, *J* 8 Hz), 2.04 (2 H, t, *J* 8 Hz), 4.84 (1 H, d, *J* 1 Hz), 6.08 (1 H, d, *J* 1 Hz); *m*/*z* 150 ($M^+$).

§ See footnote (*e*) of Table 1.

¶ The stereochemistry was determined from NOE measurements.

## References

1 T.-L. Ho, *Carbocycle Construction in Terpene Synthesis*, VCH, New York, 1988; C. D. J. Boden and G. Pattenden, *Contemp. Org. Synth.*, 1994, **1**, 433.

2 For review, see G. Majetich, in *Organic Synthesis: Theory and Application*, ed. T. Hudlicky, JAI Press, Greenwich, 1989, vol. 1, p. 173; D. Shinzer, *Synthesis*, 1988, 263; Y. Yamamoto and N. Asao, *Chem. Rev.*, 1993, **93**, 2207.

3 C. Kuroda, Y. Ohnishi and J. Y. Satoh, *Tetrahedron Lett.*, 1993, **34**, 2613; C. Kuroda, H. Nogami, Y. Ohnishi, Y. Kimura and J. Y. Satoh, *Tetrahedron*, 1997, **53**, 839.

4 For examples, see C. Kuroda, S. Shimizu and J. Y. Satoh, *J. Chem. Soc., Perkin Trans. 1*, 1990, 519; C. Kuroda, S. Inoue, R. Takemura and J. Y. Satoh, *J. Chem. Soc., Perkin Trans. 1*, 1994, 521; C. Kuroda and K. Ito, *Bull. Chem. Soc. Jpn.*, 1996, **69**, 2297; C. Kuroda, N. Mitsumata and C. Y. Tang, *Bull. Chem. Soc. Jpn.*, 1996, **69**, 1409.

5 B. M. Fraga, *Nat. Prod. Rep.*, 1996, **13**, 307; 1995, **12**, 303; 1994, **11**, 533.

6 C. Kuroda and Y. Hirono, *Tetrahedron Lett.*, 1994, **35**, 6895.

7 For related Nazarov cyclization of allylsilane derivatives, see S. E. Denmark, in *Comprehensive Organic Synthesis*, ed. B. M. Trost, Pergamon, Oxford, 1991, vol. 5, p. 751; S. E. Denmark and R. C. Klix, *Tetrahedron*, 1988, **44**, 4043; S. E. Denmark, M. A. Wallace and C. B. Walker, Jr., *J. Org. Chem.*, 1990, **55**, 5543; K.-T. Kang, S. S. Kim, J. C. Lee and J. S. U, *Tetrahedron Lett.*, 1992, **33**, 3495.

8 For example of recent synthesis of bicyclo[4.3.0]nonane, see M. Tori, M. Ikawa, T. Sagawa, H. Furuta, M. Sono and Y. Asakawa, *Tetrahedron*, 1996, **52**, 9999.

9 M. Karpf and A. S. Dreiding, *Helv. Chim. Acta*, 1979, **62**, 852.

10 For related type of ring formation, see W. L. Mock and M. E. Hartman, *J. Org. Chem.*, 1977, **42**, 459.

*Received in Cambridge, UK, 4th February 1997; Com. 7/00816C*

# Air oxidation of supercritical phase isobutane to *tert*-butyl alcohol

**Li Fan,* Yuri Nakayama and Kaoru Fujimoto**

*Department of Applied Chemistry, School of Engineering, University of Tokyo, Hongo, Bunkyo-ku, Tokyo, 113, Japan*

***tert*-2-Butyl alcohol can be synthesized efficiently on $SiO_2$–$TiO_2$ or Pd–C catalyst if air is directly introduced to the supercritical-phase isobutane.**

As the initial material in methyl *tert*-butyl ether (MTBE) production and methyl methacrylate (MMA) synthesis where MTBE is high-octane-number gasoline additive and MMA is a resin material, *tert*-butyl alcohol (TBA) is of increasing importance.[1,2] On the other hand, TBA can be used to produce isobutene *via* a dehydration reaction. Commercially, production of isobutene from isobutane *via* direct dehydrogenation needs high reaction temperatures (500–600 °C) and a catalyst which is deactivated quickly. Here we report a new synthesis of TBA where air is used directly as oxidant to convert isobutane to TBA. This synthesis can be conducted efficiently if isobutane is in the supercritical phase on selected catalysts.

Wide attention has recently been devoted to supercritical fluid applications in catalytic systems, both in homogeneous and heterogeneous systems, such as the Fischer–Tropsch reaction, alkylation and carbon dioxide conversion.[3–6] However, organic oxidation in the supercritical phase has hardly been studied until now, especially when air is used directly as oxidant. It is also of theoretic interest to pursue the reaction behaviour of oxygen species such as peroxide in supercritical fluid. It is expected that high solubility, high diffusion capacity—especially the cluster structure formed around solute molecules—and the special ionization effects of the supercritical fluid might exert a strong influence on the reaction mechanism.

Listed in Table 1 are the reaction performance data for two catalysts and a non-catalytic case, in the supercritical, gas and liquid phases.† In either the non-catalytic reaction or the catalysed reaction, changing the state of isobutane from the gas phase (44 bar) to the supercritical phase (54 bar) gave remarkably enhanced conversion of isobutane and oxygen. Meanwhile, selectivities for the target products (TBA and isobutene) increased slightly when moving from the gas phase to the supercritical phase. Exceptionally, Pd–C catalyst exhibited obvious changes in both conversion and selectivity of the reaction if the phase changed. When the total pressure was increased from 44 bar to 54 bar, the total yield of TBA and isobutene was enhanced from 0.31 to 2.70%.

All the catalysed reactions showed higher activity than the non-catalytic reactions, which proved the promotional role of the catalysts in the reaction.

More interestingly, if the total pressure of the gas phase reaction was as low as 12 bar, the reaction did not proceed, even if $SiO_2$–$TiO_2$ was utilized. Similarly, for the liquid phase reaction on $SiO_2$–$TiO_2$, the reaction rate was very low, as shown in Table 1.

Generally, the main byproduct of the reaction was acetone. The combustion product, $CO_2$, was formed only in very small amounts. CO was not detected. Lighter hydrocarbons were formed in small amounts as well, and consisted of 98% methane. The total amount of all $C_1$ species was equal to that of acetone, which indicates the decomposition of $C_4$ to $C_3$ species (acetone) and $C_1$ fractions. The carbon balance of the total products was higher than 97%, indicating remarkably low carbon deposition on the catalyst surface.

As indicated in Table 1, this reaction depended greatly on temperature and pressure, which implied the effect of the reaction phase. Fig. 1(*a*) shows a comparison of the reaction performance on $SiO_2$–$TiO_2$ catalyst under 54 bar while the reaction temperature was varied around the critical point (408 K). It is clear that isobutane and oxygen conversions were enhanced remarkably when the state of the isobutane changed from the liquid phase to the supercritical phase. Consequently, TBA yield was enhanced in the supercritical phase. The reason for the high isobutene selectivity on Pd–C catalyst in the supercritical phase is not as yet clear. It is well known that the formed TBA can be dehydrated rapidly on acidic sites of a catalyst, but the carbon support here is generally neutral.

Concerning the selectivity of the products, as exhibited in Fig. 1(*b*), TBA selectivity as well as acetone selectivity was enhanced and isobutene selectivity was suppressed in the supercritical phase reaction on $SiO_2$–$TiO_2$ catalyst.

For the oxidation mechanism in supercritical fluid, it is suggested that dioxygen can attack the most active hydrogen of isobutane to form *tert*-butyl hydroperoxide (TBHP, $Bu^tOOH$). TBHP is known as an oxygen donor in the epoxidation of alkenes.[7] It is inferred that TBHP can form in the supercritical phase from isobutane coexisting with dioxygen. This autoxidation step can proceed without catalyst,[8] which happened in the inductive period during the initial stages of the reaction.

**Table 1** Reaction performance of catalytic oxidation of isobutane by air in the supercritical phase or the gas phase[a]

| Catalyst | Total pressure/ bar | Isobutane conversion (%) | $O_2$ conversion (%) | TBA selectivity (%) | Isobutene selectivity (%) | TBA and isobutene yield (%) |
|---|---|---|---|---|---|---|
| none | 44 | 0.3 | 2.5 | 55.0 | 7.0 | 0.2 |
| none | 54 | 1.2 | 9.9 | 58.1 | 8.1 | 0.8 |
| $SiO_2$–$TiO_2$ | 44 | 2.9 | 24.0 | 59.0 | 5.2 | 1.9 |
| $SiO_2$–$TiO_2$ | 54 | 4.9 | 40.6 | 61.2 | 6.3 | 3.3 |
| $SiO_2$–$TiO_2$ | 12 | 0.0 | 0.0 | 0.0 | 0.0 | 0.0 |
| $SiO_2$–$TiO_2$[b] | 54[b] | 0.1 | 1.1 | 55.5 | 7.7 | 0.1 |
| Pd–C | 44 | 0.5 | 4.2 | 61.2 | 2.1 | 0.3 |
| Pd–C | 54 | 3.1 | 25.6 | 64.8 | 20.1 | 2.7 |

[a] Isobutane: air = 3 : 1, $W/F$ = 10 g h $mol^{-1}$, catalyst weight = 0.5 g, T = 426 K. [b] Liquid-phase reaction where the reaction temperature was 403 K.

TBHP can decompose homolytically, resulting in *tert*-butoxy radical and hydroxide radical. *tert*-Butoxy radical then combines with a third hydrogen from another isobutane to form TBA. TBA can be dehydrated on acidic sites, leading to the increase in isobutene selectivity. For the main byproduct, acetone, it could be derived from decomposition of *tert*-butoxy radical, accompanied by C1 compounds such as CO, $CO_2$ or $CH_4$.

Concerning the role of the catalyst, it is inferred that the catalyst might improve the efficiency of the oxidation of isobutane with TBHP, resulting in the enhanced conversion. Methanol is probably a byproduct, together with acetone, as in some published reports.[7,8] However, in our supercritical phase reaction, not only methanol but also $CO_2$, $CH_4$ formation accompanied acetone formation. It is suggested that the formation route of $CO_2$ and $Ch_4$ is different from that of methanol. Detailed studies on the reaction mechanism will be reported in the near future.

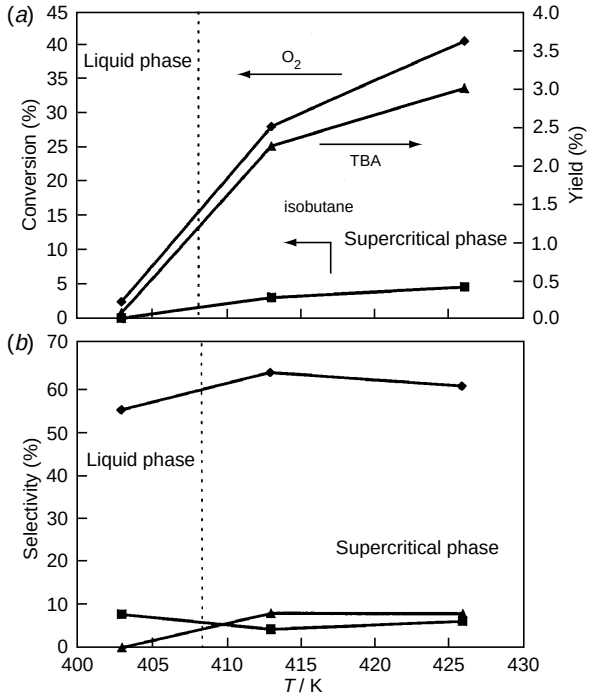



**Fig. 1** Comparison of the reaction performance around the critical point: (◆), TBA, (■) isobutane, (▲) acetone. $SiO_2$–$TiO_2$ catalyst, 54 bar, $W/F$ = 10 g h mol$^{-1}$, catalyst weight = 0.5 g, isobutane : air = 3 : 1.

Because the reactions reported above were conducted with a molar ratio of isobutane to $O_2$ = 15 : 1 (isobutane to air = 3 : 1), it is expected that the TBA yield might be enhanced further if the oxygen partial pressure was increased.[9]

Under the standard reaction conditions, the reaction required 3 h to reach a steady state from the reaction start. Catalyst deactivation was not observed during the supercritical phase reaction even after continuous reaction for 30 h.

## Footnotes

* E-mail: tfan@hongo.ecc.u-tokyo.ac.jp

† A typical flow-type fixed-bed reactor was employed, and the isobutane was fed by a high-pressure pump. Isobutane has a critical temperature of 408.13 K and a critical pressure of 36.48 bar. For the catalytic reaction, representative examples reported here are for reactions on commercially available amorphous $SiO_2$–$TiO_2$ (Fuji Silysia Chemical Co.), and a home-made palladium catalyst (2.5 wt%) supported on active carbon (Shirasagi, Takeda Pharmacy Co.). All products was analysed by gas chromatography (Shimadu GC-14B or Hitachi 163). A capillary column (TC-1) coupled with a flame ionization detector was used for analysis of the oxygenates and heavy hydrocarbons. A molecular sieve column and an active carbon column, with a thermal conductivity detector, were utilized for inorganic gas analysis. Lighter hydrocarbons with determined by an active alumina column with a flame ionization detector. The standard reaction conditions are as follows: ratio of isobutane to air = 3 : 1; $W/F$ (total) = 10 g h mol$^{-1}$; catalyst weight = 0.5 g; reaction temperature = 426 K. The total pressure for the gas phase reaction is 44 bar and that for the supercritical phase is 54 bar. Correspondingly, the partial pressure of isobutane is 33 bar and 41 bar, respectively. The feed ratio of isobutane to air was 3. When the total pressure was higher than 48 bar (36 bar of isobutane and 12 bar of air), the phase of the reaction became supercritical. The reaction at a total pressure of 54 bar was in the supercritical phase.

## References

1 *European Chemical News*, 1993, February, 15.
2 *Chemical Week*, 1993, February, 17.
3 L. Fan, K. Yokota and K. Fujimoto, *AIChE J.*, 1992, **38**, 1639.
4 P. G. Jessop, T. Ikariya and R. Noyori, *Nature*, 1994, **368**, 231.
5 P. E. Savage, S. Gopalan, T. Mizan, C. Martino and E. Brock, *AIChE J.*, 1995, **41**, 1723.
6 I. Nakamura, L. Fan, S. Ishida and K. Fujimoto, *J. Jpn. Pet. Inst.*, 1997, **40**, 61.
7 N. Emanuel, E. Denisov and Z. Maizus, *Liquid Phase Oxidation of Hydrocarbons*, Plenum, New York, 1967.
8 A. Bielanski and J. Haber, *Oxygen in Catalysis*, Marcel Dekker, New York, 1991, p. 452.
9 L. Fan and K. Fujimoto, unpublished work.

*Received in Cambridge, UK, 4th April 1997; Com. 7/02308A*

# Preparation of mesostructured lamellar zirconia

**Yinyan Huang and Wolfgang M. H. Sachtler***

*Ipatieff Laboratory, Center for Catalysis and Surface Science, Northwestern University, Evanston, IL 60201, USA*

**Mesostructured lamellar zirconia is synthesized by using anionic surfactants under hydrothermal conditions.**

Since the discovery by scientists at Mobil of the mesoporous aluminosilicate (MCM-41),[1,2] much attention has been paid not only to mesoporous aluminosilicates, but also to mesoporous oxides of other metals. Many mesoporous transition-metal oxides have been obtained. Huo *et al*.[3] and Ciesla *et al*.[4] report the syntheses of mesostructured oxides of Fe, Mn, Zn, Co, Ni, Al, Sb, W by interaction of a soluble metal solution and an anionic surfactant. Unfortunately, attempts to remove the template used for synthesis, either by leaching or by calcination, have led to the collapse of the mesostructure. Recently the syntheses of mesoporous $TiO_2$, $Nb_2O_5$ and $ThO_2$ with hexagonal pore arrangements and amorphous pore walls have been reported.[5–7] As for mesostructured zirconia, several papers report that this material can only be obtained with amorphous walls[8,9] and irregular pore arrangement. The mesoporosity is, however, lost upon crystallization of the zirconia. Another paper claims the synthesis of mesoporous zirconia with regular pore arrangement based on small-angle XRD.[10] Mesoporous lamellar zirconia was also prepared by a route using neutral amines, but the mesostructure was lost when the samples were calcined to remove the surfactant.[11] The synthesis of mesoporous zirconia using a neutral amine template that was subsequently extracted with ethanol has been reported by us; although no regular pore structure has been obtained, the mesoporosity of this material can be maintained up to 700 °C if the tetragonal modification of zirconia is stabilized by sulfation. Here, we report the synthesis of mesostructured lamellar zirconia, by using soluble zirconium chloride and an anionic surfactant.

Lamellar zirconia is obtained by hydrothermal reaction. In a typical synthesis process, 1.5 g $ZrOCl_2$ was first dissolved in 10 ml water. 1.26 g of sodium 1-hexadecanesulfonate (*n*-$C_{16}H_{33}SO_3Na$) was then dissolved in 10 ml water and mixed with the $ZrOCl_2$ solution under stirring. The surfactant/zirconium molar ratio is *ca*. 0.5 and the mixture has a pH of *ca*. 6. Stirring was continued for 30 min; the mixture was then sealed in a polyethylene bottle and heated at 90 °C for 48 h before final filtering, washing and drying in air.

Besides sodium 1-hexadecanesulfonate, 1-hexadecanesulfonyl chloride (*n*-$C_{16}H_{33}SO_2Cl$) was also used as surfactant for the synthesis of mesostructured zirconia, using the same procedure. In some cases, some $Pt(NH_3)_4(NO_3)_2$ was added to a zirconyl chloride solution before mixing it with the surfactant solution. The Pt loading is *ca*. 1 mass% based on the amount of $ZrO_2$.

The materials have been characterized by small-angle XRD and TEM. Fig. 1(*a*) and (*b*) show the small-angle XRD patterns of mesostructured zirconias synthesized using either the surfactant *n*-$C_{16}H_{33}SO_3Na$ or *n*-$C_{16}H_{33}SO_2Cl$. Their XRD patterns are very similar. The peak at $2\theta = 2°$ clearly indicates the existence of some mesostructure. The peaks at higher diffraction angles are not well resolved. In view of the inaccuracy of the XRD pattern, a *d* value of *ca*. 40 Å is estimated for the first peak.

Though many authors use small-angle XRD to determine the symmetry of the mesostructure, this procedure sometimes leads to inaccurate results. Schüth has shown that a highly resolved XRD pattern can be consistent with a chaotic structure.[12] Therefore, the present work mainly employs TEM to identify the structure of the materials. Fig. 2 shows the TEM image of mesostructured zirconia obtained by using *n*-$C_{16}H_{33}SO_3Na$ surfactant. The lamellar structure is clearly visible. The distance between two layers is estimated to be *ca*. 41 Å. This is consistent with the value obtained from XRD.

The same lamellar TEM image is found with material obtained using *n*-$C_{16}H_{33}SO_2Cl$ as the template. Incorporation of Pt does not change the mesostructure of the materials.

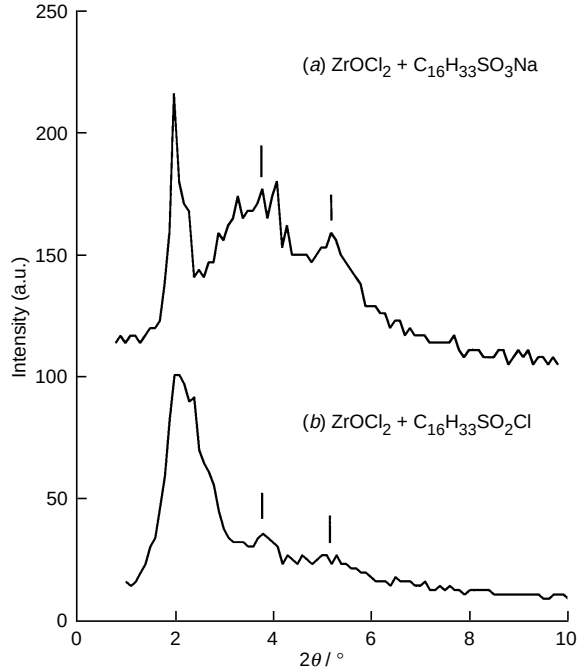



**Fig. 1** Small-angle XRD patterns of mesostructured zirconia synthesized by using surfactant *n*-$C_{16}H_{33}SO_3Na$ (*a*) and *n*-$C_{16}H_{33}SO_2Cl$ (*b*)

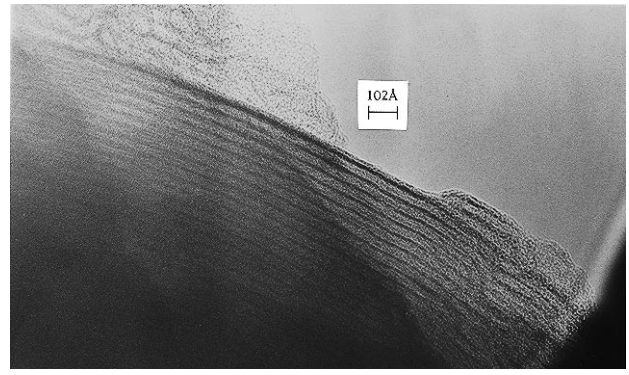



**Fig. 2** TEM image of mesostructured zirconia synthesized with *n*-$C_{16}H_{33}SO_3Na$

The materials were also analysed by thermal gravimetry (TG). As shown in Fig. 3, the surfactant is oxidized in an $O_2$ atmosphere at *ca*. 275 °C. A strong exothermic effect is observed at that temperature. The total mass loss is due to desorption of occluded materials in addition to oxidation of the surfactant. The mass loss corresponding to the oxidation of surfactant is about 50% of the total mass. Based on the TG results, a Zr/surfactant molar ratio of 1.5 is estimated. This is higher than expected for the charge balance of $ZrO^{2+}$ with *n*-$C_{16}H_{33}SO_3^-$. Apparently considerable quantities of water and other species are included in the material.

As *n*-$C_{16}H_{33}SO_3Na$ is dissolved in water, the negative *n*-$C_{16}H_{33}SO_3^-$ ion is formed. The anion can also be formed by hydrolysis of *n*-$C_{16}H_{33}SO_2Cl$. The surfactant anion will react with the $ZrO^{2+}$ cation to form a 'cation–anion composite molecule'. This composite molecule has a low solubility in water and tends to reassemble, forming an ordered structure.

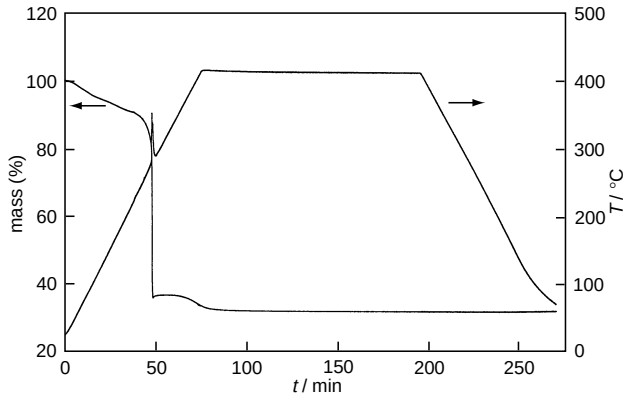



**Fig. 3** TG profile of mesostructured zirconia synthesized with *n*-$C_{16}H_{33}SO_3Na$ registered in a flow of oxygen of 20 ml $min^{-1}$

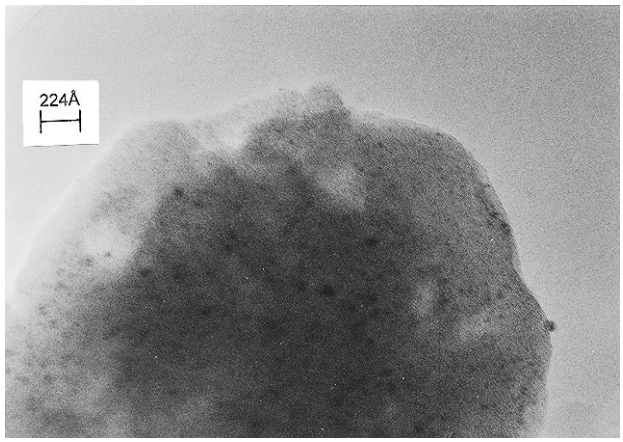



**Fig. 4** TEM image of Pt containing mesostructured zirconia by using *n*-$C_{16}H_{33}SO_3Na$ as surfactant, after calcination at 300 °C in a flow of oxygen of 100 ml $min^{-1}$

Although considerable effort was made to maintain the mesostructure by cautiously removing the surfactant, these attempts failed. Leaching of the material synthesized from *n*-$C_{16}H_{33}SO_3Na$ with an ammonia–ethanol mixture did not work either, whereas such treatment with the material from *n*-$C_{16}H_{33}SO_2Cl$ leads to the gelation of the original material.

Calcination of the materials in air at 500 °C for 6 h results in the collapse of the lamellar structure and the formation of tetragonal zirconia. The characteristic small-angle diffraction peak is lost. Upon calcining these materials in a flow of oxygen (100 ml $min^{-1}$) at 300 °C for 2 h at low ramping rate (0.5 °C $min^{-1}$), XRD analysis shows that the lamellar structure collapses and amorphous zirconia is obtained. TEM confirms that the material contains mainly amorphous zirconia particles and some small particles of tetragonal zirconia. In the case of the Pt-containing materials, highly dispersed Pt metal particles are formed. Fig. 4 shows rather uniform Pt particles dispersed on zirconia.

We gratefully acknowledge financial support from the director of the Chemistry Division, Basic Energy Sciences, US Department of Energy; Grant DE-FGO2-87ER13654 and a grant-in aid from Shell Development Company. We thank Dr Xiandong Wang for helping in TG analysis and Dr Timothy J. McCarthy and Dr Taeghwan Hyeon for taking the TEM images.

## Footnote

* E-mail: wmhs@nwu.edu

## References

1 C. T. Kresge, M. E. Leonowicz, W. J. Roth, J. C. Vartuli and J. S. Beck, *Nature*, 1992, **359**, 710.
2 J. S. Beck, J. C. Vartuli, W. J. Roth, M. E. Leonowicz, C. T. Kresge, K. D. Schmitt, C. T.-W. Chu, D. S. Olson, E. W. Sheppard, S. B. McCullen, J. B. Higgins and J. L. Schlenker, *J. Am. Chem. Soc.*, 1992, **114**, 10 834.
3 Q. Huo, D. I. Margolese, U. Ciesla, D. G. Demuth, P. Feng, T. E. Gier, P. Sieger, A. Firouzi, B. F. Chmelka, F. Schüth and G. D. Stucky, *Chem. Mater.*, 1994, **6**, 1176.
4 U. Ciesla, D. Demuth, R. Leon, P. Petroff, G. Stucky, K. Unger and F. Shüth, *J. Chem. Soc., Chem. Commun.*, 1994, 1387.
5 D. M. Antonelli and J. Y. Ying, *Angew. Chem., Int. Ed. Engl.*, 1996, **35**, 426.
6 D. M. Antonelli, A. Nakahira and J. Y. Ying, *Inorg. Chem.*, 1996, **35**, 3126.
7 D. M. Antonelli and J. Y. Ying, *Chem. Mater.*, 1996, **8**, 874.
8 M. J. Hudson and J. A. Knowles, *J. Mater. Chem.*, 1996, **6**, 89.
9 U. Ciesla, S. Schacht, G. D. Stucky, K. K. Unger and F. Schüth, *Angew. Chem., Int. Ed. Engl.*, 1996, **35**, 541.
10 J. S. Reddy and A. Sayari, *Catal. Lett.*, 1996, **38**, 219.
11 N. Ulagappan, Neeraj, B. V. N. Raju and C. N. R. Rao, *Chem. Commun.*, 1996, 2243.
12 F. Schüth, *Ber. Bunsen-Ges. Phys. Chem.*, 1995, **99**, 1306.

*Received in Columbia, MO, USA, 11th February 1997; Com. 7/00974G*

# A *gem*-aluminium(III)/antimony(III) C centre incorporated in a bimetallic six-membered heterocycle

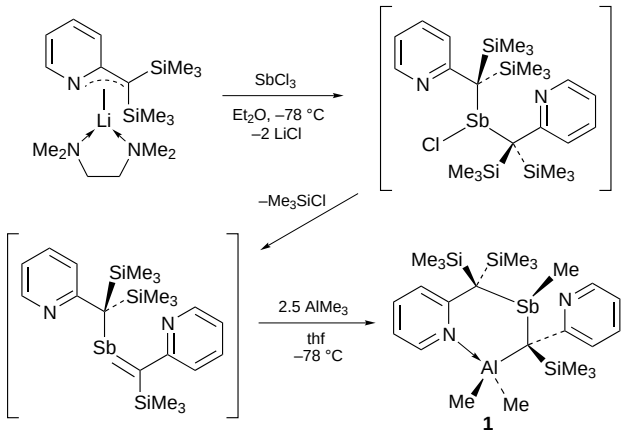
**Philip C. Andrews,[a] Colin L. Raston,*[a] Brian W. Skelton[b] and Allan H. White[b]**

[a] *Department of Chemistry, Monash University, Clayton, Victoria 3168 Australia*
[b] *Department of Chemistry, University of Western Australia, Nedlands, W.A. 6709, Australia*

**Reaction of $AlMe_3$ with the implied stibene intermediate (–Sb=C<) formed in the reaction of [(2-pyr)$(SiMe_3)_2$CLi·tmeda] with $SbCl_3$ affords the carboalumination product containing a *gem*-Al/Sb C centre as part of a six-membered heterocycle, [(2-pyr)$(SiMe_3)_2$C–Sb(Me)–(2-pyr)$(SiMe_3)$C–$Al(Me)_2$] 1, structurally authenticated as the (*RS*,*SR*) diastereoisomer.**

The main-group complexes of the bulky alkyl ligand (2-pyr)$(SiMe_3)_2C^-$, R, have been extensively investigated.[1] Such bulky ligands, devoid of a β-hydrogen, are important in the search for unusual and novel main-group chemistry such as low-valent and multiply bonded species due to the kinetic protection offered to the element in question and the presence of a potentially stabilising internal N donor. Thus the variety of complexes isolated and characterised include monomeric, subvalent, hypervalent, electron-deficient and low-coordinate species. Studies by Cowley *et al.*[2] and others[3] have shown that it is possible to stabilise double-bonded species involving group 15 elements using the tri-*tert*-butyl substituted mesityl and $(SiMe_3)_2C^-$ ligands, *e.g.* E′=E, As=P, P=As, As=As, Sb=P. Multiply bonded complexes of this type involving As and P tend to be more stable to oligomerisation than those containing Sb which appear to require a higher degree of steric protection and stabilisation.[4]

We have previously reported that it is possible to synthesise the monomeric $RSbCl_2$ complex from the 1:1 metathetical exchange reaction of $[RLi·(Et_2O)_n]$ and $SbCl_3$ in diethyl ether. However, as was also the case with the arsenic and bismuth complexes, the formation of the monochloride species from the 2:1 reaction was highly problematic with evidence for the low-temperature elimination of $SiClMe_3$ affording an intractable dark red oil.[5] Herein we now report on the synthesis and characterisation of a novel mixed group 13/15 complex **1** (Scheme 1) which was obtained *via* the addition of $AlMe_3$ to a thf solution of this red oil. Such *gem*-diorganometallics are attaining increasing recognition and importance in organic synthesis.[6]




**Scheme 1**

The dark red oil can be consistently generated from the specific 2:1 reaction of crystalline RLi·tmeda and $SbCl_3$ in thf at −78 °C. A red solution is formed over 12 h as the reaction mixture is allowed to warm to ambient temperature. The deep red oil is then obtained when all volatiles are removed *in vacuo* and LiCl removed by the addition of hexane and subsequent filtration. From initial one- and two-dimensional NMR studies it is clear that the red oil is a complex mixture of products; $^{13}C$ NMR revealed at least 5 $SiMe_3$ environments to be present. To date, attempts at obtaining a reproducible crystalline product directly from the oil have been unsuccessful despite varying the polarity of added solvents, *i.e.* hexane to thf, and cooling from 4 to −78 °C. Attempts at distilling any liquid or low-melting point products *in vacuo* (0.1 mmHg) have also been unsuccessful as decomposition to elemental antimony occurs readily above 80 °C. In an attempt to identify any of the products we have submitted the red oil to a series of reactions. One which has been successful is the addition of $AlMe_3$.

The small yellow rod-shaped crystals† of **1**‡ were obtained from the reaction of a thf solution of the red oil with a 2.5-fold excess of $AlMe_3$ (based on the initial quantity of R used) in thf at −78 °C. The crystals cocrystallised with large colourless crystals of $[(Me_3Al)_2(tmeda)]$ at 4 °C in hexane–thf over several days. That the tmeda complex is formed is indicative that all the tmeda is not removed *in vacuo* with other volatiles.

X-Ray diffraction studies on the yellow crystals revealed a novel monomeric mixed aluminium–antimony complex, space group $P2_1/n$, in which both Sb and Al are bound to the same carbon, Fig. 1. A search of the Cambridge Crystallographic Database§ confirms that this is the first mixed group 13/15 complex of its type. Importantly, a stibene (–Sb=C<) intermediate can be invoked to explain the formation of the complex as carboalumination, *viz.* the addition of $AlMe_3$ across the antimony–carbon double bond. A probable mechanism for the formation of **1** is outlined in Scheme 1.

The stibene intermediate contains a modified and an unmodified ligand as a result of $SiClMe_3$ elimination. It has to be assumed that this stibene complex is stable and present in a relatively significant quantity. $^{13}C$ NMR has been, as yet, of limited help in identifying the particular double-bonded carbon with the only markers by which to judge the chemical shift being: (*i*) stibabenzene in which the delocalised C–Sb appears at δ 178.3,[7]¶ which is coincident with both the delocalised C–N and quaternary carbon in the pyridyl ring, (*ii*) a study of several acyclic stibonium ylides[8]‖ reported the $Sb^+–C^- \leftrightarrow Sb=C$ shift to be in the region δ 74.6–93.2 which corresponds well with a lone signal at δ 78.0 in the $^{13}C$ ($C_6D_6$) NMR spectrum of the red oil. Very recently Nixon and co-workers reported[9] the first solid-state structurally characterised acyclic distibene complex, *trans*-1,4-bis(trimethylsiloxy)-1,4-bis(2,4,6-tri-*tert*-butylphenyl)-2,3-distibabutadiene, an interesting point being that the crystals are red.

The crystals of **1** are relatively air stable and melt with decomposition from 88 °C. The solid-state structure is dominated by a six-membered metallocycle [C(12)C(12′)Sb-

C(22′)AlN(11)], Scheme 1, with ring closure being secured by the dative pyridyl N–Al bond. Two chiral centres are present in the molecule, the Sb and the C centre which is *gem* with respect to the $Sb^{III}$ and $Al^{III}$ centres. These are respectively (*R*) and (*S*) or (*S*) and (*R*) in the same molecule with the solid comprised of an enantiomeric mixture.

The Sb–C(22′) distance of 2.167(7) Å is shorter than that of Sb–C(12′), *i.e.* C with two bound trimethylsilyls, which at 2.247(7) Å is longer than that found in $RSbCl_2$, 2.213(5) Å. TheAl–C(22′) bond length is 2.017(6) Å which is longer than those for the bound Me groups, av. 1.978(8) Å. The pyridyl N–Al distance of 2.062(6) Å is unremarkable. Despite the near planarity of the SbC(22′)C(22)N(21) atoms, there is little or no interaction between Sb and N(21) as confirmed by the separation of 2.914(6) Å and the close to tetrahedral angle at C(22′) [Sb–C(22′)–C(22) 106.7(4)°], which can be compared with the analogous bond angle of 94.45° in $RSbCl_2$ where there is a long but definite Sb–N [2.371(7) Å] interaction.

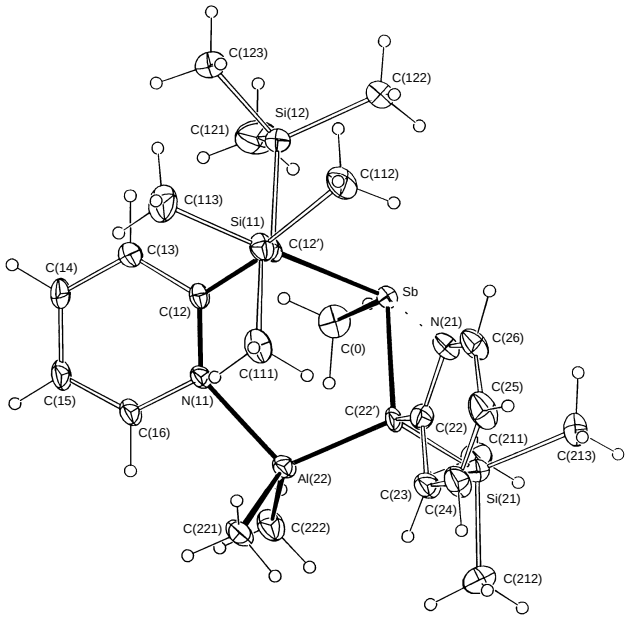



**Fig. 1** Crystal structure of **1** with selected distances (Å) and angles (°): Sb–C(0,12′,22′) 2.178(7), 2.247(7), 2.167(7); Al(22)–N(11), C(22′,221,222) 2.062(6), 2.017(6), 1.975(8), 1.982(8); C(0)–Sb–C(12′,22′) 93.0(3), 97.2(3); C(12′)–Sb–C(22′) 105.3(2); Sb–C(12′)–C(12), Si(11,12) 112.6(4), 117.1(3), 99.9(3); Sb–C(22′)–C(22), Si(21), Al(22) 106.7(4), 108.3(3), 106.7(3); N(11)–Al(22)–C(22′,221,222) 109.6(2), 102.7(3), 102.7(3); C(22′)–Al(22)–C(221,222) 118.3(3), 114.1(3); C(221)–Al(22)–C(222) 107.7(3); Al(22)–N(11)–C(12,16) 137.8(4), 106.6(4); Al(22)–C(22′)–C(22), Si(21) 114.6(4), 115.3(3).

We thank the Australian Research Council for financial support.

## Footnotes

* E-mail: c.raston@sci.monash.edu.au

† Approximate yield based on separation of sample of crystals, 32% (yield not maximised and based on consumption of ligand R). mp 88 °C (decomp.). $^1$H NMR (300 MHz, $C_6D_6$, 25 °C) δ 7.78 (d, br, 1 H), 7.67 (d, br, 1 H), 7.52 (d, 1 H), 7.05 (m, 2 H), 6.78 (t, 1 H), 6.40 (t, 1 H), 6.22 (t, 1 H), 1.08 (s, 3 H, MeSb), 0.45 (s, 9 H, $SiMe_3$), 0.25 (s, 9 H, $SiMe_3$), 0.09 (s, 9 H, $SiMe_3$), −0.37 (s, 6 H, $Me_2Al$). $^{13}$C NMR (100.6 MHz, $C_6D_6$, 25 °C) δ 168.1 (quat-C), 148.0 (CH), 145.5 (CH), 136.8 (CH), 136.2 (CH), 127.2 (CH), 125.6 (CH), 118.5 (CH), 117.7 (CH), 5.7 ($SiMe_3$), 4.8 (MeSb), 2.7, 2.1 ($SiMe_3$)$_2$, 1.2 ($Me_2Al$).

‡ *Crystallographic data* for **1**: (CAD4 diffractometer, crystals mounted in a capillaries) $C_{24}H_{44}AlN_2SbSi_3$, $M$ = 593.62; monoclinic, space group $P2_1/n$, $a$ = 11.585(6), $b$ = 14.595(13), $c$ = 18.035(12) Å, β = 102.03(5), $U$ = 2982(4) Å$^3$, $D_c$ ($Z$ = 4) = 1.322 g cm$^{-3}$; $F$(000) = 1232. $\mu_{Mo}$ = 10.9 cm$^{-1}$, specimen 0.10 × 0.28 × 0.33 mm, $A^*_{min,max}$ = 1.11, 1.34. $2\theta_{max}$ = 50°, final $R$, $R_w$ = 0.044, 0.042. $N_o$ = 3279 'observed' [$I > 3\sigma(I)$] reflections out of $N$ = 5245 unique. Al assignment based on geometry (bond lengths) and refinement of population and charge balance. Atomic coordinates, bond lengths and angles, and thermal parameters have been deposited at the Cambridge Crystallographic Data Centre (CCDC). See Information for Authors, Issue No. 1. Any request to the CCDC for this material should quote the full literature citation and the reference number 182/451.

§ Search carried out January 1997.

¶ NMR solvent $CDCl_3$ with 10% diglyme; measured at −10 °C.

‖ NMR solvent $CD_2Cl_2$.

## References

1 T. R. van den Ancker and C. L. Raston, *J. Organomet. Chem.*, 1995, **500**, 289.
2 A. H. Cowley, *Inorg. Chem.*, 1984, **23**, 2582; A. H. Cowley, N. C. Norman and M. Pakulski, *J. Chem. Soc., Dalton Trans.*, 1985, 383.
3 C. Couret, J. Escudie, Y. Madaule, H. Ranaivonjatovo and J.-G. Wolf, *Tetrahedron Lett.*, 1983, **24**, 2769; C. Couret, J. Escudie, H. Ranaivonjatovo and J.-G. Wolf, *Tetrahedron Lett.*, 1983, **24**, 3625; P. Jutzi and U. Meyer, *J. Organomet. Chem.*, 1987, **326**, C6; L. Weber and U. Sonnenberg, *Chem. Ber.*, 1989, **122**, 1809.
4 N. C. Norman, *Polyhedron*, 1993, **20**, 2431.
5 C. Jones, L. M. Engelhardt, P. C. Junk, D. S. Hutchings, W. C. Patalinghug, C. L. Raston and A. H. White, *J. Chem. Soc., Chem. Commun.*, 1991, 1560.
6 I. Marek and J.-F. Normant, *Chem. Rev.*, 1996, **96**, 3241.
7 A. J. Ashe, III, R. R. Sharp and J. W. Tolan, *J. Am. Chem. Soc.*, 1976, **98**, 5451.
8 G. Ferguson, C. Glidewell, I. Gosney, D. Lloyd, S. Metcalf and H. Lumbroso, *J. Chem. Soc., Perkin Trans. 2*, 1988, 1829.
9 P. B. Hitchcock, C. Jones and J. F. Nixon, *Angew. Chem., Int. Ed. Engl.*, 1995, **34**, 492.

*Received in Columbia, MO, USA, 11th February 1997; Com. 7/00959C*

# Cross-metathesis of alkenes with vinyl-substituted silsesquioxanes and spherosilicates: a new method for synthesizing highly-functionalized Si/O frameworks

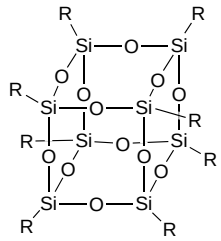
**Frank J. Feher,* Daravong Soulivong, Andrew G. Eklund and Kevin D. Wyndham**

*Department of Chemistry, University of California, Irvine, CA 92697-2025, USA*

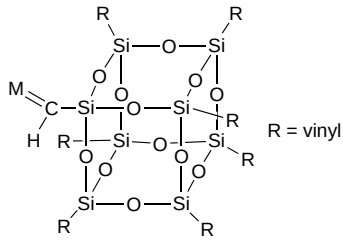
**Highly functionalized silsesquioxanes and spherosilicates of the formulae $[(RCH{=}CH)_8Si_8O_{12}]$ and $[(RCH{=}CHSiMe_2O)_8Si_8O_{12}]$ can be prepared by cross-metathesis reactions of alkenes with readily available vinyl-substituted silsesquioxane and spherosilicate frameworks, $[(vinyl)_8Si_8O_{12}]$ 1 and $[(vinylSiMe_2O)_8Si_8O_{12}]$ 2; the methodology is quite general and is not complicated by self-metathesis reactions of 1 or 2.**

Topologically spherical silsesquioxanes {*i.e.* $[RSiO_{3/2}]_n$} and silicates {*i.e.* $[ROSiO_{3/2}]_n$} have attracted widespread attention as precursors to a variety of interesting compounds and materials, and the number of known frameworks bearing synthetically useful functional groups is growing at an increasingly rapid pace.[1] Numerous methods have been reported for preparing highly functionalized silsesquioxane and spherosilicate frameworks, but the four most common routes are: (i) direct synthesis *via* hydrolytic condensation of $RSiX_3$; (ii) hydrosilylation of hydridosilsesquioxanes; (iii) silylation of spherosilicates; and (iv) synthetic manipulation of organic substituents on other readily available frameworks.

Here, we report a general new strategy for preparing highly functionalized silsesquioxanes and spherosilicates based on cross-metathesis reactions of alkenes[2] with readily available vinyl-substituted silsesquioxane[3,4] and spherosilicate frameworks.[5,6] This strategy offers access to a wide range of synthetically useful compounds, and it provides an important alternative to traditional synthetic methods based on the hydrosilylation of hydridosilsesquioxanes and the silylation of spherosilicates.



**1** R = vinyl
**2** R = $OSiMe_2$vinyl



**5** M = $Ru\{P(C_6H_{11})_3\}_2Cl_2$
**6** M = $Mo(NAr)\{OCMe(CF_3)_2\}_2$

Vinylsilsesquioxane **1**[3] reacts with both $[\{(C_6H_{11})_3P\}_2Cl_2Ru{=}CHPh]$[7] **3** and $[Mo(CHCMe_2Ph)(NC_6H_3\text{-}Pr^i_2\text{-}2,6)\{OCMe(CF_3)_2\}_2]$[8] **4** to produce new compounds exhibiting $^1$H NMR resonances consistent with the formation of new alkylidene complexes. In the case of **3**,† alkylidene resonances attributable to both **5** and $[\{(C_6H_{11})_3P\}_2Cl_2Ru{=}CH_2]$[7] grow in with nearly equal intensities at the expense of the resonance for **3**, but at longer reaction times, **5** is gradually consumed to produce $[\{(C_6H_{11})_3P\}_2Cl_2Ru{=}CH_2]$ as the major (> 95%) ruthenium-containing species. In the case of **4**,‡ $^1$H NMR resonances attributable to two new silyl-substituted alkylidenes grow in at the expense of the alkylidene resonance for **4**. The ratio of these resonances (*ca.* 2 : 1) remains constant at all times, suggesting that they are due to the *anti* (δ 13.50) and *syn* (δ 12.45) rotamers of **6**.[9]

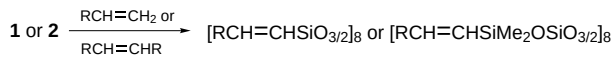
Although it is reasonable to expect the self-metathesis of **1** to be thermodynamically favourable, $^1$H NMR spectra of reaction mixtures containing **1** and either **3** or **4** never exhibit vinylic $^1$H resonances attributable to the formation of products derived from the self-metathesis of **1**. It appears that steric demands by the Si/O framework prevent the formation of metallacyclobutanes containing two adjacent silsesquioxane frameworks. Similar results are observed for spherosilicate **2**.[5] From the standpoint of synthesizing highly functionalized silsesquioxanes and spherosilicates, the practical consequences of this situation are enormous: cross-metathesis of **1** or **2** with monofunctional alkenes should never be complicated by competing oligomerization or polymerization of the vinyl-substituted Si/O frameworks.

The addition of an alkene to solutions containing **1** or **2** and an alkene metathesis catalyst quickly produces new $^1$H resonances attributable to cross-metathesis products. In the case of **1**, **4** and *cis*-oct-4-ene, for example, prominent $^1$H resonances are observed for free pent-1-ene and pent-1-enyl substituents on the $Si_8O_{12}$ framework, as well as the expected secondary metathesis products (*e.g.* $C_2H_2$ and $PhCMe_2CH{=}CHBu$). Similar results were observed upon addition of pent-1-ene, but the amount of ethene was much larger and the rate of productive cross-metathesis was slower.

Table 1 summarizes the results from a number of cross-metathesis reactions performed on a preparative scale using **3** and **4** as catalysts.§ Each reaction was performed under a slight vacuum in order to remove ethene, which greatly slows the rate of productive cross-metathesis and deactivates Schrock-type metathesis catalysts.[10,11] As expected,[12] Schrock's catalyst (*i.e.* **4**) is substantially more active than Grubbs' catalyst (*i.e.* **3**) in cases where the molybdenum alkylidene is compatible with functional groups attached to the alkene. However, the greater functional group tolerance of **3** allows the introduction of functional groups that deactivate **4**. Unfortunately, the rates of cross-metathesis with **3** are currently too slow to be of practical value for the preparation of pure octafunctional derivatives of **1** and **2**.

Both α-alkenes and internal alkenes can be used for the cross-metathesis reaction, but α-alkenes generally: (*i*) undergo cross-metathesis reactions much more readily than internal alkenes; (*ii*) offer a distinct cost advantage over internal alkenes; and (*iii*) undergo self-metathesis to internal alkenes at rates much greater than the rates of cross-metathesis with **1** or **2**. Nevertheless, internal alkenes are attractive starting materials because of their lower volatility and their inability to produce ethene. Except for reactions involving styrene, which appear to produce only *trans*-substituted products, it is important to note that the product in all cases is actually a complex mixture of substitutional isomers containing statistical distributions of *cis*- and *trans*-substituted double bonds. The same thermodynamic mixture of cross-metathesis products appears to form regardless

**Table 1** Cross-metathesis reactions of **1** and **2** with alkenes




| Entry | Si/O Framework | Alkene | Catalyst [amount (%)][a] | Conditions | Conv. (%) | Yield (%) (*trans*/*cis*)[b] |
|---|---|---|---|---|---|---|
| 1 | **1** | *cis*-Oct-4-ene (3 equiv.)[c] | **4** (1.6) | $C_6H_6$, 25 °C, 100 h | 100 | 75[d] (85/15) |
| 2 | **1** | *cis*-Oct-4-ene (3 equiv.) | **4** (5) | $C_6D_6$, 25 °C, 4.5 h | 100 | 100[e] (85/15) |
| 3 | **1** | Pent-1-ene (2 equiv.) | **4** (2.5) | Neat, 25 °C, 12 h | 100 | 100[e] (85/15) |
| 4 | **1** | Styrene (5 equiv.) | **4** (3) | $C_6D_6$, 25 °C, 12 h | 100 | 81[d] (All-*trans*) |
| 5 | **1** | Allyltrimethoxysilane (1.5 equiv.) | **4** (5) | $C_6D_6$, 25 °C, 12 h | 100 | 100[d] (88/12) |
| 6 | **1** | Ethyl undec-10-enylate (10 equiv.) | **4** (6) | $C_6D_6$, 25 °C, 22 h | 100 | 100[e] (80/20) |
| 7 | **1** | Oct-7-enyltrimethoxysilane (2 equiv.) | **4** (6) | $C_6D_6$, 25 °C, 6 h | 100 | 100[e] (84/16) |
| 8 | **1** | 5-Bromopentene (12 equiv.) | **4** (6) | $C_6H_6$, 25 °C, 16 h | 100 | 76[d] (94/6) |
| 9 | **1** | Pent-4-en-1-ol (3 equiv.) | **3** (6) | $CD_2Cl_2$, 38 °C, 48 h | 10 | — (*ca.* 4/1) |
| 10 | **1** | 5-Bromopent-1-ene (3 equiv.) | **3** (6) | $CD_2Cl_2$, 38 °C, 24 h | 25 | — (*ca.* 4/1) |
| 11 | **2** | Styrene (2 equiv.) | **4** (6) | $C_6H_6$, 25 °C, 24 h | 100 | 70[d] (All-*trans*) |
| 12 | **2** | Pent-1-ene (2 equiv.) | **4** (6) | $C_6H_6$, 25 °C, 24 h | 100 | 100[e] (86/14) |

[a] Mol% catalyst based on available $SiCH=CH_2$. [b] *trans*/*cis* ratio for SiCH=CHR groups determined by $^1H$ NMR spectroscopy. [c] Mol equiv. per $SiCH=CH_2$. [d] Isolated yield (quantified by NMR). [e] NMR yield.

of the alkene (*i.e.* internal alkene *vs.* α-alkene) used to prepare a particular octafunctional silsesquioxane. This inseparable mixture of isomers is unavoidable, but it can be transformed into a single octasubstituted product *via* catalytic hydrogenation [Pd/C, 25 °C, 160 psig) (1 psig = Pa). For example, catalytic hydrogenation of the product mixture obtained *via* cross-metathesis of **1** with pent-1-ene affords a high overall yield of $(n\text{-pentyl})_8Si_8O_{12}$ **7**.¶

We have only begun to explore the generality of this cross-metathesis procedure, but it is already clear that it offers an important new route to functionalized silsesquioxanes. It also offers intriguing possibilities for the preparation of new hybrid inorganic/organic materials, such as network polymers derived from metathesis reactions of vinyl-substituted Si/O frameworks with cyclic alkenes (ROMP) and/or dienes (ADMET). These and other potential applications are currently under investigation.

These studies were supported by the National Science Foundation and Phillips Laboratory (Edwards AFB).

## Footnotes

* E-mail: fjfeher@uci.edu

† Within 8 min of mixing at 25 °C, the reaction of **3** with a large excess of **1** in $CD_2Cl_2$ exhibits three ruthenium–alkylidene resonances with nearly equal integrated intensities: δ 20.03 (unreacted **3**), δ 18.96 {$[(C_6H_{11})_3P]_2Cl_2Ru{=}CH_2$]} and 23.35 (assigned to **5**). Characteristic resonances for styrene and both *cis* and *trans*-stilbene (derived from self-metathesis of styrene) are also observed. Within 60 min, the resonance for **3** vanishes; after 17 h, only the resonance at δ 18.96 remains.

‡ Within 15 min of mixing at 25 °C, the reaction of **4** with a large excess of **1** in $C_6D_6$ exhibits three major molybdenum alkylidene resonances with relative integrated intensities of 2 : 1 : 2: δ 13.50 (assigned on the basis of chemical shift[9] to the *anti*-rotamer of **6**), 12.45 (assigned to the *syn* rotamer of **6**) and 12.12 (unreacted **4**). Characteristic resonances for $PhCMe_2(CH{=}CH_2)$ are also observed. Within 45 min, the resonance for **4** vanishes. Provided that air is rigorously excluded from the sample, the resonances at δ 13.50 and 12.45 persist indefinitely.

§ All new compounds in Table 1 exhibited satisfactory analytical and spectroscopic data; full details will be reported elsewhere.

¶ Catalytic hydrogenation of $[CH_3CH_2CH_2CH{=}CHSiO_{3/2}]_8$ (19 mg, obtained *via* the cross-metathesis of **1** with pent-1-ene) was performed over 10% Pd/C (7 mg) in ethyl acetate (2 ml) at 160 psi $H_2$ for 2 d at 25 °C. The catalyst was removed by filtration through a short column of silica gel and washed with $CH_2Cl_2$. Rotary evaporation of the filtrate gave **7** in quantitative yield as a colourless oil. For **7**: $^1H$ NMR (500 MHz, $C_6D_6$, 25° C) δ 1.69–1.63 (m, 16 H, $CH_2$), 1.40–1.27 (m, 32H, $CH_2$), 0.88 (t, 40 H, $SiCH_2$ and $CH_3$, *J* 7.3 Hz). $^{13}C\{^1H\}$ NMR (75 MHz, $C_6D_6$, 25° C) δ 35.08 ($CH_2$), 22.84 ($CH_2$), 22.49 ($CH_2$), 14.12 ($CH_3$), 12.55 ($SiCH_2$). $^{29}Si\{^1H\}$ NMR (99 MHz, $C_6D_6$, 25° C) δ −68.2. MS (70 eV, direct inlet; rel int.): *m/z* 984 ($M^+$, 9%).

## References

1 For leading references on silsesquioxanes and spherosilicates: M. G. Voronkov and V. Lavrent'ev, *Top. Curr. Chem.*, 1982, **102**, 199; F. J. Feher and T. A. Budzichowski, *Polyhedron*, 1995, **14**, 3239; R. H. Baney, M. Itoh, A. Sakakibara, and T. Suzuki, *Chem. Rev.*, 1995, **95**, 1409; H. Bürgy, G. Calzaferri, D. Herren and A. Zhdanov, *Chimia*, 1991, **45**, 3; R. Murugavel, A. Voigt, M. G. Walawalkar and H. W. Roesky, *Chem. Rev.*, 1996, **96**, 2205; P. A. Agaskar, *Colloids Surf.*, 1992, **63**, 131; A. R. Bassindale and T. E. Gentle, *J. Mater. Chem.*, 1993, **3**, 1319; D. Hoebbel, I. Pitsch, T. Reiher, W. Hiller, H. Jancke and D. Muller, *Z. Anorg. Allg. Chem.*, 1989, **576**, 160; C. Zhang and R. M. Laine, *J. Organomet. Chem.*, 1996, **521**, 199; J. D. Lichtenhan, in *Silsesquioxane-Based Polymers*, ed. J. C. Salamone, New York, 1996; U. Dittmar, B. J. Hendan, U. Flörke and H. C. Marsmann, *J. Organomet. Chem.*, 1995, **489**, 185.

2 For leading references on cross-metathesis of alkenes: W. E. Crowe and Z. J. Zhang, *J. Am. Chem. Soc.*, 1993, **115**, 10 998; W. E. Crowe, D. R. Goldberg and Z. J. Zhang, *Tetrahedron Lett.*, 1996, **37**, 2117; B. Marciniec, C. Pietraszuk and Z. Foltynowicz, *J. Mol. Catal.*, 1992, **76**, 307.

3 M. G. Voronkov, T. N. Martynova, R. G. Mirskov and V. I. Belyi, *Zh. Obshch. Khim.*, 1979, **49**, 1522.

4 T. N. Martynova and V. P. Korchkov, *Zh. Obshch. Khim.*, 1982, **52**, 1585.

5 S. E. Yucks and K. A. Carrado, *Inorg. Chem.*, 1996, **35**, 261.

6 I. Hasegawa and S. Motojima, *J. Organomet. Chem.*, 1992, **441**, 373.

7 P. Schwab, M. B. France, J. W. Ziller and R. H. Grubbs, *Angew. Chem., Int. Ed. Engl.*, 1995, **34**, 2039.

8 R. R. Schrock, J. S. Murzdek, G. C. Bazan, J. Robbins, M. DiMare and M. O'Regan, *J. Am. Chem. Soc.*, 1990, **112**, 3875.

9 R. R. Schrock, W. E. Crowe, G. C. Bazan, M. DiMare, M. B. O'Regan and M. H. Schofield, *Organometallics*, 1991, **10**, 1832.

10 J. Robbins, G. C. Bazan, J. S. Murzdeck, M. B. O'Regan and R. R. Schrock, *Organometallics*, 1991, **10**, 2902.

11 F. J. Feher and T. L. Tajima, *J. Am. Chem. Soc.*, 1994, **116**, 2145.

12 K. Brzezinska, P. S. Wolfe, M. D. Watson and K. B. Wagener, *Macromol. Chem. Phys.*, 1996, **197**, 2065.

*Received in Bloomington, IN, USA, 24th March 1997; Com. 7/01996C*

# Oxidative carbonylation of methane to methyl acetate on a rhodium-doped iron phosphate catalyst

**Ye Wang, Masayuki Katagiri and Kiyoshi Otsuka***

*Department of Chemical Engineering, Tokyo Institute of Technology, Ookayama, Meguro-ku, Tokyo 152, Japan*

**The carbonylation of methane with carbon monoxide in the presence of nitrous oxide produces methyl acetate on a rhodium-doped iron phosphate catalyst under atmospheric pressure and at 573–673 K.**

Methane is the main constituent of the abundant natural gas resources. The direct transformation of methane to more useful chemicals or liquid fuels has long been a desirable goal for chemists. However, because methane is a very unreactive molecule, the conversion of methane to useful chemicals has proven to be a great challenge. Although there are many reports of the functionalisation of methane, the most viable process and effective catalyst are still unsettled.[1–5] Recently, we have reported that the conversion of methane is enhanced and methanol is selectively produced by co-feeding a reductant such as hydrogen over an iron phosphate ($FePO_4$) catalyst.[6–8] When nitrous oxide is used as an oxidant in the presence of hydrogen, methane can be selectively converted into methanol with high selectivity at moderate temperatures (*ca*. 620 K).[8] If carbon monoxide is used as the reductant instead of hydrogen, we can expect that the activated carbon monoxide may react with the methanol produced or with reaction intermediates such as methyl species to form acetic acid or methyl acetate. The wasteful consumption of the co-feeding reductant, which is a common problem for many biomimetic monooxygenase catalytic systems, may thus be overcome. Acetic acid is a very important chemical and is produced mainly by the carbonylation of methanol as typically demonstrated in the Monsanto process. If acetic acid or its derivatives such as methyl acetate can be produced directly from methane, the impact on the chemical industry would be significant because the production cost of many chemical products based on acetic acid will become remarkably cheaper. Reports concerning the direct carbonylation of methane to acetic acid are very scarce[9–11] and all these studies have been performed using a high pressure ( > 20 bar) liquid-phase reaction system. The use of expensive reagents such as $FHSO_3$–$SbF_5$,[9] $K_2S_2O_8$[10] and $I^-$ or perfluorobutyric acid[11] is required in these complicated systems. Furthermore, the separation of these expensive reagents or catalysts such as $RhCl_3$ from the solvents is another drawback for these homogeneous reaction systems. Therefore, a simple heterogeneous catalytic system would be more desirable and promising. This communication is the first contribution to attempt direct carbonylation of methane using a simple heterogeneous catalytic system.

The experiments were carried out using a conventional fixed-bed flow reactor (quartz tube) operated at atmospheric pressure. The Rh-doped iron phosphate catalysts with various Rh content were prepared by mixing aqueous solutions of $RhCl_3$ or $Rh(NO_3)_3$, $Fe(NO_3)_3$ and $NH_4H_2PO_4$ and evaporating water from the resultant solution to obtain the catalyst precursors. The precursors were finally calcined at 823 K for 5 h in air. The catalysts were pretreated in an oxygen flow at 723 K in the reactor and the reaction was started by introducing the reactants $CH_4$, $N_2O$ and CO. The outlet gases were bubbled into a water trap cooled with water/ice bath to collect the products, MeOH, $MeCO_2H$ and $MeCO_2Me$. These collected products were analysed by a FID-equipped gas chromatograph with acetonitrile as internal standard. Other components which could not be dissolved in the water trap were analysed by an on-line TCD-equipped gas chromatograph.

Fig. 1 compares the reaction results over $FePO_4$ and various metal-ion-doped $FePO_4$ catalysts at 648 K. Using pure $FePO_4$, a considerable amount of MeOH was formed. We have reported that oxygen species generated from the reductive activation of $N_2O$ on iron sites are responsible for the activation of $CH_4$ at such a moderate temperature.[8] However, the carbonylation products, $MeCO_2H$ and $MeCO_2Me$ were not observed at all on $FePO_4$. This result indicates that another site for the effective activation of CO for the carbonylation is required on the catalyst surface. Thus, many additives have been incorporated into $FePO_4$ to enhance the ability for the activation of CO for the carbonylation. The results in Fig. 1 suggest that rhodium is very specific for the formation of $MeCO_2Me$. Instead of $FePO_4$, a large variety of materials including $SiO_2$, $Al_2O_3$, H-ZSM-5, Ga-H-ZSM-5, H-mordenite, active carbon, $SO_4^{2-}/ZrO_2$, $MoO_3$ and $V_2O_5$ were also used as bases for rhodium. However, none of

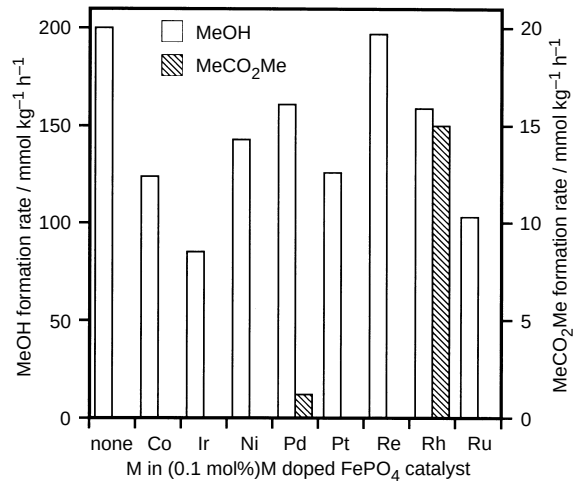



**Fig. 1** Oxidative carbonylation of methane over various metal-ion-doped $FePO_4$ catalysts. *Reaction conditions*: $T$ = 648 K, $P(CH_4)$ = $P$(CO) = 25.3 kPa, $P(N_2O)$ = 12.7 kPa, $W$ = 0.2 g, $F$ = 80 ml min$^{-1}$.

**Table 1** Effect of rhodium content on the formation of methyl acetate from methane[a]

| Rh content (%) | Formation rate/ mmol g$^{-1}$ h$^{-1}$ | | CO conv. (%) |
|---|---|---|---|
| | MeOH | $MeCO_2Me$ | |
| 0 | 200.5 | 0 | 2.5 |
| 0.1 | 125.5 | 16.0 | 2.2 |
| 0.3 | 113.0 | 26.5 | 4.3 |
| 0.5 | 92.0 | 28.5 | 2.5 |
| 1.0 | 90.0 | 21.2 | 2.5 |
| 2.0 | 126.7 | 18.3 | 2.8 |

[a] *Reaction conditions*: $T$ = 648 °C, $P(CH_4)$ = $P$(CO) = 25.3 kPa, $P(N_2O)$ = 12.7 kPa, total flow rate = 80 ml min$^{-1}$.

them showed activity for the carbonylation of $CH_4$. Therefore, $Rh/FePO_4$ is a unique catalyst. Further detailed studies were thus carried out using the $Rh/FePO_4$ catalyst.

In order to increase the rate of the carbonylation reaction, catalysts with various mol% Rh were investigated. As shown in Table 1, an increase in Rh content up to 0.5% increased the formation rate of $MeCO_2Me$ at the expense of MeOH. For the Rh (0.5%)/$FePO_4$ catalyst, the formation rate of $MeCO_2Me$ reached *ca*. one third of that of MeOH. Further increase of Rh content decreased the formation rate of $MeCO_2Me$ as well as the ratio of $MeCO_2Me$ to MeOH. This fact probably indicates that highly dispersed $Rh^{3+}$ on the surface of $FePO_4$ is responsible for the carbonylation reaction.

Naturally, the conversion of CO shown in Table 1 was mainly ascribed to the formation of $CO_2$. Only 1–5% of CO converted took part in the carbonylation reaction. Table 1 shows that the conversion of CO is not changed appreciably by the addition of Rh to $FePO_4$. This result suggests that the direct oxidation of CO into $CO_2$ occurs mainly on the host $FePO_4$.

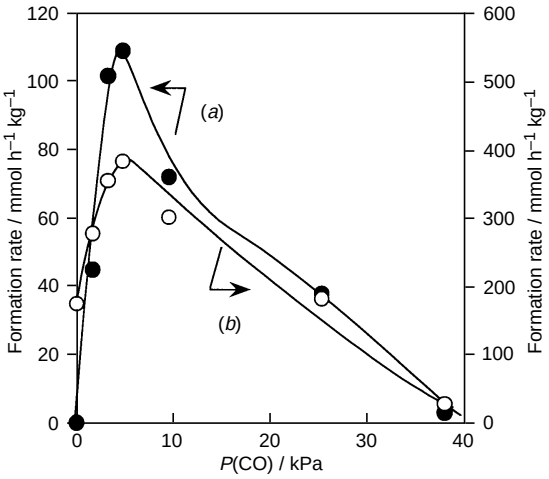



**Fig. 2** Effect of CO pressure on the formation of MeOH and $MeCO_2Me$ on Rh (0.5%)/$FePO_4$ catalyst. (*a*) $MeCO_2Me$, (*b*) MeOH. *Reaction conditions*: $T$ = 648 K, $P(CH_4)$ = $P(N_2O)$ = 25.3 kPa, $W$ = 0.2 g, $F$ = 160 ml min$^{-1}$.

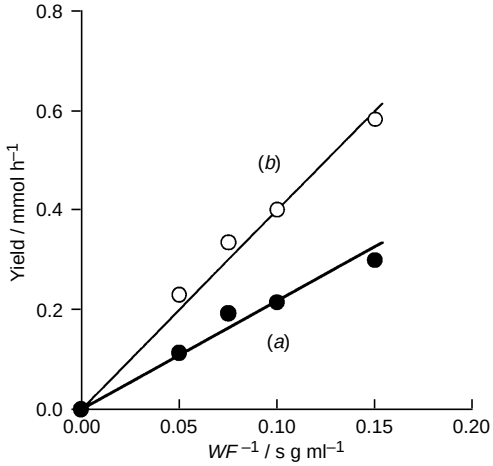



**Fig. 3** Effect of $WF^{-1}$ on the formation of MeOH and $MeCO_2Me$ on Rh (0.5%)/$FePO_4$ catalyst. (*a*) $MeCO_2Me$, (*b*) MeOH. *Reaction conditions*: $T$ = 648 K, $P(CH_4)$ = $P(N_2O)$ = 25.3 kPa, $F$ = 300 ml min$^{-1}$.

Fig. 2 shows the effect of CO pressure on the carbonylation reaction over the Rh (0.5%)/$FePO_4$ catalyst. No $MeCO_2Me$ was produced in the absence of CO. The introduction of CO caused the formation of $MeCO_2Me$. It should be noted that MeOH was also remarkably increased at low partial pressures of CO [P(CO) < 5 kPa]. This result suggests that CO functions not only as a reactant in the carbonylation reaction but also as an activator for the conversion of $CH_4$. Probably, CO reduces $Fe^{III}$ to $Fe^{II}$ on the $FePO_4$ surface and the produced $Fe^{II}$ site acts as the active site for the generation of the active oxygen species from $N_2O$.[6–8] On the other hand, higher pressures of CO are not favourable for the formation of both MeOH and $MeCO_2Me$. Competitive oxidation between CO and $CH_4$ with the active oxygen species must be the main reason.

Whether $MeCO_2Me$ is formed from the direct carbonylation of $CH_4$ or from the carbonylation of the produced MeOH is a key point in the reaction mechanism. Thus, the influence of $WF^{-1}$ (weight of catalyst/flow rate) on the yields of MeOH and $MeCO_2Me$ has been investigated. As shown in Fig. 3, the yields of both MeOH and $MeCO_2Me$ increased almost linearly with increase in $WF^{-1}$. This result indicates that MeOH and $MeCO_2Me$ are formed in parallel from $CH_4$.

The results described above allow us to speculate on a reaction mechanism as follows. $CH_4$ must be activated by the active oxygen species generated on the iron site, producing an Me species as a transient intermediate. This Me species may easily be oxidized to an MeO species on the surface of $FePO_4$. It must also migrate and adsorb on a Rh site where CO is activated. The insertion of CO into Rh–Me may occur on this Rh site, producing Rh–COMe. $MeCO_2Me$ is then formed by the reaction of Rh–COMe with the MeO species produced on $FePO_4$ near this Rh site, while the addition of a proton (probably from OH groups) to the adsorbed MeO produces MeOH. According to this mechanism, the high dispersion of Rh at sites surrounded by iron sties is a key factor for the carbonylation reaction. Further confirmation of this mechanism and the design of catalysts with high concentration of Rh sites with surrounding iron sites are underway.

## Footnote

* E-mail: kotsuka@o.cc.titech.ac.jp

## References

1 R.Pitchai and K. Klier, *Catal. Rev.-Sci. Eng.*, 1986, **28**, 13.
2 M. J. Brown and N. D. Parkyns, *Catal. Today*, 1991, **8**, 305; N. D. Parkyns, C. I. Warburton and J. D. Wilson, *Catal. Today*, 1993, **18**, 385.
3 O. V.Krylov, *Catal. Today*, 1993, **18**, 209.
4 T. J. Hall, J. S. J. Hargreaves, G. J. Hutchings, R. W. Joyner and S. H. Taylor, *Fuel Proc. Technol.*, 1995, **42**, 151.
5 R. H. Crabtree, *Chem. Rev.*, 1995, **95**, 987.
6 Y. Wang and K. Otsuka, *J. Chem. Soc., Chem. Commun.*, 1994, 2209.
7 Y. Wang and K. Otsuka, *J. Catal.*, 1995, **155**, 256.
8 Y. Wang and K. Otsuka, *Chem. Lett.*, 1994, 1893.
9 H. Hogeveen, J. Lukas and C. F. Roobeek, *Chem. Commun.*, 1969, 920.
10 K. Nakata, Y. Yamaoka, T. Miyata, Y. Taniguchi, K. Takaki and Y. Fujiwara, *J. Org. Chem.*, 1994, **473**, 329.
11 M. Lin and A. Sen, *Nature*, 1994, **368**, 613; M. Lin, T. E. Hogan and A. Sen, *J. Am. Chem. Soc.*, 1996, **118**, 4574.

*Received in Cambridge, UK, 1st April 1997; Com. 7/02159C*

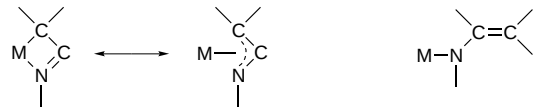
# Variation of bonding modes in homoleptic tin(II) 1-azaallyls†

**Peter B. Hitchcock, Jin Hu, Michael F. Lappert, Marcus Layh and John Severn**

*The Chemistry Laboratory, University of Sussex, Brighton, UK BN1 9QJ*

**The homoleptic tin(II) compounds Sn[N(R)C(Bu$^t$)-C(H)C$_6$H$_3$Me$_2$-2,5]$_2$ 1, Sn[N(R)C(Bu$^t$)C(H)R]$_2$ 2 and R$_2$CC(Ph)N(R)Sn[N(R)C(Ph)CR$_2$] 3 (R = SiMe$_3$) are prepared and structurally characterised.**

The important series of first-row triatom-centred, monoanionic ligands [XYZ]$^-$ include allyl, triazenide and amidinate, with the carboxylate probably the archetype. Open-chain, structurally characterised 1-azaallyl ligands are of recent date.[1] In [Li(LL′)]$_2$,[1] *rac*-[Zr(LL′)$_2$Cl$_2$][2] and *rac*-[Yb(LL′)$_2$],[3] the [LL′]$^-$ ligand behaved in an η$^3$-chelating bridging (Li) or terminal (Zr, Yb) fashion [LL′ = N(R)C(Bu$^t$)C(H)R, R = SiMe$_3$]. We now report that the latter reflects on only one possible mode of terminal 1-azaallyl–metal (M) bonding (**MA**, η$^3$-iminoalkyl), while another, **MB**, represents an η$^1$-enamidometal isomer. This is illustrated by reference to the three homoleptic 1-azaallyltin(II) complexes, having the structures Sn**B**$_2$ **1**, Sn**A**$_2$ **2** and Sn(**A**)**B 3**, the variation in structural types being due to changing the substituents on the NCC skeleton: Sn[N(R)C(Bu$^t$)C(H)C$_6$H$_3$Me$_2$-2,5]$_2$ **1**, Sn[N(R)C(Bu$^t$)C(H)R]$_2$ **2** and R$_2$CC(Ph)N(R)Sn[N(R)C(Ph)CR$_2$] **3** (R = SiMe$_3$).




**MA** **MB**

The yellow (**1**, **2**) and orange (**3**) tin complexes were readily synthesised (78–84%) from SnCl$_2$ and 2 equiv. of Li[N(R)C-(Bu$^t$)C(H)Ar] [obtained[4a] from LiCH(R)$_2$ + Bu$^t$CN, Ar = C$_6$H$_3$Me$_2$-2,5], K(LL′),[1] or Li[N(R)C(Ph)CR$_2$] [prepared[4b] from LiCR$_3$(thf)$_2$ + PhCN] in diethyl ether or pentane solution at ambient temperature. A single-crystal X-ray diffraction study‡ shows that **1** (Fig. 1) is coordinated by two

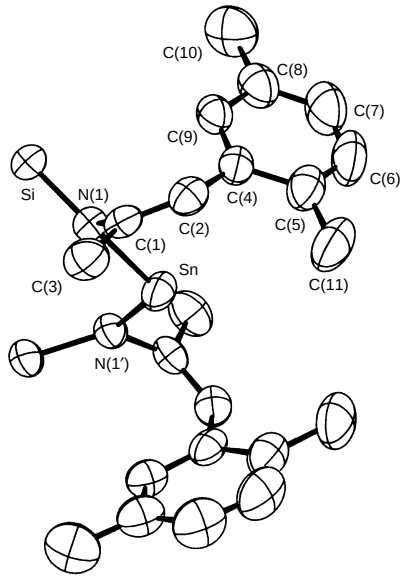



**Fig. 1** Partial molecular structure of **1** (core atoms only)

η$^1$-enamido ligands with the free electron pair pointing away from the ligands. The N(1)–Sn–N(1′) angle of 111.2° is only slightly larger than in the mononuclear tin(II) amides Sn[N(SiMe$_3$)$_2$]$_2$[5] (104.7°) or Sn[N(Me)$_2$(CH$_2$)$_3$CMe$_2$]$_2$[6] (109.7°). The arrangement of the ligands is such that the aromatic rings are within the van der Waals range above and below the Sn atom [Sn–C(2) 3.151, Sn–C(7) 3.188 Å]. A similar interaction has been reported in 1,2-C$_6$H$_4$[N(CH$_2$Bu$^t$)]$_2$Sn.[7] The enamido character of the 1-azaallyl ligand in **1** is evident from the short Sn–N(1), long N(1)–C(1) and a short C(1)–C(2) distance (Table 1), as well as $^{13}$C NMR shifts which are consistent with N(1)–C(1) being a single and C(1)–C(2) a double bond.

Changing the 2,5-dimethylphenyl group of the η$^1$-ligand system in **1** by a trimethylsilyl group alters the ligand bonding mode to η$^3$. Thus the X-ray structure of **2** (Fig. 2)‡ shows that, in contrast to **1**, C(2) and N(1) are both within bonding range of the tin atom but compared to **1** the Sn–N(1) distances are longer (Table 1). The C(1)–C(2) and C(1)–N(1) distances and the $^{13}$C NMR spectral chemical shifts show iminoalkyl rather than enamido character, as evident by comparison with Sn[NC$_5$H$_4$C(SiMe$_3$)$_2$-2]$_2$.[8] It is interesting to note that C(1) is bent towards the metal [the angle between the adjacent planes SnN(1)C(2) and N(1)C(1)C(2) is 37°] leading to a Sn–C(1) distance of 2.729(2) Å. Therefore an alternative description of **2** is as a bent sandwich complex similar to Sn(η-C$_5$Me$_5$)$_2$.[9]

The X-ray structure of crystalline **3**‡ shows that introducing a second trimethylsilyl group at C(2) or C(5) probably increases the steric demand of the ligand to such an extent that the bis(chelate) arrangement is no longer viable; thus, an intermediate situation between that of **1** and **2** is observed, wherein one ligand is η$^3$- and the other is η$^1$-coordinated. Table 1 shows relevant interatomic distances and NMR spectral chemical shifts. Important differences for the η$^3$-coordinated ligand in **3** compared with **2** are a shorter Sn–N(1) and a longer Sn–C(2) distance in **3** and a much smaller dihedral angle between the planes N(1)SnC(2) and N(1)C(1)C(2) of only 12.7°. That a higher coordination number than three in **3** is probably avoided by the increased bulk of the ligand (compared with that in **2**) is also supported by variable-temperature $^1$H and $^{13}$C NMR

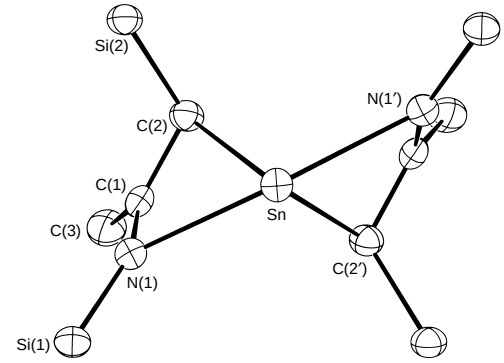



**Fig. 2** Partial molecular structure of **2** (core atoms only) with selected bond angles (°): N–Sn–N′ 146.98(6), N–Sn–C(2) 57.99(6), N–Sn–C(2′) 97.25, C(2)–Sn–C(2′) 89.44(8)

spectroscopic experiments which show the two ligands to be equivalent in solution down to −90 °C, indicating that there is a rapid intramolecular exchange between the $\eta^1$- and $\eta^3$-coordinated ligand. Comparing **2** and **3** with **1** it may be that the preference for the enamido structure in **1** is due to electronic rather than steric reasons.

In conclusion, we believe that the following features (*i*) and (*ii*) are particularly noteworthy. (*i*) Compounds **1**–**3** serve as a good example to demonstrate how comparatively small differences in the backbone of a 1-azaallyl ligand may significantly influence their metal complex bonding modes. (*ii*) Enamido–metal bonding now shown in the tin(II) complexes **1** and **3** has only recently been crystallographically established for some alkali-metal 2-methylpyridine or related derivatives,[10,11] *e.g.*[11] Li[$NC_5H_4${C(SiMe$_3$)Ph}-2](tmen); such structures are widely postulated for group 1 and 2 metal complexes, which when prepared *in situ* are valuable C–C bond-forming synthons;[12] there is NMR spectroscopic structural evidence for [M{N(H)C(Bu$^t$)CHPr$^n$}{OP(NMe$_2$)$_3$}$_x$]$_n$ (M = Li, $x$ = 1 or M = Na, $x$ = 2)[13a] and [Li{N(Ph)C=CH(CH$_2$)$_3$CH$_2$} (thf)$_x$]$_n$ ($x$ = 0, or $x$ = 1 = $n$).[13b] The [$NC_5H_4C(SiMe_3)_2$-2]$^-$ ligand has been found in an $\eta^1$-mode in the homoleptic mercury(II) complex, but it is the tautomeric (*cf.* **MB**) iminoalkyl ligated species.[14]

We thank EPSRC and SPECS-BIOSPECS for the award of a CASE studentship for J. S., EPSRC for a fellowship for J. H. and the European Commission for a category 30 HMCR fellowship for M. L.

**Table 1** Some important structural and NMR spectroscopic data on the (1-azaallyl)tin(II) complexes **1**–**3**

| | Complex | | |
|---|---|---|---|
| Property | **1** | **2** | **3** |
| CN[a] | 2 | 4 | 3 |
| $d$(Sn–N, $\eta^1$)[b]/Å | 2.130(3) | — | 2.153(4) |
| $d$(Sn–N, $\eta^3$)[b]/Å | — | 2.510(2) | 2.288(4) |
| $d$[Sn–C(1)]/Å | (2.791) | 2.729(2) | 2.775(4) |
| $d$[Sn–C(2)]/Å | (3.151) | 2.295(2) | 2.531(5) |
| C–C($\eta^1$)[b]/Å | 1.349(5) | — | 1.365(6) |
| C–C($\eta^3$)[b]/Å | — | 1.463(3) | 1.461(6) |
| C–N($\eta^1$)[b]/Å | 1.435(4) | — | 1.432(5) |
| C–N($\eta^3$)[b]/Å | — | 1.298(3) | 1.317(6) |
| δ[$^{119}$Sn{$^1$H}] | 61.5 | −387.2 | −37.3 |
| δ[$^{13}$C{$^1$H}, C(1)] | 152.6 | 202.5 | 185.7 |
| δ[$^{13}$C{$^1$H}, C(2)] | 104.4 | 50.0 | 100.6 |

[a] CN = coordination number. [b] The designations of $\eta^1$ and $\eta^3$ relate to the enamido or chelate mode of the ligand-to-metal bonding, respectively.

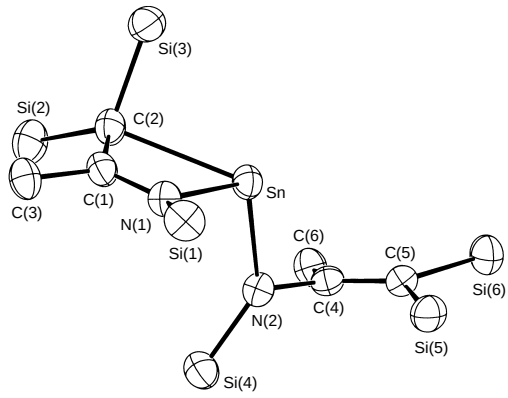



**Fig. 3** Partial molecular structure of **3** (core atoms only) with selected bond angles (°): N(1)–Sn–N(2) 109.9(1), N(1)–Sn–C(2) 59.33(1), N(2)–Sn–C(2) 113.2(2), C(4)–N(2)–Si(4) 116.4(3), C(4)–N(2)–Sn 105.0(3), Si(4)–N(2)–Sn 137.6(2)

## Footnotes

* E-mail: m.f.lappert@sussex.ac.uk

† No reprints available.

‡ *Crystal data* for **1**: $C_{34}H_{56}N_2Si_2Sn$, $M$ = 667.68, monoclinic, space group $C2/c$ (no. 15), $a$ = 13.006(4), $b$ = 15.957(3), $c$ = 17.735(10) Å, β = 98.74(3), $U$ = 3638(2) Å$^3$, $Z$ = 4, $D_c$ = 1.22 g cm$^{-3}$, $F$(000) = 1408, λ(Mo-Kα) = 0.710 73 Å, μ = 0.79 mm$^{-1}$. Data were collected at 293(2) K on a Enraf-Nonius CAD4 diffractometer in the ω–2θ mode in the range 2 < θ < 25°. The structure was solved by direct methods (SHELXS 86) and refined by full-matrix least squares on all $F^2$ (SHELXL 93) with absorption correction by ψ-scans. All non-hydrogen atoms were anisotropic, and hydrogen atoms were included in the riding mode with $U_{iso}$(H) = 1.2 $U_{eq}$(C) or 1.5 $U_{eq}$ for Me groups. Final residuals for 3190 independent reflections were $R_1$ = 0.057, $wR_2$ = 0.086 and for the 2442 with $I > 2\sigma(I)$, $R_1$ = 0.037, $wR_2$ = 0.077.

**2**: $C_{24}H_{56}N_2Si_4Sn$, $M$ = 603.8, monoclinic, space group $C2/c$ (no. 15), $a$ = 11.387(5), $b$ = 16.675(6), $c$ = 18.390(8) Å, β = 106.07(3), $U$ = 3355.4 Å$^3$, $Z$ = 4, $D_c$ = 1.20 g cm$^{-3}$, $F$(000) = 1280, λ(Mo-Kα) = 0.710 73 Å, μ = 0.92 mm$^{-1}$. 3060 independent reflections were collected at 173(2) K on a Enraf-Nonius CAD4 diffractometer in the ω–2θ mode in the range 2 < θ < 25°. The structure was solved by heavy-atom methods (SHELXS 86) and refined by full-matrix least squares on $F$ (Enraf-Nonius MolEN) with absorption correction by DIFABS. All non-hydrogen atoms were anisotropic, and hydrogen atoms were included in the riding mode with $U_{iso}$(H) = 1.2 $U_{eq}$(C) or 1.5 $U_{eq}$ for Me groups. Final residuals for 2623 reflections [with $I > 2\sigma(I)$] were $R$ = 0.025, $R'$ = 0.030.

**3**: $C_{34}H_{64}N_2Si_6Sn$, $M$ = 788.1, monoclinic, space group $P2_1/c$ (no. 14), $a$ = 19.249(4), $b$ = 12.400(3), $c$ = 19.820(5) Å, β = 112.83(2), $U$ = 4360(2) Å$^3$, $Z$ = 4, $D_c$ = 1.20 g cm$^{-3}$, $F$(000) = 1664, λ(Mo-Kα) = 0.71073 Å, μ = 0.77 mm$^{-1}$. Conditions for data collection and refinement were identical to those for **1**. Final residuals for 7663 independent reflections were $R_1$ = 0.096, $wR_2$ = 0.106 and for the 5008 with $I > 2\sigma(I)$, $R_1$ = 0.048, $wR_2$ = 0.088.

Atomic coordinates, bond lengths and angles, and thermal parameters have been deposited at the Cambridge Crystallographic Data Centre (CCDC). See Information for Authors, Issue No. 1. Any request to the CCDC for this material should quote the full literature citation and the reference number 182/463.

## References

1 P. B. Hitchcock, M. F. Lappert and D.-S. Liu, *J. Chem. Soc., Chem. Commun.*, 1994, 2637.
2 P. B. Hitchcock, S. A. Holmes, M. F. Lappert and S. Tian, *J. Chem. Soc., Chem. Commun.*, 1994, 2691.
3 P. B. Hitchcock, M. F. Lappert, D.-S. Liu and E. J. Ryan, *Polyhedron*, 1995, **14**, 2745.
4 (*a*) D.-S. Liu, unpublished work; (*b*) M. Layh, unpublished work.
5 T. Fjeldberg, H. Hope, M. F. Lappert, P. P. Power and A. J. Thorne, *J. Chem. Soc., Chem. Commun.*, 1983, 639.
6 R. W. Chorley, P. B. Hitchcock, M. F. Lappert, W.-P. Leung, P. P. Power and M. M. Olmstead, *Inorg. Chim. Acta*, 1992, **198**–**200**, 203.
7 H. Braunschweig, B. Gehrhus, P. B. Hitchcock and M. F. Lappert, *Z. Anorg. Allg. Chem.*, 1995, **621**, 1922.
8 B. S. Jolly, M. F. Lappert, L.M. Engelhardt, A. H. White and C. L. Raston, *J. Chem. Soc., Dalton Trans.*, 1993, 2653; L. M. Engelhardt, B. S. Jolly, M. F. Lappert, C. L. Raston and A. H. White, *J. Chem. Soc., Chem. Commun.*, 1988, 336.
9 P. Jutzi, F. Kohl, P. Hofmann, C. Krüger and Y.-H. Tsay, *Chem. Ber.*, 1980, **113**, 757; J. L. Atwood, W. E.Hunter, A. H. Cowley, R. A. Jones and C. A. Stewart, *J. Chem. Soc., Chem. Commun.*, 1981, 925.
10 U. Pieper and D. Stalke, *Organometallics*, 1993, **12**, 1201.
11 W.-P. Leung, L.-H. Weng, T.-J. Wang and T. C. W. Mak, *Organometallics*, 1995, **14**, 4832.
12 *cf.* J. K. Whitesell and M. A. Whitesell, *Synthesis*, 1983, 517.
13 (*a*) N. Kallman and D. B. Collum, *J. Am. Chem. Soc.*, 1987, **109**, 7466; (*b*) P. C. Andrews, D. R. Armstrong, M. MacGregor, R. E. Mulvey and D. Reed, *J. Chem. Soc., Chem. Commun.*, 1989, 1341.
14 M. J. Henderson, R. I. Papasergio, C. L. Raston, A. H. White and M. F. Lappert, *J. Chem. Soc., Chem. Commun.*, 1986, 672.

*Received in Basel, Switzerland, 20th March 1997; Com. 7/01971H*

# New sensor for dissolved dioxygen: a gold electrode modified with a condensation polymer film of β-cyclodextrin hosting cobalt tetraphenylporphyrin

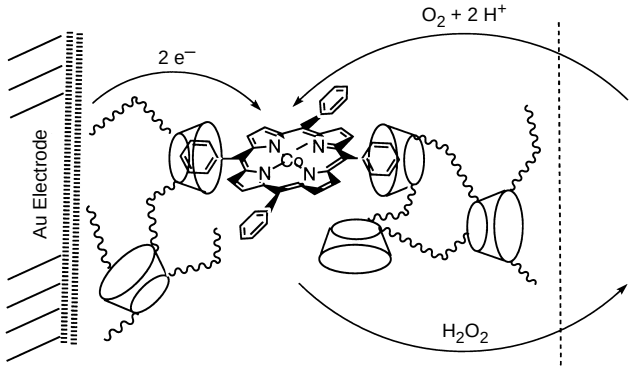
**Francis D'Souza,*[a] Yi-Ying Hsieh,[a] Heang Wickman[a] and Wlodzimierz Kutner*[a,b]**

[a] *Department of Chemistry, Wichita State University, Wichita, KS 67260-0051, USA*
[b] *Institute of Physical Chemistry, Polish Academy of Sciences, Kasprzaka 44/52, PL-01-224 Warsaw, Poland*

**A gold electrode, coated with a thin polymer film of a supramolecular complex of β-cyclodextrin and cobalt tetraphenylporphyrin, is used as an electrocatalytic sensor for determination of dioxygen dissolved in water.**

Development of supramolecular transducing systems for catalytic sensor applications is an area of active research.[1] Cyclodextrin (CD) hosts are very appealing with this respect since they can form supramolecular complexes with a broad range of organic and inorganic, both ionic and neutral compounds.[2] Additional advantages arise if a thin cyclodextrin polymer (CDP) film is cast on an electrode surface.[3,4] Importantly, the stability of supramolecular complexes of CDs embedded, *e.g.* by polycondensation, in polymer matrices is virtually the same as that of solution complexes, and in some cases the stability is even increased.[5] Moreover, CDP is soluble neither in aqueous nor in non-aqueous solvent solutions and is resistant to pH changes within a wide range (pH 2–12). The structure of CDP is relatively open, so the CDP films are readily permeable to small molecules or ions present in solution while large ones are repelled.[3,5] The shelf lifetime of CDP film coated electrodes reaches months if films are stored in air of sufficiently high humidity.

Metalloporphyrins, due to their rich and well defined redox behaviour,[6] are suitable for developing redox catalysts and sensors. For instance, monomeric cobalt porphyrins reversibly bind dioxygen and catalytically electroreduce it to peroxide both in homogeneous and heterogeneous systems.[7] Recently, formation of supramolecular complexes of β-cyclodextrin (β-CD) and free-base tetraarylporphyrins have been reported,[8] thus opening the opportunity to develop new catalytic sensor devices. In the present study, we exploit this approach (Scheme 1) by demonstrating that a polymer film of a supramolecular complex of β-CD and cobalt tetraphenylporphyrin, Co(TTP), coated on the surface of a gold electrode, (β-CDP)–[Co(TPP)]/Au, can operate as a voltammetric sensor for determination of dioxygen dissolved in aqueous solution.




**Scheme 1** Schematic representation of catalytic $O_2$ electroreduction at a gold electrode coated with a polymer film of β-cyclodextrin hosting Co(TPP)

The (β-CDP)–[Co(TPP)]/Au electrode was prepared according to a simple one-step procedure developed earlier for the β-CDP films hosting other organic compounds.[10] That is, a *ca.* 0.1 mM Co(TPP)† chloroform solution was equilibrated, by sonication for a few min, with a stock solution of 2% β-cyclodextrin soluble prepolymer (β-CDPS).‡ After partition equilibrium was attained, the stock solution turned pale red–orange. This solution was used to prepare the casting solution which was 1.5% in β-CDPS, hosting Co(TPP), 15 mM in glutaric dialdehyde and 10 mM in HCl. Then, a *ca.* 3 μm thick polymer film was prepared by dispensing a 5 μl sample of the casting solution on the Au electrode surface to form a *ca.* 4 mm diameter circular spot.[3] Polycondensation was carried out for *ca.* 1 h in a water-vapour filled container (*ca.* 40% humidity), to allow for slow water evaporation. The small thickness of the β-CDP film used in the present study is advantageous with respect to the response time of the fabricated sensor.[10b]

Cyclic voltammetry (CV)§ experiments, perofrmed with the use of the (β-CDP)–[Co(TPP)]/Au electrode in deaerated 0.1 M phosphate buffer (pH 5.6),¶ 0.1 M NaCl, exhibited an electro-oxidation peak located at $E_{pa}$ = 0.09 V (potential scan rate, $v$ = 0.1 V $s^{-1}$) corresponding to the $Co^{II}$(TPP)–$Co^{III}$(TPP) redox couple.[6] Multicyclic voltammetry experiments showed no decay of the $Co^{II}$(TPP)–$Co^{III}$(TPP) peak currents with the scan number. This indicates that Co(TPP) is not released from the film into solution, as expected for this water-insoluble catalyst. Logarithmic dependence of the $Co^{II}$(TPP)–$Co^{III}$(TPP) electro-oxidation peak current *vs.* the potential scan rate was linear, with a slope close to 0.5, indicating a semi-infinite diffusion controlled charge transport within the polymer matrix. By analogy to the earlier reported supramolecular CD–porphyrin complexes in solution,[7] one may expect that Co(TPP) is complexed predominately by inclusion of its one or more phenyl rings by the cyclodextrin host site of the polymer rather than through axial ligation of the cobalt centre. Because of the semi-infinite, and not finite, diffusion control of the CV peak current, it is also unlikely that the Co(TPP) solid is present in the form of a suspension in the film.

The voltammetric peak corresponding to electroreduction of dissolved dioxygen at a blank (β-CDP)/Au electrode, *i.e.* in the absence of the Co(TPP) catalyst in the film, occurs at $E_{pc}$ = −0.70 V ($v$ = 0.1 V $s^{-1}$). Interestingly, with the (β-CDP)–[Co(TPP)]/Au electrode, *i.e.* in the presence of the catalyst in the film, this peak is positively shifted due to electrocatalysis and occurs at $E_{pc}$ = −0.45 V ($v$ = 0.1 V $s^{-1}$). A peak current dependence on $v^{\frac{1}{2}}$ for the latter peak is linear, with zero plot intercept, for constant dioxygen concentration, indicating that dioxygen catalytic electroreduction is controlled by semi-infinite diffusion. Fig. 1 shows the effect of the dioxygen concentration on the voltammetric peak current of catalytic dioxygen electroreduction measured at the (β-CDP)–[Co(TPP)]/Au electrode. The catalytic peak current is linearly dependent on the dioxygen concentration for the entire range of

dioxygen concentration (inset in Fig. 1). Voltammetry at the rotating ring-disk (platinum–glassy carbon) electrode, with a (β-CDP)–[Co(TPP)] film coated on the disk, proved that dioxygen is catalytically electroreduced to hydrogen peroxide (Scheme 1). That is, ring current was observed corresponding to the electrooxidation of hydrogen peroxide, which is the electroreduction product at the disk when its potential is scanned from 0.2 to −0.7 V and the ring potential is kept constant at $E_R$ = 0.8 V.[11]

In summary, the Co(TPP) catalyst can be immobilized in a thin β-CDP film cast on the Au electrode surface, and the sensor thus fabricated can be successfully used for detection of dioxygen dissolved in aqueous solution. The catalyst is molecularly dispersed in the polymer matrix forming a supramolecular complex with the β-CD sites and, advantageously, this immobilization is irreversible in aqueous solutions. The catalytic peak current of dioxygen electroreduction is proportional to the dioxygen concentration in solution for the entire range of the dioxygen concentration. The (β-CDP)–[Co(TPP)]/Au electrodes show reproducible results with respect to dioxygen determination after storage for several days in air atmosphere of high humidity. Mechanistic studies on dioxygen binding to cobalt porphyrins bearing different peripheral charges, hosted by the β-CDP matrix, and hydrogen peroxide release will follow.[13]

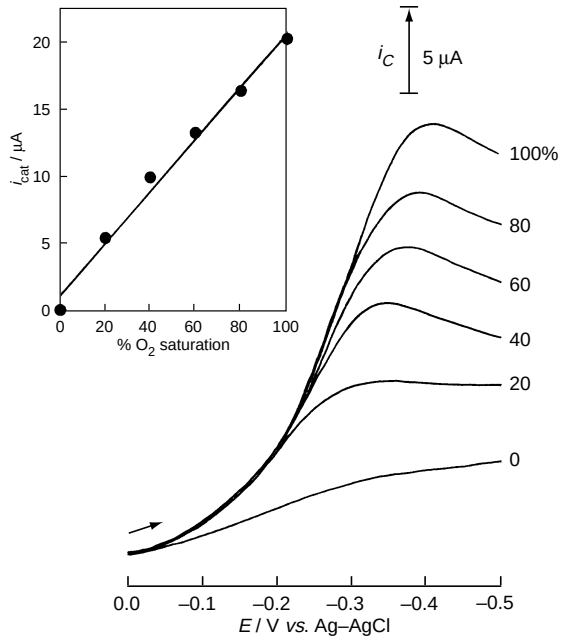



**Fig. 1** Voltammograms for the (β-CDP)–[Co(TPP)] film-coated Au disk electrode for different % $O_2$, indicated for each curve; 0.1 M phosphate buffer (pH 5.6), 0.1 M NaCl; ν 0.1 V $s^{-1}$. Inset is the dependence of the catalytic peak current, $i_{cat}$, of $O_2$ electroreduction *vs.* % $O_2$ saturation of the solution.

Financial support to F. D. from the National Science Foundation, through Grant No. EPS-9550487, and matching support from the State of Kansas, as well as to W. K. from the Polish State Committee for Scientific Research, through Grant KBN 2P 303 10 707, is gratefully acknowledged.

## Footnotes

* E-mail: dsouza@wsuhab.uc.twsu.edu; wkutner@ichf.edu.pl

† Co(TPP) was synthesized according to the literature procedure (ref. 9).

‡ β-CDPS was from Cyclolab, Cyclodextrin Research and Development Laboratory (Budapest, Hungary).

§ Cyclic voltammetry was performed by using either a Model EC/225 Voltammetric Analyzer of IBM Instruments, Inc. (Danbury, CT) or a Model 263A potentiostat/galvanostat of EG&G PAR (Princeton, NJ) and a typical three-electrode electrochemical cell. A 1.6 mm diameter disk gold electrode of Bioanalytical Systems (West Lafayette, IN) was used as the working electrode. A platinum wire and sodium chloride saturated Ag–AgCl electrode served as the auxiliary and reference electrodes, respectively. All potentials cited are against the Ag–AgCl reference electrode. All measurements were performed for a 0.1 M phosphate buffer (pH 5.6), 0.1 M NaCl solution, at 20 ± 1 °C.

¶ The pH of the working solution was chosen to be 5.6 in order to avoid hydrolysis of glycosidic bonds of the β-CDP polymer which occurs at pH < 2, and also to avoid the pH dependence of the formal redox potential of the $Co^{III}$–$Co^{II}$ couple of Co(TPP) at pH ⩾ 6, as demonstrated in ref. 12.

## References

1 *Comprehensive Supramolecular Chemistry*, ed. J. L. Atwood, J. E. D. Davies, D. D. MacNicol and R. Vogtle, Pergamon, New York, 1996; J.-M. Lehn, in *Supramolecular Chemistry*, VCH, Weinheim, 1995, ch., 5 and 8.
2 G. Wenz, *Angew. Chem., Int. Ed. Engl.*, 1994, **33**, 803.
3 W. Kutner, W. Storck and K. Doblhofer, *J. Inclusion Phenom.*, 1992, **13**, 257; W. Kutner and K. Doblhofer, *J. Electroanal. Chem.*, 1992, **326**, 139; W. Kutner, *Electrochim. Acta*, 1992, **37**, 1109.
4 J. C. Lepretre and E. Saintman, *J. Electroanal. Chem.*, 1993, **347**, 465.
5 D. Koradecki and W. Kutner, *J. Inclusion Phenom.*, 1991, **10**, 79.
6 K. M. Kadish, *Prog. Inorg. Chem.*, 1986, **34**, 435.
7 A. Bettelheim, R. J. H. Chan and T. Kuwana, *J. Electroanal. Chem.*, 1979, **99**, 93; C.-L. Ni and F. C. Anson, *Inorg. Chem.*, 1985, **24**, 4754.
8 S. Zhao and J. H. T. Luong, *J. Chem. Soc., Chem. Commun.*, 1994, 2307; F. Venema, A. E. Rowan and R. J. M. Nolte, *J. Am. Chem. Soc.*, 1996, **118**, 257.
9 J.-H. Fuhrhop and K. M. Smith, in *Porphyrins and Metalloporphyrins*, ed. K. M. Smith, Elsevier, New York, 1975, ch. 19.
10 (*a*) W. Kutner, H. Wu and K. M. Kadish, *Electroanalysis*, 1994, **6**, 934; (*b*) Q. Chen, P. V. A. Pamidi, J. Wang and W. Kutner, *Anal. Chim. Acta*, 1995, **306**, 201.
11 F. D'Souza, R. G. Deviprasad and Y.-Y. Hsieh, *J. Electroanal. Chem.*, 1996, **411**, 167.
12 R. R. Durand, Jr. and F. C. Anson, *J. Electroanal. Chem.*, 1982, **134**, 273.
13 F. D'Souza, Y.-Y. Hsieh, H. Wickman and W. Kutner, *Electroanalysis*, 1997, in press.

*Received in Columbia, MO, USA, 11th March 1997, Com. 7/01704I*

# Ultrathin oriented zeolite LTA films

**Jonas Hedlund,* Brian Schoeman and Johan Sterte**

*Department of Chemical Technology, Luleå University of Technology, SE-971 87, Luleå, Sweden*

**Ultrathin oriented films of zeolite LTA are prepared on single-crystal alumina supports by a method including adsorption of LTA seeds on the support followed by hydrothermal film crystallization.**

Molecular sieve films have great potential for example as membranes and membrane reactors as well as in sensor applications. Supported films of molecular sieves are usually synthesized by direct crystallization of the zeolite on the support.[1] Most of the work reported concerns the preparation of MFI films[2–8] because of the simplicity of this system and only a few reports treating the preparation of other types of zeolite films have appeared in the literature.[9–12] Independent of zeolite type, these films generally have a thickness exceeding 1 μm. The flux through a membrane or the response time of a chemical sensor is greatly dependent upon the film thickness and hence thin films are preferable in both membrane and sensor applications. The performance of zeolite membranes and sensors is also influenced by the orientation of the zeolite crystals constituting the film. The orientation will affect the diffusion path through the membrane and the adsorption kinetics of a chemical sensor consisting of a supported zeolite film. Recently, a novel method was presented for the preparation of ultrathin films of silicalite-1 on various substrates.[13,14]

Here, we report on the first preparation of an ultrathin oriented zeolite LTA film on a single-crystal alumina(0001) wafer. LTA seeds were prepared by hydrothermal treatment at 63 °C for 63 h of a synthesis solution with the composition $0.22Na_2O : 5.0SiO_2 : Al_2O_3 : 8.0(TMA)_2O : 400H_2O$. The synthesis solution was prepared by first dissolving aluminium isopropoxide (Sigma) and tetramethylammonium hydroxide pentahydrate (Sigma) in a sodium hydroxide solution at room temp. and then mixing this solution with a dilute silica sol (Bindzil 30/220, 31 mass% $SiO_2$ and 0.5 mass% $Na_2O$, Akzo Nobel AB). After synthesis, the seed sol was purified by repeated centrifugation and redispersion in an ammonia solution so as to maintain a pH exceeding 10.5. The sol was finally diluted to a solids content of 2.5 mass% (determined after drying at 100 °C) and adjusted to a pH of 10.7. A polished alumina(0001) wafer (10 × 10 × 0.5 mm, Coating & Crystal

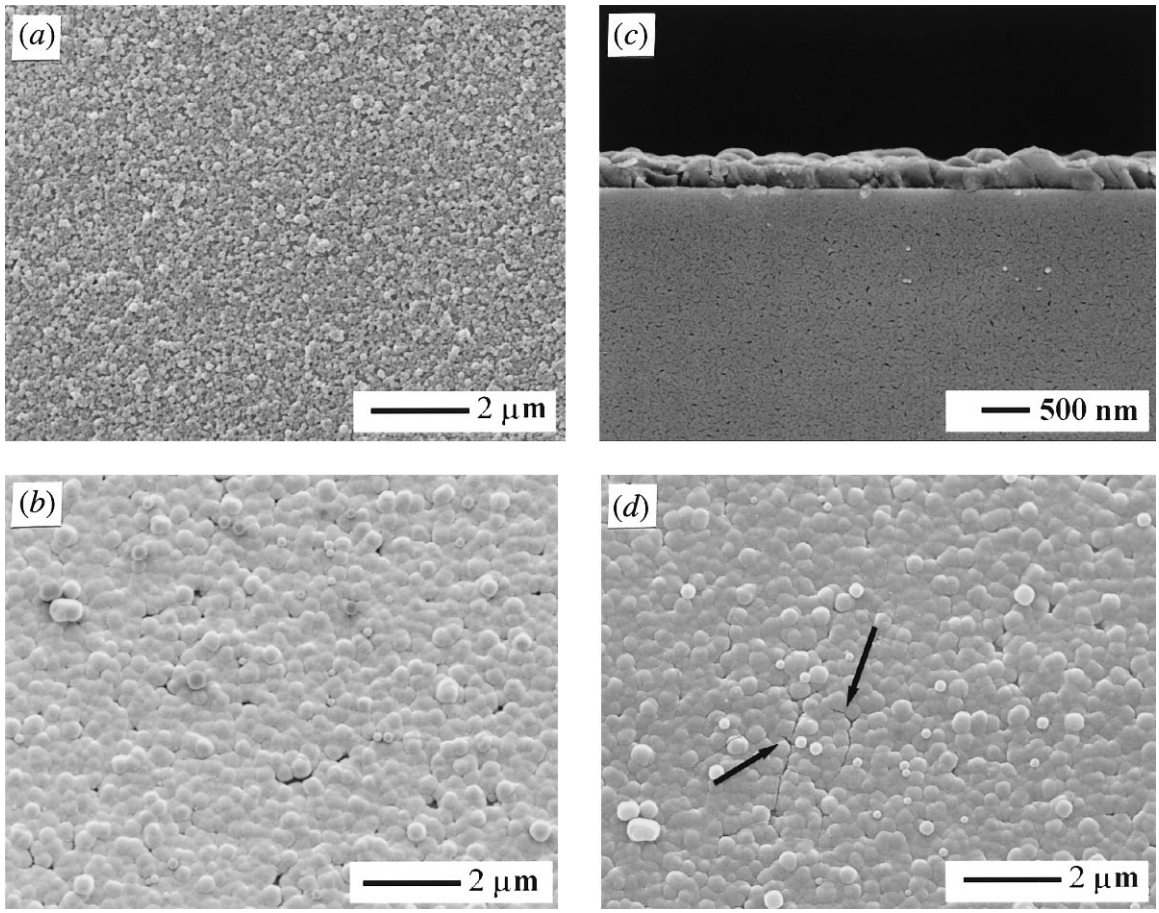



**Fig. 1** SEM micrographs showing the adsorbed zeolite LTA seed crystals after three repeated adsorptions on the substrate surface (*a*), the top view of the film after calcination recorded at an accelerating voltage of 4 kV (*b*), the side view of the film after calcination (*c*) and the top view of the film after calcination recorded at an accelerating voltage of 20 kV with arrows indicating cracks (*d*)

Technology) was mounted vertically in a Teflon holder and treated in acetone in an ultrasonic bath for 5 min followed by rinsing with distilled water. The substrate was boiled for 5 min in a mixture of $H_2O$, $H_2O_2$ and $NH_3$ (5 : 1 : 1 v/v/v of $H_2O$, 30% $H_2O_2$ and 25% $NH_3$), rinsed with distilled water and boiled for 5 min in a mixture of $H_2O$, $H_2O_2$ and HCl (6 : 1 : 1 v/v/v of $H_2O$, 30% $H_2O_2$ and 37% HCl) and finally rinsed with water and a 0.1 M ammonia solution. After the rinsing procedure the wafer was immersed in a 0.4% solution of a cationic polymer (Berocell 6100, Akzo Nobel AB, repeating unit $[CH_2CHOHCH_2NMe_2]^+_n$, $M_w$ = 50 000 g mol$^{-1}$, pH 8.0) for 5 min to reverse the surface charge of the alumina wafer from a negative to a positive value. The charge reversed wafer was rinsed in a 0.1 M ammonia solution to remove excess polymer. The substrate was treated with the LTA seed sol for 5 min to adsorb seed crystals on the charge reversed alumina surface and rinsed in a 0.1 M ammonia solution to remove excess seed crystals. This sequence, charge reversal–adsorption of seeds, was repeated twice to improve the seed coverage on the surface. Film crystallization on the seeded substrate was effected by hydrothermal treatment at 100 °C for 6.3 h in a synthesis solution prepared in the same manner and with the same composition as that used for the synthesis of the seed crystals (*vide supra*). After completion of this treatment, the sample was rinsed with a 0.1 M ammonia solution and dried in air. Samples were calcined at 425 °C for 1 h in air, using a heating and cooling rate of 1 °C min$^{-1}$. Particle size analysis by dynamic light scattering (DLS) was performed on the seed sol and on synthesis solutions after synthesis with a Brookhaven Instruments ZetaPlus. Electron micrographs were recorded with a Philips XL 30 scanning electron microscope (SEM) equipped with a $LaB_6$ emission source. X-Ray diffraction (XRD) data were collected with a Siemens D5000 powder diffractometer equipped with a Göbels mirror, 12 cm soller slit and a secondary LiF monochromator when analysing the film. A primary soller slit and variable slits to keep the illuminated area constant were used when analysing powder samples.

The average crystal size in the LTA seed sol was determined by DLS to be 130 nm with a polydisperisty of 0.1. Fig. 1(*a*) shows a SEM micrograph of the adsorbed LTA seeds on the alumina support after the three adsorption steps. Approximately 80% of the support surface is covered by seeds. The coverage after one and two adsorption steps was approximately 40 and 65%, respectively. Fig. 1(*b*) and (*c*) show top- and side-view SEM micrographs of the calcined LTA film recorded with an accelerating voltage of 4 kV. The film is essentially continuous and free of cracks with a constant thickness of *ca*. 280 nm. Fig. 1(*d*) shows essentially the same area as in Fig. 1(*b*) but recorded with an accelerating voltage of 20 kV. A comparison between the two micrographs reveals that cracks have developed, most likely due to the bombardment of the film with 20 keV electrons in the SEM when recording the micrograph in Fig. 1(*d*). Fig. 2 shows X-ray diffraction patterns of freeze-dried seeds (*a*), the purified and freeze-dried product formed in the bulk of the synthesis solution (*b*) and the film after synthesis [(*c*) and (*d*)]. The powder patterns [(*a*) and (*b*)] were recorded using a θ–2θ scan whereas patterns (*c*) and (*d*) [(*d*) is an enlargement of (*c*)] of the film were recorded with a detector scan at a grazing incidence angle of 1°. From patterns (*a*) and (*b*) in Fig. 2 it is clear that both the seeds and the bulk product consist of well crystallized zeolite LTA. The Si/Al molar ratio of the bulk product was determined by EDS analysis to be 1.1. DLS measurements showed that the average size of the final crystals obtained in the bulk phase at 100 °C was *ca*. 330 nm, *i.e.* considerably larger than the 130 nm seed crystals formed at 63 °C. The difference in crystal size explains the narrower peaks in the diffractogram recorded for the bulk product compared with the peaks in the diffractogram from the seeds. The diffractograms (*c*) and (*d*), of the final film, show that the film consists of oriented zeolite LTA crystals. The only peaks visible in this pattern are those due to (*h*00) reflections or diffraction from planes with large *h* compared with *k* and *l* indicating that the (100) plane of all crystals in the film is essentially parallel to the substrate surface.

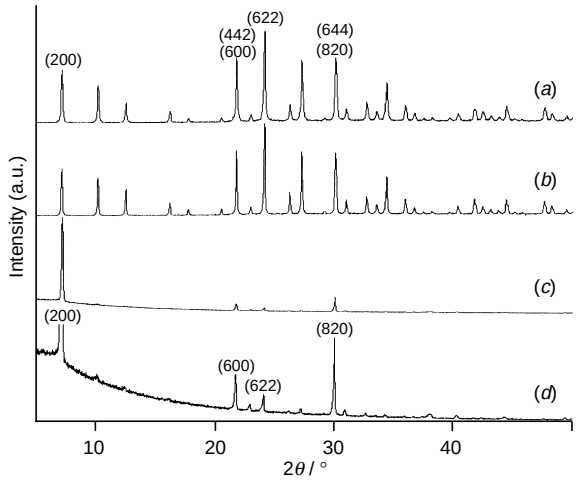



**Fig. 2** X-Ray diffraction patterns of the freeze-dried seeds (*a*), the purified and freeze-dried product formed in the bulk of the synthesis solution (*b*) and the film after synthesis (*c*) and (*d*) [(*d*) is an enlargement of (*c*)]. None of the samples were calcined prior to X-ray diffraction analysis.

The results presented show that the seed film method[13] can be used to synthesize ultrathin, oriented zeolite LTA films in a simple and elegant manner.

We wish to thank the Preem Environmental Foundation and the Swedish Research Council for Engineering Sciences (TFR) for the financial support of this project.

## Footnote

* E-mail: johe@km.luth.se

## References

1 T. Bein, *Chem. Mater.*, 1996, **8**, 1636.
2 E. Geus, M. Den Exter and H. van Bekkum, *J. Chem. Soc., Faraday Trans.*, 1992, **88**, 3109.
3 T. Masuda, A. Sato, H. Hara, M. Kouno and K. Hashimoto, *Appl. Catal. A*, 1994, **111**, 143.
4 Y. Yan, M. Tsapatsis, G. Gavalas and M. Davis, *J. Chem. Soc., Chem. Commun.*, 1995, 227.
5 Y. Yan, M. Davis and G. Gavalas, *Ind. Eng. Chem. Res.*, 1995, **34**, 1652.
6 M. Jia, K. Peinermann and R. Behling, *J. Membr. Sci.*, 1993, **82**, 15.
7 C. Bai, M. Jia, J. Falconer and R. Noble, *J. Membr. Sci.*, 1995, **105**, 79.
8 Y. Yan, S. Chaudhuri and A. Sarkar, *Chem. Mater.*, 1996, **8**, 473.
9 M. Lovallo and M. Tsapatsis, *Chem. Mater.*, 1996, **8**, 1579.
10 M. Matsukata, N. Nishiyama and K. Ueyama, *Stud. Surf. Sci. Catal.*, 1994, **84**, 1183.
11 T. Masuda, H. Hara, M. Kouno, H. Kinoshita and K. Hashimoto, *Microporous Mater.*, 1995, **3**, 565.
12 S. Yamazaki and K. Tsutsumi, *Microporous Mater.*, 1995, **4**, 205.
13 J. Hedlund, B. Schoeman and J. Sterte, *Stud. Surf. Sci. Catal.*, 1997, **105**, 2203.
14 S. Mintova, J. Hedlund, B. Schoeman, V. Valtchev and J. Sterte, *Chem. Commun.*, 1997, 15.

*Received in Bath, UK, 8th April 1997; Com. 7/02616A*

# The azido ligand: a useful tool in designing chain compounds exhibiting alternating ferro- and antiferro-magnetic interactions

**Guillaume Viau,[a] Maria Grazia Lombardi,[b] Giovanni De Munno,*[b] Miguel Julve,*[a] Francesc Lloret,[a] Juan Faus,[a] Andrea Caneschi[c] and Juan Modesto Clemente-Juan[a]**

[a] *Departament de Química Inorganica, Facultat de Química de la Universitat de València, Dr. Moliner 50, 46100 Burjassot (València), Spain*
[b] *Dipartimento di Chimica, Università degli Studi della Calabria, 87030 Arcavacata di Rende, Cosenza, Italy*
[c] *Dipartimento di Chimica, Università degli Studi di Firenze, 75/77 Via Maragliano, 50144 Firenze, Italy*

**A one-pot reaction of $Ni^{II}$ 1, $Co^{II}$ 2, $Fe^{II}$ 3 and $Mn^{II}$ 4 with 2,2′-bipyridine (bipy) and azide in water leads to $[M(bipy)(N_3)_2]_n$ chains where the metal ion is alternatively bridged by double end-on (EO) and end-to-end (EE) azido bridges; theoretical analysis of the variable-temperature magnetic susceptibility data of 1 and 4 reveals the occurrence of intrachain alternating ferro- (through EO) and antiferro-magnetic (through EE) interactions.**

A safe strategy in designing alternating chains with ferro- and antiferro-magnetic interactions has been proposed recently,[1] and the first honeycomb-layered materials of formula $[M(bipym)(N_3)_4]$ (M = Mn, Fe, Co; bipym = 2,2′-bipyrimidine)[2] with alternating ferro- (through end-on azido, EO) and antiferro-magnetic (through bischelating bipym) interactions have also been reported. Replacement of bipym by bipy (2,2′-bipyridine) yields chain compounds of formula $[M(bipy)(N_3)_4]$ (M = $Ni^{II}$ **1**, $Co^{II}$ **2**, $Fe^{II}$ **3**, $Mn^{II}$ **4**) with alternating EO and end-to-end (EE) azido bridges and exhibiting ferro- (through EO)[3] and antiferro-magnetic (EE)[4] interactions. Here, we report the synthesis, crystal structure and preliminary magnetic study of compounds **1**–**3**. The magnetic properties of **4**,[5] which is isostructural with **2** and **3**, were reinvestigated for the sake of comparison and the first theoretical analysis of the magnetic behaviour of **1** and **4** through a quantum spin model is also reported.

The one-dimensional compounds were obtained as polycrystalline green (**1**), orange (**2**) and red–brown (**3**) powders by adding an aqueous solution (25 $cm^3$) of $NaN_3$ [2 mmol (**1**) or 10 mmol (**2**, **3**)] to a methanolic solution (5 $cm^3$) containing bipy (1 mmol) and either $Ni(NO_3)_2{\cdot}6H_2O$ (1 mmol, **1**), $Co(NO_3)_2{\cdot}6H_2O$ (1 mmol, **2**) or $FeCl_2$ (1 mmol, **3**). The solid samples were filtered off and thoroughly washed with methanol and diethyl ether (yield *ca*. 50%). X-Ray quality polyhedral (**1**), arrow shaped (**2**) and prismatic (**3**) single crystals were grown by slow diffusion techniques in test (**2**, **3**) or H-shaped (**1**) tubes.†

The structures of **1**–**4** are made up of alternating chains where the metal ions are alternately linked by two EO and two EE azido bridges (Fig. 1).‡ Two nitrogen atoms of the bipy ligand complete a distorted $MN_6$ octahedral environment around each metal atom. The EE and EO bridges are propagated within the chain with a mutual perpendicular arrangement. The value of the M(1)–N(3)–M(1a) angle is 101.5(1) **1**, 100.9(1) **2** and 100.8(1)° **3** in good agreement with the value of 101.0(2)° observed in the parent compound of $Mn^{II}$ **4**.[5] The EE bridges adopt a chair conformation for the M–$(N_3)_2$–M unit. The values of the M(1)–N(6)–N(7) and N(7)–N(8)–M(1b) angles are 118.2(2) and 129.9(3)° in **1**, 127.1(2) and 129.9(2)° in **2** and 126.5(2) and 131.2(1)° in **3** [131.1(5) and 127.3(5)° in **4**]. The dihedral angle between the N(6)N(7)N(8)N(6a)N(7a)N(8a) and MN(6)N(8b) planes is 35.2(1) **1**, 24.9(1) **2** and 23.7(1)° **3** (41.9° in **4**). The intrachain metal–metal separation through EO azido is 3.248(1) **1**, 3.322(1) **2** and 3.367(1) Å **3** [3.455(6) Å in **4**] and that through EE azido is 5.117(2) **1**, 5.279(2) **2** and 5.317(2) Å **3** [5.343(5) Å in **4**]. The shortest interchain metal–metal separation is 8 Å [8.462(3) **1**, 8.115(4) **2**, 8.063(3) Å **3**].

Magnetic susceptibility measurements (290–2 K) on polycrystalline samples of **4** (Fig. 2) are consistent with overall antiferromagnetic behaviour. Least-squares analysis of the $\chi_M T$ data of **4**§ leads to $J_1 = 2.5\ cm^{-1}$, $J_2 = -6.3\ cm^{-1}$ and $g = 2.0$. $J_1$ and $J_2$ are associated with the exchange coupling through EO and EE azido bridges, respectively. The $\chi_M T$ value of **1** (Fig. 3) smoothly increases as the temperature is lowered, attains a plateau at 70 K and quickly decreases in the lower temperature region. The susceptibility curve (inset of Fig. 3) increases monotonically when cooling, attains a shoulder in the temperature range 50–20 K and then increases achieving a maximum at 8.5 K. The shape of the shoulder is field dependent at $T < 50$ K but the temperature of the maximum remains unchanged. The theoretical analysis of the magnetic data of **1**[6] matches well the experimental data in the temperature range 290–55 K. The best fit parameters are $J_1$ (coupling through EO

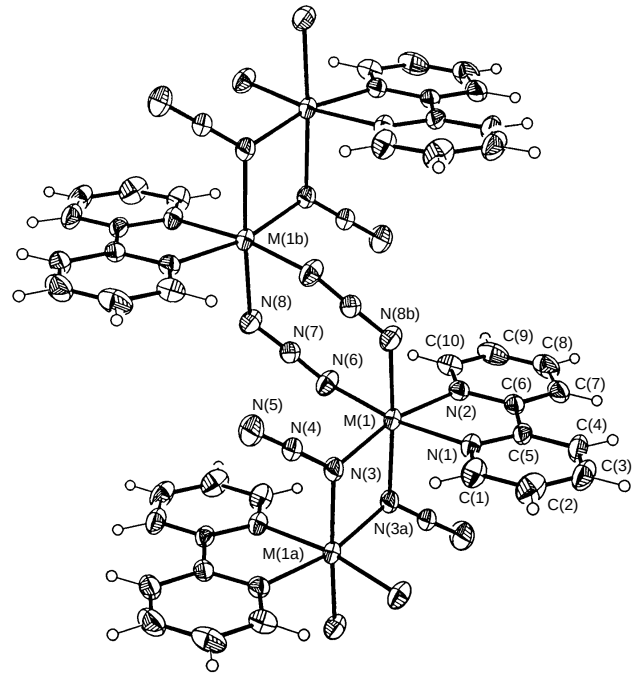



**Fig. 1** Crystal structure of $[M(bipy)(N_3)_2]_n$ (M = Ni **1**, Fe **2**, Co **3**) showing the atom numbering (ellipsoids are at the 30% probability level). The M–N bond lengths vary in the ranges 2.064(3)–2.145(4) Å for **1**, 2.118(2)–2.189(2) A for **2** and 2.132(2)–2.240(2) Å for **3**. The values of the M(1)–N(3)–M(1a) bond angles are 101.5(1) (**1**), 100.9(1) (**2**) and 100.8(1)° (**3**). The EO and EE azide groups are quasilinear [the smallest N(3)–N(4)–N(5) and N(6)–N(7)–N(8) bond angles are 178.1(3) and 176.7(2)°, respectively]. (Symmetry code for **1**: a $-x, 1-y, -z$; b $1-x, 1-y, -z$. Symmetry code for **2** and **3**: a $-x, 1-y, 1-z$; b $1-x, 1-y, 1-z$.)

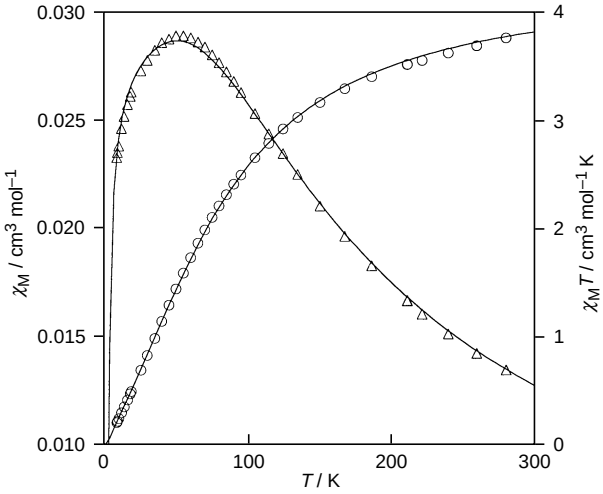



**Fig. 2** $\chi_M T$ (○) and $\chi_M$ (△) *vs. T* plots for complex **4**. The solid line corresponds to the fit to a model outlined in ref. 6.

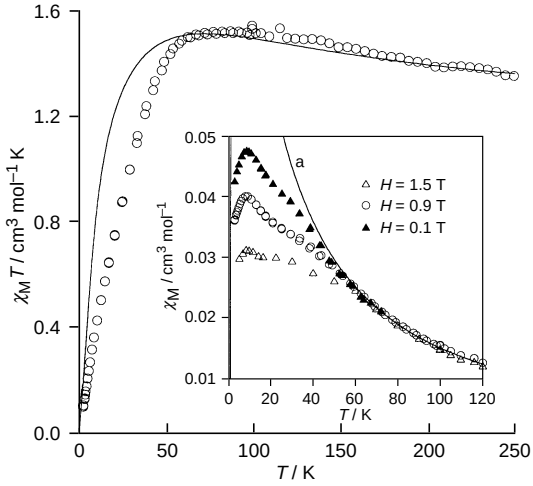



**Fig. 3** $\chi_M T$ *vs. T* plot for complex **1**. The inset shows the field dependence of the susceptibility in the low-temperature region. The solid line corresponds to the fit to a model outlined in ref. 6.

azido) = 26 $cm^{-1}$, $J_2$ (coupling through EE azido) = −2.6 $cm^{-1}$ and $g$ = 2.17. The experimental data are smaller than the calculated ones at $T$ < 55 K due to the occurrence of the mentioned shoulder precluding thus an accurate determination of the values of the exchange coupling parameters. The magnetic behaviour of **2**¶ is exotic too: $\chi_M T$ decreases when cooling down until reaching a minimum at 29 K, then increases to attain a sharp maximum at 12 K and finally decreases very quickly in the lower temperature region. As in **1**, the susceptibility curve also shows a shoulder but at higher temperatures (50–100 K), exhibiting a maximum at 8.5 K under an applied field $H$ of 0.1 T. However, this maximum disappears for $H$ > 0.5 T. Given that all the cobalt atoms in **2** are equivalent, the occurrence of a minimum in the $\chi_M T$ curve cannot be attributed to ferrimagnetism arising from a non-compensation of the local $g$-factors but to a intrachain spin canting. An interchain antiferromagnetic coupling would account for the observed maximum of susceptibility at $H$ < 0.5 T. Stronger fields overcome this antiferromagnetic coupling leading to the observed metamagnetic-like behaviour of **2**. Similar behaviour was observed for **3**. This peculiar behaviour of **1**–**3** is a fascinating feature that could be attributed to the occurrence of competing ferro- and antiferro-magnetic interactions together with a relevant local anisotropy. In the lack of a significant anisotropy, this feature is not observed (in the case of **4** and alternating $Cu^{II}$ chains).[1] Peculiar susceptibility and magnetization curves were also observed for honeycomb-layered materials with alternating intralayer ferro- and antiferro-magnetic interactions.[2] It is interesting to note that the spin vectors in the ferromagnetic chains are aligned parallel to the chain axis whereas in the case of the antiferromagnetic (or ferrimagnetic) chains they are arranged perpendicular to the chain axis in order to reconciliate both the dipolar and exchange interactions.[7] The question at hand concerning the chains exhibiting alternating ferro- and antiferro-magnetic interactions is to know the arrangement of the spin vectors for them. Our feeling is that the peculiar magnetic behaviour of **1**–**3** is related to the competition among the local anisotropy and the dipolar and exchange interactions.

This work was supported by the Spanish DGICYT (Projects PB94-1002 and PB94-0998) and the Italian Ministero dell'Università e della Ricerca Scientifica e Tecnologica.

## Footnotes

* E-mail: miguel.julve@uv.es

† Satisfactory elemental analyses (C, H, N) were obtained.

‡ *X-Ray crystal structure analyses*: Siemens R3m/V automatic diffractometer, Mo-Kα radiation, λ = 0.710 73 Å, graphite-monochromator, 295 K. Lorentz polarization and absorption corrections. Data collection, solution and refinement: ω–2θ, standard Patterson methods and subsequent Fourier recycling, SHELX-PLUS computer program. Compounds **1**–**3** have the same formula, $C_{10}H_8MN_8$ (M = Ni **1**, Co **2**, Fe **3**), triclinic, space group $P\bar{1}$ (**2** and **3** are isostructural). For **1**, $a$ = 7.017(2), $b$ = 9.662(2), $c$ = 10.279(3) Å, α = 111.12(2), β = 99.56(2), γ = 107.34(2)°, $U$ = 590.6(3) $Å^3$, $Z$ = 2, $D_c$ = 1.681 g $cm^{-3}$, crystal size 0.21 × 0.14 × 0.05 mm. 2869 reflections measured in the range 3 < 2θ < 54°, 2586 unique and 1952 assumed as observed with $I > 3\sigma(I)$; $R$ = 0.035 and $R_w$ = 0.036. For **2**, $a$ = 7.311(2), $b$ = 9.243(3), $c$ = 10.061(4) Å, α = 110.93(3), β = 102.61(3), γ = 102.93(3)°, $U$ = 584.8(3) $Å^3$, $Z$ = 2, $D_c$ = 1.699 g $cm^{-3}$, crystal size 0.40 × 0.28 × 0.24 mm. 2843 reflections measured in the range 3 < 2θ < 54°, 2589 unique and 2288 assumed as observed with $I > 3\sigma(I)$; $R$ = 0.029 and $R_w$ = 0.036. For **3**, $a$ = 7.448(2), $b$ = 9.195(3), $c$ = 10.020(3) Å, α = 111.00(2), β = 104.07(2), γ = 101.53(2)°, $U$ = 589.4(3) $Å^3$, $Z$ = 2, $D_c$ = 1.668 g $cm^{-3}$, crystal size 0.50 × 0.21 × 0.29 mm. 2856 reflections measured in the range 3 < 2θ < 54°, 2589 unique and 2277 assumed as observed with $I > 3\sigma(I)$; $R$ = 0.027 and $R_w$ = 0.031. Atomic coordinates, bond lengths and angles, and thermal parameters have been deposited at the Cambridge Crystallographic Data Centre (CCDC). See Information for Authors, Issue 1. Any request to the CCDC for this material should quote the full literature citation and the reference number 182/468.

§ The numerical expressions used for the analysis of the magnetic properties of **1** and **4** were obtained using the isotropic Hamiltonian $\hat{H} = -J \Sigma [\hat{S}_{2i}\hat{S}_{2i-1} - \alpha\hat{S}_{2i}\hat{S}_{2i+1}]$ by fitting the theoretical susceptibility curves of the rings up to ten $S$ = 1 (**1**) or six $S$ = 5/2 (**2**) local spins instead of open chains. The theoretical development has been elaborated in ref. 6.

¶ Magnetic data for complex **2** are available from the authors.

## References

1 G. De Munno, M. Julve, F. Lloret, J. Faus, M. Verdaguer and A. Caneschi, *Angew. Chem., Int. Ed. Engl.*, 1993, **32**, 1046; *Inorg. Chem.*, 1995, **34**, 157.

2 G. De Munno, M. Julve, G. Viau, F. Lloret, J. Faus and D. Viterbo, *Angew. Chem., Int. Ed. Engl.*, 1996, **35**, 1807; R. Cortés, L. Lezama, J. L. Pizarro, M. I. Arriortua and T. Fojo, *Angew. Chem., Int. Ed. Engl.*, 1996, **35**, 1810; G. De Munno, T. Poerio, G. Viau, M. Julve, F. Lloret, Y. Journaux and E. Rivière, *Chem. Commun.*, 1996, 2587.

3 R. Cortés, J. L. Pizarro, L. Lezama, M. I. Arriortua and T. Rojo, *Inorg. Chem.*, 1994, **33**, 2697; A. Escuer, R. Vicente, J. Ribas and X. Solans, *Inorg. Chem.*, 1995, **34**, 1793; M. G. Drew, C. J. Harding and J. Nelson, *Inorg. Chim. Acta*, 1996, **246**, 73.

4 O. Kahn, *Comments Inorg. Chem.*, 1984, **3**, 105; J. Ribas, M. Monfort, C. Diaz, C. Bastos and X. Solans, *Inorg. Chem.*, 1993, **32**, 3557.

5 R. Cortés, L. Lezama, J. L. Pizzaro, M. I. Arriortua, X. Solans and T. Rojo, *Angew. Chem., Int. Ed. Engl.*, 1994, **33**, 2488; R. Cortés, M. Drillon, X. Solans, L. Lezama and T. Rojo, *Inorg. Chem.*, 1997, **36**, 677.

6 J. J. Borrás-Almenar, J. M. Clemente, E. Coronado and F. Lloret, *Chem. Phys. Lett.*, in press.

7 D. Gatteschi, O. Guillou, C. Zanchini, R. Sessoli, O. Kahn, M. Verdaguer and Y. Pei, *Inorg. Chem.*, 1989, **28**, 287.

*Received in Basel, Switzerland, 21st February 1997; Com. 7/01219E*

# Oxidation using [bis(trifluoroacetoxy)]iodobenzene: a new and potentially practical approach to detection of polychlorinated phenols

**Coralie Saby and John H. T. Luong***

*Biotechnology Research Institute, National Research Council Canada, Montreal, Quebec, Canada H4P 2R2*

**A novel oxidation for pentachlorophenol, 2,4,6-trichlorophenol and 2,3,5,6-tetrachlorophenol using [bis(trifluoroacetoxy)]iodobenzene has been developed, and the oxidation products from pentachlorophenol and 2,3,5,6-tetrachlorophenol have been identified as tetrachloro-1,4-benzoquinone; this novel reaction can be applied in electrochemistry using glucose oxidase for sensitive determination and identification of PCP, one of the most toxic polychlorinated phenols.**

Considerable effort, including time-consuming immunoassay, has been directed toward the detection and quantitation of priority chlorinated pollutants such as pentachlorophenol (PCP), 2,3,5,6-tetrachlorophenol and 2,4,6-trichlorophenol.[1,2] Although electrochemical detection has frequently been used because of its simplicity and sensitivity, the oxidation products, generally believed to be quinones or radical products, are prone to polymerization, which results in electrode surface fouling.[3] Direct electrochemical oxidation of chlorophenols also requires an overpotential of +700 to +900 mV, which is sufficiently extreme so as to introduce the possibility of electroactive interference. These drawbacks can be overcome through enzymatic oxidation of chlorophenols, followed by electrochemical reduction of the chlorinated quinones. However, the two enzymes most commonly applied to this assay, tyrosinase and laccase, have been tested and found to be effective only for catechol, hydroquinone, *p*-cresol, 4-chlorophenol and 4-amino-4-chlorophenol.[4,5]

Several chlorophenols could be oxidized by ceric sulfate or chloroperoxidase. The resulting quinones were shown to efficiently recycle glucose oxidase to the oxidized form.[6] However, the PCP oxidation with ceric sulfate or hydrogen peroxide catalysed by chloroperoxidase undergoes polymerization of the oxidation product. Photochemical oxidation with hydrogen peroxide or singlet oxygen often produces a complex mixture of products including quinones, diols and triols, and polyhydroxybiphenyls.[7,8]

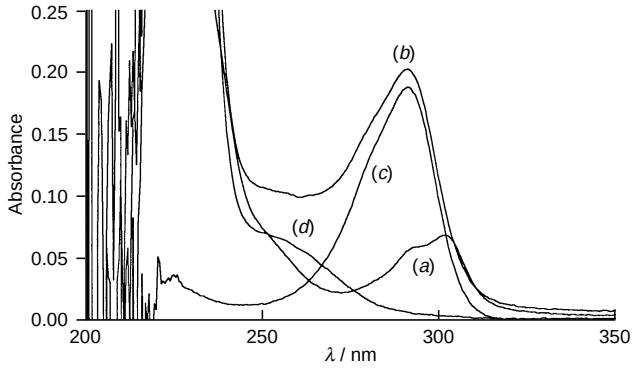



**Fig. 1** UV–Visible (Beckman DU 640 spectrometer) spectrum of (*a*) pentachlorophenol (10 μM), (*b*) the oxidation product of PCP, (*c*) the standard tetrachloro 1,4-benzoquinone (10 μM) and (*d*) [bis(trifluoroacetoxy)]iodobenzene (100 μM after hydrogen peroxide addition). Measurements were performed in 0.1 M acetic buffer, pH 3. Reaction was carried out in 0.1 M acetic buffer, pH 3 for 2 h, with 10 μM pentachlorophenol and 100 μM [bis(trifluoroacetoxy)]iodobenzene. Hydrogen peroxide (88 μM) was added to stop the reaction.

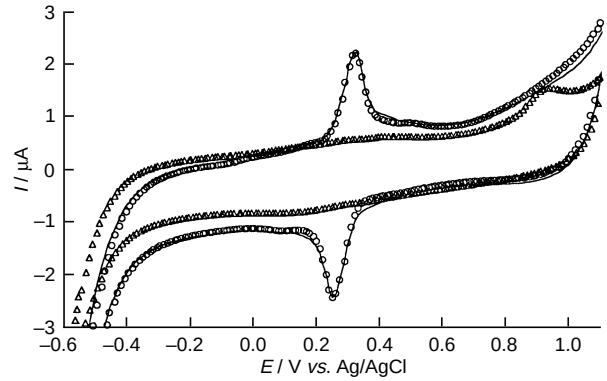
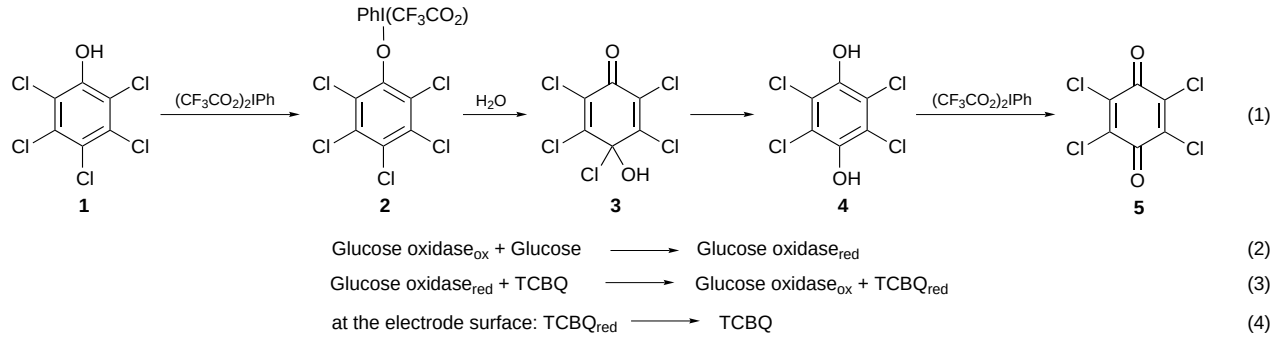



**Fig. 2** Cyclic voltammograms (0.1 M acetic acid, pH 3, 100 mV $s^{-1}$) of (Δ) pentachlorophenol (10 μM), (○) the oxidation product of PCP and (—) the standard solutions of tetrachloro-1,4-benzoquinone (10 μM). Reaction was carried out in 0.1 M acetic buffer, pH 3, for 1 h, with 10 μM pentachlorophenol and 500 μM [bis(trifluoroacetoxy)]iodobenzene. Hydrogen peroxide (440 μM) was added to stop the reaction. Equipment: CV-1B voltammograph (Bioanalytical Systems), platinum wire counter electrode, Ag/AgCl reference electrode and glassy carbon working electrode.

We report here a novel and simple reaction for the oxidation of pentachlorophenol into tetrachloro-1,4-benzoquinone (TCBQ) in aqueous media using [bis(trifluoroacetoxy)]-iodobenzene (BTIB). We also report the ability of TCBQ to oxidize reduced glucose oxidase. Although this hypervalent iodine agent.[9,10] has been used to oxidize various naphthols[11] into the corresponding quinone, no attempt has been made to oxidize chlorinated phenols with BTIB. Reaction of pentachlorophenol with BTIB was performed in 0.1 M acetate buffer, pH 3, at ambient temperature. A large excess of BTIB (molar ratio BTIB/PCP from 10 to 50) must be used to accelerate the reaction (2 h to 30 min). Neutralization of excess BTIB with hydrogen peroxide prevented further reaction of the initial products. Moreover, BTIB reaction by-products (iodobenzene and trifluoroacetate ion) are not electroactive species.

UV–VIS spectral, HPLC and cyclic voltammetric data obtained from the reacted solution demonstrated that the reaction product of pentachlorophenol with BTIB is tetrachloro-1,4-benzoquinone. Over the course of the reaction, the pentachlorophenol peaks at λ = 294 and 303 nm declined [Fig. 1, curve (*a*)] and a more intense absorption peak at 290 nm emerged and intensified [Fig. 1, curve (*b*)]. Both the absorbency profile and maximum wavelength of the PCP oxidation product were confirmed to be identical to those of standard tetrachloro-1,4-benzoquinone [Fig. 1, curve (*c*)]. The HPLC data also indicated that a significant portion of tetrachloro-1,4-benzoquinone was converted to tetrachloro-1,4-hydroquinone during the course of separation [HPLC column; 3.9 mm i.d. × 15 cm stainless steel packed with 10 μ C18 silica gel (μBondapak C18, Waters, Milford, MA), mobile phase: 25% pH 3.0, 0.1 M tartrate buffer + 25% water + 50% MeOH at a flow rate of 0.5 ml $min^{-1}$]. To facilitate the sensitive detection of tetrachloro-




1,4-benzoquinone, this oxidation product was reduced with zinc to tetrachloro-1,4-hydroquinone, which was detected by a glassy carbon electrode, +450 mV *vs.* Ag/AgCl (model LC-44 thin layer electrochemical cell connected to a model CV-1B potentiostat, Bioanalytical Systems, Lafayette, IN). The cyclic voltammogram of the product obtained from the oxidation of PCP by BTIB is identical with that of the standard tetrachloro-1,4-benzoquinone with respect to the oxidation and reduction peaks and the peak to peak separation (Fig. 2).

Another interesting result reported here is the capability of tetrachloro-1,4-benzoquinone to reoxidize glucose oxidase in the presence of excess glucose. As shown in Fig. 3(*a*), glucose oxidase immobilized on a glassy carbon electrode was readily

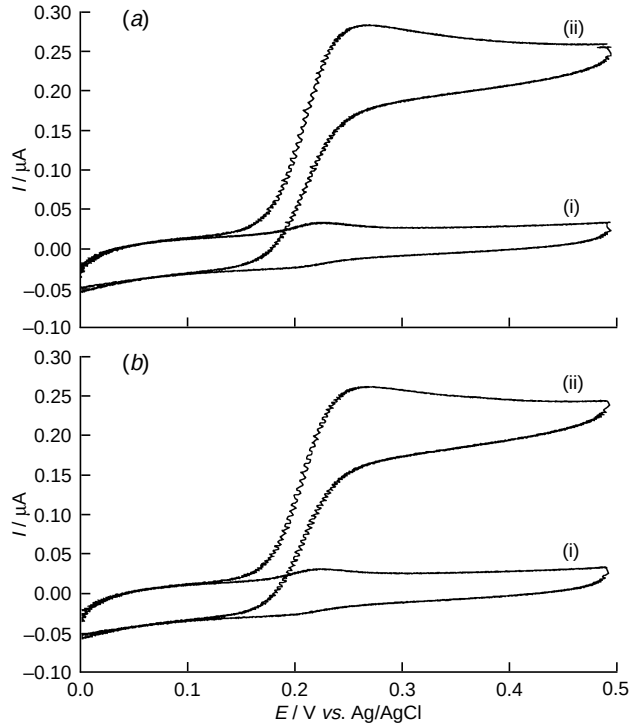



**Fig. 3** (*a*) Cyclic voltammograms of the GOD electrode in 1 μM tetrachloro-1,4-benzoquinone solution [9 ml phosphate buffer (0.3 M, pH 5) and 1 ml acetic acid (0.1 M, pH 3) containing 10 μM tetrachloro-1,4-benzoquinone, 2 mV $s^{-1}$] (i) before and (ii) after addition of 40 mM glucose. The GOD electrode was prepared as follows. After polishing of the glassy carbon electrode, 10 μl of glucose oxidase solution (glucose oxidase: 133 U, glutaraldehyde: 2.5%, 0.1 M phosphate buffer, pH 7) was placed on the surface and covered by a dialysis membrane (MWCO 14000). After drying in water saturated atmosphere for 15 min, the electrode was rinsed with 0.1 M phosphate buffer. (*b*) Cyclic voltammograms of GOD electrode in 1 μM PCP reaction solution [9 ml phosphate buffer (0.3 M, pH 5) and 1 ml 10 μM PCP reaction solution, 2 mV $s^{-1}$] (i) before and (ii) after addition of 40 mM glucose. Reaction was carried out in 0.1 M acetic buffer, pH 3, for 1 h with 10 μM pentachlorophenol and 500 μM [bis(trifluoroacetoxy)]iodobenzene. Hydrogen peroxide (440 μM) was added to stop the reaction.

reduced by its substrate, glucose. TCBQ then recycled the reduced enzyme to its original active form, *i.e.* mediating the rate-limiting electron transfer from the enzyme to the electrode. The oxidation product obtained from the PCP–BTIB reaction was also able to mediate the glucose oxidase–glucose reaction [Fig. 3(*b*)]. Based on the above findings, a mechanism for the oxidation of PCP and the mediating capability of the corresponding oxidation product can be proposed [eqns. (1)–(4)].

Oxidation of phenols often produces a mixture of isomers (1,4- and 1,2-benzoquinone). However, steric hindrance by the $(CF_3CO_2)$IPh species could be the main reason why dechlorination occurs only in position 4. In addition to PCP, BTIB also oxidized two other important chlorophenols: 2,4,6-trichlorophenol and 2,3,5,6-tetrachlorophenol. It should be noted that the 1,4-benzoquinone structure exhibited unique symmetry, and dechlorination of chlorophenols had to occur at position 4 if it was chlorinated. In view of this, both 2,3,5,6-tetrachlorophenol and PCP must yield the same oxidation product, *i.e.* tetrachloro-1,4-benzoquinone. We confirmed that the oxidation product of 2,3,5,6-tetrachlorophenol and pentachlorophenol with BTIB exhibits identical cyclic voltammetric behaviour and similar UV–visible peaks (not shown). The oxidation products of these two chlorophenols also mediated the glucose oxidase–glucose reaction, whereas BTIB and BTIB by-products did not react with reduced glucose oxidase. The detection limit of pentachlorophenol and 2,3,5,6-tetrachlorophenol was determined to be 4 nM, whereas that of 2,4,6-trichlorophenol was 8 nM; the steady state signal was attained within 2–5 min.

We have demonstrated that highly chlorinated phenols can easily be oxidized to quinones. In combination with bioelectroanalytical chemistry, this reaction offers a sensitive method for the determination of these important pollutants.

## Footnote

* luong@biotech.lan.nrc.ca

## References

1 H. Y. Neujahr, *Biotechnol. Bioeng.*, 1980, **22**, 913.
2 J. Van Emon and S. Rock, *PCP Immunoassay Technology*, U.S. Environmental Protection Agency, Washington, DC, 1995.
3 G. E. Marko-Varga, J. Emneus, L. Gorton and T. Ruzgas, *Trends Anal. Chem.*, 1995, **14**, 319.
4 R. S. Brown, K. B. Male and J. H. T. Luong, *Anal. Biochem.*, 1994, **222**, 131.
5 M. Bonakdar, J. L. Vilchez and H. A. Mottola, *J. Electroanal. Chem.*, 1989, **266**, 47.
6 S. Zhao and J. H. T. Luong, *Anal. Chim. Acta*, 1996, **327**, 235.
7 K. Omura and T. Matsuura, *Tetrahedron*, 1968, **24**, 3475.
8 A.-P. Durand, R. G. Brown, D. Worrall and F. Wilkinson, *J. Photochem. Photobiol. A: Chem.*, 1996, **96**, 35.
9 A. Pelter and S. Elgendy, *J. Chem. Soc., Perkin Trans. 1*, 1993, 1891.
10 A. McKillop, L. McLaren and R. Taylor, *J. Chem. Soc., Perkin Trans. 1*, 1994, 2047.
11 R. Barret and M. Daudon, *Tetrahedron Lett.*, 1990, **31**, 4871.

*Received in Cambridge, UK, 25th February 1997; Com. 7/01319A*

# *meso*-Arylporphyrins as dienophiles in Diels–Alder reactions: a novel approach to the synthesis of chlorins, bacteriochlorins and naphthoporphyrins

**Augusto C. Tomé, Paula S. S. Lacerda, Maria G. P. M. S. Neves and José A. S. Cavaleiro***

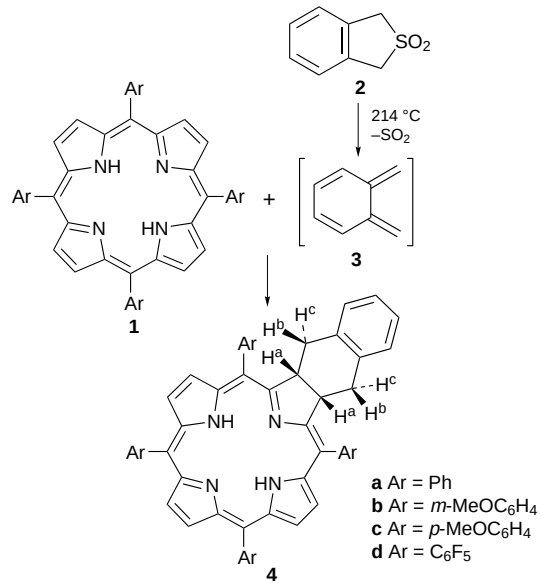
*Department of Chemistry, University of Aveiro, 3810 Aveiro, Portugal*

***meso*-Arylporphyrins participate, as dienophiles, in Diels–Alder reactions with *o*-benzoquinodimethane to yield novel chlorins, bacteriochlorins and naphtho[2,3-*b*]porphyrins.**

The use of porphyrin derivatives as photosensitizers for the photodynamic therapy (PDT) of malignant tumours received a boost with the authorisation, in several countries, of the clinical use of Photofrin, a complex mixture of porphyrins derived from haematoporphyrin.[1] In recent years, several studies related to PDT have been oriented to the search for single substances having strong absorption bands at the red end of the visible spectrum (the so-called second generation photosensitizers). This requirement is because of the greater tissue penetration of light with longer wavelengths.[2] Most of the second generation photosensitizers which have been studied are reduced porphyrins (mainly chlorins and bacteriochlorins) because of their strong absorptions near or above 700 nm.

A versatile route to the synthesis of chlorins is the Diels–Alder reaction of vinyl porphyrins with electron-deficient dienophiles.[3] Bacteriochlorins and isobacteriochlorins can also be prepared by the same type of reaction if a divinylporphyrin is used.[4] All previous studies involving Diels–Alder reactions with porphyrins have considered these macrocycles as the dienes. We now report that *meso*-arylporphyrins can also be used as dienophiles in Diels–Alder reactions.

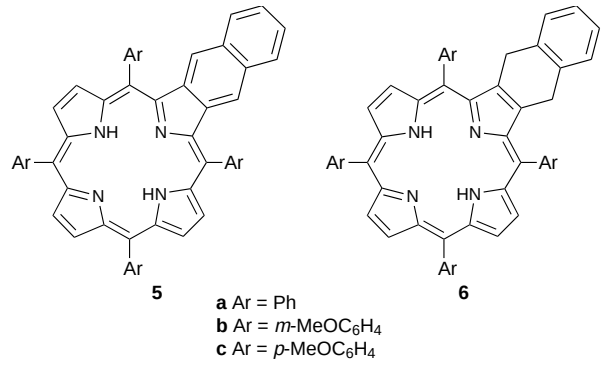
It is known that the peripheral double bonds of the porphyrin macrocycle are partially isolated from the macrocyclic conjugation pathway. The chemistry of these double bonds is, in some aspects, similar to the chemistry of normal alkenes, namely hydrogenation (to give chlorins and bacteriochlorins) and participation in pericyclic reactions (*e.g.* cheletropic reactions with carbenes[4a,5] and concerted reaction with $OsO_4$ to give β,β′-dihydroxychlorins[6]). These observations prompted us to investigate the possible participation of these peripheric double bonds in [4 + 2] cycloadditions, as the 2π electrons component, with very reactive dienes. In fact, we have found that porphyrins behave as dienophiles in the presence of *o*-benzoquinodimethane **3** (a highly reactive diene generated *in situ* by thermal extrusion of $SO_2$ from sulfone **2**) giving chlorins **4** (Scheme 1).†




**Scheme 1**

After heating a solution of *meso*-tetraphenylporphyrin (TPP **1a**, 20 mg) and sulfone **2** (55 mg, 10 equiv.) in 1,2,4-trichlorobenzene (5 ml) at reflux for 7 h under a nitrogen atmosphere, the TLC of the reaction mixture revealed unchanged starting porphyrin and three new compounds. The product with higher $R_f$ and the unchanged starting porphyrin were separated from the other two products by column chromatography (silica); in this way two fractions were obtained. The products in each fraction were then separated by preparative TLC. The main product (26% yield), the one that runs immediately below TPP, was identified as the chlorin **4a**, on basis of its mass, $^1$H and $^{13}$C NMR and visible spectra.‡ Compound **4a** displays $C_2$ symmetric $^1$H and $^{13}$C NMR spectra. The two protons H$^c$ and the two protons H$^b$ appear as doublets of doublets, respectively, at δ 2.62 (*J* 8.3 and 14.2 Hz) and 2.80 (*J* 5.8 and 14.2 Hz). The two H$^a$ protons appear as a multiplet at δ 5.32. The $^{13}$C NMR spectrum shows only 22 signals, which correspond to 'half' of the molecule. From these, two signals correspond to sp$^3$ carbons: δ 33.3 (benzylic carbons) and 48.0 (pyrroline carbons). The mass spectrum shows intense peaks at *m*/*z* 719 ([M + H]$^+$) and 718 ([M]$^+$), and one peak at *m*/*z* 614 (corresponding to TPP, formed by retro-Diels–Alder reaction). The visible spectrum of **4a** also confirms the chlorin-type structure ($\lambda_{max}$ 653 nm).

The product with higher $R_f$, the one runing slightly above TPP, was obtained in 20% yield; its mass spectrum (LSIMS) shows a base peak with *m*/*z* 715 and its visible spectrum shows a pronounced red shift of both Soret and Q bands ($\lambda_{max}$ 442, 525, 555, 606, 662 nm) relative to TPP, as expected for an extended conjugation of the porphyrin π-system. These data indicate that this compound is the naphtho[2,3-*b*]porphyrin **5a**,[7] formed by the autoxidation of chlorin **4a**. This compound was also obtained quantitatively by refluxing a $CHCl_3$ solution of chlorin **4a** with 2,3-dichloro-5,6-dicyano-1,4-benzoquinone (DDQ). The third product, the one with smaller $R_f$ obtained in 20% yield, shows a parent ion at *m*/*z* 717 ([M + H]$^+$) in its mass spectrum and a UV–VIS spectrum very similar to that of TPP.

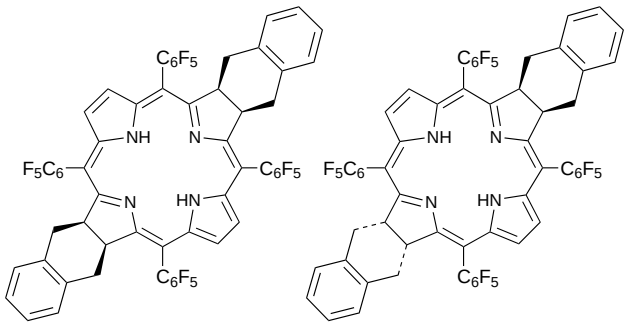


These data are in agreement with structure **6a**, a likely intermediate in the oxidation of **4a** to the naphthoporphyrin **5a**.

Similar results were obtained when porphyrins **1b** and **1c** were used. In both cases, the corresponding chlorins **4**, naphthoporphyrins **5** and porphyrins **6** could be isolated and characterized.

When *meso*-tetra(pentafluorophenyl)porphyrin **1d** was used as dienophile three products were also obtained, together with some unchanged **1d** (*ca*. 35%). The one with intermediate $R_f$ (silica) was identified as the chlorin **4d** on the basis of its $^1$H NMR, mass and electronic spectra.

The two other products show similar mass and electronic spectra, suggesting that they are diastereoisomers (**7**-*cis* and **7**-*trans*).§ Both compounds show the same parent ion at *m*/*z*




**7**-*cis* **7**-*trans*

1183 (FAB$^+$) indicating the addition of two *o*-benzoquinodimethanes per molecule of porphyrin. From the electronic spectra of these 2 : 1 adducts ($\lambda_{max}$ 747 and 761 nm, Fig. 1), it is evident that they are bacteriochlorins (opposite bis-addition) and not isobacteriochlorins (adjacent bis-addition). The $^1$H NMR spectrum of the major isomer (the one with higher $R_f$) is also in agreement with structures **7**. The formation of these bacteriochlorins is in accord with other previous studies; Callot[5] observed opposite bis-addition of methoxycarbonylcarbene to TPP and Cavaleiro *et al.*[4b] have shown that in the Diels–Alder reactions of divinylporphyrins with dienophiles, the formation of bacteriochlorins is more thermodynamically favourable than the formation of isobacteriochlorins.

The addition to porphyrin **1d**, and not to the other ones, of two *o*-benzoquinodimethane species is not an unexpected result since it is known that *o*-quinodimethanes react more easily with electron-deficient dienophiles and, in this respect, porphyrin **1d** is much more 'electron-deficient' than porphyrins **1a**–**c**.

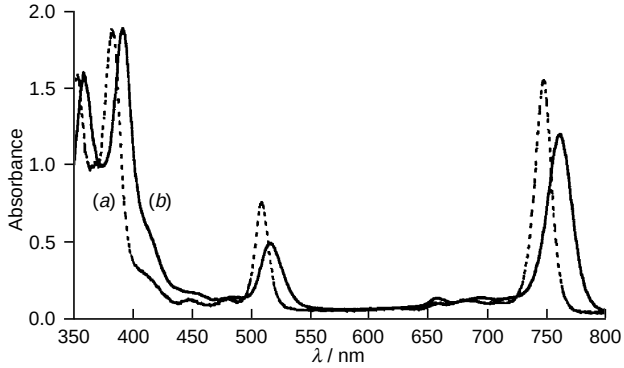



**Fig. 1** Electronic spectra of bacteriochlorins **7**: (*a*) main isomer, (*b*) minor isomer

This work was also extended to 5,15-disubstituted arylporphyrins. In this case it was found that 5,15-bis(*p*-methoxyphenyl)porphyrin also reacts with *o*-benzoquinodimethane **3** to yield the corresponding chlorin as the main product, which was characterized by $^1$H NMR, UV–VIS and mass spectral techniques.

Bacteriochlorins **7** (or other synthetic analogues), because of their strong absorption bands at 747 and 761 nm (Fig. 1) can be considered as potential new photosensitizers in PDT studies. Work is in progress in our laboratory to extend these studies to other *o*-quinodimethanes, especially certain heterocyclic ones, and to other porphyrins.

We thank JNICT, Lisbon, for funding the Research Unit No. 62/94, and the departamental MS and NMR services for spectra.

## Footnotes

* E-mail: jcavaleiro@dq.ua.pt

† Our preliminary results from the reaction of TPP with heterocyclic *o*-quinodimethanes show that this type of reaction can be successfully applied to the syntheses of heterocyclic-fused chlorins.

‡ *Spectroscopic data* for **4a**: $^1$H NMR (300 MHz, $CDCl_3$): δ −1.59 (s, 2 H, NH), 2.62 (dd, 2 H, H$^c$, *J* 8.3 and 14.2), 2.80 (dd, 2 H, H$^b$, *J* 5.8 and 14.2), 5.32 (m, 2 H, H$^a$), 6.75 (m, 2 H), 6.99 (m, 2 H), 7.62–7.85 (m, 12 H), 7.99–8.30 (m, 10 H), 8.40 (m, 2 H), 8.56 (d, 2 H, *J* 5.0); $^{13}$C NMR (75 MHz, $CDCl_3$): δ 33.3, 48.0, 112.6, 122.5, 124.0, 126.1, 126.8, 127.4, 127.6, 127.8, 128.3, 131.9, 132.2, 133.9, 134.3, 135.3, 138.9, 141.1, 142.0, 142.3, 152.5, 168.0; MS (FAB$^+$) 719 (M + H)$^+$, 718 (M)$^+$, 614 (TPP); $\lambda_{max}$($CHCl_3$)/nm (log ε) 420 (5.27), 521 (4.12), 551 (3.99), 559 (3.76), 653 (4.36).

§ *Spectroscopic data* for the most abundant isomer **7**: $^1$H NMR (300 MHz, $CDCl_3$): δ −1.65 (s, 2 H, NH), 2.78–2.96 (m, 8 H, H$^b$ + H$^c$), 5.03 (m, 4 H, H$^a$), 6.85–6.94 (m, 8 H, $C_6H_4$), 8.00 (d, 4 H, β-H, *J* 1.1 Hz); $\lambda_{max}$($CHCl_3$)/nm 747; MS (FAB$^+$) 1183 (M + H)$^+$.

## References

1 R. Bonnet, *Chem. Soc. Rev.*, 1995, **24**, 19.
2 S. Wan, J. A. Parrish, R. R. Anderson and M. Madden, *Photochem. Photobiol.*, 1991, **34**, 679.
3 R. K. DiNello and D. Dolphin, *J. Org. Chem.*, 1980, **45**, 5196; A. R. Morgan, V. S. Pangka and D. Dolphin, *J. Chem. Soc., Chem. Commun.*, 1984, 1047; V. S. Pangka, A. R. Morgan and D. Dolphin, *J. Org. Chem.*, 1986, **51**, 1094; P. Yong-Hin, T. P. Wijesekera and D. Dolphin, *Tetrahedron Lett.*, 1989, **30**, 6135; A. R. Morgan and D. H. Kohli, *Tetrahedron Lett.*, 1995, **36**, 7603; M. A. F. Faustino, M. G. P. M. S. Neves, M. G. H. Vicente, A. M. S. Silva and J. A. S. Cavaleiro, *Tetrahedron Lett.*, 1996, **37**, 3569.
4 (*a*) H. J. Callot, A. W. Johnson and A. Sweeney, *J. Chem. Soc., Perkin Trans. 1*, 1973, 1424; (*b*) J. A. S. Cavaleiro, A. H. Jackson, M. G. P. M. S. Neves and K. R. N. Rao, *J. Chem. Soc., Chem. Commun.*, 1985, 776; (*c*) P. Yong-Hin, T. P. Wijesekera and D. Dolphin, *Tetrahedron Lett.*, 1991, **32**, 2875; (*d*) R. K. Pandey, F.-Y. Shiau, K. Ramachandran, T. J. Dougherty and K. M. Smith, *J. Chem. Soc., Perkin Trans. 1*, 1992, 1377.
5 H. J. Callot, *Tetrahedron Lett.*, 1972, 1011.
6 H. Scheer and H. Inhoffen, *Hydroporphyrins: Reactivity, Spectroscopy, and Hydroporphyrin Analogues*, in *The Porphyrins*, ed. D. Dolphin, Academic Press, New York, 1978, vol. 2, part B, p. 77.
7 The synthesis and characterisation of *meso*-unsubstituted naphtho[1,2-*b*]porphyrins and dinaphthoporphyrins was recently reported: T. D. Lash and T. J. Roper, *Tetrahedron Lett.*, 1994, **35**, 7715; D. T. Lash and C. P. Denny, *Tetrahedron*, 1995, **51**, 59; T. D. Lash, C. Wijesinghe, A. T. Osuma and J. R. Patel, *Tetrahedron Lett.*, 1997, **38**, 2031.

*Received in Liverpool, UK, 11th April 1997; Com. 7/02504A*

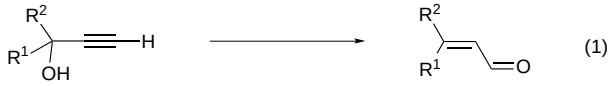
# Selective isomerisation of prop-2-yn-1-ols into α,β-unsaturated aldehydes catalysed by Ru[η³-$CH_2C(Me)CH_2]_2(Ph_2PCH_2CH_2PPh_2$)

**Michel Picquet, Christian Bruneau and Pierre H. Dixneuf***

*Laboratoire de Chimie de Coordination et Catalyse, UMR 6509: CNRS, Université de Rennes, Campus de Beaulieu, F-35042 Rennes, France*

**The complex Ru[η³-$CH_2C(Me)CH_2]_2(Ph_2PCH_2CH_2PPh_2$) is an efficient catalyst precursor for the isomerisation of prop-2-yn-1-ols into conjugated enals under mild conditions in the presence of benzoic acid *via* (*Z*)-3-hydroxyprop-1-en-1-yl benzoates.**

The isomerisation of propynylic alcohols into α,β-unsaturated aldehydes has the potential to offer access to a variety of terpenoids, *e.g.* vitamin A derivatives, as well as perfume and cosmetic components[1,2] [eqn. (1)].



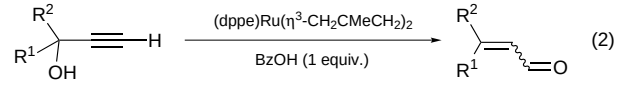
(1)

Such a transformation was first performed in the Meyer–Schuster reaction,[3] which was carried out in acidic medium and catalysed by strong acids.[4] The emergence of metal complex catalysis has allowed the use of catalytic systems based on vanadium(V) oxides[5] or the $Ti(OR)_4$–CuCl–$RCO_2H$ association,[6] operating under milder conditions but still at 125–160 °C. The system $Bu_4NReO_4$–$MeC_6H_4SO_3H$[7] gives isomerisation at room temperature with alcohol dehydration as a side reaction. A new system $MoO_2(acac)_2$–$R_2SO$–$ArCO_2H$ operates at 100 °C and appears to be efficient for the formation of prenal.[8] With these metal oxide catalysts, the suggested key steps involve the coordination of the prop-2-ynylic alcohol oxygen atom to the metal and addition of the metal oxide oxygen atom to the alkyne C(1) carbon atom to generate an allenyloxy intermediate. However, in these reactions the required presence of an acid has never been clearly taken into account in the proposed mechanisms.

We now report a new, efficient method for transformation of prop-2-yn-1-ols into α,β-unsaturated aldehydes catalysed by a (diphosphine)ruthenium(II) complex in the presence of benzoic acid, and we show that the key step involves the regioselective catalytic addition of the carboxylate to the terminal carbon atom of the C≡C triple bond, giving a (*Z*)-3-hydroxyprop-1-en-1-yl benzoate intermediate, followed by thermal elimination of the acid.

The ruthenium(II) electrophilic activation concept[9] has allowed the selective preparation of enol esters[10] and furans[11] from terminal alkynes, and β-oxopropyl esters from prop-2-yn-1-ols.[12] Modification of the catalyst precursors has recently made possible control of the regio- and stereo-selective anti-Markovnikov addition of carboxylic acids to terminal alkynes to give (*Z*)-alk-1-en-1-yl carboxylates.[13,14] An attempt to adapt the latter reaction to the addition of benzoic acid to the terminal sp carbon of prop-2-yn-1-ols in the presence of (diphosphine)-ruthenium(II) catalysts led us to discover the formal selective isomerisation of prop-2-yn-1-ylic alcohols into α,β-unsaturated aldehydes [eqn. (2)].

The reaction of the prop-2-yn-1-ol **1a** ($R^1$, $R^2$ = Me) with 1 equiv. of benzoic acid in the presence of 1 mol% of Ru[η³-$CH_2C(Me)CH_2]_2$(dppe) **I** (dppe = $Ph_2PCH_2CH_2PPh_2$) at 70 °C for 15 h led to the complete transformation of **1a**. Distillation of



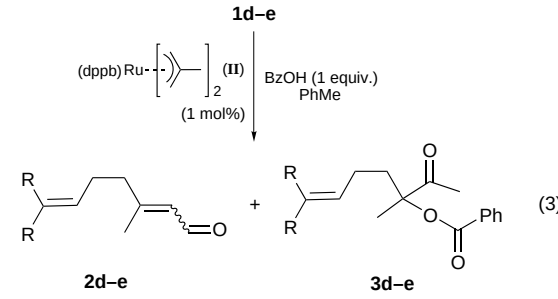
(2)

**1a–f** **2a–f**

**a** $R^1 = R^2$ = Me **d** $R^1$ = Me, $R^2 = CH_2CH_2CH{=}CH_2$
**b** $R^1$ = Me, $R^2$ = Ph **e** $R^1$ = Me, $R^2 = CH_2CH_2CH{=}CMe_2$
**c** $R^1$ = Me, $R^2 = Pr^i$ **f** $R^1 = R^2$ = Ph

the crude product led to the sole α,β-unsaturated aldehyde **2a** (prenal), isolated in 56% yield (method A). Complete transformation of the disubstituted prop-2-ynylic alcohols **1b** and **1c** in toluene under similar conditions led after distillation to the unsaturated aldehydes **2b** (68%) and **2c** (37%) (Table 1). Both isomers were formed in the respective ratios *Z*/*E* = 2 : 1 (**2b**) and 3 : 4 (**2c**). The unsaturated prop-2-yn-1-ols **1d** and **1e** were good substrates for this isomerisation as they led to the best yields in **2d** (75%) and in the terpenoid citral **2e** (73%), formed as a mixture of the *Z* and *E* isomers in the ratio 1 : 2 (Table 1).

This reaction is also catalysed by the analogous Ru[η³-$CH_2$-$C(Me)CH_2]_2$(dppb) complex **II** [dppb = $Ph_2P(CH_2)_4PPh_2$] but the competitive formation of the β-oxopropyl ester **3** was observed [eqn. (3)]. Thus, the reaction of **1e** with BzOH and 1 mol% of **II** afforded **2e** in 18% and **3e** in 50% yield, and **1d** gave 65% of **3d** only.



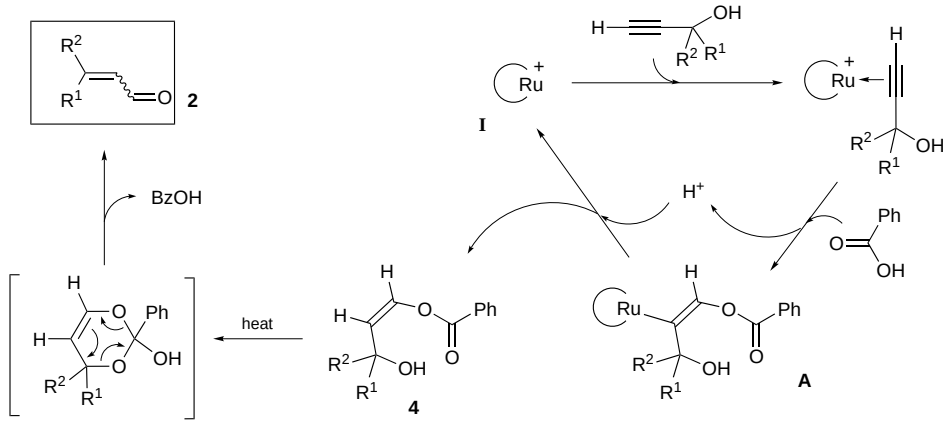
(3)

**2d–e** **3d–e**

**1e** R = Me → **2e** (18%) + **3e** (50%)
**1d** R = H → **2d** (traces) + **3d** (65%)

The formation of the keto esters **3** corresponds to the known catalytic addition of benzoate to the C(2) carbon of the triple bond followed by intramolecular transesterification.[12] By contrast, the mechanism of the isomerisation **1** → **2** can be proposed as depicted in Scheme 1. As the catalyst **I** is a known precursor favouring the *trans*-anti-Markovnikov addition of carboxylic acids to terminal alkynes,[13,14] the intermediate **A** corresponding to this first step is likely formed. Its protonolysis leads to the (*Z*)-3-hydroxyprop-1-en-1-yl benzoate **4** which gives the α,β-enal **2** *via* thermal elimination of benzoic acid during distillation (Scheme 1).

This process has been demonstrated in the case of **1a** with the following experiments which were monitored by $^1H$ NMR spectroscopy: (i) the reaction of **1a** with benzoic acid at 70 °C without a solvent in the presence of the catalyst **I** (1 mol%) gave the complete transformation of the propynol **1a** after 2 h into **2a**



**Scheme 1**

**Table 1** Ruthenium-catalysed isomerisation of prop-2-yn-1-ols[a]

| | | Yield (%) (*Z*/*E*) | |
|---|---|---|---|
| Prop-2-yn-1-ol | Enal | Method A | Method B |
| **1a** | **2a** | 56[b] | 68[b] |
| **1b** | **2b** | 68 (2:1) | 61 (2:1) |
| **1c** | **2c** | 37 (3:4) | — |
| **1d** | **2d** | 75 (1:2) | — |
| **1e** | **2e** | 73 (1:2) | 81 (2:3) |
| **1f** | **2f** | — | 79[c] |

[a] General conditions: prop-2-yn-1-ol (2.5 mmol), benzoic acid (2.5 mmol), catalyst **I** (1 mol%), toluene (2 ml). Method A: 70 °C, 15 h, distillation under reduced pressure. Method B; 70 °C, 2 h, then 100 °C for 3 h (**2a**), 15 h (**2e**), 22 h (**2b**) and 32 h (**2f**), distillation under reduced pressure. [b] Without solvent. [c] Chromatography over silica gel.

and **4a** (*Z*/*E* = 86 : 14) formed in 7 and 93% yields, respectively, as determined by $^1$H NMR of the crude mixture before distillation; (ii) heating at 100 °C for 3 h of the latter crude mixture containing **2a** and **4a** led to 96% of prenal **2a** (measured by $^1$H NMR spectroscopy) and isolated in 68% yield. These experiments show that the role of the catalyst is to generate the 3-hydroxyalk-1-en-1-yl benzoate **4a**, and that heating of the latter at 100 °C or during distillation in the presence or absence of the ruthenium derivative is the key step for the transformation of **4a** into the unsaturated aldehyde **2a**.

This sequential heating of the reaction mixture in the presence of catalyst **I**, first at 70 °C (catalytic anti-Markovnikov addition) and then at 100 °C (thermal benzoic acid elimination) appears to be the best method to selectively produce α,β-enals (method B). Thus, **1b**, **1e** and **1f** were converted into 3-hydroxyprop-1-en-1-yl benzoates **2** after treatment with benzoic acid in the presence of a catalytic amount of **I** at 70 °C for 2 h, and further heating in the same pot at 100 °C for 22, 15 and 32 h led to the complete transformation of (*Z*)-**4** and the isolation of the α,β-unsaturated aldehydes **2b**, **2e** and **2f** in 61, 81 and 79% respective yields (Table 1). The $^1$H NMR spectroscopic monitoring revealed that only the (*Z*)-esters **4** were converted into α,β-enals **2** on heating, whereas the (*E*)-isomers remained almost unchanged except in the case of **4a**. For example, from **1b**, after 2 h at 70 °C, the catalytic reaction afforded 100% of **4b** (*Z*/*E* = 70 : 30) which led after 22 h at 100 °C to 74% of **2b** (*Z*/*E* = 66 : 34) and 26% of (*E*)-**4b**.

The selective synthesis of α,β-unsaturated aldehydes requires the initial regioselective anti-Markovnikov addition of the benzoate to the triple bond, which raises the question of whether such a key step might also be involved in the previous isomerisations of propynylic alcohols promoted by metal oxides.

## Footnote

* E-mail: pierre.dixneuf@univ-rennes1.fr

## References

1 G. Ohloff, *Scent and Flagrances*, Springer-Verlag, Berlin, 1994.
2 C. Mercier and P. Chabardès, *Pure Appl. Chem.*, 1994, **66**, 1509.
3 K. H. Meyer and K. Schuster, *Chem. Ber.*, 1922, **55**, 819.
4 S. Swaminathan and K. V. Narayanan, *Chem. Rev.*, 1971, **71**, 429 and references cited therein.
5 H. Pauling, D. A. Andrews and N. C. Hindley, *Helv. Chim. Acta*, 1976, **59**, 1293; M. B. Erman, I. S. Aul'Chenko, L. A. Kheifits, V. G. Dulova, J. N. Novikov and M. E. Vol'pin, *Tetrahedron Lett.*, 1976, **34**, 2984; P. Chabardès, E. Kuntz and J. Varagnat, *Tetrahedron*, 1977, **33**, 1775.
6 P. Chabardès, *Tetrahedron Lett.*, 1988, **48**, 6253.
7 K. Narasaka, H. Kusama and Y. Hayashi, *Chem. Lett.*, 1991, 1413.
8 C. Y. Lorber and J. A. Osborn, *Tetrahedron Lett.*, 1996, **37**, 853.
9 C. Bruneau and P. H. Dixneuf, *Chem. Commun.*, 1997, 507.
10 C. Bruneau, M. Neveux, Z. Kabouche and P. H. Dixneuf, *Synlett*, 1991, 755.
11 B. Seiller, C. Bruneau and P. H. Dixneuf, *Tetrahedron*, 1995, **51**, 13 089.
12 C. Bruneau, Z. Kabouche, M. Neveux, B. Seiller and P. H. Dixneuf, *Inorg. Chim. Acta.*, 1994, **222**, 155.
13 H. Doucet, B. Martin-Vaca, C. Bruneau and P. H. Dixneuf, *J. Org. Chem.*, 1995, **60**, 7247.
14 H. Doucet, J. Höfer, N. Derrien, C. Bruneau and P. H. Dixneuf, *Bull. Soc. Chim. Fr.*, 1996, **133**, 939.

*Received in Liverpool, UK, 3rd March 1997; Com. 7/01495C*

# Environmentally friendly catalysis using supported reagents: the fast and selective bromination of aromatic substrates using supported zinc bromide[1]

**James H. Clark,*[a] Joanne C. Ross,[a] Duncan J. Macquarrie,[a] Simon J. Barlow[b] and Tony W. Bastock[b]**

[a] *Department of Chemistry, University of York, Heslington, York, UK YO1 5DD*
[b] *Contract Catalysts Ltd., Knowsley Industrial Park, Prescot, Merseyside, UK L34 9HY*

**Zinc bromide supported on mesoporous silica or acid-activated montmorillonite is a fast, efficient, selective and reusable catalyst for the *para*-bromination of activated and moderately deactivated aromatic substrates.**

Bromoaromatics are widely used as intermediates in the manufacture of pharmaceuticals, agrochemicals and other speciality chemical products. Traditional methods of aromatic bromination involve the use of non-selective hazardous acidic reagents such as mineral acids and metal halides, which can lead to separation difficulties and unacceptable levels of toxic and corrosive waste. The replacement of such reagents by non-toxic and more selective solid catalysts is very desirable and represents an important goal in the context of Clean Synthesis.[2,3] While some progress has been made in this area, notably through the use of microporous zeolites, improvements in reaction selectivity are at the expense of poor reaction rates or the need for large quantities of catalyst.[4,5] We have discovered that good regioselectivity and excellent reaction rates in the bromination of activated and moderately deactivated aromatics can be achieved through the use of supported zinc bromide catalysts.[6]

Bromination of bromobenzene using elemental bromine in $CCl_4$ in the dark proceeds slowly in the absence of an added catalyst. At 25 °C only 10% conversion of substrate is achieved after 24 h with a selectivity (*p*/*o* isomer ratio) of 4.1. Rates improve at higher temperatures but at the expense of selectivity and complete conversion of substrate within 24 h is only achieved at 76 °C when the formation of tribromobenzene further complicates the reaction. In the presence of 0.067 equiv. of zinc bromide supported on the acid-activated montmorillonite K10 (1.0 mmol $g^{-1}$; catalyst prepared from methanol in the same way as 'clayzic'[7] and dried at 200 °C before use), complete substrate conversion is achieved at 25 °C within 8 h and with a much improved selectivity of 9.6. At higher temperatures, the reaction rate increases but the selectivity falls (Table 1). We then screened a range of commonly used support materials as supports for zinc bromide (Table 1). Of these, mesoporous silica gel gives the best selectivity, along with a good rate of reaction. It is interesting to note that the same type of support proved to be the most effective in developing the Friedel–Crafts catalyst clayzic.[7]

While $CCl_4$ has commonly been used as a solvent in many halogenation reactions, environmental legislation will preclude its use in the future. We next tested likely non-polar and low-polarity alternative solvents (Table 1) and have found that of the non-halogenated solvents, hexane gives a good reaction rate and a reasonable selectivity.

As part of the catalyst optimisation studies we have examined the effect of loading of zinc bromide (Fig. 1). Loading clearly has a major effect on catalyst activity. The optimum loading for the K10 analogue is significantly lower than that for the higher surface area[7] silica gel. Catalyst activity on reuse is also an important variable and we have found that the silica-based catalyst only suffers a relatively gradual decrease in activity and selectivity on use (with an apparent increase in selectivity after the first use). It is important that the catalyst is kept solvent damp in between reactions to avoid deactivation of the catalytic sites (by decantation of the reaction liquors followed by recharging with fresh substrate solution). Total turnover efficiencies (total mole substrate converted per mole equivalent

**Table 1** Comparison of catalytic systems for the bromination of bromobenzene[a]

| Catalyst | Solvent | *T*/°C | *t*/min | Conversion of bromobenzene (GC %) | Selectivity (*p*/*o* ratio) |
|---|---|---|---|---|---|
| None | $CCl_4$ | 25 | 24 | 10 | 4.1 |
| None | $CCl_4$ | 50 | 24 | 30 | 3.4 |
| Clayzib[b] | $CCl_4$ | 25 | 8 | 100 | 9.6 |
| Clayzib | $CCl_4$ | 50 | 6 | 100 | 8.6 |
| Clayzib | $CCl_4$ | 76 | 1.5 | 100 | 6.6 |
| $ZnBr_2$ | $CCl_4$ | 25 | 7 | 3.1 | 3.0 |
| Clayzib | $CCl_4$ | 25 | 7 | 85.6 | 8.8 |
| $ZnBr_2$–silica[c] | $CCl_4$ | 25 | 7 | 93.6 | 9.7 |
| $ZnBr_2$–alumina[d] | $CCl_4$ | 25 | 7 | 93.3 | 8.2 |
| $ZnBr_2$–alumina[e] | $CCl_4$ | 25 | 7 | 98.5 | 9.3 |
| Clayzib | $CHCl_3$ | 25 | 7 | 91.5 | 9.1 |
| Clayzib | $CH_2Cl_2$ | 25 | 7 | 93.5 | 11.0 |
| Clayzib | *n*-$C_6H_{14}$ | 25 | 7 | 99.6 | 8.5 |
| Clayzib | c-$C_6H_{12}$ | 25 | 7 | 98.3 | 7.4 |
| $ZnBr_2$–silica[c,f] (1st use) | *n*-$C_6H_{14}$ | 25 | 7 | 100 | 8.7 |
| $ZnBr_2$–silica[c,f] (1st reuse) | *n*-$C_6H_{14}$ | 25 | 7 | 97.9 | 9.2 |
| $ZnBr_2$–silica[c,f] (2nd reuse) | *n*-$C_6H_{14}$ | 25 | 7 | 88.1 | 9.0 |
| $ZnBr_2$–silica[c,f] (3rd reuse) | *n*-$C_6H_{14}$ | 25 | 7 | 81.4 | 8.6 |
| $ZnBr_2$–silica[c,f] | *n*-$C_6H_{14}$ | 25 | 7 | 68.6 | 8.0 |

[a] Reactions carried out using 1.0 mmol $g^{-1}$ $ZnBr_2$ loaded on the dried support from methanol unless stated otherwise. [b] $ZnBr_2$ supported on K10. [c] 100 Å. [d] Neutral. [e] Acidic. [f] 1.75 mmol $g^{-1}$.

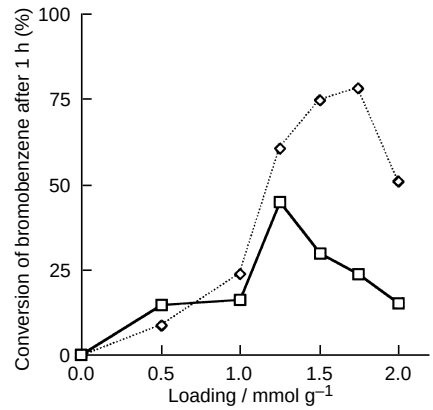



**Fig. 1** Effect of loading of $ZnBr_2$ on (◇) silica (100 Å) and (□) K10 on activity in the bromination of bromobenzene at 25 °C

**Table 2** Bromination of aromatic substrates using $ZnBr_2$–silica (100 Å)[a]

| Substrate | Catalyst | Solvent | *T*/°C | *t*/min | Conversion of substrate (GC %) | Selectivity (*p*/*o* ratio) |
|---|---|---|---|---|---|---|
| PhMe | None | *n*-$C_6H_{14}$ | 25 | 2 | 0.8 | 2.0 |
| PhMe | $ZnBr_2$–silica | *n*-$C_6H_{14}$ | 25 | 2 | 100 | 2.7 |
| PhEt | None | *n*-$C_6H_{14}$ | 25 | 5 | 0.0 | — |
| PhEt | $ZnBr_2$–silica | *n*-$C_6H_{14}$ | 25 | 5 | 68.5 | 2.4 |
| Bu$^t$Ph | None | *n*-$C_6H_{14}$ | 25 | 2 | 0.0 | — |
| Bu$^t$Ph | $ZnBr_2$–silica | *n*-$C_6H_{14}$ | 25 | 2 | 100 | ∞ |
| PhCl | None | *n*-$C_6H_{14}$ | 25 | 80 | 0.0 | — |
| PhCl | $ZnBr_2$–silica | *n*-$C_6H_{14}$ | 25 | 80 | 92.9 | 10.0 |

[a] Reactions carried out using 1.75 mmol $g^{-1}$ $ZnBr_2$ supported on silica (100 Å).

zinc bromide) of $> 40$ over 5 runs can be achieved for 1 h room temperature reactions giving selectivities of $> 8$.

The supported zinc bromide catalysts can be effectively used in the room temperature bromination of other aromatic substrates (Table 2). The bromination of toluene is very slow in the absence of an added catalyst and gives a *p*/*o* ratio (selectivity) of 2.0. On addition of the catalyst [1.75 mmol $g^{-1}$ on silica (100 Å)] there is complete conversion of the substrate within 2 min and an increase in the selectivity to 2.7. The bromination of ethylbenzene is extremely slow in the absence of a catalyst but once the silica–$ZnBr_2$ is added the reaction is complete within 5 min with a selectivity of 2.4. Bromination of *tert*-butylbenzene in the presence of the catalyst is complete within 2 min and has 100% selectivity to the *para*-isomer. For all reactions using alkylbenzene substrates we did not observe any α-brominated products. Chlorobenzene, which is mildly deactivated towards electrophiles, is unaffected by bromine at room temperature but reacts in the presence of the catalyst to give 92.9% conversion to monobrominated products within 80 min with a remarkable selectivity value of 10.

We thank Contract Chemicals Ltd, the EPSRC and the Royal Academy of Engineering (for a Clean Technology Fellowship to J. H. C.) and the Royal Society (for a Research Fellowship to D. J. M.) for financial support and other members of the Envirocats™ and York Clean Synthesis Groups for helpful discussions.

## References

1 UK patent applied for.
2 ed. J. H. Clark, *Chemistry of Waste Minimisation*, Chapman and Hall, London, 1995.
3 R. A. Sheldon, *Chem. Ind.*, 1996, **1**, 12.
4 P. Ratnasamy, A. P. Singh and S. Sharma., *Appl. Catal. A*, 1996, **135**, 25.
5 K. Smith and D. Bahzad, *Chem. Commun.*, 1996, 467.
6 J. H. Clark and D. J. Macquarrie, *Chem. Soc. Rev.*, 1996, 303.
7 J. H. Clark, S. R. Cullen, S. J. Barlow and T. W. Bastock, *J. Chem. Soc., Perkin Trans. 2*, 1994, 1117.

*Received in Cambridge, UK, 8th April 1997; Com. 7/02399E*

# Catalytic and asymmetric cyclopropanation of styrenes catalysed by ruthenium porphyrin and porphycene complexes

**Wai-Cheung Lo,[a] Chi-Ming Che,*[a] Kin-Fai Cheng*[a] and Thomas C. W. Mak[b]**

[a] *Department of Chemistry, The University of Hong Kong, Pokfulam Road, Hong Kong*
[b] *Department of Chemistry, The Chinese University of Hong Kong, Shatin, New Territories, Hong Kong*

**Ruthenium porphyrin and porphycene complexes catalyse stereospecific cyclopropanation of styrenes; high product turnovers with up to 90.8% ee were achieved with the [Ru(P*)(CO)(EtOH)] catalyst ($H_2$P* = chiral $D_4$ porphyrin).**

Metalloporphyrins are well known to be effective catalysts for alkane hydroxylation,[1] olefin epoxidation[2] and cyclopropanation.[3–5] When compared to metallosalens, porphyrin catalysts usually have a greater catalytic stability resulting in higher product turnover numbers.[6] However, their practical applications would require high regio-, stereo- and enantio-selectivities to be achieved. To our knowledge, the best reported chiral metalloporphyrins are the manganese threitol-strapped porphyrins[7] and the iron 'twin-coronet' porphyrins[8] which gave 88 and 89% ee in the epoxidation of 1,2-dihyronaphthalene and 2-nitrostyrene by iodosobenzene, respectively. Herein is described that ruthenium porphyrin and porphycene complexes are effective catalysts for stereospecific cyclopropanation of styrenes. With the $D_4$ porphyrin ($H_2$P*) reported by Halterman and Jan,[9] it is possible to achieve high product turnovers and with up to 90.8% ee which is comparable to the best ee reported with the non-porphyrin chiral metal catalysts.[10–14]

The [Ru(P)(CO)(EtOH)] catalysts (Fig. 1) used in this work were prepared by literature methods.[15,16] Refluxing [$Ru_3(CO)_{12}$] with $H_2$P* in decalin for 8 h gave [Ru(P*)(CO)] in a 90% yield, which was recrystallised from a $CH_2Cl_2$–EtOH mixture to give [Ru(P*)(CO)(EtOH)]. Its structure determined by a X-ray crystal analysis features one of the few structures of chiral ruthenium porphyrins.[17] As shown in Fig. 2, the porphyrin ligand has a pseudo $D_4$ symmetry. The ruthenium atom coordinates with one CO and one EtOH in the axial direction and is in the centre of the mean plane defined by the four nitrogen atoms of the porphyrin ligand. There are two $CH_2Cl_2$ and one EtOH solvent molecules in the unit cell with 0.5 site occupancy. Hydrogen bonding interactions exists between the coordinated EtOH and the EtOH solvent molecules with O–O distance of 2.8 Å in the unit cell. The measured C(85)–O(1) and Ru–O(Et) distances of 1.188(2) and 2.241(2) Å, respectively are comparable to the corresponding values of 1.16(3) and 2.21(2) Å found in [Ru(TPP)(CO)(EtOH)].[18]

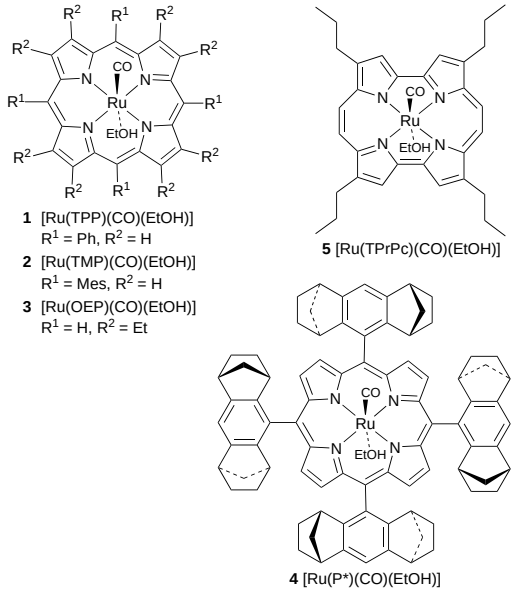



**Fig. 1** Ruthenium porphyrinoid complexes used in the catalytic cyclopropanation of alkenes

The [Ru(P)(CO)(EtOH)] complexes are excellent catalysts for the cyclopropanation of some styrenes by ethyl diazoester (EDA) with very good diastereoselectivities. The results are listed in Table 1. At a catalyst : EDA : alkene ratio of 1 : 300 : 600, the product yields based on EDA are moderate to good for **1** and **2** but the reactions become less effective for the less bulky catalysts **3** and **5**. A notable point is the high *trans* product selectivity. For example, the *trans* : *cis* ratio of 9.2 obtained from the reaction between styrene and EDA catalysed by **1** is comparable to the value of 9.5 obtained from the same reaction catalysed by [Os(TPP)(CO)(py)][3] but is considerably higher than that of 1.1 by Rh(TPP)I.[4]

In order to optimize the product yield, the reaction between 1,1-diphenylethylene and EDA catalysed by **1** was investigated. The product yield was found to increase with increasing ratio of alkene : EDA. The effectiveness of the catalyst in cyclopropanation is clearly demonstrated by the very high turnover number of 1855 and yield of 92.3% achieved at a catalyst : EDA : diphenylethylene ratio of 1 : 2000 : 20 000.

The ruthenium porphyrins catalysed the cyclopropanation of alk-1-enes and 1,1-disubstituted olefins very efficiently, but alkenes with other substitution patterns were poor substrates. *cis*- or *trans*-β-Methylstyrene could not be cyclopropanated. This shape selectivity is reminiscent of that observed for Os(TTP)-catalysed cyclopropanation[3] but constrasts with the much broader substrate compatibility of rhodium porphyrin-catalysed reactions.[5] In the latter case, only tetrasubstituted alkenes are sluggish substrates.

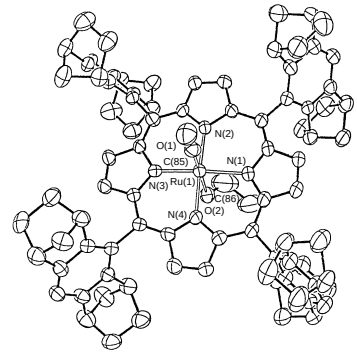


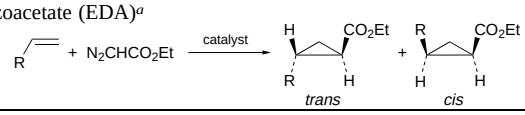

**Fig. 2** Perspective view of [Ru(P*)(CO)(EtOH)]. Selected bond lengths (Å) and angles (°): Ru(1)–N(1) 2.082(2), Ru(1)–N(2) 2.068(2), Ru(1)–N(3) 2.043(2), Ru(1)–N(4) 2.057(2), Ru(1)–C(85) 1.776(2), Ru(1)–O(2), 2.241(1), O(2)–C(86) 1.437(2), C(85)–O(1) 1.188 Å; N(1)–Ru(1)–N(2) 89.6(1), N(1)–Ru(1)–N(3) 173.7(1), N(2)–Ru(1)–N(3) 90.6(1), N(1)–Ru(1)–N(4) 88.9(1), N(2)–Ru(1)–N(4) 174.4(1), N(3)–Ru(1)–N(4) 90.3(1), Ru(1)–C(85)–O(1) 178.4(2)°.

The catalytic enantioselective cyclopropanation of alkenes was investigated using the ruthenium complex of a $D_4$-symmetric porphyrin (Fig. 1). The results are shown in Table 2. The absolute configuration of the product from the reaction between styrene and EDA was determined by comparison with literature data.[10]

With styrene as substrate and at room temperature, a product *trans* : *cis* ratio of 18 : 1 was obtained and the ee of the *trans* product was 87% with absolute configuration of (1*S*,2*S*). A high catalyst turnover number of 1665 was achieved. At 0 °C, the *trans*–*cis* selectivity improved to 24 : 1 and ee of the *trans* product increased to 91%. Similar results with very high *trans*–*cis* selectivities and high enantioselectivities for the *trans* product have also been found with other substituted styrenes. Thus, the bulky aryl groups appended on the porphyrin ring of the catalyst **4** can produce a good steric and chiral environment around the reaction site. The reactive intermediate of the cyclopropanation has also been studied. The reaction of **4** with EDA in benzene at room temperature immediately gave a species showing $\lambda_{max}$ at 407 and 534 nm observed by UV–VIS spectroscopy. This species was unstable and was observed to decay gradually. When monitored with $^1$H NMR, singlets at δ 13.79 and 8.99 were observed. This intermediate species can be tentatively assigned as the carbene complex [Ru(P*)(CH-$CO_2$Et)], with the NMR peaks at δ 13.79 and 8.99 being assigned to the carbene and the pyrrolic protons, respectively. These values are similar to the respective NMR peaks at δ 13.79 and 8.55 of [Ru(TMP)($CHCO_2$Et)].[19] The present work highlights that chiral ruthenium carbene complexes of porphyrins could be generated and spectroscopically characterised.

We acknowledge support from the University of Hong Kong and the Hong Kong Research Grants Council.

**Table 1** Ruthenium catalysed cyclopropanation of alkenes with ethyl diazoacetate (EDA)[a]




| Alkene | Catalyst | Product Yield (%)[b] | *trans* : *cis*[c] | Catalyst turnovers[d] |
|---|---|---|---|---|
| Styrene | **1** | 45 | 9.2 : 1 | 135 |
| | **2** | 68 | 7.7 : 1 | 198 |
| | **3** | 25 | 12 : 1 | 62 |
| | **5** | 39 | 11 : 1 | 117 |
| 4-Methylstyrene | **1** | 58 | 11.2 : 1 | 176 |
| | **2** | 66 | 7.5 : 1 | 208 |
| | **3** | 36 | 9.6 : 1 | 114 |
| | **5** | 52 | 9.9 : 1 | 162 |
| 4-Methoxystyrene | **1** | 71 | 8.1 : 1 | 214 |
| | **2** | 81 | 7.3 : 1 | 252 |
| | **3** | 41 | 5.8 : 1 | 121 |
| | **5** | 44 | 7.2 : 1 | 133 |
| 4-Chlorostyrene | **1** | 44 | 13.7 : 1 | 138 |
| | **2** | 53 | 10.5 : 1 | 164 |
| | **3** | 23 | 11.0 : 1 | 67 |
| | **5** | 21 | 12.3 : 1 | 63 |
| α-Methylstyrene | **1** | 50 | 2.8 : 1 | 155 |
| | **2** | 68 | 1.7 : 1 | 225 |
| | **3** | 36 | 2.0 : 1 | 106 |
| | **5** | 23 | 2.7 : 1 | 60 |

[a] Reaction conditions: catalyst : EDA : alkene = 1 : 300 : 600, $CH_2Cl_2$, room temp., *ca.* 8 h for addition of EDA then stirring for 8–12 h. [b] Isolated product yields based on EDA. [c] Determined by HPLC. [d] Calculated as the amount of cyclopropyl esters divided by the amount of catalyst.

**Table 2** Enantioselective cyclopropanation of alkenes with EDA using **2** as catalyst[a]

| Alkene | Product Yield (%) | *trans* : *cis* | *trans* % ee[c] | *cis* % ee[c] | Turnover number |
|---|---|---|---|---|---|
| Styrene | 83 | 17.8 : 1 | 86.5 (1*S*,2*S*) | 3.8 | 1665 |
| Styrene[b] | 63 | 23.6 : 1 | 90.8 (1*S*,2*S*) | 4.0 | 1267 |
| α-Methylstyrene | 69 | 3 : 1 | 87 | 35 | 1384 |
| 1,1-Diphenylethylene | 76 | — | 81 | | 1532 |
| 4-Chlorostyrene | 66 | 23.1 : 1 | 90.4 | 4.0 | 1328 |
| 4-Methylstyrene | 78 | 18.0 : 1 | 80.8 | 8.6 | 1570 |
| 4-Methoxystyrene | 61 | 15.3 : 1 | 85.4 | 8.0 | 1235 |

[a] Reaction conditions same as Table 1, except catalyst : EDA : alkene = 1 : 2000 : 10 000. [b] Reaction temp. = 0 °C. [c] Determined by chiral HPLC.

## Footnotes

* E-mail: cmche@hkucc.hku.hk

† *Crystal data* for [Ru($C_{84}H_{76}N_4$)CO·EtOH]·$CH_2Cl_2$·0.5(EtOH): $C_{89}H_{87}Cl_2N_4O_{2.5}Ru$, $M$ = 1428.6, monoclinic, space group $P2_1$, $a$ = 9.849(1), $b$ = 28.164(2), $c$ = 14.399(1) Å, β = 102.83(1)°, $U$ = 3894(2) Å$^3$, $Z$ = 2, $D_c$ = 1.214 g cm$^{-3}$, λ (Mo-Kα) = 0.71073 Å, $F$(000) = 1492, μ = 3.20 cm$^{-1}$, crystal dimensions 0.40 × 0.40 × 0.40 mm. Intensity data (3.0 < 2θ < 55.0°) were collected on a Rigaku RAXIS IIc imaging-plate system using Mo-Kα radiation (λ = 0.71073 Å) from a RU-200 rotating-anode X-ray generator at room temperature. The data were corrected for absorption and Lorentz polarisation effects. The structure was solved by direct methods and refined by full-matrix least-squares using Siemens SHELXTL PLUS (PC Version). The H-atoms were generated geometrically. 13493 Independent reflections were obtained. 12118 Reflections with $|F_0| > 6.0\sigma(|F_0|)$ were considered observed and used in the structural analysis. The last least-squares cycle was calculated with 933 parameters giving $R$ = 0.071, $R_w$ = 0.089 and goodness of fit = 2.24. The weighing scheme used was $w^{-1} = \sigma^2(F) + 0.0006F^2$. The final Fourier-difference map showed residual extrema in the range of +1.37 to −0.86 e Å$^{-3}$. Atomic coordinates, bond lengths and angles, and thermal parameters have been deposited at the Cambridge Crystallographic Centre (CCDC). See Information for Authors, Issue No. 1. Any request to the CCDC for this material should quote the full literature citation and the reference number 182/396.

## References

1 M. J. Gunter and P. Turner, *Coord. Chem. Rev*., 1991, **108**, 115.
2 B. Meunier, *Chem. Rev*., 1992, **92**, 1411.
3 D. A. Smith, D. N. Reynolds and L. K. Woo, *J. Am. Chem. Soc*., 1993, **115**, 2511.
4 H. J. Callot, F. Metz and C. Piechocki, *Tetrahedron*, 1982, **38**, 2365.
5 S. O'Malley and T. Kodadek, *Organometallics*, 1992, **11**, 2299; J. L. Maxwell, S. O'Malley, K. C. Brown and T. Kodadek, *Organometallics*, 1992, **11**, 645.
6 J. P. Collman, X. Zhang, V. J. Lee, E. S. Uffelman and J. I. Brauman, *Science*, 1993, **261**, 1404.
7 J. P. Collman, V. J. Lee, C. J. Kellen-Yuen, X. Zhang, J. A. Ibers and J. I. Brauman, *J. Am. Chem. Soc*., 1995, **117**, 692.
8 Y. Naruta, F. Tani, N. Ishihara and K. Maruyama, *J. Am. Chem. Soc*., 1991, **113**, 6865.
9 R. L. Halterman and S. T. Jan, *J. Org. Chem*., 1991, **56**, 5253.
10 H. Nishiyama, Y. Itoh, Y. Sugawara, H. Matsumoto, K. Aoki and K. Itoh, *Bull. Chem. Soc. Jpn*, 1995, **68**, 1247.
11 A. Pfaltz, *Acc. Chem. Res*., 1993, **26**, 339.
12 R. E. Lowenthal, A. Abiko and S. Masamune, *Tetrahedron Lett*., 1990, **31**, 6005.
13 D. A. Evans, K. A. Woerpel, M. M. Hinman and M. M. Faul, *J. Am. Chem. Soc*., 1991, **113**, 726.
14 M. P. Doyle, M. N. Protopopova, B. D. Brandes, H. M. L. Davies, N. J. S. Huby and J. K. Whitesell, *Synlett*, 1993, 151.
15 D. P. Rillema, J. K. Nagle, L. F. Barringer and T. J. Meyer, *J. Am. Chem. Soc*., 1981, **103**, 56.
16 Z. Y. Li, J. S. Huang, C. M. Che and C. K. Chang, *Inorg. Chem*., 1992, **31**, 2670.
17 P. Le Maux, H. Bahri, G. Simonneaux and L. Toupet, *Inorg. Chem*., 1995, **34**, 4691.
18 J. J. Bonnet, S. S. Eaton, G. R. Eaton, R. H. Holm and J. A. Ibers, *J. Am. Chem. Soc*., 1973, **95**, 2141.
19 J. P. Collman, E. Rose and G. D. Venburg, *J. Chem. Soc., Chem. Commun*., 1993, 935.

*Received in Cambridge, UK, 29th November 1996; Com. 6/08080D*

# Coexistence of both histidine tautomers in the solid state and stabilisation of the unfavourable Nδ–H form by intramolecular hydrogen bonding: crystalline L-His-Gly hemihydrate

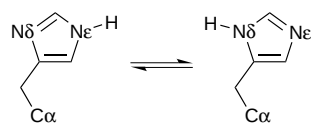
**Thomas Steiner* and Gertraud Koellner**

*Institut für Kristallographie, Freie Universität Berlin, Takustrasse 6, D-14195 Berlin, Germany*

**The crystal structure of L-His-Gly hemihydrate contains two independent peptide molecules which exhibit different histidine tautomers; the less favourable N(δ)–H form is stabilized by an intramolecular Nδ(*n*)–H···O(*n* + 1) hydrogen bond facilitated by a suitable molecular conformation.**

It is well known that the imidazole moiety of the amino acid histidine (His), if unchanged, may exist in two tautomers (Scheme 1). At pH 7, the Nε–H form is dominant. The microscopic p*K* values are 6.7 for the Nδ–H tautomer, and 6.1 for the Nε–H tautomer (determined by titration experiments on a series of suitable derivates).[1] In consequence, histidine peptide crystals grown from water are normally found with the Nε–H form of His, and if grown at low p*H*, His is positively charged with Nδ and Nε both carrying hydrogen atoms.[2,3] The present communication reports for the first time on the stable coexistence of both tautomers in one peptide crystal structure.

From solution in pure water, the dipeptide L-histidyl-glycine crystallizes as a hemihydrate (L-His-Gly·0.5$H_2O$, **1**), with two peptide molecules and one water molecule per asymmetric crystal unit† (crystal structures of the chloride and dichloride salts have been published previously[4]). Very surprisingly, the two symmetry-independent molecules are found in completely different conformations, and with different tautomers of the histidine imidazole ring (Fig. 1, selection of torsion angles given in the figure legend). The tautomeric identity has been unambiguously determined by location of the hydrogen atoms in difference Fourier calculations and subsequent isotropic refinement, but could in principle also be deduced from the crystal contacts of the non-hydrogen atoms.‡ A section of the crystal packing is shown in Fig. 2, with some geometrical hydrogen bond data given in the figure legend. Molecule **A** adopts a standard elongated conformation and the imidazole moiety is in the expected Nε-H form, very similar to the closely related molecule L-His-L-Ala crystallized from water as a dihydrate.[5] Molecule **B**, on the contrary, is found in a folded conformation as the Nδ–H histidine tautomer [Fig. 1(*b*)]. This is associated with a short and linear intramolecular side-chain to main-chain hydrogen bond Nδ(1)–H··O(2) [for N–H normalized to 1.04 Å: N··O = 2.742(5) Å, H··O = 1.71 Å, N–H··O = 170°]. This situation is exceptional not only from the chemical, but also from the crystallographic point of view: typically in crystal structures with more than one moleule per asymmetric crystal unit, the symmetry-independent molecules may have different conformations, but have the same chemical identities. It is obvious that crystal growth of **1** requires unusually complex mechanisms of molecular recognition at the crystal–solvent interface to incorporate molecules of both identities at the right places. Once incorporated in the crystal, the individual molecules are trapped in their tautomeric form.




**Scheme 1**

Previous surveys have reported that in crystal structures with uncharged His side-chains, *only* the more stable Nε–H tautomer is found[2,3] (conflicting with the present results). Since several relevant crystal structures have been published after the surveys, a new search through the Cambridge Structural Database[6] (CSD) was performed (spring 1996 version, $R$ < 0.08, all hydrogen atoms given, no metal atoms present). Of 39 His residues in 36 crystal structures, 20 are charged. Of the remaining 19 His residues, 18 are found in the Nε–H, and one in the Nδ–H form. The latter occurs in unsolvated L-His-L-Leu, **2**.[7] No previous example of the solid-state coexistence of *both* tautomers is found.

Notably, the backbone and histidine conformation of **2** is almost identical to that of molecule **1B**, and the intramolecular Nδ(1)–H··O(2) hydrogen bond is formed with very similar geometry (N··O = 2.71 Å, H··O = 1.70 Å, N–H··O = 163° for normalized hydrogen position). Since the intermolecular surroundings are very different for **1B** and **2**, it is assumed that

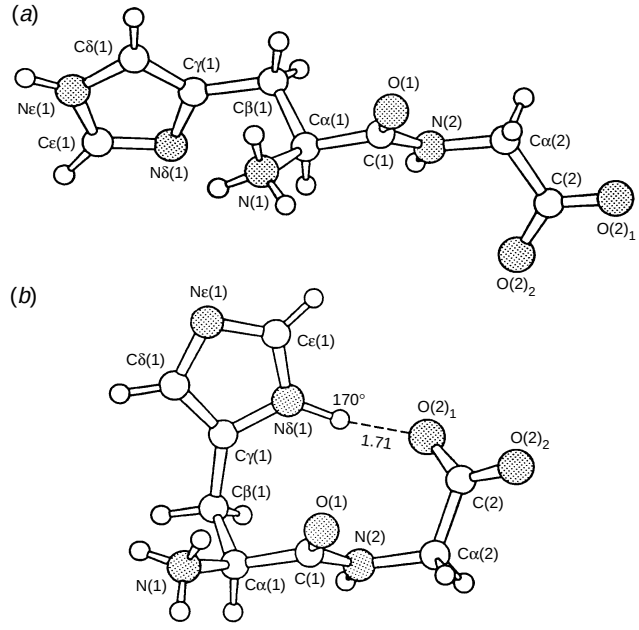



**Fig. 1** Molecular structure and atomic numbering scheme for both peptide molecules in L-His-Gly hemihydrate. (*a*) molecule **A**, (*b*) molecule **B**. The molecules are drawn in the same projection with respect to the peptide bonds. Oxygen and nitrogen atoms are drawn shaded. Selection of torsion angles defining the molecular conformation: Molecule **A**: $\psi_1$ = 147.0(4)°; $\omega_1$ = −178.1(4)°; $\varphi_2$ = 130.4(5)°; N(2)–Cα(2)–C(2)–$O(2)_1$ = −179.8(5)° (corresponds to $\psi_2$); N(2)–Cα(2)–C(2)–$O(2)_2$ = −1.1(7)°; $\chi_1^1$ = −52.4(5)°; $\chi_1^2$ = −58.2(6)°. Molecule **B**: $\psi_1$ = 166.2(4)°; $\omega_1$ = 179.1(4)°; $\varphi_2$ = −78.4(6)°; N(2)–Cα(2)–C(2)–$O(2)_1$ = −27.1(7)°; N(2)–Cα(2)–C(2)–$O(2)_2$ = 154.5(4)° (corresponds to $\psi_2$); $\chi_1^1$ = 69.5(6)°; $\chi_1^2$ = 78.4(6)°.

the occurrence of the less favourable tautomer is not induced by the crystal surrounding, but is closely associated with the conformation, in particular with the formation of a short intramolecular Nδ($n$)–H··O($n$ + 1) hydrogen bond. This interaction appears to stabilize the Nδ–H tautomer to a sufficient degree to allow crystallisation in this form. In a polypeptide chain, this kind of hydrogen bond represents an interaction of His Nδ–H with the carbonyl oxygen atom of the next residue, *i.e.* Nδ($n$)–H···O($n$ + 1). The peptide conformation is required to be close to that of **1B** ($\psi_n$ = 166°, $\varphi_{n+1}$ = −78°, $\psi_{n+1}$ = 155°, $\chi_n^1$ = 69°, $\chi_n^2$ = 78°). This is not an uncommon conformation, and several examples are quoted in ref. 7; a closer examination of these examples, however, shows that all except **1B** and **2** are formed by peptides with charged His residues, where Nδ is protonated irrespective of the conformation.

It is tempting to speculate on the relevance of such observations for proteins. Side-chain to main-chain His Nδ($n$)··O($n$ + 1) hydrogen bonds do occur in some proteins[8] (normally, however, the charge situation is not unambiguously determined), and might there stabilize the less favourable tautomeric form. More generally, it can be assumed that the Nδ–H form can be effectively stabilized also by other hydrogen bond configurations;§ this assumption is not yet backed up by peptide structure analysis.

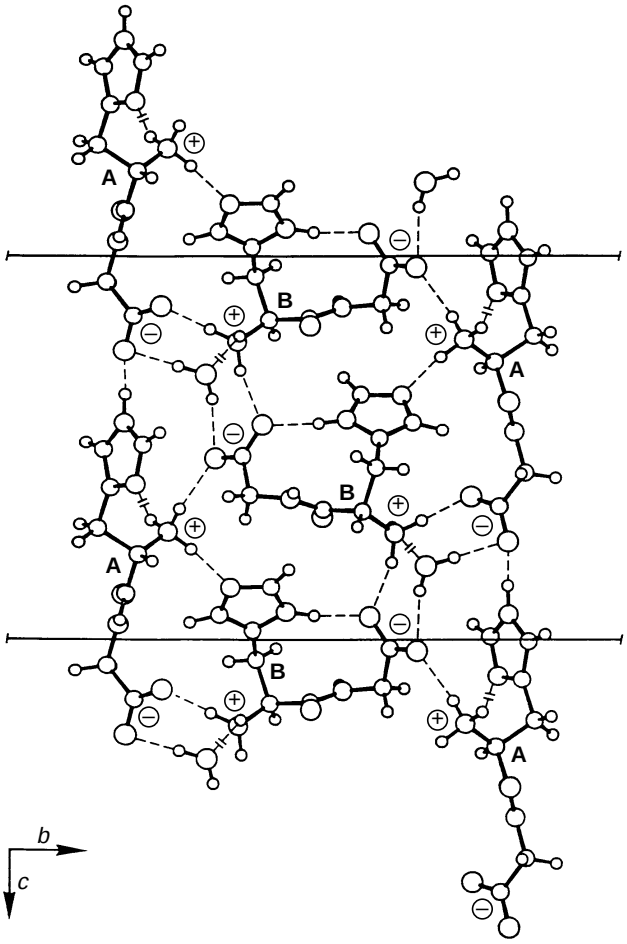



**Fig. 2** Section of the crystal packing, O/N–H··O/N hydrogen bonds are shown as dashed lines. Molecules **A** and **B** are labelled near the Cα(1) atoms. The charge situation is indicated by symbols ⊕ and ⊖. The imidazole rings are involved in the following N–H··O/N hydrogen bond interactions (for normalized hydrogen atom positions with N–H = 1.04 Å): Molecule **A**: Nδ(1) (**A**)··H$_2$–N(1) (**A**) ($x$ − 1, $y$, $z$), H··N = 1.81 Å, N··N = 2.815(6) Å, N–H··N = 160°. Nε(1) (**A**)–H··O(2)$_1$ (**A**) ($x$, $y$, $z$ − 1), H··O = 1.73 Å, N··O = 2.715(6) Å, N–H··O = 156°. Molecule **B**: Nδ(1) (**B**)–H··O(2)$_1$ (**B**) ($x$, $y$, $z$), H··O = 1.71 Å, N··O = 2.742(5) Å, N–H··O = 170°. Nε(1) (**B**)··H$_3$–N(1) (**A**) ($x$, $y$, 1 + $z$), H··N = 1.82 Å, N··N = 2.859(6) Å, N–H··N = 177°.

## Footnotes

* E-mail: steiner@chemie.fu-berlin.de

† A commercial sample of L-His-Gly (Sigma) was dissolved in water; slow evaporation yielded very thin, needle shaped colourless crystals.

*Crystal data*: L-histidyl-glycine hemihydrate, $C_8H_{12}N_4O_3 \cdot 0.5H_2O$; FW = 221.2, space group orthorhombic $P2_12_12_1$, $a$ = 4.9547(6), $b$ = 32.356(6), $c$ = 12.587(4) Å, $V$ = 2017.9(8) Å$^3$, $Z$ = 8, $Z'$ = 2, $D_c$ = 1.46 g cm$^{-3}$. Enraf-Nonius Turbo-CAD diffractometer, room temperature, Ni-filtered Cu-Kα X-rays, ω-scan mode, $\lambda/2 \sin\theta_{max}$ = 0.89 Å, 0.65 × 0.04 × 0.02 mm$^3$ crystal glued to a glass pin, 3436 reflections measured, 2999 unique, 1889 with $I > 2\sigma(I)$, no absorption correction. Structure solution and refinement with standard methods (SHELXS86[10] and SHELXL93[11]). All hydrogen atom positions were located from difference Fourier calculations; to obtain the geometrically most realistic model, the hydrogen atoms were then treated in the riding model,[11] with exception of the hisidine (N)H atoms which were refined unconstrained isotropic, the water H-atoms, which were refined with O–H bond lengths constrained to 0.90(2) Å, and the ammonium groups which were allowed to rotate. Final $R$ = 0.059 (for observed reflections), $\omega R(F^2)$ = 0.148 (for all reflections). Atomic coordinates, bond lengths and angles, and thermal parameters have been deposited at the Cambridge Crystallographic Data Centre (CCDC). See Information for Authors, Issue No. 1. Any request to the CCDC for this material should quote the full literature citation and the reference number 182/467.

‡ The tautomeric forms of molecules **A** and **B** can be deduced merely from the configuration of non-hydrogen atoms: Nε(1) (**B**) is in hydrogen bond contact with an ammonium group and can therefore only be non-protonated, and Nδ(1) (**B**) forms a hydrogen bond with a carboxylate group and must therefore carry a hydrogen atom (Fig. 2). For the 'conventional' molecule **A**, the situation is reversed: Nε(1) (**A**) is in hydrogen bond contact with a carboxylate group, and Nδ(1) (**A**) with an ammonium group, inferring the Nε–H tautomer for His(**A**).

§ In the well-defined example of a glutamic acid specific serine protease (Glu-SGP), such a case seems actually to occur: a charge-relay system involving a remarkable triad of presumably uncharged histidine residues was proposed (ref. 9). Based on the configuration of the non-hydrogen atoms, it can be inferred that in this triad, initially two residues are in the Nε–H and one in the Nδ–H form. Upon action of the charge-relay mechanism, the situation is switched to two Nδ–H and one Nε–H tautomer.

## References

1 M. Tanokura, *Biochim. Biophys. Acta*, 1983, **742**, 576.
2 R. Ramani and R. J. Boyd, *Can. J. Chem*., 1981, **59**, 3232.
3 C. H. Görbitz, *Acta Crystallogr., Sect. B*, 1989, **45**, 390.
4 T. Steiner, *Acta Crystallogr., Sect. C*, 1997, **53**, 255; *ibid*, in the press.
5 T. Steiner, *Acta Crystallogr., Sect. C*, 1996, **52**, 2554.
6 F. H. Allen, J. E. Davies, J. E. Galloy, J. J. Johnson, O. Kennard, C. F. Macrae, E. M. Mitchell, G. F. Mitchell, J. M. Smith and D. G. Watson, *J. Chem. Inf. Comput. Sci*., 1991, **31**, 187.
7 J. A. Krause, P. W. Baures and D. S. Eggleston, *Acta Crystallogr., Sect. B*, 1993, **49**, 123.
8 E. N. Baker and R. E. Hubbard, *Prog. Biophys. Mol. Biol*., 1984, **44**, 97.
9 V. L. Nienaber, K. Breddam and J. J. Birktoft, *Biochemistry*, 1993, **32**, 11469.
10 G. A. Sheldrick, SHELXS86, *Program for the solution of crystal structures*, 1986, University of Göttingen, Germany.
11 G. A. Sheldrick, SHELXL93, *Program for the refinement of crystal structures*, 1993, University of Göttingen, Germany.

*Received in Cambridge, UK, 21st November 1996; Revised manuscript received, 14th March 1997; Com. 7/01807J*

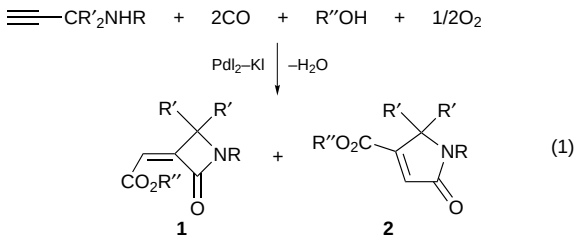
# Palladium-catalysed sequential carboxylation–alkoxycarbonylation of acetylenic amines

**Alessia Bacchi,[a] Gian Paolo Chiusoli,[b] Mirco Costa,*[b] Bartolo Gabriele,[c] Carlo Righi[b] and Giuseppe Salerno[c]**

[a] *Dipartimento di Chimica Generale, Analitica e Chimica Fisica, Università, Viale delle Scienze, 43100 Parma, Italy*
[b] *Dipartimento di Chimica Organica e Industriale, Università, Viale delle Scienze, 43100 Parma, Italy*
[c] *Dipartimento di Chimica, Università della Calabria, 87030 Arcavacata di Rende, Cosenza, Italy*

**Carbon dioxide and carbon monoxide react in sequence in an intramolecular carboxy–carbonylation reaction of *N*-alkyl-substituted dialkylpropynylamines, under the catalytic action of palladium iodide–potassium iodide in methanol in the presence of oxygen.**

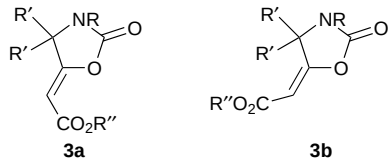
In the course of our investigation of the palladium-catalysed synthesis of β- and γ-lactams by oxidative carbonylation of acetylenic amines[1] [eqn. (1), R = alkyl, R′,R″ = alkyl], we



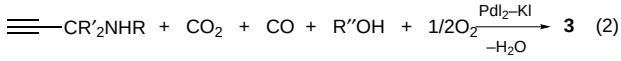

(1)

noticed the presence of small amounts of compounds containing an additional oxygen atom, the formation of which was promoted by a little water in the reaction mixture.

These compounds turned out to be (*Z*)- and (*E*)-[(alkoxycarbonyl)methylene]oxazolidin-2-ones **3a** and **3b**† in 2 : 1–3 : 1 ratio. The X-ray structure of one of them (**3a**, R = Bn; R′,R″ = methyl)‡ is shown in Fig. 1. In the crystal of **3a**, the methoxycarbonyl moiety and the five-membered ring are coplanar within 0.2 Å and oxygens O(2) and O(3) are in close contact [O(2)··O(3) 2.835(2) Å] due to the *Z* configuration of the C(2)–C(4) double bond [torsion angle C(3)–C(2)–C(4)–C(5) −175.9(2)°].

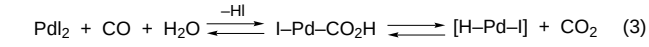



The formation of compounds **3** could be attributed to the sequential reaction of one molecule of carbon dioxide and one of carbon monoxide with the triple bond, according to eqn. (2).




(2)

In fact carbon dioxide could originate through decarboxylation of a hydroxycarbonylpalladium species[2] formed in the presence of water [eqn. (3)].




(3)

To test our hypothesis we treated a mixture of carbon dioxide (40 bar), carbon monoxide (5 bar) and air (5 bar) with *N*-(dimethylpropynyl)benzylamine in methanol (20 ml, 0.15 M), with a 100 : 1 molar ratio of amine to catalyst ($PdI_2$ or Pd–C 10% + 10 mol KI per mol of Pd). After stirring at 52 °C for 45 h products **3a** and **3b** (R = Bn; R′,R″ = Me) were obtained in an 88% yield (2 : 1 ratio) by GLC. With R = Bu the yield was 69% (3.2 : 1 ratio). Unconverted substrate (2% for R = Bn, R′ = Me; 4% for R = Bu, R′ = Me), oxazolidinone **4** (3% for R = Bn, R′ = Me; 2% for R = Bu, R′ = Me), β-lactam **1** (only traces for R = Bn; R′,R″ = Me; 4% for R = Bu; R′, R″ = Me) and compounds derived from a trimethoxycarbonylation at the nitrogen and triple bond carbons of starting propynylamines (5% for R = Bn; R′, R″ = Me; 9% for R = Bu; R′,R″ = Me) were present as by-products. A higher pressure of carbon monoxide or higher temperature led to a decrease in the yield of **3**. Under the same conditions as above the use of CO in the absence of $CO_2$ gave a less than 2% yield of **3** (R = Bu; R′,R″ = Me), which increased to 17% (**3a** : **3b** = 3) in the presence of 15% water in the reaction mixture.

The course of the reaction leading to **3a** and **3b** can be interpreted according to Scheme 1, which implies the intermediate formation of a palladium carbamate (anionic iodide ligands are omitted for simplicity).

Products **3a** and **3b** are proposed to originate from different reaction pathways, the former from *cis* attack of palladium carbamate on the triple bond, the latter from *trans* attack of the carbamate anion on the triple bond coordinated to palladium.[3] It was ascertained that isomerization of **3a** into **3b** or *vice versa* did not occur under the reaction conditions. An isomerization of the vinylpalladium precursors of **3** shown in Scheme 1 cannot be excluded but it is not likely in view of the fact that a larger availability of potassium carbamate for *trans* attack on the triple bond obtained by increasing the KI excess led to a decrease of the **3a** : **3b** ratio (for example, from 3.2 to 1.7 for R = Bu; R′,R″ = Me on passing from 10 to 100 KI : Pd molar ratio under the conditions reported in the example above).

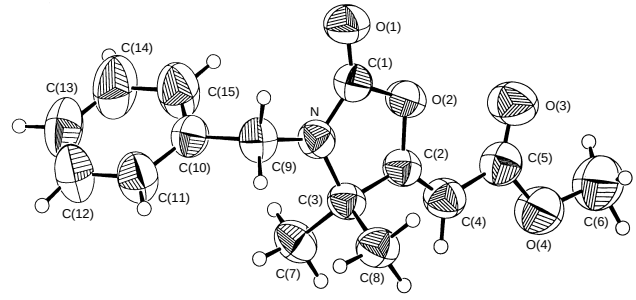
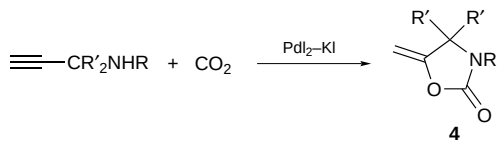



**Fig. 1** ORTEP diagram of **3a** with 50% probability thermal ellipsoids. Relevant distances (Å) and angles (°) are: N–C(1) 1.327(3), C(1)–O(2) 1.399(2), C(2)–O(2) 1.369(2), C(2)–C(3) 1.509(2), N–C(3) 1.467(2), C(2)–C(4) 1.325(3), O(2)–C(1)–N 108.7(2), O(2)–C(2)–C(3) 109.4(1), C(2)–C(3)–N 99.4(1), O(2)–C(2)–C(4) 122.9(2), C(3)–C(2)–C(4) 127.6(2). In the five-membered ring, endocyclic angles centred on the atoms N, C(1), O(2) and C(2) range from 108.7 to 112.7°, while the angle N–C(3)–C(2) is noticeably reduced [99.4(1)°].

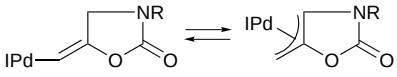
We also caused carbon dioxide (40 bar) to react with the same acetylenic amine (3.0 mmol) in MeOH (20 ml) in the presence of $PdI_2$ (100 : 1 molar ratio to the substrate) and KI (15 : 1 molar ratio to Pd) in the absence of carbon monoxide and oxygen at 75 °C for 24 h. The result was the formation of compound **4** (R = Bu, R′ = Me; 27% yield, 64% unconverted propynylamine) [eqn. (4)], which originates from protonation of the (*Z*)- or (*E*)-vinylpalladium precursor of **3**.



(4)

Although this reaction is catalytic, more satisfactory results were reached under the reported conditions in the presence of air (10 bar), a 58% yield of **4** (R = Bu, R′ = Me) being obtained at 65% conversion.

It is worth noting that in the absence of alkyl groups α to the triple bonds (R′ = H) the introduction of carbon dioxide only and not that of carbon monoxide was observed under the conditions of eqn. (2), compound **4** (61% yield; R = Bn, R′ = H) being formed exclusively. This is likely to be due to stabilization through formation of an allylpalladium complex[4] which, being poorly reactive towards carbon monoxide,[5] undergoes selectively hydrogenolysis [eqn. (5)] (the isomer with an endocyclic double bond was not detected).

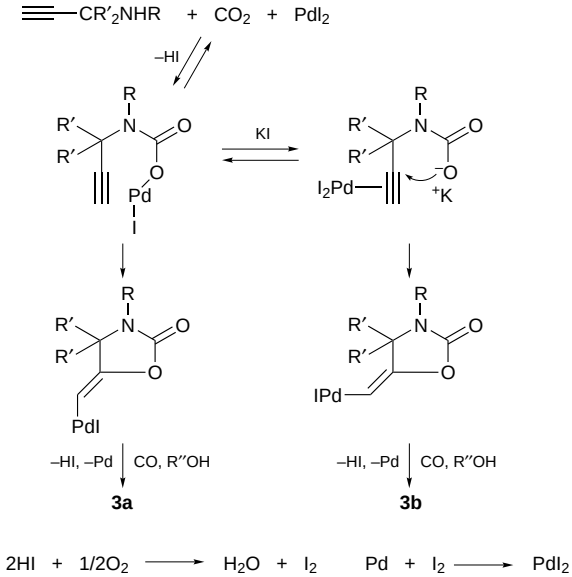


**4** (R = Bn, R′ = H) (5)

Compound **4** was previously obtained also by direct incorporation of $CO_2$ under the catalytic action of superbases in aprotic solvents.[6]

The carboxylation–alkoxycarbonylation reported here is the first catalytic reaction in which cabon dioxide and carbon monoxide are caused to react in sequence. A stoichiometric sequence in two steps was described by Carmona[7] in the formation of an anhydride from a metallacyclic complex, CO and $CO_2$.

Financial support by Ministero Pubblica Istruzione (40%) and CNR, Progetto Strategico Tecnologie Chimiche Innovative, is acknowledged. The facilities of Centro Interfacoltà di Misure of the University of Parma have been utilized for NMR determinations.



**Scheme 1**

## Footnotes

* E-mail: costa@ipruniv.cce.unipr.it

† *Selected data* for **3a** (R = Bu, R′ = Me, R″ = Me): pale yellow solid, mp 71–72 °C; $^1$H NMR (300 MHz, $CDCl_3$): δ 0.93 (t, 3 H, *J* 7.3 Hz, Me), 1.30–1.40 (m, 2 H, $CH_2$), 1.43 (s, 6 H, 2 Me), 1.57–1.67 (m, 2 H, $CH_2$), 3.17 (t, 2 H, *J* 7.9 Hz, $NCH_2$), 3.74 (s, 3 H, OMe) and 5.07 (s, 1 H, =CH); $^{13}$C NMR 75 MHz, $CDCl_3$): δ 13.52 (Me), 20.04 ($CH_2$), 27.00 (2 Me), 31.13 ($CH_2$), 40.41 ($CH_2$), 51.41 (OMe), 62.48 (qC), 91.70 (=CH), 152.65 (qC), 164.46 (qC) and 166.63 (qC); *m*/*z* 241 ($M^+$, 3%), 226 (68), 170 (52), 138 (37), 69 (100) and 59 (14); ν (KBr) cm$^{-1}$ 2930 (w), 1786 (s), 1721 (s), 1677 (m), 1401 (m), 1173 (m), 1033 (m) and 1011 (m). For **3b** (R = Bu, R′ = Me, R″ = Me, R″ = Me): colourless oil; $^1$H NMR (300 MHz, $CDCl_3$): δ 0.95 (t, 3 H, *J* 7.3 Hz, Me), 1.31–1.41 (m, 2 H, $CH_2$), 1.60–1.71 (m, 2 H, $CH_2$), 1.69 (s, 6 H, 2 Me), 3.16 (t, 2 H, *J* 7.9 Hz, $NCH_2$), 3.70 (s, 3 H, OMe) and 5.61 (s, 1 H, =CH); $^{13}$C NMR 75 MHz, $CDCl_3$): δ 13.55 (Me), 20.10 ($CH_2$), 23.02 (2 Me), 31.05 ($CH_2$), 40.09 ($CH_2$), 51.24 (OMe), 63.95 (qC), 94.91 (=CH), 152.19 (qC), 165.74 (qC) and 169.63 (qC); *m*/*z* 241 ($M^+$, 5%), 226 (83), 69 (100), 59 (26) and 55 (32); ν (film) cm$^{-1}$ 2960 (m), 2874 (w), 1801 (s), 1720 (s), 1661 (s), 1403 (m), 1267 (m), 1088 (s), 1048 (s) and 1002 (m). For **3a** (R = Bn, R′ = Me, R″ = Me): pale yellow solid, mp 125–126 °C; $^1$H NMR (300 MHz, $CDCl_3$): δ 1.32 (s, 6 H, 2 Me), 3.74 (s, 3 H, OMe), 4.48 (s, 2 H, $CH_2$), 5.07 (s, 1 H, =CH) and 7.28 (m, 5 H, Ph); $^{13}$C NMR 75 MHz, $CDCl_3$): δ 27.20 (2 Me), 44.27 ($CH_2$), 51.52 (OMe), 62.78 (qC), 92.03 (=CH), 127.76 (2 =CH), 128.04 (=CH), 128.79 (2 =CH), 136.82 (qC), 153.37 (qC), 164.46 (qC) and 166.51 (qC); *m*/*z* 275 ($M^+$, 3%), 260 (7), 132 (19), 91 (100) and 65 (11); ν (KBr) cm$^{-1}$ 2880 (w), 1787 (s), 1724 (s), 1673 (s), 1401 (s), 1209 (m), 1165 (m), 1033 (s) and 704 (m).

‡ *Crystal data* for **3a**: $C_{15}H_{17}NO_4$, *M* = 275.30, monoclinic, *a* = 19.254(5), *b* = 6.416(2), *c* = 23.592(5)Å, β = 93.27(2)° *V* = 2910(1) Å$^3$, *T* = 293 K, space group *C*2/*c* (no. 15), filtered Cu-Kα radiation, λ = 1.54178 Å, *Z* = 8, *D*c = 1.257 Mg m$^{-3}$, *F*(000) = 1168, colourless thin plates, μ(Cu-Kα) = 7.557 cm$^{-1}$, ENRAF-NONIUS CAD4 diffractometer, ω–2θ scan, 6 < 2θ < 140°, 5530 measured reflections, 2768 unique reflections, 1946 unique observed reflections [$I > 2\sigma(I)$]. The phase problem was solved by direct methods (SIR92).[8] and the structure was refined by full-matrix least-squares on all measured $F_o^2$ (SHELXL96).[9] The empirical absorption correction by Parkin, Moezzi and Hope[10] was applied on the best isotropic model as implemented in SHELXL96. All non-hydrogen atoms were refined anisotropically. Hydrogens were located in the difference Fourier map and refined isotropically. Final refinement on 249 parameters gave $R_1$ = 0.047 (on observed data), $R_1$ = 0.068 (on all data), $wR_2$ = 0.147, gof = 1.054.

Atomic coordinates, bond lengths and angles, and thermal parameters have been deposited at the Cambridge Crystallographic Data Centre (CCDC). See information for Authors, Issue No. 1. Any request to the CCDC for this material should quote the full literature citation and the reference number 182/476.

## References

1 A. Bonardi, M. Costa, B. Gabriele, G. Salerno and G. P. Chiusoli, *Tetrahedron Lett.*, 1995, **36**, 7495.
2 E. Drent and P. H. M. Budzelaar, *Chem. Rev.*, 1996, **96**, 663; B. Gabriele, G. Salerno, M. Costa and G. P. Chiusoli, *J. Mol. Catal.*, 1996, **111**, 43; V. N. Zudin, G. N. Ll'inich, V. A. Likholobov and Y. I. Yermakov, *J. Chem. Soc., Chem. Commun.*, 1984, 545.
3 C. Lambert, K. Utimoto and H. Nozaki, *Tetrahedron Lett.*, 1984, **25**, 5323.
4 B. M. Trost, *Tetrahedron*, 1977, **33**, 2615.
5 D. Medema, R. van Helden and C. F. Kohll, *Inorg. Chim. Acta*, 1969, **3**, 255.
6 M. Costa, G. P. Chiusoli and M. Rizzardi, *Chem. Commun.*, 1996, 1699.
7 E. Carmona, E. Gutiérrez-Pueblo, J. M. Martin, A. Morge, M. Paneque, M. L. Poveda and C. Rui, *J. Am. Chem. Soc.*, 1989, **111**, 2883.
8 A. Altomare, G. Cascarano, C. Giacovazzo, A. Guagliardi, M. C. Burla, G. Polidori and M. Camalli, *J. Appl. Crystallogr.*, 1994, **27**, 435.
9 G. Sheldrick, SHELXL96, Program for structure refinement. 1996, University of Goettingen, Germany.
10 S. Parkin, B. Moezzi and H. Hope, *J. Appl. Crystallogr.*, 1995, **28**, 53.

*Received in Cambridge, UK, 25th April 1997; Com. 7/02822I*

# Synthesis and X-ray structures of *N*-lithioiminophosphorane·lithium bromide adducts

**Andrei S. Batsanov, Matthew G. Davidson,* Judith A. K. Howard, Sarah Lamb, Christian Lustig and Richard D. Price**

*Department of Chemistry, Science Laboratories, South Road, Durham, UK DH1 3LE*

**Iminophosphorane anions are shown to be novel and very powerful Lewis-base donors to s-block metals by the isolation and structural characterisation of *N*-lithioiminophosphorane·lithium bromide adducts.**

We have recently been interested in the coordination of neutral phosphonium ylides **1a** to lithium compounds.[1] The isoelectronic and isonuclear iminophosphoranes **1b** possess many of the characteristics of phosphorus ylides, with the P–N bond being substantially dipolar in nature[2] which renders them theoretically capable of forming very strong complexes with

$R_3P{=}X \longleftrightarrow R_3P^{+}{-}X^{-}$ (**1**)

**1a** X = $CR'_2$
**b** X = NR′
**c** X = O

lithium compounds. Indeed, iminophosphorane–lithium complexes are calculated to be stronger even than complexes between lithium and phosphine oxides **1c**,[1] the third member of this isoelectronic and isonuclear series, and a class of compound commonly used as strong Lewis-base donors to s-block metals.[3] Furthermore, the facile deprotonation (metallation) of ylides or iminophosphoranes[4] (**1a**, **b**, R′ = H) yields species in which the negative charge on the ylidic carbon or iminic nitrogen atom is enhanced, potentially providing Lewis bases of exceptional strength. With the aim of exploring this avenue to provide unusual and potentially useful ligands for s-block metals we now report the syntheses and structural characterisation of *N*-lithoiminophosphorane compounds as their lithium halide complexes. Our results suggest that $R_3P{=}N^-$ ligands offer potential to be developed as new and powerful Lewis-basic ligands in s-block metal coordination chemistry.

Until now, the isolation and unambiguous characterisation of a *N*-(s-block-metallated) iminophosphorane has not, to our knowledge, been reported. Even the structural characterisation of a simple iminophosphorane moiety acting as a neutral donor to an s-block metal is limited to one recent example of intramolecular coordination.[5] This is surprising since *N*-lithioiminophosphoranes are well known as reagents in both organic and inorganic synthesis, for example, as synthons for $RN^{2-}$[6] and as precursors for a wide variety of *N*-substituted iminophosphoranes containing either inorganic, organometallic or organic residues.[7]

*N*-Lithioiminophosphoranes $[(Ph_3PNLi{\cdot}LiBr)_2{\cdot}4thf]{\cdot}1.5$arene (arene = benzene **3a**, toluene **3b**) were prepared by the reaction of 2 equiv. of BuLi with $Ph_3PNH_2Br$ **2** in arene–thf† and characterised by X-ray crystallography.‡

In the solid state (Fig. 1) **3a** and **3b** are isomorphous and the following discussion will be confined to **3a**, which provided the higher quality X-ray data set. The structure consists of a pseudocubane $Li_4N_2Br_2$ core in which each lithium atom is four-coordinate *via* association to three $\mu_3$-bridging anionic centres and one terminal thf molecule. Similar core structures have been found before for C–Li[8] and O–Li[9] species but complexes **3** are unique as mixed-anion tetramers incorporating organic N–Li fragments. The ability of the *N*-lithioiminophosphorane to solvate LiBr and prevent association of the lithium halide into an infinite $(LiX)_\infty$ lattice§ emphasises the powerful Lewis basicity of the iminophosphorane anion that had been anticipated. One face of the cube ($Li_2Br_2$) is distorted by a fold along the Li(1)···Li(2) axis (angle of fold 30°). This distortion is largely a steric effect due to anion–anion repulsions and has also been seen in other structures containing a $Li_4R_2X_2$ core (X = halogen).[8a,9] Comparison of inter- and intra-ring distances within the core of **3** (average inter- and intra-ring Li–Br distances, 2.738 and 2.603 Å, respectively; average inter- and intra-ring Li–N distances, 1.971 and 2.005 Å, respectively) suggests that the interactions of all four lithium atoms with iminic nitrogen atoms are favoured over those with the bromide anions. While the observed preference for Li–N over Li–Br coordination emphasises the high Lewis basicity of the iminophosphorane anion, such analysis provides no clue as to whether the core is derived from aggregation of two $Li_2Br_2$ rings or from dimerisation of two LiN·LiBr units.

The structural parameters obtained for the complexes **3** provide a useful guide to the geometry of the unknown isolated $Ph_3P{=}N^-$ anion since the interaction with $Li^+$ is substantially electrostatic in nature (which contrasts with the largely covalent interactions found for transition metal complexes). For example, the P–N bond in **3** (average P–N distance, 1.541 Å) is significantly shorter than in the dication of the structure of $\{Ph_3P{=}N[Au(PPh_3)]_3\}^{2+}2BF_4^-$ [P–N distance, 1.62(1) Å] in

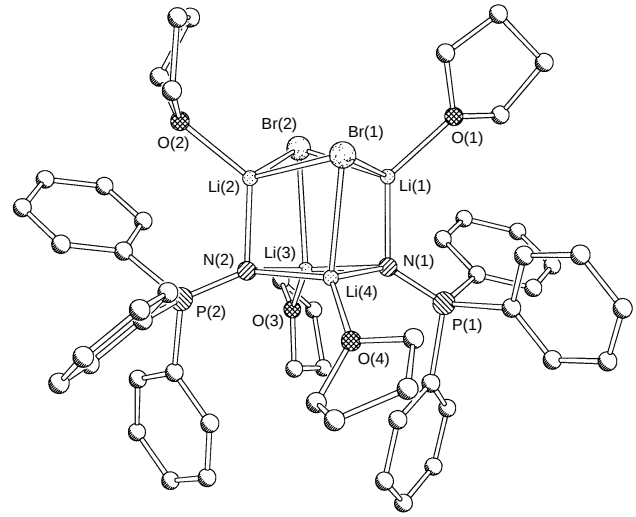



**Fig. 1** Molecular structure of **3a** and **3b** (for clarity, all H atoms and lattice solvent are omitted and only one conformation of disordered thf is shown). Selected bond distances in **3a** [**3b**] (Å): Br(1)–Li(1) 2.605(6) [2.60(1)], Br(1)–Li(2) 2.602(6) [2.60(1)], Br(1)–Li(4) 2.692(6) [2.70(1)], Br(2)–Li(1) 2.596(6) [2.59(1)], Br(2)–Li(2) 2.607(6) [2.60(1)], Br(2)Li(3) 2.784(6) [2.74(1)], N(1)–Li(1) 1.962(6) [1.97(1)], N(1)–Li(3) 1.999(6) [2.01(1)], N(1)–Li(4) 2.019(6) [2.03(1)], N(2)–Li(2) 1.979(7) [2.00(1)], N(2)–Li(3) 1.992(6) [2.02(1)], N(2)–Li(4) 2.010(6) [2.00(1)], O(1)–Li(1) 1.960(6) [1.96(1)], O(2)–Li(2) 1.953(7) [1.97(1)], O(3)–Li(3) 1.963(6) [1.95(1)], O(4)–Li(4) 1.993(6) [1.99(1)], N(1)–P(1) 1.541(3) [1.542(6)], N(2)–P(2) 1.541(3) [1.538(6)].

which the $Ph_3P{=}N^-$ unit also $\mu_3$-bridges three metal atoms.[10] Indeed, the P–N bond in **3** is shorter than in all known transition-metal compounds (distances in the range 1.59–1.66 Å).[10,11] It is also slightly shorter than in the parent iminophosphorane, $Ph_3P{=}NH$,¶ which is consistent with an increased electrostatic attraction between $P^{\delta+}$ and a more negative $N^{\delta-}$ after lithiation. As expected, the P–N bond in **3** is longer than the P–O distance in the isoelectronic but neutral $Ph_3P{=}O$ [P–O distance, 1.46(1),[12a] 1.484(1)[12b] Å].

The solution behaviour of **3** is complicated. Again, the discussion here is confined to **3a**, though the general behaviour is common to both complexes. The cryoscopically determined relative molecular mass (RMM) is concentration dependent, as are the relative intensities of resonances in the $^{31}P$ and $^{7}Li$ NMR spectra (all in benzene solution), indicating that equilibria operate in solution between two or more species. Even at room temperature, four distinct $^{31}P$ and three distinct $^{7}Li$ resonances are observed and one can easily imagine a number of thf-coordinated $(LiN{=}PPh_3)_n$, $(LiBr)_n$ and $[Li_2(Br)(N{=}PPh_3)]_n$ monomers and oligomers that may coexist in solution. Though it is difficult to assign these resonances unambiguously, it is clear from our results that, even in predominantly arene solution, dilithiation of $Ph_3P{=}NH_2Br$ does not give a solution of LiBr-free $(Ph_3P{=}NLi)_n{\cdot}xL$ as has been suggested previously in the protocol for the preparation of primary and secondary amines developed by Cristau *et al.*[6] but instead gives a well defined, stoichiometric 1:1 LiBr complex of the *N*-lithioiminophosphorane. Indeed, *N*-lithioiminophosphoranes prepared directly from *N*-unsubstituted iminophosphoranes to give only $R_3P{=}NLi$,[4] followed by reaction with R′X or $MX_n$ (X = halogen) would result in the formation of a mixed organolithium–lithium halide aggregate in solution in any case. These observations are relevant to the use of *N*-lithioiminophosphoranes in synthesis since the nature of the reactive species present in solution is well known to have an effect on the reactivity and/or selectivity of a reagent in solution.[13]

Preliminary results show that LiCl analogues of **3** are accessible, and that **3** may be used in transmetallation reactions. We are currently investigating further the use of highly polar ylidic and iminic ligands as novel complexants in s-block metal chemistry particularly with a view to achieving solvation of LiF in hydrocarbon solvents.

We thank the EPSRC (PDRA Fellowship and Quota Studentship for A. S. B. and R. D. P., respectively) and Durham University (Postgraduate Scholarship for S. L.).

## Footnotes

* E-mail: m.g.davidson@durham.ac.uk

† *Syntheses*: All manipulations were carried out under a dry $N_2$ atmosphere using Schlenk techniques and an inert atmosphere glove box. Solvents were freshly distilled prior to use. Compound **2** was prepared by slight modification of the method reported by Cristau *et al.*[6] *Typical synthetic procedure for* **3**: to a suspension of **2** (2.5 mmol, 0.90 g) in benzene (15 ml), *n*-butyllithium (5 mmol, 3.2 ml of a 1.6 M solution in hexane) was added at 25 °C. The suspension was stirred for 15 min, during which the solution turned yellow and a white precipitate persisted. Addition of 1.5 ml thf followed by warming to *ca*. 70 °C resulted in complete dissolution of the solid into a yellow solution. Upon storage of this solution for 24 h at 25 °C, colourless blocks of **3a** were obtained.

**3a**: yield 72%, mp 166 °C. $^1H$ NMR (200 MHz, $C_6D_6$): δ 8.0 (m, 6 H, *o*-Ph), 6.9–7.7 (m, 9 H, *m*,*p*-Ph, plus residual $C_6H_6$), 3.6 (qnt, 8 H, α-thf), 1.3 (qnt, 8 H, β-thf). $^{31}P$ NMR (101.2 MHz, $C_6D_6$): (0.01 M), δ 2.0 (s, 1), −1.2 (s, 3.4), −3.9 (s, 1.9), −5.5 (s, 0.4); (0.05 M), δ 1.8 (s, 1), −1.3 (s, 3.5), −4.5 (s, 4.7), −5.5 (s, 0.3); (0.09 M), δ 1.8 (s, 1), −1.3 (s, 4.5), −4.5 (s, 7.8), −5.5 (s, 1.5). $^7Li$ NMR (194.4 MHz, $C_6D_6$): δ 3.13 (s), 1.8–2.1 (m), 1.5–1.8 (m); cryoscopy (benzene, $K_b$ = 5.12 K kg $mol^{-1}$): (0.003 M), $\Delta T$ = 0.042 K, RMM 394 ± 42 [degree of association (relative to $Ph_3P{=}NLi{\cdot}LiBr{\cdot}2thf$), $n$ = 0.75]; (0.008 M), $\Delta T$ = 0.103 K, RMM = 494 ± 20 ($n$ = 0.95); (0.014 M), $\Delta T$ = 0.151 K, RMM = 549 ± 15 ($n$ = 1.05). **3b**: yield 45%, mp 166 °C. $^1H$ NMR (200 MHz, $C_6D_6$): δ 7.95 (m, 6 H, *o*-Ph), 6.9–7.7 (m, 9 H, *m*, *p*-Ph), 3.55 (qnt, 8 H, α-thf), 1.25 (qnt, 8 H, β-thf).

‡ *X-Ray structure determinations*: Yellow crystals of $C_{52}H_{62}Br_2Li_4N_2O_4P_2{\cdot}1.5$arene (arene = $C_6H_6$ **3a**, $C_6H_5Me$ **3b**), are isomorphous, triclinic, space group $P\bar{1}$ (no. 2), $M$ = 1145.7 [1166.8], $a$ = 10.682(1) [10.575(1)], $b$ = 13.758(1) [13.882(1)], $c$ = 22.280(1) [22.398(1)] Å, α = 102.91(1) [100.61(1)], β = 90.85(1) [91.33(1)], γ = 109.74(1) [109.81(1)°], $U$ = 2989.4(4) [3027.5(4) Å$^3$], $Z$ = 2, $D_c$ = 1.27 [1.28] g $cm^{-3}$, μ = 14.6[14.4] $cm^{-1}$, crystal size 0.48 × 0.44 × 0.36 [0.5 × 0.32 × 0.2 mm]. Data collection at $T$ = 150 K, Siemens CCD area detector, graphite-monochromated Mo-Kα radiation, $\bar{\lambda}$ = 0.71073 Å, ω scan mode, $2\theta \leqslant 56°$; Lorentz, polarization and semi-empirical absorption correction[14a] (on Laue equivalents) were applied; min., max. transmission 0.525, 0.638 [0.618, 0.899]; 18255 [14163] total data, 10556 [9818] unique, 8902 [7726] observed [$I \geqslant 2\sigma(I)$]; $R_{int}$ = 0.045 [0.071] before and 0.034 [0.042] after absorption correction. The structures were solved by direct methods and refined by full-matrix least squares against $F^2$, using SHELXTL (Version 5/VMS) software.[14b] Non-H atoms were refined anisotropically (disordered ones isotropically) with all H atoms, 'riding', the disordered solvent in **3b** as rigid bodies; 673 [663] variables *vs*. 10463 [9428] data, $R_w$ ($F^2$, all data) = 0.127 [0.271], $R$($F$, obs. data) = 0.045 [0.079], max. residual Δρ = 0.85 [0.94] e Å$^{-3}$. One solvent molecule is in a general position, another at an inversion centre, in **3b** both are disordered. Two thf rings in **3a** and three in **3b** are also disordered. Atomic coordinates, bond lengths and angles, and thermal parameters for **3a** and **3b** have been deposited at the Cambridge Crystallographic Data Centre (CCDC). See Information for Authors, Issue No. 1. Any request to the CCDC for this material should quote the full literature citation and the reference number 182/474.

§ Conceptually similar to the so-called ammonium salt route method of preparing Lewis base-complexed inorganic lithium salts.[15]

¶ We have determined the structure of $Ph_3PNH$ by X-ray (at 153 K) and neutron (at 20 K) diffraction and find the P–N distance to be 1.562(3) and 1.582(2) Å, respectively.[16] Another report of the X-ray structure of $Ph_3PNH$ (at 203 K) gives the P–N distance as 1.524(3) Å.[11b]

## References

1 D. R. Armstrong, M. G. Davidson and D. Moncrieff, *Angew. Chem., Int. Ed. Engl.*, 1995, **34**, 478.
2 A. W. Johnson, *Ylides and Imines of Phosphorus*, Wiley, New York, 1993.
3 W. Setzer and P. von R. Schleyer, *Adv. Organomet. Chem.*, 1985, **24**, 353; K. Gregory, P. von R. Schleyer and R. Snaith, *Adv. Inorg. Chem.*, 1991, **37**, 47.
4 H. Schmidbaur and G. Jonas, *Chem. Ber.*, 1967, **100**, 1120.
5 A. Steiner and D. Stalke, *Angew. Chem., Int. Ed. Engl.*, 1995, **34**, 1752.
6 H.-J. Cristau, J. Kadoura, L. Chiche and E. Torreilles, *Bull. Soc. Chim. Fr.*, 1989, 515.
7 Ref. 2, pp. 440–446, and references therein.
8 See for example: (*a*) H. Schmidbaur, A. Schier and U. Schubert, *Chem. Ber.*, 1983, **116**, 1938; (*b*) H. Hope and P. P. Power, *J. Am. Chem. Soc.*, 1983, **105**, 5320.
9 See for example: P. A. van der Schaaf, M. P. Hogerheide, D. M. Grove, A. L. Spek and G. van Koten, *J. Chem. Soc., Chem. Commun.*, 1992, 1703.
10 A. Bauer, F. Gabbaï, A. Schier and H. Schmidbaur, *Philos. Trans. R. Soc. London A*, 1996, **354**, 381.
11 (*a*) K. Dehnicke and J. Strähle, *Polyhedron*, 1989, **8**, 707; (*b*) M. Grün, K. Harms, R. Meyer zu Köcker, K. Dehnicke and H. Goesmann, *Z. Anorg. Allg. Chem.*, 1996, **622**, 1091.
12 (*a*) G.Bandoli, G. Bortolozzo, D. A. Clemente, U. Croatto and C. Panattoni, *J. Chem. Soc. A*, 1970, 2778; (*b*) A. L. Spek, *Acta Crystallogr., Sect. C*, 1987, **43**, 1233.
13 D. Seebach, *Angew. Chem., Int. Ed. Engl.*, 1988, **27**, 1624.
14 (*a*) G. M. Sheldrick, A. G. Orpen, B. E. Reichert and P. R. Raithby, Abstracts of ECM4, Oxford, 1977, p. 147; (*b*) G. M. Sheldrick, SHELXTL, Version 5/VMS, Siemens Analytical X-Ray Instruments Inc., Madison, WI, 1995.
15 R. Snaith and D. S. Wright, *Lithium Chemistry—A Theoretical and Experimental Overview*, ed. A. M. Sapse and P. v. R. Schleyer, Wiley, New York, 1995, ch. 5.
16 M. G. Davidson, A. E. Goeta, J. A. K. Howard, C. W. Lehmann, G. M. McIntyre and R. Price, *J. Organomet. Chem.*, in the press.

*Received in Basel, Switzerland, 3rd March 1997; Com. 7/01485F*

# Crystal structure of a flexible self-assembled two-dimensional square network complex $[Cu_2(C_3H_2O_4)_2(H_2O)_2(4,4'\text{-bpy})]\cdot H_2O$

**Jianmin Li,*[a,b] Huaqiang Zeng,[a] Jinhua Chen,[a] Quanming Wang[b] and Xintao Wu[b]**

[a] *Department of Chemical Physics, University of Science and Technology of China, Hefei, Anhui 230026, P.R. China*
[b] *State Key Laboratory of Structural Chemistry, Chinese Academy of Sciences, Fuzhou, Fujian 350002, P.R. China*

**The structure of a self-assembled two-dimensional square network complex, $[Cu_2(C_3H_2O_4)_2(H_2O)_2(4,4'\text{-bpy})]\cdot H_2O$, comprising both flexible and rigid ligands and having a large inner cavity of 15.776(3) × 15.786(2) Å, is reported.**

Since the first self-assembly of square supramolecules was reported in 1990,[1a] novel, tetranuclear, cationic macrocycles, with bond angles of *ca*. 90°, have emerged as the newest members of the family of supramolecular assemblies.[1–3] Much less is known about extended two-dimensional systems[4] based on molecular squares, on account of the lack of methods for linking monomer or molecular units. In all these cases, only rigid ligands such as 4,4′-bipyridine are chosen as the bridging ligands, although Fujita *et al.*[1d] and Slone *et al.*[3c] tried to utilize more flexible ligands to link the transition metals, they could not isolate molecular squares but only macrocyclic dinuclear complexes. Flexible organic macrocycles such as crown ethers, cyclophanes, cyclodextrins, calixarenes, clathrates are ubiquitous,[5] and this prompted us to investigate whether it is possible to combine flexible ligands with rigid ligands within a single crystal. Here we report the first X-ray crystal structure of a flexible self-assembled two-dimensional square network $[Cu_2(C_3H_2O_4)_2(H_2O)_2(4,4'\text{-bpy})]\cdot H_2O$ **1** comprising both flexible and rigid bridging ligands and having an inner cavity of 15.776(3) × 15.786(2) Å surrounded by 4,4′-bpy and malonate groups. We thus have introduced a new concept of flexible self-assembly of supramolecules.

When $Cu(C_3H_2O_4)\cdot 2H_2O$† was treated with 4.4′-bipyridine in $H_2O$–EtOH at ambient temperature [eqn. (1)], deep-blue crystals grew within several days.‡ Yields in excess of 90% were obtained and the structure of **1** was solved by single-crystal X-ray diffraction.§

$$2nCu^{2+} + 2nC_3H_2O_4^{2-} + n4,4'\text{-bpy} + 2nH_2O \xrightarrow{H_2O\text{–EtOH}} \mathbf{1} \quad (1)$$

The crystal structure of **1** is shown in Fig. 1 and can be characterized by the following features. (*i*) It consists of two-dimensional networks which are stacked parallel but in a staggered manner on each other along the *z*-axis, with an interplanar separation of 3.785 Å and angle of 45.0°. The packing of the two-dimensional polymers reveals that the small malonate rings in one layer fit exactly into the large 4,4′-bpy rings in the next, it is almost as if the two rings are acting as templates for each other. This feature is very exciting, and this complementarity of the two rings probably explains the unusually high yield of the complex (Fig. 2). (*ii*) Each network involves a small planar square with $Cu^{II}$ ions and malonate ions at each corner and side, respectively; each $Cu^{II}$ is also bridged by one 4,4′-bpy, thus forming a large square with each edge shared by one malonate group and one 4,4′-bpy ligand. The coordination geometry about each $Cu^{II}$ is a slightly distorted square pyramid (the geometric τ value is 0.15[6]). (*iii*) All the planar squares are distorted only to a small extent. The square-planar angles are 89.89(1) and 89.99(1)° in the large square and 89.25(3) and 89.35(3)° in the small one, very close to the ideal square-planar angle of 90°. The inner cavities have dimensions of 15.776(3) × 15.786(2) Å and 4.644(2) × 4.649(2) Å, respectively and no solvent molecules are clathrated in the cavities. Uncoordinated water molecules are distributed statistically. (*iv*) A malonate ion adopts a bridging position which enhances the stability of the two-dimensional network, the third coordinates to the neighbouring Cu atom. (*v*) All coordinated water molecules are nearly perpendicular to the CuNOOO base plane and two adjacent water molecules are arranged in *trans*-coordination, with two water molecules of two opposite corners being on the same side relative to the $Cu_4$ plane.

It is particularly interesting that four $Cu^{II}$ ions and four flexible malonate groups form a small planar square and four six-membered chelate rings *via* self-assembly. We define this phenomenon as flexible self-assembly of supramolecules. Recently, Tosik *et al.*[7] pointed out the conformational flexibility of chelated malonate rings through analyses of the large difference of the typical puckering of the five known $Cu^{II}$-chelated malonate rings. The conclusion can be further confirmed by the variation of bond lengths and angles belonging to the six-membered chelate ring relative to known

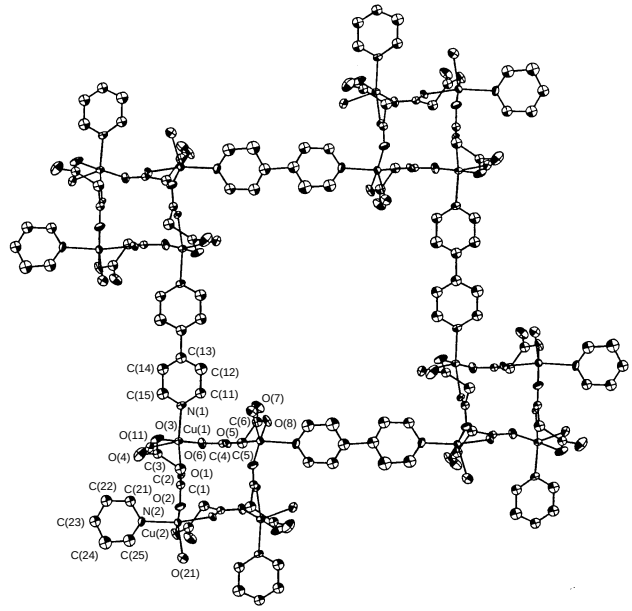



**Fig. 1** ORTEP diagram of **1** with labelling scheme. Selected bond lengths (Å) and angles (°): Cu(1)–O(1) 1.996(7), Cu(1)–O(3) 1.93(1), Cu(1)–O(6) 1.98(1), Cu(1)–O(11) 2.20(1), Cu(1)–N(1) 2.06(1), Cu(2)–O(2) 1.97(1), Cu(2)–O(5$^i$) 1.972(7), Cu(2)–O(8$^i$) 1.93(1), Cu(2)–O(21) 2.191(9), Cu(2)–N(2) 2.06(1), O(1)–Cu(1)–O(3) 89.6(4), O(1)–Cu(1)–O(6) 89.3(4), O(1)–Cu(1)–O(11) 91.4(3), O(1)–Cu(1)–N(1) 166.2(4), O(3)–Cu(1)–O(6) 174.9(4), O(3)–Cu(1)–O(11) 93.2(4), O(3)–Cu(1)–N(1) 87.1(4), O(6)–Cu(1)–O(11) 91.7(4), O(6)–Cu(1)–N(1) 92.8(4), O(11)–Cu(1)–N(1) 102.1(4), O(2)–Cu(2)–O(5$^i$) 89.5(4), O(2)–Cu(2)–O(8$^i$) 174.1(4), O(2)–Cu(2)–O(21) 92.5(4), O(2)–Cu(2)–N(2) 91.5(4), O(5$^i$)–Cu(2)–O(8$^i$) 89.8(4), O(5$^i$)–Cu(2)–O(21) 92.4(3), O(5$^i$)–Cu(2)–N(2) 167.1(5), O(8$^i$)–Cu(2)–O(21) 93.3(4), O(8$^i$)–Cu(2)–N(2) 87.8(4), O(21)–Cu(2)–N(2) 100.4(4). i: $1-x, -y, z$.

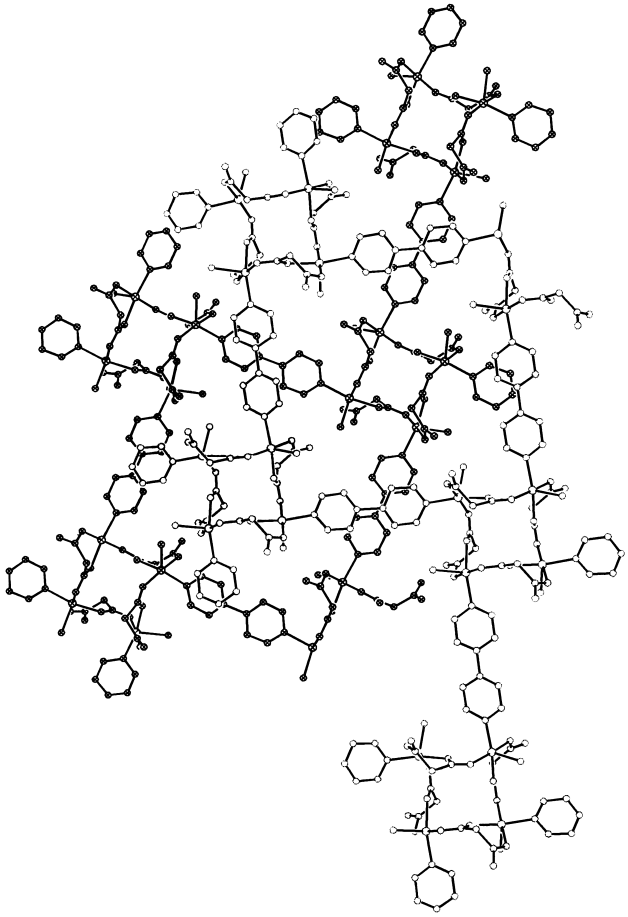


**Fig. 2** Packing diagram for **1** along the *z*-axis

compounds. Including our compound, reported Cu–O, C–O and C–C distances[7–9] are in the ranges 1.909–1.996, 1.22–1.272, and 1.48–1.530 Å, respectively, and the O–M–O angles[7–10] range from 85.0 to 94.82° in the metal-chelated malonate rings.

In summary, a novel, self-assembled two-dimensional square network complex, $[Cu_2(C_3H_2O_4)_2(H_2O)_2(4,4'\text{-bpy})]\cdot H_2O$, constitutes the first example that comprises both flexible and rigid ligands within one single crystal structure.

We thank the State Key Laboratory of Structural Chemistry, Fujian Institute of Research of Structure of Matter, Chinese Academy of Science, for financial support.

## Footnotes

* E-mail: jmli@dchp.chp.ustc.edu.cn

† *Preparation of* $Cu(C_3H_2O_4)\cdot 2H_2O$: to a mixture of copper(II) carbonate (2.0 mmol) and hot water (20 ml), malonic acid (1.9 mmol) was added and a dark blue solution was obtained. This was filtered and condensed to 5 ml and a large amount of crystals were obtained. Anal. calc. for $Cu(C_3H_2O_4)\cdot 2H_2O$: C, 17.70; H, 3.47. Found: C, 17.14; H, 3.59%.

‡ *Preparation of* **1**: to an aqueous solution (30 ml) of $Cu(C_3H_2O_4)\cdot 2H_2O$ (1.0 mmol) an ethanol solution (10 ml) of 4,4′-bpy (0.5 mmol) was added. The initially formed very small amount of fine precipitate was filtered off, and the clear filtrate was allowed to stand for several days at ambient temperature to give deep-blue crystals. Yields in excess of 90% were obtained. Anal. calc. for **1**: C, 36.43; H, 3.44, N, 5.31. Found: C, 36.50; H, 3.21; N, 5.09%.

§ *Crystal data* for **1**: $M$ = 2190.68, orthorhombic, space group $P2_12_12_1$ (no. 18), $a$ = 16.348(3), $b$ = 16.364(5), $c$ = 7.570(1) Å, $V$ = 2025.2(8) Å$^3$, $F(000)$ = 1104, $Z$ = 4, $D_c$ = 1.78 g cm$^{-3}$, $T$ = 296 K, μ(Mo-Kα) = 21.7 cm$^{-1}$, λ(Mo-Kα) = 0.710 69 Å. A crystal of approximate dimensions 0.40 × 0.40 × 0.25 mm was mounted on a Rigaku AFC5R diffractometer, using graphite-monochromated Mo-Kα radiation. Cell constants and orientation matrix for data collection were obtained from least-squares refinement, using the setting angles of 20 reflections in the range $8 < \theta < 27.5°$, measured by the computer controlled diagonal slit method of centring. Scattering factors were taken from Cromer and Waber.[11] The ω–2θ scan mode with a maximum 2θ value being 50.0° were used to collect intensity data. A total of 2075 reflections were collected, of which 2075 were unique, and 1579 had $I > 3\sigma(I)$ with 199 parameters. The data were corrected for Lorentz-polarization effects, and empirical absorption (from 0.70 to 1.00 in $I$). The structure was solved by direct methods and refined by full-matrix least-squares calculation. Cu atoms were located in the $E$ map, the remaining atoms were located in succeeding difference Fourier syntheses. H atoms of the disordered water were not included, H atoms of the coordinated water were added by difference Fourier synthesis and the other H atoms were placed at calculated positions. All H atoms were unrefined. All calculations were performed on a COMPAQ computer using Mo1EN/PC.[12] Final $R$ = 0.055, $R_w$ = 0.079 (unit weights), goodness of fit = 1.69, max. shift/e.s.d. = 0.02. The minimum and maximum peaks in the final difference Fourier map are at −0.33 and 0.87 e Å$^{-3}$, respectively. Atomic coordinates, bond lengths and angles, and thermal parameters have been deposited at the Cambridge Crystallographic Data Centre (CCDC). See Information for Authors, Issue No. 1. Any request to the CCDC for this material should quote the full literature citation and the reference number 182/464.

## References

1 (*a*) M. Fujita, J. Yakazi and K. Ogura, *J. Am. Chem. Soc.*, 1990, **112**, 5645; (*b*) M. Fujita and K. Ogura, *J. Am. Chem. Soc.*, 1993, **115**, 1574; (*c*) M. Fujita, Y. J. Kwon, S. Washizu and K. Ogura, *J. Am. Chem. Soc.*, 1994, **116**, 4981; (*d*) M. Fujita, O. Sasaki, T. Mitsuhashi and T. Fujita, *Chem. Commun.*, 1996, 1535.

2 P. J. Stang and D. H. J. Cao, *J. Am. Chem. Soc.*, 1993, **115**, 1574; P. J. Stang and J. A. Whiteford, *Organometallics*, 1994, **13**, 3776; P. J. Stang and K. Chen, *J. Am. Chem. Soc.*, 1995, **117**, 6273; P. J. Stang and B. Olenyuk, *Angew. Chem., Int. Ed. Engl.*, 1996, **35**, 732.

3 (*a*) C. M. Drain and J.-M. Lehn, *J. Chem. Soc., Chem. Commun.*, 1994, 2313; (*b*) H. Rauter, E. C. Hillgeris, A. Erxleben and B. Lippert, *J. Am. Chem. Soc.*, 1994, **116**, 616; (*c*) R. V. Slone, D. I. Yoon, R. M. Calhoun and J. T. Hupp, *J. Am. Chem. Soc.*, 1995, **117**, 11 813; (*d*) R. V. Slone, J. T.Hupp, C. L. Stern and T. E. Albrecht-Schmitt, *Inorg. Chem.*, 1996, **35**, 1096.

4 R. W. Gable, B. F. Hoskins and R. Robson, *J. Chem. Soc., Chem. Commun.*, 1990, 1677; M. Fujita, Y. J. Kwon, S. Washizu and K. Ogura, *J. Am. Chem. Soc.*, 1994, **116**, 1151; S. Subramanian and M. J. Zaworotko, *Angew. Chem., Int. Ed. Engl.*, 1995, **34**, 2127.

5 *Supramolecular Chemistry*, ed. V. Balzani and L. DeCola, Kluwer Academic Publishers, Elsevier, 1992; *Host–Guest Complex Chemistry: Synthesis, Structure, Applications*, ed. F. Vogtle and E. Weber, Springer-Verlag, Berlin, 1985; F. Diederich, *Cyclophanes*, Royal Society of Chemistry, Cambridge, 1991; *Calixarenes: A Versatile Class of Macrocyclic Compounds*, ed. J. Vicens and V. Bohmer, Kluwer Academic, Elsevier, 1990; C. D. Gutsche, *Calixarenes*, Royal Society of Chemistry, London, 1989; *Inclusion Phenomena and Molecular Recognition*, ed. J. L. Atwood, Plenum, New York, 1990; ed. E. Weber, *Top. Curr. Chem.*, 1987, **149**.

6 A. W. Addison and T.N. Rao, *J. Chem. Soc., Dalton Trans.*, 1984, 1349.

7 A. Tosik, L. Sieron and M. Bukowska-Strzyzewska, *Acta Crystallogr., Sect. C*, 1995, 1987.

8 D. Chattopadhyay, S. K. Chattopadhyay and P. R. Lowe, *J. Chem. Soc., Dalton Trans.*, 1993, 913.

9 W.-L. Kwik, K.-P. Ang and H. S.-O. Chan, *J. Chem. Soc., Dalton Trans.*, 1986, 2519.

10 K. H. Chung, E. Hong, Y. Do and C. H. Moon, *J. Chem. Soc., Chem. Commun.*, 1995, 2333.

11 D. T. Cromer and J. T. Waber, *International Tables for X-Ray Crystallography*, Kynoch Press, Birmingham, vol. 4, 1974, Table 2.2B.

12 Molen, *An Interactive Structure Solution Procedure*, Enraf-Nonius, Delft, 1990.

*Received in Cambridge, UK, 21st January 1997; Com. 7/00491E*

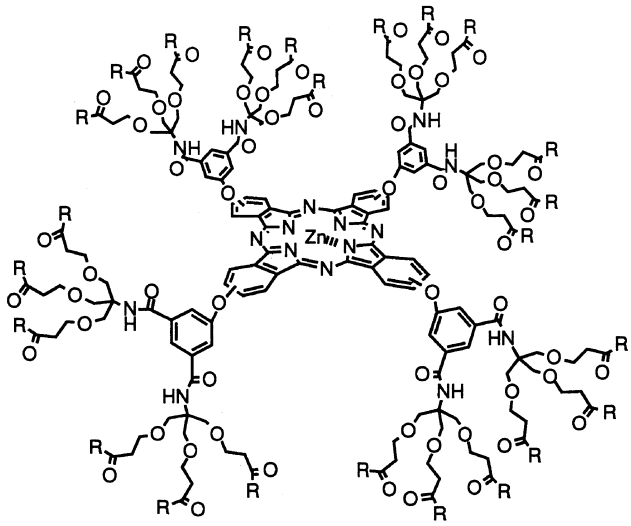
# Dendritic metallophthalocyanines: synthesis and characterization of a zinc(II) phthalocyanine[8]$^3$-arborol

**Mutsumi Kimura,*[a] Kazuaki Nakada,[a] Yuji Yamaguchi,[a] Kenji Hanabusa[a] Hirofusa Shirai[a] and Nagao Kobayashi[b]**

[a] *Department of Functional Polymer Science, Faculty of Textile Science and Technology, Shinshu University, Ueda 386, Japan*
[b] *Department of Chemistry, Graduate School of Science, Tohoku University, Sendai 980-77, Japan*

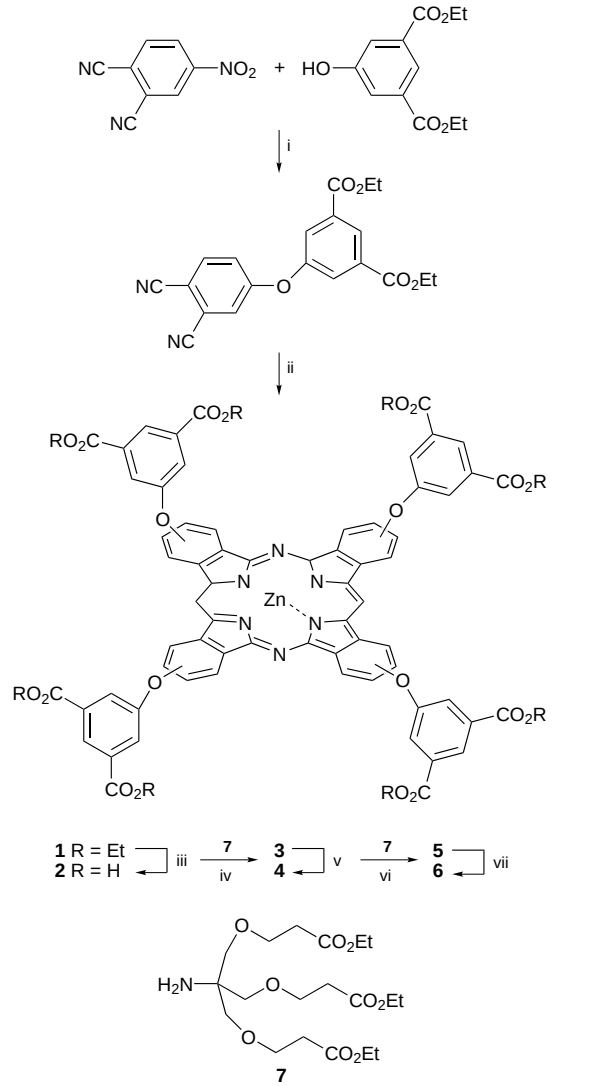
**New dendritic metallophthalocyanines are prepared on the basis of Newkome's divergent-growth approach; the number of generations within the dendrimer is found to affect the aggregation behaviour of the zinc(II) phthalocyanine moiety which forms the interior core of the dendrimers.**

The synthesis of dendrimers has recently attracted much interest. Dendrimers have a well defined globular structure with uniform molecular mass.[1] Functional dendrimers have been prepared by the introduction of functional compounds such as metal complexes, fullerenes and biomaterials to the exterior surface and the interior cores of dendrimers.[2] Highly branched dendrimers have provided a unique environment for these functional compounds, giving rise to a variety of new and modified properties.[3] Constructing a dendrimer around a phthalocyanine core could control the aggregation of the complex in aqueous media and modify its photoreactivity. Here, we report the synthesis of the first dendritic zinc(II) phthalocyanines **3**–**6** using cascade polymer methodology. The environment of photoactive zinc phthalocyanine can be controlled through encapsulation in dendrimers.



**3**; R = –OEt
**4**; R = –OLi
**5**; R = –NHC($CH_2OCH_2CH_2CO_2Et$)$_3$
**6**; R = –NHC($CH_2OCH_2CH_2CO_2Li$)$_3$

The polyether–amide dendrimers containing zinc(II) phthalocyanine derivatives were prepared by the method of Newkome *et al.*[4] according to Scheme 1.[4] The starting point for the synthesis of the dendrimers **3**–**6** was the octacarboxylic acid **2** prepared from ester **1**. Reaction of acid **2** with amine **7**, dicyclohexylcarbodiimide (DCC) and 1-hydroxybenzotriazole (HOBt) in THF at 5 °C affords the first generation dendrimer **3** in 75% yield which was purified by gel permeation chromatography (Biorad Biobeads SX-3, ethyl acetate). The hydrolysis of **3** with LiOH in MeOH–$H_2O$ afforded the first-generation dendrimer **4** bearing 24 carboxylic acid groups. A repeat of this reaction gave the second-generation dendrimers **5** and **6**. Dialysis of the reaction mixture for 2 d after hydrolysis of **3** and **5** in water, followed by freeze-drying, gave the water-soluble dendrimers **4** and **6**. The structures of these compounds were confirmed by $^1$H and $^{13}$C NMR spectroscopies, FTIR, UV–VIS



**Scheme 1** Synthesis of dendrimers **3**–**6**. *Reagents and conditions*: i, $K_2CO_3$, DMF, room temp., 72%; ii, DBU, $ZnCl_2$, *n*-pentanol, reflux, 24 h, 42%; iii, NaOH, $H_2O$–THF, 48 h, 96%; iv, DCC, HOBt, THF, 5 °C, 72 h, 75%; v, LiOH, MeOH–$H_2O$ (1 : 1), 20 °C, 48 h, 96%; vi, DCC, HOBt, THF, 5 °C, 72 h, 70%; vii, LiOH, MeOH–$H_2O$, 48 h, 81%.

and mass spectrometric analysis. Compounds **1**, **3** and **5** were soluble in organic solvents (*e.g.* chloroform, benzene, THF, DMF, acetonitrile) while **2**, **4** and **6** were water-soluble. GPC chromatograms of esters **3** and **5** show a single sharp peak for each dendrimer. These results indicate that the dendrimers are monodispersed. Dendrimer **6** (0.5 mM aqueous solution) was negatively stained, dried and examined using transmission electron microscopy (Fig. 1). The aggregates of small spheres (*ca*. 20 nm diameter) appear as light areas against a darker background. CPK models of **6** predict a highly branched, globular structure, approximately 5 nm in diameter. From the dimensions of **6** *ca*. 30 molecules of the dendrimer per aggregate is estimated.

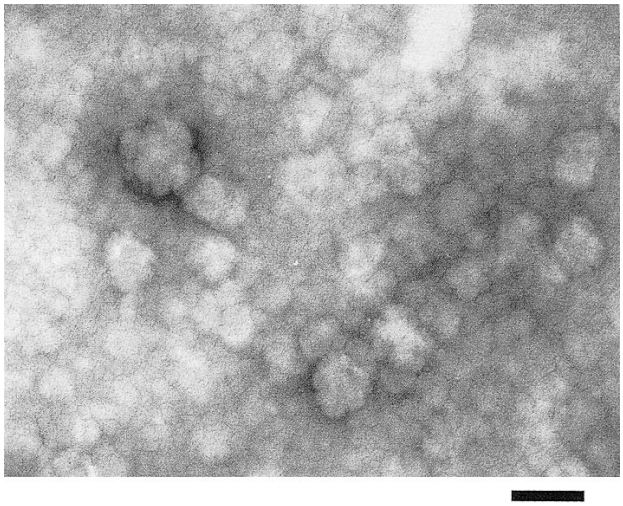


**Fig. 1** Transition electron micrograph of **6**, negatively stained with 2% phosphotungstic acid. Bar = 100 nm; 120 000 × magnification.

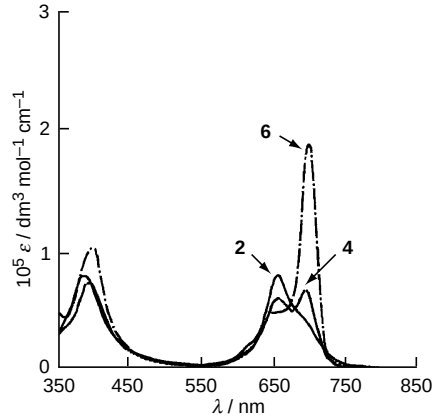



**Fig. 2** UV–VIS spectra of dendritic phthalocyanines **2**, **4** and **6** in aqueous phosphate buffer at pH 7.1

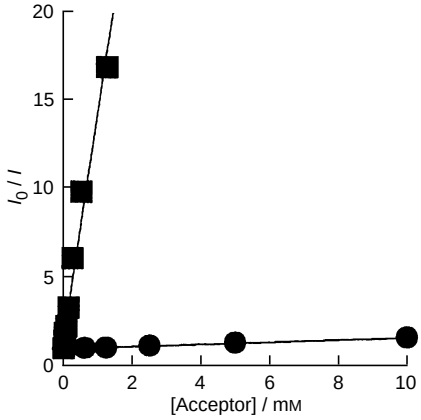



**Fig. 3** Steady-state fluorescence titration of $MV^{2+}$ (■) and SPV (●) into **6** (1.2 μM), excitation 370 nm, emission 674 nm in aqueous phosphate buffer at pH 7.1

The UV–VIS spectra indicate the inner environment of zinc phthalocyanine located within the interior core of the dendrimers. The spectra of **3** and **5** showed a sharp peak at 678.0 nm [log (ε/dm$^3$ mol$^{-1}$ cm$^{-1}$) = 5.47] with a shoulder at 621.0 nm in $CHCl_3$, and were not influenced by the number of the generations. In aqueous media, the UV–VIS spectra of **2**, **4** and **6** were quite different, reflecting the number of generations. Dendrimer **6** showed a Q band at 687.0 nm which is typical of non-aggregated Zn phthalocyanines (Fig. 2). However, a sharp peak was not observed for **2** and **4**. The spectra of **2**, **4** and **6** were little affected upon increasing the pH from 7.1 to 10.5. The broad peak at 622.0 nm, attributed to the aggregation of Zn phthalocyanine, indicates that the complexes interacted hydrophobically in aqueous media.[5] With increasing dendrimer generation, the shielding effect of the dendrimer is enhanced owing to the increased size of the molecular cage. Zinc phthalocyanine exhibits a strong fluorescence peak at 674 nm upon excitation at 370 nm, which is quenched by the addition of methyl viologen ($MV^{2+}$) and propylviologen sulfonate (SPV). Dendrimer **6** displays a strong fluorescence peak in aqueous media, however, **2** and **4** did not fluoresce because of aggregation of zinc phthalocyanine units. Stern–Volmer plots differ using $MV^{2+}$ or SPV as electron-transfer quenching agents (Fig. 3). Addition of a small amount of positively charged $MV^{2+}$ to an aqueous solution of **6** led to efficient fluorescence quenching. On the other hand, only little fluorescence quenching occurred upon addition of zwitterionic SPV. Addition of NaCl drastically diminished the fluorescence quenching by $MV^{2+}$. This behaviour can be explained by a decrease in the local concentration of $MV^{2+}$ adjacent to the dendrimer surface. This efficient quenching of the phthalocyanine fluorescence occurs *via* accumulation of $MV^{2+}$ on the negatively charged dendrimer surface. The fluorescence quenching results suggest an electron-transfer reaction between the zinc phthalocyanine and $MV^{2+}$ through the dendrimer framework. The electron-transfer quenching agents were reduced by **6** under light irradiation in the presence of triethanolamine as a sacrificial donor.

In conclusion, the number of generations affected the aggregation behaviour of the zinc phthalocyanine located in the centre of the dendrimer. The molecular cage inhibited aggregation of the zinc phthalocyanines in aqueous media, and electron transfer was observed through the dendrimer architecture from the zinc phthalocyanine core to $MV^{2+}$ accumulated on the surface of the dendrimer.

## Footnote

* E-mail: mkimura@giptc.shinshu-u.ac.jp

## References

1 D. A. Tomalia and H. D. Durst, *Top. Curr. Chem.*, 1993, **165**, 193; J. M. J. Fréchet, *Science*, 1994, **263**, 1710.
2 S. Achar and R. J. Puddephatt, *J. Chem. Soc., Chem. Commun.*, 1994, 1895; C. J. Hawker, K. L. Wooley and J. M. J. Fréchet, *J. Chem. Soc., Chem. Commun.*, 1994, 925; G. R. Newkome, X. Lin and C. D. Weis, *Tetrahedron: Asymmetry*, 1991, **2**, 957; K. Aoi, K. Itoh and M. Okada, *Macromolecules*, 1995, **28**, 5391.
3 R.-H. Jin, T. Aida and S. Inoue, *J. Chem. Soc., Chem. Commun.*, 1993, 1260; R. Sadamoto, N. Tomioka and T. Aida, *J. Am. Chem. Soc.*, 1996, **118**, 3978; P. J. Dandliker, F. Diederich, M. Gross, C. B. Knobler, A. Louati and M. E. Sanford, *Angew. Chem., Int. Ed. Engl.*, 1994, **33**, 1739.
4 G. R. Newkome and X. Lin, *Macromolecules*, 1991, **24**, 1443.
5 A. Louati, M. E. I. Meray, J. J. Andre, J. Simon, K. M. Kadish, M. Gross and A. Giraudeau, *Inorg. Chem.*, 1985, **24**, 1175; J. R. Darwent, I. MaCubbin and G. Porter, *J. Chem. Soc.*, 1982, **78**, 903.

*Received in Cambridge, UK, 24th February 1997; Com. 7/01263B*

# Metal modified carbohydrates: syntheses of furanosylidene complexes and their aza analogues[1]

**Karl Heinz Dötz,*[a] Wilm-Christian Haase,[a] Markus Klumpe[a] and Martin Nieger[b]**

[a] *Kekulé-Institut für Organische Chemie und Biochemie der Rheinischen Friedrich-Wilhelms-Universität, D-53121 Bonn, Germany*
[b] *Anorganisch-chemisches Institut der Rheinischen Friedrich-Wilhelms-Universität, D-53121 Bonn, Germany*

**Alkene metathesis and a sugar lactam electrophile/metalate nucleophile combination have been exploited in the synthesis of furanosylidene complexes and their aza analogues.**

Fischer-type carbene complexes $(CO)_5M{=}C(XR')R$ (M = Cr, W; X = O, NR″) have been developed as useful reagents in stereoselective organic synthesis. Their synthetic potential covers cycloaddition reactions,[2] including benzannulation,[2a] cyclopropanation,[2b,c] and—based on the photolytic generation of ketene equivalents[2d]—addition of imines or oxygen nucleophiles, affording β-lactams or α-amino acids, as well as aldol- and Michael-type addition reactions.[2e,f]

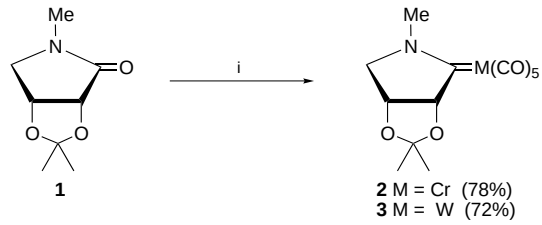
Exploiting the synthetic potential of organometallics in the developing field of C-glycoside chemistry[3] has generally been limited to stannylated and lithiated compounds. Although some encouraging examples of transition metal mediated C-glycosidations have been reported,[4b,c] well-characterized glycosyl complexes are to date only known for manganese,[4c,d] cobalt[4e] and iron.[4f] In this type of compound the anomeric centre behaves as a nucleophile; in contrast, we aimed at the incorporation of an electrophilic metal-carbene functionality into the carbohydrate skeleton. Recently, we reported on the synthesis of the first C-1 carbene complex-functionalized sugars of chromium, iron, molybdenum and tungsten[5] exploiting a strategy that can be applied to acyclic carbohydrates. We now describe two independent routes to cyclic metal glycosylidenes bearing a transition metal-stabilized carbene functionality at the former anomeric carbon atom.

Our first approach is based on the Hegedus route[6] which allows modification of amides and unsubstituted lactams into metal aminocarbenes. We have extended this strategy to a sugar lactam electrophile/metalate nucleophile combination: the reaction of *N*-methyl-2,3-*O*-isopropylidene-D-erythronolactam **1**[7] with $K_2M(CO)_5$ (M = Cr, W) affords the pentacarbonyl[1,4-dideoxy-2,3-*O*-isopropylidene-1,4-methylimino-D-erythrofuranosylidene] complexes **2** and **3** in good yields (Scheme 1).

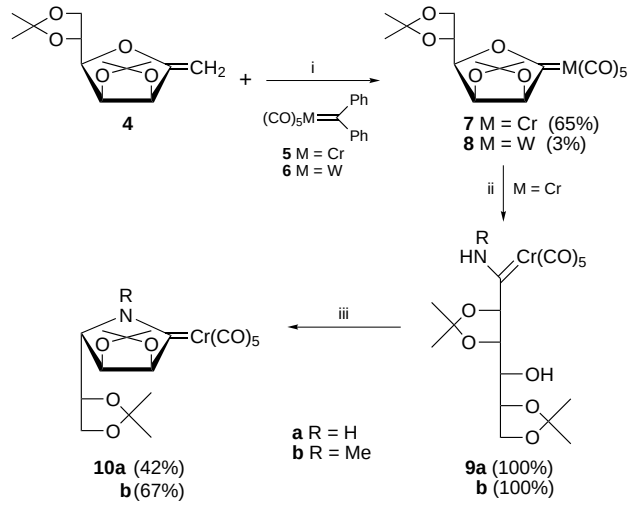
As neither the classical Fischer route[8] nor the dianion route turned out to be suited for the preparation of oxacycloalkylidene complexes, we focussed on an alkene metathesis approach.[9] The reaction of 2,5-anhydro-1-deoxy-3,4 : 6,7-di-*O*-isopropylidene-D-*manno*-hept-1-enitol **4**[10] with pentacarbonyl(diphenylcarbene) complexes of chromium and tungsten (**5** and **6**)[11] gave the pentacarbonyl(2,3 : 5,6-di-*O*-isopropylidene-D-mannofuranosylidene) complexes **7** and **8** in yields which strongly depend on the metal used (Scheme 2). Glycosylidene complexes **7** and **8** may be regarded as metal-stabilized analogues of the furanoic 'glycosylidene–carbene' intermediates reported by Vasella and co-workers.[12] The pronounced electrophilicity of the metal-carbene moiety favours the addition of nucleophiles. Thus, aminolysis of **7** with ammonia or methylamine generates the open-chain amino(glycosyl)carbene complexes **9a**,**b** offering an unprotected hydroxy group for further functionalization. They readily undergo an intramolecular Mitsunobu reaction[13] and thus provide an access to N-protected and N-deprotected azatalofuranosylidene complexes **10a**,**b** in moderate to good yields. According to X-ray structure analyses† established for **7** and **10b** (Figs. 1 and 2) both complexes adopt a similar envelope-like conformation in the solid state with C(3) being out of plane. Obviously, the epimerization at C(4), which arises from the ring opening/cyclization sequence, has no significant influence on the conformation of the glycosylidene ring. The asymmetric unit of **7** contains two independent molecules which slightly differ in their C(1)–O(1) and C(1)–C(2) bond lengths.

The novel transition metal-stabilized glycosylidene complexes are stable at room temperature and can be handled briefly in air. Their spectroscopic data‡ show the typical characteristics of electrophilic Fischer-type carbene complexes, and as such they are promising reagents for the elaboration of more complex C-glycosidic structures.

Support from the Volkswagen-Stiftung, the Graduiertenkolleg 'Spektroskopie isolierter und kondensierter Moleküle' and the Fonds der Chemischen Industrie is gratefully acknowledged.




**Scheme 1** *Reagents and conditions*: i, $K_2M(CO)_5$, THF, −78 °C, $Me_3SiCl$




**Scheme 2** *Reagents and conditions*: i, *n*-heptane, 20 °C; ii, $CH_2Cl_2$, −78 °C, $RNH_2$; iii, THF, 20 °C, $PPh_3$, diethyl azodicarboxylate

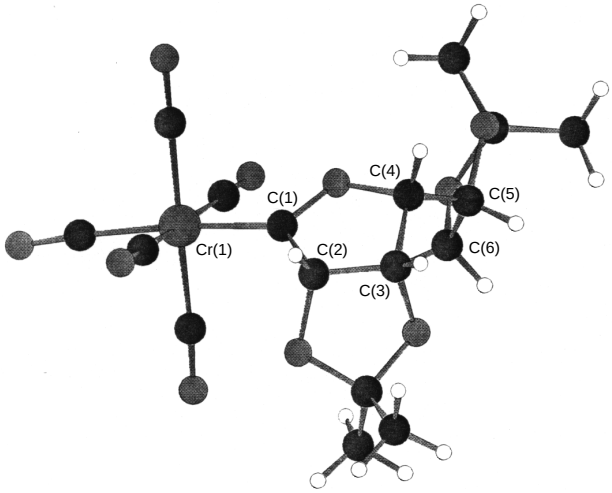



**Fig. 1** Molecular structure of furanosylidene complex **7** (one of two independent molecules). Selected distances (Å) and bond angles (°) (the second independent molecule in brackets): Cr(1)–C(1) 1.979(6) [1.980(6)], C(1)–O(1) 1.302(7) [1.332(7)], C(1)–C(2) 1.560(7) [1.535(8)], O(1)–C(4) 1.483(7) [1.482(7)], Cr(1)–C(1)–O(1) 125.0(4) [123.3(4)], Cr(1)–C(1)–C(2) 128.6(4) [121.8(4)], C(2)–C(1)–O(1) 106.4(5) [106.9(5)].

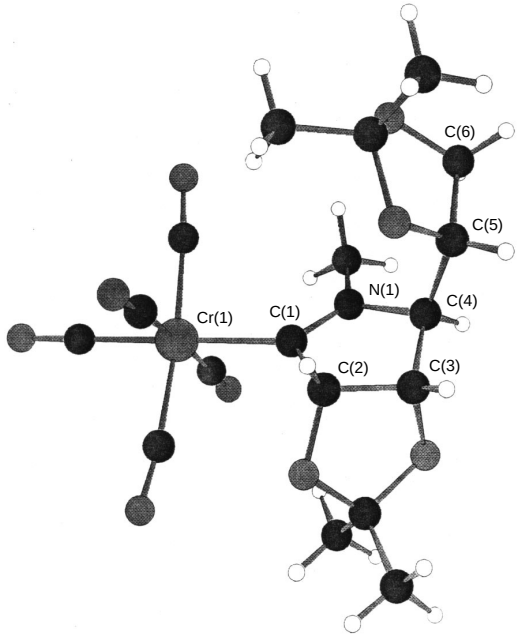



**Fig. 2** Molecular structure of 1,4-iminofuranosylidene complex **10b**. Selected distances (Å) and bond angles (°): Cr(1)–C(1) 2.097(3), C(1)–N(1) 1.313(4), C(1)–C(2) 1.524(4), N(1)–C(4) 1.495(3), Cr(1)–C(1)–N(1) 130.8(2), Cr(1)–C(1)–C(2) 123.7(2), C(2)–C(1)–N(1) 105.4(2).

## Footnotes

* E-mail: doetz@snchemie1.chemie.uni-bonn.de

† *Crystal data* for **7**: $C_{17}H_{18}O_{10}Cr$, $M$ = 434.3, monoclinic, space group $P2_1$ (no. 4), orange crystals, dimensions 0.10 × 0.18 × 0.25 mm, $a$ = 9.648(1), $b$ = 21.872(2), $c$ = 10.271(1) Å, β = 112.92(1)°, $U$ = 1996.3(3) Å$^3$, $D_c$ = 1.45 Mg m$^{-3}$, $Z$ = 4, μ(Cu-Kα) = 5.19 mm$^{-1}$, $T$ = 200(2) K, $F$(000) = 896; 3053 symmetry independent reflections were used for the structure solution (direct methods) and refinement (full-matrix least-squares on $F^2$, 523 parameters, 15 restraints), non-hydrogen atoms were refined anisotropically, H atoms localized by difference electron density and refined using a 'riding' model. $wR2$ = 0.112 {$R_1$ = 0.041 [$I > 2\sigma(I)$]}. The absolute configuration was determined by Flack's $x$-refinement $x$ = 0.00(1) (ref. 14). An empirical absorption correction and an extinction correction were applied (ref. 15).

For **10b**: $C_{18}H_{21}NO_9Cr$, $M$ = 447.4, orthorhombic, space group $P2_12_12_1$ (no. 19), yellow crystals, dimensions 0.20 × 0.30 × 0.50 mm, $a$ = 9.935(4), $b$ = 10.834(3), $c$ = 19.526(11) Å, $U$ = 2102(2) Å$^3$, $D_c$ = 1.41 Mg m$^{-3}$, $Z$ = 4, μ(Mo-Kα) = 0.59 mm$^{-1}$, $T$ = 293(2) K, $F$(000) = 928; 3718 symmetry independent reflections were used for the structure solution (direct methods) and refinement (full-matrix least-squares on $F^2$, 267 parameters), non-hydrogen atoms were refined anisotropically, H atoms localized by difference electron density and refined using a 'riding' model $wR2$ = 0.100 {$R_1$ = 0.038 [$I > 2\sigma(I)$]}. The absolute configuration was determined by Flack's $x$-refinement $x$ = 0.00(2) (ref. 14).

Atomic coordinates, bond lengths and angles, and thermal parameters have been deposited at the Cambridge Crystallographic Data Centre. See Information for Authors, Issue No. 1. Any request to the CCDC for this material should be quoted the full literature citation and the reference number 182/473.

‡ *Selected spectroscopic data* for **2**: $^{13}$C NMR (125 MHz, $CD_3OD$, 273 K): δ 265.1 (1C, C-1), 224.7 (1C, $CO_{trans}$), 219.5 (4C, $CO_{cis}$), 112.8 (1C, $C_{acetal}$), 100.2, 75.9, 69.5 (3C, C-2, C-3, C4), 43.3 (1C, NMe), 27.7, 26.2 (2C, $CH_3$). For **3**: $^{13}$C NMR (125 MHz, $CD_3OD$, 273 K): δ 247.0 (1C, C-1), 204.0 (1C, $CO_{trans}$), 199.3 (4C, $CO_{cis}$), 112.5 (1C, $C_{acetal}$), 100.9, 76.1, 68.3 (3C, C-2, C-3, C-4), 44.8 (1C, $NCH_3$), 27.5, 26.0 (2C, $CH_3$). For **7**. $^{13}$C NMR (100 MHz, $CDCl_3$, 273 K): δ 342.3 (1C, C-1), 223.9 (1C, $CO_{trans}$), 215.7 (4C, $CO_{cis}$), 114.0 (1C, $C_{acetal}$), 109.9 (1C, $C_{acetal}$), 99.1, 97.4, 74.6, 72.5, 65.9 (5C, C-2, C-3, C-4, C-5, C-6), 26.7, 26.4, 25.4, 25.3, (4C, $CH_3$). For **8**: $^{13}$C NMR (125 MHz, $CDCl_3$, 273 K): δ 314.1 (1C, C-1), 204.6 (1C, $CO_{trans}$), 196.5 (4C, $CO_{cis}$), 114.0 (1C, $C_{acetal}$), 109.9 (1C, $C_{acetal}$), 101.5, 97.8, 74.8, 72.4, 66.0 (5C, C-2, C-3, C-4, C-5, C-6), 26.75, 26.73, 25.6, 25.3 (4C, $CH_3$). For **10a**: $^{13}$C NMR (125 MHz, $CDCl_3$, 273 K): δ 279.1 (1C, C-1), 222.8 (1C, $CO_{trans}$), 217.4 (4C, $CO_{cis}$), 112.0 (1C, $CO_{acetal}$), 110.8 (1C, $C_{acetal}$), 95.2, 77.3, 75.7, 75.3, 65.9 (5C, C-2, C-3, C-4, C-5, C-6), 26.8, 26.3, 25.7, 24.8 (4C, $CH_3$). For **10b**: $^{13}$C NMR (125 MHz, $CDCl_3$, 273 K): δ 272.3 (1C, C-1), 223.1 (1C, $CO_{trans}$), 217.7 (4C, $CO_{cis}$) 111.6 (1C, $C_{acetal}$), 110.9 (1C, $C_{acetal}$), 96.6, 82.0, 78.0, 75.8, 66.3 (5C, C-2, C-3, C-4, C-5, C-6), 43.8 (1C, $NCH_3$), 27.0, 26.3, 26.1, 24.6 (4C, $CH_3$).

## References

1 Organotransition metal modified carbohydrates, part 6. For part 5, see K. H. Dötz, R. Ehlenz, O. Neuss and M. Teckenbrock, *Tetrahedron*, 1997, **53**, 5143.
2 Reviews: (*a*) K. H. Dötz, *Angew. Chem.*, 1984, **96**, 573; *Angew. Chem., Int. Ed. Engl.*, 1984, **23**, 587 (*b*) H.-U. Reissig, in *Organometallics in Organic Synthesis*, ed. H. Werner and G. Erker, Springer, Berlin, 1989, vol. 2, p. 311; (*c*) D. F. Harvey and D. M. Sigano, *Chem. Rev.*, 1996, **96**, 271; (*d*) L. S. Hegedus, in *Comprehensive Organometallic Chemistry II*, ed. E. W. Abel, F. G. A. Stone and G. Wilkinson, Pergamon, New York, 1995, vol. 12, p. 549; (*e*) W. D. Wulff, in *Comprehensive Organometallic Chemistry II*, ed. E. W. Abel, F. G. A. Stone and G. Wilkinson, Pergamon Press, New York, 1995, vol. 12, p. 470; (*f*) A. de Meijere, *Pure Appl. Chem.*, 1996, **68**, 61.
3 Review: M. H. D. Postema, *C-Glycoside Synthesis*, CRC Press, Boca Raton, 1955.
4 (*a*) T. Kametani, K. Kawamura and T. Honda, *J. Am. Chem. Soc.*, 1987, **109**, 3010; (*b*) J. C.-Y. Cheng and G. D. Daves, *J. Org. Chem.*, 1987, **52**, 3083; (*c*) P. DeShong, G. A. Slough, V. Elango and G. L. Trainor, *J. Am. Chem. Soc.*, 1985, **107**, 7788; (*d*) P. DeShong, G. A. Slough and V. Elango, *Carbohydr. Res.*, 1987, **171**, 342; (*e*) A. Rosenthal and H. J. Koch, *Tetrahedron Lett.*, 1967, 871; (*f*) G. L. Trainor and B. E. Smart, *J. Org. Chem.*, 1983, **48**, 2247.
5 K. H. Dötz, W. Straub, R. Ehlenz, K. Peseke and R. Meisel, *Angew. Chem.*, 1995, **107**, 2023; *Angew. Chem., Int. Ed. Engl.*, 1995, **34**, 1856.
6 R. Imwinkelried and L. S. Hegedus, *Organometallics*, 1988, **7**, 702; M. A. Schwindt, T. Lejon and L. S. Hegedus, *Organometallics*, 1990, **9**, 2814.
7 S. Hanessian, *J. Org. Chem.*, 1969, **34**, 675; T. Kamiya, Y. Saito, M. Hashimoto and H. Seki, *Tetrahedron*, 1972, **28**, 899.
8 E. O. Fischer and A. Maasböl, *Chem. Ber.*, 1967, **100**, 2445.
9 E. O. Fischer and K. H. Dötz, *Chem. Ber.*, 1972, **105**, 3966; J. Barluenga, F. Aznar and A. Martin, *Organometallics*, 1995, **14**, 1429.
10 R. Csuk and B. Glänzer, *Tetrahedron*, 1991, **47**, 1655.
11 C. P. Casey and T. J. Burkhardt, *J. Am. Chem. Soc.*, 1973, **95**, 5833.
12 K. Briner and A. Vasella, *Helv. Chim. Acta*, 1989, **72**, 1371; A. Vasella and S. Mangholz, *Helv. Chim. Acta*, 1995, **78**, 1020.
13 O. Mitsunobu, *Synthesis*, 1981, 1.
14 H. D. Flack, *Acta Crystallogr., Sect. A*, 1983, **39**, 876.
15 DIFABS, N. Walker and D. Stuart, *Acta Crystallogr., Sect. A*, 1983, **39**, 158.

*Received in Cambridge, UK, 1st April 1997; Com. 7/02164J*

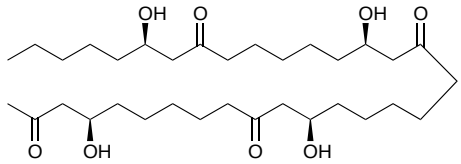
# Asymmetric total synthesis of PM-toxin A, a corn host-specific pathotoxin

**Hiroyuki Hayakawa, Makiko Ohmori, Kiyoko Takamichi, Fuyuhiko Matsuda and Masaaki Miyashita***

*Division of Chemistry, Graduate School of Science, Hokkaido University, Hokkaido 060, Japan*

**The first asymmetric total synthesis of PM-toxin A, a corn host-specific toxin produced by the fungal pathogen *Phyllosticta maydis*, starting from D-lactate is described.**

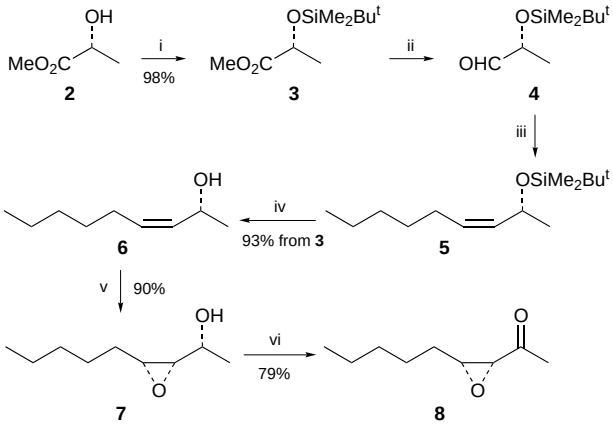
The fungal pathogen *Phyllosticta maydis* produces a corn host-specific pathotoxin, PM-toxin, which was revealed to be the cause of major epidemics of Northern T-corn leaf blight disease in the United States.[1] PM-toxin[2] and the HMT-toxin,[3] produced by the fungal pathogen *Helminthosporium maydis*, race T, are representative corn host-specific toxins.[4] PM-toxin consists of 10–15 components, of which the four major ones—PM-toxin A, B, C and D—have been isolated so far and determined to be linear $C_{33}$ and $C_{35}$ compounds containing a number of characteristic β-ketol (aldol) structures.[2] The unique structures of these corn pathotoxins as well as their marked host-specific toxicity have elicited much attention from biologists and synthetic chemists.[4,5]




PM-Toxin A **1**

We report here the first and highly stereoselective total synthesis of PM-toxin A **1** starting from D-lactate, in which three tandem aldol reactions and the regiospecific organoselenium-mediated reduction of four consecutive α,β-epoxy ketone units are involved as key steps.

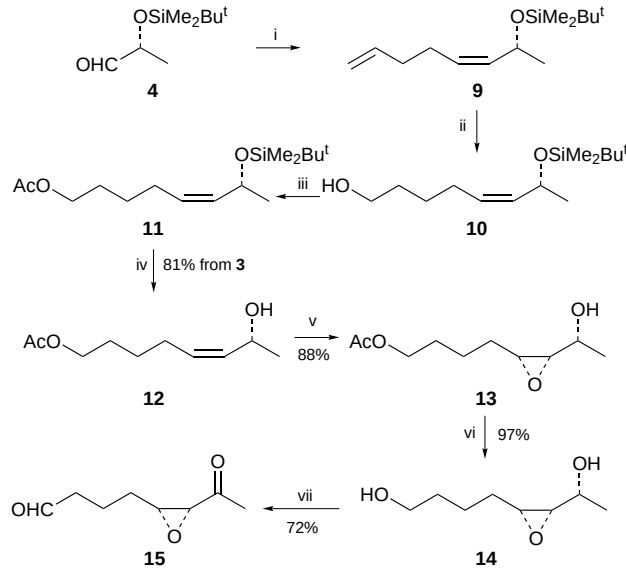
The starting methyl D-lactate **2** was treated with $Bu^tMe_2SiCl$ and imidazole in DMF to give **3** in nearly quantitative yield (Scheme 1). Reduction of **3** with DIBAL-H cleanly produced the aldehyde **4** which was subjected to the Wittig reaction with hexyltriphenylphosphonium bromide to give the (*Z*)-alkene **5** along with a trace amount of the (*E*)-isomer. Subsequent treatment of **5** with $Bu_4NF$ in THF afforded the (*Z*)-allylic alcohol **6** in 93% overall yield after purification by silica gel chromatography. Oxidation of the resulting alcohol **6** with MCPBA in $CH_2Cl_2$ gave rise to the α-epoxy alcohol **7** as the sole product in 90% yield, which was submitted to the Swern oxidation resulting in the formation of the desired epoxy ketone **8** in 79% yield. Thus a key compound for the synthesis of PM-toxin A **1** was synthesized in a stereoselective manner.



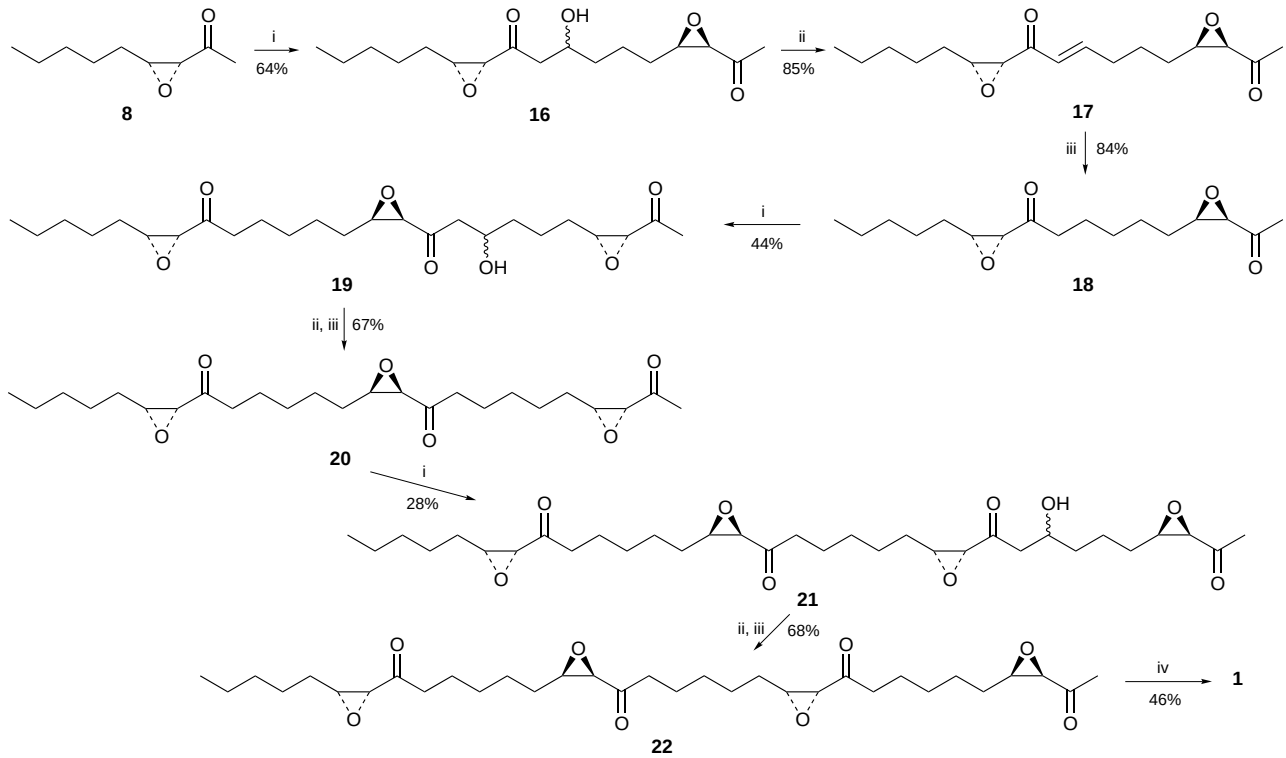

**Scheme 1** *Reagents and conditions*: i, $Bu^tMe_2SiCl$, imidazole, DMF; ii, DIBAL-H, toluene, −78 °C; iii, hexyltriphenylphosphonium bromide, BuLi, toluene; iv, $Bu_4NF$, THF; v, MCPBA, $CH_2Cl_2$, 0 °C; vi, $(COCl)_2$, DMSO, $CH_2Cl_2$, −78 °C, then $Et_3N$

Another key component **15** was synthesized according to Scheme 2. The Wittig reaction of the aldehyde **4** with pent-4-enyltriphenylphosphonium bromide gave the (*Z*)-alkene **9** along with a minor amount of the (*E*)-isomer. Since the alkenes could not be separated at this stage, the mixture was treated with 9-borabicyclo[3.3.1]nonane (9-BBN) followed by treatment with alkaline $H_2O_2$ to furnish the alcohol **10** as an inseparable mixture of isomers. Subsequent acetylation of **10** with $Ac_2O$ followed by treatment of the resulting acetate **11** with $Bu_4NF$ in THF gave rise to the desired (*Z*)-allylic alcohol **12** in 81% overall yield from **3** after purification by silica gel column chromatography.† Upon epoxidation of the allylic alcohol **12** with MCPBA in $CH_2Cl_2$ the α-epoxy alcohol **13** was exclusively formed in 88% yield. The epoxy alcohol **13** thus obtained was converted to the keto aldehyde **15**, the second key intermediate, by the two step reaction sequence: (i) hydrolysis of the acetate (97%) and (ii) Swern oxidation (72%).

With the key compounds **8** and **15** in hand, we set about the crucial tandem aldol reaction toward the synthesis of tetrakis-epoxy ketone **22**. The first aldol reaction of **8** and **15** with lithium hexamethyldisilazide (LiHMDS) as base smoothly proceeded in THF at −78 °C giving rise to the hydroxy ketone **16** as a diastereoisomeric mixture in 64% isolated yield (Scheme 3). Subsequent treatment of **16** with methanesulfonyl chloride in $CH_2Cl_2$ in the presence of DMAP directly afforded




**Scheme 2** *Reagents and conditions*: i, pent-4-enyltriphenylphosphonium bromide, BuLi, toluene; ii, 9-BBN, THF, 0 °C, then 8 M NaOH, $H_2O_2$; iii, $Ac_2O$, DMAP, pyridine; iv, $Bu_4NF$, THF; v, MCPBA, $CH_2Cl_2$, 0 °C; vi, $NH_3$, MeOH; vii, $(COCl)_2$, DMSO, $CH_2Cl_2$, −78 °C, then $Et_3N$




**Scheme 3** *Reagents and conditions*: i, LiHMDS, THF, then **15**, −78 °C; ii, $MeSO_2Cl$, DMAP, $CH_2Cl_2$; iii, $H_2$, 10% Pd–C, EtOAc; iv, $Na[PhSeB(OEt)_3]$ (16 equiv.), AcOH (24 equiv.), EtOH, 0 °C

the enone **17** in 85% yield, which was then submitted to catalytic hydrogenation over 10% Pd–C in EtOAc, resulting in the formation of the bis-epoxy ketone **18** in 84% yield. Thus the bis-epoxy ketone **18** could be synthesized *via* a three step reaction sequence. The second aldol reaction of **18** and **15** was similarly performed using LiHMDS in THF at −78 °C giving the β-hydroxy ketone **19**‡ in 44% yield. Apparently, the yield of the second aldol reaction is lower than that of the first. The products **19** were similarly converted to the tris-epoxy ketone **20** by the two step reaction sequence of mesylation (80%) and subsequent hydrogenation (84%). The third aldol reaction of **20** and **15** was, as anticipated, reluctant to proceed under similar conditions, resulting in the formation of **21** in 28% yield. The products **21**‡ thus obtained were also converted to the tetrakis-epoxy ketone **22** by the two step reaction sequence of mesylation (90%) followed by catalytic hydrogenation (76%). Although the final aldol reaction suffered from low yield, the critical compound **22** for the synthesis of PM-toxin A **1** was secured in an optically pure form *via* the tandem aldol strategy. Finally, the organoselenium-mediated reduction[6] of the tetrakis-epoxy ketone **22**, the crucial reaction in the present synthesis, was performed by treatment of **22** with benzeneselenol (PhSeH, 16 equiv.) generated *in situ* from sodium (phenylseleno)triethylborate (16 equiv.)[7] and acetic acid (24 equiv.) in ethanol.[6,8] The reduction of four consecutive epoxy ketone moieties occurred regiospecifically at the α-position as expected,[7] and the crystalline PM-toxin A **1** was obtained in 46% isolated yield (68% based on the consumed substrate) after purification by silica gel chromatography. The physical properties of the synthetic compound§ were identical with those of an authentic specimen. Furthermore, $^1H$ and $^{13}C$ NMR spectra of the corresponding tetraacetate derived from the synthetic compound were also identical with those of authentic PM-toxin A tetraacetate. Thus the stereoselective asymmetric total synthesis of PM-toxin A **1** has been achieved by employing tandem aldol reactions and the regiospecific organoselenium-mediated reduction of α,β-epoxy ketone units as key steps.

We acknowledge Professor Y. Kono (Ibaragi University) for providing us with a $^1H$ NMR spectrum of authentic PM-toxin A tetraacetate. We are grateful to the Syourai Foundation and the Hoansya Foundation for their financial support.

## Footnotes

* E-mail: miyasita@schem.ec.hokudai.ac.jp

† At this stage, it was confirmed that no racemization of the aldehyde **4** had taken place *via* $^1H$ NMR analysis of the (*S*)-mandelate ester of **12**.

‡ A diastereoisomeric mixture.

§ *Selected data* for PM toxin A **1**: mp 117–119 °C (from acetone); $[\alpha]_D^{22}$ −45 (*c* 0.16, $CHCl_3$); UV $\lambda_{max}$ 275.2 nm (MeOH); CD $\lambda_{max}$ 281 nm (MeOH); FAB-MS *m*/*z* 583 ($M-H^-$); FD-MS *m*/*z* 607 ($M + Na^+$), 623 ($M + K^+$). The $[\alpha]_D$ was measured in $CHCl_3$ since the synthetic pure compound was almost insoluble in MeOH. Data for an authentic sample: mp 118–119 °C; $[\alpha]_D^{25}$ − 11 (MeOH); UV $\lambda_{max}$ 276 nm (MeOH); CD $\lambda_{max}$ 282 nm (MeOH); FAB-MS *m*/*z* 585 ($M + H^+$); FD-MS *m*/*z* 607 ($M + Na^+$) (ref. 2).

## References

1 J. C. Comstock, C. A. Martinson and B. C. Gegenbach, *Phytopathology*, 1973, **63**, 1357; O. C. Yoder, *Phytopathology*, 1973, **63**, 1361.
2 Y. Kono, S. J. Danko, Y. Suzuki, S. Takeuchi and J. M. Daly, *Tetrahedron Lett.*, 1983, **24**, 3803; S. J. Danko, Y. Kono, J. M. Daly, Y. Suzuki, S. Takeuchi and D. A. McCrery, *Biochemistry*, 1984, **23**, 759.
3 Y. Kono, S. Takeuchi, A. Kawarada, J. M. Daly and H. W. Knoche, *Tetrahedron Lett.*, 1980, **21**, 1537; *Agric. Biol. Chem.*, 1980, **44**, 2613.
4 Y. Kono, Y. Suzuki and S. Takeuchi, *J. Synth. Org. Chem. Jpn*, 1985, **43**, 980; V. Smedegard-Peterson and R. R. Nelson, *Can. J. Botany*, 1969, **47**, 951.
5 Y. Suzuki, S. J. Danko, Y. Kono, S. Takeuchi, J. M. Daly and H. W. Knoche, *Agric. Biol. Chem.*, 1984, **48**, 2321; Y. Suzuki, S. J. Danko, Y. Kono, J. M. Daly and S. Takeuchi, *Agric. Biol. Chem.*, 1985, **49**, 149.
6 M. Miyashita, T. Suzuki and A. Yoshikoshi, *Tetrahedron Lett.*, 1987, **28**, 4293; *Chem. Lett.*, 1987, 2387; *Tetrahedron Lett.*, 1989, **30**, 1819; *J. Am. Chem. Soc.*, 1989, **111**, 3728; *Chem. Lett.*, 1990, 791.
7 M. Miyashita, M. Hoshino and A. Yoshikoshi, *Tetrahedron Lett.*, 1988, **29**, 347.
8 M. Miyashita and A. Yoshikoshi, *Synthesis*, 1980, 664.

*Received in Cambridge, UK, 2nd April 1997; Com. 7/02208E*

# Haem binding and catalytic activity of two-α-helix peptide annealed by trifluoroethanol

**Seiji Sakamoto, Shigeo Sakurai, Akihiko Ueno and Hisakazu Mihara***

*Department of Bioengineering, Faculty of Bioscience and Biotechnology, Tokyo Institute of Technology, Nagatsuta, Yokohama 226, Japan*

**A designed two-α-helix peptide His-2α binds effectively $Fe^{III}$–mesoporphyrin (haem) and enhances *N*-demethylase activity of the haem, when the 2α-helix structure is annealed by the addition of 10–20% trifluoroethanol.**

Iron porphyrins occur widely in nature as cofactors of haemproteins and display diverse functions.[1] The specific function of the haemprotein is determined by the microenvironments around the haem.[2] Thus, if we can establish the haem environments by designing polypeptide 3D structures, it will be possible to control the haem functions. So far, considerable effort has been devoted to the conjugation of porphyrin molecules by chelation[3] or covalent linkage[4–6] with designed peptide 3D structures. To develop a mini haemprotein, we here report the design and synthesis of a 2α-helix peptide His-2α, which could bind Fe–mesoporphyrin (haem) in a regulated manner. Furthermore, catalytic activity of the haem that resembled that of peroxidase was significantly increased by the binding with the peptide.

A 14-peptide segment in the peptide was designed to take an amphiphilic α-helix structure in a manner similar to that of a portion of coiled-coil proteins (Fig. 1).[7,8] The two segments were dimerized by disulfide linkage of the $Cys^{16}$ residues. As axial ligands of haem, His residues were introduced at the sixth position instead of Leu to deploy a haem parallel to the helix. The peptide was synthesized by the solid-phase method using the Fmoc strategy and purified with HPLC to high purity (> 98%). The peptide gave a molecular ion peak at *m*/*z* 3529.6 [(M + H)$^+$] (calc. 3529.1) on matrix assisted laser desorption ionization times-of-flight mass spectrometry. The monomer peptide (His-1α) was also synthesized and gave an ion peak at *m*/*z* 1836.9 [(M + H)$^+$] (calc. 1837.2).

The conformation of His-2α ($2.0 \times 10^{-5}$ mol dm$^{-3}$) in buffer (pH 7.4) was almost random due to the introduction of His residues (Fig. 2).† With increasing percentage volume of trifluoroethanol (TFE), which is known to be an α-helix stabilizing solvent,[8] the α-helicity[9] of His-2α gradually increased until it reached about 70% at 30% TFE [Fig. 2(*b*)]. Interestingly, in the presence of the haem, a further increase in α-helicity was observed at 10–20% TFE [Fig. 2(*b*), closed circles]. The largest increase of α-helicity by the addition of haem was obtained at around 15% TFE (1.4-fold). When His-2α was titrated with the haem in 15% TFE, the CD spectra of His-2α changed gradually to that of a typical α-helix structure with an isodichroic point at 204 nm (Fig. 3). The binding constant ($K_a$) in 15% TFE, which was estimated from molecular ellipticities at 222 nm using a single site binding equation,[10] was $2.8 \times 10^5$ dm$^3$ mol$^{-1}$. The addition of 1-methylimidazole (200 equiv.) inhibited the coordination of His-2α with the haem, resulting in the decrease of the α-helicity to the level without the haem. Additionally, there was no significant change in the CD spectra by the addition of haem at acidic pH (2.0–6.0). Because the p$K_a$ of imidazole is about 6.0, the pH effect is attributed to the protonation of His side chains such that they cannot act as ligands. Therefore, we concluded that the increase in α-helicity

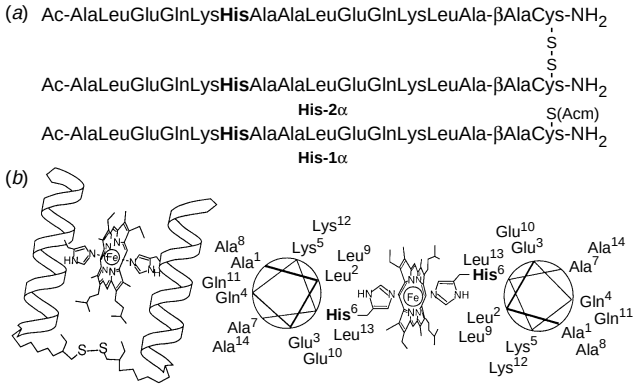



**Fig. 1** Structure of the designed peptides, His-2α and His-1α. (*a*) Amino acid sequences of His-2α and His-1α. (*b*) Illustration of two-α-helix peptide structure bound to the haem and helix wheel drawing of the two 14-peptides in coiled-coil form. Acm = acetamidomethyl.

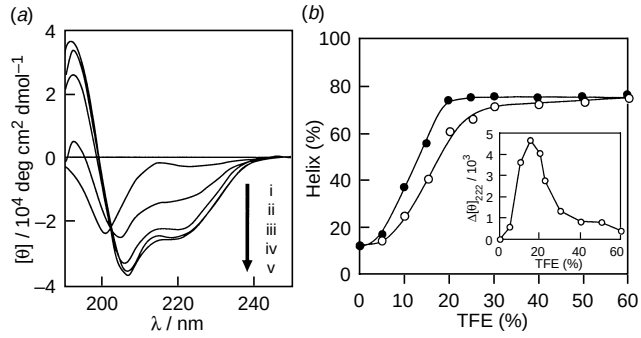



**Fig. 2** (*a*) CD spectra of His-2α with increasing percentage volume of TFE in $2.0 \times 10^{-2}$ mol dm$^{-3}$ Tris HCl buffer (pH 7.4) at 25 °C. i, 0%; ii, 15%; iii, 30%; iv, 60%; v, 97%. [His-2α ] = $2.0 \times 10^{-5}$ mol dm$^{-3}$. (*b*) Effect of TFE content on the α-helicity (○) in the absence and (●) the presence of haem ($2.0 \times 10^{-5}$ mol dm$^{-3}$). Inset: increase in ellipticity at 222 nm by the addition of haem as a function of TFE content.

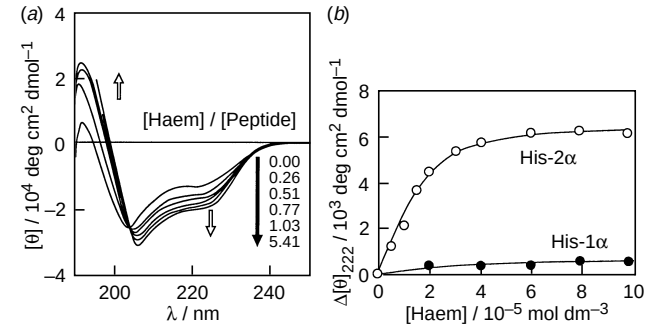



**Fig. 3** (*a*) CD spectra of His-2α with increasing haem concentration in the buffer containing 15% TFE at 25 °C. [His-2α] = $2.0 \times 10^{-5}$ mol dm$^{-3}$. (*b*) Improvement of α-helix for (○) His-2α ($2.0 \times 10^{-5}$ mol dm$^{-3}$) and (●) His-1α ($4.0 \times 10^{-5}$ mol dm$^{-3}$) by the addition of the haem.

of His-2α took place *via* the haem binding by ligation with His residues. In contrast, α-helicity of His-1α was little affected by the addition of haem at any percentage volume of TFE (0–90%), indicating that His-1α could not bind the haem in this concentration.

Titration of the haem with His-2α was also carried out in the buffer containing various amounts of TFE. At 15% TFE, the Soret band at 401 nm increased and the band at around 355 nm decreased upon the addition of His-2α [Fig. 4(*a*)]. That is, an UV–VIS spectrum of the haem was converted from the high spin to the low spin form with an isosbestic point at 390 nm. The decrease in absorbance at 355 nm indicated that the peptide acted to break up haem aggregates.[6] The binding constant for the haem with His-2α was strongly dependent on the TFE content [Fig. 4(*b*)]. His-2α showed the highest binding constant at 15% TFE ($K_a$ = 5.8 × 10$^5$ dm$^3$ mol$^{-1}$). In contrast, His-2α could not bind the haem effectively at < 10% and > 30% TFE ($K_a$ < 3.0 × 10$^4$ dm$^3$ mol$^{-1}$). These TFE titrations revealed that the 2α-helix structure annealed by TFE and the consequent formation of a hydrophobic pocket are important for the haem binding. That is, at the lower TFE content (< 10%), the hydrophobic pocket is not formed, because the conformation of His-2α is predominantly a random-coil. On the other hand, at the higher TFE content (> 30%), the 2α-helix structure is destroyed so that each α-helix segment is free to move. Because there is no hydrophobic pocket at either lower or higher TFE content, the peptide cannot bind the haem effectively. The monomer peptide His-1α and 1-methylimidazole needed a concentration of an order of *ca.* 10$^{-3}$ mol dm$^{-3}$ for the haem binding and did not show such a TFE dependence. These results also confirm that the formation of the 2α-helix structure is essential for the haem binding.

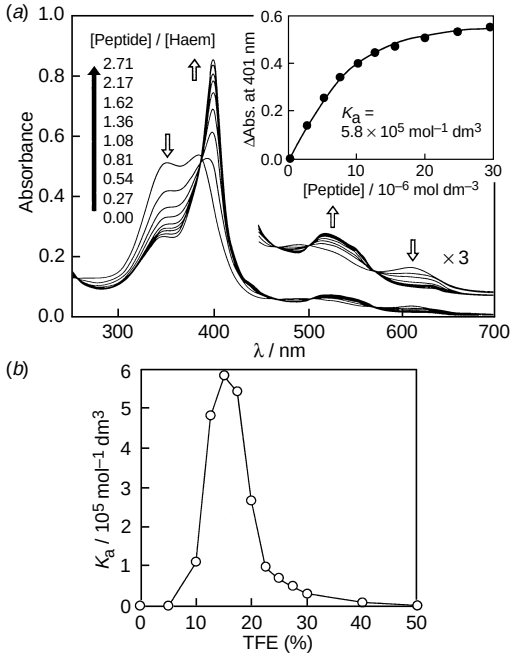



**Fig. 4** (*a*) UV–VIS spectra of the haem with increasing His-2α concentration in the buffer containing 15% TFE at 25 °C. [haem] = 1.0 × 10$^{-5}$ mol dm$^{-3}$. (*b*) Effect of TFE content on the binding constant for His-2α with the haem.

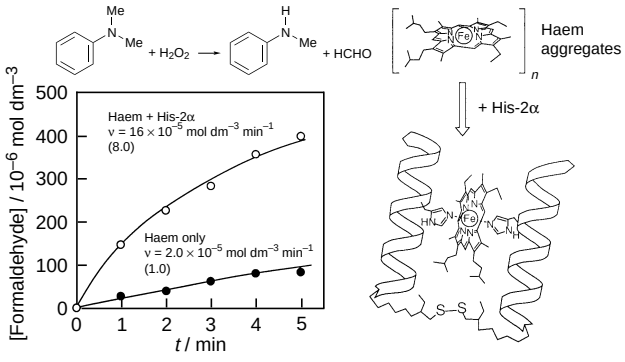



**Fig. 5** Time course of formaldehyde formation catalysed by the haem (○) in the presence and (●) absence of His-2α. The reaction was initiated by addition of hydrogen peroxide (4.9 × 10$^{-3}$ mol dm$^{-3}$) to mixtures of *N*,*N*-dimethylaniline (5.0 × 10$^{-3}$ mol dm$^{-3}$), haem (4.8 × 10$^{-6}$ mol dm$^{-3}$) and His-2α (1.0 × 10$^{-5}$ mol dm$^{-3}$) in 0.1 mol dm$^{-3}$ Tris HCl buffer (pH 7.4) containing 15% TFE at 30 °C. About 80% of the haem was bound to the peptide under the conditions according to the binding constant.

Next, demethylation catalysis of the haem bound to His-2α was demonstrated using *N*,*N*-dimethylaniline as a substrate.[11] As shown in Fig. 5, the initial rate *v* of the reaction in the presence of His-2α (*v* = 16 × 10$^{-5}$ mol dm$^{-3}$ min$^{-1}$) was accelerated by a factor of 8.0, relative to that in the absence of the peptide (*v* = 2.0 × 10$^{-5}$ mol dm$^{-3}$ min$^{-1}$). The acceleration of the reaction was dependent on the TFE content and showed a maximum value at 15% TFE. The *N*-demethylase activity was comparable to that of bilayer-bound cytochrome *c* as reported by Hamachi *et al.*[11] The initial rate was dependent on the concentration of $H_2O_2$, but not on that of *N*,*N*-dimethylaniline. Therefore, the rate-determining step is the reaction between the haem and $H_2O_2$. The peptide seems to enhance the activity by isolating the haem in the peptide structure from the haem aggregates in solution.

In conclusion, the haem binding of the His-peptide was controlled by the peptide conformation with TFE. The catalytic activity was enhanced by the formation of the haem–peptide complex, which might be another kind of catalytic molten globule.[12] The strategy using designed peptides conjugated with functional groups, such as haem, is expected to be applied to the elucidation of the roles of polypeptide 3D structure on the diverse functions of natural proteins, and the obtained information will be useful for the design artificial proteins.

## Footnotes

* E-mail: hmihara@bio.titech.ac.jp

† Leu-2α, a non-His peptide, had 55% helicity in the buffer.

## References

1 *The Porphyrins*, ed. D. Dolphin, Academic, New York, 1979, vol. 7.
2 T. L. Poulos, *Adv. Inorg. Biochem.*, 1988, **7**, 2.
3 F. Rabanal, W. F. DeGrado and P. L. Dutton, *J. Am. Chem. Soc.*, 1996, **118**, 473.
4 T. Sasaki and E. T. Kaiser, *J. Am. Chem. Soc.*, 1989, **111**, 380.
5 H. Mihara, Y. Haruta, S. Sakamoto, N. Nishino and H. Aoyagi, *Chem. Lett.*, 1996, 1; H. Mihara, K. Tomizaki, T. Fujimoto, S. Sakamoto, H. Aoyagi and N. Nishino, *Chem. Lett.*, 1996, 187.
6 D. R. Benson, B. R. Hart, X. Zhu and M. B. Doughty, *J. Am. Chem. Soc.*, 1995, **117**, 8502.
7 S. Sakamoto, H. Aoyagi, N. Nakashima and H. Mihara, *J. Chem. Soc., Perkin Trans. 2*, 1996, 2319.
8 N. E. Zhou, C. M. Kay and R. S. Hodges, *J. Biol. Chem.*, 1992, **267**, 2664.
9 J. M. Scholtz, H. Qian, E. J. York, J. M. Stewart and R. L. Baldwin, *Biopolymers*, 1991, **31**, 1463.
10 T. Kuwaraba, A. Nakamura, A. Ueno and F. Toda, *J. Phys. Chem.*, 1994, **98**, 6297.
11 I. Hamachi, A. Fujita and T. Kunitake, *J. Am. Chem. Soc.*, 1994, **116**, 8811.
12 W. F. DeGrado, *Nature*, 1993, **365**, 488; K. Johnsson, R. K. Allemann, H. Widmer and S. A. Benner, *Nature*, 1993, **365**, 530; H. Mihara, K. Tomizaki, N. Nishino and T. Fujimoto, *Chem. Lett.*, 1993, 1533; K. Broo, L. Brive, A.-C. Lundh, P. Ahlberg and L. Baltzer, *J. Am. Chem. Soc.*, 1996, **118**, 8172.

*Received in Cambridge, UK, 17th March 1997; Com. 7/01852E*

# Effect of hydrogen treatment of active carbon as a support for promoted ruthenium catalysts for ammonia synthesis

**Zhihua Zhong and Ken-ichi Aika***

*Interdisciplinary Graduate School of Science and Engineering, Tokyo Institute of Technology, 4259 Nagatsuta, Midori-ku, Yokohama 226, Japan*

**Hydrogen treatment of active carbon (A.C.) at temperatures ranging from 1073 to 1188 K for 12 h is an effective method for eliminating surface impurities, leading to the preparation of useful ruthenium catalysts; for example, 2 mass% Ru–BaO/A.C. (Ba/Ru = 5) yields 2 mmol $NH_3$ $h^{-1}$ $g^{-1}$ at 588 K under 1 atmosphere.**

Many researchers have pursued various alternatives in making pure carbon materials which are used as support material for ruthenium catalysts in the synthesis of ammonia. HSAG (high surface area graphite) was first developed in the UK[1] and the first commercial ammonia plant to use ruthenium catalysts has operated using a type of Ru/HSAG catalyst since 1992 in Canada. The catalyst used has been reported to be very efficient and stable.[2] Ruthenium catalysts supported on carbon-covered alumina (CCA) was found to be substantially improved for the synthesis of ammonia since CCA offers the purity of carbon and eliminates the acidity of alumina.[3,4] More recently, a very active Ru catalyst supported on A.C. which is treated for 2 h at 2173 K in an atmosphere of helium (400 Pa) has been reported.[5,6] The authors suggest that the high activity is due to differences in the support (A.C.) which may have similar properties to HSAG.

In this work, we have successfully eliminated the impurities such as S, N, O and Cl by treating commercial A.C. with hydrogen at moderate temperatures (1073–1188 K). We have used $Ba(NO_3)_2$ and $CsNO_3$ as the promoters because these were found to be the most effective on Ru/A.C. while $Ce(NO_3)_3$ was also used based on the results of our most recent work.[7,8]

Three kinds of granular active carbons (8–12 mesh size, 2 g) were treated in a quartz reactor by increasing the temperature to 1073 or 1188 K at a rate of 5 K $min^{-1}$ under a flow of hydrogen (30 ml $min^{-1}$) and kept at the final temperature for 12 h or more. The Ru/A.C. catalysts were prepared by impregnating A.C. with $[Ru_3(CO)_{12}]$ or $[Ru(acac)_3]$ in THF and finally heated from room temp. to 573 K in 2 h *in vacuo*.[7,8]

All the catalysts (usually 0.2 g) were pre-reduced at 473 K with hydrogen (50 ml $min^{-1}$) for 5 h, then reduced at the corresponding reduction temperatures for 3 h. The ammonia synthesis reaction was performed in a stainless-steel reactor (id = 6.5 mm) under a flow system under atmospheric pressure at 588 K.[7,8] The flow rates of $H_2$ and $N_2$ were set at 45 and 15 ml $min^{-1}$, respectively.

Elemental analysis was also carried out for these three commercially available A.C. samples and the results are shown in Table 1. We can see that the content of the carbon increases dramatically and hydrogen and nitrogen decrease when the reduction treatment is prolonged. The surface areas (BET) and the XRD patterns are only slightly different. Neither sulfur nor halogen can be detected after hydrogen treatment of A.C. (no. 76) at 1123 K for 12 h.

In this work we found that two hydrogen treatment procedures, namely, the treatment of the active carbon and the treatment of the catalyst, influenced the activity of Ru–$Ba^{2+}$/A.C. Hydrogen treatment of A.C. at high temperatures such as 1123 K enabled the elimination or reduction of the surface acidic impurities which withdraws electrons from Ru. Impregnated and decomposed $[Ru_3(CO)_{12}]$ on such active carbon proved effective in the preparation of an efficient catalyst for ammonia synthesis. However, ruthenium catalysts supported on A.C. without the promoter showed almost no activity for the synthesis reaction at 588 K. The effects of hydrogen treatment of A.C. were found to be remarkable only when a promoter such as $Ba(NO_3)_2$ was added. Moreover, the activity was also affected by the reduction temperature of the catalyst, as is shown in Fig. 1. The A.C. used for preparing these samples has been treated differently as is cited in the figure caption. The sample with A.C. which had been treated at such high temperatures as 1188 K was highly promoted by the addition of $Ba(NO_3)_2$. Those samples which had been treated for a longer time at 1188 K showed a more remarkable promotion as can be seen in Fig. 1.

The ammonia activity for the ruthenium catalysts supported on various kinds of A.C. has been shown to be a function of the reduction temperature of the catalyst as indicated in Fig. 2. We have noted here that for the catalysts with non-treated A.C. as the support, the activities varied remarkably owing to the difference in the sulfur and halogen content. However, it is most interesting to note that the catalysts performed much the same after the A.C. was treated with hydrogen at 1123 K for > 24 h. This clearly indicates that the catalytic behavior of the Ru

**Table 1** Elemental analysis (mass%) of active carbons; effect of hydrogen treatment

| Source[a] | Reduction conditions | Surface area[b]/ $m^2$ $g^{-1}$ | H | C | N | Halogen | $S(SO_4^{2-})$ | Others (ash and O) |
|---|---|---|---|---|---|---|---|---|
| #76 | No treatment | 934 | 1.11 | 88.77 | 0.21 | 3.58 | 0.57 | 5.76 |
| | Up to 1123 K for 4 h | — | 0.34 | 94.47 | — | n.d.[c] | 0.13 | 5.06 |
| | At 1123 K for 12 h | 1078 | 0.17 | 95.49 | 0.16 | n.d. | n.d. | 4.18 |
| #80 | No treatment | 1084 | 1.17 | 92.42 | — | 2.84 | 0.46 | 3.11 |
| | At 1123 K for 48 h | 914 | 1.08 | 93.29 | — | n.d. | n.d. | 5.63 |
| #75 | No treatment | 1007 | 1.00 | 92.51 | — | n.d. | n.d. | 6.49 |
| | At 1123 K for 48 h | 978 | 0.69 | 96.67 | — | n.d. | n.d. | 2.64 |

[a] #76 from Wako Chemicals (wood), #75 from Kureha Chemicals (pitch), #80 from Kanto Chemicals (coal). [b] BET surface area. [c] n.d. = Not detected.

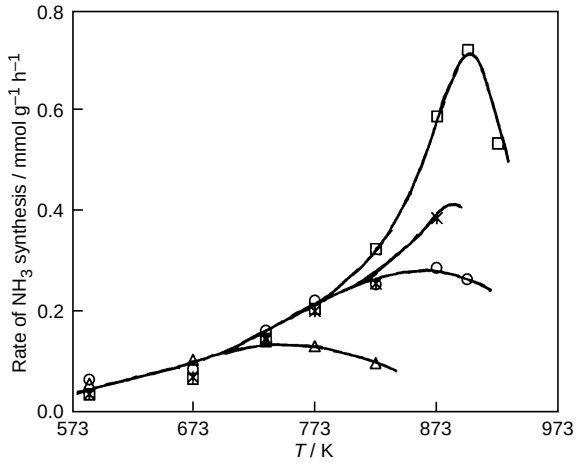



**Fig. 1** Ammonia activity of 1 mass% Ru–15$Ba^{2+}$/A.C. as a function of reduction temperature ($T$). Ru precursor [$Ru_3(CO)_{12}$]. Four kinds of A.C. (#76) were used: (△) non-treated A.C.; (○) A.C. treated at 1073 K for 14 h; (*) A.C. (○) further treated at 1188 K for 20 h; and (□) A.C. (*) further treated at 1188 K for 18 h.

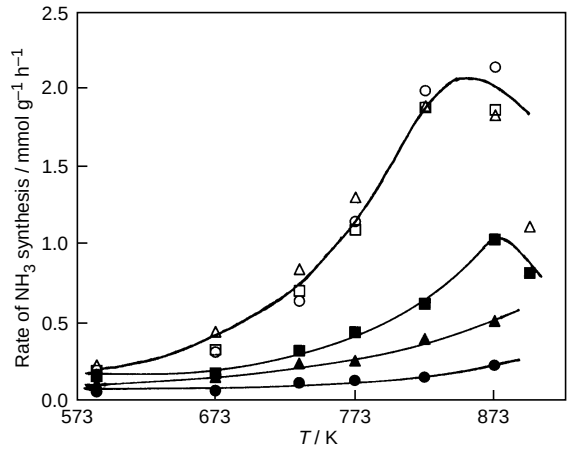



**Fig. 2** Ammonia activity of 2 mass% Ru–5$Ba^{2+}$/A.C. as a function of reduction temperature. Ru precursor [$Ru(acac)_3$]. Solid symbols represent non-treated A.C.; open symbols represent A.C. treated at 1123 K for 48 h; triangles, A.C. #76; circles, #80; squares #75.

catalysts is mainly dependent on the purity of the A.C., while not influenced by the original source or the porosity of the A.C.

The elimination of the impurity species, usually with high electronegativity, reduces the capability of A.C. to withdraw electrons from the Ru atoms and the promoter, and simultaneously enhances the electron donation of the promoter to ruthenium.

Hydrogen treatment at temperatures ranging from 1073 to 1188 K for > 12 h was found to be the significant and decisive factor in removing impurities such as sulfur and halogen left on commercial A.C. during the activation process and/or when adding the binder while the surface area and the porous structure of the A.C. was not affected. This moderate reduction treatment of A.C. (support) doubles or even triples the activities for $Cs^+$-, $Ba^{2+}$- or $Ce^{3+}$-promoted Ru catalysts for ammonia synthesis. Furthermore, the activity increases with prolonged hydrogen treatment. As supports, the different kinds of A.C. exhibited low and quite varied activity for ammonia synthesis owing to differences in impurity content. However, any A.C. treated with hydrogen was found to show equally high activity. Our studies which have been based on detailed and repeated research work have demonstrated that the removal of such impurities such as sulfur and halogens as well as the elimination of the acidic functional groups in A.C. by hydrogen treatment led to higher activity of the ruthenium catalysts, thus paving the way for the preparation of an efficient and effective catalyst for ammonia synthesis.

## Footnote

*E-mail: kenaika@chemenv.titech.ac.jp

## References

1 *US Pat.*, 4,163,775, British Petroleum, 1979.
2 S. R. Tennison, *Catalytic Ammonia Synthesis*, ed. J. R. Jennings, Plenum, New York, ch. 9, 1991.
3 S. Khaja Masthan, P. S. Sai Prasad, K. S. Rama Rao and P. Kanta Rao, *J. Mol. Catal.*, 1991, **67**, L1.
4 K. S. Rama Rao, S.Khaja Masthan, P. S. Sai Prasad and P. Kanta Rao, *Appl. Catal.*, 1991, **73**, L1.
5 Z. Kowalczyk, S. Jodzis and J. Sentek, *Appl. Catal. A*, 1996, **138**, 83.
6 Z. Kowalczyk, J. Sentek, S. Jodzis, R. Diduszko, A. Presz, A. Terzyk, Z. Kucharski and J. Suwalski, *Carbon*, 1996, **34**, 403.
7 Y. Niwa and K. Aika, *J. Catal.*, 1996, **162**, 138.
8 Y. Kadowaki and K. Aika, *J. Catal.*, 1996, **161**, 178.

*Received in Cambridge, UK, 3rd April 1997; Com. 7/02273E*

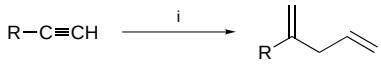
# Indium-mediated regioselective Markovnikov allylation of unactivated terminal alkynes

**Brindaban C. Ranu* and Adinath Majee**

*Department of Organic Chemistry, Indian Association for the Cultivation of Science, Jadavpur, Calcutta-700 032, India*

**Allylation of unactivated terminal alkynes by a simple treatment with allyl bromide and indium metal in THF at room temperature produces 1,4-dienes *via* regioselective Marknovnikov addition.**

Metal-mediated reactions play a significant role in organic synthesis. Of all the metals, indium has emerged in recent years as the one with most potential because of its advantages with regard to handling, toxicity, reactivity and selectivity.[1] Although indium-mediated carbonyl addition reactions have experienced tremendous growth in recent times,[2] its other interesting domains, including carboindation, still remain less well-explored.[3] Recently, a procedure for allylation of carbon–carbon triple bonds, using indium powder and allylic bromides in DMF at elevated temperature to produce allylalkenols predominantly *via* anti-Markovnikov addition, has been demonstrated.[3a] One serious limitation of this procedure is that the presence of a hydroxyl functionality near the triple bond is essential, and thus nonfunctionalised† or hydroxy-protected alkynes are not susceptible to allylation.[3a] We have observed a very significant effect on the course of the indium-mediated allylation reaction with a change of solvent and modification of the experimental conditions. Thus, unactivated (nonfunctionalised and hydroxy-protected) alkynes underwent efficient allylation *via* Markovnikov addition by simple treatment with allyl bromide and indium metal in THF at room temperature (Scheme 1).




**Scheme 1** *Reagents and conditions*: i, In, THF, room temp.

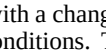
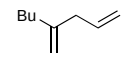
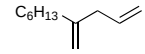
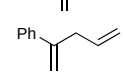
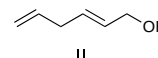
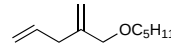
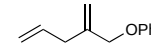
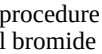
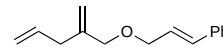
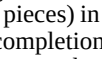
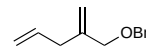
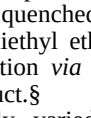
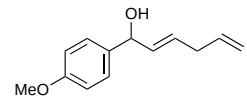
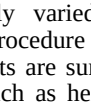
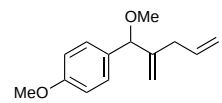
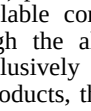
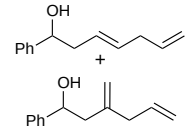
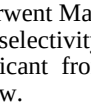
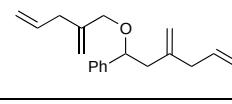
The experimental procedure is very simple. A mixture of alkyne (1 mmol), allyl bromide (8 mmol)‡ and indium metal (1 mmol, cut into small pieces) in THF (2 $cm^3$) was stirred at room temperature until completion of the reaction (TLC). The reaction mixture was quenched with a few drops of dilute HCl and extracted with diethyl ether. Evaporation of the solvent followed by purification *via* silica gel chromatography furnished the pure product.§

Several structurally varied terminal alkynes underwent allylation by this procedure to provide the corresponding 1,4-dienes. The results are summarised in Table 1. Nonfunctionalised alkynes such as hex-1-yne, oct-1-yne and phenylacetylene (entries 1–3) produced Markovnikov addition products as the sole isolable compounds in high yields. Very interestingly, although the alkynols (entries 4, 9 and 11) furnished almost exclusively or predominantly the anti-Markovnikov addition products, the corresponding ethers (entries 5–8, 10 and 12) underwent Markovnikov coupling exclusively. This reversal of regioselectivity with protection of the hydroxy group is very significant from a mechanistic as well as a synthetic point of view.

In general, the reactions are very clean, and no side products were found. No reaction occurred with internal alkynes. THF is found to be the best choice as solvent. Reactions in water and in aqueous THF are not successful. At lower temperature (0–5 °C), no efficient coupling is also observed.

In conclusion, the present procedure provides an efficient and general methodology for indium-mediated allylation of unactivated terminal alkynes. The notable advantages are the mild conditions (room temperature), operational simplicity (one-pot reaction), high yield (75–90%) and excellent regioselectivity (Markovnikov addition). To the best of our knowledge, this is the first report of indium-mediated Markovnikov allylation of uncativated alkynes. We believe this procedure will find useful application in organic synthesis. Further investigations to gain a better understanding of the criteria for selectivity and to broaden the scope of this reaction are in progress.

**Table 1** Allylation of alkynes with allyl bromide and indium metal in THF

| Entry | Alkyne | *t*/h | Product | Yield (%)[a] |
|---|---|---|---|---|
| 1 |  | 3 |  | 86 |
| 2 |  | 3 |  | 85 |
| 3 |  | 3 |  | 90 |
| 4 |  | 3 |  | 80[b] |
| 5 |  | 5 |  | 85 |
| 6 |  | 6 |  | 86 |
| 7 |  | 6 |  | 85 |
| 8 |  | 24 |  | 75 |
| 9 |  | 8 |  | 83[b] |
| 10 |  | 8 |  | 90 |
| 11 |  | 6 |  | 85 (55:45) |
| 12 |  | 7 |  | 86 |

[a] Yields refer to pure isolated products fully characterised by $^1H$ and $^{13}C$ NMR spectroscopy. [b] The corresponding Markovnikov product is formed in less than 5%.

We acknowledge financial support from CSIR, New Delhi [01(1364)/95]. A. M. also thanks CSIR for his fellowship.

## Footnotes

* E-mail: ocbcr@iacs.ernet.in

† At higher reaction temperature (150–180 °C) oct-1-yne and phenylacetylene underwent coupling with cinnamylindium in only 12–28% yield [ref. 3(*a*)].

‡ Excess allyl bromide is found to accelerate the reactions considerably; stoichiometric or a slightly larger amount (2–3 mmol) of allyl bromide makes the reactions slow.

§ The alkynes and allyl bromide were freshly distilled before use. A few alkynes, namely hex-1-yne, oct-1-yne, phenylacetylene and prop-2-ynyl alcohol, are commercial materials (E. Merck, Germany) and others were prepared *via* standard procedures. Allyl bromide was also purchased from E. Merck. Indium metal was obtained from SRL, India, as ingots and cut into small pieces whenever required. THF was procured from SD, India, and freshly distilled over sodium–benzophenone.

## References

1 P. Cintas, *Synlett*, 1995, 1087.

2 T.-P. Loh and X. R. Li, *Tetrahedron Lett.*, 1997, **38**, 869; M. Jayaraman, M. S. Manhas and A. K. Bose, *Tetrahedron Lett.*, 1997, **38**, 709; V. J. Bryan and T. H. Chan, *Tetrahedron Lett.*, 1996, **37**, 5341; S. Araki, T. Hirashita, H. Shimizu, H. Yamamura, M. Kawai and Y. Butsugan, *Tetrahedron Lett.*, 1996, **37**, 7849.

3 (*a*) S. Araki, A. Imai, K. Shimizu, M. Yamada, A. Mori and Y. Butsugan, *J. Org. Chem.*, 1995, **60**, 1841; (*b*) W. Bao, Y. Zheng, Y. Zhang and J. Zhou, *Tetrahedron Lett.*, 1996, **37**, 9333.

*Received in Cambridge, UK, 2nd April 1997; Com. 7/02241G*

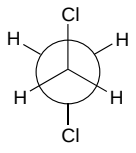
# Isolation of a nearly eclipsed chiral rotamer of 1,2-dichloroethane as an inclusion crystal with a chiral host compound

**Fumio Toda,*[a]† Koichi Tanaka[a] and Reiko Kuroda*[b]‡**

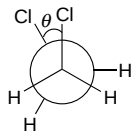
[a] *Department of Applied Chemistry, Faculty of Engineering, Ehime University, Matsuyama, Ehime 790, Japan*
[b] *Department of Life Sciences, Graduate School of Arts and Sciences, The University of Tokyo, Komaba, Meguro-ku, Tokyo 153, Japan*

**A nearly eclipsed chiral rotamer of 1,2-dichloroethane has been isolated in a pure state as an inclusion complex crystal with the chiral host compound, (*S*)-(−)-2-bromo-3,3a,8-triphenyl-1,3a-dihydrocyclopenta[*a*]inden-1-one and an X-ray crystal structure of the complex has been studied.**

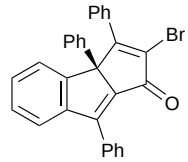
The conformation of simple acyclic molecules has long been studied, mostly spectroscopically and theoretically.[1] By these studies, it has been established that the energetically most stable rotamer (rotational isomer) around the C–C bond of 1,2-disubstituted ethane is the *trans* form. For example, 1,2-dichloroethane **1** exists in the *trans* form **1a**, the structure of which was elucidated by X-ray analysis of **1** crystallised at 212 K using a miniature zone melting procedure,[2] although the energy difference between the *trans* and *gauche* form of gaseous **1** has been estimated to be small (0.9–1.3 kcal mol$^{-1}$ by experiment and 0.91 kcal mol$^{-1}$ by calculation; 1 cal = 4.184 J).[1] The existence of **1** in the eclipsed form of the two chlorine atoms **1b** ($\theta$ = 0) is excluded, because of its instability due to strong repulsions between not only the chlorine atoms but also hydrogen atoms. The possibility of isolation of the *gauche* form **1b** ($\theta$ = 60°) would also be excluded, and isolation of the *gauche* form has never been reported.



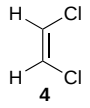

**1a**
*trans*-form



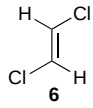

(*M*)-**1b**
eclipsed-form




(*S*)-(–)-**2**




**4**




**6**

We here report isolation of a nearly eclipsed form of **1** as a 1 : 1 inclusion complex crystal with a host compound. Recrystallisation from **1** of the optically active host compound, (*S*)-(−)-2-bromo-3,3a,8-triphenyl-1,3a-dihydrocyclopenta[*a*]-inden-1-one **2**,[3,4] gave their 1 : 1 inclusion complex **3**§ as yellow prisms in quantitative yield (mp 100–104 °C). In comparison, a 1 : 1 inclusion complex **5**§ of **2** and *cis*-1,2-dichloroethylene **4** was also prepared as pale yellow prisms by recrystallization of **2** from **4**. However, *trans*-1,2-dichloroethylene **6** did not form an inclusion complex with **2**. The 1 : 1 host–guest ratio in **3** and **5** was determined by $^1$H NMR spectroscopy, thermogravimetric measurement and elemental analyses.

In order to study the molecular conformation of **1** in **3**, an X-ray crystal structure of **3** was determined.¶ The X-ray analysis established that **1** exists as the nearly eclipsed form **1b** [$\theta$ = 36(2)°] as shown in Fig. 1. This is the first example of the isolation of the nearly eclipsed rotamer. The molecule **1b**, which adopts a conformation between the *gauche* and eclipsed form is chiral. Since **2** is an optically active (*S*)-(−)-host,‖ only one enantiomer of **1b**, the left-handed helical form (*M*)-**1b**,[6] is accommodated in **3**. This is also the first case of the isolation of an optically active rotamer of 1,2-dichloroethane. The reason for this surprising finding that sterically the very unfavourable rotamer can be trapped at room temperature in an inclusion complex was studied by comparison of the molecular and crystal structures of **3** with those of **5**.¶ The crystal structure of **5** is shown in Fig. 2. The two crystal lattice parameters are surprisingly similar, with only the 0.09–0.4% difference as shown in the footnote.¶ The two crystals adopt the same space group of $P2_12_12_1$. The location of the host and guest molecules, as well as their conformation, closely resemble to each other, as expected from the cell parameter comparison. The intramolecular Cl··Cl distance is retained, at 3.205(5) and 3.315(5) Å for **1a** in **3** and **4** in **5**, respectively. The closest contacts between the host and the guest are observed for the C=O oxygen of **2** and the Cl atom of **1b** [3.288(6) Å], and the C=O oxygen of **2** and the Cl atom of **4** [3.247(7) Å].

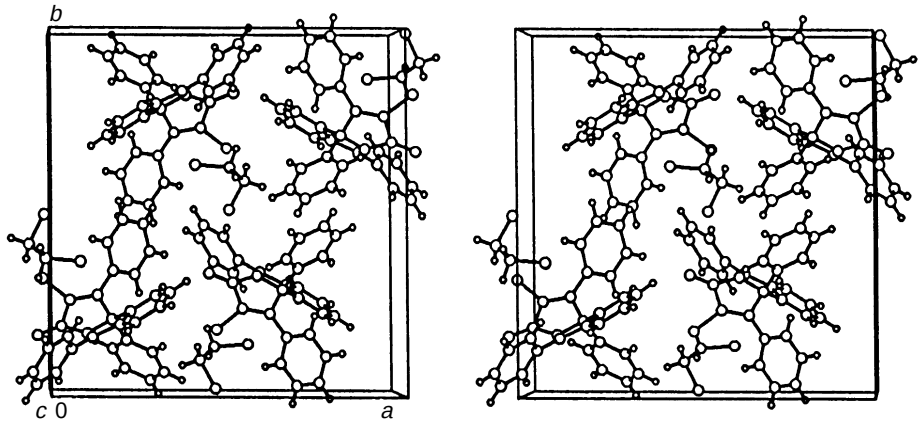



**Fig. 1** Stereoview of the 1 : 1 inclusion complex **3** of **2** and (*M*)-**1b**

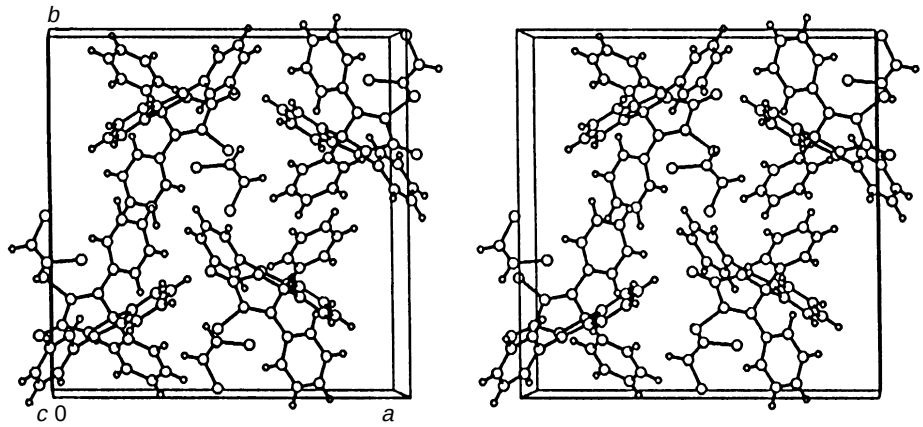



**Fig. 2** Stereoview of the 1 : 1 inclusion complex **5** of **2** and **4**

The dissociation energies of **3** (51 kJ mol$^{-1}$) and **5** (59 kJ mol$^{-1}$), which were estimated from their differential scanning calorimetry data, are also comparable, however, the slightly more stable **5** should be formed a little more readily. In fact, recrystallization of (+)-**2** (40 mg) from a 1 : 1 mixture of **1** (200 mg) and **4** (200 mg) gave **5** (32 mg, 67% yield) exclusively. This is a good example of extremely precise molecular recognition in molecular assembly.

The chlorine atoms of **1** and **4** seem to be the key to deciding whether the inclusion of the guest in the cavity occurs or not. Thus, in the two cases, the two chlorine atoms are located in similar positions. Since the *trans*-isomer of **4** (**6**) cannot be included with **2**, a guest molecule in which the two chlorine atoms are located in a *trans*-position such as **1a** would be unfavourable for accommodation in the cavity of the complex with **2**. Presence of **1b** in **2** also suggests that some electrostatic interaction between the two chlorine atoms is contributing to the stabilisation of the sterically unfavourable eclipsed-form.

## Footnotes

† E-mail: toda@en3.ehime-u.ac.jp
‡ E-mail: ckuroda@komaba.ecc.u-tokyo.ac.jp

§ *Preparation of inclusion complexes*. Compound **3**: When a solution of **2** (50 mg) in 1,2-dichloroethane (0.5 ml) was kept at room temperature for 2 h, a 1 : 1 inclusion complex **3** was obtained as yellow prisms (39 mg, 69% yield, mp 100–104 °C); $\nu_{max}$ (Nujol)/cm$^{-1}$ 1688 (C=O); $^1$H NMR ($CDCl_3$): δ 3.7 (s, $CH_2$, 4 H) and 7.1–7.8 (m, Ar, 19 H); Calc. for $C_{32}H_{23}OBrCl_2$: C, 66.92, H, 4.04. Found: C, 67.00, H, 4.11%.

Compound **5**: When a solution of **2** (50 mg) in *cis*-dichloroethylene (0.5 ml) was kept at room temperature for 2 h, a 1 : 1 inclusion complex **5** was obtained as yellow prisms (48 mg, 73% yield, mp not clear); $\nu_{max}$ (Nujol)/cm$^{-1}$ 1693 (C=O); $^1$H NMR ($CDCl_3$): δ 6.4 (s, =CH, 2 H) and 7.1–7.8 (m, Ar, 19 H); Calc. for $C_{32}H_{21}OBrCl_2$: C, 67.16, H, 3.70. Found: C, 67.22, H, 3.63%. When a solution of **2** (50 mg) in a mixture of 1,2-dichroloethane (0.25 ml) and *cis*-1,2-dichloroethylene (0.25 ml) was kept at room temperature for 2 h, **5** (45 mg, 68% yield) was obtained in the pure state.

¶ *Crystal data* for **3**: $C_{32}H_{23}OBrCl_2$, $M$ = 574.34, orthorhombic, space group $P2_12_12_1$, $a$ = 16.748(2), $b$ = 17.113(3), $c$ = 9.351(3) Å, $U$ = 2680.1(9) Å$^3$, Mo-Kα (λ = 0.71069 Å), $D_c$ = 1.423 g cm$^{-3}$, $Z$ = 4, $F$(000) = 1168, pale yellow plates, crystal dimensions 0.22 × 0.20 × 0.40 mm, μ(Mo-Kα) = 17.41 cm, 2θ–ω scan, 3480 independent reflections (5 < 2θ < 55.0°). The final $R$ = 0.045 and GOF = 1.53 for the 1775 reflections with $I > 3\sigma(I)$. Reflection data were collected on a Rigaku AFC5S four-circle diffractometer and the structure was solved by TEXSAN software using a VAXstation 3200.

*Crystal data* for **5**: $C_{32}H_{21}OBrCl_2$, $M$ = 572.343, orthorhombic, space group $P2_12_12_1$, $a$ = 16.763(2), $b$ = 17.033(1), $c$ = 9.318(1) Å, $U$ = 2660.5(6) Å$^3$, Mo-Kα (λ = 0.71069 Å), $D_c$ = 1.429 g cm$^{-3}$, $Z$ = 4, $F$(000) = 1160, pale yellow plates, crystal dimensions 0.35 × 0.25 × 0.50 mm, μ(Mo-Kα) = 17.53 cm, 2θ–ω scan, 3456 independent reflections (5 < 2θ < 55.0°). The final $R$ = 0.045 and GOF = 1.46 for the 1579 reflections with $I > 3\sigma(I)$. Reflection data were collected on a Rigaku AFC5S four-circle diffractometer and the structure was solved by TEXSAN software using a VAXstation 3200.

Atomic coordinates, bond lengths and angles, and thermal parameters have been deposited at the Cambridge Crystallographic data Centre (CCDC). See Information for Authors, Issue No. 1. Any request to the CCDC for this material should quote the full literature citation and the reference number 182/478.

‖ The absolute configuration of the host (−)-**2** has been determined to be (*S*) by comparison of the converged *R*-factors, *i.e.* 0.045 and 0.066 for the (*S*)- and (*R*)-enantiomers, respectively.

## References

1 *Stereochemistry of Organic Compounds*, ed. E. L. Eliel and S. H. Wilen, Wiley, 1994, p. 606.
2 R. Bose, D. Blaser and T. Haumann, *Z. Kristallogr.*, 1992, **198**, 311.
3 F. Toda, M. Sasaoka, Y. Todo, K. Iida, T. Hino, Y. Nishiyama, H. Ueda and T. Oshima, *Bull. Chem. Soc. Jpn.*, 1983, **56**, 3314.
4 F. Toda and K. Tanaka, *Tetrahedron: Asymmetry*, 1990, **1**, 359.
5 *IUPAC Tentative Rules for the Nomenclature of Organic Chemistry. Section E. Fundamental Stereochemistry*: See for example, *J. Org. Chem.*, 1970, **35**, 2849.

*Received in Cambridge, UK, 7th April 1997; Com. 7/02333B*

# Palladium-catalysed borylsilylation of alkynes and borylsilylative carbocyclization of diynes and an enyne compound

**Shun-ya Onozawa, Yasuo Hatanaka and Masato Tanaka***

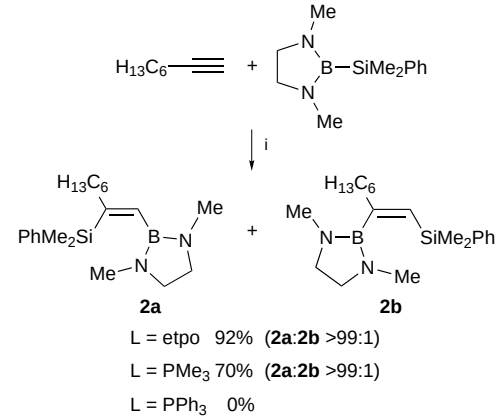
*National Institute of Materials and Chemical Research, Tsukuba, Ibaraki 305, Japan*

**Addition reactions or addition–carbocyclization reactions of a borylsilane with alkynes, α,ω-diynes or an enyne compound proceed efficiently in the presence of palladium catalysts, $P(OCH_2)_3CEt$ being the ligand of choice.**

Addition reactions of inter-heteroatom bonds such as Si–Si and Sn–Sn to unsaturated carbon bonds are extremely useful for one-step generation of two heteroatom–carbon bonds.[1] Similar chemistry starting with B–B bonds is also rapidly emerging.[2] An obvious extension is addition reactions of bonds comprising two different elements.[3] In a previous paper we disclosed palladium-catalysed addition of borylstannanes to alkynes (borylstannylation) leading to efficient synthesis of 1-boryl-2-stannyl alkenes.[4] α,ω-Diynes also react with borylstannanes, undergoing borylstannylative carbocyclization reactions to afford 1-borylmethylene-2-stannylmethylene cycloalkanes in high yields.[5a] 1,4-Addition of conjugated dienes also proceeds smoothly when $Pd(etpo)_2$ catalyst [etpo = 4-ethyl-2,6,7-trioxa-1-phosphabicyclo[2.2.2]octane, $P(OCH_2)_3CEt$] is used.[5b] As regards corresponding borylsilylation, however, only unsuccessful results have been reported by Buynak and Geng.[6] While we were studying borylsilylation as a useful extension of the borylstannylation, Ito and co-workers briefly presented successful examples of addition reactions of a borylsilane (4,4,5,5-tetramethyl-2-dimethylphenylsilyl-2-bora-1,3-dioxapentane) to alkynes, mainly using the 1,1,3,3-tetramethylbutyl isocyanide–palladium diacetate catalyst system.[7] Their communication prompted us to report our own results.

A representative procedure for the reaction of alkynes was as follows. A mixture of $Pd_2(dba)_3$ (0.005 mmol; dba = dibenzylideneacetone) and etpo (0.02 mmol), *i.e.* $Pd_2(dba)_3$–etpo catalyst system in which P/Pd = 2, in $C_6D_6$ (0.2 ml) was heated at 80 °C for 5 min, while the colour of the solution was changing from red to green. 1,3-Dimethyl-2-dimethylphenylsilyl-2-bora-1,3-diazacyclopentane **1** (0.2 mmol), oct-1-yne (0.3 mmol) and 1,4-dioxane (20 μl; internal standard for NMR analysis) were added to the resulting solution and the mixture was heated at 80 °C in a sealed NMR tube. NMR and GC–MS analyses of the reaction mixture after 2 h indicated complete consumption of **1** and adduct **2a**† being formed in 92% yield (Scheme 1). Note that the regioselectivity was >99% and that only a trace of isomer **2b** was detected by NMR analysis. Isolation of the product was simple; evaporation of the reaction mixture, addition of hexane (2 ml) to the residue, filtration and distillation of the filtrate afforded nearly pure **2a** in 84% isolated yield, which exhibited satisfactory spectral and analytical data. Observation of an 8% NOE between the allylic protons and the vinylic proton suggested that selective *cis*-addition of the B–Si bond had taken place.

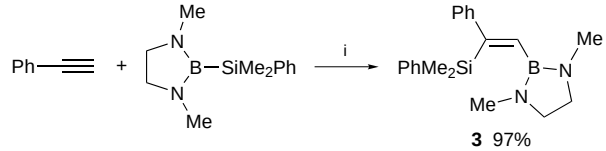
Unlike for the borylstannylation, Pd–$PPh_3$ complexes were not as efficient catalysts; the reaction of oct-1-yne with **1** did not proceed under the same conditions when either $Pd(PPh_3)_4$ or $PdCl_2(PPh_3)_2$ was used as the catalyst. The former did catalyse the reaction at higher temperatures, but the yields were still unsatisfactory, *e.g.* only 78% yield (**2a**/**2b** > 99 : 1) even after heating at 110 °C for 24 h. However the latter, which catalysed the borylstannylation at room temperature, was totally inactive even at 110 °C. We have reported that $PMe_3$ performs better than $PPh_3$ in the platinum-[8] or palladium-catalysed reactions[9] of unsaturated carbon compounds with disilanes or digermanes. The reaction of oct-1-yne with **1** was also better when catalysed by the $Pd_2(dba)_3$–$4PMe_3$ system (70% yield, 80 °C, 2 h) than by the $Pd_2(dba)_3$–$4PPh_3$ system (0% yield, 80 °C, 2 h *vs.* 18% yield, 110 °C, 7 h). However, as the foregoing typical experiment exemplifies, etpo is superior to the other phosphines as the ligand. In view of the decreasing trend of performance etpo > $PMe_3$ > $PPh_3$, the ligand effect in the borylsilylation is concluded to be similar to our previous observation made in the double silylation of acetylenes[9a,b] and quinones[9c] with disilanes and double germylation of acetylenes, dienes and alkenes.[9d]



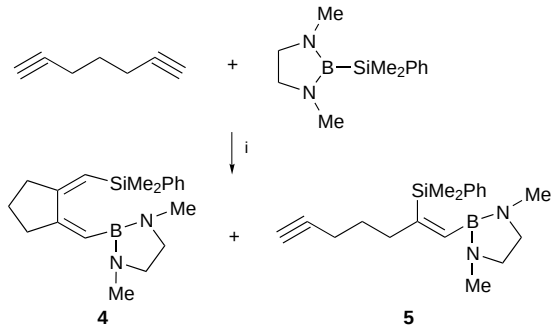

**Scheme 1** *Reagents and conditions*: i, $Pd_2(dba)_3$ (2.5 mol%), ligand (L/Pd = 2), $C_6D_6$, 80 °C, 2 h

Phenylacetylene appeared to be slightly less reactive towards **1** than oct-1-yne, but the reaction did proceed smoothly at 110 °C in the presence of the $Pd_2(dba)_3$–4etpo catalyst system to give 97% yield of **3**† as the sole product in 2 h (Scheme 2). However, the reaction of dimethyl acetylenedicarboxylate resulted in a complicated mixture.

Borylsilylative carbocyclization of hepta-1,6-diyne (0.3 mmol) with **1** (0.2 mmol) was also catalysed smoothly by the $Pd_2(dba)_3$–4etpo system in $C_6D_6$ at 110 °C to afford **4** in 81% yield.† Configurations at the silylmethylidene and borylmethylidene moieties of **4** were confirmed by 19.3 and 18.2% NOEs between the vinylic and allylic protons. A byproduct **5** coming from simple addition of **1** to one of the two acetylenic bonds without carbocyclization was also formed in 18% yield (Scheme 3). The $Pd_2(dba)_3$–$4PMe_3$ system was as active, but less selective (84% total yield after 2 h at 110 °C, **4** : **5** = 30 : 70). The $Pd_2(dba)_3$–$4PPh_3$ system was less active and even less selective (88% total yield after 7 h at 110 °C, **4** : **5** = 26 : 74). $PdCl_2(PPh_3)_2$ was totally inactive at 110 °C.




**Scheme 2** *Reagents and conditions*: i, $Pd_2(dba)_3$ (2.5 mol%), etpo (etpo/Pd = 2), $C_6D_6$, 110 °C, 2 h




**4** **5**

L = etpo, L/Pd = 2, 2 h, 98% (**4**:**5** = 81:19)

L = etpo, L/Pd = 1, 2 h, 97% (**4**:**5** = 87:13)

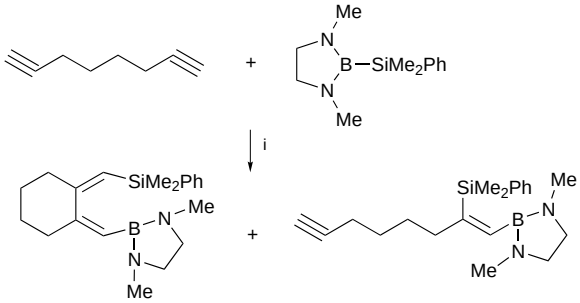
L = $PMe_3$, L/Pd = 2, 2 h, 84% (**4**:**5** = 30:70)

L = $PPh_3$, L/Pd = 2, 7 h, 98% (**4**:**5** = 26:74)

**Scheme 3** *Reagents and conditons*: i, $Pd_2(dba)_3$ (2.5 mol%), ligand (L/Pd = 2 or 1), $C_6D_6$, 110 °C

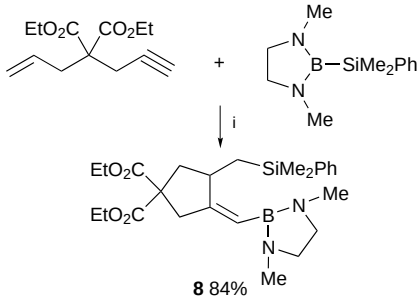
A decrease in the quantity of etpo relative to palladium is envisioned to be favourable to minimize the formation of byproduct **5** if simultaneous coordination of both acetylenic bonds to palladium is a prerequisite for the cyclization leading to **4**. Indeed, the reaction of hepta-1,6-diyne with **1** at etpo/Pd = 1 under otherwise identical conditions resulted in a slight increase in the selectivity for **4**; the **4**:**5** ratio was 87:13, obtained in a 97% combined yield. The reaction of octa-1,7-diyne with **1** was slightly less reactive and much less selective for the cyclization product **6**,† with **7** as the major product (Scheme 4). The selectivity was not appreciably improved even when etpo/Pd = 1, indicating the necessity for a new design of catalyst to circumvent the difficulty of coordination of both acetylenic bonds.

Finally an enyne compound, 4,4-bis(ethoxycarbonyl)hept-6-en-1-yne, also smoothly underwent similar cyclization with **1**




**6** 17% **7** 62%

**Scheme 4** *Reagents and conditions*: i, $Pd_2(dba)_3$ (2.5 mol%), etpo (etpo/Pd = 2), $C_6D_6$, 110 °C, 2 h




**8** 84%

**Scheme 5** *Reagents and conditions*: i, $Pd_2(dba)_3$ (2.5 mol%), etpo (etpo/Pd = 2), $C_6D_6$, 110 °C, 2 h

to give **8**† in 84% yield (Scheme 5). The $^1$H NMR spectrum of the reaction mixture displayed a weak singlet at δ 6.48, suggesting the formation of a small quantity (9%) of a byproduct, which might have come from plain addition of **1** to the triple bond.

Partial financial support from the Science and Technology Corporation (JST) through the CREST program is gratefully acknowledged. We thank Dr T. Sakakura for valuable discussions in the initial stages of the research.

## Footnotes

* E-mail: mtanaka@ccmail.nimc.go.jp

† *Selected spectral and/or physical data* for the products $^1$H NMR ($C_6D_6$), 270 MHz; *J*/Hz) for **2a**: bp 135–140 °C at $2.3 \times 10^{-3}$ Torr; $\delta_H$ 0.43 (s, 6 H, $SiCH_3$), 0.86 [t, *J* 6.8, 3 H, $CH_2(CH_2)_4CH_3$], 1.14–1.53 [m, 8 H, $CH_2(CH_2)_4CH_3$], 2.28 [t, *J* 7.2, 2 H, $CH_2(CH_2)_4CH_3$], 2.51 (s, 6 H, $NCH_3$), 2.89 (s, 4 H, $NCH_2$), 6.36 (s, 1 H, =CH), 7.10–7.33 (m, 3 H, arom), 7.50–7.65 (m, 2 H, arom). For **3**: $\delta_H$ 0.40 (s, 6 H, $SiCH_3$), 2.49 (s, 6 H, $NCH_3$), 2.84 (s, 4 H, $NCH_2$), 6.56 (s, 1 H, =CH), 6.95–7.35 (m, 8 H, arom), 7.50–7.60 (m, 2 H, arom). For **4**: bp 128–132 °C at $2.8 \times 10^{-3}$ Torr (mixture of **4** and **5**); $\delta_H$ 0.38 (s, 6 H, $SiCH_3$), 1.46–1.68 (m, 2 H), 2.31–2.41 (m, 4 H), 2.46 (s, 6 H, $NCH_3$), 2.83 (s, 4 H, $NCH_2$), 5.40 (s, 1 H, =CH), 5.62 (s, 1 H, =CH), 7.12–7.31 (m, 3 H, arom), 7.42–7.60 (m, 2 H, arom). For **6**: $\delta_H$ 0.40 and 0.43 (both s, 6 H, $SiCH_3$), 1.45–1.73 (m, 4 H), 2.20–2.40 (m, 4 H), 2.55 (s, 6 H, $NCH_3$), 2.83–2.97 (m, 4 H, $NCH_2$), 5.30 (s, 1 H, =CH), 5.47 (s, 1 H, =CH), 7.05–7.26 (m, 3 H, arom), 7.54–7.63 (m, 2 H, arom). For **8**: $\delta_H$ 0.24 (s, 3 H, $SiCH_3$), 0.26 (s, 3 H, $SiCH_3$), 0.82 (dd, *J* 11.9 and 14.6, 1 H, $SiCH_2$), 0.90 (t, *J* 7.1, 3 H, $OCH_2CH_3$), 0.91 (t, *J* 7.1, 3 H, $OCH_2CH_3$), 1.32 (dd, *J* 2.0 and 14.6, 1 H, $SiCH_2$), 1.80–1.93 (m, 1 H, $CH_2$), 2.50 (s, 6 H, $NCH_3$), 2.74–3.07 (m, 7 H, $NCH_2$, $CH_2$ and CH), 3.14 (d, *J* 17.5, 1 H, $CH_2$), 3.32 (d, *J* 17.5, 1 H, $CH_2$), 3.85–4.03 (m, 4 H, $OCH_2CH_3$), 5.43 (s, 1 H, =CBH), 7.13–7.27 (m, 3 H, arom), 7.45–7.53 (m, 2 H, arom).

## References

1 For reviews, see *Organometallic Reagents in Organic Synthesis*, ed. J. H. Bateson and M. B. Mitchell, Academic Press, New York, 1994, pp. 129–160; H. K. Sharma and K. H. Pannell, *Chem. Rev.*, 1995, **95**, 1351.

2 T. Ishiyama, N. Matsuda, N. Miyaura and A. Suzuki, *J. Am. Chem. Soc.*, 1993, **115**, 11018; R. T. Baker, P. Nguyen, T. B. Marder and S. A. Westcott, *Angew. Chem., Int. Ed. Engl.*, 1995, **34**, 1336; T. Ishiyama, N. Matsuda, M. Murata, F. Ozawa, A. Suzuki and N. Miyaura, *Organometallics*, 1996, **15**, 713; G. Lesley, P. Nguyen, N. J. Taylor, T. B. Marder, A. J. Scott, W. Clegg and N. C. Norman, *Organometallics*, 1996, **15**, 5137; C. N. Iverson and M. R. Smith, III, *Organometallics*, 1996, **15**, 5155.

3 T. Ishiyama, K.-i. Nishijima, N. Miyaura and A. Suzuki, *J. Am. Chem. Soc.*, 1993, **115**, 7219; L.-B. Han, N. Choi and M. Tanaka, *J. Am. Chem. Soc.*, 1996, **118**, 7000.

4 S.-y. Onozawa, Y. Hatanaka, T. Sakakura, S. Shimada and M. Tanaka, *Organometallics*, 1996, **15**, 5450.

5 (*a*) S.-y. Onozawa, Y. Hatanaka, T. Sakakura and M. Tanaka, presented at the 43rd Symposium on Organometallic Chemistry, Abstract PB231, Osaka, October 31–November 1st, 1996; (*b*) S.-y. Onozawa, Y. Hatanaka, T. Sakakura and M. Tanaka, presented at the 72nd Spring Annual Meeting of the Chemical Society of Japan, Abstract 3F146, Tokyo, March 27–30th, 1997.

6 J. D. Buynak and B. Geng, *Organometallics*, 1995, **14**, 3112.

7 M. Suginome, H. Nakamura, T. Matsuda and Y. Ito, presented at the 72nd Spring Annual Meeting of the Chemical Society of Japan, Abstract 2F226, Tokyo, March 27–30th, 1997.

8 T. Hayashi, A. M. Kawamoto, T.-a. Kobayashi and M. Tanaka, *J. Chem. Soc., Chem. Commun.*, 1990, 563.

9 (*a*) H. Yamashita, M. Catellani and M. Tanaka, *Chem. Lett.*, 1991, 241; (*b*) H. Yamashita and M. Tanaka, *Chem. Lett.*, 1992, 1547; (*c*) T. Hayashi, H. Yamashita, T. Sakakura, Y. Uchimaru and M. Tanaka, *Chem. Lett.*, 1991, 245; (*d*) H. Yamashita, N. P. Reddy and M. Tanaka, *Macromolecules*, 1993, **26**, 2143.

*Received in Cambridge, UK, 24th April 1997; Com. 7/02802D*

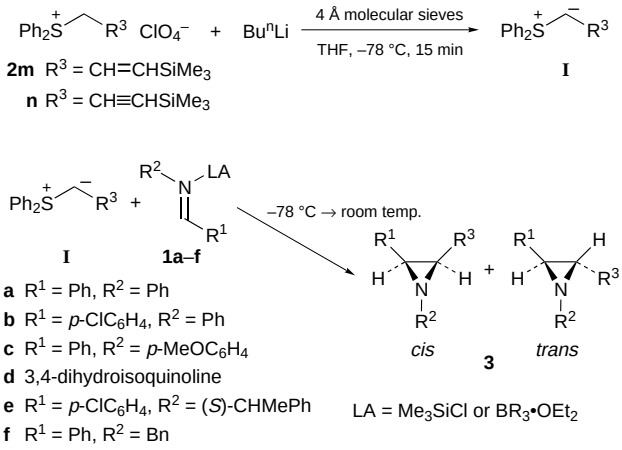
# Lewis acid promoted aziridination of imines with semistabilized sulfonium ylides: highly stereoselective synthesis of vinyl- and ethynyl-aziridines

**De-Kun Wang, Li-Xin Dai and Xue-Long Hou***

*Laboratory of Organometallic Chemistry, Shanghai Institute of Organic Chemistry, Chinese Academy of Sciences, 354 Fenglin Lu, Shanghai 200032, P.R.C.*

***cis*-Vinyl- and *cis*-ethynyl-aziridines are furnished in high yields and high stereoselectivity by aziridination of unactivated *N*-aryl or *N*-alkyl imines with S-ylides in the presence of Lewis acids.**

The addition of carbenoids[1] or ylides[2] to a C=N double bond has been demonstrated as a synthetic strategy for asymmetric aziridination in recent years, and is regarded as an alternative methodology to the reaction between nitrenoids and a C=C double bond.[3] However, the ylide and carbenoid methodologies can only be applied to an activated imine, that is to C=N double bonds with an *N*-electron withdrawing group (*N*-EWG), such as *p*-tolylsulfonyl (tosyl),[1a,2] diphenylphosphinyl (DPP)[2a,4] or 2-(trimethylsilyl) ethylsulfonyl (SES).[2a] Although the preparation of aziridines from an unactivated imine with an ylide has been documented, the ylide used is restricted to active ylides such as dimethylsulfonium methide or dimethylsulfoxonium methide, *i.e.* methylene transfer to C=N bond. No report has appeared of the reaction of an unactivated imine with a semistabilized or stabilized ylide. Considering the vigorous conditions required for the deprotection of the tosyl group from the *N*-atom[5] and the difficulties in the preparation of *N*-tosyl,[6a,b] *N*-DPP[6c] and *N*-SES[6d] imines from certain carbonyl compounds, developing a general and facile method for the aziridination of common *N*-alkyl and *N*-aryl imines with stabilized or semistabilized ylides is still a challenge. Encouraged by the successful activation of imines by Lewis acids in the allylation reaction,[7] we examined $BF_3$·$OEt_2$ and $Me_3SiCl$ activation of imines in the ylide reaction for the preparation of vinyl- and ethynyl-aziridines. In a recent paper,[8] ethyl diazoacetate was used to react with a $BF_3$·$OEt_2$ activated imine in the preparation of aziridines, which promoted us to report our own results. Thus, a new and general ylide aziridination of common *N*-alkyl and *N*-aryl imines with semistabilized allylic or prop-2-ynylic sulfonium ylides in the presence of $BF_3$·$OEt_2$ or $Me_3SiCl$ has been successfully realized not only with high yields but also with high stereoselectivity, and disclosed these results herein (Scheme 1).




**Scheme 1**

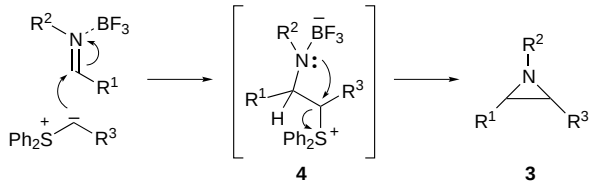
Treatment of a THF solution of sulfonium salts **2** with 1 equiv. of *n*-butyllithium at −78 °C for 15 min gave a deep-red solution of sulfonium ylide.[9] This was added to an equimolar THF solution of imine **1** and $Me_3SiCl$ (method A) or $BF_3$·$OEt_2$ (method B) at the same temperature with stirring. The temperature of the mixture was allowed to rise to room temperature, and aziridine **3** was formed as the only product. In the absence of $Me_3SiCl$ or $BF_3$·$OEt_2$, no aziridine **3** was formed even on extended stirring under the same conditions. In terms of the yield of aziridine, the reaction proceeded more efficiently using $BF_3$·$OEt_2$ as Lewis acid (method B) than $Me_3SiCl$. The ratio of the *cis*- and *trans*-products was determined by $^1H$ NMR analysis. Our best results were obtained in THF in the presence of 4 Å molecular sieves and are summarized in Table 1.†

As shown, a variety of aromatic aldimines, either *N*-aryl or *N*-alkyl, could be aziridinated with good to excellent yield, but aziridination failed when aliphatic aldimines were used as substrates. The stereoselectivity of the aziridination is strongly dependent on the nature of the group on the nitrogen atom of the imine: *N*-aryl aromatic aldimines gave purely the *cis*-aziridine (entries 1–12), while *N*-alkyl aromatic aldimines gave a mixture of *cis* and *trans* aziridines (entries 17–22). By not using an

**Table 1** Preparation of 2-vinylaziridines **3m** and 2-ethynylaziridines **3n** by the reaction of γ-trimethylsilyl-allyl and -prop-2-ynyl sulfonium ylides and aldimines mediated by Lewis acids[a]

| | **1** | | | | % | |
|---|---|---|---|---|---|---|
| Entry | $R^1$ | $R^2$ | **2** | Method[b] | Yield (**3**)[c] | *cis* : *trans*[d] |
| 1 | Ph | Ph | **2m** | A | 89 (**3ma**) | 100 : 0 |
| 2 | Ph | Ph | **2m** | B | 92 (**3ma**) | 100 : 0 |
| 3 | Ph | Ph | **2n** | A | 83 (**3na**) | 100 : 0 |
| 4 | Ph | Ph | **2n** | B | 89 (**3na**) | 100 : 0 |
| 5 | *p*-$ClC_6H_4$ | Ph | **2m** | A | 75 (**3mb**) | 100 : 0 |
| 6 | *p*-$ClC_6H_4$ | Ph | **2m** | B | 91 (**3mb**) | 100 : 0 |
| 7 | *p*-$ClC_6H_4$ | Ph | **2n** | A | 85 (**3nb**) | 100 : 0 |
| 8 | *p*-$ClC_6H_4$ | Ph | **2n** | B | 84 (**3nb**) | 100 : 0 |
| 9 | *p*-$MeOC_6H_4$ | Ph | **2m** | A | 68 (**3mc**) | 100 : 0 |
| 10 | *p*-$MeOC_6H_4$ | Ph | **2m** | B | 83 (**3mc**) | 100 : 0 |
| 11 | *p*-$MeOC_6H_4$ | Ph | **2n** | A | 69 (**3nc**) | 100 : 0 |
| 12 | *p*-$MeOC_6H_4$ | Ph | **2n** | B | 74 (**3nc**) | 100 : 0 |
| 13 | 3,4-Dihydroisoquinoline | | **2m** | A | 80 (**3md**) | 50 : 50 |
| 14 | 3,4-Dihydroisoquinoline | | **2m** | B | 82 (**3md**) | 50 : 50 |
| 15 | 3,4-Dihydroisoquinoline | | **2n** | A | 67 (**3nd**) | 60 : 40 |
| 16 | 3,4-Dihydroisoquinoline | | **2n** | B | 92 (**3nd**) | 50 : 50 |
| 17 | *p*-$ClC_6H_4$ | (*S*)-CHMePh | **2m** | B | 87 (**3me**) | 54 : 46 |
| 18 | *p*-$ClC_6H_4$ | (*S*)-CHMePh | **2n** | B | 65 (**3ne**) | 50 : 50 |
| 19 | Ph | Bn | **2m** | A | 76 (**3mf**) | 50 : 50 |
| 20 | Ph | Bn | **2m** | B | 93 (**3mf**) | 50 : 50 |
| 21 | Ph | Bn | **2n** | B | 65 (**3nf**) | 52 : 48 |
| 22 | Ph | Bn | **2n** | B | 76 (**3nf**) | 53 : 47 |

[a] All reactions were carried out at −78 °C with a ratio of imine **1**: sulfonium salt **2**: $Bu^nLi$ = 1 : 1.1 : 1.1 on a 0.5 mmol scale in THF with 4 Å molecular sieves. [b] Method A: $Me_3SiCl$ used as activator; Method B: $BF_3$·$OEt_2$ used as activator. [c] Isolated yields based on imine. [d] Determined by 300 MHz $^1H$ NMR analysis.




**Scheme 2**

*N*-tosyl imine, this reaction can be extended to include cyclic imines, such as dihydroisoquinoline (entries 13–16).

Activation of the imine by complexion with the Lewis acids, followed by nucleophilic addition of the ylide, results in the formation of intermediate **4** (Scheme 2). Subsequent ring closure and loss of diphenyl sulfide gave aziridines **3**. Aggarwal[2a] and Yamamoto[10] recently rationalized the fact that the *cis*-aziridine isomer is the thermodynamic product. In our procedure, the *cis* stereoselectivity of the reaction might come from the 1,2-steric interaction in the three-membered ring between the aryl group (this is the largest group) and either of the substitutes. The mixture of *cis* and *trans N*-alkylaziridines may result from weak steric interaction among the substituents on the three-membered ring, thus giving almost no selectivity.

In summary, we have demonstrated an efficient method for the preparation of various α-unsaturated substituted aziridines from aryl imines and semistabilized prop-2-ynylic and allylic sulfonium ylides in the presence of $BF_3$•$OEt_2$ with high *cis*-selectivity. It extends the scope of the ylide route to aziridination, without the need to prepare an *N*-EWG imine, and may also be applied to cyclic imines. In comparison to the recent work of diazoacetate with imines,[8] the present method gives higher yields with high *cis*-stereoselectivity and no sign of the formation of significant amounts of by-product. It represents an improvement over our previous routes[2b,c] and may be applied to the preparation of functionalized aziridines. The introduction of chirality into this reaction is being investigated.

Financial support from the National Natural Science Foundation of China and the Chinese Academy of Sciences is gratefully acknowledged.

## Footnotes

* E-mail: xlhou@pub.sioc.ac.cn

† *Typical experimental procedure*: A 25 ml flask containing a magnetic stirrer bar was charged with sulfonium salt **2m** (240 mg, 0.6 mmol), 4 Å molecular sieves (1 g) and anhydrous THF (4 ml), the mixture was cooled to −78 °C under $N_2$, and treated with $Bu^nLi$ (0.4 ml; 1.6 M in hexanes) (Aldrich) with stirring. After 15 min, a mixture of imine **1a** (91 mg, 0.5 mmol) and $BF_3$•$OEt_2$ (1.0 equiv.) was added at the same temperature and stirring was continued until the temperature rose to room temperature. The reaction mixture was filtered on a short column of neutral $Al_2O_3$ to remove inorganic salts. The filtrate was concentrated and chromatographed on a column of neutral $Al_2O_3$ with light petroleum (bp 60–90 °C)–EtOAc–$NEt_3$ (10 : 1 : 0.5) as eluent to give pure *cis*-**3ma** (135 mg, 92%).

## References

1 (*a*) K. B. Hansen, N. S. Finney and E. N. Jacobsen, *Angew. Chem., Int. Ed. Engl*., 1995, **34**, 676; (*b*) K. G. Rasmussen and K. A. Jørgensen, *J. Chem. Soc., Chem. Commun*., 1995, 1401; (*c*) Z. Zhu and J. H. Espenson, *J. Org. Chem*., 1995, **60**, 7090.

2 For leading references see (*a*) V. K. Aggarwal, A. Thompson, R. V. H. Jones and M. C. H. Standen, *J. Org. Chem*., 1996, **61**, 8368; (*b*) A.-H. Li, L.-X. Dai and X.-L. Hou, *Chem. Commun*., 1996, 491; (*c*) A.-H. Li, L.-X. Dai and X.-L. Hou, *J. Chem. Soc., Perkin Trans. 1*, 1996, 867; (*d*) A.-H. Li, L.-X. Dai, X.-L. Hou and M.-B. Chen, *J. Org. Chem.*, 1996, **61**, 4641; (*e*) A.-H. Li, L.-X. Dai and X.-L. Hou, *J. Chem. Soc., Perkin Trans. 1*, 1996, 2725.

3 D. A. Evans, M. M. Faul, M. T. Bilodeau, B. A. Anderson and D. M. Barnes, *J. Am. Chem. Soc*., 1993, **115**, 5328; Z. Li, K. R. Conser and E. N. Jecobsen, *J. Am. Chem. Soc*., 1993, **115**, 5326; P. Müller, C. Baud and Y. Jacquier, *Tetrahedron*, 1996, **52**, 1543.

4 X.-L. Hou, X.-F. Yang and L.-X. Dai, to be published.

5 Some methods for desulfonylation for nitrogen atom: T. Fukuyama, C.-K. Jow and M. Cheung, *Tetrahedron Lett*., 1995, **36**, 6373; E. Vedejs and S. Lin, *J. Org. Chem*., 1994, **59**, 1602; K. Bellos, H. Stamm and D. Speth, *J. Org. Chem*., 1991, **56**, 6846; R. C. Roemmele and H. Rapoport, *J. Org. Chem*., 1988, **53**, 2367 and references cited therein.

6 (*a*) B. E. Love, P. S. Raje and T. C. Williams II, *Synlett*, 1994, 493; (*b*) G. I. Georg, G. C. B. Harriman and S. A. Peterson, *J. Org. Chem*., 1995, **60**, 7366; (*c*) W. B. Jennings and C. J. Lovely, *Tetrahedron*, 1991, **47**, 5561; (*d*) S. M. Weinreb, D. M. Demko and T. A. Lessen, *Tetrahedron Lett*., 1986, **27**, 2099.

7 G. E. Keck and E. J. Enholm, *J. Org. Chem*., 1985, **50**, 146; D.-K. Wang, L.-X. Dai and X.-L. Hou, *Tetrahedron Lett*., 1995, **36**, 8649.

8 For example, the Lewis acid is necessary in the synthesis of aziridines from imines and ethyl diazoacetate, see L. Casarrubios, J. A. Pérez, M. Brookhart and J. L. Templeton, *J. Org. Chem*., 1996, **61**, 8358.

9 For the preparation of 3-trimethylsilylallyldiphenylsulfonium perchlorate **2m** and 3-trimethylsilylprop-2-ynyldiphenylsulfonium perchlorate **2n**, see T. K. Jones and S. E. Denmark, *Org. Synth*., 1990, **Coll. Vol. 7**, 524; R. W. LaRochelle, B. M. Trost and L. Krepski, *J. Org. Chem*., 1971, **36**, 1126.

10 N. Mimura, T. Ibuka, M. Akaji, Y. Miwa, T. Taga, K. Nakai, H. Tamamura, N. Fujii and Y. Yamamoto, *Chem. Commun*., 1996, 351. The *cis*-selectivity phenomenon were also found; M. Komatsu, M. Ohno, S. Tsuno and Y. Ohshiro, *Chem. Lett*., 1990, 575. The Darzens fashion; G. Cainelli, M. Panurizio and D. Giacomini, *Tetrahedron Lett*., 1991, 121.

*Received in Cambridge, UK, 30th April 1997; Com. 7/02955A*

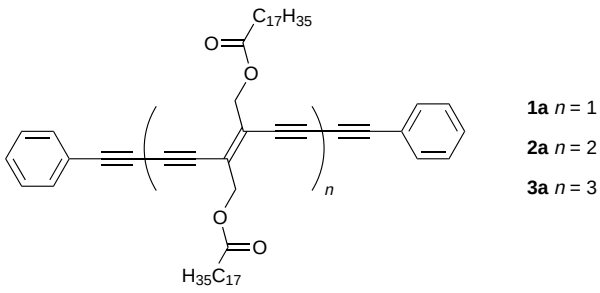
# Synthesis of liquid-crystalline oligotriacetylene derivatives

**Jean-François Nierengarten,* Daniel Guillon, Benoît Heinrich and Jean-François Nicoud**

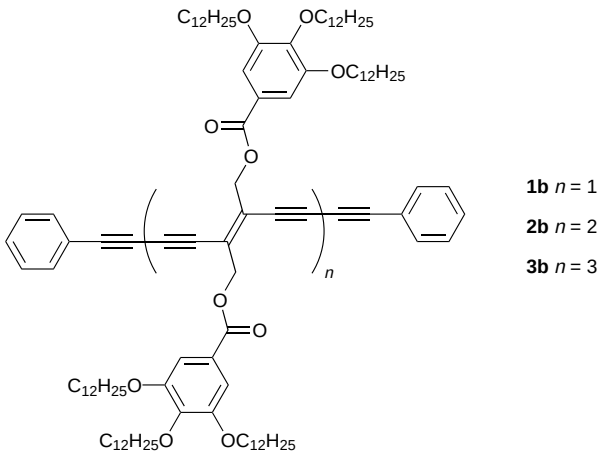
*Groupe des Matériaux Organiques, Institut de Physique et Chimie des Matériaux de Strasbourg, UMR C00460, CNRS, 23 rue du Loess, F-67037 Strasbourg, France*

**(*E*)-Hex-3-en-1,5-diyne derivatives with two or six pendant long alkyl chains have been prepared and their end-capping oligomerisation yields oligomers with a polytriacetylene conjugated backbone; whereas the end-capped mono- and di-mers do not exhibit any liquid-crystalline behaviour, the trimeric derivatives show mesomorphic properties.**

The preparation of oligomers and polymers with extended conjugated carbon cores is currently being intensively pursued,[1] with the aim of generating advanced materials for electronic,[2] photonic,[3] and non-linear optical[4] applications. For many years, polyacetylenes (PA) and polydiacetylenes (PDA) were the only known single-strand conjugated polymers with a non-aromatic all-carbon backbone; however, Diederich and co-workers succeeded recently in the preparation of oligomers and polymers with a polytriacetylene (PTA) backbone.[5] Whereas introduction of bulky substituents in PA leads to loss of conjugation due to distortion from planarity for steric reasons,[6] side chains can be attached on PDA or PTA backbones without any loss of conjugation.[5] PDAs and PTAs are also considerably more stable than PAs.[5] However, the accessibility of PDAs is limited by the requirements resulting from their preparation by topochemical polymerisation of suitably pre-organised butadiynes,[7] while PTAs can be prepared by normal chemical reactions.[5] Here we report the synthesis of PTA oligomers **1**–**3** of defined length substituted with lateral long alkyl chains. The conjugated backbone is a rigid rod that can act as a mesogenic unit and liquid crystalline properties were observed for some of the reported oligomers. The advantage of such a liquid crystal is that many properties (electroluminescence, third order optical nonlinearity *etc*.) associated with the delocalised π-electron system can be enhanced due to the orientational effect induced by the liquid crystal ordering.[8]

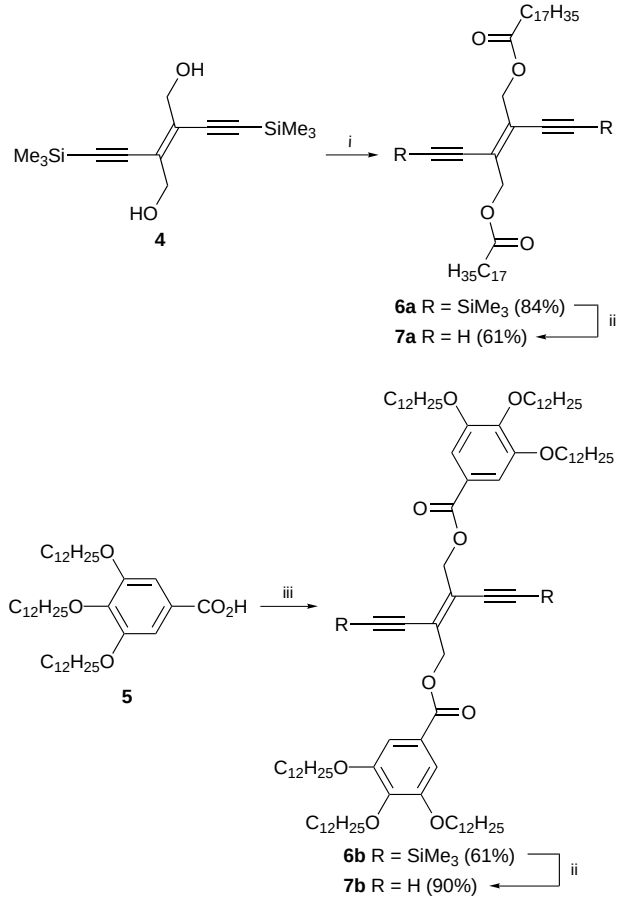



**1a** *n* = 1
**2a** *n* = 2
**3a** *n* = 3




**1b** *n* = 1
**2b** *n* = 2
**3b** *n* = 3

The synthesis of the monomers is described in Scheme 1. Diol **4** was prepared in three steps from dimethyl acetylenedicarboxylate as previously reported.[5b] The (*E*)-hex-3-en-1,5-diyne derivatives with pendant long alkyl chains were prepared by dicyclohexylcarbodiimide (DCC)-mediated esterification[9] of stearic acid and acid **5**[10] with diol **4** to give **6a** (84% yield) and **6b** (61% yield), respectively. Subsequent deprotection of **6a** and **6b** with $Bu_4NF$ in wet THF afforded *trans*-endiyne **7a** (61% yield) and **7b** (90% yield), respectively. Whereas compound **7a** is relatively unstable in the neat state, **7b** is an air-stable solid that can be stored at ambient temperature for prolonged periods of time. As previously shown by X-ray




**Scheme 1** *Reagents and conditions*: i, stearic acid, DCC, DMAP, $CH_2Cl_2$, 0 °C to room temp.; ii, $Bu_4NF$, wet THF, 0 °C; iii, **4**, DCC, DMAP, $CH_2Cl_2$, 0 °C to room temp.

crystal structure analysis of some related compounds,[11] the presence of bulky substituents in **7b** isolates the sensitive *trans*-endiyne units and prevents intermolecular reactions that would lead to decomposition.

The PTA oligomers **1a**–**3a** and **1b**–**3b** were prepared *via* end-capping oligomerisation of **7a** and **7b**, respectively. The *in situ* preparation of the Hay catalyst[12] [CuCl–TMEDA–$O_2$ (TMEDA = *N*,*N*,*N*′,*N*′-tetramethylethylenediamine)] in $CH_2Cl_2$ in the presence of **7a** and phenylacetylene furnished a mixture of oligomers, from which **1a**–**3a** were isolated by column chromatography ($SiO_2$, hexane–$CH_2Cl_2$ 3 : 2 to 1 : 2). When a large excess of phenylacetylene (10 equiv.) was used, **1a** and **2a** could be obtained in 25 and 5% yield, respectively. When **7a** and phenylacetylene were used in a 1 : 1 molar ratio, **1a** (9% yield), **2a** (5%) and **3a** (2%) could be isolated. End-capped oligomers **1b**–**3b** were prepared from **7b** and phenylacetylene under Hay coupling conditions in $CH_2Cl_2$ in a similar manner. Starting from phenylacetylene and **7b** in a 10 : 1 ratio, **1b** and **2b** were obtained in 64 and 7% yield, respectively. When a 1 : 1 molar ratio was used, **1b** (15% yield), **2b** (19%) and **3b** (12%) could be isolated by column chromatography ($SiO_2$, hexane–$CH_2Cl_2$ 2 : 1 to 1 : 1). Higher oligomers could also be eluted by using $CH_2Cl_2$ but could not be separated into pure compounds. Whereas the yields for the preparation of **1b**–**3b** are similar to that reported for related reactions,[5a] the yields of **1a**–**3a** are limited by the instability of monomer **7a** as well as by their surprisingly low solubility. All of the spectroscopic studies and elemental analysis results were consistent with the proposed molecular structures.† In spite of the presence of bulky substituents in **2b** and **3b**, their absorption spectra are similar to those of **2a** and **3a**, respectively, showing that there is no loss of conjugation as a result of a distortion from planarity for steric reasons. Compounds **2a** and **2b** show end absorption around 450 nm, and **3a** and **3b** around 500 nm.

Whereas the end-capped mono- and di-mers do not exhibit any liquid-crystalline behaviour, the trimeric derivatives **3a** and **3b** show mesomorphic properties. These have been deduced from optical and X-ray diffraction investigations. Polarised optical microscopy revealed a fluid birefringent phase at room temperature for **3b** and between 80 and 115 °C for **3a**. The clearing temperature was determined to be 40 °C for **3b**. However, in both cases, the birefringent optical textures observed on cooling the samples from the isotropic phase were non-characteristic.[13] Furthermore, the X-ray diffraction pattern of **3b** is typical of a mesomorphic phase with a sharp diffraction peak in the small angle region and a diffuse band in the wide angle region (Fig. 1). For **3a**, the diffraction patterns recorded at various temperature are more complex. The exact structure determination of these mesophases is still in progress.

The preparation of PTA oligomers with pendant long alkyl chains leads to original liquid crystalline derivatives. The synthesis of the corresponding polymers is now under investigation in our laboratory.

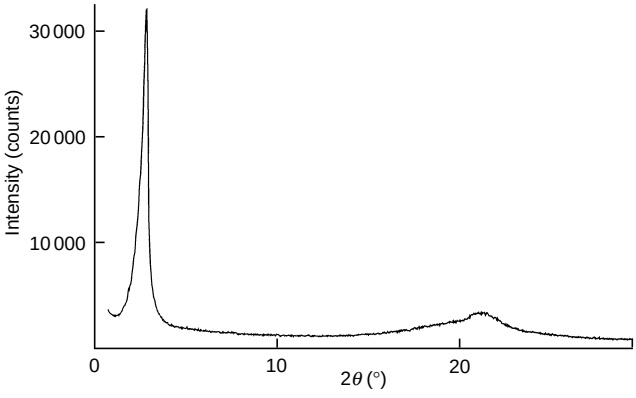



**Fig. 1** X-Ray diffraction pattern of **3b** recorded at 25 °C

We thank the CNRS for financial support. We also thank Dr A. Van Dorsellaer and R. Hueber for MS measurements and L. Oswald for technical help.

## Footnotes

* E-mail: niereng@michelangelo.u-strasbg.fr

† *Spectroscopic data* for **1b**: UV–VIS $\lambda_{max}(CH_2Cl_2)$/nm 243 (sh, 34140), 259 (49450), 360 (44560), 387 (sh, 35080); IR $\nu_{max}(CH_2Cl_2)/cm^{-1}$ 2211 (C≡C), 1718 (C=O); $^1$H NMR ($CDCl_3$, 200 MHz): 0.89 (m, 18 H), 1.26 (m, 108 H), 1.76 (m, 12 H), 4.02 (t, *J* 6.5, 4 H), 4.04 (t, *J* 6.5, 8 H), 5.21 (s, 4 H), 7.35 (s, 4 H), 7.37 (m, 6 H), 7.48 (m, 4 H); $^{13}$C NMR ($CDCl_3$, 50 MHz): 14.09, 22.68, 26.11, 29.20, 29.38, 29.64, 30.34, 31.93, 64.16, 69.11, 73.44, 76.55, 87.47, 88.68, 108.11, 121.11, 124.14, 128.48, 129.16, 129.76, 132.48, 142.55, 152.84, 165.89; FAB-MS: *m*/*z* 1650 ($MH^+$). For **2b**: UV–VIS $\lambda_{max}(CH_2Cl_2)$/nm 271 (90210), 359 (sh, 52210), 388 (67090), 419 (sh, 50270); IR $\nu_{max}(CH_2Cl_2)/cm^{-1}$ 2202 (C≡C), 1718 (C=O); $^1$H NMR ($CDCl_3$, 200 MHz): 0.89 (m, 36 H), 1.26 (m, 216 H), 1.77 (m, 24 H), 4.02 (m, 24 H), 5.15 (s, 8 H), 7.31 (s, 4 H), 7.33 (s, 4 H), 7.36 (m, 6 H), 7.47 (m, 4 H); $^{13}$C NMR ($CDCl_3$, 50 MHz): 14.09, 22.68, 26.09, 26.16, 29.38, 29.70, 30.37, 31.93, 63.95, 64.11, 69.12, 73.36, 73.47, 82.55, 87.34, 87.92, 89.54, 108.09, 108.18, 121.01, 123.95, 124.05, 127.68, 128.48, 129.83, 131.48, 132.50, 142.56, 142.68, 152.84, 165.73, 165.82; FAB-MS: *m*/*z* 3098.5 ($M^+$). For **3b**: UV–VIS $\lambda_{max}$ $(CH_2Cl_2)$/nm 273 (117850), 396 (sh, 69310), 413 (71310); IR $\nu_{max}(CHCl_3)/cm^{-1}$ 2205 (C≡C), 1715 (C=O); $^1$H NMR ($CDCl_3$, 200 MHz): 0.88 (m, 54 H), 1.25 (m, 324 H), 1.74 (m, 36 H), 3.98 (m, 36 H), 5.12 (s, 8 H), 5.16 (s, 4 H), 7.28 (s, 8 H), 7.32 (s, 4 H), 7.35 (m, 6 H), 7.42 (m, 4 H); $^{13}$C NMR ($CDCl_3$, 50 MHz): 14.09, 22.88, 26.15, 26.22, 29.38, 29.55, 29.70, 30.37, 31.93, 63.85, 63.95, 64.10, 69.12, 73.35, 73.45, 77.19, 82.27, 82.97, 87.15, 87.99 (2C), 89.67, 108.07, 108.18, 123.88, 124.04, 127.01, 127.17, 128.39, 128.48, 129.34, 129.88, 132.22, 132.49, 142.56, 142.71, 152.83, 165.66 (2C), 165.79; FAB-MS: *m*/*z* 4547 ($M^+$).

## References

1 U. H. F. Bunz, *Angew. Chem., Int. Ed. Engl.*, 1994, **33**, 1073; F. Diederich, *Nature*, 1994, **369**, 199; J. M. Tour, *Chem. Rev.*, 1996, **96**, 537.
2 *Handbook of Conducting Polymers*, ed. T. A. Skotheim, Dekker, New York, 1986, vols. 1 and 2.
3 N. C. Greenham, S. C. Moratti, D. D. C. Bradley, R. H. Friend and A. B. Holmes, *Nature*, 1993, **365**, 628.
4 C. Bosshard, K. Sutter, P. Prêtre, J. Hulliger, M. Flörsheimer, P. Kaatz and P. Günter, *Organic Nonlinear Optical Materials*, Gordon and Breach, Basel, 1995.
5 (*a*) J. Anthony, C. Boudon, F. Diederich, J.-P. Gisselbrecht, V. Gramlich, M. Gross, M. Hobi and P. Seiler, *Angew. Chem., Int. Ed. Engl.*, 1994, **33**, 763; (*b*) M. Schreiber, J. Anthony, F. Diederich, M. E. Spahr, R. Nesper, M. Hubrich, F. Bommeli, L. Degiorgi, P. Wachter, P. Kaatz, C. Bosshard, P. Günter, M. Colussi, U. W. Suter, C. Boudon, J.-P. Gisselbrecht and M. Gross, *Adv. Mater.*, 1994, **6**, 786; (*c*) A. M. Boldi, J. Anthony, V. Gramlich, C. B. Knobler, C. Boudon, J.-P. Gisselbrecht, M. Gross and F. Diederich, *Helv. Chim. Acta*, 1995, **78**, 779.
6 E. J. Ginsbrug, C. B. Gorman and R. H. Grubbs, in *Modern Acetylene Chemistry*, ed. P. J. Stang and F. Diederich, VCH, Weinheim, 1995, pp. 353–383.
7 J. Le Moigne, F. Kajzar and A. Thierry, *Macromolecules*, 1991, **24**, 2622; H. S. Nalva, *Adv. Mater.*, 1993, **5**, 341.
8 L. Yu, Z. Bao, *Adv. Mater.*, 1994, **6**, 156 and references cited therein; T. Maddux, W. Li and L. Yu, *J. Am. Chem. Soc.*, 1997, **119**, 844.
9 L. J. Matthias, *Synthesis*, 1979, 561.
10 V. Percec, M. Lee, J. Heck, H. E. Blackwell, G. Ungar and A. Alvarez-Castillo, *J. Mater. Chem.*, 1992, **2**, 931.
11 J.-F. Nierengarten, M. Schreiber, F. Diederich and V. Gramlich, *New J. Chem.*, 1996, **20**, 1273.
12 A. S. Hay, *J. Org. Chem.*, 1962, **27**, 3320.
13 D. Demus and L. Richter, *Textures of Liquid Crystals*, Verlag Chemie, Weinheim, New York, 1978; G. W. Gray, and J. W. Goodby, *Smectic Liquid Crystals: Textures and Structures*, Leonard Hill, Glasgow, London, Philadelphia, 1984.

*Received in Cambridge, UK, 10th April 1997; Com. 7/02446K*

# *In situ* generation of methylphosphonamidites for synthesis of oligonucleotide methylphosphonates

**Zhaoda Zhang,* Alexandra Nichols, Jimmy X. Tang and Jin Yan Tang**

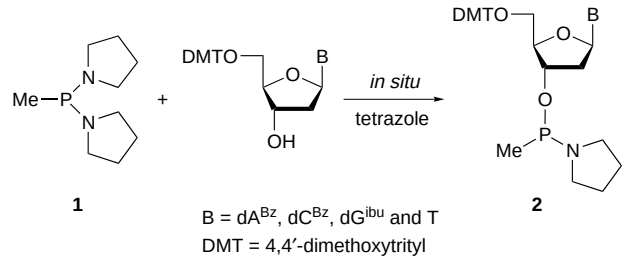
*Hybridon, Inc., 155 Fortune Boulevard, Milford, MA 01757, USA*

**5′-DMT-nucleoside methylphosphonamidites are generated *in situ* by selective activation of methylbis-(pyrrolidino)phosphine 1, and used effectively in the automated synthesis of oligonucleotide methylphosphonates.**

Methylphosphonates or the corresponding mixed backbone oligonucleotides, which contain non-ionic internucleotide linkages, have been successfully used in gene expression studies and have demonstrated their potential for development as antisense therapeutics.[1] Oligonucleotide methylphosphonates are generally prepared using methylphosphonamidite synthons. Since the methylphosphonate backbone is susceptible to hydrolysis by aqueous basic solutions, some modified methods have been developed to improve their synthesis.[2–4] However, a major limiting factor for cost efficient synthesis of oligonucleotide methylphosphonates is the time and cost required to synthesize and purify nucleoside methylphosphonamidites. One potential approach in solving this problem is to generate the methylphosphonamidite *in situ.* Although several laboratories have studied the *in situ* methodology for the syntheses of phosphodiester, phosphorothioate and radiolabelled oligonucleotides,[5–10] to the best of our knowledge none have used *in situ* methods for the synthesis of oligonucleotide methylphosphonates.

In an effort to develop oligonucleotide methylphosphonate analogues as antisense therapeutics, we have investigated the *in situ* approach in order to achieve an economical synthetic process. A series of methylphosphitylating reagents were prepared and examined.[11] We report herein our preliminary results for *in situ* generation of nucleoside methylphosphonamidites using a methylphosphordiamidite, methyl-bis-(pyrrolidino)phosphine[12]† **1**, for oligonucleotide methylphosphonates synthesis.

The *in situ* generation of nucleoside methylphosphonamidites was first studied using $^{31}$P NMR spectroscopy. The reactions were carried out at room temperature using **1** and 5′-DMT-nucleosides (dA$^{Bz}$, dC$^{Bz}$, dG$^{iBu}$ and T) in the presence of tetrazole. The results showed that although **1** was activated by 1 equiv. of tetrazole to react with 5′-DMT-nucleosides immediately, the reaction did not give the desired products (the corresponding 5′-DMT-nucleoside methylphosphonamidites) selectively under these conditions. The major side products were identified as 3′-3′ dimers.‡ To avoid this problem, a series of different reaction conditions were examined. The results show that the corresponding 5′-DMT-nucleoside methylphosphonamidites were formed exclusively by selective activation of **1** using 0.2–0.3 equiv. of tetrazole (Scheme 1). Typically, 0.10 ml (0.045 mmol) of a 0.45 M tetrazole solution in MeCN was added to a solution of 5′-DMT-thymidine (81.7 mg, 0.15 mmol) and **1** (28 mg, 0.15 mmol) in $CDCl_3$ (1.0 ml). After stirring for 10 min at room temperature, the solution was transferred into an NMR tube and examined by $^{31}$P NMR spectroscopy. The NMR results indicated that the corresponding 5′-DMT-thymidine methylphosphonamidite **2**-**T** was formed in a ratio of 97 : 3 as compared to the 3′-3′ dimer. Similar results were obtained for the other 5′-DMT-nucleosides (dA$^{Bz}$, dC$^{Bz}$ and dG$^{iBu}$).




**Scheme 1**

To further evaluate this approach, we prepared *in situ* a 0.1 M solution of 5′-DMT-thymidine methyl(pyrrolidino)phosphonamidite **2**-**T** on a 5 mmol scale.§ To make certain that 5′-DMT- thymidine was exclusively transformed into **2**-**T**, the *in situ* amidite solution was examined using $^{31}$P NMR spectroscopy. Since 5′-DMT-thymidine can not be detected in $^{31}$P NMR spectroscopy, an internal standard had to be used to determine the amount (or concentration) of **2**-**T** generated. In this way, 0.5 ml of a 0.1 M solution of 5′-DMT-thymidine methyl(diisopropylamino)phosphonamidite **3**-**T** (PerSeptive Biosystems, Framingham, MA) in $CDCl_3$ was mixed with 0.5 ml of an *in situ* generated solution of **2**-**T**, and examined by $^{31}$P NMR spectroscopy (Fig. 1).

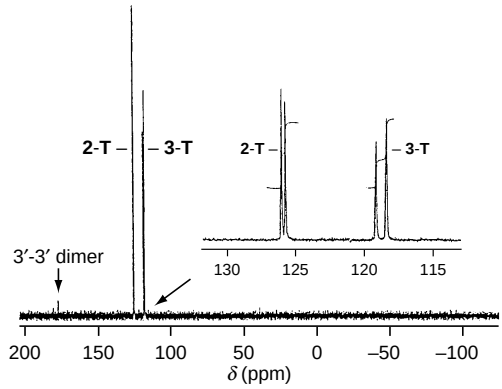



**Fig. 1** $^{31}$P NMR analysis of the methylphosphonamidite **2**-**T** solution generated *in situ*

As Fig. 1 shows, integration for compounds **2**-**T** (δ 126) and **3**-**T** (δ 119) was the same, and the 3′-3′-dimer (δ 177) was formed in less than 3% yield. The NMR results indicated that 5′-DMT-thymidine was almost quantitatively transformed into **2**-**T**, and a 0.1 M solution of **2**-**T** was prepared *in situ.*

To evaluate their effectiveness in automated solid-phase DNA synthesis, a 16-mer of oligonucleotide methylphosphonate, 5′-dT$_s$T$_s$T$_s$T$_s$T$_s$T$_{Me}$T$_{Me}$T$_{Me}$T$_{Me}$T$_{Me}$T$_{Me}$T$_{Me}$T$_{Me}$T$_{Me}$T-3′ **16T**, was synthesized as a model to test the methylphosphonamidite generated *in situ.*¶ This oligomer consists of ten methylphosphonate linkages (PMe) at the 3′-end and five phosphorothioate linkages (PS) at the 5′-end. The coupling efficiency of *in situ* amidite **2**-**T** was studied by measuring

spectrophotometrically the dimethoxytrityl cation (λ 498 nm) released at each cycle and by analysing the final product. The synthesis was carried out using a 0.1 M solution of **2-T** prepared *in situ* (used in the first ten coupling cycles) followed by a commercial 5′-DMT-thymidine-2-cyanoethoxy(*N*,*N*-diisopropylamino)phosphoramidite **T**, (PerSeptive Biosystems). The commercial methylphosphonamidite **3-T** was also examined in the synthesis of **16T** as a comparison. The results showed that methylphosphonate linkages can be synthesized using **2-T** prepared *in situ* with an average stepwise yield of 98%. The coupling yield was the same as that of the commercial methylphosphonamidite **3-T**. The *in situ* amidite 2-T was also found to be stable for at least one week. The capillary gel electrophoresis (CE) result of **16T** synthesized using one week old *in situ* amidite solution was nearly identical to that of freshly prepared *in situ* amidite solution. The CE and $^{31}$P NMR analysis results of the crude oligonucleotide **16T** are given in Figs. 2 and 3.

In summary, our studies show that the methylphosphordiamidite **1** can be selectively activated to react with deoxyribonucleosides, and chemoselectively generate the corresponding deoxyribonucleoside methylphosphonamidites *in situ*. The *in situ* methodology using **1** is easily adapted to the current phosphoramidite approach for the synthesis of oligonucleotide methylphosphonates. This method may find applications in large-scale syntheses of oligonucleotide methylphosphonates and in the synthesis of oligonucleotide methylphosphonate analogues containing modified nucleosides[13] as well as radioisotopically labelled nucleosides .

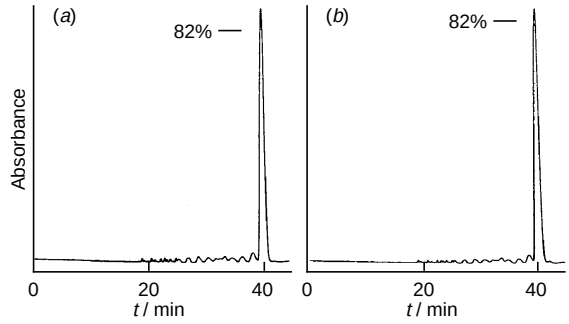



**Fig. 2** Capillary gel electrophoresis analysis of the crude oligonucleotide **16T** synthesized using (*a*) the commercial methylphosphonamidite **3-T** and (*b*) the *in situ* methylphosphonamidite **2-T**

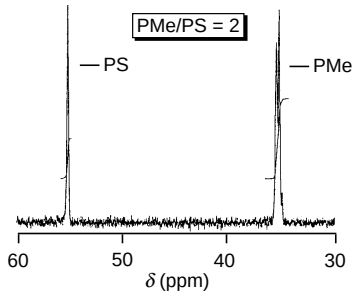



**Fig. 3** $^{31}$P NMR analysis of the crude oligonucleotide **16T** synthesized using the *in situ* methylphosphonamidite **2-T**

## Footnotes

* E-mail: zzhang@hybridon.com

† Compound **1** was prepared in 79% yield from methyldichlorophosphine and 1-(trimethylsilyl)pyrrolidine. $^{31}$P NMR ($CDCl_3$): δ 64.1.

‡ A 3′-3′ dimer was also synthesized by the reaction of methyldichlorophosphine (1.0 equiv.), 5′-DMT-thymidine (2.5 equiv.) and triethylamine (2.5 equiv) in $CH_2Cl_2$. $^{31}$P NMR ($CDCl_3$): δ 177.5.

§ To 5.0 mmol (2.72 g) of 5′-DMT-thymidine in THF (15.0 ml) was added a solution of **1** (0.93 g, 5.0 mmol) in MeCN (30.0 ml) at room temperature. The solution was stirred for 1 min. To the solution was added dropwise a 0.45 M solution of tetrazole (1.5 mmol, 3.3 ml) in MeCN. The mixture was stirred for 5 min, and then the thymidine methylphosphonamidite solution (0.1 M) was ready to use.

¶ The oligonucleotide methylphosphonate **16T** was synthesized on a 1 μmol scale using an automated synthesizer (Millipore 8909 Expedite™, Bedford, MA). For methylphosphonate linkages the synthesis was carried out using a modified protocol, in which capping was performed after the iodine oxidation step. An oxidizing agent of low water content (0.1 M $I_2$ in THF–lutidine– $H_2O$, 74.75 : 25 : 0.25) was used to minimize backbone hydrolysis.[2] Treatment (2 h) with 7 M ammonia in MeOH at 55 °C was carried out to cleave the oligomer from the support.[3] The mixture was filtered to remove the CPG. After the $NH_3$–MeOH solution was removed by lyophilisation (Speed Vac, Savant Instruments Inc., Farmingdale, NY), the remaining crude products were submitted for CE, RP-HPLC, NMR and MALDI-TOF analysis. MS (MALDI-TOF): calc. for **16T** (M + H) 4867. Found, 4868.

## References

1 For review, see P. S. Miller, P. O. P. Ts'o, R. I. Hogrefe, M. A. Reynolds and L. J. Arnold, Jr., in *Antisense Research and Applications*, ed. S. T. Crook and B. Lebleu, CRC, Ann Arbor, 1993, p. 189 and the literature cited therein.
2 R. I. Hogrefe, M. M. Vaghefi, M. A. Reynolds, K. M. Young and L. J. Arnold, Jr., *Nucleic Acids Res*., 1993, **21**, 2031.
3 N. D. Sinha, D. P. Michaud, S. J. Roy and R. A. Casale, *Nucleic Acids Res*., 1994, **22**, 3119.
4 I. Habus, T. Devlin, R. P. Iyer and S. Agrawal, *Bioorg. Med. Chem. Lett*., 1996, **6**, 1393.
5 T. M. Cao, S. E. Bingham and M. T. Sung, *Tetrahedron Lett.*, 1983, **24**, 1019.
6 S. L. Beaucage, *Tetrahedron Lett*., 1984, **25**, 375.
7 M. F. Moore and S. L. Beaucage, *J. Org. Chem*., 1985, **50**, 2019.
8 A. D. Barone, J. Y. Tang and M. H. Caruthers, *Nucleic Acids Res*., 1984, **12**, 4051.
9 W. Tan, R. P. Iyer, Z. Jiang, D. Yu and S. Agrawal, *Tetrahedron Lett.*, 1995, **36**, 5323.
10 Z. Zhang and J. Y. Tang, *Tetrahedron Lett.*, 1996, **37**, 331.
11 Z. Zhang and J. Y. Tang, patent pending.
12 J. W. Engels, T. Daum, A. Frauendorf, S. Luking, M. Mag, W. E. G. Muller, J. Muth and P. Rosmanitz, *Nucleic Acids Res*., *Symp. Ser*., 1991, **24**, 83.
13 Y. S. Sanghvi, in *Antisense Research and Applications*, ed. S. T. Crook and B. Lebleu, CRC, Ann Arbor, 1993, p. 273 and the literature cited therein.

*Received in Glasgow, UK, 14th April 1997; Com. 7/02551C*

# Hypervalent iodine-induced oxidative nucleophilic additions to alkenes: a novel acetoxy thiocyanation reaction in 1,1,1,3,3,3-hexafluoropropan-2-ol

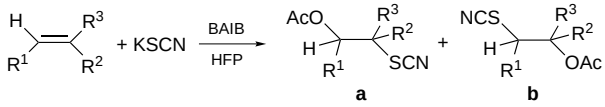
**Antonella De Mico,[a] Roberto Margarita,[a] Andrea Mariani[a] and Giovanni Piancatelli*[b]**

[a] *Centro CNR di Studio per la Chimica delle Sostanze Organiche Naturali (Associated to Istituto Nazionale di Coordinamento 'Chimica die Sistemi Biologici'), Università 'La Sapienza', P.le A. Moro 5, 00185 Roma, Italy*
[b] *Dipartimento di Chimica, Università 'La Sapienza', P.le A. Moro 5, 00185 Roma, Italy*

**The combination of [bis(acetoxy)iodo]benzene and thiocyanate anion in a polar, protic non nucleophilic solvent such as 1,1,1,3,3,3-hexafluoropropan-2-ol is able to perform an oxidative nucleophilic addition to alkenes, leading to acetoxy thiocyanate derivatives, stereoselectively and with good regioselectivity.**

1,1,1,3,3,3-Hexafluoropropan-2-ol (HFP) is described as a non-nucleophilic, strongly ionising solvent,[1] and seems to be the only solvent which is more polar than water on the Reichard $E_T$ scale.[2] The strongly stabilising influence of HFP upon electrophilic intermediates has been utilised to study chemical reactions which proceed *via* the formation of both cations and radical cations.[3,4] Additionally, the weak acidic character of HFP ($pK_a$ = 9.3) has been reported to affect the reactivity of charged nucleophiles.[5]

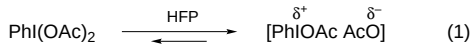
Our interest in the chemistry of hypervalent iodine(III) reagents[6] prompted us to exploit the reactivity of [bis(acetoxy)-iodo]benzene (BAIB) in HFP. We report herein the use of BAIB, HFP and thiocyanate anion, as nucleophile, to perform a novel stereospecific and regioselective acetoxy thiocyanation reaction with alkenes. The overall transformation is a fast, one-pot formal addition of AcOSCN to a double bond, which must be considered an interesting outcome. (Scheme 1).




**Scheme 1**

The BAIB–KSCN ratio plays a pivotal role on the outcome of the reaction. Since the reactivity of hard nucleophiles exhibits strong deactivation in HFP,[5] an excess of BAIB has to be added to suppress the formation of dithiocyanate derivatives. Parallel experiments in other non-nucleophilic aprotic solvents provided exclusively dithiocyanate derivatives.[6]

Our results clearly show that the reactions proceed *via* a reactive intermediate which is electrophilic in nature, and can be explained by referring to the mechanism described for the hypervalent iodine(III) reagent by Moriarty *et al.*[7] In HFP ($\varepsilon_r$ = 22.3), BAIB may undergo an ionisation process (eqn. 1) and



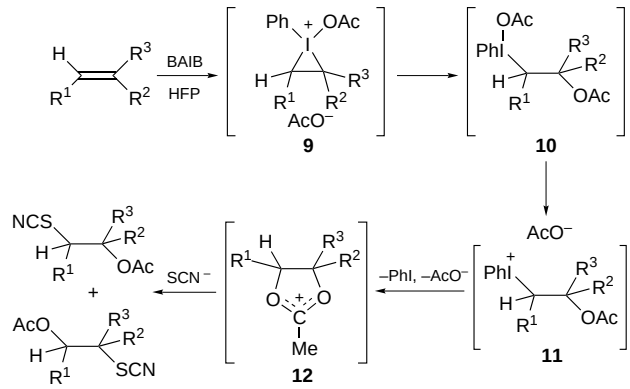

(1)

then an electrophilic addition to the alkene may follow yielding the intermediate **9**, subsequent addition of the acetoxy anion giving **10** (Scheme 2). An intramolecular $S_N2$ displacement of iodobenzene by the neighbouring acetoxy substituent leads to the cyclic intermediate **12**. Regioselective opening by thiocyanate anion furnishes the acetoxy thiocyanate derivatives.† Competing addition on **9** by thiocyanate leading to dithiocyanates may occur (Table 1, entries 6 and 7). The stereochemical outcome can be explained through the intermediate **12** since other reported mechanisms would yield the *cis* rather than *trans* products.[7,8]

The stereospecificity of the reaction seems to exclude competing radical processes. The formation of 1-(2-thiocyanoethyl)cyclohexene in entry 4, although in low yields (2–5%), reveals the occurrence of an ionic addition pathway since the above product clearly rises from an 1,2 proton shift of the initial formed secondary carbocation to the more stable tertiary one and subsequent elimination.

The acetoxy thiocyanation reaction has proven to be particularly successful with terminal alkenes (R = H), where a high regioselectivity is achieved, meanwhile it is only fair with non symmetrically substituted ones (compare Table 1 entries 2 and 5). Synthetic utility is very important with symmetrical and cyclic systems, where the addition is regio- and stereo-specific. This is also a valid method for the dissymmetrisation of olefinic compounds.

The reaction with methylcyclohexene, a more substituted system, furnishes transposition and elimination products as well as the expected acetoxy thiocyanate. Electron poor systems were recovered unreacted from the reaction medium, while




**Scheme 2**

**Table 1** Acetoxy thiocyanation of alkenes with BAIB–KSCN in HFP

| Entry | $R^1$ | $R^2$ | $R^3$ | Yield[a] (%) | Regio-selectivity (**a**/**b**) | Stereo-specificity |
|---|---|---|---|---|---|---|
| 1 | Butyl | H | H | 90 | 83/17 | — |
| 2 | Hexyl | H | H | 90 | 83/17 | — |
| 3 | Octyl | H | H | 90 | 83/17 | — |
| 4 | Cyclohexyl | H | H | 80 | 63/37 | — |
| 5 | Pentyl | H | Me | 80 | 63/37 | *anti* |
| 6 | –$(CH_2)_4$– | | H | 80[b] | > 99 | *anti* |
| 7 | –$(CH_2)_5$– | | H | 55[c] | > 99 | *anti* |

[a] The reported yields refer to isolated, chromatographically pure compounds. All the structures have been confirmed by IR, $^1$H NMR and $^{13}$C NMR analysis. [b] Additional 10% of *anti* dithiocyanate derivative was isolated. [c] Additional 30% of *anti* dithiocyanate derivative was isolated.

electron rich ones, such as dihydropyran, provided diacetoxy and dithiocyanate derivatives as the main products; this latter reactivity may be ascribed to the high stability of the cationic intermediate. Styrene derivatives immediately underwent a polymerisation process when they were dissolved in HFP; this phenomenon is probably catalysed by the acidity of the reaction medium. All the collected data are in agreement with the suggested reaction mechanism.

In conclusion, our studies on the reactivity in HFP show it to be very promising, and the results broaden the utility of BAIB, opening a route to new synthetic applications in organic chemistry. Research in this field is currently in progress, since acetoxy thiocyanate and dithiocyanate derivatives have been shown to possess good fungicidal activity.

## Footnotes

* E-mail: piancatelli@axrma.uniroma1.it

† Typical experimental procedure: a solution of the alkene (1 mmol) in 4 ml of HFP was treated with 1.2 mmol of KSCN and 4 mmol of BAIB and the resulting reaction mixture is stirred at room temperature for 20 min. The reaction was quenched with saturated aqueous $Na_2S_2O_3$ (5 ml) and extracted with EtOAc (4 × 5 ml). The combined organic extracts were washed with aqueous $NaHCO_3$ and brine, dried over anhydrous $Na_2SO_4$, and concentrated under reduced pressure. Column chromatography on $SiO_2$ (light petroleum–EtOAc) afforded pure products.

$^1$H NMR spectra ($CDCl_3$) for **2a**: 5.1 (1 H, m), 3.2 (1 H, dd, *J* 3.9 and 14.0 Hz), 3.0 (1 H, dd, *J* 6.5 and 14.0 Hz), 2.1 (3 H, s), 1.9–1.1 (10 H, m), 0.85 (3 H, t). For **2b**: 4.3 (1 H, dd, *J* 5.1 and 12.0 Hz), 4.2 (1 H, dd, *J* 7.2 and 12.0 Hz), 3.3 (1 H, m), 2.1 (3 H, s), 1.9–1.1 (10 H, m), 0.85 (3 H, t). For **6a**: 4.7 (1 H, dt, *J* 10.3 and 4.6 Hz), 3.1 (1 H, dt, *J* 10.3 and 4.3 Hz), 2.3–2.0 (2 H, m), 2.06 (3 H, s), 1.9–1.1 (6 H, m). For **7a**: 4.9 (1 H, ddd, *J* 9.0, 3.7 and 7.4 Hz), 3.4 (1 H, dt, *J* 9.0 and 3.4 Hz), 2.3–2.0 (2 H, m), 2.08 (3 H, s), 2.0 1.4 (8 H, m).

$^{13}$C NMR spectra ($CDCl_3$) for **2a**: 171.0 (C=O), 112.5 (SCN), 72.2, 37.8, 33.2, 31.4, 28.4, 29.6, 22.4, 21.0, 13.9. For **2b**: 171.0 (C=O), 110.4 (SCN), 66.1, 48.9, 33.2, 31.4, 28.4, 29.6, 22.4, 21.0, 13.9. For **6a**: 170.5 (C=O), 111.1 (SCN), 74.9, 51.5, 32.6, 32.3, 25.7, 23.8, 21.1. For **7a**: 170.5 (C=O), 111.8 (SCN), 77.8, 54.6, 32.5, 32.0, 27.8, 25.7, 22.3, 21.2.

IR spectra ($CHCl_3$, $cm^{-1}$) for **2a**: 2140 (SCN, sharp peak), 1733 (C=O, broad peak). For **2b**: 2140 (SCN, sharp peak), 1735 (C=O, broad peak). For **6a**: 2175 (SCN, sharp peak), 1730 (C=O, broad peak). For **7a**: 2145 (SCN, sharp peak), 1730 (C=O, broad peak).

## References

1 B. Allard, A. Casadevall, E. Casadevall and C. Largeau, *Nouv. J. Chem.*, 1979, **3**, 995; F. L. Schadt, T. W. Bentley and P. V. R. Schleyer, *J. Am. Chem. Soc.*, 1976, **98**, 7667.
2 C. Reichardt, *Solvent and Solvent Effect in Organic Chemistry*, Verlag Chemie, Veinhein, 1988.
3 L. Eberson, M. P. Hartshorm and O. Persson, *J. Chem. Soc., Perkin Trans 2*, 1995, 1735; 1995, 1331; L. Eberson, M. P. Hartshorm, F. Radner and O. Persson, *Chem. Commun.*, 1996, 215.
4 Y. Kita, H. Tohma, K. Hatanaka, T. Takada, S. Fujuta, S. Mitoh, H. Sakurai and S. Oka, *J. Am. Chem. Soc.*, 1994, **116**, 861.
5 L. Eberson, M. P. Hartshorm and O. Persson, *J. Chem. Soc., Perkin Trans 2*. 1996, 141; 1996, 151.
6 A. De Mico, R. Margarita, A. Mariani and G. Piancatelli, *Tetrahedron Lett.*, 1996, **37**, 1899.
7 R. A. Moriarty, R. K. Vaid and G. F. Koser, *Synlett*, 1990, **2**, 365.
8 C. A. Ramsden, *Chem Soc. Rev.*, 1994, **23**, 111.

*Received in Cambridge, UK, 24th March 1997; Com. 7/01998J*

# Zirconaindane phospholanes: key reagents for the synthesis of mono- or tri-cyclic phosphanes and related species

**M. Zablocka,[a] A. Igau,[b] B. Donnadieu,[b] J.-P. Majoral,*[b] A. Skowronska*[a] and P. Meunier*[c]**

[a] *Laboratoire de Chimie de Coordination du CNRS, 205 route de Narbonne, 31077 Toulouse Cedex, France*
[b] *Polish Academy of Sciences, Centre of Molecular and Macromolecular Studies, Sienkiewicza 112, 90-363 Lodz, Poland*
[c] *Laboratoire de Synthèse et d'Electrosynthèse Organométalliques associé au CNRS (UMR 5632), Université de Bourgogne, Faculté des Sciences Gabriel, 6 boulevard Gabriel, 21000 Dijon, France*

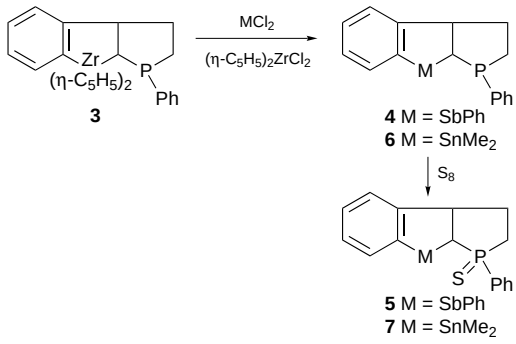
**The zirconaindane phospholane 3 reacts either with $PhSbCl_2$ or $Me_2SnCl_2$ to give tricyclic systems incorporating phosphorus, antimony or tin; the same reaction involving 3 and $R_2PCl$ (R = Ph, Et) leads to acyclic–cyclic diphosphanes.**

There is an extensive literature on the topic of cyclic phosphanes such as phospholanes, phospholenes or phospholes.[1] In contrast only a limited number of fused bicyclic and tricyclic phosphanes have been prepared and only very recently a few tricyclic 1,1-diphosphanes were described.[2] As far as we are aware, fused tricyclic systems incorporating phosphorus and other heavier main group elements, are not known. With this in mind we became interested in developing synthetic routes to these species because of the intrinsic interest in phosphane and polyphosphane derivatives as reagents for mediating organic transformations or as ligands for complex formation and use in catalysis.

This prompted us to initiate the chemistry of the zirconaindane phospholane **3** which was regioselectively prepared *via* the treatment of 1-phenyl-2-phospholene PhP–CH=CHCH$_2$CH$_2$ **1** with the transient (benzyne)zirconocene [($\eta$-$C_5H_5$)$_2$Zr($\eta^2$-$C_6H_4$)] **2**. [2] Here we will detail the formation, from **3**, of unusual phosphorus and antimony (or tin) tricyclic systems as well as that of new acyclic–cyclic diphosphanes.

Reactions of **3** with $PhSbCl_2$ in benzene at 5 °C for 1 h led to the stibaphospholane **4** [$\delta$($^{31}$P) 5.9] which was isolated in 80% yield as its sulfide adduct **5** [$\delta$($^{31}$P) 61.9] (Scheme 1). The formulation of **5** was confirmed by NMR spectroscopy,[3] mass spectrometry (FAB [M + 1]$^+$ 470) and by elemental analysis.

An analogous exchange reaction performed with **3** and $Me_2SnCl_2$ at 0 °C for 3 h gave the tin–phosphorus containing tricyclic species **6** [$\delta$($^{31}$P) 5.6] which was also fully characterized as its sulfide adduct **7** obtained in 75% yield [$\delta$($^{31}$P) 64.1)] (Scheme 1). NMR data corroborated such an assignment.† Compounds **4**–**7** are the first examples of fused tricyclic systems incorporating phosphorus and antimony or phosphorus and tin in the cyclic skeleton.



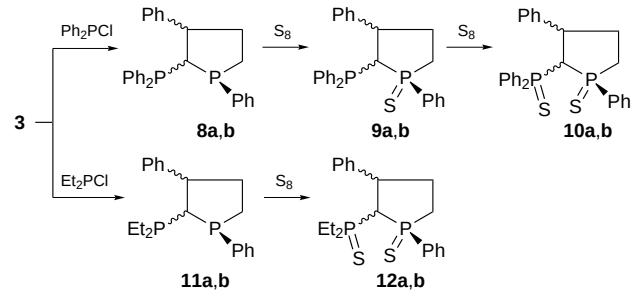

**Scheme 1**

All these reactions proceeded with ring retention. In contrast an exchange reaction with concomitant ring opening was observed when **3** was reacted with a chlorophosphane such as $Ph_2PCl$ at −40 °C for 1 h (Scheme 2). The 1,1-diphosphane **8** was obtained as two isomers **8a**,**b** in a 4 : 1 ratio as shown by $^{31}$P NMR spectroscopy: two doublets at $\delta$ 5.1 (PPh) and −12.0 ($PPh_2$) ($^2J_{PP}$ 7.8 Hz) for the major compound and $\delta$ 3.9 (PPh) and −16.3 ($PPh_2$) ($^2J_{PP}$ 19.5 Hz) for the minor one. Monosulfurization occurred regioselectively on the intracyclic phosphorus atom by adding 1 equiv. of elemental sulfur to **8a**,**b** and led to the adducts **9a**,**b** {two isomers in a 4 : 1 ratio. $\delta$($^{31}$P): 65.5 [P(S)Ph] and −9.6 ($PPh_2$), $^2J_{PP}$ 31.5 Hz (major); $\delta$ 64.1 [P(S)Ph] and −11.8 ($PPh_2$), $^2J_{PP}$ = 31.5 Hz (minor)}. Further addition of a second equivalent of sulfur led predominantly to the formation of the disulfide **10a** {$\delta$($^{31}$P) 65.2 [P(S)Ph] and 43.3 [P(S)$Ph_2$], $^2J_{PP}$ 0 Hz} isolated by silica gel column chromatography.‡ $^{13}$C and $^1$H NMR spectra coupled with mass spectrometry and microanalytical data showed clearly that cleavage of the two zirconium–carbon bonds occurred with grafting of the diphenylphosphino group in $\alpha$ position to the intracyclic P–Ph moiety.

A similar ring opening process initiated also by an exchange reaction between **3** and a chlorophosphane was detected when **3** was reacted with $Et_2PCl$. Addition of sulfur to the resulting 1,1-diphosphanes **11a**,**b** (two isomers) led to the 1,1-dithiodiphosphanes **12a**,**b** (two isomers in 9 : 1 ratio). The major isomer **12a** was isolated by chromatography and fully characterized by NMR,† mass spectrometry and elemental analysis.

X-Ray structures have been obtained for **10a**[3] and for **12a** (Fig. 1):§ they showed similar features for the two derivatives. Indeed substituents on the intracyclic carbon atoms C(1) [P(S)$Ph_2$] and C(2) (Ph) of the phospholane ring are *cis* in both cases [P(1)–C(1)–C(2)–C(21) torsion angle: 85.7° for **10a**, 73.2° for **12a**] while the substituent on C(1) and the phenyl group on the phosphorus atom P(2) are *trans* [P(1)–C(1)–P(2)–C(221) torsion angle: 3.2° for **10a**, 14.0° for **12a**].

Remarkably the regioselectivity of the reaction of phospholene **1** with a more hindered benzyne zirconocene precursor such as ($\eta^5$-Bu$^t$$C_5H_4$)$_2$Zr$Ph_2$ was found to be the same: the zirconaindane phospholane **3″** was formed nearly quantitatively




**Scheme 2**

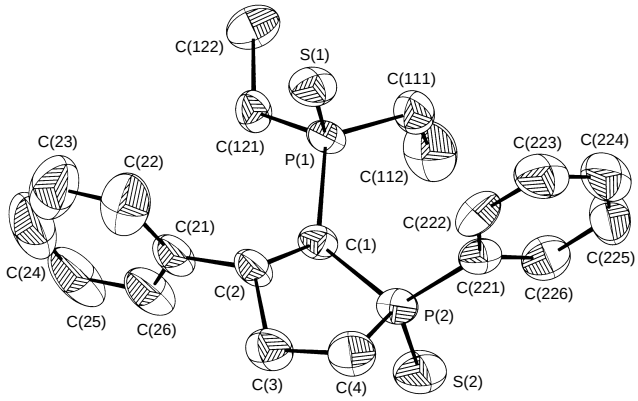
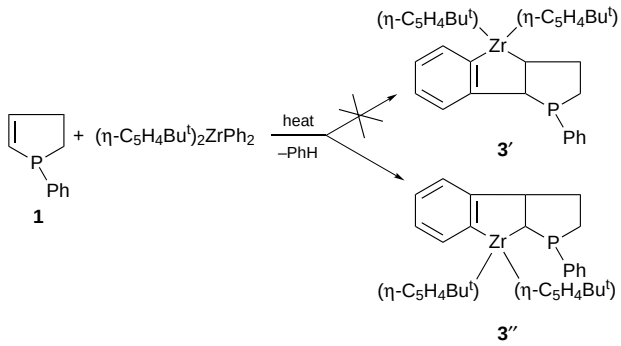



**Fig. 1** Molecular structure (CAMERON[6]) of **12a** with crystallographic numbering scheme. Selected bond lengths (Å) and angles (°): P(2)–C(1) 1.84 (1), P(2)–C(4) 1.80 (1), C(1)–C(2) 1.56 (1), C(2)–C(3) 1.53 (1), C(3)–C(4) 1.50 (2), P(2)–C(221) 1.82 (1); C(1)–P(2)–C(221) 112.8 (5), P(2)–C(1)–C(2) 105.7 (6), P(2)–C(1)–P(1) 124.0 (5).




**Scheme 3**

and no trace of **3′** was detected (Scheme 3). These results can be explained by considering that, whatever the steric hindrance encountered on zirconium, the regioselectivity of the reaction of zirconocene–benzyne complexes with phospholene **1** is governed by the transient formation of a zirconocene stabilized phosphorus benzyne complex leading in the final products **3** and **3″** to a P–Zr dative bond. Moreover, treatment of **3″** with $PhSbCl_2$ also led to the formation of the stibaphospholane **4**.

In conclusion, zirconaindane phospholanes **3** and **3″** appeared to be versatile reagents, leading to new mono- and tricyclic heavier main group element compounds *via* disubstitution reactions with ring retention (formation of **4**–**7**) or monosubstitution reactions with ring opening (formation of **10**, **12**).

Financial support of this work by the CNRS, France, and by State Committee for Scientific Research, Poland (KBN grant No. 3TO9A 03709), is gratefully acknowledged.

## Footnotes

* E-mail: majoral@lcctoul.lcc-toulouse.fr

† **5** $^{31}P\{^1H\}$ NMR ($C_6D_6$): δ 61.9. $^1H$ NMR ($C_6D_6$) (*J*/Hz): δ 1.69–2.20 (m, 4 H, $CH_2$), 3.26 [dd, $^2J$(HP) 8.0, $^3J$(HH) 6.1, 1 H, PCHSb], 3.97 (m, 1 H, CH), 6.89–7.35, 7.75–7.87 (m, 9 H, $H_{aryl}$). $^{13}C$ NMR ($CDCl_3$): δ 34.8 [d, $^2J$(CP) 6.6, $PCH_2CH_2$], 36.6 [d, $^1J$(CP) 51.8, $PCH_2$], 51.6 [d, $^1J$(CP) 46.6, PCHSb], 58.1 [d, $^2J$(CP) 8.1, PCHCH], 126.1, 128.2, 128.9, 129.4 (s, Ph), 129.3 [d, *J*(CP) 10.3, Ph], 131.4 [d, *J*(CP) 9.5, Ph], 131.6 [d, *J*(CP) 3.0, Ph], 135.8, 136.1 (s, $C_6H_4$), 136.2 [d, $^1J$(CP) 68.2, *ipso*-PPh], 140.9 [d, $^1J$(CP) 8.9, SbPh), 144.5 [d, $^3J$(CP) 2.1, *ipso*-$C_6H_4$], 156.7 [d, $^3J$(CP) 4.5, $C_6H_4$]. FABMS (MNBA–DMF): *m*/*z* 391 (100, $[M - S]^+$). **7** $^{31}P\{^1H\}$ NMR ($C_6D_6$): δ 64.1. $^1H$ NMR ($C_6D_6$): δ 0.73 (s, 6 H, $CH_3$), 1.77–2.16 (m, 4 H, $CH_2$), 3.42 [dd, $^2J$(HP) 9.6, $^3J$(HH) 9.6, 1 H, PCHSn], 4.24 (m, 1 H, PCHC*H*), 7.02–7.41, 7.65–7.96 (m, 9 H, $H_{aryl}$). $^{13}C$ NMR ($C_6D_6$): δ 4.9 (s, $CH_3$), 33.4 [d, $^2J$(CP) 6.3, $PCH_2CH_2$], 35.2 [d, $^1J$(CP) 49.8, $PCH_2$], 51.7 (s, PCH*C*H), 52.1 [d, $^1J$(CP) 33.7, PCHSn], 127.0 (s, *p*-Ph), 128.7 [d, *J*(CP) 11.9, Ph], 130.6 [d, *J*(CP) 11.4, Ph], 127.0. 127.6, 131.8, 136.0 (s, $C_6H_4$), 142.8 (s, *ipso*-$C_6H_4$), 148.1 [d, $^3J$(CP) 4.5, $C_6H_4$]. **10a** $^{31}P\{^1H\}$ NMR (thf): δ 64.2, 43.3. $^{13}C$ NMR ($CDCl_3$): δ 34.2 [dd, $^2J$(CP) 10.2, $^3J$(CP) 3.4, $PCH_2CH_2$], 34.7 [d, $^1J$(CP) 55.1, $PCH_2$], 49.1 [d, $^2J$(CP) 7.8, PCHPh], 56.2 [dd, $^1J$(CP) 38.1, $^1J$(CP) 42.9, PCHP], 127.1, 128.9, 128.6, 128.4, 131.4, 131.3 (s, Ph), 127.5 [d, *J*(CP) 13.3, Ph], 128.2 [d, *J*(CP) 12.5, Ph], 130.8 [d, *J*(CP) 2.5, Ph], 131.8 [d, *J*(CP) 9.4, Ph], 132.7 (s, *ipso*-Ph), 133.8 [d, *J*(CP) 9.8, *ipso*-Ph], 134.7 [d, *J*(CP) 11.6, Ph], 142.9 [d, *J*(CP) 8.5, *ipso*-Ph]. **12a** $^{31}P\{^1H\}$ NMR (thf): δ 62.8, 55.1 (5.1). $^{13}C$ NMR ($CDCl_3$): δ 6.8 [d, $^2J$(CP) 4.0, $PCH_2CH_3$], 7.1 [d, $^2J$(CP) 3.8, $PCH_2CH_3$], 23.0 [d, $^1J$(CP) 52.4, P*C*H$_2$CH$_3$], 25.9 [dd, $^1J$(CP) 49.7, $^3J$(CP) 4.8, P*C*H$_2$CH$_3$], 34.4 [d, $^2J$(CP) 11.3, $PCH_2CH_2$], 36.8 [d, $^1J$(CP) 54.1, $PCH_2$], 50.0 [d, $^2J$(CP) 8.0, PCHPh], 55.1 [dd, $^1J$(CP) 36.4, $^1J$(CP) 36.4, PCHP], 128.1, 128.6, 129.4 (s, Ph), 130.3 [d, *J*(CP) 69.3, *ipso*-$PPh_2$], 133.0 [d, *J*(CP) 2.8, Ph], 134.9 [d, *J*(CP) 11.4, Ph], 142.7 [d, *J*(CP) 11.6 *ipso*-PPh].

‡ The second disulfide adduct **10b** arising from sulfurisation of **9b** was not isolated.

§ *Crystal data* for $C_{20}H_{26}P_2S_2$ **12a**: $M$ = 392.49, monoclinic, space group $P2_1/n$, $a$ = 10.944 (1), $b$ = 12.033 (2), $c$ = 16.654 (1) Å, β = 107.114 (8)°, $U$ = 2096.3 Å$^3$, $Z$ = 4, $D_c$ = 1.24 g cm$^{-3}$, μ = 3.94 cm$^{-1}$. Crystal size: 0.35 × 0.15 × 0.35 mm, 1308 measured reflections (2740 independent), $R_{av}$ = 0.047, $R$ = 0.0540, $R_w$ = 0.070 from 1344 reflections with $I > 1.5\sigma(I)$. The data collection was performed at 293 K on a I.P.D.S. STOE diffractometer using graphite-monochromated Mo-Kα radiation for the two compounds. The structures were solved by direct methods using the program SIR92[4] and subsequent Fourier maps. The refinement of models were performed by using full-matrix least-squares techniques with the aid of the package CRYSTALS.[5] All hydrogen atoms were found on difference Fourier maps but they were introduced as fixed contributors with C–H = 0.96 Å and isotropic thermal parameters fixed 20% higher than those of the carbon atoms to which they were attached their positions were recalculated after each cyclic of refinement. For the two structures all non-hydrogen atoms were anisotropically refined. Atomic coordinates, bond lengths and angles, and thermal parameters have been deposited at the Cambridge Crystallographic Data Centre (CCDC). See Information for Authors, Issue No. 1. Any request to the CCDC for this material should quote the full literature citation and the reference number 182/506.

## References

1 See for example: L. D. Quin and A. N. Hughes, in *The Chemistry of Organophosphorus Compounds*, ed. F. R. Hartley, Wiley, 1990, vol. 1, ch. 10.
2 M. Zablocka, N. Cénac, A. Igau, B. Donnadieu, J.-P. Majoral, A. Skowronska and P. Meunier, *Organometallics*, 1996, **15**, 5436.
3 M. Zablocka, A. Igau, B. Donnadieu, J.-P. Majoral and A. Skowronska, unpublished work.
4 SIR92, a Program for Automatic Solution of Crystal Structures by Direct Methods. A. Altomore, G. Cascarano, G. Giacovazzo, A. Guargiardi, M. C. Burla, G. Polidori and M. Camalli, *J. Appl. Crystallogr.*, 1994, **27**, 435.
5 D. J. Watkin, C. K. Prout, R. J. Carruthers and P. Betteridge, CRYSTALS Issue 10. Chemical Crystallography Laboratory, University of Oxford, Oxford, UK, 1996.
6 D. J. Watkin, C. K. Prout and K. Pearce, CAMERON, Chemical Crystallography Laboratory, University of Oxford, Oxford, 1996.

*Received in Basel, Switzerland, 24th March 1997; Com. 7/02036H*

# Synthesis of the LTA-type $AlPO_4$ in the presence of the diazapolyoxa macrocycle 'Kryptofix 222'

**L. Schreyeck, F. D'agosto, J. Stumbe, P. Caullet* and J. C. Mougenel**

*Laboratoire de Matériaux Minéraux-ENSCMu-URA 428, 3, rue Alfred Werner, 68093 Mulhouse Cedex, France*

**The LTA-type aluminophosphate can be synthesized from aqueous mixtures in the presence of a single structuring agent, hexaoxa-4,7,13,16,21,24-diaza-1,10-bicyclo[8,8,8]-hexacosane (possibly associated with $F^-$ ion as optional co-template) and is characterized through XRD, SEM, chemical analysis, thermal analysis and solid-state NMR spectroscopy.**

Microporous materials with the LTA structure were first synthesized in their aluminosilicate forms with $Na^+$ and possibly $NMe_4^+$ as templates.[1–4] Low phosphorus-substituted LTA-type aluminosilicates [with P/(P + Si + Al) molar ratios ranging from *ca.* 0.01 to 0.04] were then prepared by Kühl[5] and Lok *et al.*[6] from alkaline media in the presence of the same templates. During the 1990s, microporous LTA-type metallophosphates could be synthesized from near-neutral reaction mixtures but only in the presence of $F^-$ ions which act as co-template by structuring the D4R units of the framework. The synthesis of the gallophosphate was thus achieved in 1992[7] with the dipropylamine as the organic template, this species being incorporated in the large $\alpha$ cage of the structure. In 1994, Sierra *et al.*[8] prepared the aluminophosphate in the presence of two organic structuring agents, namely diethanolamine and tetramethylammonium cation, these species being occluded in the $\alpha$ cage and the sodalite cage respectively.

In this work, the LTA-type aluminophosphate was prepared with the hexaoxa-4,7,13,16,21,24-diaza-1,10-bicyclo[8,8,8]-hexacosane ('Kryptofix 222', hereafter K222) as the only organic template. In opposition to the previous experimental observations concerning the LTA-type metallophosphates, the presence of the co-templating $F^-$ ions is here only optional.

The molar composition of the used gels was 0.5 $Al_2O_3$ : 0.5 $P_2O_5$ : 0.25 K222 : 0.25 or 0 HF : 40 $H_2O$. These gels were prepared by first mixing the phosphoric acid aqueous solution (85 mass% $H_3PO_4$, Prolabo, Normapur) with the aluminium source [pseudoboehmite (Catapal B, 69 mass% $Al_2O_3$–31 mass% $H_2O$, Vista Chemical Co.) or aluminium triisopropoxide (Fluka)] and the required amount of distilled water; this mixture was stirred for 30 min at room temp. before the successive addition of the (optional) HF aqueous solution [40 mass% HF (Prolabo, Normapur)] and K222 (Merck, > 99%). After stirring for 1 or 14 h (depending on whether aluminium triisopropoxide or pseudoboehmite is used, respectively), the gel was finally transferred into a Teflon-lined stainless-steel autoclave which was then heated at 170 °C without agitation in an oil-bath (the time required to reach this temperature is < 5 min). After reaction, the solids were recovered by filtration, washed with distilled water, dried at 60 °C overnight and rehydrated at room temp. for one day at 80% relative humidity. As an example, the recovered mass of solid is *ca.* 120 mg when the gel is prepared with 163 mg of aluminium triisopropoxide, 92 mg of $H_3PO_4$ solution, 10 mg of HF solution, 75 mg of K222 and 560 mg of water. The volume of the autoclave used was *ca.* 20 $cm^3$.

In the presence of HF, fully crystallized samples of LTA-type $AlPO_4$ could be easily synthesized from either aluminium source used. For instance, in the presence of aluminium triisopropoxide, crystallization was already achieved after 6 h of reaction at 170 °C, whereas a large proportion of the recovered product remains amorphous after 1 h of heating.

On the other hand, from fluoride-free reaction mixtures, the formation of pure samples of LTA-type $AlPO_4$ was only possible when pseudoboehmite was used as the aluminium source (after 5 days of heating). When aluminium triisopropoxide was employed, a mixture of the LTA-type $AlPO_4$ and of an unidentified impurity was obtained after 5 days of reaction (this impurity could correspond to a layered compound according to the XRD data and the micrographs), whereas for shorter crystallization times (one or two days) only a partial transformation of the gel into the LTA-type $AlPO_4$ occurred. The reason for this strong influence of the nature of the aluminium source is questionable, but could be related to the difference observed between the initial pH values, *i.e.* close to 3 or 7 according to whether pseudoboehmite or aluminium triisopropoxide were used, respectively (the final pH was systematically close to 7–8).

The crystals prepared from fluoride-free or fluoride-containing mixtures display the same usual cubic shape already found for the other LTA-type materials (Fig. 1). The cubes are more or less truncated, their sizes ranging from < 1 μm to *ca.* 20 μm depending on the synthesis conditions used.

X-Ray diffraction patterns [STOE STADI-P diffractometer, equipped with a curved germanium (111) primary monochromator, Cu-K$\alpha_1$ radiation] of all samples (Fig. 2) are very similar to the pattern characteristic of the cubic LTA structure (space group *Fm*3*c*). Only small differences in the relative intensities are visible between the patterns of the fluoride-containing [Fig. 2(*a*)] and fluoride-free samples [Fig. 2(*b*)], the value of the *a* parameter for the latter being slightly smaller. Both parameter values are close to the value found by Sierra *et al.*[8] for a LTA-type structure aluminophosphate (Table 1).

Only the presence of the original template K222 is detected by solution $^1H$ NMR spectroscopy (Bruker AC250 spectrometer) on samples dissolved in 6 M HCl aqueous solution

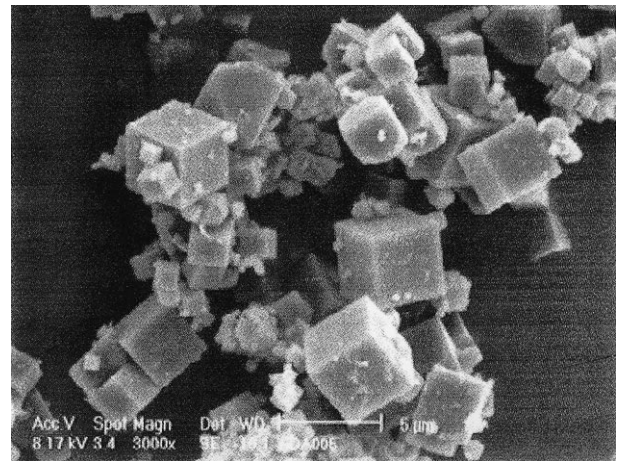



**Fig. 1** Micrographs of crystals of LTA-type $AlPO_4$ prepared at 170 °C from K222 and fluoride-containing media (Philips XL30 microscope)

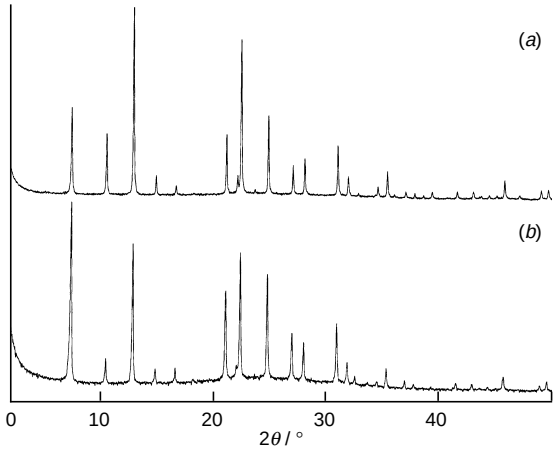



**Fig. 2** XRD patterns of the LTA-type $AlPO_4$ materials prepared in the presence of K222 from fluoride-containing (*a*) or fluoride-free media (*b*)

**Table 1** Values of the *a* parameter for as-made LTA-type $AlPO_4$ samples

| Template(s) occluded | *a*/Å |
|---|---|
| Kryptofix 222 + $F^-$ | 23.867(2) |
| Kryptofix 222 | 23.773(3) |
| Diethanolamine + $NMe_4^+$ + $F^-$[8] | 24.063(3) |

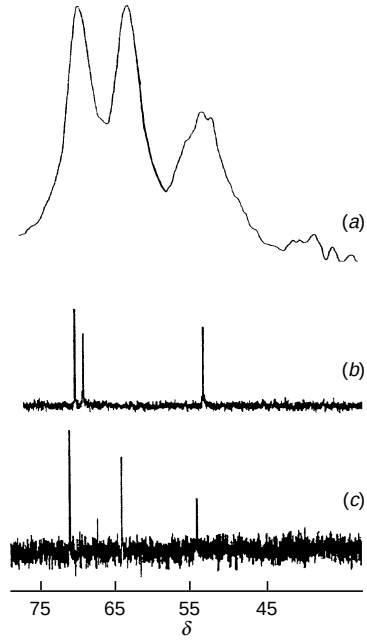



**Fig. 3** $^{13}C$ CP MAS NMR spectrum of an LTA-type $AlPO_4$ sample (*a*) and $^{13}C$ solution NMR spectra of K222 in basic (*b*) or acid (*c*) aqueous solution

(with dioxane as the internal standard). The content of K222 is close to 19 mass%, which corresponds to the incorporation of one K222 molecule per pseudocell (most probably in the large α cage). Samples prepared in the presence or absence of $F^-$ ions display the same $^{13}C$ CP MAS NMR spectrum (Bruker MSL 300 spectrometer) with three peaks at δ *ca.* 71, 65 and 55 (ref. TMS) [Fig. 3(*a*)]. These chemical shift values match more closely with those found for an acidic (pH *ca.* 3) aqueous solution of K222 [Fig. 3(*c*)] than with those measured for a basic (pH *ca.* 11) aqueous solution of K222 [Fig. 3(*b*)]. The K222 is thus probably incorporated in a diprotonated form.

According to the solution $^{19}F$ NMR spectroscopy (performed on samples dissolved in 6 M HCl solution with $CF_3CO_2H$ as the internal standard), the amount of fluoride is close to 1.8 mass% in the samples prepared from fluoride-containing mixtures, whereas, as expected, no fluoride is detectable in samples synthesized from fluoride-free media. Besides, the $^{19}F$ MAS NMR spectrum (not shown) of the fluoride-containing samples displays a unique signal (with sidebands) located at δ *ca.* −95 (relative to $CFCl_3$). Such a chemical shift value is characteristic of $F^-$ ions trapped in the D4R units of the structure of microporous aluminophosphates as previously found by Sierra *et al.*[8] (LTA-type $AlPO_4$) and Schott-Darie *et al.*[9] (AST-type $AlPO_4$). In each pseudocell, the two charges of the organic cation are compensated by two $F^-$ ions, which corresponds to the occupation of two thirds of the D4R units of the structure. In samples containing no fluoride, the positive charges of the organic species might be compensated by $OH^-$ ions.

The TG and DSC curves recorded under air (not shown) on a Setaram TG/DSC11 thermoanalyser are very similar for all samples. The first mass loss observed between 20 and 200 °C is close to 8% and can be probably attributed to the elimination of water, an endothermic signal occurring in this temperature range on the DSC curve. The remainder of the mass loss takes place between 200 and 700 °C (in two steps corresponding to two exothermic peaks at *ca.* 400 and 600 °C on the DSC curve) and amounts to *ca.* 20% which is in good agreement with the organic content determined previously from $^1H$ NMR experiments.

According to X-ray diffraction, on completion of the thermal treatment (*ca.* 750 °C) a partial amorphization occurs together with a partial conversion into tridymite. Even for calcination at lower temperatures, *e.g.* 550 °C for 4 h, a partial collapse of the structure occurs.

Finally from the experimental results above the idealized chemical formula of the unit cell can be written as

$$8\{(Al_{12}P_{12}O_{48})(X^-)_2(K222^{++})(H_2O)_8\}$$
where $X^- = F^-$ or $OH^-$

LTA-type $AlPO_4$ was previously obtained in the presence of three templates, *i.e.* diethanolamine, $F^-$ and $NMe_4^+$, each of them structuring one of the three polyhedra present, *i.e.* the α cage, the D4R unit and the sodalite cage, respectively. In this work, the LTA-type $AlPO_4$ was synthesized in the presence of Kryptofix 222 alone. This species, which is probably incorporated in the α cage, appears thus very well suited to preparation of this material. Although the presence of $F^-$ is clearly optional, the crystallization appears easier when these ions are present in the reaction mixtures. In this case $F^-$ ions are incorporated in the D4R units of the structure as co-templates.

Other organic templates of the same family are currently being tested in synthesis, possibly in association with $F^-$ ions but also with $NMe_4^+$ ions as potential co-templates.

## References

1 T. B. Reed and D. W. Breck, *J. Am. Chem. Soc*., 1956, **78**, 5972.
2 R. M. Barrer and P. J. Denny, *J. Chem. Soc.*, 1961, 971.
3 G. T. Kerr, *Inorg. Chem.*, 1966, **5**, 1537.
4 R. L. Wadlinger, E. J. Rosinski and C. J. Planck, *US Pat.*, 3375205, 1968.
5 G. H. Kühl, *Inorg. Chem.*, 1971, **10**, 2488.
6 B. M. Lok, C. A. Messina, R. L. Patton, R. T. Gajek, T. R. Cannan and E. M. Flanigen, *US Pat*., 4440871, 1984.
7 A. Merrouche, J. Patarin, M. Soulard, H. Kessler and D. Anglerot, *Molecular Sieves—Synthesis of Microporous Inorganic Materials*, Van Nostrand Reinhold, New York, vol. 1, 1992, p. 384.
8 L. Sierra, C. Deroche, H. Gies and J. L. Guth, *Microporous Mater*., 1994, **3**, 29.
8 C. Schott-Darie, J. Patarin, P. Y. Le Goff, H. Kessler and E. Benazzi, *Microporous Mater.*, 1994, **3**, 123.

*Received in Cambridge, UK, 2nd April 1997; Com. 7/02209C*

# A computational study on zeolite MCM-22

**Swie Lan Njo,* Henk van Koningsveld and Bastiaan van de Graaf**

*Laboratory of Organic Chemistry and Catalysis, Delft University of Technology, Julianalaan 136, 2628 BL Delft, The Netherlands*

**Molecular-mechanics calculations show that the framework of zeolite MCM-22 minimizes to *P*6/*m* symmetry rather than to *P*6/*mmm* or *Cmmm* symmetry.**

MCM-22, first synthesized in 1990,[1] has been applied as a catalyst in several hydrocarbon conversion reactions.[2] Although many studies[3–6] have been dedicated to the elucidation of the framework structure of MCM-22, no structure type code[7] has, as yet, been assigned.

Leonowicz *et al.*,[3] who used high-resolution electron micrographs and synchrotron X-ray diffraction powder data, proposed that MCM-22 comprises two independent multidimensional pore systems. Both systems are accessible through 10-membered rings of tetrahedral (T) atoms. One of the systems is defined by two-dimensional sinusoidal channels, the other consists of large supercages whose inner free diameter is defined by 12-membered rings of T atoms. The structure can be constructed by interconnecting modified dodecasil-1H (DOH) cages extended with a $TO_3$ cap on top $\{4^3 5^6 6^3 [4^3]\}$ and containing a framework T-atom 'buried' inside the cage. Space group *P*6/*mmm* was found to fit best and exhibits T–O–T angles of 180° (Fig. 1). Those T–O–T angles of 180° are avoided when the symmetry is reduced to *Cmmm* (Fig. 1). However, a Rietveld refinement using *Cmmm* symmetry was unsuccessful.

In this study molecular-mechanics calculations are used to get more insight into the relative stabilities of possible structures of zeolite MCM-22. The calculations were carried out on an SG Indigo workstation using the DMM force field incorporated in DELPHI.[8]

Table 1 lists the unit-cell parameters and energies of the proposed *P*6/*mmm* and *Cmmm* structures. The reduction of the symmetry from *P*6/*mmm* to *Cmmm* not only avoids T–O–T angles of 180°, but also leads to a lower energy. Energy minimization of both structures, however, converges to one and the same structure with *P*6/*m* symmetry. The energy minimized structure has T–O–T angles of 180° (as in *P*6/*mmm*) and an energy of −1817.96 kJ $mol^{-1}$ $SiO_2$ (Fig. 1 and Table 1). No structure of minimum energy with *P*6/*mmm* or *Cmmm* symmetry could be found. This might indicate that the actual symmetry of MCM-22 is lower than the proposed ones.

Structures comprising T–O–T angles of 180° should always be treated with care,[9] especially when these angles are constrained to 180° by the space-group symmetry. During minimization, however, no constraints were applied. The *P*6/*m* structure represents a minimum with T–O–T angles of 180°. The question arises whether this result can be ascribed to a force-field artefact. Although the DMM force field has already been applied successfully in earlier studies,[8] a further test on the force field was done by calculating the heats of formation of BEA, FAU, LTA, MEL, MFI and TON. Table 2 shows that the calculated heat of formation of MCM-22 with *P*6/*m* symmetry is comparable with those of the other zeolites. In Fig. 2 the

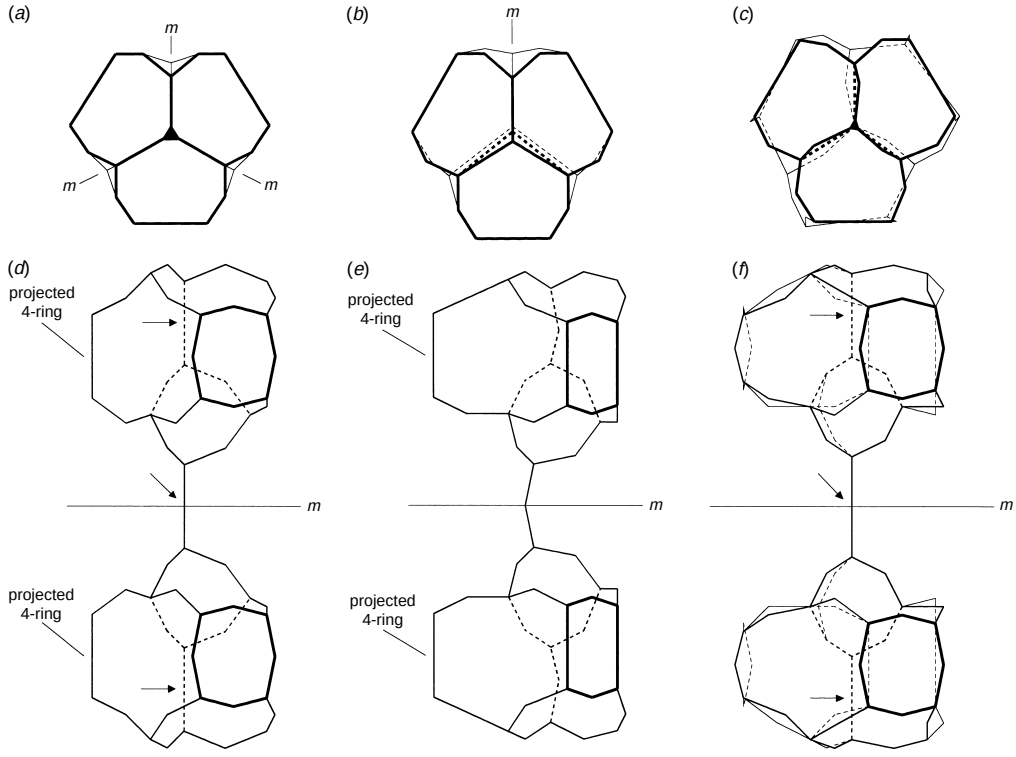



**Fig. 1** Top view (*a*)–(*c*) and side view (*d*)–(*f*) of the $\{4^3 5^6 6^3 [4^3]\}$ cages in the MCM-22 structures exhibiting *P*6/*mmm*, *Cmmm* and *P*6/*m*, respectively. Some symmetry elements are indicated. The cages in structures with *P*6/*mmm* and *P*6/*m* symmetry contain T–O–T angles of 180° (indicated by arrows). In *Cmmm* the corresponding T–O–T angles deviate from 180°.

**Table 1** Unit-cell parameters and energies of the proposed (single-point energy calculations) and minimized structures

| | Proposed[3] *P*6/*mmm* | Proposed[3] *Cmmm* | Minimized *P*6/*m* |
|---|---|---|---|
| *a*/Å | 14.1145 | 24.4470 | 14.3101 |
| *b*/Å | 14.1145 | 14.1145 | 14.3101 |
| *c*/Å | 24.8822 | 24.8822 | 24.9940 |
| $\gamma$/° | 120.0 | 90.0 | 120.0 |
| $\Delta E$/kJ mol$^{-1}$ $SiO_2$ | −1787.27 | −1815.82 | −1817.96 |

**Table 2** Calculated heats of formation in kJ mol$^{-1}$ $SiO_2$

| Zeolite | $\Delta_f H$ |
|---|---|
| BEA[10] | −870.47 |
| FAU[11] | −868.82 |
| LTA[12] | −869.52 |
| MEL[13] | −871.78 |
| MFI[14] | −872.02 |
| TON[15] | −873.46 |
| MCM-22 with *P*6/*m* | −869.96 |

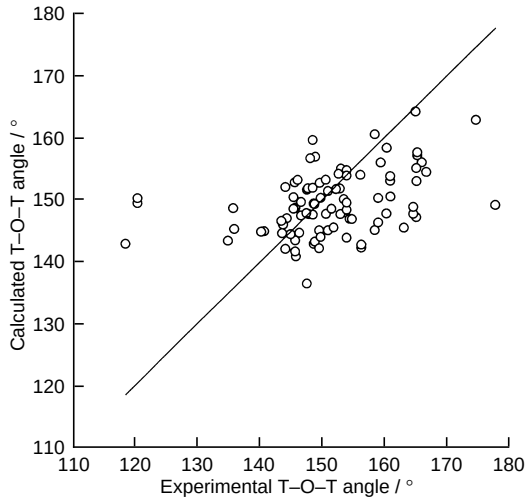



**Fig. 2** Calculated *vs.* experimental[10–15] T–O–T angles: (○) calculated T–O–T angles; (——) $y = x$

calculated T–O–T angles are given as a function of the experimental ones.[10–15] From this figure it is evident that the force field does not tend to overestimate the T–O–T angles. The range of predicted values is smaller than the range of experimental values, which indicates that the 180° angle might indeed be caused by the framework topology. A force-field artefact seems very unlikely and the *P*6/*m* structure might exist.

The calculated XRD patterns in Fig. 3 are only slightly different, which means that very accurate experimental data are necessary to elucidate the precise symmetry and topology. Owing to the size and the shape of the MCM-22 crystals, such an accurate XRD pattern might be difficult to obtain.

In conclusion, the molecular-mechanics calculations show that zeolite MCM-22 having the framework topology as proposed by Leonowicz *et al.*,[3] has *P*6/*m* symmetry. The proposed *P*6/*mmm* and *Cmmm* structures seem to be unstable

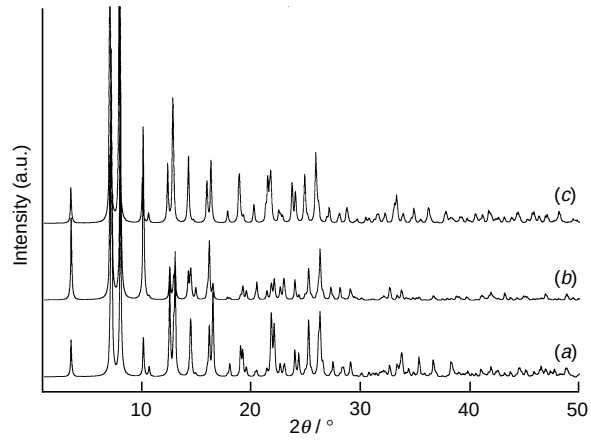



**Fig. 3** Calculated XRD patterns excluding extraframework atoms: (*a*) proposed *P*6/*mmm*;[3] (*b*) proposed *Cmmm*;[3] (*c*) calculated *P*6/*m*

systems. Zeolite MCM-22 might indeed comprise T–O–T angles of 180°.

## Footnote

* E-mail: l.njo@stm.tudelft.nl

## References

1 M. Rubin and P. Chu, *US Pat.*, 4,954,325, 1990.
2 C. T.-W. Chu, *US Pat.*, 4,956,514, 1009; A. Huss Jr., G. W. Kirker, K. M. Keville and R. T. Thomson, *US Pat.*, 4,992,615, 1991; R. P. L. Absil, E. Bowes, G. J. Green, D. O. Marler, D. S. Shihabi and R. F. Socha, *US Pat.*, 5,085,762, 1992; K. J. Del Rossi and A. Huss Jr., *US Pat.*, 5,107,047, 1992; A. Corma and J. Martinez-Triguero, *J. Catal.*, 1997, **165**, 102.
3 M. E. Leonowicz, J. A. Lawton, S. L. Lawton and M. K. Rubin, *Science*, 1994, **264**, 1910.
4 G. J. Kennedy, S. L. Lawton and M. K. Rubin, *J. Am. Chem. Soc.*, 1994, **116**, 11 000.
5 S. Nicolopoulos, J. M. González-Calbet, M. Vallet-Regí, A. Corma, C. Corell, J. M. Guil and J. Pérez-Patiente, *J. Am. Chem. Soc.*, 1995, **117**, 8947.
6 M. Hunger, S. Ernst and J. Weitkamp, *Zeolites*, 1995, **15**, 188.
7 W. M. Meier, D. H. Olson and C. Baerlocher, *Atlas of Zeolite Structure Types*, Elsevier, London, 1996.
8 E. de Vos Burchart, H. van Koningsveld and B. van de Graaf, *Microporous Mater.*, 1997, **8**, 215; S. L. Njo, J. H. Koegler, H. van Koningsveld and B. van de Graaf, *Microporous Mater.*, 1997, **8**, 223.
9 G. Vezzalini, *Z. Kristallogr.*, 1984, **166**, 63; A. Alberti, E. Galli and G. Vezzalini, *Z. Kristallogr.*, 1985, **173**, 257; A. Alberti, P. Davioli and G. Vezzalini, *Z. Kristallogr.*, 1986, **175**, 249; A. Alberti and C. Sabelli, *Z. Kristallogr.*, 1987, **178**, 249.
10 J. B. Higgins, R. B. LaPierre, J. L. Schlenker, A. C. Rohrman, J. D. Wood, G. T. Kerr and W. J. Rohrbaugh, *Zeolites*, 1988, **8**, 446.
11 P. K. Mahrer, F. D. Hunter and J. Scherzer, *Adv. Chem. Ser.*, 1971, **101**, 266.
12 V. Gramlich and W. M. Meier, *Z. Kristallogr.*, 1971, **133**, 134.
13 C. A. Fyfe, H. Gies, G. T. Kokotailo, C. Pasztor, H. Strobl and D. E. Cox, *J. Am. Chem. Soc.*, 1989, **111**, 2470.
14 H. van Koningsveld, *Acta Crystallogr., Sect. B*, 1990, **46**, 731.
15 S. A. T. Barri, G. W. Smith, D. White and D. Young, *Nature*, 1984, **312**, 533.

*Received in Bath, UK, 10th March 1997; Com. 7/01829K*

# Aggregation of carbamato ligands around the $[Co_4O]^{6+}$ core. Synthesis and structure of the cluster $[Co_4O(O_2CNC_9H_{18})_6]$ prepared by a novel oxo-transfer reaction of the nitroxyl free radical 2,2,6,6-tetramethylpiperidin-1-oxyl with $[Co_2(CO)_8]$

**Peter Jaitner,* Christopher Rieker and Klaus Wurst**

*Institute of General, Inorganic and Theoretical Chemistry, University of Innsbruck, A-6020 Innsbruck, Austria*

**The novel oxo-centred tetrahedral cobalt cluster $[Co_4O]^{6+}$ bridged by six carbamato ligands is prepared in high yield when reacting $[Co_2(CO)_8]$ with an excess of the nitroxyl radical 2,2,6,6-tetramethylpiperidin-1-oxyl; the molecular structure of the title compound is determined by a single-crystal X-ray analysis.**

The nitroxyl radical 2,2,6,6-tetramethylpiperidin-1-oxyl (tmpo) is easily oxidized electrochemically (271 mV) in a reversible one-electron step in acetonitrile to the oxoammonium ion.[1] Organic oxoammonium salts characterized by Rey and coworkers[2] have found wide application in selective oxidations of alcohols to aldehydes and ketones as reported by Ma and Bobbit[3] and Semmelhack *et al.*[4] On the other hand, tmpo is a powerful paramagnetic ligand when studying magnetic interactions between metal centres and ligands[5] or in the design of new magnetic materials.[6] We have shown that tmpo is also a valuable spin scavenger of metal carbonyl radicals generating diamagnetic electron-deficient complexes like $[V(CO)_3(tmpo)]$, $[Mn(CO)_3(tmpo)]$ and $[Co(CO)_2(tmpo)]$ **2**, containing a $\eta^2$-bonded tmpo ligand.[7] A metal ($^{51}V$, $^{55}Mn$, $^{59}Co$) NMR investigation revealed that these strained three-membered metallacycles exhibit extremely low metal shieldings.[8] Our preceding work on photolysis of $[Co_2(CO)_8]$ with tmpo in equimolar amounts proved that only the deep red 16-electron metallaoxaziridine $[Co(CO)_2(tmpo)]$ **2** is obtained.[7] But a fourfold excess of tmpo reacts at room temperature with $[Co_2(CO)_8]$ in pentane or benzene in minutes generating the blue carbamato complex $[Co_4O(O_2CNC_9H_{18})_6]$ **1** in high yield (> 80%).

None of numerous attempts to characterize **1** by spectroscopy were conclusive. Standard crystallization procedures failed as well, but suitable single crystals (deep blue plates) were obtained by means of a crystallization box equipped with a heating block described by Hulliger.[10] A single-crystal structure analysis of **1** establishes the structure† shown in Fig. 1.

The molecular structure consists of an oxo-centred tetrahedron of $Co^{II}$ atoms each edge of which is bridged by carbamato ligands. Only one structural determination of a $Co_4(\mu_4\text{-O})$ complex has been reported so far, $[\{Ir(aet)_3\}_4\text{-}Co_4]Br_6$ (aet = 2-aminoethanethiolate),[11*b*] with cobalt–oxygen bond lengths in the range 193–195 pm as found in **1**.

The mechanism of formation of **1** is not yet understood but an excess of tmpo is required for oxo transfer and simultaneously CO insertion into the radical tmpo creating carbamato ligands has to take place. When adding more tmpo to the planar coordinated compound $[Co(CO)_2(tmpo)]$ **2** an immediate colour change to blue **1** is also observed, indicating a stepwise formation of **1** and **2** as an intermediate. Surprisingly, even when performing the reaction of $[Co_2(CO)_8]$ with tmpo without solvent, **1** is formed in high yield. Attempts to identify **1** by mass spectrometry were not informative since no molecular ions or high mass fragments were observed. Only ions such as formamide and other unidentified species were detected. No EPR signal could be observed down to −196 °C. The $^{17}O$ NMR‡ spectrum exhibits two broadened signals at δ 279 and 79. Only very few comparable systems have been studied by $^{17}O$ NMR, making the assignment difficult. We attribute the signal at δ 279 to the oxygens of the carbamato ligand since carboxylates lie in this range.[9] The central $\mu_4$-oxygen at δ 79 is comparable to the shift of the dimeric oxo-bridged $[Re_2(O)_2(\mu\text{-}O)_2(\eta^5\text{-}C_5Me_5)_2]$ [Re-O–Re (δ 104), Re=O (δ 747)] reported by Herrmann and coworkers[9] or to the shift of polyoxometalates containing the $Mo_4(\mu_4\text{-O})$ group (δ 123) studied by Klemperer.[9]

The $M_4(\mu_4\text{-O})$ group is present in many binary metal oxides and is also known in some coordination complexes, such as in the basic metal acetates $[M_4(\mu_4\text{-O})(\mu\text{-}O_2CMe)_6]$ (M = Be, Zn).[11] Compounds containing such oxo bridging groups are of interest in chemistry,[11] biochemistry,[12] magnetochemistry[13] and catalysis.[14] The $Mn_4(\mu_4\text{-O})$ functional group appeared to be unknown for most heavier transition-metal elements but the groups of Puddephatt[15] and Schmidbaur[16] have reported recently new interesting examples containing the elusive $Pd(\mu_4\text{-}O)$[15] and $Au_4(\mu_4\text{-O})$[16] cluster moieties.

In conclusion, this work describes the synthesis and X-ray diffraction of the first complex containing a $Co_4(\mu_4\text{-O})$ group bridged by carbamato ligands. The facile formation of **1** from $[Co_2(CO)_8]$ and tmpo is a surprisingly easy access to a $Co_4(\mu_4\text{-}O)$ cluster; attempts to generalize this chemistry with different

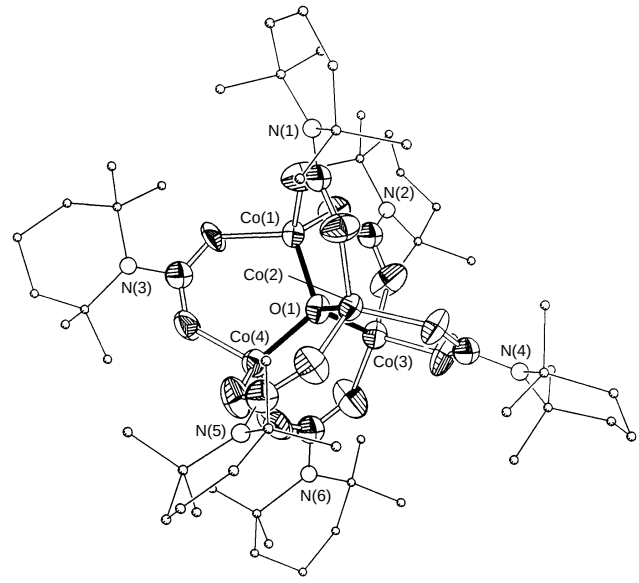



**Fig. 1** Molecular structure of **1**; selected distances (pm) and angles (°): Co(1)–O(1) 193.2(11), Co(2)–O(1) 195.5(10), Co(3)–O(1) 195.2(9), Co(4)–O(1) 193.4(9); Co(1)–O(1)–Co(4) 111.9(5), Co(4)–O(1)–Co(3) 107.8(4), Co(4)–O(1)–Co(2) 108.2(5), Co(1)–O(1)–Co(3) 108.4(5), Co(1)–O(1)–Co(2) 110.3(4), Co(3)–O(1)–Co(2) 110.2(5).

metal carbonyls and oxidizing nitroxyl radicals are under current investigation.

## Footnotes

* E-mail: peter.jaitner@uibk.ac.at

† *Crystal data* for **1**: $C_{60}H_{108}Co_4N_6O_{13}$, $M$ = 1357.24, monoclinic, space group $P2_1/n$, $a$ = 2083.8(5), $b$ = 2964.7(7), $c$ = 2540.7(6) pm, $\beta$ = 114.20(1)°, $U$ = 14.317(6) nm³, $Z$ = 8, Mo-K$\alpha$ radiation ($\lambda$ = 71.073 pm), $D_c$ = 1.259 g cm$^{-3}$ Crystal dimensions: 0.5 × 0.4 × 0.3 mm (blue prism). Data were measured on a Siemens P4 automatic diffractometer with a highly oriented graphite crystal monochromated Mo-K$\alpha$ radiation using $\breve{\omega}$ scans. The structure was solved by direct methods and refined using absorption corrected data to give $R_1$ = 0.0802 for 7092 independent observed reflections [$I > 2\,\sigma(I)$ and 897 parameters. Only the N, O and Co atoms were refined with anisotropic displacement parameters. The crystal structure has been determined and refined in the monoclinic system with X-ray data obtained from a merohedrally twinned crystal, volume ratio 23/5. The twin element can be a twofold rotation axis along $c^*$ or a mirror plane in the $b^*c^*$-plane of the reciprocal lattice (SHELXL-93; TWIN −100 0 − 10 101 or TWIN −100 010 101). The monoclinic $P$-lattice can be transformed to an orthorombic $C$-lattice $a$ = 2083, 8(5), $b$ = 4634.7(10), $c$ = 2964.7(8) pm, but no solution is available in this system.

Atomic coordinates, bond lengths and angles, and thermal parameters have been deposited at the Cambridge Crystallographic Data Centre (CCDC). See Information for Authors, Issue No. 1. Any request to the CCDC for this material should quote the full literature citation and the reference number 182/475.

‡ $^{17}$O NMR ($C_6H_6$–$C_6D_6$, ref. $H_2O$), $\delta$ 79 ($\mu_4$-O), 279 ($\mu_2O_2CNC_9H_{18}$).

## References


1 W. Sümmermann and U. Deffner, *Tetrahedron*, 1975, **31**, 593.
2 A. Caneschi, J. Laugier and P. Rey, *J. Chem. Soc., Perkin Trans. 1*, 1987, 1077.
3 Z. Ma and J. M. Bobbitt, *J. Org. Chem.*, 1991, **56**, 6110.
4 M. F. Semmelhack, C. S. Chou and D. A. Cortes, *J. Am. Chem. Soc.*, 1983, **105**, 4492.
5 Y. Y. Lim and R. S. Drago, *Inorg. Chem.*, 1972, **11**, 1334; R. M. Richman, T. C. Kuechler, S. P. Tanner and R. S. Drago, *J. Am. Chem. Soc.*, 1977, **99**, 1055; R. S. Drago, T. C. Kuechler and M. Kroeger, *Inorg. Chem.*, 1979, **18**, 2337; M. H. Dickman and R. J. Doedens, *Inorg. Chem.*, 1981, **20**, 2067; R. F. Richardson and R. W. Kreilick, *J. Am. Chem. Soc.*, 1977, **99**, 8183; O. P. Anderson and T. C. Kuechler, *Inorg. Chem.*, 1980, **19**, 1417.
6 D. Gatteschi, O. Kahn, S. Miller and F. Palacio, *Molecular Magnetic Materials*, Kluwer Academic, Dordrecht, 1991; O. Kahn, *Molecular Magnetism*, VCH, Weinheim, 1993; J. S. Miller and A. J. Epstein, *Angew. Chem., Int. Ed. Engl.*, 1994, **33**, 385; J. S. Miller, *Adv. Mater.*, 1992, **4**, 298; J. S. Miller, *Chem. Eng. News.*, 1995, **73**, 30.
7 P. Jaitner, W. Huber, G. Huttner and O. Scheidsteger, *J. Organomet. Chem.*, 1983, **259**, C1; P. Jaitner, W. Huber, A. Gieren and H. Betz, *J. Organomet. Chem.*, 1986, **311**, 379; P. Jaitner and W. Huber, *Inorg. Chim. Acta*, 1987, **129**, L45.
8 D. Rehder and P. Jaitner, *J. Organomet. Chem.*, 1987, **329**, 337.
9 W. G. Klemperer, *Angew. Chem.*, 1978, **90**, 258; H. J. Kneuper, P. Härter and W. A. Herrmann, *J. Organomet. Chem.*, 1988, **340**, 353; W. McFarlane and H. C. E. McFarlane, in *Multinuclear NMR*, ed. J. Mason, Plenum, New York, ch. 14, 1987.
10 J. Hulliger, *Angew. Chem., Int. Ed. Engl.*, 1994, **33**, 143.
11 (*a*) F. Bottomley, *Polyhedron*, 1992, **11**, 1707; B. O. West, *Polyhedron*, 1989, **8**, 219; (*b*) K. Okamoto, T. Konno and J. Hidaka, *J. Chem. Soc., Dalton Trans.*, 1994, 533.
12 K. K. Anderson and A. Graslund, *Adv. Inorg. Chem.*, 1995, **43**, 359.
13 K. S. Murray, *Adv. Inorg. Chem.*, 1995, **43**, 261.
14 S. Ladas, R. Imbihl and G. Ertl, *Surf. Sci.*, 1989, **219**, 88; 1993, **280**, 14.
15 Y. Zhang, R. J. Puddeohatt, L. Manojlovic-Muir and K. W. Muir, *Chem. Commun.*, 1966, 2599 and references therein.
16 H. Schmidbauer, S. Hofreiter and M. Paul, *Nature*, 1995, **377**, 503.


*Received in Basel, Switzerland, 24th February 1997; Com. 7/01238A*

# *In situ* probing of surface sites on supported molybdenum nitride catalyst by CO adsorption

**Shuwu Yang, Can Li*, Jiang Xu and Qin Xin***

*State Key Laboratory of Catalysis, Dalian Institute of Chemical Physics, Chinese Academy of Sciences, PO Box 110, Dalian 116023, China*

**Both molybdenum and nitrogen sites on fresh $Mo_2N/Al_2O_3$ are probed by adsorbed CO giving two characteristic IR bands at 2045 and 2200 cm$^{-1}$, respectively.**

Molybdenum nitride has unique physical and chemical properties, such as, electronic, magnetic and catalytic properties, which are similar to noble metals in many aspects. During the last decade, molybdenum nitride has attracted much attention because of its excellent catalytic activity in a number of hydrogenation reactions,[1] such as $NH_3$ synthesis, hydrotreating, hydrogenolysis and hydrogenation. Specifically supported molybdenum nitrides with high surface areas have been prepared and used in hydrotreating reactions[2–5] and show high potential in industrial applications.

Although molybdenum nitride exhibits a very good catalytic performance, the nature of the surface-active catalytic sites is not well understood. After exposure to air molybdenum nitride is partially oxidized, particularly at the surface,[6] and its surface is very difficult to reduce even with hydrogen at high temperatures, and in most cases, the surface is in an oxynitrided form. In this work, we investigated freshly prepared molybdenum nitride in order to characterize its surface.

A $MoO_3/Al_2O_3$ (10 mass% Mo) sample was prepared by the incipient wetness impregnation technique contacting γ-$Al_2O_3$ ($S_{BET}$ = 230 m$^2$ g$^{-1}$) with an aqueous solution of $(NH_4)_6Mo_7O_{24}$, followed by drying at 393 K overnight and calcination at 773 K for 4 h. The nitrided $Mo/Al_2O_3$ catalyst was prepared by temperature programmed reaction of $MoO_3/Al_2O_3$ with ammonia. The temperature was increased from room temp. to 573 K over 30 min and from 573 to 973 K for 7 h; then the temperature was maintained at 973 K for 2 h. The nitrided sample was cooled to room temperature in flowing ammonia and then passivated in a stream of 1% $O_2$–$N_2$ so as to avoid substantial oxidation. The as-prepared sample is denoted passivated $Mo_2N/Al_2O_3$. The passivated sample was pressed into a self-supporting wafer of mass *ca.* 15 mg. The wafer was placed in a quartz IR cell equipped with $CaF_2$ windows, and nitrided again in the IR cell in flowing ammonia at given temperatures for 1 h. Samples nitrided in the IR cell are denoted as freshly nitrided or renitrided samples, while the passivated $Mo_2N/Al_2O_3$ reduced with $H_2$ at 873 K is denoted reduced passivated sample. The sample was then held *in vacuo* at 773 K for 1 h. Subsequently, the sample was cooled to room temp. and exposed to 10 Torr CO for IR study. All IR spectra were collected at room temp. on a Fourier transform IR spectrometer (Bio-Rad FTS 65A) with a resolution of 4 cm$^{-1}$.

Fig. 1 shows the IR spectra of CO adsorbed on fresh $Mo_2N/Al_2O_3$ at different temperatures [Fig. 1(*b*)–(*f*)] and the IR spectrum of CO adsorbed on reduced passivated $Mo_2N/Al_2O_3$ for comparison [Fig. 1(*a*)]. A broad band at 2180 cm$^{-1}$ and two weak bands at 2100 and 2034 cm$^{-1}$ are observed for the adsorbed CO on reduced passivated $Mo_2N/Al_2O_3$. For the sample renitrided at 573 K, only a weak band appears at 2184 cm$^{-1}$ as a result of CO adsorption. This band shifts only slightly from 2184 to 2173 cm$^{-1}$ for the sample renitrided at 673 K. However, when the passivated $Mo_2N/Al_2O_3$ was renitrided at 723 K, the IR spectrum of the adsorbed CO shows a dramatic change [Fig. 1(*d*)]: four IR bands are observed at 2200, 2157, 2110 and 2045 cm$^{-1}$. For the sample renitrided at 773 K, these four IR bands appear at 2200, 2140, 2090 and 2045 cm$^{-1}$. The two bands at 2140 and 2090 cm$^{-1}$ decline in intensity while the two bands at 2200 and 2045 cm$^{-1}$ grow significantly.

For passivated $Mo_2N/Al_2O_3$ renitrided at 873 K, two IR bands can be seen for the adsorbed CO: a strong band at 2200 cm$^{-1}$ and a broad band at 2045 cm$^{-1}$, and their intensities increase considerably compared with those for $Mo_2N/Al_2O_3$ renitrided at 723 K. The IR intensities of the two bands scarcely decrease under evacuation at room temperature indicating that the adsorbed species are very stable. Both the bands at 2200 and 2045 cm$^{-1}$ can be still observed under evacuation up to 373 K. When the sample is heated to 423 K under vacuum, the band at 2045 cm$^{-1}$ diminishes while the band at 2200 cm$^{-1}$ can still be seen even the temperature is raised to 673 K and disappears only when the temperature is increased to 773 K. This result suggests that the two bands represent two different types of species formed from the CO adsorption on the fresh $Mo_2N/Al_2O_3$.

A study[7] of CO adsorption on reduced $MoO_3/Al_2O_3$ concluded that mainly $Mo^{4+}$ cations were produced when $MoO_3/Al_2O_3$ was reduced at temperatures in the range of 573–773 K. No adsorbed CO on $Mo^0$ was detected for $MoO_3/Al_2O_3$ reduced at temperatures below 973 K. A significant exposure of fully reduced Mo atoms on $MoO_3/Al_2O_3$ was seen

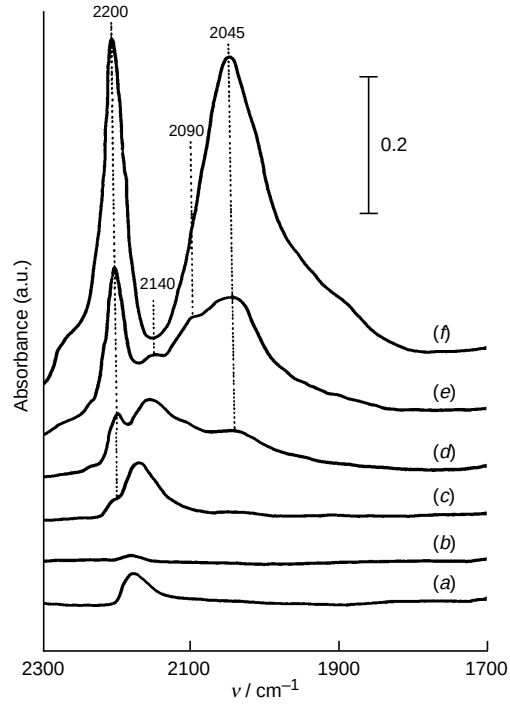



**Fig. 1** IR spectra of CO adsorbed on passivated $Mo_2N/Al_2O_3$ reduced at 873 K (*a*) and on passivated $Mo_2N/Al_2O_3$ renitrided at 573 (*b*), 673 (*c*), 723 (*d*), 773 (*e*) and 873 K (*f*)

only after a reduction above 973 K.[8] In Fig. 1(*a*), the IR band at 2180 $cm^{-1}$ indicates that CO is adsorbed mainly on $Mo^{4+}$ for the reduced passivated $Mo_2N/Al_2O_3$. The IR spectrum is similar to that for $MoO_3/Al_2O_3$ reduced at 873 K but totally different from those of CO adsorbed on the fresh $Mo_2N/Al_2O_3$ samples [Fig. 1(*b*)–(*f*)]. This leads us to conclude that the surface of reduced passivated $Mo_2N/Al_2O_3$ is in highly oxidic form, *i.e.* the surface exists mainly as the oxynitride.

The two characteristic bands at 2045 and 2200 $cm^{-1}$ appear only when the sample is renitrided at temperatures at and above 723 K, and their intensities are enhanced significantly with increase in nitriding temperature. It is obvious that these two bands are related to adsorbed CO on molybdenum nitride. The IR band at 2045 $cm^{-1}$ can be safely assigned to the linearly adsorbed CO on surface molybdenum atoms of fresh $Mo_2N/Al_2O_3$. From the band position and the chemical state of the nitride, the surface molybdenum atom may be partially positively charged.[9–11] By contrast, adsorbed CO on a reduced passivated sample shows IR bands at wavenumbers $>2100$ $cm^{-1}$, indicating that the surface molybdenum atom is in a high valence state characteristic of the oxynitride or oxide form even at a reduction temperature as high as 873 K.

It is also interesting that the strong stable band at 2200 $cm^{-1}$ is observed for fresh $Mo_2N/Al_2O_3$. This band cannot be attributed to CO adsorbed on any molybdenum cation sites since adsorbed CO on molybdenum cations at such a high frequency is easily removed by evacuation even at room temperature. From its vibrational frequency and its high stability,[12] we assign this band to NCO species formed when CO reacts with surface active nitrogen atoms created by *in situ* nitridation. A separate experiment established that the band intensity of the 2200 $cm^{-1}$ band decreased considerably while the band at 2045 $cm^{-1}$ remained unchanged when the fresh catalyst was treated with hydrogen at 773 K. The result is consistent with our assignment of the band at 2200 $cm^{-1}$ to NCO formed *via* reaction between CO and surface nitrogen atoms. Treatment with hydrogen at high temperatures can remove some of the surface active nitrogen atoms; as a result, the band intensity of NCO species is reduced. This result also suggests that a considerable amount of nitrogen atoms are present on the surface of molybdenum nitride, and that they are highly active which may play an important role in catalytic behaviour.

In summary, CO is strongly adsorbed on fresh $Mo_2N/Al_2O_3$ catalyst leading to two IR bands at 2045 and 2200 $cm^{-1}$ which can be assigned to linearly adsorbed CO on molybdenum and nitrogen sites, respectively when the catalyst is nitrided at temperatures above 723 K. Unlike CO adsorbed on reduced passivated $Mo_2N/Al_2O_3$, adsorbed CO on molybdenum nitride is very stable and behaves very similarly to that of group 8 metals. This study proves that fully nitrided molybdenum resembles noble metals; also, its surface nitrogen atoms are in a highly active form and readily react with CO to form surface NCO species. Our results also suggest that *in situ* studies of fresh nitrides are very important in the understanding of the real surface of the fresh nitride, while studies on passivated nitrides can not give correct information for the nitride, but rather, give information for the oxynitride or oxygen covered nitride.

## Footnote

* E-mail: canli@ms.dicp.ac.cn

## References

1 S. T. Oyama, *Catal. Today*, 1992, **15**, 179.
2 J. C. Schlatter, S. T. Oyama, J. E. Metcalfe, III and J. M. Lambert, Jr, *Ind. Eng. Chem. Res.*, 1988, **27**, 1648.
3 M. Nagai and T. Miyao, *Catal. Lett.*, 1992, **15**, 105.
4 M. Nagai, T. Miyao and T. Tsuboi, *Catal. Lett.*, 1992, **18**, 9.
5 C. W. Colling and L. T. Thompson, *J. Catal.*, 1994, **146**, 192.
6 E. J. Markel and J. W. Van Zee, *J. Catal.*, 1990, **126**, 643.
7 X. T. Gao and Q. Xin, *J. Catal.*, 1994, **146**, 306.
8 J. B. Peri, *J. Phys. Chem.*, 1982, **86**, 1615.
9 M. I. Zaki, B. Vielhaber and H. Knözinger, *J. Phys. Chem.*, 1986, **90**, 3176.
10 E. C. Decanio and D. A. Storm, *J. Catal.*, 1991, **130**, 653.
11 B. Müller, A. D. Van Langeveld, J. A. Moulijn and H. Knözinger, *J. Phys. Chem.*, 1993, **97**, 9028.
12 K. Nakamoto, *Infrared and Raman Spectra of Inorganic and Coordination Compounds*, Wiley-Interscience Publication, New York, 3rd edn., 1977, p. 276.

*Received in Cambridge, UK, 18th March 1997; Com. 7/01892D*

# Novel gold derivatives of titanium carbonyl and structural characterization of a compound containing an unsupported gold–titanium bond: $[Ti(CO)_6(AuPEt_3)]^-$†

**Paul J. Fischer, Victor G. Young, Jr. and John E. Ellis***

*Department of Chemistry, University of Minnesota, Minneapolis, MN 55455, USA*

**Hexacarbonyltitanate(2−) reacts with $(R_3P)AuCl$ (R = $C_6H_{11}$, Et) to provide the first anions of the general formula $[M(CO)_x(AuPR_3)_y]^z$, and a structurally characterized (for R = Et) compound containing a largely unsupported gold–titanium bond.**

Mixed gold–transition metal compounds have been known for over thirty years[1] and now hold a special position in chemistry by virtue of their often intriguing chemical and physical properties.[2] While structurally characterized compounds containing gold–metal bonds are well known for most transition-metal elements, the first example containing titanium was reported only very recently, an unusual bis(alkynyl)titanocene-gold aryl adduct; $[\{(\eta^5\text{-}C_5H_4SiMe_3)_2Ti(C{\equiv}CSiMe_3)_2\}\text{-}Au\{C_6H_2(CF_3)_3\text{-}1,3,5\}]$ **1**.[3] Since the gold atom in this complex was strongly bound to the two alkyne groups, it was required to be in close proximity to the formally $Ti^{IV}$ center. To assess whether the gold–titanium interaction was significant, as claimed,[3] we felt that it was important to obtain and determine the molecular structure of a compound containing a largely unsupported gold–titanium bond. Numerous attempts to prepare the unknown carbonyltitanate $[Ti(CO)_6(AuPPh_3)]^-$, which is analogous to the well established vanadium complex $[V(CO)_6(AuPPh_3)]$,[4,5] by the reaction of $[Ti(CO)_6]^{2-}$ with $(Ph_3P)AuCl$ were uniformly unsuccessful. However, dropwise addition of cold (−50 to −60 °C) solutions of $(R_3P)AuCl$, (R = $C_6H_{11}$, Et) to an equimolar quantity of $[K(15\text{-crown-}5)_2]_2[Ti(CO)_6]$,[6] as a finely divided cold (−50 to −80 °C) solid, provided 20–35% isolated yields of satisfactorily pure $[K(15\text{-crown-}5)_2][Ti(CO)_6(AuPR_3)]$ (R = $C_6H_{11}$ **2a**, Et **2b**), Scheme 1.‡

Compounds **2a,b** are air-sensitive brown to red–brown microcrystalline solids. Both have nearly identical IR spectra in the ν(CO) region in thf, which indicates that the carbonyl products have very similar molecular structures in solution. Carbon-13 NMR spectra of these species in thf are also very similar and show a single carbonyl resonance at $\delta_C$ *ca.* 250 from 25 to −90 °C. To confirm the presence of seven-coordinate titanium in **2a**, a 99% $^{13}CO$ enriched sample was prepared from the known $[Ti(^{13}CO)_6]^{2-}$[6] by the same procedure. The $^{13}C$ and $^{31}P$ NMR spectra of $[^{13}C_6]$**2a** showed the expected doublet ($\delta_C$, +250.3, $^3J_{PC}$ 5 Hz) and a well resolved binomial septet ($\delta_P$, 74.3, $^3J_{PC}$ 5 Hz), respectively, arising from coupling of the six equivalent carbonyl carbons to phosphorus in the coordinated tricyclohexylphosphine group. The equivalence of the carbonyl groups undoubtedly arises from the highly fluxional nature of **2a** in solution. Attempts to grow X-ray quality crystals of **2a** were unsuccessful, but suitable single crystals of **2b** were obtained.§

$$[Ti(CO)_6]^{2-} + (R_3P)AuCl \xrightarrow[-60 \text{ to } 0\ ^\circ C]{\text{thf}} [Ti(CO)_6(AuPR_3)]^- + Cl^-$$

(R = $C_6H_{11}$, Et)

**Scheme 1**

The anion in **2b** (Fig. 1) has an irregular seven-coordinate geometry about titanium. A view down the Ti–Au vector shows an approximate capped trigonal prism, where gold 'caps' carbonyl carbons C(1–4); however, the latter define a substantially non-planar face. The C(1)–Ti–C(2) and C(3)–Ti–C(4) angles of 123.1(3) and 167.1(3)°, respectively, deviate markedly from that expected for an undistorted capped trigonal prism.[7] The origin of this severe distortion is a close approach of one CO group, defined by C(1), to the gold atom. Although the Au–C(1) distance of 2.416(8) Å is outside the range of normal Au–C bond lengths and is significantly longer than the average Au–C($\eta^2$-alkyne) value of 2.23 (1) Å found in complex **1**, other structural and spectral data for crystalline **2b** point to the presence of a very weak 'semibridging' carbonyl–gold interaction. For example, the C(1)–O(1) and Ti–C(1) distances are significantly longer and shorter, respectively, than the other corresponding distances in **2b**, except that for Ti–C(4) (Fig. 1). Also, the slight non linearity of the Ti–Au–P angle of 169.45(6)° and a difference in the solid-state and solution IR spectra of **2b** in the ν(CO) region suggest that this interaction is present. Specifically, the lowest-energy ν(CO) band of **2b** decreases from 1814 $cm^{-1}$ in solution to 1791 $cm^{-1}$ as a mulled solid, which is the trend expected for a weak interaction of this type.[8] By comparison, the shortest carbonyl carbon–gold distance in the closely related $[V(CO)_6(AuPPh_3)]$ is 2.57(2) Å.[5] For the latter complex, there is no IR spectral evidence for any analogous Au–CO interaction in the solid state.[9] The average Ti–C and C–O distances are 2.05(1) and 1.16(1) Å, respectively, which are similar to corresponding values of 2.04(1) and 1.16(2) Å found in a related $Ti^0$ anionic carbonyl $[Ti(CO)_5(SnPh_3)_2]^{2-}$.[10] The Au–P distance in **2b** of 2.295(2) Å is similar to those found in other triethylphosphine gold–metal

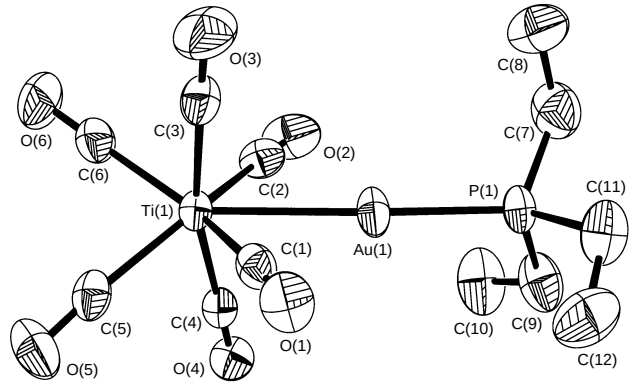



**Fig. 1** Molecular structure of the anion in **2b**. Selected dimensions (Å and °): Ti–C(1) 2.034(9), Ti–C(2) 2.065(9), Ti–C(3) 2.056(9), Ti–C(4) 2.046(8), Ti–C(5) 2.053(9), Ti–C(6) 2.060(9), Ti–Au 2.719(1), Au–P 2.295(2), Au–C(1) 2.416(8), Au–C(2) 2.599(8), C(1)–O(1) 1.175(9), C(2)–O(2) 1.141(9), C(3)–O(3) 1.155(9), C(4)–O(4) 1.155(9), C(5)–O(5) 1.147(10), C(6)–O(6) 1.155(9), P–C(av.) 1.81(1), C–C(av.) 1.48(2); Ti–Au–P 169.45(6), Ti–C(1)–O(1) 173.7(7), Ti–C(2)–O(2) 174.0(8), other Ti–C–O (av.) 177(2).

complexes; *e.g.* in $[Os_3(CO)_{10}(AuPEt_3)_2]$ the distance is 2.287(6) Å.[11] More interesting is the Ti–Au bond length of 2.719(1) Å, which, as expected, is slightly longer than the V–Au distance of 2.690(3) Å in $[V(CO)_6(AuPPh_3)]$,[5] but is 0.276 Å shorter than the Ti–Au separation of 2.995(1) Å reported for compound **1**. On this basis, although the existence of a Ti–Au bond in **1** cannot be ruled out, it is undoubtedly much weaker than that present in $[Ti(CO)_6(AuPEt_3)]^-$. The counter ion in **2b**, $[K(15\text{-crown-}5)_2]^+$, is well separated from anions in the crystalline lattice and has the usual sandwich structure containing formally ten-coordinate potassium ion, with a mean K–O distance of 2.89(5) Å. The latter number is essentially identical to the corresponding value of 2.88(9) Å, recently found in $[K(15\text{-crown-}5)_2][Zr(CO)_4(dppe)(SnMe_3)]$.[12]

Compounds **2a,b** are of additional interest in that they contain the first known anionic complexes of the general formula $[M(CO)_x(AuPR_3)_y]^z$ and may be regarded as structural models[13,14] for the presently unknown hydride, $[Ti(CO)_6H]^-$. All previously reported reactions of homoleptic carbonylmonometalates, *i.e.*, $[M(CO)_x]^{y-}$, with phosphine gold halides have given only neutral compounds of the type $[M(CO)_x(AuPR_3)_y]$. For example, the reaction of $[V(CO)_5]^{3-}$ with fewer than 3 equiv. of $(Ph_3P)AuCl$ invariably gave only the neutral gold cluster species $[V(CO)_5(AuPPh_3)_3]$ and unreacted $[V(CO)_5]^{3-}$.[15] Similar unsuccessful attempts to prepare the still unknown $[Fe(CO)_4(AuPPh_3)]^-$ by the reaction of $[Fe(CO)_4]^{2-}$ with 1 equiv. of $(Ph_3P)AuCl$ yielded only the neutral bis-gold complex, $[Fe(CO)_4(AuPPh_3)_2]$.[16] Very likely the pronounced tendency for $(R_3P)Au$ groups to bind to one another and form Au–Au bonds,[2] a phenomenon recently dubbed 'aurophilicity',[17] accounts for the favored formation of the neutral polygold–metal species in these prior studies. The relatively crowded anionic $Ti(CO)_6$ unit in **2a,b** undoubtedly inhibits attack by a second phosphine gold chloride and may be one reason why we were successful for the first time in obtaining substituted metal carbonyl anions of this type. However, substitution of trialkylphosphinegold chlorides in these reactions for the doubtlessly more electrophilic triphenylphosphinegold chloride may also have been of critical importance in this study. Extensions of this research to zirconium and hafnium will be of interest since well characterized gold derivatives of these metals are presently unknown.

We thank the National Science Foundation and donors of the Petroleum Research Fund, administered by the American Chemical Society for financial support of this research. Also we are grateful to Professor Marcetta Y. Darensbourg for a useful discussion and Ms. Christine Lundby for assistance in the preparation of the manuscript.

## Footnotes

* E-mail: ellis@chem.umn.edu

† Highly Reduced Organometallics 40; Part 39, see ref. 12.

‡ A cold (−50 °C) solution of $[(C_6H_{11})_3P]AuCl$ (0.504 g, 0.984 mmol) in thf (50 ml) was added by cannula to cold (−50 °C) and finely divided solid $[K(15\text{-crown-}5)_2]_2[Ti(CO)_6]$ (1.15 g, 0.982 mmol) with stirring. The resulting red–brown reaction mixture was stirred for 14 h while slowly warming to 0 °C. Following filtration at 0 °C, all but about 5 ml of the solvent was removed *in vacuo*. Addition of excess diethyl ether caused precipitation of the brown solid, which was recrystallized from thf–ether to provide 0.406 g (35% yield) of pure **2a**. Satisfactory elemental analysis. IR(thf): ν(CO) 1951 m, 1918 m, 1811 s $cm^{-1}$. IR (Nujol): 1959 m, 1922 (sh), 1870 (sh), 1835 (sh), 1780 s, (br) $cm^{-1}$. $^1H$ NMR (300 MHz, $[^2H_8]$thf 25 °C, $SiMe_4$): δ 3.53 (s, 40 H, 15-crown-5), 2.5-1.8 [m, 33 H, $AuP(C_6H_{11})_3$]. $^{13}C\{^1H\}$(75 MHz): δ 250.2 (d, $^3J_{PC}$ 4.6 Hz, CO), 69.7 (s, 15-crown-5), 34.3 (d, $^1J_{PC}$ = 17 Hz, $C_6H_{11}$), 31.2 (d, $^2J_{PC}$ 3 Hz, $C_6H_{11}$), 28.3 (d, $^3J_{PC}$ 11 Hz, $C_6H_{11}$), 27.1 (s, $C_6H_{11}$) $^{31}P$ (121 MHz, ref. $H_3PO_4$): δ 74.3 [s, $AuP(C_6H_{11})_3$]. Pure **2b** was obtained by a nearly identical procedure in 20% yield. IR (THF): ν(CO) = 1954m, 1918w, 1814s $cm^{-1}$. IR (Nujol): 1954m, 1838 (sh), 1791s $cm^{-1}$. $^1H$ NMR (300 MHz, $[^2H_8]$thf, 0 °C, $SiMe_4$): δ 3.53 (s, 40 H, 15-crown-5), 1.61 (m, 6 H, P**C**$H_2$CH$_3$), 1.09 (dt, *J* 7.5, $^3J_{PH}$ = 18 Hz, 9 H , PCH$_2$**C**$H_3$). $^{13}C\{^1H\}$(75 MHz): δ 249 (s, CO), 69.4 (s, 15-crown-5), 20.0 (d, $J_{PC}$ 20 Hz, P**C**$H_2$CH$_3$), 9.5 (d, $^2J_{PC}$ 4.5 Hz, PCH$_2$**C**$H_3$). $^{31}P$ (121 MHz, ref $H_3PO_4$) 56.8 [br s $AuP(C_2H_5)_3$].

§ *Crystal data* for **2b**: $C_{32}H_{55}AuKO_{16}PTi$, $M$ = 1010.7, monoclinic, space group $P2_1/c$, $a$ = 14.5279(3), $b$ = 15.8275(1), $c$ = 18.7076(3) Å, β = 93.559(1)°, $U$ = 4293.3(1) Å$^3$, $Z$ = 4, $D_c$ = 1.564 g $cm^{-3}$, $F(000)$ = 2040, μ(Mo-Kα) = 3.796 $mm^{-1}$, λ = 0.71073Å, $T$ = 173(2) K. 18 549 reflections measured on a Siemens SMART CCD area detector diffractometer yielded 7415 unique data ($2\theta_{max}$ = 50°, $R_{int}$ = 0.0350, semiempirical absorption corrections). The structure was solved by direct methods and refined by full-matrix least-squares methods on $F^2$ with statistical weighting, anisotropic displacement parameters, constrained isotropic H atoms to give $wR_2 = \{\Sigma[w(F_o^2 - F_c^2)^2]/\Sigma[w(F_o^2)^2]\}^{1/2}$ = 0.1213 on all data, conventional $R$ = 0.0531 on $F$ values of 4965 reflections having $F_o^2 > 2\sigma(F_o^2)$, goodness of fit $S$ = 1.020 for all $F^2$ values and 472 refined parameters. Largest difference peak and hole: 0.984, −1.063 e Å$^{-3}$. All calculations were performed using SGI INDY R4400-SC or pentium computers with SHEXTL-Plus V5.0 program suite. Atomic coordinates, bond lengths and angles and thermal parameters have been deposited at the Cambridge Crystallographic Data Centre (CCDC). See Information for Authors, Issue No. 1. Any request to the CCDC for this material should quote the full literature citation and the reference number 182/489.

## References

1 C. E. Coffey, J. Lewis and R. S. Nyholm, *J. Chem. Soc.*, 1964, 1741.
2 K. P. Hall and D. M. P. Mingos, *Prog. Inorg. Chem.*, 1984, **32**, 237.
3 H. Lang, K. Köhler and L. Zsolnai, *Chem. Commun.*, 1996, 2043.
4 A. S. Kasenally, R. S. Nyholm, R. S. O'Brien and M. H. B. Stiddard, *Nature*, 1964, **204**, 871.
5 M. G. B. Drew, *Acta Crystallogr., Sect. B*, 1982, **38**, 254.
6 K. M. Chi, S. R. Frerichs, S. B. Philson and J. E. Ellis, *J. Am. Chem, Soc.*, 1988, **110**, 303.
7 D. L. Kepert, *Inorganic Stereochemistry*, Springer Verlag, Berlin, 1982, pp. 116–151.
8 C. P. Horwitz and D. F. Shriver, *Adv. Organomet. Chem.* 1984, **23**, 219.
9 A. Davison and J. E. Ellis, *J. Organomet. Chem.* 1972, **36**, 113.
10 K. M. Chi, S. R. Frerichs and J. E. Ellis, *J. Chem. Soc., Chem. Commun.*, 1988, 1013.
11 B. F. G. Johnson, D. A. Kaner, J. Lewis and M. J. Rosales, *J. Organomet. Chem.*, 1982, **238**, C73.
12 J. E. Ellis, P. Yuen and M. Jang, *J. Organomet. Chem.*, 1996, **507**, 283.
13 J. W. Lauher and K. Wald, *J. Am. Chem. Soc.*, 1981, **103**, 7648.
14 D. G. Evans and D. M. P. Mingos, *J. Organomet. Chem.*, 1982, **232**, 171.
15 J. E. Ellis, *Adv. Organomet. Chem.*, 1990, **31**, 1.
16 L. W. Arndt, M. Y. Darensbourg, J. P. Fackler, Jr., R. J. Lusk, D. O. Marlen and K. A. Youngdahl, *J. Am. Chem. Soc.*, 1985, **107**, 7218.
17 A Stützer, P. Bissinger and H. Schmidbauer, *Chem. Ber.*, 1992, **125**, 367 and references therein.

*Received in Bloomington, IN, USA; 18th February 1997; Com. 7/01143A*



Typeset and printed by Black Bear Press Limited, Cambridge, England

ChemComm
FEATURE ARTICLE

# Metal chemistry relevant to the mononuclear molybdenum and tungsten pterin enzymes‡

**Charles G. Young† and Anthony G. Wedd†**

*School of Chemistry, University of Melbourne, Parkville, Victoria 3052, Australia*

**In the light of recent protein crystal structures, metal chemistry underpinning the action of oxygen-atom transfer enzymes which contain molybdenum and tungsten pterin centres is outlined.**

## Introduction

The group 6 metal molybdenum is an essential nutrient for all forms of life while its heavier congener tungsten is essential for certain anaerobic thermophilic bacteria.[1,2] The high solubility of $Mo^{VI}$ and $W^{VI}$ oxyanions in water ensures that the elements are available to biological systems ($10^{-7}$ and $10^{-9}$ mol $dm^{-3}$, respectively, in sea water), despite their low terrestrial elemental abundances.[1]

Molybdenum enzymes fall into two general classes: the nitrogenases and the molybdopterin enzymes.[3,4] The former feature the iron–molybdenum cofactor (FeMoco), a cluster of stoichiometry $Fe_7MoS_9$. The latter possess mononuclear molybdenum cofactors (Moco) with metal bound by 1,2-dithiolate links to one or two pterin ring systems [Fig. 1(*a*)].[4–6] An oxidised derivative, urothione [Fig. 1(*b*)], is excreted during normal human metabolism. Known tungsten enzymes are related to the second class.[2]

Most pterin enzymes mediate formal oxygen atom exchange between substrate X and water [eqn. (1)].[7–9]

$$X + H_2O \leftrightarrow XO + 2\,H^+ + 2\,e^- \quad (1)$$

Specific half-reactions for some of the more extensively studied systems are given in Scheme 1. Molybdenum centres operate on C, N, S and As atoms of substrate X[8–10] while the known tungsten centres operate on carbon during its assimilation from various sources.[2,11] There is usually a second reaction centre (*e.g.* flavin, iron–sulfur, cytochrome) for the complementary half-reactions and the two active sites are connected by an internal electron-transfer chain. Two identified roles for the pterin ligand are to participate directly in this intramolecular electron transfer and to tune the redox potential of the site.[6,7,12]

Molecular features of the pterin enzymes have been illuminated by recent crystal structures (Fig. 2).[12–16] These provide a basis for further progress in defining the molecular mechanisms of action. This Article concentrates on the structural and reaction chemistry at the molybdenum and tungsten sites. The value of defining the fundamental chemistry was clear from the first significant modelling experiments. Electron paramagnetic resonance (EPR) signals characteristic of $Mo^V$ appeared upon reaction of $[Mo^{VI}O_4]^{2-}$ and glycolic acids $HECH_2CO_2H$ (E = O, S).[17] Spectral parameters for the sulfur-based system were similar to the so-called 'very rapid' and 'rapid' signals of xanthine oxidase and established a major role for ligand sulfur.[18] The synthetic species generated have now been identified as square-pyramidal $[Mo^VO(SR)_4]^-$ and related species.[19–21]

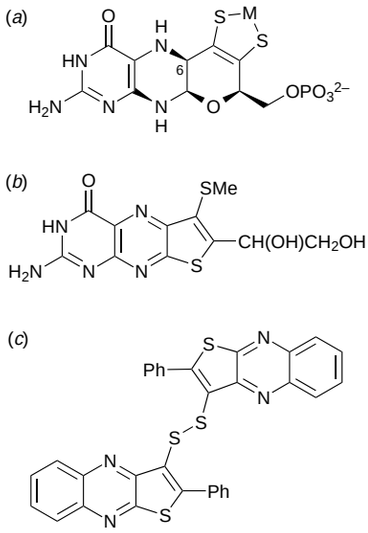
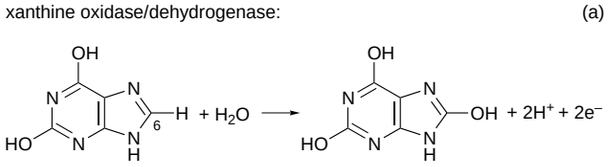



**Fig. 1** (*a*) Pterin centre with pyran ring attached at positions 6 and 7. A 1,2-dithiolate unit capable of acting as a bidentate ligand to metal M occupies positions 1′ and 2′ of the pyran ring. It is represented as an ene-1,2-dithiolate, although this point is speculative as the redox level of the pterin–pyran system is undefined at present. The phosphate substituent is elaborated to a dinucleotide in enzymes from prokaryotic organisms. (*b*) Urothione and (*c*) 2-phenylthieno[2,3-*b*]-quinoxaline.

Molybdenum enzymes

xanthine oxidase/dehydrogenase: (a)




xanthine uric acid

sulfite oxidase: $[SO_3]^{2-} + H_2O \rightarrow [SO_4]^{2-} + 2H^+ + 2e^-$ (b)

nitrate reductase: $[NO_3]^- + 2H^+ + 2e^- \rightarrow [NO_2]^- + H_2O$ (c)

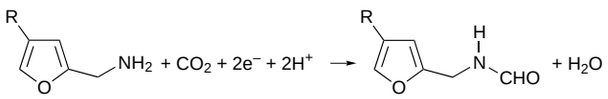
dimethyl sulfoxide reductase: $Me_2SO + 2H^+ + 2e^- \rightarrow Me_2S + H_2O$ (d)

Tungsten enzymes[a]

aldehyde oxido-reductase: $RCHO + H_2O \rightarrow RCO_2H + 2H^+ + 2e^-$ (e)

formate dehydrogenase: $HCO_2^- + H_2O \rightarrow HCO_3^- + 2H^+ + 2e^-$ (f)

formylmethanofuran dehydrogenase: (g)




**Scheme 1** [a] Molybdenum versions of these enzymes are also known [*e.g.* compare Fig. 2(*a*) and (*c*)]. In certain bacteria, both molybdenum and tungsten versions can be isolated (see, *e.g.* refs. 4 and 33).

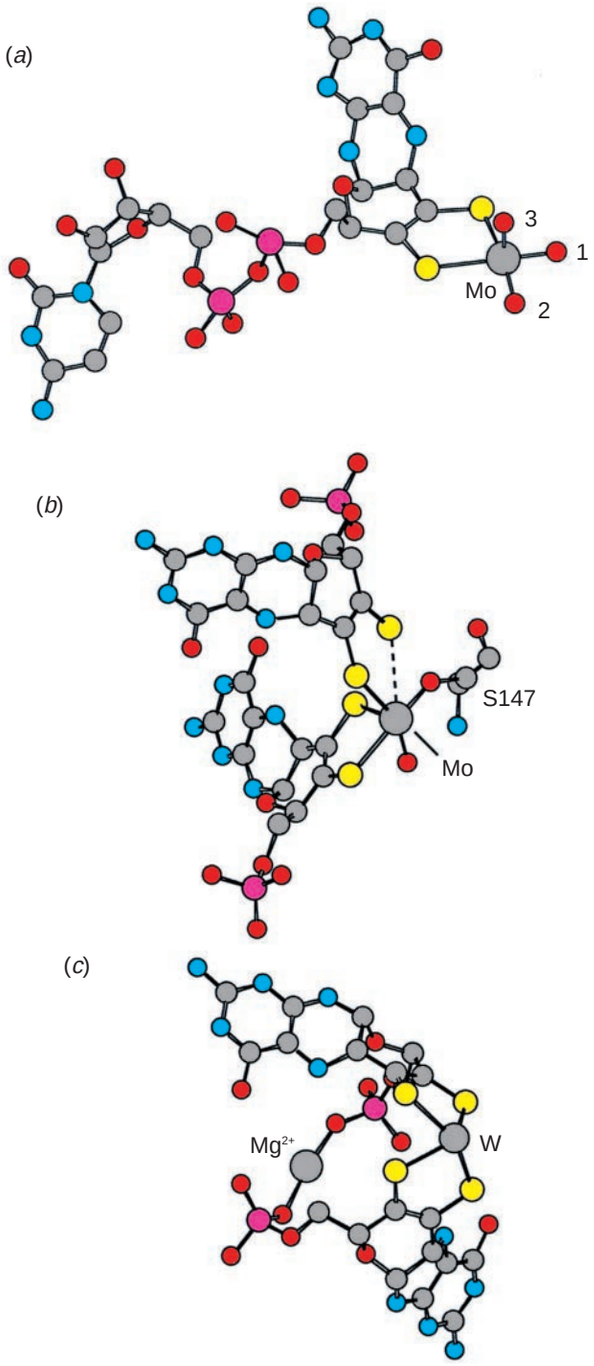



**Fig. 2** Crystal structures: representations of metal centres. Colour code: oxygen, red; nitrogen, blue; sulfur, yellow; phosphorus, magenta; metal atoms (large grey circles) are identified on the figure. (*a*) Aldehyde oxidoreductase from *Desulfovibrio gigas* (resolution = 2.25 Å): a five-coordinate site interpreted as a $Mo^{VI}O_2(OH_2)$ fragment bound to a pterin 1,2-dithiolate.[12] The ligands assigned as oxo are labelled 1 and 3 while that assigned as aqua is labelled 2. The latter has direct access to an extended solvent channel. Data at 1.8 Å resolution is now available, including that for crystals soaked in buffer containing sulfide.[13] Ligand 3 appears to be $S^{2-}$ in these latter forms. (*b*) Oxidised dimethyl sulfoxide reductase from *Rhodobacter sphaeroides* (resolution = 2.2 Å): a distorted trigonal prismatic site with a $Mo^{VI}O(OSer)$ fragment bound to two pterin 1,2-dithiolate ligands.[15] One of the latter bidentate ligands is bound asymmetrically with Mo–S distances of 2.4 and 3.1 Å. (*c*) Aldehyde oxidoreductase from *Pyrococcus furiosus* (resolution = 2.3 Å): the tungsten atom is coordinated to two pterin 1,2-dithiolate ligands whose sulfur atoms lie in an approximate square plane.[14] Two other non-protein ligands (oxo?) may be present to complete a distorted trigonal prismatic site. The two phosphate groups bind to a six-coordinate $Mg^{2+}$ ion.

## Background chemistry

High oxidation state metal-oxo chemistry is the key to catalysis of half-reaction (1) in these enzymes (for simplicity, coligands and overall charges are omitted) [eqns. (2) and (3)].

$$X + M^{VI}O \rightleftharpoons XO + M^{IV} \quad (2)$$

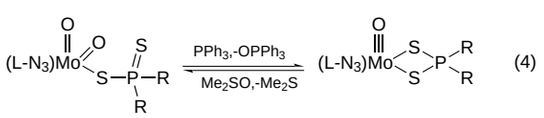
$$M^{IV} + H_2O \rightleftharpoons M^{VI}O + 2\,H^+ + 2\,e^- \quad (3)$$

$$X + H_2O \rightleftharpoons XO + 2\,H^+ + 2\,e^- \quad (1)$$

Eqn. (2) represents an oxygen atom transfer (OAT) reaction.[7,8,22] Eqn. (3) is a coupled electron–proton transfer (CEPT) reaction in which the active site is regenerated.[8,9,23] The detailed molecular mechanism employed by an enzyme varies with the nature of its substrate X.

The molybdenum enzymes seem to fall into three families, exemplified by sulfite oxidase, dimethyl sulfoxide reductase and xanthine oxidase (Scheme 1).[4]

The OAT reaction is now well established for molybdenum.[7,8,22] In particular, interconversion of *cis*-$Mo^{VI}O_2$ and $Mo^{IV}O$ complexes is promoted by a range of oxygen atom donors and acceptors *via* associative mechanisms. The ability of a dimethyl sulfoxide reductase enzyme to mediate reaction (2) in either direction has been interpreted in these terms.[24] As illustration, a structurally well characterised catalytic system based upon the trispyrazolylborate ligand L-$N_3$ [see Fig. 3(*a*) for ligand structure] is presented in eqn. (4).[25] The forward and



(4)

reverse reactions are first order with respect to both complex and substrate, consistent with bimolecular reactions involving mononuclear species. The steric bulk of ligand L-$N_3$ and the ambidentate behaviour of the dithiophosphate ligand disfavour comproportionation reaction (5) which complicates many synthetic systems.

$$Mo^{VI}O_2 + Mo^{IV}O \rightarrow [Mo^{V}O]_2(\mu\text{-}O) \quad (5)$$

The CEPT reaction depends upon π bonding in M=O systems permitting dramatic modulation of the p$K_a$ of the O atom upon change of oxidation state of metal M. Formal reduction of a *cis*-

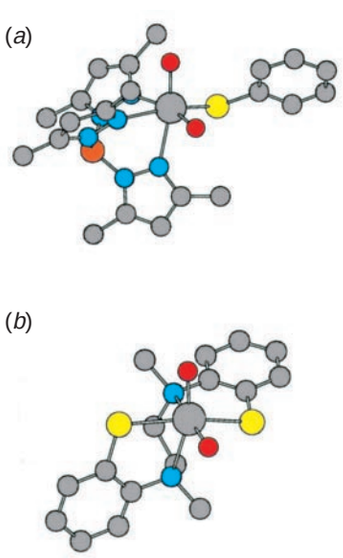



**Fig. 3** Ligands. (*a*) L-$N_3$ = hydrotris(3,5-dimethylpyrazol-1-yl)borate monoanion as present in (L-$N_3$)$MoO_2$(SPh).[36] Colour code: boron, orange. (*b*) L-$N_2S_2$ = *N*,*N*′-dimethyl-*N*,*N*′-bis(2-sulfanylphenyl)ethylenediamine dianion as present in (L-$N_2S_2$)$MoO_2$: *cis*-oxo and *trans*-thiolate ligands.[26]

$Mo^{VI}O_2$ centre increases its basicity by population of π* orbitals with significant oxo character. Simple relevant examples are provided in eqn. (6) [L = L-$N_2S_2$ or (L-$N_3$)(SPh)]; Fig. 3.[26,27]

$$LMo^{VI}O_2 + e^- \rightarrow [LMo^{V}O_2]^- \xrightarrow{H^+} LMo^{V}O(OH) \quad (6)$$

### The sulfite oxidase family: $Mo^{VI}O_2$ sites with one pterin 1,2-dithiolate ligand

A number of molybdenum pterin enzymes feature $Mo^{VI}O_2$ fragments bound to a single pterin 1,2-dithiolate [*e.g.* sulfite oxidase, assimilatory nitrate reductase; Scheme 1(b),(c)].[4] In addition, sulfite oxidase has a Mo–S–Cys linkage.[28] While active aldehyde oxidoreductase from *Desulfovibrio gigas* belongs to the [$Mo^{VI}OS$] class (*vide infra*), a crystallised form appears to contain a $Mo^{VI}O_2(OH_2)$ fragment.[12] A plausible model for the active site in sulfite oxidase would have a cysteinyl ligand substitute for $OH_2$ in position 2 of Fig. 2(*a*).

Unfortunately, catalytic intermediates are yet to be detected for enzymes in this family and so mechanism has been inferred from structural information obtained by X-ray absorption spectroscopy and EPR studies of resting forms [*e.g.* $Mo^{VI}O_2$, $Mo^{V}O(OH)$ and $Mo^{IV}O$ centres in sulfite oxidase[8]].

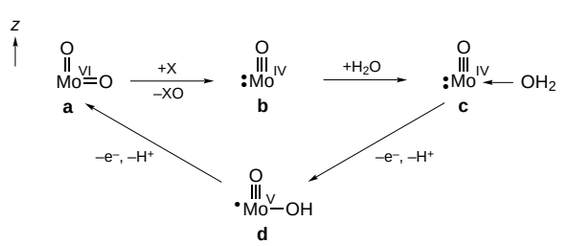
A consensus cycle has evolved in which a 'spectator' oxo ligand[29,30] controls the electronic structure allowing a second oxo ligand to participate in an OAT reaction with substrate X (Scheme 2 **a** → **b**). After coordination of ligand $H_2O$ (**b** → **c**), the catalytic site is regenerated by two CEPT steps (**c** → **d** → **a**). Reductase enzymes would cycle in the opposite direction (*cf.* assimilatory nitrate reductase[31–33]). The OAT chemistry is represented as a concerted two-electron event, the CEPT chemistry as two consecutive ($e^-$, $H^+$) transfers (rather than hydrogen-atom transfers).[34]

A synthetic model based upon $LMo^{VI}O_2Y$ (L = trispyrazolylborate ligand; Y = anionic ligand) permits fine tuning of structural and redox properties *via* variation of Y and the substituents of L.[27,34–36] In particular, complex (L-$N_3$)$Mo^{VI}$-$O_2$(SPh) [Fig. 3(*a*)] catalyses eqn. (1) (X = $PPh_3$) with $O_2$ acting as the formal oxidant.

$$PPh_3 + H_2{}^{18}O + 2O_2 \rightarrow {}^{18}OPPh_3 + 2HO_2 \quad (7)$$

Centres **a**, **b** and **d** of Scheme 2 were isolated or trapped while strong evidence for centre **c** was obtained by $^{18}O$ tracer experiments.[34] The energy profile of the cycle and its molecular mechanism have been examined theoretically.[37] Substrate $PMe_3$ is proposed to approach from a direction perpendicular to the *cis*-$MoO_2$ plane, then rotate to form intermediate $Mo^{IV}$-O($OPMe_3$) with a dihedral angle OMoOP of 0°. This imposes a $(d_{xy})^2$ configuration permitting formation of a stabilising triple bond along the *z* direction to the spectator oxo ligand (Scheme 2). Substitution of product $OPMe_3$ by $OH_2$ proceeds by an associative mechanism leading to intermediate **c**. The direction of approach of the substrate could be under tight steric control at an enzyme site.

The two CEPT steps are mediated normally by internal electron transfer to another redox enzyme site where the formal oxidant binds. In the present model system, the first CEPT step involves comproportionation between **a** and **c** (Scheme 2) to produce 2 equivalents of **d** which are then oxidised by $O_2$. The ligand steric barriers are balanced to allow hydrogen atom transfer between **a** and **c** but to disfavour formation of binuclear species [*cf.* eqn. (5)].




**Scheme 2**

The other system for which good evidence for Scheme 2 is available mimics enzymic reduction of aromatic nitro compounds, a multi-electron process [eqn. (8)].

$$ArNO_2 + 6H^+ + 6e^- \rightarrow ArNH_2 + 2\,H_2O \quad (8)$$

When intercalated into a layered double hydroxide host lattice, the $[Mo^{VI}O_2\{O_2CC(S)Ph_2\}_2]^{2-}$ ion catalyses reaction (8) cleanly.[21] An interpretation consistent with experiment has reductant PhSH inducing the initial CEPT steps (Scheme 2: **a** → **d** → **c**), followed by substitution of substrate $ArNO_2$ for ligand $H_2O$. The OAT step (**c** → **a**) then produces intermediate ArNO which is reduced directly by PhSH.

The OAT step of Scheme 2 (**a** ↔ **b**) has been demonstrated for many enzymic substrates.[7,24,38–40] For example, reduction of $[NO_3]^-$, $Me_2SO$ and $Me_3NO$ *via* electrophilic attack on $Mo^{IV}O$ has been demonstrated in systems with bi- and tridentate ligands.[7,24,38] Oxidation of $[HSO_3]^-$ is effected cleanly by $[Mo^{VI}O_2(mnt)_2]^{2-}$ (Fig. 4) in MeCN–$H_2O$.[40]

### The dimethyl sulfoxide reductase family: $Mo^{VI}O_x$ ($x$ = 1,2) sites with two pterin 1,2-dithiolate ligands

Dimethyl sulfoxide reductases had been assumed to be related to the sulfite oxidase family until recent X-ray crystallographic and absorption data for the enzyme from *Rhodobacter sphaeroides* indicated [Fig. 2(*b*)]:[15,41] (*i*) the presence of two inequivalent 1,2-dithiolate ligands. One is a symmetric bidentate ligand. The other is also bidentate but asymmetrically bound in the oxidised form and monodentate in the reduced form; (*ii*) the presence of a serine sidechain providing a Mo–alkoxo link; (*iii*) that a single oxo ligand (rather than two) is present in the oxidised form and (*iv*) that no oxo ligand (rather than one) is present in the dithionite-reduced form, and that one of the ligands is monodentate.

The situation is somewhat uncertain at the moment as two separate crystal structures of the dimethyl sulfoxide reductase from a closely related organism *R. capsulatus* suggest the presence of two oxo ligands (rather than one) in the oxidised form.[16,42] In addition, there are differences in the detail of the 1,2-dithiolate coordination modes. In one structure, both dithiolate ligands are bidentate and symmetrical,[42] while in the other, one is free and not bound to the molybdenum centre.[16] It is possible that different crystal forms have been examined.

The detailed nature of the individual sites remains to be clarified. Certainly, both $Mo^{VI}O_2$-based models and the dime-

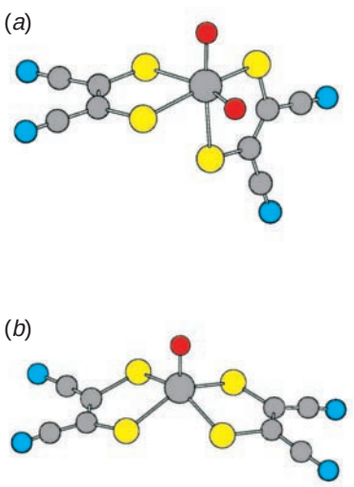



**Fig. 4** Molecular structures (M = Mo, W; mnt = dianion of 1,2-dicyano-1,2-dithioethene)[40,71,72] of (*a*) $[M^{VI}O_2(mnt)_2]^{2-}$ and (*b*) $[M^{IV}O(mnt)_2]^{2-}$

thyl sulfoxide reductase from *R. sphaeroides* can catalyse the OAT reaction (9).[7,22]

$$PR_3 + OSMe_2 \rightarrow OPR_3 + SMe_2 \quad (9)$$

This enzyme is unusual in that the molybdenum site is its sole redox site. This apparently allows efficient cycling of $PR_3$ oxidation by $Mo^{VI}$ and $OSMe_2$ reduction by $Mo^{IV}$. Equivalent processes are expected to be more difficult to achieve in other enzymes if rapid electron transfer to or from another redox site occurs after each step.

The presence of a $Mo^{VI}O$ site in the enzymes would mean that a controlling spectator oxo ligand is not necessary (*cf.* Scheme 2): the two 1,2-dithiolate ligands and their apparent ambidentate nature may impart an equivalent electronic environment. While the couple $[Mo^{VI}O_2(mnt)_2]^{2-}$–$[Mo^{IV}O(mnt)_2]^{2-}$ (Fig. 4) features two 1,2-dithiolate ligands and is active in OAT reactions, an equivalent $Mo^{VI}O$–$Mo^{IV}$ couple is not known. The $[Mo^{IV}(mnt)_3]^{2-}$ ion is known.[40,43]

Sequence homologies suggest that the serinyl ligand in dimethyl sulfoxide reductase is replaced by a cysteinyl ligand in dissimilatory nitrate reductase and in trimethylamine *N*-oxide reductase (*cf.* sulfite oxidase) and by a selenocysteinyl ligand in formate dehydrogenase.[15,44] This variation is a straightforward method of tuning the active site.

### The xanthine oxidase family: $Mo^{VI}OS$ sites with one pterin 1,2-dithiolate ligand

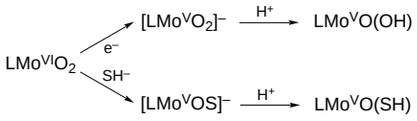
This class includes the xanthine oxidase/dehydrogenase systems [Scheme 1(*a*)] and the molybdenum aldehyde oxidoreductases which, in contrast to the other enzymes, are able to activate C–H bonds.[4,8,9] A crystal structure of the aldehyde oxidoreductase from *D. gigas* with the active site present in its hydrolysed 'desulfo' form indicates the presence of a five-coordinate site with a $Mo^{VI}O_2(OH_2)$ fragment bound to a pterin 1,2-dithiolate [Fig. 2(*a*)].[12] The aqua ligand has direct access to an extended solvent channel where substrate would be expected to bind. Structures are now available for oxidised and reduced forms of the enzyme and forms in which the thio ligand $S^{2-}$ appears to occupy the apical position in the coordination sphere.[13] X-Ray absorption spectroscopy data for the $Mo^{VI}$ and $Mo^{IV}$ levels of xanthine oxidase/dehydrogenase are consistent with $Mo^{VI}OS$ and $Mo^{IV}O(SH)$ centres. Both $Mo^{V}OS$ ('very rapid') and $Mo^{V}O(SH)$ ('rapid') centres are observed by EPR during catalytic turnover.

The complex $(L\text{-}N_3)MoOS(S_2PPr^i_2)$, synthesised with the sulfur atom donor propylene sulfide [eqn. (10)], provides a structurally characterised example of a relevant *cis*-$Mo^{VI}OS$ centre [Fig. 5(*a*)].[9,45]

$$(L\text{–}N_3)Mo^{IV}O(S_2PPr^i_2) + C_3H_6S \rightarrow (L\text{–}N_3)MoOS(S_2PPr^i_2) + MeCH{=}CH_2 \quad (10)$$

The Mo=S distance is 2.227(2) Å (compared to 2.15–2.25 Å estimated for xanthine oxidase/dehydrogenase by EXAFS) and the structure features a significant stabilising S···S interaction [2.396(3) Å] between the Mo=S and S=P functions. The apical Mo=S link observed in aldehyde oxidoreductase from *D. gigas* appears to be hydrogen bonded to a nearby histidine sidechain which may induce an equivalent stabilisation.[13]

Molybdenum(v) centres have been generated synthetically *via* Scheme 3 [L = $L\text{-}N_2S_2$ or $(L\text{-}N_3)Y$; Fig. 3) and characterised in the solid state or in solution *via* EPR hyperfine interactions in species substituted with $^2H$, $^{17}O$, $^{33}S$, $^{95}Mo$ and $^{98}Mo$.[26,27,34–36,46–48] Combination of the synthetic results with those from enzyme EPR[49,50] and single catalytic turnover experiments[51–53] led to the minimal catalytic scheme shown in Scheme 4 for xanthine oxidase/dehydrogenase under substrate limiting conditions.[9,48]




**Scheme 3**

The resting form was formulated as a *fac*-$Mo^{VI}OS(OH)$ centre.[48] This structure is supported by density functional calculations[54] and is compatible with the structural results for aldehyde oxidoreductase [Fig. 2(*a*)].[13] In this latter case, a nearby glutamic acid residue is available to act as a base for effective conversion of ligand $OH_2$ to OH during turnover. Product uric acid [Scheme 1(*a*)] bound as an anionic ligand $RO^-$ appears in both the $Mo^{IV}$ and $Mo^{V}$ (very rapid) centres of xanthine oxidase. Reduction of the resting form leads to occupation of a highly delocalised MoS $\pi_{xy}$* orbital allowing the thio ligand to become a strongly basic centre facilitating activation of the C–H bond of xanthine.[9,48]

Classification of individual steps as OAT or CEPT chemistry becomes blurred somewhat in this cycle. Generation of bound product may be classified as an OAT step while regeneration of the $Mo^{VI}$ site with $H_2O$ is a CEPT step. The state of protonation of the thio ligand and its role as a base upon reduction is also CEPT chemistry. Further complications are observed when substrate is in excess and can interact with a $Mo^{V}$ form of the enzyme generating the rapid centres [*fac*-$Mo^{V}$-O(SH)(OH)?].[4,48] A detailed molecular mechanism is still evolving.[4,13,55]

Cyanide ion inactivates xanthine oxidase/dehydrogenase under oxidising conditions to produce a 'desulfo' $Mo^{VI}O_2$ centre and $SCN^-$.[8] Complex $(L\text{-}N_3)Mo^{VI}OS(S_2PPr^i_2)$ reacts with cyanide to produce $SCN^-$ quantitatively *via* a formal sulfur atom transfer, forming $(L\text{-}N_3)Mo^{IV}O(S_2PPr^i_2)$ under dry anaerobic conditions and $(L\text{–}N_3)Mo^{VI}O_2(S_2PPr^i_2)$ in the presence of $H_2O$ and $O_2$ [eqn. (11)].[45]

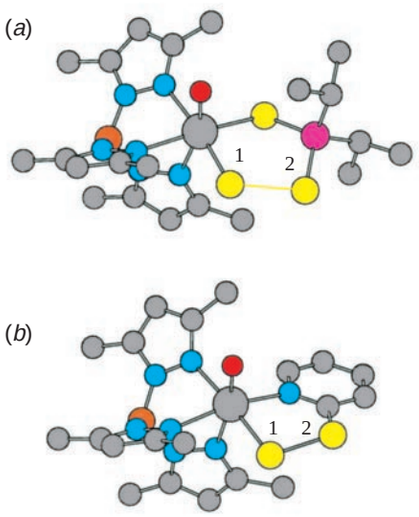
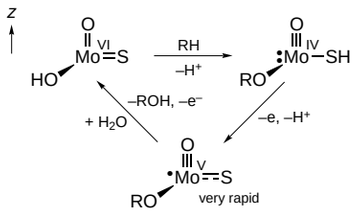



**Fig. 5** Molecular structures of (*a*) $(L\text{-}N_3)Mo^{VI}OS(S_2PPr^i_2)$[45] and (*b*) $(L\text{-}N_3)Mo^{IV}O(pyS_2)$[56]




**Scheme 4** For the very rapid centre, the Mo=S notation implies occupation of a MoS $\pi_{xy}$* orbital by the unpaired electron leading to a formal MoS bond order of 1.5[47,48]

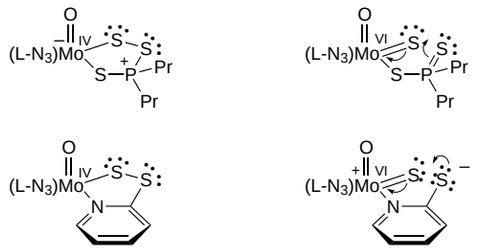
$$Mo^{VI}OS + CN^- + H_2O + O_2 \rightarrow Mo^{VI}O_2 + SCN^- + H_2O_2 \quad (11)$$

The structure of (L-$N_3$)MoO($pyS_2$), produced from (L-$N_3$)MoO(pyS) *via* a sulfur atom transfer reaction entirely similar to that of eqn. (10), is shown in Fig. 5(*b*).[56] The Mo–S and the S–S distances of 2.323(2) and 2.108(3) Å, respectively, approach those typical of a single bond (*ca.* 2.4 and 2.05 Å). The compound is best formulated as an oxodithiomolybdenum(IV) species. The alternative formulations for (L-$N_3$)$Mo^{IV}O(pyS_2)$ as a $Mo^{VI}$ species or for (L-$N_3$)$Mo^{VI}OS(S_2PPr^i_2)$ as a $Mo^{IV}$ species are less likely due to the unfavourable charge separations illustrated in Scheme 5. The redox properties of these complexes are fascinating: EPR-active $Mo^V$ species are formed upon reduction or oxidation.[56] Both (L-$N_3$)$Mo^{VI}OS(S_2PPr^i_2)$ and (L-$N_3$)$Mo^{IV}O(pyS_2)$ produce oxothiomolybdenum(V) anions upon reduction and oxodithiomolybdenum(V) cations upon oxidation (Scheme 6).

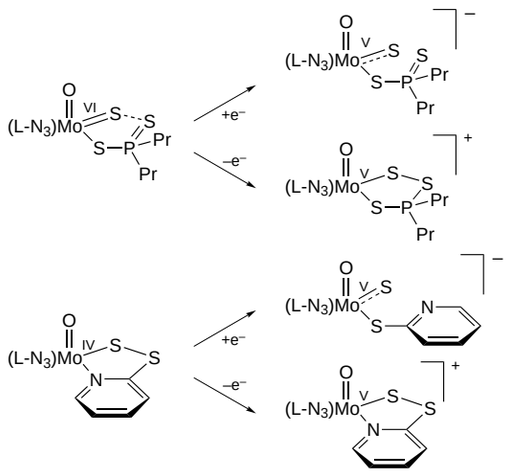
These examples highlight the facile redox interplay of molybdenum and its sulfur ligands in these systems.[57] It is apparent that the fine details of both the acid–base and redox interactions of the MoOS centre with its co-ligands (including the 1,2-dithiolate function of the pterin, in particular) and with nearby amino acid sidechains[12–16] will be crucial to a molecular understanding of each stage of catalysis in this class of enzymes.

## Tungsten enzymes

The rapid development of this field is due largely to the work of Ljungdahl, Adams, Simon and Thauer.[2,11] Tungsten enzymes are largely restricted to thermophilic organisms, which thrive in niche environments such as hot marine sediments and hydrothermal vents. In these extreme environments, the thermodynamic and kinetic attributes of tungsten appear to enhance the stability and performance of tungsten enzymes over molybdenum enzymes. The unusual biochemistry of the thermophiles is highlighted by their use of sulfur rather than dioxygen as terminal electron acceptor. However, it is in the assimilation of carbon from sources such as carbon dioxide, complex carbohydrates or proteins that the tungsten enzymes play key roles. A sample of half reactions is given in Scheme 1(e)–(g). The specific couples have very low potentials (≤400 mV *vs.* the standard hydrogen electrode[11]).



**Scheme 5**



**Scheme 6**

The best characterised enzyme is the aldehyde oxidoreductase of *Pyrococcus furiosus* [Scheme 1(e)].[58] A crystal structure has revealed a square pyramidal tungsten centre bound to two 1,2-dithiolate bidentate ligands [Fig. 2(*c*)].[14] It was not possible to identify positively the other ligands in the crystallised form. Chemical and EXAFS studies of active forms are consistent with the presence of W=O, W=S and/or W–SH functions.[58–60] These forms lose activity upon treatment with the thiophiles cyanide and arsenite. Redox titrations of active enzyme monitored by EPR suggests that some aspects of the redox chemistry may be based on the pterin ring.[61]

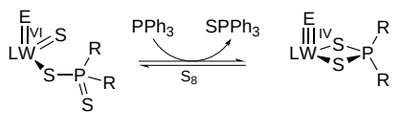
A formate dehydrogenase from *Clostridium thermoaceticum* [Scheme 1(f)] is proposed to feature selenocysteine and 1,2-dithiolate ligands [Fig. 6(*a*)].[62] The tungsten formate dehydrogenases from two *Methanobacterium* strains are resistant to cyanide inactivation.[4] Intriguingly, a molybdenum isoenzyme is not [*cf.* eqn. (11)].

Despite remarkable insights provided by EXAFS and X-ray crystallography, the detailed nature of the active sites in the tungsten enzymes remains uncertain. The presence of oxo, thio, mercapto, thiolato, selenolato and O- and N-donor ligands are all possible. The chemistry is expected to involve tungsten in oxidation states IV–VI as these dominate established compounds bearing the above ligands.

## Thiotungsten chemistry

The $W^{VI}O_2$ group is relatively unreactive and nature may exploit sulfur ligands to enhance the oxidative capacity of tungsten centres. Series of complexes featuring $W^{VI}OS$ and $W^{VI}S_2$ centres bound to ligands L-$N_3$ and L-$N_2S_2$ have been isolated using both high-valent $W^{VI}O_2$ and low-valent $W^0(CO)_x$ complexes as starting points (*e.g.* see Fig. 7).[63–66]

Under similar conditions, the reduction potentials of the $W^{VI}OS$ and $W^{VI}S_2$ complexes are 0.5–0.8 V more positive than those of the $W^{VI}O_2$ analogues and fall into the range observed for related $Mo^{VI}O_2$ species. Terminal thio ligation at $W^{VI}$ clearly facilitates reduction. The oxothio- and dithio-tungsten(VI) complexes are reducible at biologically accessible potentials whereas most of the dioxotungsten(VI) complexes are not.



(12)

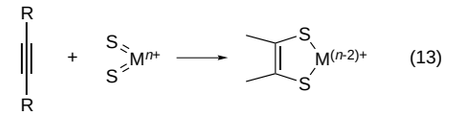
The $W^{VI}OS$ and $W^{VI}S_2$ complexes interconvert with $W^{IV}O$ and $W^{IV}S$ species by sulfur atom transfer reactions [*e.g.* eqn. (12); E = O, S; L = L-$N_3$)].

The reaction of cyanide with the $Mo^{VI}OS$ centres of xanthine oxidase/dehydrogenase and (L-$N_3$)$MoOS(S_2PR_2)$ results in the abstraction of thio ligand [eqn. (11)]. In contrast, several tungsten enzymes are not deactivated by cyanide,[4,67] and this may be interpreted to indicate the absence of thiotungsten centres in the enzymes. However, there is no reaction between (L-$N_3$)$WS_2Cl$ and $NEt_4CN$ in refluxing benzene over 24 h. The stability of this thiotungsten complex toward cyanolysis indicates that it is dangerous to dismiss the possible presence of thiotungsten centres in enzymes on the basis of their failure to react with cyanide.

## Tungsten ene-1,2-dithiolate complexes

The formate dehydrogenase enzyme from *C. thermoaceticum* is proposed to feature selenocysteine and 1,2-dithiolate ligands

[Fig. 6(*a*)]. Solutions of (L-$N_3$)$W^{VI}S_2Y$ react with alkynes to form ene-1,2-dithiolate tungsten(IV) complexes [eqn. (13)].




(13)

These remarkably facile reactions are very rapid at room temperature, even with unactivated alkynes and including acetylene. The structure of (L-$N_3$)W(OPh){$S_2C_2(CO_2Me)_2$} confirms the formation of the ene-1,2-dithiolate ligand [Fig. 6(*b*)]. The W–S bond lengths of 2.267(4) and 2.279(4) Å are considerably shorter (by 0.07 Å) than those reported previously for tungsten enedithiolates. The average W–S distance for such compounds is 2.40 Å and the W–$S_{av}$ distance for the above formate dehydrogenase is close to this average at 2.39 Å. The short W–S distances in (L-$N_3$)W(OPh){$S_2C_2(CO_2Me)_2$} are indicative of considerable $d_\pi$–$p_\pi$ bonding between the W and S atoms; the ene-1,2-dithiolate $S_2C_4$-framework is planar. Similar chemistry was recently reported for the complex [(η-$C_5Me_5$)$WS_3$]$^-$ which reacts with alkynes to give [(η-$C_5Me_5$)$WS(S_2C_2R_2)$]$^-$.[68] The complex (L-$N_3$)W(SePh){$S_2C_2$(Ph)(2-quinoxalinyl)} provides a structural and spectroscopic benchmark for the proposed site in the formate dehydrogenase [Fig. 6(*a*)]. Interestingly, it decomposes rapidly in methanolic solution in air to give (L-$N_3$)$WO_2$(OMe), diphenyldiselenide and the disulfide shown in Fig. 1(*c*). This latter species is also formed in the oxidative decomposition of [Mo{$S_2C_2$(Ph)(2-quinoxalinyl)}$_3$]$^{2-}$ in a reaction reminiscent of the formation of urothione upon degradation of the molybdenum cofactor [Fig. 1(*a*),(*b*)].[69] It is possible that degradation of pterin tungsten enzymes might produce urothione.

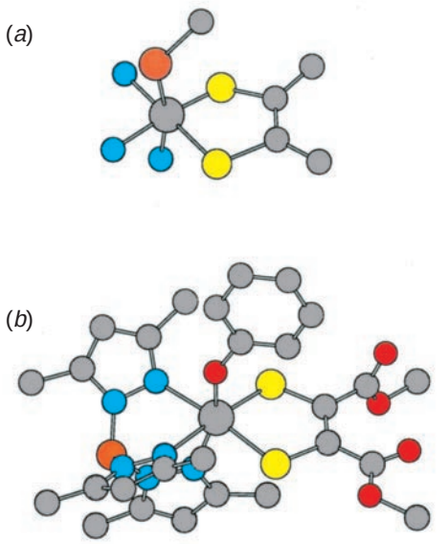



**Fig. 6** (*a*) Proposed structure at the active site of formate dehydrogenase from *Clostridium thermoaceticum*.[62] Colour code: selenium, orange. (*b*) (L-$N_3$)W(OPh){$S_2C_2(CO_2Me)_2$}.[64] Colour code: boron, orange.

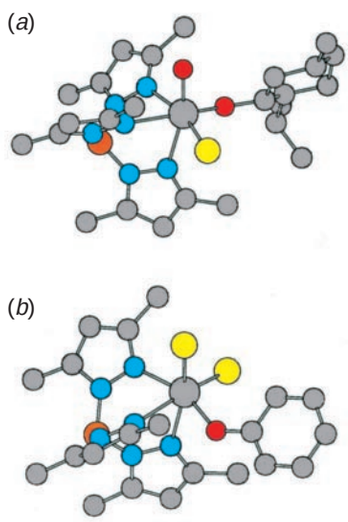



**Fig. 7** Molecular structures[64] of (*a*) (L-$N_3$)$W^{VI}$OS{(−)-mentholate} and (*b*) (L-$N_3$)$W^{VI}S_2$(OPh)

Structural and functional models for the aldehyde oxidoreductase of *P. furiosus* incorporating ene-1,2-dithiolate ligands at high-valent oxotungsten centres have been developed by Nakamura and Sarkar.[70,71] They represent exciting developments in a challenging area of coordination chemistry. The benzene-1,2-dithiolate complex $[W^{VI}O_2(bdt)_2]^{2-}$ converts benzoin to benzil [eqn. (14)].[70]

$$[W^{VI}O_2(bdt)_2]^{2-} + PhCH(OH)COPh \rightarrow [W^{IV}O(bdt)_2]^{2-} + PhCOCOPh + H_2O \quad (14)$$

The ease of this reaction contrasts with the very slow reaction of $[W^{VI}O_2(bdt)_2]^{2-}$ with $PPh_3$ and suggests that reduction of $W^{VI}O_2$ centres may be facilitated by CEPT rather than OAT reactions. Recently, the interconversion of anions $[W^{VI}O_2(mnt)_2]^{2-}$, $[W^{IV}O(mnt)_2]^{2-}$ (Fig. 4) and $[W^{VI}O(\eta^2\text{-}S_2)(mnt)_2]^{2-}$ in enzymatically relevant reactions, such as the oxidation of aldehydes to carboxylic acids, has been demonstrated.[71] The stoichiometries of these bis(ene-1,2-dithiolate)tungsten(VI) complexes are similar to the centre revealed in the aldehyde oxidoreductase [Fig. 2(*c*)] although their coordination geometries deviate from the proposed trigonal-prismatic structure at the enzyme centre. The effects of such variations on the chemistry of the tungsten centres remains to be assessed.

## Conclusions

The recent enzyme crystal structures emphasise the structural diversity available to a cofactor ligand such as the pterin 1,2-dithiolate centre. Further refinement of these structures and the anticipation of new ones in the near future (formate dehydrogenase; xanthine oxidase and dehydrogenase) will further illuminate the fundamental chemistry.

This article has but touched the surface of the chemical diversity exhibited by the molybdenum and tungsten enzymes. This diversity follows from variation of metal, ligand (oxo → thio; serine → cysteine → selenocysteine), pterin redox level and interaction with protein sidechains. Investigations will move to a new sophistication *via* synergy between the enzyme structural work, active site modification by site-directed mutagenesis and continuing development of the fundamental chemistry.


## Acknowledgements

Much of the authors' work in this area has been supported by generous grants from the Australian Research Council.


## Footnotes


† E-mail: t.wedd@chemistry.unimelb.edu.au
c.g.young@chemistry.unimelb.edu.au


‡ Abbreviations: bdt = dianion of benzene-1,2-dithiol, *C.* = *Clostridium*, CEPT = coulpled electron proton transfer, *D.* = *Desulfovibrio*, EXAFS = extended X-ray absorption fine structure, FeMoco = iron-molybdenum cofactor of nitrogenase, L-$N_2S_2$ = dianion of *N*,*N*′-dimethyl-*N*,*N*′-bis(2-sulfanylphenyl)ethylenediamine, L-$N_3$ = hydrotris(3,5-dimethylpyrazol-1-yl)borate anion, mnt = dianion of 1,2-dicyano-1,2-dithioethene, Moco = molybdenum pterin cofactor; OAT = oxygen atom transfer, *P.* = *Pyrococcus*, *R.* = *Rhodobacter*, pyS = anion of

pyridyl-2-thiol, $pyS_2$ = anion of pyridyl-2-dithiol, X = reduced substrate, Y = monoanionic ligand.

This ChemComm is also available in enhanced multi-media format *via* the World Wide Web: http://chemistry.rsc.org/rsc/cccenha.htm

**Charles Young is Reader in Chemistry at the University of Melbourne. After receiving a PhD degree from the Australian National University, he held postdoctoral appointments at the University of British Columbia and at the University of Arizona. He lectured at La Trobe University before joining the University of Melbourne in 1991. He received the Distinguished Young Chemist Award of the Federation of Asian Chemical Societies in 1995.**

**Anthony Wedd is Professor of Chemistry at the University of Melbourne. He received a PhD degree from the University of Tasmania in 1968. He joined La Trobe University in 1971 and came to the University of Melbourne in 1991.**

## References


1 J. R. R. Frausto da Silva and R. J. P. Williams, *The Biological Chemistry of the Elements*, Clarendon, Oxford, 1991, pp. 3–22 and references therein.
2 M. W. W. Adams, in *Encyclopedia of Inorganic Chemistry*, ed. R. B. King, Wiley, Chichester, UK, 1994, pp. 4284–4291.
3 *Molybdenum Enzymes, Cofactors and Model Systems*, ed. E. I. Stiefel, D. Coucouvanis and W. E. Newton, ACS Symp. Ser. 535, American Chemical Society, Washington, DC, 1993.
4 R. Hille, *Chem. Rev*., 1996, **96**, 2757.
5 J. C. Hilton and K. V. Rajagopalan, *Arch. Biochem. Biophys*., 1996, **325**, 149, and references therein.
6 D. Collison, C. D. Garner and J. A. Joule, *Chem. Soc. Rev*., 1996, 25.
7 R. H. Holm, *Coord. Chem. Rev*., 1990, **100**, 183.
8 J. H. Enemark and C. G. Young, *Adv. Inorg. Chem*., 1993, **40**, 1.
9 C. G. Young and A. G. Wedd, in *Encyclopedia of Inorganic Chemistry*, ed. R. B. King, Wiley, Chichester, UK, 1994, pp. 2330–2346.
10 J. C. Wootton, R. E. Nicolson, J. M. Cock, D. E. Walters, J. F. Burke, W. A. Doyle and R. C. Bray, *Biochim. Biophys. Acta*, 1991, **1057**, 157.
11 A. Kletzin and M. W. W. Adams, *FEMS Microbiol. Rev*., 1996, **18**, 5.
12 M. J. Ramao, M. Archer, I. Moura, J. J. G. Moura, J. LeGall, R. Engh, M. Schneider, P. Hof and R. Huber, *Science*, 1995, **270**, 1170.
13 R. Huber, P. Hof, R. O. Duarte, J. J. G. Moura, I. Moura, M.-Y. Liu, J. LeGall, R. Hille, M. Archer and M. J. Ramao, *Proc. Natl. Acad. Sci. USA*, 1996, **93**, 8846.
14 M. K. Chan, W. Mukund, A. Kletzin, M. W. W. Adams and D. C. Rees, *Science*, 1995, **267**, 1463.
15 H. Schindelin, C. Kisker, J. Hilton, K. V. Rajagopalan and D. C. Rees, *Science*, 1996, **272**, 1615.
16 F. Schneider, J. Löwe, R. Huber, H. Schindelin, C. Kisker and J. Knäblein, *J. Mol. Biol*., 1996, **263**, 53.
17 L. S. Meriwether, W. F. Marzluff and W. G. Hodgson, *Nature*, 1966, **212**, 465.
18 R. C. Bray and L. S. Meriwether, *Nature*, 1966, **212**, 467.
19 S. R. Ellis, D. Collison, C. D. Garner and W. Clegg, *J. Chem. Soc., Chem. Commun*., 1986, 1483.
20 G. R. Hanson, A. A. Brunette, A. C. McDonnell, K. S. Murray and A. G. Wedd, *J. Am. Chem. Soc*., 1981, **103**, 1953.
21 A. Cervilla, A. Corma, V. Fornes, E. Llopis, F. Perez, F. Rey and A. Ribera, *J. Am. Chem. Soc*., 1995, **117**, 6781.
22 B. E. Schultz, R. Hille, and R. H. Holm, *J. Am. Chem. Soc*., 1995, **117**, 827.
23 E. I. Stiefel, *Proc. Natl. Acad. Sci. USA*, 1973, **70**, 988.
24 B. E. Schultz, S. F. Gheller, M. C. Muetterties, M. J. Scott and R. H. Holm, *J. Am. Chem. Soc*., 1993, **115**, 2714.
25 S. A. Roberts, C. G. Young, W. E. Cleland, Jr., R. B. Ortega and J. H. Enemark, *Inorg. Chem*., 1988, **27**, 3044.
26 D. Dowerah, J. T. Spence, R. Singh, A. G. Wedd, G. L. Wilson, F. Farchione, J. H. Enemark, J. Kristofzski and M. Bruck, *J. Am. Chem. Soc*., 1987, **109**, 5655.
27 Z. Xiao, R. W. Gable, A. G. Wedd and C. G. Young, *J. Am. Chem. Soc*., 1996, **118**, 2912.
28 G. N. George, R. M. Garrett, R. C. Prince and K. V. Rajagopalan, *J. Am. Chem. Soc*., 1996, **118**, 8588.
29 A. K. Rappe and W. A. Goddard, III, *Nature*, 1980, **285**, 311.
30 A. K. Rappe and W. A. Goddard, III, *J. Am. Chem. Soc*., 1982, **104**, 448.
31 C. D. Garner, M. R. Hyde, F. E. Mabbs and V. I. Routledge, *Nature*, 1974, **252**, 579.
32 C. D. Garner, M. R. Hyde and F. E. Mabbs, *Nature*, 1975, **253**, 623.
33 M. W. W. Adams and L. E. Mortenson, in *Molybdenum Enzymes*, ed. T. G. Spiro, Wiley-Interscience, New York, 1985, pp. 519–593.
34 Z. Xiao, M. A. Bruck, J. H. Enemark, C. G. Young and A. G. Wedd, *Inorg. Chem*., 1996, **35**, 7508.
35 Z. Xiao, C. G. Young, J. H. Enemark and A. G. Wedd, *J. Am. Chem. Soc*., 1992, **114**, 9194.
36 Z. Xiao, M. A. Bruck, C. Doyle, J. H. Enemark, C. Grittini, R. W. Gable, A. G. Wedd and C. G. Young, *Inorg. Chem*., 1995, **34**, 5950.
37 M. A. Pietsch and M. B. Hall, *Inorg. Chem*., 1996, **35**, 1273.
38 J. A. Craig and R. H. Holm, *J. Am. Chem. Soc*., 1989, **111**, 2111.
39 H. Oku, N. Ueyama, M. Kondo and A. Nakamura, *Inorg. Chem*., 1994, **33**, 209.
40 S. K. Das, P. K. Chaudhury, D. Biswas and S. Sarkar, *J. Am. Chem. Soc*., 1994, **116**, 9061.
41 G. N. George, J. Hilton and K. V. Rajagopalan, *J. Am. Chem. Soc*., 1996, **118**, 1113.
42 S. Bailey, A. S. McAlpine, E. M. H. Duke, N. Benson and A. G. McEwan, *Acta Crystallogr., Sect. D*, 1996, **52**, 194; G. R. Hanson and A. G. McEwan, personal communication, October, 1996.
43 G. F. Brown and E. I. Stiefel, *Inorg. Chem*., 1973, **12**, 2140.
44 V. N. Gladyshev, S. V. Khangulov, M. J. Axley and T. C. Stadtman, *Proc. Natl. Acad. Sci. USA*, 1994, **91**, 7708.
45 A. A. Eagle, L. J. Laughlin, C. G. Young and E. R. T. Tiekink, *J. Am. Chem. Soc*., 1992, **114**, 9195.
46 G. L. Wilson, M. Kony, E. R. T. Tiekink, J. R. Pilbrow, J. T. Spence and A. G. Wedd, *J. Am. Chem. Soc*., 1988, **110**, 6923.
47 G. L. Wilson, R. J. Greenwood, J. R. Pilbrow, J. T. Spence and A. G. Wedd, *J. Am. Chem. Soc*., 1991, **113**, 6803.
48 R. J. Greenwood, G. L. Wilson, J. R. Pilbrow and A. G. Wedd, *J. Am. Chem. Soc*., 1993, **115**, 5385.
49 R. C. Bray, *Adv. Enzymol. Relat. Areas Mol. Biol*., 1980, **51**, 107.
50 G. N. George and R. C. Bray, *Biochemistry*, 1988, **27**, 3603.
51 R. Hille and H. Sprecher, *J. Biol. Chem*., 1987, **262**, 10 914.
52 R. B. McWhirter and R. Hille, *J. Biol. Chem*., 1991, **266**, 23 724.
53 J. H. Kim and R. Hille, *J. Biol. Chem*., 1993, **268**, 44.
54 M. R. Bray and R. J. Deeth, *Inorg. Chem*., 1996, **35**, 5720.
55 B. D. Howes, R. C. Bray, R. L. Richards, N. A. Turner, B. Bennett and D. J. Lowe, *Biochemistry*, 1996, **35**, 1432.
56 J. P. Hill, L. J. Laughlin, R. W. Gable and C. G. Young, *Inorg. Chem*., 1995, **35**, 3447.
57 E. I. Stiefel, in *Comprehensive Coordination Chemistry*, ed. G. Wilkinson, Pergamon, Oxford, 1987, pp. 1375–1420.
58 S. Mukund and M. W. W. Adams, *J. Biol. Chem*., 1991, **266**, 14 208.
59 G. N. George, R. C. Prince, S. Mukund and M. W. W. Adams, *J. Am. Chem. Soc*., 1992,. **114**, 3521.
60 G. N. George, personal communication, July, 1996.
61 A. F. Arendsen, M. de Vocht, Y. B. M. Bulsink and W. R. Hagen, *J. Biol. Inorg. Chem*., 1996, **1**, 292.
62 S. P. Cramer, C.-L. Liu, L. E. Mortenson, J. T. Spence, S.-M. Liu, I. Yamamoto and L. G. Ljungdahl, *J. Inorg. Biochem*., 1985, **23**, 119.
63 A. A. Eagle, E. R. T. Tiekink and C. G. Young, *J. Chem. Soc., Chem. Commun*., 1991, 1746.
64 A. A. Eagle, S. M. Harben, E. R. T. Tiekink and C. G. Young, *J. Am. Chem. Soc*., 1994, **116**, 9749.
65 S. Thomas, E. R. T. Tiekink and C. G. Young, *Organometallics*, 1996, **15**, 2428.
66 K. R. Barnard, R. W. Gable and A. G. Wedd, *J. Biol. Inorg. Chem*., submitted: complexes $(L\text{-}N_2S_2)WO_2$, $(L\text{-}N_2S_2)WOS$ and $(L\text{-}N_2S_2)WS_2$ have been characterised structurally.
67 P. A. Bertram, M. Karrasch, R. A. Schmitz, R. Bocher, S. P. J. Albracht and R. K. Thauer, *Eur. J. Biochem*., 1994, **220**, 477.
68 H. Kawaguchi and K. Tatsumi, *J. Am. Chem. Soc*., 1995, **117**, 3885.
69 C. L. Soricelli, V. A. Szalai and S. J. N. Burgmayer, *J. Am. Chem. Soc*., 1991, **113**, 9877.
70 N. Ueyama, H. Oku and A. Nakamura, *J. Am. Chem. Soc*., 1992, **114**, 7310.
71 S. K. Das, D. Biswas, R. Maiti and S. Sarkar, *J. Am. Chem. Soc*., 1996, **118**, 1387.
72 B. Götz, F. Knoch and H. Kisch, *Chem. Ber*., 1996, **1**, 33.


*6/06660G*

# A tetranuclear cluster sandwiched between edge-bridging cycloheptatrienyl rings: the synthesis and characterisation of $[Ru_4(CO)_7(\mu\text{-}C_7H_7)_2]$

**Dario Braga,[a] Paul J. Dyson,[b] Fabrizia Grepioni,*[a] Brian F. G. Johnson,*[c] Caroline M. Martin,[c] Laura Scaccianoce[c] and Alexander Steiner[d]**

[a] *Dipartimento di Chimica G. Ciamician, Università di Bologna, Via Selmi 2, 40126 Bologna, Italy*
[b] *Department of Chemistry, Imperial College of Science, Technology and Medicine, South Kensington, London, UK SW7 2AY*
[c] *Department of Chemistry, The University of Cambridge, Lensfield Road, Cambridge, UK CB2 1EW*
[d] *Department of Chemistry, The University of Liverpool, Liverpool, UK L69 3BX*

**The reaction of $[Ru_3(CO)_{12}]$ with cycloheptatriene affords $[Ru_4(CO)_7(\mu\text{-}C_7H_7)_2]$ an example of a new class of sandwich cluster which is characterised in the solid-state by single-crystal X-ray diffraction and shown to contain an unusual arrangement of two parallel edge-bridging organic rings.**

The metallocenes and other related sandwich complexes have caught the imagination of chemists since their initial discovery and continue to play an important role in the development of the subject.[1] Over the years sandwich compounds have found applications in a number of areas of technological importance.[2] For some time we have been interested in incorporating clusters of metal atoms between decks of organic rings and have made a number of sandwich clusters in which an octahedral ruthenium unit is sandwiched between two arene rings which bond to single metal atoms of the octahedron.[3–6] A further goal has been to sandwich a cluster between two face-capping rings and while this is yet to be realised a number of clusters containing one face-capping and one terminally coordinated ring have been prepared. However, in these compounds the arenes are not parallel to one another.[7–11] Here, we report the synthesis and full characterisation of a highly unusual tetranuclear cluster, in which a $Ru_4$ tetrahedron is sandwiched between two parallel edge-bridging cycloheptatrienyl rings. As such this represents a new class of sandwich compound.

The ligand-exchange reaction between $[Ru_3(CO)_{12}]$ and $[Mo(CO)_3(\eta^6\text{-}C_7H_8)]$ produced a number of products including green $[Ru_4(CO)_7(\mu\text{-}C_7H_7)_2]$ **1** in 10% yield which has been fully characterised by spectroscopy† and single-crystal X-ray crystallography.‡ Higher yields were subsequently obtained from the direct reaction of $[Ru_3(CO)_{12}]$ and cycloheptatriene.§

The structure of **1** is shown in Fig. 1 and constitutes an unprecedented example of a sandwich compound in which a tetranuclear $Ru_4$ cluster is encapsulated between two cycloheptatrienyl ligands. The ligands edge-bridge two non-contiguous Ru–Ru bonds on the tetrahedron. The Ru–C distances are in the range 1.900(9)–2.663(8) Å; the shortest bonds being with atoms C(3) and C(4) and C(2′) and C(5′) which lie just above the two pairs of Ru atoms. The almost flat rings (maximum elevation from the mean plane 0.14 Å) formally donate seven electrons to the cluster, and the bonding may be described formally as $\mu\text{-}\eta^4:\eta^3$. The $^1$H NMR spectrum in $CDCl_3$ exhibits one signal at $\delta$ 4.18 which may be taken to indicate that all the protons are equivalent on the NMR timescale suggesting the rings rotate freely in solution.

The structure is disordered in the solid state with a crystallographic twofold axis relating the two cycloheptatrienyl rings and generating two interpenetrating images of the cluster core. This disorder is reminiscent of that present in $[Co_4(CO)_{12}]$[12,13] and $[Fe_3(CO)_{12}]$.[14–16] As with these cases, the

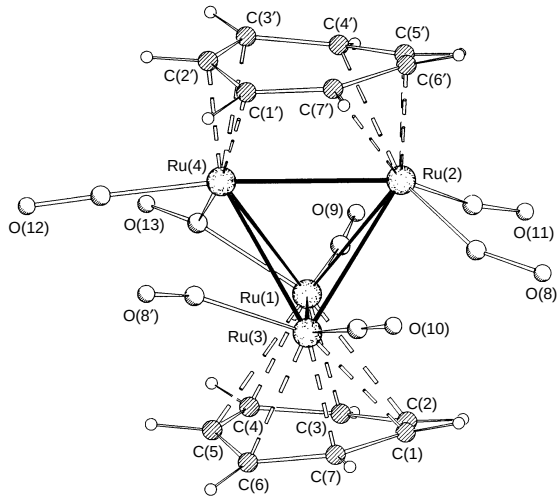



**Fig. 1** The molecular structure of **1** in the solid state showing the atomic labelling scheme, the O atoms of the carbonyl ligands bear the same numbering as their corresponding C atoms. Relevant bond lengths (Å): Ru(1)–Ru(2) 2.853(2), Ru(1)–Ru(3) 2.728(2), Ru(1)–Ru(4) 2.745(1), Ru(2)–Ru(3) 2.868(2), Ru(2)–Ru(4) 2.731(2), Ru(3)–Ru(4) 2.810(2), Ru(1)–C(2) 2.468(9), Ru(1)–C(3) 2.007(8), Ru(1)–C(4) 1.950(8), Ru(1)–Ru(5) 2.663(8), Ru(3)–C(1) 2.384(7), Ru(3)–C(6) 2.247(7), Ru(3)–C(7) 1.926(10), Ru(2)–C(4′) 2.465(8), Ru(2)–C(5′) 1.915(11), Ru(2)–C(6′) 2.175(7), Ru(2)–Ru(7′) 2.639(7), Ru(4)–C(1′) 2.183(7), Ru(4)–C(2′) 1.900(9), Ru(4)–C(3′) 2.332(8), C(1)–C(2) 1.411(1), C(1)–C(7) 1.372(11), C(2)–C(3) 1.330(11), C(3)–C(4) 1.442(11), C(4)–C(5) 1.325(11), C(5)–C(6) 1.426(11), C(6)–C(7) 1.368(11), Ru(2)–C(8) 1.849(8), Ru(3)–C(8′) 1.993(10), Ru(1)–C(9) 1.86(2), Ru(3)–Ru(10) 1.88(2), Ru(2)–C(11) 1.86(2), Ru(4)–C(12) 1.84(2), Ru(1)–C(13) 2.012(13), Ru(4)–C(13) 2.193(13), C(8)–O(8) 1.143(10), C(8′)–O(8′) 1.143(10), C(9)–O(9) 1.14(2), C(10)–O(10) 1.14(2), C(11)–O(11) 1.13(2), C(12)–O(12) 1.13(2), C(13)–O(13) 1.15(2).

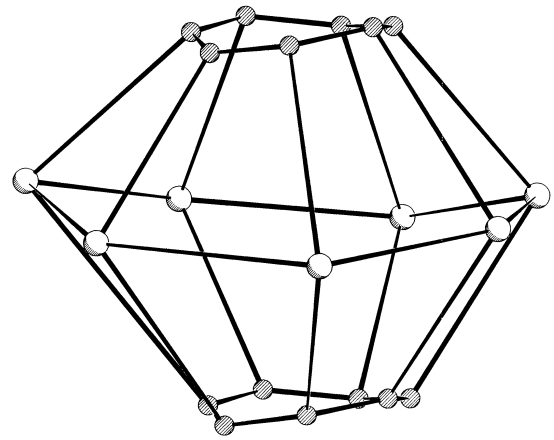


**Fig. 2** The ligand polyhedron formed by the two opposite cycloheptatrienyl ligands and by the seven O atoms of the CO ligands

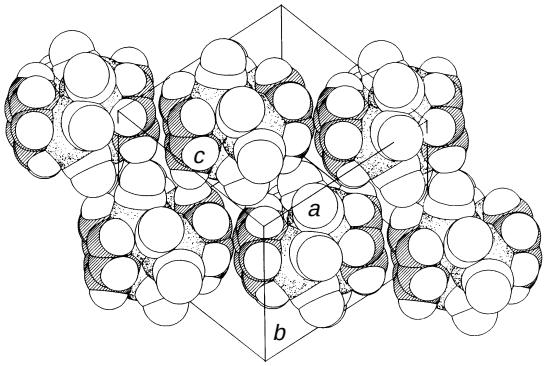



**Fig. 3** Space-filling representation of the molecular piles in the crystal structure of **1**

disorder arises from the invariance of the outer ligand polyhedron with respect to the orientation of the inner cluster unit. The ligand polyhedron is novel and Fig. 2 shows that it corresponds to a hexadecahedron formed by the two opposite cycloheptatrienyl ligands and the 'belt' of seven CO groups. Diffraction data were of sufficient quality to allow resolution of all separate images of the ligand atoms excluding C(8)O(8).

A further point of interest resides in the molecular arrangement in the solid state. Molecules pile along the 101 diagonal of the cell with direct interactions between the rings (mean distance between the ring planes 3.46 Å). This packing arrangement is illustrated in Fig. 3. Similar packing arrangements have been observed for other cluster–arene systems.[17]

We would like to thank the Royal Society for a University Research Fellowship (P. J. D.), MURST (D. B. and F. G.), the EPSRC and the EU for financial support.

## Footnotes

* E-mail: bfgj1@cam.ac.uk

† *Spectroscopic data* for **1**: IR $\nu_{CO}$ ($CH_2Cl_2$) 1961vs, 1813m $cm^{-1}$; $^1H$ NMR ($CDCl_3$) $\delta$ 4.18 (s).

‡ *Structural data* for **1**: $C_{21}H_{14}O_7Ru_4$, $M$ = 782.60, monoclinic, space group = $C2/c$, $a$ = 13.083(4), $b$ = 12.692(4), $c$ = 12.945(3) Å, $\beta$ = 93.22(2)°, $U$ = 2146.1(11) Å$^3$, $Z$ = 4, $D_c$ = 2.422 g $cm^{-3}$, $F(000)$ = 1488, crystal dimensions 0.18 × 0.16 × 0.16 mm, $2\theta_{max}$ = 50°, $\lambda$(Mo-Kα) = 0.710 69 Å, $\mu$(Mo-Kα) = 2.803 $mm^{-1}$, refinement on $(F_0)^2$ for 1886 data and 208 parameters, $wR_2$ = 0.1456 (all data), conventional $R$ = 0.0434. H-atoms were placed in geometrically calculated positions. The program SHELX 93 was used for the structure solution and refinement.[18] On decreasing the temperature to 223 K the orientation matrix is lost and the crystal diffracts poorly. This may indicate the occurrence of a phase transition, possibly associated with metal-frame reorientation, as observed in other carbonyl clusters.[19] Work is in progress to fully assess the phenomenon. Atomic coordinates, bond lengths and angles, and thermal parameters have been deposited at the Cambridge Crystallographic Data Centre (CCDC). See Information for Authors, Issue No. 1. Any request to the CCDC for this material should quote the full literature citation and the reference number 182/479.

§ *Synthesis* of **1**: $Ru_3(CO)_{12}$ (0.1 g) and cycloheptatriene (0.5 ml) were dissolved in dry octane (30 ml) and heated to reflux for 5 h and the reaction mixture turned dark brown. The solvent was removed under reduced pressure and the residue dissolved in a minimum amount of $CH_2Cl_2$ and the products purified by TLC on silica plates using $CH_2Cl_2$–hexane (1 : 4, v/v) as the eluent. The dark green band was removed and the product extracted into $CH_2Cl_2$ and characterised as **1** (50%).

## References

1 For example, see: *Advanced Inorganic Chemistry*, ed. F. A. Cotton and G. Wilkinson, Wiley, Chichester, 5th edn., 1988.
2 *Ferrocenes: homogeneous catalysis, organic synthesis, materials science*, ed. A. Togni and T. Hayashi, VCH, Weinheim, 1995.
3 D. Braga, F. Grepioni, S. Righi, B. F. G. Johnson, P. J. Bailey, P. J. Dyson, J. Lewis and M. Martinelli, *J. Chem. Soc., Dalton Trans.*, 1992, 2121.
4 R. D. Adams and W. Wu, *Polyhedron*, 1992, **2**, 2123.
5 D. Braga, F. Grepioni, C. M. Martin, E. Parisini, P. J. Dyson and B. F. G. Johnson, *Organometallics*, 1994, **13**, 2170.
6 P. J. Dyson, B. F. G. Johnson, D. Braga, F. Grepioni, C. M. Martin and E. Parisini, *Inorg. Chim. Acta*, 1995, **235**, 413.
7 M. P. Gomez-Sal, B. F. G. Johnson, J. Lewis, P. R. Raithby and A. H. Wright, *J. Chem. Soc., Chem. Commun.*, 1985, 1682.
8 P. J. Dyson, B. F. G. Johnson, D. Reed, D. Braga, F. Grepioni and E. Parisini, *J. Chem. Soc., Dalton Trans.*, 1993, 2817.
9 D. Braga, F. Grepioni, E. Parisini, P. J. Dyson, B. F. G. Johnson, D. Reed, D. S. Shepherd, P. J. Bailey and J. Lewis, *J. Organomet. Chem.*, 1993, **462**, 301.
10 P. J. Dyson, B. F. G. Johnson, C. M. Martin, A. J. Blake, D. Braga, F. Grepioni and E. Parisini, *Organometallics*, 1994, **13**, 2113.
11 S. L. Ingham, B. F. G. Johnson and J. G. M. Nairn, *J. Chem. Soc., Chem. Commun.*, 1995, 189.
12 C. H. Wei, *Inorg. Chem.*, 1969, **8**, 2384.
13 F. H. Carré, F. A. Cotton and B. A. Frenz, *Inorg. Chem.*, 1976, **15**, 380.
14 C. H. Wei and L. F. Dahl, *J. Am. Chem. Soc.*, 1969, **91**, 1351.
15 F. A. Cotton and J. M. Troup, *J. Am. Chem. Soc.*, 1974, **96**, 4155.
16 D. Braga, F. Grepioni, B. F. G. Johnson and L. Farrugia, *J. Chem. Soc., Dalton Trans.*, 1994, 2911.
17 D. Braga, P. J. Dyson, F. Grepioni and B. F. G. Johnson, *Chem. Rev.*, 1994, **94**, 1585.
18 G. M. Sheldrick, SHELX 93, Program for Crystal Structure Determination, University of Göttingen, 1993.
19 D. Braga, L. J. Farrugia, A. L. Gillon, F. Grepioni, and E. Tedesco, *Organometallics*, 1996, **15**, 4684.

*Received in Cambridge, UK, 10th April 1997; Com. 7/02448G*

# Vanadium complexes of the $N(CH_2CH_2S)_3^{3-}$ ligand with co-ligands relevant to nitrogen fixation processes

**Sian C. Davies,[a] David L. Hughes,[a] Zofia Janas,[b] Lucjan Jerzykiewicz,[b] Raymond L. Richards,*[a] J. Roger Sanders*[a] and Piotr Sobota[b]**

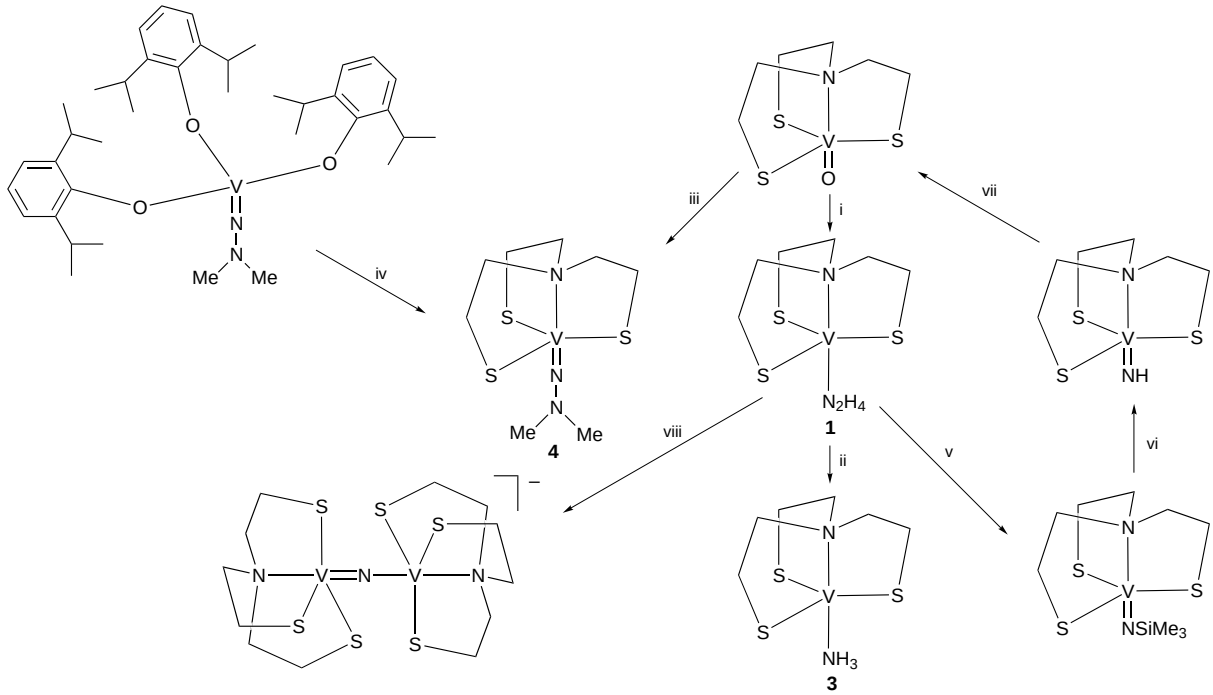
[a] *Nitrogen Fixation Laboratory, John Innes Centre, Colney Lane, Norwich, UK NR4 7UH*
[b] *Faculty of Chemistry, University of Wroclaw, 14 F. Joliot-Curie Street, 50-383 Wroclaw, Poland*

**Vanadium(III) and vanadium(V) complexes of the tris(2-thiolatoethyl)amine ligand $L^{3-}$ containing hydrazine, hydrazide, imide, ammine, cyanide and isocyanide ligands are synthesised; the complexes $[V(NH_3)L]$ and $[V(NNMe_2)L]$ have been structurally characterised.**

The cofactor of molybdenum nitrogenase contains an $MoFe_7S_9$ cluster with the Mo atom ligated by one nitrogen, three sulfurs and two oxygens[1] and it is thought that the vanadium atom in the analogous vanadium nitrogenase[2] is in a similar environment, as is possibly one of the iron atoms in the third 'iron-only' nitrogenase.[3] The chemistry of V, Mo and Fe centres which carry three sulfurs (plus other ligands) ($MS_3$ sites) is therefore of great importance in understanding the mode of action of these enzymes. In particular, reduction of $N_2$ to $NH_3$ might involve intermediate species $N_2H_m$ and $NH_n$ ($m$ = 0–4, $n$ = 0–3) bound at $MS_3$ sites.[4] Here we report use of the ligand $N(CH_2CH_2S)_3^{3-}$ [$L^{3-}$] to generate a range of complexes of $N_2H_m$ and $NH_n$ and related ligands at $MS_3$ sites, particularly for vanadium, where there is very limited chemistry of reduced nitrogen species at this metal in a sulfur-donor environment.[4,5] Key reactions to generate the vanadium series are shown in Scheme 1. All compounds described in this paper have been characterised by microanalysis and magnetic and spectroscopic data.

Treatment of $[VO(L)]$[6] with four equivalents of anhydrous hydrazine in acetonitrile removes the oxide ligand to give an almost quantitative yield of the complex $[V(NH_2NH_2)L]$ **1** as an insoluble yellow powder. When **1** is heated in suspension in tetrahydrofuran a decomposition/disproportionation reaction takes place giving a dark green, poorly soluble precipitate of composition VL **2** and a yellow solution from which $[V(NH_3)L]$ **3** crystallises on cooling. The structure of **3** is shown in Fig. 1.† The geometry around the V atom is trigonal bipyramidal with the S atoms in equatorial positions and N(4)–V–N(5) almost linear. The V–N(4) bond distance [2.155(8) Å] in **3** is considerably shorter than the corresponding distance in $[VO(L)]$[6] [2.291(6) Å], presumably reflecting the high *trans*-influence of the oxide ligand of $[VO(L)]$ relative to the $NH_3$ ligand in **3**. Individual molecules of **3** are held in chains by hydrogen bonds between the three hydrogen atoms of the ammine ligand and the S atoms of neighbouring molecules.

The formation of **1** probably involves a hydrazide intermediate such as $[V(NNH_2)L]$, since treatment of $[VO(L)]$ with $Me_3SiNHNMe_2$ gives diamagnetic $[V(NNMe_2)L]$ **4**, whose X-ray structure is shown in Fig. 2.† As far as we are aware, this is the first hydrazide of vanadium with sulfur-donor co-ligands. Compound **4** can also be prepared from $[V(OC_2H_3Pr^i_2\text{-}2,6)_3(NNMe_2)]$.[7] The V–$NNMe_2$ distance in **4** is shorter than the




**Scheme 1** *Reagents and conditions*: i, 4 equiv. $N_2H_4$, MeCN, 20 °C; ii, thf, 60 °C; iii, $Me_3SiNHNMe_2$, $CH_2Cl_2$, 20 °C; iv, 1.5 equiv. $H_3L$, hexane, 20 °C; v, excess $N_3SiMe_3$, MeCN, 80 °C; vi, MeCN–$H_2O$, 20 °C; vii, $NMe_4OH$, MeOH, 60 °C, 10 min, then HCl–$Et_2O$; viii, $NEt_4Cl$, MeCN, 80 °C, then excess $NaN_3$, MeCN, 80 °C

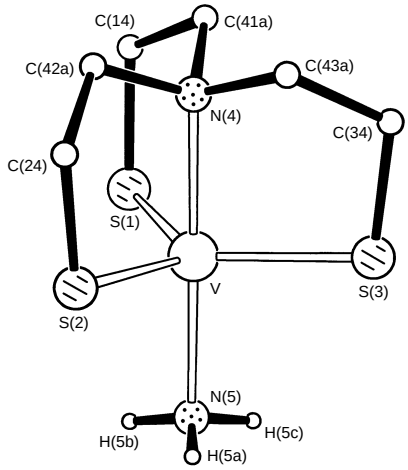



**Fig. 1** The molecular structure of **3**. There is disorder of the three C(4*n*) atoms ($n$ = 1–3); the principal component, with *ca*. 80% occupancy, C(4*n*a) is shown here. Selected bond lengths (Å) and angles (°): V–N(5) 2.154(7), V–N(4) 2.155(8), V–S(1) 2.283(3), V–S(2) 2.285(3), V–S(3) 2.301(3); N(5)–V–N(4) 178.7(3), N(5)–V–S(av.) 93.9(5), N(4)–V–S(av.) 86.1(2).

V–$NH_3$ distance in **3**, and the V–$NS_3$ distance is correspondingly longer in **4** [2.214(3) Å], approaching that in [VO(L)]. The N–N distance of the hydrazide ligand [1.305(5) Å] is in the range generally found in hydrazide complexes of the early transition metals[8,9] and in the only structurally characterised hydrazide complexes of vanadium, $[V(C_5H_5)_2\{NN(SiMe_3)_2\}]$ [1.369(9) Å],[10] the anion $[VCl_2(NH_2NMePh)_2(NNMePh)]^-$ [1.295(17) Å][11] and $[(C_9H_{18}N_2)_2(OSiMe_3)_2V(\mu\text{-}O)VO(OSiMe_3)_2]$ [1.285(3) and 1.245(4) Å].[9] However, whilst there is no doubt of the nature of the $NNMe_2$ ligand in **4**, it is unusual in that the N–C distances appear to be unequal [1.401(15), 1.502(15) Å] and N(3) lies some 0.21 Å out of the plane formed by N(2), C(7) and C(8) (Fig. 2). This phenomenon is under further investigation.

Novel nitride and imide complexes have been obtained from **1** as shown in Scheme 1. The dimer $NBu_4[LV(\mu\text{-}CN)VL]$, the salt $NEt_4[VCl(L)]$ and the adducts [V(NCMe)L] and [V(CNBu$^t$)L] have also been obtained from reaction of **3** with $NBu_4CN$, $NEt_4Cl$, MeCN and CNBu$^t$ respectively.

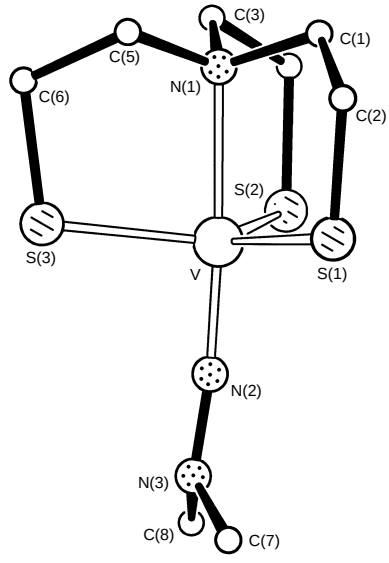



**Fig. 2** The molecular structure of **4**. Selected bond lengths (Å) and angles (°): V–N(1) 2.214(3), V–N(2) 1.681(3), N(1)–C(1) 1.514(9), V–S(1) 2.261(3), V–S(2) 2.273(3), V–S(3) 2.255(2), N(2)–N(3) 1.305(5), N(3)–C(7) 1.401(15), N(3)–C(8) 1.502(15); N(1)–V–N(2) 176.6(2), V–N(2)–N(3) 173.9(4), N(1)–V–S(av.) 84.4(3), N(2)–V–S(av.) 95.6(14)°.

The characterisation of this set of nitrogen-donor ligands at a $VS_3$ site lends further credence to the idea that fixation of $N_2$ could occur at the vanadium site of vanadium nitrogenase,[2,4,5] and we intend to probe this further by study of the interconversion of the various NR (NR = $N_2H_4$, $NH_3$, NH, *etc*.) ligands in these compounds.

We have also prepared $[Fe(NH_2NH_2)L]$ and a very insoluble compound formulated as $Mo(NH_2NH_2)L$ which appears to be polymeric; their properties will be described at a later date.

We thank the British Council, the Polish State Committee for Scientific Research and the BBSRC for support.

## Footnotes

* E-mail: richardsr@bbsrc.ac.uk

† *Crystal structure analyses*: *crystal data*: **3**: $C_6H_{15}N_2S_3V$, $M$ = 262.3, orthorhombic, space group $P2_12_12_1$ (no. 19), $a$ = 8.0612(6), $b$ = 16.6065(13), $c$ = 8.5004(12) Å, $U$ = 1137.9(2) Å$^3$, $Z$ = 4, $D_c$ = 1.531 g cm$^{-3}$, $F(000)$ = 544, $\mu$(Mo-K$\alpha$) = 13.3 cm$^{-1}$, $T$ = 293 K, $\lambda$(Mo-K$\alpha$) = 0.710 69 Å. Crystals are yellow, translucent plates. One, *ca*. 0.40 × 0.08 × 0.05 mm mounted on a glass fibre; photographic examination; Enraf-Nonius CAD4 diffractometer (with monochromated radiation) for accurate cell parameters (25 reflections, $\theta$ = 10–11°, each centred in four orientations) and diffraction intensities (1175 unique reflections to $\theta_{max}$ = 25°, 729 'observed' with $I > 2\sigma_I$). Structure determined by automated Patterson routines;[12] refined (on $F_o^2$) by full-matrix least-squares methods[13] to $wR_2$ = 0.093 and $R_1$ = 0.085 for 1170 reflections weighted $w = \sigma(F_o^2)^{-2}$.

**4**: $C_8H_{18}N_3S_3V$, $M$ = 303.4, monoclinic, space group $P2_1$ (no. 4), $a$ = 7.494(1), $b$ = 11.649(2), $c$ = 7.584(2) Å, $\beta$ = 92.03(1)°, $U$ = 661.5(2) Å$^3$. $Z$ = 2, $D_c$ = 1.523 g cm$^{-3}$, $F(000)$ = 316, $\mu$(Mo-K$\alpha$) = 12.0 cm$^{-1}$, $T$ = 300 K, $\lambda$(Mo-K$\alpha$) = 0.710 69 Å. Crystals are red, rectangular prisms. One, *ca*. 0.5 × 0.3 × 0.2 mm, sealed in a glass capillary under dinitrogen; Kuma KM-4 diffractometer (with monochromated radiation) for determination of accurate cell parameters (25 reflections, $\theta$ = 8.5–13°, each centred in four orientations) and for measurement of diffraction intensities (1218 unique reflections to $\theta_{max}$ = 25°; 1118 were 'observed' with $I > 2\sigma_I$). Structure determined by direct methods;[12] refinement on $F^2$ by full-matrix least-squares methods[13] to $wR_2$ = 0.089 and $R_1$ = 0.032 for the 'observed' reflections weighted $w = \{\sigma^2(F^2) + (0.0458P)^2 + 0.56P\}^{-1}$, with $P = (F_o^2 + 2F_c^2)/3$. Atomic coordinates, bond lengths and angles, and thermal parameters have been deposited at the Cambridge Crystallographic Data Centre (CCDC). See Information for Authors, Issue No. 1. Any request to the CCDC for this material should quote the full literature citation and the reference number 182/487.

## References

1 D. C. Rees, M. K. Chan and J. Kim, *Adv. Inorg. Chem.*, 1993, **40**, 89.
2 R. R. Eady, *Adv. Inorg. Chem.*, 1991, **36**, 77.
3 R. N. Pau, in *Biology and Biochemistry of Nitrogen Fixation*, ed. M. J. Dilworth and A. R. Glenn, Elsevier, Oxford, 1991, p. 37.
4 R. L. Richards, *Coord. Chem. Rev.*, 1996, **154**, 83.
5 S. M. Malinak, K. D. Demadis and D. Coucouvanis, *J. Am. Chem. Soc.*, 1995, **117**, 3126.
6 K. K. Nanda, E. Sinn and A. W. Addison, *Inorg. Chem.*, 1996, **35**, 1.
7 R. A. Henderson, Z. Janas, R. L. Richards and P. Sobota, unpublished work.
8 R. A. Henderson, G. J. Leigh and C. J. Pickett, *Adv. Inorg. Chem. Radiochem.*, 1984, **27**, 197.
9 A. A. Danopoulos, R. S. Hay-Motherwell, G. Wilkinson, T. K. N. Sweet and M. B. Hursthouse, *Polyhedron*, 1997, **16**, 1081 and references therein.
10 M. Veith, *Angew. Chem., Int. Ed. Engl.*, 1976, **15**, 387.
11 J. Bultitude, L. F. Larkworthy, D. C. Povey, G. W. Smith, J. R. Dilworth and G. J. Leigh, *J. Chem. Soc., Chem. Commun.*, 1986, 1748.
12 G. M. Sheldrick, *Acta Crystallogr. Sect. A*, 1990, **46**, 467.
13 G. M. Sheldrick, SHELXL—Program for crystal structure refinement, University of Göttingen, 1993.

*Received in Cambridge, UK, 28th April 1997; Com. 7/02885G*

# One-dimensional alignment of organometallic donor–acceptor compounds *via* coordination polymerization. Synthesis and structures of $[W(\equiv CC_6H_4X\text{-}4)(OBu^t)_3]_\infty$ (X = $NMe_2$, SMe)

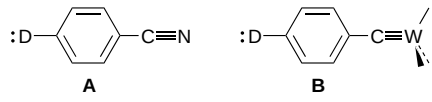
**Holly A. Brison, Timothy P. Pollagi, Timothy C. Stoner, Steven J. Geib and Michael D. Hopkins***

*Department of Chemistry and Materials Research Center, University of Pittsburgh, Pittsburgh, Pennsylvania 15260, USA*

**Metal–alkylidyne complexes of the type $W(\equiv CC_6H_4X\text{-}4)(OBu^t)_3$ (X = $NMe_2$, SMe), which are analogues of classic organic donor–acceptor compounds, form infinite-chain structures in the solid state through weak intermolecular dative bonds between the tungsten and donor atoms.**

A design prerequisite for bulk molecular materials that possess second-order non-linear optical responses is that the individual chromophores of which they are composed must be non-centrosymmetrically ordered. One strategy for achieving this order is to incorporate the chromophore, typically a conjugated organic molecule with electron-donor (D) and -acceptor (A) substituents, into a polymer host, upon which the host–guest material is processed to induce temporary alignment of the chromophore dipoles, or *via* chemical bonds into a lattice of appropriate three-dimensional structure.[1] A second approach is to design chromophores that 'self-assemble' into ordered arrays, such as hydrogen-bonded networks of organic compounds[2] or metal coordination polymers.[3]

Our interest in developing transition-metal analogues of conjugated organic compounds and polymers[4] led us to inquire if replacing the ubiquitous cyano groups of organic donor–acceptor compounds **A** with metal–alkylidyne groups **B** would serve the dual purposes of broadening the electronic tunability of the acceptor and of affecting one-dimensional A–D···A–D ordering of the chromophores. Alkylidyne complexes of the type $M(\equiv CR)X_3$ (M = Mo, W)[5] are especially interesting in this context because the metal centres are potential electron acceptors (formally $M^{VI}$), and because they weakly coordinate neutral ligands *trans* to the M≡C bond, which can lead to one-dimensional polymeric structures if the alkylidyne R group contains a ligating substituent.[6] Herein we report the syntheses of $W(\equiv CC_6H_4NMe_2\text{-}4)(OBu^t)_3$ **1** and $W(\equiv CC_6H_4SMe\text{-}4)(OBu^t)_3$ **2**, and that these complexes exhibit one-dimensional A–D···A–D polymeric structures in the solid state.




**A** **B**

Compounds **1** and **2** can be prepared from the reaction between $4\text{-}XC_6H_4CN$ (X = $NMe_2$, SMe) and $W_2(OBu^t)_6$[7] in pentane at room temp. Within minutes of combining the reagents the reaction mixture changes from deep red to brown, and white $[WN(OBu^t)_3]_\infty$[8] precipitates. Filtration of the solution and removal of solvent *in vacuo* yields a brown powder. Recrystallization of this material from pentane at −35 °C provides yellow–orange **1** and **2** in 73 and 74% yield (based on $4\text{-}XC_6H_4CN$), respectively.† The $^1H$ and $^{13}C$ NMR data for **1** and **2** are similar to those for the related compound $W(\equiv CPh)(OBu^t)_3$.[9] There is no evidence from the NMR data for static intermolecular interactions among monomers in solution.

Single-crystal X-ray diffraction studies of **1** and **2** reveal them to be polymeric in the solid state, consisting of one-dimensional zigzag chains of monomers connected by weak dative bonds between the donor and tungsten atoms of adjacent molecules.‡ The structures of the repeat units of $[\mathbf{1}]_\infty$ and $[\mathbf{2}]_\infty$ are shown in Fig. 1, and a view of an extended fragment of $[\mathbf{1}]_\infty$ is provided in Fig. 2. The assembly of **1** and **2** into infinite-chain structures does not result in significant structural perturbations to their $WCO_3$ cores: the W≡C bond distances of $[\mathbf{1}]_\infty$ [1.754(7) Å] and $[\mathbf{2}]_\infty$ [1.757(6) Å] are essentially identical to that of $W(\equiv CPh)(OBu^t)_3$ [1.758(5) Å],[10] and there is only a slight flattening of the pyramidal $WO_3$ units of $[\mathbf{1}]_\infty$ and $[\mathbf{2}]_\infty$ as a result of the axial ligation in the polymers [O–W–$O_{av}$: $[\mathbf{1}]_\infty$ 115(1)°, $[\mathbf{2}]_\infty$ 114(2)°, $W(\equiv CPh)(OBu^t)_3$ 111(2)°]. From an electronic standpoint, only small structural perturbations are expected because the intermolecular W···E bonds in $[\mathbf{1}]_\infty$ and $[\mathbf{2}]_\infty$ are extremely long [W···N 2.767(4), W···S 3.079(2) Å]. Steric interactions and packing forces are presumably responsible for the more noticeable distortions, such as the slight 'bowing' of the $E\text{–}C_6H_4\text{–}C{\equiv}W$ unit (Fig. 2).

Despite the long W···N bond distance, the electronic structure of the aniline moiety in $[\mathbf{1}]_\infty$ is significantly altered from that expected for monomeric **1**. Specifically, the nitrogen centres in $[\mathbf{1}]_\infty$ are pyramidal [C(5)–N–C(6) 113.9(3)°, C(6)–N–C(6a) 110.9(6)°], in contrast to the expected planar structure, and the C(5)–N bond distance [1.438(8) Å] is consistent with $sp^3$ hybridization for nitrogen rather than $sp^2$ hybridization [$d(C_{aryl}\text{–}N_{sp^3})$ = 1.43 Å, $d(C_{aryl}\text{–}N_{sp^2})$ = 1.37 Å].[11] This

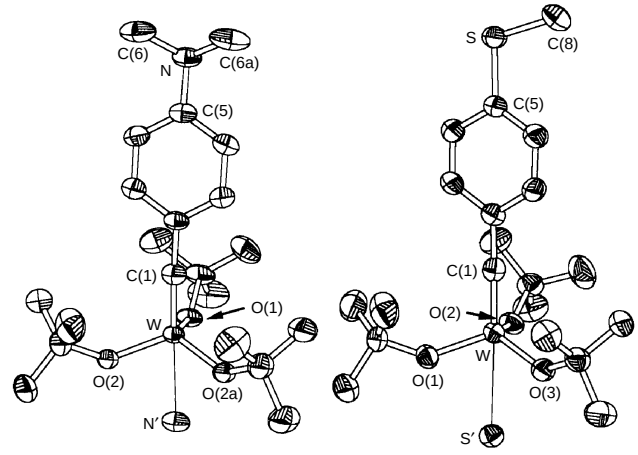


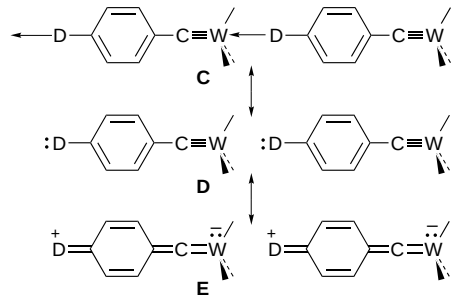

**Fig. 1** Thermal ellipsoid representations (50% probability) of the structures of **1** (left) and **2** (right). The donor atoms of the adjacent molecules are also shown. Selected bond distances (Å) and bond angles (°): for **1**: W–C(1) 1.754(7), W···N 2.767(4), W–O(1) 1.868(4), W–O(2) 1.876(3), C(5)–N 1.438(8); C(5′)–N′–W 107.5(4), N′–W–C(1) 174.2(3), O(1)–W–O(2) 115.2(1), O(2)–W–O(2a) 113.2(2), C(1)–W–O(1) 101.4(3), C(1)–W–O(2) 104.9(1), W–C(1)–C(2) 170.8(5), C(5)–N–C(6) 113.9(3), C(6)–N–C(6a) 110.9(6); for **2**: W–C(1) 1.757(6), W···S 3.079(2), W–O(1) 1.873(4), W–O(2) 1.881(4), W–O(3) 1.894(4), C(5)–S 1.772(5); C(5′)–S′–W 101.9(2), S′–W–C(1) 173.6(2), O(1)–W–O(2) 115.3(2), O(1)–W–O(3) 111.4(2), O(2)–W–O(3) 115.3(2), W–C(1)–C(2) 174.0(4), C(5)–S–C(8) 103.9(3).



**Fig. 2** Tetrameric section of $[W(\equiv CC_6H_4NMe_2\text{-}4)(OBu^t)_3]_\infty$. Atoms are shaded as follows: tungsten, black; oxygen, dotted; carbon, grey; nitrogen, hatched.

indicates that the π interaction between the $NMe_2$ and aryl groups is significantly diminished from what it would be in the monomeric compound. For $[\mathbf{2}]_\infty$, in contrast, the C(5)–S bond distance [1.772(5) Å] is typical of that for an organic thioanisol [$d(C_{aryl}–S)$ = 1.77 Å],[11] suggesting that the S–aryl π-interactions are of comparable magnitude in both the polymer and monomer forms. In principle, strong $D \rightarrow \{C{\equiv}W(OBu^t)_3\}$ interactions should be manifested as a quinoidal distortion of the aryl rings, but the C–C distances {$[\mathbf{1}]_\infty$ 1.378(6)–1.386(6) Å, $[\mathbf{2}]_\infty$ 1.369(8)–1.411(8) Å} are not known with sufficient precision to draw any conclusions on this point. We are presently studying the electronic spectra of these materials to deduce the extent of their $D \rightarrow \{C{\equiv}W(OBu^t)_3\}$ charge transfer.

In summary, we have discovered a class of organometallic analogues of classic organic *para*-phenylene D–A compounds that form one-dimensional solid-state structures. Qualitatively describing the bonding in these polymers requires the use of a third valence-bond canonical structure (**C**) in addition to the two typically invoked for monomeric D–A compounds (**D**, **E**).




From the standpoint of designing non-linear optical materials, achieving the optimum balance among these structures through chemical modifications involves trade offs; attempting to favour intramolecular $D \rightarrow A$ charge transfer (**E**) by increasing the electron-withdrawing capacity of the metal (*e.g.* the use of less strongly donating ancillary ligands) will also strengthen, detrimentally, the intermolecular interactions (**C**). Fortunately, the extremely long W···E bond distances in $[\mathbf{1}]_\infty$ and $[\mathbf{2}]_\infty$ suggest that even a very weak dative interaction is sufficient to affect one-dimensional organization of this class of compounds, and thus that steric modification of the ancillary ligands or of the donor group may allow independent tuning of intra- and inter-molecular charge transfer. Experiments to test this hypothesis are in progress. An additional challenge is to engineer non-centrosymmetric space groups for these materials, as those for **1** and **2** are centrosymmetric; derivatives with chiral ancillary ligands should be important in this context.

We thank the National Science Foundation for supporting this research (Grant CHE-9307013).

## Footnotes

* E-mail: mdh1@vms.cis.pitt.edu

† For **1**: $^1$H NMR ($C_6D_6$): δ 7.34 (d, 2 H, $C_6H_4$), 6.60 (d, 2 H, $C_6H_4$), 2.54 [s, 6 H, $N(CH_3)_2$], 1.56 [s, 27 H, $OC(CH_3)_3$]. $^{13}$C{$^1$H} NMR ($C_6D_6$): δ 258.5 (s with satellites $^1J_{CW}$ 309.4 Hz, W≡C), 149.3 (s, $C_6H_4$), 139.3 (s, $C_6H_4$), 133.6 (s, $C_6H_4$), 112.2 (s, $C_6H_4$), 81.1 [s, $OC(CH_3)_3$], 40.6 [s, $N(CH_3)_2$], 33.1 [s, $OC(CH_3)_3$]. For **2**: $^1$H NMR ($C_6D_6$): δ 7.22 (d, 2 H, $C_6H_4$), 2.00 [s, 3 H, $S(CH_3)$], 1.49 [s, 27 H, $OC(CH_3)_3$]; the second $C_6H_4$ resonance was obscured by the solvent. $^{13}$C{$^1$H} NMR ($C_6D_6$): δ 257.3 (s with satellites $^1J_{CW}$ 305.2 Hz, W≡C), 145.8 (s, $C_6H_4$), 136.6 (s, $C_6H_4$), 133.1 (s, $C_6H_4$), 126.5 (s, $C_6H_4$), 81.5 [s, $OC(CH_3)_3$], 33.0 [s, $OC(CH_3)_3$], 16.2 [s, $S(CH_3)$].

‡ *Crystal data*: for **1**: $C_{21}H_{37}NO_3W$, $M$ = 535.37, orthorhombic, space group *Pnma*, $a$ = 16.389(11), $b$ = 15.529(9), $c$ = 9.336(6) Å, $V$ = 2376(3) Å$^3$, $Z$ = 4, $D_c$ = 1.497 g cm$^{-3}$, $F(000)$ = 1072. 2827 independent reflections were collected and used in structure solution and subsequent least-squares refinement on $F^2$. $R1$ = 0.0515 (all data), $wR2$ = 0.0780 (all data), GOF = 1.023. For **2**: $C_{20}H_{34}O_3SW$, $M$ = 538.38, monoclinic, space group $P2_1/n$, $a$ = 8.527(1), $b$ = 16.409(3), $c$ = 16.746(3) Å, β = 97.11(3)°, $V$ = 2325.1(7) Å$^3$, $Z$ = 4, $D_c$ = 1.538 g cm$^{-3}$, $F(000)$ = 1072. Of 5677 reflections collected, 5326 independent reflections were used in structure solution and subsequent least-squares refinement on $F^2$. $R1$ = 0.0521 (all data), $wR2$ = 0.0987 (all data), GOF = 1.024. Data for both crystals were collected at −65 °C with Mo-Kα radiation and were corrected for absorption. Direct-method solutions yielded positions of all non-hydrogen atoms, which were refined anisotropically. Hydrogen-atom positions were calculated [$d$(C–H) = 0.96 Å]. Atomic coordinates, bond lengths and angles, and thermal parameters have been deposited at the Cambridge Crystallographic Data Centre (CCDC). See Information for Authors, Issue No. 1. Any request to the CCDC for this material should quote the full literature citation and the reference number 182/453.

## References

1 *Polymers for Second-Order Nonlinear Optics*, ed. G. A. Lindsay and K. D. Singer, American Chemical Society, Washington, DC, 1995; T. J. Marks and M. A. Ratner, *Angew. Chem., Int. Ed. Engl.*, 1995, **34**, 155; L. R. Dalton, A. W. Harper, R. Ghosn, W. H. Steier, M. Ziari, H. Fetterman, Y. Shi, R. V. Mustacich, A. K.-Y. Jen and K. J. Shea, *Chem. Mater.*, 1995, **7**, 1060.
2 G. R. Desiraju, *Angew. Chem., Int. Ed. Engl.*, 1995, **34**, 2311; J. C. MacDonald and G. M. Whitesides, *Chem. Rev.*, 1994, **94**, 2383.
3 C.-T. Chen and K. S. Suslick, *Coord. Chem. Rev.*, 1993, **128**, 293.
4 T. P. Pollagi, J. Manna, S. J. Geib and M. D. Hopkins, *Inorg. Chim. Acta*, 1996, **243**, 177 and references therein.
5 J. S. Murdzek and R. R. Schrock, in *Carbyne Complexes*, ed. H. Fischer, P. Hofmann, F. R. Kreissl, R. R. Schrock, U. Schubert and K. Weiss, VCH, Weinheim, 1988, pp. 147.
6 T. P. Pollagi, S. J. Geib and M. D. Hopkins, *J. Am. Chem. Soc.*, 1994, **116**, 6051.
7 M. H. Chisholm, B. W. Eichhorn, K. Folting, J. C. Huffman, C. D. Ontiveros, W. E. Streib and W. G. Van Der Sluys, *Inorg. Chem.*, 1987, **26**, 3182.
8 R. R. Schrock, M. L. Listemann and L. G. Sturgeoff, *J. Am. Chem. Soc.*, 1982, **104**, 4291.
9 M. L. Listemann and R. R. Schrock, *Organometallics*, 1985, **4**, 74.
10 F. A. Cotton, W. Schwotzer and E. S. Shamshoum, *Organometallics*, 1984, **3**, 1770; *J. Organomet. Chem.*, 1985, **296**, 55.
11 F. H. Allen, O. Kennard, D. G. Watson, L. Brammer, A. G. Orpen and R. Taylor, *J. Chem. Soc., Perkin Trans. 2*, 1987, S1.

*Received in Bloomington, IN, USA, 13th February 1997; Com. 7/01046J*

# X-Ray absorption and photoelectron spectroscopic observation of intrazeolitic silicon nanoclusters

**J. He, D. D. Klug, J. S. Tse* and K. F. Preston**

*Steacie Institute for Molecular Sciences, National Research Council of Canada, 100 Sussex Drive, Ottawa, Canada K1A 0R6*

**The Si-K near-edge absorption spectra and X-ray photoelectron spectra of silicon nanoclusters encapsulated in the pores of zeolite Y are measured; the intrazeolitic Si clusters display a blue shift of the K-edge (0.5 eV) relative to that of bulk Si and a strong room-temperature photoluminescence, which is consistent with the quantum confinement effect; the number of Si in the as-prepared sample is estimated to be 20 atoms per unit cell of zeolite Y from both XPS and Si K NEXAFS analysis.**

The drive towards nanoscale technology has motivated intense research on Si clusters and nanocrystals.[1] These are new forms of Si that exhibit quantum confinement effects and novel optoelectronic properties, such as efficient room-temperature photoluminescence. Several chemical approaches have been used to prepare these nanostructured forms of Si, including solution-phase synthesis *via* the dehalogenation of halosilanes by alkali metals[2,3] or by the Zintl compound KSi,[4] ultrasonic fracture of electrochemically etched Si wafers (porous Si),[5] gas-phase depositions by either slow combustion[6] or microwave plasma[7] of silanes and molecular sieve encapsulation *via* chemical vapour deposition of gaseous silanes.[8] Except for the molecular sieve encapsulation, these methods produce Si clusters with broad size distribution ranging from several Ångstroms to hundreds of nanometres. With well defined and well ordered cavities and channels, molecular sieves provide a ready access for synthesizing single-sized clusters and assembling cluster arrays periodically.[9]

Recently, Ozin *et al.* reported the synthesis of intrazeolitic Si nanoclusters.[8a] Dehydrated zeolite HY was employed to anchor disilane. FTIR spectroscopy showed that the disilane selectively reacted with the hydroxy group of the Brønsted-acid sites within the supercages. Subsequent thermal treatment of the silane-containing zeolite precursor led, *via* $H_2$ elimination and Si clustering reactions to intrazeolitic Si nanoclusters. The overall process is believed to occur *via* eqn. (1), where Z represents the zeolite framework and Y is zeolite Y.

$$Z{-}OH + Si_2H_6 \xrightarrow[-H_2]{} Z{-}OHSi_2H_5 \xrightarrow[-H_2]{\text{heat}} (Si_nH_m)Y \quad (1)$$

The dimensions of such nanoclusters are too small for standard microscopic (*e.g.* TEM) and diffraction (*e.g.* XRD) techniques to provide detailed structural information. Here, for the first time, we describe direct evidence for the formation of intrazeolitic Si clusters, their electronic properties and average cluster size from the study of Si-K near-edge absorption fine structure and core-level X-ray photoelectron spectroscopy.

The intrazeolitic silicon clusters used in this work were prepared by a procedure similar to that reported previously.[8a] Known quantities of disilane gas were transferred into a closed vessel containing zeolite HY through a vacuum line equipped with a pressure meter.† The mixture was then heated at 100 °C for 40 h. After removing the generated $H_2$ and unreacted disilane, the sample was heated to 550 °C at 1 °C $min^{-1}$ and held at this temperature for 2 h under vacuum ($10^{-3}$ Torr). The resulting solid is an air-stable pale yellow powder. X-Ray diffraction analysis showed that the long-range lattice of the zeolite framework was distorted but that the order of zeolite cavities remained intact.

Si K-edge absorption measurements were performed at the Syncrotron Radiation Center at University of Wisconsin at Madison, WI, using the CSRF beamline and a double-crystal monochromator with InSb(111) crystals.[10] All data were obtained with total electron yield detection and an effective sampling depth of *ca.* 700 Å.[11] Fig. 1 shows Si-K near-edge X-ray absorption fine structure (NEXAFS) data from both as-prepared intrazeolitic silicon clusters and zeolite HY. The edge at 1847 eV is due to the framework $SiO_2$ in zeolite. Two additional absorptions are found in the as-prepared intrazeolitic silicon clusters, *i.e.* at *ca.* 1839 and 1845 eV, respectively. The former is characteristic of a non-oxidized form of silicon and can be unambiguously attributed to the presence of silicon clusters. The intensity of this absorption is size-dependent and increases with the disilane loadings.[12] In their NEXAFS study of surface-oxidized silicon nanocrystals, Schuppler *et al.* assigned the absorption edges at ⩾1843 eV between the crystalline Si (c-Si) and $SiO_2$ thresholds to the interfacial $SiO_x$ ($x < 2$) species.[13] Similarly, the absorption edge at 1845 eV can be attributed to ≡SiO and $=SiO_2$ species which connect silicon clusters to the framework. This assignment was further supported by the *in situ* FTIR study of the encapsulation process indirating that both $HSiO(Si)_2$ and $HSiO_2(Si)$ were found in the intrazeolitic Si clusters.[12] Soft X-ray photoemission spectroscopy of the as-prepared sample showed the presence of $SiO_2$ only and no detectable non-oxidized form of Si in the outer 25 Å of the zeolite particles. This provides confirmation that essentially all of the silicon clusters are within the zeolite pore structure.

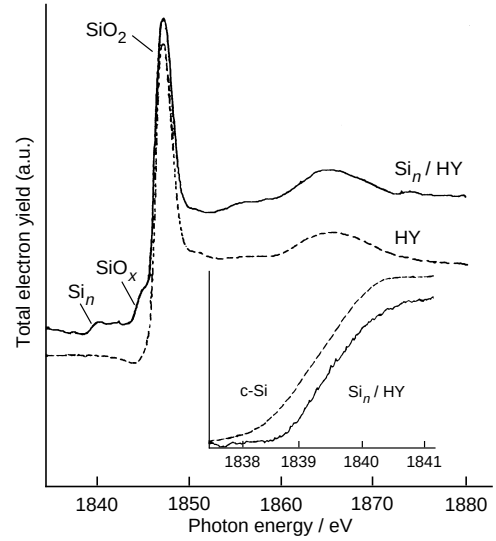



**Fig. 1** Si K-edge NEXAFS data from intrazeolitic silicon clusters ($Si_n$/HY) and zeolite HY. Inset shows the comparison of the Si absorption edges between crystalline Si (c-Si) and silicon clusters.

A detail of the Si K-edge absorption for as-prepared intrazeolitic silicon clusters and c-Si is presented in the inset of Fig. 1. From this it can be seen that the absoption edge for the silicon clusters is *ca*. 0.5 eV higher than that of c-Si. A blue shift in the absorption edge is indicative of a quantum confinement effect where the bottom of the LUMO orbitals (or conduction band) is raised relative to the 1s core level. A similar observation has been reported in the Si K-edge absorption studies of porous-Si (p-Si) samples, whose absorption edge is *ca*. 0.4–0.5 eV higher than that of c-Si.[14]

X-Ray photoelectron spectroscopy (XPS) was used to determine the chemical composition. Fig. 2 shows the XPS spectra from both intrazeolitic silicon clusters and zeolite HY samples. In addition to the peak at the Si 2p binding energy of 102.9 eV, corresponding to $SiO_2$, a weak peak centred at 99.2 eV appears in the intrazeolitic silicon clusters. This peak is characteristic of the Si 2p binding energy for unoxidized Si, reflecting the presence of silicon clusters. The SiO species, indentified by the NEXAFS above, is not observed because its concentration is so low that its peak is overlapped by that of $SiO_2$ in the XPS spectrum. Within the XPS detectable range (the outer 50 Å of the zeolite particles), the contents of $SiO_2$ (framework of zeolite) and Si (silicon clusters) were determined to be 93.19 and 6.81 atom%, respectively. This comparison enables an approximate estimate of the minimum occupancy of Si (as silicon clusters) in the zeolite pores, *i.e. ca.* 20 Si atoms per unit cell.‡ This number is similar to that obtained from the edge jump of the X-ray absorption spectrum.‡

The as-prepared intrazeolitic silicon clusters exhibit a strong room-temperature photoluminescence. Remarkably, its broad spectrum with a peak energy of 2.28 eV (with 488 nm excitation) closely resembles that of the organosilicon cluster, *syn*-tricyclooctasilane (2.25 eV).[15] This tentatively suggests that the structure of the intrazeolitic silicon clusters resembles that of *syn*-tricyclooctasilane. Further investigation into the cluster size and shape is in progress.

In summary, we have demonstrated that Si K-edge absorption spectroscopy is a useful tool for the direct observation of the encapsulation of silicon clusters in zeolite Y and for the study of their electronic properties. XPS provides a means of estimating the content of Si in each unit cell of zeolite.

We are grateful to Mr Regent Dutrisac and Mr Gerald Pleizier for excellent technical assistance, Dr Chris Ratcliffe for valuable discussions, and to Dr Anne McPhee of UOP (Des Plaines, Illinois, USA) for the provision of Y-zeolites.

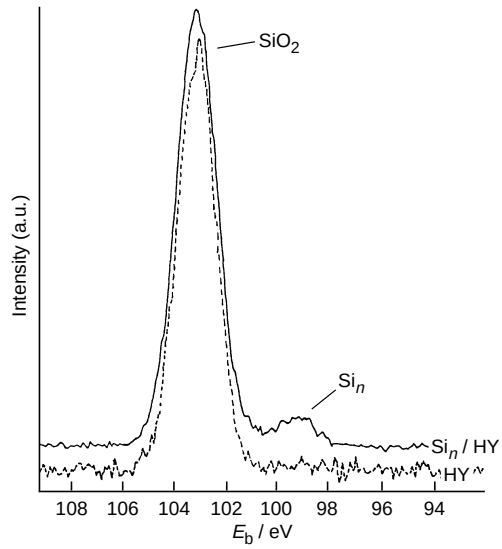



**Fig. 2** XPS data from intrazeolitic silicon clusters and zeolite HY

## Footnotes

* E-mail: tse@ned1.sims.nrc.ca

† Zeolite HY was prepared from commercial zeolite Y (LZ-Y52, $SiO_2/Al_2O_3$ = 4.74) by (*i*) fully exchanging the Na content with $NH_4$ cations to generate $NH_4Y$, (*ii*) slowly heating the $NH_4Y$ to 460 °C at 1 °C $min^{-1}$ increments, (*iii*) maintaining this temperature for 10 h, and then (*iv*) gradually cooling to room temperature; all steps at a pressure $< 10^{-3}$ Torr except (*i*). The HY zeolite contains eight supercages per unit cell. The disilane loadings were calculated according to $4Si_2H_6$ per supercage.

‡ XPS spectra were recorded on the XPS Kratos Axis Instrument, using monochromated Al-Kα radiation. The effective sampling depth is 50 Å. The unit-cell formula for a dehydrated zeolite HY can be expressed as $H_{56}(AlO_2)_{56}(SiO_2)_{136}$. Because the photoemission experiment shows that the non-oxidized form of Si is undetectable in the outer 25 Å of the zeolite, the actual Si content in the body of zeolite should be at least twice as much as that measured by XPS, when compared with the measured $SiO_2$ content in the same sampling depth (50 Å). Therefore, the number of Si atoms per unit cell can be calculated as follows: $2 \times 6.81 \times (135/93.19) \approx 20$.

In Si K-edge absorption spectra, the relative concentrations of Si and $SiO_2$ in the intrazeolitic Si clusters are also directly proportional to their individual edge jumps.[16] Since each unit cell of zeolite contains 136 units of $SiO_2$, the number of Si can thus be estimated to be 13 atoms per unit cell from its edge jump relative to that of $SiO_2$. By adding the contribution of $SiO_x$ species to Si clusters, the Si atoms per unit cell would be *ca*. 20, in agreement with the estimation by XPS data.

## References

1 For reviews: M. F. Jarrod, *Science*, 1991, **252**, 1085; A. P. Alivisatos, *Science*, 1996, **271**, 933; Ö. Dag, A. Kuperman and G. A. Ozin, *Adv. Mater.*, 1995, **7**, 72; L. E. Brus, *Adv. Mater*., 1993, **5**, 286.
2 J. R. Heath, *Science*, 1992, **258**, 1131.
3 For review of organosilicon-cluster synthesis see: A. Sekiguchi and H. Sakurai, *Adv. Organomet. Chem.*, 1995, **37**, 1.
4 R. A. Bley and S. M. Kauzlarich, *J. Am. Chem. Soc.*, 1996, **118**, 12461.
5 J. L. Heinrich, C. L. Curtis, G. M. Credo, K. L. Kavanagh and M. J. Sailor, *Science*, 1992, **255**, 66.
6 A. Fojtik, H. Weller, S. Fiechter and A. Henglein, *Chem. Phys. Lett.* 1987, **134**, 477; K. A. Littau, P. F. Szajowski, A. J. Muller, A. R. Kortan and L. E. Brus, *J. Phys. Chem.*, 1993, **97**, 1224.
7 H. Takagi, H. Ogawa, Y. Yamazaki, A. Ishizaki and T. Nakagiri, *Appl. Phys. Lett.*, 1990, **56**, 2379.
8 (*a*) G. A. Ozin, Ö. Dag, A. Kuperman and P. M. Macdonald, *Stud. Surf. Sci. Catal.*, 1994, **84**, 1107; (*b*) E. Chomski, Ö. Dag, A. Kuperman, N. Coombs and G. A. Ozin, *Chem. Vap. Deposition*, 1996, **2**, 8.
9 For reviews see: G. D. Stucky and J. E. MacDougall, *Science*, 1990, **247**, 669; N. Herron, *J. Inclusion Phenom. Mol. Recognit. Chem.*, 1995, **21**, 283.
10 B. X. Yang, F. H. Middleton, B. G. Olsson, G. M. Bancroft, J. M. Chen, T. K. Sham, K. Tan and D. J. Wallace, *Nucl. Instrum. Met. A*, 1992, **316**, 422.
11 M. Kasrai, W. N. Lennard, R. W. Brunner, G. M. Bancroft, J. A. Bardwell and K. H. Tan, *Appl. Surf. Sci.*, 1996, **99**, 303.
12 J. He, D. D. Klug, J. S. Tse and K. F. Preston, to be published.
13 S. Schuppler, S. L. Friedman, M. A. Marcus, D. L. Adler, Y. H. Xie, F. M. Ross, Y. J. Chabal, T. D. Harris, L. E. Brus, W. L. Browm, E. E. Chaban, P. F. Szajoski, S. B. Christman and P. H. Citrin, *Phys. Rev. B*, 1995, **52**, 4910.
14 J. R. Dahn, B. M. Way, E. W. Fuller, W. J. Weydanz, J. S. Tse, D. D. Klug, T. Van Buuren and T. Tiedje, *J. Appl. Phys.*, 1994, **75**, 1946.
15 Y. Kanemitsu, K. Suzuki, H. Uto, Y. Masumoto, T. Matsumoto, S. Kyushin, K. Higuchi and H. Matsumoto, *Appl. Phys. Lett.*, 1992, **61**, 2446; S. Kyushin, H. Matsumoto, Y. Kanemitsu and M. Goto, *J. Phys. Soc. Jpn.*, 1994, **63**, 46.
16 P. A. Lee, P. H. Citrin, P. Eisenberger and B. M. Kincaid, *Rev. Mod. Phys.*, 1981, **53**, 769.

*Received in Bloomington, IN, USA, 27th September 1996; Revised manuscript received, 9th April 1997; Com. 7/03001K*

# Ruthenium(III)-promoted oxidative dimerization of aniline to *N*-phenyl-1,2-phenylenediimine. Definitive proof for the template reaction

**Kedar Nath Mitra,[a] Partha Majumdar,[a] Shie-Ming Peng,[b] Alfonso Castiñeiras[c] and Sreebrata Goswami*[a]**

[a] *Department of Inorganic Chemistry, Indian Association for the Cultivation of Science, Calcutta 700 032, India*
[b] *Department of Chemistry, National Taiwan University, Taipei, Taiwan, Republic of China*
[c] *Departmento de Química Inorgánica, Facultad de Farmacia, Universidad de Santiago de Compostela, 15706-Santiago de Compostela, Spain*

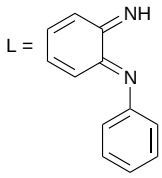
**Two novel examples of ruthenium-promoted oxidative *ortho*-dimerization of aniline are described which demonstrate that the dimerization reaction proceeds *via* coordination of anilines to the metal ion.**

In a recent communication[1] we described unusual examples of osmium-promoted oxidative dimerization of primary aromatic amines [eqn. (1)] to *N*-aryl-1,2-arylenediimine (L). It was

$$[Os^{IV}Br_6]^{2-} \xrightarrow{PhNH_2} [Os^{II}L_2Br_2] \quad (1)$$

**1**

L =




proposed that prior *cis*-coordination of amines to the metal ion is the key step for the dimerization reaction.

Here, we further demonstrate two more novel examples of ruthenium-promoted oxidative dimerization reactions of aniline which established that coordination of amines takes place during the course of reaction.

The first reaction [eqn. (2)] is the reaction of $[Ru(acac)]_3$[2]

$$[Ru(acac)_3] \xrightarrow{PhNH_2} [Ru(acac)_2L] \quad (2)$$

**2**

with neat aniline at 130 °C. Chromatographic work-up of the reaction mixture afforded $[Ru(acac)_2L]$, which was recrystallised from an aqueous acetonitrile solution and obtained as bown needles in 30% yield. Addition of $NEt_3$, which acts as a proton sink, to the reaction mixture increases the yield considerably to 65%. The compound $[Ru(acac)_2L]$ is soluble in common organic solvents and is diamagnetic. The N–H stretch occurs[3] as a sharp feature of moderate intensity in the range 3300–3200 $cm^{-1}$. The presence of a strong C=N stretch near 1600 $cm^{-1}$ characterizes the presence of diimine chromophore in the compound. The $^1H$ NMR spectrum of the complex consists of three methyl resonances at $\delta$ 1.76(3 H), 1.83(6 H) and 2.35 (3 H); resolved aromatic proton resonances between $\delta$ 6.5 and 7.4 and the N–H resonance is observed[4] as a relatively broad singlet at $\delta$ 10.8. Suitable crystals for an X-ray structure determination† were obtained upon slow evaporation of a saturated solution of the compound in hexane, and a view of the molecule is shown in Fig. 1. Ruthenium is coordinated by the four oxygens of two acetylacetonato ligands and by the two nitrogens of a diimine ligand in a distorted octahedral geometry. The imine, C–N bond lengths, average 1.341(8) Å, are considerably shorter than a C–N single bond, 1.433(9) Å. The analytical, spectral and X-ray data collectively conform to the formulation of **2** as $[Ru(acac)_2L$.]

To gain a better insight into the course of above metal-promoted oxidation reaction, we used $RuCl_3 \cdot 3H_2O$ as a starting material to carry out a similar reaction. $RuCl_3 \cdot 3H_2O$ was selected since first, as in $[Ru(acac)_3]$, ruthenium is trivalent and secondly, the chloride salt is much more labile towards substitution than is $Ru(acac)_3$. Therefore, a higher degree of amine coordination was anticipated.

This reaction proceeded very smoothly and recrystallisation of the crude product from dichloromethane–hexane [eqn. (3)]

$$RuCl_3 \bullet 3H_2O \xrightarrow{PhNH_2} [RuCl_2(PhNH_2)_2L] \quad (3)$$

**3**

resulted a highly crystalline compound **3** (yield, 60%), which contains one diimine (L), two *trans*-anilines and two *cis*-chlorides in the co-ordination sphere.

Unlike **2**, compound **3** is sparingly soluble in common organic solvents. The IR spectrum shows[3] multiple sharp $\nu_{NH}$ between 3300 and 3100 $cm^{-1}$, sharp $\nu_{C=C}$ and $\nu_{C=N}$ at 1600 and 1580 $cm^{-1}$ and two $\nu_{Ru-Cl}$ stretches[5] at 360 and 340 $cm^{-1}$. The

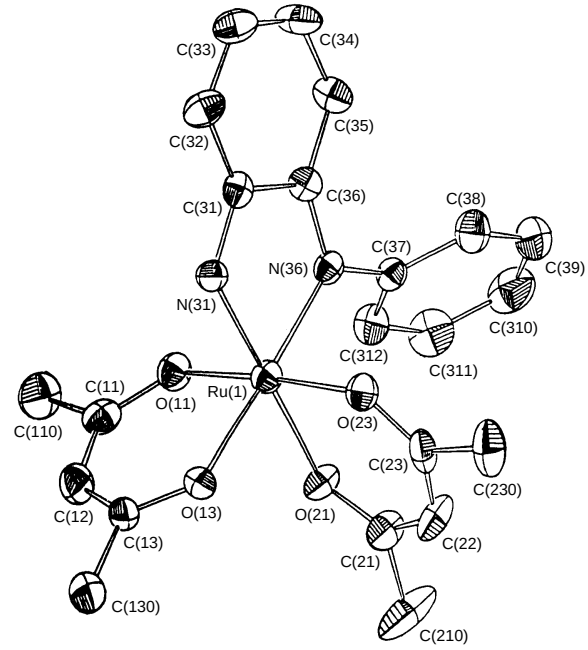



**Fig. 1** Molecular structure of $[Ru(acac)_2L]$ **2** showing the atom numbering scheme. The asymmetric unit consists of two crystallographically distinct molecules. The figure shows a view of molecule 1. Selected bond distances (Å): Ru(1)–N(31) 1.958(5), Ru(1)–N(36) 1.996(5), Ru(1)–O(11) 2.019(5), Ru(1)–O(13) 2.068(4), Ru(1)–O(21) 2.050(4), Ru(1)–O(23) 2.031(5), N(31)–C(31) 1.333(8), N(36)–C(36) 1.352(8), N(36)–C(37) 1.429(8).

$^1$H NMR spectrum shows two doublet NH resonances[6] at $\delta$ 5.09 and 4.84 assigned to $NH_2$. Verification of the composition as well as the geometry of the compound was ascertained by single-crystal X-ray diffraction,† and a view of the molecule is shown in Fig. 2. There are three types of Ru–N distances in the molecule. The two Ru–N(aniline) single bonds are identical and are longer than the Ru–N(imine) bonds indicating a relatively weak bond between Ru and aniline. The two diimine, C=N bonds are much shorter than the C–N bonds. To the best of our knowledge compound **3** represents the first authentic example of aniline coordinated to ruthenium. Indications are strong that it can act as a good starting compound for substitution reactions and for performing reactions at the coordinated aniline.

It is worthwhile to compare the results of the three reactions (1)–(3). For osmium [eqn. (1)] a bis(diimine) complex was obtained whereas only a monodiimine complex resulted from reaction (2). It is noteworthy that the difference of the oxidation states of the metal ions in the starting compound and the end product is two in reaction (1) but is one in reaction (2). Interestingly, in reaction (3) only two of the four coordinated anilines have undergone oxidative dimerization and notably, the metal centre has undergone only a one-step reduction. From the above results it appears reasonable that the difference in the oxidation levels of the reactant and the product is equal to the number of diimine ligands formed in the reaction.

In conclusion, it may be stated that the above results are a clear manifestation of template dimerization of primary aromatic amines to yield novel coordination complexes of arylene diimines which otherwise are not achievable.[7]

Financial support received from the CSIR, New Delhi is acknowledged. We thank Dr Samaresh Bhattacharya for his suggestions.

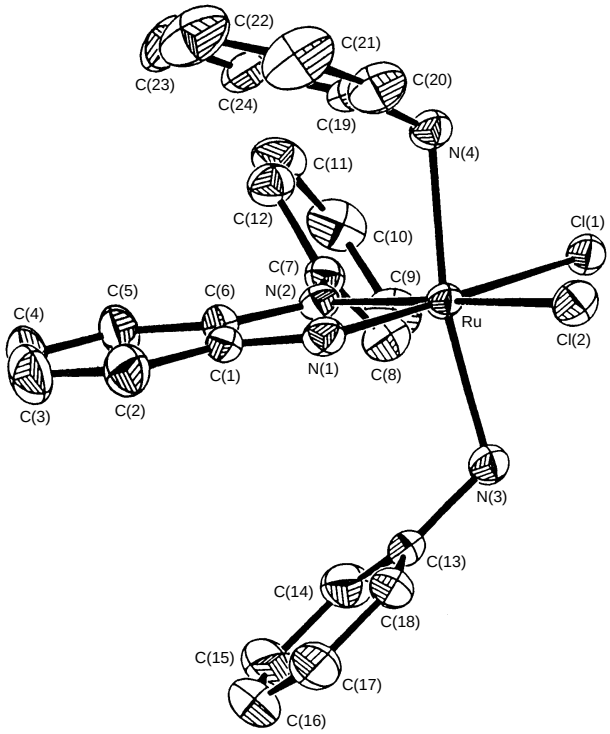



**Fig. 2** Molecular structure of $[RuCl_2(PhNH_2)_2L]$ **3** showing the atom numbering scheme. Selected bond distances (Å): Ru–N(1) 1.940(4), Ru–N(2) 1.997(4), Ru–N(3) 2.135(4), Ru–N(4) 2.135(4), Ru–Cl(1) 2.422(1), Ru–Cl(2) 2.429(1), N(1)–C(1) 1.319(7), N(2)–C(6) 1.343(7), N(2)–C(7) 1.445(6), N(3)–C(13) 1.451(7), N(4)–C(19) 1.449(7).

## Footnotes

* E-mail: icsg@iacs.ernet.in

† *Crystal data*: $[Ru(acac)_2L]\cdot 0.25H_2O$ **2**: $C_{22}H_{25}N_2O_{4.25}Ru$, $M$ = 486.51, monoclinic, space group $C2/c$, $a$ = 33.578(9), $b$ = 9.922(2), $c$ = 26.354(5) Å, $\beta$ = 93.114(10)°, $U$ = 8768(3) Å$^3$, $Z$ = 16, $D_c$ = 1.474 g cm$^{-3}$, crystal dimensions 0.20 × 0.25 × 0.30 mm. Intensity data were collected on Enraf-Nonius CAD4 diffractometer with graphite-monochromated Mo-Kα radiation ($\lambda$ = 0.710 73 Å) using the $\omega$–2$\theta$ scan mode with $2\theta_{max}$ = 32.4°. 12 707 unique reflections were measured and 12 705 with $I \geqslant 2\sigma(I)$ were used in the refinement. The structure was solved by direct methods[8] by a full-matrix least-squares procedure based on $F^2$ which smoothly converged to $R$ = 0.0805. The final Fourier difference map showed residual extrema at 0.62, −0.80 e Å$^{-3}$.

$[RuCl_2(PhNH_2)_2L]\cdot CH_2Cl_2$ **3**: $C_{25}H_{26}N_4Cl_4Ru$, $M$ = 625.38, monoclinic, space group $P2_1/n$, $a$ = 9.390(5), $b$ = 19.225(2), $c$ = 15.631(3) Å, $\beta$ = 101.91(3)°, $U$ = 2761(16) Å$^3$, $Z$ = 4, $D_c$ = 1.504 g cm$^{-3}$, crystal dimensions 0.25 × 0.45 × 0.60 mm. Intensity data were collected on Enraf-Nonius CAD4 diffractometer with graphite-monochromated Mo-Kα radiation ($\lambda$ = 0.710 73 Å) using the $\omega$–2$\theta$ scan mode with $2\theta_{max}$ = 50.0°. 4848 unique reflections were measured and 3093 with $I \geqslant 2\sigma(I)$ were used in the refinement. Refinement of positional and anisotropic thermal parameters for all non-hydrogen atoms converged to $R$ = 0.040. The final Fourier difference map showed residual extrema at 0.680, −0.510 e Å$^{-3}$. Atomic coordinates, bond lengths and angles, and thermal parameters have been deposited at the Cambridge Crystallographic Data Centre (CCDC). See Information for Authors, Issue No. 1. Any request to the CCDC for this material should quote the full literature citation and the reference number 182/486.

## References

1 K. N. Mitra and S. Goswami, *Chem. Commun.*, 1997, 49.
2 A. Endo, M. Watanbe, S. Hayashi, Shimizu and G. P. Sato, *Bull. Chem. Soc. Jpn.*, 1978, **51**, 800.
3 A. Danopoulos, A. C. C. Wong, G. Wilkinson, M. Hursthouse and B. Hussain, *J. Chem. Soc., Dalton Trans.*, 1990, 315.
4 L. F. Warren, *Inorg. Chem.*, 1977, **16**, 2814.
5 S. Choudhury, M. Kakoti, A. K. Deb and S. Goswami, *Polyhedron*, 1992, **11**, 3183.
6 H. Y. Cheng and S.-M. Peng, *Inorg. Chim. Acta*, 1990, **169**, 23.
7 J. March, *Advanced Organic Chemistry*, Wiley Interscience, New York, 3rd edn., 1985, p. 1034.
8 G. M. Sheldrick, SHELXS 86, Program for the solution of crystal structures, University of Göttingen, 1986.

*Received in Cambridge, UK, 25th March 1997; Com. 7/02047C*

# Phosphorus–sulfur–nitrogen heterocycles from diferrocenyl dithiadiphosphetane disulfide

**Mark R. StJ. Foreman, Alexandra M. Z. Slawin and J. Derek Woollins***

*Department of Chemistry, Loughborough University, Loughborough, UK LE11 3TU*

**$FcP(S)S_2P(S)Fc$ undergoes cycloaddition reactions with C–N bonds to generate C–P–N rings including the novel, boat shaped, $PN_2C_2S$ system as well as four-membered $P_2CN$ rings.**

Cycloaddition reactions provide one of the most exciting entries into heterocyclic compounds. We have recently developed[1] a facile synthesis of $FcP(S)S_2P(S)Fc$ **1** (Fc = ferrocenyl) which can be considered as consisting of two $FcPS_2$ units (capable of a wide range of cycloaddition reactions) in solution [eqn. (1)].




(1)

Very few cycloaddition reactions of phosphetane disulfides have been described, though some reactions of Lawesson's reagent **2** with amines,[2] ureas[3] and cyanamides[4] to form sulfur–phosphorus–nitrogen compounds are known. Here we describe the results of our studies into the reactions of cyanamides, and related systems with **1**. The first example of the synthesis (and X-ray structure) of a $PN_2C_2S$ is reported together with a novel, readily generalised, synthesis of the $P_2SN$ ring system.

Thus, the reaction of **1** with dimethylcyanamide gives *P*-ferrocenyl 2,6-bis(dimethylamino)1,3,5,4-thiadiazaphosphorine-4-sulfide **3** in good yield and *P*-ferrocenyl *P*-dimethylamino thiophosphoroisothiocyanate **4** in lower yield.† Both **3** and **4** displayed the expected spectroscopic properties. The X-ray structure‡ of **3** (Fig. 1) confirms the identity of the heterocycle, the $PC_2N_2S$ ring adopts a distorted boat conformation with the P and S(2) atoms at the prow and stern of the boat. The P and S(2) atoms lie 0.48 and 0.30 Å, respectively above the C(1)N(1)C(2)N(2) mean plane [max. deviation 0.007 Å for C(1)] with the C(1)C(2)S(2) and PN(1)N(2) planes being inclined by 15.7 and 30.0°, respectively, to this plane. Within the six-membered ring the bond lengths are in accord with the localised structure drawn in Scheme 1, *i.e.* short C–N bonds [C(1)–N(1) 1.289(6), C(2)–N(2) 1.290(6) Å] and 'normal' single P–N and C–S bond lengths. The angles at the ring nitrogen atoms are close to trigonal whilst the C(1)–S(2)–C(2) angle is significantly contracted at 101.0(2)° and the N(1)–P(1)–N(2) is close to tetrahedral [108.2(2)°]. The exocyclic P=S and ferrocenyl groups occupy (approximate) axial and equatorial sites whilst the $NMe_2$ groups are only slightly out of the central $C_2N_2$ plane of the ring [N(3) and N(4) lie 0.16 and 0.25 Å below the $C_2N_2$ plane and on the opposite side to S(2) and P(1)]. The coplanarity of the $NMe_2$ groups is accompanied by short C–N bond lengths [C(2)–N(4) 1.365(6), C(1)–N(3) 1.335(6) Å] suggesting some degree of delocalisation in this part of the molecule. The cyclopentadienyl rings in the ferrocenyl group are twisted by *ca.* 72° with respect to (w.r.t.) the $C_2N_2$ ring plane. In the structure of **4** (Fig. 2)‡ the phosphorus centre is approximately tetra-

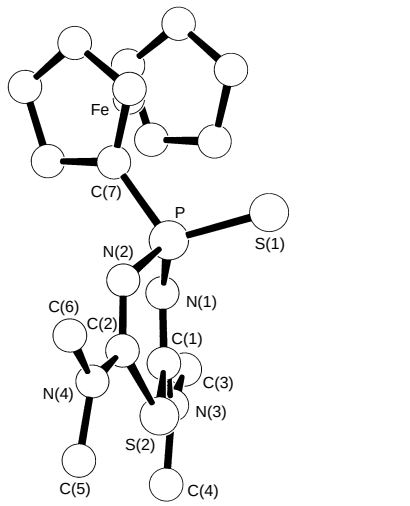
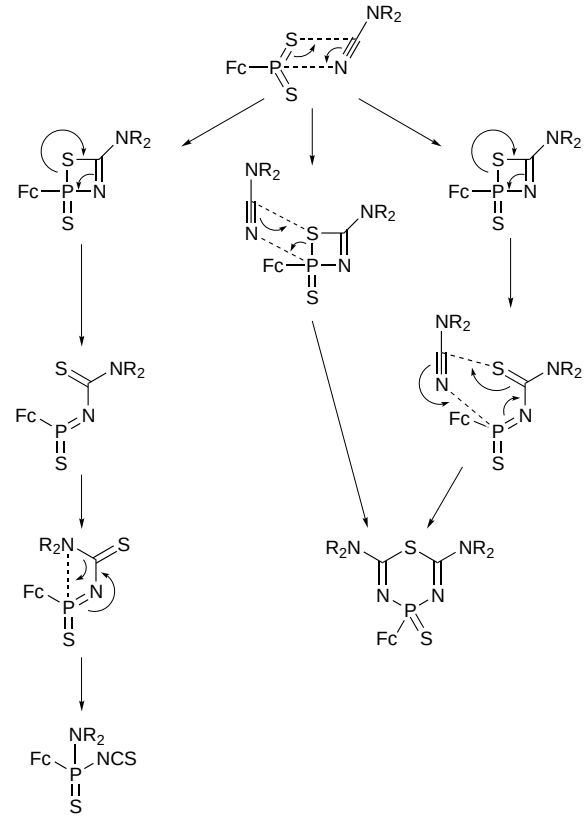


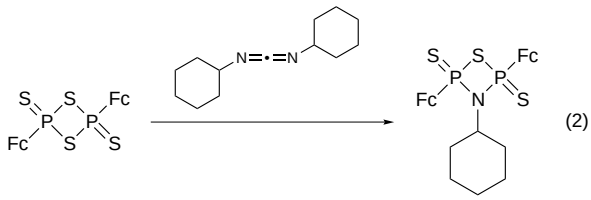

**Fig. 1** X-Ray crystal structure of **3**. Important bond lengths (Å) and angles (°): P–N(1) 1.648(6), P–N(2) 1.664(4), P–S(1) 1.941(2), P(1)–C(7) 1.783(5), N(1)–C(1) 1.289(6), N(2)–C(2) 1.290(6), C(1)–S(2) 1.788(5), C(2)–S(2) 1.771(5), C(1)–N(3) 1.335(6), C(2)–N(4) 1.365(6); N(1)–P–N(2) 108.2(2), P–N(1)–C(1) 122.6(4), P–N(2)–C(2) 121.0(4), N(1)–C(1)–S(2) 125.4(5), N(2)–C(2)–S(2) 127.3(4), C(1)–S(2)–C(2) 101.0(2), S(1)–P–C(7) 111.1(2), N(1)–P–S(1) 114.6(1), N(2)–P–S(1) 113.6(2), N(1)–P–C(7) 104.4(4), N(2)–P–C(7) 103.9(2).



**Scheme 1**

hedral, interestingly P–N(1) is substantially shorter [1.631(4) Å] than P–N(11) [1.700(5) Å] reflecting the difference in electronegativities of the $NMe_2$ and NCS groups. The formation of these products presents a challenge mechanistically; we believe that a series of [2 + 2] reactions are a reasonable explanation for the formation of **3** and **4** (Scheme 1).

The reaction of dicyclohexylcarbodimide with **1** gives [eqn. (2)] 2,4-diferrocenyl-3-cyclohexyl-1,3,2,4-thiaazadiphosphorine-2,4-disulfide **5**.† Alternatively reaction of **1** with



(2)

*N*-(benzylidene)aniline yields the phenyl analogue **6**.† Compounds **5** and **6** display the expected spectroscopic properties. There are only two previous reported examples[5,6] of the crystallographic characterisation of the RP(S)SNP(S)R rings. The X-ray structures‡ of **5** and **6** are isomorphous and we shall only discuss **6**. The molecule (Fig. 3) has crystallographic twofold symmetry and the central $P_2NS$ ring is thus flat with the S(1) and S(1*) atoms lying on opposite sides of the ring. Within the rings the bond lengths are appropriate for P–N and P–S single bonds whilst the internal ring angles [S(2)–P(1)–N(1) 87.8(2), P(1)–N(1)–P(1*) 104.5(4), P(1)–S(2)–P(1*) 79.9(2)°] indicate substantial ring strain. The phenyl substituent is twisted by *ca*. 14° w.r.t. the $P_2NS$ plane in **6**.

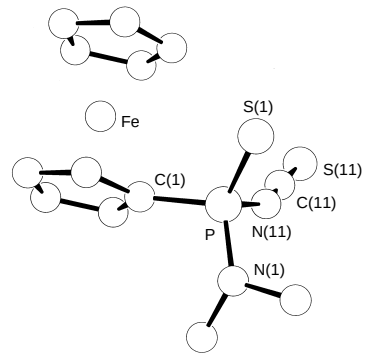



**Fig. 2** X-Ray crystal structure of **4**. Important bond lengths (Å) and angles (°): P–C(1) 1.766(5), P–S(1) 1.914(2), P–N(1) 1.631(4), P–N(11) 1.700(5), N(11)–C(11) 1.166(6), C(11)–S(11) 1.538(7); C(1)–P–S(1) 116.7(2), C(1)–P–N(1) 107.3(2), C(1)–P–N(11) 101.2(2), N(1)–P–S(1) 113.2(2), N(1)–P–N(11) 104.9(3), N(11)–P–S(1) 113.2(2), P–N(11)–C(11) 156.5(6), N(11)–C(11)–S(11) 177.1(6).

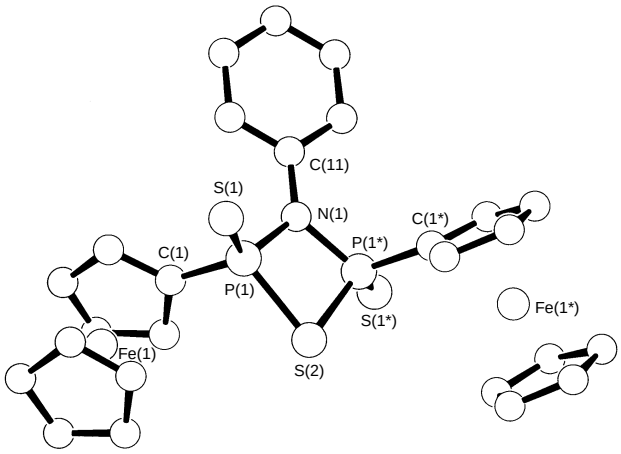



**Fig. 3** X-Ray structure of **6**, **5** is isomorphous (and is not illustrated). Important bond lengths (Å) and angles (°) with values for **5** given in square brackets: P(1)–C(1) 1.789(5) [1.785(6)], P(1)–S(1) 1.917(3) [1.918(3)], P(1)–S(2) 2.098(3) [2.095(3)], P(1)–N(1) 1.704(5) [1.675(5)]; C(1)–P(1)–S(1) 114.3(3) [114.1(2)], C(1)–P(1)–N(1) 108.4(3) [109.2(2)], C(1)–P(1)–S(2) 106.6(3) [105.9(3)], S(1)–P(1)–S(2) 120.1(1) [119.9(1)], S(1)–P(1)–N(1) 116.5(2) [116.7(2)], S(2)–P(2)–N(1) 87.8(2) [87.9(2)], P(1)–N(1)–P(1*) 104.5(4) [105.3(5)], P(1)–S(2)–P(1*) 79.9(2) [79.0(2)].

## Footnotes

* E-mail: J.D.Woollins@lboro.ac.uk

† **3** and **4**: **1** (2.91 g, 5.2 mmol) and dimethylcyanamide (1.5 g, 21 mmol) were refluxed together in toluene (50 ml) for 8 min. Silica gel chromatography using firstly light petroleum–toluene and then $CH_2Cl_2$ as the eluent gave **3** and **4** (2.6 g, 60 and 0.57 g 15% yields respectively).

**5**: *N*,*N*′-Dicyclohexylcarbodiimide (0.72 g, 3.5 mmol) and **1** (1.9 g, 3.4 mmol) were refluxed in toluene (10 ml) for 7 days. After removal of solvent and chromatography (light petroleum) an orange solid was obtained. This was washed with boiling ethyl acetate to give after filtration **5** (77 mg, 101 μmol, 3%) as a orange solid.

**6**: **1** (3.0 g, 5.36 mmol) and *N*-(benzylidene)aniline (2.0 g, 11.0 mmol) were refluxed in toluene (150 ml) (24 h). After addition of xylenes (100 ml) the reaction was refluxed for a further 64 h. Chromatography on silica, elution with 500 ml of 40% $CH_2Cl_2$ in light petroleum followed by 500 ml of $CH_2Cl_2$, gave a red solid. Recrystallisation from ethyl acetate yielded 0.97 g. 1.57 mmol, 29%.

‡ *Crystal data* Common to all determinations: Diffractometer Rigaku AFC7S $2\theta_{max}$ 120°, Cu-Kα radiation, $\lambda$ = 1.541 78 Å, $T$ = 296 K, structure solutions by direct methods, refinements employed teXsan. **3**: $C_{16}H_{21}FeN_4PS_2$, $M$ = 420.3, monoclinic, space group $P2_1/c$ (no. 14), $a$ = 13.084(4), $b$ = 7.897(6), $c$ = 18.364(5) Å, $\beta$ = 97.31(2)°, $U$ = 1882(1) Å$^3$, $D_c$ = 1.483 g cm$^{-3}$, $Z$ = 4, 3184 reflections measured, 1820 with $I > 2\sigma(I)$. All non-H atoms refined anisotropically to yield $R$ = 0.040 and $R_w$ = 0.038 for 218 parameters. **4**: $C_{13}H_{15}FeN_2PS_2$, $M$ = 350.2, monoclinic, space group $P2_1/n$ (no. 14), $a$ = 7.6883(9), $b$ = 20.6140(9), $c$ = 9.8804(9) Å, $\beta$ = 90.700(9)°, $U$ = 1566(2) Å$^3$, $D_c$ = 1.486 g cm$^{-3}$, $Z$ = 4, 2162 reflections measured, 1359 with $I > 2\sigma(I)$. All non-H atoms refined anisotropically to yield $R$ = 0.037 and $R_w$ = 0.037 for 173 parameters. **5**: $C_{26}H_{29}Fe_2NPS_3$, $M$ = 625.3, orthorhombic, space group *Pbcn* (no. 60), $a$ = 17.260(5), $b$ = 15.020(3), $c$ = 10.333(4) Å, $U$ = 2678(1) Å$^3$, $D_c$ 1.550 g cm$^{-3}$, $Z$ = 4, 2304 reflections measured, 840 with $I > 2\sigma(I)$. The cyclohexyl group was disordered and the two sites were refined anisotropically with 0.6 and 0.4 occupancies, only the H-atoms on the higher occupancy site were included in the refinement. The remaining non-H atoms were refined anisotropically to yield $R$ = 0.041 and $R_w$ = 0.049 for 170 parameters. **6** $C_{26}H_{23}Fe_2NPS_3$, $M$ = 619.3, orthorhombic, space group *Pbcn* (no. 60), $a$ = 16.723(2), $b$ = 14.861(2), $c$ = 10.216(3) Å, $U$ = 2538(1) Å$^3$, $D_c$ = 1.620 g cm$^{-3}$, $Z$ = 4, 2186 reflections measured, 948 with $I > 2\sigma(I)$. $R$ = 0.048 and $R_w$ = 0.035 for 152 parameters. Atomic coordinates, bond lengths and angles, and thermal parameters have been deposited at the Cambridge Crystallographic Data Centre (CCDC). See Information for Authors, Issue No. 1. Any request to the CCDC for this material should quote the full literature citation and the reference number 182/480.

## References

1 M. R. StJ. Foreman, A. M. Z. Slawin and J. D. Woollins, *J. Chem. Soc., Dalton Trans.*, 1996, 3653.
2 K. Clausen, A. A. Ei-Barbary and S. O. Lawesson, *Tetrahedron*, 1981, **37**, 1019.
3 A. A. El-Barbary and S. O. Lawesson, *Indian J. Chem. Sect. B*, 1984, **23**, 655.
4 A. Schmidpeter and N. Schindler, *Angew. Chem., Int. Ed. Engl.*, 1968, **7**, 943.
5 W. Zeiss, H. Jenjes, D. Lux, W. Schwarz and H. Hess, *Z. Naturforsch., Teil B*, 1979, **34**, 1334.
6 C. Donath, B. Wallis, M. Meisel and P. Leibnitz, *Z. Anorg. Allg. Chem.*, 1989, **576**, 33.

*Received in Cambridge, UK, 28th April 1997; Com. 7/02857A*

# Transition-state structural refinement with GRACE and CHARMM: realistic modelling of lactate dehydrogenase using a combined quantum/classical method

**Vicente Moliner,† Alexander J. Turner and Ian H. Williams***

*School of Chemistry, University of Bath, Bath, UK BA2 7AY*

**A transition structure for reduction of pyruvate catalysed by lactate dehydrogenase is refined and characterised in hybrid quantum mechanical/molecular mechanical (AM1/CHARMM) calculations involving a fully flexible active-site region by means of a novel procedure (GRACE), and is remarkably similar to that calculated *in vacuo*.**

The key to understanding of the fundamental processes of enzyme catalysis, or to designing transition-state analogues (as potential drugs) or modified enzymes (with new specificities), is knowledge of transition-state structure and properties. Computational simulation of enzymic reactions[1] provides a valuable tool for investigation of these issues. We report the results of a combined classical/quantum modelling study of a transition structure (TS) for reduction of pyruvate catalysed by lactate dehydrogenase (LDH). A novel computational procedure is employed, which allows the TS to be located with full gradient relaxation of the positions of 1900 atoms of a solvated enzyme–substrate complex utilising a hessian involving displacements of 147 atoms in the active site. The resulting TS shows remarkable structural similarity to that determined in earlier molecular orbital (MO) calculations[2–4] for the reaction *in vacuo*.

LDH is an NAD-dependent enzyme catalysing the interconversion of pyruvate and lactate. The X-ray crystal structure of its inhibitor-bound ternary complex has been determined,[5] and its mechanism has been the subject of many experimental[6] and several theoretical studies.[2–4,7–9] Although the reaction rate of the wild-type enzyme with pyruvate at room temperature is actually limited by a conformational transition, the chemical step involves hydride transfer (HT) from the nicotinamide ring of NADH to the carbonyl C atom of the substrate. The Empirical Valence-Bond theoretical study by Warshel[7] presupposed that HT to pyruvate occurs first, followed by protonation on the carbonyl O atom of the substrate from His-195. However, all previous MO studies,[2–4,8,9] performed using a variety of *in vacuo* models, concur that proton transfer (PT) precedes HT. These contradictory conclusions beg the question: what influence does the protein environment have upon the reaction mechanism?

We have employed a hybrid theoretical technique in which a quantum mechanical (QM) description of the chemical bond making and breaking events is combined with a molecular mechanics (MM) treatment of the surrounding protein and solvent. The first phase of this work used the CHARMM24 program[10] as described previously for reactions in aqueous solution[11] and in a solvated enzyme active site.[12] Computational limitations made it impractical to include the entire LDH protein in the calculations, so we selected a pseudo-sphere of 1900 atoms of enzyme, co-factor, substrate and solvent centred around the substrate, hydride donor and proton donor groups. This system was divided into a QM region of 39 atoms (the shaded portion of Fig. 1 comprising pyruvate, the nicotinamide ring of NADH and part of His-195), treated by the AM1 semiempirical MO method,[13] and a MM region, comprising the rest of the protein (CHARMM24 potentials) and the solvent water (TIP3P).[14] Two link atoms were inserted where the QM/MM boundary intersected covalent bonds (indicated as ● in Fig. 1). The QM/MM total energy surface shown in Fig. 2 was

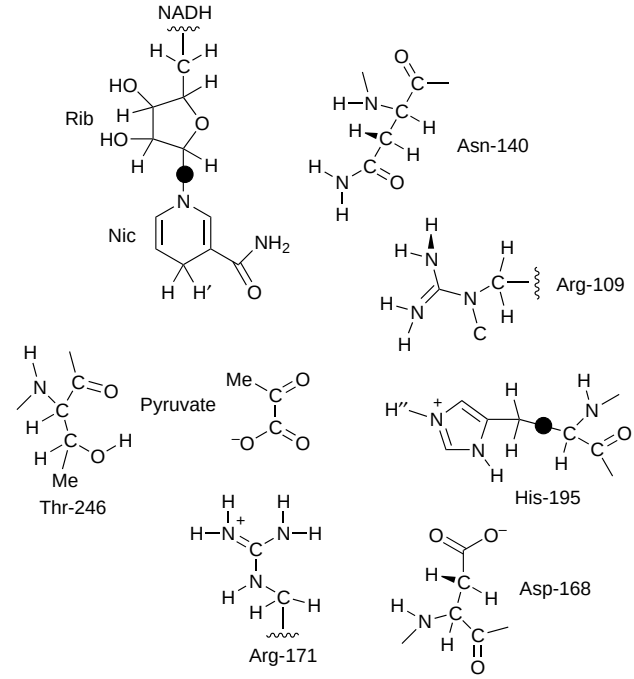



**Fig. 1** LDH active site. The shaded region corresponds to the QM atoms; the two link atoms are indicated as ●.

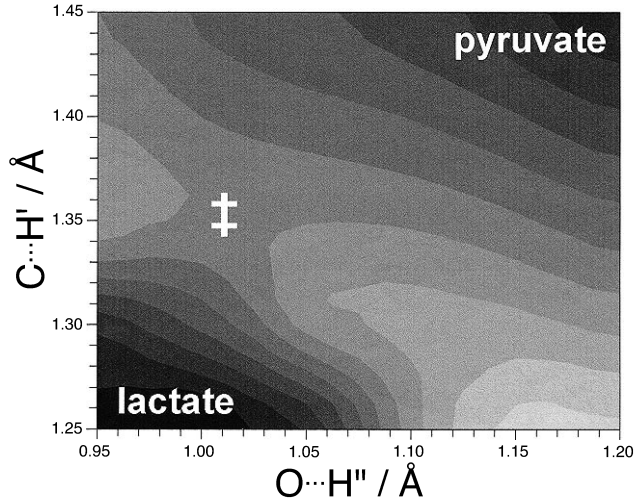



**Fig. 2** QM/MM total energy contour map (dark = low energy; light = high energy) for LDH-catalysed pyruvate reduction by NADH obtained as a function of hydride transfer and proton transfer coordinates by means of grid searches using CHARMM

constructed from a grid formed by pairs of rigid internal-constraint values for the making bond distances C··H′ and O··H″, from the carbonyl C atom of pyruvate to the H′ atom of the nicotinamide ring (hydride donor), and from the carbonyl O atom of pyruvate to the H″ atom of His-195 (proton donor), respectively. At each grid point relaxation of the entire hybrid QM/MM potential was performed to the constrained local minimum. At the surface of the pseudo-sphere, a solvent boundary potential was employed to prevent evaporation of water molecules, and harmonic restraints were applied to protein atoms disconnected from the backbone, owing to truncation, in order to preserve the enzyme structure. All non-bonded interactions were included.

The approximate TS, corresponding to the saddle point on Fig. 2, was then refined, using our newly developed GRACE‡ software. A partial-rational-function-operator/adopted-basis-Newton-Raphson method was employed, utilising a hessian matrix of order 441 × 441, describing the curvature of the QM/MM energy hypersurface for a sub-set of the system (larger than that shown in Fig. 1), together with a diagonal hessian plus updates for the rest of the system. A detail of the refined TS is shown in Fig. 3. The r.m.s. residual gradient on the 147 atoms in the sub-set is less than 0.1 kcal $mol^{-1}$ $Å^{-1}$ in the optimized structure, while on the remaining 1753 atoms it is less than 0.005 kcal $mol^{-1}$ $Å^{-1}$; these residual gradients are lower than the commonly accepted convergence criterion for optimized geometries of small molecules in quantum chemistry.[15] Finally, the intrinsic reaction coordinate[15] path was determined from the TS in each direction, leading to pyruvate and to lactate, in order to demonstrate conclusively that the reported structure is indeed a TS for the correct reaction. It is this capability to refine and characterise TSs precisely within a large flexible domain of the reacting system which distinguishes the present work from other recently published QM/MM applications to enzymic reactions.[16]

The transition vector ($\nu^{\ddagger}$ = 568*i* $cm^{-1}$) for the TS of the LDH-catalysed reaction involves motion of both the transferring hydride H′ and proton H″, indicating a concerted mechanism. However, PT is much further advanced (Pauling bond order $n_{O\cdots H''}$ = 0.81) than HT ($n_{C\cdots H'}$ = 0.33). This is remarkably similar to the TS found in a gas-phase AM1 supermolecule calculation for a *N*-methyl-1,4-dihydronicotinamide–pyruvate–(methylguanidinium)–methylimidazolium complex.[3] The PT and HT components occur in perpendicular planes, the degree of HT is essentially the same (*cf.* 0.31),[3] but PT is slightly earlier (*cf.* 0.93 for specific acid catalysis).[3] The TS for this reaction appears to be a robust entity, the essential features of whose structure are invariant to the nature of its environment.

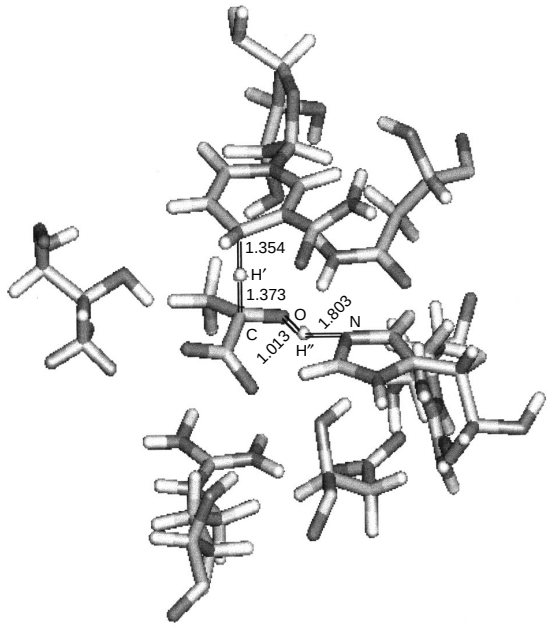



**Fig. 3** QM/MM transition structure refined using GRACE for LDH-catalysed pyruvate reduction by NADH (distances in Å)

Finally, several active site residues, notably Arg-109 and Asn-140, display considerable mobility over the range of structures spanned by the energy surface in Fig. 2. We have evidence that the TS reported here is only one of a family of structures of similar energy which differ in regard to conformations of amino acid sidechains; the transition state for the enzymic reaction represents an average of the properties of these many, nearly degenerate TSs. This insight emerges only as a consequence of the flexible model of the active site employed in this study.

We are grateful to the Leverhulme Trust for a Visiting Fellowship (V. M.), the BBSRC for a Studentship (A. J. T.), SmithKline Beecham for an equipment donation, and Glaxo-Wellcome and the EPSRC for financial support. We thank Dr Tim Dafforn for supplying us with initial coordinates for the LDH–NADH–pyruvate ternary complex.

## Footnotes

* E-mail: i.h.williams@bath.ac.uk
† On leave from the Departament de Ciencies Experimentals, Universitat Jaume I, Castelló, Spain.
‡ GRACE is a powerful extension to Tool Control Language (TCL), which uses free format data structures and cache technology to interface QM packages (like CADPAC, GAMESS or GAUSSIAN) with CHARMM (or CHARMm) or with its own routines for investigation of QM/MM energy surfaces. The structured programming advantages of TCL are augmented by many novel features including a range of powerful optimisers for minima and saddle points, IRC paths and vibrational frequencies.

## References

1 A. J. Mulholland, G. H. Grant and W. G. Richards, *Protein Eng.*, 1993, **6**, 133; A. J. Mulholland and M. Karplus, *Biochem. Soc. Trans*., 1996, **24**, 254.
2 J. Wilkie and I. H. Williams, *J. Am. Chem. Soc.*, 1992, **114**, 5243.
3 J. Andrés, V. Moliner, J. Krechl and E. Silla, *J. Chem. Soc., Perkin Trans. 2*, 1995, 1551.
4 J. Wilkie and I. H. Williams, *J. Chem. Soc., Perkin. Trans. 2*, 1995, 1559.
5 D. B. Wigley, S. J. Gamblin, S. P. Turkenburg, E. J. Dodson, K. Piontek, H. Muirhead and J. J. Holbrook, *J. Mol. Biol.*, 1992, **223**, 317.
6 A. R. Clarke, T. Atkinson and J. J. Holbrook, *Trends Biochem. Sci.*, 1989, **14**, 101 and 145.
7 A. Yadav, R. M. Jackson, J. J. Holbrook and A. Warshel, *J. Am. Chem. Soc.*, 1991, **113**, 4800.
8 J. Andrés, V. Moliner, J. Krechl and E. Silla, *Bioorg. Chem.*, 1993, **21**, 260; J. Andrés, V. Moliner and V. S. Safont, *J. Chem. Soc., Faraday Trans.*, 1994, **90**, 1703.
9 S. Ranganathan and J. E. Gready, *J. Chem. Soc., Faraday Trans.*, 1994, **90**, 2047.
10 B. R. Brooks, R. E. Bruccoleri, B. D. Olafson, D. J. States, S. Swaminathan and M. Karplus, *J. Comput. Chem.*, 1983, **4**, 187; CHARMM24b2, M. Karplus, Harvard University, 1996.
11 J. A. Barnes and I. H. Williams, *Chem. Commun.*, 1996, 193.
12 J. A. Barnes and I. H. Williams, *Biochem. Soc. Trans*., 1996, **24**, 263.
13 M. J. S. Dewar, E. G. Zoebisch, E. F. Healy and J. J. P. Stewart, *J. Am. Chem. Soc.*, 1985, **107**, 390.
14 W. L. Jorgensen, J. Chandrasekhar, J. Madura, R. W. Impey and M. L. Klein, *J. Chem. Phys.*, 1983, **79**, 926.
15 J. B. Foresman and Æ. Frisch, *Exploring Chemistry with Electronic Structure Methods*, Gaussian, Inc., Pittsburgh, PA, 1993.
16 *E.g.* M. J. Harrison, N. A. Burton, I. H. Hillier and I. R. Gould, *Chem. Commun.*, 1996, 2769; M. Peräkylä and P. A. Kollman, *J. Am. Chem. Soc.*, 1997, **119**, 1189.

*Received in Exeter, UK, 16th April 1997; Com. 7/02600E*

# New chain architecture for a one-dimensional aluminophosphate, $[H_3NCH_2CH_2NH_3][AlP_2O_8H]$

**Ian D. Williams,*[a] Jihong Yu,[a,b] Qiuming Gao,[b] Jiesheng Chen[b] and Ruren Xu*[b]**

[a] *Department of Chemistry, Hong Kong University of Science and Technology, Clear Water Bay, Kowloon, Hong Kong*
[b] *Key Laboratory of Inorganic Hydrothermal Synthesis, Department of Chemistry, Jilin University, Changchun, China*

**A new type of one-dimensional aluminophosphate polymer chain is found for $[H_3NCH_2CH_2NH_3][AlP_2O_8H]$ containing fused $Al_2P_2$ four-membered rings, with terminal $PO_4H$ side-groups.**

The chemistry of aluminophosphates templated by organic amines continues to yield unexpected results, with the recent report of a new stoichiometry ($Al_3P_5$) from an alcoholic system,[1] and that through use of basic conditions, the known $[AlP_2O_8]^{3-}$ formulation can exist as a two-dimensional sheet with large 20-membered rings.[2] Previously aluminophosphates based on $[AlP_2O_8]^{3-}$ were only found as variably protonated one-dimensional polymer chains consisting of $Al_2P_2$ rings corner shared at Al [Fig. 1(*a*)].[3–5] We now report a new type of chain architecture for the one-dimensional ALPO $[H_3NCH_2CH_2NH_3][AlP_2O_8H]$ **1** which has a linear arrangement of fused (edge-shared) $Al_2P_2$ four-membered rings, and ($PO_4H$) side groups [Fig. 1(*b*)].

Compound **1** was synthesised from a predominantly alcoholic solvent system, utilising a gel composition of 1.0 $Al(OPr^i)_3$ : 12.5 $H_3PO_4$ : 5.0 en : 80 EG : 12.5 $H_2O$. Crystals of **1** suitable for a single-crystal X-ray structure determination† were obtained after heating this mixture for 14 days at 180 °C under autogeneous pressure in a Teflon-lined autoclave. The compound formed is essentially phase-pure, based on powder X-ray diffraction.

The structure of **1** is shown in polyhedral representation in Fig. 2. It consists of one-dimensional $[AlP_2O_8H]^{2-}$ polymeric anions, made up of tetrahedral $AlO_4$ and $PO_4$ units. These are connected in a zigzag ladder arrangement of fused $Al_2P_2$ four-membered rings, with pendant $PO_4H$ side groups. Thus there are both terminal and triply bridging phosphate groups, with connectivities to Al of one and three. This is different from the previously published structures of $[AlP_2O_8]^{3-}$ type anions in which both phosphates are chemically similar simple bridges linked to two Al. The $Al_2P_2$ rings in **1** have all four Al and P coplanar with two bridging oxygens (adjacent) above and two below the ring plane. The ring has dihedral angles of 75.4° to its adjoining neighbours, to create the zigzag effect.

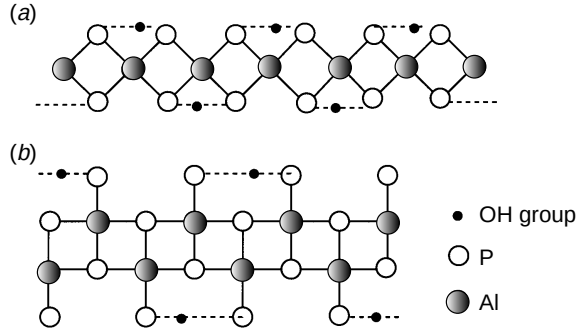



**Fig. 1** Schematic representation of $[AlP_2O_8H]^{2-}$ polymers; (*a*) corner- and (*b*) edge-shared four-membered ring chain

The metric parameters for this compound are well determined (data : parameter ratio *ca.* 20 : 1) and allow reasonably detailed analysis of the aluminophosphate bonding. Fig. 3 shows a fragment of the chain with atom labelling scheme. The aluminate group has one short Al–O distance [Al(1)–O(4) 1.685(1) Å] associated with an almost linear bridge to the terminal phosphate [Al(1)–O(4)–P(1) 171.8(1)°]. The other three Al–O bonds are in the range 1.741–1.746(1) Å and have angles at oxygen of 137.5–139.7(1)°. The shortening implies stronger p–d π bonding between Al and O for the sp hybridised oxygen bridge; interestingly no shortening is observed for P(1)–O(4) compared to the other P–$O_{bridge}$ bonds [P–O 1.535–1.544(1) Å]. There are four oxygens terminal to the phosphorus atoms, three on the $PO_4H$ side group. One of these has a longer bond [P(1)–O(1) 1.578(1) Å], and an associated hydrogen atom, so is assigned as P–OH. The other three P–$O_{terminal}$ bonds, which involve the oxygen atoms O(2), O(3) and O(8), are shorter [1.499–1.509(2) Å] and can be thought of as a mixture of P=O and P–$O^-$ canonical forms.

The one-dimensional chains are hydrogen-bonded to and separated by ethylene diammonium ions, with all six $NH_3$ protons acting as simple hydrogen-bond donors to the O(2), O(3) and O(8) terminal oxygens which carry substantial negative charge. The chains are also in van der Waals contact with two neighbours through the terminal phosphates, but there are no intermolecular P–OH···O=P (or P–OH···$^-$O–P) hydrogen bonds. Rather these are intramolecular [O(1)–H(1)···O(2) 2.641 Å] along the individual one-dimensional strand, as indicated in the Figures.

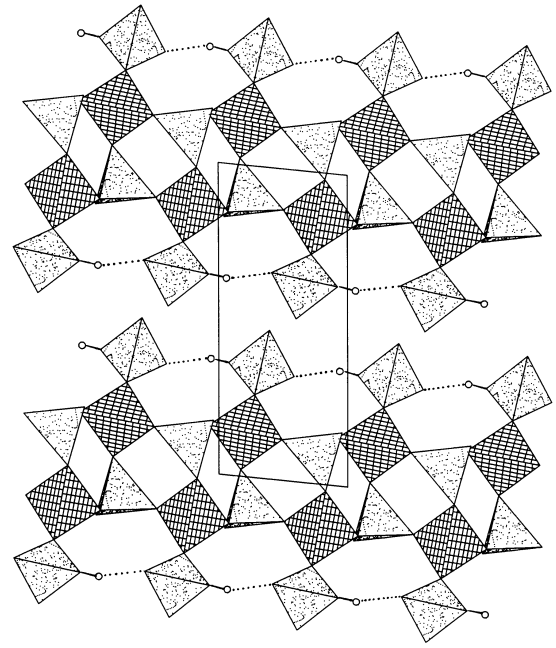


**Fig. 2** Polyhedral view of $[H_3NCH_2CH_2NH_3][AlP_2O_8H]$ **1** along the *b*-axis showing neighbouring anion chains

Isomerism within ALPO systems is a well known phenomenon, with a wealth of structures known for the neutral three-dimensional $AlPO_4$-*n*,[6] and the two-dimensional $[Al_2P_3O_{12}]^{3-}$ [7,8] and $[Al_3P_4O_{16}]^{3-}$ systems.[9] The isomer types are affected by the organo-templates which are usually amines, as well as the reaction conditions. Variables such as temperature, pressure, time and solvent system, as well as gel composition and concentration have profound effects, even for the same organic template. Thus, in addition to compound **1**, a number of other low-dimensional ALPOs have been formed using ethylenediamine (en), including a $[Al_3P_4O_{16}]^{3-}$ phase,[10] the isostructural one-dimensional polymers of the classical type [Fig.1(*a*)] $[H_3NCH_2CH_2NH_3][AlP_2O_8H]\cdot H_2O$[11] and $[NH_4][H_3NCH_2CH_2NH_3][AlP_2O_8]$,[5] as well as the salt $[NH_4][H_3NCH_2CH_2NH_3]_4[Al(PO_4)_4]$.[11] These last two also require the decomposition of en to form ammonia.

The promotion of low dimensionality in aluminophosphate materials by use of non-aqueous solvent systems has been discussed by Ozin and coworkers,[1] who also demonstrated that the one-dimensional polymer $[H_3NC_5H_9]_5[Al_3P_5O_{20}H]$ can be transformed in the solid state to the two-dimensional compound $[H_3NC_5H_9]_2[Al_2P_3O_{12}H]$. In the present case, the solvent system is predominantly ethylene glycol and a large excess of phosphoric acid is used, which may account for the low Al : P ratio of 1 : 2, compared to the other phases templated by ethylenediamine.

The existence of the $PO_4H$ side-groups in **1** indicates a low level of polyhedral condensation, which may have implications for the mechanism of build-up of ALPO polymers with higher levels of complexity. It should be noted that ribbons of fused four-membered rings, topologically equivalent to the 'ladder' structure of **1**, may be found in various higher dimensional ALPOs, for example in many of the $[Al_3P_4O_{16}]^{3-}$ and $AlPO_4$-*n* phases. The current structure would seem to be ideally set up for condensation of $AlO_4$ units across the P′–OH···O–P hydrogen bonded bridges (Fig. 3) to form new $Al_3P_3$ six-membered rings, another commonly featured ALPO structural sub-unit.

To our knowledge, however, terminal phosphate groups have not been seen previously for polymeric ALPO systems, although they exist in the molecular ion $[Al(PO_4)_4]^{9-}$.[11] We predict the recent findings of novel stoichiometries and dimensionalities in ALPO materials is likely to continue, if the phosphate components may also exist in this terminal mode, connected to a single aluminate, rather than as two-, three- or four-connected tetrahedral building blocks.

The authors wish to thank the Research Grants Council (H. K.) and National Natural Science Foundation of China for financial support and Dr. Zhenyang Lin for useful discussions.

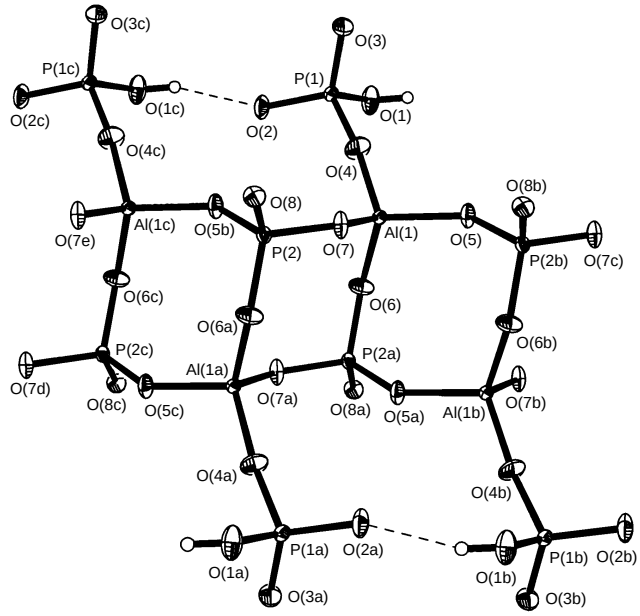



**Fig. 3** Thermal ellipsoid (40%) plot of **1** with labelling scheme for the anion

## Footnotes

* E-mail: chwill@usthk.ust.hk

† A colourless bar of dimensions 300 × 120 × 80 μm was selected. Structure carried out using a Siemens P4-RA diffractometer and solution and refinement by SHELXTL-PLUS; *Crystal data*: $C_2H_{11}AlN_2O_8P_2$, $M_w$ = 280.0, triclinic, $P\bar{1}$, $a$ = 4.901(1), $b$ = 9.032(1), $c$ = 11.691(1) Å, $\alpha$ = 81.38, $\beta$ = 82.27(1), $\gamma$ = 75.83(1)°, $U$ = 493.5(1) Å$^3$, $Z$ = 2, $D_c$ = 1.89 Mg m$^{-3}$, $R$ = 0.034, $R_w$ = 0.042 for 3486 data with $F \geqslant 4\sigma(F)$. Atomic coordinates, bond lengths and angles, and thermal parameters have been deposited at the Cambridge Crystallographic Data Centre (CCDC). See Information for Authors, Issue No. 1. Any request to the CCDC for this material should quote the full literature citation and the reference number 182/442.

## References

1 S. Oliver, A. Kuperman, A. Lough and G. A. Ozin, *Chem. Mater*., 1996, **8**, 2391.
2 K. R. Morgan, G. J. Gainsford and N. B. Milestone, *Chem. Commun*., 1997, 61.
3 T. Wang, L. Yu and W. Pang, *J. Solid State Chem*., 1990, **89**, 392.
4 R. H. Jones, J. M. Thomas, R. Xu, Q. Huo, Y. Xu, A. K. Cheetham and D. Bieber, *J. Chem. Soc., Chem. Commun*., 1990, 1170.
5 Q. Gao, J. Chen, S. Li, R. Xu, J. M. Thomas, M. Light and M. B. Hursthouse, *J. Solid State Chem*., 1996, **127**, 145.
6 S. T. Wilson, T. R. Cannan, E. M. Flanigen, B. M. Lok and C. A. Messina, *ACS Symp. Ser*., 1983, **218**, 79.
7 A. M. Chippindale, A. V. Powell, L. M. Bull, R. H. Jones, A. K. Cheetham, J. M. Thomas and R. Xu, *J. Solid State Chem*., 1992, **96**, 199.
8 S. Oliver, A. Kuperman, A. Lough and G. A. Ozin, *Chem. Commun.*, 1996, 1761.
9 I. D. Williams, Q. Gao, J. Chen, L-Y. Ngai, Z. Lin and R. Xu, *Chem. Commun.*, 1996, 1781.
10 R. H. Jones, J. M. Thomas, R. Xu, Q. Huo, A. K. Cheetham and A. V. Powell, *J. Chem. Soc., Chem. Commun*., 1991, 1266.
11 D. Riou, Th. Loiseau and G. Ferey, *J. Solid State Chem*., 1992, **99**, 414.

*Received in Bath, UK, 14th March 1977; Com. 7/01830D*

# The use of palladium on porous glass for catalytic coupling reactions

**Jintong Li, Albert W.-H. Mau and Christopher R. Strauss***

*CSIRO Division of Molecular Sciences, Private Bag 10, Clayton South MDC, Victoria 3169, Australia*

**Palladium on porous glass is a useful heterogeneous catalyst for liquid phase organic coupling reactions which can be carried out in the presence of air, without the need for solubilizing and activating ligands.**

Catalysts of palladium, its complexes and its salts, are well recognized for activation of C–H bonds towards coupling reactions.[1–3] In this regard, the Heck reaction of an aryl or vinyl halide with an alkene in the presence of palladium derivatives has been the subject of intensive study and there is growing interest in synthetic transformations of terminal alkynes *via* homo- or hetero-couplings of the Glaser, Eglington or Chodkiewicz–Cadiot type.[4–6]

However, commercial development, particularly of Heck reactions, has not progressed as rapidly as could have been expected, most likely because of low turnover numbers and low turnover frequencies.[7] The susceptibility of palladium catalysts to poisoning also necessitates the use of relatively large amounts (1–5 mol%) of expensive metal to ensure acceptable conversions.[8] Attempts at overcoming these disadvantages have involved the use of organopalladium complexes, usually containing phosphine ligands, as homogeneous catalysts.[1–3] Although such complexes can be difficult to separate from product mixtures and to recover from reaction media,[9] some recent success has been obtained with methods employing homogeneous two-phase catalysis.[10] Nonetheless, many phosphine ligands are thermally unstable, even at temperatures as low as 120 °C,[11] so maximum reaction temperatures are limited. In some cases, aryl groups emanating from degraded phosphines can react with olefinic starting materials, thereby affecting the course of the reaction.[12,13] Benefits of phosphine-free palladium catalysts have been discussed.[14]

In ongoing research into the development of technologies for environmentally benign chemistry,[15] we have investigated palladium metal on porous glass tubing as a catalyst for chemical syntheses. The catalyst may be similar to the membrane developed for hydrogen separation by Uemiya *et al.*,[16] and analogous to the platinum on porous glass used by Sun and Khang for dehydrogenation of cyclohexane.[17] Although such catalysts do not appear to have been employed for coupling reactions their potential advantages, including mechanical and thermal stability, solvent resistance, reusability, longevity, and obviation of air- and temperature-sensitive ligands have strong appeal.

Our *ca.* 0.18% palladium on porous glass tubing could be used for reactions conducted continuously or batchwise. It offered resistance to oxidative deterioration and could be re-used several times for repeat or different reactions. Examples, mostly carried out in the presence of air, with either conventional heating or under microwave irradiation in a novel pressure-tight batch reactor (MBR),[18] are compiled in Table 1.† Turnover numbers for entries 1–8 in this table were calculated from single, non-exhaustive reaction runs and have been compiled to show that the palladium was catalytic. For the Heck coupling of 4-bromoacetophenone with styrene, when the same sample of catalyst was re-used several times, or when the molar ratio of catalyst to reactants was substantially decreased (*e.g.* 0.02 mol% Pd was used for entry 9, Table 1), the turnover

**Table 1** Example reactions and conditions (*N*,*N*-dimethylacetamide as solvent)

| Entry | Starting material(s) | *T*/°C | *t*/h | Major product(s) | Conversion (%) | Turnover number |
|---|---|---|---|---|---|---|
| 1 | PhI + $CH_2$=CH–$CH_2$OH | 120[a] | 3 | $PhCH_2CH_2CHO$ + PhCH=CHCHO + by-products (52 : 30 : 18) | 99 | > 100 |
| 2 | PhI + $PhCH=CH_2$ | 180[a] | 1.5 | *trans*- + *cis*-PhCH=CHPh + $(Ph)_2CH=CH_2$ (83 : 1 : 16) | 100 | > 100 |
| 3 | PhI + phenylacetylene | 100[b] | 88 | 1,2-diphenylacetylene | 95[c] | > 100 |
| 4 | 4-bromobenzaldehyde + phenylacetylene | 100[b] | 24/72/96 | 4′-formyl-1,2-diphenylacetylene | 79[c]/86[c]/100[c] | > 100 |
| 5 | 4-bromoacetophenone + phenylacetylene | 140[b] | 12/100 | 4′-acetyl-1,2-diphenylacetylene | 55[c]/87[c] | > 100 |
| 6 | 4-bromoacetophenone + 1-hexyne | 100[a]/ 140[a] | 6/2 | 1-(4′-acetyl)phenylhex-1-yne + by-products[d] (51 : 49) | 16/73 | *ca.* 100 |
| 7 | 2-bromopyridine + phenylacetylene | 140[b] | 48/100 | 2-(2-pyridyl)-1-phenylacetylene | 55[c]/83[c] | *ca.* 100 |
| 8 | phenylacetylene | 150[b] | 48 | 1,4-diphenylbuta-1,3-diyne + homo-addition product (93 : 7) | 71 | *ca.* 100 |
| 9 | 4-bromoacetophenone + styrene | 180[e] | 12 | *trans*- + *cis*-4′-acetyl-1,2-diphenylethylene + 1-(4-acetylphenyl)-1-phenylethylene (91 : 2 : 7) | 98 | 4000 |

[a] Carried out in air, with the MBR. [b] Carried out in air, with conventional heating. [c] 1,4-diphenylbuta-1,3-diyne and a homo-addition product ($M_w$ 204) of phenylacetylene were present. [d] Some of these were formed by addition of hex-1-yne to the product. [e] Conventional heating, under argon.

numbers were an order of magnitude greater than the other values shown in Table 1.

The regioselectivity of Heck reactions was consistent with Heck's observation that terminal alkenes yield about 80 : 20 mixtures of 1- and 2-arylated alkenes when there are no major steric influences (see entries 2 and 9, Table 1).[3] Also in agreement with previous findings,[19] Heck reaction of iodobenzene with allyl alcohol afforded 3-phenylpropionaldehyde as the major product (entry 1, Table 1). However, *trans*-3-phenylprop-2-enal was also produced and in greater abundance than the expected regioisomer 2-phenylpropionaldehyde.[3] To our knowledge, this olefinic aldehyde has not been reported from the same reactants under Heck conditions. Air present during the reaction may have played a role, an aspect which will require further investigation.

Similarly with Heck reactions, internal alkynes can be obtained by coupling of aryl iodides or bromides with terminal acetylenes under palladium catalysis.[5] However, typical requirements for high amounts of catalyst (1–5 mol% Pd) and co-addition of copper salts (also 1–5 mol% in Cu) can diminish the industrial viability of such procedures.[8] New moisture-stable phosphapalladocycles, without copper salts, recently afforded a high yielding coupling of 4-bromoacetophenone with phenylacetylene, albeit under a single set of satisfactory conditions. When alternative starting aryl halides and alkynes were used, reaction either did not proceed or was only moderately successful in most cases.[8]

With palladium on porous glass, neither copper salts nor activating ligands were necessary. Conversions for the coupling of phenylacetylene with iodobenzene and with 4-bromobenzaldehyde were nearly quantitative (entries 3 and 4, respectively, Table 1) and were satisfactory for phenylacetylene with 4-bromoacetophenone (entry 5, Table 1) and 2-bromopyridine (entry 7, Table 1). Although several of these results were comparable with those of Herrmann *et al.*, the coupling of 4-bromoacetophenone with phenylacetylene in dimethylacetamide (DMA) with NaOAc as base and also the reaction of this ketone with hexyne proceeded with palladium on porous glass (see entries 5 and 6, Table 1) where it had failed with the phosphapalladocycles.[8]

Homocoupling of phenylacetylene[20] was apparent in all reactions involving this alkyne, so not surprisingly, 1,4-diphenylbuta-1,3-diyne was formed quite efficiently in the absence of other reactants (entry 8, Table 1). Thermal addition products of ($M_w$ 204) were also formed in relatively low amounts in all reactions involving phenylacetylene.

The above results show that palladium on porous glass is a useful catalyst for synthetic coupling reactions, and suggest that it could have applications in other reactions catalysed by palladium, *e.g.* dehydrogenation[17] and hydrogenation.

We thank Mr L. Bagnell for carrying out experiments for entry 9 in Table 1.

## Footnotes

* E-mail: chris.strauss@molsci.csiro.au

† Prewashed porous glass tubing (7 mm o.d., 4.8 mm i.d. tubing with 250 $m^2\ g^{-1}$ internal surface area, 28% porosity; 2.54 g) was allowed to stand overnight in an aqueous solution (50 ml) of $[Pd(NH_3)_4]Cl_2$, containing 110 ppm in palladium. It was then removed, washed three times with deionised water and immersed in a solution comprising $NaBH_4$ (2.0 g) in deionised water (100 ml), at room temperature for up to 5 h. In a typical experiment, a mixture of 4-bromoacetophenone (5 mmol) and phenylacetylene (8 mmol) in *N*,*N*-dimethylacetamide (50 ml) containing NaOAc (8 mmol) and 0.18% Pd on porous glass (2.54 g glass; 0.043 mmol Pd) was heated with stirring for 100 h in air at 140 °C. At regular intervals, samples were withdrawn for analysis by GC and GC–MS. See entry 5, Table 1.

## References

1 L. S. Hegedus, *Tetrahedron*, 1984, **40**, 2415; R. F. Heck, *Org. React.*, 1982, **27**, 345; R. F. Heck, *Palladium Reagents in Organic Chemistry*, Academic Press, London, 1985; B. M. Trost, *Angew. Chem., Int. Ed. Engl.*, 1995, **34**, 259.
2 A. de Meijere and F. E. Meyer, *Angew. Chem., Int. Ed. Engl.*, 1994, **33**, 2379.
3 R. F. Heck, in *Comprehensive Organic Synthesis*, series ed. B. M. Trost and I. Fleming, vol. ed. M. F. Semmelhack, Pergamon, Oxford, 1993, vol. 4, p. 833.
4 K. Sonogashira, in *Comprehensive Organic Synthesis*, series ed. B. M. Trost and I. Fleming, vol. ed. G. Pattenden, Pergamon, Oxford, 1993, vol. 3, p. 551; T. Sakamoto, H. Nagata, Y. Kondo, M. Shiraiwa and H. Yamanaka, *Chem. Pharm. Bull.*, 1987, **35**, 823; A. Vidal-Ferran, C. M. Muller and J. K. M. Sanders, *J. Chem. Soc., Chem. Commun.*, 1994, 2657; S. Y. Cho, S. S. Kim, K.-H. Park, S. K. Kang, J.-K. Choi, K.-J. Hwang and E. K. Yum, *Heterocycles*, 1996, **43**, 1641; T. Okita and M. Isobe, *Synlett*, 1994, 589; A.P. Melissaris and M. H. Litt, *J. Org. Chem.*, 1994, **59**, 5818.
5 L. Cassar, *J. Organomet. Chem.*, 1975, **93**, 253.
6 H. A. Dieck and R. F. Heck, *J. Organomet. Chem.*, 1975, **93**, 259.
7 M. Beller and T. H. Riermeier, *Tetrahedron Lett.*, 1996, **37**, 6535.
8 W. A. Herrmann, C.-P. Reisinger, K. Ofele, C. Brossmer, M. Beller and H. Fischer, *J. Mol. Catal.*, 1996, **108**, 51.
9 J. Kiviaho, T. Hanaoka, Y. Kubota and Y. Sugi, *J. Mol. Catal.*, 1995, **101**, 25.
10 B. Cornils, *Angew. Chem., Int. Ed. Engl.*, 1995, **34**, 1575.
11 W. A. Herrmann, C. Brossmer, K. Ofele, C.-P. Reisinger, T. Priermeier, M. Beller and H. Fischer, *Angew. Chem., Int. Ed. Engl.*, 1995, **34**, 1844; D. R. Coulson, *J. Chem. Soc., Chem. Commun.*, 1968, 1530; P. Fitton and E. A. Rick, *J. Organomet. Chem.*, 1971, **28**, 287.
12 W. A. Herrmann, C. Brossmer, K. Ofele, M. Beller and H. Fischer, *J. Mol. Catal.*, 1995, **103**, 133.
13 M. Sakamoto, I. Shimizu and A. Yamamoto, *Chem. Lett.*, 1995, 1101.
14 T. I. Wallow and B. M. Novak, *J. Org. Chem.*, 1994, **59**, 5034.
15 L. Bagnell, K. Cavell, A. M. Hodges, A. W.-H. Mau and A. J. Seen, *J. Membrane Sci.*, 1993, **85**, 291; A. J. Seen, K. J. Cavell, A. W.-H. Mau and A. M. Hodges, *J. Membrane Sci.*, 1994, **87**, 149; J. Li, K. Tachihara, K. Nagai, T. Nakagawa and S. Wang, *J. Appl. Polym. Sci.*, 1996, **60**, 1645; J. Li, K. Nagai, T. Nakagawa and S. Wang, *J. Appl. Polym. Sci.*, 1996, **61**, 2467; C. R. Strauss and R. W. Trainor, *Aust. J. Chem.*, 1995, **48**, 1665; J. An, L. Bagnell, T. Cablewski, C. R. Strauss and R. W. Trainor, *J. Org. Chem.*, 1997, **62**, 2505.
16 S. Uemiya, Y. Kude, K. Sugino, N. Sato, T. Matsuda and E. Kikuchi, *Chem. Lett.*, 1988, 1687; S. Uemiya, N. Sato, H. Ando, Y. Kude, T. Matsuda and E. Kikuchi, *J. Membrane Sci.*, 1991, **56**, 303.
17 Y.-M. Sun and S.-J. Khang, *Ind. Eng. Chem. Res.*, 1988, **27**, 1136.
18 K. D. Raner, C. R. Strauss, R. W. Trainor and J. S. Thorn, *J. Org. Chem.*, 1995, **60**, 2456.
19 J. B. Melpolder and R. F. Heck, *J. Org. Chem.*, 1976, **41**, 265; G. Dyker and P. Grundt, *Tetrahedron Lett.*, 1996, **37**, 619 and references cited therein.
20 C. Amatore, E. Blart, J. P. Genet, A. Jutand, S. Lemaire-Audoire and M. Savignac, *J. Org. Chem.*, 1995, **60**, 6829.

*Received in Cambridge, UK, 10th April 1997; Com. 7/02457F*

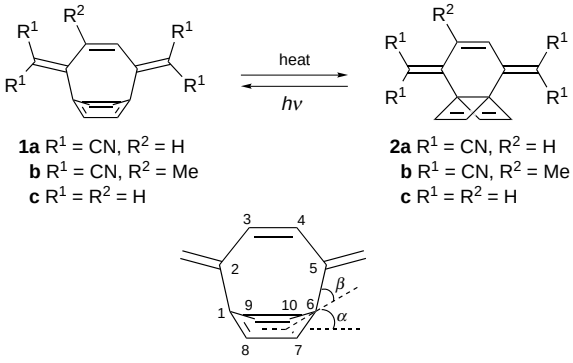
# The first observation of thermal transformation of strained paracyclophane into the Dewar isomer

**Masahiro Okuyama, Masakazu Ohkita and Takashi Tsuji***

*Division of Chemistry, Graduate School of Science, Hokkaido University, Sapporo 060, Japan*

**The kinetic stabilization of the [4]paracyclophane structure in the 2,5-bis(dicyanomethylene)-2-ene derivative permits the first observation of thermal isomerization of a strained paracyclophane to the Dewar valence tautomer; the activation free energy for the process is 18.3 ± 0.3 kcal mol$^{-1}$ at −20 °C.**

Isomerization of benzene to the Dewar valence tautomer is a highly endothermic process and the benzene ring is expected to be extremely bent in its late transition state.[1,2] A similar distortion of the benzene ring is effected in paracyclophane bridged by a short side chain,† and recent theoretical calculations suggest that the Dewar form becomes almost isoenergetic to or slightly higher in energy than the benzene form when the bridging chain is shortened to tetramethylene [–$(CH_2)_4$–].[3] Thus, it is suggested that thermal isomerization of the latter to the former is, at least, energetically feasible in [4]paracyclophane. [4]Paracyclophane and its derivatives have successfully been generated,[4,5] but their extreme thermal instability has impeded the observation of their possible cyclization to the Dewar forms.[4] We recently succeeded in stabilizing the skeleton of [4]paracyclophane in the 2,4-bis(dicyanomethylene)-2-ene derivative **1a** to permit the measurement of its $^1$H NMR spectrum for the first time.[6] We report here that **1a** and **1b** undergo thermal isomerization to the Dewar forms **2a**,**b**, respectively, and that their lifetimes in dilute solution are essentially limited by the above reactivity in the absence of air.




Compound **2a** in diethyl ether–isopentane glass at 77 K exhibits a characteristic absorption band with fine structure in the wavelength region of λ = 300–390 nm [Fig. 1(*a*)]. Irradiation of the glassy mixture with a 365 nm light source leads to the generation of **1a** exhibiting broad absorption in the 280–420 nm range at the expense of **2a**, as clearly displayed in the difference spectrum [Fig. 1(*b*)].[6] When the resulting mixture was thawed, briefly warmed up to room temperature, and refrozen at 77 K in the dark, the difference spectrum obtained from the absorptions before and after the heating was a near mirror image to the first one, as shown in Fig. 1(*c*), indicating the nearly quantitative thermal reversion of **1a** to **2a**. The half-life of **1a** at −20 °C is 15 ± 5 min and, accordingly, the activation free energy for the isomerization of **1a** to **2a** is $\Delta G^{\ddagger}$ = 18.3 ± 0.3 kcal mol$^{-1}$ at the same temperature.‡ The agreement of this energy barrier with a recent theoretical value (22 kcal mol$^{-1}$) for the isomerization of parent [4]paracyclophane **3** to 1,4-tetramethylene Dewar benzene **4**[3b] is extremely good, especially when a slightly higher exothermicity for the process from **1a** to **2a** as compared to that from **3** to **4** is taken into account. Similar photochemical generation of **1b** from **2b** and its clean thermal reversion at ambient temperature was also observed by UV–VIS spectrometry.

For such thermal unimolecular transformation to be observed the process must be exothermic. To gain information on the structures and energetics of **1** and **2**, computational analysis was undertaken. Geometrical optimization was carried out for truncated systems **1c** and **2c** using the GAUSSIAN 94 program package[7] since *ab initio* computations for **1a** and **2a** to reasonable accuracy exceeded the capacity of available computers. The optimized structures of **1c** and **2c** at the MP2/6-31G* and B3LYP/6-31G* levels are all $C_{2v}$ symmetric and the former lies higher in energy than the latter by 14.3 kcal mol$^{-1}$ at the MP2/6-13G* level and by 14.4 kcal mol$^{-1}$ at the B3LYP/6-13G* level, proving the exothermicity of the process from **1** to **2**.§ The deformation angles α and β, which give a measure of the degree to which the benzene ring is bent, and the interatomic distance between the bridgehead carbons, C(1) and C(6), in **1c** are 27.4 and 44.5°, and 2.700 Å at the MP2/6-31G* level and 28.6 and 43.0°, and 2.686 Å at the B3LYP/6-31G* level.¶ The diminution of this interatomic distance by further distortion of the benzene ring as compared to that in **1a** will certainly result in a lowered energy barrier to isomerization to the Dewar form, and hence in a diminished lifetime of the

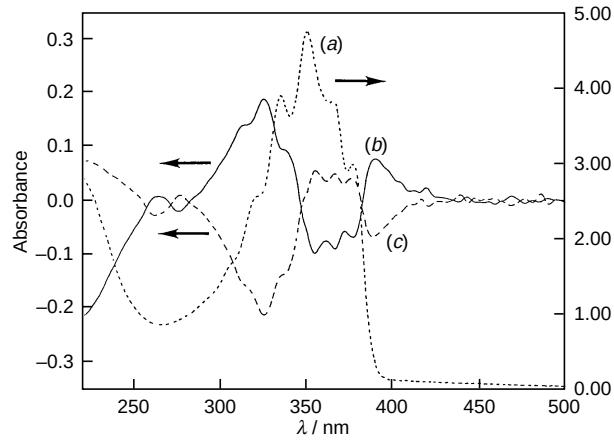



**Fig. 1** UV–VIS absorption spectra in diethyl ether–isopentane (1 : 1) at 77 K: (*a*) for **2a**; (*b*) difference spectrum obtained from the spectra before and after the irradiation of **2a** with 365 nm light; (*c*) difference spectrum obtained from those before and after the subsequent brief heating of the photolysed mixture to room temperature

benzene form.‖ Thus, **1** represents almost a limiting case of experimentally accessible strained paracyclophanes.

We acknowledge the Ministry of Education, Science and Culture of Japan for a Grant-in-Aid for Scientific Research (No. 06453031). T. T. thanks the Computer Center of the Institute for Molecular Science for the use of the NEC HSP computer.

## Footnotes

* E-mail: tsuji@science.hokudai.ac.jp

† The isomerization path has been predicted by calculations to have $C_{2v}$ symmetry (ref. 2).

‡ The photochemical isomerization of **2a** to **1a** is reversible and the latter constitutes only *ca*. 6% of the mixture in a photostationary state. The observation of the cycloreversion by another method, *e.g.* $^1$H NMR spectroscopy, was, therefore, experimentally difficult.

§ The total electronic energies of **1c** and **2c** are −461.563666 and −461.586464 a.u. at the MP2/6-31G* level and −463.095426 and −463.118401 a.u. at the B3LYP/6-31G* level, respectively.

¶ Other geometrical parameters for **1c** calculated at the MP2/6-31G* level (those at the B3LYP/6-31G* level in parenthesis; bond length in Å and bond angle in degrees): C(1)–C(2) = 1.496 (1.507), C(2)–C(3) = 1.497 (1.505), C(3)–C(4) = 1.385 (1.377), C(1)–C(8) = 1.413 (1.410), C(7)–C(8) = 1.391 (1.392), C(1)–C(2)–C(3) = 113.31 (113.00), C(2)–C(3)–C(4) = 138.58 (138.64), C(8)–C(1)–C(9) = 117.10 (116.98), C(1)–C(8)–C(7) = 117.60 (117.32).

‖ The interatomic distance between the reaction centres in the transition state for the benzene–Dewar benzene isomerization has been calculated to be in a range of 2.0–2.2 Å (refs. 2, 3).

## References

1 Reviews: D. Bryce-Smith and A. Gilbert, *Tetrahedron*, 1976, **32**, 1309; *Rearrangements in Ground and Excited States*, ed. P. de Mayo, Academic Press, New York, 1980, pp. 349–379.

2 M. Tsuda, S. Oikawa and K. Kimura, *Int. J. Quantum Chem.*, 1980, **18**, 157; M. Meisel and R. Janoschek, *J. Chem. Soc., Chem. Commun.*, 1986, 1066; M. von Arnim and S. D. Peyerimhoff, *Theor. Chim. Acta*, 1993, **85**, 43; F. Bockisch, J.-C. Rayez, H. Dreeskamp, D. Liotard and B. Duguay, *Theor. Chim. Acta*, 1993, **85**, 69.

3 (*a*) S. Grimme, *J. Am. Chem. Soc.*, 1992, **114**, 10 542; (*b*) B. Ma, H. M. Sulzbach, R. B. Remington and H. F. Schaefer, III, *J. Am. Chem. Soc.*, 1995, **117**, 8392.

4 T. Tsuji and S. Nishida, *J. Chem. Soc., Chem. Commun.*, 1987, 1189; *J. Am. Chem. Soc.*, 1988, **110**, 2157; *J. Am. Chem. Soc.*, 1989, **111**, 368; T. Tsuji, S. Nishida, M. Okuyama and E. Osawa, *J. Am. Chem. Soc.*, 1995, **117**, 9804.

5 B. G. M. Kostermans, M. Bobeldijk, W. H. De Wolf and F. Bickelhaupt, *J. Am. Chem. Soc.*, 1987, **109**, 2471.

6 M. Okuyama and T. Tsuji, *Angew. Chem., Int. Ed. Engl.*, 1997, **36**, 1085.

7 M. J. Frisch, G. W. Trucks, H.B. Schlegel, P. M. W. Gill, B. G. Johnson, M. A. Robb, J. R. Cheeseman, T. Keith, G. A. Petersson, J. A. Montgomery, K. Rachavachari, M. A. Al-Laham, V. G. Zackrewski, J. V. Ortiz, J. B. Foresman, J. Cioslowski, B. B. Stefanov, A. Nanayakkara, M. Challacombe, C. Y. Peng, P. Y. Ayala, W. Chen, M. W. Wong, J. L. Andres, E. S. Replogle, R. Gomperts, R. L. Martin, D. J. Fox, J. S. Binkley, D. J. Defrees, J. Baker, J. P. Steward, M. Head-Gordon, C. Gonzales and J. A. Pople, Gaussian Inc., Pittsburgh PA, 1995.

*Received in Cambridge, UK, 18th April 1997; Com. 7/02663C*

# Anodic co-oxidation of urazole and ferrocenes: first trapping of cyclopentadienols

**Jocelyn Lorans,[a] Fabrice Pierre,[a] Loïc Toupet[b] and Claude Moinet*[a]**

[a] *Laboratoire 'Electrochimie et Organométalliques', UMR CNRS 6509, Université de Rennes 1, 35042 Rennes cedex, France*
[b] *Laboratoire de Physique Cristalline, Université de Rennes 1, 35042 Rennes cedex, France*

**Cyclopentadien-5-ols, the major products resulting from decomposition of some ferrocenium cations by molecular oxygen, are regio- and stereo-selectively trapped by 4-phenyl-1,2,4-triazoline-3,5-dione.**

In oxygenated organic solvents, ferrocenium cations are unstable[1] and can easily be used for generating substituted cyclopentadienes in the presence of very reactive dienophiles. The strong dienophilic character of cyclic α-carbonyl azo compounds is well known.[2–6] These are generally prepared by chemical oxidation of the corresponding hydrazino compounds using lead(IV) acetate[7,8] or *tert*-butyl hypochlorite.[9–11] We report herein the co-oxidation of ferrocenes and a triazolidine-dione (urazole) in a flow cell fitted with a graphite felt porous anode.[12] Electrolyses were performed in acidified MeCN (2% $H_2SO_4$); solid sodium carbonate and oxygen were added to the solution of triazolinedione and ferrocenium cations at the outlet of the cell. Decomposition of ferrocenium cations proceeded *via* unexpected cyclopentadien-5-ols as major products which were trapped *in situ* with 4-phenyl-1,2,4-triazoline-3,5-dione (Scheme 1). To the best of our knowledge, this reaction has never been reported before. Theoretical calculations show that the three cyclopentadienol isomers should be very unstable.[13] Previously, cyclopentadienol has only been postulated as an intermediate during a thermal retro-Diels–Alder reaction.[14]

Decomposition of ferrocenium cation **1a** in the presence of triazolinedione **2** was complete after 1 h and gave a mixture of **3a** and **4a**. The yield of **3a** increased as the molar ratio triazolinedione : ferrocenium cation increased, whereas the yield of **4a** was practically unchanged (Table 1). The $^1$H and $^{13}$C NMR spectra of **3a** show a regio- and stereo-selective addition. X-Ray analyses show that **3a** results from an *exo* addition (Fig. 1) and **4a** from an *endo* addition. Compound **4a** is identical to the Diels–Alder adduct prepared by a different method using **2** and freshly distillated cyclopentadiene.[8]

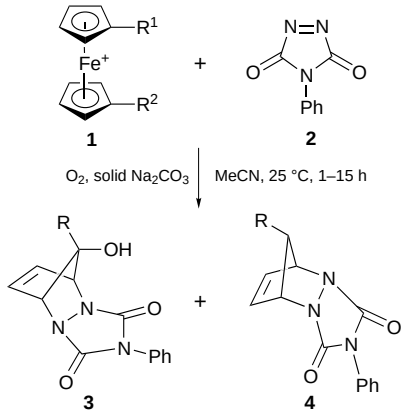
1,1′-Dialkylated ferrocenium cations **1b** and **1d** decomposed more slowly than **1a** and gave, after reaction with **2**, compounds **3b** and **3d** respectively. The $^1$H and $^{13}$C NMR spectra of **3b** and **3d** and the X-ray analysis of **3b** (Fig. 2) indicate a regioselective *exo*-addition like that for **3a**. After decomposition of mono-alkylated ferrocenium cation **1c** and reaction with **2**, a mixture of **3a** and **3d** was isolated. Compounds **3a** and **3d** were separated by column chromatography. Adduct **4a** was not detected.

The rate of decomposition of acetylferrocenium **1e** and 1,1′-diacetylferrocenium **1f** was much faster. Thus **1f** gave a mixture of unidentified products and **1e** gave **3a** in poor yield (12%).

**Table 1** Composition of mixtures from decomposition of ferrocenium cations **1** in the presence of 4-phenyl-1,2,4-triazoline-3,5-dione **2**

| Substrates (molar ratio) | Products (% yield[a]) |
|---|---|
| **1a** + **2** (1 : 1) | **3a** (46) + **4a** (12) |
| **1a** + **2** (1 : 2) | **3a** (69) + **4a** (14) |
| **1a** + **2** (1 : 3) | **3a** (80) + **4a** (15) |
| **1b** + **2** (1 : 2) | **3b** (41) |
| **1c** + **2** (1 : 2) | **3a** (24) + **3d** (45) |
| **1d** + **2** (1 : 2) | **3d** (52) |
| **1e** + **2** (1 : 2) | **3a** (12) |
| **1f** + **2** (1 : 2) | — |

[a] Calculated from initial ferrocene.




**Scheme 1**

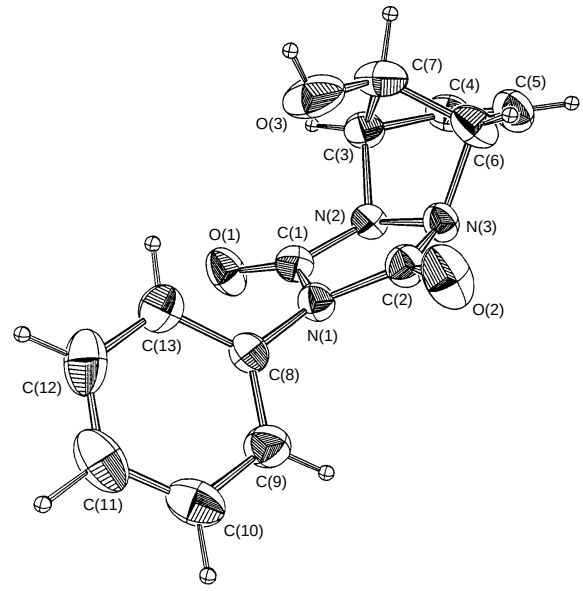



**Fig. 1** X-Ray structure of **3a**

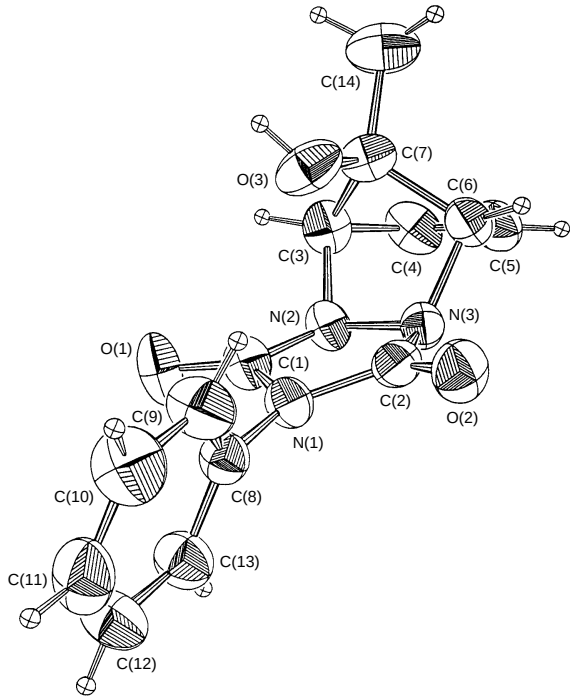



**Fig. 2** X-Ray structure of **3b**

Decomposition of ferrocenium cation is probably initiated *via* radical coupling with molecular oxygen as previously suggested.[1] After rearrangement and chemical evolution, cleavage of the iron and the formed cyclopentadienol ligand takes place, whereas only limited decomplexation of the second ligand (in case of **1a**) leads to free cyclopentadiene. To support this hypothesis, we note that the oxygen decomposition of ferrocenium cations in MeCN gave a brown precipitate characterised as an iron salt; elemental analyses of this salt showed the presence of one cyclopentadienyl ligand.[15]

## Footnotes

* E-mail: claude.moinet@univ-rennes1.fr

† *Selected data* for **3a**, **3b** *and* **3d**. Satisfactory elemental analyses were obtained for these new compounds. For **3a**: mp 214 °C; $\nu(CH_2Cl_2)/cm^{-1}$ 1726 (CO); HRMS: *m/z* 241.084 ($M^+$); $\delta_H$ (300 MHz, $CD_3COCD_3$) −4.15 (dt, 1 H, C*H*OH), 4.80 (m, 2 H, CH), 5.65 (d, 1 H, OH), 6.53 (t, 2 H, =CH), 7.35–7.51 (m, 5 H, $C_6H_5$); $\delta_C$ (75 MHz, $CD_3COCD_3$) −69.14 (d, CH), 83.29 (d, CHOH), 134.00 (d, C=C), 160.34 (s, C=O), 133.73 (s), 126.86 (d), 128.68 (d), 129.62 (d) ($C_6H_5$). For **3b**: mp 213–214 °C; $\nu(CH_2Cl_2)/cm^{-1}$ 1724 (CO); HRMS: *m/z* 271.095 ($M^+$). $\delta_H$ (300 MHz, $CD_3COCD_3$) −1.40 (s, 3 H, $CH_3$), 3.36 (s, 1 H, OH), 4.63 (t, 2 H, CH), 6.50 (t, 2 H, =CH), 7.3–7.5 (m, 5 H, $C_6H_5$); $\delta_C$ (75 MHz, $CD_3COCD_3$) −17.57 (q, $CH_3$), 71.03 (d, CH), 90.26 (d, COH), 132.80 (d, C=C), 158.88 (s, C=O), 131.30 (s), 125.67 (d), 128.62 (d), 129.22 (d) ($C_6H_5$). For **3d** mp 197–198 °C; $\nu(CH_2Cl_2)/cm^{-1}$ 1725 (CO); HRMS: *m/z* 285.110 ($M^+$); $\delta_H$ (300 MHz, $CD_3COCD_3$) −0.98 (t, 3 H, $CH_3$), 1.71 (q, 2 H, $CH_2$), 3.34 (s, 1 H, OH), 4.67 (t, 2 H, CH), 6.48 (t, 2 H, =CH), 7.3–7.5 (m, 5 H, $C_6H_5$); $\delta_C$ (75 MHz, $CD_3COCD_3$) −9.29 (q, $CH_3$), 23.98 (t, $CH_2$), 69.89 (d, CH), 93.76 (s, COH), 132.46 (d, C=C), 158.93 (s, C=O), 131.35 (s), 125.70 (d), 128.59 (d), 129.21 (d) ($C_6H_5$).

‡ *X-Ray crystal data* for **3a**: $C_{13}H_{11}N_3O_3$: MW = 257.25, Orthorhombic, *Pbca*, *a* = 11.386(2), *b* = 12.706(2), *c* = 16.275(3) Å, *V* = 2354.4(7) Å$^3$, *Z* = 8, *R* = 0.030, *Rw* = 0.029 for 1354 observations and 206 variables. For **3b**: $C_{14}H_{13}N_3O_3$: MW = 271.28, monoclinic, $P2_1/n$, *a* = 16.440(8), *b* = 8.490(7), *c* = 9.580(4) Å, β = 105.07(3)°, *V* = 1291(1) Å$^3$, *Z* = 4, *R* = 0.036, *Rw* = 0.034 for 1278 observations and 221 variables.

Data at 294 K were collected on an automatic diffractometer CAD4 Enrar-Nonius with graphite monochromatized Mo-Kα radiation. Atomic coordinates, bond lengths and angles, and thermal parameters have been deposited at the Cambridge Crystallographic Data Centre (CCDC). See Information for Authors, Issue No. 1. Any request to the CCDC for this material should quote the full literature citation and the reference number 182/484.

## References

1 W. P. Fehlhammer and C. Moinet, *J. Electroanal. Chem. Interfacial Electrochem.*, 1983, **158**, 187.
2 E. Fahr and H. Lind, *Angew. Chem., Int. Ed. Engl.*, 1966, **5**, 372.
3 K. MacKenzie, in *The Chemistry of the Hydrazo, Azo and Azoxy Groups*, ed. S. Patai, Wiley, New York, 1975, ch. 11.
4 G. Bianchi, C. De Micheli and R. Gandolfi, in *The Chemistry of the Double Bonded Functional Groups*, ed. S. Patai, Wiley, New York, 1977, part 1, ch. 6.
5 M. Quinteiro, C. Seoane and J. L. Soto, *Heterocycles*, 1978, **9**, 1771.
6 C. J. Moody, *Azo Dicarbonyl Compounds Advances in Heterocyclic Chemistry*, Academic Press Inc., 1982, vol. 30.
7 R. A. Clement, *J. Org. Chem.*, 1960, **25**, 1724; 1962, **27**, 1115.
8 R. C. Cookson, S. S. H. Gilani and I. D. R. Stevens, *Tetrahedron Lett.*, 1962, **14**, 615; *J. Chem. Soc., C*,1967, 1905.
9 E. F. Ullman and E. A. Barktus, *Chem. Ind.*, 1962, 93.
10 T. J. Kealy, *J. Am. Chem. Soc.*, 1962, **84**, 966.
11 J. Sauër and B. Schröder, *Angew. Chem., Int. Ed. Engl.*, 1965, **4**, 711.
12 C. Moinet and E. Raoult, *Bull. Soc. Chim. Fr.*, 1991, 214.
13 F. Turecek, *J. Org. Chem.*, 1986, **51**, 1563.
14 K. Alder and F. H. Flock, *Chem. Ber.*, 1956, 1732.
15 C. Moinet, unpublished results.

*Received in Cambridge, UK, 14th April 1997; Com. 7/02516E*

# Locked-in methyl groups in 1,5-dimethylnaphthalene close to the melting point

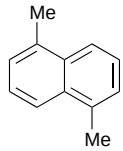
**Chick C. Wilson***

*ISIS Department, CLRC Rutherford Appleton Laboratory, Chilton, Didcot, Oxon, UK OX11 0QX*

**Single crystal neutron diffraction shows that the methyl group conformations in 1,5-dimethylnaphthalene are unchanged, with a hydrogen atom in the molecular plane, even as the crystal approaches the melting point.**

Our recent work on variable temperature single crystal neutron diffraction using rapid data collection methods is aimed at changing the overall energy content of the system and monitoring structural changes. These can involve either the internal vibrations of the molecule as indicated by anisotropic thermal parameters, or the order-disorder characteristics of parts of the molecule. These neutron studies have focused on hydrogen atom motions[1] and ordering,[2,3] and the present work represents our first attempt at examining a steric effect using this technique.

We have chosen to study 1,5-dimethylnaphthalene **1**, in which a steric interaction between the methyl groups and the neighbouring hydrogen atoms is likely to occur, reducing the propensity of the methyl groups to freely rotate in the crystal structure. The aim of the present work was to extend previous neutron diffraction measurements of the structure of **1** to higher temperatures and to use the hydrogen thermal parameters to examine the methyl group rotation as the temperature approaches the melting point. The original X-ray study[4] found that the methyl groups in the title compound are sterically 'frozen' into a single orientation, a conclusion supported by room temperature neutron diffraction measurements.[5] There was, however, the expectation that these methyl groups would start to rotate from this orientation before the crystal melts ($T_m$ = 353 K) with the rotation predicted to set in above 290 K, but this has not been examined until now.




**1**

To this end, we have collected single crystal neutron diffraction data from the title compound at a series of temperatures, on the SXD at ISIS.[6]† Large single crystals were grown by repeated recrystallisation from an acetone solution of **1** purchased from the Aldrich Chemical Company. Since the samples are volatile, a crystal of dimension 3 × 2 × 2 mm was sealed in a glass capillary and mounted in standard fashion on a Displex helium refrigerator. Initial data frames confirmed the unit cell and space group to be in agreement with previous work. A limited data set was collected at 100 K, followed by full data sets at 290 and 320 K. To allow the final data set to be collected as close to the melting point as practicable, a second crystal was mounted identically to the first and placed into the same cooling device on the instrument. A series of data frames were then collected as the sample was heated from room temperature through the melting point. The intensities of a group of strong reflections in this frame were monitored and significant reduction in intensity found to set in at around 340 K, approximately 10 K below the melting point. It was therefore decided to collect the data at 340 K and the original sample was remounted in identical fashion, heated to this temperature and diffraction data collected.

At all temperatures data were collected and reduced to structure factors in the standard fashion.[6] The structural model from which refinement began was that of ref. 5, but in addition the methyl hydrogens were located in all cases using Fourier calculations, which were computed using the GSAS program.[7] Refinement of the crystal structure at each temperature was carried out by least-squares methods in GSAS, using anisotropic thermal parameters on all atoms (Fig. 1). The data/

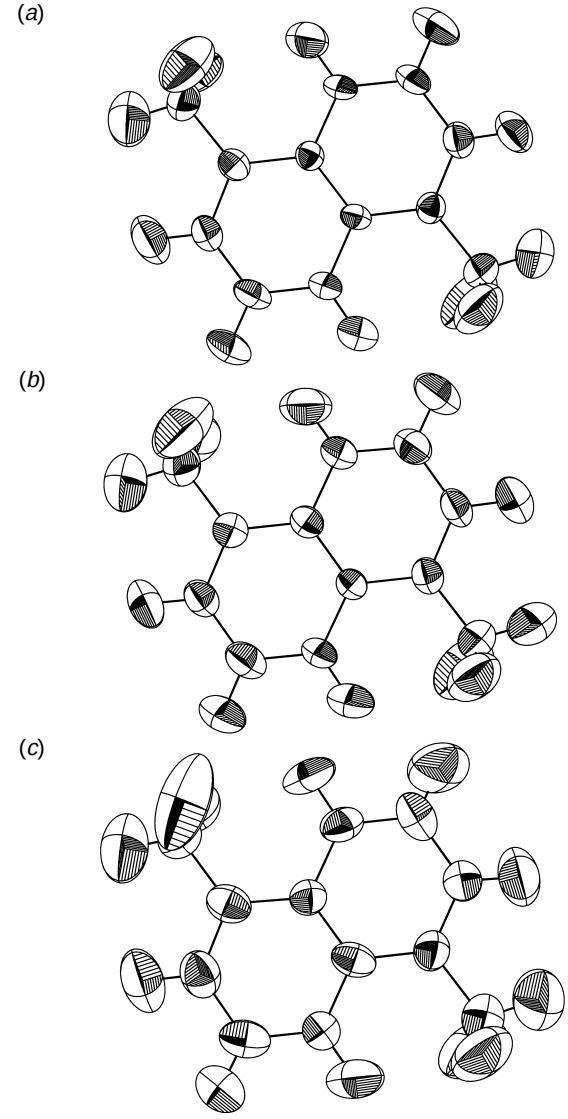



**Fig. 1** ORTEP (ref. 10) views of the refined structure of 1,5-dimethylnaphthalene at (*a*) 290, (*b*) 320 and (*c*) 340 K. The ellipsoids are plotted at 50% probability. The plot shows the equilibrium orientation of the methyl groups to be unchanged with increasing temperature.

parameter ratio for the 340 K data set is rather low, due to the fact that the crystal was progressively decreasing in volume as the data collection proceeded; in fact the inter-frame scale factors show that approximately 50% of the crystal was lost during the two days of data collection at 340 K.

The refined anisotropic thermal displacement parameters were subjected to rigid body analysis using the TLS method,[8,9] in which the two methyl groups were treated as undergoing torsional motions about the C–C bonds connecting them to the naphthalene ring. Although the precision of the TLS analysis is rather low, particularly at 340 K because of the low data/parameter ratio, it permits the general trend with temperature to be observed (Fig. 2).

Two major points emerge from the refinements. First, the equilibrium orientation of the methyl groups is essentially the same at all temperatures, and the in-plane hydrogen atom found at room temperature[5] remains in-plane even at 340 K. This observation was confirmed both from the refinements using the room temperature structural model as starting point, and also was clearly indicated by the Fourier calculations, in which the six methyl hydrogens were unambiguously located at all temperatures with no indication of significant atomic density in any other chemically plausible position around these groups.

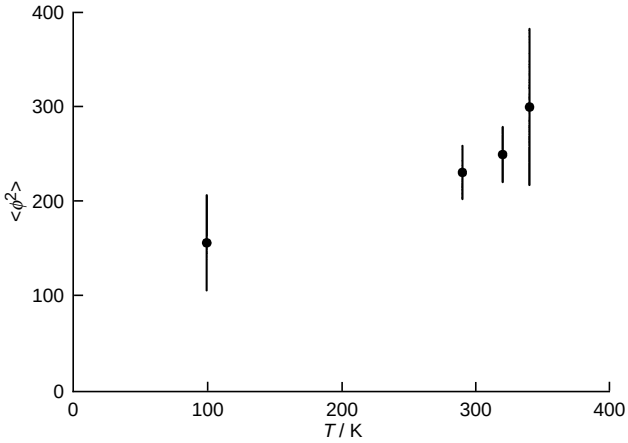



**Fig. 2** The average mean square torsional amplitude $<\phi^2>$ for the two methyl groups in 1,5-dimethylnaphthalene as a function of temperature

Secondly, the torsional motions of both methyl groups broadly increase with temperature as expected. However, there is an indication of the effect of steric clashes in the relatively low magnitude of these librations even close to melting (compare $<\phi^2>_{340\ K} = 300°^2$ for **1** with $<\phi^2>_{330\ K} = 940°^2$ for a molecule with a methyl group undergoing unhindered rotation, *e.g.* paracetamol[1]).

In conclusion, we clearly have in 1,5-dimethylnaphthalene a sterically hindered molecule in which the propensity of the methyl groups to undergo large torsional oscillations at high temperature is frustrated by steric effects. The methyl groups appear to be restrained in a single equilibrium orientation even close to the melting point, undergoing progressively larger but still hindered vibrations.

## Footnotes

* E-mail: ccw@isise.rl.ac.uk

† Atomic coordinates, bond lengths and angles, and thermal parameters have been deposited at the Cambridge Crystallographic Data Centre (CCDC). See Information for Authors, Issue No. 1. Any request to the CCDC for this material should quote the full literature citation and the reference number 182/481.

## References

1 C. C. Wilson, unpublished work.
2 C. C. Wilson, N. Shankland and A. J. Florence, *Chem. Phys. Lett.*, 1996, **253**, 103.
3 C. C. Wilson, N. Shankland and A. J. Florence, *Faraday Trans.*, 1996, **92**, 5051.
4 J. Beintema, *Acta Crystallogr.*, 1965, **18**, 647.
5 G. Ferraris, D. W. Jones, J. Yerkess and K. D. Bartle, *J. Chem. Soc., Perkin Trans. 2*, 1972, 1628.
6 C. C. Wilson, *J. Mol. Struct.*, 1997, **405**, 207.
7 A. C. Larsen and R. B. von Dreele, GSAS, General Structure Analysis System, Los Alamos National Laboratory Report, 1994, LAUR-86-748, New Mexico, USA.
8 V. Schomaker and K. N. Trueblood, *Acta Crystallogr.*, 1968, **B24**, 63.
9 K. N. Trueblood and E. Huber-Buser, THMA11, program for analysing thermal parameters, 1987, UCLA.
10 C. K. Johnson, ORTEP, Thermal Ellipsoid Plotting program, Oak Ridge National Laboratory Report, 1994, ORNL-3794, Tennessee, USA.

*Received in Cambridge, UK, 11th April 1997; Com. 7/02479G*

# Stereochemical observations on the bromate induced monobromopentahydroxylation of benzene by catalytic photoinduced charge transfer osmylation. A concise synthesis of (±)-pinitol

**Pierre M. J. Jung, William B. Motherwell* and Alvin S. Williams**

*Christopher Ingold Laboratories, Department of Chemistry, University College London, 20 Gordon Street, London, UK WC1H 0AJ*

**The use of lower temperatures in the title reaction favours the formation of the *neo* diastereoisomer of the deoxybromoinositol whose diisopropylidene derivative can be converted in three steps to (±)-pinitol.**

We have recently described the first examples of a direct stereocontrolled polyhydroxylation pathway from arenes to cyclitols based on catalytic photoinduced charge-transfer osmylation and featuring the use of barium chlorate as a stoichiometric reoxidant.[1] Here we also reported the single unoptimised experiment shown in Scheme 1, whereby the selection of sodium bromate as an alternative 'co-oxidant' led to apparent suppression of the normal third osmylation sequence leading to the *meso* derivative, *allo*-inositol hexaacetate **1**, and formation of the two deoxybromoinositols **2** and **3** in a highly diastereoselective manner and in a combined yield of 18.8%. We now present the results of a study which was designed to probe the stereochemical origins of this unusual monobromopentahydroxylation reaction, together with the elaboration of these readily available products in a concise synthesis of (±)-pinitol.

Casual inspection of the products formed in Scheme 1 clearly suggests that they may be formally derived by the *trans* addition of hypobromous acid at some intermediate stage following the initial formation of the osmate ester of benzene diol. In the first instance, we were therefore intrigued to discover whether bromohydrin formation could be encouraged at the diene stage through an increase in the concentration of bromate anion, particularly since the isolation of minor amounts of the bromoconduritols C **4** and F **5** implied that such a pathway was possible. A systematic study revealed, however, that even at very high concentrations of bromate (2.65 M *cf.* 0.22 M Scheme 1) there was no essential change, either in the relative ratio of *allo*-inositol hexaacetate **1** to brominated products **2** and **3**, or in the diastereoisomeric ratio **2**:**3**.

By way of contrast however, as shown in Table 1, the influence of temperature on the reaction was shown to exert a highly significant effect, with the *neo* diastereoisomer **2** predominating at lower temperature and the *chiro* derivative **3** favoured at higher temperatures.

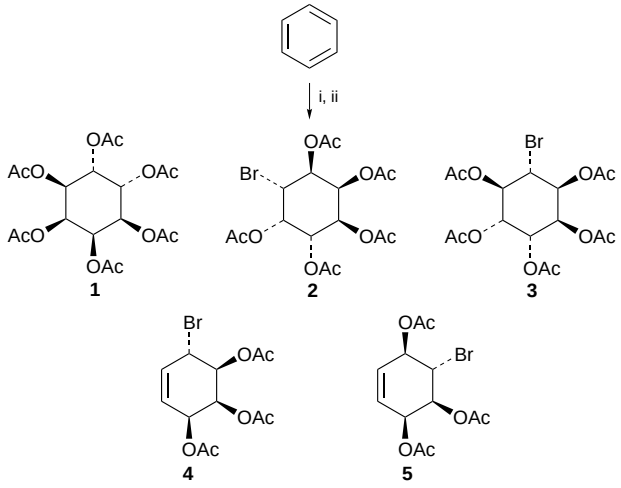
**Table 1** Yields and relative ratios of products as a function of temperature[a]

| | Product yield (%) | | Relative ratio |
|---|---|---|---|
| *T*/°C | **1** | **2** + **3** | **2**:**3** |
| 2 | 5.1 | 12.6 | 2:1 |
| 15 | 7.4 | 16.3 | 1:1 |
| 30 | 7.7 | 18.8 | 1:5 |
| 45 | 5.7 | 16.4 | 1:5 |

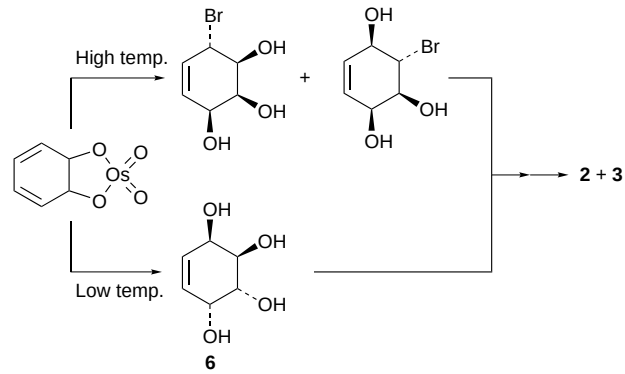
[a] All reactions were run at 0.36 M concentration of bromate using $OsO_4$ (1.3 mol%) as catalyst with irradiation for 43 h.

A variety of reasons lead us to believe that this crossover in the diastereoisomeric ratio may be explained by the bifurcated reaction pathway shown in Scheme 2, whereby the low temperature reactions tend to pass *via* the intermediacy of conduritol E **6**, or an osmate ester derived therefrom, while formation of bromoconduritols **4** and **5** intervenes effectively at higher temperature.

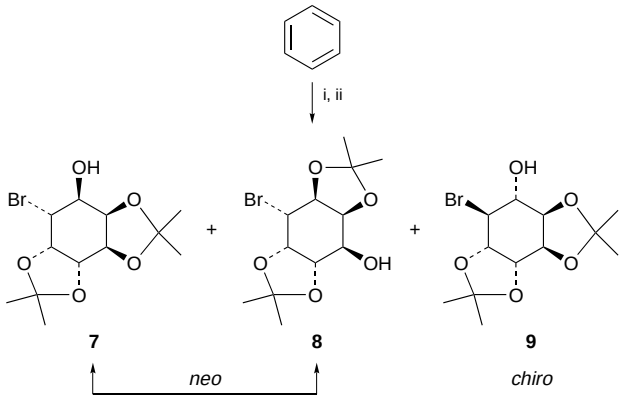
Thus, a significant clue was provided in a parallel low temperature experiment (2 °C) using chlorate anion (0.22 M) as the oxygen atom transfer reagent. Under these conditions, chlorohydrin formation is not observed, and osmylation of the third double bond in the *anti*-tetrol is sufficiently slow to permit isolation of significant amounts of both the inositol and conduritol acetates [**1** 6.1%, **6** (tetraacetate) 4.1%]. We therefore speculated that bromate disproportionation was




**Scheme 1** *Reagents and conditions*: i, $OsO_4$ (cat.), *h*ν, $NaBrO_3$ (0.22 M), 45 °C; ii, AcOH, $Ac_2O$, (**1**) 7.7%, **2**:**3** 5.1:1, 18.8%, **4**:**5**, 1:5, 2.3%




**Scheme 2**




**Scheme 3** *Reagents and conditions*: i, $OsO_4$ (cat.), *h*ν, $NaBrO_3$ (0.22 M), 15 °C; ii, acetone, TsOH, $H_2O$, (**7**) 8%, (**8**) 6.7%, (**9**) 2.5%

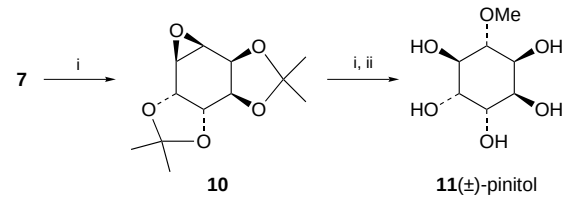
slower at lower temperatures and that the deoxybromoinositols **2** and **3** were formed by addition of hypobromous acid to conduritol E **6** during the work up stage, which involved a reductive quench of bromate residues with sodium metabisulfite. Indeed, this very combination has recently been shown to be an excellent method for bromohydrin formation.[2] Some support for this hypothesis came from an experiment in which a vast excess of cyclohexene was added as a sacrificial alkene following a photoosmylation at 2 °C, and prior to the addition of metabisulfite. In this instance, the relative proportion of the isolated bromohydrin acetates was significantly lower than before [**2** + **3**; 6.2%, compare 12.6% (Table 1)], and counterbalanced by the corresponding isolation of conduritol E (tetraacetate, 8.6%).

While the results presented in Table 1 clearly demonstrate that diastereoisomeric crossover has occurred, it should be noted that the strongly ionising conditions employed in the acetylation step almost certainly promote neighbouring group participation.[3] This aspect was highlighted when the products from a bromate driven photoosmylation reaction at 15 °C were isolated as their isopropylidene derivatives by treatment of the crude reaction mixture with acetone and toluene-*p*-sulfonic acid. (Scheme 3).

The supposition that the isolated ratio of deoxybromocyclitols from this experiment [**7** + **8** (*neo*, 14.7%) : **9** (*chiro*, 2.5%); 5.9 : 1] is probably a more appropriate reflection of the initial product distribution prior to derivatisation was also supported by a further blank experiment in which reaction of conduritol E **6** with sodium bromage–sodium metabisulfite was followed by neutralisation with sodium hydroxide and subsequent acetylation under less ionising acidic conditions with acetic anhydride in acetic acid to give **2** and **3** (72%, ratio **2** : **3**, 6.3 : 1).

From a preparative standpoint, irrespective of the fact that two competing pathways are operating, it is apparent that experimental conditions can be selected to favour either the *neo* or the *chiro* series as the major diastereoisomer. Moreover, in practical terms, a single recrystallisation of a mixture of **2** and **3** from EtOH at room temperature gives pure **3**, while advantage can be taken of the known relative insolubility of *neo*-inositol[4] to precipitate the parent bromocyclitol from **2** by simple acid catalysed hydrolysis using HCl in MeOH.

The ready availability of these protected building blocks in a single one-pot operation offers a variety of possibilities for further synthetic manipulation in the important cyclitol area. By way of illustration, we elected to prepare (±)-pinitol **11**, the




**Scheme 4** *Reagents and conditions*: i, $K_2CO_3$, MeOH, heat 2 h, 83%; ii, $Al_2O_3$, MeOH, heat 24 h; iii, $H_2O$, THF, HCl (cat), 60% from **10**

3-*O*-methyl ether of *chiro*-inositol, with both enantiomers occurring in various plant sources. (+)-Pinitol has been shown to possess significant hypoglycemic and antidiabetic activity in diabetic albino mice.[5] Previous syntheses of pinitol, either in racemic form[6] or of either antipode,[7,8] have relied on the use of *cis*-dienediols available by microbial oxidation of arenes using *Pseudomonas putida*.

Thus, as shown in Scheme 4, ring closure of the bromohydrin **7** to epoxide **10** was smoothly accomplished using $K_2CO_3$ in MeOH (83%). The regiospecificity of the subsequent ring-opening of the epoxide with alumina in MeOH is governed by the necessity for a *trans* opening *anti* to the neighbouring isopropylidene groups and finds precedent in Hudlicky's elegant enantiodivergent synthesis of both antipodes.[8] An acidic work up to this reaction led to *in situ* deprotection to afford (±)-pinitol **11** in 60% isolated yield from **10**. The overall sequence therefore requires three operations and five discrete steps from benzene.

In summary, the present study has shown that the influence of temperature in the catalytic photoinduced charge transfer osmylation of benzene may be usefully controlled, either in the reaction using chlorate anion as oxidant to suppress tertiary osmylation at lower temperature and hence favourer conduritol E production, or to influence the stereochemical outcome in the bromate reaction leading to *neo* and *chiro* deoxybromoinositols.

We thank the EPSRC for the award of a postdoctoral fellowship (P. M. J. J.) and B. P. for the award of a studentship (A. S. W.). We also wish to acknowledge stimulating and helpful discussions with Dr H. A. J. Carless.

## Footnote

* E-mail: w.b.motherwell@ucl.ac.uk

## References

1 W. B. Motherwell and A. S. Williams, *Angew. Chem., Int. Ed. Engl.*, 1995, **34**, 280.
2 H. Masuda, K. Takase, M. Nishio, A. Hasegawa, Y. Nishiyama and Y. Ishii, *J. Org. Chem.*, 1994, **59**, 5550.
3 For examples in the cyclitol area, see G. E. McCasland and E. C. Horswill, *J. Am. Chem. Soc.*, 1953, **75**, 4020 and references cited therein.
4 S. J. Angyal and D. C. Craig, *Carbohydr. Res.*, 1994, **263**, 149.
5 C. R. Narayanan, D. D. Joshi, A. M. Mujumdar and V. V. Dhekne, *Curr. Sci.*, 1987, **56**, 139.
6 S. V. Ley, F. Sternfeld and S. Taylor, *Tetrahedron Lett.*, 1987, **28**, 225; H. A. J. Carless, J. R. Billinge and O. Z. Oak, *Tetrahedron Lett.*, 1989, **30**, 3113.
7 S. V. Ley, F. Sternfeld and S. Taylor, *Tetrahedron*, 1989, **45**, 3463.
8 T. Hudlicky, J. D. Price, F. Rulin and T. Tsunoda, *J. Am. Chem. Soc.*, 1990, **112**, 9439.

*Received in Cambridge, UK, 6th May 1997; Com. 7/03071A*

# Chiral salen manganese complex encapsulated within zeolite Y: a heterogeneous enantioselective catalyst for the epoxidation of alkenes

**María J. Sabater, Avelino Corma,* Antonio Domenech, Vicente Fornés and Hermenegildo García**

*Instituto de Tecnología Química C.S.I.C.-U.P.V., Apartado 22012, 46071-Valencia, Spain*

**A chiral (salen)$Mn^{III}$ complex [salen: *trans*-(*R*,*R*)-1,2-bis(salicylideneamino)cyclohexane] analogous to Jacobsen's catalyst is prepared inside the supercages of zeolite Y, showing catalytic activity very similar to that of the chloride complex in the homogeneous phase.**

The use of chiral catalysts has become a powerful methodology in modern synthetic organic chemistry.[1] In this regard, the Sharpless epoxidation of allylic alcohols constituted an authentic breakthrough in this field.[2,3] More recently, Jacobsen and co-workers expanded the scope of the catalytic asymmetric epoxidation to unfunctionalized alkenes with high stereocontrol by using chiral (salen)Mn complexes.[4]

A further logical improvement of this homogeneous catalytic method would consist of the incorporation of the catalyst on to an inorganic support, making it possible to perform the reaction heterogeneously.[5,6] In the present work, we have successfully accomplished for the first time the preparation of a chiral (salen)manganese complex analogous to the Jacobsen catalyst into the supercages of large pore Y zeolite.† The resulting (salen)Mn complex entrapped within Y zeolite exhibits similar catalytic activity as the same complex under homogeneous conditions.

The pore structure of Y zeolite consists of almost spherical 13 Å cavities interconnected tetrahedrally through smaller apertures of 7.4 Å diameter. Molecular modelling predicts that both the salen ligand [salen: *trans*-(*R*,*R*)-1,2-bis(salicylideneamino)-cyclohexane] or the corresponding (salen)$Mn^{III}$ complex can be easily accomodated inside the supercages of Y zeolites. Analogously, it is predicted that the actual Jacobsen's catalyst having four *tert*-butyl groups on the phenyl rings does not fit into the Y zeolite supercages.

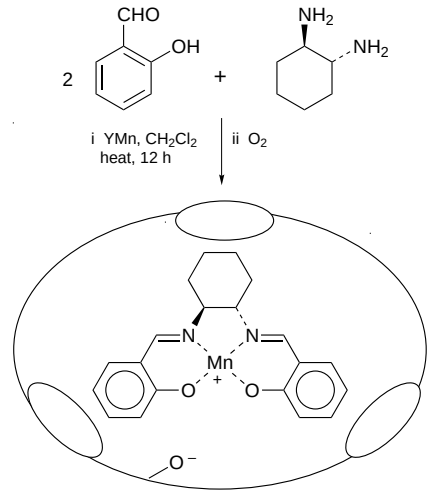
The synthesis of the (salen)$Mn^{III+}$ in the intracrystalline cages of zeolite Y is outlined in Scheme 1. Basically it consists of the condensation of optically active *trans*-(*R*,*R*)-1,2-diamino-cyclohexane and salicylaldehyde around $Mn^{II}$ metal ions resident in the supercages (1 $Mn^{2+}$ every 5 supercages) and a final oxidation step.

Other alternative protocols were found to be less efficient. If both reagents were added simultaneously, an unfavourably large excess of uncomplexed ligand was formed. On the other hand, if chiral diaminocyclohexane was the first reactant added to MnY, the IR spectrum of the corresponding zeolite predominatly showed the bands of unreacted amine.

Samples of (salen)$Mn^{III}$ complex in zeolite Y were fully characterized by thermogravimetry–differential scanning calorimetry (TG–DSC), diffuse reflectance and FTIR spectroscopies and cyclic voltammetry (CV). Thus, the salen/$Mn^{III}$ ratio of the solids quantified by TG–DSC was 1.3 indicating a slight excess of the uncomplexed ligand. The IR spectrum of the zeolite guest after the synthesis shown in Scheme 1 was compared with those recorded for authentic samples of the salen ligand and (salen)$Mn^{III}$Cl (Fig. 1).

As it can be seen from Fig. 1, the spectrum of the (salen)$Mn^{III}$-Y sample coincides with that of the chloride salt of the same complex, thus establishing the purity and identity of the (salen)$Mn^{III}$-Y zeolite. In contrast, the most characteristic band associated with the salen ligand appearing at 1500 $cm^{-1}$ is absent for the zeolite sample, indicating that the amount of uncomplexed ligand is below the detection limit of this technique.

Direct support for the +3 oxidation state of Mn ions as well as their complexation by salen was obtained by electrochemical techniques.[7] The electrochemical behaviour of the (salen)$Mn^{III}$ intrazeolite complex in $Me_2SO$ showed an equilibrium potential of −0.32 V *vs.* SCE. This value matches that recorded for the same complex in a homogeneous phase. Notably, the redox potential of the uncomplexed $Mn^{3+}/Mn^{2+}$ pair would be far more positive. Accordingly, MnY did not show any electrochemical activity .




**Scheme 1**

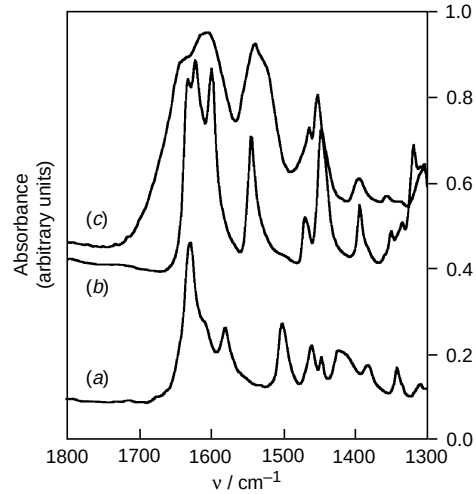



**Fig. 1** Aromatic region of the FTIR spectra of (*a*) the salen ligand, (*b*) (salen)$Mn^{III}$Cl and (*c*) (salen)$Mn^{III}$-Y complexes. Note that the 1535 $cm^{-1}$ absorption characteristic of the complex is present in the spectrum of (salen)$Mn^{III}$-Y sample. In contrast, the salen ligand has a specific 1500 $cm^{-1}$ band as the most distinctive absorption.

EPR measurements confirmed the disappearance of the majority of $Mn^{2+}$ ions from the initial MnY to the final (salen)$Mn^{III}$-Y sample.

In order to determine the performance of the (salen)manganese complexes encapsulated in Y zeolite, the epoxidation of four prochiral alkenes was tested and the results compared with those obtained under homogeneous conditions (Table 1).

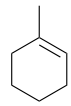
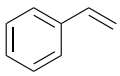
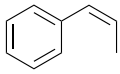
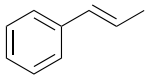
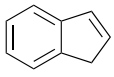
The oxidations were carried out in the presence of catalytic amounts of the (salen)$Mn^{III}Cl$ complex (5 mol%) or 90 mg of the heterogeneous (salen)$Mn^{III}$-Y system by using NaOCl in $CH_2Cl_2$ at 5 °C. Higher reaction temperatures led to a significant decrease in asymmetric induction as well as a dramatic decrease in the epoxide selectivity.

The reactions showed a high chemoselectivity except for compound **1**. Indeed, in most of the cases at 5 °C epoxides were obtained as the main or sole products as detected by GC analysis. Notably, by-products commonly observed for other non-enantioselective zeolite-catalysed epoxidations arising from epoxide scission were absent.[8]

The lower reaction rates obtained with the (salen)$Mn^{III}$-Y heterogeneous catalyst compared to the homogenous counterpart could have been anticipated in view of the restrictions imposed on the diffusion substrate and products through the micropores of the solid, especially when the reaction is run at low temperatures.

With regard to the enantioselectivity, the trisubstituted olefin **1** and styrene **2** gave poor enantiomeric excess. This agrees with previous data on the performance of the Jacobsen's catalyst.[9,10] In contrast, conjugated *trans* olefin **3** and the cyclic indene **4** were epoxidized in moderate to good enantioselectivity both in the homogeneous and the heterogeneous catalysis.

**Table 1** Asymmetric epoxidation of alkenes **1**–**4** catalysed by the (*R*,*R*)-(salen)$Mn^{III}$ complex and NaOCl as oxidant in the homogeneous and heterogeneous phases

| Entry | Olefin[a] | Catalyst[b] | Conversion (%)[c,d] | Epoxide selectivity (%)[c] | Ee (%) |
|---|---|---|---|---|---|
| 1 |  | (salen)$Mn^{III}Cl$ | 37 | 65 | 8 |
| 2 | **1** | (salen)$Mn^{III}$-Y | 11 | 65 | 5 |
| 3 |  | (salen)$Mn^{III}Cl$ | 47 | 80 | 27 |
| 4 | **2** | (salen)$Mn^{III}$-Y | 40 | 61 | 20 |
| 5 |  | (salen)$Mn^{III}Cl$ | 28 | 100 | 74[e] |
| 6 | *cis*-**3** | (salen)$Mn^{III}$-Y | 5 | 76 | 58[e] |
| 7 |  | (salen)$Mn^{III}Cl$ | 23 | 90 | 41 |
| 8 | *trans*-**3** | (salen)$Mn^{III}$-Y | 11 | 100 | 24 |
| 9 |  | (salen)$Mn^{III}Cl$ | 30 | 100 | 60 |
| 10 | **4** | (salen)$Mn^{III}$-Y | 20 | 96 | 50 |

[a] Reactions were run at 5 °C in $CH_2Cl_2$. [b] (salen)$Mn^{III}Cl$, 5% mol; (salen)Mn-Y, 90 mg of catalyst with a complex content of 3.8%. [c] Determined by quantitative capillary GC analysis. [d] Reaction time: 2–3 h using (salen)$Mn^{III}Cl$ and 12–15 h for (salen)$Mn^{III}$-Y catalyst. [e] Ee of *trans* epoxide.

Although the ees obtained using (salen)$Mn^{III}$-Y and (salen)-$Mn^{III}Cl$ follow the same pattern, we consistently noticed somewhat lower values for the zeolite-bound catalyst. This can be interpreted as a combination of two unfavourable factors: (i) the occurrence of a non-catalysed, unselective epoxidation route in the liquid phase and/or (ii) the existence of residual amounts of uncomplexed $Mn^{2+}$ acting as catalytic sites.

The above point raises the question of how to assess that the reaction is taking place inside the zeolite micropores. The simplest straightforward way to address this point is to determine the inactivity of the heterogeneous (salen)$Mn^{III}$-Y catalyst by using reagents of larger dimensions than the pore windows of zeolite host. Under these conditions the homogeneous (salen)$Mn^{III}Cl$ counterpart must be still an efficient epoxidation catalyst.

Thus, we found that a iodosylbenzene derivative obtained by basic hydrolysis of [bis(trifluoroacetoxy)iodo]benzene[11] gives very similar results to those presented in Table 1 using NaOCl in the presence of (salen)$Mn^{III}Cl$. However, FABMS established that the structure of this iodosylbenzene sample was not monomeric but likely to be a cyclic oligomeric precursor of PhIO. Therefore, this bulky reagent would be size excluded from the 7.4 Å faujasite pore windows. Accordingly, no conversion could be observed in the epoxidation of alkenes **2**–**4** in the presence of (salen)$Mn^{III}$-Y catalyst. In addition, this lack of activity of the (salen)$Mn^{III}$-Y catalyst compared to the 43% conversion achieved using (salen)$Mn^{III}Cl$ indicates that no leaching of Mn ions from the interior of the zeolite to the solution occurs and also that the external surface sites play a very minute role in the overall catalytic process. To further establish the lack of Mn leaching, we performed chemical analysis of the liquid phase after the reaction. No Mn ions could be detected.

All the enantioselective enzymatic systems in nature have in common the incorporation of the active sites into a confined space defined by the tertiary protein structure. Our chiral (salen)$Mn^{III}$-Y catalyst mimics this strategy: the rigid, inorganic framework of the zeolite determines the reaction cavity surrounding the active complex.

## Footnotes

* E-mail: itq@upv.es

† Although no article has been published yet, a referee has indicated that a similar chiral (salen)Mn complex inside zeolite EMT has been claimed by T. Bein, ACS Chiral Catalysis Symposium, Orlando, 1996.

## References

1 J. D. Morrison, *Asymmetric Synthesis*, Academic Press, New York, 1983.
2 T. Katsuki and K. B. Sharpless, *J. Am. Chem. Soc.*, 1980, **102**, 5974.
3 R. M. Hanson, *Chem. Rev.*, 1991, **91**, 437.
4 E. N. Jacobsen and W. Zhang, *J. Org. Chem.*, 1991, **56**, 2296.
5 F. Minutolo, D. Pini and P. Salvadori, *Tetrahedron Lett.*, 1996, **37**, 3375.
6 I. E. J. Vankelecom, D. Tas, R. F. Parton, V. Vandevyver and P. A. Jacobs, *Angew. Chem., Int. Ed. Engl.*, 1996, **35**, 1346.
7 F. Bedioui, K. J. Devynck and K. J. Balkus Jr., *J. Phys. Chem.*, 1996, **100**, 8607.
8 M. Alvaro, A. Corma, H. García, S. Valencia, *Appl. Catal. A*, 1995, **128**, L7.
9 E. N. Jacobsen, W. Zhang and M. L. Güller, *J. Am. Chem. Soc.*, 1991, **113**, 6703.
10 E. N. Jacobsen, W. Zhang, A. R. Muci, J. R. Ecker and L. Deng, *J. Am. Chem. Soc.*, 1991, **113**, 7063.
11 H. J. Lucas, E. R. Kennedy and M. W. Formo, *Org. Synth.*, 1963, **3**, 483.

*Received in Liverpool, UK, 25th February 1997; Com. 7/01337J*

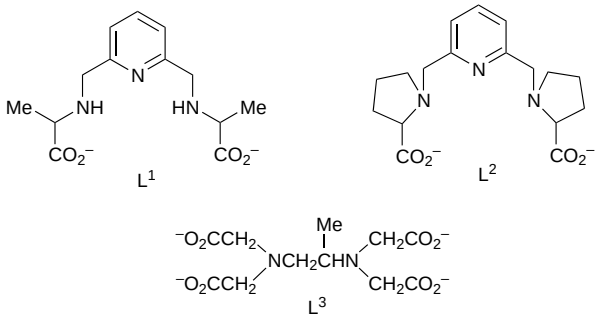
# Stereoselectivity and mechanism of $Cu^{2+}$ transfer between chiral, multidentate ligands

**Klaus Bernauer* and Marie-Fabiola Gilet**

*Laboratoire de Chimie Inorganique et Analytique, Institut de Chimie, Université de Neuchâtel, Av. de Bellevaux 51, 2000 Neuchâtel, Switzerland*

**The ligand-exchange kinetics between the enantiomers of [Cu(alamp)] or [Cu(promp)] and (*S*)-pdta are measured by CD spectroscopy; three different reaction intermediates are proposed, involving the three different states of N-protonation of pdta; at pH < 7 an associative mechanism involving a cage-like, hydrogen-bonded intermediate is suggested for [Cu(alamp)] in which the metal ion is transferred in a single rate limiting step from one ligand to the other.**

Stereoselectivity has not been used to investigate metal-ion-transfer reactions in aqueous solutions. Only two communications concerning stereoselective metal-ion transfer in organic solvents are reported in the literature. Kurganov *et al.*[1] observed rate differences in the dismutation of copper(II) complexes with N-substituted optically active diamines in acetonitrile and in nitrobenzene and Warmuth and Elias[2] reported stereoselective ligand exchange of nickel(II) Schiff-base complexes in acetone. In the following, we present some preliminary results of the stereoselective ligand exchange between the chiral copper(II) complexes of deprotonated *N*,*N*′-[(pyridine-2,6-diyl)bis(methylene)]bis(alanine) [alamp ($L^1$)] or *N*,*N*′-[(pyridine-2,6-diyl)bis(methylene)]bis(proline) [promp, ($L^2$)] and (*S*)-1,2-diaminopropanetetraacetic acid [(*S*)-$H_4$pdta ($H_4L^3$)] according to eqn. (1). From the known protonation constants of the ligands[3] and




$$[CuL] + (S)\text{-}H_n\text{pdta}^{(4-n)-} \rightleftharpoons [Cu\{(S)\text{-pdta}\}]^{2-} + H_mL^{(2-m)-}$$

$$L = (R,R)\text{- or } (S,S)\text{-}L^1,\ (R,R)\text{- or } (S,S)\text{-}L^2 \qquad (1)$$

the formation constants of $[CuL^1]$, $[CuL^2]$[4] and $[CuL^3]^{2-}$,[5] it can be calculated that the equilibrium (1) lies to more than 96% to the right, and that the concentration of free $Cu^{2+}$ is < 1% over the whole pH range from 4 to 11 under the measurement conditions. Reaction rates are determined under pseudo-first-order conditions, the exchange ligand $H_n\text{pdta}^{(4-n)-}$ being initially present in a tenfold excess. The rate of the reaction is best measured by the change of the intensity of the circular dichroism (CD) at $\lambda$ = 607 nm, at which the product complex has no CD signal.

From the observed rate constants, represented as a function of pH in Fig. 1,† the following conclusions can be drawn: (*i*) for both $[CuL^1]$ and $[CuL^2]$ the reaction takes place by at least three different pathways corresponding to the two protonated and the entirely deprotonated form of pdta as indicated in Scheme 1; (*ii*) with $L^1$ as the ligand the reaction is fastest with $H_2pdta^{2-}$, whereas the relative rates with $[CuL^2]$ are $Hpdta^{3-} > H_2pdta^{2-} > pdta^{4-}$; (*iii*) all the reactions show small but significant stereoselectivity, which is highest for the exchange reaction between $[CuL^1]$ and $H_2pdta^{2-}$ in the pH range 4–7. The ratio of the observed rate constants for the two diastereoisomeric couples is $k_\Delta/k_\Lambda = 1.3 \pm 0.1$ {$k_\Delta$ stands for the reaction between [Cu{(*R*,*R*)-$L^1$}] and (*S*)-pdta}.

The observed stereoselectivity clearly indicates an associative mechanism but the concentration of the intermediate must be low, the rate of the reaction having linear dependence up to a pdta concentration of 0.03 M ($K_i \leqslant 3$ dm$^3$ mol$^{-1}$). However, the most interesting observations are: (*i*) the acceleration of the reaction involving $[CuL^1]$ by the presence of the two N–H protons on the exchange ligand, protons which have to be replaced by the metal ion, and (*ii*) the striking difference in the selection of the most favourable reaction pathway for $[CuL^1]$ and $[CuL^2]$. The only difference between the two complexes able to influence this mechanistic selection is the presence of the two N–H groups in the former, groups which are replaced by alkyl residues in the latter. It becomes therefore evident that in

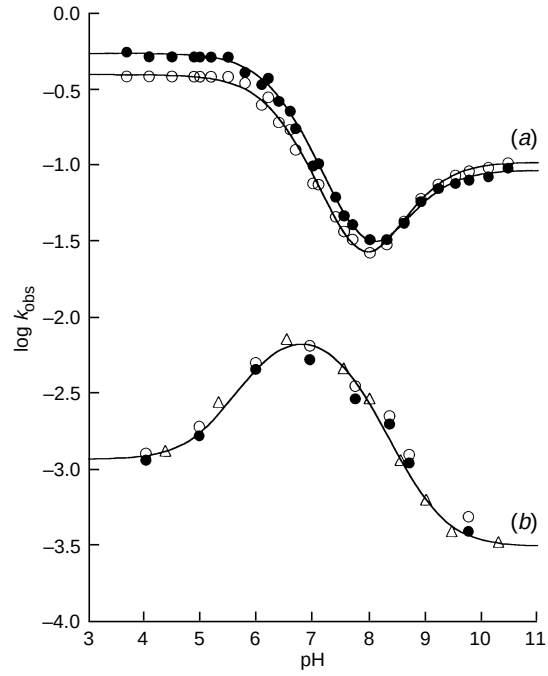
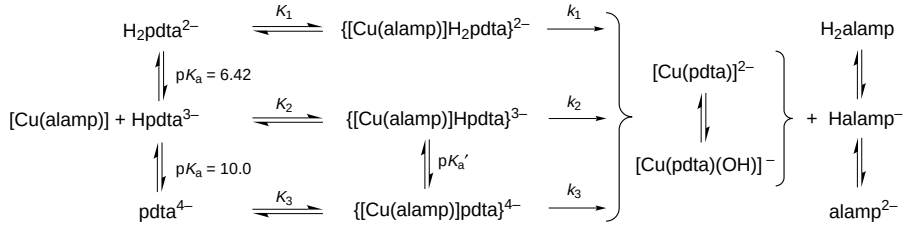



**Fig. 1** Observed rate constants for the reaction between [Cu(alamp)] (*a*) or [Cu(promp)] (*b*), with (*S*)-pdta as a function of pH. $[Cu^{2+}] = 1 \times 10^{-3}$ M, [alamp] or [promp] $= 1 \times 10^{-3}$ M, [(*S*)-pdta] $= 1 \times 10^{-2}$ M, [buffer] = 0.2 M {pH = 4.0–5.5 (acetate, values extrapolated to zero buffer concentration), 5.6–6.5 [2-morpholinoethanesulfonic acid monohydrate (MES)], 6.6–7.9 [3-morpholino-2-hydroxypropanesulfonic acid (MOPSO)], 8.1–10.1 (borate)}. Buffer concentration refers to the ionic constituent. $T$ = 20 °C; (○) (*R*,*R*)-ligand, (●) (*S*,*S*)-ligand, (△) *rac*-pdta.




**Scheme 1**

the exchange with [CuL[1]] the N–H groups of both ligands, $H_2pdta^{2-}$ and alamp are important for stabilising an intermediate containing four hydrogen bridges, a possible structure of which is shown in Fig. 2. Such an intermediate cannot be formed with [CuL[2]].

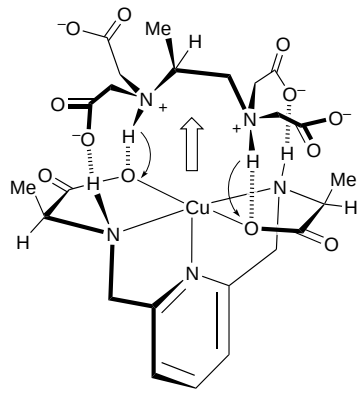


**Fig. 2** Possible transition state in metal-ion transfer between [Cu{(*S*,*S*)-alamp}] and (*S*)-$H_2pdta^{2-}$

Whereas metal-ion transfer between multidentate ligands usually takes place by multistep substitutions, involving intermediates containing dangling groups,[6,7] the proposed hydrogen-bonded intermediate allows a transfer in a concerted single-step reaction avoiding any intermediate solvation and desolvation steps except the elimination of the coordinated water molecule from the starting copper(II) complex. Furthermore, the simultaneous transfer of the two protons ensures the conservation of the local charge distribution during the reaction.

We thank the Swiss National Science Foundation for financial support (Grant No. 20-48′270.96).

## Footnotes

* E-mail: klaus.bernauer@ich.unine.ch

† The lines in Fig. 1 represent best fits of the measurements, according to Scheme 1, by using the following values {only mean values were used for the two enantiomers of [Cu(promp)]}

| | | $K_1k_1$ | $K_2k_2$ | $K_3k_3$ |
|---|---|---|---|---|
| | p$K_a$′ | dm$^3$ mol$^{-1}$s$^{-1}$ | | |
| [Cu{(*R*,*R*)-alamp}] | 8.85 | 39 | 0.6 | 10.5 |
| [Cu{(*S*,*S*)-alamp}] | 8.85 | 54 | 0.95 | 9.3 |
| [Cu(promp)] | 7.6 | 0.115 | 0.87 | 0.031 |

## References

1 A. A. Kurganov, T. M. Ponomareva and W. A. Dawankov, *Dolk. Akad. Nauk. SSSR*, 1986, **293**, 623.
2 R. Warmuth and H. Elias, *Inorg. Chem.*, 1991, **30**, 5027.
3 K. Bernauer, H. Stoeckli-Evans, D. Hugi-Cleary, J. Hermann Hilgers, H. Abd-el-kalek, J. Porret and J.-J. Sauvain, *Helv. Chim. Acta*, 1992, **75**, 2335.
4 K. Bernauer and L. Verardo, to be published.
5 *Critical Stability Constants*, ed. R. M. Smith and A. E. Martell, Plenum, New York, London, 1974, vol. 1, p. 212.
6 P. E. Reinbold and K. H. Pearson, *Inorg. Chem.*, 1970, **9**, 2330.
7 R. G. Wilkins, in *Kinetics and Mechanism of Reactions of Transition Metal Complexes*, VHC Weinheim, 2nd edn., 1991, p. 219 ff and references therein.

*Received in Basel, Switzerland, 17th March 1997; Com. 7/01832K*

# Stereocontrolled synthesis of the HIJ ring system of ciguatoxin

**Tohru Oishi, Kenji Maeda and Masahiro Hirama***

*Department of Chemistry, Graduate School of Science, Tohoku University, Sendai 980-77, Japan*

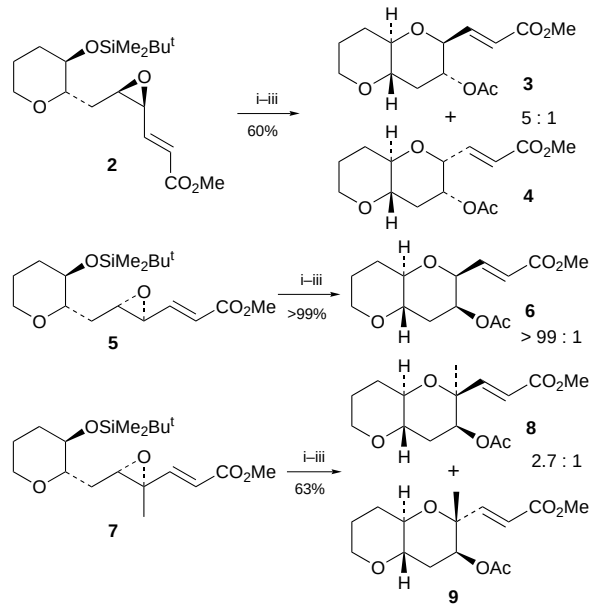
**Divergent synthesis of the HIJ ring framework 21 of ciguatoxin 1 starting with oxocane 10 is achieved using the palladium- and acid-catalysed cyclization reactions of hydroxy epoxides.**

Ciguatoxin **1** is the principal toxin which causes ciguatera poisoning.[1] Its unique structure and agonist activity against $Na^+$ channels have attracted considerable attention from synthetic organic chemists.[2] Although numerous synthetic studies of fragments of **1** have been reported, the central medium rings, such as the F and I rings, have eluded synthesis until very recently.[3,4] We describe herein the first divergent synthesis of the HIJ ring system of **1** *via* stereocontrolled palladium-[5] and acid-catalysed[6] cyclization reactions of hydroxy epoxides starting with the methyl oxocane I ring.[3]

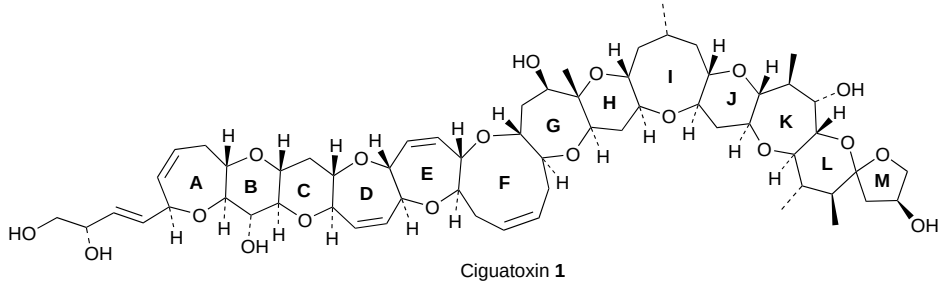
The palladium-catalysed cyclization procedure[5] was examined first to construct the H and J rings. *cis*-Epoxide **2** and *trans*-epoxide **5**, and trisubstituted *trans*-epoxide **7** were subjected to a cyclization reaction as models for constructing the J and H rings, respectively (Scheme 1).† While complete stereocontrol was realized for **5** to give **6** (> 99 : 1), lower selectivities were observed for **2** and **7** to give mixtures of **3** and **4** (5 : 1), and **8** and **9** (2.7 : 1), respectively. The *trans*-epoxide **15** was therefore used to construct the J ring, and we chose acid-catalysed cyclization technology to prepare the H ring.

Optically active oxocane **10**[3] was converted to **11** *via* protection of the primary alcohol as a benzyloxymethyl (BOM) ether, removal of the acyl groups and subsequent protection of the 1,3-diol as the acetonide and of the remaining secondary alcohol as a triisopropylsilyl ether in 83% overall yield (Scheme 2). The BOM group of **11** was removed by hydrogenolysis and the resulting primary alcohol was converted to the trifluoromethanesulfonate, which was immediately treated with the lithium acetylide generated from **22** in THF–dimethylpropyleneurea (DMPU) (6 : 1) at −78 °C[7] to give the adduct **12** in 68% overall yield. Selective removal of the ethoxyethyl (EE) group with pyridinium toluene-*p*-sulfonate (PPTS) in propanol[8] produced **13** in quantitative yield. The prop-2-ynyl alcohol **13** was partially reduced with sodium dihydrobis(2-methoxyethoxy)aluminate (Red-Al)[9] to give the *trans*-allylic alcohol **14**. Sharpless asymmetric epoxidation of **14** using D-(−)-diethyl tartrate (DET) gave the corresponding α-epoxide exclusively, and successive oxidation of the primary alcohol with a $SO_3$–pyridine complex and Wittig olefination gave **15** in 88% overall yield. Stereospecific construction of the J ring was achieved by the palladium-catalysed cyclization.[5] Treatment of **15** with tetrabutylammonium fluoride in THF, followed by solvent exchange to $CH_2Cl_2$ and addition of a catalytic amount of $Pd(PPh_3)_4$, gave **16** within 5 min as a single diastereoisomer in 93% yield in two steps.‡ The stereochemistry of the resulting alcohol with a non-natural orientation could be readily inverted by reduction of the corresponding ketone with $NaBH_4$.[10]

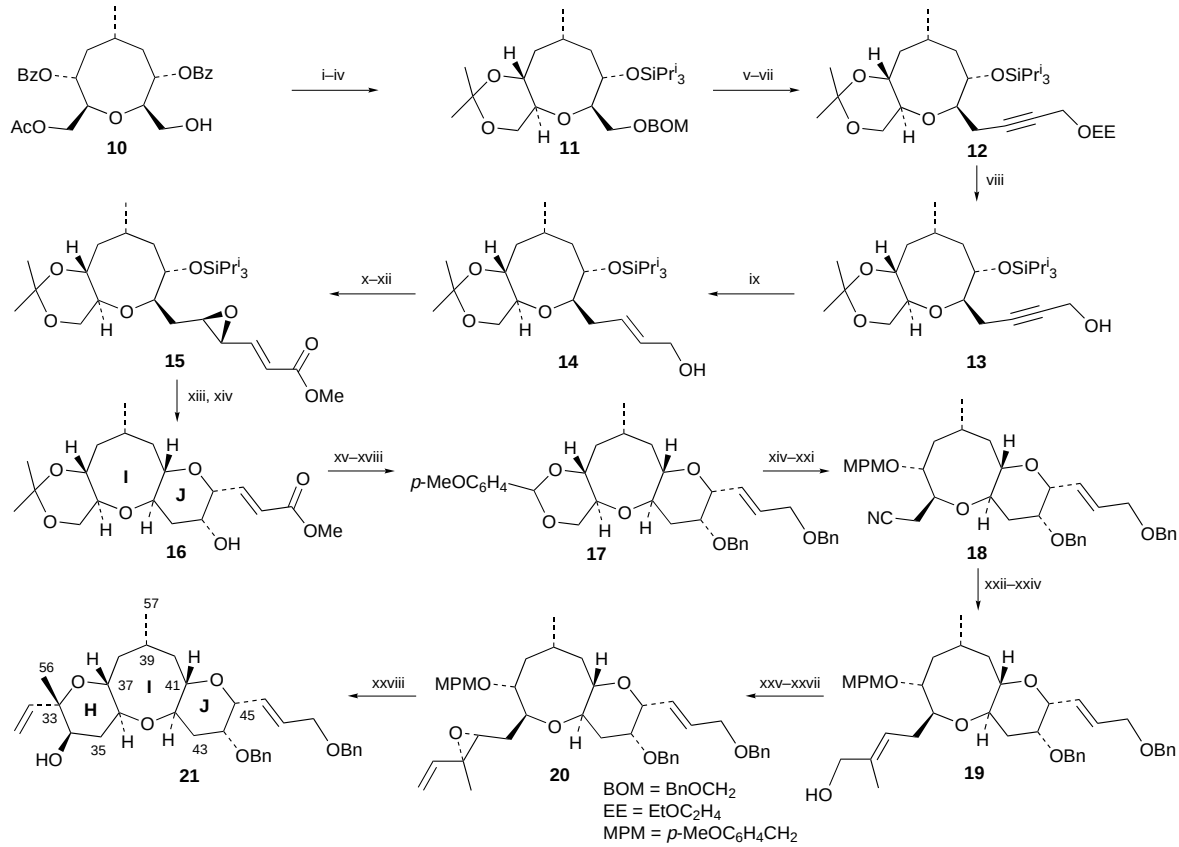
Having completed the synthesis of the I and J ring system, we were now in a position to construct the H ring. The ester **16** was reduced with DIBAL-H, the resulting alcohols were protected as benzyl ethers, and transformation of the acetonide into *p*-methoxybenzylidene acetal gave **17** in 90% overall yield. Regiospecific reductive cleavage of the benzylidene acetal with DIBAL-H furnished the *p*-methoxybenzyl (MPM) ether, and the resulting primary alcohol was converted to the methanesulfonate, which was then treated with sodium cyanide to yield the nitrile **18** in 91% overall yield. Extension of the side chain *via* DIBAL-H reduction and Wittig olefination with (carbethoxyethylene)triphenylphosphorane gave the α,β-unsaturated ester, which was reduced to allylic alcohol **19** in 98% overall yield. Sharpless asymmetric epoxidation of **19** furnished the corresponding hydroxy epoxide and further oxidation to the aldehyde and Wittig olefination gave **20** in 75% overall yield. Finally, treatment of **20** with 2,3-dichloro-5,6-dicyano-




**Scheme 1** *Reagents and conditions*: i, $Bu_4NF$, THF; ii, $Pd(PPh_3)_4$ (cat.), $PPh_3$ (cat.), $CH_2Cl_2$; iii, $Ac_2O$, pyridine




Ciguatoxin **1**




**Scheme 2** *Reagents and conditions*: i, $BnOCH_2Cl$, $Pr^i_2EtN$, $Bu_4NI$ (cat.), $(CH_2Cl)_2$, 40 °C, 99%; ii, $K_2CO_3$, MeOH, 99%; iii, 2,2-dimethoxypropane, PPTS (cat.), MeCN, 85%; iv, $Pr^i_3SiOSO_2CF_2$, 2,6-lutidine, $(CH_2Cl)_2$, −30 °C, quant.; v, $H_2$, $Pd(OH)_2$–C (cat.), AcOEt, 87%; vi, $(CF_3SO_2)_2O$, $Et_3N$, $(CH_2Cl)_2$, −15 °C; vii, HC≡$CCH_2C_2H_4OEt$ **22**, BuLi, THF–DMPU (6 : 1), −78 °C, 78% (2 steps); viii, PPTS (cat.), PrOH; ix, Red-Al, $Et_2O$, 0 °C to room temp., 97% (2 steps); x, (−)-DET, $Ti(OPr^i)_4$, $Bu^tOOH$, molecular sieves 4A, $CH_2Cl_2$, −20 °C, 97%; xi, $SO_3$·pyridine, $Et_3N$, DMSO, $(CH_2Cl)_2$, 0 °C to room temp.; xii, $Ph_3P$=$CHCO_2Me$, toluene, 94% (2 steps); xiii, $Bu_4NF$, THF; xiv, $Pd(PPh_3)_4$ (cat.), $PPh_3$ (cat.), $CH_2Cl_2$, 93% (2 steps); xv, DIBAL-H, $CH_2Cl_2$, −78 °C, 98%; xvi, BnBr, NaH, DMF–THF (1 : 1), 0 °C, 92%; xvii, *p*-$MeC_6H_4SO_3H$·$H_2O$ (cat.), MeOH; xviii, *p*-$MeOC_6H_4CH(OMe)_2$, PPTS (cat.), $(CH_2Cl)_2$, quant. (2 steps); xix, DIBAL-H, $CH_2Cl_2$, −40 °C, 97%; xx, $MeSO_2Cl$, $Et_3N$, $CH_2Cl_2$, 0 °C, quant.; xxi, NaCN, 18-crown-6 (cat.), DMF, 50 °C, 94%; xxii, DIBAL-H, $CH_2Cl_2$, −60 °C; xxiii, $Ph_3P$=$CMeCO_2Et$, toluene, 98% (2 steps); xxiv, DIBAL-H, $CH_2Cl_2$, −78 °C, quant.; xxv, (−)-DET, $Ti(OPr^i)_4$, $Bu^tOOH$, molecular sieves 4A, $CH_2Cl_2$, −20 °C, 90%; xxvi, $SO_3$·pyridine, $Et_3N$, DMSO, $(CH_2Cl)_2$, 0 °C to room temp.; xxvii, $Ph_3P^+CH_3Br^-$, $NaN(SiMe_3)_2$, THF, 0 °C, 83% (2 steps); xxviii, DDQ, $CH_2Cl_2$–$H_2O$ (20 : 1), 88%.

1,4-benzoquinone (DDQ) in $CH_2Cl_2$ and water (20 : 1) resulted in cleavage of the MPM ether, and spontaneous cyclization of the resulting hydroxy epoxide prevailed under the weakly acidic conditions to afford **21** in 88% yield.§ The overall yield of **21** from **10** was 25% in 28 steps. Thus each step effectively proceeded in good yield (⩾95% yield).

In conclusion, we have demonstrated that the appropriate combination of stereoselective pyran formation methodologies allows us to synthesize the central HIJ ring system of **1** starting with oxocane **10**. Further synthetic studies directed towards **1** are in progress in our laboratory. We thank the Uehara Memorial Foundation, The Naito Foundation, and the Ministry of Education, Science and Culture, Japan for financial support.

## Footnotes

* E-mail: hirama@ykbsc.chem.tohoku.ac.jp

† Epoxides **2**, **5** and **7** were prepared from (2*S*,3*R*)-2-ethenyl-3-hydroxytetrahydropyran (ref. 6).

‡ On the other hand, acid-catalysed cyclization (ref. 6) of the **15** gave the 5-*exo* cyclization product (tetrahydrofuran) exclusively.

§ *Representative data* for **21**: $[\alpha]_D^{25}$ −2.14 (*c* 0.35, $CHCl_3$); $^1$H NMR (600 MHz, $CDCl_3$): δ 1.04 (3 H, d, *J* 7.2 Hz, H57), 1.26 (3 H, s, H56), 1.51 (1 H, ddd, *J* 13.5, 11.2, 2.7 Hz, H43ax), 1.52 (1 H, ddd, *J* 14.3, 9.5, 6.2 Hz, H38ax), 1.59 (1 H, d, *J* 3.6 Hz, OH), 1.63 (1 H, td, *J* 12.2, 11.0 Hz, H35ax), 1.74 (1 H, ddd, *J* 14.4, 10.6, 8.0 Hz, H40ax), 1.84 (1 H, br dd, *J* 14.3, 3.6 Hz, H38eq), 1.84–1.89 (1 H, m, H39), 1.88 (1 H, br d, *J* 14.4 Hz, H40eq), 2.12 (1 H, ddd, *J* 12.2, 5.0, 4.6 Hz, H35eq), 2.28 (1 H, ddd, *J* 13.5, 4.7, 3.1 Hz, H43eq), 3.20 (1 H, ddd, *J* 10.6, 9.2, 3.1 Hz, H41), 3.23 (1 H, ddd, *J* 11.0, 10.5, 5.0 Hz, H36), 3.40 (1 H, ddd, *J* 10.5, 9.5, 3.6 Hz, H37), 3.46 (1 H, ddd, *J* 12.2, 4.6, 3.6 Hz, H34), 3.52 (1 H, ddd, *J* 11.2, 9.2, 4.7 Hz, H42), 3.56–3.58 (1 H, m, H44), 3.86–3.88 (1 H, m, H45). The relative stereochemistry was unambiguously determined by NOE experiments.

## References

1 M. Murata, A. M. Legrand, Y. Ishibashi and T. Yasumoto, *J. Am. Chem. Soc*., 1989, **111**, 8929; M. Murata, A. M. Legrand, Y. Ishibashi, M. Fukui, and T. Yasumoto, *J. Am. Chem. Soc.*, 1990, **112**, 4380.

2 E. Alvarez, M.-L. Candenas, R. Pérez, J. L. Ravelo and J. D. Martín, *Chem. Rev.*, 1995, **95**, 1953 and references cited therin; H. Oguri, S. Hishiyama, T. Oishi and M. Hirama, *Synlett*, 1995, 1252; H. Oguri, S. Hishiyama, O. Sato, T. Oishi, M. Hirama, M. Murata, T. Yasumoto and N. Harada, *Tetrahedron*, 1997, **53**, 3057.

3 Oishi, M. Shoji, K. Maeda, N. Kumahara and M. Hirama, *Synlett*, 1996, 1165.

4 M. Inoue, M. Sasaki and K. Tachibana, *Tetrahedron Lett.*, 1997, **38**, 1611.

5 T. Suzuki, O. Sato and M. Hirama, *Tetrahedron Lett.*, 1990, **31**, 4747.

6 K. C. Nicolaou, C. V. C. Prasad, P. K. Somers and C.-K. Hwang, *J. Am. Chem. Soc.*, 1989, **111**, 5330.

7 H. Kotsuki, I. Kadota and M. Ochi, *Tetrahedron Lett.*, 1990, **31**, 4609.

8 H. A. Tius and A. H. Faug, *J. Am. Chem. Soc.*, 1986, **108**, 1035.

9 S. E. Denmark and T. K. Jones, *J. Org. Chem.*, 1982, **47**, 4595.

10 Y. Mori, K. Yaegashi and H. Furukawa, *J. Am. Chem. Soc.*, 1996, **118**, 8158.

*Received in Cambridge, UK, 1st April 1997; Com. 7/02158E*

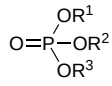
# Photoinduced electron-transfer reactions of tri-1-naphthyl phosphate and di-1-naphthyl methylphosphonate sensitised by 9,10-dicyanoanthracene

**Mitsunobu Nakamura,*[a]† the late Reizo Dohno[a] and Tetsuro Majima*[b]**

[a] *Department of Engineering Science, Himeji Institute of Technology, Shosha 2167, Himeji, Hyogo 671-22, Japan*
[b] *The Institute of Scientific and Industrial Research, Osaka University, Mihogaoka 8-1, Ibaraki, Osaka 567, Japan*

**1,1′-Binaphthyl is formed by photoinduced electron-transfer reactions of tri-1-naphthyl phosphate and di-1-naphthyl methylphosphonate sensitised by 9,10-dicyanoanthracene in MeCN, while no reaction occurs in the case of mono-1-naphthyl and di- or tri-phenyl esters.**

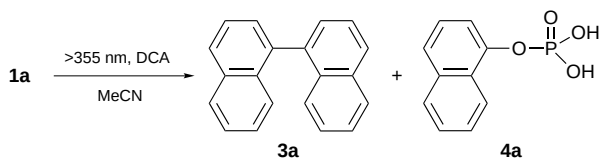
Photochemical reactions of organophosphorus compounds have been widely studied from the mechanistic and synthetic points of view.[1] Recently much attention has been paid to the photoreactivities of caged compounds of phosphates and phosphonates with an aryl substituent as a chromophore *in vivo*.[2] Radical cations of trivalent phosphorous compounds such as phosphines or phosphites generated in photoinduced electron-transfer reactions have been found to be oxidised by MeOH.[3] Although photoinduced electron-transfer reactions of organic compounds have been extensively investigated,[4,5] little is known about aryl phosphates and phosphonates. Electron-transfer reactions of aryl phosphates and phosphonates are of particular importance in relation to the caged compounds *in vivo*. We report here the photoinduced electron-transfer reactions of phosphates **1** and methylphosphonates **2** with aromatic substituents sensitised by 9,10-dicyanoanthracene.



**1a** $R^1 = R^2 = R^3$ = 1-naphthyl
**b** $R^1 = R^2 = R^3$ = 4-methoxy-1-naphthyl
**c** $R^1 = R^2$ = Et, $R^3$ = 1-naphthyl
**d** $R^1 = R^2$ = Et, $R^3$ = 4-methoxy-1-naphthyl
**e** $R^1$ = H, $R^2 = R^3$ = 4-$MeOC_6H_4$
**f** $R^1$ = Me, $R^2 = R^3$ = 4-$MeOC_6H_4$

An argon-saturated MeCN solution containing of $5 \times 10^{-5}$ M of 9,10-dicyanoanthracene (DCA) and $1 \times 10^{-3}$ M of tri-1-naphthyl phosphate **1a** was irradiated with a medium-pressure Hg lamp using a $BiCl_3$–HCl filter (cutoff < 355 nm) for 1 h (conversion 15%) to give 1,1′-binaphthyl **3a** and 1-naphthyl phosphate **4a** with a 1 : 1 ratio and a qunatum yield of 0.0013 (Scheme 1). Similarly both **3a** and **4a** were formed as the main products in the photoreaction of a di-1-naphthyl methylphosphonate **2a** and DCA mixture.

4,4′-Dimethoxy-1,1′-binaphthyl **3b** was formed in the cases of tris(4-methoxy-1-naphthyl) phosphate **1b** and bis(4-methoxy-1-naphthyl) methylphosphonate **2b**, while no reaction




**Scheme 1**

occurred in the cases of mono-1-naphthyl (**1c**, **1d**) and diphenyl derivatives (**1e**, **1f**, **2c**, **2d**). These results show that the photoreaction occurs only in the compounds with two or three naphthyl substituents linked by an O–P(O)–O chain. Since fluorescence of $^1$DCA* was completely quenched with **1** or **2** and the free-energy change of the quenching is exergonic with $\Delta G_{et} = -15$ or $-25$ kcal mol$^{-1}$ (1 cal = 4.184 J), respectively, electron transfer proceeds from **1** or **2** to $^1$DCA* to give radical cations of **1** or **2** (**1**$^{\cdot+}$ or **2**$^{\cdot+}$) and radical anion of DCA (DCA$^{\cdot-}$) at the diffusion-controlled rate.‡

Laser flash photolyses of a mixture of DCA and **1a** were performed to clarify the reaction mechanism of the formation of **3a** and **4a**.§ The transient absorption spectrum in the range of 430–750 nm with a peak at around 700 nm was observed at 20 ns after a 4 ns flash in argon-saturated MeCN (Fig. 1). The 700 nm peak was completely quenched, while an absorption in the range of 430–500 nm was observed even in oxygen-saturated MeCN. The 430–500 nm band disappeared in the presence of *trans*-4,4′-dimethoxystilbene (DMS) with formation of DMS$^{\cdot+}$.[5] The 700 nm band is assigned to DCA$^{\cdot-}$, while the 430–500 nm band is assigned to **1a**$^{\cdot+}$. The assignments were confirmed by the measurement of **1a**$^{\cdot+}$ formed during γ-radiolysis of **1a** in a butyl chloride rigid matrix at 77 K.¶ The quantum yield of **1a**$^{\cdot+}$ formation was measured to be $\phi = 0.04$–$0.07$ from that of DMS$^{\cdot+}$ fromation in the presence of DMS. The smaller value suggests that the back electron-transfer in the radical ion pair of DCA$^{\cdot-}$ and **1a**$^{\cdot+}$ is significantly exergonic with $\Delta G_{-et} = -50$ kcal mol$^{-1}$ and occurs more favourably than the solvent separation to give DCA$^{\cdot-}$ and **1a**$^{\cdot+}$.

The decay of **1a**$^{\cdot+}$ should correspond to the formation of **3a**. Unfortunately, the optical densities of the 430–500 nm band due to **1a**$^{\cdot+}$ were too small to be analysed. Pulse radiolysis of **1a** in 1,2-dichloroethane at room temperature (Fig. 2) was performed to clarify the formation of **3a** from **1a**$^{\cdot+}$.‖ The transient absorption spectrum assigned to **1a**$^{\cdot+}$ with sharp bands at 400 and 430 nm and a broad band at 550–750 nm was observed

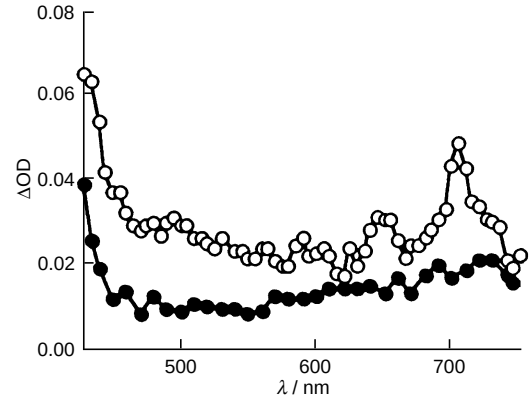
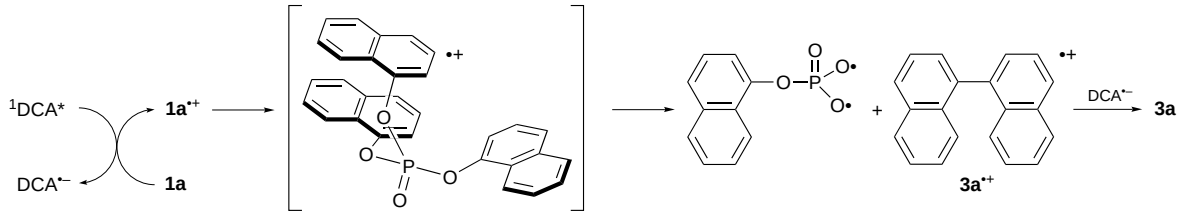



**Fig. 1** Transient absorption spectra immediately after a flash during laser flash photolysis of **1a**–DCA in (○) argon-saturated and (●) oxygen-saturated MeCN




**Scheme 2**

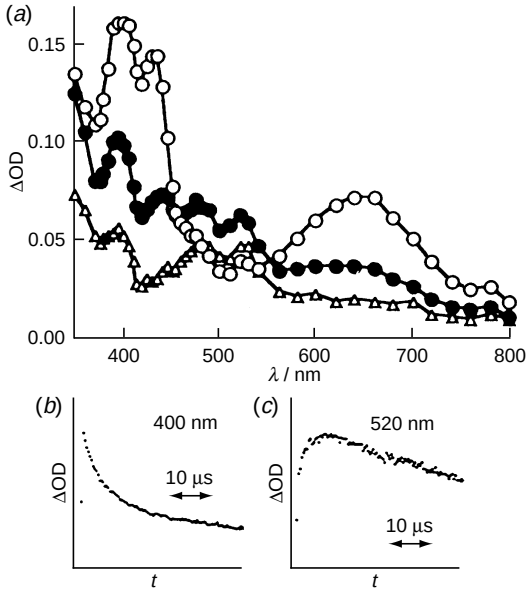



**Fig. 2** (*a*) Transient absorption spectral changes during pulse radiolysis of **1a** in argon-saturated 1,2-dichloroethane: (○) immediately after the pulse, (●) 5 μs after the pulse, and (Δ) 20 μs after the pulse. Kinetic traces illustrating the time profiles of (*b*) $\Delta OD_{400}$ and (*c*) $\Delta OD_{520}$.

immediately after an 8 ns pulse, and decayed with formation of new bands at 480 and 520 nm assigned to **3a**$^{\bullet+}$ at the first-order rate constant of $k = 8.9 \times 10^4$ s$^{-1}$.

On the other hand, the spectrum of **1c**$^{\bullet+}$ showed sharp bands at 390 and 440 nm and a broad band at 550–700 nm, was slightly different in the shape and peak wavelength from that for **1a**$^{\bullet+}$, and decayed without formation of any new bands. It is well known that naphthalene$^{\bullet+}$ dimerises with a neutral naphthalene to form a π-dimer radical cation with a 580 nm band at the equilibrium constant of $K = 520$ M$^{-1}$ in PhCN,[6] and that 1,3-di-1-naphthylpropane$^{\bullet+}$ forms a stable intramolecular dimer radical cation.[7] Phosphate **1a** in the singlet excited state forms intramolecularly a face-to-face excimer between two naphthyl groups.[1c] Therefore, a face-to-face structure between two naphthyl groups is suggested to be present in **1a**$^{\bullet+}$, decomposing into **3a**$^{\bullet+}$.

Consequently, electron transfer from **1a** to $^1$DCA* occurs to give **1a**$^{\bullet+}$ and DCA$^{\bullet-}$, **1a**$^{\bullet+}$ with the face-to-face structure between two naphthyl groups decomposes to **3a**$^{\bullet+}$ and the residue, and **3a** is finally formed as the stable product from the reduction of **3a**$^{\bullet+}$ with DCA$^{\bullet-}$ (Scheme 2).

We thank Professor Setsuo Takamuku and Professor Yoshiki Okamoto for helpful discussions, Dr Akito Ishida, Mrs Sachiko Tojo and Miss Tomoko Hashikawa for their help with the experiments, and the members of the Radiation Laboratory of ISIR, Osaka University, for running the linear accelerator. This work was partly supported by the Saneyoshi Scholarship Foundation (M. N.) and a Grant-in-Aid (No. 08240229) from the Ministry of Education, Science, Sport and Culture of Japan (T. M.).

## Footnotes

† E-mail: nakamura@esci.eng.himeji-tech.ac.jp

‡ Since the Stern–Volmer constants, $k_q\tau$, in the fluorescence quenching of $^1$DCA* by **1** and **2** were found to be 270–320 M$^{-1}$ for **1** and **2**, $k_q$ = (1.6–2.1) × 10$^{10}$ M$^{-1}$ s$^{-1}$ was calculated to be approximately equal to the diffusion-controlled rate constant from the lifetime of $^1$DCA*, τ = 14.9 ns using the literature value (ref. 5). The oxidation potentials, $E^{ox}_{1/2}$, of **1** and **2** were measured by cyclic voltammetry at a platinum electrode in dry MeCN with 0.1 M $Et_4NClO_4$ as a supporting electrolyte. The free energy changes, $\Delta G_{et}$, were calculated by using the Rehm–Weller equation (refs. 5 and 8).

§ Laser flash photolyses of the sample solutions were performed at room temperature by a flash at 355 nm (5 ns, 20 mJ pulse$^{-1}$) obtained by the third-harmonic oscillation from a Nd : YAG laser (ref. 9).

¶ γ-Radiolyses of the samples in degassed butyl chloride at 77 K were performed by a $^{60}$Co γ source; concentration of substrate, 10$^{-3}$ to 10$^{-2}$ M (ref. 10).

‖ Pulse radiolyses of the sample solutions were performed at room temperature using an electron pulse (8 ns, 28 MeV) obtained from a linear accelerator at Osaka University (ref. 11).

## References

1 (*a*) G. W. Sluggett, P. F. McGarry, I. V. Koptyug and N. J. Turro, *J. Am. Chem. Soc.*, 1996, **118**, 7367; (*b*) M. Nakamura, Y. Okamoto and S. Takamuku, *Chem. Commun.*, 1996, 209; (*c*) M. Nakamura, K. Sawasaki, Y. Okamoto and S. Takamuku, *Bull. Chem. Soc. Jpn.*, 1995, **68**, 3189; (*d*) S. Ganapathy, K. P. Dockery, A. E. Sopchik and W. G. Bentrude, *J. Am. Chem. Soc.*, 1993, **115**, 8863.

2 T. Furuta, H. Torigai, M. Sugimoto and M. Iwamura, *J. Org. Chem.*, 1995, **60**, 3953; M. C. Pirrung and S. W. Shuey, *J. Org. Chem.*, 1994, **59**, 3890; R. S. Givens and L. W. Kuepper, III, *Chem. Rev.*, 1993, **93**, 55.

3 S. Yasui, K. Shioji, A. Ohno and M. Yoshihara, *J. Org. Chem.*, 1995, **60**, 2099.

4 *Photoinduced Electron Transfer*, ed. M. A. Fox and M. Chanon, Elsevier, Amsterdam, The Netherlands, 1988; S. L. Mattes and S. Farid, in *Organic Photochemistry*, ed. A. Padwa, Marcel Deckker, New York, 1983; vol. 6, pp. 233–326; U. C. Yoon and P. S. Mariano, *Acc. Chem. Res.*, 1992, **25**, 233; V. D. Parker, *Acc. Chem. Res.*, 1984, **17**, 243; L. Eberson, *Adv. Phys. Org. Chem.*, 1982, **18**, 79; J. Mattay, *Top. Curr. Chem.*, 1990, **156**, 219; G. J. Kavarnos and N. J. Turro, *Chem. Rev.*, 1986, **86**, 401.

5 I. G. Gould, D. Ege, J. E. Moser and S. Farid, *J. Am. Chem. Soc.*, 1990, **112**, 4290.

6 A. Kira, S. Arai and M. Imamura, *J. Phys. Chem.*, 1972, **76**, 1119.

7 Y. Tsujii, A. Tsuchida, S. Ito and M. Yamamoto, *Macromolecules*, 1991, **24**, 4061.

8 D. Rehm and A. Weller, *Isr. J. Chem.*, 1970, **8**, 259; A. Weller, *Z. Phys. Chem. (Munich)*, 1982, **133**, 93.

9 T. Majima, S. Tojo, A. Ishida and S. Takamuku, *J. Org. Chem.*, 1996, **61**, 7793.

10 S. Tojo, K. Morishima, A. Ishida, T. Majima and S. Takamuku, *Bull. Chem. Soc. Jpn.*, 1995, **68**, 958.

11 A. Ishida, M. Fukui, H. Ogawa, S. Tojo, T. Majima and S. Takamuku, *J. Phys. Chem.*, 1995, **99**, 10808; T. Majima, M. Fukui, A. Ishida and S. Takamuku, *J. Phys. Chem.*, 1996, **100**, 8913; T. Majima, S. Tojo, A. Ishida and S. Takamuku, *J. Phys. Chem.*, 1996, **100**, 13615; T. Majima, S. Tojo, A. Ishida and S. Takamuku, *J. Phys. Chem. A*, 1997, **101**, 1048.

*Received in Cambridge, UK, 2nd April 1997; Com. 7/02230A*

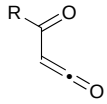
# New thermal rearrangements of vinylogous ketoketenes and related intermediates

**Gary A. Cartwright, Robert O. Gould and Hamish McNab***

*Department of Chemistry, The University of Edinburgh, West Mains Road, Edinburgh, UK EH9 3JJ*

**2-Oxopyran-5-carbaldehydes (*e.g.* 3) containing a trapping group in the 5-position rearrange thermally by a sequence involving electrocyclic ring opening, *E*/*Z* isomerisation and ring closure; a similar strategy has enabled the first cases of thermal interconversion of pyran-2-ones and 2-pyridones, and of automerisation of 2-pyridones to be identified.**

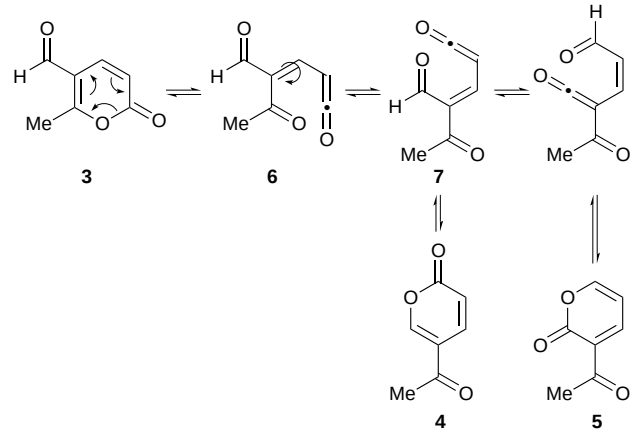
Studies of the thermal chemistry of unsaturated ketenes have provided in recent years many examples of unusual molecular rearrangements.[1] The ketoketene system **1** (R = Ph) undergoes 1,3-aryl shifts,[2] and its vinylogue **2**, which can be generated by ring opening of pyran-2-ones under flash vacuum pyrolysis (FVP) conditions,[3] shows 1,5-hydrogen shifts which serve to equilibrate 3- and 5-substituted pyran-2-one isomers (Scheme 1). Pyran-2-thione similarly rearranges quantitatively to thiapyran-2-one.[3] Here we demonstrate that in the presence of an appropriate trapping group the potential for thermal rearrangement in vinylogous ketoketenes is more extensive than has been previously recognised, due to the possibility of thermal *E*–*Z* isomerisation.[4] In addition, this strategy has provided the first examples of equilibration of pyran-2-ones and 2-pyridones, and of automerisation in the 2-pyridone system.



**1**

Thus 6-methyl-2-oxopyran-5-carboxaldehyde **3**† was synthesised in 79% yield by the reaction of diazomethane with 2-oxopyran-5-carbaldehyde[5] (*cf.* ref. 6). This compound lacks a good migrating substituent at the 6-position and therefore cannot give rearrangement products by the standard Pirkle mechanism (Scheme 1). Nevertheless, FVP of **3** at 550–750 °C gave rise to a quantitative mixture of the isomers **3**, **4** and **5** which were not separated but could be readily identified by characteristic[7] coupling constants in the $^1$H NMR spectra of the mixtures. Thus the 5-acetyl compound **4** showed $^3J_{3,4}$ (10.0 Hz), and the 3-acetyl derivative **5** showed typical values of $^3J_{4,5}$ (6.8 Hz) and $^3J_{5,6}$ (5.0 Hz) which compare well with data for α-pyrone itself ($^3J_{3,4}$ 9.4, $^3J_{4,5}$ 6.3 and $^3J_{5,6}$ 5.0 Hz).[7] Methyl signals of **4** and **5** occurred at $\delta_H$ 2.42 and 2.61 respectively, positions typical of acetyl groups. The formation of **4** is readily explained by *Z* to *E* isomerisation[4] of the alkene function of the ring-opened intermediate **6**, followed by collapse *via* electrocyclisation involving the initial aldehyde substituent (Scheme 2). An extension of the mechanism by 1,5-H-shift in the newly generated intermediate **7** gives the third isomer **5** after similar electrocyclic ring closure. The ratio of **3**:**4**:**5** at equilibrium (> 700 °C; Fig. 1) presumably reflects the relative stereoelectronic effects of the ring substituents; pyrones with certain other 5-carbonyl-containing substituents apparently do not rearrange significantly to the 3-isomers at high temperatures.[3]

In order to apply this methodology to pyran-2-one–2-pyridone equilibria, a 5-imino-substituted pyrone was required. The substrate **8** was therefore synthesised by condensation of the appropriate aldehyde (prepared in 60% yield by Rosenmund



**3** **6** **7** **4** **5**

**Scheme 2**

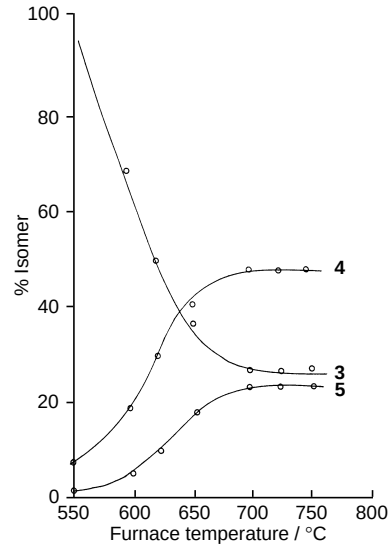
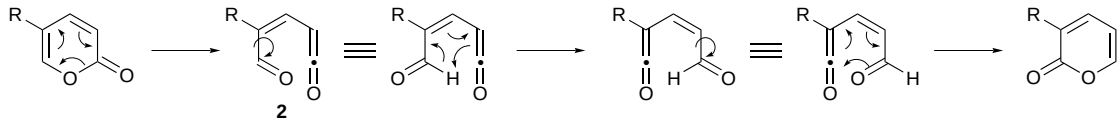


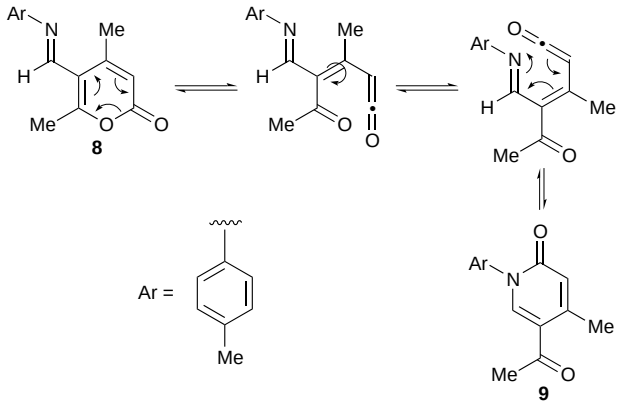

**Fig. 1** Equilibration of **3**, **4** and **5** by FVP of **3** at different furnace temperatures



**2**

**Scheme 1**

reduction of the corresponding acyl chloride) with *p*-toluidine (90%). FVP of **8** at 650 °C gave a quantitative yield of a single rearranged pyridone **9** (Scheme 3) whose structure was confirmed by X-ray crystallography‡ (Fig. 2). Assuming that there is little significant difference in the thermodynamic properties of the acetyl and aldimine substituents, the pyridone ring system appears to be overwhelmingly favoured thermodynamically with respect to the related pyrone.




**Scheme 3**

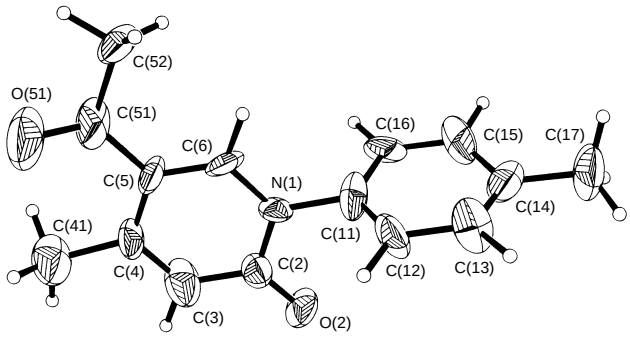
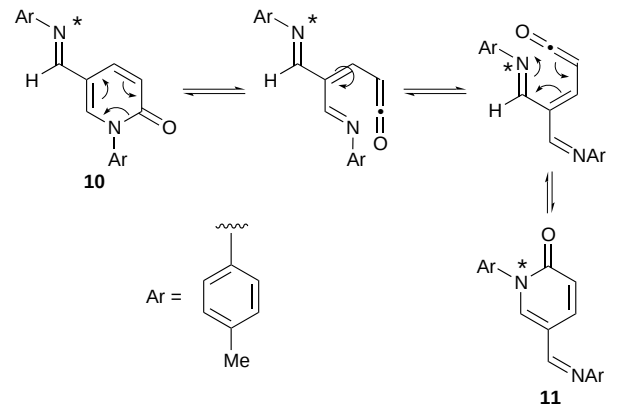



**Fig. 2** Thermal ellipsoid plot of **9** showing the crystallographic numbering scheme

In contrast to the situation with pyran-2-one and thiopyran-2-one systems,[3] very little is known of the thermal behaviour of 2-pyridones except for some fragmentation reactions under forcing conditions.[8] It is clear from the above result that 2-pyridones are unlikely to ring open under such mild conditions as their *O*-analogues, but we were interested to determine the general feasibility of this process. Accordingly, we reacted *p*-toluidine with 2-oxopyran-5-carbaldehyde and condensed the resulting oxopyridine carbaldehyde (56%) with $^{15}$N-labelled *p*-toluidine to give the imine **10** (96%) ($\delta_N$ −63.76 relative to external nitromethane). Reversing this sequence gave an authentic sample of the labelled pyridone **11** ($\delta_N$ −198.19). FVP of **10** at 750 °C, conditions under which the pyrones were completely equilibrated, gave just 4% of the automerised species **11** as shown by the small peak at $\delta_N$ −198.19 in the $^{15}$N NMR spectrum of the pyrolysate (Scheme 4). This result nevertheless establishes for the first time that thermal electrocyclic ring opening of the 2-pyridone system is a viable, albeit high energy, process. The rearrangement was much more pronounced (37%) at 850 °C, but the $^{15}$N NMR spectrum was confused by many other peaks due to decomposition products.




**Scheme 4**

We are grateful to British Petroleum International Ltd. for a Research Studentship (to G. A. C.) and to Dr D. Reed for the $^{15}$N NMR spectra, which were obtained through the S.E.R.C. (now E.P.S.R.C.) supported University of Edinburgh high-field NMR service.

## Footnotes

* E-mail: h.mcnab@ed.ac.uk

† All new compounds were characterised by their spectra and by elemental analyses, unless otherwise stated.

‡ *Crystal data* for **9**. $C_{15}H_{15}NO_2$, $M$ = 241.28, orthorhombic, space group $P2_12_12_1$, $a$ = 5.557(4), $b$ = 9.645(4), $c$ = 24.272(10) Å, $V$ = 1300.9 Å$^3$ (from setting angles for 10 *h*0*l* and 10 0*kl* data, 2θ = 8–24°, λ = 0.71073 Å), $Z$ = 4, $D_{calc}$ = 1.232 g cm$^{-3}$, $T$ = 295K, colourless needle, 0.85 × 0.2 × 0.08 mm, μ = 0.077 mm$^{-1}$, $F$(000) = 512. Data collection and processing—Stoë STADI-2 2-circle diffractometer, graphite monochromated Mo-Kα X-radiation, $T$ = 295K, ω-scans with ω-range (2.0 + 0.5 sinμ/tanθ)°, 1039 unique reflections ($2\theta_{max}$ 50°, $0 \leqslant h \leqslant 6$, $0 \leqslant k \leqslant 10$, $0 \leqslant l \leqslant 26$) giving 547 with $F \geqslant 4\sigma(F)$ for use in all calculations. No significant crystal decay or movement was apparent, and no absorption correction was made. Structure solution and refinement—automatic direct methods[9] located all non-hydrogen atoms which were then refined anisotropically; hydrogen atoms were inserted in calculated positions with fixed atomic displacement parameters of $U$ = 0.05 Å$^2$ (C–H = 1.08 Å). Only the torsion angles of the methyl groups were refined. At final convergence, $R$, $R_w$ = 0.075, 0.026 respectively, $S$ = 1.12 for 173 refined parameters and the final difference synthesis showed no peak or trough outside ±0.3 e Å$^{-3}$. An extinction parameter was refined, converging to 4.0 × 10$^{-4}$. No absorption corrections were made. The weighting scheme $w^{-1} = \sigma^2(F)$ gave satisfactory agreement analyses; in the final cycle, the maximum δ/σ was 0.07. Inlaid[10] atomic scattering factors were used, molecular geometry calculations utilised CALC,[11] and Fig. 2 was produced by SHELXTL.[12] Atomic coordinates, bond lengths and angles, and thermal parameters have been deposited at the Cambridge Crystallographic Data Centre (CCDC). See Information for Authors, Issue No. 1. Any request to the CCDC for this material should quote the full literature citation and the reference number 182/477.

## References

1 C. Wentrup, W. Heilmayer and G. Kollenz, *Synthesis*, 1994, 1219.
2 C. Wentrup and K.-P. Netsch, *Angew. Chem., Int. Ed. Engl.*, 1984, **23**, 802.
3 W. H. Pirkle and W. V. Turner, *J. Org. Chem.*, 1975, **40**, 1617.
4 C. L. Hickson and H. McNab, *J. Chem. Res. (S)*, 1989, 176.
5 J. T. Kurek and G. Vogel, *J. Heterocycl. Chem.*, 1968, **5**, 275.
6 J. Fried and R. C. Elderfield, *J. Org. Chem.*, 1941, **6**, 577.
7 For example, W. H. Pirkle and M. Dines, *J. Heterocycl. Chem.*, 1969, **6**, 1.
8 D. A. Brent, J. D. Hribar and D. C. DeJongh, *J. Org. Chem.*, 1970, **35**, 135.
9 SHELX86, program for crystal structure solution, G. M. Sheldrick, University of Göttingen, F.R.G., 1986.
10 SHELX76, program for crystal structure refinement, G. M. Sheldrick, University of Cambridge, England, 1976.
11 CALC, program for molecular geometry calculations, R. O. Gould and P. Taylor, University of Edinburgh, Scotland, 1985.
12 SHELXTL/PC, Version 4.3, Siemens Analytical X-ray Instruments Inc., Madison, Wisconsin, USA, 1992.

*Received in Cambridge, UK, 8th April 1997; Com. 7/02395B*

# Low-temperature oxygenation of methane into formic acid with molecular oxygen in the presence of hydrogen catalysed by $Pd_{0.08}Cs_{2.5}H_{1.34}PVMo_{11}O_{40}$

**Noritaka Mizuno,*[a] Hiromi Ishige,[a] Yasuhiro Seki,[a] Makoto Misono,[a] Don-Jin Suh,[b] Wonchull Han[b] and Tetsuichi Kudo[b]**

[a] *Department of Applied Chemistry, Graduate School of Engineering, The University of Tokyo, Hongo, Bunkyo-ku, Tokyo 113, Japan*

[b] *Institute of Industrial Science, The University of Tokyo, Minato-ku, Roppongi, Tokyo 106, Japan*

**The title reaction is catalysed by $Pd_{0.08}Cs_{2.5}H_{1.34}PVMo_{11}O_{40}$ at temperatures as low as 423–593 K, and the catalytic rate, which reached a maximum at 573 K, is $1.2 \times 10^{-4}$ mol $h^{-1}$ $g^{-1}$, *ca.* $3 \times 10^2$ times higher than $FePO_4$, the most active catalyst previously reported.**

The activation and functionalization of methane has attracted much attention owing to its abundance in natural gas and low reactivity.[1–8] Recently, there has been a renewed interest in the direct conversion of methane into oxygenates.[6–19] Various catalysts have been tested with a variety of oxidants in heterogeneous[9–17] and homogeneous systems.[18–20]

The utilization of molecular oxygen for the oxidation of methane is a rewarding goal since it has the highest content of active oxygen and forms no by-products. However, direct oxidation with molecular oxygen cannot be achieved using heterogeneous catalysts under atmospheric pressure because the high temperatures and pressures required, which induce radical formation, needed for the activation of methane and/or oxygen leads to overoxidation of the oxygenated products. Therefore, a lowering of the reaction temperature is a key requirement for selective oxidation. We have reported the direct oxidation of lower alkanes with molecular oxygen catalysed by heteropoly compounds, but oxidation of methane was unsuccessful.[21]

On the other hand, reductants such as aldehyde,[22] hydrogen[23] and zinc[24] promoted the oxidation of alkanes and alkenes with molecular oxygen and significantly lowered the reaction temperature in homogeneous systems. However, concerning catalytic oxygenation of methane with dioxygen in the presence of reductants in heterogeneous systems, only the $FePO_4$–$O_2$–$H_2$ system has been studied;[15] Even in this system, a temperature as high as 623 K was required which is much higher than for homogeneous systems. Here we report the selective oxygenation of methane into formic acid with a $O_2$–$H_2$ mixture at temperatures as low as 423–593 K.

$H_{3+x}PV_xMo_{12-x}O_{40}$ heteropolyacids were obtained commercially from Nippon Inorganic Colour and Chemical Co., Ltd. The other reagents used were of analytical grade and used without further purification.

The catalysts were prepared as follows: 3.6 $cm^3$ of an aqueous solution of palladium nitrate (0.08 mol $dm^{-3}$) was added dropwise to 60.0 $cm^3$ of an aqueous solution of $H_4PVMo_{11}O_{40}$ (0.06 mol $dm^{-3}$), followed by the addition of 56.3 $cm^3$ of an aqueous solution of caesium carbonate (0.08 mol $dm^{-3}$) at 323 K and the powder samples were carefully collected and the resulting suspension evaporated to dryness at 323 K. The actual composition of the powder is $Pd_{0.08}Cs_{2.5}H_yPVMo_{11}O_z$, but are designated $Pd_{0.08}Cs_{2.5}H_{1.34}PVMo_{11}O_{40}$ according to the stoichiometry of the starting materials.

Catalytic reactions were performed in a flow reactor. Prior to the reaction, 120 mg of catalyst was treated in an O2 stream (60 $cm^3$ $min^{-1}$) for 1 h at 573 K. The reactions were performed at atmospheric pressure and the feed gas typically consisted of 28 vol% methane, 14 vol% $O_2$ with the balance $N_2$, and the total flow rate was 22 $cm^3$ $min^{-1}$. The gases at the outlet of the reactor were analysed by FID (equipped with methanizer) and a TCD gas chromatograph. Selectivity was calculated on the $C_1$ (methane)-basis. The products were formic acid, methanol and $CO_x$. Similar products were observed for the other heteropoly catalysts used. The conversion and the selectivity data were collected after 2–5 h of reaction, when nearly steady-state conversion and selectivity were obtained for each catalyst.

Fig. 1 shows the temperature dependency of the conversion and selectivity for $Pd_{0.08}Cs_{2.5}H_{1.34}PVMo_{11}O_{40}$. It is noted that the reaction proceeded even at 423 K. The conversion of methane monotonously increased with increase in the reaction temperature and reached a maximum at 573 K. The rate for the methane conversion at 573 K was $1.2 \times 10^{-4}$, *ca.* $3 \times 10^2$ greater than that of the most active heterogeneous catalyst ($FePO_4$) reported previously.[15] The selectivity to formic acid was > 67%. Such high selectivity towards formic acid has not been reported previously in heterogeneous oxidation of methane.[1–8] The highest yield of formic acid was obtained at 573 K. $Pd_{0.08}Cs_{2.5}H_{1.34}PVMo_{11}O_{40}$ also catalysed the oxidation of ethane into acetic acid under similar conditions. Similar conversion and selectivity with reaction temperature were observed for $Pd_{0.08}Cs_{2.5}H_{3.34}PV_3Mo_9O_{40}$.

An increase in the yield of formic acid was achieved by further $V^{5+}$-substitution. The conversions for $Pd_{0.08}Cs_{2.5}H_{0.34+x}PV_xMo_{12-x}O_{40}$ ($x$ = 0, 1, 2 and 3) were 0.08, 0.08, 0.10 and 0.14%, respectively and increased with $V^{5+}$ substitution. The selectivities to formic acid were 46, 70, 76 and 60% for $x$ = 0, 1, 2 and 3, respectively, and the highest selectivity to formic acid was observed at $x$ *ca.* 2. It follows that the substitution of $V^{5+}$ for $Mo^{6+}$ in $Pd_{0.08}Cs_{2.5}H_{0.34}PMo_{12}O_{40}$ resulted in the enhancement of formic acid production and the yield reached a maximum at $x$ = 2–3.

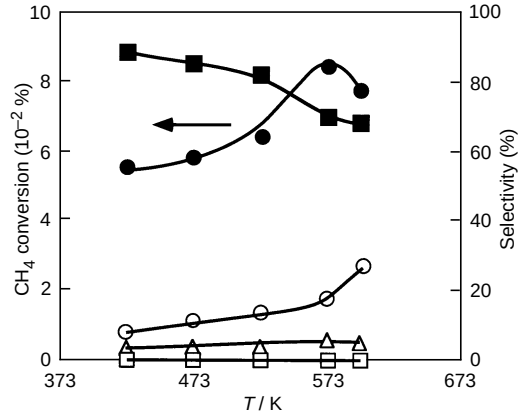



**Fig. 1** Temperature dependence of conversion and selectivity; catalyst, $Pd_{0.08}Cs_{2.5}H_{1.34}PVMo_{11}O_{40}$. Conversion of methane (●) and selectivities towards formic acid (■), methanol (□), CO (△) and $CO_2$ (○).

No selective oxidation proceeded in the absence of Pd or when carbon monoxide was used instead of hydrogen. The addition of 1.9 vol% hydrogen peroxide instead of a gaseous mixture of $H_2$ and $O_2$ led to similar conversion and selectivity to oxygenates. This suggests that the active oxygen species arises from hydrogen peroxide formed by an $H_2$–$O_2$ reaction catalysed by Pd. Reports that Pd in acidic medium catalyses the reaction of dioxygen with dihydrogen to form hydrogen peroxide,[25] and the fact that heterpolyacids and their caesium salts are strongly acidic[26] supports this hypothesis. Formic acid is formed by the liquid-phase oxidation of methane with hydrogen peroxide catalysed by $H_4PVMo_{11}O_{40}$;[27] this suggests that successive oxidation of methane *via* hydrogen peroxide can be catalysed by heteropolyacids.

This work was supported in part by a Grant-in-Aid for Scientific Research from the Ministry of Education, Science, Sports and Culture of Japan.

## Footnote

* E-mail: tmizuno@hongo.ecc.u-tokyo.ac.jp

## References

1 R. Pitchai and K. Klier, *Catal. Rev.-Sci. Eng.*, 1986, **28**, 13.
2 H. D. Gesser, N. R. Hunter and C. B. Prakash, *Chem. Rev.*, 1985, **85**, 235.
3 G. J. Hutchings, M. S. Scurrell and J. R. Woodhouse, *Chem. Soc. Rev.*, 1989, **18**, 251.
4 R. D. Srivastava, P. Zhou, G. J. Stiegel, V. U. S. Rao and G. Cinquegrane, *Catalysis (London)*, 1992, **9**, 1993.
5 J. L. G. Fierro, *Catal. Lett.*, 1993, **22**, 67.
6 R. H. Crabtree, *Chem. Rev.*, 1995, **95**, 987.
7 M. G. Axelrod, A. M. Gaffney, R. Pitchai and J. A. Sofranko, *Natural Gas Conversion II*, Elsevier, New York, 1994, p. 93.
8 R. D. Srivastava, S. V. Gollakota, G. J. Stiegel and A. C. Bose, *Methane and Alkane Conversion Chemistry*, Plenum, New York, 1995, p. 291.
9 J. S. J. Hargreaves, G. J. Hutchings, R. W. Joyner and S. H. Taylor, *Chem. Commun.*, 1996, 523.
10 C. Shi, Q. Sun, H. Hu, R. G. Herman, K. Klier and I. E. Wachs, *Chem. Commun.*, 1996, 663.
11 M. Faraldos, M. A. Banares, J. A. Anderson, H. Hu, I. E. Wachs and J. L. G. Fierro, *J. Catal.*, 1996, **160**, 214.
12 C. T. Au, H. He, S. Y. Lai and C. F. Ng, *J. Catal.*, 1996, **163**, 399.
13 Y. S. Lin and Y. Zeng, *J. Catal.*, 1996, **164**, 220.
14 P. M. Witt and L. D. Schmidt, *J. Catal.*, 1996, **163**, 465.
15 Y. Wang and K. Otsuka, *J. Catal.*, 1995, **155**, 256.
16 W. Li and S. T. Oyama, *Heterogeneous Hydrocarbon Oxidation*, ACS, Washington, 1996, p. 364.
17 M. A. Banares, L. A. Alemany, F. M.-Jimenez, J. M. Blasco, M. L. Granados, M. A. Pena and J. L. G. Fierro, *Heterogeneous Hydrocarbon Oxidation*, ACS, Washington, 1996, p. 78.
18 N. Basickes, T. E. Hogan and A. Sen, *J. Am. Chem. Soc.*, 1996, **118**, 13 111.
19 Y. Fujiwara, K. Takai and Y. Taniguchi, *Chem. Lett.*, 1996, 591.
20 A. Bagno, H. Bukala and G. A. Olah, *J. Org. Chem.*, 1990, **55**, 4284.
21 N. Mizuno, D.-J. Suh, W. Han and T. Kudo, *J. Mol. Catal. A: Chem.*, 1996, 114, 309; N. Mizuno, D.-J. Suh, W. Han, T. Kudo and M. Iwamoto, *Stud. Surf. Sci. Catal. B*, 1996, **101**, 1001.
22 S. Murahashi, Y. Oda and T. Naota, *J. Am. Chem. Soc.*, 1992, **114**, 7913.
23 M. T. Atlay, M. Preece, G. Strukal and B. R. James, *J. Chem. Soc., Chem. Commun.*, 1982, 406.
24 I. Yamanaka, M. Soma and K. Otsuka, *J. Chem. Soc., Chem. Commun.*, 1995, 2235.
25 Y. Izumi, H. Miyazaki and S. Kawahara, *Jpn. Pat.*, 47121, 1981; G. L. Wayne, *Eur. Pat.*, 132294, 1983.
26 T. Okuhara, N. Mizuno and M. Misono, *Adv. Catal.*, 1996, **41**, 113.
27 Y. Seki, N. Mizuno and M. Misono, *72th Symposium of the Chemical Society of Japan*, Tokyo, March, 1997, 1D237.

*Received in Cambridge, UK, 14th April 1997; Com. 7/02514I*

# NMR structural analysis of a β-hairpin peptide designed for DNA binding

**Allister J. Maynard and Mark S. Searle***

*Department of Chemistry, University of Nottingham, University Park, Nottingham, UK NG7 2RD*

**NMR and circular dichroism (CD) spectroscopy shows that an unconstrained 16 residue linear peptide folds autonomously in water into a β-hairpin: the designed peptide adopts a conformation that mimics the anti-parallel β-sheet DNA binding motif of the *met* repressor protein dimer with key residues for DNA recognition presented in the same positions and orientations principally on one face of the β-hairpin template.**

Recent studies have shown that small peptides of 14 to 17 residues, derived from the Bovine Immunodeficiency Virus (BIV) Tat protein[1] and HIV Rev protein,[2] can bind to nucleic acids with high affinity as β-hairpin or α-helical structures inserted into the major groove of RNA. Such model systems open up the possibility of using designed peptides or non-peptidic analogues for sequence specific recognition of nucleic acids in a therapeutically beneficial manner, either through blocking transcription factor binding[3] or by delivering some reactive functional group to the surface of DNA or RNA where single or double strand damage could be inflicted.[4]

The *met* repressor protein dimer represents a novel class of DNA binding proteins that recognise DNA in a sequence specific manner through insertion of a two stranded anti-parallel β-sheet into the major groove.[5] The key residues for binding and recognition by the *met* repressor are shown in Fig. 1(*a*). We have designed a linear 16-residue peptide analogue of this binding motif, that incorporates all of these key residues, by linking two β-strands *via* a two residue turn sequence such that the 16-mer can fold to form a β-hairpin structure [Fig. 1(*b*)] with the correct anti-parallel alignment of β-strands. The most abundant two residue turns in the protein structure data base are of the type I′ variety with the sequence NG particularly favoured.[6,7] To remove some of the sequence degeneracy inherent in the peptide and aid structural analysis by NMR, a tyrosine has been introduced at position 3 on the non-binding face (in place of Ile in the native sequence) to provide a good NMR probe for folding through long range NOEs. Here we describe the characterisation of the 16-mer [Fig. 1(*b*)], which we show by NMR and CD is appreciably folded in aqueous solution, representing one of only a few examples of short peptides that adopt compact folded β-structures in water.[6,8]

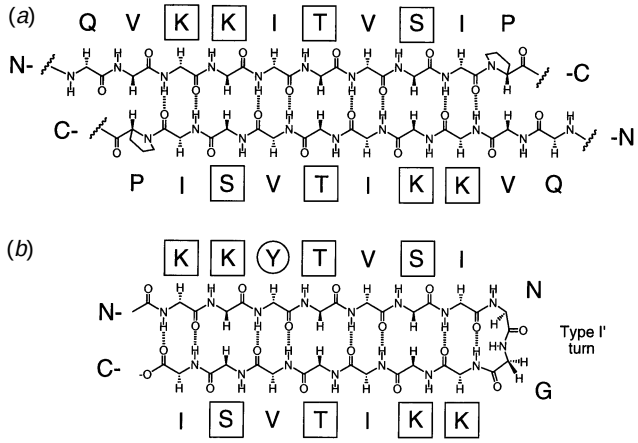



**Fig. 1** (*a*) Anti-parallel alignment of the two β-strands of the DNA recognition motif of the *met* repressor protein dimer. Key residues for DNA binding and recognition are highlighted in square boxes. (*b*) Designed 16 residue β-hairpin analogue of (*a*). Peptides were synthesised on a 0.1 mM scale using standard F-moc solid-phase protocols followed by purification by reverse phase HPLC using an Applied Biosystems Aquaphore Octyl column (10 mm × 100 mm). Purity was assessed by mass spectral analysis and $^1$H NMR spectroscopy.

The *N*-acetylated 16-mer [Fig. 1(*b*)] has been studied by far-UV circular dichroism (CD) spectroscopy in aqueous solution at pH 4.0 and 7.5 μM concentration. A significant negative ellipticity at 216 nm suggests that the peptide forms a high proportion of folded structure in purely aqueous solution with the absorption profile reminiscent of β-structure (both turn and sheet) in equilibrium with some random coil (negative ellipticity below 198 nm)[9] (data not shown). Addition to the peptide of small amounts of methanol (< 20% v/v) produces a significant deepening of the minimum at 216 nm and formation of a maximum at 200 nm indicative of a displacement of the equilibrium already present in aqueous solution further towards the folded state, as has been reported for a number of other model peptide systems.[10]

The most conclusive evidence for folded structure is the observation of long range NOEs between residues in the anti-parallel strands of the β-hairpin. A full resonance assignment has been possible using established procedures,[11] allowing such

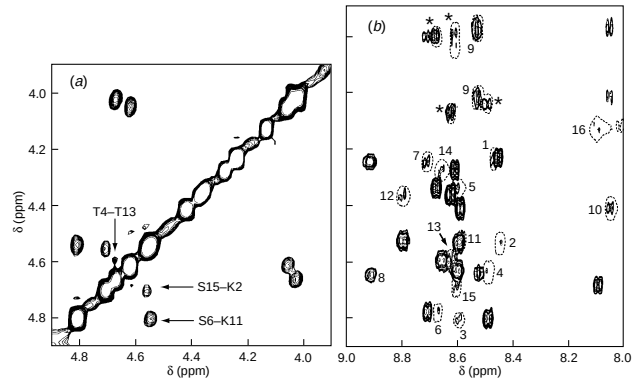



**Fig. 2** (*a*) Portion of the NOESY spectrum (200 ms mixing time) of the 16-mer at 278 K illustrating cross-strand αα(i,j) NOEs as highlighted. The intensity of the T4–T13 NOE cross-peak is distorted due to its position close to the diagonal; (*b*) Finger-print regions (NH to Hα) of NOESY (200 ms) and TOCSY spectra (overlayed) of the 16-mer. TOCSY data are plotted as a single broken contour. In general, αN(i,i) NOEs (occuring at the same positions as TOCSY cross-peaks) are very weak for residues in extended β-strands (residues 1–7 and 10–16), while αN(i,i + 1) sequential interresidue NOEs are much more intense. Note: for N8 and G9 NOEs αN(i,i) and αN(i,i + 1) are of comparable intensity reflecting their positions in the β-turn. Asterisks mark the position of NH to Hβ cross-peaks in both NOESY and TOCSY. TOCSY NH to Hα cross-peaks are numbered according to the sequence: N-Ac-K$^1$K$^2$Y$^3$T$^4$V$^5$S$^6$I$^7$N$^8$G$^9$K-$^{10}$K$^{11}$I$^{12}$T$^{13}$V$^{14}$S$^{15}$I$^{16}$. $^1$H NMR spectra were recorded at 500 MHz on a Bruker DRX500 spectrometer using standard phase sensitive 2D NMR pulse sequences. Attenuation of the residual solvent peak in NOESY and TOCSY spectra recorded in 90% $H_2O$ solution was achieved by presaturation. The sodium salt of trimethylsilyl propionate was used as an internal chemical shift reference.

long range interactions to be identified. The main chain alignment shown in Fig. 1(*b*) brings a number of Hαs of non-hydrogen bonded residues into close proximity. Accordingly, several intense interstrand αα(i,j)† interactions are readily detected in both NOESY and ROESY spectra recorded in aqueous solution. In Fig. 2(*a*), NOEs are identified between Ser6-Lys11, Thr4-Thr13 and Lys2-Ser15 that are fully consistent with the proposed anti-parallel alignment of the peptide chain. These observations are substantiated by studies in 90% $H_2O$ solution were cross-strand long-range NN(i,j)† interactions between residues involved in hydrogen bonding are also evident (Lys1-Ile16, Val5-Ile12 and Ile7-Lys10). The first of these interactions (Lys1-Ile16) illustrates that even the two terminal residues are held in close proximity for an appreciable proportion of the time, indicative of the peptide adopting a well-defined conformation in aqueous solution. While these NOEs provide evidence for long range order in the peptide chain, the intensity of NOEs between adjacent residues provide additional support for local order between nearest neighbours. The majority of residues give rise to intense αN(i,i + 1) sequential NOEs but very weak (or undetected) NN(i,i + 1) and αN(i,i) interactions [Fig. 2(*b*)], consistent with the involvement of many residues in an extended β-strand conformation.[12] In the random coil these NOEs are expected to be much more similar in intensity due to averaging over a large number of conformational states.[12] Significantly different NOE intensities are observed for residues at the centre of the sequence where, for example, a strong sequential NN(i,i + 1) NOE between G9 and K10, together with similar intensity αN(i,i) and αN(i,i + 1) NOEs for N8 and G9 [Fig. 2(*b*)], are diagnostic of the involvement of these residues in a β-turn.

Chemical shift values for Hα resonances have been widely used as an indicator of folded structure in solution.[6,8,10] Positive deviations from tabulated random coil values[11] generally correlate with residues found in extended β-strand conformations, while negative (upfield) shifts are associated with residues in α-helices or β-turn conformations.[13] In the present case, positive deviations (Δδ) are evident for residues 2–7 and 10–15, while negative (upfield) shifts are identified for residues at the centre of the sequence. The plot of Δδ *versus* amino acid sequence clearly has the characteristic appearance of a β-hairpin, that is, two β-strands separated at the centre of the sequence by a turn. More pronounced effects are apparent in the presence of low concentrations of methanol reflecting the effects of the organic solvent in displacing the equilibrium towards the folded state (Fig. 3). We have established that all

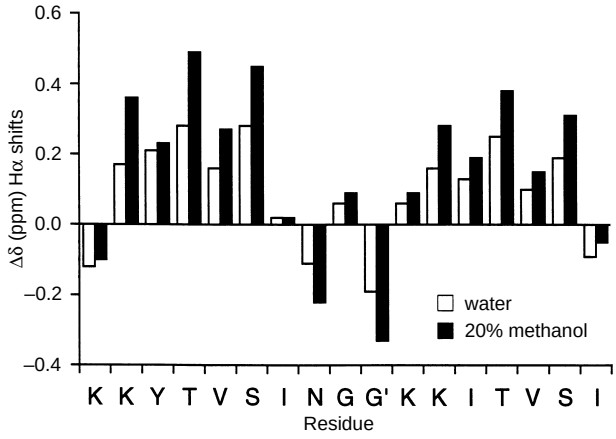



**Fig. 3** Deviations of CαH chemical shifts from random coil values in aqueous solution and 20% v/v methanol, pH 4.5 and 278 K

chemical shifts and line widths are independent of sample concentration over a *ca*. 300-fold dilution range (8.0 to 0.03 mM), indicating that the reported effects are a consequence of folding of the monomeric peptide rather than the formation of aggregates.

We have shown unambiguously by CD and NMR experiments that the designed peptide forms a high proportion of folded structure in purely aqueous solution with the desired alignment of the peptide backbone. The 16-mer represents one of only a few examples of short linear peptides that are able to adopt compact folded β-hairpin structures in water, providing a useful model system for probing β-sheet forming interactions relevant to protein folding mechanisms, with the added potential for DNA recognition.

We acknowledge the EPSRC (studentship to A. J. M.), The Royal Society, Nuffield Foundation and the Department of Chemistry at the University of Nottingham for financial support. We thank John Keyte for peptide synthesis and Dr Gary Sharman for helpful discussions.

## Footnotes

* E-mail: mark.searle@nottingham.ac.uk

† αα(i,j) interresidue NOE between Hαs of residues i and j; NN(i,j)-NH to NH NOE between residues i and j; αN(i,i + 1)-NOE between Hα of residue i and NH of residue i + 1.

## References

1 J. D. Puglisi, L. Chen, S. Blanchard and A. D. Frankel, *Science*, 1995, **270**, 1200; X. Ye, R. A. Kumar and D. J. Patel, *Chem. Biol.*, 1995, **2**, 827.
2 J. L. Battiste, R. A. D. Tan and J. R. Williamson, *J. Biomol. NMR*, 1995, **6**, 375; R. D. Peterson, D. P. Bartel, J. W. Szostak, S. J. Horvath and J. Feigon, *Biochemistry*, 1994, **33**, 5357.
3 J. J. Welch, F. J. Rauscher II and T. A. Beerman, *J. Biol. Chem.*, 1994, **269**, 31 051; D. Henderson and L. H. Hurley, *Nature Med.*, 1995, **1**, 525.
4 P. G. Schultz, J. S. Taylor and P. B. Dervan, *J. Am. Chem. Soc.*, 1982, **104**, 6861; R. P. Herzberg and P. B. Dervan, *J. Am. Chem. Soc.*, 1982, **104**, 313.
5 W. S. Somers and S. E. V. Philips, *Nature*, 1992, **359**, 387.
6 F.J. Blanco, G. Rivas and L. Serrano, *Nat. Struct. Biol.*, 1994, **1**, 584.
7 E. G. Hutchinson and J. M. Thornton, *Protein Sci.*, 1994, **3**, 2207.
8 F. J. Blanco, M. A. Jimenez, J. Herranz, M. Rico, J. Santoro and J. L. Nieto, *J. Am. Chem. Soc.*, 1993, **115**, 5887; F. J. Blanco and L. Serrano, *Eur. J. Biochem.*, 1995, **230**, 634; M. S. Searle, D. H. Williams and L. C. Packman, *Nat. Struct. Biol.*, 1995, **2**, 999; V. Sieber and G. R. Moe, *Biochemistry*, 1996, **35**, 181; E. de Alba, M. A. Jimenez, M. Rico and J. L. Nieto, *Folding and Design*, 1996, **1**, 133.
9 J. T. Yang, C.-S. C. Wu and H. M. Martinez, *Methods Enzymol.*, 1986, **130**, 208; W. C. Johnson, Jr. *Annu. Rev. Biophys. Biophys. Chem.*, 1988, **17**, 145; H. J. Dyson and P. E. Wright, *Annu. Rev. Biophys. Biophys. Chem.*, 1991, **20**, 519.
10 F. J. Blanco, M. A. Jimenez, A. Pineda, M. Rico, J. Santoro and J. L. Nieto, *Biochemistry*, 1994, **33**, 6004; J. P. L. Cox, P. A. Evans, L. C. Packman, D. H. Williams and D. N. Woolfson, *J. Mol. Biol.*, 1993, **234**, 483; M. S. Searle, R. Zerella, D. H. Williams and L. C. Packman, *Protein Eng.*, 1996, **9**, 559.
11 K. Wuthrich, *NMR of Proteins and Nucleic Acids*, Wiley, New York, 1986.
12 L. J. Smith, K. A. Bolin, H. Schwalbe, M. W. MacArthur, J. M. Thornton and C. M. Dobson, *J. Mol. Biol.*, 1996, **255**, 494; L. J. Smith, K. M. Fiebig, H. Schwalbe and C. M. Dobson, *Folding and Design*, 1996, **1**, R95.
13 D. S. Wishart, B. D. Sykes and F. M. Richards, *Biochemistry*, 1992, **31**, 1647.

*Received in Glasgow, UK, 16th April 1997; Com. 7/02593I*

# A new synthetic route to allylsilanes: the reaction of silyllithium reagents with aromatic carbonyl compounds and aluminium tris(2,6-diphenylphenoxide) (ATPH)

**Susumu Saito,[a] Kazuto Shimada,[a] Hisashi Yamamoto,*†[a] Eduardo Martínez de Marigorta[b] and Ian Fleming*[b]**

[a] *Graduate School of Engineering, Nagoya University, CREST, Japan Science and Technology Corporation (JST), Furo-Cho, Chikusa, Nagoya 464-01, Japan*
[b] *Department of Chemistry, Lensfield Road, Cambridge, UK CB2 1EW*

**Conjugate 1,6-addition of silyllithium reagents to aromatic carbonyl substrates in the presence of the carbonyl protector aluminium tris(2,6-diphenylphenoxide) (ATPH) gives allylsilanes.**

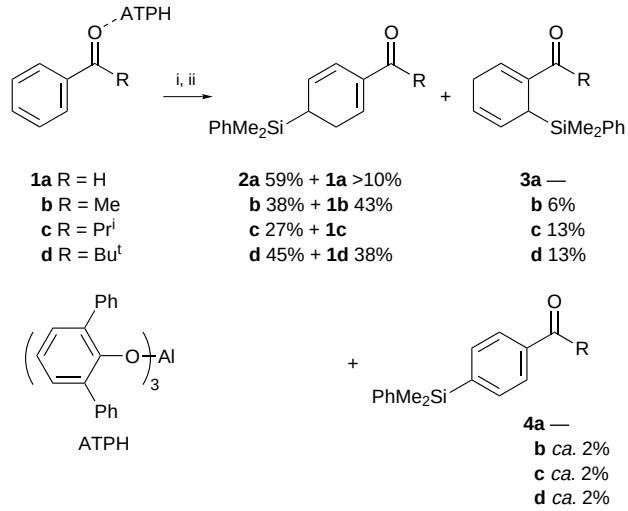
Allylsilanes are versatile synthetic intermediates,[1] and several methods are available to prepare these reagents.[2] We recently described the conjugate addition of several alkyllithiums to aromatic carbonyl compounds complexed with aluminium tris(2,6-diphenylphenoxide) (ATPH),[3] in which the Lewis acid effectively blocks carbonyl carbons from nucleophilic attack. This result led us to explore the possibility of using this strategy for the synthesis of allylsilanes using silyllithium reagents[4,5] in place of the alkyllithium reagents. We report here that the 1,6-addition of silyllithium reagents to the aromatic carbonyl compound–ATPH complex, and subsequent enolate capture with an appropriate electrophilic reagent, does provide a route to functionalised allylsilanes (Scheme 1).

Treatment of the precomplexed salt **1a** of benzaldehyde and ATPH with phenyldimethylsilyllithium ($PhMe_2SiLi$)[5] at −78 °C produced, after stirring for 30 min and quenching with concentrated hydrochloric acid at −78 °C, selective 1,6-addition to give allylsilane **2a** in 59% yield.‡ When a similar procedure was applied to aromatic ketones **1b**–**d**, 1,6-addition products **2b**–**d** were accompanied by small amounts of the 1,4-addition products **3b**–**d**§ and the aromatised silylated products **4b**–**d** (Scheme 1). These results suggest that the γ-carbon of the carbonyl substrate was selectively protonated by way of dienolate intermediates, which was confirmed by quenching the intermediates **5** in the acetophenone series at low-temperature with deuterated acid to give the monodeuterated products **6** (Scheme 2).

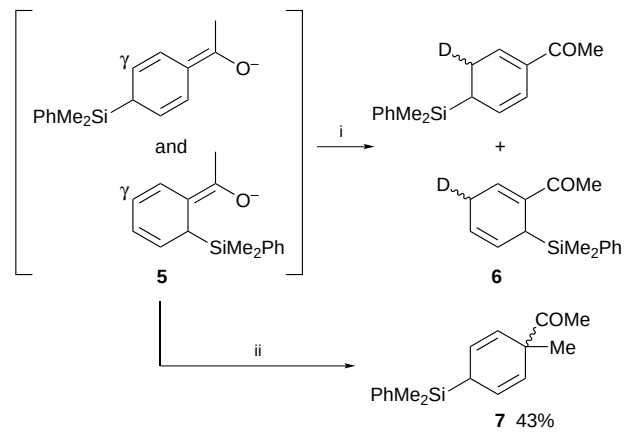
When the generation of dienolate **5** was followed by treatment with an excess of methyl trifluoromethanesulfonate (10 equiv.) at −78 °C for 1 h, the α-methylated product **7** was formed in 43% yield after the usual low-temperature acidic work-up. Methylation occurred predominantly at the α-carbon, in contrast to the exclusive γ-protonation with hydrochloric acid (Scheme 2).

Similarly, phenyldimethylsilyllithium underwent conjugate addition to methyl benzoate in the presence of ATPH with high 1,6-selectivity (1,6 : 1,4 = 87 : 13), but relatively low regioselectivity on protonation to give a mixture (52 : 35 : 13) of the regioisomeric pentadienyl silanes **9** (Scheme 3), including a stereoisomeric mixture (*cis* : *trans* = 1 : 3.1) in the case of the α-protonated product **9b**. The *cis* : *trans* ratio was determined by $^1$H NMR spectroscopy and assigned by a NOESY measurement. In contrast, methylation of the dienolate intermediates **8** gave *cis*-**10** regio- and stereo-selectively, with the methyl group entering *anti* to the resident silyl group. This finding is similar to the alkylation of cyclic enolates having a silyl group adjacent to the nucleophilic centre, which are highly selective for attack by the incoming electrophile *anti* to the silyl group.[6] The relative stereochemistry of *cis*-**10** was assigned by a NOESY measurement by converting the mixture **10** into the alcohols **11** by reduction with diisobutylaluminium hydride (DIBAL-H).

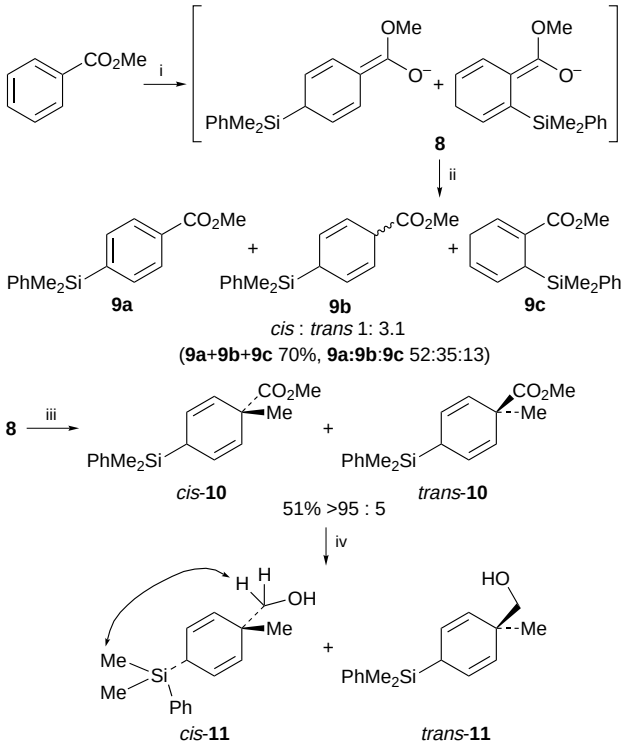
1,6-Addition also took place, in somewhat higher yield, with 1-naphthaldehyde **12a** and with 1-acetonaphthone **12b** to give the adducts **13** (Scheme 4). In an attempt to prepare the hydrate of an aromatic ring, we also carried out the reaction with the latter substrate using the more easily functionalised 2-methylbut-2-enyldiphenylsilyl group[7] to give the adduct **14**. Functionalisation of the silyl group was carried out using protodesilylation at the exocyclic allylsilane unit to give the



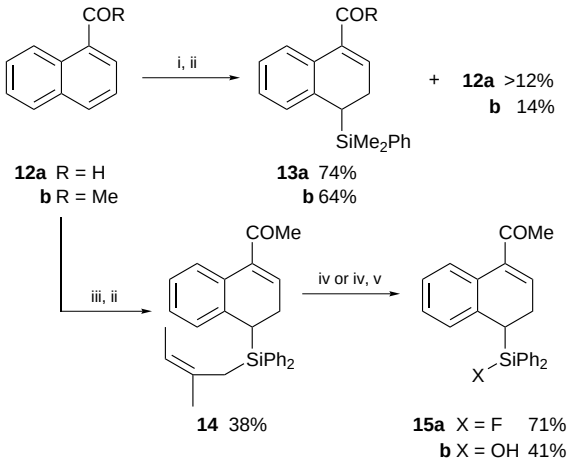

**Scheme 1** *Reagents*: i, $PhMe_2SiLi$; ii, HCl, $H_2O$




**Scheme 2** *Reagents*: i, DCl, $D_2O$; ii, $MeOSO_2CF_3$




**Scheme 3** *Reagents and conditions*: i, ATPH, toluene, $PhMe_2SiLi$, −78 °C, 30 min; ii, conc. HCl, −78 °C to room temp.; iii, $MeOSO_2CF_3$ (10 equiv.), −78 °C, 1 h; iv, DIBAL-H, 0 °C




**Scheme 4** *Reagents and conditions*: i, ATPH, toluene, $PhMe_2SiLi$, −78 °C; ii, conc. HCl, −78 °C to room temp.; iii, ATPH, toluene, 2-methylbut-2-enyldiphenylsilyllithium, −78 °C; iv, $BF_3$·AcOH, $CH_2Cl_2$, −10 °C; v, KF, $H_2O_2$, MeOH–THF, 0 °C

silyl fluoride **15a** in 71% yield. Subsequent treatment under Tamao's conditions[8] with potassium fluoride and hydrogen peroxide in THF–MeOH produced hydroxy silane **15b** in fair yield, but not the naphthalene hydrate (Scheme 4). A method for efficiently transforming the silyl group into a hydroxy group is still under investigation.

We thank the Ministry of Culture, Science, Education and Sports of Japan and the Basque Government for providing financial support.

## Footnotes

† E-mail: j45988a@nucc.cc.nagoya-u.ac.jp

‡ *Typical experimental procedure*: benzaldehyde ($51 \times 10^{-3}$ cm³, 0.5 mmol) was added to a solution of ATPH (0.55 mmol) in toluene (4.0 cm³) at −78 °C under argon, and the resulting orange solution of the ATPH–benzaldehyde complex was stirred at this temperature for 10 min. A solution of phenyldimethylsilyllithium (0.35 mol dm⁻³ in THF, 2.86 cm³, 1.0 mmol) was added at −78 °C, and the reaction mixture was stirred at this temperature for 30 min. The reaction was quenched with concentrated hydrochloric acid (12 mol dm⁻³; 1.5 cm³) at −78 °C, stirred at room temperature for 15 min, diluted with water (4.5 cm³) and extracted with diethyl ether ($3 \times 15$ cm³). The organic layer was dried ($Na_2SO_4$) and concentrated. The residue was purified by column chromatography on silica gel ($CH_2Cl_2$–hexane to give the 1,6-adduct **2a** (59% isolated). *Selected data* for **2a**: $R_f$ = 0.35 ($CH_2Cl_2$–hexane, 1 : 2); $\nu_{max}$ (film)/cm⁻¹ 1682, 1250, 1115. $\delta_H$ ($CDCl_3$, 300 MHz) 9.22 (1 H, s, CHO), 7.55–7.30 (5 H, m, SiCPh), 6.44 (1 H, t, *J* 5.6, SiCHCH$_2$C*H*), 6.28 (1 H, d, *J* 9.6, SiCHCHC*H*), 5.92 (1 H, dd, *J* 5.2 and 9.6, SiCHC*H*), 2.77 (1 H, ddd, *J* 3.9, 10.8 and 18.9, C$H_A$H$_B$), 2.48 (1 H, ddd, *J* 5.7, 5.7 and 18.9, CH$_A$$H_B$), 2.07 (1 H, m, SiCH), 0.32 (6 H, s, $SiMe_2$); $\delta_C$($CDCl_3$) 190.7, 145.7, 138.2, 136.6, 133.8, 131.1, 129.3, 127.8, 116.6, 24.5, 23.9, −4.8 and −5.0 (Found: C, 74.2; H, 7.6. $C_{15}H_{18}OSi$ requires C, 74.3; H, 7.5%).

§ *Selected data* for **3b**: $R_f$ = 0.28 ($CH_2Cl_2$–hexane, 4 : 1); $\nu_{max}$(film)/cm⁻¹ 1671(C=O), 1612 (conjugated C=C) and 1239 (C–Si); $\delta_H$($CDCl_3$, 250 MHz) 7.50–7.26 (5 H, m, SiPh), 6.63 (1 H, ddd, *J* 1.25, 2.5 and 5.7, CH=CCO), 5.75 (1 H, ddd, *J* 2.9, 5.2 and 9.6, C*H*=CHCHSi), 5.44 (1 H, br dd, *J* 4.6 and 9.6, CH=C*H*CHSi), 3.23 (1 H, dt, *J* 3.6 and 5.7, C*H*Si), 2.73 (1 H, dddd, *J* 4.5, 4.7, 4.7 and 23, CH$_A$$H_B$, equatorial), 2.39 (1 H, dddd, *J* 22.9, 8.8, 2.6 and 2.6, C$H_A$H$_B$, axial), 2.24 (3 H, s, MeCO), 0.24 (6 H, s, $SiMe_2$); $\delta_C$($CDCl_3$) 198.2, 140.8, 135.4, 134.5, 134.2, 129.4, 128.2, 127.8, 119.7, 30.03, 29.5, 25.6, −3.2 and −4.2 (Found: M⁺, 256.1280. $C_{16}H_{20}OSi$ requires *M*, 256.1283).

## References

1 E. W. Colvin, *Silicon in Organic Synthesis*, Butterworths, London, 1981, ch. 9; W. P. Weber, *Silicon Reagents for Organic Synthesis*, Springer-Verlag, 1983, ch. 11; I. Fleming, J. Dunoguès and R. Smithers, *Org. React.* (*N.Y.*), 1989, **37**, 57.

2 T. K. Sarkar, *Synthesis*, 1990, 969 and 1101; I. Fleming, in *Comprehensive Organic Synthesis*, ed. B. M. Trost and I. Fleming, Pergamon, Oxford, 1991, vol. 2, ed. C. H. Heathcock, ch. 2.2, pp. 563–593. Allylsilanes derived by silylation of allyl-metal species: M. C. Henry and J. G. Nortes, *J. Am. Chem. Soc.*, 1960, **82**, 555; V. F. Mironov and V. V. Nepomnina, *Izv. Akad. Nauk SSSR, Ser. Khim.*, 1960, 1419 (*Chem. Abstr.*, 1961, **55**, 358); J.-P. Pillot, J. Dunoguès and R. Calas, *Tetrahedron Lett.*, 1976, 1871. Allylsilanes derived from silylmethyl anions: K. Ito, M. Fukui and Y. Kurachi, *J. Chem. Soc., Chem. Commun.*, 1977, 500; D. Seyferth, K. R. Wursthorn and R. E. Mammarella, *J. Org. Chem.*, 1977, **42**, 3104. Allylsilanes derived by nucleophilic allylic substitutions with silyl anions: I. Fleming and D. Marchi, *Synthesis*, 1981, 560; I. Fleming, D. Higgins, N. J. Lawrence and A. P. Thomas, *J. Chem. Soc., Perkin Trans. 1*, 1992, 3331; J. G. Smith, S. E. Drozda, S. P. Petraglia, N. R. Quinn, E. M. Rice, B. S. Taylor and M. Viswanathan, *J. Org. Chem.*, 1984, **49**, 4112. Allylsilanes from β-silylcarbonyl compounds: I. Fleming, S. Gil, A. K. Sarkar and T. Schmidlin, *J. Chem. Soc., Perkin Trans. 1*, 1992, 3351.

3 K. Maruoka, M. Ito and H. Yamamoto, *J. Am. Chem. Soc.*, 1995, **117**, 9091; S. Saito and H. Yamamoto, *Chem. Commun.*, in the press.

4 Preparation of silyl-lithium species: W. C. Still, *J. Org. Chem.*, 1976, **41**, 3063; H. Gilman and G. D. Lichtenwalter, *J. Am. Chem. Soc.*, 1958, **80**, 608; R. Balasubramanian and J. P. Oliver, *J. Organomet. Chem.*, 1980, **197**, C7; G. Gutekunst and A. G. Brook, *J. Organomet. Chem.*, 1982, **225**, 1.

5 D. J. Ager, I. Fleming and S. K. Patel, *J. Chem. Soc., Perkin Trans. 1*, 1981, 2520; I. Fleming, T. W. Newton and F. Roessler, *J. Chem. Soc., Perkin Trans. 1*, 1981, 2527; I. Fleming, R. Roberts and S. C. Smith, *Tetrahedron Lett.*, 1996, **37**, 9395.

6 H.-F. Chow and I. Fleming, *J. Chem. Soc., Perkin Trans. 1*, 1984, 1815; I. Fleming, N. L. Reddy, K. Takaki and A. C. Ware, *J. Chem. Soc., Chem. Commun.*, 1987, 1472; I. Fleming and S. K. Ghosh, *J. Chem. Soc., Chem. Commun.*, 1994, 2285.

7 I. Fleming and S. B. D. Winter, *Tetrahedron Lett.*, 1993, **37**, 7287; 1995, **36**, 1733; I. Fleming and D. Lee, *Tetrahedron Lett.*, 1996, **38**, 6929.

8 K. Tamao, N. Ishida, T. Tanaka and M. Kumada, *Organometallics*, 1983, **2**, 1694; K. Tamao and N. Ishida, *J. Organomet. Chem.*, 1984, **269**, C37; K. Tamao, M. Kumada and K. Maeda, *Tetrahedron Lett.*, 1984, **25**, 321; K. Tamao, N. Ishida, Y. Ito and M. Kumada, *Org. Synth.* (*N.Y.*), 1990, **69**, 96.

*Received in Cambridge, UK, 21st April 1997; Com. 7/02684F*

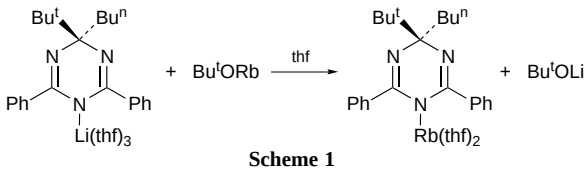
# Exploiting a substituted dihydrotriazinide as a novel bulky ligand: synthesis and crystal structure of a rubidium complex with an unprecedented tetrameric cyclic core

**William Clegg,[a] Allison M. Drummond,[b] Robert E. Mulvey*[b] and Paul O'Shaughnessy[a]**

[a] *Department of Chemistry, University of Newcastle, Newcastle-upon-Tyne, UK NE1 7RU*
[b] *Department of Pure and Applied Chemistry, University of Strathclyde, Glasgow, UK G1 1XL*

**A metal exchange reaction between the alkoxide Bu$^t$ORb and a dihydrotriazinidolithium complex in tetrahydrofuran (thf) has yielded the first reported triazinidorubidium species, in the bis(thf) solvate of 4-*n*-butyl-4-*tert*-butyl-2,6-diphenyl-1,4-dihydro-*s*-triazinido-1-rubidium, which exists as a unique cyclic tetramer in the solid state having an unprecedented sixteen-membered (NCNRb)$_4$ ring core.**

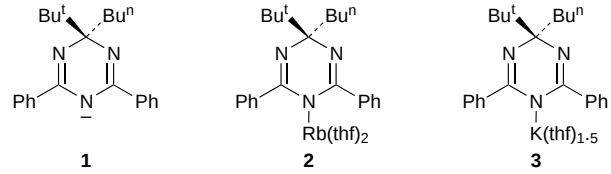
We introduced the dihydrotriazinide **1** in 1993 with a view to shedding light on the intermediate steps involved in alkyllithium-induced cyclotrimerisation reactions of aromatic nitriles.[1] More recently our focus has shifted towards developing this anion as a novel, sterically-encumbered ligand on account of its interesting combination of features. These include (*i*) three heteroatom (N) binding sites; (*ii*) two sterically-flexible Ph sidearms available for π and/or agostic bonding; (*iii*) a bulky, branched [Bu$^n$(Bu$^t$)C] tail, and (*iv*) the possibility of inducing chirality at the saturated ring C atom by metallating only one adjacent N site. **1** made an immediate impact in this role through its participation in the metal derivative, **3**, which established a new type of structure formally designated a 'potassium potassate'.[2] In attempting to extend this work to other metals, we have succeeded in synthesising a rubidium complex employing **1** as a ligand, the surprising structure of which provides the basis for this communication. Structural information on air-sensitive Rb compounds[3] is meagre in comparison to the mountain of data available on lighter alkali-metal congeners (particularly those of lithium[4]), reflecting the lower stability of the former and the greater handling difficulties that this presents. Hitherto only two tetrameric Rb complexes have been reported, as most other aggregates have polymeric constitutions. Moreover, both tetramers, [(Bu$^t$ORb)$_4$][5] and [(Me$_3$SiORb)$_4$],[6] display cubane-based architectures. This background serves to put the novelty of the new complex **2** into perspective, as it, in contrast, adopts an unprecedented cyclic, sixteen-membered (NCNRb)$_4$ ring arrangement. Furthermore, its tetrameric constitution also sets it apart from all other known dihydrotriazinidoalkali-metal structures, which exist as monomers, dimers or polymers.[7]




**Scheme 1**

Scheme 1 shows the simple metal exchange strategy used in the synthesis of **2** (anhydrous and anaerobic conditions were employed throughout). Upon isolation the colourless/pale yellow crystals of **2** were taken directly from the mother-liquor and coated in an inert oil prior to undergoing an X-ray diffraction examination. Characterisation of air- and moisture-sensitive **2** was completed by elemental analyses and a $^1$H NMR spectroscopic study.†

Anion–cation contacts [N(1)–Rb(1) 2.978(3)Å] alternate with longer dative N(2A)–Rb(1) ones [3.033(3)Å] to make up the cyclic tetramer within the crystal structure of **2** (Fig. 1).‡ The molecule possesses tetragonal ($S_4$ or $\bar{4}$) symmetry. With respect to its N centres, the dihydrotriazinide assumes a bis-monodentate, bridging role leaving the N(3) centre unligated. Dimensions within the $C_3N_3$ ring show that there is a degree of π-delocalisation about the N(2)C(2)N(1)C(1)N(3) fragment, such that the structural formula of **2** as written represents only one possible mesomeric form, though the dominant one. The $C_3N_3$ ring is essentially planar (root mean square deviation



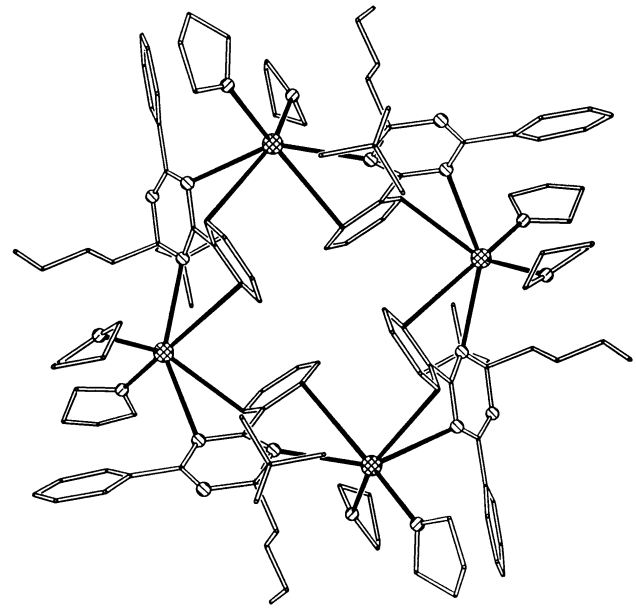



**Fig. 1** The structure of the tetrameric molecule without hydrogen atoms. Selected dimensions (Å and °): Rb(1)–N(1) 2.978(3), Rb(1)–N(2A) 3.033(3), Rb(1)–O(1) 2.824(3), Rb(1)–O(2) 2.811(3), Rb(1)–C(11) 3.352(3), Rb(1)–C(15A) 3.380(3), N(1)–C(1) 1.369(4), N(1)–C(2) 1.362(4), N(2)–C(2) 1.304(4), N(2)–C(3) 1.471(4), N(3)–C(3) 1.481(4), N(3)–C(1) 1.295(4), N(1)–Rb(1)–N(2A) 148.19(7), O(1)–Rb(1)–O(2) 110.00(10), C(11)–Rb(1)–C(15A) 90.17(9); symmetry operator A: $\frac{1}{2}+y$, $\frac{1}{2}-x$, $\frac{1}{2}-z$.

0.017 Å). The coordination sphere of the Rb cation involves opposing sides of two equivalent triazinide ligands (Fig. 2). A pair of thf molecules also bind to Rb. Accompanying these Rb–heteroatom bonds are a number of Rb–C interactions. As is often the case with organometallic derivatives of alkali metals, the coordination number and geometry are not entirely clearly defined, with a range of Rb–C distances and with some close contacts a necessary consequence of others. In this structure, however, one phenyl group on each triazine ring lies between two Rb cations in such an orientation that each *ortho* C atom forms a bond with one metal ion [C(11)–Rb(1) 3.352(3) Å, C(15)–Rb(1B) 3.380(3) Å], giving a primary coordination number of six for Rb. Each Rb cation is thus chelated by one N atom and one phenyl *ortho*-C atom of two triazinide ligands. The disposition of the ligands relative to the cations generates other close Rb–C contacts, notably 3.450(3) Å for C(10) and 3.573(3) Å for C(2), which presumably also contribute to the overall ligand–metal bonding. All other Rb–C distances are > 3.6 Å. The second phenyl group on each triazine is not involved in metal coordination; these four groups occupy positions at the periphery of the structure and form a 'paddle wheel' arrangement. In effect, the thf ligands lie *cis* to each other in view of the relatively small O–Rb–O bond angle [110.12(10)° *cf* 180° in an ideal *trans* situation]. More open, but still well short of being linear, are the N-Rb-N contacts [angle 148.12(7)°] which link the four monomeric fragments together into a cyclic ring. To achieve this ring closure, the Rb cation sits out of the mean planes of both attached $C_3N_3$ rings, by 1.750 and 1.160 Å.

Turning to a comparison of bond dimensions with those in other structures, the N–Rb distances in **2** lie between those of the two asymmetric N–Rb bonds in the amide $[\{[RbN(SiMe_3)_2{\cdot}1.5\ dioxane]_2\}_\infty]$ (2.946, 3.141 Å).[8] The C–Rb contact distances in **2** are also typical of those found in structures with delocalised aryl groups, *e.g.* 3.351–3.643 Å in $[(Ph_3CRb{\cdot}pmdeta)_\infty]$;[9] 3.14–3.57 Å in $[(PhCH_2Rb{\cdot}pmdeta)_\infty]$.[10]

The cyclic, oligomeric nature of the structure of **2** provides an interesting contrast with the zigzag, polymeric chain arrangement preferred by the potassium counterpart **3**.[2] Given that the precursor to **2**, $[(Bu^tORb)_4]$ is isostructural with $[(Bu^tOK)_4]$,[5] it would not have been unreasonable to assume that **2** and **3** might adopt a common structural motif. However, it is important to recognise that these butoxides are three-dimensional 'stacked-ring' structures, which are not greatly affected by the size differential between the metals (ionic radii: $Rb^+$ 1.52 Å, $K^+$ 1.38 Å). On the other hand, structures with one-dimensional heteroatom–metal connectivities, as in **2** and **3**, can be profoundly affected. In **2** this is manifested in the addition of extra solvent ligands (metal : thf ratio 1 : 2, *cf* 1 : 1.5 in **3**), and in an increased number of metal–ligand interactions (primary coordination number of Rb = 6; *cf*. 4 or 5 for K in **3**).

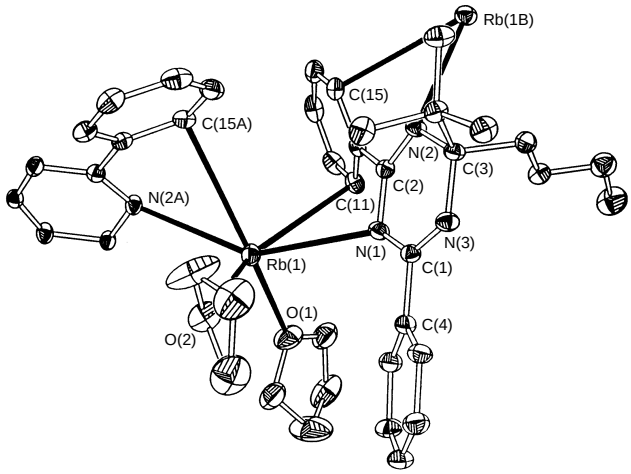



**Fig. 2** Thermal ellipsoid plot at 30% probability, showing the asymmetric unit of **2**, together with one adjacent $PhC_3N_3$ unit to complete the coordination of Rb(1), and the adjacent Rb atom to complete the bonding environment of the triazine ligand. Hydrogen atoms are omitted, and key atoms are labelled.

In conclusion, the special ligating ability of **1** has been further demonstrated by the determination of the crystal structure of a rubidium complex exhibiting a novel cyclic tetrameric arrangement. From this evidence, **1** can be regarded as a novel alternative to conventional bulky nitrogen ligands such as the amide $[(Me_3Si)_2N^-]$. This prospect now calls for a full investigation of the coordination chemistry of **1** with other metal partners.

We thank the EPSRC and the University of Strathclyde for supporting this work.

## Footnotes

* E-mail: r.e.mulvey@strath.ac.uk

† Yield (first batch), 28%; mp 70–72 °C. Anal ($C_{31}H_{44}N_3O_2Rb$)C, H, N, Rb. $^1$H NMR (400 MHz, [$^2H_5$]pyridine) $\delta$ 0.73 (t, $CH_3$ of $Bu^n$), 1.41 (m, $\gamma$-$CH_2$ of $Bu^n$), 1.55 (s, $Bu^t$), 1.67 (m, $CH_2$ of thf), 1.84 (m, $\beta$-$CH_2$ of $Bu^n$), 2.12 (m, $\alpha$-$CH_2$ of $Bu^n$), 3.70 (t, $OCH_2$ of thf), 7.38(t, *p*-Ph), 7.47 (m, *m*-Ph), 8.94 (d, *o*-Ph).

‡ *Crystal data* for **2**: $C_{124}H_{176}N_{12}O_8Rb_4$, $M$ = 2304.6, tetragonal, space group $I\bar{4}$, $a$ = 25.225(2), $c$ = 11.1115(9) Å, $U$ = 7070.3(10) Å$^3$, $Z$ = 2, $D_c$ = 1.083 g cm$^{-3}$, $\mu$ = 1.43 mm$^{-1}$ (Mo-K$\alpha$, $\lambda$ = 0.710 73 Å), $F$(000) = 2432, $T$ = 160 K. Siemens SMART CCD area-detector diffractometer, crystal size 0.56 × 0.50 × 0.38 mm, $\theta_{max}$ 28.5°, 22406 reflections measured, 8002 unique ($R_{int}$ = 0.0236). Structure solution by direct methods, full-matrix least-squares refinement on $F^2$ with weighting $w^{-1} = \sigma^2(F_o^2) + (0.0683P)^2$, where $P = (2F_c^2 + F_o^2)/3$, anisotropic displacement parameters, riding hydrogen atoms, no absorption correction, extinction parameter $x$ = 0.000 40(16), where $F_c' = F_c/(1 + 0.001\, x\, F_c^2\lambda^3/\sin 2\theta)^{\frac{1}{4}}$, absolute structure parameter = 0.042(7). Final $R_w = \{\Sigma[w(F_o^2 - F_c^2)^2]/\Sigma[w(F_o^2)^2]^{\frac{1}{2}}\}$ = 0.1194 for all data, conventional $R$ = 0.0423 on $F$ values of 6506 reflections with $F_o^2 > 2\sigma(F_o^2)$, $S$ = 1.074 on $F^2$ for all data and 339 parameters. Final difference map between +0.70 and −0.41 e Å$^{-3}$. Programs: Siemens SMART and SAINT control and integration software, SHELXTL (G. M. Sheldrick, University of Göttingen, Germany), and local programs. Atomic coordinates, bond lengths and angles, and thermal parameters have been deposited at the Cambridge Crystallogaphic Data Centre (CCDC). See Information for Authors, Issue No. 1. Any request to the CCDC for this material should quote the full literature citation and reference number 182/488.

## References

1 D. R. Armstrong, W. Clegg, M. MacGregor, R. E. Mulvey and P. A. O'Neil, *J. Chem. Soc., Chem. Commun.*, 1993, 608.
2 W. Clegg, L. Horsburgh, R. E. Mulvey and M. J. Ross, *J. Chem. Soc., Chem. Commun.* 1994, 2393.
3 C. Schade and P. v. R. Schleyer, *Adv. Organomet. Chem.*, 1987, **27**, 169.
4 W. Setzer and P. v. R. Schleyer, *Adv. Organomet. Chem.*, 1985, **24**, 353.
5 M. H. Chisholm, S. R. Drake, A. A. Naiini and W. E. Streib, *Polyhedron*, 1991, **10**, 337.
6 E. Weiss, K. Hoffmann and H.-F. Grützmacher, *Chem. Ber.*, 1970, **103**, 1190.
7 D. R. Armstrong, K. W. Henderson, M. MacGregor, R. E. Mulvey, M. J. Ross, W. Clegg and P. A. O'Neil, *J. Organomet. Chem.*, 1995, **486**, 79.
8 F. T. Edelmann, F. Pauer, M. Wedler and D. Stalke, *Inorg. Chem.*, 1992, **31**, 4143.
9 D. Hoffmann, W. Bauer, P. v. R Schleyer, U. Pieper and D. Stalke, *Organometallics*, 1993, **12**, 1193.
10 D. Hoffmann, W. Bauer, F. Hampel, N. J. R. v. E. Hommes, P. v. R. Schleyer, P. Otto, U. Pieper, D. Stalke, D. S. Wright and R. Snaith, *J. Am. Chem. Soc.*, 1994, **116**, 528.

*Received in Cambridge, UK, 2nd May 1997; Com. 7/03009F*

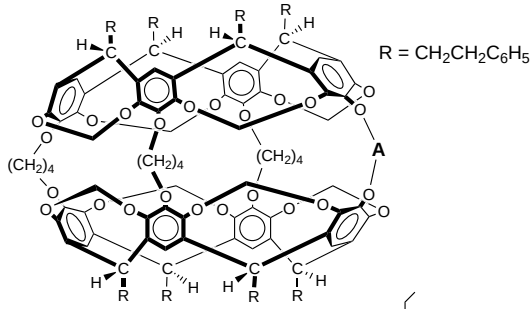
# Dissymmetric new hemicarcerands containing four bridges of different lengths

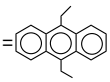
**Juyoung Yoon, Carolyn B. Knobler, Emily F. Maverick and Donald J. Cram***

*Department of Chemistry and Biochemistry, University of California, Los Angeles, CA 90095-1569, USA*

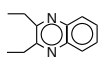
**Three new hemicarcerands 1–3 each with one unique eight-atom-long bridge and three identical six-atom-long bridges are reported along with a crystal structure of 2⊙$PhNO_2$, a totally dissymmetric host with nitrobenzene as encapsulated guest.**

A prior paper reported the syntheses and characterizations of seven new hemicarcerands **4**–**6**, **8**–**11** and 36 new hemicarceplexes with diol **12** as starting material.[1] The crystal structure of **8**⊙4-$MeC_6H_4OMe$ indicated it to be somewhat disordered but essentially isostructural with more than 25 hemicarceplexes of **7**⊙guest containing 4 $O(CH_2)_4O$ bridges.[2,3]




**1**, A = $(CH_2)_6$; **2**, A = 4-$CH_2C_6H_4CH_2$; **3**, A =  ; **4**, A = $CH_2$;

**5**, A = $(CH_2)_2$; **6**, A = $(CH_2)_3$; **7**, A = $(CH_2)_4$; **8**, A = $(CH_2)_5$;

**9**, A =  ; **10**, A =  ; **11**, A =  ; **12**, A = H H

Examination of Corey–Pauling–Koltun (CPK) models of possible unique bridges whose lengths, steric requirements and rigidities would seriously disrupt the isostructural pattern of the standard $[O(CH_2)_4O]_3$ bridges provided $O(CH_2)_6O$, *p*-$OCH_2C_6H_4CH_2O$ and 9,10-$(OCH_2)_2$-anthracene as candidate moieties. In *N*-methylpyrrolidinone (NMP) as solvent and $Cs_2CO_3$ as base, at temperatures of 55–70 °C, diol **12** reacted respectively with $TsO(CH_2)_6OTs$ (Ts = tosyl), 4-$ClCH_2C_6H_4CH_2Cl$ and 9,10-$(ClCH_2)_2$-anthracene to give after chromatographic purification (thick layer plate, $CHCl_3$/silica gel), **1**⊙$CHCl_3$ (78%), **2**⊙$CHCl_3$ (80%) and **3** (empty, 78%).†,‡ In **1**–**3** the unique bridges are all eight atoms long and of varying degrees of rigidity and steric requirements. Formally, the two portals that flank the unique bridge are 28-membered rings, while the other two are 26-membered rings.

The fact that **1** and **2** were isolated as their complexes with $CHCl_3$ rather than with NMP inside indicates either that the final bond-making process occurred in an empty cavity, or that guest exchange, host⊙NMP + $CHCl_3$ → host⊙$CHCl_3$ + NMP, took place during the chromatographic purification conducted at 25 °C. In contrast, empty **3** was isolated as the product of completing the shell closure. In CPK models, both NMP and $CHCl_3$ easily enter and depart the inner phase of **1**–**3**, although the two benzo groups of the anthracene-containing bridge in **3** substantially narrow its two flanking portals. Experimentally a 400 MHz $^1H$ NMR spectrum of **3** in $CDCl_3$ at 25 °C gave two sets of host signals ($OCH_2O$ protons) in an intensity ratio of 2.8 : 1 attributed to empty **3** (2.8) and **3**⊙$CDCl_3$ (1). When the solution was warmed to 55 °C, the signals due to **3**⊙$CDCl_3$ disappeared, but reappeared when the solution was cooled to 25 °C. When $CDCl_2CDCl_2$ and $(CD_2)_4O$ were each substituted for $CDCl_3$ in similar experiments, only signals for empty **3** were observed at both 25 and 55 °C. Apparently, these two molecules are too large to enter **3** at these temperatures.

When **2**⊙$CHCl_3$ was heated in $PhNO_2$ as solvent at 150 °C for 3 days, **2**⊙$PhNO_2$ was formed.† The complex crystallized as **2**⊙$PhNO_2$·5$PhNO_2$, whose crystal structure was determined at −98 °C. The remarkable feature of the crystal structure is not that *R* (0.22) is so large, but that a solvated complex of molecular mass 3037 which contains no symmetry element and is disordered could be determined at all. Fortunately the disorder is concentrated in the least interesting parts of the structure (the eight feet and the five solvate molecules).§ In Fig. 1 are shown a stereo side-view of **2**⊙$PhNO_2$ (*a*) a stereo end-view of the bridges and guest (*b*), and a side-view of the bridges and guest (*c*). Included for comparison is a side-view of the bridges and guest of **7**⊙$PhNO_2$ (*d*), reported earlier.[2]

Substitution of one conformationally mobile, six-atom-long $O(CH_2)_4O$ bridge in **7** by the relatively rigid eight-atom-long *p*-$OCH_2C_6H_4CH_2O$ bridge in **2** both desymmetrizes and

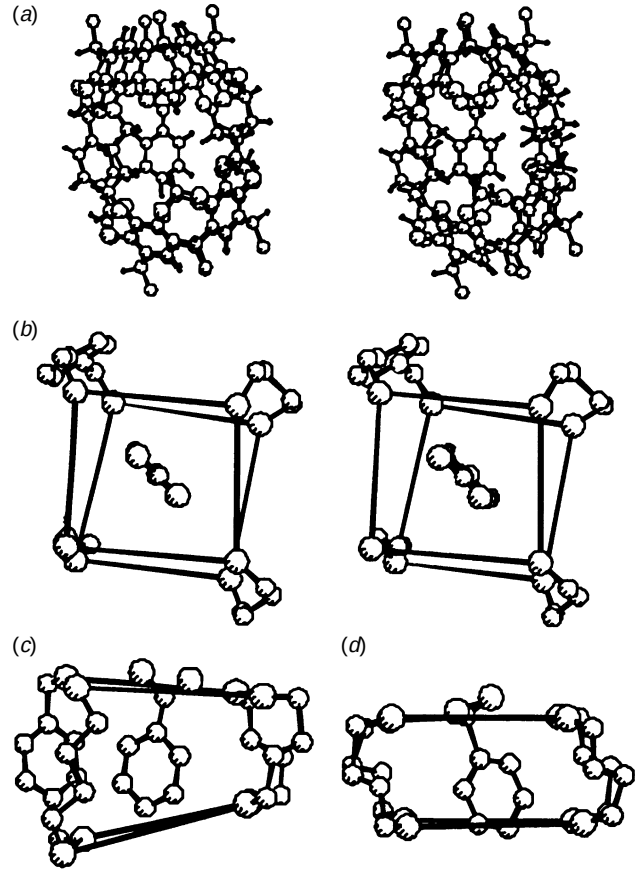
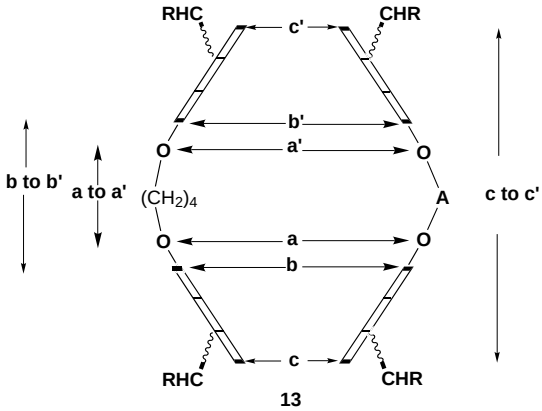



**Fig. 1** (*a*) Side stereoview of **2**⊙$PhNO_2$. R groups in host **2** are represented by C atoms. (*b*) Top stereoview of bridges and guest. (*c*) Side-view of bridges and guest. (*d*) Side-view of bridges and guest of **7**⊙$PhNO_2$.

introduces strain into those parts of the host that define its cavity. Although strain distributes itself as evenly as possible, the polycyclic aryl-rich character of the bowls resists deformation more than the more linear bridges. The distances defined in diagram **13** substantiate this expectation. For example, the lengths (and maximum spread in values) of the four edges of the oxygen best planes **a** and **a′** visible in Fig. 1(*b*) average 6.25 (0.57) and 6.46 (0.49) Å, respectively, in **2**⊙$PhNO_2$, as compared to 6.31 (0.09) Å in **7**⊙$PhNO_2$. The lengths (and maximum spread in values) of the two diagonals of planes **a** and **a′** average 8.84 (0.47) and 9.12 (0.79) Å respectively in **2**⊙$PhNO_2$, as compared to 8.92 (0.07) Å for plane **a** (and **a′**) in **7**⊙$PhNO_2$. Thus the maximum spread in edge and diagonal distances for planes **a** and **a′** are 5 to 11 times larger for **2**⊙$PhNO_2$ than for **7**⊙$PhNO_2$. The **b**–**c** and **b′**–**c′** average bowl depths for **2**⊙$PhNO_2$ and **7**⊙$PhNO_2$ vary only from 2.47 and 2.44 for the former to 2.43 Å in the latter complex. Likewise, the maximum out-of-planes **a** and **a′** oxygen distances and spreads are small, 0.06 and 0.11 Å (spreads, 0.12 and 0.20 Å) respectively for **2**⊙$PhNO_2$, and 0.04 Å (spread, 0.08 Å) for **7**⊙$PhNO_2$.




**13**

The bowl-to-bowl bridge lengths **b**–**b′** for **2**⊙$PhNO_2$ average 7.46 with a maximum spread of 2.00 Å, whereas **7**⊙$PhNO_2$ gives values of 6.46 and 0.14 Å, respectively. Thus the stressed **2**⊙$PhNO_2$ complex gives a factor of 14 more spread in its bridge lengths than does **7**⊙$PhNO_2$. More interestingly, one of the two $O(CH_2)_4O$ bridges that flank the *p*-$OCH_2C_6H_4CH_2O$ bridge (length, 8.51 Å) in **2**⊙$PhNO_2$ is 7.98 Å long, compared to the 6.46 Å average length of the four bridges in **7**⊙$PhNO_2$, and the other two $O(CH_2)_4O$ bridges in **2**⊙$PhNO_2$ (6.51 and 6.82 Å). The two oxygen squares in the views of the bridges resemble a slightly opened book in **2**⊙$PhNO_2$, whereas in **7**⊙$PhNO_2$, the similar side-view resembles a closed book [Fig. 1(*b*)–(*d*)].

How does the long $O(CH_2)_4O$ bridge in **2**⊙$PhNO_2$ become that way, and what are the consequences for the cavity shape? In all but two [all four bridges were $O(CH_2)_5O$[5] or $OCH_2CH_2OCH_2CH_2O$[6]] of our prior crystal structures involving tetrol bowls of the type incorporated in **1**–**12**, the unshared electron pairs of the oxygens that terminate the four bridges face inward toward the cavity. This places their attached carbon chains outside the cube defined by the eight oxygens, as in **7**⊙$PhNO_2$. CPK molecular model examinations show that such conformations minimize bridge lengths, whereas when the electron pairs face outward, the carbon chains turn inward, the bridge lengths increase, and the cavities narrow in their equatorial dimensions because the methylenes encroach on the corners of the cavities. The top and side views of the bridges show that in contrast to the other three bridges of **2**⊙$PhNO_2$, two of the methylenes of the long $O(CH_2)_4O$ bridge are turned inward to accommodate its adjacent, outward-turned but longer *p*-$OCH_2C_6H_4CH_2O$ bridge. As a result of the longer bridge lengths (av., 7.46 Å) in **2**⊙$PhNO_2$ as compared to **7**⊙$PhNO_2$ (av., 6.46 Å), the average **c**–**c′** distance which measures cavity length in the former complex is 12.15 Å, significantly longer than the 11.28 Å length in the latter complex.

The $PhNO_2$ guest's best plane is diagonally arranged in the cavities so as to be roughly coplanar with the oxygens of diagonally located bridges. Molecular model examination indicates that diagonal arrangements avoid collisions of the guest atoms with the enforced inward-turned single hydrogens of the eight $OCH_2O$ spanners. Of the two possible diagonal locations, the one including the *p*-$OCH_2C_6H_4CH_2O$ bridge (length, 8.51 Å) is occupied by the $PhNO_2$ guest (see both top- and side-views in Fig. 1), thus avoiding the inward-turned $O(CH_2)_4O$ bridge (length 7.98 Å).

The ways in which **2** modifies its structure to accommodate its single longer bridge provide insights about the degrees of freedom available to transition states for entries and exits of guests from the inner phases of hemicarcerands.

Attempts to obtain crystals suitable for structure determination of host **3** failed. However, a molecular model of **3** can be assembled only in a conformation whose 9,10-$(OCH_2)_2$-anthracene bridge resembles that found for the *p*-$OCH_2C_6H_4CH_2O$ bridge of **2**⊙$PhNO_2$. A comparison of the complexing properties of hosts **1**–**3**, **8** and **10** will be reported in a future paper.

The authors warmly thank the NIH for Grant GM 12640 which supported this research.

## Footnotes

* E-mail: maverick@chem.ucla.edu

† These new compounds have elemental analyses within 0.30% of theory, and the expected $^1$H NMR spectra and FAB (*m*/*z*, $M^+ + H$) mass spectra.

‡ These procedures were patterned after those leading to **4**–**6** and **8**–**11**.[1] Probably initially NMP solvent molecules served as guests during addition of the fourth bridge, but underwent exchange with $CHCl_3$ during chromatographic purification to provide **1**⊙$CHCl_3$ and **2**⊙$CHCl_3$.

§ *Crystal data*: the crystal structure of **2**⊙$PhNO_2$·5$PhNO_2$ (crystallized from $CHCl_3$–$PhNO_2$, determined at 175 K): triclinic, space group $P\bar{1}$, $a$ = 20.241(5), $b$ = 26.350(5), $c$ = 15.143(3) Å, $\alpha$ = 98.84(2)°, $\beta$ = 95.01(2)°, $\gamma$ = 94.26(2)°, $V$ = 7918(3) Å$^3$, $Z$ = 2, 20676 unique reflections, 11944 > 4$\sigma(F)$, maximum $2\theta$ = 120°, Cu-K$\alpha$ radiation, and was refined to $R$ = 0.22 (SHELXL93[4a]). The precision of the intensities is severely affected by the high background, due to the capillary containing the crystal and the ice that collected on it. The structure was solved by direct methods (SHELXS90[4b]). All non-hydrogen atoms have been refined isotropically. All hydrogen atoms were refined with fixed C–H distances (0.93–0.98 Å) and with fixed displacement parameters (1.2 $U_{iso}$ of the attached C atom). One molecule of $PhNO_2$ is located in the host cavity; there are five additional molecules of $PhNO_2$ per host molecule, two of which are probably disordered or low occupancy. In addition, high displacement parameters for three of the eight 'feet' ($CH_2CH_2Ph$ groups) indicate disorder.

Atomic coordinates, bond lengths and angles, and displacement parameters have been deposited at the Cambridge Crystallographic Data Centre (CCDC). See Information for Authors, Issue No. 1. Any request to the CCDC for this material should quote the full literature citation and the reference number 182/466.

## References

1 J. Yoon, C. B. Knobler and D. J. Cram, *J. Org. Chem.*, 1996, **61**, 9323.

2 T. A. Robbins, C. B. Knobler, D. R. Bellew and D. J. Cram, *J. Am. Chem. Soc.*, 1994, **116**, 111.

3 D. J. Cram and J. M. Cram, *Container Molecules and Their Guests*, *Monographs in Supramolecular Chemistry*, ed. J. F. Stoddart, The Royal Society of Chemistry, Cambridge, 1994, pp. 131–216.

4 (*a*) G. M. Sheldrick, SHELXL93, Program for Crystal Structure Refinement, University of Göttingen, Germany, 1993; (*b*) *Acta Crystallogr., Sect. A*, 1990, **46**, 467.

5 Y.-S. Byun, T. A. Robbins, C. B. Knobler and D. J. Cram, *J. Chem. Soc., Chem. Commun.*, 1995, 1947.

6 Y.-S. Byun, O. Vadhat, M. T. Blanda, C. B. Knobler and D. J. Cram, *J. Chem. Soc., Chem. Commun.*, 1995, 1825.

*Received, in Columbia, MO, USA, 19th February 1997; Com. 7/01187C*

# First syntheses, structural and theoretical studies of $\eta^5$-1,2,4-triphosphole metal tricarbonyl complexes of Cr, Mo and W

**Vinicius Caliman,[a] Peter B. Hitchcock,[a] John F. Nixon,*[a] Laszlo Nyulaszi*[b] and Nurgun Sakarya[a]**

[a] *School of Chemistry, Physics, and Environmental Science, University of Sussex, Brighton, UK BN1 9QJ*
[b] *Department of Inorganic Chemistry, Technical University of Budapest, H-1521 Budapest, Hungary*

**Evidence for an $\eta^5$-ligated 1,2,4-triphosphole ring system which exhibits some aromatic character is presented *via* the first syntheses, structural and theoretical studies of $\eta^5$-1,2,4-triphosphole metal tricarbonyl complexes of zero-valent Cr, Mo and W.**

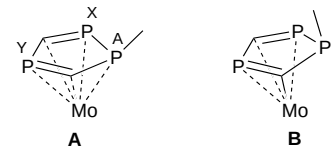
Although phospholes, $RPC_4H_4$, are known to be non-aromatic ring systems,[1] it has recently been shown by theoretical calculations[2] that stepwise replacement of the C=C double bonds by conjugatively similar P=C units[3] increases the planarity and aromatic character of the five-membered ring system owing to a combination of ring strain effects and a lower inversion barrier at the $\sigma^3\lambda^3$-phosphorus. Thus, the recently synthesized[4] di-*tert*-butyl-1,2,4-triphosphole $P_3C_2Bu^t_2CH(SiMe_3)_2$ **1** (which to date is the only known triphosphole), is expected to exhibit greater aromatic character than the parent phosphole. Here we present the first results which support this proposal exemplified by (*i*) the synthesis and structural characterisation of the compounds $[M(CO)_3\{\eta^5\text{-}P_3C_2Bu^t_2CH(SiMe_3)_2\}]$ (M = Cr **2**, Mo **3**, W **4**) in which the ring acts as a 6e donor to the metal and (*ii*) theoretical calculations on the parent 1,2,4-triphosphole $HP_3C_2H_2$ **5** and its hypothetical complex $[M(CO)_3(\eta^5\text{-}HP_3C_2H_2)]$ (M = Mo) **6**. These triphosphole metal tricarbonyl complexes can therefore be considered as being closely related to the long-known $[M(CO)_3(\eta^6\text{-arene})]$ compounds.

Treatment of $P_3C_2Bu^t_2CH(SiMe_3)_2$ **1** with $[M(CO)_4(\eta^4\text{-nbd})]$ (M = Cr, Mo; nbd = norbornadiene) in tetrahydrofuran affords the red complexes $[M(CO)_3\{\eta^5\text{-}P_3C_2Bu^t_2CH(SiMe_3)_2\}]$ (M = Cr **2**, Mo **3**).† Likewise reacting **1** with $[W(CO)_5(thf)]$ gives $[W(CO)_3\{\eta^5\text{-}P_3C_2Bu^t_2CH(SiMe_3)_2\}]$ **4**. Complexes **2** and **3** were also prepared directly from **1** and the appropriate $[M(CO)_3(\eta^6\text{-chp})]$ complex, (M = Cr, Mo; chp = cycloheptatriene).

The $^{31}P\{^1H\}$ NMR spectra of **2**–**4**† each showed the characteristic pattern of lines expected for [AXY] spin systems, significantly chemically shifted from **1** but with $^1J_{PAPX}$, $^2J_{PAPY}$ and $^2J_{PXPY}$ coupling constants similar in magnitude to values found for the free di-*tert*-butyl-1,2,4-triphosphole **1**.[4]

Compounds **2** and **3** were also fully structurally characterised by single-crystal X-ray diffraction studies‡ and the molecular structure of **3** is shown in Fig. 1. Specially noteworthy is the observation that in both **2** and **3** the metal tricarbonyl fragment is coordinated to all five atoms of the 1,2,4-triphosphole ring system which is planar. The distances between the metal and the plane of the ring defined by P(1)P(2)P(3)C(1)C(2) are 1.799 and 1.962 Å for **2** and **3** respectively, and the sums of the bond angles around the formally $sp^3$-hybridised phosphorus atom are 356.6° for **2** and 352.2° for **3**. The metal to $\sigma^3\lambda^3$-phosphorus [P(2)] distance in both structures **2** and **3** is significantly shorter than to the $\sigma^2\lambda^3$ phosphorus ring atoms P(1) and P(3). The 1,2,4-triphosphole rings in complexes **2**–**4** can therefore be considered as donating six electrons to the metal centre. As expected the P–C and P···P bond lengths within the coordinated 1,2,4-triphosphole lie between the values expected for single and double bonds, and are quite close to those found in both the penta- and hexa-phosphaferrocenes $[Fe(\eta^5\text{-}P_3C_2Bu^t_2)(\eta^5\text{-}P_2C_3Bu^t_3)]$ and $[Fe(\eta^5\text{-}P_3C_2Bu^t_2)_2]$ which contain the $\eta^5$-ligated aromatic di- and tri-phospholyl anions.[5] Prior to this work transition-metal complexes of phospholes had only involved ligation of the ring *via* the phosphorus lone pair electrons and/or through the diene system.[1]

We have also carried out theoretical studies in order to better understand the interaction between the 1,2,4-triphosphole ring system and the group 6 metal tricarbonyl moieties. Geometry optimization§ of the tricarbonyl Mo complex **6** of the hypothetical H-substituted triphosphole $HP_3C_2H_2$ **5** resulted in two different structures at the Hartree–Fock level (HF) of the theory. One of them involved $\eta^5$-ligation of the ring to the metal (A) while the other utilised $\eta^4$-coordination (B). The




$\eta^4$-coordinated compound was more stable only by 0.02 kcal $mol^{-1}$ (1 cal = 4.184 J) however on reoptimization using the density functional method, only the $\eta^5$-structure was obtained, even when starting from the $\eta^4$-HF optimized geometry. Although only the $\eta^5$-complex was also obtained experimentally (*vide infra*), in agreement with the density functional calculations, this computational behaviour indicates that the $\eta^4$-complex should not be much less stable than its $\eta^5$-counterpart, and furthermore the 1,2,4-triphosphole ring

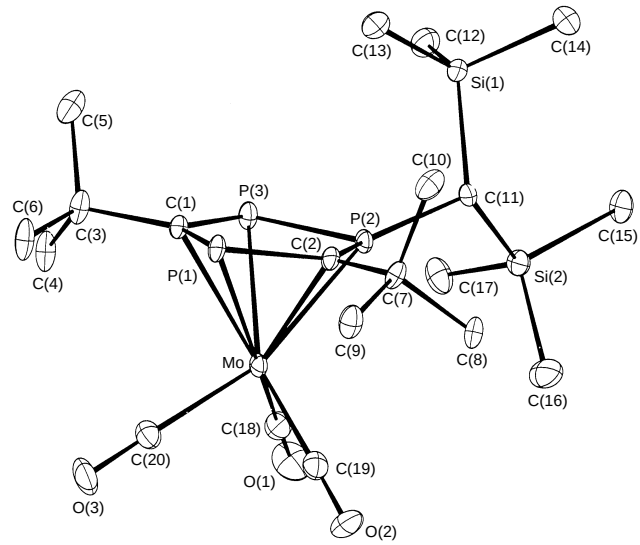



**Fig. 1** Molecular structure of **3**. Selected bond lengths (Å) and angles (°): P(2)–P(3) 2.105(3), P(2)–C(2) 1.745(7), P(3)–C(1) 1.767(7), P(1)–C(2) 1.761(7), P(1)–C(1) 1.777(8), P(2)–C(3) 1.799(7); P(2)–P(3)–C(1) 94.2(3), P(1)–C(1)–P(3) 124.1(4), C(1)–P(1)–C(2) 99.6(3), P(1)–C(2)–P(2) 116.6(4), P(3)–P(2)–C(2) 105.5(3), P(3)–P(2)–C(3) 120.7(3), C(2)–P(2)–C(3) 126.0(4).

**Table 1** Experimental (X-ray), HF and B3LYP optimized structural parameters (in Å) and Wiberg bond indices for 1,2,4-triphosphole **5** and its $Mo(CO)_3$ complex **6**

| | 1,2,4-Triphosphole **5** | | | | $Mo(CO)_3$ complex **6** | | | |
|---|---|---|---|---|---|---|---|---|
| | Exptl.[a] | HF | B3LYP | $I_{Wib}$ | Exptl.[b] | HF | B3LYP | $I_{Wib}$ |
| $P^1P^2$ | 2.098 | 2.173 | 2.187 | 1.065 | 2.105 | 2.168 | 2.204 | 1.017 |
| $P^2C^3$ | 1.734 | 1.791 | 1.780 | 1.031 | 1.745 | 1.782 | 1.794 | 1.006 |
| $C^3P^4$ | 1.720 | 1.672 | 1.710 | 1.667 | 1.761 | 1.726 | 1.736 | 1.278 |
| $P^4C^5$ | 1.763 | 1.803 | 1.797 | 1.020 | 1.777 | 1.767 | 1.798 | 1.051 |
| $C^5P^1$ | 1.718 | 1.675 | 1.713 | 1.707 | 1.767 | 1.734 | 1.739 | 1.315 |
| $MoP_1$ | | — | — | — | 2.585 | 2.652 | 2.525 | 0.388 |
| $MoP_2$ | | — | — | — | 2.424 | 2.545 | 2.654 | 0.328 |
| $MoC_3$ | | — | — | — | 2.472 | 2.374 | 2.691 | 0.321 |
| $MoP_4$ | | — | — | — | 2.609 | 2.599 | 2.514 | 0.403 |
| $MoC_5$ | | — | — | — | 2.426 | 2.407 | 2.784 | 0.288 |

[a] X-Ray structural data for **1** from ref. 4. [b] X-Ray structural data refers to complex **3**.

systems are borderline cases between aromatic and non-aromatic molecules. Interestingly attempts to synthesise complexes involving different ligating modes of the di-*tert*-butyl-1,2,4-triphosphole ring, for example $[M(CO)_5(\eta^1\text{-}RP_3C_2Bu^t_2)]$ or $[M(CO)_4(\eta^4\text{-}RP_3C_2Bu^t_2)]$ [R = $CH(SiMe_3)_2$; M = Cr, Mo, W] using either $[M(CO)_5(thf)]$, $[M(CO)_4(\eta^4\text{-nbd})]$, or $[M(CO)_3(\eta^6\text{-chp})]$ as precursors, only led to the tricarbonyl complexes **2**–**4** and no other intermediates could be detected when the reactions were carefully monitored by $^{31}P$ NMR spectroscopy.

Calculations on the hypothetical complex $[Mo(CO)_3(\eta^5\text{-}HP_3C_2H_2)]$ **6** show that it exhibits remarkable stability towards dissociation to 1,2,4-triphosphole **5** and $Mo(CO)_3$ (39.91 and 27.22 kcal $mol^{-1}$ at the HF and DFT levels respectively); and for comparison the stabilization of the corresponding benzene complex $[Mo(CO)_3(\eta^6\text{-}C_6H_6)]$ was calculated to be 33.82 and 24.21 kcal $mol^{-1}$ respectively at the above two levels.

The calculated structural characteristics§ (Table 1) of the $\eta^5$-complex (A) are comparable to the values obtained experimentally from the X-ray structural analyses on **2** and **3**, however, the P···P separation and some of the Mo–P and Mo–C bond lengths are not reproduced particularly well by the calculations. Similarly, the structures of the parent triphosphole calculated at the HF and B3LYP levels had considerably longer single bond lengths than in the X-ray structure of the alkylated derivative (Table 1). This behaviour is in accordance with an increased aromaticity, due to the alkylation. Indeed, the bis(trimethylsilyl)methyl group has a partial flattening effect on the $\sigma^3.\lambda^3$-phosphorus.[6] The increased planarity then enhances the aromaticity of the system. Changes in bond lengths upon complexation of the 1,2,4-triphosphole ring to the metal centre are well accounted for by the calculations, *i.e.* the formal double bonds become slightly longer, while the other bond lengths only undergo small changes. The $\eta^5$-nature of complex **6** is also clearly shown by the Wiberg covalent bond indices[7] listed in Table 1, from which it is evident that all Mo–C and Mo–P indices are of similar magnitude. Comparing the parent and the complexed triphosphole, the largest change is again in the Wiberg indices of the formal double bond, in accordance with its increasing length noted above.

The present results clearly provide the first evidence for an $\eta^5$-ligated 1,2,4-triphosphole ring system which exhibits some aromatic character, and complements the recently reported[8] ready displacement of naphthalene by the di-*tert*-butyl-1,2,4-triphosphole **1** from the zerovalent ruthenium complex $[Ru(\eta^6\text{-}C_{10}H_8)(\eta^4\text{-}C_8H_{12})]$ to afford $[Ru\{\eta^5\text{-}P_3C_2Bu^t_2[CH(SiMe_3)_2]\}(\eta^4\text{-}C_8H_{12})]$, in which the triphosphole also behaves as a 6e donor.

We wish to thank the Brazilian Government (*via* CNPq) and the Turkish Government for financial support (to V. C. and N. S. respectively); EPSRC for general support for phosphaalkyne chemistry; to OTKA T 014555 and to the Royal Society for financing our collaborative UK–Hungary studies.

## Footnotes

* E-mail: j.nixon@sussex.ac.uk

† *NMR data*. **2**: $\delta_P{}^A$ −59.2, $\delta_P{}^X$ 106.6, $\delta_P{}^Y$ 35.6; $^1J_{PAPX}$ 502.9, $^2J_{PAPY}$ 32.6, $^2J_{PXPY}$ 54.9. **3**: $\delta_P{}^A$ −44.4, $\delta_P{}^X$ 99.8, $\delta_P{}^Y$ 46.9; $^1J_{PAPX}$ 507.7, $^2J_{PAPY}$ 30.5, $^2J_{PXPY}$ 50.5. **4** $\delta_P{}^A$ −72.8, $\delta_P{}^X$ 76.3, $\delta_P{}^Y$ 24.2; $^1J_{PAPX}$ 496.8, $^2J_{PAPY}$ 31.4, $^2J_{PXPY}$ 53.4. (*J* in Hz.)

‡ *Crystal data*: **2**: $T$ = 173 K; $C_{20}H_{37}CrO_3P_3Si_2$, orthorhombic, space group $P2_12_12_1$ (no. 19), $a$ = 9.858(4), $b$ = 16.288(5), $c$ = 16.972(3) Å, $Z$ = 4, $D_c$ = 1.28 g $cm^{-3}$, $U$ = 2725(2) $Å^3$, Mo-K$\alpha$ ($\lambda$ = 0.710 73 Å), $F$(000) = 1112, crystal dimensions 0.40 × 0.40 × 0.25 mm, the structure was solved by direct methods and refined to $R_1$ = 0.078, $wR2$ = 0.215 for 2425 observed reflections with $I > 2\sigma(I)$ (total unique reflections 2708), no of parameters = 262, on an Enraf-Nonius CAD4 diffractometer. Max., min. residual electron density = 0.78, −1.69 e $Å^{-3}$ (near Cr), programs used SHELXS-86, SHELXL-93, MolEN.

**3**: $C_{20}H_{37}MoO_3P_3Si_2$, monoclinic, space group $P2_1/n$ (no. 14), $a$ = 9.704(3), $b$ = 16.558(8), $c$ = 17.040(4) Å, $\beta$ = 95.58(2)°, $Z$ = 4, $D_c$ = 1.39 g $cm^{-3}$, $U$ = 2725(2) $Å^3$, $F$(000) = 1184, crystal dimensions 0.40 × 0.40 × 0.20 mm, other details as above; $R_1$ = 0.065, $wR2$ = 0.160 for 3772 observed reflections (total unique reflections 4777), no of parameters = 262. Max., min residual electron density = 1.31, −1.04 e $Å^{-3}$.

Atomic coordinates, bond lengths and angles, and thermal parameters have been deposited at the Cambridge Crystallographic Data Centre (CCDC). See Information for Authors, Issue No. 1. Any request to the CCDC for this material should quote the full literature citation and the reference number 182/454.

§ Please consult the authors for full details of the calculations.

## References

1 F. Mathey, *Chem. Rev*., 1988, **88**, 437; A. N. Hughes, in *Handbook of Organophosphorus Chemistry*, ed. R. Engel, Marcell Dekker, New York, 1992.
2 L. Nyulászi, *J. Phys. Chem*., 1996, **100**, 6194.
3 L. Nyulászi, J. Réffy and T. Veszprémi, *J. Phys. Chem*., 1993, **97**, 4011.
4 V. Caliman, P. B. Hitchcock and J. F. Nixon, *J. Chem. Soc., Chem. Commun*., 1995, 1661.
5 R. Bartsch, P. B. Hitchcock and J. F. Nixon, *J. Chem. Soc., Chem. Commun*., 1987, 1146.
6 L. Nyulászi and J. F. Nixon, to be published.
7 K. B. Wiberg, *Tetrahedron*, 1968, **24**, 1083.
8 P. B. Hitchcock, J. F. Nixon and N. Sakarya, *Chem. Commun*., 1996, 2751.

*Received, in Cambridge, UK, 28th February 1997; Com. 7/01412K*

# Carbon dioxide activation: synthesis and characterization of a cadmium(II) dinuclear complex with a novel μ-carbonato bridge

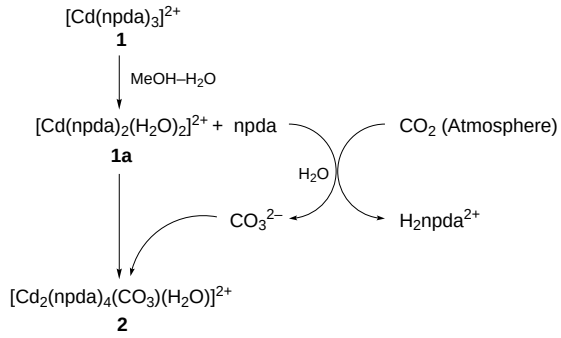
**Chandi Pariya,*[a]† Vedavati G. Puranik[b] and Nirmalendu Ray Chaudhuri*[a]‡**

[a] *Department of Inorganic Chemistry, Indian Association for the Cultivation of Science, Calcutta 700 032, India*
[b] *Division of Physical Chemistry, National Chemical Laboratory, Pune 411 008, India*

**The cadmium(II) complex of *N′*-isopropyl-2-methylpropane-1,2-diamine (npda), $[Cd(npda)_3][ClO_4]_2$ 1 in aqueous methanol absorbs $CO_2$ from air to form a cadmium(II) dinuclear complex, $[Cd(npda)_4(CO_3)(H_2O)][ClO_4]_2{\cdot}H_2O$ 2, the first ever example of a μ-carbonato cadmium(II) diamine complex which is characterized by elemental analysis, IR and crystal structure determination.**

Transition metals bound to $CO_2$ and reactions of the resulting complexes have been of much interest in connection with utilization of $CO_2$.[1–3] A large-scale method of reducing $CO_2$ similar to photosynthesis in green plants, has, as yet, not been developed. The benefit of reduction of $CO_2$ in the atmosphere can be doubled if $CO_2$ can be absorbed and harvested as a chemical feedstock.[4,5] Development of metal–$CO_2$ chemistry derived much of its inspiration from such a challenging possibility. However, most prepared and characterized transition-metal complexes containing $CO_2$[6–12] and a variety of bridging carbonates[13–17] are air-sensitive. Here we describe: (*a*) the first example of a cadmium complex which can spontaneously react with $CO_2$ under atmospheric conditions in the presence of a base, and (*b*) structural characterization of the resultant dinuclear complex featuring a novel μ-carbonato group bridging two cadmium ions.

In the course of our studies[18–21] on the synthesis, characterization and thermal investigation of transition-metal (nickel, copper, zinc and cadmium) complexes of *N′*-isopropyl-2-methylpropane-1,2-diamine (npda), we reported[20] that only cadmium(II) perchlorate generates tris-diamine species with excess npda, $[Cd(npda)_3][ClO_4]_2$ **1** being obtained as a white powder. When a methanolic solution of **1** was stirred in air and its volume reduced, colourless crystals formulated as $[Cd_2(npda)_4(CO_3)(H_2O)][ClO_4]_2{\cdot}H_2O$ **2** were obtained in good yield.§ Complex **2** was also prepared from $[Cd(npda)_3][ClO_4]_2$ by passing a stream of carbon dioxide or by addition of carbonate in methanolic solution. The ease of formation of this unusual bimetallic complex may be attributed to the unique steric features of npda, since no effort was made to promote reaction with $CO_2$, nor has such bridging been observed previously for other cadmium complexes featuring different ligands.




**Scheme 1**

Complex **2** gave satisfactory elemental analysis and its IR spectrum showed the presence of amine as well as carbonate[16] groups, the latter being absent in **1**. The tris-diamine complex **1**, when dissolved in an aqueous medium, dissociates into $[Cd(npda)_2(H_2O)_2][ClO_4]_2$ **1a**[20b] and npda, to release the excessive steric congestion owing to the bulky substituents of a third npda ligand. It appears that complex **1a** is a very active species for reaction with $CO_2$ in the presence of npda; the latter is supposed to act also as a base, which would raise the concentration of $CO_2$ in solution. Although at a first glance it might appear that the complex **2** is generated by the interaction of the bis-complex and $CO_2$ as the metal : npda ratio in **2** was 1 : 2, the formation of **2** from a simple bis-complex was not observed. The proposed mechanistic pathway for this reaction is shown in Scheme 1.

The initial loss of a ligand unit leads to a coordinatively unsaturated intermediate, $[Cd(npda)_2]^{2+}$ which coordinates to two molecules of water to form $[Cd(npda)_2(H_2O)_2]^{2+}$. The released npda reacts with $CO_2$ to form $CO_3^{2-}$ [$CO_2 + H_2O +$ npda $\rightarrow$ $CO_3^{2-}$ (aq) + $H_2npda^{2+}$] and eventually yields $[Cd_2(npda)_4(CO_3)(H_2O)]^{2+}$.[14]

The crystal structure of **2** revealed the presence of a novel, bridging tridentate carbonate, and presented an excellent opportunity to study the configuration and interactions of the two npda ligands in an octahedral configuration. Fig. 1 shows a view and atom-numbering scheme of the dication $[Cd_2(npda)_4(CO_3)(H_2O)]^{2+}$ containing a novel μ-carbonato bridge, which is associated in the crystal with two perchlorate ions and a water molecule of crystallization.

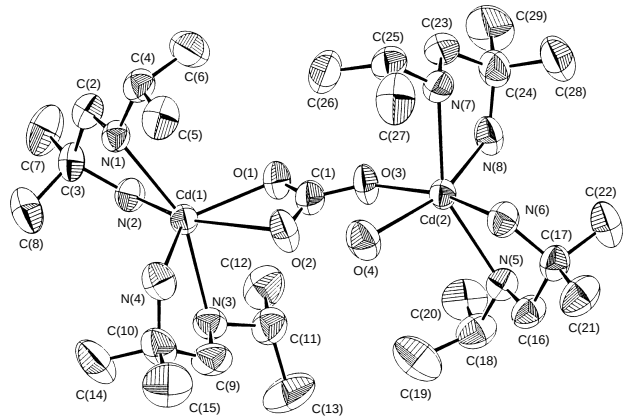



**Fig. 1** ORTEP diagram of complex **2**. Thermal elipsoid are drawn at 50% probability, the water molecule and perchlorate ions are not shown for clarity. Selected bond distances (Å) and angles (°): Cd(1)–O(1) 2.172(4), Cd(1)–O(2) 2.768(4), Cd(1)–N(1) 2.389(4), Cd(1)–N(2) 2.324(4), Cd(1)–N(3) 2.407(5), Cd(1)–N(4) 2.324(4), Cd(2)–O(3) 2.238(3), Cd(2)–O(4) 2.351(4), Cd(2)–N(5) 2.385(5), Cd(2)–N(6) 2.386(4), Cd(2)–N(7) 2.403(5), Cd(2)–N(8) 2.309(4), C(1)–O(1) 1.278(6), C(1)–O(2) 1.279(7), C(1)–O(3) 1.268(6); O(1)–Cd(1)–O(2) 51.46(3), O(3)–Cd(2)–O(4) 82.8(2), N(2)–Cd(1)–N(1) 75.0(2), N(4)–Cd(1)–N(3) 75.8(2), N(5)–Cd(2)–N(6) 75.0(2), N(8)–Cd(2)–N(7) 73.7(2), O(1)–C(1)–O(2) 119.7(4), O(1)–C(1)–O(3) 118.7(5), O(2)–C(1)–O(3) 121.6(5).

In the dinuclear complex cation both cadmium atoms have a significantly distorted octahedral coordination with $N_4O_2$ chromophores. Distortions from ideal octahedral geometry are due to the two bidentate diamines and the asymmetric nature of the bridging carbonato ion, the smallest *cis* angle being 51.46(3)° [O(1)–Cd(1)–O(1)]. The carbonato moiety is planar and the C–O bond distances are almost equal [av. 1.278(6) Å] unlike those in bidentate carbonate systems.[17] A three-dimensional network of intra- and inter-molecular hydrogen bonds involving water molecules, amine nitrogen atoms and perchlorate ions stabilizes the crystal packing; the shortest hydrogen bond is O(1w)···O(1) (1 +*x*, *y*, *z*) 2.812(3) Å.

We thank Dr A. Sarkar, Division of Organic Chemistry (Synthesis), National Chemical Laboratory, Pune for helpful discussions and also Professor T. P. Singh, All India Institute of Medical Science, New Delhi is acknowledged for preliminary data (complex **2**) on the crystal structure determination. One of us (C. P.) thanks Professor Chung-Sun Chung, Department of Chemistry, National Tsing Hua University, Hsinchu, Taiwan, ROC for encouragement.

## Footnotes

† Present address: Department of Chemistry, National Tsing Hua University, Hsinchu, Taiwan 30043, ROC.
E-mail: pariya@chem.nthu.edu.tw
‡ E-mail: icnrc@iacs.ernet.in

§ *X-Ray structure determination*: a colourless crystal of approximate dimensions 0.2 × 0.3 × 0.6 mm was used for the data collection on a PC controlled Enraf-Nonius CAD-4 single-crystal X-ray diffractometer (293 K) with graphite-monochromated Mo-Kα radiation using ω–2θ scan mode and 1° $min^{-1}$ scan speed. Unit-cell parameters were refined from 25 least-squares fitted machine-centred reflections in the range 18 < 2θ < 30°. Three standard reflections measured every hour showed < 4% variation in intensity. The structure was solved by direct methods using NRCVAX[22] and refined by full-matrix least-squares techniques on $F^2$ using SHELXL-93[23] to $R$ = 0.0280, $R_w$ = 0.075 from 5358 unique reflections, from a total number of 5558 reflections collected. Least-squares refinement of scale, position and anisotropic thermal parameters for non-hydrogen atoms was carried out. The hydrogen-atom positions were geometrically fixed and confirmed by difference Fourier analysis. Each hydrogen atom was assigned the same isotropic thermal parameter as the atom to which it was bonded.

*Crystal data* for **2**: $C_{29}H_{76}Cd_2Cl_2N_8O_{13}$, $M$ = 1036.6, monoclinic, space group $P2_1$, $a$ = 9.338(8), $b$ = 12.888(1), $c$ = 20.493(3) Å, $\beta$ = 101.78(4)°, $U$ = 2414(2) Å$^3$, $Z$ = 2, $D_c$ = 1.426 Mg $m^{-3}$. Final $R$ [$I > 2\sigma(I)$] $R_1$ = 0.0280 and $R_w$ = 0.0754; $w = 1/\sigma^2[(F_o^2) + (0.0499p)^2 + 0.6831p]$, where $p = (F_o^2 + 2F_c^2)/3$. Number of refined parameters is 486. The 'Flack parameter' is 0.083(3).[24] CCDC 510.

## References

1 D. J. Darensbourg and R. Kuetosic, *Adv. Organomet. Chem.*, 1983, **22**, 129; D. A. Palmer and R. V. Eldik, *Chem. Rev.*, 1983, **83**, 651; R. Eisenberg and D. E. Hendricksen, *Adv. Catal.*, 1979, **28**, 79.
2 T. Ito and A. Yamamto, *Organic and Bio-organic Chemistry of Carbon Dioxide*, ed. S. Inoue and S. Yamazaki, Wiley, New York, 1980; J. Cramer and A. L. Meyers, *Atmos. Environ.*, 1972, **6**, 563; C. F. Base, Jr., H. E. Goeller, J. S. Oison and R. M. Rotty, *Am. J. Sci.*, 1977, **65**, 310.
3 J. R. Bolton, *Science*, 1978, **202**, 705; R. William, R. S. Bloom and A. Bloom, *Appl. Phys. Lett.*, 1978, **33**, 381.
4 A. Naitoh, K. Otha, T. Mizuno, H. Yoshida, M. Sakai and H. Noda, *Electrochim. Acta*, 1993, **38**, 2177.
5 J. Costamagna, G. Ferraudi, J. Canales and J. Vargas, *Coord. Chem. Rev.*, 1996, **148**, 221.
6 M. Aresta, C. F. Nobile, V. G. Albano, E. Forni and M. Manassero, *J. Chem. Soc., Chem. Commun.*, 1975, 636; M. Aresta and C. F. Nobile, *J. Chem. Soc., Dalton Trans.*, 1977, 708.
7 S. Gambarotta, F. Arena, C. Floriani and P. F. Zanazzi, *J. Am. Chem. Soc.*, 1982, **104**, 5082.
8 G. S. Bristow, P. B. Hitchcock and M. F. Lappert, *J. Chem. Soc., Chem. Commun.*, 1981, 1145.
9 J. C. Calabrese, T. Herskovitz and J. B. Kinney, *J. Am. Chem. Soc.*, 1983, **105**, 5914.
10 S. Gambarotta, C. Floriani, A. Chiesi-Villa and C. Guastini, *J. Am. Chem. Soc.*, 1985, **107**, 2985; R. Alvarez, E. Carmona, J. M. Marin, M. L. Poveda, E. Gutierrez-Puebla and A. Monge, *J. Am. Chem. Soc.*, 1986, **108**, 2286.
11 B. Demerseman, R. Mahé and P. H. Dixneuf, *J. Chem. Soc., Chem. Commun.*, 1984, 1394.
12 M. Kato and T. Ito, *Inorg. Chem.*, 1985, **24**, 509.
13 S. Cenini, F. Porta, M. Pizzotti and C. Crotti, *J. Chem. Soc., Dalton Trans.*, 1985, 163; H. H. Karsch, *Chem. Ber.*, 1977, **210**, 2213.
14 This type of mechanism was originally proposed by Tanase *et al.* in $[Ni(Me_2en)_3](ClO_4)_2$ ($Me_2en$ = *N*,*N*-dimethylethane-1,2-diamine) where the final complex was $[Ni_3(Me_2en)_6(CO_3)(H_2O)_4][ClO_4]_4$; T. Tanase, S. Nitta, S. Yoshikawa, K. Kobayashi, T. Sakurai and S. Yano, *Inorg. Chem.*, 1992, **31**, 1058.
15 S. C. Rawle, C. J. Harding, P. Moore and N. W. Alcock, *J. Chem. Soc., Chem. Commun.*, 1992, 1701.
16 E. Carmona, F. Gonzalez, M. L. Poveda, J. M. Marin, J. L. Atwood and R. D. Rogers, *J. Am. Chem. Soc.*, 1983, **105**, 3365.
17 R. J. Geue and M. R. Snow, *J. Chem. Soc., A*, 1971, 2981; M. R. Churchill, G. M. Harris, R. A. Lashewycz, T. P. Dasgupta and K. Koshy, *Inorg. Chem.*, 1979, **18**, 2290.
18 C. Pariya, A. Ghosh and N. Ray Chaudhuri, *J. Chem. Res.* (*S*), 1994, 428; C. Pariya, S. Ghosh, A. Ghosh, M. Mukherjee, A. K. Mukherjee and N. Ray Chaudhuri, *J. Chem. Soc., Dalton Trans.*, 1995, 337; C. Pariya, A. Ghosh and N. Ray Chaudhuri, *Thermochim. Acta*, 1995, **268**, 153.
19 C. Pariya, M. M. Bhadbhade, A. Ghosh, B. Narayanan and N. Ray Chaudhuri, *J. Chem. Soc., Dalton Trans.*, submitted.
20 (*a*) C. Pariya, A. Ghosh, S. Ganguli and N. Ray Chaudhuri, *Thermochim. Acta*, 1994, **242**, 195; (*b*) Complexes with a cadmium : ligand ratio of 1 : 2 are characterized and reported in ref. 20(*a*). Based on previous experience and the presence of ligated water molecule in the binuclear product, an octahedral, bis-aquo structure has been formulated for **1a**.
21 C. Pariya, N. Ray Chaudhuri, S. Seth and A. Das, *Acta Crystallogr., Sect. C*, 1996, **52**, 358; C. Pariya, N. Ray Chaudhuri, A. Das and S. Seth, *Acta Chem. Scand.*, 1995, **49**, 859.
22 E. J. Gabe, Y. L. Page, J. P. Charland, F. L. Lee and P. S. White, *J. Appl. Crystallogr.*, 1989, **22**, 384.
23 G. M. Sheldrick, SHELXL-93, Program for refinement of crystal structure, University of Göttingen, 1993.
24 H. D. Flack, *Acta Crystallogr., Sect. A*, 1983, **39**, 876.

*Received in Basel, Switzerland, 10th March 1997; Com. 7/01676J*

# Preparation of functionalized biaryl compounds *via* cross-coupling reactions of aryltrialkoxysilanes with aryl bromides

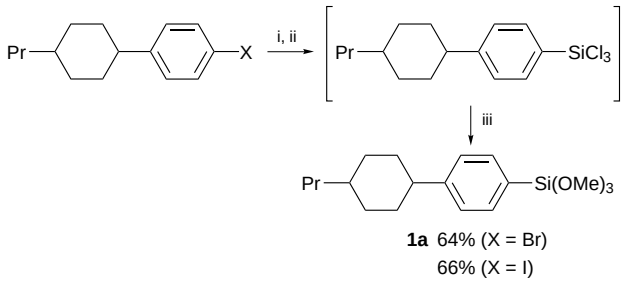
**Koichi Shibata,* Kazutoshi Miyazawa and Yasuyuki Goto**

*Chisso Petrochemical Corporation, Specialty Chemicals Research Center, 5-1 Goi Kaigan, Ichihara, Chiba 290, Japan*

**Aryltrimethoxysilanes react with aryl bromides in the presence of fluoride ion and palladium catalysts to give the corresponding biaryl compounds in good yields with high chemoselectivity.**

Many functional organic materials and natural bioactive organic compounds contain biaryl units in their structures. In particular, the proportion of biaryl compounds in liquid crystalline compounds is high, and many biaryl-type liquid crystalline compounds have been developed.[1] In recent years, considerable interest in the construction of functionalized biaryl components *via* aryl–aryl coupling reactions has been aroused.[2]

Arylboronic acids are known to undergo cross-coupling reactions with aryl halides.[3] Recently, pentacoordinate aryl silicates activated by fluoride ion have been shown to exhibit high reactivity in coupling reactions, and different kinds of pentacoordinate aryl silicates have been used for aryl–aryl cross-coupling reactions.[2c,2f,4]




**Scheme 1** *Reagents and conditions*: i (X = Br) Mg (1.1 equiv.), THF, 50 °C, 2 h; (X = I) BuLi (1.0 equiv.), hexane, −70 °C, 2 h; ii (X = Br) $SiCl_4$ (1.5 equiv.), 0 °C to room temp., 17 h; (X = I) $SiCl_4$ (2 equiv.), −70 °C to room temp., 17 h; iii, MeOH (8.0 equiv.), pyridine (8.0 equiv.), 0 °C, 30 min

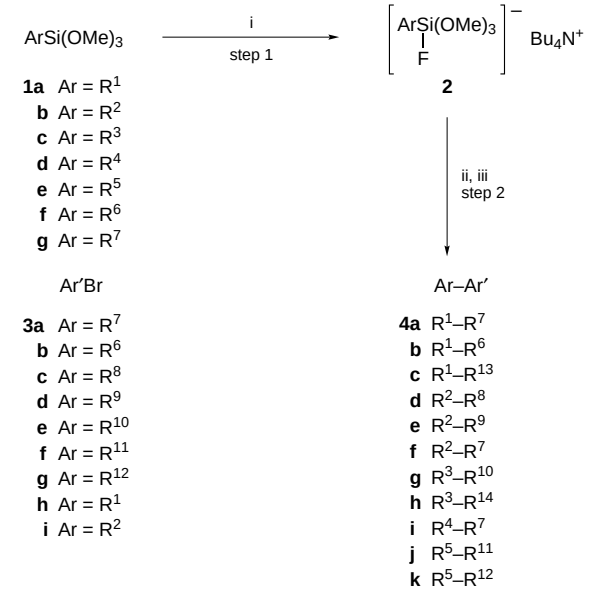
**Table 1** Preparation of biphenyl **4a** from **1a** and **3a**[a]

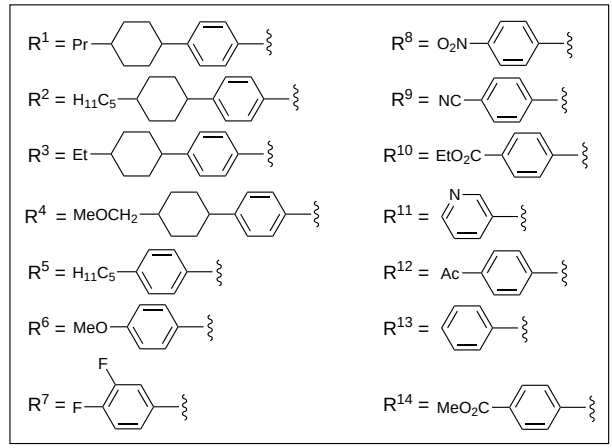
| Entry | Catalyst (mol%) | Step 2 Solvent | *t*/h | Yield of **4a** (%) |
|---|---|---|---|---|
| 1[b] | $Pd(OAc)_2$ (5) | DMF | 3 | 2 |
| 2 | $Pd(OAc)_2$ (10) | THF–DMF | 3 | 49 |
| 3 | $Pd(Ph_3P)_4$ (5) | THF–DMF | 3 | 71 |
| 4[c] | $Pd(Ph_3P)_4$ (5) | THF-Toluene | 10 | 91 |
| 5 | $Pd(Ph_3P)_4$ (5) | THF | 3 | 19 |
| 6 | $Pd(Ph_3P)_4$ (5) | Toluene[d] | 3 | 94 |
| 7 | $Pd(OAc)_2$ (5) | Toluene[d] | 3 | 46 |
| 8 | $Pd(OAc)_2$ (5)–$Ph_3P$ (5) | Toluene[d] | 3 | 83 |
| 9 | $Pd(OAc)_2$ (5)–$Ph_3P$ (10) | Toluene[d] | 3 | 89 |
| 10 | $Pd(OAc)_2$ (5)–$Ph_3P$ (15) | Toluene[d] | 3 | 90 |
| 11 | $Pd(OAc)_2$ (5)–$Ph_3P$ (20) | Toluene[d] | 3 | 80 |

[a] TBAF (1.05 equiv.) was used as a fluoride ion source, and Step 1 was carried out in THF for 30 min at room temperature, unless otherwise noted. [b] Step 1: KF (5 equiv.) was used instead of TBAF and the reaction was carried out for 3 h at 100 °C in DMF; Step 2: Reaction was carried out for 3 h at 120 °C. [c] Reaction time of Step 2 was 10 h. [d] Before Step 2, THF was removed under reduced pressure.

Here we report the reactivity of a new type of pentacoordinate aryl silicate, aryl(fluoro)trimethoxosilicate(1−) **2**, which was easily obtained from aryltrimethoxysilane **1** and a fluoride ion source. At the outset, preparation of **1a** was attempted in several ways, and reactions using tetrachlorosilane gave **1a** in acceptable yields after distillation (Scheme 1).[4] Other arylsilanes **1b**–**g** were also prepared using this method and they were so stable that no decomposition occurred during ordinary aqueous work-up. Although direct reaction of the aryl Grignard or lithium reagent with tetramethoxysilane could afford **1a**, its yield was low (*ca.* 35%).[5] The main product of the reaction was diaryl(dimethoxy)silane.

4-(*trans*-4-*n*-Propylcyclohexyl)-3′,4′-difluorobiphenyl **4a**, which is used in active matrix liquid crystal displays, was




**Scheme 2** *Reagents and conditions*: i, $Bu_4NF$ (1.05 equiv.); ii, Ar'Br (**3a**–**i**) (1.2 equiv.); iii, Pd catalyst, reflux

chosen as a model compound, and cross-coupling reactions of 4-(*trans*-4-*n*-propylcyclohexyl)phenyltrimethoxysilane **1a** with 1-bromo-3,4-difluorobenzene **3a** were attempted.[6] Arylsilane **1a** was stirred with KF in DMF and then the reaction mixture was reacted with **3a** for 3 h at 120 °C in the presence of a catalytic amount of palladium(II) acetate [$Pd(OAc)_2$]. However, the yield of the desired product **4a** was only 2% (Table 1, entry 1). When the fluoride ion source and the solvent were changed to tetrabutylammonium fluoride (TBAF)† and THF–DMF mixed solvents, respectively, the yield of **4a** increased to 49% (entry 2). In addition, changing of the catalyst to tetrakis-(triphenylphosphine)palladium(0) [$(Ph_3P)_4Pd$] gave **4a** in 71% yield (entry 3). Under theses conditions, reactions were carried out in several solvents (entries 4–6), and toluene was found to be the best solvent (entry 6).

Although the yield of **4a** was 46% when $Pd(OAc)_2$ was used as a catalyst, the addition of $Ph_3P$ had a remarkable effect (entries 8–11). The best molar ratio of $Pd(OAc)_2$ and $Ph_3P$ was 1 : 3, which gave **4a** in 90% yield (entry 10). From the above results, it can be seen that $(Ph_3P)_4Pd$ and $Pd(OAc)_2$–$Ph_3P$ are good catalysts for the reaction. Taking the price, stability and simplicity of handling into account, $Pd(OAc)_2$–$Ph_3P$ is the more practical.

The reactions of several arylsilanes **1** with aryl bromides were investigated next under the conditions used in Table 1, entry 10 (Scheme 2). They proceeded with high chemoselectivity and the results are summarized in Table 2.

All reactions gave the desired biaryl derivatives in good yields except entry 2. In particular, when **3a** was used, **4a**, **4f**, and **4i** were obtained in more than 82% yield within 10 h (entries 1, 5 and 7). In general, as liquid crystalline compounds having fluorine atoms on their aromatic rings are known to exhibit good properties, the present reaction is very useful for the preparation of fluorinated liquid crystalline compounds.[6,7]

**Table 2** Preparation of a variety of biaryl compounds[a] **4**

| Entry | **1** | **3** | *t*/h | Product (% yield) |
|---|---|---|---|---|
| 1[b] | **1a** | **3a** | 3 | **4a** (90) |
| 2 | **1a** | **3b** | 10 | **4b** (61), **4c** (29) |
| 3 | **1b** | **3c** | 25 | **4d** (74) |
| 4 | **1b** | **3d** | 30 | **4e** (87) |
| 5 | **1b** | **3a** | 10 | **4f** (92) |
| 6 | **1c** | **3e** | 30 | **4g** (84), **4h** (4) |
| 7 | **1d** | **3a** | 30 | **4i** (82) |
| 8 | **1e** | **3f** | 30 | **4j** (72) |
| 9 | **1e** | **3g** | 30 | **4k** (84) |
| 10 | **1f** | **3h** | 30 | **4b** (75) |
| 11 | **1g** | **3i** | 30 | **4f** (78) |

[a] $Pd(OAc)_2$ (5 mol%)-$Ph_3P$ (15 mol%) was used as catalyst and the reactions were carried out in toluene. [b] The same data as shown in Table 1, entry 10.

The reaction of 4-bromoanisole **3b** with **1a** gave not only the desired **4b** (61%) but also the demethoxylated product **4c** (29%; entry 2). Although the mechanism of demethoxylation has not been elucidated, it is most probable that demethoxylation occurs before the formation of the new $sp^2$–$sp^2$ bond because the reaction of the reverse combination of entry 2 showed no formation of **4c** (entry 10).

In these reactions, homo-coupling products were not detected and other byproducts were also very rare, which made purification of the products straightforward. Another advantage of this reaction system is that **1** is very resistant to hydrolysis, and thus can be stored for a long time without special precautions to exclude moisture.

## Footnotes

* E-mail: qyk13654@niftyserve.or.jp

† TBAF containing 5 mass% water was purchased from Aldrich and used after drying with molecular sieves 4 Å.

## References

1 D. Demus, H. Demus and H. Zaschke, *Flüssige Kristalle in Tabellen*, VEB Deutsche Verlag für Grundstoff Industrie, Leipzig, 1976; D. Demus and H. Zaschke, *Flüssige Kristalle in Tabellen II*, VEB Deutsche Verlag für Grundstoff Industrie, Leipzig, 1984; G. W. Gray and G. R. Luckhurst, *The Molecular Physics of Liquid Crystal*, Academic Press, New York, London, Toronto, Sydney and San Francisco, 1979.

2 For reviews of the preparation of biaryls, see (*a*) M. T. Sainsbury, *Tetrahedron*, 1980, **36**, 3327; (*b*) G. Bringmann, R. Walter and R. Weirich, *Angew. Chem., Int. Ed. Engl*., 1990, **29**, 977;. (*c*) T. Hiyama and Y. Hatanaka, *Pure Appl. Chem*., 1994, **66**, 1471; (*d*) D. W. Knight, *Comprehensive Organic Synthesis*, Pergamon Press, Oxford, New York, Seoul and Tokyo, vol. 3, pp. 499-516, 1991; (*e*) N. Miyaura and A. Suzuki, *Synth. Org. Chem. Jpn*., 1988, **46**, 848; (*f*) A. Suzuki and N. Miyaura, *J. Synth. Org. Chem. Jpn*., 1993, **51**, 1043.

3 Y. Hatanaka and T. Hiyama, *J. Synth. Org. Chem. Jpn.*, 1990, **48**, 834; Y. Hatanaka, K. Goda, Y. Okahara and T. Hiyama, *Tetrahedron*, 1994, **50**, 8301.

4 For the reactions of organometallic reagents with tetrachlorosilane, see: L. W. Breed and W. J. Haggerty, *J. Org. Chem*., 1960, **25**, 126; W. Laarz, M. Schulten, R. Boese and D. Blaeser, *Z. Naturforsch. B, Chem. Sci.*, 1992, **47**, 1233; N. Auner, R. Probst, F. Hahn and E. Herdtweck, *J. Organomet. Chem*., 1993, **459**, 25.

5 For the reactions of organometallic reagents with tetramethoxysilane, see: T. G. Selin and R. West, *J. Am. Chem. Soc*., 1962, **84**, 1856; R. Tacke, A. Mentlage-Falten, H. Linoh and S. Magada, *Z. Naturforsch., B: Anorg Chem., Org. Chem*., 1986, **41B**, 649;A. Hosomi, S. Kohra, K. Ogata, T. Yanagi and Y. Tominaga, *J. Org. Chem*., 1990, **55**, 2415.

6 Y. Goto, T. Ogawa, S. Sawada and S. Sugimori, *Mol. Cryst. Liq. Cryst.*, 1991, **209**, 1.

7 H. J. Plach, B. Rieger, E. Poetsch and V. Reiffenrath, *Proc. 10th Int. Disp. Res. Conf.*, 1990, 136; G. Weber, U. Finkenzeller, T. Geelhaar, H. J. Plach, B. Rieger and L. Pohl, *Liq. Cryst.*, 1989, **5**, 1381; H. J. Plach, G. Weber and B. Rieger, *Proc. SID Int. Symp.*, 1990, 91.

*Received in Cambridge, UK, 13th March 1997; Com. 7/01770G*

# $[H_3N(CH_2)_3NH_3]Fe_2O(PO_4)_2$: a novel layered iron phosphate containing tetramers of $FeO_5$ trigonal bipyramids

**Kwang-Hwa Lii* and Yuh-Feng Huang**

*Institute of Chemistry, Academia Sinica, Taipei, Taiwan*

**The synthesis and characterization of a layered iron phosphate is described; the structure consists of novel $Fe_4O_{16}$ clusters formed of four $FeO_5$ trigonal bipyramids, which are linked into two-dimensional sheets through phosphate tetrahedra with propanediammonium cations between the sheets.**

A large variety of molybdenum and vanadium phosphates with layered and open frameworks have been synthesized under mild hydrothermal conditions using organic amines as templates.[1,2] It is reasonable to assume that the formation of these solids will occur with other d-block elements. Iron phosphates exist as minerals and have a rich crystal chemistry. A large number of ternary iron phosphates have been synthesized under high temperature, high pressure hydrothermal conditions.[3] Little work, however, has been carried out on the organically templated iron phosphates and, to our knowledge, only three phases, namely $[H_3N(CH_2)_2NH_3]_{0.5}[Fe(OH)PO_4]$,[4] $[HN(CH_2CH_2)_3NH]_3[Fe_8(HPO_4)_{12}(PO_4)_2(H_2O)_6]$[5] and $[H_3N(CH_2)_3NH_3]_2[Fe_4(OH)_3(HPO_4)_2(PO_4)_3]\cdot xH_2O$,[6] have been synthesized. The latter is particularly interesting because the structure contains large tunnels with 20-ring windows and its framework metal atom density is smaller than the very open faujasite. Here we describe the synthesis and characterization of a novel amine encapsulating FePO, which has a layer structure and contains a hitherto unknown tetramer of $FeO_5$ trigonal bipyramids.

Hydrothermal treatment of $FeCl_3\cdot 6H_2O$ (2.5 mmol), $H_3PO_4$ (7.5 mmol), $H_2N(CH_2)_3NH_2$ (14 mmol), *n*-butanol (7 ml) and water (3 ml) for 3 days at 160 °C followed by slow cooling at 5 °C $h^{-1}$ to room temperature produced $[H_3N(CH_2)_3NH_3]Fe_2O(PO_4)_2$, **1**, as orange plate crystals and a very small amount of a pale yellow material. The yellow material was $[H_3N(CH_2)_3NH_3]_2[Fe_4(OH)_3(HPO_4)_2(PO_4)_3]\cdot xH_2O$,[5] as indicated from powder X-ray diffraction measurements. A small orange crystal was used to determine its structure by single-crystal X-ray diffraction.† The orange crystals were manually separated from the yellow material to give pure **1** as judged by visual microscopic examination and by comparison of the X-ray powder pattern to the pattern simulated from the atomic coordinates derived from single-crystal study. The yield of **1** was 94% based on iron. Chemical analysis confirmed the amount of 1,3-diaminopropane (Found: C, 9.22; H, 2.99; N, 7.08. Calc. C, 9.15; H, 3.07; N, 7.11%). The IR spectrum (KBr) showed N–H and C–H stretches at 3090 and 2945 $cm^{-1}$, respectively Thermal gravimetry in air showed a mass loss in two steps. In the first step over 280–400 °C a mass loss of 11.0% was observed which corresponded to the release of one mol of $C_3H_4$ (Calc. 10.2%) due to the decomposition of diprotonated 1,3-diaminopropane. The product contained $NH_4^+$ as confirmed by the presence of a band at 3360 $cm^{-1}$ for the N–H stretch and disappearance of the band at 2945 $cm^{-1}$ for the C–H stretch in the IR spectrum of the sample heated to 350 °C. A powder X-ray pattern of the sample indicated that it was amorphous. The second step in TG (400–750 °C, mass loss 13.0%) was attributed to the release of one mol of $H_2O$ and two mol of $NH_3$ (Calc. 13.2%). The final decomposition product at 800 °C was $FePO_4$. The room-temperature Mössbauer spectrum of **1** is a doublet with $\delta$ (isomer shift) = 0.35 mm $s^{-1}$ (relative to iron foil at 300 K), $\Delta E_Q$ (quadrupole splitting) = 0.92 mm $s^{-1}$, and $\Gamma$ (full width at half-height) = 0.32 mm $s^{-1}$. The isomer shift is consistent for iron(III) phosphates.[7] Variable-temperature magnetic susceptibility measurements on a powder sample showed that $\chi_M T$ decreased with decreasing temperature and the value at 300 K was only 19% of the spin-only value, indicating large antiferromagnetic interactions so that $\chi_M$ is significantly reduced from the expected non-interacting moment even at room temperature.

The structure consists of anionic sheets of formula $[Fe_2O(PO_4)_2]^{2-}$ in the *bc*-plane with charge compensating propanediammonium cations between the sheets (Fig. 1). The sheets are constructed from tetramers of $FeO_5$ trigonal bipyramids, which are joined to four other tetramers by the bridging phosphate ligands as shown in Fig. 2. Each sheet has a double-layered structure. Within a layer, $FeO_5$ trigonal bipyramids share corners with $PO_4$ tetrahedra, in an alternating manner to form eight-sided windows. Infinite tunnels are formed along the [100] direction, in which the organic molecules are located. The molecules are locked in their positions by hydrogen bonds to phosphate oxygens [$d_{N(1)-O(5)}$ = 2.81, $d_{N(2)-O(1)}$ = 2.84, $d_{N(2)-O(4)}$ = 2.83 Å]. The tetramer contains a dimer of edge-sharing trigonal bipyramids which further links at the shared

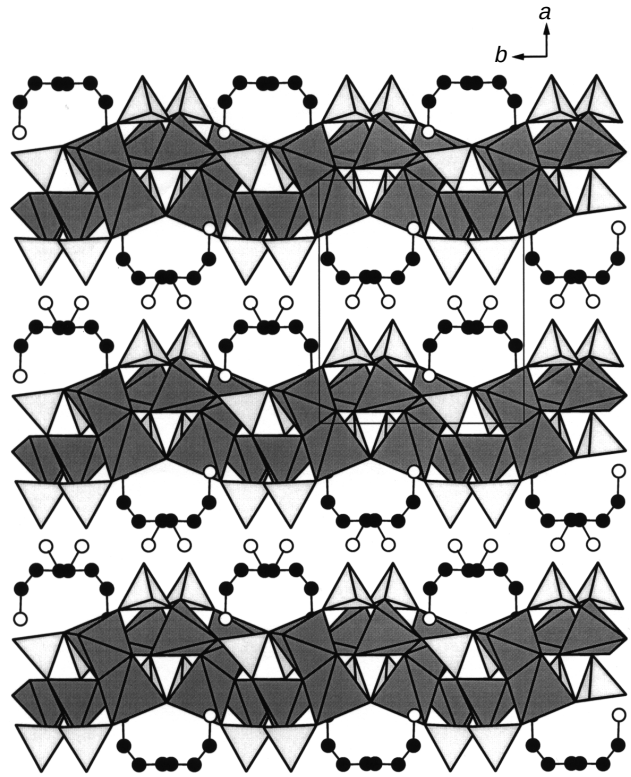



**Fig. 1** Polyhedral view of the structure of **1** along the [001] direction. Polyhedra with darker shade, $FeO_5$ trigonal bipyramids; tetrahedra with lighter shade, $PO_4$; solid circles, C atoms; open circles, N atoms.

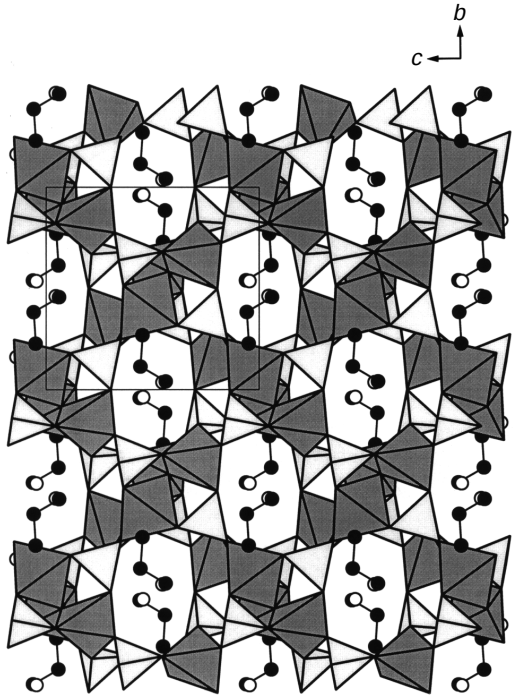



**Fig. 2** Section of a sheet in **1** showing the connectivity between the iron–oxygen clusters

corners to two other trigonal bipyramids forming a $Fe_4O_{16}$ cluster (Fig. 3). The tetramer possesses $\bar{1}$ symmetry located at the midpoint of the shared edge. The $P(1)O_4$ group is tetradentate. Two of the phosphate oxygens bond to two Fe atoms of a cluster in a bridging mode, while the other two bridge to two Fe atoms of an adjacent cluster. The $P(2)O_4$ group coordinates to three Fe atoms of two different clusters through three oxygen donors; the fourth oxygen, O(5), is present as a pendant P=O unit and projects into the interlamellar region. Average Fe–O and P–O bond lengths are typical for their polyhedra, with Fe(1)–O 1.934, Fe(2)–O 1.949, P(1)–O 1.538 and P(2)–O 1.542 Å, in accord with the sum of ionic radii, $r(^{V}Fe^{3+})$ = 0.58, $r(^{IV}P^{5+})$ = 0.17 and $r(^{III}O^{2-})$ = 1.36 Å.[8]

The most remarkable structural feature of $[H_3N(CH_2)_3NH_3]Fe_2O(PO_4)_2$ is the presence of a novel $Fe_4O_{16}$ cluster formed of four $FeO_5$ trigonal bipyramids. Although five-coordination with trigonal-bipyramidal geometry is frequently found in iron phosphates, iron–oxygen clusters formed of only $FeO_5$ trigonal bipyramids are very rare. To our knowledge, $Fe_3PO_7$ is the only other iron phosphate which contains clusters

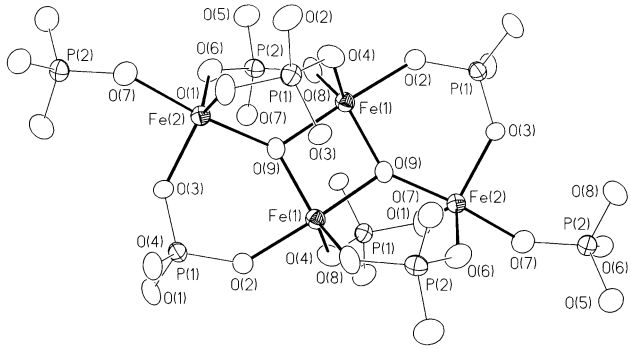



**Fig. 3** The tetranuclear iron cluster in **1**; thermal ellipsoids are shown at 60% probability

of $FeO_5$ trigonal bipyramids.[9] The $Fe_3PO_7$ structure consists of $Fe_3O_{10}$ clusters of edge-sharing $FeO_5$ trigonal bipyramids. The polyhedral linkage in the octahedral tetramers in the mineral leucophosphite, $K_2[Fe_4(OH)_2(H_2O)_2(PO_4)_4]\cdot 2H_2O$[10] and the organically templated iron phosphate $[H_3N(CH_2)_3NH_3]_2[Fe_4(OH)_3(HPO_4)_2(PO_4)_3]\cdot xH_2O$[5] is similar to that in **1**. The tetranuclear $Fe_4O_{16}$ core in the iron arsenate $Cs_3Fe_5O(OH)(AsO_4)_5$[10] has the same structure as that of the molecular tetramer $[\{Ti(OEt)_4\}]$,[12] in which four $MO_6$ octahedra are joined by shared edges. This new phosphate, $[H_3N(CH_2)_3NH_3]Fe_2O(PO_4)_2$, further expands the variety of structures in the iron phosphate phase space which contain clusters of Fe–O polyhedra linked *via* phosphate tetrahedra. The incorporation of bulky organic templates, as compared to cations like the alkali metals, apparently increases the size and complexity of the framework. We are continuing the exploratory synthesis of new FePO frameworks with structure directing organic templates.

The authors thank the Institute of Chemistry, Academia Sinica and the National Science Council of Taiwan for support, Professor S.-L. Wang and Ms. F.-L. Liao at National Tsing Hua University for X-ray intensity data collection, and Professor T.-Y. Dong at National Sun Yat-Sen University for Mössbauer spectroscopy measurements.

## Footnotes

* E-mail: lii@chem.sinica.edu.tw

† *Crystal data* for $[H_3N(CH_2)_3NH_3]Fe_2O(PO_4)_2$: monoclinic, space group $P2_1/c$, $a$ = 11.6591(8), $b$ = 9.5718(7), $c$ = 10.1158(7) Å, $\beta$ = 99.963(2)°, $U$ = 1111.9(2) Å$^3$, $Z$ = 4, $M_r$ = 393.79, $D_c$ = 2.352 g cm$^{-3}$, $\mu$(Mo-K$\alpha$) = 29.4 cm$^{-1}$, $\lambda$ = 0.710 73 Å, graphite monochromator, crystal dimensions: 0.075 × 0.075 × 0.012 mm. The crystal was mounted on a Siemens Smart-CCD diffractometer equipped with a normal focus, 3 kW sealed-tube X-ray source. Intensity data were collected in 1200 frames with increasing $\omega$ (width of 0.30° per frame). Of the 2603 unique reflections collected ($2\theta_{max}$ = 57.5°), 1770 reflections were considered observed [$I > 3.0\sigma(I)$] after Lorentz polarization and semiempirical absorption corrections using the SHELXTL-PC program package ($T_{min, max}$ = 0.773, 0.912).[13] The structure was solved by direct methods: the Fe and P atoms were first located and the C, N, and O atoms were found in the final difference Fourier map. The H atoms were not located. Refinement (164 variables) was performed by full-matrix least-squares analysis, with anisotropic thermal parameters for all atoms. $(\Delta\rho)_{max, min}$ = 0.90, −0.80 e Å$^{-3}$. The reliability factors converged to $R(F)$ = 0.055, $R_w(F)$ = 0.063 and GOF = 1.39. CCDC 182/508.

## References

1 R. C. Haushalter and L. A. Mundi, *Chem. Mater.*, 1992, **4**, 31 and references therein.
2 M. I. Khan, L. M. Meyer, R. C. Haushalter, A. L. Schweitzer, J. Zubieta and J. L. Dye, *Chem. Mater.*, 1996, **8**, 43 and references therein.
3 K.-H. Lii, *J. Chem. Soc., Dalton Trans.*, 1996, 819 and references cited therein.
4 M. Cavellec, D. Riou and G. Ferey, *Acta Crystallogr., Sect. C*, 1995, **51**, 2242; J. R. D. DeBord, W. M. Reiff, R. C. Haushalter and J. Zubieta, *J. Solid State Chem.*, 1996, **125**, 185.
5 K.-H. Lii and Y.-F. Huang, *J. Chem. Soc., Dalton Trans.*, in press.
6 K.-H. Lii and Y.-F. Huang, *Chem Commun*, 1997, 839.
7 C. Gleitzer, *Eur. J. Solid State Inorg. Chem.*, 1991, **28**, 77.
8 R. D. Shannon, *Acta Crystallogr., Sect. A*, 1976, **32**, 751.
9 A. Modaressi, A. Courtois, R. Gerardin, B. Malaman and C. Gleitzer, *J. Solid State Chem.*, 1983, **47**, 245.
10 P. B. Moore, *Am. Mineral.*, 1972, **57**, 397.
11 B. Wang, S.-L. Wang and K.-H. Lii, *Chem. Commun.*, 1996, 1061.
12 J. A. Ibers, *Nature*, 1963, **197**, 686.
13 G. M. Sheldrick, SHELXTL PC, Version 5, Siemens Analytical X-Ray Instruments, Inc., Madison, WI, USA, 1995.

*Received in Cambridge, UK, 17th March 1997; Com. 7/01847I*

# New rhodacyclopentane with phenylvinylidene substituents, *mer*-[Rh{$CH_2C(=CHPh)C(=CHPh)CH_2$}Cl($PMe_3$)$_3$]. Structure and formation through concerted cycloaddition of phenylallene molecules to [RhCl($PMe_3$)$_3$]

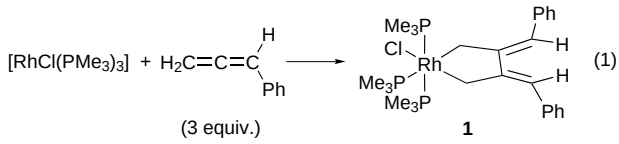
**Kohtaro Osakada,* Jun-Chul Choi, Susumu Sarai, Take-aki Koizumi and Takakazu Yamamoto***

*Research Laboratory of Resources Utilization, Tokyo Institute of Technology, 4259 Nagatsuta, Midori-ku, Yokohama 226, Japan*

**[RhCl($PMe_3$)$_3$] reacts with an excess of phenylallene to give a new rhodacyclopentane, *mer*-[Rh{$CH_2C(=CHPh)C(=CHPh)CH_2$}Cl($PMe_3$)$_3$] 1, which is not obtained *via* the reaction of [RhCl(η²-$CH_2$=C=CHPh)($PMe_3$)$_3$] 2 with phenylallene.**

Several complexes of Ti, Ta, Co, Ir and Ni have been reported to undergo addition of two alkene molecules to give the corresponding saturated metallacyclopentanes.[1] Similar formation of metallacycles from the 2 : 1 reaction of allene and transition-metal complexes is much less common,[2] while the reaction is involved as a crucial step in cyclooligomerization of allene or substituted allene promoted by metal complexes.[3] Chlororhodium(I) complexes catalyze polymerization[4] or cyclooligomerization[5] of 1,2-dienes depending on the ligands bonded to the Rh center. Formation of a rhodacyclopentane from allene would be intriguing in relation to the the mechanism of the above cyclooligomerization of the 1,2-dienes catalyzed by Rh complexes. Here, we report the addition of phenylallene to [RhCl($PMe_3$)$_3$], to give a novel rhodacyclopentane which is structurally characterized.

[RhCl($PMe_3$)$_3$] reacts with 3 equiv. of phenylallene to give *mer*-[Rh{$CH_2C(=CHPh)C(=CHPh)CH_2$}Cl($PMe_3$)$_3$] **1** as shown in eqn. (1).†




The reaction mixture does not contain any other rhodacyclopentanes that would be formed through addition of phenylallene in a different orientation of the double bonds. Fig. 1 shows the molecular structure of **1** which has an octahedral coordination around the Rh center with three $PMe_3$ ligands at meridional coordination sites.‡ Three C–C bond distances in the five-membered chelate ring are quite similar, while the Rh–C(1) bond [2.16(1) Å] is longer than the Rh–C(10) bond [2.061(1) Å] owing to a larger *trans* influence of $PMe_3$ relative to Cl. The C–C bond distances [1.49(2) Å] are significantly longer than the corresponding bond of the platinacyclopentane prepared from dimerization of cycloheptatetraene in the presence of a platinum(0) complex.[2b] Both of the two C=C double bonds in **1** have *Z* structure owing to less steric congestion around the *s-cis* diene moiety than the other possible geometry of the double bonds.

The $^{13}C\{^1H\}$ NMR spectrum gives rise to signals due to the $CH_2$ carbons at $\delta$ 22.26 and 13.21. The former peak, with a large $J$(CP) value (77 Hz), is assigned to the carbon bonded *trans* to $PMe_3$ and the latter to carbon *trans* to Cl. Two $^1H$ NMR signals due to the $CH_2$ hydrogens are observed at $\delta$ 3.02 and 2.11, which are assigned to the $CH_2$ group *trans* to $PMe_3$ and *trans* to Cl, respectively, based on the $^1H$–$^{13}C$ COSY spectrum. The other $^1H$ and $^{13}C$ NMR signals as well as the $^{31}P\{^1H\}$ NMR spectrum are in accord with the structure obtained by X-ray crystallography.

Reaction of a reduced amount of phenylallene with [RhCl($PMe_3$)$_3$] has been examined in order to obtain an insight for the pathway of reaction (1). Reaction in a 1.2 : 1 ratio in hexane results in the formation of [RhCl(η²-$CH_2$=C=CHPh)($PMe_3$)$_3$] **2** which is isolated as the hexane insoluble product.§

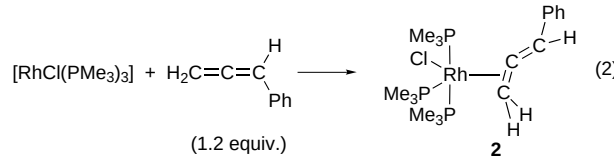



Fig. 2 shows the molecular structure of **2** which shows a trigonal-bipyramidal coordination around the Rh centre with P(1) and P(3) at the apical positions.‡ Elongation of the π-coordinated C=C double bond [$CH_2$=C 1.406(9), C=CHPh

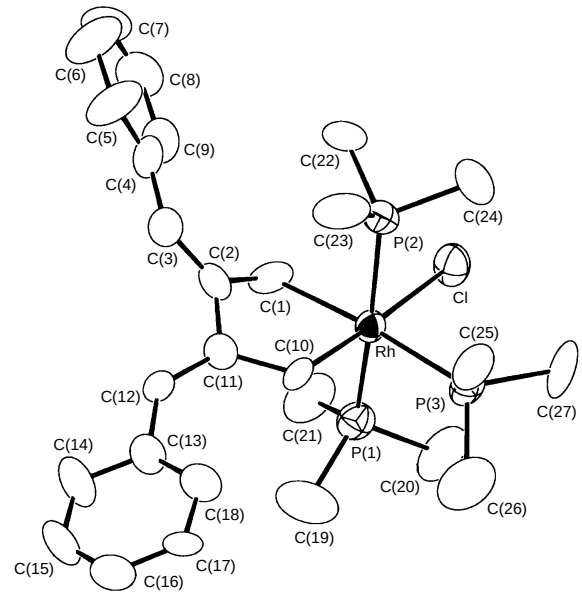



**Fig. 1** ORTEP drawing of **1** at 30% probability level. Selected bond distances (Å) and angles (°): Rh–Cl 2.503(3), Rh–P(1) 2.331(5), Rh–P(2) 2.326(4), Rh–P(3) 2.368(3), Rh–C(1) 2.16(1), Rh–C(10) 2.06(1), C(1)–C(2) 1.49(2), C(2)–C(3) 1.38(2), C(2)–C(11) 1.49(2), C(10)–C(11) 1.49(2), C(11)–C(12) 1.35(2); Cl–Rh–P(1) 86.9(1), Cl–Rh–P(2) 85.5(1), Cl–Rh–P(3) 95.8(1), Cl–Rh–C(1) 94.3(4), Cl–Rh–C(10) 176.3(3), P(1)–Rh–P(2) 168.9(1), P(2)–Rh–P(3) 94.6(2), P(1)–Rh–P(3) 94.1(2), P(1)–Rh–C(1) 88.4(4), P(1)–Rh–C(10) 92.7(4), P(2)–Rh–C(1) 84.1(4), P(2)–Rh–C(10) 94.3(4), P(3)–Rh–C(1) 169.6(4), P(3)–Rh–C(10) 87.8(3), C(1)–Rh–C(10) 82.0(5), Rh–C(1)–C(2) 107.6(9), C(1)–C(2)–C(3) 125(1), C(1)–C(2)–C(11) 111(1), C(11)–C(2)–C(3) 122(1), Rh–C(10)–C(11) 112.6(8), C(10)–C(11)–C(12) 128(1), C(2)–C(11)–C(10) 112(1), C(2)–C(11)–C(12) 119(1).

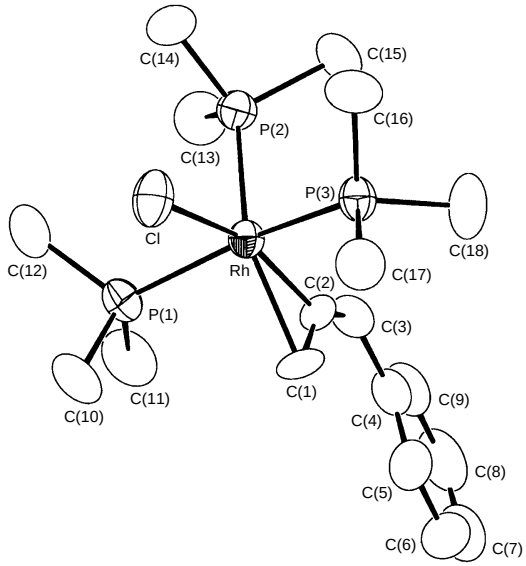
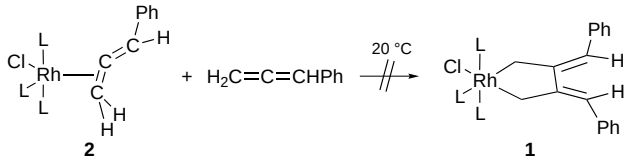



**Fig. 2** ORTEP drawing of **2** at 50% probability level. Selected bond distances (Å) and angles (°): Rh–Cl 2.540(2), Rh–P(1) 2.320(2), Rh–P(2) 2.323(2), Rh–P(3) 2.325(2), Rh–C(1) 2.126(7), Rh–C(2) 1.988(6), C(1)–C(2) 1.406(9), C(2)–C(3) 1.353(9); Cl–Rh–P(1) 84.79(7), Cl–Rh–P(2) 97.80(7), Cl–Rh–P(3) 83.36(7), Cl–Rh–C(1) 118.3(2), Cl–Rh–C(2) 158.0(2), C(1)–Rh–C(2) 39.8(3), P(1)–Rh–P(2) 96.74(7), P(2)–Rh–P(3) 96.94(7), P(1)–Rh–P(3) 162.98(7), C(1)–C(2)–C(3) 142.1(7).




**Scheme 1**

1.353(9) Å] as well as a bend of the cumulated double bonds [C(1)–C(2)–C(3) 142.1(7)°] indicate the presence of significant back-donation from the Rh center to the phenylallene ligand. The $^1$H NMR spectrum of **2** above 25 °C shows partial liberation of a $PMe_3$ ligand to afford a square-planar rhodium(I) complex [Rh($\eta^2$-$CH_2$=C=CHPh)Cl($PMe_3$)$_2$] **3** which is isolated from the mixture and characterized by X-ray crystallography.¶

Reaction of **2** and phenylallene in a 1 : 2 molar ratio in toluene for 8 h at 20 °C does not give **1** but causes quantitative recovery of **2** as shown in Scheme 1.

The results are in contrast with previous reports indicating that several transition-metal complexes containing π-coordinated alkenes react further with alkenes to give the corresponding metallacyclopentane.[1*d*,*f*,*g*] The present study has disclosed that the π-coordinated phenylallene complex **2**, with an 18 electron Rh center, is not a precursor of the metallacycle **1** in reaction (1) and that formation of **1** proceeds through direct cycloaddition of two phenylallene molecules to [RhCl($PMe_3$)$_3$].

This work was financially supported by a Grant-in-Aid for Scientific Research from the Ministry of Education, Science, Sports and Culture, Japan.

## Footnotes

* E-mail: kosakada@res.titech.ac.jp

† To a toluene (8 ml) solution of [RhCl($PMe_3$)$_3$] (158 mg, 0.43 mmol) was added phenylallene (150 mg, 1.3 mmol) at room temp. The initial pale yellow solution gradually turned pale brown accompanied by deposition of an off-white solid which was collected by filtration after the reaction for 8 h, and dried *in vacuo* to give **1** (203 mg, 79%).

‡ *Crystal data*: for **1**: $C_{27}H_{43}ClP_3Rh$, $M_r$ = 598.92, orthorhombic, space group *Pbca* (no. 61), $a$ = 35.023(6), $b$ = 13.823(3), $c$ = 12.155(2) Å, $U$ = 5884 Å$^3$, $Z$ = 8, $D_c$ = 1.353 g cm$^{-3}$, $\mu$(Mo-Kα) = 8.37 cm$^{-1}$ (graphite-monochromated radiation, $\lambda$ = 0.71069 Å), $F$(000) = 2496. The data collection was made on a Rigaku AFC5R diffractometer at ambient temperature (293 K) using $\omega$ scan mode for Lorentz and polarization effects. An empirical absorption correction ($\psi$ scan) was applied. Of the unique 5877 reflections with $2\theta \leqslant 55°$, 1959 reflections with $I > 3\sigma(I)$ were used in the refinement. A total of 289 parameters (non-hydrogen atoms modelled anisotropically) were refined with $w = [\sigma(F_o)]^{-2}$. Hydrogen atoms were placed in idealised geometries and included in the structure calculation without refinement of the parameters. The structure converged to $R$ = 0.054 and $R_w$ = 0.044. For **2**: $C_{18}H_{35}ClP_3Rh$, $M_r$ = 482.75, orthorhombic, space group $P2_12_12_1$ (no. 19), $a$ = 12.926(2), $b$ = 15.979(2), $c$ = 11.307(3) Å, $U$ = 2336 Å$^3$, $Z$ = 4, $D_c$ = 1.373 g cm$^{-3}$, $\mu$(Mo-Kα) = 10.36 cm$^{-1}$ (graphite-monochromated radiation, $\lambda$ = 0.71069 Å), $F$(000) = 1000. The data collection and absorption correction were carried out similarly to **1**. Of the unique 2528 reflections with $2\theta \leqslant 55°$, 2066 reflections with $I > 3\sigma(I)$ were used in the refinement. A total of 208 parameters were refined with $w = [\sigma(F_o)]^{-2}$ and the structure converged to $R$ = 0.038 and $R_w$ = 0.029. Treatment of hydrogen atoms is similar to **1**. CCDC 182/513.

§ To a hexane (8 ml) dispersion of [RhCl($PMe_3$)$_3$] (115 mg, 0.31 mmol) was added phenylallene (44 mg, 0.38 mmol) at room temp. Stirring the mixture for 26 h led to separation of a yellow solid which was collected by filtration and dried *in vacuo*. Recrystallization from thf–hexane afforded **2** as yellow crystals (85 mg, 57%).

¶ Dissociation of $PMe_3$ from **2** is not thermodynamically favoured. The equilibrium constant for **2** = **3** + $PMe_3$ is 5.1 × 10$^{-4}$ l mol$^{-1}$ even at 60 °C and is probably much smaller near 25 °C although precise equilibrium constant was not feasible. Crystallographic results of **3** which show a square-planar coordination around the Rh center will be reported separately.

## References

1 (*a*) A. R. Fraser, P. H. Bird, S. A. Bezman, J. R. Shapley, R. White and J. A. Osborn, *J. Am. Chem. Soc.*, 1973, **95**, 597; (*b*) J. X. McDermott, M. E. Wilson and G. M. Whitesides, *J. Am. Chem. Soc.*, 1976, **98**, 6529; (*c*) R. H. Grubbs and A. Miyashita, *J. Organomet. Chem.*, 1978, **161**, 371; (*d*) S. J. McLain, C. D. Wood and R. R. Schrock, *J. Am. Chem. Soc.*, 1979, **101**, 4558; (*e*) S. A. Cohen, P. R. Auburn and J. E. Bercaw, *J. Am. Chem. Soc.*, 1983, **105**, 1136; (*f*) P. Binger, T. R. Martin, R. Benn, A. Rufinska and G. Schroth, *Z. Naturforsch. Teil B*, 1984, **39**, 993; (*g*) K. Mashima and H. Takaya, *Organometallics*, 1985, **4**, 1464.

2 (*a*) G. K. Barker, M. Green, J. A. K. Howard, J. L. Spencer and F. G. A. Stone, *J. Chem. Soc., Dalton Trans.*, 1978, 1839; (*b*) W. R. Winchester, M. Gawron, G. J. Palenik and W. M. Jones, *Organometallics*, 1985, **4**, 1894.

3 D. J. Pasto, N.-Z. Huang and C. W. Eigenbrot, *J. Am. Chem. Soc.*, 1985, **107**, 3160.

4 S. Otsuka and A. Nakamura, *J. Polym. Sci., Part B: Polym. Lett. Ed.*, 1967, **5**, 973; J. P. Scholten and H. J. van der Ploeg, *J. Polym. Sci., Polym. Chem. Ed.*, 1972, **10**, 3067; J. P. Scholten and H. J. van der Ploeg, *J. Polym. Sci., Polym. Chem. Ed.*, 1973, **11**, 3205; J. Leland, J. Boucher and K. Anderson, *J. Polym. Sci., Polym. Chem. Ed.*, 1977, **15**, 2785.

5 F. N. Jones and R. V. Lindsey, *J. Org. Chem.*, 1968, **33**, 3838; S. Otsuka, A. Nakamura and H. Minamida, *Chem. Commun.*, 1969, 191; J. P. Scholten and H. J. van der Ploeg, *Tetrahedron Lett.*, 1972, 1685.

*Received in Cambridge, UK, 17th March 1997; Com. 7/01859B*

# Uracil quartet formation through non-covalent interaction with a neutral metal ammine complex

**Holger Witkowski, Eva Freisinger and Bernhard Lippert***

*Fachbereich Chemie, Universität Dortmund, D-44221 Dortmund, Germany*

**Cocrystallization of 1-methyluracil (Hmura) and *trans*-$[PtCl_4(NH_3)_2]$ yields an adduct of composition $[PtCl_4(NH_3)_2]\cdot 2$ Hmura with two types of uracil quartets, one of which is relevant to that formed in tetraplex RNA.**

Nucleobase quartets, in particular of guanine (G), have been the subject of considerable interest.[1] More recently, the existence of uracil (U)[2] and thymine (T)[3,4] quartets in four-stranded RNA and DNA helices has been demonstrated applying NMR spectroscopy. Both $G_4$ and $T_4$ quartets require the presence of alkali- or alkaline-earth metal cations in their center for stabilization. Although probably more stable than $T_4$ quartets owing to the absence of the 5-methyl group, $U_4$ quartets appear not to have been considered intrinsically stable entities. Their formation in RNA is certainly aided by an existing $(G_4)_n$ core, with $U_4$ layered on top.

Here we report the X-ray crystal structure analysis of a 1-methyluracil (Hmura) adduct of the neutral metal complex *trans*-$[PtCl_4(NH_3)_2]$† which reveals the presence of two types of uracil quartet structures.‡ There are two crystallographically independent $Pt^{IV}$ entities, Pt(1) (on a fourfold axis) and Pt(1′) (on a *S*4 axis), the structures of which are normal (Fig. 1). Both octahedral metal complexes are sandwiched between two uracil quartets (I, II), each in such a way that the $NH_3$ groups form hydrogen bonds to four exocyclic oxygen atoms of the Hmura bases. Specifically, in quartet I N(7) and N(8) ammine protons of two Pt units form hydrogen bonds with four O(2) oxygens (Fig. 2). In quartet II N(7′) ammine protons are hydrogen bonded to four O(4) oxygens (Fig. 3). In both cases, the four oxygens form a square [dimensions 3.643(4) × 3.643(4) Å between O(2) sites in I; 3.443(5) × 3.443(5) Å between O(4) sites in II]. Distances between the ammine N atoms and these oxygens are 3.052(4) Å [N(7)–O(2)] and 3.149(5) Å [N(8)–O(2)] for I, as well as 2.948(4) and 3.047(4) Å [N(7′)–O(4)] for II. Although protons at the $NH_3$ ligands were not located, the scenario, $NH_3$ group above a square of acceptor sites, probably indicates dynamically disordered H atoms of the $NH_3$ groups.[5] Both quartets are strongly non-planar. Quartet I has roughly the shape of a cup, with O(2) atoms representing its bottom, while quartet II is saddle-shaped. Only II displays the four cyclic H bonds between N(3) and O(4) sites of adjacent nucleobases [3.059(6) Å] seen in RNA uracil quartets and therefore can be considered a model of it.[6] It is to be noted that each Hmura takes part in both types of quartets.

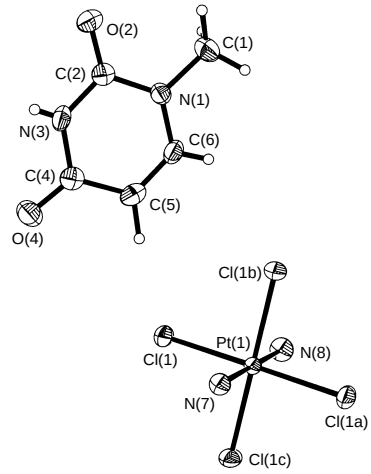



**Fig. 1** Molecular structure of the *trans*-$[PtCl_4(NH_3)_2]$ entity and of the Hmura ring. Selected bond lengths (Å) and angles (°) for the Pt complex: Pt(1)–N(7) 2.069(6), Pt(1)–N(8) 2.064(7), Pt(1)–Cl(1) 2.3137(10), N(7)–Pt(1)–N(8) 180.000(1), N(7)–Pt(1)–Cl(1) 89.85(3), N(8)–Pt(1)–Cl(1) 90.15(3). The geometry of the Hmura ring does not differ significantly from published data.[7]

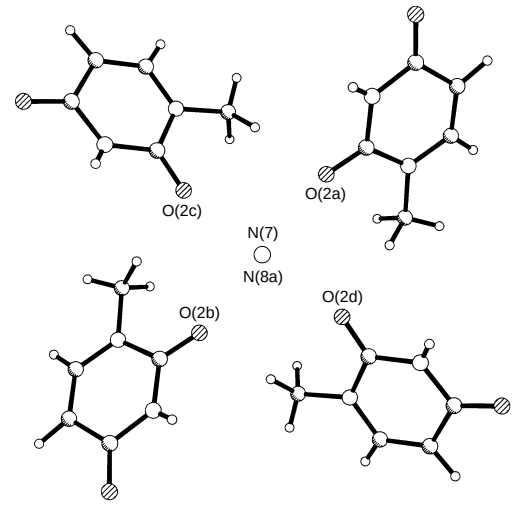



**Fig. 2** View of quartet I; N(7) and N(8) ammine groups are 1.636(7) Å above and 1.810(7) Å below the plane formed by the four O(2) oxygen atoms

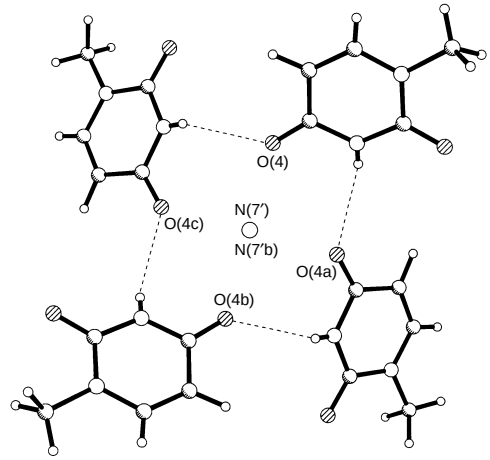



**Fig. 3** View of quartet II with cyclic N(3)H···O(4) hydrogen bonds indicated. The N(7′) ammine groups of Pt(1) are 1.751(5) Å each below and above the plane formed by the four O(4) oxygen atoms. The four uracil bases are markedly non-planar and form angles of 44° between each other.

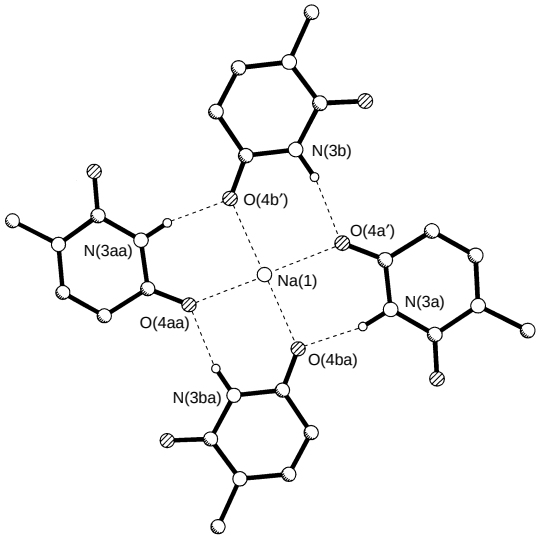



**Fig. 4** View of quartet III as found in $[Na(Hmura)_4][AuCl_4]$. The four Hmura bases are coplanar with Na(1). The protons at the N(3) sites are at calculated positions. Selected interatomic distances (Å): O(4a′)···N(3b) 2.83(2), O(4a′)···O(4b′) 3.28(2), O(4a′)···Na(1) 2.336(7), O(4b′)···Na(1) 2.301(8).

The difference in hydrogen-bond formation between Hmura [pairwise N(3)H···O(4) hydrogen bonds of 2.814(2) Å] and that observed in $[PtCl_4(NH_3)_2]\cdot 2$Hmura is also reflected in differences in the IR spectra.§

In the course of this work, it occurred to us that we had, without recognizing it then,[8] prepared a planar uracil quartet III already two years prior to the first report of $U_4$ in a RNA tetraplex.[2] In $[Na(Hmura)_4][AuCl_4]$[8] (Fig. 4) the four O(4) oxygens form a square of 3.28 Å and four hydrogen bonds, between N(3) and O(4) sites of *ca.* 2.83 Å, with $Na^+$ in the center.

In summary, the apparent ease of quartet formation of Hmura in the presence of suitable partners (Pt–$NH_3$ groups, $Na^+$) suggests that $U_4$ structures in RNA may be more readily formed than generally anticipated. Stabilization may not only be brought about by a $G_4$ support and/or alkali-metal ion binding, but also by additional hydrogen bonding. The $NH_3^+$ group of lysine, which is ubiquitous in many nucleic acid binding proteins, could be a candidate in this respect. Finally, $[PtCl_4(NH_3)_2]\cdot 2$Hmura represents, to the best of our knowledge, the first example of a neutral metal ammine complex interacting with a nucleobase in a specific manner. Hydrogen bonding of cationic metal complexes, *e.g.* of $[Co(NH_3)_6]^{3+}$ with DNA is known to have dramatic effects on the DNA stucture.[9]

We thank the Deutsche Forschungsgemeinschaft (DFG) and the Fonds der Chemischen Industrie (FCI) for financial support of this work.

## Footnotes

* E-mail: lippert@pop.uni-dortmund.de

† *trans*-$[PtCl_4(NH_3)_2]\cdot 2$Hmura was obtained in two ways: (*a*) *trans*-$[Pt(NH_3)_2$(mura-$N^3$)$_2]$ (0.65 mmol; obtained from *trans*-$[Pt(NH_3)_2(H_2O)_2][NO_3]_2$ and 2–3 equiv. of Hmura in a similar way to the *cis*-isomer)[10] was suspended in water (10 ml) at 40 °C; 4 M HCl (4 ml) was added dropwise until all the solid was dissolved. Heating was continued for 1 h and a pale yellow precipitate {*trans*-$[PtCl_2(NH_3)_2]$ identified by IR spectroscopy} was removed by filtration. Slow evaporation of the filtrate at room temp. gave crystals of *trans*-$[PtCl_4(NH_3)_2]\cdot 2$Hmura in 12% yield. Oxidation has apparently been brought about by air. Satisfactory elemental analyses were obtained for C, H and N {*trans*-$[PtCl_4(NH_3)_2]\cdot 2$Hmura, $C_{10}H_{18}Cl_4N_6O_4Pt$. Found (Calc.) C, 19.1 (19.27); H, 2.9 (2.91); N, 13.5 (13.49)%}.

(*b*) To a solution of *trans*-$[PtCl_4(NH_3)_2]$[11] (0.3 mmol) in water (10 ml) was added Hmura (0.6 mmol); the mixture was briefly heated until all solid material had dissolved. Slow evaporation at room temp. gave crystals of *trans*-$[PtCl_4(NH_3)_2]\cdot 2$Hmura (identified by IR spectroscopy) in 93% yield.

‡ *Crystal data*: $C_{10}H_{18}Cl_4O_4N_6Pt$; $M$ = 623.19, tetragonal, space group $P4/n$, $a = b$ = 15.496(2), $c$ = 7.580(2) Å, $U$ = 1820.2(6) Å$^3$, $Z$ = 4, $F(000)$ = 1192; $D_c$ = 2.274 Mg m$^{-3}$; $\mu$(Mo-K$\alpha$) = 8.326 mm$^{-1}$ yellow cube; size, 0.15 × 0.15 × 0.15 mm. Data collection and processing: Enraf-Nonius-Mach3 diffractometer (graphite-monochromated Mo-K$\alpha$ radiation), $T$ = 293(2) K; $\omega$–2$\theta$ scans; $\theta$ range 2.63–24.97°; index ranges $-13 \leqslant h \leqslant 18$, $-13 \leqslant k \leqslant 18$, $0 \leqslant l \leqslant 9$; 3280 reflections measured, 1600 independent ($R_{int}$ = 0.0259); 1356 observed [$F_o > 4\sigma(F_o)$]. Structure solution and refinement: Patterson syntheses (SHELXS-86[12]), full-matrix least squares on $F^2$ (SHELXL-93[13]); hydrogen atoms found in difference Fourier synthesis and refined isotropically, all other atoms anisotropic; 140 parameters refined; empirical absorption correction ($\psi$-scans); min., max. corrections 0.5515, 0.9972; $R_1$ = 0.0306; $wR_2$ = 0.0496 (all data); max., min. residual electron density 0.596, −0.764 e Å$^{-3}$. Atomic coordinates, bond length and angles, and thermal parameters have been deposited at the Cambridge Crystallographic Data Centre (CCDC). Any request to the CCDC for this material should quote the full literature citation and the reference number 182/505.

§ The IR spectrum of *trans*-$[PtCl_4(NH_3)_2]\cdot 2$Hmura (KBr pellet; Bruker FTIR spectrometer IFS 28) and that of Hmura[14] differ, as expected, but the former is not a simple superposition of spectra of Hmura and *trans*-$[PtCl_4(NH_3)_2]$.[15] This is particularly well seen in the 900–700 cm$^{-1}$ region, *e.g.* Hmura: 870s (br), 805s, 757s, 722m; *trans*-$[PtCl_4(NH_3)_2]$: 878m (br); *trans*-$[PtCl_4(NH_3)_2]\cdot 2$Hmura: 823s, 782s, 758m, 738w, 719m. Similarly, in the Raman spectra (solid state; Jobin Yvon, T 64000; Spectra Physics laser, $\lambda$ = 514.5 nm) both the intense $\nu$(Pt–Cl) and $\nu$(Pt–N) modes[15] of *trans*-$[PtCl_4(NH_3)_2]$ and the characteristic Hmura ring modes have undergone shifts as compared to the pure components.

## References

1 J. R. Williamson, *Annu. Rev. Biophys. Biomol. Struct.*, 1994, **23**, 703 and references therein.
2 C. Cheong and P. B. Moore, *Biochemistry*, 1992, **31**, 8406.
3 G. Gupta, A. E. Garcia, Q. Guo, M. Lu and N. R. Kallenbach, *Biochemistry*, 1993, **32**, 7098.
4 M. H. Sarma, J. Luo, K. Umemoto, R.-d. Yuan and R. H. Sarma, *J. Biomol. Struct., Dyn.*, 1992, **9**, 1131.
5 P. Scheibel, A. Hoser, W. Prandl, G. Heger, W. Paulus and P. Schweiss, *J. Phys. Condens. Mater.*, 1994, **11**, 10989; R. Essmann, G. Kreiner, A. Niemann, D. Rechenbach, A. Schmiedering, T. Sichla, U. Zachwieja and H. Jacobs, *Z. Anorg. Allg. Chem.*, 1996, **622**, 1161.
6 From a strictly geometrical point of view, I could be considered a model of a T quartet. If atoms are interchanged, *e.g.* N(1)$CH_3$ is considered a C(5)$CH_3$ group of T, O(2) a O(4) in T *etc.*, the resulting entity would correspond to $T_4$ with the methyl groups pointing to the center of the quartet and no hydrogen bonds between the four thymines; *cf.* also discussions in ref. 3.
7 W. Micklitz, B. Lippert, H. Schöllhorn and U. Thewalt, *J. Heterocycl. Chem.*, 1989, **26**, 1499.
8 B. Fischer, H. Preut, B. Lippert, H. Schöllhorn and U. Thewalt, *Polyhedron*, 1990, **9**, 2199.
9 R. V. Gessner, G. J. Quigley, A. H.-J. Wang, G. A. Van der Marel, J. H. van Boom and A. Rich, *Biochemistry*, 1985, **24**, 237.
10 D. Neugebauer and B. Lippert, *J. Am. Chem. Soc.*, 1982, **104**, 6596.
11 G. B. Kauffman and D. O. Cowan, *Inorg. Synth.*, 1963, **7**, 237.
12 G. M. Sheldrick, *Acta Crystallogr., Sect. A*, 1990, **46**, 467.
13 G. M. Sheldrick, SHELXL-93, Program for crystal structure refinement, University of Göttingen, 1993.
14 H. Susi and J. S. Ard, *Spectrochim. Acta Part A*, 1974, **30**, 1843.
15 D. W. James and M. J. Nolan, *J. Raman Spectrosc.*, 1973, **1**, 271.

*Received in Basel, Switzerland, 24th March 1997; Com. 7/02035J*

# Chiral phosphorus(III) triflates†

**Victoria A. Jones, Mark Thornton-Pett and Terence P. Kee***

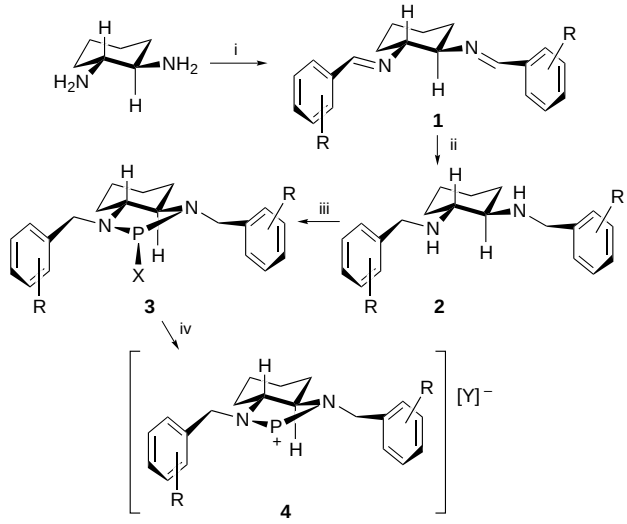
*School of Chemistry, University of Leeds, Woodhouse Lane, Leeds, UK LS2 9JT*

**A $C_2$-symmetric bicyclic diazaphospholidine framework supports a phosphorus centre within an inherently chiral environment which displays both solution- and solid-phase behaviour consistent with ambiphilic phosphenium character.**

In recent years, chemists have become increasingly interested in main-group analogues of carbenes,[1] principally those of Si,[2] Ge,[3] Sn,[4] As[5] and P.[6] Indeed of these heterocarbenes, the phosphorus analogues, $\sigma^2\lambda^3$ phosphenium cations, have received significant attention over the past 20 years and much is known of their organic and coordination chemistry.[7] However, we report here a class of phosphenium compound which possesses the significant 'added value' of chirality; an effective $\sigma^2\lambda^3$ phosphorus atom possessing both electrophilic and nucleophilic properties contained within a chiral, $C_2$-symmetric, coordination sphere; an environment which, for the first time, opens up significant possibilities in asymmetric synthesis, analysis and catalysis.[8]

The appropriate synthetic procedures are outlined in Scheme 1.[9]

Various experiments shed light upon the nature of the interaction between phosphorus and trifluoromethylsulfonate (triflate) in **4a**[OTf]. A single $^{31}$P NMR resonance is observed at $\delta$ +271.1 (0.54 mol dm$^{-3}$, 300 K, $CH_2Cl_2$), well within the range expected for two-coordinate phosphenium cations ($\delta$ 110–515)[7] along with intriguing, non-linear concentration-dependent $^{31}$P NMR behaviour at room temp.; a 24-fold increase in concentration from 0.025–0.6 M results in a $\Delta\delta$ of +5.98 ppm. We interpret such behaviour as evidence of a dynamic interaction between phosphorus and triflate oxygen(s) at room temperature leading to a more 'naked' phosphenium cation with slightly lower frequency $\delta_P$ at higher dilution. Consistently, $^{31}$P NMR chemical shifts of **4a**[OTf] (0.3 mol dm$^{-3}$, $CH_2Cl_2$), reveal a linear dependence upon temperature between 295 K ($\delta_P$ 269.2) and 203 K ($\delta_P$ 274.2) with a slope of $-5.4 \times 10^{-2}$ ppm K$^{-1}$; higher temperatures presumably favouring uncoordinated phosphenium cation as suggested by the low-frequency perturbation of $\delta_P$. This behaviour contrasts with the configurationally stable $\sigma^3\lambda^3$ phosphorus derivative **3a**-Ph which shows linear behaviour but in the opposite direction with $\Delta\delta$ of +4.2 ppm between 203 and 298 K and slope $+4.6 \times 10^{-2}$ ppm K$^{-1}$.



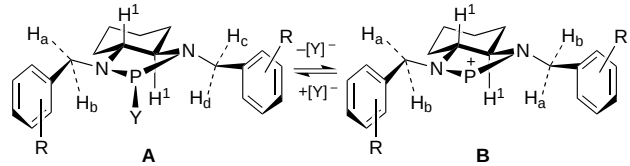

**Scheme 1** *Reagents and conditions*: i, ArCHO; Ar = functionalised phenyl (Ph **a**, 4-NMe$_2$C$_6$H$_4$ **b**, 1-C$_{10}$H$_7$ **c**, 2-C$_{10}$H$_7$ **d**, 4-MeOC$_6$H$_4$ **e**); ii, LiAlH$_4$, thf; iii, PX$_3$ (X = Cl, Br, I), NEt$_3$ (2 equiv.); iv, AlCl$_3$ or Me$_3$SiOSO$_2$CF$_3$ (TMSOTf). [Y] = [AlCl$_4$]$^-$, [OTf]$^-$

Further evidence for a dynamic interaction between phosphorus and triflate in **4a**[OTf] is revealed upon examination of the $^1$H NMR spectrum. Should **4a**[OTf] possess a static covalent or slowly exchanging configuration at phosphorus, then the methylene hydrogens on each benzyl substituent (H$_a$, H$_b$) should express themselves as two distinct [ABX] patterns (Scheme 2; **A**, X = P Y = triflate). Indeed, in the configurationally fixed derivative **3a**-Ph (Y = Ph; Scheme 2; **A**, Y = Ph), two [ABX] patterns are indeed observed centred at $\delta$ 4.31 ($^2J_{HH}$ 14.7, $^3J_{PH}$ 14.6 Hz) and 3.67 ($^2J_{HH}$ 14,9, $^3J_{PH}$ 12.7 Hz). However, between 300 and 200 K only a single [ABX] pattern is observable for the methylene hydrogens of **4a**[OTf] centred at $\delta$ 4.55 ($^2J_{HH}$ 14.5, $^3J_{PH}$ 11.3 Hz), behaviour consistent with local $C_2$ symmetry at the phosphorus atom of **4a**[OTf] caused presumably by rapid exchange of coordinated (Scheme 2, **A**) and uncoordinated triflate (Scheme 2, **B**). It is possible to perturb the interaction between phosphorus and triflate in solution *via* $^{31}$P NMR titration experiments. Thus, addition of 10 equiv. of NBu$^n_4$[OTf] to a $CH_2Cl_2$ solution of **4a**[OTf] (0.02 mol dm$^{-3}$, 300 K) results in a small perturbation to $\delta_P$ $\Delta\delta$ of +4.4 ppm.

Presumably, this perturbation reflects a dynamic process such that higher concentrations of triflate favour increased interactions with phosphorus and consequently, a shift in $\delta_P$ to high frequency.

$^{19}$F NMR and solution conductivity studies are also supportive of this conclusion. Variable-temperature $^{19}$F NMR studies on **4a**[OTf] ($CD_2Cl_2$, 203–293 K, referenced to $C_6F_6$ at $\delta$ −162.9) reveal behaviour which parallels that of ionic NBu$^n_4$[OTf] more closely than covalent Me$_3$SiOTf (Fig. 1). Me$_3$SiOTf and NBu$^n_4$[OTf] possess solution molar conductivities $\Lambda$ (thf, 296 K, 0.11 mol dm$^{-3}$) of 0.03 and 3.14 $\Omega^{-1}$ cm$^2$ mol$^{-1}$, respectively, whilst the corresponding measurements under the same conditions for **4a**[OTf] reveal a molar conductivity $\Lambda$ of 0.43 $\Omega^{-1}$ cm$^2$ mol$^{-1}$. It is clear that **4a**[OTf], although formally a weak electrolyte and less conducting than the ionic triflate NBu$^n_4$[OTf], is a stronger electrolyte than Me$_3$SiOTf by a factor of 14; consistent with significant yet dynamic solution interaction between phosphorus and trfilate in **4a**[OTf].[10]

A single-crystal X-ray study of racemic **4a**[OTf] reveals a formally two-coordinate trivalent phosphorus centre in which




**Scheme 2** Relationship between coordinated (**A**) and uncoordinated (**B**) in **4**[Y]; Y = *e.g.* [AlCl$_4$]$^-$, [O$_3$SCF$_3$]$^-$, [C$_5$H$_5$N]

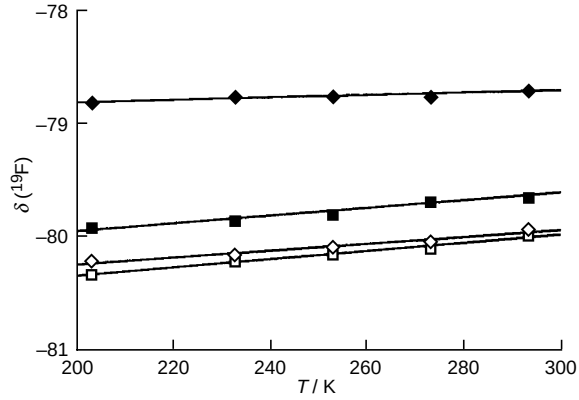



**Fig. 1** Plot of $^{19}F$ NMR chemical shifts of **4a**[OTf] (■), **4a**-Py[OTf] (◇), $NBu^n_4$[OTf] (□) and $Me_3SiO_3SCF_3$ (◆) *vs.* temperature ($CH_2Cl_2$, 0.1 mol $dm^{-3}$)

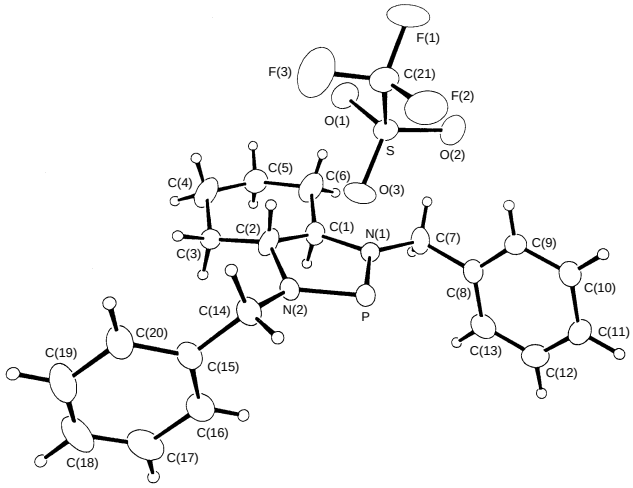



**Fig. 2** Molecular structure of **4a**[OTf] with atom numbering scheme. Selected bond lengths (Å) and angles (°): P–N(1) 1.616(3), P–N(2) 1.625(3), N(1)–C(1) 1.465(5), N(1)–C(7) 1.468(5), N(2)–C(2) 1.470(5), N(2)–C(14) 1.469(5), P–O(1) 2.841(5), P–O(3′) 2.755(5). N(1)–P–N(2) 94.9(2), C(1)–N(1)–C(7) 119.6(3), C(1)–N(1)–P 113.5(3), C(7)–N(1)–P 126.5(3), C(2)–N(2)–C(14) 121.0(3), C(2)–N(2)–P 112.8(3), C(14)–N(2)–P 121.4(3).

both nitrogen atoms possess significant $sp^2$ character as evidenced by their trigonal-planar environment, the deviations of N(1) and N(2) from the best-fit planes connecting atoms P(1)C(1)C(7) and P(1)C(2)C(14) are −0.05 and +0.19 Å, respectively [sum of angles around N(1) and N(2), 359.6 and 355.2°, respectively (Fig. 2)]. Such trigonal planarity is expected to facilitate effective delocalisation of formal positive charge on phosphorus through P–N π-bonding. Arguably the most interesting features are connected with the phosphorus–triflate interaction. P(1) has close contacts to one oxygen atom of each of two triflate groups in the crystal at distances of 2.841 and 2.755 Å; these interactions are well within the van der Waals distance for a phosphorus–oxygen interaction (*ca*. 3.35 Å) but are nevertheless > 1 Å longer than expected for a single P–O covalent bond (*ca*. 1.63 Å).[11] Furthermore, the two O–P bond vectors are directed along the axes expected for interaction with opposite lobes of a vacant phosphorus 3p orbital of a formally $\sigma^2\lambda^3$ phosphenium cation [the angles between the P–O vectors and normals to the plane N(1)P(1)N(2) are 11.5 and 10.2°]. The conclusion from the solid state is that phosphorus–triflate interactions are present although likely to be significantly weaker than for a formal P–O single covalent bond,[12] in agreement with solution data.

Ambiphilic behaviour may be demonstrated for **4a**[OTf] by its interaction with (*i*) $BH_3$·thf to afford a species with a direct P–B linkage, presumably {*N*,*N*′-[*trans*-1,2-$C_6H_{10}(NCH_2Ph)_2$]-$PBH_3$(thf)}[OTf] ($\delta_P$ 96.2, peak separationn 85 Hz resulting from $^1J_{PB}$, thf, 0.34 mol $dm^{-3}$) and (*ii*) pyridine to afford the adduct {*N*,*N*′-[*trans*-1,2-$C_6H_{10}(NCH_2Ph)_2$]P-$NC_5H_5$}[OTf] ($\delta_P$ 168.3, $CH_2Cl_2$, 0.075 mol $dm^{-3}$).[12] Variable-temperature $^{19}F$ NMR experiments on the latter reveal behaviour commensurate with ionic triflate character (Fig. 1) whilst $^1H$ NMR spectroscopy reveals that pyridine exchange is rapid on the NMR timescale at 300 K; a single [ABX] pattern being observed for the benzyl methylene hydrogens. We are currently building upon these preliminary observations to examine the potential of chiral phosphenium salts such as **4a**[OTf] in asymmetric synthesis, analysis, coordination chemistry and catalysis.

We thank the EPSRC for financial support, Albright and Wilson Ltd, for generous gifts of chemicals, Dr Mimi Hii (Dyson Perrins) for several valuable suggestions and Professeur Sylvain Juge (Cergy-Pontoise, France) for most enlightening exchanges of information.

## Footnotes

† This ChemComm is also available in enhanced multi-media format *via* the World Wide Web: http://chemistry.rsc.org/rsc/cccenha.htm. Supplementary material (including synthetic, analytical and spectroscopic details for compounds **1**–**4**) is available electronically upon e-mail request to T.P.Kee@chem.leeds.ac.uk

‡ All new compounds returned satisfactory microanalyses.

§ *Crystal structure data* for **4a**[OTf]: $C_{21}H_{24}F_3N_2PS$, $M$ = 472.45, monoclinic, space group $P2_1/a$, $a$ = 13.961(2), $b$ = 11.292(2), $c$ = 15.742(2) Å, $\beta$ = 114.846(12)°, $U$ = 2251.9(6) Å$^3$, $Z$ = 4, $D_c$ = 1.39 Mg $m^{-3}$, $F(000)$ = 984, $\mu$ = 2.399 $mm^{-1}$, $T$ = 160 K; crystal size 0.70 × 0.34 × 0.08 mm. 3472 reflections were measured at 190 K on a Stoe STADI4 4-circle diffractometer operating in the $\omega$–$\theta$ scan mode using graphite monochromated Cu-Kα radiation ($\lambda$ = 1.541 84 Å). Data were corrected for absorption empirically using azimuthal $\psi$-scans (max., min. transmission factors 0.215, 0.559, respectively). The structure was solved by direct methods[13] and was refined by full-matrix least-squares analysis on $F^2$ using all the unique data.[14] $wR = \{\Sigma[w(F_o^2 - F_c^2)^2]/\Sigma[w(F_o^2)^2]\}^{\frac{1}{2}}$ = 0.1598 for all data, conventional $R$ [on $F$ values of 3280 reflections with $F_o^2 > 2\sigma(F_o^2)$] = 0.0713, goodness of fit $S$ = 1.183 on all $F^2$ for 275 parameters. All non-hydrogen atoms were refined with anisotropic displacement parameters. All hydrogen atoms were constrained to idealised positions using a riding model. Atomic coordinates, bond lengths and angles, and thermal parameters have been deposited at the Cambridge Crystallographic Data Centre (CCDC). See Information for Authors, Issue No. 1. Any request to the CCDC for his material should quote the full literature citation and the reference number 182/483.

## References

1 W. A. Herrmann, L. J. Goossen, C. Kocher and G. R. J. Artus, *Angew. Chem., Int. Ed. Engl.*, 1997, **35**, 2805.
2 P. Blakeman, B. Gehrhus, J. C. Green, J. Heinicke, M. F. Lappert, M. Kindermann and T. Veszpremi, *J. Chem. Soc., Dalton Trans.*, 1996, 1475.
3 H. Suzuki, K. Okabe, S. Uchida, H. Watanabe and M. Goto, *J. Organomet. Chem.*, 1996, **509**, 177.
4 H. Nakazawa, Y. Yamaguchi and K. Miyoshi, *Organometallics*, 1996, **15**, 1337.
5 N. Burford, J. A. C. Clyburne, P. Losier, T. M. Parks and T. S. Cameron, *Phosphorus, Sulfur, Silicon*, 1994, **93**, 301.
6 P. Dyer, A. Baceiredo and G. Bertrand, *Inorg. Chem.*, 1996, **35**, 46.
7 See for example: A. H. Cowley and R. A. Kemp, *Chem. Rev.*, 1985, **85**, 367 and references therein.
8 *UK Pat. Appl.* 9624997.4.
9 V. A. Jones, A. Cawley, H. G. Butler, M. J. Cain, D. S. Brown, M. Thornton-Pett and T. P. Kee, manuscript in preparation.
10 O. Dahl, *Tetrahedron Lett.*, 1982, **23**, 1493.
11 J. E. Huheey, *Inorganic Chemistry. Principles of Structure and Reactivity*, Harper, New York, 3rd edn., 1983, p. A38.
12 For related structural studies see: N. Burford, P. Losier, C. MacDonald, V. Kyrimis, P. K. Bakshi and T. S. Cameron, *Inorg. Chem.*, 1994, **33**, 1434 and references therein.
13 G. M. Sheldrick, *Acta. Crystallogr., Sect. A*, 1990, **46**, 467.
14 G. M. Sheldrick, SHELXL-93, program for refinement of crystal structures, University of Gottingen, 1993.

*Received in Cambridge, UK, 9th April 1997; Com. 7/02419C*

# First example of a copper(I)–water bond. Synthesis and structure of polymeric poly-μ-2,3-diphenylquinoxaline–(aqua)copper(I) cation

**Jnan P.Naskar,[a] Sanchita Hati,[a] Dipankar Datta*[a] and Derek A. Tocher*[b]**

[a] *Department of Inorganic Chemistry, Indian Association for the Cultivation of Science, Calcutta 700 032, India*
[b] *Department of Chemistry, University College London, 20 Gordon Street, London, UK WC1H 0AJ*

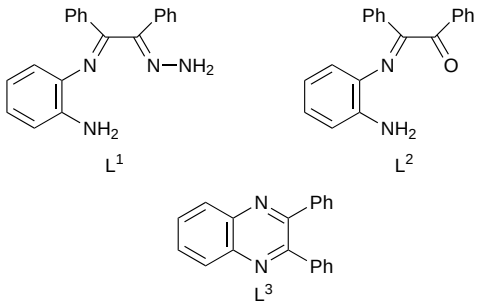
**The perchlorate salt of the poly-μ-2,3-diphenylquinoxaline(aqua)copper(I) cation containing a discrete $Cu^+$–$OH_2$ bond is synthesised and characterised structurally.**

In terms of Pearson's hard–soft classification of Lewis acids and bases, $Cu^+$ is generally accepted as 'soft' while $H_2O$ is 'hard'.[1] Consequently, according to the hard–soft acid–base (HSAB) principle of Pearson,[1–3] there is an inherent incompatibility between the $Cu^+$ ion and $H_2O$. This statement is supported by the experimental observation that the $Cu^+$ ion disproportionates in water ($\log K = 6.00$) into metallic copper and $Cu^{2+}$ [eqn. (1)].[4] Hence while water is a very common ligand in the

$$2Cu^+ \overset{K}{\rightleftharpoons} Cu^{2+} + Cu^0(s) \quad (1)$$

chemistry of the 'borderline' $Cu^{2+}$ ion, ligation of water to a copper(I) center is hitherto unknown.[5] However, the HSAB principle only considers relative stability and does not preclude the possibility of a bond between $Cu^+$ and $H_2O$ altogether. Herein for the first time we report a copper(I) complex having a discrete $Cu^+$–$OH_2$ bond.

The novel copper(I) complex has been obtained during attempts to develop the copper(II) chemistry of the Schiff base $L^1$ of 1,2-phenylenediamine (opda) and benzilmonohydrazone (bmh). When copper(II) perchlorate hexahydrate is reacted with an equimolar quantity of $L^1$, generated *in situ* in ethanol, the C=N bonds are hydrolysed giving rise to $L^2$ and free hydrazine, opda and benzil. Subsequently $L^2$ cyclises with the elimination of a water molecule resulting in formation of 2,3-diphenylquinoxaline $L^3$. Reaction of opda with benzil also yields $L^3$.[6] The hydrazine formed *in situ* reduces $Cu^{2+}$ to $Cu^+$. One of the products isolated from this reaction mixture is the perchlorate salt of the polymeric cationic copper(I) complex of $L^3$ and water, $\{[CuL^3(H_2O)]ClO_4 \cdot 0.5C_2H_5OH\}_n$ **1**. Subsequent investigation demonstrates that compound **1** is formed in good yield by reaction of copper(II) perchlorate hexahydrate with $L^3$ in the presence of excess hydrazine hydrate.†




Compound **1** is diamagnetic and orange–red [$\lambda_{max}$ (Nujol mull): 390 nm]. It is indefinitely stable in air in the solid state. However, in solution, it is almost immediately oxidised to give a faint green solution. Its structure, as revealed by X-ray crystallography,‡ consists of an infinite polymeric chain cation (Fig. 1), where adjacent copper(I) centers are bridged by the aromatic nitrogens of $L^3$, and perchlorate anions which are not coordinated to the copper. Each copper atom is coordinated through nitrogen to two molecules of $L^3$ and a water molecule completes the coordination sphere (Fig. 2). The coordination of the copper is best described as distorted linear $CuN_2$ with a weak interaction with water. Alternatively the coordination might be viewed as distorted trigonal planar. The three angles around copper vary considerably from those expected in a regular environment [N(1)–Cu(1)–N(2) 152.5(2)°, N(1)–Cu(1)–O(1) 107.6(2)°, N(2)–Cu(1)–O(1) 99.8(2)°]. There is no precedent for a $Cu^+$–$OH_2$ bond in the literature with which the Cu(1)–O(1) bond length [2.154(6) Å] observed here can be compared. However, from the bond valence sum models,[7,8] in a symmetric $CuO_3^+$ chromophore, the ideal $Cu^+$–O bond length is calculated to be 1.99 Å. Thus the Cu(1)–O(1) bond in **1** is longer than expected. On the other hand, the $Cu^+$–N bonds [Cu(1)–N(1) 1.952(4) Å, Cu(1)–N(2) 1.968(5) Å] in **1** are slightly shorter than that expected (1.98 Å) for a symmetric $CuN_3^+$ moiety.

Compound **1** provides a rare example of a copper(I) complex with a neutral oxygen donor coordinated to the metal. There are, to the best of our knowledge, only two other examples[9,10] and in these the O donor atom belongs to acetone, which is much

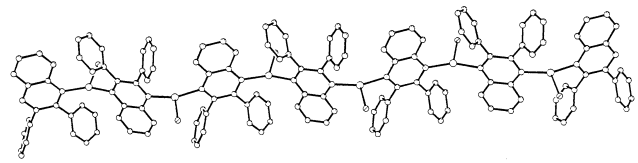


**Fig. 1** The polymeric cation in **1**; H atoms are omitted for clarity

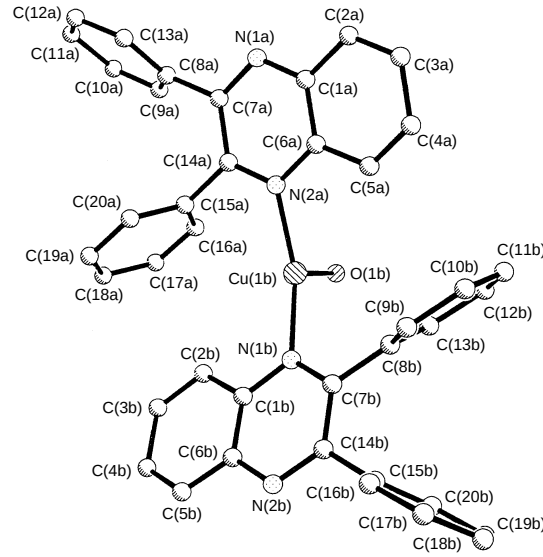



**Fig. 2** The coordination sphere of the copper(I) ion in **1**; H atoms are omitted for clarity

'softer' than water. It may be noted in passing that the $Cu^+$ ion does not disproportionate in acetone to any significant extent (log $K$ − 1.50).[4]

D. D. gratefully acknowledges the financial support received from the Department of Science and Technology, New Delhi, India.

## Footnotes

* E-mail: d.a.tocher@ucl.ac.uk

† A 5 ml ethanolic solution of 0.370 g (1 mmol) of $Cu(ClO_4)_2·6H_2O$ was added to a 20 ml ethanolic solution of 0.282 g of L[3] (1 mmol). The resulting bluish green solution was heated to boiling. To this hot solution, 0.05 ml of hydrazine hydrate (4 mmol) diluted in 5 ml of ethanol was added dropwise with constant stirring. The resulting deep orange reaction mixture was stirred for 5 min and then left in the air. (Initially a small amount of white precipitate appeared which dissolved during stirring.) After 30 min, the deep orange–red crystalline compound precipitated was filtered, washed with 2 ml of ethanol and dried *in vacuo* over fused $CaCl_2$. Yield, 0.290 g (60%). Satisfactory analytical data was obtained.

‡ *Crystal data* for $C_{21}H_{19}ClCuN_2O_{5.5}$ **1**: $M_w$ = 486.37, orthorhombic, space group $P2_12_12$, $a$ = 12.996(3), $b$ = 17.392(3), $c$ = 9.183(2) Å, $U$ = 2075.6(7) Å$^3$, $Z$ = 4, $D_c$ = 1.56 g cm$^{-3}$, $\mu$ = 1.22 mm$^{-1}$. 2685 reflections collected on an automated four-circle diffractometer (Nicolet R3mV; Mo-Kα, $\lambda$ = 0.710 73 Å, 2$\theta$ 5–55° at 20 °C) and were corrected for Lorentz and polarisation effects, and empirically for absorption. The structure was solved by Patterson methods (SHELXS-86[11]) and refined using alternating least-squares and difference-Fourier techniques (SHELXL-93,[12] refinement based on $F^2$). In the latter stages a disordered solvent molecule (ethanol) was observed to lie about the twofold axis at (1.0, 0.5, $z$). The best refinement was obtained with a net occupancy of 0.5 for this molecule. The non-hydrogen atoms (except those of the ethanol) were refined anisotropically while the hydrogens of the organic ligand were placed in idealised positions. The final cycle of least-squares refinement included 268 parameters and did not shift any parameter by more than 0.01 times its standard deviation. The final residuals were $R$ = 0.0564 and $wR_2$ = 0.1538, observed data [$I \geqslant 2\sigma(I)$] and $R$ = 0.0675 and $wR_2$ = 0.1742, for all data. The absolute structure was determined using SHELXL-93 procedures [absolute structure parameter −0.02(3)]. CCDC 182/520.

## References

1 R. G. Pearson, *Inorg. Chim. Acta*, 1995, **240**, 93 and references therein.
2 B. Douglas, D. McDaniel and J. Alexander, *Concepts and Models of Inorganic Chemistry*, 3rd edn., Wiley, New York, 1994, pp. 337–343.
3 S. Hati and D. Datta, *Proc. Indian Acad. Sci.* (*Chem. Sci.*), 1996, **108**, 143 and references therein.
4 D. Datta, *Indian J. Chem., Sect. A*, 1987, **26**, 605 and references therein.
5 B. J. Hathaway, in *Comprehensive Coordination Chemistry: The Synthesis, Reactions, Properties and Applications of Coordination Compounds*, ed. G. Wilkinson, Pergamon, Oxford, 1987, vol. 5, ch. 53.
6 A. R. Ahmed, L. K. Mehta and J. Parrick, *J. Chem. Soc., Perkin Trans. 1*, 1996, 2443.
7 S. Hati and D. Datta, *J. Chem. Soc., Dalton Trans.*, 1995, 1177.
8 J. P. Naskar, S. Hati and D. Datta, *Acta Crystallogr., Sect. B*, in press.
9 M. Munakata, S. Kitagawa and T. Emori, *J. Chem. Soc., Chem. Commun.*, 1991, 1244.
10 M. Munakata, T. Kuroda-Sowa, M. Maekawa, M. Nakamura, S. Akiyama and S. Kitagawa, *Inorg. Chem.*, 1994, **33**, 1284.
11 G. M. Sheldrick, SHELXS-86, Program for crystal structure solution, *Acta Crystallogr., Sect. A*, 1990, **46**, 467.
12 G. M. Sheldrick, SHELXL-93, University of Göttingen, 1993.

*Received in Basel, Switzerland, 17th April 1997; Com. 7/02622F*

# Tandem insertion of allenyl carbenoids and aldehydes into zirconacycles: an unexpected cyclisation

**George J. Gordon and Richard J. Whitby***

*Department of Chemistry, Southampton University, Southampton, Hants, UK SO17 1BJ*

**Allenyl carbenoids (3-chloro-1-lithioalk-1-ynes) insert into zirconacyclopentanes and zirconacyclopentenes to afford cyclic η³-allenyl/prop-2-ynyl zirconocene complexes which give allenyl, alkynyl or cyclised-alcohol products on addition of aldehydes activated with boron trifluoride–diethyl ether.**

The formation of zirconacyclo-pentanes and -pentenes by co-cyclisation of 1,*n*-dienes and 1-en-*n*-ynes, or reaction of zirconocene η²-alkene or -alkyne complexes with alkenes or alkynes comprises a useful C–C bond forming method.[1] For efficient use in organic synthesis methods for further elaboration of the carbon–zirconium bonds in these intermediates are required. Carbonylation,[2] isocyanide insertion,[3] addition of aldehydes,[4] and copper catalysed reactions[5] have been reported recently. We have described the tandem insertion of lithium chloroallylides and a variety of electrophiles into mono- and bi-cyclic zirconacyclo-pentanes and -pentenes to provide highly elaborated organic products.[6] We have also reported the insertion of prop-2-ynyl carbenoids (1-chloro-1-lithioalk-2-ynes) into zirconacycles.[7] We now describe the tandem insertion of allenyl carbenoids (3-chloro-1-lithioalk-1-ynes) and aldehydes into zirconacycles to afford a variety of alkyne, allene, and unexpected cyclised products.

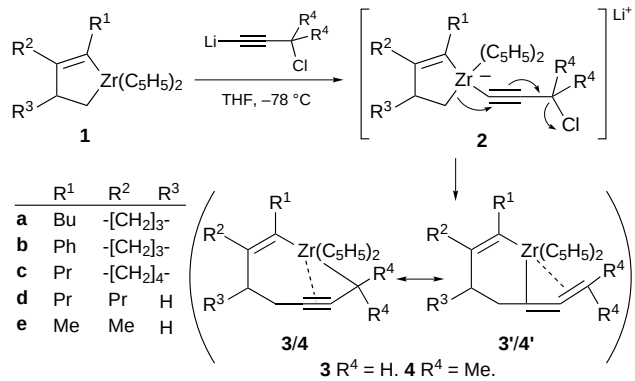
A variety of zirconacyclopentenes **1** were synthesised, either by intramolecular co-cyclisation of 1,6- or 1,7-enynes induced by zirconocene but-1-ene,[8] or by addition of alkynes to *in situ* generated zirconocene ethylene.[9] After cooling to −78 °C, dropwise addition of 3-choroprop-1-yne followed by lithium 2,2,6,6-tetramethylpiperidide generated the unstable allenyl carbenoid, 1-lithio-3-chloroprop-1-yne, which underwent insertion into the alkyl C–Zr bond of the zirconacyclopentenes **1**, presumably *via* an 18 electron zirconate intermediate **2**, to afford the ring expanded products **3a–e** (Scheme 1). In the same way insertion of 1-lithio-3-chloro-3-methylbut-1-yne gave the zirconacycles **4a** and **4e**. The bonding in the zirconocene η³-prop-2-ynyl/allenyl complexes **3** and **4** may be described in terms of the two contributing resonance structures **3**/**4** and **3′**/**4′** (Scheme 1).[7,10] Relative contributions of the two structures vary. The $^{13}C$ NMR shifts of the prop-2-ynyl/allenyl components of **3a** ($\delta_C$ = 103.3, 104.3 and 46.8) and **4a** ($\delta_C$ = 127.9, 176.6 and 87.3) demonstrate the much greater contribution of the allenyl form when $R^4$ = Me. η³-Prop-2-ynyl/allenyl complexes of transition metals are rare, and have recently been reviewed.[11]

Protonation of **3a**,**b**, and **e** required several hours stirring with excess methanol and gave a mixture of terminal allene **5** and internal alkyne **6** products,† favouring the later (Scheme 1). Protonation of **4a** was fast, and gave exclusively the allene **7**.

Reaction of the η³-prop-2-ynyl complexes **3** and **4** with aldehydes activated with boron trifluoride–diethyl ether was examined. For example **3a** gave an excellent overall yield (based on the starting enyne) of the allenol **8a** ($R^5$ = Pr) when reacted with butyraldehyde (Scheme 2). The regiochemistry of addition to the η³-moiety is the opposite of that observed in the elaboration of analogous η³-allyl complexes.[6] Much to our surprise reaction of **3a** with benzaldehyde gave a quite different product which proved to be the cyclised dienol alcohol **9a** ($R^5$ = Ph). Generally, reaction of complexes **3** with alkyl aldehydes gave only the allene product **8**, whereas benzaldehyde gave either the dienol **9**, or a mixture of **8** and **9** (Table 1). The *gem*-dimethyl substituted complexes **4a** and **4e** gave only the dienols **10** with either aliphatic, or aromatic aldehydes (Table 1).

In addition to extensive NMR studies (including H–H and C–H COSY) on most of the allenol and dienol products, the structure of **9d** ($R^5$ = Ph) was further proven through degradation. Ozonolysis followed by dimethyl sulfide work-up gave undeca-4,5,8-trione and 3-phenyl-3-hydroxypropanal. The stereochemistry of the exocyclic alkene in **10e** ($R^5$ = Ph) was proven by NOE studies, in particular a 9.6% enhancement between the vinylic methyl group and the adjacent vinylic hydrogen. All the dienol products were formed as single isomers.

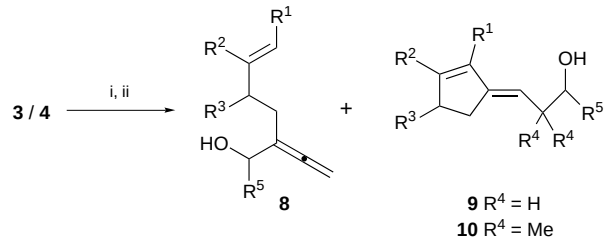
A likely mechanism for the cyclisation to afford the dienol products **9** and **10** is given in Scheme 3. Addition of the boron trifluoride complex of the aldehyde to the terminus of the prop-2-ynyl system generates both an alkyne, and a cationic




| | $R^1$ | $R^2$ | $R^3$ |
|---|---|---|---|
| **a** | Bu | -$[CH_2]_3$- | |
| **b** | Ph | -$[CH_2]_3$- | |
| **c** | Pr | -$[CH_2]_4$- | |
| **d** | Pr | Pr | H |
| **e** | Me | Me | H |

| Protonation of **3** / **4** | | | |
|---|---|---|---|
| | **5** : **6**[a] | Yield (%) | |
| **3a** | 1 : 1.5 | 70 | |
| **4a** | **7** only | 65 | |
| **3b** | 1 : 1.8 | 88 | |
| **3d** | 1 : 1.4 | 87 | |

**Scheme 1** Ratios determined from $^1H$ NMR of the crude products



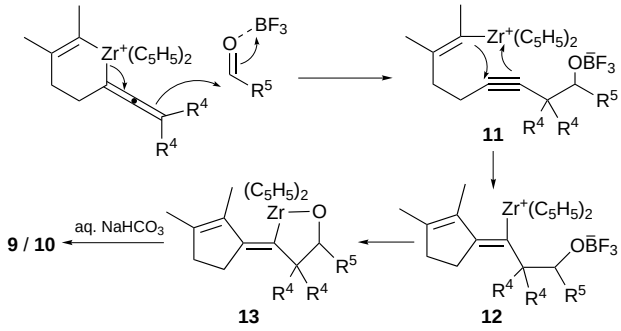

**Scheme 2** *Reagents and conditions*: i, $R^5CHO$, $BF_3{\cdot}Et_2O$, −78 °C to room temp., 2 h; ii, aq. $NaHCO_3$, room temp., 16 h

zirconium species. Intramolecular insertion of the pendant alkyne into the carbon–cationic zirconocene bond in **11** to give **12** has some precedent.[12] The final step, formation of the oxazirconacycle **13** (which is likely to be relatively stable towards hydrolysis), is speculation, but may explain why work-up with $D_2O$ or MeOD fails to give deuterated product (DCl causes decomposition).

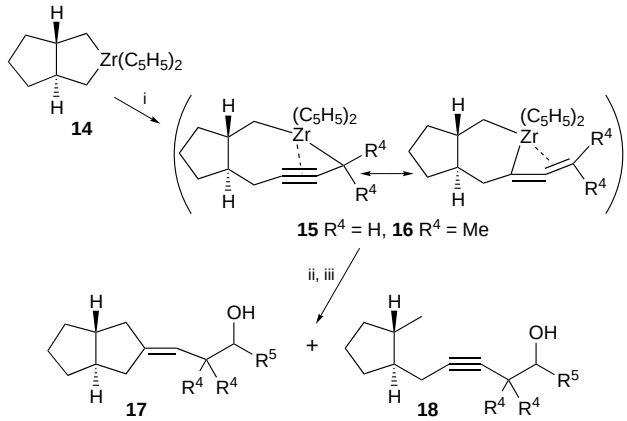
**Table 1.** Results of $R^5CHO/BF_3{\cdot}Et_2O$ addition to **3/4**

| Substrate | $R^5$ | Product | Yield (%)[a] |
|---|---|---|---|
| **3a** | Pr | **8** | 83 |
| **3a** | Ph | **9** | 51[c] |
| **3a** | Bu$^i$ | **8** | 74 |
| **4a** | Ph | **10** | 61 |
| **4a** | Bu$^i$ | **10** | 74 |
| **3c** | Ph | **8** : **9** :: 2.4 : 1.0[b] | 61 |
| **3d** | Ph | **8** : **9** :: 1.0 : 5.0[b] | 71 |
| **3d** | Pr | **8** | 76 |
| **3e** | Pr | **8** | 84 |
| **4e** | Ph | **10** | 68 |

[a] Of **8** + **9**, or **10** based on enyne for **a** and **c**, and $(C_5H_5)_2ZrCl_2$ for **d** and **e**. 1.5 equiv. of aldehyde/$BF_3{\cdot}Et_2O$ used with aromatic aldehydes, 3.0 equiv. with aliphatic. [b] Determined from $^1$H NMR of crude product. [c] Unstable to chromatography.




**Scheme 3** Possible mechanism for dienol formation




**Scheme 4** *Reagents and conditions*: i, $R^4{}_2ClCC{\equiv}CH$, LiTMP, −78 °C, THF; ii, $R^5CHO$, $BF_3{\cdot}Et_2O$, −78 °C to room temp.; iii, aq. $NaHCO_3$

**Table 2.** Aldehyde addition to **15** and **16**

| Substrate | $R^4$ | $R^5$ | Products | Yield (%)[a] | **17** : **18** |
|---|---|---|---|---|---|
| **15** | H | Bu$^i$ | **17a/18a** | 23 | 1 : 1.3 |
| **15** | H | Ph | **18b** | 75 | 0 : 1 |
| **16** | Me | Bu$^i$ | **17c/18c** | 72 | 1 : 1.3 |
| **16** | Me | Ph | **17d/18d** | 81 | 1[b] : 10.6 |

[a] Combined yield of pure **17** + **18** before separation. [b] Not isolated pure.

Application of the tandem insertion of 1-lithio-3-chloroalk-1-ynes and aldehydes to zirconacyclopentane systems highlighted further reactivity and product selectivity variations. Co-cyclisation of hepta-1,6-diene using zirconocene but-1-ene gave the zirconacycle **14**. Insertion of 1-lithio-3-chloroprop-1-yne or 1-lithio-3-chloro-3-methylbut-1-yne afforded the ring expanded zirconacycles **15** and **16** respectively (Scheme 4). Addition of aldehydes activated with boron trifluoride–diethyl ether gave the bicyclic enol products **17** and/or the alkynols **18** (Table 2). Both products arise from insertion at the terminus of the prop-2-ynyl system in marked contrast to the results from unsaturated zirconacycles (Table 1). The structure of **17c** was proven by ozonolysis to give bicyclo[3.3.0]octan-3-one and 2,2,5-trimethyl-3-hydroxyhexanal, each prepared by independent synthesis.

In summary, we have shown that the insertion of 1-lithio-3-chloroalk-1-ynes (allenyl carbenoids) into zirconacyclopentenes and pentanes affords unusual cyclic $\eta^3$-prop-2-ynyl/allenyl complexes. Further elaboration by the addition of boron trifluoride activated aldehydes gives a variety of products, some of which result from intramolecular insertion into a proposed intermediate cationic zirconocene.

We thank the EPSRC for a quota award. R. J. W. thanks Pfizer UK and Zeneca for generous uncommitted financial support.

## Footnotes

* E-mail: RJW1@soton.ac.uk

† All organic compounds were characterised ($^1$H and $^{13}$C NMR, IR, MS and HRMS) as pure compounds with the exception of **17a** which decomposed during seperation from **18a**. The compounds **18a**, **c** and **d** were seperated *via* their $Co_2(CO)_6$ adducts.

## References

1 E.-I. Negishi and T. Takahashi, *Acc. Chem. Res.*, 1994, **27**, 124; R. D. Broene and S. L. Buchwald, *Science*, 1993, **261**, 1696; E. Negishi, in *Comprehensive Organic Synthesis*, ed. B. M. Trost and I. Fleming, Pergamon Press, Oxford, 1991, vol. 5, p. 1163; S. L. Buchwald and R. D. Broene, in *Comprehensive Organometallic Chemistry II*, ed. E. W. Abel, F. G. A. Stone and G. Wilkinson, Pergamon, Oxford, UK, 1995, Vol. 12; p. 771 and R. D. Broene, p. 323.

2 D. Swanson, C. Rousset, E. Negishi, T. Takahashi, T. Seki, M. Saburi and Y. Uchida, *J. Org. Chem.*, 1989, **54**, 3521; E. Negishi, S. J. Holmes, J. M. Tour, J. A. Miller, F. E. Cederbaum, D. R. Swanson and T. Takahashi, *J. Am. Chem. Soc.*, 1989, **111**, 3336.

3 J. M. Davis, R. J. Whitby and A. Jaxa-Chamiec, *Tetrahedron Lett.*, 1992, **33**, 5655; G. D. Probert, R. J. Whitby and S. J. Coote, *Tetrahedron Lett.*, 1995, **36**, 4113; K. Aoyagi, K. Kasai, D. Y. Kondakov, R. Hara, N. Suzuki and T. Takahashi, *Inorg. Chim. Acta*, 1994, **220**, 319.

4 C. Coperet, E. I. Negishi, Z. F. Xi and T. Takahashi, *Tetrahedron Lett.*, 1994, **35**, 695.

5 T. Takahashi, M. Kotora and Z. F. Xi, *J. Chem. Soc., Chem. Commun.*, 1995, 1503; T. Takahashi, R. Hara, Y. Nishihara and M. Kotora, *J. Am. Chem. Soc.*, 1996, **118**, 5154; K. Kasai, M. Kotora, N. Suzuki and T. Takahashi, *J. Chem. Soc., Chem. Commun.*, 1995, 109; B. H. Lipshutz and M. Segi, *Tetrahedron*, 1995, **51**, 4407.

6 T. Luker and R. J. Whitby, *Tetrahedron Lett.*, 1994, **35**, 785, 9465; 1995, **36**, 4109; G. J. Gordon and R. J. Whitby, *Synlett*, 1995, 77.

7 G. J. Gordon and R. J. Whitby, *Chem. Commun.*, 1997, 1045.

8 E. Negishi, F. E. Cederbaum and T. Takahashi, *Tetrahedron Lett.*, 1986, **27**, 2829.

9 T. Takahashi, M. Kageyama, V. Denisov, R. Hara and E. Negishi, *Tetrahedron Lett.*, 1993, **34**, 687.

10 P. W. Blosser, J. C. Gallucci and A. Wojcicki, *J. Am. Chem. Soc.*, 1993, **115**, 2994.

11 A. Wojcicki, *New J. Chem.*, 1994, **18**, 61.

12 J. A. Miller and E. Negishi, *Israel J. Chem.*, 1984, **24**, 76; A. E. Harms and J. R. Stille, *Tetrahedron Lett.*, 1992, **33**, 6565; K. H. Shaughnessy and R. M. Waymouth, *J. Am. Chem. Soc.*, 1995, **117**, 5873.

*Received in Cambridge, UK, 22nd April 1997; Com. 7/02732J*

# Generation of an equilibrating collection of circular inorganic copper(I) architectures and solid-state stabilisation of the dicopper helicate component

**P. N. W. Baxter,[a] J.-M. Lehn*[a] and K. Rissanen[b]**

[a] *Laboratoire de Chimie Supramoléculaire, (CNRS-URA 422) Institut Le Bel, Université Louis Pasteur, 4 rue Blaise Pascal, 67000, Strasbourg, France*

[b] *Department of Chemistry, University of Jyväskylä, Jyväskylä, Finland*

**$Cu^{I}$ ions and ligand L self-assemble to generate in solution a mixture of the double helical 1, triangular 2 and square grid 3 complexes, from which 1 has been crystallized and its crystal structure determined.**

Within the field of supramolecular inorganic chemistry, self-assembly provides direct access to complex architectures comprising spatially and geometrically well defined arrays of metal ions.[1,2] Widely diverse morphologies have been obtained, such as helicates,[1,2c] pseudorotaxane racks,[3] ladders,[4] grids,[5] rings[6] and cages.[7] In order to design species presenting specific structural and functional features, it is of great importance to establish the rules by which control of the self-assembly process can be achieved through chemical programming by means of suitable components and assembling algorithms. Mixtures of ligands and metal ions that combine preferentially into one out of a range of possible self-assembled species provide an opportunity for studying how ligand design and choice of metal ion can influence the product distribution and thus the self-assembly pathway.[6,8]

On the other hand, mixtures of ligands and metal ions may yield mixtures of complexes resulting from the reversible combination of the different constituents. Such a situation represents a process of dynamic combinatorial chemistry (DCC) of inorganic supramolecular type, making potentially available a wide variety of combinations representing the members of a virtual combinatorial library (VCL).[6a,b,9] Of special interest is then the possibility to select and express a given member of the VCL for specific purposes, for instance by means of external factors. In the inorganic domain, such behaviour has been observed in the assembly of circular helicates.[6a,b]

We present here a case where a mixture of a ligand and of metal ions yields in solution a collection of self-assembled species, from which a single product can be isolated in the solid state by appropriate adjustment of the conditions.

When nitromethane was added to a 1 : 1 mixture of ligand L† and $[Cu(MeCN)_4]PF_6$ and the mixture stirred at ambient temperature under argon for 24 h, a dark brown–orange colour rapidly developed indicative of the coordination of $Cu^{I}$ to L. Removal of solvent under vacuum yielded a dark brown solid which upon analysis by electrospray mass spectrometry showed clearly the formation of the oligomeric complexes $[Cu_nL_n]^{n+}$ ($n$ = 2, 3, 4) as the dominant species present at $1 \times 10^{-4}$ mol $dm^{-3}$ in $CH_2Cl_2$.‡ The $^1H$ NMR spectrum of the product in $CD_2Cl_2$ consisted of a complicated pattern of sharp peaks characteristic of an equilibrium mixture of slowly exchanging species. Detailed analysis of the data ($^1H$–$^1H$ COSY measurements) indicated the presence of three major species in proportions roughly equal to 6 : 4 : 3 for **1**, **2** and **3**, respectively. In addition a minor compound was also present (*ca.* 5%); the relative amounts appeared to be insensitive to changes in concentration. In $CD_3NO_2$ solution, the spectrum simplified to give nine broad bands corresponding to ligand L in a single chemical environment and indicative of medium-fast exchange between different copper(I) containing entities. In $CD_3CN$ solution, the peaks sharpened indicating rapid equilibration of the species on the NMR timescale.

When a nitromethane solution of the above reaction mixture was layered with benzene and left to stand, all the material present crystallised as large dark brown blocks. A crystal structure determination§ showed that the product was the binuclear complex **1** composed of two ligands L wrapped in a helical arrangement around two $Cu^{I}$ ions separated by 7.579 Å (Fig. 1). Both ligands are seen to be curved when viewed perpendicular to their mean planes and have therefore to adopt a strained conformation in order to coordinate both $Cu^{I}$ ions. There are four intramolecular stacking interactions (within 3.5 Å) between each phenyl ring and a terminal pyridine ring of the partner ligand. The coordination polyhedron about each $Cu^{I}$ ion is highly distorted and intermediate between tetrahedral and square-planar geometries, with Cu–N bond lengths of 2.017(9)–2.132(9) Å and N–Cu–N angles of 75.9(4)–78.8(4)° (chelate ring) and 110.9(4)–144.6(4)° (interligand). In addition, the crystals were found to be homochiral, so that the complex has undergone spontaneous resolution upon crystallisation.

Redissolution of the crystals in $CD_2Cl_2$ results in instant regeneration of a $^1H$ NMR spectrum identical to that of the crude reaction mixture prior to crystal growth as described above, showing that complex **1** rapidly opens in solution to form an equilibrium mixture of products. The proportions of each species and the preferential crystallisation of only **1** result from an interplay of enthalpic, entropic and crystal packing factors.

On the basis of the structure of **1** as well as of the spectrometric data, the other two substances present in solution may be considered to be the triangular complex **2** and the square [2 × 2] grid type structure **3** (Scheme 1).

In conclusion, a 1 : 1 combination of L with $Cu^{I}$ generates in solution an equilibrating mixture of the self-assembled inorganic architectures **1**, **2** and **3**, which converts into the single species **1** in the solid state upon crystallisation. These features represent an attractive illustration of a dynamic combinatorial chemistry process, yielding an inorganic supramolecular library of complexes from which a single member may be trapped by crystallisation. The latter result is also of interest with respect to

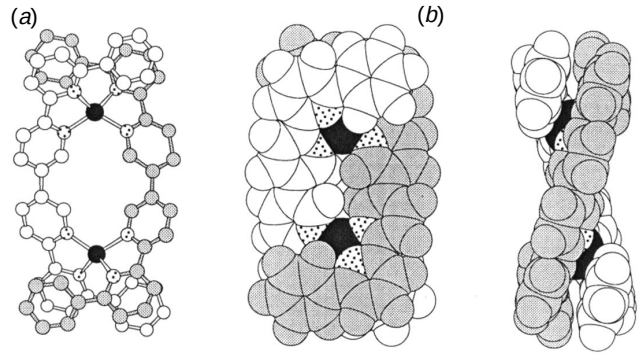
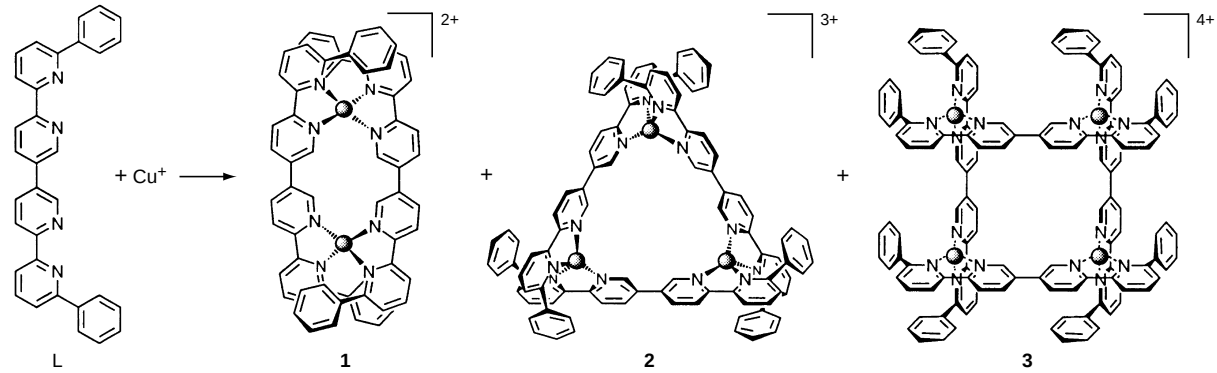



**Fig. 1** Crystal structure of the double-helical complex **1**; (*a*) ball-and-stick, (*b*) space-filling representations




**Scheme 1** Self-assembly of an equilibrating mixture of the double-helical **1**, triangular **2** and square [2 × 2] grid **3** complexes from L and $Cu^{I}$. Complexes **2** and **3** can in principle exist in different interwoven structures; only one structure is shown here.

crystal engineering and the investigation of the factors that dictate solid state selection processes.

We thank Annick Dupont-Gervais, Emmanuelle Leize and Alain Van Dorsselaer for the electrospray mass spectrometric measurements.

## Footnotes

* E-mail: lehn@chimie.u.strasbg.fr

† Ligand L was prepared following the same synthetic route as the analog bearing methyl groups in place of the phenyl groups.[5b]

‡ ESMS ($10^{-4}$ mol $dm^{-3}$ $CH_2Cl_2$) *m/z* (rel. intensity %); 1868 (2) $\{[Cu_3L_3](PF_6)_2\}^+$, 1196.8 (5) $\{[Cu_2L_2]PF_6\}^+$, $\{[Cu_4L_4](PF_6)_2\}^{2+}$, 861.5 (82) $\{[Cu_3L_3]PF_6\}^{2+}$, 749.8 (12) $\{[Cu_4L_4]PF_6\}^{3+}$, 526.2 (100) $[Cu_2L_2]^{2+}$, $[Cu_3L_3]^{3+}$, $[Cu_4L_4]^{4+}$. Very weak peaks are also present, which could correspond to the minor species observed in the NMR spectrum. Microanal. Calc. for $C_{32}H_{22}CuF_6N_4P$, $\{CuLPF_6\}$: C, 57.27; H, 3.30; N 8.35. Found C, 57.32; H 3.29; N 8.57%.

§ *Crystal data* for **1**: $C_{64}H_{44}Cu_2F_{12}N_8P_2{\cdot}2C_3H_6O{\cdot}C_6H_6$, $M_r$ = 1536.36, monoclinic, space group *Cc*, *a* = 30.374(1), *b* = 8.092(1), *c* = 34.132(3) Å, $\beta$ = 123.15(1)°, *U* = 7023(1) Å$^3$, *Z* = 4, $D_c$ = 1.453 Mg $m^{-3}$, *F*(000) = 3144, *T* = 293 ± 1 K, crystal dimensions 0.3 × 0.4 × 0.4 mm, dark red–brown, 4703 collected reflections, of which 4226 unique ($R_{int}$ = 0.027) were recorded on an Enraf-Nonius CAD4 diffractometer using graphite monochromatised Mo-K$\alpha$ radiation ($\lambda$ = 0.7017 Å) and $\omega$–2$\theta$ scan mode (scan width ° 0.65 × 0.35 tan$\theta$) to 2$\theta$ = 45° (*h* 0 → 32, *k* 0 → 8 and *l* −36 → 36). $L_p$ correction, absorption correction based on $\psi$-scans was applied [max., min. abs. corr. 1.44 and 1.16, respectively, $\mu$(Mo-K$\alpha$) = 0.737 $mm^{-1}$]. The structure was solved by direct methods (SHELXS)[10] and subjected to full-matrix least-squares refinement (SHELXL)[11] on $F_o^2$. All non-H atoms were refined anisotropically. The H-atoms were calculated in idealised positions and refined as riding atoms with fixed isotropic temperature factors. Eight geometrical restraints were used to keep feasible geometry for the solvent molecules. Final *R* indices: [$I > 2\sigma(I)$] $R_1$ = 0.0537, $wR_2$ = 0.1386; (all data) $R_1$ = 0.0711, $wR_2$ = 0.1518 for 907 parameters. Owing to the acentric space group a Flack's absolute structure parameter was refined to 0.03(2). Goodness-of-fit on $F_o^2$ = 1.099. Convergence max. shift/error < 0.01, largest diff. peak and hole 0.539 and −0.352 e Å$^{-3}$. Atomic coordinates, bond lengths, and thermal parameters have been deposited at the Cambridge Crystallographic Data Centre (CCDC). See Information for Authors, Issue No. 1. Any request to the CCDC for this material should quote the full literature citation and the reference number 182/501.

## References

1 J.-M. Lehn, *Supramolecular Chemistry: Concepts and Perspectives*, VCH, Weinheim, 1995.
2 *Comprehensive Supramolecular Chemistry*, ed. J. L. Atwood, J. E. D. Davies, D. D. MacNicol, F. Vögtle and J.-M. Lehn, Pergamon, Oxford, 1996; (*a*) P. N. W. Baxter, vol. 9, ch. 5, pp. 165–211; (*b*) M. Fujita, vol. 9, ch. 7, pp. 253–282; (*c*) E. C. Constable, vol. 9, ch. 6, pp 213–252.
3 H. Sleiman, P. N. W. Baxter, J.-M. Lehn and K. Rissanen, *J. Chem. Soc., Chem. Commun.*, 1995, 715.
4 P. N. W. Baxter, G. S. Hanan and J.-M. Lehn, *Chem. Commun.*, 1996, 2019.
5 (*a*) M.-T. Youinou, N. Rahmouni, J. Fischer and J. A. Osborn, *Angew. Chem., Int. Ed. Engl.*, 1992, **31**, 733; (*b*) P. N. W. Baxter, J.-M. Lehn, J. Fischer and M.-T. Youinou, *Angew. Chem., Int. Ed. Engl.*, 1994, **33**, 2284.
6 (*a*) B. Hasenknopf, J.-M. Lehn, B. O. Kneisel, G. Baum and D. Fenske, *Angew. Chem., Int. Ed. Engl.*, 1996, **35**, 1838; (*b*) B. Hasenknopf, J.-M. Lehn, N. Boumediene, A. Dupont-Gervais, A. Van Dorsselaer, B. Kneisel and D. Fenske, to be published; (*c*) D. P. Funeriu, J.-M. Lehn, G. Baum and D. Fenske, *Chem. Eur. J.*, 1997, **3**, 99.
7 P. N. W. Baxter, J.-M. Lehn, A. De Cian and J. Fischer, *Angew. Chem., Int. Ed. Engl.*, 1993, **32**, 69.
8 M. Fujita, O. Sasaki, T. Mitsuhashi, T. Fujita, J. Yazaki, K. Yamaguchi and K. Ogura, *Chem. Commun.*, 1996, 1535; F. M. Romero, R. Ziessel, A. Dupont-Gervais and A. Van Dorsselaer, *Chem. Commun.*, 1996, 551.
9 I. Huc and J.-M. Lehn, *Proc. Natl. Acad. Sci. USA*, 1997, **94**, 2106.
10 G. M. Sheldrick, SHELXS86, in *Crystallographic Computing 3*, ed. G. M. Sheldrick, C. Kruger and R. Goddard, Oxford University Press, 1993, pp. 175–189.
11 G. M. Sheldrick, SHELXL93, Program for crystal structure refinement, University of Göttingen, 1993.

*Received in Cambridge, UK, 6th May 1997; Com. 7/03083E*

# Synthesis of μ-oxo-bridged group 15 element–aluminium heterodinuclear porphyrins [(oep)(Me)M–O–Al(oep)]$ClO_4$ (M = P, As, Sb) and X-ray crystal structure of [(oep)(Me)As–O–Al(oep)]$ClO_4$

**Go Yamamoto, Ryo Nadano, Wataru Satoh, Yohsuke Yamamoto* and Kin-ya Akiba***

*Department of Chemistry, Faculty of Science, Hiroshima University, 1-3-1 Kagamiyama, Higashi-Hiroshima, 739, Japan*

**μ-Oxo-bridged group 15 element–aluminium heterodinuclear porphyrins, [(oep)(Me)M–O–Al(oep)]$ClO_4$ (M = P, As, Sb), are synthesized by the reaction of [(oep)(Me)M(OH)]-$ClO_4$ with (oep)AlMe.**

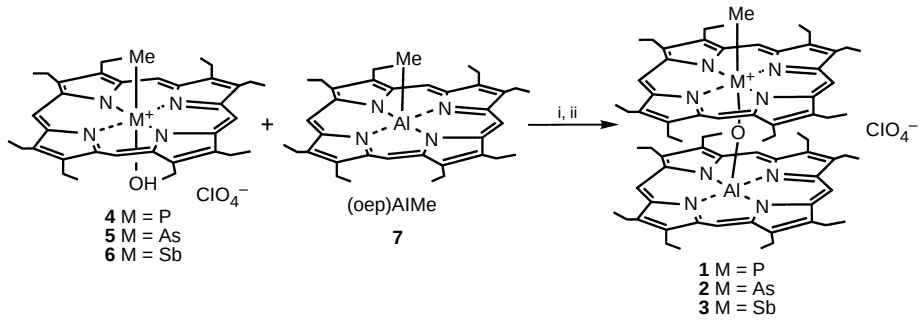
μ-Oxo-bridged dinuclear porphyrins bearing a transition metal such as Fe, Ru, Mn, V, or Ti have been investigated extensively because of their relation to biological systems.[1,2] Recently, a μ-oxo-bridged dinuclear porphyrin skeleton containing boronic acids has been reported to be useful for molecular recognition of saccharides.[3] However, only a few synthetic methods are available for the synthesis of μ-oxo-bridged dinuclear transition-metal porphyrins, and μ-oxo-bridged dinuclear porphyrins bearing main-group elements have not been reported. Here we report a new synthetic route to μ-oxo-bridged group 15 element–aluminium heterodinuclear porphyrins, [(oep)(Me)M–O–Al(oep)]$ClO_4$ (M = P **1**, As **2**, Sb **3**), and the X-ray crystallographic structure of **2**.

Recently we reported that the hydroxy protons of [(oep)(R)-P(OH)]$^+X^-$ were relatively acidic and easily removed by treatment with DBU to generate (oep)(R)P=O which were stable, and the double bond character of the P=O bond was confirmed by an X-ray analysis of (oep)(Et)P=O. In fact, the p$K_a$ value of [(oep)(Et)P(OH)]$^+X^-$ was determined to be *ca.* 7–8 in water.[4] The corresponding arsenic porphyrins also showed similar behavior in acid–base treatment[5] although the corresponding antimony porphyrins did not show the formation of such double-bonded compounds.[6] Since aluminium porphyrins bearing an alkyl group are known to be reactive towards alcohols and phenols bearing acidic protons,[7] it was of interest to examine whether the acidic hydroxy groups in [(oep)(R)-M(OH)]$^+X^-$ (M = P, As) were reactive toward (oep)AlMe in spite of the anticipated steric hindrance.

To our delight the reaction of [(oep)(Me)P(OH)]$ClO_4$ **4** with (oep)AlMe **7** proceeded smoothly under reflux in dichloromethane for 1.5 days, and the expected μ-oxo-bridged P/Al heterodinuclear porphyrin **1** was isolated in 62% yield (Scheme 1). The compound was stable to atmospheric moisture and chromatographic treatment [neutral $Al_2O_3$, benzene–$CH_2Cl_2$–MeOH (15 : 6 : 1)] and characterization was carried out by elemental analysis and NMR spectroscopy.† The reaction of the corresponding arsenic porphyrin **5** with **7** proceeded slowly and **2** was obtained in 49% yield after 4 days in refluxing dichloromethane. The difference of the reactivity between **4** and **5** can be related to the acidity of the hydroxy group in **4** and **5**, **4** being more acidic than **5** since the methyl protons of **4** shifted upfield faster than those of **5** upon addition of DBU (in portions) to a mixture of **4** and **5** in $CDCl_3$. As expected, the reaction of the least acidic antimony porphyrin [(oep)(Me)-Sb(OH)]$ClO_4$ **6** with **7** was very sluggish and only 7% of **3** was obtained after 2 weeks in refluxing 1,2-dichloroethane. $^1$H NMR of the μ-oxo-bridged heterodinuclear porphyrin [(oep)-(Me)M–O–Al(oep)]$ClO_4$ showed characteristic methyl signals at very high fields ($\delta$ −7.96 in **1**, −7.94 in **2**, −7.92 in **3**) which were even higher than those of the starting [(oep)(Me)M-(OH)]$ClO_4$ ($\delta$ −5.79 in **4**, −5.63 in **5**, −6.13 in **6**) probably due to the ring current effect of the aluminium porphyrin nucleus.

Crystals of **2** suitable for X-ray analysis were obtained by recrystallization from dichloromethane–dibutyl ether. X-Ray structural analysis‡ of the compound was carried out on the basis of the centrosymmetric *C*2/*c* group, showing the required twofold axis passed through the C–As–O–Al bond. Fig. 1 shows an ORTEP drawing of a single molecule of **2** (solvent dichloromethane omitted for clarity). Since the As, O and Al atoms lie on the crystallographic twofold axis the As–O–Al bond is explicitly linear. The average torsional angle between N(1)–As–Al–N(3) and N(2)–As–Al–N(4) is 15.3°, the structure of **2** can be represented in terms of a near-eclipsed conformation.[2] The interplanar distance between the mean planes of the porphinato cores is 3.71 Å.

It is interesting that the As–O [1.690(3) Å] and Al–O [1.731(3) Å] bond distances in **2** are shorter than the As–O distance [1.826(6) Å] in **5**,[5] and the reported Al–O distance [1.789(3) Å] in [(diporphyrin biphenylene)CoAl(OEt)],[8] respectively. Similar shortening has been considered to be due to sp hybridization of the oxo oxygen and $d_\pi$(M)–$p_\pi$(O)–$d_\pi$(M)




**Scheme 1** *Reagents and Conditions:* i, see text; ii, $NaClO_4$, $CH_2Cl_2$, MeCN

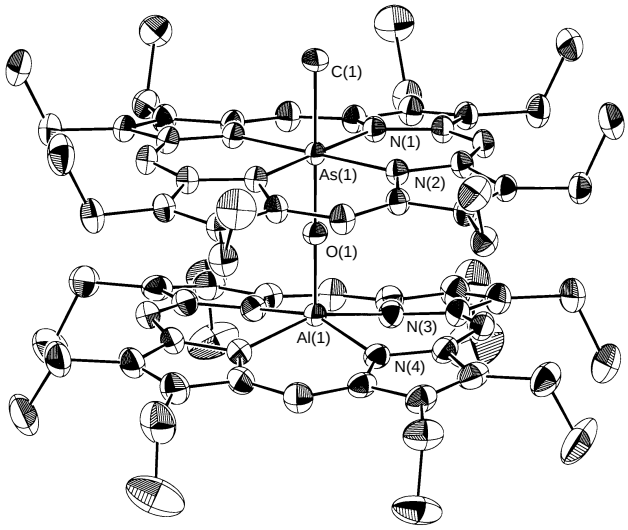



**Fig. 1** Molecular structure of **2**. Selected bond lengths (Å) and angles (°): As–C(1) 1.971(4), As–O(1) 1.690(3), As–N(1) 2.028(3), As–N(2) 2.034(3), Al(1)–O(1) 1.731(3), Al(1)–N(3) 2.005(3), Al(1)–N(4) 2.017(3); C(1)–As–N(1) 90.5(1), C(1)–As–N(2) 90.2(1), O(1)–As–N(1) 89.5(1), O(1)–As–N(2) 89.8(1), N(1)–As–N(2) 89.6(1), O(1)–Al(1)–N(3) 101.3(1), O(1)–Al(1)–N(4) 100.8(1), N(3)–Al(1)–N(4) 87.9(2).

interaction in [{(oep)Ru(OH)}$_2$O],[9] however, there is no formal contribution of a d-orbital in **5**. Further synthetic and structural studies are now in progress.

## Footnotes

* E-mail: akiba@sci.hiroshima-u.ac.jp

† Compounds, **1**, **2** and **3** gave satisfactory elemental analyses for C, H and N. *Spectroscopic data*: **1**; $^1$H NMR ($CDCl_3$), $\delta$ 9.06 (s, 4 H), 8.42 (s, 4 H), 3.83–4.22 (m, 32 H), 1.82 (t, 24 H), 1.67 (t, 24 H), −7.96 (d, 3 H). **2**; $^1$H NMR ($CDCl_3$), $\delta$ 9.24 (s, 4 H), 9.05 (s, 4 H), 4.09–4.28 (m, 24 H), 3.98 (dq, 8 H), 1.91 (t, 24 H), 1.58 (t, 24 H), −7.94 (s, 3 H). **3**; $^1$H NMR ($CDCl_3$), $\delta$ 9.37 (s, 4 H), 8.90 (s, 4 H), 3.80–4.25 (m, 32 H), 1.91 (t, 24 H), 1.58 (t, 24 H), −7.92 (s, 3 H).

‡ *Crystal data* for **2**·$CH_2Cl_2$: $C_{74}H_{93}AlAsCl_3N_8O_5$, $M$ = 1381.8, monoclinic, space group $C2/c$, $a$ = 15.5820(7), $b$ = 35.578(1), $c$ = 15.1920(7) Å, $\beta$ = 114.305(2)°, $U$ = 7675.5 Å$^3$, $Z$ = 4, $D_c$ = 1.20 g cm$^{-3}$, $T$ = 297 K. Data were collected on a Mac Science DIP2030 imaging plate equipped with graphite-monochromated Mo-K$\alpha$ radiation ($\lambda$ = 0.710 73 Å). Unit-cell parameters were determined by autoindexing several images in each data set separately with the program DENZO.[10] From the cell constants and systematic absences, the space group was chosen to be $C2/c$. For each data set, rotation images were collected in 6° increments with a total rotation of 180° about $\phi$. Data were processed by using SCALEPACK.[10] The structure was solved using the MAXUS (Mac Science) system and refined by full-matrix least-squares. Final $R_1$ = 0.085 ($R_w$ = 0.097) for 5703 observed reflections with $I > 5\sigma(I)$. Atomic coordinates, bond lengths and angles, and thermal parameters have been deposited at the Cambridge Crystallographic Data Centre (CCDC). See Information for Authors, Issue No.1. Any request to the CCDC for this material should quote the full literature citation and the reference number 182/502.

## References

1 For recent reports: K. M. Kadish, M. Autret, Z. Ou, P. Tagliatesta, T. Boschi and V. Fares, *Inorg. Chem.*, 1997, **36**, 204; J. A. Hays, C. L. Day, V. G. Young, Jr. and L. K. Woo, *Inorg. Chem.*, 1996, **35**, 7601.
2 B. Cheng, J. D. Hobbs, P. G. Debrunner, J. Erlebacher, J. A. Shelnutt and W. R. Scheidt, *Inorg. Chem.*, 1995, **34**, 102.
3 M. Takeuchi, T. Imada and S. Shinkai, *J. Am. Chem. Soc.*, 1996, **118**, 10658.
4 Y. Yamamoto, R. Nadano, M. Itagaki and K.-y. Akiba, *J. Am. Chem. Soc.*, 1995, **117**, 8287.
5 W. Satoh, R. Nadano, Y. Yamamoto and K.-y. Akiba, *Chem. Commun.*, 1996, 2451.
6 K.-y. Akiba, Y. Onzuka, M. Itagaki, H. Hirota and Y. Yamamoto, *Organometallics*, 1994, **13**, 2800; K. M. Kadish, M. Autret, Z. Ou, K.-y. Akiba, S. Masumoto, R. Wada and Y. Yamamoto, *Inorg. Chem.*, 1996, **35**, 5564.
7 N. Takeda and S. Inoue, *Bull. Chem. Soc. Jpn.*, 1978, **51**, 3564.
8 R. Guilard, M. A. Lopez, A. Tabard, P. Richard, C. Lecomte, S. Brandes, J. E. Hutchison and J. P. Collman, *J. Am. Chem. Soc.*, 1992, **114**, 9877.
9 H. Matsuda, T. Taga, K. Osaki, H. Sugimoto, M. Mori and H. Ogoshi, *J. Am. Chem. Soc.*, 1981, **103**, 2199.
10 Z. Otwinowski, University of Texas, Southwestern Medical Center.

*Received in Cambridge, UK, 8th May 1997; Com. 7/03160B*

# Hydrozirconation of an η²-ligated phosphaalkyne. A new synthetic route to η²-ligated phosphaalkenes

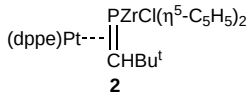
**Maria Helena A. Benvenutti, Nathalie Cenac and John F. Nixon***

*School of Chemistry, Physics and Environmental Science, University of Sussex, Brighton, Sussex, UK, BN1 9QJ*

**The phosphaalkyne complex [Pt(dppe)(η²-Bu$^t$C≡P)] undergoes ready hydrozirconation with [ZrHCl(η⁵-$C_5H_5$)$_2$] to give the metallaphosphaalkene complex [Pt(dppe){η²-Bu$^t$CH=PZrCl(η⁵-$C_5H_5$)$_2$}] which is a useful precursor for the synthesis of η²-phosphaalkene complexes.**

The recent report of the formation of a phosphaalkenyl ruthenium(II) complex by hydroruthenation of the phosphaalkyne Bu$^t$C≡P[1,2] prompts us to describe the first examples of the facile conversion of the η²-ligated Bu$^t$C≡P by a synthetic route which offers considerable potential for the synthesis of a range of η²-ligated Bu$^t$CH=PX derivatives.

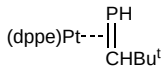
Thus treatment of [Pt(dppe)(η²-Bu$^t$C≡P)] **1**[3] with the Schwartz reagent, [ZrHCl(η⁵-$C_5H_5$)$_2$], quantitatively affords the η²-ligated metallaphosphaalkene complex [Pt(dppe){η²-Bu$^t$CH=PZrCl(η⁵-$C_5H_5$)$_2$}] **2** which occurs as a single isomer.†




**2**

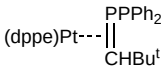
It is interesting to note that the [ZrCl(η⁵-$C_5H_5$)$_2$] fragment adds solely to the phosphorus atom which is at the positive end of the dipole in uncoordinated Bu$^t$C≡P. Hydrozirconation of phosphaalkenes $R_2C{=}PR'$ has been the subject of a very recent review,[3] where it was pointed out that the course of these reactions depends strongly on the nature of the substituents attached to phosphorus or carbon.

Treatment of **2** with $H_2O$ at −60 °C in thf for 1 h readily affords the yellow η²-phosphaalkene complex [Pt(dppe)(η²-Bu$^t$CH=PH)] as a 3 : 1 mixture of *cis*- and *trans*-isomers **3a** and **3b**.‡ The uncoordinated phosphaalkene is unknown.




**3**

The synthetic potential of the intermediate **2** in the generation of other phosphaalkene complexes is illustrated by its reaction with $Ph_2PCl$ leading to ready elimination of [$ZrCl_2$(η⁵-$C_5H_5$)$_2$] and formation of the diphenylphosphino-phosphaalkene complex [Pt(dppe)(η²-Bu$^t$CH=P$Ph_2$)] **4** as a mixture of *cis*- and *trans*-isomers.§




**4**

The field of metallaphosphaalkene complexes has recently been reviewed by Weber[4] but the synthesis of **2** represents a new approach; furthermore as discussed elsewhere,[5] the reactivity of **2** towards halogeno-compounds offers considerable synthetic potential to generate other metallaphosphaalkene complexes by treatment with appropriate metal halides.

We thank both the EPSRC and the EEC/CNPq for their financial support of other aspects of phosphaalkyne chemistry research at Sussex.

## Footnotes

* E-mail: j.nixon@sussex.ac.uk

† NMR data for **2**: $^{31}$P {$^1$H} (121.4 MHz, $C_6D_6$); δ 47.7 (dd, $CH_2PPh_2$, $^2J_{PP}$ 53.9, $^2J_{PP}$ 35.5, $^1J_{PPt}$ 3233.6 Hz), 52.7 (dd, PCBu$^t$, $^2J_{PP}$ 35.5, $^2J_{PP}$ 15.3, $^1J_{PPt}$ 282.2 Hz). $^{13}$C{$^1$H} (75.4 MHz, $C_6D_6$); δ 30.5 (dd, $CH_2$, $J_{CP}$ 33.0, $J_{CP}$ 15.9, $^2J_{CPt}$ 16.0 Hz), 33.2 (dd, $CH_2$, $J_{CP}$ 32.4, $J_{CP}$ 14.7, $^2J_{CPt}$ 19.0 Hz), 33.8 (dd, $CH_3$, $J_{CP}$ 6.1, $J_{CP}$ 5.7, $^3J_{CPt}$ 32.9 Hz), 74.1 (ddd, CH, $J_{CP}$ 83.6, $J_{CP}$ 50.0, $^2J_{CP}$ 3.7, $J_{CPt}$ 341.3 Hz), 109.6–109.7 (m, $C_5H_5$), 126.5 (s, Ph), 126.9 (dd, Ph, $J_{CP}$ 8.4, $J_{CP}$ 0.8 Hz), 127.3 (d, Ph, $J_{CP}$ 6.0 Hz), 127.6 (d, Ph, $J_{CP}$ 9.9 Hz), 128.1 (dd, Ph, $J_{CP}$ 42.5, $J_{CP}$ 1.1, $J_{CPt}$ 54.7 Hz), 129.3 (dd, Ph, $J_{CP}$ 38.8, $J_{CP}$ 10.0 Hz), 130.9 (d, Ph, $J_{CP}$ 11.0, $J_{CPt}$ 11.2 Hz), 131.4 (d, Ph, $J_{CP}$ 12.6, $J_{CPt}$ 19.0 Hz), 133.1 (d, Ph, $J_{CP}$ 12.6, $J_{CPt}$ 21.8 Hz), 134.4 (dd, Ph, $J_{CP}$ 13.7, $J_{CP}$ 2.4, $J_{CPt}$ 24.2 Hz); quaternary carbons unidentified. $^1$H (300 MHz, $C_6D_6$); δ 1.28 (s, 9 H, $CH_3$), 2.00 (m, 4 H, $CH_2$), 4.19 (ddd, 1 H, CH, $J_{HP}$ 7.5, $J_{HP}$ 7.5, $J_{HP}$ 3.8, $^2J_{HPt}$ 55.6 Hz), 5.80–6.01 (m, 10 H, $C_5H_5$), 6.80–8.21 (m, 20 H, Ph).

‡ *NMR data for* **3a** *and* **3b**: **3a** $^{31}$P{$^1$H} ($C_6D_6$); δ 154.7 (dd, PH, $J_{PP}$ 52.1, $J_{PP}$ 11.0, $J_{PPt}$ 286.7, $J_{PH}$ 138.5 Hz), 51.8 (dd, $PPh_2$, $J_{PP}$ 52.1, $J_{PP}$ 45.8, $J_{PPt}$ 3226.1 Hz), 56.9 (dd, $PPh_2$, $J_{PP}$ 45.8, $J_{PP}$ 11.0, $J_{PPt}$ 2929.7 Hz). $^{13}$C{$^1$H} (thf); δ 27.5 (dd, $CH_2$, $J_{CP}$ 32.6, $J_{CP}$ 14.1, $^2J_{CPt}$ 13.9 Hz), 31.5 (dd, $CH_2$, $J_{CP}$ 33.6, $J_{CP}$ 18.1, $^2J_{CPt}$ 20.5 Hz), 33.8 (dd, $CH_3$, $J_{CP}$ 8.5, $J_{CP}$ 5.8, $^3J_{CPt}$ 30.7 Hz), 69.6 (ddd, CH, $J_{CP}$ 65.9, $J_{CP}$ 52.0, $J_{CP}$ 4.2 Hz), 126.5–134.3 (m, Ph); quaternary carbons unidentified. $^1$H ($C_6D_6$); δ 1.41 (s, 9 H, $CH_3$), 2.00 (m, 4 H, $CH_2$), 2.70 (ddd, PH, $^1J_{HP}$ 150, $^3J_{HP}$ 12.5, $^3J_{HH}$ 9.6, $^2J_{HPt}$ 51.8 Hz), 4.38 (dddd, 1 H, CH, $^2J_{HP}$ 18.8, $^3J_{HH}$ 9.6, $^3J_{HP}$ 3.0, $^3J_{HP}$ 3.1, $^2J_{HPt}$ 58.0 Hz), 6.99–8.15 (m, 2 Ph). **3b** $^{31}$P{$^1$H} for the minor product: δ −167.0 (dd, PH, $^3J_{PP}$ 49.9, $J_{PP}$ 6.2, $J_{PPt}$ 325.6, $J_{PH}$ 145.8 Hz), 50.3 (dd, $PPh_2$, $J_{PP}$ 49.9, $J_{PP}$ 48.0, $J_{PPt}$ 3237.7 Hz), 56.9 (dd, $PPh_2$, $J_{PP}$ 48.0, $J_{PP}$ 6.2, $J_{PPt}$ 2929.7 Hz).

§ *NMR data for* **4**: $^{31}$P{$^1$H} ($CD_2Cl_2$) δ −80.0 (ddd, PCH, $^1J_{PP}$ 213.2, $^2J_{PP}$ 54.0, $^2J_{PP}$ 9.6, $^1J_{PPt}$ 297.9 Hz), −12.7 (ddd, $PPh_2$, $^1J_{PP}$ 213.2, $^3J_{PP}$ 9.4, $^3J_{PP}$ 5.8, $^2J_{PPt}$ 38.0 Hz), 51.5 (ddd, $CH_2PPh_2$, $^2J_{PP}$ 54.0, $^2J_{PP}$ 39.8, $^3J_{PP}$ 5.8, $^1J_{PPt}$ 3198.0 Hz), 53.9 (ddd, $CH_2PPh_2$, $^2J_{PP}$ 39.8, $^2J_{PP}$ 9.6, $^3J_{PP}$ 5.4, $^1J_{PPt}$ 2951.5 Hz).

## References

1 R. B. Bedford, A. F. Hill and C. Jones, *Angew. Chem., Int. Ed. Engl.*, 1996, **35**, 547.
2 R. B. Bedford, A. F. Hill, C. Jones, A. J. P. White, D. J. Williams and J. D. E. T. Wilton-Ely, *Chem. Commun.*, 1997, 179.
3 J.-P. Majoral, M. Zablocka, A. Igau and N. Cenac, *Chem. Ber.*, 1996, **129**, 879.
4 L. Weber, *Angew. Chem., Int. Ed. Engl.*, 1996, **35**, 271.
5 M. H. A. Benvenutti, N. Cenac, S. D'Arbeloff and J. F. Nixon, paper in preparation.

*Received in Cambridge, UK, 9th May 1997; Com. 7/03201C*

# The photochemistry of lomefloxacin. An aromatic carbene as the key intermediate in photodecomposition

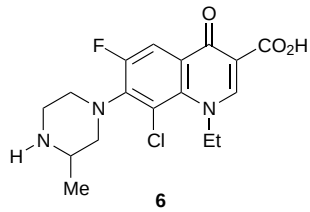
**E. Fasani, M. Mella, D. Caccia, S. Tassi, M. Fagnoni and A. Albini***

*Department of Organic Chemistry, University of Pavia, Via Taramelli 10, 27100 Pavia, Italy*

**Irradiation of the 6,8-difluoroquinolone antibiotic lomefloxacin causes selective heterolytic defluorination from position 8 and leads to products rationalized as arising from the cation either *via* nucleophile addition or intramolecular carbene C–H insertion and hydrogen transfer.**

The strong antibacterial activity of fluoroquinoles (FQ) has led to their large-scale use in medicine.[1] A major drawback of this relatively new class of antibiotics is their phototoxic effects.[2–8] There are indications that reactive oxygen species, such as singlet oxygen, superoxide anion or hydroxyl radical, play a role in some cases.[9–14] However, this is not necessarily the main mechanism underlying such an effect. As an example, it has recently been reported that in the case of lomefloxacin **1**, which is not only more phototoxic than other FQs but also more photomutagenic and carcinogenic,[15,16] the phototoxic effect is not related to singlet oxygen and superoxide anion generation[17] and furthermore photoinduced single strand breaks in plasmid DNA are actually *decreased* in the presence of oxygen.[18] This suggests that oxygen activation is not involved, and that a different mechanism operates; it has also been noted that fluoride ion is liberated during the photolysis of **1**.[18] An investigation of the photochemistry of **1** was thus warranted. As is shown in the following, a detailed product study demonstrates the unusual photochemical behaviour of this molecule and suggests a mechanism for the toxic and particularly the carcinogenic/mutagenic activity.

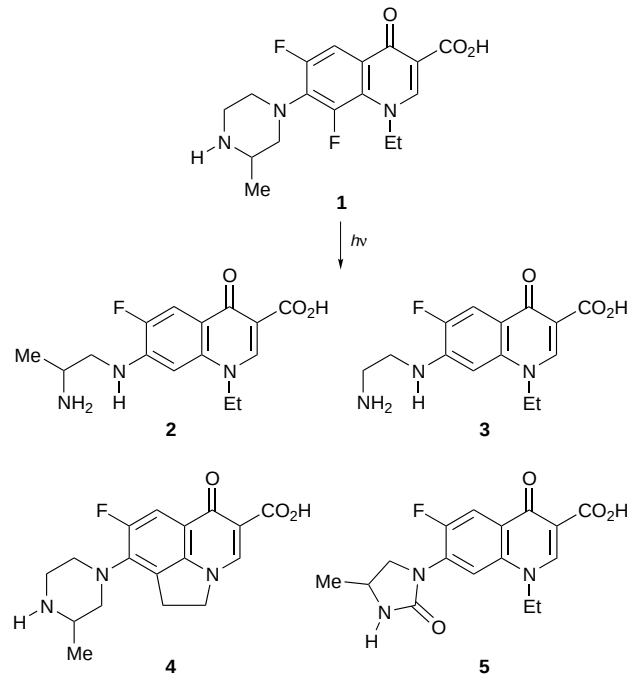
Irradiation ($\lambda$ > 310 nm) of lomefloxacin **1** ($10^{-4}$ M) in argon-flushed phosphate buffer (pH 7.4) up to 90% conversion gave several products. These were transformed into the corresponding *N*′-ethylcarbamates by treatment with ethyl chloroformate, extracted with chloroform, esterified by treatment with diazomethane and chromatographically separated. In this way, the main photolysis products were recognised as the two diamines **2** and **3**, accompanied by minor amounts of the tricyclic derivative **4** and a trace of the imidazolonyl derivative **5** (Scheme 1). Irradiation of the hydrochloride of **1** in argon-flushed water (pH 4.3) gave the 8-chloro derivative **6** as one of the main products.†



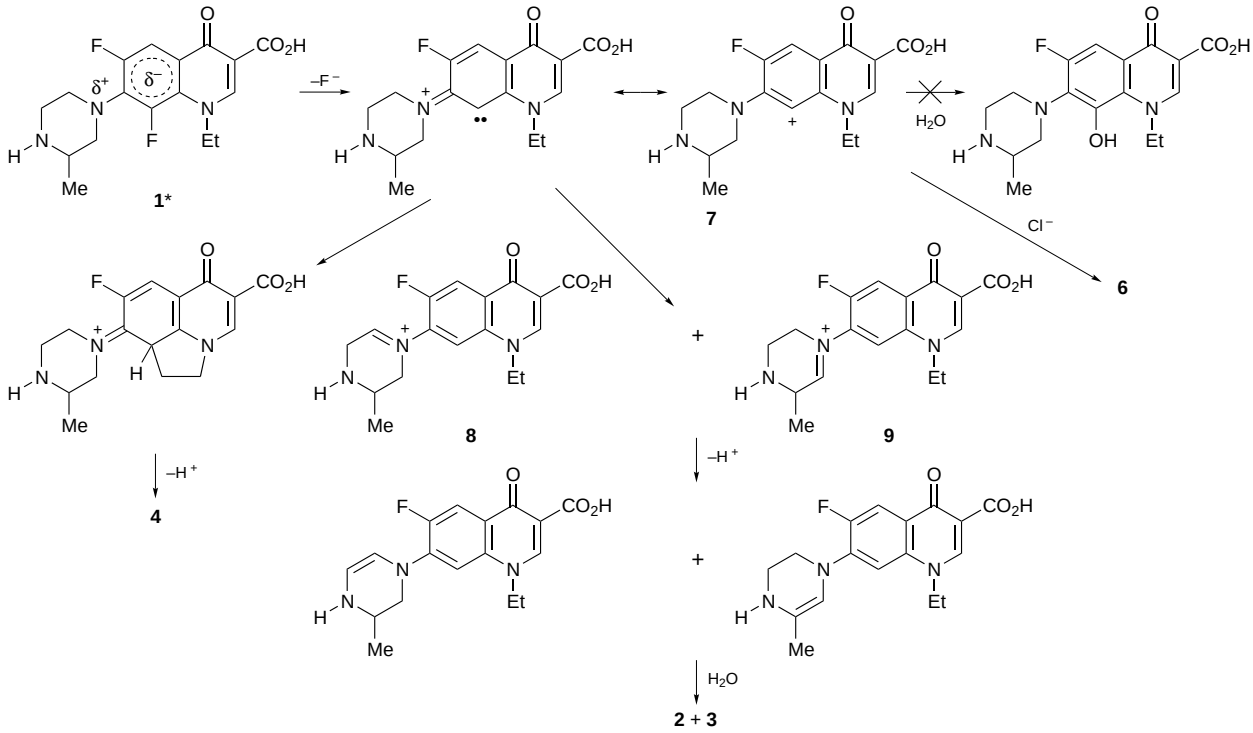
**6**

Inspection of **2**–**5** shows that two processes occurred in all cases, *viz* (i) reductive defluorination selectively at position 8, and (ii) modification of an *N*-alkyl chain, either the piperazinyl group (products **2**, **3** and **5**) or the 1-ethyl group (product **4**). Since the photoproducts are themselves FQs, competitive light-absorption by the products and the starting material occurred. However, when the irradiation was limited to a lower conversion (35%) the ratio of products was essentially the same. Furthermore, we found that **1** ($\Phi_{dec}$ 0.65) was far more sensitive to irradiation than all the monofluoro FQs we examined under these conditions ($\Phi_{dec}$ < 0.03) and also than compounds **2**–**5**, which are monofluoro derivatives. Thus, these products arose from a monophotonic reaction, and both processes (i) and (ii) occurred in a single reaction rather than *via* two sequential photoinitiated steps. Furthermore the product distribution was again similar in air-equilibrated solution. On the other hand, irradiation of the monohydrochloride omitting the buffer gave product **6**, conserving the piperazine ring intact and with substitution of a chloro group for the 8-fluoro atom.

The mechanism we propose is indicated in Scheme 2. The reaction proceeds from the short-lived singlet excited state and is by far the main decay path ($\Phi_{react} \approx 0.65$, $\tau_{fluo}$ < 1 ns, little influence of dissolved oxygen, thus $\Phi_{isc}$ is low and the triplet has little role in the reaction). Homolysis of the C–F bond is obviously out of question (bond dissociation energy C–F = 125 kcal $mol^{-1}$, energy of signlet excited **1** = 81 kcal $mol^{-1}$). Thus heterolytic loss of $F^-$ is involved, and the mechanism proposed must explain also the other modification occurring concurrently. The singlet state has an internal charge transfer character (strong Stokes shift, 6000 $cm^{-1}$) and the zwitterionic form is important in **1***. Loss of fluoride leads to cation **7**, for which mesomeric carbocationic and carbene forms can be considered. In phosphate buffer we isolated no product arising from the carbocation (such as phenols), but that product **6** formed when the nucleophile is chloride substantiates this path. On the other hand a striking indication for carbene reactivity comes from the structure of product **4**, obviously resulting from well precedented carbene C–H insertion[19] into the conforma-



**Scheme 1**



**Scheme 2**

tionally suitable δ position. Products **2** and **3** also arise from the carbene *via* intramolecular hydrogen transfer to give the rearranged cations **8** and **9**. These deprotonate to enediamines, which in turn are hydrolysed, whether in solution or during work up, to the observed diamines. Compound **5** also results from demolition of the piperazinyl chain coupled with defluorination.

There are only a few precedents for photoinduced defluorination in aromatic or heterocyclic chemistry, *viz* those of *N*-formyl-4-fluorotryptophan methyl ester[20] and of some dimethoxyfluorobenzenes,[21] both involving related activation by electron-donating groups. The peculiarly high photoreactivity of lomefloxacin with respect to other FQs (see above) is certainly due to the selective defluorination from position 8, apparently due to activation by both the adjacent amino groups, which increase the zwitterionic character of the singlet excited state and facilitate the fragmentation indicated in Scheme 2. Studies in progress in this laboratory show however that this type of reactivity is rather general, and defluorination accompanied by alkylamino chain degradation also takes place in FQs containing only the 6-fluoro group, although with a lower efficiency.‡

The fact that cation **7** exhibits carbene chemistry dominated by *intramolecular* C–H insertion and hydrogen transfer strongly suggests that the cause of the observed carcinogenic/mutagenic effect of this drug is formation of a covalent bond by direct reaction of excited **1** with DNA through a related *intermolecular* process.

Partial support of this work by the Istituto Superiore di Sanità, Rome, is gratefully acknowledged.

## Footnotes

* E-mail: albini@chifis.unipv.it

† All products have been fully characterised by elemental analysis and spectroscopic means as the corresponding *N*′-ethylcarbamate methyl esters.

‡ Release of fluoride by irradiation of enoxacin has been detected (ref. 22).

## References

1 H. C. Neu, in *The 4-Quinolones*, ed. G. C. Crumplin, Springer Verlag, London, 1990, p. 1.
2 W. Christ, T. Lehnert and B. Ulbrich, *Rev. Infect. Dis.*, 1988, **1**, 5141.
3 N. Wagai, F. Yamagughi, M. Sekiguchi and K. Tawara, *Toxicol. Lett.*, 1990, **54**, 299.
4 K. S. Loveday, *Photochem. Photobiol*., 1996, **63**, 369.
5 P. D. Forbes, C. P. Sambuco, R. M. Parker and A. H. Hoberman, 23rd Annual Meeting of the American Society of Photobiology, 1995, June 17–22, Washington, DC.
6 E. Fernandez and A. M. Cardenas, *J. Photochem. Photobiol. B., Biol.*, 1990, **4**, 329.
7 N. Wagai and K. Tawara, *Arch. Toxicol.*, 1991, **66**, 392.
8 N. Wagai and K. Tawara, *Free Radical Res. Commun.*, 1992, **17**, 387.
9 S. Raoul, J. E. Rosen, G. M. Williams and J. Cadet, *Photochem. Photobiol.*, 1995, **61**, 108.
10 P. Dayhaw-Berker and T. G. Truscott, *Photochem. Photobiol*., 1988, **47**, 765.
11 G. Vermeersch, J. C. Ronfard-Haret, M. Bazin, V. Carillet, P. Morliere and R. Santus, *Photochem. Photobiol.*, 1991, **54**, 661.
12 N. Wagai and K. Tawara, *Arch. Toxicol.*, 1991, **65**, 495.
13 P. Bliski, L. J. Martinez, E. B. Koker and C. F. Chignell, *Photochem. Photobiol.*, 1996, **64**, 496.
14 L. Martinez, P. Bliski and C. F. Chignell, *Photochem. Photobiol*., 1996, **64**, 911.
15 J. M. Domagala, *J. Antimicrob. Chemother*., 1994, **33**, 685.
16 A. A. Chatelet, S. Albertini and E. Gocko, *Mutagenesis*, 1996, **11**, 497.
17 L. Martinez, R. Sik and C. F. Chignell, *Photochem. Photobiol*., 1966, **63**, 29S.
18 L. J. Martinez, G. Li and C. F. Chignell, *Photochem. Photobiol*., 1997, **65**, 599.
19 Z. Majerski, Z. Hamersak and R. Sarac-Aneri, *J. Org. Chem.*, 1988, **53**, 5053 and references cited therein.
20 N. C. Yang, A. Huang and D. H. Yang, *J. Am. Chem. Soc.*, 1989, **111**, 8060.
21 G. Zhang and P. Wan, *J. Chem. Soc., Chem. Commun.*, 1994, 19.
22 G. Condorelli, G. De Guidi, S. Giuffrida, P. Miano, A. Velardita and S. Sortino, *Photochem. Photobiol.*, 1996, **63**, 75S.

*Received in Cambridge, UK, 12th May 1997; Com. 7/03226I*



Typeset and printed by Black Bear Press Limited, Cambridge, England

ChemComm
FEATURE ARTICLE

# A new generation of homogeneous arene hydrogenation catalysts†

**Ian P. Rothwell**

*Department of Chemistry, 1393 Brown Building, Purdue University, West Lafayette, IN 47907-1393, USA*

**The homogeneous hydrogenation of a variety of arene substrates can be catalysed by hydride derivatives of niobium and tantalum. A key feature of these catalysts is the presence of bulky ancillary aryloxide ligation. The systems demonstrate high regio- and stereo-selectivity in the hydrogenation of benzenes and polynuclear aromatic hydrocarbons. A unique characteristic of the niobium compounds is an ability to rapidly hydrogenate arylphosphine ligands, providing a new procedure for the synthesis of cyclohexylphosphine ligands.**

## Introduction

The field of arene hydrogenation chemistry will soon be entering its second century. The initial work of Sabatier on the interaction of finely divided nickel with ethylene was stimulated by Mond's earlier discovery of $[Ni(CO)_4]$.[1] Instead of isolating an ethylene derivative of nickel, serendipity led Sabatier to uncover the high activity of finely divided nickel for carrying out the hydrogenation of a variety of unsaturated organic substrates.[2] In 1901 with co-worker Senderens he 'attacked a case of hydrogenation, which up to that time had not been realized by any method, that of benzene'.[1] Not only did the experiment succeed, but the product obtained by the complete hydrogenation of benzene was, in fact, much purer (mp of 6 °C) than the sample of cyclohexane previously isolated by Markovnikov from Caucasian petroleum that had a mp of −11 °C![1,3] In subsequent papers Sabatier applied the method to a variety of mononuclear and polynuclear aromatic hydrocarbons with great success.[3] The discovery and development of this 'Sabatier method' led to the Nobel Prize (shared with Grignard) in 1912.

Following Sabatier's work, a variety of heterogeneous catalysts for arene hydrogenation was developed. Historically significant was the work of Adams on finely divided 'platinum-oxide, platinum black' (Adam's catalyst)[4] and the process of selectively digesting alloys to generate finely divided samples of metals (*e.g.* Raney nickel) by the industrial chemist Murray Raney.[5] The conversion of benzene to cyclohexane still represents the most important industrial hydrogenation reaction and is today carried out chiefly using a combination of Raney nickel and $Ni/Al_2O_3$ catalysts.[6] The product cyclohexane is primarily utilized in the production of adipic acid.

A more efficient utilization of sometimes expensive metals involves depositing the metal or its compounds onto suitable supports. Recently a number of materials obtained by attaching organometallic compounds to oxide surfaces have been shown to be highly active arene hydrogenation catalysts.[7]

The development of homogeneous catalysts capable of hydrogenating arene substrates has lagged well behind the heterogeneous systems. Following the original discovery of the so-called Wilkinson's catalyst[8] the field of homogeneous transition-metal catalysed alkene hydrogenation has grown into a large and sophisticated area of chemistry.[9] Despite this there is a relative dearth of systems that will hydrogenate benzene rings.[10,11] The majority of these systems are based upon middle and later transition metals and in some situations successful reactivity is limited to polynuclear aromatic hydrocarbon substrates. In certain cases, valuable mechanistic studies have been carried out,[10,12] although not all of these systems have been proven to be homogeneous. One system of particular note is an allyl–cobalt catalyst developed by Muetterties *et al.*[10] where NMR experiments led to the conclusion that the $C_6D_6H_6$ obtained by treating $C_6D_6$ with $H_2$ was an all-*cis* isotopomer.[13] This result has recently been confirmed using ion–molecule chemistry.[14] The hydrogenation of aromatics by Ziegler type catalysts utilizing nickel or cobalt alkoxides, acetylacetoates or carboxylates and trialkylaluminium activators has been known for some time.[15] The most significant of these is the 'Dimersol' process developed by the Institut Francais du Petrole (IFP), a homogeneous system that appears to be a viable alternative to heterogeneous technology for the large scale hydrogenation of benzene.[15]

During our studies of the early d-block metal chemistry that can be supported by sterically bulky aryloxide ligation[16] we discovered that mixed hydrido aryloxide derivatives of niobium and tantalum would carry out the intra- and inter-molecular hydrogenation of arene rings. This Feature Article highlights both the synthetic utility of the new catalysts as well as our present mechanistic knowledge.

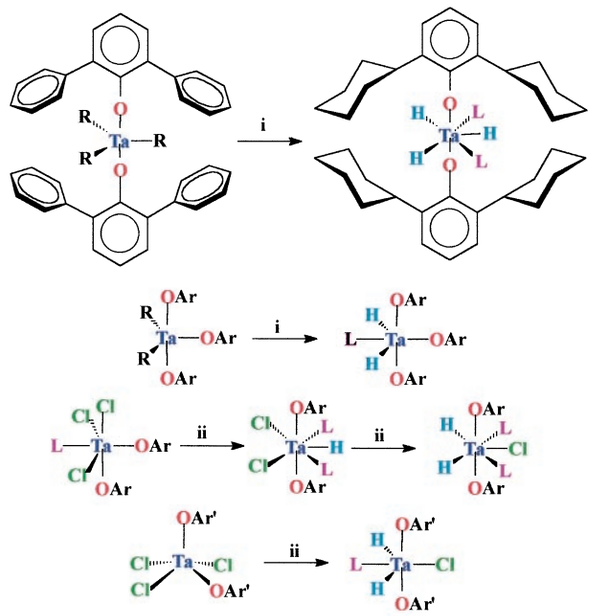
## Synthesis and characterization of niobium and tantalum hydrido aryloxides

Of the many strategies available for the synthesis of transition-metal hydrides, two procedures are successful at generating mixed hydrido aryloxide derivatives of niobium and in particular tantalum (Scheme 1).[17] The first involves the high-pressure hydrogenolysis[18] of hydrocarbon solutions of mixed alkyl/aryloxides, typically in the presence of phosphine donor ligation. In some instances the hydrogenolysis is slow even under forcing conditions and only the alkyl precursor is reclaimed. In the case of aryloxide ligation containing *ortho*-phenyl substituents, the products isolated contain 2,6-dicyclohexylphenoxide groups (Scheme 1).[19] Under no circumstances have we detected the hydrogenation of phenyl rings either *meta* or *para* to the aryloxide oxygen or of the phenoxide nucleus itself. This is a highly significant result as it shows that these reaction mixtures do not contain small amounts of indiscriminate, possibly heterogeneous, arene hydrogenation catalysts. This selectivity coupled with an analysis of the stereochemistry of the reaction utilizing $D_2$ reagent gas and isolation of intermediates (*vide infra*) shows that the hydrogenation occurs in an intramolecular fashion within the niobium or tantalum compound itself.[19]

The second route to hydride derivatives involves treatment of the corresponding chloro aryloxides with $Bu^n_3SnH$ in the presence of a donor phosphine (Scheme 1).[17] In the case of niobium, evolution of $H_2$ and formation of hydrogenation inactive $d^1$ species such as all-*trans*-$[Nb(OC_6H_3Pr^i_2\text{-}2,6)_2Cl_2(L)_2]$ (L = tertiary phosphine) takes place,[20] whereas discrete $d^0$ hydride compounds can be isolated for tantalum. The reaction does not lead to total substitution of all Ta–Cl bonds, but the procedure can be readily scaled up as well as modified by the use of commercially available $Bu^n_3SnD$ to produce the corresponding deuteriated derivatives.[17]

The $d^0$ hydrides so far isolated fall into two broad categories. With two moderately bulky aryloxides, seven coordinate bis(phosphine) derivatives are isolated. These compounds contain a pentagonal-bipyramidal structure with mutually *trans*-axial phenoxide oxygen atoms (Scheme 1). The characteristically low field chemical shift of the Ta–H resonances not only aids in characterization, but careful analysis of the hydride signals shows these molecules to be stereochemically rigid on the NMR timescale.[17]

With the bulkier 2,6-di-*tert*-butylphenoxide or with three 2,6-diisopropylphenoxide ligands, six-coordinate mono(phosphine) species are generated (Scheme 1). The two structurally characterized examples show a distinct distortion away from octahedral geometry (*e.g.* Fig. 1).[17] In both cases the mutually *trans* hydride ligands are bent towards the Ta–P bond. These X-ray diffraction results are supported by IR studies which confirm the acute H–Ta–H angles (intensities of the symmetric and asymmetric stretching vibrations).[17] The origins of these distortions are beyond the scope of this review, but theoretical analysis points to σ bonding effects (not π bonding) as being important.[21]




**Scheme 1** OAr = 2,6-diisopropyl, OAr′ = 2,6-di-*tert*-butylphenoxide, L = tertiary phosphine, R = $CH_2C_6H_4Me$-4. *Reagents and conditions*: i, $H_2$ (1200 psi), 80 °C; ii, $Bu^n_3SnH$, L.

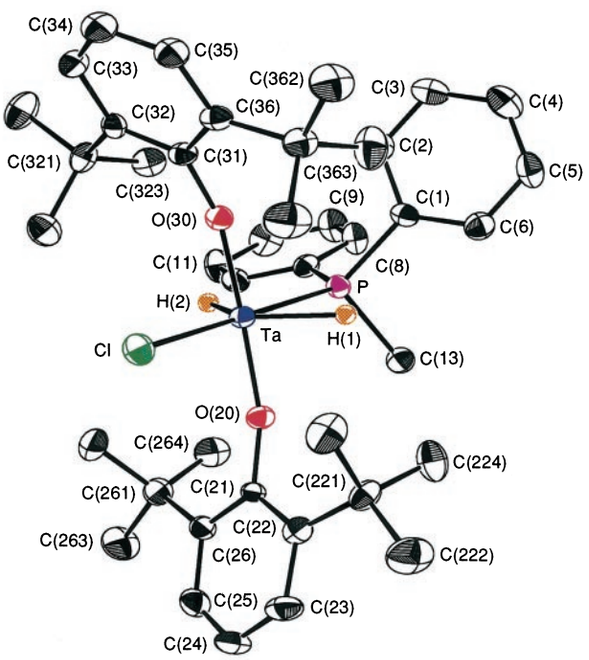


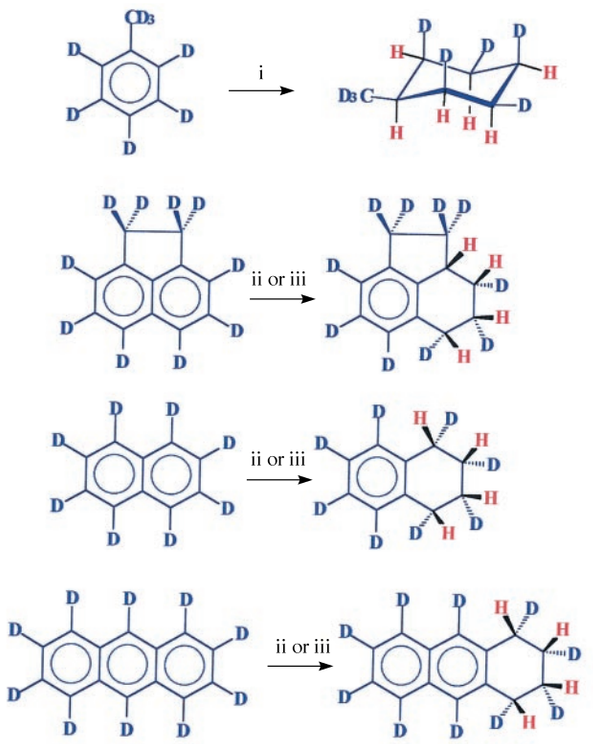

**Fig. 1** ORTEP view of $[Ta(OC_6H_3Bu^t_2\text{-}2,6)_2Cl(H)_2(PMePh_2)]$

## Intermolecular hydrogenation of arene rings: regio- and stereo-selectivities

Hydrocarbon solutions of the isolated tantalum trihydrides $[Ta\{OC_6H_3(C_6H_{11})_2\text{-}2,6\}_2(H)_3(PMe_2Ph)_2]$ and $[Ta(OC_6H_3\text{-}Pr^i_2\text{-}2,6)\}_2(H)_3(PMe_2Ph)_2]$ will catalyse the hydrogenation of naphthalene and anthracene at 80 °C under a hydrogen pressure of 50–1500 psi (psi ≈ $6.895 \times 10^3$ Pa).[24] When the hydrogenation of naphthalene is carried out in $C_6D_6$ solvent in a high-pressure 5 mm $^1H$ NMR tube, complete conversion of 20 equiv. of naphthalene to tetralin occurs with no decrease in the intensity of the tantalum hydride signals in the $^1H$ NMR spectrum. Only trace amounts of cyclohexane are formed in this reaction, indicating a much slower attack on the benzene solvent. In the cases of anthracene, almost exclusive formation of 1,2,3,4-tetrahydroanthracene precedes formation of 1,2,3,4,5,6,7,8-octahydroanthracene with no detectable quantities of 9,10-dihydroanthracene (typical of radical catalysts[22] and Birch type reductions[23]) being formed.

These hydride catalysts exhibit strong inhibition by added phosphine and this sensitivity to even trace amounts of free phosphine hinders kinetic analysis of the reactivity. This observation is consistent with an initial dissociation of at least one Ta–$PR_3$ bond in the seven-coordinate hydrides prior to substrate hydrogenation.

The hydrogenation of $[^2H_8]$naphthalene, $[^2H_{10}]$anthracene and $[^2H_{10}]$acenaphthene by hydride $[Ta\{OC_6H_3(C_6H_{11})_2\text{-}2,6\}_2(H)_3(PMe_2Ph)_2]$ produced single isotopomers as shown (Scheme 2).[24] Analysis of the $^1H$ and $^{13}C$ NMR spectra confirmed a highly selective, all-*cis* hydrogenation had oc-



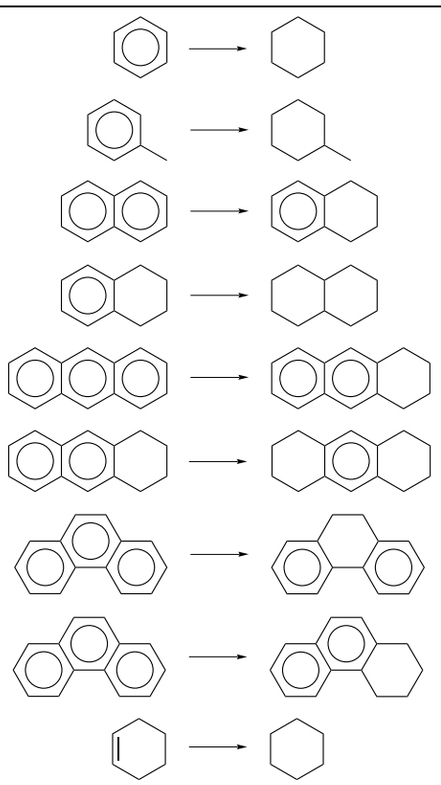

**Scheme 2** *Reagent and conditions*: i, $[Nb(OC_6HPh_4\text{-}2,3,5,6)_2Cl_3]/3Bu^nLi$, 80 °C, 1200 psi $H_2$, ii, $[Ta(OC_6H_3Pr^i\text{-}2,6)_3(H)_3(PMePh_2)_2]$, 80 °C, 1200 psi $H_2$; iii, $[Nb(OC_6H_3Ph_2\text{-}2,6)_2(CH_2C_6H_4Me\text{-}4)_3]$, 80 °C, 1200 psi $H_2$

curred with no H/D scrambling within either unreacted substrate or products. The all-*cis* nature of [$^2H_8$]tetralin has also been confirmed by ion–molecule techniques.[25]

The hydrogenolysis of alkyls of stoichiometry $[M(OAr)_2R_3]$ and $[M(OAr)_3R_2]$ (M = Nb, Ta) would be expected to generate base-free tri- and di-hydrides respectively. Although hydrides of this stoichiometry have not been isolated, the solutions thus generated are more active arene hydrogenation catalysts than the phosphine adducts, with niobium showing higher activity than tantalum and a stereoselectivity identical to that found for isolated tantalum catalysts such as $[Ta\{OC_6H_3(C_6H_{11})_2\text{-}2,6\}_2(H)_3(PMe_2Ph)_2]$ (Scheme 2).

An alternative, more synthetically straightforward procedure for carrying out the hydrogenation of arene substrates involves mixing the chloride precursors $[Nb(OAr)_3Cl_2]$ and $[Nb(OAr)_2Cl_3]$ (ArO = 2,6-diisopropyl-, 2,6-diphenyl- or 2,3,5,6-tetraphenyl-phenoxide) with 2–3 equiv. of Bu$^n$Li followed by exposure to $H_2$.[26] This procedure allows the hydrogenation to be carried out under milder conditions where hydrogenolysis of Nb–$CH_2SiMe_3$ and Nb–$CH_2Ph$ bonds is slow. The niobium catalysts obtained by these methods demonstrate almost identical regio- and stereo-selectivity compared to the tantalum hydride systems.[24] Individual experiments as well as competition reactions show the relative rates of attack on arene substrates shown (Table 1).

**Table 1** Relative rates of hydrogenation of aromatic hydrocarbons compared to benzene at 100 °C



| | |
|---|---|
| | 1[a] |
| | 0.4[b] |
| | 7[c] |
| | 0.35[c] |
| | 21[c] |
| | 3[c] |
| | 1.3[c] |
| | 0.7[c] |
| | 25 (25 °C)[d] |

[a] $[Nb(OC_6HPh_4\text{-}2,3,5,6)_2Cl_3]$/3Bu$^n$Li, 100 °C, 0.464 mmol Nb, 190 mmol $C_6H_6$ (409 per Nb), volume 20 ml, 1 h, 1200 psi $H_2$, analysed by GC. [b] $[Nb(OC_6HPh_4\text{-}2,3,5,6)_2Cl_3]$/3Bu$^n$Li, 100 °C, 0.464 mmol Nb, 95 mmol $C_6H_6$ (200 per Nb), 95 mmol $C_6H_5Me$ (200 per Nb), volume 20 ml, 1 h, 1200 psi $H_2$, analysed by GC. [c] $[Nb(OC_6HPh_4\text{-}2,3,5,6)_2Cl_3]$/3Bu$^n$Li, 100 °C, 0.464 mmol Nb, 190 mmol $C_6H_6$ (409 per Nb), 9.5 mmol substrate (20 per Nb), volume 20 ml, 1–6 h, 1200 psi $H_2$, analysed by GC and corrected for concentration of substrate. [d] $[Nb(OC_6HPh_4\text{-}2,3,5,6)_2Cl_3]$/3Bu$^n$Li, 25 °C, 0.464 mmol Nb, 95 mmol $C_6H_6$ (200 per Nb), 95 mmol Nb, 95 mmol $C_6H_8$ (200 per Nb), volume 20 ml, 1–6 h, 1200 psi $H_2$, analysed by GC.

These results indicate that selectivity is determined by the coordination affinity of the arene ring and steric factors. Anthracene is hydrogenated faster than naphthalene to initially produce 1,2,3,4-tetrahydroanthracene. Attack on this (essentially a 2,3-disubstituted naphthalene) yields exclusively octahydroanthracene. Consistent with this is the preference for attack on the unsubstituted ring of 2-methylnaphthalene.[24] The hydrogenation of naphthalene by the alkyl precursors $[Nb(OC_6H_3Ph_2\text{-}2,6)_2(CH_2C_6H_4Me\text{-}4)_3]$ in cyclohexane only occurs at temperatures above 50 °C but reaches a plateau of maximum activity above 100 °C (Fig. 2).

Further hydrogenation of tetralin produces predominantly *cis*-decalin (*cis*/*trans* = 9) but at a rate an order of magnitude slower than the formation of tetralin. The hydrogenation of benzene by the $[Nb(OC_6HPh_4\text{-}2,3,5,6)_2Cl_3]$/3Bu$^n$Li system is slower than initial attack on naphthalene. A drop in activity is again observed at too high a temperature, possibly indicative of thermal instability of the catalyst. Toluene undergoes hydrogenation 2.5 times slower than benzene and the methylcyclohexane produced by hydrogenation of [$^2H_8$]toluene has been shown by NMR methods to be the all-*cis* isotopomer (Scheme 2).

These catalysts also show high activity for the hydrogenation of alkenes and dienes. The hydrogenation of cyclohexene occurs much faster and under much milder conditions than the corresponding hydrogenation of aromatic substrates (Table 1).

All of these catalysts/precursors suffer from a sensitivity to protic impurities and dioxygen. In order for catalytic activity to be achieved and maintained the substrates, solvents and equipment must be thoroughly dried and the reaction set up with precautions being taken to prevent contamination by air or moisture. This normally requires the pressure reactors being charged and assembled within a Dri-Lab facility.

## Mechanistic considerations

A preference to undergo substitution reactions rather than addition chemistry is a defining characteristic of aromatic compounds. Consideration of the heats of formation (kcal mol$^{-1}$, cal = 4.184 J) of gaseous benzene (19.8), cyclohexa-1,3-diene (25.6), cyclohexene (−0.9) and cyclohexane (−29.4)[27] show that the generation of cyclohexa-1,3-diene is the problematic (endothermic) step in the hydrogenation of benzene. Furthermore, on purely thermodynamic arguments it appears a daunting task to design a combination of catalyst and conditions which will lead to only the partial hydrogenation of benzene. The success of Birch reductions[23] and related reactions at stoichiometrically generating partially hydrogenated products (typically 1,4-dienes) is due to the much higher electron affinity of the arene substrate over the products. The conversion of benzene to cyclohexene is thermodynamically favourable, and the monoene is a highly desired product. Recently there has been some success in the development of heterogeneous catalysts for converting benzene into cyclohexene.[28] Thermodynamic analysis of the stoichiometric reaction of a transition-metal dihydride with ethylene followed by oxidative addition of $H_2$ shows that both steps can be exothermic leading to a viable catalytic cycle. In contrast although the corresponding reaction with benzene to produce cyclohexa-1,3-diene may conceivably be exothermic, such a dihydride must be thermodynamically unstable with respect to loss of $H_2$. The partial saturation of fused-ring aromatic compounds does not suffer from as dramatic a loss of resonance stabilization, *e.g.* conversion of naphthalene to 1,2-dihydronaphthalene is exothermic. This accounts for the more facile hydrogenation of polynuclear aromatic hydrocarbons by heterogeneous and homogeneous systems compared to single ring aromatics. This hypothesis is given strong support in the reaction chemistry of main-group hydride reagents. In particular the mammoth body of work dealing with the stoichiometric hydroboration of alkenes[29] contrasts with the Lilliputian studies

involving arene substrates.[30] A large number of transition-metal hydride compounds are stable in aromatic solvents. When reactivity does occur, it commonly involves aromatic C–H bond activation either *via* oxidative-addition pathways (sometimes preceded by $H_2$ elimination)[31] or else by σ-bond metathesis with highly electrophilic $d^0$ metal hydrides.[32]

Our attempts to understand these Group 5 metal-catalysed reactions has led us to volunteer the mechanistic pathways shown in Scheme 3. We have attempted with some success to isolate and study some of the reasonable intermediates in this catalytic cycle. Considerable experimental evidence has been obtained that the niobium and tantalum aryloxides can strongly bind to cyclohexa-1,3-diene intermediates produced by transfer of two hydrogen atoms to an arene ring. An intramolecular example of this is the formation of a chelated cyclohexadiene species generated *via* attack on an *ortho*-phenyl phenoxide ligand by an intermediate niobium dihydride.[19] Although we have as yet not detected the stoichiometric, intermolecular attack of an isolated niobium or tantalum hydride on a benzene ring, a series of cyclohexa-1,3-diene derivatives can be readily obtained by reduction methods (Scheme 4).[33] The structural parameters for these species indicate a significant contribution

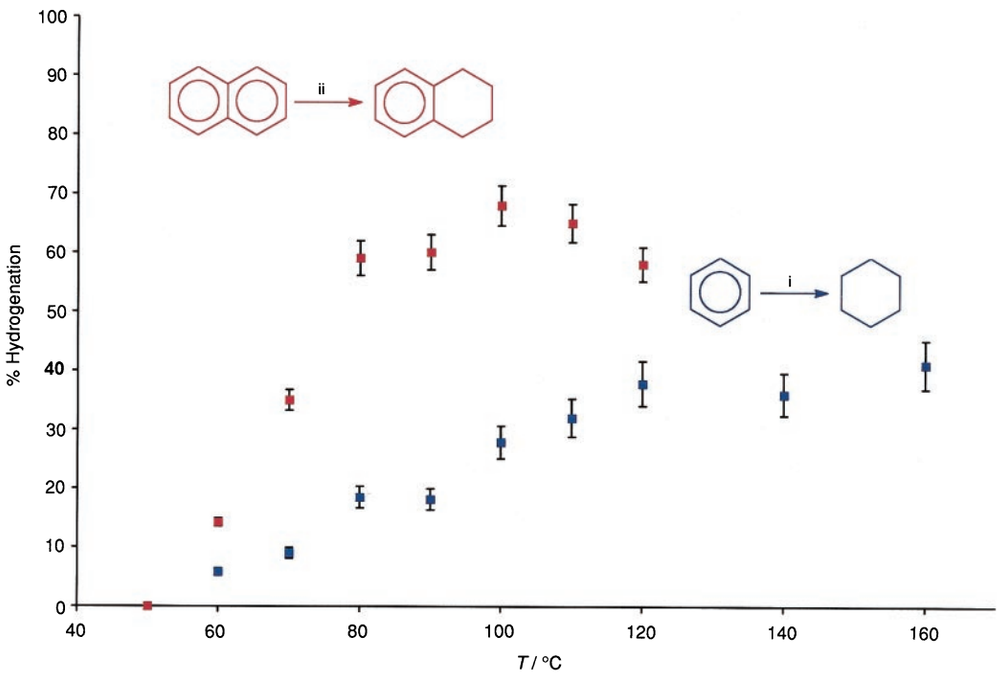
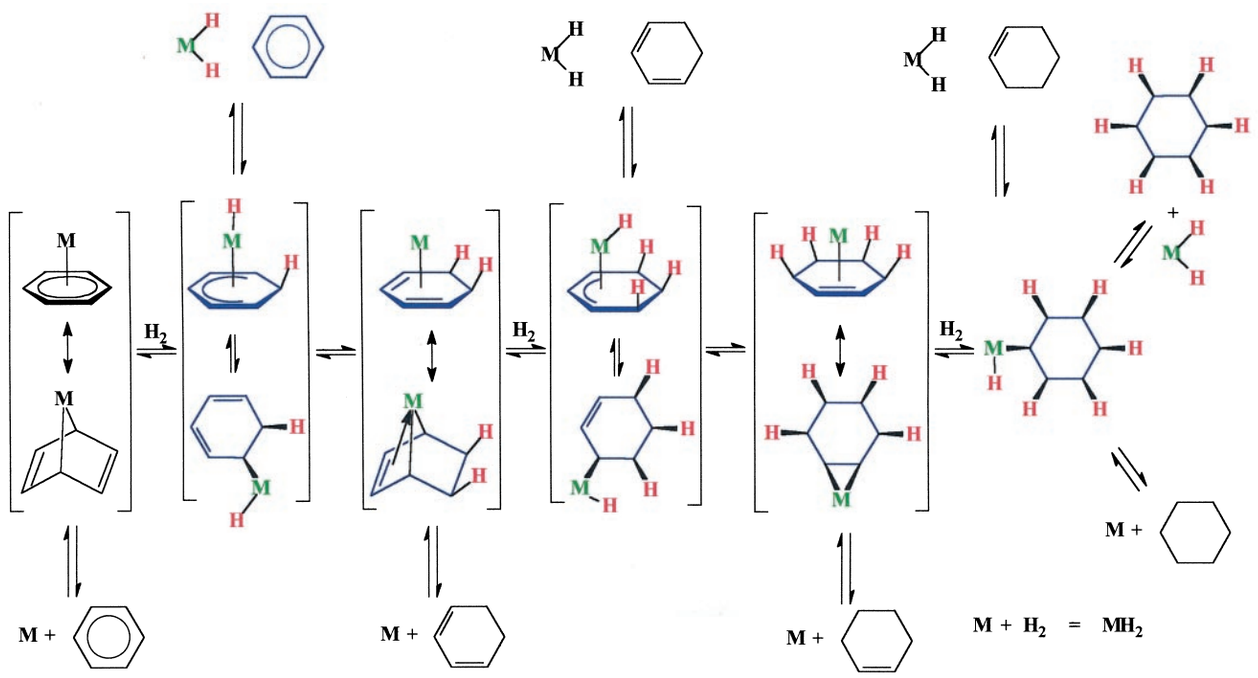



**Fig. 2** Temperature dependence of the hydrogenation of benzene and naphthalene. *Reagents and conditions*: i, $[Nb(OC_6HPh_4-2,3,5,6)_2Cl_3]/3Bu^nLi$, 0.464 mmol Nb, 190 mmol $C_6H_6$ (409 per Nb), volume 20 ml, 6 h, 1200 psi $H_2$; ii, $[Nb(OC_6H_3Ph_2-2,6)_2(CH_2C_6H_4Me-4)_3]$, 0.1 mmol, 20 mmol $C_{10}H_8$ (200 per Nb), volume 3 ml, $C_6H_{12}$ solvent, 6 h, 1200 psi $H_2$.

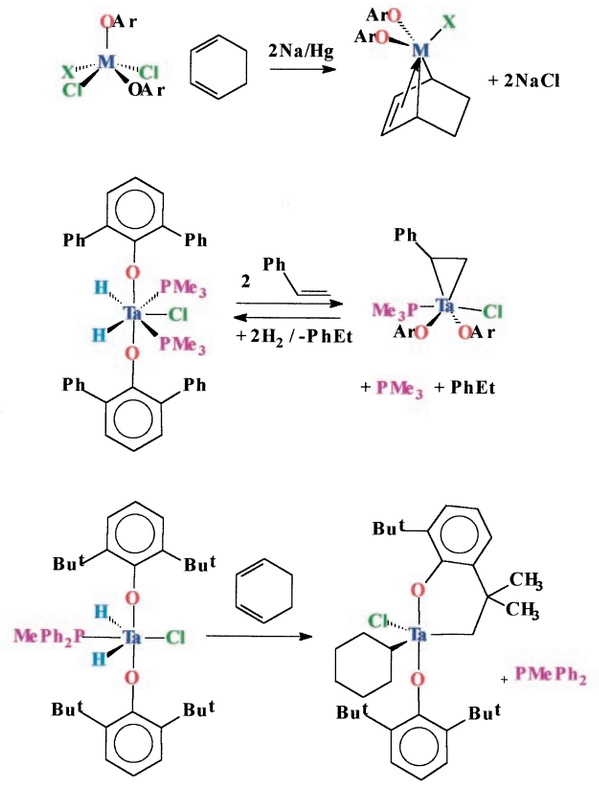



**Scheme 3**

from a metallanorbornene ($d^0$ metal) bonding picture.[34] Some important observations are the fact that dissociation or displacement of cyclohexa-1,3-diene from these compounds is difficult and that they react with $H_2$ under very mild conditions to liberate cyclohexane. Species of this type are, therefore, reasonable intermediates during the catalytic cycle, but are found to react rapidly with $H_2$ under the conditions at which arene hydrogenation is carried out.[33] The strong binding of the cyclohexa-1,3-diene fragment to niobium and tantalum metal centres also accounts for the preference for an all-*cis* hydrogenation in intermolecular arene hydrogenation. The niobium compound [Nb($OC_6H_3Pr^i_2$-2,6)$_3$($\eta^4$-$C_6H_8$)] will catalyse the hydrogenation of cyclohexa-1,3-diene and cyclohexene under very mild conditions. Mechanistic studies show that cyclohexa-1,3-diene is hydrogenated selectively over cyclohexene. Furthermore labelling studies show that intermediate cyclohexene is not released during the hydrogenation of cyclohexa-1,3-diene.[33,35] In contrast the less active catalyst [Nb($OC_6H_3$-$Pr^i_2$-2,6)$_2$Cl($\eta^4$-$C_6H_8$)] converts cyclohexa-1,3-diene into cyclohexene prior to formation of cyclohexane. These results show how slight changes in the ligand environment of a homogeneous catalyst can lead to dramatically different selectivity.

The proposed mechanistic pathway (Scheme 3) proceeds next *via* a cyclohexene complex. Although no cyclohexene complex has yet been isolated, the stoichiometric reaction of the tantalum dihydride [Ta($OC_6H_3Ph_2$-2,6)$_2$Cl(H)$_2$($PMe_3$)$_2$] with styrene has been shown to produce 1 equiv. of ethylbenzene and a styrene complex (Scheme 4).[36]

The solid-state structure of this product shows the presence of a tantacyclopropane ring and in solution dissociation or exchange of bound styrene is slow, again showing how formally $d^2$ fragments such as [M(OAr)$_3$] or [M(OAr)$_2$Cl] will strongly bind to unsaturated groups.[36] Treatment of the styrene complex with $H_2$ regenerates the initial dihydride along with another equivalent of ethylbenzene (Scheme 4). The final, partially hydrogenated intermediate in the catalytic cycle is a cyclohexyl–metal species (Scheme 3). The stoichiometric reaction of




**Scheme 4** M = Nb, Ta; OAr = 2,6-diisopropylphenoxide; X = Cl, OAr

cyclohexa-1,3-diene with dihydride [Ta($OC_6H_3Bu^t_2$-2,6)-Cl(H)$_2$($PMePh_2$)] produces a stable cyclohexyl compound (Scheme 4); the third equivalent of hydrogen originating by C–H bond activation (cyclometallation) of one of the 2,6-di-*tert*-butyl phenoxide ligands.[37]

Clearly much more mechanistic work is needed on these and other model systems to gain a better understanding of the arene hydrogenation chemistry. In particular mention should be made of an alternative mechanistic pathway involving initial activation of the arene by coordination to a $d^2$ metal fragment. This reaction certainly has precedence in Group 5 metal chemistry, particularly in the work of the Wolczanski[38] and Wigley[34,39] groups. The extremely reactive $d^2$ [Ta(silox)$_3$] species will coordinate and activate a multitude of unsaturated substrates including benzene and heterocyclic compounds.[38] During studies of alkyne oligomerization, Wigley and co-workers have shown that strong bonding of arenes takes place to $d^2$ [Ta(OAr)$_2$Cl] fragments and a tantalanorbornadiene bonding picture has been proposed.[34] The hydrogenolysis of one of the metal–carbon bonds in this species would generate the same cyclohexadienyl hydride as formed by insertion of a $d^0$ metal–hydride bond across benzene (Scheme 3). During our studies of the chemistry of low-valent aryloxides of tungsten we have isolated a series of 16-electron compounds in which $\eta^6$-binding of an *ortho*-phenyl ring of a 2,3,5,6-tetraphenylphenoxide ligand occurs.[40] These compounds react with certain ketones to produce products that can be considered as originating from a tungstanorbornadiene ground-state structure.[41] Reaction with $H_2$ takes place under very mild conditions to produce an *ortho*-cyclohexene ring.[40] Our present knowledge of species such as [Nb($OC_6H_3Pr^i_2$-2,6)$_3$] and [Ta($OC_6H_3Pr^i_2$-2,6)$_2$Cl] is that they undergo rapid intramolecular dehydrogenation of *ortho* $Pr^i$ groups even in the presence of benzene.[36,42] Clearly further studies are needed to determine conclusively whether one or both of these pathways are operating in these catalytic systems.

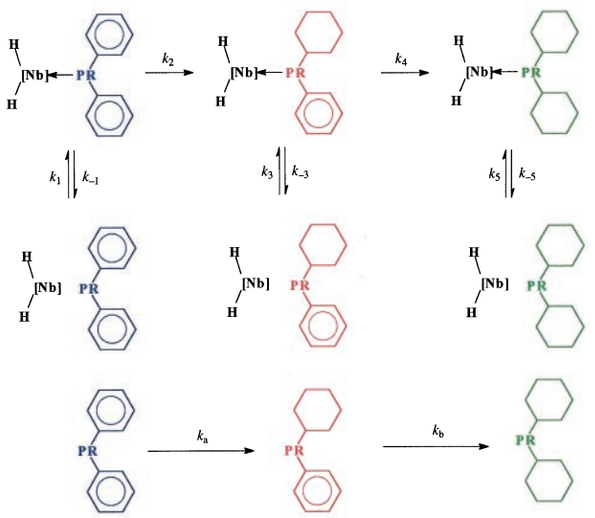
## Catalytic hydrogenation of arylphosphines: a novel case of heteroatom insensitivity

When the tantalum dihydride [Ta($OC_6H_3Pr^i_2$-2,6)$_3$-(H)$_2$($PMePh_2$)] is heated under hydrogen pressures for days, the stepwise formation of the cyclohexylphosphine species [Ta($OC_6H_3Pr^i_2$-2,6)$_3$(H)$_2${PMe($C_6H_{11}$Ph)}] and [Ta($OC_6H_3$-$Pr^i_2$-2,6)$_3$(H)$_2${PMe($C_6H_{11}$)$_2$}] is observed by $^1$H and $^{31}$P NMR spectroscopy.[17] In the field of transition-metal mono-, di- and poly-hydride chemistry the phosphine ligand is a dominant ancillary.[43] Furthermore, by far the vast majority of alkene hydrogenation catalysts contain phosphine ligation as a critical component, particularly systems where a chiral phosphine auxiliary causes asymmetric hydrogenation of a prochiral substrate. In none of these situations has the hydrogenation of aryl groups attached to phosphorus been documented. Any vexing interference by arylphosphines typically involves cyclometallation of arene CH bonds,[44] $\pi$-complexation with the metal[45] or hydrogenolysis of P–C bonds leading to inert metal phosphide species.[46] The niobium arene hydrogenation systems exhibit much greater activity than the tantalum hydrides for the hydrogenation of arylphosphines. This reactivity has been utilized to develop a new synthetic procedure for the formation of cyclohexylphosphines from their cheaper, readily available phenylphosphine counterparts.[47] The success of the niobium compounds for carrying out the reaction is remarkable and must rely on a number of important features. The coordination of the substrate phosphine ligand acts as a 'Trojan Horse' bringing in close proximity to the metal the aryl group. However, carrying out the total saturation of the phenyl ring undoubtedly necessitates breaking at various stages the Nb–P bond. The success of the reaction not only depends on facile exchange of substrate/product phosphine groups within the metal coordination sphere, but also on the fact that the much greater basicity

of cyclohexylphosphines must be offset by their larger cone angle.[48] A much stronger binding of one of the product phosphine ligands could effectively shut down the catalysis. We have also studies the course of these reactions by $^{31}P$ NMR analysis at intermediate stages of hydrogenation. In no cases have we been able to detect significant quantities of cyclohexadienyl- or cyclohexenyl-phosphine compounds. The build up and decay of intermediate cyclohexylphenylphosphines can be readily illustrated by a reaction profile in which the fraction of products is plotted against the fraction hydrogenation of the sample. Some interesting information can be gained from these plots. In the case of the hydrogenation of $PPh_3$ by the catalyst system $[Nb(OC_6HPh_4\text{-}2,3,5,6)_2Cl_3]/3Bu^nLi$ the dramatic build up of the final intermediate $PPh(C_6H_{11})_2$ can be seen (Fig. 3).

This reaction profile can be simulated accurately using a simple kinetic model involving sequential first-order rate constants.[26] The success of this kinetic model for the reaction places constraints on the rate constants within a more complex model in which rates of phosphine coordination and dissociation are included. Although many regimes can exist for this model, the restraint that the rates of phosphine association/dissociation are faster than the rate of saturation of the arene ring means that the first-order constants from the simple model are proportional to the product of the formation constants of the metal phosphine and the rate of arene ring hydrogenation. This is highlighted in Scheme 5 for an alkyldiphenylphosphine. The low relative rate of hydrogenation of $PPh(C_6H_{11})_2$ (Fig. 3) may, therefore, be ascribed either to a low formation constant for the bulky phosphine and/or relatively slow attack on the P–Ph group within this particular ligand. By exploiting this reaction profile we have been able to synthesize the deuteriated compounds $[P(C_6H_5)(C_6H_5D_6)_2]$ and $[P(C_6D_5)(C_6D_5H_6)_2]$ and show that the reaction occurs in a predominantly all-*cis* fashion for attack at both phenyl rings.[26] The detection of non-all-*cis* stereoisomers is almost certainly a consequence of the intermediate regiochemistry of the reaction.[19]

Due to the much documented lack of inversion of configuration at phosphorus under ambient conditions, substrates of stoichiometry $RPPh_2$ are prochiral. We find that the build up of the intermediate, chiral (unresolved) alkyl, phenyl, cyclohexylphosphine can be enhanced by increasing the bulk of the alkyl substituent (Table 2). In the case of $[Pr^iPPh(C_6H_5D_6)]$, labelling studies again show a predominance of all-*cis* hydrogenation.[26] The use of phosphines with chiral alkyl groups leads to diastereomeric pairs. Analysis by $^{31}P$ NMR indicates a slight diastereomeric excess for the alkyls so far examined (Fig. 4, Table 2), showing the successful transfer of chirality from a carbon atom to an adjacent phosphorus centre.[49]




**Scheme 5** If $k_1$, $k_{-1}$, $k_3$, $k_{-3} \gg k_2$, $k_4$ then $k_a/k_b = (k_1/k_{-1})k_2/(k_3/k_{-3})k_4$

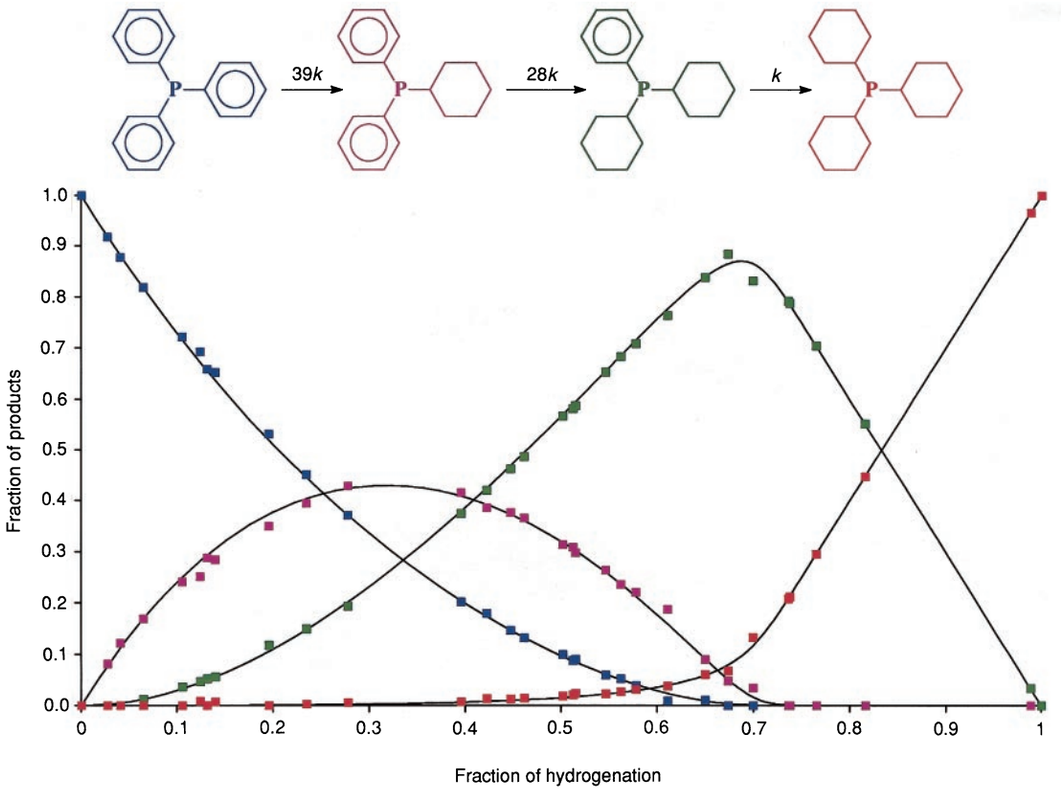



**Fig. 3** Reaction profile for the hydrogenation of $PPh_3$ by $[Nb(OC_6HPh_4\text{-}2,3,5,6)_2Cl_3]/3Bu^nLi$, 0.464 mmol Nb, 190 mmol $C_6H_6$ (409 per Nb), 9.5 mmol $PPh_3$ (20 per Nb), volume 20 ml, 60 °C, 1200 psi $H_2$

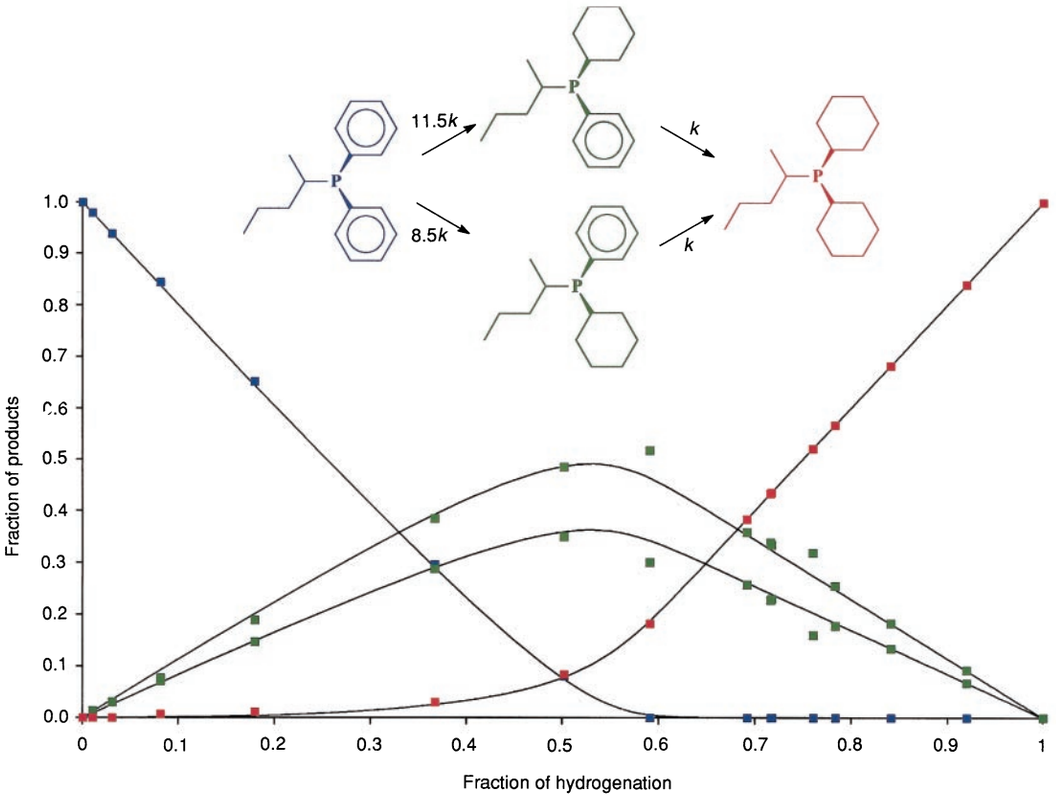
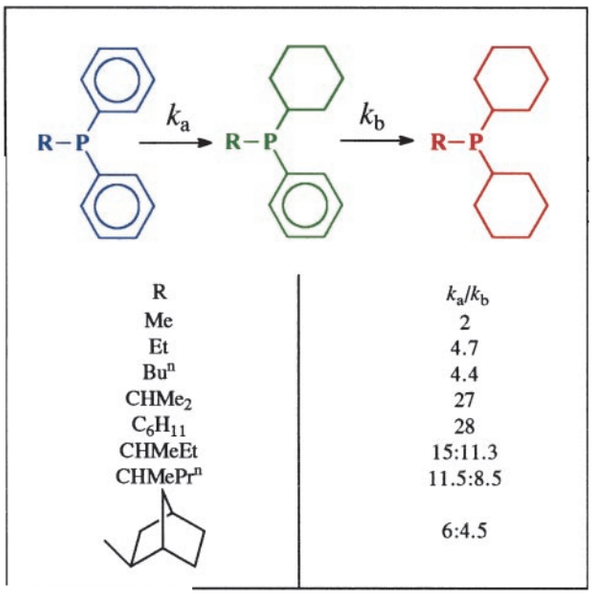



**Fig. 4** Reaction profile for the hydrogenation of [(s-$C_5H_{11}$)$PPh_2$] by [Nb($OC_6HPh_4$-2,3,5,6)$_2Cl_3$]/3Bu$^n$Li, 0.464 mmol Nb, 190 mmol $C_6H_6$ (409 per Nb), 9.5 mmol [(s-$C_5H_{11}$)$PPh_2$] (20 per Nb), volume 20 ml, 60 °C, 1200 psi $H_2$

**Table 2** Ratio of rate constants for hydrogenation of alkyldiphenylphosphines[a]




| R | $k_a/k_b$ |
|---|---|
| Me | 2 |
| Et | 4.7 |
| Bu$^n$ | 4.4 |
| $CHMe_2$ | 27 |
| $C_6H_{11}$ | 28 |
| CHMeEt | 15:11.3 |
| $CHMePr^n$ | 11.5:8.5 |
|  | 6:4.5 |

[a] [Nb($OC_6HPh_4$-2,3,5,6)$_2Cl_3$]/3Bu$^n$Li, 60 °C, 0.464 mmol Nb, 190 mmol $C_6H_6$ (409 per Nb), 9.5 mmol $RPPh_2$ (20 per Nb), volume 20 ml, 1200 psi $H_2$, analysed by $^{31}$P NMR and $k_a/k_b$ obtained by simulation.

The mild conditions used in these studies will not lead to racemization on the timescale of the experiment. It is clearly possible to envision adapting these systems for catalytically generating enantiomeric excesses of chiral phosphine ligands.

The hydrogenation of the bis(phosphine) substrates $Ph_2P(CH_2)_nPPh_2$ ($n$ = 1–6) leads to the corresponding cyclohexyl derivatives. The reactions profile for the hydrogenation of dppm by [Nb($OC_6H_3Pr^i_2$-2,6)$_2Cl_3$]/3Bu$^n$Li shows the build up of product dcpm even at low fraction hydrogenation.[26] This indicates that in this case the rate of hydrogenation of the P–Ph group is faster than the rate of dissociation from the catalytically active site.


## Acknowledgements

I thank my enthusiastic and gifted co-workers whose names appear in the appropriate references and the Department of Energy for financial support.



**Ian P. Rothwell is Professor of Chemistry at Purdue University. He was born in Manchester and educated at Marple Hall Grammar School in Cheshire and University College London where he obtained his PhD under the supervision of Professor A. J. Deeming. Following a postdoctoral appointment at Indiana University with Professor M. H. Chisholm he joined the faculty of Purdue University in 1981. He has received the Meldola Medal and Prize (1984) and the Corday Morgan Medal and Prize (1990) of the Royal Society of Chemistry.**


## Footnote

† This ChemComm is also available in enhanced multi-media format *via* the World Wide Web: http://chemistry.rsc.org/rsc.cccenha.htm

## References


1 P. Sabatier, *How I Have Been Led to the Direct Hydrogenation Method by Metallic Catalysts, Ind. Eng. Chem.*, 1926, **18**, 1004.
2 P. Sabatier and J.-B. Senderens, *Compt. Rend.*, 1897, **124**, 616.
3 P. Sabatier and J.-B. Senderens, *Compt. Rend.*, 1901, **132**, 210; 566; 1254.

4 R. Adams and J. R. Marshall, *J. Am. Chem. Soc.*, 1928, **50**, 1970; V. Voorhees and R. Adams, *J. Am. Chem. Soc.*, 1922, **44**, 1397.
5 M. Raney, *Catalysts from Alloys, Ind. Eng. Chem.*, 1940, **32**, 1199; *US Pat.* 1 628 190, May 19th, 1927 to the Gilman Paint and Varnish Company.
6 K. Weissermel and H.-J. Arpe, in *Industrial Organic Chemistry*, VCH, New York, 2nd edn., 1993, p. 343.
7 M. S. Eisen and T. J. Marks, *J. Am. Chem. Soc.*, 1992, **114**, 10 358; R. D. Profilet, A. P. Rothwell and I. P. Rothwell, *J. Chem. Soc., Chem. Commun.*, 1993, 42; M. D. Ward and J. Schwartz, *J. Am. Chem. Soc.*, 1981, **103**, 5253.
8 J. F. Young, J. A. Osborn, F. H. Jardine and G. Wilkinson, *Chem. Commun.*, 1965, 131; J. A. Osborn, F. H. Jardine, J. F. Young and G. Wilkinson, *J. Chem. Soc. A*, 1966, 1711.
9 F. A. Cotton and G. Wilkinson, *Advanced Inorganic Chemistry*, Wiley, New York, 5th edn. 1988 p. 1244.
10 E. L. Muetterties and J. R. Bleeke, *Acc. Chem. Res.*, 1979, **12**, 324; L. S. Stuhl, M. Rakowski DuBois, F. J. Hirsekorn, J. R. Bleeke, A. E. Stevens and E. L. Muetterties, *J. Am. Chem. Soc.*, 1978, **100**, 2405.
11 G. A. Olah and A. Molnar, *Hydrocarbon Chemistry*, Wiley, New York, 1985; G. W. Parshall and S. D. Ittel, *Homogeneous Catalysis*, Wiley, New York, 2nd edn., 1992; B. R. James, *Homogeneous Hydrogenation*, Wiley, New York, 1973; M. Bennett, *CHEMTECH*, 1980, 444; P. M. Maitlis, *Acc. Chem. Res.*, 1978, **100**, 2405; J. P. Collman, K. M. Kosydar, M. Bressan, W. Lamanna and T. Garrett, *J. Am. Chem. Soc.*, 1984, **106**, 2569; I. Amer, H. Amer, R. Ascher, J. Blum and Y. Sasson, *J. Mol. Catal.*, 1987, **39**, 185; K. R. Januszkiewicz and H. Alper, *Organometallics*, 1983, **2**, 1055; E. Baralt, S. J. Smith, J. Hurwitz, I. T. Horvath and R. H. Fish, *J. Am. Chem. Soc.*, 1992, **114**, 5187; R. H. Fish, E. Baralt and S. J. Smith, *Organometallics*, 1991, **10**, 54; R. A. Sanchez-Delgado, D. Rondon, A. Andriollo, V. Herrera, G. Martin and B. Chaudret, *Organometallics*, 1993, **12**, 4291; P. Abley, I. Jardine and F. J. McQuillin, *J. Chem. Soc. C*, 1971, 840; P. D. Taylor and M. Orchin, *J. Org. Chem.*, 1972, **37**, 3913.
12 J. Halpern, *Pure Appl. Chem.*, 1987, **59**, 173; D. E. Linn and J. Halpern, *J. Am. Chem. Soc.*, 1987, **109**, 2969.
13 E. L. Muetterties, M. C. Rakowski, F. J. Hirsekorn, W. D. Larson, V. J. Basus and F. A. L. Anet, *J. Am. Chem. Soc.*, 1975, **97**, 1266.
14 K. Seemeyer, D. Schroder, M. Kempf, O. Lettau, J. Muller and H. Schwarz, *Organometallics*, 1995, **14**, 4465.
15 *Applied Homogeneous Catalysis with Organometallic Compounds*, ed. B. Cornils and W. A. Herrmann, VCH, New York, 1996, vol. 1; Y. Chauvin, J. Gaillard, J. Leonard, P. Booifay and J. W. Andrews, *Hydrocarbon Processing*, 1982 (May), 110; A. Alvanipour and L. D. Kispert, *J. Mol. Catal.*, 1988, **48**, 277; M. F. Sloan, A. S. Matlack and D. S. Breslow, *J. Am. Chem. Soc.*, 1963, **85**, 4014; S. J. Lapporte and W. R. Schuett, *J. Org. Chem.*, 1963, **28**, 1947.
16 I. P. Rothwell, *Acc. Chem. Res.*, 1988, **21**, 153; M. A. Lockwood, P. E. Fanwick, O. Eisenstein and I. P. Rothwell, *J. Am. Chem. Soc.*, 1996, **118**, 2762; M. A. Lockwood, J. R. Clark, B. C. Parkin and I. P. Rothwell, *Chem. Commun.*, 1996, 1973; S. A. Waratuke, E. S. Johnson, M. G. Thorn, P. E. Fanwick and I. P. Rothwell, *Chem. Commun.*, 1996, 2617.
17 B. C. Parkin, J. C. Clark, V. M. Visciglio, P. E. Fanwick and I. P. Rothwell, *Organometallics*, 1995, **14**, 3002; V. M. Visciglio, P. E. Fanwick and I. P. Rothwell, *J. Chem. Soc., Chem. Commun.*, 1992, 1505; B. C. Ankianiec, P. E. Fanwick and I. P. Rothwell, *J. Am. Chem. Soc.*, 1991, **113**, 4710.
18 J. M. Mayer, P. T. Wolczanski, B. D. Santarsiero, W. A. Olson and J. E. Bercaw, *Inorg. Chem.*, 1983, **22**, 1149;
19 M. A. Lockwood, M. C. Potyen, B. D. Steffey and P. E. Fanwick, *Polyhedron*, 1995, **14**, 3293; B. D. Steffey and I. P. Rothwell, *J. Chem. Soc., Chem. Commun.*, 1990, 213; B. D. Steffey, R. W. Chesnut, J. L. Kerschner, P. Pellechia, P. E. Fanwick and I. P. Rothwell, *J. Am. Chem. Soc.*, 1989, **111**, 378.
20 K. D. Allen, M. A. Bruck, S. D. Gray, R. P. Kingsborough, D. P. Smith, K. J. Weller and D. E. Wigley, *Polyhedron*, 1995, **14**, 3315.
21 D. G. Gusev, R. Kuhlman, G. Sini, O. Eisenstein and K. G. Caulton, *J. Am. Chem. Soc.*, 1994, **116**, 2685.
22 H. M. Feder and J. Halpern, *J. Am. Chem. Soc.*, 1975, **97**, 7186.
23 A. J. Birch, *Quart. Rev.*, 1950, **4**, 69.
24 J. S. Yu, B. C. Ankianiec, M. T. Nguyen and I. P. Rothwell, *J. Am. Chem. Soc.*, 1992, **114**, 1927.
25 Y. Huang, R. D. Profilet, J. H. Ng, Y. Ranasinghe, I. P. Rothwell and B. S. Freiser, *Anal. Chem.*, 1994, **66**, 1050.
26 M. C. Potyen and I. P. Rothwell, *J. Chem. Soc., Chem. Commun.*, 1995, 849.
27 G. M. Loudon, *Organic Chemistry*, Benjamin Cummings, Menlo Park, CA, 2nd edn., 1988.
28 R. L. Burwell, *Chemtracts-Inorg. Chem.*, 1993, **5**, 330; H. Imamura, T. Konishi, Y. Sakata and S. Tsuchiya, *J. Chem. Soc., Chem. Commun.*, 1993, 1852.
29 H. C. Brown, *Boranes in Organic Chemistry*, Cornell University Press, Ithaca, New York, 1972.
30 M. Yalpani, *Chem. Ber.*, 1990, **123**, 983; R. Koster, W. Schüßler and M. Yalpani, *Chem. Ber.*, 1989, **122**, 677; M. Yalpani, T. Lunow and R. Köster, *Chem. Ber.*, 1989, **122**, 687.
31 *Selective Hydrocarbon Activation*, ed. J. A. Davis, P. L. Watson, J. F. Liebman and A. Greenberg, VCH, New York, 1990.
32 M. E. Thompson, S. M. Baxter, A. R. Bulls, B. J. Burger, M. C. Nolan, B. D. Santarsiero, W. P. Schaefer and J. E. Bercaw, *J. Am. Chem. Soc.*, 1987, **109**, 203.
33 V. M. Visciglio, M. T. Nguyen, J. R. Clark, P. E. Fanwick and I. P. Rothwell, *Polyhedron*, 1996,. **15**, 551.
34 P. A. Wexler, D. E. Wigley, J. B. Koerner and T. A. Albright, *Organometallics*, 1991, **10**, 2319.
35 J. T. Barry and M. H. Chishom, *J. Chem. Soc., Chem. Commun.*, 1995, 1599.
36 J. R. Clark, P. E. Fanwick and I. P. Rothwell, *J. Chem. Soc., Chem. Commun.*, 1995, 553.
37 J. R. Clark, P. E. Fanwick and I. P. Rothwell, unpublished work.
38 P. T. Wolczanski, *Polyhedron*, 1995, **14**, 3335.
39 S. D. Gray, K. J. Weller, M. A. Bruck, P. M. Briggs and D. E. Wigley, *J. Am. Chem. Soc.*, 1995, **117**, 10 678.
40 M. A. Lockwood, P. E. Fanwick and I. P. Rothwell, *Polyhedron*, 1995, **14**, 3363.
41 M. A. Lockwood, P. E. Fanwick and I. P. Rothwell, *Chem. Commun.*, 1996, 2013.
42 J. S. Yu, L. Felter, M. C. Potyen, J. R. Clark, V. M. Visciglio, P. E. Fanwick and I. P. Rothwell, *Organometallics* 1996, **15**, 4443; J. S. Yu, P. E. Fanwick and I. P. Rothwell, *J. Am. Chem. Soc.*, 1990, **112**, 8171.
43 R. H. Crabtree, in *Comprehensive Coordination Chemistry*, ed. G. Wilkinson, R. D. Gillard and J. A. McCleverty, Pergamon, New York, 1987, vol. 2, p. 689.
44 E. C. Constable, *Polyhedron*, 1984, **3**, 1037; M. I. Bruce, *Angew. Chem., Int. Ed. Engl.*, 1977, **16**, 73.
45 R. L. Luck, R. H. Morris and J. F. Sawyer, *Organometallics*, 1984, **3**, 247.
46 P. E. Garrou, *Chem. Rev.*, 1985, **85**, 171.
47 I. P. Rothwell and J. S. Yu, *US Pat.* 5 530 162, 1996; J. S. Yu and I. P. Rothwell, *J. Chem. Soc., Chem. Commun.*, 1992, 632.
48 C. A. Tolman, *Chem. Rev.*, 1977, **77**, 313.
49 M. C Potyen and I. P. Rothwell, unpublished work.


*6/06985A*

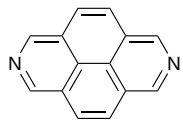
# Crystal engineering: the effects of π–π interactions in copper(I) and silver(I) complexes of 2,7-diazapyrene

**Alexander J. Blake,[a] Neil R. Champness,*[a] Andrei N. Khlobystov,[a,b] Dmitri A. Lemenovskii,[b] Wan-Sheung Li[a] and Martin Schröder*[a]**

[a] *Department of Chemistry, The University of Nottingham, University Park, Nottingham, UK NG7 2RD*
[b] *Department of Chemistry, Moscow State University, 119899 Moscow, Russia*

**The ligand 2,7-diazapyrene (L) is used to construct three- and two-dimensional arrays with $Cu^{I}$ and $Ag^{I}$ ions: $\{[Cu^{I}L_2]PF_6\}_\infty$ shows an adamantoid network with three interpenetrating networks, while $\{[Ag^{I}L_2(MeCN)_2]BF_4\}_\infty$ forms linear chains of $[AgL]_\infty$ units linked by apparent π–π stacking and Ag···Ag interactions between adjacent diazapyrene ligands to form two-dimensional sheets.**

Crystal engineering and the design of solid-state architectures has become an area of increasing interest over recent years.[1–4] Much study has been centred upon the use of supramolecular contacts, particularly hydrogen-bonding, between suitable molecules to generate multi-dimensional arrays or networks.[1–3] In comparison, the design of inorganic networks has been less well developed.[4–8] We have been investigating the effect of ligand functionality upon the construction of two- and three-dimensional arrays and, in particular, adamantoid or super-diamondoid networks based upon copper(I) complexes.[8] We were interested in monitoring the effects of ligand bulk and the potential of π–π stacking interactions in controlling network geometry. With this in mind we chose the ligand 2,7-diazapyrene (L)[9] as a potentially useful building block in the construction of multi-dimensional architectures. We report herein the first structurally characterised examples of metal complexes with L.



2,7-diazapyrene L

The reaction of $[Cu(MeCN)_4]PF_6$ with L in MeCN–PhCN afforded unusual triangular-shaped red crystals suitable for X-ray analysis. The crystal structure shows† the complex $\{[CuL_2]PF_6\}_\infty$ to form a three-dimensional adamantoid network in which each $Cu^{I}$ centre is co-ordinated in a tetrahedral geometry to four diazapyrene ligands, Cu–N 2.044(9)Å. The spaces within each adamantoid network are filled by two other adamantoid networks and the three interpenetrating arrays related to each other by a 90° rotation (Fig. 1). This form of interpenetration contrasts with that observed for other copper(I) adamantoid networks which are related to each other by simple translation.[5,6,8] Adjacent lattices interact with each other *via* face-to-face π–π interactions between 2,7-diazapyrene ligands which are arranged so that the N···N axes of the ligand are at 90° to one another. The distance between aromatic rings is 3.469 Å, compared with a value of 3.450 Å for the free ligand which we have structurally characterised.[10] The positive charge of the metallo-ligand lattice is balanced by $PF_6^-$ counter anions which were found to be disordered around a threefold axis. The counter anion site was also found to be partially occupied with three-quarters of the $PF_6^-$ anion sites filled.†

The three independent interpenetrating lattices observed for $\{[CuL_2]PF_6\}_\infty$ contrasts with the four observed for $\{[Cu(4,4'\text{-bipy})_2]BF_4\}_\infty$[5] and five for $\{[Cu(bpe)_2]BF_4\}_\infty$ [bpe = 1,2-*trans*-(4-pyridyl)ethene].[8] 2,7-Diazapyrene is a slightly shorter linker than 4,4′-bipy, giving a Cu···Cu distance of 10.904 Å along the edges of each adamantoid unit in $\{[CuL_2]PF_6\}_\infty$ compared to 11.166 Å for $\{[Cu(4,4'\text{-bipy})_2]BF_4\}_\infty$.[5] Athough the decrease in the number of interpenetrating lattices might in principle be explained by the decrease in the length of the linking ligand, this seems unlikely given such a small decrease in Cu···Cu distance. Increasedπ–π interactions between adjacent lattices should encourage more

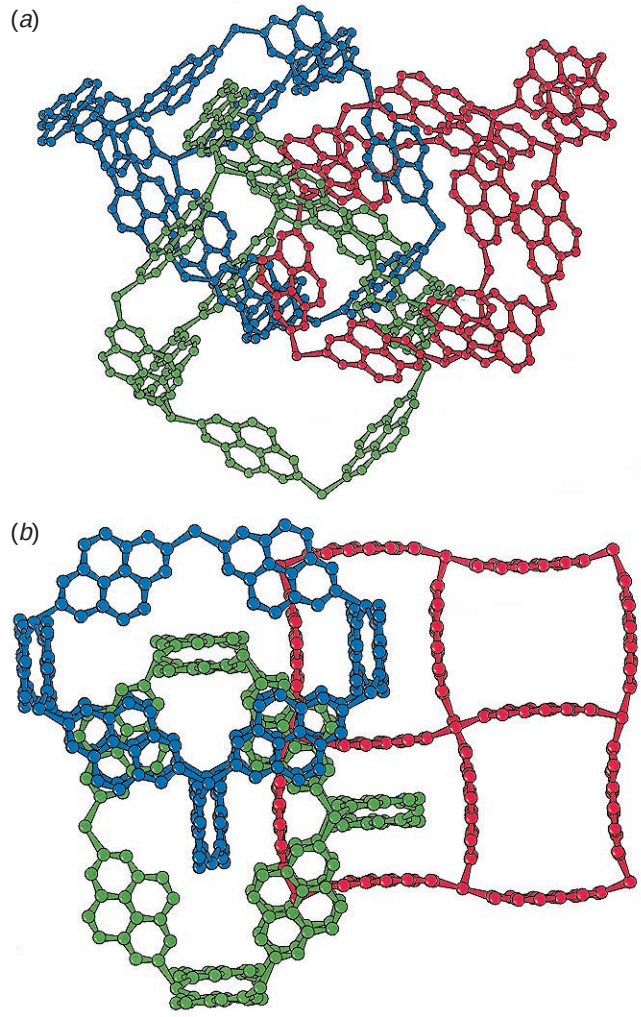


**Fig. 1** Two views of the structure of $\{[CuL_2]PF_6\}_\infty$ (L = 2,7-diazapyrene) showing three interlocking adamantoid cages. $PF_6^-$ anions omitted for clarity.

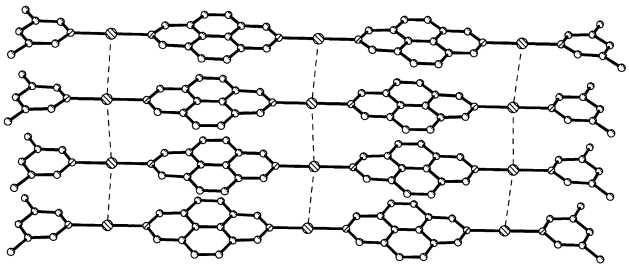


**Fig. 2** View of the structure of $\{[AgL(MeCN)_2]BF_4\}_\infty$ (L = 2,7-diazapyrene); MeCN molecules and $BF_4^-$ anions have been omitted for clarity

efficient packing which would be expected to lead to increased numbers of independent lattices rather than the decrease observed here. Thus, the decrease in the number of interpenetrating lattices in $\{[CuL_2]PF_6\}_\infty$ can be rationalised by the greater lateral steric bulk of L reducing the volume within any given adamantoid lattice that can be filled by other symmetry related lattices. This represents the identification of another factor controlling the degree of interpenetration in adamantoid lattices.[8,11]

The related silver(I) complex $\{[AgL(MeCN)_2]BF_4\}_\infty$ was obtained by reaction of L with $AgBF_4$ in 1 : 1 or 2 : 1 ligand-to-metal ratios. The structure of the complex shows† linear chains of alternating $Ag^I$ ions and L (Fig. 2). These chains are linked together *via* face-to-face π–π interactions between 2,7-diazapyrene ligands in which the ligand N···N axes are parallel to each other with a separation of 3.380 Å: a separation of 3.450 Å is observed in the X-ray structure of the metal-free L.[10] This π–π interaction also enforces the formation of apparent Ag···Ag interactions of 3.641(2) Å. Bonding between adjacent chains is further strengthened by MeCN ligands which bridge adjacent Ag centres, Ag–N 2.871(4), 2.926(4) Å, to form two-dimensional sheets. The enforced formation of Ag···Ag interactions in this structure is in sharp contrast to the analogous complex $\{[Ag(4,4'\text{-bipy})]BF_4\}_\infty$ in which $Ag^I$ ions on adjacent linear chains are staggered thereby precluding the formation of Ag···Ag interactions or π–π stacking between bipyridyl ligands.[12]

We thank the EPSRC for support.

## Footnotes

* E-mail: m.schroder@nottingham.ac.uk

† Stoe Stadi-4 four-circle diffractometer, graphite-monochromated Mo-Kα radiation, $\omega$–$\theta$ scans, $\theta_{max}$ = 25°. Both structures were solved using direct methods[13] and all non-H atoms were located using subsequent difference-Fourier methods.[14] In both cases hydrogen atoms were placed in calculated positions and were allowed to ride on their parent atoms.

*Crystal data* for $\{[CuL_2]PF_6\}_\infty$: $C_{28}H_{16}CuF_6N_4P$, $M$ = 616.96, cubic, space group $I\bar{4}3d$ (no. 220), $a$ = 19.505(7) Å, $U$ = 7421(5) Å$^3$, $Z$ = 12, $F$(000) = 3720, $D_c$ = 1.657 g cm$^{-3}$, $\mu$(Mo-Kα) = 1.020 mm$^{-1}$. A red triangular crystal (0.28 × 0.27 × 0.23 mm). Numerical absorption corrections were applied to the data ($T_{min}$ 0.7004, $T_{max}$ 0.7487), 603 unique reflections [$R_{int}$ = 0.096], of which 485 had $I \geqslant 2\sigma(I)$, were used in all calculations. A correction for crystal decay (4%) was applied during data reduction. The $PF_6^-$ anion was found to be disordered around a threefold axis and the equatorial F atoms were split over four sites of occupancy 0.15, 0.11, 0.22, 0.52. In order to balance charges the occupancy of the $PF_6^-$ anion was required to be 0.25 (rather than 0.333 on a threefold site), see main text. This was further justified by the improvements which resulted in the overall refinement model, for example $R_1$ decreased from 0.068 to 0.063. The weighting scheme $w^{-1} = [\sigma^2(F_o^2) + (0.052P)^2 + 51.4P]$, $P = (\max(F_o^2,0) + 2F_c^2)/3$ was adopted. At final convergence[14] $R_1$ [$I > 2\sigma(I)$] = 0.0629, $wR_2$ (all data) = 0.1509 for 104 parameters, $S$ = 1.20, $(\Delta/\sigma)_{max}$ = 0.003, $\Delta\rho_{max}$ = 0.40 e Å$^{-3}$.

For $\{[AgL(MeCN)_2]BF_4\}_\infty$: $C_{18}H_{14}AgBF_4N_4$, $M$ = 481.01, monoclinic, space group $C2/c$ (no. 15), $a$ = 21.660(7), $b$ = 11.380(2), $c$ = 7.263(3) Å, $\beta$ = 100.93(3)°, $U$ = 1757.8(10) Å$^3$, $Z$ = 4, $F$(000) = 952, $D_c$ = 1.818 g cm$^{-3}$, $\mu$(Mo-Kα) = 1.198 mm$^{-1}$. A pale yellow plate (0.23 × 0.15 × 0.05 mm). Absorption corrections based upon $\psi$-scans were applied to the data ($T_{min}$ 0.8202, $T_{max}$ 0.9336), 1283 unique reflections [$R_{int}$ = 0.030], of which 1283 had $F_o \geqslant 4\sigma(F_o)$, were used in all calculations.The methyl carbon of the acetonitrile solvent molecule was found to be disordered over two equally occupied sites.The weighting scheme $w^{-1} = [\sigma^2(F_o^2) + (0.0246P)^2 + 8.19P]$, $P = [\max(F_o^2,0) + 2F_c^2]/3$ was adopted. At final convergence[14] $R_1$ [$I > 2\sigma(I)$] = 0.0393, $wR_2$ (all data) = 0.0809 for 148 parameters, $S$ = 1.04, $(\Delta/\sigma)_{max}$ = 0.002, $\Delta\rho_{max}$ = 0.58 e Å$^{-3}$.

Atomic coordinates, bond lengths and angles, and thermal parameters have been deposited at the Cambridge Crystallographic Data Centre (CCDC). See Information for Authors, Issue No. 1. Any request to the CCDC for this material should quote the full literature citation and the reference number 182/472.

## References

1 G. R. Desiraju, in *Crystal Engineering: Design of Organic Solids*, Elsevier, Amsterdam, 1989.
2 *The Crystal as a Supramolecular Entity*, ed. G. R. Desiraju, Wiley, 1995.
3 G. R. Desiraju, *Angew. Chem., Int. Ed. Engl.*, 1995, **34**, 2311.
4 R. Robson, B. F. Abrahams, S. R. Batten, R. W. Gable, B. F. Hoskins and J. Liu, *Supramolecular Architecture*, ACS publications, 1992, ch. 19.
5 L. R. MacGillivary, S. Subramanian and M. J. Zaworotko, *J. Chem. Soc., Chem. Commun.*, 1994, 1325.
6 L. Carlucci, G. Ciani, D. M. Proserpio and A. Sironi, *J. Chem. Soc., Chem. Commun.*, 1994, 2755.
7 S. B. Copp, S. Subramanian and M. J. Zaworotko, *J. Am. Chem. Soc.*, 1992, **114**, 8719; S. B. Copp, S. Subramanian and M. J. Zaworotko, *J. Chem. Soc., Chem. Commun.*, 1993, 1078; S. B. Copp, K. T. Holman, J. O. S. Sangster, S. Subramanian and M. J. Zaworotko, *J. Chem. Soc., Dalton Trans.*, 1995, 2233; S. Subramanian and M. J. Zaworotko, *Angew. Chem., Int. Ed. Engl.*, 1995, **34**, 2127; P. Losier and M. J. Zaworotko, *Angew. Chem., Int. Ed. Engl.*, 1996, **35**, 2779; B. F. Abrahams, S. R. Batten, H. Hamit, B. F. Hoskins and R. Robson, *Angew. Chem., Int. Ed. Engl.*, 1996, **35**, 1691; D. Venkataraman, S. Lee, J. S. Moore, P. Zhang, K. A. Hirsch, G. B. Gardner, A. C. Covey and C. L. Prentice, *Chem. Mater.*, 1996, **8**, 2030; D. M. L. Goodgame, S. Menzer, A. M. Smith and D. J. Williams, *Angew. Chem., Int. Ed. Engl.*, 1995, **34**, 574; P. C. M. Duncan, D. M. L. Goodgame, S. Menzer and D. J. Williams, *Chem. Commun.*, 1996, 2127.
8 A. J. Blake, N. R. Champness, S. S. M. Chung, W.-S. Li and M. Schröder, *Chem. Commun.*, 1997, 1005.
9 P. J. Stang, D. H. Cao, S. Saito and A. M. Arif, *J. Am. Chem. Soc.*, 1995, **117**, 6273.
10 A. J. Blake, N. R. Champness, A. Khlobystov, W.-S. Li and M. Schröder, unpublished work.
11 O. Ermer, *J. Am. Chem. Soc.*, 1988, **110**, 3747.
12 A. J. Blake, N. R. Champness, S. S. M. Chung, W.-S. Li and M. Schröder, unpublished work
13 G. M. Sheldrick, SHELXS-86, *Acta Crystallogr., Sect. A*, 1990, **46**, 467.
14 G. M. Sheldrick, SHELXL-93, University of Göttingen, Germany, 1993.

*Received in Cambridge, UK, 25th March 1997, 7/02050C*

# A tetranickel(II) macrocyclic complex incorporating five different bridging groups‡

**Paul E. Kruger† and Vickie McKee***

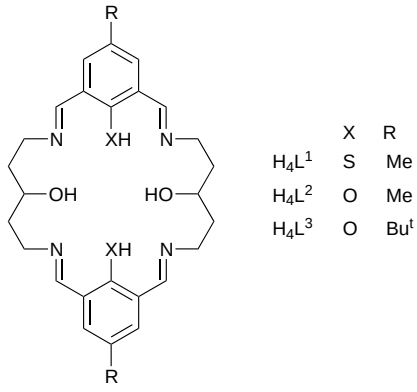
*Chemistry Department, Queen's University, Belfast, Northern Ireland, UK, BT9 5AG*

**The synthesis and crystal structure of the tetranickel(II) complex $[Ni_4(L^1)(OH)(MeCO_2)_3(MeCO_2H)]$ is reported, where $H_4L^1$ is a macrocyclic ligand incorporating thiophenolate, alkoxo and imine donors; the faces of the tetranickel array are differentiated and two of the nickel ions share three monatomic bridges (S,O,O).**

As part of a programme to synthesise and investigate polynuclear arrays, we have characterised tetranuclear macrocyclic complexes of ligands $H_4L^2$ and $H_4L^3$ containing phenoxo and alkoxo bridging groups.[1] The properties of these arrays can, in principle, be modified by varying the donor groups, size of the macrocycle, nature of the metal ions *etc*. In this way the assemblies can be tuned to give control over various aspects of metal–metal interactions, redox properties and exogenous ligand binding. Here, we report the synthesis and characterisation of a neutral tetranickel(II) complex of $H_4L^1$, a new ligand in which the phenol donors are replaced by the larger and softer thiophenol group.

The tetranickel(II) complex was prepared by a template route. Solid $Ni(MeCO_2)_2{\cdot}4H_2O$ was added to 2,6-diformyl-4-methylthiophenol[2,3] in refluxing isopropyl alcohol under an inert atmosphere, followed by dropwise addition of 1,5-diamino-3-hydroxypentane[4] in methanol–isopropyl alcohol solution. After refluxing for 20 h, the volume of the solution was reduced, the brown powder filtered off, and recrystallised from chloroform–dichloromethane containing a small amount of methanol (yield *ca*. 30%). Microanalytical data were consistent with the formulation $[Ni_4L^1(OH)(MeCO_2)_3(MeCO_2H)]{\cdot}1.5\ H_2O$. The secondary ion mass spectrum confirms the presence of fragments containing the $[Ni_4L^1(OH)]^{3+}$ core. Clusters centred at: *m*/*z* 924 (15), 888 (20), 829 (100, base peak) and 770 (35) are assigned to $[Ni_4L^1(OH)(MeCO_2)_2(H_2O)_2]^+$, $[Ni_4L^1(OH)(MeCO_2)_2]^+$, $[Ni_4L^1(OH)(MeCO_2)]^+$ and $[Ni_4L^1(OH)]^+$, respectively. Dark brown crystals of the methanol solvate, $[Ni_4L^1(OH)MeCO_2)_3(MeCO_2H)]{\cdot}MeOH$, suitable for X-ray diffraction studies§ were obtained by slow diffusion of diethyl ether into a dmf–methanol solution of the complex. The asymmetric unit contains one $[Ni_4L^1(OH)(MeCO_2)_3(MeCO_2H)]{\cdot}MeOH$ complex (Fig. 1). The four coplanar nickel(II) ions are each coordinated to one thiophenolate sulfur, one alkoxy oxygen and one imine from the macrocycle and to a central $\mu_4$-hydroxo group, O(3). Six-coordination is completed by three bridging acetate ligands and one acetic acid group. The macrocyclic donors are *fac* for Ni(1) and Ni(4) but *mer* for Ni(2) and Ni(3). The coordinated acetic acid molecule forms a one-atom bridge between Ni(2) and Ni(3) and is also quite strongly hydrogen-bonded to a macrocyclic alkoxy donor [O(62)···O(2) 2.516(7) Å]. The description of this bond as $RCO_2H{\cdots}OR'$ rather than $RCO_2^-{\cdots}HOR'$ is made on the basis of an electron density peak 1.14 Å from O(62) and 1.46 Å from O(2) which is assigned to the carboxylic acid hydrogen. Similar coordinated acetic acid molecules are found in the related phenolate complex,[5] $[Ni_4L^3(OH)(MeCO_2)_3(MeCO_2H)_2]{\cdot}DMF{\cdot}H_2O$. The three acetate ligands act as conventional *syn-syn* three-atom bridges between pairs of nickel ions on the same side of the macrocyclic ring; one of the acetate ions is hydrogen-bonded to the solvent methanol [O(41)···O(71), 2.806(7) Å]. The oxygen atom of the central $\mu_4$-hydroxo group projects 0.581(4) Å from the plane of the four nickel ions into the cavity bounded by the three acetate ligands (Fig. 2) and is prevented from interacting with any other species. A sharp peak at 3598 $cm^{-1}$ in the infrared spectrum is consistent with this environment and assigned to the $\nu_{OH}$ vibration.[6] The hydroxo hydrogen atom was located unambiguously from difference Fourier maps.

Each nickel ion is linked to the next *via* three bridging groups. For Ni(1)···Ni(2) and Ni(3)···Ni(4) these are one alkoxo, one hydroxo, one 1,3-acetato group; for Ni(1)···Ni(4), thiophenolato, hydroxo and 1,3-acetato, while Ni(2) and Ni(3) are linked by three single-atom bridges [S(2), O(3) and O(61)], so that they share one octahedral face (Fig. 3). This geometry is not unusual where all three bridges are light atoms and there are several examples where all three are sulfur donors.[7] However, the only other example containing three mixed sulfur/light atom bridges is at the active site of the [NiFe] hydrogenase from *Desulfovibrio gigas* where two cysteine thiolates and a putative oxo species form three monatomic bridges between the Ni and Fe centres.[8] While the complex described in this paper is not




| | X | R |
|---|---|---|
| $H_4L^1$ | S | Me |
| $H_4L^2$ | O | Me |
| $H_4L^3$ | O | $Bu^t$ |

**Scheme 1**

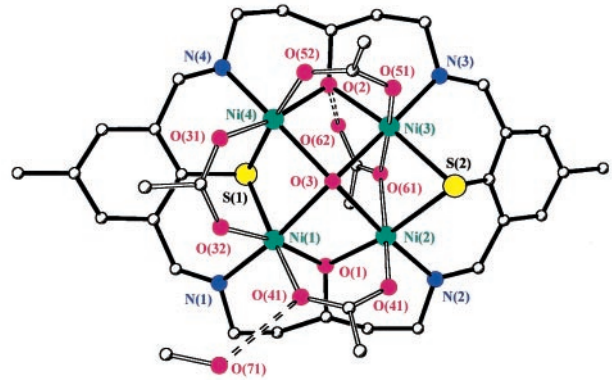



**Fig. 1** Perspective view of $[Ni_4L^1(OH)(MeCO_2)_3(MeCO_2H)]{\cdot}MeOH$, hydrogen atoms are omitted. Selected interatomic distances (Å): Ni(1)–Ni(2) 2.998(1), Ni(2)–Ni(3) 2.910(1), Ni(3)–Ni(4) 3.061(1), Ni(4)–Ni(1) 3.170(1).

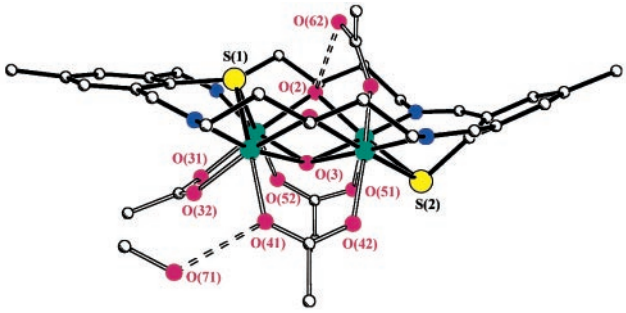



**Fig. 2** View perpendicular to the $Ni_4$ plane showing the non-planar conformation of the macrocycle. Selected bond angles (°): Ni(1)–O(3)–Ni(2) 83.5(2), Ni(2)–O(3)–Ni(3) 82.1(2), Ni(3)–O(3)–Ni(4) 88.3(2), Ni(4)–O(3)–Ni(1) 90.4(2), Ni(4)–S(1)–Ni(1) 84.17(7), Ni(3)–S(2)–Ni(2) 76.29(6), Ni(2)–O(1)–Ni(1) 97.0(2), Ni(3)–O(2)–Ni(4) 93.1(2).

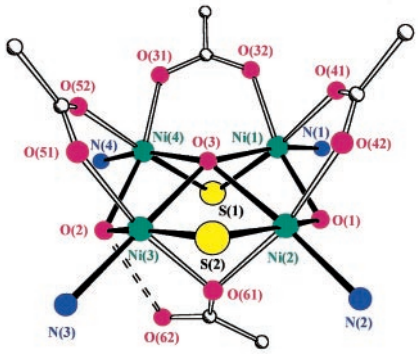



**Fig. 3** The coordination spheres of the nickel ions. Selected bond distances (Å): Ni(1)–O(3) 2.237(4), Ni(2)–O(3) 2.263(5), Ni(3)–O(3) 2.165(4), Ni(4)–O(3) 2.231(5), Ni(1)–S(1) 2.366(2), Ni(4)–S(1) 2.363(2), Ni(2)–S(2) 2.365(2), Ni(3)–S(2) 2.347(2), Ni(1)–O(1), 2.029(5), Ni(2)–O(1) 1.973(4), Ni(3)–O(2) 2.094(5), Ni(4)–O(2) 2.124(5), Ni(1)–N(1), 2.057(6), Ni(2)–N(2) 2.062(6), Ni(3)–N(3) 2.066(5), Ni(4)–N(4) 2.072(6), Ni(1)–O(32) 2.059(5), Ni(1)–O(41) 2.111(5), Ni(2)–O(42) 2.048(5), Ni(2)–O(61) 2.166(4), Ni(3)–O(51) 2.025(5), Ni(3)–O(61) 2.120(5), Ni(4)–O(31) 2.002(5), Ni(4)–O(52) 2.074(5).

intended to model the biosite, it does provide some indications as to how accurate active site mimics could be achieved.

In Schiff-base ligands derived from 2,6-diformylthiophenols the large sulfur donor must be accommodated without appreciable expansion of the relatively inflexible thiophenol–diimine unit. This requirement generally causes the sulfur atom and the imine groups to lie on opposite sides of the plane of the phenyl ring with geometry similar to that at S(1).[3,9–11] The deviations from the plane of the phenyl ring (Fig. 2) are much greater at S(2), presumably as a consequence of the face-sharing geometry of Ni(2) and Ni(3). Overall, the complex is markedly unsymmetric; the faces of the tetranickel array can be distinguished and two different Ni sites can be identified. One face is closed by the three acetato ligands; on the other side access to Ni(1) and Ni(4) is blocked by the apical thiolate donor S(1) but Ni(2) and Ni(3) have one site occupied only by the neutral acetic acid group. The solubility of the neutral complex in chloroform–dichloromethane suggests that the anionic ligands remain coordinated in solution, at least in these solvents.

Details of the magnetic properties of the present complex will be discussed along with those of related complexes[5] but, in summary, the nickel ions are high-spin and the complex shows net antiferromagnetic coupling, very similar in magnitude to that observed in more symmetrical tetranickel(II) arrays.[5,12,13] Murray and coworkers[12,13] have modelled this behaviour in terms of isolated pairs of dimers each with a single $J$ of *ca.* $-30$ $cm^{-1}$.

We are grateful to the EPSRC for financial support and to Boujemaa Moubaraki and Keith S. Murray, Monash University, for the magnetic data.

## Footnotes

* E-mail: v.mckee@qub.ac.uk
† Present address: Department of Chemistry, Trinity College, Dublin, Ireland, E-mail: paul.kruger@tcd.ie
‡ This ChemComm is also available in enhanced multi-media format *via* the World Wide Web: http://chemistry.rsc.org/rsc/cccenha.htm
§ *Crystal data*: $[Ni_4L^1(OH)(MeCO_2)_3(MeCO_2H)]\cdot MeOH$, $C_{37}H_{50}N_4Ni_4O_{12}S_2$, brown–green block, 0.60 × 0.53 × 0.32 mm, monoclinic, space group $P2_1/n$, $a$ = 11.105(2), $b$ = 18.297(3), $c$ = 20.027(3) Å, $\beta$ = 93.52(1)°, $U$ = 4061(1) $Å^{-3}$, $Z$ = 4, $\mu$ = 1.996 $mm^{-1}$, $F(000)$ = 2160. Using graphite-monochromated Mo-K$\alpha$ radiation ($\lambda$ = 0.710 73 Å) at 153(2) K, a total of 6009 reflections was collected in the range $4 < 2\theta < 50°$. Data were corrected for Lorentz and polarisation effects and a semiempirical aborption correction, based on $\psi$-scans, was applied ($T_{max}$ = 0.980, $T_{min}$ = 0.558). The structure was solved by direct methods[14] and refined by full-matrix least squares on $F^2$, using all 5278 independent reflections ($R_{int}$ = 0.0583). All the non-hydrogen atoms were refined with anisotropic atomic displacement parameters and hydrogen atoms bonded to carbon were inserted at calculated positions, hydrogen atoms bonded to oxygen were located from difference Fourier maps and not further refined. Refinement converged with $wR_2$ = 0.1351, GOF = 1.124 (all data) and $R_1$ = 0.0481 ($2\sigma$ data). All programs used in the structure refinement are contained in the SHELXL-93 package.[15] Atomic coordinates, bond lengths and angles, and thermal parameters have been deposited at the Cambridge Crystallographic Data Centre (CCDC). See Information for Authors, Issue No. 1. Any request to the CCDC for this material should quote the full literature citation and the reference number 182/507.

## References

1 V. McKee and S. S. Tandon, *J. Chem. Soc., Dalton Trans*., 1991, 221; *Inorg. Chem*., 1989, **28**, 2901; *J. Chem. Soc., Chem. Commun*., 1988, 1334.
2 M. S. Newman and H. A. Karnes, *J. Org. Chem*., 1966, **31**, 3980; C. J. McKenzie, personal communication.
3 S. Brooker, P. D. Croucher and F. M. Roxburgh, *J. Chem. Soc., Dalton Trans*., 1996, 3031.
4 G. R. Owen and C. B. Reese, *J. Chem. Soc., C*, 1970, 2401; I. Murese, M. Hatano, M. Tanaka, S. Ueno, H. Okawa and S. Kida, *Bull. Chem. Soc. Jpn*., 1982, **55**, 2404.
5 P. E. Kruger, V. McKee, B. Moubaraki, K. S. Murray and S. S. Tandon, in preparation.
6 M. Bell, A. J. Edwards, B. F. Hoskins, E. H. Kachab and R. Robson, *J. Am. Chem. Soc*., 1989, **111**, 3603.
7 A. Silver and M. Millar, *J. Chem. Soc., Chem. Commun*., 1992, 948; T. Konno, K. Okamoto and J. Hidaka, *Acta Crystallogr., Sect. C*, 1993, **49**, 222; T. Konno and K. Okamoto, *Bull. Chem. Soc. Jpn*., 1995, **68**, 610; T. Beissel, F. Birkelbach, E. Bill, T. Glaser, F. Kesting, C. Krebs, T.Weyhermüller, K. Wieghardt, C. Butzlaff and A. X. Trautwein, *J. Am. Chem. Soc*., 1996, **118**, 12 376.
8 A. Volbeda, E. Garcin, C. Piras, A. L.-deLacey, V. M. Fernandez, E. C. Hatchikian, M. Frey and J. C. Fontecilla-Camps, *J. Am. Chem. Soc*., 1996, **118**, 12989; A. Volbeda, M. H. Charon, C. Piras, E. C. Hatchikian, M. Frey and J. C. Fontecilla-Camps, *Nature*, 1995, **373**, 580.
9 B. F. Hoskins and I. A. S. McDonald, *Aust. J. Chem*., 1984, **37**, 1395; P. Iliopoulos, K. S. Murray, R. Robson, J. Wilson and G. A. Williams, *J. Chem. Soc., Dalton Trans*., 1987, 1585.
10 A. J. Atkins, A. J. Blake and M. Schröder, *J. Chem. Soc., Chem. Commun*., 1993, 1662; A. J. Atkins, D. Black, A. J. Blake, A. Marin-Becerra, S. Parsons, L. Ruiz-Ramirez and M. Schröder, *Chem. Commun*., 1996, 457; N. D. J. Branscombe, A. J. Blake, A. Marin-Becerra, Wan-Sheung Li, S. Parsons, L. Ruiz-Ramirez and M. Schröder, *Chem. Commun*., 1996, 2573.
11 S. Brooker and P. D. Croucher, *J. Chem. Soc., Chem. Commun*., 1995, 2075.
12 A. J. Edwards, B. F. Hoskins, E. H. Kachab, A. Markiewicz, K. S. Murray and R. Robson, *Inorg. Chem*., 1992, **31**, 3585.
13 K. S. Murray, *Adv. Inorg. Chem*., 1995, **43**, 261.
14 G. M. Sheldrick, SHELXS-86, *Acta Crystallogr. Sect. A*, 1990, **46**, 467.
15 G. M. Sheldrick, SHELXL-93, Universität Göttingen, 1993.

*Received in Basel, Switzerland, 23rd April 1997; 7/02788E*

# Mesoporous M41S materials in capillary gas chromatography

**M. Raimondo, G. Perez,* M. Sinibaldi, A. De Stefanis and A. A. G. Tomlinson***

*Institutes of Chromatography and Materials Chemistry, Rome Research Area, CNR, C.P. 10 Monterotondo Staz., 00016 Rome, Italy*

**M-41S materials anchored to glass capillary columns *via* sol–gel techniques can be advantageously utilised for gas chromatographic separations.**

Rapid advances in preparing mesoporous materials such as those of the M41S class (particularly MCM-41[1]), pillared clays (PILCs) and analogues are due to their use as catalysts, especially in clean technology. However, MCMs have still to find practical application in this field, and it is possible they may instead be useful in others, such as separation technology. PILCs (pillared clays, which are micro/mesoporous) can separate inert gas mixtures and hydrocarbons,[2] which suggested using M41S solids in chromatographic separations, and in particular as stationary phases for gas–solid chromatography (GSC). Apart from benthone 34,[3] and differently from packed columns (where zeolites have been in use for some time)[4] other attempts to analyse liquid hydrocarbon mixtures by GSC on zeolites or expanded solids in general have failed, because strong sorption of individual components and/or their catalytic transformation due to intrinsic high acidity (at the relatively high temperatures required for elution) constitute limitations. Following successful use of mordenite in ion-exclusion chromatography,[5] we have found that it is possible to coat GC capillary columns with mesoporous silica-based MCM-41, which can separate organic molecules.

The MCM-41 used was prepared as in the original patent[6] and gave the reported XRPD and BET $N_2$ (specific surface area = 995 $m^2\ g^{-1}$). Fig. 1 shows both XRPD and an AFM image of the material. The latter shows that from toluene MCM-41 aggregates to form roughly platelet-shaped bundles of varying dimensions (typically 50–80 × 150–200 nm).

In a typical column preparation, a fused silica capillary (1 m long, 200 μm id; Composite Metal Services, UK) was modified with the silanizing agent, sulfanylpropyltrimethoxysilane [$(MeO_3)Si(CH_2)_3SH$, Aldrich] as follows. One end of the capillary was immersed in a vial containing 6 mol $dm^{-3}$ HCl and the solution allowed to flow through under pressure for 3 h. The capillary was then washed with water and silanizing agent

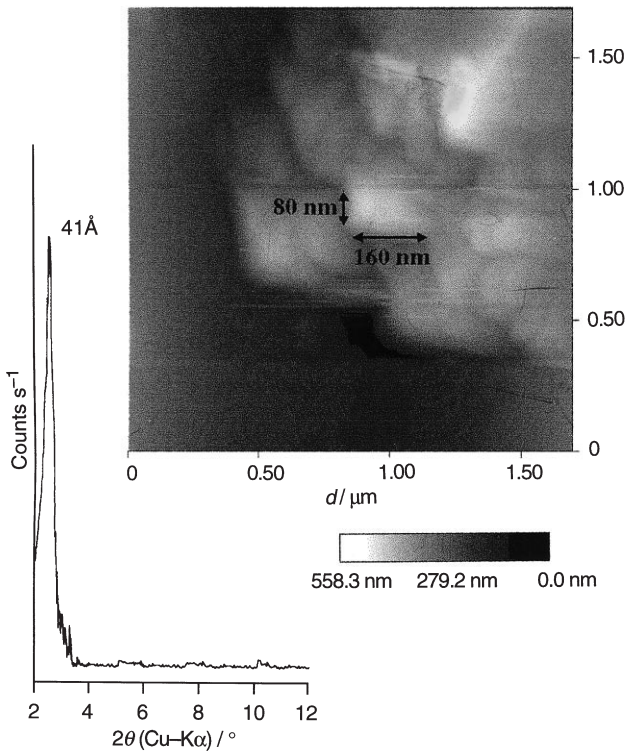



**Fig. 1** XRPD of MCM-41 utilised and AFM image showing the MCM morphology [conditions: Digital Nanoscope III instrument, deposit from ambient toluene suspension onto muscovite mica (001), followed by heating at 200 °C for 3 h; tapping mode]

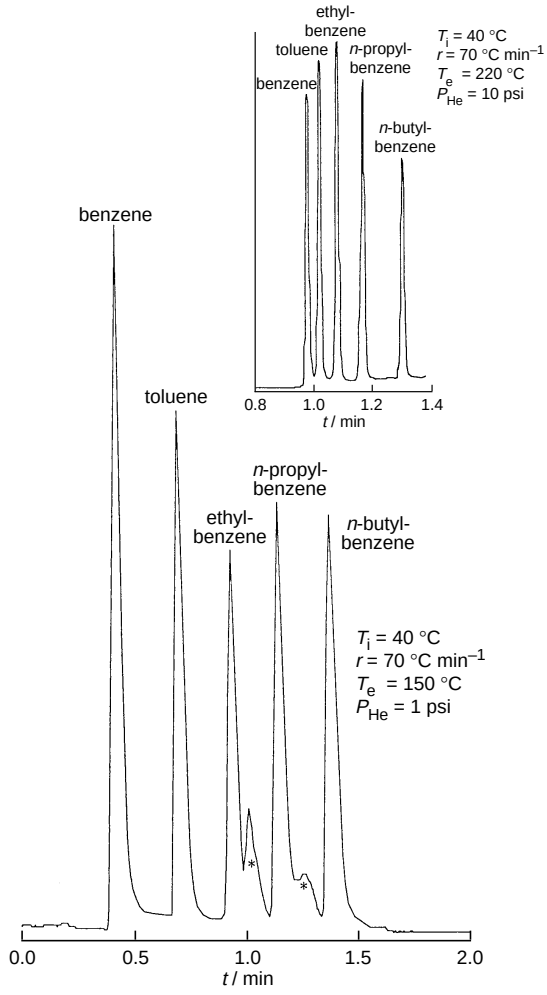



**Fig. 2** GC separation of hydrocarbon mixture on the MCM-41 film capillary column. Inset shows separations performed on a HP-1 type (polydimethylsiloxane) column; conditions: $l$ = 25 m, id = 0.53 mm. * = impurities.

by dipping one end of the tube, kept *ca*. 20 cm higher than the other end, into the reagent. The capillary was sealed using a sodium silicate solution and heated overnight (100 °C). After cooling, both ends of the capillary were cut, the solution decanted, and the capillary was dried, and then filled with a well shaken suspension of 0.5 g of the MCM-41 in dry toluene. The capillary was sealed and left to react at 60 °C overnight. After completion of the reaction, both ends of the capillary were cut and it was connected to a chromatographic delivery pump (Perkin Elmer, series 400 model) washed with hexane and $Pr^iOH$ and dried under He.

Fig. 2 shows a typical separation of a light hydrocarbon mixture (1 : 1 : 1 : 1 : 1): separation is achieved at much lower temperatures, with much shorter retention times and on shorter columns (1 m) rather than the 25–30 m of conventional capillary columns (inset). In control experiments, no separation was possible on capillaries which were identical, except for the MCM-41 attachment step. That separation indeed occurs within the MCM-41 cavities and by a mechanism depending on the proton affinities of the compounds, is neatly demonstrated in Fig. 3. For both benzene–diethyl ether and benzene–heptane mixtures there is inversion in elution order compared with standard GC on polydimethylsiloxane (insets). It is well known that oxygen-containing molecules are retained strongly on zeolites due to onium ion formation,[7] as is also benzene (*via* arenium ion formation[8]). It appears this is also the case for M41S materials. The generality of the behaviour (whether other porous silicas can be used) and other anchoring agents and separations are under investigation and the acidity of anchored MCM-41 is being modulated by cation exchange in order to maximise peak symmetry and separation factors.

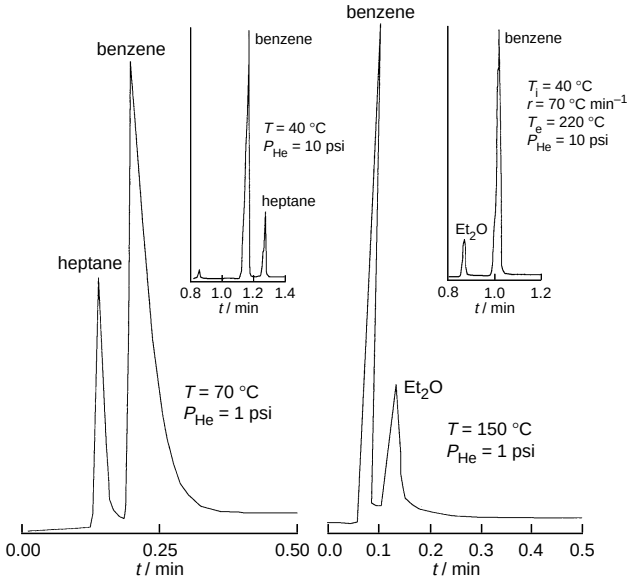



**Fig. 3** GC separation of benezene–diethyl ether and benzene–heptane on the MCM-41 film capillary column. Insets, standard GC on polydimethoxysilane (conditions as in Fig. 2).

## Footnote

* E-mail: gus@nserv.icmat.mlib.cnr.it

## References

1 J. S. Beck, J. C. Vartuli, W. J. Roth, M. E. Leonowicz, C. T. Kresge, K. D. Schmitt, C. T-W. Chu, D. H. Olson, E. W. Sheppard, S. B. McCullen, J. B. Higgins and J. L. Schlenker, *J. Am. Chem. Soc*., 1992, **114,** 10 834.
2 A. De Stefanis, G. Perez and A. A. G. Tomlinson, *J. Mater. Chem*., 1994, **4**, 959 and unpublished work.
3 V. D. Nefedov, E. N. Sinotova, G. P. Akulov and M. V. Korsakov, *Zh. Org. Khim*., 1973, **9**, 629.
4 T. G. Andronikashvili and G. V. Tsitsishvili, *J. Chromatogr*., 1984, **292**, 3.
5 B. K. Glod, G. Perez and A. A. G. Tomlinson, *J. Chromatogr*., 1997, **760**, 292.
6 C. T. Kresge, M. E. Leonowicz, W. J. Roth and J. C. Vartuli, *US Pat.*, 5 102 643, 1992.
7 J. G. Kremer and R. A. Van Santen, *Chem. Rev*., 1995, **95**, 638.
8 D. M. Brouwer, E. L. Mackor and C. MacLean, in *Carbonium Ions*, ed. G. A. Olah and P. v. R. Schleyer, Wiley-Interscience, New York, 1970, vol. 2, p. 864.

*Received in Bath, UK, 16th April 1997; 7/02849K*

# Ionic liquid–polymer gel catalytic membrane

**Richard T. Carlin* and Joan Fuller**

*Covalent Associates, Inc., 10 State Street, Woburn, Massachusetts, 01801, USA*

**A novel catalytic membrane for heterogeneous hydrogenation is fabricated by incorporating palladium into a gas-permeable ionic liquid–polymer gel composed of 1-*n*-butyl-3-methylimidazolium hexafluorophosphate and poly(vinylidene fluoride)–hexafluoropropylene copolymer.**

We have recently described the preparation and properties of novel ionic liquid–polymer gel electrolytes for application in a variety of electrochemical devices.[1] The gels are freestanding, flexible films composed of an air-stable, room-temperature ionic liquid and poly(vinylidene fluoride)–hexafluoropropylene copolymer [PVdF(HFP)]. The ionic liquids consist of a perfluorinated anion (*e.g.* $BF_4^-$, $CF_3SO_3^-$, $PF_6^-$) and a 1,3-dialkylimidazolium cation (*e.g.* 1-ethyl-3-methylimidazolium) and can have either hydrophilic or hydrophobic character.[2] Although many of the synthetic routes to the ionic liquids require expensive, environmentally undesirable reagents, such as silver salts, we have developed convenient, low-cost routes to high-purity hydrophilic and hydrophobic ionic liquids which make them readily available for research and commercial applications.[3]

A series of ionic liquids based on the 1-*n*-butyl-3-methylimidazolium cation ($BMI^+$) were recently demonstrated to be versatile solvents for homogeneous catalysis.[4] The catalysis was performed in a two-phase liquid–liquid design which greatly facilitates product recovery while maintaining the catalyst in the reactive ionic liquid phase. Gas-permeable membranes can also function as two-phase catalyst systems and can be engineered to enhance the desired chemical reactions.[5] The non-volatile ionic liquids have already been demonstrated as effective membrane materials for gas separations when supported within a porous polymer support.[6] Additionally, while ionic liquids composed of perfluorinated anions have only recently garnered interest as reaction media, other ionic liquids, particularly moisture-sensitive chloroaluminates, are well documented to be effective solvents for organic, inorganic and electrochemical reactions.[7] The efficacy of chloroaluminates as media for organometallic preparations is illustrated by recent reports of reductive carbonylation[8] and Friedel–Crafts acylation[9] of cyclopentadienyl complexes.

To take advantage of the ionic liquids as catalyst solvents and of the ruggedness of the ionic liquid–polymer gels, we have prepared ionic liquid–polymer gels containing a heterogeneous palladium catalyst. These composite materials were tested as a propene hydrogenation catalyst in a membrane configuration.

A typical ionic liquid–polymer catalytic membrane was prepared by mixing 0.044 g 10 mass% Pd on activated carbon (Pd/C, Aldrich), 1.08 g $BMIPF_6$,[3,4] and 0.576 g PVdF(HFP) (Kynar Flex 2801-00, Elf Atochem) with 3 ml 4-methylpentan-2-one (MP) under ambient conditions. This mixture was poured into an aluminium weighing pan of 5 cm diameter and was gelled by heating on a hot plate set at *ca.* 75 °C. The MP was allowed to evaporate overnight in ambient air. The final composite membrane was a flexible, dimensionally stable film with thickness *ca.* 0.06 cm and area *ca.* 14 $cm^2$, giving a total palladium metal loading of only *ca.* 0.3 mg $cm^2$. The ionic liquid imparts ionic conductivity and flexibility to the otherwise insulating, rigid PVdF(HFP) copolymer.

Fig. 1 shows two optical images of the membrane taken at 200× magnification with an inverted metallurgical microscope. The left-hand image was taken using reflected light and shows a few black Pd/C catalyst particles protuding through the otherwise featureless polymer gel surface. The right-hand image, taken in transmitted light with the focal plan positioned inside the membrane, clearly shows individual Pd/C particles dispersed throughout the membrane interior.

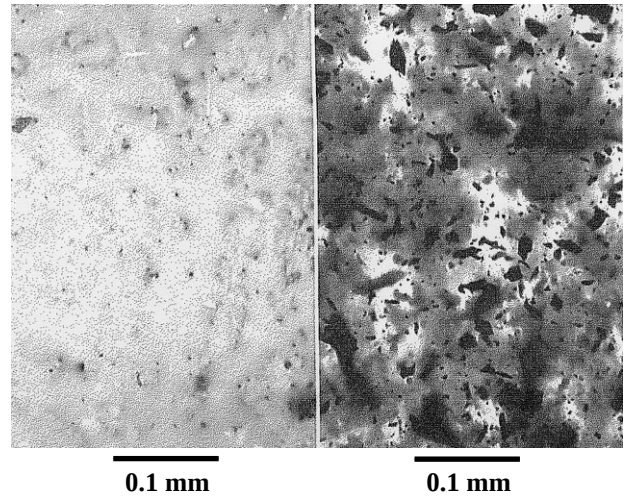



**Fig. 1** Optical images at 200× magnification showing the surface (left, reflected light) and interior (right, transmitted light) of the ionic liquid–polymer catalytic membrane

The ionic liquid–polymer membrane was loaded into a catalyst membrane reactor† and evaluated using propene hydrogenation as a model reaction. The propene permeability coefficient ($P_{propene}$) for the membrane was 300 barrers.‡ Fig. 2 summarizes the data collected for propene hydrogenation as a function of time, where $t_R = 0$ corresponds to the initial introduction of $H_2$ over the permeate side of the membrane. The flux of propene through the membrane decreased as the flux of propane increased, while the total flux (flux propene + flux

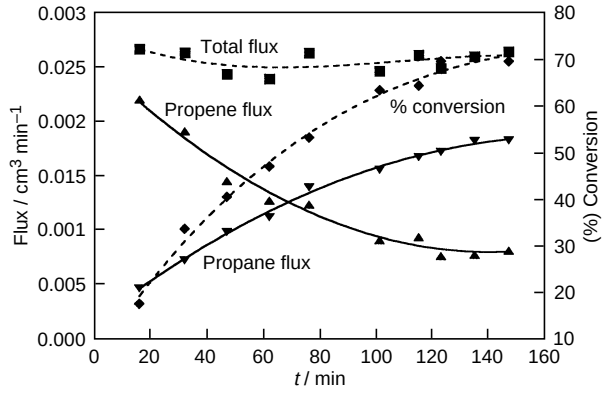



**Fig. 2** Plots of propene flux ( ▲ ), propane flux (▼), total flux (■) and % conversion (◆) as a function of time

propane) remained constant throughout the experiment. The conversion reached 70% after 2 h and remained constant after this time. We attribute the gradual rise in catalytic activity to the fact that the Pd/C particles are uniformly distributed throughout the ionic liquid–polymer gel structure, and so $H_2$ on the permeate side of the membrane must diffuse through the membrane interior to the catalyst sites. The time dependence of the fluxes for propene and propane follows $t^{1/2}$ behaviour, consistent with a diffusion-controlled model.

Ionic liquid–polymer gel membranes are a versatile matrix for exploring catalytic processes in the presence of a variety of ionic liquids.[1] Also, because the high ion concentration (*ca*. 3 M) is not detrimental to catalytic activity, these gel electrolytes may be useful for electrocatalytic applications.

This work was sponsored by the Air Force Office of Scientific Research, and the Department of Energy. Opinions, interpretations, conclusions, and recommendations are those of the authors and are not necessarily endorsed by the United States Air Force or the Department of Energy.

## Footnotes

* E-mail: 73474.64@compuserve.com

† The membrane reactor was a Gelman 47 mm inline filter holder fitted with Swagelock Quick-Connect couplings for connection to feed and permeate gases. The filter holder used an O-ring sealing mechanism which gave an effective membrane area of 9.6 $cm^2$. During membrane experiments, the feed side of the membrane was contacted with static propene gas at 1 atm, while the permeate side was swept with $H_2$ at 10.5 $cm^3\ s^{-1}$ STP. The permeate gases were vented through a manual sample loop which was used to inject 1 ml samples into a gas chromatograph for analysis with a silica gel column and a TCD detector.

‡ 1 barrer = $10^{-10} \times 1\ cm^3$ (STP) cm $cm^{-2}\ s^{-1}\ cmHg^{-1}$.

## References

1 J. Fuller, A. C. Breda and R. T. Carlin, *J. Electrochem. Soc.*, 1997, **144**, L69.
2 E. I. Cooper and E. J. M. O'Sullivan, in *Proceedings of the 8th International Symposium on Molten Salts*, ed. R. J. Gale, G. Blomgren and H. Kojima, The Electrochemical Society Proceedings Series, Pennington, NJ, 1992, PV 92–16, p. 386; J. S. Wilkes and M. J. Zaworotko, *J. Chem. Soc., Chem. Commun.*, 1992, 965; J. Fuller, R. T. Carlin, H. C. De Long and D. Haworth, *J. Chem. Soc., Chem. Commun.*, 1994, 299; R. T. Carlin, H. C. De Long, J. Fuller and P. C. Trulove, *J. Electrochem. Soc.*, 1994, **141**, L73; P. Bonhôte, A.-P. Dias, N. Papageorgiou, K. Kalyanasundaram and M. Grätzel, *Inorg. Chem.*, 1996, **35**, 1168.
3 J. Fuller and R. T. Carlin, *J. Electroanal. Chem.*, submitted.
4 Y. Chauvin, L. Maussmann and H. Olivier, *Angew. Chem., Int. Ed. Engl.*, 1995, **34**, 2698; Y. Chauvin and H. Olivier-Bourbigou, *CHEMTECH*, 1995, **25**, 26.
5 M. P. Harold, C. Lee, A. J. Burggraaf, K. Keizer, V. T. Zaspalis and R. S. A. de Lange, *MRS Bull.*, 1994, **4**, 34.
6 G. P. Pez, R. T. Carlin, D. V. Laciak and C. Sorenson, *US Pat.*, 4,761,164.
7 For reviews see: R. M. Pagni, in *Advances in Molten Salt Chemistry*, ed. G. Mamantov, C. B. Mamantov and J. Braunstein, Elsevier, Amsterdam, 1987, vol. 6, p. 211; R. A. Osteryoung, in *Molten Salts Chemistry*, ed. G. Mamantov and R. Marrasi, NATO ASI, Series C, Mathematical and Physical Sciences, D. Reidel, Dordrecht, 1987, vol. 202, p. 329; C. L. Hussey, in *Advances in Non-aqueous Chemistry*, ed. G. Mamantov and A. Popov, VCH, New York, 1994, ch. 4, p. 227; R. T. Carlin and J. S. Wilkes, in *Advances in Non-aqueous Chemistry*, ed. G. Mamantov and A. Popov, VCH, New York, 1994, ch. 5, p. 277.
8 R. T. Carlin and J. Fuller, *Inorg. Chim. Acta*, 1997, **255**, 189.
9 J. K. D. Surette, L. Green and R. D. Singer, *Chem. Commun.*, 1996, 2753.

*Received in Columbia, MO, USA; 1st April 1997; 7/02195J*

# Photo-Stevens rearrangement reaction of *S*-naphthylmethyl-*N*-*p*-tosylsulfimides

**Hiroyuki Morita,* Hideo Kamiyama, Miho Kyotani, Takayoshi Fujii, Toshiaki Yoshimura, Shin Ono and Choichiro Shimasaki**

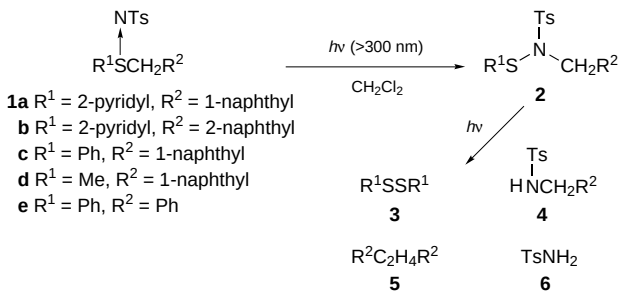
*Department of Chemical and Biochemical Engineering, Faculty of Engineering, Toyama University, 3190 Gofuku, Toyama 930, Japan*

**Photolysis sulfimides unexpectedly led to Stevens rearrangement products.**

In the thermal reaction of sulfimides, the products derived *via* Stevens rearrangement were reported to be formed.[1] In the photolysis of sulfimides, however, it is reported that nitrenes are initially generated *via* a photo-induced cleavage of the S–N linkage.[2] In contrast to this mechanistic route for photolytic decomposition of sulfimides, another route *via* Stevens rearrangement was recently reported for the particular case of a cyclic sulfimide derivative, *i.e.* *N*-tosylnaphtho[1,8-*de*]-1λ⁴,3-dithiin-1-imine, which rearranged to naphtho[1,8-*ef*]-[1,4,2]dithiaazepine, followed by de-imination to give *N*-*p*-tosylaldimines and naphtho[1,8-*cd*]-1,2-dithiole quantitatively.[3] In this reaction the driving force apparently results from formation of a stable cyclic disulfide *via* the through-space interaction between the two sulfur atoms at the 1,8-positions of naphthalene.

In order to study more precisely and photolytic behaviour of acyclic sulfimide derivatives, we prepared several *S*-naphthylmethyl-*N*-*p*-tosylsulfimides and carried out their photolysis using a high-pressure mercury lamp with a Pyrex filter under nitrogen.† When **1a**‡ was irradiated in degassed MeOH under these conditions, the major products were dipyridyl disulfide **3a** and *N*-(naphthylmethyl)toluene-*p*-sulfonamide **4a**.§ In view of the formation of **4a**, the reaction is considered to pass through a rearrangement mechanism, *i.e.* a Stevens-type rearrangement as depicted in Scheme 1. Here we report the first examples of this photo-induced Stevens rearrangement reaction in *S*-naphthylmethyl-*N*-*p*-tosylsulfimide derivatives.

*S*-Aryl- or *S*-alkyl-*S*-naphthylmethyl-*N*-*p*-tosylsulfimides **1a**–**e** were prepared by the reaction of the corresponding sulfides with the sodium salt of *N*-chlorotoluene-*p*-sulfonamide (Chloramine T) in MeCN in high yields. Photolysis of *S*-naphthylmethyl-*N*-*p*-tosylsulfimides in degassed $CH_2Cl_2$ was carried out under the previously described conditions for 2 h. The results are summarized in Table 1. The photolyses of *S*-pyridyl-, *S*-phenyl- and even *S*-methyl-*S*-(1-naphthylmethyl)- or *S*-(2-naphthyl-methyl)-*N*-*p*-tosylsulfimide derivatives **1a**–**d** (entries 1–4) were found to lead to the Stevens rearrangement product **2**, as well as **3** and **4**, which are formed by photolysis of **2** in a secondary photochemical step, while in the photolysis of *S*-benzyl-*S*-phenyl-*N*-*p*-tosylsulfimide **1e** (entry 5), the reaction




**Scheme 1**

did not proceed at all. This result suggests that a napthyl group is necessary in this reaction as a useful chromophore to accept photoirradiation and to initiate the photoreaction. Therefore, measurements of the UV–VIS spectra of **1a**–**d** were carried out and showed, as expected, the existence of a strong absorption band ($\log\varepsilon = 4.9$) around 230 nm, extending beyond the 300 nm region as shoulders, while **1e** showed no absorption beyond 300 nm.

A further study of the photolysis of *S*-(2-pyridyl)-*S*-(1-naphthylmethyl)-*N*-*p*-tosylsulfimide **1a** in several solvents was carried out under the same conditions. The products formed were found to depend significantly on the nature of solvents used. In aprotic solvents such as $CH_2Cl_2$ and MeCN, the primary rearranged product **2a**¶ was formed as the major product; however, in acetone the secondary products **3a** and **4a** were the major products, presumably due to acceleration of the photochemical excitation of **2a** by probable triplet sensitization of acetone, as suggested by Guo and Jenks in the photolysis of sulfoxide.[4] Meanwhile, in alcoholic solvents, another mechanistic path is apparently involved and toluene-*p*-sulfonamide **6**, as well as the products **3a** and **4a** *via* Stevens-type rearrangement, was formed predominantly. One possibility for this mechanism is the nitrene pathway, which would immediately lead to sulfonamide **6** and the corresponding sulfide, which is observed to decompose to **3a** and **5a** under the same conditions. Another possibility is a pathway involving the initial protonation at the iminonitrogen atom of the sulfimide and subsequent

**Table 1** Photolysis of *N*-tosylsulfimides **1** in $CH_2Cl_2$[a]

| | | | Yield (%)[b] | | |
|---|---|---|---|---|---|
| Entry | Compound | Conversion (%) | **2** | **3** | **4** |
| 1 | **1a** | 100 | 27 | 45 | 72 |
| 2 | **1b** | 92 | 47 | 37 | 46 |
| 3 | **1c** | 94 | 40 | 33 | 30 |
| 4 | **1d** | 63 | 54 | —[c] | 42 |
| 5 | **1e** | 0 | — | — | — |

[a] Irradiation with a 400 W high-pressure Hg lamp; concentration: 0.2 mmol; reaction time = 2 h. [b] Isolated yield. [c] Dimethyl disulfide not isolated.

**Table 2** Photolysis of *S*-(2-pyridyl)-*S*-(naphthylmethyl)-*N*-*p*-tosylsulfimide **1a** in different solvents[a]

| | Yield (%)[b] | | | | |
|---|---|---|---|---|---|
| Solvent | **2a** | **3a** | **4a** | **5a** | **6** |
| MeOH | 0 | 25 | 15 | 7 | 64 |
| Pr$^i$OH | 0 | 38 | 34 | 21 | 57 |
| $CH_2Cl_2$ | 27 | 45 | 72 | trace | 0 |
| MeCN | 15 | 33 | 54 | trace | 0 |
| $Me_2CO$ | 0 | 41 | 74 | 4 | 0 |

[a] Irradiation with a 400 W high-pressure Hg lamp: concentration: 0.2 mmol; reaction time = 2 h. Isolated yield.

formation of an alkoxysulfonium salt (counter anion $TsNH^-$) which eventually decomposes to the corresponding sulfide and a carbonyl compound.‖ A similar mechanism was suggested by Oae in the case of the thermolysis of *N*-*p*-tosylsulfimides in MeOH.[1a]

In order to confirm the mechanistic pathway of this photoreaction, the product distribution in the course of photolysis of **1a** in $CH_2Cl_2$ under the previously described conditions was determined by quantitative analysis with HPLC. The result is illustrated in Fig. 1; the amount of starting sulfimide **1a** decreased gradually, and three new species appeared. Two were found to be di(2-pyridyl) disulfide **3a** and *N*-(1-naphthylmethyl)toluene-*p*-sulfonamide **4a** by comparing their HPLC retention times and their spectral data with those of authentic compounds prepared or separated by chromatography. The third species showed a maximum after 40 min and then gradually decreased. This probably points to the existence of the intermediate **2** in this reaction, which apparently reacted to give the products **3a** and **4a**. Therefore, the reaction mixture was separated by HPLC after 40 min photolysis and the product corresponding to this intermediate was identified as **2a**. Further, in order to clarify that **2a** is exactly the intermediate of this reaction, photolysis of **2a** thus separated was carried out under the same conditions to afford the expected products **3a** and **4a** in good yields. All these results indicate clearly that this reaction proceeds *via* a photo-induced Stevens rearrangement to afford the intermediate **2a**, which subsequently decomposes to dipyridyl disulfide **3a** and *N*-(1-naphthylmethyl)toluene-*p*-sulfonamide **4a** together with a small amount of product **5a** *via* direct cleavage of the S–$CH_2$ linkage.

We are now pursuing further studies to clarify the limitations and the detailed mechanism of this reaction.

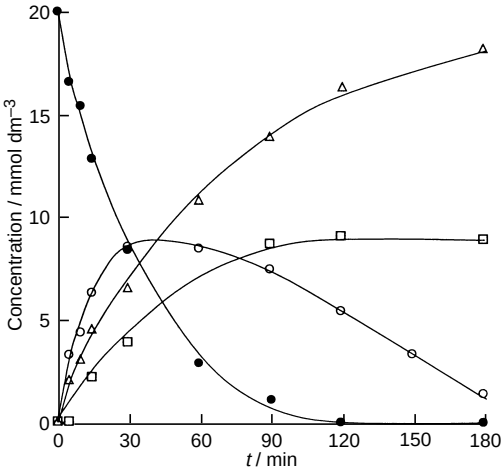



**Fig. 1** Product distribution in the course of photolysis of **1a**; (●) **1a**, (○) **2a**, (□) **3a** and (△) **4a**

## Footnotes

* E-mail: morita@sci.toyama-u.ac.jp

† All photolyses were carried out in 9 mm i.d. Pyrex glass tubes, sealed with a septum under nitrogen atmosphere at room temperature, with irradiation from a 400 W high-pressure mercury lamp.

‡ Compound **1a** was prepared by the following procedure: a solution of pyridyl naphthylmethyl sulfide and Chloramine T (1.5 equiv.) in 100 ml of MeCN was refluxed for 6 h. After removal of MeCN, washing with water to remove excess Chloramine T and drying, *S*-pyridyl-*S*-naphthylmethyl-*N*-*p*-tosylsulfimide was obtained in 88% yield, mp 164 °C (AcOEt–hexane). *Selected data* for **1a**: $^1$H NMR (400 MHz, $CDCl_3$): $\delta$ 2.20 (s, Me, 3 H), 4.46 (dd, *J* 13 Hz, 1 H), 5.34 (dd, *J* 13 Hz, 1 H), 6.63–6.65 (m, 2 H), 7.17–7.34 (m, 5 H), 7.48–7.58 (m, 3 H), 7.75–7.84 (m, 2 H), 7.97–8.08 (m, 2 H), 8.31–8.33 (m, 1 H), 8.70–8.72 (m, 1 H); $^{13}$C NMR (100 MHz, $CDCl_3$): $\delta$ 21.3, 54.8, 122.1, 122.9, 123.7, 125.1, 125.5, 125.7, 126.1, 127.0, 127.8, 128.8, 128.8, 129.5, 130.0, 131.2, 131.3, 133.6, 138.9, 140.8, 149.9; $\nu_{max}$ (KBr)/cm$^{-1}$ 1280, 1100 ($SO_2$), 980 (SN); Calc. for $C_{23}H_{20}N_2O_2S_2$: C, 65.68; H, 4.79; N, 6.66. Found: C, 65.52; H, 4.84; N, 6.49%.

§ *Selected data* for **4a**: $^1$H NMR (400 MHz, $CDCl_3$): $\delta$ 2.45 (s, Me, 3 H), 4.53 (d, *J* 1 Hz, $CH_2$, 2 H), 4.63 (d, *J* 2 Hz, NH, 1 H), 7.25–7.35 (m, 4 H), 7.46–7.51 (m, 2 H), 7.77–7.90 (m, 5 H); $^{13}$C NMR (100 MHz, $CDCl_3$); $\delta$ 21.5, 45.4, 123.2, 125.1, 126.0, 126.7, 126.9, 127.2, 128.7, 129.1, 129.7, 131.1, 133.7, 136.4, 143.5; $\nu_{max}$ (KBr)/cm$^{-1}$ 1330, 1160 ($SO_2$), 3300 (NH); *m/z* 311 ($M^+$); Calc. for $C_{18}H_{17}NO_2S$: C, 69.42; H, 5.50; N, 4.49. Found: C, 69.51; H, 5.62; N, 4.33%.

¶ *Selected data* for **2a**: $^1$H NMR (400 MHz, $CDCl_3$): $\delta$ 2.44 (s, Me, 3 H), 6.70—6.73 (m, 1 H), 6.81–6.83 (m, 1 H), 6.99–7.03 (m, 1 H), 7.30–7.36 (m, 3 H), 7.47–7.49 (m, 1 H), 7.57–7.61 (m, 1 H), 7.65–7.67 (d, *J* 2 Hz, 1 H), 7.74–7.76 (d, *J* 2 Hz, 1 H), 7.85–7.88 (m, 2 H), 8.08–8.10 (m, 1 H), 8.44–8.47 (m, 1 H); $^{13}$C NMR (100 MHz, $CDCl_3$): $\delta$ 21.6, 55.8, 118.3, 119.9, 123.8, 124.8, 125.7, 126.7, 127.9, 128.5, 129.3, 129.6, 129.7, 130.0, 131.9, 133.5, 135.0, 136.1, 144.3, 148.1, 160.6; $\nu_{max}$(KBr)/cm$^{-1}$ 1351, 1165 ($SO_2$); *m/z* 78 ($C_5H_5N^+$), 127 ($C_{10}H_7^+$), 141 ($C_{10}H_7CH_2^+$), 155 ($Ts^+$), 156 ($C_{10}H_7CH_2NH^+$), 311 ($TsNHCH_2C_{10}H_7^+$), 420 ($M^+$); Calc. for $C_{23}H_{20}N_2O_2S_2$: C, 65.68; H, 4.79; N, 6.66. Found: C, 65.86; H, 4.79; N, 6.60%. The methylene protons ($CH_2C_{10}H_7$) were not observed in the $^1$H NMR spectrum, even after varying the solvent, although all other analytical and combustion data confirmed this structure.

‖ In MeOH the formation of paraformaldehyde was observed.

## References

1 (*a*) T. Aida, N. Furukawa and S. Oae, *J. Chem. Soc., Perkin Trans. 2*, 1976, 1433; (*b*) H. Kise, G. F. Whitefield and D. J. Swern, *J. Org. Chem.*, 1972, **37**, 1125; (*c*) T. L. Gilchrist, C. J. Rees and C. W. Moody, *J. Chem. Soc., Perkin Trans. 1*, 1975, 1964; (*d*) M. Hori, T. Kataoka, H. Shimizu and K. Matsuo, *Tetrahedron Lett.*, 1979, 3969; (*e*) Y. Tamura, S. M. Bayomi, C. Mukai, M. Ikeda, M. Murase and M. Kise, *Tetrahedron Lett.*, 1980, **21**, 553.

2 Y. Hayashi and D. J. Swern, *J. Am. Chem. Soc.*, 1973, **95**, 5205; N. Furukawa, M. Fukumura, T. Nishio and S. Oae, *J. Chem. Soc., Perkin Trans. 1*, 1977, 96; T. L. Gilchrist, C. J. Moody and C. W. Rees, *J. Chem. Soc., Perkin Trans. 1*, 1978, 1871.

3 T. Fujii, T. Kimura and N. Furukawa, *Tetrahedron Lett.*, 1995, **36**, 1075.

4 Y. Guo and W. S. Jenks, *J. Org. Chem.*, 1995, **60**, 5480.

*Received in Corvallis, OR, USA, 27th January 1997; revised MS received 19th May 1997; 7/03455E*

# Synthesis and characterization of the first dodecanuclear M–Ag–S cage cluster: $[NEt_4]_2[\{M_2Ag_2S_2O_2(S_2C_2H_4)_2\}_3(\mu_6\text{-}S)]\cdot CH_2Cl_2\cdot MeCN$ (M = Mo, W)

**Ping Lin, Xintao Wu,* Wenjian Zhang, Jun Guo, Tianlu Sheng, Quanming Wang and Jiaxi Lu**

*State Key Laboratory of Structural Chemistry, Fujian Institute of Research on the Structure of Matter, The Chinese Academy of Sciences, Fuzhou, Fujian 350002, P.R. China*

**The first dodecanuclear heterobimetallic cage cluster with a central $\mu_6$-S ligand, containing the core $[\{M_2Ag_2S_2O_2(edt)_2\}_3(\mu_6\text{-}S)]^{2-}$ (M = Mo, W; $H_2$edt = ethane-1,2-dithiol), is synthesized and characterized; the average Ag–$\mu_6$-S bond length of the core $[\{Mo(W)_2Ag_2S_2O_2(edt)_2\}_3(\mu_6\text{-}S)]^{2-}$ is 2.528 (2.531) Å.**

The chemistry of heterometallic cluster compounds has attracted considerable attention for their uses as models for the active sites in a variety of metalloenzymes and their potential applications as functional materials in several fields.[1] Heterometallic cluster compounds containing $[MS_4]^{2-}/M'^{+}$ (M = Mo, W; M′ = Cu, Ag) have been extensively studied.[2] At present, some polynuclear $M^{VI}$–Ag–S (M = Mo, W) cluster compounds such as $NEt_4[(PPh_3)_2Ag(\mu\text{-}S)_2Mo(\mu\text{-}S)OCu(CN)]$ (butterfly),[3] $[\{Ag(PPh_3)\}_3MoS_4Cl]$ (cubane-like),[4] $[Ag_6M_2S_6O_2(Me_3CS)_2(PPh_3)_4]$ (double-cubane-like),[5] $[M_2S_8Ag_4(PPh_3)_4]$ (cage),[6] $[W_4Ag_5S_{16}\cdot Nd(dmf)_8]_n$ (one-dimensional chain)[7] and $[WS_4Ag\cdot NH_3C(CH_2OH)_3\cdot H_2O]_n$ (double chain)[8] have been characterized. A few $M^{V}$–Ag–S complexes such as $[M_2AgS_4(edt)_2(PPh_3)]^-$ (incomplete cubane-like)[9] and $[\{(PPh_3)Ag\}_2Mo_2S_4(tdt)_2]$ (cubane-like)[10] have been reported. However, no non-polymeric M–Ag–S (M = Mo, W) complexes with more than nine metal centers have, as yet, been synthesized.

Herein the syntheses and characterization of novel dodecanuclear heterobimetallic clusters $[NEt_4]_2[\{M_2Ag_2S_2O_2(S_2C_2H_4)_2\}_3(\mu_6\text{-}S)]\cdot CH_2Cl_2\cdot MeCN$ (M = Mo **1**, W **2**) with cage cores $[\{M_2Ag_2S_2O_2(S_2C_2H_4)_2\}_3(\mu_6\text{-}S)]^{2-}$ (M = Mo, W) are described, the first molybdenum(v) or tungsten(v)–silver clusters containing a $\mu_6$-S ligand. To our knowledge, this type of cluster containing $\mu_6$-S is rare in molybdenum or tungsten(v)–copper(silver) clusters, the only example being $[NEt_4]_2[Mo_6Cu_6S_6(\mu_6\text{-}S)O_6(S_2)_6]$ synthesized by our group;[11] reaction of $AgNO_3$ with $[NEt_4]_2[Mo_2S_2O_2(S_2)_2]$ did not lead to an analogous Mo–Ag complex.

The starting material $[NEt_4]_2[Mo_2O_2S_2edt_2]$ **3** was prepared according to ref. 12 and $[NEt_4]_2[W_2S_4(edt)_2]$ **4** was obtained by published procedure;[13] all other chemicals were purchased. Both compounds **1** and **2** were synthesized in the air by the 'spontaneous self-assembly' method. To the solution of $[NEt_4]_2[Mo_2S_2O_2(edt)_2]$ **3** (0.356 g, 0.5 mmol in 20 ml MeCN–20 ml $CH_2Cl_2$) was added $AgNO_3$ (0.17 g, 1.0 mmol in 20 ml MeCN–20 ml $CH_2Cl_2$), and the mixture was stirred for 0.5 min. Then two drops of an $(NH_4)_2S$ solution (containing 8% S) were added, the reaction mixture was stirred for 5 min, and the resulting brown precipitate was filtered off. The orange filtrate was allowed to stand at room temp. in the air for 5 days after which 0.06 g of red crystals of **1** were obtained.† Similarly, to a solution of $[NEt_4]_2[W_2S_4(edt)_2]$ **4** (0.470 g, 0.5 mmol in 20 ml MeCN–20 ml $CH_2Cl_2$) was added four drops of aqueous $H_2O_2$ (30% $H_2O_2$) under stirring for 2 h, $AgNO_3$ (0.17 g, 1.0 mmol in 20 ml MeCN–20 ml $CH_2Cl_2$) was then added and the mixture was stirred for 0.5 min. Two drops of $(NH_4)S$ solution were added and the reaction mixture stirred for 5 min, and the resulting brown precipitate was filtered off. The yellow filtrate was allowed to stand at room temp. in the air for 5 days after which 0.07 g of orange crystals of **2** were obtained.†

X-Ray structure analysis‡ revealed the existence of the cage core of $[\{M_2Ag_2S_2O_2(edt)_2\}_3(\mu_6\text{-}S)]^{2-}$ (M = Mo, W), a tripolymer consisting of three $[M_2S_2O_2(edt)_2]^{2-}$ and two $Ag^+$ fragments, with an S atom in the center binding to six Ag atoms. Cluster **1** is isomorphous with the corresponding tungsten cluster **2** and only the structure of **1** is thus described. An ORTEP drawing of the anion of **1** is shown in Fig. 1. From the configuration of the twelve metal atoms and all the S atoms, the core can be described as a cage with an $S^{2-}$ at its center. The cage has two windows each composed of a puckered $Ag_3S_6C_6$ 15-membered ring which is composed of three Ag atoms combining three $^-SC_2H_4S^-$ units; the $S^{2-}$ ion can enter the cage through the window and is coordinated to six Ag atoms, forming $\mu_6$-S. The Ag–$\mu_6$-S distances range from 2.504 to 2.556 Å, av. 2.528 Å (in **2** the av. Ag–$\mu_6$-S length is 2.531 Å). There are three weak Ag–Ag metal–metal bonds with Ag(1)–Ag(2), Ag(3)–Ag(4), Ag(5)–Ag(6) 3.0652, 3.0354, 3.0799 Å, respectively; angles Ag(1)–$\mu_6$-S–Ag(2), Ag(3)–$\mu_6$-S–Ag(4), Ag(5)–$\mu_6$-S–Ag(6) are 74.24, 74.13, 75.18°, respectively.

Each Mo atom displays tetragonal-pyramid (*TPY*) coordination geometry, with two S atoms of $^-SC_2H_4S^-$ ($S_{edt}$), two bridging S atoms of binuclear molybdenum ($S_{br}$) and one terminal oxygen atom. The oxygen atom occupies the axial position of each *TPY* and the four remaining sulfido atoms are

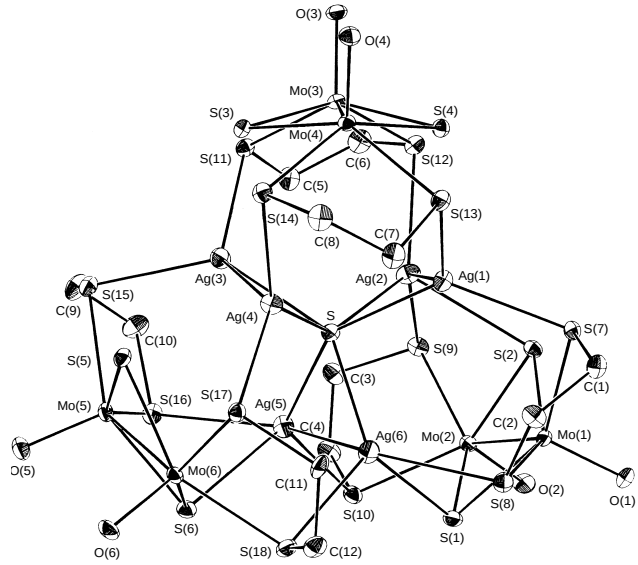



**Fig. 1** ORTEP diagram of $[\{Mo_2Ag_2S_2O_2(edt)_2\}_3(\mu_6\text{-}S)]^{2-}$ (10% displacement ellipsoids). Selected distances (Å) and angles (°): Mo(1)–Mo(2) 2.8861(14), Mo(3)–Mo(4) 2.8859(13), Mo(5)–Mo(6) 2.8802(14), Mo–$S_{edt}$ (av) 2.438(3), Ag(1)–Ag(2) 3.0652(14), Ag(3)–Ag(4) 3.0354(14), Ag(5)–Ag(6) 3.0799(15), Ag(1)–S 2.556(3), Ag(2)–S 2.523(3), Ag(3)–S 2.533(3), Ag(4)–S 2.504(3), Ag(5)–S 2.539(3), Ag(6)–S 2.510(3), Ag(5)–S(16) 2.694(3), Ag–$S_{edt}$ (av) 2.584(3), S(1)–Ag(6) 2.794(3), S(2)–Ag(2) 2.721(3), S(3)–Ag(3) 2.863(3), S(4)–Ag(1) 2.853(3), S(5)–Ag(4) 2.889(3), S(6)–Ag(5) 2.758(3); Ag(1)–S–Ag(2) 74.24(8), Ag(3)–S–Ag(4) 74.13(9), Ag(5)–S–Ag(6) 75.18(9), $S_{br}$–Mo–$S_{br}$ (av) 101.73(11), $S_{edt}$–Mo–$S_{edt}$ (av) 81.27(11).

equatorial. The average $S_{br}$–Mo–$S_{br}$ angle is 101.73°. Each Mo atom is chelated by one $^{-}SC_2H_4S^{-}$ forming a five-membered ring, and the average Mo–$S_{edt}$ and average $S_{edt}$–Mo–$S_{edt}$ angle are 2.438 Å and 81.27°, respectively. The average Mo–Mo distance of 2.8841 Å is almost the same as in $[M_2Ag$-$S_4(edt)_2(PPh_3)]^{-}$[9] (2.881 Å) and slightly longer than in $[NEt_4]_2[Mo_2S_4(edt)_2]$[17] (2.863 Å).

Each $^{-}SC_2H_4S^{-}$ is coordinated by two Ag atoms through its two S atoms with Ag–$S_{edt}$ ranging from 2.496 to 2.694 Å, and the average Ag–$S_{edt}$ distance is 2.584 Å.

It is interesting that the distances of six $S_{br}$ atoms of the three $[Mo_2S_2O_2(edt)_2]$ moieties of cluster **1** to the corresponding Ag atoms are different, and all are longer than the longest Ag–$S_{edt}$ [Ag(5)–S(16) 2.694(3) Å] or the longest Ag–$\mu_6$-S distance [Ag(1)–S, 2.556(3) Å]. Two $S_{br}$ atoms of one $[Mo_2S_2O_2(edt)_2]$ are also weakly bonded to the corresponding Ag atoms [S(1)–Ag(6) 2.794(3), S(1)–Ag(2) 2.721(3) Å] while only one $S_{br}$ atom of a second $[Mo_2S_2O_2(edt)_2]$ is bonded [S(6)–Ag(5) 2.758(3) Å], the other $S_{br}$ atom of this $[Mo_2S_2O_2(edt)_2]$ shows a longer Ag···$S_{br}$ non-bonding distance [S(5)–Ag(4) 2.889(3) Å]; for the third $[Mo_2S_2O_2(edt)_2]$, none of $S_{br}$ atom bonds to Ag [S(4)···Ag(1) 2.853(3), S(3)···Ag(3) 2.863(3) Å]. The three longer Ag···$S_{br}$ non-bonding distances suggest that there is only weak interaction between Ag(1) and S(4), Ag(3) and S(3), Ag(4) and S(5). Therefore, there are three four-coordinate Ag atoms in compound **1** [Ag(2), Ag(5), Ag(6)]; (two $S_{edt}$, one $S_{br}$ and $\mu_6$-S atom) to give a distorted tetrahedral geometry [angles S–Ag–S are in the wide range 68.00(10)–128.11(10)°]. The other Ag atoms [Ag(1), Ag(3), Ag(4)] are three-coordinate, each being coordinated by three S atoms ($\mu_6$-S and two $S_{edt}$).

This research was supported by grants from the State Key Laboratory of Structural Chemistry, Fujian Institute of Research on the Structure of Matter, the Chinese Academy of Sciences, and the Science Foundations of the Nation and Fujian Province.

## Footnotes

* E-mail: wxt@ms.fjirsm.ac.ch

† *Spectroscopic data* for **1**: IR (KBr pellet): $\nu$/cm$^{-1}$: $\nu$(Mo–μ-S) and $\nu$(Mo–$\mu_3$-S) 468.6 m, 439.7 m; $\nu$(Mo–O) 954.6 s. UV (dmf solution): $\lambda$/nm ($\varepsilon$/dm$^3$ mol$^{-1}$ cm$^{-1}$): 266 ($3.7 \times 10^4$), 302 ($3.8 \times 10^4$).

For **2**: IR (KBr pellet): $\nu$/cm$^{-1}$: $\nu$(W–μ-S) and $\nu$(W–$\mu_3$-S) 464.8 m, 424.3 m; $\nu$(W–O) 962.3 s. UV (dmf solution): $\lambda$/nm ($\varepsilon$/dm$^3$ mol$^{-1}$ cm$^{-1}$): 280 ($3.17 \times 10^4$), 340 ($1.45 \times 10^4$).

‡ For all structural analyses, all calculations were performed on a Indyworkstation of a silicon Graphics instrument with SHELXTL program.[14] The structure was solved by direct methods, and the positions of Mo/W and Ag atoms were obtained from E maps. The remaining non-hydrogen atoms were located from successive difference Fourier maps. The refinement of structures was performed by full least-squares techniques on $F^2$ using SHELXL-93.[15] Data were corrected with program SADABS.[16]

*Crystal data*: **1**: $C_{31}H_{69}Ag_6Cl_2Mo_6N_3O_6S_{19}$, $M_r$ = 2482.29, tetragonal, space group $I4_1/a$, $a = b$ = 42.013(4), $c$ = 16.034(2) Å, $U$ = 28301.4 Å$^3$, $Z$ = 16, $D_c$ = 2.331 g cm$^{-3}$, $T$ = 293(2) K; $\lambda$(Mo-Kα) = 0.710 73 Å, $\theta$ range 1.93–23.26°. Siemens Smart CCD diffractometer, ω scan. 10 141 unique reflections were used in the refinement and 7231 reflections with $I > 2\sigma(I)$ used to calculate $R$ and $R_w$. The last successful full-matrix least-squares refinement with anisotropic thermal parameters for Mo, Ag, S, O, C atoms of the cluster core, isotropic thermal parameters for all N, C, Cl atoms of the cations and the solution molecule (538 variables) converged to $R$ = 0.0499, $R_w$ = 0.1062, GOF = 1.079 (no attempt was made to locate hydrogen atoms).

**2**: $C_{31}H_{69}Ag_6Cl_2N_3O_6S_{19}W_6$, $M_r$ = 3010.26. $a = b$ = 42.0176(6), $c$ = 16.0098(3) Å, $U$ = 28265.0 Å$^3$, $D_c$ = 2.830 g cm$^{-3}$, $T$ = 293(2) K, $\theta$ range 1.37–23.24°. 10 126 unique reflections were used in the refinement and 7609 reflections with $I > 2\sigma(I)$ used to calculate $R$ and $R_w$. Anisotropic thermal parameters for W with other details as above. $R$ = 0.0586, $R_w$ = 0.1440, GOF = 1.020. CCDC 182/517.

## References

1 E. I. Stiefl and R. R. Chianelli, *Nitrogen Fixation*, Plenum, New York, 1993; C. L. Coyle, T. R. Halbert and E. I. Stiefl, *US Pat.*, 4978464, 1990; U. Riaz, O. Curnow and M. D. Curtis, *J. Am. Chem. Soc.*, 1991, **113**, 1416.
2 A. Müller, E. Diemann, R. Jostes and H. Bögge, *Angew. Chem.*, 1981, **93**, 957; *Angew. Chem., Int. Ed. Engl.*, 1981, **20**, 934; S. Sarkar and S. B. S. Mishra, *Coord. Chem. Rev.*, 1984, 59, 239; X.-T. Wu, P.-C. Chen, S.-W. Du, N-Y. Zhu and J.-X. Lu, *J. Cluster Sci.*, 1994, **5**, 265; C. E. Holloway and M. Melnik, *Rev. Inorg. Chem.*, 1993, **13**, 233; H.-W. Hou, X.-Q. Xin and S. Shi, *Coord. Chem. Rev.*, 1996, **53**, 25.
3 S.-W. Du, N.-Y. Zhu, P.-C. Chen, X.-T. Wu and J.-X. Lu, *J. Chem. Soc., Dalton Trans.*, 1992, 339.
4 N.-Y. Zhu, J.-H. Wu, S.-W. Du, X.-T. Wu and J.-X. Lu, *Inorg. Chim. Acta*, 1992, **11**, 1201.
5 S.-W. Du, N.-Y. Zhu, P.-C. Chen and X.-T. Wu, *Polyhedron*, 1992, **11**, 2489; S.-W. Du and X.-T. Wu, *J. Coord. Chem.*, 1993, **30**, 183.
6 A. Müller, H. Bögge, E. Koniger-Ahlborn and W. Hellmann, *Inorg. Chem.*, 1979, **18**, 2301; A. Müller, H. Bögge and E. Koniger-Ahlborn, *J. Chem. Soc., Chem. Commun.*, 1978, 739.
7 Q. Huang, X.-T. Wu, Q.-M, Wang, T.-L. Sheng and J.-X. Lu, *Angew. Chem., Int. Ed. Engl.*, 1996, **35**, 868.
8 Q. Huang, X.-T. Wu, T.-L. Sheng and Q.-M. Wang, *Inorg. Chem.*, 1995, **27**, 4931.
9 N.-Y. Zhu, X.-T. Wu and J.-X. Lu, *J. Chem. Soc., Chem. Commun.*, 1991, 235.
10 H.-B. Chen, S.-F. Lu, J.-Q. Huang, Q.-J. Wu and X.-Y. Huang, *Phys. Chem. Lett.*, 1994, 732.
11 X.-T. Wu, Wang, B. Wang, Zheng, Y.-F. Zheng and J.-X. Lu, *Jiegou Huaxue* (*Chin. J. Struct. Chem.*), 1988, **71**, 47.
12 W.-J. Zhang, Master thesis, Fujian Institute of Research, 1996, p. 11.
13 W. H. Pan, T. Chandler, J. H. Enemark and E. I. Stiefel, *Inorg. Chem.*, 1984, **23**, 4265.
14 G. M. Sheldrick, SHELXTL Version 5.03, Siemens Analytical X-Ray Instruments Inc., Madison, WI, 1990.
15 G. M. Sheldrick, SHELXTL93, Program for the Refinement of crystal structure. University of Göttingen, 1993.
16 G. M. Sheldrick, SADABS, University of Göttingen, 1996.
17 G. Bunzey and J. H. Enemark, *Inorg. Chem.*, 1978, **17**, 682.

*Received in Cambridge, UK, 20th May 1997; 7/03468G*

# Chiral arene ruthenium complexes as asymmetric Diels–Alder catalysts

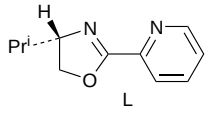
**David L. Davies,* John Fawcett, Shaun A. Garratt and David R. Russell**

*Department of Chemistry, University of Leicester, Leicester, UK LE1 7RH*

**The cation [RuCl(L)(η⁶-mes)]⁺ [L = 4-isopropyl-2-(2-pyridyl)-1,3-oxazoline] is synthesised diastereoselectively; treatment with $AgSbF_6$ gives a dication which is an enantioselective catalyst for the asymmetric Diels–Alder reaction between methacrolein and cyclopentadiene.**

Recently, much attention has focussed on the development of chiral Lewis-acid catalysts for a variety of carbon–carbon bond-forming reactions.[1] Impressive results have been reported for Diels–Alder reactions mostly with titanium, aluminium or boron based catalysts.[2] Such catalysts have a number of drawbacks *viz*. they are often extremely sensitive to water, hence are generally employed at high catalytic loadings (often *ca*. 20%); also, attempts to understand the mechanisms of catalysis and selectivity are hampered by the complexity of the chemical behaviour of the catalyst, *e.g.* formation of oligomers, ligand-exchange reactions. Recently some transition-metal and lanthanide complexes have been described as promising catalysts for these reactions.[3] Half-sandwich complexes have been extensively used in stoichiometric and catalytic organic transformations often with impressive asymmetric induction. Indeed, half-sandwich complexes of Rh and Fe with chiral phosphorus ligands have recently been shown to be asymmetric catalysts for Diels–Alder reactions.[4]

Bisoxazolines have given high enantioselectivity in a number of asymmetric catalytic processes, for example copper catalysed cyclopropanation and aziridination[5] and more recently Diels–Alder reactions;[3b,c,f] whilst phosphino-oxazolines work well in palladium-catalysed allylic substitution.[5c,6] However, the use of these types of ligands with half-sandwich complexes is less well studied, the first arene ruthenium complexes with bisoxazoline ligands having been reported recently.[7]




L

Refluxing L with $[RuCl_2(\eta^6\text{-mes})]_2$ (mes = 1,3,5-trimethylbenzene) in methanol in the presence of $NaSbF_6$ or $KPF_6$ gives [RuClL(η⁶-mes)]X (X = $SbF_6$, $PF_6$) in good yield.† The complexation of the ligand is highly diastereostereoselective, only one of two possible diastereomers being observed by $^1H$ NMR spectroscopy. The X-ray structure was carried out to determine which diastereomer was formed. The structure of the cation with selected bond distances and angles is shown in Fig. 1.‡ The ruthenium has a pseudo-octahedral geometry with L coordinated such that the isopropyl substituent is on the same side as the chloride rather than the arene to miminise unfavourable steric interactions. The Ru–N(1) oxazoline and Ru–N(2) pyridine bond lengths are the same, as found previously for other 2-iminopyridine complexes.[8] The use of L-valine in the ligand preparation means that the configuration at the chiral carbon is (*S*) and the structure shows that the ruthenium is also (*S*) (based on the priority arene > Cl > $N_{ox}$ > $N_{py}$).[9] There is no evidence for formation of the other diastereomer in the NMR spectrum and thus it is assumed that this geometry is retained in solution and the configuration at ruthenium is stable in $CD_2Cl_2$ solution as found for related iminopyridine complexes.[8b]

In order for the complex to be used as a Lewis-acid catalyst the chloride must be removed, this is easily done by treating with $AgSbF_6$ in acetone–water to give $[Ru(H_2O)L(\eta^6\text{-mes})][SbF_6]_2$ **2**.† The $^1H$ NMR spectrum of **2** in $[CD_2Cl_2$–$(CD_3)_2CO$ 10 : 1] shows a broad singlet at $\delta$ 5.40 due to coordinated water with free water from the NMR solvent at $\delta$ 1.81. The observation of separate signals for free and co-ordinated water indicates that water exchange is relatively slow on the NMR timescale.

Complex **2** catalyses the Diels–Alder reaction between methacrolein and cyclopentadiene (Table 1).§ The reaction proceeds rapidly at room temp. (essentially quantitative conversion in < 45 min monitored by $^1H$ NMR) at low catalyst loading (as little as 0.5 mol%) and with good *exo* : *endo* selectivity (⩾95 : 5) and good enantioselectivity (ee 70%) (entry 1). As can be seen from entries 2, 5 and 7 increasing the catalyst ratio to 5 mol% has very little effect on the *exo* : *endo* ratio or on the enantioselectivity. However, reducing the temperature of the reaction to 0 °C (entries 3, 6 and 8) or −20 °C (4 and 9) leads to small improvements in the enantioselectivity. The major product is identified as (1*R*,2*S*,4*R*)-2-methylbicyclo[2.2.1]hept-5-ene-2-carbaldehyde by comparison of the sign of the optical rotation [$\alpha$], and the GC behaviour of the acetal formed from (2*R*,4*R*)-pentanediol with literature values.[3b] The absolute configuration of the major *exo* product can be rationalised by assuming that the methacrolein coordinates in the preferred *S–trans* conformation with the aldehyde H pointing towards the

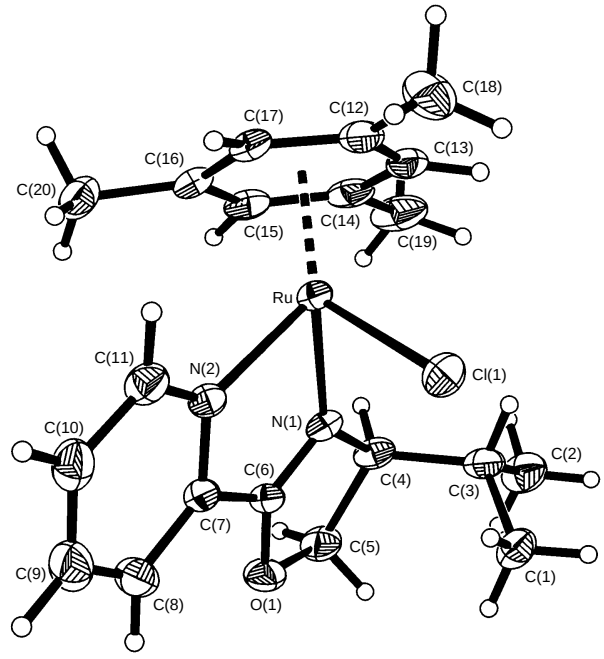
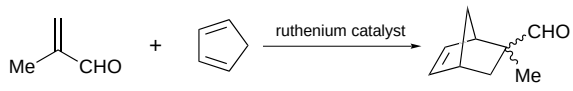



**Fig. 1** Molecular structure and atom numbering scheme for the cation of **1**. Selected bond distances (Å) and angles (°): Ru–N(1) 2.118(4), Ru–N(2) 2.117(4), Ru–Cl(1) 2.402(2), N(2)–C(7) 1.351(7), C(7)–C(6) 1.449(8), C(6)–N(1) 1.280(7), N(2)–Ru–N(1) 76.4(2).

**Table 1** Enantioselective Diels–Alder reaction of methacrolein with cyclopentadiene catalysed by complex **2** in dichloromethane




| Entry | Catalyst (mol%) | *T*/°C | *t*/h | Yield[a] (%) | Isomer ratio (*exo : endo*) | Ee (%) |
|---|---|---|---|---|---|---|
| 1 | 0.5 | r.t.[b] | 0.25 | > 95 | 95 : 5 | 70 |
| 2 | 1 | r.t. | 0.2 | > 95 | 95 : 5 | 70 |
| 3 | 1 | 0 | 3 | 72[c] | 96 : 4 | 76 |
| 4 | 1 | −20 | 24 | 30[c] | 96 : 4 | 78 |
| 5 | 2 | r.t. | 0.33 | > 95 | 95 : 5 | 71 |
| 6 | 2 | 0 | 24 | 92[c] | 95 : 5 | 75 |
| 7 | 5 | r.t. | 1 | > 95 | 94 : 6 | 72 |
| 8 | 5 | 0 | 6 | 53[c] | 95 : 5 | 75 |
| 9 | 5 | −20 | 72 | 90[c] | 96 : 4 | 81 |

[a] NMR tube reaction, yield from integration. [b] r.t. = Room temperature. [c] Isolated yield.

arene ring; the alternative orientation formally obtained by a 180° rotation about the Ru–O bond would be disfavoured due to steric interactions between the vinyl substituent and the arene. Attack of the cyclopentadiene is expected to occur at the *Re* face of the methacrolein, the *Si* face being shielded by the isopropyl of L which is consistent with the observed major product. Further studies to try and identify the actual catalyst, *i.e.* with methacrolein coordinated, to extend the range of substrates and to optimise the enantioselectivity are currently underway.

We thank the University of Leicester for a studentship (S. A. G.) and Johnson Matthey for a loan of $RuCl_3$.

## Footnotes

* E-mail: dld3@le.ac.uk

† *Selected spectroscopic data*: for **1**: $^1$H NMR (300 MHz, $CD_2Cl_2$, 20 °C, $SiMe_4$); $\delta$ 0.77 (d, 3 H, *J* 7 Hz, CH*Me*′Me′), 1.02 (d, 3 H, *J* 7 Hz, CHMe*Me*′), 2.25 (s, 9 H, $C_6Me_3$), 4.82 (m, 2 H, OCH + NCH), 5.00 (t, 1 H, *J* 11 Hz, OCH), 5.33 (s, 3 H, $C_6H_3$), 7.75 (m, 1 H, pyr), 7.88 (d, 1 H, *J* 7 Hz, pyr), 8.10 (dt, 1 H, *J* 1.5, 7.5 Hz, pyr), 9.05 (d, 1 H, *J* 5 Hz, pyr). Satisfactory elemental analysis (C, H, N). For **2**: $^1$H NMR [300 MHz, $CD_2Cl_2$–$(CD_3)_2CO$ (10 : 1), 20 °C, $SiMe_4$], $\delta$ 0.57 (d, 3 H, *J* 7 Hz, CH*Me*′Me′), 1.01 (d, 3 H, *J* 7 Hz, CHMe*Me*′), 2.22 (s, 9 H, $C_6Me_3$), 4.78 (dd, 1 H, *J* 5, 8.5 Hz, OCH), 4.92 (m, 1 H, NCH), 5.03 (t, 1 H, *J* 10 Hz, OCH), 5.40 (s, 2 H, $H_2O$), 5.55 (s, 3 H, $C_6H_3$), 7.87 (m, 2 H, pyr), 8.15 (t, 1 H, *J* 8 Hz, pyr), 9.40 (d, 1 H, *J* 5 Hz, pyr). Satisfactory elemental analysis (C, H, N).

‡ *Crystal data* for **1**: $C_{20}H_{26}ClF_6N_2OPRu$, $M$ = 591.92, orthorhombic, space group $P2_12_12_1$, $a$ = 8.461(1), $b$ = 9.330(1), $c$ = 29.347(4) Å, $U$ = 2316.5 Å$^3$, $Z$ = 4, $D_c$ = 1.697 g cm$^{-3}$, $\mu$ = 0.925 mm$^{-1}$, $F$(000) = 1192, graphite-monochromated Mo-K$\alpha$ radiation ($\lambda$ = 0.710 73 Å). Data collected on a Siemens P4 diffractometer at 190 K. 3080 reflections collected with 5 < $\theta$ < 25°, 2881 unique ($R_{int}$ = 0.027). A $\psi$-scan absorption correction was applied. The structure was solved by Patterson methods and refined using full-matrix least squares on $F^2$ (SHELXL-96). Anisotropic displacement parameters used for all atoms, hydrogens included in calculated positions (C–H 0.96 Å), with isotropic displacement parameters set to 1.2 $U_{eq}$(C). Final $R_1$ = 0.0406, $wR_2$ = 0.0838 for all data). CCDC 182/521.

§ NMR tube experiments (in air): methacrolein (*ca.* 0.25 mmol) was added to a suspension of **2** (1.25, 2.5, 5, or 12.5 μmol) in $CD_2Cl_2$ (0.5 cm$^3$) which lead to rapid dissolution of **2** to give a yellow solution. The solution was transferred to an NMR tube and 2,6-di-*tert*-butylpyridine (1 equiv./mol catalyst) and cyclopentadiene (0.5 mmol) were added. The $^1$H NMR spectrum was run immediately and then repeated after suitable time intervals. Schlenk reactions (under $N_2$). Methacrolein (1 mmol) and 2,6-di-*tert*-butylpyridine (1 equiv./mol catalyst) were added to a suspension of **2** (0.01, 0.02, or 0.05 mmol) in $CH_2Cl_2$ (2 cm$^3$). The resulting yellow solution was cooled to the appropriate temperature before addition of cyclopentadiene (2 mmol). At the end of the reactions, the mixture was passed through a silica plug, the solvent was removed and the product was obtained as a colourless oil. The *exo : endo* ratio was determined by NMR spectroscopy and the enantiomeric excess was determined by GC after conversion to the acetal with (2*R*,4*R*)-pentanediol.[3b] The catalyst could also be prepared *in situ* from complex **1** and 1 equiv. of $AgSbF_6$ in $CH_2Cl_2$, filtration through Celite into a Schlenk tube to remove AgCl and then addition of the reagents as described above.

## References

1 *Catalytic Asymmetric Synthesis*, ed. I. Ojima, VCH, Weinheim, 1993; R. Noyori, *Asymmetric Catalysis in Organic Synthesis*, Wiley, New York, 1994.
2 H. B. Kagan and O. Riant, *Chem. Rev.*, 1992, **92**, 1007; K. Narasaka, *Synthesis*, 1991, 1.
3 (*a*) S. Kobayashi and H. Ishitani, *J. Am. Chem. Soc.*, 1994, **116**, 4083; (*b*) D. A. Evans, J. A. Murry, P. von Matt, R. D. Norcross and S. J. Miller, *Angew. Chem., Int. Ed. Engl.*, 1995, **34**, 798; (*c*) D. A. Evans, S. J. Miller and T. Lectka, *J. Am. Chem. Soc.*, 1993, **115**, 6460; (*d*) J. Jaquith, J. Guan, S. Wang and S. Collins, *Organometallics*, 1995, **14**, 1079; (*e*) S. Kobayashi, H. Ishitani, I. Hachiya and M. Araki, *Tetrahedron*, 1994, **50**, 11623; (*f*) E. J. Corey, N. Imai and H.-Y. Zhang, *J. Am. Chem. Soc.*, 1991, **113**, 728.
4 D. Carmona, C. Cativiela, R. Garcia-Correas, F. J. Lahoz, M. P. Lamata, J. A. Lopez, M. P. Lopez-Ram de Viu, L. A. Oro, E. San Jose and F. Viguri, *Chem. Commun.*, 1996, 1247; E. P. Kundig, B. Bourdin and G. Bernardinelli, *Angew. Chem., Int. Ed. Engl.*, 1994, **33**, 1856.
5 (*a*) A. Pfaltz, *Acc. Chem. Res.*, 1993, **26**, 339; (*b*) D. A. Evans, K. A. Woerpel, M. M. Hinman and M. M. Faul, *J. Am. Chem. Soc.*, 1991, **113**, 726; (*c*) A. Pfaltz, *Acta Chem. Scand.*, 1996, **50**, 189.
6 G. J. Dawson, J. M. J. Williams and S. J. Coote, *Tetrahedron. Lett.*, 1995, **36**, 461 and references therein.
7 H. Asano, K. Katayama and H. Kurosawa, *Inorg. Chem.*, 1996, **35**, 5760.
8 (*a*) S. K. Mandal and A. R. Chakravarty, *Polyhedron*, 1992, **11**, 823; (*b*) D. L. Davies, J. Fawcett, R.Krafczyk and D. R. Russell, submitted for publication.
9 T. E. Sloan, *Top. Stereochem.*, 1981, **12**, 1; K. Stanley and M. C. Baird, *J. Am. Chem. Soc.*, 1975, **97**, 6598.

*Received in Cambridge, UK, 16th May 1997; 7/03386I*

# The synthesis of a symmetrically substituted α-octa(isopentoxy)anthralocyanine

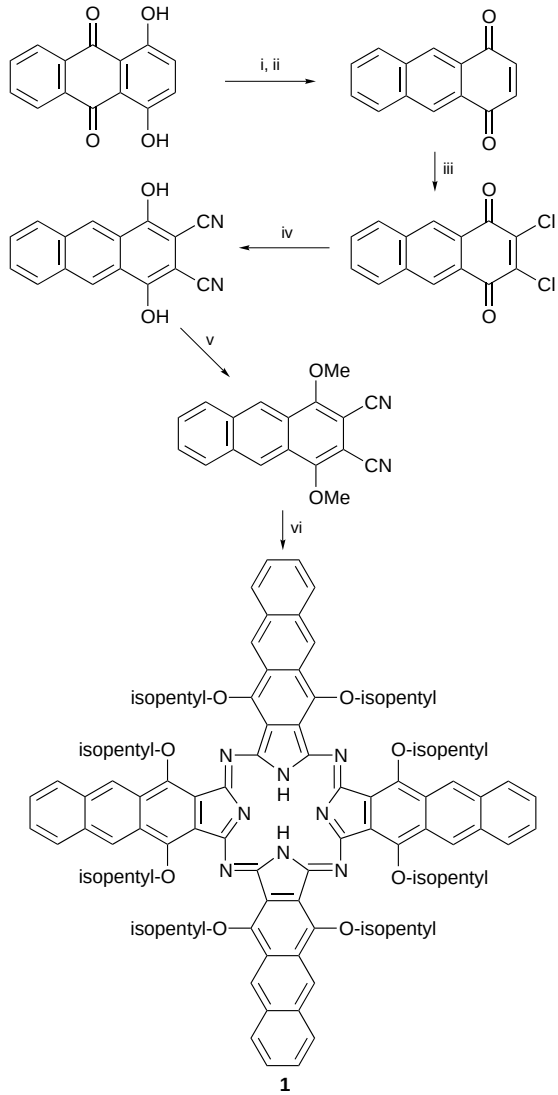
**Peter V. Bedworth,[a] Joseph W. Perry[a,b] and Seth R. Marder*[a,b]**

[a] *Beckman Institute, 139-74 California Institute of Technology, Pasadena, CA 91125, USA*
[b] *Jet Propulsion Laboratory, California Institute of Technology, Pasadena, CA 91109, USA*

**α-Octa(isopentoxy)anthralocyanine has been synthesized and is found to have an unprecedented low-energy Q-band absorption and a low first oxidation potential.**

In an effort to synthesize dyes that may find use in optical limiting devices[1,2] we have been investigating phthalocyanine complexes (Pcs). The Pcs have a region of relatively weak absorption from *ca*. 450–650 nm which falls between their Q and B bands. In addition, in this same spectral region they have strong excited-state absorption in their singlet manifold and even stronger absorption in their triplet manifold.[1] Consequently, in this spectral range the molecules are relatively transparent under weak irradiation, but under intense irradiation, such as from a pulsed laser source, it is possible to create a significant excited-state population that will be relatively opaque in the same spectral range. When the Pcs are functionalized with heavy atoms it is also possible to enhance the intersystem crossing rate so as to generate a large triplet population. Since the excited-states of these molecules are strongly absorbing, and it is possible to saturate the ground to excited-state transition, they are referred to as reverse saturable absorbers (RSAs) and are useful in optical limiting devices.[1,3,4] For certain applications where it is important to protect sensors from intense laser pulses in the 600–900 nm range, it is necessary to move the transparency window (the region between the high energy side of the Q band and the low energy side of the B band) to lower energy. It has been demonstrated that the transparency window of the phthalocyanines can be tuned by a number of structural modifications.[5] One approach is to benzannulate the phthalocyanine molecules and another is to substitute the rings with electron donors, thereby shifting the Q and B bands and therefore the transparency window to lower energy. We have also attempted to make these molecules soluble in common organic solvents despite structural features that would impart limited solubility. This is necessary in order to make dyes that are useful for many device configurations. Octaalkoxyphthalocyanines and octaalkoxynaphthalocyanines,[5] as well as a number of alkyl substituted anthralocyanines,[6–9] have been previously described. Here we describe the synthesis, linear optical properties and electrochemistry of α-octaisopentoxyanthralocyanine **1**.

The synthetic pathway to octaalkoxyanthralocyanine **1** is shown in Scheme 1. The method is analogous to the synthesis of the octaalkoxynaphthalocyanines and tetra-*tert*-butylanthralocyanine.[9] The anthracene-1,4-dione was prepared by literature methods.[10,11] For 2,3-dichloroanthracene-1,4-dione, the method of Langa was modified. Chlorine gas was added in a vigorous stream to a solution of anthracene-1,4-dione in boiling acetic acid, which was interrupted for 20 min every 5 min, until the reaction was deemed complete as evidenced by $^1$H NMR spectroscopy. The red solution with yellow crystalline precipitate was allowed to cool to ambient temperature and then filtered. The yellow crystalline solid was dried under vacuum (0.01 Torr) over KOH, to give the title compound in 75% yield.[10,11] 2,3-Dicyano-1,4-dihydroxyanthracene was prepared in moderate yield by treating 2,3-dichloroanthracene-1,4-dione with an excess of KCN in hot EtOH.[12] *O*-Methylation was accomplished with dimethyl sulfate in the presence of $K_2CO_3$. The synthesis of **1** from 2,3-dicyano-1,4-dimethoxyanthracene was analogous to the synthesis of the corresponding α-octaalkoxynaphthalocyanine to yield 15% of the desired product after purification. As was consistent with the reactivity of other alkoxy Pcs,[13] we observed complete *trans* alkoxylation of the methyl group by the isopentyl group from the solvent (there were no observable singlet methyl resonances by $^1$H NMR spectroscopy) under the reaction conditions.[13] It is also important to note that **1** is fairly sensitive to silica gel. Thus, the isolated yield of **1** is significantly reduced if chromatography is performed at conventional flow rates and accordingly, flash




**1**

**Scheme 1** *Reagents and conditions*: i, $NaBH_4$, MeOH; ii, $H_2O$, HCl; iii, $Cl_2$, AcOH, reflux; iv, KCN, EtOH; v, dimethyl sulfate, $K_2CO_3$, acetone; vi, lithium isopentoxide, isopentyl alcohol, reflux

chromatography techniques are necessary. All compounds gave satisfactory spectroscopic and analytical data.†

The UV–VIS/NIR spectrum of **1** (Fig. 1) shows a small splitting between the $Q_x$ and $Q_y$ bands and the bands are sharp, characteristic of phthalocyanines. The Q bands for **1** occur at 980 and 954 nm. These bands are red shifted about 110 nm compared to the analogous octaalkoxynaphthalocyanine and red shifted 80 nm compared to the tetra-*tert*-butylanthralocyanine.[6] The B bands of **1** are bathochromically shifted compared to the B bands of the octabutoxynaphthalocyanine, giving solutions of **1** a pleasant violet hue. The transparency window has moved about 100 nm bathochromically compared to the Npcs.[6]

The cyclic voltammogram of **1** (Fig. 2) shows four quasi-reversible redox events; those at $E_{1/2}$ = −1279 and −1039 mV we attribute to sequential one electron reductions and those at 35 and 366 mV we attribute to sequential one electron oxidations. The separation of the inner-most redox events correlates well with the energy of the Q band. We have shown that through a systematic approach we have moved the transparency window of a Pc to a region centred about 700 mm. This will allow for the investigation of the utility of this compound and derivatives thereof as the active elements for optical limiters in a particularly important spectral range.

We thank the Air Force Office of Scientific Research and the US Wright Patterson Air Force Base for funding this effort. P. V. B. thanks The James Irvine Foundation for a postdoctoral fellowship.

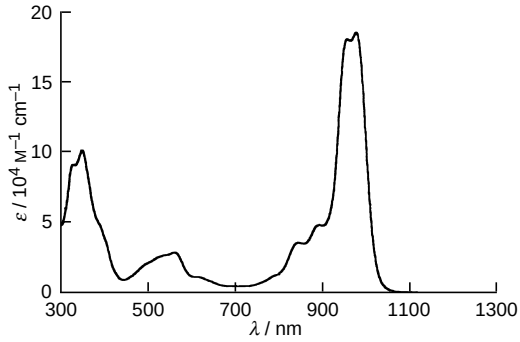



**Fig. 1** The absorption spectrum of **1** in toluene

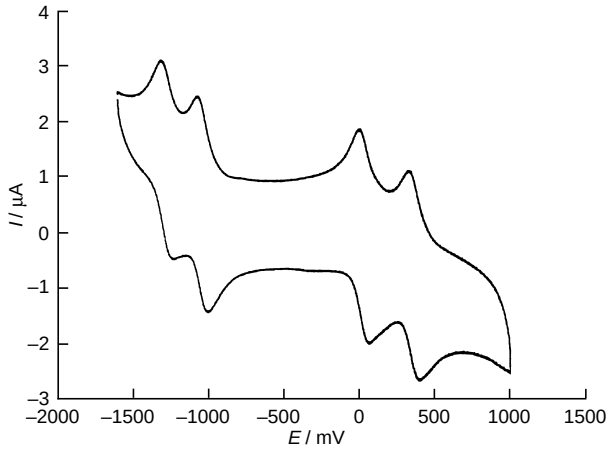



**Fig. 2** Cyclic voltammogram of **1** in $CH_2Cl_2$, Ag/AgCl (aq.), 0.1 M $Bu_4NPF_6$, 500 mV $s^{-1}$, $V_{init.}$ = −600 mV. Four quasi-reversible redox events at $E_{1/2}$ = −1279, −1039, 35 and 366 mV are observed. The $E_{1/2}$ of ferrocene was found to be 514 mV under these conditions.

## Footnotes

* E-mail: srm@cco.caltech.edu

† *2,3-Dicyano-1,4-dimethoxyanthracene*. To a slurry of 2,3-dichloroanthracene-1,4-dione (50 g, 185 mmol) in EtOH (1 l) at 60 °C under argon was added a solution of KCN (61 g, 925 mmol) in water (240 ml). The mixture was stirred at 60 °C for 2 h then filtered. The solution was then cooled and neutralized with 3 M HCl (carefully in a hood with a sodium hypochlorite trap). The brown solid precipitate was collected and dried overnight over KOH under vacuum. To a mixture the crude 2,3-dicyano-1,4-dihydroxyanthracene (34 g) and $K_2CO_3$ (76 g, 548 mmol) in acetone (150 ml) was added dimethyl sulfate (40 ml, 411 mmol). The mixture was heated to reflux for 3 h then poured into water. The brown solid residue was further washed with water then dried under vacuum over $P_2O_5$. The bright yellow product was collected by sublimation then recrystallized from MeOH to give 5 g of the title product. $^1$H NMR (300 MHz, $CD_2Cl_2$): $\delta$ 8.85 (s, 2 H), 8.14 (4 line m, 2 H), 7.69 (4 line m, 2 H), 4.39 (s, 6 H); $\nu_{max}$(KBr)/cm$^{-1}$ 3062, 2949, 2226, 1452, 1351, 1029, 886, 749; $\lambda_{max}$($CHCl_3$)/nm 404, 388, 370.

*Compound 1*. To a slurry of 2,3-dicyano-1,4-dimethoxyanthracene (2 g, 6.9 mmol) in anhydrous isopentyl alcohol (40 ml) at 25 °C under argon was added lithium (5 mg). The mixture was heated to reflux for 1 h then allowed to cool to room temperature and acetic acid (10 ml) was added and stirred overnight at room temperature under argon. The mixture was neutralized with deoxygenated saturated aqueus $NaHCO_3$ and extracted with deoxygenated methylene $CH_2Cl_2$. The organic layer was washed with deoxygenated water then dried with $Na_2SO_4$ (if $MgSO_4$ was used a considerable amount of AncMg was formed). The solvent was removed *in vacuo* and the residue was quickly chromatographed (solvent flow rate was about four times as fast as a standard flash column, if chromatography was run at a conventional rate the yield was greatly attenuated) on a short (125 × 45 mm) silica gel column with deoxygenated solvent (1 : 1, cyclohexane–$CH_2Cl_2$) to give 10% yield (0.29 g, 0.18 mmol) of the title compound; $^1$H NMR (300 MHz, $CD_2Cl_2$): $\delta$ 9.6 (br m, 8 H), 8.44 (br m, 8 H), 7.76 (br m, 8 H), 5.35 (m, 16 H), 2.19 (br q, *J* 7 Hz, 16 H), 2.26 (nonet, *J* 7 Hz, 4 H), 1.5 (br s, 24 H), 1.1 (br d, *J* 6 Hz, 36 H), 0.92 (br s, 12 H); $^{13}$C NMR (75 MHz, [$^2H_6$]THF): $\delta$ 151.2, 133.4, 130.1, 129.9, 127.4, 124.8, 76.5, 40.5, 26.4, 23.4 (two quarternary carbons not observed); $^{13}$C NMR DEPT 90 (125 MHz, [$^2H_6$]THF): $\delta$ 129.88, 127.36, 124.84, 26.43; FAB MS $C_{105}H_{116}N_8O_8$: Calc., 1602.87. Found ($MH^+$), 1603.9. Elemental analysis $C_{105}H_{116}N_8O_8$: Calc., C, 77.94; H, 7.23; N, 6.92; Found, C, 78.00; H, 7.27; N, 6.84%.

## References

1 J. W. Perry, K. Mansour, I. Y. S. Lee, X. L. Wu, P. V. Bedworth, C. T. Chen, D. Ng, S. R. Marder, P. Miles, T. Wada, M. Tian and H. Sasabe, *Science*, 1996, **273**, 1533.
2 J. W. Perry, *Organic and Metal Containing Reverse Saturable Absorber for Optical Limiting*, in *Nonlinear Optics of Organic Molecules and Polymers*, ed. H. S. Nalwa, and S. Miyata, CRC Press, Boca Raton, FL, 1997, p. 813.
3 D. J. Hagen, T. Xia, A. A. Said, T. H. Wei and E. W. Van Stryland, *Int. J. Nonlinear Opt. Phys.*, 1994, **2**, 483.
4 J. W. Perry, K. Mansour, S. R. Marder, K. J. Perry, D. Alvarez and I. Choong, *Optics Lett.*, 1994, **19**, 625.
5 A. B. P. Lever and C. C. Leznoff, *Phthalocyanines Properties and Applications*, VCH, Weinheim, 1989.
6 N. Kobayashi, S. Nakajima and T. Osa, *Inorg. Chim. Acta*, 1993, **210**, 131.
7 W. Freyer and L. Q. Minh, *Monatsh. Chem.*, 1986, **117**, 475.
8 M. Hanack, R. Dieing and U. Rohrig, *Chem. Lett.*, 1993, 399.
9 W. Freyer, H. Stiel, K. Teuchner and D. Leupold, *J. Photochem. Photobiol. A, Chem.*, 1994, **80**, 161.
10 E. Barranco, N. Martin, J. L. Segura, C. Seoane, P. Delacruz, F. Langa, A. Gonzalez and J. M. Pingarron, *Tetrahedron*, 1993, **49**, 4881.
11 N. Martin, J. L. Segura, C. Seoane, P. Delacruz, F. Langa, E. Orti, P. M. Viruela and R. Viruela, *J. Org. Chem.*, 1995, **60**, 4077.
12 G. A. Reynolds and C. VanAllen, *J. Am. Chem. Soc.*, 1964, **29**, 3591.
13 M. J. Cook, A. J. Dunn, S. D. Howe, D. J. Thomson and K. J. Harrison, *J. Chem. Soc., Perkin. Trans. 1*, 1988, 2453.

*Received in Corvallis, OR, USA, 21st January 1997; revised MS received 19th May 1997; 7/03454G*

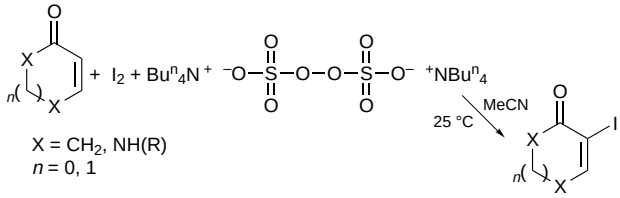
# Novel α-iodination of functionalized ketones with iodine mediated by bis(tetra-*n*-butylammonium) peroxydisulfate

**Je Pil Whang, Seung Gak Yang and Yong Hae Kim***

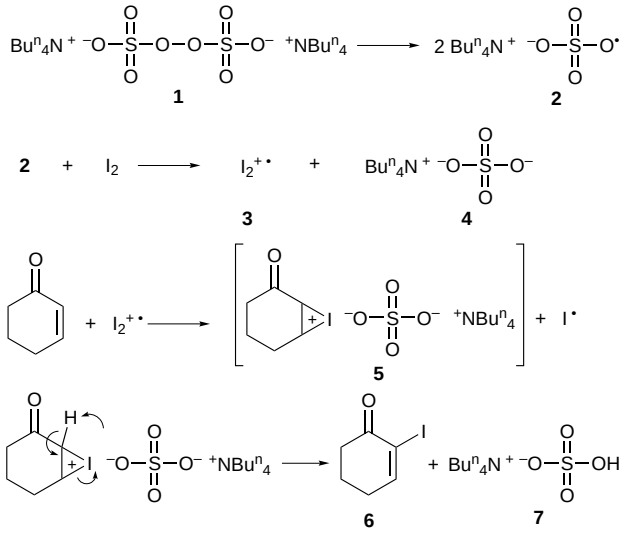
*Department of Chemistry, Korea Advanced Institute of Science and Technology, Taejon, 305-701, Korea*

**α,β-Unsaturated ketones, β-keto esters and uracil derivatives react with iodine in the presence of bis(tetra-*n*-butylammonium) peroxydisulfate under mild conditions in MeCN at 25 °C to give the corresponding α-iodinated products in good yields.**

α-Haloenones and α-halo ketones are highly reactive and versatile intermediates for the generation of α-carbon substituted enones[1] and ketones.[2] α-Halo ketones have been well studied and documented, but only a few reports on the preparation of α-iodoenones have been reported, which employ iodine–ceric ammonium nitrate[3] and $I_2$–pyridine–$CCl_4$.[4] The reactivity of α-iodine is higher, especially in transition metal mediated reactions, than the corresponding bromo or chloro derivatives, while functionalization of the 5-position of uracils or uridines is important for the synthesis of chemotherapeutic agents[5] and synthetic oligonucleotide probes.[6] Bis(tetra-*n*-butylammonium) peroxydisulfate **1** has been successfully prepared and turns out to be a useful source of tetra-*n*-butylammonium sulfate radical **2**,[7]† which is readily convertible to sulfate anion by one electron transfer from a substrate. Working on the supposition that activation of iodine by **2** might be possible, various enones, ketones, and uracils were examined in the reaction system.




**Scheme 1**

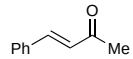
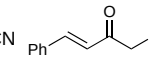
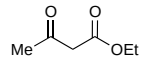
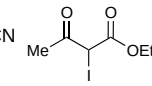
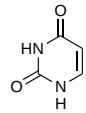
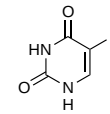
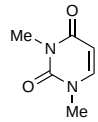
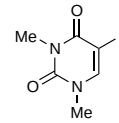
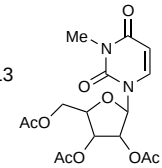
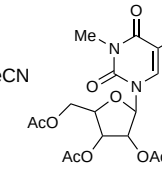


**Scheme 2**

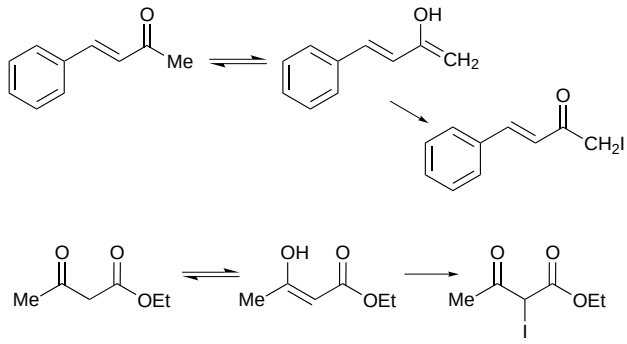
We have found that α,β-unsaturated ketones, β-keto esters and uracil derivatives reacted with $I_2$ in the presence of **1** to give the corresponding α-iodo α,β-unsaturated ketones, α-iodo β-keto esters and 5-iodouracil products respectively in good yields (Scheme 1).

An example of the procedure is as follows. A solution of cyclohex-2-ene-1-one (1.0 mmol, 1.0 equiv.) in 5 ml of dried MeCN was added at room temperature to a solution of bis(tetra-*n*-butylammonium) peroxydisulfate (1.0 mmol, 1.0 equiv.) and $I_2$ (1.0 mmol, 1.0 equiv.) in 5 ml of dried MeCN. The reaction mixture was monitored by thin layer chromatography with stirring at room temperature. When the reaction was completed,

**Table 1** α-Iodinations with $I_2$ and bis(tetra-*n*-butylammonium) peroxydisulfate in MeCN at 25 °C

| Entry | Reactant | $I_2$/ equiv. | **1** equiv. | *t*/h | Solvent | Product | Yield (%)[a] |
|---|---|---|---|---|---|---|---|
| 1 |  | 0.5 | 0.5 | 5 | MeCN |  | 48 |
| 2 | | 0.5 | 1.0 | 5 | MeCN | | 60 |
| 3 | | 1.0 | 0.5 | 5 | MeCN | | 54 |
| 4 | | 1.0 | 1.0 | 5 | $CCl_4$ | | 25 |
| 5 | | 1.0 | 1.0 | 5 | $CH_2Cl_2$ | | 65 |
| 6 | | 1.0 | 1.0 | 5 | $CHCl_3$ | | 34 |
| 7 | | 1.0 | 1.0 | 5 | MeCN | | 85 |
| 8 |  | 1.0 | 1.0 | 3.5 | MeCN |  | 83 |
| 9 |  | 1.0 | 1.0 | 24 | MeCN |  | 95 |
| 10 |  | 1.0 | 1.0 | 2 | MeCN |  | 90 |
| 11 |  | 1.0 | 1.0 | 1 | MeCN |  | 72 |
| 12 |  | 1.0 | 1.0 | 3.5 | MeCN |  | 75 |
| 13 |  | 1.0 | 1.0 | 12 | MeCN |  | 82 |

[a] Isolated yield; purified by column chromatography.




**Scheme 3**

the mixture was poured into 10% aqueous sodium bisulfate (30 ml) and extracted with ethyl acetate (30 ml × 3). The organic layer was washed with $H_2O$ (40 ml × 3) and dried over anhydrous $MgSO_4$. After filtration and concentration under reduced pressure, the residue was purified by flash column chromatography (silica gel 230–400 mesh, EtOAc–*n*-hexane, 1 : 10, v/v) to give 2-iodocyclohex-2-en-1-one (85%). All the products were identified by their $^1$H NMR and/or $^{13}$C NMR and mass spectra.

Optimization of the iodinations indicates that 1 equiv. each of substrate, iodine and **1** affords the best results. The results obtained are summarized in Table 1.

The reaction mechanism is not clear. It appears to be initiated by cleavage of **1** to give **2**.[7]† The sulfate radical **2** may react with $I_2$ to form a cationic iodine radical **3** and the sulfate anion **4**. The cyclic enone then reacts with **3** to form an iodine-bridged intermediate **5**. A sulfate anion **4** may abstract the α-proton from intermediate **5** to form the products **6** and **7**,‡ as shown in Scheme 2.

It is of interest that α,β-unsaturated methyl ketones gave the methyl-iodinated products (95%, entry 9) instead of iodination at the double bond, and a β-keto ester afforded an α-iodinated product (90%, entry 10). These reactions appears to proceed *via* their enol forms (Scheme 3).

This work was supported by generous grants from the Center for Biofunctional Molecules of KOSEF.

## Footnotes

* E-mail: kimyh@sorak.kaist.ac.kr

† Bis(tetra-*n*-butylammonium) peroxydisulfate was prepared from 2.0 equiv. of tetra-*n*-butylammonium hydrogen sulfate and 1.0 equiv. of potassium peroxydisulfate in water at room temperature. It was extracted with $CH_2Cl_2$, dried over anhydrous $MgSO_4$ and then concentrated to give **1**, which was dried under vacuum for one day.

‡ In the iodination of cyclohex-2-en-1-one, **7** was isolated in 80% and its identity confirmed; mp 170–172 °C (*Aldrich Catalogue Hand Book of Fine Chemicals*, 1996–1997, mp 171–173 °C).

## References

1 E. Negishi, Z. R. Owczarczyk and D. R. Swanson, *Tetrahedron Lett.*, 1991, **32**, 4453; M. Kabat, J. Kiegiel, N. Cohen, K. Toth, P. M. Wovkulich and M. R. Uskokovic, *Tetrahedron Lett.*, 1991, **32**, 2343; L. S. Liebeskind and J. Wang, *Tetrahedron Lett.*, 1990, **31**, 4293; A. B. Smith, S. J. Brancs, M. A. Guaciaro, P. M. Wovkulich and A. Korn, *Org. Synth.*, 1996, **Coll. Vol. VII**, 271.

2 H. O. House, *Modern Synthetic Reactions*, W. A. Benjamin Inc., Menlo Park, California, 1972, pp. 459–478.

3 C. R. Johnson, J. P. Adams, M. P. Braun, C. B. W. Senanayake, P. M. Wovkulich and M. R. Uskokovic, *Tetrahedron Lett.*, 1992, **33**, 917.

4 K. M. Kim, K. H. Chung, J. N. Kim and E. K. Ryu, *Synthesis*, 1993, 283.

5 H. Misuya and S. Broder, *Nature*, 1987, **325**, 773; D. Bergstrom, X. Lin, G. Wang, D. Rotstein, P. Beal, P. Norrix and J. Ruth, *Synlett*, 1992, 179.

6 G. B. Dryer and P. B. Dervan, *Proc. Natl. Acad. Sci. USA*, 1981, **5**, 6633; J. T. Goodwin and G. D. Glick, *Tetrahedron Lett.*, 1993, **34**, 5549; T. L. Ruth, *Oligonucleotides and Their Analogs*, IRL Press, London, 1991.

7 Y. H. Kim, *Sulfur and Phosphorous Peroxides*, ed. W. Ando, Wiley New York, 1992, ch. 8, pp. 387.

*Received in Cambridge, UK, 14th April 1997; 7/02524F*

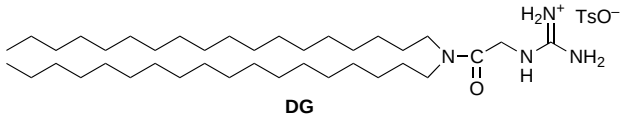
# Control of molecular ordering in guanidinium-functionalized monolayer by carboxylate template molecules

**Yushi Oishi,*[a] Takayuki Kato,[a] Miyuki Kuramori,[a] Kazuaki Suehiro,[a] Katsuhiko Ariga,[b] Ayumi Kamino,[b] Hiroshi Koyano[b] and Toyoki Kunitake[b]**

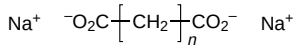
[a] *Department of Applied Chemistry, Faculty of Science and Engineering, Saga University, 1 Honjo-machi, Saga 840, Japan*
[b] *Supermolecules Project, JST, Kurume Research Park, 2432 Aikawa, Kurume, Fukuoka 839, Japan*

**Electron diffraction studies of a [(dioctadecyl)carbamoylmethyl]guanidinium toluene-*p*-sulfonate (DG) monolayer reveal that the regularity of the molecular arrangement and the size of crystalline domains are controlled through binding of aqueous α,ω-dicarboxylates with various spacer lengths.**

Morphological and structural control of monolayers at the air–water interface is crucial for their applications in molecular electronics, optical devices and biomedical uses.[1,2] It has been demonstrated that patterning of monolayer components within a monolayer is realized through molecular recognition between monolayer components and aqueous templates.[3,4] We describe here that this concept is extended to control of regularity of the molecular arrangement in a monolayer. Dialkylguanidinium monolayers have been shown to strongly bind aqueous sodium α,ω-dicarboxylates through hydrogen and ionic bonding.[5] These interactions are expected to affect molecular packing, as inferred from π-*A* isotherms. Diffraction techniques are a powerful tool for evaluating the molecular packing in a monolayer.[3,6,7]




**DG**




dicarboxylate

Figs. 1(*a*)–(*f*) show electron diffraction (ED) patterns† of a **DG** monolayer‡ on pure water and on 0.1 mM aqueous solutions of sodium oxalate ($n$ = 0), malonate ($n$ = 1), succinate ($n$ = 2), glutarate ($n$ = 3) and adipate ($n$ = 4).§ Each monolayer was transferred by the horizontal drawing-up method[6] onto a hydrophilic SiO substrate,¶ after compressing up to a surface pressure of 30 mN m$^{-1}$.‖ The ED pattern of the **DG** monolayer on pure water was an amorphous halo, indicating that the monolayer is in an amorphous state. This may be caused by electrostatic repulsion among ionic hydrophilic groups of the **DG** molecules.[7] The elemental ratio of oxygen and nitrogen atoms (O/N) obtained by X-ray photoelectron spectroscopic analysis of a multilayered film of the monolayer revealed that the hydrophilic groups of the **DG** molecules are dissociated, with $TsO^-$ replaced with a $OH^-$ counterion.** On the other hand, the ED pattern of the monolayer on aqueous sodium oxalate displays a crystalline arc, indicating that crystallization of the monolayer is induced by the oxalate template. Apparently, electrostatic repulsion among the positive hydrophilic groups is weakened by tight binding of the rigid oxalate template, inducing transformation from the amorphous to the crystalline state. **DG** monolayers on aqueous malonate and succinate are also in the crystalline state. However, the arc of these ED patterns is broader along the azimuthal direction than that of the monolayer on oxalate. This broadening suggests reduction in the size of the crystallites†† formed in the monolayer and a random alignment of the crystallographical axes of the crystallites. It appears that the bridging effect of two neighbouring monolayer components is lessened owing to the relatively flexible methylene spacers connecting the two carboxylate groups in malonate and succinate. In the cases of glutarate and adipate with longer methylene spacers, the corresponding ED patterns are again amorphous haloes. The bridging effect must be reduced even more due to the longer methylene chains between the two carboxylate units. These

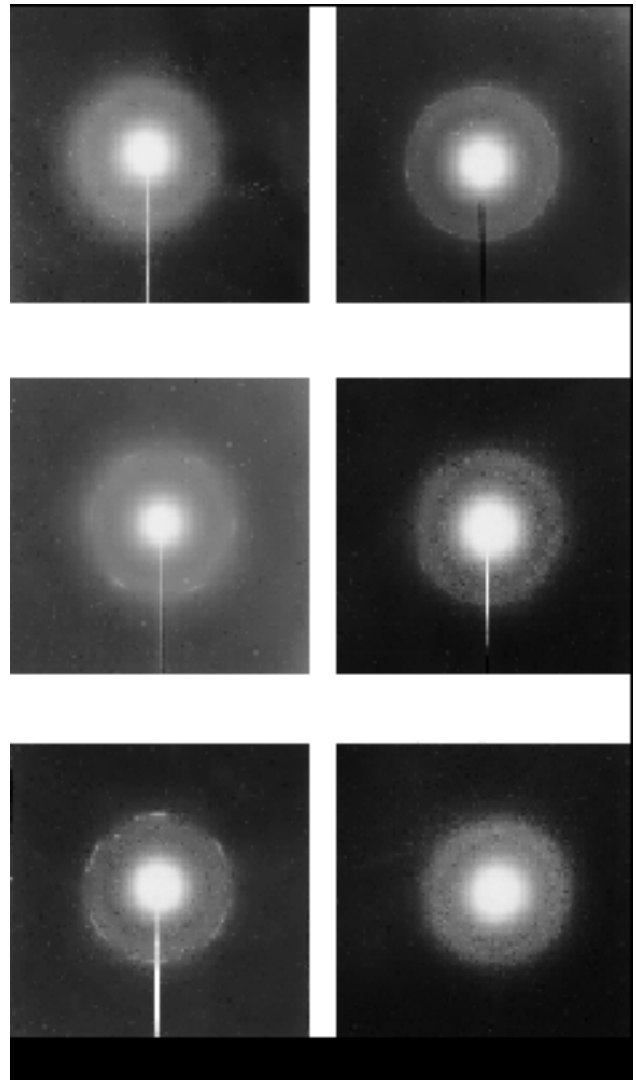


**Fig. 1** ED patterns of each **DG** monolayer (*a*) on pure water, (*b*) on aqueous oxalate, (*c*) on aqueous malonate, (*d*) on aqueous succinate, (*e*) on aqueous glutarate and (*f*) on aqueous adipate

structural changes based on ED pattern analyses were reflected in the π-*A* isotherms, as shown in Fig. 2. The shapes of these π-*A* isotherms‡‡ are affected by the presence and the nature of the dicarboxylates: the averaged molecular area of the monolayers on oxalate and malonate at a surface pressure of 30 mN $m^{-1}$ was smaller than that on pure water, and again increased as the number of the spacer methylene groups in the dicarboxylates increased from succinate to adipate. Therefore, the molecular area of the monolayer, evaluated from π-*A* isotherms, is smaller in the crystalline state (on aqueous oxalate, malonate and succinate) than that in the amorphous one (on pure water, aqueous glutarate and adipate). The expanded region observed in the π-*A* isotherm on pure water was much reduced on aqueous dicarboxylates. This change supposedly comes from suppression of free molecular translational movement at low surface pressures by binding of the hydrophilic groups of the **DG** molecules to dicarboxylates.

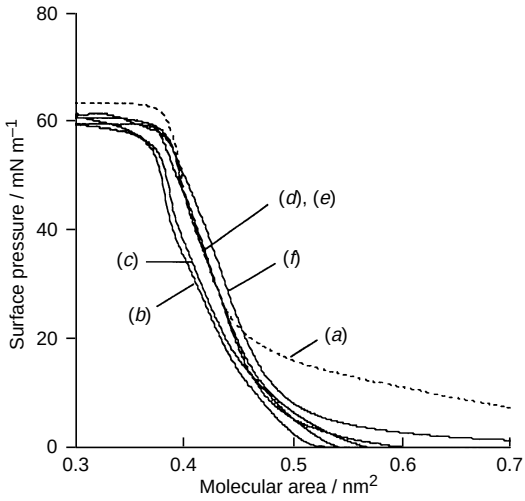



**Fig. 2** π-*A* Isotherms of each **DG** monolayer (*a*) on pure water, (*b*) on aqueous oxalate, (*c*) on aqueous malonate, (*d*) on aqueous succinate, (*e*) on aqueous glutarate and (*f*) on aqueous adipate

Fig. 3 shows a schematic representation of the relationship between the mode of host–guest interaction and the monolayer morphology. **DG** molecules are randomly arranged in the monolayer on pure water, because the **DG** monolayer can not crystallize owing to electrostatic repulsion among the cationic head groups. In the case of the **DG** monolayer on a template molecule without a spacer group, the **DG** monolayer crystallizes and the molecules form large crystalline domains, because the cohesive effect among the hydrophobic groups in **DG** molecules and the tight bridging of the two monolayer components act cooperatively. In the case of the **DG** monolayer on template molecules with spacer groups, the bridging effect is lessened, and the monolayer is composed of small crystalline domains and/or the positional order in the monolayer deteriorates.

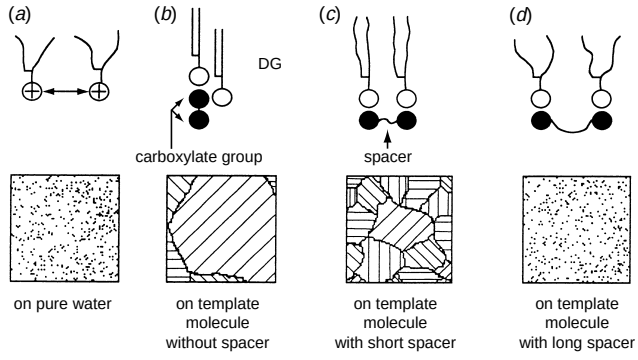



**Fig. 3** Schematic representation of the aggregation structure of each **DG** monolayer. Points and lines express the random and the regular molecular arrangement of **DG** molecules in the monolayer, respectively.

In summary, the molecular ordering and the size of crystalline domains in guanidinium monolayers can be controlled by aqueous dicarboxylates with different methylene bridge lengths. Preliminary observation of the monolayer by atomic force microscopy also confirms the presented results. The details on their molecular images are now under investigation.

## Footnotes

* E-mail: oishiy@cc.saga-u.ac.jp

† ED patterns in this study are for a monolayer transferred onto the hydrophilic SiO substrate, not for a floating monolayer on a water surface. However, the structure of the transferred monolayer is considered to be the same as that of the floating monolayer (see ref. 6). ED patterns were recorded with a Hitachi H-600S transmission electron microscope, operating at an acceleration voltage of 75 kV and with a beam current of several μA. The electron beam was several μm in diameter.

‡ Benzene–ethanol (80 : 20) was used as the spreading solvent. Compression was started 10 min after spreading at a rate of 0.2 mm $s^{-1}$ by using a computer-controlled film balance system FSD-50 (USI System, Fukuoka). The subphase temperature was kept at 293 ± 0.2 K. Surface pressures were measured by a Wilhelmy plate which was calibrated with the transition pressure of an octadecanoic acid monolayer.

§ Subphase pH was *ca.* 6 and the strongly basic **DG** was protonated. Dicarboxylates were added with equivalent NaOH into subphase, thus they must be the sodium salt (see ref. 5).

¶ The hydrophilic SiO substrate was prepared by vapour deposition of SiO onto a Formvar thin layer, with which an electron microscope grid was covered on a glass slide.

‖ The transfer ratio for each monolayer was unity, indicating that the SiO substrate is completely covered with each monolayer.

** Replacement of the $TsO^-$ counterion by $OH^-$ was strongly suggested by the absence of an S atom and the O/N ratio of 0.44 in the XPS data of the transferred LB film.

†† The broadness of arc along the azimuthal direction on the ED pattern results from the existence of a large number of crystalline domains with different crystallographical axes. The diameter of the electron beam was constant in this study. Therefore, the broader arc observed on the present ED pattern indicates a size reduction of the crystalline domain in monolayer.

‡‡ Highly water-soluble dicarboxylates do not make any contribution to the molecular area. Thus, the molecular area (abscissa in Fig. 2) is based on the number of **DG** molecules.

## References

1 A. Ulman, *An Introduction to Ultrathin Organic Films, from Langmuir-Blodgett to Self-Assembly*, Academic, San Diego, 1991.
2 R. H. Tredgold, *Order in Thin Organic Films*, Cambridge University Press, New York, 1995.
3 Y. Oishi, Y. Torii, M. Kuramori, K. Suehiro, K. Ariga, K. Taguchi, A. Kamino and T. Kunitake, *Chem. Lett.*, 1996, 411; Y. Oishi, Y. Torii, T. Kato, M. Kuramori, K. Suehiro, K. Ariga, K. Taguchi, A. Kamino, H. Koyano and T. Kunitake, *Langmuir*, 1997, **13**, 519.
4 H. Koyano, K. Yoshihara, K. Ariga, T. Kunitake, Y. Oishi, O. Kawano, M. Kuramori and K. Suehiro, *Chem. Commun.*, 1996, 1769.
5 With all of the dicarboxylates, excluding oxalate, FT–IR and XPS measurements of the LB films indicated the formation of 1 : 1 guanidinium–carboxylate pairs with hydrogen bonding interactions. Oxalate produced an asymmetric complex where one guanidinium was bound to oxalate through hydrogen bonding and the other guanidinium existed as a non-hydrogen bonded counterion; A. Kamino, H.Koyano, K. Ariga and T. Kunitake, *Bull. Chem. Soc. Jpn.*, 1996, **69**, 3619.
6 Y. Oishi, T. Kuri, Y. Takashima and T. Kajiyama, *Chem. Lett.*, 1994, 1445.
7 T. Kajiyama, H. Kozuru, Y. Takashima, Y. Oishi and K. Suehiro, *Supramol. Sci.*, 1995, **2**, 107; Y. Oishi, Y. Takashima, K. Suehiro and T. Kajiyama, *Langmuir*, in the press.

*Received in Cambridge, UK, 28th April 1997; 7/02880F*

# Preparation of 5-trimethylsilyl-1,3-phenylenebis[diazo(4-pyridyl)methane] and magnetic properties of its 1:1 copper(II) complex after photolysis

**Satoru Karasawa,[a] Masakazu Tanaka,[a] Noboru Koga*[a] and Hiizu Iwamura*[b]**

[a] *Faculty of Pharmaceutical Sciences, Kyushu University, Maidashi, Higashi-ku, Fukuoka 812-82, Japan*
[b] *Institute for Fundamental Research in Organic Chemistry, Kyushu University, Hakozaki, Higashi-ku, Fukuoka 812-81, Japan*

**Photolysis of a paramagnetic 1:1 complex of copper(II) with 5-trimethylsilyl-1,3-phenylenebis[diazo(4-pyridyl)methane] produces a ferromagnetic chain consisting of an alternating array of 3d spins of $Cu^{II}$ and 2p spins of the quintet dicarbenes.**

Formation of metal complexes carrying free radical ligands has been proved to be a powerful design strategy for ordering heterospin systems consisting of 2p and 3d spins.[1,2] Based on this strategy, diazobis(4-pyridyl)methane **1** was designed and prepared.[3] The pyridine units are used to construct a polymeric chain structure by ligation with metal ions and the diazo moiety is photolyzed to produce the carbene unit which plays an important role as a triplet spin source as well as a magnetic coupling unit. 1 : 1 complexes of bis(hexafluoroacetylacetonato)-manganese(II) and -copper(II), $Mn(hfac)_2$ and $Cu(hfac)_2$, with **1** became one-dimensional ferri- and ferro-magnetic chains, respectively, upon photolysis.

To extend and improve these metal–carbene spin systems, we designed a 1,3-benzenediylbis[diazo(4-pyridyl)methane] derivative **2** carrying a bulky trimethylsilyl group at position 5 to attenuate the interchain antiferromagnetic interaction and also coupled this photoresponsive ligand with $Cu(hfac)_2$ to give $[Cu(hfac)_2{\cdot}\mathbf{2}]$ in which the generated quintet carbenes are expected to interact with the copper ions ferromagnetically, as illustrated in Scheme 1.

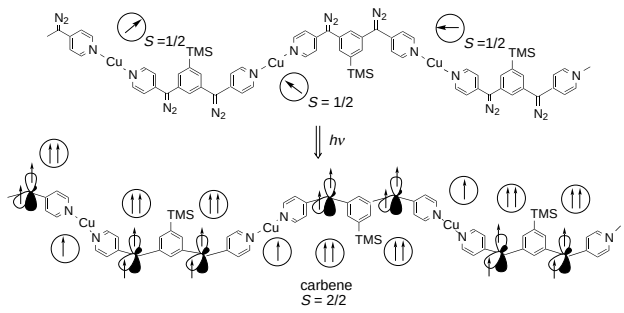
1,3-Dibromo-5-trimethylsilylbenzene was lithiated with $Bu^tLi$ in anhydrous diethyl ether and reacted with 4-cyanopyridine, followed by hydrolysis with aq. $H_2SO_4$. The dipyridyl diketone thus obtained was converted to diazo compound **2** by a usual procedure[3] *via* the corresponding dihydrazone. Compound **2** was crystallized from diethyl ether as red bricks [mp = 109 °C (decomp.)] and its molecular structure was investigated by X-ray analysis.† The molecular structure of **2** has a mirror plane passing through C(8) and C(10) in the benzene ring and the pyridyl groups are directed to the opposite side of the trimethylsilyl group. The dihedral angle between the pyridyl groups and the benzene ring is 44.86° (Fig. 1).

In the EPR spectrum after photolysis of **2** in frozen 2-methyltetrahydrofuran, signals characteristic of quintet dicarbene[4] with a zero-field splitting parameter $D$ in the range 0.07–0.13 $cm^{-1}$ were observed in addition to weak signals due to a monocarbene. The intensities of the quintet signals decreased according to Curie behaviour in the temperature range 10–74 K, suggesting that the quintet is a ground state. By mixing a solution of $Cu(hfac)_2$ in MeOH and **2** in MeOH–$CH_2Cl_2$, the 1 : 1 complex $[Cu(hfac)_2{\cdot}\mathbf{2}]$ was obtained as brown microcrystals. Although no structural information‡ for the complex was obtained, it is reasonable to assume an infinite chain structure since in the two pyridyl nitrogens are ligated to two different metal ions to produce chain structures in the corresponding manganese(II) complex, $[Mn(hfac)_2{\cdot}\mathbf{2}]$† (Fig. 2), prepared under similar conditions and the analogous $[Cu(hfac)_2{\cdot}\mathbf{1}]$.[5]

A microcrystalline sample (*ca*. 0.5 mg) of $[Cu(hfac)_2{\cdot}\mathbf{2}]$ was used for magnetic measurements on a SQUID susceptometer. The sample placed inside the sample compartment of the susceptometer was irradiated at 5–7 K with second harmonic light ($\lambda$ = 532 nm) from a Nd/YAG laser through an optical fiber.[5] After iradiation for 10 h, followed by SQUID measurements, IR absorptions of the sample at 2068 $cm^{-1}$ due to the diazo groups of $[Cu(hfac)_2{\cdot}\mathbf{2}]$ disappeared completely.

The temperature dependences of the molar magnetic susceptibility $\chi_{mol}$ per formula unit of $[Cu(hfac)_2{\cdot}\mathbf{2}]$ are shown in Fig. 3 in the form of $\chi_{mol}T$ *vs.* $T$ plots before and after irradiation, and subsequent annealing at 300 K. Before irradiation, $\chi_{mol}T$ values are nearly constant at 0.55 ± 0.03 emu K $mol^{-1}$ in the temperature range 2–200 K. These values are close to that ($\chi_{mol}T$ = 0.38 emu K $mol^{-1}$) calculated for a dilute $S = \frac{1}{2}$ paramagnet, indicating that the d electrons of $Cu^{II}$ are magnetically isolated.

The $\chi_{mol}T$ values after the photolysis of $[Cu(hfac)_2{\cdot}\mathbf{2}]$ for 10 h increased continuously with decrease in temperature from 100 K, reached a maximum value of 23.4 emu K $mol^{-1}$ at 5.0 K, and decreased below 5 K. This behavior is reversible up to 100 K after which the $\chi_{mol}T$ values decreased at different rates as observed in Fig. 3. In a consecutive measurement for the same sample left at 300 K, $\chi_{mol}T$ showed the behavior prior to




**Scheme 1**

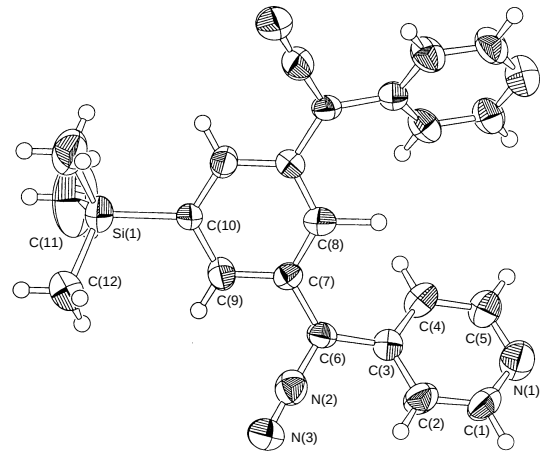



**Fig. 1** ORTEP drawing of ligand **2** at 30% probability

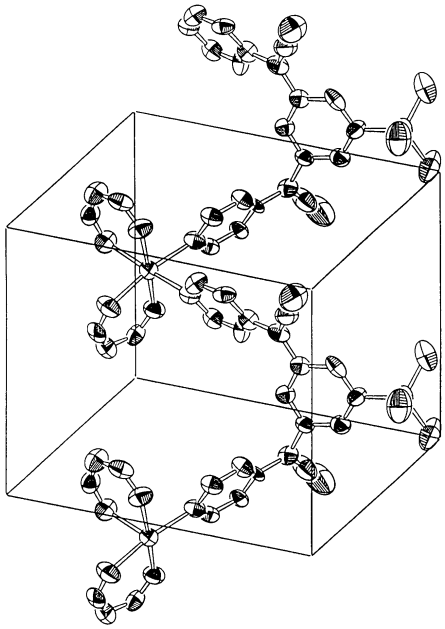


**Fig. 2** ORTEP drawing of [Mn(hfac)$_2$·**2**] at 30% probability

irradiation. A maximum value of 23.4 emu K mol$^{-1}$ after irradiation for 10 h far surpasses the theoretical value of 4.37 emu K mol$^{-1}$ for an $S = 5/2$ species expected for a single unit produced by ferromagnetic interaction between Cu$^{II}$ ($S = 1/2$) and a quintet carbene ($S = 4/2$) in the complex. The increase of $\chi_{mol}T$ as the temperature was decreased from 100 to 5 K clearly demonstrates an increase of the correlation length of the ferromagnetic coupling along the one-dimensional heterospin chain with decreasing temperature. The decrease of $\chi_{mol}T$ below 5 K might be caused by an interchain antiferromagnetic interaction.

Taking into account the temperature independent $\chi_{mol}T$ values above 100 K and those in a consecutive measurement after annealing the sample at 300 K, we interpret the irreversible

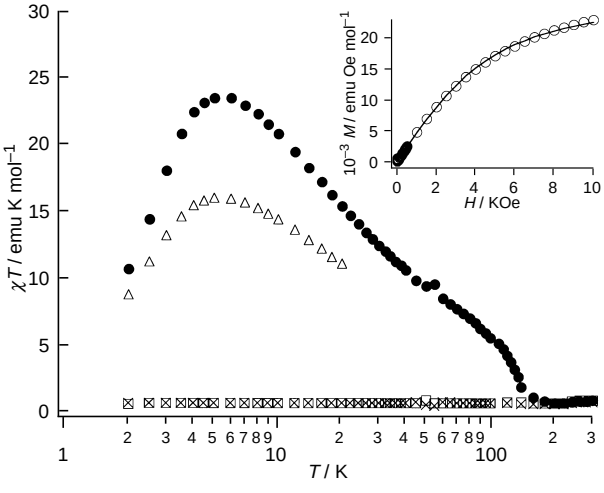



**Fig. 3** Temperature dependences of $\chi_{mol}T$ per formula [Cu(hfac)$_2$·**2**] for a powder sample before (□) and after irradiation for 2 (△) and 10 h (●), and then annealing at 300 K for 1 h (×). The field dependence of magnetization $M$ for [Cu(hfac)$_2$·**2**] at 5 K is given in the inset. The solid curve is the theoretical fit § ($S = 17.25 \pm 0.01$).

change of $\chi_{mol}T$ at 100 K as indicating a chemical loss of the generated carbene centers.

In order to estimate the ferromagnetic correlation length, the field dependences of magnetization $M$ for the same sample of [Cu(hfac)$_2$·**2**] after irradiation for 10 h at 5 K were investigated. A theoretical curve represented by a Brillouin function§ was fitted to the experimental data by a least-squares method to give $S = 17.25 \pm 0.06$, as indicated by the solid curve in the inset of Fig. 3. This value corresponds to a ferromagnetic coupling of *ca*. seven units at 5 K along the chains. This estimate of the correlation length obtained from the $M$–$H$ plots is consistent with that (*ca*. 7 units)¶ from the maximum value at 5 K in the $\chi_{mol}T$–$T$ plot.

Although it can not be stated at the present stage if the bulkiness of the trimethylsilyl group was effective in weakening the antiferromagnetic interchain interaction, [Cu(hfac)$_2$·**2**] did show a higher maximum $\chi_{mol}T$ compared to the corresponding unsubstituted copper complex.[6] It is concluded that the photochemical generation of two triplet carbene centers coupled ferromagnetically to each other through the *m*-phenylene ring and consequent magnetic coupling of these 2p spins with 3d spins of Cu$^{II}$ through the pyridine rings established a one-dimensional ferromagnetic chain (Scheme 1).

## Footnotes

* E-mail: koga@yakukaws.phar.kyushu-u.ac.jp

† *Crystal data*: **2**: $C_{21}H_{20}N_6Si$, $M = 384.51$, orthorhombic, space group *Pnma* (no. 62), $a = 19.205(3)$, $b = 17.308(3)$, $c = 6.137(3)$ Å, $U = 2039(1)$ Å$^3$, $T = 296$ K, $Z = 4$, $D_c = 1.252$ g cm$^{-3}$, $\mu$(Cu-K$\alpha$) = 11.59 cm$^{-1}$, 1845 total (1800 independent) reflections, $R = 0.062$ and $R_w = 0.044$ for 595 reflections with $I > 3\sigma(I)$. [Mn(hfac)$_2$·**2**]: $C_{31}H_{22}O_4F_{12}MnN_6Si$, $M = 853.56$, triclinic, space group $P\bar{1}$ (no. 2), $a = 13.069(1)$, $b = 13.284(2)$, $c = 10.917(2)$ Å, $\alpha = 91.07(1)$, $\beta = 90.50(1)$, $\gamma = 81.975(9)°$, $U = 1876.4(4)$ Å$^3$, $T = 296$ K, $Z = 2$, $D_c = 1.511$ g cm$^{-3}$, $\mu$(Cu-K$\alpha$) = 41.19 cm$^{-1}$, 4393 total (4110 independent) reflections, $R = 0.060$ and $R_w = 0.048$ for 497 reflections with $I > 3\sigma(I)$. Atomic coordinates, bond lengths and angles, and thermal parameters have been deposited at the Cambridge Crystallographic Data Centre (CCDC). See Information for Authors, Issue No. 1. Any request to the CCDC for this material should quote the full literature citation and the reference number 182/503.

‡ In solution diazo moieties of the complex was relatively unstable at room temperature and growth of a single crystal for X-ray analysis was prevented by this instability.

§ $M = NgS\mu_B B(x)$ where $B(x)$ is a Brillouin function, where $x = gS\mu_B H/(k_B T)$, and the other symbols have their usual meanings.

¶ The correlation length ($n$ = number of units) was estimated by the following equation: $n\chi_{mol}T = 0.125\, g^2 nS\,(nS + 1)$, where $\chi_{mol}T = 23.4$, $g = 2$, and $S = 5/2$.

## References

1 G. R. Eaton and S. S. Eaton, *Acc. Chem. Res*., 1988, **21**, 107; A. Caneschi, D. Gatteschi, J. P. Renard, P. Rey and R. Sessoli, *Inorg. Chem*., 1989, **28**, 1976; A. Caneschi, D. Gatteschi and P. Rey, *Prog. Inorg. Chem*., 1991, **39**, 331; A. B. Burdukov, V. I. Ovcharenko, V. N. Ikorski, N. V. Pervukhina, N. V. Podberezskaya, I. A. Grigor'ev, S. V. Larionov and L. B. Volodarsky, *Inorg. Chem*., 1991, **30**, 972; K. Inoue and H. Iwamura, *J. Am. Chem. Soc*., 1994, **116**, 3173.

2 M. Kitano, Y. Ishimaru, K. Inoue, N. Koga and H. Iwamura, *Inorg. Chem*., 1994, **33**, 6012.

3 N. Koga, Y. Ishimaru and H. Iwamura, *Angew. Chem., Int. Ed. Engl*., 1996, **36**, 755.

4 A. Izuoka, S. Murata, T. Sugawara and H. Iwamura,, *J. Am. Chem. Soc*., 1987, **109**, 2631.

5 Y. Sano, M. Tanaka, N. Koga, K. Matsuda and H. Iwamura, *J. Am. Chem. Soc*., in press.

6 S. Karasawa, M. Tanaka, N. Koga and H. Iwamura, unpublished work.

*Received in Cambridge, UK, 1st April 1997; 7/02168B*

# A cyclic supramolecular complex containing eight metal ions, twelve bridging ligands, and an anion encapsulated in the central cavity

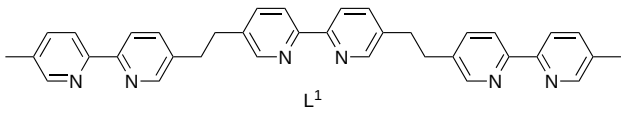
**Peter L. Jones, Kate J. Byrom, John C. Jeffery, Jon A. McCleverty* and Michael D. Ward***

*School of Chemistry, University of Bristol, Cantock's Close, Bristol, UK BS8 1TS*

**Reaction of the bis-bidentate ligand bis{3-(2-pyridyl)pyrazol-1-yl}dihydroborate ($L^-$) with cobalt(II) or nickel(II) salts results in formation of complexes $[M_8L_{12}X]X_3$ (X = $ClO_4$, $PF_6$), which have a cyclic structure with one anion encapsulated in the central cavity.**

The assembly of structurally sophisticated, high-nuclearity coordination complexes from the reactions of relatively simple ligands with suitable metal ions is a burgeoning field. The principles of molecular recognition between components, and how the steric information contained in the number/orientation of ligand binding sites and the stereoelectronic preferences of the metal ion combine to give the final structure, are becoming better understood.[1]

In some systems there is only one optimal structure for the supramolecular species defined by a particular metal/ligand combination. Such systems are exemplified by Lehn's molecular grids[2] and molecular cylinders:[3] there is only one way in which the twin conditions (*i*) all of the ligand binding sites being occupied, and (*ii*) all of the metal ions being coordinated in their preferred coordination environment, can be fulfilled. In contrast in other systems a wide variety of stoichiometries and therefore structures are possible, all of which can fulfil the above requirements. These systems are exemplified by Lehn's molecular rings.[4,5] For example the ligand $L^1$ has three bidentate chelating binding sites with flexible spacers between them. Coordination to metal ions having a preference for six coordination gave various complexes with a 1 : 1 metal : ligand stoichiometry but with very different structures: notably the triple helicate $[Ni_3(L^1)_3]^{6+}$ and the molecular ring $[Fe_5(L^1)_5Cl]^{9+}$, which contains a chloride ion tightly bound in the cavity at the centre of the ring.[5]




$L^1$

We describe here the preparation and characterisation of complexes of bis{3-(2-pyridyl)pyrazol-1-yl}dihydroborate} ($L^-$) with $Ni^{2+}$ and $Co^{2+}$ which are octanuclear molecular rings containing encapsulated anions. The ligand $L^-$ was prepared† as its potassium salt in high yield by reaction of 3-(2-pyridyl)pyrazole with $KBH_4$.[6] Since it contains two bidentate compartments linked by a flexible spacer, it could act as a tetradentate chelate to one large metal ion, or act as a bridge in oligonuclear species.[7] With $Ni^{II}$ and $Co^{II}$, both of which prefer pseudo-octahedral tris-chelate coordination, a 2 : 3 metal : $L^-$ stoichiometry is likely in the absence of other ligands.

Reaction of KL with $Co(O_2CMe)_2{\cdot}4H_2O$ (1 : 1 ratio) in MeOH afforded a red–brown solution from which a solid precipitated on addition of $KPF_6$. Analytical data suggested the empirical formulation $[Co_2L_3][PF_6]$. A material analysing as $[Ni_2L_3][PF_6]$ was similarly prepared from KL and $Ni(NO_3)_2{\cdot}6H_2O$ in MeOH followed by precipitation with $KPF_6$. The yields of these were subsequently optimised (50–60%) by use of a 2 : 3 metal : ligand ratio in the preparation. Examination of both complexes by electrospray (ES) mass spectrometry (MeCN; 5 V cone voltage) showed a strong peak at *m/z* 1410 in each case. These correspond to the species $[Co_8L_{12}(PF_6)]^{3+}$ (calc. for most abundant peak: 1409.7) and $[Ni_8L_{12}(PF_6)]^{3+}$ (calc. for most abundant peak: 1409.0); no other reasonable combination of metal, ligand, counter ion and charge corresponds to these values, and the +3 charge was confirmed by the $\frac{1}{3}$-integral spacing between isotopic components of the peaks. Numerous fragmentation peaks were also observed. The highest mass peaks indicate in both cases formation of a $\{M_8L_{12}\}$ species which is associated with one anion; no anion-free peaks corresponding to $[M_8L_{12}]^{4+}$ were observed. Exactly similar behaviour was observed for $[Fe_5(L^1)_5Cl]^{9+}$, where loss of chloride was never observed by ESMS.[5]

This result suggested that a $\{M_8L_{12}\}$ molecular ring may have formed, containing one tightly bound anion in the central cavity. Accordingly we attempted to crystallise these complexes, but crystals of the hexafluorophosphate salts could not be obtained. The cobalt(II) complex was therefore re-prepared as the perchlorate salt, $\{[Co_2L_3][ClO_4]\}_n$. After several attempts small crystals were grown from MeCN–diethyl ether which were just suitable for X-ray diffraction, and a partial structral determination showed the complex to be $[Co_8L_{12}(ClO_4)][ClO_4]_3$ in agreement with the ESMS data.‡ Despite the poor quality of the data the gross structure of the complex cation is quite clear (Fig. 1), consisting of a $\{Co_8L_{12}\}$ ring with a perchlorate ion in the central cavity, and bears obvious similarities to Lehn's $[Fe_5(L^1)_5Cl]^{9+}$ complex. Each ligand L acts as a bridge between two adjacent metal ions, with an alternating pattern of one and then two bridging ligands

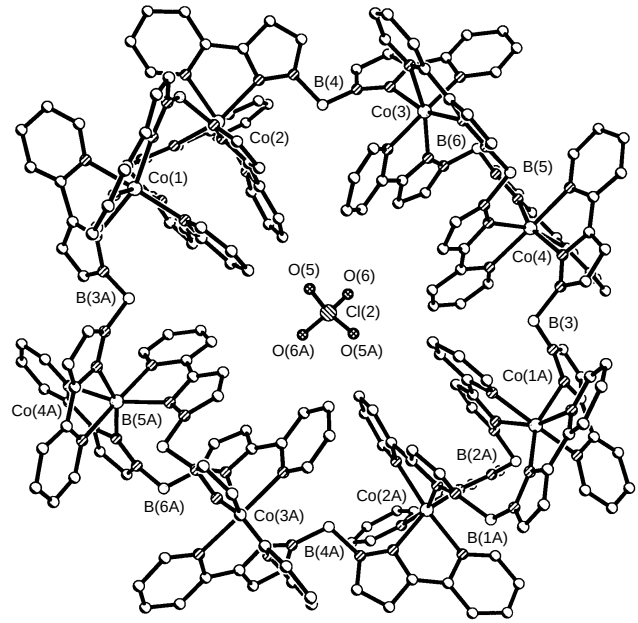



**Fig. 1** Crystal structure of the $[Co_8L_{12}(ClO_4)]^{3+}$ cation

between each adjacent pair of metals (see Fig. 2). Each metal is six-coordinated by three bidentate chelating fragments, each from a different ligand, and all ligand binding sites are used. The complex cation lies astride a twofold axis which is perpendicular to the plane of the ring and passes through the Cl atom of the encapsulated perchlorate anion; it is chiral, with all eight metal centres having the same absolute chirality (△ in the figure) and is therefore a helical ring.

Attempts to examine the solution properties of $[Co_8L_{12}(ClO_4)][ClO_4]_3$ by NMR spectroscopy were not very successful. Although $^1$H NMR spectra of high-spin cobalt(II) complexes can give useful structural information,[8] the $^1$H NMR spectrum of $[Co_8L_{12}(ClO_4)][ClO_4]_3$ in $CD_3CN$ was broadened to the point where individual signals were not detectable. $^{31}$P and $^{19}$F NMR spectra of $[Ni_8L_{12}][PF_6]_4$ showed only one signal in each case at the same position observed for $NH_4PF_6$. If one anion remained in the ring and did not exchange in the NMR timescale, then two resonances in a 3:1 ratio would be expected; if the ring were intact but exchange of the anion fast, a single shifted signal would be seen. These observations suggest that the kinetic lability of the metal centres results in dissociation of the ring in solution, and that its formation with the encapsulated anion occurs during crystallisation (or at least evaporation of the solvent, as in ESMS).

The formation of this structure raises an important question: does the central anion (perchlorate or hexafluorophosphate) act as a template to control the size of the ring by dictating the assembly pathway, or is the ring a particularly stable structure which forms on its own and then subsequently traps whatever appropriately sized guest can be found in the reaction medium? In the former case the use of a different templating anion could lead to the assembly of a differently sized ring (at least in the solid state); in the latter case, formation of a particular ring size means that a size-specific host is formed which could be of use in, for example, selective extraction or recognition of anions. We note that poly(guanidinium) strands can assemble around templating sulfate anions to give double helicates,[9] and that other examples of molecular recognition of small guest species by cyclic coordination complexes having large central cavities are known.[10]

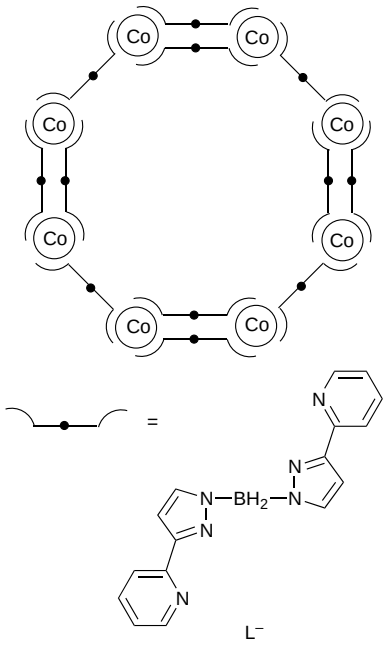



**Fig. 2** Schematic drawing of the octanuclear ring showing the alternating disposition of bridging ligands along the edges

We thank the EPSRC and Unilever Research for financial support, and Mr C. Carraz and Dr J. Fleming for the NMR experiments.

## Footnotes

* E-mail: mike.ward@bristol.ac.uk

† Potassium bis[3-(2-pyridyl)pyrazolyl]dihydroborate KL. A mixture of 3-(2-pyridyl)pyrazole (3.50 g, 24.1 mmol) and $KBH_4$ (0.49 g, 9.0 mmol) was ground together finely with a mortar and pestle and then gradually heated to 150 °C. Melting occurred at *ca*. 120 °C, at which point evolution of $H_2$ commenced. The temperature was maintained at 150 °C for 30 min, after which time $H_2$ evolution had ceased. The solid white mixture was cooled and 100 cm$^3$ of warm toluene was added. The suspension was stirred vigorously overnight to allow the excess unreacted 3-(2-pyridyl)pyrazole to dissolve. The product was filtered off as a white solid, which was washed further with several portions of toluene and then hexane, and dried. Yield of KL: 2.48 g (81%). Negative-ion FAB MS: *m/z* 301 [$L^-$]. Satisfactory analytical and $^1$H NMR data were obtained.

‡ *Crystallographic details*. $[Co_8L_{12}(ClO_4)][ClO_4]_3 \cdot n$(disordered solvent), small orange blocks grown from MeCN–diethyl ether. A crystal of dimensions 0.1 × 0.1 × 0.05 mm was mounted on a Siemens SMART diffractometer under a stream of $N_2$ at −100 °C. Orthorhombic, space group *Pbcn*; $a$ = 31.89(2), $b$ = 18.719(4), $c$ = 41.11(1) Å; $U$ = 24 540(27) Å$^3$; $Z$ = 4; $\mu$ = 0.72 mm$^{-1}$. 108 409 reflections were measured with $2\theta_{max}$ = 46.5°; after merging these gave 17 602 unique data with $R$(sigma) = 0.223. Many factors combined to make this a poor structure. The crystals were small and diffracted weakly; they lost solvent instantly on removal from the mother-liquor and decomposed partially during the transfer to the diffractometer, even when coated with paraffin oil saturated with the recrystallisation solvent mixture; there was substantial disorder in the free counter ions and the large number of lattice solvent molecules; the number of parameters was large (174 non-hydrogen atoms in the asymmetric unit). The lattice solvents were best approximated as four MeCN and two $Et_2O$ molecules per asymmetric unit (*i.e.* eight MeCN and four $Et_2O$ per $\{Co_8L_{12}(ClO_4)\}^{3+}$ unit). The best level of refinement achievable so far was $R_1$ = 0.19, goodness-of-fit 1.233. Consequently the full structural details are not of publishable quality, and it is not possible to extract precise bond lengths and angles. However the complex cation is sufficiently well defined to be quite certain about its gross structure.

## References

1 D. Philip and J. F. Stoddart, *Angew. Chem., Int. Ed. Engl.*, 1996, **35**, 1155; D. S. Lawrence, T. Jiang and M. Levett, *Chem. Rev.*, 1995, **95**, 2229; D. B. Amabilino and J. F. Stoddart, *Chem. Rev.*, 1995, **95**, 2725; J.-M. Lehn, *Supramolecular Chemistry*, VCH, Weinheim, 1995; T.Biessel, R. E. Powers and K. N. Raymond, *Angew. Chem., Int. Ed. Engl.*, 1996, **35**, 1084.

2 P. N. W. Baxter, J.-M. Lehn, J. Fischer and M.-T. Youinou, *Angew. Chem., Int. Ed. Engl.*, 1994, **33**, 2284.

3 P. N. W. Baxter, J.-M. Lehn, A. De Cian and J. Fischer, *Angew. Chem., Int. Ed. Engl.*, 1993, **32**, 69.

4 D. Funeriu, J.-M. Lehn, G. Baum and D. Fenske, *Chem. Eur. J.*, 1997, **3**, 99.

5 B. Hasenknopf, J.-M. Lehn, B. O. Kneisel, G. Baum and D. Fenske, *Angew. Chem., Int. Ed. Engl.*, 1996, **35**, 1838.

6 S. Trofimenko, J. C. Calabrese and J. S. Thompson, *Inorg. Chem.*, 1992, **31**, 974 and references therein.

7 E. Psillakis, J. C. Jeffery, J. A. McCleverty and M. D. Ward, *Chem. Commun.*, 1997, 479; E. Psillakis, J. C. Jeffery, J. A. McCleverty and M. D. Ward, *J. Chem. Soc., Dalton Trans.*, in press.

8 E. C. Constable, M. A. M. Daniels, M. G. B. Drew, D. A. Tocher, J. V. Walker and P. D. Wood, *J. Chem. Soc., Dalton Trans.*, 1993, 1947.

9 J. Sánchez-Quesada, C. Seel, P. Prados, J. de Mendoza, I. Dalcol and E. Giralt, *J. Am. Chem. Soc.*, 1996, **118**, 277.

10 M. Fujita, J. Yazaki and K. Ogura, *J. Am. Chem. Soc.*, 1990, **112**, 5345; A. Bilyk and M. M. Harding, *J. Chem. Soc., Chem. Commun.*, 1995, 1697; A. W. Maverick, S. C. Buckingham, Q. Yao, J. R. Bradbury and G. G. Stanley, *J. Am. Chem. Soc.*, 1986, **108**, 7430; M. Fujita, S. Nagao and K. Ogura, *J. Am. Chem. Soc.*, 1995, **117**, 1649.

*Received in Basel, Switzerland, 19th February 1997; 7/01192J*

# Intramolecular proton transfer from a cation to the associated, structurally characterised, hydride-containing anion $[(PPh_3)_2(H)Ru(\mu\text{-}H)(\mu\text{-}Cl)_2Ru(H)(PPh_3)_2]^-$ to give an $\eta^2$-$H_2$ complex

**Kenneth S. MacFarlane, Ajey M. Joshi, Steven J. Rettig and Brian R. James***

*Department of Chemistry, University of British Columbia, Vancouver, British Columbia, V6T 1Z1, Canada*

**The previously unknown, dinuclear, ionic ruthenium(II) species [Hdma][$(PPh_3)_2$(H)Ru(μ-H)(μ-Cl)$_2$Ru(H)-($PPh_3$)$_2$]·dma 1 (dma = *N*,*N*-dimethylacetamide) is characterised by X-ray crystallography; in solution, intramolecular proton transfer from the cation to the anion gives the known molecular hydrogen complex [$(PPh_3)_2(\eta^2\text{-}H_2)$Ru(μ-H)(μ-Cl)$_2$Ru(H)($PPh_3$)$_2$] 2.**

A general method for preparing dihydrogen complexes is protonation of transition-metal hydride species,[1] a process that can be viewed as the reverse of heterolytic cleavage of $H_2$. There are reported examples of an equilibrium between a molecular hydrogen complex and the corresponding hydride [*i.e.* M($\eta^2$-$H_2$) ⇌ M($H^-$) + $H^+$], and some include intramolecular proton transfer from the $\eta^2$-$H_2$ ligand to a co-ligand, which acts as a base.[2] To our knowledge, there are no examples where this proton transfer is from a cation to the associated anion of a transition-metal complex. The closest related example is proton transfer from cyclohexanol to the anionic $[RuH_3(PPh_3)_3]^-$ to generate $[Ru(\eta^2\text{-}H_2)(H)_2(PPh_3)_3]$.[3] We report here, the X-ray crystal structure of the ionic complex [Hdma][$(PPh_3)_2$(H)Ru(μ-H)(μ-Cl)$_2$Ru(H)($PPh_3$)$_2$]·dma **1**,† which in solution undergoes proton transfer to give the known complex [$(PPh_3)_2(\eta^2\text{-}H_2)$Ru(μ-H)(μ-Cl)$_2$Ru(H)($PPh_3$)$_2$] **2**.[4]

Red prisms of **1** were serendipitously grown in a dma filtrate that was left at *ca*. 20 °C for several months. The reactants were $[RuCl_3(PPh_3)_2(dma)]$·dma,[5] and 1 equiv. of dppb [1,4-bis(diphenylphosphino)butane], left under 1 atm $H_2$. A pink coproduct, established by $^1H$ and $^{31}P\{^1H\}$ NMR spectroscopy and elemental analysis‡ to be the ionic complex [Hdma][(dppb)Cl-Ru(μ-Cl)$_3$RuCl(dppb)] **3**, was also isolated; the anion of **3** has been previously characterised by X-ray crystallography within a complex where the associated cation was 1,1,3-trimethyl-2,3-dihydroperimidinium.[6]

The molecular structure of **1** is shown in Fig. 1. The dinuclear anion, with a $C_2$ axis, contains one bridging and two terminal hydrides. The cation $[Hdma]^+$, the proton of which was not located or included in the model, has been studied previously by X-ray diffraction within *N*,*N*-dimethylacetamidonium chloride;[7] the cation here is different from that found for **1**, as the $H^+$ is located between the O and Cl, with strong hydrogen bonds. The dma sites in **1** are occupied 50% by a neutral molecule and 50% by a $[Hdma]^+$ moiety. The IR spectrum (KBr pellet) of crystalline **1** shows a strong broad $\nu_{C=O}$ at 1647 $cm^{-1}$, close to that found for free dma solvent (1640 $cm^{-1}$). For comparison purposes, the $\nu_{C=O}$ band in [Hdma]Cl was observed at 1670 $cm^{-1}$.[7]

The Ru–μ-H bond length of 1.72 Å observed in **1** is similar to that observed for one side of the unsymmetrical hydride bridge in [L($\eta^2$-$H_2$)Ru(μ-H)(μ-Cl)$_2$Ru(H)($PPh_3$)$_2$] (1.71 Å); L = a phosphorus–nitrogen chelating, ferrocene-based ligand,[4] but is significantly longer than the other Ru–μ-H bond length in the $\eta^2$-$H_2$ species (1.49 Å). The Ru–terminal hydride bond length (1.59 Å) is similar to that in the species containing L.[4] The locations of the hydrogen atoms in **2** and the analogous [{P($C_6H_4$Me-*p*)$_3$}$_2$($\eta^2$-$H_2$)Ru(μ-H)(μ-Cl)$_2$Ru(H){P($C_6H_4$Me-*p*)$_3$}$_2$] complex were not established in earlier X-ray crystallographic studies; however, these complexes did not contain a $C_2$ axis.[4,8,9] For **1** and the molecular (L)($\eta^2$-$H_2$) complex,[4] the hydride and the $\eta^2$-$H_2$ ligands were located. Of note, complex **2** has recently been studied by X-ray crystallography using CCD detection with all the hydride and $\eta^2$-$H_2$ hydrogens now located.[10] Comparison of the bond lengths and angles of **1** with those of **2**[10] are entirely consistent with the formulation of **1** as [Hdma][$(PPh_3)_2$(H)Ru(μ-H)(μ-Cl)$_2$Ru(H)($PPh_3$)$_2$]·dma.

The Ru–Ru bond length of 2.83 Å in **1** is the same as that in **2** (from the partial structure) and is in the range generally reported for a Ru–Ru single bond (2.632–3.034 Å).[4] The Ru–Cl–Ru (69.20°) and Cl–Ru–Cl (81.58°) bond angles of **1** are also indicative of a Ru–Ru single bond within the general class of dinuclear $Ru_2$ complexes containing face-sharing bioctahedra.[11]

$^{31}P\{^1H\}$ and $^1H$ NMR spectroscopic studies on $[^2H_8]$toluene solutions of the crystalline sample of **1** show spectra essentially

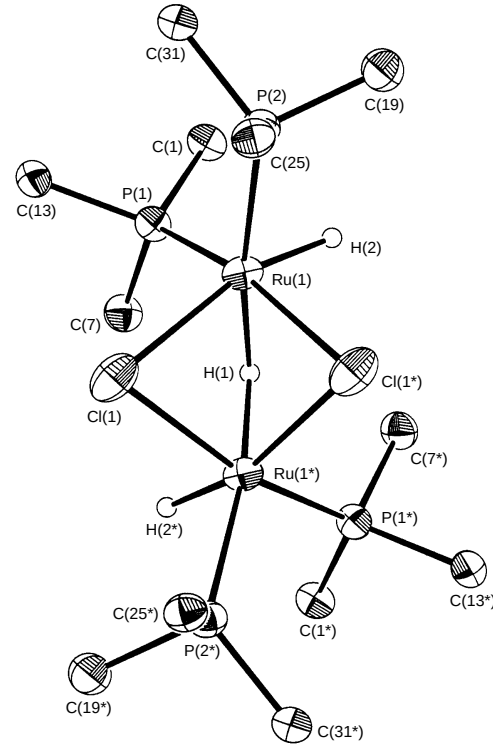



**Fig. 1** ORTEP plot of the anion of [Hdma][$(PPh_3)_2$(H)Ru(μ-H)(μ-Cl)$_2$Ru(H)($PPh_3$)$_2$]·dma **1**. Thermal ellipsoids for non-hydrogen atoms are drawn at 33% probability (some of the phenyl carbons have been omitted for clarity); * refers to the symmetry operation: $-x$, $y$, $\frac{1}{2} - z$. Selected bond lengths (Å) and angles (°): Ru(1)–Ru(1*) 2.8251(5), Ru(1)–Cl(1) 2.510(1), Ru(1)–Cl(1*) 2.4649(9), Ru(1)–P(1) 2.2576(9), Ru(1)–P(2) 2.3483(9), Ru(1)–H(2) 1.59(3), Ru(1)–H(1) 1.72(3); Cl(1)–Ru(1)–Cl(1*) 81.58(4), Ru(1)–Cl(1)–Ru(1*) 69.20(3), Ru(1*)–Ru(1)–H(2) 109.1(9), Ru(1*)–Ru(1)–H(1) 35(1), H(1)–Ru(1)–H(2) 86(1).

identical to those of the neutral $\eta^2$-$H_2$ complex **2**, thus demonstrating conversion of **1** into **2** in this solvent (Scheme 1). The $^{31}P\{^1H\}$ spectrum of **1** in $C_7D_8$ at 20 °C shows two broad resonances at $\delta$ 71.3 and 46.3, while at −89 °C the spectrum gives an ABCD spin system, the data corresponding exactly to those previously observed for **2**;[4,8,9] the 20 °C spectrum also shows a small amount (*ca*. 5%) of another species associated with an AB pattern ($\delta_A$ 56.8, $\delta_B$ 54.7, $^2J_{AB}$ 30 Hz) and this possibly results from the presence of **1**.

$$[Hdma]^+[(PPh_3)_2(H)Ru(\mu\text{-}H)(\mu\text{-}Cl)_2Ru(H)(PPh_3)_2]^-\bullet dma$$

**1**

$$\downarrow$$

$$2\ dma + [(PPh_3)_2(\eta^2\text{-}H_2)Ru(\mu\text{-}H)(\mu\text{-}Cl)_2Ru(H)(PPh_3)_2]$$

**2**

**Scheme 1**

The $^1H$ NMR spectrum of **1** in $C_7D_8$ at 20 °C shows a single broad resonance in the hydride region at $\delta$ −12.8, but at −79 °C signals are seen at $\delta$ −8.7 (br d), −12.6 (br s) and −17.3 (br s), and these data correspond to those for the μ-hydride, $\eta^2$-$H_2$ and terminal hydride, respectively, of **2**, as established by the $T_1$ measurements and exchange-spectra simulations for these protons [similar data are found for the $P(C_6H_4Me\text{-}p)_3$ analogue].[4,8,9] Two other resonances of lower intensity observed at $\delta$ −14.9 (t, $^2J_{PH}$ 31.1 Hz) and $\delta$ −17.7 (br s) could again be attributed to the terminal- and bridging-hydrides of **1**. We have been unable to detect the $^1H$ resonance for the proton of $[Hdma]^+$. {Of interest, the resonance for the proton of this cation in a $CH_2Cl_2$ solution of [Hdma]Cl has been reported at $\delta$ 12.[7] The $[H(dma)_2]^+$ cation is also known, *e.g.* within $[H(dma)_2][AuCl_4]$ where $\delta_H$ was reported at −17.45,[12,13] but we have repeated this work and find $\delta_H$ at +18}.

The observation of NMR signals that are consistent with the presence of small amounts of **1** in Scheme 1 implies an equilibrium reaction, but unfortunately this could not be confirmed by measuring the $^{31}P\{^1H\}$ NMR spectra of **2** in $C_7D_8$ solutions containing several equivalents of dma; only signals due to **2** were seen (trace water in the added dma could complicate these measurements on the 'reverse' process).

Nevertheless, despite our failure to establish Scheme 1 as an equilibrium, the spectral and X-ray structural data taken together demonstrate unequivocally the proton-transfer reaction shown in the forward reaction.

(*a*) $2\ [RuCl_3(PPh_3)_2(dma)]\bullet dma + 4\ H_2$

$\downarrow$ Proton sponge (PS), dma, 24 h

$[(PPh_3)_2(\eta^2\text{-}H_2)Ru(\mu\text{-}H)(\mu\text{-}Cl)_2Ru(H)(PPh_3)_2]\bullet 2dma + 4\ PSH^+\ Cl^-$

(*b*) $[\{RuCl(PPh_3)_2\}_2(\mu\text{-}Cl)_2] + 3\ H_2$

$\downarrow$ PS, $C_7H_8$, 24 h

$[(PPh_3)_2(\eta^2\text{-}H_2)Ru(\mu\text{-}H)(\mu\text{-}Cl)_2Ru(H)(PPh_3)_2] + 2\ PSH^+\ Cl^-$

**Scheme 2**

Of note, we have reported two synthetic routes to the $\eta^2$-$H_2$ complex **2** (Scheme 2).[4,8] In retrospect, in light of the data given here, the solid-state product from Scheme 2(*a*) should be reformulated as the ionic complex **1**, while in solution the neutral species **2** would be present. Reaction in the absence of dma allows the isolation of the neutral complex **2** in the solid state [Scheme 2(*b*)].

A key step in the mechanism of the well known hydrogenation catalyst $[Ru(H)Cl(PPh_3)_3]$ is initial dissociation of a phosphine ligand to generate species containing the '$Ru(PPh_3)_2$' moiety,[8,9] but whether dinuclear species such as the anion of **1**, or the $\eta^2$-$H_2$ complex **2**, play any role in the catalysis still remains to be established.

We thank the Natural Sciences and Engineering Council of Canada for financial support, and Johnson Matthey Co. and Colonial Metals Inc. for loans of $RuCl_3\cdot 3H_2O$.

## Footnotes

* E-mail: brj@chem.ubc.ca

† Crystals of **1** are monoclinic, space group *C*2/*c*, $a$ = 23.762(3), $b$ = 13.372(2), $c$ = 25.937(3) Å, $\beta$ = 119.575(7)°, $Z$ = 4; $\mu$(Mo-Kα) = 6.34 $cm^{-1}$, $T$ = 21 °C. The structure was solved by the Patterson method and was refined by full-matrix least-squares procedures to $R$ = 0.036 ($R_w$ = 0.033) for 5504 reflections with $I \geqslant 3\sigma(I)$. Satisfactory elemental analysis was obtained for **1**. CCDC no. 182/519.

‡ *Data* for **3**: $^1H$ NMR (300 MHz, $CDCl_3$, 20 °C): $\delta$ 1.58 (br m, 4 H, $CH_2$), 1.65 (br m, 4 H, $CH_2$), 2.05 (s, 3 H, $CH_3$), 2.15 (br m, 2 H, $CH_2$), 2.55 (br m, 4 H, $CH_2$), 2.88 (br m, 2 H, $CH_2$), 2.90 (s, 3 H, $CH_3$), 3.00 (s, 3 H, $CH_3$), 6.7–7.6 (m, 40 H, Ph), 8.2 (br s, 1 H, *H*dma). $^{31}P\{^1H\}$ NMR (121.42 MHz, $CDCl_3$, 20 °C): $\delta$ 48.9 (s). Satisfactory elemental analysis was obtained for **3**.

## References

1 P. G. Jessop and R. H. Morris, *Coord. Chem. Rev.*, 1992, **121**, 155.
2 M. Schlaf and R. H. Morris, *J. Chem. Soc., Chem. Commun.*, 1995, 625; M. Schlaf, A. J. Lough and R. H. Morris, *Organometallics*, 1996, **15**, 4423.
3 D. E. Linn, Jr. and J. Halpern, *J. Am. Chem. Soc.*, 1987, **109**, 2969.
4 C. R. S. M. Hampton, I. R. Butler, W. R. Cullen, B. R. James, J.-P. Charland and J. Simpson, *Inorg. Chem.*, 1992, **31**, 5509.
5 I. S. Thorburn, S. J. Rettig and B. R. James, *Inorg. Chem.*, 1986, **25**, 234.
6 S. N. Gamage, R. H. Morris, S. J. Rettig, D. C. Thackray, I. S. Thorburn and B. R. James, *J. Chem. Soc., Chem. Commun.*, 1987, 894.
7 E. Benedetti, B. Di Blasio and P. Baine, *J. Chem. Soc., Perkin Trans. 2*, 1980, 500.
8 T. W. Dekleva, I. S. Thorburn and B. R. James, *Inorg. Chim. Acta*, 1985, **100**, 49.
9 C. Hampton, T. W. Dekleva, B. R. James and W. R. Cullen, *Inorg. Chim. Acta*, 1988, **145**, 165.
10 K. S. MacFarlane, S. J. Rettig, B. R. James, J. D. Ferrara, T. L. Hendrixon, J. W. Pflugrath and B. R. Vincent, unpublished work.
11 F. A. Cotton and R. C. Torralba, *Inorg. Chem.*, 1991, **30**, 2196.
12 M. Ziegler, P. Barth and H. Winkler, *Angew. Chem., Int. Ed. Engl.*, 1969, **8**, 980.
13 M. S. Hussain and E. O. Schlemper, *J. Chem. Soc., Dalton Trans.*, 1980, 750.

*Received in Bloomington, IN, USA; 23rd May 1997; 7/03593D*

# Hydrothermal synthesis and structural characterization of $[Cu(en)_2]_2Cu_7Cl_{11}$: a three-dimensional open-framework copper halide with occluded $[Cu(en)_2]^{2+}$ cations

**Jeffrey R. D. DeBord,[a] Ying-jie Lu,[a] Christopher J. Warren,[a] Robert C. Haushalter*[a] and Jon Zubieta*[b]**

[a] *NEC Research Institute, 4 Independence Way, Princeton, NJ 08540, USA*
[b] *Department of Chemistry, Syracuse University, Syracuse, NY 13244, USA*

**A new type of three-dimensional open-framework copper chloride, prepared simply by the hydrothermal treatment of $CuCl_2 \cdot H_2O$ and en, is built up from unusual chloride bridged $Cu_4$ tetramers connected by $CuCl_{3/3}$ units and has voids in the framework that are filled with charge-compensating $[Cu(en)_2]^{2+}$ cations.**

While the utility of the aluminosilicate zeolites[1] derived from their shape selective absorptivities, reactive acid sites and substantial chemical and thermal stability remains unsurpassed, recent synthetic efforts have sought to expand the chemical reactivity and catalysis associated with open framework inorganic materials to a variety of new systems. Early efforts produced the large class of aluminophosphate materials.[1d,2] In hopes of increasing the chances of observing new types of shape selective catalysis by incorporating d-block elements into these materials as stoichiometric framework constituents, organically templated solids such as molybdenum phosphates,[3] vanadium phosphates,[4] cobalt phosphates[5] and vanadium oxides[6] have recently been prepared. It appears that the organic templates used in the syntheses not only fulfill the requirement of leaving a molecular sized void in the framework upon post-synthesis removal, but are essential for the synthesis by providing a species that can allow the crystal to grow *via* charge neutralization at the crystal/solution interface by virtue of possessing a suitable shape and charge to volume ratio. Such incorporation of an organic molecule will necessarily induce a large degree of structural complexity into the system by virtue of the relatively large number of framework atoms required to totally encapsulate the large molecule. We report here an extension of this concept of templating a three-dimensional anionic framework with bulky cations to the copper halide system with the hydrothermal synthesis and structural characterization of $[Cu(en)_2]_2Cu_7Cl_{11}$ **1** (en = ethylenediamine), a three-dimensional copper halide open-framework material with entrained $[Cu(en)_2]^{2+}$ cations.

The halide $[Cu(en)_2]_2Cu_7Cl_{11}$ **1** is prepared from the extremely simple reaction of $CuCl_2 \cdot 2H_2O$, en and water in a mole ratio of 1 : 1.4 : 148 at 170 °C for 4 days, and is isolated as purple crystals.† The X-ray structural analysis of **1**‡ shows the material to be an open-framework solid with a topologically unique framework composed of copper and chlorine. The formulation of the framework as all diamagnetic $Cu^+$ with entrained $Cu(en)_2^{2+}$ ($d^9$ S = 1/2) centers is supported by magnetic measurements which show the compound to be paramagnetic with $\mu_{eff}$ (300 K) = 2.43(1) $\mu_B$ and $\theta = -4.0(3)$ K.

The framework of **1** is constructed from the unusual $Cu_4$ tetrameric building blocks (Fig. 1) which contain copper tetrahedrally coordinated by chloride ligands. The tetramer is composed of a dimer of edge-sharing $CuCl_4$ tetrahedra, with the two Cl atoms which form the shared edge also coordinated to two copper atoms from a corner-sharing dimer of $CuCl_4$ tetrahedra, which results in these two Cl atoms connecting the dimers in a $\mu_3$ fashion. The tetramers are linked into a covalently bonded three-dimensional lattice by three coordinate Cu atoms (Fig. 2). The Cu atoms in these three-coordinate sites display slightly pyramidal trigonal coordination, with the Cu displaced 0.41 Å above the least-square plane of the three Cl atoms, and are crystallographically disordered into two sites on either side of this plane.

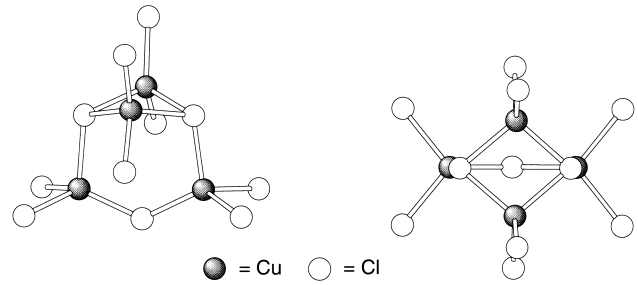



**Fig. 1** Two views of the $Cu_4$ tetramer found in $[Cu(en)_2]_2Cu_7Cl_{11}$ **1** which is composed of two-edge sharing $CuCl_4$ tetrahedra, the two bridging chloride ligands of which also form two vertices from a corner-sharing pair of $CuCl_4$ tetrahedra, thereby adapting a $\mu_3$ coordination mode

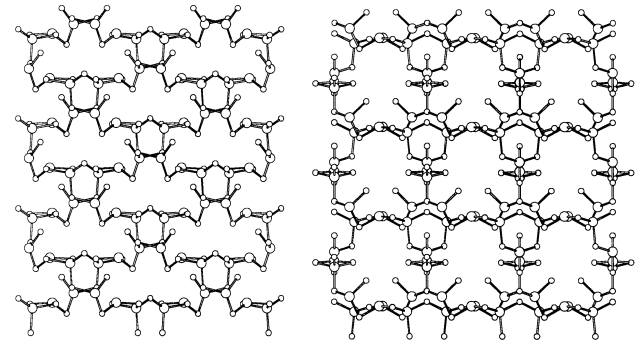


**Fig. 2** Two views of the structure of $[Cu(en)_2]_2Cu_7Cl_{11}$ **1** 45° apart and parallel to the *ab* plane showing the manner in which the $Cu_4$ tetramers are linked by the $CuCl_{3/3}$ groups; the $[Cu(en)_2]^{2+}$ cations have been omitted for clarity

The three-dimensional copper halide framework can be conceptually envisioned as being built up in space group $P4_2nm$ from the aforementioned tetramers connected along the $4_2$ screw axis *via* the trigonal $CuCl_{3/3}$ bridges into rectangular spirals. These spirals are in turn intertwined with another crystallographically identical spiral to give copper halide double helices as shown in Fig. 3. Unlike the recent example of chiral inorganic double helices found in the vanadium phosphate $[NH_2Me_2]K_4[V_{10}O_{10}(H_2O)_2(OH)_4(PO_4)_7] \cdot 4H_2O$[7] mirror images of the double helix in the title compound must also exist in the crystal since $P4_2nm$ is not an enantiomorphic space group. In fact, each double helix is fused with and is surrounded by four identical double helices of the opposite handedness that

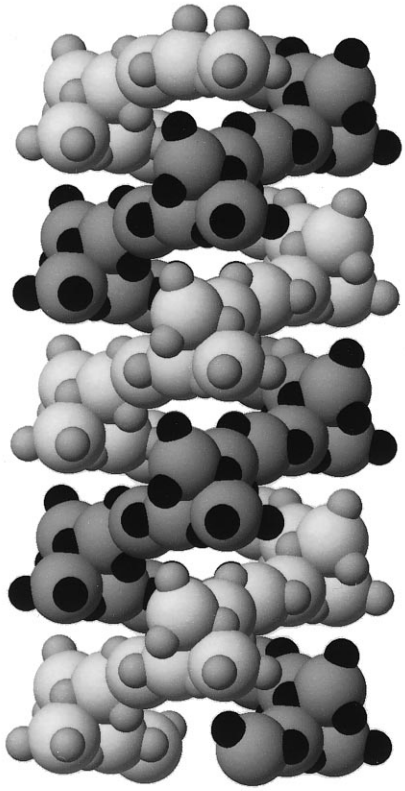


**Fig. 3** The copper halide double helices in $[Cu(en)_2]_2Cu_7Cl_{11}$ **1**

are related to one another by the mirror planes present on (110) and $(\bar{1}10)$.

This connectivity generates voids in the framework that are filled by charge-compensating $[Cu(en)_2]^{2+}$ cations. The $[Cu(en)_2]^{2+}$ cations interact with the framework not only *via* two long axial Cu–Cl interactions at 2.77 and 2.80 Å, but also with numerous interactions in the range 3.3–3.6 Å from the N atoms of the en to the Cl atoms of the framework which are presumably N–H···Cl hydrogen bonds. Bond angles for these N–H···Cl interactions range from 153.3 to 171.7°, further supporting the existance of hydrogen bonds.

The hydrothermally mediated, cation-directed crystallization of covalently bonded three-dimensional framework materials with large occluded cations has been extended to the halide system with the synthesis and structural characterization of $[Cu(en)_2]_2Cu_7Cl_{11}$ **1**. It is clear that highly crystalline materials with covalently bonded three-dimensional frameworks as reported here would be very difficult to prepare at room temp. The increased solvating ability of water at higher temperatures is definitely necessary to provide the environment required for the assembly of covalent three-dimensional solids from simple precursor crystal growth. Since these reaction conditions or starting materials could hardly be simpler, this method should be applicable to the preparation of a very large number of new solids with potentially interesting or useful molecular seiving, photochemical or catalytic properties. This method has yielded a variety of large copper halide clusters, one-dimensional polymers and layered solids with coordinated organic ligands, which will be reported shortly.

The work at Syracuse University was supported by NSF Grant CHE-9318824.

## Footnotes

* E-mails: bhaushalter@symyx.com, jazubiet@mailbox.syr.edu

† *Experimental procedure*: ethylenediamine (0.20 ml, 0.0042 mol) was added to a solution of $CuCl_2 \cdot 2H_2O$ (0.51 g, 0.003 mol) in 8 ml water contained in a 23 ml polytetrafluoroethylene-lined Parr acid digestion vessel. The vessel was sealed and heated to 170 °C for four days under autogeneous pressure. After cooling, purple crystal were isolated and washed with water. Powder X-ray diffraction shows the product to be monophasic.

‡ *Crystal data for* **1**: Tetragonal, space group $P4_2nm$, $a$ = 13.241(2), $c$ = 8.953(2) Å, $V$ = 1569.7(5) Å$^3$, $Z$ = 8, $M_w$ = 300.56 g mol$^{-1}$, $D_c$ = 2.544 g cm$^{-3}$. The structure was solved by direct methods and refined using full-matrix least squares on $F^2$ with SHELXTL. All of the non-hydrogen atoms were refined with anisotropic thermal parameters. The final refinement was based on 1294 reflections with $I > 2.0\sigma(I)$ and converged with $R(R_w)$ = 0.0362(0.0843). Atomic coordinates, bond lengths and angles, and thermal parameters have been deposited at the Cambridge Crystallographic Data Centre (CCDC). See Information for Authors, Issue No. 1. Any request to the CCDC for this material should quote the full literature citation and the reference number 182/490.

## References

1 (*a*) M. Occelli and H. Robson, *Zeolite Synthesis*, American Chemical Society, Washington, DC, 1989; (*b*) D. Breck, *Zeolite Molecular Sieves*, Krieger, Malabar, FL, 1974; (*c*) D. Vaughan, in *Zeolites: Facts, Figures, Future*, ed. P. Jacobs and R. van Santen, Elsevier, Amsterdam, 1989, pp. 95–116; (*d*) W. Meier and D. Olson, *Atlas of Zeolite Structure Types*, Butterworth, London, 1987; (*e*) R. Barrer, *Hydrothermal Chemistry of Zeolites*, Academic Press, New York, 1982.

2 R. Szostak, *Molecular Sieves Principles of Synthesis and Identification*, Van Nostrant Reinhold, New York, 1989; M. Occelli and H. Robson, *Zeolite Synthesis*, ACS, Washington, DC, 1989, ch. 23.

3 R. Haushalter and L. Mundi, *Chem. Mater*., 1992, **4**, 31.

4 V. Soghomonian, Q. Chen, R. Haushalter and J. Zubieta, *Angew. Chem., Int. Ed. Engl*., 1995, **34**, 223; V. Soghomonian, R. Haushalter, Q. Chen and J. Zubieta, *Inorg. Chem*., 1994, **33**, 1700; V. Soghomonian, R. Haushalter, Q. Chen and J. Zubieta, *Angew. Chem., Int. Ed. Engl*., 1993, **32**, 610; V. Soghomonian, R. Haushalter, Q. Chen and J. Zubieta, *Chem. Mater*., 1993, **5**, 1690; V. Soghomonian, R. Haushalter, Q. Chen and J. Zubieta, *Chem. Mater*., 1993, **5**, 1595.

5 J. Chen, R. Jones, S. Natarajan, M. Hursthouse and J. Thomas, *Angew. Chem., Int. Ed. Engl*., 1994, **33**, 639; J. DeBord, R. Haushalter and J. Zubieta, *J. Solid State Chem.*, 1996, **125**, 270.

6 Y. Zhang, C. O'Connor, A. Clearfield and R. Haushalter, *Chem. Mater*., 1996, **8**, 595; Y. Zhang, J. DeBord, C. O'Connor, R. Haushalter, A. Clearfield and J. Zubieta, *Angew. Chem., Int. Ed. Engl*., 1996, **35**, 989; J. DeBord, Y. Zhang, R. Haushalter, J. Zubieta and C. O'Connor, *J. Solid State Chem.*, 1996, **122**, 251; Y. Zhang, R. Haushalter and A. Clearfield, *Chem. Commun.*, 1996, 1055; Y. Zhang, R. Haushalter and A. Clearfield, *Inorg. Chem.*, 1996, **35**, 4950.

7 V. Soghomonian, Q. Chen, R. Haushalter, J. Zubieta and C. O'Connor, *Science*, 1993, **259**, 1596.

*Received in Cambridge, UK, 25th March 1997; 7/02053H*

# New molecular superconductor containing paramagnetic chromium(III) ions

**Lee Martin,[a] Scott S. Turner,[a] Peter Day,*[a] Frank E. Mabbs[b] and Eric J. L. McInnes[b]**

[a] *Davy Faraday Research Laboratory, The Royal Institution of Great Britain, 21 Albemarle Street, London, UK W1X 4BS*
[b] *EPSRC cw EPR Service Centre, Department of Chemistry, University of Manchester, UK M13 9PL*

**The molecular charge-transfer salt β″-(bedt-ttf)$_4$[(H$_2$O)Cr(C$_2$O$_4$)$_3$]·PhCN [bedt-ttf = bis(ethylenedithio)tetrathiafulvalene], containing paramagnetic Cr$^{III}$ ions ($S$ = 3/2), is a superconductor with $T_c$ = 6.0(5) K.**

Superconductivity can be destroyed by magnetic fields, through break up of $S$ = 0 Cooper pair charge carriers. This is true whether the field is applied externally by a magnet, or arises internally from magnetic moments within the lattice.[1] However there is evidence to suggest that $S$ = 1 Cooper pairs can coexist with strong magnetic fields. To explore this antagonism between magnetism and superconductivity we have been systematically preparing molecular charge-transfer salts in which layers consisting of stacks of the organic donor molecule bedt-ttf [bis(ethylenedithio)tetrathiafulvalene] are interleaved by layers containing anionic transition-metal complexes which are paramagnetic. Among many bedt-ttf charge-transfer salts we found one containing paramagnetic high-spin Fe$^{III}$ ions which was a superconductor below 8.5(3) K.[2] The compound in question, β″-(bedt-ttf)$_4$[(H$_2$O)Fe(C$_2$O$_4$)$_3$]·PhCN **1**, contains the trigonally distorted-octahedral [Fe(C$_2$O$_4$)$_3$]$^{3-}$ with $S$ = 5/2, which is one of numerous known oxalate complexes of d-block elements. It is therefore pertinent to seek other examples with different magnetic moments to compare the effect of such a change on the superconducting critical temperature. Here we report that the corresponding Cr$^{III}$ compound, with a lower magnetic moment ($S$ = 3/2) is indeed a superconductor, but with a slightly lower $T_c$ that the Fe$^{III}$ compound.

Crystals of (bedt-ttf)$_4$[(H$_2$O)Cr(C$_2$O$_4$)$_3$]·PhCN **2** were grown from solutions generated electrochemically in H-shaped cells at a constant current of 1 μA using wet PhCN as solvent and [NH$_4$]$_3$[Cr(C$_2$O$_4$)$_3$]·3H$_2$O as supporting electrolyte. The solvent was saturated with bedt-ttf, excess solid being placed at the base of the anode arm of the H-cell. Black needle shaped crystals grew on the Pt anode. The structure of this new charge-transfer salt[3] is isostructural to that of **1**, featuring alternate layers of bedt-ttf cations, and layers containing [Cr(C$_2$O$_4$)$_3$]$^{3-}$, H$_2$O and PhCN. The cation layers adopt the β″ packing arrangement, with stacks of bedt-ttf having numerous short intermolecular S···S distances. The anion layers have a honeycomb arrangement of [Cr(C$_2$O$_4$)$_3$]$^{3-}$ with their outer oxygens hydrogen-bonded to the water molecules. Within each layer there is exclusively one chiral form of [Cr(C$_2$O$_4$)$_3$]$^{3-}$ and successive layers contain alternating Δ and Λ enantiomers. The PhCN molecules occupy hexagonal cavities with the CN groups parallel, causing an elongation of the hexagonal network along the *b*-axis.

Susceptibility measurements were performed on a Quantum Design MPSM7 SQUID magnetometer on randomly oriented polycrystalline samples within a gelatin capsule, and the data was collected on a Hewlett-Packard 486/33N PC. In fields > 0.01 T the susceptibility from 300 to 4 K is well fitted by the Curie–Weiss law together with a temperature-independent Pauli contribution to give a Curie constant of 1.956(2) emu K mol$^{-1}$ (1.875 is expected for Cr$^{3+}$, $S$ = 3/2). The fitted Weiss constant of −0.21(1) K indicates a very weak antiferromagnetic interaction between Cr centres. The Pauli contribution is 0.0016(3). In a plot of $\chi^{-1}$ *vs.* T there is a distinct change of slope near 150 K, probably indicative of a minor structural phase transition. In contrast, upon cooling the sample in zero applied field and measuring the susceptibility in a field of 5 × 10$^{-4}$ T whilst warming, the response is diamagnetic from 1.75 to 6.0 K indicating the presence of superconductivity. Type II superconducting behaviour is observed upon recooling as flux is trapped inside the sample and the susceptibility is less negative (Fig. 1). As the applied field is increased, the diamagnetism decreases, until at 0.002 T a Curie tail begins to develop as the high susceptibility of the Cr$^{3+}$ obscures the superconducting transition. The superconducting transition is completely suppressed by fields greater than 0.01 T, when the susceptibility obeys the Curie–Weiss law from 1.75 K to room temperature.

Polarised optical reflectivity of single crystals was recorded at room temp. using a Perkin Elmer 1710 spectrometer fitted with a Spectra Tech microscope and a KRS5 polariser. When the electric vector is both parallel and perpendicular to the needles axis of the crystal, the spectrum of **2** shows a high metallic reflectivity at frequencies below *ca.* 3800 cm$^{-1}$ with weak sharp vibrational features superimposed (Fig. 2). Several of the latter are assigned[4] to the [Cr(C$_2$O$_4$)$_3$]$^{3-}$: an O–C–O stretching vibration as 1270 and 1320 cm$^{-1}$, an O–C–O symmetric stretching vibration at 1390 cm$^{-1}$ and an O–C–O asymmetric stretching vibration at 1645 cm$^{-1}$. The other weak vibrational modes due to bedt-ttf and PhCN can be assigned by comparison with published data.[5] The metallic reflectivity has been fitted to a Drude expression[6] for free electrons with a damping term for the charge carrier motion. A value of 3570 cm$^{-1}$ is calculated for the plasma frequency.

The EPR spectra of a polycrystalline sample were recorded at X- and K-band from 4 to 300 K on a Bruker ESP300E spectrometer. Cooling was achieved *via* a BVT2000 variable-temperature unit (300–100 K) or an Oxford Instruments ESR910 cryostat (< 100 K). Spectrum simulations were achieved *via* in-house software.[7] At each temperature the spectrum consisted of separate resonances attributable to the localised Cr$^{3+}$ and to the conduction electrons. The relative

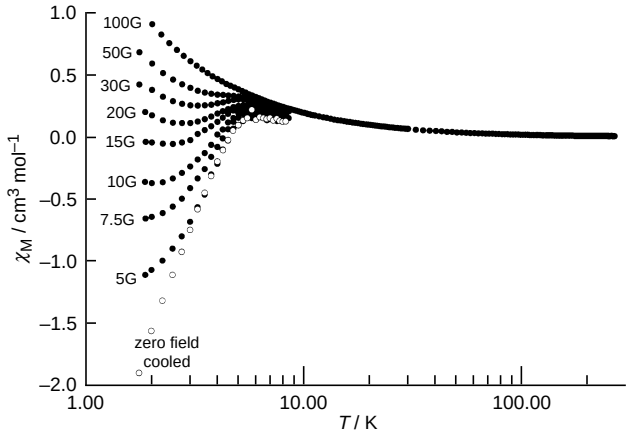



**Fig. 1** Temperature variation of the magnetic susceptibility of **2** in fields from 0 to 0.01 T. Open circles are zero-field cooled data and filled circles are field-cooled data.

intensities of the resonances arising from each of these vary with temperature, see Fig. 3. Those for the conduction electrons decrease with decreasing temperature, in contrast to those due to the chromium centres which increase. The observation of spectra from the two different centres indicates that interaction between them remains weak over the whole temperature range. The resonance due to the conduction electrons consists of a single line at $g = 2.006(1)$ comparable with the free-electron $g$ value, whereas the spectrum relating to $Cr^{3+}$ is complex. Simulations of the $Cr^{3+}$ resonances at both X- and K-band resulted in acceptable fits only if the presence of two different Cr centres in a 1 : 1 ratio was assumed. These two centres have the same $g$ values (2.00) but significantly different zero-field splitting parameters; $|D| = 0.52$ cm$^{-1}$, $|E/D| = 0.07$ cm$^{-1}$ and $|D| = 0.70$ cm$^{-1}$, $|E/D| = 0.16$ cm$^{-1}$. Since $|D|$ is more sensitive to changes in the electronic environment about Cr than $g$, there are two types of coordinated chromium differentiated by very small structural changes, probably in the O–Cr–O angles rather than bond distances. This is apparently in contradiction to the crystal structure. However the latter was refined from room-temperature data and it is likely that there is a structural phase transition to a lower symmetry on cooling, as already indicated by the bulk susceptibility data. The fact that the ratio of the two metal centres is 1 : 1 points to the possibility that the origin of this effect may be the interaction of each chiral form with the bedt-ttf layers.

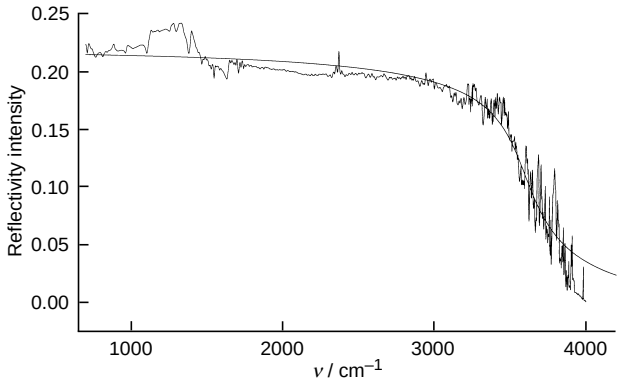



**Fig. 2** Reflectivity of a crystal of **2** with the electric vector of the incident light parallel and perpendicular to the needle axis. The line is a fit to a damped Drude expression.

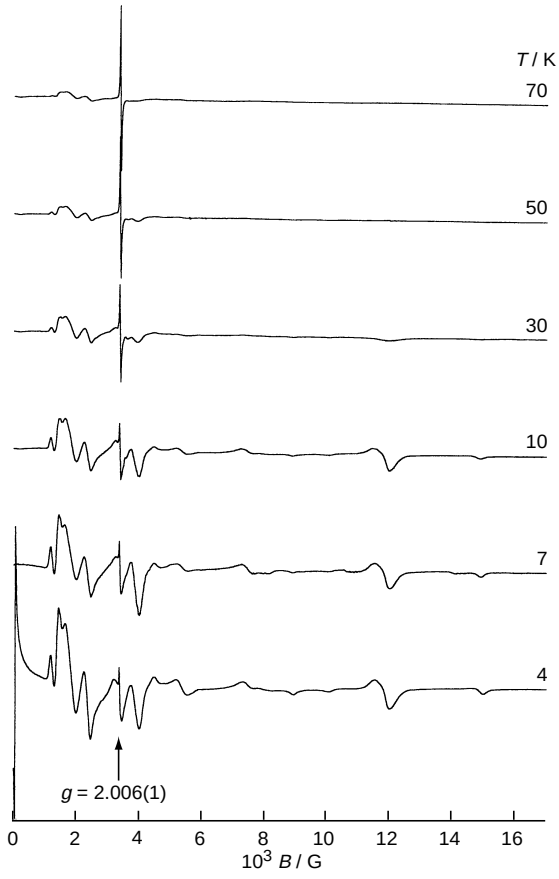



**Fig. 3** X-Band EPR spectra of a polycrystalline sample of **2** in the temperature range 70–4 K

An interesting feature of the EPR at X-band is a line with inverted phase compared to the rest of the spectrum near to zero frequency at the lowest temperatures. The origin of this feature is unknown and is the subject of further investigations. However, similar features have been observed in the EPR of high-temperature cuprate[8] superconductors as well as bedt-ttf[9] and $C_{60}$[10] based superconductors. It has been suggested to be due to the formation of weak links and closed superconducting loops between grains and is considered to be a marker for the onset of superconductivity.[11] Detailed investigations of the EPR spectra of **1** and similar materials will be reported in subsequent articles.

In conclusion we have found that replacing Fe by Cr in the paramagnetic molecular superconductor **1** brings about a small decrease in $T_c$ and $H_c$ despite the smaller magnitude of the paramagnetic moment embedded in the lattice. Thus, given that the unit-cell constants of **1** and **2** are essentially identical, there is no simple relationship between the strength of the local magnetic binding energy of the Cooper pairs. We are continuing to explore this intriguing family of superconductors, including synthesis of examples containing only closed-shell metal ions.

We are grateful to Professor W. Hayes of the Clarendon Laboratory, Oxford, for access to IR reflectivity equipment. We thank Professor M. B. Hursthouse and Dr S. J. Coles of the EPSRC X-ray Crystallography Service, Cardiff, for communication of results. One of us (S. S. T.) thanks Dr P. Harper for discussions on Drude theory. The work is supported by the EPSRC.

## Footnote

* E-mail: pday@ri.ac.uk

## References

1 See for example: *Superconductivity in Magnetic and Exotic Materials*, ed. T. Matsubara and A. Kotani, Springer Series in Solid State Science, Springer, Berlin, 1984, vol. 42, p. 1.
2 A. W. Graham, M. Kurmoo and P. Day, *J. Chem. Soc., Chem. Commun.*, 1995, 2061; M. Kurmoo, A. W. Graham, P. Day, S. J. Coles, M. B. Hursthouse, J. L. Caulfield, J. Singleton, F. L. Pratt, W. Hayes, L. Ducasse and P. Guionneau, *J. Am. Chem. Soc.*, 1995, **117**, 12 209.
3 Solved by M. B. Hursthouse and S. J. Coles of the EPSRC X-ray Crystallography Service, Cardiff, UK, unpublished work.
4 K. Nakamoto, *Infrared and Raman Spectra of Inorganic and Coordination Compounds*, Wiley, New York, 1978.
5 J. E. Eldridge, C. C. Homes, H. H. Wang, A. M. Kini and J. M. Williams, *Synth. Met.*, 1995, **70**, 983.
6 R. E. Hummel, *Electronic Properties of Materials*, Springer-Verlag, Berlin, 1993, ch. 10 and 11.
7 F. E. Mabbs and D. Collison, *Electron Paramagnetic Resonance of d-Transition Compounds*, Elsevier, Amsterdam, 1992, ch. 6.
8 A. Dulcic, R. H. Crepeau and J. H. Freed, *Phys. Rev. B*, 1989, **39**, 4249.
9 V. Kataev, G. Winkel, N. Knauf, A. Gruetz, D. Khomskii, D. Wohllebene, W. Crump, J. Hahn and K. F. Tebbe, *Physica B*, 1992, **179**, 24.
10 A. A. Zakhidov, H. Araki, K. Tada, K. Yakushi and K. Yoshino, *Phys. Lett. A*, 1995, **205**, 317.
11 T. K. Xia and D. Stround, *Phys. Rev. B*, 1989, **39**, 4792.

*Received in Cambridge, UK, 15th May 1997; 7/03352D*

# Chemoselective backbone cyclization of unprotected peptides

**Julio A. Camarero and Tom W. Muir***

*Laboratory of Synthetic Protein Chemistry, The Rockefeller University, 1230 York Avenue, New York, NY 10021, USA*

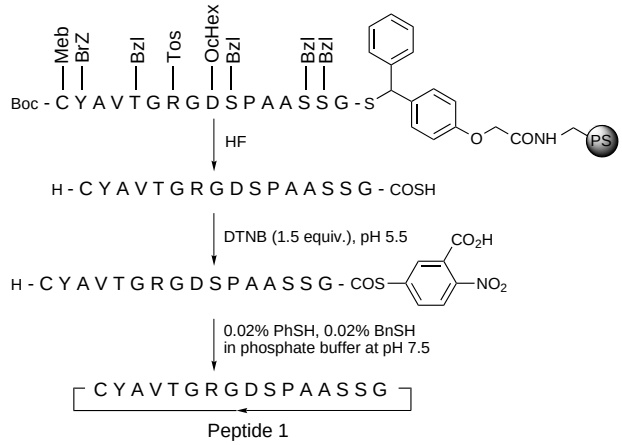
**A fully unprotected 15 residue peptide containing an N-terminal Cys residue and a C-terminal thioester moiety is cleanly converted to the corresponding head-to-tail cyclic peptide in aqueous buffers at around neutral pH.**

Cyclic peptides have restricted conformational flexibility compared to their linear counterparts, a feature which makes them of great interest in studying the structure–activity relationships of bioactive peptides.[1,2,3] Classical solution-based approaches to the synthesis of amide-cyclized peptides rely on fully protected linear precursors which are selectively activated and cyclized under conditions of high dilution.[4] Although this methodology has been used with satisfactory results in the synthesis of small cyclic peptides,[5] its application to the cyclization of larger peptides is constrained by the decreasing solubility of fully protected peptides as their size increases. To overcome these solubility problems, many researchers have utilized a variety of minimal protection strategies.[6] However, cyclization of minimally protected fragments *via* conventional carboxylate activation chemistries can lead to the accumulation of unwanted side-products, resulting in the desired material being generated in only moderate yield.[6]

In a recent report, Tam and co-workers describe a powerful new route to cyclic peptides in which unprotected peptide precursors are chemoselectively cyclized in aqueous solution.[7] This approach utilizes a thiazolidine-forming[8] intramolecular chemical ligation reaction, and was used to generate a series of cyclic peptides in good yield from soluble linear peptide precursors.[7] Here we describe a complementary methodology which facilitates the rapid and quantitative backbone cyclization of fully unprotected peptides in aqueous solution. Our cyclization strategy is based on an intramolecular native chemical ligation reaction,[9] and therefore requires the presence of an N-terminal Cys† residue and a C-terminal thioester moiety within the linear peptide precursor. We have successfully applied this new cyclization approach to the generation of backbone cyclized model peptide **1**, the sequence of which is derived from the tenth type 3 module of Fibronectin, and contains the RGD motif known to be involved in binding to the integrin class of cell adhesion receptor.[10]

The synthetic strategy used to generate cyclic peptide **1** is illustrated in Scheme 1. The fully protected linear precursor was assembled manually by stepwise SPPS using the *in situ* neutralization/HBTU [2-(1*H*-benzotriazole-1-yl)-1,1,3,3-tetramethyluronium hexafluorophosphate] activation protocol for Boc chemistry.[11] The synthesis was carried out on a Boc-Gly-(thioester handle)-aminomethyl-polystyrene resin[12,13] on a 0.1 mmol scale. After the synthesis was complete, the cleavage and total deprotection was accomplished by treatment with anhydrous HF–*p*-cresol (95 : 5, 10 ml, 0 °C for 1 h). Following trituration with cold diethyl ether, the crude peptide-$^{\alpha}$thioacid was extracted with 0.1% TFA in MeCN–$H_2O$ (1 : 1, 15–20 ml) and lyophilised. Analysis of the crude material by analytical C18 reverse-phase HPLC (10–40% B‡ over 30 min) gave a major peak whose mass was consistent with that of the expected peptide-$^{\alpha}$COSH [calculated molecular weight (av. isotope comp.) = 1444.5 Da; found = 1443.9 ± 0.1 Da]. In order to transform the $^{\alpha}$thioacid function into an active $^{\alpha}$thioester, the lyophilised crude material (65 mg, 45 μmol) was dissolved in a buffer containing 6 M GuHCl, 0.1 M sodium phosphate, pH 5.5 (30 ml), and a solution of DTNB [5,5′-dithiobis(2-nitrobenzoic acid)] in 0.1 M phosphate buffer, pH 5.5 (15 ml of a 5 mM solution, 1.5 equiv.) was added at room temperature. The thioesterification reaction was complete after 30 min,§ and the major product was characterized by ESMS (electrospray mass spectrometry) as being the desired peptide-$^{\alpha}$thioester [calculated molecular weight (av. isotope comp.) = 1607.6; found = 1605.9 ± 0.1 Da]. Upon completion, the reaction was quenched by the addition of 0.1% TFA in $H_2O$, and the peptide-$^{\alpha}$thioester product purified by preparative HPLC (C18 reverse-phase HPLC column, 18–23% B over 45 min at 50 ml min$^{-1}$) in high purity [10 mg, 6.2 μmol, Fig. 1(*a*)]. It is worth noting that the lower p$K_a$ of the $^{\alpha}$thioacid group relative to the cysteine sulfhydryl group ensures that the predominant reaction with DTNB at pH 5.5 is thioesterification and not disulfide formation.[14]

Cyclization of the linear peptide precursor (containing the necessary N-terminal Cys and C-terminal thioester group) to give peptide **1** was accomplished under high dilution conditions as follows. The purified peptide-$^{\alpha}$thioester was dissolved to a final concentration of *ca*. 50 μM in a freshly degassed buffer (pH 7.5) containing 0.1 M sodium phosphate, 1 mM EDTA, and both PhSH and BnSH at a concentration of 0.02% v/v.¶ In order to monitor the course of the reaction, small aliquots (100 μl) of the reaction mixture were periodically removed, quickly quenched by addition of 10% TFA in $H_2O$ (20 μl), and then analysed by analytical C18 reverse-phase HPLC. Under these conditions, the backbone cyclization reaction was found to be completely chemoselective, since only the desired cyclomonomeric peptide **1** was obtained [Fig. 1(*b*)]. Moreover, cyclization proceeded extremely fast and the linear starting material was cleanly converted to the cyclic product within 10 min [Fig. 1(*c*)]. Cyclic peptide **1** was purified by semipreparative C18 reverse-phase HPLC (10–40% B over 45 min at ml min$^{-1}$) and characterized by ESMS [calculated molecular weight (av.




**Scheme 1**

isotope comp.) = 1408.5 Da; found = 1408.4 ± 0.6 Da] and tryptic digestion.‖

In summary, we have described a practical new strategy which allows fully unprotected peptides to be cyclized in a head-to-tail manner in aqueous solution at neutral pH. In the example described, cyclization was observed to be both clean and rapid, and afforded the desired cyclic peptide **1** in excellent yield. As with intermolecular native chemical ligation,[9] this intramolecular cyclization reaction can be performed in the presence of all naturally occurring amino acid side-chains, including additional cysteine sulfhydryls. The compatibility of this cyclization chemistry with native protein folding conditions coupled with recent advances in the total chemical synthesis of proteins,[15] suggests a potentially straightforward route to circular versions of small proteins and protein domains.

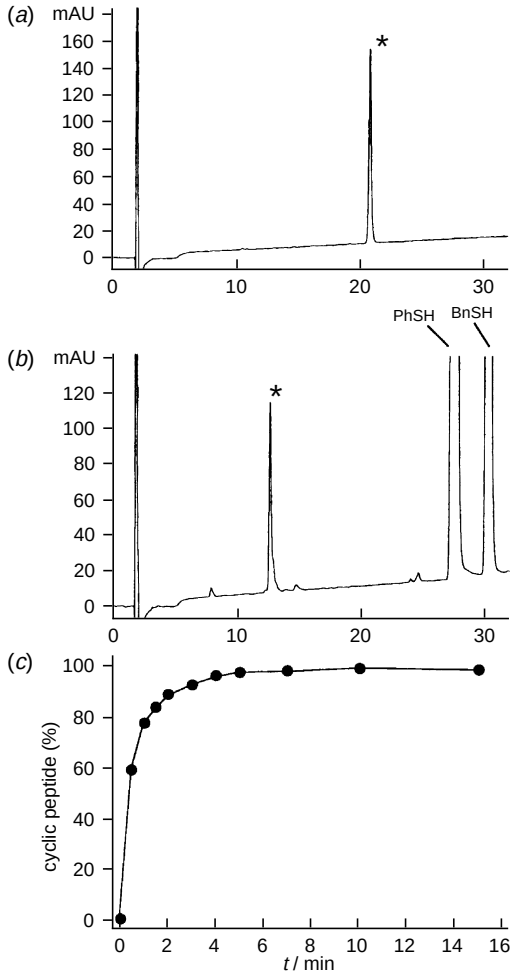



**Fig. 1** Reverse-phase HPLC analysis of peptide **1** cyclization. (*a*) peptide-$^{\alpha}$COSNB after HPLC purification. (*b*) cyclization reaction after 15 min. (*c*) progress of the cyclization reaction. The desired product in each panel is indicated by an asterisk.

We thank The Rockefeller University for financial support and the Ministerio de Educación y Ciencia of Spain for a postdoctoral fellowship (J. A. C.).

## Footnotes

* E-mail: muirt@rockvax.rockefeller.edu

† A more general approach to native (amide-forming) chemical ligation that extends the technique beyond the originally reported X-Cys ligation site to X-Gly and Gly-X ligation sites has been described recently.[16]

‡ Where A = 0.1% TFA in $H_2O$ and B = 0.1% TFA in MeCN : $H_2O$ (9 : 1 v/v).

§ Thioesterification of peptide-$^{\alpha}$thioacids with aryl disulfides such as DTNB goes *via* an acyl disulfide intermediate.[17]

¶ Inclusion of BnSH and PhSH in the ligation buffer results in the *in situ* conversion of the 2-nitrobenzoic peptide-$^{\alpha}$thioester (peptide-$^{\alpha}$COSNB) into the corresponding benzyl and phenyl peptide-$^{\alpha}$thioesters through trans-thioesterification.[18] The presence of these aromatic thio cofactors was found to eliminate unwanted peptide-$^{\alpha}$thioester hydrolysis.

‖ Trypsin hydrolysis in 0.1 M Tris HCl buffer pH 8.5 at the unique Arg residue yielded only a single product, as expected for a cyclomonomeric structure, that did not co-elute with the peptide **1** and gave a molecular peak 18 Da higher than the cyclic peptide [molecular weight calculated (av. isotope comp.) = 1426.5 Da; found = 1426.4 ± 0.6 Da].

## References

1 V. J. Hruby, *Life Sci.*, 1982, **31**, 189.
2 V. J. Hruby, F. Al-Obeidi and W. Kazmierski, *Biochem. J.*, 1990, **268**, 249.
3 J. Rizo and L. M. Gierasch, *Annu. Rev. Biochem.*, 1992, **61**, 387.
4 M. Bodanszky, *Principles of Peptide Synthesis*, Springer, Berlin, 1984.
5 R. Schmidt and K. Neubert, *Int. J. Peptide Protein Res.*, 1991, **37**, 502; J. S. McMurray, R. J. A. Budde and F. Dyckes, *Int. J. Peptide Protein Res.*, 1993, **42**, 209.
6 F. Al-Obeidi, M. E. Hadley, B. M. Pettit and V. J. Hruby, *J. Am. Chem. Soc.*, 1989, **111**, 3413; A. G. Beck-Sickinger, E. Grouzmann, E. Hoffmann, W. Gaida, E. G. Van Meir, B. Waeber and G. Jung, *Eur. J. Biochem.*, 1992, **206**, 957; R. Tolman, B. A. Bednarek, B. A. Johnson, W. J. Leanza, S. Marburg, D. J. Underwood, E. A. Emini and A. J. Conley, *Int. J. Peptide Protein Res.*, 1993, **41**, 455; J. A. Camarero, J. J. Cairo, E. Giralt and D. Andreu, *J. Peptide Sci.*, 1995, **1**, 241.
7 P. Botti, T. D. Pallin and J. P. Tam, *J. Am. Chem. Soc.*, 1996, **118**, 10 018.
8 C.-F. Liu and J. P. Tam, *Proc. Natl. Acad. Sci. USA*, 1994, **91**, 6584.
9 P. E. Dawson, T. W. Muir, I. Clark-Lewis and S. B. H. Kent, *Science*, 1994, **266**, 776.
10 M. D. Pierschbacher and E. Ruoslathi, *Nature*, 1984, **309**, 30.
11 M. Schnolzer, P. Alewood, A. Jones, D. Alewood and S. B.H. Kent, *Int. J. Peptide Prot. Res.*, 1992, **40**, 180.
12 D. Yamashiro and C. H. Li, *Int. J. Peptide Prot. Res.*, 1988, **31**, 322.
13 L. E. Canne, S. M. Walker and S. B. H. Kent, *Tetrahedron Lett.*, 1995, **36**, 1217.
14 M. Baca, T. W. Muir, M. Schnolzer and S. B. H. Kent, *J. Am. Chem. Soc.*, 1995, **117**, 1881.
15 T. W. Muir, *Structure*, 1995, **3**, 649.
16 L. Canne, S. J. Bark and S. B. H. Kent, *J. Am. Chem. Soc.*, 1996, **25**, 5891.
17 L. Zhang and J. P. Tam, *Tetrahedron Lett.*, 1997, **1**, 3.
18 P. E. Dawson, T. W. Muir and S. B. H. Kent, *J. Am. Chem. Soc.*, 1997, **119**, 4325.

*Received in Glasgow, UK, 19th March 1997; 7/02083J*

# Enhancement of *endo* selectivity in Diels–Alder reactions of methyl (*E*)-3-nitroacrylate with (*E*)-1-oxybuta-1,3-dienes

**Richard J. Stoodley* and Wai-Hung Yuen**

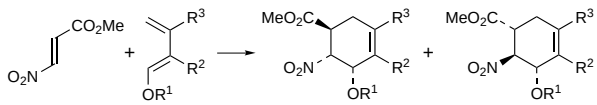
*Department of Chemistry, UMIST, PO Box 88, Manchester, UK M60 1QD*

**(*E*)-1-Acetoxybuta-1,3-dienes show enhanced *endo* selectivity in Diels–Alder reactions with methyl (*E*)-3-nitroacrylate compared with (*E*)-1-methoxybuta-1,3-dienes and (*E*)-1-trimethylsilyloxybuta-1,3-dienes.**

In foundation studies, Danishefsky[1] established that Diels–Alder reactions of the nitroacrylate **1** with 1-oxybuta-1,3-dienes are highly regioselective but poorly stereoselective. For example, the cycloaddition involving the diene **2a** (in PhH) led to a 50 : 50 mixture of the *endo*-nitro cycloadduct **3a** and the *exo*-nitro cycloadduct **4a**; mixtures of the cycloadducts **3b**/**4b** and **3d**/**4d** were also produced in the corresponding reactions of the dienes **2b** and **2d**, although the ratios were not specified. With the intention of utilising cycloadducts of types **3** and/or **4** for the synthesis of carbasugars (particularly, 4-aminocarbapyranoses), we have sought to control the stereochemical outcome of the cycloadditions. The results described herein illustrate a means of producing *endo*-nitro cycloadducts of type **3** in preference to their *exo*-nitro counterparts of type **4**.

Table 1 summarises the outcome of Diels–Alder reactions of the nitroacrylate **1**[2] with the 1-oxybuta-1,3-dienes **2a**,† **2b**,† **2c**,†‡ **2d**,† **2e**,[3]§ **2f**,¶ **2g**,[4] **2h**,[5] **2i**,[6] **2j**,[7] **2k**,[8] **2l**[9] and **2m**.‖ From the results, it is clear that the *O*-substituent plays a significant role in determining the *endo* : *exo* selectivity.** Thus, an *O*-acetyl substituent is considerately more effective than an *O*-methyl or *O*-trimethylsilyl group (which are comparable) in promoting the formation of *endo*-nitro cycloadducts. It is also evident that the 3-substituent is influential. Thus, for dienes with comparable *O*-substituents, *endo*-nitro group selectivity increases in the order H > Me > OAc > $OSiMe_2R$. Finally, it should be noted that dienes featuring a 2-methyl group generally show a higher *endo*-nitro group selectivity than their 2-unsubstituted counterparts.

**Table 1** Selectivity of Diels–Alder reactions involving the nitroacrylate **1** and the dienes **2a**–**m**[a]

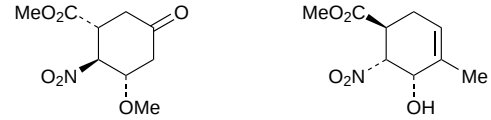


**1** **2** **3** **4**

| Diene **2** | $R^1$ | $R^2$ | $R^3$ | Cyclo-adducts | Ratio[b] | Yield (%)[c] |
|---|---|---|---|---|---|---|
| **a** | Me | H | H | **3a/4a** | 67 : 33 | 67 |
| **b** | $SiMe_3$ | H | H | **3b/4b** | 68 : 32 | — |
| **c** | Ac | H | H | **3c/4c** | > 95 : 5 | 71 |
| **d** | Me | H | $OSiMe_3$ | **3d/4d** | 35 : 65 | — |
| **e** | Me | H | $OSiMe_2Bu^t$ | **3e/4e** | 33 : 67 | — |
| **f** | Ac | H | $OSiMe_2Bu^t$ | **3f/4f** | 74 : 26 | 73 |
| **g** | Ac | H | OAc | **3g/4g** | 82 : 18 | 57 |
| **h** | $SiMe_3$ | H | Me | **3h/4h** | 50 : 50 | — |
| **i** | Ac | H | Me | **3i/4i** | 85 : 15 | 69 |
| **j** | $SiMe_3$ | Me | H | **3j/4j** | 85 : 15 | — |
| **k** | Ac | Me | H | **3k/4k** | 92 : 8 | 64 |
| **l** | Me | Me | $OSiMe_3$ | **3l/4l** | 52 : 48 | — |
| **m** | Ac | Me | $OSiMe_2Bu^t$ | **3m/4m** | 83 : 17 | 71 |

[a] The reactions were performed in dry dichloromethane (*ca*. 5 $cm^3$) using the nitroacrylate (1 mmol) and the diene (1 mmol). [b] The cycloadduct ratio was determined by 300 MHz $^1H$ NMR spectroscopic analysis of the crude product. [c] The yield refers to the purified cycloadduct mixture (the ratio was unaltered) isolated after silica gel column chromatography.

From a preparative context, the following points are of note. It was possible to isolate the ensuing cycloadducts in a pure state by crystallisation: **3a**†† (17% yield), mp 68–70 °C; **3c**†† (68% yield), mp 88–90 °C; **3i**†† (54% yield), mp 118–120 °C; and **3k**†† (60% yield), mp 88–90 °C. When the crude silylated cycloadduct mixtures **3d**/**4d** and **3j**/**4j** were subjected to hydrolysis, crystallisation of the products gave compound **5** (34% yield), mp 110–112 °C (lit.,[1] 110–112 °C), and compound **6**†† (42% yield), mp 108–110 °C, in pure states.



**5** **6**

The results reported are of both synthetic and mechanistic interest. In a synthetic context, they illustrate that *O*-substituent tuning can have a notable impact on *endo* : *exo* selectivity in cycloaddition reactions involving (*E*)-1-oxybuta-1,3-dienes of type **2** and the nitroacrylate **1**. Specifically, *O*-acetyl substituents are more effective than *O*-methyl/silyl groups in promoting the formation of *endo*-nitro cycloadducts of type **3**. From a mechanistic standpoint, the results suggest that the degree of 'electron richness' of a diene is an important consideration in *endo* : *exo* selectivity issues. In particular, electron-rich dienes favour the formation of *exo*-nitro cycloadducts of type **4**. Recently, Node and co-workers have noted[10] that *exo*-nitro group selectivity is a feature of Diels–Alder reactions of Danishefsky's diene **2d** and (*E*)-nitroalkenes (bearing alkyl or aryl groups) but they suggest that the *endo* transition state is destabilised by electrostatic repulsion between the silyloxy group of the diene and the nitro group of the dienophile.

## Footnotes

* E-mail: richard.stoodley@umist.ac.uk

† The dienes **2a**–**d** were purchased from Aldrich.

‡ The reaction of the diene **2c** with the ethyl ester counterpart of the nitroacrylate **1** has been studied by Shin and co-workers (ref. 11). Although the cycloadduct ratio was not specified, the ethyl ester analogue of the *endo*-nitro cycloadduct **3c** was isolated in 57% yield.

§ The diene **2e** was prepared by a modification of the literature route (ref. 3) in which (*E*)-4-methoxybut-3-en-2-one was treated with *tert*-butyldimethylsilyl triflate and triethylamine (ref. 12).

¶ The diene **2f** was prepared from (*E*)-4-acetoxybut-3-en-2-one (ref. 4) in a manner analogous to that employed in the synthesis of the diene **2e**.

‖ The diene **2m** was prepared from (*E*)-4-acetoxy-3-methylbut-3-en-2-one [obtained by acetylation (ref. 4) of the sodium salt of (*E*)-4-hydroxy-3-methylbut-3-en-2-one (ref. 13)] in a manner similar to that used in the synthesis of the diene **2e**.

** In general, the cycloadducts were differentiated by the appearance in the NMR spectrum of the double doublet at *ca*. δ 4.90, attributed to the nitro-bearing methine proton; coupling constants (*J*) of *ca*. 4 and 12 Hz were

observed for *endo*-nitro cycloadducts of type **3** and of *ca*. 8 and 11 Hz for *exo*-nitro cycloadducts of type **4**.

†† All new compounds displayed analytical and spectral properties that supported their assigned structures.

## References


1 S. Danishefsky, M. P. Prisbylla and S. Hiner, *J. Am. Chem. Soc*., 1978, **100**, 2918.
2 J. E. McMurray, J. H. Musser, I. Fleming, J. Fortunak and C. Nübling, *Org. Synth*., 1988, **Coll. Vol. VI**, 799.
3 R. E. Ireland, P. A. Aristoff and C. F. Hoyng, *J. Org. Chem*., 1979, **44**, 4318.
4 R. P. Potman, F. J. van Kleef and H. W. Scheeren, *J. Org. Chem*., 1985, **50**, 1955.
5 E. W. Colvin and I. G. Thom, *Tetrahedron*, 1986, **42**, 3137.
6 J. F. W. Keana, J. S. Bland, P. E. Eckler, V. Nelson and J. Z. Gougoutas, *J. Org. Chem*., 1976, **41**, 2124.
7 K. Krohn, K. Tolkiehn, V. Lehne, H. W. Schmalle and H.–F. Grützmacher, *Liebigs Ann. Chem*., 1985, 1311.
8 P.–Y. Blanc, *Helv. Chim. Acta*, 1961, **44**, 1.
9 S. Danishefsky, C.–F. Yan, R. K. Singh, R. B. Gammill, P. M. McCurry, Jr., N. Fritsch and J. Clardy, *J. Am. Chem. Soc*., 1979, **101**, 7001.
10 M. Node, K. Nishide, H. Imazato, R. Kurosaki, T. Inoue and T. Ikariya, *Chem. Commun*., 1996, 2559.
11 C.–g. Shin, M. Yamaura, E. Inui, Y. Ishida and J. Yoshimura, *Bull. Chem. Soc. Jpn.*, 1978, **51**, 2618.
12 H. Emde, D. Domsch, H. Feger, U. Frick, A. Götz, H. H. Hergott, K. Hofmann, W. Kober, K. Krägeloh, T. Oesterle, W. Steppan, W. West and G. Simchen, *Synthesis*, 1982, 1.
13 R. Kaushal, S. Sorani and S. S. Despande, *J. Indian Chem. Soc.*, 1942, **19**, 107; R. C. Gupta, D. S. Larsen, R. J. Stoodley, A. M. Z. Slawin and D. J. Williams, *J. Chem. Soc., Perkin Trans. 1*, 1989, 739.



*Received in Cambridge, UK, 18th April 1997; 7/02658G*

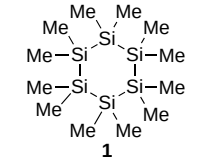
# Photo-induced silylene-transfer reactions of cyclic organosilanes to phenanthraquinone

**Masahiro Kako, Masumi Ninomiya and Yasuhiro Nakadaira***

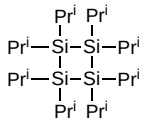
*Department of Chemistry, The University of Electro-Communications, Chofu, Tokyo, 182, Japan*

**Cophotolysis of cyclic organosilanes 1–4 with phenanthraquinone gave silylene insertion products *via* radical displacement at the silicon atoms of organosilanes by the photochemically excited phenanthraquinone.**

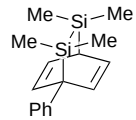
Electron-transfer reactions of heavier group 14 organometallic compounds have been studied extensively from the mechanistic and synthetic viewpoints.[1] For these reactions, electron-deficient carbonyl compounds, especially *p*-benzoquinones, are frequently used as electron acceptors.[2,3] We and the other groups found that the photoreactions of some disilane and digermane derivatives with *p*-benzoquinones underwent electron-transfer processes to produce *O*-silylated and *O*-germylated *p*-benzoquinones.[2] On the other hand, it was reported that the photolysis of α-diketones with alkyl and allylic stannanes afforded exclusively the alkylated and allylated α-ketols without giving any stannylated products.[3] These previous results prompted us to investigate the photoreaction of organosilanes and *o*-benzoquinones, which serve as good silylene traps due to their s-*cis* α-diketone structures.[4] We now report the photoreaction of cyclic organosilanes **1–4** with phenanthraquinone (PQ), providing the first example of silylene transfer reactions induced by photoexcited triplet *o*-benzoquinones.



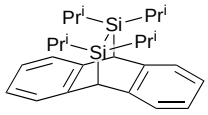
**1**



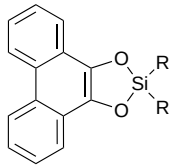
**2**



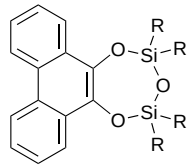
**3**



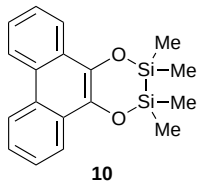
**4**



**5** R = Me
**7** R = Pr$^i$



**6** R = Me
**8** R = Pr$^i$



**10**

Irradiation of a solution (MeCN–$CH_2Cl_2$ = 4 : 1) of dodecamethylcyclohexasilane **1** ($1.1 \times 10^{-2}$ M) and PQ ($3.5 \times 10^{-2}$ M) in a sealed tube with two 500 W tungsten-halogen lamps (passing through an aqueous $NaNO_2$ filter, cutoff < 400 nm) afforded dioxasilolene **5**,† as a silylene adduct of PQ, along with a minor amount of trioxadisilepine **6**. In the case of photolysis of cyclotetrasilane **2**, dioxasilolene **7** was produced, whereas the corresponding trioxadisilepine **8** was not formed at all, as summarized in Table 1. We detected no other product derived from PQ while substantial amounts of PQ were recovered after the photolyses.

It is well-known that ultraviolet photolysis of **1** produces free dimethylsilylene, which can be trapped readily by α-diketones to afford trioxadisilepine derivatives.[4] However, **1** is entirely inert to the visible light employed in the present photolyses. Furthermore, the present reaction does not seem to involve free dimethylsilylene because the cophotolysis of **1** and PQ in the presence of $Et_3SiH$, a common silylene trap, did not give any $Et_3SiMe_2SiH$.[4b]

Since the reaction was efficiently quenched by addition of anthracene, the triplet PQ is suggested to be the key intermediate as judged by the comparison of the singlet and the triplet energies of PQ ($E_S$ = *ca.* 54, $E_T$ = *ca.* 48 kcal mol$^{-1}$)[5] and those of anthracene ($E_S$ = *ca.* 76, $E_T$ = *ca.* 43 kcal mol$^{-1}$).[6] Meanwhile, the consumption of **1** was suppressed by addition of 1,4-diazabicyclo[2.2.2]octane (DABCO), which has a lower oxidation potential ($E_{ox}$ = +0.70 V *vs.* SCE) than that of **1** ($E_{ox}$ = +1.45 V *vs.* SCE). The free energy changes ($\Delta G$) for the electron-transfer from cyclosilanes to the triplet PQ are given in Table 2.‡ These data suggest that the reaction may proceed *via* a partial or complete electron-transfer from the cyclosilanes to the photoexcited PQ at least in a polar solvent, such as MeCN. In fact, the silylene-transfer reactions were found to proceed substantially faster in MeCN than in benzene, as shown in Table 1.

We propose the following mechanism on the basis of Pedulli's result that photoexcited ketones are capable of cleaving Si–Si bonds of polysilanes *via* $S_H2$ type radical displacement at the silicon atoms.[8] Thus, the photochemically

**Table 1** Photo-induced silylene-transfer reactions of cyclosilanes to PQ

| Silane | Conditions | *t*/h | Conversion (%) | Product (% yield)[a] |
|---|---|---|---|---|
| **1** | *h*ν/PQ/$CH_3CN$/$CH_2Cl_2$ | 4.5 | 61 | **5** (138), **6** (33) |
| **1** | *h*ν/PQ/$CH_6H_6$ | 10.5 | 49 | **5** (161), **6** (31) |
| **2** | *h*ν/PQ/$CH_2Cl_2$l | 0.5 | 70 | **7** (82) |
| **2** | *h*ν/PQ/$CH_6H_6$ | 1.5 | 70 | **7** (57) |
| **3** | *h*ν/PQ/$CH_3CN$/$CH_2Cl_2$ | 0.5 | 89 | **5** (28), **6** (11), biphenyl (100) |
| **3** | *h*ν/PQ/$CH_6H_6$ | 1.5 | 65 | **5** (62), **6** (13), biphenyl (94) |
| **4** | *h*ν/PQ/$CH_3CN$ | 3.0 | 100 | **7** (85), anthracene (97) |
| **4** | *h*ν/PQ/$CH_6H_6$ | 18.0 | 70 | **7** (69), anthracene (100) |

[a] Based on the consumption of silanes.

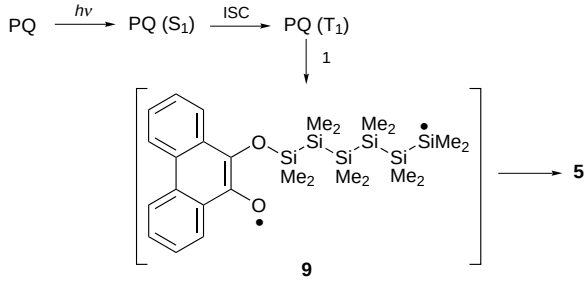
**Table 2** The free energy changes ($\Delta G$) for the electron-transfer from cyclosilanes to PQ

| | $E_{ox}$/V *vs.* SCE | $\Delta G$/kcal mol$^{-1}$ in MeCN | in $C_6H_6$ |
|---|---|---|---|
| **1** | +1.45 | −1.41 | +17.84 |
| **2** | +1.00 | −11.79 | +7.47 |
| **3** | +0.42 | −25.16 | −6.0 |
| **4** | +1.17 | −7.9 | +11.4 |

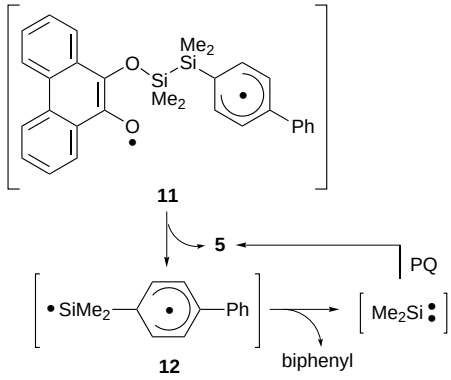
excited PQ attacks one of the silicon atoms of **1** to afford a biradical intermediate **9**. At the initial interaction, a partial or complete electron-transfer from **1** to the triplet PQ may take place in polar solvents as mentioned above. Subsequent intramolecular O–Si bond formation in **9** would provide **5** as illustrated in Scheme 1. The yields of **5** indicate that a molecule of **1** donates more than an equimolar amount of silylene units to PQ. We obtained polymeric products containing silane fragments in these reactions, which might have arisen from framentation of the starting materials. In addition, the photoreaction of **1** and PQ in the presence of $CCl_4$ gave $Cl(Me_2Si)_nCl$ ($n$ = 4–6), which would substantiate the present mechanism involving the silyl radical intermediates.[9]

There seemed to be three possible pathways leading to **6**: (i) intramolecular cyclization in **9** could afford **10**, which would be susceptible to atmospheric oxidation to give **6**, (ii) addition of free dimethylsilylene to **5** could give rise to **6** *via* **10**, and (iii) dimethylsilanone,[10] if formed in the course of reaction, could insert into **5** to produce **6**. However, the intermediate **10** was never detected in the photolysates while all trapping experiments for free dimethylsilylene and dimethylsilanone were not successful. When the reaction was carried out under an aerobic atmosphere, the yields of **6** increased while those of **5** decreased. The residual molecular oxygen plays an important role in the formation of **6**. Since **5** is stable in the air, it is suggested that molecular oxygen should be incorporated, probably as some radical species, to afford **6** during the photoreactions. Further investigations are in progress to clarify the mechanism.

Recently, it has been demonstrated that 7,8-disilabicyclo[2.2.2]octa-2,5-diene **3**, which is known as a disilene precursor,[10] also acts as a good electron donor.[11] Therefore, we anticipated that cophotolysis of **3** with PQ would produce selectively the corresponding disilanylene adduct **10**. Interestingly, the silylene adduct **5** was obtained along with **6** instead of **10**. Moreover, in contrast to the case of **1**, the intermediacy of free dimethylsilylene was evidenced by the formation of $Et_3SiMe_2SiH$ in the cophotolysis of **3** with PQ in the presence of $Et_3SiH$. Based on the mechanism proposed for **1**, the reaction of **3** is interpreted as shown in Scheme 2. The initially formed adduct **11** would collapse to afford **5**, **12**, free dimethylsilylene and biphenyl successivley. It should be noted that free dimethylsilylene could contribute to the formation of **5** and **6**. Compound **4** gave a similar result, although no trioxadisilepine **8** was obtained as the case of **2**.




**Scheme 1**




**Scheme 2**

In summary, we have indicated that silylene-transfer reactions take place between cyclic organosilanes **1**–**4** and the photochemically excited triplet PQ. The formation of free dimethylsilylene is noteworthy since there has been no precedent of generation of free silylenes induced by photoexcited carbonyl compounds as far as we know.

This work was supported in part by Grants-in-Aid from the Ministry of Education, Science, and Culture in Japan. We thank Toshiba Silicon Co. Ltd. for a gift of organosilicon reagents.

## Footnotes

† *Selected spectral data* for **5**: $^1$H NMR ($C_6D_6$): $\delta$ 8.54 (d, 2H, *J* 8.0 Hz), 8.46 (6, 2H, *J* 8.0 Hz), 7.53 (t, 2H, *J* 8.0 Hz) 7.40 (t, 2H, *J* 8.0 Hz), 0.20 (s, 6H); $^{13}$C NMR ($CDCl_3$): $\delta$ 139.35 (s), 127.38 (s), 126.97 (d), 125.39 (s), 124.81 (d), 123.50 (d), 121.06 (d), −0.80 (q); *m/z* 266 ($M^+$, 6%), 252 (21), 210 (100), 181 (34), 152 (35), 43 (20). For **6**: $^1$H NMR ($CDCl_3$): $\delta$ 8.62 (d, 2H, *J* 8.0 Hz), 8.16 (d, 2H, *J* 8.0 Hz), 7.62–7.58(m, 4H), 0.36 (s, 12H); $^{13}$C NMR($CDCl_3$): $\delta$ 135.43 (s), 129.00 (s), 127.73 (s), 126.65 (d), 125.20 (d), 122.39 (d), 122.14 (d), −0.90 (q); *m/z* 340 ($M^+$, 100%), 325 (30), 266 (82), 236 (44), 133 (58), 73 (21). For **7**: $^1$H NMR ($CDCl_3$): $\delta$ 8.67 (d, 2H, *J* 8.0 Hz), 8.15 (d, 2H, *J* 8.0 Hz), 7.65–7.53 (m, 4H), 1.43 (sept, 2H, *J* 7.5 Hz), 1.16 (d, 12H, *J* 7.5 Hz); $^{13}$C NMR ($CDCl_3$): $\delta$ 139.66 (s), 126.55(s), 126.46 (d), 124.63 (s), 124.25 (d), 120.88 (d), 120.71 (d), 15.80 (q), 13.04 (d); *m/z* 322($M^+$, 100%), 236 (28), 208 (10), 43 (20).

‡ The $\Delta G$ values were calculated according to the Rehm–Weller equation (ref. 7) {$\Delta G$/kcal mol$^{-1}$ = 23.06[$E$(D/D$^+$)−$E$(A$^-$/A)−$\Delta E_{excit.}$ + $\Delta E_{coul.}$)]}. The reduction potential of PQ is −0.66 V (*vs.* SCE) and the triplet energy of PQ was used as the excitation energy ($\Delta E_{excit.}$) (ref. 5). The Coulomb interaction energies ($\Delta E_{coul.}$) are −0.06 and +0.78 eV for MeCN and benzene, respectively [ref. 7(*b*)].

## References

1 M. Kako, M. Mori, K. Hatakenaka, S. Kakuma, Y. Nakadaira, M. Yasui and P. Iwasaki, *Tetrahedron*, 1997, **53**, 1265 and references cited therein.
2 M. Igarashi, T. Ueda, M. Wakasa and Y. Sakaguchi, *J. Organomet. Chem.*, 1991, **421**, 9; H. Komoriya, M. Kako, Y. Nakadaira, K. Mochida, M. Tonogaki-Kubota and T. Kobayashi, *Chem. Lett.*, 1984, 1213; *J. Organomet. Chem.*, 1995, **499**, 123; E. Baciocchi, T. D. Giacco, F. Elisei and M. Ioele, *J. Org. Chem.*, 1995, **60**, 7974.
3 A. Takuwa, Y. Nishigaichi, K. Yamashita and H. Iwamoto, *Chem. Lett.*, 1990, 639; 1990, 1761; A. Takuwa, Y. Nishigaichi, T. Yamaoka and K. Iihama, *J. Chem. Soc., Chem. Commun.*, 1991, 1359.
4 (*a*) W. Ando and M. Ikeno, *J. Chem. Soc., Chem. Commun.*, 1979, 655; (*b*) P. P. Gasper, in *Reactive Intermediates*, ed. M. Jones, Jr. and R. A. Moss, Wiley, New York, 1978, vol. 1, p. 229; 1981, vol. 2, p. 335; 1985, vol. 3, p. 333.
5 R. Foster and M. I. Foreman, in *The Chemistry of the Quinonoid Compounds*, ed. S. Patai, Wiley, New York, 1974, ch. 6, p. 257.
6 S. L. Murov, *Handbook of Photochemistry*, Marcel Dekker, New York, 1973.
7 (*a*) D. Rehm and A. Weller, *Isr. J. Chem.*, 1970, **8**, 259; (*b*) J. Mattay, J. Runsink, J. Gersdorf, T. Rumbach and C. Ly, *Helv. Chem. Acta*, 1986, **69**, 442.
8 A. Alberti, S. Dellonte, C. Paradisi, S. Roffia and G. F. Pedulli, *J. Am. Chem. Soc.*, 1990, **112**, 1123.
9 H. Sakurai, K. Sakamoto and M. Kira, *Chem., Lett.*, 1984, 1213; Y. Nakadaira, N. Komatsu and H. Sakurai, *Chem. Lett.*, 1985, 1781.
10 G. Raabe and J. Michl, *Chem. Rev.*, 1985, **85**, 419; in *The Chemistry of Organosilicon Compounds*, ed. S. Patai and Z. Rappoport, Wiley, New York, 1989, ch. 17, p. 1015.
11 Y. Nakadaira, Y. Gomi, H. Hosoe, S. Kyushin, M. Kako, K. Hatakenaka and M. Ohashi, *Bull. Chem. Soc. Jpn.*, 1993, **66**, 344.

*Received in Cambridge, UK, 1st April 1997; 7/02161E*

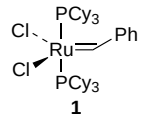
# Enyne metathesis for the facile synthesis of highly functionalised novel bicyclic β-lactams

**Anthony G. M. Barrett,*[a]† Simon P. D. Baugh,[a] D. Christopher Braddock,[a] Kevin Flack,[a] Vernon C. Gibson*[a]‡ and Panayiotis A. Procopiou[b]**

[a] *Department of Chemistry, Imperial College of Science, Technology and Medicine, London, UK SW7 2AY*
[b] *Department of Medicinal Chemistry, Glaxo Wellcome Research and Development Ltd, Gunnels Wood Road, Stevenage, Hertfordshire, UK SG1 2NY*

**A wide range of bicyclic β-lactam systems have been prepared *via* the enyne metathesis reaction using catalytic quantities of *trans*-$(Cy_3P)_2Cl_2Ru{=}CHPh$ (Cy = cyclohexyl).**

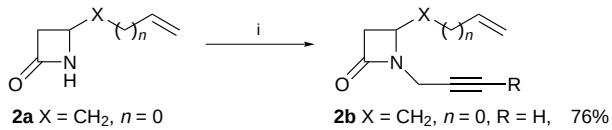
The elaboration of carbon skeletons *via* the construction of carbon–carbon bonds represents one of the most important endeavours in synthetic organic chemistry. The use of catalytic quantities of ruthenium[1] and molybdenum[2] carbenes as pioneered by Grubbs *et al.* for ring-closing metathesis (RCM)[3] is exemplary in this respect and is finding increasing use as the key synthetic step *en route* to polyfunctional natural products.[4] As a variant on RCM of dienes, Kinoshita and Mori have demonstrated the catalytic ability of ruthenium carbene **1** to generate conjugated dienes (with concomitant rearrangement of the carbon skeleton) from enynes.[5] Recently we have reported the use of ring-closing and cross metathesis for the preparation of novel monocyclic and bicyclic β-lactams in a synthetically fast and efficient manner.[6,7] The possibility of utilising enyne metathesis as a route into highly functionalised bicyclic β-lactams appeared attractive and herein we disclose our results in this arena.




**1**

Cy = cyclohexyl

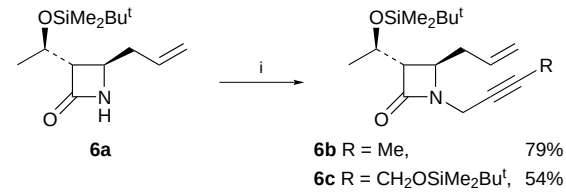
A broad range of enyne substrates were synthesised by two general routes. The previously prepared 4-substituted lactams **2a**–**5a**[6–8] were treated with prop-2-ynyl bromides in the presence of potassium hydroxide and tetrabutylammonium bromide to give variously functionalised enyne substrates **2b**–**5b**, **2c** (Scheme 1).§ Chiral, non-racemic enynes **6b** and **6c** were produced in an analogous fashion (Scheme 2). The *N*-allylated azetidinones **9** and **10** were synthesised using a modified procedure of Basak and Khamrai[9] for the introduction of the prop-2-ynyl group followed by *N*-allylation in the usual manner (Scheme 3).




**2a** X = $CH_2$, *n* = 0
**3a** X = $CH_2$, *n* = 1
**4a** X = O, *n* = 1
**5a** X = NTs, *n* = 1

**2b** X = $CH_2$, *n* = 0, R = H, 76%
**2c** X = $CH_2$, *n* = 0, R = Me, 58%
**3b** X = $CH_2$, *n* = 1, R = Me, 83%
**4b** X = O, *n* = 1, R = Me, 60%
**5b** X = NTs, *n* = 1, R = Me, 51%

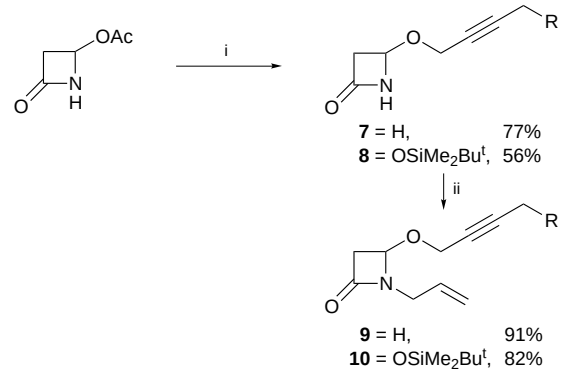
**Scheme 1** *Reagents and conditions*: i, $BrCH_2C{\equiv}CR$, KOH, $Bu_4N^+Br^-$, THF, 0 °C, 2 h




**6a**

**6b** R = Me, 79%
**6c** R = $CH_2OSiMe_2Bu^t$, 54%

**Scheme 2** *Reagents and conditions*: i, $BrCH_2C{\equiv}CR$, KOH, $Bu_4N^+Br^-$, THF, 0 °C, 2 h




**7** = H, 77%
**8** = $OSiMe_2Bu^t$, 56%

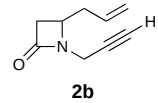
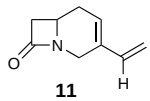
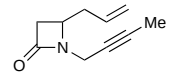
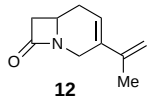
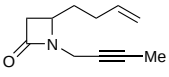
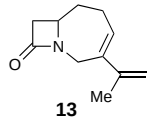
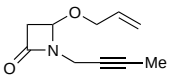
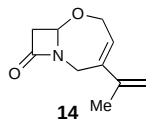
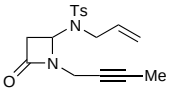
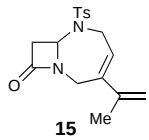
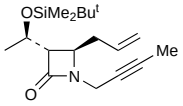
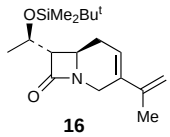
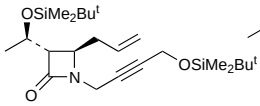
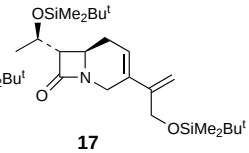
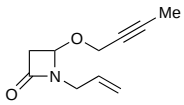
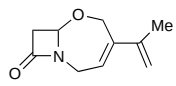
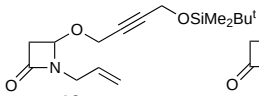
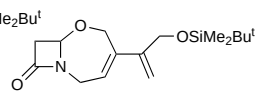
**9** = H, 91%
**10** = $OSiMe_2Bu^t$, 82%

**Scheme 3** *Reagents and conditions*: i, $HOCH_2C{\equiv}CH_2R$, $Zn(OAc)_2$, PhMe, 120 °C; ii, $BrCH_2CH{=}CH_2$, NaH, DMF, 0 °C, 2 h

Attempts to bring about the cyclisation of the parent enyne **2b** were unsuccessful even with catalyst loadings of up to 10 mol% **1**: only starting material was recovered (Table 1, entry 1). However, the non-terminal enyne **2c** was found to undergo metathesis with as little as 1 mol% carbene **1**, albeit in 20% yield. Increasing amounts of catalyst gave increasing quantities of products and at 10 mol% catalyst **1** an 88% yield of **12** was obtained (Table 1, entry 2).¶ Under similar conditions enyne substrates **3b**–**6b**, **6c**, **9** and **10** furnished dienes **13**–**19** in similarly excellent yields (Table 1, entries 3–9). The range of

functionalities and steric bulk tolerated by this reaction, combined with the high yields obtainable for these cyclisations, make this a valuable addition to the procedures currently available for synthesising such complex β-lactam structures. Further applications of alkene and enyne metathesis will be reported in due course.

**Table 1** Enyne metathesis using ruthenium carbene **1**[a]

| Entry | Enyne | Product | **1** (Mol%) | Yield[b] (%) |
|---|---|---|---|---|
| 1 |  **2b** |  **11** | 1 | 0 |
| | | | 10 | 0 |
| 2 |  **2c** |  **12** | 1 | 20 |
| | | | 5 | 52 |
| | | | 10 | 88 |
| 3 |  **3b** |  **13** | 10 | 82 |
| 4 |  **4b** |  **14** | 10 | 88 |
| 5 |  **5b** |  **15** | 10 | 70 |
| 6 |  **6b** |  **16** | 10 | 100 |
| 7 |  **6c** |  **17** | 15 | 72 |
| 8 |  **9** |  **18** | 5 | 48 |
| | | | 10 | 74 |
| 9 |  **10** |  **19** | 10 | 82 |

[a] All reactions carried out on *ca*. 0.25 mmol scale as a 0.1 M solution in $CH_2Cl_2$ with catalyst for 3 h. [b] Isolated yield after column chromatography.

We thank Glaxo Wellcome Research Ltd. for the most generous endowment (to A. G. M. B.) and for a CASE grant (to S. P. D. B.), the Wolfson Foundation for establishing the Wolfson Centre for Organic Chemistry in Medical Science at Imperial College, and the Engineering and Physical Sciences Research Council for studentships (to S. P. D. B. and K. F.).

## Footnotes

† E-mail: m.stow@ic.ac.uk
‡ E-mail: v.gibson@ic.ac.uk
§ All new compounds were fully characterised by spectroscopic data, microanalysis and/or HRMS.
¶ Typical experimental procedure: to enyne **2c** (50 mg, 0.30 mmol) was added a solution of catalyst **1** (21 mg, 0.03 mmol) in $CH_2Cl_2$ (3 ml). The solution was heated to reflux for 3 h, concentrated and chromatographed on silica (4 : 1 diethyl ether–hexane) to produce carbacephem **12** (44 mg, 88%) as a colourless oil.

## References

1 P. Schwab, M. B. France, J. W. Ziller and R. H. Grubbs, *Angew. Chem., Int. Ed. Engl.*, 1995, **34**, 2039.
2 R. R. Schrock, J. S. Murdzek, G. C. Bazan, J. Robbins, M. DiMare and M. O'Regan, *J. Am. Chem. Soc.*, 1990, **112**, 3875.
3 For a recent review, see R. H. Grubbs, S. J. Miller and G. C. Fu, *Acc. Chem. Res.*, 1995, **28**, 446.
4 For example, see D. Schinzer, A. Limberg, A. Bauer, O. M. Böhm and M. Cordes, *Angew. Chem., Int. Ed. Engl.*, 1997, **36**, 523; Z. Yang, Y. He, D. Vourloumis, H. Vallberg and K. C. Nicolaou, *Angew. Chem., Int. Ed. Engl.*, 1997, **36**, 166; R. E. Taylor and J. D. Haley, *Tetrahedron Lett.*, 1997, **38**, 2061; F. P. J. T. Rutjes and H. E. Shoemaker, *Tetrahedron Lett.*, 1997, **38**, 677; J. S. Clark and J. G. Kettle, *Tetrahedron Lett.*, 1997, **38**, 123; A. Fürstner and K. Langemann, *J. Org. Chem.*, 1996, **61**, 8746; P. Bertinato, E. J. Sorensen, D. Meng and S. J. Danishefsky, *J. Org. Chem.*, 1996, **61**, 8000; A. G. M. Barrett, J. C. Beall, V. C. Gibson, M. R. Giles and G. L. P. Walker, *Chem. Commun.*, 1996, 2229; H. S. Overkleeft and U. K. Pandit, *Tetrahedron Lett.*, 1996, **37**, 547.
5 A. Kinoshita and M. Mori, *J. Org. Chem.*, 1996, **61**, 8356; A. Kinoshita and M. Mori, *Synlett*, 1994, 1020.
6 A. G. M. Barrett, S. P. D. Baugh, V. C. Gibson, M. R. Giles, E. L. Marshall and P. A. Procopiou, *Chem. Commun.*, 1996, 2231.
7 A. G. M. Barrett, S. P. D. Baugh, V. C. Gibson, M. R. Giles, E. L. Marshall and P. A. Procopiou, *Chem. Commun.*, 1997, 155.
8 For the preparation of **3a**, see J. H. Bateson, A. J. G. Baxter, P. M. Roberts, T. C. Smale and R. Southgate, *J. Chem. Soc., Perkin Trans. 1*, 1981, 3242.
9 A. Basak and U. Khamrai, *Synth. Commun.*, 1994, **24**, 131.

*Received in Cambridge, UK, 30th April 1997; 7/02952G*

# (BEDT-TTF)($F_1$TCNQ) and (BEDT-TTF)($F_2$TCNQ)$_x$(TCNQ)$_{1-x}$ (*x ca.* 0.5): all-organic metals down to 2 K

**T. Hasegawa,[a] K. Inukai,[a] S. Kagoshima,[a] T. Sugawara,[a] T. Mochida,[b] S. Sugiura[c] and Y. Iwasa[c]**

[a] *Department of Pure and Applied Sciences, The University of Tokyo, Komaba, Meguro, Tokyo 153, Japan*
[b] *Institute for Molecular Sciences, Myodaiji, Okazaki 444, Japan*
[c] *Japan Advanced Institute of Science and Technology, Tatsunokuchi, Ishikawa 923-12, Japan*

**Crystal structures and solid-state properties are reported for all-organic metals, (ET)(F1) and (ET)(F2)$_x$(TCNQ)$_{1-x}$ (*x ca.* 0.5), which are isostructural with each other and preserve metallic states down to 2 K.**

Cation-radical salts derived from the organic donor, bis(ethylenedithio)tetrathiafulvalene (BEDT-TTF or ET), have attracted considerable interest because of the rich variations of the crystal structures and the two-dimensionality of their electronic structures, affording various solid-state properties such as superconductivity,[1] fermiology,[2] *etc.* In contrast to most ET salts, represented as (ET)$_2$X (X = inorganic counter anion), investigated so far, the advantage of the title materials, which are ET-based donor–acceptor (DA) type charge-transfer (CT) complexes, is that the organic acceptor molecules can be designed by chemical modification to have variable electron affinity or molecular polarizability, which may enable control of the crystal structures and electronic properties.

TCNQ and its fluorinated derivatives, 2-fluorotetracyanoquinodimethane ($F_1$TCNQ, abbreviated F1) and 2,5-difluorotetracyanoquinodimethane ($F_2$TCNQ, F2), are chosen for this purpose. Among these CT complexes, the structure and properties of (ET)(TCNQ) have been investigated, and the strong electron–electron correlations are found to be responsible for its metal–insulator transition at *ca.* $T$ = 330 K.[3,4] To investigate the fluorine-substitution effect on (ET)(TCNQ), the following two types of single crystals for the DA complexes have been synthesized; the CT compounds (ET)($F_n$TCNQ) ($n$ = 0, 1, 2) and the ternary CT compounds (ET)($F_n$TCNQ)$_x$(TCNQ)$_{1-x}$ ($0 < x < 1$). It is noted that the electron affinity of $F_n$TCNQ can be controlled by the number ($n$), without changing the molecular volume significantly.[5]

$F_1$TCNQ and $F_2$TCNQ were synthesized using a new route reported by Uno *et al.*[6] Single crystals of (ET)($F_n$TCNQ) ($n$ = 0, 1, 2) were obtained by slow cooling of concentrated solutions of the salts in chlorobenzene or 1,1,2-trichloroethane. Among (ET)($F_n$TCNQ) ($n$ = 0, 1, 2), a low electrical resistivity was observed in (ET)(F1), of the order of $10^{-2}$ Ω cm at room temp. Conversely, the resistivity of a single crystal of (ET)(F2) is extremely high, *ca.* $10^5$ Ω cm. Such dependence of the resisitivty on $n$ is not directly associated with change of the electron affinity of $F_n$TCNQ,[7] but is attributed to the drastic variation of their crystal structures.

Fig. 1 shows the crystal structure of (ET)(F1)† from which it is seen that the donors and acceptors form sheets independently along the 010 plane. The ET molecules are stacked face-to-face along the *c*-axis, and arranged side-by-side along the [100] and the [101] directions [Fig. 1(*b*)]. The intermolecular S···S distance is found to be 3.48 Å between ETs aligned along [101] and 3.71 Å along [100], indicating the two-dimensional nature of the conducting sheet. Molecular packing of ETs is uniform in the sheets, which is in contrast to most other ET-based conductors. In (ET)(TCNQ), for example, ET molecules are dimerized in their two-dimensional donor sheets.[3]

The effect of fluorine substitution becomes more apparent in (ET)(F2)$_x$(TCNQ)$_{1-x}$ ($0 < x < 1$). The electrical resistivity of the compaction sample becomes lowest (*ca.* $10^{-2}$ Ω cm) at *x ca.* 0.5 being 50 times smaller than that of (ET)(TCNQ), and *ca.* $10^5$ times smaller than that of (ET)(F2), as seen in the inset of Fig. 3.

X-Ray powder diffraction patterns were measured to investigate the crystal structures of (ET)(F2)$_x$(TCNQ)$_{1-x}$. The samples used for the measurements were obtained by evaporating the solvent from the whole concentration solution, ensuring that the nominal ratio of the ingredients in solution is identical to the chemical composition of the sample.‡ The results are presented in Fig. 2 for (ET)(F2)$_x$(TCNQ)$_{1-x}$ **2′** at *x ca.* 0.5, together with those of (ET)(F2) **1**, (ET)(F1) **2** and (ET)(TCNQ) **3**. The structures of **1**, **2** and **3** are clearly different from each other. In the ternary system, on the other hand, the highest conductive compound, (ET)(F2)$_x$(TCNQ)$_{1-x}$ **2′** (*x ca.* 0.5), is considered to be isostructural with **2**.§ This means that the introduction of a fluorine into each TCNQ, on the average, commonly gives isostructural compounds. The diffractograms for the samples at *x ca.* 0.25 and 0.75 clearly show that they are composed of two phases, *e.g.* **1** + **2′**.

Fig. 3 shows the temperature dependence of the electrical resistivity of single crystals of (ET)(F1) and of the crystalline flake samples of (ET)(F2)$_x$(TCNQ)$_{1-x}$ (*x ca.* 0.5), obtained by slow cooling of concentrated solutions. Metallic properties are preserved down to 2 K. $R$(room temp.)/$R$(4.2 K) is *ca.* 70 and 30 for (ET)(F1) and (ET)(F2)$_x$(TCNQ)$_{1-x}$ (*x ca.* 0.5), respectively, providing unambiguous evidence for good metallic character down to 4.2 K.

Finally we speculate as to why the introduction of a fluorine into TCNQ commonly stabilizes the structure of a highly conducting phase. Although the orientation of $F_1$TCNQ is

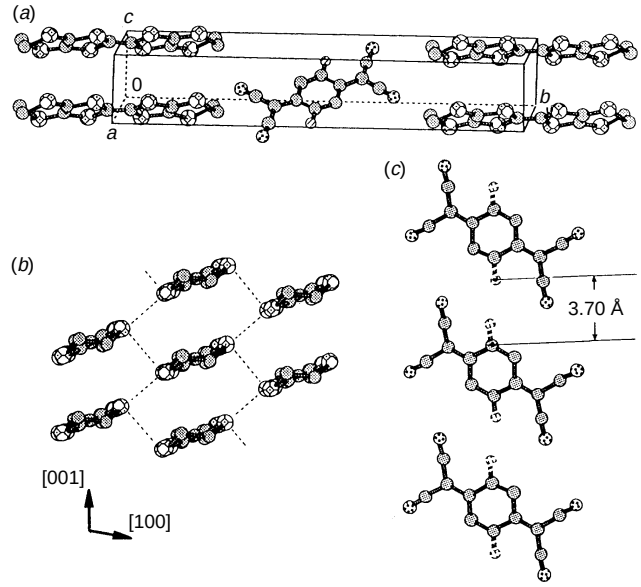



**Fig. 1** (*a*) Crystal structure of (ET)(F1); (*b*) view of molecular packing of ETs along the long molecular axis; (*c*) molecular arrangement of F1

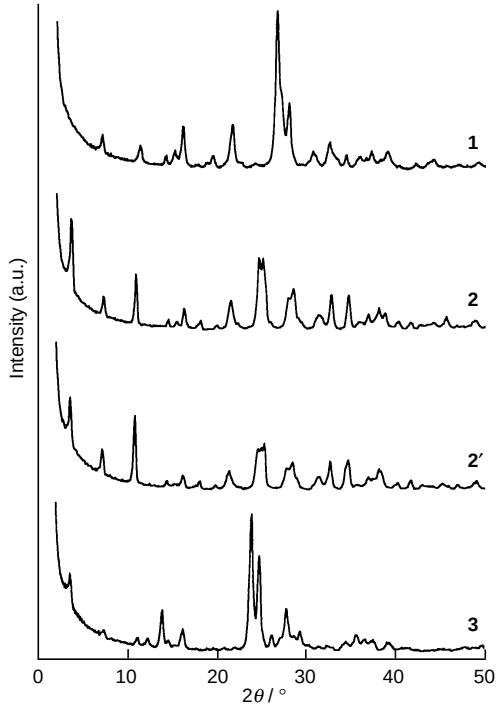



**Fig. 2** X-Ray powder diffraction pattern of (ET)(F2)$_x$(TCNQ)$_{1-x}$ **2′** (*x ca.* 0.5) in comparison with those of (ET)(F$_n$TCNQ) (*n* = 0, 1, 2). (ET)(F2) **1**, (ET)(F1) **2** and (ET)(TCNQ) **3**. The structure of (ET)(F2)$_x$(TCNQ)$_{1-x}$ **2′** (*x ca.* 0.5) is similar to that of (ET)(F1) **2**.

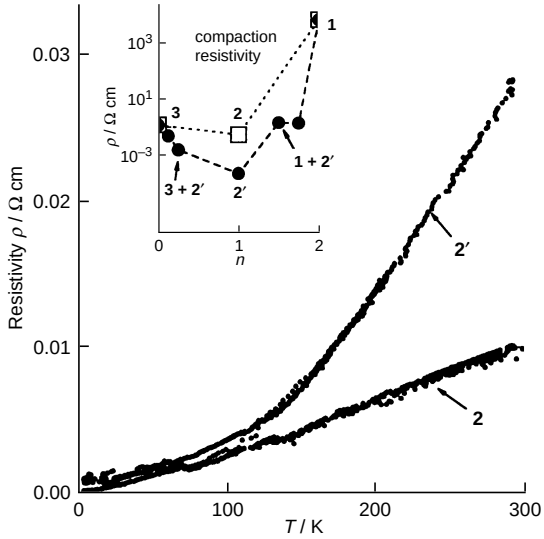



**Fig. 3** Temperature dependence of electrical resistivity for an (ET)(F1) single crystal and (ET)(F2)$_x$(TCNQ)$_{1-x}$ (*x ca.* 0.5) crystalline flake sample. Inset shows compaction electrical resistivity *vs.* average number (*n*) of F atoms per TCNQ. Open squares are for (Et)(F$_n$TCNQ) (*n* = 0, 1, 2) and filled squares for (ET)(F2)$_x$(TCNQ)$_{1-x}$.

disordered in (ET)(F1), the intermolecular F···C distance of 3.70 Å [Fig. 1(*c*)], which is shorter than the sum of the van der Waals radii of the F···H–C arrangement,[8] strongly suggests the presence of a local structure represented as ···(TCNQ)F···(TCNQ)F···(TCNQ)F···, based on the hydrogen-bond-like interaction between CH and F. A similar local structure is also expected in (ET)(F2)$_x$(TCNQ)$_{1-x}$ to form a ···F(TCNQ)F···(TCNQ)···F(TCNQ)F···(TCNQ)··· arrangement, which accounts for the exclusive formation of the (ET)(F1) structure when one fluorine is introduced per TCNQ (at *x ca.* 0.5).

In summary, we obtained two kinds of ET-based all-organic metals, (ET)(F1) and (ET)(F2)$_x$(TCNQ)$_{1-x}$ (*x ca.* 0.5), preserving metallic states down to 2 K. Between them, (ET)(F2)$_x$(TCNQ)$_{1-x}$ (*x ca.* 0.5) is an all-organic ternary metal and is isostructural with (ET)(F1), in both of which the specific hydrogen-bond-like interaction is suggested to stabilize the structures affording highly conductive compounds.

The authors are grateful to N. Itoh and A. Sasaki for their experimental assistance. This work is supported by a Grant-in-Aid for Scientific Research on Priority Area from the Ministry of Education, Science and Culture of Japan.

## Footnotes

* E-mail: chasega@komaba.ecc.u-tokyo.ac.jp

† *Crystal data* for (ET)(F1): triclinic, space group $P\bar{1}$, $a$ = 5.893(2), $b$ = 24.866(8), $c$ = 4.237(2) Å, α = 90.53(2), $\beta$ = 98.35(2), $\gamma$ = 97.14(1), $Z$ = 1, $U$ = 609.53 Å$^3$, $T$ = 300 K. The structure was solved by direct methods (SHELXS86; G. M. Sheldrick, in *Crystallographic Computing 3*) and refined using 1531 reflections. The final $R$ value was 0.08. Atomic coordinates, bond lengths and angles, and thermal parameters have been deposited at the Cambridge Crystallographic Data Centre (CCDC). See Information for Authors, Issue No. 1. Any request to the CCDC for this material should quote the full literature citation and the reference number 182/485.

‡ The results of elemental analysis (mass ratio) at the nominal ratio of $x$ = 0.5 is C, 43.24; H, 1.94; N, 9.20; S, 42.42; F, 3.31% which corresponds to the nominal composition C, 43.54; H, 1.827; N, 9.23; S, 42.27; F, 3.13%. The observed difference may be due to some impurities such as decomposed material as well as small amounts of (ET)(F2) crystals.

§ All the peaks are indexed in terms of a single phase with triclinic cell parameters obtained from powder diffraction, assuming the space group $P\bar{1}$, (300 K): $a$ = 5.884, $b$ = 24.841, $c$ = 4.246 Å, $\alpha$ = 92.94, $\beta$ = 97.87, $\gamma$ = 96.96°, $U$ = 603.63 Å$^3$.

## References

1 See for example: J. M. Williams, *et al.*, *Science*, 1991, **252**, 1501.
2 See for example: *Organic Conductors*, ed. J. P. Farges, Marcel Dekker, New York, 1994.
3 T. Mori and H. Inokuchi, *Solid State Commun.*, 1986, **59**, 355.
4 Y. Iwasa, *et al.*, *Phys. Rev. B*, 1994, **49**, 3580.
5 J. P. Ferraris and G. Saito, *J. Chem. Soc., Chem. Commun.*, 1978, 993; G. Saito and J. P. Ferraris, *J. Chem. Soc., Chem. Commun.*, 1979, 1027.
6 K. Uno, *et al.*, *Tetrahedron Lett.*, 1985, **26**, 1553.
7 G. Saito and J. P. Ferraris, *Bull. Chem. Soc. Jpn.*, 1980, **53**, 2141.
8 A. J. Bondi, *Phys. Chem.*, 1964, **68**, 441.

*Received in Cambridge, UK, 11th February 1997; 7/00994A*

# Configurationally guided peptide conformational motifs: crystal structure of a $L^{\alpha}D^{\beta}L^{\beta}D^{\alpha}D^{\beta}L^{\alpha}$ type hexapeptide fold

**F. Fabiola,[a] V. Pattabhi,[a] S. Rawale,[b] E. B. Raju[b] and S. Durani*[b]**

[a] *Department of Crystallography and Biophysics, University of Madras, India*
[b] *Department of Chemistry and Biotechnology Center, I.I.T., Bombay, India*

**A new concept in macromolecular design is described, using sequence configuration as the tool to control the topology of a compact polymer chain fold.**

Residue configuration as a sequence variable provides a promising tool for the design of novel peptide conformational motifs. Illustrating the concept, we describe here a configurationally guided $L^{\alpha}D^{\beta}L^{\beta}D^{\alpha}D^{\beta}L^{\alpha}$ type peptide conformational motif. Residue preferences in the Ramachandran diagram[1] remain fundamental to the stereochemical outcome of peptide chain folding. Genetically encodable poly-L-configurational peptides are required in forming the familiar α-helix and β-sheet motifs,[2] because every residue needs to occur in the same left half of the Ramachandran diagram. The alternating L,D-configurational gramicidin A forms β-helical channel or β-double helical pore motifs,[3,4] while the alternating L,D-configurational cyclic peptides of Ghadiri and co-workers are self-organizing nanotubular structures,[5] because consecutive residues occur in the opposite halves of the Ramachandran diagram [see Fig. 1(*a*)]. The type II and type II' β-hairpins, being $L^{\beta}L^{\beta}D^{\alpha}L^{\beta}$ and $L^{\beta}D^{\beta}L^{\alpha}L^{\beta}$ type motifs based on the positional preferences for L- or D-configurational residues and their conformational states,[6] are most reliably approached by using sequence configuration as the design strategy.[7–9] Control of peptide chain folding *via* sequence configuration is thus a promising tool to achieve the design of unnatural peptide conformational motifs.

The L- and D-configurational residues in the hexapeptide Boc-L-Leu[1]-D-Val[2]-L-Pro[3]-D-Asp[4](OMe)-D-Val[5]-L-Leu[6]-NHMe† are noted to occur in the preferred halves of the Ramachandran diagram [Fig. 1(*b*)]. The configurational sequence LDLDDL combines with the conformational sequence αββαβα to produce the $L^{\alpha}D^{\beta}L^{\beta}D^{\alpha}D^{\beta}L^{\alpha}$ type motif, which has a compact backbone fold and a specific pattern of interpeptide hydrogen bonds‡ (Fig. 2). In its architectural plan, the motif may either be recognized as a consecutive type II-II' β-turn anchoring an unusual $L^{\alpha}D^{\beta}$ type dipeptide fold, or as a type II' β-hairpin with D configurational arms bracketed by L configurational residues in α type conformational states. An almost ideal type II' β-turn has Val[5]-Leu[6] as its corner residues ($\phi$ = 72, $\psi$ = −117° for D-Val[5] against the ideal values 60 and −120°, and −81 and −14° for L-Leu[6] against the ideal values −90 and 0°) and the $i + 3 \rightarrow i$ type hydrogen bond between the methylamide NH and the Asp[4] CO. An almost ideal type II β-turn has Pro[3]-Asp[4] as its corner residues ($\phi$ = −64, $\psi$ = 129° for L-Pro[3] against the required −60 and 120 , and 72 and 19° for D-Asp[4] against the requirement 90 and 0°) and the $i + 3 \rightarrow i$ type hydrogen bond between the Val[2] CO and the Val[5] NH. The D-configurational valines in the first and fourth position of this β-turn element are in the β region of the right half of the Ramachandran diagram ($\phi$ = 126, $\psi$ = −92° for Val[2] and 72 and −117° for Val[5]) and with an additional hydrogen bond between the Val[2] NH and the Val[5] CO. The segment Val-Pro-Asp(OMe)-Val is thus a $D^{\beta}L^{\beta}D^{\alpha}D^{\beta}$ type β-hairpin, being an enantiomer of the naturally occurring $L^{\beta}D^{\beta}L^{\alpha}L^{\beta}$ type hairpin with a type II' β-turn and L-configurational arms and a diastereoisomer of another naturally occurring but stereochemically less preferred $L^{\beta}L^{\beta}D^{\alpha}L^{\beta}$ type hairpin with a type II β-turn and L-configurational arms.[10] Leu[1] at the N-terminal end has α-helical type torsional angles ($\phi$ = −66, $\psi$ = −45° against the ideal values −57 and −48°) and has its NH hydrogen bonded to the Val[5] CO, which also participates in a bifurcated hydrogen bond with the Val[2] NH.

The Val[2] and Val[5] side chains are in a stack-like arrangement, while the Leu[6] side chain and Boc group are in a parallel arrangement, together describing a molecular cleft which accommodates the side chain of an Asp[4](OMe) from another molecule, providing for intermolecular packing. The masking of the Asp carboxylate and consequent suppression of its

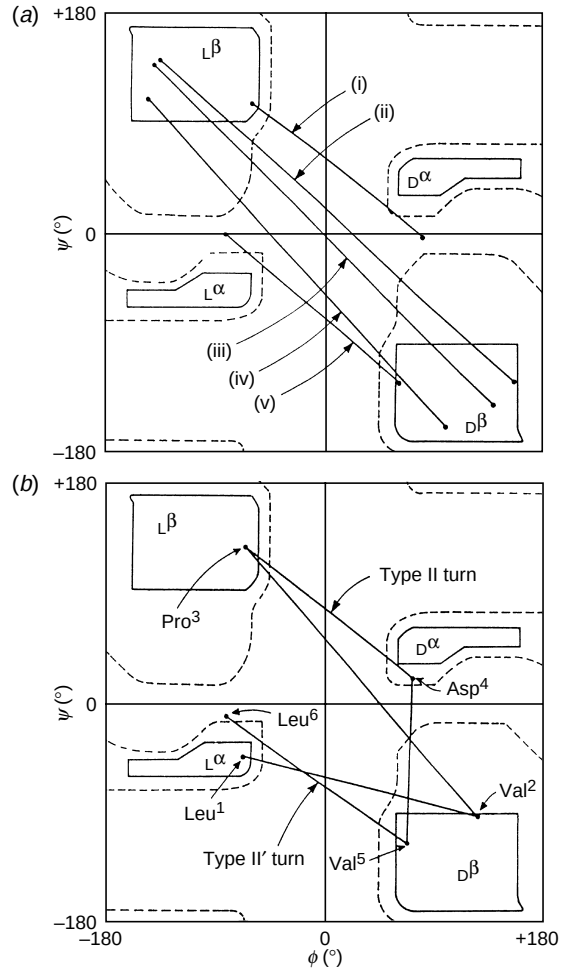



**Fig. 1** The regions in the Ramachandran diagram favoured for L- and D-configurational residues. (*a*) The requirement of $\phi$ and $\psi$ angles for (i) type II β-turn, (ii) gramicidin β-double helical pore, (iii) Ghadiri's octapeptide nanotubular structure, (iv) gramicidin β-helical channel and (v) type II' β-turn. (*b*) The $\phi$ and $\psi$ angles in the hexapeptide Boc-L-Leu-D-Val-L-Pro-D-Asp(OMe)-D-Val-L-Leu-NHMe.

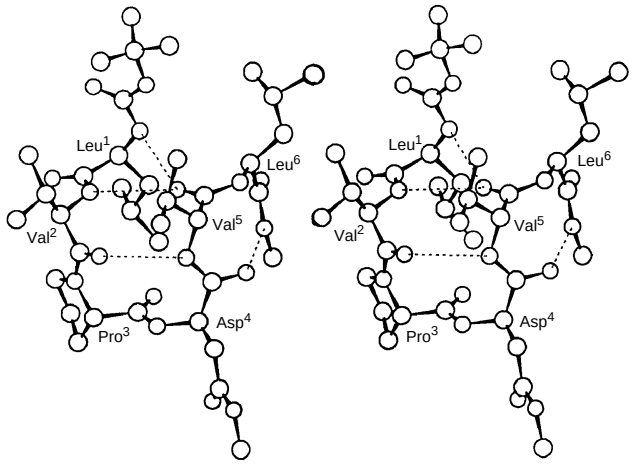



**Fig. 2** Stereodiagram of the molecular structure of the hexapeptide Boc-L-Leu-D-Val-L-Pro-D-Asp(OMe)-D-Val-L-Leu-NHMe

tendency to hydrogen bond with a main chain NH is apparently a factor in the extended conformation of the Asp side chain and in its participation in this specific intermolecular packing arrangement. Intermolecular packing also features hydrogen bonds involving the Leu[6] NH and the CO group of Boc moiety from one molecule and, respectively, the Leu[1] CO and Asp[4] NH groups from two different molecules.

A most remarkable feature of the $L^{\alpha}D^{\beta}L^{\beta}D^{\alpha}D^{\beta}L^{\alpha}$ type motif is that its α-helix-favouring leucines occur in the $\alpha$ conformational region and its β-sheet-favouring valines occur in the β conformational region, while its turn-favouring Pro and Asp moieties occur in a β-turn element.[11] Thus the effects of structural origin, manifested in protein folding, are possibly operative over and above the effects of configurational origin, and will require consideration as part of the overall design strategy for the approach to other possible configurationally-guided peptide conformational motifs.

The project funding was from Department of Science and Technology, and Department of Atomic Energy, Government of India.

## Footnotes

* E-mail: sdurani@biotec.btc.iitb.ernet.in

† The peptide synthesis was by solution phase methodology, the purification was by RP-HPLC on a C-18 column eluting with water–MeOH, and characterization was by NMR and mass spectrometry.

‡ Colourless rectangular crystals (0.75 × 0.15 × 0.2 mm) obtained from aq. MeOH were used for intensity data collection on an Enarf-Nonius CAD4 diffractometer with Cu-Kα ($\lambda$ = 1.5418 Å) radiation. The crystals were monoclinic, space group $P2_1$, with cell parameters $a$ = 10.059(1), $b$ = 18.864(2), $c$ = 12.586(1) Å; $\beta$ = 91.62(5)°, $V$ = 2383.9 Å, $Z$ = 2, and diffracted up to 63°. The structure was solved using SHELXS-86 (ref. 12) and refined using SHELXS-93 (ref. 13). Hydrogens were refined as riding over the heavier atoms. The final $R$-factor was 0.046 ($wR$ = 0.1254) for 3415 observed reflections with $F_o \geqslant 4\sigma(F_o)$. CCDC 182/504.

## References

1 G. N. Ramachandran, C. Ramakrishnan and V. Sasiekaran, *J. Mol. Biol.*, 1963, **7**, 95.
2 L. Pauling and R. B. Corey, *Proc. Natl. Acad. Sci. USA*, 1953, **39**, 247; L. Pauling, R. B. Corey and H. R. Barnson, *Proc. Natl. Acad. Sci. USA*, 1951, **37**, 205.
3 B. A. Wallace and K. Ravikumar, *Science*, 1988, **241**, 182; B. A. Wallace, *Annu. Rev. Biophys. Biophys. Chem.*, 1990, **19**, 127.
4 D. A. Langes, *Science*, 1988, **241**, 188.
5 J. D. Harterink, J. R. Granja, R. A. Milligen and M. R. Ghadiri, *J. Am. Chem. Soc.*, 1996, **118**, 43; N. Khazanovich, J. R. Granja, D. E. McRee, R. A. Milligen and M. R. Ghadiri, *J. Am. Chem. Soc.*, 1994, **116**, 6011; M. R. Ghadiri, J. R. Granja, R. A. Milligen, D. E. McRee and N. Khazanovich, *Nature*, 1993, **366**, 324.
6 G. D. Rose, L. M. Gierasch and J. A. Smith, *Adv. Protein. Chem.*, 1985, **37**, 1.
7 T. S. Haque, J. C. Little and S. H. Gelleman, *J. Am. Chem. Soc.*, 1996, **118**, 6975.
8 I. L. Karle, S. K. Awasti and P. Balaram, *Proc. Natl. Acad. Sci. USA*, 1996, **37**, 205.
9 M. D. Struthers, R. P. Cheng and B. Imperialli, *Science*, 1996, **217**, 342; B. Imperialli, S. L. Fisher, R. A. Moats and T. J. Prins, *J. Am. Chem. Soc.*, 1992, **114**, 3182.
10 D. J. Barlow and J. M. Thornton *J. Mol. Biol.*, 1988, **201**, 601.
11 P. Y. Chou and G. D. Fasman, *J. Mol. Biol.*, 1977, **115**, 135.
12 M. Sheldrick, SHELXS-86. Program for crystal structure determination, 1986, Inorganic Chemistry Institute, Gottingen University, Germany.
13 M. Sheldrick, SHELXS-93, Program for crystal structure determination, 1993, Inorganic Chemistry Institute, Gottingen University, Germany.

*Received in Cambridge, UK, 15th April 1997; 7/02562I*

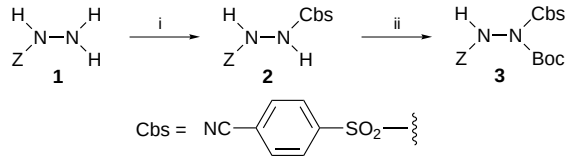
# Stepwise synthesis of tetrasubstituted hydrazines

**Leif Grehn,[a] Hans Lönn[b] and Ulf Ragnarsson*[a]**

[a] *Department of Biochemistry, University of Uppsala, Biomedical Center, Box 576, S-751 23 Uppsala, Sweden*
[b] *Astra Draco AB, Medicinal Chemistry, PO Box 34, S-221 00 Lund, Sweden*

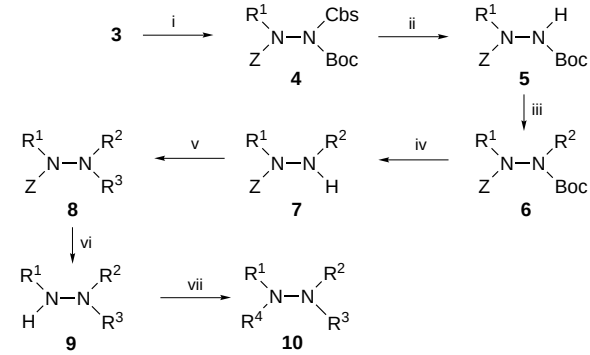
**A new triprotected hydrazine reagent has been made and applied in alkylation/acylation reactions for stepwise synthesis of tetrasubstituted derivatives in high purity and yield.**

In continuation of our efforts aiming at the simple synthesis of substituted hydrazines by a repetitive method,[1] we now present a first, easily made hydrazine derivative **3** with three *orthogonal* protecting groups. This reagent and products thereof allow alkylation and acylation and intermediate selective removal of protecting groups to take place under mild conditions and essentially quantitatively in all individual steps. Although, so far, our major efforts have been directed towards optimizing the overall reaction scheme with respect to the yield and purity of the intermediates **5**–**8** and products **10**, it is evident that this procedure affords simultaneously a high degree of molecular diversity.




**Scheme 1** *Reagents and conditions*: i, CbsCl, pyridine, 94%; ii, $Boc_2O$, DMAP, MeCN, 93%

The starting material for the key reagent **3** is Z-substituted hydrazine **1**, liberated from the corresponding hydrochloride.[2] Using commercially available 4-cyanobenzenesulfonyl (Cbs) chloride,[3] this is easily converted to **2** with two amide functions of obviously different acidity (Scheme 1),[4] which therefore allows regioselective reaction with $Boc_2O$ in the presence of DMAP at the sulfonamide nitrogen[5] to give the triprotected




**Scheme 2** *Reagents and conditions*: i, $R^1OH$, $PPh_3$, DEAD, THF, 80–99%; ii, Al(Hg), $CO_2$, aq. $Et_2O$, 92–99%; iii, $R^2X$ (X = Br or I), $K_2CO_3$–NaOH, $Bu_4NHSO_4$, $C_6H_6$, 92–100% or 2,4-$(O_2N)_2C_6H_3F$, $K_2CO_3$, $Bu_4NHSO_4$, MeCN, 85–97%; iv, TFA, $CH_2Cl_2$, 93–99%; v, $R^3Cl$, pyridine, 86–99%; vi, TFA (reflux); vii, $R^4{}_2O$ or 4-$FC_6H_4SO_2Cl$ (reflux), 72–98%

**Table 1** Synthesis of hydrazines **4**–**10**

| | $R^1$ | $R^2$ | $R^3$ | $R^4$ | Yield (%) | Mp/°C |
|---|---|---|---|---|---|---|
| **4a** | Bn | — | — | — | 98 | 105–105.5 |
| **4b** | 4-$ClC_6H_4CH_2$ | — | — | — | 99 | 93.5–94 |
| **4c** | 4-$MeOC_6H_4CH_2$ | — | — | — | 97 | 111–111.5 |
| **4d** | (*S*)-EtMeCHCH$_2$ | — | — | — | 80 | oil |
| **5a** | Bn | — | — | — | 92 | 65–65.5 |
| **5b** | 4-$ClC_6H_4CH_2$ | — | — | — | 99 | 89.5–90 |
| **5c** | 4-$MeOC_6H_4CH_2$ | — | — | — | 92 | 103.5–104 |
| **5d** | (*S*)-EtMeCHCH$_2$ | — | — | — | 94 | 80.5–81 |
| **6aa** | Bn | Me | — | — | 100 | oil |
| **6ab** | Bn | $CH_2CO_2Et$ | — | — | 97 | oil |
| **6ac** | Bn | 2,4-$(O_2N)_2C_6H_3$ | — | — | 95 | 129–130 |
| **6ba** | 4-$ClC_6H_4CH_2$ | Me | — | — | 99 | oil |
| **6bb** | 4-$ClC_6H_4CH_2$ | 2,4-$(O_2N)_2C_6H_3$ | — | — | 85 | 105–106 |
| **6ca** | 4-$MeOC_6H_4CH_2$ | $CH_2CO_2Et$ | — | — | 93 | oil |
| **6cb** | 4-$MeOC_6H_4CH_2$ | 2,4-$(O_2N)_2C_6H_3$ | — | — | 97 | 121.5–122 |
| **6cc** | 4-$MeOC_6H_4CH_2$ | Me | — | — | 99 | oil |
| **6d** | (*S*)-EtMeCHCH$_2$ | 4-$O_2NC_6H_4CH_2$ | — | — | 92 | oil |
| **7aa** | Bn | Me | — | — | 99 | oil |
| **7ab** | Bn | $CH_2CO_2Et$ | — | — | 93 | oil |
| **7b** | 4-$ClC_6H_4CH_2$ | Me | — | — | 99 | oil |
| **7d** | (*S*)-EtMeCHCH$_2$ | 4-$O_2NC_6H_4CH_2$ | — | — | 95 | oil |
| **8aa** | Bn | Me | 4-$FC_6H_4CO$ | — | 99 | 101.5–102.5 |
| **8ab** | Bn | $CH_2CO_2Et$ | Bu$^t$CO | — | 94 | oil |
| **8b** | 4-$ClC_6H_4CH_2$ | Me | Bz | — | 99 | 68–68.5 |
| **8d** | (*S*)-EtMeCHCH$_2$ | 4-$O_2NC_6H_4CH_2$ | $C_{10}H_7CO$ | — | 86 | foam |
| **10a** | Bn | Me | 4-$FC_6H_4CO$ | 4-$FC_6H_4SO_2$ | 72[a] | 113.5–114.5 |
| **10b** | 4-$ClC_6H_4CH_2$ | Me | Bz | Ac | 98[b] | 97–97.5 |
| **10d** | (*S*)-EtMeCHCH$_2$ | 4-$O_2NC_6H_4CH_2$ | $C_{10}H_7CO$ | $ClCH_2CO$ | 96[c] | 79–80 |

[a] From **8a**. [b] From **8b**. [c] From **8d**.

derivative **3** with three different protecting groups. The overall yield of **3** from **1** is 87%.†

Compound **3** easily undergoes the Mitsunobu reaction with alcohols,[6] thereby giving rise to triprotected monosubstituted hydrazines **4** (Scheme 2). From compounds of this type the Cbs group can be cleaved reductively with Hg-activated aluminium to provide crystalline intermediates **5**, which are alkylated as previously described[1] under phase transfer conditions to give 1,2-diprotected 1,2-disubstituted hydrazine intermediates **6**. These differ from those described earlier in one important respect, namely, that their Boc and Z groups can be removed selectively in optional order. So far, we prefer to remove the Boc group first under mild acidic conditions *via* compounds **7** and subsequently acylate the latter to **8**. Finally, these can be deprotected under stronger acidic or catalytic hydrogenolysis conditions to give substances **9**, although we normally prefer to acylate them without isolation directly to the final products **10**.

A relatively large number of compounds **4**–**10** have been prepared to investigate and exemplify this scheme, all of which are listed in Table 1. No indication whatsoever of incomplete selectivity in the removal of the protecting groups in intermediates **4** and **6** has been detected. Alkylations and acylations of **5**, **7** and **9** were performed as described previously.[1] As can be seen from the table, all steps proceed very satisfactorily and few intermediates are obtained in less than 90% yield.

Mono- and di-alkylated hydrazines are extensively used as precursors in the synthesis of heterocycles.[7] Recently, Han and Janda also applied this methodology in their synthesis of α-aza amino acids.[8] Highly substituted hydrazines have found a number of practical applications.[9]

Although not demonstrated experimentally here, several other reactions of the amino group in addition to alkylation and acylation can be envisaged to be useful in this context, but we have confined ourselves to exemplify a few additional functional groups which can be introduced easily using the present conditions. Considering the large number of alkylating and acylating agents available, it seems reasonable to assume that the new reagent can be used for construction of chemical libraries. Further modification of functional groups present in compounds such as **10** could additionally increase the potential for molecular diversity inherent in these, at first glance, simple compounds.

We thank the Swedish Natural Science Research Council, the National Board for Industrial and Technical Development and Astra Draco AB for generous financial support.

## Footnotes

* E-mail: urbki@bmc.uu.se

† *Selected data* for **3**: $^1$H NMR (400 MHz, $CDCl_3$, major conformer): δ 1.34 (s, 9 H, Boc), 5.18 and 5.24 (AB quartet, *J* 12.1 Hz, 2 H, $CH_2$), 7.14 (br s, 1 H, NH), 7.37 (perturbed signal, 5 H, Ph), 7.80 (d, *J* 8.3 Hz, 2 H, Cbs $H_{3,5}$), 8.24 (d, *J* 8.3 Hz, 2 H, Cbs $H_{2,6}$).

## References

1 U. Mäeorg, L. Grehn and U. Ragnarsson, *Angew. Chem.*, 1996, **108**, 2802; *Angew. Chem., Int. Ed. Engl.*, 1996, **35**, 2626.
2 E. Wünsch, *Chem. Ber.*, 1965, **98**, 797.
3 T. Hamada and O.Yonemitzu, *Synthesis*, 1986, 852.
4 I. Koppel, J. Koppel, F. Degerbeck, L. Grehn and U. Ragnarsson, *J. Org. Chem.*, 1991, **56**, 7172.
5 L. Grehn, K. Gunnarsson and U. Ragnarsson, *Acta Chem. Scand., Ser. B*, 1986, **40**, 745.
6 O. Mitsunobu, *Synthesis*, 1981, 1; D. L. Hughes, *Org. React.*, 1992, **42**, 335.
7 U. Jensen-Korte and N. Müller, *Methoden Org. Chem.* (*Houben-Weyl*), 4th edn. 1952–1990, vol. E16a, pp. 807–815; J. Elguero, in *Comprehensive Heterocyclic Chemistry*, ed. A. R. Katritzky, C. W. Rees and K. T. Potts, Pergamon, Oxford, 1984, vol. 5, pp. 291–301; J. B. Polya, *ibid.*, pp. 762–768.
8 H. Han and K. D.Janda, *J. Am. Chem. Soc.*, 1996, **118**, 2539.
9 A. R. Katritzky, J. Wu and S. V. Verin, *Synthesis*, 1995, 651.

*Received in Cambridge, UK, 2nd May 1997; 7/03008H*

# The photogeneration of aryltropylium ions: a potential photo-switch for supramolecular assemblies based on donor–acceptor interaction

**Uwe Pischel,[a] Werner Abraham,*[a] Wolfram Schnabel[b] and Uwe Müller[c]**

[a] *Humboldt-University, Institute of Chemistry, Hessische Str. 1-2, D-10115 Berlin, Germany*
[b] *Hahn-Meitner-Institut Berlin GmbH, Department of Physical Chemistry, Glienicker Str. 100, D-14109 Berlin, Germany*
[c] *Martin-Luther-University Halle, Institute of Organic Chemistry, Geusaer Str., D-06217 Merseburg, Germany*

**The photogeneration of aryltropylium cations with lifetimes strongly depending on the donor capacity of the aryl substituent has been achieved by photolysing the corresponding 7-methoxycycloheptatrienes 2, 3 and 4.**

Switchable supramolecular assemblies such as rotaxanes[1] and catenanes[2] comprise a fascinating challenge in the field of supramolecular chemistry.[3] We are designing macrocycles[4] and rotaxanes with arylcycloheptatriene building blocks which can easily be transformed to tropylium ions by thermal hydride transfer.[5] In contrast to cycloheptatyrienes, tropylium ions are strong electron-acceptors which can be used to recognize donor partners within rotaxanes or catenanes.

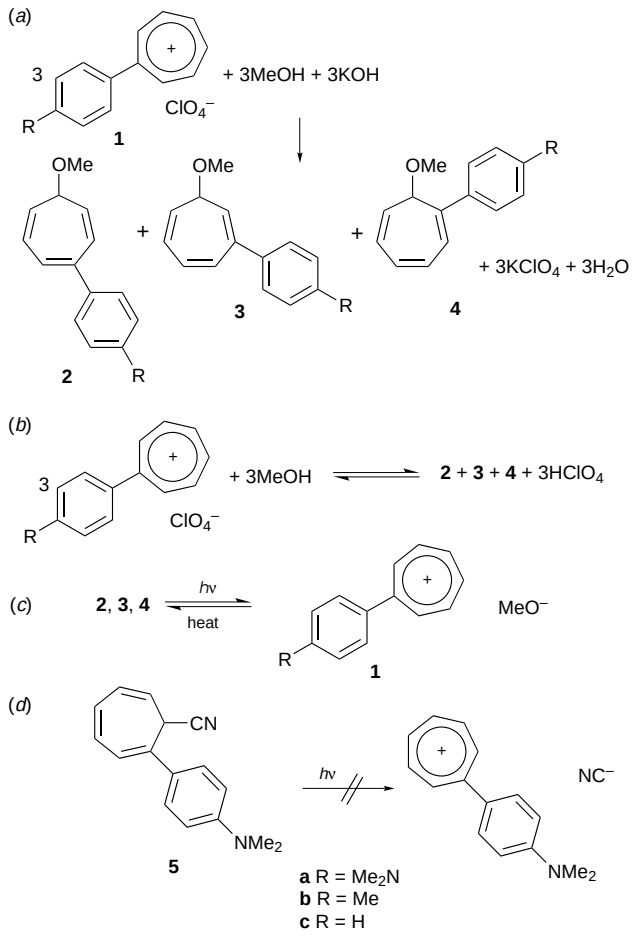
Here we report on the generation of tropylium ions by photochemical heterolytic cleavage of the C–O bond in cycloheptatriene derivatives **2**, **3** and **4**. Provided the cycloheptatriene is regenerated by the fast nucleophilic attack of the methoxy ion or methanol (see Scheme 1), the acceptor can be switched 'on' and 'off' by a photochemical and a thermal step, respectively.

So far the only known example is the dibenzosuberenyl cation, which can be obtained by laser flash photolysis of the parent alcohol in trifluoroethanol.[6] Our design of precursors of tropylium cations is based on cycloheptatriene derivatives containing effective leaving groups and substituents capable of stabilizing tropylium ions. Halides and azide are inappropriate leaving groups because cycloheptatriene derivatives containing these groups are converted into tropylium ions upon dissolution in polar solvents.[7] In the present work CN and MeO were chosen as leaving groups and aryl groups as stabilizing substituents. 7-Methoxy-*x*-aryl cycloheptatrienes ($x$ = 1, 2, 3) were prepared by the reaction of the corresponding aryltropylium ions with a base in methanol solution. Typically, the reaction of 4-dimethylaminophenyltropylium perchlorate **1a** with KOH results in the formation 3-(4-dimethylaminophenyl)-7-methoxycyclohepta-1,3,5-triene **2a** and the isomers **3a** and **4a** in the ratio **2a**:**3a**:**4a** = 1:1:0.7. Compound **2a** was isolated from the isomeric mixture, obtained by reaction of **1a**, by recrystallization from hexane at low temperature.

Three experiments were performed to study the photogeneration of aryltropylium ions with the aid of a ruby laser (Korad Model K1 QS2, $\lambda$ = 347 nm, flash duration 20 ns) or a flashed xenon lamp (band filter 1602 and 810, Jenaer Glaswerk Schott & Gen., nominal wavelength $\lambda_{ex}$ = 340–380 nm, flash duration 15 μs): (i) Compounds **2a** or **5** were irradiated in MeCN or MeOH solution. (ii) The mixture of isomers (**2**, **3** and **4**) obtained by the reaction of **1** with KOH in MeOH according to reaction (*a*) in Scheme 1 was irradiated *in situ*. (iii) A dilute solution of **1a** in MeOH ($2 \times 10^{-5}$ mol $l^{-1}$) was irradiated in the absence of a base. Under these conditions the equilibrium (*b*) in Scheme 1 is shifted almost completely to the right side, *i.e.* the solution contains the isomers **2a**, **3a** and **4a** apart from a very small amount of the tropylium ion.

Notably, apart from **5** all other cycloheptatriene derivatives yielded the tropylium ion upon UV irradiation. Obviously, CN is not as effective a leaving group as the methoxy group.

In the case of **2a** [experiment (i)] the photogeneration of **1a** according to reaction (*c*) in Scheme 1 was evidenced by the formation of the characteristic optical absorption of the tropylium ion ($\lambda_{max}$ = 570 nm) during the flash (see Fig. 1). Simultaneously with the transient absorption a photocurrent was formed indicating the generation of ionic species (**1a** and $MeO^-$). The quantum yield $\Phi$(ion) = 0.1 for the generation of **1a** in MeOH solution was determined† with the aid of the extinction coefficient of **1a** $\varepsilon_{567} = 4.7 \times 10^4$ l mol$^{-1}$ cm$^{-1}$. The transient absorption at $\lambda_{max} \approx 570$ nm increased linearly with the absorbed dose per flash, indicating that the heterolytic bond cleavage in **2a** is not due to a biphotonic effect but results from a one photon excitation. Noticeably, at constant absorbed dose, the transient absorption at $\lambda_{max} \approx 570$ nm is much weaker in MeCN than in MeOH indicating different ion yields in the two solvents. In this connection it is interesting to note that other carbenium ions were also found to be generated with higher yields in MeOH than in MeCN solution.[8]




**Scheme 1**

Irradiation of the isomers **2a**, **3a** and **4a** *in situ* [experiment (ii)] also resulted in the formation of the transient absorption spectrum of **1a**.

The tropylium ion generated as described above turned out to be unusually long-lived. Compound **1a**, generated by photoexcitation of **2a** in MeOH solution [experiment (i)] disappeared according to second order kinetics: $k_2 = 2 \times 10^6$ mol$^{-1}$ s$^{-1}$, corresponding to a first half-life of 0.3 s at [**1a**] = $1.7 \times 10^{-6}$ mol l$^{-1}$. Obviously, the rate of decay of **1a** is determined by the neutralization reaction, **1a** + MeO$^-$ in this case. In the case of experiment (iii) the disappearance followed exactly first order kinetics with a pseudo-first order rate constant: $k_1 = 0.3$ s$^{-1}$. In this case the rate of disappearance is determined by the reaction of **1a** with MeOH because methoxy anions produced in the primary photolytic act are scavenged by protons [see reaction (*b*) in Scheme 1]. With aid of $k_1 = 0.3$ s$^{-1}$, the bimolecular rate constant $k_2 = k_1$/[MeOH] = $1.2 \times 10^{-2}$ l mol$^{-1}$ s$^{-1}$ is obtained for the reaction **1a** + MeOH.

Compounds with substitutents **b** and **c** on the aryl group were examined *via* experiment (ii), *i.e.* **1b** and **1c** were converted into the corresponding isomer mixtures **2b**, **3b**, **4b** and **2c**, **3c**, **4c**, respectively, by reaction with KOH (1 equiv.) in MeOH, and the reaction mixtures were irradiated. The transient absorption spectra recorded in these cases posses maxima at the positions expected[5] for the tropylium ions **1b** and **1c** ($\lambda$ = 370 and 395 nm, respectively). The first-order lifetimes are definitely shorter than in the case of **1a**: $\tau$ = 270 μs (**1b**) and 190 μs (**1c**). The large differences in the lifetimes of **1a**, **1b** and **1c** are explained in terms of an increased stability of the tropylium ion with increasing electron-donor power of the substituent at the aryl group. This assumption is substantiated by the reduction potentials measured *vs.* SCE: −0.40 (**1a**), −0.19 (**1b**) and −0.17 V (**1c**).[9]

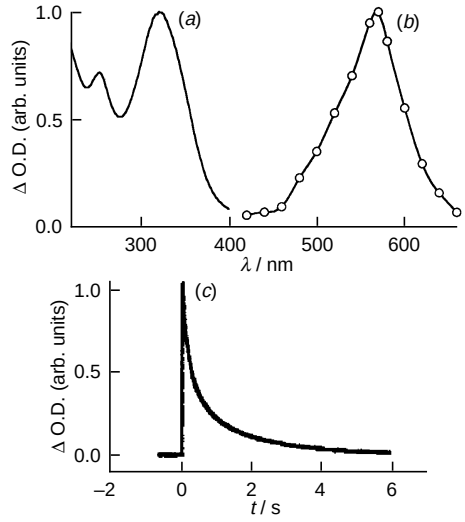



**Fig. 1** (*a*) Optical absorption spectrum of **2a** in MeOH; (*b*) transient absorption spectrum recorded 250 ms after irradiation of **2a** in MeOH with a 15 μs flash ($\lambda_{ex}$ = 340–380 nm); (*c*) decay of the transient absorption at 570 nm

In conclusion, the quantum yield of ion generation is large enough and the lifetime of photogenerated tropylium ions is long enough to allow intramolecular rearrangements in rotaxanes or catenanes containing arylcycloheptatriene building blocks. Concerning the applicability of such systems as photoswitches, system-optimizing appears necessary with respect to long-term performance. Regarding compound **2a**, the switch cycle can be repeated several times. However, irradiation of **2a** with 10 laser flashes ($5.7 \times 10^{-5}$ E l$^{-1}$ flash$^{-1}$, flash duration 20 ns) reduces the intensity of the transient optical absorption due to **1a** by a factor of 2.

## Footnotes

* E-mail: abraham@chemie.hu-berlin.de

† A benzophenone–naphthalene actinometer was used with $\varepsilon_{T-T} = 1.5 \times 10^{-4}$ l mol$^{-1}$ cm$^{-1}$ at $\lambda_{obs}$ = 425 nm.

## References

1 R. Ballardini, V. Balzani, M. T. Gandolfi, L. Prodi, M. Venturi, D. Philip, H. G. Ricketts and J. F. Stoddart, *Angew. Chem.*, 1993, **105**, 1362.
2 D. B. Amabilino, C. O. Dietrich-Buchecker, A. Livoreil, L. Perez-Garcia, J.-P. Sauvage and J. F. Stoddart, *J. Am. Chem. Soc.*, 1996, **118**, 3905.
3 D. Philip and J. F. Stoddart, *Angew. Chem.*, 1996, **108**, 1243.
4 V. Wendel and W. Abraham, *Tetrahedron Lett.*, 1997, **43**, 1177.
5 C. Jutz and F. Voithenleitner, *Chem. Ber.*, 1964, **94**, 29.
6 L. J. Johnston, J. Lobough and V. Wintgens, *J. Phys. Chem.*, 1989, **93**, 7370.
7 T. Asao and M. Oda, *Cycloheptatrienylium (Tropylium)-Salze*, in *Methoden der Organischen Chemie*, Georg Thieme Verlag, Stuttgart, New York, vol. V/2c, 1985, pp. 49–85.
8 R. A. McClelland, *Tetrahedron*, 1996, **52**, 6823.
9 B. Dreher, W. Abraham and F. Pragst, *J. Prakt, Chem.*, 1983, **325**, 104.

*Received in Cambridge, UK, 28th April 1997; 7/02892J*

# Diastereoselective intramolecular photochemical [2 + 2] cycloaddition reactions of tethered L-(+)-valinol derived tetrahydrophthalimides

**Kevin I. Booker-Milburn,* Sirin Gulten and Andrew Sharpe**

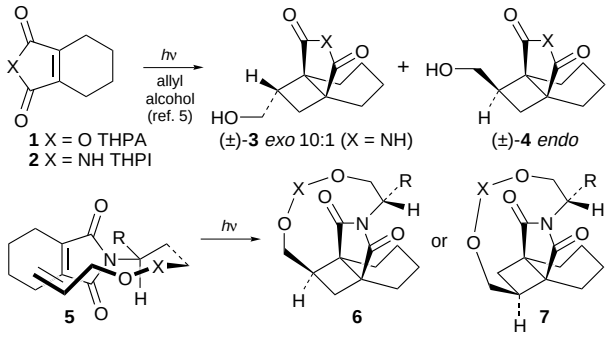
*School of Chemical Sciences, University of East Anglia, Norwich, Norfolk, England, UK NR4 7TJ*

**Intramolecular photochemical [2 + 2] cycloaddition of allyl alcohol linked to amino acid derived 3,4,5,6-tetrahydrophthalimides, either *via* a carbonate or silicon tether, gives the corresponding cyclobutanes in excellent yield with diastereoselectivities as high as 8 : 1.**

Asymmetric [2 + 2] photocycloaddition using chiral auxiliaries and chiral additives is far less developed than other areas of asymmetric synthesis. Although a number of systems have been studied,[1] there exist very few methods for the preparation of enantiomerically pure cyclobutanes compared to the corresponding thermal [4 + 2] and [3 + 2] cycloaddition reactions. Both Fleming[2] and Crimmins[3] have reported the use of silicon tethers in controlling regio- and stereo-selectivity in [2 + 2] photocycloadditions. Very recently Piva and Pete[4] reported some promising results using chiral hydroxy acids as spacers for controlling asymmetric intramolecular [2 + 2] photocycloadditions. We now disclose our own results in this area involving the diastereoselective intramolecular [2 + 2] cycloaddition reactions of alkenols tethered to L-(+)-valinol derived tetrahydrophthalimides.

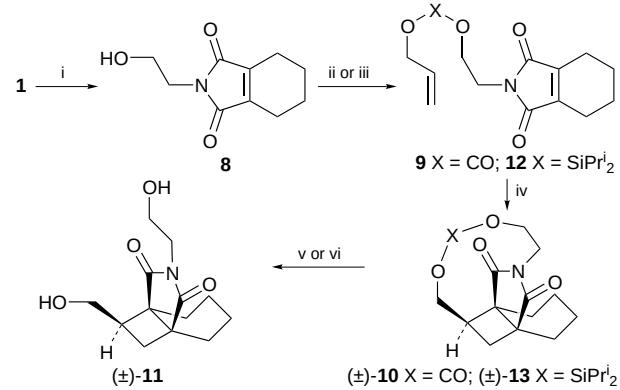
We recently reported[5] that 3,4,5,6-tetrahydrophthalic anhydride (THPA, **1**) and the corresponding imide (THPI, **2**) underwent efficient intermolecular photocycloaddition with alkenols to give the corresponding cyclobutanes in excellent yields with diastereoselectivities as high as 10 : 1. The major isomer in all cases was the *exo* isomer **3** which, due to the absence of any absolute stereochemical control, was formed as a racemic mixture (only one enantiomer drawn for clarity). We then elected to study the cycloaddition reactions of alkenols linked to THPI derivatives in order to achieve two goals: (i) the selective formation of the *endo* isomer **4** and (ii) by the use of chiral linkers, control the absolute stereochemistry of **4**. If the cycloadducts **6** or **7** could be formed selectively from **5** then cleavage of the tether (X) would lead to the synthesis of enantiopure *endo* cycloadducts (Scheme 1).

Initially we investigated the use of ethanolamine as a linker and found that heating THPA with ethanolamine in toluene gave the tetrahydrophthalimide derivative **8** in 96% yield. Reaction of **8** with allyl chloroformate gave the carbonate tethered tetrahydrophthalimide **9** in good yield (84%). Irradiation† of **9** in MeCN for just 90 min resulted in the exclusive formation of the (±)-*endo* cycloadduct **10** in excellent yield (95%, only one enantiomer drawn for clarity). Hydrolysis to the diol **11**, followed by NOE studies, confirmed the highly selective *endo* mode of cycloaddition obtained by use of a carbonate tether. Synthesis of the silicon tethered[2] variant **12** (X = $SiPr^i_2$) was achieved by treatment of **8** with 2 equiv. of $Cl_2SiPr^i_2$ followed by an excess of allyl alcohol (53% overall). Irradiation of **12** again gave the (±)-*endo* cycloadduct **13** as the sole product in 74% yield. Treatment of **13** with $Bu_4NF$ yielded the diol **11** in excellent yield (82%) (Scheme 2).



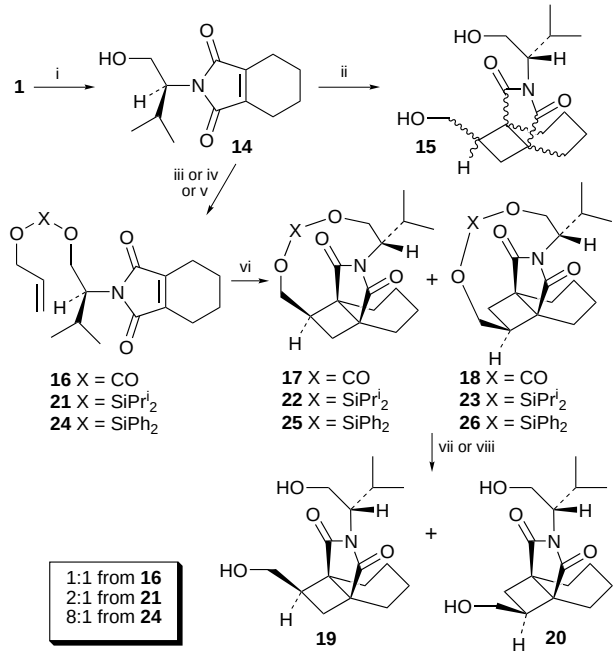

**Scheme 1**

With the *exo*/*endo* selectivity problem solved we then turned our attention to the use of tethered chiral ethanolamines to control the diastereoselectivity of the *endo* selective cycloadditions and ultimately the enantioselectivity upon removal of the chiral ethanolamine. Treatment of **1** with L-(+)-valinol gave the tetrahydrophthalimide **14** in excellent yield (95%). Irradiation of **14** with allyl alcohol gave rise to a complex mixture (75%) of four cycloadducts which by NMR spectroscopy appeared to be the various possible *exo* and *endo* diastereoisomers of **15**. This was not too surprising as it would be expected that there would be little stereochemical control exerted by the valinol unit during an intermolecular photocycloaddition. Reaction of **14** with allyl chloroformate as before gave the carbonate **16** in moderate yield (61%). Irradiation of **16** gave two cycloadducts (**17** and **18**) which upon hydrolysis (74%) were shown by $^1$H NMR spectroscopy to be an inseparable 1 : 1 mixture‡ of the diastereomeric diols **19** and **20**. Although this result was disappointing in terms of asymmetric induction, the overall yield in the photocycloaddition step was high (90%) and the irradiation times were short (60 min), thus indicating that the basic photocycloaddition was not hampered by the introduction of a chiral centre in the linker. Synthesis of the $SiPr^i_2$ tethered variant was carried out as before to give **21** in 71% yield. Irradiation (90 min) of **21** gave a mixture of the cycloadducts **22** and **23** (74%) which, upon treatment with $Bu_4NF$, gave the diols **19** and **20** as an inseparable mixture of diastereoisomers (87%) in a ratio of 2 : 1 although it was not possible to assign which was the major isomer. Encouraged by these results we decided

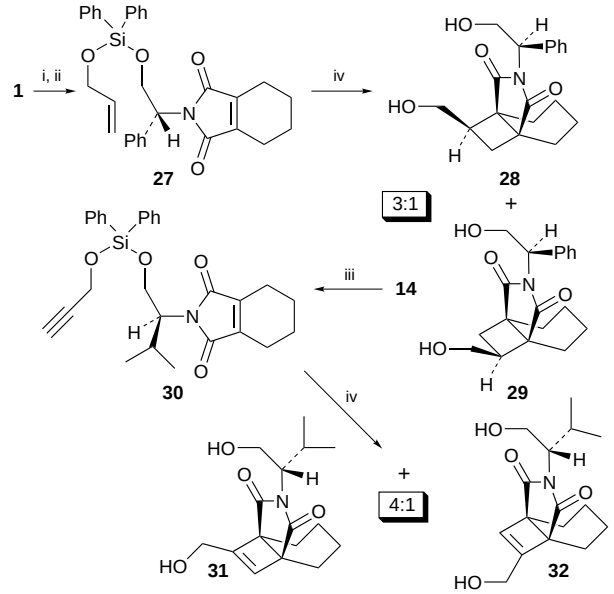



**Scheme 2** *Reagents and conditions*: i, ethanolamine, toluene, heat, 96%; ii, allyl chloroformate, pyridine, THF, 0 °C, 84% for **9**; iii, $Cl_2SiPr^i_2$ (2 equiv.), $Et_3N$, $CH_2Cl_2$, then allyl alcohol (4 equiv.), 53% for **12**; iv, *h*ν, MeCN, 95% for **10**, 74% for **13**; v, KOH (1.2 equiv.), EtOH–$H_2O$ (1 : 1), 64% from **10**; vi, $Bu_4NF$, THF, 82% from **13**

to try and increase the diastereoselectivity of the cycloaddition by changing the nature of the groups on silicon. Thus treatment of **14** with $Cl_2SiPh_2$ in DMF followed by treatment with an excess of allyl alcohol gave the $SiPh_2$ tethered variant **24** in 60% overall yield. Irradiation (60 min) of **24** gave an excellent yield (82%) of the two cycloadducts **25** and **26** which, upon treatment with $Bu_4NF$, gave the diastereomeric diols **19** and **20** in 97% yield and in a very pleasing ratio of 8 : 1. Again it was not possible to assign which was the major diastereoisomer, although it was the same as that obtained with the diisopropyl tether (Scheme 3).




**Scheme 3** *Reagents and conditions*: i, L-(+)-valinol, toluene, heat, 95%; ii, *h*ν, allyl alcohol, MeCN, 6 h, 75%; iii, allyl chloroformate, pyridine, THF, 3 h, 0 °C, 61% for **16**; iv, $Cl_2SiPr^i_2$, $Et_3N$, $CH_2Cl_2$, then allyl alcohol (4 equiv.), 71% for **21**; v, $Cl_2SiPh_2$ (2 equiv.), $Et_3N$, DMF, then allyl alcohol (4 equiv.), 60% for **24**; vi, *h*ν, MeCN, 60–90 min, 90% for **17**/**18**, 74% for **22**/**23**, 82% for **25**/**26**; vii, KOH (1.2 equiv.), EtOH–$H_2O$ (1 : 1), 74% from **17**/**18**; viii, $Bu_4NF$, THF, 87% from **22**/**23**, 97% from **25**/**26**




**Scheme 4** *Reagents and conditions*: i, (*R*)-(−)-2-phenylglycinol, toluene, heat, 97%; ii, $Cl_2SiPh_2$ (2 equiv.), $Et_3N$, MeCN, then allyl alcohol (4 equiv.), 46%; iii, $Cl_2SiPh_2$ (2 equiv.), $Et_3N$, MeCN, then prop-2-yn-1-ol (4 equiv.), 58%; iv, *h*ν, MeCN, 5–6 h, then $Bu_4NF$, THF, 83% overall for **28**/**29** and 38% overall for **31**/**32**

In order to study the effects of other chiral ethanolamines, **1** was treated with (*R*)-(−)-2-phenylglycinol to give the corresponding tetrahydrophthalimide (97%). Treatment of this with $Cl_2SiPh_2$ in DMF followed by an excess of allyl alcohol gave the $SiPh_2$ tethered phthalimide **27** in 46% overall yield. Irradiation gave a high yield of cycloaddition products (89%) which, upon cleavage with $Bu_4NF$ (93%), afforded the diastereoisomeric diols **28** and **29** in a ratio of 3 : 1. This clearly demonstrates that the valinol unit is superior to phenylglycinol in controlling diastereoselectivity during photocycloaddition. Finally, treatment of the valinol derivative **14** with $Cl_2SiPh_2$ followed by treatment with an excess of prop-2-ynyl alcohol gave the $SiPh_2$ tethered alkynol variant **30** in moderate overall yield (58%). Irradiation of **30** gave a 46% yield of the corresponding cyclobutenes which, upon desilylation with $Bu_4NF$ (81%), gave the diastereoisomeric diols **31** and **32** in a ratio of 4 : 1. Although the ratio was not as good as in the allyl alcohol case (**24**) this is, to the best of our knowledge, the first example of this type of diastereoselective cyclobutene formation (Scheme 4).

In summary, L-(+)-valinol derived tetrahydrophthalimides containing silicon tethered alkenol and alkynol units have been shown to undergo efficient, diastereoselective intramolecular [2 + 2] photocycloadditions. Present studies are concerned with the assignment of the absolute configuration of the major diastereoisomer from these cycloadditions in order gain some information about the transition state, and hopefully increase the diastereoselectivity by investigating different reaction conditions. We are also investigating the efficient hydrolytic removal of the valinol linker so that ultimately it can be used as a true chiral auxiliary in the enantioselective, photochemical synthesis of highly substituted cyclo-butanes and -butenes.

We would like to thank the Canakkale Onsekiz Mart University, Turkey (S. G.) and the EPSRC (GR/K15985) (A. S.) for financial support of this work.

## Footnotes

* E-mail: k.booker-milburn@uea.ac.uk

† Glassware consisted of a standard, water cooled, pyrex immersion well photochemical apparatus of 100 ml reaction volume. All reactions were carried out in dry, degassed MeCN (100 ml) with concentrations of between 0.01–0.036 M in substrate. Irradiations were performed using a 125 W medium-pressure mercury vapour lamp obtained from Osram HQL (MBF-U) bulbs. All new compounds were fully characterised by IR, $^1$H NMR and $^{13}$C NMR spectroscopy, and either elemental analysis or HRMS.

‡ The diastereoisomeric ratio was readily ascertained by $^1$H NMR spectroscopy from comparison of the integrals of the two pairs of diastereotopic Me groups present in the various mixtures of **19** and **20**.

## References

1 B. S. Green, Y. Rabinsohn and M. Rejtö, *Carbohydr. Res.*, 1975, **45**, 115; B. S. Green, A. T. Hagler, Y. Rabinsohn and M. Rejtö, *Isr. J. Chem.*, 1976/77, **15**, 124; G. L. Lange, C. Decicco and M. Lee, *Tetrahedron Lett.*, 1987, **28**, 2833; A. I. Meyers and S. A. Fleming, *J. Am. Chem. Soc.*, 1986, **108**, 306; H. Herzog, H. D. Koch, H. D. Scharf and J. Runsink, *Tetrahedron*, 1986, **42**, 3547; M. Demuth, A. Palomer, H. D. Sluma, A. K. Dey, C. Kruger and Y. H. Tsay, *Angew. Chem., Int. Ed. Engl.*, 1986, **25**, 1117; M. Sato, K. Takayama, Y. Abe, T. Furuya, N. Inukai and C. Kaneko, *Chem. Pharm. Bull.*, 1990, **38**, 336; D. Haag and H. D. Scharf, *J. Org. Chem.*, 1966, **61**, 6127; M. T. Crimmins and T. L. Reinhold, *Org. React.*, 1993, **44**, 297.

2 S. A. Fleming and S. C. Ward, *Tetrahedron Lett.*, 1992, **33**, 1013; C. L. Bradford, S. A. Fleming and S. C. Ward, *Tetrahedron Lett.*, 1995, **36**, 4189,

3 M. T. Crimmins and L. E. Guise, *Tetrahedron Lett.*, 1994, **35**, 1657.

4 S. Faure, S. Piva-Le Blanc, O. Piva and J.-P. Pete, *Tetrahedron Lett.*, 1997, **38**, 1045.

5 K. I. Booker-Milburn, J. K. Cowell and L. J. Harris, *Tetrahedron Lett.*, 1994, **35**, 3883; K. I. Booker-Milburn, F. Delgado Jiménez and A. Sharpe, *Synlett*, 1995, 735; K. I. Booker-Milburn, J. K. Cowell, A. Sharpe and F. Delgado Jiménez, *Chem. Commun.*, 1996, 249.

*Received in Liverpool, UK, 8th April 1997; 7/02386C*

# A novel efficient sulfenylation method using quinone mono-*O,S*-acetals under mild conditions

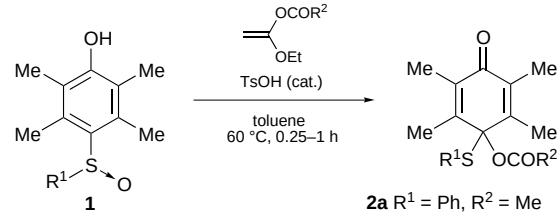
**Masato Matsugi, Kentoku Gotanda, Kenji Murata and Yasuyuki Kita***

*Faculty of Pharmaceutical Sciences, Osaka University, 1-6 Yamada-oka, Suita, Osaka 565, Japan*

**A novel method for sulfenylation induced by aromatization of quinone mono-*O,S*-acetals is described.**

It is important to introduce sulfur effectively into organic compounds, as many biologically active compounds contain sulfur functions.[1] Although many methods for sulfenylation have been reported to date,[2] a mild sulfenylation reaction under neutral conditions is not readily available. Under these circumstances, we report here a novel sulfenylation reaction using quinone mono-*O,S*-acetals which gives high yields under almost neutral conditions.

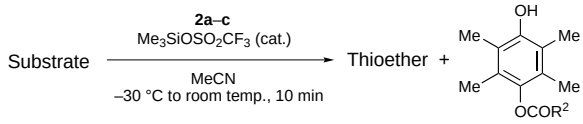
We have already reported that various quinone mono-*O,S*-acetals **2**, which are intermediates in aromatic Pummerer rearrangement, could be isolated easily in high yields.[3] These compounds readily aromatize by reaction with various nucleophiles, giving sulfenylation products. Therefore, we examined




**2a** $R^1$ = Ph, $R^2$ = Me 70%
**b** $R^1$ = Ph, $R^2$ = $CH_2Cl$ 87%
**c** $R^1$ = Me, $R^2$ = Me 86%

**Scheme 1**

**Table 1** Sulfenylation by quinone mono-*O,S*-acetals **2a**–**c**




**3a** $R^2$ = Me
**b** $R^2$ = $CH_2Cl$

| Entry | Substrate | *O,S*-Acetals | Thioethers | Yield (%)[a] |
|---|---|---|---|---|
| 1 | **4a** *n* = 0 | **2a** | **5a** *n* = 0, $R^1$ = Ph | 98 |
| 2 | **4a** *n* = 0 | **2b** | **5a** *n* = 0, $R^1$ = Ph | 99 |
| 3 | **4a** *n* = 0 | **2c** | **5b** *n* = 0, $R^1$ = Me | 94 |
| 4 | **4b** *n* = 1 | **2b** | **5c** *n* = 1, $R^1$ = Ph | 95 |
| 5 | **6a** $R^3$ = H, $R^4$ = OMe | **2b** | **7a** | 99 |
| 6 | **6b** $R^3$ = Me, $R^4$ = OMe | **2b** | **7b** | 100 |
| 7 | **6c** $R^3$ = Ph, $R^4$ = OMe | **2b** | **7c** | 98 |
| 8 | **6d** $R^3$ = OMe, $R^4$ = OMe | **2b** | **7d** | 99 |
| 9 | **6e** $R^3$ = H, $R^4$ = Ph | **2b** | **7e** | 96 |
| 10 | **8a** $R^5$ = H, $R^6$ = OMe, $R^7$ = OMe, $R^8$ = OMe | **2b** | **9a** | 99 |
| 11 | **8b** $R^5$ = OMe, $R^6$ = H, $R^7$ = OMe, $R^8$ = OMe | **2b** | **9b** | 99 |
| 12 | **8c** $R^5$ = Me, $R^6$ = H, $R^7$ = OMe, $R^8$ = OMe | **2b** | **9c** | 99 |
| 13 | **8d** $R^5$ = Me, $R^6$ = H, $R^7$ = OMe, $R^8$ = Me | **2b** | **9d** | 67[b] |
| 14 | **8e** $R^5$ = H, $R^6$ = H, $R^7$ = $NMe_2$, $R^8$ = H | **2b** | **9e** | 64[b] |
| 15 | **10a** $R^9$ = H, $R^{10}$ = Me | **2b** | **11a** | 99 |
| 16 | **10b** $R^9$ = OMe, $R^{10}$ = Me | **2b** | **11b** | 99 |
| 17 | **10c** $R^9$ = H, $R^{10}$ = Ph | **2b** | **11c** | 94 |

[a] Yields refer to pure isolated products by column chromatography; phenol derivatives **3a** or **3b** were almost quantitatively formed as by-products in all cases.
[b] Diphenyl disulfide was formed as a by-product.

the possibility that **2** might act as an effective reagent for the sulfenylation of various nucleophiles under mild conditions. The starting quinone mono-*O*,*S*-acetals **2a–c** were prepared by Pummerer reaction of the corresponding sulfoxide **1** with 1-ethoxyvinyl esters.[4] A higher yield was obtained with **2b** and **2c** than **2a** (Scheme 1).[3]

First we examined the ability of quinone mono-*O*,*S*-acetals **2a–c** for sulfenylation by the use of cyclic silyl enol ethers **4a**,**b** and found that **2a–c** were excellent sulfenylating reagents which gave the target thioethers in quantitative yields (Table 1, entries 1–4).† The generality of this sulfenylation reaction was confirmed using various acyclic silyl enol ethers **6a–e** with **2b** (Table 1, entries 5–9). This sulfenylating reagent also reacted easily with electron-rich aromatic compounds such as **8a–e** and heteroaromatic compounds **10a–c**, and the corresponding thioethers were obtained by direct sulfenylation (Table 1, entries 10–17). These sulfenylation reactions were completed within 10 min at −30 °C to room temperature under nearly neutral conditions, giving thioether derivatives in almost quantitative yields. In addition, as a side product, the hydroquinone derivative **3** was easily removed by treatment with weak aqueous alkali.

In conclusion, we have succeeded in developing novel sulfenylating reagents by taking advantage of activation on the sulfur atom based on aromatization. These reagents might be applied to the synthesis of biologically active substances having sulfur functions and labile functions that are sensitive to basic or acidic conditions.

## Footnotes

* E-mail: kita@em.phs.osaka-u.ac.jp

† Typical procedure: a mixture of **4** (1 mmol), **2a–c** (1 mmol) and $Me_3SiOSO_2CF_3$ (cat.) in MeCN (5 ml) was stirred at room temperature under a positive atmosphere of dry nitrogen. After 10 min, the mixture was concentrated *in vacuo*. Purification by column chromatography on silica gel (eluent: AcOEt–hexane = 1 : 5) gave **5a–c** in 94–99% yield.

## References

1 For recent reviews, see R. D. Norcross and I. Paterson, *Chem. Rev.*, 1995, **95**, 2041; D. J. Faulkner, *Nat. Prod. Rep.*, 1995, **12**, 223.

2 For example: H. Behforouz and J. E. Kerwood, *J. Org. Chem.*, 1969, **34**, 51; E. J. Corey and S. Knapp, *Tetrahedron Lett.*, 1976, 4687; R. J. Goodridge, T. W. Hambley, R. K. Haynes Gilbert and W. C. Berkeley, Jr., *J. Am. Chem. Soc.*, 1974, **96**, 5495; P. G. Gassman, D. P. Gilbert and S. M. Cole, *J. Org. Chem.*, 1977, **42**, 3233; D. Scholz, *Synthesis*, 1983, 944; D. Scholz, *Liebigs Ann. Chem.*, 1984, 259; S. Andreades, J. F. Harris, Jr. and W. A. Sheppard, *J. Org. Chem.*, 1964, **29**, 898; R. M. Scribner, *J. Org. Chem.*, 1966, **31**, 3671; H. P. Kaufman and K. Kuchler, *Chem. Ber.*, 1934, **67B**, 944; Y. Tamura, S. Kwon, M. W. Chun and M. Ikeda, *J. Heterocycl. Chem.*, 1978, **15**, 425; K. Tomita, A. Terada and R. Tachikawa, *Heterocycles*, 1976, **4**, 733; D. S. Reno and R. J. Pariza, *Org. Synth.*, 1996, **74**, 124.

3 Y. Kita, Y. Takeda, M. Matsugi, K. Iio, K. Gotanda, K. Murata and S. Akai, *Angew. Chem., Int. Ed. Engl.*, in the press.

4 Y. Kita and N. Shibata, *Synlett*, 1996, 273; N. Shibata, M. Matsugi, N. Kawano, S. Fukui, C. Fujimori, K. Gotanda, K. Murata and Y. Kita, *Tetrahedron: Asymmetry*, 1997, **8**, 303.

*Received in Cambridge, UK, 29th April 1997; 7/02912H*

# Montmorillonite K-10 and KSF as remarkable acetylation catalysts

**Ai-Xiao Li, Tong-Shuang Li* and Tian-Hui Ding**

*Department of Chemistry, Hebei University, Boading 071002, Hebei Province, P.R. China*

**Montmorillonite K-10 and KSF catalyse the acetylation of alcohols, thiols, phenols and amines with acetic anhydride in excellent yield.**

The protection of hydroxy, thiol and amino groups by the formation of esters and amides is of great importance in organic synthesis.[1] Although a variety of procedures use the transesterification methodology,[2] the acylation of alcohols and phenols is routinely carried out using acid anhydrides or acid chlorides in the presence of tertiary amines such as triethylamine and pyridine.[3] DMAP is particularly noteworthy as an efficient catalyst for the acylation of tertiary alcohols.[4] Recently, Vedejs and co-workers reported tributylphosphine to be a similar catalyst for the acylation of alcohols.[5] In addition to the above catalysts, protonic acids such as toluene-*p*-sulfonic acid[6] and Lewis acids such as zinc chloride,[7] cobalt chloride[8] and scandium trifluoromethanesulfonate[9] are also known to catalyse the acylation of alcohols and phenols. Nevertheless, there is still a great demand for acid catalysts to generate esters under mild conditions.

Montmorillonite clays, a class of inexpensive and noncorrosive solid acids, have been used as efficient catalysts for a variety of organic reactions.[10] In a recent study on the preparation of 1,1-diacetates from aldehydes catalysed by montmorillonite clays, we found that hydroxy groups were protected as acetates in hydroxy-containing aromatic aldehydes.[11] In connection with our ongoing work on montmorillonite clay catalysis,[12] we now give a preliminary account of our study of the acetylation of alcohols, phenols, thiols and amines catalysed by montmorillonite K-10 and KSF.

As shown in Table 1, a series of alcohols, phenols, thiols and amines were acetylated with acetic anhydride under catalysis by montmorillonite K-10 and KSF. Generally K-10 worked better than KSF in terms of reaction time, temperature and/or yield

**Table 1** Acetylation of alcohols, phenols, thiols and amines with acetic anhydride catalysed by K-10 and KSF

| Entry | Substrate | Catalyst | Solvent | Ratio[a] | *T*/°C | *t*/h | Product[b] | Yield[c] (%) |
|---|---|---|---|---|---|---|---|---|
| 1 | Octanol | K-10 | none | 2 : 1 | room temp. | 1 | Octyl acetate | 96 |
| | | KSF | none | 2 : 1 | room temp. | 4 | Octyl acetate | 96 |
| 2 | Benzyl alcohol | KSF | none | 2 : 1 | room temp. | 1 | Benzyl acetate | 90 |
| 3 | Ethylene glycol | KSF | $CHCl_3$ | 4 : 1 | 62 | 2 | Ethane-1,2-diyl diacetate | 76 |
| 4 | Glycerol | KSF | $CHCl_3$ | 6 : 1 | 62 | 1.5 | Propane-1,2,3-triyl triacetate | 95 |
| 5 | Cholesterol | K-10 | $CH_2Cl_2$ | 2 : 1 | room temp. | 2 | Cholesteryl acetate | 98 |
| | | KSF | $CHCl_3$ | 2 : 1 | 62 | 2 | Cholesteryl acetate | 98 |
| 6 | Dihydrobetulin | K-10 | $CH_2Cl_2$ | 4 : 1 | 40 | 3 | 3β,28-Diacetoxylupane | 94 |
| 7 | Triphenylmethanol | KSF | $CCl_4$ | 2 : 1 | 76 | 2 | No reaction | — |
| 8 | *tert*-Butyl alcohol | KSF | none | 2 : 1 | 80 | 0.25 | 2-Methylpropene | 94 |
| 9 | 3α-Methyl-5α-cholestan-3β-ol | K-10 | $CH_2Cl_2$ | 2 : 1 | 40 | 2 | 3β-Acetoxy-3α-methyl-5α-cholestane | 23 |
| | | | | | | | 3-Methyl-5α-cholest-2-ene | 49 |
| 10 | 3β-Methyl-5α-cholestan-3α-ol | K-10 | $CH_2Cl_2$ | 2 : 1 | 35 | 1 | 3α-Acetoxy-3β-methyl-5α-cholestane | 27[d] |
| | | | | | | | 3-Methyl-5α-cholest-2-ene | 49[d] |
| 11 | 2-Mercaptoethanol | KSF | $CH_2Cl_2$ | 1 : 1 | 40 | 0.25 | Ethyl 2-mercaptoacetate | 20 |
| 12 | 2-Mercaptoethanol | KSF | $CH_2Cl_2$ | 4 : 1 | 40 | 1.5 | 2-Acetylthioethyl acetate | 92 |
| 13 | Benzenethiol | K-10 | none | 2 : 1 | room temp. | 2 | *S*-Phenyl thioacetate | 97 |
| | | KSF | none | 2 : 1 | room temp. | 5 | *S*-Phenyl thioacetate | 92 |
| 14 | Phenol | KSF | none | 2 : 1 | room temp. | 3.5 | Phenyl acetate | 83 |
| 15 | α-Naphthol | KSF | $CHCl_3$ | 2 : 1 | 62 | 4 | α-Naphthyl acetate | 87 |
| 16 | β-Naphthol | K-10 | $CH_2Cl_2$ | 2 : 1 | room temp. | 2.5 | β-Naphthyl acetate | 98 |
| | | KSF | $CH_2Cl_2$ | 2 : 1 | 40 | 2 | β-Naphthyl acetate | 98 |
| 17 | 3-Nitrophenol | KSF | none | 2 : 1 | room temp. | 5 | 3-Nitrophenyl acetate | 98 |
| 18 | 2-Nitrophenol | KSF | $CHCl_3$ | 2 : 1 | 62 | 7 | 2-Nitrophenyl acetate | 93 |
| 19 | 4-Nitrophenol | KSF | $CH_2Cl_2$ | 2 : 1 | 40 | 2.5 | 4-Nitrophenyl acetate | 98 |
| 20 | 2-Methylphenol | KSF | none | 2 : 1 | room temp. | 3.5 | 2-Methylphenyl acetate | 90 |
| 21 | 4-Methoxyphenol | KSF | none | 2 : 1 | room temp. | 4.5 | 4-Methoxyphenyl acetate | 92 |
| 22 | Hydroquinone | KSF | none | 4 : 1 | room temp. | 2 | Benzene-1,4-diyl diacetate | 98 |
| 23 | Catechol | KSF | none | 4 : 1 | room temp. | 3 | Benzene-1,2-diyl diacetate | 98 |
| 24 | Resorcinol | KSF | $CHCl_3$ | 4 : 1 | 62 | 3 | Benzene-1,3-diyl diacetate | 78 |
| 25 | Benzene-1,3,5-triol | KSF | $CHCl_3$ | 6 : 1 | 62 | 4.5 | Benzene-1,3,5-triyl triacetate | 83 |
| 26 | 2-Aminophenol | KSF | $CH_2Cl_2$ | 2 : 1 | 40 | 1 | *N*-(2-Hydroxyphenyl)acetamide | 72 |
| 27 | 2-Aminophenol | KSF | $CH_2Cl_2$ | 4 : 1 | 40 | 3 | *N*-(2-Acetoxyphenyl)acetamide | 70 |
| 28 | Diisopropylamine | KSF | $CH_2Cl_2$ | 4 : 1 | 40 | 2 | *N*-Diisopropylacetamide | 98 |
| 29 | 2-Nitroaniline | K-10 | $CH_2Cl_2$ | 2 : 1 | 40 | 3.5 | 2-Nitroacetanilide | 98 |
| | | KSF | $CH_2Cl_2$ | 2 : 1 | 40 | 3.5 | 2-Nitroacetanilide | 87 |

[a] Acetic anhydride: substrate (mol : mol). [b] All products were identified by their $^1$H NMR spectra and/or by comparison of their bp or mp with authentic samples. [c] Isolated yield. [d] Net yield, conversion rate of the material is 27.5%.

(entries 1, 5, 13, 16 and 29). Primary and secondary alcohols and phenols can be easily acetylated at room temperature or in refluxing $CH_2Cl_2$ or $CHCl_3$. No selectivity between primary and secondary hydroxy groups was observed (entries 4 and 6). Different results were obtained for several tertiary alcohols. For example, triphenylmethanol remained unchanged even when the reaction was performed in refluxing $CCl_4$ for 2 h (entry 7). *tert*-Butyl alcohol gave 2-methylpropene (entry 8). 3β-Methyl-5α-cholestan-3α-ol afforded mainly 3-methyl-5α-cholest-2-ene, with a minor amount of 3α-acetoxy-3β-methyl-5α-cholestane (27% net yield based on 27.5% conversion rate) (entry 10). The hydroxy equatorial epimer, 3α-methyl-5α-cholestan-3β-ol, gave the corresponding acetate in better yield (23%) and 3-methyl-5α-cholest-2-ene (entry 9). It is noteworthy that 3-methyl-5α-cholest-2-ene was the exclusive dehydration product in both reactions. These results indicated that K-10 and KSF were not efficient catalysts for acetylation of tertiary alcohols. Polyhydroxy compounds were transformed into the corresponding polyacetates (entries 3, 4, 6, 22, 23, 24 and 25). In the presence of K-10 or KSF, thiols and amines were also converted into the corresponding acetamides and thioacetates (entries 12, 13, 26, 27, 28 and 29). Acetylation of thiols was slower than hydroxy groups (entry 11). Amino groups could be preferentially acetylated in the presence of hydroxy groups (entry 26).

In a typical procedure, a mixture of octan-1-ol (650 mg, 5.00 mmol), K-10 (or KSF) (purchased from Fluka and used directly) (100 mg) and acetic anhydride (1.02 g, 10.0 mmol) was stirred at room temperature for 1 h (or 4 h). The catalyst was removed by filtration and washed with $CH_2Cl_2$. The solvent was evaporated under reduced pressure. The residue was purified by column chromatography on silica gel to give octyl acetate (813 mg, 96%).

In conclusion, K-10 and KSF are good acetylation catalysts for primary and secondary alcohols, phenols, thiols and amines but not for tertiary alcohols. The present method has the additional advantages of mild conditions, high yield, easy separation and inexpensive and environmentally friendly catalysts.

This project was supported by the NSFC (29572039), the Education Commission of Hebei Province and the Science and Technology Commission of Hebei Province.

## References

1 S. S. Rana, J. J. Barlow and K. L. Matta, *Tetrahedron Lett.*, 1981, **22**, 5007; T.-S. Li, Y.-L. Li and X.-T. Liang, *Steroids*, 1990, **55**, 263; T. W. Greene and P. G. M. Wuts, *Protective Groups in Organic Synthesis*, Wiley, New York, 2nd edn., 1991; A. A. Mourabit, H. Poujol, C. Poupat, A. Ahond and P. Potier, *Tetrahedron Lett.*, 1996, **37**, 9189; K. Takeda, A. Nakajima and E. Yoshii, *Synlett*, 1997, 255.

2 J. Otera, *Chem. Rev.*, 1993, **93**, 1449 and references cited therein; A. Loupy, A. Petit, M. Ramdani, C. Yvanaeff, M. Majdoub, B. Labiad and D. Villemin, *Can. J. Chem.*, 1993, **71**, 90; Y. Ishii, M. Takeno, Y. Kawasaki, A. Muromachi, Y. Nishiyama and S. Sakaguchi, *J. Org. Chem.*, 1996, **61**, 3088; B. S. Balaji, M. Sasidharan, R. Kumar and B. Chanda, *Chem. Commun.*, 1996, 707.

3 R. I. Zhdanov and S. M. Zhenodarova, *Synthesis*, 1975, 222; D. Horton, *Org. Synth.*, 1973, **Coll. Vol. 5**, 1.

4 G. Hofle, V. Steglich and H. Vorbruggen, *Angew. Chem., Int. Ed. Engl.*, 1978, **17**, 569; E. F. V. Scriven, *Chem. Soc. Rev.*, 1983, **12**, 129.

5 E. Vedejs and S. T. Diver, *J. Am. Chem. Soc.*, 1993, **115**, 3358; E. Vedejs, N. S. Bennett, L. M. Conn, S. T. Diver, M. Gingras, S. Lin, P. A. Oliver and M. J. Peterson, *J. Org. Chem.*, 1993, **58**, 7286.

6 A. C. Cope and E. C. Herrick, *Org. Synth.*, 1963, **Coll. Vol. 4**, 304.

7 R. H. Baker and F. G. Bordwell, *Org. Synth.*, 1955, **Coll. Vol. 3**, 141.

8 J. Iqbal and R. R. Srivastava, *J. Org. Chem.*, 1992, **57**, 2001.

9 K. Ishihara, M. Kubota, H. Kurihara and H. Yamamoto, *J. Org. Chem.*, 1996, **61**, 4560.

10 T.-S. Li and T.-S. Jin, *Youji Huaxue*, 1996, **16**, 385.

11 Z.-H. Zhang, T.-S. Li and C.-G. Fu, *J. Chem. Res.* (*S*), 1997, 174.

12 T.-S. Li, Y.-T. Yang and Y.-L. Li, *J. Chem. Res.* (*S*), 1993, 30; T.-S. Li, H.-Z. Li, J.-L. Guo and T.-S. Jin, *Synth. Commun.*, 1996, **26**, 2497; T.-S. Li, S.-H. Li, J.-T. Li and H.-Z. Li, *J. Chem. Res* (*S*), 1997, 26; T.-S. Li and S.-H. Li, *Synth. Commun.*, 1997, **27**, in the press; T.-S. Li, Z.-H. Zhang and C.-G. Fu, *Tetrahedron Lett.*, 1997, **38**, 3285.

*Received in Cambridge, UK, 16th May 1997; 7/03389C*

# Aggregation of fluoroalkyl units: synthesis of gelling fluoroalkylated end-capped oligomers containing hydroxy segments possessing metal ion binding and releasing abilities

**Hideo Sawada,*[a,b] Toshihiro Tanimura,[a] Shinsuke Katayama[b] and Tokuzo Kawase[c]**

[a] *Department of Chemistry, Nara National College of Technology, Yamatokoriyama, Nara 639-11, Japan*
[b] *Department of Chemistry, Faculty of Advanced Engineering, Nara National College of Technology, Yamatokoriyama, Nara 639-11, Japan*
[c] *Faculty of Human Life Science, Osaka City University, Sumiyoshi, Osaka 558, Japan*

**New fluoroalkylated end-capped oligomers containing 2-hydroxypropyltrimethylammonium or carboxy(hydroxy)-methylamido segments, which are prepared from the reaction of fluoroalkanoyl peroxides with the corresponding monomers, can cause gelation where strong aggregation of the fluoroalkyl segments is involved in establishing the physical gel network, not only in water but also in organic media under the non-crosslinked conditions, and had a high metal ion binding and releasing power.**

Recently there has been increased interest in organofluorinated polymeric materials, especially partially fluoroalkylated macromolecules, because of their unique properties such as high solubility, surface activity and biological activity, which cannot be achieved using the corresponding non-fluorinated macromolecules or perfluorinated polymers.[1] From such a viewpoint, we have been studying the synthesis of fluoroalkylated end-capped oligomers using fluoroalkanoyl peroxides as key intermediates,[2] and these partially fluoroalkylated compounds have been demonstrated to be able to reduce the surface tension of water,[3] and to be potent and selective inhibitors of HIV type-1 *in vitro*.[4] Therefore, it is of interest to develop such compounds. In the course of our studies for the synthesis and applications of fluoroalkylated end-capped oligomers, we have found that fluoroalkylated oligomers containing not only trimethylammonium and hydroxy segments but also hydroxy and carboxy segments can cause gelation in aqueous and organic media under non-crosslinked conditions. More interestingly, these fluoroalkylated oligomers were also found to have high metal ion binding and releasing power. The results are described herein.

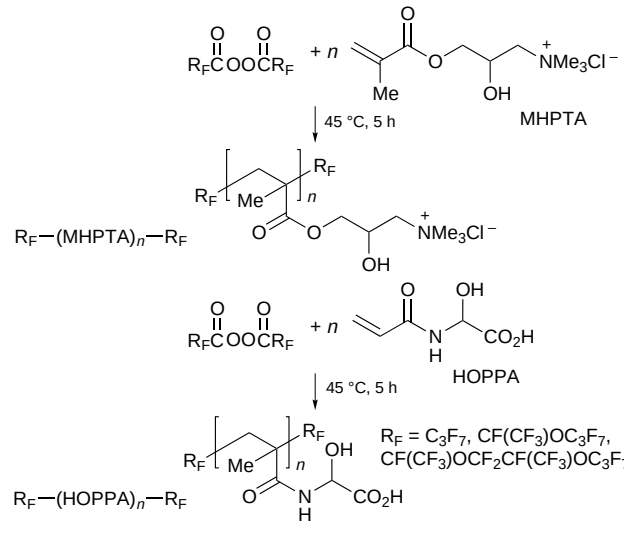
A series of fluoroalkylated oligomers containing trimethylammonium and hydroxy segments [$R_F$–(MHPTA)$_n$–$R_F$] were prepared *via* the reactions of fluoroalkanoyl peroxides with 3-methacryloxy-2-hydroxypropyltrimethylammonium chloride (MHPTA).† Similarly, we succeeded in preparing a series of fluoroalkylated oligomers containing hydroxy and carboxy segments *via* the reaction of fluoroalkanoyl peroxides with 2-hydroxy-2-[(1-oxoprop-2-enyl)amino]acetic acid (HOPPA), as shown in Scheme 1.‡

The results for the reaction of fluoroalkanoyl peroxides with MHPTA and HOPPA are shown in Table 1. As shown, perfluoropropylated and perfluorooxaalkylated MHPTA or HOPPA oligomers were obtained in moderate to excellent yields under very mild conditions. The perfluoropropylated and perfluoro-1-methyl-2-oxapentylated MHPTA oligomers (entries 1–3, Table 1) were soluble in water, and we were able to measure their molecular weights by GPC analyses [$\bar{M}_n$ ($\bar{M}_w$/$\bar{M}_n$) = 2630 (3.02) (entry 1); 2060 (3.86) (entry 2); 6760 (11.0) (entry 3)]. However, in perfluoro-1-methyl-2-oxapentylated MHPTA oligomers, the oligomers with larger molar ratios of MHPTA to peroxide (entries 4–9) formed gels or became 'gel-like' with not only water but also MeOH, EtOH, DMF and DMSO, and we were unable to measure their molecular weights owing to the high viscoelacticity of the fluids or the gel formation. A corresponding non-fluorinated MHPTA oligomer [–(MHPTA)$_n$–] was completely soluble in these solvents.

In fluoroalkylated HOPPA oligomers, not only perfluoropropylated but also perfluorooxaalkylated HOPPA oligomers were found to cause gelation with water, DMF and DMSO under non-crosslinked conditions. It is important to note that the corresponding non-fluorinated HOPPA oligomers [–(HOPPA)$_n$–] forms no gels with these solvents.

We have measured the minimum concentrations ($C_{min}$) of these oligomers necessary for gelation in water at 30 °C according to the method reported by Hanabusa *et al.*,[5] and the results are shown in Table 1.

As shown, the amount ($C_{min}$) of a fluoroalkylated oligomer necessary to gel 1 l of water was 7–330 g, and the oligomers with greater molar ratios of MHPTA (or HOPPA) to peroxide or longer perfluorooxaalkylated oligomers were found to exhibit higher gelling ability. These results strongly suggest that the main driving forces for gelation are the synergistic interactions between aggregations of fluoroalkyl units in oligomers and the intermolecular hydrogen bonding between hydroxy or carboxy segments, including the interactions of OH and $N^+$ groups. On the other hand, the corresponding non-fluorinated oligomers could not form a physical gel network in these media owing to the absence of the aggregation of fluoroalkyl units. Hitherto, it was known that some macromolecules cause chemical and physical gelation in aqueous solutions, but the application of these compounds to organogels has been limited. The striking characteristic of our present oligomers as gelling agents is the




**Scheme 1**

**Table 1** Reactions of fluoroalkanoyl peroxides $R_FC(O)OOC(O)R_F$ with MHPTA or HOPPA and minimum gel concentration of fluoroalkylated MHPTA or HOPPA oligomers for gelation at 30 °C

| Entry | Peroxide $R_F$ | Central segment | Ratio peroxide : central segment | Yield (%)[a] | $C_{min}$/g dm$^{-3}$ [b] |
|---|---|---|---|---|---|
| 1 | $C_3F_7$ | MHPTA | 4 : 21 | 21 | soluble |
| 2 | $C_3F_7$ | MHPTA | 4 : 42 | 30 | soluble |
| 3 | $CF(CF_3)OC_3F_7$ | MHPTA | 4 : 11 | 17 | soluble |
| 4 | $CF(CF_3)OC_3F_7$ | MHPTA | 5 : 25 | 36 | gel-like |
| 5 | $CF(CF_3)OC_3F_7$ | MHPTA | 4 : 42 | 12 | gel-like |
| 6 | $CF(CF_3)OC_3F_7$ | MHPTA | 4 : 65 | 39 | 102 |
| 7 | $CF(CF_3)OC_3F_7$ | MHPTA | 4 : 85 | 25 | 7 |
| 8 | $CF(CF_3)OCF_2CF(CF_3)OC_3F_7$ | MHPTA | 4 : 22 | 32 | 330 |
| 9 | $CF(CF_3)OCF_2CF(CF_3)OC_3F_7$ | MHPTA | 4 : 43 | 88 | 51 |
| 10 | $C_3F_7$ | HOPPA | 4 : 41 | 83 | 88 |
| 11 | $CF(CF_3)OC_3F_7$ | HOPPA | 4 : 8 | 8 | 100 |
| 12 | $CF(CF_3)OC_3F_7$ | HOPPA | 4 : 20 | 20 | 93 |
| 13 | $CF(CF_3)OC_3F_7$ | HOPPA | 5 : 50 | 71 | 91 |
| 14 | $CF(CF_3)OCF_2CF(CF_3)OC_3F_7$ | HOPPA | 3 : 5 | 15 | 94 |
| 15 | $CF(CF_3)OCF_2CF(CF_3)OC_3F_7$ | HOPPA | 3 : 13 | 50 | 87 |
| 16 | $CF(CF_3)OCF_2CF(CF_3)OC_3F_7$ | HOPPA | 3 : 26 | 85 | 53 |

[a] Yields are based on the starting materials (MHPTA or HOPPA) and the decarboxylated peroxide unit ($R_F$–$R_F$). [b] gel-like = highly vicoelastic fluid.

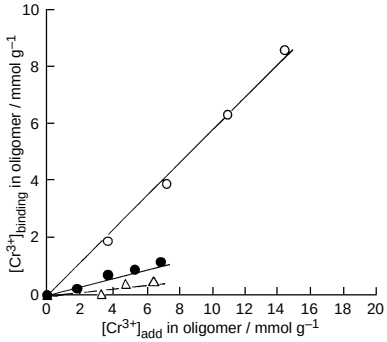



**Fig. 1** Relationship between relative amounts of $Cr^{3+}$ binding to fluoroalkylated oligomers and initial $Cr^{3+}$: (○) $R_F$–$(MHPTA)_n$–$R_F$ [$R_F$ = $CF(CF_3)OC_3F_7$ (entry 7)], (●) $R_F$–$(HOPPA)_n$–$R_F$ [$R_F$ = $CF(CF_3)OCF_2CF(CF_3)OC_3F_7$ (entry 16) and (△) $R_F$–$(MHPTA)_n$–$R_F$ [$R_F$ = $CF(CF_3)OC_3F_7$ (entry 6)]

ability to harden not only water but also organic polar solvents. This feature is attributable to the fact that fluoroalkyl segments are solvophobic in aqueous and organic media, and enhance aggregation due to strong interaction between the fluoroalkyl segments.

From both fundamental and technological standpoints, it is interesting to study the adsorptive properties against metal ions of our new fluoroalkylated oligomer gels. Thus, we performed quantitative measurements of the uptake of $Cr^{3+}$ (15–60 mmol dm$^{-3}$) by the $R_F$–$(MHPTA)_n$–$R_F$ (entry 7, Table 1) hydrogel. The metal ion concentration of the supernatant liquid after the incubation (at 25 °C for 24 h) was determined spectrophotometrically using a calibration curve, and the results are shown in Fig. 1.

As shown, $Cr^{3+}$ was found to bind strongly to the fluoroalkylated oligomer hydrogel with *ca.* 60% binding ratio [based on the relative amount of $Cr^{3+}$ binding to gel ($[Cr^{3+}]_{binding}$/oligomer) and relative amount of initial $Cr^{3+}$($[Cr^{3+}]_{add}$/oligomer)]. The $R_F$–$(MHPTA)_n$–$R_F$ (entry 6, Table 1) hydrogel possessing a higher $C_{min}$ value than entry 7 had a weaker $Cr^{3+}$ binding power (*ca.* 10% binding ratio) under similar conditions. The $R_F$–$(HOPPA)_n$–$R_F$ (entry 16, Table 1) hydrogel was also shown to have a $Cr^{3+}$ binding power (*ca.* 17% binding ratio) as shown in Fig. 1. However, fluoroalkylated oligomers (entries 8 and 11) possessing higher $C_{min}$ values than entries 6, 7 or 16 were found to have poor $Cr^{3+}$ binding power. From these results, it can be said that the fluoroalkylated oligomer networks in the hydrogels possessing lower $C_{min}$ values are likely to bind strongly to the metal ion, since stronger aggregation of the fluoroalkyl segments is necessary for the establishment of the physical gel network to exhibit lower $C_{min}$ value.

More interestingly, it was found that $Cr^{3+}$ can be easily released from the $Cr^{3+}$-bound $R_F$–$(MHPTA)_n$–$R_F$ (entry 7, Table 1) hydrogel into water with *ca.* 60% releasing ratio (the ratio based on the relative amount of $Cr^{3+}$ released into water and relative amount of $Cr^{3+}$ binding to gel) after the incubation at 25 °C for 24 h. On the other hand, $Cr^{3+}$ was not released from the $Cr^{3+}$-bound $R_F$–$(HOPPA)_n$–$R_F$ hydrogels under similar conditions. This is because the interaction of $Cr^{3+}$ and $R_F$–$(HOPPA)_n$–$R_F$ hydrogels is ionic, whereas the main driving force for $Cr^{3+}$ binding to $R_F$–$(MHPTA)_n$–$R_F$ is coordination between $Cr^{3+}$ and OH segments.

Thus it has been demonstrated that our new fluoroalkylated oligomers containing hydroxy segments can cause gelation under non-crosslinked conditions, and that the aggregation of fluoroalkyl units in water and/or organic media becomes a new driving factor for gelation in addition to well-known interactions such as hydrogen bond and ionic interactions. In addition, it has been shown that these new fluoroalkylated oligomer hydrogels have high metal-binding or releasing power. Thus, these fluorinated oligomer gels are expected to prove useful in various fields as novel fluorinated functional materials.

## Footnotes

* E-mail: sawada@center.nara-k.ac.jp

† *Selected data* for $R_F$–$(MHPTA)_n$–$R_F$ [$R_F$ = $CF(CF_3)OC_3F_7$] $\nu_{max}$/cm$^{-1}$ 3457 (OH), 1725 (C=O), 1321 ($CF_3$), 1241 ($CF_2$); $\delta_H(D_2O)$ 0.68–1.11 ($CH_3$), 1.61–2.15 ($CH_2$), 3.05–3.19 ($CH_3$), 3.31–3.54 ($CH_2$), 4.43–4.55 (CH); $\delta_F(D_2O$, ext. $CF_3CO_2H)$: −5.63 to −6.93 (16 F), −53.25 (6 F).

‡ *Selected data* for $R_F$–$(HOPPA)_n$–$R_F$ [$R_F$ = $CF(CF_3)OC_3F_7$] $\nu_{max}$/cm$^{-1}$ 3465 (OH), 3187 (NH), 1745 (C=O), 1336 ($CF_3$), 1257 ($CF_2$); $\delta_H(D_2O)$ 0.98–2.48 ($CH_2$, CH), 5.09–5.62 (CH); $\delta_F(D_2O$, ext. $CF_3CO_2H)$: −6.96 to −7.76 (16 F), −54.15 (6 F).

## References

1 *Organofluorine Chemistry*, ed. R. E. Banks, B. E. Smart and J. C. Tatlow, Plenum, New York, 1994; Z.-Y. Yang, A. E. Feiring and B. E. Smart, *J. Am. Chem. Soc.*, 1994, **116**, 4135.
2 H. Sawada, *Chem. Rev.*, 1996, **96**, 1779.
3 H. Sawada, Y.-F. Gong, Y. Minoshima, T. Matsumoto, M. Nakayama, M. Kosugi and T. Migita, *J. Chem. Soc., Chem. Commun.*, 1992, 537; H. Sawada, Y. Minoshima and H. Nakajima, *J. Fluorine Chem.*, 1992, **65**, 169.
4 M. Baba, T. Kira, S. Shigeta, T. Matsumoto and H. Sawada, *J. Acquired Immune Defic. Syndr.*, 1994, **7**, 24.
5 K. Hanabusa, Y. Watanabe, M. Kimura, T. Koyama and H. Shirai, *Sen'i Gakkaishi*, 1996, **52**, 129.

*Received in Cambridge, UK, 24th April 1997; 7/02800H*

# Efficient coupling reactions of allylamines with soft nucleophiles using nickel-based catalysts

**Hervé Bricout, Jean-François Carpentier and André Mortreux***

*Laboratoire de Catalyse Hétérogène et Homogène, Groupe de Chimie Organique Appliquée, URA CNRS 402, ENSCL, BP 108-59652 Villeneuve d'Ascq Cedex, France*

**Substitution reactions of *N,N*-diethylallylamine 1 with soft nucleophiles such as active methylene compounds 2a–c and piperidine 5 proceed much more rapidly in the presence of Ni(dppb)$_2$ [dppb = 1,4-bis(diphenylphosphino)butane] as catalyst than with comparable palladium systems.**

Recently we reported the effectiveness of preformed Ni$^0$-bisphosphine catalysts for the rearrangement of dialkyl allylmalonate derivatives,[1a] a recently discovered case of nucleophilic allylic substitution which proceeds *via* C–C bond cleavage.[1b] In this special reaction, nickel catalysts proved to be more active than comparable palladium systems, suggesting the superior ability of the former to activate allylic substrates having a poor leaving group. Here we report that such nickel-based systems are much more efficient than palladium catalysts for coupling of allylamines[2] with so-called 'soft' nucleophiles.[3]

The comparative study was performed using the simple *N,N*-diethylallylamine **1** and active methylene compounds **2a–c** as shown in eqn. (1). The results are summarized in Table 1. In all cases, the reaction was totally selective for allylation products, although a mixture of monoallylation (**3a–c**) and diallylation (**4a–c**) products was obtained. Using 2 mol% of Ni(dppb)$_2$ generated from Ni(COD)$_2$ and 2 mol equiv. of the diphosphine gave allylation products of dimethyl malonate **2a** in virtually quantitative yield with an initial activity of 50 h$^{-1}$ (turnover frequency, TOF) at 80 °C in THF (entry 1). Additional base such as BSA [BSA = *N,O*-bis(trimethylsilyl)acetamide] did not affect the reaction (entry 2). On the other hand, a significant increase in the catalytic activity arose upon adding tetrabutylammonium perchlorate as a promoter (5 equiv. with respect to Ni) (entry 3), in direct line with our previous observations on nickel-catalysed coupling reactions of allylic alcohol derivatives.[4] Changing the solvent to DMF further increased the catalytic activity, so that the completion time decreased to 20 min at 80 °C (entry 4), allowing the reaction to be performed at 50 °C (entry 5). At this temperature, the best catalytic activity was observed by combining the solvent effect of DMF and the promoting effect of [NBu$_4$][ClO$_4$] (entry 6). Surprisingly, in light of palladium literature,[2b–h] the *in situ* formation of the allyl ammonium salt *via* addition of acetic acid proved somewhat detrimental (entry 7). The use of palladium catalysts led to poorer results. As a matter of fact, no reaction at all occurred using the *in situ* combination Pd(OAc)$_2$–PPh$_3$ (1 : 5) in THF with BSA as a base (entry 8). Modest activity was obtained with this catalytic system in DMF, which was slightly improved upon adding acetic acid (entries 9 and 10). The *in situ* combination Pd(OAc)$_2$–dppb (1 : 3) showed the best performance of the palladium catalysts tested (entry 11), but the latter is still at least ten times less active than the best nickel-based

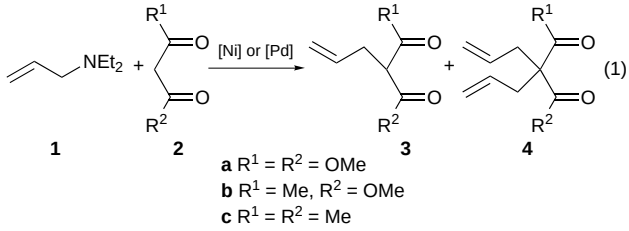



**Table 1** Catalysed coupling reactions of *N,N*-diethylallylamine **1** with methylene active compounds **2a–c**

| Entry | **2** | Catalytic system[a] | Solvent | Additive (equiv.) | *T*/°C | Conv. (%) | *t*/h[b] | **3** : **4** | TOF[c]/h$^{-1}$ |
|---|---|---|---|---|---|---|---|---|---|
| 1 | **2a** | Ni$^0$/dppb | THF | — | 80 | 100 | 12 | 87 : 13 | 35 |
| 2 | **2a** | Ni$^0$/dppb | THF | BSA (75) | 80 | 100 | 12 | 88 : 12 | 10 |
| 3 | **2a** | Ni$^0$/dppb | THF | [NBu$_4$][ClO$_4$] (5) | 80 | 100 | 2 | 90 : 10 | 200 |
| 4 | **2a** | Ni$^0$/dppb | DMF | — | 80 | 100 | 0.3 | 87 : 13 | ≫ 170 |
| 5 | **2a** | Ni$^0$/dppb | DMF | — | 50 | 95 | 3.5 | 87 : 13 | 85 |
| 6 | **2a** | Ni$^0$/dppb | DMF | [NBu$_4$][ClO$_4$] (5) | 50 | 95 | 2.8 | 88 : 12 | 100 |
| 7 | **2a** | Ni$^0$/dppb | DMF | AcOH (10) | 80 | 100 | 3 | 88 : 12 | 40 |
| 8 | **2a** | Pd$^{II}$/PPh$_3$ | THF | BSA (75) | 80 | 0 | 15 | — | 0 |
| 9 | **2a** | Pd$^{II}$/PPh$_3$ | DMF | — | 80 | 54 | 17 | 90 : 10 | 6 |
| 10 | **2a** | Pd$^{II}$/PPh$_3$ | DMF | AcOH (10) | 80 | 64 | 15 | 94 : 6 | 8 |
| 11 | **2a** | Pd$^{II}$/dppb | DMF | — | 80 | 100 | 5 | 90 : 10 | 45 |
| 12 | **2b** | Ni$^0$/dppb | DMF | — | 80 | 100 | < 0.1 | 73 : 27 | ≫ 600 |
| 13 | **2b** | Ni$^0$/dppb | DMF | — | 50 | 100 | 0.5 | 72 : 28 | 350 |
| 14 | **2b** | Pd$^{II}$/PPh$_3$ | DMF | — | 80 | 93 | 9 | 77 : 23 | 25 |
| 15 | **2b** | Pd$^{II}$/dppb | DMF | — | 80 | 100 | 1 | 75 : 25 | 215 |
| 16 | **2b** | Pd$^0$/dppb | DMF | — | 80 | 95 | 1.5 | 81 : 19 | 110 |
| 17 | **2b** | Pd$^0$/dppb | THF | — | 80 | 80 | 15 | 76 : 24 | 5 |
| 18 | **2c** | Ni$^0$/dppb | DMF | — | 80 | 10 | 0.25[d] | 97 : 3 | 20 |
| 19 | **2c** | Pd$^{II}$/dppb | DMF | — | 80 | 100 | 1 | 78 : 22 | 150 |

[a] [Metal]/[**1**]/[**2**] = 1 : 50 : 75; Ni$^0$/dppb: prepared from Ni(COD)$_2$ and 2 equiv. of the phosphine ligand; Pd$^{II}$/PPh$_3$: prepared *in situ* from Pd(OAc)$_2$ and 5 equiv. of PPh$_3$; Pd$^{II}$/dppb: prepared *in situ* from Pd(OAc)$_2$ and 3 equiv. of dppb. [b] Optimized time for conversion of **1** into **3** and **4** as indicated by quantitative GLC; No side products were observed. [c] Initial catalytic activity (< 10% conversion). [d] 10% yield after 15 min as after 16 h.

**Table 2** Catalysed exchange reactions of *N*,*N*-diethylallylamine **1** with piperidine **5**[a]

| Entry | Catalytic system | Solvent | Additive (equiv.) | Conv. (%)[b] | *t*/min | TOF/$h^{-1}$ |
|---|---|---|---|---|---|---|
| 1 | $Ni^0$/dppb | DMF | — | 100 | 360 | 35 |
| 2 | $Ni^0$/dppb | DMF | $[NBu_4][ClO_4]$ (5) | 100 | 150 | 60 |
| 3 | $Ni^0$/dppb | DMF | AcOH (5) | 100 | 40 | 400 |
| 4 | $Ni^0$/dppb | THF | AcOH (5) | 45 | 1020 | 4 |
| 5 | $Ni^0$/dppb | DMF | AcOH (50) | 100 | 5 | ≫ 600 |
| 6 | $Pd^{II}$/dppb | DMF | AcOH (50) | 92 | 120 | 60 |

[a] [Metal]/[**1**]/[**5**] = 1 : 50 : 500; $T$ = 50 °C. [b] Conversion of **1** into *N*-allylpiperidine **6** as indicated by quantitative GLC.

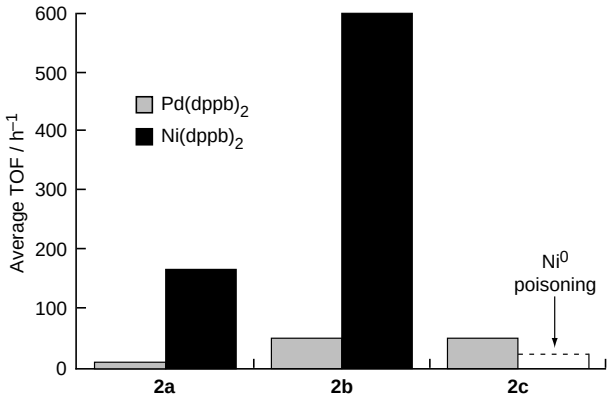
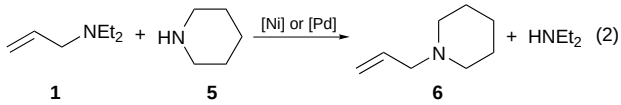



**Fig. 1** Average turnover frequencies of nickel and palladium catalysts for the coupling of **1** with **2a**–**c** (see Table 1 for reaction conditions)

system for this reaction. A similar trend, with even more marked differences between nickel and palladium catalysts, was observed for the alkylation of **1** with methyl acetoacetate **2b**. The simple system using $Ni(dppb)_2$ as the catalyst and DMF as the solvent allowed the reaction carried out with 2 mol% to Ni to be completed within 5 min at 80 °C and with an average activity of 100 $h^{-1}$ at 50 °C (entries 12 and 13).† The *in situ* combination $Pd(OAc)_2$–dppb proved once again to be the most effective palladium catalyst (entries 14–17), but its performance at 80 °C was still lower than that of the above nickel system at 50 °C. However, nickel catalysts proved inefficient for the coupling of **1** with acetylacetone **2c** (entry 18), because of a rapid catalyst poisoning evidenced by the gradual shift in the colour of the solution from orange–yellow [typical colour of $Ni(dppb)_2$] to pale green [$Ni^{II}$ species, possibly $Ni(acac)_2$]. Although it must be pointed out that **2c** is the most acidic compound among active methylene compounds **2a**–**c**, there is no definitive evidence that this catalyst decay occurs *via* an oxidative protolysis of nickel intermediates.‡ Anyway, the catalyst poisoning was still observed in the presence of an excess of **1** ([Ni] : [**1**] : [**2c**] = 1 : 75 : 50). No comparable phenomenon was observed with palladium catalysts, such as the *in situ* combination $Pd(OAc)_2$–dppb, which afforded alkylation products **3c**/**4c** with performance similar to that observed for the coupling of **1** with **2b** (entry 19). Fig. 1 summarises the overall performance of best Ni–dppb and Pd–dppb systems.

The results of the exchange reaction between **1** and piperidine **5** to give *N*-allylpiperidine **6** (eqn. 2) bring further evidence of




the general ability of nickel catalysts to promote nucleophilic substitution of allylamines (Table 2). We found that the aforementioned trends for the nickel-catalysed coupling of **1** with active methylene compounds **2a**, **b** proved also to be true for this exchange reaction. A notable exception arose from the beneficial effect of added acetic acid as expected from the literature.[2b–h] Namely, the formation of **6** was best conducted by using $Ni(dppb)_2$ as the catalyst, DMF as the solvent and by adding 1 equiv., of AcOH with respect to **1** (Table 2, entry 5). The most efficient palladium catalyst found [*in situ* combination $Pd(OAc)_2$–dppb, 1 : 3] took at least 20 times longer for the exchange reaction to go to completion than the latter nickel-based system under the same conditions (entry 6).

In conclusion we have demonstrated that $Ni(dppb)_2$ easily generated from $Ni(COD)_2$ and 2 equiv. of the bisphosphine is generally a much more active catalyst than comparable palladium systems for substitution of allylamines with 'soft' nucleophiles. Two explanations can be proposed for this trend: (i) the higher ability of nickel catalysts to activate allylic substrates having a poor leaving group, *i.e.* here the C–N bond, and/or (ii) the lower propensity of Ni to be coordinated by amines, thus resulting in larger amounts of active Ni–phosphine species. The limitation of these nickel-based systems lies in the sensitivity of nickel intermediates towards acetylacetone.

## Footnotes

* E-mail: mortreux@ensc-lille.fr

† In a typical experiment (Table 1, entry 13), to $Ni(COD)_2$ (36 mg, 0.13 mmol) in a 50 ml glass reactor equipped with a Teflon cap was added a degassed solution of dppb (111 mg, 0.26 mmol) in DMF (12.5 ml) under nitrogen. After 15 min of magnetic stirring, **1** (0.74 g, 6.5 mmol), **2b** (1.13 g, 9.75 mmol) and heptane (1.00 g, 10 mmol, GLC internal standard) were added. The solution was stirred at 50 °C and the reaction was monitored by quantitative GLC analysis of aliquot samples. Coupling reactions involving a co-reagent and exchange reactions of **1** with piperidine were carried out in a similar manner. *In situ* palladium catalysts were prepared by mixing $Pd(OAc)_2$ with a degassed solution (THF or DMF) of the phosphine ligand. The resulting yellow solution was stirred for 15 min at room temperature before use.

‡ Such a degradation of nickel intermediates could be rationalised as follows:

$$Ni^0(dppb) + 2\ acacH \rightarrow Ni(acac)_2 + H_2 + dppb$$

## References

1 (*a*) H. Bricout, J.-F. Carpentier and A. Mortreux, *Tetrahedron Lett.*, 1997, **38**, 1053; (*b*) Y. I. M. Nilsson, P. G. Andersson and J.-E. Bäckvall, *J. Am. Chem. Soc.*, 1993, **115**, 6609.

2 Palladium-catalysed nucleophilic substitution of allylamines and related derivatives: (*a*) K. E. Atkins, W. E. Walker and R. M. Manyik, *Tetrahedron Lett.*, 1970, **43**, 3821; (*b*) B. M. Trost and E. Keinan, *J. Org. Chem.*, 1980, **45**, 2741; (*c*) A. Hosomi, K. Hoashi, S. Kohra, Y. Tominaga, K. Otaka and H. Sakurai, *J. Chem. Soc., Chem. Commun.*, 1987, 570; (*d*) F. Garro-Helion, A. Merzouk and F. Guibé, *J. Org. Chem.*, 1993, **58**, 6109; (*e*) S. Murahashi, Y. Imada and K. Nishimura, *Tetrahedron*, 1994, **50**, 453; (*f*) M. Grellier, M. Pfeffer and G. Van Koten, *Tetrahedron Lett.*, 1994, **35**, 2877; (*g*) S. Lemaire-Audoire, M. Savignac, J.-P. Genêt and J.-M. Bernard, *Tetrahedron Lett.*, 1995, **36**, 1267; (*h*) S. Lemaire-Audoire, M. Savignac, C. Dupuis and J.-P. Genêt, *Bull. Soc. Chim. Fr.*, 1995, **132**, 1157.

3 To the best of our knowledge, the cross-coupling of allylamines with boronic acids ('hard' nucleophiles) is the sole example of the use of nickel catalysts: B. M. Trost and M. D. Spagnol, *J. Chem. Soc., Perkin Trans. 1*, 1995, 2083.

4 H. Bricout, J.-F. Carpentier and A. Mortreux, *J. Chem. Soc., Chem. Commun.*, 1995, 1863.

*Received in Cambridge, UK, 30th April 1997; 7/02954C*

# Partial separation of enantiomeric 1,2-diols *via* ketal formation with a polymer-supported chiral ketone

**Ian D. Clarke and Philip Hodge***

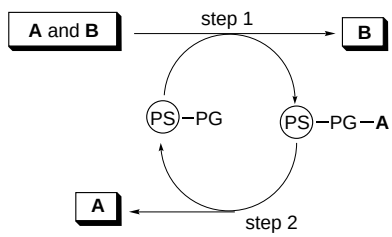
*Department of Chemistry, University of Manchester, Oxford Road, Manchester, UK M13 9PL*

**Partial separations of the (*R*,*R*)- and (*S*,*S*)-enantiomers of butane-2,3-diol, *trans*-cyclohexane-1,2-diol and dimethyl tartrate were achieved *via* ketal formation with a polymer-supported 7-keto steroid; in each case one enantiomer reacted in higher yield than the other and release of the diols from the support gave diol fractions significantly enriched in one enantiomer**

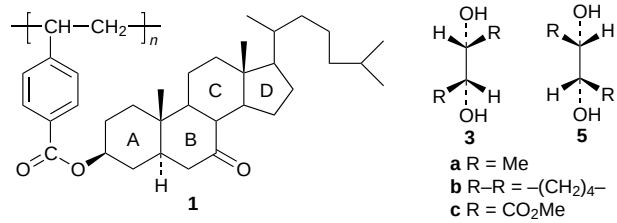
In recent years many organic reactions have been carried out which involve polymer-supported (PS) species.[1] The most well known examples are those involved in 'solid phase' peptide syntheses.[2] The latter can be viewed as examples of organic reactions using PS substrates and also as examples of the use of PS protecting groups (PS-PGs),[3] in this case for carboxylic acids. Reactions involving PS substrates are currently of great interest in combinatorial chemistry.[4,5] Organic reactions involving PS reagents and PS catalysts have also been studied extensively.[1]

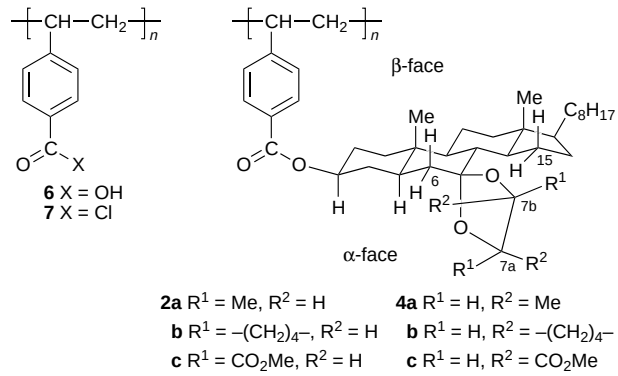
An application of PS species which has received little attention is the use of PS-PGs to achieve separations by the procedure summarised in Scheme 1. In step 1 the mixture of compounds to be separated, **A** and **B**, is treated with a PS-PG which selectively binds **A** to the support. Those components, **B**, of the mixture that fail to bind to the support are recovered. In step 2, the components of the original mixture, **A**, bound to the support are released by carrying out the appropriate 'deprotection' procedure. Thus, **A** is separated from **B** and the PS-PG is available for re-use. This method of achieving separations is less laborious than column chromatography and potentially it could be automated. Examples of this separation procedure being used in organic chemistry include the use of a PS-diol to separate 3-keto steroids from 17- and 20-keto steroids,[6] and of a PS-boronic acid to separate the *cis*- and *trans*-isomers of cyclohexane-1,2- and -1,3-diols.[7]

This communication is concerned with the separation of mixtures of *enantiomeric* diols *via* ketal formation with a PS chiral ketone. The PS chiral ketone selected for this initial study was an ester **1** of 3β-hydroxy-5α-cholestan-7-one. Inspection of Dreiding models of the ketals **2** derived from PS-ketone **1** and diols **3** indicates that the **R¹** groups at the 7b-position will experience significant steric interactions with the D-ring (especially the 15α-hydrogen) whilst the **R¹** groups at the 7a-position will not experience any significant non-bonding interactions with other parts of the steroid nucleus. In the ketals **4** derived from diols **5** the **R²** groups at the 7b-position may experience minor non-bonding interactions with the 6α-hydrogen whilst those at the 7a-position will again not experience any significant interactions. Thus, the PS ketone **1** is expected to bind diols **5** more readily than diols **3**. The presence of two **R** groups in each diol is necessary to ensure that one **R** group is present at the crucial 7b-position.




**Scheme 1**




Gel-type polystyrene beads crosslinked with 2% of divinylbenzene and containing carboxylic acid residues **6** (1.10 mmol $g^{-1}$), were prepared from commercial blank crosslinked beads *via* lithiated polystyrene.[8,9] The carboxylic acid groups **6** were converted into acid chloride residues **7**, the latter reacted with 3β-hydroxy-5α-cholestan-7-one,† and the unreacted residues **7** capped with MeOH essentially as described before.[13] This gave polymer beads containing residues **1** with a loading (0.60 mmol $g^{-1}$), similar to that reported before.[13]

Ketal formation (step 1) was achieved by treating mixtures of enantiomeric diols in toluene at reflux temperature with PS ketone **1** in the presence of a catalytic amount of toluene-*p*-sulfonic acid (PTSA). The reaction was carried out for 56 h in an apparatus equipped with a Dean–Stark trap. At the end of the reaction period the beads were filtered off and unbound diol recovered. The ketalisation yield, *i.e.* the percentage of supported ketone converted into the ketals, was estimated from the amount of unbound diol. The bound diol was released (> 97% recovered) by treating the PS ketal at 20 °C for 22 h with wet dioxane containing a catalytic amount of PTSA. All diol fractions were shown to be > 98% pure by $^1$H NMR spectroscopy. The percentage enantiomeric excesses of diol samples (ees) were estimated by polarimetry and/or chiral GC. The results are summarised in Table 1.

The separation of the (*R*,*R*)- and (*S*,*S*)-butane-2,3-diols was studied initially: see entries 1–7. It is evident that both diols

bound to the beads, but that, as expected, the (*S*,*S*)-diol **5a** bound in higher yields. The ketalisation yield was, however, only 57% even when equimolar amounts of (*S*,*S*)-diol **5a** and ketone **1** were used (entry 1). This may be due in part to some of the bound ketone being inaccessible due to steric crowding.[13] The diol recovered from the beads had a 42% ee of the (*S*,*S*)-diol **5a**. With an equimolar amount of racemate (*i.e.* 0% ee) as the starting material (entry 2) the diol recovered from the beads had a 39% ee of the (*S*,*S*)-diol **5a**. This rose to a 47% ee when the recovered diol was recycled (entry 3). The initial result (entry 2) indicates that 65% of the original (*S*,*S*)-diol **5a** bound to the beads whereas 29% of the (*R*,*R*)-diol **3a** bound, *i.e.* the yield ratio for the enantiomers was 2.2 : 1.

Apart from resolving racemates, other useful applications of the present type of system could involve raising the ee of reaction products from asymmetric syntheses. This might be achieved either by *concentrating* the major enantiomer or by *removing* the minor enantiomer. Starting with a mixture of butane-2,3-diol enantiomers having an 80% ee of the (*S*,*S*)-isomer **5a**, see entry 4, the diol recovered from the beads had a 90% ee. Similarly a starting material with 90% ee gave a product of 94% ee. This rose to a 97% ee when the recovered diol was recycled (entry 6). Thus through three cycles (entries 4–6) the ee of the (*S*,*S*)-diol **5a** was raised from 80 to 97%. Attempts to remove the (*S*,*S*)-enantiomer **5a** from a mixture having an 80 ee of the (*R*,*R*)-enantiomer **3a** was less successful (entry 7). After treating a five-fold excess of the mixture with the beads, the ee of recovered *unbound* diol had increased to only 82%. Evidently the binding of the preferred (*S*,*S*)-diol **5a** was almost entirely offset by the large proportion of the (*R*,*R*)-diol **3a** present.

**Table 1** Separation *via* ketal formation with PS keto steroid **1**

| | Starting material[a] | | | | Recovered diol[b] | |
|---|---|---|---|---|---|---|
| Entry | **3**,**5** | Ee (%) | Enantiomer in excess | Ketalisation yield (%) | Ee (%)[c] | Enantiomer in excess |
| 1[d] | **a** | 0 | — | 57 | 42 | *S*,*S* |
| 2 | **a** | 0 | — | 47 | 39 | *S*,*S* |
| 3 | **a** | 39 | *S*,*S* | 37 | 47[e] | *S*,*S* |
| 4 | **a** | 80 | *S*,*S* | 43 | 90[f] | *S*,*S* |
| 5 | **a** | 90 | *S*,*S* | 49 | 94 | *S*,*S* |
| 6 | **a** | 94 | *S*,*S* | 42 | 97[e] | *S*,*S* |
| 7[g] | **a** | 80 | *R*,*R* | 90[h] | 82[i] | *R*,*R*[g] |
| 8 | **b** | 0 | — | 11 | 55[f] | *S*,*S* |
| 9 | **b** | 80 | *S*,*S* | 20 | 92 | *S*,*S* |
| 10 | **c** | 0 | — | 9 | 72[e] | *R*,*R* |

[a] Except where indicated otherwise, ratio of diol to ketone was 1 : 1. [b] Except where indicated otherwise, the diol fraction examined was that obtained by deketalisation. The recoveries were > 97%. [c] Unless indicated otherwise, the ees were determined both by polarimetry and chiral GC. The results were in close agreement (±1%). Polarimetry was based literature values (ref. 14): $[\alpha]_D^{20}$ +13.0 (neat) for **5a**; $[\alpha]_D^{20}$ + 36.7 (*c* 0.45 in $H_2O$) for **5b**; $[\alpha]_D^{20}$ + 20.0 (*c* 20 in $H_2O$) for **5c**. Chiral GC was carried out using a CP-Chirosil-DEX CB stationary phase. [d] Ratio of diol to ketone was 2 : 1. [e] Ee determined by polarimetry only. [f] Ee determined by GC only. [g] This experiment used a five-fold excess of the diol and focused on the *unbound* diol. [h] Percentage of starting material *not* bound. [i] The *unbound* diol fraction was examined.

The ketalisation yields were lower starting with racemic mixtures of the (*R*,*R*)- and (*S*,*S*)-*trans*-cyclohexane-1,2-diols and dimethyl (*R*,*R*)- and (*S*,*S*)-tartrates (entries 8–10) but the recovered diols had higher ee, 55 and 72% respectively, than with butan-2,3-diol. Thus, the more significant the steric interactions the greater the discrimination between the enantiomers but the lower the chemical yield. It should be noted here that with a perfect discrimination between the enantiomers and all the ketone residues of **1** fully available, starting with racemates the ketalisation yields would be only 50%. As expected the enantiomers which bound in the higher yields were the (*S*,*S*)-enantiomer **5b** and (*R*,*R*)-enantiomer **5c**. The results using the racemates as starting materials indicate yield ratios of 6.9 : 1 with the enantiomeric diols **5b** and **3b** and 6.1 : 1 with the enantiomeric diols **5c** and **3c**.

The keto steroid had no tendency to detach from the beads under the reaction conditions used in this study. Thus, no steroid was detected by $^1$H NMR spectroscopy in any of the diol fractions. Indeed, the FT–IR spectrum of the PS ketone **1** at the end of the experiments was indistinguisable from that when first prepared. All the above results were obtained with one batch of resin, thus demonstrating that the PS ketone **1** can be recycled.

This initial study shows that significant separations of enantiomers can be achieved using the procedure outlined in Scheme 1. The procedure could undoubtedly be automated. Future work is being directed towards identifying chiral molecules which are more discriminating between the enantiomers and which permit higher loadings to be achieved.

We thank the EPSRC for financial support.

## Footnotes

* E-mail: philip.hodge@man.ac.uk

† 3β-Hydroxy-5α-cholestan-7-one, mp 168 °C (lit.,[10] 170.5–171.5) and $[\alpha]_D^{20}$ −33 (*c* 2 in chloroform) {lit.,[11] $[\alpha]_D^{20}$ −36 (*c* 1.6 in chloroform)}, was prepared by oxidising cholesteryl acetate with chromic acid,[12] hydrogenating (Pd–charcoal) the product, then hydrolysing the ester group.

## References

1 (*a*) *Polymer-supported Reactions in Organic Synthesis*, ed. P. Hodge and D. C. Sherrington, Wiley, Chichester, 1980; (*b*) *Syntheses and Separations Using Functional Polymers*, ed. D. C. Sherrington and P. Hodge, Wiley, Chichester, 1988; (*c*) *Polymeric Reagents and Catalysts*, ed. W. T. Ford, ACS Symposium Series 308, Washington D.C., 1986.
2 R. B. Merrifield, *J. Am. Chem. Soc.*, 1963, **85**, 2149.
3 P. Hodge, *Chem. Ind.*, 1979, 624; J. M. J. Fréchet, ch. 6 in ref. 1(*a*).
4 G. Lowe, *Chem. Soc. Rev.*, 1996, **25**, 309.
5 N. K. Terrett, M. Gardner, D. W. Gordon, R. J. Kobylecki and J. Steele, *Tetrahedron*, 1995, **51**, 8135.
6 P. Hodge and J. Waterhouse, *J. Chem. Soc., Perkin Trans. 1*, 1983, 2319.
7 E. Seymour and J. M. J. Fréchet, *Tetrahedron Lett.*, 1976, 3669.
8 T. M. Fyles and C. C. Leznoff, *Can. J. Chem.*, 1976, **54**, 935.
9 M. J. Farrall and J. M. J. Fréchet, *J. Org. Chem.*, 1976, **41**, 3877.
10 H. R. Nace and G. A. Crosby, *J. Org. Chem.*, 1979, **44**, 3105.
11 D. H. R. Barton and J. D. Cox, *J. Chem. Soc.*, 1948, 783.
12 H. C. Meuley, US Pat. 2 505 646, (*Chem. Abstr.*, 1950, **44**, 6894).
13 P. Hodge, J. Kemp, E. Khoshdel and G. M. Perry, *Reactive Polymers*, 1985, **3**, 299.
14 *Dictionary of Organic Compounds*, 5th edn.,, Chapman and Hall, New York, 1982.

*Received in Cambridge, UK, 15th April 1997; 7/02567J*

# A pH cleavable linker for zone diffusion assays and single bead solution screens in combinatorial chemistry

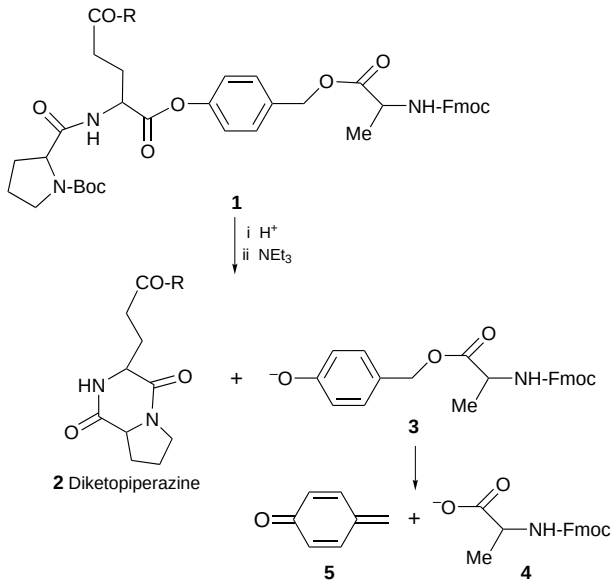
**Butrus Atrash and Mark Bradley***

*Department of Chemistry, University of Southampton, Southampton, UK SO17 1BJ*

**A safety catch linker has been developed that allows efficient compound release into buffered aqueous solutions and agarose gels.**

Linkers, acting as the selectively cleavable bridge between the solid support and the compound of interest, play a pivotal role in solid phase, combinatorial and peptide chemistry. This role is fundamental, not only in dictating the range of chemistry which can be carried out, but also in determining the particular screening approach to the library in question.[1] At the present time there are a limited number of linkers available that are 'biocompatible' in terms of linkers being directly cleavable within the assay. The best known examples are light cleavable linkers;[2] the internal imidazole catalysed, ester cleavable linkers of Frank[3] and the iminodiacetic acid based linkers of Lebl.[4] All of these have a number of attractive features but also limitations for screening.

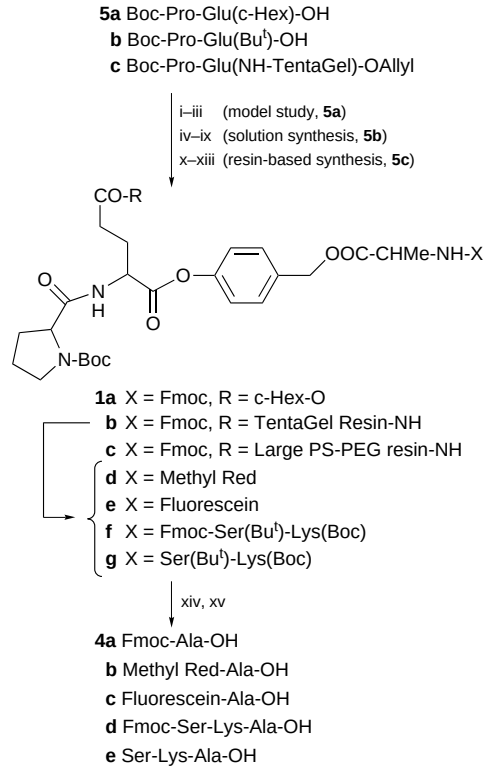
We now report the development of a highly efficient linker which cleaves at pH 8, following acidic (safety catch) activation. The activated linker rapidly cleaves in buffered solution and within agarose gel within a time frame that allows the gel to set before compound release but fast enough to allow complete cleavage within a few hours. The key mechanistic features of the linker **1** are diketopiperazine **2** formation, taking place at pH 7–8, which releases a derivatised hydroxymethylphenol(ate) **3**. This then undergoes a facile 1,6-elimination process to give the product **4** and the quinone methide by-product **5** (see Scheme 1). The process was initially investigated in solution using **1a** (R = cyclohexylO) which was synthesised as shown in Scheme 2. Cleavage was monitored by TLC following removal of the Boc group and treatment with $NEt_3$, and resulted in rapid cleavage (< 1 h) of the linker and quantitative release of Fmoc-Ala-OH.




**Scheme 1**

Having ascertained the practicalities of cleavage the first resin-based experiments were initiated by the synthesis of **1b** and by its simple derivatisation to give **1d**–**g**† to look at the ensuing release of **4a**–**e**. The linkers were initially synthesised in solution and attached to the resin prior to derivatisation since in our view quantification of linker efficiency/kinetics is most reliable with homogeneous material coupled to the solid support. Subsequently the solution synthesis was replaced by an efficient resin based synthesis as shown in Scheme 2.

Cleavage from the resin was followed by UV analysis in real time, RP-HPLC [with samples being removed and quenched (0.1% TFA) before injection] and quantification using internal standards. Although TentaGel is compatible with most solvents and hence a wide range of compounds, we were interested in the variation of cleavage rate with a number of different compounds. Compounds released in this study included Fmoc-Ala-OH, Methyl Red-Ala-OH, Fluorescein-Ala-OH and two tripeptides Fmoc-Ser-Lys-Ala-OH and H-Ser-Lys-Ala-OH. The




**Scheme 2** *Reagents and conditions*: i, 4-$HOC_6H_4CHO$, DCC, 98%; ii, $NaBH_3CN$, 65%; iii, Fmoc-Ala, DCC, DMAP, 68%; iv, 4-$HOC_6H_4CHO$, DCC, 90%; v, $NaBH_3CN$, 80%; vi, Fmoc-Ala, DCC, DMAP, 79%; vii, $CF_3CO_2H$–$CH_2Cl_2$ (1 : 1), 100%; viii, $Boc_2O$, 60%; ix, TentaGel Resin-S $NH_2$ or 'big' PS-PEG-$NH_2$ beads, DIC, HOBt; x, $Pd(PPh_3)_4$, dimedone; xi, 4-$HOC_6H_4CHO$, DCC; xii, $NaBH_3CN$; xiii, Fmoc-Ala, DCC, DMAP; xiv, $CF_3CO_2H$–$CH_2Cl_2$ (1 : 1); xv, $K_2HPO_4$ (50 mM, pH 8)

resins used were TentaGel-S-$NH_2$ and aminomethyl polystyrene beads (150–300 μm, 2 mmol $g^{-1}$) made water-compatible by the method of Hudson.[5] Cleavage results are shown in Fig. 1.

The half-lives of cleavage from TentaGel-S-$NH_2$ in 50 mM phosphate buffer (pH 8.0) ranged from 10–75 min depending on the compound being cleaved with yields greater than 70% in all cases.‡ As with photocleavable linkers[6] we observed that hydrophobic compounds were released much more slowly into the aqueous assay solution than hydrophilic, a factor which must have implications for single bead library screening. The intermediate **3** was identified by HPLC and ES-MS in the cleavage of **1b**. The large water compatible beads **1c** were studied for the release of Fmoc-Ala-OH. The half-life for cleavage in this case was 800 min, which compares with 75 min for Fmoc-Ala-OH being released from TentaGel resin. Clearly the difference illustrates the effect of bead size on the diffusion of materials into and out of the large beads (these beads swell to about 600–700 μm in water), but also we believe it is associated with the smaller PEG chains on our larger beads compared to those found on TentaGel.

Beads **1b**,**e** were used in a zone diffusion type assay. The Boc safety catch was removed and the beads added to molten agarose (45 °C) and poured into petri dishes. Fluorescent zones were clearly visible around beads **1e** after 2–3 h in the agarose gel. Beads **1b** were left in the gel for 12 h, following which 5% TFA–$H_2O$ was added, the gel melted and the beads removed and thoroughly washed. Fmoc analysis indicated that 70% of the material had been cleaved from the resin. Since the half-life of cleavage for **1b** in solution is 75 min this experiment demonstrates that materials are cleaved into the agarose gel with relatively good efficiency, although as expected more slowly than into free solution.

In summary, we have developed what we believe is a practical example of a "pH" labile linker for solid phase and combinatorial chemistry. Importantly we have shown that the linker is stable to the base treatments required during Fmoc peptide chemistry and that it is efficiently cleaved in buffered aqueous solutions following synthesis. The one negative side is the quinone methine that may need quenching in the assay. We believe that linkers of this type have huge potential in solid phase chemistry for the screening of compound libraries using single bead solution screens and zone diffusion assays.

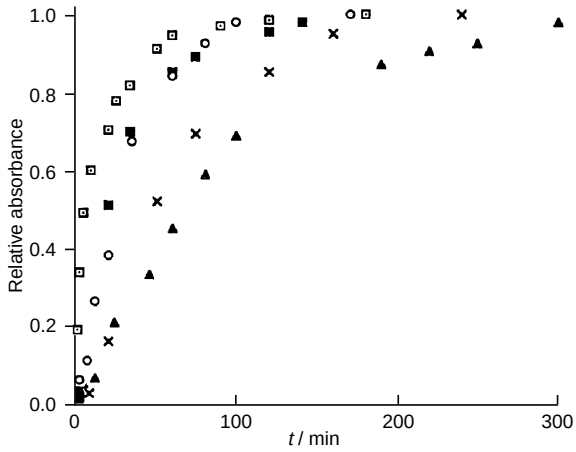



**Fig. 1** Kinetics of compound release from **1b**,**d**–**g**: (x) Methyl Red-Ala, (▲) Fmoc-Ala, (■) Fluor-Ala, (○) Fmoc-Ser-Lys-Ala, (⊡) Ser-Lys-Ala

We thank the EPSRC for a ROPA award and the Royal Society for a University Research Fellowship (M. B.).

## Footnotes

* E-mail: mb14@soton.ac.uk

† *Selected data* for Boc-Pro-Glu(OH)OPh$CH_2$OAla-Fmoc (*E*/*Z* forms exist about the Boc-Pro urethane): $\delta_H$(300 MHz, $CD_3OD$) 1.38–1.51 (12 H, m, *Boc*-Pro and C*H*$_3$CH), 1.65–2.06 and 2.08–2.45 [6 H, 4 br m, Pro-$CH_2$ (β and γ) and Glu-$CH_2$ (β)], 2.48–2.63 [2 H, m, Glu-$CH_2$ (γ)], 3.37–3.48 and 3.49–3.64 [2 H, 2 br m, Pro-$CH_2$ (δ)], 4.15–4.20 (1 H, t, *J* 7, FmocCH), 4.26–4.41 [2 H, 2 m, Ala and Pro CH (α)], 4.30 (2 H, d, *J* 7, Fmoc$CH_2$), 4.68 [1 H, m, Glu-CH (α)], 5.16 (2 H, ABq, *J* 7, Ar$CH_2$), 7.07 (2 H, d, *J* 8, Ar), 7.30 (2 H, t, *J* 8, Fmoc), 7.39 (2 H, d, *J* 8, Ar), 7.40 (2 H, t, *J* 7, Fmoc), 7.66 (2 H, d, *J* 7, Fmoc), 7.79 (2 H, d, *J* 7, Fmoc); $\delta_C$(75 MHz, $CD_3OD$) 17.45 (*C*$H_3$-Ala), 24.46 [Pro-*C*$H_2$ (γ)], 27.24 [Glu-*C*$H_2$ (β)], 28.63 ($Me_3$), 31.07 [Glu-*C*$H_2$ (γ)], 32.47 [Pro-*C*$H_2$ (β)], 47.86 [Pro-*C*$H_2$ (δ)], 48.23 [Ala-*C*H (α)], 51.10 (Fmoc-*C*H), 53.38 [Glu-*C*H (α)], 61.52 [Pro-*C*H (α)], 67.05 (*C*$H_2$Ar), 67.95 (Fmoc-*C*$H_2$), 81.53 (*C*$Me_3$), 120.90, 122.63, 126.16, 128.12, 128.74, 130.30 (ArCH), 135.16, 142.48, 145.14, 151.84, (ArC), 156.0, 158.33 (urethanes), 171.46, 171.62, 174.34 (esters and amide), 176.05 (acid); TLC $R_f$ 0.3 (49 : 1 EtOAc–AcOH); mp 102–104 °C; ES-MS (+ve): *m*/*z* 766.3 $(M + Na)^+$, 781.4 $(M + K)^+$; $\nu_{max}(CHCl_3)/cm^{-1}$ 3424, 3351, 2979, 1725, 1681, 1508; HRMS: expected for $C_{40}H_{46}O_{11}N_3$, 744.3132. Found, 744.3166. Compounds **1d**,**f**,**g** were synthesised from **1b** in a conventional manner using DIC–HOBt couplings and 20% piperidine–DMF deprotections. Compound **1e** was prepared using Fluorescein isocyanate.

‡ Based on the initial dry weight substitution of TentaGel. We have found it very hard to return TentaGel to its free flowing form after solvation, thus yields probably represent a minimum value. A control cleavage in which the safety catch had not been removed showed no compound release after 4 h.

## References

1 M. A. Gallop, R. W. Barrett, W. J. Dower, S. P. A. Fodor and E. M. Gordon, *J. Med. Chem.*, 1994, **37**, 1233; N. K. Terrett, M. Gardner, D. W. Gordon, R. J. Kobylecki and J. Steele, *Tetrahedron*, 1995, **51**, 8135; M. Rinnova and M. Lebl, *Collect. Czech. Chem. Commun.*, 1996, **61**, 171.

2 J. J. Burbaum, M. H. Ohlmeyer, J. C. Reader, I. Henderson, L. W. Dillard, G. Li Troy, T. L. Randle, N. H. Sigal, D. Chelsky and J. J. Baldwin, *Proc. Natl. Acad. Sci. USA*, 1995, **91**, 6027; J. J. Baldwin, J. J. Burbaum, I. Henderson and M. H. Ohlmeyer, *J. Am. Chem. Soc.*, 1995, **117**, 5588; C. P. Holmes and D. G. Jones, *J. Org. Chem.*, 1995, **60**, 2318.

3 S. Hoffmann and R. Frank, *Tetrahedron Lett.*, 1994, **35**, 7763.

4 M. Lebl, M. Patek, P. Kocis, V. Krchnak, V. J. Hruby, S. E. Salmon and K. S. Lam, *Int. J. Pept. Protein Res.*, 1993, **41**, 201; S. E. Salmon, K. S. Lam, M. Lebl, A. Kandola, P. S. Khattri, S. Wade, M. Patek, P. Kocis, V. Krchnak, D. Thorpe and S. Felder, *Proc. Natl. Acad. Sci. USA*, 1993, **90**, 11 708; P. Kocis, V. Krchnak and M. Lebl, *Tetrahedron Lett.*, 1993, **34**, 7251.

5 R. M. Cook, J. H. Adams and D. Hudson, *Tetrahedron Lett.*, 1994, **35**, 6777.

6 N. Bouloc, M. Phil Thesis, *Diffusion Zone Assays for Bio-Active libraries—Light Mediated Compound Release*, University of Southampton, 1996.

*Received in Glasgow, UK, 18th April 1997; 7/02677C*

# Lipase–triethylamine-mediated dynamic transesterification of a tricyclic acyloin having a latent *meso*-structure: a new route to optically pure oxodicyclopentadiene

**Takahiko Taniguchi and Kunio Ogasawara***

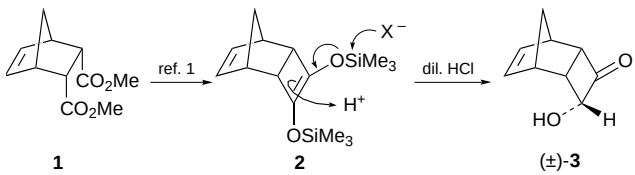
*Pharmaceutical Institute, Tohoku University, Aobayama, Sendai 980-77, Japan*

**The racemic tricyclic acyloin (±)-*endo*-3-hydroxytricyclo[4.2.1.0$^{2,5}$]non-7-en-4-one has been dynamically resolved *via* the transient formation of the *meso*-enediol isomer under lipase–triethylamine-mediated kinetic transesterification conditions to give the single chiral acetate (−)-*endo*-3-acetoxytricyclo[4.2.1.0$^{2,5}$]non-7-en-4-one, serving as a precursor of (−)-oxodicyclopentadiene, in excellent optical and chemical yields.**

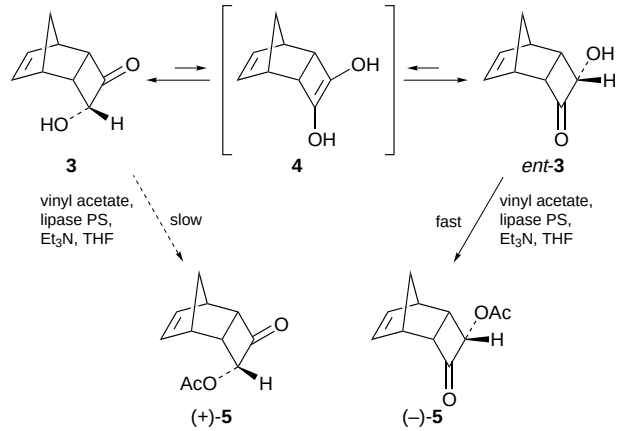
During the preparation of the racemic tricyclic acyloin 3-hydroxytricyclo[4.2.1.0$^{2,5}$]non-7-en-4-one (±)-**3** starting from *endo*-2,3-bis(methoxycarbonyl)bicyclo[2.2.1]hept-5-ene **1** by employing the acyloin condensation,[1] we observed[2] that an acid hydrolysis of the bis-trimethylsilyloxy intermediate **2** furnished stereoselectively the single racemic acyloin (±)-**3** having an *endo*-hydroxy group (Scheme 1).† The *endo*-hydroxy configuration of **3** did not change even in the presence of triethylamine, which brought about complete deuterium exchange of the methine hydrogen on the acyloin functionality with deuterium oxide within 10 h. This seemed to be due to facile equilibration between the acyloin **3** and the transient *meso*-1,2-enediol intermediate **4** followed by convex-face selective protonation of the latter under weak basic conditions. Since the analogues of **3** having cyclopentenol and cyclohexenol rings in place of the four-membered ring have been found to be kinetically better discriminated than those having an *exo*-hydroxy group under lipase-mediated transesterification conditions,[3] we assumed that dynamic kinetic resolution[4,5] should take place in a facile manner to give a single enantiomeric *endo*-acetate **5**. The racemic acyloin (±)-**3** might be subjected to the transesterification conditions in the presence of an appropriate lipase under favourable equilibrium conditions,[6] thus generating the transient enediol **4** having *meso* symmetry. We report herein the first example of the lipase-mediated dynamic transesterification of the racemic acyloin **3** leading to the highly optically enriched single *endo*-acetate (−)-**5** *via* the transient generation of the *meso*-enediol **4** in reaction with vinyl acetate in THF containing a catalytic amount of triethylamine (Scheme 2).

When the racemic acyloin **3** was stirred with vinyl acetate (1.2 equiv.) in THF containing triethylamine[3b,5a,7] (0.1 equiv.) in the presence of lipase PS‡ (*Pseudomonas* sp. immobilized on Celite, Amano) for 48 h at room temperature, transesterification occurred to give the optically active *endo*-acetate (−)-**5**, $[\alpha]_D^{24}$ −120.7 (*c* 2.0, $CHCl_3$), in 75% yield accompanied by a minor amount of 5-hydroxy-4-oxatricyclo[5.2.1.0$^{2,6}$]dec-8-en-3-one§ (10%) which was separated by silica gel column chromatography. The optical yield of the product was determined to be 97% ee by HPLC (chiral column CHIRALCEL OD, 5% Pr$^i$OH–hexane) indicating clearly that the dynamic kinetic resolution took place as expected. When the reaction was carried out without triethylamine, simple kinetic resolution occurred to give the same *endo*-acetate (−)-**5**, $[\alpha]_D^{26}$ −120.3 (*c* 1.0, $CHCl_3$), (> 99% ee, CHIRALCEL OD, 5% Pr$^i$OH–hexane) in 45% yield leaving 53% of the optically enriched starting acyloin (+)-**3**, $[\alpha]_D^{27}$ + 190.5 (*c* 0.9, $CHCl_3$) (92% ee, CHIRALCEL OD, 5% Pr$^i$OH–hexane); thus, this result indicates that the amine accelerated the equilibrium between **3** and *ent*-**3** *via* the *meso*-1,2-enediol **4**. When the racemic acyloin (±)-**3** was stirred with vinyl acetate in the same THF–triethylamine medium without the lipase, the transesterification which competes with the enzymatic reaction, although it occurred, proceeded very slowly to give the racemic *endo*-acetate (±)-**5** in less than 3% yield, leaving most of the starting material untouched after 48 h at room temperature. Taking these observations into account, we concluded that triethylamine is requisite for the present dynamic transesterification and the actual enantioselectivity exerted by the enzyme was higher than that observed.

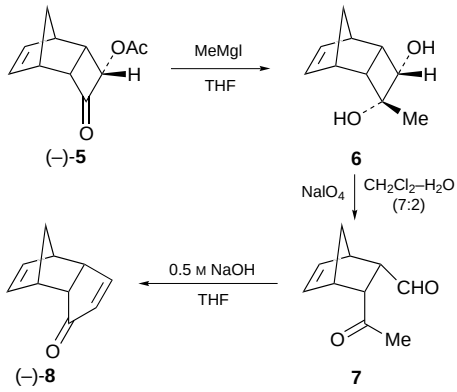
Having established the efficient dynamic kinetic transesterification of the racemic acyloin (±)-**3** having a latent *meso*-structure, the optically active acetate (−)-**5** thus obtained was next transformed into optically active oxodicyclopentadiene **8** so as to determine the absolute configuration of the resolved product as well as to probe its synthetic utility. Thus (−)-**5** was treated with excess MeMgI in THF to give the diol **6**, $[\alpha]_D^{26}$ −15.7 (*c* 0.6, $CHCl_3$), in nearly quantitative yield. Treatment of the diol **6** with sodium periodate gave the keto aldehyde **7** which was immediately exposed to diluted aqueous sodium hydroxide[8] to give the known oxodicyclopentadiene (−)-**8**, mp 74 °C, $[\alpha]_D^{26}$ −154.0 (*c* 1.0, $CHCl_3$) [lit.,[3b] mp 76 °C, $[\alpha]_D^{29}$ −158.5 (*c* 1.0, $CHCl_3$)] (> 99% ee by HPLC: CHIRALCEL OB, 10% Pr$^i$OH–hexane), in 50% overall yield by intramolecular aldolization.[8] Since optically active oxodicyclopentadiene **8** is




**Scheme 1**




**Scheme 2**




**Scheme 3**

interconvertible into the enantiomer[8] and used as a versatile chiral building block,[9] the present transformation constitutes the determination of the absolute structure of the chiral acetate (−)-**5** as shown and an alternative synthesis of optically active oxodicyclopentadiene[3b,9,10] **8** (Scheme 3).

In conclusion, we have demonstrated that the tricyclic racemic acyloin *endo*-3-hydroxytricyclo[4.2.1.0$^{2,5}$]non-7-en-4-one (±)-**3** is dynamically acylated with vinyl acetate in an enantiospecific manner *via* the transient *meso*-enediol **4** in THF containing triethylamine in the presence of lipase to give the single *endo*-acetate (−)-**5**, proving itself as a potential chiral building block[2] and serving at the same time as the precursor of versatile chiral oxodicyclopentadiene **8**. We are currently working on extension of the present dynamic kinetic resolution to other acyloins having latent *meso* structure as well as to the acyloins having latent prochirality, and on exploitation of the chiral acyloin acetates obtained for the construction of a variety of optically active molecules.

## Footnotes

* E-mail: konol@ mail.cc.tohoku.ac.jp
† The stereochemistry of **3** was determined by NOE measurements.
‡ Lipase LIP (*Pseudomonas aeruginosa*, TOYOBO) also gave the same acetate (−)-**5** (97% ee) in 60% yield without leaving the starting acyloin (±)-**3**.
§ The same compound was generated from **3** on reaction with 30% $H_2O_2$–0.5 M NaOH.

## References

1 R. D. Miller, D. L. Dolce and V. Y. Merritt, *J. Org. Chem.*, 1976, **41**, 1221.
2 *cf*. T. Taniguchi, Y. Goto and K. Ogasawara, *Synlett*, in the press.
3 (*a*) K. Tanaka and K. Ogasawara, *Synthesis*, 1995, 1237; (*b*) T. Sugahara, Y. Kuroyanagi and K. Ogasawara, *Synthesis*, 1996, 1101.
4 For reviews on dynamic kinetic resolution, see R. S. Ward, *Tetrahedron: Asymmetry*, 1995, **6**, 1475; H. Stecher and K. Faber, *Synthesis*, 1997, 1.
5 For recent examples, see (*a*) N. J. Turner, J. R. Winterman, R. NcCague, J. S. Paratt and J. C. Taylor, *Tetrahedron Lett.*, 1995, **36**, 1113; (*b*) J. V. Allen and J. M. J. Williams, *Tetrahedron Lett.*, 1996, **37**, 1859; (*c*) M. van den Heuvel, A. D. Cuiper, H. van der Deen, R. M. Kellogg and B. L. Feringa, *Tetrahedron Lett.*, 1997, **38**, 1655.
6 For a non-dynamic kinetic resolution of acyloins, see D. Gala, D. J. DiBenedetto, J. E. Clark, B. L. Murphy, D. P. Schumacher and M. Steinman, *Tetrahedron Lett.*, 1996, **37**, 611; W. Adam, M. T. Maria, R. T. Fell and C. R. Saha-Moeller, *Tetrahedron: Asymmetry*, 1996, **7**, 2207.
7 *cf*. F. Theil, S. Ballschuh, A. Kunath and H. Schick, *Tetrahedron: Asymmetry*, 1991, **2**, 1031; F. Theil, J. Weidner, S. Ballschuh, A. Kunath and H. Schick, *Tetrahedron Lett.*, 1993, **34**, 305; T. Sugahara and K. Ogasawara, *Tetrahedron Lett.*, 1996, **37**, 205.
8 S. Takano, K. Inomata and K. Ogasawara, *Chem. Lett.*, 1989, 359.
9 For a pertinent review, see K. Ogasawara, *J. Synth. Org. Chem. Jpn.*, 1996, **54**, 15.
10 For a recent synthesis of optically active **8**, see J. Knol and B. L. Feringa, *Tetrahedron Lett.*, 1997, **38**, 2527 and references cited therein.

*Received in Cambridge, UK, 29th April 1997; 7/02910A*

# Luminescence from ytterbium(III) and its complexes in solution†

**Andrew Beeby, Rachel S. Dickins, Stephen Faulkner, David Parker* and J. A. Gareth Williams**

*Department of Chemistry, University of Durham, South Road, Durham, UK DH1 3LE*

**Time-resolved studies of luminescence from ytterbium in solution are reported offering opportunities for luminescent imaging in the near IR, and allowing the use of a wide range of aromatic antennae to sensitise the metal centre; the luminescence of the solvated ion and of a wide variety of complexes is examined, both by direct excitation and by inter- and intra-molecular energy transfer.**

Time-resolved luminescence of lanthanide complexes has been of interest for some years.[1–3] However, interest has centred almost exclusively on the sensitised luminescence of complexes of $Eu^{III}$ and $Tb^{III}$. Such complexes have the advantage of possessing long luminescent lifetimes, but they are excited by long-wavelength UV radiation over the same range ($\lambda$ < 360 nm) as biological molecules. This seriously limits the utility of such complexes for direct *in vivo* applications. An additional problem arises from the relatively large energy gap between the emissive and ground states, which requires the use of aromatic antennae with relatively high triplet state energies to sensitise the metal efficiently.[4]

Lanthanides which emit at longer wavelengths have relatively small energy gaps between the excited and the ground state. This allows the use of antennae with much lower triplet state energies, avoiding the competitive excitation of biological chromophores. Time-resolved luminescence from neodymium has been studied recently by deconvolution of the detector response from a nitrogen-cooled germanium diode, allowing the resolution of lifetimes as short as 30 ns. Emission spectra over the range 800–1800 nm were obtained.[5] Ytterbium is another lanthanide which offers the possibility of long-wavelength luminescence. There is only one excited state and it is luminescent ($^2F_{5/2}$) emitting at 980 nm $^2F_{5/2}$–$^2F_{7/2}$). The $Yb^{III}$ ion is not readily reduced ($E_{1/2}$ = −1.35 V, *cf.* −0.35 V for $Eu^{III/II}$), so that competitive photoinduced electron transfer to the Yb from an excited singlet state of an antenna is not likely to occur. Ytterbium luminescence in the solution state has been largely neglected, and reports have concentrated on measurement of the emission spectra of simple systems with no time resolution.[6,7] We have examined the time-resolved luminescence from the ytterbium ion in a variety of solvents by direct excitation or energy transfer from co-dissolved chromophores, and describe examples of intramolecular energy transfer from energy-matched aryl groups in stable complexes with aza-macrocycle based ligands.

Initially, the possibility of intermolecular energy transfer from co-dissolved 4-carboxypropylpyrene ($\lambda_{exc}$ = 355 nm, $\tau$ = 0.34 μs in 50 : 50 MeOH–$H_2O$) and 9-hydroxymethylanthracene ($\lambda_{exc}$ = 266 nm, $\tau$ = 0.81 μs in MeOH) was investigated. Deconvolution and fitting of the decay curves was used to establish the lifetime of emission from the ytterbium centre. Deconvolution from the detector response was made possible by measuring the detector response using a short-lived pump (in our case the laser dye **DCM**). The lifetime was determined by minimising residuals and reduced $\chi^2$ over a range of lifetimes.‡[5] The lifetimes shown in Table 1 are much longer than those of neodymium in aqueous and methanolic solutions {*cf.* $\tau_{H_2O}[Nd(NO_3)_3]$ = 30 ns, $\tau_{MeOH}[Nd(NO_3)_3]$ = 70 ns}.[5] These differences relate to the more facile quenching of $Nd^{3+}$ by energy-matched O–H and C–H oscillators.[5]

Demonstration of direct excitation with ytterbium is more difficult. The absorption and emission spectra of ytterbium are very similar owing to the fact that there is only one readily populated excited state of ytterbium. The ytterbium ion was selectively excited using the output from a YAG driven optical parametric oscillator (OPO) producing photons at 970 nm. Emission was observed in the low energy tail of the emission band by using a 1055 nm interference filter with a 40 nm bandpass.§ As can be seen from the data in Table 1, the lifetimes are solvent dependent. The lifetime is longer in strongly coordinating solvents, such as $Me_2SO$, in which the ligating group stretching harmonics do not correspond well to the energy of the Yb $^2F_{5/2}$ state.

Meshkova and coworkers have reported the use of (2-pyridazo)-2-naphthol in the luminescent determination of ytterbium, but reported no time-resolved studies.[7,8] The 1 : 1 complex of the azo dye with ytterbium was prepared and the lifetime of the luminescence measured. Deconvolution techniques were employed to obtain the lifetime of the known 3 : 1 complex[9] with dibenzoylmethane ($\lambda_{exc}$ = 532 nm, $H_2O$). The luminescent lifetime of the pyridazo complex increased from 557 to 1250 ns on solvent deuteriation. This effect occurs

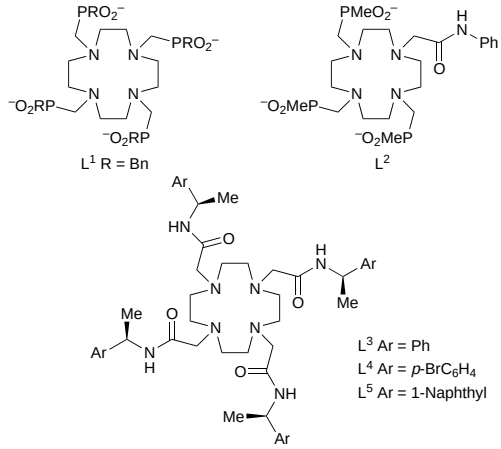
**Table 1** Lifetimes of ytterbium complexes and salts in protiated and deuteriated solvents (293 K; errors on lifetimes are ± 15%)

| Complex[c] | Solvent | Lifetime[a,b]/μs | $\lambda_{exc}$/nm |
|---|---|---|---|
| $Yb(CF_3SO_3)_3$ | $D_2O$ | 3.95 | 970 |
| | $Me_2SO$ | 5.26 | 970 |
| | $(CD_3)_2SO$ | 9.45 | 970 |
| $Yb(O_2CMe)_3$ | $D_2O$ | 3.84 | 970 |
| $Yb(dbm)_3$ | $CH_3OH$ | 0.50 | 355 |
| | $CD_3OD$ | 7.55 | 355 |
| | $CD_3OD$ | 7.33 | 970 |
| $[YbL^1]^-$ | $H_2O$ | 4.53 | 266 |
| | $D_2O$ | 8.90 | 266 |
| | $D_2O$[d] | 9.03 | 970 |
| $[YbL^2]$ | $H_2O$ | 1.87 | 266 |
| | $D_2O$[d] | 6.70 | 266 |
| $[YbL^3]^{3+}$ | $H_2O$ | 0.70 | 266 |
| | $D_2O$ | 6.18 | 266 |
| $[YbL^4]^{3+}$ | $H_2O$ | 0.77 | 266 |
| | $D_2O$ | 7.48 | 266 |
| $[YbL^5]^{3+}$ | $H_2O$ | 0.83 | 266 |
| | $D_2O$ | 5.00 | 266 |
| $[Yb(nta)_2]^{3-}$ | $D_2O$ | 8.10 | 970 |
| $[Yb(edta)_2]^{5-}$ | $D_2O$[d] | 10.9 | 970 |
| | $H_2O$ | 2.18 | 970 |
| $[Yb(dtpa)]^{2-}$ | $D_2O$[d] | 8.23 | 970 |
| | $H_2O$ | 0.73 | 970 |

[a] For excitation at 970 nm, decay curves were observed using a 1050 nm interference filter with a 40 nm bandpass with the aid of a polariser to block scattered light from the laser source. [b] Lifetimes were independent of the concentration of dissolved oxygen. [c] dbm = dibenzoylmethane anion, nta = nitrilotriacetate and dtpa = diethylenetriamine pentaacetate. [d] The rate constant for luminescent quenching in these cases was shown to be directly proportional to the mole fraction of $H_2O$ present in $H_2O$–$D_2O$ mixtures.

because the complex formed in solution does not completely encapsulate the metal centre. This allows close diffusion of solvent molecules which quench the luminescence due to coupling between the O–H oscillators and the metal centre. Relaxation *via* O–D oscillators is much less efficient, since only higher harmonics overlap with the metal excited state and the Frank–Condon overlap factor is less favourable. The lifetime of the dibenzoylmethane complex was similarly affected by the nature of the solvent.

In developing probes for long-wavelength luminescence one aim is to provide new methods for the imaging of biological systems. It is necessary that the complexes formed should be kinetically stable and that vibrational quenching by energy-matched oscillators should be minimised. With this in mind, we have investigated the behaviour of complexes of a variety of [12]aneN$_4$ based ligands (L$^1$–L$^5$) and selected acyclic chelating agents . The lifetimes of these complexes have been determined




and are reported in Table 1. The longest lifetimes were observed for the complex of the tetrabenzyl phosphinate, [YbL$^1$]$^-$, ($\tau_{H_2O}$ = 4.5 μs; $\tau_{D_2O}$ = 9.0 μs independent of [O$_2$]) and may be related to the complete encapsulation of the metal centre by the ligand. Recent crystallographic studies on complexes of L$^1$ with Y, Eu, Gd and Yb have shown that there are no coordinated water molecules.[10] Thus quenching of the metal centre is greatly reduced, and a relatively long lifetime is observed, with a small difference between the lifetimes in protiated and deuteriated solvents.[13] The residual quenching effect ($\Delta k_{H_2O/D_2O} = 1.11 \times 10^5\ s^{-1}$) can be assigned to a contribution from closely diffusing, unbound water molecules. This complex is particularly hydrophobic and probably sets a lower limit on this 'outer-sphere' quenching effect.[2,3] Complexes of the related mono-amide triphosphinate L$^2$ with Eu and Tb allow a hydrogen-bonded water molecule to approach the metal centre more closely.[11] This leads to an increased difference between the lifetimes in protiated and deuteriated solvents, and results in slightly shorter lifetimes in water than are observed with the tetraphosphinate. The ytterbium complexes of the tetramide ligands L$^3$–L$^5$ (ref. 12) and dtpa show considerably shorter lifetimes. The presence of one Yb-bound water molecule in these cases is in accord with published crystallographic information on related structures.[14]

The quenching effect of O–H oscillators on the rate constants for ytterbium luminescence may be fitted to eqn. (1),

$$q = A(k_{H_2O} - k_{D_2O}) - B \qquad (1)$$

where $q$ is the number of water molecules coordinated to the metal, $k_{H_2O}$ the quenching rate constant in H$_2$O, $k_{D_2O}$ that in D$_2$O, $A$ is a constant reflecting quenching sensitivity and $B$ is a term representing the quenching effect of outer-sphere water molecules ($0.1 < B < 0.3$). The results in Table 1 allow $A$ to be estimated to be 1.0 μs. Similar empirical relationships have been devised for analogous complexes of europium and terbium,[13] and were modified recently in light of the definition of an outer-sphere quenching effect.[2,3]

In summary, stable complexes of ytterbium have been shown to undergo emission in the near-IR on a microsecond timescale. Such behaviour renders ytterbium complexes attractive candidates for luminescent imaging *in vivo*, particularly since time-gating is possible using existing technologies and sensitised excitation is possible in the range 450–600 nm. In addition, the luminescence method allows the assessment of the hydration state of ytterbium complexes in solution. The results of selected *in vivo* imaging experiments using such systems are under investigation.

The authors thank Dr Robert Clark of the Department of Archaeology, University of Durham, for assistance with use of the MOPO, EPSRC for funding (R. S. D., J. A. G. W.) the University of Durham for a fellowship (S. F.), and the Durham Centre for Time Resolved Spectroscopy for access to equipment.

## Footnotes

* E-mail: david.parker@durham.ac.uk

† This ChemComm is also available in enhanced multi-media format *via* the World Wide Web: http://chemistry.rsc.org/rsc/ccenha.htm

‡ Measurement of lifetimes was carried out using the signal observed with a nitrogen-cooled germanium photodiode/amplifier (North Coast EO-817-P) operating in high-sensitivity mode. Decays were analysed by iterative reconvolution and non-linear least-squares analysis of the instrument response profile with a single exponential function, and in all cases gave good fits, as judged by the randomness of three residuals and a satisfactory reduced $\chi$-squared value. Further experimental details and a discussion of the validity of the method can be found in ref. 5.

§ However, the short duration spike arising from scattered light was still sufficiently intense that short lifetimes could not be measured by direct excitation of the metal centre using the established procedures, since the decay was completely subsumed by the spike. Lifetimes in deuteriated solvents or in H$_2$O–D$_2$O mixtures (see Table 1) could, however, be determined by discarding the early data points and fitting the remaining points to an exponential decay.

## References

1 A. Beeby, M. Murru, D. Parker and G. Williams, *J. Chem. Soc., Chem. Commun.*, 1993, 1116; G. Mathis, *Clin. Chem.*, 1995, **41**, 1391; E. Soini, L. Hemmila and P. Dhalen, *Ann. Biol. Clin. (Paris)*, 1990, **48**, 567; E. F. G. Dickson, A. Pollak and E. P. Diamandis, *J. Photochem. Photobiol. B, Biol.*, 1995, **27**, 3.

2 R. S. Dickins, D. Parker, A. S. deSousa and J. A. G. Williams, *Chem. Commun*., 1996, 697.

3 D. Parker and J. A. G. Williams, *J. Chem. Soc., Dalton Trans.*, 1996, 3613.

4 A. Beeby, D. Parker and J. A. G. Williams, *J. Chem. Soc., Perkin Trans. 2*, 1996, 1565.

5 A. Beeby and S. Faulkner, *Chem. Phys. Lett.*, 1997, 116.

6 A. Heller, *J. Am. Chem. Soc.*, 1966, 88, 2058; G. Stein and E. Wurzberg, *J. Chem. Phys.*, 1975, **62**, 208; E. B. Sveshnikova, S. P. Naumov and T. A. Shakhverdov, *Opt. Spectrosc.* (*USSR*), 1977, **40**, 529.

7 Y. V. Korovin, S. B. Meshkova and N. S. Poluektov, *Zh. Anal. Khim.*, 1984, **39**, 300.

8 N. S. Poluetkov, S. B. Meshkova and Yu V. Korovin, *Ukr. Khim. Zn.*, 1987, **53**, 844.

9 The complex was prepared according to the reported procedure and gave a satisfactory combustion analysis and electrospray mass spectrum, as did the complexes reported in Table 1; H. S. Amoli, G. G. Aziz and F. Mohanazadeh, *Indian J. Chem., Sect. A*, 1996, **35**, 11.

10 S. Aime, A. Batsanov, M. Botta, J. A. K. Howard, D. Parker, K. Pulukkody and J. A. G. Williams, *Inorg. Chem.*, 1994, **33**, 4696; S. Aime, A. S. Batsanov, M. Botta, R. S. Dickins, S. Faulkner, C. E. Foster, A. Harrison, J. A. K. Howard, J. Moloney, T. J. Norman, D. Parker, L. Royle and J. A. G. Williams, *J. Chem. Soc., Dalton Trans.*, 1997, submitted.

11 S. Aime, M. Botta, D. Parker and J. A. G. Williams, *J. Chem. Soc., Dalton Trans.*, 1996, 17.

12 R. S. Dickins, J. A. K. Howard, C. Lehmann, J. Moloney, D. Parker and R. D. Peacock, *Angew. Chem., Int. Ed. Engl.*, 1997, 521.

13 W. D. Horrocks and D. R. Sudnick, *Acc. Chem. Res.* , 1981, **14**, 384

14 G. R. Choppin, *Pure Appl. Chem.*, 1971, **27**, 23; F. A. Hart in *Comprehensive Coordination Chemistry*, Pergamon, Oxford, 1987, vol. 3 ch. 39; S. Aime, M. Barge, M. Botta, D. Parker and A. S. de Sousa, *J. Am. Chem. Soc.*, 1997, **119**, 4767.

*Received in Liverpool, UK, 8th April 1997; 7/02388J*

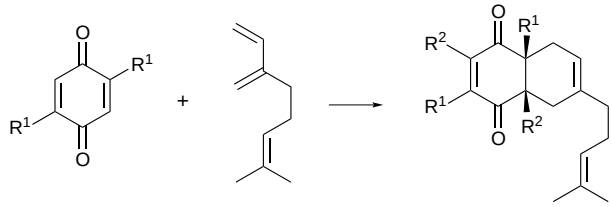
# Accelerated Diels–Alder reaction of quinones generated *in situ* by a modified electrode in an aqueous sodium dodecyl sulfate micellar system

**Kazuhiro Chiba,* Madoka Jinno, Ayako Nozaki and Masahiro Tada**

*Laboratory of Bio-organic Chemistry, Tokyo University of Agriculture and Technology, 3-5-8 Saiwai-cho, Fuchu, Tokyo 183, Japan*

**Diels–Alder reaction of *in situ* generated quinones with dienes is accomplished in excellent yield in an aqueous sodium dodecyl sulfate solution by selective electrooxidation on a glassy carbon electrode modified by cation-exchange resin.**

A solvent system which possesses internal solvent pressures induces rate acceleration of intermolecular cycloaddition processes.[1] Previously we produced varied cycloadducts *via* electrochemically-generated intermediates in a lithium perchlorate–nitroalkane solution, which was found to accelerate cycloaddition reactions.[2] Aqueous solutions were also shown to be powerful media for Diels–Alder reactions which involved hydrophilic dienes and/or dienophiles.[3] An aqueous solution can also be a facile electrolytic medium for large scale reaction systems, although the acceleration properties of aqueous media are less effective for many organic compounds which are insoluble in water. In addition, dispersion of lipophilic or easily oxidizable compounds in the electrolytic medium often prevents electron transfer by coating, and oxidatively decomposing on, the electrodes. We therefore envisioned that the desired cycloaddition reaction should proceed at the interface of or inside of a micelle in which less polar, easily oxidizable dienes



**1** $R^1$ = H
**2** $R^1$ = Me

**3**

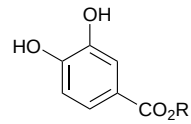
**4** $R^1$ = $R^2$ = H
**5** $R^1$ = Me, $R^2$ = H
**6** $R^1$ = H, $R^2$ = Me

**Scheme 1**

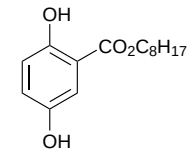
**Table 1** Effect of emulsifiers on the acceleration of Diels–Alder reaction in aqueous media[a]

| Quinone | Products | Emulsifier | Concentration/ mM | T/°C | Yield (%) |
|---|---|---|---|---|---|
| **1** | **4** | — | — | 25 | 5.2 |
| **1** | **4** | sodium toluene-*p*-sulfonate | 20 | 25 | 12.8 |
| **1** | **4** | sodium dodecylsulfonate | 20 | 25 | 8.0 |
| **1** | **4** | sodium dodecylbenzenesulfonate | 20 | 25 | 15.4 |
| **1** | **4** | sodium dodecylbenzenesulfonate | 200 | 25 | 18.6 |
| **1** | **4** | sodium dodecyl sulfate | 20 | 25 | 35.1 |
| **1** | **4** | sodium dodecyl sulfate | 200 | 25 | 99.8 |
| **2** | **5** + **6** (1:1) | — | — | 25 | ND[b] |
| **2** | **5** + **6** (1:1) | — | — | 40 | 12.1 |
| **2** | **5** + **6** (1:1) | sodium dodecyl sulfate | 20 | 25 | 43.0 |
| **2** | **5** + **6** (1:1) | sodium dodecyl sulfate | 20 | 40 | 82.2 |

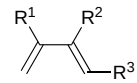
[a] All reactions were performed with dienophile and diene (10 mM each) in 0.1% aq. acetic acid. The reaction mixtures were allowed to stand for 40 h. Yields were determined by NMR by using internal standards. [b] ND = Not detected.



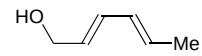
**7** R = Et
**8** R = $C_8H_{17}$



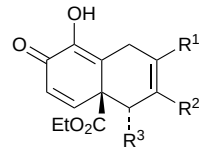
**9**



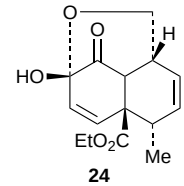
**10** $R^1$ = $R^3$ = H, $R^2$ = Me
**11** $R^1$ = $R^2$ = Me, $R^3$ = H
**12** $R^1$ = $R^2$ = H, $R^3$ = $CH_2CO_2Et$
**13** $R^1$ = H, $R^2$ = Me, $R^3$ = $CH_2CO_2Et$
**14** $R^1$ = H, $R^2$ = Me, $R^2$ = $CH_2CH{=}CMe_2$



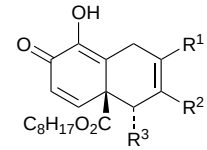
**15**



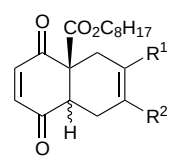
**16** $R^1$ = $R^3$ = H, $R^2$ = Me
**17** $R^1$ = Me, $R^2$ = $R^3$ = H
**18** $R^1$ = $R^3$ = H, $R^2$ = $(CH_2)_2CH{=}CMe_2$
**19** $R^1$ = $(CH_2)_2CH{=}CMe_2$, $R^2$ = $R^3$ = H
**20** $R^1$ = $R^2$ = Me, $R^3$ = H
**21** $R^1$ = $R^2$ = H, $R^3$ = $CH_2CO_2Et$
**22** $R^1$ = H, $R^2$ = Me, $R^3$ = $CH_2CO_2Et$
**23** $R^1$ = H, $R^2$ = Me, $R^3$ = $CH_2CH{=}CMe_2$



**24**



**25** $R^1$ = $R^3$ = H, $R^2$ = $(CH_2)_2CH{=}CMe_2$
**26** $R^1$ = $(CH_2)_2CH{=}CMe_2$, $R^2$ = $R^3$ = H
**27** $R^1$ = $R^2$ = Me, $R^3$ = H
**28** $R^1$ = H, $R^2$ = Me, $R^3$ = $CH_2CH{=}CMe_2$



**29** $R^1$ = H, $R^2$ = $(CH_2)_2CH{=}CMe_2$
**30** $R^1$ = $R^2$ = Me

could be maintained. Here we report our findings, which show that an aqueous sodium dodecyl sulfate (SDS) micellar system can realize the oxidative generation of unstable quinones and the marked acceleration of their cycloaddition with varied dienes.

In a preliminary study, the acceleration properties of emulsifiers for Diels–Alder reactions were examined. An equimolar mixture of quinone (**1** or **2**) and myrcene **3** in benzene or MeCN gave no product after 40 h standing at 25 °C,[4] but very small amounts of cycloadducts were obtained in water even though the starting materials scarcely dissolved (Scheme 1). Although the Diels–Alder reaction was slightly accelerated by some emulsifiers, only SDS was found to accelerate significantly the cycloaddition reaction, which was further promoted by an increase in SDS concentration (Table 1).

As SDS also played a role as supporting electrolyte in water, the dispersion of SDS could be directly applied to the electrolytic system. The anode (glassy carbon, 60 × 20 mm) was firstly coated with Nafion,† and surface sulfonic acid moieties were converted to sulfonamide groups by treating with phenyl(ethyl)amine and DCC in dry MeCN (2 h at room temp.). Electrochemical oxidation was performed in a dispersion of ethyl 3,4-dihydroxybenzoate **7** (1.0 mM) and **10** (1.5 equiv.) in 20 mM SDS in 15 ml of 0.5% acetic acid using the modified anode and a Pt plate (10 × 10 mm) as the cathode in an undivided cell (2.2 F $mol^{-1}$, 0.8 V *vs.* SCE). In this reaction system, water soluble hydroquinones were directly oxidized on the electrode in the presence of dienes to yield the desired cycloadducts **16-24** (Table 2). Although dienes **12**, **13** and **14** were labile on a bare glassy carbon anode, giving cycloadducts in low yield (0–30%), the modified electrode successfully gave the desired products **20**–**23**. Hydrophobic hydroquinones **8** and **9** were barely oxidized in the micellar system, although the selective oxidation of hydroquinones followed by the cycloaddition reaction with dienes proceeded after addition of cerium(III) sulfate (0.02 equiv.) to the electrolytic system (1.2 V *vs.* SCE). It is presumed that $Ce^{IV}$ was effectively generated at the electrode, thus oxidizing the hydrophobic hydroquinones at the interface of the SDS micelle (Fig. 1). Although hydrophilic *p*-quinones which possess electron withdrawing groups were unstable in aqueous media due to Michael addition of $H_2O$, it was found that hydrophobic *p*-quinone generated by cerium oxidation in the SDS micelle gave the desired cycloadducts in excellent yields **29** and **30**. This result showed that decomposition of quinones by the addition of $H_2O$ was prevented in the hydrophobic micelle to give cycloadducts with dienes selectively.

**Table 2** Electrochemical generation and cycloaddition of quinones with dienes in the micellar solution

| Hydroquinone | Diene | Products | Yield (%) | |
|---|---|---|---|---|
| **7** | **10** | **16** + **17** | quant. | (**16**:**17** 1:1) |
| **7** | **3** | **18** + **19** | 96 | (**18**:**19** 1:2) |
| **7** | **11** | **20** | quant. | |
| **7** | **12** | **21** | 88 | |
| **7** | **13** | **22** | 94 | |
| **7** | **14** | **23** | 96 | |
| **7** | **15** | **24** | 84 | |
| **8** | **3** | **25** + **26** | 96 | (**25**:**26** 1:2) |
| **8** | **11** | **27** | quant. | |
| **8** | **14** | **28** | 94 | |
| **9** | **3** | **29** | 92 | |
| **9** | **11** | **30** | 95 | |

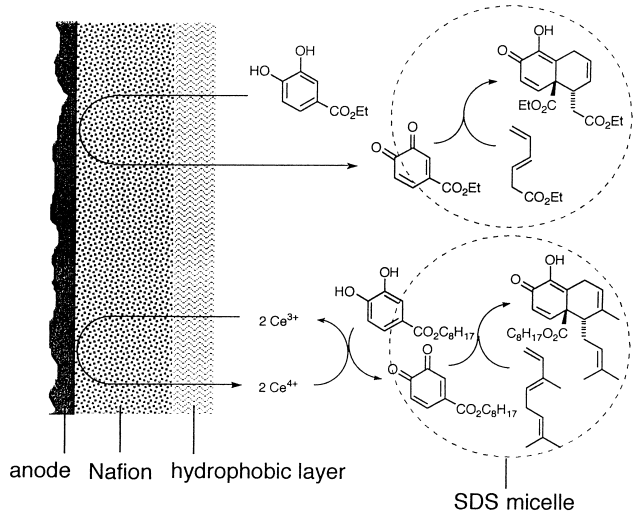



**Fig. 1** Proposed mechanism of Diels–Alder reaction of *in situ* generated quinones in the SDS micellar system using the modified electrode

In conclusion, the electrochemical generation of quinones and subsequent Diels–Alder reaction was accomplished to give varied cycloadducts in a simple, moderate aqueous SDS solution in which the Diels–Alder reaction was markedly accelerated. The modified anode in the SDS micellar solution provided selective oxidation of hydroquinones to give the desired products in high yields (84–100%) and current efficiency (88–96%).

## Footnotes

* E-mail: chiba@cc.tuat.ac.jp

† A 5 wt% solution of Nafion in a mixture of alcohol and water (Aldrich) was coated and dried on the glassy carbon plate (0.05 ml $cm^{-2}$).

## References

1 P. A. Grieco, J. J. Nunes and M. D. Gaul, *J. Am. Chem. Soc*., 1990, **112**, 4595; M. A. Forman and W. P. Dailey, *J. Am. Chem. Soc*., 1991, **113**, 2761.

2 K. Chiba and M. Tada, *J. Chem. Soc., Chem. Commun*., 1994, 2485; K. Chiba, J. Sonoyama and M. Tada, *J. Chem. Soc., Chem. Commun*., 1995, 1381; *J. Chem. Soc., Perkin Trans. 1*, 1996, 1435.

3 R. Breslow, U. Maitra and Darry Rideout, *Tetrahedron Lett.*, 1983, **24**, 1901; D. A. Jaegler, H. Shinozuka and P. Goodson, *J. Org. Chem*., 1991, **56**, 2482; P. A. Grieco, P. Garner and Z. He, *Tetrahedron Lett*., 1983, **24**, 1897; D. A. Jaeger and J Wang, *Tetrahedron Lett.*, 1992, **33**, 6415; W. Blokzijl, M. J. Blandamer and J. B. F. N. Engberts, *J. Am. Chem. Soc.*, 1991, **113**, 4241.

4 J. B. Hendrickson and V. Singh, *J. Chem. Soc., Chem. Commun*., 1983, 837.

*Received in Cambridge, UK, 7th May 1997; 7/03113K*

# Ruthenium catalysed formation of 2-alkoxy-5-methylenetetrahydropyrans

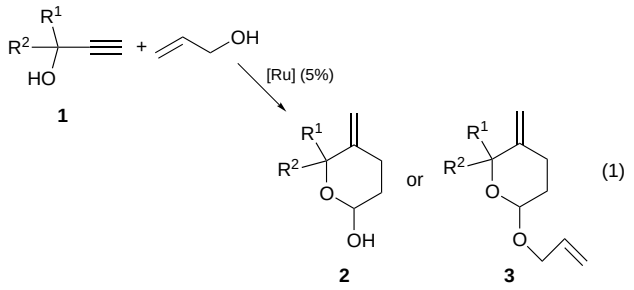
**Sylvie Dérien, Beatriz Gomez Vicente and Pierre H. Dixneuf***

*UMR 6509 CNRS-Université de Rennes 1, Laboratoire de Chimie de Coordination et Catalyse, Campus de Beaulieu, 35042 Rennes, France*

**The regioselective carbon–carbon coupling of prop-2-yn-1-ols with allyl alcohol is achieved in the presence of the ruthenium(II) catalyst RuCl(cod)($C_5Me_5$) and leads to either 2-hydroxy- or 2-allyloxy-5-methylenetetrahydropyrans.**

The tetrahydropyran skeleton is a key structure in intermediates for the synthesis of natural products such as terpenoids, pheromones, antibiotics and other biologically active compounds.[1] The 2-alkoxy-5-methylenetetrahydropyrans have been used to give access to 3-hydroxypyran-4-ones, flavouring components,[2] aggregation pheromones,[3] members of the tricothecanes[4] and to precursors of cytotoxic and antitumour active vernolepin.[5] The 2-alkoxytetrahydropyrans are usually conveniently constructed from sugars.[3,4]

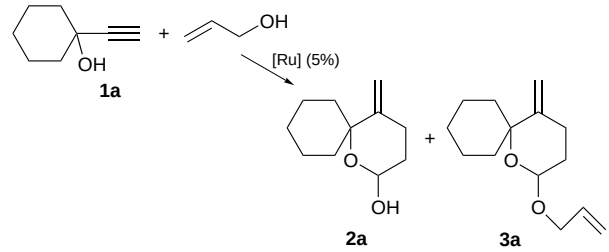
We now report a novel, general method leading to new 2-hydroxy- or 2-alkoxy-5-methylenetetrahydropyrans. It is based on a regioselective ruthenium catalysed C–C coupling of prop-2-yn-1-ols with allyl alcohol, with atom economy, according to eqn. (1).




The carbon–carbon bond coupling of C≡C and C=C bonds on a ruthenium(II) centre has already been reported to preferentially lead to linear derivatives[6] and we have shown by contrast that the reaction of terminal alkynes with allyl alcohol in the presence of ruthenium(IV) and ruthenium(II) catalyst precursors led to γ,δ-unsaturated aldehydes[7] with a branched/linear ratio up to 4 : 1.

The reaction of the prop-2-yn-1-ol **1a** (2.5 mmol) with 3 equiv. of allyl alcohol, in the presence of 5 mol% of RuCl(cod)($C_5Me_5$) catalyst[8] (cod = cycloocta-1,5-diene) affords a mixture of **2a** and **3a** below 90 °C. However, when a large excess of allyl alcohol is used (5 ml) the same reaction, performed above 45 °C, leads to the selective formation of the mixed acetal **3a** (Scheme 1). The latter was obtained after 1 h at 80 °C in 80% yield; by contrast, when the reaction was performed at 25 °C (30 min), only the hemiacetal **2a** (80%) was obtained.

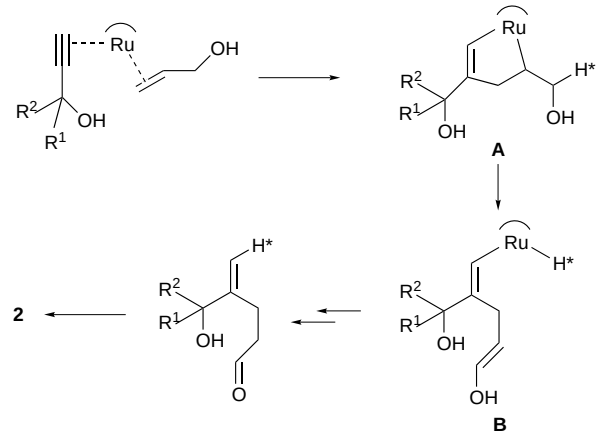
These results show that the hemiacetal **2a** is first selectively produced and that further heating in an excess of allyl alcohol selectively leads to the 2-allyloxy acetal **3a**. The reaction corresponds, after displacement of the cod ligand, to the *regioselective* oxidative coupling of the alkyne C≡C and allyl alcohol C=C bonds on the ruthenium centre, leading to **A**, followed by β-elimination involving the exocyclic methylene group, giving the intermediate **B** (Scheme 2). The latter, on reductive elimination, should form a branched γ,δ-unsaturated aldehyde which cyclises into the six-membered hemiacetal **2**. It is noteworthy that the presence of a hydroxy group at the α-position of a terminal C≡CH bond allows the regioselective coupling leading only to the branched isomer, a regioselectivity phenomenon not observed before.[6,7] A ruthenium allenylidene intermediate (Ru=C=C=$CR_2$) usually produced by metal activation of prop-2-yn-1-ols (HC≡$CR_2$OH) followed by water elimination[9] can be ruled out. Indeed the reaction of MeC≡C-$CH_2$OH with allyl alcohol according to the conditions shown in Table 1 also affords the cyclic hemiacetal of type **2** with an exocyclic ethylidene group.




| | | | |
|---|---|---|---|
| allyl alcohol: 3 equiv. | 90 °C, 5 h | — | 30% |
| allyl alcohol: 5 ml | 45 °C, 3 h | 45% | 35% |
| | 45 °C, 20 h | — | 77% |
| | 80 °C, 1 h | — | 80% |
| | room temp., 30 min | 80% | — |

**Scheme 1**

The conditions in Table 1, applied to a variety of prop-2-yn-1-ols with an excess of allyl alcohol, can be used to produce selectively either the corresponding 2-hydroxy- **2** or 2-allyloxy-tetrahydropyrans **3**, respectively. Prop-2-ynyl alcohol **1b** leads to a low yield of **2b** (42%) but **1c** affords selectively **2c** (70%) or **3c** (55%). When unsymmetrically substituted derivatives **1d**–**f** ($R^1 \neq R^2$) were used, diastereoisomers were formed in good yields (51–78%) in the ratio 60 : 40 for both **2d**–**f** and **3d**–**f**




**Scheme 2**

**Table 1** Results of reaction of **1** and allyl alcohol to give **2** and **3**[a]

| | | | Reaction at room temp. | | Reaction at 80 °C | |
|---|---|---|---|---|---|---|
| Alkynol | $R^1$ | $R^2$ | *t*/h | Product (% yield)[b] | *t*/h | Product (% yield)[b] |
| **1a** | $-[CH_2]_5-$ | | 0.5 | **2a** (80) | 1 | **3a** (80) |
| **1b** | H | H | 1 | **2b** (42) | 7 | **2b** (28) **3b** (15) |
| **1c** | Me | Me | 2 | **2c** (70) | 1 | **3c** (55) |
| **1d** | Me | Et | 2 | **2d** (64)[c] | 4 | **3d** (61)[c] |
| **1e** | Me | $CH_2CHMe_2$ | 2 | **2e** (78)[c] | 5 | **3e** (51)[c] |
| **1f** | Me | $[CH_2]_2CH{=}CMe_2$ | 2 | **2f** (68)[c] | 3 | **3f** (72)[c] |
| **1g** | Me | Ph | 3 | **2g** (73) | 5 | **2g** (60) **3g** (11) |

[a] Reaction conditions: **1** (2.5 mmol) in allyl alcohol (5 ml) was treated with [RuCl(cod)($C_5Me_5$)] (0.125 mmol, 5 mol%) under the conditions shown. [b] Isolated yields after silica gel chromatography. All compounds were fully characterised by spectroscopic methods. [c] Diastereomeric ratio of 60 : 40 determined by $^1$H NMR.

derivatives. This ratio corresponds to the anomer ratio usually obtained from sugar derivatives. However, from the phenyl derivative **1g** only one diastereoisomer **2g** was obtained either at 25 °C (3 h) in 73% yield or at 80 °C (5 h) in 60% yield. In that case the presence of the aryl group slowed down the formation of the allyloxy acetal, and the derivative **3g** could only be observed in 11% yield at 80 °C for 5 h. NOE experiments showed the relative *trans* arrangement of the phenyl group and the OH group of **2g**.

This one-pot ruthenium catalysed regioselective C–C coupling reaction followed by cyclisation takes place with atom economy,[10] and offers a new route to functional tetrahydropyran derivatives. On the basis of the known reactions involving 2-alkoxytetrahydropyrans obtained from sugars,[1] this selective catalytic formation of 2-alkoxy-5-methylenetetrahydropyrans has potential for organic synthesis.

## Footnote

* E-mail: pierre.dixneuf@univ-rennes1.fr

## References

1 M. H. D. Postema, *Tetrahedron*, 1992, **48**, 8545.
2 K. Sato, S. Inoue, T. Tanami and M. Ohasi, *J. Chem. Soc., Perkin Trans. 1*, 1981, 1015.
3 D. E. Plaumann, B. J. Fitzsimmons, B. M. Ritchie and B. Fraser-Reid, *J. Org. Chem.*, 1982, **47**, 941.
4 D. B. Tulshian and B. Fraser-Reid, *Tetrahedron*, 1984, **40**, 2083.
5 F. Kido, T. Abiko and M. Kato, *J. Chem. Soc., Perkin Trans. 1*, 1995, 2989.
6 B. M. Trost, A. F. Indolese, T. J. J. Müller and B. Treptow, *J. Am. Chem. Soc*., 1995, **117**, 615; B. M. Trost, J. A. Martinez, R. J. Kulawiec and A. F. Indolese, *J. Am. Chem. Soc*., 1993, **115**, 10402.
7 S. Dérien, D. Jan and P. H. Dixneuf, *Tetrahedron*, 1996, **52**, 5511.
8 P. J. Fagan, W. S. Mahoney, J. C. Calabrese and I. D. Williams, *Organometallics*, 1990, **9**, 1849.
9 D. Touchard, N. Pirio and P. H. Dixneuf, *Organometallics*, 1995, **14**, 4920 and references cited therein.
10 B. M. Trost, *Angew. Chem., Int. Ed. Engl.*, 1995, **34**, 259.

*Received in Cambridge, UK, 24th May 1997; 7/02799K*

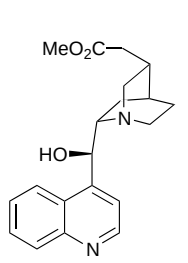
# Building thermodynamic combinatorial libraries of quinine macrocycles

**Stuart J. Rowan and Jeremy K. M. Sanders***

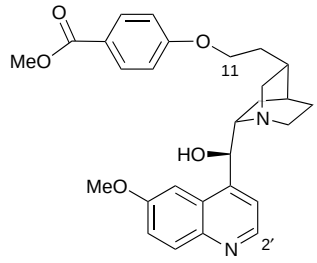
*Cambridge Centre for Molecular Recognition, University Chemical Laboratory, Lensfield Road, Cambridge, UK CB2 1EW*

**Thermodynamically-controlled transesterification of a predisposed cinchonidine building block with a more flexible extended quinine monomer leads to a combinatorial mixture of 11 macrocyclic receptors which is analysed by electrospray mass spectrometry; similar results with alkaloid–cholate mixtures demonstrate the generality of the approach.**

We have recently shown that thermodynamically-controlled transesterification can lead to efficient synthesis of oligomeric macrocycles,[1,2] and that when the monomeric building blocks are suitably predisposed a single product may dominate even when other oligomers are kinetically accessible.[3] For example, the cinchonidine monomer **1** (HO–Cc–OMe) is



**1** HO–Cc–OMe



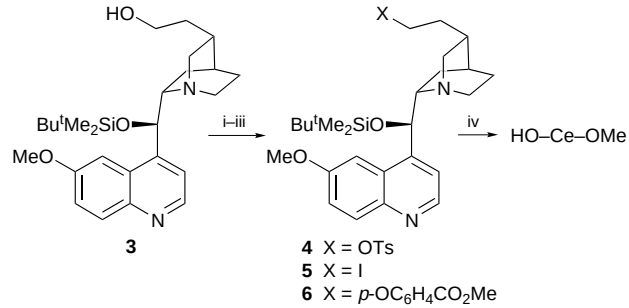
**2** HO–Ce–OMe

predisposed to give almost exclusively the cyclic trimer under thermodynamic control. We now report that the extended quinine monomer **2** (HO–Ce–OMe), in which this predisposition is slightly relaxed, gives access to a wider range of homomacrocycles; more importantly it allows the development of thermodynamically-controlled receptor libraries by combination with other building blocks such as **1**.

In order to relax the predisposition of **1**, we elected to extend the cinchonidine monomer at the 11-position. The chosen extension, a methyl 4-hydroxybenzoate moiety, serves several functions: it is compatible with our transesterification conditions; it programs into the molecule added length to increase the size of any cavity formed and allow access to cyclic dimer; introduces a little extra flexibility; and is still rigid enough to prevent formation of cyclic lactone monomer. Synthesis of **2** started from the previously prepared 11-alcohol **3**.[2] This was converted into the tosylate **4** with tosyl chloride and triethylamine (77% yield), which on heating with NaI in acetone gave 9-*O*-*tert*-butyldimethylsilyl-10,11-dihydro-11-iodo quinine **5** in 86% yield. Compound **5** was converted into **6** (75%) by stirring with methyl 4-hydroxybenzoate, 18-crown-6 and $K_2CO_3$, and removal of the $Bu^tMe_2Si$ group using $Bu_4NF$–THF gave the extended monomer **2** in 78% yield (Scheme 1).

The result of submitting monomer **2** to transesterification under thermodynamic control[2] was a mixture of mainly cyclic dimer ($Ce_2$) : trimer ($Ce_3$) : tetramer ($Ce_4$) and higher oligomeric quinines, with a mass ratio of 30 : 41 : 29 respectively† (Scheme 2). Even though there is still a distinct preference for cyclic trimer,‡ the extension unit has allowed access to cyclic dimer (not previously seen even in kinetic cyclisations of **1**[4]) and tetramer under thermodynamic control, demonstrating the expected relaxation of predisposition.

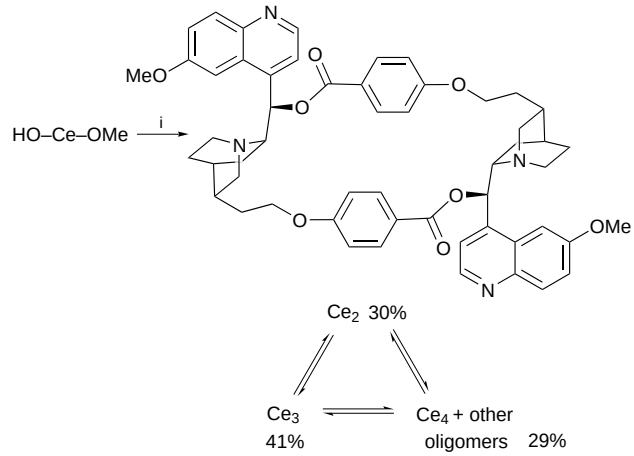
Under thermodynamic control, mixtures of cinchonidine monomer **1** and preorganised xanthenes self-sort to give good yields of cyclic trimer and dimer respectively because the homo-products are stabilised.[3] However, the relaxed constraints of the extended monomer **2** combined with predisposed **1** lead to quite a different outcome: thermodynamic transesterification of **1** and **2** under the usual conditions led to a combinatorial library of macrocycles, as observed by electrospray mass spectrometry§ (Fig. 1). The mass spectrum contains two of the three possible dimers, all possible trimers and small amounts of all the possible tetramers. It is unwise to draw precise quantitative conclusions from peak intensities since individual species have different inherent detectabilities in electrospray mass spectra, but there are systematic and interpretable deviations from the expected statistical distribution of hetero : homo oligomers. The extended quinine homo-dimer is seemingly favoured over the hetero dimer, which is not surprising given that **1** cannot form homo dimer at all. The trimers show the expected weighting towards the cinchonidine homo trimer but the more promiscuous monomer **2** gives access to two new hetero trimers. To a first approximation, it appears that the tetramers are formed in statistical proportions.




**3**

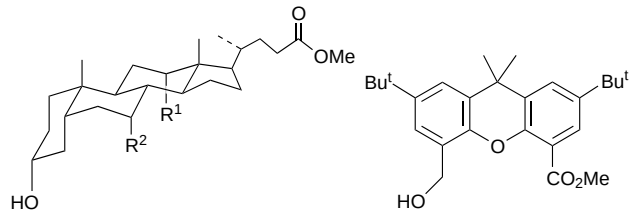
**4** X = OTs
**5** X = I
**6** X = *p*-$OC_6H_4CO_2Me$

**Scheme 1** *Reagents and conditons*: i, TsCl, $Et_3N$, room temp., 4 h; ii, NaI, acetone, reflux, 16 h; iii, 4-$HOC_6H_4CO_2Me$, 18-crown-6, $K_2CO_3$, room temp., 16 h; iv, $Bu_4NF$, THF, room temp., 4 h.




**Scheme 2** *Reagents and conditions*: i, KOMe, 18-crown-6, toluene, reflux, 1 h.

To further examine the idea of relaxation of predisposition monomers **1** and **2** were individually mixed with the cholate monomer **7**, which has enough flexibility to allow access to a




**7** **8**

$R^1$ = OBn
$R^2$ = $OCH_2OCH_2CH_2OMe$

range of cyclic oligomers.[1] Transesterification produced a cocktail of all the possible hetero oligomers of both **1** and **2** with **7**, which is consistent with the idea that if there is enough flexibility in one component then that is generally sufficient to give a range of macrocycles. We had already demonstrated that mixing of **1** with the highly preorganised xanthene monomer **8** leads to self-sorting.[3] To examine how powerfully preorganised **8** is we allowed it to react in the presence of extended quinine monomer **2**: the result was predominantly self-sorting, indicating that preorganised monomers such as **8** find it difficult to form mixtures with monomers that do not have the correct 'bite size' or flexibility.

These results demonstrate that it is possible to generate combinatorial libraries of macrocyclic receptors even when one of the building blocks is predisposed to produce just a single product. By mixing only two monomers we observe 11 cyclic products, showing how large libraries of macrocycles can be

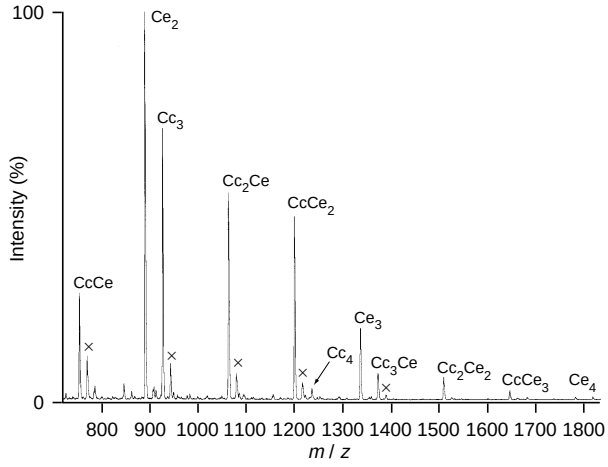



**Figure 1** Electrospray mass spectrum of the thermodynamic cyclisation reaction mixture of **1** (HO–Cc–OMe) and **2** (HO–Ce–OMe). Peaks marked (×) are $NH_4^+$ adducts of molecular ions.

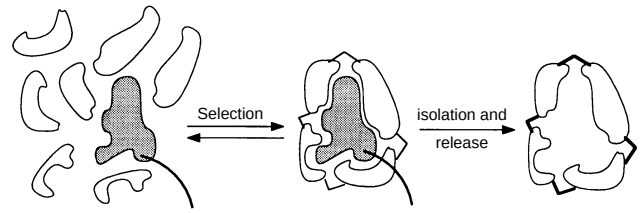



**Fig 2** Schematic representation of a thermodynamic selection approach to receptors

obtained quickly from a small number of monomers. The way is now open for creating thermodynamically controlled macrocyclic receptor libraries (Fig. 2), with the possibility of thermodynamic templating to bias the library towards robust, covalent receptors with good binding properties.[5-7] If the guest is tethered in some way it should also be possible to isolate the receptors from an otherwise hopelessly complex mixture.

We thank Merck, Sharp and Dohme and the EPSRC for generous financial support. We also thank Drs P. A. Brady and D. G. Hamilton for cholate and xanthene samples.

## Footnotes

* E-mail: jkms@cam.ac.uk

† Determined by 400 MHz $^1$H NMR spectroscopy of the reaction mixture after work up and dissolution in $CDCl_3$: The chemical shifts for $H_{2'}$ were: dimer ($Ce_2$: δ 8.77), trimer ($Ce_3$: δ 8.74) and higher oligomers ($Ce_{4+}$: δ 8.70–8.73).

‡ In the absence of significant enthalpic differences in the stability of oligomers, simple entropic considerations lead to an expected order of abundance monomer > dimer > trimer > tetramer *etc*.

§ ES-MS were obtained on a VG BioQ triple quadrupole apparatus (VG Bio Tech Ltd, Altrincham, UK). The electrospray source was heated to 70 °C and the sampling cone voltage ($V_c$) was 105 V. Samples were introduced into the mass spectrometer source with an LC pump (Shimadzu LC-9A LC pump) at a flow rate of 4 μl $min^{-1}$ of MeCN–$H_2O$ (1 : 1). Calibration was performed using protonated horse myoglobin. Scanning was performed from *m/z* 200 to 2000 in 10 s. The data system was operated as a multichannel analyser, and several scans were summed to obtain the final spectrum. No hetero oligomers are detected in the electrospray mass spectra of control mixtures of homo oligomers.

## References

1 P. A. Brady, R. P. Bonar-Law, S. J. Rowan, C. J. Suckling and J. K. M. Sanders, *Chem. Commun.*, 1996, 319.
2 S. J. Rowan, P. A. Brady and J. K. M. Sanders, *Angew. Chem., Int. Ed. Engl.*, 1996, **35**, 2143.
3 S. J. Rowan, D. G. Hamilton, P. A. Brady and J. K. M. Sanders, *J. Am. Chem. Soc.*, 1997, **119**, 2578.
4 S. J. Rowan, P. A. Brady and J. K. M. Sanders, *Tetrahedron Lett.*, 1996, **37**, 6013.
5 W. C. Still, P. Hauck and D. Kempf, *Tetrahedron Lett.*, 1987, **28**, 2817.
6 A. V. Eliseev and M. I. Nelen, *J. Am. Chem. Soc.*, 1997, **119**, 1147.
7 I. Huc and J.-M. Lehn, *Proc. Natl. Acad. Sci. USA*, 1997, **94**, 2106 and references cited therein.

*Received in Liverpool, UK, 13th May 1997; 7/03291I*

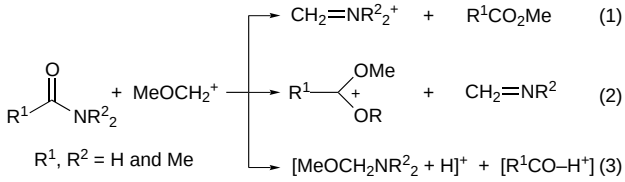
# The methoxymethyl cation cleaves peptide bonds in the gas phase†

**Michael A. Freitas,[a] Richard A. J. O'Hair,*[a] Suresh Dua[b] and John H. Bowie[b]**

[a] *School of Chemistry, The University of Melbourne, Parkville, Victoria 3052, Australia*
[b] *Department of Chemistry, The University of Adelaide, Adelaide, S.A. 5005, Australia*

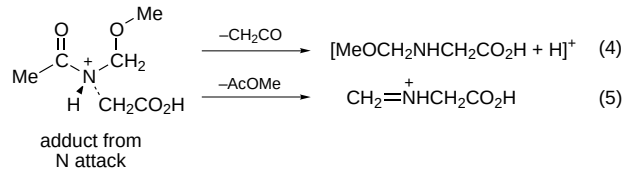
**Methoxymethyl cations and simple *N*-acyl amino acids and dipeptides react in the gas phase to form $[M + MeOCH_2]^+$ ions which fragment *via* a number of pathways including amide bond cleavage.**

A major goal in modern mass spectrometry is the development of techniques to structurally characterize molecules of biological significance. As part of our ongoing research into the gas phase electrophilic modification of biomolecules and model compounds,[1,2] we became interested in designing reagents to sequence biomolecules *via* specific *gas phase* ion–molecule reactions. Thus for peptides, the ultimate aim is to develop site specific ion–molecule reactions to cleave the peptide bonds in an analogous fashion to solution phase chemistry such as the Edman technique.[3–5] Although at first glance such an effort may seem ambitious, we were encouraged during a recent flowing afterglow study on the rates of ion–molecule reactions of the methoxymethyl cation. In particular, we rediscovered a reaction[6] which leads to products arising from amide bond cleavage [eqns. (1)–(3)].

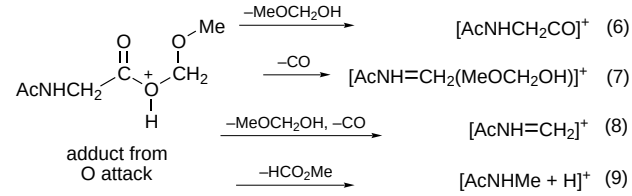



Here we present preliminary results designed to address the question: can the methoxymethyl cation be used to cleave peptide bonds in the gas phase? Experiments were performed on a VG ZAB-2HF reverse sector tandem mass spectrometer.[7] Methoxymethyl cations, which were generated in the chemical ionization source using $MeOCH_2CH_2OMe$ as the CI gas, were allowed to react with peptides and model systems introduced *via* a direct insertion probe. Typical source conditions were: source temperature = 250 °C; electron energy = 70 eV; emission current = 200 mA; source pressure = $7 \times 10^{-4}$ Torr, measured on the source ion gauge. In each case, three major alkylated product ions $[M + MeOCH_2]^+$, $[M + Me]^+$ and $[M + CH]^+$ were formed, consistent with previous studies.[2b,6] In order to gain some insights into the regioselectivity of attack by $MeOCH_2^+$, collisional activated mass-analysed ion kinetic energy (CA-MIKE) spectra were carried out on each of the $[M + MeOCH_2]^+$ ions using argon as the collision gas (at a pressure of $2 \times 10^{-6}$ Torr).

The first model systems we chose to study were the *N*-acyl derivatives of glycine and alanine (Table 1).‡ The $[M + MeOCH_2]^+$ ions of these systems both fragment *via* loss of $CH_2CO$ and $MeCO_2CH_3$. These losses are best rationalized as occuring *via* attack at the amide nitrogen atom to give a nitrogen adduct which then undergoes amide bond cleavage as shown in eqn. (4) [*c.f.* eqn. (3)] and eqn. (5) [*c.f.* eqn. (1)]. Further




products due to loss of $MeOCH_2OH$, $[MeOCH_2OH + CO]$ and $HCO_2Me$ (this loss might arise from hydride ion transfer followed by a proton transfer[8]) are also observed which may arise from initial attack at the C terminus to give an oxygen adduct which then undergoes the fragmentations shown in eqns. (6)–(9). Thus the methoxymethyl cation not only cleaves amide




bonds, but also cleaves the C–OH bond of the carboxylic acid group.

We next turned our attention to the $[M + MeOCH_2]^+$ ions of the free dipeptides glycylglycine, glycylalanine and alanylglycine, which all only fragment to form $[M + CH]^+$ ions as the major product with $[M + Me]^+$ ion formation as a minor reaction channel (Table 1). The lack of attack by the methoxymethyl

**Table 1** CID MS/MS Spectra of $[M + MeOCH_2]^+$ ions of peptides and model systems

| Neutral species (*m/z* of $[M + MeOCH_2]^+$) | Daughter ions (intensity)[a] |
|---|---|
| $MeC(O)NHCH_2CO_2H$ (162) | 132(54), 130(100), 120(2.5), 100(2.5), 88(5), 74(5), 72(17), 45(1) |
| $MeC(O)^{15}NHCH_2CO_2H$ (163) | 133(15), 131(100), 121(2), 101(1.5), 89(3.5), 75(2), 73(5), 45(1) |
| $MeC(O)NHCD_2CO_2H$ (164) | 134(21), 130(100), 122(3), 102(2), 90(5), 76(5), 74(9), 45(1) |
| $MeC(O)NHCHMeCO_2H$ (176) | 146(24), 144(100), 134(1.5), 114(16), 102(11), 86(4), 45(*) |
| $H_2NCH_2C(O)NHCH_2CO_2H$ (177) | 147(2), 145(100) |
| $H_2NCH_2C(O)NHCHMeCO_2H$ (191) | 161(2), 159(100) |
| $H_2NCHMeC(O)NHCH_2CO_2H$ (191) | 161(3), 159(100) |
| $MeC(O)NHCH_2C(O)NHCH_2CO_2H$ (219) | 201(4), 189(6), 187(100), 176(*), 157(*), 145(2), 120(1), 88(1) |

[a] (*) Designates an ion with an intensity of less than 1.

cation onto the peptide bond with concomitant fragmentation is consistent with the known gas phase reactivity of glycine[2a] as well as the basicity of the various functional groups within dipeptides. For example, *ab initio* calculations have shown the following basicity order for glycylglycine: N-terminal amino group > oxygen of amide group > nitrogen of amide group > carboxyl carbonyl oxygen).[9]

In order to make the peptide bonds in these dipeptides more susceptible to attack by the $MeOCH_2^+$ ion, we have examined the effects of moderating the gas phase reactivity of the N-terminal amino group *via N*-acetylation. Thus the $[M + MeOCH_2]^+$ ions of *N*-acetyl derivatives‡ of glycylglycine, glycylalanine and alanylglycine not only decompose to form $[M + CH]^+$ and $[M + Me]^+$ ions, but more importantly, several other product ions resulting from amide bond cleavage were observed (Table 1 and Fig. 1). In particular, the CA-MIKE spectra of the $[M + MeOCH_2]^+$ ions of these *N*-acetyl derivatives indicate that attack by the methoxymethyl cation onto the heteroatom adjacent to a C=O group followed by bond cleavage are general. Thus attack at all three sites (labelled as 1–3 in Fig. 2) occurs, thereby providing *complete* sequence information. Consequently distinction between *N*-acetylglycylalanine and *N*-acetylalanylglycine is readily made (Fig. 1). Interestingly, cleavage of the peptide bonds in these instances gives rise to fragments ions (Fig. 2) where the charge is retained at the C terminus (*i.e.* modified Y ions such as $[Y_n + CH]^+$ and $[Y_1 + CH_3OCH_2]^+$ are formed), while the only fragment ion in which the charge is retained at the N terminus is that due to cleavage of the C terminus OH bond to give a $B_3$ ion [for sequence ion nomenclature, see ref. 4(*a*)]. Thus not only does the methoxymethyl cation cleave the peptide bonds, but it cleaves them in a specific fashion, thereby simplifying the mass spectra.

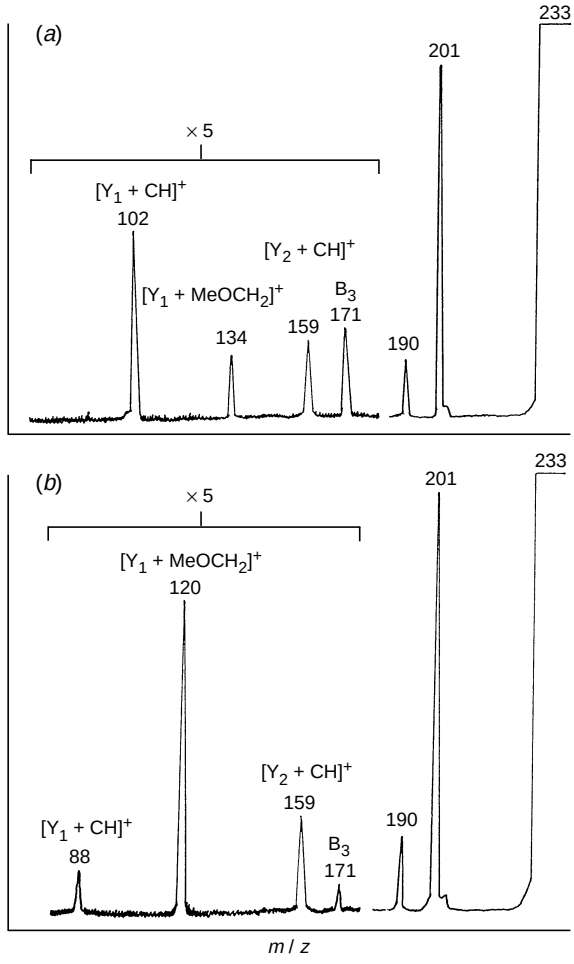



**Fig. 1** CA-MIKE spectra of the $[M + MeOCH_2]^+$ ions of (*a*) *N*-acetylglycylalanine and (*b*) *N*-acetylalanylglycine

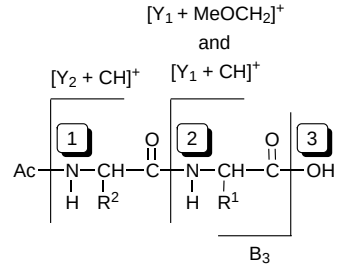



**Fig. 2**

Further work is required to determine the general utility of these reactions to sequence small peptides in the gas phase *via* cleavage of their peptide bonds (the inherent limitations of volatility of the peptide could potentially be overcome using laser desorption CI[10]). In particular the effects of residues with potentially reactive side chains (*e.g.* lysine, aspartic acid *etc*.) need to be investigated. Future studies will also examine the modes of reactivity of other reagent ions such as $ClCH_2^+$.

R. A. J. O. and J. H. B. both thank the ARC for financial support. M. F. thanks the School of Chemistry at the University of Melbourne for a Research Fellowship.

## Footnotes

* E-mail: r.ohair@mail.chemistry.unimelb.edu.au

† Part 8 of the Series 'Gas Phase Ion Chemistry of Biomolecules'.

‡ *N*-Acetyl derivatives were prepared *via* a modified literature procedure (D. P. Knapp, *Methods Enzymol.*, 1990, **193**, 314): The α-amino acid or dipeptide (0.002 mol) was dissolved in 2 ml of 2 M NaOH and chilled in an ice bath. Upon complete dropwise addition of acetic anhydride (2 ml), the mixture was stirred for a further 10 min followed by careful acidification to pH < 4 with $H_2SO_4$. The solution was allowed to warm to room temperature and extracted with EtOAc (3 × 25 ml). The combined EtOAc layers were dried with anhydrous $Na_2SO_4$ and the solvent was removed *in vacuo*. The resultant *N*-acetyl derivatives were purified *via* recrystallization from MeOH. All other compounds were of reagent grade obtained commercially and were used without further purification. $H_2{}^{15}NCH_2CO_2H$ (99 atom% $^{15}N$) and $H_2NCD_2CO_2H$ (98 atom% D) were both obtained from Cambridge Isotope Laboratories.

## References

1 M. A. Freitas, R. A. J. O'Hair, J. A. R. Schmidt, S. E. Tichy, B. E. Plashko and T. D. Williams, *J. Mass Spectrom.*, 1996, **31**, 1086.

2 For gas phase reactions of $MeOCH_2^+$ with glycine and cysteine, see (*a*) R. A. J. O'Hair, M. A. Freitas, S. Gronert, J. A. R. Schmidt and T. D. Williams, *J. Org. Chem.*, 1995, **60**, 1990; (*b*) M. A. Freitas, R. A. J. O'Hair and T. D. Williams, submitted to *J. Org. Chem.*

3 *Sequencing of Proteins and Peptides*, in *Laboratory Techniques in Biochemistry and Molecular Biology*, 2nd edn., ed. G. Allen, Elsevier, Amsterdam, 1989, ch. 6.

4 Mass spectrometry has been used to sequence small peptides. For some leading references, see (*a*) K. Biemann and I. A. Papayannopoulos, *Acc. Chem. Res.*, 1994, **27**, 370; (*b*) R. J. Waugh and J. H. Bowie, *Rapid Commun. Mass Spectrom.*, 1994, **8**, 169.

5 The only other report of a peptide bond cleavage reaction involved reacting the $[M - H]^-$ ion of some peptide models $[MeC(O)NHCH_2C(O)X; X = OEt and NHMe]$ with a neutral electrophile: X. Cheng and J. J. Grabowski, *Proceedings of the 39th ASMS Conference on Mass Spectrometry and Allied Topics*, Nashville, Tennesee, May 19–24, 1991, p. 477.

6 The methoxymethyl cation cleaves the acyl bond in acids, esters and amides: M. C. Caserio and J. K. Kim, *J. Org. Chem.*, 1982, **47**, 2940.

7 K. L. Busch, G. L. Glish and S. A. McLuckey, *Mass Spectrometry/Mass Spectrometry. Techniques and Applications of Tandem Mass Spectrometry*, VCH, New York, 1988.

8 H. E. Audier, F. Dahhani, A. Millet and D. Kuck, *Chem. Commun.*, 1997, 429.

9 K. Zhang, D. M. Zimmerman, A. Chung-Phillips and C. J. Cassady, *J. Am. Chem. Soc.*, 1993, **115**, 10 812.

10 See for example: J. P. Speir and I. J. Amster, *J. Am. Soc. Mass Spectrom.*, 1995, **6**, 1069.

*Received in Cambridge, UK, 14th May 1997; 7/03335D*

# Enantioselective catalytic Diels–Alder reaction of ethyl 2-benzoylacrylate with chiral bis(oxazoline)– or mono(oxazoline)–magnesium complex

**Yuko Honda,[a] Tadamasa Date,[b] Hajime Hiramatsu[b] and Masashige Yamauchi*[a]**

[a] *Faculty of Pharmaceutical Sciences, Josai University, Keyakidai, Sakado, Saitama 350-02, Japan*
[b] *Analytical Research Laboratory, Tanabe Seiyaku C., Ltd, Kashima, Yodogawaku, Osaka 352, Japan*

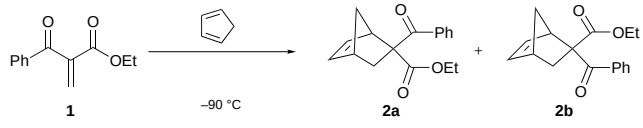
**The magnesium catalysed Diels–Alder reaction of 2-benzoylacrylate gave the *endo*-adduct enantioselectively with bis(oxazoline) 5 as a $C_2$-symmetric ligand or mono-(oxazoline) 4 as a non-$C_2$-symmetric ligand.**

A great deal of effort has been invested in enantioselective Diels–Alder reactions catalysed by chiral Lewis acids, and tremendous advances have been achieved in recent years.[1] $C_2$-Symmetric ligand–metal complexes have proven to be excellent catalysts, and in most cases *N*-α,β-unsaturated acyloxazolidinones have been used as two-point dienophile binding agents in these reactions.[2] Recently, non-$C_2$-symmetric phosphinoaryloxazolines have been shown to be effective ligands for Pd-catalysed asymmetric allylic substitution.[3] We have reported a highly diastereoselective and *endo/exo* selective Diels–Alder reaction of (1′*R*,2′*S*,5*R*)-5-methyl-2-methyl-2-(1-phenylethyl)cyclohexyl 2-benzoylacrylate with cyclopentadiene catalysed by a Lewis acid.[4] This suggests that an enantioselective Diels–Alder reaction should occur using ethyl 2-benzoylacrylate **1**,[5] a two-point binding dienophile, in the presence of a chiral Lewis acid. Herein, we describe the magnesium-catalysed Diels–Alder reaction of **1**, as dienophile, with cyclopentadiene using *N*-[(1*R*)-2-chloro-1-phenylethyl]-2-ethyl-2-[(4*R*)-4-phenyl-4,5-dihydro-1,3-oxazol-2-yl]butyramide **4** as a non-$C_2$-symmetric chiral ligand and bis(oxazoline) **5** as a $C_2$-symmetric chiral ligand.

Our initial efforts were focussed on the possibility that ethyl 2-benzoylacrylate **1** should be a good two-point binding dienophile in an enantiomeric Diels–Alder reaction with cyclopentadiene by use of bis(oxazoline) **5**–magnesium complex. In the reaction with the complex prepared from **5**, $MgI_2$ and $I_2$ (co-catalyst) in $CH_2Cl_2$ at room temperature by Corey's procedure,[2b] the enantioselectivity was not particularly high (Table 1, entry 1), but the selectivity was much improved with the complex prepared in refluxing MeCN (entry 2). The diastereoisomers showed one spot by TLC and could not be resolved by column or medium pressure chromatography, but the ratio was determined by $^1$H NMR spectroscopy as mentioned in our previous report,[4] and in most cases only the *endo*-isomer was obtained (Table 1).

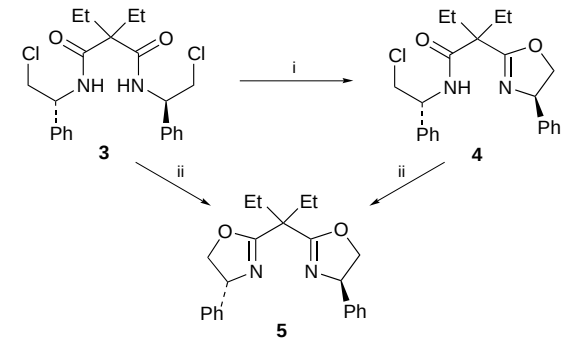
As **1** proved to be a suitable dienophile, we next examined the reaction using *N*-[(1*R*)-2-chloro-1-phenylethyl]-2-ethyl-2-[(4*R*)-4-phenyl-4,5-dihydrooxazol-2-yl]butyramide **4** as a chiral ligand. Compound **4** was synthesized by treatment of dichloride **3** with an equimolar amount of NaOH in MeOH–$H_2O$ at 60 °C. In contrast to the fact that most of the bis(oxazoline)s used as chiral ligands are oily materials, the mono(oxazoline) **4** exists as colourless prisms (mp 127–128 °C from EtOAc) and is therefore easy to handle. The reaction with the complex prepared from **4**:$MgI_2$:$I_2$ (1:1:1) in $CH_2Cl_2$ at room temperature also gave poor enantioselectivity (entry 3). When the reaction was performed with the complex prepared in refluxing MeCN, the ee increased to 87% (entry 4). Interestingly, the enantioselectivities of the reactions with the complex prepared from $MgI_2$:**4**:$I_2$ (1:2:2) were almost equal or slightly higher (entries 5,6). It is well known that head or tail enrichment may occur during chromatography on achiral columns of samples containing an excess of one enantiomer.[2i,6] We therefore collected all the Diels–Alder adducts before $^1$H NMR and HPLC analyses. After separation of the *endo* adduct by preparative HPLC, if necessary, the enantioselectivities were determined by analytical HPLC.‡ Furthermore, the ligands

**Table 1** Asymmetric catalytic Diels–Alder reaction of ethyl 2-benzoylacrylate

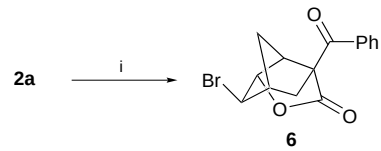



**1** **2a** **2b**

| | Catalyst | | | Diels–Alder adduct | | |
|---|---|---|---|---|---|---|
| Entry | $MgI_2$ (equiv.) | Ligand (equiv.) | Conditions | Yield (%) | **2a**:**2b** | %Ee of **2a** |
| 1 | 0.2 | **5** (0.2) | $CH_2Cl_2$, room temp., 3 h | 74 | 97:3 | 69.8 |
| 2 | 0.2 | **5** (0.2) | MeCN, reflux, 1 h | 81 | >99:1 | 85.3 |
| 3 | 0.2 | **4** (0.2) | $CH_2Cl_2$, room temp., 3 h | 76 | >99:1 | 18.3 |
| 4 | 0.2 | **4** (0.2) | MeCN, reflux, 1 h | 88 | >99:1 | 87.0 |
| 5 | 0.1 | **4** (0.2) | MeCN, reflux, 1 h | 88 | >99:1 | 87.3 |
| 6 | 0.2 | **4** (0.4) | MeCN, reflux, 1 h | 75 | >99:1 | 88.6 |




**Scheme 1** *Reagents*: i, NaOH (1 equiv.), MeOH–$H_2O$; ii, NaOH (excess), MeOH–$H_2O$




**Scheme 2** *Reagents*: i, $Br_2$, $CCl_4$

were recovered almost quantitatively from column chromatography as the last fraction. The absolute configuration of **2a** was confirmed by treatment of **2a** with bromine in $CCl_4$ to give bromo-lactone **6**, whose absolute structure was determined by X-ray crystallography (Fig. 1).§

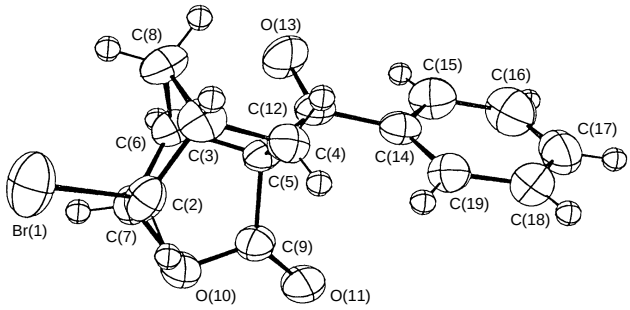



**Fig. 1** ORTEP diagram of **6**

The almost perfect diastereoselectivity of the reaction can be rationalised to be due to the steric hindrance of the benzene ring situated nearly perpendicular to the ene in the fixed metal-chelated enedione as mentioned earlier.[4] However, the reaction mechanism giving high enantioselectivity using mono(oxazoline) is unclear. An attempt to capture the complex of the Lewis acid–chiral ligand or Lewis acid–ligand–dienophile in crystal form has not been successful. Further investigations to clarify the precise structures of the catalysts formed from **4** : $MgI_2$ : $I_2$ (1 : 1 : 1 and 2 : 1 : 2) and the reaction mechanism as well as to develop other asymmetric reactions using this complex are now in progress.

## Footnotes

* E-mail: yamauchi@josai.ac.jp

† General experimental procedure: a mixture of the ligand, $MgI_2$ and $I_2$ in the solvent was treated under the conditions shown in Table 1. The solvent was removed and the resulting complex was dissolved in $CH_2Cl_2$ (1.0 ml) and cooled at −90 °C. To this solution **1** (1 mmol) in $CH_2Cl_2$ (1.5 ml) was added and stirred for 30 min, then cyclopentadiene (1.5 mmol) in $CH_2Cl_2$ (2.5 ml) was added slowly for a period of 3 h. After the reaction was completed the reaction mixture was quenched with water and washed with 5% aqueous $Na_2S_2O_3$. The organic layer was dried and evaporated. The resulting residue was subjected to column chromatography to yield the adducts.

‡ Preparative HPLC was carried out with a JASCO Megapak SIL-10 column (1.0 × 25 cm; eluate 5% AcOEt in hexane) and analytical HPLC with a Daisel CHIRALCEL OD column (0.46 × 25 cm; eluate 0.1% propan-2-ol in hexane).

§ *Crystal data* for **6**: $C_{15}H_{13}O_3Br$, $M$ = 321.16, orthorhombic, space group $P2_12_12_1$, $a$ = 10.935(1), $b$ = 18.884(1), $c$ = 6.326 (1) Å, $U$ = 1287.7(2) Å$^3$, $Z$ = 4, $D_c$ = 1.66 g cm$^{-3}$, $\mu$(Cu-K$\alpha$) = 4.37 mm$^{-1}$. Reflections were measured on a Rigaku AFC5R diffractometer in the range 4.7 < $\theta$ < 65.1° (Cu-K$\alpha$ radiation) with the $\omega$–2$\theta$ scan technique, 2154 reflections were used for all calculations. The structure was solved by direct methods [SHELX-86 (ref. 7)] and refined anisotropically on $F^2$ (SHELXL-93 (ref. 8)]. All hydrogen atoms were refined for all parameters; $wR_2(F^2)$ = 0.0773 with $R(F)$ = 0.0303 for 225 parameters. The absolute configuration was determined Flack's $\chi$-parameter (ref. 9) −0.02(2). CCDC 182/514.

## References

1 R. Noyori, *Asymmetric Catalysis in Organic Synthesis*, Wiley, New York, 1994; K. Ishihara and H. Yamamoto, in *Advances in Catalytic Processes*, ed. M. P. Doyle, JAI Press, London, 1995.
2 (*a*) E. J. Corey, N. Imai and H.-Y. Zhang, *J. Am. Chem. Soc.*, 1991, **113**, 728; (*b*) E. J. Corey and K. Ishihara, *Tetrahedron Lett.*, 1992, **33**, 6807; (*c*) D. A. Evans, S. J. Miller and T. Lectka, *J. Am. Chem. Soc.*, 1993, **115**, 6460; (*d*) D. A. Evans and D. M. Barnes, *Tetrahedron Lett.*, 1997, **38**, 57; (*e*) PS. Kobayashi and H. Ishitani, *J. Am. Chem. Soc.*, 1994, **116**, 4083; (*f*) K. V. Gothelf and K. A. Jørgensen, *J. Org. Chem.*, 1995, **60**, 6847; (*g*) C. Haase, C. Sarko and M. DiMare, *J. Org. Chem.*, 1995, **60**, 1777; (*h*) K. Narasaka, N. Iwasawa, M. Inoue, T. Yamada, M. Nakashima and J. Suginori, *J. Am. Chem. Soc.*, 1989, **111**, 5340; (*i*) D. Seebach, R. Dahinden, R. E. Mart, A. K. Beck, D. A. Plattner, and N. M. Kühnle, *J. Org. Chem.*, 1995, **60**, 1788.
3 P. Matt and A. Pfaltz, *Angew. Chem., Int. Ed. Engl.*, 1993, **32**, 566; P. Matt, O. Loiseleur, G. Koch and A. Pfaltz, *Tetrahedron: Asymmetry*, 1994, **5**, 573; G. Koch and A. Pfaltz, *Tetrahedron: Asymmetry*, 1996, **7**, 2213; H. Rieck and G. Helmchen, *Angew. Chem., Int. Ed. Engl.*, 1995, **34**, 2687.
4 M. Yamauchi, Y. Honda, N. Matsuki, T. Watanabe, T. Date and H. Hiramatsu, *J. Org. Chem.*, 1996, **61**, 2719.
5 M. Yamauchi, S. Katayama and T. Watanabe, *Synthesis*, 1982, 935.
6 W.-L. Tsai, K. Hermann, E. Hug, B. Rohde and A. S. Dreiding, *Helv. Chim. Acta*, 1985, **68**, 2238; P. Diter, S. Tandien, O. Samuel and H. B. Kagan, *J. Org. Chem.*, 1994, **59**, 370.
7 G. M. Sheldrick, *Acta Crystallogr., Sect. A*, 1990, 46, 467.
8 G. M. Sheldrick, SHELXL-93, University of Göttingen, Germany, 1993.
9 H. D. Flack, *Acta Crystallogr., Sect. A*, 1983, 39, 676.

*Received in Cambridge, UK, 29th April 1997; 7/02920I*

# Non-ionic [2]rotaxanes containing methylated α-cyclodextrins

**Akira Harada,* Jun Li and Mikiharu Kamachi**

*Department of Macromolecular Science, Graduate School of Science, Osaka University, Toyonaka, Osaka 560, Japan*

**Non-ionic [2]rotaxanes have been prepared from complexes of oligoethylene derivatives with methylated α-cyclodextrins by capping them with trinitrophenyl groups as stoppers.**

Recently, much attention has been focused on the construction of interlocked molecular structures, such as rotaxanes and catenanes, because of their unique structures and properties.[1] Crown ethers,[2] cyclodextrins (CD),[3] cyclophanes[4] and cucurbituril[5] have been used as ring components of rotaxanes. Symmetric[6] and asymmetric[7] [2]rotaxanes containing α-CD and methylated β-CD have been prepared and characterized. However, all the [2]rotaxanes are ionic and in some cases their stoppers are metal complexes which are in equilibrium with dissociation states, so rings may come off. To obtain non-ionic [2]rotaxanes, it is necessary to design a dumbbell part which consists of neutral stoppers and a neutral axle. We chose a 2,4,6-trinitrobenzenesulfonic acid sodium salt (TNBS) as a stopping agent and diaminohexaethylene dihydrochloride (DAHE-2HCl) as an axle because TNBS is large enough to prevent dethreading and DAHE-2HCl is long enough to penetrate a methylated α-CD cavity. Moreover, TNBS and the amino groups of DAHE react easily with each other to give a covalent C–N bond in aqueous solution under mild conditions. 2,6-Di-*O*-methyl-α-CD (DM-α-CD) and 2,3,6-tri-*O*-methyl-α-CD (TM-α-CD) were chosen as ring molecules, because they are highly soluble in water and are able to form complexes with oligoethylene derivatives in aqueous solutions. Here we report the first preparation of non-ionic [2]rotaxanes based on the formation of the inclusion complexes.

α-CD forms complexes with ω, ω′-diaminoalkanes to give crystalline complexes. However, DM-α-CD and TM-α-CD did not form crystalline complexes, forming instead soluble complexes with ω, ω′-diaminoalkanes in an aqueous solution, although DAHE is insoluble in water. DAHE could be dissolved in aqueous solutions of DM-α-CD or TM-α-CD. The molar ratio of DAHE dissolved to the methylated α-CD is 1 : 1, indicating formation of 1 : 1 complexes. The complexes were allowed to react with TNBS to prevent dethreading of the cyclodextrins (Scheme 1). The products precipitated from water and were collected and purified by preparative thin layer chromatography (TLC) on $SiO_2$. This gave two kinds of [2]rotaxanes containing DM-α-CD and TM-α-CD, respectively. The [2]rotaxanes were obtained in high yields; 42% for DM-α-CD-[2]rotaxane and 48% for TM-α-CD-[2]rotaxane.

The products were characterized by elemental analysis, UV–VIS, $^1$H NMR, $^{13}$C NMR and FAB mass spectra.† TLC of the products on $SiO_2$ plates (90 : 10, $CHCl_3$–MeOH) revealed single spots in each case. The products showed absorptions at 417 and 347 nm, indicating that the 2,4,6-trinitrophenyl groups were substituted on the axles. The UV–VIS spectra as well as the $^1$H NMR spectra and elemental analyses revealed that the ratio between the methylated α-CD and DAHE-$TNP_2$ was 1 : 1.

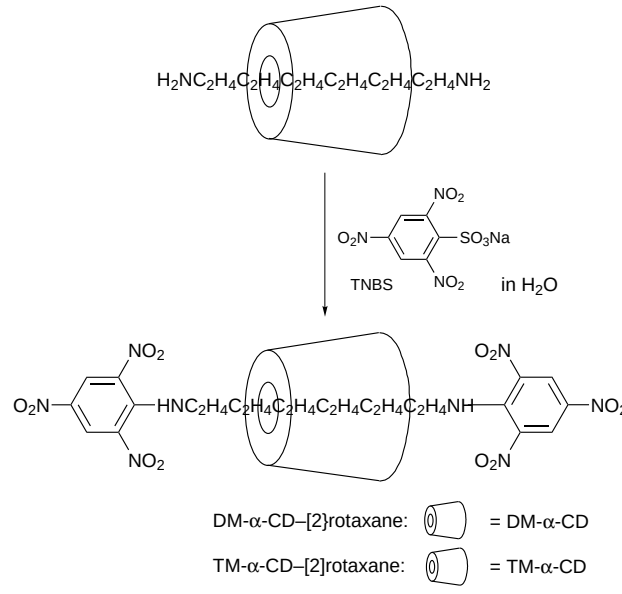
The $^1$H NMR spectrum of TM-α-CD-[2]rotaxane shows that it is composed of TM-α-CD, an HE chain and trinitrophenyl end groups in the proper ratios, that is, a single TM-α-CD unit, one HE chain and two TNP end groups. The peaks of TM-α-CD and DAHE-$TNP_2$ in the spectrum of [2]rotaxane show some shifts compared with those of its components, indicating that TM-α-CD and a HE chain are imprisoned in a single molecule. The $^1$H NMR spectrum of DM-α-CD-[2]rotaxane showed similar results.

Fig. 1 shows the $^{13}$C NMR spectrum of DM-α-CD-[2]rotaxane together with those of DM-α-CD and DAHE-$TNP_2$. The spectrum shows that the compound is composed of a single DM-α-CD and a single DAHE-$TNP_2$ unit. The C(c) and C(d) resonances of the TNP group split into two peaks, respectively. One is due to the TNP group at the small side of DM-α-CD and another is due to the TNP group at the larger cavity side. The C(e) resonance of the HE chain also separates into two peaks for the same reason. The resonances of the HE backbone split into a more complex pattern indicating that the HE chain is included in the cavity of DM-α-CD.

The FAB MS spectra of the two [2]rotaxanes are characteristic of DM-α-CD-[2]rotaxane and TM-α-CD-[2]rotaxane, respectively. In addition to peaks for the molecular ions and those with sodium, fragmentation peaks for the components are also observed.

The solubilities of the two [2]rotaxanes are quite different from those of their components. The [2]rotaxanes are insoluble in water, although DM-α-CD, TM-α-CD, TNBS and even complexes of DAHE with methylated α-CDs are soluble in water. The rotaxanes are soluble in most organic solvents such as chloroform, benzene, DMSO and DMF. The solubilities of the rotaxanes in organic solvents are higher than the thread and stopper molecule DAHE-$TNP_2$. The rotaxanes do not dethread into their components in any solvents, because the stopper group is covalently bound to the thread.

In conclusion, new neutral non-ionic [2]rotaxanes containing methylated CDs were prepared by utilizing the complex formation of derivatives of ω,ω′-diaminoalkane and methylated α-CDs in high yields. The rotaxanes obtained here have the simplest structures of such supramolecular compounds containing CDs reported, which enables us to study the basis of




**Scheme 1**

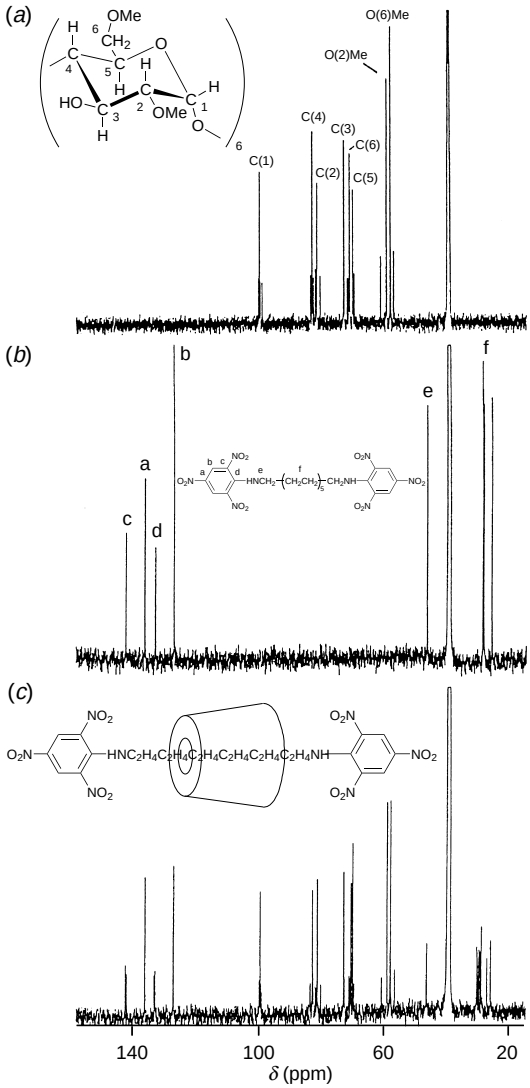



**Fig. 1** 125.65 MHz $^{13}$C CP MAS NMR spectra of (*a*) DM-α-CD, (*b*) DAHE-TNP$_2$ and (*c*) DM-α-CD–[2]rotaxane in [$^2$H$_6$]DMSO at 30 °C

rotaxane chemistry. This work also provides new methods for the synthesis of more complexed rotaxanes and catenanes using such non-covalent self-assembly processes.

## Footnotes

* E-mail: harada@chem.sci.osaka-u.ac.jp

† *Selected data* for **DM-α-CD-[2]rotaxane**: $^1$H NMR (CDCl$_3$, 270 MHz): δ 9.02 (d, 4 H, Ph), 8.94 (d, 2 H, PhNH), 4.95 [m, 12 H, C(2)OH and C(1)H of CD], 3.69–3.98 [m, 18 H, C(3)H and C(6)H of CD], 3.61 [s, 18 H, C(2)OCH$_3$ of CD], 3.40–3.57 [m, 6 H, C(5)H of CD], 3.36 [s, 18 H, C(6)OCH$_3$ of CD], 3.11–3.27 [m, 12 H, C(2)H and C(4)H of CD], 3.03 [d, 4 H, H(α) of hexaethylene chain], 1.24–1.77 (m, 20 H, hexaethylene backbone); $^{13}$C NMR ([$^2$H$_6$]DMSO, 125.65 MHz): δ 141.87 [C(2) of Ph], 136.00 [C(4) of Ph], 132.94 [C(1) of Ph], 127.07 [C(3) of Ph], 99.61 [C(1) of CD], 82.91 [C(4) of CD], 81.36 [C(2) of CD], 72.99 [C(3) of CD], 70.75 [C(6) of CD], 70.17 [C(5) of CD], 59.39 [MeO of C(2) of CD], 58.28 [MeO of C(6) of CD], 46.62 [C(α) of HE chain], 26.12–30.50 (HE backbone); Positive ion FAB MS: *m/z* 1799.7 (M + CH$_2$ + Na$^+$), 1777.7 (M$^+$ + CH$_2$), 1763.7 (M$^+$ + 1), 1759.7, 1745.7, 1729.7, 1714.7. Calc. for $C_{72}H_{115}N_8O_{42}$: C, 49.00; H, 6.57; N, 6.35. Found: C, 49.01; H, 6.53; N, 6.36%.

For **TM-α-CD-[2]rotaxane**: $^1$H NMR (CDCl$_3$, 270 MHz): δ 9.01 (d, 4 H, Ph), 8.91 (d, 2 H, PhNH), 5.02 [d, 6 H, C(1)OH of CD], 3.40–3.85 [m, 24 H, C(3)H, C(5)H and C(6)H of CD], 3.48 [s, 18 H, C(3)OCH$_3$ of CD], 3.37 [C(6)OCH$_3$ of CD], 3.11–3.18 [m, 12 H, C(2)H and C(4)H of CD], 3.03 [m, 4 H, H(α) of hexaethylene chain], 1.25–1.70 (m, 20 H, hexaethylene backbone); $^{13}$C NMR ([$^2$H$_6$]DMSO, 125.65 MHz): δ 141.67 [C(2) of Ph], 136.07 [C(4) of Ph], 133.02 [C(1) of Phenyl], 126.99 [C(3) of Ph], 99.18 [C(1) of CD], 82.09 [C(4) of CD], 81.82 [C(2) of CD], 80.75 [C(3) of CD], 70.91 [C(6) of CD], 70.86 [C(5) of CD], 60.94 [MeO of C(3) of CD], 58.26 [MeO of C(2) of CD], 56.93 [MeO of C(6) of CD], 46.31 [C(α) of HE chain], 26.40–30.85 (HE backbone); Positive ion FAB MS: *m/z* 1869.8 (M + Na$^+$), 1848.8 (M$^+$ + 1), 1847.8 (M$^+$), 1831.8 (M − CH$_3$), 1830.8, 1829.9, 1814.8. Calc. for $C_{78}H_{126}N_8O_{42}$: C, 50.70; H, 6.87; N, 6.06. Found: C, 50.47; H, 6.84; N, 6.09%.

## References

1 D. Philp and J. F. Stoddart, *Angew. Chem., Int. Ed. Engl.*, 1996, **35**, 1154; H. W. Gibson, M. C. Bheda and P. T. Engen, *Prog. Polym. Sci.*, 1994, **19**, 843; A. Harada, *Large Ring Molecules*, ed. J. A. Semlyen, Wiley, Chichester, 1996, p. 407.

2 D. B. Amabilino and J. F. Stoddart, *Chem. Rev.*, 1995, **95**, 2725; H. W. Gibson, *Large Ring Molecules*, ed. J. A. Semlyen, Wiley Chichester, 1996, p. 191.

3 A. Harada, *Polym. News*, 1993, **18**, 358; G. Wenz, *Angew. Chem., Int. Ed. Engl.*, 1994, **33**, 803; I. Yamaguchi, K. Osakada and T. Yamamoto, *J. Am. Chem. Soc.*, 1996, **118**, 1811; A. Harada, J. Li and M. Kamachi, *Nature* (*London*), 1992, **356**, 325.

4 R. A. Bissell, E. Córdova, A. E.Kaifer and J. F. Stoddart, *Nature* (*London*), 1994, **369**, 133; P. L. Anelli, N. Spencer and J. F. Stoddart, *J. Am. Chem. Soc.*, 1991, **113**, 5131.

5 D. Whang and K. Kim, *J. Am. Chem. Soc.*, 1997, **119**, 451; D. Whang. Y.-M. Jeon, J. Heo and K. Kim, *J. Am. Chem. Soc.*, 1996, **118**, 11 333.

6 H. Ogino, *J. Am. Chem. Soc.*, 1981, **103**, 1303; H. Ogino and K. Ohata, *Inorg. Chem.*, 1984, **23**, 3312; J. S. Manka and D. S. Lawrence, *J. Am. Chem. Soc.*, 1990, **112**, 2440; T. V. S. Rao and D. S. Lawrence, *J. Am. Chem. Soc.*, 1990, **112**, 3614; D. L. Dick, T. V. S. Rao, D. Sukumaran and D. S. Lawrence, *J. Am. Chem. Soc.*, 1992, **114**, 2664; R. S. Wylie and D. H. Macartney, *J. Am. Chem. Soc.*, 1992, **114**, 3136; (*g*) After submitting this manuscript, the synthesis and characterization of an α-CD [2]rotaxane containing a cob(III)alamin stoppered decamethylene chain has been reported: R. B. Hannak, G. Färber, R. Konrat and B. Kräutler, *J. Am. Chem. Soc.*, 1997, **119**, 2313.

7 R. Isnin and A. E. Kaifer, *J. Am. Chem. Soc.*, 1991, **113**, 8188; G. Wenz, E. Bey and L. Schmidt, *Angew. Chem., Int. Ed. Engl.*, 1992, **31**, 783.

*Received in Columbia, MO, USA, 11th April 1997; 7/02498C*

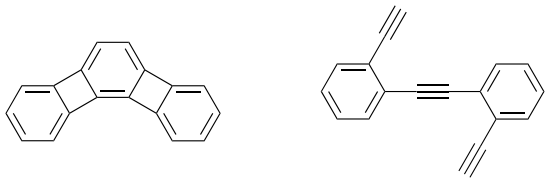
# From phenylenes to acenes: flash vacuum pyrolytic isomerization of angular [3]phenylene to benzo[*ghi*]fluoranthene

**Adam J. Matzger and K. Peter C. Vollhardt***

*Department of Chemistry, University of California at Berkeley and the Chemical Sciences Division, Lawrence Berkeley National Laboratory, Berkeley, CA, 94720-1460, USA*

**The flash vacuum pyrolysis of angular [3]phenylene and bis(2-ethynylphenyl)ethyne produces benzo[*ghi*]fluoranthene and chrysene, respectively.**

Recently there has been much attention focused on the thermal interconversion of aromatic hydrocarbons because of its relevance to the formation of fullerenes[1] and environmental pollutants.[2] In connection with this, the fate of **1**[3] was of great interest because of its inherent strain and thus, its potential to equilibrate with its linear conterpart,[4] undergo retrocyclization to **2**,[5] or cascade into known $C_{18}H_{10}$ manifolds.[1,2]

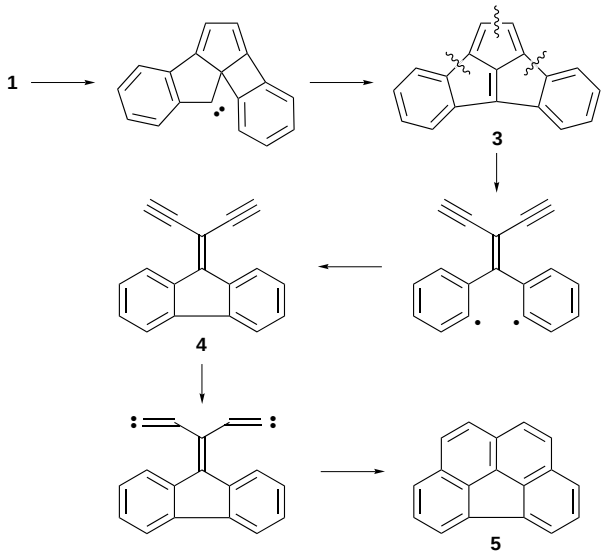


**1** **2**

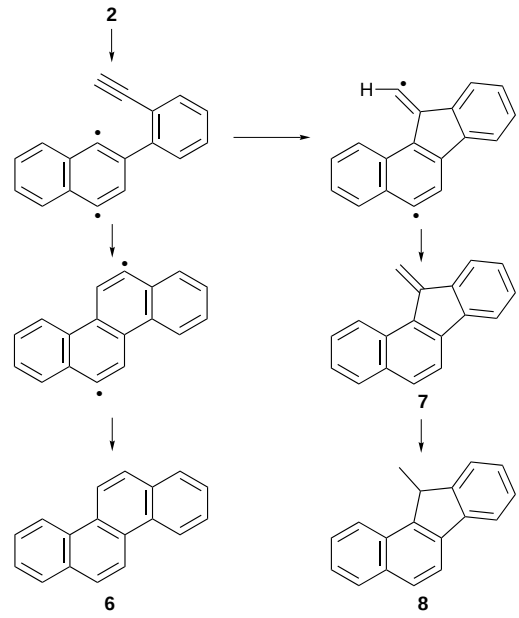
Initial experiments, in which **1** was sublimed through a quartz tube at 780 °C, resulted in essentially complete recovery of starting material. This result is not surprising, considering that **1** was first synthesized by pyrolytic methods at 800 °C.[6] Remarkably, however, at 1000 °C, the major isolable product was the unanticipated isomer benzo[*ghi*]fluoranthene **5** (10%),[7] in addition to minor quantities of chrysene ($C_{18}H_{12}$) **6** (2.5%) and fluoranthene ($C_{16}H_{10}$) (1%). A proposed mechanism for the transformation of **1** to **5** is outlined in Scheme 1. The first steps involve isomerization to dibenzoacepentalene **3**,[8] a formal Stone–Wales rearrangement.[1*a*] Stepwise or concerted cleavage of the five membered rings would afford diethynyldibenzofulvene **4** after phenyl radical recombination. The last two steps have their closest analogy in the synthesis of corannulene by flash vacuum pyrolysis (FVP) of an etheno-bridged, trimethylsilyl-protected derivative of **4**.[9]† The origin of chrysene may be **2** (*vide infra*). Significantly, **5** is not the product that might be expected on the basis of the results of the pyrolysis of biphenylene,[10] namely cyclopent[*hi*]acephenanthrylene (which has been shown to be inert to rearrangement to **5** under our conditions),[1*d*] presumably a consequence of the regioselectivity of the initial 1,2-shifts enforced by the proximity of the two four-membered rings.

As a control experiment, the FVP of **2** was executed. At 780 °C, all of the starting material had been consumed and chrysene **6** constituted the major isolated product (1.9% yield), none of **5** being present. A possible pathway from **2** to **6** is patterned after that proposed by Bergman in the solution thermolysis of the corresponding parent dienetriyne to form naphthalene (Scheme 2).[11] In the latter, the added hydrogen in the product is supplied by the solvent. The absence of an obvious hydrogen source in the FVP of **2** explains the low yield of **6**. Deuterium labelling of the terminal triple bonds‡ supported the proposed mechanism by furnishing only [5,11-$^2H_2$]chrysene. Note that neither **1** nor **3** are formed even at 1000 °C.

To further corroborate the fate of **2**, it was heated in benzene solution (205 °C) in the presence of cyclohexa-1,4-diene. Surprisingly, the major product was not **6** (2.5%), but rather 11-methyl-11*H*-benzo[*a*]fluorene **8** (19%).[12]§ We propose that the initially formed 1,4-didehydronaphthalene from **2** bifurcates to not only undergo 6-*endo*-digonal but also 5-*exo*-digonal




**Scheme 1**




**Scheme 2**

closure to form the five membered ring (Scheme 2). The resultant diradical would then be capped with hydrogen from cyclohexa-1,4-diene to provide the reactive fulvene **7** which undergoes fast transfer hydrogenation under the reaction conditions to yield **8**.[13] Further evidence for the intermediacy of **7** is found in the thermolysis of **2** in MeOH at 217 °C, in which the methyl group of the solvent is the hydrogen source. In this case 11-(2-hydroxyethyl)-1*H*-benzo[*a*]fluorene¶ is formed (26%) along with **6** (4.3%). This product is suggested to arise by trapping of **7** with ·$CH_2OH$, followed by H abstraction from MeOH. The absence of products arising from 5-*exo* closure in the gas phase pyrolysis suggests that equilibration of the two diradicals to give the more stable didehydrochrysene is rapid under the conditions employed and/or that decomposition of the dibenzofulvene occurs in the absence of a good hydrogen donor.

Finally, we note that the observed conversion of phenylene **1** to the cyclopenta fused polycyclic benzenoid **5** constitutes the first of a series of potential conversions of larger phenylenes to semifullerenes.

This work was supported by the National Science Foundation (CHE-9202152). A. J. M. was a Syntex predoctoral fellow (1994–1995) and an ACS Division of Organic Chemistry Graduate Fellow (sponsored by Rohm and Haas Co.) (1995–1996).

## Footnotes

* E-mail: vollhard@cchem.berkeley.edu

† This report describes **5** as a side product, resulting from loss of $C_2$. Consistent with this finding is our observation of fluoranthene in the pyrolysis of **1**.

‡ Synthesized from bis[2-(trimethylsilylethynyl)phenyl]ethyne using MeOD and $K_2CO_3$.

§ GC–MS indicates that most of the diradicals formed add to cyclohexadiene or benzene rather than being trapped as **4** or **5**, thus accounting for the low combined yield of these products (21.5%).

¶ 11-(2-Hydroxyethyl)-1*H*-benzo[*a*]fluorene: *m/z* (EI-MS) 260 ($M^+$, 71%), 242 (49), 241 (30), 229 (16), 228 (19), 226 (15), 215 (100); $^1$H NMR (500 MHz, $CDCl_3$): $\delta$ 2.40 (dq, *J* 13.4, 6.7 Hz, 1 H), 2.69 (dtd, *J* 13.9, 7.1, 3.6 Hz, 1 H), 3.38 (m, 2 H), 4.55 (dd, *J* 7.0, 3.6 Hz, 2 H), 7.32 (t, *J* 7.3 Hz, 1 H), 7.40 (t, *J* 7.4 Hz, 1 H), 7.45 (t, *J* 7.5 Hz, 1 H), 7.55 (t, *J* 7.4 Hz, 1 H), 7.62 (d, *J* 7.4 Hz, 1 H), 7.80 (d, *J* 7.5 Hz, 1 H), 7.88 (m, 2 H), 7.92 (d, *J* 8.2 Hz, 1 H), 8.17 (d, *J* 7.3 Hz, 1 H); $\nu_{max}$(neat)/cm$^{-1}$ 3353, 3053, 2927, 1466, 1022, 909, 821, 760.

## References

1 (*a*) L. T. Scott, *Pure Appl. Chem.*, 1996, **68**, 291; (*b*) P. W. Rabideau and A. Sygula, *Acc. Chem. Res.*, 1996, **29**, 235; (*c*) R. F. C. Brown and F. W. Eastwood, *Pure Appl. Chem.*, 1996, **68**, 261; (*d*) L. W. Jenneskens, M. Sarobe and J. W. Zwikker, *Pure Appl. Chem.*, 1996, **68**, 219.
2 U. E. Wiersum, *Janssen Chim. Acta*, 1992, **10**, 3.
3 R. Diercks and K. P. C. Vollhardt, *Angew. Chem.*, 1986, **98**, 268; *Angew. Chem., Int. Ed. Engl.*, 1986, **25**, 266.
4 B. C. Berris, G. H. Hovakeemian, Y.-H. Lai, H. Mestdagh and K. P. C. Vollhardt, *J. Am. Chem. Soc.*, 1985, **107**, 5670.
5 R. Diercks and K. P. C. Vollhardt, *J. Am. Chem. Soc.*, 1986, **108**, 3150
6 J. W. Barton and R. B. Walker, *Tetrahedron Lett.*, 1978, 1005.
7 W. Karcher, R. J. Fordham, J. J. Dubois, P. G. J. M. Glaude and J. A. M. Ligthart, *Spectral Atlas of Polycyclic Aromatic Compounds*, Reidel, Dordrecht, 1985.
8 The synthesis of acepentalene and its tribenzo derivative have recently been reported: R. Haag, D. Schröder, T. Zywietz, H. Jiao, H. Schwarz, P. von R. Schleyer and A. de Meijere, *Angew. Chem.*, 1996, **108**, 1413; *Angew. Chem., Int. Ed. Engl.*, 1996, **35**, 1317; R. Haag, B. Ohlhorst, M. Noltemeyer, R. Fleischer, D. Stalke, A. Schuster, D. Kuck and A. de Meijere, *J. Am. Chem. Soc.*, 1995, **117**, 10474.
9 G. Zimmermann, U. Nuechter, S. Hagen and M. Nuechter, *Tetrahedron Lett.*, 1994, **35**, 4747; R. F. C. Brown, N. Choi, K. J. Coulston, F. W. Eastwood, U. E. Wiersum and L. J. Jenneskens, *Tetrahedron Lett.*, 1994, **35**, 4405.
10 U. E. Wiersum and L. W. Jenneskens, *Tetrahedron Lett.*, 1993, **34**, 6615.
11 K. N. Bharucha, R. M. Marsh, R. E. Minto and R. G. Bergman, *J. Am. Chem. Soc.*, 1992, **114**, 3120.
12 G. M. Badger, *J. Chem. Soc.*, 1941, 535.
13 The rapid hydrogenation of dibenzofulvene by a radical mechanism has been observed: T. E. Nalesnik, J. H. Freudenberger and M. Orchin, *J. Organomet. Chem.*, 1981, **221**, 193.

*Received in Corvallis, OR, USA, 17th April 1997; 7/02680C*

# Drastic metal-ion enhancement in photoinduced aggregation of copolymers carrying crown ether and spirobenzopyran moieties

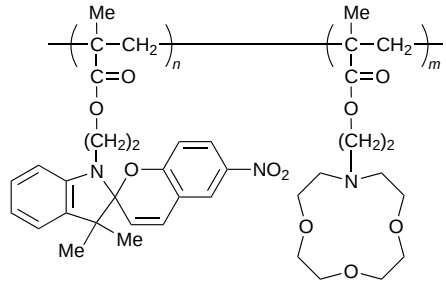
**Keiichi Kimura,* Miwa Sumida and Masaaki Yokoyama**

*Chemical Process Engineering, Faculty of Engineering, Osaka University, Yamada-oka 2-1, Suita, Osaka 565, Japan*

**Metal ion complexation of the crown ether moiety of crown ether–spiropyran copolymer 1 brings about the enhanced aggregation of its merocyanine moiety, formed by photoisomerization of its spiropyran, which results in reversible polymer precipitation.**

Spirobenzopyran derivatives, typical photochromic compounds,[1] when isomerized to their corresponding merocyanine forms, tend to aggregate.[2] The aggregation of the merocyanine isomers is enhanced in polymers carrying spirobenzopyran moieties on their side chains.[3]

Spirobenzopyran derivatives incorporating a monoazacrown ether moiety are attractive materials which can realize photochemical control of cation complexation.[4,5] Since an easy way to combine a spirobenzopyran moiety with a crown ether moiety is copolymerization of vinyl monomers carrying their corresponding functional moieties, we have designed such polymers **1** carrying side chains with monoaza-12-crown-4 and spirobenzopyran moieties. During the course of investigating the cation complexation and photochromism of the crown ether–spiropyran copolymer **1**, we have discovered an intriguing phenomenon. Herein we report the reversible photoinduced aggregation and precipitation of polymer **1** enhanced dramatically by cation complexation of its crown ether moieties.




**1** *n* / *m* = 1

Radical copolymerization of an equimolar amount of the corresponding vinyl monomers of monoaza-12-crown-4 and spirobenzopyran[6] afforded crown ether–spiropyran copolymer **1** which possessed a composition of almost 1 : 1 (spiropyran–crown ether unit) and a number average molecular weight of $1.3 \times 10^4$ (polystyrene standard). The cation complexing ability of **1** toward alkali metal ions, which was estimated by a conventional solvent extraction technique, is in the order $Na^+ > K^+ > Li^+$, as shown in Fig. 1. The crown ether–spiropyran copolymer **1** has a very different ion selectivity from its corresponding monomeric crown ether, *N*-benzylmonoaza-12-crown-4 (10-benzyl-1,4,7-trioxa-10-azacyclododecane). The higher cation complexing ability toward $Na^+$ and $K^+$ than $Li^+$ is probably due to the easy formation of intrapolymer 2 : 1 (crown ether ring–metal ion) complexes with $Na^+$ and $K^+$ by cooperative action of two neighbouring crown ether rings, as was the case with poly(12-crown-4) derivatives.[7] Intrapolymer sandwich-type complex formation promotes cation binding and thereby cation extraction.

UV irradiation (300–400 nm) causes isomerization of the spiropyran moiety of **1** to its corresponding merocyanine from, which in turn brings about aggregation of the resulting zwitterionic merocyanine moieties. This phenomenon was suggested in absorption spectral changes of a THF solution of crown ether–spiropyran copolymer **1**. The behaviour of the merocyanine aggregation of **1** in the presence of an equimolar amount of alkali metal perchlorate is distinct from that in the absence of any metal salt, as illustrated by the absorption maximum difference for its merocyanine moiety after 5 min of UV irradiation (Fig. 2). In the absence of metal ions, the photoirradiation caused an increase in the absorption peak around 600 nm assigned to the non-aggregated merocyanine moiety, which shifted gradually to shorter wavelength (560 nm) after prolonged photoirradiation. The blue shift of the merocyanine absorption peak can be attributed to the formation of H-type aggregates.[3] Further UV irradiation caused little change in the absorption spectrum. In a solution containing $Li^+$ ions, on the other hand, the absorption around 560 nm attributed to H-type aggregation appeared after only 5 min of irradiation, with a colour change of the solution from colourless to purple. Further irradiation decreased the absorption with a slight red shift, and then purple-coloured polymer started to precipitate from the solution. The modest blue shift in a solution containing $Na^+$ ions indicates that the H-type aggregate formation is sluggish in the system containing $Na^+$ ions as compared with that containing $Li^+$ ions. Since, in a solvent in which they are moderately soluble (*e.g.* THF), polymer molecules of **1** generally cast in a contracted form in the absence of metal ions, the photoisomerized merocyanine moieties are likely to form intramolecular aggregates in a polymer chain. In the presence of

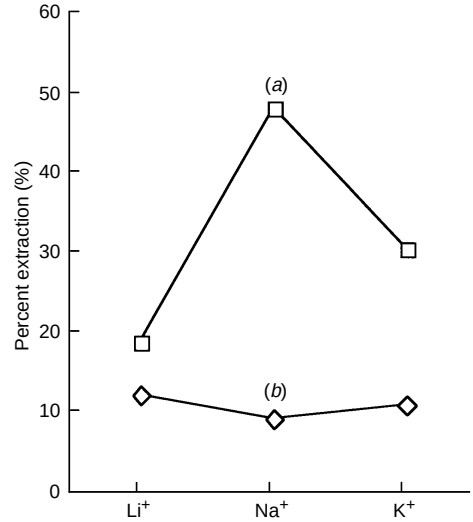



**Fig. 1** Cation extraction (*a*) by crown ether–spiropyran copolymer **1** and (*b*) comparison with *N*-benzylmonoaza-12-crown-4. Aqueous phase: 0.1 mol $dm^{-3}$ alkali metal hydroxide, $7 \times 10^{-5}$ mol $dm^{-3}$ picric acid. Organic phase: $2.1 \times 10^{-3}$ mol $dm^{-3}$ crown ether unit in 1,2-dichloroethane. Extracted for 15 min in the dark.

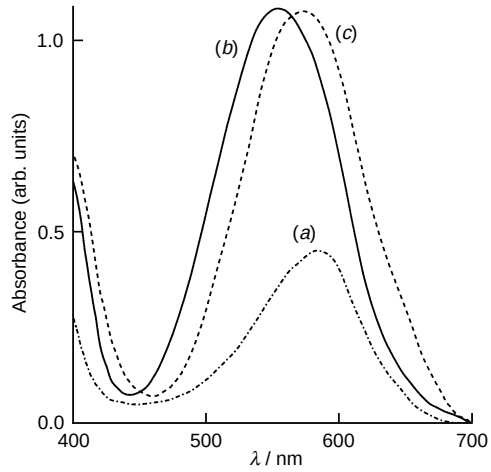



**Fig. 2** Absorption spectra of crown ether–spiropyran copolymer **1** in THF (*a*) without metal ion, (*b*) with $LiClO_4$, and (*c*) with $NaClO_4$, after UV irradiation for 5 min. Polymer **1** and metal perchlorate: $4 \times 10^{-4}$ mol $dm^{-3}$ each in THF. UV light: 300–400 nm.

metal ions, however, the polymer chains carry positive electric charges due to cation complexation with its crown ether moieties, and therefore the polymer chains expand due to intramolecular electrostatic repulsion among the cationic charges.[8,9] The expansion of the polymer chains increases the probability of formation of an interpolymer merocyanine aggregate while suppressing the intramolecular (intrapolymer) one. Thus, the interpolymer merocyanine aggregation induces crosslinking of **1**, finally leading to the polymer precipitation.

Very interestingly, the polymer precipitate formed on UV irradiation in the presence of the metal ion can be dissolved again by subsequent visible light irradiation (for 20 min), leaving the solution almost transparent. This means that the UV-induced precipitation and visible light-induced dissolution of polymer **1** in the presence of $Li^+$ ions is quite reversible. This is also the case in the presence of $Na^+$ ions, although the UV-induced merocyanine aggregation and precipitation is not as easy as in the $Li^+$ system. This is probably because polymers carrying a 12-crown-4 moiety at the side chain tend to form intramolecular 2 : 1 (crown ether ring–metal ion) complexes with $Na^+$.[7,10] This intramolecular formation of the sandwich-type complexes suppresses more or less the polymer chain expansion which is required for the interpolymer merocyanine aggregation.

Thus, reversible photocontrol in the precipitate formation of crown ether–spiropyran copolymer **1**, based on cation complexation-induced merocyanine aggregation, has been realized in THF solutions containing metal ions. Further studies are now under way to elucidate the properties of the polymer precipitate.

This work was partially supported by a Grant-in-Aid for Scientific Research from the Ministry of Education, Science, Sports, and Culture, Japan. Financial support from the Nagase Science and Technology Foundation is also acknowledged.

## Footnote

* E-mail: kimura@chem.eng.osaka-u.ac.jp

## References

1 R. C. Bertelson, in *Photochromism*, ed. G. H. Brown, Wiley Interscience, New York, 1971, p. 45.
2 V. A. Krongauz and E. S. Goldburst, *Nature*, 1978, **271**, 43.
3 V. A. Krongauz and E. S. Goldburst, *Macromolecules*, 1981, **14**, 1382.
4 K. Kimura, T. Yamashita and M. Yokoyama, *J. Chem. Soc., Perkin Trans. 2*, 1992, 613.
5 K. Kimura, T. Yamashita and M. Yokoyama, *J. Phys. Chem.*, 1992, **96**, 5614.
6 E. I. Zaitseva, A. L. Prokhoda, L. N. Kurkovskaya, R. R. Shifrina, N. S. Kardash, D. A. Drapkina and V. A. Krongauz, *Chem. Heterocycl. Compd.* (*Engl. Transl.*), 1973, **12**, 1233.
7 T. Maeda, M. Ouchi, K. Kimura and T. Shono, *Chem. Lett.*, 1981, 1573.
8 M. Irie, A. Menju and K. Hayashi, *Macromolecules*, 1979, **12**, 1176.
9 M. Irie and W. Schnabel, *Macromolecules*, 1986, **19**, 2846.
10 M. Bourgoin, K. H. Wong, J. Y. Hui and J. Smid, *J. Am. Chem. Soc.*, 1975, **97**, 3462.

*Received in Cambridge, UK, 13th May 1997; 7/03293E*

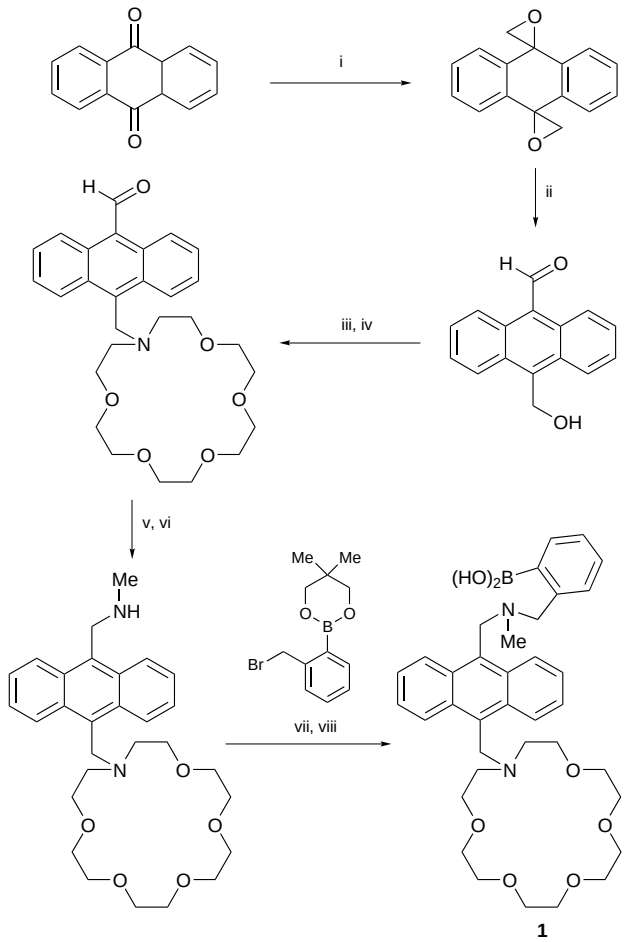
# Selective D-glucosamine hydrochloride fluorescence signalling based on ammonium cation and diol recognition

**Christopher R. Cooper and Tony D. James***

*The University of Birmingham, School of Chemistry, Edgbaston, Birmingham, UK B15 2TT*

**Fluorescent photoinduced electron transfer sensor 1 with monoaza-18-crown-6 ether and boronic acid receptor units shows selective fluorescent enhancement with D-glucosamine hydrochloride in aqueous solution at pH 7.18.**

The development of fluorescent receptors for saccharides has recently gained much attention.[1] In a series of recent papers the interaction of boronic acid and amine[2–6] has been used to create photoinduced electron transfer (PET)[7,8] sensory systems for saccharides. When saccharides from cyclic boronate esters with boronic acids, the acidity of the boronic acid is enhanced[9] and therefore the Lewis acid–base interaction between the boronic acid and the tertiary amine is strengthened. The strength of this acid–base interaction modulates the PET from the amine (acting as a quencher) to anthracene (acting as a fluorophore). These compounds show increased fluorescence at neutral pH through suppression of the photoinduced electron transfer from nitrogen to anthracene on saccharide binding; a direct result of the stronger boron–nitrogen interaction.[2–7]



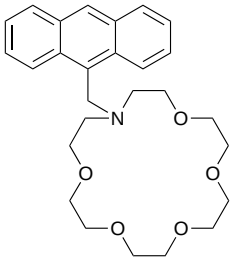

**Scheme 1** *Reagents and conditions*: i, NaH, $Me_3SI$, DMSO, room temp., 80%; ii, LiBr, MeCN, 60 °C, quant.; iii, $MeSO_2Cl$, $Et_3N$, $CH_2Cl_2$, −10 °C, 93%; iv, 1-aza-18-crown-6, $K_2CO_3$, NaI, MeCN, reflux, 50%; v, MeOH, $MeNH_2$, room temp., quant.; vi, $NaBH_4$, MeOH, room temp., quant.; vii, $K_2CO_3$, MeCN, reflux, 30%; viii, EtOH–$H_2O$ (1 : 2), pH 7.3, quant.

In a recent paper de Silva reports[10] on how two different binding sites can be used to develop a selective fluorescent sensor for γ-aminobutyric acid. The system consists of an azacrown ether (ammonium binding site) and guanadinium (carboxylate binding site). This work shows how two different receptor sites can be used to obtain high selectivities for molecules containing multiple functional groups. We have previously shown how two boronic acid binding units can be used in the selective recognition of glucose[3] and the chiral discrimination of monosaccharides.[4] Here we extend our work on boronic acid fluorescent sensors by the incorporation of a second and *different* binding site. The incorporation of a second binding site will allow the development of sensors for a variety of biologically important molecules containing saccharide fragments.

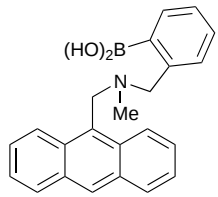
Sensor **1** consists of monoaza-18-crown-6 ether as a binding site for the ammonium terminal of D-glucosamine hydrochloride, while a boronic acid serves as a binding site for the diol (carbohydrate) part of D-glucosamine hydrochloride. The nitrogen of the azacrown ether unit can participate in PET with the anthracene fluorophore; ammonium ion binding can then cause fluorescence recovery. This recovery is due to hydrogen bonding from the ammonium ion to the nitrogen of the azacrown ether. The strength of this hydrogen bonding interaction modulates the PET from the amine to anthracene. As explained above, the boronic acid unit can also participate in PET with the anthracene fluorophore, and diol binding can also cause fluorescence recovery. The anthracene unit serves as a rigid spacer between the two receptor units, with the appropriate spacing for the glucose moiety.[3] This system is expected to behave like an AND logic gate[11] in that fluorescence recovery will only be observed when two chemical inputs are supplied; for this system the two chemical inputs are an ammonium cation and a diol group. Compound **1** was synthesised as outlined in Scheme 1. The fluorescence of compound **1** varies as a function of pH giving a p$K_a$ of 7.32 (water, 0.05 $mol^{-1}$ $dm^{-3}$ tetramethylammonium chloride); under the same conditions the p$K_a$ of D-glucosamine hydrochloride is 7.56. Binding studies were carried out in a 33.2% (w/w) ethanol–water buffer[12] at pH 7.18. This pH was chosen to balance the protonation of the azacrown ether and deprotonation of the D-glucosamine hydrochloride. At low pH the sensor is protonated and no signal is observed, conversely at higher pH the D-glucosamine hydrochloride is present predominantly as free amine and will not bind strongly with the azacrown ether.

The stability constants for compounds **1**, **2** and **3** with D-glucose and D-glucosamine hydrochloride are given in Table 1. The curves from which the constants were calculated are shown in Fig. 1 and 2.

Compound **2**[13] does not display any fluorescence enhancement or have a binding constant with D-glucose because it has no saccharide binding site. D-glucosamine hydrochloride binding with compound **2** is also not observed under the experimental conditions, because the buffer solution saturates with




**2**




**3**

**Table 1** Stability constants for D-glucose and D-glucosamine hydrochloride with **1**, **2** and **3**

| | log $K_a$ ($r^2$; data points) | | |
|---|---|---|---|
| | **1** | **2** | **3** |
| D-Glucose | —[a] | —[a] | 2.92 (0.996; 8) |
| D-Glucosamine hydrochloride | 3.31 (0.997; 8) | < 1[b] | 2.70 (0.999; 7) |

[a] No fluorescence switching is possible. [b] No fluorescence change observed up to the solubility limit (0.1 mol $dm^{-3}$).

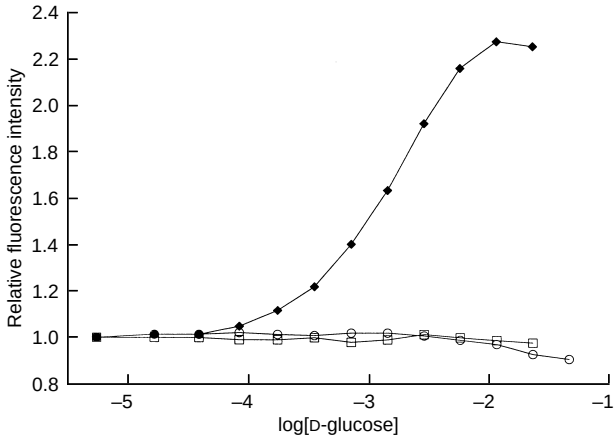



**Fig. 1** Fluorescence intensity–log[D-glucose] profile of (○) **1**, (□) **2** and (◆) **3** at 25 °C; $3.33 \times 10^{-6}$ M of **1**, **2** or **3** in EtOH–$H_2O$ (1 : 2), pH 7.18, $\lambda_{ex}$ 372 nm, $\lambda_{em}$ 425 nm

D-glucosamine hydrochloride before the binding event can be observed, giving an upper limit on the log$K_a$ for D-glucosamine hydrochloride of 1. As expected compound **3** shows a fluorescence enhancement with D-glucose (log$K_a$ = 2.92) and D-glucosamine hydrochloride (log$K_a$ = 2.70). With D-glucose the boronic acid has a choice of binding either the 1,2- or 4,6-diols, but with D-glucosamine hydrochloride binding with just the 4,6-diol is possible. The stability constant of **3** with D-glucose is higher than that observed with D-glucosamine hydrochloride, reflecting the known selectivity of boronic acids for the 1,2-diol of D-glucose.[14] Compound **1** shows a fluorescence increase with D-glucosamine hydrochloride (log$K_a$ = 3.31), but no increase with D-glucose. The result clearly demonstrates that for a fluorescent output *both* a diol *and* ammonium group must be present in the guest. The stability of the D-glucosamine hydrochloride complex with compound **1** is greater than that with compound **3**. (log$K_a$ = 3.31 *versus* 2.70) This increase in stability can be attributed to co-operative binding by the boronic acid and azacrown ether.

With this work we have demonstrated that the boronic acid PET system can be used in combination with other binding sites

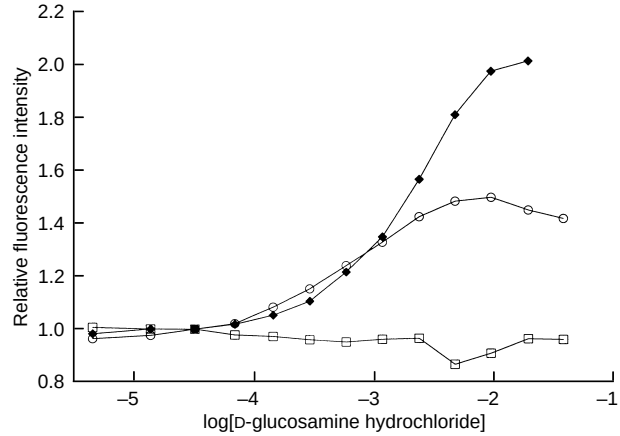



**Fig. 2** Fluorescence intensity–log[D-glucosamine hydrochloride] profile of (○) **1**, (□) **2** and (◆) **3** at 25 °C; $3.33 \times 10^{-6}$ M of **1**, **2** or **3** in EtOH–$H_2O$ (1 : 2), pH 7.18, $\lambda_{ex}$ 372 nm, $\lambda_{em}$ 425 nm

to create new and selective receptors for important biological molecules. We believe that this unit will be increasingly used as a general building block in molecular receptor design.

T. D. J. acknowledges the Royal Society for support through the award of a University Fellowship. C. R. C. acknowledges the School of Chemistry for support through the award of a School Studentship.

## Footnote

* E-mail: tdjames@chemistry.bham.ac.uk

## References

1 G. Deng, T. D. James and S. Shinkai, *J. Am. Chem. Soc.*, 1994, **116**, 4567 and references cited therein; J. Yoon and A. W. Czarnik, *J. Am. Chem. Soc.*, 1992, **114**, 5874; G. T. Morin, M. P. Hughes, M.-F. Paugam and B. D. Smith, *J. Am. Chem. Soc.*, 1994, **116**, 8895 and references cited therein.
2 T. D. James, K. R. A. S. Sandanayake and S. Shinkai, *J. Chem. Soc., Chem. Commun.*, 1994, 477.
3 T. D. James, K. R. A. S. Sandanayake and S. Shinkai, *Angew. Chem., Int. Ed. Engl.*, 1994, **33**, 2207.
4 T. D. James, K. R. A. S. Sandanayake and S. Shinkai, *Nature*, 1995, **374**, 345.
5 T. D. James and S. Shinkai, *J. Chem. Soc., Chem. Commun.*, 1995, 1483.
6 T. D. James, P. Linnane and S. Shinkai, *Chem. Commun.*, 1996, 281; T. D. James, K. R. A. S. Sandanayake and S. Shinkai, *Angew. Chem., Int. Ed. Engl.*, 1996, **35**, 1910.
7 R. A. Bissel, A. P. de Silva, H. Q. N. Gunaratna, P. L. M. Lynch, G. E. M. Maguire, C. P. McCoy and K. R. A. S. Sandanayake, *Top. Curr. Chem.*, 1993, **168**, 223.
8 A. W. Czarnik, *Fluorescent Chemosensors for Ion and Molecular Recognition*, ACS Books, Washington, 1993.
9 J. P. Lorand and J. D. Edwards, *J. Org. Chem.*, 1959, **24**, 769.
10 A. P. de Silva, H. Q. N. Gunaratna, C. McVeigh, G. E. M. Maguire, P. R. S. Maxwell and E. O'Hanion, *Chem. Commun.*, 1996, 2191.
11 A. P. de Silva, H. Q. N. Gunaratna and C. P. McCoy, *Nature*, 1993, **264**, 42; S. Iwata and K. Tanaka, *J. Chem. Soc., Chem. Commun.*, 1995, 1491.
12 D. D. Perrin and B. Dempsey, *Buffers for pH and Metal Ion Control*, Chapman and Hall, London, 1974, ch. 6.
13 A. P. deSilva and S. A. deSilva, *J. Chem. Soc., Chem. Commun.*, 1986, 1709.
14 S. Shinkai, K. Tsukagoshi, Y. Ishikawa and T. Kunitake, *J. Chem. Soc., Chem. Commun.*, 1991, 1039.

*Received in Cambridge, UK, 13th May 1997; 7/03300A*

# Synthesis and solid-state polymerization of a diacetylene containing a tetrathiafulvalene group

**Satoru Shimada,*[a]† Atsushi Masaki,[a] Kikuko Hayamizu,[a] Hiro Matsuda,*[a] Shuji Okada[b] and Hachiro Nakanishi[b]**

[a] *National Institute of Materials and Chemical Research, 1-1 Higashi, Tsukuba, Ibaraki 305, Japan*
[b] *Institute for Chemical Reaction Science, Tohoku University, 2-1-1 Katahira, Aoba-ku, Sendai, Miyagi 980, Japan*

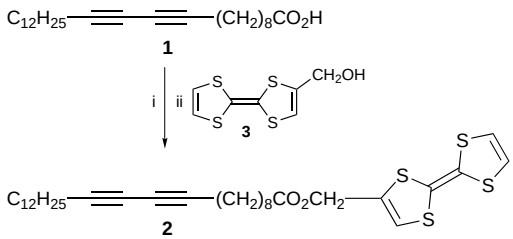
**A diacetylene containing a tetrathiafulvalene substituent has been synthesized and can be readily polymerized in the solid state to yield a novel polydiacetylene.**

Polydiaceteylenes (PDAs), which are highly regular conjugated polymers produced by solid-state polymerization, have been attracting much attention because of their electrical transportation and third-order nonlinear optical properties.[1] We have investigated the synthesis of PDAs having aromatic[2] and alkynyl groups,[3] and heteroatoms[4] directly bound to $sp^2$ carbons of the conjugated main chain in order to modulate the electronic structures and thereby modify the electrical and optical properties. Meanwhile, tetrathiafulvalene (TTF) and analogous derivatives are also of interest because they have large electron-donating properties and form highly conductive charge-transfer complexes, which in some cases can be superconducting. Therefore we designed a PDA, obtained by solid-state polymerization, with TTF moieties contained in the side groups. Such a molecular design would have both a conjugated polymer main chain and electron-donating side chains. However, the incorporation of TTF units into the side chains of PDAs has been essentially unexplored so far.[5] Here we report the first example of a PDA derivative containing TTF groups in the substituents.

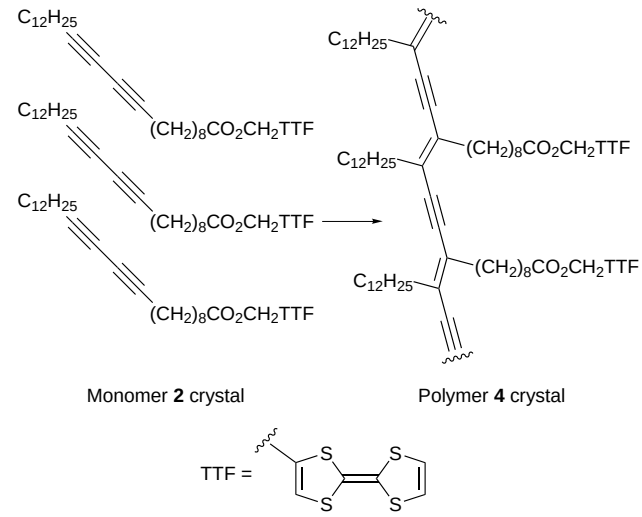
The monomer **2** of PDA was prepared in two steps as shown in Scheme 1. 4-(Hydroxymethyl)tetrathiafulvalene **3**[6] was used as a building block for TTF. Treatment of pentacosa-10,12-diynoic acid **1** with oxalyl chloride in $CH_2Cl_2$ quantitatively afforded the corresponding acid chloride. Addition of the acid chloride of **1** to a $CH_2Cl_2$ solution of hydroxymethyltetrathiafulvalene **3** with triethylamine at room temperature gave the diacetylene derivatives **2**‡ in poor yield (< 10%). However, the condensation reaction proceeded more smoothly to give **2** in 80% yield when 4-dimethylaminopyridine was used as base at 40 °C.[7]

The redox behaviour of monomer **2** was investigated by cyclic voltammetry. (electrolyte $Bu_4NPF_6$, *vs.* SCE, in MeCN at 25 °C) The monomer **2** exhibits two quasi-reversible redox couples at approximately $E^{1/2}{}_1$ +0.30 and $E^{1/2}{}_2$ +0.67 V, redox behaviour typical of the TTF system.[7]

The colour of the bulk crystals of monomer **2** changed to dark blue from light yellow after exposure to UV with a low-pressure mercury lamp (4 W) or $^{60}$Co γ-ray irradiation. This indicated clearly that the crystal structures of the monomers were suitable for solid-state polymerization, proceeding *via* 1,4-addition as shown in Scheme 2.[1]




**Scheme 1** *Reagents and conditions*: i, $(COCl)_2$, $CH_2Cl_2$, room temp., 3 h; ii, DMAP, $CH_2Cl_2$, reflux, 12 h




**Scheme 2**

A detailed study of the solid-state polymerization of monomer **2** stimulated by $^{60}$Co γ-ray irradiation (dose rate *ca.* 9.8 KGyh$^{-1}$) was achieved by gravimetry after extraction of the unreacted monomer using benzene, the polymer being insoluble in this solvent, as shown in Fig. 1. The polymer content of the crystals increased with the γ-ray dose up to 250 KGy, to about 72% conversion. However, the rate of polymerization became slow for doses in excess of 250 KGy. This polymerization curve for the monomer **2** is similar to that reported for nonadeca-2,4-diynoic acid[8] and tricosa-10,12-diynoic acid.[9]

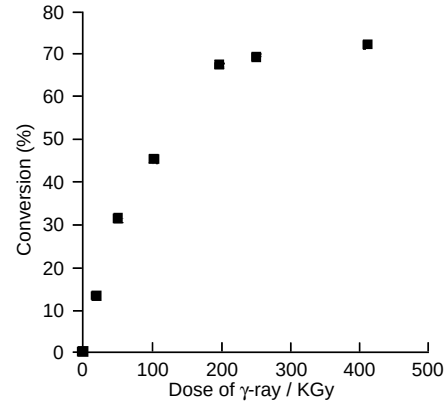



**Fig. 1** Time–conversion curve for solid-state polymerization of diacetylene **2** induced by $^{60}$Co γ-ray irradiation

The decoupled magic angle cross-polarised solid-state high resolution $^{13}C$ NMR spectrum of the reaction product after a 500 KGy radiation dose was measured at 50.2 MHz. The spectrum is consistent with the chemical structure of polymer **4** shown in Scheme 2. In particular, the carbon signals at $\delta$ 102 and 130 correspond to the acetylenic and alkenic carbons of the conjugated backbone of the polymer **4**, respectively, and are comparable to those found in poly(dodeca-5,7-diyne-1,12-diol bis{[(butoxycarbonyl)methyl]urethane}) in the red phase.[10]

By X-ray diffraction techniques it was established that polymer **4** produced by 500 KGy radiation is still similar in crystal structure to monomer **2**.

In conclusion, a novel diacetylene containing a TTF moiety was synthesized and subsequently polymerized in the solid state to yield a novel PDA with TTF groups located in the polymer side chains. Investigations into the physical properties of this PDA are in progress.

## Footnotes

† E-mail: sshimada@ccmail.nimc.go.jp

‡ Compound **2** gave satisfactory analytical and spectral data. *Selected data* for **2**: light yellow crystals, mp 52 °C; $^1H$ NMR ($CDCl_3$): $\delta$ 0.81 (t, 3 H, *J* 6.7 Hz), 1.19–1.29 (m, 32 H), 2.17 (t, 4 H, *J* 6.7 Hz), 2.27 (t, 2 H, *J* 7.5 Hz), 4.74 (s, 2 H), 6.24 (s, 3 H); $^{13}C$ NMR ($CDCl_3$): $\delta$ 14.11, 19.18, 22.67, 24.78, 28.28, 28.33, 28.73, 28.83, 28.97, 29.03, 29.08, 29.32, 29.46, 29.61, 29.68, 31.89, 33.99, 60.55, 65.19, 65.26, 77.43, 77.59, 111.66, 118.94, 119.06, 131.25, 173.18; Calc. for $C_{32}H_{46}O_2S_4$: C, 65.04; H, 7.85; S, 21.70. Found: C, 65.08; H, 7.97; S, 21.20%. *m/z* (EI-MS) m/z 590.2320 (calc. for $C_{32}H_{46}O_2S_4$, 590.2383).

## References

1 H. Bassler, *Polydiacetylenes*, ed. H. J. Cantow, Springer Verlag, Berlin, 1984, p. 1.
2 H. Matsuda, H. Nakanishi, T. Hosomi and M. Kato, *Macromolecules*, 1988, **21**, 1238.
3 S. Okada, K. Hayamizu, H. Matsuda, A. Masaki, N. Minami and H. Nakanishi, *Macromolecules*, 1994, **27**, 6259 and references cited therein.
4 S. Shimada, A. Masaki, S. Okada and H. Nakanishi, *Nonlinear Opt.*, 1995, **13**, 57.
5 V. Y. Khodorkovsky, G. V. Tormos, O. Y. Neilands, N. V. Kolotilo and A. Y. Il'chenko, *Tetrahedron Lett.*, 1992, **33**, 973.
6 J. Garin, J. Orduna, S. Uriel, A. J. Moore, M. R. Bryce, S. Wegener, D. S. Yufit and J. A. K. Howard, *Synthesis*, 1994, **489**.
7 M. R. Bryce, W. Devonport and A. J. Moore, *Angew. Chem., Int. Ed. Engl.*, 1994, **33**, 1761.
8 B. Tieke and D. Bloor, *Makromol. Chem.*, 1981, **182**, 133.
9 B. Tieke, D. Bloor and R. J. Young, *J. Mater. Sci.*, 1982, **17**, 1156.
10 A. D. Nava, M. Thakur and A. E. Tonelli, *Macromolecules*, 1990, **23**, 3055.

*Received in Cambridge, UK, 3rd April 1997; 7/02274C*

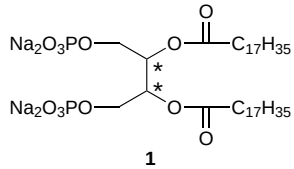
# Supramolecular expression of chirality in assemblies of gemini surfactants

**Nico A. J. M. Sommerdijk, Mark H. L. Lambermon, Martinus C. Feiters, Roeland J.M. Nolte*† and Binne Zwanenburg***

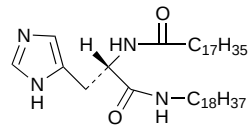
*Department of Organic Chemistry, NSR-Institute for Molecular Structure, Design and Synthesis, University of Nijmegen, Toernooiveld, 6525 ED Nijmegen, The Netherlands*

**Supramolecular expression of chirality occurs in mixtures of an L-histidine derivative and the (*S*,*S*) isomer of a phosphatidic acid-based gemini surfactant, but not in mixtures of this histidine derivative and the (*R*,*R*)- or (*R*,*S*)-gemini surfactant.**

Gemini surfactants are amphiphilic molecules containing two hydrophilic head groups and two long aliphatic chains, which are linked by a rigid[1,2] or flexible spacer,[3,4] and as such have potentially interesting properties.[1] Theoretical calculations[5] and recent experimental results[6,7] indeed indicate that 'geminis' behave differently from normal surfactants, which opens the way for new applications.




**1**




**2**

In a previous paper we showed that gemini surfactants based on phosphatidic acid (see **1**) can undergo stereodependent fission or fusion in the presence of calcium ions.[8] Here we report that these surfactants are capable of recognising a long chain L-histidine derivative, leading to a stereodependent expression of molecular chirality at the supramolecular level.

The (*R*,*R*), (*S*,*S*) and (*R*,*S*) forms of compound **1** were synthesised as described elsewhere.[8] All three stereoisomers of **1** formed bilayer aggregates when they were dispersed in water. Histidine surfactant **2** alone could not be dispersed in water to form distinct aggregates due to its low solubility.‡ When **2** (25 or 50 mol%) was mixed with the (*R*,*S*) isomer of **1** and dispersed in water at pH 6.5, vesicles with diameters ranging from 150 to 750 nm were generated. Increasing the concentration of **2** to 75 mol% led to the formation of extended bilayers and multilayer structures. In contrast, at all concentrations aqueous dispersions of **2** and the (*R*,*R*) isomer of **1** yielded irregularly shaped, rod-like structures with an average diameter of 30 nm and a length of 0.2–2.0 μm [Fig. 1(*a*)]. When **2** and the (*S*,*S*) isomer of **1** were mixed, helical structures together with planar bilayer aggregates were found in samples containing 25 mol% of **2** [Fig. 1(*b*)]. In samples containing 50 and 75 mol% of **2**, the aggregates tended to form twisted structures [Fig. 1(*c*)], but no distinct morphologies could be detected in the bulk of the material.

Further experiments revealed that the helical structures were only generated when the concentration of **2** was between 25 and 35 mol%, with the optimum lying at 30 mol%. Right-handed helices with a pitch of approximately 90 nm and a thickness of *ca*. 40 nm were observed exclusively [Fig. 1(*d*)].§ When the concentration of **1** deviated from 30 mol%, the observed helices were shorter and many of them contained defects [Fig. 1(*c*)]. The fact that the pitch and the thickness of the helices were similar in all cases suggests that their formation occurred in a precise manner, requiring a distinct ratio of the two surfactants, rather than a variable one. Since a concentration of 30 mol% of **2** appeared to be optimal, 1 : 2 complexes of **2** and (*S*,*S*)-**1** are probably the building blocks from which the helices are constructed.

Monolayer experiments revealed that **2** forms stable monolayers at the air–water interface. The surface area–surface pressure isotherms displayed a transition to a non-compressible state at relatively low surface pressure (Fig. 2). This suggests

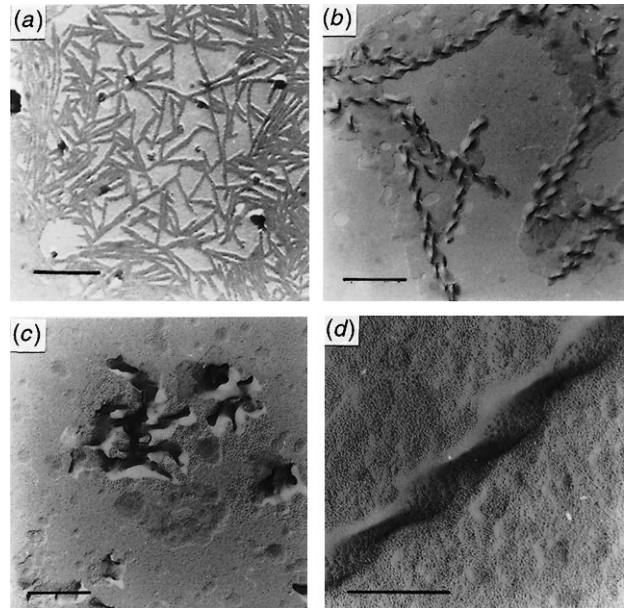



**Fig. 1** Transmission electron micrographs [Pt shadowing, (*a*)–(*c*) bars represent 400 nm, (*d*) bar represents 100 nm] of mixtures of (*a*) (*R*,*R*)-**1** and **2** (75 mol%), (*b*) (*S*,*S*)-**1** and **2** (25 mol%), (*c*) (*S*,*S*)-**1** and **2** (50 mol%) and (*d*) (*S*,*S*)-**1** and **2** (30 mol%)

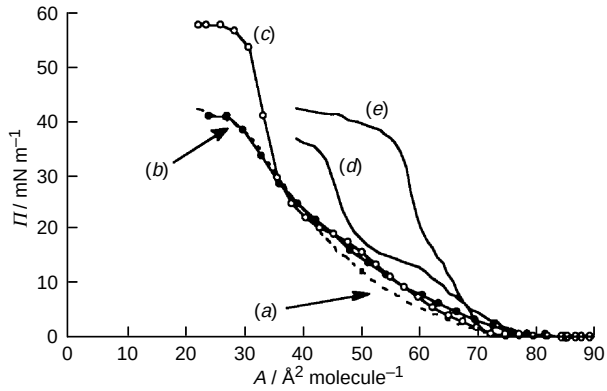



**Fig. 2** Monolayer isotherms recorded at 20 °C of mixtures of (*S*,*S*)-**1** and **2** on a sub-phase of pH 6.5: (*a*) 25, (*b*) 33, (*c*) 50, (*d*) 75 and (*e*) 100 mol% **2**

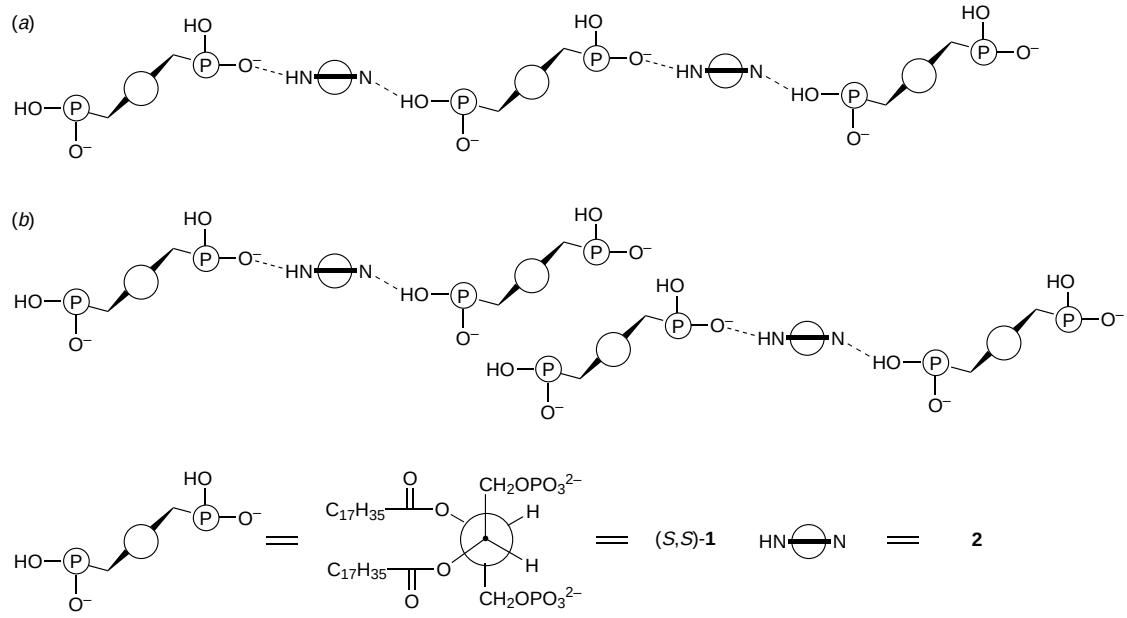



**Fig. 3** Schematic representation of (*a*) a 1 : 1 complex and (*b*) a 1 : 2 complex of **2** and (*S*,*S*)-**1**

that in the monolayer the molecules of **2** have a high degree of organisation, probably because they are linked by strong intermolecular hydrogen bonds *via* their imidazole groups, assisted by the formation of so-called amide polymers, *i.e.* linear arrays of hydrogen bonds between the amide groups of **2**. Mixing **2** with an increasing amount of (*S*,*S*)-**1** led to a gradual increase in the compressibility of the monolayer and to a gradual change in the overall shape of the isotherm. At a concentration of 33 mol% of **2**—this is the concentration at which helices start to be observed—the isotherm did not change further and showed the highest degree of compressibility.¶ These results can be rationalised as follows: the (*S*,*S*) isomer of **1** preferentially adopts an extended conformation in which the phosphate groups have an *anti* orientation.[8]‖ It is likely therefore that in a 1 : 1 mixture highly ordered, linear arrays of pairs of (*S*,*S*)-**1** and **2** are present, interconnected by hydrogen bonds, both between the head groups and the neighbouring amide groups [Fig. 3(*a*)]. In this way the molecules will be confined to their positions in a two dimensional lattice. In a mixture containing 33 mol% of **2**, however, individual 2 : 1 complexes of (*S*,*S*)-**1** and **2** may be formed, allowing both translational and rotational freedom of the complexes with respect to each other [Fig. 3(*b*)]. The complexes are thus free to adopt orientations in which the average molecular area is minimised, and in which chirality is accumulated by close packing of the stereogenic centres. This asymmetric packing of the building blocks probably extends over long distances, leading to the formation of helical aggregates.

The authors thank H. P. M. Geurts for assistance in performing the electron microscopy experiments and Professor G. I. Tesser and P. J. H. M. Adams for the kind donation of Boc-protected L-histidine and for helpful discussions.

## Footnotes

† E-mail: tijdink@sci.kun.nl

‡ Surfactant **2** was prepared from Boc-protected L-histidine. One alkyl chain was introduced by a DCC coupling with octadecylamine (yield 60%). Deprotection of the Boc-amide with trifluoroacetic acid and subsequent acylation with *N*-(stearoyloxy)succinimide resulted in the introduction of the second alkyl chain (yield 75%). Calc. for **2** ($C_{42}H_{80}O_2N_4$): C, 74.9; H, 12.0; N, 8.3. Found: C, 74.2; H, 11.5; N, 8.4%.

§ In mixtures containing 1–10 mol% of **2** planar bilayers and a small amount of fibres were observed, suggesting that only a small fraction of (*S*,*S*)-**1** is interacting with **2**, leading to the formation of these fibres.

¶ Monolayers of mixtures of **1** and **2** were inspected by Brewster angle microscopy. No chiral domains were detected.

‖ The p$K_a$ values of (*S*,*S*)-**1** were determined to be 1.8 and 10.2, implying that at pH 6.5 the molecules are in the monoprotonated state (ref. 9).

## References

1 F. M. Menger and C. A. Littau, *J. Am. Chem. Soc.*, 1991, **113**, 1451.
2 F. M. Menger and C. A. Littau, *J. Am. Chem. Soc.*, 1993, **15**, 10 083.
3 R. Zana, M. Benrraou and R. Rueff, *Langmuir*, 1991, **7**, 1072.
4 R. Zana and Y. Talmon, *Nature*, 1993, **362**, 228.
5 S. Karaborni, K. Esselink, P. A. J. Hilbers, B. Smit, J. Karthauser, N. M. van Os and R. Zana, *Science*, 1994, **266**, 5183.
6 Q. Hue, R. Leon, P. M. Petroff and G. D. Stucky, *Science*, 1995, **268**, 5215.
7 L. Perez, J. L. Torres, A. Manresa, C. Solans and M. R. Infante, *Langmuir*, 1996, **12**, 5296.
8 N. A. J. M. Sommerdijk, T. H. L. Hoeks, M. Synak, M. C. Feiters, R. J. M. Nolte and B. Zwanenburg, *J. Am. Chem. Soc.*, 1997, **119**, 4338.
9 N. A. J. M. Sommerdijk, M. C. Feiters, R. J. M. Nolte and B. Zwanenburg, *Recl. Trav. Chim. Pays-Bas*, 1994, **113**, 194.

*Received in Cambridge, UK, 8th May 1997; 7/03161K*

# A self-cleaving DNA nucleoside

**Vineet Gupta and Eric T. Kool***

*Department of Chemistry, University of Rochester, Rochester, NY 14627, USA*

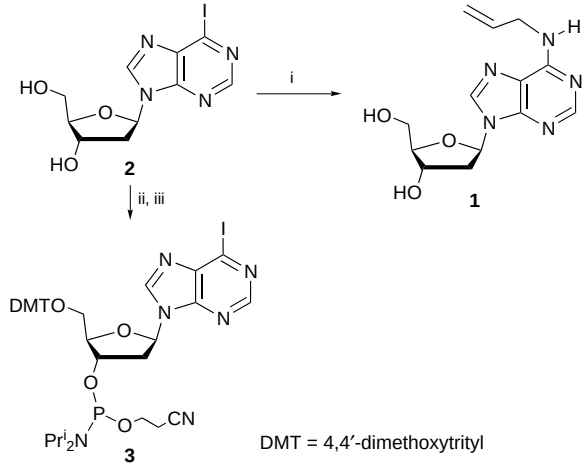
**An allyl-modified nucleoside has been shown to self-alkylate and depurinate on treatment with iodine and heat; placement in DNA strands yields site-directed cleavage of the DNA.**

Much attention has been focused on the development of methods for cleavage of DNA or RNA strands at specific sites. One common approach taken is the use of a reactive group which is delivered to specific sequences in a nucleic acid target by attachment of the reactive group to a DNA-binding ligand with known sequence preference.[1] One goal of such work has been the hybridization-directed cleavage of biologically harmful nucleic acid sequences, resulting in possible therapeutic applications.[2] Another application is the cutting of chemically- or enzymatically-synthesized DNA at positions which cannot be processed by known restriction endonuclease enzymes,[3] which can also be useful as a tool in the study of nucleic acid structure and function.

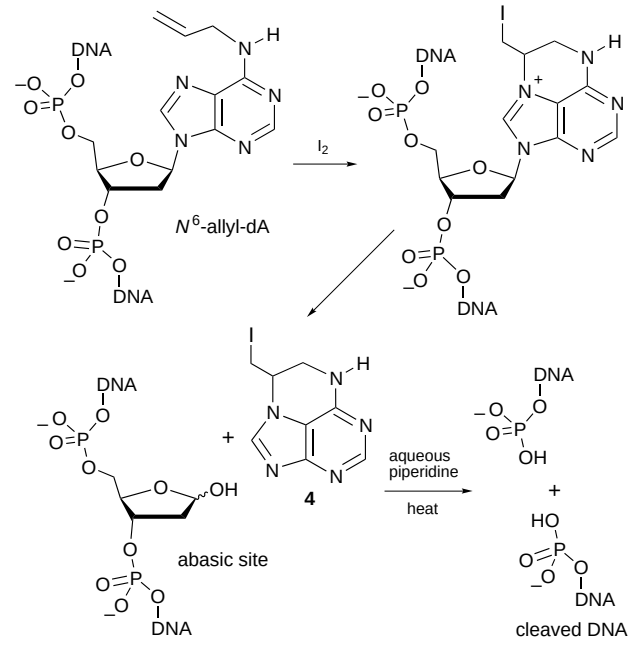
Our design of a self-cleaving DNA base was inspired by Maxam–Gilbert alkylation of purines. Alkylation at $N^7$ (or other ring nitrogens) by dimethyl sulfate results in depurination with formation of an abasic deoxyribose, and subsequent heating in aqueous base gives strand cleavage with loss of the sugar residue. In principle, direction of an alkylating group to a specific purine under mild conditions could enable facile and specific chain cleavage. We envisioned that placement of an allyl function near nucleophilic ring nitrogens might allow for such alkylation if a mild electrophilic activating reagent could be found. The reagent must be reactive enough to activate the alkylation functionality, but not so reactive that it modifies natural DNA.

We synthesized the nucleoside $N^6$-allyl-dA **1** to test this possibility (Scheme 1). This compound was obtained from iodopurinedeoxyriboside **2** by substitution with allylamine. After some experimentation we arrived at iodine as a mild electrophilic reagent for activating the double bond.[4] We found that $I_2$ reacts rapidly with $N^6$-allyl-dA in neutral aqueous solution or in DMSO at room temperature. This reaction was monitored by 300 MHz proton NMR in [$^2H_6$]DMSO. In addition, nuclear Overhauser enhancements were observed between H-8 and protons on methyl substituents added to the terminus of the allyl group (data not shown), establishing that the cyclization occurs on the $N^7$ nitrogen rather than the $N^1$ position. The $^{13}$C NMR spectrum confirms the structure having the 6-membered-ring product. After 24 h at room temperature, or after 30 min heating (90 °C), a second new adenine-derived compound is observed in the NMR spectrum. We surmised that this is the cyclized base **4** which had been eliminated from the sugar; to test this we independently synthesized this compound by treating allyladenine with iodine. NMR and HPLC studies confirmed its identity. The second byproduct of the reaction in DMSO is hydroxymethylfuran, also identified by comparison to an authentic sample. The four natural DNA nucleosides did not react under these conditions as monitored by NMR spectroscopy; this is not unexpected, since iodine is a commonly-used reagent in the oxidative step of DNA synthesis.

We then incorporated $N^6$-allyl-dA into synthetic DNA strands to test whether this chemistry could be carried out in the polymer. Since iodine is used in the standard synthesis cycle, we added the allyl functionality immediately after synthesis of the DNA chain, by first incorporating the iodopurine phosphoramidite **3**.[5] We treated the resulting DNA attached to the solid CPG-support with neat allylamine (65 °C, 18 h) and followed this with a standard 12 h ammonia treatment to remove any remaining protecting groups. Two different sequences, containing one and two allyl-modified dAs respectively, were synthesized. Enzymatic digestion of these strands to the nucleosides followed by HPLC analysis showed that the $N^6$-allyl-dA was present in these strands in the expected ratio, with no evidence




**Scheme 1** *Reagents and conditions*: i, allylamine (neat), room temp.; ii, 4,4′-dimethoxytrityl chloride, $Pr^i_2EtN$, $CH_2Cl_2$; iii, *N*,*N*-diisopropyl-*O*-cyanoethylphosphoramidic chloride, $Pr^i_2EtN$, $CH_2Cl_2$




**Scheme 2**

of any other derivatives such as deoxyadenosine or deoxyinosine (data not shown). This establishes that the postsynthetic addition of the amine proceeds with high (≥95%) conversion. The iodopurine **3** is thus an efficient vehicle for incorporation of amine nucleophiles into DNA.[6]

The expected products of self-cleavage of the sequence 5′-dTTTTTTA*TTTTT are 5′-dTTTTTTp and 5′-pdTTTTT (Scheme 2). We synthesized these fragments as authentic samples for comparison on high-resolution gels. The second modified strand had the sequence 5′-dTTTTTTTA*TTTTTTA*TTTTT, containing two possible cleavage sites. The result of iodine treatment with ABI oxidizing solution followed by heating with piperidine was efficient and clean chain cleavage for both sequences (Scheme 2). Experimentation with solvents and reaction conditions established that most selective cleavage occurred using 20 mM $I_2$ and 66 μM DNA strand concentration.† High-resolution polyacrylamide gels show the cleavage (Fig. 1), and separate gels show that the products co-migrate with the authentically synthesized fragments. Reversed-phase HPLC analysis also confirmed this finding. Control reactions show (Fig. 1) that the presence of the allyl function in the DNA is necessary for cleavage, as is iodine treatment of the DNA. Examination of the reaction products indicates that cleavage is not completely selective for the allyl-substituted base, with some background cleavage also occurring at other bases. Experiments with a third oligonucleotide of mixed sequence (5′-pdGTCAGTCAA*GTCAGTCAp) (data not shown) showed that this was more pronounced for purine-containing DNA. This nonselective iodine reaction was somewhat surprising because of the common use of iodine in DNA synthesis; however, it seems possible that altering conditions beyond those we examined, or using a more selective electrophile, might lead to increased specificity for allyladenine.

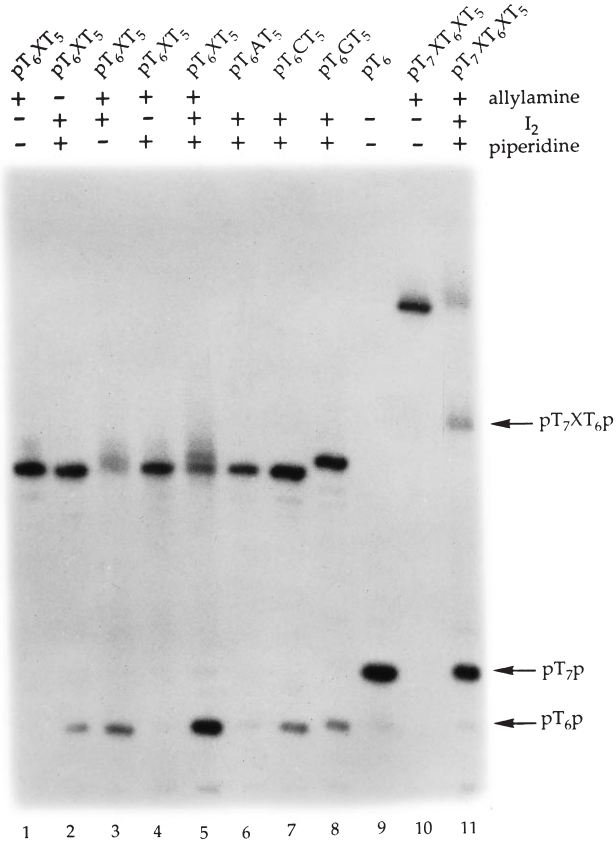



**Fig. 1** Cleavage assay of two DNA sequences containing **1** by denaturing gel electrophoresis. All the sequences were 5′-$^{32}$P labelled. Lanes 1–5 show the reactions with the sequence 5′-$T_6A^*T_5$, lanes 6–8 the reactions with control DNA molecules, lane 9 the product marker and lanes 10–11 the reactions with DNA sequence 5′-$T_7A^*T_6A^*T_5$. Lane 1: no reaction. Lane 2: reaction of allyl untreated 5′-$T_6A^*T_5$ with both $I_2$ and piperidine. Lane 3: reaction of 5′-$T_6A^*T_5$ only with $I_2$. Lane 4: reaction of 5′-$T_6A^*T_5$ only with piperidine. Lane 5: reaction of 5′-$T_6A^*T_5$ with $I_2$ as well as piperidine. Lanes 6–8: reaction of 5′-$T_6AT_5$, 5′-$T_6CT_5$ and 5′-$T_6GT_5$ respectively with both $I_2$ and piperidine. Lane 10: no reaction. Lane 11: reaction of 5′-$T_7A^*T_6A^*T_5$ with both $I_2$ and piperidine. Lanes 3, 5 and 11 clearly show the cleavage of modified DNA to the expected products. Some non-specific cleavage can be seen in lanes 2, 6, 7 and 8.

A few other reports of methods for generating abasic (depurinated or depyrimidinated) sites or for site-directed cleavage in DNA exist in the literature.[7] The present method represents an alternative cleavage strategy which, unlike most of the previous approaches, allows essentially normal base pairing prior to the cleavage. Studies aimed at finding strategies for decreasing associated nonspecific cleavage are currently underway.

## Footnotes

* E-mail: etk@etk.chem.rochester.edu

† Conditions for reactions on DNA: (1) Allylamine treatment—1 ml of allylamine (neat) was added to CPG bound DNA (1 μmol synthesis) and the mixture was kept at 65 °C for 18 h. It was lyophilised and treated with $NH_4OH$ at 55 °C for 12 h, lyophilised and gel purified. (2) Iodine treatment—5′-$^{32}$P labelled DNA sequence (200 pmol, 66 μM) was dissolved in 3 μl of 20 mM $I_2$ solution (20% v/v pyridine, 10% v/v water, 70% v/v THF), and incubated at 4 °C for 10 min. The mixture was then diluted with 150 μl $H_2O$ and heated at 90 °C for 6 h. (3) Piperidine treatment—100 μl of a 1.0 M aq. piperidine solution in $H_2O$ was added and the mixture heated at 90 °C for 30 min, and lyophilised.

## References

1 V. V. Vlassov, S. A. Gaidamakov, V. V. Gorn and S. A. Grachev, *FEBS Lett.*, 1985, **182**, 415; J.-C. Francois, T. S.-Behmoaras, C. Barbier, M. Chassignol, N. T. Thuong and C. Hélène, *Proc. Natl. Acad. Sci. USA*, 1989, **86**, 9702; B. C. F. Chu and L. E. Orgel, *Proc. Natl. Acad. Sci. USA*, 1985, **82**, 963; G. F. Dreyer and P. B. Dervan, *Proc. Natl. Acad. Sci. USA*, 1985, **82**, 968; C.-H. B. Chen and D. S. Sigman, *Proc. Natl. Acad. Sci. USA*, 1986, **83**, 7147; D. E. Bergstrom and N. P. Gerry, *J. Am. Chem. Soc.*, 1994, **116**, 12067; T. LeDoan, L. Perrouault, D. Praseuth, N. Habhoub, J.-L. Decout, N. T. Thuong, J. Lhomme and C. Hélène, *Nucleic Acids Res.*, 1987, **15**, 7749; C. J. Murphy, M. R. Arkin, Y. Jenkins, N. D. Ghatlia, S. H. Bossman, N. J. Turro and J. K. Barton, *Science*, 1993, **262**, 1025; M. Komiyama, *J. Biochem.*, 1995, **118**, 665; T. P. Prakash and K. N. Ganesh, *J. Chem. Soc., Chem. Commun.*, 1994, 1357; E. H. Chang, P. S. Miller, C. Cushman, K. Devadas, K. F. Pirollo, P. O. P. Ts'O and Z. P. Yu, *Biochemistry*, 1991, **30**, 8283; J. Hovin, A. Guzaev, E. Azhayeva, A. Azhayev and H. Lönnberg, *J. Org. Chem.*, 1995, **60**, 2205; V. N. Soyfer and V. N. Potaman, *Triple-Helical Nucleic Acids*, Springer, 1996, 93.

2 C. Hélène, *Pure Appl. Chem.*, 1994, **66**, 663.

3 G. Gish and F. Eckstein, *Science*, 1988, **240**, 1520; M. Mag, S. Luking and J. W. Engels, *Nucleic Acids Res.*, 1991, **19**, 1437; M. C. Pirrung and J.-C. Bradley, *J. Org. Chem.*, 1995, **60**, 6270; D. Liu, S. L. Daubendiek, M. A. Zillman, K. Ryan and E. T. Kool, *J. Am. Chem. Soc.*, 1996, **118**, 1587.

4 M. J. Robins, R. H. Hall and R. Thedford, *Biochemistry*, 1967, **6**, 1837.

5 It may be possible to directly place the allyl-dA in the strand during synthesis if a different oxidizing reagent is used in the synthesis cycle. See, for example J.-L. Fourrey and J. Varenne, *Tetrahedron Lett.*, 1985, **26**, 1217.

6 The ribofuranose version of iodopurine has been synthesized previously. See V. Nair and S. G. Richardson, *J. Org. Chem.*, 1980, **45**, 3969.

7 J. A. Iocono, B. Gildea and L. W. McLaughlin, *Tetrahedron Lett.*, 1990, **31**, 175; A. Laayoun, J.-L. Decout, E. Defrancq and J. Lhomme, *Tetrahedron Lett.*, 1994, **35**, 4991; D. Peoc'h, A. Meyer, J.-L. Imbach and B. Rayner, *Tetrahedron Lett.*, 1991, **32**, 207; T. Horn, K. Downing, Y. Gee and M. S. Urdea, *Nucleosides Nucleotides*, 1991, **10**, 299; M. M. Greenberg, *Tetrahedron*, 1995, **51**, 29; T. Horn and M. S. Urdea, *Tetrahedron Lett.*, 1986, **27**, 4705; B. Giese, A. Dussy, C. Elie, P. Erdmann and U. Schwitter, *Angew. Chem., Int. Ed. Engl.*, 1994, **33**, 1861; P. M. Hardy, D. Holland, S. Scott, A. J. Garman, C. R. Newton and M. J. McLean, *Nucleic Acids Res.*, 1994, **22**, 2998.

*Received in Corvallis, OR, USA, 27th January 1997; 7/00626H*

# An unusual imine (N=C) alkylalumination reaction

**Pingrong Wei and David Atwood***

*Center for Main Group Chemistry, Department of Chemistry, North Dakota State University, Fargo, North Dakota 58105, USA*

**Addition of 3 equiv. of $AlMe_3$ to a heptadentate Schiff-base ligand made from salicylaldehyde and bis(2-aminoethyl)-ethylenediamine ($H_3L^1$) results in an unusual alkylalumination of one of the imine bonds; addition of 2 equiv. of $B(OMe)_3$ or $AlMe_3$ to one of these ligands leads to the formation of bimetallic derivatives containing four- and five-coordinate metals, respectively.**

In the course of our explorations of group 13 Schiff-base chelate complexes we have discovered an unusual imine (N=C) alkylalumination reaction. Schiff-base ligands (and the salen class, in particular) form a wide range of complexes with transition[1] and main-group metals.[2] One of the reasons why these ligands are so useful is because they do not undergo further reactions after coordinating a metal. In fact, transition-metal complexes of the reduced form of the salen ligand (the salan class)[3] are difficult to isolate because they dehydrogenate back to the Schiff-base derivative when exposed to air.[4]

In turning our attention to ligands possessing multiple (more than four) binding sites we examined those derived from the condensation of 3 equiv. of salicylaldehyde (with H or Bu$^t$ at the 2,4-positions, or Cl at the 4-position, of the aryl ring) with bis(2-aminoethyl)ethylenediamine. The resulting ligands are denoted $H_3L^1$, $H_3L^2$ and $H_3L^3$, respectively. We had intended to prepare neutral bi- and tri-metallic derivatives of these ligands for potential catalytic applications. Previously reported group 13 complexes with this[5] and related systems[6] have focused on charged compounds useful in medicinal applications.

In the present work, two neutral bimetallic derivatives, $(HL^2)[B(OMe)_2]_2$ **1** and $L^1AlMe(AlMe_2)$ **2**, could be prepared in good yields using the appropriate stoichiometry (Scheme 1).† The X-ray data for **1** was such that a full solution could not be obtained. However, the overall morphology of the molecule is clear (Fig. 1). The formation of **1** follows similar reactions for bimetallic salen derivatives.[7] This is not the case for **2** for which the $^{27}Al$ NMR data indicates that only five-coordinate aluminium is present ($\delta$ 65.40). In the $^1H$ NMR there are two Al–Me shifts in a 1 : 2 ratio. This data can tentatively be attributed to the structure shown in Scheme 1. Surprisingly, in reactions with 3 equiv. of the aluminium reagent, one of the N=C bonds undergoes an unusual alkyalumination reaction in the formation of trimetallic derivative **3** (Scheme 1, Fig. 2).

In the structure‡ one portion of the molecule coordinates an $AlMe_2$ unit by an oxygen and imine nitrogen, forming a six-

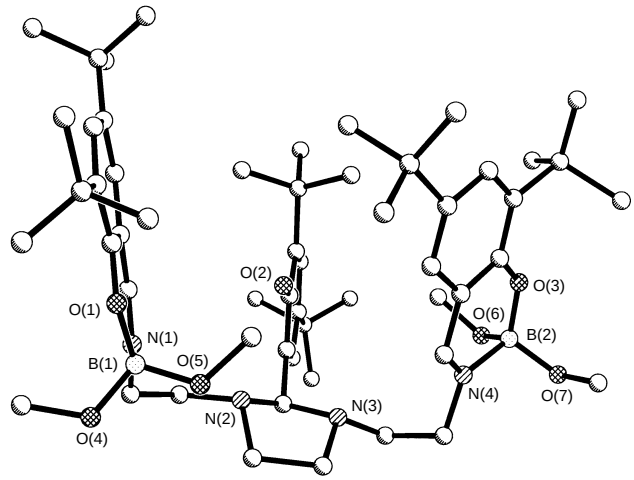
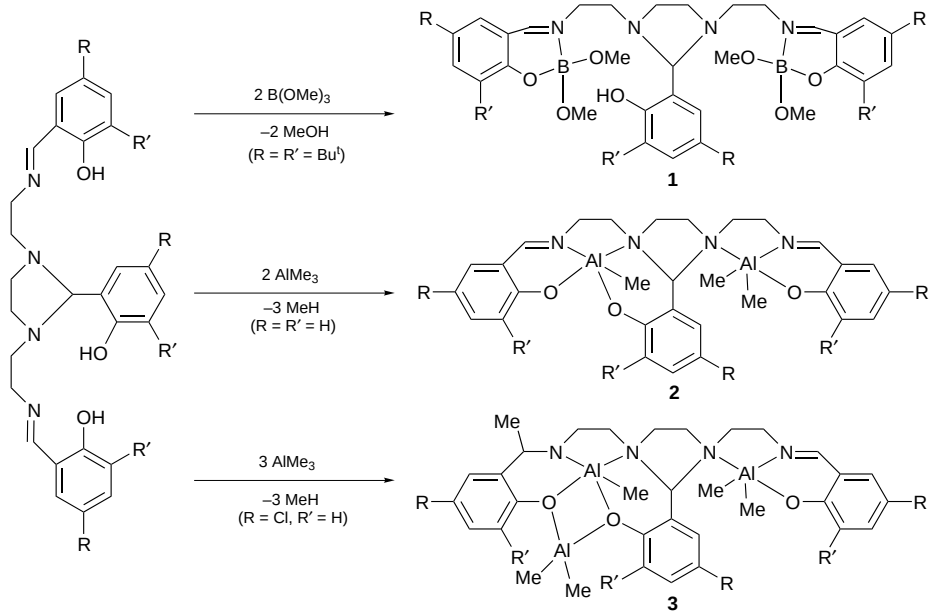



**Fig. 1** Preliminary structure of **1** demonstrating the overall morphology of the molecule




**Scheme 1** General syntheses of group 13 compounds with $H_3L^n$ ($n$ = 1–3)

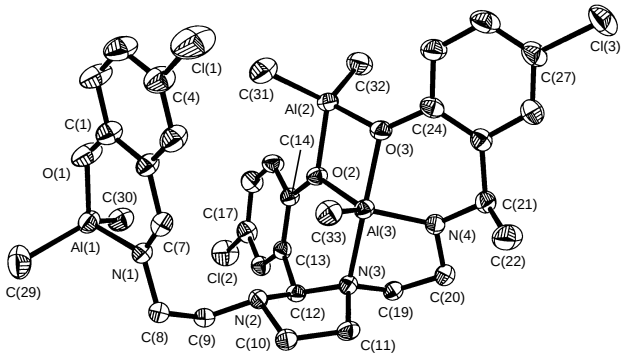



**Fig. 2** Molecular structure and atom numbering scheme for **3**. Selected bond distances (Å) and angles (°): Al(1)–O(1) 1.769(3), Al(1)–C(30) 1.945(5), Al(1)–C(29) 1.947(5), Al(1)–N(1) 1.961(3), Al(2)–O(3) 1.816(3), Al(2)–O(2) 1.884(3), Al(2)–C(31) 1.935(5), Al(2)–C(32) 1.943(5), Al(3)–N(4) 1.822(3), Al(3)–O(2) 1.912(3), Al(3)–O(3) 1.944(3), Al(3)–C(33) 1.966(4), Al(3)–N(3) 2.091(3), N(4)–C(21) 1.459(5), C(21)–C(22) 1.524(6); O(1)–Al(1)–C(30) 110.6(2), O(1)–Al(1)–C(29) 112.2(2), C(30)–Al(1)–C(29) 119.1(2), O(1)–Al(1)–N(1) 95.77(14), C(30)–Al(1)–N(1) 110.5(2), C(29)–Al(1)–N(1) 106.1(2), O(3)–Al(2)–O(2) 79.95(11), O(3)–Al(2)–C(31) 115.9(2), O(2)–Al(2)–C(31) 108.8(2), O(3)–Al(2)–C(32) 110.6(2), O(2)–Al(2)–C(32) 116.9(2), C(31)–Al(2)–C(32) 118.7(2), N(4)–Al(3)–O(2) 120.37(13), N(4)–Al(3)–O(3) 90.82(13), O(2)–Al(3)–O(3) 76.15(11), N(4)–Al(3)–C(33) 127.4(2), O(2)–Al(3)–C(33) 111.6(2), O(3)–Al(3)–C(33) 93.9(2), N(4)–Al(3)–N(3) 83.96(13), O(2)–Al(3)–N(3) 89.82(11), O(3)–Al(3)–N(3) 159.98(12), C(33)–Al(3)–N(3) 104.7(2), Al(2)–O(2)–A(31) 100.78(12), Al(2)–O(3)–Al(3) 102.05(13), N(4)–C(21)–C(22) 112.0(3), N(4)–C(21)–C(23) 113.6(3), C(22)–C(21)–C(23) 110.3(3).

membered ring. This is a familiar coordination mode for Schiff-base ligands. The second portion of the molecule contains two aluminium atoms linked by bridging oxygens. The terminal $AlMe_2$ group adopts a geometry that is structurally similar to the other $AlMe_2$ group. The central, five-coordinate aluminium atom is in a distorted trigonal-bipyramidal geometry. The equatorial bond distances are systematically shorter than the axial distances. This is exemplified in the distances for axial, Al(3)–N(3) [2.091(3) Å] compared to equatorial, Al(3)–N(4) [1.822(3) Å] atoms. The oxygens follow a similar trend [Al(3)–O(2) 1.912(3), Al(3)–O(3) 1.944(3) Å]. Closely related to **3** is the trimetallic complex (salean)AlMe$(AlMe_2)_2$ [salean = *N*,*N*′-bis(*o*-hydroxybenzyl)-1,2-diaminoethane].[8] It also contains four- and five-coordinate (trigonal bipyramidal) aluminiums bridged by oxygen atoms. In this complex the axial atoms are oxygen and form an angle of 163.0(1)° at distances of 1.982(3) and 1.959(3) Å. The differences in the N=C and N–C(Me) linkages are reflected in the N–C bond distances of 1.290(5) and 1.459(5) Å, respectively. Furthermore, the imine group appears as a singlet in the $^1$H NMR ($\delta$ 7.94) while the amine NC*H*(Me) appears as a multiplet ($\delta$ 4.14).

The use of group 13 reagents in the reduction of alkynes, alkenes and carbonyl substituents is a well known, yet still expanding area of chemistry.[9] Alkylalumination reactions generally require the intermediacy of a group 4 catalyst.[10] The catalyst acts to activate the substrate in a manner that is still being defined. That an aluminium species is being produced in **3** that can alkylate carbon–nitrogen multiple bonds in the absence of a metal catalyst is an intriguing prospect. Based upon the fact that a compound containing two five-coordinate aluminium atoms can be isolated (**2**), the third equivalent of $AlMe_3$ presumably effects the alkylation in **3**. The coordination of the first two $AlR_n$ units makes the imine linkage vulnerable to this addition. This type of reaction bears some resemblance to the alkylation of nitriles in which the first step is the formation of an organoaluminium–nitrile adduct.[11] Whether the formation of **3** is through an intra- or intermolecular alkylation remains to be determined.

This work was supported by the National Science Foundation (Grant 9452892) and the donors of the Petroleum Research Fund, administered by the American Chemical Society (Grant 31901-AC3). Partial support was provided by Union Carbide. The receipt of an NSF-CAREER (CHE-9625376) award is also gratefully acknowledged.

## Footnotes

* E-mail: emgc@plains.nodak.edu

† Full experimental details will be published in due course. Only a partial list of data is given here. **1**: mp 182–184 °C. $^1$H NMR ($CDCl_3$): $\delta$ 1.13–1.41 (m, 54 H, $CCH_3$), 2.85 (s, 6 H, $OCH_3$), 3.16 (s, 6 H, $OCH_3$) 2.72, 2.93, 3.35, 3.50 (m, 12 H, $NCH_2$), 3.81 (s, 1H, NCHN), 6.84 (d, 1 H, Ph H), 7.06 (d, 2 H, Ph H), 7.17 (d, 1 H, Ph H), 7.51 (d, 2 H, Ph H), 8.07 (s, 2 H, N=CH). Analysis, Calc: C, 70.34; H, 9.38. Found: C, 69.95; H, 9.28%. **2**: mp > 260 °C. $^1$H NMR ($CDCl_3$): $\delta$ −0.92 to −0.73 (m, 9 H, $AlCH_3$), 2.46–3.02, 3.28–3.71 (m, 12 H, $NCH_2$), 3.86 (s, 1 H, NCHN), 6.63–7.41 (m, 12H, Ph H), 8.14 (s, 1 H, N=CH), 8.21 (s, 1 H, N=CH). $^{27}$Al ($CDCl_3$): $\delta$ 65.40. Analysis, Calc: C, 65.00; H, 6.49. Found: C, 65.13; H, 6.24%. **3**·1.5$C_6H_5Me$: mp > 260 °C. $^1$H NMR ($CDCl_3$): $\delta$ −0.99 to −0.53 (m, 15 H, $AlCH_3$), 1.38 (d, 3 H, $CCH_3$), 2.35 (s, 3 H, $PhCH_3$), 2.73–2.77, 3.08, 3.48 (m, 12 H, $NCH_2$), 3.53 (s, 1 H, NCHN), 4.14 (m, 1H, NC*H*$CH_3$), 7.11 (m, 9 H, Ph H), 7.94 (s, 1 H, N=CH). $^{27}$Al ($CDCl_3$): $\delta$ 54.50, 163.95. Analysis Calc. for **3**·$C_6H_5Me$: C, 58.46; H, 6.08. Found: C, 58.15; H, 6.26%.

‡ *Crystallographic data*: **1**, monoclinic, $P2_1/c$, $a$ = 15.4330(14), $b$ = 20.6409(19), $c$ = 22.7704(20) Å, $\beta$ = 98.779(2)°, $U$ = 7168.5(5) Å$^3$, $Z$ = 4, 2670 observed [$I > 4.0\sigma(I)$], $R_1$ = 0.1932, $wR_2$ = 0.5439. **3**·1.5$C_6H_5Me$, monoclinic, $P2_1/n$, $a$ = 11.8994(6), $b$ = 31.498(2), $c$ = 13.7396(7) Å, $\beta$ = 115.006(1)°, $U$ = 4667.0(4) Å$^3$, $Z$ = 4, 6024 observed [$I > 2.0\sigma(I)$], $R_1$ = 0.0620, $wR_2$ = 0.1218. CCDC 182/515.

## References

1 R. H. Holm, G. W. Everett Jr. and A. Chakravorty, *Prog. Inorg. Chem*., 1966, **7**, 83; M. D. Hobday and T. D. Smith, *Coord. Chem. Rev*., 1972, **9**, 311.
2 S. J. Dzugan and V. L. Goedken, *Inorg. Chem*., 1986, **25**, 2858; K. S. Chong, S. J. Rettig, A. Storr and J. Trotter, *Can. J. Chem*., 1977, **55**, 2540; P. L. Gurian, L. K. Cheatham, J. W. Ziller and A. R. Barron, *J. Chem. Soc., Dalton Trans*., 1991, 1449; D. A. Atwood, J. A. Jegier and D. Rutherford, *J. Am. Chem. Soc*., 1995, **117**, 6779; M. G. Davidson, C. Lambert, I. Lopez-Solera, P. R. Raithby, P. R. and R. Snaith, *Inorg. Chem*., 1995, **34**, 3765; D. A. Atwood, J. A. Jegier and D. Rutherford, *Inorg. Chem*., 1996, **35**, 63.
3 D. A. Atwood, J. Benson, J. A. Jegier, N. F. Lindholm, K. J. Martin, R. J. Pitura and D. Rutherford, *Main Group Chem*., 1995, **1**, 99; D. A. Atwood, *Coord. Chem. Rev*., 1997, in the press.
4 A. Berkessel, J. W. Bats and C. Schwarz, *Angew. Chem., Int. Ed. Engl.*, 1990, **29**, 106; A. Böttcher, H. Elias, E.-G. Jäger, H. Langfelderova, M. Mazur, L. Müller, H. Paulus, P. Pelikan, M. Rudolph and M. Valko, *Inorg. Chem.*, 1993, **32**, 4131; A. Böttcher, H. Elias, L. Müller and H. Paulus, *Angew. Chem., Int. Ed. Engl*., 1992, **31**, 623; D. A. Atwood, J. A. Jegier, N. F. Lindholm, K. J. Martin and D. Rutherford, *J. Coord. Chem*., 1996, **38**, 305.
5 B. W. Tsang, C. J. Mathias, P. E. Fanwick and M. A. Green, *J. Med. Chem.*, 1994, **37**, 4400.
6 E. Wong, P. Caravan, S. Liu, S. J. Rettig and C. Orvig, *Inorg. Chem.*, 1996, **35**, 715 and references therein.
7 P. Wei and D. A. Atwood, *Inorg. Chem*., 1997, in press.
8 D. A. Atwood, J. A. Jegier, K. J. Martin and D. Rutherford, *Organometallics*, 1995, **14**, 1453; D. A. Atwood and D. Rutherford, *Comments Inorg. Chem*., 1995, **19**, 25.
9 J. A. Miller, in *Chemistry of Aluminum, Gallium, Indium and Thallium*, ed. A. J. Downs, Chapman and Hall, New York, p. 372.
10 E.-I. Negishi, D. Y. Kondakov, D. Choueiry, K. Kasai and T. Takahashi, *J. Am. Chem. Soc*., 1996, **118**, 9577.
11 T. Mole and E. A. Jeffery, *Organoaluminum Compounds*, Elsevier, New York, 1972, p. 240.

*Received in Columbia, MO, USA; 19th February 1997; 7/01185G*

# Carbenoid transfer to imines: a new heterogeneous catalytic synthesis of aziridines

**J. Madan Mohan, B. S. Uphade, V. R. Choudhary, T. Ravindranathan and A. Sudalai***

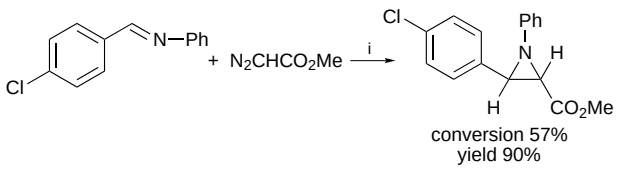
*National Chemistry Laboratory, Pune 411 008, India*

**A heterogeneous catalytic method for the preparation of *trans*-aziridines from imines and methyl diazoacetate is described using $Rh^{III}$- and $Mn^{III}$-exchanged montmorillonite K10 clays as catalysts.**

The aziridinine ring is a versatile building block for organic synthesis, not only because the ring opening of aziridines provides a convenient entry to the stereoselective preparation of functionalized amino compounds but also because the exocyclic N-substitutent modulates the properties and reactivity of the 3-membered ring.[1] The chemistry and preparation of enantiomerically pure aziridine-2-carboxylates have been the targets of many synthetic efforts in recent years for the preparation of both α- and β-amino acids.[2] Classical methods[3] for the synthesis of aziridines are ring closure of amino alcohols, ring opening of epoxides with sodium azide and addition of α-halo ester enolates to *N*-(trimethylsilyl)imines. Although potentially a very useful method for the preparation of aziridines, the cycloaddition of carbenes to imines has not been investigated extensively. In fact very few methods have been reported for the catalytic preparation of aziridines from aromatic imines and diazo esters. These methods employ catalysts such as copper complexes[4] and methylrhenium trioxide[5] under homogeneous conditions. More recently, $BF_3{\cdot}OEt_2$-catalysed aziridination of imines with diazoacetate has been reported.[6] The other important catalytic method, *viz*. the addition of [*N*-(toluene-*p*-sulfonyl)imino]phenyliodinane (PhI=NTs) as nitrene precursor onto alkenes, has been used for the direct synthesis of aziridines using soluble $Cu^{I}$ and $Cu^{II}$ complexes.[7] However, the yields and selectivities reported are far from satisfactory. For example, Cu-catalysed addition of diazo esters to imines proceeds in low yields (15–30%) and is of limited use.[8] Further, copper triflate-catalysed carbene addition to imines proceeds to give a mixture of *cis*- and *trans*-aziridines and shows poor selectivity in terms of product distribution. Recently Aggarwal *et al*.[9] has also shown an effective asymmetric aziridination process mediated by sulfur ylides and working in a catalytic fashion.

Currently, acid catalysed organic transformations by transition metal-exchanged aluminosilicate clays is an area of considerable potential and interest due to ease of handling and workup, non-corrosiveness and low cost of clays.[10] Here we report that the $Rh^{III}$-exchanged acid activated montmorillonite clay, K10, catalyses cycloaddition reactions between methyl diazoacetate and imines to form *trans*-aziridines with good conversion and yield (Scheme 1).

Rh- and Mn-exchanged montmorillonite K10 clay catalysts were prepared by exchanging the clay with dilute solutions of $RhCl_3$ and $Mn(NO_3)_3$, respectively. For example, a mixture containing $RhCl_3$ (0.3 g) and clay (25 g) in distilled water (600 ml) was stirred vigorously at room temperature for 24 h. It was centrifuged and the clay was washed repeatedly with distilled water until the discarded filtrate was free from $Cl^-$ ions. Finally, the clay was dried at 110 °C for 12 h. A 5% Rh/C catalyst was obtained from Degussa. The 0.5 wt% $Rh/Al_2O_3$ and $Rh/SiO_2$ gel catalysts for comparison purpose were prepared using the incipient wetness impregnation technique.




**Scheme 1** *Reagents and conditions*: i, Rh-clay (10% m/m), dry benzene, 353 K, 3 h

In a typical experiment, a mixture of imine ($R^1$ = 4-$ClC_6H_4$, $R^2$ = Ph; 2.15 g, 10 mmol), methyl diazoacetate (1.2 g, 12 mmol) and Rh-clay (200 mg; 10% m/m) in dry benzene (30 ml) was heated under reflux for 5 h. The progress of the reaction was monitored by TLC. The catalyst was filtered off and the product purified by flash chromatography to afford the corresponding *trans*-aziridine† (1.63 g, 57%).

The results of aziridination of the imine ($R^1$ = 4-$ClC_6H_4$, $R^2$ = Ph) over various supported metal catalysts (Table 1) indicate that $Rh^{III}$-exchanged montmorillonite K10 clay exhibits significantly higher activity and selectivity than the $Rh/SiO_2$ and $Rh/Al_2O_3$ catalysts. However, it is to be noted that catalysts such as Cu-exchanged K10 and Rh/C failed to catalyse the reaction. Although Mn-clay also exhibited good conversion and yield in this case, it surprisingly failed to catalyse the aziridination reaction when applied to other types of imines.

Table 2 lists the results of the various imines which have been successfully aziridinated with $N_2CHCO_2Me$ catalysed by the $Rh^{III}$-clay. The yield in the process is in the range 30–75%; products other than aziridine are not formed. A novel feature of this catalytic system is that only a single isomer of the aziridine was obtained as determined by GC–MS and $^1H$ and $^{13}C$ NMR spectroscopy. The coupling constant for the aziridine ring protons for these products are in the range 3.6–3.8 Hz, which confirms that the only product is the isomer with *trans* configuration (*E*-isomer) with respect to the C–C bond. This *trans*-selective aziridination is therefore complementry to the earlier technique of Casarrubios *et al*.[6] which is *cis*-selective. A variety of aromatic imines and one aliphatic imine have undergone cycloaddition with $N_2CHCO_2Me$ over the $Rh^{III}$-clay to give aziridines in good yields and excellent selectivity. It is noteworthy that the product survives the acidic environment and does not yield side products arising out of cleavage by protonation of the aziridine ring nitrogen because of its poor

**Table 1** Aziridination of aryl imine ($R^1$ = 4-$ClC_6H_4$, $R^2$ = Ph) with $N_2CHCO_2Me$ over various catalysts[a]

| Entry | Catalysts | *t*/h | Yield[b] (%) |
|---|---|---|---|
| 1 | Rh-clay | 5 | 57 |
| 2 | Mn-clay | 10 | 46 |
| 3 | Cu-clay | 10 | 0 |
| 4 | $Rh/SiO_2$ gel | 12 | 52 |
| 5 | $Rh/Al_2O_3$ | 12 | 40 |
| 6 | Rh/C[c] | 12 | 0 |

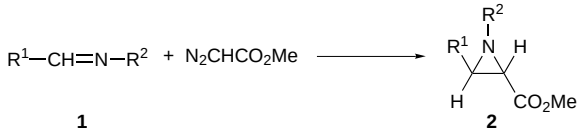
[a] Reaction conditions: imine (10 mmol), diazo ester (12 mmol), catalyst (10% m/m), dry benzene, reflux. [b] Isolated and purified yield. [c] Commercial catalyst from Degussa.

basicity (aromatic amine). Also this result contrasts with that using methylrhenium trioxide, which is effective only for aromatic imines.[5] The catalyst, recovered by filtration, was reused at least three times without affecting the reactivity and selectivity of the process.

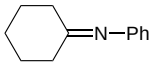
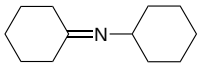
In conclusion, this study was demonstrated that $Rh^{III}$-montmorillonite K10 is an efficient and reusable solid catalyst for imine aziridination using methyl diazoacetate as the carbene precursor.

B. S. U. is grateful to CSIR, New Delhi, India, for the award of a Senior Research Fellowship. J. M. M. is thankful to the Director, NCL, for allowing him to carry out work in NCL.

**Table 2** Rh-clay catalysed aziridination of imines[a]




**1** **2**

| Entry | $R^1$ | $R^2$ | *t*/h | Yield[b] (%) |
|---|---|---|---|---|
| 1 | 4-$ClC_6H_4$ | Ph | 5 | 57 |
| 2 | 4-$MeOC_6H_4$ | Ph | 3 | 32 |
| 3 | 3,4-$(OMe)_2C_6H_3$ | Ph | 7 | 42 |
| 4 | 3,4,5-$(OMe)_3C_6H_2$ | Ph | 10 | 75 |
| 5 | 4-$ClC_6H_4$ | 2,5-$Cl_2C_6H_3$ | 6 | 40 |
| 6 | 4-$ClC_6H_4$ | 3-$NO_2$-4-$MeC_6H_3$ | 9 | 50 |
| 7 | 2-Furyl | Ph | 7 | 38 |
| 8 | 2-Furyl | Cyclohexyl | 5.5 | 48 |
| 9 | Bn | Ph | 8 | 30 |
| 10 | $Pr^i$ | Ph | 8 | 48 |
| 11 |  | | 10 | 41 |
| 12 |  | | 6 | 37 |

[a] Reaction conditions: imine (10 mmol), diazo ester (12 mmol), Rh-clay (10% m/m), dry benzene, reflux. [b] Isolated and purified yield; the selectivity was nearly 100% and no other product could be seen by TLC.

## Footnotes

* E-mail: prs@ncl.ernet.in

† *Selected data* for **2** ($R^1$ = 4-$ClC_6H_4$, $R^2$ = Ph): $^1H$ NMR (200 MHz, $CDCl_3$): $\delta$ 3.2 (1 H, d, *J* 3.8 Hz), 3.6 (3 H, s), 3.8 (1 H, d, *J* 3.8 Hz), 7.0 (2 H, d, *J* 8 Hz), 7.3 (5 H, m) and 7.6 (2 H, d, *J* 8 Hz); $^{13}C$ NMR (50 MHz, $CDCl_3$): $\delta$ 45.52, 45.65, 51.96, 119.82, 122.95, 123.62, 128.17, 128.29, 128.65, 128.96, 129.91, 130.83, 130.83, 133.72, 133.83, 152.0 and 167.65; *m*/*z* 286 ($M^+$, 25%), 256 (30), 228 (90), 193 (55), 165 (35), 155 (20), 150 (15), 125 (35), 104 (50), 89 (55), 77 (100), 63 (25) and 59 (15).

## References

1 W. H. Pearson, B. W. Lian and S. C. Bergmeier, in *Comprehensive Heterocyclic Chemistry II*, ed. A. Padwa, Pergamon Press, USA, 1996, vol. 1A, pp. 1–60.
2 D. Tanner, *Angew. Chem., Int. Ed. Engl.*, 1994, **33**, 599.
3 J. A. Deyrup, in *The Chemistry of Heterocyclic Compounds*, ed. A. Hassner, Wiley, New York, 1983, vol. 42, part 1, ch. 1.
4 K. B. Hansen, N. S. Finney and E. N. Jacobsen, *Angew. Chem., Int. Ed. Engl.*, 1995, **34**, 676; K. G. Rasmussen and K. A. Jorgensen, *J. Chem. Soc., Chem. Commun.*, 1995, 1401.
5 Z. Zhu and J. H. Espenson, *J. Org. Chem.*, 1995, **60**, 7090; *J. Am. Chem. Soc.*, 1996, **118**, 9901.
6 L. Casarrubios, J. A. Perez, M. Brookhart and J. L. Templeton, *J. Org. Chem.*, 1996, **61**, 8358.
7 D. A. Evans, M. M. Faul and M. T. Bilodeau, *J. Am. Chem. Soc.*, 1994, **116**, 2742.
8 P. Baret, H. Buffet and J. L. Pierre, *Bull. Soc. Chim. Fr.*, 1972, 2493.
9 V. K. Aggarwal, A. Thompson, R. V. H. Jones and M. C. H. Standen, *J. Org. Chem.*, 1996, **61**, 8368.
10 *Solid Supports and Catalysts in Organic Synthesis*, ed. K. Smith, Ellis Horwood, Chichester, 1992.

*Received in Cambridge, UK, 22nd April 1997; 7/02745A*

# Prediction of transition state structure in protein tyrosine phosphatase catalysis using a hybrid QM/MM potential

**Jason C. Hart,[a] Neil A. Burton,[a] Ian H Hillier,*[a] Martin J. Harrison[a] and Philip Jewsbury[b]**

[a] *Department of Chemistry, University of Manchester, Manchester, UK M13 9PL*
[b] *Zeneca Pharmaceuticals, Alderley Park, Macclesfield, Cheshire, UK SK10 4TG*

**The transition state for tyrosine phosphate hydrolysis by the enzyme protein tyrosine phosphatase (PTP1B) has been determined using a hybrid QM(PM3)/MM potential, showing that the reaction is dissociative with essentially no P–S bond formation in the transition state.**

The reversible phosphorylation of proteins is the major form of post-translational modification and is a key control mechanism in biochemistry for processes such as cell regulation.[1,2] Protein tyrosine phosphatases (PTPases) are a large family of enzymes that catalyse the hydrolysis of phosphotyrosine (pTyr) residues in specific proteins.[3,4] Structural[5] and kinetic[6] studies have provided a molecular understanding of PTPase activity. In brief, the enzyme active site is conserved for all PTPases and contains catalytic Cys (215 in PTP1B) and Asp (181 in PTP1B) residues. The former residue exists as the anion and acts as the nucleophile, the latter having the role of a general acid. The reaction involves the formation of a phosphoenzyme intermediate (with Cys 215 in PTP1B). Hydrolysis of this intermediate results in the regeneration of the active site.[4]

Two extreme mechanisms of phosphate ester hydrolysis are usually invoked, either dissociative or associative[3,7] which depend on the size of the negative charge on the phosphate group. In aqueous solution, kinetic data have led to the conclusion that phosphate monoesters hydrolyse *via* a transition state with little bond formation to the attacking nucleophile and extensive bond cleavage to the leaving group characteristic of a dissociative mechanism.[8] Retention of chiral properties rules out a true diffusable metaphosphate intermediate. At physiological pH monoesters such as pTyr exist as dianions and kinetic data, particularly heavy atom isotope measurements, have led to the general conclusion that PTPase catalysis proceeds *via* a dissociative transition state[6] similar to that observed in solution.[8] The characterisation of the transition state at a molecular level is naturally central to understanding the mode of action of PTPases and to the design of PTPase specific inhibitors.

The use of combined quantum mechanical/molecular mechanical (QM/MM) methods to model macromolecular reactivity is now well established,[9–13] and we have shown how such methods can be used to locate transition states for enzyme catalysed reactions[14] employing our hybrid QM/MM code[15] which couples the QM code GAUSSIAN94[16] with the MM code AMBER 4.0.[17] To further aid the understanding of the mode of action of PTPases we here describe a hybrid QM/MM study of the mechanism of phosphate hydrolysis by the enzyme PTP1B. We utilise the crystal structure of PTP1B (Ser-215) and a phosphotyrosine substrate[5] to study phosphoryl transfer between pTyr and the Cys residue (replacing Ser-215), involving proton transfer from Asp-181 to the Tyr leaving group. In our model, the pTyr substrate in the crystal structure was replaced by 4–methylphenyl phosphate to allow for substrate mobility. This enzyme–substrate structure was first energy minimised (using the AMBER 4.0 force field) and was then employed in a QM(PM3)/MM calculation, the QM part of the structure being shown in Fig. 1. The bulk of the enzyme was kept fixed during the modelling of the reaction, with the positions of the majority of the QM atoms, including the whole substrate, being allowed to vary. The QM link atoms, as well as the QM atoms of the protein backbone, were kept fixed. We chose to use the PM3[18] Hamiltonian due to its success in modelling studies of phosphate hydrolysis.[7]

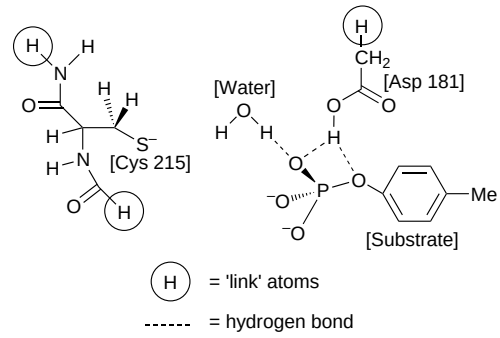



**Fig. 1** QM region of active site–substrate

We have mapped out the potential energy surface for the dissociative reaction by minimising the substrate active site structure for a range of P–O (bridge) distances (while allowing the remaining QM atoms to optimise). This led to an approximate structure of the transition state, which was subsequently refined and characterised by calculation of the harmonic frequencies. The reactant and transition state structures thus obtained are shown in Fig. 2. It is clear that the transition state is largely dissociative, with a lengthened P–O bond and effectively no increase in S–P interaction compared to the reactant structure. The calculated partial atomic charges reveal a developing negative charge on the Tyr leaving group during the course of the reaction. The formal charge on this group increases from 0.80e in the reactant to 0.92e in the transition state, 0.07e of the total increase of 0.12e being associated with the bridge oxygen. In both reactant and transition state structures the proton of Asp-181 interacts with two oxygen atoms of the substrate (Fig. 2). The effect of this developing negative charge on the leaving group is to increase the interaction with the bridge oxygen compared to that

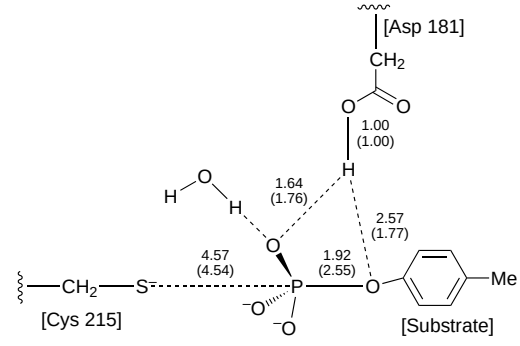



**Fig. 2** Active site–substrate geometry. Reactant structure (Å) and, in parenthesis, transition state structure.

involving the terminal oxygen. However, we do not find proton transfer from the asparate group to have occurred at the transition state. The energy barrier between the reactant and transition state structures is 27.2 kJ mol$^{-1}$. Further along the reaction pathway to the product, there is a second barrier corresponding to proton transfer to the leaving OPh group along with S–P bond formation. However, this second barrier is at lower energy than the dissociative transition state that we have identified so that the P–O bond cleavage is rate determining in line with experiment.[6]

Thus, the first theoretical prediction of the nature of the transition state for a PTP–catalysed reaction, which we have presented here where the transition state corresponds to considerable P–O bond lengthening, with little P–S bond formation, is in general agreement with the conclusions from kinetic measurements. Of particular interest is the quite flat potential energy profile in the region of the transition state with a change of only 7 kJ mol$^{-1}$ when the P–O length changes from 2.10 Å to the optimal value of 2.55 Å in the transition state (Fig. 2). This flat energy surface is also reflected in the low value of the imaginary frequency of the transition state (114*i* cm$^{-1}$). Such a flat surface suggests that there will be considerable geometric freedom in the design of suitable inhibitors of this enzymic reaction.

We thank the EPSRC for support of this research.

## Footnote

* E-mail: ian.hillier@man.ac.uk

## References

1 E. G. Krebs, *Angew. Chem., Int. Ed. Engl.*, 1993, **32**, 1122.
2 E. H. Fischer, *Angew. Chem., Int. Ed. Engl.*, 1993, **32**, 1130.
3 J. B. Vincent and M. W. Crowder, *Phosphatases in Cell Metabolism and Signal Transduction: Structure, Function and Mechanism*, Springer, New York, 1995.
4 D. Barford, Z. Jia and N. K. Tonks, *Nat. Struct. Biol.*, 1995, **2**, 1043.
5 Z. Jia, D. Barford, A. J. Flint and N. K. Tonks, *Science*, 1995, **268**, 1754.
6 A. C. Hengge, G. A. Sowa, L. Wu and Z. Y. Zhang, *Biochemistry.*, 1995, **34**, 13982.
7 J. Wilkie and D. Gani, *J. Chem. Soc., Perkin Trans. 2*, 1996, 783.
8 A. C. Hengge, W. A. Edens and H. Elsing, *J. Am. Chem. Soc.*, 1994, **116**, 5045.
9 A. Warshel and M. Levitt, *J. Mol. Biol.*, 1976, **103**, 227.
10 M. J. Field, P. A. Bash and M. Karplus, *J. Comput. Chem.*, 1990, **11**, 700.
11 J. Aqvist and A. Warshel, *Chem. Rev.*, 1993, **93**, 2523.
12 U. C. Singh and P. A. Kollman, *J. Comput. Chem.*, 1986, **7**, 718.
13 B. Waszkowycz, I. H. Hillier, N. Gensmantel and D. W. Payling, *J. Chem. Soc., Perkin Trans. 2*, 1991, 225.
14 M. J. Harrison, N. A. Burton, I. H. Hillier and I. R. Gould, *Chem. Commun.*, 1996, 2769.
15 M. J. Harrison, PhD Thesis, The University of Manchester, 1997.
16 M. J. Frisch, G. W. Trucks, H. B. Schlegel, P. M. W. Gill, B. G. Johnson, M. A. Robb, J . R. Cheeseman, T. A. Keith, G. A. Petersson, J. A. Montgomery, K. Raghavachari, M. A. Al-Laham, V. G. Zakrzewski, J. V. Ortiz, J. B. Foresman, J. Cioslowski, B. B. Stefanov, A. Nanayakkara, M. Challacombe, C. Y. Peng, P. Y. Ayala, W. Chen, M. W. Wong, J. L. Andres, E. S. Replogle, R. Gomberts, R. L. Martin, D. J. Fox, J. S. Binkley, D. J. Defrees, J. Baker, J. P. Stewart, M. Head-Gordon, C. Gonzalez and J. A. Pople, GAUSSIAN94 , Gaussian Inc., Pittsburgh PA, 1995.
17 D. A. Pearlman, D. A. Case, J. C. Caldwell, G. L. Seibel, U. C. Singh, P. Weiner and P. A. Kollman, AMBER 4.0, University of California, San Francisco, 1994.
18 J. J. P. Stewart, *J. Comput. Chem.*, 1989, **10**, 209

*Received in Cambridge, UK, 4th April 1997; 7/02304I*

# Phosphadisilacyclobutenes by stepwise silylene additions to phosphaalkynes

**Manfred Weidenbruch,*[a] Susanne Olthoff,[a] Karl Peters[b] and Hans Georg von Schnering[b]**

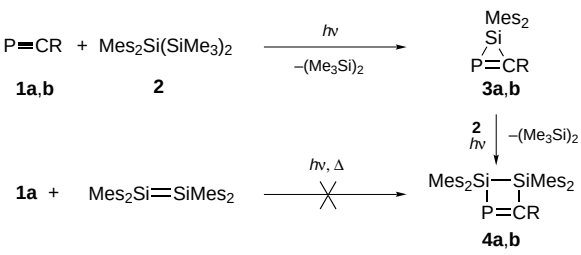
[a] *Fachbereich Chemie, Universität Oldenburg, D-26111 Oldenburg, Germany*
[b] *Max-Planck-Institut für Festkörperforschung, D-70506 Stuttgart, Germany*

**The phosphaalkynes RC≡P [R = 1-adamantyl (1a) or R = 2-methylcyclohexyl (1b)] react with dimesitylsilylene, presumably by [2+1] cycloaddition followed by silylene insertion, to furnish phosphadisilacyclobutenes; the molecular structure of the adamantyl derivative was determined by X-ray crystallography.**

Since the synthesis of the first thermally stable phosphaalkyne[1] in 1981, the chemistry of this class of compounds has experienced an explosive development which is reflected in several review articles.[2] However, there are only a few examples of [2+1] cycloadditions to the P≡C triple bond and concrete evidence for [2+2] cycloadditons is still lacking. It has been shown that reaction of the silylene $R_2Si$: (R = $CMe_3$) with **1a** proceeds smoothly to furnish the phosphasilirene[3] as an oily liquid, similar to the 2*H*-phosphirenes[4] accessible by other routes and for which crystals suitable for X-ray structural analyses can only be obtained after formation of the corresponding $W(CO)_5$ complexes. A crystalline germaphosphirene has been prepared by addition of the germylene $R_2Ge$: [R = $CH(SiMe_3)_2$][5] to *tert*-butylphosphaacetylene.[6] Addition of the stannylene $R_2Sn$: [R = $CH(SiMe_3)_2$] to the same triple bond system appears to proceed by a different course since the formation of the phosphadistannacyclobutene obtained was interpreted as being more indicative of a [2+2] addition of the distannene,[7] $R_2Sn{=}SnR_2$, to the phosphaalkyne.[8] However, as can be seen from the present results, the formation of this four-membered ring system may also be explained in terms of an initial [2+1] cycloaddition and subsequent insertion of a further stannylene unit into an intermediate three-membered ring system.

Reaction of dimesitylsilylene, generated photochemically from the trisilane **2**, with the phosphaalkynes **1a,b**[9,10] afforded the phosphadisilacyclobutenes **4a** (pale yellow crystals, mp 285 °C, yield 18 %) and **4b** (yellow crystals, mp 275 °C, yield 14%) (Scheme 1). The structures of these two representatives of a new four-membered ring system were confirmed by their analytical and spectroscopic data.† Of high diagnostic value are the positions of their $^{31}P$ NMR signals, which are strongly deshielded and appear at $\delta$ 441 (**4a**) and 443 (**4b**) in the region typical of silyl-substituted phosphaalkenes.[11] In the $^{29}Si$ NMR spectra the two silicon atoms give rise to doublets with $^1J_{^{29}Si,^{31}P}$ and $^2J_{^{29}Si,^{31}P}$ couplings.

Final confirmation of the structures of these molecules was provided by an X-ray crystallographic analysis of **4a** (Fig. 1) which revealed an almost planar ring (angular sum: 359.1°).‡




**Scheme 1**

The largest endocyclic angle occurred at the carbon atom and the two smallest at the silicon atoms. In comparison to the only currently known phosphasilirene,[3] all endocyclic bond lengths are elongated to some extent, indicating the differing bonding situations in the three- and four-membered ring systems.

The different behaviour of di-*tert*-butylsilylene and dimesitylsilylene towards **1a** are assumed to be due to the larger spatial requirements of the *tert*-butyl groups which effectively shield the three-membered ring from further attack. The reactions of **1a,b** with **2** probably also proceed through the three-membered ring intermediates **3**, which undergo subsequent insertion of a second silylene molecule to furnish the four-membered ring products isolated. However, a second possibility, in which the photochemically generated silylene **2** undergoes primary dimerisation to the disilene with a Si=Si double bond and subsequent [2+2] cycloaddition with the phosphaalkyne, is also feasible. Thus, we have prepared tetramesityldisilene[12] and examined its behaviour towards **1a** under both photochemical and thermal conditions. In neither case could any reaction be detected. Hence, not only have we obtained evidence in favour of the proposed [2+1] cycloaddition to the P≡C triple bond with subsequent rapid silylene insertion into the three-membered ring, but also further illustrated the absence of unequivocally demonstrated [2+2] cycloadditions to phosphaalkynes.[2]

However, an alternative mechanism for the formation of **4a,b**, in which—according to Scheme 2—the silylene is trapped by addition to the phosphorus atoms of **1a,b** to furnish an ylide intermediate, followed by the addition of a second silylene molecule and ring closure cannot be excluded.§

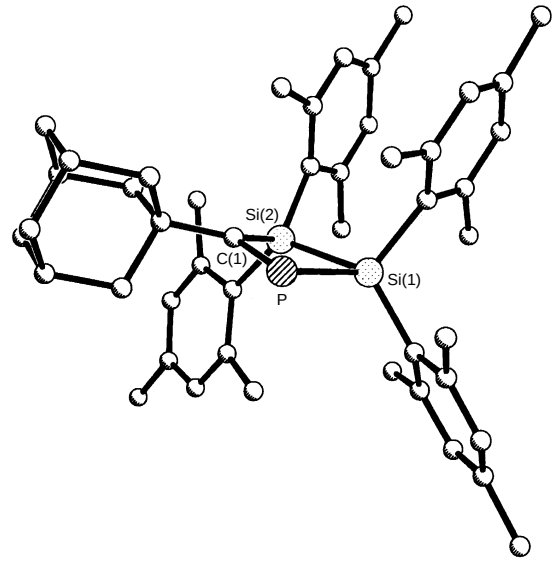
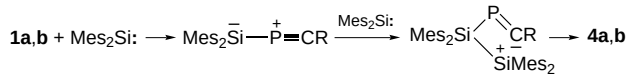



**Fig. 1** Molecular structure of **4a** in the crystal (hydrogen atoms omitted). Selected bond lengths (pm) and angles (°): C(1)–P 170.1(3), P–Si(1) 228.8(1), Si(1)–Si(2) 239.1(1), Si(2)–C(1) 190.3(3), Si(1)–P–C(1) 90.1(1), P–Si(1)–Si(2) 77.6(1), Si(1)–Si(2)–C(1) 85.5(1), P–C(1)–Si(2) 108.9(2).



**Scheme 2**

Financial support by the Deutsche Forschungsgemeinschaft and the Fonds der Chemischen Industrie is gratefully acknowledged. We thank Professor Marsmann, Paderborn, for the $^{29}$Si NMR spectra.

## Footnotes

† *Selected spectroscopic data* for **4a**: $\delta_H$ 1.55 (m, 6 H), 1.87 (m, 3 H), 2.04 (s, 6 H), 2.06 (s, 6 H), 2.18 (m, 6 H), 2.43 (s, 12 H), 2.63 (s, 12 H), 6.59 (s, 8 H); $\delta_C$ 20.89 ($C_p$), 26.04 ($C_p$), 26.17 ($C_p$), 29.82 (CH), 36.88 ($CH_2$), 46.05 ($CH_2$), 46.20 ($CH_2$), 129.05 (CH), 138.22 ($C_q$), 143.37 ($C_q$), 144.87 ($C_q$) ($C_p$ and $C_q$ refer to primary and quaternary carbon atoms); $\delta_P$ 441.2 (s); $\delta_{Si}$ 2.15 (d, $^2J_{^{29}Si,^{31}P}$ 8 Hz), −20.2 (d, $^1J_{^{29}Si,^{31}P}$ 67 Hz); MS (CI, isobutane) *m/z* 711 ($MH^+$, 48%). For **4b**: $\delta_H$ 1.40 (m, 10H), 1.45 (s, 3 H), 2.02 (s, 6 H), 2.06 (s, 6 H), 2.44 (s, 12 H), 2.62 (s, 12 H), 6.59 (s, 8 H); $\delta_C$ 20.95, 23.23, 25.99, 26.30, 41.75, 48.29, 129.18, 129.73, 132.57, 134.29, 138.29, 143.41, 144.89; $\delta_P$ 442; $\delta_{Si}$ 2.2 (d, $^2J_{^{29}Si,^{31}P}$ 8.2 Hz), −22.7 (d, $^1J_{^{29}Si,^{31}P}$ 42 Hz); MS (CI, isobutane) *m/z* 673 ($MH^+$, 100 = %).

‡ *Crystal data* for **4a**: $C_{47}H_{59}PSi_2$, $M$ = 711.1, crystal dimensions 0.70 × 0.60 × 0.30 mm, monoclinic, space group $P2_1/n$, $a$ = 1318.3(1), $b$ = 1923.2(1), $c$ = 1652.4(1) pm, $\beta$ = 98.589(6)°, $V$ = 4142.4(5) pm$^3$, $Z$ = 4, $D_c$ = 1.140 g cm$^{-3}$, $\lambda$(Mo-K$\alpha$) = 71.073 pm, $T$ = 296(2) K, $2\theta_{max}$ = 55°, unique reflections 9513, observed [$F > 2\sigma(F)$] 6884, data-to-parameter ratio 15.23. The structure was solved by direct phase determination using the Siemens SHELXTL PLUS program system and refined by full-matrix least-squares techniques. Hydrogen atoms were placed in calculated positions, and all other atoms were refined anisotropically; $R$ = 0.066, $R_w$ = 0.062. CCDC 182/516.

§ We thank one of the referees for drawing our attention to this possibility.

## References

1 G. Becker, G. Gresser and W. Uhl, *Z. Naturforsch.*, 1981, **B36**, 16.
2 Reviews: M. Regitz, in *Multiple Bonds and Low Coordination in Phosphorus Chemistry*, ed. M. Regitz and O. J. Scherer, Thieme Verlag, Stuttgart, 1990, p. 58; J. F. Nixon, *Chem. Rev.*, 1988, **88**, 1327; M. Regitz and P. Binger, *Angew. Chem.* 1988, **100**, 1541; *Angew. Chem., Int. Ed. Engl.*, 1988, **27**, 1485; R. Appel, F. Knoll and I. Ruppert, *Angew. Chem.*, 1981, **93**, 771; *Angew. Chem., Int. Ed. Engl.*, 1981, **20**, 731.
3 A. Schäfer, M. Weidenbruch, W. Saak and S. Pohl, *Angew. Chem.*, 1987, **99**, 806; *Angew. Chem., Int. Ed. Engl.*, 1987, **26**, 776; see also D. W. H. Rankin, in *Organosilicon Chemistry*, ed. N. Auner and J. Weis, VCH, Weinheim, 1994, p. 3.
4 O. Wagner, G. Maas and M. Regitz, *Angew. Chem.*, 1987, **99**, 1328; *Angew. Chem. Int. Ed. Engl.*, 1987, **26**, 1257.
5 P. J. Davidson, D. H. Harris and M. F. Lappert, *J. Chem. Soc., Dalton Trans.*, 1976, 2268.
6 A. H. Cowley, S. W. Hall, C. M. Nunn and J. M. Power, *J. Chem. Soc., Chem. Commun.*, 1988, 753.
7 D. E. Goldberg, D. H. Harris, M. F. Lappert and K. M. Thomas, *J. Chem. Soc., Chem. Commun.*, 1976, 261; D. E. Goldberg, P. B. Hitchcock, M. F. Lappert, K. M. Thomas, T. Fjeldberg, A. Haaland and B. E. R. Schilling, *J. Chem. Soc., Dalton Trans.*, 1986, 2387.
8 A. H. Cowley, S. W. Hall, C. M. Nunn and J. M. Power, *Angew. Chem.*, 1988, **100**, 874; *Angew. Chem., Int., Ed. Engl.*, 1988, **27**, 838.
9 T. Allspach, M. Regitz and G. Becker, *Synthesis*, 1986, 31.
10 W. Rösch, U. Vogelbacher, T. Allspach and M. Regitz, *J. Organomet. Chem.*, 1986, **306**, 39.
11 K. R. Dixon, in *Multinuclear NMR*, ed. J. Mason, Plenum Press, New York and London, 1987, p. 369.
12 R. West, M. J. Fink and J. Michl, *Science*, 1981, **214**, 1343.

*Received in Cambridge, UK, 6th May 1997; 7/03054A*

# Self-association of poly(aramide) dendrimers

**Frank Osterod and Arno Kraft***

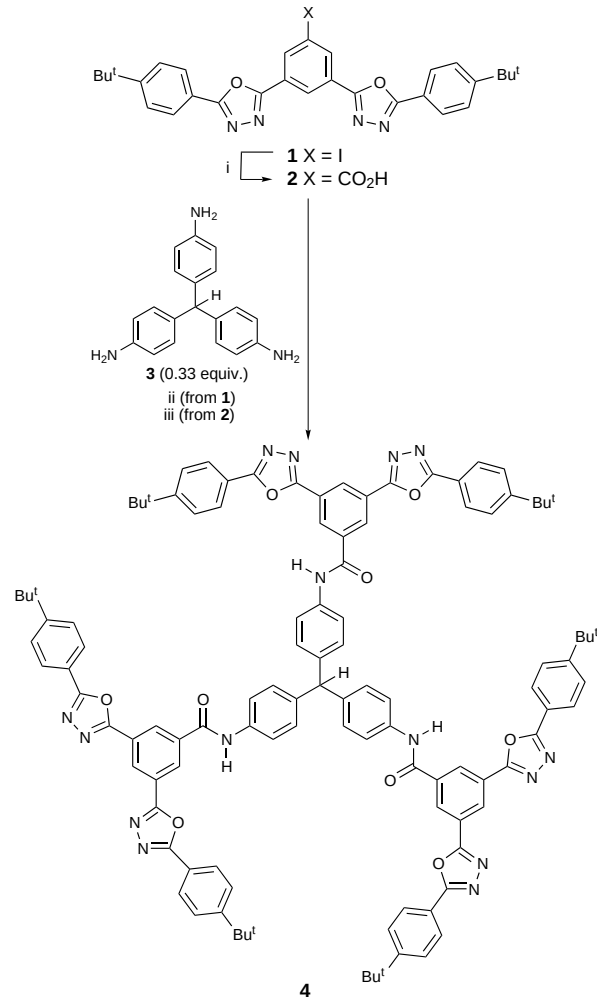
*Department of Organic Chemistry and Macromolecular Chemistry II, Heinrich Heine University of Düsseldorf, Universitätsstr. 1, D-40225 Düsseldorf, Germany*

**Two poly(aramide) dendrimers, which possess electron-deficient 1,3,4-oxadiazole and aromatic systems linked by amide units to a triphenylmethane core, strongly self-associate in chloroform solution through hydrogen bonding.**

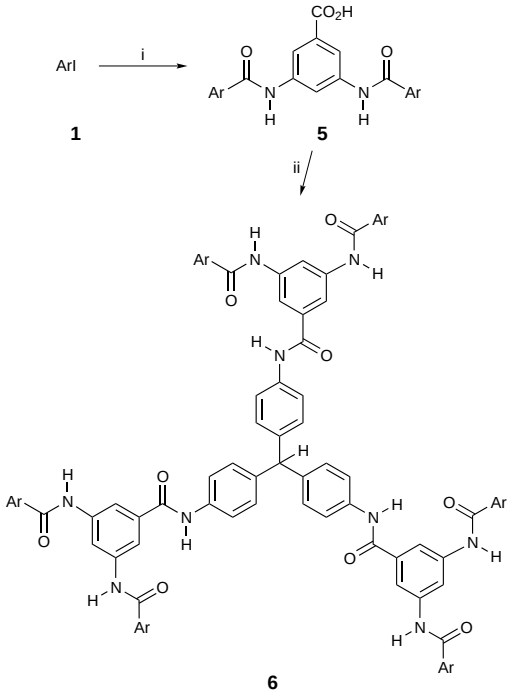
During the last decade, dendrimers with highly branched, spherical structures have attracted much attention.[1] They often possess unique properties, such as unusually good solubility. Linear poly(aramide)s, for example, are well-known high-performance fibre materials which owe their high tensile strength to a large degree of hydrogen bonding between aligned polymer chains; however, these polycondensates dissolve only in highly polar solvents such as concentrated sulfuric acid. In contrast, the few hitherto known dendritic or hyperbranched poly(aramide)s are soluble in DMF, DMSO and THF, yet the attempts towards their synthesis were hampered by side reactions.[2,3] We have recently embarked on a programme to synthesise dendrimers containing 1,3,4-oxadiazole systems.[4] These heterocycles are notable for their potential application as electron-transporting materials in electroluminescent devices based on organic fluorescent dyes and polymers.[5] The star-branched and dendritic derivatives with $\geqslant$3 oxadiazoles per molecule dissolve well in chlorinated and aromatic solvents, form amorphous glasses[6,7] and tend towards π-stacking in solution.[4] We now report the synthesis of oxadiazole-containing poly(aramide) dendrimers that are soluble in organic solvents such as chloroform. So far, our efforts have concentrated on structures with a triphenylmethane core, starting with triamine **3**.[8]

Palladium-catalysed carbonylations[9] form the key step in the syntheses of dendritic poly(aramide)s **4** and **6**. Branched compound **4** is thus obtained in a single step from aryl iodide **1**, **3** and carbon monoxide with *N*-methyl-2-pyrrolidone (NMP) as solvent, 1,8-diazabicyclo[5.4.0]undec-7-ene (DBU) as base and $PdCl_2$–$Ph_2P(m\text{-}C_6H_4SO_3Na)$[10] as catalyst (Scheme 1). The seven-component reaction furnished **4** in 45% yield after purification by column chromatography.† However, it proved very difficult to remove the last traces of the NMP residues, and we therefore sought a different method that avoided the use of a high-boiling solvent in the last step of the synthesis. Conversion of **1** into carboxylic acid **2** was accomplished by another palladium-catalysed carbonylation. In a subsequent step, acid **2** and triamine **3** were coupled with triphenyl phosphite[11] in pyridine. Carbonylation reactions were also effective for the preparation of acid **5** and had the particular advantage that no protecting groups were required. Coupling of the acid with **3** finally furnished **6** (Scheme 2).

As usually for dendrimers, solubility is mainly determined by the substitutents at the periphery (in our case, these are *tert*-butyl substituted aromatic systems) whereas the amide groups in the centre of **4** and **6** induce hydrogen-bonding interactions. In fact, the solubility of dendrimer **4** in chloroform extends to 50–60 mg $ml^{-1}$. It was at first surprising to find that **6**, which has nine amide groups, dissolves with even more ease in chloroform (over 200 mg $ml^{-1}$). This is one of the advantages of the branched dendrimer structure.[1,2] While a linear aramide structure in poly(aramide)s has a detrimental effect on solubility, the higher degree of branching in **6** counteracts the solvophobic effect of the extra amide groups. The $^1H$ NMR spectra of **4** and **6** depend strongly on concentration, temperature and solvent while lineshapes are not influenced by the NMR frequency. This rules out dynamic processes and is a strong indication of self-association.[12] The $^1H$ NMR signals of **4** in $CDCl_3$ are all broad and without fine structure. The fact that they become sharp on addition of [$^2H_6$]DMSO (15%) underlines that hydrogen-bonding is responsible for the self-association of **4**. We estimated the association constant $K_a$ of **4** in $CDCl_3$ by a dilution experiment. A decrease in concentration below $10^{-3}$ mol $dm^{-3}$ led to a significant increase in resolution of the $^1H$ NMR signals. Most chemical shifts were only slightly dependent on concentration ($\Delta\delta \leqslant 0.25$) with the exception of the NH singlet. In the concentration range investigated ($10^{-1}$ to $10^{-3}$ mol $dm^{-3}$), $\delta_{NH}$ varied from 9.91 to 9.11 and allowed $K_a$




**Scheme 1** *Reagents and conditions:* i, $LiOH{\cdot}H_2O$ (2 equiv.), $PdCl_2$ (0.03 equiv.), $Ph_2P(m\text{-}C_6H_4SO_3Na)$ (0.09 equiv.), NMP, CO, 100 °C, 1–2 d, then HCl, 79–95%; ii, $PdCl_2$ (0.03 equiv.), $Ph_2P(m\text{-}C_6H_4SO_3Na)$ (0.09 equiv.), DBU (1.2 equiv.), NMP, CO, 100 °C, 1–2 d, then HCl, 31%; iii, $P(OPh)_3$ (1.2 equiv), pyridine, 100 °C, 12 h, then HCl, 45%



**Scheme 2** *Reagents and conditions:* i, 3,5-diaminobenzoic acid (0.5 equiv.), $PdCl_2$ (0.6 equiv.), $Ph_2P(m\text{-}C_6H_4SO_3Na)$ (0.18 equiv.), DBU (1.8 equiv.), NMP, CO, 100 °C, 4 d, then HCl, 38%; ii, **3** (0.33 equiv.), $P(OPh)_3$ (1.2 equiv.), pyridine, 100 °C, 12 h, then HCl, 37%

to be estimated to 790 ± 100 $dm^3$ $mol^{-1}$ in dry chloroform at 30 °C, assuming the isodesmic model of indefinite self-association.[13] Hydrogen bonds weaken also at higher temperature: the $^1H$ NMR spectrum of a 0.005 mol $dm^{-3}$ solution of **4** in $CDCl_3$–$C_2D_2Cl_4$ (1:2) revealed sharp signals and the expected multiplicity pattern for the aromatic protons upon raising the temperature to 80 °C. Vapour-pressure osmometry (VPO) studies in chloroform at 30 °C gave evidence of an association degree ⩾4 and a number average molar mass exceeding 3500 g $mol^{-1}$ (over twice as high as expected for non-associated **4**) at concentrations ⩾0.02 mol $dm^{-3}$. At comparatively low concentrations, a significant amount of **4** is present in solution in the form of higher oligomers. Although self-association generally counteracts solubility, the branched structure of **4** successfully suppresses precipitation of the compound. Only after chromatography could a small amount of **4** be induced to crystallise from a $CH_2Cl_2$–MeOH.

Association becomes even more dominant for **6** with its nine amide groups. The $^1H$ NMR spectrum of the dendrimer in $CDCl_3$ is characterised by broad signals, and even the *tert*-butyl 'singlet' has a linewidth of $\Delta\delta \approx 0.4$ (at 0.002 mol $dm^{-3}$) at half maximum. Addition of $[^2H_6]$DMSO no longer suffices to break up all hydrogen bonds. In fact, this demands the addition of a much more polar cosolvent such as trifluoroacetic acid. The remarkably strong association is also deduced from the $^1H$ NMR spectrum of **6** in $C_2D_2Cl_4$ (0.01 mol $dm^{-3}$) at 138 °C, which still displays broadened signals for the aromatic protons and a complicated pattern for the *tert*-butyl protons between $\delta$ 0.95 and 1.50. It seems unlikely that all amide groups will be involved in hydrogen bonding because the propeller configuration of the triphenylmethane[14] core and the disordered structure of the branched periphery prevent such a fit. Nevertheless, a larger number of amide groups per dendrimer molecule enhance the probability of multiple interactions and therefore contributes to an increased association constant. In addition, the electron-deficient oxadiazole and aromatic systems also take part in aromatic–aromatic interactions, judging from the upfield $^1H$ NMR shifts of several aromatic proton signals.[15]

At first glance the molar masses of dendrimers **4** and **6** seem to be comparitively low, yet the tendency of these compounds to strongly self-associate in solution makes them behave like polymers, as is apparent by an increased viscosity and effective molar mass even in dilute solutions. Whereas polymers suffer from a lack of purification methods that makes it difficult to remedy any incorporated structural defects, dendrimers can be much more easily purified. We expect that self-associating poly(aramide) dendrimers with solubilising and electroactive functional groups at the periphery will have promising material properties, which are the subject of further investigations.

We thank the Deutsche Forschungsgemeinschaft, the Fonds der Chemischen Industrie and Professor G. Wulff for generous support, Dr H. Luftmann (University of Münster) for MALDI-TOF MS measurements, and Ms H. Fürtges for assistance in the preparation of starting materials.

## Footnotes

* E-mail: kraft@iris-oc2.oc2.uni-duesseldorf.de

† All compounds were characterised by microanalysis, IR, NMR and mass spectroscopy. *Selected data* for **4**: $^1H$ NMR (500 MHz, $CDCl_3$–$[^2H_6]$DMSO, 6:1) 1.40 (s, $CH_3$), 5.63 (s, 1 H, $Ar_3CH$), 7.24, 7.88 [AA'XX', 12 H, $(C_6H_4)_3C$], 7.60, 8.11 (AA'XX', 24 H, $Bu^tC_6H_4$), 8.96 (t, *J* 1.6 Hz, 3 H), 8.99 (d, 6 H, $C_6H_3$), 10.50 (s, NH); $R_f$ ($CH_2Cl_2$–MeOH, 15:1) 0.75. For **6**: $^1H$ NMR (500 MHz, $CDCl_3$–$CF_3CO_2D$, 6:1) 1.38 (s, $CH_3$), 5.71 (s, 1 H, $Ar_3CH$), 7.27, 7.63 [AA'XX', $(C_6H_4)_3C$], 7.67, 8.16 (AA'XX', $Bu^tC_6H_4$), 8.37 (br s, 6 H), 8.68 [br s, 3 H, $(CONH)_2C_6H_3CO$], 9.18 (br s, 2 H), 9.23 (br s, 1 H, $C_6H_3$); $R_f$($CH_2Cl_2$–MeOH, 9:1) 0.5.

## References

1 For a recent monograph on dendrimers, see G. R. Newkome, C. N. Moorefield and F. Vögtle, *Dendritic Molecules: Concepts, Synthesis, Perspectives*, VCH, Weinheim, 1996.
2 S. C. E. Backson, P. M. Bayliff, W. J. Feast, A. M. Kenwright, D. Parker and R. W. Richards, *Macromol. Symp.*, 1994, **77**, 1.
3 Y. H. Kim, *J. Am. Chem. Soc.*, 1992, **114**, 4947.
4 A. Kraft, *Chem. Commun.*, 1996, 77.
5 Application of 1,3,4-oxadiazole derivatives in electroluminescent devices: Y. Hamada, C. Adachi, T. Tsutsui and S. Saito, *Jpn. J. Appl. Phys.*, 1992, **31**, 1812; A. R. Brown, D. D. C. Bradley, J. H. Burroughes, R. H. Friend, N. C. Greenham, P. L. Burn, A. B. Holmes and A. Kraft, *Appl. Phys. Lett.*, 1992, **61**, 2793.
6 X.-C. Li, A. Kraft, R. Cervini, G. C. W. Spencer, F. Cacialli, R. H. Friend, J. Grüner, A. B. Holmes, J. C. DeMello and S. C. Moratti, *Mater. Res. Soc. Symp. Proc.*, 1996, **413**, 13.
7 J. Bettenhausen and P. Strohriegl, *Adv. Mater.* 1996, **8**, 507; J. Bettenhausen and P. Strohriegl, *Makromol. Chem., Commun.*, 1996, **17**, 623.
8 D. Hellwinkel and H. Fritsch, *Chem. Ber.*, 1990, **123**, 2207.
9 For other syntheses of poly(aramide)s by palladium-catalysed carbonylations, see M. Yoneyama, M. Kakimoto and Y. Imai, *Macromolecules*, 1988, **21**, 1908; S. R. Turner, R. J. Perry and R. W. Blevins, *Macromolecules*, 1992, **25**, 4819; V. R. Reichert and L. J. Mathias, *Macromolecules*, 1994, **27**, 7024.
10 S. Ahrland, J. Chatt, N. R. Davies and A. A. Williams, *J. Chem. Soc.*, 1958, 276.
11 N. Yamazaki, M. Matsumoto and F. Higashi, *J. Polym. Sci., Polym. Chem. Ed.*, 1975, **13**, 1373.
12 Until now, dendrimer–dendrimer interactions involved mainly micelle formation, aggregation or self-assembly in solution, and liquid-crystalline phase transition in the absence of solvent: G. R. Newkome, C. N. Moorefield, G. R. Baker, R. K. Behera, G. H. Escamillia and M. J. Saunders, *Angew. Chem., Int. Ed. Engl.*, 1992, **31**, 917; J. M. J. Fréchet and I. Gitsov, *Macromol. Symp.*, 1995, **98**, 441; V. Percec, P. Chu, G. Ungar and J. Zhou, *J. Am. Chem. Soc.*, 1995, **117**, 11441; J. C. M. van Hest, D. A. P. Delnoye, M. W. P. L. Baars, C. Elissen-Román, M. H. P. van Genderen and E. W. Meijer, *Chem. Eur. J.*, 1996, **2**, 1616; S. C. Zimmerman, F. Zeng, D. E. C. Reichert and S. V. Kolotuchin, *Science*, 1996, **271**, 1095.
13 R. B. Martin, *Chem. Rev.*, 1996, **96**, 3043.
14 N. Veldman, A. L. Spek, J. J. H. Schlotter, J. W. Zwikker and L. W. Jenneskens, *Acta Crystallogr., Sect. C*, 1996, **52**, 174.
15 For hydrogen-bonding in aramides and attractive π-interactions between electron-poor aromatic compounds, see A. P. Bisson and C. A. Hunter, *Chem. Commun.*, 1996, 1723; C. A. Hunter and J. K. M. Sanders, *J. Am. Chem. Soc.*, 1990, **112**, 5525.

*Received in Cambridge, UK, 6th May 1997; 7/03072J*

# Direct electrochemistry of horseradish peroxidase adsorbed on glassy carbon electrode from organic solutions

**Yizhu Guo and Ana R. Guadalupe***

*Department of Chemistry, PO Box 23346, University of Puerto Rico, Río Piedras Campus, San Juan, Puerto Rico 00931-3346*

**Using a 'solvent engineering' approach, the direct electrochemistry of catalytically active horseradish peroxidase (HRP) adsorbed on glassy carbon electrodes from HRP–DMSO and HRP–formamide solutions has been readily obtained in aqueous phosphate buffer (pH 7.0), with a surface formal potential of −0.365 V *vs.* Ag/AgCl and an apparent electron transfer rate constant of 0.655 $s^{-1}$.**

Study of the direct heterogeneous electron transfer of proteins and enzymes is a convenient and informative means for understanding the kinetics and thermodynamics of biological redox processes.[1] Work on direct electron transfer involving biomolecules has largely focused on relatively small proteins,[2] most notably cytochromes, microperoxidases, ferredoxins and myoglobin. Direct electron transfer between the electrode and the prosthetic group of catalytically active protein-enzymes possessing a considerably greater molar mass is prevented by exceedingly large electron hopping distances, by improper orientation of the adsorbed enzyme, or by adsorptive denaturation.[3a] Mediators or promoters are generally employed to study the electron-transfer kinetics of large proteins.[3] We report here preliminary results on the use of 'solvent engineering' for the direct electrochemistry of *catalytically active* horseradish peroxidase (HRP). 'Solvent engineering' has attracted much interest in nonaqueous enzymology in the last decade.[4] Many interesting findings and advances have been made in these areas.[5] Here we demonstrate the feasibility of this approach in bioelectrochemistry.

Amperometric peroxidase-modified electrodes have been one of the most extensively studied biosensors for the detection of hydrogen peroxide, organic hydroperoxides, phenols, aromatic amines and hazardous compounds. Many of these sensors are reported to be based on an apparent direct electron transfer between the immobilized peroxidase and the electrode surface.[6] Only one observation of the direct redox process of HRP adsorbed on electrochemically activated carbon electrodes has been claimed,[7] providing only the redox potentials in the range of −0.33 to −0.25 V *vs.* SCE. Little is known of the rate of electron transfer of HRP at electrode surfaces. Using the 'solvent engineering' approach we have readily obtained the direct electrochemistry of HRP adsorbed on glassy carbon electrodes by cyclic voltammetry.

The glassy carbon electrodes (BAS, $d$ = 1.6 mm) were polished with 0.05 μm $Al_2O_3$ and 1 micron diamond paste, respectively, sonicated in water, acetone and water successively, then dried in air at room temperature. Horseradish peroxidase solutions (2 mg $ml^{-1}$) were prepared by dissolving HRP (E.C. 1.11.1.7, 90 units $mg^{-1}$, Sigma) in pure DMSO or formamide (FA). The glassy carbon electrodes were soaked in these solutions for 15 min, then rinsed with copious amounts of phosphate buffer (pH 7.0, 20 mM) and ultrapure water. It has been demonstrated that enzymes (*e.g.* trypsin, chymotrypsin, lysozyme, ribonuclease) dissolved in pure organic solvents, such as DMSO and FA, do not inactivate irreversibly.[8] Nearly all original enzymatic activity is restored from organic solution not only upon immediate dilution with aqueous buffer but even after a 24 h incubation of the enzyme in organic solvents at 25 °C. Voltammograms were recorded with a BAS Electroanalyzer 100W/B interfaced to a 33 MHz Gateway 2000 computer. All the voltammetric experiments were performed with Ag/AgCl (3 M NaCl) reference and platinum auxiliary electrodes in 20 mM potassium phosphate buffer at pH 7.0.

Fig. 1 shows a typical cyclic voltammogram obtained for HRP adsorbed on a glassy carbon electrode from HRP–DMSO solution. The modified electrodes are quite stable, with little change in the voltammogram during cycling, as demonstrated by the first cycle and the fiftieth cycle shown in Fig. 1. The broadness of these peaks suggests an HRP adsorbate distribution[9] perhaps resulting from multiple conformations of adsorbed HRP from the organic solution or differential adsorption energies, and the full-width at half-maximum ($E_{FWHM}$) is 0.175 V. The redox potentials are in the range of −0.3 to −0.42 V with scan rate varying from 20 to 500 mV $s^{-1}$, and the surface formal potential [$E^{\circ\prime}$ = ($E_{pc}$ + $E_{pa}$)/2] was around −0.365 V. The position of the cathodic maximum is close to the value of the redox potential of the $Fe^{2+}/Fe^{3+}$ electron transfer in the active centre of peroxidase obtained by potentiometric studies (−0.3 to −0.45 V).[1c,10] The peak current $I_p$ was found to be proportional to scan rate ($v$), indicative of a surface-confined redox process. The surface coverage ($\Gamma$) was calculated to be $5.2 \times 10^{-11}$ mol $cm^{-2}$, consistent with the high intensity of the nitrogen signal in the X-ray photoelectron spectra of the modified electrodes. From the variation of $E_{pc}$ with $v$,[11] an apparent electron transfer rate constant $k_s$ was calculated to be 0.655 $s^{-1}$.

Besides DMSO, direct electrochemistry of HRP has been also observed for electrodes modified in HRP–FA solution, with $E^{\circ\prime}$ = −0.348 V, $E_{FWHM}$ = 0.190 V, $\Gamma$ = $4.4 \times 10^{-11}$

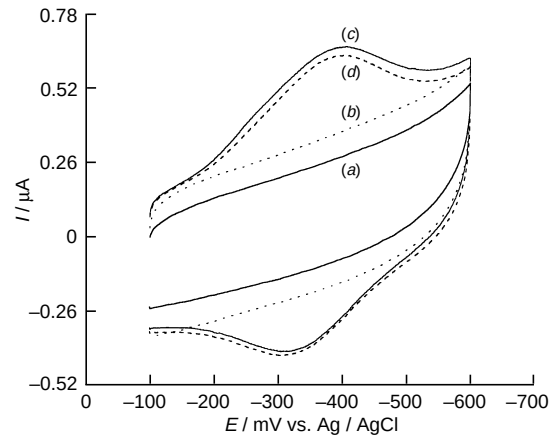



**Fig. 1** Cyclic voltammograms of a glassy carbon electrode at a scan rate of 100 mV $s^{-1}$ before and after soaking for 15 min in pure DMSO or in 2 mg $ml^{-1}$ HRP–DMSO solution: (*a*) before soaking, (*b*) after soaking in DMSO, (*c*) the first cycle after soaking in HRP–DMSO, (*d*) the fiftieth cycle after soaking in HRP–DMSO. The supporting electrolyte is 20 mM potassium phosphate buffer at pH 7.0.

mol $cm^{-2}$ and $k_s$ = 0.60 $s^{-1}$. Considering the distinctly different characters of DMSO and FA toward proteins, that is, DMSO is destructive to a protein's structural integrity[12] while FA is a solvent similar to water where there exists solvophobic interactions,[13] we might expect to observe different conformations for HRP in DMSO and in FA, and it is surprising to find that the electrochemical performance of HRP adsorbed on glassy carbon electrodes from HRP–DMSO and HRP–FA solutions is nearly the same. However, considering the reversible inactivation of dissolved enzymes in organic solvent and the complete restoration of their original catalytic activities upon dilution, these results are reasonable and expected. It is reported that a higher degree of haem exposure lowers the redox potential of a haemoprotein,[14] and there is only a few millivolt difference in the redox potentials of HRP adsorbed from HRP–DMSO and HRP–FA solutions, indicating that the restored conformation of the adsorbed enzyme upon dilution with aqueous buffer is independent of the solvent from which it was adsorbed. Furthermore, the heterogeneous electron transfer rates for HRP adsorbed on a glassy carbon electrode from organic solutions are very close to that of HRP adsorbed on a graphite electrode from aqueous solution (0.66 $s^{-1}$), which was obtained as the rate of electron transfer of the electrocatalytic reduction of $H_2O_2$ in phosphate buffer by rotating disk technique.[15] This suggests that the enzyme conformation and catalytic activity might be the same as that when the enzyme is adsorbed from aqueous solutions. As expected, these modified electrodes show catalytic activity for the reduction of hydrogen peroxide, with an onset potential at around 0.0 V and levelling off at around −0.25 V. When the peroxide inhibitor KCN was introduced into the buffer solution, the peaks of the current–voltage curve disappeared and no catalytic activity was observed after $H_2O_2$ addition. As we noticed a small direct reaction occurs between peroxide and the naked electrode and cyanide poisons the electrode, but the current on the enzyme modified electrode is much higher and the biocatalytic process is inhibited substantially by cyanide. The facts above demonstrate that the redox process of the *active* enzyme's prosthetic group has been obtained by cyclic voltammetry using 'solvent engineering'. The exact role of the organic solvents is not clear at present. Proteins dissolved in organic solvents are at least partially unfolded, resulting in a more intimate contact of the proteins with the electrode surface, a shorter electron transfer distance and a favourable orientation for the restored conformation upon rinsing with aqueous buffer. That is, one of the significant advantages of this approach is the possibility of reorganization of the conformation of adsorbed proteins on electrode surface from their organic solutions. Another possibility is to operate protein modification in protein-dissolving organic solvents, allowing inner core modification on the unfolded proteins. The latter has yet to be exploited.

In summary, we have demonstrated the feasibility of using a 'solvent engineering' approach to study the electron transfer reaction of adsorbed HRP. Applications for the direct electrochemistry of other large proteins and enzymes, and the construction of mediatorless biosensors, can be readily envisaged.

The financial support of NIH-MBRS (Grant Number S06 GM08102) is greatly appreciated.

## Footnote

* E-mail: agudalu@upracd.upr.clu.edu

## References

1 (*a*) R. A. Marcus and N. Sutin, *Biochim. Biophys. Acta*, 1985, **811**, 265; (*b*) H. B. Gray and B. Malmstrom, *Biochemistry*, 1989, **28**, 7499; (*c*) G. Dryhurst, K. M. Kadish, F. Scheller and R. Rennerberg, *Biological Electrochemistry*, Academic Press, New York, 1982; (*d*) L. H. Guo and H. A. O. Hill, *Direct Electrochemistry of Proteins and Enzymes*, in *Advances in Inorganic Chemistry*, ed. A. G. Sykes, Academic Press, San Diego, CA, 1990, vol. 36, pp. 341–375.

2 F. A. Armstrong, P. A. Cox, H. A. O. Hill, V. J. Lowe and B. N. Oliver, *J. Electroanal. Chem.*, 1986, **217**, 331; H. A. O. Hill, *Pure Appl. Chem.*, 1987, **59**, 734; P. Yeh and T. Kuwana, *Chem. Lett.*, 1977, 1145; E. F. Bowden, F. M. Hawkridge, J. F. Chebowski, E. E. Bancroft, C. Thorpe and H. N. Blount, *J. Am. Chem. Soc.*, 1982, **104**, 7641; D. E. Reed and F. M. Hawkridge, *Anal. Chem.*, 1987, **59**, 2334; R. Santucci, H. Reinhard and M. Brunori, *J. Am. Chem. Soc.*, 1988, **110**, 8536; B. C. King, F. M. Hawkridge and B. M. Hoffman, *J. Am. Chem. Soc.*, 1992, **114**, 10 603.

3 (*a*) C. Bourdrillon, C. Demaille, J. Moiroux and J. M. Saveant, *Acc. Chem. Res.*, 1996, **26**, 529; (*b*) V. J. Razumas, A. v. Gudavicius and J. J. Kukys, *J. Electroanal Chem.*, 1986, **198**, 81; (*c*) M. J. Eddows and H. A. O. Hill, *J. Chem. Soc., Chem. Commun.*, 1977, 771; (*d*) P. M. Allen, H. A. O. Hill and N. J. Walton, *J. Electroanal Chem.*, 1984, **178**, 69; (*e*) M. J. Eddows and H. A. O. Hill, *J. Am. Chem. Soc.*, 1979, **101**, 4461; (*f*) H. C. Landrum, R. T. Salmon and F. M. Hawkridge, *J. Am. Chem. Soc.*, 1977, **99**, 3154; (*g*) T. Sagara, K. Niwa, A. Sone, C. Hinnen and K. Niki, *Langmuir*, 1990, **6**, 254.

4 A. Zaks and A. M. Klibanov, *J. Biol. Chem.*, 1988, **263**, 3194; A. M. Klibanov, *CHEMTECH*, 1986, **6**, 354; A. M. Klibanov, *Trends Biochem. Sci.*, 1989, 141.

5 K. Ryu and J. S. Dordick, *Biochemistry*, 1992, **31**, 2588; R. H. Valivety, P. J. Hailing and A. R. MaCrae, *Biochim. Biophys. Acta*, 1992, **1118**, 218; A. E. M. Janssen, A. V. Padt, H. M. Sonsbeek and K. V. Riet, *Biotechnol. Bioeng.*, 1993, **41**, 95; P. J. Halling, *Biochim. Biophys. Acta*, 1990, **1040**, 225; R. H. Valivety, G. A. Johnston, C. J. Suckling and R. J. Halling, *Biotechnol. Bioeng.*, 1991, **38**, 1137; S. Saini, G. F. Hall, M. E. A. Downs and A. P. F. Turner, *Anal. Chim. Acta*, 1991, **249**, 1; A. J. Russell, S. Chatterjee and S. Bambot, *Indian J. Chem.*, 1992, **31B**, 934; C. Lanne, S. Boeren, K. Vos and C. Veeger, *Biotechnol. Bioeng.*, 1987, **30**, 81.

6 V. Razumas, J. Jasaitis and J. Kulys, *Bioelectrochem. Bioenerg.*, 1984, **12**, 297; G. Jonsson and L. Gorton, *Electroanalysis*, 1989, **1**, 465; W. O. Ho, D. Athey, C. J. McNeil, H. J. Hager, G. P. Evans and W. H. Mullen, *J. Electroanal. Chem.*, 1993, **351**, 185; V. A. Bogdanovskaya, V. A. Fridman, M. R. Tarasevich and F. Scheller, *Anal. Lett.*, 1994, **27**, 2823; L. Gorton, G. Bremle, E. Csoregi, G. Jonsson-Pettersson and B. Persson, *Anal. Chim Acta*, 1991, **249**, 43; E. Csoregi, G. Jonsson-Pettersson and L. Gorton, *J. Biotechnol.*, 1993, **30**, 315; C. Wang and J. Mulchandani, *Anal. Chem.*, 1995, **67**, 1109; S. Dong and Y. Guo, *J. Chem. Soc., Chem. Commun.*, 1995, 483; T. Lotzbeyer, W. Schuhmann and H. L. Schmidt, *Sens. Actuators B*, 1996, **33**, 50.

7 V. A. Bogdanovskaya, M. R. Tarsevich, R. Hintsche and F. Scheller, *Bioelectrochem. Bioenerg.*, 1988, **19**, 581.

8 N. Chang, S. J. Hen and A. M. Klibanov, *Biochem. Biophys. Res. Commun.*, 1991, **176**, 1462; N. Chang and A. M. Klibanov, *Biotechnol. Bioeng.*, 1992, **39**, 575.

9 M. J. Tarlov and E. F. Bowden, *J. Am. Chem. Soc.*, 1991, **113**, 1847; R. A. Clark and E. F. Bowden, *Langmuir*, 1997, **13**, 559.

10 F. A. Armstrong and A. M. Lannon, *J. Am. Chem. Soc.*, 1987, **109**, 7211.

11 E. Laviron, *J. Electroanal. Chem.*, 1979, **101**, 19.

12 A. A. Klyosov, N. Van Viet and I. V. Berezin, *Eur. J. Biochem.*, 1975, **59**, 3; A. L. Fink, *J. Biol. Chem.*, 1974, **249**, 5027; M. Hofmann, G. Bovermann and M.Nilges, *Eur. J. Biochem.*, 1989, **186**, 95.

13 A. Ray, *Nature*, 1971, **231**, 313.

14 R. Santucci, H. Reinhard and M. Brunori, *J. Am. Chem. Soc.*, 1988, **110**, 8536; E. Stellwagen, *Nature* (*London*), 1978, **275**, 73.

15 T. Ruzgas, L. Gorton, J. Emnus and G. Mavko-Varga, *J. Electroanal. Chem.*, 1995, **391**, 41.

*Received in Cambridge, UK, 12th May 1997; 7/03254D*

# Supramolecular intercalation of $C_{60}$ into a calixarene bilayer—a well-ordered solid-state structure dominated by van der Waals contacts

**Leonard J. Barbour, G. William Orr and Jerry L. Atwood***

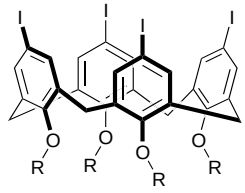
*Department of Chemistry, University of Missouri-Columbia, Columbia MO 65211, USA*

**$C_{60}$ co-crystallizes with *p*-iodocalix[4]arene benzyl ether to form a layered structure in which the $C_{60}$ molecule is ordered without the presence of appreciably strong intermolecular interactions.**

There has been much interest in the supramolecular complexation of fullerenes, both in solution[1–4] and in the solid state.[5–11] Crystallographic characterization of crystals containing $C_{60}$ is often confounded by twinning[12] and orientational disorder,[9–11,13,14] the latter being mainly due to the lack of anisotropy of the molecule, and to its inability to interact strongly with other species. It is well-established that important considerations in the design of systems for molecular recognition include shape and size discrimination, as well as the exploitation of relatively weak non-covalent forces[15] (*e.g.* hydrogen bonding, π··π interactions). That these criteria are usually complementary makes the prediction of solid-state structures extremely difficult, thus forcing one to produce multicomponent materials by trial and error in order to examine the resulting structures for clues relating to their formation and stability.

Several crystal structures containing ordered $C_{60}$ molecules have been reported to date.[6,7,16,17] From these studies we are able to deduce the nature of the weak interactions which can be used to hold the molecule in place. In this context, there have been reports of interactions between six-membered aromatic rings and the electron-poor 6:5 $C_{60}$ ring fusion,[16,18] $C_5H_5$ or $C_5Me_5$ rings and the electron-rich 6:6 ring fusion,[17] $C_5$··$C_5$ interactions,[6,19] aromatic C–H··$C_6$ hydrogen-π bonds[16] and C··I interactions.[13]

We are interested in forming supramolecular complexes between fullerenes and calixarenes and have recently achieved some success in this area.[1,2] The supramolecular chemistry of calixarenes is mainly associated with a bowlic cavity which may act as a receptor site for molecular inclusion. Chemical substitution at the lower rim of calix[4]arenes invaribly results in a significant reduction in the size of the molecular cavity as the molecule adopts the so-called 'pinched-cone' conformation. However, despite the loss of the cavity, such substitution can lead to molecules with interesting solid-state packing properties relating to their shape and functionality. In an effort to gain a better understanding of some of the factors affecting the formation of stable solid-state structures, we are investigating the interaction of $C_{60}$ with a series of calix[4]arene compounds which have been modified to include both halogen and phenyl moieties. We present here the results of one such structure with a particularly interesting solid-state architecture.




**1** R = benzyl

Slow diffusion of propan-2-ol into a solution of **1** and $C_{60}$ (5:1 molar ratio) in *o*-dichlorobenzene yielded dark red crystals suitable for single-crystal X-ray diffraction analysis.† The asymmetric unit consists of one half of the calixarene molecule, which is situated on a $\bar{4}$ axis, and one quarter of a $C_{60}$ molecule which is positioned with its centre on the intersection of three mutually orthogonal two-fold rotation axes. No atoms occupy special positions in the unit cell. Although the $C_{60}$ molecule does not exhibit orientational disorder, the thermal ellipsoids of its atoms have large amplitudes parallel to its surface (Fig. 1). As shown in Fig. 2, the most striking feature of the overall structure is that $C_{60}$ molecules are intercalated into calixarene bilayers running parallel to (001). The calixarene molecule possesses $C_2$ symmetry and within each calixarene monolayer there are two distinct molecular orientations. These two orientations are rotated by 90° relative to one another and alternate like the squares on a chess board as shown in Fig. 2(*a*). The calixarene bilayer consists of two such monolayers associated with one another in a head-to-head fashion, *i.e.* where the upper rim of each calixarene molecule is one layer faces the upper rim of a calixarene molecule of the second layer across a $\bar{4}$ symmetry site. This arrangement gives rise to large intermolecular cavities which are occupied by the $C_{60}$ molecules. Fig. 2(*b*) shows a cross-section of the bilayers which are stacked along the crystallographic *c* axis with the calixarene molecules in adjacent bilayers associated with one another in a tail-to-tail arrangement. Thus the calixarene molecules are arranged in . . . a b c d a . . . columns parallel to the *c* axis.

At first glance, it would appear that the head-to-head association of the calixarenes may be facilitated by I··I interactions, while the tail-to-tail association can be attributed to π··π interactions between the benzyl moieties. However, the closest I··I approach in the structure is 4.26(2) Å. A recent survey[20] of halogen··halogen interactions, based on data from the Cambridge Crystallographic Database, suggests that symmetrical I··I distances of ⩾4.0 Å probably only correspond to van der Waals contacts which occur as a consequence of molecular packing, and thus contribute little to the energy of the crystal. Similarly, the shortest benzyl centroid··centroid dis-

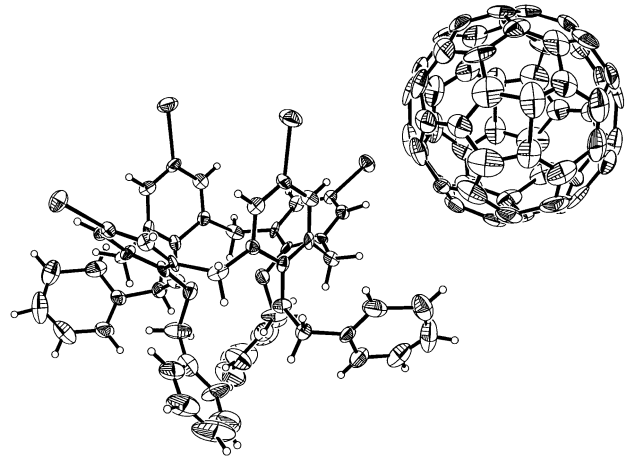


**Fig. 1** ORTEP diagram showing 30% thermal ellipsoids

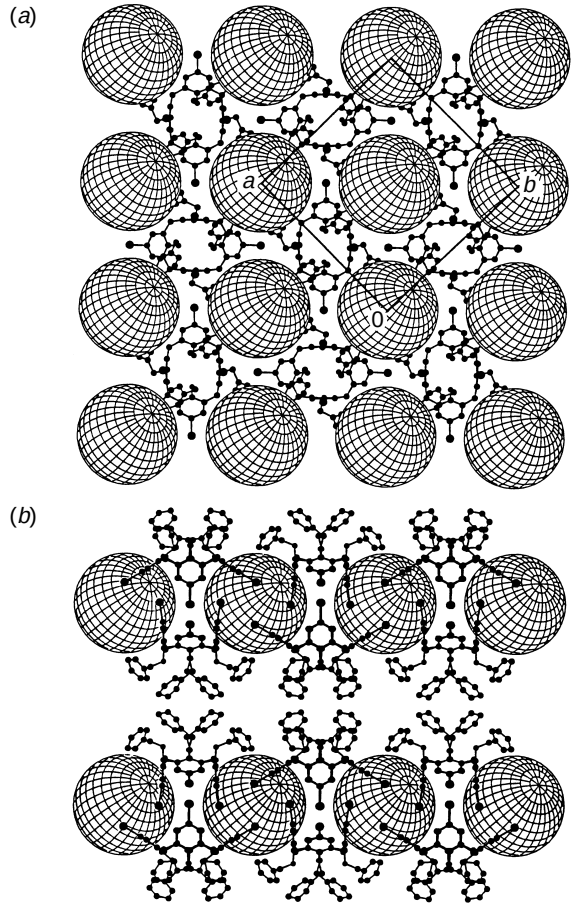



**Fig. 2** Packing diagrams (hydrogen atoms omitted) viewed along (*a*) [001], looking down the calixarene cavities and showing the $C_{60}$ molecules resting on a 2-dimensional calixarene monolyer, and (*b*) [−110], showing a cross-section of two adjacent $C_{60}$-intercalated calixarene bilayers centred at $x,y,\frac{3}{4}$, and $x,y,\frac{1}{4}$

tance of 5.28(3) Å is much too long to be attributed to an appreciably strong aromatic π··π interaction.[21]

The shortest $C_{60}$ C··I distance of 3.67(3) Å is comparable to the sum of the van der Waals radii[22] (3.68 Å) and is considerably longer than the value of 3.09 Å reported for the solvated structure $C_{60}$·$I_2$·toluene.[13] In an earlier study, $C_{60}$ C··I values of 3.29 and 3.54 Å were reported for the solvate $C_{60}$·$C_6H_6$·$CH_2I_2$,[23] implying that these interactios contribute to ordering of the $C_{60}$ molecule. Furthermore, in the present structure, the closest approach of iodine to any centroid of the fullerene rings is 3.84(4) Å. There are no calixarene aromatic centroids within 5 Å of any 6 : 5 bond of the $C_{60}$ and all fullerene ring centroids are > 3.8 Å from any calixarene atoms or ring centroids. The closest calixarene–fullerene C··C contact of 3.55 Å compares favourably with the sum of their van der Waals radii (3.54 Å). It therefore appears that the only contact between the calixarene and $C_{60}$ which may feasibly be construed as an interaction is that between an aromatic hydrogen atom (*ortho* to the iodine) of the calixarene and a carbon atom of the fullerene. This distance is 2.63(2) Å while the C–H··C angle is 168(1)°.

The closest $C_{60}$··$C_{60}$ approach is 13.46 Å within the intercalated layers and 21.18 Å between layers. The average 5 : 6 and 6 : 6 bond lengths [1.46(8) and 1.31(8) Å respectively] are in good agreement with values reported in the literature. Despite the apparent absence of any appreciable interactions between the $C_{60}$ and calixarene, it is intriguing that the structure has yielded such a well-ordered $C_{60}$ molecule.

We are grateful for funding from the National Science Foundation.

## Footnotes

* E-mail: chenja@mizzou1.missouri.edu

† *Crystal data* for $2(C_{56}H_{44}I_4O_4)$·$C_{60}$: $M$ = 3297.62, tetragonal, $a = b$ = 19.0353(7), $c$ = 42.372(2) Å, $V$ = 15353(1) Å$^3$, space group $I\bar{4}c2$, $Z$ = 4, $D_c$ = 1.427 g cm$^{-3}$, $\mu$(Mo-Kα) = 16.71 cm$^{-1}$, $F$(000) = 6423. A dark red crystal of dimensions 0.45 × 0.25 × 0.20 mm was used. Intensity data were collected on a Siemens SMART CDD diffractometer using the omega scan mode. Data were corrected for absorption using the program SADABS which is based on the method of Blessing (ref. 24). The positions of the iodine atoms were located by the Patterson method and the structure was expanded by difference synthesis. All non-hydrogen atoms were refined anisotropically while hydrogen atoms were placed in calculated positions. A peak of 1.93 e Å$^{-3}$ in the final difference Fourier map was unaccounted for. NMR analysis of the crystals did not reveal the presence of *o*-dichlorobenzene or propan-2-ol, and the peak was thus attributed to being an artifact of the structure. Final refinement converged with $R_1$ = 0.089 for 4522 unique reflections [$I > 2\sigma(I)$, $2\theta \leqslant 46°$], 425 parameters and 12 restraints. Atomic coordinates, bond lengths and angles, and thermal parameters have been deposited at the Cambridge Crystallographic Data Centre (CCDC). See Information for Authors, Issue No. 1. Any request to the CCDC for this material should quote the full literature citation and the reference number 182/471.

## References

1 J. L. Atwood, G. A. Koutsantonis and C. L. Raston, *Nature*, 1994, **368**, 229.
2 J. L. Atwood, M. J. Barnes, M. G. Gardiner and C. L. Raston, *Chem. Commun.*, 1996, 1449.
3 T. Andersson, K. Nilsson, M. Sundahl, G. Westman and O. Wennerström, *J. Chem. Soc., Chem. Commun.*, 1992, 604.
4 Z. Yoshida, H. Takekuma, S. Takekuma and Y. Matsubara, *Angew. Chem., Int. Ed., Engl.*, 1994, **33**, 1597.
5 T. Haino, M. Yanase and Y. Fukazawa, *Angew. Chem., Int. Ed. Engl.*, 1997, **36**, 259.
6 J. D. Crane, P. B. Hitchcock, H. W. Kroto, R. Taylor and D. R. M. Walton, *J. Chem. Soc., Chem. Commun.*, 1992, 1764.
7 J. D. Crane and P. B. Hitchcock, *J. Chem. Soc., Dalton Trans.*, 1993, 2537.
8 M. M. Olmstead, A. S. Ginwalla, B. C. Noll, D. S. Tinti and A. L. Balch, *J. Am. Chem. Soc.*, 1996, **118**, 7737.
9 L. Y. Chiang, J. W. Swirczewski, K. Liang and J. Millar, *Chem. Lett.*, 1994, 981.
10 D. M. Eichhorn, S. Yang, W. Jarrell, T. F. Baumann, L. S. Beall, A. J. P. White, D. J. Williams, A. G. M. Barrett and B. M. Hoffmann, *J. Chem. Soc., Chem. Commun.*, 1995, 1703.
11 O. Ermer, *Helv. Chim. Acta*, 1991, **74**, 1339.
12 S. Liu, Y. Lu, M. M. Kappes and J. A. Ibers, *Science*, 1991, **254**, 408.
13 P. R. Birkett, C. Christides, P. B. Hitchcock, H. W. Kroto, K. Prassides, R. Taylor and D. R. M. Walton, *J. Chem. Soc., Perkin Trans. 2*, 1993, 1407.
14 H.-B. Bürgi, E. Blanc, D. Schwarzenbach, S. Liu, Y. Lu, M. M. Kappes and J. A. Ibers, *Angew. Chem., Int. Ed. Engl.*, 1992, **31**, 640.
15 G. R. Desiraju, *Crystal Engineering: The Design of Organic Solids*, Elsevier, Amsterdam, 1989.
16 M. Fedurco, M. M. Olmstead and W. R. Fawcett, *Inorg. Chem.*, 1995, **34**, 390.
17 W. I. F. David, R. M. Ibberson, J. C. Matthewman, K. Prassides, T. J. S. Dennis, J. P. Hare, H. W. Kroto, R. Taylor and D. R. M. Walton, *Nature*, **353**, 147.
18 A. L. Bach, V. J. Catalano, J. W. Lee and M. M. Olmstead, *J. Am. Chem. Soc.*, 1992, **114**, 5455.
19 W. C. Wan, X. Liu, G. M. Sweeney and W. E. Broderick, *J. Am. Chem. Soc.*, 1995, **117**, 9580.
20 R. Pedireddi, D. S. Reddy, B. S. Goud, D. C. Craig, A. D. Rae and G. R. Desiraju, *J. Chem. Soc., Perkin Trans. 2*, 1994, 2353.
21 C. A. Hunter, *Angew. Chem., Int. Ed. Engl.*, 1993, **32**, 1594.
22 A. Bondi, *J. Phys. Chem.*, 1964, **68**, 441.
23 U. Geiser, S. K. Kumar, B. M. Savall, S. S. Harried, K. D. Carlson, P. R. Mobley, H. H. Wang, J. M. Williams, R. E. Botto, W. Liang and M.-H. Whangbo, *Chem. Mater.*, 1992, **4**, 1077.
24 R. H. Blessing, *Acta Crystallogr., Sect. A*, 1995, **51**, 33.

*Received in Cambridge, UK, 25th March 1997; 7/02075I*

# First synthesis of cyclotrihydrazino peptides

**Sophie Carret, Michèle Baudy-Floc'h, Albert Robert and Philippe Le Grel***

*Groupe de Recherches Synthèse et Electrosynthèse Organiques Université de Rennes I, UMR CNRS 6510 Avenue du Général Leclerc, F-35042 Rennes Cédex, France*

**Synthesis of novel cyclotrihydrazino peptides using an original cyclisation method at high dilution.**

A growing number of peptides are regularly isolated from animal and human tissues. Most exhibit interesting biological effects as hormones or neuromediators. From this point of view they appear to possess high potential as therapeutic agents. However, among other reasons, their low bioavailability represents a strong limitation on their use in this field. To solve this problem peptide analogues have been synthesised and screened to produce active peptidomimetic compounds with enhanced enzyme resistance.[1] Among them, pseudo-peptides, in which the peptidic linkage is modified, are the object of great interest and have already lead to some concrete applications. For example 'Zoladex' is a powerful anticancer drug in the azapeptide class.[2]

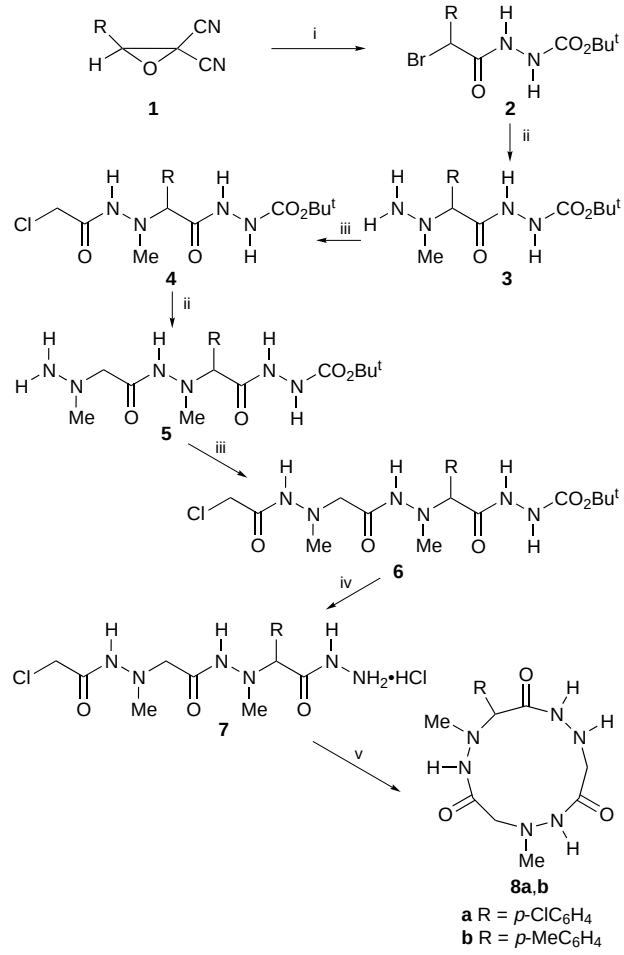
Peptidase action is also generally lower on cyclic peptides and some, like Bottromycin, have found good use as antibiotics.[3] However, obtaining cyclic derivatives remains a problematic aspect of peptidic synthesis; yields are generally low and various factors influence the success or failure of cyclisation, including the nature and the connections of amino acid residues, solvent effects, concentration and also the type of reaction involved to induce ring closure.[4,5]

Here we report preliminary results of the synthesis of, to the best of our knowledge, the first cyclohydrazino peptides. The linear precursors were prepared using improvements to a methodology that we have already described in a previous paper.[6] To achieve the ring closure we perfected an original strategy which supplements classical methods of peptide cyclisation such as azide activation,[7] activated esters[8] or coupling reagents.[9] Scheme 1 summarizes the synthesis. Reacting *gem*-dicyano epoxides[10] **1** with $Bu^tCO_2NHNH_2{\cdot}HBr$ leads to α-halo hydrazides **2**.[11] Substitution of the halogen by methylhydrazine gives **3** which is then acylated by chloroacetyl chloride to afford **4**. Reiteration of these two steps gives **6** which includes a terminal azaglycine ester linked to an aryl hydrazinosarcosine, itself connected to an *N*-chloroacylated hydrazinosarcosine.

We took advantage of the high lability of the halogen atom in α-halo hydrazides. Indeed, we have shown that such halogens are easily displaced by nucleophiles when the reaction takes place in the presence of an additional base.[12] After elimination of the Boc function we get the polyhalo compound **7** (with undetermined HCl stoichiometry); this was then treated in high dilution in MeCN with pyridine (5 equiv.). Cyclotrihydrazino peptide **8** precipitated slowly as an amorphous powder (20% yield after purification). Compound **8** was characterized by $^1H$ and $^{13}C$ NMR spectroscopy, and its monomeric structure was established by FAB mass spectroscopy (formation of the cyclodimer had to be ruled out). Microanalysis confirmed the high purity of the compound.† At the time we undertook this work, Gani used a similar method to synthesise 1,2,5-triazepine-3,6-diones.[13]

It has been shown by X-ray and model studies that hydrazino acid residues can stabilize the folded conformation of small pseudo-peptidic patterns by hydrogen bonding.[14] The success of our synthesis of pseudo-peptide **8** may arise from such a favourable conformation bringing nearer the two reactive ends (Fig. 1).

It is worth noting that despite the high solubility of **7** and the insolubility of **8** in water, this solvent failed to allow cyclisation, possibly because competitive hydrogen bonding with water




**Scheme 1** *Reagents and conditions* (for R = *p*-$ClC_6H_4$): i, $Bu^t$-$CO_2NHNH_2{\cdot}HBr$, MeCN, room temp., 8 h, 99%; ii, $NH_2NHMe$, MeCN, 0 °C, 2 h, 93%; iii, $ClCH_2COCl$, pyridine, $CH_2Cl_2$, 0 °C, 84%; iv, HCl (g), $CH_2Cl_2$, 5 min., room temp., 99%; v, pyridine, MeCN, room temp. 2 d, 20%

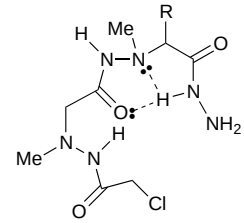


**Fig. 1**

destroys the favourable conformation for closure. This result emphasizes the crucial role played by the solvent in determining the precursor's geometry.

This preliminary work opens the way to the preparation of other original cyclopseudo-peptides of smaller or larger size, with different arrangements and various side chains. We also plan to investigate solvent effects in more detail; in particular we will examine the influence of adding ions to the reactions carried out in water.

## Footnotes

* E-mail: michele.baudy-floch@univ-rennes1.fr

† *Selected data* for **8a**: 20%; mp > 260 °C; $^1$H NMR (200 MHz, $D_2O$–$CF_3CO_2H$) 2.24 (s, 3 H), 2.58 (s, 3 H), 3.27 (m, 2 H), 3.36 (m, 2 H), 4.24 (s, 1 H), 7.37 (m, 4 H); $^{13}$C NMR (200 MHz, $D_2O$–[$^2H_6$]DMSO) 43 (q, *J* 142 Hz), 44 (q, *J* 142 Hz), 53 (t, *J* 147 Hz), 59 (t, *J* 150 Hz), 70 (d, *J* 142 Hz), 128.5 (d, *J* 168 Hz), 129 (d, *J* 168 Hz), 132, 135, 166, 168, 172; $\nu_{max}$ (Nujol)/cm$^{-1}$ 3290, 3240 br (NH), 1700, 1650, 1620 br (CO); HRMS (FAB) ($MH^+$) Calc. for $C_{14}H_{20}N_6O_3Cl$: 355.1284. Found: 355.1263. Calc.: C, 47.39; H, 5.40; N, 23.69; Cl, 9.90. Found: C, 47.45; H, 5.36; N, 23.66; Cl, 10.00%.

## References

1 A. Giannis and T. Kolter, *Angew. Chem., Int. Ed. Engl.*, 1993, **32**, 1244.
2 J. Gante, *Synthesis*, 1989, 405.
3 Y. A. Ovchinnikov and V. T. Ivanov, *Tetrahedron*, 1989, **31**, 2177.
4 M. Bodanszky, *Principles of Peptide Synthesis*, Springer Verlag, 1984.
5 K. D. Kopple, *J. Pharm. Sci.*, 1972, **61**, 1345.
6 C. Barré, P. Le Grel, A. Robert and M. Baudy-Floc'h, *J. Chem. Soc., Chem. Commun.*, 1994, 607.
7 Y. S. Klausner and M. Bodansky, *Synthesis*, 1974, 549.
8 M. Waki and N. Izumiyia, *J. Am. Chem. Soc.*, 1967, **89**, 1278.
9 R. Paul and G. W. Anderson, *J. Am. Chem. Soc.*, 1960, **82**, 4596; B. Neises and W. Steglich, *Angew. Chem., Int. Ed. Engl.*, 1978, **17**, 522; B. Castro, J. R. Dormoy, G. Evin and C. Selve, *Tetrahedron Lett.*, 1975, 1219; R. Knorr, A. Trzeciak, W. Bannwarth and D. Gillessen, *Tetrahedron Lett.*, 1989, **30**, 1927.
10 Epoxides **1** were prepared in a two step procedure. For the first one, a Knoevenagel–Cope condensation, see P. D. Gardner and R. L. Brandon, *J. Org. Chem.*, 1957, **22**, 1704. For the second step, a stereospecific epoxidation of the alkene by sodium hypochlorite, see M. Baudy, A. Robert and A. Foucaud, *J. Org. Chem.*, 1978, **43**, 3732.
11 P. Le Grel, M. Baudy-Floc'h and A. Robert, *Synthesis*, 1987, 306.
12 P. LeGrel, M. Baudy-Floc'h and A. Robert, *Tetrahedron*, 1988, **44**, 4805.
13 M. M. Lenman, S. L. Ingham and D. Gani, *Chem. Commun.*, 1996, 85.
14 M. Marraud, V. Dupont, V. Grand, S. Zerkout, A. Lecoq, G. Boussard, J. Vidal, A. Collet and A. Aubry, *Biopolymers*, 1993, **33**, 1135.

*Received in Glasgow, UK, 6th February 1997; 7/01932G*

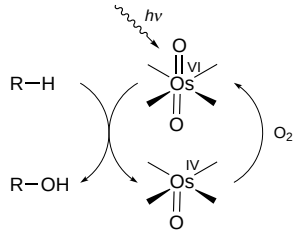
# Photocatalytic and aerobic oxidation of saturated alkanes by a neutral luminescent *trans*-dioxoosmium(VI) complex $[OsO_2(CN)_2(dpphen)]$

**Jack Y. K. Cheng,[a] Kung-Kai Cheung,[a] Chi-Ming Che*[a] and Tai-Chu Lau[b]**

[a] *Department of Chemistry, The University of Hong Kong, Pokfulam Road, Hong Kong*
[b] *Department of Biology and Chemistry, City University of Hong Kong, Tat Chee Avenue, Kowloon Tong, Hong Kong*

**A neutral *trans*-dioxoosmium(VI) complex $[OsO_2(CN)_2(dpphen)]$ (dpphen = 4,7-diphenyl-1,10-phenanthroline) is prepared and characterized by X-ray crystal analysis; the excited state is long-lived, emissive and oxidizing [$E°(Os^{VI–V})$ = 2.15 V *vs*. NHE; lifetime = 0.95 μs; quantum yield = $5 \times 10^{-4}$; $\lambda_{em}$(max.) = 650 nm]; under UV–VIS irradiation and in the presence of dioxygen, cyclohexane is oxidized to cyclohexanol and cyclohexanone with a turnover number of 16; secondary C–H bonds of propane and primary C–H bonds of *n*-hexane are also oxidized.**

The search for new metal catalysts for aerobic oxidation of saturated alkanes has continued to receive general interest.[1] One approach to this area is to develop highly oxidizing metal–oxo complexes through irradiation with UV light as represented in Scheme 1.[2,3]




**Scheme 1**

Previous studies revealed that *trans*-$[Os^{VI}(tmc)O_2]^{2+}$ (tmc = 1,4,8,11-tetramethyl-1,4,8,11-tetraazacyclotetradecane) is capable of oxidizing a wide variety of organic substrates in acetonitrile upon UV–VIS irradiation.[2,4] However, the photoreduced product *trans*-$[Os^{II}(tmc)(MeCN)_2]^{2+}$ is stable with regard to aerobic oxidation back to the starting $[Os^{VI}(tmc)O_2]^{2+}$.[5] Herein is described a neutral *trans*-dioxoosmium(VI) complex $[OsO_2(CN)_2(dpphen)]$ **1** (dpphen = 4,7-diphenyl-1,10-phenanthroline) which can mediate photocatalytic oxidation of saturated alkanes in the presence of dioxygen.

Addition of dpphen in $CH_2Cl_2$ to a freshly prepared aqueous solution of $K_2[OsO_2(OH)_2(CN)_2]$[6] and in the presence of $NBu_4Cl$ at room temp. gave complex **1** in 85% yield.† A perspective view of the molecule is shown in Fig. 1.‡ Similarly to most octahedral *trans*-dioxoosmium(VI) complexes,[2d] the $OsO_2$ moiety is close to linear with the average Os–O distance and O=Os=O angle being 1.722(6) Å and 172.6(2)°, respectively.

Complex **1** is soluble in acetonitrile, dichloromethane and benzene. In MeCN, it shows an intense high energy absorption at $\lambda$ = 290 nm ($\varepsilon$ = 35 840 $dm^3\ mol^{-1}\ cm^{-1}$) and a shoulder at 360 (970). Compared with *trans*-$[Os^{VI}(tmc)O_2]^{2+}$, it has a much higher absorptivity in the UV region and this is attributed to the mixing of intraligand π–π* and spin-allowed $p_\pi(O^{2-})$–$d_{\pi^*}(Os^{VI})$ charge-transfer transitions.[7] In this regard, dpphen serves as an antenna for UV light. As with other *trans*-dioxoosmium(VI) complexes,[2] **1** is emissive in the solid state and in solution at room temp. Emission occurs at 635 nm with an excited state lifetime of 0.95 μs in MeCN. The $E_{0–0}$ value, estimated from the 77 K solid-state emission spectrum is 2.11 eV and the $E°(Os^{VI–V})$ by cyclic voltammetry in MeCN is 0.04 V *vs*. NHE. Using the equation, $E°(Os^{VI*–V}) = E°(Os^{VI–V}) + E_{0–0}$, the excited state is oxidizing with $E°(Os^{VI*–V})$ = 2.15 V *vs*. NHE. Upon excitation with UV–VIS light, **1** can oxidize saturated hydrocarbons such as cyclohexane, *n*-hexane, propane, adamantane and cumene. This features the first well defined metal–oxo complexes capable of oxidizing such unreactive C–H bonds. Results of photoreactions undertaken in MeCN or $CH_2Cl_2$ are summarized in Table 1. The organic products were either alcohols, ketones or aldehydes. The product yield for adamantane oxidation is low, presumably due to competitive secondary photochemical oxidation of the solvent by the excited osmium–oxo complex, the concentration of adamantane in $CH_2Cl_2$–MeCN being limited by its solubility. It is striking to find that the secondary C–H bonds of propane and primary C–H bonds of *n*-hexane could also be oxidized. Importantly, the oxidation of cyclohexane and *n*-hexane became catalytic in the presence of air. For cyclohexane oxidation, 16 turnovers were found after 12 h of reaction. The excited osmium–oxo species in this work has a significantly different reactivity from other highly oxidizing metal–oxo complexes. It is known that oxidation of adamantane by highly oxidizing Ru=O complexes takes place almost exclusively at the tertiary position.[8,9] In this work, both secondary and tertiary C–H bonds of adamantane were photochemically oxidized by **1**. Fur-

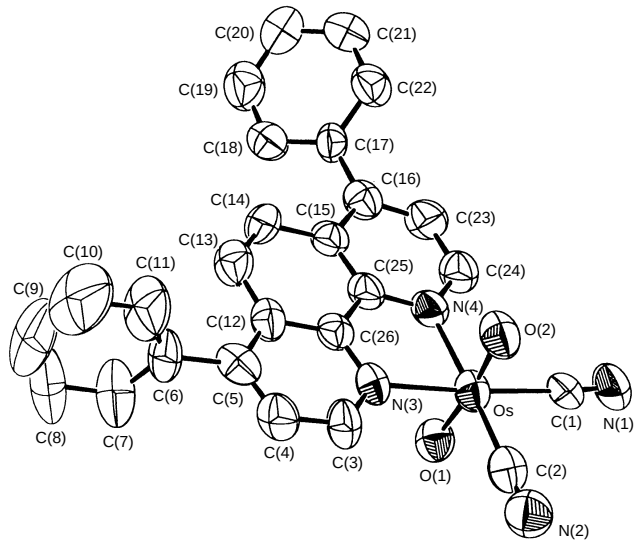



**Fig. 1** Perspective view of **1** (50% thermal ellipsoids): Os–O(1) 1.721(5), Os–O(2) 1.723(6), Os–N(3) 2.127(7), Os–N(4) 2.157(6), Os–C(1) 2.02(1), Os–C(2) 2.053(8); O(1)–Os–O(2) 172.6(2), O(1)–Os–N(3) 87.0(2), O(1)–Os–C(1) 92.7(3), O(2)–Os–N(3) 87.5(3), O(2)–Os–C(1) 94.4(4), N(3)–Os–N(4) 77.5(2), N(3)–Os–C(1) 176.3(3), N(3)–Os–C(2) 95.3(3), C(1)–Os–C(2) 88.4(3)

**Table 1** Photochemical oxidations of various organic substrates by **1**[a]

| Substrate | Solvent | Product(s) | Yield (%) (degassed) | Yield (%) (aerobic) |
|---|---|---|---|---|
| *n*-Hexane | MeCN (5 ml)–$CH_2Cl_2$ (2 ml) | Hexan-3-one | 26 | 160 |
| | | Hexan-2-one | 32 | 195 |
| | | Hexan-3-ol | 5 | 113 |
| | | Hexan-2-ol | 10 | 171 |
| | | Hexaldehyde } Hexan-1-ol } | 0.5 | 20 |
| Cyclohexane | MeCN (5 ml) | Cyclohexanol | 4 | 227[b] |
| | | Cyclohexanone | 35 | 225 |
| Cyclohexane | MeCN (5 ml)–$CH_2Cl_2$ (2 ml) | Cyclohexanol | 6 | 765[c] |
| | | Cyclohexanone | 30 | 800 |
| Propane | MeCN (4 ml)–propane (2 atm) | Propanone | 16.4 | |
| | | Propan-2-ol | 7.3 | |
| Cumene | $CH_2Cl_2$ (5 ml) | 2-Phenylpropan-2-ol | 115 | |
| | | Acetophenone | 77 | |
| Adamantane[d] | $CH_2Cl_2$ (8 ml)–MeCN (2 ml) | 1-Adamantanol | 10.6 | |
| | | 2-Adamantanol | 10.2 | |

[a] Complex **1** (30 mg for degassed and 10 mg for aerobic) was used with 5 ml of organic substrate; reaction time = 12 h. Yield based on **1** by GC analysis with an internal standard. [b] The yield for cyclohexanol and cyclohexanone after 2 days was 396 and 370%, respectively. [c] 2 atm $O_2$. [d] 0.2 g of adamantane used.

thermore, a small primary kinetic isotope effect ($k_H/k_D$) of *ca.* 2.2 was found for cyclohexane oxidation,which is smaller than that of 5.3 for $[Ru^{V}L(O)]^{2+}$ {HL = [2-hydroxy-2-(2-pyridyl)ethyl]bis[2-(2-pyridylethyl)]amine}.[10] The small kinetic isotopic effect and the lower tertiary C–H/secondary C–H selectivity suggests that the excited Os=O species could be regarded as a highly reactive 'ligated oxygen atom' species and Sawyer used the term 'oxene' to denote such a species.[11] A trace amount of cyclohexyl chloride was detected in the photochemical oxidation of cyclohexane in the presence of $CCl_4$.

An orange–brown solution was usually obtained after the photochemical reactions of **1** in MeCN, which slowly re-oxidized back to **1** by air. Interestingly, it gave an intense orange emission at 590 nm, the intensity of which is 20 times higher than the emission of **1** recorded under similar conditions. Our previous study revealed that $[Os^{II}I(CN)_2(X)_2L]$ complexes are highly emissive (quantum yield = 0.4–0.06) at similar energy (L = dpphen; $\lambda_{max}$/nm, X = $Me_2SO$, 625; $PPh_3$, 660).[12] We tentatively assign the photoproduct as $[Os^{II}(CN)_2(dpphen)(MeCN)_2]$. It is likely that the coordinated MeCN in $[Os^{II}(CN)_2(dpphen)(MeCN)_2]$ is more labile than in *trans*-$[Os^{II}(tmc)(MeCN)_2]^{2+}$, thus accounting the observed aerobic reoxidation of the former back to the starting *trans*-dioxoosmium(VI) complex. For the aerobic photochemical oxidations, there could be other reactive pathway(s) besides the one by the excited osmium–oxo species, since the cyclohexanone/cyclohexanol ratio for the aerobic and anaerobic oxidation of cyclohexane are different (1 : 1 *cf.* 10 : 1).

We acknowledge support from the University of Hong Kong, the Croucher Foundation, and the Hong Kong Research Grants Council.

## Footnotes

* E-mail: cmche@hkucc.hku.uk

† Proton NMR ($CDCl_3$): $\delta$ 10.17 (d, 2), 8.24 (s, 2), 8.10 (d, 2), 7.69–7.52 (m, 5). IR (Nujol): $\nu$ (Os=O) 856.1 $cm^{-1}$. UV–VIS: $\lambda$/nm ($\varepsilon$/$dm^3$ $mol^{-1}$ $cm^{-1}$), 290 (35 835), 330(sh) (8492), 367(sh) (966).

‡ *Crystal data*: $C_{26}H_{16}N_4O_2Os$, $M_r$ = 606.64, orthorhombic, space group *Pbca* (no. 61), $a$ = 27.385(4), $b$ = 13.025(2), $c$ = 12.635(2) Å, $U$ = 4508(1) $Å^3$, $Z$ = 8, $D_c$ = 1.788 g $cm^{-3}$, $\mu$(Mo-K$\alpha$) = 56.86 $cm^{-1}$, $F$(000) = 2336, $T$ = 301 K. A brown crystal of dimensions 0.20 × 0.15 × 0.30 mm was used for data collection on a Rigaku AFC7R diffractometer with graphite monochromatized Mo-K$\alpha$ radiation ($\lambda$ = 0.71073 Å) using $\omega$–2$\theta$ scans with $\omega$-scan angle (0.63 + 0.35 tan$\theta$)° at a scan speed of 4.0 $min^{-1}$. 4452 reflections were uniquely measured, of which 2307 reflections with $I > 1.5\sigma(I)$ were considered observed and used in the structural analysis. A crystallographic asymmetric unit consists of one molecule and all 33 non-H atoms were refined anisotropically. 16 H atoms at calculated positions with thermal parameters equal to 1.3 times that of the attached C atoms were not refined. Convergence for 298 variable parameters by least-squares refinement on $F$ with $\omega = 4F_o^2/\sigma^2(F_o^2)$, where $\sigma^2(F_o^2) = [\sigma^2(I) + (0.018F_o^2)^2]$ for 2307 reflections with $I > 1.5\sigma(I)$ was reached at $R$ = 0.035 and $R_w$ = 0.030 with a goodness-of-fit of 1.32 ($\Delta/\sigma_{max}$ = 0.01). CCDC 182/509.

## References

1 S. Davis and R. S. Drago, *J. Chem. Soc., Chem. Commun.*, 1990, 250; D. N. Hendrickson, M. G. Kinnaird and K. S. Suslick, *J. Am. Chem. Soc.*, 1987, **109**, 1243.
2 (*a*) C. M. Che, V. W. W. Yam, K. C. Cho and H. B. Gray, *J. Chem. Soc., Chem. Commun.*, 1987, 948; (*b*) V. W. W. Yam and C. M. Che, *New. J. Chem.*, 1989, **13**, 707; (*c*) V. W. W. Yam and C. M. Che, *Coord. Chem. Rev.*, 1990, **97**, 93; (*d*) K. F. Chin, Y. K. Cheng, K. K. Cheung, C. X. Guo and C. M. Che, *J. Chem. Soc., Dalton Trans.*, 1995, 2967.
3 H. Arzoumanian, G. Agrifoglio, H. Krentzien and M. Capparelli, *J. Chem. Soc., Chem. Commun.*, 1995, 655.
4 C. Creutz and M. H. Chou, *Inorg. Chem.*, 1994, **33**, 3199; S. Schindler, E. W. Castner, C. Creutz and N. Sutin, *Inorg. Chem.*, 1993, **32**, 4200.
5 C. M. Che, W. K. Cheng and V. W. W. Yam, *J. Chem. Soc., Dalton Trans.*, 1990, 3095.
6 C. Sartori and W. Preetz, *Z. Anorg. Allg. Chem.*, 1989, 151.
7 V. M. Miskowski, H.B. Gray and M. D. Hopkins, *Adv. Transition Met. Chem.*, 1996, **1**, 159.
8 C. M. Che, V. W. W. Yam and T. C. W. Mak, *J. Am. Chem. Soc.*, 1990, **112**, 2284.
9 T. C. Lau and C. K. Mak, *J. Chem. Soc., Chem. Commun.*, 1995, 943; A. S. Goldstein, R. H. Beer and R. S. Drago, *J. Am. Chem. Soc.*, 1994, **116**, 2424; M. S. Thompson and T. J. Meyer, *J. Am. Chem. Soc.*, 1982, **104**, 5076.
10 C. M. Che, C. Ho and T. C. Lau, *J. Chem. Soc., Dalton Trans.*, 1991, 1259.
11 D. T. Sawyer, *Comments Inorg. Chem.*, 1990, **10**, 129.
12 J. Y. K. Cheng, K. K. Cheung and C. M. Che, *J. Chem. Soc., Chem. Commun.*, 1997, **6**, 623.

*Received in Cambridge, UK, 30th January, 1997; 7/00702G*

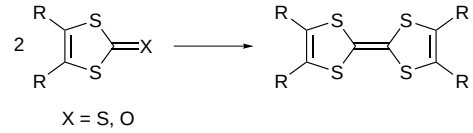
# Desulfurisation and ring opening of cyclic trithiocarbonates at a dimolybdenum centre

**Harry Adams, Matthew N. Bancroft and Michael J. Morris***

*Department of Chemistry, University of Sheffield, Sheffield, UK S3 7HF*

**The dimolybdenum alkyne complexes $[Mo_2(\mu\text{-}R^1C{\equiv}CR^1)(CO)_4(\eta\text{-}C_5H_5)_2]$ ($R^1$ = $CO_2Me$, Ph) react with 1,3-dithiole-2-thiones by cleavage of the C=S bond, ring opening of the resulting carbene and coupling with the alkyne ligand; one of the products, $[Mo_2(\mu\text{-}S)(\mu\text{-}SCR^2{=}CR^2SCCR^1CR^1)(\eta\text{-}C_5H_5)_2]$ ($R^1$ = $R^2$ = $CO_2Me$), is structurally characterised.**

The chemistry of 1,3-dithiole-2-thiones and related sulfur heterocycles has undergone a massive expansion in the last twenty years following the observation that certain charge-transfer salts of tetrathiafulvalene (TTF) and bis(ethylenedithio)-tetrathiafulvalene (BEDT-TTF) (and their selenium analogues) exhibit conducting and superconducting properties.[1–3] The coupling of two five-membered 1,3-dithiole rings to form the central double bond is an important step in most TTF syntheses (Scheme 1), and is usually performed with $P(OEt)_3$; however yields can be variable, and the reaction often works better if X = O than if X = S, thus necessitating an extra synthetic step as the thiones are usually more easily available. Some time ago, metal carbonyls, most successfully $[Co_2(CO)_8]$, were reported to effect desulfurisation and coupling of 1,3-dithiole-2-thiones to the corresponding TTF derivatives, with moderate yields.[4] In some cases, intermediate species were observed but no organometallic products were isolated.[5] We have therefore decided to examine the chemistry of such desulfurisation reactions with the ultimate aim of discovering an efficient, widely applicable reagent to effect thione coupling.



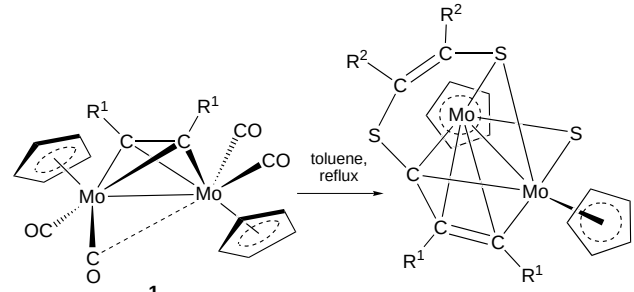

**Scheme 1**

During our investigation of the chemistry of the alkyne complexes $[Mo_2(\mu\text{-}R^1C{\equiv}CR^1)(CO)_4(\eta\text{-}C_5H_5)_2]$ **1** ($R^1$ = H, alkyl, aryl, $CO_2Me$, *etc*.), we have shown that their reactions with thiols differ markedly from those of the parent compounds $[Mo_2(CO)_n(\eta\text{-}C_5H_5)_2]$ ($n$ = 4, 6) in that C–S bond cleavage is a common occurrence, leading to sulfido-bridged complexes.[6,7] Here we demonstrate that cleavage of the C=S bond of 1,3-dithiole-2-thiones is also possible in this system, and moreover that it leads to the construction of novel sulfur-based ligands which incorporate the alkyne bridge.

Reaction of **1** ($R^1$ = $CO_2Me$) with 1 equiv. of 4,5-bis(carbomethoxy)-1,3-dithiole-2-thione **2a** in refluxing toluene over 5.5 h resulted in the formation of a single green product, **3a**, which was isolated by chromatography in 67% yield (Scheme 2). This complex displayed no metal carbonyl absorptions in its IR spectrum, and mass spectrometry indicated incorporation of one molecule of the heterocycle into the dimolybdenum complex with retention of the alkyne ligand. Its NMR spectra† displayed equivalent $C_5H_5$ ligands and four different methyl resonances (two of them coincident in the room-temperature $^1H$ NMR spectrum). Analogous complexes **3b** ($R^2$ = SMe) and **3c** ($R^2$ = SCOPh) were formed from **1** and heterocycles **2b** and **2c** {derived from methylation or acylation of $[NEt_4]_2[Zn(dmit)_2]$ respectively[2]} in comparable yields. Ethylene trithiocarbonate **4** also reacts with **1** to produce a similar complex, formulated as $[Mo_2(\mu\text{-}S)(\mu\text{-}SCH_2CH_2SCCR^1CR^1)(\eta\text{-}C_5H_5)_2]$ **5**, showing that a saturated group linking the two sulfur atoms can be tolerated. Non-cyclic trithiocarbonates such as $(BuS)_2C{=}S$ react with **1** over a longer time period to give closely related complexes, which will be described elsewhere.[8]

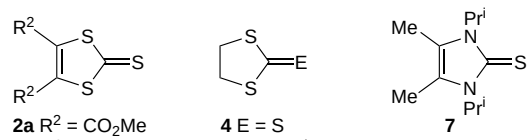
The result of an X-ray crystal structure determination of **3a** is shown in Fig. 1.‡ The two molybdenum atoms, which are linked by a rather short bond of 2.5825(7) Å, are bridged virtually symmetrically by the sulfur atom S(3), which has arisen through C=S bond cleavage of the thione group. The other bridging ligand is formed by ring opening of the five-membered heterocycle and linking of the original thione carbon to the alkyne; it is bonded through the bridging sulfur atom S(1) and through carbon atoms C(11)–C(13). This latter portion bridges the two metals in an allyl-type coordination, σ-bound to Mo(2) and π-bound to Mo(1). The observation of only one $C_5H_5$ resonance in the $^1H$ NMR spectrum of **3a** at both room temperature and low temperature (218 K) implies that there is a rapid fluxional process which interchanges the σ, π coordination modes of the allyl portion of the bridging ligand.

The newly assembled ligand is formally tetraanionic, with the result that the two molybdenum atoms are both formally $Mo^{IV}$. Indeed, the molecular geometry is strongly reminiscent of that found in the quadruply bridged $Mo^{IV}$ compounds $[Mo_2(\mu\text{-}S)_2(\mu\text{-}SMe)_2(\eta\text{-}C_5H_5)_2]$[9] and $[Mo_2(\mu\text{-}S)_2(\mu\text{-}SPr^i)(\mu\text{-}PPh_2)(\eta\text{-}C_5H_5)_2]$.[10] Thus, the atoms Mo(1), Mo(2), S(1) and C(11) form a plane (maximum deviation 0.0000 Å) which within experimental error intersects at an angle of 90° with the plane formed by Mo(1), Mo(2), S(3) and C(13) (maximum deviation 0.0176 Å).




**1**

**3a** $R^1$ = $R^2$ = $CO_2Me$
**b** $R^1$ = $CO_2Me$, $R^2$ = SMe
**c** $R^1$ = $CO_2Me$, $R^2$ = SCOPh
**d** $R^1$ = Ph, $R^2$ = $CO_2Me$



**2a** $R^2$ = $CO_2Me$
**b** $R^2$ = SMe
**c** $R^2$ = SCOPh

**4** E = S
**6** E = $NPr^i$

**7**

**Scheme 2**

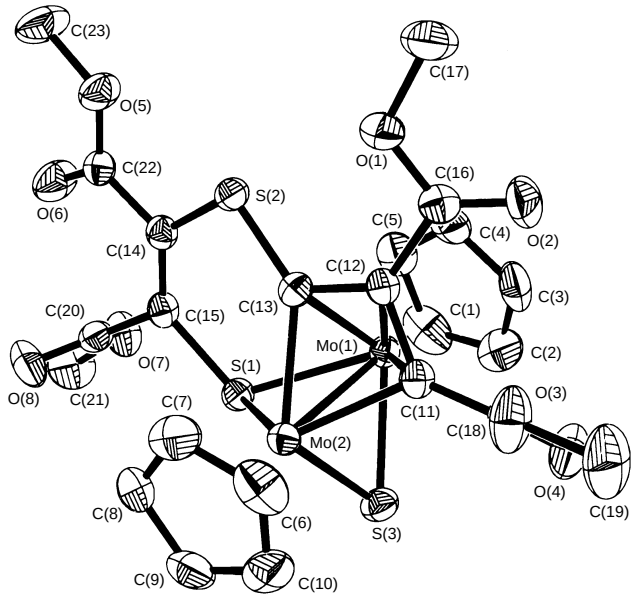



**Fig. 1** Molecular structure of complex **3a** in the crystal. Selected bond lengths (Å): Mo(1)–Mo(2) 2.5825(7), Mo(1)–S(3) 2.343(2), Mo(2)–S(3) 2.325(2), Mo(1)–S(1) 2.4594(14), Mo(2)–S(1) 2.471(2), Mo(1)–C(11) 2.176(5), Mo(1)–C(12) 2.360(5), Mo(1)–C(13) 2.223(5), Mo(2)–C(11) 2.162(5), Mo(2)–C(13) 2.200(5), C(11)–C(12) 1.416(7), C(12)–C(13) 1.415(7), C(14)–C(15) 1.349(7).

We propose that the initial step in the reaction is loss of a CO ligand and coordination of the heterocycle followed by cleavage of the C=S bond to produce the sulfido ligand and a coordinated dithiocarbene; coupling of the carbene ligand to the alkyne and ring opening by cleavage of one C–S bond would give the observed product. Dithiolium carbenes such as those derived from **2a**–**c** are pseudo-aromatic and thought to be relatively stable: they can be trapped in the reactions of $CS_2$ with activated alkynes[11] and can also be stabilised at a variety of metal centres.[12] Moreover formation of dithiocarbene ligands by desulfurisation of trithiocarbonates, including **4**, has previously been observed in reactions with iron carbonyls,[13] and an example of thioketone C=S bond cleavage at an alkoxide-ligated dimolybdenum centre leading to a bridging sulfido ligand and a terminal diarylcarbene has recently been reported.[14]

Further experiments to delineate the scope of the reaction have shown that all three sulfur atoms of the trithiocarbonate group appear to be necessary for successful product formation. Thus, neither the related 2-imino-1,3-dithiole **6** nor the tetraalkyl imidazole 2-thione **7** gave any tractable product. Changing the alkyne ligand in complex **1** also has a detrimental effect: so far only $[Mo_2(\mu\text{-}C_2Ph_2)(CO)_4(\eta\text{-}C_5H_5)_2]$ has given an analogous complex $[Mo_2(\mu\text{-}S)\{\mu\text{-}SC(CO_2Me)=C(CO_2Me)\text{-}SCCPhCPh\}(\eta\text{-}C_5H_5)_2]$ **3d** on treatment with **2a**.

Further studies on the reactivity of these novel compounds are currently in progress.

We thank the EPSRC for a studentship (M. N. B.).

## Footnotes

* E-mail: M.Morris@sheffield.ac.uk

† *Spectroscopic data* (NMR in $CDCl_3$, all signals are singlets unless otherwise stated). Satisfactory elemental analyses were obtained for all new compounds.

**3a**: mp 200–203 °C. $^1$H NMR $\delta$ 5.75 (10 H, $C_5H_5$), 3.88 (3 H, Me), 3.87 (6 H, 2 × Me), 3.60 (3 H, Me); $^{13}$C NMR $\delta$ 173.4, 168.5, 164.1, 161.5 (all *C*$O_2$Me), 134.5, 132.6 (both *C*$CO_2$Me), 112.9, 111.4 (2 *C*$CO_2$Me), 108.4 (μ-C), 99.8 ($C_5H_5$), 53.3, 53.2, 52.8, 52.2 (all Me); MS *m/z* 715 ($M^+$), 572. **3b**: mp 200–202 °C. $^1$H NMR $\delta$ 5.78 (10 H, $C_5H_5$), 3.85, 3.58 (both 3 H, OMe), 2.52, 2.48 (both 3 H, SMe); $^{13}$C NMR $\delta$ 174.0, 161.9 (both *C*$O_2$Me), 137.0, 124.3 (both *C*SMe), 110.7, 110.4 (both *C*$CO_2$Me), 109.9 (μ-C), 99.7 ($C_5H_5$), 52.6, 52.0 (both OMe), 20.2, 19.8 (both SMe); MS *m/z* 691 ($M^+$), 572. **3c**: mp 168–170 °C. $^1$H NMR $\delta$ 7.96–7.37 (m, 10 H, Ph), 5.94 (10 H, $C_5H_5$), 3.85, 3.60 (both 3 H, Me); $^{13}$C NMR $\delta$ 189.3, 188.1 (both *C*OPh), 173.8, 161.5 (both *C*$O_2$Me), 136.4–127.6 (m, Ph), 136.2, 125.4 (both *C*SCOPh), 112.1, 110.7, 110.2 (2 *C*$CO_2$Me + μ-C), 100.2 ($C_5H_5$), 52.7, 52.1 (both Me); MS *m/z* 871 ($M^+$), 573. **5**: mp 172–173 °C. $^1$H NMR $\delta$ 6.03 (10 H, $C_5H_5$), 3.75, 3.48 (both 3 H, Me), 2.72, 2.29 (both m, 2 H, $CH_2$); $^{13}$C NMR $\delta$ 174.5, 162 3 (both *C*$O_2$Me), 123.1, 111.4 (both *C*$CO_2$Me), 104.6 (μ-C), 99.7 ($C_5H_5$), 52.2, 51.7 (both Me), 35.9, 29.8 (both $CH_2$); MS *m/z* 601 ($M^+$), 573.

‡ *Crystal data* for **3a**: $C_{23}H_{22}Mo_2O_8S_3$, $M$ = 714.47, monoclinic, space group $P2_1/c$ ($C_2^5h$, no. 14), $a$ = 17.994(4), $b$ = 8.4820(10), $c$ = 16.713(4) Å, $\beta$ = 98.97(3)°, $U$ = 2519.6(9) Å$^3$, $F$(000) = 1424, Mo-Kα radiation ($\bar{\lambda}$ = 0.71073 Å), $\mu$(Mo-Kα) = 1.291 mm$^{-1}$, $Z$ = 4, $D_c$ = 1.883 g cm$^{-3}$.

Three-dimensional, room-temperature X-ray data were collected in the range $3.5 < 2\theta < 50°$ on a Siemens P4 diffractometer by the $\omega$-scan method. Of the 5513 reflections measured, all of which were corrected for Lorentz and polarisation effects and for absorption by the analysis of 10 azimuthal scans (minimum and maximum transmission coefficients 0.486 and 0.908), 3605 independent reflections exceeded the significance level $|F|/\sigma(|F|) > 4.0$. The structure was solved by direct methods and refined by full-matrix least-squares methods on $F^2$. Hydrogen atoms were included in calculated positions and refined in riding mode. Refinement converged at a final $R$ = 0.0393 ($wR_2$ = 0.1625 for all 4377 unique data, 325 parameters, mean and maximum $\delta/\sigma$ 0.000, 0.000), with allowance for the thermal anisotropy of all non-hydrogen atoms. Minimum and maximum final electron density −0.775 and 0.827 e A$^{-3}$. A weighting scheme $w = 1/[\sigma^2(F_o^2) + (0.0748P)^2 + 0.00P]$ where $P = (F_o^2 + 2F_c^2)/3$ was used in the latter stages of refinement. Complex scattering factors were taken from the program package SHELXL93[15] as implemented on the Viglen 486dx computer. CCDC 182/493.

## References

1 M. Narita and C. U. Pittman, Jr., *Synthesis*, 1976, 489; A. Krief, *Tetrahedron*, 1986, **42**, 1209; J. M. Williams, J. R. Ferraro, R. J. Thorn, K. D. Carlson, U. Geiser, H. H. Wang, A. M. Kini and M.-H. Whangbo, *Organic Superconductors: Synthesis, Structure, Properties and Theory*, Prentice Hall, Englewood Cliffs, NJ, 1992.
2 N. Svenstrup and J. Becher, *Synthesis*, 1995, 215.
3 P. Cassoux, L. Valade, H. Kobayashi, A. Kobayashi, R. A. Clark and A. E. Underhill, *Coord. Chem. Rev.*, 1991, **110**, 115; R. M. Olk, B. Olk, W. Dietzsch, R. Kirmse and E. Hoyer, *Coord. Chem. Rev.*, 1992, **117**, 99.
4 G. Le Coustumer and Y. Mollier, *J. Chem. Soc., Chem. Commun.*, 1980, 38; T. K. Hansen, I. Hawkins, K. S. Varma, S. Edge, S. Larsen, J. Becher and A. E. Underhill, *J. Chem. Soc., Perkin Trans. 1*, 1991, 1963.
5 A. Gorgues, P. Batail and A. Le Coq, *J. Chem. Soc., Chem. Commun.*, 1983, 405.
6 H. Adams, N. A. Bailey, S. R. Gay, T. Hamilton and M. J. Morris, *J. Organomet. Chem.*, 1995, **493**, C25.
7 H. Adams, N. A. Bailey, S. R. Gay, L. J. Gill, T. Hamilton and M. J. Morris, *J. Chem. Soc., Dalton Trans.*, 1996, 2403, 3341.
8 M. N. Bancroft and M. J. Morris, unpublished work.
9 M. Rakowski Dubois, M. C. Van Derveer, D. L. Dubois, R. C. Haltiwanger and W. K. Miller, *J. Am. Chem. Soc.*, 1980, **102**, 7456.
10 H. Adams, N. A. Bailey, A. P. Bisson and M. J. Morris, *J. Organomet. Chem.*, 1993, **444**, C34.
11 H. D. Hartzler, *J. Am. Chem. Soc.*, 1970, **92**, 1412, 1413; 1973, **95**, 4379.
12 H. Le Bozec, A. Gorgues and P. H. Dixneuf, *Inorg. Chem.*, 1981, **20**, 2486; M. Ngounda, H. Le Bozec and P. H. Dixneuf, *J. Org. Chem.*, 1982, **47**, 4000; H. Le Bozec and P. H. Dixneuf, *J. Chem. Soc., Chem. Commun.*, 1983, 1462.
13 A. Benoit, J. Y. Le Marouille, C. Mahe and H. Patin, *J. Organomet. Chem.*, 1982, **233**, C51; G. J. Kruger, L. Linford, H. G. Raubenheimer and A. A. Chalmers, *J. Organomet. Chem.*, 1984, **262**, 69; A. Lagadec, B. Misterkiewicz, A. Darchen, D. Grandjean, A. Mousser and H. Patin, *Organometallics*, 1988, **7**, 242.
14 T. A. Budzichowski, M. H. Chisholm and K. Folting, *Chem. Eur. J.*, 1996, **2**, 110.
15 G. M. Sheldrick, SHELXL93, An integrated system for solving and refining crystal structures from diffraction data, University of Göttingen, 1993.

*Received in Cambridge, UK, 14th May 1997; 7/03336B*

# Moulding a honeycomb framework around $[Co(\eta^5\text{-}C_5H_5)_2]^+$ *via* charge-assisted C–H···O hydrogen bonds

**Dario Braga,* Alessandro Angeloni, Fabrizia Grepioni and Emilio Tagliavini**

*Dipartimento di Chimica G. Ciamician, Università di Bologna, Via Selmi 2, 40126 Bologna, Italy*

**Strong O–H···O hydrogen bonds between $[(Hta)(H_2ta)]^-$ anions derived from D,L-tartaric acid $[H_2ta]$ hold together a honeycomb superanion templated around the cation $[Co(\eta^5\text{-}C_5H_5)_2]^+$ *via* charge-assisted C–H···O hydrogen bonds.**

Organic–organometallic crystal engineering is a means to combine physical and chemical features of organic and organometallic molecules and ions in the solid state. Organic–organometallic crystals can be constructed by taking advantage of the complementary role of strong and directional O–H···O hydrogen bonds to selectively and tightly link together organic molecules, and of diffuse networks of C–H···O hydrogen bonds and anion–cation interactions to link the organic and organometallic fragments in the crystal.[1]

Along this line, we have designed, synthesized and characterized supramolecular aggregates of the paramagnetic cations $[Cr(\eta^6\text{-arene})_2]^+$ (arene = benzene and toluene) with cyclohexane-1,3-dione (CHD). The aggregation of the CHD systems in superanions is based on strong hydrogen bonds, whereas the interaction between organic fragments and organometallic complexes is based on weak C–H···O hydrogen bonds reinforced by the different polarity.[2] The participation of water oxygens in C–H···$O_{water}$ bonds has been evidenced by the structure of the hydrated $[Cr(C_6H_6)_2][CHD]\cdot 3H_2O$ and by the polar structure of the hydrated hydroxide $[Cr(C_6H_6)_2]OH\cdot 3H_2O$.[3]

Here we report that the reaction of the hydroxide $[Co(\eta^5\text{-}C_5H_5)_2]OH$ with D,L-tartaric acid $[H_2ta]$ in water (or THF) affords the novel supramolecular systems $[Co(\eta^5\text{-}C_5H_5)_2]^+[(Hta)(H_2ta)]^-$ **1** and $[Co(\eta^5\text{-}C_5H_5)_2]^+[Hta]^-\cdot H_2O$ **2** depending on the stoichiometric ratio between cobaltocenium hydroxide and tartaric acid. The hydroxide is obtained *in situ* by bubbling oxygen through a water solution of cobaltocene.† Crystals suitable for X-ray diffraction‡ are obtained by evaporation of the solvent in the air at room temp.

The cobaltocenium cation in crystalline **1** is encapsulated within an anionic organic honeycomb framework (Fig. 1) of stoichiometry [tartrate·tartaric acid]$_n$ generated by the aggregation of dimeric monoanions $[(Hta)(H_2ta)]^-$. The supramolecular monoanion $[(Hta)(H_2ta)]^-$ is formed as a consequence of the loss of one proton every two tartaric acid molecules, with the two units bonded *via* a strong –C(O)O–H···O(O)C– hydrogen bond [2.434(1) Å]. The dimers are then linked in the honeycomb framework *via* O–H···O bonds involving the two external carboxyl groups and the hydroxyl groups. The interaction between the supramolecular anionic network and the encapsulated $[Co(\eta^5\text{-}C_5H_5)_2]^+$ cations occurs *via* C–H···O hydrogen bonds[4] between the staggered cyclopentadienyl ligands of the cations and the –CO and the –OH groups of the anionic framework. Six independent C–H···O interactions are observed in the range 2.10–2.35 Å.† These values fall towards the lower limit for interactions of this type clearly indicating that the electrostatic interaction $C\text{–}H^{\delta+}\cdots O^{\delta-}$ is reinforced by the difference in charge between host and guest.[5]

The umbalance between the number of –OH and C=O acceptor sites and the number of 'conventional' donors (four –OH groups out of five participate in intramolecular –OH···O bonds) is likely to be the driving force towards aggregation around the $[Co(\eta^5\text{-}C_5H_5)_2]^+$ cations in **1**.

If the stoichiometry ratio between $[Co(\eta^5\text{-}C_5H_5)_2]OH$ and tartaric acid in the acid–base reaction is changed from 1 : 2 to 1 : 1, the hydrated crystalline salt $[Co(\eta^5\text{-}C_5H_5)_2]^+[Hta]^-\cdot H_2O$ **2** is obtained. In contrast to **1**, the $[Co(\eta^5\text{-}C_5H_5)_2]^+$ cations are in eclipsed conformation. Crystalline **2** can be described as a layered structure in which a corrugated anionic network of $[Hta]^-$ ions and water molecules alternates with layers of cobaltocenium cations (Fig. 2). The water molecules form O–H···O hydrogen-bond tetramers involving two hydroxyl groups of two neighbouring tartrate anions. As in **1**, the

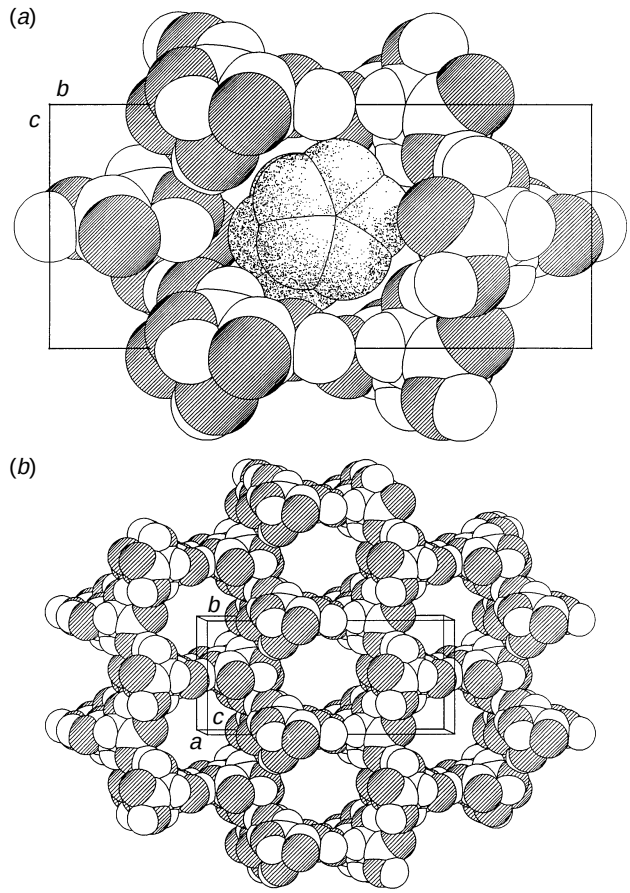



**Fig. 1** (*a*) Space-filling representation of the tartaric acid template in crystalline $[Co(\eta^5\text{-}C_5H_5)_2]^+[(Hta)(H_2ta)]^-$ **1**. (*b*) Space-filling representation of the anionic honeycomb framework formed by the $[(Hta)(H_2ta)]^-$ units, the cobaltocenium cations pile inside the channels extending along the *a*-axis. Relevant hydrogen-bonding parameters (in Å; O···O < 2.8, C–H···O < 2.5): intra, $O_{OH}\cdots Q_{CO)OH}$ 2.711, 2.638; inter, $O_{OH}\cdots Q_{CO)OH}$ 2.677; $O_{OH}\cdots Q_{OH}$ 2.776; $O^-\cdots Q_{OH}$ 2.434; $C\text{–}H_{Cp}\cdots O$ 2.396, 2.302, 2.333, 2.097, 2.354, 2.341, 2.253.† Relevant bonding parameters (in Å): mean Co–C 2.042(4); C=O 1.197(3), 1.222(3); $C{=}O_{(CO)OH}$ 1.319(2), 1.280(3); $C\text{–}O_{OH}$ 1.415(2), 1.417(2); mean C–C 1.521(6).

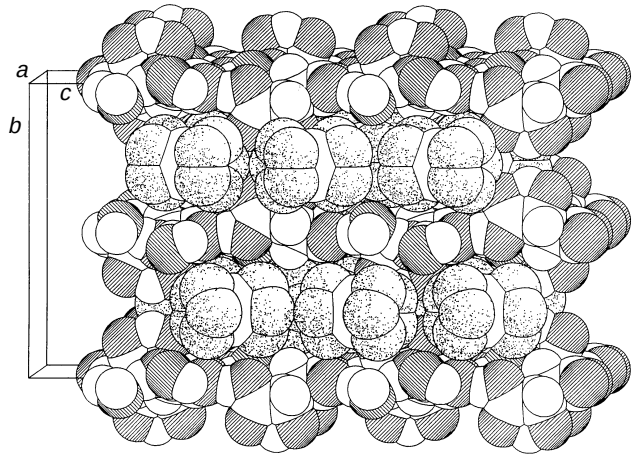



**Fig. 2** Space-filling outline of the layered structure in crystalline $[Co(\eta^5\text{-}C_5H_5)_2]^+[Hta]^-\cdot H_2O$ **2**. Relevant hydrogen bonding parameters (in Å, O···O < 2.8, C–H···O < 2.5 Å): intra $O_{OH}\cdots O_{CO/O^-}$ 2.550, 2.640; inter $O_{(CO)OH}\cdots O_W$ 2.725; $O_{OH}\cdots O_W$ 2.640, 2.784; $O^-\cdots O_{OH}$ 2.479; $C\text{–}H_{Cp}\cdots O$ 2.222, 2.338, 2.238, 2.425, 2.445. Relevant bonding parameters (in Å): mean Co–C (over the two cations) 2.016(10); mean $C_{Cp}\text{–}C_{Cp}$ 1.394(19); C=O 1.225(8), 1.220(8); $C\text{–}O_{(CO)OH}$ 1.279(8), 1.251(8); $C\text{–}O_{OH}$ 1.402(8), 1.410(8); mean C–C 1.528(14).

interaction between anion and cation is based on C–H···O hydrogen bonds (of which three in the range 2.20–2.35 Å) between the cyclopentadienyl hydrogens and the –OH and $–CO_2H$ groups. Interestingly, the two sets of C–H···O bonds in **1** and **2** stabilize, respectively, the staggered and eclipsed conformations of the organometallic cation.

With this study we have provided evidence that charge-assisted C–H···O hydrogen bonds can be used to mould O–H···O hydrogen-bond networks around organometallic cations. We have also demonstrated that it is possible to promote supramolecular aggregation of common organic acids *via* acid–base reaction with organometallic hydroxides produced *in situ*. This simple strategy opens a simple route to the preparation of a number of organic–organometallic crystalline aggregates.

Work is in progress to isolate and characterize other crystalline salts based on the utilization of chiral acids,[7] including natural amino acids, to obtain chiral organometallic crystals potentially useful for non-linear optical studies.[8]

Financial support by MURST and by the University of Bologna (project: intelligent molecules and molecular aggregates) is acknowledged.

## Footnotes

* E-mail: dbraga@ciam.unibo.it

† Powdered $[Co(\eta^5\text{-}C_5H_5)_2]$ (28 mg, 1.5 mmol) was added to 8 ml of bidistilled water at room temp. Oxygen was bubbled to completely oxidize cobaltocene into bright yellow $[Co(\eta^5\text{-}C_5H_5)_2]^+$. Powdered D,L-tartaric acid (45 mg, 3 mmol for **1**, 22.5 mg, 1.5 mmol for **2**) was then added and **1** and **2** were crystallized by evaporation at room temp. in air. The same materials can be obtained by oxidizing cobaltocene in THF at room temp. in the presence of the appropriate stoichiometric amount of solid D,L-tartaric acid. The resulting insoluble materials separate out as yellow solids, which were filtered off and dissolved in a minimum quantity of water for recrystallization. The reaction in THF very likely proceeds *via* formation of the peroxide anion $\{[Co(\eta^5\text{-}C_5H_5)_2] + O_2 \rightarrow [Co(\eta^5\text{-}C_5H_5)_2]^+ + O_2^{\cdot -}\}$ which deprotonates the acid as in the reaction between $[Cr(\eta^6\text{-}C_6H_6)_2]$ and cyclohexane-1,3-dione.[2b]

‡ *Crystal data*: $[Co(\eta^5\text{-}C_5H_5)_2]^+[(Hta)(H_2ta)]^-$ **1**: $C_{18}H_{21}CoO_{12}$, $M$ = 488.28, monoclinic, space group $P2_1/n$, $a$ = 6.589(2), $b$ = 18.210(4), $c$ = 8.208(2) Å, $\beta$ = 92.19(2)°, $U$ = 984.1(4) Å$^3$, $Z$ = 2, $D_c$ = 1.648 g cm$^{-3}$, $F(000)$ = 504, $\mu$ = 0.939 mm$^{-1}$, $\theta$ range 3.0–28°, 2606 reflections measured, 2362 of which were independent, refinement on $F^2$ for 169 parameters, $R_w$ ($F^2$, all reflections) = 0.0920, $R_1$ [1839 reflections with $I > 2\sigma(I)$] = 0.0333. Two disordered positions were found for the cyclopentadienal rings with site occupancy of 0.60 and 0.40, respectively that did not change with temperature indicating a static disorder. The two orientations correspond to two alternative sets of C–H···O interactions.

$[Co(\eta^5\text{-}C_5H_5)_2]^+[Hta]^-\cdot H_2O$ **2**: $C_{14}H_{17}CoO_7$, $M$ = 356.21, orthorhombic, space group *Pnma*, $a$ = 12.048(9), $b$ = 16.683(5), $c$ = 14.458(5) Å, $U$ = 2906(2) Å$^3$, $Z$ = 8, $D_c$ = 1.628 g cm$^{-3}$, $F(000)$ = 1472, $\mu$ = 1.214 mm$^{-1}$, $\theta$ range 3.0–28°, 3353 reflections measured, 3050 of which were independent, refinement on $F^2$ for 209 parameters, $R_w$ ($F^2$, all reflections) = 0.1778, $R_1$ [1153 reflections with $I > 2\theta(I)$] = 0.0526. Common to both compounds: graphite monochromated Mo-Kα radiation, $\lambda$ = 0.71069 Å, $T$ = 223(2) K. All non-H atoms were refined anisotropically. (O)H atoms directly located from Fourier maps and not refined. H atoms bound to C atoms were added in calculated positions. The computer programs SHELX86[6a] and SHELXL92[6b] were used for structure solution and refinement. The computer program SCHAKAL92 was used for all graphical representations.[6c] In order to evaluate the C–H···O bonds the C–H distances were normalized to the neutron derived value of 1.08 Å. CCDC 182/492.

## References

1 D. Braga and F. Grepioni, *Acc. Chem. Res.*, 1994, **27**, 51; *Chem. Commun.*, 1996, 571.
2 (*a*) D. Braga, F. Grepioni, J. J. Byrne and A. Wolf, *J. Chem. Soc., Chem. Commun.*, 1995, 1023; (*b*) D. Braga, A. L. Costa, F. Grepioni, L. Scaccianoce and E. Tagliavini, *Organometallics*, 1997, **16**, 2070.
3 D.Braga, A. L. Costa, F. Grepioni, L. Scaccianoce and E. Tagliavini, *Organometallics*, 1996, **15**, 1084.
4 G. R. Desiraju, *Acc. Chem. Res.*, 1991, **24**, 290; 1996, **29**, 441.
5 T. Steiner, *Cryst. Rev.*, 1996, **6**, 1; P. Gilli, V. Bertolasi, V. Ferretti and G. Gilli, *J. Am. Chem. Soc.*, 1994, **116**, 909.
6 (*a*) G. M. Sheldrick, *Acta Crystallogr., Sect. A*, 1990, **46**, 467; (*b*) G.M. Sheldrick, SHELXL92, Program for Crystal Structure Determination; University of Göttingen, Göttingen, 1992; (*c*) E. Keller, SCHAKAL92 Graphical Representation of Molecular Models, University of Freiburg, 1992.
7 D. Braga, A. Angeloni, F. Grepioni and E. Tagliavini, *Organometallics*, submitted.
8 N. J. Long, *Angew. Chem., Int. Ed. Engl.*, 1995, **34**, 21.

*Received in Basel, Switzerland, 3rd March 1997; 7/01484J*

# Dependence of metal-to-metal distances on Mo–Mo multiple bond orders; a new triple bond

**F. Albert Cotton,*[a] Lee M. Daniels,[a] Carlos A. Murillo,*[a,b] and Daren J. Timmons[a]**

[a] *Laboratory for Molecular Structure and Bonding, Department of Chemistry, Texas A&M University, College Station, TX 77843-3255, USA*

[b] *Department of Chemistry, Universidad de Costa Rica, Ciudad Universitaria, Costa Rica*

**A paddlewheel compound with a triply bonded $Mo_2^{6+}$ core is reported and used to reexamine and correct a previously reported $Mo_2^{5+}$ distance that was too long.**

The question of how the Mo–Mo distance will change when the formal Mo–Mo bond order changes in the range of three to four is not quite as simple as might naively be expected.[1] The reason is that the usual way of changing bond order also changes the average oxidation state of the metal atoms in the $Mo_2^{n+}$ core, and this in itself also affects the strength of the Mo–Mo bond. Specifically, in going through the series $Mo_2^{4+}$, $Mo_2^{5+}$, $Mo_2^{6+}$, the bonding electron configuration changes in the order $\sigma^2\pi^4\delta^2$, $\sigma^2\pi^4\delta$, $\sigma^2\pi^4$, which should progressively weaken the bond. However, in the same series, the increased charge should contract the σ and π orbitals of the metal atoms, thus also weakening the bond.† The two effects act in the same direction, so the net effect can be qualitatively predicted, namely, bond length will increase in the order $Mo_2^{4+}$, $Mo_2^{5+}$, $Mo_2^{6+}$. But by how much?

To approach the problem quantitatively, it is necessary to prepare compounds in which the core changes but the surrounding ligands do not. There has not heretofore been any such series for $Mo_2^{n+}$ although the series $[Mo_2(SO_4)_4]^{4-}$, $[Mo_2(SO_4)_4]^{3-}$, $[Mo_2(HPO_4)_4]^{2-}$ comes close.[2] The Mo–Mo distances in that case are 2.11, 2.17, 2.22 Å, respectively. The $SO_4^{2-}$ and $HPO_4^{2-}$ ligands are rather hard and would not tend to compensate very much for the effect of increasing charge, and thus the charge effect might be contributing as much (or more) than the bond order effect in this series.

One would predict that in a similar series where the ligands are much softer (more basic and/or more polarizable) the charge effect would be mitigated and the net changes would be smaller and due more to the bond order changes. We have now obtained a compound that allows us to test this prediction and correct a recently published report. This compound is $[Mo_2(hpp)_4(BF_4)_2]\cdot 4CH_2Cl_2$,‡,§ **1**$\cdot 4CH_2Cl_2$, and its structure¶ is presented in Fig. 1.

We have previously[3] prepared and structurally characterized the neutral molecule $[Mo_2(hpp)_4]$ and found the Mo–Mo bond (of order 4) to have a length of 2.067(1) Å. Thus, as shown in Table 1, the change in going from bond order 4 to bond order 3 is +0.075 Å. Similarly, earlier work in this laboratory[4] showed that with the very similar ligand, $[(p\text{-}C_6H_4Me)NC(H)N(p\text{-}C_6H_4Me)]^-$, the change in going from the neutral (quadruply bonded) compound to the +1 cation is 0.037 Å (see Table 1). Thus, the changes found on going from the $Mo_2^{4+}$ to $Mo_2^{5+}$ to $Mo_2^{6+}$ species with soft, basic ligands are only about 60% of those with the hard ligands.

However, Table 1 also shows a disturbing observation: the difference in the Mo–Mo distance in a recently reported guanidinate derivative is 0.206 Å in changing from $Mo_2^{4+}$ to $Mo_2^{5+}$.[5] Is our prediction incorrect?

A careful analysis of the supporting information provided with the structural report of the cationic guanidinate complex

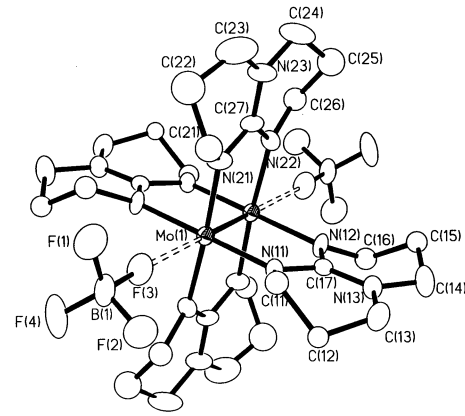



**Fig. 1** A drawing of the centrosymmetric ionic compound **1** showing the atom labelling scheme and displacement ellipsoids at the 30% probability level. The hpp ligands are conformationally disordered; only one orientation is shown. Selected bond distances (Å) are Mo(1)–Mo(1′) 2.142(2), Mo–N(11) 2.075(7), Mo(1)–N(21) 2.088(8), Mo(1′)–N(22) 2.073(8), Mo(1′)–N(12) 2.083(7), Mo(1)···F(3) 2.768(6).

**Table 1** Variations of the Mo–Mo and Mo–N distances (Å) for dimolybdenum species bridged by amidinate ligands and differences in the metal–metal distance between the corresponding cationic and neutral species

| Compound | Mo–Mo | Δ(Mo–Mo) cationic–neutral species | | Mo–N (av.) | Charge of $Mo_2^{n+}$ unit | Ref. |
|---|---|---|---|---|---|---|
| $[Mo_2(DTolF)_4]$[a] | 2.085(4) | 0.037 | | 2.17 | 4 | 4 |
| $[Mo_2(DTolF)_4]PF_6$ | 2.122(3) | | | 2.15 | 5 | 4 |
| $[Mo_2\{\mu\text{-}\eta^2\text{-}(NPh)_2CNHPh\}_4]$ | 2.0839(9) | 0.206 | 0.037 | 2.17 | 4 | 5 |
| $[Mo_2\{\mu\text{-}\eta^2\text{-}(NPh)_2CNHPh\}_4]BF_4$[b] | 2.290(1) | | | 2.14 | 5 | 5 |
| $[Mo_2\{\mu\text{-}\eta^2\text{-}(NPh)_2CNHPh\}_4]BF_4$[c] | 2.121(1) | | | 2.14 | 5 | [d] |
| $[Mo_2(hpp)_4]$ | 2.067(1) | 0.075 | | 2.16 | 4 | 3 |
| $[Mo_2(hpp)_4(BF_4)_2]$ | 2.142(2) | | | 2.08 | 6 | [d] |

[a] DTolF = N,N′-di-*p*-tolylformamidinate anion. [b] Uncorrected. [c] Corrected. [d] This work.

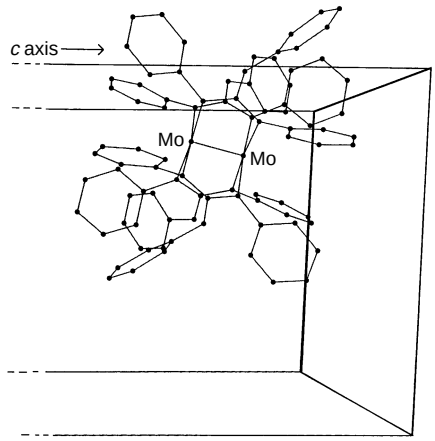



**Fig. 2** A drawing of one cation of the molecule $[Mo_2\{\mu\text{-}\eta^2\text{-}(NPh)_2CNHPh\}]BF_4$ (from ref. 5) in a box representing the unit cell, showing that the Mo–Mo unit is more or less aligned along the *c* axis

showed that the geometry of the phenyl groups in the ligands had significant distortions. In many cases the C–C distances were as long as 1.50 Å; the internal C–C–C angles varied from 115 to 125°. Furthermore, a plot of the unit cell for this compound (Fig. 2) shows that the Mo–Mo units are nearly aligned parallel to the *c* axis. Significantly, most of the long C–C bonds of the phenyl groups were more or less along the same direction. We therefore suspected that an error had been made in the input data‖ of the *c* axis used for the calculation of the bond distances and angles. Indeed, when the length of 23.573(7) Å for the *c* axis reported in the abstract given in ref. 5 is used for the calculation of the bond distances and angles, as opposed to 25.573(7) Å given in their crystallographic data and subsequently used by Bailey *et al*. for their calculations, the phenyl rings are found to be very regular. The internal bond angles vary from 119 to 121° and the C–C distances are found in the normal range 1.36–1.41 Å. Such calculation gives a Mo–Mo distance of 2.121 Å which is entirely consistent with our prediction. We are currently working on the preparation of a compound containing the $[Mo_2(hpp)_4]^+$ species which we expect to have a Mo–Mo distance similar to that of the $[Mo_2(DTolF)_4]^+$ analog.

Support from the National Science Foundation and the University of Costa Rica is gratefully appreciated.

## Footnotes

* E-mails: cotton@tamu.edu; murillo@tamu.edn

† An equivalent explanation is that an increase in the metal charge also increases intermetal repulsions, an opposite effect to that observed for the metal-to-ligand interactions.

‡ hpp = 1,3,4,6,7,8-hexahydro-2*H*-pyrimido[1,2-a]pyrimidinate.

§ *Preparation*: Under a nitrogen atmosphere, a solution of $[Mo_2(hpp)_4]^3$ (0.74 g 1.0 mmol) in 15 ml $CH_2Cl_2$ was added to $AgBF_4^-$ (0.20 g 1.0 mmol). The reaction mixture was stirred for 30 min at room temp. and filtered. The resulting dark brown solution was carefully layered with hexanes. Within a few days, the slow diffusion of the layers afforded dark brown crystals of **1**·$4CH_2Cl_2$. Yield: 22% (based on $[Mo_2(hpp)_4]$); 44% (based on $AgBF_4$). Elemental analysis was satisfactory.

¶ *Crystal data* for **1**·$4CH_2Cl_2$: crystal dimensions 0.3 × 0.2 × 0.05 mm, $C_{32}H_{56}N_{12}B_2Cl_8F_8Mo_2$, $M$ = 1257.99, orthorhombic, space group *Pbca*, $a$ = 15.783(8), $b$ = 15.456(8), $c$ = 20.657(6) Å, $Z$ = 4, $D_c$ = 1.658 g cm$^{-3}$, $\mu$(Mo-K$\alpha$) = 0.991 mm$^{-1}$. Data were obtained at 213(2) K on a Nonius FAST diffractometer. A total of 3306 unique reflections were collected using ellipsoid-mask fitting within a $2\theta$ range of 4.72–45.1°. The structure was solved by direct methods and refined by full-matrix least squares using all 3301 reflections for 288 parameters. The hpp ligands are conformationally disordered and adjacent $CH_2$ groups deviate in opposite directions. Disordered atoms were refined isotropically. Chemically identical bonds were constrained to have identical distances. The final refinement converged to $R_1(F_o)$ = 0.081 and $wR_2(F_o^2)$ = 0.152. CCDC 186/528.

‖ Similar errors have been made before. See for example our earlier report: F. A. Cotton, L. M. Daniels, C. A. Murillo and X. Wang, *J. Am. Chem. Soc.*, 1996, **118**, 12449.

*Note added in proof*: We have been informed by the authors of ref. 5 that they concur with our discussion of the error in the bond length in their compound.

## References

1 F. A. Cotton and R. A. Walton, *Multiple Bonds between Metal Atoms*, Oxford University Press, 1993.
2 Ref 1, p. 632.
3 F. A. Cotton and D. J. Timmons, *Polyhedron*, in the press.
4 F. A. Cotton, X. Feng and M. Matusz, *Inorg. Chem.*, 1989, **28**, 594.
5 P. J. Bailey, S. F. Bone, L. A. Mitchell, S. Parsons, K. J. Taylor and L. J. Yellowlees, *Inorg. Chem*., 1997, **36**, 867.

*Received in Bloomington, IN, USA; 8th April 1997; 7/02384G*

# Supramolecular assembling of the cationic complex (2,2′:6′,2″-terpyridine)methylplatinum(II) ion on α-helical poly(L-glutamic acid)

**Luigi Monsu' Scolaro,* Andrea Romeo and Antonio Terracina**

*Dipartimento di Chimica Inorganica, Chimica Analitica e Chimica Fisica, Universita' di Messina, and Istituto di Chimica dei Prodotti Naturali (ICTPN-CNR), Sezione di Messina, Messina, Italy*

**The cationic organometallic platinum(II) complex ion [Pt(terpy)Me]$^+$ aggregates on α-helical poly(L-glutamic acid) through a multistep process leading to highly organised supramolecular assemblies.**

Planar dyes, such as porphyrins and acridines, bind to helical biopolymers leading to adducts which exhibit induced circular dichroism (ICD) in the wavelength region where the bound molecules absorb light.[1–3] The biological matrix acts as a template support for the formation of short- or long-range organised assemblies of chromophores, stabilised by an interplay of electrostatic, hydrogen bonding and dispersive forces. Different types of biopolymers have been reported to behave as template systems including double-stranded DNA,[3] single-stranded DNA and RNA[4] and polypeptides.[5,6] The kinetics of the supramolecular aggregation are in general multiphasic[7] and the use of simple matrices offers a way of reducing the difficulty in assessing the mechanism of interaction. In this respect, poly(glutamic acid) is an interesting biopolymer, because the only interaction modes are electrostatic and hydrogen bonding. Furthermore, it undergoes a transition from α-helix to random-coil above pH 5[8] so that it is possible to control the structure and the nature of the resulting adduct by modulating the pH and the ionic strength.

In a previous study,[9] we reported on the strong tendency for self-aggregation of the complex ion [Pt(terpy)Me]$^+$ **1** in contrast with the well studied [Pt(terpy)(het)]$^+$ (het = 2-hydroxyethanethiolate).[10] The addition of low concentrations of nucleic acids, such as DNA[9] or single-stranded poly(rA),[11] leads to a distribution of complex **1** between its free self-aggregated form in solution and on the backbone of the DNA. The very weak ICD and resonance light-scattering (RLS)[12] signals of these adducts indicate that the aggregation on these matrices is not well structured over extended lengths.

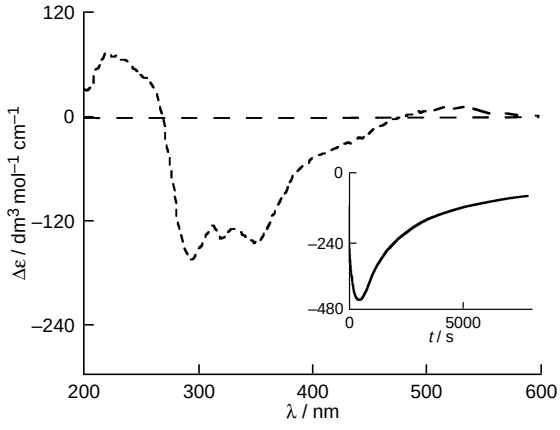
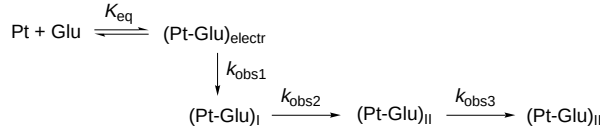



**Fig. 1** CD spectrum of the final adduct between the complex [Pt(terpy)-Me]Cl and poly(L-glutamate). The inset shows the kinetic trace recorded at 280 nm. Experimental conditions: [Pt] = $2.5 \times 10^{-5}$ M, [Glu] = $5 \times 10^{-5}$ M, pH 4.5 in 5 mM acetate buffer, $T$ = 298 K. ($k_{obs1}$ = 0.25 ± 0.03 s$^{-1}$, $k_{obs2}$ = 0.016 ± 0.002 s$^{-1}$, $k_{obs3}$ = 0.0008 ± 0.0001 s$^{-1}$, as derived from the best fitting analysis of the overall kinetic trace, see text).

Here we report a preliminary kinetic investigation of the interaction between **1** and the poly(L-glutamic acid) in the α-helical conformation. To the best of our knowledge this is the first example of a supramolecular aggregate formed by an organometallic platinum(II) complex.

On adding a solution of complex to a prethermostated solution of poly(L-glutamic acid) at pH 4.5,† the absorption spectrum shows an instantaneous and small bathochromic shift (< 2 nm) associated with a slight hypochromicity of the 313 and 331 nm bands of the complex. The spectral changes are rapidly masked by an increase in Rayleigh scattering. The time behaviour of the scattered intensity can be monitored by conventional light-scattering techniques and shows an initial rapid increase followed by slower steps. The time evolution of the process can be monitored more conveniently by CD spectroscopy (Fig. 1). On addition of the polymer, the sequence of CD spectra reveals a multiphasic process which involves the formation of at least four different species (Scheme 1), characterised by large values of $\Delta\varepsilon$ (*ca.* −180 dm$^3$ mol$^{-1}$ cm$^{-1}$ at 300 nm for the final adduct). Kinetic runs were performed at 280 nm (inset in Fig. 1) and were analysed as three coupled consecutive first-order steps. The initial CD spectral change is faster than the mixing time.




**Scheme 1**

The observed rate constants ($k_{obs1}$, $k_{obs2}$, $k_{obs3}$) exhibit a bell-shaped dependence on the concentration of the polymer (Fig. 2). The $k_{obs}$ values increase to reach a maximum corresponding to a ratio $r_f$ = 0.5 ($r_f$ = [Pt]$_o$/[poly(Glu)]$_o$). Therefore, when the concentration of the matrix is below a threshold, an increase of its concentration determines an acceleration of the rates, as a result of the increased availability of binding sites. A further increase of the concentration provokes a dispersion of the complex on the matrix and leads to a decrease in the rate. A similar concentration dependence is shown by the intensity of the ellipticity corresponding to the final adduct. In order to establish the importance of the α-helical conformation of the polymer, the dependence of the kinetic rate constants and ellipticity intensities on the pH was investigated. It has been found that these parameters exhibit, also in this case, a bell-shaped profile with the maximum centred at pH 4.5 and 4.8 for the rate and the ellipticity, respectively. An experiment performed at pH 7.0, well above the helix to coil transition, showed that the ICD spectrum is very weak and it is reversed in phase with respect to lower pH.[13]

According to the experimental findings, the following mechanism can be suggested (see Scheme 1). The first step

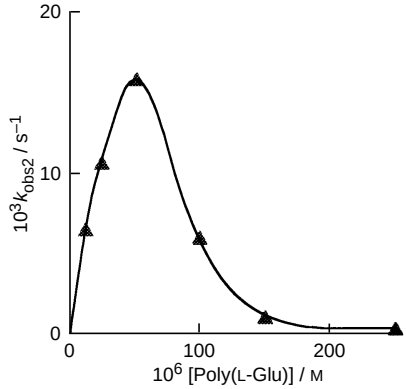



**Fig. 2** Dependence of the observed first-order rate constant ($k_{obs2}$/$s^{-1}$) for the second stage of the assembling on the concentration of poly(L-glutamate) (in molar glutamate residues). Experimental conditions: [Pt] = $2.5 \times 10^{-5}$ M, pH 4.5 in 5 mM acetate buffer, 298 K.

involves a fast electrostatic pre-equilibrium between oppositely charged species leading to a low-ordered adduct. The fairly high initial value of the ellipticity suggests the formation of dimers or higher aggregates (nucleation step). These small aggregates serve as promoters for the subsequent growth of the assembly. The following steps can be ascribed to conformational re-arrangements owing to changes in the relative orientation of the chromophores with respect to the matrix backbone or to a conformational change of the matrix itself caused by the aggregation.[14]

The reaction intermediate $(Pt–Glu)_{II}$ and the final adduct are characterised by large values of ellipticity. The value of $|\Delta\varepsilon/\varepsilon| \approx 2.3\%$ for the final adduct and resonance light scattering measurements[12] indicate the presence of extended arrays of strongly coupled chromophores forming a highly organised assembly in which the biopolymer acts as a template matrix.[5] A structural model for the supramolecular assembling can be inferred from the presence of maxima in the rate and ellipticity profiles, as shown by the glutamate concentration and pH dependences. At pH 4.5 the negative charges on the side chains are half-neutralised and, given the observed maxima at $r_f = 0.5$, a stoichiometric ratio of 1 : 1 (cationic complex to unprotonated glutamate residues) is indicated. Taking into account the translational rise of 1.5 Å for a residue in the α-helix,[15] it is possible to assume the presence of a negative charge every 3 Å. This distance is that expected for π–π stacking interactions between two terpyridine moieties.[16] Therefore, we are inclined to think that the polypeptide acts as template support to form an α-helix of chromophores, which is stabilised by electrostatic interactions with the polymer and by π–π stacking interactions between the aromatic region of the complexes.

The remarkable tendency to give supramolecular assemblies is peculiar to $[Pt(terpy)Me]^+$, as demonstrated by the fact that the closely related cation $[Pt(terpy)Cl]^+$, under the same experimental conditions, does not lead to any organised adduct. The higher hydrophobicity together with the higher extent of electron density on the metal center, in the case of the organometallic species, could be responsible for this behaviour.

The possibility of tuning the electronic and steric properties of the chromophore‡ and of the supporting biopolymer opens the way to control the molecular recognition between the interacting species.

We thank the CNR, MURST and a NATO grant #SRG 950676 for financial support. The authors are grateful to Professors Robert F. Pasternack and Raffaello Romeo for stimulating discussions.

## Footnotes

* E-mail: Monsu@chem.unime.it

† Poly(L-glutamic acid) was obtained from Sigma as its sodium salt ($M_W \approx 13\,600$; polydispersity = 1.2). The pH of the reaction mixtures was adjusted to the desired value using 5 mM acetate buffer.

‡ The organometallic compound [Pt(Phterpy)Me]Cl (Phterpy = 4′-phenyl-2,2′ : 6′,2″-terpyridine), under the same experimental conditions, leads to ICD spectra four times less intense than those of complex **1**, as a consequence of the steric congestion brought about by the phenyl substituent on the terpyridine ring. Steric effects are crucial in determining the behaviour of the complexes [Pt(terpy)Ph]Cl and [Pt(Phterpy)Ph]Cl, where the phenyl ring is directly bound to the metal center and out of the coordination plane. These latter compounds show no detectable interaction with the polypeptide.

## References

1 L. Stryer and E. R. Blout, *J. Am. Chem. Soc.*, 1961, **83**, 1411; R. E. Ballard, A. J. McCaffery and S. F. Mason, *Biopolymers*, 1966, **4**, 97; Y. Sato, M. Hatano and M. Yoneyama, *Bull. Chem. Soc. Jpn.*, 1973, **46**, 1980; Y. Sato and M. Hatano, *Bull. Chem. Soc. Jpn.*, 1973, **46**, 3339.

2 S. Ikeda, T. Nezu and G. Ebert, *Biopolymers*, 1991, **31**, 1257; T. Nezu and S. Ikeda, *Bull. Chem. Soc. Jpn.*, 1993, **66**, 25.

3 E. J. Gibbs, I. Tinoco, Jr., M. F. Maestre, P. A. Ellinas and R. F. Pasternack, *Biochem. Biophys. Res. Commun.*, 1988, **157**, 350; R. F. Pasternack, C. Bustamante, P. J. Collings, A. Giannetto and E. J. Gibbs, *J. Am. Chem. Soc.*, 1993, **115**, 5393; N. E. Mukundan, G. Petho, D. W. Dixon, M. S. Kim and L. G. Marzilli, *Inorg. Chem.*, 1994, **33**, 4676.

4 R. F. Pasternack, R. A. Brigandi, M. J. Abrams, A. P. Williams and E. J. Gibbs, *Inorg. Chem.*, 1990, **29**, 4483; R. F. Pasternack, S. Gurrieri, R. Lauceri and R. Purrello, *Inorg. Chim. Acta*, 1996, **246**, 7.

5 E. J. Gibbs and R. F. Pasternack, *J. Inorg. Organomet. Polym.*, 1993, **3**, 77.

6 P. Pancoska, M. Urbanova, L. Bednarova, K. Vacek, V. Z. Panschenko, S. Vasiliev, P. Malon and M. Kral, *Chem. Phys.*, 1990, **147**, 401.

7 G. Schwarz and W. Balthsar, *Eur. J. Biochem.*, 1970, **12**, 461; G. Schwarz and S. Kose, *Eur. J. Biochem.*, 1972, **29**, 249; G. Schwarz and A. Seelig-Loffler, *Biochim. Biophys. Acta*, 1975, **379**, 125; M. Tsuda, *Bull. Chem. Soc. Jpn.*, 1975, **48**, 1709; M. Dourlent and J. F. Hogrel, *Biopolymers*, 1976, **15**, 29; F. Watanabe, *Biopolymers*, 1977, **16**, 1827; K. Murakami, T. Sano, N. Kure, K. Ishii and T. Yasunaga, *Biopolymers*, 1983, **22**, 2035.

8 A. Wada, *Mol. Phys.*, 1960, **3**, 409; D. S. Olander and A. Holtzer, *J. Am. Chem. Soc.*, 1968, **90**, 4549.

9 G. E. Arena, L. Monsu' Scolaro, R. F. Pasternack and R. Romeo, *Inorg. Chem.*, 1995, **34**, 2994.

10 S. J. Lippard, *Acc. Chem. Res.*, 1978, **11**, 211 and references therein; J. K. Barton and S. J. Lippard, *Biochemistry*, 1979, **18**, 2661.

11 G. E. Arena, M. Casamento, L. Monsu' Scolaro and R. Romeo, unpublished work.

12 R. F. Pasternack and P. J. Collings, *Science*, 1995, **269**, 935.

13 At this pH the poly(glutamic acid) is reported as a left-handed helix; S. S. Birke, I. Agbaje and M. Diem, *Biochemistry*, 1992, **31**, 450.

14 B. Pispisa, M. Barteri and M. Farinella, *Inorg. Chem.*, 1983, **22**, 3166.

15 C. R. Cantor and P. R. Schimmel, in *Biophysical Chemistry, Part I*, W. H. Freeman and Co., New York, 1980, p. 91.

16 J. A. Bailey, M. G. Hill, R. E. Marsch, V. M. Miskowski, W. P. Schaefer and H. B. Gray, *Inorg. Chem.*, 1995, **34**, 4591.

*Received in Basel, Switzerland, 20th March 1997; 7/01972F*

# Molecular architecture *via* coordination: self-assembly of cyclic cationic porphyrin aggregates *via* transition-metal bisphosphane auxiliaries

**Peter J. Stang,* Jun Fan and Bogdan Olenyuk**

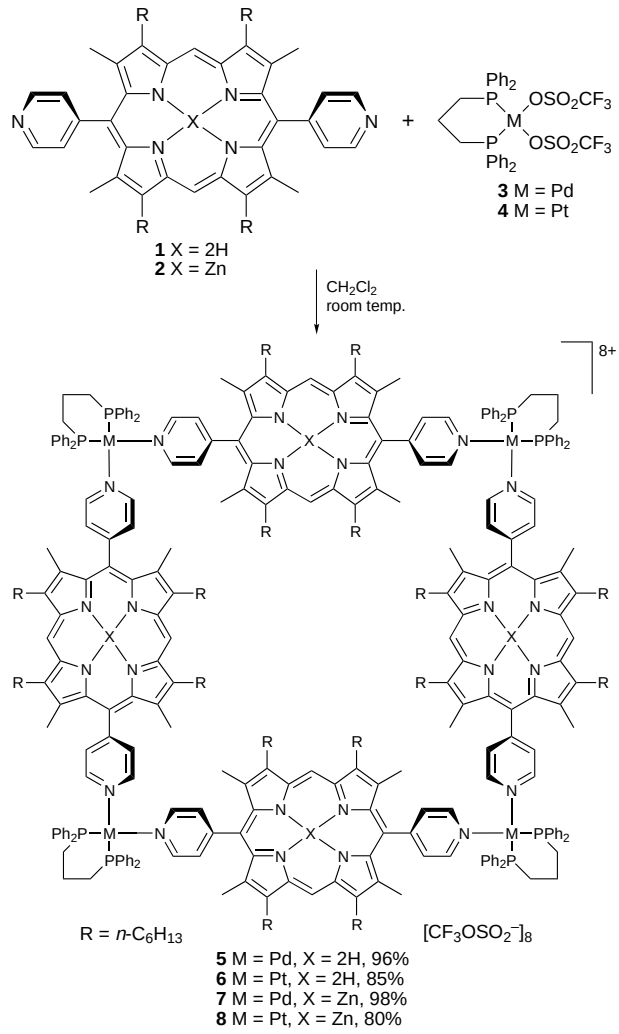
*Department of Chemistry, The University of Utah, Salt Lake City, Utah 84112, USA*

**Self-assembly and non-covalent interactions are employed for the preparation of a new family of cationic artificial supramolecular multiporphyrin aggregates incorporating $Pd^{II}$ and $Pt^{II}$ bisphosphane complexes as auxiliaries.**

Among the variety of naturally occurring self-assembling supramolecular species the photosynthetic reaction centre[1] and light harvesting complex of purple bacteria[2] represent excellent examples of well defined multichromophore aggregates whose structure and properties and most likely function are essentially determined by the nature and positioning of their constituent components. In recent years many examples of self-assembled multiporphyrin arrays were made by employing hydrogen bonding,[3] transition-metal-mediated self-coordination,[4] self-aggregation in non-polar organic solvents[5] as well as transition-metal-directed cyclic oligomerization[6] and threading,[7] to name only a few. Combined with recent advances in the studies of directional energy transport in chromophore-labelled supramolecular assemblies,[8] they provide useful insights in the development of a completely functional artificial photosynthetic centre. An intriguing way to further extend this topic is to construct a conformationally rigid photoactive aggregate with the constituent chromophores linked together or combined with redox-active species by employing coordination to square-planar late transition-metal (namely $Pd^{II}$ or $Pt^{II}$) bisphosphanes in a *cis*-manner. Such a tetranuclear assembly will have the geometry of a square with transition metals in the corners serving as the auxiliaries. Since both the chemistry and structure of many simple examples of such molecular square complexes are currently relatively well understood,[9,10] the possible application of this type of self-assembly principle to the construction of large multiporphyrin arrays is an especially attractive task. Herein, we report the formation, characterization and absorbance characteristics of several new cationic multiporphyrin aggregates based on these concepts.

We chose to prepare porphyrin[11] **1** and its Zn complex **2** for this study owing to their relatively straightforward preparation and, most important, high solubility in common organic solvents which facilitates the self-assembly process. Interaction of the porphyrin molecule **1** with the reactive bistriflates **3** or **4**,[9d] in dichloromethane at room temperature results in the formation of the desired tetranuclear complexes **5** and **6** in excellent isolated yields (Scheme 1).† These aggregates are isolated and characterized as air-stable robust (though hygroscopic) microcrystalline solids with high decomposition points. Their NMR spectra revealed several interesting features. Both the $^1H$ and $^{13}C$ NMR spectra indicate one set of signals for the pyridine rings but two sets for the porphyrin moiety with the second set being considerably high-field shifted. The $^{31}P$ NMR of **5** and **6** however, show a single signal, supporting the formation of a single highly symmetrical entity. Compared to the starting bistriflates **3** and **4**, these $^{31}P$ signals are shifted upfield by *ca*. 10 ppm, indicative of the coordination of the nitrogen lone pair to the transition metal.‡ Taken together, these data suggest that (*i*) the porphyrin moieties in **1** are restricted in rotation around both the pyridine–porphyrin and the metal–pyridine nitrogen bonds[12] and (*ii*) the porphyrin rings are most likely coplanar with respect to each transition-metal coordination plane.§ As a consequence, each porphyrin moiety has part of the ring located 'inside' the cyclic tetranuclear assembly, which therefore is subject to the ring current effects formed by the entire large cyclic assembly as no such high-field shifts are observed for more common acyclic porphyrin aggregates and oligomers.[13] Moreover, molecular models indicate that the individual porphyrin units are coplanar and located too far apart from each other to be influenced by the ring currents of their neighbours (Fig. 1).[14]¶ These considerations along with the above discussed NMR spectroscopic data confirm the cyclic nature of aggregates **5** and **6**.

When the Zn complex of porphyrin **2** was employed under these self-assembly conditions the heterobimetallic assemblies **7** and **8** were isolated (Scheme 1). Interestingly, in the absence of the transition metal auxiliary the Zn-porphyrin **2** itself exists in solution mainly as a mixture of self-coordinated oligomers.




**Scheme 1**

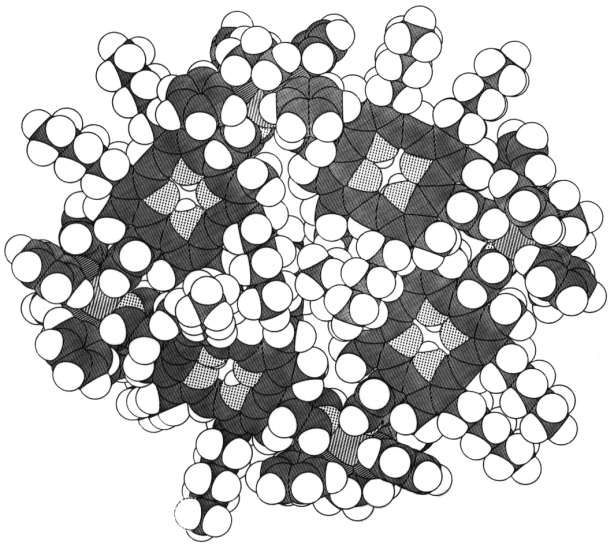


**Fig. 1** Space-filling model of tetramer **6**, derived from force-field calculations (Biosym/MSI, ESFF)

The proton signals of the pyridyl hydrogens of **2** in chloroform solution are shifted upfield and completely absent from the aromatic region of its $^1$H NMR spectrum. This large upfield shift of the pyridyl protons coordinated to the inner Zn atom of a neighbouring porphyrin moiety is indicative of their proximity to the porphyrin ring current.[4] When **3** or **4** are added to the porphyrin solution the NMR spectra indicate the coordination of pyridyl protons exclusively to $Pd^{II}$ or $Pt^{II}$, presumably due to the greater M–N bond strength compared to the Zn–N bond as well as possibly enthalpic factors which favour the formation of these cyclic tetramers more than the open-chain oligomers of the porphyrin alone.[4b] Because of this greater Pd–N, Pt–N bond strength assemblies **5**, **6** and **7**, **8** are found to be stable in a wide concentration range from $10^{-9}$ to at least $10^{-2}$ mol $dm^{-3}$. This feature makes them particularly interesting targets for spectroscopic studies in highly dilute solutions, where most of the self-coordinated Zn-containing aggregates as well as hydrogen-bonded assemblies exist in monomeric forms.[3,4] Assemblies **7** and **8** are isolated in excellent yields (Scheme 1) and are air and thermally stable. The similarity of all the NMR spectroscopic data of **7** and **8** to tetramers **5** and **6** suggests that all the above considerations regarding the solution structures **5** and **6** also apply to Zn-containing assemblies **7** and **8**.

The UV–VIS spectra of the assemblies **5** and **6** show a 8–12 nm red shift of their Soret and Q-bands as compared to **1** along with considerable decrease of their intensity. As seen, the $Pt^{II}$ tetramer **6** decreases the intensities of these absorption bands by more than a factor of two as compared to its $Pd^{II}$ counterpart **5**. Moreover, the fluorescence of the porphyrin moiety **1** is quenched to a large degree when they are assembled in tetramers **5** and **6**. The absorbance maxima in **7** and **8** are red shifted by 10–12 nm, much like in squares **5** and **6**. Interestingly, the spectra for the Zn-containing tetramers indicate an increase in the Soret and Q-band intensities, as compared to porphyrin **2** itself. Furthermore, the influence of the transition metal on the absorbance intensities seems to be reversed in **7** and **8** as compared to **5** and **6**: the $Pt^{II}$ tetramer has a higher absorbance for both the Soret and Q-bands than the $Pd^{II}$ analogue. The explanation of this phenomenon may be in the fact, that unlike porphyrin **1**, its Zn-containing counterpart largely exists in solution in the form of self-coordinated oligomers. When the auxiliary complexes of $Pd^{II}$ or $Pt^{II}$ are added, the oligomers are converted to the assemblies **7** and **8**, respectively. Since the decrease in absorbance in self-coordinated Zn-containing porphyrin oligomers as compared to free porphyrin is well documented,[4] this effect may account for the unusual spectroscopic behaviour of Zn-containing species **2** and **7**, **8**.

In conclusion, a new family of artificial cationic supramolecular multiporphyrin aggregates can be readily assembled *via* non-covalent interactions by using $Pd^{II}$ and $Pt^{II}$ bisphosphane complexes as auxiliaries. These large stable aggregates may serve as both useful models for intrasupramolecular energy transfer as well as provide useful insights for future self-assembly of photoactive supramolecular systems.

Financial support by the National Science Foundation (CHE-9529093) and University of Utah Graduate Research Fellowship to Bogdan Olenyuk are gratefully acknowledged. We also thank Johnson-Matthey for a generous loan of Pd and Pt salts.

## Footnotes

† *Preparation of aggregates* **5**–**8**: To a solution of 0.017 mmol of porphyrins **1** or **2** in 10 ml of $CH_2Cl_2$, 0.017 mmol of **3** or **4** was added and the resulting solution was stirred at room temp. from 1 h (for **5** and **7**) to 4 or 5 days (**6** and **8**, respectively). The solvent was reduced in volume to 1 ml *in vacuo* and pentane or diethyl ether were added resulting in the formation of a dark-red solids, which were collected, washed and dried *in vacuo*.

‡ Both the magnitude and the direction of the chemical shifts are comparable to those observed for the $(dppp)_2Pd^{II}$ and $(dppp)_2Pt^{II}$-based tetranuclear squares (geometry established by X-ray structural data[9d]).

§ The MM2 calculation indicates hindered rotation at room temperature. The minimum steric energy corresponds to the pyridine ring being oriented nearly perpendicularly to the porphyrin plane.

¶ ESFF force-field calculations were performed on a Biosym/MSI 95.0 package.

## References

1 J. Deisenhofer, O. Epp, K. Miki, R. Huber and H. Michel, *J. Mol. Biol*., 1984, **80**, 385.
2 H. Zuber and R. A. Brunisholz, in *Chlorophylls*, ed. H. Scheer, CRC Press, Boca Raton, FL, 1991, p. 627.
3 P. Tecilla, R. P. Dixon, G. Slobodkin, D. S. Alavi, D. H. Waldeck and A. D. Hamilton, *J. Am. Chem. Soc*., 1990, **112**, 9408; C. M. Drain, R. Fischer, E. C. Nolen and J.-M. Lehn, *J. Chem. Soc., Chem. Commun*., 1993, 243; C. M. Drain, C. K. Russell and J.-M. Lehn, *Chem. Commun*., 1996, 337.
4 C. A. Hunter and R. K. Hyde, *Angew. Chem., Int. Ed. Engl*., 1996, **35**, 1936 and references therein.
5 H. Tamiaki, T. Miyatake, R. Tanikaga, A. R. Holzwarth and K. Schaffner, *Angew. Chem., Int. Ed. Engl*., 1996, **35**, 772.
6 C. M. Drain and J.-M. Lehn, *J. Chem. Soc., Chem. Commun*., 1994, 2313.
7 D. B. Amabilino, C. O. Dietrich-Buchecker and J.-P. Sauvage, *J. Am. Chem. Soc*., 1996, **118**, 3285.
8 S. E. Webber, *Chem. Rev*., 1990, **90**, 1469; M. R. Wasiliewski, *Chem. Rev*., 1992, **92**, 435; M. A. Fox, *Acc. Chem. Res*., 1992, **25**, 569.
9 B. Olenyuk, J. A. Whiteford and P. J. Stang, *J. Am. Chem. Soc*., 1996, **118**, 8132 and references therein.
10 M. Fujita, *J. Synth. Org. Chem., Jpn*., 1996, **54**, 953 and references therein.
11 J. S. Manka and D. S. Lawrence, *Tetrahedron Lett*., 1989, **30**, 6989.
12 P. J. Stang, B. Olenyuk and A. M. Arif, *Organometallics*, 1995, **14**, 5281; J. M. Brown, J. J. Pérez-Torrente and N. W. Alcock, *Organometallics*, 1995, **14**, 1195.
13 H. L. Anderson, *Inorg. Chem*., 1994, **33**, 972.
14 U. Dinur, A. T. Hagler, in *Review of Computational Chemistry*, ed. K. B. Lipkwowitz and D. B. Boyd, VCH, New York, 1991, vol. 2, ch. 4; O. Ermer, *Struct. Bonding (Berlin)*, 1976, **27**, 161.

*Received in Columbia, MO, USA, 22nd January 1997; 7/00506G*

# Remarkable non-oxidative conversion of methane to naphthalene and benzene on Co and Fe modified Mo/HZSM-5 catalysts

**Shetian Liu, Qun Dong, Ryuichiro Ohnishi and Masaru Ichikawa***

*Catalysis Research Center, Hakkaido University, Kita-Ku, N-11, W-10, Sapporo 060, Japan*

**Remarkable production of naphthalene and benzene is found in the dehydrocondensation of methane under non-oxidative conditions on Co- and Fe-modified Mo/HZSM-5 catalysts at 973 K and 1 atm pressure of methane.**

Recently there is an increasing interest to activate methane under non-oxidative conditions and convert it to higher hydrocarbons and aromatic compounds as alternative feedstocks for the petrochemical industry.[1,2] Some supported Pt and Ru catalysts yield $C_2$–$C_5$ hydrocarbons and even benzene in the low-temperature homologation of methane[3–5] but continuous catalytic reaction does not proceed. It has been previously reported that on Mo-supported ZSM-5 zeolite catalysts, a considerable amount of benzene was produced at 973 K in 60–70% selectivity in the gas-phase products at lower methane conversion while only benzene and toluene have been observed as the aromatic products.[6,7] Nevertheless, methane conversion was drastically decreased owing to irreversible coke formation on the catalysts.

Here, we describe that Fe- and Co-modified Mo/HZSM-5 catalysts exhibit remarkable production of naphthalene and benzene as the major aromatic products together with a small amount of their derivatives such as toluene, xylene and methylnaphthalene in the dehydrocondensation of methane at 973 K and 1 atm pressure. Furthermore, it was found that the addition of cobalt and iron to Mo/HZSM-5 catalyst markedly improved the yield of naphthalene and benzene along with effective reduction of coke formation.

The Mo/HZSM-5 and Fe/Co-modified Mo/HZSM-5 catalysts were prepared by the conventional impregnation (incipient wetness) of $NH_4$ZSM-5 (Si/Al = 79, Toso Co.) with $(NH_4)_6Mo_7O_{24}\cdot 4H_2O$ (Kanto Chem. Co.), $Co(NO_3)_2\cdot 6H_2O$ (Wako Pure Chem. Ind. Ltd.) or $Fe(NO_3)_3\cdot 6H_2O$ (Wako) aqueous solutions. After the impregnated samples were dried at 393 K and calcined at 773 K in air, catalytic tests were carried out under atmospheric pressure of methane in a continuous flow microreactor system equipped with a quartz tube (8 mm id) packed with 0.3 g of catalyst pellets of 20–42 mesh. After flushing with He at 973 K for 40 min, a feed gas mixture (99.99% purity, Sumitomo Seika Co.) of 98% $CH_4$ with 2% Ar as internal standard for analysis was introduced into the fixed-bed reactor at a flow rate of 7.5 ml $min^{-1}$ [space velocity = 1500 ml (g cat. h)$^{-1}$, contact time = 3.8 s] through a mass flow controller (Brooks 5850E).

Hydrocarbon products including $C_2$–$C_4$ alkanes (and/or alkenes) and condensable $C_6$–$C_{12}$ aromatics such as benzene, toluene, xylene, naphthalene and methylnaphthalenes were removed by a six-way sampling valve heating at 500 K and analyzed by on-line gas chromatography (Shimadzu GC-14A) equipped with a flame ionization detector (FID) using a 4 mm × 1 m Porapak-P column. Another GC (Shimadzu GC-8A) with a thermoconductive detector (TCD) was employed for on-line product analysis of $H_2$, Ar, CO, $CH_4$ and $CO_2$ using a 4 mm × 2 m activated carbon column. All products were identified by using GC–MS (Perkin-Elmer, Auto System GC, 910 Q-Mass).

Using an internal standard analyzing method, conversion of methane, selectivities of hydrocarbon products and coke formed on the catalyst were evaluated according to the mass balance for carbon and hydrogen. The total gas flow rate at the outlet of the reactor ($F^{\text{outlet}}$) can be calibrated by eqn. (1). The methane

$$F^{\text{inlet}} X_{\text{Ar}}^{\text{inlet}} = F^{\text{outlet}} X_{\text{Ar}}^{\text{outlet}} \tag{1}$$

conversion (Conv.) and selectivity ($S_{\text{product}}^{\text{carbon}}$) of hydrocarbon products in gas phase on carbon base were calculated from eqns. (2) and (3). The selectivity of coke including undetected heavy

$$\begin{aligned}\text{Conv.} &= \frac{F^{\text{inlet}} X_{\text{methane}}^{\text{inlet}} - F^{\text{outlet}} X_{\text{methane}}^{\text{outlet}}}{F^{\text{inlet}} X_{\text{methane}}^{\text{inlet}}} \\ &= 1 - \frac{X_{\text{methane}}^{\text{outlet}} X_{\text{Ar}}^{\text{inlet}}}{X_{\text{methane}}^{\text{inlet}} X_{\text{Ar}}^{\text{outlet}}}\end{aligned} \tag{2}$$

$$\begin{aligned}S_{\text{product}}^{\text{carbon}} &= \frac{F^{\text{outlet}} X_{\text{product}}^{\text{outlet}} N_{\text{product}}^{\text{carbon}}}{F^{\text{inlet}} X_{\text{methane}}^{\text{inlet}} - F^{\text{outlet}} X_{\text{methane}}^{\text{outlet}}} \\ &= \frac{X_{\text{Ar}}^{\text{inlet}} X_{\text{product}}^{\text{outlet}} N_{\text{product}}^{\text{carbon}}}{X_{\text{Ar}}^{\text{outlet}} X_{\text{methane}}^{\text{inlet}} - X_{\text{Ar}}^{\text{inlet}} X_{\text{methane}}^{\text{outlet}}}\end{aligned} \tag{3}$$

aromatics, amorphous carbon and graphitic carbon on the catalysts is given by $1 - \Sigma S_{\text{product}}^{\text{carbon}}$. Here, $F$, $X$ and $N^{\text{carbon}}$ represent total gas flow rate, mole fraction and carbon number in a molecule, respectively.

The non-oxidative conversion of methane was conducted by flowing methane on the catalyst in the fixed bed at 973 K. $C_2$-hydrocarbons and aromatic compounds were continuously obtained with a considerable evolution of hydrogen on the Mo/HZSM-5 and Co/Fe-modified Mo/HZSM-5 catalysts. The major aromatic compounds produced in the reaction are benzene and naphthalene with other aromatics produced only in trace amounts. Fig. 1 shows the conversion of methane and the selectivity of hydrocarbon products such as benzene and naphthalene with time on stream of the reaction at 973 K. The selectivity of hydrocarbon products in the gas phase increases and reaches a value of 68% on carbon basis and then keeps constant, while the selectivity of coke was *ca*. 32% on the Mo/HZSM-5 catalyst. The conversion of methane decreases rapidly from 12 to 8% at the initial stage of the reaction in forming a large amount of hydrogen and CO where $MoO_3$ supported on HZSM-5 was converted to reduced Mo species and $Mo_2C$.[2,8] Methane conversion shows a moderate decrease (6–8%) upon prolonged reaction time (30 h) to give a stable selectivity of the hydrocarbon products including $C_2$–$C_4$ compounds and aromatics such as benzene and naphthalene. The thermodynamic equilibrium conversion of methane for $6CH_4 = C_6H_6 + 9H_2$ is calculated as 11.8% at 973 K and 1 atm of methane. The constant selectivity of hydrocarbon products (68%) and coke (32%) in the stationary stage of the reaction may suggest that both products are derived from a common intermediate $CH_x$ formed on the Mo/HZSM-5 catalysts. In the initial stage of the reaction, the composition of gas-phase hydrocarbons comprised 31 and 62% of naphthalene and benzene on carbon basis, respectively, and after 20 h of reaction time changed to 6 and 67% while the $C_2$ products increased to 20%. This may suggest that benzene, naphthalene and their derivatives may

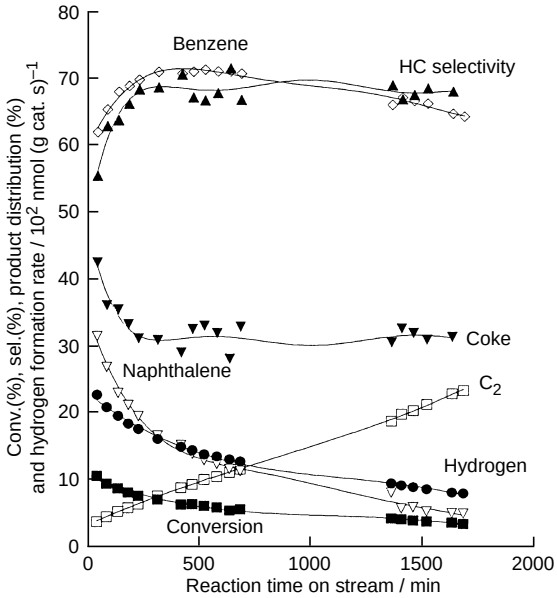
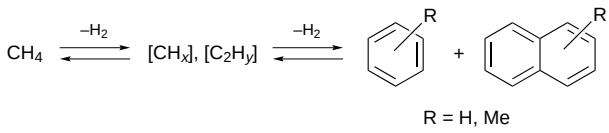



**Fig. 1** Catalytic performances of 3% Mo/HZSM-5 zeolite catalyst for methane non-oxidative dehydrocondensation reaction at 973 K. (■) Methane conversion, (▲) selectivity of hydrocarbon products, (▼) selectivity of coke, (●) formation rate of hydrogen, (◇) percentage of benzene in hydrocarbon products, (▽) percentage of naphthalene in hydrocarbon products, (□) percentage of ethane + ethene in hydrocarbon products.

consequently be produced *via* $[CH_x]$ and/or $C_2H_y$ intermediates as proposed previously[7,8] and the reaction may occur *via* Scheme 1.




**Scheme 1**

From Fig. 2 it is clear that addition of Fe, as for Co, to Mo/HZSM-5 catalysts yields a considerable enhancement of aromatic products such as naphthalene and benzene in the reaction at 973 K. It is of interest to observe that a maximum yield of benzene and naphthalene was attained in low concentrations of Fe or Co in Mo/HZSM-5 [atomic ratio *ca.* 0.2–0.4 for M/(M + Mo) (M = Fe, Co)]. 1% Co loading into 3% Mo/HZSM-5 resulted in an increase of benzene yield from 3.2 to 4.7% owing to higher conversion of methane and higher benzene selectivity in gas-phase hydrocarbon products as compared with 3% Mo/HZSM-5. On the other hand, the promotion of benzene yield upon addition of Fe to Mo/ZSM-5 is due to the suppression of coke formation from 31 to 21%, although the Fe/HZSM-5 catalyst showed preferential formation of coke (75% selectivity) in the reaction. Further addition of Fe or Co to Mo/HZSM-5 resulted in a decrease of the aromatic products owing to substantial increase of coke formation in methane conversion. The results suggest that the binary FeMo and CoMo oxide/carbides formed on the ZSM-5 support are active for the dehydrogenation of methane towards aromatics

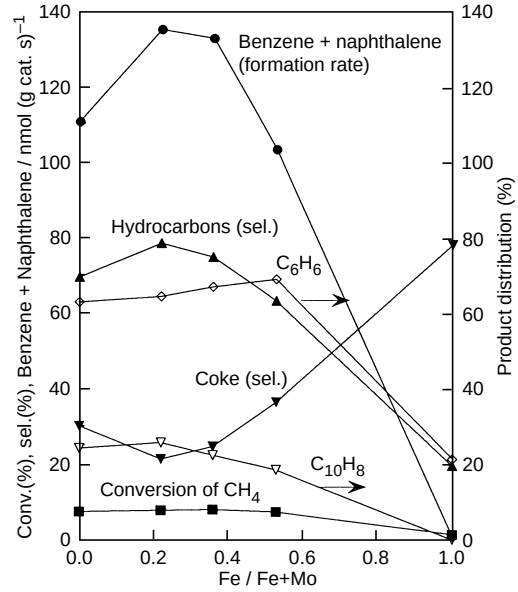



**Fig. 2** Catalytic performances of Fe-Mo/HZSM-5 zeolite catalysts for methane non-oxidative dehydrocondensation reaction at 973 K (data are taken at 160 min of the reaction time on stream). (■) Methane conversion, (▲) selectivity of hydrocarbon products, (▼) selectivity of coke, (●) formation rate of benzene and naphthalene, (◇) percentage of benzene in hydrocarbon products, (▽) percentage of naphthalene in hydrocarbon products.

such as naphthalene and benzene. In this regard, it was of interest to find that a $Fe_2(MoO_4)_3$ powdered sample prepared by coprecipitation[9] gave a remarkable evolution of hydrogen to form coke, whereas a negligible amount of hydrocarbon was produced upon admission of methane at 973 K. This implies that the FeMo binary site may highly active for the dehydrogenation of methane to promote the formation of $CH_x$ as the common species to be converted to aromatic compounds on the FeMo/HZSM-5 supported catalysts.

## Footnote

* E-mail: michi@ct.hines.hokudai.ac.jp

## References

1 A. Szoke and F. Solymosi, *Appl. Catal. A: General*, 1996, **142**, 361.
2 K. Murata and H. Ushijima, *J. Chem. Soc., Chem. Commun.*, 1994, 1157.
3 T. Koerts, P. A. Leclercq and R. A. van Santen, *J. Am. Chem. Soc.*, 1992, **114**, 7272.
4 M. Ichikawa, T. Tanaka, W. Pan, T. Otani, R. Ohnishi and T. Shido, *Stud. Surf. Sci. Cat.*, 1996, **101**, 1075.
5 C. Ovales, V. Leon, S. Reyes and F. Rosa, *J. Catal.*, 1991, **129**, 368.
6 L. Wang, L. Tao, M. Xie, G. Xu, J. Huang and Y. Xu, *Catal. Lett.*, 1993, **21**, 35.
7 Y. Xu, S. Liu, L. Wang, M. Xie and X. Guo, *Catal. Lett.*, 1995, **30**, 135.
8 F. Solymosi, J. Cserenyi, A. Szoke, T. Bansagi and A. Oszko, *J. Catal.*, 1997, **165**, 150.
9 M. Cannizzaro, P. Forzatti, I. Pasquon and P. L. Villa, *React. Kinet. Catal. Lett.*, 1981, **17**, 57.

*Received in Cambridge, UK; 22nd April 1997; 7/02731A*

# A discrete cubane-like $[Cu_7Te]$ cluster: synthesis and structural characterization of $(NBu_4)_4Cu_7As_3Te_{13}$

**Chwanchin Wang and Robert C. Haushalter*†**

*NEC Research Institute, 4 Independence Way, Princeton, NJ 08540, USA*

**The structure of the $[Cu_7As_3Te_{13}]^{4-}$ anion contains a discrete cubane-like $[Cu_7Te]$ cluster which is surrounded exclusively by three $[As(Te_2)Te_2]^{3-}$ ligands and resembles the close packing of the Cu metal along the [111] direction.**

Recently, much attention has been focused on the soluble binary chalcogenides and polychalcogenides which exhibit a great deal of structural diversity due mainly to the variety of catenation and bonding modes of the chalcogen atoms.[1–5] In contrast to the large number of binary chalcogenides, comparatively few ternary chalcogenides were reported. Investigation of the ternary M–As–E (M = transition metals and main-group elements; E = S, Se) systems by using the solventothermal technique has produced several compounds.[6,7] There is a common feature in these structures, that is, a varied degree of condensation of the basic structural units, $[AsE_3]^{3-}$ (E = S and Se) through the chalcogen atoms acting as ligands toward both transition metals and main-group elements. The $[AsS_3]^{3-}$ ligand coordinated to transition-metal compounds was also reported.[8] While research has been concentrated on the sulfide and selenide systems, only one telluride compound, $(NEt_4)_4Cu_4SbTe_{12}$,[9] containing a $[Sb(Te_2)_2Te]^{3-}$ structural unit was reported. To further the investigation of the telluride systems, we have examined the Cu–As–Te system using the extractive method and report the first telluride containing a $[As(Te_2)Te_2]^{3-}$ ligand which is exclusively used as a tridentate ligand to the Cu atoms.

One gram of an alloy with a nominal composition of $K_2CuAsTe_4$, prepared from the fusion of $K_2Te$, KAs, Cu, and Te in stoichiometric proportions, was extracted by dissolving in 10 ml of ethylenediamine that had been freshly distilled from a red $K_4Sn_9$ solution. The brown extract was filtered and layered with an equal volume of a saturated solution of tetrabutylammonium bromide in ethylenediamine. After one week, $(NBu_4)_4Cu_7As_3Te_{13}$ was isolated in *ca.* 12% yield (based on Cu) as small, black elongated hexagonal-like crystals. The composition of the alloy does not seem to be crucial, as the extraction of a more Cu-rich alloy of the composition $K_2Cu_3AsTe_4$ also yielded the title compound.

The structure‡ of $(NBu_4)_4Cu_7As_3Te_{13}$ consists an unprecedented, discrete cubane-like $[Cu_7Te]$ cluster which is exclusively coordinated by three $[As(Te_2)Te_2]^{3-}$ ligands as shown in Fig. 1, **1a**. The As atom in the $[As(Te_2)Te_2]^{3-}$ ligand is bound to a $Te_2^{2-}$ and two $Te^{2-}$ ligands in a trigonal-pyramidal fashion. This ligand is observed in the title compound for the first time but is structurally quite similar to $(NBu_4)_3SbTe_4$.[10] The As–Te bond distances range from 2.561 to 2.639 Å, comparable to those of $[K(2,2,2\text{-crypt})]_2As_2Te_6$[11] and $(NEt_4)_2As_2Te_5$.[12] The Te–Te bond distances ranging from 2.720 to 2.735 Å are close to those of $(NBu_4)_3SbTe_4$[10] and $CsAs_2Te_6$,[13] in good agreement with the Te–Te covalent bond distance, 2.74 Å.[14] The three terminal Te atoms from each $[As(Te_2)Te_2]^{3-}$ ligand are bound to a rhombus-like $Cu_4$ unit with each Te atom coordinated to two Cu atoms having Cu–Te distances in the range 2.523–2.728 Å. The structure of the $[Cu_7As_3Te_{13}]^{4-}$ anion is constructed in such fashion that shows a pseudo-threefold axis running through Cu(1) and Te(13) atoms [Fig. 1, **1b**]. The most striking feature of the anion is that the inner core, which is surrounded by the three $[As(Te_2)Te_2]^{3-}$ ligands, is a cubane-like $[Cu_7Te]$ cluster [Fig. 1, **1c**]. In the $[Cu_7Te]$ cluster, there are two coordination environments of Cu atoms: Cu(1) bound to four Te atoms has a distorted tetrahedral geometry, while the rest of the Cu atoms, each bound to three Te atoms, have a nearly trigonal-planar geometry. It is somewhat surprising that, based on the charge balance, all Cu atoms bear a 1+ charge. Both tetrahedral and trigonal-planar coodination environments of $Cu^I$ ions have been previously reported.[4,9] The average Cu–Te distance [2.72(3) Å] of the $CuTe_4$ tetrahedron is

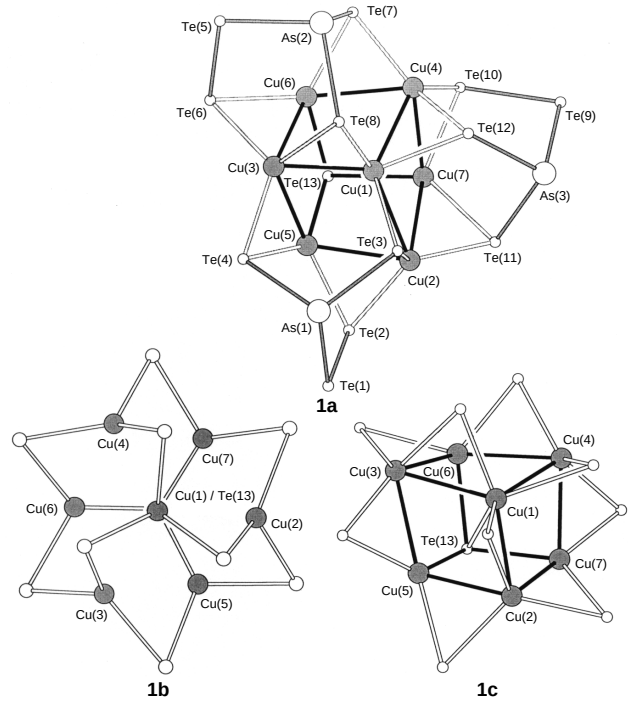



**Fig. 1** Structure of the $[Cu_7As_3Te_{13}]^{4-}$ anion **1a** which shows a pseudo-threefold axis running through Cu(1) and Te(13) atoms **1b**. Some selected bond distances (Å): Te(1)–Te(2) 2.735(3), Te(1)–As(1) 2.632(4), Te(2)–Cu(2) 2,552(4), Te(2)–Cu(5) 2.599(4), Te(3)–As(1) 2.615(4), Te(3)–Cu(2) 2.549(4), Te(3)–Cu(1) 2.685(4), Te(4)–As(1) 2.603(4), Te(4)–Cu(5) 2.534(4), Te(4)–Cu(3) 2.523(4), Te(5)–Te(6) 2.738(3), Te(5)–As(2) 2.608(4), Te(6)–Cu(3) 2.543(4), Te(6)–Cu(6) 2.614(4), Te(7)–As(2) 2.625(4), Te(7)–Cu(6) 2.542(4), Te(7)–Cu(4) 2.542(4), Te(8)–As(2) 2.602(4), Te(8)–Cu(3) 2.544(4), Te(8)–Cu(1) 2.728(5), Te(9)–Te(10) 2.720(4), Te(9)–As(3) 2.639(4), Te(10)–Cu(4) 2.560(4), Te(10)–Cu(7) 2.623(4), Te(11)–As(3) 2.619(4), Te(11)–Cu(2) 2.544(4), Te(11)–Cu(7) 2.546(4), Te(12)–As(3) 2.561(4), Te(12)–Cu(4) 2.553(4), Te(12)–Cu(1) 2.702(4), Te(13)–Cu(5) 2.501(4), Te(13)–Cu(6) 2.491(4), Te(13)–Cu(7) 2.500(4), Te(13)–Cu(1) 2.764(4), Cu(1)–Cu(2) 2.698(5), Cu(1)–Cu(3) 2.660(5), Cu(1)–Cu(4) 2.667(5), Cu(1)–Cu(5) 2.764(5), Cu(1)–Cu(6) 2.770(5), Cu(1)–Cu(7) 2.814(7), Cu(2)–Cu(5) 2.691(5), Cu(2)–Cu(7) 2.764(5), Cu(3)–Cu(5) 2.785(6), Cu(3)–Cu(6) 2.659(5), Cu(4)–Cu(6) 2.760(5), Cu(4)–Cu(7) 2.683(5). The inner core of the anion shows a cubane-like $[Cu_7Te]$ cluster in which both the Cu–Cu contacts and the Cu–Te bonds are highlighted with bold lines **1c**. Some of the atoms are omitted for clarity.

slightly longer than that [2.55(4) Å] of the trigonal planar $CuTe_3$. Another interesting feature is that the $Cu_7$ unit resembles close packing of the Cu metal along the [111] direction. The average Cu–Cu distance is 2.73(5) which is about 0.17 Å longer than that in Cu metal. The $Cu_7$ unit is then capped with a Te(13) atom at the bottom corner to complete a cube. The Te(13) atom within the cube has an umbrella-shaped coordination to a $Cu_4$ unit which shows one long [2.764(4) Å] and three short (2.491–2.501 Å) Te–Cu distances. This results in a compression of a regular cube along the body diagonal containing Cu(1) and Te(13) and, concomitantly, in the formation of two different coordination environments of Cu atoms. The cube is compressed to the extent that a bonding interaction of 2.764(4) Å develops between Cu(1) and Te(13). It is also notable that the Te atoms in the structure exhibit two [Te(1), Te(5), Te(11)], three {all the terminal Te atoms in $[As(Te_2)Te_2]^{3-}$ ligand} and four [Te(13)] coordination environments.

To our knowledge, the 23-atom anionic cluster of the title compound represents the largest ternary telluride Zintl anion that has been synthesized to-date. We and others[9] have demonstrated that both $[As(Te_2)Te_2]^{3-}$ and $[Sb(Te_2)_2Te]^{3-}$ ligands can be used as building blocks in the construction of larger Zintl anions. Our results further suggest the possibility of obtaining much larger clusters or extended structures by the use of ligands with formulae $[M(Te_2)_{3-x}Te_x]^{3-}$ (M = As, Sb; $x$ = 0–3).

## Footnotes

* E-mail: bobh@symyx.com
† Present address: Symyx Technologies, 420 Oakmead Parkway, Sunnyvale CA 94086, USA.

‡ *Crystal data* for $C_{64}H_{144}As_3Cu_7N_4Te_{13}$: space group $Pna2_1$ (no. 33), $a$ = 18.473(3), $b$ = 22.809(6), $c$ = 24.443(6) Å, $U$ = 10299(3) Å$^3$, $Z$ = 4, $D_c$ = 2.096 g cm$^{-3}$, $\mu$(Mo-K$\alpha$) = 60.16 cm$^{-1}$. 9916 unique reflections were collected of which 3964 had $I \geqslant 3\sigma(I)$. An empirical absorption correction was applied. The structure was solved by direct method and refined by full-matrix least-squares to a final $R$ = 0.039 ($R_w$ = 0.038) with anisotropic thermal parameters for As, Cu, and Te atoms and isotropic thermal parameters for non-hydrogen atoms. CCDC 182/495.

## References

1 M. A. Ansari and J. A. Ibers, *Coord. Chem. Rev*., 1990, **100**, 223.
2 M. A. Ansari, J. M. McConnachie and J. A. Ibers, *Acc. Chem. Res*., 1993, **26**, 574.
3 M. G. Kanatzidis, *Chem. Mater*., 1990, **2**, 353.
4 M. G. Kanatzidis and S.-P. Huang, *Coord. Chem. Rev*., 1994, **130**, 509.
5 C. J. Warren, R. C. Haushalter and A. B. Bocarsly, *J. Alloys Compd*., 1995, **229**, 175.
6 J.-H. Chou and M. G. Kanatzidis, *Inorg. Chem*., 1994, **33**, 1001.
7 J.-H. Chou and M. G. Kanatzidis, *Inorg. Chem*., 1997, **36**, 4.
8 G. A. Zank, T. B. Rauchfuss and S. R. Wilson, *J. Am. Chem. Soc*., 1984, **106**, 7621.
9 S. Dhingra and R. C. Haushalter, *J. Am. Chem. Soc*., 1994, **116**, 3651.
10 J. L. Shreeve-Keyer and R. C. Haushalter, *Polyhedron*, 1996, **15**, 1213.
11 C. Belin, *C. R. Acad. Sci. Ser. C*, 1984, **298**, 691.
12 C. J. Warren, R. C. Haushalter and A. B. Bocarsly, *Chem. Mater*., 1994, **6**, 780.
13 M. Wachhold and W. S. Sheldrick, *Z. Naturforsch., Teil B*, 1996, **51**, 1235.
14 L. Pauling, *The Nature of the Chemical Bond*, Cornell University Press, 1960.

*Received in Cambridge, UK, 17th April 1997; 7/02646C*

# Probing peristatic chirality of alkaline cations: NMR study of alkaline borocryptates

**Ernest Graf,[a] Roland Graff,[b] Mir Wais Hosseini,*[a] Clarisse Huguenard[c] and Francis Taulelle[c]**

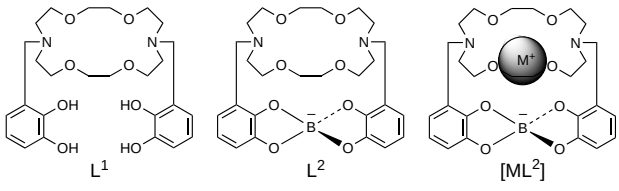
[a] *Laboratoire de Chimie de Coordination Organique (URA 422 CNRS), Université Louis Pasteur, F-67000 Strasbourg, France*
[b] *Service Commun de RMN, Université Louis Pasteur, F-67000 Strasbourg, France*
[c] *Laboratoire de RMN et Chimie du Solide (UMR 50 CNRS), Université Louis Pasteur, F-67000 Strasbourg, France*

**Enantiomeric differentiation of chiral borocryptates using NMR spectroscopy in a chiral liquid crystalline medium is achieved using different NMR probes localised both on the receptor and on the substrate; the observed chirality at the substrate is described as being induced by the spiroborate junction and mediated by the peristatic chirality of the cavity.**

For more than a century, chemists have been dealing with chirality which appears to be one of the most subtle aspects of chemistry.[1] On one hand, synthetic chemists use their skill to prepare compounds presenting either established[2] or new types of chirality.[3] On the other hand, physical chemists develop methods allowing measurement of chirality. Amongst such methods, NMR appears to be one of the most useful techniques.[4] In particular, NMR spectroscopy in oriented nematic phases has been shown to be a powerful method for the differentiation of enantiomers.[5]

Recently, inspired by naturally occurring antibiotics such as boromycin[6a] and aplasmomycin[6b] as well as by cryptands such as [222],[7] compound $L^1$ was designed.[8a] In the presence of a equimolar mixture of $B(OH)_3$ and MOH (M = alkali metal) in EtOH–$H_2O$, $L^1$ affords neutral binuclear complexes of the type $[ML^2]$ (Scheme 1). The binding ability of $L^2$ towards alkali-metal cations has been studied both in solution by NMR spectroscopy[8b] and in the solid state by X-ray analysis.[8c]

In dealing with chirality, the binding of boron by $L^1$ with a tetrahedral coordination geometry, affords the chiral cryptand $L^2$ (Fig. 1). The latter upon complexation with alkali-metal cations leads to chiral cryptates $[ML^2]$. The X-ray analysis of complexes with $M^+$ = $K^+$, $Rb^+$ or $Cs^+$ revealed the presence of both (*R*) and (*S*) enantiomers as a racemic mixture in the solid state.[8c] Whereas the free cryptand $L^2$ possesses an inherent chirality of the enantiomorphic type (*R* and *S*), for the labile and exchangeable complexed alkali-metal cation, the chirality is being imposed by the chiral cavity of the receptor through non-covalent interactions, and is therefore not inherent, and may be described as peristatic chirality[9] (peristasis = environment).† This type of chirality has been also recognised in a compound in which polyethyleneglycol was used to connect two catechol units.[10]




**Scheme 1**

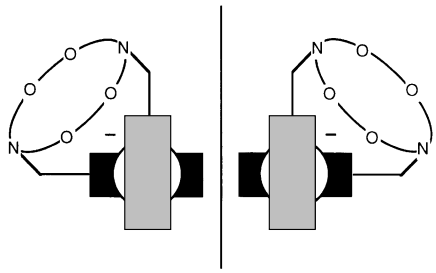


**Fig. 1** Schematic representation of chirality arising from the spiroborate junction in the borocryptand $L^2$

Enantiomeric differentiation of chiral molecules has been demonstrated using NMR spectroscopy in oriented chiral liquid crystals[5a] in particular in a poly(γ-benzyl L-glutamate) (PBLG)–$CH_2Cl_2$ (11–12% m/m) mixture[5b] forming cholesteric lyotropic mesophases.[5c]

Here, we report the extension of this method to the enantiomeric differentiation of complex molecules formed by non-covalent interactions between a receptor and a substrate.

For the chiral borocryptate $[ML^2]$, the receptor $L^2$ contains, in addition to classical $^1H$ and $^{13}C$ NMR active nuclei, both $^{10}B$ ($I$ = 3) and $^{11}B$ ($I$ = 3/2) possessing quadrupolar moments. On the other hand, the alkali-metal cations, being also NMR active, and possessing a quadrupolar moment, can also be studied by the same technique. Thus, enantiomeric differentiation in the $[ML^2]$ complexes can be studied in PBLG–$CH_2Cl_2$ (11–12% m/m), both at the level of the receptor $L^2$ and the substrate by combining the NMR data collected for the receptor part ($^{10}B$, $^{11}B$) and for the cationic substrates ($^{133}Cs$ and $^{14}N$).‡

The $^{10}B$ NMR spectrum of $[CsL^2]$ [Fig. 2(*a*)] can be deconvoluted into two sets of signals [Fig. 2(*b*), (*c*)] in 1 : 1 ratio as expected for a racemic mixture. The two distinct signals arise from each enantiomer. Whereas for one of the enantiomers [Fig. 2(*b*)], the signal was a broad singlet with a linewidth ($\Delta\nu_{1/2}$) of 51.9 Hz, the signal for the other enantiomer appeared as a sextet ($^{10}B$, $I$ = 3) with values of 221.6 and 73.3 Hz for the quadrupolar splitting ($\nu_Q$) and $\Delta n_{1/2}$, respectively [Fig. 2(*c*)].

$[CsL^2]$ was also studied by $^{11}B$ NMR. Again, the observed spectrum [Fig. 2(*d*)] could be deconvoluted into a broad signal ($\Delta\nu_{1/2}$ = 48.1) [Fig. 2(*e*)] and a triplet ($^{11}B$, $I$ = 3/2) with $\nu_Q$ = 503.2 Hz and $\Delta\nu_{1/2}$ = 48.7 Hz [Fig. 2(*f*)]. For both $^{10}B$ and $^{11}B$, the non-observation of a quadrupolar splitting for one of the enantiomers remains to be explained.

Interestingly, when investigating $[CsL^2]$ by $^{133}Cs$ NMR, the observed spectrum [Fig. 2(*g*)] was also composed of two sets of signals corresponding to two enantiomers. The spectrum could be deconvoluted into two septets ($^{133}Cs$, $I$ = 7/2), one with a small quadrupolar splitting constant ($\nu_{Q1}$ = 73.0 Hz, $\Delta\nu_{1/2}$ = 25.0 Hz) [Fig. 2(*h*)] and the other with a larger quadrupolar splitting constant ($\nu_{Q2}$ = 188.2 Hz, $\Delta\nu_{1/2}$ = 28.7 Hz) [Fig. 2(*i*)].

The binding ability of $L^2$ towards cations such as $NH_4^+$ has been previously established by an X-ray study,[11] and $NH_4L^2$ has been investigated by $^{10}B$, $^{11}B$ and $^{14}N$ NMR.

$^{10}B$ NMR observations [Fig. 3(*a*–*c*)] were similar to those obtained for $[CsL^2]$ ($\nu_{Q1}$ = 120.0 Hz, $\Delta\nu_{1/2}$ = 55.1 Hz). However, for $^{11}B$ the observed spectrum [Fig. 3(*d*)] appeared to be a superimposition of two triplets of the same intensity with

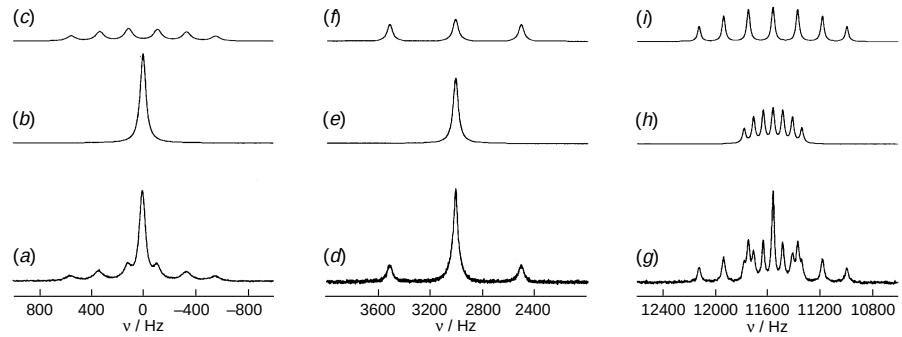



**Fig. 2** NMR spectra of [CsL²] in a chiral liquid-crystalline solvent : $^{10}$B (53.73 MHz) observed (*a*) and deconvoluted signals for both enantiomers (*b*), (*c*); $^{11}$B (160.42 MHz) observed (*d*) and deconvoluted signals for both enantiomers (*e*), (*f*); $^{133}$Cs (65.58 MHz) observed (*g*) and deconvoluted signals for both enantiomers (*h*), (*i*). $^{10}$B, $^{11}$B and $^{133}$Cs chemical shifts were referenced to $BF_3{\cdot}Et_2O$ and aqueous saturated $CsNO_3$, respectively as external references.

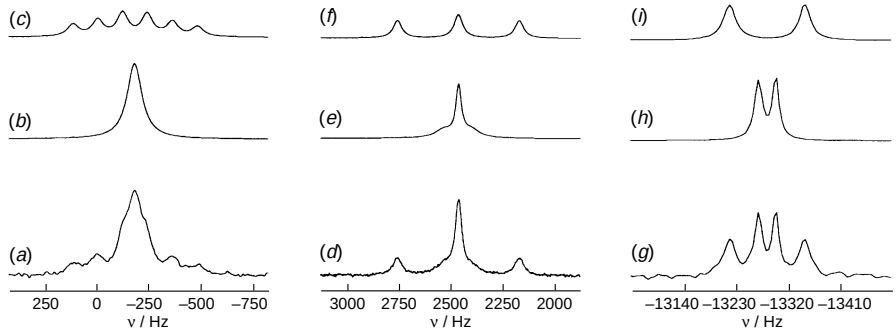



**Fig. 3** NMR spectra of [$NH_4L^2$] in chiral liquid-crystalline solvent: $^{10}$B (53.73 MHz) observed (*a*) and deconvoluted signals for both enantiomers (*b*), (*c*); $^{11}$B (160.42 MHz) observed (*d*) and deconvoluted signals for both enantiomers (*e*), (*f*); $^{14}$N (36.12 MHz) observed (*g*) and deconvoluted signals for both enantiomers (*h*), (*i*). $^{14}$N chemical shifts were referenced to neat $MeNO_2$ as external reference.

$\nu_{Q1}$ = 66.7 Hz [Fig. 3(*e*)] and $\nu_{Q2}$ = 293.2 Hz [Fig. 3(*f*)] corresponding to both enantiomers.

In $^{14}$N NMR studies, probably owing to the unsymmetrical environment around the two bridgehead nitrogen atoms leading to large quadrupolar interactions, the amino groups could not be observed. Nevertheless, the signal for the symmetrical $NH_4^+$ substrate was observed [Fig. 3(*f*)] as a superimposition of two doublets ($^{14}$N, $I$ = 1) in 1 : 1 ratio [Fig. 3(*h*), (*i*)]. Again, the two enantiomers were differentiated by large ($\nu_{Q1}$ = 128.7 Hz, $\Delta\nu_{1/2}$ = 18.0 Hz) and small ($\nu_{Q2}$ = 30.7 Hz, $\Delta\nu_{1/2}$ = 6.0 Hz) quadrupolar splitting constants.

Although not reported here, complexes formed between the cryptand L² and other cations such as $Rb^+$ and $K^+$ behaved similarly.

Enantiomeric differentiation of chiral molecules based on NMR studies in liquid-crystalline media was elegantly demonstrated by Courtieu and coworkers.[5a,b] Using different NMR probes on both the receptor and the substrate, we were able to detect, for the first time, the chirality of the ensemble, on different locations of the complex molecule. Based on our observations, we can describe the observed chirality at the cation site as induced by the spiroborate junction and mediated by the peristatic chirality of the cavity.

We thank the CNRS and the Institut Universitaire de France (IUF) for financial support.

## Footnotes

* E-mail: hosseini@chimie.u-strasbg.fr

† The adjective 'peristatic' (peristasis = environment) has been suggested at the EUCHEM Conference on Stereochemistry (Bürgenstock, May, 1966) by Professor S. D. Atkins (see ref. 11).

‡ The experiments were performed on dissolved single racemate crystals (the racemic nature was established by X-ray analysis). The deconvolution of the observed signal as two sets of signals was based on the observation of the quadrupolar splitting for one of the enantiomers which allowed abstraction of its contribution from the observed signal. The remaining signal was assigned to the other enantiomer. The ratio of the two signals was found to be 1 : 1 (±2%), as expected for a racemic mixture.

## References

1 V. Prelog, *Science*., 1976, **193**, 17.
2 R. S. Cahn, C. Ingold and V. Prelog, *Angew. Chem., Int. Ed. Engl.*, 1966, **5**, 385.
3 J. C. Chambron, C. Dietrich-Buchecker and J.-P. Sauvage, *Top. Curr. Chem.*, 1993, **165**, 132.
4 D. Parker, *Chem. Rev.*, 1991, **91**, 1441.
5 (*a*) E. Lafontaine, J.-P. Bayle and J. Courtieu, *J. Am. Chem. Soc.*, 1989, **111**, 829; (*b*) J.-P. Bayle, J. Courtieu, E. Gabetty, A. Lowenstein and J. M. Péchiné, *New J. Chem.*, 1992, **16**, 837; I. Canet, A. Meddour, J. Courtieu, J. L. Canet and J. Salaün, *J. Am. Chem. Soc.*, 1994, **116**, 2155; (*c*) R. W. Duke, D. B. Du Pré, W. A. Hines and E. T. Samulski, *J. Am. Chem. Soc.*, 1976, **98**, 3094.
6 (*a*) R. Hütter, W. Keller-Schierlein, F. Knüsel, V. Prelog, G. C. Rodgers, P. Sutter, G. Vogel, W. Voser and H. Zähner, *Helv. Chim. Acta*, 1967, **50**, 1533; (*b*) T. Okazaki, T. Kitahara and Y. Okami, *J. Antibiot.*, 1975, **28**, 176.
7 B. Dietrich, J.-M. Lehn and J.-P. Sauvage, *Tetrahedron Lett.*, 1969, 2885; 2889.
8 (*a*) E. Graf, M. W. Hosseini and R. Ruppert, *Tetrahedron Lett.*, 1994, **35**, 7779; (*b*) E. Graf, M. W. Hosseini, R. Ruppert, N. Kyritsakas, A. De Cian, J. Fischer, C. Estournès and F. Taulelle, *Angew. Chem., Int. Ed. Engl.*, 1995, **34**, 1115; (*c*) E. Graf, M. W. Hosseini, A. De Cian and J. Fischer, *Bull. Soc. Chim. Fr.*, 1996, **133**, 743.
9 K. Mislow and M. Raban, *Top. Stereochem.*, 1967, **1**, 1.
10 Y. Kobuke, Y. Sumida, M. Hayashi and H. Ogoshi, *Angew. Chem.*, 1991, **103**, 1513; *Angew. Chem., Int. Ed. Engl.*, 1991, **30**, 1496.
11 E. Graf, M. W. Hosseini, R. Ruppert, A. De Cian and J. Fischer, *J. Chem. Soc., Chem. Commun.*, 1995, 1505.

*Received in Cambridge, UK, 11th April 1997; 7/02495I*

# Odd-membered higher heterocalixarene architecture featuring cage conformation. Synthesis and X-ray structure analysis of a 1 : 2 : 2 inclusion cascade complex with acetone and dichloromethane

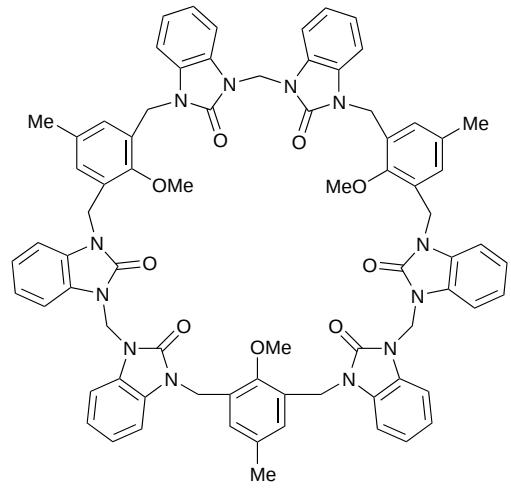
**Jörg Trepte,[a] Mátyás Czugler,[b]† Karsten Gloe[a] and Edwin Weber*[b]**

[a] *Institut für Anorganische Chemie, Technische Universität Dresden, Mommsenstrasse 13, D-01062 Dresden, Germany*
[b] *Institut für Organische Chemie, Technische Universität Bergakademie Freiberg, Leipziger Strasse 29, D-09596 Freiberg/Sachs, Germany*

**The first crystal structure of a heterocalix[9]arene host molecule created from six benzimidazol-2-one and three *p*-methylanisole units displays guest binding *via* a cascade of interactions of the two acetone and two dichloromethane guest molecules with the host and with each other as well.**

Calixarenes and their analogues have emerged as an important topic of supramolecular chemistry.[1] In the past decade a great many structural modifications involving ring sizes and functionalization of the calixarenes have been performed and studied in terms of conformational flexibility, hollow space effects and inclusion behaviour.[2] Current directions focus on the use of calixarene frameworks as modular building blocks in order to construct higher molecular architectures.[3] Notwithstanding the great structural variety in calixarene chemistry, odd-membered higher calixarene homologues having more than eight arene subunits are very rare, to say nothing of derivatives containing heterocycles[4] instead of the conventional phenol subunits. The following study considers both items. Compared with hydrogen-bond stabilized conformations of conventional calixarene systems of the same ring size the alternate arrangement of the subunits in the new metacyclophane causes the formation of a cavity. We report the versatile synthesis of a novel heterocalix[9]arene **1** and the remarkable crystal structure of its supramolecular complex with acetone and dichloromethane, **1**·$Me_2CO$·$CH_2Cl_2$ (1 : 2 : 2). The heterocalix[9]arene host molecule **1**, in which benzimidazol-2-one moieties as heterocyclic units are involved, was obtained *via* two-step fragment condensation[4] from 2,6-bis(bromomethyl)-6-methylanisole and methylene-1,1′-bis(benzimidazol-2-one) building elements using blocking/deblocking, high dilution and template (3 equiv. $Cs_2CO_3$) techniques in dry DMF to yield 26% of **1** (mp 249–250 °C). On recrystallization from a solvent mixture of acetone and dichloromethane (1 : 1), **1** readily forms a crystalline complex composed of **1** and the two solvents in a 1 : 2 : 2 stoichiometric ratio.

An X-ray structure model‡ of the present complex in the crystal (Fig. 1) reveals typical calix-inclusion formation as one of the acetone guest molecules sits in the cavity and is visibly held fixed by a C–H··O interaction from a benzimidazolone entity.§ Steric and electrostatic matching with other neighbouring residues is also important. The second acetone molecule is bound on the perimeter *via* another C–H··O interaction, again from a benzimidazolone residue. The enhanced activity of the benzimidazolones is also shown by the cascade-like binding of the two further dichloromethane guests. These are located on the host molecular surface, kept by C–H··Cl interactions to each other and to the host in a consecutive manner. The cascade ends on a Cl··π interaction[5] with a chlorine atom to anisole ring centre distance of 3.55 Å. This anisole moiety is the only one that plays a role in the active fixing of guest molecules. As reported recently for other smaller-ring hetero-calixarene cases,[4] the side-on-side stacking of symmetry centre-related host molecules with reference to the benzimidazolone plane (interplanar distances 3.4–3.6 Å) appears repeatedly. This is also visible in the crystal packing (Fig. 2). Thus stacking of the hetero-units is an important motif, apparently contributing to crystal formation for this type of host molecule.




**1**

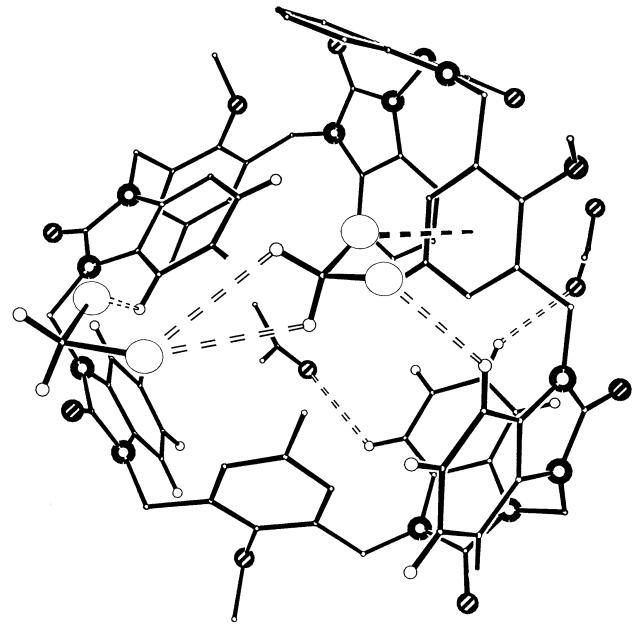


**Fig. 1** View of the **1**·acetone·dichloromethane (1 : 2 : 2) inclusion complex, with the principal cooperative interactions shown in broken lines. Only relevant hydrogen atoms are retained in the picture.

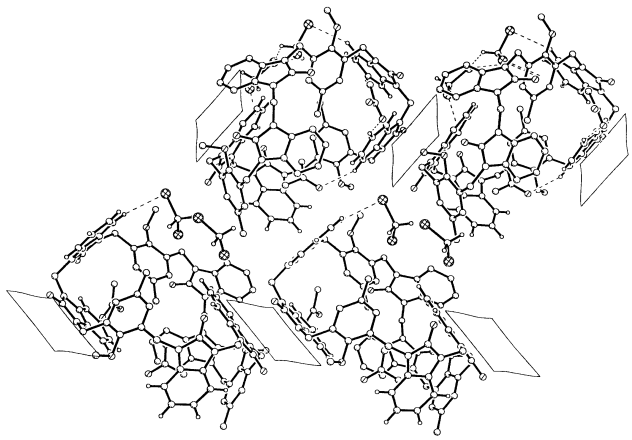


**Fig. 2** Packing in the **1**·acetone·dichloromethane (1 : 2 : 2) crystal illustrating stacking on the benzimidazolone sides (highlighted by irregular rectangles) and C–H··Cl interactions (broken lines)

We thus conclude that the unusual activity of the benzimidazol-2 one moiety renders it a particularly interesting building block for new calix frameworks, not only due to its ability to exaggerate ring dimensions and make such large rings somewhat stiffer than anisole units usually do alone, but also for its enhanced cooperativity in interactions with guest molecules.

E. W. and M. C. are indebted to an INTAS Grant (No. 94-972) for financial support. M. C. and E. W. also thank the Hungarian Research Fund (Grant OTKA 015181) and the Fonds der Chemischen Indüstrie, respectively for support-in-part. The authors in Dresden greatly acknowledge financial support by the Deutsche Forschungsgemeinschaft (GK 155).

## Footnotes

* E-mail: weber@tu-Freiberg.de
† On leave from the Central Research Institute of Chemistry, Budapest, Hungary.

‡ *X-Ray structure analysis* of **1**·acetone·dichloromethane (1 : 2 : 2): monoclinic, $P2_1/c$ space group, $a$ = 13.127(3), $b$ = 23.977(5), $c$ = 25.526(5) Å, $\beta$ = 96.75(3)°, $Z$ = 4, total data collected (refs. 6,7) = 16 388, independent reflections = 16 098 $R_{(int)}$ = 0.179. Crystals were of poor quality, soft, air-sensitive, and could only be exposed to moderate cooling ($T$ = 203 K, they became brittle below −80 °C). The initial structure model, obtained by direct methods [SHELXS-86 (ref. 8)], was refined against 11 943 non-negative observations (using alternating conjugate gradient and full-matrix least-squares refinement on $F^2$ data) to convergence at relative poor $R$ values [final $R$ indices $I > 2\sigma(I)$: $R_1$ = 0.151, $wR_2$ = 0.395, $R$ (all data): $R_1$ = 0.289, $wR_2$ = 0.548, program SHELXL-93 (ref. 9)]. Atomic assignments in the critical regions were checked by scrutinizing $U_{iso}$ values. All non-hydrogen atoms were treated with anisotropic displacement parameters. Hydrogen atom positions were generated from geometric evidence and were kept riding on their mother atoms. Atomic coordinates, bond lengths and angles, and thermal parameters have been deposited at the Cambridge Crystallograpic Data Centre (CCDC). See Information for Authors, Issue No. 1. Any request to the CCDC for this material should quote the full literature citation and the reference number 182/500.

§ The hydrogen-bonding cascade in this crystal structure is maintained in part by weak C–H··Cl interactions [C(78)–H(78)··Cl(1) = 0.94(2), 2.94(1) Å, 136(1)°; C(1e)–H(1ec)··Cl(2) = 0.98(2), 3.12(2) Å, 106(2)°; C(1e)–H(1ed)··Cl(2) = 0.98(2), 3.05(2) Å, 111(2)°] and by C(1e)–Cl(2)··X(1a) = 3.537(7) Å, 152(1)°, where X(1a) denotes a benzimidazolone ring centre. The C(49)–O(1a) = 3.07(2) Å distance is indicative of the electrostaic attraction between a benzimidazole carbon and the acetone oxygen. The long H··O distance of 2.8 Å [C(49)–H(49)··O(1a) 0.94 (2), 2.8(2) Å, 122(1)°] indicates that this is not a C–H··O interaction (ref. 10). The acetone binding also occurs *via* the benzimidazolone C–H and guest O interactions [C(69)–H(69)··O(1n) 0.96(2), 2.497 Å, 152(1)°].

## References

1 D. N. Reinhoudt, *9th Int. Symp. Mol. Recognit. Inclusion, Coll. Abstr. Pl. 01*, 1996, Lyon, France; J. Vicens and V. Böhmer, *Calixarenes: A Versatile Class of Macrocyclic Compounds*, Topics in Inclusion Science, Kluwer Academic Publishers, Dordrecht, 1991, vol. 3.
2 B.-H. Huisman, D. M. Rudkevich, F. C. J. M. Van Veggel and D. N. Reinhoudt, *J. Am. Chem. Soc.*, 1996, **118**, 3523.
3 V. Böhmer, G. Wasikiewicz, G. Rohicki and T. Kielkiewicz, *Angew. Chem., Int. Ed. Engl.*, 1994, **33**, 214; D. N. Reinhoudt, P. Timmermann, W. Verboom, F. C. J. van Veggel and W. P. van Hoorn, *Angew. Chem., Int. Ed. Engl.*, 1994, **33**, 1292.
4 E. Weber, J. Trepte, K. Gloe, M. Piel, M. Czugler, V. C. Kravtsov, Yu. A. Simonov, J. Lipkowski and E. V. Ganin, *J. Chem. Soc., Perkin Trans. 2*, 1996, 2359.
5 I. Csöregh, E. Weber and M. Czugler, *J. Chem. Soc., Perkin Trans. 2*, 1997, 23.
6 *CAD4 Operations Manual*, Enraf-Nonius, Delft, 1977.
7 HELENA V14.12, a program for data reduction of CAD4 data, A.L. Spek, University of Utrecht, Laboratory for Crystal and Structural Chemistry, Bijvoet Center for Biomolecular Research, 1993.
8 SHELXS-86, a program for the solution of crystal structures, G. M. Sheldrick, *Acta Crystallogr., Sect. A*, 1990, **46**, 467.
9 SHELXL-93, a program for crystal structure refinement, G. M. Sheldrick, University of Göttingen, Germany, 1993.
10 J. D. Chaney, C. R. Goss, K. Folting, B. D.Santarsiero and M. D. Hollingsworth, *J. Am. Chem. Soc.*, 1996, **118**, 9432; M. D. Hollingsworth, personal communication.

*Received in Cambridge, UK, 28th April 1997; 7/02861J*

# Photochemical cleavage of duplex DNA by *N*-benzoyloxy-2-thiopyridone linked to 9-aminoacridine

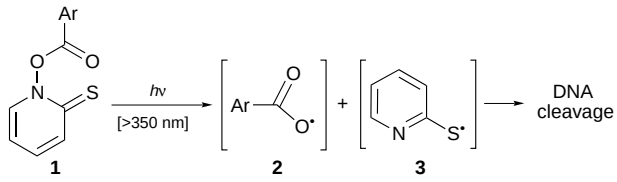
**Emmanuel A. Theodorakis,* Xin Xiang and Petra Blom**

*Department of Chemistry and Biochemistry, University of California, San Diego, 9500 Gilman Drive, La Jolla, California 92093-0358, USA*

**Upon illumination *N*-aroyloxy-2-thiopyridones induce non-specific single-strand nicks in duplex DNA at micromolar concentrations.**

Synthetic reagents that cleave DNA are of great interest as tools in biochemical sciences. The design of such molecules constitutes a timely and challenging research topic and has led to the development of both sequence-specific DNA cleavers[1] and DNA footprinting reagents.[2]

Our studies are directed towards the development of conceptually new approaches to DNA cleavage, induced by photoactivation of *N*-aroyloxy-2-thiopyridone derivatives, such as **1** (Scheme 1).[3,4] To this end, we were guided by the operational advantages offered by the photoinducible DNA cleavage using the *N*-benzoyloxy-2-thiopyridone **4**.[5] These

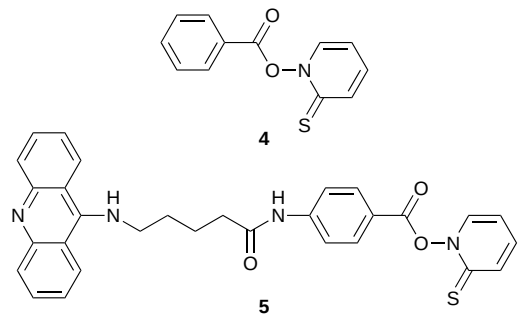


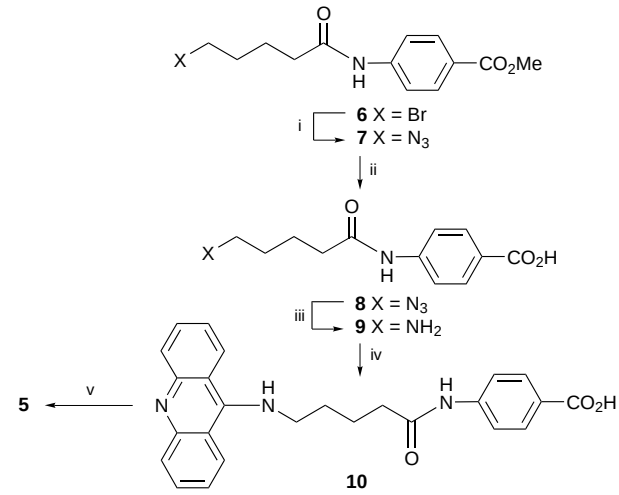

**Scheme 1**

molecules could be ideal nucleic acid cleavers since they possess the following characteristics: a purely organic structure, facile preparation, prolonged stability in the absence of light, and well documented radical chemistry.[3] The observed nucleic acid strand scission occurs upon a simple irradiation ($\lambda$ > 350 nm), presumably *via* the generation of aroyloxyl radicals **2** and without the need of a metal or external oxidants.

Herein we describe our preliminary data on a novel family of photoactivated DNA-cleavers represented by **5**. The reagent design is based on linking a DNA photocleaving ligand to the 9-aminoacridine *via* a polymethylene chain. The aminoacridinyl group could assure high affinity for duplex DNA *via* intercalation,[6] while the thiopyridone entity could account for the DNA cleavage. Indeed, upon irradiation ($\lambda$ > 350 nm), compound **5** produces single strand breaks in duplex DNA with no intrinsic sequence selectivity.

The synthesis of compound **5** commences with bromide **6**, itself readily available by the condensation of 5-bromovaleroyl chloride with methyl *p*-amino benzoate. Azidation of **6**,




**Scheme 2** *Reagents and conditions*: i, $NaN_3$ (2.0 equiv.), 18-crown-6 (0.05 equiv.) DMF, 25 °C, 3 h, 91%; ii, KOH (2.0 equiv.), THF–$H_2O$ (1 : 1), 25 °C, 24 h, 98%; iii, 10% Pd/C (0.1 equiv.), $H_2$, MeOH, 24 h, 89%; iv, 9-chloroacridine (1.0 equiv.), PhOH, 110 °C, 1 h, 90%; v, 2-mercaptopyridine *N*-oxide (1.0 equiv.), EDC (1.0 equiv.), DMF, 25 °C, 1 h, 43%

(Scheme 2), followed by saponification of the methyl ester moiety and reduction of the azido group gave rise to amino acid **9** in 79% overall yield, through intermediates **7** and **8**. Coupling of **9** with 9-chloroacridine followed by esterification with 2-mercaptopyridine *N*-oxide using 1-(3-dimethylaminopropyl)-3-ethylcarbodiimide hydrochloride (EDC) afforded conjugate **5** in 38% overall yield.

We further compared the visible light photolysis of **5** and **4** in the presence of supercoiled circular φX174 DNA (Fig. 1). Control experiments indicated that both light and the thiopyridone derivatives **5** or **4** are necessary for the DNA cleavage (lanes 1–3). Complete inhibition of the cleavage by glutathione (lanes 11, 12) further supports the notion that free radicals are responsible for the DNA damage. Moreover, compound **5**

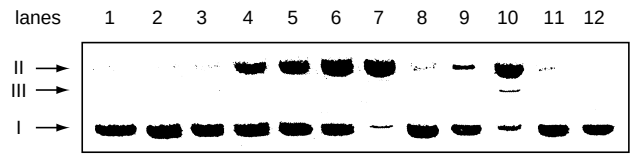



**Fig. 1** Concentration-dependent photocleavage of φX174 DNA induced by **4** and **5**. The φX174 DNA (50 μM/base pair) was incubated for 1 h at 25 °C with 4 or 5 (30 mM Tris-HCl, 20 mM NaCl), then subjected to irradiation at 4 °C (lanes 1 and 4–12) with one lamp (GE 300 W) placed at approximately 20 cm from the samples. The results were analysed on 1% agarose gel (Tris-acetate buffer) stained with ethidium bromide. Lane 1: φX174DNA (control); lane 2: DNA and 60 μM of **5** (no *h*ν); lane 3: DNA and 1 mM of **4** (no *h*ν) lanes 4–7: DNA and **5** at concentrations of 5: 5, 10, 30 and 60 μM, respectively; lanes 8–10: DNA and **4** at concentrations of **4**: 30, 60 and 1.0 mM, respectively; lane 11: DNA, 60 mM of **5**, and 3.0 mM of glutathione; lane 12: DNA, 1.0 mM of **4** and 3.0 mM of glutathione.

cleaves DNA at concentrations as low as $5 \times 10^{-6}$ M, while at $6 \times 10^{-5}$ M complete conversion of the form I to form II is observed. In comparison, derivative **4** produces similar results at $1 \times 10^{-3}$ M concentration. This substantial increase in efficiency of cleavage is attributed to the intercalating properties of 9-aminoacridine.[6]

An autoradiogram illustrating the results obtained upon irradiation of **5** in the presense of the 5′-$^{32}$P labelled 93-mer duplex DNA is shown in Fig. 2. Our data show that both **4** and **5** generate identical DNA ladders upon irradiation and the photocleavage is indisputably neither base- nor sequence-specific. Furthermore, comparison of lanes 8–12 indicate that **5** is more efficient than **4** in cleaving DNA and can accurately cut the duplex at concentrations as low as $5 \times 10^{-6}$ M. This increase in efficiency of cleavage is attributed to the presence of the 9-aminoacridinyl group. We ruled out the possibility that the 9-aminoacridinyl group enhances cleavage by altering the conformation of the DNA, since less cleavage was detected when 9-aminoacridine was added as an external intercalator (compare lines 12,13). Interestingly, the cleavage is more enhanced upon subsequent treatment with piperidine at 90 °C for 30 min without any change in sequence or base specificity (lines 7,8). Based on the above data we believe that in the case of **5** the DNA cleavage is performed by the intercalation complex and is probably mediated by aroyloxyl radicals.

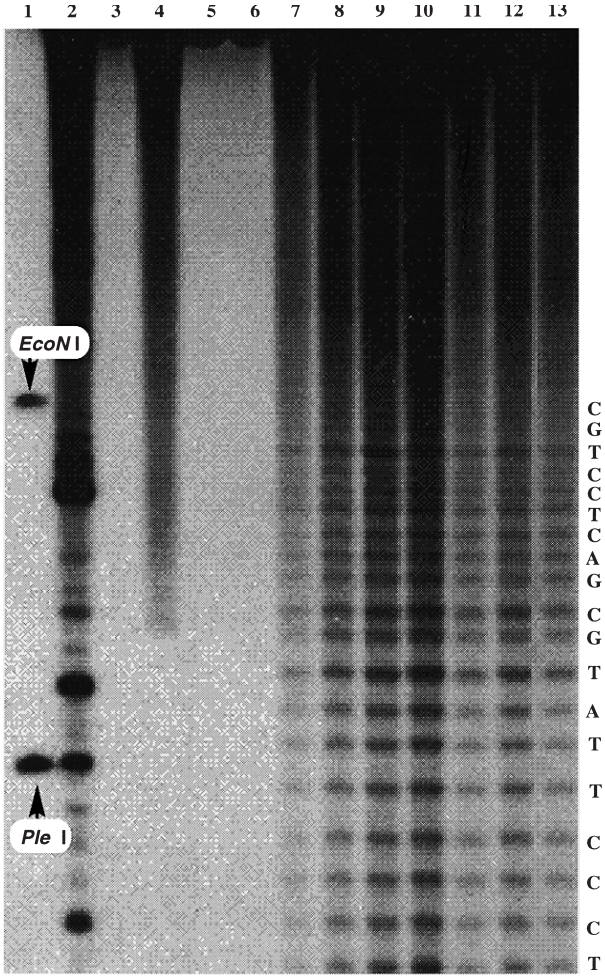



**Fig. 2** Autoradiogram of a 10% denaturing polyacrylamide gel showing photocleavage of 5′-32P end-labeled Sal I / Sph I restriction fragment of pBR322 duplex DNA (93-mer), induced by **4** and **5**. DNA was incubated for 1 h at 25 °C with compounds **4** or **5** in buffered solution (30 mM Tris-HCl, 20 mM NaCl) and then irradiated (with one GE 300 W lamp placed 20 cm from the samples) for another 2 h at 4 °C (lanes 3,4 and 7–13). The resulted solution was treated with piperidine (1 M) at 90 °C for 30 min, followed by EtOH precipitation (lanes 8–13). Lane 1: DNA cut by PIe I (14 base pairs) and EcoN I (28 base pairs); lane 2: DNase footprinting; lane 3: DNA (control); lane 4: DNA irradiated and piperidine treated without **4** or **5**; lane 5: DNA and 200 μM of **4** (no *hν*); lane 6: DNA and 60 μM of **5** (no *hν*); lane 7: DNA and 5 μM of **5** (no piperidine treatment); lanes 8–10: DNA and **5** at concentrations of **5**: 10 and 20 μM respectively; lanes 11,12: DNA and **4** at concentrations of **4**: 40 and 60 μM respectively; lane 13: DNA, **4** (60 μM) and 9-aminoacridine (30 μM).

It is evident from the above studies that the *N*-aroyloxy-2-thiopyridones **1** can induce non-specific single strand nicks in duplex DNA in a light-dependent reaction. The efficiency and/or selectivity of the cleavage could be tuned by the proper choice of the DNA recognition element. In addition the light intensity that is responsible for the photoactivation could be tuned by structurally modifying the thiopyridone core. Thus, the *N*-benzoyloxy-2-thiopyridone moiety can be used for the design of new DNA photocleaving reagents with potential use as 'photofootprinting reagents' or as 'site-directed photonucleases'. Studies across these lines are now under investigation in our laboratories.

We thank Dr T. Li and Professors Y. Tor and K. C. Nicolaou of this department for useful discussions and the Donors of The Petroleum Research Fund, administered by the American Chemical Society, for partial support of this research.

## Footnote

* E-mail: etheodor@ucsd.edu

## References

1 A. M. Maxam and W. Gilbert, *Methods Enzymol.*, 1980, **65**, 499; S. A. Kane, H. Sasaki and S. M. Hecht, *J. Am. Chem. Soc.*, 1995, **117**, 9107; T. Li, Z. Zeng, V. A. Estevez, K. U. Baldenius, K. C. Nicolaou and G. F. Joyce, *J. Am. Chem. Soc.*, 1994, **116**, 3709; J. G. Muller, P. Zheng, S. E. Rokita and C. J. Burrows, *J. Am. Chem. Soc.*, 1996, **118**, 2320; M. J. Absalon, J. W. Kozarich and J. Stubbe, *Biochemistry*, 1995, **34**, 2065.

2 R. P. Hertzberg and P. B. Dervan, *J. Am. Chem. Soc.*, 1982, **104**, 313; M. D. Kuwabara and D. S. Sigman, *Biochemistry*, 1987, **26**, 7234; T. D. Tullius, *Nature*, 1988, **18**, 213; N. Schmid and J.-P. Behr, *Biochemistry*, 1991, **30**, 4357; P. B. Dervan, *Nature*, 1992, **359**, 87.

3 J. Boivin, E. Crepon and S. Z. Zard, *Tetrahedron*, 1990, **31**, 6869; D. H. R. Barton, B. Lacher and S. Z. Zard, *Tetrahedron*, 1987, **43**, 4321; W. Adam, D. Ballmaier, B. Epe, G. N. Grimm and C. R. Saha-Moller, *Angew. Chem., Int. Ed. Engl.*, 1995, **34**, 2156; B. M. Aveline, I. E. Kochevar and R. W. Redmond, *J. Am. Chem. Soc.*, 1996, **118**, 289; K. M. Hess and T. A. Dix, *Anal. Biochem.*, 1992, **206**, 309.

4 For selected reports on light-induced DNA cleaving agents, see M. M. Becker and J. C. Wang, *Nature*, 1984, **309**, 682; K. Uchida, A. M. Pyle, T. Morii and J. K. Barton, *Nucleic Acids Res.*, 1989, **17**, 10 259; W. Adam, J. Cadet, F. Dall′Acqua, B. Epe, D. Ramaiah and C. R. Saha-Moller, *Angew. Chem. Int. Ed. Engl.*, 1995, **34**, 107; I. Saito, M. Takayama, T. Matsuura, S. Matsugo and S. Kawanishi, *J. Am. Chem. Soc.*, 1990, **112**, 883; A. J. Blacker, J. Jazwinski, J.-M. Lehn and F. X. Wilhelm, *J. Chem. Soc., Chem., Commun.*, 1986, 1035; J. C. Quada, M. J. Levy and S. M. Hecht, *J. Am. Chem. Soc.*, 1993, **115**, 12 171; P. A. Wender, S. M. Touami, C. Alayrac and U. C. Philipp, *J. Am. Chem. Soc.*, 1996, **118**, 6522; G. A. Neuhart, C. C. Cheng and H. H. Thorp, *J. Am. Chem. Soc.*, 1995, **117**, 1463.

5 E. A. Theodorakis and K. M. Wilkoxen, *Chem. Commun.*, 1996, 1927.

6 9-Aminoacridine displays strong intercalating properties onto DNA with no intrinsic sequence selectivity. For selected literature on this topic, see C. Bailly and J.-P. Henichart, *Perspect. Bioconj. Chem.*, 1991, 112; A. H. J. Wang, *Curr. Opin. Struct. Biol.*, 1992, **2**, 361; P. E. Nielsen, C. Jeppesen, M. Egholm and O. Buchardt, *Biochemistry*, 1988, **27**, 6338; A. Lorente, J. F. Espinosa, M. F. Saiz, J.-M. Lehn, W. D. Wilson and Y. Y. Zhong, *Tetrahedron Lett.*, 1996, **37**, 4417; F. C. K. Chiu, R. T. C. Brownlee, K. Mitchell and D. R. Phillips, *Bioorg. Med. Chem. Lett.*, 1995, **5**, 1689.

*Received in Corvallis, OR, USA, 28th April 1997; 7/02913F*

# Syntheses and single-crystal X-ray structures of $[(Bu^tNP)_2(Bu^tN)_2]MCl_2$ (M = Zr, Hf): the first transition-metal bis(alkylamido)cyclodiphosphazane complexes

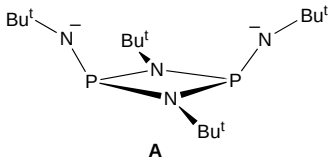
**Luke Grocholl,[a] Lothar Stahl*[a] and Richard J. Staples[b]**

[a] *Department of Chemistry, University of North Dakota, Grand Forks, ND 58202-9024, USA*
[b] *Department of Chemistry and Chemical Biology, Harvard University, Cambridge, MA 02138, USA*

**The interaction of $[(Bu^tNP)\{Bu^tNLi(thf)\}_2]$ with $ZrCl_4$ and $HfCl_4$ produces the remarkably stable monomeric $[(Bu^tNP)_2(Bu^tN)_2]MCl_2$ (M = Zr, Hf) complexes.**

The organometallic chemistry of the group 4 metals is dominated by compounds of the type $(\eta\text{-}C_5H_5)_2MCl_2$ and variations thereof.[1] The ubiquity of these bent metallocenes is largely due to the cyclopentadienyl ligand's ability to stabilise large, electropositive metals sterically and electronically and to create monomeric complexes with a well defined coordination environment. Because of the success of the 'constrained-geometry catalysts', *i.e.*, hybrid complexes with a mixed $(\eta\text{-}C_5Me_4)SiMe_2NBu^t$ ligand, in the Ziegler–Natta polymerization alkenes,[2] there has in recent years been a tremendous synthetic interest in group 4 amide complexes. This research has produced a large number of early-transition-metal complexes with bi-, tri-, and tetra-dentate amide ligands.[3] Many of these new compounds are structurally interesting and some have shown outstanding reactivity.[4] Due to their small bite angles most of these chelating amides are unable to stabilize the heavier group 4 metals as monomeric complexes, however, thereby reducing potential catalytic activity.

To synthesise monomeric amide complexes of zirconium and hafnium we have used bis(*tert*-butylamido)cyclodiphosphazane, **A**, as a ligand.[5] Although these cyclic phosphorus–nitrogen molecules have been known for some time,[6] their metal chemistry is not well developed and their use as chelating bis(amide) ligands is all but unknown.[7] The obscurity of cyclodiphosphazanes is surprising, because their flexible bite angle and multidentate nature make them ideal ligands for transition- and main-group-metals alike.




**A**

The prolonged (24 h) interaction of $[(Bu^tNP)_2(Bu^tNLi{\cdot}thf)_2]$ with $MCl_4$ in hot toluene (Scheme 1) afforded $[(Bu^tNP)_2(Bu^tN)_2]MCl_2$ (M = Zr **1**, Hf **2**), in yields of *ca.* 80%.† These colourless compounds have remarkable thermal and chemical stability, being unaffected by oxygen and sulfur in hot toluene solutions even after 12 h. NMR spectral data show conclusively that the metal complexes have $C_{2v}$ symmetry in solution. Thus, for example, the $^1H$ NMR spectra of **1**(**2**) display two singlets at $\delta$ 1.41(1.40) and 1.27(1.27), for the amido and imido *tert*-butyl groups, respectively, while the $^{31}P\{^1H\}$ NMR spectra consist of only one sharp singlet at $\delta$ 101.7 and 99.9, respectively, indicative of equivalent $P^{III}$ centres.

$[(Bu^tNP)_2(Bu^tNLi{\cdot}thf)_2] + MCl_4$

toluene, 80 °C; –2 LiCl

$[(Bu^tNP)_2(Bu^tN)_2]MCl_2$

M = Zr **1**
Hf **2**

**Scheme 1**

A single-crystal X-ray analysis confirmed the solid-state structure of **1** as that shown in Fig. 1;‡ the hafnium analogue is isostructural. These compounds crystallise racemically twinned as discrete molecules in the acentric orthorhombic space group $P2_12_12_1$. The metal–chloride and metal–amide bonds define to a first approximation a pseudo-tetrahedral coordination geometry about the zirconium atom. An additional fifth, long Zr–N(1) interaction, however, reduces the molecular symmetry from $C_{2v}$ to $C_s$ in the solid state to create a highly distorted trigonal-bipyramidally coordinated zirconium atom. Alternatively the central moiety of the molecule may be described as two almost perpendicular inorganic heterocycles, consisting of phosphorus, nitrogen and zirconium atoms. Symmetry-related zirconium–nitrogen and phosphorus–nitrogen bonds are, within experimental errors, equivalent. Thus, the two zirconium–nitrogen bonds are 2.060(3) and 2.067(3) Å long, making them quite comparable to those in related compounds with monodentate

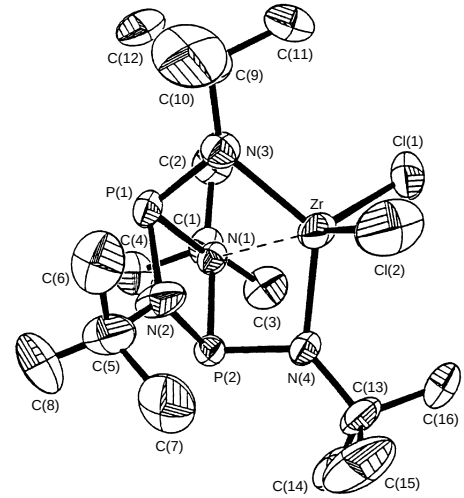



**Fig. 1** Molecular structure and labeling scheme for **1**. Selected bond distances (Å) and angles (°) not mentioned in the text: P(1)–N(1) 1.790(3), P(1)–N(2) 1.729(4), P(1)–N(3) 1.682(3), P(2)–N(1) 1.780(3), P(2)–N(2) 1.743(4), P(2)–N(4) 1.681(3), Cl(1)–Zr–Cl(2) 104.51(8), N(3)–Zr–Cl(1) 110.6(1), N(3)–Zr–Cl(2) 102.4(1), N(4)–Zr–Cl(1) 110.4(1), N(4)–Zr–Cl(2) 102.6(1). The corresponding values for **2** are: P(1)–N(1) 1.785(10), P(1)–N(2) 1.734(9), P(1)–N(3) 1.632(9), P(2)–N(1) 1.790(9), P(2)–N(2) 1.752(11), P(2)–N(4) 1.665(9), Cl(1)–Hf–Cl(2) 103.7(2), N(3)–Hf–Cl(1) 110.5(3), N(3)–Hf–Cl(2) 103.0(3), N(4)–Hf–Cl(1) 109.7(3), N(4)–Hf–Cl(2) 102.4(3).

amides.[8] The zirconium–chloride bonds, however, are shorter than those in $(\eta\text{-}C_5H_5)_2ZrCl_2$, and this may reflect the lesser steric crowding of these bonds in **1**, or perhaps a small amount of Cl to Zr π-electron donation. The slight bond asymmetry, 2.375(2) and 2.397(2) Å, is presumably the result of the ring–zirconium interaction, and it is notable that the Zr–Cl bond *trans* to the Zr–N(1) bond is the longer of the two. In keeping with the trends normally observed for isostructural zirconium and hafnium species,[1] the metal–ligand bonds in the hafnium analogue are slightly shorter than those in the zirconium complex. The hafnium compound has equidistant metal–amide bonds of 2.053(9) and 2.081(10) Å, and slightly inequivalent Hf–Cl bonds of 2.355(5) and 2.382(4) Å.

Unlike the majority of the more common chelating diamides, cyclodiphosphazane **A** can effectively envelop the central metal atom through additional bonds. This is clearly demonstrated by both the secondary N(1)–Zr donor bond of 2.398(3) Å and the extremely short non-bonding distance of 2.891(1) Å between the phosphorus atoms and the zirconium centre. Because the rigidity of the ligand prevents a closer approach between metal and phosphazane ring, it is difficult to assess the strength of this ring–metal interaction. Lone-pair donation by ring–nitrogen atoms in the related cyclophosphazenes is well documented, however, and usually forms bonds of considerable strength.[9]

Only comparatively minor structural changes are displayed by the ligand upon coordination to the metals. There is a slight puckering in the cyclodiphosphazane portion of the molecule that is also observed in the pristine ligand, resulting in a slight folding along the N(1)···N(2) line[10] The exocyclic phosphorus–nitrogen distances are significantly shorter than the endocyclic ones, a feature we believe to be due to steric factors. The trends in the P–N bond distances of N(1) and N(2) are those expected based on the differences in their coordination numbers, the four-coordinate N(1) having the longer bonds.

Like many successful ancillary ligands, cyclodiphosphazane **A** is able to impose a well defined coordination environment on its complexes. In **1** and **2**, for example, it has produced a steric pocket that is quite reminiscent of that in bent metallocenes and related compounds. The bulky *tert*-butyl substituents of the ligand form a rather wide gap in the equatorial plane of the complexes that may allow selective access of substrate molecules to the Lewis-acidic metal centres. The cyclodiphosphazane ligand subtends identical angles of 124.6(1) and 124.8(4) Å at the metal in **1** and **2**, respectively; these values are well above that of a regular tetrahedron but comparable to those found in metallocenes.

Because of their unique structural features, **1** and **2** appear to be excellent candidates for catalytic applications which demand low-coordinate, highly Lewis-acidic metal centres with well defined coordination environments and the desirable *cis*-arrangement of the chloride ligands. Whether ligand-centred reactions caused by the phosphorus and equatorial nitrogen centres compromise this reactivity, however, remains to be seen. Catalytic studies are currently under way, and they should provide insight into the reaction chemistry of the title compounds.

## Footnotes

* E-mail: lothar.stahl@mail.chem.und.nodak.edu

† Anal. Found for **1**: C, 37.55; H, 6.89; N, 10.87. Calc. for $C_{16}H_{36}Cl_2N_4P_2Zr$: C, 37.79; H, 7.13; N, 11.02%. Mp 215 °C. Positive chemical ionisation (PCI) MS, 509.708 $[M + H]^+$. Anal. Found for **2**: C, 32.34; H, 6.05; N, 9.20. Calc. for $C_{16}H_{36}Cl_2HfN_4P_2$: C, 32.25; H, 6.09; N, 9.40%. Mp 201 °C. PCI MS, 597.1 $[M + H]^+$.

‡ *Crystal data*: for **1**: $C_{16}H_{36}Cl_2N_4P_2Zr$, $M_r$ = 508.55; orthorhombic, space group $P2_12_12_1$, $a$ = 9.921(2), $b$ = 15.129(3), $c$ = 16.331(4) Å, $U$ = 2451.2(8) Å$^3$, $D_c$ = 1.378 g cm$^{-3}$, $Z$ = 4, $F(000)$ = 1056. Intensity measurements were made with a Siemens SMART CCD (charge-coupled device) X-ray diffractometer equipped with an LT-2 low-temperature apparatus operating at 213 K using Mo-Kα radiation, $\lambda$ = 0.710 73 Å and $\omega$-scans of 0.3° per frame for 10 s, until a complete hemisphere was collected. A total of 9072 reflections in 1271 frames were collected in the $4° < 2\theta < 56°$ range with a final resolution of 0.84 Å. Of these reflections, 4921 were unique ($R_{int}$ = 0.0248) and observed [$I > 2\sigma(I)$] and used in the refinement. An absorption correction based on $\psi$-scans was applied to the data set, $T_{min, max}$ = 0.683, 0.962. The first 50 frames were recollected at the end of data acquisition to monitor for decay which was <1%. Cell parameters were retrieved using SMART[11] software and refined using SAINT[12] on all observed reflections. Data reduction was performed with the SAINT software which corrects for $L_p$ and decay. The absorption correction was applied using SADABS which was supplied with the program. The structure was solved in the uniquely determined space group $P2_12_12_1$ (no. 19) by using the direct methods option of the SHELX-90[13] program and refined by least-squares on $F^2$ with SHELXL-93,[14] incorporated in SHELXTL-PC V 5.03.[15] Hydrogen atom positions were calculated by geometrical methods and refined as a riding model. The refinement converged at $R_1$ = 0.0412 and $wR_2$ = 0.1017 and a final GOF = 1.016. The final difference map showed no peaks(holes) greater than 0.373(−1.039) e Å$^{-3}$.

For **2**: $C_{16}H_{36}Cl_2HfN_4P_2$, $M_r$ = 595.82; orthorhombic, space group $P2_12_12_1$, $a$ = 9.937(3), $b$ = 15.132(4), $c$ = 16.414(5) Å, $U$ = 2468(1) Å$^3$, $D_c$ = 1.603 g cm$^{-3}$, $Z$ = 4, $F(000)$ = 1184. Hardware configurations and software programs were identical to those used for **1.** A total of 6141 data were collected at 293 K in the range $4 < 2\theta < 45°$. Upon merging, $R_{int}$ = 0.0221, these yielded 3078 unique and observed [$I > 2\sigma(I)$] data which were used in the refinement. An absorption correction based on $\psi$-scans was applied, $T_{min, max}$ = 0.738, 0.942. The crystal showed no decay during the data collection. Refinement converged at $R_1$ = 0.0472, $wR_2$ = 0.1138. The largest residual electron densities in the final difference map were peaks and holes of 0.774 and −1.795 e Å$^{-3}$, respectively. CCDC 182/494.

## References


1 D. J. Cardin, M. F. Lappert and C. L. Raston, *Chemistry of Organo-Zirconium and Organo-Hafnium Compounds*, Wiley, New York, 1986.

2 J. C. Stevens, F. J. Timmers, D. R. Wilson, G. F. Schmidt, P. N. Nickias, R. K. Rosen, G. W. Knight and S. Lai, *Eur. Pat. Appl.*, EP-416-815-A2; P. J. Shapiro, E. Bunel, W. P. Schaefer and J. E. Bercaw, *Organometallics*, 1990, **9**, 867.

3 F. G. N. Cloke, P. B. Hitchcock and J. B. Love, *J. Chem. Soc., Dalton Trans.*, 1995, 25; H. Memmler, K. Walsh, L. H. Gade and J. W. Lauher, *Inorg. Chem.*, 1995, **34**, 4062; C. Floriani, S. Ciurli, A. Chiesi-Villa and C. Guastini, *Angew. Chem., Int. Ed. Engl.*, 1987, **26**, 70; H. Brand and J. Arnold, *J. Am. Chem. Soc.*, 1992, **114,** 2266; R. Uhrhammer, D. G. Black, T. G. Gardner, J. D. Olsen and R. F. Jordan, *J. Am. Chem. Soc.*, 1993, **115**, 8493; K. Aoyagi, P. K. Gantzel, K. Kalai and T. D. Tilley, *Organometallics*, 1996, **15**, 923; J. D. Scollard, D. H. McConville and J. J. Vittal, *Organometallics*, 1995, **14**, 5478.

4 J. D. Scollard and D. H. McConville, *J. Am. Chem. Soc.*, 1996, **118**, 10 008; J. D. Scollard, D. H. McConville, N. C. Payne and J. J. Vittal, *Macromolecules*, 1996, **29**, 5241.

5 R. R. Holmes and J. A. Forstner, *Inorg. Chem.*, 1963, **2**, 380.

6 T. G. Hill, R. C. Haltiwanger, M. L. Thompson, S. A. Katz and A. D. Norman, *Inorg. Chem.*, 1994, **33**, 1770; G. Bulloch and R. Keat, *J. Chem. Soc., Dalton Trans.*, 1974, 2010; G. Bulloch, R. Keat and D. G. Thompson, *J. Chem. Soc., Dalton Trans.*, 1977, 99.

7 O. J. Scherer, G. Wolmershäuser and H. Conrad, *Angew. Chem., Int. Ed. Engl.*, 1983, **22**, 404.

8 C. Arioldi, D. C. Bradley, H. Chudzynska, M. B. Hursthouse, K. M. Abdul Malik and P. R. Raithby, *J. Chem. Soc., Dalton Trans.*, 1980, 2010.

9 H. P. Calhoun, N. L. Paddock and J. Trotter, *J. Chem. Soc., Dalton Trans.*, 1973, 2708; W. Harrison and J. Trotter, *J. Chem. Soc., Dalton Trans.*, 1973, 61.

10 L. Grocholl, L. Stahl and R. J. Staples, manuscript in preparation.

11 SMART V 4.043 Software for the CCD Detector System, Siemens Analytical Instruments Division, Madison, WI, 1995.

12 SAINT V 4.035 Software for the CCD Detector System, Siemens Analytical Instruments Division, Madison, WI, 1995.

13 G. M. Sheldrick, SHELXS-90, Program for the Solution of Crystal Structures, University of Göttingen, 1986.

14 G. M. Sheldrick, SHELXL-93, Program for the Refinement of Crystal Structures, University of Göttingen, 1993.

15 SHELXTL 5.03 (PC-Version), Program Library for Structure Solution and Molecular Graphics, Siemens Analytical Instruments Division, Madison, WI, 1995.


*Received in Bloomington, IN, USA, 16th April 1997; 7/02606D*

# Synthesis of a new titanosilicate: an analogue of the mineral penkvilksite

**Yunling Liu, Hongbin Du, Fengqi Zhou and Wenqin Pang***

*Key Laboratory of Inorganic Synthesis and Preparative Chemistry, Department of Chemistry, Jilin University, Changchun, 130023, China*

**A new titanosilicate which is a structural analogue of the mineral penkvilksite, is obtained from $SiO_2$–$TiO_2$–$Na_2O$–$H_2O$–$(TMA)_2O$ and characterized by powder X-ray diffraction (XRD), TGA, SEM, $^{29}$Si CP MAS NMR, ion exchange and adsorption measurements.**

Titanium silicates such as TS-1,[1,2] TS-2[3] Ti-β,[4,5] *etc*., have attracted considerable research attention since they have been found to have remarkable catalytic activity and selectivity in the hydroxylation of organic compounds in the presence of dilute aqueous hydrogen peroxide. Recently, two novel titanium silicates ETS-4[6,7] and ETS-10[6–8] have been discovered, which have interesting structures and exhibited unique ion-exchange and adsorption properties. More recently, we synthesized a novel layered titanium silicate JDF-Ll[9,10] with five-coordinate titanium, which has potential in catalysis, intercalation and ion-exchange.

There are many natural titanium silicates occurring in the Earth's crust, but only a few such as pharmacosiderite[11,12] and zorite[13] could be synthesized. Penkvilksite was originally described by Bussen *et al*.,[14] as a new titanosilicate mineral, with chemical formula $Na_4Ti_2Si_8O_{22}{\cdot}5H_2O$ and space group indexed as orthorhombic or monoclinic. After the second polytype was found in nature, the orthorhombic penkvilksite was denoted penkvilksite-2O and the monoclinic penkvilksite as penkvilksite-1M.[15] Both penkvilksite-2O and penkvilksite-1M have minor substitutions of Ca, Zr, Fe and Al for Na, Ti and Si, respectively. The structure consists of $TiO_6$ octahedra and $SiO_4$ tetrahedra connected to each other to form a three-dimensional framework.

Here we report, for the first time, the synthesis of a penkvilksite-type titanium silicate. The samples were synthesized hydrothermally using tetrabutyltitanium(IV) (98%), tetramethylammonium hydroxide (TMAOH, 25%), fumed silica (99.9%), sodium hydroxide (96%) and distilled water as reactants. The chemical composition of the initial gel was $3.7SiO_2 : 5.9TiO_2 : 1.0Na_2O : 100H_2O : 0.6(TMA)_2O$. In a typical preparation, the following procedure was followed: sodium hydroxide (0.27 g) was first dissolved in distilled water (12 ml) and then $Ti(OBu^n)_4$ (5.1 g) was added slowly to the solution under vigorous stirring, to which aqueous TMAOH (2.5 ml) was added, followed by fumed silica (0.6 g). The mixture was stirred until it became homogeneous, then transferred into a Teflon-lined stainless-steel autoclave, and heated at 473 K for *ca*. 15 days. The products were recovered by filtration, washed and dried at 353 K. The sample was characterized by X-ray diffraction (Rigaku D/MAX-IIIA), thermal analysis (Perkin-Elmer, TGA-7), scanning electron microscopy (Hitachi X-650B), and $^{29}$Si CP MAS NMR (Bruker MSL-400).

The XRD pattern of the as-synthesized crystalline product is similar to that of the mineral penkvilksite, but showing different relative intensities (Fig. 1). SEM showed that the sample consisted of plate-like crystals of *ca*. 20 × 50 μm (Fig. 2).

Thermogravimetry of the product showed a total mass loss of 7.8% from 328 to 588 K. This was considered to be mainly due to the removal of waste located on the external surface and in the pores. The product is stable up to 873 K and converts into a dense phase at *ca.* 973 K, as indicated by XRD analysis.

In the $^{29}$Si CP MAS NMR study of the as-synthesized penkvilksite, three signals with chemical shifts of $\delta$ −85.2, −96.0 and −101.6 referenced to tetramethylsilane were

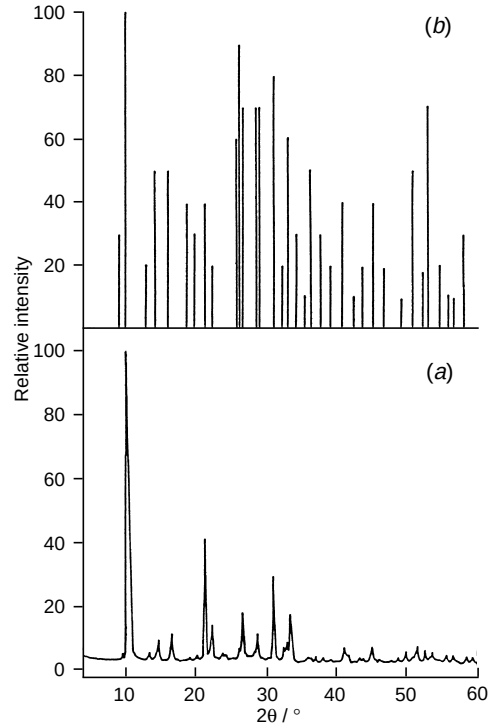



**Fig. 1.** X-Ray diffraction patterns of (*a*) as-synthesized penkvilksite and (*b*) the mineral penkvilksite

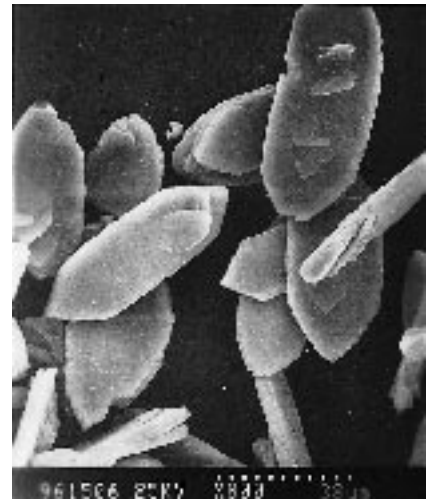


**Fig. 2.** Scanning electron micrograph of as-synthesized penkvilksite

observed. According to refs. 8 and 13, the resonance at $\delta$ −85.2 can be attributed to Si(2Si, 2Ti) and that at $\delta$ −96.0 to Si(3Si, 1Ti). These assignments are consistent with the framework connectivity of penkvilksite. The additional resonance at $\delta$ −101.6 may be due to small amount of impurities in the sample.

The ion-exchange behaviour of penkvilksite was measured in 1 M $KNO_3$ at 80 °C sitrring for 24 h. It was found that 18% of the potassium ions could be exchanged into the penkvilksite. The ion-exchange capacity of $K^+$ is 0.72 mequiv $g^{-1}$ which is lower than that of other minerals. This may be due to the short reaction time employed.

Adsorption studies were performed isothermally in a Cahn 2000 balance. Before the test, the calcined sample was dehydrated at 473 K at $10^{-3}$ Torr for 2 h, and then cooled to room temp. under vacuum. Brunauer–Emmett–Teller (BET) adsorption experiments showed type 1 adsorption behaviour and indicated that the adsorption capacity of water was 6.0 mass% at $p/p_0 = 0.2$.

In the synthesis of titanosilicate penkvilksite, we found that alkali-metal ions have an important effect on its formation. In fact, several titanosilicates were produced in $SiO_2$–$TiO_2$–$M_2O$–$H_2O$–$(TMA)_2O$ (M = $Na^+$ or $K^+$ or $Na^+ + K^+$) systems, dependent on the content of alkali-metal ions in the gel. In the presence of $K^+$, ETS-10 was readily obtained, while with $Na^+$ ions alone in the gel, penkvilksite and ETS-4 were synthesized. The former was favoured at low $Na^+$ concentration and the latter at high $Na^+$ concentration. In addition, the titanium content was also an important factor for the formation of penkvilksite. Appropriate titanium content in the gel was found to be essential in the crystallization of the pure products. Higher or lower titanium content resulted in the formation of amorphous phases or quartz impurities.

In conclusion, a titanosilicate penkvilksite analogue has been synthesized for the first time under hydrothermal conditions. Its successful synthesis provides possibilities in the synthesis of other new types of titanium silicate materials by varying various synthesis factors such as alkali-metal ions used, titanium content and templates, *etc*.

The authors would like to thank the National Natural Science Foundation of China, the Doctorial Program Foundation of the State Education Commission of China and the Key Laboratory of Inorganic Synthesis and Preparative Chemistry of Jilin University for support.

## References

1 M. Taramasso, G. Perego and B. Notari, *US Pat.*, 4 410 501, 1983.
2 S. Bordiga, S. Coluccia, C. Lamberti, L. Marchese, A. Zecchina, F. Boscherini, F, Genoni, G. Leofanti, G. Petrini and G. Vlaic, *J. Phys. Chem.*, 1994, **98**, 4125.
3 J. S. Reddy, R. Kumar and P. Ratnasany, *Appl. Catal.*, 1990, **58**, L1.
4 T. Blasco, M. A. Camblor, A. Corma and J. Perez-Pariente, *J. Am. Chem. Soc.*, 1993, **115**, 11 806.
5 M. A. Camblor, A. Corma and J. Perez-Pariente, *Zeolites*, 1993, **13**, 82.
6 S. M. Kuznicki, *US Pat.*, 4 853 202, 1989.
7 S. M. Kuznicki, *US Pat.*, 4 938 939, 1990.
8 M. W. Anderson, O. Terasaki, T. Ohsuna, A. Philippou, S. P. MacKay, A. Ferreira, J. Rocha and S. Lidin, *Nature*, 1994, **367**, 347.
9 H. Du, M. Fang, J. Chen and W. Pang, *J. Mater. Chem.*, 1996, **6**, 1827.
10 M. A. Roberts, G. Sankar, J. M. Thomas, R. H. Jones, H. Du, J. Chen, W. Pang and R. Xu, *Nature*, 1996, **381**, 401.
11 W. T. A. Harrison, T. E. Gier and G. D. Stucky, *Zeolites*, 1995, **15**, 408.
12 E. A. Behrens, D. M. Poojary and A. Clearfield, *Chem. Mater.*, 1996, **8**, 1236.
13 H. Du, F. Zhou, W. Pang and Y. Yue, *Microporous Mater.*, 1996, **7**, 73.
14 I. V. Bussen, Yu. P. Men'shikov, A. N. Mer'kov, A. P. Nedorezova, Yc. I. Uspenksaya and A. P. Khomyakov, *Dokl. Earth Sci. Sect.*, 1975, **217**, 126.
15 S. Merlino, M. Pasero, G. Artioli and A. P. Khomyakov, *Am. Miner.*, 1994, **79**, 1185.

*Received in Cambridge, UK, 10th April 1997; 7/02452E*

# Stereoselective synthesis of the *C*-analogue of β-D-glucopyranosyl serine

**Luigi Lay,[a] Morten Meldal,[b] Francesco Nicotra,[a] Luigi Panza*[a] and Giovanni Russo[a]**

[a] *Dipartimento di Chimica Organica e Industriale, Centro per lo Studio delle Sostanze Organiche Naturali del CNR, Università di Milano, via Venezian 21, I-20133 Milano, Italy*
[b] *Carlsberg Laboratory, Department of Chemistry, Gamle Carlsberg Vej 10, DK-2500 Valby, Copenhagen, Denmark*

**The [2,3]-Wittig sigmatropic rearrangement of an appropriate glucose derivative followed by further chemical modification afforded stereoselectively the *C*-analogue of β-D-glucopyranosyl serine.**

Protein glycosylation plays fundamental roles in inter- and intra-cellular recognition.[1] Thus, *N*-linked protein glycosylation is involved in protein sorting and the ability of the immune system to recognize and discriminate *O*-linked tumour associated glycoprotein antigens of malignant tissue as foreign structures has been well documented.[1] Furthermore, *O*-glycosylation of a peptide or a protein can increase their solubility and their resistance towards enzymatic degradation, can modify the conformation of the peptide backbone and modulate the biological activity. These properties have recently stimulated great interest in glycopeptides as therapeutic agents.[2]

One limitation of the use of these compounds as potential drugs is the sensitivity of the glycosidic linkage between the sugar and the peptide towards both chemical and enzymatic deglycosylation.[1] For these reasons it is of great interest to have access to stable analogues of *O*-glycosylated amino acids, such as *C*-glycosyl amino acids, in which the glycosidic oxygen atom can be substituted with a methylene group or omitted to give nor analogues. Few examples of the synthesis of *C*-glycosyl amino acids as well as their incorporation in biologically active peptides appear in the literature.[3] However, such compounds are not easily obtainable, particularly by direct carbon–carbon bond forming reactions between a sugar and an amino acid,[4] and have usually been prepared as diastereoisomeric mixtures at the α-carbon of the amino acid moiety.[3]

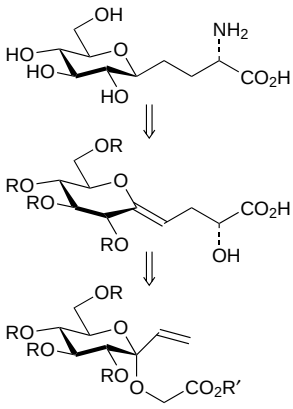
Here we describe the synthesis of the *C*-analogue of glucopyranosyl serine using a [2,3]-Wittig sigmatropic rearrangement[5] in which the chirality of the sugar induces the stereoselective formation of the amino acid moiety, according to the retrosynthetic pathway in Scheme 1.

The appropriate precursor **2**† for Wittig rearrangement was prepared in 70% yield (Scheme 2) from known compound **1**[5] by treatment with methyl glycolate (5 equiv.) and $BF_3{\cdot}Et_2O$ (1.5 equiv.) in the presence of 4 Å molecular sieves.

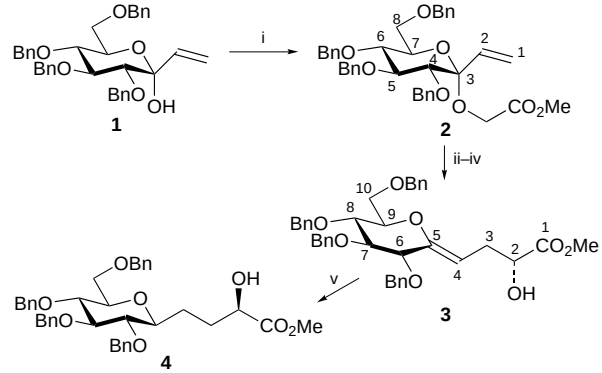
Since preliminary attempts to effect silyl trifluoromethanesulfonate-mediated Wittig rearrangement[6] on **2** were unsuccessful, the dianionic [2,3]-Wittig rearrangement[7] was considered. Compound **2** was then hydrolysed with 2% NaOH in MeOH. The carboxylic acid obtained was treated with excess LDA (3 equiv.) in THF at −78 °C and the reaction mixture was allowed to warm to 0 °C. The crude product was then treated wih $CH_2N_2$ in $Et_2O$–MeOH and the α-hydroxy ester **3** was isolated in 70% yield from **2** (de > 95%). The geometry of the newly formed double bond was shown to be *Z* by an NOE experiment.‡ Compound **3** was hydrogenated with freshly prepared Raney-Ni in EtOH to give **4** in 80% yield. The absolute configuration of the stereocentre at C-2 was determined converting **4** into the (*R*)- and (*S*)-MTPA esters by treatment with (*R*)- and (*S*)-MTPA chloride, respectively, in $CH_2Cl_2$–pyridine. The $^1$H NMR spectrum of the MTPA esters showed a $\Delta\delta$ value ($\delta S - \delta R$) of +0.1 ppm for the signals of the hydrogen atoms at C-3 and C-4, allowing the assigment of the absolute configuration *R* at C-2.[8]

Moreover, the chemical shift of the hydrogen atom at C-5 of **4**, which resonates at $\delta$ 3.27, suggests the presence of an equatorial substituent which was confirmed subsequently on compound **8**.

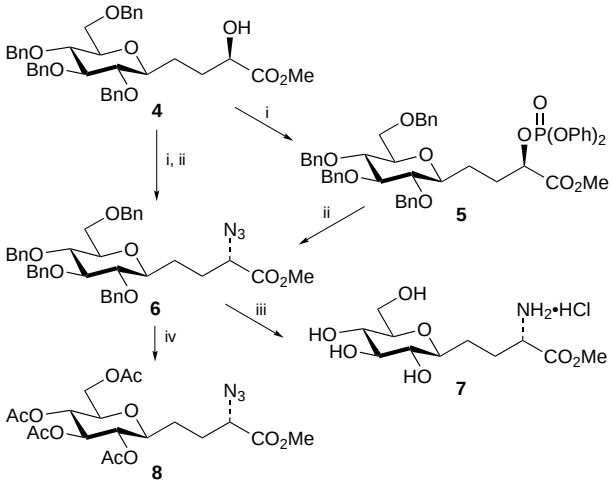
The substitution of the hydroxy group with a nitrogen was attempted using diphenylphosphoryl azide (DPPA),[9] which should have allowed the direct conversion of an α-hydroxy ester to the corresponding azide with inversion of configuration. When compound **4** was treated with DPPA (2.5 equiv.) and DBU (0.98 equiv.) in toluene at 20 °C, only the intermediate phosphate **5** was isolated in good yield (Scheme 3). Moreover, when the reaction mixture was heated, the substitution reaction with the azide was incomplete even at reflux (110 °C) and gave many byproducts. However, treatment of the phosphate with




**Scheme 1**




**Scheme 2** *Reagents and conditions*: i, $HOCH_2CO_2Me$, $BF_3{\cdot}Et_2O$, 20 °C, 70%; ii, NaOH, MeOH, room temp.; iii, LDA, THF, −78 → 0 °C; iv, $CH_2N_2$, $Et_2O$–MeOH, 70% from **2**; v, $H_2$, Raney-Ni, MeOH, 80%



**Scheme 3** *Reagents and conditions*: i, DPPA, DBU, toluene; ii, $Bu_4NN_3$, toluene; iii, $H_2$, $Pd(OH)_2$, EtOH, quant.; iv, $Ac_2O$, $Me_3SiOSO_2CF_3$, 67%

$Bu_4NN_3$ in toluene gave the desired substitution product **6** in 88% yield. The reaction conditions were then modified as follows to obtain a one-pot transformation: the phosphate ester was formed as described above, but with heating to 55 °C. Then a solution of $Bu_4NN_3$[10] (3 equiv., 0.2 M solution in toluene) was added and the mixture was stirred at the same temperature until the phosphate ester disappeared on TLC: in this way the desired azido ester **6** was obtained in 92% yield.§

Reduction of the azido group and contemporary hydrogenolysis of the benzyl ethers was carried out with $Pd(OH)_2$ in EtOH containing few drops of 5% aq. HCl to finally afford the deprotected compound **7** in an almost quantitative yield.

In order to incorporate the obtained analogue into glycopeptides using either solution or solid phase synthesis, it would be useful to maintain the azido group[11] and to change the protecting groups on the sugar moiety. The benzylated analogue **6** was thus submitted to acetolysis[12] by treatment with trimethylsilyl trifluoromethanesulfonate in $Ac_2O$ at room temp. for 40 h to give the acetylated derivative **8** in 67% yield.

The $^1$H NMR spectrum of compound **8** showed a signal at $\delta$ 3.42 due to the hydrogen atom at C-5 in which the coupling constant with the adjacent ring hydrogen at C-6 (*J* 9.5 Hz) clearly confirmed that the equatorial configuration had been obtained at position 5, corresponding to the β-anomer of the *O*-linked analogue.

The reported procedure allows a simple and stereoselective access to the *C*-linked analogue of glucopyranosyl serine which can be incorporated in synthetic peptides. As the sugar moiety is not directly involved into chemical modifications, the procedure could be, in principle, applicable to other monosaccharides. Work is in progress to extend the scope of the procedure.

Part of the present work was supported by the EU-Carenet 2 program (ERB4061PL95-0372).

## Footnotes

* E-mail: panza@imiucca.csi.unimi.it

† All new compounds gave satisfactory elemental analysis and specroscopic data. *Selected data*: $[\alpha]_D$: **2**, 25.3 (*c* 0.8, $CHCl_3$); **3**: 45.6 (*c* 1.0, $CHCl_3$); **4**, 4.5 (*c* 0.9, $CHCl_3$); **5**, 5.4 (*c* 1.0, $CHCl_3$); **6**, 8.9 (*c* 1.0, $CHCl_3$); **7**, −8.1 (*c* 1.0, MeOH); **8**, 16.4 (*c* 1.0, $CHCl_3$). $^1$H NMR ($CDCl_3$): **2**, 5.96 (dd, 1 H, *J* 17.5, 10.8 Hz, H-2), 5.60 (dd, 1 H, *J* 17.5, 1.7 Hz, H-1a), 5.30 (dd, 1 H, *J* 10.8, 1.7 Hz, H-1b), 4.22 (t, 1 H, *J* 9.5 Hz, H-5), 4.10 and 4.02 (2 d, 2 H, *J* 16.1 Hz, C*H*$_2$CO$_2$Me), 3.72 (s, 3 H, Me), 3.42 (d, 1 H, *J* 9.5 Hz, H-4); **3**, 4.94 (t, 1 H, *J* 7.4 Hz, H-4), 4.26 (br t, 1 H, *J* 5.1 Hz, H-2), 3.91 (d, 1 H, *J* 5.7 Hz, H-6), 3.71 (s, 3 H, Me), 2.94 (br s, 1 H, OH), 2.67–2.58 (m, 2 H, H-3); **4**, 4.18 (dd, 1 H, *J* 7.5, 4.4 Hz, H-2), 3.72 (s, 3 H, Me), 3.27 (m, 1 H, H-5), 3.04 (br s, 1 H, OH), 2.03 (m, 1 H, H-4a), 1.88 (m, 2 H, H-3), 1.57 (m, 1 H, H-4b); **5**, 5.04 (dt, 1 H, *J* 7.7, 4 Hz, H-2), 3.65 (s, 3 H, Me), 3.18 (m, 1 H, H-5), 2.15 (m, 1 H, H-3a), 1.93 (m, 2 H, H-3b and H-4a), 1.57 (m, 1 H, H-4b); **6**, 3.94 (dd, 1 H, *J* 8.8, 4.6 Hz, H-2), 3.74 (s, 3 H, Me), 3.26 (m, 1 H, H-5), 2.03 (m, 1 H, H-3a), 1.81 (m, 2 H, H-3b and H-4a), 1.56 (m, 1 H, H-4b); **7** ($D_2O$, 50 °C), 4.39 (t, 1 H, *J* 6.3 Hz, H-2), 4.02 (s, 3 H, Me), 3.48 (m, 1 H, H-5), 2.38 (m, 1 H, H-3a), 2.21 (m, 2 H, H-3b and H-4a), 1.73 (m, 1 H, H-4b); **8**, 5.14 (t, 1 H, *J* 9.5 Hz, H-7), 5.01 (t, 1 H, *J* 9.5 Hz, H-8), 4.85 (t, 1 H, *J* 9.5 Hz, H-6), 4.18 (dd, 1 H, *J* 12.4, 5.2 Hz, H-10a), 4.08 (dd, 1 H, *J* 12.4, 2.3 Hz, H-10b), 3.89 (dd, 1 H, *J* 8.8, 4.5 Hz, H-2), 3.77 (s, 3 H, Me), 3.60 (ddd, 1 H, *J* 9.5, 5.2, 2.3 Hz, H-9), 3.42 (dt, 1 H, *J* 9.5, 2.4 Hz, H-5), 2.1–1.9 (m, 13 H, H-3a and 4 Ac), 1.8–1.6 (m, 2 H, H-3b and H-4a), 1.57 (m, 1 H, H-4b).

‡ By irradiation of the vinylic hydrogen, an NOE of 4.5% was observed on the hydrogen atom at C-6 for compound **3**.

§ $^1$H and $^{13}$C NMR spectra of compounds **6**-**8** each showed a single set of peaks indicating the formation of a single diastereoisomer.

## References

1 H. Lis and N. Sharon, *Eur. J. Biochem.*, 1993, **218**, 1; R. A. Dwek, *Chem. Rev.*, 1996, **96**, 683; S.-I., Hakmori, *Adv. Cancer Res.*, 1989, **52,** 257; G. W. Hart, K. D. Greis, D. L.-Y. Dong, M. A. Blomberg, T.-Y. Chou, M.-S. Jiang, E. P. Roquemore, D. M. Snow, L. K. Kreppel, R. N. Cole, F. I. Comer, C. S. Arnold and B. K. Hayes, in *Glycoimmunology*, ed. A. Alavi and J. S. Axford, Plenum Press, New York, 1995, pp. 115–123.

2 J. F. Fisher, A. W. Harrison, G. L. Bundy, K. F. Wilkinson, B. D. Rush and M. J. Ruwart, *J. Med. Chem.*, 1991, **34**, 3140; J. Kihlberg, J. Ahman, B. Walse, T. Drakenberg, A Nilsson, C. Söderberg-Ahlm, B. Bengtsson and H. Olsson, *J. Med. Chem.*, 1995, **38**, 161.

3 K. Michael, V. Wittmann, W. König, J. Sandow and H. Kessler, *Int. J. Pept. Protein Res.*, 1996, **48**, 59 and references cited therein.

4 B. J. Dorgan and R. F. W. Jackson, *Synlett*, 1996, 859.

5 A paper in which glucose is used in a Wittig rearrangement for the stereoselective synthesis of chiral prop-2-ynylic alcohols has recently been published: K. Tomooka, Y. Nakamura and T. Nakai, *Synlett*, 1995, 321.

6 K. Mikami, O. Takahashi, T. Tabei and T. Nakai, *Tetrahedron Lett.*, 1986, **27**, 4511.

7 K. Kakinuma and H.-Y. Li, *Tetrahedron Lett.*, 1989, **31**, 4157.

8 I. Ohtani, T. Kusumi, Y. Kashman and H. Kakisawa, *J. Am. Chem. Soc.*, 1991, **113**, 4092.

9 A. S. Thompson, G. R. Humphrey, A. M. DeMarco, D. J. Mathre and E. J. J. Grabowski, *J. Org. Chem.*, 1993, **58**, 5886.

10 A. Brändström, B. Lamm and I. Palmertz, *Acta Chem. Scand. Ser. B*, 1974, **28**, 699.

11 M. Meldal, M. A. Juliano and A. M. Jansson, *Tetrahedron Lett.*, 1997, **38**, 2531.

12 J. Alzeer and A. Vasella, *Helv. Chim. Acta*, 1995, **78**, 177.

*Received in Cambridge, UK, 6th May 1997; 7/03063K*

# A short highly stereoselective synthesis of the fluorinated natural product (2*S*,3*S*)-4-fluorothreonine

**Muhammad R. Amin,[a] David B. Harper,[b] Janet M. Moloney,[a] Cormac D. Murphy,[b] Judith A. K. Howard[a] and David O'Hagan*[a]**

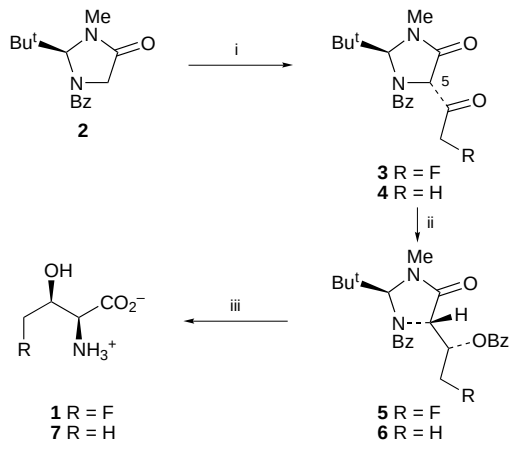
[a] *Department of Chemistry, University of Durham, Science Laboratories, South Road, Durham, UK DH1 3LE*
[b] *Department of Food Science, The Queen's University of Belfast, Newforge Lane, Belfast, UK BT9 5PX*

**A three step stereoselective route to the fluorinated natural product (2*S*,3*S*)-4-fluorothreonine is described; the route is amenable to the preparation of (2*S*,3*S*)-4-fluoro[3-$^2$H]threonine and (2*S*,3*R*)-[4,4,4-$^2H_3$]threonine.**

4-Fluorothreonine **1** is a secondary metabolite of *Streptomyces cattleya* and is one of the few natural products that contain fluorine. The compound was first isolated[1] in 1986 in the course of studies aimed at improving thienamycin production by the organism. It was reported to be a single stereoisomer but the relative or absolute stereochemistry was not established at that time. Two syntheses of (2*S*,3*S*)-4-fluorothreonine **1** have been reported,[2] one prior[3] to its isolation from *S. cattleya*, and in each case the optical rotation values were close to that of the natural amino acid **1** ($[\alpha]_D$ −20) implying a 2*S*,3*S* absolute configuration. In our current programme[4–6] focused on evaluating the biosynthetic origin of fluoroacetate and 4-fluorothreonine in *S. cattleya* it proved necessary to confirm the absolute stereochemistry of **1**. As the two published syntheses are lengthy we have developed a new and more direct approach to (2*S*,3*S*)-4-fluorothreonine **1** which exploits Seebach's imidazolidinone methodology for the synthesis of α-amino-β-hydroxy acids.[7] This appeared attractive at the outset as a straightforward condensation between **2** and fluoroacetaldehyde should deliver the required framework. However, fluoroacetaldehyde is not readily prepared and despite several attempts we were not able to devise a suitable synthesis. The literature preparations[8] for fluoroacetaldehyde generated aqueous solutions which are inadequate for the current purpose.

The route was therefore modified as shown in Scheme 1 such that **2** was treated with fluoroacetyl chloride[9] (**WARNING**: highly toxic) to generate the resultant β-ketone **3**,† a crystalline solid. From the X-ray structure of **3** it is noteworthy that the geometry at C-5 is fully tetrahedral and that the β-carbonyl system is non-planar. This is an important feature as C-5 is rendered configurationally stable, a situation that is revealed again in the X-ray structure of the analogous defluorohydro compound **4**,‡ an intermediate in our synthesis of (2*S*,3*R*)-threonine (Fig. 1). It was not clear at the outset if the subsequent reduction of the β-carbonyls of **3** and **4** would be stereoselective and deliver the desired *threo* products, however in the event this proved to be the case. Treatment of **3** and **4** with $NaBH_4$ in MeOH generated the benzoate esters **5**§ and **6** respectively as single diastereoisomers. The benzoates **5** and **6** and not the *N*-benzoyl derivatives were the sole products, indicating a facile transacylation after carbonyl reduction. This transacylation is consistent with Seebach's observations[7b] after the direct condensation of **2** with acetaldehyde. The *allo*-diastereoisomers were not detectable by $^{13}C$, $^1H$ and $^{19}F$ (for **5** only) NMR spectroscopy of the crude reaction products, indicating that the reduction is highly stereoselective with hydride delivered exclusively to the *si* face of **3** (*re* face of **4** due to a change in assignment priorities). If the transition state conformation of **3** bears a resemblence to the ground state structure as shown in Fig. 1 then the *si* face of the carbonyl is the more exposed of the two as the *N*-benzoyl aromatic ring hinders access to the *re* face.

The benzoates **5** and **6** were subjected to hydrolysis (10 M HCl at 100 °C) and the resultant (2*S*,3*S*)-4-fluorothreonine **1**¶ and (2*S*,3*R*)-threonine **7** [identical in all respects to natural (2*S*,3*R*)-threonine] were recovered after purification on Dowex $H^+$. The *threo* relative stereochemistry of **1** was confirmed by an




**Scheme 1** *Reagents and conditions*: i, LDA, $FCH_2COCl$ (acetyl chloride for **4**), THF, −100 °C, 57%; ii, $NaBH_4$, MeOH, 20 °C, 5 min, 67%; iii, 10 M HCl, 100 °C, 72 h, 64%

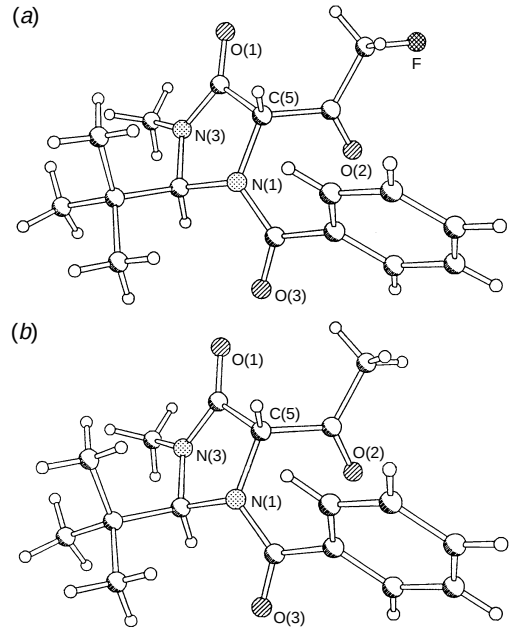



**Fig. 1** X-Ray structures of **3** (*a*) and **4** (*b*). The geometry at C-5 of the β-ketone is tetrahedral in each case.

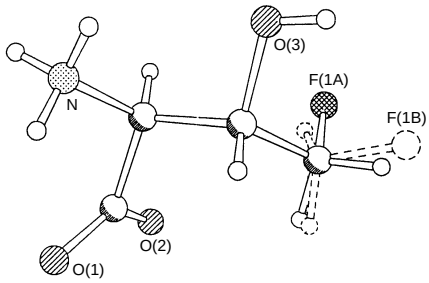
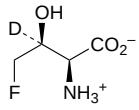
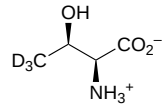



**Fig. 2** X-Ray structure of synthetic (2*S*,3*S*)-4-fluorothreonine **1**, showing two positions for the disordered $CH_2F$ group with occupancies of 66(2)% (solid) and 34(2)% (dashed)

X-ray structural study‖ (Fig. 2). The 2*S*,3*S* assignment for **1** follows from the structure of **3** where the known absolute stereochemistry of the auxiliary allows a 2*S* designation to be made at C-5 and subsequently at the α-position of the amino acid. All analytical data ($[\alpha]_D$ −20, $^{19}F$ NMR, HPLC, GC–MS of MSTFA derivative) were identical to a sample of 4-fluorothreonine **1** isolated[4] from *Streptomyces cattleya*, confirming the absolute stereochemistry of the natural product. Additionally this route to (2*S*,3*S*)-4-fluorothreonine is amenable to isotope labelling and (2*S*,3*S*)-4-fluoro[3-$^2$H]threonine **1a** was prepared by employing $NaB^2H_4$ in the reduction step. This material is being used to probe the anabolic and catabolic flux of (2*S*,3*S*)-4-fluorothreonine in *S. cattleya*.




**1a**




**7a**

The modified methodology offers an alternative route to *threo* amino acids and it displays a higher stereoselectivity to that previously described for (2*S*,3*R*)-threonine.[7b] The method has the additional advantage of using acid chlorides in place of aldehydes when the requisite aldehyde is unavailable, as in the case of fluoroacetaldehyde, or is expensive, as in the case of isotopic labelling. For example, a sample of racemic [4,4,4-$^2H_3$]threonine **7a** was prepared from [$^2H_3$]acetyl chloride, a cheaper and more highly stereoselective route to the labelled amino acid than that using [$^2H_3$]acetaldehyde with racemic imidazolidinone **2**.

We thank Dr A. S. Batsanov (University of Durham, Department of Chemistry) for help in the X-ray structural work. We are also grateful to Drs Roy Bowden, Harry Eccles and Peter Binks of BNFL for their interest in this work and to BNFL Company Research Laboratories, Springfields, for financial support.

## Footnotes

* E-mail: david.O'hagan@durham.ac.uk

† *Selected data* for **3**: mp 197 °C; $[\alpha]_D$ +140 (*c* 1, $CHCl_3$); $\nu_{max}(CDCl_3)$/cm$^{-1}$ 3360m, 2960s, 1715s, 1695s, 1665m; $\delta_H(CDCl_3)$ 7.60–7.35 (5 H, m, Ar), 5.75 [1 H, s, HC(2)], 5.39 [1 H, s, HC(5)], 4.45 (2 H, m, $FCH_2$), 3.06 (3 H, s, NMe), 1.08 (9 H, s, Bu$^t$); $\delta_C(CDCl_3)$ 197.7 (C-1′, d, $J_{CF}$ 18.6), 170.6 (*C*OPh), 165.0 (C-4), 135.8 (Ar), 131.6 (Ar), 128.8 (Ar), 127.6 (Ar), 83.8 (C-2′, d, *J* 187), 80.4 (C-2), 66.2 (C-5), 40.3 [*C*$(CH_3)_3$], 32.2 (NMe), 26.1 [C(*C*$H_3)_3$]; $\delta_F(CDCl_3)$ −230.8 (t, *J* 46.3); Found: C, 63.52; H, 6.63; N, 8.63. $C_{17}H_{21}N_2O_3F$ requires: C, 63.68; H, 6.55; N, 8.74%.

‡ *Selected data* for **4**: mp 188–189 °C (decomp.); $[\alpha]_D^{25}$ +120 (*c* 0.01, $CHCl_3$); $\nu_{max}(CDCl_3)$/cm$^{-1}$ 2984s (br), 2940s (br), 2287s (br), 1732s, 1700s, 1397s; $\delta_H(CDCl_3)$ 7.60–7.23 (5 H, m, Ar), 5.64 (1 H, s, HC-2), 5.11 [1 H, s, HC(5)], 3.00 (3 H, s, NMe), 1.82 (3 H, s, $CH_3CO$), 0.99 (9 H, s, Bu$^t$); $\delta_C(CDCl_3)$ 199.7 (C-1″), 171.3 (*C*OPh), 165.3 (C-4), 136.3 (Ar), 131.3 (Ar), 128.6 (Ar), 127.7 (Ar), 79.9 (C-2′), 70.5 (C-5), 40.3 [*C*$(CH_3)_3$], 32.1 (NMe), 28.7 (C-2′), 26.1 [C(*C*$H_3)_3$]; Found: C, 56.18; H, 7.27; N, 9.21. $C_{17}H_{22}N_2O_3$ requires: C, 56.29; H, 7.28; N, 9.27%.

§ *Selected data* for **5**: (0.32 g, 67%): an oil; $[\alpha]_D$ −13 (*c* 1, $CHCl_3$); $\nu_{max}$ $(CDCl_3)$/cm$^{-1}$ 3360m (br), 2958s, 1675s, 1645m; $\delta_H(CDCl_3)$ 8.10–7.60 (5 H, m, Ar), 5.62 (1 H, m, HCObz), 4.91 (2 H, dm, *J* 47, $FH_2C$), 4.31 [1 H, d, *J* 2.1, HC(2)], 4.15 [1 H, m, HC(5)], 3.02 (3 H, s, NMe), 1.15 (9 H, s, Bu$^t$; $\delta_C(CDCl_3)$ 172.5 (*C*OPh), 165.4 (CO), 133.2 (Ar), 129.6 (Ar), 129.4 (Ar), 128.3 (Ar), 83.7 (C-2), 81.8 (C-2′, d, *J* 172.4, $CH_2F$), 72.1 (C-1′, d, *J* 19.4, *C*OBz), 58.2 (C-5), 37.2 [*C*$(CH_3)_3$], 31.1 (NMe), 25.3 [C(*c*$H_3)_3$]; $\delta_F$ $(CDCl_3)$ −233.1 (dt, *J* 47.4, 25); Found: 323.17628. $C_{17}H_{23}N_2O_3F$ requires: 323.17709 (M + H$^+$).

¶ *Selected data* for **1** (90 mg, 64%): white crystalline solid; mp 182–183 °C (lit.,[1,2] 181–182 °C); $[\alpha]_D$ −20 (*c* 5, $H_2O$) [lit.,[2] −20 (*c* 0.06, $H_2O$]; $\nu_{max}$(KBr)/cm$^{-1}$ 3500s, 3000s, 2800s, 1435m, 1130m; $\delta_H$ ($D_2O$) 4.52 (2 H, ddd, *J* 46.5, 10.5, 3.9, $CH_2F$), 4.22 (1 H, dq, *J* 25, 4.6, HC(3), 3.72 [1 H, d, *J* 4.8, HC(2)]; $\delta_C(D_2O)$ 175.5 (C-1), 87.8 (d, *J* 167.5, C-4), 70.8 (d, *J* 19.1, C-3), 59.2 (C-2); $\delta_F(D_2O)$ −229.7 (dt, *J* 47, 25).

‖ X-Ray diffraction experiments were performed on a Rigaku AFC6S 4-circle diffractometer (graphite-monochromated Cu-Kα radiation, $\lambda$ = 1.54184 Å, $\omega$ scan mode) for **1** and on a Siemens SMART 3-circle diffractometer with a CCD area detector (graphite-monochromated Mo-Kα radiation, $\lambda$ = 0.71073 Å, $\omega$ scan mode in 0.3° frames) for **3** and **4**. The structures were solved by direct methods and refined by full-matrix least-squares (non-H atoms anisotropic, H isotropic) against $F^2$ of all data, using SHELXTL ver. 5/VMS software (G. M. Sheldrick, Siemens Analytical X-Ray Instruments Inc., Madison, WI, USA, 1995). Absolute configurations were assigned according to those of the starting materials. CCDC 182/499.

*Crystal data* for **1**: $C_4H_8FNO_3$, *M* = 137.1, *T* = 296 K, orthorhombic, space group $P2_12_12_1$ (No. 19), *a* = 5.231(1), *b* = 7.870(2), *c* = 13.603(3) Å, *U* = 560.0(2) Å$^3$, *Z* = 4, $D_x$ = 1.63 g cm$^{-3}$, $\mu$ = 13.9 cm$^{-1}$, crystal size 0.15 × 0.15 × 0.05 mm, 730 data total ($2\theta \leqslant 100°$), 549 unique, 447 observed with $I > 2\sigma(I)$, $R_{int}$ = 0.029, 93 variables, *R* (*F*, obs. data) = 0.059, *wR* ($F^2$, all data) = 0.163, goodness-of-fit *S* = 1.02, $\Delta\rho_{min,max}$ = 0.27, −0.22 e Å$^{-3}$.

For **3**: $C_{17}H_{21}FN_2O_3$, *M* = 320.4, *T* = 296 K, orthorhombic, space group $P2_12_12$ (No. 18), *a* = 13.294(1), *b* = 21.437(2), *c* = 6.037(1) Å, *U* = 1720.5(3) Å$^3$, *Z* = 4, $D_x$ = 1.24 g cm$^{-3}$, $\mu$ = 0.9 cm$^{-1}$, crystal size 0.4 × 0.2 × 0.15 mm, 12 388 data total ($2\theta \leqslant 55°$), 3916 unique, 2909 observed, $R_{int}$ = 0.041, 225 variables, *R* = 0.050, *wR* = 0.142, *S* = 1.14, $\Delta\rho_{min,max}$ = 0.19, −0.19 e Å$^{-3}$.

For **4**: $C_{17}H_{22}N_2O_3$, *M* = 302.4, *T* = 150 K, orthorhombic, space group $P2_12_12$ (No. 18), *a* = 12.636(1), *b* = 21.459(2), *c* = 6.059(1) Å, *U* = 1642.9(3) Å$^3$, *Z* = 4, $D_x$ 1.22 g cm$^{-3}$, $\mu$ = 0.8 cm$^{-1}$, crystal size 0.4 × 0.2 × 0.1 mm, 9842 data total ($2\theta \leqslant 50°$), 2866 unique, 2289 observed, $R_{int}$ = 0.064, 216 variables, *R* = 0.050, *wR* = 0.115, *S* = 1.14, $\Delta\rho_{min,max}$ = 0.15, −0.19 e Å$^{-3}$.

## References

1 M. Sanada, T. Miyano, S. Iwadare, J. M. Williamson, B. H. Arison, J. L. Smith, A. W. Douglas, J. M. Liesch and E. Inamine, *J. Antibiot.*, 1986, **39**, 259.
2 M. Shimizu, T. Yokota, K. Fujimori and T. Fujisawa, *Tetrahedron: Asymmetry*, 1993, **4**, 835.
3 C. Scolastico, E. Conca, L. Prati, G. Guanti, L. Banfi, A. Berti, P. Farina and U. Valcavi, *Synthesis*, 1985, 850.
4 K. A. Reid, J. T. G. Hamilton, R. D. Bowden, D. O'Hagan, L. Dasaradhi, M. R. Amin and D. B. Harper, *Microbiology*, 1995, **141**, 1385.
5 J. T. G. Hamilton, M. R. Amin, D. B. Harper and D. O'Hagan, *Chem. Commun.*, 1997, 797.
6 J. Nieschalk, J. T. G. Hamilton, C. D. Murphy, D. B. Harper and D. O'Hagan, *Chem. Commun.*, 1997, 799.
7 (*a*) D. Blaser and D. Seebach, *Liebigs Ann. Chem.*, 1991, 1067; (*b*) D. Seebach, E. Juaristi, D. D. Miller, C. Schickli and T. Weber, *Helv. Chim. Acta*, 1987, **70**, 237; (*c*) D. Seebach, J. D. Aebi, R. Naef and T. Weber, *Helv. Chim. Acta.*, 1985, **68**, 144.
8 G. Teutsch and A. Bonnet, *Tetrahedron Lett.*, 1984, **25**, 1561; B. C. Saunders, G. J. Stacey and I. G. E. Wilding, *J. Chem. Soc.*, 1949, 773.
9 Fluoroacetyl chloride is prepared in a straightforward manner from fluoroacetic acid and thionyl chloride and can be distilled prior to use: D. O'Hagan, J. White and D. A. Jones, *J. Labelled Cmpd. Radiopharm.*, 1994, **34**, 871.

*Received in Cambridge, UK, 7th May 1997; 7/03121A*

ChemComm
FEATURE ARTICLE

# Designer crystals: intermolecular interactions, network structures and supramolecular synthons

**Gautam R. Desiraju**

*School of Chemistry, University of Hyderabad, Hyderabad 500 046, India*

**Questions relating to the prediction of the crystal structure or structures of a given organic molecule may be more gainfully reversed so that retrosynthetic analysis of a target crystal network leads to the identification of molecular precursors. Crystal engineering is solid state supramolecular synthesis and supramolecular synthons, units formed by synthetic operations involving intermolecular interactions, may be used to focus efforts in such logic-driven retrosynthesis.**

## Introduction

Crystal engineering has been defined as the understanding of intermolecular interactions in the context of crystal packing and in the utilisation of such understanding in the design of new solids with desired physical and chemical properties.[1] The origins of this subject lie in the work of Gerhard Schmidt who realised, more than 25 years ago, that the systematic development of organic solid state chemistry required a proper theory of crystal packing.[2] The term 'crystal engineering' was also introduced by Schmidt in the context of solid state reactions and early papers in the subject,[3] including the first *Chemical Communications* from my research group in 1983,[4] were concerned almost exclusively with crystal engineering as a means of developing better organic reactions.

Crystal structures are mediated by intermolecular interactions and the easiest way of obtaining reliable information on these interactions is through crystallography. With the ever-increasing number of accurate X-ray and neutron diffraction analyses, a distinct change in perception occurred with regard to crystal engineering during the late eighties.[1] Instead of concentrating exclusively on topochemical reactions, structural chemists also began to conceive of organic crystals that could act as catalysts, microporous materials, frequency doublers, ferromagnets and superconductors. A particular crystal packing may also be attractive for aesthetic reasons, just as targets like cubane or dodecahedrane have been attractive molecular targets in the past. A crystal is as respectable a synthetic target as a molecule and form and function motivate current efforts in crystal design.

The awareness that a crystal is the supermolecule *par excellence* further heightened interest in crystal engineering and brought the subject into the mainstream of supramolecular chemistry.[5] Crystal engineering is recognised today as an important form of supramolecular synthesis and the full rigour of synthetic methodology and strategy may now be brought to bear in the quest for complex and general supramolecular synthetic targets in the solid state. An important consequence of these developments is the identification of a crystal as a retrosynthetic target.[6]

This article is a personal view of the development and growth of crystal engineering, seen mainly through the 25 or so *Chemical Communications* from my research group.

## From molecular to crystal structure

Crystals are built from molecules and the natural question that has been posed with respect to crystal engineering is, 'given the molecular structure of an organic substance, what is its crystal structure?' The molecular basis of organic chemistry makes such a question seem almost intuitive and much progress was made and is continuing to be made in seeking answers here. The first well-documented attempt in this direction is the correlation, established in 1951 by the great chemical crystallographer J. Monteath Robertson, between the molecular structures of planar fused-ring aromatic hydrocarbons and their packing type as revealed by the crystallographic short axis.[7] Robertson divided such hydrocarbons into two rather broad but fairly distinct types. He observed that disk-like molecules with an area large compared with their thickness (coronene, ovalene) tend to stack in columns and that the periodicity along this short axis, which is usually the monoclinic *b* axis, is about 4.7 Å. In the second class he included molecules which are still flat and disk-like, but of smaller area (naphthalene, anthracene) and noted that there is a tendency for such molecules to be steeply inclined to the symmetry plane and for the periodicity to be about 6.0 Å. It is remarkable that a statement of such prescience was made more than 45 years ago.

In 1988, Angelo Gavezzotti of the University of Milan and I re-examined Robertson's correlation and further amplified it.[8–10] With hindsight of knowledge on intermolecular forces, notably the ubiquitous herringbone and stacking forces, that are prevalent in all types of crystals of aromatic compounds, it was possible to divide fused aromatic hydrocarbons into four categories that are illustrated in Fig. 1: (*a*) the pure herringbone structure (naphthalene, anthracene) contains nearest-neighbour molecules which are related *only* by the inclined T-geometry and have short axes in the 5.4–8.0 Å region; (*b*) the coronene group of Roberston was designated as γ-packing and was shown to contain *both* herringbone and stacking geometries. The short axis range for this group is between 4.6–5.4 Å; (*c*) another group of structures with a monoclinic axis greater than 8.0 Å was also found to exhibit both herringbone and stacking geometries but here, molecular dimers were observed. This group is exemplified by pyrene and perylene and was designated the 'sandwich-herringbone' structure; (*d*) planar hydrocarbons do not crystallise so that *only* stacking interactions are found between nearest-neighbours, but such a possibility exists for cup-shaped molecules like tribenzopyrene. This category was designated as β-packing and it has short axes less than 4.2 Å.

With such an analysis it became possible to predict the packing pattern of any given aromatic hydrocarbon. It was recognised that the herringbone interaction (glide or screw-forming tendency) was promoted by the presence of hydrogen atoms and rim-carbon atoms, while the stacking interactions would be favoured by the presence of many internal carbon atoms in the molecular structure. Glide-stack ratios were therefore derived on the basis of empirically designated glide and stack-forming propensities for each atom in the molecular structure. Plotting these ratios against molecular surface area introduces the idea of molecular shape and with it a mapping from molecular to crystal structure. Our predictions of crystal structure from molecular structure were satisfying but even at the time we were well aware that they are accurate only because the forces in hydrocarbon crystals are isotropic.

Hydrocarbon crystals are exceptional in this regard. Most organic compounds contain heteroatoms and the intermolecular interactions in their crystals are a complex mosaic of forces of varying strengths, directionalities and distance dependence characteristics.[1] Anisotropic, long-range forces tend to dominate crystallisation preferences even as the isotropic forces contribute to the bulk of the crystal sublimation energy. These anisotropic forces are not minor irritants but conspire to render almost impossible direct and simple extrapolations from molecular to crystal structure. A functional group approach is unsuitable because the molecular recognition events during crystallisation depend on the complementarity of molecular structural features rather than on their identity. This is a fundamental problem. Suppose a general molecule to have recognition sites A, B, C, ... and so on. Then, possible recognition patterns could be found from among combinations such as A··B, B··C, A··C or from more complex patterns such as (A,C)··(B,D) or (A,B,C)··(D,E). Each favourable pattern would limit the possibilities for subsequent, subsidiary patterns, but in general the presence of even a moderate number of competitive recognition sites in a molecule, say three of four functional groups capable of hydrogen bonding, could result in a large number of crystal structures $C_1$, $C_2$, $C_3$ ... $C_n$ from a single molecular structure $M_1$. Most of these structures $C_1$–$C_n$ are not routinely realisable in the solid state because polymorphism is not a universal phenomenon. However, even in this mitigating circumstance, the prediction of the experimentally observed structure $C_m$ is not trivial.[11] Computer simulations show that structures $C_1$–$C_n$ are often closely related enthalpically and the global minimum structure is not always the one that is obtained experimentally, either because the computations are approximate or because the crystallisation process is subject to both kinetic and thermodynamic factors.

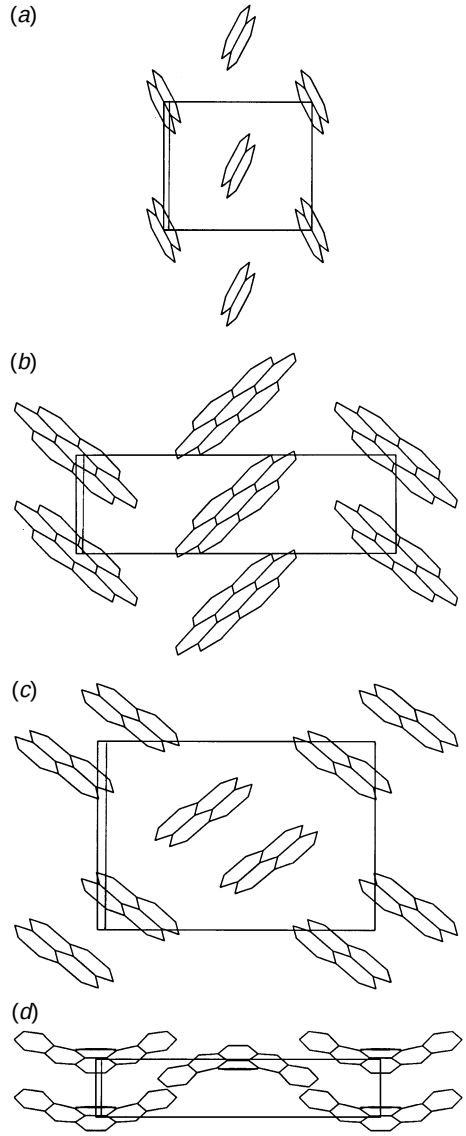
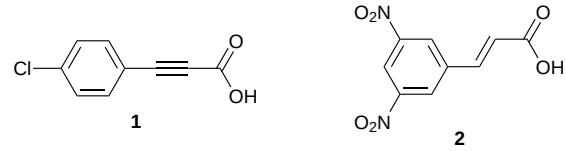
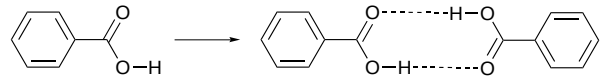



**Fig. 1** The four basic aromatic crystal packings: (*a*) naphthalene, (*b*) coronene, (*c*) pyrene, and (*d*) tribenzopyrene. The short axes are vertical in each case.

A typical manifestation of these problems is illustrated by the anomalous crystal structures of 4-chlorophenylprop-2-ynoic acid **1** and 3,5-dinitrocinnamic acid **2**. Usually it is expected that




carboxylic acids, especially those containing aromatic groups, crystallise with the dimer structure. A few acids adopt the catemer structure but such occurrences have been well-rationalised.[12] This molecular monomer → crystalline dimer transform is the basis of several recent experiments in crystal engineering and many would accept this transform as an article of faith.




However, acid **1** adopts a rare crystal structure with two symmetry independent molecules (Fig. 2).[13] In one, the carboxy group has a *syn* conformation while in the other, it is *anti*. The hydrogen bonding pattern is not quite a catemer but contains alternating molecules with the *syn* and *anti*-conformations. To compound the confusion, each hydrogen bond lies on a centre of inversion and the resulting hydrogen atom disorder does not disappear even at low temperature. In contrast, the almost identical (in molecular terms) 4-chlorocinnamic acid, adopts the 'normal' dimer structure. Again, while acid **2** (space group *C*2/*c*) forms an O–H··O dimer ring, this ring lies on the 2-fold axis rather than on the inversion centre.[14] These anomalous occurrences have been rationalised on the basis of C–H··O hydrogen bonding. In acid **2**, C–H··O hydrogen bonds are dominant and numerous and seem to be so significant that they are able to change the site symmetry of the carboxylic acid O–H··O dimer ring. In **1**, however, their absence (because of the lack of a critically large number of acidic C–H groups in the molecular structure) seems to lead to the unusual *quasi*-catemer structure. C– H··O hydrogen bonds are just one of the several secondary features that can influence, often unpredictably, crystal packing and they have been discussed extensively elsewhere.[15–17]

To summarise, a molecular functional group approach is often difficult in attempting to answer the question, 'given the

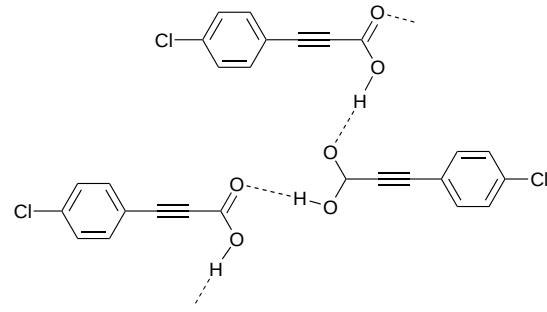



**Fig. 2**

molecular structure of an organic substance, what is its crystal structure?' Of course, this question betrays the molecular basis of classical organic chemistry. Crystals are supermolecules and their structural features are best described in terms of supramolecular descriptors, that is patterns of interactions rather than in terms of molecular descriptors, that is functional groups. A one-to-one correspondence does not exist between functional groups and patterns of interactions and so questions relating to the prediction of supramolecular (crystal) structure from molecular structure (i) are difficult to answer, (ii) may have multiple answers, and (iii) may not even be the most relevant questions one might want to ask.

## The crystal as a supramolecular entity

The term 'supramolecular' signifies that which is beyond the molecule and supramolecular concepts have had the greatest influence in organic chemistry where the molecule is paramount. Supermolecules are not merely collections of molecules but they have structural features and properties that are characteristic not of the molecules themselves but of larger, more extended assemblies.[18] In keeping with this, structural chemists and crystallographers have had little difficulty in recognising an organic crystal as the ultimate example of a supermolecule.[5,19] Indeed, crystals constitute one end of the supramolecular continuum and may be viewed as 'hard' supermolecules in contrast to the 'softer' supramolecular aggregates which exist in solution. Atoms, covalent bonds and molecules have their counterparts in molecules, intermolecular interactions and supermolecules. Accordingly, it is not hard to visualise polymorphism as superisomerism and to identify structural homologous series such as benzene, naphthalene and anthracene.

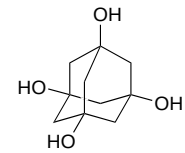
If a crystal is a supermolecule, then crystal engineering is the solid state supramolecular equivalent of organic synthesis.[6] Synthesis is the distinctive feature that demarcates chemistry from the other physical sciences—*la chimie crée son objet*;[20] yet it is only in recent times that synthetic supramolecular chemistry has assumed definite contours. If studies of supramolecular systems should even be a part of chemistry, then the time-tested principles of synthesis should be found to be applicable to them. In this regard, the role of the solid state is especially relevant. Unlike solution supermolecules whose formation could often be influenced by solvent effects, the formation of stable crystal forms permits the establishment of even weak interactions which, when numerous, may affect supramolecular structure decisively. So, crystal structure as defined as a networking of intermolecular interactions is the supramolecular equivalent of molecular structure as defined as a networking of covalent bonds.

## Crystal engineering and organic synthesis

In general, any synthetic activity, in chemistry or elsewhere, may be said to possess three attributes: target identification, strategy and methodology. In loose terms, these attributes amount to knowing the job at hand, what to do, and how to do it. It is pertinent to examine the subject of crystal engineering from this standpoint.

Target identification in traditional organic synthesis consists in knowing the molecular formula of the goal molecule with all the attendant stereochemistry. Crystal engineering is supramolecular synthesis and so targets here must be defined supramolecularly, that is as networks. This is not a familiar exercise. Traditionally, structural chemists have viewed a molecular crystal as an assembly of atoms in which the distances between atoms in certain groups (molecules) are much smaller than the distances between atoms in different groups.[21] This depiction owes to Kitaigorodskii but again betrays the molecular view of organic chemistry. Even the title of Kitaigorodskii's classic *Molecular Crystals and Molecules* reflects this bias. Yet, any organic crystal may be depicted as a network with the molecules as nodes. Such a depiction, although unusual, is not completely new. In Powell's 1948 illustrations of the β hydroquinone clathrates, for example, only the network structures are shown.[22] The molecules have been reduced to points. If such an operation is carried out on the orthorhombic polymorph of benzene, the result is not far from a face-centred cubic lattice. Of course, hydrogen bonded structures lend themselves easily to a network depiction but in the end, *any* organic structure may be thus viewed.

The development of network theory to organic crystal chemistry is novel but this is hardly the case for inorganic crystal structures. Thus the logical step after depicting an organic crystal structure as a network is to search for its inorganic counterpart. Such comparisons are not just chemical curiosities but play a very important part in the development of a proper theory of crystal engineering, because one is able to draw from the very considerable literature which exists in the inorganic structural domain to choose new target networks. In this context, the structure of 1,3,5,7-tetrahydroxyadamantane **3**




**3**

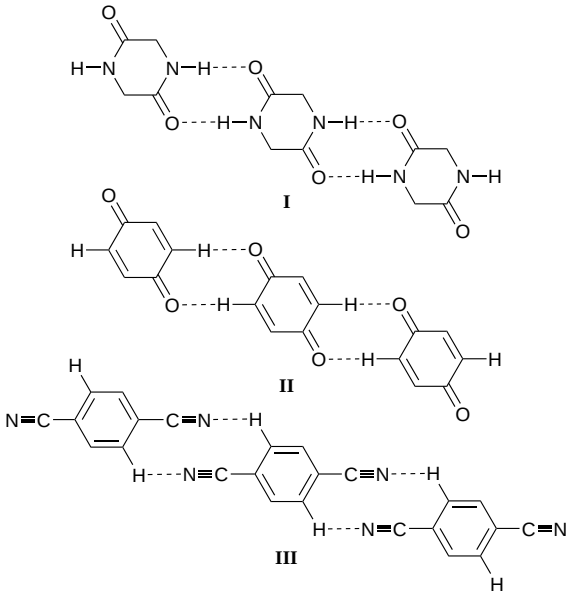
is especially interesting.[23] The crystal packing of this compound may be clearly understood only when it is simplified and reduced in terms of its hydrogen bond network. The structure is intricate and belongs to the uncommon space group *Pbcn* with molecules in both general and special positions. The structure also contains many strong O–H···O hydrogen bonds and our attempts to decipher the packing by conventional methods (plots, geometrical calculations) proved unsuccessful. As an alternative strategy, we sought to develop a structural analogy between **3** and a simple inorganic structure. Now, a hydroxy group has a supramolecular valence of two, corresponding to a pair of hydrogen bonds, one donated and the other accepted. Therefore the packing of **3** should be derivable in terms of an eight-connected net. So we simplified the structure of **3** by reducing the molecules to spheres and displaying only the hydrogen bond connections. The result is shown in Fig. 3 which is easily recognisable as a *quasi*-BCC packing. If one distinguishes between the symmetry independent molecules, one could liken this structure to CsCl or, more strictly speaking, to $Cr_2Al$.

Supramolecular synthetic methodology amounts to a knowledge of the strength and directional characteristics of the intermolecular interactions. Much has been written and said about this topic[1] and I will merely list some of the more important interactions here. Yet, as in molecular synthesis, this is the most arduous component in the synthetic exercise, requiring much knowledge and experience. In addition to the well-understood strong hydrogen bonds of the O–H···O, N–H···O and N–H···N type, weak hydrogen bonds of the C–H···O(N) and O(N)–H···π type should also be considered. A number of other weak heteroatom interactions such as N···halogen, S···S and halogen···halogen are known to have specific effects upon crystal packing, while the more exotic organometallic interactions (O–H···M, M–H···O, Au···Au) are only now beginning to be noticed.[6] A mention must be made of interactions in hydrocarbon systems. It is known for instance that phenyl groups pack with very specific geometries, leading to crystals that are characterised by high crystallinity and low solubility—the so called 'phenyl factor'.[24] In this context, it is still not clear if the C–H···π 'hydrogen bond' is an extreme case of the herringbone interaction.

The node connections in the network depiction of an organic crystal structure are of greater significance than the nodes. These connections consist of recognisable groups of inter-

molecular interactions and the term *supramolecular synthon* has been suggested in analogy to molecular synthons in organic synthesis.[6,25] Like molecular synthons, supramolecular synthons enable a focussing of synthetic strategy and allow the synthetic chemist to attack general supramolecular targets. Supramolecular synthons incorporate both chemical and geometrical aspects of molecular recognition. In principle, a given supramolecular structure contains a very large number of supramolecular synthons. However, in the most useful and significant of these, a maximum of structural information is encapsulated within the most economically-sized unit. If information is a measure of the amount of form— *Information ist das Mass einer Menge von Form*[26] the most useful synthons combine smallness with form.

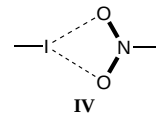
Consider for instance the linear ribbon structures of piperazine-2,5-dione, 1,4-benzoquinone and 1,4-dicyanobenzene. The network depictions of each of these structures are identical. The supramolecular synthons **I**, **II** and **III** are equivalent though




they are constituted with strong (**I**) and weak hydrogen bonds (**II**, **III**) respectively. A knowledge of the piperazine-2,5-dione structure and the directional properties of C–H··O and C–H··N hydrogen bonds allows an anticipation of the benzoquinone and dicyanobenzene crystal structures. Widely different substances can have the same or similar crystal structures and in this manner, supramolecular synthons may be invoked in crystal design strategies.

## From network to molecular structures—retrosynthesis

Implicit in the supramolecular synthon approach to crystal engineering is the identification of a crystal as a retrosynthetic target. As stated above, a target is defined in terms of a network and a typical example of supramolecular retrosynthesis is now illustrated with reference to structures based on the polarisation induced iodo··nitro synthon **IV**.[27,28] Previous work showed that




there is a definite tendency for I atoms to make short, attractive contacts with nitro groups and a possible synthetic target is a linear ribbon (Fig. 4). If one alternates synthon **IV** with phenyl rings, 4-iodonitrobenzene **4** suggests itself retrosynthetically as a molecule that has few other crystallisation options. In the crystal structure of **4**, the desired ribbon pattern is obtained. The

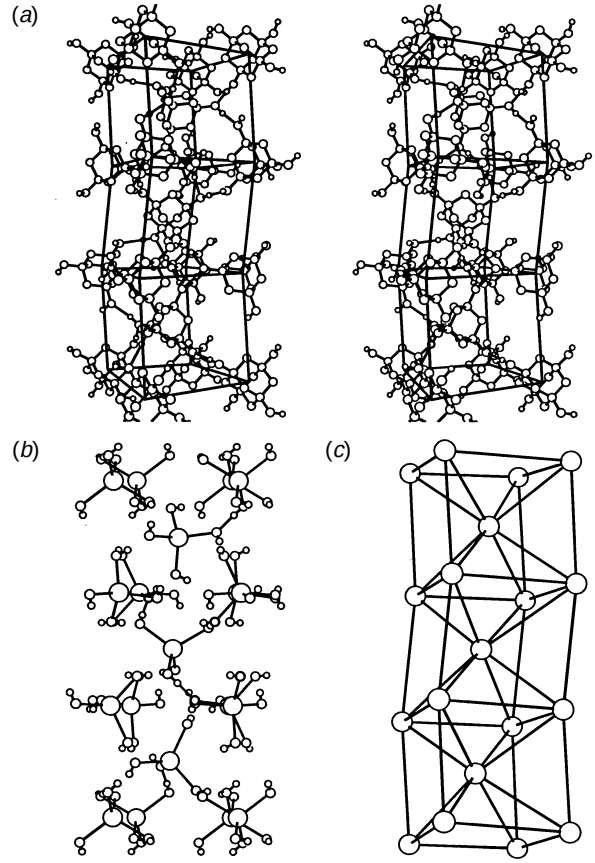



**Fig. 3** (*a*) Stereoview of the crystal structure of 1,3,5,7-tetrahydroxyadamantane **3**; (*b*) same as (*a*), with the adamantyl skeleton reduced to a sphere; (*c*) same as (*b*) with the entire molecule reduced to a sphere and hydrogen bonds shown as lines. Notice the similarity of (*c*) to the CsCl structure.

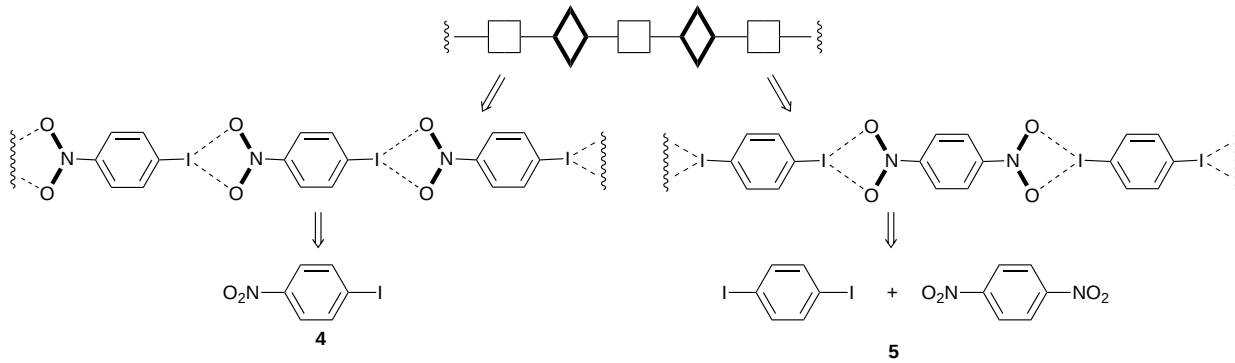


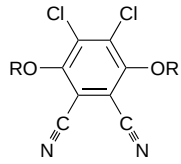

**Fig. 4**

strategy may be extended to the crystal structure of the 1:1 complex **5** of 1,4-diiodobenzene, and 1,4-dinitrobenzene where again synthon **IV** alternates, but in opposite senses, with the phenyl rings. Retrosynthetic analysis of the linear ribbon target shows that the crystal structures of compound **4** and complex **5** are equivalent. Such observations reiterate that distinct molecular structures $M_1$, $M_2$, $M_3$, ... may in general be associated with the same crystal structure $C_m$.

## The future—designer crystals

Crystal engineering is poised today at an exciting intersection of structural and supramolecular chemistry and combines scientific rigour with artistry and skill. If truly designer crystals are to become a reality, progress will become necessary in each of the three synthetic aspects: target identification, methodology and strategy.

Unlike in molecular synthesis, target identification (network designation) in crystal engineering is a non-trivial exercise. Progress in network theory and information science, coupled with technical advances in current database software such as the Cambridge Structural Database,[29] will probably become indispensable if crystal structures are to be routinely notated as networks. Consider for instance the similar networking of molecules in the 1,4-diethoxy **6** and 1,4-dihydroxy derivative **7**




**6** R = Et
**7** R = H

of 2,3-dicyano-5,6-dichlorobenzene (Fig. 5).[30] In both cases, tetrameric loops are formed. In **6** the relevant interaction is the polarisation-induced C≡N··Cl–C, while in **7**, conventional hydrogen bonding of the C≡N··H–O type is involved. Interestingly, the O–H··O bonded tetramers in α-oxalic acid and squaric acid are topologically related to **6** and **7**. It would be desirable if comparisons such as these could be generated routinely through database protocols.

Improved supramolecular synthetic methodology will consist of obtaining more accurate and reliable information on intermolecular interactions. It is clear that a very large number of precise, low temperature X-ray structure determinations will be obtained in the future. Neutron diffraction analysis will become increasingly common as a means of studying and characterising unusual types of hydrogen bonding. We have recently collaborated with Judith Howard of the University of Durham on the neutron diffraction analysis of 2-ethynyladamantan-2-ol, which contains an O–H··π hydrogen bond and have shown that the O–H group points to the centre of the alkyne bond rather than towards one of the carbon atoms that form this bond.[31] Joint studies with Dario Braga of the University of Bologna have confirmed the existence of a number of soft hydrogen bond-like interactions: M–H··O, O–H··M, C–H··O≡C– M and the *pseudo*-agostic C–H··M.[32] How useful all these interactions will be in a general sense remains to be seen. However, it is worthwhile to note that molecular synthesis progressed greatly with an array of novel reactions and if the molecule–supermolecule analogy continues to be a reliable predictor of future events, then it is only a matter of time before the exotic interactions begin to be exploited in crystal engineering.

Another compelling need is to be able to visualise a crystal structure in its entirety, not just look at selected intermolecular interactions which have been deemed to be important. The vast majority of organic crystal structures are best considered as an interplay between the medium range, isotropic forces and the long range, anisotropic forces. Sometimes, the directional requirements of these forces act in consonance, at other times in conflict and it is hard in any given situation to predict if the isotropic or anisotropic forces will dominate. This variable and subtle interplay of intermolecular forces is both confusing and annoying. It is simplistic at best and grossly misleading at worst to try and analyse, even more so to try and design, crystal structures on the basis of only a single type of intermolecular interaction. The understanding of the interplay of intermolecular interactions is a major challenge in the practice of crystal engineering today because secondary and tertiary features often control structurally important attributes of a crystal, for example, the presence or absence of an inversion centre. Along these lines, we have been collaborating with Frank Allen of the Cambridge Crystallographic Data Centre in the use of an interaction display program, NIPMAT.[33] This program creates a pictorial matrix using the atoms in the molecular skeleton ($A_1$, $A_2$, ... $A_m$, ... $A_n$) in which the matrix element $A_mA_n$ is defined as representing the shortest intermolecular contact $A_m$··$A_n$ in the crystal. Each matrix element is shown in terms of a grey scale The shorter the contact, the greyer the square which represents that particular contact. Therefore, the plot obtained (see Fig. 6 for the NIPMAT plots of naphthalene and terephthalic acid) is a visual representation of *all* the intermolecular interactions *simultaneously*. These plots show the utter difference in packing in these two structures. In naphthalene, C··H interactions are important coupled with an overall isotropic packing. This is shown by the overall greyness of the plot. In terephthalic acid, O–H··O hydrogen bonding and C··C stacking are important and the packing is more directional. This is shown by the more black-and-white appearance of the plot.

It is in the area of new synthetic strategies that the most exciting developments may be expected. An appreciation of supramolecular synthons not only as structural units but also as

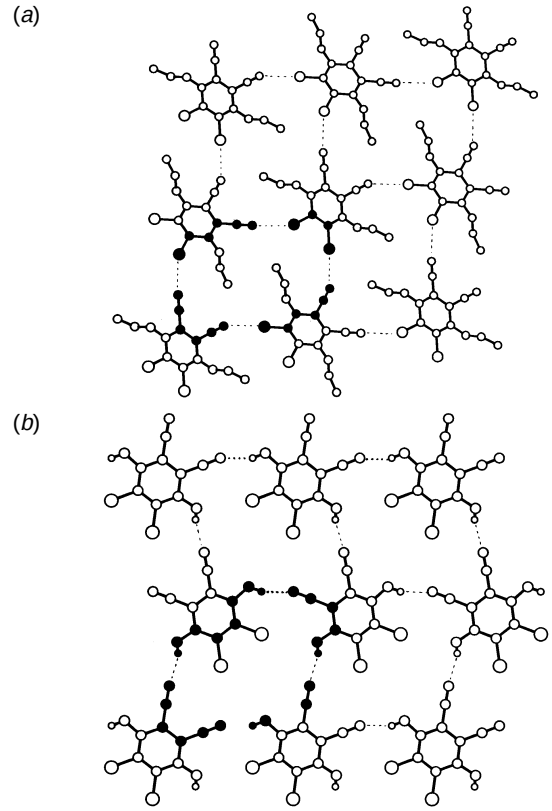
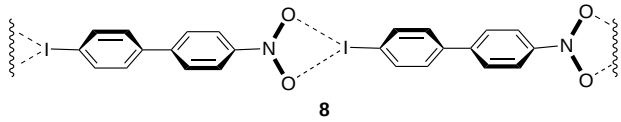



**Fig. 5** Networking of molecules in (*a*) 1,4-diethoxy-2,3-dicyano-5,6-dichlorobenzene **6** *via* C≡N··Cl interactions and (*b*) 1,4-dihydroxy- 2,3-dicyano-5,6-dichlorobenzene **7** *via* C≡N··H–O hydrogen bonds. These networks are topologically similar although the interactions are quite different.

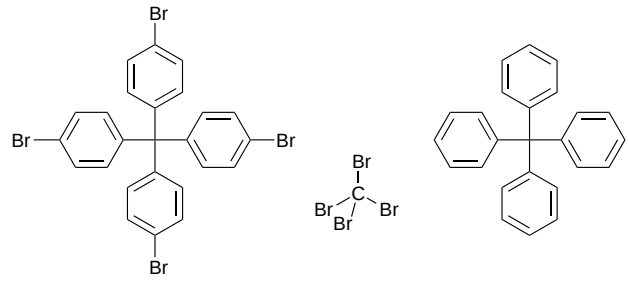
being responsible for characteristic supramolecular properties may lead to novel and unexpected solid state structures. In a recent report, we have shown that the linear ribbon structure of 4-nitro-4′-iodobiphenyl **8** may be retrosynthetically derived by



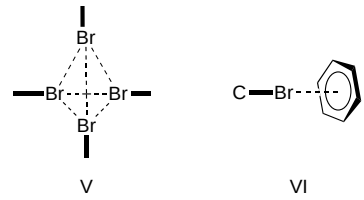
**8**

an interleaving of the iodo–nitro synthon **IV** and the twisted biphenyl molecular synthon.[34] The chiral ribbons that result pack in the non-centrosymmetric space group *Fdd2* and the crystals display moderate SHG activity (×6 urea). The term 'supramolecular chiron' has been suggested.[35] More interestingly, the calculated molecular hyperpolarisability β, of **8** is only $4.3 \times 10^{-30}$ esu. This observation hints that the crystal SHG has contributions also from the polarisation-based synthons **IV**. Many useful crystal properties are a consequence of molecular *and* supramolecular structure. It is therefore not surprising that supramolecular hyperpolarisability as manifested in synthons such as **IV** are important.

A final example demonstrates the equivalence of appropriate molecular and supramolecular synthons in crystals of tetrakis-(4-bromophenyl)methane **9** and the 1 : 1 molecular complex of $CBr_4$ **10** and tetraphenylmethane **11** (Fig. 7).[36] In **9**, a diamondoid network is formed by linking the tetraphenylmethane units with the tetrahedral supramolecular synthon **V**. Four bromine atoms are arranged in a tetrahedral fashion and the distance between any two of them is 3.91 Å. If the empty centroid in **V** is considered as a phantom 'carbon' atom, then the cluster approximates to a super-$CBr_4$ molecule.



**9** **10** **11**



V VI

One can now interchange the molecular and supramolecular synthons in the structure of **9**. The $Br_4$ clusters **V** are connected to the tetraphenyl moieties through C–Br covalent bonds. It was expected that these Ph–Br molecular synthons could be replaced with the supramolecular synthon **VI**, which is based on the Br··phenyl interaction. In other words, the replacement of **V** with $CBr_4$ accompanied by the concomitant replacement of **9** by **11** should lead to no major structural change. In practice, co-crystallisation of $CBr_4$ **10** and **11** led exclusively to the formation of a complex which is nearly isostructural with **9**. In

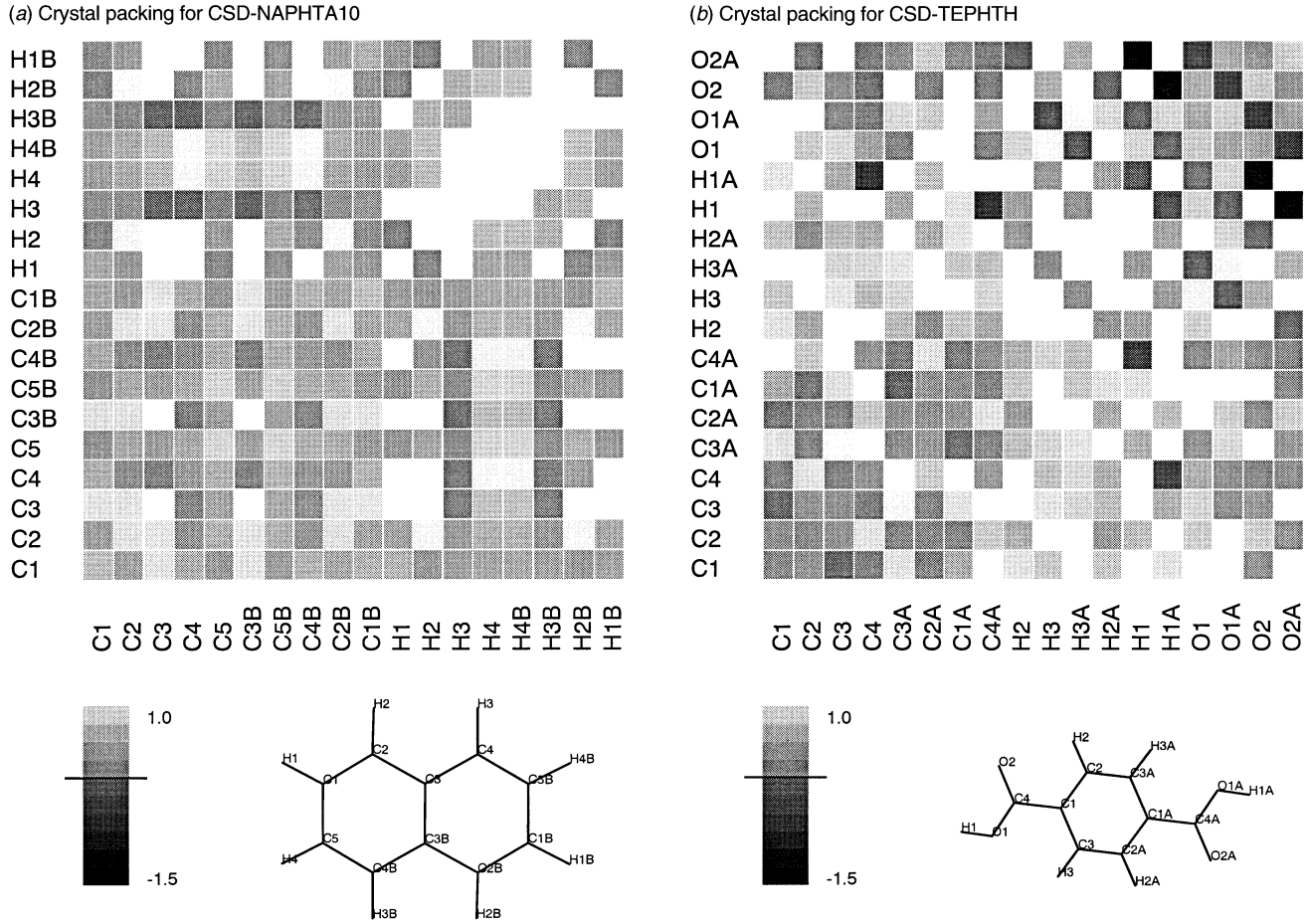



**Fig. 6** NIPMAT plots of (*a*) naphthalene (NAPHTA10) and (*b*) terephthalic acid (TEPHTH). Notice that the packing in the former is of a more isotropic nature.

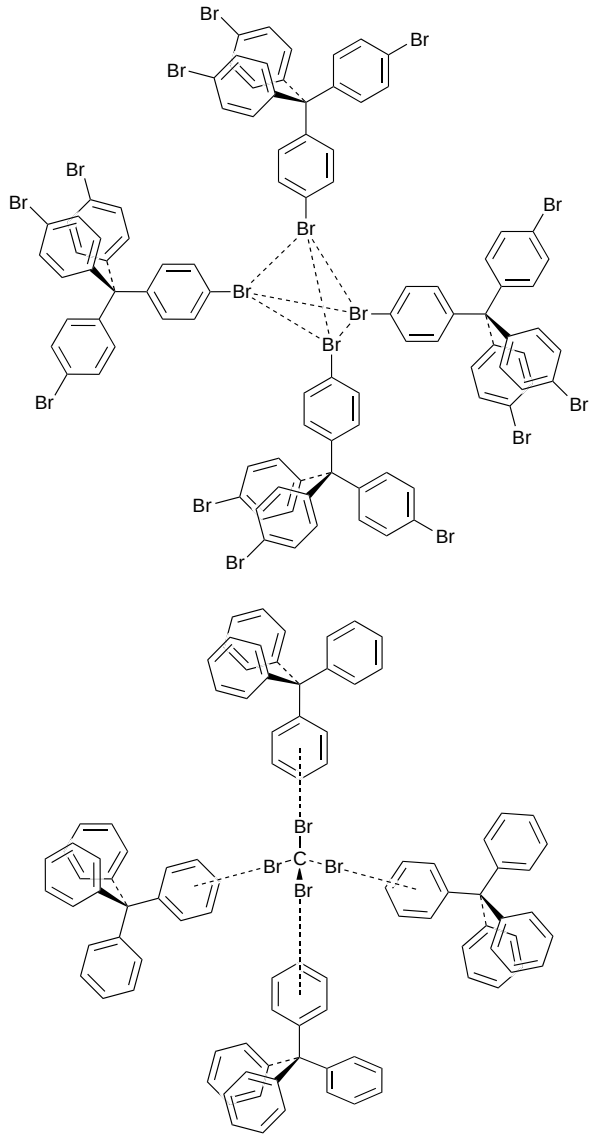



**Fig. 7**

the complex, four molecules of **11** are linked to a $CBr_4$ molecule through synthon **VI** (Br··phenyl ring centre 3.67 Å). There are no major differences in the crystal structures of **9** and the complex of **10** and **11**, and both may be simplified to distorted diamondoid networks. Although these crystal structures are formed from widely different components (**9** is a one-component crystal while the complex is a two-component crystal), they have close similarities at the supramolecular level. Most intriguingly, the distance between the bromine in the tetrahedral synthon **V** is only 12% greater than the Br··Br distance in the $CBr_4$ molecule. Observations such as this almost seem to challenge Kitaigorodskii's definition of a molecular crystal as one in which the distances between certain groups of atoms (molecules) are much smaller than the distances between atoms in different groups.[21]

## Crystallography and organic chemistry

The research described in this article is but another statement in the dialogue that has existed between X-ray crystallography and organic chemistry throughout this century.[37] This dialogue has been sometimes friendly and sometimes not, but it has always led to unexpected and fruitful developments in both subjects. Schmidt, in general, did not differentiate between these subjects when he extended the topochemical principle to organic reactions,[2] nor did say Bürgi and Dunitz when they developed the idea of structure correlation.[38] This article began with a reference to the tremendous strides in the practice of crystallography today and it has hopefully gone on to show that with the corresponding reduction of experimental burden, the endeavours of the chemical crystallographer may profitably be harnessed towards supramolecular synthesis. Crystallographers have always been confounded by technical strides in their subject and yet have always responded successfully by redefining their subject. It was J. M. Robertson who, while commenting on new methods in crystallography in the early fifties, predicted that, '*In the future, it is to be expected that the new methods will outstrip the standard degradative procedures of organic chemistry and the energies of the chemist will then be freed to concentrate on his second major problem, that of synthesis, which* ***at present*** *lie beyond the scope of crystallography*'.[39] It is with a keen sense of pleasure therefore that I draw the attention of the reader to how accurately Robertson was looking into the distant future, to a time when the subject of synthesis would come well within the ambit of X-ray crystallography.


## Acknowledgements

I thank my students, post-doctoral researchers and collaborators for their cooperation and enthusiasm. Financial support from the Department of Science and Technology, Government of India, is acknowledged. This paper is adapted from a keynote lecture delivered at the XVII Congress of the International Union of Crystallography, Seattle, in August, 1996.



**Gautam R. Desiraju was born in Madras (now Chennai) in 1952. He obtained a BSc degree from the University of Bombay in 1972 and a PhD degree from the University of Illinois at Urbana-Champaign in 1976 working with David Curtin and Iain Paul. After two years as a member of the research staff of the Eastman Kodak Company, Rochester, he returned to India where he is now a Professor of Chemistry at the University of Hyderabad. His research interests are centred in the area of structural chemistry and include crystal engineering, supramolecular chemistry, solid state reactivity and drug design.** ***Chemical Communications*** **remains one of his favourite scientific journals.**


## References


1 G. R. Desiraju, *Crystal Engineering. The Design of Organic Solids*, Materials Science Monographs 54, Elsevier, Amsterdam, 1989.
2 G. M. J. Schmidt, *Pure Appl. Chem.*, 1971, **27**, 647.
3 *Organic Solid State Chemistry*, ed. G. R. Desiraju, Studies in Organic Chemistry 32, Elsevier, Amsterdam, 1987.
4 G. R. Desiraju and J. A. R. P. Sarma, *J. Chem. Soc., Chem. Commun.*, 1983, 45.
5 *The Crystal as a Supramolecular Entity*, ed. G. R. Desiraju, Perspectives in Supramolecular Chemistry 2, Wiley, Chichester, 1996.
6 G. R. Desiraju, *Angew. Chem., Int. Ed. Engl.*, 1995, **34**, 2311.
7 J. M. Robertson, *Proc. R. Soc. London*, 1951, **A207**, 101.
8 A. Gavezzotti and G. R. Desiraju, *Acta Crystallogr., Sect. B*, 1988, **44**, 427.
9 G. R. Desiraju and A. Gavezzotti, *J. Chem. Soc., Chem. Commun.*, 1989, 621.
10 G. R. Desiraju and A. Gavezzotti, *Acta Crystallogr., Sect.B*, 1989, **45**, 473.
11 A. Gavezzotti, *Acc. Chem. Res.*, 1994, **27**, 309.
12 L. Leiserowitz, *Acta Crystallogr., Sect. B*, 1976, **32**, 775.
13 G. R. Desiraju, B. N. Murty and K. V. R. Kishan, *Chem. Mater.*, 1990, **2**, 447.
14 G. R. Desiraju and C. V. K. Sharma, *J. Chem. Soc., Chem. Commun.* 1991, 1239.
15 J. A. R. P. Sarma and G. R. Desiraju, *Acc. Chem. Res.*, 1986, **19**, 222.
16 G. R. Desiraju, *Acc. Chem. Res.*, 1991, **24**, 290.

17 G. R. Desiraju, *Acc. Chem. Res*., 1996, **29**, 441.
18 J.-M. Lehn, *Supramolecular Chemistry: Concepts and Perspectives*, VCH, Weinheim, 1995.
19 J. D. Dunitz, *Pure Appl. Chem*., 1991, **63**, 177.
20 See ref. 18, p. 206. This is cited from M. Berthelot, *Chimie Organique Fondée sur la Synthèse*, Mallet-Bachelier, Paris, 1860, vol. 2, p. 811.
21 A. I. Kitaigorodskii, *Molecular Crystal and Molecules*, Academic Press, New York, 1973.
22 D. E. Palin and H. M. Powell, *J. Chem. Soc.*, 1947, 208.
23 D. S. Reddy, D. C. Craig and G. R. Desiraju, *J. Chem. Soc., Chem. Commun.*, 1995, 339.
24 I. G. Dance, in *Perspectives in Supramolecular Chemistry: The Crystal as a Supramolecular Entity*, ed. G. R. Desiraju, Wiley, Chichester, 1996, vol. 2.
25 E. J. Corey, *Pure Appl. Chem*. 1967, **14**, 19.
26 C. F. von Weizsäcker, *Aufbau der Physik (Structure of Physics)*, 1st edn., dtv, Stuttgart, 1988, p. 167. This definition of 'information' has also been mentioned by A. Müller, H. Reuter and S. Dillinger, *Angew. Chem., Int. Ed. Engl.*, 1995, **34**, 2328 and I thank Professor Müller for bringing von Weizsäcker's paper to my attention.
27 F. H. Allen, B. S. Goud, V. J. Hoy, J. A. K. Howard and G. R. Desiraju, *J. Chem. Soc., Chem. Commun.*, 1994, 2729.
28 V. R. Thalladi, V. J. Hoy, F. H. Allen, J. A. K. Howard and G. R. Desiraju, *Chem. Commun.*, 1996, 401.
29 F. H. Allen, J. E. Davies, J. J. Galloy, O. Johnson, O. Kennard, C. F. Macrae and D. G. Watson, *J. Chem. Inf. Comput. Sci.*, 1991, **31**, 204.
30 D. S. Reddy, Y. E. Ovchinnikov, O. V. Shishkin, Y. T. Struchkov and G. R. Desiraju, *J. Am. Chem. Soc.*, 1996, **118**, 4085.
31 F. H. Allen, J. A. K. Howard, V. J. Hoy, G. R. Desiraju, D. S. Reddy and C. C. Wilson, *J. Am. Chem. Soc*., 1996, **118**, 4081.
32 D. Braga, F. Grepioni, E. Tedesco, K. Biradha and G. R. Desiraju, *Organometallics*, 1996, **15**, 2692.
33 R. S. Rowland, *Am. Crystallogr. Assoc. Abstr.*, 1995, **23**, 63.
34 J. A. R. P. Sarma, F. H. Allen, V. J. Hoy, J. A. K. Howard, R. Thaimattam, K. Biradha and G. R. Desiraju, *Chem. Commun.*, 1996, 101.
35 S. Hanessian, personal communication.
36 D. S. Reddy, D. C. Craig and G. R. Desiraju, *J.Am.Chem.Soc.*, 1996, **118**, 4090.
37 J. D. Dunitz, in *Structural Studies on Molecules of Biological Interest*, ed. G. Dodson, J. P. Glusker and D. Sayre, Clarendon, Oxford, 1981, pp. 47–59.
38 H.-B. Bürgi and J. D. Dunitz, *Acc.Chem.Res.*, 1983, **16**, 153.
39 J. M. Robertson, *Organic Crystals and Molecules*, Cornell University Press, Ithaca, New York, 1953, p. 7.

*6/07149J*

# Fluorapatite coatings by metal organic chemical vapor deposition

**Enrico Ciliberto and Giuseppe Spoto**

*Dipartimento di Scienze Chimiche, Università di Catania, Viale A. Doria 6, Catania, 95125 Italy*

**The metal organic chemical vapor deposition technique is used for the production of fluorapatite coatings using titanium as substrate and yttrium oxide as a passive diffusion barrier.**

There has currently been tremendous interest in designing new materials to be used in repairing and reconstructing diseased or damaged parts of the human body. In this context great interest has been devoted to the study of some calcium phosphate-based materials, initially chosen for their chemical similarity to the main bone-constituting inorganic compounds,[1] whose *in vivo* behavior has been defined as bioactive.[2] Hydroxyapatite [HAP, $Ca_{10}(PO_4)_6OH_2$] and fluorapatite [FAP, $Ca_5(PO_4)_3F$] are two of the more commonly used ceramics for clinical applications. They show typical bioactive behavior *in vivo* generating direct contact between the bone and the ceramic surface with no fibrous tissue layer intervention.[3] Unfortunately though, poor mechanical properties prevent their use as load-bearing implants and considerable research has thus been directed towards the development of calcium phosphate-based coatings on high strength substrates for prosthetic applications involving complex loading arrangements.[4] In the last few years equal efforts have been made in the study and optimisation of HAP-based coatings and, more recently, FAP coatings have been produced. FAP is more stable than HAP at high temperatures[5] and has been seen to have favorable biological characteristics.[6,7]

The plasma spraying technique (PLS), first introduced by De Groot *et al*.,[8] is the most thoroughly investigated method for the production of calcium phosphate-based coatings. However, the high temperature (in the region of 10 000 K) at which the ceramic powder is maintained during the process, generates the partial decomposition of the precursor compounds. This is not easily controlled and amorphous phases are formed.[9,10] The above limitations have led to the development of new synthetic routes with the aim of increasing control of the different chemical and physical characteristics of the coatings such as stoichiometry, crystallinity, thickness and surface composition.

We report the use of metal organic chemical vapor deposition (MOCVD) as a new technique for the production of FAP coatings and as an alternative to PLS. The MOCVD technique is a widely used technique in both applicative and research fields, being based on the production of solid coatings from the chemical reactions of gaseous or vaporized metal–organic compounds.[11] Various features make this useful for the production of thick coatings on complex shaped objects. The possibility of 'chemically' and kinetically controlling the deposition process throughout its course and the scope for large-scale production[11,12] are also important aspects which make this technique extremely promising for bioceramic coating production. When compared to PLS, MOCVD allows improved control of coating characteristics as the type of nucleation and growth, the deposition rate and the final stoichiometry of the coating can be modulated.[11]

The experiments were carried out with a horizontal hot-wall reactor† using $Ca(hfa)_2$·tetraglyme (Hhfa = 1,1,1,5,5,5-hexafluoropentane-2,4-dione, tetraglyme = 2,5,8,11,14-pentaoxapentadecane) and diphenylphosphinic acid (dppa) (Aldrich) as volatile precursors. Titanium was used as the substrate (Goodfellow). To prevent deleterious effects due to the formation of an interfacial layer made up of titanium oxide, the exposed surface was modified by the application of an MOCVD-deposited diffusion barrier constituted of yttrium oxide ($Y_2O_3$).‡ For all the samples, coatings of FAP were obtained, following a double-step deposition process. The coatings made up of calcium fluoride ($CaF_2$),§ obtained after the first step, were transformed into FAP after treatment with dppa vapor. During the latter step the highest substrate temperature throughout the process was reached (550 °C). This double step made a modulation of the FAP/$CaF_2$ ratio possible by controlling the time of exposure to dppa vapor.

For all the samples X-ray diffraction (XRD)¶ patterns clearly showed the presence of polycrystalline FAP (Fig. 1) whose average crystallite size was estimated using the Scherrer formula: $t = 0.9\lambda/(B\cos\theta)$ where $t$ is the crystallite size, $\lambda$ is the X-ray wavelength, $B$ is the full width at half maximum (FWHM) and $\theta$ is the X-ray angle of incidence at the Bragg condition angle for the selected peak. This formula roughly evaluates the size of the coherent crystallite domains by considering how the decrease in size of the crystallite causes an extension of the diffracted line beyond instrumental broadening. When considering the (002) reflection an average crystallite size of *ca*. 400 Å was estimated for the coatings deposited in the reported conditions.† Surface morphology was probed by atomic force microscopy (AFM).‖ The investigation showed the presence of round particles with a diameter in the range of a few hundred nanometers. Distortion effects, induced by the tip geometry and by tip–sample interactions, that could partially alter the real particle diameters, have not been considered.[13]

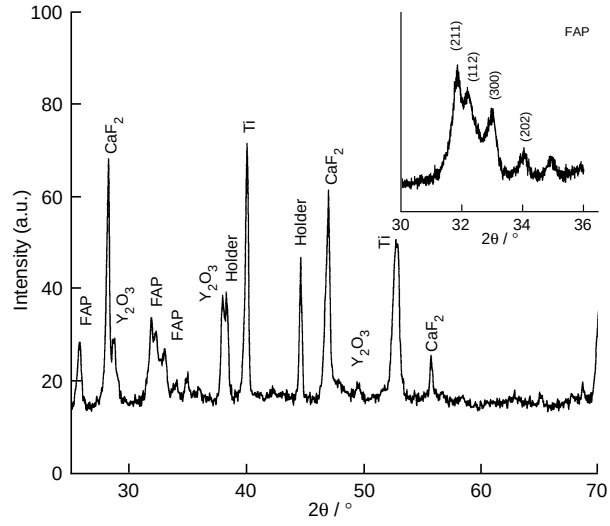



**Fig. 1** X-Ray diffraction pattern obtained from $Y_2O_3$-coated titanium after fluorapatite deposition. The spectrum obtained using Cu-Kα radiation clearly shows the presence of titanium and $Y_2O_3$ together with $CaF_2$ and FAP. Two peaks attributed to the aluminium holder are also shown. The transformation of $CaF_2$ to the crystalline FAP is a consequence of exposure to diphenylphosphinic acid vapor at 550 °C. The characteristic features of the FAP reflections included in the range $2\theta$ = 30–36° are highlighted.

This evidence, together with the XRD results, suggests that crystallites bind to form these particles.

Deposition rate, evaluated in the range of 0.5–1 μm $h^{-1}$, was estimated by examining X-ray photoelectron spectroscopy (XPS) depth profiles** after calibrating the sputter rate for the coatings using the Rutherford backscattering spectroscopy.††

The study of substrate/coating interfaces is of great relevance for problems concerning adhesion to the substrate. X-Ray photoelectron spectroscopy depth profiles were used to investigate the FAP/substrate interface when titanium was the substrate and $Y_2O_3$ was the diffusion barrier. The analyses (Fig. 2) showed the presence of an yttrium-containing layer which slowed titanium diffusion. This was a consequence of the thermodynamic stability of $Y_2O_3$ which is more stable than titanium and therefore allows a passive diffusion barrier to form for the titanium itself.[14] The relatively broad distribution of the yttrium layer and the presence of calcium, oxygen and phosphorus with only a slight decrease in concentration with depth (sputtering time) may indicate a partial substitution of the yttrium in the FAP structure. Unfortunately, no evidence for this substitution was observed in the XRD pattern.

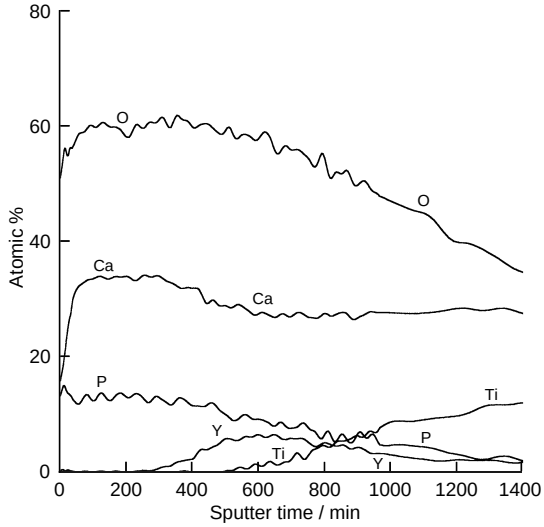



**Fig. 2** X-Ray photoelectron spectroscopy depth profile of a $Y_2O_3$-coated titanium substrate after fluorapatite deposition. Signals due to the yttrium layer appear after 200 min of $Ar^+$ sputtering, increasing in intensity up to 600 min of sputtering. Titanium diffusion towards the surface is stopped according to maximum yttrium concentration.

MOCVD is thus proposed as a new technique for the production of FAP coatings. This technique makes it possible to produce FAP coatings whose properties fit relevant properties for biomaterial coatings. In fact, the coatings are crystalline with a particle diameter in the same range as that of suitable biomaterials.[15] The use of proper diffusion barriers also reduces unwanted effects due to the formation of a brittle interface between the substrate and the coating. A positive point to be underlined is the lower temperature maintained during deposition in comparison with the temperature reached with the PLS technique.

We are now further optimizing the deposition parameters with the aim to increase the deposition rate. We are also testing various diffusion barriers in an attempt to produce coatings with increased performances.

The authors acknowledge with thanks Professors G. C. Allen, K. DeGroot, R. Langer and S. Mann for valuable discussions and interest.

## Footnotes and References

* E-mail: eciliberto@dipchi.unict.it

† The reactor chamber was constituted by a quartz tube. During the depositions a total pressure of 10 Torr was maintained in the chamber while a continuous flux of Ar (50 ml $min^{-1}$) was used as carrier for the sublimed precursors. A temperature of 85 °C was maintained in the sublimation region of the reactor for the $Ca(hfa)_2$·tetraglyme adduct and dppa was sublimed at a temperature of 185 °C. The highest temperature reached during the experiments in in the deposition region in which the substrate to be coated was placed was 550 °C. For a detailed description of the synthetic procedure used for $Ca(hfa)_2$·tetraglyme adduct see: G. Malandrino, F. Castelli and I. L. Fragalà, *Inorg. Chim. Acta*, 1994, **224**, 203.

‡ Yttrium oxide was deposited using $[Y(dpm)_3]$ (Aldrich) as the volatile precursor maintaining the substrate to be coated at 300 °C with Ar flux (50 ml $min^{-1}$) used as carrier. The total pressure in the reactor during deposition was 10 Torr. A temperature of 165 °C was maintained in the sublimation region of the reactor during deposition.

§ The $CaF_2$ coatings were characterized by XRD and XPS; XRD spectra showed their highly crystalline nature with no preferred orientation structure. XPS confirmed the presence of Ca and F on the surface of the coatings with carbon, oxygen and silicon impurities. The atomic ratio Ca/F was *ca.* 0.5.

¶ X-Ray diffraction measurements (Ni-filtered Cu-Kα radiation) were made for the coated samples placed in aluminium sample holders, and scanned with a Philips PW1820 $\theta$–$2\theta$ goniometer. A 0.5° scatter slit and a 0.2° receiving slit were used during all the acquisitions.

‖ AFM images were recorded in air with a NanoScope III (Digital Instruments Inc.) in the constant-force mode on the as-deposited samples. The detection scheme of this instrument is based on the laser beam deflection of a microfabricated $Si_3N_4$ cantilever (spring constant 0.58 N $m^{-1}$, scan rate 8.72 Hz) with an integrated $Si_3N_4$ pyramidal tip and subsequent detection by means of a split photo diode.

** X-Ray photoelectron spectroscopy depth profiles were obtained with a PHI5600 ESCA/SAM monochromator system obtaining X-ray photoelectron spectra (Al-Kα = 1486.6 eV), anode voltage 14 kV, power setting 350 W) for the energy ranges in which the main photoemission processes for the elements of interest occur (30 second bursts of $Ar^+$ sputtering, $Ar^+$ accelerator voltage 3 kV, ion current 0.5 nA, rastered area 3 × 3 mm). The spectra were performed at a 45° takeoff angle with a pass energy of 23.58 eV for the wide scans and 5.85 eV for the narrow scans. The typical operating pressure was in the range $10^{-9}$–$10^{-10}$ Torr. The XPS spectrometer was calibrated using the Ag 3d region of an etched Ag sheet. The separation between Ag $3d_{3/2}$ (368.3 eV) and the Ag $3d_{1/2}$ was 6.00 eV. The energy resolution was 0.48 eV. The binding energy of the experimental spectra was calibrated on the basis of the most intense peak of the C 1s region at 284.5 eV.

†† Rutherford backscattering spectra were obtained using a 2 MeV $He^+$ beam (van de Graaff generator). The beam current was 8 nA and the backscattering angle was 160°.

1 F. Betts, N. C. Blumenthal and A. S. Posner, *J. Cryst. Growth*, 1981, **53**, 63.
2 L. L. Hench, R. J. Splinter, W. C. Allen and T. K. Greenlee Jr., *J. Biomed. Mater. Res*, 1972, **2**, 117.
3 L. L. Hench, *Chem. Ind.*, 1995, **14**, 547.
4 R. G. T. Geesink, K. de Groot and A. K. T. Christel, *Clin. Orthop*., 1987, **225**, 147.
5 J. C. Elliot, *Structure and Chemistry of the Apatites and other Calcium Orthophosphates*, Elsevier, Amsterdam, 1994, pp. 63–110.
6 W. J. A. Dhert, C. P. A. T. Klein, J. A. Jansen, E. A. ven der Velde, R. C. Vriesde, P. M. Rozing and K. De Groot, *J. Biomed. Mater. Res*., 1993, **27**, 127.
7 L. Heling, R. Heindel and B. Merin, *J. Oral Implantol*. 1981, **9**, 548.
8 K. de Groot, R. Geesink, C. P. A. T. Klein and P. Serekain, *J. Biomed. Mater. Res*., 1987, **21**, 1375.
9 P. Cheang and K. A. Khor, *Biomaterials*, 1996, **17**, 537.
10 L. G. Ellies, D. G. A. Nelson and J. D. B. Featherstone, *Biomaterials*, 1992, **13**, 313.
11 M. L. Hitchman and K. F. Jensen, *Chemical Vapor Deposition: Principles and Applications*, Accademic Press, London, 1993, pp. 1–90.
12 J. T. Spencer, *Prog. Inorg. Chem.*, 1994, **41**, 145; T. T. Kodas and M. J. Hampden-Smith, *The Chemistry of Metal CVD*, VCH Verlagsgesellschaft, 1994, pp.1–43.
13 P. M. Williams, K. M. Shakesheff, M. C. Davies, D. E. Jackson, C. J. Roberts and S. J. B. Tendler, *Langmuir*, 1996, **12**, 3468.
14 R. R. Kieschke and T. W. Clyne, *Mater. Sci. Eng. A*, 1991, **135**, 145.
15 B. R. Constantz, I. C. Ison, M. T. Fulmer, R. D. Poser, S. T. Smith, M. Van Wagoner, J. Ross, S. A. Goldstein, J. B. Jupiter and D. I. Rosenthal, *Science*, 1995, **267**, 1796.

*Received in Bath, UK, 6th May 1997; 7/03318D*

# A new manganese cluster topology capable of yielding high-spin species: mixed-valence $[Mn_7(OH)_3Cl_3(hmp)_9]^{2+}$ with $S \geqslant 10$

**Milissa A. Bolcar,[a] Sheila M. J. Aubin,[b] Kirsten Folting,[a] David N. Hendrickson*[b] and George Christou*[a]**

[a] *Department of Chemistry and Molecular Structure Center, Indiana University, Bloomington, IN 47405-4001, USA*
[b] *Department of Chemistry-0358, University of California at San Diego, La Jolla, CA 92093-0358, USA*

**The reaction between $MnCl_2{\cdot}4H_2O$, Hhmp (Hhmp = 2-hydroxymethylpyridine) and $NEt_4MnO_4$ in MeCN gives $NEt_4[Mn_7(OH)_3Cl_3(hmp)_9]Cl[MnCl_4]$ 1; the 4 $Mn^{II}$, 3 $Mn^{III}$ cation comprises a $Mn_6$ hexagon containing a central Mn ion, and it possesses a $S \geqslant 10$ ground state.**

The study of molecules possessing unusually large spin values in their ground state is an area of intense current research.[1–6] These efforts are driven by a number of considerations, not least of which is the desire to elucidate the various factors responsible for yielding high-spin molecules. These include the topological arrangement of the paramagnetic ions, the nature (ferro- or antiferro-magnetic) of the inter-ion exchange interactions, and the presence of competing exchange interactions of comparable magnitude.[7] Further, it has recently become apparent that a relatively high ground-state spin value is one of the necessary requirements for molecules to be able to exhibit the new phenomenon of single-molecule magnetism.[1,8,9] The synthesis of new high-spin molecules is thus of interest. However, it is difficult to predict in advance for clusters what kind of topology and structure will lead to a high-spin species and even more difficult to then achieve a deliberate synthesis of such a species. We herein describe a new heptanuclear mixed-valence manganese complex with $hmp^-$ ligation (Hhmp = 2-hydroxymethylpyridine) and a new core topology for $Mn_7$ species, and show that this topology yields a high-spin ground state. Further, we show that these results suggest means whereby additional high-spin molecules might be accessed by small changes to currently available species containing a hexagon of metal ions.

Treatment of a stirred yellow slurry of $MnCl_2{\cdot}4H_2O$ (3 equiv.) and Hhmp (10 equiv.) in MeCN with solid $NEt_4MnO_4$ (2 equiv.) resulted in a dark brown solution. After 1 h, the solvent was removed *in vacuo* and the residue recrystallized twice (or more) from $CH_2Cl_2$–$Et_2O$ to give dark brown crystals of $NEt_4[Mn_7(OH)_3Cl_3(hmp)_9]Cl[MnCl_4]$ **1** in typical yields of *ca.* 40%; dried solid analyzed as $\mathbf{1}{\cdot}CH_2Cl_2{\cdot}3H_2O$.† The crystallographic sample of $\mathbf{1}{\cdot}3CH_2Cl_2$ was grown from $CH_2Cl_2$–toluene. The structure‡ of the $[Mn_7(OH)_3Cl_3(hmp)_9]^{2+}$ cation (Fig. 1) consists of a nearly planar $Mn_7$ unit comprising a central Mn(1) held within a $Mn_6$ hexagon by three $\mu_3$-$OH^-$ [O(8), O(9), O(10)] and three $\mu_3$-OR [O(29), O(53), O(77)] groups, the latter from three $hmp^-$ chelates. The remaining $hmp^-$ O atoms doubly bridge $Mn_2$ pairs of the hexagon. Three terminal $Cl^-$ ions complete peripheral ligation. Charge considerations require a 4 $Mn^{II}$, 3 $Mn^{III}$ mixed-valence description and, on the basis of $Mn^{III}$ Jahn–Teller (JT) distortions and bond valence sum calculations,[10] the $Mn^{III}$ ions are Mn(2), Mn(4) and Mn(6). The JT elongation axes contain O(29), O(53), O(77) and N(14), N(38), N(62). The cation has virtual $C_3$ symmetry. The $Cl^-$ anion is hydrogen-bonded to the $\mu_3$-$OH^-$ groups [O···Cl 3.049(16)–3.187(16) Å], but the $NEt_4^+$ and $MnCl_4^{2-}$ ions are well separated from the $Mn_7$ cation. A side view (Fig. 1) shows a Mn/O layered structure, with layers of O atoms above and below the $Mn_7$ layer, reminiscent of the hexagonal close-packed layered structure in, *e.g.* $CdI_2$.[11] The structure is different from that of other $Mn_7$ complexes, but similar to that of $[M_6NaL_{12}]^+$ (M = $Co^{II}$, $Cu^{II}$; HL = 6-methyl-2-hydroxypyridine)[12] and $[Fe_6Na(OMe)_{12}(dbm)_6]^+$ ($6Fe^{III}$; Hdbm = dibenzoylmethane),[13] where a $Na^+$ ion occupies the central position, and also $[Cu_7L_{12}]^{2+}$ ($7Cu^{II}$)[14] and $[Fe_7(OMe)_6(OPh)_6(MeCN)_{12}]^{2+}$ ($7Fe^{II}$),[15] which are homometallic.

Magnetic susceptibilities ($\chi_M$) of $\mathbf{1}{\cdot}CH_2Cl_2{\cdot}3H_2O$ have been measured in a 10.0 kG dc field and a 1.0 G ac field oscillating at 1000 Hz and corrected for the presence of the $MnCl_4^{2-}$ ($S$ = 5/2) ion, which is assumed, based on the crystal structure, to not be interacting with the $Mn_7$ cation. The dc $\chi_mT$ is essentially temperature independent at *ca.* 26.4 $cm^3$ K $mol^{-1}$ until *ca.* 100 K, and then increases to a maximum of 27.70 $cm^3$ K $mol^{-1}$ at 30.0 K and then decreases to 12.28 $cm^3$ K $mol^{-1}$ at 2.00 K. Similar values are seen for the ac $\chi_MT$ data, although it does not decrease as much at low temperatures. The data suggest a large ground-state spin value, and magnetization *vs.*

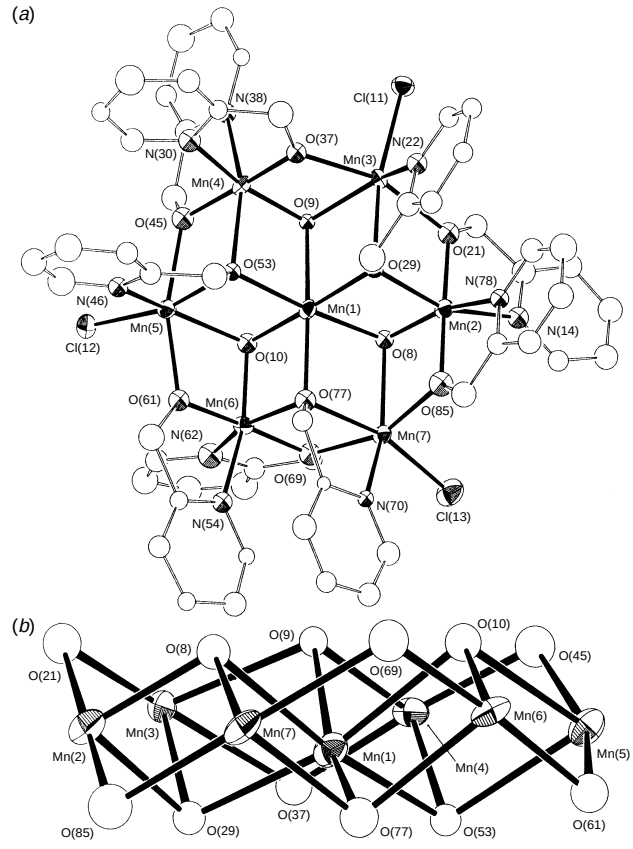



**Fig. 1** (*a*) The structure of the $[Mn_7(OH)_3Cl_3(hmp)_9]^{2+}$ cation of **1** viewed approximately along the virtual $C_2$ axis. Selected distances (Å): Mn(1)···Mn(2) 3.196(6), Mn(1)···Mn(3) 3.376(5), Mn(1)···Mn(4) 3.184(5), Mn(1)···Mn(5) 3.353(6), Mn(1)···Mn(6) 3.180(5), Mn(1)···Mn(7) 3.362(5), Mn(2)···Mn(3) 3.291(5), Mn(3)···Mn(4) 3.232(5), Mn(4)···Mn(5) 3.297(5), Mn(5)···Mn(6) 3.202(5), Mn(6)···Mn(7) 3.295(5), Mn(2)···Mn(7) 3.234(5). (*b*) A side view emphasizing the O/Mn/O layers. Displacement of Mn(1) from the $Mn_6$ least-squares plane is 0.388 Å.

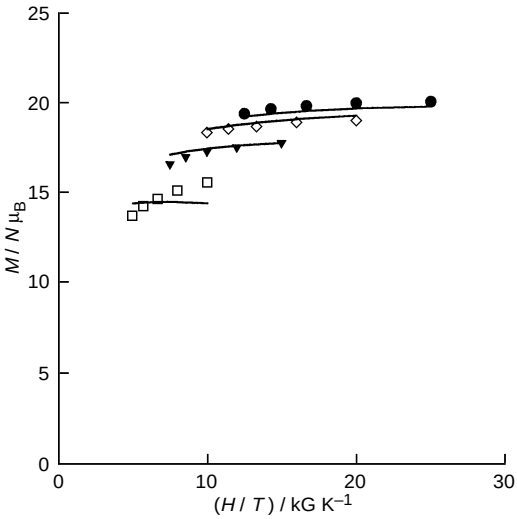



**Fig. 2** Reduced magnetization ($M/N\mu_B$) *vs.* $H/T$ data for complex **1**. The solid lines are the fit to a $S = 11$ state with $g = 1.85$ and $D = -0.15$ cm$^{-1}$.

field data were therefore collected in the 20–50 kG and 2.00–4.00 K ranges (Fig. 2). Fitting of these data, employing a spin-Hamiltonian matrix diagonalization approach, gave $S = 11$, $g = 1.85$ and $D = -0.15$ cm$^{-1}$; an equally good fit was obtained with $S = 10$, $g = 2.03$ and $D = -0.18$ cm$^{-1}$, which, however, is slightly less favored by the $g > 2$ value. Attempts to fit magnetization data measured at temperatures above *ca*. 4 K resulted in poor fits assuming only one state is populated. We conclude that in the 2–4 K range, the lowest energy state in a 20–50 kG field has $S = 11$. At temperatures above *ca*. 4 K, other states with smaller $S$ values are presumably populated and this is why the maximum in $\chi_M T$ at *ca*. 30 K falls short of the value expected for a molecule with $S = 10$ or 11; weak, intermolecular antiferromagnetic exchange interactions likely also serve to decrease the $\chi_M T$ value at low temperature. No out-of-phase ac signals were observed in the ac studies in the 2.00–50 K range.

A ground-state spin value for **1** of $S \geqslant 10$ makes this complex a new member of the small family of high-spin ($S \geqslant 8$) complexes.[1–8] With 4 $Mn^{II}$ and 3 $Mn^{III}$ ions, **1** could have ground-state values in the range $S = 2$–16. The intermediate value of $S \geqslant 10$ can be rationalized as due to competing exchange interactions of comparable magnitude.[7] The pairwise exchange interactions are of two types: $J_{io}$ and $J_{oo}$ (i = inner, o = outer), the former comprising both $J_{22}$ ($Mn^{II}$–$Mn^{II}$) and $J_{23}$ ($Mn^{II}$–$Mn^{III}$) interactions and the latter only $J_{23}$. The ground state of **1** will be dependent on the relative magnitudes of the competing $J_{io}$ and $J_{oo}$ interactions, since literature precedent indicates that $J_{22}$ and $J_{23}$ interactions are essentially always weakly antiferromagnetic and of comparable magnitude.[16] Thus, as a result of the $J_{io}$ *vs.* $J_{oo}$ competition, it is impossible for the spins in **1** to align antiparallel to each of their neighboring spins and the ground state consequently adopts an intermediate spin value, one of the highest yet observed.

The above analysis predicts that if the central Mn(1) ion of **1** were missing (or replaced by, *e.g.* $Na^+$), there would be no competing exchange interactions and the ground state would be $S = 15/2 - 6 = 3/2$. These species are currently not known and are being sought to test this prediction, but we note that $[Fe_6Na(OMe)_{12}(dbm)_6]^+$ (6 $Fe^{III}$) has an $S = 0$ ground state[13] consistent with antiparallel alignments of six $S = 5/2$ spins around the ring. Replacement of the $Na^+$ in this complex with a seventh $Fe^{III}$ or any other paramagnetic ion should give relatively high ground-state spin values as competing exchange interactions are introduced. This introduction of a seventh paramagnetic centre into preformed $M_6Na$ (or $M_6$) species may or may not prove synthetically challenging; however, challenging or not, it certainly warrants investigation since success would be extremely beneficial for the future health of the field of high-spin molecules, which is currently heavily dependent on serendipity. We also note that exactly the above kind of $Fe^{III}_7$ unit {*i.e.* $[Fe_7(\mu_3\text{-}OH)_6(\mu_2\text{-}OH)_6]^{9+}$} is a recognizable fragment within the cores of cocrystallized $[Fe_{17}O_4(OH)_{16}(heidi)_8(H_2O)_{12}](NO_3)_3/[Fe_{19}O_6(OH)_{14}(heidi)_{10}(H_2O)_{12}](NO_3)$ [heidi = $N(CH_2CO_2H)_2(CH_2CH_2OH)$] and is undoubtedly a major contributor to the *S ca.* 33/2 ground state of one of them.[2]

*Note added in proof:* the related cation $[Zn_7(hmp)_{12}]^{2+}$ has very recently been reported.[17]

This work was supported by the National Science Foundation and the National Institutes of Health.

## Footnotes and References

* E-mail: christou@indiana.edu

† The complex analysed satisfactorily (C, H, N, Cl) as $\mathbf{1}\cdot CH_2Cl_2\cdot 3H_2O$.

‡ *Crystal data*: $\mathbf{1}\cdot 3CH_2Cl_2$, triclinic, space group $P\bar{1}$, $a = 17.592(6)$, $b = 19.393(6)$, $c = 12.735(3)$ Å, $\alpha = 95.99(2)$, $\beta = 95.72(1)$, $\gamma = 82.89(1)°$, $U = 4271$ Å$^3$, $Z = 2$, $T = -153$ °C, $\mu = 15.985$ cm$^{-1}$, $D_c = 1.658$ g cm$^{-3}$. The structure was solved using MULTAN-78 and refined on $F$ to $R(F) = 0.0936$ and $R_w(F) = 0.0891$ using 4183 unique reflections with $F > 2.33\sigma(F)$. CCDC 182/512.

1 H. J. Eppley, H.-L. Tsai, N. de Vries, K. Folting, G. Christou and D. N. Hendrickson, *J. Am. Chem. Soc.*, 1995, **117**, 301; H.-L. Tsai, S. Wang, K. Folting, W. E. Streib, D. N. Hendrickson and G. Christou, *J. Am. Chem. Soc.*, 1995, **117**, 2503; H. J. Eppley, S. Wang, H.-L. Tsai, S. M. Aubin, K. Folting, W. E. Streib, D. N. Hendrickson and G. Christou, *Mol. Cryst. Liq. Cryst.*, 1995, **274**, 159.
2 A. K. Powell, S. L. Heath, D. Gatteschi, L. Pardi, R. Sessoli, G. Spina, F. Del Giallo and F. Pieralli, *J. Am. Chem. Soc.*, 1995, **117**, 2491.
3 A. Scuiller, T. Mallah, M. Verdaguer, A. Nivorozkhin, J.-L. Tholence and P. Veillet, *New J. Chem.*, 1996, **20**, 1.
4 C. D. Delfs, D. Gatteschi, L. Pardi, R. Sessoli, K. Weighardt and D. Hanke, *Inorg. Chem.*, 1993, **32**, 3099; A. Caneschi, D. Gatteschi, J. Laugier, P. Rey, R. Sessoli and C. Zanchini, *J. Am. Chem. Soc.*, 1988, **110**, 2795.
5 D. P. Goldberg, A. Caneschi, C. D. Delfs, R. Sessoli and S. J. Lippard, *J. Am. Chem. Soc.*, 1995, **117**, 5789.
6 A. J. Blake, C. M. Grant, S. Parsons, J. M. Rawson and R. E. P. Winpenny, *J. Chem. Soc., Chem. Commun.*, 1994, 2363.
7 D. N. Hendrickson in *Research Frontiers in Magnetochemistry*, ed. C. J. O'Connor, World Scientific, Singapore, 1993.
8 R. Sessoli, D. Gatteschi, A. Caneschi and M. A. Novak, *Nature*, 1993, **365**, 141; D. Gatteschi, A. Caneschi, L. Pardi and R. Sessoli, *Science*, 1994, **265**, 1054.
9 S. M. J. Aubin, M. W. Wemple, D. M. Adams, H.-L. Tsai, G. Christou and D. N. Hendrickson, *J. Am. Chem. Soc.*, 1996, **118**, 7746.
10 I. D. Brown and D. Altermatt, *Acta Crystallogr., Sect. B*, 1985, **41**, 244.
11 *Inorganic Structural Chemistry*, ed. U. Muller, Wiley, New York, 1993.
12 S. McConnell, M. Motevalli and P. Thornton, *Polyhedron*, 1995, **14**, 459; A. J. Blake, R. O. Gould, P. E. Y. Milne and R. E. P. Winpenny, *J. Chem. Soc., Chem. Commun.*, 1991, 1453.
13 A. Caneschi, A. Cornia and S. J. Lippard, *Angew. Chem., Int. Ed. Engl.*, 1995, **34**, 467.
14 A. J. Blake, R. O. Gould, C. M. Grant, P. E. Y. Milne, D. Reed and R. E. P. Winpenny, *Angew. Chem., Int. Ed. Engl.*, 1994, **33**, 195.
15 V. S. Nair, A. Kitaygorodskiy and K. S. Hagen, *Abstracts of Papers, 206th National Meeting of the American Chemical Society*, Washington, DC, 1993, INOR 525.
16 L. Que, Jr. and A. E. True, *Prog. Inorg. Chem.*, 1990, **38**, 97.
17 M. Tesmer, B. Muller and H. Vahrenkamp, *Chem. Commun.*, 1997, 721.

*Received in Cambridge, UK, 2nd May 1997; 7/03007J*

# Two-photon processes in the photo-Claisen and photo-Fries rearrangements. Direct observation of dienic ketenes generated by photolysis of transient cyclohexa-2,4-dienones

**M. Consuelo Jiménez,[a] Miguel A. Miranda,*[b] J. C. Scaiano*[b] and Rosa Tormos[a]**

[a] *Departamento de Química/Instituto de Tecnología Química UPV-CSIC, Universidad Politécnica de Valencia, Camino de Vera s/n, Apdo 22012, 46071, Valencia, Spain*
[b] *Department of Chemistry, University of Ottawa, Ottawa, Canada K1N 6N5*

**Using the two-laser two-colour technique it has been possible to promote two photon chemistry in the cases of benzyl phenyl ether 1a and phenyl acetate 1b; this is based on the photolysis of the transient cyclohexa-2,4-dienone intermediates 2a,b of the photo-Claisen and photo-Fries rearrangement to the dienic ketenes 4a and 4b.**

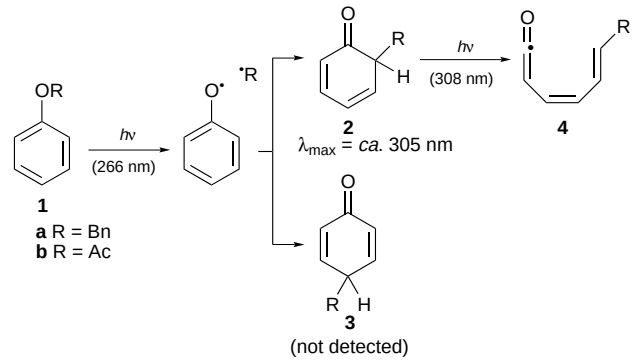
The classical Claisen and Fries rearrangements have been known for nearly 90 years.[1] Their photochemical equivalents were first reported in 1952 and 1960, respectively.[2] Since then, a considerable number of reports have appeared in connection with the synthetic as well as mechanistic aspects of both photorearrangements. Much of this work was done during the first two decades since their discovery and is summarized in several reviews.[3] A satisfactory understanding of the mechanism has been achieved by using laser flash photolysis,[4] CIDNP[4e,5] and transient Raman spectroscopy,[6] as well as studies on magnetic isotope effects and magnetic fields effects.[7]

The above contributions support the idea that photo-Claisen and photo-Fries rearrangements occur from an excited singlet state, *via* homolysis of the aryloxy–alkyl (or acyl) bond, to give radical pairs enclosed in a solvent cage. Radical recombination leads to the rearranged alkyl (or acyl) migration products, while out-of-cage hydrogen abstraction by the aryloxy radical leads to the formation of phenols. This picture has been confirmed by independent generation of the involved radicals *via* Norrish type I photoreaction of ketones in the presence of phenols, which leads to aryl ethers (or esters) plus *C*-alkyl (or *C*-acyl) phenols.[8]

Being the prototypes for geminate cage recombination/escape of relatively large radicals, both photorearrangements have attracted recent attention as model reactions to study the influence of constraining media such as cyclodextrins,[9] micelles,[10] zeolites,[11] supercritical carbon dioxide[12] and stretched low-density polyethylene films.[13]

There is some spectroscopic evidence for the involvement of non-enolized cyclohexadienones as intermediates.[4] If such transient species were actually intervening, it should be possible in principle to photolyse them at their absorption maxima using the recently developed two-laser two-colour technique.[14] If the typical photoproducts of cyclohexadienones were thus formed,[15] this could constitute an additional proof for their involvement in the photo-Claisen and photo-Fries rearrangements. Besides, this methodology could provide a direct entry to two-photon chemistry of aryl ethers and esters, which still remains to be explored.

Laser flash photolysis of deareated 5 mM solutions of benzyl phenyl ether **1a** in methylcyclohexane was carried out with a Nd-YAG laser (fourth harmonic, 266 nm, < 10 ns, ⩽ 20 mJ pulse$^{-1}$) using a 90° excitation geometry and a quartz beam diffuser in front of the sample (Scheme 1). A transient signal appeared, which was assigned to the cyclohexa-2,4-dienone **2a** by comparison with the known properties of these species.[4] In a second experiment, two-laser two-colour laser flash photolysis was employed to examine the effect of laser excitation on the above mentioned reaction intermediate. The same 266 nm laser was used as synthesis laser to generate **2a**, while a 308 nm excimer laser (HCl/Xe/Ne, 6 ns, 70 mJ pulse$^{-1}$) was used to photolyse the intermediate. The wavelength of the latter was selected to match the optical absorption of cyclohexa-2,4-dienone (maximum at *ca.* 300 nm). The synthesis laser was incident from the front face, while for the photolysis laser a 90° geometry was adopted. The most remarkable result was a permanent and irreversible bleaching of the transient signal as monitored at 295 nm (Fig. 1, insert). In the absorption spectrum obtained after photolysis of **2a**, an enhancement was observed at 260–270 nm, accompanied by a decrease at 300–320 nm. The difference spectrum displayed a well-defined maximum at 270




**Scheme 1**

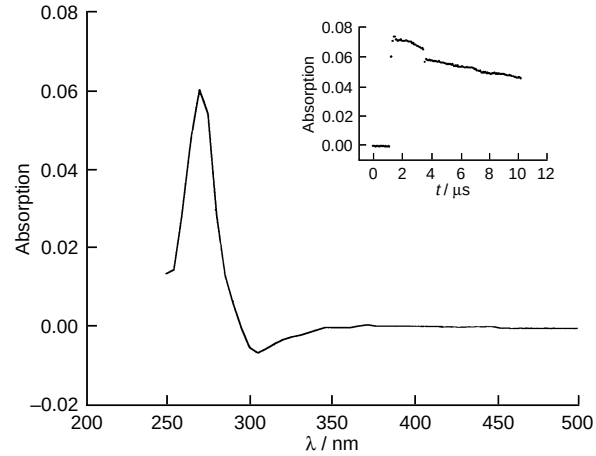



**Fig. 1** Absorption spectrum of the dienic ketene **4a** obtained from the difference between the spectra of the reaction of **1a** after and before the 308 nm laser pulse. The insert shows the bleaching of the transient signal monitored at 295 nm.

nm and a less marked emission at 305 nm (Fig. 1). Taking into account the possibility of electrocyclic ring opening in the case of **2a**, a plausible structure of the intermediate absorbing at 270 nm would be that of a dienic ketene such as **4a**. This assignment was confirmed by comparison with the spectra of similar ketenes generated by photolysis of stable 6,6-disubstituted cyclohexa-2,4-dienones.[16]

The same experiments were carried out with phenyl acetate **1b**. Flash photolysis with the 266 nm laser gave rise to a transient signal whose structure was assigned to be **2b**. When this intermediate was photolysed at 308 nm in the two-laser two-colour experiment, a sharp enhancement of the signal monitored at 330 nm was observed (Fig. 2, insert). This was somewhat surprising as, in the case of the benzyl ether **1a**, the result was bleaching of the signal. The spectrum of the new intermediate was obtained in the usual way, by examining the difference between the spectra after and before the 308 nm laser pulse. This spectrum showed a maximum at longer wavelength (330 nm) than **4a** (Fig. 2). In principle, photochemical opening of 6-acetylcyclohexa-2,4-dienone **2b** to the corresponding dienic ketene **4b** was expected to occur, by analogy with the behaviour of the 6-benzyl derivative **2a** upon photolysis at 308 nm. Transient **4b** presents an extended conjugation, owing to attachment of the acetyl group at the end of the polyunsaturated system. This would explain the position of its absorption maximum and is in agreement with the proposed structure.

In summary, using the two-laser two-colour technique it has been possible to promote two photon chemistry in the case of benzyl phenyl ether **1a** and phenyl acetate **1b**. This is based on the photolysis of the proposed cyclohexa-2,4-dienone intermediates **2a**,**b** of the photo-Claisen and photo-Fries rearrangements and involves direct detection of the electrocyclic ring opening products, the dienic ketenes **4a** and **4b**.

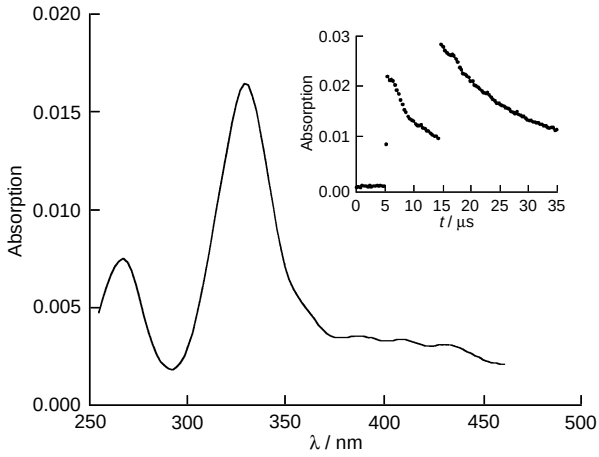



**Fig. 2** Absorption spectrum of the dienic ketene **4b** obtained from the difference between the spectra of the reaction of **1b** after and before the 308 nm laser pulse. The insert shows the jump of the transient signal monitored at 330 nm.

Financial support by the Spanish Government (fellowships to M. C. J. and R. T.) is gratefully acknowledged. We also thank Mr André Simard for skillful technical assistance.

## Footnotes and References

† E-mail: mmiranda@qim.upv.es

1 L. Claisen, *Chem. Ber.*, 1912, **45**, 3157; K. Fries and G. Finck, *Ber. Dtsch. Chem. Ges.*, 1908, **41**, 4271.
2 M. S. Kharasch, G. Stampa and W. Nudenberg, *Science*, 1952, **116**, 309; J. C. Anderson and C. B. Reese, *Proc. Chem. Soc., London*, 1960, 217.
3 V. I. Stenberg, *Org. Photochem.*, 1967, **1**, 127; D. Bellus, *Adv. Photochem.*, 1971, **8**, 109; M. A. Miranda, *Photo-Fries Reactions and related processes*, in *Handbook of Organic Photochemistry and Photobiology*, ed. W. M. Horspool and P. S. Song, CRC Press, Boca Raton, 1995, p. 570.
4 (*a*) K. Heimi, S. Naruto, K. Hirao and O. Yonemitsu, *Chem. Pharm. Bull.*, 1974, **22**, 718; (*b*) H. J. Timpe and H. J. Friedrich, *Z. Chem.*, 1976, **16**, 369; (*c*) C. E. Kalmus and D. M. Hercules, *J. Am. Chem. Soc.*, 1974, **96**, 449; (*d*) T. T. Arai, S. Tobita and H. Shizuka, *J. Am. Chem. Soc.*, 1995, **117**, 3968; (*e*) N. P. Gritsan, Y. P. Tsentalovich, A. V. Yurkovskaya and R. Z. Sagdeev, *J. Phys. Chem.*, 1996, **100**, 4448.
5 W. Adam, H. Fischer, H. J. Hansen, H. Heimgartner, H. Schmid and H. R. Waespe, *Angew. Chem.*, 1973, **85**, 669; W. Adam, *J. Chem. Soc., Chem. Commun.*, 1974, 289; W. Adam, J. A. de Sanabia and H. J. Fischer, *J. Org. Chem.*, 1973, **38**, 2571.
6 S. M. Beck and L. E. Brus, *J. Am. Chem. Soc.*, 1982, **104**, 1805.
7 P. Nakagaki, M. Hiramatsu, T. Watanabe, Y. Tanimoto and S. Nagakura, *J. Phys. Chem.*, 1985, **89**, 3222; H. J. Shine and W. Subotkowsky, *J. Org. Chem.*, 1987, **52**, 3815.
8 M. C. Jiménez, P. Leal, M. A. Miranda and R. Tormos, *J. Chem. Soc., Chem. Commun.*, 1995, 2009.
9 M. S. Syamala, B. N. Rao and V. Ramamurthy, *Tetrahedron*, 1988, **44**, 7234; A. V. Veglia, A. M. Sánchez and R. H. Rossi, *J. Org. Chem.*, 1990, **55**, 4083.
10 A. K. Singh and S. N. Sonar, *Synth. Commun.*, 1985, **15**, 1113.
11 R. Suau, G. Torres and M. Valpuesta, *Tetrahedron Lett.*, 1995, **36**, 1311; K. Pitchumani, M. Warrier and V. Ramamurthy, *J. Am. Chem. Soc.*, 1996, **118**, 9428.
12 D. Andrew, B. T. Des Islet, A. Margaritis and A. C. Weedon, *J. Am. Chem. Soc.*, 1995, **117**, 6132.
13 C. Cui and R. G. Weiss, *J. Am. Chem. Soc.*, 1993, **115**, 9820.
14 J. C. Scaiano, L. J. Johnston, W. G. McGimpsey and D. Weir, *Acc. Chem. Res.*, 1988, **21**, 22.
15 A. G. Schultz, *Photorearrangement Reactions of Linearly Conjugated Cyclohexadienones*, in *Handbook of Photochemistry and Photobiology*, ed. W. M. Horspool and P. S. Song, CRC Press, Boca Raton, 1995, p. 728.
16 G. Quinkert, E. Kleiner, B. Freitag, J. Glenneberg, U. Billhardt, F. Cech, K. R. Schmieder, C. Schudok, H. Steinmetzer, J. W. Bats, G. Zimmermann, G. Dürner and D. Rehm, *Helv. Chim. Acta*, 1986, **69**, 469.

*Received in Liverpool, UK, 23rd May 1997; 7/03606J*

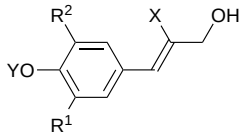
# Rational design, synthesis and biological evaluation of the first inhibitor of lignin polymerization

**Nicolas Daubresse,[a] Yves Chupeau,[b] Charlette Francesch,[a] Catherine Lapierre,[c] Brigitte Pollet[c] and Christian Rolando*[a]**

[a] *Ecole Normale Supérieure, Département de Chimie, URA 1679 du CNRS, Processus d'Activation Moléculaire, 24 rue Lhomond, 75231 Paris Cedex 05, France*
[b] *Laboratoire de Biologie Cellulaire, INRA, Centre de Versailles, 78026 Versailles, France*
[c] *Laboratoire de Chimie Biologique, INRA-CBAI, Institut National Agronomique Paris-Grignon, 78850 Thiverval-Grignon, France*

**A fluorinated analogue of coniferin (the glucoside of coniferyl alcohol) has been synthesized in three steps from vanillin tetraacetyl glucoside; bearing a fluorine atom on the β position of the propenyl side chain which is involved in the main site of coupling, it is designed as a potential inhibitor of oxidases involved in the biosynthesis of lignin, and *in vivo* experiments show a pronounced inhibition of lignin biosynthesis in poplar plantlets, with a five-fold decrease in lignin formed.**

Lignins, the second major natural biopolymer on earth after cellulose, are biosynthesized by polycondensation of cinnamyl alcohols **1a**–**c**.[1–3] The crucial step consists of an oxidative




**1a** X = Y = $R^1$ = H, $R^2$ = OMe
**b** X = Y = H, $R^1$ = $R^2$ = OMe
**c** X = Y = $R^1$ = $R^2$ = H
**2** X = F, Y = $R^1$ = H, $R^2$ = OMe
**3** X = H, Y = glucose, $R^1$ = H, $R^2$ = OMe
**4** X = F, Y = glucose, $R^1$ = H, $R^2$ = OMe

coupling of these phenols, *via* the formation of radicals[4] by a radical–radical or a radical–anion mechanism.[5,6] The enzymatic route remains unclear, since peroxidases and laccases can both, in artificial medium, catalyse the oxidation step and lead to lignin-like dehydropolymers (DHP).[7–9] To the best of our knowledge, there has been no report on specific inhibition of the polymerization step *in vivo*. Coloration tests on microcuttings, however, have shown that fluoroferulic acid is able to inhibit the activity of peroxidases.[10–12]

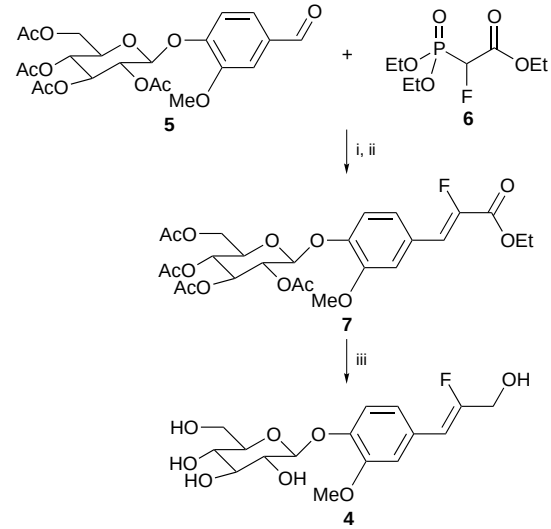
We herein describe the first *in vivo* inhibition of lignin biosynthesis by use of the fluorinated analogue **2** of coniferyl alcohol **1a**, the main natural precursor of lignin. A fluorine atom has been substituted for one hydrogen in the β-vinyl position. The structures of **1a** and **2** are very close, and thus we can expect similar affinities for the enzymes.[13,14] Compounds **1a** and **2** have similar redox potentials [0.11 and 0.16 V respectively](SHE),[15] as might be supposed based on the reported slightly destabilizing effect of fluorine on radical centres.[16,17] Thus no difference should be observed in the ability of the enzyme to oxidize **1a** or **2**. On the other hand, the reactivity of the radical obtained from **2** is expected to be dramatically changed, owing to the interaction between the stabilizing effect of the methoxy group on the aromatic ring[15] and the strong electron-withdrawing effect of the fluorine atom.[18]

Glucosides **3** are the natural protected forms of cinnamyl alcohols **1** and have been extensively used for radiolabelling experiments,[19,20] the glucosyl residue being cleaved *in situ* by a β-glucosidase before the polymerization step.[21–23] β-Fluoroconiferin **4** was thus designed as the stable protected form of fluoroconiferyl alcohol, the actual inhibitor.

Synthesis of **4** was easily achieved, with high yields, from the tetra-*O*-acetylglucoside of vanillin **5** (Scheme 1).[24,25] A Wadsworth–Edmons reaction with triethylfluorophosphonate **6**[26, 27] under phase transfer conditions catalysed by tris[2-(2-methoxyethoxy)ethyl]amine (TDA-1)[28] led, after isomerization of the *E/Z* mixture with bromine,[29] to pure *Z* β-fluoro α,β-unsaturated ester **7**.† The five ester groups were reduced with *in situ* generated lithium borohydride leading to pure **4**.‡

The biochemical assay was performed according to a standard test we have developed on poplar plantlets grown *in vitro* under controlled conditions.§[30] This test is based on the assimilation of the glucosides of cinnamyl alcohols which are administered to the plantlets through the growing artificial medium. Artificial substrates **3** (sample 1) and **4** (sample 2) were delivered to lignifiying zones after diffusion in the medium and crossing of the root barrier. After allowing a three week growing phase, incorporation was followed by a standard lignin analysis of the new stems: lignin was chemically degraded by thioacidolysis and residues were analysed by GC–MS and quantified by GC after silylation.¶[31,32]

After three weeks of growing, no difference was observed on the aspect of plantlets from blanks (no feeding), samples 1 (fed **3**) and 2 (fed **4**). The extent of lignification was, however,




**Scheme 1** *Reagents and conditions*: i, TDA-1, aq. $K_2CO_3$, $CH_2Cl_2$, reflux, 24 h, 91%; ii, $Br_2$ (0.05 equiv.), $CCl_4$, 4 h, 88%; iii, $NaBH_4$ (7.4 equiv.), LiCl (10 equiv.), glyme, 80 °C, 18 h, 69%

**Table 1** Thioacidolysis yields in μmol $g^{-1}$ of dried stems in main G (guaiacyl) and S (syringyl) lignin-derived monomers recovered from poplar plantlets cultured *in vitro*

| Sample | Precursor administered | G | S | S+ G | S/G |
|---|---|---|---|---|---|
| Blank | None | 21 | 10 | 31 | 0.50 |
| 1 | Coniferin | 26 | 15 | 41 | 0.58 |
| 2 | Fluoroconiferin | 4 | 3 | 7 | 0.78 |

significantly lowered in sample 2: the thioacidolysis yield (a reflection of the lignin concentration) was only 7 μmol $g^{-1}$, compared to a 31 μmol $g^{-1}$ yield for the blank and sample 1 (Table 1).

These results suggest that the designed compound fluoroconiferyl alcohol **2** acts as an inhibitor of the lignification process. As the catalytic activity of the β-glucosidase is most probably unchanged, the lignin biosynthesis must be affected at the oxidative polymerization step. Lignin precursors such as coniferyl alcohol **1a** are oxidized by any kind of oxidizing enzymes, and no specificity has yet been established. The use of labelled derivatives of **4** should allow the identification of the enzymes specifically involved in the oxidative biosynthesis of lignin.

## Footnotes and References

* E-mail: chr@roxane.ens.fr

† *Selected data* for **7**: $^1$H NMR (250 MHz, $CDCl_3$): 7.42–7.28 (m, 3 H, $H_{ar}$), 7.01 (d, 1 H, ArCH, $J_{HF}$ 34.8), 5.44–5.26 (m, 3 H, H2,3,4), 5.16 (m, 1 H, H1), 4.50 (q, 2H, C$H_2$CH$_3$, *J* 7.1), 4.43 (dd, 1 H, H6b, *J* 12.3, 5.0), 4.32 (dd, 1 H, H6a, *J* 12.3, 2.6), 3.99 (s, 3 H, MeO), 3.95 (ddd, 1 H, H5, *J* 10.0, 5.0, 2.6), 2.21 (s, 6 H, Ac), 2.19 (s, 6 H, Ac), 1.53 (t, 3 H, CH$_2$C$H_3$ *J* 7.1); MS (CI, $NH_3$) *m/z* 588 (100%, M + 18), 331 (23), 240 (14), 110 (43).

‡ *Selected data* for **4**: mp 142–144 °C (Found: C, 48.51; H, 6.32. $C_{16}H_{21}FO_8.2H_2O$ requires C, 48.48, H, 6.36%); $^1$H NMR (250 MHz, $CD_3OD$): 7.18 (br s, 1 H, $H_{ar}$2), 7.09 (d, 1 H, $H_{ar}$5, *J* 8.5), 7.02 (br d, 1 H, $H_{ar}$6, *J* 8.5), 5.78 (d, 1 H, ArC*H*CF, $J_{HF}$ 39.1), 4.86 (d, 1 H, H1, *J* 7.0), 4.13 (d, 2 H, ArCHCFC$H_2$, $J_{HF}$ 15.0), 3.72 (s, 3 H, MeO), 3.67 (m, 1 H, H6b), 3.63 (m, 1 H, H6a), 3.55–3.35 (m, 4 H, H2,3,4,5); $^{13}$C NMR (62.5MHz, $CD_3OD$): 158.1 (d, ArCH*C*F, $J_{CF}$ 265), 148.8 ($C_{ar}$4), 145.6 ($C_{ar}$3), 127.8 ($C_{ar}$1), 121.4 (d, Ar*C*H, $J_{CF}$ 7.0), 116.0 ($C_{ar}$5), 112.3 (d, $C_{ar}$6, $J_{CF}$ 7.9), 106.0 (d, $C_{ar}$2, $J_{CF}$ 6.1), 100.9 (C1), 76.6 (C3), 76.1 (C5), 73.2 (C2), 69.7 (C4), 60.9 (C6), 60.8 (d, CF*C*H$_2$OH, $J_{CF}$ 32.3), 55.1 (MeO). MS (CI, $NH_3$) *m/z* 378 (83%), 360 (10), 198 (74), 182 (14), 181 (100), 180 (48), 163 (12), 102 (22).

§ *Plant material and administration* of **3** and **4**. Microcuttings from hybrid poplar (*Populus alba* × *Populus tremula*, clone 717-B4) were cultured aseptically on solid medium as previously described (ref. 30). One day after the sterile deposition of nodes into culture tubes, 2.5 mg of coniferin **3** (sample 1) or fluoroconiferin **4** (sample 2) in DMSO (30 μl) were added carefully on the surface of the solid medium without any contact with the nodes. After three weeks of controlled growing, samples were collected, new shoots were detached, freeze-dried and directly subjected to thioacidolysis. Each administration was repeated for five culture tubes, and the amount of collected sample varied from 3 to 5 mg.

¶ *Thioacidolysis and GC–MS analysis*. Thioacidolysis was performed as previously described (refs. 31, 32). The amount of C22 docosane internal standard was 0.02 mg per analysis of *ca.* 3 mg of dried sample.


1 K. Freudenberg and A. C. Neish, 1968, in *Constitution and Biosynthesis of Lignin*, ed. K. Freudenberg and A. C. Neish, Springler, Berlin.
2 K. V. Sarkanen and C. H. Ludwig, *Precursors and their Polymerization*, in *Lignins. Occurrence, Formaion, Structure and Reactions*, ed. K. V. Sarkanen and C. H. Ludwig, Wiley-Interscience, New-York, ch. 4, p. 95.
3 T. Higushi, *Wood Sci. Technol.*, 1990, **24**, 23.
4 K. Freudenberg, *Angew. Chem.*, 1956, **68**, 508.
5 P. Hapiot, P. Neta, J. Pinson, C. Rolando and S. Schneider, *New J. Chem.*, 1993, **17**, 211.
6 P. Hapiot, J. Pinson, P. Neta, C. Francesch, F. Mhamdi, C. Rolando and S. Schneider, *Phytochem.*, 1994, **36**, 1013.
7 R. A. Savidge, *Biochem. Soc. Trans.*, 1992, **20**, 229.
8 R. Sterjades, J. F. D. Dean and K. E. L. Ericksson, *Planta*, 1992, **190**, 75.
9 W. Bao, D. O'Malley, R. Whetten and R. Sederoff, *Science*, 1993, **260**, 672.
10 R. Goldberg, A. Pang, M. Pierron, A. M. Catesson, Y. Czaninski, C. Francesch and C. Rolando, *Phytochem.*, 1988, **27**, 1647.
11 A.-M. Catesson, A. Pang, C. Francesch, C. Rolando and R. Goldberg, *Inhibition of Cell Wall Peroxydases with Ferulic Salts and Fluorinated Analogues*, in *Plant Cell Wall Polymers, 399*, Wiley, New York, 1989, p. 193.
12 C. Kevers, T. Gaspar, C. Lapierre, D. Jouin, B. Monties, C. Francesch, C. Rolando, R. Goldberg and A.-M. Catesson, *Phytochem.*, 1990, **29**, 1543.
13 M. Schlosser, *Tetrahedron*, 1978, **34**, 3.
14 J. Welch, *Tetrahedron*, 1987, **43**, 3123.
15 P. Hapiot, J. Pinson, C. Francesch, F. Mhamdi, C. Rolando and S. Schneider, *J. Electroanal. Chem.*, 1992, **328**.
16 X. Creary, *J. Org. Chem.*, 1980, **45**, 280.
17 J. M. Dust and D. R. Arnold *J. Am. Chem. Soc.*, 1983, **105**, 1221.
18 H. G. Viehe, Z. Janousek and R. Merenyi, *Acc. Chem. Res.*, 1985, **18**, 148.
19 Y. Xie, D. Robert and N. Terashima, *Plant Physiol. Biochem.*, 1994, **32**, 243.
20 N. Terashima, K. Fukushima, Y. Sano and K. Takabe, *Holzforschung*, 1988, **42**, 347.
21 K. Freudenberg and J. M. Harkin, *Phytochem.*, 1963, **2**, 189.
22 E. Surholt and W. Hoesl, *Z. Plantzenphysiol.*, 1981, **10**, 207.
23 S. Marcinowski, H. Falk, D. K. Hammer, B. Hoyer and H. Grisebach, *Planta*, 1979, **144**, 161.
24 K. Krohn and J. Thiem, *J. Chem. Soc., Perkin Trans.*, 1977, 1186.
25 E. Fischer and K. Raske, *Chem. Ber.*, 1909, **42**, 1465.
26 E. Elkik and M. Imbeaux, *Synthesis*, 1989, 861.
27 G. Etemad-Moghadam and J. Seyden-Penne, *Bull. Soc. Chim. Fr.*, 1985, 448.
28 G. Soula, *J. Org. Chem.*, 1985, **50**, 3717.
29 I. Sataty and C. Y. Meyers, *Tetrahedron Lett.*, 1974, 4161.
30 Y. Chupeau, M. C. Chupeau and M. Lemoine, *J. Plant. Physiol.*, 1993, **141**, 601.
31 C. Lapierre, B. Pollet and C. Rolando, *Res. Chem. Inter*, 1995, **21**, 397.
32 C. Rolando, B. Monties and C. Lapierre, 1992, *Thioacidolysis*, in *Methods in Lignin Chemistry*, ed. S. Y. Lin and C. W. Dence, Springer-Verlag, Berlin, 1992, p. 334.


*Received in Glasgow, UK, 6th February 1997; 7/02464I*

# The enantioselective total synthesis of (−)-myltaylenol

**Sven Doye, Torsten Hotopp and Ekkehard Winterfeldt***

*Institute of Organic Chemistry, University of Hannover, Schneiderberg 1b, 30167 Hannover, Germany*

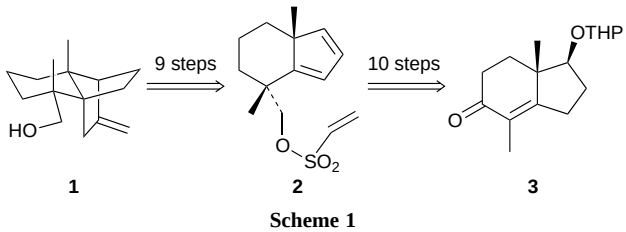
**Using an intramolecular Diels–Alder cycloaddition followed by an oxidative rupture of the connective unit as the key step, the unusual carbon framework of (−)-myltaylenol was established.**

In 1985 Matsuo[1] and his colleagues reported the isolation of the unusual sesquiterpenoid alcohol (−)-myltaylenol **1** from the liverwort *Mylia taylorii*. The compound is characterized by a novel polycyclic terpenoid framework containing three consecutive quartenary carbon atoms and although Srikrishna[2] and his group in 1994 briefly described a remarkable biomimetic transformation, which finally gave rise to the corresponding racemic desoxy compound starting from cyclogeraniol, no enantioselective approach to this type of molecule has been reported.

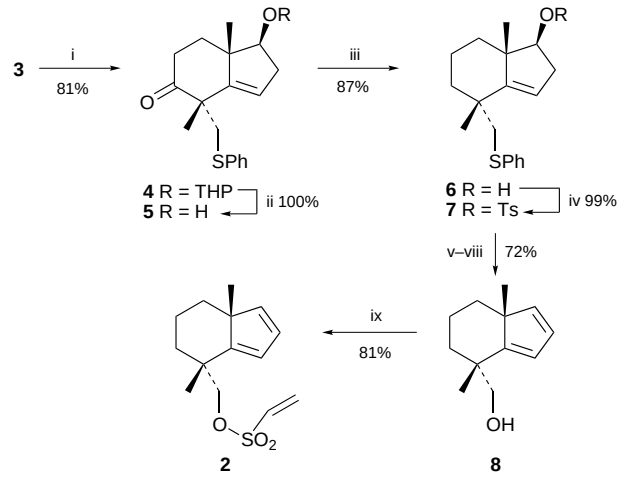
As retrosynthetic planning disclosed an intramolecular Diels–Alder cycloaddition employing cyclopentadiene **2** to be a potential key step and since we had in recent years gained some experience with dienes of this type, the enantioselective preparation of this compound was considered our first target.

For hydrindane derivatives of this structure the pure enantiomers of the Hajos–Wiechert ketone had been shown in our group to be an ideal starting material[3] and as the monoalkylated derivative **3** is well described in the literature[4] we employed the highly selective alkylation of this unsaturated ketone with thiophenylmethyl iodide followed by a Wolff–Kishner reduction to prepare the cyclopentenol **5**. To generate the corresponding cyclopentadiene, the tosylate **7** was formed and treated with potassium *tert*-butoxide in THF at 65 °C. Subsequent Pummerer rearrangement followed by a borohydride reduction gave rise to the primary alcohol **8**, which after treatment with ethenesulfonyl chloride was ready for the intramolecular cycloaddition. For this process and the accompanying oxidative ring fission of the sulfonate we had decided on the Metz protocol.[5] This worked nicely as far as the intramolecular cycloaddition was concerned. The oxidation employing 2-methoxy-4,4,5,5-tetramethyl-1,3,2-dioxaborolane, however, which had been successfully applied by Metz and his colleagues in various instances, failed. Since the electrophilic attack has to take place next to a quarternary carbon atom we came to the conclusion that steric hindrance may be the cause for this failure. We thus treated the carbanion of **9**, generated using Bu$^s$Li, with molecular oxygen and were pleased to note the clear formation of hydroxy ketone **10**. As the yield under various conditions, however, barely exceeded 40% we investigated the relationship between the amount of Bu$^s$Li used and the yield under standard reaction conditions and noticed that a large surplus of the deprotonating species (10–11 equiv.) reliably gave a 65% yield of the hydroxy ketone. With this piece of information at hand one may speculate about the formation of *sec*-butyl hydroperoxide and its possible role as an oxidant. We hesitate, however, to discuss the mechanism of this useful process at this stage of our investigation.

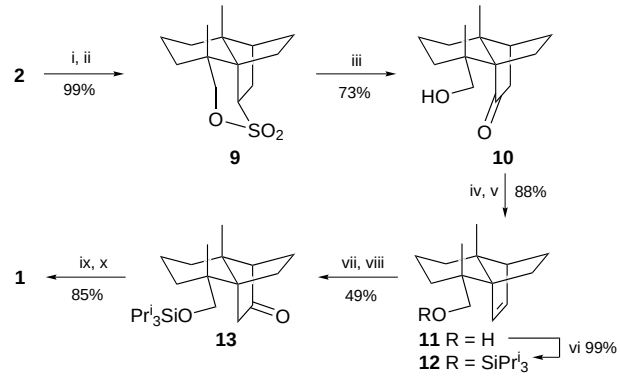
Without collecting further information about this oxidation we converted the keto group into the corresponding olefin **11** in a Shapiro reaction. Since it was hoped that a very bulky protecting group on the primary alcohol would change it into a large inert moiety, thus rendering the subsequent borane addition/oxidation sequence highly regioselective, triisopropylsilyl triflate in the presence of triethylamine was used as




**Scheme 1**




**Scheme 2** *Reagents and conditions*: i, KOBu$^t$, THF, 0 °C, then $PhSCH_2I$, THF, −78 °C, 30 min; ii, HCl·EtOH, room temp., 16 h; iii, KOH, $N_2H_4$, diglycol, 200 °C, 4 h; iv, TsCl, DMAP, $CH_2Cl_2$, room temp., 16 h; v, KOBu$^t$, THF, 65 °C, 3.5 h; vi, $NaIO_4$, MeOH, 0 °C → room temp., 16 h; vii, $Ac_2O$, 100 °C, 62 h; viii, KOH, MeOH, room temp., 2 h, then $NaBH_4$, 0 °C, 30 min; ix, $ClSO_2CH{=}CH_2$, $EtNPr^i_2$, $CH_2Cl_2$, −15 °C, 1.5 h




**Scheme 3** *Reagents and conditions*: i, toluene, 111 °C, 20 h; ii, Pd/C, $H_2$, THF, room temp., 16 h; iii, Bu$^s$Li, $O_2$, THF–HMPA (7 : 1), −78 °C, 3 h; iv, $TsN_2H_3$, TsOH, EtOH, MS 3 Å, 78 °C, 2 h; v, BuLi, THF, 75 °C, 50 min; vi, $Pr^i_3SiOTf$, $NEt_3$, THF, −78 °C, 2 h; vii, $BH_3$·THF, THF, 0 °C, 24 h, then NaOH, $H_2O_2$, EtOH, 50 °C, 3 h; viii, DMSO, $(COCl)_2$,$NEt_3$, $CH_2Cl_2$, −60 °C; ix, $Ph_3PMeBr$, KOBu$^t$, benzene, room temp., 48 h; x, $Bu_4NF$, THF, room temp., 18 h

the silylating reagent. Although models indicate a remarkable regional shielding of the cyclopentene **12** the observed selectivity was less than 1.5 : 1 in favour of the desired ketone **13**.

As the chromatographic separation of the intermediate pairs of epimeric secondary alcohols did not pose any problems and the subsequent Swern oxidation gave a high yield of the corresponding ketone, we were at this stage ready to use a Wittig reaction for the introduction of the exocyclic double bond. This operation as well as the subsequent deprotection with tetrabutylammonium fluoride proceeded in very high yield and gave rise to (−)-myltaylenol **1**, which by comparison with authentic spectra kindly provided by Dr Matsuo proved to be the desired natural compound.

The kind help provided by Dr Matsuo is highly appreciated. The work described was supported by the Fonds der Chemischen Industrie, and S. Doye is grateful for a Kekulé scholarship from this institution.

## Footnote and References

* E-mail: winterfeldt@mbox.oci.uni-hannover.de

1 D. Takaoka, A. Matsuo, J. Kuramoto, M. Nakayama and S. Hayashi, *J. Chem. Soc., Chem. Commun.*, 1985, 482.
2 A. Srikrishna, C. V. Yelamaggad, K. Krishnan and M. Nethaji, *J. Chem. Soc., Chem. Commun.*, 1994, 2259.
3 K. Matcheva, M. Beckmann, D. Schomburg and E. Winterfeldt, *Synthesis*, 1989, 814.
4 D. J. Crispin, A. E. Vanstone and J. S. Whitehurst, *J. Chem. Soc.* (*C*), 1970, 10.
5 P. Metz, M. Fleischer and R. Fröhlich, *Tetrahedron*, 1995, **51**, 711.

*Received in Cambridge, UK, 8th May 1997; 7/03164E*

# Conversion of pyrroles into bis-1,2,5-thiadiazoles: a new route to biheterocycles

**Xiao-Guang Duan and Charles W. Rees**

*Department of Chemistry, Imperial College of Science, Technology and Medicine, London, UK SW7 2AY*

**Trithiazyl trichloride 1 converts 1-aryl-2,5-diphenylpyrroles 2c into isothiazole imines 3c, but 1-alkyl-2,5-diphenylpyrroles (*e.g.* 4) react very differently to give the bis-1,2,5-thiadiazole 5 in which two N–S–N units have been fused onto the pyrrole and the alkyl–N unit has been excised, in a new dissection of the pyrrole ring, thus providing a novel route to an aromatic biheterocycle.**

There has recently been a marked revival of interest in biheterocyclic systems (known for over a hundred years[1]) since they appear as structural subunits in many natural products and in conducting polymers like polypyrrole and polythiophene, and they have provided a wide range of finely tuned chelating ligands in coordination and organometallic chemistry.[1] The many different biheterocycles reported have been prepared by standard coupling, cyclisation and cycloaddition reactions, together with a few reactions involving the extrusion of sulfur or dinitrogen. We now describe an entirely new and unusually short route to such a system, the bis-1,2,5-thiadiazoles.

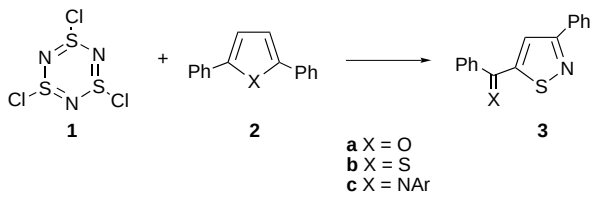
We have shown that trithiazyl trichloride **1** reacts with 2,5-diphenylfuran **2a** to give 5-benzoyl-3-phenylisothiazole **3a** regiospecifically and in high yield; 2,5-diphenylthiophene **2b** and **1** gave the same product, by formation and oxidation of the analogous thiobenzoyl compound **3b** (Scheme 1).[2] We have also shown that **1** reacts with 2,3-unsubstituted pyrroles by fusing an N–S–N unit across this bond to give pyrrolo-[1,2,5]thiadiazoles (*e.g.* **7** below), often in high yield.[3]

We now find that 1-aryl-2,5-diphenylpyrroles **2c** react with **1** in the same way as **2a** and **2b** to give the analogous products, the imines **3c**† (Scheme 1), together with the 3,4-dichloropyrroles† reflecting the high reactivity of pyrroles towards electrophilic substitution. However, when the *N*-aryl groups were replaced by alkyl groups a new and unexpected reaction was observed. Thus treatment of 1-methyl-2,5-diphenylpyrrole **4** with trimer **1** (2 equiv.) in refluxing $CCl_4$ gave a colourless crystalline solid, mp 82–83 °C, with one less carbon and with four nitrogen and two sulfur atoms in its molecular formula ($C_{16}H_{10}N_4S_2$) (45%). Assuming that the MeN unit has been lost and the remaining carbon connectivity retained, the bis-1,2,5-thiadiazole structure **5**† seemed possible. This structure was supported by all the analytical and spectroscopic data and by formation of the same product from 1,4-diphenylbuta-1,3-diyne or (*E*)-1,4-diphenylbut-1-en-3-yne with **1** under the same conditions, in similar yields (43–44%) (Scheme 2).

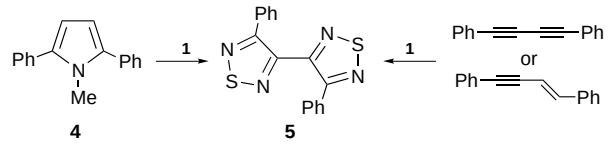
We have explained the formation of 1,2,5-thiadiazoles from such alkenes and alkynes by overall 1,3-cycloaddition of an N–S–N unit in the trimer, followed by loss of the remaining S–N–S unit as $[ClSNSCl]^+ Cl^-$ or $[SNS]^+ Cl^-$.[4] This mechanism is directly applicable to 2,3-unsubstituted pyrroles to give the observed pyrrolothiadiazoles.[3] With *N*-methylpyrrole this process can occur twice *via* an intermediate such as **6**‡ which would rapidly aromatise by elimination of HCl to give the observed product **7** (Scheme 3). The analogous intermediate, **8**,‡ from 1-methyl-2,5-diphenylpyrrole **4** cannot aromatise similarly, but it can do so by loss of two protons from the methyl group which has to be accompanied by cleavage of the *N*–C(α) pyrrole bonds (arrows in **8**) to give the very stable bis-thiadiazole **5** and HCN (Scheme 4).

With the *N*-aryl compounds, the intermediate analogous to **8** cannot aromatise by any such elimination and, if formed at all, would probably be in equilibrium with its precursors; the reaction therefore takes the different pathway described above (Scheme 1). Thus the dominant role of the *N*-substituent, and the extensive rearrangement involved in the conversion of **4** into **5**, whilst initially puzzling, appear to be mechanistically reasonable.

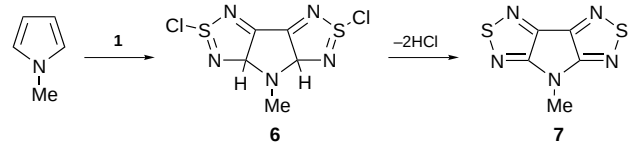
Hydrogen cyanide was shown to be a product of the reaction of trimer **1** with pyrrole **4** by using commercial HCN length-of-stain detector tubes.§ Blank experiments showed that this method was not sensitive to the hydrogen chloride formed in the reaction but that the monomer, NSCl, in thermal equilibrium with the trimer, did interfere if it were not efficiently condensed



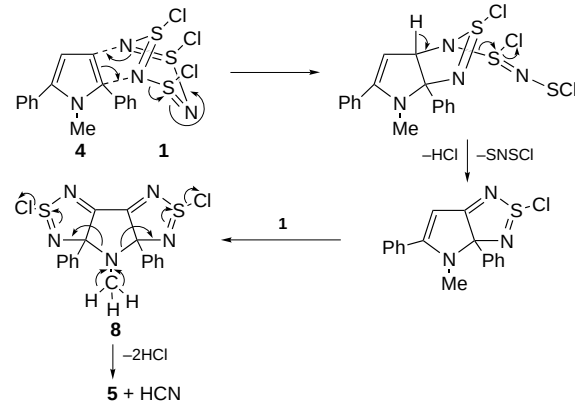

**Scheme 1**




**Scheme 2**




**Scheme 3**




**Scheme 4**

out before the exit gases passed through the detector tube. Other *N*-alkyl-2,5-diphenylpyrroles reacted with **1** to give the bis-thiadiazole **5**, accompanied by 3,4-dichlorination of the pyrrole ring. The best yields of **5** were obtained from the *N*-methyl **4** and the *N*-ethyl compounds, and were improved further (to 70%) in the presence of 4 Å molecular sieves. Conversion of 1-ethyl-2,5-diphenylpyrrole into bis-thiadiazole **5** is presumably accompanied by the formation of methyl cyanide (*cf.* **8**), but certainly not HCN, and no colour change was observed in the detector tube for this reaction.

Formation of bis-1,2,5-thiadiazole **5** form *N*-alkylpyrroles and **1** represents a new dissection of the pyrrole ring and provides a novel and short route to an aromatic biheterocycle; very few bis-1,2,5-thiadiazoles have been reported,[5] and hitherto they were not readily available.

We thank Zeneca Specialties and MDL Information Systems (UK) Ltd for financial support, the Wolfson Foundation for establishing the Wolfson Centre for Organic Chemistry in Medical Science at Imperial College, and Dr Tai-Yuen Yue for valuable discussions.

## Footnotes and References

† All new compounds have been fully characterised by elemental analysis, spectroscopy and mass spectrometry.
‡ In **6** and **8** the sulfur–chlorine bonds are shown as covalent, but these would be partly ionised, at least, to the thiadiazolium chlorides.
§ Kitagawa HCN length-of-stain detector tubes (Type SB) supplied by Sabre Gas Detection, Unit 1, Blackwater Way, Aldershot, Hampshire.

1 For a comprehensive review, see P. J. Steel, *Adv. Heterocycl. Chem.*, 1996, **67**, 1.
2 X.-L. Duan, C. W. Rees and T.-Y. Yue, *Chem. Commun.*, 1997, 367; X.-L. Duan, R. Perrins and C. W. Rees, *J. Chem. Soc., Perkin Trans. 1*, 1997, 1617.
3 X.-G. Duan and C. W. Rees, *J. Chem. Soc., Perkin Trans. 1*, 1997, in the press.
4 X.-G. Duan, X.-L. Duan, C. W. Rees and T.-Y. Yue, *J. Chem. Soc., Perkin Trans. 1*, 1997, in the press.
5 J. Sundermeyer and H. W. Roesky, *Chem. Ber.*, 1991, **124**, 1517; S. Mataka, Y. Ikezaki, Y. Shimojo, A. Torii and M. Tashiro, *Chem. Ber.*, 1993, **126**, 2767.

*Received in Liverpool, UK, 20th May 1997; 7/03484I*

# Self-replication in a Diels–Alder reaction

**Bing Wang and Ian O. Sutherland***

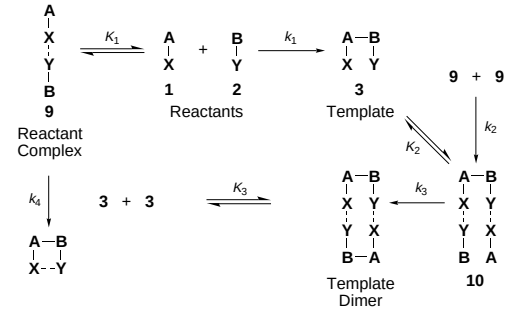
*Department of Chemistry, University of Liverpool, PO Box 147, Liverpool, UK L69 3BX*

**The Diels–Alder reaction between ene 1 and diene 2 at 23 and 40 °C shows sigmoidal characteristics for the formation of product 3 and a response to added 3 that indicates that it is an efficient catalyst for the reaction.**

Replication is an essential feature of biological systems and simple chemical analogues have been studied, usually as possible models for prebiotic replication.[1,2] The simplest example of a self-replicating system is the autocatalytic synthesis of a self-complementary molecular template (Scheme 1) and examples of such systems involving self-complementary oligonucleotides have been described[1,3] by von Kiedrowski and Orgel. Other examples which have been developed have been based upon amide formation, studied[4] by Rebek and co-workers and recently the subject[5] of a careful kinetic analysis, and anil formation studied[6] by von Kiedrowski's group. Recently Rebek has described[7] a more complex system based upon four different reactants giving two complementary templates.

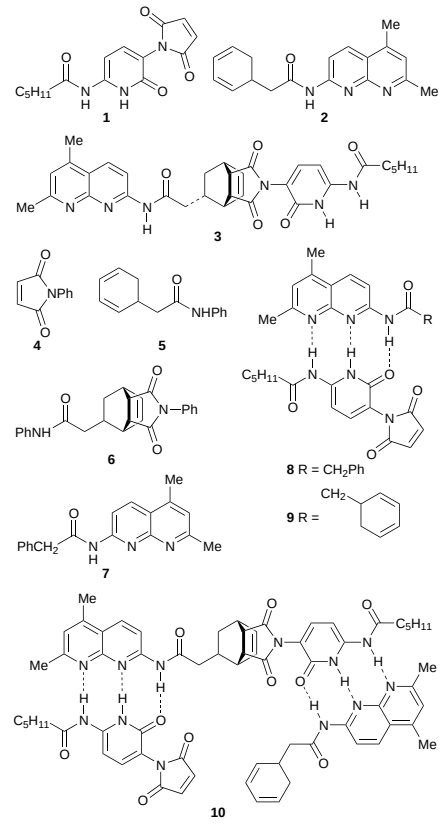
Here we describe a novel self-replicating system of the type shown in Scheme 1 which is very different from the original examples inspired by consideration of prebiotic evolution. The reaction centres (**A** and **B** in Scheme 1) were selected as the ene and diene components of the classical Diels–Alder reaction because it is known[8] that the Diels–Alder reaction can be catalysed effectively by complexation of the reactants in a suitably designed ditopic host. The binding sites (**X** and **Y** in Scheme 1) were selected on the basis of work[9] by Kelly and co-workers. After careful consideration of molecular models,[10] the existing kinetic data for Diels–Alder reactions, solubility requirements and synthetic accessibility, the 6-acylamino-2-pyridone derivative **1** and the 2-acylaminonaphthyridine **2** were selected as target ene and diene systems and were synthesised by conventional procedures.

The model compounds **4** and **5** lacking the binding sites reacted very slowly in $CD_2Cl_2$ at 23 and 40 °C and the course of the reaction could be followed by $^1$H NMR spectroscopy; the product **6** is assumed to have *endo*-stereochemistry but may consist of one or both of the two possible *endo*-diastereoisomers. Reactant pairs **4** and **2** and **5** and **1** reacted together at similar rates but the pair of reactants **1** and **2** with complementary binding sites reacted relatively rapidly at both 23 and 40 °C to give product **3**, probably a mixture of *endo*-diastereoisomers, in good yield. Fig. 1, based upon integration of alkenic $^1$H NMR signals in diene **2** and product **3**, shows the rate of product formation at 40 °C; the signals of the diastereoisomers of **3** overlap and no attempt has been made to separate the diastereoisomeric reaction pathways. The sigmoidal character of the reaction curves at both temperatures indicates that an autocatalytic process of the type shown in Scheme 1 could be operating, whereas the reaction of **4** and **5** shows simple second order characteristics. The catalysis of the reaction of **1** and **2** by product **3** was confirmed by carrying out the reaction in the presence of 0.05 and 0.1 equiv. of product **3** (see Fig. 1 which shows the results); the reaction under these conditions shows initial catalysis and a loss of the induction period associated with sigmoidal character.




**Scheme 1** A simple self-replication cycle. **A** and **B** represent reacting groups attached to complementary binding sites **X** and **Y**. The full lines represent covalent attachment and the broken lines represent hydrogen bonding interactions.

The results at 40 °C were analysed in terms of the reactions and equilibria shown in Scheme 1 using a computer model† including all of the reactions and equilibria and the insertion of trial values for the rate constants and the equilibrium constants. The value of $K_1$ was found by a study of the association between pyridone **1** and the acylaminonaphthyridine **7** using an $^1$H NMR titration procedure, in which increments of **7** were added to a 0.02 M solution of **1** in $CD_2Cl_2$, and the chemical shifts of the NH protons were used in association with a simple computational procedure for finding a 'best fit' value for the association constant. The values of $K_1$ (228 mol l$^{-1}$ at 23 °C and 163 mol l$^{-1}$ at 40 °C) are consistent with some inhibition of binding (*cf.* ref. 9) between the two components of the complex **8** as a result of non-bonding interactions between the 7-methyl substituent on the naphthyridine and the alkyl group of the pyridone side-chain at position 6. These interactions, which are



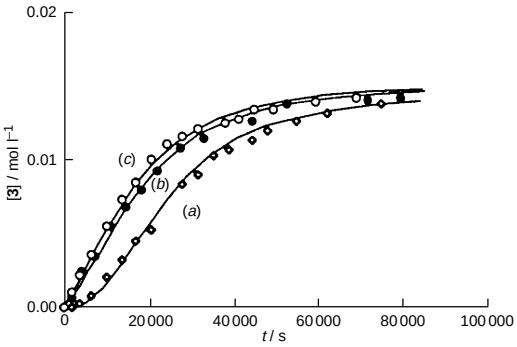



**Fig. 1** Observed and calculated reaction curves for the Diels–Alder reaction between **1** and **2** at 40 °C based upon Scheme 1: (*a*) 0%, (*b*) 5% and (*c*) 10% added template. The best fit for observed and calculated data is obtained with $k_1 = k_2 = 3.5 \times 10^{-5}$ l mol$^{-1}$ s$^{-1}$, $K_1 = 163$ l mol$^{-1}$, $K_2 = 2.66 \times 10^4$ l$^2$ mol$^{-2}$, $k_3 = 2.0 \times 10^{-3}$ s$^{-1}$, $K_3 = 2.66 \times 10^4$ l mol$^{-1}$, $k_4 = 0$ s$^{-1}$. Experimental errors in the concentrations of product **3** derived from NMR spectra are probably of the order ±0.0005 mol l$^{-1}$.

evident in molecular mechanics calculations,[10] are also expected to inhibit the dimerisation of product **3** and the formation of the templated reaction complex **10**. Accordingly a value of $K_1^2$ was assigned to the equilibrium constant $K_2$ and values of $K_3$ were chosen in the range $K_2/10$ to $10K_2$. Assignment of values to $k_4$ greater than $10^{-7}$ s$^{-1}$ did not reproduce the observed induction period for the reaction and, as expected, this reaction does not appear to make a significant contribution to the formation of product **3**. The value for $k_1$ was based initially upon the second order rate constant for the reaction of the model ene **4** and diene **5** and the reaction between complexed pairs of reactants was assumed to have a rate constant $k_2$ with the same value as $k_1$. Trial values for the first order rate constant $k_3$ for the catalysed reaction were selected in association with trial values of $K_3$. Eventually it was found that a good fit between observed and calculated reaction curves could not be obtained unless a considerably lower value than that obtained from the reaction of **4** and **5** was selected for $k_1$ and $k_2$, and the final values for rate constants and equilibrium constants are summarised below Fig. 1 which shows the comparison of observed and calculated results. It is not clear why the reaction of **4** and **5** is not a good model for the uncatalysed reaction of **1** and **2**. We note that the experimental data points have the lack of precision associated with integration of NMR signals but in spite of this the agreement between observed and calculated data is satisfactory for the reaction at 40 °C. The results at 23 °C were more difficult to analyse in the same way and satisfactory agreement between observed and calculated data has not yet been obtained, although the data does fit the simpler reaction scheme discussed below.

The calculated effective molarity of the catalysed reaction (7 mol l$^{-1}$ at 40 °C) is based upon the value of $k_3$ and the value of the bimolecular rate constant $k$ for the model reaction of **4** and **5** ($6.98 \times 10^{-5}$ mol$^{-1}$ s$^{-1}$ at 23 °C and $2.81 \times 10^{-4}$ mol$^{-1}$ l s$^{-1}$ at 40 °C) rather than the rate constant $k_1$ which cannot be measured directly, although the value of the latter suggests that this effective molarity may be an underestimate. It indicates that transition state binding by the template is reasonably efficient since it is of the same order as the effective molarity (4 mol l$^{-1}$) observed for the acceleration of a Diels–Alder reaction within a well designed cavity as reported by Sanders and co-workers.[8] It is evident from the calculations that a good sigmoidal reaction curve for the reaction in the absence of added template (see Fig. 1) requires both a moderately high effective molarity in the template catalysed reaction and a reasonably low value for the dimerisation constant $K_3$. That the Diels–Alder reaction allows this is a consequence of a transition state that resembles product but has partial bonds that are more flexible than those of the rigid bicyclic system in the product. Furthermore the template **3** holds the reactive groups of the ene **1** and diene **2** in close proximity and the intramolecular reaction in the reactant complex **9** is prevented by preference for an *endo*-transition state which requires the extended arrangement for reactants shown in **10**.

Other self-replicating systems have often been analysed[1b,3c,4] in terms of Scheme 2 involving only two reactions with a value for α of 0.5. This simple scheme with $\alpha = 0.5$ did not produce calculated reaction curves in accord with our results but more extended calculations using values for α between 0.5 and 1.0 gave a good fit for a rate law of the type shown in Scheme 2 and a value for α of 0.8 (details of calculated rate constants are given below the scheme). This value for α is based upon a value for $k_1$ equal to that computed for rate constants $k_1$ and $k_2$ in Scheme 1 and we note that the 'best fit' value for α varies as $k_1$ varies. An ideal system would have a value for α close to 1.0 which would require a value for $K_3$ much lower than that for $K_1^2$.

$$\mathbf{A} + \mathbf{B} \xrightarrow{k_1} \mathbf{C}$$

$$\mathbf{A} + \mathbf{B} + \alpha\mathbf{C} \xrightarrow{k_2} (1+\alpha)\mathbf{C}$$

Overall rate: $dC/dt = k_1[A][B] + k_2[A][B][C]^{\alpha}$

**Scheme 2** A simplified reaction scheme for a self replication cycle. **A** and **B** are the two reactants giving **C** which is a catalytic template for the reaction, and α lies between 0 and 1. A satisfactory agreement between observed and experimental data is obtained with the following values of rate constants and a value for α of 0.8: at 23 °C, $k_1 = 6.98 \times 10^{-6}$ l mol$^{-1}$ s$^{-1}$ and $k_2 = 0.133$ l$^{1.8}$ mol$^{-1.8}$ s$^{-1}$; at 40 °C, $k_1 = 3.5 \times 10^{-5}$ and $k_2 = 0.350$ l$^{1.8}$ mol$^{-1.8}$ s$^{-1}$.

The Diels–Alder reaction of **1** and **2** differs from reactions reported in other work in that reactant **2** and product **3** are chiral and that **3** can, in principle, be formed as four possible diastereoisomers. These stereochemical features, which will be discussed in the full paper, lead to diastereoisomeric reaction pathways which have not been separated in the kinetic analysis above.

We conclude that the Diels–Alder reaction with a well-defined bicyclic transition state offers a basis for efficient self-replicating systems that could be investigated for transfer of chemical information coded in terms of the regio- and stereo-selectivity[1b] of template catalysed bond formation. Other reactions with well-defined transition states which generate stereo- and regio-isomers may offer similar possibilities.

## Footnotes and References

* E-mail: ios@liverpool.ac.uk

† We thank Dr S. Walker of this Department for the use of this program which is based upon numerical integration of the rate equation.

1 (*a*) L. E. Orgel, *Nature*, 1992, **358**, 203; (*b*) L. E. Orgel, *Acc. Chem. Res.*, 1995, **28**, 109.
2 S. Hoffman, *Angew. Chem., Int. Ed. Engl.*, 1992, **31**, 1013.
3 (*a*) G. von Kiedrowski, *Angew. Chem., Int. Ed. Engl.*, 1986, **25**, 932; (*b*) G. von Kiedrowski, B. Wlotzka and J. Helbing, *Angew. Chem., Int. Ed. Engl.*, 1989, **28**, 1235; (*c*) G. von Kiedrowski, B. Wlotzka, J. Helbing, M. Matzen and S. Jordan, *Angew. Chem., Int. Ed. Engl.*, 1991, **30**, 423.
4 T. Tjivikua, P. Ballester and J. Rebek, Jr., *J. Am. Chem. Soc.*, 1990, **112**, 1249; J. S. Nowick, Q. Feng, T. Tjivikua, P. Ballester and J. Rebek, Jr., *J. Am. Chem. Soc.*, 1991, **113**, 8831; V. Rotello, Jong-In Hong and J. Rebek, Jr., *J. Am. Chem. Soc.*, 1991, **113**, 6880.
5 D. N. Reinhoudt, D. M. Rudkevich and F. de Jong, *J. Am. Chem. Soc.*, 1996, **118**, 6880.
6 A. Terfort and G. von Kiedrowski, *Angew. Chem., Int. Ed. Engl.*, 1992, **31**, 654.
7 M. M. Conn, E. A. Wintner and J. Rebek, Jr., *Angew. Chem., Int. Ed. Engl.*, 1994, **33**, 1577; R. J. Peters, J. Huc and J. Rebek, Jr., *Angew. Chem., Int. Ed. Engl.*, 1994, **33**, 1579.
8 C. J. Walter, H. L. Anderson and J. K. M. Sanders, *J. Chem. Soc., Chem. Commun.*, 1993, 458; C. J. Walker and J. K. M. Sanders, *Angew. Chem., Int. Ed. Engl.*, 1995, **34**, 217.
9 T. R. Kelly, C. Zhao and G. J. Bridger, *J. Am. Chem. Soc.*, 1989, **111**, 3744; T. R. Kelly, G. J. Bridger and C. Zhao, *J. Am. Chem. Soc.*, 1990, **112**, 8024.
10 MACROMODEL 4.0, Columbia University, New York, 1993.

*Received in Liverpool, UK, 6th March 1997; 7/01573I*

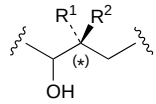
# Highly regio- and stereo-selective alkyl substitution with copper reagents for the construction of chiral trifluoromethylated quaternary carbon centres

**Shuichi Hiraoka, Takashi Yamazaki* and Tomoya Kitazume**

*Department of Bioengineering, Tokyo Institute of Technology, 4259 Nagatsuta-cho, Midori-ku, Yokohama 226, Japan*

**A new route for the asymmetric construction of quaternary carbon centres containing a trifluoromethyl group has been established using a highly regio- and stereo-selective $S_N2'$ reaction of organocopper and organocuprate reagents with allylic mesylates 4 and 8.**

Enhancement of biological activity in many natural product classes by the selective introduction of one, two or three fluorine atoms is a proven cornerstone strategy for medicinal and bioorganic chemists.[1] We were intrigued by the stereospecific replacement of either methyl group in the structure **1**, as found

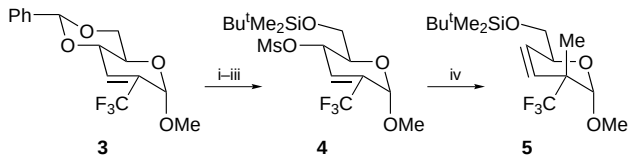



**1** $R^1 = R^2 = Me$
**2a** $R^1 = CF_3$, $R^2 = Me$
**2b** $R^1 = Me$, $R^2 = CF_3$

in Epothilone A[2] and antitumour active Shikoccidine derivatives,[3] by a trifluoromethyl moiety, which would lead to the sterically as well as electronically modified structures **2a** or **2b** with an additional asymmetric carbon centre. However, as far as we are aware, the Diels–Alder reaction of 2-(trifluoromethyl)acrylate[4] is the only reported procedure to access such a target structure, possibly due to the difficulty of alkyl substitution at a $CF_3$-attached carbon centre.[5] Although in general the $S_N2'$ reaction and 1,4-addition of cuprates are among the most efficient methods for the synthesis of quaternary centres,[6] such an approach has not yet been attempted in this context.

Recently we reported a novel strategy for the synthesis of optically active compounds with variously fluorinated methyl groups ($CH_{3-n}F_n$: $n$ = 1–3) *via exo*-difluoromethylene compounds synthesised from commercially available D-glucose.[7,8] Utilization of the readily accessible allylic alcohol **3** *via* $S_N2'$ reaction with copper reagents is an attractive way to create diastereoselectively a quaternary centre. An additional synthetic advantage of this approach is the possibility of controlling the alkene stereochemistry as *Z*, an outcome which is not easily obtainable otherwise. Here we describe the regio- and stereoselective alkyl substitution of allylic mesylates **4** and **8** using organocopper and organocuprate chemistry.

At the initial stages of this investigation, we chose the substrate **4** depicted in Scheme 1. To our surprise, reaction of allylic mesylate **4**, easily prepared from **3** in three steps, with

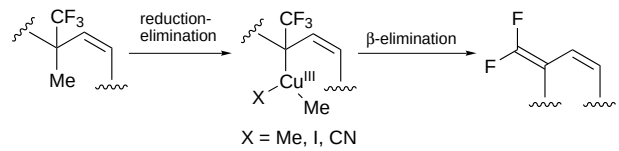



**Scheme 1** *Reagents and conditions*: i, TFA, MeOH–$H_2O$; ii, $Bu^tMe_2SiCl$, imidazole; iii, MsCl, $Et_3N$; iv, organocopper and organocuprate reagents

Gilman cuprate $Me_2CuLi$–LiI in $Et_2O$ gave the unexpected diene **6** in 98% yield, rather than either the $S_N2'$ product or the common $S_N2$ type byproduct (Table 1, entry 1). Although the desired $S_N2'$ material **5** was furnished in 35% yield after changing the solvent to THF, **6** was still the main product (54% yield, entry 2). Formation of **6** may be rationalized by the preferential Cu–F elimination because of the relatively poor reductive elimination ability of the Me ligand on the intermediary σ-copper(III) adduct (Scheme 2).† One result which supported this assumption was obtained by the addition of the electron-donating bidentate amine tetramethylethylenediamine (TMEDA) to the conditions used in entry 2: TMEDA was considered to make the ground state more stable than the corresponding transition state by analogy with HMPA,‡ and the yield of **6** was significantly increased from 54 to 92% (entry 2 *vs.* 6).

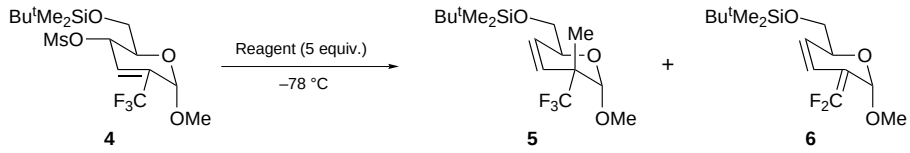
The above unfavourable pathway giving the difluorinated diene **6** was avoided by the use of cyanocuprate, known to undergo a facile reductive elimination,[9,10] resulting in complete $S_N2'$ displacement (entry 5). Moreover, it was also found that addition of $BF_3$ to the Gilman cuprate $Me_2CuLi$–LiI effectively suppressed the Cu–F elimination irrespective of the solvent (entries 3 and 4). Treatment of **4** with organocopper reagent, MeCu–LiI, yielded **5** with high stereoselectivity and complete γ-selectivity (entry 7). On the other hand, in sharp contrast to the case of the Gilman reagent, significant retardation of the reaction by $BF_3$ was observed, and this system furnished the $S_N2'$ product **5** in a disappointing 18% yield (entry 8).

It is well-known that the use of an organocopper reagent in a different solvent and/or in the presence (or absence) of ligands or Lewis acids sometimes leads to the formation of different species or equilibration mixture, and Table 1 collects the proposed reactive species in each specific conditions. Lipshutz *et al.* claimed that in $Et_2O$ solution $Me_2CuLi$ exists in the dimeric form $Me_4Cu_2Li_2$ (entry 1), while further addition of 2 equiv. of $BF_3$ affords a mixture of $Me_5Cu_3Li_2$ and MeLi–$BF_3$ (entry 3).[11] In THF, $Me_2CuLi$ forms an equilibrium mixture of MeLi, $Me_3Cu_2Li$ and $Me_4Cu_2Li_2$ (entry 2), which is converted to $Me_3Cu_2Li$ and MeLi–$BF_3$ when such a solution is treated with $BF_3$ (entry 4).[12] It should be noted that the dimeric Gilman cuprate $Me_4Cu_2Li_2$ is the reactive species leading to *exo*-difluoromethylene compounds **6** (entries 1 and 2). On the basis of chemical and NMR spectroscopic experiments, Lipshutz also proposed that MeCu–LiI was in an equilibrium with a MeLi–$BF_3$ complex and $I_2CuLi$ in the presence of $BF_3$[13] and thus, comparison of entries 7 and 8 suggests only low reactivity of MeLi–$BF_3$ in this procedure. Consequently, it is concluded that both $Me_5Cu_3Li_2$ and $Me_3Cu_2Li$ should be the 'true' reacting species giving **5** by smooth reductive elimination.




**Scheme 2**

**Table 1** Substitution of allylic mesylate **4** with organocopper and organocuprate reagents




**4** **5** **6**

| Entry | Reagent[a] | Solvent | Additive | *t*/h | Proposed species | Product (%)[b] **5** | **6** |
|---|---|---|---|---|---|---|---|
| 1 | $Me_2CuL$–LiI | $Et_2O$ | — | 0.25 | $Me_4Cu_2Li_2$[c] | 0 | 98 |
| 2 | $Me_2CuLi$–LiI | THF | — | 0.25 | MeLi + $Me_3Cu_2Li$ + $Me_4Cu_2Li_2$[c] | 35 | 54 |
| 3 | $Me_2CuLi$–LiI | $Et_2O$ | $BF_3$[d] | 0.25 | $Me_5Cu_3Li_2$ + MeLi·$BF_3$[e] | 96 | 0 |
| 4[f] | $Me_2CuLi$–LiI | THF | $BF_3$[d] | 0.25 | $Me_3Cu_2Li$ + MeLi·$BF_3$[e] | 95 | 0 |
| 5 | $Me_2CuCNLi$ | $Et_2O$ | — | 2 | | 98 | 0 |
| 6 | $Me_2CuL$–LiI | THF | TMEDA[d] | 0.25 | | 5 | 92 |
| 7 | MeCu–LiI | $Et_2O$ | — | 1.5 | | 95 | 0 |
| 8 | MeCu–LiI | $Et_2O$ | $BF_3$[g] | 3 | MeLi·$BF_3$[h] | 18[i] | 0 |

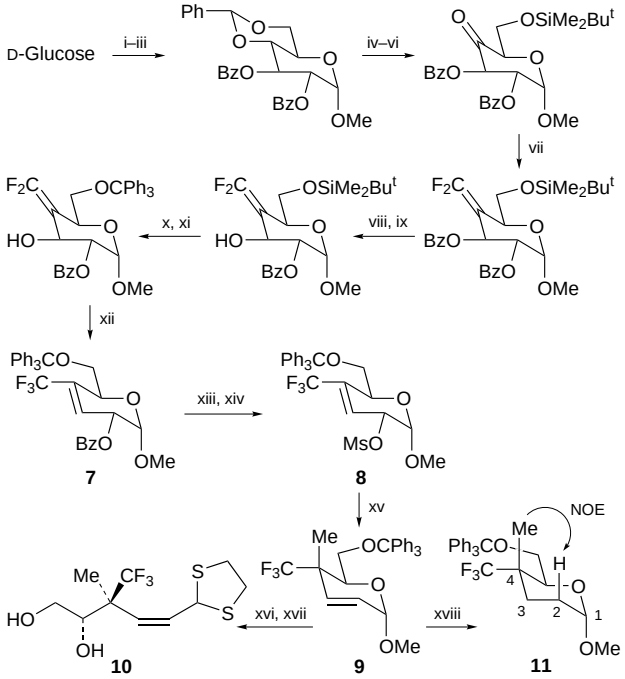
[a] 5 quiv. based on **4**. [b] Determined by $^{19}F$ NMR spectroscopy. [c] Ref. 12. [d] 10 equiv. [e] Ref. 11. [f] $BF_3$ was added at −60 °C. [g] 5 equiv. [h] Ref. 13. [i] Starting material (76%) was recovered.

Next, we performed the same reaction with a different substrate containing a $CF_3$ group at the 4-position. The requisite allylic mesylate **8** was prepared as shown in Scheme 3.

As was our expectation, treatment of **8** with cyanocuprate MeCuCNLi, the best reagent with the allylic mesylate **4**, furnished **9** again as a single stereoisomer in 96% yield. For the determination of the stereochemical course of this $S_N2'$ reaction, **9** was subjected to hydrogenation and the C-4 methyl group of thus obtained **11** was concluded to be axially oriented from NOE measurements (Scheme 3). This result is rationalized in terms of the well-accepted *anti* $S_N2'$ mechanism.[14] Deprotection of methyl glucoside **9** with $BBr_3$ and formation of the dithioacetal allowed us to readily transform **9** into the corresponding acyclic form **10** with complete retention of (*Z*) stereochemistry (11.6 Hz between H-2 and H-3).

In conclusion, a novel pathway for the highly regio- and stereo-selective $S_N2'$ reaction of allylic mesylates **4** and **8** has been realized, which forms a unique strategy for the construction of chiral quaternary carbon centres containing a trifluoromethyl group. Further application of the present reaction to mono- as well as di-fluoromethylated allylic mesylates is currently being pursued in our laboratories.

This work was financially supported by the Ministry of Education, Science, Sports and Culture of Japan [Grant-in-Aid No. 085269]. One of the authors (S. H.) is grateful for a JSPS research fellowship for young scientists.




**Scheme 3** *Reagents and conditions*: i, MeOH, HCl; ii, PhCH $(OMe)_2$, TsOH (cat.); iii, BzCl, pyridine, room temp.; iv, TsOH (cat.), MeOH; v, Bu$^t$Me$_2$SiCl, imidazole; vi, PDC, $Ac_2O$; vii, $CF_2Br_2$–$(Me_2N)_3P$; viii, DIBAL-H; ix, BzCl, pyridine, 0 °C; x, AcOH–$H_2O$; xi, $Ph_3CCl$, $Et_3N$; xii, DAST; xiii, $K_2CO_3$, MeOH; xiv, MsCl, $Et_3N$; xv, MeCuCNLi; xvi, $BBr_3$; xvii, $HS(CH_2)_2SH$, $BF_3$·$Et_2O$; xviii, $H_2$, Pd/C

## Footnotes and References

* E-mail: tyamazak@bio.titech.ac.jp

† This type of elimination was reported in the case of allylic sulfinyl mesylates: see ref. 9.

‡ Strongly electron-donating HMPA was calculated to increase the energy barrier to reductive elimination when added to $Me_3Cu$: S. H. Bertz, G. Miao, B. E. Rossiter and J. P. Snyder, *J. Am. Chem. Soc.*, 1995, **117**, 11023.

1 J. T. Welch, *Fluorine in Bioorganic Chemistry*, Wiley, New York, 1991.
2 A. Balog, D. Meng, T. Kamenecka, P. Bertinato, P. Su, E. J. Sorensen and S. J. Danishefsky, *Angew. Chem., Int. Ed. Engl.*, 1996, **35**, 2801.
3 D. Backhaus and L. A. Paquette, *Tetrahedron Lett.*, 1997, **38**, 29.
4 Y. Hanzawa, M. Suzuki, Y. Kobayashi and T. Taguchi, *J. Org. Chem.*, 1991, **56**, 1718.
5 N. Shinohara, J. Haga, T. Yamazaki, T. Kitazume and S. Nakamura, *J. Org. Chem.*, 1995, **60**, 4363.
6 J. Mulzer, G. Dürner and D. Trauner, *Angew. Chem., Int. Ed. Engl.*, 1996, **35**, 2830.
7 T. Yamazaki, S. Hiraoka and T. Kitazume, *Tetrahedron: Asymmetry*, 1997, **8**, 1157.
8 S. Hiraoka, T. Yamazaki and T. Kitazume, *Synlett*, 1997, 669.
9 R. F. de la Pradilla, M. B. Rubio, J. P. Marino and A. Viso, *Tetrahedron Lett.*, 1992, **33**, 4985.
10 L. Hamon and J. Levisalles, *Tetrahedron*, 1989, **45**, 489.
11 B. H. Lipshutz, E. L. Ellsworth and T. J. Siahaan, *J. Am. Chem. Soc.*, 1989, **111**, 1351.
12 B. H. Lipshutz, J. A. Kozlowski and C. M. Breneman, *J. Am. Chem. Soc.*, 1985, **107**, 3197.
13 B. H. Lipshutz, E. L. Ellsworth and S. H. Dimock, *J. Am. Chem. Soc.*, 1990, **112**, 5869.
14 J. A. Marshall, *Chem. Rev.*, 1989, **89**, 1503.

*Received in Cambridge, UK, 12th May 1997; 7/03223D*

# Lariat ethers with a novel proton-ionizable group. Synthesis and solvent extraction of alkali metal cations

**Vincent J. Huber, Sheryl N. Ivy, Jianping Lu and Richard A. Bartsch***

*Department of Chemistry and Biochemistry, Texas Tech University, Lubbock, Texas 79409-1061, USA*

**Novel lariat ethers with pendent *N*-alkyl- and *N*-aryl-sulfonyl carbamoyl groups are synthesized in two steps from *sym*-(decyl)dibenzo-16-crown-5-oxyacetic acid; for competitive solvent extraction of alkali metal cations from aqueous solutions into chloroform by these proton-ionizable lariat ethers with 'tunable' acidity, the selectivity order is $Na^+ \gg K^+$ with no detectable extraction of $Li^+$, $Rb^+$ or $Cs^+$.**

A wide variety of macrocyclic polyether compounds (crown ethers) has been developed for the complexation and separation of metal ions. Many of these crown compounds show superior binding and selectivity towards Group 1 and 2 metal cations compared to other ligands.[1–3] The binding efficiency and selectivity of crown compounds may be increased by the addition of a ligand-bearing side arm to form a lariat ether.[4] Unlike their crown ether analogues, lariat ethers possess three-dimensional cavities for the coordination of metal cations.[5] The properties of these pendent ligation sites, *i.e*. their Lewis basicity and whether they are neutral or ionizable, plays an important role in determining the metal-ion binding properties of the lariat ether.

Previously we have prepared substituted lariat ethers **1** and investigated their applications in solvent extraction and liquid membrane transport of alkali metal cations, as well as their use in polymeric membrane electrodes.[6–8] The $R^1$ substituent on the three-carbon bridge (hydrogen, alkyl, perfluoroalkyl or aryl) affects not only the lipophilicity of the lariat ether, but also the preorganization of the binding site.[9] Moreover, the ligand substituent $R^2$ can be ionizable or neutral, *e.g*. a carboxylic acid or an amide, respectively, depending on the target metal ion and the particular application of interest.[10,11] Proton-ionizable lariat ether carboxylic acids and phosphonic acid monoethyl esters are particularly effective in metal ion separation processes.[12]

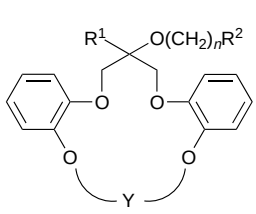
We are now investigating a novel type of proton-ionizable lariat ether in which the acidity of the pendant function is 'tunable'. In *N*-alkyl- or *N*-aryl-sulfonylcarbamoyl lariat ethers such as **2**, variation of the X group (alkyl, perfluoroalkyl or aryl) should influence the acidity of the pendent group. We now report a synthetic route to dibenzo lariat ethers **3**–**6** and the application of these novel lipophilic proton-ionizable lariat ethers in the solvent extraction of alkali metal cations.

The lariat ether **3**–**6** are prepared in two steps from the lipophilic lariat ether oxyacetic acid **7**.[13] A general procedure for the conversion of lariat ether carboxylic acid **7** into the corresponding *N*-trifluoromethylsulfonyl amide **3** is as follows: Benzene (25 ml) was added to **7** (2.00 g, 3.68 mmol) followed by oxalyl chloride (1.90 ml, 22.0 mmol). The resulting mixture was stirred at room temperature under nitrogen for 6 h then evaporated *in vacuo*. The resultant acid chloride was dissolved in dry THF (25 ml) and added to a mixture of pentane–washed potassium hydride (2.10 g, 18.4 mmol) and trifluoromethane sulfonamide (0.66 g, 4.40 mmol) in dry THF (25 ml). The mixture was stirred at room temperature for 10 h under nitrogen and then water (10 ml) was carefully added to destroy the remaining potassium hydride. The THF solution was separated from the aqueous layer and diluted with ethyl acetate (100 ml). The resulting organic solution was washed with 10% aqueous potassium carbonate (2 × 30 ml), dried over magnesium sulfate and evaporated *in vacuo*. The residue was washed with hexanes and purified by column chromatography ($Al_2O_3$, $CH_2Cl_2 \rightarrow 2\%$ MeOH–$CH_2Cl_2$) to give the potassium salt of ionized **3** as a white solid which was dissolved in $CHCl_3$ and washed with 1 M HCl (50 ml). Evaporation of the $CHCl_3$ *in vacuo* gave **3** as a white solid (2.03 g, 82% yield).† Similar procedures were utilized to prepare acetamides **4**–**6**. (For the preparation of **6**, a shorter, 1 h reaction of the lariat ether oxyacetyl chloride with the potassium sulfonamidate gave a cleaner crude product.)

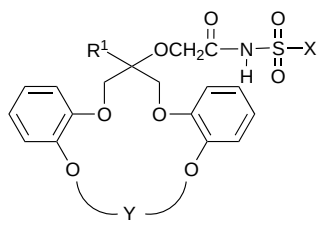
A single crystal of the proton-ionizable lariat ether **3** suitable for X-ray diffraction analysis was grown and its solid-state structure determined. In the structure, the functional side arm is oriented over the polyether cavity, as noted previously for lariat ether carboxylic acid **7**.[14] Thus the presence of the geminal decyl group in **3** preorganizes the coordinating side arm for metal ion complexation.[9]

Solvent extractions of alkali metal cations from aqueous solutions into chloroform by the lariat ether carboxamides were performed.‡ Results from competitive extractions of aqueous solutions containing 20 mM (each) of the alkali metal cations with 5 mM chloroform solutions of **3**–**6** are presented in Fig. 1. Metal ion loadings at pH 11 and selectivity factors are given in Table 1.

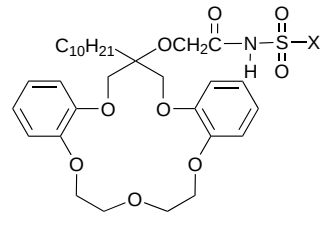
The lariat ether oxyacetamide **3**–**6** are found to be efficient extractants with very high selectivity for $Na^+$. The maximal loading is 96–100% as calculated for the formation of 1 : 1 ionized lariat ether–metal ion complexes. Only $Na^+$ and $K^+$ are detectably extracted into the chloroform phase and the $Na^+/K^+$ selectivity is 47–49 under conditions of high loading. The similarity of extraction selectivities for the four extractants indicates that changing X does not exert an appreciable steric



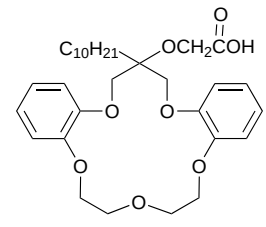

**1**




**2**




**3** R = $CF_3$
**4** R = Me
**5** R = Ph
**6** R = 4-$NO_2C_6H_4$




**7**

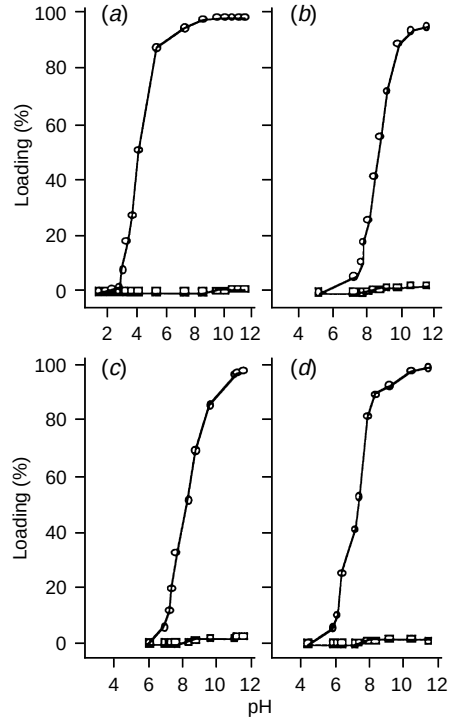



**Fig. 1** Metal loadings of the organic phase *vs.* the pH of the aqueous phase for competitive solvent extractions of 20 mM (each) solutions of alkali metal cations with 5 mM chloroform solutions of (*a*) **3**, (*b*) **4**, (*c*) **5** and (*d*) **6**, with (○) $Na^+$ and (□) $K^+$

**Table 1** Loading and selectivity factors for extraction of alkali metal cations by proton-ionizable lariat ethers **3**–**6** at pH 11[a]

| Extractant | Total loading (%) | Selectivity $Na^+/K^+$ |
|---|---|---|
| **3** | 100 | 49 |
| **4** | 96 | 47 |
| **5** | 97 | 48 |
| **6** | 100 | 49 |

[a] Concentrations of extracted $Li^+$, $Rb^+$ and $Cs^+$ were below detection limits.

effect. However, the variation of X does appreciably influence the side arm acidity. As judged from the extraction profiles, the acidities of the proton-ionizable lariat ethers decrease in the order: **3** > **6** > **4**, **5**. The efficiency with which **3** extracts $Na^+$ from acidic aqueous solutions is noteworthy.

Further investigations of metal ion separations with such 'tunable' proton-ionizable lariat ethers are in progress.

This research was supported by the Division of Chemical Sciences of the Office of Basic Energy Sciences of the U.S. Department of Energy. We thank Dr Frederick J. Brown of Zeneca Pharmaceuticals for the suggestion that *N*-alkyl- and *N*-aryl-sulfonylcarbamoyl groups be incorporated into proton-ionizable lariat ethers. We also thank Dr Carey E. Bauer of Northern Illinois University and Dr Robin D. Rogers of the University of Alabama, Tuscaloosa, for determining the X-ray crystal structure of **3**.

## Footnotes and References

* E-mail: rabartsch@ttu.edu

† Spectra ($^1H$ and $^{13}C$ NMR and IR) of compounds **3**–**6** are consistent with their structural assignments and will be reported in a more detailed publication. *Selected data* for **3**: mp 100 °C; calc. for $C_{32}H_{49}F_3NO_9S$: C, 56.88; H, 6.56; N, 2.07. Found: C, 56.99; H, 6.83; N, 2.06%. For **4**: 75% yield of white solid, mp 43–45 °C; calc. for $C_{32}H_{47}NO_9S{\cdot}0.1\ CH_2Cl_2$: C, 61.17; H, 7.55; N, 2.22. Found: C, 61.36; H, 7.76; N, 2.10%. For **5**: 81% yield of white solid, mp 52–54 °C; calc. for $C_{37}H_{49}NO_9S$: C, 64.99; H, 7.22; N, 2.05. Found: C, 64.75; H, 7.32; N, 2.00%. For **6**: 80% yield of yellow solid, mp 54–57 °C; calc. for $C_{37}H_{48}N_2O_{11}S$: C, 60.97; H, 6.64; N, 3.84. Found: C, 60.62; H, 6.69; N, 3.72%.

‡ Into a capped, metal-free, plastic 15 ml centrifuge tube was added 2.0 ml of an aqueous solution which was 20.0 mM (each) in sodium, potassium, rubidium and cesium chlorides and 20.0 mM in lithium (chloride + hydroxide). [Due to the higher acidity of **3**, some of the extracted aqueous solutions for this ligand were 20.0 mM (each) in lithium, sodium, potassium, rubidium and cesium chlorides with added HCl.] A 5.0 mM solution of the proton-ionizable lariat ether (2.0 ml) was added and the tube was shaken on a vortex mixer for 4 min and then centrifuged for 4 min to promote complete phase separation. The aqueous phase was removed with a syringe and the equilibrium pH of this aqueous phase was measured with a combination microelectrode. Of the organic phase, 1.5 ml was transferred by syringe into a new plastic centrifuge tube. After adding 3.0 ml of 0.1 M HCl, the tube was shaken on a vortex mixer for 4 min and then centrifuged for 4 min. A portion of the aqueous phase was removed with a syringe and diluted with deionized water for alkali metal cation analysis by ion chromatography.

1 M. Hiraoka, *Crown Compounds. Their Characteristics and Applications*, Elsevier, New York, 1982.
2 *Host Guest Complex Chemistry, Macrocycles*, ed. F. Vögtle and E. Weber, Springer-Verlag, New York, 1990.
3 *Crown Binding by Macrocycles, Complexation of Cationic Species by Crown Ethers*, ed. Y. Inoue and G. W. Gokel, Marcel Dekker, New York, 1990.
4 G. W. Gokel, D. M. Dishong and C. J. Diamond, *J. Chem. Soc., Chem. Commun.*,1980, 1051.
5 G. W. Gokel, in *Cation Binding by Macrocycles, Complexation of Cationic Species by Crown Ethers*, ed. Y. Inoue and G. W. Gokel, Marcel Dekker, New York, 1990, pp. 253–310.
6 A. Ohki, J.-P. Lu and R. A. Bartsch, *Anal. Chem.*, 1994, **66**, 651.
7 A. Ohki, J.-P. Lu, X. Hwang and R. A. Bartsch, *Anal. Chem.*, 1994, **66**, 4332.
8 A. Ohki, S. Maeda, J.-P. Lu and R. A. Bartsch, *Anal. Chem.*, 1994, **66**, 1743.
9 D. J. Cram, *Angew. Chem., Int. Ed. Engl.*, 1986, **25**, 1039.
10 S. P. Kasprzyk and R. A. Bartsch *J. Heterocycl. Chem.*, 1993, **30**, 119.
11 Y. Jang and R. A. Bartsch, *J. Heterocycl. Chem.*, 1995, **32**, 1441.
12 R. A. Bartsch, *Solvent Extr. Ion Exch.*, 1989, **7**, 829.
13 W. Walkowiak, W. A. Charewicz, S. I. Kang, I.-W. Yang, M. J. Pugia and R. A. Bartsch, *Anal. Chem.*, 1990, **62**, 2018.
14 R. A. Bartsch, J. S. Kim, U. Olsher, D. W. Purkiss, V. Ramesh, N. K. Dalley and T. Hayashita, *Pure Appl. Chem.*, 1993, **65**, 399.

*Received in Corvallis, OR, USA, 6th May 1997; 7/03106H*

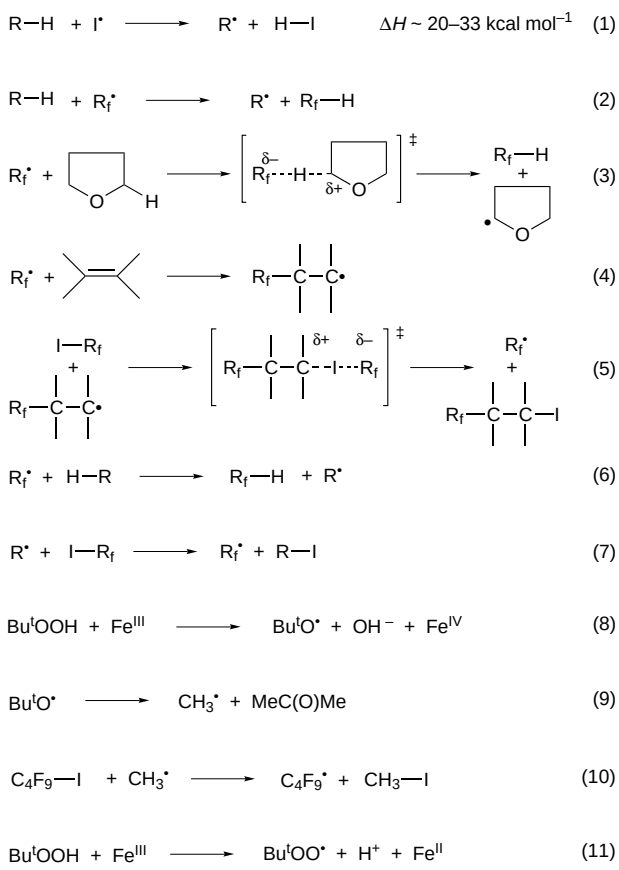
# A new direct homolytic iodination reaction of alkanes by perfluoroalkyl iodides

**Lucia Liguori, Hans-René Bjørsvik, Anna Bravo, Francesca Fontana and Francesco Minisci***

*Dipartimento di Chimica del Politecnico, via Mancinelli 7, I-20131 Milano, Italy*

**A new method for the direct free-radical chain iodination of alkanes by perfluoroalkyl iodides is described.**

The direct free-radical iodination of alkanes by iodine, unlike the other halogens, is not feasible owing to its large positive enthalpy of hydrogen abstraction [eqn. (1)]. The rates of




hydrogen abstraction from C–H bonds [eqn. (2)] by perfluoroalkyl radicals ($R_f$·) are $>10^3$ times larger than those of the analogous hydrocarbon radicals.[1] Enthalpic (the higher energy of $R_f$–H compared to R–H bonds) and polar (the electrophilic character of $R_f$·) effects influence the rates of hydrogen abstraction. Thus, the rate of hydrogen abstraction by $C_7F_{15}$· from THF, whose α-position is particularly activated by both enthalpic and polar [eqn. (3)] factors, has been evaluated[1] at $6.1 \times 10^5$ M$^{-1}$ s$^{-1}$. On the other hand, alkyl radicals easily abstract iodine atom from $R_f$–I, as shown by the effective free-radical addition of $R_f$–I to alkenes[2] [eqns. (4) and (5)], with the polar effect playing a significant role.

Thus, the conditions of alkane iodination according to the radical chain of eqns. (6) and (7) appeared to be fulfilled.

Iodocyclohexane was obtained in 70% yield, based on $C_4F_9I$, by refluxing a solution of cyclohexane and $C_4F_9I$ in acetic acid in the presence of catalytic amounts of Bu$^t$OOH and $Fe(OAc)_3$. The reaction is explained by the radical chain of eqns. (6) and (7), initiated by a redox system [eqns. (8)–(10)] and represents a new simple, direct iodination of alkanes; we believe[3] eqn. (8) to be operating in this case, rather than eqn. (11).

In order to probe the reactivity–selectivity relationship of the reaction, an investigation was carried out with heptane, adamantane and 1-chlorohexane; heptane gave a mixture of all the iodoheptane isomers (Table 1, including a comparison with chlorination by *N*-chloroamines).

Enthalpic and steric effects contribute to the regioselectivity: the $CH_2$ groups in positions 3 and 4 have substantially the same reactivity, while the $CH_2$ in position 2 is more reactive due to steric factors and the methyl group is less reactive for enthalpic reasons. The behaviour is qualitatively similar to that for chlorination by protonated *N*-chloroamines[4] (Minisci chlorination),[5] in which the selectivity is determined by hydrogen abstraction by $R_2NH^{+\cdot}$.

The free-radical reactivity of adamantane is interesting because the selectivity of hydrogen abstraction is little affected by enthalpic factors, but it is greatly influenced by polar effects[6] (high selectivity with $R_2NH^{+\cdot}$[6] and $ArC(O)OO^{\cdot}$[7] radicals and in electron-transfer processes[8]). The yields obtained according to eqns. (6) and (7) (84.7% 1-iodo- and 15.3% 2-iodo-ada-

**Table 1** Iodination of heptane

| Iodinating agent | Iodination per hydrogen (%)[a] | | | |
|---|---|---|---|---|
| | 1-iodo | 2-iodo | 3-iodo | 4-iodo |
| $C_4F_9I$ | 1 (4.1) | 18.7 (51.0) | 11.1 (30.3) | 10.7 (14.6) |
| $Me_2NHCl^+$ | 1 | 75.8 | 39.5 | 39.0 |
| $Bu^i{}_2NCl$ | 1 | 75.3 | 26.4 | 26.1 |

[a] Figures in brackets indicate the yield of each isomer.

**Table 2** Iodination of 1-chlorohexane

| Iodinating agent | Iodination per hydrogen (%)[a] | | | | | |
|---|---|---|---|---|---|---|
| | 1-iodo | 2-iodo | 3-iodo | 4-iodo | 5-iodo | 6-iodo |
| $C_4F_9I$ | 0.2 (2.1) | 0.3 (3.5) | 1 (12.0) | 2.2 (26.7) | 4.2 (50.0) | 0.3 (5.7) |
| $Me_2NHCl^+$ | — | — | 1 | 2.9 | 10.5 | 0.2 |
| $Cl_2$ | 0.09 | 0.4 | 1 | 1.1 | 1.2 | 0.5 |

[a] Figures in brackets indicate the yield of each isomer.

mantane) confirm the expected influence of the polar effect, due to the electrophilic character of $C_4F_9^{\cdot}$, the higher stability of 1-adamantyl$^+$ with respect to its (secondary) 2-isomer[9] and the oxidation potential of adamantane ($E_{ox}$ = 2.72 V *vs*. SCE), which is lower than that of 2,3-dimethylbutane ($E_{ox}$ = 3.45 V *vs*. SCE).[8]

The iodination of 1-chlorohexane, reported in Table 2 and compared with chlorination by $Me_2NHCl^+$ and $Cl_2$, further supports our ideas about the influence of enthalpic and polar effects in hydrogen abstraction by $C_4F_9^{\cdot}$.

The σ-inductive and field effects of the chlorine atom in 1-chlorohexane are significant in the iodination, but they are lower than in chlorination by $Me_2NHCl^+$. This result suggests that the increase in hydrogen abstraction rates for $R_f^{\cdot}$ compared to the analogous hydrocarbon radicals must be mainly ascribed to the enthalpic effect (higher energy of the $R_f$–H bonds), the polar effect being a significant but minor factor.

We have recently[10] reached the same conclusion concerning the increase in addition rates of $R_f^{\cdot}$ to aromatic substrates, compared to addition of alkyl radicals, which is due mainly to the enthalpic effect, with a significant but minor polar contribution.

## Footnote and References

* E-mail: fontana@dept.chem.polimi.it

1 W. R. Dolbier, Jr., *Chem. Rev.*, 1996, **96**, 1557.
2 M. Yoshida, N. Kamigata, H. Sawada and M. Nakayama, *J. Fluorine Chem.*, 1990, **49**, 1.
3 F. Minisci, E. Vismara and F. Fontana, *J. Org. Chem.*, 1989, **54**, 5224; F. Minisci, F. Fontana, S. Araneo, F. Recupero, S. Banfi and S. Quici, *J. Am. Chem. Soc.*, 1995, **117**, 226; F. Minisci, F. Fontana, S. Araneo, F. Recupero and L. Zhao, *Synlett*, 1996, 119.
4 R. Bernardi, R. Galli and F. Minisci, *J. Chem. Soc. B*, 1968, 324.
5 N. C. Deno, *Methods in Free Radical Chemistry*, ed. E. S. Huyser, Marcel Dekker, New York, 1975, p. 143.
6 F. Minisci, F. Fontana, L. Zhao, S. Banfi and S. Quici, *Tetrahedron Lett.*, 1994, **35**, 8033.
7 A. Bravo, H. R. Bjørsvik, F. Fontana, F. Minisci and A. Serri, *J. Org. Chem.*, 1996, **61**, 940.
8 F. Mella, M. Freccero, T. Soldi, E. Fasani and A. Albini, *J. Org. Chem.*, 1996, **61**, 1413.
9 G. A. Olah, G. Liang and G. D. Mateesen, *J. Org. Chem.*, 1974, **39**, 3750.
10 A. Bravo, H. R. Bjørsvik, F. Fontana, L. Liguori and F. Minisci, *J. Org. Chem.*, in the press.

*Received in Liverpool, UK, 14th May 1997; 7/03332J*

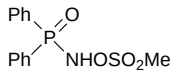
# Base induced rearrangement of *N,O*-bis(diphenylphosphinoyl)hydroxylamine: $^{18}$O-labelling evidence on how the phosphonamidic-phosphinic anhydride product is formed

**Martin J. P. Harger***

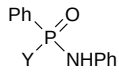
*Department of Chemistry, The University, Leicester, UK LE1 7RH*

**The $^{18}$O-labelled substrate $Ph_2P(O)NHOP(^{18}O)Ph_2$ rearranges with base (KOBu$^t$) to give $Ph(PhNH)P(O)O-P(^{18}O)Ph_2$ but not $Ph(PhNH)P(O)^{18}OP(O)Ph_2$, in accord with a concerted mechanism rather than one involving a metaphosphonimidate intermediate; $Ph(PhNH)P(^{18}O)-OP(O)Ph_2$ is also formed, but only because the substrate rapidly equilibrates with $Ph_2P(^{18}O)NHOP(O)Ph_2$ prior to rearrangement.**

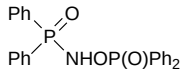
When suitably activated, *N*-phosphinoylhydroxylamines undergo base-induced reactions in which an aryl or alkyl group migrates from phosphorus to nitrogen.[1] Thus, for example, the *O*-sulfonyl compound **1** reacts readily with amines and alkoxides to give the phosphonamidic acid derivative **2** (Y = RNH or RO).[2] The *O*-phosphinoyl compound **3** is much less reactive but with *tert*-butoxide it does rearrange, giving the phosphonamidic-phosphinic mixed anhydride **4**.[3] The formation of **4** is important, adding weight to the circumstantial evidence than an analogous but short-lived phosphonamidic-sulfonic anhydride is formed initially in the rearrangement reactions of **1**.[4] Thus by studying the mechanism of the rearrangement of **3** to **4**, the more versatile and useful rearrangement reactions of **1** and related sulfonyl compounds may also be better understood.



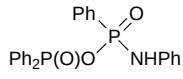

**1**




**2**

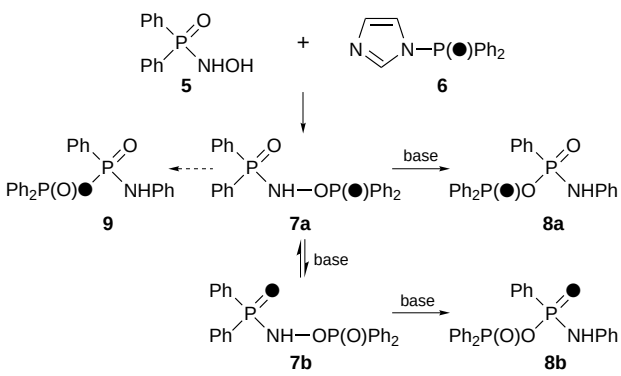



**3**



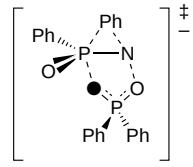

**4**

Isotopically enriched $Ph_2P(^{18}O)Cl$ was obtained from $Ph_2PCl$ (in $CH_2Cl_2$) by hydrolysis with [$^{18}$O]water (1 equiv.) followed by treatment with chlorine (slight excess). Reaction with *N*-(trimethylsilyl)imidazole then afforded the phosphinylating agent **6** (Scheme 1) and this, on stirring with *N*-(diphenylphosphinoyl)hydroxylamine **5** in $CH_2Cl_2$ (4 h at room temp.), gave the $^{18}$O-labelled substrate **7a**, mp 181–183 °C (from $CHCl_3$–diethyl ether). The mass spectrum of **7a** indicated 78% enrichment with one $^{18}$O atom [*m/z* (FAB) 434 and 436 $(M + H)^+$] and the $^{31}$P NMR spectrum [Fig. 1(*a*)] confirmed the location of the label: $\delta_P$ ($CDCl_3$; 162 MHz) 39.38 or 39.33 (both d, $J_{PP}$ 19 Hz; ratio 22 : 78; $^{18}$O-induced shift 0.048 ppm) and 29.68 (d, $J_{PP}$ 19 Hz).

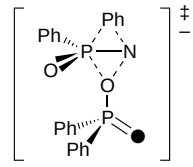



**Scheme 1**

The labelled substrate **7a** (0.07 mmol) was shaken with KOBu$^t$ (0.10 mmol) in *tert*-butyl alcohol (containing 10% $C_6D_6$ for NMR lock) (0.5 ml) and the $^{31}$P NMR spectrum of the reaction mixture was recorded. For the anhydride rearrangement product, $^{18}$O-induced high-field peaks, of equal intensity, were seen in both the phosphinoyl and phosphonamidoyl resonances [Fig. 1(*b*); *t* = 40 min]: $\delta_P$ (reaction mixture; 162 MHz) 24.12 or 24.08 (both d, $J_{PP}$ 35 Hz; $^{18}$O-induced shift 0.044 ppm) and 7.74 or 7.70 (both d, $J_{PP}$ 35 Hz; $^{18}$O-induced shift 0.037 ppm.† This might suggest structure **9** (Scheme 1), with the label located in the bridging (P–O–P) position, and a reaction mechanism in which the conjugate base of the substrate rearranges concertedly *via* a transition state such as **10**. However, the intensities of the isotope-induced high-field peaks (*ca*. 40% of the total signal) are only about half of what they should be for **9**, given the $^{18}$O-enrichment (78%) of the substrate. This points instead to an even distribution of the label between the two non-bridging (P=O) positions of the anhydride product, corresponding to an equal mixture of the structures **8a** and **8b**. Such a labelling pattern is difficult to reconcile with any reasonable rearrangement mechanism, but degradation of the product showed it to be true: reaction with methoxide gave some $Ph_2P(O)OMe$ by attack at one of the phosphorus atoms of the anhydride and some PhP(O)(NHPh)OMe by attack at the other, and these both had $^{18}$O-enrichments (40 and 37% respectively by GC–MS) equal to about half that (78%) of the substrate.




**10**




**11**

The reaction of the labelled substrate **7a** was repeated but with quenching ($CF_3CO_2H$) after just 2 min, at *ca*. 10% completion. The $^{31}$P NMR spectrum of the remaining substrate showed the $^{18}$O label to be equally shared between the P=O groups of the *O*- and *N*-phosphinoyl moieties. Apparently, under the conditions of the rearrangement, the two phosphoryl (P=O) oxygen atoms in the substrate rapidly equilibrate, *i.e.* **7a** ⇌ **7b** (Scheme 1).‡ The product resulting from the rearrangement of **7b** can only be **8b**, with the label in the phosphonamidic non-bridging position, so from **7b** we can learn nothing about the mechanism of the rearrangement. Attention must therefore be focussed on the behaviour of **7a** (half the total $^{18}$O after

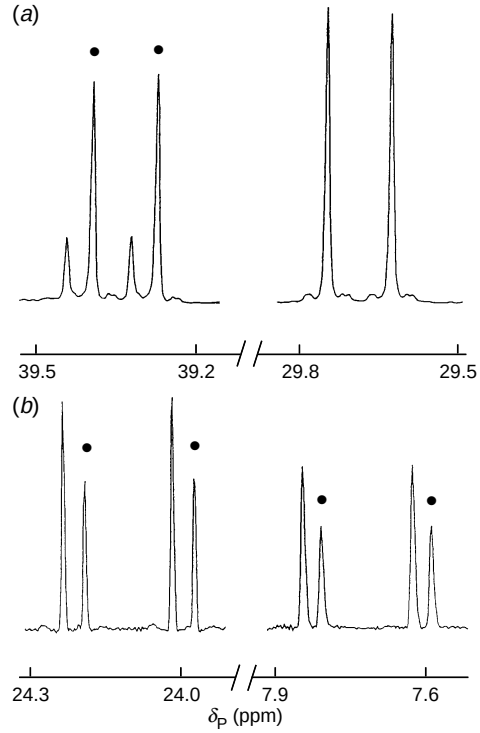
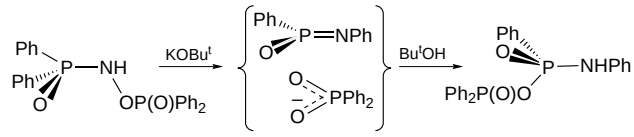



**Fig. 1** $^{31}$P NMR spectra (162 MHz; $^{1}$H decoupled) of (*a*) $^{18}$O-enriched substrate **7a** (in $CDCl_3$) and (*b*) rearrangement product **8a** + **8b** [in Bu$^t$OH–$C_6D_6$ containing KOBu$^t$]; isotope-shifted peaks (●) at high field

equilibration with **7b**). When **7a** rearranges it is a labelled phospinate group [OP($^{18}$O)$Ph_2$] that is transferred from nitrogen to phosphorus, so formation of the new O–P bond might involve the labelled or the unlabelled oxygen atom. The latter seems actually to be the case. In the $^{31}$P NMR spectrum of the rearrangement product [Fig. 1(*b*)] there are substantial high-field isotope-induced peaks for structure **8a** ($\delta_P$ 24.08; $\Delta\delta$ 0.044 ppm), derived from **7a**, and for **8b** ($\delta_P$ 7.70; $\Delta\delta$ 0.037 ppm), derived from **7b**, but not for **9**. In the case of **9** the isotope-induced shifts, due to P–$^{18}$O single bonds, would be relatively small.[5] Appropriate peaks ($\delta_P$ 24.09; $\Delta\delta$ 0.033 ppm) may just be detectable in the phosphinoyl resonance [Fig. 1(*b*)], but they are hardly significant.§ The conclusion must be that, in the rearrangement, the phosphinate group is transferred from nitrogen to phosphorus without any appreciable incorporation of the phosphoryl (P=O) oxygen atom into the new O–P bond. If the rearrangement of the conjugate base of the substrate is concerted, it must proceed *via* a transition state that resembles **11** rather than **10**.

In principle the rearrangement could be non-concerted, with a three-coordinate metaphosphonimidate intermediate, but in that case the phosphinate group would be set free and would become a fully-formed anion (Scheme 2). In the limit the two




**Scheme 2**

oxygen atoms in the anion would be equivalent and involved equally in the formation of the new O–P bond, *i.e.* **7a** would give equal amounts of **8a** and **9**. Initially, when first released from nitrogen, the oxygen atoms of the phosphinate anion might be non-equivalent, because of differences in solvation (by Bu$^t$OH) and/or association with the counterion ($K^+$), but it seems unlikely that they could remain distinct to the extent that only one of them plays any part in forming the new bond to phosphorus. We therefore feel bound to favour a concerted mechanism for the rearrangement, with a transition state resembling **11**, and also to reconsider our preference for a non-concerted mechanism in the case of sulfonyl compounds such as **1**.[6]

We thank Dr G. A. Griffith for recording NMR spectra and Professor P. M. Cullis for advice and encouragement.

## Footnotes and References

† The mixed anhydride reacts very readily with traces of water in basic media. Moisture was excluded as far as possible but some formation of the hydrolysis products $Ph_2P(O)O^-$ ($\delta_P$ 17.53 or 17.49; $^{18}$O-induced shift 0.036 ppm) and Ph(PhNH)P(O)O$^-$ ($\delta_P$ 7.05 or 7.02; $^{18}$O-induced shift 0.035 ppm) could not be avoided.

‡ The unexpected equilibration of the phosphoryl oxygen atoms (or the phosphinoyl groups) is interesting but peripheral to the present investigation.

§ The magnitude of an $^{18}$O-induced shift depends on the environment of the phosphorus atom, but the single bond (P–$^{18}$O) shift is generally in the range 0.3 to 0.7 times the double bond (P=$^{18}$O) shift (ref. 5). That being so, any appreciable amount of **9** would certainly be detectable in the presence of **8a** and **8b**. An attempt to confirm this experimentally, by treating $Ph_2P(O)^{18}O^-$ with Ph(PhNH)P(O)Cl in Bu$^t$OH, was complicated by side reactions but the phosphinoyl resonance of the mixed anhydride clearly showed a single bond shift 0.7 times the double bond shift.

1 M. J. P. Harger and A. Smith, *J. Chem. Soc., Perkin Trans. 1*, 1987, 683; M. J. P. Harger and P. A. Shimmin, *Tetrahedron*, 1992, **48**, 7539 and references cited therein.
2 M. J. P. Harger, *J. Chem. Soc., Perkin Trans. 1*, 1983, 2699.
3 M. J. P. Harger, *Tetrahedron Lett.*, 1990, **31**, 1451.
4 M. J. P. Harger and A. Smith, *J. Chem. Soc., Perkin Trans. 1*, 1990, 2507; M. J. P. Harger and R. Sreedharan-Menon, *J. Chem. Soc., Perkin Trans. 1*, 1994, 3261.
5 P. M. Cullis, in *Phosphorus-31 NMR Spectral Properties in Compound Characterisation and Structural Analysis*, ed. L. D. Quin and J. G. Verkade, VCH, Weinheim, New York and Cambridge, 1994, pp. 315–331.
6 M. J. P. Harger, *Chem. Commun.*, 1997, 403.

*Received in Cambridge, UK, 28th April 1997; 7/2856C*

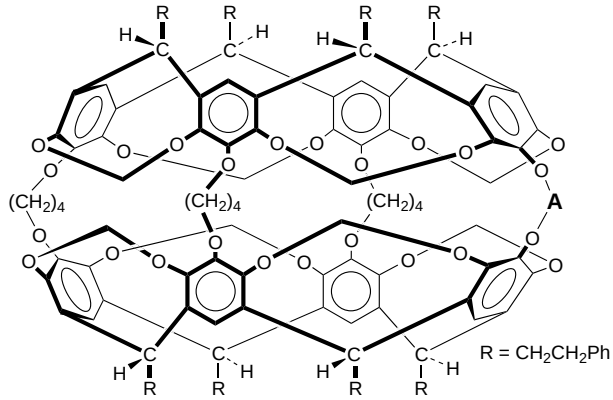
# Decomplexation rate comparisons of hemicarceplexes whose single unique host bridge is changed in length and blocking power

**Juyoung Yoon and Donald J. Cram***

*Department of Chemistry and Biochemistry, University of California, Los Angeles, CA 90095-1569, USA*

**Decomplexation rates of hemicarceplexes can be manipulated by changes in solvent, guest, one of four host-bridge lengths and one of four host-bridge's blocking power.**

Prior papers reported the syntheses and characterizations of hosts **1**–**6**, as well as crystal structures of **1**⊙4-$MeC_6H_4OMe$, **2**⊙$CHCl_3$, **4**⊙$PhNO_2$ and **6**⊙guests.[1–3] In five crystalline complexes of **6**, the host parts were essentially isostructural and changed only in minor ways when guests of generally similar size were involved (*e.g.* 1,4-$I_2C_6H_4$, 1,4-$Me_2C_6H_4$, $PhNO_2$, 2-$BrC_6H_4OH$ and $Me_2NCOMe$). Decomplexation rates for **7**⊙guests were generally on the human time scale only at temperatures of 100–200 °C, indicating that considerable constrictive binding must be overcome during the decomplexation process.[4,5]




**1**, A = $(CH_2)_5$; **2**, A = 1,3-$(CH_2)_2C_6H_4$; **3**, A = $(CH_2)_6$; **4**, A = 1,4-$(CH_2)_2C_6H_4$; **5**, A = 9,10-$(CH_2)_2$anthracene; **6**, A = $(CH_2)_4$; **7**, all four bridging units are 1,2-$(CH_2)_2C_6H_4$

We report here the results of a survey of decomplexation rates as a function of host structure (**1**–**5**), guest structure (4-MeO-$C_6H_4OMe$, 3-$MeOC_6H_4OMe$, 4-$MeOC_6H_4Me$ and 4-$MeC_6H_4Me$), temperature (25–120 °C) and solvent ($CDCl_3$ and $CDCl_2CDCl_2$).† Hemicarceplex **2**⊙4-$MeOC_6H_4OMe$ was selected as a standard complex, whose first order rate constants were determined by following the appearance in their $^1H$ NMR spectra of methyl proton signals for free guest in $CDCl_3$ at four temperatures (25, 35, 45 and 55 °C) and in $CDCl_2CDCl_2$ at four temperatures (90, 100, 110, 120 °C). The decomplexations exhibited good first order behaviour over several half-lives. The technique and treatment of the data are described in a prior publication as applied to decomplexation kinetics of **7**⊙guests, in which empty host was demonstrated to be the initial product.[4]‡ Table 1 records the activation parameters ($\Delta H^‡$, $\Delta S^‡$ and $\Delta G^‡_{308}$) and $t_{1/2}$ values for decomplexations of **2**⊙4-$MeOC_6H_4OMe$ in the two solvents at 35 °C.§

First order rate constants were also determined for decomplexations involving hosts **1**–**4** and the four disubstituted benzene guests at 35 °C in $CDCl_3$. With use of eqn. 1, $k_{relative}$

$$k_{relative} = k_{H⊙G}/k_{\mathbf{2}⊙4\text{-}MeOC_6H_4OMe} \quad (1)$$

values were obtained, from which $\Delta G^‡$ values for nine complexes were calculated, and a lower limit of $\Delta G^‡$ for **5**⊙4-$MeOC_6H_4OMe$ was estimated. Table 2 provides the structures of the eleven complexes, the values of rate constants, and $\Delta G^‡_{308}$.

The most striking feature of the results is that the simple change of solvent from $CDCl_3$ to $CDCl_2CDCl_2$ resulted in an increase of activation free energy for decomplexation of **2**⊙4-$MeOC_6H_4OMe$ of $\Delta(\Delta G^‡_{308})$ = 4.1 kcal $mol^{-1}$. The enthalpy, $\Delta(\Delta H^‡)$ = 6.2, and entropy changes, $\Delta(T\Delta S^‡)_{308}$ = 2.1, both contribute to the change in free energy, but the enthalpy change is the larger contributor by 4.1 kcal $mol^{-1}$. The decomplexation half-life for **2**⊙4-$MeOC_6H_4OMe$ is 800 times *longer* in $CDCl_2CDCl_2$ than in $CDCl_3$. The fact that solvation plays such a large role in the transition state for decomplexation suggests that it resembles in structure the dissociated rather than the starting state of the complex. Models (Corey–Pauling–Koltun or CPK) of possible transition states show that to be significantly solvated, the guest must protrude substantially from the portal for multiple guest–solvent contacts to be made. The fact that $CDCl_2CDCl_2$ is much larger than $CDCl_3$ suggests that steric inhibition of solvation of the transition state for decomplexation is responsible for this very large effect of solvent on rate. The only other study of the effects of solvent on rates of decomplexation of hemicarceplexes involved **7**⊙$Me_2NCOMe$ (100 °C).[4] The rate constants decreased by an overall factor of about 45, and in the following order as solvent was changed: $C_6D_5Br$ > $C_6D_5Cl$ > 1,2-$(CD_3)_2C_6D_4$ > 1,4-$(CD_3)_2C_6D_4$ > $CDCl_2CDCl_2$ > $C_6D_5CD_3$. The six solvents vary considerably in their polarity and polarizability, but little in their overall size, compared to $CDCl_3$ *vs.* $CDCl_2CDCl_2$.

An examination of a CPK model of host **6** which contains four $O(CH_2)_4O$ bridges indicates that although the four portals are 26-membered rings, there is little chance of the substituted benzenes of this study entering or departing the inner phase of this hemicarcerand except at very high temperatures. Experimentally, **6**⊙4-$MeC_6H_4OMe$ was formed only when **6** was heated in molten guest at 170 °C for 3.5 days.[3] Decomplexation of **6**⊙$Me_2NCOMe$ required heating a solution of the complex in $Ph_2O$ at 195 °C for 5 days. We conclude that the complexations and decomplexations of **1**–**5** occur through the two 27- or 28-membered ring portals partially defined by the unique bridge.

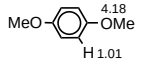
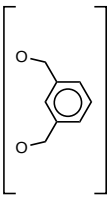
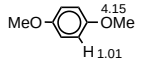
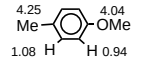
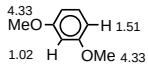
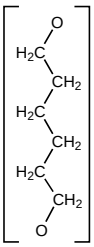
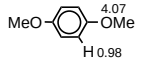
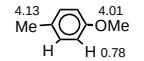
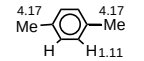
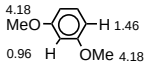
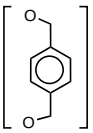
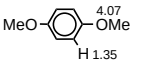
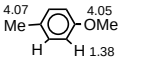
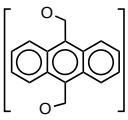
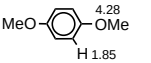
Comparisons of the activation free energies (Table 2) for decomplexations in $CDCl_3$ at 35 °C of various complexes of 4-$MeOC_6H_4OMe$ as a common guest show the effects of portal

**Table 1** Activation parameters and half-lives for decomplexation of **2**⊙4-$MeOC_6H_4OMe$ in $CDCl_3$ and $CDCl_2CDCl_2$

| Solvent | $t_{1/2}$/min[a] | $\Delta H^‡$/ kcal $mol^{-1}$ | $\Delta S^‡$/cal $mol^{-1}$ $K^{-1}$ | $\Delta G^‡_{308}$/ kcal $mol^{-1}$ |
|---|---|---|---|---|
| $CDCl_3$ | 182 | 19.0 | −15.3 | 23.7 |
| $CDCl_2CDCl_2$ | 147 000 | 25.2 | −8.4 | 27.8 |

[a] At 35 °C.

**Table 2** Decomplexation rate constants and activation free energies for host⊙guest at 35 °C in $CDCl_3$, and $^1H$ NMR spectral $\Delta\delta$ values ($\delta_{free\ guest} - \delta_{complexed}$, ppm)[a]

| Host No. | Bridge O–A–O | Guest | $k$/ $10^{-3}$ min$^{-1}$ | $\Delta G^{\ddagger b}$/ kcal mol$^{-1}$ |
|---|---|---|---|---|
| 1 | [O(CH$_2$)$_5$O] |  | 0.324 | 25.2 |
| 2 |  |  | 3.81 | 23.7 |
| 2 | |  | 1.12 | 24.5 |
| 2 | |  | 0.257 | 25.4 |
| 3 |  |  | 57.2 | 22.0 |
| 3 | |  | 48.0 | 22.2 |
| 3 | |  | 22.4 | 22.6 |
| 3 | |  | 16.9 | 22.8 |
| 4 |  |  | 6.00 | 23.4 |
| 4 | |  | 5.35 | 23.5 |
| 5 |  |  | ≪0.1 | > 27 |

[a] 400 MHz in $CDCl_3$ at 25 °C. [b] $\Delta G^{\ddagger}_{308} = 23.7 - RT\ln k_{relative}$.

size and blocking power of the unique bridge. For example, $\Delta G^{\ddagger}$ is 25.2 kcal mol$^{-1}$ with O(CH$_2$)$_5$O as the unique bridge, but decreases to 22.0 kcal mol$^{-1}$ with O(CH$_2$)$_6$O as the unique bridge. This decrease of 3.2 kcal mol$^{-1}$ reflects the increase of portal size by one $CH_2$ group added to the portal ring members (27 increased to 28), and corresponds to an increase in rate constant by a factor of 177. When the unique bridge is not increased in portal ring members but is decreased in blocking power by substitution of a 1,3-C$_6$H$_4$ for the internal (CH$_2$)$_3$ of the O(CH$_2$)$_5$O bridge, the $\Delta G^{\ddagger}$ value decreases by 1.5 kcal mol$^{-1}$, and the rate constant increases by a factor of 12. When the unique bridge is not changed from 28 portal ring members, but is increased in blocking power by substitution of a 1,4-C$_6$H$_4$ group for the central (CH$_2$)$_4$ moiety of O(CH$_2$)$_6$O, the $\Delta G^{\ddagger}$ value increases by 1.4 kcal mol$^{-1}$, and the rate constant decreases by a factor of 9.5. These trends correlate with the near-planarity of the 3-OCH$_2$C$_6$H$_4$CH$_2$O bridges in crystal structures of complexes containing these bridges,[6] and the near-perpendicularity of the aryl plane and the OCH$_2$··CH$_2$O plane in the crystal structure of **4**⊙C$_6$H$_5$NO$_2$.[2] When the 9,10-(OCH$_2$)$_2$-anthracenyl bridge is substituted for the O(CH$_2$)$_6$O bridge, the $\Delta G^{\ddagger}$ value increases by > 5 kcal mol$^{-1}$, and the rate constant decreases by a factor of at least 600. Model examination of **5** shows that the near perpendicularity of the two near planes of this bridge is enforced, and that the blocking ability of this bridge is greatly increased by the extension of its central ring by the two attached benzo groups. Model examination shows that in spite of this additional blocking effect, the 28-membered rings are still more available for use as portals than are the two 26-membered rings present in **5**.

Notice that independent of whether the host is **2**, **3** or **4** the increasing order of activation energy correlates with guest structural changes as follows: 4-MeOC$_6$H$_4$OMe < 4-MeC$_6$H$_4$OMe < 4-MeC$_6$H$_4$Me < 3-MeOC$_6$H$_4$OMe (see Table 2). For host **2** (27-membered ring portals), the $\Delta G^{\ddagger}$ values provide a spread of only 1.7 kcal mol$^{-1}$. For **3** (28-membered ring portals) an even lower spread of 0.8 kcal mol$^{-1}$ is observed. The more confined entryway is the more selective, as expected.

We interpret the above correlations in terms of the relative contributions of *intrinsic* and *constrictive* binding that must be overcome for decomplexation to occur.[4] The five hosts have similarly shaped cavities generally complementary to the similarly shaped guests, suggesting that the intrinsic binding energies for the complexes are close to one another. In the transition states for decomplexation, the portals of each host must become slot-shaped and complementary to the slot-shaped cross section of the departing guest. Also, by guest rotation, the Me groups must pass from occupying the hosts' axial bowls to being aligned with the equatorially disposed portals. These shape and location adaptations in the transition state must overcome constrictive binding, which should be sensitive to portal-guest complementarity, and to exposure of protruding guest parts to bulk solution.

The authors warmly thank the U.S. Public Health Service for Supporting Grant GM-12640.

## Footnotes and References

* E-mail: maverick@chem.ucla.edu

† All new complexes gave elemental analyses within 0.30% of theory, and expected $^1H$ NMR and FAB (*m/z*, M + H$^+$) mass spectra.

‡ The reaction G′ + H⊙G → H⊙G′ + G, where G′ is solvent, should give first order kinetics for appearance of G. Formally, a mechanism might apply in which G′ enters H in the same transition state that G departs. When H has multiple potential entryways whose equilibrium dimensions are comparable to cross sections of G′, activation energies for guest substitution are very low, and concerted mechanisms might apply. However, $\Delta G^{\ddagger}$ values for **2**⊙4-MeOC$_6$H$_4$OMe are rather high. Molecular model examinations show that for one portal to become large enough to accommodate guest departure, the other three must decrease their apertures through many small conformational adjustments, thus becoming unavailable for simultaneous solvent entry.

§ Decomplexation kinetics were conducted on 0.5 ml samples of 2 mM solutions of complexes in degassed $CDCl_3$ or $CDCl_2CDCl_2$ in sealed $^1H$ NMR tubes in the probe of a 400 MHz spectrometer adjusted to the desired temperature (±1 °C) after the probe temperature was calibrated with HOCH$_2$CH$_2$OH (ref. 7). The $CDCl_3$ or $CDCl_2CDCl_2$ had recently been passed through a plug of neutral activated alumina. About 20–25 spectra were recorded at appropriate time intervals. The first order rate constants were calculated from the strong signals of the guest methyl groups upon decomplexation. Tables 1 and 2 record the results.

1 J. Yoon, C. Sheu, K. N. Houk, C. B. Knobler and D. J. Cram, *J. Org. Chem.*, 1996, **61**, 9323.
2 J. Yoon, C. B. Knobler, E. F. Maverick and D. J. Cram, *Chem. Commun.*, in the press.
3 T. A. Robbins, C. B. Knobler, D. R. Bellew and D. J. Cram, *J. Am. Chem. Soc.*, 1994, **116**, 111.
4 D. J. Cram, M. T. Blanda, K. Paek and C. B. Knobler, *J. Am. Chem. Soc.*, 1992, **114**, 7765.
5 D. J. Cram and J. M. Cram, *Container Molecules and Their Guests*, Monographs in Supramolecular Chemistry, ed. J. Fraser Stoddart, The Royal Society of Chemistry, Cambridge, 1994, pp. 131–216.
6 R. C. Helgeson, K. Paek, C. B. Knobler, E. F. Maverick and D. J. Cram, *J. Am. Chem. Soc.*, 1996, **118**, 5590.
7 A. L. Van Geet, *Anal. Chem.*, 1968, **40**, 2227

*Received in Columbia, MO, USA, 7th April 1997; 7/02380D*

# Immobilization and cleavage of DNA at cationic, self-assembled monolayers containing $C_{60}$ on gold

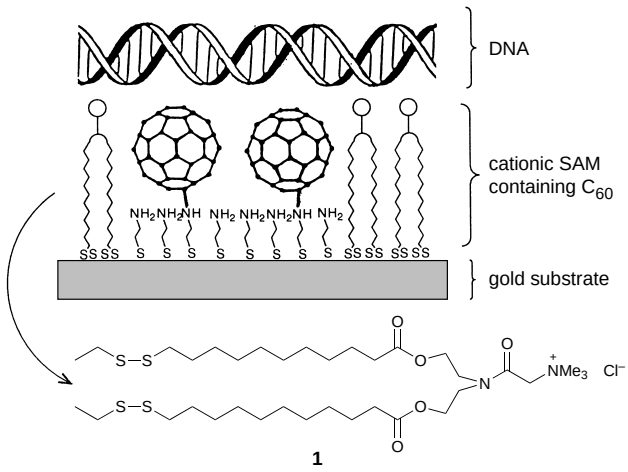
**Nobuyuki Higashi,*† Takayo Inoue and Masazo Niwa***

*Department of Molecular Science & Technology, Faculty of Engineering, Doshisha University, Kyotanabe, Kyoto 610-03, Japan*

**A cationic, self-assembled monolayer on gold substrate can immobilize DNA without impairing its native structure; the site-specific photocleavage of the DNA is achieved by incorporation of [60]fullerene into the monolayer.**

The immobilization of DNA on a two-dimensional solid surface is of interest both in studies of DNA itself and in various applications. For instance, in atomic force microscopy, the DNA must be firmly affixed to a surface to minimize the effects of tip interactions during scanning.[1] Immobilization of DNA on an electrode is also used to produce biosensors.[2,3] The strategy employed in this study was to prepare, on a gold surface, a well-ordered monolayer assembly that contained cationic groups, such as quaternary ammonium salts, that would interact electrostatically with the phosphate groups of DNA. Monolayer assemblies of this type have been described previously.[4–6] Here we report immobilization of DNA on a self-assembled monolayer (SAM) of **1** and cleavage of the DNA, which is important from biological and clinical viewpoints. Recently, [60]fullerene ($C_{60}$) was found to have a G (guanine base)-selective DNA cleaving ability in the presence of visible light.[7] If $C_{60}$ could be successfully incorporated in the SAMs of **1** (Fig. 1), the immobilized DNA might be expected to cleave site-specifically.

The preparation of **1** and its adsorption property on gold substrate have been described elsewhere.[4,6] The monolayers were first formed by soaking gold mirror plates (prepared by evaporation of gold onto one side of a glass plate, 2 × 2 cm) in solutions of **1** in EtOH for 1 h. Calf thymus DNA was immobilized on the surface by soaking the SAM film in a buffer solution (50 mmol $dm^{-3}$ tris buffer, pH 7.4) of DNA (1 mg $ml^{-1}$) for 2 h. The film was then rinsed several times with the tris buffer to remove free DNA, and dried at room temperature. The reflection–absorption spectrum of this film on gold, which was measured using a multi-channel photodetector (Otsuka Electronics, MCPD–100, Japan), gave an absorption maximum at 263 nm assigned to the π–π* transition of nucleic acid bases of DNA, suggesting the binding of DNA onto the monolayer surface through electrostatic interaction. To estimate the stoichiometry of such an ion complex, the XPS spectra were measured before and after DNA binding. As a result, the phosphorous (phosphate anion in DNA) : nitrogen (ammonium group and amide bond of **1**) ratio was determined to be 2 : 1.7 (±0.3); the ammonium cation : phosphate anion ratio is thus calculated to be 1 : 1.7. This result implies that about half of the total phosphate anions of DNA contributed to the complexation with the cationic surface of **1**-SAM; in other words, half of the anions remained free.




**1**

**Fig. 1** Schematic illustration for immobilization of DNA on the cationic SAM containing $C_{60}$ on gold

Subsequently, the intercalation of Methylene Blue was examined by spectroscopic means. In aqueous solution, intercalation of Methylene Blue into DNA base pairs is known to cause both hypochromism and red shifting of the absorption maximum.[8] These observations are explained by stacking interactions of intercalated dye with base pairs in DNA and electrostatic interactions with phosphate anions of DNA, respectively.[9] In the case of the monolayer-bound DNA, the spectrum of Methylene Blue showed a 6 nm red shift of the absorption maximum. This spectral feature suggests that Methylene Blue was trapped in the monolayer-bound DNA through intercalation, although we were not able to obtain information regarding hypochromism because of difficulty in comparing the absolute absorbance of Methylene Blue before and after intercalation.

To locate $C_{60}$ close to the DNA immobilized at the monolayer surface, mixed monolayers of **1** and 2-mercaptoethylamine (cysteamine) were prepared on gold substrates. Cysteamine, which can form a SAM on gold, was employed since Caldwell *et al.*[10] described that $C_{60}$ could be bound covalently onto cysteamine-modified gold substrates. The mixed monolayer (mole fraction of **1** in the mixture, $f_1$ = 0.2) was prepared by soaking the gold plate in a 1 mmol $dm^{-3}$ EtOH solution containing **1** and cysteamine for 24 h. The monolayer-modified gold plate thus obtained was then soaked in a 1 mmol $dm^{-3}$ benzene solution of $C_{60}$ for 24 h at room temperature. The resulting substrates were thoroughly rinsed in benzene to remove residual physisorbed $C_{60}$. Incorporation of $C_{60}$ in the monolayers was confirmed by measuring the contact angle of water.‡ When the same procedure was performed on a pure **1** monolayer ($f_1$ = 1)-modified gold plate, no binding of $C_{60}$ was observed, as expected. Immobilization of DNA on the mixed monolayer-modified gold plates was carried out in the same manner as described above. To reveal the site-specificity of photocleavage, several types of DNA {salmon sperm DNA, calf thymus DNA, poly[$(dGdC)_2$] and poly[$(dAdT)_2$]} which were different in base pair composition were used. Irradiation experiments were performed under the same condition for all samples. If cleavage of DNA took place, the resultant short fragments, such as oligonucleotides and nucleotides, readily diffused into the bulk phase and were then detectable by spectroscopy.§ Fig. 2 shows UV spectra of the bulk aqueous phases from which poly[$(dGdC)_2$]-immobilized monolayer plates ($f_1$ = 0.2 and added 1) were withdrawn after 3 h irradiation. For comparison, the UV spectrum of an aqueous solution of poly[$(dGdC)_2$] itself at a concentration of 6 × $10^2$

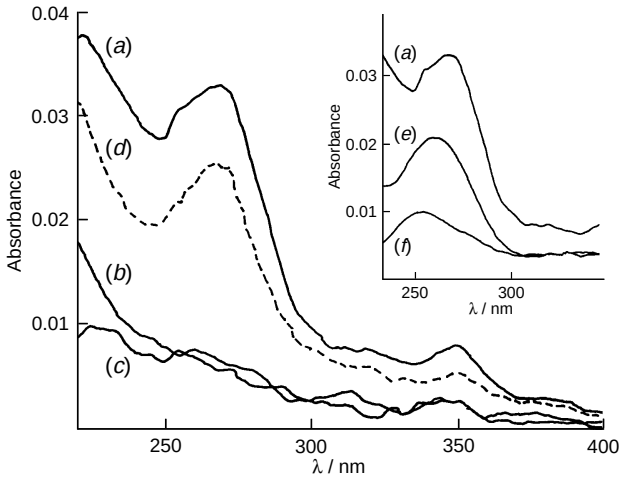



**Fig. 2** UV absorption spectra of aqueous solutions resulting from irradiation of poly[(dGdC)$_2$] monolayers under standard conditions; (*a*) $f_1$ = 0.2 monolayer; (*b*) $f_1$ = 1 monolayer; (*c*) $f_1$ = 0.2 monolayer shielded from the visible light; (*d*) aqueous solution of poly[(dGdC)$_2$] itself at a concentration of $6 \times 10^2$ ng ml$^{-1}$. Inset: spectra of aqueous solutions of DNA monolayers; (*e*) salmon sperm DNA; (*f*) calf thymus DNA, compared with (*a*) treated under the same conditions.

ng ml$^{-1}$ is included in the figure. In the case of $f_1$ = 1 without $C_{60}$, no peak was observed at around 260 nm based on the $\pi$–$\pi$* transition of nucleic acid bases. In contrast, the mixed monolayer ($f_1$ = 0.2)-bound poly[(dGdC)$_2$] gave an absorption peak at 260 nm due to cleaving although the same poly[(dGdC)$_2$] shielded from the visible light did not. These results strongly suggest that the DNA cleavage was caused by singlet oxygen[11] generated by interaction of the photoexcited $C_{60}$ group with molecular oxygen. For the mixed monolayer ($f_1$ = 0.2)-bound poly[(dAdT)$_2$], light irradiation led to no cleavage (data not shown here). Fig. 2 (inset) displays a comparison of UV spectra for different DNA samples. The absorbance at around 260 nm was found to decrease in the following order: ply[(dGdC)$_2$] > salmon sperm DNA > calf thymus DNA, which implies G-selective cleavage of DNA because this order corresponds well to the guanine content in these DNA samples.[12]

In summary, we have demonstrated that cationic SAMs can immobilize DNA without disrupting its intrinsic higher-order structure, and that site-specific cleavage of the DNA is successfully achieved by incorporation of $C_{60}$ into the SAM. A more detailed examination of the cleaved fragments is now in progress.

This work was supported by the Nano-structure Hybrid program at the Advanced Research Center for Engineering and Technology of Doshisha University.

## Footnotes and References

† E-mail: nhigashi@mail.doshisha.ac.jp

‡ The mixed monolayer ($f_1$ = 0.2) gave a hydrophilic surface ($\theta_{H_2O}$ = 49°) before adsorption of $C_{60}$. After soaking this mixed monolayer plate in the $C_{60}$ solution, the increased hydrophobicity of the resulting surface ($\theta_{H_2O}$ = 62°) was confirmed *via* contact angle measurements.

§ Immobilization of the DNA samples on the mixed monolayer-modified gold plates (2 × 2 cm) was first carried out, and then the plates were immersed in 2 ml tris buffer solutions (pH 7.4). After 3 h irradiation with visible light ($\lambda$ > 500 nm), UV spectra of the aqueous phases (2 ml) were measured.

1 A. L. Weisenhorn, M. Egger, F. Ohnesorge, S. A. C. Gould, S.-P. Heyn, H. G. Hansma, R. L. Sinsheimer, H. E. Gaub and P. K. Hansma, *Langmuir*, 1991, **7**, 8.
2 *E.g.*: H. Su, M. R. Kallury, M. Thompson and A. Roach, *Anal. Chem.*, 1994, **66**, 769 and references cited therein.
3 X.-H. Xu, H. C. Yang, T. E. Mallouk and A. J. Bard, *J. Am. Chem. Soc.*, 1994, **116**, 8386.
4 N. Higashi, T. Mori and M. Niwa, *J. Chem. Soc., Chem. Commun.*, 1990, 225.
5 M. Niwa, T. Mori, E. Nishio, H. Nishimura and N. Higashi, *J. Chem. Soc., Chem. Commun.*, 1992, 547.
6 M. Niwa, T. Mori and N. Higashi, *J. Mater. Chem.*, 1992, **2**, 245.
7 H. Tokuyama, S. Yamaga, E. Nakamura, T. Shiraki and Y. Sugiyama, *J. Am. Chem. Soc.*, 1993, **115**, 7918.
8 E. Tuite and B. Norden, *J. Am. Chem. Soc.*, 1994, **116**, 7548.
9 H. Porumb, *Prog. Biophys. Mol. Biol.*, 1978, **34**, 175.
10 W. B. Caldwell, K. Chen, C. A. Mirkin and S. J. Babinec, *Langmuir*, 1993, **9**, 1945.
11 J. Piett and P. D. Moore, *Photochem. Photobiol.*, 1982, **35**, 705.
12 J. Marmur and P. Doty, *J. Mol. Biol.*, 1962, **5**, 109.

*Received in Cambridge, UK, 24th February 1997; 7/01265I*

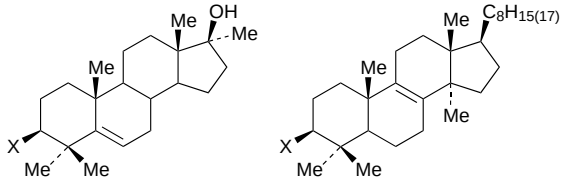
# Unusual generation of methoxy groups in Barton deoxygenations of alcohols

**Caroline S. Bensasson, Sir John Cornforth,*† Ming-Hui Du and James R. Hanson***

*School of Chemistry, Physics and Environmental Science, University of Sussex, Brighton, UK BN1 9QJ*

**Reaction of the *S*-methyl dithiocarbonate of lanosterol with excess of tributyltin deuteride and azoisobutyronitrile in benzene afforded lanosteryl methyl ether in which all hydrogen in the methoxy group originated from the organotin reagent.**

In mid-1996 C. S. B. prepared 4,4,17-trimethylandrost-5-en-17β-ol **1** from the *S*-methyl dithiocarbonate **2** in refluxing benzene with tributyltin hydride and the initiator AIBN, an unexpected product, methyl ether **3**, was formed in 28% yield. The ether was thought at the time to be a contaminant, inadvertently formed by a Williamson synthesis, of xanthate **2** which had been prepared by the usual treatment of alcohol **4** with sodium hydride, carbon disulfide and then iodomethane. However, spectra of **2** showed only slight contamination with **3**. Some months later, M. H. D. informed J. C. that an unrelated xanthate had yielded principally the analogous methoxy compound on attempted Barton deoxygenation, and that the corresponding imidazolylthiocarbamate (prepared without use of a methylating agent) gave the same methoxy compound. J. C. mentioned his view of this result to J. R. H., who recalled C. S. B.'s expermiment. We decided to investigate the matter by an experiment with lanosterol.




**1** X = H
**2** X = OC(=S)SMe
**3** X = OMe
**4** X = OH

**5** X = OC(=S)SMe
**6** X = OMe
**7** X = H

The lanosterol available was a commercial preparation containing the 24,25-dihydro compound. The *S*-methyl dithiocarbonate **5**, prepared by Barton and McCombie's[1] procedure, contained *ca*. 40% dihydro compound and only traces of methyl ether **6** (by $^1$H NMR spectroscopy). On reduction with tributyltin hydride (5 equiv.; initial concentration 0.17 mol dm$^{-3}$) and AIBN (0.36 equiv.) in boiling benzene for 6 h, a 42% yield of methyl ether **6**, along with deoxygenated product **7**, was formed. With tributyltin deuteride (95 atom%) the yield of **6** was 14%. The $^1$H NMR spectrum of the labelled compound at 500 MHz showed, instead of the sharp 3H singlet of **6** at $\delta$ 3.37, three signals (total 0.75H) at $\delta$ 3.33, 3.35 and 3.37. The $^2$H NMR spectrum showed that all excess deuterium was in the methoxy group and that the $CHD_2$ and $CD_3$ concentrations were about equal, as required by statistical distribution of H and D in a 1 : 3 ratio. This agrees with the total H content and corresponds to an average isotope effect ($k_H/k_D$) of *ca*. 5 for the three hydrogen transfers. The molecular ions in the EI mass spectrum were grouped in eight peaks showing minor amounts of the OMe species **6** with larger proportions of $OCH_2D$, $OCHD_2$ and $OCD_3$ species along with 24,25-dihydro analogues and $^{13}$C companions. The peak pattern was accurately matched (Fig. 1) by the distribution calculated for random substitution of 75% of the methoxy protium by deuterium (as observed by NMR spectroscopy) combined with a 70 : 30 ratio of methoxylanostadienyl ions to methoxylanostenyl ions.‡ The major peak, principally lanostadienyl trideuteromethyl ether ion, had an exact mass of 443.4210 (Calc. for $^{12}C_{31}{}^1H_{49}{}^2H_3{}^{16}O$: 443.4206). The excess of deuterium-free species indicates slight (*ca*. 0.2%) contamination of **5** with pre-existing **6**. These results demonstrate that all three hydrogen atoms in the methoxy group of the reduction product **6** originated from the tin hydride. It follows that the carbon source of this methoxy group was the –OC(=S)S– group.

Barton and co-workers[1–3] have shown that octadecyloxythiocarbonylimidazole with 2 equiv. of tributyltin hydride in boiling toluene gave the hemithioformal $C_{18}H_{37}OCH_2SSnBu_3$, and analogous by-products were also formed from various dithiocarbonates (including *S*-methyl) of cholestanol. Formation of methoxy groups has not been reported until now, although it might well have been observed and misinterpreted as we initially did. As applied to an *S*-methyl dithiocarbonate **8** the mechanism for Barton deoxygenation preferred at first by its originator[3] postulates reversible addition of tributylstannyl radical to the C=S bond (Scheme 1). The ensuing radical **9** can either undergo thermal cleavage to dithiocarbonate **10** and alkyl radical **11** leading to deoxygenated product **12** (route a), or accept a hydrogen from $Bu_3SnH$ to form **13** which is then cleaved (thermally?) to thioformate *O*-ester **14** which finally adds $Bu_3SnH$ yielding hemithioformal **15** (route b). The last step was supported by a separate experiment with *O*-ethyl thioformate which gave the hemithioformal $EtOCH_2SSnBu_3$. When later experiments[4] indicated that radicals of type **9** are thermally very unstable, a non-radical mechanism of hydride transfer was preferred for generation of **13** from **8** and presumably of **15** from **14**.

In these mechanisms both methylene hydrogens are supplied from $Bu_3SnH$ by additions, radical or non-radical, to thiocarbonyl groups. For addition of the third hydrogen no thiocarbonyl intermediate is possible. It seems necessary to postulate that

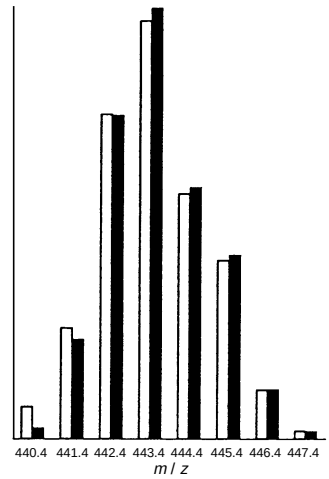
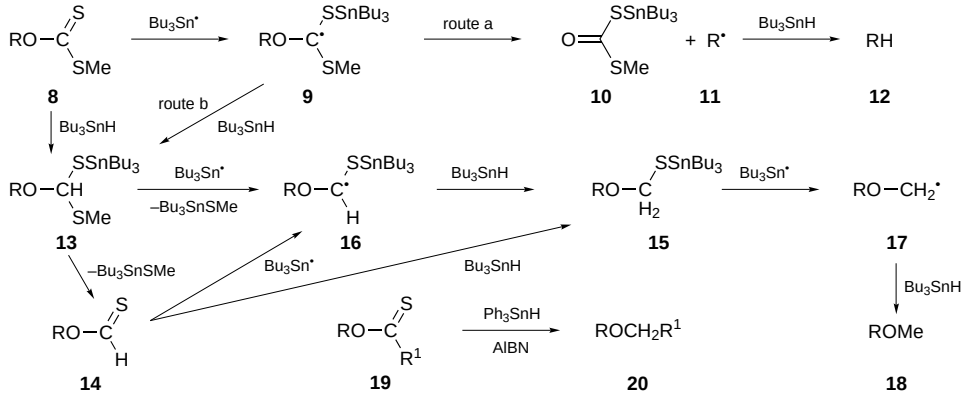



**Fig. 1** Molecular ions from deuteriated **6**: (□) measured and (■) calculated. See text for basis of calculation.



**Scheme 1**

hemithioformals **15** can generate radicals **17** either by thermolysis or (more probably, we think) by attack of $Bu_3Sn^{\cdot}$ on the sulfur atom leading to elimination of $(Bu_3Sn)_2S$. The radical product **17** then accepts its third hydrogen from $Bu_3SnH$, forming **18**. Nicolaou *et al.*§ showed[5] that thioesters **19** with triphenyltin hydride–AIBN (and in one example, less efficiently, with tributyltin hydride–AIBN) yielded ethers **20**; thioformate *O*-esters were not tried but there seems little doubt that these could yield methyl ethers. The reaction, as we also prefer, was represented as addition of $Bu_3Sn^{\cdot}$ and elimination of $(Bu_3Sn)_2S$. A similar mechanism might apply also to addition of the *second* hydrogen, attack of $Bu_3Sn^{\cdot}$ on the SMe sulfur atom of the earlier intermediate **13** leading to elimination of $Bu_3SnSMe$ and formation of the oxygen-stabilized radical **16**, which then accepts hydrogen from $Bu_3SnH$. Such a mechanism could apply to addition of the *first* hydrogen only if the initial attack of $Bu_3Sn^{\cdot}$ on **8** is at SMe instead of S=C, as Barker and Beckwith[6] suggested on the basis of experiments with $Bu_3Sn^{\cdot}$ in the absence of $Bu_3SnH$. Barton's later work[4] controverts this mechanism.

Deoxygenation to RH species by (unpromoted) $Bu_3SnH$ is favoured[1] by higher dilutions and higher temperatures: the branching to give routes a and b, whatever the mechanisms, is due to competition between a unimolecular thermolysis and a bimolecular hydrogen-transfer. Conversely, higher concentrations of $Bu_3SnH$ should favour the pathways leading to hydrogen additions. In fact an excess of $Bu_3SnH$ over the 3 equiv. theoretically required was used in all experiments where formation of ROMe was observed, and **5** with only 1.5 equiv. of $Bu_3SnD$ formed no measurable **6**. The step preceding addition of the third hydrogen is therefore the slowest.

## Footnotes and References

† E-mail: j.w.cornforth@sussex.ac.uk

‡ In the molecular ions the dienyl species appears to be enriched. The two heaviest fragment ions ($M-15$ containing methoxy, and methoxy-free $M-47$) show the opposite effect and their peak patterns are both matched by assuming a 55 : 45 ratio. The base peak in the spectrum is at *m*/*z* 69, indicating favoured cleavage of the dienyl species to $Me_2C{=}CHCH_2^{+\cdot}$. The observed patterns are consistent with the dienyl species being preferentially ionized, but also preferentially cleaved so as to be under-represented in the heavier fragments.

§ We are indebted to a referee for drawing attention to this work.

1 D. H. R. Barton and S. W. McCombie, *J. Chem. Soc., Perkin Trans. 1*, 1975, 1574.
2 D. H. R. Barton, D. Crich, A. Löbberding and S. Z. Zard, *J. Chem. Soc., Chem. Commun.*, 1985, 646.
3 D. H. R. Barton, D. Crich, A. Löbberding and S. Z. Zard,*Tetrahedron*, 1986, **42**, 2329.
4 D. H. R. Barton, D. O. Jang and J. C. Jaszberenyi, *Tetrahedron Lett.*, 1990, **31**, 3991.
5 K. C. Nicolaou, M. Sato, E. A. Theodorakis and N. D. Miller, *J. Chem. Soc., Chem. Commun.*, 1995, 1583.
6 P. J. Barker and A. L. J. Beckwith, *J. Chem. Soc., Chem. Commun.*, 1984, 683.

*Received in Liverpool, UK, 8th May 1997; 7/03156D*

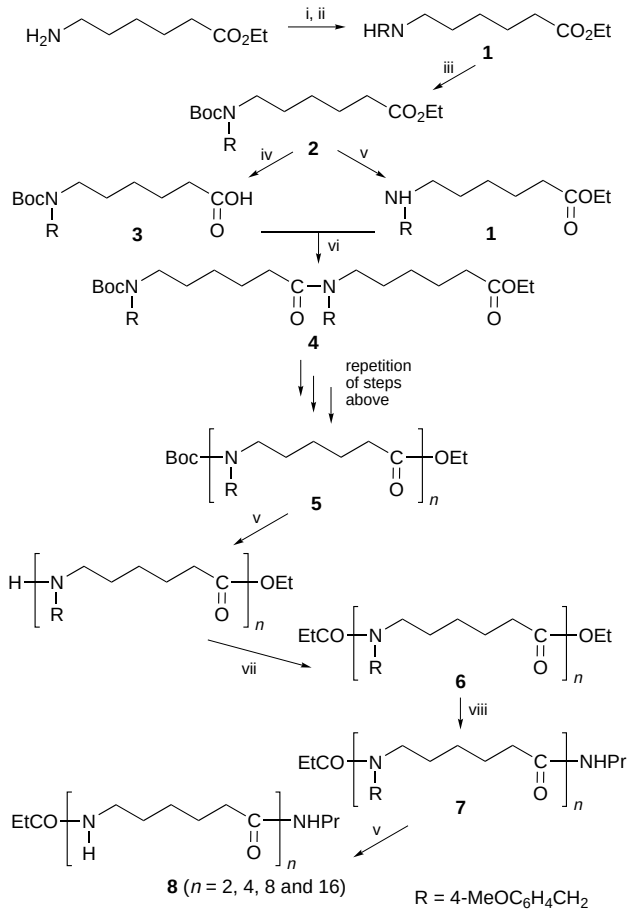
# A simple amide protecting group: synthesis of oligoamides of Nylon 6

**Gerald M. Brooke,*[a] S. Mohammed[a] and Mark C. Whiting[b]**

[a] *Chemistry Department, Science Laboratories, South Road, Durham, UK DH1 3LE*
[b] *School of Chemistry, University of Bristol, Cantock's Close, Bristol, UK BS8 1TS*

**The 4-methoxybenzyl group (R) in amide groups NR(C=O) renders all intermediates in the synthesis of oligomers of Nylon 6 soluble in common solvents and is readily removed in boiling trifluoroacetic acid.**

Wallace Carothers described the first use of a disecondary diamine to introduce 'rubberiness' into a polyamide in an early patent—the preparation of poly(N,N'-dimethylpentamethylenesuccinamide), $\{N(Me)(CH_2)_5N(Me)(C{=}O)(CH_2)_2(C{=}O)]_n\}$;[1] the hydrogen-bonding properties due to the NH(C=O) group, which confer many of the desirable properties of Nylons, were lost from the point of view of normal use at that time, textiles. Soon afterwards, other workers investigated the use of *N*,*N*′-dialkyl derivatives of 1,6-hexamethylenediamine (alkyl = methyl, ethyl, isobutyl and benzyl) for incorporation into alkyl Nylon 6,10 polymer,[2] but very little has been published since in this area. The most noticeable physical property affected in these polymers compared with the non-alkylated materials was a marked increase in solubility in common organic solvents.




**Scheme 1** *Reagents and conditions*: i, 4-$MeOC_6H_4CHO$; ii, $NaBH_4$; iii, $Boc_2O$; iv, NaOH, the $H^+$; v, TFA, 25 °C; vi, DCC, 1-hydroxybenzotriazole; vii, EtCOCl; viii, $PrNH_2$, KCN(cat.); ix, TFA, reflux

The best science is carried out on pure compounds. Recently, the preparation of some monodisperse linear long-chain alkanes was described,[3] materials of interest for relating their properties as models to those of commercial polythene, a polydisperse substance; the folding of the molecular chains in these compounds is of particular interest.[4] The study of pure oligoamides of the Nylon family is expected to provide even more insights into the nature of the chain-folding process since both amide and alkyl folds are possible.

We have exploited the lack of inter-chain hydrogen-bonding in *N*-alkylated amides to make soluble intermediates which were purified by chromatography on silica to produce pure 'end-capped' Nylon 6 oligomers. These compounds have been made previously,[5] but their purity could not be monitored. While relatively little work has been carried out on amide protecting groups,[6] we have now discovered that the 4-methoxybenzyl group in an amide $[N(CH_2C_6H_4OMe\text{-}4)(C{=}O)]$ is an excellent protecting group, conferring solubility in common solvents† on all derivatives, and being readily removed by boiling TFA. Scheme 1 shows the initial formation of the partially protected ethyl ester of acid **1** and its final protection to give the *N*-Boc derivative **2**, the starting material for an iterative synthesis. The first protected amide linkage in **4** was formed from **3** and **1** by a method used in peptide chemistry.[7] The Boc group in **4** was removed by TFA at room temperature and the chain-doubling reaction repeated successively to give first the fully protected dimer **5** ($n$ = 2), then the tetramer **5** ($n$ = 4) *etc.* up to the hexadecamer **5** ($n$ = 16). Individual 'end-capped' amides were obtained by deprotection of the *N*-terminus in **5**, followed by propanoylation to give **6**, and conversion of the ethoxycarbonyl terminus to the propylamide derivative **7**.‡ Finally, removal of the amide protecting group gave 'end-capped' oligomers **8** ($n$ = 2, 4, 8 and 16) of Nylon 6.§ The purity of the intermediates, formed in high yielding reactions, could be monitored by HPLC and their structures confirmed by $^1H$ NMR spectroscopy. The final end-capped Nylon 6 oligomers **8** were found to be soluble in $CD_3CO_2D$ at 80 °C, which enabled the complete confirmation of their structures to be carried out by $^1H$ NMR spectroscopy at 500 MHz. Currently, we are employing similar methodology for the synthesis of oligomers of Nylon 6,6 and Nylon 4,6.

The 4-methoxybenzyl group as a protecting group on nitrogen in an amide not only renders the parent molecule more soluble (the property exploited in this work); it also removes a potentially acidic hydrogen which could be incompatible in further types of reaction. It would then assume the role of a classical protecting group, and could be introduced into a NH(C=O) bond *via* treatment with LDA–4-methoxybenzyl bromide.

## Footnotes and References

* E-mail: g.m.brooke@durham.ac.uk

† Binary mixtures of appropriate solvents for chromatography were selected from the following: $CH_2Cl_2$, MeOH, EtOAc, $Et_2O$ and light petroleum (bp 40–60 °C).

‡ All the intermediates **2**–**7** in Scheme 1 were viscous liquids/gums; compound **1** was a liquid, bp 148–151 °C/0.01 mm Hg.

§ An unidentified solid precipitated during the final deprotection of the amide groups in **7**. The TFA was removed *in vacuo* and the residue was

found to dissolve completely in $CH_2Cl_2$, the oligoamide being rendered soluble by traces of trifluoroacetic acid. Treatment of the solution with dilute sodium hydrogen carbonate solution brought about the immediate precipitation of **8** in each case.


1 W. H. Carothers, *US Pat.*, 2 130 523, 1938.
2 W. O. Baker and C. S. Fuller, *J. Am. Chem. Soc.*, 1943, **65**, 1120; B. S. Briggs, C. J. Frosch and R. H. Erickson, *Ind. Eng. Chem.*, 1946, **38**, 1016; E. L. Wittbecker, R. C. Houtz and W. W. Watkins, *Ind. Eng. Chem.*, 1948, **40**, 875; J. R. Lewis and R. J. W. Reynolds, *Chem. Ind. (London)*, 1951, 958.
3 G. M. Brooke, S. Burnett, S. Mohammed, D. Proctor and M. Whiting, *J. Chem. Soc., Perkin Trans. 1*, 1996, 1635.
4 C. S. Bassett, R. H. Olley, S. J. Sutton and A. S. Vaughan, *Macromolecules*, 1996, **29**, 1852.
5 H. Zahn and G. B. Gleitsman, *Angew. Chem., Int. Ed. Engl.*, 1963, **2**, 410.
6 T. W. Greene and P. G. M. Wuts, *Protective Groups in Organic Synthesis*, 2nd edn., Wiley, New York, 1991, p. 397.
7 M. Bodanszky and A. Bodanszky, *The Practice of Peptide Synthesis*, Springer, Berlin, 1984, p. 145.


*Received in Liverpool, UK, 23rd May 1997; 7/03607H*

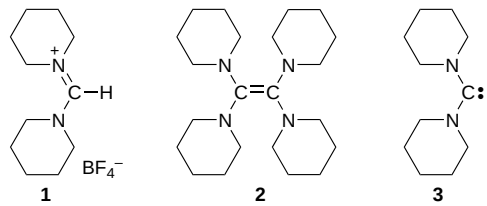
# Bis(*N*-piperidyl)carbene and its slow dimerisation to tetrakis(*N*-piperidyl)ethene

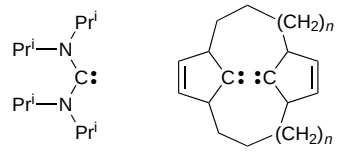
**Roger W. Alder* and Michael E. Blake**

*School of Chemistry, University of Bristol, Cantock's Close, Bristol, UK BS8 1TS*

**An unhindered bis(*sec*-amino)carbene can be generated by deprotonation of an amidinium ion with lithium diisopropylamide, and undergoes remarkably slow dimerisation to the corresponding tetraaminoethene.**

When amidinium salt **1** is treated with lithium diisopropylamide in THF at −80 °C, allowed to warm to room temperature, the THF removed and the residue dissolved in [$^2H_8$]toluene (all operations conducted under dry nitrogen), signals for two species are seen in the $^{13}C$ NMR spectrum. One of these is readily identified as the known[1] tetrakis(*N*-piperidyl)-ethene **2** ($\delta$ 25.7, 27.4, 51.6 and 134.6). The other species has lines at $\delta$ 24.8, 27.2, 53.1 and 236.8, and we assign this to bis(*N*-piperidyl)carbene **3**, on the basis of the chemical shift for the unique carbon [the central carbon in **4** absorbs at $\delta$ 255,[2] and other known[3] ylidic bis(*sec*-amino)carbene derivatives all absorb in the range $\delta$ 210–270]. All likely alternatives absorb at much lower chemical shifts (the central carbon of **1** occurs at $\delta$ 154, the carbonyl carbon in the urea absorbs at $\delta$ 171, and triaminomethane derivatives typically absorb at about $\delta$ 100). The subsequent behaviour of **2** and **3** is conveniently monitored by following the $CH_2$–N absorptions in the $^1H$ NMR spectrum, which come at $\delta$ 2.90 for **2** and $\delta$ 3.15 for **3**. Careful purification of all reagents and rigorous exclusion of air and water leads to solutions where the signals for **2** increase proportionally as those for **3** disappear (integration with respect to the residual protons in the solvent);† however, even under these conditions the reaction rate is only first order with respect to the carbene **3**. Signals for **3** persist for > 24 h in [$^2H_8$]toluene, but conversion to **2** occurs within 3 h in [$^2H_8$]THF.

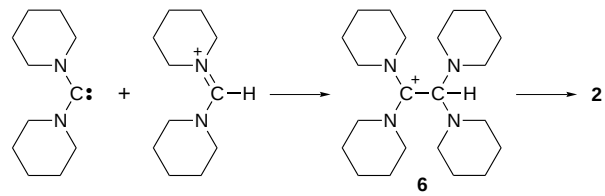



Why is some dimer generated in the initial reaction with base, and why is dimerisation first order in carbene? We suggest that, during the initial reaction, carbene **3** attacks precursor **1** to generate substituted amidinium ion **6**, which is then deprotonated to give **2** (see Scheme 1). This is the reverse of the mechanism proposed by Lemal[4] to account for reactions of the tetraaminoethene derivatives studied by Wanzlick which give products apparently derived from bis(*sec*-amino)carbenes. Wanzlick[5] had proposed that there was reversible dissociation of the tetraaminoethenes, but Lemal showed that this was not the case through a crossover experiment. The subsequent slow conversion of **3** to **2** may occur by rate-limiting regeneration of low concentrations of **1** from **3** (*e.g.* by reaction with residual diisopropylamine), followed by the steps in Scheme 1. Clearly uncatalysed dimerisation of **3** is too slow to be competitive; we estimate that $\Delta G^{\ddagger} \geqslant 100$ kJ mol$^{-1}$ for this process in [$^2H_8$]toluene. Arduengo *et al.*[6] have recently reported the generation of a stable thiazol-2-ylidene and its dimer; they find that the carbene only dimerises in the presence of the thiazolium ion precursor, further supporting Scheme 1.

Why is dimerisation of **3** so sluggish? Both thermodynamic and kinetic factors must be considered. Recent calculations[7,8] and experimental results[9] with imidazol-2-ylidenes show that dimerisation of these carbenes can actually be thermodynamically unfavourable. In particular, Taton and Chen[9] have shown that intramolecular double bond formation is favourable for **5a**, but that equilibrium favours the bis-carbene for **5b**. These remarkable observations are partially due to loss of aromaticity in the tetraazafulvalene dimers and calculations predict a dissociation energy of about 200 kJ mol$^{-1}$ for the parent tetraaminoethene,[8] still much lower than for ethene itself (710 kJ mol$^{-1}$). Steric effects will reduce the dissociation energy in **2** somewhat, but the conversion of **3** to **2** is clearly favourable, and so there must be a high intrinsic barrier to the dimerisation. Hoffmann *et al.*[10] pointed out that dimerisation of singlet methylene to ethene is forbidden along the least motion pathway. They proposed a non-least motion pathway in which the sp$^2$ lone pair of one methylene approached the empty p orbital of the other. In their extended Hückel calculations, this approach led to ground state ethene without activation energy. More sophisticated theoretical calculations[11] suggest a barrier of about 170 kJ mol$^{-1}$ for this non-least motion process and moreover that it leads to an excited state of ethene. There are therefore good theoretical grounds for expecting a very significant electronic barrier in this sort of process. In addition, there could be significant steric interactions between the piperidyl rings of **3** in the non-least motion approach. We note that both rate-limiting proton transfer (as suggested above) and the uncatalysed non-least motion process are likely to involve considerable charge separation in the transition state, and so will occur faster in more polar solvents.

The persistence of the diaminocarbene **3** is very striking and it now seems that almost any bis(*sec*-amino)carbene should be observable‡ at ambient temperatures under conditions which take account of the strong basicity[12] and nucleophilicity of these species. In fact, $(Me_2N)_2C$ ($\delta_C$ 244.4) has now been generated




**Scheme 1**

using similar procedures and a study of its behaviour is currently in progress.

We thank the EPSRC for a studentship (to M. E. B.) and Professor Michael E. Denk for an exchange of information before publication.

## Footnotes and References

* E-mail: Rog.Alder@bristol.ac.uk

† Carbene **3** is extremely sensitive to reaction with impurities. In early experiments, even with the usual precautions, signals for **3** disappeared over 1–3 h without a concomitant increase in the absorptions due to **2**.

‡ Unhindered 1,3-dialkyl-4,5-dihydroimidazol-2-ylidenes with isopropyl and methyl substituents have been generated and observed to dimerise slowly: M. K. Denk, A. Thadani, K. Hatano and A. Lough, *Angew. Chem*., in the press.

1 J. W. Scheeren and R. J. F. Nivard, *Recl. Trav. Chim. Pay-Bas*, 1969, **88**, 289; O. Tsuge, K. Yanagi and M. Horie, *Bull. Chem. Soc. Jpn*., 1971, **44**, 2171.
2 R. W. Alder, P. R. Allen, M. Murray and A. G. Orpen, *Angew. Chem., Int. Ed. Engl.*, 1996, **35**, 1121.
3 Imidazol-2-ylidenes: A. J. Arduengo III, R. L. Harlow and M. Kline, *J. Am. Chem. Soc*., 1991, **113**, 361; A. J. Arduengo III, H. V. R. Dias, R. L. Harlow and M. Kline, *J. Am. Chem. Soc*., 1992, **114**, 5530; 4,5-dihydroimidazol-2-ylidenes: A. J. Arduengo III, J. R. Goerlich and W. J. Marshall, *J. Am. Chem. Soc*., 1995, **117**, 11 027.
4 D. M. Lemal, R. A. Lovald and K. I. Kawano, *J. Am. Chem. Soc*., 1964, **86**, 2518; for a review, see: D. M. Lemal, in *The Chemistry of the Amino Group*, ed. S. Patai, Interscience, New York, 1968, pp. 701–748.
5 H.-W. Wanzlick and E. Schikora, *Angew. Chem*., 1960, **72**, 494; H.-W. Wanzlick, *Angew. Chem., Int. Ed. Engl*., 1962, **1**, 75; see also: H.-J. Schönherr and H.-W. Wanzlick, *Chem. Ber*., 1970, **103**, 1037 and intervening papers.
6 A. J. Arduengo III, J. R. Goerlich and W. J. Marshall, *Liebigs Ann. Recl*., 1997, 365.
7 D. A. Dixon and A. J. Arduengo III, *J. Phys. Chem*., 1991, **95**, 4180.
8 C. Heinemann and W. Theil, *Chem. Phys. Lett*., 1994, **217**, 11.
9 T. A. Taton and P. Chen, *Angew. Chem., Int. Ed. Engl*., 1996, **35**, 1011.
10 R. Hoffmann, R. Gleiter and F. B. Mallory, *J. Am. Chem. Soc*., 1970, **92**, 1460.
11 K. Ohta, E. R. Davidson and K. Morokuma, *J. Am. Chem. Soc*., 1985, **107**, 3466.
12 R. W. Alder, P. R. Allen and S. J. Williams, *J. Chem. Soc., Chem. Commun*., 1995, 1267.

*Received in Cambridge, UK, 27th June 1997; 7/03610H*

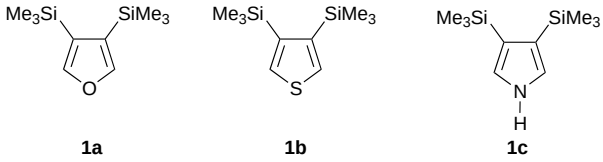
# 3,4-Bis(trimethylsilyl)-1*H*-pyrrole: a versatile building block for unsymmetrically 3,4-disubstituted pyrroles

**Ho-Wai Chan, Po-Ching Chan, Jian-Hui Liu and Henry N. C. Wong***

*Department of Chemistry, The Chinese University of Hong Kong, Shatin, New Territories, Hong Kong*

**3,4-Bis(trimethylsilyl)-1*H*-pyrrole 1c functions as a versatile building block for the construction of unsymmetrically 3,4-disubstituted pyrroles through the use of stepwise regiospecific *ipso* mono-halogenation, Sonogashira cross-coupling reactions and Suzuki cross-coupling reactions; the advantages of this strategy lie in its stepwise manner as well as in its prospect of yielding 3,4-disubstituted pyrroles with diverse substitution patterns.**

Pyrroles occur abundantly as structural units in many non-natural and natural molecules, including conducting poly(pyrroles),[1] antimitotics,[2] antitumour agents,[3] fungicides,[4] marine alkaloids[5] and porphyrins.[6] In the literature, several approaches to 3,4-disubstituted pyrroles have been recorded.[7–14] These approaches are generally not suitable for pyrroles containing elaborate substituents. With routes for the preparation of structurally diversified 3,4-disubstituted furans and thiophenes[15] from 3,4-bis(trimethylsilyl)furan **1a** and



**1a** **1b** **1c**

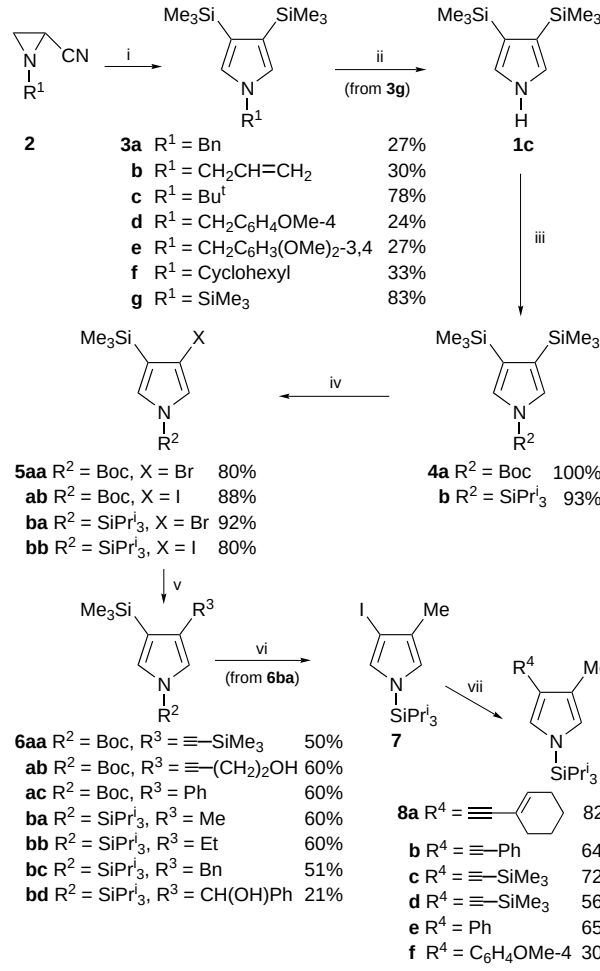
3,4-bis(trimethylsilyl)thiophene **1b** now at our disposal, we focused our attention on the synthesis of 3,4-disubstituted pyrroles. Herein we report our strategy for synthesizing unsymmetrically 3,4-disubstituted pyrroles utilizing 3,4-bis(trimethylsilyl)-1*H*-pyrrole **1c** as a building block.

By utilizing the [2 + 3] cycloaddition reported by La Porta *et al.*,[16] a number of *N*-protected 3,4-bis(trimethylsilyl)pyrroles were synthesized (Scheme 1) *via* thermal reactions of 2-cyanoaziridines **2**[17] with bis(trimethylsilyl)acetylene.† It is noteworthy that the preparation of **3c**, **3f** and **3g** did not require the use of sealed tubes. Amongst all the *N*-protected pyrroles prepared, only 1,3,4-tris(trimethylsilyl)pyrrole **3g** could be deprotected by a simple protodesilylation in MeOH, providing the desired molecule **1c** in good yield.

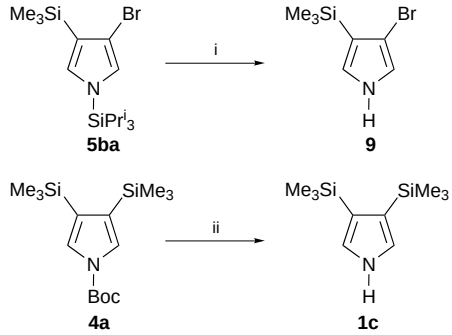
Due to the instability of **1c** as well as to the necessity for further transformation, **4a** and **4b** were synthesized by employing *tert*-butoxycarbonyl[18] and triisopropylsilyl groups[11b,c] as *N*-protecting groups. The role of a trimethylsilyl group in the *ipso*-directing substitution of aromatic compounds has been well documented.[19] In order to test the versatility of **4a** and **4b** in the realization of 3,4-disubstituted pyrroles, and the *ipso*-directing role of the trimethylsilyl groups, several halides **5** were regiospecifically prepared *via* literature procedures (Scheme 1).[20] Sonogashira reaction[21] was utilized to convert **5ab** into alkynes **6aa** and **6ab**. On the other hand, **5ab** was also successfully transformed to **6ac** by way of a Suzuki cross-coupling reaction.[22] A combined procedure involving lithiation and alkylation also converted **5ba** to **6ba**, **6bb**, **6bc** and **6bd**. In order to complete our initial plan of securing unsymmetrically 3,4-disubstituted pyrroles, **6ba** was allowed to undergo a regiospecific iodination, yielding iodide **7**. Sonogashira reaction of **7** again gave alkynes **8a**–**d**. Moreover, compounds **8e** and **8f** were also obtained from **7** *via* a Suzuki reaction pathway.

It is noteworthy that mild deprotection of **5ba** and **4a** was accomplished by using NaOMe in MeOH, affording 1*H*-pyrroles **9** and **1c**, respectively (Scheme 2).

In conclusion, making use of 3,4-bis(trimethylsilyl)-1*H*-pyrrole **1c** as a building block, an efficient and stepwise




**Scheme 1** *Reagents and conditions*: i, (for **3a**, **3b**, **3d** and **3e**) $Me_3SiC{\equiv}CSiMe_3$, DBU, PhMe, sealed tube, 170 °C; (for **3c**, **3f** and **3g**) $Me_3SiC{\equiv}CSiMe_3$, xylene, reflux; ii, MeOH, 95%; iii, (for **4a**) $BOC_2O$, DMAP, $CH_2Cl_2$, 30 min; (for **4b**) BuLi, THF, −78 °C, 30 min, then $Pr^i_3SiCl$; iv (for **5aa**) NBS, THF, 0 °C, 1 h; (for **5ab**) $I_2$, $CF_3CO_2Ag$, THF, −78 °C, 1 h; (for **5ba**) NBS, THF, −10 °C, 1 h; (for **5bb**) $I_2$, $CF_3CO_2Ag$, THF, −78 °C, 1 h; v, (for **6aa** and **6ab**) $R^3H$, $PdCl_2(PPh_3)_2$, CuI, $Et_2NH$, 22–24 h; (for **6ac**) $PhB(OH)_2$, $Pd(PPh_3)_4$, 2 M $Na_2Co_3$, MeOH–PhMe; (for **6bb** and **6bc**) BuLi, THF, −20 °C, then $R^3Br$; (for **6bd**) $Bu^tLi$, THF, −78 °C, 15 min, then PhCHO, HMPA, −78 to 0 °C; vi, $I_2$, $CF_3CO_2Ag$, THF, 55%; vii, (for **8a**–**d**) $R^4H$, $Pd(PPh_3)_4$, CuI, $Et_2NH$, reflux; (for **8e** and **8f**) $R^4B(OH)_2$, $Pd(PPh_3)_4$, 2 M $Na_2CO_3$, MeOH–PhMe, 80 °C




**Scheme 2** *Reagents and conditions*: i, NaOMe, MeOH, reflux, 1 h, 98%; ii, NaOMe, MeOH, THF, 80%

procedure for the synthesis of a number of unsymmetrically 3,4-disubstituted protected pyrroles has been established.

Financial support from the Research Grants Council (Hong Kong) Earmarked Grants for Research (CUHK 93/7.01, CUHK 21/92M) is gratefully acknowledged.

## Footnotes and References

* E-mail: hncwong@cuhk.edu.hk

† All new compounds were identified by means of $^{1}$H NMR and $^{13}$C NMR spectroscopy and mass spectrometry, as well as elemental analyses.

1 J. M. Cooper, D. G. Morris and K. S. Ryderr, *J. Chem. Soc., Chem. Commun.*, 1995, 697; H.-H. Anh, F. Fache and M. Lemaire, *New J. Chem.*, 1992, **16**, 1017.
2 J. K. Groves, N. E. Cundasawmy and H. J. Anderson, *Can. J. Chem.*, 1973, **51**, 1089.
3 S. Halazy and P. Magnus, *Tetrahedron Lett.*, 1984, **25**, 1421.
4 N. E. Heard and J. Turner, *J. Org. Chem.*, 1995, **69**, 4302.
5 A. Fürstner, H. Weintritt and A. Hupperts, *J. Org. Chem.*, 1995, **60**, 6637; M. G. Banwell, B. L. Flynn, E. Hamel and D. C. R. Hockless, *Chem. Commun.*, 1997, 207.
6 B. Franck and A. Nonn, *Angew. Chem., Int. Ed. Engl.*, 1995, **43**, 1795.
7 N. P. Pavri and M. L. Trudell, *J. Org. Chem.*, 1997, **62**, 2649; R. ten Have, F. R. Leusink and A. M. van Leusen, *Synthesis*, 1996, 871; C. Dell'Erba, A. Giglio, A. Mugnoli, M. Novi, G. Petrillo and P. Stagnaro, *Tetrahedron*, 1995, **51**, 5181; D. van Leusen, E. van Echten and A. M. van Leusen, *J. Org. Chem.*, 1992, **57**, 2245; D. van Leusen, E. Flentge and A. M. van Leusen, *Tetrahedron*, 1991, **47**, 4639; S. P. J. M. van Nispen, C. Mensink and A. M. van Leusen, *Tetrahedron Lett.*, 1980, **21**, 3723; A. M. van Leusen, H. Siderius, B. E. Hoogenboom and D. van Leusen, *Tetrahedron Lett.*, 1972, **13**, 5337.
8 K. Ichimur, S. Ichikawa and K. Imamura, *Bull. Chem. Soc. Jpn.*, 1976, **49**, 1157.
9 D. H. R. Barton, J. Kervagoret and S. Z. Zard, *Tetrahedron*, 1990, **46**, 7587.
10 H. Seino, Y. Ishii, T. Sasagawa and M.Hidai, *J. Am. Chem. Soc.*, 1995, **117**, 12 181; H. Seino, Y. Ishii, T. Sasagawa and M. Hidai, *J. Am. Chem. Soc.*, 1994, **116**, 7433.
11 (*a*) A. Alvarez, A. Guzmán, A. Ruiz and E. Velarde, *J. Org. Chem.*, 1992, **57**, 1653; (*b*) B. L. Bray, P. H. Mathies, R. Naef, D. R. Solas, T. T. Tidwell, D. R. Artis and J. M. Muchowski, *J. Org. Chem.*, 1990, **55**, 6317; (*c*) J. M. Muchowski and R. Naef, *Helv. Chim. Acta*, 1984, **67**, 1168.
12 N. W. Gabel, *J. Org. Chem.*, 1962, **27**, 301.
13 Y. Gao, M. Shirai and F. Sato, *Tetrahedron Lett.*, 1996, **37**, 7787.
14 T. J. Barton and G. P. Hussmann, *J. Org. Chem.*, 1985, **50**, 5881.
15 X.-S. Ye, P. Yu and H. N. C. Wong, *Liebigs. Ann.*, 1997, **3**, 459.
16 P. La Porta, L. Capuzzi and F. Bettarini, *Synthesis*, 1994, **5**, 287.
17 G. Bonteville, Y. Gelas-Mialke and R. Vessière, *Bull. Soc. Chim. Fr.*, 1971, 3264; B. A. Arbuzov and B. P. Lugovkin, *J. Gen. Chem. USSR (Engl. Trans,.)*, 1951, **21**, 99.
18 L. Grehn and U. Ragnarsson, *Angew. Chem., Int. Ed. Engl.*, 1984, **23**, 296.
19 N. C. Cutress, A. R. Katritziky, C. Eaborn, D. R. M. Walton and R. D. Topsom, *J. Organomet. Chem.*, 1975, **43**, 131; B. Bennetau and J. Dunogues, *Synlett.*, 1993, 171; H. Ishibashi, H. Sakashita and M. Ikeda, *J. Chem. Soc., Perkin Trans. 1*, 1992, 1953.
20 L. A. Jacob, B.-L. Chen and D. Stec, *Synthesis*, 1993, **4**, 611; S. R. Wilson and L. A. Jacob, *J. Org. Chem.*, 1986, **51**, 4833.
21 K. Sonogashira, Y. Tohda and N. Nagihara, *Tetrahedron Lett.*, 1975, **16**, 4467.
22 A. Suzuki, *Pure Appl. Chem.*, 1991, **63**, 419.

*Received in Cambridge, UK, 5th June 1997; 7/03921B*

# A cyclodextrin to reverse the regioselectivity of nitrile oxide cycloaddition to a terminal alkene

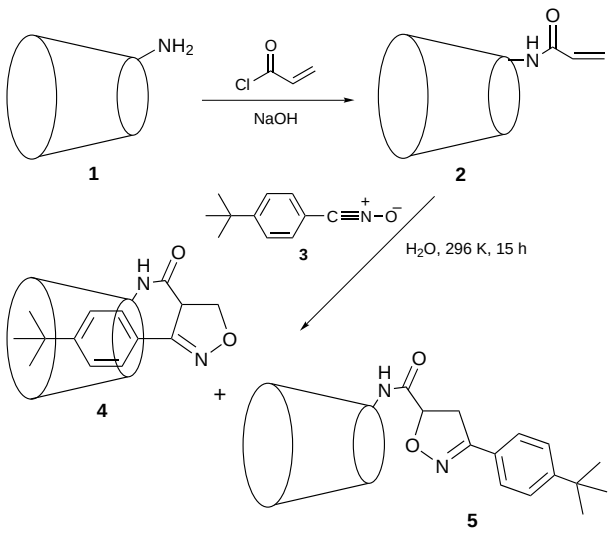
**Adam G. Meyer,[a] Christopher J. Easton,*[a] Stephen F. Lincoln[b] and Gregory W. Simpson[c]**

[a] *Research School of Chemistry, Australian National University, Canberra ACT 0200, Australia*
[b] *Department of Chemistry, University of Adelaide, Adelaide SA 5005, Australia*
[c] *CSIRO Division of Chemical and Polymers, Private Bag 10, Rosebank MDC, Clayton Vic 3169, Australia*

**The 1,3-dipolar cycloaddition of 4-*tert*-butylbenzonitrile oxide with 6$^A$-acrylamido-6$^A$-deoxy-β-cyclodextrin in aqueous solution favours formation of the 4-substituted isoxazoline, in contrast to the normal predominance of the 5-substituted regioisomer from reactions of monosubstituted alkenes.**

Nitrile oxide cycloaddition reactions with alkenes afford isoxazolines, which are of interest as versatile precursors of a range of 1,3-bifunctional compounds.[1] With mono- and trisubstituted alkenes the regioselectivity is usually determined by steric effects and the reactions afford almost exclusively 5- and 4,5,5-substituted isoxazolines, respectively. In order to reverse this regioselectivity, we envisaged that inclusion complexes of modified cyclodextrins[2] could be exploited. There have been reports that β-cyclodextrin affects the regioselectivity of nitrile oxide cycloadditions,[3] but it has now been demonstrated that these are in error and the cyclodextrin has no affect on the course of reaction in these examples.[4] Natural cyclodextrins have been used to accelerate Diels–Alder reactions of included guests and affect the distribution of products.[5] This occurs through self-assembly of the reactants within the cyclodextrin annulus, however our aim was to control the orientation of interaction between the reactants.

To develop this strategy, the dipolarophile was tethered to the cyclodextrin as the acrylamide **2** (Scheme 1). 4-*tert*-Butylbenzonitrile oxide **3** was selected as the dipole since alkyl-substituted aromatic compounds of this type are known to form thermodynamically stable inclusion complexes with β-cyclodextrin.[6] It was anticipated that inclusion of the hydrophobic moiety of the dipole **3** within the annulus of the modified cyclodextrin **2** would then establish the alignment for the cycloaddition (Fig. 1).




**Scheme 1**

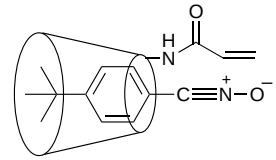
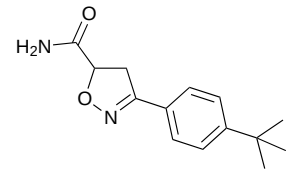


**Fig. 1** Alignment of the dipole **3** and the dipolarophile **2** in the host–guest complex

Treatment of the amino-substituted cyclodextrin **1**[7] with acryloyl chloride under basic conditions gave the acrylamide **2**.† 4-*tert*-Butylbenzaldehyde reacted with hydroxylamine, then *N*-chlorosuccinimide,[8] to give the corresponding hydroximinoyl chloride, from which the nitrile oxide **3** was generated *in situ* by reaction with triethylamine. Thus the cycloaddition involved rapidly stirring a mixture of the acrylamide **2** (0.03 mmol) and the hydroximinoyl chloride (0.12 mmol) in water (2.5 ml) at 296 K for 1 h, then adding triethylamine (0.12 mmol) and stirring that mixture for a further 15 h. After work-up, this afforded a quantitative yield of a 2.3 : 1 mixture of the isoxazolines **4** and **5**,† which were separated using HPLC (Scheme 1). The $^1$H NMR resonances due to the isoxazoline ring protons were assigned with the aid of double quantum filtered COSY experiments. When the cycloaddition reaction was repeated in DMF instead of water, the isoxazolines **4** and **5** were produced in 87% yield, as a 1 : 4 mixture.

The effect of the cyclodextrin annulus of the dipolarophile **2** was established by performing the cycloaddition of the nitrile oxide **3** with acrylamide. As expected, in either water or DMF, this reaction afforded only the 5-substituted isoxazoline **6**.†




**6**

Therefore, the production of the 4-substituted isoxazoline **4** in the reactions of the cyclodextrin derivative **2** highlights the effect of dipole **3**–dipolarophile **2** host–guest complex formation. As expected, this effect is greater in water than in DMF because the formation of cyclodextrin inclusion complexes is favoured in aqueous solutions.

### Footnotes and References

* E-mail: easton@rsc.anu.edu.au

† *Selected data* for **2**: 79%; $^1$H NMR (500 MHz; [$^2H_6$]DMSO): $\delta$ 7.95 (1 H, br s, NH), 6.26 (1 H, dd, *J* 11.0, 17.5), 6.03 (1 H, *J* 17.5), 5.55 (1 H, d, *J* 11.0). For **4**: HPLC (Waters carbohydrate analysis column with 80% MeCN in $H_2O$): $t_R$ = 25 min; $^1$H NMR (500 MHz; [$^2H_6$]DMSO): $\delta$ 7.96 (1 H, br s, NH), 7.46 (2 H, d, *J* 8.0, ArH), 7.37 (2 H, d, *J* 8.0, ArH), 4.63 [1 H, m, isoxazoline C(5)-H], 4.60 [1 H, m, isoxazoline C(5)-H′], 4.37 [1 H, m,

isoxazoline C(4)-H]. For **5**: HPLC (as for **4**): $t_R$ = 20 min; $^1$H NMR (500 MHz; [$^2H_6$]DMSO): $\delta$ 7.93 (1 H, br s, NH), 7.61 (2 H, d, *J* 8.5, ArH), 7.47 (2 H, d, *J* 8.5, ArH), 5.09 [1 H, m, isoxazoline C(5)-H], 3.62 [1 H, dd, isoxazoline C(4)-H], 3.50 [1 H, dd, *J* 6.5, 17.0, isoxazoline C(4)-H′]. For **6**: $^1$H NMR (500 MHz; [$^2H_6$]DMSO): $\delta$ 7.60 (2 H, d, *J* 8.5, ArH), 7.46 (2 H, d, *J* 8.5, ArH), 5.01 [1 H, dd, *J* 6.5, 11.5, isoxazoline C(5)-H], 3.62 [1 H, dd, isoxazoline C(4)-H], 3.50 [1 H, dd, *J* 6.5, 17.0, isoxazoline C(4)-H′].


1 C. J. Easton, C. M. M. Hughes, G. P. Savage and G. W. Simpson, *Adv. Heterocycl. Chem.*, 1994, **60**, 261; G. Bianchi, R. Gandolfi and P. Grünanger, in *The Chemistry of Functional Groups*, ed. S. Patai and Z. Rappoport, Wiley, New York, 1983, suppl. C, pt. 2, pp. 752–778.

2 M. L. Bender and M. Komiyama, *Cyclodextrin Chemistry*, Springer-Verlag, Berlin, 1978; J. Szejtl, *Cyclodextrins and their Inclusion Complexes*, Akademiai Kiado, Budapest, 1982; R. J. Clarke, J. H. Coates and S. F. Lincoln, *Adv. Carbohydr. Chem. Biochem.*, 1989, **46**, 205; C. J. Easton and S. F. Lincoln, *Chem. Soc. Rev.*, 1996, **25**, 163.

3 K. Rama Rao, N. Bhanumathi, T. N. Srinivasan and P. B. Sattur, *Tetrahedron Lett.*, 1990, **31**, 899; K. Rama Rao, *Pure Appl. Chem.*, 1992, **64**, 141; K. Rama Rao, N. Bhanumathi, T. N. Srinivasan and P. B. Sattur, *Tetrahedron Lett.*, 1990, **31**, 3201.

4 C. J. Easton, C. M. M. Hughes, E. R. T. Tiekink, G. P. Savage and G. W. Simpson, *Tetrahedron Lett.*, 1995, **36**, 629.

5 D. C. Rideout and R. Breslow, *J. Am. Chem. Soc.*, 1980, **102**, 7816; D. D. Sternbach and D. M. Rossana, *J. Am. Chem. Soc.*, 1982, **104**, 5853; H.-J. Schneider and N. K. Sangwan, *Angew. Chem., Int. Ed. Engl.*, 1987, **26**, 896; N. K. Sangwan and H.-J. Schneider, *J. Chem. Soc., Perkin Trans. 2*, 1989, 1223; I. Hunt and C. D. Johnson, *J. Chem. Soc., Perkin Trans. 2*, 1991, 1051.

6 Y. Matsui, T. Nishioka and T. Fujita, *Top. Curr. Chem.*, 1985, **128**, 61.

7 S. E. Brown, J. H. Coates, D. R. Coghlan, C. J. Easton, S. J. van Eyk, W. Janowski, A. Lepore, S. F. Lincoln, Y. Luo, B. L. May, D. S. Schiesser, P. Wang and M. L. Williams, *Aust. J. Chem.*, 1993, **46**, 953; L. D. Melton and K. N. Slessor, *Carbohydr. Res.*, 1971, **18**, 29.

8 K.-C. Liu, B. R. Shelton and R. K. Howe, *J. Org. Chem.*, 1980, **45**, 3916.



*Received in Cambridge, UK, 23rd May 1997; 7/03575F*

# Structure investigation of a dimethylaluminium derivative of ethyl *rac*-lactate in the solid state and solution. First evidence for stereoselective association of a dialkylaluminium *O,O′*-chelate complex

**Janusz Lewiński,* Janusz Zachara and Iwona Justyniak**

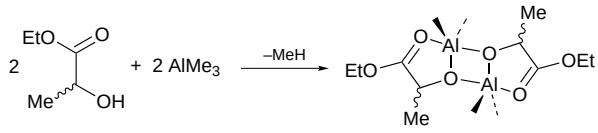
*Department of Chemistry, Warsaw University of Technology, Noakowskiego 3, PL-00-664 Warsaw, Poland*

**The reaction of $AlMe_3$ with an equimolar amount of ethyl *rac*-lactate (Helac) affords *rac*-[$Me_2Al${(*S**)-elac}]$_2$; the X-ray structure shows that the adduct is formed in a highly stereoselective manner and variable-temperature $^1H$ NMR spectra indicates that the five-coordinated complex is non-rigid in solution.**

Organoaluminium derivatives of *O,O′*-bifunctional ligands have been under investigation for many years owing to their practical and fundamental importance. For example, these compounds have been reported as organometallic intermediates in carbon–carbon bond formation reactions,[1] as precursors of catalysts in polymerisation processes[2,3] or precursors for MOCVD.[4] Although five-coordination in diorganoaluminium chelate complexes has been frequently postulated and as early as 1972 the [$R_2Al(O,O′)$]$_2$-type adduct has been reported as the first crystallographically characterised five-coordinated organoaluminium compound,[3a] there are not many examples of structurally characterised [$R_2Al(O,O′)$]$_2$-type complexes.[3a,4,5] Recently, we have described the structure characterisation of the first simple monomeric five-coordinate monoalkyaluminium chelate complex.[6] Due to the potential utility of organoaluminium derivative of *O,O′*-bifunctional ligands in organic synthesis and polymerisation processes, the investigation into the chemistry of organoaluminium chelate compounds, especially complexes bearing chiral centres,[7] has become an important challenge. The results concerning the structure of the dimethylaluminium derivative of racemic ethyl lactate are presented here as part of our studies on the structure of dialkylaluminium chelate compounds in solid state and solution. We report here that the formation of the [$R_2Al(O,O′)$]$_2$ adduct is a stereoselective reaction and show that this type of five-coordinated complex is non-rigid in solution.

The interaction of $Me_3Al$ with an equimolar amount of ethyl *rac*-lactate (Helac) results in quantitative evolution of methane and formation of *rac*-[$Me_2Al${(*S**)-elac}]$_2$ **1** (Scheme 1).†

The molecular structure of **1** has been determined by X-ray diffraction‡ and its solution structure has been characterised by $^1H$ and $^{27}Al$ NMR as well as cryoscopic molecular mass determination.§ The molecule is a dimer with two five-coordinate aluminium atoms (Fig. 1). The monomeric units are bonded *via* alkoxide oxygen atoms O(1) and O(1′) with the formation of a central four-membered ring $Al_2(\mu\text{-}O)_2$. The ethyl lactate anions form two five-membered chelate rings with aluminium, which lie approximately in one plane with a central bridging ring. The root mean square deviation of the atoms from this plane is 0.086 Å. The geometry of the aluminium atom coordination sphere can be described as a distorted trigonal bipyramid. The equatorial plane is defined by the C(6) and C(7) carbon atoms and the alkoxide oxygen. The axial positions are occupied by the O(2) oxygen atom of the carbonyl group and the alkoxide O(1′) oxygen atom of the second monomeric unit. The angle between the axial substituents is 164.74(6)°. As is shown in Fig. 1, the methyl groups bonded to the chiral C atom in the chelating ligand lie on the same side of the plane outlined by three fused heterocyclic rings, and the dimer molecule has $C_2$ symmetry. This indicates that only monomeric units of the same configuration as the chiral centre in the chelating ligand associate with each other giving exclusively (*R,R*) and (*S,S*) diastereoisomers. Thus, the formation of the dimeric five-coordinate complex **1** is a stereoselective reaction.




**Scheme 1**

It should be noted that the Al–O distances within the central $Al_2(\mu\text{–}O)_2$ ring in **1** [Al(1)–O(1) 1.848(2) Å and Al(1)–O(1′) 1.936(2) Å] differ significantly despite the fact that the same bridging oxygen atoms are bonded to the equivalent aluminium atoms. It is apparent that this results from the geometry of the dimeric five-coordinate molecules, which imposes that each bridging oxygen atom is in the equatorial position of one

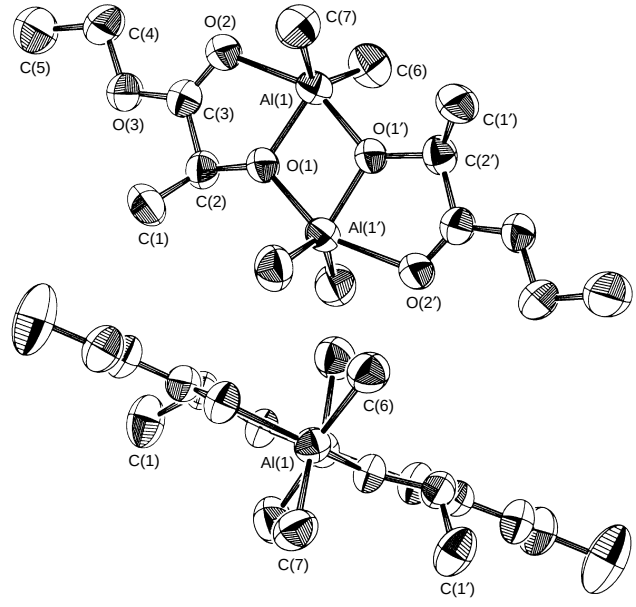



**Fig. 1** ORTEP view of the molecular structure of [$Me_2Al${(*S*)-elac}]$_2$ **1** with thermal ellipsoids drawn at 50% probability level. Bottom: view of the molecule along a mean plane formed by heterocyclic rings. Selected bond lengths (Å) and angles (°): Al(1)–O(1) 1.848(2), Al(1)–O(1′) 1.936(2), Al(1)–O(2) 2.157(2), Al(1)–C(6) 1.954(4), Al(1)–C(7) 1.956(4), O(2)–C(3) 1.224(3), O(1)–C(2) 1.405(3), O(1)–Al(1)–O(1′) 75.6(1), O(1)–Al(1)–C(6) 117.9(2), O(1)–Al(1)–C(7) 117.0(2), C(6)–Al(1)–C(7) 124.3(2), O(1)–Al(1)–O(2) 78.20(9), O(1′)–Al(1)–O(2) 153.8(1), C(3)–O(2)–Al(1) 111.4(2), C(2)–O(1)–Al(1) 122.9(2), Al(1)–O(1)–Al(1′) 104.2(1), O(1)–C(2)–C(3) 106.0(3), O(2)–C(3)–C(2) 120.4(3). Atoms labelled with a prime belong to the counterpart of dimeric units generated by two-fold axis (*y, x, −z*).

aluminium atom and in the axial position with respect to the other. Although non-equivalence of Al–O distances within the $Al_2(\mu\text{-}O)_2$ ring is usually noted in the description of structural data of compounds consisting of such a symmetrical four-centred bridging system, it is commonly interpreted as resulting from the different characters of these bridging bonds; for example, one Al–O bond is of a covalent and the other of a donor–acceptor or partial dative/covalent character.[8,9] We would like to emphasise at this point that the Al–O bonds in the $Al_2(\mu\text{-}O)_2$ ring are of the same character (σ two-centre–two-electron bonds) and the differences in the bridging Al–O bonds length are due to the different geometrical locations in the coordination sphere of the Al atoms.

The dimeric structure of **1** is retained in solution as found from a cryometric molecular mass determination in benzene. The NMR spectra of **1** are consistent with the structure found in the solid state. The $^{27}$Al NMR spectrum of **1** consists of a single resonance at $\delta$ 114 indicative of five-coordinate aluminium.[5a,10] The $^1$H NMR spectrum of **1** in $CD_2Cl_2$ solution at 20 °C displays a single resonance for the Al–$CH_3$ protons, and a doublet and quartet for the C–$CH_3$ and C–H protons, respectively, associated with the chiral centre as well as two resonances of the ester ethyl group; the methylene protons of the ethyl group are diastereotopic giving rise to an eight-line pattern. As the temperature is decreased the resonance associated with Al–$CH_3$ protons broadens (*ca.* −80 °C) and splits into two well separated resonances at −93 °C. This result can be best interpreted in terms of a dissociative process in which the Al–O chelate bond undergoes cleavage giving rise to the interchange of the chelating groups between the two aluminium centres and permitting the Al–$CH_3$ groups to become equivalent on the NMR timescale.

Additionally, we chose ethyl lactate for structure investigation in the expectation that IR spectroscopy could be a sensitive probe for detecting an equilibrium between five- and four-coordinate dimeric organoaluminium species with chelated and dangling *O,O′*-bifunctional ligand carbonyl groups. However, the IR spectrum of **1** in $CH_2Cl_2$ solution shows only one carbonyl group stretching vibration at 1690 cm$^{-1}$. The observed decrease in comparison to that in free Helac (1728 cm$^{-1}$) is consistent with the coordination of the carbonyl group to aluminium. Furthermore, the presence of the strong band of the chelate carbonyl group and lack of uncoordinated carbonyl groups bands can be interpreted in terms of dangling ligands being present at non-detectable concentrations or that intermediate species involving dangling ligands have different geometry and corresponding bands occur with non-appreciable intensities.

Further studies are required in order to determine the nature of five-coordinate $[R_2Al(O,O')]_2$ adduct formation in a highly stereoselective manner and the structural characterisation of this type of adducts derived from $AlR_3$ and racemic *O,OH* bifunctional ligands is currently in progress.

We thank Professor D. J. Stufkens (Universiteit van Amsterdam) for helpful discussion of IR spectra and the National Research Committee (Grant 3 T09A 108 12) for financial support.

## Footnotes and References

* E-mail: lewin@ch.pw.edu.pl

† *Preparation* of **1**: ethyl *rac*-lactate (7.0 mmol) was dissolved in toluene (10 cm$^3$) and $AlMe_3$ (7.0 mmol) was added dropwise at −78 °C. After the addition was complete the reaction mixture was allowed to warm to room temp. The solvent was then removed under vacuum, leaving a white solid that was crystallised from toluene–hexane at 0 °C. The yield was essentially quantitative.

‡ *Crystal data* for **1**: $C_{14}H_{30}Al_2O_6$: tetragonal, space group $P4_12_12$ (no. 92) and $P4_32_12$ (no. 96) for (*S,S*) and (*R,R*) diastereoisomers, respectively; *D*c = 1.137 g cm$^{-3}$, $Z$ = 4, $a$ = 7.6188(7), $c$ = 35.055(6) Å, $U$ = 2034.8(4) Å$^3$, $T$ = 20 °C, Mo-K$\alpha$ radiation ($\lambda$ = 0.71073 Å), $\mu$ = 1.64 cm$^{-1}$, Siemens P3 diffractometer, $2\theta_{max}$ = 50°, $\theta$–$2\theta$ scans, 4171 reflections collected (1801 unique, $R_{int}$ = 0.0694). The structure was solved by direct methods[11] in the $P4_12_12$ space group and was refined by full-matrix least-squares on $F^2$.[12] Hydrogen atoms were included in idealised positions and refined isotropically. Refinement converged at $wR_2$ = 0.1082 for 1697 data and 112 parameters [$R_1$ = 0.0477 for 1021 unique reflections with $F_o > 4\sigma(F_o)$]. Absolute structure could not be determined reliably due to the high e.s.d. for the refined Flack $x$ parameter 0.3(4).[13] A weighting scheme $w = [\sigma^2(F_o^2) + (0.0280P)^2]^{-1}$ where $P = (F_o^2 + 2F_c^2)/3$ was used in the final stage of refinement. Residual electron density = +0.17, −0.16 e Å$^{-3}$. CCDC 182/529.

§ *Selected data* for **1**: $^1$H NMR ($CD_2Cl_2$, 20 °C), $\delta$ −0.72 (12H, s, $AlCH_3$), 0.94 (6H, t, $CH_2CH_3$), 1.35 (6H, d, $CHCH_3$), 3.90 (4H, qd, $CH_2CH_3$), 4.40 (1H, q, $CHCH_3$); (−90 °C), −0.62 (6H, s, $AlCH_3$), −0.56 (6H, s, $AlCH_3$), 0.78 (6H, t, $CH_2CH_3$), 1.32 (6H, d, $CHCH_3$), 3.61 (4H, q, $CH_2CH_3$), 4.33 (1H, q, $CHCH_3$), $^{27}$Al NMR ($C_6D_6$, 20 °C) $\delta$ 114 ($\Delta H_{\frac{1}{2}}$ = 5780 Hz); molecular mass (cryoscopy in benzene): found 350, calc. 348.4.

1 See for example: M. Gerster, K. Schenk and P. Renaud, *Angew. Chem., Int. Ed. Engl.*, 1996, **35**, 2396; T. Arai, H. Sasai, K. Aoe, K. Okamura, T. Date and M. Shibasaki, *Angew. Chem., Int. Ed. Engl.*, 1996, **35**, 104; P. Renaud and M. Gerster, *J. Am. Chem. Soc*., 1995, **117**, 6607; F. H. van Steen, G. P. M. van Mier, A. L. Spek, J. Kroon and G. van Koten, *J. Am. Chem. Soc*., 1991, **113**, 5742; E. A. Jeffery, A. Meisters and T. Mole, *J. Organomet. Chem*., 1974, **74**, 373.

2 E. J. Vandenberg in *Catalysis in Polymer Synthesis*, ACS Symp. Ser. 496, ed. E. J. Vandenberg and J. C. Salamone, Washington, DC, 1992.

3 Y. Kai, N. Yasuoka, N. Kasai and M. Kakudo, *Bull. Chem. Soc. Jpn.* 1972, **45**, (*a*) 3397; (*b*) 3403.

4 See for example: H. Schuman, M. Fric, B. Heymer and F. Girgsdies, *J. Organomet. Chem*., 1996, **512**, 117.

5 (*a*) R. Benn, A. Rufińska, H. Lehmkuhl, E. Janssen and C. Kruger, *Angew. Chem., Int. Ed. Engl.*, 1983, **22**, 779; (*b*) D. G. Hendershot, M. Barber, R. Kumar and J. P. Oliver, *Organometallics*, 1991, **10**, 3302.

6 J. Lewiński, J. Zachara, B. Mańk and S. Pasynkiewicz, *J. Organomet. Chem*., 1993, **454**, 5; J. Lewiński, J. Zachara, T. Kopeć and Z. Ochal, *Polyhedron*, 1997, **16**, 1337.

7 Recently the synthesis and structure investigation of dialkylaluminium derivative of optically active amino alcohols have been described: M. L. Sierra, V. S. J. de Mel and J. P. Oliver, *Organometallics*, 1989, **8**, 2486; R. Kumar, M. L. Sierra and J. P. Oliver, *Organometallics*, 1994, **13**, 4285; D. A. Atwood, F. P. Gabai, J. Lu, M. P. Reminghton, D. Rutherford and M. P. Sibi, *Organometallics*, 1996, **15**, 2308.

8 A. Haaland, *Angew. Chem., Int. Ed. Engl.*, 1989, **28**, 992; A. Haaland, *Coordination Chemistry of Aluminum*, ed. G. H. Robinson, VCH, New York, 1993, pp. 1–56.

9 The appropriate description of M–O differentiation in asymmetric bridges is really the subject of the discussion for other metal alkoxides, see for example: M. A. Matchett, M. Y. Chiang and W. E. Buhro, *Inorg. Chem.*, 1990, **29**, 360.

10 R. Benn and A. Rufińska, *Angew. Chem., Int. Ed. Engl.*, 1986, **25**, 851; R. Benn, A. Rufińska, H. Lehmkuhl and E. Janssen, *J. Organomet. Chem*., 1987, **333**, 155.

11 G. M. Sheldrick, SHELXS-86, *Acta Crystallogr., Sect. A*, 1990, **46**, 467.

12 G. M. Sheldrick, SHELXL-93, University of Göttingen, 1993.

13 H. D. Flack, *Acta Crystallogr., Sect. A*, 1983, **39**, 876.

*Received in Cambridge, UK, 28th April 1997; 7/02855E*

# Application of chelating diphosphine ligands in the nickel-catalysed hydrocyanation of alk-l-enes and ω-unsaturated fatty acid esters

**Wolfgang Goertz,[a] Paul C. J. Kamer[b], Piet W. N. M. van Leeuwen[b] and Dieter Vogt*[a]**

[a] *Institut für Technische Chemie und Petrolchemie, Rheinisch-Westfälische Technische Hochschule, Templergraben 55, D-52056 Aachen, Germany*

[b] *J. H. van't Hoff Research Institute, Department of Inorganic Chemistry, University of Amsterdam, Nieuwe Achtergracht 166, 1018 WV Amsterdam, The Netherlands*

**The hydrocyanation of alk-l-enes and ω-unsaturated fatty acid esters using zerovalent nickel complexes yields the corresponding nitriles and cyanoesters, which can be useful starting materials in organic synthesis.**

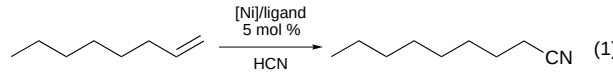
The nickel-catalysed addition of HCN to butadiene, known as the DuPont ADN Process, is the most important hydrocyanation reaction today at an industrial scale.[1] Many investigations have been made to understand its mechanism and to improve activity and selectivity.[2] A major problem still arises from the formation of inactive nickel cyanides when the zero-valent metal centre is exposed to an excess of HCN.

Recently we reported the successful application of diphosphines in the hydrocyanation of styrene.[3] These newly developed Xantphos ligands[4] have large bite angles and rigid backbones (Fig. 1). It is likely that they enhance the final reductive elimination step in the catalytic cycle by supporting a tetrahedral geometry. Dicyano nickel(II) species with a square-planar geometry affording P–Ni–P angles of about 90° are disfavoured. Moreover, the Xantphos ligands allow a large excess of HCN by providing more stable $Ni^0$ complexes compared to monodentates due to the chelate effect.

Although the first homogeneously catalysed hydrocyanation of linear alkenes was published by Arthur and Pratt[6] in 1954, only a few more examples representing this class of substrates can be found in the literature.[7] Nevertheless alkyl nitriles are valuable intermediates for the synthesis of amides, amines, carboxylic acids and esters.

Using *n*-octenes as starting materials, Keim *et al.* have found in earlier work that, irrespective of the position of the double bond, the anti-Markovnikov product 1-cyanooctane is formed with 80% regioselectivity.[8] However, in order to avoid fast deactivation of the catalyst, the monodentate phosphite ligands like $P(OC_6H_4Me\text{-}p)_3$ had to be employed in ratios (relative to Ni) > *ca*. 15 to 1. Recent efforts were made with diphosphites in the hydrocyanation of butadiene[9] and with diphosphinites in the hydrocyanation of vinylarenes.[10]

We report here the catalytic hydrocyanation of long-chain substrates having a non-conjugated double bond with $Ni^0$ complexes. This work represents the first successful hydrocyanation of alk-l-enes and ω-unsaturated fatty acid esters applying chelating diphosphines, with a ligand to metal ratio of only 1.05 [eqn. (1)].‡ These systems were shown to be stable

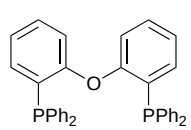



(1)

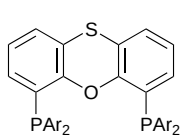
against an excess of HCN up to 1000 in a batch reaction. $AlCl_3$ was added to the reaction mixtures as a cocatalyst. The role of the Lewis acid is to activate the catalyst precursor when non-conjugated alkenes are used as substrates.[11]

The use of diphosphines with large bite angles induces yields that are comparable to those obtained with the commercial *ortho*-tolylphosphite system in the hydrocyanation of oct-1-ene (Table 1, entries 1–4). The hydrocyanation of dec-1-ene with the same catalysts leads to similar results. Ligands with electron-withdrawing substituents on the phosphorus atom give rise to more stable $Ni^0$ complexes, since back-donation of d electrons from the metal is favoured in this case. For that reason the Thixantphos ligand was derivatised by introducing trifluoromethyl groups at the *meta* positions in the PPh moiety (Fig. 1). Increased yields and excellent selectivities with this system clearly indicate a higher complex stability and better performance of the catalyst (Table 1, entry 4).

When dealing with monodentate phosphite ligands in hydrocyanation catalysis the Tolman angle $\theta$ is the important factor,[12] whereas with bidentate ligands the bite angle is decisive. The use of common diphosphine ligands with bite angles between 78 and 98° like dppe, dppp, dppb or binap in the hydrocyanation of styrene results in almost no conversion.[3] We observed the same behaviour in the hydrocyanation of substrates dealt with in the present communication. Best activities are obtained with bite angles around 109°.




DPEphos, bite angle = 105°




Thixantphos, Ar = Ph, bite angle = 113°
$CF_3$-Thixantphos, Ar = $C_6H_3(CF_3)_2$-3,5, bite angle = 115°

**Fig. 1** Xantphos type ligands. Bite angles were calculated using molecular mechanics.† The natural bite angle is defined as the preferred chelation angle determined only by ligand backbone constraints and not by metal valence angles.[5]

**Table 1** Nickel-catalysed hydrocyanation of oct-1-ene and methyl dec-9-enoate[a]

| Entry | Ligand | Oct-1-ene | | Methyl 9-dec-1-enoate |
|---|---|---|---|---|
| | | Yield[b] (%) | Selectivity[c] (%) | yield[b] (%) |
| 1 | DPEphos | 36 | 82 | 13 |
| 2 | Thixantphos | 42 | 91 | 10 |
| 3[d] | $P(OC_6H_4Me)_3$ | 51 | 82 | 33 |
| 4 | $CF_3$-Thixantphos | 51 | 96 | 36 |

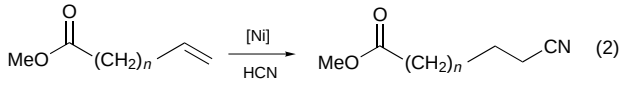
[a] *Reaction conditions*: Ni:$AlCl_3$:ligand:substrate:HCN = 1:1:1.05:20:25, 333 K, 16 h. [b] Yields are based on the substrate and were determined by temperature-controlled gas chromatography with added standard compounds. [c] Selectivity = chemical yield of nitriles / conversion (substrate). [d] Ligand to nickel ratio = 20.

**Table 2** Regioselectivity[a] towards the terminal nitriles obtained in the hydrocyanation of oct-1-ene and methyl dec-9-enoate

| Ligand | Oct-1-ene | Methyl 9-dec-1-enoate |
|---|---|---|
| DPEphos | 29 | 39 |
| Thixantphos | 84 | 75 |
| $P(OC_6H_4Me\text{-}p)_3$ | 82 | 77 |

[a] Regioselectivity is defined as the % of linear nitrile.

Hydrocyanation of functionalised alkenes leads to interesting chemical building blocks. Reaction of ω-unsaturated fatty acid esters with HCN gives the corresponding cyanoesters [eqn. (2),



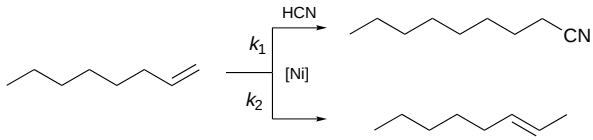
(2)

$n$ = 7–11]. The substrate acid esters are readily available from natural resources.[13] To the best of our knowledge this is the first example of a catalytic hydrocyanation using this class of substrates.

For methyl dec-9-enoate the obtained yields and selectivities are similar to the unfunctionalised alkenic substrates (Table 1, entries 1–4). The presence of the ester group does not inhibit the catalytic reaction. However, with fatty acid esters containing a longer chain, such as methyl undec-10-enoate or methyl tetradec-13-enoate, the yields decrease slightly.

The Xantphos type diphosphines DPEphos and Thixantphos have almost identical electronic properties but different bite angles. Moreover, for DPEphos, the S-bridge in the backbone is missing which makes the ligand flexible. These characteristics influence the regioselectivity towards the nitrile products (Table 2). We suggest that the more rigid ligand backbones disfavour conformational changes in the metal complexes formed. With Thixantphos the observed linearity reaches 84%.

The formation of branched nitriles mainly takes place when the double bond of the starting unsaturated substrate is isomerised *via* an intermediate nickel hydride species to give an internal alkene. Usually, isomerisation and β-elimination of a thermodynamically favoured internal alkene ($k_2$) is much faster than hydrocyanation ($k_1$) (Scheme 1). Thus another approach to explain the difference in regioselectivity with DPEphos and Thixantphos is a kinetic one. The more rigid a ligand is, the more favoured is hydrocyanation ($k_1$).




**Scheme 1**

The results reported here clearly indicate the unique properties of the Xantphos type diphosphine ligands possessing large bite angles in hydrocyanation reactions. Effective nickel-catalysed hydrocyanation of long-chain unsaturated substrates can be achieved. The regioselectivity can be controlled by providing a rigid ligand backbone.

We would like to thank Professor Dr Wilhelm Keim for kindly supporting our work and Professor Dr Siegfried Warwel, H. P. Kaufmann-Institut Münster, for the donation of the fatty acid esters.

## Footnotes and References

* E-mail: dieter.vogt@post.rwth-aachen.de

† The molecular mechanics calculations were performed on a Silicon Graphics Indigo*2* workstation using SYBYL[14] software version 6.3 and a modified TRIPOS force field with a Ni–P bond length of 2.177 Å and a P–Ni–P bending force constant of 0 kcal $mol^{-1}$ $degree^{-2}$.

§ In a typical experiment, 1 ml of a bright yellow 0.0325 mM solution of $[Ni(cod)_2]$ in toluene was added to a Schlenk tube containing a stirring bar and 1.05 equiv. of ligand. The mixture was stirred for 30 min to ensure complete formation of the catalyst precursor. Then 0.65 mmol of the substrate and 0.0325 mmol of Lewis acid ($AlCl_3$ as a stock solution) was added. The solution was then cooled to *ca*. 220 K, 30 μl of liquid HCN (0.78 mmol) was added at once and the tube was placed in a heating bath. After 16 h at 333 K, the excess of HCN was removed by a gentle stream of argon, solid particles were removed by centrifugation and the remaining solution was analysed by temperature-controlled gas chromatography.

1 R. J. McKinney, in *Homogeneous Catalysis*, ed. G. W. Parshall, Wiley, New York, 1992, p. 42.
2 C. A. Tolman, R. J. McKinney, W. C. Seidel, J. D. Druliner and W. R. Stevens, *Adv. Catal*., 1985, **33**, 1.
3 M. Kranenburg, P. C. J. Kamer, P. W. N. M. van Leeuwen, D. Vogt and W. Keim, *J. Chem. Soc., Chem. Commun.*, 1995, 2177.
4 M. Kranenburg, Y. E. M. van der Burgt, P. C. J. Kamer, P. W. N. M. van Leeuwen, K. Goubitz and J. Fraanje, *Organometallics*, 1995, **14**, 3081.
5 C. P. Casey and G. T. Whiteker, *Isr. J. Chem*., 1990, **30**, 299.
6 P. Arthur, Jr., D. C. England, B. C. Pratt and G. M. Whitman, *J. Am. Chem. Soc*., 1954, **76**, 5364.
7 B. W. Taylor and H. E. Swift, *Erdöl Kohle Erdgas Petrochem*., 1974, **27**, 93; E. S. Brown, in *Aspects of Homogeneous Catalysis*, ed. R. Ugo, Reidel, Dordrecht, 1974, vol. 2, p. 57.
8 W. Keim, A. Behr, J. P. Bioul and J. Weisser, *Erdöl Kohle Erdgas Petrochem*., 1982, **35**, 436.
9 M. J. Baker, K. N. Harrison, A. G. Orpen, P. G. Pringle and G. Shaw, *J. Chem. Soc., Chem. Commun*. 1991, 803.
10 T. V. RajanBabu and A. L. Casalnuovo, *J. Am. Chem. Soc.*, 1996, **118**, 6325.
11 C. A. Tolman, W. C. Seidel, J. D. Druliner and P. J. Domaille, *Organometallics*, 1984, **3**, 33.
12 C. A. Tolman, *J. Chem. Educ*., 1986, **63**, 199.
13 S. Warwel, H.-G. Jägers and S. Thomas, *Fat Sci. Technol.*, 1992, **94**, 323; S. Warwel, P. Bavaj, B. Ercklentz, M. Harperscheid, M. Rüsch gen. Klaas and S. Thomas in *Nachwachsende Rohstoffe*, ed. M. Eggersdorfer, S. Warwel and G. Wulff, VCH, Weinheim, 1993, p. 69.
14 SYBYL version 6.3, TRIPOS Associates, St. Louis, MO 63144, USA.

*Received in Bloomington, IN, USA; 24th April 1997; 7/02811C*

# Phosphorus monoxide as a terminal ligand

**Marc J. A. Johnson, Aaron L. Odom and Christopher C. Cummins*†**

*Department of Chemistry, 2-227, Massachusetts Institute of Technology, 77 Massachusetts Avenue, Cambridge, MA 02139-4307, USA*

**Dimethyldioxirane oxidation of phosphide PMo[N(R)Ar]$_3$ [R = C(CD$_3$)$_2$Me, Ar = C$_6$H$_3$Me$_2$-3,5] efficiently provides (OP)Mo[N(R)Ar]$_3$, a complex shown by X-ray crystallography to contain a terminal phosphorus monoxide ligand, and which reacts with dimethylzirconocene to give addition of a Zr–Me bond across the phosphoryl moiety.**

Known phosphorus monoxide complexes[1–3] are those in which PO[4–10] serves as a triply bridging ligand. These have been prepared by oxo transfer to a $P_2Ni_2W$ cluster,[1] and by hydrolysis of a $\mu_3$-P(NPr$^i_2$) functional group.[3] Recent reports of terminal phosphide ($P^{3-}$) complexes[11–15] hint at the possibility of preparing terminal PO complexes by oxygen-atom transfer to the terminal P ligand. Accordingly, dimethyldioxirane oxidation[16,17] has been found to effect the desired conversion of PMo[N(R)Ar]$_3$ **1** to (OP)Mo[N(R)Ar]$_3$ **2**. Synthetic, structural, and initial reactivity data pertaining to **2** are detailed herein.

Treatment of a −78 °C gold-colored solution of **1** (1.0009 g, 1.4853 mmol) in dichloromethane (50 ml) with dimethyldioxirane (20 ml of a 0.075 M solution in acetone[18]) elicited a rapid color change to purple, the color of **2**.‡ Workup consisted of cold-filtration, precipitation of **2** by addition of acetonitrile (75 ml, pre-chilled to just above its melting point), and collection of solid **2** (73.8% yield) by filtration. Once thus obtained in pure form, solid **2** can be manipulated and maintained at 25 °C for at least *ca.* 5 days without noticeable decomposition. When dissolved in various solvents (*e.g.* benzene, diethyl ether, heptane and dichloromethane) **2** is more sensitive, undergoing gradual reversion to **1** according to $^1$H and $^{31}$P NMR spectroscopic monitoring.

Diamagnetic **2** exhibits a single $^{31}$P NMR signal at $\delta$ 269.8, shifted dramatically upfield relative to **1** but in a range typical of two-coordinate phosphorus compounds.[19] Proton NMR data for **2** are indicative of a single environment for the N(R)Ar ligands, consistent with the threefold (propellor) symmetry typical of complexes containing three N(R)Ar ligands.[20–25]

Single crystals of **2** suitable for an X-ray diffraction study§ were obtained by slow cooling to −35 °C of a diisopropyl ether solution. Molecular **2** evinces pseudo-threefold symmetry about the near-linear [177.6(8)°] Mo–P–O moiety, which is flanked by the three *tert*-butyl substituents (Fig. 1). An intriguing feature of the structure is the molybdenum–phosphorus distance *d*(MoP) = 2.079(5) Å, which is shorter by 0.04 Å than *d*(MoP) for terminal phosphide **1**.[11] Contraction of the molybdenum–phosphorus distance in this manner is explicable in terms of rehybridization at P upon addition of a terminal substituent.[26] The phosphorus–oxygen distance [1.49(2) Å] in **2** is comparable to that measured by IR diode laser spectroscopy for gaseous PO [1.476 370(15) Å)],[27,28] and to *d*(PO) values for $\mu_3$-PO complexes: 1.509(3),[3] 1.462(9) and 1.480(10).[1] Phosphoryl halide species such as $OPCl_3$ contrastingly exhibit longer phosphorus–oxygen distances, on the order of 1.54–1.58 Å,[29] while *d*(PO) for OP(C$_6$H$_{11}$)$_3$ is 1.490(2) Å.[30] Other metrical parameters pertaining to the structure of **2** are unexceptional.

Previously reported (SP)Mo[N(R)Ar]$_3$ **3**[11] was shown recently by X-ray crystallography to resemble **2** in terms of its monomeric nature and gross structural characteristics.[31] The rough similarity of **2** and **3** was used to advantage to obtain assignment of the $\nu_{PO}$ (1232 cm$^{-1}$) and $\nu_{PS}$ (782 cm$^{-1}$) IR stretching frequencies for the two complexes, by digital subtraction of solution FTIR spectra. The $\nu_{PO}$ value for **2** is similar to that reported for gaseous PO (1220.25 cm$^{-1}$), and also is comparable to values reported for $\mu_3$-PO complexes (1260, 1169 cm$^{-1}$).

Initial reactivity studies indicate that the phosphoryl phosphorus in **2** is susceptible to nucleophilic attack in a manner reminiscent of the Fischer carbene synthesis.[32] Accordingly, treatment of **2** (282.0 mg, 0.4088 mmol) with dimethylzirconocene[33] (103.3 mg, 0.4108 mmol) in benzene (7.5 ml) led to formation of [(R$^1$)(R$^2$O)P]Mo[N(R)Ar]$_3$ [**4**, R$^1$ = Me, R$^2$ = Zr(Me)($\eta$-C$_5$H$_5$)$_2$], which was isolated by crystallization

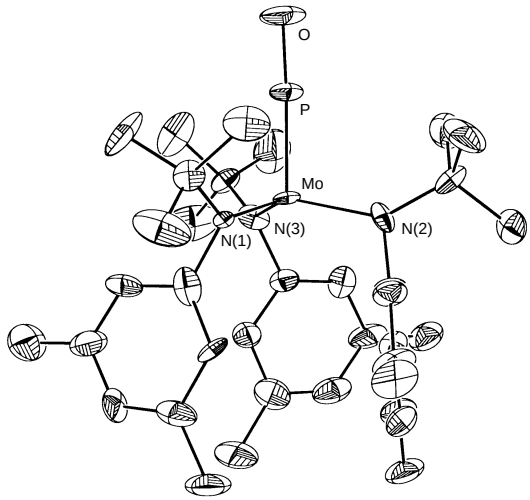
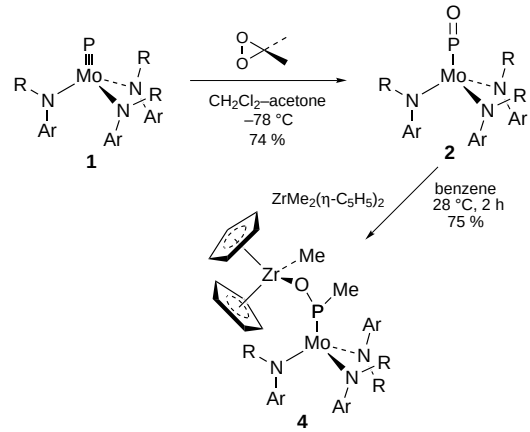



**Fig. 1** ORTEP drawing of the molecular structure of **2** with 35% probability ellipsoids. Selected bond lengths (Å) and angles (°): Mo–P 2.079(5), Mo–N(1) 1.95(2), Mo–N(2) 1.94(2), Mo–N(3) 1.994(13), P–O 1.49(2); Mo–P–O 177.6(8), P–Mo–N(1) 101.7(4), P–Mo–N(2) 101.4(5), P–Mo–N(3) 101.6(5), N(1)–Mo–N(2) 113.1(6), N(1)–Mo–N(3) 117.2(6), N(2)–Mo–N(3) 118.0(6).




**Scheme 1**

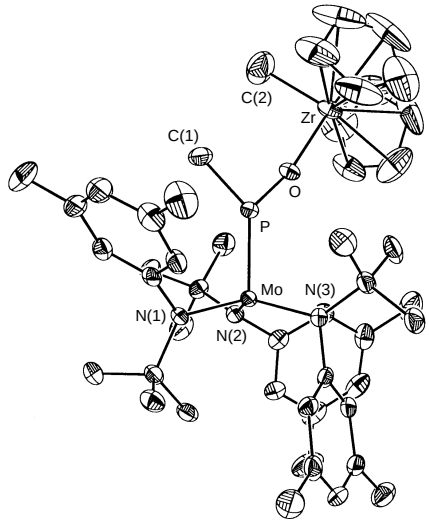



**Fig. 2** ORTEP drawing of the molecular structure of **4** with 35% probability ellipsoids. Selected bond lengths (Å) and angles (°): Mo–P 2.169(2), Mo–N(1) 1.995(5), Mo–N(2) 2.011(5), Mo–N(3) 1.993(5), P–O 1.613(5), P–C(1) 1.832(8), Zr–O 2.000(4), Zr–C(2) 2.253(11); Mo–P–O 127.7(2), Mo–P–C(1) 133.9(3), O–P–C(1) 97.6(3), Zr–O–P 163.6(3), O–Zr–C(2) 97.1(4), P–Mo–N(1) 101.6(2), P–Mo–N(2) 103.2(2), P–Mo–N(3) 101.7(2), N(1)–Mo–N(2) 109.1(2), N(1)–Mo–N(3) 112.6(2), N(2)–Mo–N(3) 125.0(2).

from a 1 : 1 diethyl ether–heptane mixture as orange–brown plates in 75.0% yield (Scheme 1). Diamagnetic **4** exhibits a single $^{31}$P NMR signal at $\delta$ 284.4 {*cf.* $\delta$ 312 for $Mo[P(C_6H_{11})_2]_4$[34]}. A reasonable oxidation state assignment for the Mo centre in **4** is +4. Proton NMR data for **4** are indicative of a single N(R)Ar ligand environment on the NMR timescale, although the solid-state structure of **4** reveals a low-symmetry conformation. A doublet ($^2J_{PH}$ 14 Hz) at $\delta$ 1.535 is attributed to the PMe moiety.

The three-coordinate phosphorus in **4** was shown by X-ray diffraction§ to be essentially planar [sum of angles = 359.2(3)°], consistent with Mo–P π bonding in the complex (Fig. 2). The observed *d*(MoP) of 2.169(2) Å is also consistent with a molybdenum–phosphorus multiple bond {*cf.* *d*(MoP) of 2.265(2) Å for $Mo[P(C_6H_{11})_2]_4$[34]}. The conformation of **4** is noteworthy in that one of the N(R)Ar ligands is oriented with its *tert*-butyl group distal from phosphorus, presenting an Ar π cloud to the methyl substituent on phosphorus. The Zr–O–P(Me)–Mo core in **4** is reminiscent of Zr–O–C(R′)–M cores in zirconoxy carbenes prepared by addition of Zr–R′ (R′ = H, alkyl) bonds across the CO unit in metal carbonyl complexes.[35]

We thank Monsanto Company for support of this work, and Michael K. Stern for helpful discussions. M. J. A. J. thanks NSERC for a predoctoral fellowship.

## Footnotes and References

* E-mail: ccummins@mit.edu

† Alfred P. Sloan Fellow, 1997–2000.

‡ All manipulations were carried out under an atmosphere of dry nitrogen using solvents purified by standard methods. The new compounds **2** and **4** gave satisfactory elemental analyses (C, H and N).

§ *Crystallographic data*: For **2**: triclinic, space group $P\bar{1}$, $a$ = 10.7615(8), $b$ = 11.4942(9), $c$ = 15.1899(11) Å, $\alpha$ = 89.865(2), $\beta$ = 80.838(2), $\gamma$ = 89.4900(10)°, $U$ = 1854.9(2) Å$^3$, $Z$ = 2, 2988 unique reflections, data/parameter ratio = 7.9, $R_1$ = 0.1207, $wR_2$ = 0.2683, GOF 1.050, residuals based on $I > 2\sigma(I)$.

For **4**: orthorhombic, space group *Pbca*, $a$ = 11.3996(2), $b$ = 23.2075(4), $c$ = 39.2443(7) Å, $U$ = 10382.3(3) Å$^3$, $Z$ = 8, 7456 unique reflections, data/parameter ratio 15, $R_1$ = 0.0669, $wR_2$ = 0.2023, GOF = 1.269, residuals based on $I > 2\sigma(I)$. CCDC 182/527.

1 O. J. Scherer, J. Braun, P. Walther, G. Heckmann and G. Wolmershäuser, *Angew. Chem., Int. Ed. Engl.*, 1991, **30**, 852.
2 W. A. Herrmann, *Angew. Chem., Int. Ed. Engl.*, 1991, **30**, 818.
3 J. F. Corrigan, S. Doherty, N. J. Taylor and A. J. Carty, *J. Am. Chem. Soc.*, 1994, **116**, 9799.
4 R. M. Atalla and P. D. Singh, *Astrophys. Space Sci.*, 1987, **133**, 267.
5 G. A. Blake, E. C. Sutton, C. R. Masson and T. G. Phillips, *Astrophys. J.*, 1987, **315**, 621.
6 H. E. Matthews, P. A. Feldman and P. F. Bernath, *Astrophys. J.*, 1987, **312**, 358.
7 Z. Mielke, M. McCluskey and L. Andrews, *Chem. Phys. Lett.*, 1990, **165**, 146.
8 H.-B. Qian, P. B. Davies and P. A. Hamilton, *J. Chem. Soc., Faraday Trans.*, 1995, **91**, 2993.
9 L. R. Thorne, V. G. Anicich, S. S. Prasad and W. T. Huntress Jr., *Astrophys. J.*, 1984, **280**, 139.
10 R. J. Vanzee and A. U. Khan, *Chem. Phys. Lett.*, 1975, **36**, 123.
11 C. E. Laplaza, W. M. Davis and C. C. Cummins, *Angew. Chem., Int. Ed. Engl.*, 1995, **34**, 2042.
12 N. C. Zanetti, R. R. Schrock and W. M. Davis, *Angew. Chem., Int. Ed. Engl.*, 1995, **34**, 2044.
13 G. Wu, D. Rovnyak, M. J. A. Johnson, N. C. Zanetti, D. G. Musaev, K. Morokuma, R. R. Schrock, R. G. Griffin and C. C. Cummins, *J. Am. Chem. Soc.*, 1996, **118**, 10 654.
14 M. Scheer, *Angew. Chem., Int. Ed. Engl.*, 1995, **34**, 1997.
15 M. Scheer, J. Müller and M. Häser, *Angew. Chem., Int. Ed. Engl.*, 1996, **35**, 2492.
16 R. W. Murray, *Chem. Rev.*, 1989, **89**, 1187.
17 W. Adam, R. Curci and J. O. Edwards, *Acc. Chem. Res.*, 1989, **22**, 205.
18 W. Adam, J. Bialas and L. Hadjiarapoglou, *Chem. Ber.*, 1991, **124**, 2377.
19 M. Regitz and O. J. Scherer, *Multiple Bonds and Low Coordination in Phosphorus Chemistry*, Georg Thieme Verlag, Stuttgart, 1990.
20 A. R. Johnson, P. W. Wanandi, C. C. Cummins and W. M. Davis, *Organometallics*, 1994, **13**, 2907.
21 M. J. A. Johnson, P. M. Lee, A. L. Odom, W. M. Davis and C. C. Cummins, *Angew. Chem., Int. Ed. Engl.*, 1997, **36**, 87.
22 C. E. Laplaza, W. M. Davis and C. C. Cummins, *Organometallics*, 1995, **14**, 577.
23 C. E. Laplaza, A. L. Odom, W. M. Davis, C. C. Cummins and J. D. Protasiewicz, *J. Am. Chem. Soc.*, 1995, **117**, 4999.
24 C. E. Laplaza, M. J. A. Johnson, J. C. Peters, A. L. Odom, E. Kim, C. C. Cummins, G. N. George and I. J. Pickering, *J. Am. Chem. Soc.*, 1996, **118**, 8623.
25 J. C. Peters, A. R. Johnson, A. L. Odom, P. W. Wanandi, W. M. Davis and C. C. Cummins, *J. Am. Chem. Soc.*, 1996, **118**, 10 175.
26 W. Kutzelnigg, *Angew. Chem., Int. Ed. Engl.*, 1984, **23**, 272.
27 J. E. Butler, K. Kawaguchi and E. Hirota, *J. Mol. Spectrosc.*, 1983, **101**, 161.
28 H.-B. Qian, *J. Mol. Spectrosc.*, 1995, **174**, 599.
29 N. N. Greenwood and A. Earnshaw, *Chemistry of the Elements*, Pergamon, Oxford, 1984.
30 J. A. Davies, S. Dutremez and A. A. Pinkerton, *Inorg. Chem.*, 1991, **30**, 2380.
31 M. J. A. Johnson, A. L. Odom and C. C. Cummins, manuscript in preparation.
32 E. O. Fischer, in *Nobel Lectures in Chemistry*, ed. T. Frängsmyr, World Scientific, Singapore, 1993, p. 105.
33 E. Samuel and M. D. Rausch, *J. Am. Chem. Soc.*, 1973, **95**, 6263.
34 R. T. Baker, P. J. Krusic, T. H. Tulip, J. C. Calabrese and S. S. Wreford, *J. Am. Chem. Soc.*, 1983, **105**, 6763.
35 P. T. Wolczanski and J. E. Bercaw, *Acc. Chem. Res.*, 1980, **13**, 121.

*Received in Bloomington, IN, USA, 7th May 1997; 7/03105J*

# Template synthesis and X-ray crystal structure of a trinuclear complex with four- and five-coordinate silver(I) centres

**Wai-Kwok Wong,*[a] Lilu Zhang,[a] Feng Xue[b] and Thomas C. W. Mak[b]**

[a] *Department of Chemistry,Hong Kong Baptist University, Kowloon, Hong Kong*
[b] *Department of Chemistry, The Chinese University of Hong Kong, Shatin, N.T., Hong Kong*

**Single-crystal X-ray analysis of the trinuclear complex $[Ag_3L_2][CF_3SO_3]_3$ [L = {(*o*-$Ph_2C_6H_4$)CH = $NCH_2CH_2$}$_3$N], synthesized by interaction of $Ag(CF_3SO_3)$, $N(CH_2CH_2NH_2)_3$ and *o*-$Ph_2PC_6H_4$(CHO) in 3 : 2 : 6 molar ratio in ethanol, shows that the complex has approximate $C_2$ symmetry and is composed of a four- and two five-coordinate silver(I) centres.**

We have been interested in the preparation of diimino-, diamino- and diamido-diphosphine ligands and demonstrated that these ligands do indeed exhibit a very rich coordination chemistry.[1,2] We have extended our study to the preparation of polydentate ligands containing three or more iminophosphino groups. Herein we report the template synthesis of the heptadentate ligand {(*o*-$Ph_2PC_6H_4$)CH=$NCH_2CH_2$}$_3$N and the structure of its silver(I) complex.

Attempts to synthesize the heptadentate ligand {(*o*-$Ph_2PC_6H_4$)CH=$NCH_2CH_2$}$_3$N *via* direct condensation of $N(CH_2CH_2NH_2)_3$ with 3 equiv. of *o*-$Ph_2PC_6H_4$(CHO) were unsuccessful. However, when $Ag(CF_3SO_3)$, $N(CH_2CH_2NH_2)_3$ and *o*-$Ph_2PC_6H_4$(CHO) were allowed to react in 3 : 2 : 6 molar ratio in ethanol for 12 h at room temp., work-up gave the trinuclear silver complex $[Ag_3L_2][CF_3SO_3]_3$ **1**,† [L = {(*o*-$Ph_2PC_6H_4$)CH=$NCH_2CH_2$}$_3$N], as yellow crystals in moderate yield. Crystals of **1**·2EtOH·2$CH_2Cl_2$·$H_2O$ suitable for X-ray diffraction study‡ were grown from dichloromethane-diethyl ether–ethanol. A perspective drawing of the cation $[Ag_3L_2]^{3+}$ of **1** is shown in Fig. 1 with selected bond lengths and bond angles given in the caption. The structure analysis reveals that the trinuclear complex has approximately $C_2$ symmetry and is composed of a four- and two five-coordinated silver(I) centres. The two five-coordinate silver centres [Ag(1), Ag(3)] adopt a distorted trigonal-bipyramidal geometry with the equatorial positions occupied by two phosphino [P(1), P(2) for Ag(1); P(5), P(6) for Ag(3)] and an amino [N(1) for Ag(1), N(5) for Ag(3)] groups, and the axial positions by two imino [N(2), N(3) for Ag(1); N(7), N(8) for Ag(3)] groups of the heptadentate ligand L. Their equatorial bond angles [114.8(3), 118.8(3), 126.2(1)° summing to *ca*. 360° for Ag(1); 114.8(3), 118.7(3), 126.2(1)° summing to *ca*. 360° for Ag(3)] and axial bond angle [139.5(3)° for Ag(1); 140.2(3)° for Ag(3)] are almost identical. The Ag–P distances [Ag(1)–P(1) 2.430(5), Ag(1)–P(2) 2.429(4), Ag(3)–P(5) 2.429(5), Ag(3)–P(6) 2.440(4) Å] are normal and comparable to those of analogous silver diimino- and diamino-diphosphine complexes.[2] The Ag–amino distances [Ag(1)–N(1) 2.456(9), Ag(3)–N(5) 2.479(8) Å] are comparable to the long Ag–N distance [2.411(4) Å] in [Ag{P($C_6H_4$Me-*p*)$_3$}{$BPh_2$(pz)$_2$}] (pz = pyrazolyl).[3] The Ag–imino distances [Ag(1)–N(2) 2.580(8), Ag(1)–N(3) 2.608(9), Ag(3)–N(7) 2.661(9), Ag(3)–N(8) 2.654(7) Å] are significantly longer and comparable to the Ag–N distance [2.56(1) Å] in [Ag(Binap-$P_2N_2$)][$BF_4$] (Binap = binaphthylene).[2] The tetra-coordinated silver atom [Ag(2)] adopts a distorted tetrahedral geometry by coordinating to the two heptadentate ligands *via* pairs of imino [N(4), N(6)] and phosphino [P(3), P(4)] groups. The Ag–P distances [Ag(2)–P(3) 2.370(5); Ag(2)–P(4) 2.366(4) Å] are normal. The Ag–imino distances [Ag(2)–N(4) 2.604(9), Ag(2)–N(6), 2.643(8) Å] are comparable to those of Ag(1). The P(3)–Ag(2)–P(4) and N(4)–Ag(2)–N(6) angles are 164.8(1) and 83.1(3)°, respectively. The observed structural feature shows that the imino groups only interact weakly with the silver centres.

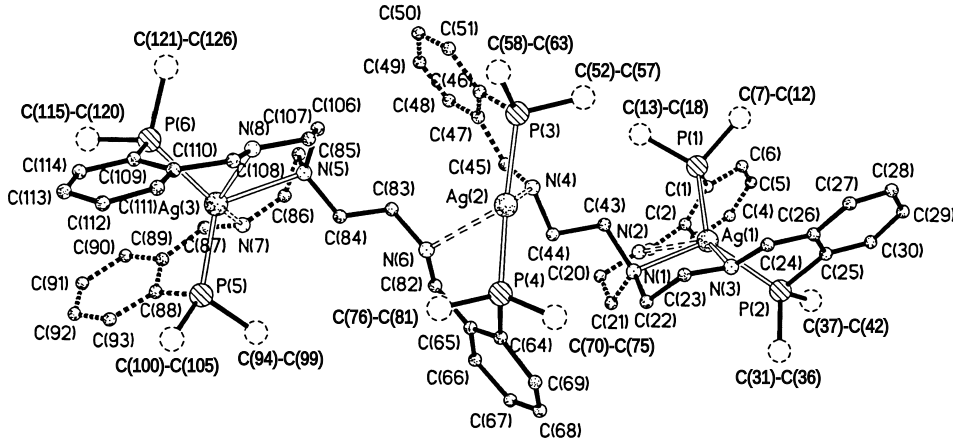
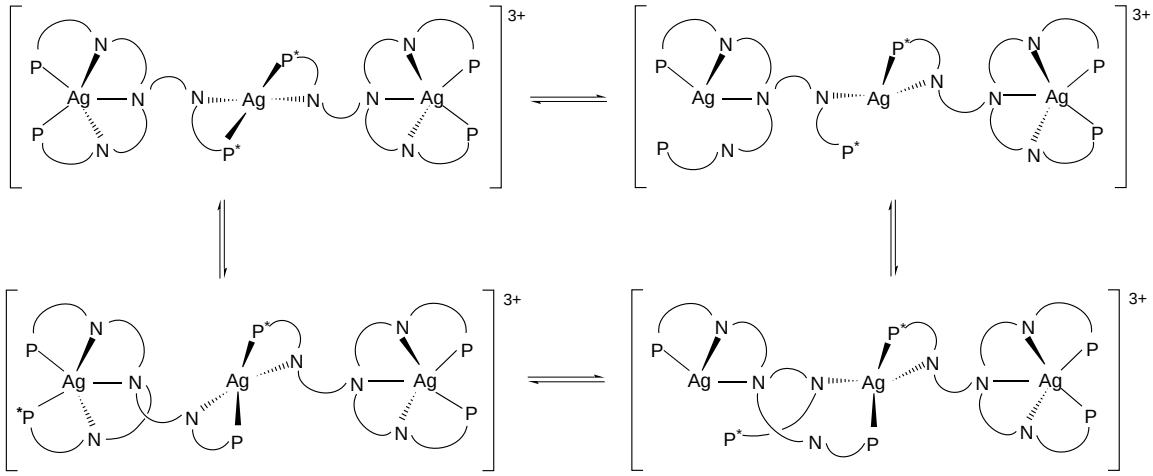



**Fig. 1** A perspective drawing of the trinuclear cation $[Ag_3L_2]^{3+}$ of compound **1**. For clarity, the hydrogen atoms are omitted and the phenyl rings of the $PPh_2$ groups are each represented by a circle with broken outline. Selected bond lengths (Å) and angles (°): Ag(1)–P(1) 2.432(5), Ag(1)–P(2) 2.435(4), Ag(1)–N(1) 2.443(9), Ag(1)–N(2) 2.580(8) , Ag(1)–N(3) 2.608(9), Ag(2)–P(3) 2.370(5), Ag(2)–P(4) 2.366(4), Ag(2)–N(4) 2.604(9), Ag(2)–N(6) 2.643(8), Ag(3)–P(5) 2.429(5), Ag(3)–P(6) 2.440(4), Ag(3)–N(5) 2.479(8), Ag(3)–N(7) 2.661(9), Ag(3)–N(8) 2.654(7), N(2)–C(19) 1.181(14), N(3)–C(24) 1.219(16), N(4)–C(45) 1.221(13), N(6)–C(82) 1.288(17), N(7)–C987) 1.294(11), N(8)–C(108) 1.154(15); P(1)–Ag(1)–P(2) 126.2(1), P(1)–Ag(1)–N(1) 114.8(3), P(2)–Ag(1)–N(1) 118.8(3), N(2)–Ag(1)–N(3) 139.5(3), P(3)–Ag(2)–P(4) 164.8(1), P(3)–Ag(2)–N(4) 73.1(3), P(3)–Ag(2)–N(6) 119.2(3), P(4)–Ag(2)–N(4) 120.1(3), P(4)–Ag(2)–N(6) 72.4(3), N(4)–Ag(2)–N(6) 83.1(3), P(5)–Ag(3)–P(6) 126.2(1), P(5)–Ag(3)–N(5) 114.8(3), P(6)–Ag(3)–N(5) 118.7(3), N(7)–Ag(3)–N(8) 140.2(3).



**Scheme 1** Proposed mechanism for the dynamic behaviour of the cation $[Ag_3L]^{3+}$

Complex **1** exhibited temperature-dependent $^{31}P\{^1H\}$ NMR spectra. At room temp. in $CD_2Cl_2$, two broad peaks centred at $\delta$ 6.5 and 10.6 appeared, which at −80 °C broadened into complex multiplets in the range $\delta$ 3.0–14.0, indicating non-equivalence of all phosphorus atoms. On the other hand, in $[^2H_7]$DMF at 120 °C the two broad peaks centred at $\delta$ 6.9 and 10.4 at 25 °C coalesced into a sharp singlet at $\delta$ 7.4, indicating that all the phosphorus atoms were equivalent. The variable-temperature $^{31}P\{^1H\}$ NMR study shows that the phosphino groups undergo facile intramolecular exchange. The observed solution dynamic behaviour can be explained by the proposed mechanism in Scheme 1 which shows that both the imino and the phosphino groups undergo rapid dissociation and association with the metal centres. The free heptadentate ligand $\{(o\text{-}Ph_2PC_6H_4)CH{=}NCH_2CH_2\}_3N$ can be liberated from **1** quantitatively by reacting **1** with an excess of KCN.

Thanks are due to the Hong Kong Baptist University and the Hong Kong Research Grants Council (HKBU 131/94P and CUHK 311/94P) for financial support.

## Footnotes and References

* E-mail: wkwong@sci.hkbu.edu.hk

† Crystals of **1** were obtained by the interaction of $Ag(CF_3SO_3)$, $N(CH_2CH_2NH_2)_3$ and $o\text{-}Ph_2PC_6H_4(CHO)$ in 3 : 2 : 6 molar ratio in ethanol for 12 h at room temp. Recrystallization in dichloromethane gave yellow crystals, yield: 0.21 g, 55%, mp 240–242 °C (decomp.) (Found: C, 54.7; H, 4.1; N, 3.9. Calc. for $C_{135}H_{132}Ag_3Cl_4F_9N_8O_{12}P_6S_3$: C, 54.5; H, 4.4; N, 3.8%.) IR ($cm^{-1}$, in KBr): 3063w, 2841w, 1708w, 1647s, 1560w, 1480w, 1435s, 1263vs, 1223s, 1150s, 1098m, 1086w, 1030vs, 911w, 747s, 696s, 637vs, 575w, 505s. NMR ($CD_2Cl_2$): $^{31}P\{^1H\}$, $\delta$ 8.2 (br, m) and 10.2 (br, m); $^{19}F\{^1H\}$, $\delta$ −78.5 (s); $^1H$, *H*C=N protons, $\delta$ 8.53 (4H, br, s) and 8.60 (2H, br, *s*); phenyl protons, 6.85–7.69 (84H, br, m); $NCH_2CH_2N$ protons, 2.65 (12H, m) and 3.55 (12H, m).

‡ *Crystal data* for **1**·$2C_2H_5OH$·$2CH_2Cl_2$·$H_2O$: $C_{135}H_{132}Ag_3Cl_4F_9N_8O_{12}P_6S_3$, $M$ = 2976.9, triclinic, space group $P\bar{1}$ (no. 2), $a$ = 13.900(2), $b$ = 22.495(2), $c$ = 25.202(2) Å, $\alpha$ = 112.54(2), $\beta$ = 93.04(2), $\gamma$ = 94.46(2)°, $U$ = 7226.8(14) Å$^3$, $Z$ = 2, $D_c$ = 1.368 g $cm^{-3}$, $F$(000) = 3044, 294 K, Mo-K$\alpha$ radiation, $\lambda$ = 0.71073 Å, $\mu$(Mo-K$\alpha$) = 6.56 $cm^{-1}$, yellow plate 0.10×0.30×0.40 mm, 15731 unique data measured on a MSC/Rigaku RAXIS IIC imaging plate system with a rotating anode (50 kV, 90 mA, 46 3° oscillation frames in the range 0–138°, exposure 10 min per frame),[4] absorption correction using the ABSCOR program,[5] 8731 observed reflections [$F > 6\sigma(F)$]. The structure was solved by direct methods and refined by full matrix least-squares analysis to give $R$ = 0.088, $R_w$ = 0.123. The solvate molecules and the anions exhibit positional disorder and the atoms were each assigned an occupancy factor of 0.5. All non-hydrogen atoms including disordered atoms were refined anisotropically. The total number of refined parameters is 1611. Hydrogen atoms were generated in their idealized positions (C–H bond fixed at 0.96 Å) and allowed to ride on their respective parent carbon atoms. These hydrogen atoms were assigned appropriate isotropic thermal parameters and included in structure-factor calculations but not in the refinement. Computations were performed using the SHELTXL-PLUS (PC version) program package.[6] CCDC 182/496.

1 W. K. Wong, J.-X. Gao, Z.-Y. Zhou and T. C. W. Mak, *Polyhedron*, 1992, **11**, 2965; W. K. Wong, J.-X. Gao and W. T. Wong, *Polyhedron*, 1993, **12**, 1647; W. K. Wong, J.-X. Gao, Z.-Y. Zhou and T. C. W. Mak, *Polyhedron*, 1993, **12**, 1415; J.-X. Gao, H.-L. Wan, W. K. Wong, M. C. Tse and W. T. Wong, *Polyhedron*, 1996, **15**, 1241.

2 W. K. Wong, J.-X. Gao, W. T. Wong, W. C. Cheng and C. M. Che, *J. Organomet. Chem*., 1994, **471**, 277; W. K. Wong, T. W. Chik, K. N. Hui, I. Williams, X. Feng, T. C. W. Mak and C. M. Che, *Polyhedron*, 1996, **15**, 4447.

3 M. I. Bruce, J. D. Walsh, B. W. Skelton and A. H. White, *J. Chem. Soc., Dalton Trans.*, 1981, 956.

4 J. Tanner and K. Krause, *Rigaku J*, 1994, **11**, 4; 1990, **7**, 28; K. L. Krause and G. N. Phillips, Jr., *J. Appl. Crystallogr.*, 1992, **25**, 146; M. Sato, M. Yamamoto, K. Imada, Y. Katsube, N. Tanaka and T. Higashi, *J. Appl. Crystallogr.*, 1992, **25**, 348.

5 T. Higashi, *ABSCOR - An Empirical Absorption Correction Based on Fourier Coefficient Fitting*, Rigaku Corporation, Tokyo, 1995.

6 G. M. Sheldrick, *SHELXL PC Manual*, Siemens Analytical X-Ray Instruments, Inc., Madison, Wisconsin, 1990; *Computational Crystallography*, ed. D. Sayre, Oxford University Press, New York, 1982, p. 506; *Crystallographic Computing 3: Data Collection, Structure Determination, Proteins, and Databases* ed. G. M. Sheldrick, C. Kruger and R. Goddard, Oxford University Press, New York, 1985, p. 175.

*Received in Cambridge, UK, 22nd April 1997; 7/02749D*

# A simple procedure for the separation of the catalytically important phosphabicyclononane isomers

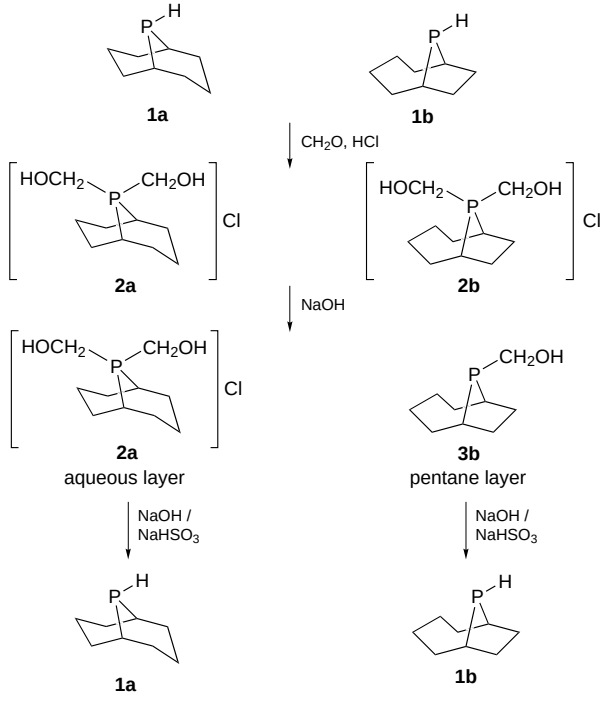
**Joanne H. Downing, Victoria Gee and Paul G. Pringle***

*School of Chemistry, University of Bristol, Cantocks Close, Bristol, UK BS8 1TS*

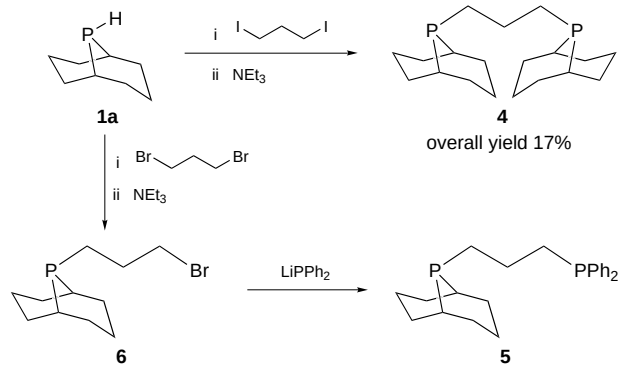
**The isomeric [3.3.1]- and [4.2.1]-phosphabicyclononanes are readily separated by a sequence of hydrophosphination/dehydrophosphination steps; new diphosphine ligands derived from the [3.3.1] isomer are described.**

Phosphine ($PH_3$) adds to cycloocta-1,5-diene to give a mixture of the bicyclic secondary phosphines **1a** and **1b**, sometimes referred to as 'phobane'.[1,2] Tertiary phosphines made from this mixture are ligands for the cobalt-catalysed hydroformylation process[3] currently carried out on a large scale industrially.[4] Recently derivatives of **1a** and **1b** have attracted attention as ligands for hydroformylation,[5] carbonylation,[6] and asymmetric catalysis.[2,7] To date there have been no reports of the separation of the isomers **1a** and **1b** although, by exploiting the difference in reactivity between the isomers, ligands derived from the symmetrical isomer **1a** have been isolated.[2,8] Here we report an easy method for separating **1a** and **1b** and the use of pure **1a** in further ligand synthesis.

The reactions which form the basis for the separation are summarised in Scheme 1. The crystalline, air-stable phosphonium salts **2a** and **2b** are readily made from the mixture of **1a** and **1b** with $CH_2O$ in the presence of HCl. Loss of $CH_2O$ from **2a**/**b** is promoted by NaOH but we have found that one hydroxymethyl group in **2b** is much more reactive than any of the others. Thus an aqueous solution of a **2a**/**b** mixture reacted selectively with NaOH to give neutral phosphine **3b** which was then extracted into pentane to leave pure **2a** in the aqueous layer. The crystal structure of the complex *cis*-[$PtCl_2$(**3b**)$_2$] suggests that it is the hydroxymethyl group lying over the seven-membered ring that is the reactive one.[8]




**Scheme 1**




**Scheme 2** (Overall yield 50%)

Treatment of an aqueous solution of **2a** with NaOH and $NaHSO_3$ (to trap the generated $CH_2O$) gave the symmetrical secondary phosphine **1a** which was then extracted into pentane. Similarly the unsymmetrical isomer **1b** was made by treatment of a pentane solution of **3b** with aqueous NaOH and $NaHSO_3$. The separation can be carried out efficiently on a multigram scale† and both **1a** and **1b** have been isolated and fully characterised.‡

Access to **1a** has allowed us to synthesise the diphosphine derivatives **4** and **5** by the routes shown in Scheme 2; the modest overall yields reported reflect the small scale (0.1–1 g) of these preliminary reactions. Treatment of **1a** with $I(CH_2)_3I$ followed by $NEt_3$ gave **4**[5] exclusively in contrast to the mixture of isomers formed when $H_2P(CH_2)_3PH_2$ adds to cycloocta-1,5-diene. Treatment of **1a** with $Br(CH_2)_3Br$ gave the intermediate **6** which reacts with $LiPPh_2$ to give the unsymmetrical diphosphine **5**. The application of these new ligands in coordination chemistry and catalysis is in progress.

We thank EPSRC and Albright and Wilson for supporting this work.

## Footnotes and References

* E-mail: paul.pringle@bristol.ac.uk

† The separation of **1a** and **1b** was carried out as follows (under nitrogen except where specified). To a stirred solution of a crude mixture of **1a** and **1b** supplied by Albright and Wilson Ltd (77 g, *ca*. 60% **1a**/**b** by $^{31}$P NMR with the ratio of **1a** to **1b** of *ca*. 1.1 : 1) in aqueous $CH_2O$ (95 cm$^3$, 35% m/m, 1.20 mol) was added aqueous HCl (120 cm$^3$, 5 M, 0.60 mol) dropwise over 30 min. After 1 h, the volatiles were removed on a rotary evaporator in air to give a viscous white oil. In air, trituration with propan-2-ol (400 cm$^3$) gave a white solid which was filtered off, washed with cold propan-2-ol (50 cm$^3$) and diethyl ether (50 cm$^3$); the yield of salts **2a** and **2b** was 56 g which represents *ca*. 72% yield. The solid was dissolved in hot (*ca*. 60 °C) water (*ca*. 20 cm$^3$) and then when the solution had cooled to *ca*. 40 °C, acetone was added until the solution turned cloudy (*ca*. 50 cm$^3$). Then the mixture was refrigerated (0 °C) for 16 h to give crystalline **2a**/**b** in > 80% recovery. To a rapidly stirred solution of **2a**/**b** (8.5 g, 36 mmol) in water (20 cm$^3$) with a layer of pentane (35 cm$^3$), was added aqueous NaOH (16 cm$^3$, 1 M, 16 mmol) dropwise by syringe over 5 min. After a further 10 min, the pentane layer was separated and the aqueous layer washed with pentane (2 × 10

cm$^3$). To the aqueous layer, more aqueous NaOH (1 M, 1 cm$^3$) was added (to remove the final traces of **2b**) and then in a separating funnel (in air), the aqueous layer was washed with pentane (2 × 30 cm$^3$) and then separated. The aqueous layer was then deaerated, pentane (50 cm$^3$) was added, then aqueous NaOH (37.6 cm$^3$, 1 M, 37.6 mmol) added dropwise over 5 min and finally solid $NaHSO_3$ (7.8 g, 75 mmol) was added and the mixture stirred for 1 h. Then the pentane layer was separated and the aqueous layer washed with pentane (2 × 20 cm$^3$). The pentane extracts were combined, dried over $MgSO_4$, filtered and then evaporated to dryness to give a white solid **1a** (2.32 g, 87%) which was 99.5% pure **1a** (by $^{31}$P NMR).

In a separate experiment a pentane solution (*ca.* 30 cm$^3$) of **3b** (obtained as described above but from 1.78 g of **2a**/**b**, 7.5 mmol) was treated with water (20 cm$^3$) and NaOH (3.25 cm$^3$, 1 M, 3.25 mmol) followed by solid $NaHSO_3$ (3.44 g, 33 mmol) and the mixture rapidly stirred for 44 h. Then the pentane layer was separated and the aqueous layer washed with pentane (3 × 10 cm$^3$). The pentane extracts were combined, dried over $MgSO_4$, filtered and then evaporated to dryness to give a white solid **1b** (0.26 g, 55%) which was 99% pure **1b** (by $^{31}$P NMR).

‡ *Selected spectroscopic data*. **1a**: $^{31}$P NMR ($CDCl_3$, 162 MHz) $\delta$ −54.1 [$^1J$(PH) 192.1 Hz]; $^1$H ($CDCl_3$, 400 MHz) $\delta$ 3.20 [d, 1 H, $^1J$(PH) 192.1 Hz], 1.55–2.55 (br m, 14 H); $^{13}$C ($CDCl_3$, 100 MHz) $\delta$ 33.9 [d, $J$(PC) 6.1 Hz], 30.0 [d, $J$(PC) 9.2 Hz], 22.6 (s), 22.4 [d, $J$(PC) 42.7 Hz], 22.1 (s); mass spectrum (EI) $m/z$ 142 ($M^+$). **1b**: $^{31}$P NMR ($CDCl_3$, 162 MHz) $\delta$ −48.4 [$^1J$(PH) 188.1 Hz]; $^1$H ($CDCl_3$, 400 MHz) $\delta$ 2.70 [d, 1H, $^1J$(PH) 188.0 Hz], 2.59 (br s, 2 H), 2.06 (m, 2 H), 1.35–1.82 (m, 10 H). $^{13}$C ($CDCl_3$, 100 MHz) $\delta$ 37.1 [d, $J$(PC) 7.6 Hz], 35.5 [d, $J$(PC) 7.6 Hz], 35.3 [d, $J$(PC) 15.3 Hz], 25.8 [d, $J$(PC) 7.6 Hz]; mass spectrum (EI) $m/z$ 142 ($M^+$). $^{31}$P NMR data (162 MHz): **2a** ($D_2O$) $\delta$ +23.1; **2b** ($D_2O$) $\delta$ 55.4; **3a** ($CDCl_3$) $\delta$ −31.7; **3b** ($CDCl_3$) $\delta$ 4.3; **4** ($C_6D_6$) $\delta$ −37.6; **5** ($C_6D_6$) $\delta$ −38.1 (s, $PC_8H_{14}$), −17.2 (s, $PPh_2$); **6** ($C_6D_6$) $\delta$ −37.8.


1 R. F. Mason and J. L. Van Winkle, *US Pat*., 3 400 163, 1968, to Shell Oil Co.
2 H. C. L. Abbenhuis, U. Burckhardt, V. Gramlich, C. Köllner, P. S. Pregosin, R. Salzmann and A. Togni, *Organometallics*, 1995, **14**, 759.
3 Shell International Research, *Chem. Abstr*., 1967, **66**, 65101r; *Neth. Pat*., 6 604 094, 1966; Mitsubishi Petrochemical Co. Ltd., *Chem. Abstr*., 1981, **95**, 186 627z; *Jpn. Kokai Tokkyo Koho*, JP 80 113 731, 1980.
4 K. Weisselmel and H-J. Arpe, *Industrial Organic Chemistry*, VCH, New York, 1993.
5 E. Drent, D. H. L. Pello, J. C. L. J. Suykerbuyk and J. Van Gogh, *World Pat*., 5354, 1995, to Shell International Research.
6 R. P. Tooze, *World Pat*., 15 938, 1995, to ICI; S. T. Howard, J. P. Foreman and P. G. Edwards, *Inorg. Chem*., 1996, **35**, 5805.
7 H. C. L. Abbenhuis, U. Burckhardt, V. Gramlich, A. Martelletti, J. Spencer, I. Steiner and A. Togni, *Organometallics*, 1996, **15**, 1614; H. C. L. Abbenhuis, U. Burckhardt, V. Gramlich, A. Togni, A. Albinati and B. Müller, *Organometallics*, 1994, **13**, 4481.
8 J. Fawcett, P. A. T. Hoye, R. D. W. Kemmitt, D. J. Law and D. R. Russell, *J. Chem. Soc., Dalton Trans*., 1993, 2563.
9 J. H. Downing, PhD thesis, University of Bristol, 1992.



*Received in Cambridge, UK, 9th May 1997; 7/03204H*

# A novel acridone derivative for the fluorescence tagging and mass spectrometric sequencing of peptides

**Thomas Faller,[a] Kathryn Hutton,[b] George Okafo,[a] Andy Gribble,[a] Patrick Camilleri*[a] and David E. Games[b]**

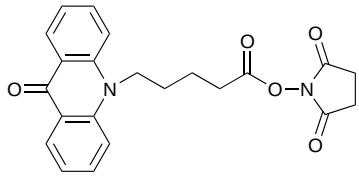
[a] *SmithKline Beecham Pharmaceuticals, New Frontiers Science Park, Third Avenue, Harlow, Essex, UK CM19 5AW*
[b] *University of Wales, Swansea, Singleton Park, Swansea, Wales, UK SA2 8PP*

**An acridone derivative containing an activated carboxylic group is highly reactive towards primary amine groups, and allows selective analysis either using absorbance at a wavelength of 410 nm or fluorescence at excitation and emission wavelengths of 400 and 418 nm, respectively; MS–MS analysis of peptides tagged with this reagent gives fragmentation patterns which are usually considerably more intense than background.**

Peptides tagged with a fluorescent label offer a major advantage in that they can be selectively analysed or localised even in complex biological fluids. Such derivatives have proved to be especially useful in bio- and immuno-assays. Fluorescent labels have included fluorescein, methylanthranylate, a number of cyanine dyes and succinimidyl pyrene-1-butyrate.[1–4]. These molecules can have disadvantages, such as sensitivity to light and fluorescence quenching in acidic or basic conditions. Moreover, the cyanine dyes are bulky molecules (molecular weight *ca*. 1000) which carry three to five charges at neutral pH; such properties can interfere with biological activity.

The acridone moiety is highly fluorescent and is stable to light, heat and oxidation. In earlier studies we have used 2-aminoacridone extensively in the reductive amination of monosaccharides and a variety of complex oligosaccharides.[5,6] A general and highly sensitive assay for antibody catalysis has also been demonstrated recently by using a number of acridone labelled compounds.[7]

We have now synthesised the succinimide ester **1** in three



**1**

$F^{1}VNQHLC(SO_3H)GSH^{10}LVEALYLVC(SO_3H)G^{20}ERGFFYTPKA^{30}$

**2**

steps from relatively inexpensive starting materials. Acridone was reacted with methyl 5-bromopentanoate to give methyl 9,10-dihydro-9-oxoacridine-10-pentanoate **3** (31%). Ester **3** was then hydrolysed with 10% aqueous NaOH to give the corresponding pentanoic acid **4** in (80%). Finally, to a solution of **4** and *N*-hydroxysuccinamide was added DCC to give **1** (34%) as a yellow solid (mp 181–182 °C). None of the yields mentioned have been optimised.

Compound **1** absorbs visible light at 410 nm and fluoresces intensely at excitation and emission wavelengths of 400 and 418 nm, respectively. It is neutral over the widest possible pH range and reacts rapidly with primary amines and, to a lesser extent, with phenolic hydroxy groups. To show the diversity in the use of **1** in the labelling and tracking of peptides, we have derivatised insulin chain B (oxidised) **2**, and carried out MS and enzymic digestion studies on material tagged in one or more positions. About 5 nmol of **2** were used in these experiments in 20 μl of solution. In separate experiments we have shown that a 20–50 pmol level of protein could be derivatised especially by performing the derivatisation reaction in volumes as low as 2 μl of solution. We used higher amounts for this study as it was necessary to collect derivatives of **2** for the tryptic digestion experiments which we describe later.

The extent of labelling by **1** can be controlled by its molar ratio to the peptide to be derivatised. Reactions were carried out by mixing the peptide in 10 μl of $NaHCO_3$ buffer (pH 8.5) with a solution (10 μl) of **1** in MeCN. The resulting mixture was left at room temperature for 1 h prior to analysis. For single labelling a 1:1 molar ratio is used, whereas multiple labelling is obtained in the presence of 10 molar excess of **1**. From the preliminary studies carried out on a number of peptides it appears that the ε-amino group in lysine is the first to be derivatised, followed by the amino group at the N-terminal end of the peptide and tyrosine residues. Multiple labelled peptides are easily separated and isolated by HPLC, using a reversed-phase C18 column and a mobile phase consisting of a gradient of 0.1% TFA in water and 0.1% TFA in MeCN.

Derivatisation of **2** with excess **1** yields four major products, one of which is single-tagged and the remainder of which are double tagged. We carried out LC–MS–MS analysis of triply charged parent ions using a Finnigan MAT LCQ ion trap mass spectrometer. Fig. 1 shows the total ion current for all product ions from an MS–MS experiment after derivatisation of **2** using excess **1**. Electrospray mass spectrometric and MS–MS analysis showed that peak 1 was related to **2** containing a single acridone moiety at the lysine residue in position 29. As expected this molecule elutes first as it is less hydrophobic than the double-labelled peptides. The latter peptides are again labelled at the same lysine and in addition contain a tag at the N-terminal phenylalanine (peak 2) or at a tyrosine in positions 26 (peak 3) and 16 (peak 4). It is interesting that these double labelled peptides also differ in hydrophobicity, and this may be partly due to conformational changes.

The product ion spectra from the fragmentation of the triply charged underivatised (*m/z* 1166) and double tagged **2** (*m/z*

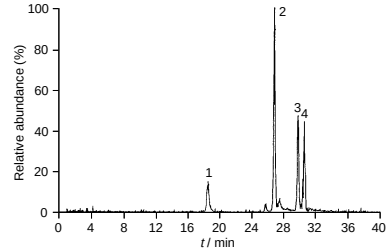



**Fig. 1** Reversed-phase HPLC–MS–MS analysis of insulin chain B derivatised with excess **1**. Detection of peaks was by monitoring total ion current for all product ions produced from triply charged parent ions. Peak 1 is related to a derivative of **2** labelled only at $^{29}$Lys, whereas peaks 2–4 are double tagged derivatives, again labelled at $^{29}$Lys and at $^{1}$Phe, $^{26}$Tyr and $^{16}$Tyr, respectively.

**Table 1** Fragment ions from triple protonated **2**, single tagged

| Fragment | Mass | *m/z* observed | Charge |
|---|---|---|---|
| FVNQHLC($SO_3H$)GSHLVEALYLVC($SO_3H$)GERGFFYTPK(tag)A[a] | 3772 | 1259 | 3+ |
| FVNQHLC($SO_3H$)GSHLVEALYLVC($SO_3H$)GERGFFYTPK(tag) | 3684 | 1229 | 3+ |
| FVNQHLC($SO_3H$)GSHLVEALYLVC($SO_3H$)GERGFFYT | 3182 | 1592 | 2+ |
| FVNQHLC($SO_3H$)GSHLVEALYLVC($SO_3H$)GERGFFY | 3080 | 1541 | 2+ |
| FVNQHLC($SO_3H$)GSHLVEALYLVC($SO_3H$)GERGFF | 2917 | 1459 | 2+ |
| FVNQHLC($SO_3H$)GSHLVEALYLVC($SO_3H$)GERGF | 2770 | 1386 | 2+ |
| FVNQHLC($SO_3H$)GSHLVEALYLVC($SO_3H$)GER | 2566 | 1284 | 2+ |
| FVNQHLC($SO_3H$)GSHLVEALYLV | 2073 | 1038 | 2+ |
| FVNQHLC($SO_3H$)GSHLVEALYL | 1973 | 988 | 2+ |
| FVNQHLC($SO_3H$)GSHLVEALY | 1860 | 931 | 2+ |
| FVNQHLC($SO_3H$)GSHLVEAL | 1696 | 849/1697 | 2+/1+ |
| FVNQHLC($SO_3H$)GSHLVEA | 1583 | 793/1584 | 2+/1+ |
| FVNQHLC($SO_3H$)GSHLV | 1383 | 1384 | 1+ |
| VC($SO_3H$)GERGFFYTPK(tag)A | 1799 | 1800 | 1+ |
| FYTPK(tag)A | 1002 | 1003 | 1+ |
| TPK(tag)A | 692 | 693 | 1+ |
| PK(tag)A | 591 | 592 | 1+ |

[a] Parent ion (single tag, peak 1).

1351) are shown in Fig. 2(*a*) and (*b*), respectively. Signals from the single and multiple tagged peptides are more intense than those from intact **2**. Product ions obtained from the fragmentation of the single tagged derivative of **2** are collected in Table 1. It is clear that besides confirming the positions of the acridone labels on **2** these data provide an abundance of sequencing information. Moreover, covalent tagging of the acridone derivative to **2** *via* a stable amide bond appears to have simplified the distribution of fragment ions compared to those obtained from **2** itself, most probably due to a decrease of the number of basic sites.

Due to the intense fluorescence of the acridone moiety we also investigated the ease of adaptation of this fluorophore as a label useful in assaying the bioactivity of an enzyme. We were especially interested to find out whether labelling hinders biological activity. For this purpose we followed the hydrolysis of single and double labelled **2** by the proteolytic enzyme trypsin. The single (peak 1) and double labelled (peak 2) insulin derivatives were isolated by HPLC and about half of the solvent was removed *in vacuo*. The volume of the remaining solution was doubled by adding 50 mM $NH_4HCO_3$ buffer (pH 7.8). Trypsin in water was added to give a derivatised peptide to enzyme ratio of 200 : 1. The hydrolysis was monitored with time

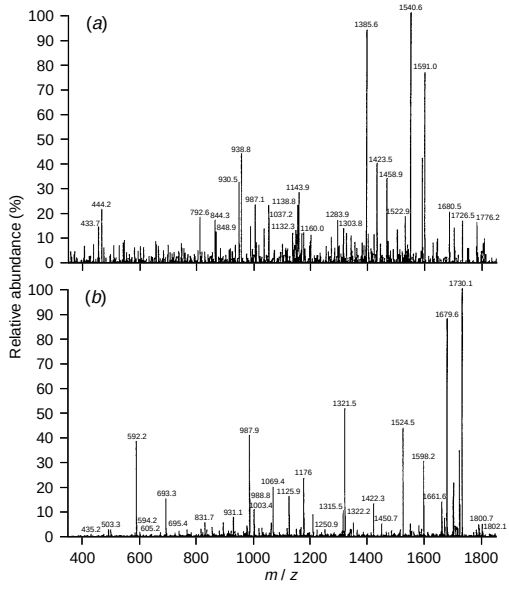



**Fig. 2** Influence of the presence of label on the product ion spectrum from the fragmentation of triply charged (*a*) original insulin chain B and (*b*) peptide labelled in positions 1 and 29

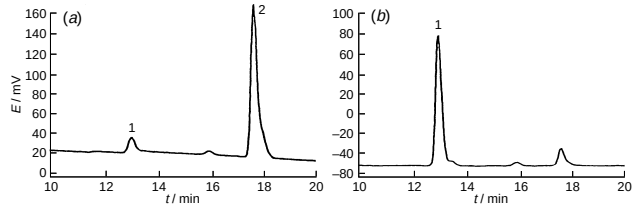



**Fig. 3** HPLC analysis of the mixture from the enzymic hydrolysis of single tagged insulin chain B. Starting material (peak 2) disappears leading to the formation of one product (peak 1) with time: (*a*) 0 and (*b*) 60 min.

by direct HPLC analysis of the reaction mixture and fluorescence detection, and was found to be complete in about 60 min.

As expected, in the case of single tagged **2** only one fluorescent product was obtained (Fig. 3). MS confirmed that the fluorescence signal was related to the peptide GFFYTPK-(tag)A (*m/z* 1206), as a result of hydrolysis at the arginine residue in position 22. The remainder of **2**, that is FVNQ...GER (*m/z* 2584), had a retention time shorter than that containing the acridone moiety, which emphasises the hydrophobic character imparted by this tag.

The tryptic digestion of double labelled **2** showed the simultaneous formation of two fluorescent signals. This confirmed that the arginine residue was located in between the two tags in the sequence. One of the signals again corresponded to the peptide GFFYTPK(tag)A. The other peptide, now with a longer retention time, corresponded to F(tag)V NQ...GER (*m/z* 2860). From these studies it is clear that derivatised lysine residues are not susceptible to tryptic digestion. However, hydrolysis on the carbonyl end of the arginine residue was not affected by this labelling procedure.

## Footnote and References

* E-mail: patrick_camilleri@sbphrd.com

1 K. R. Anumula, R. P. Schulz and N. Back, *Peptides*, 1992, **13**, 663.
2 C. G. Bradshaw, K. Ceszkowski, G. Turcatti, I. J. Beresford and A. Chollet, *J. Med. Chem.*, 1994, **37**, 1991.
3 N. W. Bunnett, P. F. Dazin, D. G. Payan and E. F. Grady, *Peptides*, 1995, **16**, 733.
4 G. Panigrahi, B. Zhao, J. J. Krepinsky and P. Sadowski, *J. Am. Chem. Soc.*, 1996, **118**, 12004.
5 M. Greenaway, G. N. Okafo, P. Camilleri and D. Dhanak, *J. Chem. Soc., Chem. Commun.*, 1994, 1691.
6 G. Okafo, L. Burrow, S. A. Carr, G. D. Roberts, W. Johnson and P. Camilleri, *Anal. Chem.*, 1996, **68**, 4424.
7 J. L. Reymond, T. Koch, J. Schroer and E. Tierney, *Proc. Natl. Acad. Sci. USA*, 1996, *93*, 4251.

*Received in Cambridge, UK, 14th March 1997; 7/01787A*

# A soluble fluorous phase polymer support

**David E. Bergbreiter* and Justine G. Franchina**

*Department of Chemistry, Texas A&M University, College Station, TX 77843-3255, USA*

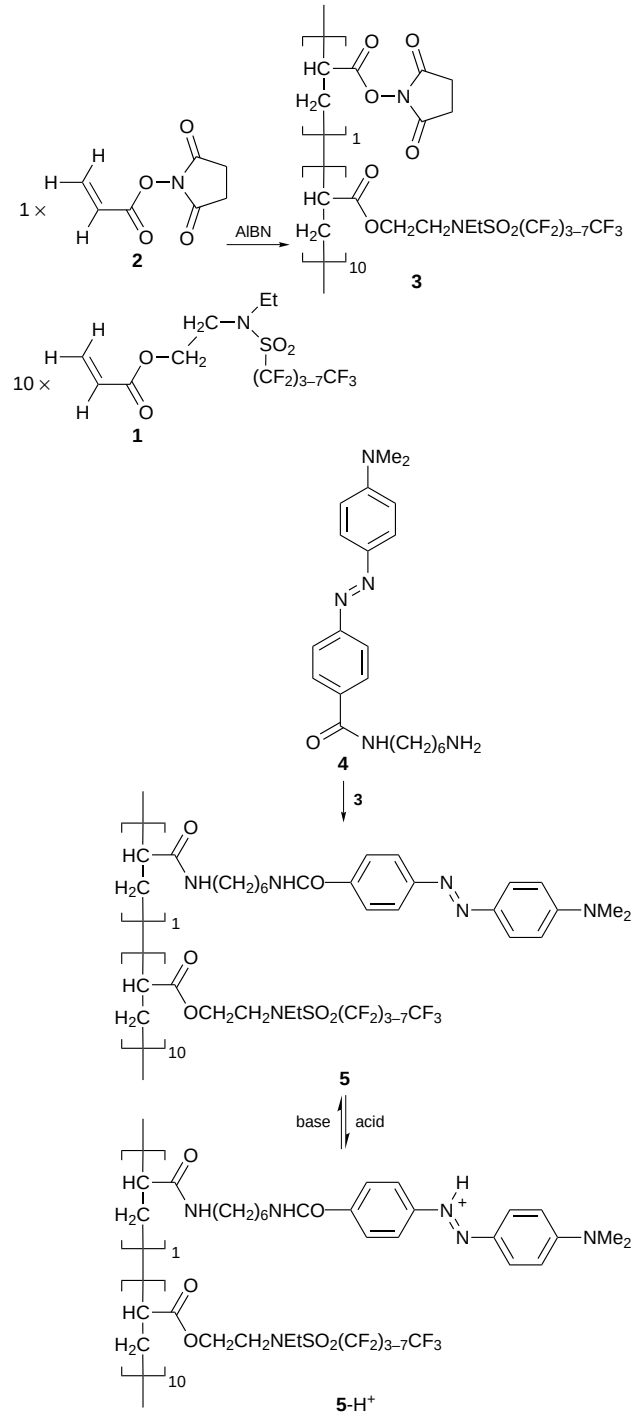
**The synthesis of fluorous phase soluble fluoropolymer supports that readily covalently bind amine-containing reagents and that react with and separate from reagents in aqueous and hydrocarbon solvents is described.**

Fluorous phase chemistry is the most recent of several strategies that have been developed to facilitate separation of catalysts or reagents from products or one another.[1–5] Such separation processes are of increasing interest for environmental reasons and as a basis for the recovery, separation and processing of intermediates or products in synthetic chemistry.[2,6] As originally described by Horváth,[1] this chemistry consists of essentially three elements; a fluorocarbon solvent, a hydrocarbon solvent and a fluorous tag that renders something fluorous phase soluble. Here we describe an alternative approach to synthesis of fluorous labels. The idea was to prepare a soluble fluorocarbon polymer that has reactive sites that can be used to covalently bind reagents and to render them soluble in the fluorous phase as a polymer-bound reagent.

A soluble polymer support for fluorous phase chemistry has several requirements beyond those generally expected in a polymer support. Such a polymer should be selectively soluble in a fluorous phase as opposed to an aqueous or hydrocarbon solvent phase. It should be easy to attach or remove reagents, catalysts or ligands. Moreover, if a fluoropolymer support were to be practically useful, emulsions formed by shaking a hydrocarbon solution with the fluoropolymer in the fluorous phase should quickly and easily phase separate. Finally, a fluorous phase soluble fluoropolymer supported reagent has to react readily with species in a non-fluorocarbon aqueous or hydrocarbon phase. The preliminary experiments outlined here show that these goals can be achieved with simple fluorocarbon polymers derived from acrylic acid.

To test our ideas, we prepared a fluoropolymer-bound dye as shown in Scheme 1. The requisite fluoropolymer-bound dye is prepared in two steps. First, we prepared a fluoroacrylate–*N*-acryloyloxysuccinimide (NASI) copolymer **3**. The active ester in this copolymer was in turn used to attach an amino-containing *p*-Methyl Red derivative **4** to yield a highly coloured pH-sensitive fluoropolymer-bound dye **5**.

The copolymerization of the fluorinated acrylate **1** and the *N*-acryloyloxysuccinimide **2** was accomplished using AIBN as the initiator in *tert*-butyl alcohol. After 48 h, the copolymer precipitated. After decantation of the remaining reaction solution, any residual monomers in the fluoropolymer were removed by THF extraction. The product was characterized by IR spectroscopy (imide peaks at 1818 and 1788 $cm^{-1}$, an intense but broad carbonyl peak at 1746 $cm^{-1}$ and C–F peaks in the 1150–1250 $cm^{-1}$ region). The absence of vinyl peaks at $\delta$ 5.8–6.8 in the $^1H$ NMR spectrum of the polymer confirmed that there was no monomer in the polymeric product. The polymer's molecular weight was measured by end group titration for samples of the homopolymer of **1** and for **1**–NASI copolymers produced using 4,4′-azobis(4-cyanovaleric acid) as the initiator. These $M_n$ values were 120 345 and 107 705 Da, respectively. Viscometry was also carried out and the intrinsic viscosity of the **1**–NASI copolymer produced with AIBN initiation was 1.56 dl $g^{-1}$ in $Cl_2CFCClF_2$ at 29 °C (*K* and *a* values for this polymer are not available) (a structurally similar fluorinated polyacrylate of reasonably high molecular weight had a reported intrinsic viscosity of 0.25–0.49 dl $g^{-1}$).[7]




**Scheme 1**

Derivatization of this active ester-containing polymer with functional amines was carried out in a biphasic reaction mixture. For example, reaction of **3** with the Methyl Red derivative **4** was carried out by dissolving **3** in a fluorocarbon solvent (FC77, 3M Co., a fluorinated cyclic ether, $C_8F_{16}O$) and vigorously mixing this solution with a THF solution of the amine-containing Methyl Red derivative **4**. The yield in this reaction was high (> 90%) based on the observed complete disappearance of the broad $CH_2$ singlet of the succinimide at $\delta$ 2.9. The product copolymer **5** was isolated by simple separation of fluorocarbon phase and removal of the FC77 solvent. The product polymer's IR spectrum showed a complete loss of the active ester imide peaks (confirming the NMR results, *vide supra*) and a new amide carbonyl peak at 1638 $cm^{-1}$. The loading of Methyl Red on this polymer was estimated to be $0.075 \times 10^{-3}$ equiv. of Methyl Red per gram of polymer.

The Methyl Red-containing fluoropolymer **5** was not soluble in ordinary organic solvents (THF, alcohols, chloroform, DMSO, toluene) but **5** like **3**, was soluble in fluorinated solvents such as FC77 or $PhCF_3$.[8,9] Solutions of **5** or **5**-$H^+$ in FC77 were immiscible with water and organic solvents. Separation of this fluoropolymer-bound dye from these solvents appeared visually to be quantitative. A more quantitative estimate of > 99.9% of **5** being retained in the fluorous phase was obtained by UV–visible spectroscopy of the THF or water layer, which showed no Methyl Red present in this second phase.

Shaking solutions of **5** in FC77 with THF produces emulsions that separate within 10 min. In the case of mixtures of **5**–FC77 and water, the emulsion of **5**-$H^+$–FC77 and water required up to 60 min to separate on standing.

Reaction of the fluoropolymer-bound Methyl Red with aqueous HCl or with HCl that had been added to an immiscible THF phase led to an immediate protonation of the fluoropolymer-bound dye as evidenced by the instantaneous change in the fluorous phase colour from yellow to red. Similarly, addition of a base to the THF or water solution produced a change back to yellow. Bases like NaOH–$H_2O$ or $Et_3N$ in THF were equally effective.

Another advantage of this fluorocarbon polymer support is that the so-called 'Teflon pony-tails' are well insulated from the reacting group. However, it is worth noting that this alone is not sufficient to make ionic chemistry in a fluorous phase equivalent to that in an aqueous phase. Equilibration of **5** in FC77 with buffer solutions of varying pH and with THF solutions of **4** show that **5** is a weaker base than **4**. We estimate that the p$K_a$ of the fluorous phase Methyl Red **5** is between 1.0 and 1.5 based on the colour change for fluorocarbon solutions of **5** equilibrated with aqueous buffer solutions. This greater than one hundred-fold decrease in the acidity of **4** on covalent binding to **3** is most likely due to decreased solvation of the cation in the fluorous phase.

In summary, vinyl fluoropolymers copolymerize with other vinyl monomers that contain reactive groups to form starting materials for synthesis of polymer-supported reagents that will be fluorous phase soluble. The product polymer-supported species can easily be separated from organic or aqueous solutions but still have excellent reactivity as judged by the fast protonation/deprotonation experiments described here. Continuing work will explore other fluoropolymer supports and exploit this reactivity in catalytic chemistry.

Support of this work by the National Science Foundation (CHE-9222717) and the Robert A. Welch Foundation is gratefully acknowledged. We are also indebted to Drs D. W. Zhu and N. L. Franchina of 3M for supplying us with the necessary monomer and fluorocarbon solvents.

## Footnotes and References

* E-mail: bergbreiter@chemvx.tamu.edu

1 I. T. Horváth and J. Rábai, *Science*, 1994, **266**, 72.
2 A. Studer, S. Hadida, R. Ferritto, S. Y. Kim, P. Jeger, P. Wipf and D. P. Curran, *Science*, 1997, **275**, 823.
3 R. P. Hughes and H. A. Trujillo, *Organometallics*, 1996, **15**, 286.
4 S. G. DiMagno, P. H. Dussault and J. A. Schultz, *J. Am. Chem. Soc.*, 1996, **118**, 5312.
5 G. Pozzi, F. Montanari and S. Quici, *Chem. Commun.*, 1997, 69.
6 D. P. Curran, *Chemtracts: Org. Chem.*, 1996, **9**, 75.
7 C. P. Jariwala, P. E. G. Sundell, C. E. Hoyle and L. J. Mathias, *Macromolecules*, 1991, **24**, 6352–6353.
8 D. W. Zhu, *Synthesis*, 1993, 953; D. W. Zhu, *Macromolecules*, 1996, **29**, 2813.
9 A. Ogawa and D. P. Curran, *J. Org. Chem.*, 1997, **62**, 450.

*Received in Corvallis, OR, USA, 12th March 1997; 7/01754E*

# Ring-closing depolymerisation of aromatic polyethers

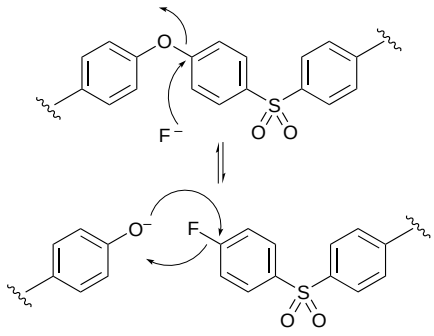
**Abderrazak Ben-Haida,[a] Ian Baxter,[b] Howard M. Colquhoun,*[a]† Philip Hodge,*[a]‡ Franz H. Kohnke[a]§ and David J. Williams*[b]**

[a] *Department of Chemistry, University of Manchester, Manchester, UK M13 9PL*
[b] *Department of Chemistry, Imperial College, South Kensington, London, UK SW7 2AY*

**Equilibration of aromatic poly(ether sulfone)s and poly(ether ketone)s under conditions of fluoride-catalysed ether exchange leads, at low polymer concentrations in dipolar aprotic solvents, to efficient ring-closing depolymerisation.**

Ring-opening polymerisation of macrocyclic aromatic ether ketones and ether sulfones offers a potentially valuable route to high-performance aromatic polymers,[1–3] and such chemistry has recently become the focus of significant research activity.[4] Advantages of this approach, in the production of composite structures for example, include the very much lower initial viscosities of macrocyclic oligomers relative to the corresponding high molecular weight polymers, the complete absence of by-products, and the fact that ring-opening polymerisations of strain-free macrocycles are largely entropy-driven and thermally neutral.

The synthesis and ring-opening polymerisation of macrocyclic aromatic ethers was first reported in 1989,[1] but the key reaction which would enable recycling of such materials (ring-closing depolymerisation)[5] has not so far been demonstrated. Aromatic poly(ether sulfone)s and poly(ether ketone)s do however undergo catalytic transetherification at high temperatures in the presence of strong but kinetically labile nucleophiles such as fluoride ion,[6] and the existence of this process (Scheme 1) strongly suggests a potential mechanism for polymer–macrocycle interconversion.

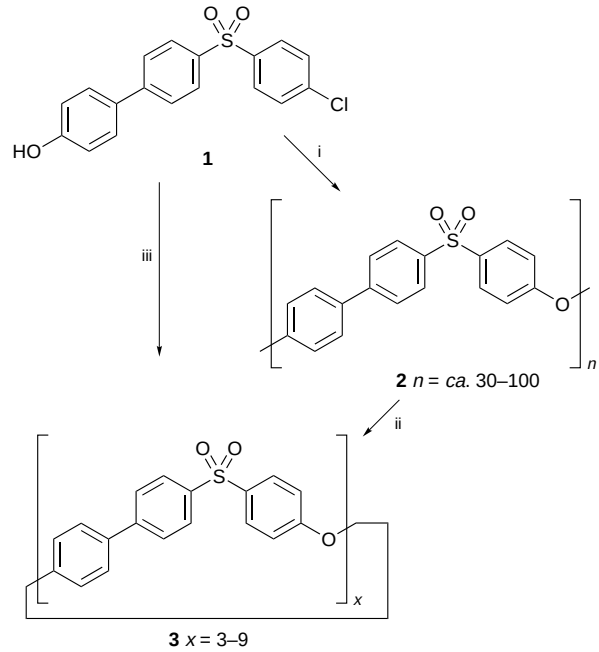


**Scheme 1**

We now report that efficient ring-closing depolymerisation of the aromatic poly(ether sulfone) **2** ($M_w$ = 29 000, $M_n$ = 8500 Da) can be achieved in dimethylacetamide (DMA) solution at 0.03 M monomer-equivalent concentration and at a temperature of 150 °C, using CsF (0.02 M) as catalyst (Scheme 2). Under these conditions the broad GPC peak associated with the starting polymer disappears over the course of about 12 h, and is progressively replaced by a series of sharp peaks representing macrocyclic oligomers in the approximate molecular weight range $M_w$ = 800–4000 (Fig. 1). It should be noted that the macrocylic oligomers are present (as is often the case for condensation polymers) at a low level even in the starting polymer **2**. Indeed, when polycondensation of monomer **1** is carried out under high-dilution conditions these same macrocyles, identified by FAB-MS, come to represent the major fraction of the product (Scheme 2).

After equilibration of polymer **2** for 48 h in the presence of CsF there is no further change in the molar mass distribution, and the oligomers can be recovered in *ca*. 95% yield by precipitation in aqueous MeOH. Elemental analysis for fluorine (after repeated extraction with water to remove residual inorganics) reveals only very low levels of fluoride ion incorporation (*ca*. one fluorine for every thirty polymer repeat units) consistent with the formation of mainly cyclic species. Peak positions in the GPC and HPLC chromatograms of the depolymerised product are superimposable on those of the macrocyclic oligomers formed by polycondensation of monomer **1**. Moreover, FAB mass spectra of the products from macrocyclisation of **1** and from depolymerisation of **2** show an identical series of parent ions associated exclusively with cyclic species, from cyclotrimer ($[M + H]^+$ 925) to cycloheptamer ($[M + H]^+$ 2158).

The cyclic trimer, tetramer, pentamer and hexamer were isolated from the products of depolymerisation by column chromatography (silica gel; $ClHC{=}CCl_2$ : $CH_2Cl_2$ : EtOAc, 64 : 33 : 3) and were characterised by FAB mass spectrometry, $^1H$ and $^{13}C$ NMR spectroscopy, GPC, HPLC and DSC. Their well-resolved $^1H$ NMR spectra confirm that, as expected for pure cyclic oligomers, only three AA′BB′ systems are present in the aromatic region. Resonances assigned to protons *ortho* to the biphenyl linkage show significant variations of chemical shift as a function of ring-size, and are for example shifted upfield by *ca*. 0.1 ppm in the cyclic trimer **3** ($x$ = 3), relative to the higher ring sizes. Crystals of **3** ($x$ = 3) suitable for X-ray



**Scheme 2** *Reagents and conditions*: i, $K_2CO_3$, $PhSO_2Ph$, 280 °C; ii, CsF, DMA, 150 °C; iii, $K_2CO_3$, DMA, 150 °C

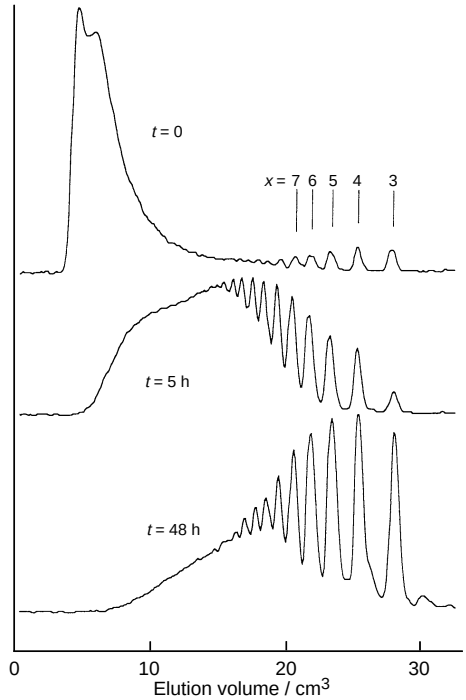



**Fig. 1** Gel permeation chromatograms (eluent $CHCl_3$) showing progressive ring-closing depolymerisation of polymer **2** and formation of the macrocyclic oligomers $[OArArSO_2Ar]_x$ (Ar = 1,4-phenylene)

analysis, were isolated from $CHCl_3$. These melted sharply at 475 °C, but higher cyclic oligomers decomposed above 500 °C without melting. The structure of **3** ($x$ = 3), determined by single-crystal X-ray diffraction,¶ is shown in Fig. 2. There is evidence for a slight degree of ring-strain in this macrocycle, in that all three C–S–C bond angles (101.6 ± 0.1°) are compressed by about 3.3° from their normal open-chain value of 104.9°. The biphenyl unit, which frequently adopts a coplanar conformation as a consequence of crystal packing and symmetry considerations,[7] here takes up a conformation close to its isolated

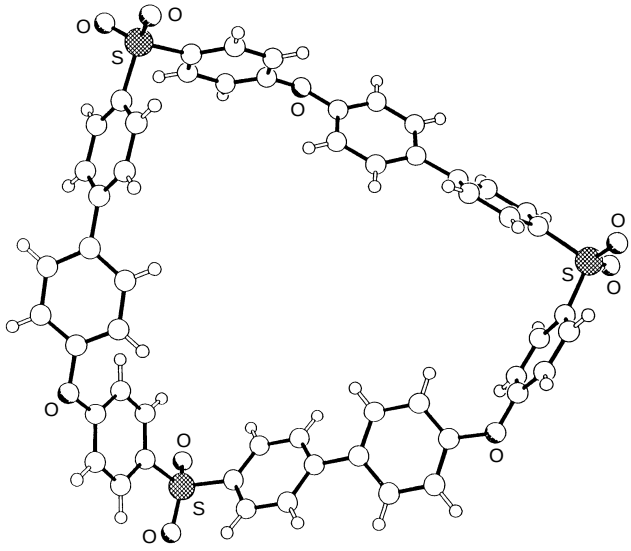
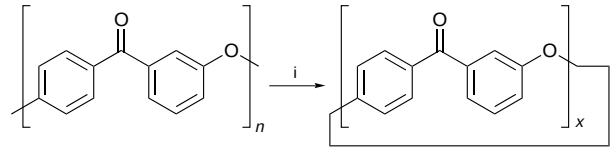



**Fig. 2** Molecular geometry of the cyclic trimer **3** ($x$ = 3) (the solvating molecule of $CHCl_3$, which partly fills the molecular cavity, has been omitted for clarity)




**4** $x$ = 2–11

**Scheme 3** *Reagents and conditions*: i, CsF, DMA, 155 °C

minimum-energy position,[8] with inter-ring torsion angles for the three independent biphenyl residues in the range 34–38°.

Ring-closing depolymerisation appears to be a quite general reaction for activated aromatic polyethers. The poly(ether ketone) **4** (Scheme 3), for example,[9] is cleaved to form macrocyclic species under very similar conditions and on much the same timescale as polymer **2**. Analysis of the product mixture by GPC, HPLC and FAB-MS demonstrates formation of macrocyclic ether ketone oligomers up to at least the cycloundecamer, and lower oligomers from cyclic dimer to cyclic hexamer have been isolated in pure form by column chromatography.

The potential of ring-closing depolymerisation chemistry for recycling (in every sense!) high-performance aromatic polyethers has thus been demonstrated for the first time. The possibility that non-equilibrium conditions might circumvent the current requirement for very low polymer concentrations in such reactions is now under investigation.

We wish to thank the Royal Society and the EPSRC for financial support of this research.

## Footnotes and References

† Present address: Department of Chemistry and Applied Chemistry, University of Salford, Salford, UK M5 4WT.
E-mail: h.m.colquhoun@chemistry.salford.ac.uk
‡ E-mail: philip.hodge@man.ac.uk
§ On leave from the Department of Organic and Biological Chemistry, University of Messina, I-98166, Messina, Italy.

¶ *Crystal data* for **3** ($x$ = 3): $C_{54}H_{36}O_9S_3{\cdot}CHCl_3$, $M$ = 1044.38, monoclinic, space group $P2_1/n$, $a$ = 7.468(2), $b$ = 20.110(3), $c$ = 34.099(5) Å, $\beta$ = 95.68(2)°, $Z$ = 4, $U$ = 5096(2) Å$^3$, $T$ = 213 K, $D_c$ = 1.361 g cm$^{-3}$, $\mu$(Cu-Kα) = 3.25 mm$^{-1}$, $F(000)$ = 2152. A total of 7560 independent reflections ($2\theta \leqslant 120°$) were measured on a Siemens P4 rotating-anode diffractometer, with graphite-monochromated Cu-Kα radiation, using ω-scans. The structure was solved by direct methods and refined anisotropically using $F^2$ data to give $R_1$ = 0.062, $wR_2$ = 0.136 for 4988 independent observed reflections [$I > 2\sigma(I)$]. CCDC 182/533.

1 J. A. Cella, J. J. Talley and J. M. Fukuyama, *Polym. Prepr. Am. Chem. Soc., Div. Polym. Chem.*, 1989, **30** (2), 581.
2 H. M. Colquhoun, C. C. Dudman, M. Thomas, C. A. O'Mahoney and D. J. Williams, *J. Chem. Soc., Chem. Commun.*, 1990, 336.
3 M. J. Mullins, E. P. Woo, D. J. Murray and M. T. Bishop, *Chemtech*, 1993, August, 25.
4 D. Xie and H. W. Gibson, *Polym. Prepr. Am. Chem. Soc., Div. Polym. Chem.*, 1994, **35** (1), 401; K. P. Chan, Y.-F. Wang, A. S. Hay, X. L. Hronowski and R. J. Cotter, *Macromolecules*, 1995, **28**, 6705; Y. Ding and A. S. Hay, *Macromolecules*, 1996, **29**, 3090; Y.-F. Wang, M. Paventi and A. S. Hay, *Polymer*, 1997, **38**, 469 and references cited therein.
5 M. Melchiors, H. Keul and H. Höcker, *Macromolecules*, 1996, **29**, 6442; B. R. Wood, J. A. Semlyen and P. Hodge, *Polymer*, 1997, **38**, 2287.
6 T. E. Attwood, A. B. Newton and J. B. Rose, *Br. Polym. J.*, 1972, **4**, 391.
7 C. P. Brock and R. P. Minton, *J. Am. Chem. Soc.*, 1989, **111**, 4586.
8 W. R. Busing, *J. Am. Chem. Soc.*, 1982, **104**, 4829.
9 M. F. Teasley and B. S. Hsaio, *Macromolecules*, 1996, **29**, 6432.

*Received in Cambridge, UK, 3rd June 1997; 7/03854B*

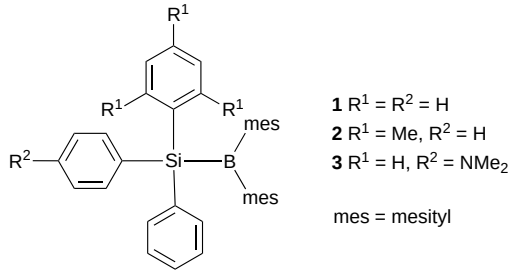
# First evidence of visible-range absorbing Si–B chromophores

**J.-P. Pillot,*[a] M. Birot,*[a] E. Bonnefon,[a] J. Dunoguès,[a] J.-C. Rayez,[b] M.-T. Rayez,[b] D. Liotard[b] and J.-P. Desvergne[c]**

[a] *Laboratoire de Chimie Organique et Organométallique (URA 35-CNRS), Université Bordeaux 1, 351, Cours de la Libération, 33405 Talence Cédex, France*
[b] *Laboratoire de Physicochimie Théorique (URA 503-CNRS), Université Bordeaux 1, 351, Cours de la Libération, 33405 Talence Cédex, France*
[c] *Laboratoire de Photophysique et Photochimie Moléculaire (URA 348-CNRS), Université Bordeaux 1, 351, Cours de la Libération, 33405 Talence Cédex, France*

**Novel aromatic silylboranes involving trigonally bonded boron display absorption and fluorescence emission in the visible range due to the Si–B bond; these results are supported by MNDO calculations.**

We have recently described the synthesis and characterisation of novel organosilylboranes (compounds **1**–**3**) possessing a dimesitylboryl moiety linked to a triarylsilyl group.[1]




**1** $R^1 = R^2 = H$
**2** $R^1 = Me$, $R^2 = H$
**3** $R^1 = H$, $R^2 = NMe_2$

mes = mesityl

Surprisingly, these reasonably stable silylboranes strongly absorb in the visible region as evidenced by their yellow or yellow–green colour. Meanwhile, it has been pointed out by others[2] that a toluene solution of a bis(amino)silylene–tris(pentafluorophenyl)borane adduct exhibits a deep yellow colour. This Lewis adduct slowly isomerizes into a new silylborane possessing a trigonally bonded boron, but no information was given concerning the origin of the coloration of this compound. Here we report our preliminary results demonstrating the close connection between the electronic absorption and fluorescence emission properties of silylboranes and the presence of the Si–B bond.

The UV spectra of organosilylboranes **1**–**3** and two reference compounds, $Ph_3SiMe$ **4** and $(mes)_2BPh$ **5** in a non-polar solvent, are shown in Fig. 1. Compounds **1**–**3** display a broad absorption band around 400 nm which is independent of the concentration. This band does not appear in phenylsilanes and phenylboranes which usually present $\lambda_{max}$ at appreciably shorter wavelengths.[3,4] Thus, the UV spectra of both reference compounds **4** and **5** in *n*-hexane (insert of Fig. 1) only exhibit absorption bands around 270 and 320 nm, respectively, and the spectrum of an equimolar mixture of these two compounds roughly corresponds to the sum of the spectra of each component. Therefore, the new band peaking in the visible range for derivatives **1**–**3** is due to the presence of the Si–B bond.

Interestingly, this long-wavelength absorption shifts from 397 nm for **2** to 405 nm for **1**. This bathochromic effect might be connected to a stronger interaction between boron and silicon in **1**. For **3**, a marked bathochromic effect is revealed ($\lambda_{max}$ = 409 nm), anticipating a much larger interaction between Si and B: the presence of the dimethylamino group probably augments the electron-donating ability of the silyl group to boron. This is consistent with the strong electron-acceptor ability of the dimesitylboryl group which was reported to behave in an analogous manner to a nitrile one.[5] Likely, these electronic factors might contribute to increase the electron density on the Si–B link and therefore the strength of this bond. The UV absorption spectra of compounds **1**–**3** are weakly sensitive to the polarity of the solvent, suggesting that their ground state does not exhibit a significant charge-transfer character.

The fluorescence emission of compounds **1**–**3** is characterised with a low fluorescence quantum yield ($\Phi_f$ *ca.* $5 \times 10^{-3}$ for **1**) indicating efficient non-radiative deactivation pathways for the singlet excited state. Upon excitation at 300 nm, **1**–**3** display two fluorescence emission bands ($\lambda_{max}$ *ca.* 340 and 480 nm) and only one (*ca.* 480 nm) upon excitation at 400 nm. On the other hand, the two reference compounds **4** and **5** present an emission band at 320 and 370 nm respectively, when excited at 300 nm. Addition of their spectra results in a broad band around 350 nm, which roughly matches the position of the high energy band observed for organosilylboranes **1**–**3** when excited at the same wavelength. Therefore, the second emission band at 480 nm can be attributed to the Si–B chromophore. Moreover, excitation spectra recorded in the 480 nm region indicate that an efficient intramolecular energy transfer occurs from aromatics to the Si–B bond.

The fluorescence emission spectra of **1** in solvents of increasing polarity are shown in Fig. 2.

In contrast to the UV absorption, the fluorescence emission of compounds **1**–**3** is very sensitive to the polarity of the solvent (Table 1). Thus, a marked solvatochromic effect is found for compound **1,** even stronger for **3**, as the values of $\lambda_{max}$ shift from

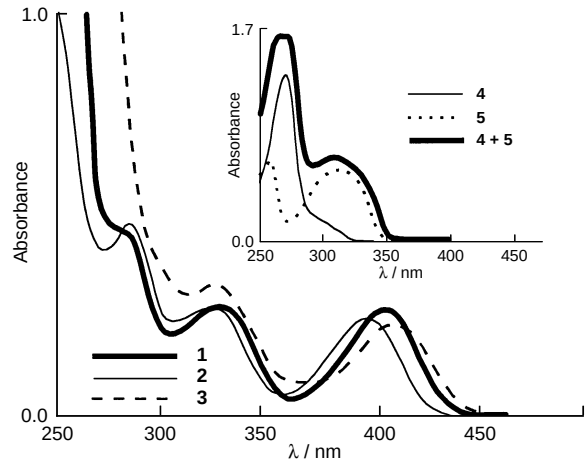



**Fig. 1** Electronic absorption spectra of organosilylboranes **1**–**3** in *n*-hexane, room temp., conc. $5.8 \times 10^{-5}$ (**1**), $6.4 \times 10^{-5}$ (**2**) and $8.4 \times 10^{-5}$ M (**3**). Insert: spectra of the reference compounds in *n*-hexane, room temp., conc. $7.7 \times 10^{-5}$ (**4**), $8.4 \times 10^{-5}$ (**5**) and $4.1 \times 10^{-5}$ M for each component of the mixture **4** + **5**.

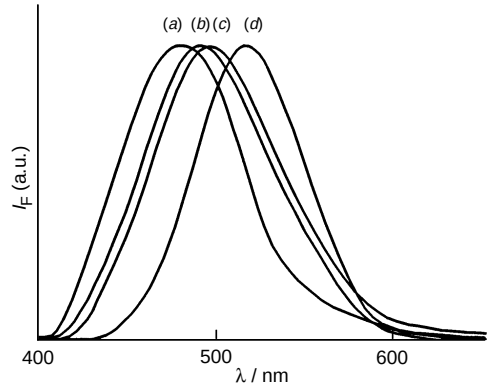



**Fig. 2** Emission fluorescence spectra of **1** in various solvent ($\lambda_{exc}$ = 400 nm): *n*-hexane (*a*); diethyl ether (*b*); chloroform (*c*); acetonitrile (*d*)

480 nm in *n*-hexane to 640 nm in acetonitrile. From the relationship[6] between the variation of $\nu_{max}$, the polarity factor $\Delta f$, and the radius of the solvent cavity $\rho$ (estimated from space-filling molecular models), it is possible to estimate the dipole moment $\Delta\mu$ in the excited state (on the assumption that $\mu \approx 0$ in the ground state).[7–9] The calculated values are relatively high as they range from 11.3 D (**1**) to 19.5 D (**3**), pointing out the large charge-transfer character of the fluorescent excited singlet state.

To rationalise the photoelectronic properties of silylboranes **1**–**3**, MNDO/CI (single excitations and single and double excitations CI) calculations[10] based on 10 occupied and 10 unoccupied MOs around the Fermi level have been performed on **1**, **4** and **5,** using the AMPAC program.[11] In reference compounds **4** and **5**, theoretical singlet absorption wavelengths $\lambda$ and relative oscillator strengths *f* (**4**: $\lambda$ = 225 nm, *f ca.* 1.5; **5**: $\lambda$ = 260 nm, *f ca.* 0.25; $\lambda$ = 230 nm, *f ca.* 0.5) appear to be in good semi-quantitative agreement with the experimental spectra shown in the insert of Fig.1, although the theoretical wavelengths are systematically blue-shifted by *ca*. 50 nm with respect to the experimental ones. Similar determinations performed on **1** reveal three singlet absorptions: 357 (0.08), 296 (0.08) and 233 nm (1.03) which are in good agreement with the experimental spectrum (Fig. 1) within the 50 nm blue-shift range. Analysis of the relevant wavefunctions shows that (*i*) in **4**, the 225 nm transition corresponds to a $\pi$–$\pi^*$ excitation involving the aromatic rings, the positively charged silicon atom being unchanged by this transition; (*ii*) in compound **5**, the 260 and 230 nm transitions are associated with a significant electronic transfer from the phenyl and mesityl groups to the boron atom (slightly positively charged in the ground singlet state); and (*iii*) in **1**, the first band (357 nm) corresponds to a noticeable charge transfer from silicon to boron atom, the second one (296 nm) to a transfer from mesityl groups to boron atom and the third one (233 nm) to a $\pi$–$\pi^*$ excitation in the aromatic rings with a slight electronic depletion on silicon atom. Analogous studies using the MNDO/d method,[12] which take into account Si d atomic orbitals, do not qualitatively change these results.

**Table 1** Maxima of the fluorescence emission bands of compounds **1** and **3** *vs.* polarity of the solvent ($\lambda_{exc}$ = 400 nm, room temp.)

| | | λ/nm | |
|---|---|---|---|
| Solvent | $\Delta f^a$ | **1** | **3** |
| Cyclohexane | 0.09 | 480 | 480 |
| Benzene | 0.10 | 480 | 525 |
| Diethyl ether | 0.25 | 492 | 560 |
| Chloroform | 0.25 | 495 | 580 |
| Acetonitrile | 0.39 | 515 | 640 |

[a] $\Delta f = f - \frac{1}{2}f'$; $f = (\varepsilon - 1)/(2\varepsilon + 1)$; $f' = (n^2 - 1)/(2n^2 + 1)$.

To examine the role of the solvent polarity on the emission spectrum of **1**, calculations have also been performed on UV absorption and emission transitions with a continuum solvation model, the COSMO approach,[13] coupled to the MNDO/CI method. It turns out that the theoretical absorption spectrum of **1** is unaltered by the presence of a polar solvent, even a very high polar one like acetonitrile. Conversely, calculation indicates a bathochromic shift on the emission spectrum. This result is in excellent accord with the experimental findings.

The authors are indebted to the Conseil Régional Aquitaine for financial support.

## Footnote and References

* E-mail: j-p.pillot@lcoo.u-bordeaux.fr; m.birot@lcoo.u-bordeaux.fr

1 E. Bonnefon, M. Birot, J. Dunoguès, J.-P. Pillot, C. Courseille and F. Taulelle, *Main Group Metal Chem.*, 1996, **19**, 761.
2 N. Metzler and M. Denk, *Chem. Commun*., 1996, 2657.
3 J. C. Doty, B. Babb, P. J. Grisdale, M. Glogowski and J. L. R. Williams, *J. Organomet. Chem*., 1972, **38**, 229.
4 J. Nagý, J. Réffy, A. Kuszmann-Borbély and K. Pálossy-Becker, *J. Organomet. Chem*., 1967, **7**, 393.
5 A. Shultz and W. Kaim, *Chem. Ber*., 1989, **122**, 1863.
6 N. Mataga, Y. Kaifu and M. Koizumi, *Bull. Chem. Soc. Jpn.*, 1956, **29**, 465; C. Reichardt, *Solvent Effects in Organic Chemistry*, VCH, Weinheim, 1990 and references therein.
7 A. Onkelinx, F. C. De Schryver, L. Viaene, M. Van der Auweraer, K. Iwai, M. Yamamoto, M. Ichikawa, H. Masuhara, M. Maus and W. Rettig, *J. Am. Chem. Soc.*, 1996, **118**, 2892 and references therein.
8 E. Lippert, *Z. Naturforsch*., 1956, **29**, 465.
9 E. Lippert, *Ber. Bunsen-Ges. Phys. Chem. (Z. Elecktrochem.)*, 1957, **61**, 962.
10 M. J. S. Dewar and W. Thiel, *J. Am. Chem. Soc*., 1977, **99**, 4899; *Oranometallics*, 1986, **5**, 375.
11 AMPAC 6.0, 1994 Semichem, 7128 Summit, Shawnee, KS 66216, 1994.
12 W. Thiel and A. A. Voityuk, *J. Mol. Struct.*, 1994, **313**, 141.
13 A. Klamt and G. Schüürmann, *J. Chem. Soc., Perkin Trans. 2*, 1993, 799; A. Klamt, *J. Phys. Chem.*, 1996, **100**, 3349.

*Received in Basel, Switzerland, 26th March 1997; 7/02106B*

# 5-*endo*-Trigonal cyclization of *o*-substituted *gem*-difluorostyrenes: syntheses of 2-fluorinated indoles, benzo[*b*]furans and benzo[*b*]thiophenes

**Junji Ichikawa,*† Yukinori Wada, Tatsuo Okauchi and Toru Minami***

*Department of Applied Chemistry, Kyushu Institute of Technology, Sensui-cho, Tobata, Kitakyushu 804, Japan*

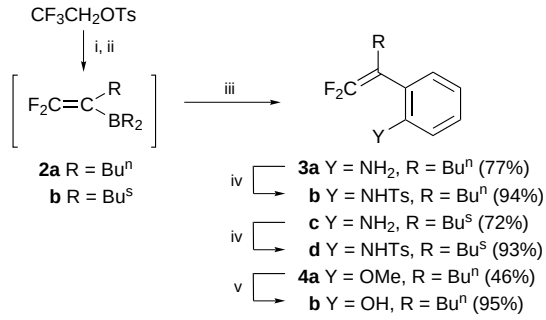
**β,β-Difluorostyrenes bearing tosylamido, hydroxy or methylsulfinyl groups at the *o*-position undergo intramolecular substitution of the nitrogen, oxygen or sulfur with loss of fluorine *via* a 5-*endo*-trigonal process leading to 2-fluorinated heterocyclic systems in high yields.**

*gem*-Difluoroalkenes possess remarkable reactivity toward nucleophilic substitution for their fluorine atoms *via* addition–elimination processes.[1] This reactivity is due to (i) the electrophilic activation of the carbon–carbon double bond by the two fluorines and (ii) the leaving-group ability of the fluoride ion. This chemical reactivity renders these alkenes valuable as synthetic building blocks[2] as well as mechanism-based enzyme inhibitors.[3] We have recently reported the reactions of 2,2-difluorovinyl ketones with external nucleophiles leading to facile syntheses of α,β-unsaturated ketones,[4] α-oxo ketene derivatives[5] and 3- or 5-fluoropyrazoles.[6] Our interest in the further application of *gem*-difluoroalkene chemistry led us to explore an intramolecular version of such vinylic fluorine substitution reactions. Here we report the construction of ring-fluorinated heterocyclic systems starting from *o*-substituted β,β-difluorostyrenes.[7]

β,β-Difluorostyrenes **1** bearing nucleophilic *ortho* nitrogen, oxygen or sulfur heteroatoms were designed as substrates for the intramolecular substitution. We sought to effect the 5-*endo*-trigonal ring closure of **1** to afford 5-membered 2-fluoro heterocycles despite this cyclization being disfavoured in Baldwin's rules.[8] Among 5-*endo*-trigonal cyclizations, such nucleophile-driven ring closures have only rarely been observed in synthetic chemistry,[9] in contrast with electrophile-driven[10]‡ and radical-initiated ring closures.[11] We expected that the unique properties of *gem*-difluoroalkenes could make a nucleophilic approach feasible. Specifically, we thought that (i) the highly polarized difluorovinylidene alkenic bond displays significant single bond character ($^{13}$C NMR: *ca.* $\delta$ 150 and 90 for $CF_2$=C) and would allow initial ring formation, and (ii) the successive elimination of fluoride ion could suppress the reverse ring opening. Such a process would provide an efficient access to 2-fluorinated indoles, benzo[*b*]furans, and benzo[*b*]-thiophenes, of which synthetic methods are quite limited in spite of the potential uses of 2-fluoro heterocycles as components of agrochemicals, pharmaceuticals and dyestuffs.[12] On the basis of these considerations, we investigated the cyclization of **1**.

The starting materials were easily prepared as outlined in Scheme 1 by using the one-pot sequence which we have previously developed for the preparation of *gem*-difluorostyrenes.[13] The coupling reactions of 2,2-difluorovinylboranes **2a** and **2b** (generated *in situ* from 2,2,2-trifluoroethyl toluene-*p*-sulfonate) with *N*-butylmagnesio-*o*-iodoaniline were effected in the presence of CuI with palladium catalysis to prepare *o*-amino-β,β-difluorostyrenes **3a** and **3c** as precursors of 2-fluoroindoles. *o*-Hydroxy-β,β-difluorostyrene **4b**, a precursor of 2-fluorobenzo[*b*]furan, was similarly obtained by the coupling of **2a** with *o*-iodoanisole, followed by demethylation with $BBr_3$.

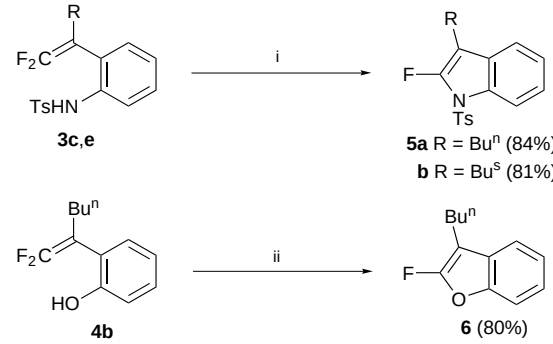
The attempted cyclization of **3a** by treatment with 1.2 equiv. of Bu$^n$Li failed, while treatment of toluene-*p*-sulfonamide **3b** with 1.2 equiv. of NaH in DMF successfully promoted the



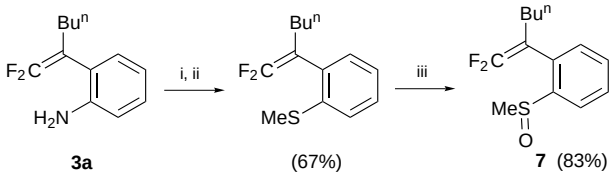

**Scheme 1** *Reagents and conditions*: i, Bu$^n$Li (2.1 equiv.), THF, −78 °C, 0.5 h; ii, $BR_3$ (1.1 equiv.), THF, −78 °C, 1 h then room temp., 3 h; iii, ArI (0.9 equiv.), CuI (1.0 equiv.), $Pd_2(dba)_3$·$CHCl_3$ (0.02 equiv.), $PPh_3$ (0.08 equiv.), THF–HMPA (4 : 1), room temp. 1 h; iv, TsCl (1.1 equiv.), pyridine, 0 °C to room temp., 11 h; v, $BBr_3$ (1.1 equiv.), $CH_2Cl_2$, −15 °C to room temp., 2 h

'disfavoured' 5-*endo*-trigonal cyclization to afford 2-fluoroindole **5a** in 84% yield (Scheme 2).[14]§ Successful ring closure did not necessitate the use of high-dilution conditions, and proceeded smoothly even in the case of the starting styrene **3d** which bore a secondary alkyl group at the α-position. Moreover, when the hydroxystyrene **4b** was treated under similar conditions, 5-*endo*-trigonal cyclization of the corresponding alkoxide occurred leading to 2-fluorobenzo[*b*]furan **6** in 80% yield (Scheme 2).[15]¶

As a further example of the cyclization we next tried the intramolecular substitution utilizing a sulfur nucleophile. For the purposes of generating a thiolate moiety, the methlysulfinyl group was selected as an *ortho* substituent of β,β-difluorostyrene. The Pummerer rearrangement of *o*-methylsulfinyl-β,β-difluorostyrene **7** followed by solvolysis would allow the cyclization *via* the unisolated intermediate, hemiacetal trifluoroacetate **8**.[16] Thus, **7** was readily derived from **3a** *via* diazotization as depicted in Scheme 3. Successive treatment of **7** with (i) trifluoroacetic anhydride and $Et_3N$ and (ii) $K_2CO_3$ in MeOH provided 2-fluorobenzo[*b*]thiophene **9** in 82% yield as expected (Scheme 4).[17]‖

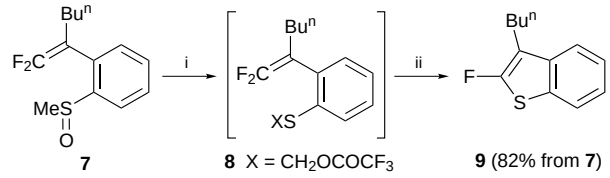



**Scheme 2** *Reagents and conditions*: i, NaH (1.2 equiv.), DMF, 80 °C, 7 h; ii, NaH (1.2 equiv.), DMF, 0 to 60 °C, 2 h




**3a** (67%) **7** (83%)

**Scheme 3** *Reagents and conditions*: i, $CF_3CO_2H$ (2 equiv.), $Me_2CHCH_2CH_2ONO$ (2 equiv.), MeCN, 0 °C, 0.5 h; ii, aq. NaSMe (3 equiv.), MeCN, 0 °C to room temp., 1.5 h; iii, aq. $TiCl_3$ (2 equiv.), aq. $H_2O_2$ (3 equiv.), MeOH–$H_2O$, room temp., 2 h




**7** **8** X = $CH_2OCOCF_3$ **9** (82% from **7**)

**Scheme 4** *Reagents and conditions*: i, $(CF_3CO)_2O$ (3 equiv.), $Et_3N$ (3 equiv.), $CH_2Cl_2$, 0 °C, 0.5 h; ii, $K_2CO_3$ (6 equiv.), MeOH, 0 °C to reflux, 2 h

In conclusion, nucleophilic addition–elimination reactions with the β,β-difluorovinylidene moiety allows normally 'disfavoured' 5-*endo*-trigonal cyclizations to occur. This cyclization process affords ring-fluorinated indoles, benzo[*b*]furans, and benzo[*b*]thiophenes in high yields. These 'anti-Baldwin' results indicate that some of the unique reactivity of *gem*-difluoroalkenes may be derived from a partial single bond character of the alkene.

We gratefully acknowledge financial support for this research in the form of a grant from the Ministry of Education, Science, Sports, and Culture, Japan (Grant-in-Aid for Scientific Research No. 09640641), and Central Glass Co. Ltd. to J. I. We also thank the Center for Instrumental Analysis KIT for the measurement of analytical data.

## Footnotes and References

† E-mail: ichikawa@che.kyutech.ac.jp

‡ Electrophile-driven cyclizations refer to ring closure initiated by the coordination of the double bond in a substrate to an external electrophile such as $I_2$ and PhSeCl. Strictly speaking, this type of cyclization does not seem likely to be an exception to Baldwin's rules.

§ **5a**: $^1$H NMR (500 MHz, $CDCl_3$): δ 0.86 (3H, t, *J* 7.4 Hz), 1.21 (2H, tq, *J* 7.4, 7.4 Hz), 1.53 (2H, tt, *J* 7.4, 7.4 Hz), 2.34 (3H, s), 2.52 (2H, td, *J* 7.4 Hz, $J_{HF}$ 0.8 Hz), 7.20 (2H, d, *J* 8.4 Hz), 7.23 (1H, ddd, *J* 7.7, 7.7, 1.2 Hz), 7.28 (1H, ddd, *J* 7.7, 7.7, 1.4 Hz), 7.33 (1H, dd, *J* 7.7, 1.2 Hz), 7.73 (2H, d, *J* 8.4 Hz), 8.08 (1H, d, *J* 7.7 Hz). $^{13}$C NMR (126 MHz, $CDCl_3$): $\delta$ 13.6, 21.3 (d, $J_{CF}$ 3 Hz), 21.5, 22.1, 30.5, 99.7 (d, $J_{CF}$ 11 Hz), 114.4, 118.9 (d, $J_{CF}$ 7 Hz), 124.0, 124.0 (d, $J_{CF}$ 4 Hz), 126.8, 128.1 (d, $J_{CF}$ 6 Hz), 129.8, 130.6, 134.7, 145.2, 147.4 (d, $J_{CF}$ 276 Hz). $^{19}$F NMR (470 MHz, $CDCl_3$–$C_6F_6$): $\delta$ 29.1 (1F, s). $\nu_{max}$(neat)/cm$^{-1}$ 2960, 2930, 2860, 1660, 1455, 1395, 1190, 1180, 745, 690, 665. *m/z* (20 eV) 345 ($M^+$, 100%), 190 (68), 148 (92). HRMS: calc. for $C_{19}H_{20}O_2SNF$, 345.1199 ($M^+$). Found, 345.1188.

¶ *Selected data* for **6**: $^1$H NMR (500 MHz, $CDCl_3$): $\delta$ 0.94 (3H, t, *J* 7.4 Hz), 1.39 (2H, tq, *J* 7.4, 7.4 Hz), 1.66 (2H, tt, *J* 7.4, 7.4 Hz), 2.57 (2H, td, *J* 7.4 Hz, $J_{HF}$ 1.0 Hz), 7.19–7.25 (2H, m), 7.32–7.36 (1H, m), 7.40–7.45 (1H, m). $^{13}$C NMR (126 MHz, $CDCl_3$): $\delta$ 13.8, 21.0 (d, $J_{CF}$ 3 Hz), 22.4, 30.7 (d, $J_{CF}$ 2 Hz), 90.6 (d, $J_{CF}$ 12 Hz), 110.8, 119.2 (d, $J_{CF}$ 6 Hz), 123.1 (d, $J_{CF}$ 4 Hz), 123.2, 129.3 (d, $J_{CF}$ 3 Hz), 147.1, 157.1 (d, $J_{CF}$ 278 Hz). $^{19}$F NMR (470 MHz, $CDCl_3$–$C_6F_6$): $\delta$ 42.0 (1F, s). $\nu_{max}$ (neat)/cm$^{-1}$ 2960, 2940, 2860, 1675, 1455, 1380, 1295, 1260, 1185, 1140, 740. *m/z* (20 eV) 192 ($M^+$, 43%), 149 (100). HRMS: calc. for $C_{12}H_{13}OF$, 192.0950 ($M^+$). Found, 192.0918.

‖ This formation of benzothiophenes is favoured by Baldwin's rules since second-row elements are permitted 5-*endo*-trigonal processes [ref. 8(*b*)]. *Selected data* for **9**: $^1$H NMR (500 MHz, $CDCl_3$): $\delta$ 0.94 (3H, t, *J* 7.5 Hz), 1.39 (2H, tq, *J* 7.5, 7.5 Hz), 1.64 (2H, tt, *J* 7.5, 7.5 Hz), 2.75 (2H, td, *J* 7.5 Hz, $J_{HF}$ 1.3 Hz), 7.28 (1H, ddd, *J* 7.6, 7.6, 1.4 Hz), 7.35 (1H, ddd, *J* 7.6, 7.6, 0.9 Hz), 7.58 (1H, d, *J* 7.9 Hz), 7.64 (1H, d, *J* 7.9 Hz). $^{13}$C NMR (126 MHz, $CDCl_3$): $\delta$ 13.8, 22.5, 23.6, 31.0 (d, $J_{CF}$ 2 Hz), 115.5 (d, $J_{CF}$ 10 Hz), 121.5 (d, $J_{CF}$ 6 Hz), 122.6, 124.0 (d, $J_{CF}$ 4 Hz), 124.6, 131.3 (d, $J_{CF}$ 2 Hz), 136.8 (d, $J_{CF}$ 6 Hz), 159.2 (d, $J_{CF}$ 289 Hz). $^{19}$F NMR (470 MHz, $CDCl_3$–$C_6F_6$): $\delta$ 29.1 (1F, s). $\nu_{max}$(neat)/cm$^{-1}$ 2960, 2930, 2860, 1610, 1460, 1435, 1265, 1190, 1065, 755, 730. *m/z* (20 eV) 208 ($M^+$, 50%), 165 (100). HRMS: calc. for $C_{12}H_{13}SF$, 208.0722 ($M^+$). Found 208.0694.

1 L. G. Sprague, K. B. Baucom, S. F. Sellers and R. A. DuBoisson, in *Chemistry of Organic Fluorine Compounds II*, ed. M. Hudlicky and A. E. Pavlath, ACS Monograph 187, American Chemical Society, Washington, DC, 1995, pp. 729–756.
2 M. J. Tozer and T. F. Herpin, *Tetrahedron* 1996, **52**, 8619.
3 J. R. McCarthy, P. S. Sunkara, D. P. Matthews, A. J. Bitonti, E. T. Jarvi, J. F. Sabol, R. J. Resvick, E. W. Huber, W. A. v. d. Donk, G. Yu and J. Stubbe, in *Biomedical Frontiers of Fluorine Chemistry*, ed. I. Ojima, J. R. McCarthy and J. T. Welch, ACS Symposium Series 639, American Chemical Society, Washington, DC, 1996, ch. 18; P. Bey, J. R. McCarthy and I. A. McDonald, in *Selective Fluorination in Organic and Bioorganic Chemistry*, ed. J. T. Welch, ACS Symposium Series 456, American Chemical Society, Washington, DC, 1991, pp. 105–133.
4 J. Ichikawa, N. Yokota, M. Kobayashi and T. Minami, *Synlett*, 1993, 186.
5 J. Ichikawa, M. Kobayashi, N. Yokota, Y. Noda and T. Minami, *Tetrahedron*, 1994, **50**, 11637; J. Ichikawa, N. Yokota, M. Kobayashi, K. Amano and T. Minami, *Synlett*, 1996, 243.
6 J. Ichikawa, M. Kobayashi, Y. Noda, N. Yokota, K. Amano and T. Minami, *J. Org. Chem.*, 1996, **61**, 2763.
7 *o*-Substituted β,β-dichloro- and -dibromo-styrenes have recently been reported to undergo intramolecular cyclization *via* electrophilic carbenoids: M. Topolski, *J. Org. Chem.*, 1995, **60**, 5588.
8 (*a*) J. E. Baldwin, *J. Chem. Soc., Chem. Commun*., 1976, 734; (*b*) J. E. Baldwin, J. Cutting, W. Dupont, L. Kruse, L. Silberman and R. C. Thomas, *ibid.*, 1976, 736; (*c*) J. E. Baldwin, R. C. Thomas, L. I. Kruse and L. Silberman, *J. Org. Chem.*, 1977, **42**, 3846.
9 D. Craig and A. M. Smith, *Tetrahedron Lett.*, 1992, **33**, 695; P. Auvray, P. Knochel and J. F. Normant, *Tetrahedron Lett.*, 1985, **26**, 4455; R. Grigg, J. Kemp, J. F. Malone, S. Rajviroongit and A. Tangthongkum, *Tetrahedron*, 1988, **44**, 5361. For a related example, see: R. D. Chambers and M. P. Greenhall, *J. Chem. Soc., Chem. Commun.*, 1990, 1128.
10 A. D. Jones and D. W. Knight, *Chem. Commun*., 1996, 915; Y. Landais and D. Planchenault, *Synlett*, 1995, 1191 and references cited therein; B. H. Lipshutz and T. Gross, *J. Org. Chem.*, 1995, **60**, 3572 and references cited therein; M. Kimura, H. Harayama, S. Tanaka and Y. Tamaru, *J. Chem. Soc., Chem. Commun*., 1994, 2531.
11 For 5-*endo* radical cyclizations onto an unsaturated carbon, see T. Gimisis and C. Chatgilialoglu, *J. Org. Chem.*, 1996, **61**, 1908; T. Sato, N. Chono, H. Ishibashi and M. Ikeda, *J. Chem. Soc., Perkin Trans. 1*, 1995, 1115; A. V. R. Rao, A. K. Singh, K. M. Reddy and K. Ravikumar, *J. Chem. Soc., Perkin Trans. 1*, 1993, 3171. See, also: D. L. J. Clive and W. Yang, *Chem. Commun.*, 1996, 1605. For 5-*endo* radical cyclizations onto a multiple-bonded, first-row heteroatom, see: Y. Yamamoto, M. Ohno and S. Eguchi, *J. Org. Chem.*, 1996, **61**, 9264 and references cited therein.
12 M. J. Silvester, *Adv. Heterocycl. Chem.*, 1994, **59**, 1; *Aldrichim. Acta*, 1991, **24**, 31; *Organofluorine Chemistry, Principles and Commercial Applications*, ed. R. E. Banks, B. E. Smart and J. C. Tatlow, Plenum Press, New York, 1994.
13 J. Ichikawa, T. Minami, T. Sonoda and H. Kobayashi, *Tetrahedron Lett.*, 1992, **33**, 3779; see also: J. Ichikawa, M. Fujiwara, H. Nawata, T. Okauchi and T. Minami, *Tetrahedron Lett.*, 1996, **37**, 8799.
14 For the synthesis of fluoroindoles, see H. F. Hodson, D. J. Madge, A. N. Z. Slawin, D. A. Widdowson and D. J. Williams, *Tetrahedron*, 1994, **50**, 1899. For the synthesis of fluoropyrroles, see Z.-M. Qiu and D. J. Burton, *Tetrahedron Lett.*, 1995, **36**, 5119; J. Leroy and C. Wakselman, *Tetrahedron Lett.*, 1994, **35**, 8605 and references cited therein.
15 For the synthesis of fluorobenzo[*b*]furans, see: D. H. R. Barton, R. H. Hesse, G. P. Jackman and M. M. Pechet, *J. Chem. Soc., Perkin Trans. 1*, 1977, 2604. For the synthesis of fluorofurans, see A. K. Forrest and P. J. O'Hanlon, *Tetrahedron Lett.*, 1995, **36**, 2117; K. Burger and B. Helmreich, *J. Chem. Soc., Chem. Commun*., 1992, 348; H. L. Sham and D. A. Betebenner, *J. Chem. Soc., Chem. Commun*., 1991, 1134.
16 R. N. Young, J. Y. Gauthier and W. Coombs, *Tetrahedron Lett.*, 1984, **25**, 1753.
17 For the synthesis of fluorobenzo[*b*]thiophenes, see; P. Nussbaumer, G. Petrenyi and A. Stütz, *J. Med. Chem.*, 1991, **34**, 65. For the synthesis of fluorothiophenes, see K. Burger and B. Helmreich, *Heterocycles*, 1994, **39**, 819.

*Received in Cambridge, UK, 7th May 1997; 7/03110F*

# Carbon monoxide–phosphaalkyne coupling and C–H activation of an N–Me group in the 4e-$\eta^2$-phosphaalkyne complex $[WF(C_6H_4CH_2NMeCH_2CH_2NMe_2)(CO)(\eta^2\text{-}P{\equiv}CBu^t)]$. Crystal and molecular structure of $[WF\{CH_2N(CH_2Ph)CH_2CH_2NMe_2\}(CO)\{\eta^4\text{-}PCBu^t(CO)CBu^tP\}]$

**Maria Helena A. Benvenutti,[a] Peter B. Hitchcock,[a] Jaqueline L. Kiplinger,[b] John F. Nixon*[a] and Thomas G. Richmond*[b]**

[a] *School of Chemistry, Physics and Environmental Science, University of Sussex, Brighton, UK BN1 9QJ*
[b] *Department of Chemistry, University of Utah, Salt Lake City, Utah 84112, USA*

**An unusual series of reactions involving an intermediate 4e $\eta^2$-phosphaalkyne tungsten complex is described.**

There is current interest in the coordination chemistry of phosphaalkynes, RC≡P, and transition-metal compounds containing phosphorus analogues of unsaturated ring systems such as 1,2- and 1,3-diphosphacyclobutadiene, 1,2- and 1,2,4- di- and tri-phosphacyclopentadienyl, and most recently 1,3,5-triphosphabenzene, which can all be derived from the parent phosphaalkyne.[1–3]

The number of examples of phosphaalkynes acting as $\eta^2$-(4e) ligands to transition-metal centres is very limited and to date none have been structurally characterised owing to their ready further reaction to afford 1,3-diphosphacyclobutadiene complexes.[4] In order to extend the range of such complexes we have now synthesised the $Bu^tC{\equiv}P$ analogue of the recently described[5] structurally related $\eta^2$-(4e) nitrile complex $[WF(C_6H_4CH_2NMeCH_2CH_2NMe_2)(CO)(\eta^2\text{-}N{\equiv}CC_6F_5)]$. Although NMR spectroscopic evidence† (P≡C, $\delta_P$ 452.4, $\delta_C$ 315.2; $^1J_{PC}$ 117.7, $^1J_{PW}$ 82.0 Hz) fully confirmed[4] the expected formation of the green $\eta^2$-(4e) phosphaalkyne complex $[WF(C_6H_4CH_2NMeCH_2CH_2NMe_2)(CO)(\eta^2\text{-}P{\equiv}CBu^t)]$ **2**, when $[WF(C_6H_4CH_2NMeCH_2CH_2NMe_2)(CO)_3]$ **1**,[6] was treated with $Bu^tC{\equiv}P$ for 3 h in toluene at room temp. it proved impossible to isolate it in crystalline form. A facile further reaction of **2** with $Bu^tC{\equiv}P$ (5 equiv. at 90 °C for 2 h in toluene in a closed system) affords the novel red complex $[WF\{CH_2N(CH_2Ph)CH_2CH_2NMe_2\}(CO)\{\eta^4\text{-}PCBu^t(CO)CBu^tP\}]$ **3**, (30% yield), containing an $\eta^4$-ligated 3,4-diphosphacyclopentadieneone and a three-membered $NCH_2W$ ring system. Complex **3** has been structurally characterised by spectroscopic data‡ and by a single-crystal X-ray diffraction study§ (Fig. 1). The reactivity of **2** contrasts with the behaviour of the analogous $\eta^2$-(4e) nitrile complex which does not undergo coupling reactions and whose chemistry is dominated by ready dissociation of the nitrile ligand.

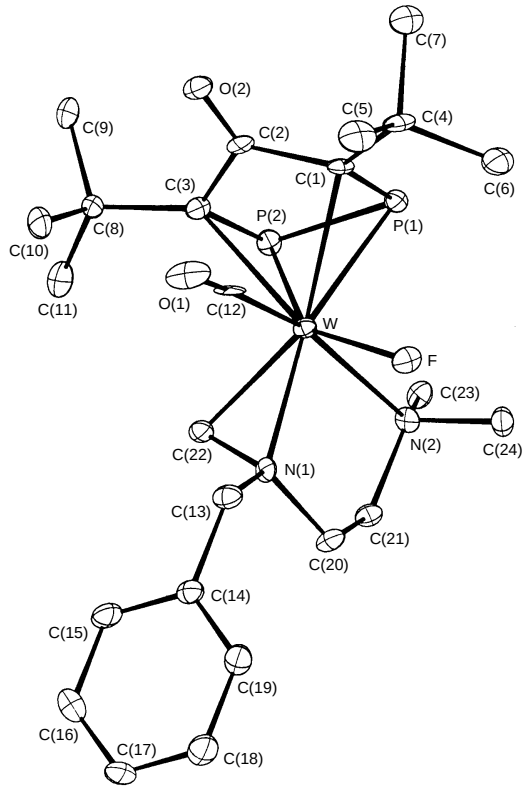
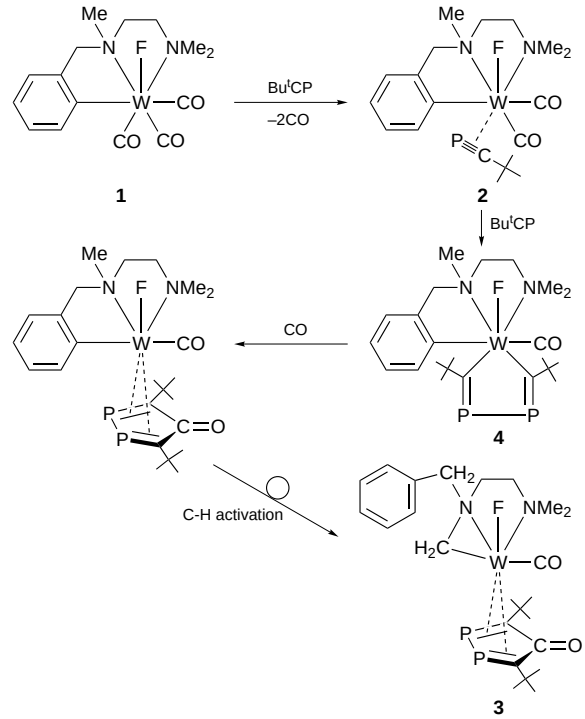



**Fig. 1** Molecular structure of **3**. Selected bond lengths (Å) and angles (°): W–P(1) 2.504(2), W–P(2) 2.490(2), W–C(1) 2.412(7), W–C(3) 2.443(8), W–C(12) 1.992(9), W–C(22) 2.169(9), W–F 1.997(4), W–N(1) 2.175(6), W–N(2) 2.408(6), P(1)–P(2) 2.173(3), P(1)–C(1) 1.740(8), P(2)–C(3) 1.769(8), O(1)–C(12) 1.158(10), O(2)–C(2) 1.233(9), N(1)–C(22) 1.441(10), C(1)–P(1)–P(2) 94.6(3), C(3)–C(2)–C(1) 109.4(6), C(3)–P(2)–P(1) 93.8(3).




**Scheme 1**

We believe that **3** results either from CO insertion into an intermediate $\eta^4$-ligated 1,2-diphosphacyclobutadiene complex formed from **2** and $Bu^tC{\equiv}P$, or alternatively into the five-membered tungstadiphosphacyclopentadiene ring of complex **4**, followed by reductive elimination (Scheme 1). No such intermediates could be detected spectroscopically, however we showed previously[7] that carbonyl insertion and reductive elimination occurs in the closely related tungsten(II) alkoxide. Presumably the bulky $\eta^4$-ligated 3,4-diphosphacyclopentadieneone ring system generated from **2** causes crowding at the metal centre, and subsequent relief of steric strain results in the formation of **3** *via* (*i*) C–H activation of the uncoordinated $NCH_3$ group to generate the $NCH_2W$ ring system and (*ii*) hydrogen transfer to the metallated $C_6H_4$ fragment.

Previously we described (*i*) CO coupling of two phosphaalkynes to give rhodium(I) complexes of the six membered ring system RhPCORCRP, (R = $Bu^t$, adamantyl),[8] and (*ii*) carbonylation of coordinated phosphaalkynes to give phosphinidene $[Bu^t(CO)P]$ complexes,[9,10] however the formation of the 3,4-diphosphacyclopentadienone ring in **3** is unprecedented, although Cowley and coworkers[11] have structurally characterised the isomeric diphosphatricyclo[1.2.0.$0^{2,5}$]pentane ring system. Likewise, reports of C–H activation of an N–Me group are also rare in organometallic systems. A recent report by van Koten *et al.*[12] described the stereoselective C–H activation of an N–Me group in the tantalum complex $[TaCl_2(CH_2Ph)_2\{C_6H_4(Me)NMe\text{-}2\}]$, in which the key step proceeds by a σ-bond metathesis which also involves the relief of steric strain.

## Footnotes and References

* E-mail: j.nixon@sussex.ac.uk

† *Spectroscopic data* for **2**: $^1$H NMR (300 MHz, $CDCl_3$) $\delta$ 1.73 (s, $Bu^t$, 9 H). $^{31}P\{^1H\}$ NMR (121.4 MHz, $CDCl_3$, 85% $H_3PO_4$ external ref. $\delta$ 0.00) $\delta$ 452.42 (s, $^1J_{PW}$ 82.0). $^{13}C\{^1H\}$ (75.4 MHz, $CDCl_3$) $\delta$ 315.18 (d, P≡C, $^1J_{PC}$ 117.7 Hz), 225.60 (d, CO, $^2J_{CF}$ 21.0, $^1J_{CW}$ 137.0), 124.50 (s, $C_6H_5$), 125.17 (s, $C_6H_5$), 128.98 (s, $C_6H_5$), 144.02 (s, $C_6H_5$), 143.45 (s, $C_6H_5$), 188.25 (d, W–C, $^2J_{CF}$ 4.0 Hz), 34.33 (d, C*C*H$_3$, $J_{PC}$ 5.2 Hz), 30.40 (s, *C*CH$_3$), 57.20 (s, $CH_2$), 61.35 (s, $CH_2$), 66.14 (s, $CH_2$), 56.25 (s, $CH_3$), 47.41 (d, $CH_3$, $J_{CF}$ 8.7 Hz), 48.51 (d, $CH_3$, $J_{CF}$ 20.6 Hz).

‡ *Spectroscopic data* for **3**: IR ($CHCl_3$) $\nu_{CO}$ 1966s, 1611m cm$^{-1}$. MS (70 eV, EI) *m/z* (%) 650 (2) [M$^+$], 622 (25) [M$^+$ − CO]. $^1$H NMR (300 MHz, $CDCl_3$) $\delta$ 1.82 (dd, $CH_2$, 1 H, *J* 13.6, 4.1 Hz), 2.40 (dt, $CH_2$, 1 H, *J* 13.7, 4.5 Hz), 2.70 (dd, $CH_2$, 1 H, *J* 12.5, 4.3), 2.85 (dt, $CH_2$ 1 H, *J* 13.1, 4.5 Hz), 3.10 (d, $CH_2$, 1 H, *J* 4.7 Hz), 3.33 (d, $CH_2$, 1 H, *J* 6.2 Hz), 4.70 (d, $CH_2$, 2 H, *J* 32.8, 5.3 Hz), 2.27 (d, $CH_3$, 3 H, *J* 5.8 Hz), 2.77 (d, $CH_3$, 3 H, *J* 2.2 Hz), 1.21 (s, $Bu^t$, 9 H), 0.98 (s, $Bu^t$, 9 H), 7.35–7.26 (m, Ph, 5 H). $^{31}P\{^1H\}$ NMR (121.4 MHz, $CDCl_3$) $\delta$ −62.02 (dd, $^1J_{PP}$ 263.0, $^2J_{PF}$ 15.0 Hz) −87.60 (dd, $^1J_{PW}$ 29.0, $^2J_{PF}$ 15.0 Hz). $^{13}C\{^1H\}$ (75.4 MHz, $CDCl_3$) $\delta$ 216.26 (d, CO, $J_{CP}$ 8.1 Hz), 186.67 (s, CO), 134.24 (s, $C_6H_5$, *ipso*), 128.81 (s, $C_6H_5$), 128.50 (s, $C_6H_5$, *para*), 128.43 (s, $C_6H_5$), 58.39 (dd, $CH_3$, *J* 23.6, 12.0 Hz, $J_{CF}$ or $J_{CP}$), 49.31 (dd, $CH_3$ *J* 21.4, 7.1 Hz, $J_{CF}$ or $J_{CP}$), 30.52 (dd, C*C*H$_3$, $J_{PC}$ 2.2, 8.7 Hz), 30.27 (d, C*C*H$_3$, $J_{PC}$ 8.8 Hz), 38.40 (d, *C*CH$_3$, $J_{PC}$ 13.6 Hz), 37.09 (d, *C*CH$_3$, $J_{PC}$ 14.6 Hz), 65.02 (s, $CH_2$), 55.96 (s, $CH_2$), 48.63 (s, $CH_2$), 44.00 (dd, $CH_2$, *J* 9.4, 5.7 Hz, $J_{CF}$ or $J_{CP}$), 125.55 (d, PCP, $J_{PC}$ 85.7 Hz), 109.02 (d, PCP, $J_{PC}$ 81.2 Hz). $^{19}$F NMR (376.3 MHz, $CD_2Cl_2$, $CFCl_3$ external ref., $\delta$ 0.00) $\delta$ 42.05 (m, $^2J_{FP}$ 15.0 Hz).

§ *Crystal data* for **3**: $C_{24}H_{37}FN_2O_2P_2W{\cdot}CH_2Cl_2$, *M* = 735.27, monoclinic, space group *C*2/*c* (no. 15), *a* = 34.036(9), *b* = 9.861(2), *c* = 18.313(8) Å, $\beta$ = 112.05(3)°, *U* = 5697(3) Å$^3$, *Z* = 8, $D_c$ = 1.72 Mg m$^{-3}$, *F*(000) = 2928. The data were obtained with an Enraf-Nonius CAD4, diffractometer using Mo-K$\alpha$ radiation, $\lambda$ = 0.71073 Å, $\mu$ = 4.39 mm$^{-1}$, on a crystal 0.25 × 0.25 × 0.10 mm. 4031 reflections measured for $2 < \theta < 23°$ giving 3962 unique. Refinement on $F^2$ using SHELXL-93, non-H atoms anisotropic, H atoms in riding mode, except for those on C(22) which were freely refined. $R_1$ = 0.035 [for 3202 reflections with $I > 2\sigma(I)$], $wR_2$ = 0.093 (all data). CCDC 182/498.


1 J. F. Nixon, *Chem. Soc. Rev.*, 1995, **24**, 319 and references therein.
2 J. F. Nixon, *Coord. Chem. Rev.*, 1995, **145**, 201 and references therein.
3 P. L. Arnold, F. G. N. Cloke, P. B. Hitchcock and J. F. Nixon, *J. Am. Chem. Soc.*, 1996, **118**, 7630.
4 G.Brauers, M. Green, C. Jones and J. F. Nixon, *J. Chem. Soc., Chem. Commun.*, 1995, 1125.
5 J. L. Kiplinger, A. M. Arif and T. G. Richmond, *Organometallics*, 1997, **16**, 246.
6 B. P. Buffin, M. J. Poss, A. M. Arif and T. G. Richmond, *Inorg. Chem.*, 1993, **32**, 3805.
7 B. P. Buffin, A. M. Arif and T. G. Richmond, *J. Chem. Soc., Chem. Commun.*, 1993, 1432.
8 P. B. Hitchcock, M. J. Maah and J. F. Nixon, *Heteroatom Chem.*, 1991, **2**, 243.
9 P. Gaede, B. F. G. Johnson, J. F. Nixon, M. Nowotny and S. Parsons, *Chem. Commun.*, 1996, 1455.
10 S. I. Al-Resayes, P. B. Hitchcock and J. F. Nixon, *J. Chem. Soc., Chem. Commun.*, 1987, 928.
11 A. R. Barron, A. H. Cowley, S. W. Hall and C. M. Nunn, *Angew. Chem., Int. Ed. Engl.*, 1988, **27**, 837.
12 H. C. L. Abbenhuis, R. van Belzen, D. M. Grove, A. J. A. Klomp, G. P. M. van Mier, A. L. Spek and G. van Koten, *Organometallics*, 1993, **12**, 210.


*Received in Cambridge, UK, 13 May 1997; 7/03303F*

# The first mononuclear η⁸-coordinated pentalene complex: synthesis and molecular structure of [Ta{η⁸-$C_8H_4(SiMe_3)_2$-1,4}$Cl_3$]

**Qasim A. Abbasali, F. Geoffrey N. Cloke,* Peter B. Hitchcock and Stephen C. P. Joseph**

*The Chemistry Laboratory, School of Chemistry, Physics and Environmental Science, University of Sussex, Brighton, UK BN1 9QJ*

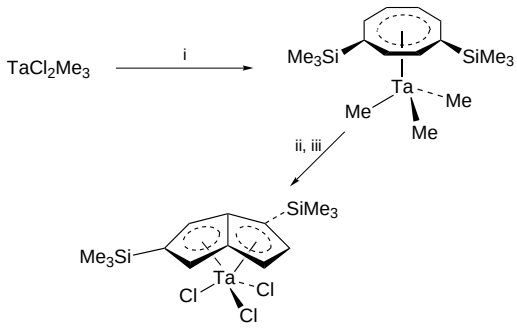
**Treatment of [$TaCl_2Me_3$] with $Li_2$(cot″) (cot″ = 1,4-bis(trimethylsilyl)cyclooctatetraene] affords [Ta(η-cot″)$Me_3$], which reacts with [$NHPr^i_2Et$]Cl in dichloromethane to yield the complex [Ta{η⁸-$C_8H_4(SiMe_3)_2$-1,4}$Cl_3$]; X-ray crystallography shows the latter to contain a pentalene ligand bound through all eight carbons to a single tantalum centre.**

Transition-metal complexes derived from pentalene, or its dianion, are somewhat rare, and presently known examples fall into two categories: (*a*) binuclear systems which contain the planar pentalene dianion *e.g.* [$M_2$(η⁵,η⁵-$C_8H_6$)$_2$] (M = Co, Ni),[1] [(η³-$C_3H_5$)Ni(η⁵,η⁵-$C_8H_6$)Ni(η³-$C_3H_5$)][2] and [(η⁵-$C_5Me_5$)M(η⁵,η⁵-$C_8H_6$)M(η⁵-$C_5Me_5$)] (M = Fe, Co, Ni);[3] (*b*) binuclear systems in which two metal carbonyl fragments are bound to the five-membered rings of a folded pentalene ring system, formed by *in situ* elimination of dihydrogen from a cyclooctatetraene ligand, *e.g.* [{Ru($MMe_3$)(CO)$_2$)}$_2$(η⁵,η⁵-$C_8H_6$)] (M = Si, Ge), [$Ru_3$(CO)$_8$(η⁵,η⁵-$C_8H_6$)] and [$Ru_3$(CO)$_8${η⁵,η⁵-$C_8H_4(SiMe_3)_2$-1,4}].[4]

Recently, we have been exploring the chemistry of group 4 metal complexes incorporating the cot″ ligand [cot″ = 1,4-bis(trimethylsilyl)cyclooctatetraene] and were interested in extending this work to the group 5 elements.[5] Here we report the surprising conversion of an η⁸-cot″ ligand into an η⁸-pentalene ligand on a single tantalum centre.

Attempts to prepare a complex of the type [Ta(η-cot″)$Cl_3$] starting from $TaCl_5$, as an entry into mono-cot″ tantalum chemistry, were uniformly unsuccessful, persistently producing brown intractable solids. As an alternative starting material, dark purple [Ta(η-cot″)$Me_3$] **1** was prepared from the reaction between $Li_2$(cot″) and [$TaCl_2Me_3$] in hexane at −78 °C (Scheme 1) in 70% yield,† in an analogous fashion to that described by Schrock and coworkers for the synthesis of [Ta(η-cot)$Me_3$].[6] The $^1$H and $^{13}$C{$^1$H} NMR spectra of **1** show the typical resonances for a planar η⁸-cot″ ring and the Ta–Me groups.‡

In an attempt to prepare [Ta(η-cot″)$Cl_3$], the complex [Ta(η-cot″)$Me_3$] was treated with 3 equiv. of [$NHPr^i_2Et$]Cl in $CH_2Cl_2$; however, after work up air-sensitive red needles of the pentalene complex [Ta{η⁸-$C_8H_4(SiMe_3)_2$-1,4}$Cl_3$] **2** (Scheme 1) were obtained in 10% yield.§




**Scheme 1** i, $Li_2$[(cot″)(thf)$_x$], *n*-pentane; ii, 3 [$NHPr^i_2Et$]Cl, $CH_2Cl_2$; iii, vacuum sublimation ($10^{-5}$ mbar, 140 °C)

The $^1$H NMR spectrum of **2** exhibits four downfield signals ($\delta$ 6.51–5.32) attributable to four distinct ring proton environments and two upfield singlets ($\delta$ 0.4 and 0.3) assignable to two distinct trimethylsilyl groups. The $^{13}$C{$^1$H} NMR spectrum shows ten resonances, eight of which are at low field and as such can be attributed to the carbon ring framework, whilst those carbons associated with the trimethylsilyl substituents are identified by two singlets at $\delta$ −0.2 and −0.7.¶

Single crystals of **2**, suitable for X-ray diffraction studies,‖ were grown by vapour-phase diffusion in an evacuated sealed tube at 160 °C. The molecular structure of **2**, as shown in Fig. 1, shows the complex to contain the first example of a pentalene ligand η⁸-coordinated to a single metal centre. The pentalene ring in **2** is folded about the bridgehead [C(2)–C(6)] bond, with a fold angle of 33°; in the metal–metal bonded binuclear complex [{Ru($GeMe_3$)(CO)$_2$}$_2$(η⁵,η⁵-$C_8H_6$)] the fold angle is 9°.[7] The tantalum–ring carbon distances of **2** range from 2.182(13), for the bridgehead carbons to 2.583(13) Å for the 'wingtip' carbons, and may be compared to the tantalum–ring carbon distances in [Ta(cot″)$Me_3$] **1** which lie between 2.424(6) and 2.488(5) Å.[8] The pentalene ring C–C bond lengths in **2** range from 1.36(2) [C(7)–C(8)] to 1.48(2) [C(1)–C(2)] Å with a bridgehead [C(2)–C(6)] bond length of 1.47(2) Å. In the planar pentalene ring system found in [(η⁵-$C_5Me_5$)Fe(η⁵,η⁵-$C_8H_6$)Fe(η⁵-$C_5Me_5$)], the ring C–C distances lie between 1.464(5) (for the bridgehead) and 1.408(5) Å. For the folded (9°) ligand in [{Ru($GeMe_3$)(CO)$_2$}$_2$(η⁵,η⁵-$C_8H_6$)],[6] the ring C–C distances range from 1.32(5) to 1.51(4) with a bridgehead C–C distance of 1.43(5) Å. The Ta–Cl bond lengths in **2** range from 2.362(3) to 2.386(3) Å and can be compared to the Ta–Cl

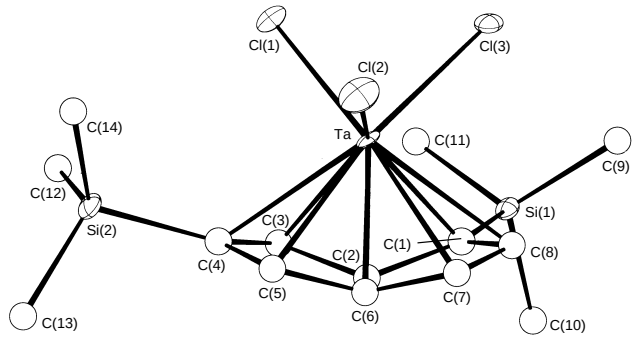



**Fig. 1** CAMERON[12] representation of the crystal structure of **2**. Selected bond lengths (Å) and angles (°): Ta–C(1) 2.351(12), Ta–C(2) 2.182(13), Ta–C(3) 2.358(12), Ta–C(4) 2.583(12), Ta–C(5) 2.469 (13), Ta–C(6) 2.217(12), Ta–C(7) 2.488(13), Ta–C(8) 2.539(13), Ta–Cl(1) 2.362(3), Ta–Cl(2) 2.374(4), Ta–Cl(3) 2.386 (3), C(1)–C(2) 1.48(2), C(2)–C(6) 1.47(2), C(2)–C(3) 1.40(2), C(3)–C(4) 1.43(2), C(4)–C(5) 1.41(2), C(5)–C(6) 1.43(2), C(6)–C(7) 1.43(2), C(7)–C(8) 1.36(2), C(8)–C(1) 1.45(2); C(1)–C(2)–C(3) 129.8(11), C(2)–C(3)–C(4) 109.7(11), C(4)–C(5)–C(6) 108.9(12), C(7)–C(6)–C(2) 108.2(10), C(8)–C(7)–C(6) 107.8 (11), C(8)–C(1)–C(2) 104.0 (10), C(3)–C(2)–C(6) 106.8(11), C(6)–C(2)–C(1) 106.7(10), C(5)–C(4)–C(3) 107.8 (11), C(7)–C(6)–C(5) 133.8(12), C(5)–C(6)–C(2) 106.7(11), C(1)–C(8)–C(1) 113.0(11).

distance of 2.387(11) Å in [Ta($\eta^5$-$C_5Me_5$)$Me_2Cl_2$].[9] Further comparisons are difficult due to the lack of other, related compounds.

Attempts are currently underway to study the mechanism of this reaction and to improve the yield of **2**; the latter promises to be a versatile precursor to monopentalene tantalum chemistry.

We thank the EPSRC and BP Chemicals for CASE Studentships (to Q. A. A. and S. C. P. J.), Dr A. G. Avent for the NMR studies and Dr A. Abdul-Sada for mass spectral analysis.

## Footnotes and References

* E-mail: f.g.cloke@sussex.ac.uk

† *Preparation of* [Ta(η-cot″)$Me_3$] **1**: to a pentane (40 ml) solution of [$TaCl_2Me_3$] (0.25 g, 0.84 mmol) at −40 °C was added a pentane (40 ml) suspension of [$Li_2$(cot″)] (0.284 g, 0.9 mmol) dropwise over a period of 45 min during which the reaction mixture darkened to brown. Once the addition was complete, the brown suspension was stirred at −40 °C for 60 min before being warmed to room temp. and left to stir overnight. Filtration through Celite on a frit, and concentration and cooling of the red filtrate to −30 °C yielded **1** as purple crystals (0.28 g, yield = 70%).

‡ *NMR and mass spectral data* for complex **1**. $^1$H NMR ($C_6D_6$, 298 K); $\delta$ 6.39 (2 H, m, CH ring), 6.33 (2 H, s, CH ring), 5.95 (2 H, m, CH ring), 0.67 (9 H, s, TaMe), 0.49 (18 H, s, $SiMe_3$). $^{13}$C{$^1$H} NMR ($C_7D_8$, 298 K); $\delta$ 102.82 (CH ring), 100.62 (CH ring), 96.96 (CH ring), 93.84 (*C*$SiMe_3$ ring), 65.55 (TaMe), 0.36 ($SiMe_3$). Mass spectrum (EI). *m*/*z* 459 ([M]$^+$ − Me, 50%).

§ *Preparation of* [Ta{$\eta^8$-$C_8H_4$($SiMe_3$)$_2$-1,4}$Cl_3$] **2**: to a solid mixture of [Ta(cot″)$Me_3$] (0.195 g, 0.41 mmol) and [NH$Pr^i_2$Et]Cl (0.204 g, 1.23 mmol) in a sublimer tube was added $CH_2Cl_2$ (*ca.* 20 ml) at room temp. After the mixture was allowed to stir for 15 min, the solvent was removed *in vacuo*. The residue was then sublimed at 140 °C ($10^{-5}$ mbar) to afford a red solid. Recrystallisation of this solid from pentane–diethyl ether (9 : 1) produced long red needle crystals of **2** (0.022 g, yield = 10%). Microanalysis: Calc.: C, 31.50; H, 4.15. Found: C, 31.89; H, 4.24%.

¶ *NMR and mass spectral data* for complex **2**: $^1$H NMR ($CD_2Cl_2$, 298 K): $\delta$ 6.51 (1 H, d, $J_{HH}$ 4.3, CH ring), 5.86 (1 H, d, $J_{HH}$ 0.9, CH ring), 5.68 (1 H, dd, $J_{HH}$ 4.3, 0.9, CH ring), 5.32 (1 H, s, CH ring), 0.4 (9 H, s, $SiMe_3$), 0.3 (9 H, s, $SiMe_3$). $^{13}$C{$^1$H} NMR ($CD_2Cl_2$, 298 K); $\delta$ 142.7 (C ring), 139.4 (CH ring), 133.0 (C ring), 126.0 (CH ring), 118.0 (CH ring), 112.3 (CH ring), 107.5 (*C*$SiMe_3$), 106.3 (*C*$SiMe_3$), −0.2 ($SiMe_3$), −0.7 ($SiMe_3$). Mass spectrum (EI). *m*/*z* 534 ([M]$^+$, 23%).

‖ *Crystal data*: $C_{14}H_{22}Cl_3Si_2Ta$, *M* = 533.80, triclinic, space group $P\bar{1}$ (no. 2), *a* = 7.206(2), *b* = 11.245(4), *c* = 12.233(4) Å, $\alpha$ = 88.85(3), $\beta$ = 75.08(3), $\gamma$ = 83.69(3)°, *U* = 952.0(5) Å$^3$, *Z* = 2, $D_c$ = 1.86 cm$^{-3}$, *F*(000) = 516. Monochromated Mo-Kα radiation, $\lambda$ = 0.71073 Å, $\mu$ = 63.1 cm$^{-1}$, *T* = 173 K. Data were collected on an Enraf–Nonius CAD 4 diffractometer in the $\theta$–2$\theta$ mode using a crystal of *ca.* 0.4 × 0.2 × 0.05 mm. A total of 3341 unique reflections were measured for 2 < $\theta$ < 25° and +*h*, ±*k*, ±*l*, and used in the refinement based on $F^2$ using SHELXL-93.[10] The structure was solved by direct methods using SHELXS-86[11] and Ta, Cl, Si atoms were refined anisotropically by full-matrix lest-squares methods. Hydrogen atoms were included in the riding mode with $U_{iso}$ = 1.2 or 1.5 $U_{eq}$(C) for the methyl groups. An absorption correction ($\psi$ scan, $T_{max}$ = 1.00, $T_{min}$ = 0.58) was applied. The final residuals were $R_1$ = 0.068 [for 2948 reflections with $I > 2\sigma(I)$] and $wR_2$ = 0.179 (for all data). CCDC 182/530.

1 T. J. Katz and N. Acton, *J. Am. Chem. Soc.*, 1972, **94**, 3281; T. J. Katz, N. Acton and J. McGinnis, *J. Am. Chem. Soc.*, 1972, **94**, 6205.
2 A. Miyake and A. Kanai, *Angew. Chem., Int. Ed. Engl.*, 1971, **10**, 801.
3 E. E. Bunel, L. Valle, N. L. Jones, P. J. Carroll, C. Barra, M. Gonzalez, N. Munoz, G. Visconti, A. Aizman and J. M. Manriquez, *J. Am. Chem. Soc.*, 1988, **110**, 6597.
4 S. A. R. Knox and F. G. A. Stone, *Acc. Chem. Res.*, 1974, **7**, 321.
5 N. C. Burton, F. G. N. Cloke, P. B. Hitchcock, H. C. de Lemosand and A. A. Sameh, *J. Chem. Soc., Chem. Commun.*, 1989, 1462; F. G. N. Cloke, P. B. Hitchcock and S. C. P. Joseph, *J. Chem. Soc., Chem. Commun.*, 1994, 1207; F. G. N. Cloke, P. B. Hitchcock, N. Kaltsoyannis, S. C. P. Joseph, A. McCamley and P. Mountford, *J. Chem. Soc., Dalton Trans.*, 1994, 2867; C. J. Cardin, F. G. N. Cloke, P. B. Hitchcock and S. C. P. Joseph, *Organometallics*, 1995, **14**, 3556; Q. A. Abbasali, F. G. N. Cloke, P. B. Hitchcock, S. C. P. Joseph and D. Peron, *J. Mol. Catal.*, submitted.
6 A. D. English, L. J. Guggenberger and R. R. Schrock, *J. Am. Chem. Soc.*, 1976, **98**, 903.
7 J. A. K. Howard and P. Woodward, *J. Chem. Soc., Dalton Trans.*, 1978, 412.
8 S. C. P. Joseph, D.Phil. Thesis, University of Sussex, 1994.
9 M. Gomez, G. Jimenez, P. Royo and J. M. Selas, *J. Organomet. Chem.*, 1992, **439**, 147.
10 G. M. Sheldrick, SHELXL-93, Program for Crystal Structure Refinement, University of Göttingen, 1993.
11 G. M. Sheldrick, SHELXS-86, Program for the Solution of Crystal Structures, University of Göttingen, 1986.
12 D. J. Watkin and L. J. Pearce, CAMERON, An Interactive Graphics Editor, University of Oxford, 1993.

*Received in Basel, Switzerland, 2nd May 1997; 7/03031B*

# One- and two-dimensional organic–inorganic composite solids constructed from molybdenum oxide clusters and chains linked through {M(2,2′-bpy)}$^{2+}$ fragments (M = Co, Ni, Cu)

**Pamela J. Zapf,[a] Christopher J. Warren,[b] Robert C. Haushalter[b] and Jon Zubieta*[a]**

[a] *Department of Chemistry, Syracuse University, Syracuse, NY 13244, USA*
[b] *NEC Research Institute, 4 Independence Way, Princeton, NJ 08540, USA*

**Hydrothermal reactions of $Na_2MoO_4·2H_2O$ and $MoO_3$ with $MCl_2·xH_2O$ (M = Co, Ni, Cu) and 2,2′-bipyridine yield one- and two-dimensional solids, characterized by molybdenum oxide monomers, clusters and chains linked by {M(2,2′-bpy)}$^{2+}$ groups and represented by the formulae $[M(bpy)_x(H_2O)_yMo_nO_{3n+1}]$ ($n$ = 2, M = Cu, $x$ = 1, $y$ = 0; $n$ = 3, M = Co, $x$ = 1, $y$ = 0; $n$ = 4, M = Ni, $x$ = 2, $y$ = 0).**

Metal oxide-based solids have provoked significant contemporary interest by virtue of their applications to areas as diverse as catalysis, sorption, molecular electronics, energy storage, optical materials and ceramics.[1,2] While the rational synthesis of new solids possessing unique structures and properties remains a challenge,[3] the structure-directing properties of organic components have been successfully exploited in the synthesis of metastable composite materials which retain the structural characteristics of the starting materials.[4,5] These organic constituents are most commonly present in the roles of tethers between metal sites, a mode adopted by 4,4′-bipyridine and related ligand types,[6] of charge-compensating cations such as organoammonium units,[7] or of ligands covalently linked to the inorganic backbone of the solid.[8] We recently demonstrated an additional type of composite material based on amine-ligated transition- or post-transition-metal cation complexes intercalated between mixed-valence vanadium oxide layers.[9] This observation suggested that appropriate transition-metal coordination compounds could also be incorporated directly into the covalent backbone of the solid either as peripheral metal/organic components or as complex bridging ligands. This expectation has been realized in the preparation and characterization of the one-dimensional solids $[Ni(2,2′\text{-bpy})_2Mo_4O_{13}]$ **1** and $[Cu(2,2′\text{-bpy})Mo_2O_7]$ **2** and the two-dimensional phase $[Co(2,2′\text{-bpy})Mo_3O_{10}]$ **3**.

Compounds **1**–**3** were prepared from mixtures of $Na_2MoO_4·2H_2O$, $MoO_3$, $MCl_2·xH_2O$, and 2,2′-bpy, heated to 160 °C for 72–120 h.† The IR spectra of **1**–**3** exhibit strong bands in the range 910–970 cm$^{-1}$ attributed to $\upsilon$(Mo=O), and a series of bands characteristic of 2,2′-bpy in the range 1100–1600 cm$^{-1}$.

The structure of $[Ni(2,2′\text{-bpy})_2Mo_4O_{13}]$ **1** (Fig. 1) is constructed from the common β-molybdate clusters $[Mo_8O_{26}]^{4-}$, linked through $\{Ni(bpy)_2O_2\}^{2+}$ octahedra into a one-dimensional ribbon. The molybdenum core consists of edge-sharing $\{MoO_6\}$ octahedra in the compact β-molybdate geometry.[10] Two adjacent molybdenum sites on either side of the cluster engage in corner-sharing interactions through bridging oxo-groups to a $\{NiN_4O_2\}$ octahedron, such that each $\{Mo_8O_{26}\}^{4-}$ cluster is linked through four $\{NiN_4O_2\}$ octahedra to the two neighboring clusters of the ribbon. The nickel site is defined by four nitrogen donors from two 2,2′-bpy ligands and *cis*-oxo groups from two adjacent molybdenum clusters.

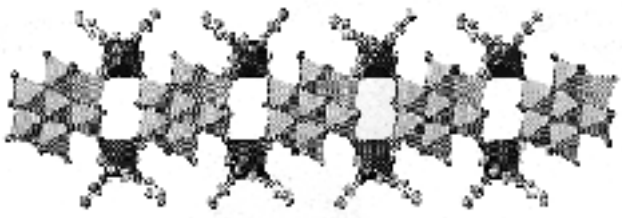


**Fig. 1** A polyhedral representation of the one-dimensional structure of **1**. The lighter polyhedra represent the molybdenum sites and the darker the nickel octahedra. The carbon atoms of the bipyridyl ligands are shown as light spheres. Selected bond lengths (Å): Ni–N, 2.053(7), 2.058(7), 2.060(6), 2.072(7); Ni–O, 2.056(6), 2.090(5).

Examination of the structure of **1** would suggest that further condensation of molybdenum oligomers into one-dimensional molybdenum oxide motifs should be feasible. As illustrated in Fig. 2, the structure of $[Cu(2,2′\text{-bpy})Mo_2O_7]$ **2** consists of a buckled one-dimensional molybdenum oxide chain linked to peripheral $\{CuN_2O_4\}$ octahedra. The $\{Mo_2O_7\}$ chain is constructed from edge-sharing $\{MoO_6\}$ octahedra and $\{MoO_5\}$ square pyramids. Each molybdenum octahedron shares common edges with a neighboring molybdenum octahedron, a

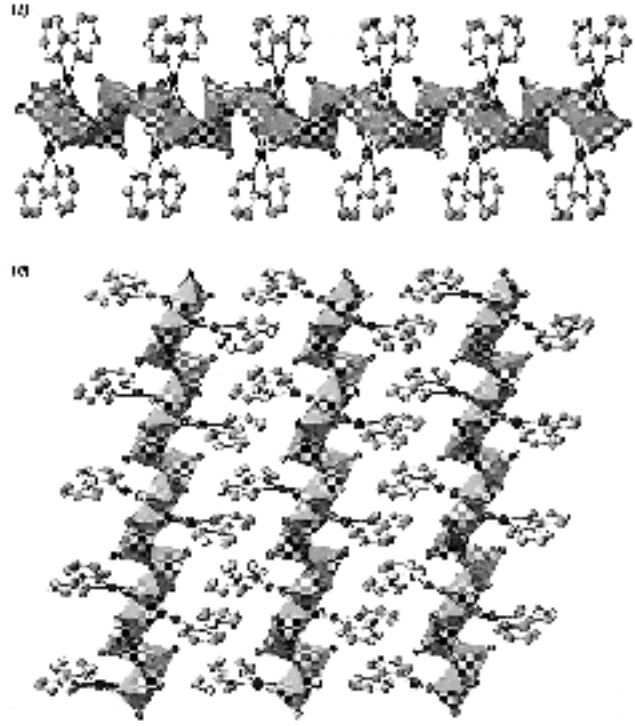


**Fig. 2** (*a*) A view of the one-dimensional structure of **2**. The molybdenum sites are represented as polyhedra, while the Cu centers are shown as dark spheres. (*b*) The packing of adjacent one-dimensional strands, showing the stacking of bipyridyl rings from adjacent chains. Selected bond lengths (Å): Cu(1)–N, 2.011(14), 2.003(14); Cu(1)–O, 1.989(11), 1.995(10), 2.355(11), 2;405(10); Cu(2)–N, 1.974(14), 1.976(14); Cu(2)–O, 1.995(11), 1.997(11), 2.355(11), 2.360(11). The longer Cu–axial oxygen bonds have been omitted for clarity.

molybdenum square pyramid, and two copper octahedra, and a common corner with one square-pyramidal unit. One square-pyramidal site engages in edge-sharing with an adjacent square pyramid and a molybdenum octahedron and displays corner-sharing with a second molybdenum octahedron and two $\{CuN_2O_4\}$ octahedra, while the second $\{MoO_5\}$ site exhibits edge-sharing to a square-pyramidal and an octahedral molybdenum site and corner-sharing to a $\{MoO_6\}$ site and a $\{CuN_2O_4\}$ octahedron. Consequently, each $\{CuN_2O_4\}$ unit links to four molybdenum polyhedra of the chain, sharing four vertices in two edge and two corner interactions with the molybdenum sites. The folding of the molybdenum chain reflects the incorporation of the $\{CuN_2O_4\}$ units through four-point, two-edge attachments and illustrates the role of the $M^{2+}$ site in defining chain geometry.

Since one-dimensional molybdenum oxide chains are a recurring theme in oxide structural chemistry,[16,17] the incorporation of appropriate metal–ligand subunits should allow bridging into higher dimensional solids. The structure of $[Co(2,2'\text{-bpy})Mo_3O_{10}]$ **3** (Fig. 3) illustrates this point. The structure consists of one-dimensional molybdenum oxide chains, constructed of molybdenum tetrahedra, octahedra and square pyramids, linked through $\{CoN_2O_4\}$ octahedra into a two-dimensional covalent network. The oxide chain itself results from the edge-sharing of $\{MoO_6\}$ octahedra and $\{MoO_5\}$ square pyramids. The $\{MoO_4\}$ tetrahedra link to the chain through a single corner-sharing interaction, but bridge two $\{CoN_2O_4\}$ octahedra through two additional corner-sharing linkages. Each Co site is defined by the nitrogen donors of the bpy ligand and four oxygen donors from three $\{MoO_4\}$ groups and one $\{MoO_6\}$ octahedron. The overall structure may be described as folded chains of edge-sharing molybdenum polyhedra linked through double chains of alternating $\{CoN_2O_4\}$ octahedra and $\{MoO_4\}$ tetrahedra into a two-dimensional network.

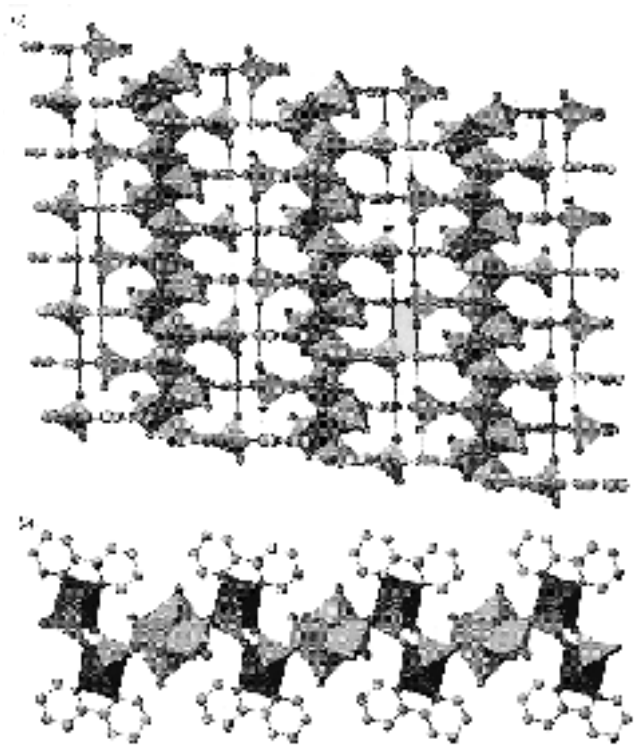


**Fig. 3** (*a*) A view of the two-dimensional structure of **3** parallel to the crystallographic *c* axis. The molybdenum sites are represented as polyhedra, while the cobalt sites are illustrated as larger darkened spheres. (*b*) A view down the *a* axis showing the linking of molybdenum polyhedral chains through $\{(MoO_4)_2[Co(bipy)]_2\}$ units in parallel chains. Selected bond lengths (Å): Co–N, 2.082(9), 2.105(9); Co–O, 2.092(8), 2.094(8) ×2, 2.119(7).

Molybdenum oxides have received considerable attention for their catalytic properties in organic oxidations[13,14] and for their intercalation properties.[15,16] Recent studies[11,12] have focused on structural modification and design of metal oxides through the introduction of organic components as templates, charge-compensating cations, tethers, or covalently linked network constituents. Another approach to composite metal oxide/organic solids is that illustrated in the preparation of **1**–**3**, which employs metal–organic ligand fragments as covalent linkers to metal oxide components of various nuclearities or dimensionalities. A curious feature of these initial investigations is the range of structural types which evolve from the introduction of $\{M'(bpy)_n\}^{2+}$ units as the divalent d-block element is varied. A degree of primitive synthetic design appears inherent in the systematic variation of the divalent metal, the diamine ligand, and the hydrothermal conditions employed.

This work was supported by NSF grant CHE9617232.

## Footnotes and References

† Reactions were carried out in Teflon-lined Parr acid digestion bombs at 30% fill volume. *Reaction conditions summary*: **1**, mole ratio for $Na_2MoO_4{\cdot}2H_2O : MoO_3$: $NiCl_2$ : 2,2′-bpy : $H_2O$ of 1.0 : 1.1 : 6.0 : 2.0 : 1990; 160 °C, 72 h; **2**, $Na_2MoO_4{\cdot}2H_2O : MoO_3 : CuCl_2$ : 2,2′-bpy : $H_2O$ of 1.0 : 1.0 : 4.1 : 2.1 : 2068; 160 °C, 72 h; **3**, $Na_2MoO_4{\cdot}2H_2O : MoO_3 : CoCl_2$ : 2,2′-bpy : $H_2O$ of 1.0 : 1.0 : 1.7 : 1.4 : 881; 160 °C, 117 h.

‡ *Crystal data*: $C_{20}H_{16}Mo_4N_4NiO_{13}$ **1**: monoclinic, space group $P2_1/n$, $a$ = 10.0516(3), $b$ = 16.2988(5), $c$ = 15.8084(5) Å, $\beta$ = 100.074(1)°, $U$ = 2550.0(1) Å$^3$, $R_1$ = 0.0705 for 6000 reflections. $C_{10}H_8CuMo_2N_2O_7$ **2**: triclinic, space group $P\bar{1}$, $a$ = 7.1835(3), $b$ = 11.5682(5), $c$ = 16.9615(7) Å, $\alpha$ = 89.568(1), $\beta$ = 79.995(1), $\gamma$ = 81.739(1)°, $U$ = 1373.5(1) Å$^3$, $Z$ = 4, $R_1$ = 0.065 for 3821 reflections. $C_{10}H_8CoMo_3N_2O_{10}$ **3**: triclinic, space group $P\bar{1}$, $a$ = 6.9889(6), $b$ = 10.5877(9), $c$ = 11.0077(9) Å, $\alpha$ = 88.674(2), $\beta$ = 89.930(2), $\gamma$ = 79.985(1)°, $U$ = 801.9(1) Å$^3$, $Z$ = 2, $R_1$ = 0.064 for 3567 reflections. CCDC 182/534.


1 A. K. Cheetham, *Science*, 1994, **264** and references therein.
2 P. A. Cox, *Transition Metal Oxides*, Clarendon Press, Oxford, 1995.
3 T. E. Mallouk and H. Lee, *J. Chem. Educ.*, 1990, **67**, 829.
4 M. Fujita, Y. J. Kwon, O. Sasahi, K. Yamaguchi and K. Ogura, *J. Am. Chem. Soc.*, 1995, **117**, 7287 and references therein.
5 N. Masciocchi, D. Cairati, L. Carlucci, G. Mezza, G. Ciani and A. Sireni, *J. Chem. Soc., Dalton Trans*, 1996, 2739.
6 P. Losier and M. J. Zaworotko, *Angew. Chem., Int. Ed. Engl.*, 1996, **35**, 2779 and references therein.
7 M. E. Davis, A. Katz and W. R. Ahmad, *Chem. Mater.*, 1996, **8**, 1820 and references therein.
8 S. Wang, D. B. Mitzi, G. A. Landrum, H. Genin and R. Hoffmann, *J. Am. Chem. Soc.*, 1997, **119**, 724.
9 Y. Zhang, J. R. D. DeBord, C. J. O'Connor, R. C. Haushalter, A. Clearfield and J. Zubieta, *Angew. Chem., Int. Ed. Engl.*, 1996, **35**, 989.
10 M. Inoue and T. Yamase, *Bull. Chem. Soc. Jpn.*, 1995, **68**, 3055 and references therein.
11 M. I. Khan, Q. Chen and J. Zubieta, *Inorg. Chim. Acta*, 1993, **213**, 328 and references therein.
12 Y. Xu, L. H. An and L.-L. Koh, *Chem. Mater*., 1996, **8**, 814.
13 E. M. McCarron, III and A. W. Sleight, *Polyhedron*, 1986, **5**, 129.
14 D. O'Hare in *Inorganic Materials*, ed. D. W. Bruce and D. O'Hare, Wiley, New York, 1992.
15 R. C. T. Slade, T. K. Halstead and P. G. Dickens, *J. Solid State Chem.*, 1980, **34**, 183.
16 J. W. Johnson, A. J. Jacobson, S. M. Rich and J. F. Brody, *J. Am. Chem. Soc.*, 1981, **103**, 8246.


*Received in Columbia, Mo, USA, 22nd April 1997; 7/02765F*

# Oxygen buffering capacity of mixed cerium terbium oxide: a new material with potential applications in three-way catalysts

**Serafín Bernal, Ginesa Blanco, Miguel A. Cauqui, Pilar Corchado, José M. Pintado and José M. Rodríguez-Izquierdo***

*Departamento de Ciencia de los Materiales e Ingeniería Metalúrgica y Química Inorgánica, Universidad de Cádiz, Apartado 40, Puerto Real, 11510, Spain*

**A new method to compare the oxygen buffering capacity (OBC) of catalysts shows that Ce–Tb mixed oxide presents an exceptional capability for attenuating fast oscillations of oxygen partial pressure.**

Ceria has been for years one of the components of catalytic automobile exhaust converters (TWC). The capacity and the rate of response to buffer the oscillations of the oxygen partial pressure in the waste gases are recognised among its key properties.[1] However, improvements in such features are currently demanded for designing better catalytic cartridges for cleaner cars.[2,3]

The present paper reports on a simple technique to compare the oxygen buffering capacity (OBC) of catalysts. We illustrate the working principle of this new method with results given by four samples: $CeO_2$, Rh (3 mass%)/$CeO_2$, Rh (3 mass%)/$SiO_2$, and a Ce–Tb mixed oxide (20 mol% Tb), hereafter referred to as CT-80/20.

The results reported here show that the performance of CT-80/20 is much better than that of the other studied systems. We highlight the overlying properties of CT-80/20 in the following conditions: (*a*) at low temperature, with the catalyst starting to work effectively from 473 K, (*b*) over a very broad range, including temperatures higher than 873 K, (*c*) in the absence of noble metal, CT-80/20 being superior to the two Rh-containing tested catalysts, and (*d*) following severe ageing and sintering treatments. The new method described herein was useful to reveal and discriminate the advantages of CT-80/20, giving in a single test valuable information both of the capacity and rate of response of the samples as oxygen buffers.

The ceria and silica supports were high surface area samples, with 100 and 180 $m^2\ g^{-1}$ BET surface area, respectively. Rhodium was dispersed in both cases by conventional impregnation from aqueous nitrate solutions. The metal dispersion obtained in both cases by HREM is higher than 70%. The Ce–Tb mixed oxide was prepared by precipitation with ammonia from a solution of the nitrates. The terbium-modified ceria was obtained by calcination at 873 K, showing fluorite-like structure and a BET surface area of 45 $m^2\ g^{-1}$. The pretreatment for $CeO_2$ and CT-80/20 samples consisted of oxidation at 873 K in a flow of $O_2$(5%)–He, followed by slow cooling to 293 K. The rhodium-containing samples were first reduced in hydrogen at 623 K, flowed with helium from 623 up to 673 K, cooled in helium to 293 K, and reoxidized in a flow of $O_2$(5%)–He up to 373 K. After these pretreatments, the gas flow, in each case, is turned to He, and the temperature is tuned to the value selected for carrying out the test.

The experimental method consists of injecting 0.25 ml $O_2$(5%)–He pulses, at 10 s intervals, over the 60 ml $min^{-1}$ inert gas stream. The $O_2$ content at the outlet of the reactor is measured with a thermal conductivity (TC) detector. The $O_2$ content is the result of the balance of the oxygen injected, consumed and released by the sample.

The amount of catalyst used in the experiments was 200 mg. We focus the comparative study of the four catalyst samples at 673 K, this rather low value being relevant because of the particular interest of improving the TWC efficiency during the cold start period of operation of motor vehicles.[2,3]

If the sample does not have any oxygen buffer capacity at the selected operating conditions, we detect oscillations in the TC signal with a maximum height of 0.75 mV. This is found for pure ceria, as shown in Fig. 1(*a*). A blank test without sample leads to a pattern of oscillations coincident with that shown in Fig. 1(*a*).

Conversely, Fig. 1(*b*) clearly illustrates how the Rh/$CeO_2$ catalyst attenuates the oscillations of the oxygen partial pressure induced by the pulses. Those injected during the first minute are partially consumed increasing the oxidation level of the sample and making it active for buffering; after this the catalyst reaches a steady response to the oxygen pressure oscillations. When the injections cease after 8 min the sample gradually returns to its initial equilibrium state in the flowing He carrier. The efficiency of a sample as an oxygen buffer can be accounted by the attenuation factor, defined as the ratios of the steady-state amplitude of the oscillations in the absence of sample (0.75 mV) and in its presence. For Rh/$CeO_2$ the attenuation factor is 2.1.

The Rh/$SiO_2$ sample is tested as a representative case of a catalyst in which it is assumed that the support does not have the

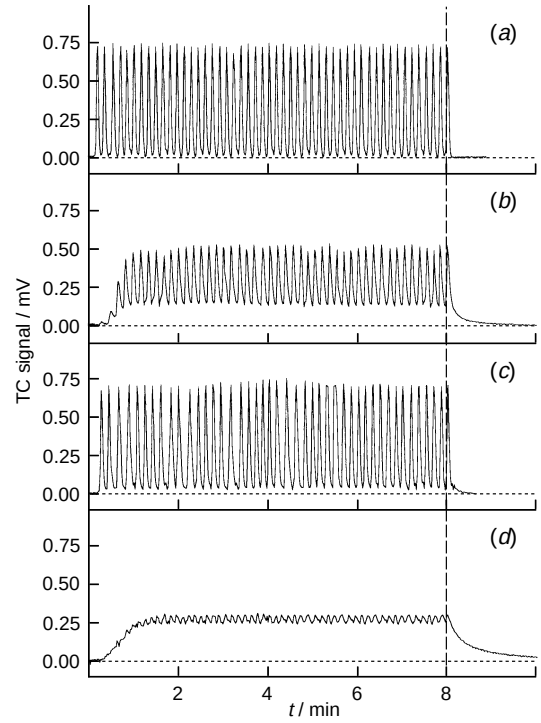



**Fig. 1** TC signals for OBC experiments carried out at 673 K on: (*a*) $CeO_2$, (*b*) Rh/$CeO_2$, (*c*) Rh/$SiO_2$ and (*d*) CT-80/20. The dotted vertical line corresponds to the time at which we stopped the injection of pulses.

ability to contribute to the OBC. In this case, Fig. 1(*c*), the oxygen signal oscillations show only a tiny level of attenuation, with an attenuation factor of 1.06. Such an effect must be attributed to the influence of the oxygen partial pressure on its chemisorption–desorption on the oxidised rhodium.

The above experiments [Fig. 1(*a*)–(*c*)] allow one to conclude that the OBC of the $Rh/CeO_2$ catalyst is not the result of the simple overlap of Rh and $CeO_2$ buffering capacities, and that a synergetic effect must be invoked to understand its behaviour. This observation is in agreement with the well known existence of singular metal-support interactions for noble metals supported on ceria,[1,4–8] thus giving credence to the reliability of the experimental technique.

Fig. 1(*d*) shows the behaviour of the Ce–Tb mixed oxide, CT-80/20. This catalyst gradually varies its oxidation level retaining part of the oxygen injected in the starting pulses. After this, the CT-80/20 oxide reaches a state in which its oxygen buffering ability is extremely high. The attenuation factor of the oxygen pressure oscillations in this case is 10.8. This behaviour is related to the ability of the mixed oxide to rapidly change its composition in response to the pulses. It is through these changes that CT-80/20 can attenuate the $O_2$ pressure oscillations, undergoing oxidation when the atmosphere is rich in oxygen and reduction when the $O_2$ partial pressure in the flowing gas is low.

The performance of CT-80/20 was also outstanding when the temperature was changed within very broad limits. This can be checked by analysing the results of a similar pulse experiment carried out at a linear heating rate of 20 K $min^{-1}$, from 323 up to 873 K. In this way rapid collection of OBC data was possible. Fig. 2 shows the temperature range in which the catalyst does not have the ability to attenuate pulses ($T$ < 473 K). From 473 to 573 K the attenuation of the pulses rapidly increases while from 573 to 873 K the attenuation factor remains high and almost constant.

The very high rate of response of the CT-80/20 mixed oxide in the whole temperature range in which the oxygen pressure oscillations attenuation is effective is remarkable. Because of experimental constraints the frequency of the pulses, 0.1 Hz, could not be increased; however, it is not far from the typical frequency of such oscillations in real TWC converters, of the order of 1 Hz.[2,3]

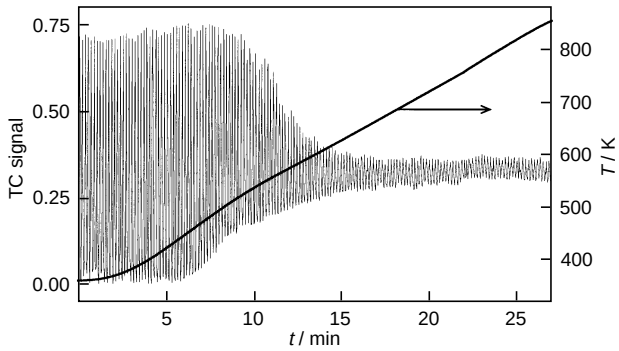



**Fig. 2** TC signal for an OBC experiment on CT-80/20, at a heating rate of 20 K $min^{-1}$

Some other available results show that the performance of CT-80/20 is maintained for low surface area samples (8 $m^2$ $g^{-1}$), obtained by ageing the starting mixed oxide for 2 h at 1123 K in a flow of He. In this case the attenuation factor of the oxygen pulses remains > 8. This result suggests the participation of oxygen from the bulk in the buffering mechanism. The lack of a proportional dependence between the OBC of CT-80/20 and the surface area of the sample is a very valuable feature for catalysts like TWCs which must operate under high temperature conditions for prolonged periods, thus potentially contributing to extension of its useful lifetime.[8]

One additional comment is that, like pure ceria, the buffering abilities of pure terbia are very different from those for the terbia modified cerium oxide, CT-80/20. The mixed oxide presents a much better performance than those of its individual components.

The details of the experimental conditions used in these tests have been adapted to obtain a good discrimination among the essayed samples. However, it would be possible to change some of the experimental settings, such as loop volume, amount of sample, inert gas flow rate, *etc.*, to obtain a good level of discrimination for other catalysts or temperature testing conditions.

In conclusion, we have proposed a new method to compare, in a fast and simple way, the OBCs of catalysts. Using this method we find that the modification of pure ceria by addition of 20 mol% of terbia increases dramatically its capability for attenuating fast oscillations of the oxygen partial pressure. This makes the terbia-modified cerium oxide CT-80/20, which shows superior properties over $Rh/CeO_2$, a potential candidate for inclusion in improved TWC formulations.

## Footnote and References

* E-mail: josemaria.izquierdo@uca.es

1 B. T. Kilbourn, *Cerium. A Guide to its Role in Chemical Technology*, Molycorp Inc., 1992.
2 P. Degobert, *Automobiles and Pollution*, Society of Automotive Engineers, Inc., 1995.
3 A. Trovarelli, *Catal. Rev. Sci. Eng.*, 1996, **38**, 439.
4 T. Bunluesin, E. S. Putna and R. J. Gorte, *Catal. Lett.*, 1996, **41**, 1.
5 J. Soria, A. Martínez-Arias and J. C. Conesa, *Vacuum*, 1992, **43**, 437.
6 S. Bernal, J. J. Calvino, G. A. Cifredo, J. M. Rodríguez-Izquierdo, V. Perrichon and A. Laachir, *J. Chem. Soc., Chem. Commun.*, 1992, 460.
7 S. Bernal, F. J. Botana, J. J. Calvino, M. A. Cauqui, G. A. Cifredo, A. Jobacho, J. M. Pintado and J. M. Rodríguez-Izquierdo, *J. Phys. Chem.*, 1993, **97**, 4118.
8 B. Engler, E. Koberstein and P. Schubert, *Appl. Catal.*, 1989, **48**, 71.

*Received in Bath, UK, 16th April 1997; 7/02617J*

# Vibrational properties of ethyltitanium trichloride and its 1,2-bis(dimethylphosphino)ethane adduct: characterisation of isolated $\nu$(C–H) modes and implications for agostic bonding

**G. Sean McGrady,[a] Anthony J. Downs,[a] Arne Haaland,[b] Wolfgang Scherer[c] and Donald C. McKean[d]**

[a] *Inorganic Chemistry Laboratory, University of Oxford, South Parks Road, Oxford, UK OX1 3QR*
[b] *Department of Chemistry, University of Oslo, Box 1033 Blindern, N-0315 Oslo, Norway*
[c] *Anorganisch-chemisches Institut, Technische Universität München, Lichtenbergstrasse 4, D-85747 Garching, Germany*
[d] *Department of Chemistry, University of Edinburgh, King's Buildings, West Mains Road, Edinburgh, UK EH9 3JJ*

**The IR spectra of normal and specifically deuteriated [$CH_3CH_2TiCl_3$] show that coordination by $Me_2PCH_2CH_2PMe_2$ (dmpe) results in an unusually low stretching frequency for one of the β-C–H bonds in the ethyltitanium fragment; the results are analysed for their relevance to the bonding in the β-agostic unit in the light of quantum chemical calculations.**

Despite their potential significance,[1] so-called agostic interactions can be tormentingly difficult to pin down in transition-metal alkyls. Whilst the presence of M···H–C interactions (M = metal) may often be inferred from a distorted M–alkyl geometry, the true degree and nature of the effect are hard to ascertain. Diffraction with X-rays, if not with neutrons, and NMR and (particularly) vibrational spectroscopies have failed in most cases to afford clearcut results.

Vibrational studies of the coordinated alkyl group have mostly been impaired by the lack of any definitive analysis aimed at establishing the true natures of the various transitions. In principle, the C–H stretching modes should be a highly sensitive index to the bonding and geometry of the alkyl group: in practice, coupling with, or masking by, other modes, and notably $2 \times \delta_{asym}(CH_3)$, tends to cloud the picture. In an extensive study of small organic molecules, partial deuteriation has been exploited to decouple C–H stretching fundamentals from other modes.[2] The 'isolated' C–H stretching modes [$\nu^{is}$(CH)] thus identified provide an unusual insight into conformational, stereoelectronic and bonding effects, and prove to be an extremely sensitive measure of C–H bond strength. As part of a comprehensive, systematic enquiry into the nature of β-agostic interactions in transition-metal alkyls,[3] we have investigated the IR spectra of the base-free molecule [$EtTiCl_3$] **1** and its adduct **2** with $Me_2PCH_2CH_2PMe_2$ (dmpe), each incorporating either normal $CH_3CH_2$ or specifically deuteriated $CHD_2CD_2$ groups. Complex **2** has been deliberately chosen in view of its seminal rôle in relation to notions about β-agostic interactions, X-ray diffraction having identified a $TiCH_2CH_3$ fragment with a curiously tight TiCC angle (86°).[4]

The low volatility and thermal instability of [$EtTiCl_3$] poses serious problems in the measurement and interpretation of the IR spectrum of the molecule in the gas phase. Notwithstanding these complications, we have obtained and assigned spectra for several isotopomers. The IR spectrum of the gaseous [$CH_3CH_2TiCl_3$] molecule, **1**, [Fig. 1(*a*)] shows all the C–H stretching fundamentals to occur in the 'normal' region, *i.e.* 2800–3100 $cm^{-1}$. The spectrum of the $CHD_2CD_2$ isotopomer, **1**-$h_1$, [Fig. 1(*b*)] shows just two proximal bands attributable to $\nu^{is}$(CH) modes and corresponding to conformers with the unique C–H bond disposed either out of or within the mirror plane of the $C_s$-symmetric molecule [C–H″ 2953 (A) or C–H′ 2927 $cm^{-1}$ (B), respectively; Fig. 1(*b*), Scheme 1]. The spectra bear a close resemblance to those reported for [($\eta$-$C_5H_5$)$TiCl_2Et$][5] and clearly imply a normal or anagostic structure for **1**, in keeping with the findings of an electron diffraction study.[3]

By contrast, the IR spectrum of solid [$CH_3CH_2TiCl_3$(dmpe)] [Fig. 1(*c*)] exhibits, in addition to bands in the region 2800–3100 $cm^{-1}$, a broad absorption centred at 2615 $cm^{-1}$ (C). The spectrum of the $CHD_2CD_2$ isotopomer **2**-$h_1$ [Fig. 1(*d*), Scheme 1] resembles that of **1**-$h_1$ in containing just two features identifiable with $\nu^{is}$(CH) modes, but with frequencies of 2933 (D) and 2585 $cm^{-1}$ (E) for the out-of-plane (C–H″) and in-plane

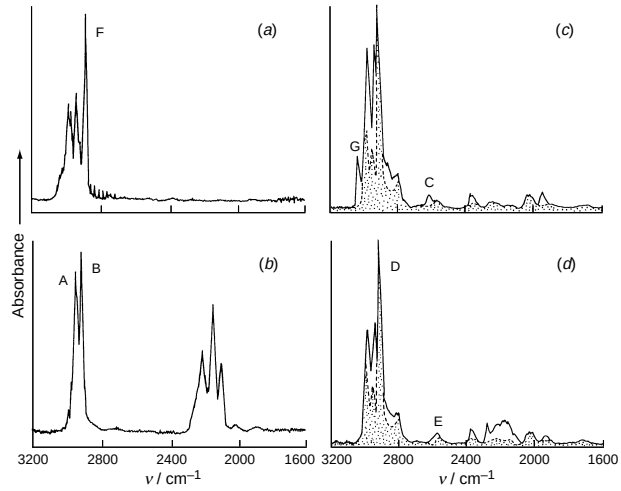
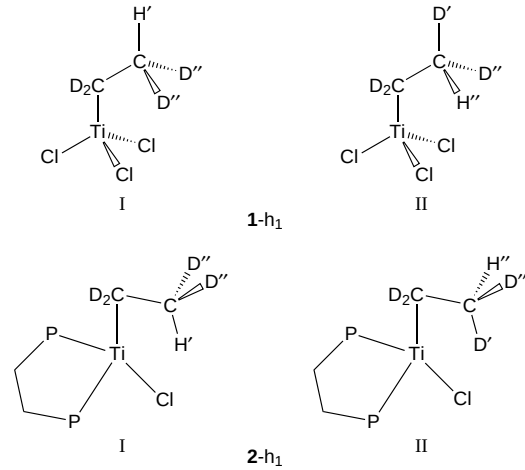



**Fig. 1** IR spectra of **1** (*a*), **1**-$h_1$ (*b*), **2** (*c*), and **2**-$h_1$ (*d*) in the region corresponding to C–H(D) stretching vibrations. In (*c*) and (*d*) the spectrum of [$TiCl_4$(dmpe)] has been overlaid (stippled) to aid identification of the internal modes of the ethyl moiety.




**Scheme 1**

**Table 1** Observed C–H(D) stretching frequencies (in $cm^{-1}$) for the ethyl groups of **1**, **1**-$h_1$ and **2**-$h_1$, and calculated scaled harmonic frequencies (in $cm^{-1}$) for **1**, **1**-$h_1$, **2a** and **2a**-$h_1$[a]

| | $[CH_3CH_2TiCl_3]$ | | | $[CHD_2CD_2TiCl_3]$ | | | $[CH_3CH_2TiCl_3$(diphosphine)] | | | $[CHD_2CD_2TiCl_3$(diphosphine)] | | |
|---|---|---|---|---|---|---|---|---|---|---|---|---|
| Group | $\nu_{obs}$ | $\nu_{calc}$ | Assignment (local sym.) | $\nu_{obs}$ | $\nu_{calc}$ | Assignment (conformer)[b] | $\nu_{obs}$ (**2**) | $\nu_{calc}$ (**2a**) | Assignment (local sym.) | $\nu_{obs}$ (**2**) | $\nu_{calc}$ (**2a**) | Assignment (conformer)[b] |
| $C_\alpha H_2$ | 2933[c] | 2929 | $\nu_{as}(CH_2'')$ (a″) | 2199(sh) | 2192 | $\nu_{as}(CD_2'')$ (II) | 3028(G)[c] | 3028 | $\nu_{as}(CH_2'')$ (a″) | 2275 | 2274 | $\nu_{as}(CD_2'')$ (I) |
| | | | | | 2191 | $\nu_{as}(CD_2'')$ (I) | | | | | 2273 | $\nu_{as}(CD_2'')$ (II) |
| | 2878(F)[c] | 2879 | $\nu_s(CH_2'')$ (a′) | 2105 | 2112 | $\nu_s(CD_2'')$ (I) | 2933 | 2960 | $\nu_s(CH_2'')$ (a′) | 2172 | 2169 | $\nu_s(CD_2'')$ (II)[e] |
| | | | | | 2112 | $\nu_s(CD_2'')$ (II) | | | | 2172 | 2173 | $\nu_s(CD_2'')$ (I) |
| $C_\beta H_3$ | 2980[d] | 2978 | $\nu_{as}(CH_3)$ (a″) | 2953(A)[c] | 2953 | $\nu^{is}(CH'')$ (II) | 2970 | 2964 | $\nu_{as}(CH_2'')$ (a″) | 2933(D)[c] | 2933 | $\nu^{is}(CH'')$ (II) |
| | | | | 2927(B)[c] | 2927 | $\nu^{is}(CH')$ (I) | | | | | | |
| | | | | | | | | | | 2225 | 2225 | $\nu_{as}(CD_2'')$ (I) |
| | 2963[d] | 2956 | $\nu_{as}(CH_3)$ (a′)[e] | 2235(sh) | 2230 | $\nu_{as}(CD_2'')$ (I) | ol[f] | 2899 | $\nu_s(CH_2'')$ (a′) | 2172 | 2180 | $\nu(CD'')$ (II)[e] |
| | | | | 2216 | 2217 | $\nu_{as}(CD'D'')$ (II)[e] | | | | 2100 | 2125 | $\nu_s(CD_2'')$ (I) |
| | 2878[d] | 2898 | $\nu_s(CH_3)$ (a′)[e] | 2150 | 2147 | $\nu_s(CD_2'')$ (I) | 2615(C) | 2585 | $\nu(CH')$ (a′) | 2585(E)[c] | 2585 | $\nu^{is}(CH')$ (I) |
| | | | | 2150 | 2139 | $\nu_s(CD'D'')$ (II)[e] | | | | 1929 | 1907 | $\nu(CD')$ (II) |

[a] Scale factors: $[EtTiCl_3]$, methyl, CH″ 0.951, CH′ 0.968; methylene, 0.971; $[EtTiCl_3(H_2PCH_2CH_2PH_2)]$, methyl, CH″ 0.930, CH′ 0.917; methylene, 0.953. The very small differences between the two CH″ bonds in both the methyl and methylene groups have been ignored. Calculated $\nu$(CD) values have been multiplied by 1.011 to offset anharmonicity. [b] Conformers specified by I and II as in Scheme 1. [c] Frequency used for scaling the DFT force field. [d] Likely to be affected by Fermi resonance. [e] These descriptions are approximate. [f] ol signifies overlay by features arising from the dmpe ligand.

(C–H′) modes, respectively; the separation between them is an order of magnitude greater than that found for **1**-$h_1$. These observations point unmistakably to the presence of two chemically distinct types of C–H bond attached to the β-carbon atom of the ethyl ligand in **2** [*viz*. two terminal (C–H″) and one agostic (C–H′)]. For the C–H′ bond in **2**-$h_1$, $\nu^{is}$(CH) thus has a frequency comparable with those reported for the normal (coupled) $\nu$(CH) modes in other β-agostic complexes.[3] To our knowledge, the $\nu^{is}$(CH) frequency of 2585 $cm^{-1}$ in **2**-$h_1$ is the first to be determined in a complex whose β-agostic structure has been verified by diffraction methods. It is remarkable for being some 200 $cm^{-1}$ lower than that of any $\nu^{is}$(CH) reported hitherto (*cf*. 2799 $cm^{-1}$ in $NMe_3$ where the C–H bonds are weakened through interaction with the antiperiplanar lone pair[2]).

Drawing on the empirical equations developed elsewhere[2,6] leads from the values of $\nu^{is}$(CH) displayed by **2**-$h_1$ to the following estimates of spectroscopic bond length ($r_0$ in pm) and adiabatic bond dissociation enthalpy ($D_0$ in kJ $mol^{-1}$): $r_0$(C–H″) = 109.8, $D_0$(C–H″) = 410; $r_0$(C–H′) = 113.4, $D_0$(C–H′) = 280. At face value, therefore, the results imply that, as the β-$CH_3$ unit of the ethyl group approaches the Ti centre, the in-plane C–H′ bond suffers an appreciable weakening, being 3.6 pm longer and having a dissociation enthalpy 130 kJ $mol^{-1}$ smaller than its out-of-plane (C–H″) counterparts.† However, there is no suggestion of significant chemical activation of the C–H′ bond, nor of any significant degree of alkene hydride character to the ethyl unit on the evidence of $^2H$ NMR measurements on samples of **2** in the presence of $D_2$, $CD_4$ and $C_2D_4$.

There is a second noteworthy feature of the IR spectra. Coordination of $[EtTiCl_3]$ by dmpe results also in a significant increase in the frequencies of the $\nu$(CH) modes associated with the methylene portion of the ethyl ligand [from 2878 (F), 2933 $cm^{-1}$ in **1** to 2933, 3028 $cm^{-1}$ (G) in **2**]. A concomitant widening of the HCH angle can be inferred from the increase in the ratio $\nu_{as}/\nu_s$ for the $C_\alpha H_2$ unit. Complexation thus appears to give a methylene group with C–H bonds roughly 1.3 pm shorter and 20 kJ $mol^{-1}$ stronger than those in base-free $[EtTiCl_3]$.[7] Simultaneously the methylene $^{13}C$ resonance of the solution species undergoes a substantial low-frequency shift, while $^1J$(CH) increases from 134.3 to 147.3 Hz.[1,3]

The interpretation of the IR spectra has been underpinned by density functional theory (DFT) calculations on $[EtTiCl_3]$ and the model compound $[EtTiCl_3(H_2PCH_2CH_2PH_2)]$ **2a**. Since optimisation yields equilibrium structures in good agreement with those determined experimentally for **1** and **2**,[3,4] replacement of the methyl groups in dmpe by hydrogen appears to have very little effect on the overall structure of the complex. Accordingly, the calculated (harmonic) frequencies of the EtTi group of **2a** may reasonably be expected, with due allowance for scaling, to approximate those determined by experiment for **2**. The results listed in Table 1 for the $\nu$(CH) and $\nu$(CD) modes of **1**, **2**, and **2a** bear out this expectation. Inspection of the calculated force field shows the normal mode characterising the $C_\beta$–H′ stretching vibration to consist exclusively of a rectilinear motion almost perpendicular to the Ti–H directrix. Computational evidence indicates that the Ti–$C_\alpha$ bonding electrons are delocalised over both $C_\alpha$ and $C_\beta$ atoms as well as over their appended H atoms, and that reduction of the TiCC valence angle allows the establishment of covalent bonding between Ti and $C_\beta$, and to a lesser extent, one of its H atoms.[3] The spectroscopic evidence is fully consistent with such a model.

## Footnotes and References

* E-mail: smcgrady@jesus.ox.ac.uk

† Against these quantitative estimates certain caveats need to be entered. Firstly, the empirical correlations between $\nu^{is}$(CH) and (*i*) bond length and (*ii*) bond enthalpy are founded on the assumptions of a C–H potential well whose curvature varies in a linear manner with the C–H distance and well depth, respectively. These conditions are likely to be met only for C–H bonds which are very similar in nature, with but small deviations from a 'norm'. Secondly, a low $\nu^{is}$(CH) frequency increases the likelihood of coupling of this mode, *e.g.* with the symmetric $\nu$(CD) mode of the terminal $CHD_2$ group (at *ca.* 2120 $cm^{-1}$), and so putting its vibrational isolation at risk.

1 M. Brookhart, M. L. H. Green and L.-L. Wong, *Prog. Inorg. Chem.*, 1988, **36**, 1.
2 D. C. McKean, *Chem. Soc. Rev.*, 1978, **7**, 399; *Croat. Chem. Acta*, 1988, **61**, 447.
3 A. Haaland, W. Scherer, H. V. Volden, K. Ruud, O. Swang, G. S. McGrady, A. J. Downs, W. A. Herrmann, M. Geisberger, T. Priermeier, R. Boese and D. Bläser, *J. Am. Chem. Soc.*, submitted.
4 Z. Dawoodi, M. L. H. Green, V. S. B. Mtetwa, K. Prout, A. J. Schultz, J. M. Williams and T. F. Koetzle, *J. Chem. Soc., Dalton Trans.*, 1986, 1629.
5 A. H. J. Robertson, G. P. McQuillan and D. C. McKean, *J. Chem. Soc., Dalton Trans.*, 1995, 3941.
6 D. C. McKean, *Int. J. Chem. Kinet.*, 1989, **21**, 445.
7 H. J. Bernstein, *Spectrochim. Acta*, 1962, **18**, 161.

*Received in Cambridge, UK, 9th June 1997; 7/03975A*

# A novel pentadentate ligand 2,6-bis[methoxybis(2-pyridyl)methyl]pyridine L for mononuclear iron(II) and manganese(II) compounds; synthesis and crystal structures of $[FeL(MeCN)][ClO_4]_2$ and $[(MnL(H_2O)][ClO_4]_2$

**Maartje E. de Vries,[a] Rene M. La Crois,[a] Gerard Roelfes,[a] Huub Kooijman,[b] Anthony L. Spek,†[b] Ronald Hage[c] and Ben L. Feringa*[a]**

[a] *Department of Organic and Molecular Inorganic Chemistry, University of Groningen, Nijenborgh 4, 9747 AG Groningen, The Netherlands*
[b] *Bijvoet Centre for Biomolecular Research, Crystal and Structural Chemistry, University of Utrecht, Padulalaan 8, 3584 CH Utrecht, The Netherlands*
[c] *Unilever Research Laboratory Vlaardingen, PO Box 144, 3130 AC Vlaardingen, The Netherlands*

**A novel pentadentate ligand L is capable of stabilising $Fe^{II}$ and $Mn^{II}$ centres, the first of which gives a transient iron hydroperoxide species upon treatment with hydrogen peroxide.**

Mononuclear iron and manganese centres are common in oxygenases and the synthesis of low molecular mass complexes that show structural and functional similarities to natural systems is of great current interest.[1,2] An approach to novel biomimetic catalysts for selective oxygenations is based on the design of multidentate ligands that can accommodate low-valent iron[1,2] or manganese[1,3] and are capable of stabilising intermediates in the oxygenation cycles. We wish to present a unique ligand L with a fivefold pyridine donor set which is particularly effective for this purpose. This is demonstrated by the synthesis and structural characterisation of the corresponding iron $[FeL(MeCN)][ClO_4]_2$ **1** and manganese $[MnL(H_2O)][ClO_4]_2$ **2** complexes.

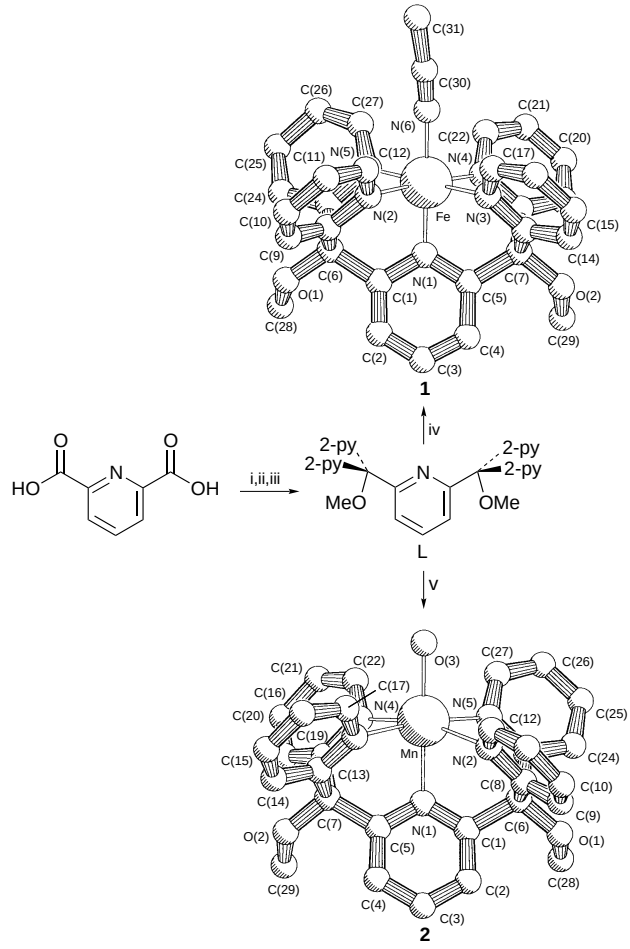
Ligand L was prepared in a three step procedure, from pyridine-2,6-dicarboxylic acid (Scheme 1). Treatment with $SOCl_2$ was followed by reaction of the acid chloride with 6 equiv. of 2-pyridyllithium. The resulting 2,6-bis[hydroxybis(2-pyridyl)methyl]pyridine was methylated to afford L.

Complexation of L with $Fe(ClO_4)_2 \cdot 6H_2O$ in MeCN–$CH_3OH$ (1 : 1) gave **1** in 86% yield. Red–brown crystals were obtained by slow diffusion of ethyl acetate into the product solution. Complex **1** is a low-spin iron(II) complex as deduced from its diamagnetic $^1H$ NMR spectrum‡ and absence of EPR signals. Furthermore in acetonitrile the complex has an absorption maximum at 425 nm. Cyclic voltammetry of **1** in acetonitrile shows reversible oxidation at 1.21 V *vs*. SCE corresponding to the $Fe^{III}$–$Fe^{II}$ couple.

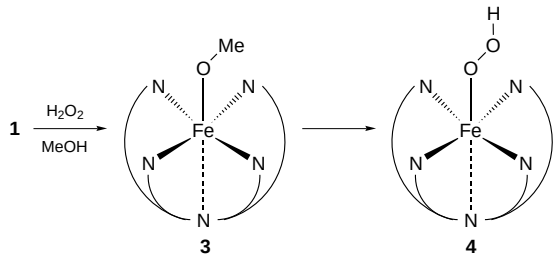
The crystal structure of **1** shows a six-coordinate $Fe^{II}$ centre surrounded by nitrogen atoms from four equatorial and one apical pyridine moieties.§ The second apical position is occupied by an acetonitrile molecule. The four equatorial pyridine rings are not positioned perpendicular to the basal plane but are folded outwards to provide a cleft-type of arrangement. The Fe–N bond lengths to N(1), N(4), N(5) and N(6) of 1.93–2.00 Å are characteristic for a low-spin $Fe^{II}$ centre.[4–6] The Fe–N(2) and Fe–N(3) bond lengths of 2.08 Å are long for a low-spin iron(II) complex, which is probably due to the fact that the cleft formed by the four equatorial pyridine rings is slightly too large to accommodate a low-spin $Fe^{II}$ with equal Fe–N distances.

Treatment of **1** in methanol with an excess (100 equiv.) of hydrogen peroxide at 25 °C (Scheme 2) causes the appearance of a blue species ($\lambda_{max}$ = 592 nm) with a half-life of 3 h.

The nature of this intermediate was examined by electrospray ionisation mass spectrometry (nozzle = 70 V). The results show that immediately after addition of $H_2O_2$ a prominent ion, with a peak cluster at *m/z* 661 is formed which can be formulated as $\{[FeL(OCH_3)](ClO_4)\}^+$ **3**.¶ This indicates initial oxidation of iron(II) complex **1** to an iron(III) species. In the course of the reaction with hydrogen peroxide an ion with *m/z* 663 is formed at the expense of **3** which corresponds to $\{[FeL(OOH)](ClO_4)\}^+$ **4**.




**Scheme 1** Synthesis of L, complexes **1** and **2** and X-ray crystal structures of the cations of **1** and **2**. Hydrogens have been omitted for clarity. *Reagents and conditions*: i, $SOCl_2$, reflux, 4 h; ii, $Bu^nLi$, 2-bromopyridine, thf; iii, NaH,MeI, thf; iv, $Fe(ClO_4)_2 \cdot 6H_2O$, MeCN, MeOH; v, $Mn(ClO_4)_2 \cdot 6H_2O$, MeCN. Selected interatomic distances (Å): for **2**: Fe–N(1) 1.927(8), Fe–N(2) 2.078(8), Fe–N(3) 2.076(9), Fe–N(4) 1.995(9), Fe–N(5) 1.957(8), Fe–N(6) 1.952(8). For **3**: Mn–O(3) 2.100(3), Mn–N(1) 2.223(3), Mn–N(2) 2.297(3), Mn–N(3) 2.248(3), Mn–N(4) 2.230(3), Mn–N(5) 2.214(3).




**Scheme 2** Formation of the blue iron(II) hydroperoxide complex **4**

The assignment of the blue species as a hydroperoxide complex **4** is furthermore based on similar spectroscopic data as reported recently for an iron(III) hydroperoxide intermediate.[5,6] It is also corroborated by the results from EPR measurements at 77 K which exhibit *g* values at 2.15, 2.13 and 1.98 indicative of a low-spin iron(III) species.[2,5–7] Based on the available coordination site and the pentadentate nature of L an end-on hydroperoxide structure for **4** is proposed.

Preliminary investigations show that complex **1** is catalytically active in the oxidation of alkanols. For example, treatment of benzyl alcohol in acetone with 100 equiv. of $H_2O_2$ in the presence of **1** gave a clean and fast conversion to benzaldehyde (65 equiv. with respect to **1** within 0.5 h).‖

Treatment of a solution of L in acetonitrile with $Mn(ClO_4)_2{\cdot}6H_2O$ followed by vapour diffusion of diethyl ether resulted in greyish crystals of $[MnL(H_2O)][ClO_4]_2$ **2** (35% yield). Complex **2** shows no absorptions in the visible spectrum which points to a high-spin manganese(II) complex.[3,8]

Electrospray ionisation mass spectrometry (nozzle = 70 V) affords prominent peaks at *m/z* 265, 629, corresponding to the ions $[MnL]^{2+}$ and $\{[MnL](ClO_4)\}^+$, respectively. The crystal structure of **2** exhibits similar features as found for **1** including six-coordination of manganese with four pyridines in the equatorial positions.§ In contrast to complex **1**, one apical position is occupied by a water molecule, which donates two hydrogen bonds to the two independent $ClO_4^-$ anions. The Mn–N bond lengths of 2.21–2.30 Å are typical for the Mn–N(pyridyl) distances observed in six-coordinated manganese(II) complexes.[3,8] The Mn–O distance is 2.10 Å.

In conclusion, a new pentadentate ligand L has been designed. The pentadentate nature of L is evident from the structures of **1** and **2** leaving a sixth coordination site free to accommodate weakly bonded ligands such as acetonitrile and water. This ligand is effective in the formation of iron(II) and manganese(II) complexes and capable of stabilising a transient hydroperoxide species. Catalytic oxidation experiments with these new complexes are in progress.

We gratefully acknowledge stimulating discussions with Professor L. Que, Jr. and we thank M. Jeronimus-Stratingh for the ES–MS measurements. This work was supported in part (A. L. S.) by the Netherlands Foundation of Chemical Research (SON) with financial aid from the Netherlands Organisation for Scientific Research (NWO) and in part (R. M. La C.) by IOP catalysis.

## Footnotes and References

* E-mail: feringa@chem.rug.nl
† Address correspondence concerning crystallography to this author.

‡ $^1$H NMR (200 MHz, $CD_3CN$, 25 °C): $\delta$ 2.11 (m, 3 H, MeCN), 4.04 (s, 6 H, $OCH_3$), 8.01 (m, 15 H, py), 9.94 (m, 4 H, py).

§ *Crystal data*: for **2**, $C_{31}H_{28}Cl_2FeN_6O_{10}$, $M_r$ = 771.35, red–brown, block-shaped crystal (0.2 × 0.2 × 0.1 mm), monoclinic, space group $P2_1$ (no. 4), $a$ = 9.751(2), $b$ = 19.326(5), $c$ = 9.7986(17) Å, $\beta$ = 101.427(17)°, $U$ = 1809.9(7) Å$^3$, $Z$ = 2, $D_c$ = 1.415 g cm$^{-3}$, $F(000)$ = 792, $\mu$(Mo-K$\alpha$) = 6.3 cm$^{-1}$, 3495 reflections measured, 3293 independent, ($1.05 < \theta < 25.00°$, $\omega$ scan, $T$ = 150 K, Mo-K$\alpha$ radiation, graphite monochromator, $\lambda$ = 0.71073 Å) on an Enraf-Nonius CAD4 Turbo diffractometer on rotating anode. Data were corrected for $L_p$ effects and for linear decay of 3% of the reference reflections, but not for absorption. The structure was solved by automated Patterson methods (DIRDIF96). Refinement on $F^2$ was carried out by full-matrix least-squares techniques (SHELXL-96); no observance criterion was applied during refinement. Electron density in a disordered solvent area (164 Å$^3$, 47.9 e per asymmetric unit) was taken into account in the refinement *via* PLATON/SQUEEZE. Where relevant, data cited above are given without disordered solvent contribution. Hydrogen atoms were included in the refinement on calculated positions riding on their carrier atoms. Refinements of a racemic twin model resulted in slightly lower $wR_2$ values and a component ratio of 0.84(10) : 0.16. Refinements converged at a final $wR_2$ value of 0.1674, $R_1$ = 0.0669 [for 2282 reflections with $F_\sigma > 4\sigma(F_\sigma)$], $S$ = 0.985, for 455 parameters. A final difference Fourier showed no residual density outside −0.76 and 0.59 e Å$^{-3}$.

For **3**, $C_{29}H_{27}Cl_2MnN_5O_{11}$, $M_r$ = 747.40, greyish, block-shaped crystal (0.4 × 0.2 × 0.1 mm), monoclinic, space group $P2_1/c$ (no. 14), $a$ = 12.5605(12), $b$ = 12.8173(12), $c$ = 19.3461(17) Å, $\beta$ = 93.360(8)°, $U$ = 3109.2(5) Å$^3$, $Z$ = 4, $D_c$ = 1.597 g cm$^{-3}$, $F(000)$ = 1532, $\mu$(Mo-K$\alpha$) = 6.7 cm$^{-1}$, 8433 reflections measured, 7119 independent, ($1.06 < \theta < 27.50°$). Data collection and handling were performed as described for compound **2**. The reference reflections displayed a linear decay of 2%. The structure was solved by automated Patterson methods (SHELXS-86). The water hydrogen atoms were located on a Fourier map and subsequently included in the refinement. Refinement converged at a final $wR_2$ value of 0.1331, $R_1$ = 0.0564 [for 4676 reflections with $F_\sigma > 4\sigma(F_\sigma)$], $S$ = 1.021, for 462 parameters. A final difference Fourier showed no residual density outside −0.66 and 0.50 e Å$^{-3}$. CCDC 182/491.

¶ A related iron(III) methoxy species was observed by ES–MS for $[FeL'(MeCN)](ClO_4)_2]$ [L′ = *N*,*N*-bis(2-pyridylmethyl)-*N*-bis(2-pyridyl)-methylamine] and the crystal structure of the corresponding methoxy complex was recently solved; manuscript is in preparation.

‖ For selective catalytic oxidation of alkanols to aldehydes with manganese complexes and hydrogen peroxides, see ref. 9.

1 S. J. Lippard and J. M. Berg, *Principles of Bioinorganic Chemistry*, University Science Books, Mill Valley, CA, 1994; *Bioinorganic Catalysis*, ed. J. Reedijk, M. Dekker, New York, 1993; A. L. Feig and S. J. Lippard, *Chem. Rev.*, 1994, **94**, 759.
2 L. Que, Jr. and R. Y. N. Ho, *Chem. Rev.*, 1996, **96**, 2607.
3 R. Hage, *Recl. Trav. Chim. Pays-Bas*, 1996, **115**, 385.
4 P. N. Hawker and M. V. Twigg, *Comprehensive Coordination Chemistry*, ed. G. Wilkinson, Pergamon, Oxford, 1987, vol. IV.
5 M. Lubben, A. Meetsma, E. C. Wilkinson, B. L. Feringa and L. Que, Jr., *Angew. Chem., Int. Ed. Engl.*, 1995, **34**, 1512.
6 S. Menage, E. C. Wilkinson, L. Que, Jr. and M. Fontecave, *Angew. Chem., Int. Ed. Engl.*, 1995, **34**, 203; J. Kim, E. Larka, E. C. Wilkinson and L. Que, Jr., *Angew. Chem., Int. Ed. Engl.*, 1995, **34**, 2048; L. Que Jr. and Y. Dong, *Acc. Chem. Res.*, 1996, **29**, 190.
7 I. Bernal, I. M. Jensen, K. B. Jensen, C. J. McKenzie, H. Toftlund and J. Tuchagues, *J. Chem. Soc., Dalton Trans.*, 1995, 3667.
8 Y. Gultneh, A. Farooq, K. D. Karlin, S. Liu and J. Zubieta, *Inorg. Chim. Acta*, 1993, **211**, 171.
9 I. E. Markó, P. R. Giles, M. Tsukazaki, S. M. Brown and C. J. Urch, *Science*, 1996, **274**, 2044; C. Zondervan, R. Hage and B. L. Feringa, *Chem. Commun.*, 1997, 419.

*Received in Cambridge, UK, 24th April 1997; 7/02804K*

# Azaheteroalkene metathesis: reaction of imines with molybdenum(VI) bis(imide) complexes

**Gidget K. Cantrell and Tara Y. Meyer***

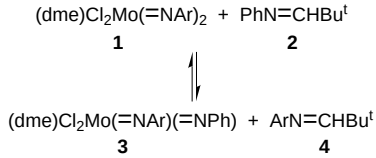
*Department of Chemistry, University of Pittsburgh, Pittsburgh, Pennsylvania 15260, USA*

**Bis(imide) complexes (dme)$Cl_2$Mo(=NR)$_2$ (R = $Bu^t$, $C_6H_3Pr^i_2$-2,6) and ($Bu^tO$)$_2$Mo(=NAr)$_2$ (Ar = $C_6H_3Pr^i_2$-2,6) undergo imide/imine metathesis with PhN=CH($Bu^t$) or ($Pr^n$)N=CHPh.**

Transition-metal-mediated reactions offer many potential advantages over traditional approaches to carbon–heteroatom bond formation including selectivity, mild reaction conditions, varied functional group tolerances, and increased reaction rates. A promising strategy for the development of these coupling reactions involves the extension of metal–alkylidene-mediated alkene metathesis, which is used extensively in polymer synthesis and increasingly in the preparation of natural products,[1–3] to heteroalkenes. We are particularly interested in carbon–nitrogen bond formation through metal–imide-mediated imine metathesis.

Reports of catalytic metathesis of azaheteroalkenes are rare and no system of general utility has been described.[4,5] Carbodiimides have been metathesized by $Cl_4Mo$=NR[6] and isocyanates by [(η-$C_5H_4$Me)Mo(=NR)$_2$]$_2$.[7] Only one example exists, however, of the metathesis of the less activated, but more versatile imine substrates. The early transition-metal imide complex, (η-$C_5H_5$)$_2$Zr(=$NBu^t$)(thf), reacted with *N*-phenylimines to give diazametallacycles that underwent further metathetical exchange with external imines, presumably *via* imide intermediates.[8,9] Although this reagent is an imine metathesis catalyst, it suffers from significant limitations, the reaction is inhibited by high imine concentrations and the reagent is reported to undergo a competing dimerization that deactivates it towards further reaction. Herein, we identify a class of metal complexes that exhibit the key step of catalytic imine metathesis, imide/imine metathesis, without such substrate inhibition or terminal dimer formation.

Treatment of (dme)$Cl_2$Mo(=NAr)$_2$[10] (Ar = $C_6H_3Pr^i_2$-2,6) **1**, with 0.8 equiv. of *tert*-butylanil **2**† in $C_6D_6$ at 100 °C produced metathesis product **4** over the course of several days as observed by $^1$H NMR spectroscopy (Scheme 1). After 18 days the ratio of **2** to **4** was *ca.* 1 : 1.‡ When the reaction was repeated with 12 equiv. of imine **2** to 1 equiv. of bis(imide) **1**, the reaction proceeded much more rapidly, producing 1.4 equiv. of imine **4** after 8 days at 85 °C.§ Inversion of the stoichiometry, 9 equiv. of **1** to 1 equiv. of imine **2**, slowed the reaction to the degree that only a trace of product imine **4** was observed after 8 days at 85 °C. Unambiguous identification of product imine **4** was achieved by comparison of the $^1$H NMR spectrum with that of an authentic sample and by GC–MS analysis of the reaction mixture. Increasing the temperature results in a concomitant increase in rate; the optimum reaction conditions have not yet been determined.



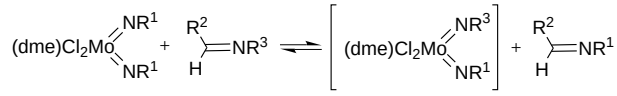

**Scheme 1**

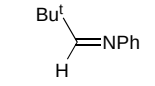
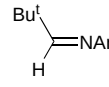
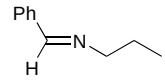
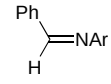
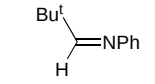
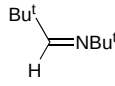
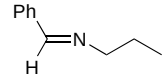
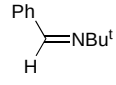
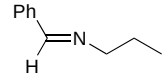
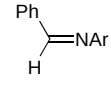
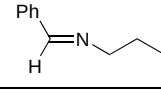
These reactions proceeded cleanly. No evidence for precoordination or for metallacyclic intermediates was observed by $^1$H NMR spectroscopy for any of the stoichiometric combinations;¶ nor were alkenes detected. Competing intermolecular imide/imide metathesis,[11] which in these systems equilibrates all bis(imide) complexes, prevented isolation and complete characterization of the mixed imide product (dme)$Cl_2$Mo(=NAr)(=NPh) **3**. $^1$H NMR resonances associated with **3** were, however, identified in the reaction mixture by comparison with those from a spectrum of an authentic sample.‖,**

Imide/imine metathesis is remarkably general for this class of bis(imides). The reaction proceeds despite changes in substrate imine, imide-nitrogen substituent, or ancillary ligand (Table 1). Specifically, imides **1** and (dme)$Cl_2$Mo(=$NBu^t$)$_2$, **5**,[10] react with imine **2**. Imides **1**, **5**, and ($Bu^tO$)$_2$Mo(=NAr)$_2$, **6**,[12] also react with *N*-propylbenzaldimine **8**, to give the expected exchange products. Only the sterically crowded (ArO)$_2$Mo(=NAr)$_2$, **7**, is unreactive.†† The fact that imide/imine metathesis occurs in all but one of the examples investigated to date suggests that these catalysts can be 'tuned' by varying the ancillary ligands.

One goal of this work was to identify a catalyst that does not undergo significant termination reactions. Compelling evidence for a lack of such termination reactions in the systems we have described can be found by examining the $^1$H NMR spectra; no significant amount of any species other than those described above was present. Specifically, we did not observe any stable

**Table 1**. Imide/imine metathesis




| Bis(imide) | | Substrate imine | | Product imine[a] |
|---|---|---|---|---|
| (dme)$Cl_2$Mo(=NAr)$_2$ | **1** |  | **2** |  |
| | |  | **8** |  |
| (dme)$Cl_2$Mo(=$NBu^t$)$_2$ | **5** |  | **2** |  |
| | |  | **8** |  |
| ($Bu^tO$)$_2$Mo(=NAr)$_2$ | **6** |  | **8** |  |
| (ArO)$_2$Mo(=NAr)$_2$ | **7** |  | **8** | No reaction |

[a] Characterized by $^1$H NMR spectroscopy and/or GC–MS analysis.

imide-bridged dimers, a particular concern since similar dimer formation limited the utility of $(\eta\text{-}C_5H_4Me)_2Zr(=NBu^t)(thf)$ as an imine metathesis catalyst.[8,9] Previous workers, who have examined these molybdenum bis(imide) complexes for other applications, have also found them to be primarily monomeric in solution. In a particularly relevant and elegant study, Gibson and coworkers observed intermolecular imide/imide exchange of $(Bu^tO)_2Mo(=NBu^t)_2$ with $(Bu^tO)_2Mo(=NAr)_2$.[11] Although the most likely mechanism for exchange would involve an imide-bridged dimer, no spectral evidence for a significant concentration of this intermediate could be found. Also germane is the observation by Chisholm *et al.* that an analogous bis(imide) dimer $[(Bu^tO)_2Mo(=NPh)(\mu\text{-}NPh)]_2$,[13] characterized by X-ray crystallography, exhibited a monomeric solution molecular mass.[14] Based on our data and these reports we can conclude that, although imide-bridged dimers are likely to be present in our reaction mixture, they do not represent a termination step for imide/imine metathesis.

Although these preliminary studies do not provide a complete picture of the metathesis, the data do provide some insights into the mechanism. It is clear, for example, that the imine products do not arise from a pathway involving initial decomposition of the metal imide. In control experiments, catalysts **1** and **5** were observed to be stable for weeks at 100 °C in $C_6D_6$. Moreover, integration of imide $^1$H NMR resonances *vs.* an internal standard showed that there was very little diversion of metal–imide complexes to insoluble or unidentified species.

We also do not believe that the reaction we are observing is water catalyzed. No acceleration was observed when trace water was added to the reaction mixture, nor was the reaction retarded when the reaction mixture was pre-dried for 3 days over molecular sieves before it was decanted and combined with bis(imide) complex **1**.

Like many of the alkylidene catalysts, the bis(imide) catalysts described herein do not exhibit precoordinated nor metallacyclic intermediates in their reaction with unsaturated substrates.[1c] Further studies are required to ascertain if, in fact, the metathesis proceeds through a [2 + 2] mechanism as would be expected by analogy to alkene metathesis systems. These studies are currently being pursued.

In summary, we have identified the first potential catalysts for imine metathesis. These bis(imide) catalysts undergo a general metathesis with imines without termination by dimer formation.

We thank the National Science Foundation (CHE-9624138) and The University of Pittsburgh (CRDF) for financial support. G. K. C. thanks the Pennsylvania Space Grant Consortium for fellowship support.

## Footnotes and References

* E-mail: tmeyer+@pitt.edu

† Imines were prepared by condensation of the parent aldehyde and amine in benzene over molecular sieves, followed by purification by vacuum distillation. The procedure was analogous to that described for imine preparation by S. R. Sandler, and W. Karo, in *Organic Functional Group Preparations*, Academic Press, New York, 1986, vol. II, p. 302.

‡ The ratio of products reported reflects the equilibrium reached after complete metathesis of the first and partial metathesis of the second imide reactive site.

§ *Typical NMR experiment*: reaction of $(dme)Cl_2Mo(NAr)_2$ **1** and $PhN{=}CH(Bu^t)$ **2**. Complex **1** (0.005 g, 0.008 mmol, 1 equiv.) was dissolved in *ca.* 0.5 ml $C_6D_6$ in an NMR tube equipped with a Teflon stopcock. Hexamethylbenzene in $C_6D_6$ and imine **2** (*ca.* 12 equiv.) were added. The sample was maintained for 24 h at room temp. to verify the stoichiometry and stability of the reaction mixture. The sample was heated and maintained at 85 °C for 18 d. The progress of the reaction was monitored by $^1$H NMR spectroscopy. $^1$H NMR ($C_6D_6$) of $ArN{=}CH(Bu^t)$ (unisolated) $\delta$ 7.25 (s, 1, C*H*$Bu^t$), 3.05 (spt, 2, C*H*$Me_2$, $J_{CH}$ 6.7 Hz), 1.17 (d, 12, CH*Me*$_2$, $J_{CH}$ 6.6 Hz), 1.07 (s, 9, $Bu^t$); mass spectrum (EI) *m/z* 245 ($M^+$), 188 ($M^+ - Bu^t$). $^1$H NMR ($C_6D_6$) $(dme)Cl_2Mo(NAr)(NPh)$ (unisolated) $\delta$ 4.40 (spt, 2, C*H*$Me_2$, $J_{CH}$ 7.1 Hz), 1.30 (d, 12, CH*Me*$_2$, $J_{CH}$ 6.8 Hz). Phenyl and aryl resonances could not be definitively assigned owing to the complexity of the spectrum in this region.

¶ The diazametallacycle, if present, exists only in trace amounts since the total imine concentration (substrate + product) remains nearly constant throughout the reaction.

‖ Compound **3** was independently prepared by the reaction of bis(imide) **1** with phenyl isocyanate.

** $(dme)Cl_2Mo(=NPh)_2$ should be present as well, arising from metathesis of both imido groups and, also, from intermolecular imide/imide metathesis. The complexity of the phenyl region of the spectrum precludes the assignment of resonances for this species.

†† $(ArO)_2Mo(NAr)_2$ was prepared by analogy to $(Bu^tO)_2Mo(NAr)_2$ by reaction of $(dme)Cl_2Mo(NAr)_2$ with 2 equiv. of LiOAr. $^1$H NMR ($C_6D_6$) $\delta$ 6.87–7.08 (m, 12, aryl), 3.82 (spt, 4, C*H*$Me_2$, $J_{CH}$ 6.8 Hz), 3.48 (spt, 4, C*H*$Me_2$, $J_{CH}$ 6.8 Hz), 1.25 (d, 24, CH*Me*$_2$, $J_{CH}$ 6.8 Hz), 1.00 (d, 24, CH*Me*$_2$, $J_{CH}$ 6.8 Hz); $^{13}$C NMR ($C_6D_6$) $\delta$ 160.7 ($C_{ipso}$, OAr), 154.4 ($C_{ipso}$, NAr), 143.6, 138.2, 127.6, 124.3, 123.9, 123.1 (aryl), 29.4 (C*H*$Me_2$, OAr), 28.0 (C*H*$Me_2$, NAr), 24.5 (CH*Me*$_2$, OAr), 24.2 (CH*Me*$_2$, NAr). Anal. Calc. for $C_{48}H_{68}N_2O_2Mo$: C, 71.87; H, 8.56; N, 3.50. Found: C, 71.91; H, 8.74; N, 3.50%.

1 For reviews of alkene metathesis see: (*a*) R. H. Grubbs and W. Tumas, *Science*, 1989, **243**, 907; (*b*) R. R. Schrock, *Acc. Chem. Res.*, 1990, **23**, 158; (*c*) A. J. Amass, in *New Methods of Polymer Synthesis*, ed. J. R. Ebdon, Chapman and Hall, New York, 1991, p. 76.
2 S.-H. Kim, N. Bowden and R. H. Grubbs, *J. Am. Chem. Soc.*, 1994, **116**, 10801.
3 G. C. Fu and R. H. Grubbs, *J. Am. Chem. Soc.*, 1992, **114**, 7324.
4 W. A. Nugent, *Metal-Ligand Multiple Bonds*, Wiley, New York, 1988.
5 For a recent review of transition metal imido complexes, see D. E. Wigley, *Prog. Inorg. Chem.*, 1994, **42**, 239.
6 I. Meisel, G. Hertel and K. Weiss, *J. Mol. Catal.*, 1986, **36**, 159.
7 M. L. H. Green, G. Hogarth, P. C. Konidaris and P. Mountford, *J. Organomet. Chem.*, 1990, **394**, C9.
8 K. E. Meyer, P. J. Walsh and R. G. Bergman, *J. Am. Chem. Soc.*, 1994, **116**, 2669.
9 K. E. Meyer, P. J. Walsh and R. G. Bergman, *J. Am. Chem. Soc.*, 1995, **117**, 974.
10 H. H. Fox, K. B. Yap, J. Robbins, S. Cai and R. R. Schrock, *Inorg. Chem.*, 1992, **31**, 2287.
11 M. Jolly, J. P. Mitchell and V. C. Gibson, *J. Chem. Soc., Dalton Trans.*, 1992, 1331.
12 M. Jolly, J. P. Mitchell and V. C. Gibson, *J. Chem. Soc., Dalton Trans.*, 1992, 1329.
13 M. H. Chisholm, K. Folting, J. C. Huffman, C. C. Kirkpatrick and A. L. Ratermann, *J. Am. Chem. Soc.*, 1981, **103**, 1305.
14 M. H. Chisholm, K. Folting, J. C. Huffman and A. L. Raterman, *Inorg. Chem.*, 1982, **21**, 978.

*Received in Bloomington, IN, USA, 23rd April 1997; 7/02780J*

# First oxazagermete: synthesis, structure and thermal cycloreversion into a germanone

**Tsuyoshi Matsumoto, Norihiro Tokitoh and Renji Okazaki***

*Department of Chemistry, Graduate School of Science, The University of Tokyo, 7-3-1 Hongo, Bunkyo-ku, Tokyo 113, Japan*

**A novel four-membered ring compound, 1,2,4-oxazagermete, is obtained by the reaction of diarylgermylene tbt(tip)Ge: with mesitonitrile oxide; its thermolysis generates germanone tbt(tip)Ge=O as evidenced by trapping reactions with dimethylbutadiene and ethanol.**

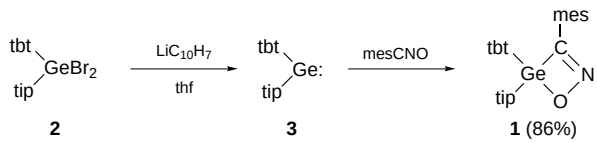
Small-ring compounds containing a group 14 element have been of current interest because of their intriguing structural properties and potential utility as precursors of reactive intermediates taking advantage of their ring strain. Since many such small-ring compounds are highly reactive under ambient conditions, some stabilization is often necessary for their isolation, for example, the use of a very bulky substituent.[1]

Here we report the synthesis of kinetically stabilized 1,2,4-oxazagermete **1**, a novel four-membered ring compound containing germanium, by an efficient steric protecting group, 2,4,6-tris[bis(trimethylsilyl)methyl]phenyl (tbt).[2] There have been several reports on 1,2-oxazetes. They were observed as reactive intermediates in the thermal and photochemical reactions of α,β-unsaturated nitro compounds or in the reaction of vinyl radicals and NO,[3] and some oxazetes having bulky substituents have been isolated although their molecular structures were not established.[4] In contrast, there has been no report so far on the heavier group 14 element analogue of an 1,2-oxazete.

Oxazagermete **1** was synthesized as stable colourless crystals in 87% by the reaction of diarylgermylene tbt(tip)Ge: **3** (tip = 2,4,6-triisopropylphenyl), generated from dibromogermane **2** and lithium naphthalenide in thf,[5] with mesitonitrile oxide (Scheme 1). This represents the first synthesis of an oxazagermete as well as the first isolation of a [1 + 3]-cycloaddition reaction product of a germylene with 1,3-dipolar reagents.[6]

Oxazagermete **1** showed characteristic spectral data.† The C=N bond stretching was observed at 1612 $cm^{-1}$ in the IR spectrum, which is similar to those reported for 1,2-oxazetes.[4] In the $^{13}C$ NMR spectrum, a singlet peak was observed at $\delta$ 174.8 assignable to the carbon in the four-membered ring, which is more shielded than that of an oxazete owing to the more electropositive Ge atom on the carbon.[4c]

The molecular structure of **1** has been determined by X-ray crystallographic analysis and an ORTEP drawing is shown in Fig. 1.‡ The bond angle C(34)–Ge–O considerably shrinks from that of normal $sp^3$ configuration to 68.7(2)°, suggesting the large ring strain of the four-membered ring, which is also reflected on the long Ge–O bond length [1.872(4) Å] compared with that of a typical Ge–O single bond (1.75–1.85 Å).[7] The four-membered ring of **1** is perfectly planar with the sum of the bond angles being 360°.




**Scheme 1**

Thermolysis of **1** was carried out in the expectation that it would dissociate into a germanium–oxygen double-bond species (germanone) tbt(tip)Ge=O **4** and mesitonitrile, since an 1,2-oxazete is known to undergo thermal cycloreversion into the corresponding ketone and nitrile.[3,4] The chemistry of germanones has not been fully disclosed yet, although they have been a fascinating subject of considerable attention in recent years.[1b,8]

When a [$^2H_6$]benzene solution of **1** and 2,3-dimethylbuta-1,3-diene in a sealed NMR tube was heated at 120 °C for 12 h, the starting materials were consumed completely ($^1H$ NMR) to afford **5**–**7** and mesitonitrile (Scheme 2).§ Formation of compounds **5**–**7** and an almost quantitative yield of mesitonitrile clearly indicates the generation of intermediary germanone **4**, since we previously reported the formation of **7** from germanone **4** generated from by the reaction of germylene **3** with tribenzylamine *N*-oxide.[8]

Compounds **6** and **7** are most likely produced from germanone **4** *via* intramolecular cyclization,[9] while the formation of compound **5** is reasonably explained in terms of an ene

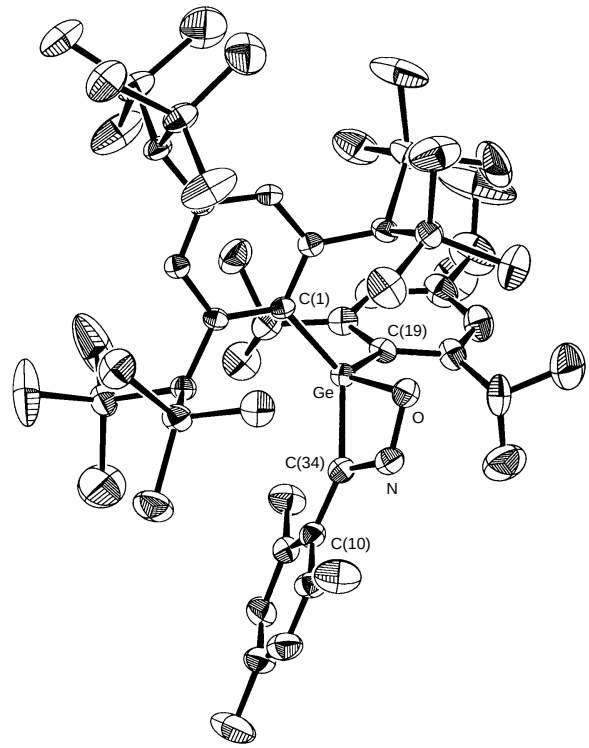
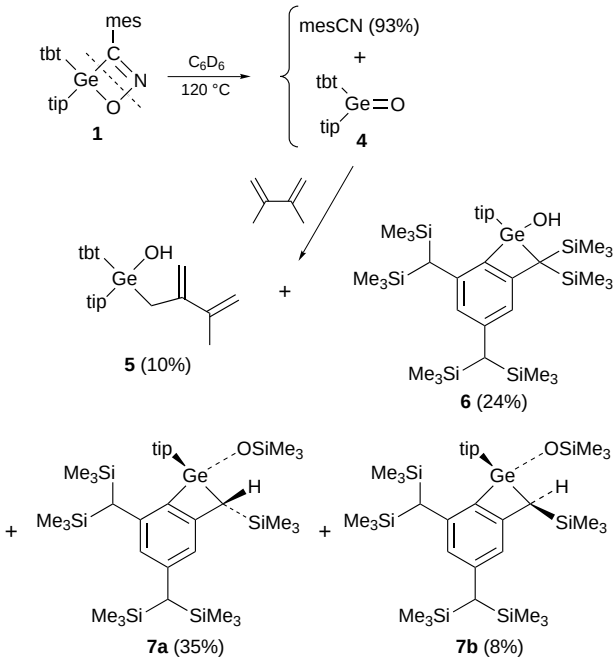



**Fig. 1** ORTEP drawing of oxazagermete **1** with thermal ellipsoid plots (30% probability). Selected bond lengths (Å) and angles (°): Ge–O 1.872(4), Ge–C(1) 1.968(6), Ge–C(19) 1.974(6), Ge–C(34) 2.001(6), C(34)–N 1.291(9), N–O 1.418(8), C(10)–C(34) 1.459(10); C(1)–Ge–O 105.9(2), C(1)–Ge–C(19) 114.9(2), C(1)–Ge–C(34) 123.0(3), C(19)–Ge–O 112.9(3), C(19)–Ge–C(34) 119.1(3), O–Ge–C(34) 68.7(2), Ge–O–N 92.7(3), O–N–C(34) 107.6(5), Ge–C(34)–N 91.1(5), Ge–C(34)–C(10) 146.2(5), N–C(34)–C(10) 122.7(6).




**Scheme 2**

reaction of germanone **4** with the butadiene. In the cases of chalcogen double-bond species, tbt(tip)Ge=X (X = S, Se, Te), the corresponding [4 + 2] cycloadducts were obtained in the reactions with dienes.[2] The reason for this difference is not clear at present.

The total yield of the silyl-migrated compounds **7a** and **7b** is higher than that of the hydrogen-migrated compound **6**, which is probably due to the higher affinity of silicon for oxygen. The product ratio of **7a** to **7b** is considered to be kinetically determined since no isomerization from **7a** to **7b** is observed even at 180 °C.

The generation of germanone **4** was also confirmed by the thermal reaction of **1** in benzene (at 120 °C, in a sealed tube) in the presence of ethanol, in which ethoxy(hydroxy)germane tbt(tip)Ge(OH)(OEt) **8**, an ethanol adduct of **4**, was obtained in 82%. This finding indicates that the intermolecular reaction with ethanol was faster than the intramolecular silyl or hydrogen migration mentioned above. It was also confirmed by thermolysis (120 °C) of a [$^2H_6$]benzene solution of oxazagermete **1** in the presence of 0.3 equiv of ethanol while being monitored by $^1$H NMR. In the initial stage, the ethanol adduct **8** was observed exclusively, and, after consumption of ethanol, the rearrangement reaction to **6**, **7a** and **7b** occurred.

In summary, we have succeeded in the isolation and crystallographic analysis of the first 1,2,4-oxazagermete **1**, which undergoes thermal cycloreversion into mesitonitrile and germanone tbt(tip)Ge=O.

## Footnotes and References

* E-mail: okazaki:@chem.s.u-tokyo.ac.jp

† *Spectral data* for **1**: white crystals; mp 196–197 °C (decomp.) ($CH_2Cl_2$–EtOH); $^1$H NMR ($CDCl_3$, 500 MHz, 350 K) $\delta$ −0.12 (s, 18 H), 0.07 (s, 18 H), 0.09 (s, 18 H), 1.03 (br s, 6 H), 1.24 (d, *J* 6.9 Hz, 6 H), 1.25 (br s, 6 H), 1.39 (s, 1 H), 1.58 (br s, 2 H), 2.25 (s, 3 H), 2.39 (s, 6 H), 2.87 (spt, *J* 6.9 Hz, 1 H), 3.37 (br s, 2 H), 6.39 (br s, 2 H), 6.81 (s, 2 H), 7.06 (s, 2 H); $^{13}$C NMR ($CDCl_3$, 125 MHz, 340 K) $\delta$ 1.00 (q), 1.08 (q), 1.97 (q), 2.21 (q), 2.23 (q), 20.86 (q), 23.68 (q), 23.73 (q), 24.03 (q), 24.93 (q), 26.94 (q), 29.36 (d), 31.04 (d), 33.99 (d), 34.32 (d), 123.41 (d), 128.71 (d), 129.86 (d), 133.43 (s), 134.28 (s), 137.49 (s), 137.90 (s), 145.58 (s), 149.96 (s), 151.69 (s), 155.17 (s). High-resolution FABMS: observed *m/z* 990.5158 ([M + H]$^+$). Calc. for $C_{52}H_{94}{}^{74}GeNOSi_6$ 990.5163.

‡ *Crystallographic data* for **1**: $C_{52}H_{93}GeNOSi_6$, *M* = 989.42, triclinic, space group $P\bar{1}$, *a* = 13.002(3), *b* = 19.433(4), *c* = 12.503(5) Å, $\alpha$ = 101.48(2), $\beta$ = 91.22(2), $\gamma$ = 77.17(1)°, *U* = 3018(1) Å$^3$, *Z* = 2, $D_c$ = 1.083 g cm$^{-3}$, *T* = 296 K, *F*(000) = 1072, colourless prism with dimensions 0.60 × 0.50 × 0.40, μ(Mo-Kα) = 6.48 cm$^{-1}$, $R(R_w)$ = 0.056(0.062). Weighting scheme; $w = 1/\sigma^2(F_o)$. The intensity data ($2\theta$ < 55°) for **1** were collected on a Rigaku AFC5R diffractometer with graphite-monochromated Mo-K$\alpha$ radiation ($\lambda$ = 0.710 69 Å), and 14 509 reflections (13 892 unique) were measured. The structure of **1** was solved by direct methods (structure solution methods; MITHRIL[10] and DIRDIF[11]), and refined by full-matrix least squares using the TEXSAN crystallographic software package.[12] All the non-hydrogen atoms were refined anisotropically, while the hydrogen atoms were placed in calculated positions. The final cycles of the least-squares refinement were based on 5387 observed reflections [$I > 3\sigma|I|$] and 550 variable parameters. The maximum and minimum peaks on the final difference Fourier map correspond to 0.40 and −0.37 e Å$^{-3}$, respectively. CCDC 182/526.

§ New compounds **5** and **6** here obtained gave satisfactory spectral and analytical data. For **5**: white crystals; mp 189–191 °C (deccomp.) ($CH_2Cl_2$–EtOH); $^1$H NMR ($CDCl_3$, 500 MHz, 300 K) $\delta$ −0.17 (s, 9 H), 0.00 (s, 9 H), 0.03 (s, 9 H), 0.05 (s, 9 H), 0.06 (s, 9 H), 0.13 (s, 9 H), 0.82 (d, *J* 6.9 Hz, 3 H), 1.02 (d, *J* 6.9 Hz, 3 H), 1.13 (s, 1 H), 1.173 (d, *J* 6.9 Hz, 3 H), 1.174 (d, *J* 6.9 Hz, 3 H), 1.27 (br s, 6 H), 1.84 (s, 3 H), 2.09 (s, 1 H), 2.13 (s, 1 H), 2.37 (d, *J* 12.3 Hz, 1 H), 2.66 (br s, 1 H), 2.79 (spt, *J* 6.9 Hz, 1 H), 2.85 (d, *J* 12.3 Hz, 1 H), 3.95 (br s, 1 H), 4.28 (s, 1 H), 4.86 (s, 1 H), 5.00 (s, 1 H), 5.17 (s, 1 H), 6.29 (s, 1 H), 6.40 (s, 1 H), 6.89 (s, 1 H), 6.93 (s, 1 H). High-resolution FABMS: observed *m/z* 927.5016 ([M + H]$^+$). Calc. for $C_{48}H_{92}{}^{74}GeOSi_6$ 927.5054. For **6**: white crystals; mp 177–179 °C ($CH_2Cl_2$–EtOH); $^1$H NMR ($CDCl_3$, 500 MHz, 300 K) $\delta$ −0.09 (s, 9 H), 0.04 (s, 18 H), 0.06 (s, 9 H), 0.16 (s, 9 H), 0.17 (s, 9 H), 1.24 (d, *J* 6.9 Hz, 6 H), 1.29 (br s, 6 H), 1.33 (d, *J* 6.9 Hz, 6 H), 1.66 (s, 1 H), 1.72 (br s, 1 H), 2.87 (spt, *J* 6.9 Hz, 1 H), 3.29 (br s, 2 H), 6.44 (s, 1 H), 6.46 (s, 1 H). High-resolution FABMS: observed *m/z* 845.4339 ([M+H]$^+$); calc. for $C_{42}H_{83}{}^{74}GeOSi_6$ 845.4271.

1 Recent reviews; see (*a*) T. Tsumuraya, S. A. Batcheller and S. Masamune, *Angew. Chem., Int. Ed. Engl.*, 1991, **30**, 902; (*b*) J. Barrau, J. Escudié and J. Satgé, *Chem. Rev.*, 1990, **90**, 283; (*c*) M. Driess and H. Grützmacher, *Angew. Chem., Int. Ed. Engl.*, 1996, **35**, 828; (*d*) K. M. Baines and W. G. Stibbs, *Adv. Organomet. Chem.*, 1996, **39**, 275.

2 For the other examples of kinetic stabilization by tbt, see: H. Suzuki, N. Tokitoh, S. Nagase and R. Okazaki, *J. Am. Chem. Soc.*, 1994, **116**, 11 578; N. Tokitoh, T. Matsumoto, K. Manmaru and R. Okazaki, *J. Am. Chem. Soc.*, 1993, **115**, 8855; T. Matsumoto, N. Tokitoh and R. Okazaki, *Angew. Chem., Int. Ed. Engl.*, 1994, **33**, 2316; N. Tokitoh, T. Matsumoto and R. Okazaki, *J. Am. Chem. Soc.*, 1997, **119**, 2337; N. Tokitoh, M. Saito and R. Okazaki, *J. Am. Chem. Soc.*, 1993, **115**, 2065.

3 T. H. Kinstle and J. G. Stam, *J. Org. Chem.*, 1970, **35**, 1771; J. T. Pinhey and E. Rizzardo, *Tetrahedron Lett.*, 1973, 4057; A. G. Sherwood and H. E. Qunning, *J. Am. Chem. Soc.*, 1963, **85**, 3506; J. M. Surzur, C. Dupy, M. P. Bertrand and R. Nousier, *J. Org. Chem.*, 1972, **37**, 2782.

4 (*a*) K. Wieser and A. Berndt, *Angew. Chem., Int. Ed. Engl.*, 1975, **14**, 69; (*b*) 1975, **14**, 70; (*c*) H. G. Corkins, L. Storace and E. R. Osgood, *Tetrahedron Lett.*, 1980, **21**, 2025.

5 N. Tokitoh, K. Kishikawa, T. Matsumoto and R. Okazaki, *Chem. Lett.*, 1995, 827.

6 For the reaction of a germylene with 1,3-dipolar reagents, see, for example: C. Glidewell, D. Lloyd and K. W. Lumbard, *J. Chem. Soc., Dalton Trans.*, 1987, 501.

7 K. M. Baines and W. G. Stibbs, *Coord. Chem. Rev.*, 1995, **145**, 157.

8 N. Tokitoh, T. Matsumoto and R. Okazaki, *Chem. Lett.*, 1995, 1087.

9 For a similar cyclization of bis(2,4,6-tri-*tert*-butylphenyl)germanone, see: P. Jutzi, H. Schmidt, B. Neumann and H.-G. Stammler, *Organometallics*, 1996, **15**, 741.

10 C. J. Gilmore, MITHRIL. An integrated direct methods computer program, *J. Appl. Crystallogr.*, 1984, **17**, 42 (University of Glasgow).

11 P. T. Beuskens, DIRDIF. Direct methods for difference structures—an automatic procedure for phase extension and refinement of difference structure factors, Technical Report 1984/1 Crystallography Laboratory, Toernooiveld, 6525 Ed Nijmegen, 1984.

12 TEXSAN: TEXRAY Structure Analysis Package, Molecular Structure Corporation, 1985.

*Received in Cambridge, UK, 12th May 1997; 7/03241B*

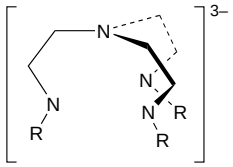
# Highly selective trimerisation of MeNC by a novel titanium imido complex containing a tridentate dianionic ligand

**Alexander J. Blake,[a] Philip E. Collier,[a] Lutz H. Gade,*[b] Mary McPartlin,[c] Philip Mountford,*[a] Martin Schubart[b] and Ian J. Scowen[c]**

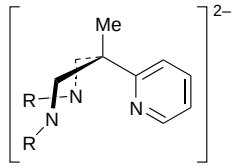
[a] *Department of Chemistry, University of Nottingham, University Park, Nottingham, UK NG7 2RD*
[b] *Institut für Anorganische Chemie der Universität Würzburg, Am Hubland, D-97074 Würzburg, Germany*
[c] *School of Applied Chemistry, University of North London, Holloway Road, London, UK N7 8DB*

**A new type of imido compound [Ti(NBu$^t$)L(py)] 1 containing a tripodal dianionic ligand is reported which effects the remarkably selective trimerisation of MeNC; the crystal structures of 1 and [TiL{N(Me)N(Bu$^t$)($C_4H_3N_2$Me)}] 2 are described [L = MeC(2-$C_5H_4N$)($CH_2NSiMe_3$)$_2$].**

Transition-metal imido complexes are relevant to industrially important processes such as acrylonitrile synthesis and ring-opening metathesis polymerisation, and also to biological processes such as nitrogen fixation.[1] Highly reactive transition-metal imido transients, in particular, have demonstrated a rich chemistry including cycloaddition reactions, catalytic hydroammination and C–H bond activation.[1b] Imido complexes that have reactive {M=NR} functionalities but yet are sufficiently kinetically stable to be isolated are extremely rare. Cognisant of the very successful use of the trianionic triamidoamine ligands [($RNCH_2CH_2$)$_3$N]$^{3-}$ **A** in developing groups 5–7 metal–ligand multiple bond chemistry,[2] we wished to explore the potential of the dianionic tripodal ligands [MeC(2-$C_5H_4N$)($CH_2NR$)$_2$]$^{2-}$ **B**.




**A**




**B**

The ligand system **B** is related to **A**, but features several important differences. Firstly, the pyridyl nitrogen donor function in **B** is only relatively weakly coordinating (compared to amide donor groups in **A**) and this 'arm' can potentially dissociate[3] from the metal centre during reactions to open up a larger reactive site. Furthermore, **B** is only a dianionic ligand and thus allows access to neutral metal–ligand multiply bonded complexes of the group 4 metals. Here, we report the synthesis of a novel titanium imido complex containing a tridentate ligand of the type **B**, along with an example of its reactivity.

Reaction of the previously described complex [Ti(NBu$^t$)Cl$_2$(py)$_3$][4] with the dilithiated diamidopyridine ligand [Li$_2$L]$_2$[5] in benzene followed by standard work-up afforded [Ti(NBu$^t$)L(py)] **1** in good yield [L = MeC(2-$C_5H_4N$)($CH_2NSiMe_3$)$_2$]. The X-ray structure of **1** is shown in Fig. 1† and is consistent with the solution $^1$H and $^{13}$C NMR data.‡ Compound **1** comprises an approximately trigonal-bipyramidal titanium centre with the *tert*-butylimide and the amide donor groups of the diamidopyridine ligand occupying the equatorial sites. The pyridyl-N atom of the diamidopyridine ligand lies in one of the apical sites and a pyridine ligand completes the coordination sphere. Compound **1** is the first fully characterised example of a terminal titanium imido complex supported by an amido ligand, although complexes of the type [Ti(NR)(NHR)$_2$] (R = SiBu$^t_3$) have been proposed as reactive

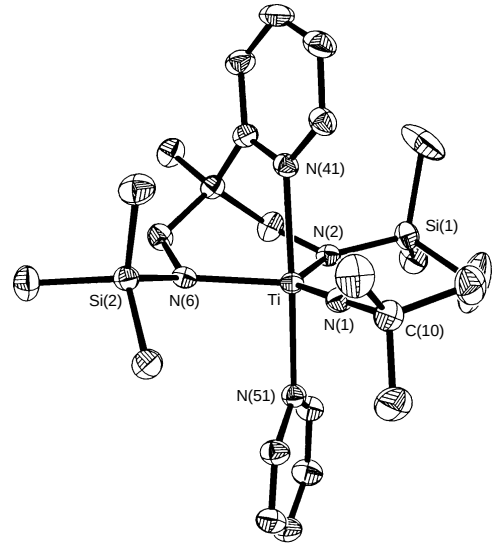
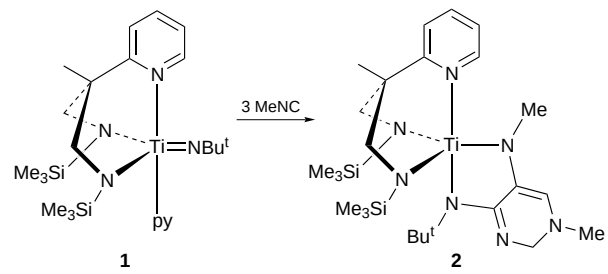



**Fig. 1** Molecular structure of [Ti(NBu$^t$)L(py)] **1**. Hydrogen atoms are omitted for clarity and thermal ellipsoids are drawn at the 50% probability level. Selected bond lengths (Å) and angles (°): Ti–N(1) 1.724(2), Ti–N(2) 2.025(2), Ti–N(6) 1.983(2), Ti–N(41) 2.203(2), Ti–N(51) 2.278(2); Ti–N(1)–C(10) 175.10(17), N(1)–Ti–N(2) 130.09(9), N(1)–Ti–N(6) 115.84(9), N(2)–Ti–N(6) 113.33(8), N(41)–Ti–N(51) 165.83(7).

transients.[6] The Ti=NBu$^t$ bond length of 1.724(2) Å lies at the long end of the range of known titanium–*tert*-butylimido bond lengths.[1b] The pyridine molecule is substantially less tightly bound [Ti–N(51) 2.278(2) Å] than the pyridyl fragment [Ti–N(41) 2.203(2) Å] of the diamidopyridine ligand and is readily lost in reactions of **1**.

Preliminary reactivity studies of [Ti(NBu$^t$)L(py)] **1** with a range of unsaturated substrates have indicated that this complex possesses a very reactive Ti=NBu$^t$ linkage. By way of example, we describe here the novel reaction of **1** with methyl isocyanide. Thus compound **1** reacts with 3 mol equiv. of MeNC at room temp. to yield a single product [TiL{N(Me)N(Bu$^t$)($C_4H_3N_2$Me)}] **2** (Scheme 1). On titration of **1** with




**1** **2**

**Scheme 1**

MeNC in $C_6D_6$, $^1$H NMR spectroscopy indicated complete cooperativity in the trimerisation (*vide infra*) of the isocyanide molecules as no intermediates were observed.

The solid-state structure of **2** was established unambiguously by X-ray crystallography (Fig. 2) which revealed a central five-coordinate Ti atom with a distorted trigonal-bipyramidal arrangement of N-donor atoms. The apical positions are occupied by the pyridyl [Ti–N(41) 2.282(2) Å] and *tert*-butyl amide fragment N-donor atoms. The Ti=NBu$^t$ linkage of **1** has clearly undergone C–N and C–C coupling (with concomitant C–H bond migration) with three molecules of MeNC to form a coordinated 3-methyl-5,6-diamino-2,3-dihydropyrimidine derivative. The type of reaction giving rise to **2** is unprecendented in group 4 imido chemistry. Reactions of later transition-metal imido complexes with aryl isocyanides have very recently been described[7] but pyrimidine-type rings were not formed.

In conclusion, we have shown that the type of trifunctional amido-supported imido complex described can generate novel chemistry. The instantaneous formation of **2** and the absence of detectable intermediates precludes the proposal of a mechanistic pathway at this stage, but such studies will be included in further investigations into this new type of metal-mediated isocyanide cyclisation. Further preliminary results in these laboratories indicate that compounds analogous to **1** can be formed for other tridenate diamidoamines and transition metals, and work is in progress to establish the overall scope of this chemistry.

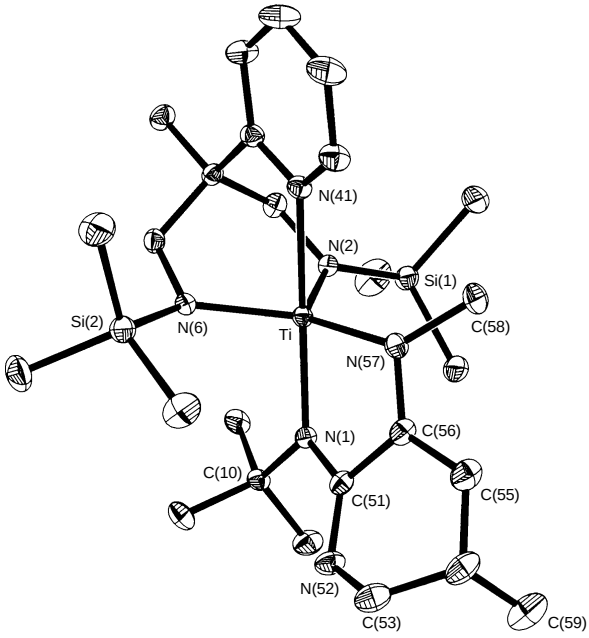



**Fig. 2** Molecular structure of [TiL{N(Me)N(Bu$^t$)($C_4H_3N_2$Me)}] **2**. Hydrogen atoms are omitted for clarity and thermal ellipsoids are drawn at the 20% probability level. Selected bond lengths (Å) and angles (°): Ti–N(1) 2.034(2), Ti–N(2) 1.890(2), Ti–N(6) 1.936(2), Ti–N(41) 2.282(2), Ti–N(57) 1.965(2), N(1)–C(51) 1.379(3), C(51)–N(52) 1.299(4), N(52)–C(53) 1.457(4), C(53)–N(54) 1.448(4), N(54)–C(55) 1.414(4), C(55)–C(56) 1.349(4), C(51)–C(56) 1.484(4); N(1)–Ti–N(1)–N(2) 109.87(9), N(1)–Ti–N(6) 98.66(9), N(2)–Ti–N(6) 108.53(10), N(1)–Ti–N(41) 163.94(9).

This work was supported by grants from the EPSRC (to P. M. and M. McP.), the Deutsche Forschungsgemeinschaft (SFB 347 to L. H. G.) and the Leverhulme Trust (to P. M.). L. H. G., P. M. and M. McP. thank the British Council and DADD for support under the ARC programme.

## Footnotes and References

* E-mail: philip.mountford@nottingham.ac.uk

† *Crystal data* for [Ti(NBu$^t$)L(py)] **1**: $C_{24}H_{43}N_5Si_2Ti$, $M$ = 505.71, triclinic, space group $P\bar{1}$, $a$ = 9.535(3), $b$ = 10.125(3), $c$ = 15.948(3) Å, $\alpha$ = 90.63(3), $\beta$ = 99.22(3), $\gamma$ = 105.40(2)°, $U$ = 1416.1(7) Å$^3$, $Z$ = 2, $D_c$ = 1.186 g cm$^{-3}$, $F(000)$ = 544, $T$ = 150 K, Mo-K$\alpha$, $5.2 \leqslant 2\theta \leqslant 50°$. The structure was solved by direct methods (SHELXS = 96) and 289 parameters were refined (SHELXL-96) on $F^2$ for 4983 data to give final conventional $R_1$ = 0.0416 [for 4308 data with $F_o > 4\sigma(F_o)$] and $wR_2$ = 0.1084 (all data). For [TiL{N(Me)N(Bu$^t$)($C_4H_3N_2$Me)}] **2**: $C_{25}H_{47}N_7Si_2Ti$, $M$ = 549.78, triclinic, space group $P\bar{1}$, $a$ = 10.031(2), $b$ = 11.4608(14), $c$ = 15.465(2) Å, $\alpha$ = 94.333(8), $\beta$ = 108.378(13), $\gamma$ = 111.976(11), $U$ = 1526.4(4) Å$^3$, $Z$ = 2, $D_c$ = 1.196 g cm$^{-3}$, $F(000)$ = 592, $T$ = 298 K, Mo-K$\alpha$, $2.85 \leqslant 2\theta \leqslant 50°$. The structure was solved by direct methods and 316 parameters were refined on $F^2$ for 5346 data. All computations were performed with SHELXTL PC 5.03. Refinement converged at $R_1$ = 0.0437 [for 3900 data with $F_o > 4\sigma(F_o)$] and $wR_2$ = 0.1102 (all data). CCDC 182/525.

‡ NMR spectroscopic and elemental analytical data for the new compounds have been deposited for scrutiny by the referees.

1 (*a*) V. C. Gibson, *Adv. Mater.*, 1994, **6**, 37; (*b*) D. E. Wigley, *Prog. Inorg. Chem.*, 1994, **42**, 239; (*c*) W. A. Nugent and J. M. Mayer, *Metal–Ligand Multiple Bonds*, Wiley-Interscience, New York, 1988; (*d*) W. A. Nugent and B. L. Haymore, *Coord. Chem. Rev.*, 1980, **31**, 123.

2 R. R. Schrock, *Acc. Chem. Res.*, 1997, **30**, 9.

3 S. Friedrich, L. H. Gade, A. J. Edwards and M. McPartlin, *J. Chem. Soc., Dalton Trans.*, 1993, 2861.

4 S. C. Dunn, A. S. Batsanov and P. Mountford, *J. Chem. Soc., Chem. Commun.*, 1994, 2007; A. J. Blake, P. E. Collier, S. C. Dunn, W.-S. Li, P. Mountford and O. V. Shishkin, *J. Chem. Soc., Dalton Trans.*, 1997, in the press.

5 S. Friedrich, M. Schubart, L. H. Gade, I. J. Scowen and M. McPartlin, manuscript in preparation.

6 C. C. Cummins, C. P. Schaller, G. D. Van Duyne, P. T. Wolczanski, A. W. E. Chan and R. Hoffmann, *J. Am. Chem. Soc.*, 1991, **113**, 2985. These authors describe spectroscopic evidence for [Ti(NR)(NHR)$_2$(OEt$_2$)] (R = SiBu$^t_3$).

7 A. D. Danopoulos, G. Wilkinson, T. K. N. Sweet and M. B. Hursthouse, *J. Chem. Soc., Dalton Trans.*, 1996, 271; A. D. Danopoulos, G. Wilkinson, T. K. N. Sweet and M. B. Hursthouse, *J. Chem. Soc., Dalton Trans.*, 1996, 3771.

*Received in Basel, Switzerland, 12th May 1997; 7/03275G*

# Synthesis and structural characterization of a tetrahedral sp³ carbide cluster compound

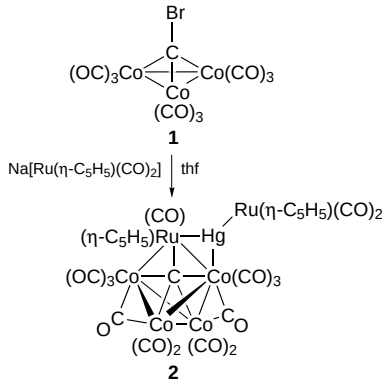
**Yoshiaki Takahashi, Munetaka Akita* and Yoshihiko Moro-oka***

*Research Laboratory of Resources Utilization, Tokyo Institute of Technology, 4259 Nagatsuta, Midori-ku, Yokohama 226, Japan*

**Treatment of the ($\mu_3$-halomethylidyne)tricobalt cluster compound ($\mu_3$-X–C)$Co_3(CO)_6L_3$ with Na[Ru($\eta$-$C_5H_5$)$(CO)_2$] produces the heptanuclear ($\mu_5$-C)($\eta$-$C_5H_5$)$_2Ru_2Co_4Hg(CO)_{13}$ 2 [X = Br; $L_3$ = $(CO)_3$] and tetranuclear carbide cluster compound ($\eta$-$C_5H_5$)$(CO)_2Ru(\mu_4$-C)$Co_3(CO)_6$(tdpm) 4 [X = Cl; $L_3$ = $CH(PPh_2)_3$ (tdpm)], *via* substitution of $\mu_3$-X–C; the latter complex 4 is the first example of a structurally characterized tetrahedral sp³ carbide cluster compound.**

Transition-metal carbide cluster compounds have been studied extensively over twenty years as model compounds for a carbide species adsorbed on a metal surface.[1,2] Previous studies have revealed various aspects of such a species as a pivotal intermediate in catalytic transformations of hydrocarbons and carbon monoxide (*e.g.* conversion to $CH_x$ species through H-addition).[3] However, the carbido carbon atoms in the previous examples are partly or completely encapsulated in a metal array such as butterfly and octahedral structures.[1] To the best of our knowledge, no example of a structurally characterized carbide cluster compound with an sp³-hybridized carbido carbon atom has been reported so far,[4,5] although it would be the most probable structure that an organic chemist expects. Our research interest has been focused on synthetic study toward polymetallic compounds with a simple carbon linkage such as permetallated ethane, ethene and ethyne,[6] and herein we report the synthesis of the first structurally characterized example of a tetrahedral sp³ carbide cluster compound, a permetallated methane.

The synthetic method that we have employed is nucleophilic substitution of the classical ($\mu_3$-halomethylidyne)tricobalt cluster derivatives, ($\mu_3$-X–C)$Co_3(CO)_6L_3$,[7] by a metal anion.[5a,8] When the ($\mu_3$-bromomethylidyne)nonacarbonyl derivative, ($\mu_3$-Br–C)$Co_3(CO)_9$ **1** [X = Br; $L_3$ = $(CO)_3$] was treated with the ruthenate, Na[Ru($\eta$-$C_5H_5$)$(CO)_2$], in thf, a heptanuclear carbide cluster compound ($\mu_5$-C)($\eta$-$C_5H_5$)$_2Ru_2Co_4Hg(CO)_{13}$ **2** was obtained in low yield (*ca.* 10%) by way of replacement of Br and addition of metal fragments (Scheme 1).† The molecular structure determined by X-ray crystallography (Fig. 1) contains a carbido carbon atom which is encapsulated in the pentanuclear




**Scheme 1**

$RuCo_4$ wingtip-bridged butterfly structure.‡ Interaction of one of the two Ru–Co edges with the [HgRu($\eta$-$C_5H_5$)$(CO)_2$]$^+$ fragment, which is isolobal with $H^+$, causes slight elongation of the Ru(1)–Co(1) bond [2.937(2) Å; *cf.* Ru(1)–Co(4) 2.837(3) Å] owing to a three-center–two-electron interaction. Judging from the Co(1)–C(1)–Co(4) [165.0(10)°] and $M_{ax}$–C(1)–$M_{eq}$ angles [82–99°: $M_{ax}$ = Co(1), Co(4)], the coordination structure of the central carbido carbon atom can be described as distorted trigonal bipyramidal with a Ru(1)–Co(2)–Co(3) equatorial plane. This type of ($\mu_5$-C)$M_5$ structure has several precedents.[8] The mechanism of formation of **2** should involve initial nucleophilic substitution of **1** with the ruthenate giving a tetrahedral carbide intermediate, which picks up $Co(CO)_n$ and [HgRu($\eta$-$C_5H_5$)$(CO)_2$]$^+$ fragments present in a reaction mixture§ to form the electron-precise species **2** with 76 cluster valence electrons (the wingtip-bridged butterfly $RuCo_4$ core). The formation of **2** suggests susceptibility of the $\mu_3$-CBr moiety in **1** toward nucleophilic substitution, and similar reactions affording encapsulated carbide cluster compounds have already been reported.[9]

In order to prevent the tricobalt unit from fragmentation and cluster core expansion, the three cobalt atoms were linked together by a tripodal ligand, tris(diphenylphosphino)methane (tdpm). Treatment of the $\mu_3$-chloromethylidyne cluster supported by tdpm, ($\mu_3$-Cl–C)$Co_3(CO)_6$(tdpm) **3** [X = Cl; $L_3$ = tdpm],¶ with Na[Ru($\eta$-$C_5H_5$)$(CO)_2$] in thf gave the brown complex **4** (5–10%) along with the $\mu_3$-methylidyne complex, ($\mu_3$-H–C)$Co_3(CO)_6$(tdpm) **5**, after chromatographic separation (Scheme 2).† A $^1$H NMR spectrum of **4** containing a $\eta$-$C_5H_5$ signal ($\delta$ 5.81) in addition to signals from tdpm [$\delta$ 5.77 (1 H, q, $J_{PH}$ 6.1 Hz, $P_3CH$), 6.7–7.3 (30 H, m, $Ph_6$)] is consistent with

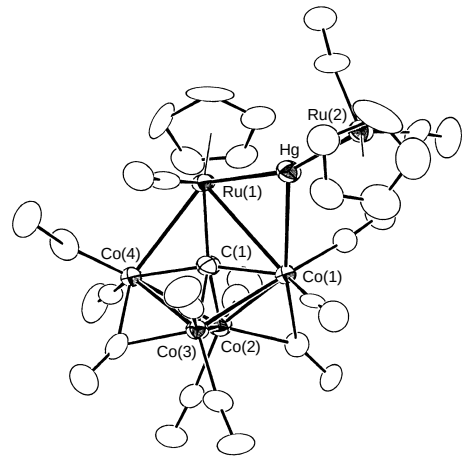
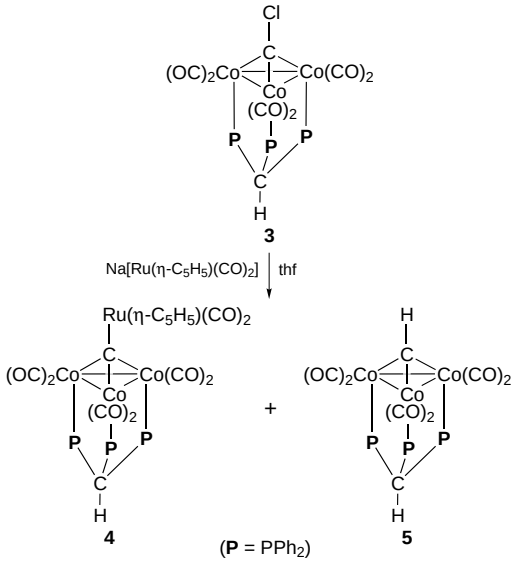



**Fig. 1** Molecular structure of **2** drawn at the 30% probability level. Important bond lengths (Å) and angles (°): C(1)–Ru(1) 1.97(2), C(1)–Co(1) 1.86(2), C(1)–Co(2) 1.95(2), C(1)–Co(3) 1.93(2), C(1)–Co(4) 1.87(2), Ru(1)–C(1)–Co(1) 99.6(7), Ru(1)–C(1)–Co(2) 139.1(9), Ru(1)–C(1)–Co(3) 142.2(9), Ru(1)–C(1)–Co(4) 95.4(7), Co(1)–C(1)–Co(2) 82.7(6), Co(1)–C(1)–Co(3) 86.6(6), Co(1)–C(1)–Co(4) 165.0(10), Co(2)–C(1)–Co(3) 78.6(6), Co(2)–C(1)–Co(4) 85.4(6), Co(3)–C(1)–Co(4) 82.1(6).




**Scheme 2**

the expected structure, $(\eta\text{-}C_5H_5)(CO)_2Ru(\mu_4\text{-}C)Co_3(CO)_6(tdpm)$, which is supported by the single $^{31}P$ NMR resonance ($\delta$ 39.0) and established by X-ray crystallography (Fig. 2).‡ The central carbido carbon atom [C(1)] is bonded to the distal Ru atom and the basal $Co_3$ triangle through σ bonds [C(1)–Ru 2.122(8) Å, C(1)–Co 1.887–1.924(9) Å]. Although the Ru–C(1)–Co [129.2–132.9(5)°] and Co–C(1)–Co angles [80.4–81.6(3)°] deviate from the ideal tetrahedral angle (109.4°) owing to the fact that the Co atoms are linked together by metal–metal bonds, the hybridization of the central carbido carbon atom is found to be close to $sp^3$. Thus the tetranuclear complex **4** has been characterized as a tetrahedral $sp^3$ carbide cluster compound, a permetallated methane. The formation of the $\mu_3$-CH compound **5** suggests participation of a radical mechanism initiated by electron transfer from the ruthenate to **3**. Coupling of the resulting radical species, $\cdot(\mu_3\text{-}C)Co_3(CO)_6(tdpm)$ and $\cdot Ru(\eta\text{-}C_5H_5)(CO)_2$, would furnish **4**, but H-abstraction from the reaction medium may give rise to **5**.

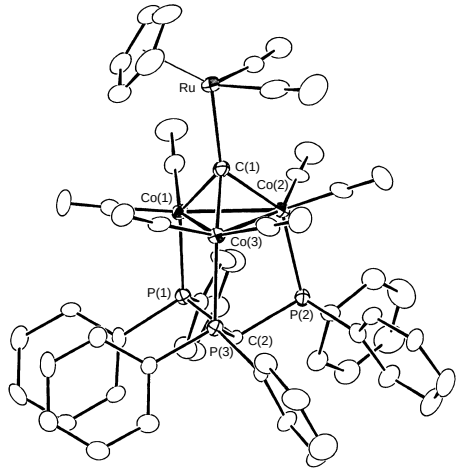



**Fig. 2** Molecular structure of **4** drawn at the 30% probability level. Important bond lengths (Å) and angles (°): C(1)–Ru 2.122(8), C(1)–Co(1) 1.887(9), C(1)–Co(2) 1.924(8), C(1)–Co(3) 1.912(9), Ru–C(1)–Co(1) 129.2(4), Ru–C(1)–Co(2) 132.9(5), Ru–C(1)–Co(3) 132.2(5), Co(1)–C(1)–Co(2) 80.9(3), Co(2)–C(1)–Co(3) 80.4(3), Co(3)–C(1)–Co(1) 81.6(3).

In conclusion, the present study has revealed the versatility of the synthetic method for carbide cluster compounds *via* nucleophilic displacement of halogenomethylidyne clusters with metalates, and the first example of a structurally characterized tetrahedral $sp^3$ carbide cluster has been prepared successfully by this method.

This work was supported by grants from the Ministry of Education, Science, Sports and Culture of the Japanese Government.

## Footnotes and References

* E-mail: makita@res.titech.ac.jp

† *Spectral data*: for **2**: $\delta_H(CDCl_3)$ 5.20, 5.22 (s, $C_5H_5 \times 2$); IR ($CH_2Cl_2$); $\nu$(C≡O) 2073, 2037, 2021, 1974, 1948, 1848 $cm^{-1}$; FDMS: *m/z* 1145 ($M^+$). For **4**: IR ($CH_2Cl_2$), $\nu$(C≡O) 2034, 1986, 1972, 1938 $cm^{-1}$; FDMS: *m/z* 1146 ($M^+$). Attempted measurement of $\delta_C$(μ-C) of **2** and **4** was unsuccessful owing to the $^{59}Co$ quadrapole moment and $^{31}P$ coupling.

‡ X-Ray diffraction measurements of **2** were made on a Rigaku RAXIS IV imaging plate area detector with graphite-monochromated Mo-Kα radiation. *Crystal data* for **2**: $C_{24}H_{10}Co_4HgO_{13}Ru_2$ $M$ = 1144.8, $T$ = 25 °C, monoclinic, space group $C2/c$, $a$ = 39.95(1), $b$ = 8.606(2), $c$ = 18.22(2) Å, $\beta$ = 101.44(7)°, $U$ = 6139(5) $Å^3$, $Z$ = 8, $D_c$ = 2.48 g $cm^{-3}$, $\mu$ = 81.2 $cm^{-1}$, $R(R_w)$ = 0.110(0.161) for all the 5773 unique data and 392 parameters (on $F^2$). X-Ray diffraction measurements of **4** were made on a Rigaku AFC7R automated four-circle diffractometer with graphite-monochromated Mo-Kα radiation. *Crystal data* for **4**·$2C_6H_5Me$: $C_{65}H_{52}Co_3O_8P_3Ru$, $M$ = 1331.9, $T$ = −70 °C, orthorhombic, space group $P2_12_12_1$, $a$ = 19.565(3), $b$ = 23.763(5), $c$ = 12.544(3) Å, $U$ = 5832(4) $Å^3$, $Z$ = 8, $D_c$ = 1.52 g $cm^{-3}$, $\mu$ = 12.3 $cm^{-1}$ $R(R_w)$ = 0.085(0.087) for all the 5677 unique data and 635 parameters (on $F^2$). CCDC 182/524.

§ The $[HgRu(\eta\text{-}C_5H_5)(CO)_2]^+$ fragment may arise from $Hg[Ru(\eta\text{-}C_5H_5)(CO)_2]_2$, a byproduct of the synthesis of $Na[Ru(\eta\text{-}C_5H_5)(CO)_2]$ by Na-amalgam reduction. $Hg[Ru(\eta\text{-}C_5H_5)(CO)_2]_2$ was isolated from the reaction mixture and characterized by X-ray crystallography.

¶ Complex **3** was prepared by thermal reaction of $(\mu_3\text{-Cl–C})Co_3(CO)_9$ with tdpm. Attempted synthesis of the bromo derivative by reaction of **1** with tdpm did not afford the expected product but the zwitterionic cyclic adduct, $Co_3(CO)_6(\mu\text{-}PPh_2)(\mu_3\text{-}CPPh_2CH_2PPh_2)$, the formation of which also involved nucleophilic displacement at the $\mu_3$-Br–C moiety. M. Akita, Y. Takahashi and Y. Moro-oka, unpublished work.

1 M. Tachikawa and E. L. Muetterties, *Prog. Inorg. Chem.*, 1981, **28**, 203; J. S. Bradley, *Adv. Organomet. Chem.*, 1982, **22**, 1.
2 For related metal complexes with polycarbon ligands, see: (*a*) W. Beck, B. Niemer and M. Wieser, *Angew. Chem., Int. Ed. Engl.*, 1993, **32**, 923; (*b*) H. Lang, *Angew. Chem., Int. Ed. Engl.*, 1994, **33**, 547; (*c*) M. Akita and Y. Moro-oka, *Bull. Chem. Soc. Jpn.*, 1995, **68**, 420; (*d*) M. Brady, W. Weng, Y. Zhou, J. W. Seyler, A. J. Amoroso, A. M. Arif, M. Böhme, G. Frenking and J. A. Gladysz, *J. Am. Chem. Soc.*, 1997, **119**, 775.
3 D. F. Shriver and M. P. Jensen, *Acc. Chem. Res.*, 1988, **21**, 374.
4 A tetragold carbide complex was reported by Schmidbauer *et al.*, but its molecular structure has not been determined. H. Schmidbauer and O. Steigelman, *Z. Naturforsch., Teil B*, 1992, **47**, 1721. See also: H. Schmidbauer, *Gold Bull.*, 1990, **23**, 1.
5 Attempts to synthesize a tetrahedral carbide cluster and related tetranuclear complexes have appeared. (*a*) N. D. Duffy, N. M. Kassis and A. D. Rae, *J. Organomet. Chem.*, 1993, **460**, 97; (*b*) A. M. Crespi, M. J. Went, S. S. Sunshine and D. F. Shriver, *Organometallics*, 1988, **7**, 214; (*c*) T. Beringhelli, G. Ciani, G. D'Alfonso, A. Sironi and M. Freni, *J. Chem. Soc., Chem. Commun.*, 1985, 978.
6 M. Akita, S. Sugimoto, M. Tanaka and Y. Moro-oka, *J. Am. Chem. Soc.*, 1992, **114**, 7581. See also ref. 2(*b*).
7 D. Seyferth, *Adv. Organomet. Chem.*, 1976, **14**, 97.
8 See, for example: J. S. Bradley, E. W. Hill, G. B. Ansell and M. A. Madrick, *Organometallics*, 1982, **1**, 1634.
9 V. G. Albano, P. Chini, S. Martinengo, M. Sansoni and D. Strumolo, *J. Chem. Soc., Chem. Commun.*, 1974, 299; A. Ceriotti, G. Longoni, M. Manassero, P. R. Della and S. Mirella, *J. Chem. Soc., Dalton Trans.*, 1984, 299.

*Received in Cambridge, UK, 24th April 1997; 7/02806G*

# Interdigitated supramolecular laminates

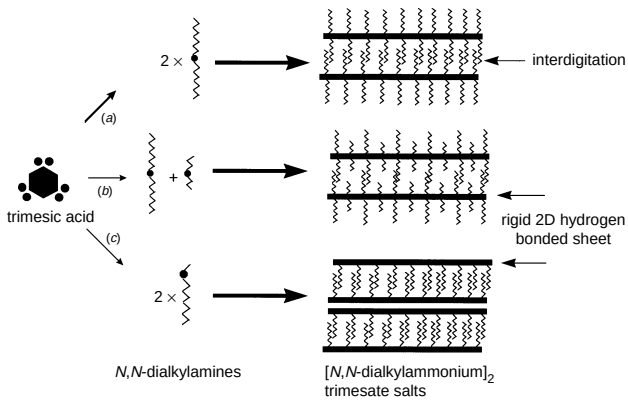
**C. V. Krishnamohan Sharma,[a] Cary B. Bauer,[b] Robin D. Rogers[b] and Michael J. Zaworotko*[a]**

[a] *Department of Chemistry, Saint Mary's University, Halifax, Nova Scotia, B3H 3C3, Canada*
[b] *Department of Chemistry, The University of Alabama, Tuscaloosa, AL, 35487, USA*

**Secondary ammonium salts of trimesic acid form robust interdigitated lamellar structures which are sustained by a combination of strong hydrogen bonds in two dimensions and hydrophobic interactions in the third dimension.**

Various types of lamellar, bilayer and monolayer architectures have been investigated for applications in membranes, mesogens, surfactants and Langmuir–Blodgett (LB) films.[1] A better understanding of the structural details of these systems and their relationship to specific chemical processes and functions requires structural information from the crystalline state. Rational design of such organized molecular assemblies in the solid state is also a fundamental and contemporary problem of crystal engineering[2,3] and the use of hydrogen bonds to impart dimensional control over network structures is now well established.[4] We report herein a novel two-dimensional hydrogen bonded motif which forms lamellar crystal structures because of strong hydrogen bonds between complementary organic cations and anions. Furthermore, the entire three-dimensional molecular arrangement is predictable with reasonable accuracy as a consequence of hydrophobic interactions between interdigitated alkyl or aryl groups in the third dimension.

Partially or fully deprotonated salts of 1,3,5-benzenetricarboxylic acid (trimesic acid, $H_3TMA$) invariably react with amines to afford salts with flat hydrogen-bonded sheet structures.[5] These rigid hydrogen-bonding patterns are robust and the presence of ammonium cations in the sheet makes such structures ideal for designing interdigitated supramolecular lamellar structures since long-chain alkyl groups can be substituted at the ammonium moiety. Scheme 1 depicts various possible layered structures that one might design using secondary alkylammonium salts of $HTMA^{2-}$. The series of dialkylammonium salts, $[NHPr_2]_2[HTMA]$ **1**, $[NH(C_6H_{13})_2]_2[HTMA]$ **2**, $[NH(C_8H_{17})_2]_2[HTMA]$ **3** and $[NH(C_{10}H_{21})_2]_2[HTMA]$ **4**, were synthesized by slow addition of 2 equiv. of the appropriate amine to 1 equiv. of $H_3TMA$ in MeOH and, in order to prevent precipitation of non-stoichiometric products, refluxing for 2 h. Quantitative yields of the colourless solids **1**–**4** were obtained by slow evaporation of MeOH. Crystals of **1** and **2**–**4** suitable for single-crystal X-ray crystallography were obtained from butan-1-ol and MeOH, respectively (**1**, mp > 300 °C; **2**, mp 243 °C; **3**, mp 248 °C; **4**, mp 265 °C).




**Scheme 1**

The crystal structures† of **1**–**4** exhibit identical two-dimensional hydrogen-bonding networks stabilized by $N^+–H\cdots O^-$ and $O–H\cdots O^-$ hydrogen bonds as shown in Fig. 1. Table 1 is a compilation of hydrogen bond lengths of **1**–**4** and indicates that the relevant hydrogen bond lengths are almost identical. The ammonium protons in the sheet are engaged in a robust hydrogen-bonding network and are arranged in alternating columns (Fig. 1). The hydrophobic alkyl substituents of the ammonium cations project above and below the sheet and the space between the protruding columns of alkyl groups facilitates interdigitation or close-packing of the adjacent layers (Fig. 2). The geometrical arrangement of the cations in the layer is

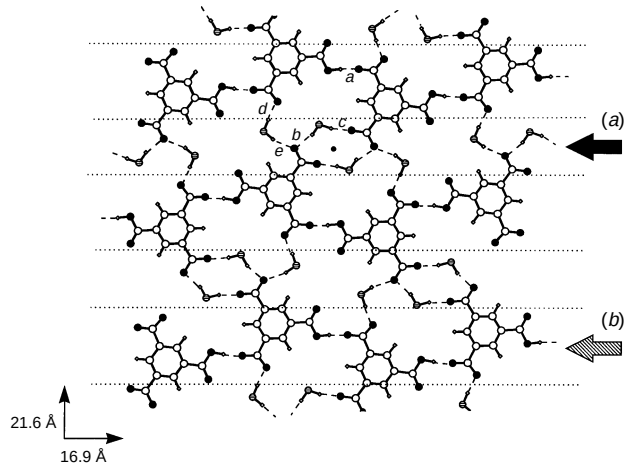



**Fig. 1** The two-dimensional hydrogen bonding network observed in **1**–**4**. Five different hydrogen bonds are marked (shown as dashed lines, *a*–*e*, Table 1). The alkyl substituents of the ammonium cations are omitted for clarity. N and O atoms are shown as hatched and filled circles, respectively. The dotted lines are marked on the sheet to show the alternating columns of alkyl subsituents. (*a*) Substituents of the ammonium cation project perpendicular to this plane; (*b*) space suitable for interdigitation of alkyl groups from neighbouring layers.

**Table 1** Hydrogen bonding distances (Å) in the two-dimensional layers of **1**–**5**

| | O···O | N···O | | | |
|---|---|---|---|---|---|
| | *a* | *b* | *c* | *d* | *e* |
| **1** | 2.540(6) | 2.773(8) | 2.732(6) | 2.887(8) | 2.654(8) |
| **2** | 2.511(10) | 2.765(12) | 2.728(11) | 2.834(12) | 2.635(15) |
| **3** | 2.543(4) | 2.772(5) | 2.701(4) | 2.829(4) | 2.654(4) |
| **4** | 2.524(12) | 2.766(13) | 2.696(11) | 2.818(13) | 2.690(13) |
| **5**[a] | 2.567(7) | 2.751(8) | 2.709(8) | 2.809(8) | 2.687(7) |
| | | 2.777(8) | 2.769(7) | | |

[a] **5** crystallizes in a non-centrosymmetric space group ($P2_1$). Consequently, unlike **1**–**4**, there is no crystallographic inversion center across *b* and *c*.

critical and controls the stacking in the third direction. The interlayer separations of **1**–**4** are *ca*. 7.0, 10.3, 12.4, 14.6 Å, respectively, and are directly related to the alkyl chain lengths and the interdigitation of the alkyl groups that facilitates close packing. There is a recognizable tilt in the octyl and decyl chains of **3** and **4** with respect to the surface of the sheet (77.2, 73.9°), especially when compared to that seen for the propyl and hexyl groups in **1** and **2**, respectively (87.4, 89.0°). Such an observation is to be expected.[6] The dimensions of the repeating unit of the plane are *ca*. 16.9 × 21.6 Å in all five compounds, but only correspond to unit-cell parameters, *i.e*. the *bc* plane, in **3**–**5**.

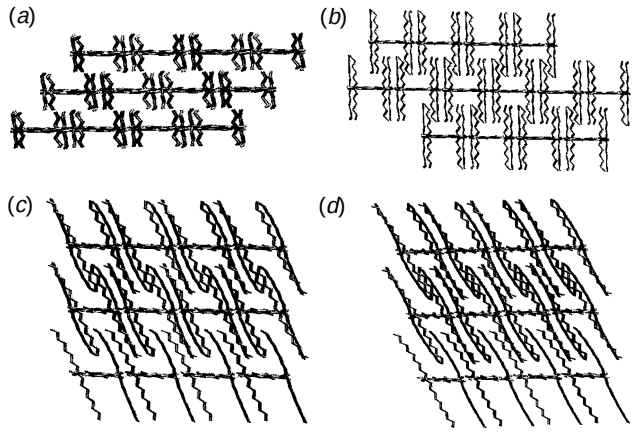



**Fig. 2** Perspective views of the supramolecular laminates **1**–**4** [(*a*)–(*d*)]. Note that interdigitation and tilt of the alkyl groups occurs as the chain length increases.

We have also been able to synthesize a mixed-cation supramolecular laminate of $HTMA^{2-}$ with *N*,*N*-dibenyzlammonium and *N*,*N*-dipropylammonium, **5** [Scheme 1(*b*)].[6] **5** is a doubly deprotonated salt and the asymmetric unit contains four $HTMA^{2-}$ anions, six *N*,*N*-dibenzylammonium cations, two *N*,*N*-dipropylammonium cations and one molecule of MeOH. The crystal structure reveals an interdigitated supramolecular laminate architecture with alternating layers of different composition (Fig. 3). The hydrogen-bonding pattern of layer A, a mixed-cation supramolecular laminate, is similar to **1**–**4** (Fig. 1, Table 1). However, layer B, which contains dibenzylammonium cations, has a slightly different hydrogen-bonding pattern as the MeOH molecule is also involved in the hydrogen-bonding scheme. This observation suggests that a wide range of new supramolecular laminates is at hand, possibly with interesting properties such as liquid crystallinity and the ability to intercalate guest molecules.[7]

In conclusion, **1**–**5** serve as good examples of rationally designed solids and should be of help for the general study and understanding of laminate packing arrangements. The results reported herein further suggest that the complex problem of controlling three-dimensional architecture in solids can successfully be reduced to a simple one-dimensional problem by using the strategy of choosing a suitably substituted rigid two-dimensional layer as a starting point.[4]

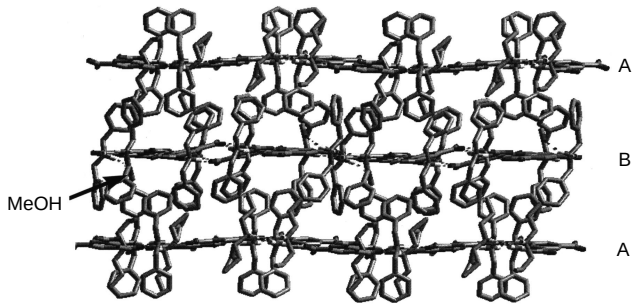



**Fig. 3** The interdigitated mixed supramolecular laminate structure of **5**. Layer A contains *N*,*N*-dibenzylammonium and *N*,*N*-dipropylammonium cations. Layer B contains dibenzylammonium cations only. Note that MeOH is involved in the hydrogen bonding in layer B.

We acknowledge the generous financial support of the NSERC and ESTAC (Canada) in the form of research grants.

## Footnotes and References

* E-mail: mike.zaworotko@stmarys.ca

† *Crystal data* for **1**–**5**: $C_{21}H_{36}N_2O_6$ **1**, $M_w$ = 412.5, monoclinic, space group $P2_1/c$, $a$ = 8.734(3), $b$ = 16.951(7), $c$ = 17.811(7), $\beta$ = 103.99(4)°, $U$ = 2558.70(14) Å$^3$, $Z$ = 4, $D_c$ = 1.07 Mg m$^{-3}$, $T$ = 290 K, $\mu$ = 0.07 mm$^{-1}$. 1427 reflections out of 3349 unique reflections with $I > 2.5\sigma(I)$ were considered, $R_f$ = 0.083, $R_w$ = 0.068. $C_{33}H_{60}N_2O_6$ **2**, $M_w$ = 580.9, monoclinic, space group $P2_1/n$, $a$ = 11.531(3), $b$ = 16.942(2), $c$ = 19.952(6), $\beta$ = 98.07(3)°, $U$ = 3859.2(16) Å$^3$, $Z$ = 4, $D_c$ = 1.00 Mg m$^{-3}$, $T$ = 290 K, $\mu$ = 0.06 mm$^{-1}$. 1339 reflections out of 5042 unique reflections with $I > 2.5\sigma(I)$ were considered, $R_f$ = 0.090, $R_w$ = 0.086. The data for **1** and **2** were measured on an Enraf-Nonius CAD-4 diffractometer at 290 K using the $\omega$ scan mode. $C_{41}H_{76}N_2O_6$, **3**, $M_w$ = 693.1, monoclinic, space group $P2_1/c$, $a$ = 12.4771(7), $b$ = 16.8788(9), $c$ = 21.5789(11), $\beta$ = 91.992(1)°, $U$ = 4541.7(4) Å$^3$, $Z$ = 4, $D_c$ = 1.01 Mg m$^{-3}$, $T$ = 173 K, $\mu$ = 0.06 mm$^{-1}$. 4222 reflections out of 6333 unique reflections with $I > 3.0\sigma(I)$ were considered, $R_f$ = 0.114, $R_w$ = 0.101. $C_{49}H_{92}N_2O_6$ **4**, $M_w$ = 805.3, monoclinic, space group $P2_1/c$, $a$ = 14.6856(8), $b$ = 16.8941(11), $c$ = 21.5929(13), $\beta$ = 97.970(2)°, $U$ = 5305.5(6) Å$^3$, $Z$ = 4, $D_c$ = 1.01 Mg m$^{-3}$, $T$ = 173 K, $\mu$ = 0.06 mm$^{-1}$. 2064 reflections out of 4291 unique reflections with $I > 3.0\sigma(I)$ were considered, $R_f$ = 0.117, $R_w$ = 0.115 $C_{133}H_{148}N_8O_{25}$ **5**, $M_w$ = 2256.2, monoclinic, space group $P2_1$, $a$ = 16.7901(3), $b$ = 16.8905(2), $c$ = 21.9464(2), $\beta$ = 96.384(1), $U$ = 6185.3(4), $Z$ = 2, $D_c$ = 1.211 Mg m$^{-3}$, $T$ = 173 K, $\mu$ = 0.08 mm$^{-1}$. 18350 reflections out of 20 242 unique reflections with $I > 4.0\sigma(I)$ were considered, $R_f$ = 0.083, $R_w$ = 0.086. The intensity data for **3**–**5** were collected on a Siemens SMART/CCD diffractometer at 173 K using the $\theta$ scan mode. The thermal parameters for the terminal C atoms in the alkyl chains of **1**-**5** are high, probably a manifestation of unresolvable disorder, and account for the relatively high $R$ values. CCDC 182/518.

1 F. M. Menger, J. Lee and K.S. Hagen, *J. Am. Chem. Soc.*, 1991, **113**, 4017 and references therein; J. L. Slater and C. H. Huang, *Prog. Lipid. Res.*, 1988, **27**, 325; F. Neve, M. Ghedini, G. D. Munno and A. Levelut, *Chem. Mater.*, 1995, **7**, 688; C. M. Paleos and D. Tsiourvas, *Angew. Chem., Int. Ed. Engl.*, 1995, **34**, 1696; G. A. Jeffrey, *Mol. Cryst. Liq. Cryst.*, 1990, **185**, 209; G. J. Ashwell, T. W. Walker, I. R. Gentle, G. J. Foran, G. S. Bahra and C. R. Brown, *J. Mater. Chem.*, 1996, **6**, 969; K. Eichhorst-Gerner, A. Stabel, G. Moessner, D. Declerq, S. Valiyaveettil, V. Enkelmann, K. Mullen and J.P. Rabe, *Angew. Chem., Int. Ed. Engl.*, 1996, **35**, 1492.

2 G. R. Desiraju, *Crystal Engineering The Design of Organic Solids*, Elsevier, Amsterdam, 1989; *Angew. Chem., Int. Ed. Engl.*, 1995, **34**, 2328.

3 J.-M. Lehn, *Angew. Chem., Int. Ed. Engl.*, 1990, **29**, 1304; F. Garcia-Tellado, S. J Geib, S. Goswami and A. D. Hamilton, *J. Am. Chem. Soc.*, 1991, **113**, 9265; J. A. Zerkowski, J. C. MacDonald, T. Seto, D. A. Wierda and G. M. Whitesides, *J. Am. Chem. Soc.*, 1994, **116**, 2382; C. B. Aakeröy, D. P. Hughes and M. Niewenhuyzen, *J. Am. Chem. Soc.*, 1996, **118**, 10134.

4 V. A. Russell, M. C. Etter and M. D. Ward, *J. Am. Chem. Soc.*, 1994, **116**, 1941; V. A. Russell and M. D. Ward, *Chem. Mater.*, 1996, **8**, 1654 and references therein; J. J. Kane, R. Liao, J. W. Lauher and F. W. Fowler, *J. Am. Chem. Soc.*, 1995, **117**, 12003.

5 R. E. Melendez, C. V. K. Sharma, M. J. Zaworotko, C. Bauer and R. D. Rogers, *Angew. Chem., Int. Ed. Engl.*, 1996, **35**, 2213; R. E. Melendez and M. J. Zaworotko, *Supramolecular Chem.*, 1997, **8**, 157.

6 J. Wang, F. Leveiller, D. Jacquemain, K. Kjaer, J. Als-Nielsen, M. Lahav and L. Leiserowitz, *J. Am. Chem. Soc.*, 1994, **116**, 1192; D. M. Small, *The Physical Chemistry of Lipids: From Alkanes to Phospholipids*, Plenum, New York and London, 1986, vol. 4; K. Okuyama, H. Watanabe, M. Shimoura, K. Hirabayashi, T. Kunitake, T. Kajiyama and N. Yasuoka, *Bull. Chem. Soc. Jpn.*, 1986, **59**, 3351; O. J. Almeida and B. G. Dixon, *Chem. Mater.*, 1995, **7**, 2039.

7 K. Sawada, Y. Ohashi, N. Limura and H. Hirata, *International Union of Crystallography, XVII Congress and General Assembly*, Seattle, Washington, USA, 8–17, 1996, Abstract PS11.07.17.

*Received in Columbia, MO, USA, 14th March 1997; 7/01827D*

# Bis(β-diketonate) ligands for the synthesis of bimetallic complexes of $Ti^{III}$, $V^{III}$, $Mn^{III}$ and $Fe^{III}$ with a triple-helix structure

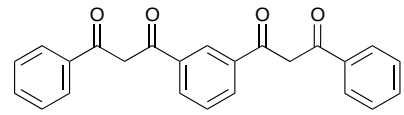
**Vincent A. Grillo, Elisa J. Seddon, Craig M. Grant, Guillem Aromí, John C. Bollinger, Kirsten Folting and George Christou***

*Department of Chemistry and the Molecular Structure Center, Indiana University, Bloomington, IN 47405-4001, USA*

**Addition of the bis(β-diketone) ligand L [L = 1,3-bis(3-phenyl-3-oxopropanoyl)benzene] to a suitable source of $M^{III}$ ions (M = Ti, V, Mn, Fe) in a L : M = 3 : 2 ratio gives the dinuclear products $[M_2L_3]$, which have a triple-helical structure.**

The use of oligopyridyl, oligo-2,2′-bipyridyl and related ligands in transition-metal chemistry has been receiving a great deal of attention in recent years.[1–7] Their products with mononuclear metal ions have displayed a variety of fascinating structures such as double[1,2,4,8] or triple helices,[1,2,3,6,9] and 'cylindrical',[10] 'capped'[11] or 'circular'[12] architectures. As such, these ligands have been amongst the central players in the supramolecular chemistry field.

Bis(β-diketonate) ligands offer similar potential for the preparation of supramolecular assemblies, and we herein report the initial use of the ligand L for the synthesis of bimetallic complexes of formula $[M_2L_3]$ (M = $Ti^{III}$, $V^{III}$, $Mn^{III}$, $Fe^{III}$) with a triple-helix structure. Ligand L† was prepared from a Claisen condensation employing dimethyl isophthalate and acetophenone in the presence of NaH, a method related to that in the early literature of bis(β-diketonates).[13] Addition of L to a convenient source of $M^{III}$ [$MCl_3(thf)_3$[14] (M = Ti, V), $Mn(O_2CMe)_2{\cdot}4H_2O$/$NBu^n_4MnO_4$, $Fe(ClO_4)_2{\cdot}6H_2O$/air] in dmf or $CH_2Cl_2$ gave dark coloured solutions from which could be isolated crystalline $[M_2L_3]$ (M = Ti **1**, V **2**, Mn **3**, Fe **4**) in 30–70% yields, followed by recrystallisation from dmf–MeOH (**1**–**3**) or thf–$Me_2CO$ (**4**).‡ Complexes **1**–**4** are isostructural§ (Fig. 1) and consist of two six-coordinate $M^{III}$ ions chelated and bridged by three $L^{2-}$ groups. The M···M separations are very similar [7.222(2) **1**, 7.224(2) **2**, 7.350(2) **3**, 7.262(4) Å **4**] and the molecules are in a triple-helix conformation, as emphasized by the view along the M···M vector (Fig. 2). The average ligand twist angles (defined as the angles between the two M–M–C(methine) planes for each ligand) are 42.8 **1**, 44.0 **2**, 47.4 **3** and 40.8° **4**. The structural parameters show only the small differences expected from varying the $M^{III}$ ion and the presence in **3** of a Jahn–Teller axial elongation along the O(3)–Mn(1)–O(35) and O(8)–Mn(2)–O(40) axes. The metal geometries are essentially octahedral. The series could undoubtedly be extended to other $M^{III}$ ions (*e.g.*, $Cr^{III}$, $Co^{III}$) and this is currently being explored. The triple-helix structures of **1**–**4** with the ligand $L^{2-}$ are new additions to the relatively small but growing family of dinuclear metal complexes with a triple-helix structure, hitherto with ligands other than β-diketonates.[2,3,6,9,15–17]




L

Detailed characterisation of **1**–**4** by a variety of spectroscopic and physical methods is in progress. Preliminary electrochemical studies by cyclic voltammetry in dmf confirm that the two $M^{III}$ ions are interacting. The 'richest' CV scans belong to **1** and **2** which show very similar electrochemical behaviour (Fig. 3). Both exhibit two pairs of closely spaced reversible reductions: −1.076, −1.212 V ($\Delta E$ = 0.136 V) and −1.720,

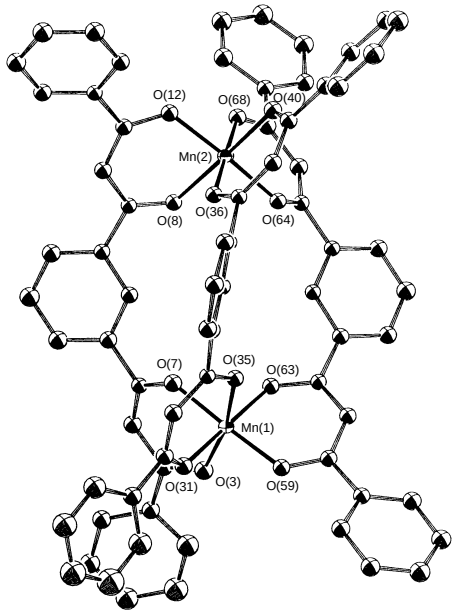



**Fig. 1** The structure of $[Mn_2L_3]$ **3**; complexes **1**, **2** and **4** are isostructural

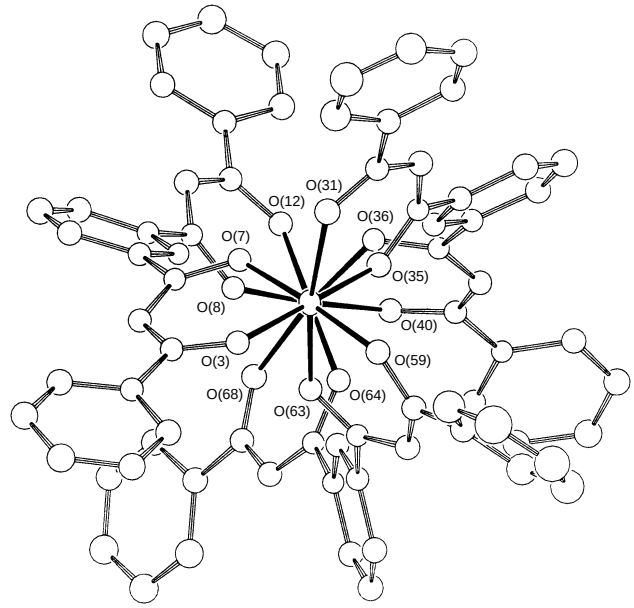



**Fig. 2** A view down the Mn···Mn vector of **3** emphasizing the triple-helical conformation of the molecule

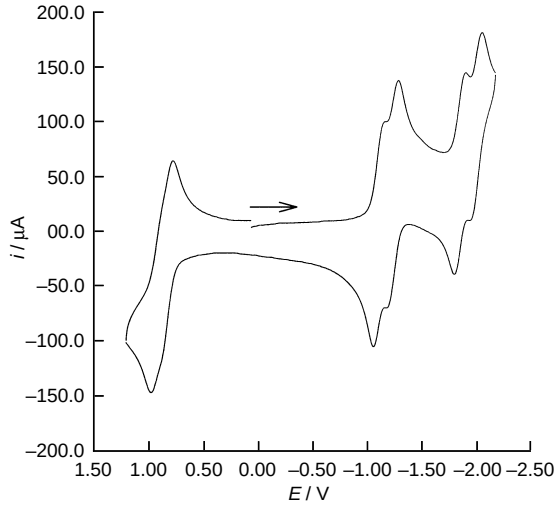



**Fig. 3** Cyclic voltammogram at 100 mV $s^{-1}$ for complex **2** in dmf at a glassy carbon electrode and with $NBu^n_4PF_6$ as supporting electrolyte

−1.900 V ($\Delta E$ = 0.180 V) for **1** and −1.104, −1.240 V ($\Delta E$ = 0.136 V) and −1.840, −2.000 V ($\Delta E$ = 0.160 V) for **2** *vs.* SCE. In addition, for both complexes, there is a less well resolved pair of oxidation processes: +0.016, +0.092 V for **1** ($\Delta E$ = 0.076 V) and +0.808, +0.884 V for **2** ($\Delta E$ = 0.080 V). The large $\Delta E$ values are indicative of intramolecular interactions between the two $M^{III}$ ions. Complex **4** shows only a single pair of reversible reductions, at −0.460 and −0.584 V. Complex **3** shows a broad, quasi-reversible reduction process at −0.018 V ($E_{pc} - E_{pa}$ = 0.520 V), with an additional irreversible oxidation at approximately +1.238 V. For all four species, additional reductions are observed at < −2.0 V. The redox behaviour of **1**–**4** is related to that of the corresponding mononuclear $M(dbm)_3$ (dbm = anion of dibenzoylmethane), which exhibit single redox processes at similar processes to **1**–**4**. Variable-temperature magnetic susceptibility studies on **1**–**4** are currently in progress to quantitate the strength of intramolecular interactions within these molecules.

This work was supported by the National Science Foundation.

## Footnotes and References

* E-mail: christou@indiana.edu

† *Selected spectroscopic data* for L: $^1$H NMR ($CD_2Cl_2$, 500 MHz): $\delta$ 6.98 (s, 2 H), 7.53 (t, *J* 8 Hz, 4 H), 7.61 (t, *J* 8 Hz, 2 H), 7.66 (t, *J* 8 Hz, 1 H), 8.04 (d, *J* 8 Hz, 4 H), 8.19 (d, *J* 8 Hz, 2 H), 8.60 (s, 1 H); EI-MS ($M^+$) 370.1 ($C_{24}H_{18}O_4$ requires 370.1).

‡ The complexes analysed satisfactorily.

§ *Crystal data* **1**: $C_{72}H_{48}O_{12}Ti_2$, $M_r$ = 1200.90, monoclinic, space group *C*2/*c*, *a* = 22.924(3), *b* = 17.721(2), *c* = 18.870(2) Å, $\beta$ = 129.60(1)°, *U* = 5906.7 Å$^3$, *Z* = 4, *T* = 106 K, $\mu$ = 3.293 $cm^{-1}$, 1689 reflections with $F > 4\sigma(F)$, $R(F)$ = 0.0645, $R_w(F^2)$ = 0.1030. **2**·0.72 MeOH: $C_{72}H_{48}O_{12}V_2$·0.72 MeOH, $M_r$ = 1207.06 (excl. solv), monoclinic, space group *C*2/*c*, *a* = 22.982(4), *b* = 17.906(3), *c* = 18.057(3) Å, $\beta$ = 127.09(1)°, *U* = 5945.7 Å$^3$, *Z* = 4, *T* = 106 K, $\mu$ = 3.829 $cm^{-1}$, 3038 reflections with $F > 3\sigma(F)$, $R(F)$ = 0.0481, $R_w(F)$ = 0.0510. **3**·$CH_2Cl_2$: $C_{73}H_{50}O_{12}Cl_2Mn_2$, $M_r$ = 1300.0, triclinic, space group $P\bar{1}$, *a* = 15.682(3), *b* = 16.850(4), *c* = 13.843(3) Å, $\alpha$ = 105.63(1), $\beta$ = 102.92(1), $\gamma$ = 113.93(1)°, *U* = 2980.5 Å$^3$, *Z* = 2, *T* = 102 K, $\mu$ = 5.806 $cm^{-1}$, 8025 reflections with $F > 3\sigma(F)$, $R(F)$ = 0.0657, $R_w(F)$ = 0.0589. **4**·thf: $C_{76}H_{56}O_{13}Fe_2$, $M_r$ = 1293.00, triclinic, space group $P\bar{1}$, *a* = 16.151(5), *b* = 16.982(6), *c* = 11.817(4) Å, $\alpha$ = 108.50(2), $\beta$ = 103.54(2), $\gamma$ = 87.24(2)°, *U* = 2987.0 Å$^3$, *Z* = 2, *T* = 103 K, $\mu$ = 5.561 $cm^{-1}$, 4128 reflections with $F > 3\sigma(F)$, $R(F)$ = 0.0911, $R_w(F)$ = 0.0835. CCDC 182/522.

1 J.-M. Lehn, *Supramolecular Chemistry*, VCH, Weinheim, 1995.
2 C. Piguet, G. Bernardinelli, B. Bocquet, A. Quattropani and A. F. Williams, *J. Am. Chem. Soc.*, 1992, **114**, 7440; C. Piguet, J.-C. G. Bünzli, G. Bernardinelli, G. Hopfgartner and A. F. Williams, *J. Am. Chem. Soc.*, 1993, **115**, 8197; C. Piguet, G. Bernardinelli, B. Bocquet, O. Schaad and A. F. Williams, *Inorg. Chem.*, 1994, **33**, 4112.
3 M.-T. Youinou, R. Ziessel and J.-M. Lehn, *Inorg. Chem.*, 1991, **30**, 2144.
4 T. M. Garrett, U. Koert, J.-M. Lehn, A. Rigault, D. Meyer and J. Fischer, *J. Chem. Soc., Chem. Commun.*, 1990, 557; J.-M. Lehn, A. Rigault, J. Siegal, J. Harrowfield, B. Chevrier and D. Moras, *Proc. Natl. Acad. Sci. USA*, 1987, **84**, 2565; W. Zarges, J. Hall, J.-M. Lehn and C. Bolm, *Helv. Chim. Acta*, 1991, **74**, 1843.
5 R. C. Scarrow, D. L. White and K. N. Raymond, *J. Am. Chem. Soc.*, 1985, **107**, 6540.
6 B. R. Serr, K. A. Andersen, C. M. Elliot and O. P. Anderson, *Inorg. Chem.*, 1988, **27**, 4499; S. Ferrere and C. M. Elliot, *Inorg. Chem.*, 1995, **34**, 5818.
7 K. T. Potts, K. A. Gheysen Raiford and M. Keshavarz-K, *J. Am. Chem. Soc.*, 1993, **115**, 2793.
8 R. Chotalia, E. C. Constable, M. Neuburger, D. R. Smith and M. Zehnder, *J. Chem. Soc., Dalton Trans.*, 1996, 4207; C. Piguet, G. Hopfgartner, B. Bocquet, O. Schaad and A. F. Williams, *J. Am. Chem. Soc.*, 1994, **116**, 9092.
9 R. Krämer, J.-M. Lehn, A. De Cian and J. Fischer, *Angew. Chem., Int. Ed. Engl.*, 1993, **32**, 703.
10 P. Baxter, J.-M. Lehn, A. De Cian and J. Fischer, *Angew. Chem., Int. Ed. Engl.*, 1993, **32**, 69.
11 E. Leize, A. Van Dorsselaer, R. Krämer and J.-M. Lehn, *J. Chem. Soc., Chem. Commun.*, 1993, 990; M. Albrecht, S. J. Franklin and K. N. Raymond, *Inorg. Chem.*, 1994, **33**, 5785.
12 B. Hasenknopf, J.-M. Lehn, B. O. Kneisel, G. Baum and D. Fenske, *Angew. Chem., Int. Ed. Engl.*, 1996, **35**, 1838.
13 D. F. Martin, M. Shamma and W. C. Fernelius, *J. Am. Chem. Soc.*, 1958, **80**, 4891.
14 L. E. Manzer, *Inorg. Synth.*, 1982, **21**, 138.
15 T. B. Karpishin, T. D. P. Stack and K. N. Raymond, *J. Am. Chem. Soc.*, 1993, **115**, 6115; B. Kersting, M. Meyer, R. E. Powers and K. N. Raymond, *J. Am. Chem. Soc.*, 1996, **118**, 7221.
16 E. J. Enemark and T. D. P. Stack, *Angew. Chem., Int. Ed. Engl.*, 1995, **34**, 996.
17 M. Albrecht and S. Kotila, *Angew. Chem., Int. Ed. Engl.*, 1995, **34**, 2134; M. Albrecht and S. Kotila, *Chem. Commun.*, 1996, 2309; M. Albrecht, H. Rottele and P. Burger, *Chem. Eur. J.*, 1996, **2**, 1264.

*Received in Cambridge, UK, 1st May 1997; 7/02971C*

# First identification by EPR spectra of lanthanum(II) organometallic intermediates (and $E_{\frac{1}{2}}$ for $La^{3+} \rightarrow La^{2+}$) in the C–O bond activation of dimethoxyethane†

**M. Cristina Cassani,[a] Michael F. Lappert*[a] and Franco Laschi[b]**

[a] *The Chemistry Laboratory, University of Sussex, Brighton, UK BN1 9QJ*
[b] *Universita' di Siena, Dipartimento di Chimica, Siena, Italy I-53100*

**The reaction of [La(Cp″)$_3$] with K in dimethoxyethane (dme) at ambient temperature leads to the formation of lanthanocene(III) methoxides *via* persistent paramagnetic lanthanum(II) intermediates that are characterised by EPR spectroscopy and tentatively assigned to [K(dme)$_x$]-[La(Cp″)$_3$] and [La(Cp″)$_2$(dme)$_y$] [Cp″ = η$^5$-C$_5$H$_3$(SiMe$_3$)$_2$-1,3]; the cyclic voltammogram of [La(Cp″)$_3$] in thf is also reported, $E_{\frac{1}{2}}^{red}$ = −2.8 V.**

Recently we showed that the reaction of [Ln(Cp″)$_3$] [Ln = Ce or Nd, Cp″ = η$^5$-C$_5$H$_3$(SiMe$_3$)$_2$-1,3] with K in dimethoxyethane (dme) gave the lanthanocene(III) methoxide [{Ln(Cp″)$_2$(μ-OMe)(}$_2$].[1] It was postulated that a Ln$^{II}$ complex was a plausible transient intermediate involved in the C–O bond cleavage.

We now report that treatment of [La(Cp″)$_3$] **1** with a K mirror in dme led to the immediate formation of a dark royal blue solution **2** from which a white crystalline mixture was obtained. The latter contained K(Cp″), [{La(Cp″)$_2$(μ-OMe)}$_2$] **3**, and an as yet unidentified polynuclear lanthanum methoxide **4**, Scheme 1.‡

The particularly striking feature of this reaction is that the blue solution **2** was paramagnetic and its EPR spectrum revealed it to contain two lanthanum(II) complexes.§ Fig. 1(*a*) shows the ambient-temperature EPR spectrum which consisted of two sets **A** and **B** of well resolved $S$ = 1/2 metal-centred octuplets with **A** : **B** *ca.* 1.5 : 1. In each of **A** and **B**, the height of the EPR lines progressively decreased from their centre while concomitantly their peak separation increased from left to right. Each of the **A** and **B** sets arises from the hyperfine coupling of the unpaired electron with the $^{139}$La nucleus (99.91% natural abundance, $\mu_1$ = +2.776, $I$ = 7/2), with $g_{\mathbf{A}}$ = 1.972(8), $a_{\mathbf{A}}$($^{139}$La) = 134.0(5) G and $g_{\mathbf{B}}$ = 1.970(8), $a_{\mathbf{B}}$($^{139}$La) = 145.0(5) G. These hyperfine couplings are of similar magnitude but intermediate between (*i*) the calculated value of 186 G (using spin-polarised unrestricted Hartree–Fock wavefunctions),[2a] and (*ii*) that measured (*ca.* 50 G at 20 K) for a La$^{2+}$ defect in a CaF$_2$ lattice; this being, as far as we are aware, the only prior experimental literature value.[3] These data strongly contrasted with those from the EPR spectrum of (*i*) [La$^{3+}$@C$_{82}^{3-}$] which consists of eight extremely narrow ($\Delta H$ = 0.125 G) equally spaced [$a$($^{139}$La) = 1.25 G] lines of equal height centred at $g$ = 2.0010 (1,1,2,2-tetrachloroethane, 293 K);[2a–d] and (*ii*) [LaI$_2$(bipy)$_2$(dme)] [$a$($^{139}$La) = 7.4 G, $g$ = 2.0031 (dme, 293 K)], [LaI$_2$(bipy)$_2$(thf)$_2$] [$a$($^{139}$La) = 5.9 G, $g$ = 2.0009 (thf, 293 K)] or [LaI$_2$(bipy)(dme)$_2$] [$a$($^{139}$La) = 7.0 G, $g$ = 2.0015 (thf, 293 K)] containing one radical anion ligand (bipy = 2,2-bipyridyl)[4] and underline the significant La orbital character of the actual isotropic spectral pattern.

The EPR spectra recorded at the melting point (200–220 K) of the glassy blue solution **2**, exhibited the isotropic spectral features of **A**, that of **B** being undetected up to 275 K. Fig. 1(*b*) shows the EPR spectrum at 275 K. Upon gradually increasing the temperature, the signals due to **B** started appearing and their intensity steadily increased until at 330 K, **B** became the major species. This behaviour was reversed upon cooling. We conclude that in **2**, **A** and **B** represent distinct species in thermal equilibrium, and a plausible interpretation is that the EPR signals **A** and **B** be assigned to the lanthanum(II) species [K(dme)$_x$][La(Cp″)$_3$] and [La(Cp″)$_2$(dme)$_y$], respectively.

Similar features to those described above for the [La(Cp″)$_3$]–K system in dme were observed for those in thf, except that no reaction product involving solvent fragmentation was observed; K(Cp″) was isolated. The EPR spectral data for the thf system showed two octuplets at 295 K (**A** : **B**, *ca.* 4 : 1): $g_{\mathbf{A}}$ = 1.969(8), $a_{\mathbf{A}}$($^{139}$La) = 136.0(8) G and $g_{\mathbf{B}}$ = 1.971(8), $a_{\mathbf{B}}$($^{139}$La) = 146.0(8) G.

In order to investigate the reduction of [La(Cp″)$_3$] in an alternative fashion, and to obtain a value for the La$^{3+}$–La$^{2+}$ reduction potential, the electrochemical reduction of [La(Cp″)$_3$] was examined. The cyclic voltammogram of [La(Cp″)$_3$] in thf at a vitreous carbon electrode is shown in Fig. 2. The reduction potential $E_{\frac{1}{2}}$ (La$^{3+}$ → La$^{2+}$) was found to be −2.8 V and the process was reversible. The cited $E_{\frac{1}{2}}$ value is relative to the Fc$^+$–Fc couple, ferrocene (Fc) being used as the internal standard.

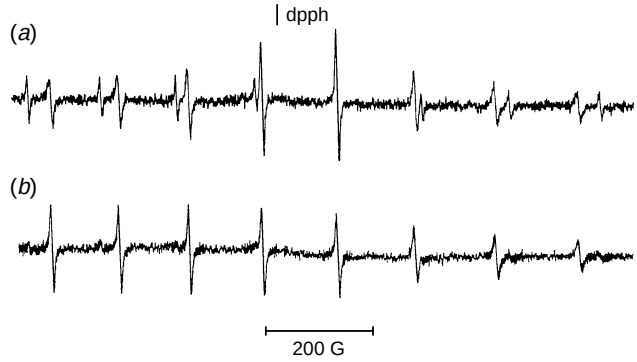
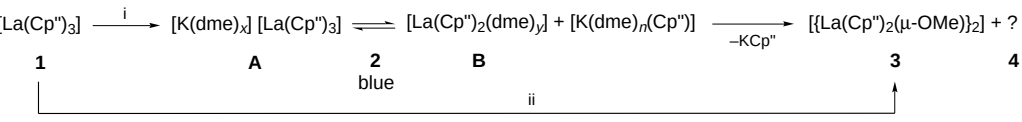



**Fig. 1** EPR spectrum of solution **2** in dme at (*a*) 295 and (*b*) 275 K




**Scheme 1** *Reagents and conditions*: i, K mirror, dme, 3 h at −40 °C and then 45 h at 25 °C; ii, MeOH, toluene, 2 h −40 °C. The yield of crystalline **3** (not optimised) was 46% (i) or 50% (ii).

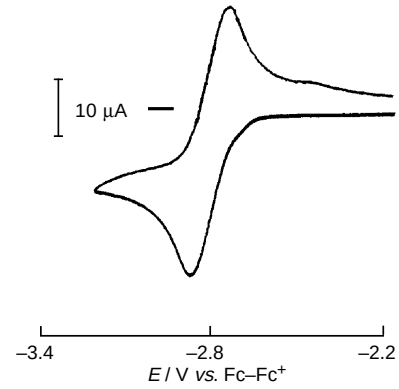



**Fig. 2** Cyclic voltammogram of **1** in thf with 0.2 mol $dm^{-3}$ $[NBu_4][PF_6]$ as supporting electrolyte at a vitreous carbon working electrode; scan rate 50 mV $s^{-1}$, 25 °C

By using the NMR-accessible, diamagnetic $La^{III}$ ($f^0$), it was further shown that in the reduction of $[La(Cp'')_3]$ in dme by K, the nature of the final product (like that of the intermediate **A** and **B**) was temperature dependent. When the reduction was initiated at −40 °C, the $^1H$ NMR spectrum in $C_6D_6$ of the eventually isolated crystalline white solid showed signals attributed not only to K(Cp″) and $[\{La(Cp'')_2(\mu\text{-}OMe)\}_2]$,‡¶ but also to another species (or mixture) **4** comprising a doublet at $\delta$ 6.99 and a singlet at $\delta$ 3.47 having *ca.* 10% of the intensity of the corresponding signals in **3**. Repeating the same reaction at ambient temperature, integration showed that the relative abundance of **4** : **3** was *ca.* 1 : 1. A similar trend was observed in the $^{13}C$ NMR spectra. Homonuclear decoupling and NOE experiments confirmed that the $^1H$ NMR spectral doublet at $\delta$ 6.99 and singlet at $\delta$ 3.47 be attributed to a second bis(cyclopentadienyl)lanthanum(III) methoxide (the expected triplet for the Cp″ and singlet for the $SiMe_3$ protons of **4** overlapped with those of **3**); from their relative intensity it is estimated that **4** has three $Cp''^-$ ligands for each $OMe^-$. One possible molecular formula, consistent with a $La^{3+}$ oxidation state, is $[La_6(Cp'')_{12}(OMe)_4O]$.

From equimolar portions of $[La(Cp'')_3]$ and methanol, a similar mixture of **3** and **4** was obtained and their relative proportions showed a comparable temperature dependence. Evans *et al.* have previously demonstrated that the reaction of $[Y(\eta\text{-}C_5H_5)_2Cl(thf)]$ with KOMe gave the polynuclear organo-yttrium methoxide oxide $[\{Y(\eta\text{-}C_5H_5)_2(\mu\text{-}OMe)\}_2\{Y(\eta\text{-}C_5H_5)_2\}(\mu_3\text{-}O)]^-$.[5]

Among organolanthanide compounds, stable +2 oxidation state complexes were unambiguously established only for those of Yb ($f^{14}$), Eu($f^7$) and Sm($f^6$), although claims have been made for $Ce^{II}$[6] and $Nd^{II}$.[7] The present results provide definitive evidence for thermally stable organolanthanide(II) complexes, which being oxophilic and powerful reducing agents are able to cleave the C–O bond of dme at ambient temperature (as previously postulated for related Ce and Nd systems).[1]

We thank Drs S. K. Ibrahim and C. J. Pickett for the cyclic voltammetric data, Dr A. G. Avent for the NOE experiment, the European Union for the provision of a Marie Curie Fellowship for M. C. C. and EPSRC for other support.

## Footnotes and References

* E-mail: m.f.lappert@sussex.ac.uk

† No reprints available.

‡ *General experimental procedure*: **1** was added to a K mirror in dme at −40 °C. The colour changed immediately to dark blue and after 3 h the mixture was warmed to room temp. and then stirred for 45 h. After filtration, the filtrate was concentrated to a small volume and cooled at −30 °C to give a white crystalline mixture (desolvated by heating for 5 h at 70–80 °C/$10^{-2}$ mmHg). Alternatively, after filtration the solvent was evaporated *in vacuo* and pentane added: a thermolabile, dark green, insoluble product separated from the colourless solution. The nature of the exceedingly air- and moisture-sensitive green product is currently under investigation, while the colourless solution contained K(Cp″), **3** and **4**. After complete removal of coordinated dme the lanthanum(III) methoxides were separated from the K(Cp″) by extraction with toluene.

§ EPR data were taken on an ER 200-D Bruker spectrometer operating at X-band (9.43 GHz); UV–VIS (dme, 298 k): $\lambda_{max}$ 578.9, 689.8(sh) nm.

¶ *Spectroscopic and analytical data*: K(Cp″) was identified by elemental analysis and by comparing its NMR spectra with those of a separately prepared compound (from HCp″ + KH in thf). The EIMS spectra of the crystalline lanthanum methoxide mixture, obtained either from the reduction in dme or from the protolytic reaction with methanol did not show the dinuclear molecular ion $M^+$ at $m/z$ = 1178 but the following principal fragments were observed: $m/z$ 1147 $[M - OCH_3]^+$, 1133, 1115, 967 $[M - Cp'']^+$, 953, 939, 921, 729 and 557 $[La(Cp'')_2]^+$. $^1H$ NMR ($C_6D_6$, 293 K) of **3**: $\delta$ 7.08 (t, $^4J$ 1.8 Hz), 6.96 (d, $^4J$ 1.8 Hz), 3.53 (s), 0.39 (s). DEPT $^{13}C$ NMR ($C_6D_6$, 293 K) of **3**: cyclopentadienyl region partially obscured by solvent, $\delta$ 130.0 (CH), 125.6 (CH), 54.2 ($OCH_3$), 1.3 ($SiCH_3$). IR (Nujol): 3069m, 3042m, 1316m, 1246s, 1208m, 1176w, 1078s, 1051s, 922s, 834vs br, 773s, 751s br, 689s, 640s, 625s $cm^{-1}$.

1 Yu. K. Gun'ko, P. B. Hitchcock and M. F. Lappert, *J.Organomet. Chem.*, 1995, **499**, 213.
2 (*a*) R. D. Johnson, M. S. de Vries, J. R. Salem, D. S. Bethune and C. S. Yannoni, *Nature*, 1992, **355**, 239; (*b*) R. D. Johnson, D. S. Bethune and C. S. Yannoni, *Acc. Chem. Res.*, 1992, **25**, 169; (*c*) S. Bandow, H. Shinohara, Y. Saito, M. Ohkohchi and Y. Ando, *J. Phys. Chem.*, 1993, **97**, 6101; (*d*) C. S. Yannoni, H. R. Wendt, M. S. de Vries, R. L. Siemens, J. R. Salem, J. Lyerla, R. D. Johnson, M. Hoinkis, M. S. Crowder, C. A. Brown, D. S. Bethune, L. Taylor, D. Nguyen, P. Jedrzejewsky and H. C. Dorn, *Synthetic Met.*, 1993, **59**, 279.
3 H. Bill and O. Pilla, *J. Phys. C: Solid State Phys.*, 1984, **17**, 3263.
4 M. N. Bochkarev, I. L. Fedushkin, V. I. Nevodchikov, V. K. Cherkasov, H. Schumann, H. Hemling and R. Weimann, *J. Organomet. Chem.*, 1996, **524**, 125.
5 W. J. Evans, M. S. Sollberger, J. L. Shreeve, J. M. Olofson, J. H. Hain and J. W. Ziller, *Inorg. Chem.*, 1992, **31**, 2492.
6 A. Greco, S. Cesca and G. Bertolini, *J. Organomet. Chem.*, 1976, **113**, 321.
7 M. Wedler, A. Recknagel and F. T. Edelmann, *J. Organomet. Chem.*, 1990, **395**, C26.

*Received in Basel, Switzerland, 11th April 1997; 7/02493B*

# A simple and efficient method for epoxidation of terminal alkenes

**Christophe Copéret, Hans Adolfsson and K. Barry Sharpless***

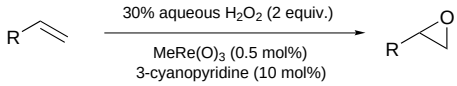
*Department of Chemistry, The Scripps Research Institute, 10550 N. Torrey Pines Road, La Jolla, California 92037, USA*

**The use of a catalytic amount of 3-cyanopyridine in the methyltrioxorhenium catalysed epoxidation of terminal alkenes with aqueous hydrogen peroxide speeds turnover, which results in the formation of many functionalized epoxides in high yields.**

Despite numerous literature precedents, the epoxidation of terminal alkenes remains a challenge in organic synthesis.[1] While screening for other examples of ligand accelerated catalysis (LAC),[2] our group has recently discovered that pyridine enhances the rate of the methyltrioxorhenium (MTO)-catalysed epoxidation of alkenes, while also tempering the Lewis acidity of the metal centre and thereby protecting the epoxide from destruction.[3] This method gives high yields of epoxides for di-, tri- and tetra-substituted alkenes; however, the epoxidation of terminal alkenes requires prolonged reaction times (3–5 days) and the conversion rarely exceeds 60–80%. Therefore, we decided to investigate the epoxidation of styrene, which is both a terminal alkene and the progenitor of a sensitive epoxide. The intention was to probe the relationship between the basicity of various pyridine ligands and their effectiveness.† We found that while basic pyridines (pyridine, 4-*tert*-butyl- and 4-methoxy-pyridine) protected the epoxide from ring opening, they also diminished the catalyst lifetime. On the other hand, less basic pyridines, and especially the ones bearing electron-withdrawing substituents in the meta position, *e.g.* 3-cyano-pyridine, 3-fluoropyridine, methyl nicotinate and even nicotinic acid, allowed high conversions (90–100%), but provided little or no protection for the epoxide. As a result mixtures of benzaldehyde, benzoic acid, styrene diol and only trace amounts of styrene oxide were obtained.

With these two facts in hand, epoxidation with a mixture of the two types of pyridines was attempted. Thus, treatment of a mixture of styrene (20 mmol), pyridine (2 mmol), 3-cyanopyridine (2 mmol) and MTO (0.1 mmol) in $CH_2Cl_2$ (14 ml) with 30% aqueous $H_2O_2$ (4 ml, 40 mmol) at room temperature gave, after 17 h, a 76% yield of styrene oxide along with 10% recovered styrene according to GC analysis. Using 2.5 ml instead of 14 ml of $CH_2Cl_2$—increasing the concentration from 1.2 to 5.0 M—allowed a better conversion (97–99%) in a shorter time (6 h) and gave an 89–92% yield of styrene oxide.‡ Other combinations of pyridines were less effective and presence of the parent pyridine was essential for the protection of the epoxide. In fact, even under the best conditions, benzaldehyde (0–0.5%), benzoic acid (0–1%) and styrene diol (2–3%) were always detected.

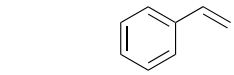
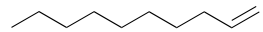
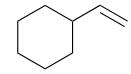
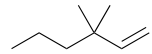
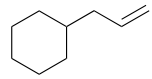
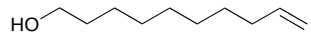
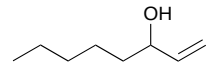
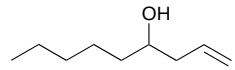
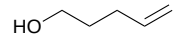
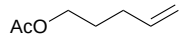
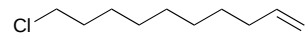
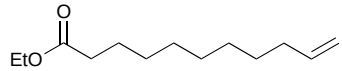
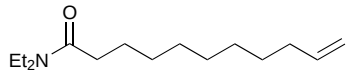
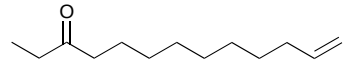
The other terminal alkenes in Table 1 give epoxides which are much less acid sensitive and their epoxidation did not require the use of a mixture of pyridines [eqn. (1)].§



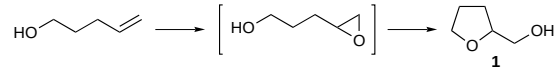
(1)

3-Cyanopyridine proved to be the optimal ligand in these cases.¶ A representative procedure for the epoxidation of such terminal alkenes is as follows: a mixture of dec-1-ene (28.0 g, 200 mmol), 3-cyanopyridine (2.08 g, 20 mmol) and MTO (249 mg, 1 mmol) in $CH_2Cl_2$ (120 ml) was treated with 40 ml of 30% aqueous $H_2O_2$ (400 mmol) and stirred for 17 h at 24 °C.‖ The biphasic reaction mixture was then treated with crushed ice (20 g) and a catalytic amount of $MnO_2$ (25 mg) and stirred until

**Table 1** MTO-catalysed epoxidations of terminal alkenes with hydrogen peroxide in the presence of 3-cyanopyridine[a]

| Entry | Alkene | Yield (%)[b,c] | *t*/h |
|---|---|---|---|
| 1[d] |  | 85 | 6 |
| 2 |  | 94 | 17 |
| 3 |  | 86 | 30 |
| 4 |  | 78 | 30 |
| 5 |  | 89 | 20 |
| 6 |  | 89 | 19 |
| 7[e] |  | 94 | 27 |
| 8[e] |  | 88 | 17 |
| 9 |  | 97[f] | 18 |
| 10 |  | 94 | 20 |
| 11 |  | 86 | 30 |
| 12 |  | 89 | 20 |
| 13 |  | 90 | 19 |
| 14 |  | 96 | 24 |

[a] Reaction conditions: Alkene (1 equiv.), MTO (0.5 mol%), 3-cyanopyridine (10 mol%), 30% $H_2O_2$ (aq.) (2 equiv.) in $CH_2Cl_2$. Alkene concentration: 1.3 M. See footnote §. [b] Conversions are > 99%. [c] Isolated yield. [d] A mixture of 3-cyanopyridine and pyridine (10 mol% of each) was employed. Alkene concentration: 4 M. [e] The epoxides were formed as a 1 : 1 mixture of diastereomers. [f] The initially formed epoxy alcohol cyclized completely to the tetrahydrofurfuryl alcohol **1**, which was isolated in 97% yield.



**1**

oxygen evolution ceased (1 h). Following phase separation, the water layer was extracted with $CH_2Cl_2$, the combined organic layers were dried over $Na_2SO_4$ and concentrated to an oil. Hexane was added to this crude product, and the resulting white precipitate was removed by filtration.** The filtrate was concentrated, and the crude colourless oil was distilled to yield 31.4 g of decene oxide (94% yield, 96.5% purity).††

This method is general and quite independent of the steric bulk at the α-position of the alkene (entries 3 and 4). Moreover, the presence of alcohol functionalities did not significantly affect the yield of epoxidation (entries 6–8) or its diastereoselectivity (entries 7 and 8).‡‡ However, the bis(homoallylic) alcohol (entry 9) gave only the furan **1** in high yields, but the epoxide is isolated in excellent yield if the hydroxy group is protected (entry 10). Other remote functionalities (amides, chlorides, esters and ketones) are also compatible with this epoxidation method (entries 11–14), and it is noteworthy that in the epoxidation of the ω-alkenone (entry 14) the possible Baeyer–Villiger products were not detected (*i.e.* < 1%) based on NMR spectroscopy of the crude reaction mixture.[4]

In summary, a remarkable, albeit poorly understood, beneficial effect of 3-cyanopyridine on MTO-catalysed epoxidations of terminal alkenes has been established. For this challenging class of substrates, this method of epoxidation could prove to be one of the most convenient because (i) it shows good functional group compatibility (wide scope), (ii) it is mild (*i.e.* neutral conditions, room temperature), (iii) it uses a readily available, safe and environmentally friendly oxidizing agent (30% aqueous $H_2O_2$), and (iv) it is easy to perform on the scales common (1 to 200 mmol) in the laboratory (no tedious work-up, no by-products). We are currently investigating ways to increase turnover numbers as well as trying to understand the special nature of the 3-cyanopyridine ligand.

We are grateful to the National Institutes of Health (GM 28384), the National Science Foundation (CHE 9521152), the W. M. Keck Foundation, and the Skaggs Institute for Chemical Biology for financial support. H. A. and C. C. are also grateful to the Swedish Natural Science Research Council and the Association des Amis des Sciences for post-doctoral fellowships, respectively. We also want to thank Drs Wallace Pringle, Yuji Tokunaga and Andrei Yudin for helpful discussions.

## Footnotes and References

* E-mail: sharples@scripps.edu

† Studies on the effect of various pyridine ligands (substituent effect) for the MTO–pyridine derivatives system are still underway.

‡ Longer reaction time did not increase conversion, and favoured formation of the by-products.

§ All compounds were isolated and characterized by standard techniques. All reactions proceeded to > 99% conversion unless otherwise noted.

¶ In the absence of 3-cyanopyridine, the reaction was slower and showed evidence of catalyst deactivation (*i.e.* only 93% conversion after 40 h). Anhydrous $H_2O_2$—reaction in *tert*-butyl alcohol— resulted in lower yields and prolonged reaction times, see ref. 1(*b*) and especially W. A. Herrmann, R. W. Fischer, M. U. Rauch and W. Scherer *J. Mol. Catal.*, 1994, **86**, 243.

‖ The reaction is slightly exothermic, and should be kept around 24 °C with a water bath.

** It is worth pointing out that 90–100% of the 3-cyanopyridine is consumed by the end of the reaction, and the white precipitate formed was identified as 3-cyanopyridine *N*-oxide. Monitoring the reaction with NMR spectroscopy showed that its formation became significant only late in the reaction, when the amount of alkene remaining was close to the amount of 3-cyanopyridine. For oxidations of amines using MTO, see Z. Zhu and J. H. Espenson, *J. Org. Chem.*, 1995, **60**, 1326; R. W. Murray; K. Iyanar, J. Chen and J. T. Wearing, *Tetrahedron Lett.*, 1996, **37**, 805; A. Goti and L. Nannelli, *Tetrahedron Lett.*, 1996, **37**, 6025; S. Yamazaki, *Bull. Soc. Chem. Jpn.*, 1997, **70**, 877.

†† This yield does not take into account the purity of the starting material; Aldrich dec-1-ene is 94% pure.

‡‡ No or little diastereoselectivity is usually observed in the MTO-catalysed epoxidation of allylic and homoallylic alcohols (W. Adam and C. M. Mitchell, *Angew. Chem., Int. Ed. Engl.*, 1996, **35**, 533; T. R. Boehlow and C. D. Spilling, *Tetrahedron Lett.*, 1996, **37**, 2717). This is in sharp contrast to some other transition metal-catalysed epoxidation reactions, see K. B. Sharpless and T. R. Verhoeven, *Aldrichim. Acta*, 1979, **12**, 63.

1 Terminal alkenes are much less reactive, and only few reactions give good conversion. (*a*) For seminal papers and some recent advances in epoxidation of alkenes other than the MTO-catalysed ones, see G. Berti, F. Bottari, B. Macchia and F. Macchia, *Tetrahedron*, 1965, **21**, 3277; G. Venturello, E. Alneri and M. Ricci, *J. Org. Chem.*, 1983, **48**, 3831; C. Venturello and R. D'Aloisio, *J. Org. Chem.*, 1988, **53**, 1553; J. Prandi, H. B. Kagan and H. Mimoun, *Tetrahedron Lett.*, 1986, **27**, 2617; W. Adam and A. K. Smerz, *J. Org. Chem.*, 1996, **61**, 3506; R. W. Murray and M. Singh, *Org Synth.*, 1996, **74**, 91; K. Sato, M. Aoki, M. Ogawa, T. Hashimoto and R. Noyori, *J. Org. Chem.*, 1996, **61**, 8310; K. Sato, M. Aoki, M. Ogawa, T. Hashimoto, D. Paneyella and R. Noyori, *Bull Soc. Chem. Jpn.*, 1997, **70**, 905; R. Murugavel and H. W. Roesky, *Angew. Chem., Int. Ed. Engl.*, 1997, **36**, 477; (*b*) For MTO-catalysed epoxidation of alkenes, see Hoechst AG (W. A. Herrmann, D. W. Marz, J. G. Kuchler, G. Weichselbaumer and R. W. Fischer) DE 3,902,357, 1989; W. A. Herrmann, R. W. Fischer and D. W. Marz, *Angew. Chem., Int. Ed. Engl.*, 1991, **30**, 1638; W. A. Herrmann, R. W. Fischer, M. U. Rauch and W. Scherer, *J. Mol. Catal.*, 1994, **86**, 243; A. M. Al-Ajlouni and J. H. Espenson, *J. Am. Chem. Soc.*, 1995, **117**, 9243; O. Pestovsky, R. van Eldik, P. Huston and J. H. Espenson, *J. Chem. Soc., Dalton Trans. 2*, 1995, 133; W. A. Herrmann, *J. Organomet. Chem.*, 1995, **500**, 149; W. Adam and C. M. Mitchell, *Angew. Chem., Int. Ed. Engl.*, 1996, **35**, 533; T. R. Boelow and C. S. Spilling, *Tetrahedron Lett.*, 1996, **37**, 2717; A. M. Al-Ajlouni and J. H. Espenson, *J. Org. Chem.*, 1996, **61**, 3969; W. A. Herrmann, J. D. G. Correia, M. U. Rauch, G. R. J. Artus and F. E. Kühn, *J. Mol. Cat.*, 1997, **118**, 33; ARCO Chemical Technology (G. L. Crocco, W. P. Shum, J. G. Zajacek and H. S. Kesling, Jr.) US 5,166,372, 1992; (*c*) For reviews on epoxidation of alkenes, see G. Strukul, *In Catalytic Oxidation with Hydrogen Peroxide as Oxidant*, Kluwer, Dordrecht, 1992; R. A. Sheldon, *In Applied Homogeneous Catalysis with Organometallic Compounds*, ed. B. Cornils and W. A. Herrmann, VCH, Weinheim, 1996.

2 D. J. Berrisford, C. Bolm and K. B. Sharpless, *Angew. Chem., Int. Ed. Engl.*, 1995, **34**, 1059.

3 J. Rudolph, K. L. Reddy, J. P. Chiang and K. B. Sharpless, *J. Am. Chem. Soc.*, 1997, **119**, 6185.

4 W. A. Herrmann, R. W. Fischer and J. D. G. Correia, *J. Mol. Catal.*, 1994, **94**, 213.

*Received in Corvallis, OR, USA, 19th May 1997; 7/03542J*

# Graphite as an effective catalyst for Friedel–Crafts acylation

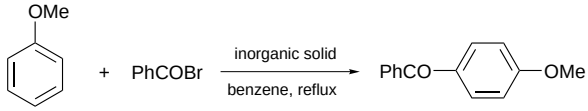
**Mitsuo Kodomari,* Yoshitada Suzuki and Kouji Yoshida**

*Department of Industrial Chemistry, Faculty of Engineering, Shibaura Institute of Technology, Shibaura, Minato-ku, Tokyo 108, Japan*

**Graphite is found to promote Friedel–Crafts acylation of aromatic compounds such as anisole, toluene and *o*-xylene with acyl halides to give the corresponding acylated products in high yields.**

Friedel–Crafts acylation of aromatic compounds is one of the most important syntheses of aryl ketones. In contrast to Friedel–Crafts alkylation, which proceeds readily in the presence of catalytic amounts of Lewis acid, acylation requires more than one equivalent, *e.g.* of $AlCl_3$. This is due to the complexation of $AlCl_3$ by the ketone product. The catalyst used cannot easily be recovered and recycled; therefore, a large amount of toxic waste is generated. In order to solve this problem, some catalytic Friedel–Crafts acylations have recently been developed. $Ln(OTf)_3$–$LiClO_4$,[1] $TiCl(OTf)_3$–TfOH [2] and $ReBr(CO)_5$[3] have been reported as catalysts for Friedel–Crafts acylation. In addition, the use of inorganic solid supported reagents[4] or solid acids[5] as catalysts, resulting in higher selectivity, easier work-up and environmentally safe reactions, has been reported. For instance, HZSM-5 zeolite has been reported to promote the liquid-phase acylation of anisole with carboxylic acid.[5b] However, it has limitations with regard to generality and efficiency. Recently, it has also shown that alumina promotes the acylation of reactive aromatics such as anisole and

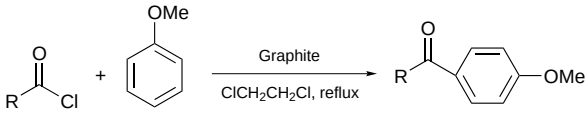
**Table 1** Acylation of anisole using the various inorganic solids[a]




| Inorganic solid | Yield (%)[b] |
|---|---|
| None | 0 |
| Graphite | 89 |
| Active charcoal | trace |
| Molecular sieves (5 Å) | 41 |
| $Al_2O_3$ (neutral) | 9 |
| Silica gel | 0 |

[a] A mixture of anisole (2 mmol), benzoyl bromide (3 mmol) and inorganic solid (1 g) in benzene (5 ml) was refluxed for 8 h. [b] Yields were determined by GLC.

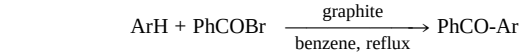
**Table 2** Acylation of anisole with acyl chlorides[a]

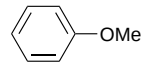
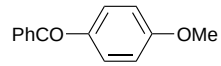
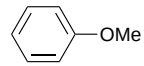
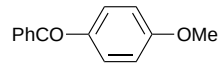
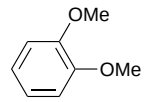
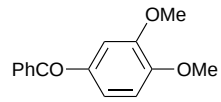
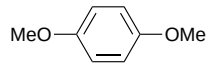
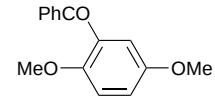
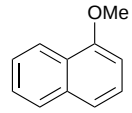
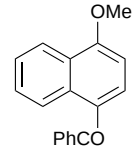
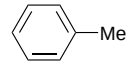
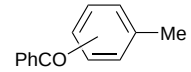
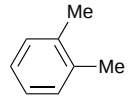
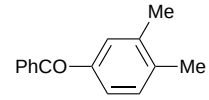
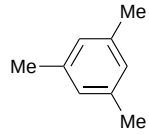
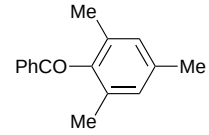
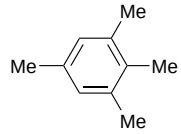
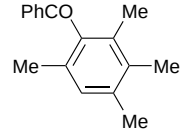
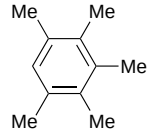
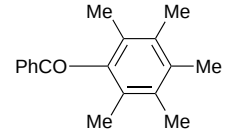



| R | *t*/h | Yield (%)[b] |
|---|---|---|
| Ph[c] | 8 | 85 |
| Cyclohexyl | 8 | 84 |
| Pr$^i$ | 3 | 89 |
| $C_5H_{11}$ | 8 | 66 |
| $C_{12}H_{25}$ | 8 | 63 |
| $PhCH_2$ | 8 | 61 |

[a] Conditions: anisole (2 mmol), acyl chloride (3 mmol), graphite (1 g), $ClCH_2CH_2Cl$ (5 ml). [b] Yields were determined by GLC. [c] The reaction was carried out at 120 °C in chlorobenzene.

**Table 3** Graphite catalysed Friedel–Crafts acylation[a]




| Run | ArH | *t*/h | Product | Yield (%)[b] |
|---|---|---|---|---|
| 1 |  | 8 |  | 89 |
| 2[c] |  | 16 |  | 70 |
| 3 |  | 8 |  | 92 |
| 4 |  | 8 |  | 60 |
| 5 |  | 8 |  | 93 |
| 6[d] |  | 24 |  | 86 ($o$ :$p$ = 1:4) |
| 7[e] |  | 24 |  | 97 |
| 8 |  | 3 |  | 84 |
| 9 |  | 3 |  | 85 |
| 10 |  | 3 |  | 83 |

[a] ArH (2 mmol), benzoyl bromide (3 mmol), graphite (1 g) and benzene (5 ml). [b] Yields were determined by the internal standard method *via* GLC. [c] Addition of sodium carbonate (6 mmol). [d] Solvent: toluene (5 ml). [e] Solvent: *o*-xylene (5 ml).

thiophene with carboxylic acid in the presence of trifluoroacetic anhydride.[6] During the course of our studies aimed at developing supported reagents as catalysts for Friedel–Crafts reaction,[7] we found that graphite, without any treatment, promotes the Friedel–Crafts acylation of aromatic compounds with acyl halides to afford the corresponding acylated products in high yields.

Graphite was shown to have a remarkably high activity for the acylation of active aromatic compounds such as anisoles and polymethylbenzenes with acyl halide to give the corresponding acylated compounds in high yields, without any of the environmental disadvantages of using toxic homogeneous reagents such as $AlCl_3$. In a typical experiment, graphite† was added to a mixture of anisole (2 mmol) and benzoyl bromide (3 mmol) in benzene. The mixture was heated under reflux for 8 h. Graphite was removed by filtration, and the filtrate was washed with aqueous sodium hydrogen carbonate, to remove the excess benzoyl bromide, and concentrated under reduced pressure. The crude product was chromatographed on silica gel to afford *p*-methoxybenzophenone (80%). The products obtained were analysed by GLC, IR and NMR spectroscopy. The amount of graphite used relative to benzoyl bromide was between 0.5 and 2 g. The optimum yield of *p*-methoxybenzophenone was obtained with 1 g of graphite, whereas 2 g gave a slightly lower yield. When a large amount of graphite was used, the yields were decreased due to absorption of an appreciable amount of the product and starting material on the graphite. Empirical testing of five inorganic solids revealed that graphite was most effective in promoting the reaction. MS-5A, though less effective than graphite, was also effective, whereas active charcoal, silica gel and alumina were entirely ineffective (see Table 1). Alkanoyl and cycloalkanecarbonyl chlorides could be used as acylating reagents in the reactions, and the corresponding acylated products were obtained in good yield (Table 2). The reaction of anisole with isobutyl chloride and with cyclohexanecarbonyl chloride gave isopropyl 4-methoxyphenyl ketone and cyclohexyl 4-methoxyphenyl ketone, respectively, in high yields. However, the acylation of anisole with acetyl chloride gave *p*-methylacetophenone in low yield. This is probably due to evaporation (low boiling point of acetyl chloride). Benzoylation of several anisoles and polymethylbenzenes with benzoyl bromide in the presence of graphite was carried out and the results are summarised in Table 3. Anisole, veratrole and α-methoxynaphthalene reacted with benzoyl bromide to give the corresponding benzoylated products in high yields. In the present reactions, benzoyl bromide was a better acylating reagent than benzoyl chloride. For example, anisole reacted with benzoyl bromide to afford *p*-methoxybenzophenone in 89% yield, whereas a 50% yield was obtained in the reaction with benzoyl chloride under the same conditions; the yield was improved to 85% when the reaction was carried out at 120 °C in chlorobenzene. These graphite-promoted acylations proceeded even after addition of sodium carbonate, which traps hydrogen bromide generated during the reaction, although the rate of the reaction was slower than that in the reaction without sodium carbonate (Table 3, run 2). Polymethylbenzenes such as mesitylene, 1,2,3,5-tetramethylbenzene and pentamethylbenzene gave the corresponding benzoylated products in high yields. However, benzoylation of toluene and *o*-xylene was very slow in refluxing benzene, giving methylbenzophenone (a mixture of *o*- and *p*-isomers) and 3,4-dimethylbenzophenone in low yield, respectively; the yields were improved when the reaction was performed using toluene and *o*-xylene as both substrate and solvent. Benzene was hardly benzoylated under similar conditions. The reaction of benzene with benzoyl bromide was heated to reflux for 24 h to give benzophenone in 20% yield.

Further understanding of the catalysis by graphite and the application of graphite to other synthetic reactions are now under investigation.

## Footnotes and References

* E-mail: kodomari@sic.shibaura-it.ar.jp

† Graphite powder was from Aldrich (Catalogue no. 28, 286-3) and was employed without further purification.

1 A. Kawada, S. Mitamura and S. Kobayashi, *Chem. Commun.*, 1996, 183.
2 J. Izumi and T. Mukaiyama, *Chem. Lett.*, 1996, 739.
3 H. Kusama and K. Narasaka, *Bull. Chem. Soc. Jpn.*, 1995, **68**, 2379.
4 Y. Izumi, N. Natsume, H. Takamine, I. Takamori and K. Urabe, *Bull. Chem. Soc. Jpn.*, 1989, **62**, 2159; T. W. Bastock, J. H. Clark, P. Landon and K. Martin, *J. Chem. Res.* (*S*), 1994, 104.
5 (*a*) B. Chiche, A. Finiels, G. Gauthier and P. Geneste, *J. Org. Chem.*, 1986, **51**, 2128; (*b*) Q. L. Wang, Y. Ma, X. Ji, H. Yan and Q. Qiu, *J. Chem. Soc., Chem. Commun.*, 1995, 2307.
6 B. C. Ranu, K. Ghosk and U. Jana, *J. Org. Chem.*, 1996, **61**, 9546.
7 M. Kodomari and S. Taguchi, *J. Chem. Res.* (*S*), 1996, 241.

*Received in in Cambridge, UK, 6th June 1997; 7/03947F*

# Palladium catalysed polymerization of aryl diodides with acetylene gas in aqueous medium: a novel synthesis of areneethynylene polymers and oligomers

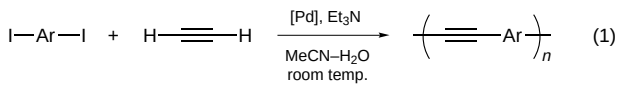
**Chao-Jun Li,*[a] William T. Slaven IV,[a] Vijay T. John[b] and Sukanta Banerjee[b]**

[a] *Department of Chemistry, Tulane University, New Orleans, LA 70118, USA*
[b] *Department of Chemical Engineering, Tulane University, New Orleans, LA 70118, USA*

**Palladium catalysed copolymerization of aryl iodides with acetylene gas in an aqueous medium provides areneethynylene polymers and oligomers.**

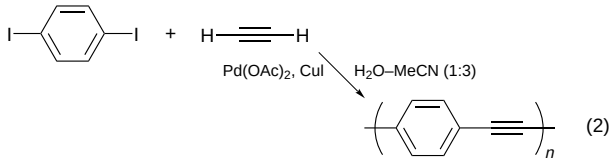
Poly(areneethynylene) is an important class of conjugated polymer exhibiting properties such as photoluminescence,[1] electronic conductivity and nonlinear optics.[2] These polymers also exhibit exceptionally high quantum yields of fluorescence in comparison to other conjugated polymers.[3] Such properties render the polymers potentially useful for applications in constructing light emitting diodes (polymer LEDs)[4] and fluorescence sensors.[5] Previously, areneethynylene polymers and oligomers have been synthesized by the polymerization of aryl dihalides with aryl diacetylenes (requiring multistep syntheses) through Sonogashira coupling.[6] The reaction also requires the use of triethylamine as solvent and refluxing conditions.

As part of our continuing interest in synthesizing areneethynylene-type polymers and oligomers,[7] we required a simple and practical method for ready access to these materials. Conceptually, a convenient and economical way of generating these polymers is *via* the copolymerization of aryl dihalides with acetylene gas. During our studies of aqueous organic reactions,[8] we became interested in synthesizing poly(areneethynylene)s *via* polymerization of aryl halides with acetylene gas in aqueous medium [eqn. (1)].



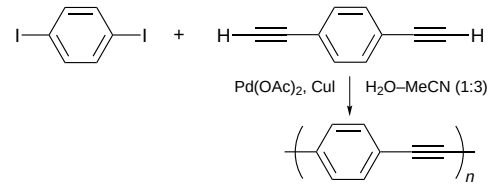
(1)

To ensure that the reactants were soluble, a mixture of water–MeCN was used as the reaction solvent. The average molecular weights ($M_w$ and $M_n$) of the polymer were characterized by gel permeation chromatography (GPC) using polystyrene as standard and THF as the eluent. Thus, 1,4-diiodobenzene was stirred with acetylene gas in a mixture of MeCN and water (3 : 1) in the presence of a catalytic amount of palladium acetate and cuprous iodide, together with 3 equiv. of triethylamine at room temperature. After three days, a dark brown polymeric solid was generated quantitatively [eqn. (2)]. The polymer thus



(2)

generated had very low solubility in common solvents, *e.g.* THF, benzene, $CH_2Cl_2$. We were unable to determine the molecular weight of this insoluble polymer. However, the molecular weights of the soluble fraction indicate oligomers with $M_n$ = 828 and $M_w$ = 4326. The polymer generated through this method appears very similar to those prepared by the polymerization of aryl dihalides with aryl diacetylenes [eqn. (3)]. The effectiveness of this preliminary investigation led us

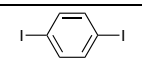
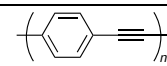
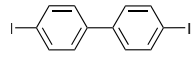
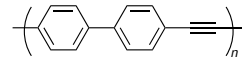
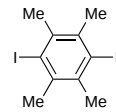
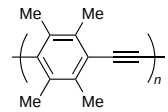
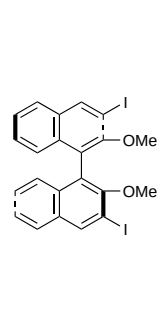
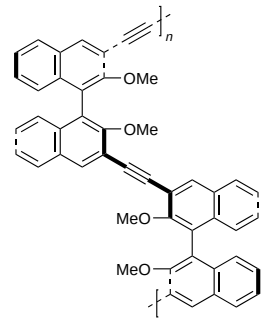


(3)

investigate the preparation of other areneethynylene polymers and oligomers by this convenient method. The results are listed in Table 1.[9]

The polymerization of 1,4-diiodo-2,3,5,6-tetramethylbenzene and acetylene gas generated a polymer (yield 51%) which is slightly more soluble in THF than the phenylethynylene polymer. GPC measurement of the soluble portion showed $M_n$ = 1185 and $M_w$ = 3495. Polymerization of 4,4′-diiodobiphenyl and acetylene gas again generated an insoluble polymer. The soluble, low molecular weight portion

**Table 1** Data for areneethynylene polymers and oligomers[a]

| Entry | Diiodoarene | Polymer (oligomer) | Reaction conditions[b] | $M_n$ | $M_w$ |
|---|---|---|---|---|---|
| |  |  | A | 828 | 4326 |
| |  |  | B | 504 | 1291 |
| |  |  | B | 1185 | 3495 |
| |  |  | C | 1250 | 3180 |

[a] All reactions were carried out at room temperature under an atmosphere of acetylene gas. $M_n$ and $M_w$ distributions are based only on the soluble portion of the polymerized material. [b] Reaction conditions: A = $Pd(OAc)_2$ (5%), $PPh_3$ (10%), CuI (5%), $Et_3N$ (5 equiv.), 3 days, in MeCN–$H_2O$ (3 : 1); B = $Pd(OAc)_2$ (5%), $PPh_3$ (10%), CuI (5%), $Et_3N$ (5 equiv.), 3 days in THF–$H_2O$ (3 : 1); C = Pd(OAc) (5%), P(*m*-$PhSO_3Na)_3$ (10%), CuI (5%), $Et_3N$ (5 equiv.), 5 days, in THF–MeCN–$H_2O$ (1 : 1 : 2).

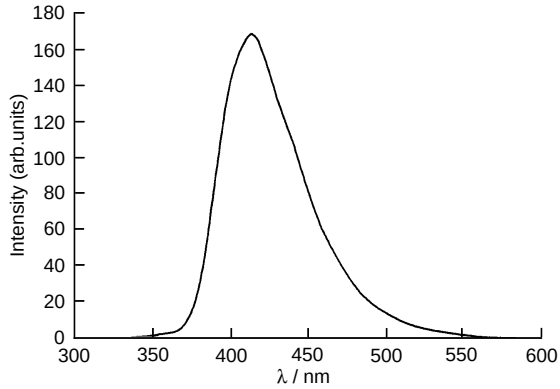



**Fig. 1** Fluorescence of the binaphthyl polymer in THF (excitation wavelength = 324 nm)

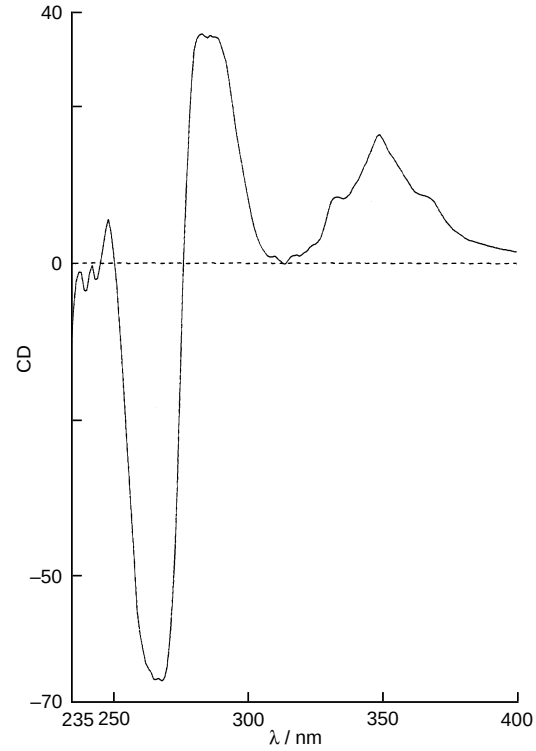



**Fig. 2** Circular dichroism spectrum of the binaphthyl polymer

showed $M_n$ = 504 and $M_w$ = 1291. On the other hand, polymerization of 3,3′-diiodo-2,2′-dimethoxy-1,1′-binaphthyl and acetylene gas generated a polymer (yield 48%) which is soluble in a variety of common organic solvents (*e.g.* THF, $CH_2Cl_2$, $CHCl_3$). Characterization showed $M_n$ = 1250 and $M_w$ = 3180, which are similar to those of the corresponding polymer that was prepared *via* the palladium-catalysed Stille reaction[10] by a modified procedure of Cummins[11] using bis(tributylstannyl)acetylene in refluxing 1,4-dioxane ($M_n$ = 1860 and $M_w$ = 3200). The polymer shows a strong fluorescence, which suggests the potential for LED applications. The fluorescence spectrum of the polymer (Fig. 1) shows an emission maxima of 435 nm when excited at 324 nm. Both $^1H$ and $^{13}C$ NMR showed significant broadening of all the corresponding peaks. The circular dichroism (CD) spectrum of the polymer in chloroform (Fig. 2) shows a negative Cotton effect at λ = 245 nm and a positive effect at λ = 277 nm. Attempts to obtain information about the endgroups of the oligomers *via* MALDI MS were not successful. Further evaluation of the method for synthesis of areneethynylene polymers and oligomers as well as the characterization of the polymers and oligomers is in progress.

## Footnotes and References

* E-mail: cjli@mailhost.tcs.tulane.edu

1 T. Yamamoto, M. Takagi, K. Kizu, T. Maruyama, K. Kubota, H. Kanbara, T. Kurihara and T. Kaino, *J. Chem. Soc., Chem. Commun.*, 1993, 797.
2 R. H. Baughman, J. L. Bredas, R. R. Chance, R. L. Elsenbaumer and L. W. Shacklette, *Chem. Rev.*, 1982, **82**, 209.
3 A. P. Davey, S. Elliott, O. O'Conner and W. Blau, *J. Chem. Soc., Chem. Commun.*, 1995, 1433.
4 D. D. C. Bradley, *Adv. Mater.*, 1992, **4**, 756.
5 Q. Zhou and T. M. Swager, *J. Am. Chem. Soc.*, 1995, **117**, 7017.
6 K. Sonogashira, Y. Tohda and N. Hagira, *Tetrahedron Lett.*, 1975, 4467.
7 C. J. Li, D. Wang and W. T. Slaven, IV, *Tetrahedron Lett.*, 1996, **37**, 4459.
8 C. J. Li, *Chem. Rev.*, 1993, **93**, 2023; C. J. Li, *Tetrahedron*, 1996, **52**, 5643.
9 For palladium catalysed coupling of terminal acetylenes with aryl halides in aqueous medium, see A. L. Calsalnuovo and J. C. Calabreze, *J. Am. Chem. Soc.*, 1990, **112**, 4324; J. P. Genet, E. Blart and M. Savignac, *Synlett*, 1992, 715; D. V. Davydov and I. P. Beletskaya, *Russ. Chem. Bull.*, 1995, **44**, 965. A rhodium catalysed polymerization of phenylacetylene in aqueous medium was recently reported, see B. Z. Tang, W. H. Poon, S. M. Leung, W. H. Leung and H. Peng, *Macromolecules*, 1997, **30**, 2209; *Polym. Mater. Sci. Eng.*, 1997, **76**, 385.
10 For reviews, see: J. F. Stille, *Angew. Chem., Int. Ed. Engl.*, 1986, **25**, 508; W. J. Scoot and J. E. McMurry, *Acc. Chem. Res.*, 1988, **21**, 47.
11 C. H. Cummins, *Tetrahedron Lett.*, 1994, **35**, 857.

*Received in Cambridge, UK, 29th May 1997; 7/03723F*

# Isotopic labelling studies of the deaminative fragmentation of *N*-nitrosohydroxylamines and related compounds by kinetics, millimetre-wave spectroscopy and $^{17}O$ NMR spectroscopy

**Johanna Haider, M. N. Stuart Hill, Iain D. Menneer, Howard Maskill* and John G. Smith**

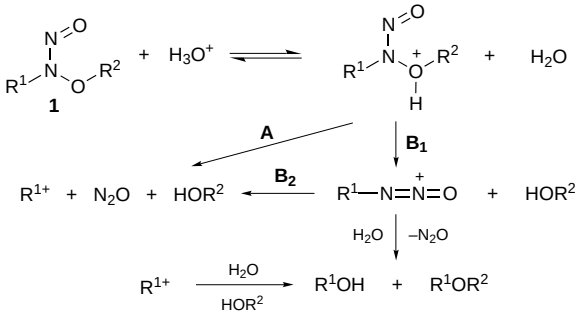
*Department of Chemistry, Bedson Building, University of Newcastle upon Tyne, Newcastle upon Tyne, UK NE1 7RU*

**Nitrous oxide enriched with $^{18}O$ has been identified by millimetre-wave spectroscopy from the acid-induced hydrolysis of $N^1$-(2-adamantyl)-$N^2$-[$^{18}O$]hydroxydiazen-1-ium $N^1$-oxide 2 which, along with $^{17}O$ NMR studies and an α-deuterium kinetic isotope effect of $k_H/k_D$ = 0.98 (±0.02) for *N*-nitroso-*N*-(2-[2-$^2$H]adamantyl)-*O*-benzylhydroxylamine 4, confirms (i) that nitrous oxide is liberated in these reactions, and (ii) that the fragmentations in these reactions are step-wise and not concerted.**

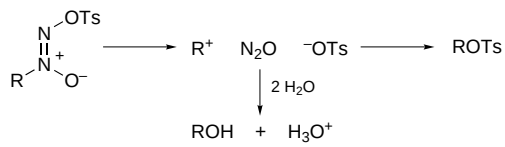
A decade ago, the biological importance of nitric oxide (NO) was first recognised,[1] and this led to the search for compounds capable of releasing NO under mild physiological conditions. Promising first results were reported for some rather complex *N*-nitrosohydroxylamine derivatives,[2] whereas simpler analogues were shown to undergo a new deamination type of reaction.[3] Since related *N*-nitrosamines are known to be carcinogenic,[4] and deamination reactions involve highly reactive electrophilic intermediates with mutagenic potential, the borderline between the possibly benevolent homolytic reaction and the almost certainly hazardous heterolytic alternative from *N*-nitrosohydroxylamines required exploration, and both mechanisms need better characterization.

The mechanism we proposed for the acid-induced deamination type of solvolysis of *N*-nitroso-*N*,*O*-dialkylhydroxylamines **1** is shown in Scheme 1.[3] Our earlier results did not allow us to distinguish between the concerted fragmentation (path A) and the step-wise alternative (path B). We had previously established, however, that the related fragmentation of alkylazoxy arenesulfonates, shown in Scheme 2 for azoxy tosylates, is concerted.[5] $N^1$-(2-Adamantyl)-$N^2$-hydroxydiazene-1-ium $N^1$-oxide **2**, the product of nitrosation of *N*-(2-adamantyl)hydroxylamine, also undergoes acid-induced hydrolysis with kinetic features very similar indeed to those of several *N*-nitroso-*N*,*O*-dialkylhydroxylamines.[3] Consequently, a mechanism involving isomerization of **2** into its *N*-nitroso isomer **3** followed by protonation and fragmentation was proposed, and is shown in Scheme 3. In this mechanism also, the fragmentation could be concerted (path A) or step-wise (path B). Additionally, however, the direct mechanism from **2** shown in Scheme 4 in which the other oxygen departs as part of the nucleofuge appeared a viable alternative, especially in view of the above-mentioned fragmentation of alkylazoxy tosylates (Scheme 2). We now report that, by a combination of isotopic studies and spectroscopic methods, we have been able to distinguish between the concerted and step-wise alternatives for compounds **1**, and between the mechanisms of Schemes 3 and 4 for $N^1$-(2-adamantyl)-$N^2$-hydroxydiazene-1-ium $N^1$-oxide **2**.

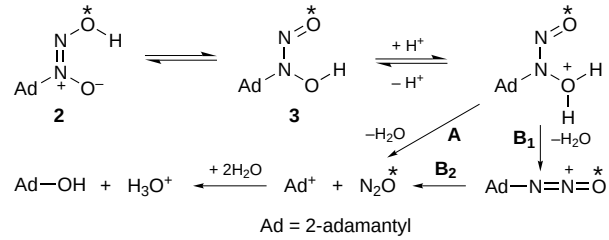
Compound **2** was prepared by reaction of *N*-(2-adamantyl)-hydroxylamine with aqueous nitrous acid enriched with $^{17}O$ following a procedure established by Dahn,[6] and the labelled atom, marked with an asterisk in Scheme 3, was confirmed by $^{17}O$ NMR spectroscopy [$\delta_O$ 198 (relative to $^{17}OH_2$), the other oxygen giving a signal at $\delta_O$ 334].[3]† The $^{17}O$ NMR spectrum of the adamantan-2-ol ($\delta_O$ = 30), isolated from acid-induced hydrolysis of this labelled substrate, was then recorded and shown to be identical to a sample of natural abundance adamantan-2-ol,‡ *i.e.* none of the $^{17}O$ in the substrate ended up in the adamantanol. Since appreciable quantities of the ether R–O–R′ are formed from the hydrolysis of the *N*-nitroso-*N*,*O*-dialkylhydroxylamines **1**, we are confident that the water molecule which departs as nucleofuge from **2** (or from **3**–whichever is involved) would be trapped to some extent by the 2-adamantyl cation. We concluded on the basis of this admittedly negative evidence that the isotopically labelled oxygen departs entirely as nitrous oxide according to the mechanism in Scheme 3. To obtain positive evidence, we also



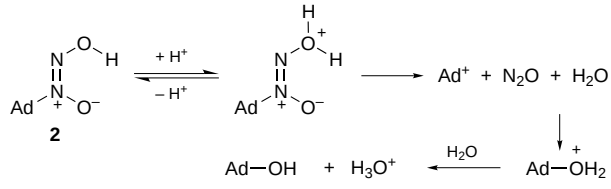
**Scheme 1**



**Scheme 2**



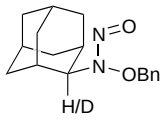
**Scheme 3**



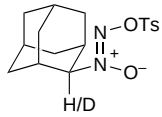
**Scheme 4**

prepared compound **2** specifically enriched with $^{18}O$ at the oxygen marked with an asterisk in Scheme 3. The acid-induced hydrolysis was then carried out for more than eight half-lives at 65 °C, and the evolved gas was flushed through by a stream of nitrogen, dried by a potassium hydroxide tower, and trapped at liquid nitrogen temperature. It was then transferred *via* normal vacuum line procedures to a millimetre-wave spectrometer and part of its rotational spectrum was recorded.[7] In addition to the band at 125 614 MHz due to the $J$ 5 ← 4 rotational transition in the $N_2O$ containing $^{16}O$, we also observed the band at 71 155 MHz corresponding to the $J$ 3 ← 2 transition of the $N_2O$ molecule containing $^{18}O$; both frequencies are in excellent agreement with values calculated from literature data.[8] This result corroborates the $^{17}O$ NMR result described above, and together they are compatible with the mechanism of Scheme 3 and rule out that in Scheme 4.

We also prepared *N*-nitroso-*N*-(2-adamantyl)-*O*-benzylhydroxylamine **4** specifically labelled with deuterium at C-2 of the



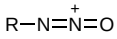

**4**



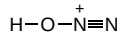

**5**




**6a** R = 2-adamantyl
**b** R = H




**7a** R = H
**b** R = 2-adamantyl




**8**

adamantyl system, and measured the α-deuterium kinetic isotope effect (KIE). Results of $k_H/k_D$ = 1.09–1.13 for the α-deuterium KIE for solvolysis of 2-adamantylazoxy tosylate **5** were part of the evidence that cleavage of the C–N bond is involved in the rate-limiting transition state for the solvolysis of **5** (Scheme 2).[5] Similar results would be expected for **4** if the mechanism follows path A in Scheme 1 (or if the reaction is step-wise with step $B_2$ rate limiting). The step-wise mechanism with the initial step $B_1$ rate limiting would be expected to have an α-deuterium KIE of approximately unity since only minor perturbations of the α-C–H vibrations are expected in the formation of the transition structure from the reactant molecule. Reactions were measured at two temperatures and two acid concentrations as shown in Table 1, and results of $k_H/k_D$ = 0.98 (±0.02) were obtained; these are compatible only with the stepwise mechanism and rate-limiting departure of the nucleofuge.

The protonated form of **2** in Scheme 4 is clearly analogous to **5** in that both have good nucleofuges, $H_2O$ and $TsO^-$ respectively, bonded to the terminal nitrogen of the azoxy group. Stepwise fragmentation of **5** and of the protonated form of **2** would involve **6a** as an intermediate. In a theoretical investigation, however, we have already shown that **6b** exists only as a transition structure in the gas-phase isomerization of **7a** into **8**,[9] and that no bonded structure corresponding to **6a** is expected to exist. So, whereas **5** avoids formation of **6a** by a concerted fragmentation, we have now shown that formation of **6a** from **2** in acidic solution is avoided by rearrangement and a step-wise route involving **7b** (Scheme 3, path B).

**Table 1** Rate constants and α-deuterium kinetic isotope effects for the acid-induced hydrolysis of *N*-nitroso-*N*-(2-adamantyl)-*O*-benzylhydroxylamine[a]

| Compound | $T$/°C | $[HClO_4]$/mol dm$^{-3}$ | $k/10^{-3}$ s$^{-1}$ | $k_H/k_D$ |
|---|---|---|---|---|
| **4**-H | 34.68 | 0.10 | 1.14 | |
| **4**-D | 34.68 | 0.10 | 1.16 | 0.98 |
| **4**-H | 44.67 | 0.10 | 2.90 | |
| **4**-D | 44.67 | 0.10 | 2.92 | 0.99 |
| **4**-H | 44.68 | 0.50 | 4.86 | |
| **4**-D | 44.68 | 0.50 | 5.04 | 0.96 |

[a] Reaction rates were measured by our normal UV spectrophotometric method which has already been described (refs. 3, 5). Simultaneous reactions were monitored for about three half-lives with two cells containing the protium compound and two cells containing the deuterium analogue in the same thermostatted four-cell block. Identical solvolytic media were used for H and D compounds in one four-cell experiment, and the ionic strength in all reactions was 1.0 mol dm$^{-3}$ ($NaClO_4$). The rate constant for a given compound was reproducible to within 1%, and standard deviations on individual rate constants were always less than 1%. The maximum error in $k_H/k_D$ is estimated to be 0.02.

## Footnotes and References

* E-mail: h.maskill@ncl.ac.uk

† $^{17}O$ NMR spectra were recorded using a Bruker WM 300 WB spectrometer operating at 300 MHz for $^1H$ and 40.670 MHz for $^{17}O$; the solvent was deuteriochloroform.

‡ For both the natural abundance (non-solvolytic) sample of adamantan-2-ol and that isolated from the hydrolysis of 2-Ad-N(O)$^{17}$OH, practically the same signal-to-noise ratio was achieved for the signal at $\delta_O$ 30 after 880 000 scans using identical spectrometer conditions and similar substrate solution concentrations.

1 A. R. Butler, *Chem. Br.*, 1990, 419; A. R. Butler and D. L. H. Williams, *Chem. Soc. Rev.*, 1993, 233; P. L. Feldman, O. W. Griffith and D. J. Stuehr, *Chem. Eng. News*, December 20, 1993, p. 26.
2 See, for example, C. M. Maragos, D. Morley, D. A. Wink, T. M. Dunams, J. E. Saavedra, A. Hoffman, A. A. Bove, L. Isaac, J. A. Hrabie and I. K. Keefer, *J. Med. Chem.*, 1991, **34**, 3242 and citations in ref. 1.
3 I. D. Menneer, H. Maskill and D. I. Smith, *J. Chem. Soc., Chem. Commun.*, 1995, 1855; I. D. Menneer, PhD Thesis, Newcastle, 1996.
4 D. L. H. Williams, *Nitrosation*, Cambridge University Press, Cambridge, 1988.
5 H. Maskill, J. T. Thompson and A. A. Wilson, *J. Chem. Soc., Perkin Trans. 2*, 1984, 1693; I. M. Gordon and H. Maskill, *J. Chem. Soc., Chem. Commun.*, 1989, 1358.
6 H. Dahn and M.-N. Ung-Truong, *Helv. Chim. Acta*, 1988, **71**, 241.
7 J. H. Carpenter, J. D. Cooper, J. B. Simpson, J. G. Smith and D. H. Whiffen, *J. Phys. E.*, 1974, **7**, 678.
8 B. A. Andreev, A. V. Burenin, E. N. Karyakin, A. F. Krupnov and S. M. Shapin, *J. Mol. Spectrosc.*, 1976, **62**, 125.
9 P. M. W. Gill, H. Maskill, D. Poppinger and L. Radom, *J. Chem. Res. (S)*, 1987, 54.

*Received in Cambridge, UK, 2nd June 1997; 7/03801A*

# The synthesis of (*S*)-(+)-gossypol *via* an asymmetric Ullmann coupling

**A. I. Meyers* and Jeffrey J. Willemsen**

*Department of Chemistry, Colorado State University, Fort Collins, Colorado 80523-1872, USA*

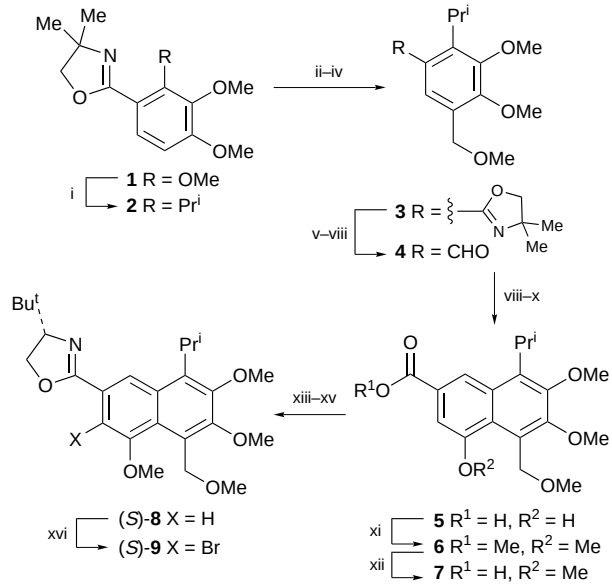
**The first asymmetric total synthesis of (*S*)-(+)-gossypol is described using chiral oxazolines as the naphthyl substituent in a highly diastereoselective aryl–aryl coupling.**

In 1886, racemic gossypol **13** was isolated[1] from cotton seeds and its structure elucidated in 1938 by Adams.[2] It is known to be active as an oral anti-spermatogenic agent[3] and has recently been tested on male subjects in China.[4] Additionally, (*R*)-gossypol was shown to be ten times more effective than its *S* antipode against tumour cells[5] and also showed inhibitory activity against HIV type 1.[6] The *S* antipode, on the other hand, has exhibited activity against herpes simplex virus,[7] and influenza[8] and parainfluenza virus.[7] The *S* enantiomer also induces DNA strand breaks in human leukocytes.[9]

Synthetic efforts to reach this axially chiral system have thus far only led to racemic gossypol, along with various analogues in the search for further biological activity.[10] The synthetic routes to gossypol feature mainly phenolic oxidative coupling, although in one instance an organolithium–$CoBr_2$ oxidative coupling was reported to proceed in poor (25%) yield.[10*c*]

Our approach to gossypol in enantiomerically pure form (either *R* or *S*) was based upon our earlier reports on asymmetric Ullmann couplings of 2-phenyl[11] or several naphthyl oxazolines.[12,13] In these earlier studies we showed that biaryl atropisomers could be accessed in high enantiomeric purity by either a thermodynamically controlled reaction[11] or a kinetically controlled process.[12,13] Due to the ample *ortho* substitution present in gossypol, restricted rotation about the symmetrically structural aryl–aryl bond showed relatively stable axially chiral enantiomers and indeed both have been isolated from natural sources.[14,15]

From the rich chemistry that has been developed[16] for the oxazoline moiety, both chiral and achiral, we felt this was a further opportunity to highlight a number of different reactions exhibited by the oxazolines. The route to (*S*)-**13** was initiated by transforming 2,3,4-trimethoxybenzene into the oxazoline **1** and displacing the 2-methoxy with isopropylmagnesium bromide as described previously (Scheme 1).[13] However, the route to gossypol required a pentasubstituted benzene **3** and, unlike the previous report, its preparation was not a trivial matter. We found that **2** could be metallated with ethoxyvinyllithium–HMPA[17] followed by addition of DMF to afford the intermediate formyl derivative. Reduction of the latter with $LiAlH_4$ and conversion to the methyl ether gave the tetrasubstituted phenyl oxazoline **3**. The oxazoline was removed, as described in previous studies,[16] to furnish the tetrasubstituted benzaldehyde **4** in 89% yield from **2**. A Stobbe condensation[18] followed by cyclization ($Ac_2O$–AcOH) and hydrolysis afforded the properly substituted naphthoic acid **5**. Our previous report on a model system[13] lacked the crucial substituent at C-5 in the naphthalene moiety. The naphthoic acid **5** was transformed, *via* its methyl ester **6**, to the tetramethoxynaphthoic acid **7** in 34% overall yield from starting oxazoline **1**. Conversion of **7** to the chiral oxazoline **8**[16*c*]† was performed with (*S*)-(+)-*tert*-leucinol[19] and then brominated in good yield to the bromonaphthalene **9**. This now represented the completely substituted precursor to gossypol and was subjected to the asymmetric Ullmann conditions. Heating a 40% solution of **9** in freshly distilled DMF and activated copper[20] (2 equiv.) at reflux for 1 h gave the

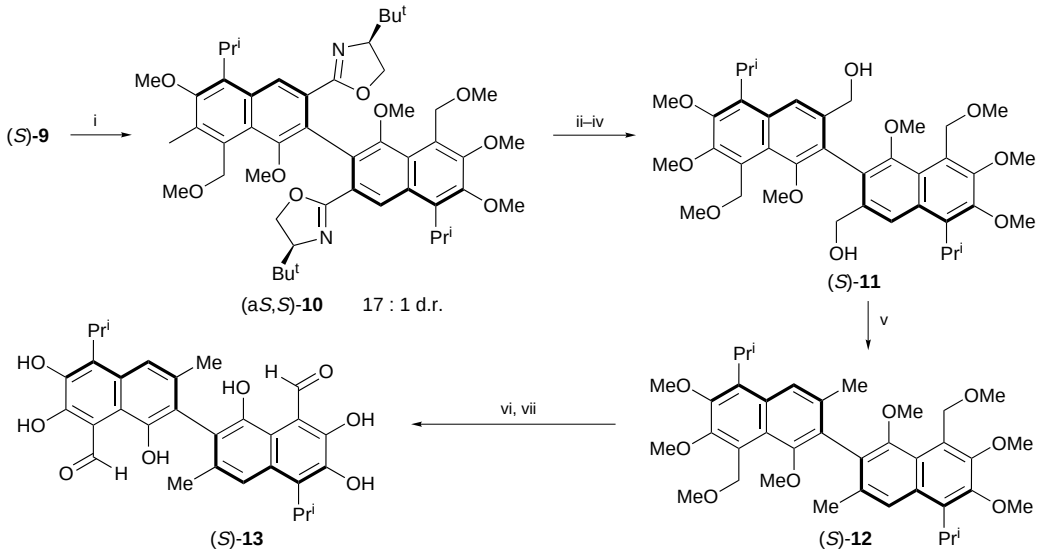



**Scheme 1** *Reagents and conditions*: i, $Pr^iMgCl$, 96%; ii, EtOCH=CHLi, DMF; iii, $LiAlH_4$; iv, NaH, MeI, 72% over 3 steps; v, $MeOSO_2CF_3$; vi, $NaBH_4$; vii, $H_2O^+$, 89% from **2**; viii, NaH, dimethyl succinate; ix, AcOH, $Ac_2O$; x, KOH, 59% over 3 steps; xi, $K_2CO_3$, $Me_2SO_4$, 97%; xii, KOH, 98%; xiii, $(COCl)_2$; xiv, (*S*)-*tert*-leucine; xv, $SOCl_2$, 87% over 3 steps; xvi, $Br_2$, AcOH, 74%

binaphthyl system **10**‡ in 80% yield (Scheme 2) as a 17 : 1 diastereoisomeric mixture (NMR; *tert*-butyl singlets integrated between $\delta$ 0.50–0.55, ± 1% after several determinations). This is in contrast to the earlier report[13] where only a 11 : 1 diastereomeric ratio was obtained using a model system. After chromatography, the pure (a*S*,*S*)-**10** was relieved of its chiral auxiliary using previously described procedures[16*c*] to afford the diol (*S*)-**11**, which was immediately reduced to the requisite dimethyl derivative (*S*)-**12**.§ The *S* configuration assigned to **12** is based upon the previous transition state models[11,12] and had to await confirmation when gossypol was reached, since its X-ray structure and chiroptical properties have been reported.[21] The final approach to (*S*)-gossypol was accomplished by cleaving all eight methyl ethers with $BBr_3$ in $CH_2Cl_2$ at −78 °C for 24 h and immediatley transforming the polyhydroxy system to the bis(formyl) derivative using Swern conditions. The product (*S*)-**13**, reached in 9% overall yield from **1**, showed all The properties¶ for gossypol described in the literature[22,23] and was reached in only six steps from the bromonaphthyl oxazoline **9**. The enantiomeric purity of synthetic gossypol, as prepared above, was assessed as 99.2 : 0.8 by preparing the Schiff base from (*S*)-phenylalanine methyl ester and comparing it to racemic gossypol.[15]‖

Although the *S* enantiomer is known to be inactive as a male fertility agent,[3] simply carrying out the above syntheses using (*R*)-(−)-*tert*-leucinol would give the other gossypol antipode.

The authors are grateful to the National Institutes of Health and the U.S. Department of Education for a fellowship




**Scheme 2** *Reagents and conditions*: i, $Cu^0$, DMF, reflux, 80%; ii, TFA; iii, $Ac_2O$; iv, $LiAlH_4$, 72% over 3 steps; v, Pd/C, $H_2$, 84%; vi, $BBr_3$; vii, DMSO, $(COCl)_2$, 81% over 2 steps

(J. W. W.). The authors also thank Dr K. Drauz of Degussa AG for generous samples of (*S*)-*tert*-leucine.

## Footnotes and References

* E-mail: aimeyers@lamar.colostate.edu

† *Selected data* for (*S*)-**8**: light yellow oil $[\alpha]_D$ −61 (*c* 1.2, $CHCl_3$); $^1$H NMR (300 MHz, $CDCl_3$) $\delta$ 0.96 (s, 9 H), 1.47 (d, 6 H, *J* 7.3), 3.40 (s, 3 H), 3.89 (s, 3 H), 3.99 (s, 3 H), 4.02–4.14 {m, 5 H [therein 4.07 (s, 3 H)]}, 4.23–4.34 (m, 2 H), 4.98 (s, 2 H), 7.49 (s, 1 H), 8.16 (s, 1 H); $^{13}$C NMR (75 MHz, $CDCl_3$) $\delta$ 31.8, 32.5, 34.9, 32.0, 43.0, 57.6, 62.1, 78.4, 75.2, 85.2, 103.9, 105.0, 119.2, 124.0, 126.3, 128.4, 133.6, 143.3, 148.6, 149.8, 158.1; $\nu_{max}$(thin film)/cm$^{-1}$ 2952, 1655, 1450, 1263, 1183, 1042; HRMS: calc. for $C_{25}H_{35}NO_5$: 429.2515. Found: 429.2520.

‡ *Selected data* for (a*S*,*S*)-**10**: light yellow oil: $[\alpha]_D$ 228 (*c* 1.9, $CHCl_3$); $^1$H NMR (300 MHz, $CDCl_3$) $\delta$ 0.55 (s, 18 H), 1.48 (d, 12 H, *J* 7.4), 3.29 (s, 6 H), 3.85 (s, 6 H), 3.98–4.04 {m, 16 H [therein 3.98 (s, 6 H), 4.03 (s, 6 H)]}, 4.30–4.37 (m, 4 H), 5.16 (s, 4 H), 7.50 (s, 2 H); $^{13}$C NMR (75 MHz, $CDCl_3$) $\delta$ 21.0, 22.1, 24.9, 27.5, 47.3, 49.3, 52.4, 59.1, 67.1, 70.6, 81.4, 109.6, 119.2, 120.8, 123.1, 132.4, 145.2, 147.9, 146.0, 150.5, 151.9, 160.1; $\nu_{max}$ (thin film)/cm$^{-1}$ 2957, 1644, 1594, 1463, 1341, 1242, 1030; calc. for $C_{50}H_{68}N_2O_{10}$: C, 70.07; H, 7.99. Found: C, 70.25; H, 7.89%.

§ *Selected data* for (*S*)-**12**: colorless oil: $[\alpha]_D$ 193 (*c* 1.4, $CHCl_3$); $^1$H NMR (300 MHz, $CDCl_3$) $\delta$ 1.51 (d, 12 H, *J* 7.3), 2.16 (s, 6 H), 3.13 (s, 6 H), 3.65 (s, 6 H), 4.08 {m, 14 H [therein 4.02 (s, 6 H), 4.11 (s, 6 H)]}, 5.35 (s, 4 H), 7.39 (s, 2 H); $^{13}$C NMR (75 MHz, $CDCl_3$) $\delta$ 24.2, 25.9, 29.1, 57.8, 62.0, 62.6, 68.4, 82.8, 103.3, 112.3, 117.2, 118.6, 120.5, 124.3, 125.9, 130.0, 134.1, 136.9; $\nu_{max}$(thin film)/cm$^{-1}$ 2957, 1654, 1602, 1459, 1290, 1246, 1034; calc. for $C_{38}H_{50}O_8$: C, 71.90; H, 7.94. Found: C, 71.95; H, 7.91%.

¶ *Selected data* for (*S*)-gossypol (*S*)-**13**: yellow powder: mp 186.1–186.9 °C (lit.,[2] 184 °C); $[\alpha]_D$ 371 (*c* 1.1, $CHCl_3$); $^1$H NMR (300 MHz, $CDCl_3$) $\delta$ 1.54 (d, 12 H, *J* 7.0), 2.14 (s, 6 H), 3.88 (septet, 2 H, *J* 6.9), 5.85 (s, 2 H), 6.39 (s, 2 H), 7.77 (s, 2 H), 11.11 (s, 2 H), 15.11 (s, 2 H); $^{13}$C NMR (75 MHz, $CDCl_3$) $\delta$ 20.5, 20.5, 28.1, 111.9, 114.9, 116.5, 118.2, 129.8, 134.0, 134.4, 143.4, 150.8, 156.0, 199.5; $\nu_{max}$(KBr)/cm$^{-1}$ 3377 (br), 1615, 1601, 1440, 1335, 1168 cm$^{-1}$; HRMS (LSIMS): calc. for $C_{30}H_{30}O_8$: 518.1941. Found: 518.1949.

‖ Racemic gossypol came from (i) a synthesis as above using achiral oxazolines, and (ii) purchased from Sigma. HPLC of the phenylalanine Schiff base from the Sigma material showed a 60 : 40 ratio of isomers, an indication that it originated from natural sources. The synthetic racemic material gave a 49 : 51 ± 1 ratio of diastereoisomers from (*S*)-phenylalanine. HPLC conditions: $C_{18}$ reverse phase, 5 μm Hypersil®-ODS, gradient MeCN–$KH_2PO_4$ (0.01 M aq.) 91 : 9 to 82 : 18; monitored at 254 nm.

1 J. Longmore, *Indian J. Chem.*, 1886, **5**, 200.
2 R. Adams, R. C. Morris, D. J. Butterbaugh and E. C. Kirkpatrick, *J. Am. Chem. Soc.*, 1938, **60**, 2191 and earlier papers.
3 National Coordinating Group on Male Fertility Agents, *China's Med.*, 1978, **6**, 417.
4 S. Z. Qian and Z. G. Wang, *Annu. Rev. Pharmacol. Toxicol.*, 1984, **24**, 329.
5 A. E. A. Joseph, S. A. Martin and P. Knox, *Br. J. Cancer*, 1986, **54**, 511.
6 T. S. Lin, R. Schinazi, B. P. Griffith, E. M. August, B. H. F. Eriksson, D. K. Zheng and W. H. Prusoff, *Antimicrob. Agents Chemother.*, 1989, **33**, 2149.
7 P. H. Dorsett and E. E. Kerstine, *J. Pharm. Sci.*, 1975, **64**, 1073; R. J. Radloff, L. M. Deck, R. E. Royer and P. L. Vanderjagt, *Pharmacol. Res. Commun.*, 1986, **18**, 1063.
8 L. V. Goryunova and S. A. Vichkanova, *Farmakol. Toksikol.*, 1969, **32**, 615.
9 C. Yu, M. Sten, M. Nordenskjold, B. Lambert, S. A. Matlin and R. H. Zhou, *Mutat. Res.*, 1986, **164**, 71.
10 (*a*) J. D. Edwards and J. L. Cashaw, *J. Am. Chem. Soc.*, 1957, **79**, 2283; (*b*) M. C. Venati, *J. Org. Chem.*, 1981, **46**, 3124; (*c*) D. A. Shirley and W. L. Dean, *J. Am. Chem. Soc.*, 1957, **79**, 1205; (*d*) P. C. Meltzer, P. H. Bickford and G. H. Lambert, *J. Org. Chem.*, 1985, **50**, 3121; (*e*) V. I. Oguyonov, O. S. Petrov, E. P. Tiholov and N. M. Mollov, *Helv. Chim. Acta*, 1989, **72**, 353.
11 T. D. Nelson and A. I. Meyers, *Tetrahedron Lett.*, 1993, **34**, 3061.
12 T. D. Nelson and A. I. Meyers, *J. Org. Chem.*, 1994, **59**, 2577; A. I. Meyers and M. J. McKennon, *Tetrahedron Lett.*, 1995, **36**, 5869.
13 A brief report on the asymmetric Ullmann coupling leading to the (+)-apogossypol hexamethyl ether, a degradation product of **13**, has appeared: A. I. Meyers and J. J. Willemsen, *Tetrahedron Lett.*, 1996, **37**, 791.
14 S. A. Matlin, R. H. Zhou, G. Bialy, R. P. Bialy, R. H. Naqvi and M. C. Lindberg, *Contraception*, 1985, **31**, 141.
15 S. A. Matlin, A. G. Belengue, R. Tyson and R. G. Brooks, *J. High Resolut. Chromatogr.*, 1987, **10**, 86.
16 Three reviews on oxazolines and their synthetic utility have appeared (*a*) A. I. Meyers and E. D. Mihelich, *Angew. Chem., Int. Ed. Engl.*, 1976, **15**, 270; (*b*) M. Reuman and A. I. Meyers, *Tetrahedron Reports*, 1985, 837; (*c*) T. G. Gant and A. I. Meyers, *Tetrahedron Reports*, 1994, 2297.
17 M. Shimano and A. I. Meyers, *J. Am. Chem. Soc.*, 1994, **116**, 10 815.
18 W. S. Johnson and G. H. Daub, *Org. React.*, Wiley, New York, 1950, vol. 1.
19 M. L. McKennon, A. I. Meyers, K. Drauz and M. Schwarm, *J. Org. Chem.*, 1993, **58**, 3568.
20 R. C. Fuson and E. A. Cleveland, *Org. Synth.*, 1955, **Coll. Vol. III**, 339.
21 L. Huang, S. Yi-Kang, G. Snatzke, D. K. Zheng and J. Zhou, *Collect. Czech. Chem. Commun.*, 1988, **53**, 2664.
22 J. W. Jarozewski, T. Strom-Hausen and L. L. Hansen, *Chirality*, 1992, **4**, 216; D. K. Zheng, Y. K. Si, J. K. Meng, L. Huang, *J. Chem. Soc., Chem. Commun.*, 1985, 168; D. S. Sampath and P. Balarem, *J. Chem. Soc., Chem. Commun.*, 1986, 649.
23 B. Brzezinski, J. Olejnk, S. Paszyc and T. F. Aripov, *J. Mol. Struct.*, 1990, **220**, 261; B. Brycki, B. Brzezinski, B. Marciniak and S. Paszyc, *Spectrosc. Lett.*, 1991, **24**, 509.

*Received in Corvallis, OR, USA, 5th May 1997; 7/03043F*

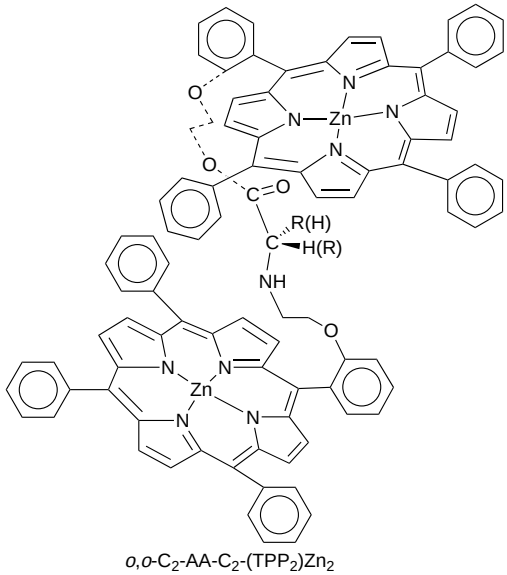
# Chiral linear assembly of amino acid bridged dimeric porphyrin hosts

**Hai-yang Liu,[a] Jin-wang Huang,[a] Xuan Tian,[b] Xiang-dong Jiao,[a] Guo-tian Luo,[a] and Liang-nian Ji*[a]**

[a] *Department of Chemistry, Zhongshan University, Guangzhou 510275, China*
[b] *National Laboratory of Applied Organic Chemistry, Lanzhou University, Lanzhou 730000, China*

**Chiral linear zinc porphyrin arrays are constructed from amino acid bridged zinc porphyrin dimers and ethylenediamine *via* self-assembly in $CHCl_3$; the induced CD sign and shape of the array are different from that of the porphyrin subunit.**

In photosynthesis, plant cells utilize arrays of up to three hundred porphyrin molecules (chlorophyll) for light capture.[1] These porphyrin chromophores are fixed spatially and orientationally by the skeleton material of the cells. The design and synthesis of artifical molecular systems aimed at mimicking the structure and/or function of photosynthetic centres has attracted much recent interest.[2] In order to construct large porphyrin arrays, a 'building block' strategy has been developed.[3] It was considered that unidimensional porphyrin arrays were particularly well-adapted to accommodate multistep electron-transfer (ET) reactions, eventually leading to long-lived and spatially-remote charge separation states. Each module consists of a porphyrin covalently attached to a chelate and transition metals have been used for making these one-dimensional multicomponent molecular systems.[4] We have synthesized a number of amino acid bridged chiral zinc porphyrin dimers *o,o*-$C_2$-AA-$C_2$-$(TPP)_2Zn_2$,[5] and here we report a facile approach to the construction of chiral linear zinc porphyrin arrays from these zinc porphyrin dimers and a bidentate ligand (ethylenediamine) in $CHCl_3$. Our 'module–linker' strategy for making one-dimensional porphyrin arrays is illustrated in Fig. 1.




*o,o*-$C_2$-AA-$C_2$-$(TPP_2)Zn_2$

R = H (AA = Gly)
R = Me (AA = Ala)
R = CH(OH)Me (AA = Thr)
R = Bn (AA = Phe)

UV–VIS spectra of metal-free porphyrin dimers *o,o*-$C_2$-AA-$C_2$-$(TPP)_2$ exhibited the usual free base porphyrin bands and the $\lambda_{max}$ values were close to those of tetraphenylporphyrin. However, Q band red-shifting (*ca.* 10–15 nm) occurred for zinc

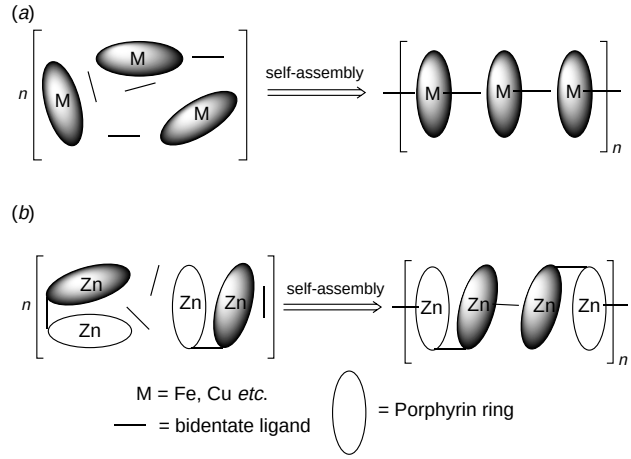



**Fig. 1** 'Module–linker' strategy used to assemble one-dimensional porphyrin arrays. The basic module is metalloporphrin monomer (*a*) or zinc porphyrin dimer (*b*) and the linker is a suitable linear bidentate ligand.

porphyrin dimers *o,o*-$C_2$-AA-$C_2$-$(TPP)_2Zn_2$ (Table 1). As the π–π interaction between two porphyrin chromophores is enhanced by metallaton,[6] the red shift indicated π–π attraction made the two zinc porphyrins adopt a head to tail arrangement in the dimer and an intramolecular exciton coupling interaction[7] existed between the two zinc porphyrins.

Split induced circular dichroism (ICD) at the soret absorption band was observed for chiral amino acid (Ala, Thr, Phe) bridged zinc porphyrin dimers *o,o*-$C_2$-AA-$C_2$-$(TPP)_2Zn_2$ and the L- and D-amino acid bridged zinc porphyrin dimers constituted pairs of enantiomers (Fig. 2). No significant ICD was observed for the corresponding free base porphyrin dimers. This strongly suggested that the ICD of these complexes was correlated to the chiral π–π stacking of the zinc porphyrins in the dimers. Namely, the observed ICD was caused by chiral exciton coupling interactions.[8]

Molecular orientation in porphyrin-based aggregates can be conveniently monitored by CD spectroscopy.[9] Here CD titration methods were used to detect the formation of the chiral porphyrin array. The ICD spectra of chiral zinc porphyrin dimers *o,o*-$C_2$-AA-$C_2$-$(TPP)_2Zn_2$ is dramatically reduced upon the addition of propylamine; this suggests that the coordination of propylamine to *o,o*-$C_2$-AA-$C_2$-$(TPP)_2Zn_2$ blocked much of

**Table 1** Electronic absorption spectrum data of *o,o*-$C_2$-AA-$C_2$-$(TPP)_2Zn_2$ (in $CHCl_3$, room temp.)

| | UV–VIS $\lambda_{max}$/nm | | |
|---|---|---|---|
| Zinc porphyrin | Soret | Q | |
| (TPP)Zn[a] | 418.3 | 547.1 | 583.9 |
| *o,o*-$C_2$-Gly-$C_2$-$(TPP)_2Zn_2$ | 418.5 | 557.1 | 599.3 |
| *o,o*-$C_2$-Ala-$C_2$-$(TPP)_2Zn_2$ | 419.9 | 556.1 | 598.1 |
| *o,o*-$C_2$-Thr-$C_2$-$(TPP)_2Zn_2$ | 421.9 | 554.9 | 594.5 |
| *o,o*-$C_2$-Phe-$C_2$-$(TPP)_2Zn_2$ | 420.1 | 553.3 | 595.3 |

[a] This work.

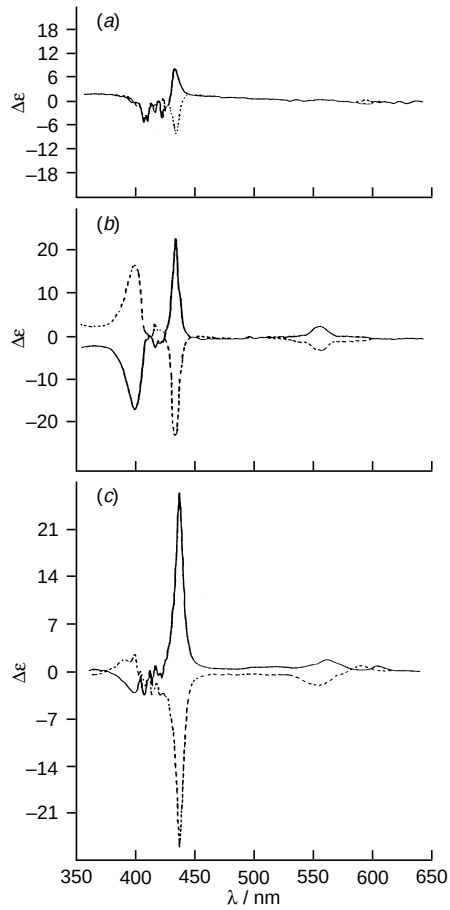



**Fig. 2** CD spectra of *o,o*-$C_2$-(L-AA)-$C_2$-$(TPP)_2Zn_2$ (——) and *o,o*-$C_2$-(D-AA)-$C_2$-$(TPP)_2Zn_2$ (- - -) in $CHCl_3$ at room temperature: (*a*) *o,o*-$C_2$-Ala-$C_2$-$(TPP)_2Zn_2$, (*b*) *o,o*-$C_2$-(Thr)-$C_2$-$(TPP)_2Zn_2$ and (*c*) *o,o*-$C_2$-Phe-$C_2$-$(TPP)_2Zn_2$

the exciton interaction.[6] The change in the ICD spectra of the system might also be due to changes in dimer conformation arising from coordination of the metal of the porphyrin, for coordination of the metal by a ligand reduces the magnitude of the π–π interaction in metalloporphyrins and generally leads to disaggregation.[10] When bidentate ligand ethylenediamine was added to a solution of *o,o*-$C_2$-AA-$C_2$-$(TPP)_2Zn_2$, however, this was not the case (Fig. 3). At the first stage of the addition (ethylenediamine : zinc porphyrin ≤ *ca.* 1 : 1), the CD sign at *ca.* 436 nm was gradually reversed with increasing ethylenediamine. With further addition of ethylenediamine, the ellipticities gradually decreased, and finally disappeared when a large excess of ethylenediamine was added. Surprisingly, when a diamine having a long connecting chain, such as 1,10-diaminodecane, was added to the solution of *o,o*-$C_2$-AA-$C_2$-$(TPP)_2Zn_2$, the ICD of the system gradually reduced and finally disappeared. No reversed ICD was observed at any [1,10-diaminodecane] : [zinc porphyrin] molar ratio. We suggest that the reversed ICD of ethylenediamine–*o,o*-$C_2$-AA-$C_2$-$(TPP)_2Zn_2$ complexes is due to the formation of relatively rigid chiral linear porphyrin arrays [Fig. 1(*b*)], since reversed ICD should have been observed for the 1,10-diaminodecane–*o,o*-$C_2$-AA-$C_2$-$(TPP)_2Zn_2$ complex if it were due to the formation of the species with the bidentate ligand binding inside the cavity of the zinc porphyrin dimer. The CD ethylenediamine titration experiments revealed that the chiral linear zinc porphyrin array [Fig. 1(*b*)] reached a maximum concentration when [ethylenediamine] : [zinc porphyrin] was *ca.* 1 : 1. At higher ethylenediamine content, this bidentate ligand would act as a monodentate ligand and would result in the dissociation of the arrays.

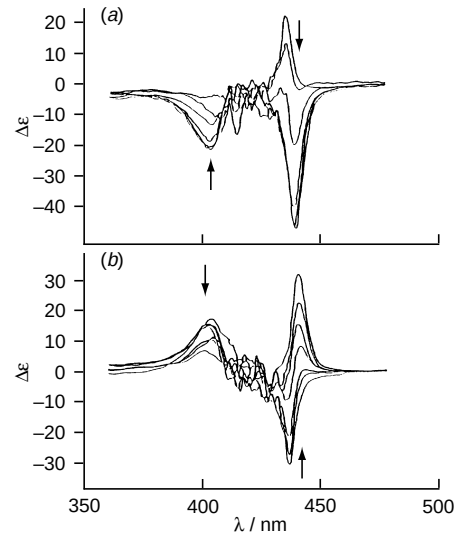



**Fig. 3** Changes in the CD spectra upon addition of ethylenediamine to a solution of *o,o*-$C_2$-Thr-$C_2$-$(TPP)_2Zn_2$ (in $CHCl_3$ at room temp., [ethylenediamine] : [zinc porphyrin] ≤ 1 : 1); (*a*) *o,o*-$C_2$(L-Thr)-$C_2$-$(TPP)_2$ and (*b*) *o,o*-$C_2$-(D-THr)-$C_2$-$(TPP)_2Zn_2$

In conclusion, we have demonstrated that chiral linear zinc porphyrin arrays can easily be built with amino acid bridged zinc porphyrin dimer and the bidentate ligand ethylenediamine in solution *via* a 'module–linker' self-assembling strategy. The present study should also be helpful for the investigation of ICD of porphyrins.[8]

This work was supported by the National Natural Science Foundation of China and Chan-an MA Education Foundation of Zhongshan University.

## Footnote and References

* E-mail: cesjln@zsulink.zsu.edu.cn

1 J. Barber and B. Anderson, *Nature*, 1994, **370**, 31.
2 E. Alessio, M. Macchi, S. Heath and L. G. Marzilli, *Chem. Commun.*, 1996, 1411; D. L. Officer, A. K. Burrell and D. C. W. Reid, *Chem. Commun.*, 1996, 1657; C. A. Hunter and R. J. Shannon, *Chem. Commun.*, 1996, 1361; H. Imohori, E. Yoshizawa, K. Yamada, K. Hagiwara, T. Okada and Y. Sakata, *J. Chem. Soc., Chem. Commun.*, 1995, 1133.
3 E. E. Bonfantini and D. L. Officer, *Tetrahedron Lett.*, 1993, **34**, 8531; H. L. Anderson, *Inorg. Chem.*, 1994, **33**, 972; V. S.-Y. Lin, S. G. Dimagno and M. J. Therien, *Science*, 1994, **264**, 1105.
4 A. Harriman and J.-P. Sauvage, *Chem. Soc. Rev.*, 1996, **25**, 41.
5 H.-y. Liu, J.-w. Huang, B. Pen, X. Tian and L.-n. Ji, *Acta Sci. Nat. Univ. Sunyatseni*, 1996, **35**, 131; Synthesis of other chiral porphyrin dimers, see T. Ema, S. Nemugaki, S. Tsuboi and M. Utaka, *Tetrahedron Lett.*, 1995, 5905; M. J. Crossley, L. G. Mackay and A. C. Try, *J. Chem. Soc., Chem. Commun.*, 1995, 1925; V. Flores, C. Nguyen, C. A. Sindelar, L. D. Vasquez and A. M. Shachter, *Tetrahedron Lett.*, 1996, 8633.
6 C. A. Hunter, P. Leighton and J. K. M. Sanders, *J. Chem. Soc., Perkin Trans. 1*, 1989, 547.
7 M. Kasha, H. R. Rawls and M. Ashraf El-Bayoumi, *Pure Appl. Chem.*, 1965, **11**, 371.
8 S. Matile, N. BeBerova, K. Nakanishi, J. Fleischhauer and R. W. Woody, *J. Am. Chem. Soc.*, 1996, **118**, 5198; T. Arai, K. Takei, N. Nishino and T. Fujimoto, *Chem. Commun.*, 1996, 2133.
9 S. Arimori, M. Takeuchi and S. Shinkai, *J. Am. Chem. Soc.*, 1996, **118**, 245; T. Imada, H. Murakami and S. Shinkai, *J. Chem. Soc., Chem. Commun.*, 1994, 1557.
10 C. A. Hunter and J. K. M. Sanders, *J. Am. Chem. Soc.*, 1990, **112**, 5525.

*Received in Cambridge, UK, 28th April 1997; 7/02876H*

# Ferrocene-containing liquid-crystalline dendrimers: a novel family of mesomorphic macromolecules

**Robert Deschenaux,*[a] Elisabeth Serrano[a] and Anne-Marie Levelut[b]**

[a] *Institut de Chimie, Université de Neuchâtel, Av. de Bellevaux 51, 2000 Neuchâtel, Switzerland*
[b] *Université Paris-Sud, Laboratoire de Physique des Solides, Bâtiment 510, 91405 Orsay Cedex, France*

**The synthesis and liquid-crystalline properties of a first-generation dendritic core substituted with six mesomorphic ferrocene units are reported; the investigated compound exhibited a broad enantiotropic smectic A phase (polarized optical microscopy, DSC, and XRD studies) and good thermal stability (thermogravimetry).**

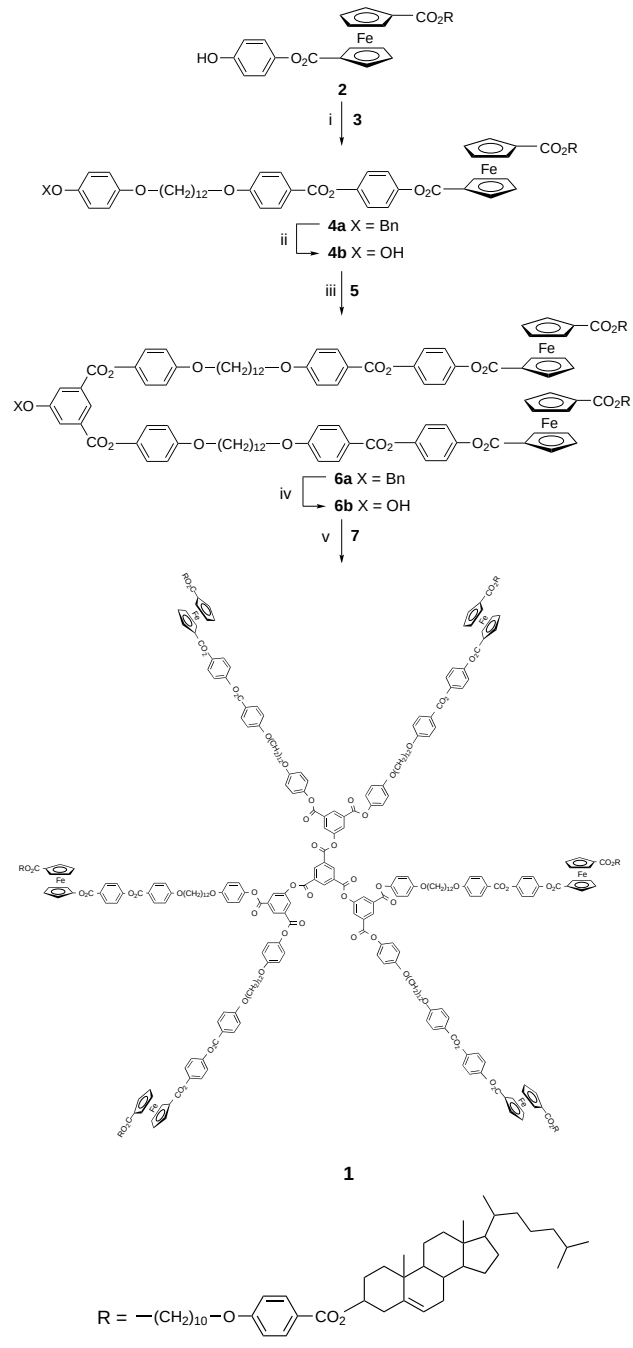
Increasing interest is currently accorded to the design and synthesis of dendrimers.[1] The possibility of creating new materials, characterized by a well defined and aesthetic macromolecular structure, displaying unique properties (such as catalysis,[2] encapsulation,[3] chiroptical activity[4] and redox activity[5]) strongly motivated these studies.

Liquid-crystalline dendrimers have been recently reported. An $AB_2$ rod-like mesogenic monomer was used to synthesize dendrimers up to the fourth generation.[6] Nematic and smectic phases were observed for these materials. First-[7] and second-generation[8] polysiloxane dendrimers were functionalized by mesogenic moieties, and showed smectic A or smectic C phases. Metal complexes were prepared from various metal ions and first- or second-generation ethyleneimine dendrimers and a hexagonal columnar phase was identified for a $Cu^{II}$ complex.[9] These novel structures form a most interesting class of anisotropic materials from a fundamental and practical viewpoint: the structural features of such compounds should lead to important basic information for a better understanding of the structure–mesomorphic properties relationship for liquid-crystalline macromolecules and, ultimately, could be exploited for elaborating new liquid-crystalline devices. To our knowledge, organometallic-type liquid-crystalline dendrimers have not been reported.

To further explore the capability of mesogenic ferrocene derivatives to act as mesomorphic building blocks for the construction of liquid-crystalline macromolecules,[10] we extended our interest to ferrocene-containing thermotropic dendrimers. This communication describes the synthesis and mesomorphic properties of the ferrocene-containing thermotropic dendrimer **1**, which represents the first organometallic-type liquid-crystalline dendrimer.

A first-generation dendrimer was selected to explore the thermal and liquid-crystalline behavior of such a new structure. A ferrocene-based cholesterol framework was used as a mesomorphic promoter owing to the high liquid-crystalline tendency of cholesterol derivatives: recently, we reported the first fullerene[60]-containing thermotropic liquid crystal obtained by derivatizing the $C_{60}$ core with a twin-cholesterol derivative.[11]

The synthesis of **1** is outlined in Scheme 1. Condensation of ferrocene derivative **2**† with 4-(4′-benzyloxyphenoxy)-dodecyloxybenzoic acid chloride **3**† gave the protected ferrocene-containing unramified sub-unit **4a**. Deprotection of the latter species under standard conditions gave the phenol derivative **4b**, which was subsequently reacted with 5-benzyloxyisophthaloyl dichloride **5**† to furnish the protected ferrocene-containing ramified branch **6a**. Removal of the benzyl protecting group under standard conditions led to the phenol intermediate **6b**. Finally, treatment of **6b** with 1,3,5-ben-




**Scheme 1** *Reagents and conditions*: i, 4-(4′-Benzyloxyphenoxy)-dodecyloxybenzoic acid chloride **3**, $Et_3N$, $CH_2Cl_2$, reflux, overnight, 96%; ii, $H_2$, Pd/C, $CH_2Cl_2$–EtOH, room temp., overnight, 96%; iii, 5-Benzyloxyisophthaloyl dichloride **5**, $Et_3N$, $CH_2Cl_2$, reflux, overnight, 73%; iv, $H_2$, Pd/C, $CH_2Cl_2$–EtOH, room temp., 2 d, 63%; v, 1,3,5-benzenetricarbonyl trichloride **7**, $Et_3N$, $CH_2Cl_2$, reflux, 24 h, 86%.

zenetricarbonyl trichloride **7** gave the targeted ferrocene-containing dendrimer **1** as an orange solid. The latter species was purified by column chromatography (silica gel, eluent: $CH_2Cl_2$–acetone–heptane 10 : 0.5 : 2 v/v/v) and crystallization ($CH_2Cl_2$–heptane). Its structure and purity were confirmed by $^1$H NMR spectroscopy and elemental analysis.‡

The thermal and liquid-crystalline properties of **1** were investigated by a combination of differential scanning calorimetry (DSC), polarized optical microscopy (POM), and X-ray diffraction studies.§

A glass transition temperature ($T_g$) was detected by DSC (second heating run) at 47 °C (onset transition) followed by an endotherm at 150 °C (peak transition, $\Delta H$ = 69.6 kJ mol$^{-1}$).

POM examinations clearly revealed the formation of a liquid-crystalline phase between $T_g$ and the endothermic peak. The latter corresponded to the clearing point. Slow cooling of the sample from the isotropic liquid into the mesophase gave rise to a focal conic texture and homeotropic areas. From these observations, the mesophase was identified as an enantiotropic smectic A phase.

The nature of the liquid-crystalline phase was clearly and unambiguously established from X-ray data. Firstly, diffraction patterns typical of disordered smectic phases, characterized by a sharp diffraction peak at the low-angle region (a second-order diffraction peak was observed in some cases) and a diffuse peak at the wide-angle region, were obtained. The layered structure was retained below $T_g$. The *d*-layer spacing was found to be 40.7 Å at room temperature and 41.3 Å at 86 °C (the sample was heated to the isotropic liquid, cooled to room temperature, and re-heated to the desired temperature). Secondly, a sample was oriented by mechanical shearing on mica close to the clearing point, and was analysed at room temperature. A diffraction pattern typical of a smectic phase, consisting of aligned equidistant sharp spots at small angles and of two diffuse arcs at wide angles, was obtained. The sharp spots are aligned along the shearing direction (meridian) and the points of highest intensity in the diffuse arcs are located in the equatorial plane. Therefore the director is parallel to the shearing direction and perpendicular to the layer planes. The mesophase is actually smectic A.

Finally, compound **1** showed good thermal stability as confirmed by thermogravimetry (10 °C min$^{-1}$, under $N_2$), which indicated that no decomposition occurred up to *ca*. 250 °C. Mass losses of 1, 5 and 10% were detected at 258, 281 and 322 °C, respectively.

The above results demonstrate that ferrocene-containing liquid-crystalline dendrimers represent a valuable family of mesomorphic macromolecules, showing a pronounced liquid-crystalline tendency and good thermal stability. Furthermore, ferrocenyl functionalized dendrimers have emerged as an interesting class of electro-active macromolecules.[5a,b] The presence of the ferrocene unit in mesomorphic dendrimers is particularly attractive with potential for elaborating dendrimer-based switchable molecular units: we have recently shown that electron transfer can be used to generate mesomorphism in the ferrocene–ferrocenium redox system.[13]

R. D. acknowledges the Swiss National Science Foundation (grant 20-45588.95) for financial support.

## Footnotes and References

† The syntheses of **2** [from ferrocene-1,1′-dicarboxylic acid chloride,[12] cholest-5-en-3β-yl-4-(10-hydroxydecyloxy)benzoate[11] and hydroquinone monobenzyl ether], **3** (from 12-bromododecanol, 4-hydroxymethyl benzoate, and hydroquinone monobenzyl ether), and **5** (from dimethyl 5-hydroxyisophthalate and hydroquinone monobenzyl ether) and thermal and liquid-crystalline properties (smectic A and/or chiral nematic phases) of all ferrocene intermediates will be described in a full report.

‡ *Selected data* for **1**: $^1$H NMR (400 MHz, $CDCl_3$): $\delta$ 9.33 (s, 3 H, arom.), 8.96 (s, 3 H, arom.), 8.37 (s, 6 H, arom.), 8.14 (d, 12 H, arom.), 7.97 (d, 12 H, arom.), 7.28 (s, 24 H, arom.), 7.15 (d, 12 H, arom.), 6.96–6.86 (m, 36 H, arom.), 5.42 (d, 6 H, C=CH, cholesteryl), 4.97 (t, 12 H, Cp), 4.91 (t, 12 H, Cp), 4.90–4.70 (sh, 6 H, CHO, cholesteryl), 4.51 (m, 24 H, Cp), 4.20 [t, 12 H, $CO_2CH_2(CH_2)_9$], 4.11–3.97 [3×t, 36 H, $(CH_2)_9CH_2O$ and $OCH_2(CH_2)_{10}CH_2O$], 2.45 (d, 12 H, cholesteryl), 2.04–0.65 (series of m, 462 H, 246 cholesteryl protons and 216 aliphatic protons). Anal. Calc. for $C_{555}H_{687}Fe_6O_{84}$ (9037.56): C, 73.76; H, 7.66. Found: C, 73.48; H, 7.69%.

§ For instrumentation, see: R. Deschenaux, I. Kosztics and B. Nicolet, *J. Mater. Chem.*, 1995, **5**, 2291; M. Veber, P. Sotta, P. Davidson, A.-M. Levelut, C. Jallabert and H. Strzelecka, *J. Phys. Fr.*, 1990, **51**, 1283.


1 D. A. Tomalia, *Adv. Mater.*, 1994, **6**, 529; G. R. Newkome, C. N. Moorefield and F. Vögtle in *Dendritic Molecules: Concepts, Syntheses, Perspectives*, VCH Verlagsgesellschaft, Weinheim, 1996.

2 C. C. Mak and H.-F. Chow, *Macromolecules*, 1997, **30**, 1228; J. W. J. Knapen, A. W. van der Made, J. C. de Wilde, P. W. N. M. van Leeuwen, P. Wijkens, D. M. Grove and G. van Koten, *Nature*, 1994, **372**, 659.

3 J. F. G. A. Jansen, E. M. M. de Brabander-van den Berg and E. W. Meijer, *Science*, 1994, **266**, 1226.

4 J. R. McElhanon, M.-J. Wu, M. Escobar and D. V. McGrath, *Macromolecules*, 1996, **29**, 8979; C. C. Mak and H.-F. Chow, *Chem. Commun*., 1996, 1185; J. F. G. A. Jansen, H. W. I. Peerlings, E. M. M. de Brabander-van den Berg and E. W. Meijer, *Angew. Chem., Int. Ed. Engl.*, 1995, **34**, 1206; D. Seebach, J.-M. Lapierre, G. Greiveldinger and K. Skobridis, *Helv. Chim. Acta*, 1994, **77**, 1673.

5 (*a*) C.-F. Shu and H.-M. Shen, *J. Mater. Chem.*, 1997, **7**, 47; (*b*) I. Cuadrado, M. Moran, C. M. Casado, B. Alonso, F. Lobete, B. Garcia, M. Ibisate and J. Losada, *Organometallics*, 1996, **15**, 5278; (*c*) M. R. Bryce, W. Devonport and A. J. Moore, *Angew. Chem., Int. Ed. Engl.*, 1994, **33**, 1761.

6 V. Percec, P. Chu, G. Ungar and J. Zhou, *J. Am. Chem. Soc.*, 1995, **117**, 11 441.

7 S. A. Ponomaremko, E. A. Rebrov, A. Yu. Bobrovsky, N. I. Boiko, A. M. Muzafarov and V. P. Shibaev, *Liq. Cryst.*, 1996, **21**, 1.

8 K. Lorenz, D. Hölter, B. Stühn, R. Mülhaupt and H. Frey, *Adv. Mater.*, 1996, **8**, 414.

9 U. Stebani, G. Lattermann, M. Wittenberg and J. H. Wendorff, *Angew. Chem., Int. Ed. Engl.*, 1996, **35**, 1858.

10 R. Deschenaux, I. Kosztics, U. Scholten, D. Guillon and M. Ibn-Elhaj, *J. Mater. Chem.*, 1994, **4**, 1351; R. Deschenaux, V. Izvolenski, F. Turpin, D. Guillon and B. Heinrich, *Chem. Commun.*, 1996, 439.

11 Th. Chuard and R. Deschenaux, *Helv. Chim. Acta*, 1996, **79**, 736.

12 F. W. Knobloch and W. H. Rauscher, *J. Polym. Sci.*, 1961, **54**, 651.

13 R. Deschenaux, M. Schweissguth and A.-M. Levelut, *Chem. Commun.*, 1996, 1275.


*Received in Bath, UK, 25th April 1997; 7/02850D*

# Spontaneous oxidation of $C_{60}Ph_5X$ (X = H, Cl) to a benzo[*b*]furanyl[60]fullerene

**Anthony G. Avent, Paul R. Birkett, Adam D. Darwish, Harold W. Kroto, Roger Taylor* and David R. M. Walton**

*The Chemistry Laboratory, CPES School, University of Sussex, Brighton, UK BN1 9QJ*

**On exposure to air, both $C_{60}Ph_5H$ and $C_{60}Ph_5Cl$ spontaneously oxidise with elimination of the hydrogen or chlorine attached to the cage and the *ortho* hydrogen of the adjacent phenyl group, giving a benzo[*b*]furanyl[60]fullerene; a second oxygen is located in the pentagon that is surrounded by phenyl groups.**

Various fused five-membered heterocyclic derivatives of fullerenes, each prepared by [3 + 2] cycloaddition reactions, have been described. The parent heterocyclic rings (or derivatives thereof) are pyrrole,[1] pyrazole,[2] triazole,[3] isoxazole,[4] oxazole,[5] isothiazole,[6] disilolane,[7] azirine[8] and furan;[9] a bis(fullerene) derivative of furan has also been described.[10] We now report the formation of a benzo[*b*]furan derivative (Fig. 1) *via* an entirely different route, involving spontaneous oxidation.

Pure $C_{60}Ph_5H$ was prepared as described previously.[11] A sample which had been in air for *ca*. one year was found to have changed colour from bright red to orange–brown. A minor component (*ca*. 10%), soluble only in acetone, contained C=O and OH groups (IR) but could not be identified further. Analysis of the remainder by HPLC (4.6 mm × 25 cm Cosmosil Buckyprep column, 1 : 1 toluene–hexane eluent at 0.25 ml $min^{-1}$) showed it to consist of two new compounds of 1060 and 1136 amu (respective retention times 46.8 and 35.8 min *cf*. 29.7 min for $C_{60}Ph_5H$). The 1060 amu species (*ca*. 30%) is unsymmetrical $C_{60}Ph_4O_2$, which fragments during EI mass spectrometry to $C_{60}Ph_n$ ($n$ = 0–4) and $C_{58}Ph_n$ ($n$ = 0–4) species, the latter arising from 2 × CO loss.[12] The structure of the 1136 amu species (*ca*. 60%) is described below, but it can also be produced by an alternative and more rapid route, involving easier purification. In this, a benzene solution of $C_{60}Ph_5Cl$ (87 mg) was exposed to sunlight for two weeks, whence all of the reagent was consumed. Chromatography ($SiO_2$, $CCl_4$) of a $CCl_4$ solution of the product gave a small quantity of orange material. Elution with toluene produced the orange–red 1136 amu species ($R_f$ = 0.57, 30 mg, 34%, needles from $CCl_4$). An OH-containing product co-eluted with a small amount of this, and there was a considerable amount of unidentified residue on the column which was removed with $CH_2Cl_2$–MeOH (9 : 1).

The EI mass spectrum (Fig. 2) of the 1136 amu species showed reproducible fragmentation involving successive loss of 16 and 14 amu species. The 16 amu fragment is clearly

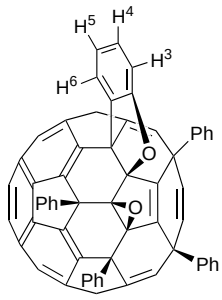



**Fig. 1** The proposed structure of $C_{60}Ph_4C_6H_4O_2$; the second oxygen probably forms an epoxide across one bond of the central pentagon, thereby introducing the required asymmetry

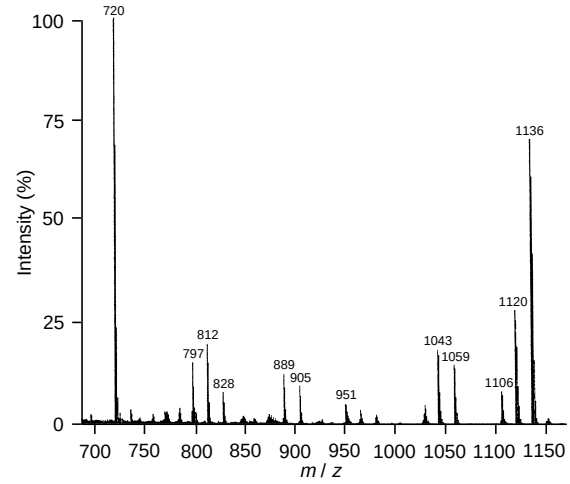



**Fig. 2** EI mass spectrum (70 eV) for $C_{60}Ph_4C_6H_4O_2$

oxygen; the 14 amu loss was shown by $^1$H NMR analysis not to be due to a methylene species. There remained the possibility that in the structure two hydrogens had been replaced by an oxygen bridge either between two *ortho* positions of adjacent phenyl groups, or between one *ortho* position and the hydrogen on the cage (in the derivation from $C_{60}Ph_5H$). The latter conjecture was proven by the $^1$H NMR spectrum (Fig. 3) with 2D-COSY analysis, and by $^{13}$C NMR spectroscopy. (In the derivation from $C_{60}Ph_5Cl$, the second oxygen replaces one *ortho* hydrogen and the chlorine on the cage.)

The *ortho*, *meta* and *para* hydrogens of four of the phenyl rings (designated A, B, C, and D) are indicated on the spectrum (Fig. 3). The spread of resonances between the positions of the rings is greater, the more downfield the signal for the *ortho*-hydrogen as noted previously for phenylated fullerenes. There

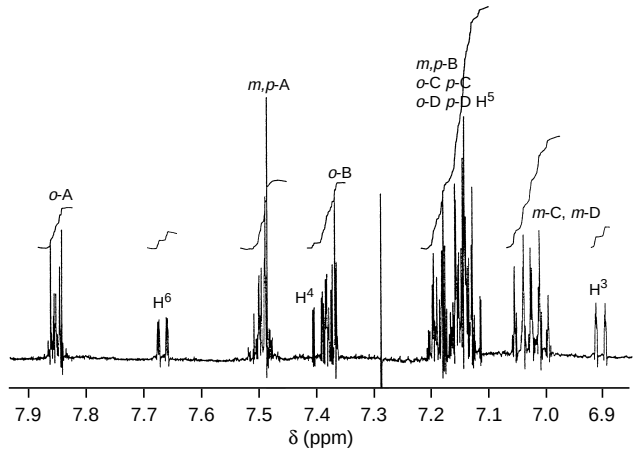



**Fig. 3** $^1$H NMR spectrum for $C_{60}Ph_4C_6H_4O_2$

are only four hydrogens present in the fifth ring and these appear at $\delta$ 7.66 (dd, *J* 7.5 and 1.3 Hz), 7.40 (dd, *J* 7.75 and 1.15 Hz), 7.12 (dd, *J* 7.40 and 1.0 Hz) and 6.90 (dt, *J* 8.12 and 0.8 Hz). These peaks are assigned (2D-COSY) to $H^6$, $H^4$, $H^5$ and $H^3$ respectively; the most downfield resonance is attributed to $H^6$, *cf.* the spectrum of 2-methylanisole.[13] Since the structure is unsymmetrical, it is probable that the remaining oxygen forms an epoxide across one of the double bonds in the pentagon at the epicentre of the phenyl groups, thereby reducing strain in this ring. One might *a priori* then expect to observe the attachment of a second oxygen across the remaining double bond in this pentagon, but this will be unfavourable due to p-orbital repulsions arising from the adjacent oxygens. This conjecture is not discounted by the indication that diepoxide formation occurs across the 1,2- and 3,4-positions of a six-membered ring (in an iridium derivative)[14] because here the greater ring size places the oxygens substantially further apart.

The 2D analysis shows that the 1,4 relationship of the four phenyl groups is D→A→C→B, but the positions relative to the epoxide in the pentagonal ring of the cage are uncertain.

The proposed structure requires that eight resonances be observed in the $sp^3$ region of the $^{13}C$ NMR spectrum. These are found at $\delta_C$ 55.86, 55.87, 58.77, 58.80, 60.24, 74.98, 81.30,and 94.49 (all 1 C). The latter two resonances can be assigned to the epoxide carbons, since reported $\delta$ values for fullerene epoxides are $\delta$ 90.18 for $C_{60}O$,[15] and 85.78 (5,6-isomer) and 92.42, 90.99 (1,2-isomer) for $C_{70}O$;[16] the resonance at $\delta$ 74.98 probably refers to the other cage carbon that bears oxygen, and that at $\delta$ 60.24 to the carbon bearing the unique aryl group. The remaining four resonances occur as two pairs, consistent with the structure.

The structure requires 52 peaks in the $sp^2$ region and these are found (all 1 C except for indicated coincidences) at $\delta_C$ 152.81, 151.44, 150.86, 150.00, 148.94, 148.92, 148.89 (2 C), 148.86, 148.73, 148.68, 148.66, 148.59, 148.53, 148.45, 148.41, 148.33, 148.27, 147.97, 147.86 (3 C), 147.81, 147.80, 147.68, 147.67, 147.60, 147.58, 145.27, 144.83, 144.75, 144.66, 144.60, 144.47, 144.46, 144.44, 144.16, 144.13, 144.09, 144.03, 143.96, 143.90, 143.86, 143.77, 143.74, 143.69, 143.62, 143.44, 143.33, 143.29, 142.63, 142.42. It requires eight pairs of resonances of 2 C intensity due to the *ortho* and *meta* carbons of the four phenyl rings, and these (confirmed by proton decoupling) occur at $\delta_C$ 129.40, 129.08, 128.92, 128.51, 128.33, 128.22, 128.18 and 128.15. The fourteen remaining 1 C resonances for the other carbons of the aryl rings occur at $\delta_C$ 157.91 (*C*–O, *cf.* 159.8 for the *ipso* carbon in anisole[17]), 138.50, 138.36, 137.25, 136.73, 130.57, 128.46, 127.74, 127.71, 127.63, 125.84, 124.59, 122.47 and 110.76.

The mechanism involved in the reactions is unclear, but a rationale can be provided for the formation of the benzo[*b*]fullerene from $C_{60}Ph_5H$. The facile light-catalysed oxidation of hydrofullerenes to fullerenols[18] is a typical alkane oxidation to alkanol which proceeds *via* intermediate formation of a hydroperoxide followed by disproportionation with a second alkane molecule. For $C_{60}Ph_5H$, this disproportionation will be sterically hindered by the adjacent phenyl groups, whereas elimination of water between the hydroperoxide and the *ortho* hydrogen of the adjacent phenyl group is sterically favourable (and also reduces steric interactions between the phenyl groups). Consistent with this explanation is the fact that preformed $C_{60}Ph_5OH$ does not form the benzo[*b*]furan derivative on standing.[19] The epoxidation of one of the double bonds in the second pentagon is a typical fullerene reaction, which may here proceed *via* intermediate formation of an endoperoxide by a standard [2 + 4] cycloaddition involving singlet oxygen (readily produced by fullerenes) as dienophile.[20]

The mechanism for the formation of the same product from the chloro precursor is presently obscure, and we plan to investigate the effect of substituents in the aryl rings upon the reaction rate, in order to clarify the mechanism.

We thank the Royal Society and the EPSRC for support.

## Footnotes and References

* E-mail: r.taylor@sussex.ac.uk


1 X. Zhang, M. Willems and C. S. Foote, *Tetrahedron Lett.*, 1993, **34**, 8187; M. Maggini, G. Scorrano, A. Bianco, C. Toniolo, R. P. Sijbesma, F. Wudl and M. Prato, *J. Chem. Soc., Chem. Commun.*, 1994, 305; X. Shi, W. B. Caldwell, K. Chen and C. A. Mirkin, *J. Am. Chem. Soc.*, 1994, **116**, 11598; T. Drovetskaya, C. A. Reed and P. Boyd, *Tetrahedron Lett.*, 1995, 7971; L.-H. Shu, G.-W. Wang, H.-M. Wu and X.-F. Lao, *Tetrahedron Lett.*, 1995, 3871; S. R. Wilson, Y. Wang, J. Cao and X. Tan, *Tetrahedron Lett.*, 1996, 775; N. Martin, L. Sanchez, C. Seoane, R. Andreu, J. Garin and J. Orduna, *Tetrahedron Lett.*, 1996, 5979; H. Imahori and Y. Sakata, *Chem. Lett.*, 1996, 199; L. Gan, D. Zhou, C. Luo, H., Tan, C. Huang, M. Lü, J. Pan and Y. Wu, *J. Org. Chem.*, 1996, **61**, 1954.

2 T. Suzuki, Q. Li, K. C. Khemani and F. Wudl, *J. Am. Chem. Soc.*, 1992, **114**, 7301; A. B. Smith, R. M. Strongin, L. Brard, G. T. Furst, W. J. Romanov, K. G. Owens and R. J. Goldschmidt, *J. Chem. Soc., Chem. Commun.*, 1994, 2187; W. Duczek and H.-J. Niclas, *Tetrahedron Lett.*, 1995, 2457; Y. Matsubara, H. Tada, S. Nagase and Z. Yoshida, *J. Org. Chem.*, 1995, **60**, 5372.

3 B. Nuber, F. Hampel and A. Hirsch, *Chem. Commun.*, 1996, 1799; J. Averdung, G. Torres-Garcia, H. Luftmann, I. Schlachter and J. Mattay, *Fullerene Sci. Technol.*, 1996, **4**, 633.

4 M. S. Meier, M. Poplawska, A. L. Compton, J. Shaw, J. P. Selegue and T. F. Guarr, *J. Am. Chem. Soc.*, 1994, **116**, 7044; H. Irngartinger, C.-M. Köhler, U. Huber-Patz and W. Krätschmer, *Chem. Ber.*, 1994, **127**, 581.

5 M. R. Banks, J. I. G. Cadogan, I. Gosney, P. K. G. Hodgson, P. R. R. Langridge-Smith and D. R. Rankin, *J. Chem. Soc., Chem. Commun.*, 1994, 1365; L.-L. Shiu, K.-M. Chien, T.-Y. Lin, G.-R. Her, S.-L. Huang and T.-Y. Luh, *J. Chem. Soc., Perkin Trans. 1*, 1994, 3355; J. Averdung, J. Mattay, D. Jacobi and W. Abraham, *Tetrahedron*, 1995, **51**, 2543.

6 D. Brizzolara, J. T. Ahlemann and H. W. Roesky, *Bull. Soc. Chim. Fr.*, 1993, **130**, 745.

7 T. Akasaka, W. Ando, K. Kobayashi and S. Nagase, *J. Am. Chem. Soc.*, 1993, **115**, 10 366.

8 J. Averdung, C. Weolff and J. Mattay, *Tetrahedron Lett.*, 1996, 4683.

9 M. Prato, T. Suzuki, H. Foroudian, G. Li, K. Khemani, F. Wudl, J. Leonetti, R. D. Little, T. White, R. Rickborn, S. Yamago and E. Nakamura, *J. Am. Chem. Soc.*, 1993, **115**, 1594; R. Gonzalez, B. W. Knight and F. Wudl, *J. Org. Chem.*, 1994, **59**, 7949; C. K. F. Shen, K.-M. Chien, T.-Y. Liu, T.-I. Lin, G.-R. Her and T.-Y. Luh, *Tetrahedron Lett.*, 1995, **36**, 5383; M. Ohno, A. Yashiro and S. Eguchi, *Chem. Commun.*, 1996, 291; N. Jagerovic, J. Elguero and J.-L. Aubagnac, *J. Chem. Soc., Perkin Trans. 1*, 1996, 499.

10 S. Lebedkin, S. Ballenweg, J. Gross, R. Taylor and W. Krätschmer, *Tetrahedron Lett.*, 1995, 4971.

11 A. G. Avent, P. R. Birkett, J. D. Crane, A. D. Darwich, G. J. Langley, H. W. Kroto, R. Taylor and D. R. M. Walton, *J. Chem. Soc., Chem. Commun.*, 1994, 1463.

12 A. D. Darwich, P. R. Birkett, G. J. Langley, H. W. Kroto, R. Taylor and D. R. M. Walton, *Fullerene Sci. Technol.*, in the press.

13 W. Brugel, *Handbook of NMR Spectral Parameters*, Heyden, London, 1979.

14 A. L. Balch, D. A. Costa, B. C. Noll and M. M. Olmstead, *J. Am. Chem. Soc.*, 1995, **117**, 8926.

15 K. M. Kreegan, J. L. Robbins, W. K. Robbins, J. M. Millar, R. D. Sherwood, P. J. Tindall, D. M. Cox, J. M. McCaulay, D. R. Jones, R. Gallagher and A. B. Smith, *J. Am. Chem. Soc.*, 1992, **114**, 1103.

16 V. N. Bezmelnitsin, A. V. Eletskii, N. G. Schepetov, A. G. Avent and R. Taylor, *J. Chem. Soc., Perkin Trans. 2*, 1997, 683.

17 P. C. Lauterbur, *J. Am. Chem. Soc.*, 1961, **83**, 1846.

18 A. D. Darwish, A. K. Abdul-Sada, G. J. Langley, H. W. Kroto, R. Taylor and D. R. M. Walton, *J. Chem. Soc., Perkin Trans. 2*, 1995, 2359.

19 P. R. Birkett, unpublished results.

20 J. March, *Advanced Organic Chemistry*, 4th edn., Wiley, Chichester, 1992, p. 830.


*Received in Cambridge, UK, 2nd June 1997; 7/03803H*

# Zirconia nanotubes

**C. N. R. Rao,* B. C. Satishkumar and A. Govindaraj**

*Solid State and Structural Chemistry Unit and CSIR Centre of Excellence in Chemistry, Indian Institute of Science, Bangalore 560 012, India*
*Jawaharlal Nehru Centre for Advanced Scientific Research, Jakkur, Bangalore 560 064, India*

**Hollow nanotubes of zirconia as well as of yttria-stabilized zirconia are successfully prepared by first coating the carbon nanotubes appropriately with the oxidic material and then burning off the carbon of the template.**

Preparation of hollow nanotubes of ceramic metal oxides is an important and challenging problem. Hollow nanotubes of silica have been recently prepared by the hydrolysis of tetraethylorthosilicate (TEOS) in a mixture of ethanol, ammonia, water and tartaric acid.[1] We were able to prepare silica nanotubes by calcining acid-treated carbon nanotubes coated with TEOS and then oxidizing the carbon at higher temperatures. The silica comprising the nanotubes was however amorphous. We considered that it would be most rewarding if we could prepare hollow nanotubes of important ceramic oxides. Here we report the first successful preparation of hollow nanotubes of both zirconia and yttria-stabilized zirconia through the use of carbon nanotubes as templates.

The procedure employed by us for preparing zirconia nanotubes is as follows. In a typical preparation, 200 mg of multi-walled carbon nanotubes (prepared by the arc evaporation of graphite[2] and subjected to heat treatment at 973 K in air for 20 min to remove other forms of carbon[3]) were refluxed in nitric acid (16 M) for 12 h to create acidic sites on the surface.[4,5] The acid-treated carbon nanotubes were reacted with 2 ml of $Zr(OPr^n)_4$ in an argon atmosphere, sonicated for 2 min and the mixture was stored in a desiccator for 48 h. The product was then washed with dilute HF (48%) followed by dry methanol, to remove the excess alkoxide, followed by drying at 373 K and calcination at 723 K in air for 12 h. This procedure yielded zirconia-coated carbon nanotubes. Fig. 1(*a*) shows a typical scanning electron microscope (SEM) image of carbon nanotubes coated with $ZrO_2$ in this manner. A transmission electron microscope (TEM) image of a zirconia-coated nanotube is shown in Fig. 1(*c*). The $ZrO_2$-coated carbon nanotubes were heated at 973 K in air for 48 h to oxidize the carbon. Thermogravimetry indicated that the carbon is oxidized around 973 K. By this means, we could obtain pure zirconia nanotubes as revealed in the SEM and TEM images of Fig. 2(*a*) and (*b*), respectively. The tube diameter is generally *ca*. 40 nm and the wall thickness is *ca.* 6 nm. The hollow nature of the nanotubes is clearly indicated by the TEM image. Electron and X-ray diffraction patterns showed the material to be composed of a 50 : 50 mixture of monoclinic and tetragonal phases. Heating to

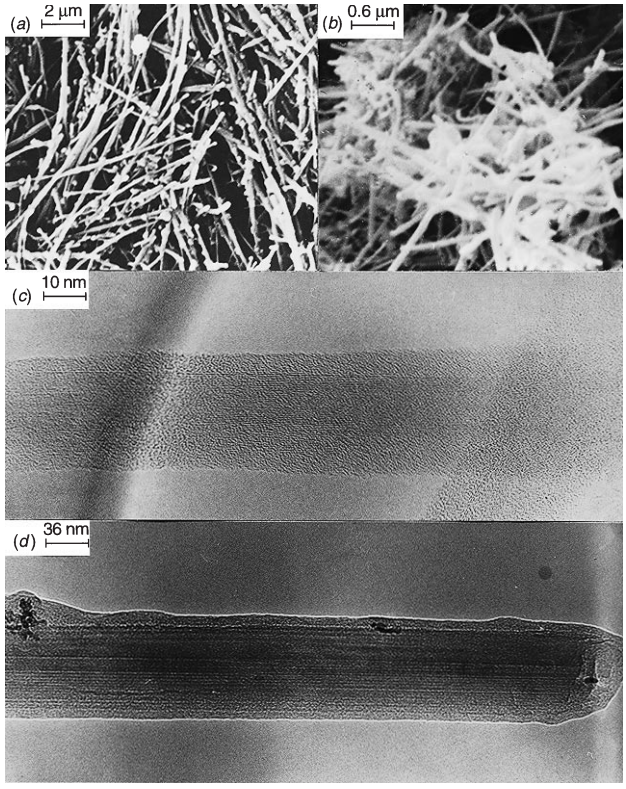



**Fig. 1** (*a*) SEM image of zirconia-coated carbon nanotubes, (*b*) SEM image of carbon nanotubes coated with stabilized zirconia, (*c*) TEM image of a zirconia-coated carbon nanotube and (*d*) TEM image of a carbon nanotube coated with stabilized zirconia

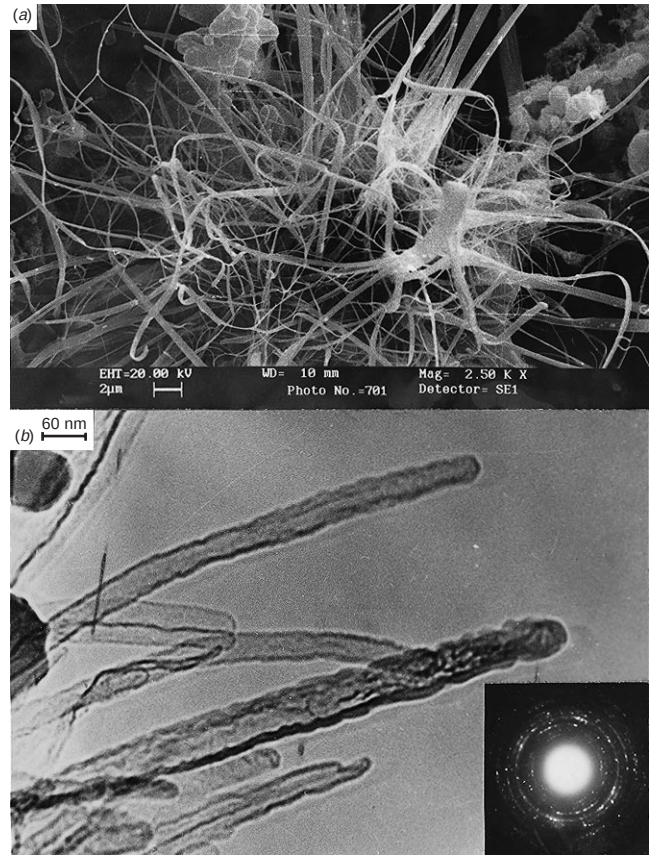



**Fig. 2** (*a*) SEM image of zirconia nanotubes, (*b*) TEM image showing hollow nanotubes of zirconia. Inset gives the electron diffraction pattern.

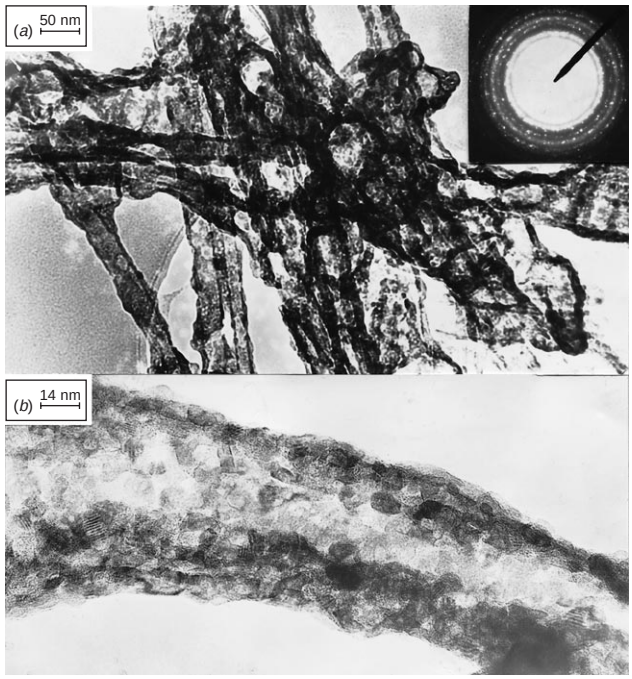



**Fig. 3** TEM images showing hollow nanotubes of stabilized zirconia. The electron diffraction pattern is shown in the inset.

high temperatures to obtain monophasic nanotubes resulted in the collapse of the nanotubes, because of the first-order nature of the monoclinic–tetragonal transformation.[6] Since this would not be a problem with stabilized zirconia, we proceeded to prepare the nanotubes of yttria-stabilized zirconia (0.92 $ZrO_2$–0.08 $Y_2O_3$) by a similar procedure.

In order to prepare the nanotubes of yttria-stabilized zirconia, 1.5 g of $ZrOCl_2 \cdot 8H_2O$ was dissolved in 10 ml of distilled water, to which 3 ml of a solution of 0.1 g of $Y_2O_3$ in 16 M $HNO_3$ was added. After cooling the solution to 273 K, the pH of solution was adjusted to 9 by the addition of ammonia, to obtain a gel. The gel was washed thoroughly with distilled water and dissolved in $HNO_3$ (1 M). 300 mg of acid-treated carbon nanotubes were stirred with this solution for 24 h. The solvent was slowly evaporated in a hot air oven, the product dried at 373 K for 12 h and then calcined at 723 K in air for 12 h. This procedure yielded carbon nanotubes coated with stabilized zirconia. Thermogravimetry showed that the carbon in the coated tubes is oxidized completely around 970 K in air.

A typical SEM image of carbon nanotubes coated with stabilized zirconia is shown in Fig. 1(*b*) and a TEM image of one such nanotube is shown in Fig. 1(*d*). We have found it desirable to treat the nanotubes coated with stabilized zirconia with ethylene glycol followed by dilute $HNO_3$, before burning off the carbon, in order to stabilize the tubular structure of stabilized zirconia. After oxidizing the carbon at 973 K, we obtained hollow nanotubes of stabilized zirconia. The TEM images in Fig. 3 show the outer diameter to vary between 40 and 50 nm, and the wall thickness to be *ca.* 6 nm. The image in Fig. 3(*b*) shows the lattice fringes of the oxide in some regions. The hollow nature of the nanotubes is also revealed in the images. The electron diffraction and X-ray diffraction patterns showed the material to possess the known cubic structure of stabilized zirconia ($a$ = 5.1164 Å). We believe that such hollow ceramic nanotubes may have several applications. We are now in the process of preparing such ceramic nanotubes starting with single-walled carbon nanotubes.

## Footnote and References

* E-mail: cnrrao@sscu.iisc.ernet.in

1 H. Nakamura and Y. Matsui, *J. Am. Chem. Soc.*, 1995, **117**, 2651; H. Nakamura and Y. Matsui, *Adv. Mater.*, 1995, **7**, 871.
2 S. Iijima, *Nature*, 1991, **354**, 56.
3 C. N. R. Rao, R. Seshadri, A. Govindaraj and R. Sen, *Mater. Sci. Eng.*, 1995, **R15**, 209.
4 R. M. Lago, S. C. Tsang, K. L. Lu, Y. K. Chen and M. L. Green, *J. Chem. Soc., Chem. Commun.*, 1995, 135.
5 C. N. R. Rao, A. Govindaraj and B. C. Satishkumar, *Chem. Commun.*, 1996, 1525.
6 C. N. R. Rao and K. J. Rao, *Phase Transitions in Solids*, McGraw-Hill, New York, 1978.

*Received in Cambridge, UK, 26th February 1997; 7/01354J*

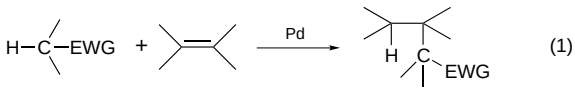
# Palladium catalysed alkylative dimerization between pronucleophiles and vinyltins

**Itaru Nakamura, Naofumi Tsukada, Mohammad Al-Masum and Yoshinori Yamamoto***

*Department of Chemistry, Graduate School of Science, and Research Center for Organic Resources and Materials Chemistry, Institute for Chemical Reaction Science, Tohoku University, Sendai 980-77, Japan*

**In the presence of catalytic amounts of $Pd_2(dba)_3$·$CHCl_3$ and dppb, the reaction of pronucleophiles 1 with vinyltins 2 gives the corresponding alkylative dimerization products of the vinyl group, 1,4-disubstituted butene derivatives 3, in good to high yields.**

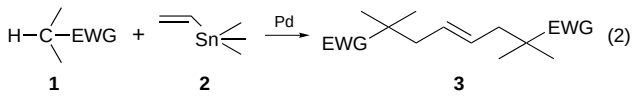
Palladium catalysed addition of carbon pronucleophiles to unactivated C–C double bonds is becoming an important new procedure for C–C bond formation[1–4] [eqn. (1)]. It has been



(1)

reported that allenes,[2] dienes[3] and enynes[4] can be used as the unactivated olefinic compounds for the pronucleophile addition.

However, until now, it was not known that simple alkenes undergo this type of addition in the presence of palladium catalysts. During this investigation, we have found that the palladium catalysed reaction of vinyltins **2** with certain pronucleophiles **1** gives the corresponding alkylative dimerization products of the vinyl group, 1,4-disubstituted butene derivatives **3** [eqn. (2)].

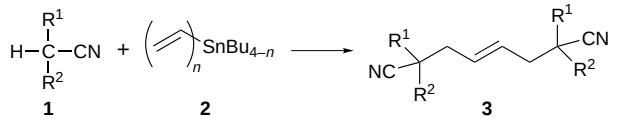


(2)

The results are summarized in the Table 1. The reaction of ethyl 2-phenyl-2-cyanoacetate **1a** (1 equiv.) with vinyltributyltin **2a** (1 equiv.) in the presence of $Pd_2(dba)_3$·$CHCl_3$ (10 mol%) dppb (20 mol%) in THF at room temperature gave the alkylative dimerization product **3a** in 51% yield (entry 1). Very interestingly, the yield of **3a** increased to 81% using divinyldibutyltin **2b** instead of **2a** (entry 2). The reaction of **1a** (1 equiv.) with **2a** (2 equiv.) produced **3a** in 51% yield, indicating that the increase of the yield in the reaction with **2b** was not due to the presence of two vinyl groups in **2b**. The reaction of **1a** with tetravinyltin **2c** afforded **3a** in 78% yield (entry 3), pointing out that the presence of two vinyl groups in the reagent molecule is enough to enhance the chemical yield. The reaction of phenylmalononitrile **1b** with **2b** produced **3b** in 89% yield (entry 4). To investigate the influence of electronic effect of phenyl substituents upon the product yield, the *para*-substituted arylcyanoacetates **1c**, **1d** and **1e** were treated with **2b** and the corresponding alkylative dimerization products **3c**, **3d** and **3e** were obtained in 75, 71 and 65% yield, respectively (entries 5–7). Therefore, electronic effects did not exert a significant influence upon the product yield. The reaction of isopropylmalononitrile **1f** with **2b** gave **3f** in 43% (entry 8). The *trans* stereochemistry of the products **3** was determined unambiguously by comparison with authentic samples prepared independently.[5] No *cis*-isomers were detected in all reactions. Other pronucleophiles, such as malononitrile, diethyl malonate and diethyl phenylmalonate, did not react with vinyltins **2**. The alkylative dimerization took place with other catalysts such as $Pd(PPh_3)_4$ and $Pd(dba)_2$, but the use of $Pd_2(dba)_3$·$CHCl_3$ gave the best result. The reaction did not proceed at all with $PdCl_2(PPh_3)_2$, $Pd(OAc)_2$, and $Pt(PPh_3)_4$ as catalyst.

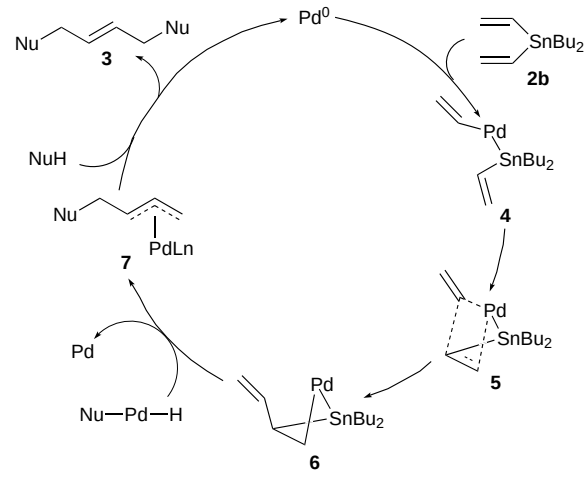
The reaction of **1a** with **2b** is representative. A mixture of $Pd_2(dba)_3$·$CHCl_3$ (51.7 mg, 0.05 mmol), dppb (42.6 mg, 0.1 mmol), ethyl 2-phenyl-2-cyanoacetate **1a** (0.09 ml, 0.52 mmol) and divinyldibutyltin **2b** (0.13 ml, 0.51 mmol) in dry THF (3 ml) was stirred under an argon atmosphere at room temperature for 2 days. The reaction was monitored by TLC analysis, and the

**Table 1** Palladium catalysed alkylative dimerization of vinyltins[a]




| Entry | Pronucleophile | | | Vinyltin | | Product | Isolated yield (%) |
|---|---|---|---|---|---|---|---|
| | | $R^1$ | $R^2$ | | *n* | | |
| 1 | **1a** | Ph | $CO_2Et$ | **2a** | 1 | **3a** | 51 |
| 2 | **1a** | Ph | $CO_2Et$ | **2b** | 2 | **3a** | 81 |
| 3 | **1a** | Ph | $CO_2Et$ | **2c** | 4 | **3a** | 78 |
| 4 | **1b** | Ph | CN | **2b** | 2 | **3b** | 89 |
| 5 | **1c** | *p*-$MeOC_6H_4$ | $CO_2Et$ | **2b** | 2 | **3c** | 75 |
| 6 | **1d** | *p*-$ClC_6H_4$ | $CO_2Et$ | **2b** | 2 | **3d** | 71 |
| 7 | **1e** | *p*-$CF_3C_6H_4$ | $CO_2Et$ | **2b** | 2 | **3e** | 65 |
| 8 | **1f** | $Pr^i$ | CN | **2b** | 2 | **3f** | 43 |

[a] The reaction of **1** (0.5 mmol) with **2** (0.5 mmol) was carried out in the presence of $Pd_2(dba)_3$·$CHCl_3$ (10 mol%) and dppb (20 mol%) in THF at room temperature.

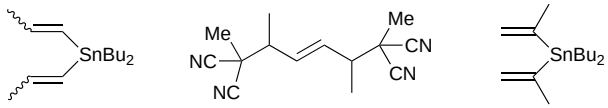



**Scheme 1**

starting materials disappeared after 2 days. The reaction mixture was purified by silica gel flash column chromatography using hexane–ethyl acetate (10 : 1) as eluent, giving the alkylative dimerization product **3a** (88.5 mg, 0.21 mmol) in 81% yield.

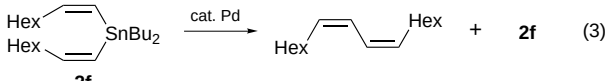
A plausible mechanism for this unprecedented alkylative dimerization reaction is shown in Scheme 1, although it is speculative. The oxidative insertion of $Pd^0$ into the carbon–tin bond of **2b** would produce the vinylpalladium intermediate **4**. The intramolecular carbopalladation to the double bond of a vinyl group would afford the allyltin–palladium complex **6** *via* **5**. It is known that the palladium catalysed reaction of allyltin with certain pronucleophiles (NuH) gives the corresponding allylation product ($CH_2$=$CHCH_2$Nu).[6] Accordingly, it is probable that **6** would react with pronucleophiles to give the π-allylpalladium complex **7**. The Trost–Tsuji type reaction of **7** with pronucleophiles (NuH) would give the butene derivatives **3**.

In order to gain an insight into the mechanism for the alkylative dimerization, the reaction of dibutyldiprop-1-enyltin **2d** with methylmalononitrile **1g** was carried out under similar




**2d** **3g** **2e**

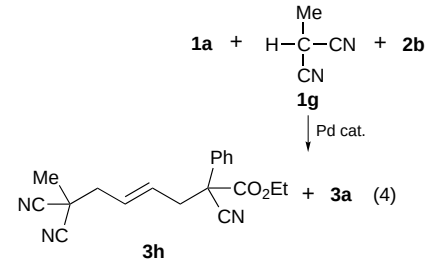
conditions as above. The alkylative dimerization product **3g** was obtained as a mixture of diastereoisomers in only 10% yield; the ratio of the diastereomers was not determined. Furthermore, the reaction of dibutyldi(1-methylethenyl)tin **2e** with **1a** did not proceed at all and the starting materials were recovered. Perhaps the carbopalladation step becomes sluggish in the reaction of **2d** (the similar step for **2b** is shown in Scheme 1, from **4** to **6**) because of the steric effect of a β-methyl subsituent, and an α-methyl substituent would stop the carbopalladation step completely, as was observed in the reaction of **2e**. Dibutyldi(*cis*-oct-1-enyl)tin **2f**, which was synthesized in our laboratory by the method reported recently,[7] was treated with $Pd_2(dba)_3$·CHCl (10 mol%) and dppb (20 mol%) in dry THF at room temperature for 1 day, and *cis,cis*-hexadeca-7,9-diene **8** was obtained in 23% yield along with recovered **2f** [eqn. (3)]. This result clearly indicates that the




**2f** 23% 14%

oxidative insertion of $Pd^0$ into the carbon–tin bond of **2f** takes place readily, although it is not clear at present how the stereoselective dimerization of the *cis*-octenyl group proceeds under the reaction conditions.[8] Although the reaction of **8** with pronucleophiles was not investigated, the reaction of certain dienes, such as buta-1,3-diene and 2-methylbuta-1,3-diene, with pronucleophiles (**1a** and **1g**) under the same reaction conditions as above gave only mono-adducts in high yields:[9] no traces of the double addition products **3** were found. This result clearly indicated that the palladium catalysed reaction of vinyltins with pronucleophiles does not form dienes as intermediates.

Finally, the reaction of **2b** in the presence of two different kinds of pronucleophiles was carried out in order to ascertain whether a second pronucleophile (Nu'H) can participate at the stage from **7** to **3** [eqn. (4)]. A mixture of **1g** (0.5 mmol), **2b** (1.0




**3h**

mmol), $Pd_2(dba)_3$·$CHCl_3$ (0.1 mmol) and dppb (0.2 mmol) in dry THF was stirred at room temperature for 30 min and then the second pronucleophile **1a** (0.5 mmol) was added. The mixture was stirred for 2 days. The cross-coupling product **3h** was obtained in 5% yield along with **3a** (50%). Since the reactivity of **1g** is lower than **1a**, the homo-coupling product **3a** was afforded as the major product. There is still room for improvement in order to produce a synthetically useful cross-coupling procedure, but the experimental results suggests that the process shown in **7**→**3** would intervene in the alkylative dimerization.

Although further investigation is needed to establish the mechanism for this unprecedented reaction, the coupling is useful for the synthesis of functionalized but-2-ene derivatives.

## Footnotes and References

* E-mail: yoshi@yamamoto1.chem.tohoku.ac.jp

1 For a review, see B. M. Trost, *Angew. Chem., Int. Ed. Engl.*, 1995, **34**, 259.
2 For allenes: Y. Yamamoto, M. Al-Masum and N. Asao, *J. Am. Chem. Soc.*, 1994, **116**, 6019; Y. Yamamoto, M. Al-Masum, N. Fujiwara and N. Asao, *Tetrahedron Lett.*, 1995, **36**, 2811; Y. Yamamoto and M. Al-Masum, *Synlett*, 1995, 969; Y. Yamamoto, M. Al-Masum and N. Fujiwara, *Chem. Commun.*, 1996, 381; Y. Yamamoto, M. Al-Masum and A. Takeda, *Chem. Commun.*, 1996, 831; M. Meguro, S. Kamijo and Y. Yamamoto, *Tetrahedron Lett.*, 1996, **37**, 7453. For other types of allene addition: B. M. Trost and V. J. Gerusz, *J. Am. Chem. Soc.*, 1995, **117**, 5156; L. Besson, J. Goré and B. Cazes, *Tetrahedron Lett.*, 1995, **36**, 3853.
3 For 1,3-dienes: K. Takahashi, A. Miyake and G. Hata, *Chem. Ind.* (*London*), 1971, 488; K. Takahashi, A. Miyake and G. Hata, *Bull. Chem. Soc. Jpn.*, 1972, **45**, 1183; O. S. Andell, J. E. Bäckvall and C. Moberg, *Acta Chem. Scand., Ser. B*, 1986, **40**, 184; P. W. Jolly and N. Kokel, *Synthesis*, 1990, 771; C. Mercier, G. Mignani, M. Aufrand and G. Allmang, *Tetrahedron Lett.*, 1991, **32**, 1433; B. M. Trost and L. Zhi, *Tetrahedron Lett.*, 1992, **33**, 1831.
4 For enynes: M. M. Salter, V. Gevorgyan, S. Saito and Y. Yamamoto, *Chem. Commun.*, 1996, 17.
5 The Mitsunobu type reaction between *trans*-but-2-en-1,4-diol and pronucleophiles produced the corresponding 1,4-disubstituted butenes. Those authentic samples were compared with the alkylative dimerization products **3**; O. Mitsunobu, *Synthesis*, 1981, 1.
6 Y. Yamamoto and N. Fujiwara, *J. Chem. Soc., Chem. Commun.*, 1995, 2013.
7 N. Asao, J.-X. Liu, T. Sudoh and Y. Yamamoto, *J. Org. Chem.*, 1996, **61**, 4568.
8 For palladium catalysed dimerization of alkenylstannanes, see S. Kanemoto, S. Matsubara, K. Oshima, K. Utimoto and H. Nozaki, *Chem. Lett.*, 1987, 5; G. A. Tolstikov, M. S. Miftakhov, N. A. Danilova, Ya. L. Vel'der and L. V. Spirikhin, *Synthesis*, 1989, 633.
9 Y. Yamamoto and N. Tsukada, unpublished work. see also ref. 3.

*Received in Cambridge, UK, 20th May 1997; 7/03463F*



Typeset and printed by Black Bear Press Limited, Cambridge, England

ChemComm
FEATURE ARTICLE

# Designer Lewis acid catalysts—bulky aluminium reagents for selective organic synthesis

**Susumu Saito and Hisashi Yamamoto***

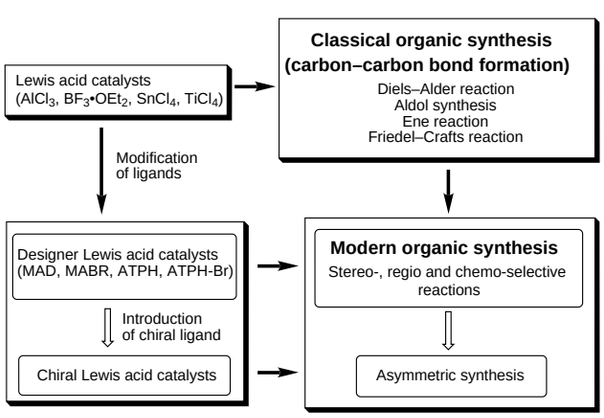
*Graduate School of Engineering, Nagoya University, Chikusa, Nagoya 464-01, Japan*

**Sterically hindered aluminium aryloxides have been developed as designer Lewis acid catalysts for stereo-, regio- and chemo-selective carbon–carbon bond-forming reactions. Compared with classical Lewis acids, these aluminium reagents coordinate strongly with various oxygen-containing substrates, and this coordination is affected by the steric environment of their ligands. The carbonyl groups of the bound substrates are either electronically activated or sterically deactivated depending on the aluminium reagent used and the type of reaction. Designer chiral catalysts based on the structure of these bulky aluminium reagents have also been examined.**

## Introduction

Lewis acid-promoted carbon–carbon bond-forming reactions are some of the most important processes in organic synthesis. Traditionally, the Friedel–Crafts reaction,[1] the ene reaction,[2] the Diels–Alder reaction[3] and the Mukaiyama aldol synthesis[4] are catalysed by ordinary Lewis acids such as $AlCl_3$, $TiCl_4$, $BF_3$, and $SnCl_4$. These classical Lewis acids activate a wide variety of functional groups and the reactions usually proceed efficiently but with relatively low stereo-, regio- and chemoselectivities. The relatively simple design of ligands for these Lewis acids leads to monomeric Lewis acids in organic solvent and consequently to high Lewis acidity and reactivity. Furthermore, upon coordination with designed ligand(s), the well designed Lewis acid exhibits new selectivity (Scheme 1).

Several bulky aluminium reagents can be prepared from sterically hindered phenols. Most aluminium reagents in solution exist as dimeric, trimeric, or higher oligomeric structures.[5] In contrast, methylaluminium bis(2,6-di-*tert*-butyl-4-methylphenoxide) (MAD)[6] and aluminium tris(2,6-diphenylphenoxide) (ATPH)[7] are monomeric in organic solvents. The Lewis acidity of these reagents decreases with the coordination of more electron-donating aryloxides, but this can be compensated for by loosening of the aggregation. Compared with classical Lewis acids, the steric effect of our aluminium reagents also plays an important role in selective organic synthesis, which is the subject of this article.



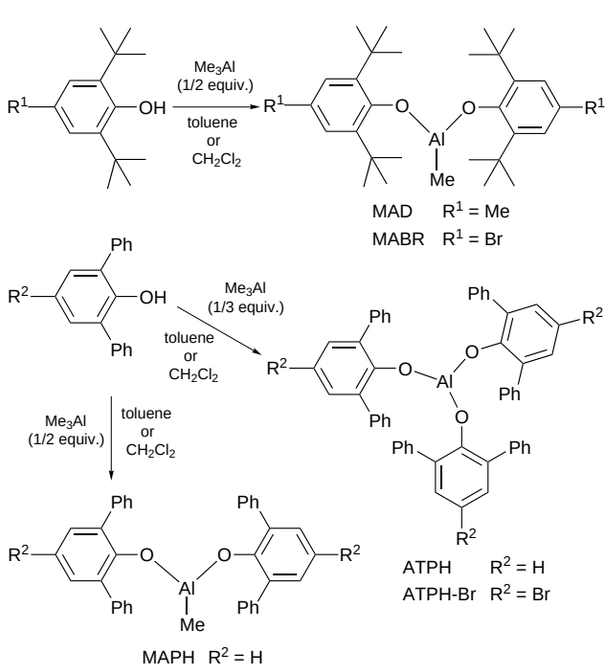

**Scheme 1**

## Preparation of various aluminium phenoxides

MAD, ATPH, methylaluminium bis(4-bromo-2,6-di-*tert*-butylphenoxide) (MABR)[8] and methylaluminium bis(2,6-diphenylphenoxide) (MAPH)[9] are readily prepared by treatment of $Me_3Al$ with a corresponding amount of the phenol in toluene (or in $CH_2Cl_2$) at room temperature for 0.5–1 h with rigorous exclusion of air and moisture. These reagents can be used without further purification for all of the reactions described here. The reactivity of a phenol toward $Me_3Al$ largely depends on the steric limitations of the phenol. For example, treatment of 3 equiv. of 2,6-di-*tert*-butyl-4-methylphenol with $Me_3Al$ in $CH_2Cl_2$ at room temperature under argon results in the generation of bis(phenoxide) MAD together with the unreacted phenol. In contrast, 3 equiv. of 2,6-diphenylphenol react completely with 1 equiv. of $Me_3Al$ to produce the tris(phenoxide) ATPH (Scheme 2).

## Structural features of ATPH

The X-ray crystal structure of the *N*,*N*-dimethylformamide (DMF)–ATPH complex[7] disclosed that the three arene rings of ATPH form a propeller-like arrangement around the aluminium centre, and hence ATPH has a cavity with $C_3$ symmetry. By contrast, the X-ray crystal structure of the benzaldehyde–ATPH complex shows that the cavity surrounds the carbonyl substrate upon complexation with slight distortion from $C_3$ symmetry. A




**Scheme 2**

particularly notable structural feature of these aluminium–carbonyl complexes is the Al–O–C angles and Al–O distances (Fig. 1), which clarify that the size and the shape of the cavity changes flexibly depending on the substrates. According to these models, the cavity should be able to differentiate between carbonyl substrates, which, when accepted into the cavity, should exhibit unprecedented reactivity under the steric and electronic environment of the arene rings. $^1$H NMR analysis of the crotonaldehyde–ATPH complex (300 MHz, $CD_2Cl_2$) revealed that the original chemical shifts of the aldehydic proton ($H_a$) at $\delta$ 9.50, and the α- and β-carbon protons ($H_b$ and $H_c$) at $\delta$ 6.13 and 6.89, were significantly shifted upfield to $\delta$ 6.21, 4.92 and 6.40, respectively. The largest $\Delta\delta$ value of $H_a$ of 3.29 suggests that the carbonyl is effectively shielded by the arene rings of the cavity. This observation is in contrast to the resonance frequencies of the crotonaldehyde–$Et_2AlCl$ complex at −60 °C ($H_a$: $\delta$ 9.32; $H_b$: $\delta$ 6.65; $H_c$: $\delta$ 7.84), and those of crotonaldehyde complexes with other ordinary Lewis acids.[10]

**Molecular recognition with bulky aluminium reagents**

The monomeric aluminium phenoxides have sufficient Lewis acidity and thus bind with polar functionalities. The complexation is heavily dependent on the structural features of these functional groups. Thus, functional groups on the outside of a molecule bind to bulky aluminium reagents rather tightly, while functional groups on the inside of a molecule will not form stable complexes. In other words, the steric bulk of aluminium reagents appears to play a crucial role in discriminating between structurally or electronically similar substrates.

*Discrimination of two different ethers*

The 125 MHz $^{13}$C NMR spectrum of a mixture of 1 equiv. each of MAD, methyl 3-phenylpropyl ether **1**, and ethyl 3-phenylpropyl ether **2** in $CDCl_3$ (0.4 M solution) at −50 °C (Scheme 3) showed that the original signal of methyl ether **1** at $\delta$ 58.7 shifted downfield to $\delta$ 60.1, whereas the signal of the α-methylene carbon of ethyl ether **2** remained unchanged. This unusual selectivity could not be observed with other Lewis acids as shown below. This method could be extended to the use of a polymeric aluminium aryloxide in complexation chromatography: heteroatom-containing solutes can be separated by complexation with a stationary, insolubilized organoaluminium polymer.[11]

*Discrimination of two different ketones*

Selective reduction of more hindered or electronically less polarizable ketones can be accomplished using MAD as a selective stabilizer of the carbonyls of less hindered or electronically more polarizable ketones.[12] Treatment of 1.0 equiv. each of acetophenone **3** and pivalophenone **4** in $CH_2Cl_2$ with 1.0 equiv of MAD at −78 °C, followed by subsequent addition of diisobutylaluminium hydride (DIBAL-H) at this temperature yielded alcohols **5** and **6** in a ratio of 1 : 10 (Scheme 4). Selective coordination of MAD with **3** was observed by $^{13}$C NMR spectroscopy. These results suggest that the tight binding of MAD with sterically less congested **3** inhibited the attack of DIBAL-H at the carbonyl of **3**.

*Discrimination of two different esters*

Discrimination between two different ester carbonyls can be similarly achieved with MAD.[13] For example, reaction of *tert*-butyl methyl fumarate **7** with 1.1 equiv. of MAD in $CH_2Cl_2$ at −78 °C gave organoaluminium–fumarate complex **8** exclusively (Scheme 5), the structure of which was rigorously established by low-temperature $^{13}$C NMR spectroscopy. Diels–Alder reaction of complex **8** with cyclopentadiene at −78 °C in

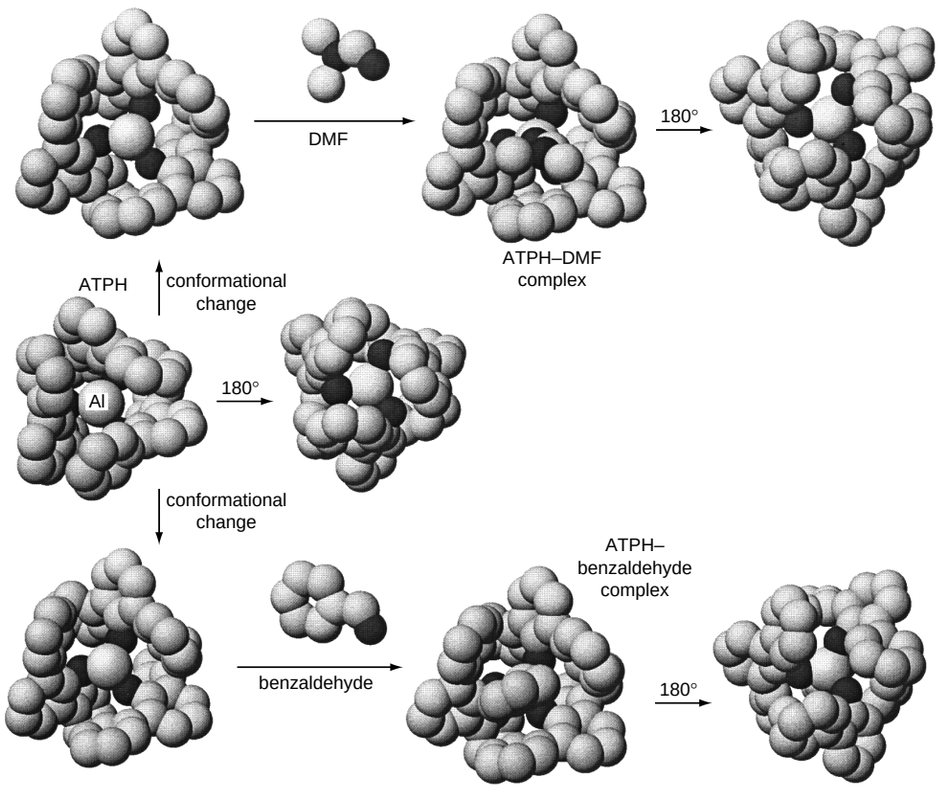
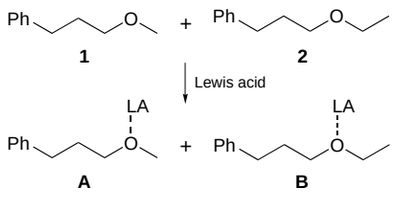


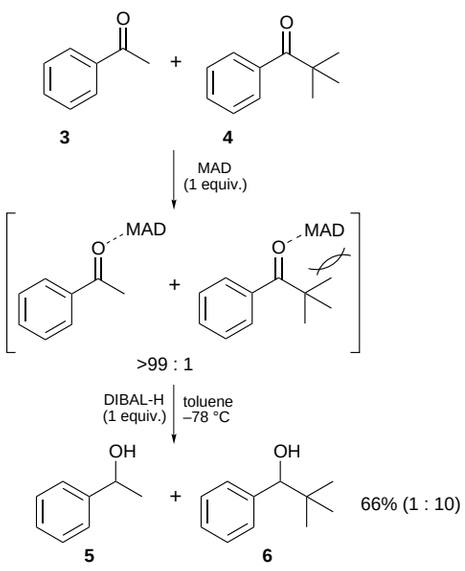

**Fig. 1** Schematic complexation processes of DMF and benzaldehyde with ATPH, and the X-ray crystal structures of the ATPH–DMF and ATPH–benzaldehyde complexes. The protons are omitted for clarity. Front side view [looking down the O($sp^2$)–Al bond] and back side view [180° rotation from the front side view around the axis perpendicular to the O($sp^2$)–Al bond] are shown. Selected distances (Å) and angles (°): ATPH–DMF: Al–O($sp^3$)–C 135.6(8), Al–O($sp^2$)–C 138.1(3), Al–O($sp^3$) 1.711(3), Al–O($sp^2$) 1.795. ATPH-benzaldehyde: Al–O($sp^3$)–C 149.6(5), 136.1(5) and 144.1(5), Al–O($sp^2$)–C 135.7(9), Al–O($sp^3$) 1.694(3), 1.728(5) and 1.709(5), Al–O($sp^2$) 1.856(5).

toluene gave, after 1 h, cycloadduct **9**, predominantly with *endo* orientation of the methoxycarbonyl group. Thus, the methyl ester coordinated with the aluminium reagent gave us high *endo*-selectivity of the Diels–Alder reaction. Even methyl and isopropyl or methyl and ethyl can be fairly well discriminated with MAD.




| Lewis acid | **A** : **B** |
|---|---|
| MAD | >99:1 |
| $Bu^i_3Al$ | 4 : 1 |
| $SnCl_4$ | 2 : 1 (ether : Lewis acid = 2:1) |
| $BF_3{\bullet}OEt_2$ | no complexation |
| $BEt_3$ | 5 : 3 |

**Scheme 3**

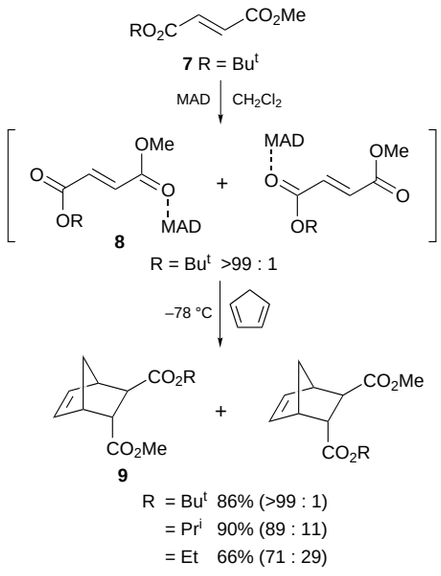



**Scheme 4**

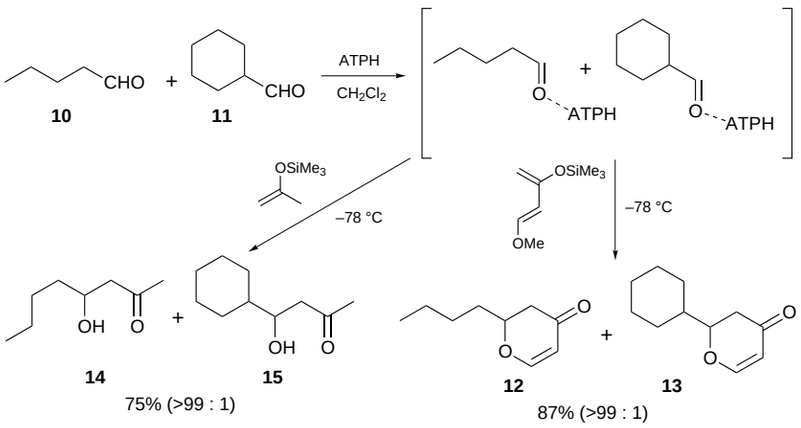
*Discrimination of two different aldehydes*

ATPH can discriminate between structurally similar aldehydes, thereby facilitating the selective functionalization of the less hindered aldehyde carbonyl.[14] Treatment of an equimolar mixture of valeraldehyde **10** and cyclohexanecarboxaldehyde **11** with 1.1 equiv. of ATPH in $CH_2Cl_2$ at −78 °C, followed by addition of Danishefsky's diene at this temperature, gave hetero-Diels–Alder adducts **12** and **13** in a ratio of >99 : 1 (Scheme 6). It should be noted that only the complexed aldehyde could react with the diene. The reaction gave relatively low chemoselectivity with other typical Lewis acids: [**12** : **13** ratios: $(Pr^iO)_2TiCl_2$ = 6.2 : 1; $Me_3Al$ = 5 : 1; MAD = 3.7 : 1; $TiCl_4$ = 2 : 1; $BF_3{\cdot}OEt_2$ = 1.3 : 1; MAPH = 1 : 3.4]. This fact emphasizes that the cavity of ATPH plays an important role in differentiating between the reactivities of the two different aldehydes. In a similar manner, the aldol reaction of a mixture of **10** and **11** was effected equally well with ATPH to furnish 4-hydroxyoctan-2-one **14** without **15**.

Obviously, the coordinated aldehyde is electronically activated but sterically deactivated with bulky aluminium reagents. The selective functionalization of more sterically hindered aldehydes was accomplished by the combined use of MAPH and alkyllithiums (RLi; R = $Bu^n$ or Ph) (Scheme 7).[15] In this system, MAPH acted as a carbonyl protector of a less hindered aldehyde such as **10**, and therefore the carbanions preferentially




**Scheme 5**




**Scheme 6**

react with more hindered carbonyl groups. It should be noted that alkyllithium reagents could react with aldehydes in the absence of the aluminium reagent.

**Bulky aluminium reagents for selective organic syntheses**

So far we have discussed the discriminating abilities of aluminium reagents. In this section, we will focus on the reactions promoted with bulky aluminium reagents which could not be achieved with ordinary Lewis acid catalysts.

*Conjugate addition to α,β-unsaturated carbonyl compounds*

Organocuprates are the most widely used reagents for Michael addition to α,β-unsaturated ketones, one of the most powerful and important carbon–carbon bond-forming reactions. ATPH can be used as a carbonyl protector upon complexation, which facilitates 1,4-addition to even α,β-unsaturated aldehydes,[10] for which 1,4-addition is virtually unexplored. Complexation of cinnamaldehyde **12** with 1.1 equiv. of ATPH in $CH_2Cl_2$ at −78 °C, followed by subsequent addition of 1.5 equiv. of *n*-butylmagnesium bromide ($Bu^nMgBr$), gave the 1,4-addition product preferentially (Scheme 8). The alkylation of **12** with MAD and $Bu^nMgBr$ gave unsatisfactory results (95%; 1,4 : 1,2 adduct ratio = 7 : 93). The combination of MAPH with the same butylating agent gave an equal mixture of 1,4- and 1,2-adducts (98%; ratio = 49 : 51). Replacing organomagnesium reagents with organo-calcium, -strontium and -barium reagents enhanced 1,4-selectivity. One of the advantages of this method over organocopper-mediated conjugate addition is the availability of lithium alkynides and thermally unstable lithium carbenoids as Michael donors. With alkynides, raising the reaction temperature after the Michael addition triggered cyclopropanation to give a sole diastereoisomer (Scheme 9).

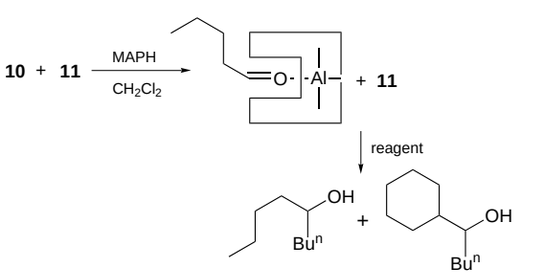
Application of this system to α,β-unsaturated ketones gave even more general and pronounced 1,4-selectivity ( > 99 : 1).[16] In this case, various alkyllithiums can be used as Michael donors, and this ATPH–RLi system enables the introduction of perfluoroalkyl or perfluoroaryl substituents at the β-positions of carbonyl functions (Scheme 10).[17]

Several ketone lithium enolates and the dianions of β-dicarbonyl substrates similarly undergo highly selective 1,4-addition to various α-enones. Thus, tandem inter- and intramolecular Michael addition using the enolates of α,β-unsaturated ketones as Michael donors[18] was achieved successfully: treatment of **13**–ATPH complex in toluene with a THF solution of the benzylideneacetone lithium enolate at −78 °C, followed by refluxing for 13 h, gave stereochemically homogeneous annulation product **14** in 50% yield ( > 84% de) (Scheme 11).

Michael addition of the dianions derived from β-dicarbonyl compounds facilitated another annulation: Michael addition of a dianion, followed by intramolecular aldol condensation.[19] Complexation of ATPH with *trans*-chalcone **15** in $CH_2Cl_2$ at −78 °C, followed by treatment with the dianion of methyl acetoacetate gave, after quenching with aq. HCl, bicyclic product **16** in high yield (Scheme 12). This system can also be used for elaboration of the bicyclo[3.5.1]undecane ring system in **17**, which can be found in the backbones of terpenoids[20] and the taxol family.[21]

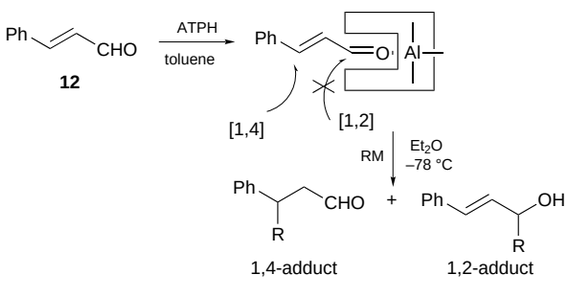
The exceedingly bulky aluminium reagent aluminium tris(2,6-di-*tert*-butyl-4-methylphenoxide) (ATD)[22] was superior to ATPH or MAD as a carbonyl protector in ynones.[23] Initial complexation of oct-3-yn-2-one **18** in toluene with ATD and subsequent addition of a hexane solution of $Bu^nLi$ at −78 °C generated 1,4-adduct **19** in 92% yield together with a small amount of the 1,2-adduct (Scheme 13).

Selective 1,6-addition of alkyllithiums to aromatic carbonyl substrates such as benzaldehyde or acetophenone was achieved with ATPH to give cyclohexadienyl compounds **20** and **21**, respectively (Scheme 14).[24] According to the molecular structure of the benzaldehyde–ATPH complex (Fig. 2), it is



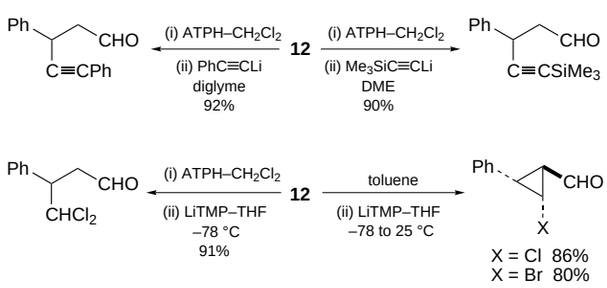

| | |
|---|---|
| $Bu^nTi(OPr^i)_3$ (1 equiv.) | 31% (2.5:1) |
| MAPH (1 equiv.)/ $Bu^nLi$ (1 equiv.) | 76% (1:6.5) |
| MAPH (2 equiv.)/ $Bu^nLi$ (2 equiv.) | 45% (1:14) |

**Scheme 7**

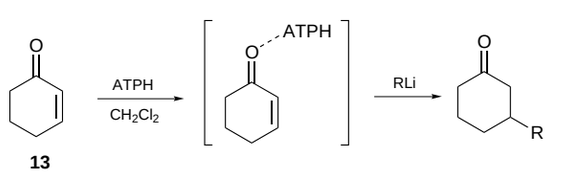



| | | |
|---|---|---|
| RM = | $Bu^nLi$ | 92% (49:51) |
| | $Bu^nMgCl$ | 99% (90:10) |
| | $Bu^nCal$ | 88% (98:2) |
| | $Bu^nSrI$ | 60% (95:5) |
| | $Bu^nBal$ | 97% (97:3) |

**Scheme 8**

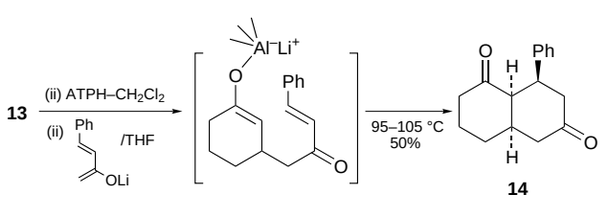



**Scheme 9**

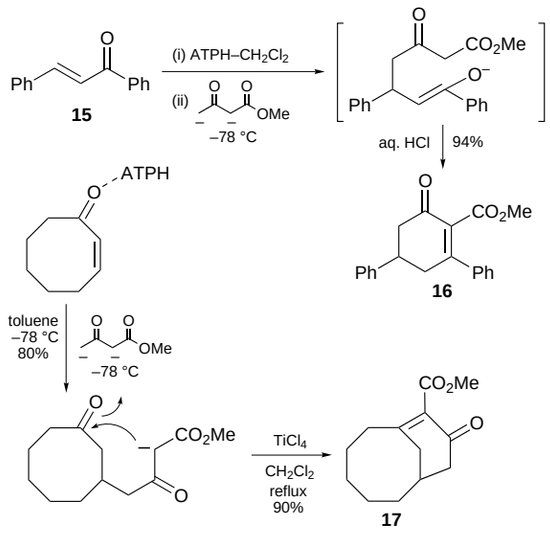



RLi = MeLi (83%), PhLi (86%), PhC≡CLi (99%), $Cl_3CLi$ (60%), $CF_3CF_2Li$ (75%)

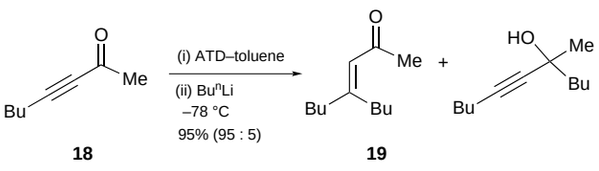
**Scheme 10**




**Scheme 11**

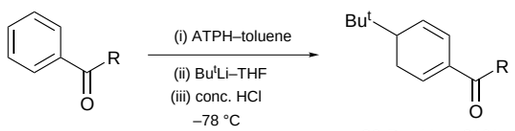



**Scheme 12**




**18** **19**

**Scheme 13**




**20** R = H 81%
**21** R = Me 93%

**Scheme 14**

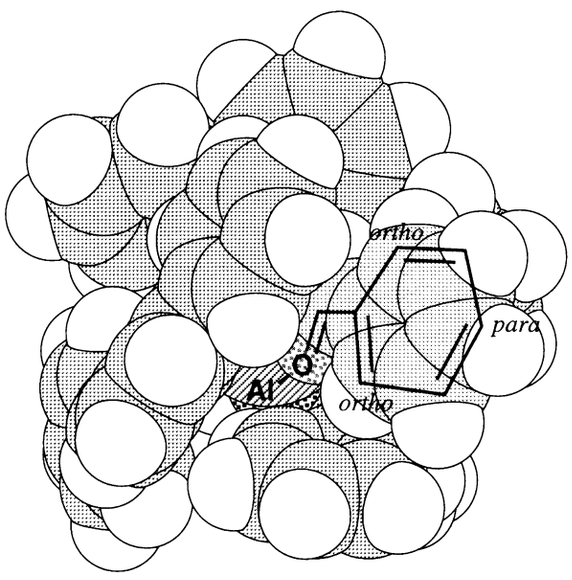



**Fig. 2** X-Ray crystal structure (space-filling model) of the ATPH–benzaldehyde complex, which shows the more facile nucleophilic attack at the *para*-position

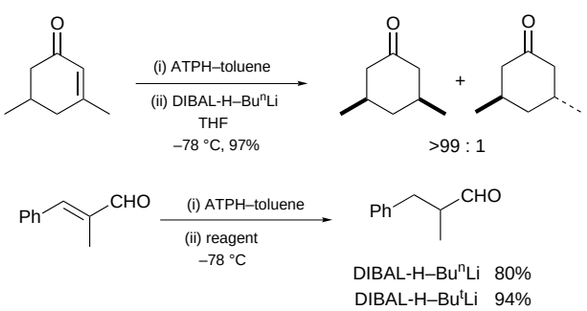
obvious that the *para* position of benzaldehyde is deshielded by the three arene rings, which effectively block the *ortho* position and the carbonyl carbon from nucleophilic attack.

Efficient conjugate reduction of several α,β-unsaturated carbonyl substrates was similarly realized by the combined use of ATPH and diisobutylaluminium hydride–butyllithium 'ate' complex (DIBAL-H–BunLi) as a reducing agent (Scheme 15).[25] Diisobutylaluminium hydride–*tert*-butyllithium (DIBAL-H-ButLi) was more effective for the 1,4-reduction of α,β-unsaturated aldehydes.

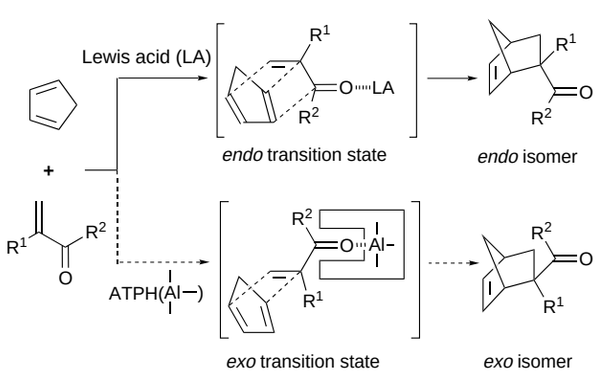
*exo-Selective Diels–Alder reaction*

One characteristic stereochemical feature of the Diels–Alder reaction is *endo* selectivity. The origin of the *endo* preference in Diels–Alder reactions can be ascribed to 'secondary orbital interactions'. If the carbonyl functions of dienophilic α,β-unsaturated carbonyl substrates are effectively shielded by complexation with ATPH, secondary interaction is decreased, thereby disfavouring the hitherto preferred *endo* transition state (Scheme 16).

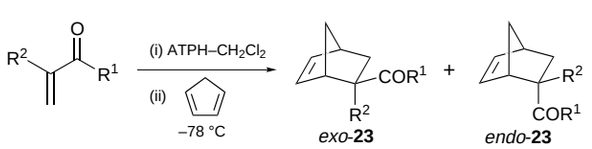
As expected, precomplexation of α,β-unsaturated ketone **22a** with ATPH in $CH_2Cl_2$ at −78 °C, followed by cyclization with cyclopentadiene, resulted in stereochemical reversal to furnish *exo*-**23a** as a major product (Scheme 17). Similarly, the Diels–Alder reaction with other dienophiles **22b,c** complexed with ATPH exhibited *exo* selectivity.[26]




**Scheme 15**




**Scheme 16**




**22a** $R^1$ = Ph, $R^2$ = H **a** 81% (73:27)
**b** $R^1$ = Ph, $R^2$ = Me **b** 81% (96:4)
**c** $R^1$ = $R^2$ = Me **c** 87% (87:13)

**Scheme 17**

This concept was extended intramolecularly to give *trans*-fused stereoisomer **25**, while an ordinary aluminium reagent gave *cis*-isomer **24** *via* an *endo* transition state (Scheme 18).

*Stereoselective and asymmetric Claisen rearrangement*

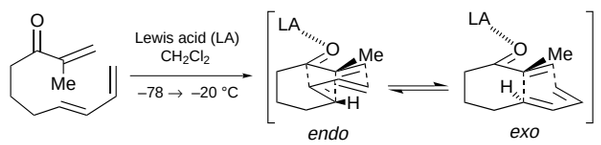
Claisen rearrangement[27] is accelerated significantly with bulky aluminium reagents. With MABR, the rearrangement of 1-substitutedprop-2-enyl vinyl ether derivatives **26**–**28** takes place in a few seconds even at −78 °C to give the (*Z*)-alk-4-enols after reduction with $NaBH_4$ (Scheme 19). When MABR is replaced by MAPH, (*E*)-isomers are formed preferentially.[28] This stereochemical reversal observed with MABR and MAPH can be accounted for by the two possible chair-like transition state structures *ax*-**29** and *eq*-**29**, respectively,[28,29] which are suggested by the absolute configuration of the double bonds and the allylic carbons of the produced aldehydes (Scheme 20).

Optically pure aluminium reagent (*R*)-**30** was synthesized from 1 equiv. each of (*R*)-(+)-3,3′-bis(triarylsilyl)-1,1′-bi-2-naphthol and $Me_3Al$,[30] based on the structure of MAPH. Chiral (*R*)-**30** is an excellent promoter for the asymmetric Claisen rearrangement of allyl vinyl ethers **31** or **32** which possess bulky substituents such as trialkylsilyl or trialkylgermyl groups,[31] but is totally ineffective for sterically less hindered substrates (Scheme 21).

Claisen rearrangement is considered to proceed *via* a six-membered transition state.[27,32] The preferential conformation of the reactant in the transition state might be due to the shape and the size of the cavity of ATPH. This hypothesis can be verified by treatment of 1-butylprop-2-enyl vinyl ether **33** with ATPH at 0 °C to give isomeric rearrangement products (*E*)- and (*Z*)-**34** in 87% yield in a ratio of 16 : 1 (Scheme 22). MAPH-mediated rearrangement of **33** gave fairly good stereoselectivity [(*E*)-**34** : (*Z*)-**34** = 5 : 1].

The effect of the electron-withdrawing group of the ATPH ligands on stereoselectivity and acceleration of the rearrangement was also investigated.[33] The rearrangement of **33** with ATPH-Br proceeded with prominent stereoselectivity [−78 °C, 13 h; (*E*)-**34** : (*Z*)-**34** = > 200 : 1], which suggests that both the cavity and the high Lewis acidity are responsible for the high degree of stereocontrol. The rearrangement of (*E*)-**35** and (*Z*)-**35** with various aluminium reagents indicates that the reaction rate was significantly enhanced with ATPH-Br to give **36** almost quantitatively (Scheme 23).

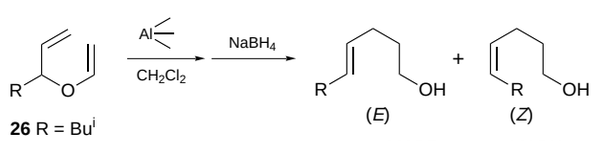
The catalytic Claisen rearrangement of 1,1-dimethyl-3-phenylprop-2-enyl vinyl ether **37** was achieved with 5–10 mol% of ATPH-Br by taking advantage of its high Lewis acidity




**24** *cis* isomer **25** *trans* isomer

| Lewis acid = | $Me_3Al$ | 75% (88:12) |
|---|---|---|
| | ATPH | 69% (4:96) |

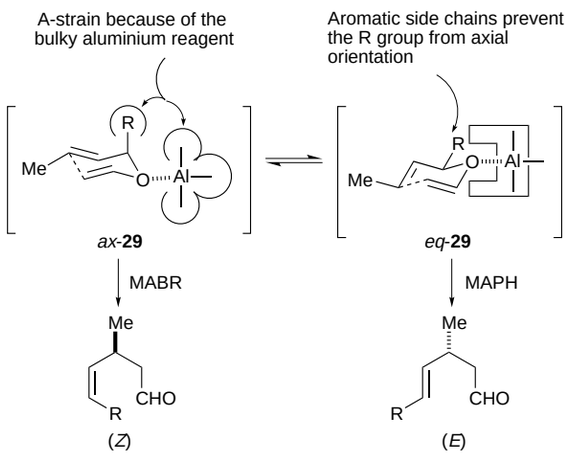
**Scheme 18**



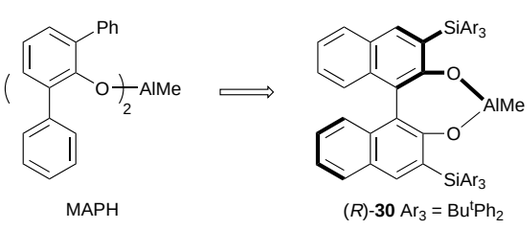

**26** R = $Bu^i$
**27** R = vinyl
**28** R = allyl

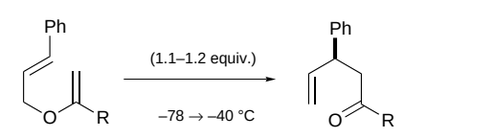
| | MABR | MAPH |
|---|---|---|
| R = $Bu^i$ | 64% (7:93) | 85% (97:3) |
| R = vinyl | 97% (24:76) | 91% (90:10) |
| R = allyl | 40% (7:93) | 97% (95:5) |

**Scheme 19**




**Scheme 20**

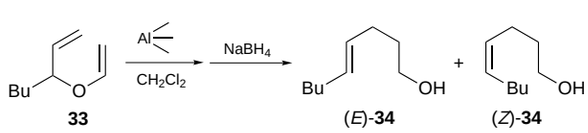



**31** R = $SiMe_3$
**32** R = $GeMe_3$

| R = $SiMe_3$ | 76% (90% ee) |
|---|---|
| R = $GeMe_3$ | 68% (93% ee) |

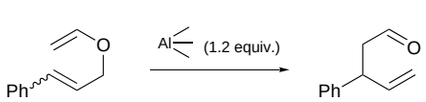
**Scheme 21**




**33** (*E*)-**34** (*Z*)-**34**

| MAPH | 75% (5:1) |
|---|---|
| ATPH | 87% (16:1) |

**Scheme 22**




(*E*)- and (*Z*)-**35** **36**

| −78 °C, 1 h, toluene | MAD | 37% |
|---|---|---|
| | MABR | 76% |
| | ATPH | 93% |
| | ATPH-Br | 98% |
| −20 °C, 1 h, $CH_2Cl_2$ | ATPH | 48% |
| | ATPH-Br | 93% |

**Scheme 23**

(Scheme 24). MABR was entirely ineffective for the catalytic rearrangement.

Based on the structure of ATPH, an optically active catalyst, aluminium tris[(*R*)-1-(1-naphthyl)-3-phenyl-2-naphthoxide] [(*R*)-ATBN], was synthesized, and was subjected to the asymmetric Claisen rearrangement of (*E*)-**35** and **38**–**40** to give the corresponding aldehydes in moderate enantioselectivities (> 60% ee) (Scheme 25). In contrast, the more elaborated (*R*)-ATBN analogue, aluminium tris[(*R*)-1-(1-naphthyl)-3-(*p*-fluorophenyl)-2-naphthoxide] [(*R*)-ATBN-F], generated products with up to 92% ee. Taking in account the decomposition of (*E*)-**35** which took precedence over the rearrangement with (*R*)-**30**, adequate design of Lewis acid catalysts was proven to be important for the stereoselective and asymmetric Claisen rearrangement.

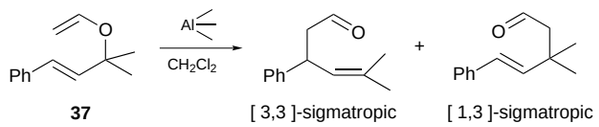
*Selective alkylation at the α-carbon of unsymmetrical ketones*

An unsymmetrical dialkyl ketone can form two regioisomeric enolates upon deprotonation under either kinetic or thermodynamic control. Ideal conditions for the kinetic control of less-substituted enolate formation are those in which deprotonation is irreversible using lithium diisopropylamide (LDA). On the other hand, at equilibrium, the more substituted enolate is the dominant species with moderate selectivity. A hitherto unknown method, *i.e.* the kinetically controlled generation of the more substituted enolate, was realized by the combined use of ATPH and LDA.[34]

Precomplexation of ATPH with 2-methylcyclohexanone **41** at −78 °C in toluene was followed by treatment with LDA in THF, and the mixture was stirred for 1 h (Scheme 26). Subsequent treatment with methyl trifluoromethanesulfonate (MeOTf) furnished 2,2-dimethylcyclohexanone **43** and 2,6-dimethylcyclohexanone **42** in an isolated yield of 53% in a ratio of 32 : 1. Similarly, highly regiocontrolled alkylation of unsymmetrical **44** and **46** with octyl trifluoromethanesulfonate ($C_8H_{17}OTf$) was achieved to give **45** and **47**, respectively (> 99 : 1) (Scheme 27). Replacing ATPH with MAD resulted in a lack of regioselectivity (**42** : **43** = *ca* 1 : 1).

Using *tert*-butyldimethylsilyl trifluoromethanesulfonate ($Bu^tMe_2SiOTf$) in place of alkyl trifluoromethanesulfonates in the present alkylation system produced silyoxybutylated product **48** as a result of THF ring-opening, where alkylation similarly occurred at the more hindered α-carbon of unsymmetrical ketone **41** (Scheme 28).[35]

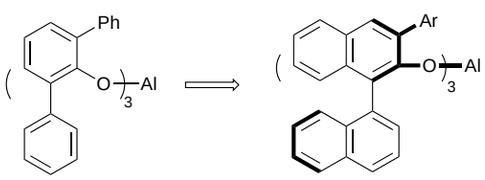
Generation of the kinetically deprotonated more substituted enolate can be explained in terms of the effect of ATPH on the inherent coordination preference of unsymmetrical ketones. Most likely, the bulky aluminium reagent ATPH prefers coordination with one of the lone pairs *anti* to the more hindered α-carbon of the unsymmetrical ketones. As a consequence, the aluminium reagent surrounds the less hindered site of the carbonyl group, thus obstructing the trajectory of the nucleophilic attack of LDA (Fig. 3).



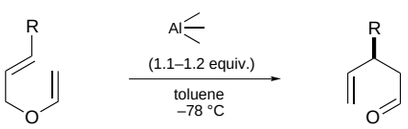

**37** [3,3]-sigmatropic [1,3]-sigmatropic

| | | |
|---|---|---|
| ATPH-Br | (10 mol%), –78 °C, 2.5 h | 90% (5:1) |
| ATPH-Br | (5 mol%), –78 °C, 20 h | 82% (4.8:1) |
| MABR | (5 mol%), –78 °C, 20 h | <9% |

**Scheme 24**



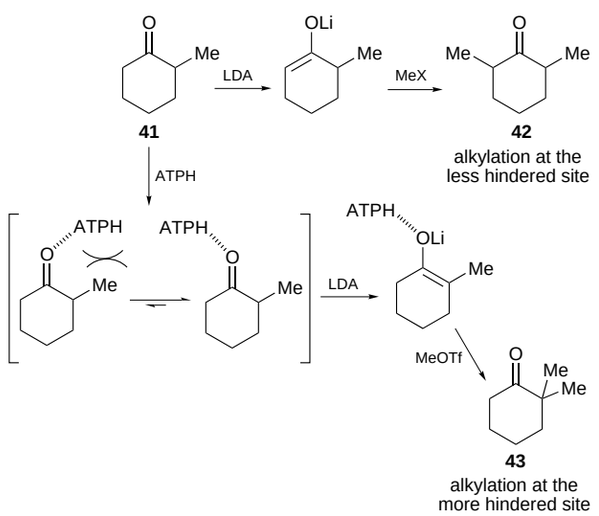

ATPH (*R*)-ATBN Ar = Ph
(*R*)-ATBN-F Ar = *p*-FPh



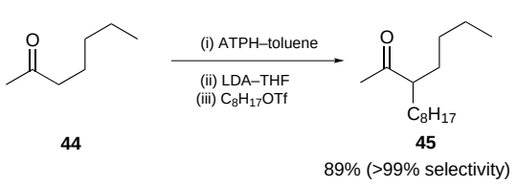

(*E*)- **35** R = Ph
**38** R = c-hexyl
**39** R = $Bu^t$
**40** R = $Me_3Si$

| | | |
|---|---|---|
| R = Ph | (*R*)-ATBN | 93% (61% ee) |
| R = Ph | (*R*)-ATBN-F | 97% (76% ee) |
| R = c-hexyl | (*R*)-ATBN-F | 85% (86% ee) |
| R = $Bu^t$ | (*R*)-ATBN-F | 70% (91% ee) |
| R = $Me_3Si$ | (*R*)-ATBN-F | 78% (92% ee) |

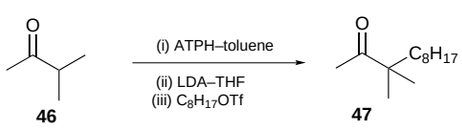
**Scheme 25**




**Scheme 26**

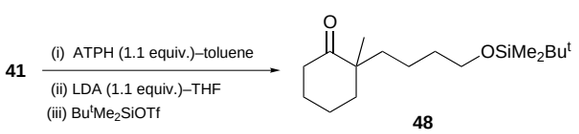



**44** **45**
89% (>99% selectivity)




**46** **47**
71% (>99% selectivity)

**Scheme 27**




**Scheme 28**

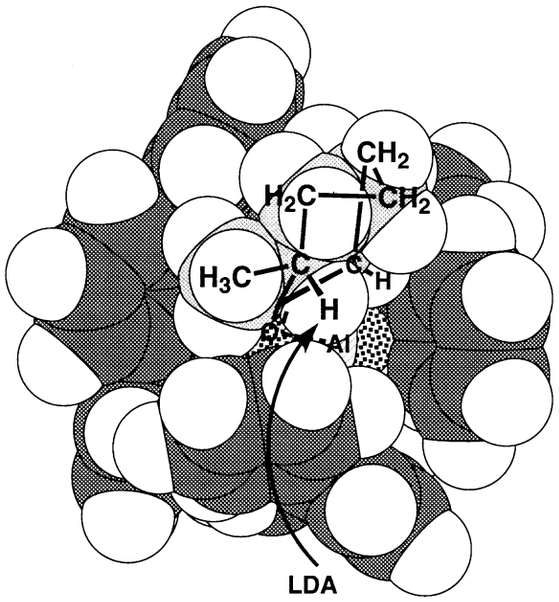



**Fig. 3** Space-filling model of the ATPH–**41** complex. LDA attack is more feasible at the more substituted α-carbon.

## Conclusion

The designer Lewis acids described here show several unique characteristics. In particular, these designer Lewis acids can (i) discriminate between structurally and electronically similar oxygen functionalities, (ii) protect the carbonyl groups of α,β-unsaturated carbonyl compounds from nucleophiles (this observation was extended to selective 1,4- and 1,6-additions, as well as new annulation processes), (iii) promote stereoselective Claisen rearrangement, and the chiral catalysts lead to an asymmetric rearrangement, (iv) selectively coordinate with unsymmetrical carbonyl compounds to generate more substituted enolates. The designer Lewis acid catalysts described here are only a few examples of what is possible. Thus, the search for a new and practical designer Lewis acid still remains a challenge in selective organic synthesis.

## Acknowledgments

We are indebted to our co-workers whose names appear in the references. In particular, we gratefully acknowledge the contribution of Professor Keiji Maruoka, who has since moved to Hokkaido University. We appreciate the support of Mr T. Inohara of the Ono Pharmaceutical Company for performing the single crystal X-ray analysis of the benzaldehyde–ATPH complex, and acknowledge the finacial support of the Ministry of Education, Science, and Culture of Japan.

**Susumu Saito, born in 1969, was educated at the Department of Applied Chemistry, Nagoya University, between 1991 and 1995 under the supervision of Professor H. Yamamoto. He has been a Research Associate in organic chemistry at the Graduate School of Engineering, Nagoya University, since 1995.**

**Professor Hisashi Yamamoto received his bachelor's degree from Kyoto University in 1967 under Professor H. Nozaki, and he attended Harvard University for his PhD studies under the direction of Professor E. J. Corey. His first academic position was as Instructor and then Lecturer at Kyoto University, and in 1977 he became Associate Professor of chemistry at the University of Hawaii. In 1980, he became an Associate Professor at Nagoya University and became Professor there in 1983. He was recipient of the Chemical Society of Japan Award in 1995.**

## References

1 G. A. Olah, R. Krishnamuri and G. K. Surya Prakash, in *Comprehensive Organic Synthesis*, ed. B. M. Trost, Pergamon, Oxford, 1991, vol. 3, ch. 1.8.
2 B. B. Snider, in *Comprehensive Organic Synthesis*, ed. B. M. Trost, Pergamon, Oxford, 1991, vol. 5, ch. 1.1.
3 W. Oppolzer, in *Comprehensive Organic Synthesis*, ed. B. M. Trost, Pergamon, Oxford, 1991, vol. 5, ch. 4.1.
4 T. Mukaiyama, K. Banno and K. Narasaka, *J. Am. Chem. Soc.*, 1974, **96**, 7503; T. Mukaiyama, *Angew. Chem., Int. Ed. Engl.*, 1977, **16**, 817.
5 *Organometallics*, ed. C. Elschenbroich and A. Salzer, VCH, Weinheim, 1992, ch. 7.2.
6 K. Maruoka, T. Itoh, M. Sakurai, K. Nonosita and H. Yamamoto, *J. Am. Chem. Soc.*, 1988, **110**, 3588.; M. B. Power, S. G. Bott, J. L. Atwood and A. R. Barron, *J. Am. Chem. Soc.*, 1990, **112**, 3446.
7 K. Maruoka, H. Imoto, S. Saito and H. Yamamoto, *J. Am. Chem. Soc.*, 1994, **116**, 4131.
8 K. Maruoka, T. Ooi and H. Yamamoto, *J. Am. Chem. Soc.*, 1989, **111**, 6431; K. Maruoka, T. Ooi and H. Yamamoto, *J. Am. Chem. Soc.*, 1990, **112**, 9011.
9 K. Maruoka, A. B. Concepcion, N. Murase, M. Oishi, N. Hirayama and H. Yamamoto, *J. Am. Chem. Soc.*, 1993, **115**, 3943.
10 R. F. Childs, D. L. Mulholland and A. Nixon, *Can. J. Chem.*, 1982, **60**, 801.
11 K. Maruoka, S. Nagahara and H. Yamamoto, *J. Am. Chem. Soc.*, 1990, **112**, 6115.
12 K. Maruoka, Y. Araki and H. Yamamoto, *J. Am. Chem. Soc.*, 1988, **110**, 2650.
13 K. Maruoka, S. Saito and H. Yamamoto, *J. Am. Chem. Soc.*, 1992, **114**, 1089; K. Maruoka, H. Imoto, S. Saito and H. Yamamoto, *Synlett*, 1993, 197.
14 K. Maruoka, S. Saito and H. Yamamoto, *Synlett*, 1994, 439.
15 K. Maruoka, S. Saito, A. B. Concepcion and H. Yamamoto, *J. Am. Chem. Soc.*, 1993, **115**, 1183.
16 K. Maruoka, I. Shimada, H. Imoto and H. Yamamoto, *Synlett*, 1994, 519.
17 K. Maruoka, I. Shimada, M. Akakura and H. Yamamoto, *Synlett*, 1994, 611.
18 S. Saito, I. Shimada, Y. Takamori, M. Tanaka, K. Maruoka and H. Yamamoto, *Bull. Chem. Soc., Jpn.*, in the press.
19 S. Saito, M. Shiozawa, Y. Takamori and H. Yamamoto, *Synlett.*, 1997, 359.
20 L. A. Paquette, *Chem. Soc. Rev.*, 1995, 9.
21 K. C. Nicolau, W.-M. Dai and R. K. Guy, *Angew. Chem., Int. Ed. Engl.*, 1994, **33**, 15.
22 M. D. Healy and A. R. Barron, *Angew. Chem., Int. Ed. Engl.*, 1992, **31**, 921.
23 K. Maruoka, H. Imoto and H. Yamamoto, *Synlett*, 1995, 719.
24 K. Maruoka, M. Ito and H. Yamamoto, *J. Am. Chem. Soc.*, 1995, **117**, 9091.
25 S. Saito and H. Yamamoto, *J. Org. Chem.*, 1996, **61**, 2928.
26 K. Maruoka, H. Imoto and H. Yamamoto, *J. Am. Chem. Soc.*, 1994, **116**, 12 115.
27 P. Wipf, in *Comprehensive Organic Synthesis*, ed. B. M. Trost, Pergamon, Oxford, 1991, vol. 5, ch. 7.2.
28 K. Nonoshita, H. Banno, K. Maruoka and H. Yamamoto, *J. Am. Chem. Soc.*, 1990, **112**, 316.
29 K. Nonoshita, K. Maruoka and H. Yamamoto, *Bull. Chem. Soc. Jpn.*, 1992, **65**, 541.
30 K. Maruoka, A. B. Concepcion and H. Yamamoto, *Bull. Chem. Soc. Jpn.*, 1992, **65**, 3501.
31 K. Maruoka, H. Banno and H. Yamamoto, *Tetrahedron: Asymmetry*, 1991, **2**, 647.
32 K. Maruoka, S. Saito and H. Yamamoto, *J. Am. Chem. Soc.*, 1995, **117**, 1165.
33 S. Saito, K. Shimada and H. Yamamoto, *Synlett*, 1996, 720.
34 S. Saito, M. Ito and H. Yamamoto, *J. Am. Chem. Soc.*, 1997, **119**, 611.
35 S. Saito, M. Ito, K. Maruoka and H. Yamamoto, *Synlett*, 1997, 357.

*6/07464B*

# A new rhenium(I) tricarbonylpolypyridine donor–acceptor complex featuring a long-lived charge-separated excited state

**Raymond Ziessel,*[a] Alberto Juris*[b] and Margherita Venturi[b]**

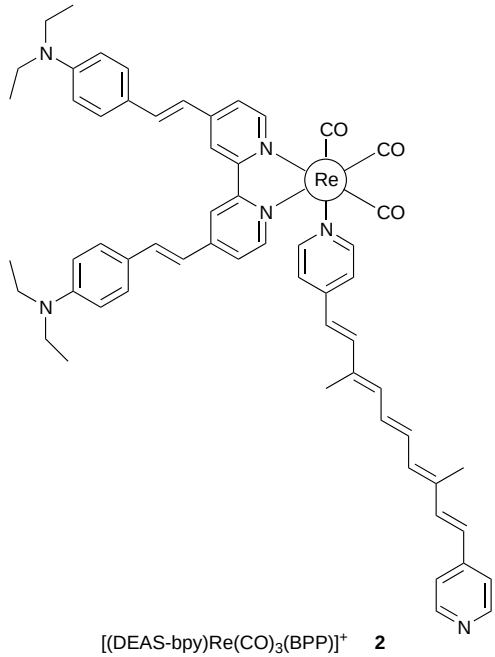
[a] *Laboratoire de Chimie, d'Électronique et de Photonique Moléculaires, Ecole Chimie, Polymères, Matériaux, 1 rue Blaise Pascal, BP 296F, 67008 Strasbourg Cédex, France*

[b] *Dipartimento di Chimica "G. Ciamician", Università di Bologna, via Selmi 2, 40126 Bologna, Italy*

**The new mononuclear complex [(DEAS-bpy)Re(CO)$_3$(BPP)]$^+$ is prepared {DEAS-bpy = 4,4′-bis[*p*-(diethylamino)-α-styryl]-2,2′-bipyridine, BPP = 1,10-bis(4-pyridyl)-3,8-dimethyl-1,3,5,7,9-decapentaene} in which electrochemical and photophysical properties clearly indicate the presence of a long-lived charge-separated excited state at room temperature upon light excitation.**

Photoinduced charge separation is a pivotal process in natural photosynthesis. Archetypal examples of artificial systems include porphyrin triads and polypyridyl complexes of d$^6$ transition-metal complexes.[1–10] The rhenium(I) tricarbonyl complexes appear particularly interesting not only for their photophysical properties, but also because it is quite easy to synthesize species containing two different ligands connected to the same *fac*-Re$^I$(CO)$_3$ core.

We have now prepared the new mononuclear *fac*-[(DEAS-bpy)Re(CO)$_3$(BPP)]CF$_3$SO$_3$ complex **2** starting from *fac*-[(DEAS-bpy)Re(CO)$_3$Cl],[11] **1**, by introducing the electron-




[(DEAS-bpy)Re(CO)$_3$(BPP)]$^+$ **2**

acceptor BPP ligand in the axial position.† The simultaneous coordination of BPP and DEAS-bpy on the same metal center gives rise to a very interesting donor–acceptor complex, which forms a long-lived charge-separated state upon light excitation.

Table 1 collects the electrochemical, absorption, and luminescence data of **1** and **2**, and of the free DEAS-bpy and BPP ligands. Electrochemical characterization of complex **2** indicates that the first reduction process occurs at −0.88 V. This process can be assigned to BPP reduction by comparison with the reduction potentials of the two free DEAS-bpy and BPP ligands. The first oxidation process observed for complex **2** (+0.75 V) is bielectronic and irreversible, indicating that this process involves DEAS-bpy amine oxidation as indeed found in the free DEAS-bpy ligand (bielectronic irreversible wave at +0.66 V). On the other hand, it is known that the coordinated bpy unit is oxidized only at very high potential ($E$ > 2 V),[13] and oxidation of the free ligand BPP features a monoelectronic process at +1.00 V.

Fig. 1 illustrates absorption and emission spectra of complexes **1** and **2**. The photophysical properties of **2** in a rigid matrix at 77 K are very similar to those shown by **1**. Indeed, the two complexes show emission spectra almost identical in position and shape, and with similar lifetime values (Table 1). As in **1** the 77 K emission is known to originate from a DEAS-

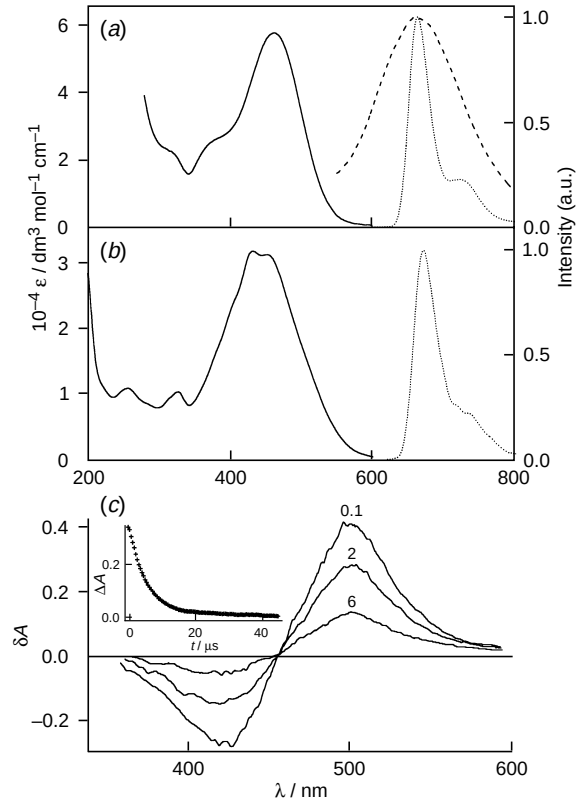



**Fig. 1** Absorption spectrum (——), and uncorrected luminescence spectra at room temp. (- - - -) and at 77 K (dotted line) for complexes **1** (*a*) and **2** (*b*); solvents are DMF at room temperature and DMF–$CH_2Cl_2$ (9 : 1 v/v) at 77 K for **1**; for complex **2** acetonitrile and methanol–ethanol (4 : 1 v/v) were used at 293 and 77 K, respectively. (*c*) Transient absorption spectra at room temp. in deaerated acetonitrile solution for **2**. $\lambda_{exc}$ 355 nm. The spectra were acquired with a delay of 0.1, 2 or 6 μs after the pulse, and a width of 0.5 μs. Inset: decay of the transient signal, monitored at 510 nm.

**Table 1** Electrochemical, absorption and emission data

| Compound | Electrochemistry[a] $E_{red}$/V | Electrochemistry[a] $E_{ox}$/V | Absorption[b] $\lambda_{max}$/nm ($\varepsilon$/dm$^3$ mol$^{-1}$ cm$^{-1}$) | Luminescence[c] $\lambda_{max}$ (298 K)/ nm ($\tau$/ns) | Luminescence[c] $\lambda_{max}$ (77 K)/nm ($\tau$/μs) |
|---|---|---|---|---|---|
| **1**[d] | −1.27 | +0.69[e] | 455 (57100)[e] | 674 (33)[e] | 665 (630)[f] |
| **2** | −0.88 [1] | +0.75 i[g] [2] | 454 (31100) | — | 675 (360) |
| DEAS-bpy | −2.00 [4] | +0.66 i[g] [2] | 394 (53200) | 516 (< 1) | 632 (≈ 2000)[h]<br>490 (0.028) |
| BPP | −0.86 [3] | +1.00 i[g] [1] | 428 (52500)[i] | 557 (< 1) | 490 (< 0.001) |

[a] Argon-purged acetonitrile solution containing 0.05 M $NEt_4PF_6$, room temp.; potentials *vs.* SCE; unless otherwise noted, the waves are reversible or quasi-reversible; number of exchanged electrons in square brackets. [b] Room temp., in MeCN solution, unless otherwise stated. [c] Emission maxima and luminescence lifetimes in deaerated acetonitrile solution at room temp. and in MeOH–EtOH (4 : 1, v/v) rigid matrix at 77 K, unless otherwise noted. [d] Ref. 11. [e] In DMF. [f] DMF–$CH_2Cl_2$ (9 : 1, v/v). [g] i = Irreversible. [h] In $C_3H_7I$ glass. [i] $\varepsilon$ value in EtOH, from ref. 12.

bpy ligand centered (LC) phosphorescence emission, the same should hold also for **2**. The photophysical properties at room temp. in fluid solution are, on the contrary, completely different. Complex **1** features an emission band again due to a DEAS-bpy LC phosphorescence emission, whereas **2** does not show any luminescence emission.‡

Further experiments at room temp. showed that in **2** a transient species is formed following laser flash excitation in deaerated acetonitrile (Fig. 1). An absorption band with $\lambda_{max}$ *ca.* 520 nm is observed arising from the new transient species formed, together with the bleaching of the ground-state absorption around 430 nm. The kinetic of the back reaction to the ground state was followed both at 510 nm (decay of the transient species) and at 430 nm (ground state recovery), obtaining in both cases a good first-order fit, with the same kinetic constant within experimental error ($k = 0.23 \times 10^6$ s$^{-1}$). No sign of decomposition was observed.

In an additional experiment, absorption of the triplet state of the free BPP ligand was measured populating it by energy transfer using anthracene as the triplet donor. The spectrum measured 2 μs after the excitation pulse features a single absorption band at 640 nm. This excludes that the transient spectrum observed in complex **2** may arise from triplet energy transfer to the BPP subunit.

The photophysical behavior of complex **2** can be rationalized by considering the energy position of the relevant states that can be reached after light excitation.

At room temp., the energy of the DEAS-bpy LC phosphorescence can be taken from the 77 K emission (corresponding to $E = 1.83$ eV), by considering that the energy of a LC state is essentially temperature independent. Electrochemical data (Table 1) indicate that the simultaneous presence of DEAS-bpy and BPP modules, which are both electroactive units, gives rise to a redox-separated state, corresponding to BPP reduction and DEAS-bpy oxidation, with $E = 0.88 + 0.75 = 1.63$ eV. Given the relative energy position of these two states, at room temp., **2** is not emissive because of the presence of this redox-separated state as the lowest excited state, thus deactivating the LC state. The transient observed for complex **2** in laser flash experiments is assigned to this redox-separated species.

At 77 K, complex **2** features emission from the lowest-lying LC state, as the level corresponding to the charge-separated state moves to higher energy. Indeed it is known that in rigid media, charge-separated states are normally trapped in a non-equilibrium condition, so that their energy content is higher with respect to the room temp. situation.[14]

The simultaneous coordination of the bidentate DEAS-bpy and the monodentate BPP ligands to a *fac*-$Re^I(CO)_3$ center leads to a donor–acceptor complex which at room temp. gives rise to a 4.3 μs charge-separated state upon light excitation. It is worth noting that this charge-separated state is noticeably long-lived compared to those observed in other donor–acceptor complexes in homogeneous solution.[4,5,9,10] The slowness of the intramolecular back-electron-transfer reaction to the ground state can be justified by considering that its energy content (1.63 eV) places it in the so called 'Marcus inverted region'.[15]

This work was supported by Ministero dell'Università e della Ricerca Scientifica e Tecnologica, and partially supported by the Centre National de la Recherche Scientifique.

## Footnotes and References

* E-mail: juris@ciam.unibo.it

† Complex **2** has been prepared by reacting **1** with $AgCF_3SO_3$ followed by subsequent addition of the BPP ligand. The deep-red crude product was then purified by chromatography and recrystallization. Elemental analysis, IR, NMR, and $FAB^+$ spectra were performed with satisfactory results.

‡ Note that, whereas MLCT states are usually important to determine the spectroscopic properties of $Re^I(CO)_3$ complexes, in **1** and **2** the behavior is dominated by LC states.

1 M. P. O'Neil, M. P. Niemczyk, W. A. Svec, D. Gosztola, G. L. Gaines III and M. R. Wasielewski, *Science*, 1992, **257**, 63 and references therein.
2 J.-P. Collin, A. Harriman, V. Heitz, F. Odobel and J.-P. Sauvage, *J. Am. Chem. Soc.*, 1994, **116**, 5679.
3 A. Harriman, F. Odobel and J.-P. Sauvage, *J. Am. Chem. Soc.*, 1994, **116**, 5481.
4 S. L. Mecklenburg, D. G. McCafferty, J. R. Schoonover, B. M. Peek, B. W. Erickson and T. J. Meyer, *Inorg. Chem.*, 1994, **33**, 2974.
5 K. A. Opperman, S. L. Mecklenburg and T. J. Meyer, *Inorg. Chem.*, 1994, **33**, 5295.
6 M. Seiler, H. Dürr, I. Willner, E. Joselevich, A. Doron and J. F. Stoddart, *J. Am. Chem. Soc.*, 1994, **116**, 3399.
7 E. H. Yonemoto, G. B. Saupe, R. H. Schmehl, S. M. Hubig, R. L. Riley, B. L. Iverson and T. E. Mallouk, *J. Am. Chem. Soc.*, 1994, **116**, 4786.
8 L. A. Kelly and M. A. J. Rodgers, *J. Phys. Chem.*, 1995, **99**, 13 132.
9 M. Frank, M. Nieger, F. Vögtle, P. Belser, A. von Zelewsky, L. De Cola, V. Balzani, F. Barigelletti and L. Flamigni, *Inorg. Chim. Acta*, 1996, **242**, 281.
10 M. Kropf, E. Joselevich, H. Dürr and I. Willner, *J. Am. Chem. Soc.*, 1996, **118**, 655.
11 A. Juris, S. Campagna, I. Bidd, J.-M. Lehn and R. Ziessel, *Inorg. Chem.*, 1988, **27**, 4007.
12 M. Blanchard-Desce, T. S. Arrhenius and J.-M. Lehn, *Bull. Soc. Chim. Fr.*, 1993, **130**, 266.
13 J. B. Chlistunoff and A. J. Bard, *Inorg. Chem.*, 1993, **32**, 3521.
14 P. Chen and T. Meyer, *Inorg. Chem.*, 1996, **35**, 5520.
15 P. F. Barbara, T. J. Meyer and M. A. Ratner, *J. Phys. Chem.*, 1996, **100**, 13 148.

*Received in Basel, Switzerland, 28th April 1997; 7/02902K*

# Reduction of $Ge(Cl)C_6H_3mes_2$-2,6 to give the cyclotrigermenyl radical $(GeC_6H_3mes_2\text{-}2,6)_3^{\cdot}$ and the trigermenyl anion salt $K(GeC_6H_3mes_2\text{-}2,6)_3$

**Marilyn M. Olmstead, Lihung Pu, Richard S. Simons and Philip P. Power***

*Department of Chemistry, University of California, Davis, California 95616, USA*

**Treatment of $Ge(Cl)C_6H_3mes_2$-2,6 1 with 1 equiv. of $KC_8$ furnishes the new cyclotrigermenyl radical $(GeC_6H_3mes_2\text{-}2,6)_3^{\cdot}$, 2) which is characterized by EPR and X-ray crystallography; reduction with a further equivalent of $KC_8$ gives the new trigermenyl allyl anion analogue $K(GeC_6H_3mes_2\text{-}2,6)_3$ which has an open $Ge_3$ framework with a wide Ge–Ge–Ge angle of 159.19(10)° at the central Ge and a Ge–Ge distance of 2.422(2) Å.**

Recent reports have shown that sterically crowding ligands with terphenyl substituents can stabilize coordination and bonding not readily observed with other ligands. Prominent examples include low-coordinate metal thiolates such as the monomeric $Fe(SC_6H_3mes_2\text{-}2,6)_2$[1] (mes = $C_6H_2Me_3$-2,4,6), the formally aromatic cyclotrigallane $M_3(GaC_6H_3mes_2\text{-}2,6)_3$ (M = Na[2a] or K[2b]), or the germylyne complex $(\eta^5\text{-}C_5H_5)(CO)_2MoGeC_6H_3mes_2$-2,6 featuring a MoGe triple bond.[3] The synthesis of the latter species by the reaction of $Na[Mo(\eta^5\text{-}C_5H_5)(CO)_3]$[4] with $Ge(Cl)C_6H_3mes_2$-2,6, **1**,[5] has prompted further investigation of the chemistry of the $Ge(Cl)C_6H_3mes_2$-2,6 species. Here, its reduction to form either the neutral radical $(GeC_6H_3mes_2\text{-}2,6)_3^{\cdot}$, which has a three-membered $Ge_3$ ring, or the salt $K(GeC_6H_3mes_2\text{-}2,6)_3$, with an open $Ge_3$ core structure, is described.

Treatment of $Ge(Cl)C_6H_3mes_2$-2,6, **1**,[5] with slightly less than 1 equiv. of $KC_8$[6] affords the radical $(GeC_6H_3mes_2\text{-}2,6)_3^{\cdot}$ **2**, as dark blue crystals in moderate yield.† In a similar manner, the addition of excess $KC_8$ (2 equiv. per germanium) gives the anionic trigermanium species $(GeC_6H_3mes_2\text{-}2,6)_3^-$ as its potassium salt $K(GeC_6H_3mes_2\text{-}2,6)$, **3**, which was isolated as dark green crystals.

The structures of both **2** and **3** have been determined by X-ray crystallography.‡ The data for **2** showed that it crystallizes as crystallographically independent trimeric units which feature a cyclic triangular arrangement of three germaniums (Fig. 1) in which the average Ge–Ge distance is 2.35(7) Å. Unfortunately, the structure displayed disorder problems involving the important core atoms, which adopt a number of slightly different positions such that several plausible $Ge_3$ triangular arrays are possible which leave the organic ligand atoms unmoved. Nonetheless, the structure could be refined to an overall residual ($R_1$) value of 0.064. The presence of a disordered core unit is consistent with the formulation of **2** as a substituted cyclogermenyl radical (*i.e.* a germanium analogue of a cyclopropenyl radical). In valence bond terms, the ring in such a species is expected to involve a double bond between two members with the unpaired electron located on the remaining atom. Thus, three orientations (**A**, **B**, **C**) may be written since each germanium bears the same $C_6H_3mes_2$-2,6 substituent.

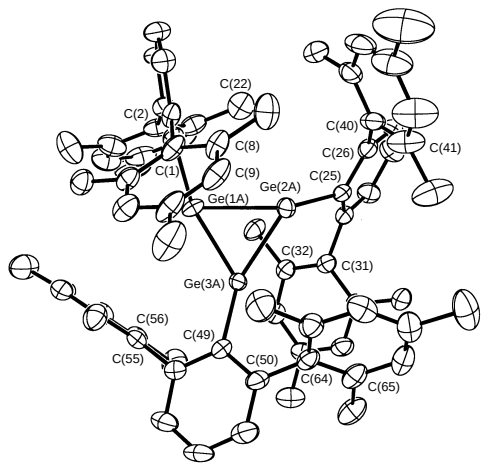
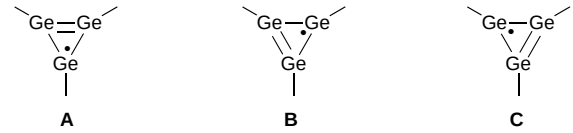



**Fig. 1** Crystal strucutre of **2** featuring one possible arrangmeent of the $Ge_3$ core. The average Ge–Ge distance is 2.35(7) Å.




The EPR spectrum of **2** in hexane solution at room temp. displays a major signal with $g$ = 2.0069 and has a hyperfine coupling to a single $^{73}Ge$ ($I$ = 9/2, 7.8% natural abundance) nucleus. The relative intensity of the hyperfine lines in the EPR spectrum is consistent with the location of the unpaired electron on one germanium atom. The π-molecular orbital picture of the ring features a molecular orbital of a symmetry occupied by a pair of electrons and the doubly degenerate e antibonding level occupied by the unpaired electron. The relatively low hyperfine coupling, a ($^{73}Ge$) = 16 G, is consistent with the location of the unpaired electron in an orbital of π-symmetry indicating planar or near-planar geometry at the germanium center.

Treatment of **1** with 2 equiv. of $KC_8$[6] affords the anionic species **3** (Fig. 2) as its potassium salt. Apparently, the addition of a further electron to **2** results in the opening of the $Ge_3$ ring to afford a trigermenyl analogue of the allyl anion (Scheme 1).

The structure of **3** is characterized by a two-fold rotation axis of symmetry along the C(1)–Ge(1) axis implying planar geometry at Ge(1). The torsion angle between the C(1) ring and the coordination plane at Ge(1) is 81.2°. The potassium countercation is complexed in a π fashion by the C(5) (K–centroid 2.68 Å) and C(20) (K–centroid 2.84 Å) mesityl rings and occupies the two possible coordination sites with equal probability (*i.e.* 50% occupancy of each site). The complexing mesityl rings form a bent sandwich structure at the $K^+$ ion which also interacts very closely with a methyl group [$K^+\cdots C(35)$ 2.81Å] from the C(29) methyl ring. The $K^+\cdots\pi$-interactions are at the lower end of the range previously observed [*cf.* K–C range 3.142(5)–3.253(4) Å and K–centroid of 2.87 Å in (pmdeta)(thf)$KCPh_3$;[7] K–C 3.167(2)–3.288(2) Å in {(pmdeta)$KCH_2Ph_\infty$}.[8]]. The $Ge_3$ array is characterized by a wide Ge(2)–Ge(1)–Ge(2a) angle of 159.19(10) Å and a Ge(1)–Ge(2) distance of 2.422(2) Å. The Ge(1)–C(1) and Ge(2)–C(14) distances are 2.048(14) and 2.022(10) Å. In addition, the Ge(1)–Ge(2)–C(14) angle is

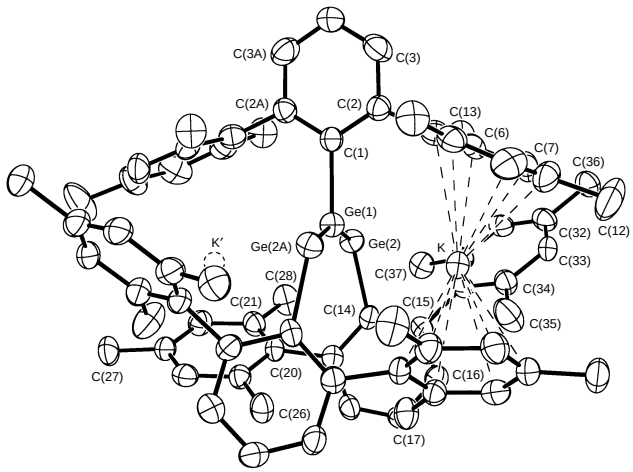
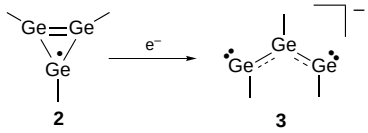



**Fig. 2** Crystal structure of **3**. The 50% $K^+$ occupancy of each site is indicated by displaying only one set of $K^+$ mesityl interactions. Some important bond distances (Å) and angles (°) are: Ge(1)–Ge(2) 2.422(2), Ge(2)–Ge(1)–Ge(2A) 159.19(10), Ge(1)–Ge(2)–C(14) 111.3(3). Further data are given in the text.




**Scheme 1**

111.3(3)° and there is a torsion angle of 20.6° in the C(14)–Ge(2)···Ge(2a)–C(14a) array. These geometrical features are consistent with the description of the $(GeC_6H_3mes_2\text{-}2,6)_3^-$ ion as an allyl anion analogue in which the (*Z*-oriented) lone pairs of the two outer germaniums behave as phantom ligands.

In many respects the structures of **2** and **3** complement that of the recently reported cyclotrigermenium cation $[GeSiBu^t_3]_3^+$ **4**[9] which has a formally aromatic 2π-electron system with an average Ge–Ge bond distance of 2.326(4) Å, *cf*. Ge–Ge double bond distance of 2.239(4) Å in the $Ge_3$ ring species *c*-$[\{GeSiBu^t_3\}_2\{Ge(SiBu^t_3)_2\}]$.[10] The addition of a further electron may afford a neutral cyclotrigermenyl radical species exemplified by **2**, which contains an unpaired electron in a doubly degenerate antibonding π orbital. The average Ge–Ge bond length observed in **2** is 2.327(12) Å which is very similar to that in **4** and *ca*. 0.1 Å shorter than a normal Ge–Ge single bond, 2.44 Å.[11] However, the large standard deviations in the structural parameters of **2**, as well as the different type of substituent, make such a comparison of limited value. Further reduction of **2** affords **3**. Presumably, the addition of a second electron to **2** results in sufficient destabilization of the structure to effect its rearrangement to give **3**. In MO terms the HOMO in the open structure is non-bonding rather than antibonding as it would be if the ring structure were retained. The average Ge–Ge bond length in **3** is *ca*. 0.1 Å longer than that seen in **4**. It is probable that the increased interelectronic repulsion owing to the negative charge, coupled with the 20.6° torsion angle between the planes at Ge(2) and Ge(2a), contributes to the lengthening of the Ge–Ge bonds which are only marginally shorter than a normal Ge–Ge single bond.[11] Further investigation of the chemical and spectroscopic properties of **2** and **3** and their tin analogues is in progress.

We thank the National Science Foundation and the Donors of the Petroleum Fund administered by the American Chemical Society for generous financial support.

## Footnotes and References

* E-mail: pppower@ucdavis.edu

† All manipulations were carried out under anaerobic and anhydrous conditions. The compound $Ge(Cl)C_6H_3mes_2$-2,6,[5] which exists as Ge–Ge bonded dimer in the solid, and $KC_8$ [6] were synthesized as described in the literature.

**2**·0.5thf. To a well stirred solution of **1** (0.42 g, 1.0 mmol) in thf (15 ml) was added $KC_8$ (0.135 g, 0.85 mmol) *via* a solids-addition tube. The solution which was initially yellow became a very dark red, almost black, color. After 3 h all the $KC_8$ appeared to have been consumed, whereupon the volatile materials were removed under reduced pressure. The black residue was extracted with hexane (2×20 ml) and the solution was filtered through Celite. The volume was reduced to *ca*. 20 ml and the solution was placed in a −20 °C freezer for 4 days to afford a mixture of a minor amount of microcrystalline orange crystals (*i.e.* **1**) together with large dark blue, almost black, crystals which could be easily separated by suspending the microcrystals in the solution and decanting rapidly with a cannula to afford X-ray quality crystals of **2**·thf [mp > 100 °C (decomp.)]. Yield 0.13 g, 28.5%. The thf in **2**·0.5thf may be removed by prolonged (12 h) pumping at 0.01 mmHg.

**3**·$0.5C_6H_{14}$, $LiC_6H_3mes_2$-2,6[12] (1.2 g, 3.73 mmol) was added *via* a solids-addition funnel to $GeCl_2$·dioxane (0.86 g, 3.73 mmol) in thf (30 ml) and stirred for 3 h. $KC_8$ (1.01 g, 7.4 mmol) was then added *via* a solids-addition funnel and the mixture was stirred for a further 2 h. The volatile materials were then removed under reduced pressure and the residue was extracted with 30 ml of hexane–toluene (4 : 1). The solution was filtered through Celite and concentrated to *ca*. 20 ml. Storage of 2 days in a −20 °C freezer afforded the product **3** as dark green crystals. Yield 0.35 g, 0.29 mmol, 23.5%. Mp 180–2 °C, $^1$H NMR($C_7D_8$) $\delta$ 2.02 (s, 24H, *o*-$CH_3$), 2.03 (s, 12H, *o*-$CH_3$), 2.21 (s, 6H, *p*-$CH_3$), 2.26 (s, 12H, *p*-$CH_3$), 6.63 (s, 8H, *m*-mes), 6.767 (d, 6H, $J_{HH}$ 6.9 Hz), 6.84 (s, 4H, m-mes), 7.08 (t, 3H, $J_{HH}$ 7.0 Hz), *p*-$C_6H_3$). $^{13}$C{$^1$H} NMR ($C_6D_6$) $\delta$ 21.16, 22.69 (*o*-$CH_3$), 22.89, 23.19 (*p*-$CH_3$), 135.02, 135.82, 130.45, 137.96, 138.55, 139.14, 139.62, 141.18, 142.19, 143.23, 143.91, 145.55, 145.85 (aryl). UV–VIS ($\lambda_{max}$, ε: 266 nm, $\varepsilon$ = 7000 $dm^3\ mol^{-1}\ cm^{-1}$).

‡ *Crystal data* for **2**·0.5thf and **3** (*T* = 130 K, Cu-Kα = 1.54178Å): **2**·0.5thf, $C_{74}H_{79}GeO_{0.5}$, *M* = 1194.14, monoclinic, space group *C*2/*c*, *a* = 43.284 (5), *b* = 12.921(2), *c* = 22.746(3) Å, $\beta$ = 102.78(1)°, *V* = 12 435(3) Å$^3$, abs. coeff. = 2.022 $mm^{-1}$, *Z* = 8, $wR_2$ = 0.1756 for all 8408 data, $R_1$ = 0.064 for 6387 [$I > 2\sigma(I)$] data.

**3**.0.5 $C_6H_{14}$, $C_{75}H_{82}Ge_3K$, *M* = 1240.28, monoclinic, space group *C*2/*c*, *a* = 17.865(6), *b* = 17.994(5), *c* = 23.323(9) Å, $\beta$ = 108.06(3)°, *V* = 71 284 Å$^3$, abs. coeff. = 2.288 $mm^{-1}$, *Z* = 4, $wR_2$ = 0.2453 for all 4665 data, $R_1$ = 0.09 for 3170 [$I > 2\sigma(I)$] data. CCDC 182/523.

1 J. J. Ellison, K. Ruhlandt-Senge and P. P. Power, *Angew. Chem.*, 1994, **106**, 1248; *Angew. Chem., Int. Ed. Engl.*, 1994, **33**, 1000.
2 (*a*) X.-W. Li, W. T. Pennington and G. H. Robinson, *J. Am. Chem. Soc.*, 1995, **117**, 7578; (*b*) X.-W. Li, Y. Xie, P. R. Schreiner, K. D. Gripper, R. C. Crittendon, C. F. Campana, H. F. Schaefer and G. H. Robinson, *Organometallics*, 1996, **15**, 3798.
3 R. S. Simons and P. P. Power, *J. Am. Chem. Soc.*, 1996, **118**, 11966.
4 R. G. Hayter, *Inorg. Chem.*, 1963, **2**, 1031.
5 R. S. Simons, L. Pu, M. M. Olmstead and P. P. Power, *Organometallics*, 1997, **16**, 1920.
6 I. S. Weitz and M. Rabinovitz, *J. Chem. Soc., Perkin Trans. 1*, 1993, 117.
7 D. Hoffmann, W. Bauer, P.v.R. Schleyer, U. Pieper and D. Stalke, *Organometallics*, 1993, **12**, 1193.
8 D. Hoffmann, W. Bauer, F. Hampel, N. J. R. van Eikema Hommes, P.v.R. Schleyer, P. Otto, U. Pieper, D. Stalke, D. S. Wright and R. Snaith, *J. Am. Chem. Soc.*, 1996, **116**, 528.
9 A. Sekiguchi, M. Tsukamoto and M. Ichinohe, *Science*, 1997, **275**, 5296.
10 A. Sekiguchi, H. Yamazaki, C. Kabuto and H. Sakurai, *J. Am. Chem. Soc.*, 1995, **117**, 8025.
11 A. F. Wells, *Structural Inorganic Chemistry*, Clarendon, Oxford, 3rd edn., 1986, p. 1279.
12 K. Ruhlandt-Senge, J. J. Ellison, R. J. Wehmschulte, F. Pauer and P. P. Power, *J. Am. Chem. Soc.*, 1993, **115**, 11 353.

*Received in Bloomington, IN, USA, 2nd May 1997; 7/03037A*

# Novel base-dopable poly(2,7-fluorenylene) derivatives

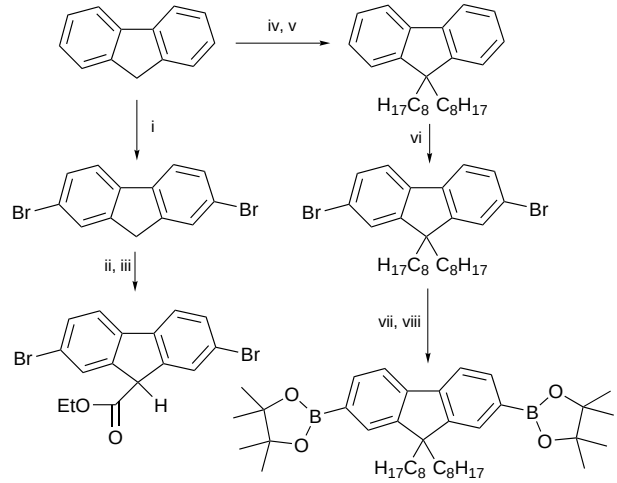
**Maxime Ranger and Mario Leclerc***

*Département de Chimie, Université de Montréal, Montréal, Québec, Canada H3C 3J7*

**A novel acidic poly(fluorenylene) derivative has been synthesized which, upon base-doping, shows electrical conductivities of $10^{-6}$–$10^{-5}$ S cm$^{-1}$; this new doping method for conjugated polymers opens the way to the preparation of air-stable n-type conducting polymers.**

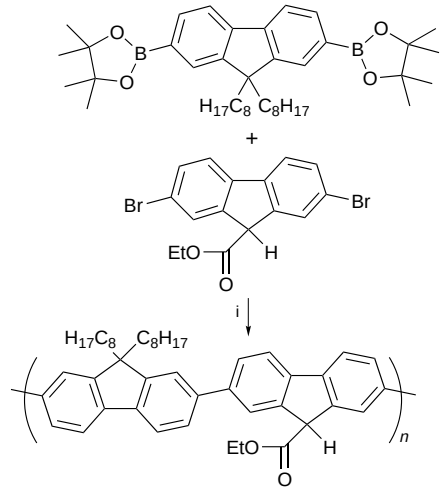
Conjugated polymers, such as poly(acetylene)s, poly(pyrrole)s, poly(thiophene)s, *etc.*, can undergo redox processes (partial oxidation or reduction) which create mobile charge carriers (radical cations, dications or their negative analogs) and lead to high electrical conductivities.[1] These reversible redox reactions (also called doping reactions) modify the electronic structure of the conjugated polymers and are also accompanied by colour changes (electrochromism). Another major development in the field of conducting polymers appeared with the possibility of creating positive charge carriers through the protonation of basic conjugated polymers. For instance, poly(aniline)s can exhibit an insulating-to-conducting transition through a simple protonation of the imine moieties (without any external redox process).[2] Once again, this doping reaction induces colour changes which are related to the formation of the charge carriers. Conversely, acidic conjugated polymers could be base-dopable and this approach should lead to negative charge carriers which could be particularly interesting for the development of electron-injecting electrodes in light-emitting or electrochemical devices. Along these lines, interesting work on poly(2-hydroxy-1,4-phenylene) was recently published by Pei *et al.*,[3] where delocalization of negative charges on the side chains onto the conjugated main chain led to conductivities of 5 $\times$ $10^{-9}$ S cm$^{-1}$. However, it could be more interesting to create charge carriers directly on the backbone and for this purpose, 9-monosubstituted poly(2,7-fluorenylene)s are certainly promising candidates. Indeed, fluorenes bearing a cyano or an ester group at the 9-position exhibit relatively low p$K_a$ (8–10) values in organic solvents, which can be rationalized by the fact that the deprotonation reaction induces the aromatization of the inner ring.[4] Therefore, we report here the first synthesis of a well-defined acidic poly(2,7-fluorenylene) derivative and the characterization of its electrical and optical properties upon base-doping.

As shown in Scheme 1, ethyl 2,7-dibromofluorene-9-carboxylate was easily synthesized in two steps from fluorene. Recently, Pei and Yang[5] reported the nickel-catalysed reduction with metallic zinc of 2,7-dibromo 9,9-disubstituted fluorenes to yield well-defined 9,9-disubstituted poly(2,7-fluorenylene)s, but first attempts with this method were found to be inefficient in the case of acidic 2,7-dibromofluorene-9-carboxylates. The oxidative synthesis of fluorene-9-carboxylates, following the method reported by Yoshino and co-workers,[6] gave only highly cross-linked polymers. Finally, as reported for the synthesis of well-defined processable poly(*p*-phenylene)s,[7] it has been found that palladium-catalysed Suzuki couplings between 2,7-dibromofluorene-9-carboxylates and fluorene derivatives bearing diboronic moieties lead to well-defined poly(2,7-fluorenylene) derivatives. For this purpose, as also described in Scheme 1, 2,7-bis(4,4,5,5-tetramethyl-1,3,2-dioxaborolan-2-yl)-9,9-dioctylfluorene was synthesized, in good yield, in three steps from fluorene. This synthetic procedure could not be applied to 2,7-dibromofluorene-9-carboxylate because of the use of organolithium compounds in the preparation of the boron derivatives. All monomers were characterized by NMR spectroscopy and mass spectrometry and complete details of their synthesis will be published in a forthcoming publication. As shown in Scheme 2, this method yields a well-defined alternating copolymer where 50% of the repeat units can be base-doped. Nevertheless, this alternating structure can indeed be useful since it has been shown that fully protonated polyanilines are less conducting than 50% acid-doped polyanilines.[8]




**Scheme 1** *Reagents and conditions*: i, $CuBr_2$, $Al_2O_3$, $CCl_4$, reflux, 5 h, 97%; ii, LDA (2.1 equiv.), THF, −78 °C; iii, $ClCO_2Et$ (1 equiv.), 92% over two steps; iv, Bu$^n$Li (2 equiv.), THF, −78 °C; v, $C_8H_{17}Br$ (3 equiv.), 99% over two steps; vi, $Br_2$ (2 equiv.), $FeCl_3$ (2 mol%), $CHCl_3$, O→25 °C, 24 h, 99%; vii, Bu$^n$Li (2.1 equiv.), THF, −78 °C; viii, 2-isopropoxy-4,4,5,5-tetramethyl-1,3,2-dioxaborolane (2.5 equiv.), 65% over two steps

The synthesis of this alternated poly(2,7-fluorenylene) derivative gives a pale yellow polymer, completely soluble in THF




**Scheme 2** *Reagents and conditions*: i, $[(PPh_3)_4]Pd$ (2 mol%), PhMe–$Na_2CO_3$ (2 M aq.), Ar, reflux, 48 h, 65%

and $CHCl_3$. On the basis of size exclusion chromatography measurements performed in THF, and using a calibration curve obtained with monodispersed polystyrene standards, this polymer has a weight-average molecular weight of 8000 and a polydispersity index of 1.4. This class of materials should show some acidic properties. Indeed, fluorene-9-carboxylate has a $pK_a$ of around 10 in a mixture of DMSO–$H_2O$ (90 : 10 v/v), the deprotonated form giving an absorption maximum around 400 nm.[4] Accordingly, the corresponding neutral polymer exhibits an absorption maximum at 376 nm in THF while a new broad absorption band appears around 430 nm in the presence of potassium *tert*-butoxide. Consequently, this base-doping of the polymer induces a yellow-to-orange colour change. This phenomenon is reversible and, upon protonation, the polymer recovers its initial colour.

Four-probe electrical measurements on dried pressed pellets of the base-doped polymer revealed conductivities of $10^{-6}$–$10^{-5}$ S cm$^{-1}$. This electrical conductivity is excellent for an n-doped polymer considering that the conducting state has been obtained from a simple deprotonation reaction and that all measurements have been carried out in air. Moreover, it is worth noting that poly(fluorenylene)s are not particularly good conducting materials (probably due to weak interchain interactions); for instance, oxidized poly(fluorenylene) derivatives show electrical conductivities of $10^{-3}$ S cm$^{-1}$[6,9] whereas neutral poly(fluorenylene) derivatives show conductivities lower than $10^{-9}$ S cm$^{-1}$. However, these promising results obtained with a base-dopable poly(fluorenylene) derivative opens a new route for the preparation of n-doped conducting polymers. It is believed that the synthesis of cyano-monosubstituted poly(fluorenylene)s could lead to more conducting materials since, as reported for the monomers, the deprotonated form of fluorene-9-carboxylate may involve a partial localisation of the negative charge on the enolate form of the ester group, which is impossible with a cyano substituent.[4] Moreover, 9-cyanofluorene is more acidic than the carboxylate derivatives. Finally, the preparation of double-stranded, fully soluble poly(fluoreneacene)s, as developed by Scherf and Müllen,[10] bearing strong electron-withdrawing substituents could also lead to conducting, base-doped polymers.

This work was supported by research grants from the Natural Sciences and Engineering Research Council (NSERC) of Canada. The authors acknowledge D. Rondeau for his help in the synthesis of some monomers and C. Mellon and Professor L. Breau for much helpful advice.

## Footnote and References

* E-mail: leclerma@ere.umontreal.ca

1 *Handbook of Conducting Polymers*, ed. T. A. Skotheim, Marcel Dekker, New York, 1986.
2 W. S. Huang, B. D. Humphrey and A. G. MacDiarmid, *J. Chem. Soc., Faraday Trans. 1*, 1986, **82**, 2385.
3 Q. Pei, F. Klavetter and Y. Yang, *Polym. Prepr.*, 1995, **36**, 213.
4 C. F. Bernasconi and F. Terrier, *J. Am. Chem. Soc.*, 1987, **109**, 7115.
5 Q. Pei and Y. Yang, *J. Am. Chem. Soc.*, 1996, **118**, 7416.
6 M. Fukuda, K. Sawada and K. Yoshino, *Jpn. J. Appl. Phys.*, 1989, **28**, L1433.
7 M. Rehahn, A. D. Schluter, G. Wegner and W. J. Feast, *Polymer*, 1989, **30**, 1054.
8 G. D'Aprano, M. Leclerc and G. Zotti, *Macromolecules*, 1992, **25**, 2145.
9 J. Rault-Berthelot and J. Simonet, *New. J. Chem.*, 1986, **10**, 169.
10 U. Scherf and K. Müllen, *Adv. Polym. Sci.*, 1995, **123**, 1.

*Received in Corvallis, OR, USA, 6th May 1997; 7/03076B*

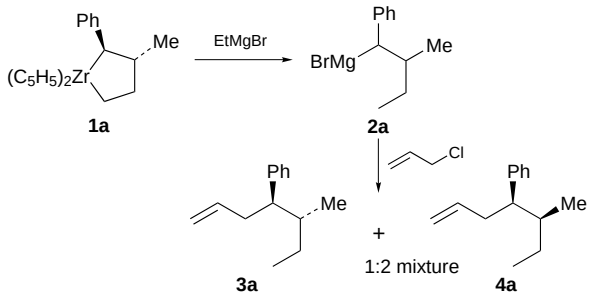
# Highly regio- and diastereo-selective carbon–carbon bond formation reaction of unsymmetrical zirconacyclopentanes using copper salt

**Tamotsu Takahashi,* Yasushi Nishihara, Ryuichiro Hara, Shouquan Huo and Martin Kotora**

*Catalysis Research Center and Graduate School of Pharmaceutical Sciences, Hokkaido University, Kita-ku, Sapporo 060, Japan*

**Reaction of unsymmetrical zirconacyclopentanes with allyl chloride or benzoyl chloride in the presence of copper chloride gave allylated or benzoylated products with high regio- and diastereo-selectivities.**

Regio- and stereo-selective reactions are attractive and useful for organic synthesis. Recently we reported the unprecedented highly regioselective transmetalation of zirconacyclopentanes such as **1a** with EtMgBr to afford Grignard compound **2a**.[1] It is known that zirconacyclopentane **1a** is prepared by the reaction of $(C_5H_5)_2Zr(CH_2{=}CH_2)$,[2] which is generated from $(C_5H_5)_2ZrCl_2$, 2 equiv. of EtMgBr and β-methylstyrene with high stereo- and regio-selectivity.[3] However, further reaction of **1a**, for example with allyl chloride by transmetalation from zirconium to magnesium, gave a mixture of two diastereomers **3a** and **4a** in a ratio of almost 1 : 2 (Scheme 1). Here we report the regio- and diastereo-selective C–C bond formation reactions of unsymmetrical zirconacyclopentanes.

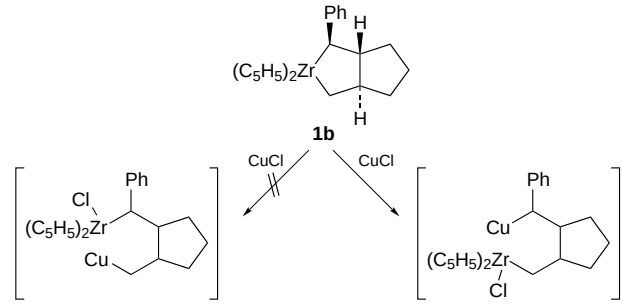



**Scheme 1**

Unsymmetrical zirconacyclopentanes **1a**–**d** were prepared by the reaction of β-methylstyrene with $(C_5H_5)_2ZrEt_2$[1,3] or by the reaction of dienes[3] or trienes[4] with $(C_5H_5)_2ZrBu_2$ (the Negishi reagent).[5] The unsymmetrical zirconacyclopentanes have two different Zr–C bonds. One of the most attractive aspects of these species is the regioselective C–C bond formation reactions of these two different Zr–C bonds. Reaction of zirconacyclopentane **1a** with allyl chloride in the presence of a stoichiometric amount of copper(I) chloride gave product **3a** in 64% yield as the sole product. The C–C bond formation reaction selectively proceeded at the carbon which had a phenyl substituent. The formation of the regioisomer was not observed (regioselectivity > 98%). More interestingly, the $^{13}C$ NMR spectrum of **3a** showed that the only one diastereoisomer was formed. This is in sharp contrast to the case with EtMgBr.

The stereochemistry of the product **3a** was determined by comparison of the $^{13}C$ NMR spectrum of its hydrogenation product with those of the two diastereomers **5** and **6** which were prepared as authentic samples. The $^{13}C$ NMR spectrum of the hydrogenation product of **3a** was identical to that of **5**. This result clearly indicated that this type of copper mediated C–C bond formation reaction of **1a** with allyl chloride gave diastereomerically pure product **3a** and no formation of its stereoisomer **4a** was observed. The stereochemistry between the Ph and Me substituents was maintained during this allylation reaction of **1a**.

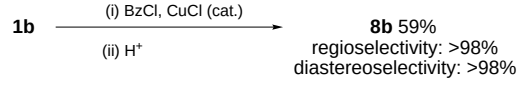
Unsymmetrical bicyclic zirconacyclopentane **1b** also showed the same selectivity for the copper catalysed allylation reaction as shown in Table 1. Allylation product **3b** was obtained in 94% yield after hydrolysis. Iodinolysis instead of hydrolysis afforded **7b** in 90% yield. The allylation selectively occurred at the carbon which had a phenyl substituent. In the reaction of **1b** with BzCl the regioselectivity was very high ( > 98%). The first step of this reaction is a transmetalation reaction from zirconium to copper as reported.[6–10] This suggests that this step is highly regioselective. The more sterically hindered carbon attached to zirconium is transferred to copper (Scheme 2) due to the repulsion between cyclopentadienyl ligands and the substituent. Even a methyl group at the β-position has a remarkable effect on the regioselectivity, as shown in the case of **1c** and **1d**. Allylation product **3c** and benzoylation product **8d** were obtained with > 98% regioselectivity.




**Scheme 2**

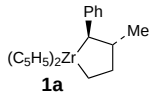
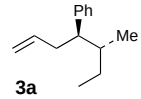
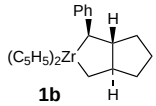
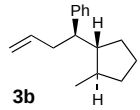
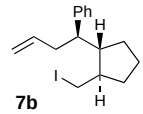
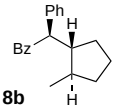
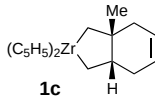
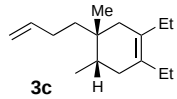
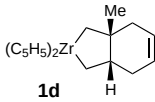
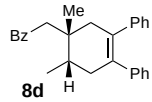
When **1b** reacted with allyl chloride or benzoyl chloride (Scheme 3), only one diastereomer was obtained as observed in the case of **1a**. The stereochemistry of the product **8b** was determined by X-ray analysis as shown in Fig. 1. It clearly showed that the stereochemistry of **1b** was also maintained during the reactions. There are two possible paths to explain this stereochemistry (Scheme 4). One is a retention-retention path for the transmetalation step and the C–C bond formation step. The other is an inversion-inversion path. The former path is more likely, although the mechanism is not clear yet.




**Scheme 3**

**Table 1** Regio- and diastereo-selective carbon–carbon bond formation reactions of unsymmetrical zirconacyclopentanes[a]

| Zircona-cyclopentane | Chloride | *t*/h | *T*/°C | Product | Yield (%)[b] | Regio-selectivity | Diastereo-selectivity |
|---|---|---|---|---|---|---|---|
|  **1a** |  | 1 | 0 |  **3a** | 64[c] (48) | >98 | >98 |
|  **1b** |  | 6 | 0 |  **3b** | 94 (83) | >98 | >98 |
| |  | 6 | 0 |  **7b** | 90 (78) | >98 | >98 |
| | BzCl | 1 | 0 |  **8b** | 59 (49) | >98 | >98 |
|  **1c** |  | 1 | 0 |  **3c** | 74 (58) | >98 | *d* |
|  **1d** | BzCl | 1 | 0 |  **8d** | 70 (59) | >98 | *d* |

[a] Catalytic amount (0.1 equiv.) of CuCl was used. [b] Yields were determined by GC. Isolated yields are shown in parentheses. [c] One equivalent of CuCl was used. [d] Product was diasteromerically pure.

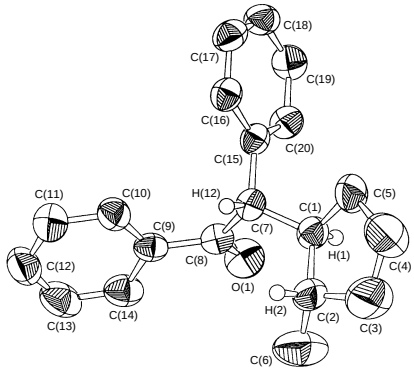
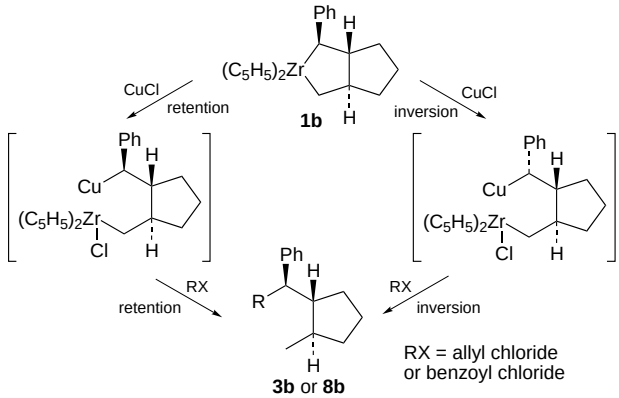



**Fig. 1** ORTEP Drawing of **8b**




**Scheme 4**

Further investigations on the selective C–C bond formation characteristics of zirconacycles are in progress.

## Footnotes and References

* E-mail: tamotsu@cat.hokudai.ac.jp

† *Selected crystallographic data* for **8b**: CCDC 182/511.

1 T. Takahashi, T. Seki, M. Saburi and E. Negishi, XIVth International Conference on Organometallic Chemistry, Detroit, MI, 1990, B17; T. Takahashi, T. Seki, Y. Nitto, M. Saburi, C. J. Rousset and E. Negishi, *J. Am. Chem. Soc.*, 1991, **113**, 6266. For related catalytic reactions involving the transmetalation step of zirconacyclopentanes with RMgX, see also U. M. Dzhemilev, O. S. Vostrikova and G. A. Tolstikov, *J. Organomet. Chem.*, 1985, **285**, 43; A. H. Hoveyda and Z. Xu, *J. Am. Chem. Soc.*, 1991, **113**, 5079; K. S. Knight and R. H. Waymouth, *J. Am. Chem. Soc.*, 1991, **113**, 6268; D. P. Lewis, P. M. Muller and R. J. Whitby, *Tetrahedron Lett.*, 1991, **32**, 6297.

2 T. Takahashi, N. Suzuki, M. Kageyama, Y. Nitto, M. Saburi and E. Negishi, *Chem. Lett.*, 1991, 1579.

3 E. Negishi, D. Choueiry, T. B. Nguyen, D. R. Swanson, N. Suzuki and T. Takahashi, *J. Am. Chem. Soc.*, 1994, **116**, 9751.

4 T. Takahashi, M. Kotora, K. Kasai and N. Suzuki, *J. Chem. Soc., Chem. Commun.*, 1994, 2693.

5 E. Negishi, F. E. Cederbaum and T. Takahashi, *Tetrahedron Lett.*, 1986, **27**, 2829.

6 T. Takahashi, M. Kotora and Z. Xi, *J. Chem. Soc., Chem. Commun.*, 1995, 1503.

7 K. Kasai, M. Kotora, N. Suzuki and T. Takahashi, *J. Chem. Soc., Chem. Commun.*, 1995, 109; B. H. Lipshutz and M. Segi, *Tetrahedron*, 1995, **51**, 4407.

8 L. M. Venanzi, R. Lehman, R. Keil and B. H. Lipshutz, *Tetrahedron Lett.*, 1992, **33**, 5857; T. Takahashi, M. Kotora, K. Kasai and N. Suzuki, *Tetrahedron Lett.*, 1994, **35**, 5685.

9 T. Takahashi, M. Kotora, K. Kasai and N. Suzuki, *Organometallics*, 1994, **13**, 4183.

10 T. Takahashi, R. Hara, Y. Nishihara and M. Kotora, *J. Am. Chem. Soc.*, 1996, **118**, 5154.

*Received in Cambridge, UK, 12th May 1997; 7/03227G*

# A silicon controlled total synthesis of the antifungal agent (+)-preussin

**Rekha Verma and Sunil K. Ghosh***

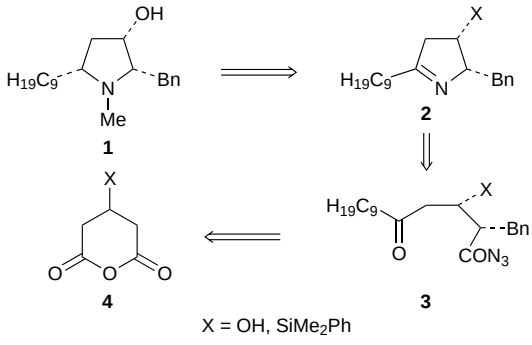
*Bio-Organic Division, Bhabha Atomic Research Centre, Trombay, Mumbai 400 085, India*

**A stereoselective total synthesis of (+)-preussin has been achieved from a *meso* anhydride featuring a dimethyl(phenyl)silyl group as a masked hydroxy group which also restricts elimination reactions, stereodirects hydrogenation and ester enolate alkylation, and facilitates Curtius reaction.**

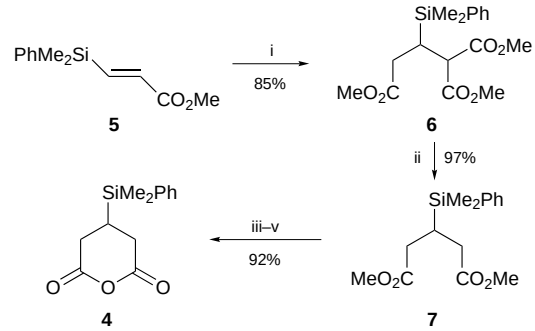
(+)-Preussin, (2*S*,3*S*,5*R*)-1-methyl-5-nonyl-2-benzylpyrrolidin-3-ol (also known as L-657,398), **1** was isolated from the fermentation broths of *Aspergillus ochraceus* ATCC 22947 and *Preussia sp.*[1] This structurally novel pyrrolidine alkaloid has broader spectrum antifungal activity against both filamentous fungi and yeasts than the structurally related antibiotic anisomycin. The first total synthesis of (+)-preussin was reported by Pak and Lee[2] taking D-glucose as a substrate. Four more syntheses have been published subsequently using (*S*)-phenylalanine[3] and its enantiomer[4] as starting materials.

A simple retrosynthetic analysis could be postulated for (+)-preussin **1** from *meso* anhydride **4**[5] *via* $\Delta^1$-pyrroline **2** as shown in Scheme 1 (X = OH). However, as pointed out by Livinghouse,[3a] an intermediate like **2** is unstable due to the ease of elimination of the protected or unprotected OH group to provide a pyrrole derivative. Therefore, a substitute for this group is desirable which would resist elimination, could be stereospecifically converted to a hydroxy group when desired, could possibly stereodirect both saturation of the $\Delta^1$-pyrroline system and introduction of the benzyl group, and possibly facilitate the Curtius reaction of **3**. Considering all these requirements, we envisaged that a dimethyl(phenyl)silyl ($PhMe_2Si$) group would be an ideal substitute. It is known to be a poor leaving group and, as shown by Fleming,[6] it can be stereospecifically converted to a hydroxy group with retention of configuration. They have further shown that β-silyl ester enolate alkylations occur with high *anti* stereoselectivity.[7] Moreover, we have found that a β-silicon group facilitates the Curtius reaction of acyl azides‡ in close analogy to silicon directed Bayer–Villiger oxidation of β-silyl ketones.[8]

The starting *meso* anhydride **4** could easily be obtained in a few steps from β-silyl acrylate **5**[9] *via* the triester **6** and Fleming's *meso* diester **7**[10] as depicted in Scheme 2. When **4** was opened up with (±)-naphthylethanol **8**, it was expected to show good diastereocontrol, as observed by Fleming and Ghosh[11] for the opening up of a 3,4-bis-silyl substituted *meso* adipic anhydride. However, we obtained an inseparable 85 : 15



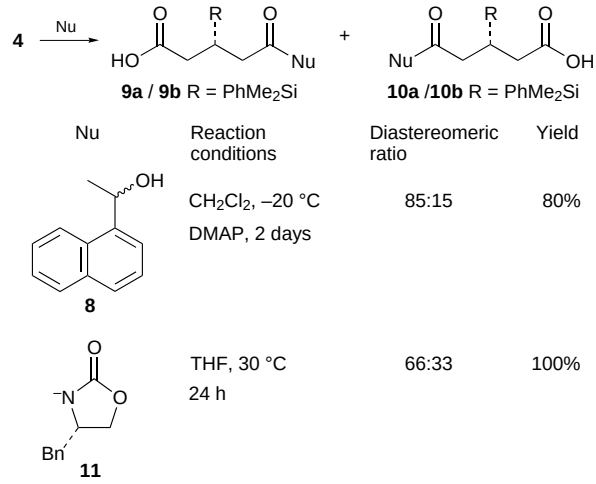

**Scheme 1**



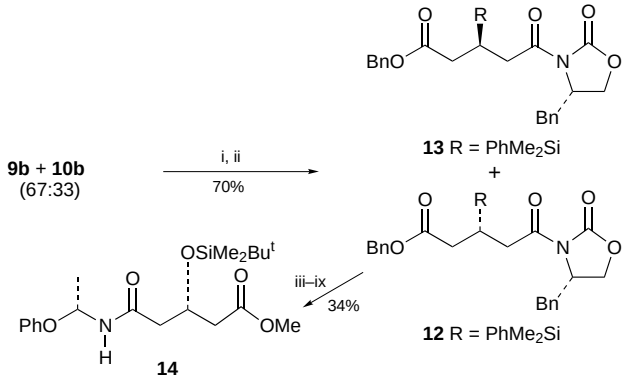

**Scheme 2** *Reagents and conditions*: i, NaOMe, dimethyl malonate, room temp., 48 h; ii, NaCl, DMSO, $H_2O$, heat, 2.5 h; iii, KOH, MeOH, $H_2O$, room temp., 48 h; iv, dil. HCl; v, $Ac_2O$, reflux, 2.5 h

mixture of diastereoisomeric acids **9a** and **10a** (stereochemistry not determined) (Scheme 3) in 80% yield. In a related study, Theisen and Heathcock[5a] have also observed that 3-alkyl substituted glutaric anhydrides show poor diastereocontrol with increasing size of the alkyl groups. Alternatively, we opened up the anhydride with the lithium anion of the Evans' auxiliary[12] **11** which quantitatively provided a mixture of diastereoisomeric acids **9b** and **10b** in a ratio of *ca.* 67 : 33 (analysed as their methyl esters by NMR spectroscopy). To the best of our knowledge, this forms the first example of the desymmetrization of a *meso* anhydride using an anion of a chiral imide. Although the selectivity was low, the benzyl esters **12** and **13**‡ of these acids were easily separable by chromatography. The absolute stereochemistry of the major acid **9b** was established by converting it to a known derivative **14**[5b] following the reactions depicted in Scheme 4.

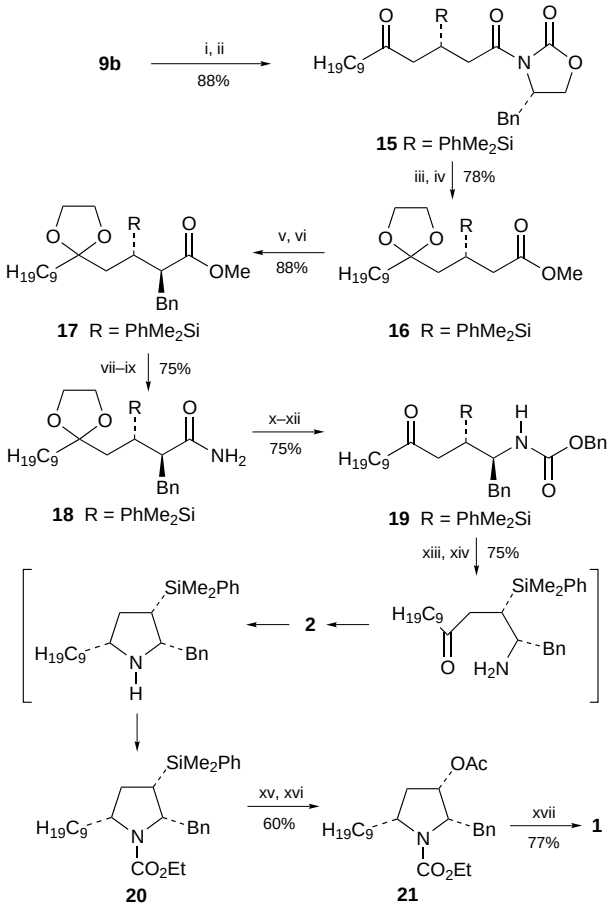
The major acid **9b** was converted to the ketone **15** in 60% yield (88% based on recovered **9b**) (Scheme 5), which was quantitatively protected[13] as the acetal and the auxiliary was removed[12] to provide the homochiral methyl ester **16** in 78% yield.§ We could recover the auxiliary in 78% yield (> 99% considering the wrong attack on the auxiliary) without any loss




**Scheme 3**




**Scheme 4** *Reagents and conditions*: i, $Et_3N$, PivCl, −78 to 0 °C, 1 h; ii, BnOH, DMAP, room temp., 24 h; iii, chromatographic removal of **13**; iv, $H_2$, 10% Pd–C; room temp., 24 h; v, KBr, NaOAc, AcOOH, room temp., 24 h; vi, (*S*)-phenylethylamine, DCC, DMAP, room temp., 24 h; vii, LiOOH, THF, 0 °C, 40 min; viii, $CH_2N_2$; ix, $Bu^tMe_2SiCl$, DMF, imidazole, room temp., 15 h




**Scheme 5** *Reagents and conditions*: i, $Et_3N$, PivCl, −78 to 0 °C, 1 h; ii, $C_9H_{19}MgBr$, −25 °C, 48 h; iii, 1,2-bis(trimethylsilyloxy)ethane, $Me_3SiOSO_2CF_3$, −20 °C, 48 h; iv, MgOMeBr, THF, 30 °C, 18 h; v, LiTMP, THF–DMPU, −78 °C, 1 h; vi, BnBr, −78 to −10 °C, 60 h; vii, KOH, MeOH, $H_2O$, 80 °C, 32 h; viii, $Im_2CO$, room temp., 30 min; ix, liq. $NH_3$; x, $Pb(OAc)_4$, BnOH, DMF, 100 °C, 15 h; xi, TsOH, acetone, $H_2O$, reflux, 2.5 h; xii, chromatographic removal of minor diastereoisomer; xiii, $H_2$, 10% Pd–C, EtOH, AcOH, 7 h; xiv, EtOCOCl, $Et_3N$, 0 °C, 15 h; xv, KBr, NaOAc, AcOOH, room temp., 20 h; xvi, $Ac_2O$, DMAP, $CH_2Cl_2$, room temp., 20 h; xvii, $LiAlH_4$, THF, room temp., 24 h

of optical purity. The ester enolate *C*-benzylation took place with high *anti* selectivity[7] (*anti*:*syn* = 93:7) to give ester **17** which was resistant to hydrazinolysis. This ester was hydrolysed, converted to primary amide **18** *via* its acid imidazolide and was subjected to modified Curtius reaction conditions[14] which smoothly† provided the expected benzyloxycarbonyl protected amine in good yield. The acetal protection was subsequently removed to give the ketone **19** in overall 75% yield from **17**. At this stage we could easily separate the unwanted minor diastereoisomer by chromatography. The ketone **19** was subjected to hydrogenolysis whereupon removal of the benzyloxycarbonyl group took place. The generated amino group condensed intramolecularly with the carbonyl group spontaneously to provide the $\Delta^1$-pyrroline **2** (X = $PhMe_2Si$) which was *in situ* hydrogenated with hydrogens coming from the least hindered surface, *i.e*. away from the silicon and benzyl groups, to provide the pyrrolidine derivative with all three substituents having *cis* stereochemistry. Subsequently, the NH group was protected as ethoxycarbonyl derivative **20** and the silyl group in the molecule was converted to a hydroxy group[6] and then to its acetate **21**.¶ Lithium aluminium hydride reduction of this acetate provided (+)-preussin **1** in 77% yield. Since we started with the homochiral methyl ester **16,** and the synthetic sequence does not cause any epimerisation, the enatiomeric purity of (+)-preussin should undoubtedly be very high (>99%). This was confirmed from its specific rotation value ($[\alpha]_D^{25}$ + 31.1, *c* 1, $CHCl_3$) and spectral data.[2] The overall yield of (+)-preussin from the homochiral ester **16** was 17.2%.

We acknowledge RSIC, Mumbai for the NMR facility, and Dr A. Banerji and Dr V. R. Mamdapur for their support.

## Footnotes and References

* E-mail: bod@magnum.barct1.ernet.in

† A silicon group at the β-position enhances the rate of Curtius reaction of acyl azides; details will be published elsewhere.

‡ We are in the process of converting this diastereoisomer to acetal **16**.

§ During the process, an undesired product (about 22%) was also formed by attack of the methoxide ion on the wrong carbonyl of the auxiliary.

¶ The NMR spectra of **20** and **21** could not be fully interpreted as these are known to be mixtures of amide geometrical isomers as well as atropisomers.

1 R. E. Schwartz, J. Liesch, O. Hensens, L. Zitano, S. Honeycutt, G. Garrity, R. A. Fromtling, J. Onishi and R. Monaghan, *J. Antibiot.*, 1988, **41**, 1774; R. E. Schwartz, J. C. Onishi, R. L. Monaghan, J. M. Liesch and O. D. Hensens, *US* P 4 847 284, 1989; J. H. Johnson, D. W. Phillipson and A. D. Kahle, *J. Antibiot.*, 1989, **42**, 1184.

2 C. S. Pak and G. H. Lee, *J. Org. Chem.*, 1991, **56**, 1128.

3 (*a*) P. L. McGrane and T. Livinghouse, *J. Am. Chem. Soc.*, 1993, **115**, 11 485; (*b*) M. Overhand and S. M. Hecht, *J. Org. Chem.*, 1994, **59**, 4721; (*c*) W. Deng and L. E. Overman, *J. Am. Chem. Soc.*, 1994, **116**, 11 241.

4 M.Shimazaki, F. Okazaki, F. Nakajima, T. Ishikawa and A. Ohta, *Heterocycles*, 1993, **36**, 1823.

5 (*a*) P. D. Theisen and C. H. Heathcock, *J. Org. Chem.*, 1993, **58**, 142, and references cited; (*b*) D. S. Karanewsky, M. F. Malley and J. Z. Gougoutas, *J. Org. Chem.*, 1991, **56**, 3744.

6 I. Fleming, R. Henning, D. C. Parker, H. E. Plaut and P. E. J. Sanderson, *J. Chem. Soc., Perkin Trans. 1*, 1995, 317.

7 R. A. N. C. Crump, I. Fleming, J. H. M. Hill, D. Parker, N. L Reddy and D. Waterson, *J. Chem. Soc., Perkin Trans. 1*, 1992, 3277.

8 P. F. Hudrlik, A. M. Hudrlik, T. Yimenu, M. A. Waugh and G. Nagendrappa, *Tetrahedron*, 1988, **44**, 3791.

9 K. Takeshita, Y. Seki, K. Kawamoto, S. Murai and N. Sonoda, *J. Org. Chem.*, 1987, **52**, 4864.

10 I. Fleming, *Stereocontrol in Organic Synthesis Using Silicon Compounds*, Conferencias Plenarias de la XXIII Reunio'n Bienal de Qui'mica, Salamanca, 1990, p. 89.

11 I. Fleming and S. K. Ghosh, *J. Chem. Soc., Chem. Commun.*, 1994, 2285.

12 D. A. Evans, T. C. Britton, R. L. Dorow and J. F. Dellaria, Jr., *Tetrahedron*, 1988, **44**, 5525.

13 T. H. Chan, M. A. Brook and T. Chaly, *Synthesis*, 1983, 203.

14 H. E. Baumgarten, H. L. Smith and A. Staklis, *J. Org. Chem.*, 1975, **40**, 3554.

*Received in Cambridge, UK, 16th May 1997; 7/03387G*

# *exo*-Binding of $Na^+$ between two fused calix[4]arenes and *endo* binding of $Na^+$ within the calix[4]arene cones in the disodium salt of 1,3-dimethyl ether *p-tert*-butylcalix[4]arene

**Stuart R. Dubberley, Alexander J. Blake and Philip Mountford***

*Department of Chemistry, University of Nottingham, Nottingham, UK NG7 2RD*

**Reaction of 1,3-dimethyl ether *p-tert*-butylcalix[4]arene ($H_2L$) with sodium hydride in tetrahydrofuran affords the dimeric metallocalixarene species $[Na_2L]_2$ which possesses a novel structure in which the $Na^+$ ions are coordinated in two very different environments.**

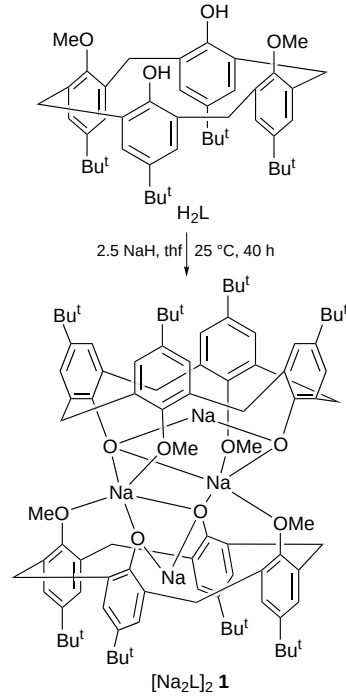
The study of calixarenes (and their derivatives) as receptor molecules *via endo*-binding of substrates within their cavities is a very active area of current research.[1] Furthermore, calixarenes can also act as polydentate O-donor ligands to main-group and transition-metal centres forming mononuclear[2] and fused binuclear[3] derivatives. O-Derivatised calixarenes with pendant arms containing Lewis-basic amide, ester, or polyether functionalities have also been widely studied for their ion-binding properties.[1b,c] In contrast, the simple O-alkylated calix[4]arenes have received very little attention and only a handful of metallo derivatives have been reported; these include mononuclear organometallic zirconium,[4] zinc,[3a] aluminium and gallium[5] derivatives of 1,3-dimethyl ether *p-tert*-butylcalix[4]arene ($H_2L$) and an $Na^+$ complex of tetramethyl ether *p-tert*-butylcalix[4]arene with the metal cation bonded in an *exo* fashion (with respect to the cavity of the cone) to the four ethereal oxygen atoms.[6]

Recent spectroscopic and structural studies have shown that complexation of alkali-metal cations within the calix[4]arene cavity involves cation–π interactions.[7] Furthermore, O-coordination of a transition metal at the lower rim of mononuclear *p-tert*-butylcalix[4]arenes can also allow for alkali-metal binding within the cavity.[2f] Binuclear derivatives wtih metals bridging the lower rims of two fused calixarene ligands may bind organic substrates within the divergent cavities.[3b,c] Here we show that simple metallation of 1,3-dimethyl ether *p-tert*-butylcalix[4]arene affords a lipophilic binuclear structure with both *exo* binding of $Na^+$ between the fused calixarene units and *endo* binding of $Na^+$ within the two calixarene cones.

A tetrahydrofuran (thf) solution of 1,3-dimethyl ether *p-tert*-butylcalix[4]arene ($H_2L$)[8] and sodium hydride (2.5 equiv.) was stirred at room temp. for 40 h (Scheme 1). Filtration and concentration afforded colourless crystals of the poly(thf) solvate of $[Na_2L]_2$ **1** suitable for X-ray diffraction analysis (*vide infra*). These crystals very readily lose thf; the total yield of pure base-free **1** on removal of all residual thf was 70%. The molecular structure of $[Na_2L]_2$ **1** is shown in Fig. 1.† Molecules of **1** lie on crystallographic twofold axes; the thf molecules of crystallisation (not shown) exhibit no unusual contacts to the $Na^+$ ions or calix[4]arene ligand and occupy lattice interstitial sites.

Molecules of $[Na_2L]_2$ **1** comprise two doubly deprotonated 1,3-dimethyl ether *p-tert*-butylcalix[4]arene dianions fused at the lower rim by two bridging sodium cations [Na(2) and Na(2A)], each of which possesses an approximately trigonal-bipyramidal coordination geometry. Each bridging sodium is coordinated to two ethereal O-donors and to three phenolate anionic O-donors, with three of the oxygen atoms belonging to one $L^{2-}$ unit and the remainder to the other. The second pair of sodium cations [Na(1) and Na(1A)] are situated *endo* to the lower rim within the calixarene cone. Na(1) is tightly bonded to the two mutually opposite phenolate O-donors [namely O(2) and O(4)] and has bonding[9] contacts to all four phenol ring *ipso* (with respect to oxygen) carbons at < *ca.* 2.9 Å [range 2.792(3)–2.900(5) Å]. There are further Na···C(arene) π-contacts in the range 2.918(6)–3.056(6) Å to the two arene rings bearing O(1) and O(3) (Fig. 1). The former ring appears to be $\eta^3$-bonded (the *m* and *p*-carbons are not strongly bound) to Na(1) while the latter has effectively $\eta^5$-coordination (the *p*-carbon is significantly less closely bound). The Na(1)···ring centroid distances for the two coordinated rings are 2.76 [for that supporting O(1)] and 2.65 Å. The normals to the least-squares planes of the two coordinated rings form an angle of 3.8°, whereas the non-coordinated rings are somewhat flattened with an angle of 75.1° between the normals to their planes. The four sodium ions and the oxygen donor atoms O(2), O(4), O(2A) and O(4A) in **1** comprise an unusual short, twisted ladder structure which may be viewed as an $Na_4O_4$ cubane that has been opened up along two of the Na···O vectors![10a] Furthermore, **1** is a rare example of a structurally characterised, base-free sodium phenoxide.[10b,c] A search of the Cambridge Structural Database showed that the individual Na–O and Na···C distances in **1** lie within the ranges previously observed for non-calixarene systems.

The structure of $[Na_2L]_2$ is unusual in calixarene metal complex chemistry since it exhibits simultaneous bonding of




**Scheme 1**

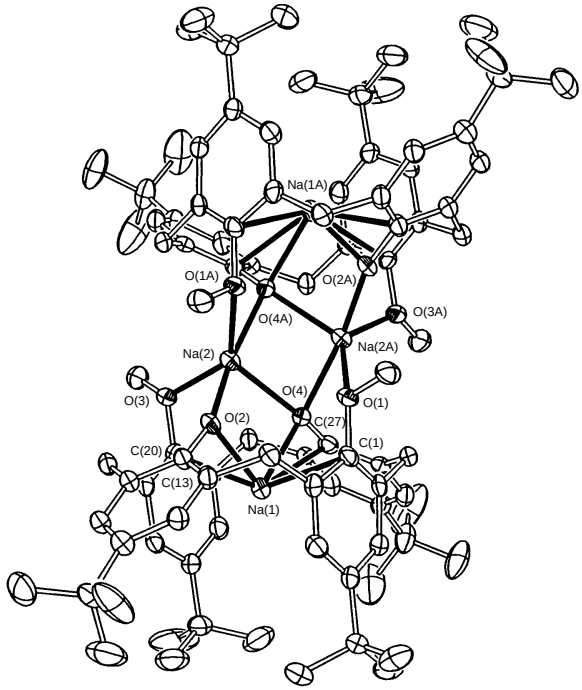



**Fig. 1** Molecular structure of $[Na_2L]_2$ **1**. Hydrogen atoms and thf molecules of crystallisation omitted for clarity, principal bonds to the sodium ions are shown in black and thermal ellipsoids are drawn at the 50% probability level. Selected bond lengths (Å) and angles (°): Na(1)–C(1) 2.792(3), Na(1)–C(13) 2.800(6), Na(1)–C(20) 2.900(5), Na(1)–C(27) 2.797(5), Na(1)–O(2) 2.281(4), Na(1)–O(4) 2.283(4), Na(2)–O(1A) 2.538(4), Na(2)–O(2) 2.129(4), Na(2)–O(3) 2.343(4), Na(2)–O(4) 2.376(4), Na(2)–O(4A) 2.259(4); O(2)–N(2)–O(4A) 163.32(17), O(2)–Na(2)–O(1A) 90.84(15), O(2)–Na(2)–O(3) 89.86(15), O(2)–Na(2)–O(4) 88.55(15), O(1A)–Na(2)–O(3) 138.53(15), O(1A)–Na(2)–O(4) 127.84(14), O(3)–Na(2)–O(4) 93.63(15). Atoms denoted A are related to their counterparts by the symmetry operator: $1 - x, y, 3/2 - z$.

two pairs of otherwise Lewis-base free sodium ions in both possible coordination modes, namely between the fused calixarene units and also within the cones. It is also the first example of a fused dicalix[4]arene bridged by alkali (or alkaline earth) metals; only transition-metal- or post-transition-metal-fused dicalix[4]arenes have been reported previously.[2c–e] A fused derivative of the tetraanion of *p-tert*-butylcalix[4]arene featuring three bridging Zn or Zn(tmeda) units with *endo* ZnEt groups has very recently been described.[3a] Other examples of calix[4]arenes having an *endo* coordinated metal ion have also generally featured additional ligation by Lewis-base donors or other substituents.[2f,7b] In addition, Floriani has recently suggested that coordination of a transition metal to the lower rim O-donors can provide a general strategy for binding alkali-metal ions inside the calix[4]arene cavity.[2f] The homoleptic structure of **1** demonstrates that straightforward encapsulation of sodium ions within the cavity is achieved in a simple one-pot system without the need for transition-metal complexation or additional Lewis-base ligands. The structure of **1** also confirms that cation binding by deprotonated calix[4]arenes within the cone involves a substantial degree of metal–oxygen binding in addition to metal–π-ring interactions.

Preliminary experiments have indicated that $[Na_2L]_2$ is a precursor to new group 2 and early transition-metal complexes *via* sodium halide elimination reactions. We are currently studying the synthesis and structures of other base-free, group 1 and group 2 homoleptic derivatives of 1,3-dialkyl ether *p-tert*-butylcalix[4]arenes, and of *p-tert*-butylcalix[4]arene itself, to explore the relative importance of the metal–phenolate and metal–π-ring interactions.

This work was supported by grants from the EPSRC, Leverhulme Trust and Royal Society (to P. M.). We also thank the EPSRC for a studentship (to S. R. D.) and the provision of a diffractometer and Dr M. G. Davidson (University of Durham) and Professor V. C. Gibson (Imperial College, London) for sharing their results with us prior to publication (see pages 1605 and 1607 of this issue).

## Footnotes and References

* E-mail: philip.mountford@nottingham.ac.uk

† *Crystal data* for $[Na_2L]_2 \cdot 6thf$: $C_{84}H_{116}Na_4O_8 \cdot 6C_4H_8O$, $M$ = 1778.43, monoclinic, space group $C2/c$, $a$ = 18.606(5), $b$ = 30.461(10), $c$ = 20.228(5) Å, $\beta$ = 99.22(3)°, $U$ = 11316(6) Å$^3$, $Z$ = 4, $D_c$ = 1.044 g cm$^{-3}$, $F(000)$ = 3872, $T$ = 150 K, Mo-Kα radiation, $5.7 \leqslant 2\theta \leqslant 47.1°$. The structure was solved by direct methods (SHELXS-96[11a]) and 591 parameters were refined (SHELXL-96[11b]) on $F^2$ for 8351 data to give final conventional $R_1$ = 0.1097 [for data with $F_o > 4\sigma(F_o)$] and $wR_2$ = 0.3436 (all data). Notes on the refinement: phenyl rings were restrained to have local $C_{2v}$ symmetry and to be coplanar with their 1- and 4-substituent atoms. The fully occupied thf solvate molecules were refined with local $C_2$ symmetry. H atoms were included in geometrically calculated positions or located from Fourier difference syntheses; H atoms for partially occupied thf solvates were not included. All full-site occupancy, non-H atoms were refined anisotropically with extensive rigid bond restraints applied to the $U^{ij}$ components. Atomic coordinates, bond lengths and angles, and thermal parameters have been deposited at the Cambridge Crystallographic Data Centre (CCDC). See Information for Authors, Issue No. 1. Any request to the CCDC for this material should quote the full literature citation and the reference number 182/469.

1 (*a*) C. D. Gutsche, *Calixarenes*, Royal Society of Chemistry, Cambridge, 1989; (*b*) V. Böhmer, *Angew. Chem., Int. Ed. Engl.*, 1995, **34**, 713; (*c*) *Calixarenes: A Versatile Class of Macrocyclic Compounds*, ed. J. Vicens and V. Böhmer, Kluwer Academic, Dordrecht, 1991.

2 (*a*) J. M. Harrowfield, M. I. Ogden, W. R. Richmond and A. H. White, *J. Chem. Soc., Dalton Trans.*, 1991, 2153; (*b*) A. Zanotti-Gerosa, E. Solari, L. Giannini, C. Floriani, A. Chiesi-Villa and C. Rizzoli, *Chem. Commun.*, 1996, 119; (*c*) F. Corazza, C. Floriani, A. Chiesi-Villa and C. Rizzoli, *Inorg. Chem.*, 1991, **30**, 4465; (*d*) V. C. Gibson, C. Redshaw, W. Clegg and M. R. J. Elsegood, *J. Chem. Soc., Chem. Commun.*, 1995, 2371; (*e*) F. Corazza, C. Floriani, A. Chiesi-Villa and C. Guastini, *J. Chem. Soc., Chem. Commun.*, 1990, 640; (*f*) A. Zanotti-Gerosa, E. Solari, L. Giannini, C. Floriani, A. Chiesi-Villa and C. Rizzoli, *Chem. Commun.*, 1997, 183; (*g*) J. A. Acho, L. H. Doerrer and S. J. Lippard, *Inorg. Chem.*, 1995, **34**, 2542.

3 (*a*) M. G. Gardiner, S. M. Lawrence, C. L. Ratson, B. W. Skelton and A. H. White, *Chem. Commun.*, 1996, 2491; (*b*) J. L. Atwood, P. C. Junk, S. M. Lawrence and C. L. Raston, *Supramol. Chem.*, 1996, **7**, 15; (*c*) J. L. Atwood, S. G. Bott, C. Jones and C. L. Raston, *J. Chem. Soc., Chem. Commun.*, 1992, 1349; (*d*) F. Corazza, C. Floriani, A. Chiesi-Villa and C. Guastini, *J. Chem. Soc., Chem. Commun.*, 1990, 1083; (*e*) M. M. Olmstead, G. Sigel, H. Hope, X. Xu and P. P. Power, *J. Am. Chem. Soc.*, 1985, **107**, 8087.

4 L. Giannini, E. Solari, A. Zanotti-Gerosa, C. Floriani, A. Chiesi-Villa and C. Rizzoli, *Angew. Chem., Int. Ed. Engl.*, 1996, **35**, 85.

5 J. L. Atwood, M. G. Gardiner, C. Jones, C. L. Raston, B. W. Skelton and A. W. White, *Chem. Commun.*, 1996, 2487.

6 S. G. Bott, A. W. Coleman and J. L. Atwood, *J. Am. Chem. Soc.*, 1986, **108**, 1709.

7 (*a*) F. Inokuchi, Y. Miyahara, T. Inazu and S. Shinkai, *Angew. Chem., Int. Ed. Engl.*, 1995, **34**, 1364; (*b*) J. M. Harrowfield, M. I. Ogden, W. R. Richmond and A. H. White, *J. Chem. Soc., Chem. Commun.*, 1991, 1159.

8 A. Casnati, A. E. Arduini, A. Pochini and R. Ungaro, *Tetrahedron*, 1991, **47**, 2221.

9 E. Weiss, *Angew. Chem., Int. Ed. Engl.*, 1993, **32**, 1501.

10 (*a*) An example of a related $Na_4O_4$ ladder is found for the cyclohexano-15-crown-5 adduct of NaOPh: K. A. Watson, S. Forthier, M. P. Murchie and J. W. Bovenkamp, *Can. J. Chem.*, 1991, **69**, 687; (*b*) I. Cragg-Hine, M. G. Davidson, O. Kocian, T. Kottke, F. S. Mair, R. S. Snaith and J. F. Stoddart, *J. Chem. Soc., Chem. Commun.*, 1993, 1355; (*c*) M. P. Hogerheide, S. N. Ringelberg, M. D. Janssen, J. Boersma, A. L. Spek and G. van Koten, *Inorg. Chem.*, 1996, **35**, 1195.

11 (*a*) G. M. Sheldrick, *Acta Crystallogr., Sect. A*, 1990, **46**, 467; (*b*) SHELXL-96, Institut für Anorganische Chemie der Universität Göttingen, Germany, 1996.

*Received in Basel, Switzerland, 7th March 1997; Com. 7/01639E*

# Can alkali-metal ions influence the coordination and reactivity of calix[4]arenes at transition-metal centres?†

**Vernon C. Gibson,*[a] Carl Redshaw,[a] William Clegg[b] and Mark R. J. Elsegood[b]**

[a] *Department of Chemistry, Imperial College, South Kensington, London, UK SW7 2AY*
[b] *Department of Chemistry, University of Newcastle, Newcastle upon Tyne, UK NE1 7RU*

**Novel chromium and molybdenum calix[4]arene complexes are described in which the calixarene coordination is constrained by alkali-metal ion interactions with the phenoxide units; in the chromium example, an unprecedented calixarene C–H bond activation is found.**

There is currently much interest in the synthesis and characterisation of new metallocalixarenes.[1–6] The simplest of the calixarenes, the calix[4]arene system, usually binds in tetradentate fashion and retains its cone-like appearance.[1–9] In recent examples, however, it has been found that the calix[4]arene is capable of adopting alternative conformations in binding at metal centres, for example a partially flattened cone arrangement identified in aluminium[10] and zinc compounds[11] and an alkali-metal-constrained elliptical conformation in which the calixarene oxygens occupy mutually *cis* and *trans* sites in an octahedral geometry.[2] There has also been a report of an elliptical calixarene arrangement in the absence of alkali-metal ions;[8] it is thus unclear whether it is the transition metal or the alkali-metal ions that exert the more substantial influence on calix[4]arene conformation. Here, we describe two unusual structures that contain alkali-metal ions within elliptical calixarene ligands; in one case an unprecedented C–H bond activation of the calixarene ligand results, providing the first indication that highly reactive metal centres may arise from these constrained geometry ligand–metal environments.

Treatment of $[Mo(NAr)(CHCMe_2Ph)(O_3SCF_3)_2(dme)]$ (Ar = $C_6H_3Me_2$-2,6) with 1 equiv. of $K_4L$ ($H_4L$ = *p-tert*-butylcalix[4]arene) in tetrahydrofuran (thf) affords, after work-up, orange prisms of $[Mo(NAr)(L)K_2(NCMe)_3O]_2$ **1**‡ in 70% yield. Crystals of **1** suitable for an X-ray determination§ were grown from acetonitrile at room temp. The asymmetric unit comprises one half of a dimeric molecule and two non-coordinated molecules of acetonitrile. The molecular structure is shown in Fig. 1 and selected bond lengths are given in the caption. The molecule is a centrosymmetric dimer in which each molybdenum atom possesses a pseudo-octahedral geometry. The calixarene 'cones' are distorted in such a way that two opposing phenoxide rings are drawn together by π interactions with potassium atom K(1) which is also bonded to the oxygens of the remaining two phenoxide units. One of the latter two rings is also involved in a π interaction with a bridging potassium atom, K(2), which forms part of a ladder motif. The Mo–O(5) bond distance within this motif, at 1.752(2) Å, is consistent with substantial multiple bond character.[12] The origin of the ladder oxygen atoms is most likely the thf solvent since the reaction and subsequent work-up were conducted under rigorous air- and moisture-free conditions.

In extending our investigations to chromium, $[Cr(NBu^t)_2Cl_2]$ was reacted with 2 equiv. of $LiOBu^t$ in thf to generate $[Cr(NBu^t)_2(OBu^t)_2]$ which was then treated *in situ* with 2 equiv. of $H_4L$. This led after work-up to the formation of large green needles of **2** in 60% yield. Crystals suitable for an X-ray determination§ were grown from acetonitrile solution at room temp.; they incorporate four uncoordinated molecules of acetonitrile per molecule of the complex. The molecular structure is shown in Fig. 2; selected bond lengths and angles are given in the caption. All of the *tert*-butylimido and *tert*-butoxide ligands of the starting chromium species are sacrificed, as *tert*-butylamine and *tert*-butyl alcohol, respectively, and two calix[4]arene units are coordinated to the chromium centre. One possesses a similar coordination geometry to that observed in **1** with the exception that the smaller lithium ion interacts with just one of the arene rings and the interaction is strongest with the *ipso* and *ortho* ring carbons [Li···C(*ipso*) 2.599(10) Å, Li···C(*ortho*) 2.716(10), 2.797(10) Å]. A remarkable feature of the complex is the joining of this calixarene to a second calixarene unit *via* an ether [O(1)] linkage. This formally arises from the activation of a bridging methylene C–H bond of the second calixarene, to our knowledge the first time such reactivity has been observed in a metallocalixarene complex. The resultant ether oxygen atom is then bonded to an axial coordination site in the chromium complex.

The remainder of the second calixarene unit is bonded to the metal centre through two phenoxide linkages whose oxygen atoms are hydrogen bonded to atoms O(5) and O(6), which in turn are coordinated to a lithium atom bound to O(3). The net result is the encapsulation of an octahedral chromium(III) centre by two fused calix[4]arene rings. While it is not possible to establish with any degree of certainty the mechanism of C–H bond activation in **2**, it is possible that it may be a consequence of the constrained calixarene coordination geometry which leads to severe bending at the axial oxygens O(1) and O(3) [120.0(3), 112.6(3)°, respectively]. Future studies will be directed towards probing the influence of the constrained

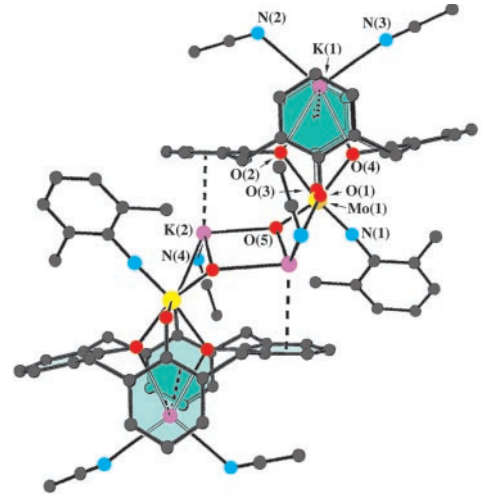



**Fig. 1** The molecular structure of **1** with H atoms and $Bu^t$ groups omitted. Selected distances (Å) and angles (°): Mo(1)–O(1) 2.059(2), Mo(1)–O(2) 2.108(2), Mo(1)–O(3) 2.037(2), Mo(1)–O(4) 2.053(2), Mo(1)–O(5) 1.752(2), Mo(1)–N(1) 1.768(3), K(1)–O(2) 2.639(2), K(1)–O(4) 2.607(2), K(1)–N(2) 2.832(4), K(1)–N(3) 2.819(4), K(1)–ring centroids 3.129(3), 3.164(3), K(2)–O(5) 2.632(2), K(2)–O(5A) 2.832(2), K(2)–O(1A) 2.642(2), K(2)–N(4) 2.741(4), K(2)–ring centroid 2.862(3); Mo(1)–O(1)–C(9) 119.6(2), Mo(1)–O(2)–C(20) 126.7(2), Mo(1)–O(3)–C(31) 119.8(2), Mo(1)–O(4)–C(42) 137.2(2).

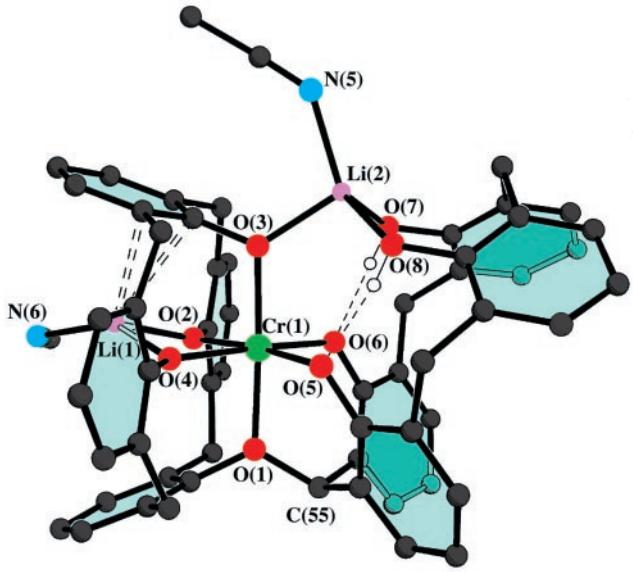



**Fig. 2** Molecular structure of **2** with Bu$^t$ groups and most H atoms omitted; OH groups are shown. Selected distances (Å) and angles (°): Cr–O(1) 1.995(3), Cr–O(2) 1.935(3), Cr–O(3) 1.972(3), Cr–O(4) 1.924(3), Cr–O(5) 1.959(3), Cr–O(6) 1.945(3), Li(1)–O(2) 1.857(9), Li(1)–O(4) 1.896(10), Li(1)–N(6) 2.000(11), shortest Li(1)–C 2.599(10), Li(2)–O(3) 1.920(8), Li(2)–O(7) 1.917(9), Li(2)–O(8) 1.922(9), Li(2)–N(5) 2.018(10); Cr–O(1)–C(1) 120.0(3), Cr–O(2)–C(12) 128.0(3), Cr–O(3)–C(23) 112.6(3), Cr–O(4)–C(34) 134.5(3), Cr–O(1)–C(55) 117.8(2), Cr–O(5)–C(45) 127.5(3), Cr–O(6)–C(56) 129.3(3).

calixarene coordination geometry on the reactivity of calixarene-complexed metal centres.

The Engineering and Physical Sciences Research Council is thanked for financial support. Dr P. Mountford (University of Nottingham) is thanked for sharing results prior to publication.

## Footnotes and References

* E-mail: v.gibson@ic.ac.uk

† This ChemComm is also available in enhanced multi-media format *via* the World Wide Web: http://chemistry.rsc.org/rsc/cccenha.htm

‡ Satisfactory elemental analyses have been obtained. *Selected spectroscopic data* for **1**: $^1$H NMR ($CDCl_3$, 500 MHz, 298 K) $\delta$ 7.00 −6.65 (overlapping m, 22 H, aryl), 4.42 (d, 4 H, $^3J_{HH}$ 13.8 Hz, $CH_2$), 4.31 (d, 4 H, $^3J_{HH}$ 14.3 Hz, $CH_2$), 3.27 (d, 4 H, $^3J_{HH}$ 14.5 Hz, $CH_2$), 3.07 (d, 4 H, $^3J_{HH}$ 14.0 Hz, $CH_2$), 2.37 (s, 12 H, $CH_3$Ar), 1.31 (m, 18 H, MeCN), 1.19 − 1.11 (overlapping m, 72 H, [$(CH_3)_3$C]). $^{13}$C{$^1$H} NMR ($CDCl_3$, 100.6 MHz, 298 K) $\delta$ 165.5, 164.2, 162.7, 154.1 (4 × s, *ipso*-aryl), 140.2, 138.7, 138.2, 134.8, 134.3, 134.1, 133.8, 132.2, 131.1, 130.9, 130.6, 128.2, 127.2, 124.1, 123.8, 123.6, 123.1, 122.9, 122.8, 122.5, 36.2 (Ar$CH_2$Ar), 35.4 (Ar$CH_2$Ar), 32.0 [C($CH_3$)$_3$], 31.9 [C($CH_3$)$_3$], 31.8 [C($CH_3$)$_3$], 31.7 [C($CH_3$)$_3$], 28.0, 22.5, 18.5 ($C_6H_3Me_2$-2,6) [quaternary $(CH_3)_3C$ not observed]. $^1$H NMR spectra of **2** are broad and uninformative; the X-band EPR spectrum (solid, 298 K) is complex comprising broad low-field features centred at $g$ = 3.35 and several weaker features out to $g$ = 1.19.

§ *Crystal data*: **1**·4MeCN: $C_{116}H_{140}K_4Mo_2N_8O_{10}$·4$CH_3CN$, $M$ = 2318.9, monoclinic, space group $P2_1/n$, $a$ = 20.2461(12), $b$ = 12.0202(7), $c$ = 27.1727(15) Å, $\beta$ = 110.700(2)°, $U$ = 6185.9(6) Å$^3$, $Z$ = 2, $D_c$ = 1.245 g cm$^{-3}$, $\mu$ = 0.40 mm$^{-1}$ (Mo-K$\alpha$, $\lambda$ = 0.710 73 Å), $T$ = 160 K. 37 557 reflections were measured on a Siemens SMART CCD area-detector diffractometer and corrected semiempirically for absorption (transmission 0.761–0.917), yielding 13 952 unique data ($2\theta_{max}$ = 55.0°, $R_{int}$ = 0.0479). The structure was determined by direct methods and refined by $F^2$ for all data, with anisotropic displacement parameters, and riding isotropic H atoms. Final $R_w$ = $\{\Sigma[w(F_o^2 - F_c^2)^2]/\Sigma[w(F_o^2)^2]\}^{1/2}$ = 0.1135 for all data, conventional $R$ = 0.0571 on $F$ values of 11 481 reflections with $F_o^2 > 2\sigma(F_o^2)$; goodness of fit = 1.232 on $F^2$ values for 715 refined parameters. All final difference map features were within ± 0.5 e Å$^{-3}$.

**2**·4MeCN: $C_{92}H_{111}CrLi_2N_2O_8$·4$CH_3CN$, $M$ = 1602.9, monoclinic, space group $P2_1/c$, $a$ = 17.5630(7), $b$ = 46.3196(18), $c$ = 13.0311(5) Å, $\beta$ = 108.796(2)°, $U$ = 10 035.6(7) Å$^3$, $Z$ = 4, $D_c$ = 1.061 g cm$^{-3}$, $\mu$ = 0.17 mm$^{-1}$ (Mo-K$\alpha$, $\lambda$ = 0.710 73 Å), $T$ = 160 K. Experimental and computational methods were as for **1**, with 47 608 measured data, transmission 0.448–0.962, 13 090 unique data ($2\theta_{max}$ = 45.0°, $R_{int}$ = 0.0681), disorder in some Bu$^t$ groups modelled with restraints, $R_w$ = 0.2646 for all data, $R$ = 0.0873 for 9667 data having $F_o^2 > 2\sigma(F_o^2)$; goodness of fit = 1.067 for 1136 refined parameters and 306 restraints, extremes of difference map +1.29 and −0.39 e Å$^{-3}$. The hydroxyl hydrogens were located in a difference map and freely refined. Programs: Siemens SMART (control), SAINT (integration) and SHELXTL, and local programs. CCDC 182/537.

1 L. Giannini, E. Solari, A. Zanotti-Gerosa, C. Floriani, A. Chiesi-Villa and C. Rizzoli, *Angew. Chem., Int. Ed. Engl.*, 1996, **35**, 2825; B. Castellano, A. Zanotti-Gerosa, E. Solari and C. Floriani, *Angew. Chem., Int. Ed. Engl.*, 1996, **15**, 4894.
2 A. Zanotti-Gerosa, E. Solari, L. Giannini, C. Floriani, A. Chiesi-Villa and C. Rizoli, *Chem. Commun.*, 1997, 183.
3 J. A. Acho, L. H. Doerrer and S. J. Lippard, *Inorg. Chem.*, 1995, **34**, 2542.
4 V. C. Gibson, C. Redshaw, W. Clegg and M. R. J. Elsegood, *J. Chem. Soc., Chem. Commun.*, 1995, 2371.
5 J. A. Acho and S. J. Lippard, *Inorg. Chim. Acta*, 1995, **229**, 5.
6 A. Zanotti-Gerosa, E. Solari, L. Giannini, C. Floriani, A. Chiesi-Villa and C. Rizzoli, *Chem. Commun.*, 1996, 119.
7 F. Corazza, C. Florianni, A. Chiesi-Villa and C. Guastini, *J. Chem. Soc., Chem. Commun.*, 1990, 640.
8 F. Corazza, C. Florianni, A. Chiesi-Villa and C. Rizzoli, *Inorg. Chem.*, 1991, **30**, 4465.
9 F. Corazza, C. Floriani, A. Chiesi-Villa and C. Guastini, *J. Chem. Soc., Chem. Commun.*, 1990, 1083.
10 J. L. Atwood, M. G. Gardiner, C. Jones, C. L. Raston, B. W. Skelton and A. H. White, *Chem. Commun.*, 1996, 2487.
11 M. G. Gardiner, S. M. Lawrence, C. L. Raston, B. W. Skelton and A. H. White, *Chem. Commun.*, 1996, 2491.
12 W. A. Nugent and J. M. Mayer, *Metal–Ligand Multiple Bonds*, Wiley Interscience, New York, 1988.

*Received in Basel, Switzerland, 3rd April 1997; 7/02272G*

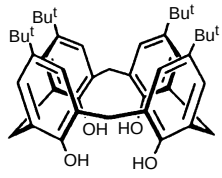
# Synthesis and X-ray structures of tetralithium derivatives of *tert*-butylcalix[4]arene containing unique Li–O cores based on a square-pyramidal geometry

**Matthew G. Davidson,* Judith A. K. Howard, Sarah Lamb and Christian W. Lehmann**

*University of Durham, Department of Chemistry, Science Laboratories, Durham, UK DH1 3LE*

**Tetralithiation of *tert*-butylcalix[4]arene in the presence of hmpa (hexamethylphosphoramide) results in the isolation of either a monomeric complex in which LiOH is incorporated into an $Li_5O_5$ core based on an isolated square pyramid of Li atoms, or a dimeric LiOH-free species containing an $Li_8O_8$ core in which the same structural motif is maintained by edge-sharing of two square pyramids of Li atoms.**

Both underivatised and partially O-alkylated calixarenes have attracted much attention as phenolic ligands for both transition and p-block metals. The flexible orientation of the coordinating phenolic oxygen atoms, coupled with the potential for multi-metallations has recently led to reports of some fascinating and unique structures.[1,2] Although the interaction of alkali metals with neutral lower-rim-modified calixarenes is well known,[1] the isolation and characterisation of homometallic phenoxy-bound alkali-metal derivatives of calixarenes is restricted to only one Cs-[3] and one Na-containing[4] example. Floriani *et al*. have very recently reported the syntheses and X-ray structures of some mixed alkali-metal–transition metal–calixarene complexes[5] although in these cases solvation of the alkali metal is exclusively in the cavity of the calixarene. In the light of these considerations and also in view of the unusual structural chemistry that has recently been found to result from multilithiations of organic molecules[6] we felt it was timely to consider the simple metallation of calixarenes with s-block metals. We herein report our preliminary results concerning the simple reaction of $Bu^nLi$ with *tert*-butylcalix[4]arene $H_4L$ (below) which has resulted in the isolation and X-ray structural characterisation of two related tetralithiated calixarenes.




$H_4L$

Reaction of $H_4L$ in toluene solution with 4 equiv. of $Bu^nLi$ in the presence of an excess of hexamethylphosphoramide hmpa (used as received, without pre-drying, *vide infra*) resulted in the formation of a fine white precipitate suspended in a pale yellow solution. Dissolution of this solid by warming to 100 °C and then cooling to room temp. afforded a crop of colourless, air-sensitive crystals. Preliminary characterisation by IR (in particular a strong sharp O–H stretch at 3612 $cm^{-1}$) and $^1H$ NMR spectroscopies, and then an X-ray crystal structure† revealed the isolated product to be $Li_4L{\cdot}LiOH{\cdot}4hmpa$ **1**. In the solid state (Fig. 1) the molecule lies on a crystallographic twofold axis. The four coplanar Li atoms which formally metallate the calixarene lie below the plane defined by the O atoms of the calixarene's lower rim. Each of the Li atoms is coordinated to a neutral hmpa molecule. Together, the four hmpa ligands create a lower rim cavity of similar dimensions to that defined by the four aryl groups of the calixarene on the opposite side of the macrocycle, which itself retains a normal cone configuration. In spite of their similar proportions the two cavities are electronically very different. The bottom of the upper cavity is anionic ($O^-$ lined) while the lower one is cationic ($Li^+$ lined) in nature, which facilitates the complementary binding of a $Li^+$ cation [Li(3) bound to all four phenolic oxygen atoms] and an $OH^-$ anion [O(99), $\mu_4$-bridged to the four coplanar Li atoms]. An additional feature of the structure of **1** is that both the normal upper rim cavity and the novel lower rim cavity (defined by the hmpa ligands) act as hosts for guest toluene molecules (not shown in the figure), emphasising their similar dimensions. Thus overall, the structure of **1** may be viewed as resulting from the incorporation of LiOH into a $Li_4L$ moiety; Li(3)···O(99) [2.25(1) Å] is longer than other Li–O bonds within the core of **1** [1.92(1)–2.089(4) Å] though an interaction between the two is still probable.

The incorporation of LiOH and $Li_2O$ into organolithium compounds, whether deliberately or serendipitously, has been reported before,[7] and in order to probe the source of the LiOH unexpectedly incorporated into **1**, and to obtain an LiOH free complex, similar reactions were carried out using a freshly dried (over activated 13X molecular sieve) sample of hmpa. Analysis of the resulting crystalline solid, again ultimately by X-ray crystallography,† revealed the composition of complex **2** to be $(Li_4L{\cdot}2hmpa)_2$. In the solid state **2** is dimeric, is free from LiOH, and has only two rather than four hmpa molecules per calixarene (Fig. 2). The crystallographic asymmetric unit consists of two independent but geometrically and chemically similar $Li_4O_4$ 'monomeric' units which then give centrosymmetric 'dimeric' aggregates. Within the $Li_8O_8$ core there are

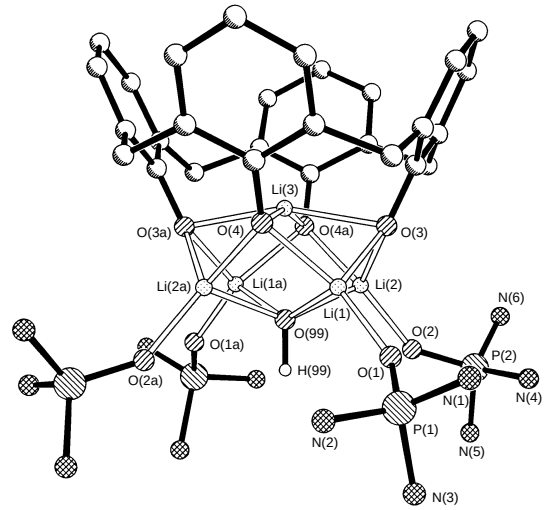



**Fig. 1** Molecular structure of **1**; for clarity, all hydrogen atoms, calixarene Bu$^t$ groups, hmpa methyl groups and lattice solvent are omitted

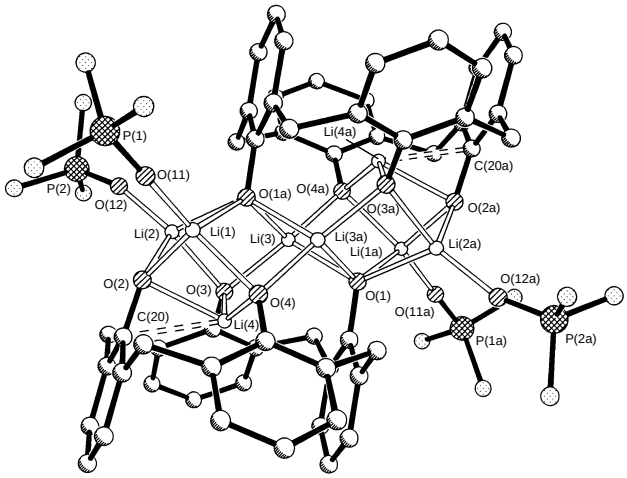



**Fig. 2** Molecular structure of **2** (only one of two crystallographically independent but chemically similar molecules is shown). For clarity, all hydrogen atoms, calixarene Bu$^t$ groups, hmpa methyl groups and lattice solvent are omitted.

three distinct lithium environments: two Li atoms [Li(1) and Li(2)] are complexed by hmpa and retain a similar environment to that found for the four coplanar Li atoms of **1**; Li(3) is uncomplexed by hmpa and bridges the two calixarenes; and Li(4) lies within the calixarene cavity. One oxygen atom [O(1)] fulfils the $\mu_4$-capping role played by O(99) in **2**, resulting in a distortion of the original cone conformation of the calixarene. Thus, Li(4) is bound to only three O atoms which prompts an interaction with the $\pi$-system of one of the calixarene aryl groups [Li(4)–C(20) 2.31(1) Å]. The distance between O(1) and Li(4a) ( > 2.8 Å) is considerably longer than the corresponding Li···O separation found in **1**. Other Li–O distances within the core of **2** [1.91(1)–2.11(1) Å] are comparable to those found in **1**. Thus, despite being free of LiOH, in **2** the same general structural features are present as in **1**: a $Li^+$ cation lies in the O lined cavity of the calixarene and an $O^-$ anion caps four Li atoms. The $^1$H NMR spectrum of **2** suggests that the complex retains a distorted cone configuration in solution: three resonances assigned to Bu$^t$ groups (relative integrals 2 : 1 : 1) and three corresponding Ar–H resonances are observed, which is consistent with the asymmetry of the calixarene seen in the solid state, and contrasts with the equivalence of Bu$^t$ groups (and Ar–H protons) in the $^1$H NMR spectrum of **1**.

In the light of the structures of **1** and **2**, one can envisage the latter as being suited to act as a carrier for inorganic salts by binding the ion-separated components of the salt in two complementary cavities, resulting in a complex for which **1** is a model. In contrast to the work described by Floriani,[5] in which the shape of the calixarene cavity was modified using Nb or Ta in order to accommodate alkali-metal cations, the structures of **1** and **2** suggest that significant deviation from the normal cone configuration is unnecessary in order to bind lithium within the cavity.

Although **2** can be reproducibly prepared using dried hmpa, the synthesis of **1** has not to date been reproduced, even though spectroscopic evidence suggests that its crystal structure is representative of the bulk product obtained. The source of LiOH incorporated in **1** remains an open question. Although the use of 'wet' hmpa is consistent with the product obtained, it is possible that LiOH present in the sample of Bu$^n$Li used,[7c] or contamination from another source was responsible. We are currently investigating the incorporation, by controlled and reproducible means, of s-block metal salts (including LiOH) into lithiated calixarene derivatives.

Also of note in these structures are the geometries of the $Li_5O_5$ and $Li_8O_8$ cores of **2** and **3**. Both are best viewed as derived from a square-pyramidal structural motif (Fig. 3). In **2**

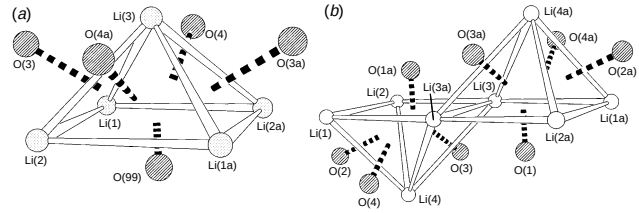



**Fig. 3** Li–O cores of (*a*) **1** and (*b*) **2**; connections between lithium atoms are not intended to imply bonding interactions

all five faces of an isolated square pyramid of lithium atoms are capped by oxygen atoms [four $\mu_3$ and one $\mu_4$, Fig. 3(*a*)]. In **2**, the same motif persists, though here two square pyramids of lithium share one edge and the inner triangular face of each is uncapped leaving the eight oxygen atoms to cap the other eight faces [six $\mu_3$ and two $\mu_4$, Fig. 3(*a*)]. To our knowledge, these are the first observations of such a structural motif in organolithium chemistry, though pentanuclear organolithium species of any geometry are extremely rare.[8] The arrangement of a square plane of lithium atoms capped by a $\mu_4$ oxygen atom is, however, reminiscent of an isolated fragment of the polymeric layered structure of LiOMe.[9]

We thank Durham (University Scholarship for S. L), The Royal Society (Leverhulme Trust Senior Research Fellowship for J. A. K. H.), and Dr P. Mountford (Nottingham) for communication of unpublished results.

## Footnotes and References

* E-mail: m.g.davidson@durham.ac.uk

† *Crystal data*: **2**: colourless crystals of $C_{68}H_{125}Li_5N_{12}O_9P_4 : 3.9\ C_5H_5CH_3 \cdot 0.1H_2O$, orthorhombic, space group *Pbca*, M = 1771.28, *a* = 18.380(3), *b* = 28.436(6), *c* = 19.724(3) Å, *U* = 10309(3) Å$^3$, *Z* = 4. Data collection at *T* = 150 K, *wR*(*F*$^2$, all data) = 0.2484, *R*(*F*, obs. data) = 0.0887.

**3**: colourless crystals of $C_{136}H_{200}Li_8N_{12}O_{12}P_4$ triclinic, space group $P\bar{1}$ (no. 2), *M* = 2374.48 *a* = 15.435(2), *b* = 16.891(2), *c* = 30.674(3) Å, $\alpha$ = 95.66(1), $\beta$ = 90.68(1), $\gamma$ = 116.71(4), *U* = 7094(1), *Z* = 2. Data collection at *T* = 150 K, *wR*(*F*$^2$, all data) = 0.4154, *R*(*F*, obs. data) = 0.1322.

CCDC 182/482.

1 V. Böhmer, *Angew. Chem., Int. Ed. Engl.*, 1995, **34**, 713 and references therein.
2 A. Zanotti-Gerosa, E. Solari, L. Giannini, C. Floriani, A. Chiesi-Villa and C. Rizzoli, *Chem. Commun.*, 1996, 119; J. M. Smith and S. G. Bott, *Chem. Commun.*, 1996, 377; J. L. Atwood, M. G. Gardiner, C. Jones, C. L. Raston, B. W. Skelton and A. H. White, *Chem. Commun.*, 1996, 2487; M. G. Gardiner, S. M. Lawrence, C. L. Raston, B. W. Skelton and A. H. White, *Chem. Commun.*, 1996, 2491.
3 R. Assmus, V. Böhmer, J. M. Harrowfield, M. I. Ogden, W. R. Richmond, B. W. Skelton and A. H. White, *J. Chem. Soc., Dalton Trans.*, 1993, 2427.
4 S. R. Dubberley, A. J. Blake and P. Mountford, *Chem. Commun.*, 1997, 1603.
5 A. Zanotti-Gerosa, E. Solari, L. Giannini, C. Floriani, A. Chiesi-Villa and C. Rizzoli, *Chem. Commun.*, 1997, 183.
6 See for example: I. Cragg-Hine, M. G. Davidson, O. Kocian, F. S. Mair, E. Pohl, P. R. Raithby, R. Snaith, N. Spencer and J. F. Stoddart, *Angew. Chem., Int. Ed. Engl.*, 193, **32**, 1182 and references therein; W. Clegg, L. Horsburgh, R. E. Mulvey and M. J. Moss, *Angew. Chem., Int. Ed. Engl.*, 1995, **34**, 1233.
7 (*a*) C. Lambert, F. Hampel, P. v. R. Schleyer, M. G. Davidson and R. Snaith, *J. Organomet. Chem.*, 1995, **487**, 139; (*b*) S. C. Ball, I. Cragg-Hine, M. G. Davidson, R. P. Davies, M. I. Lopez-Solara, P. R. Raithby, D. Reed, R. Snaith and E. M. Vogl, *J. Chem. Soc., Chem. Commun.*, 1995, 247; (*c*) M. Driess, H. Pritzkow, S. Martin, S. Rell, D. Fenske and G. Baum, *Angew. Chem., Int. Ed. Engl.*, 1996, **35**, 986.
8 D. Barr, W. Clegg, R. E. Mulvey and R. Snaith, *J. Chem. Soc., Chem. Commun.*, 1984, 226; Search of Cambridge Structural Database.
9 E. Weiss, *Angew. Chem., Int. Ed. Engl.*, 1993, **32**, 1501 and references therein.

*Received in Cambridge, UK, 3rd April 1997; 7/02280H*

# Gene sensor using ferrocenyl oligonucleotide

**Toshihiro Ihara,*† Masamichi Nakayama, Mitsuru Murata, Koji Nakano and Mizuo Maeda***

*Department of Chemical Science and Technology, Faculty of Engineering, Kyushu University, Hakozaki, Higashi-ku, Fukuoka 812-81, Japan*

**An electrochemical gene sensing system has been developed using a redox-active ferrocene-modified oligonucleotide and an oligonucleotide anchored on a gold electrode, both of which formed a sandwich-type ternary complex with the target DNA to give a redox current.**

Radioactive isotopes (RI) such as $^{32}P$ are widely used as labels of DNA because of their high detection sensitivity. However, due to their hazardous nature and short shelf life, the development of an alternative detection system that is convenient and practical without relying on RI is eagerly hoped for. We have proposed electrochemical methods as the alternative[1–3] and proved their potential using a high performance liquid chromatography–electrochemical detector system.[4] Recently, several systems for electrochemical detection of DNA have been reported.[5–11] Here we describe a novel electrochemical technique for gene detection in which a sandwich-type complex from an oligodeoxynucleotide (ODN) immobilized on a gold electrode, the target DNA and a ferrocenyl ODN is formed to give a response (Fig. 1).

All ODNs used in this study were prepared on a fully automated DNA synthesizer (Parmacia, Gene Assembler Plus). The ferrocenyl ODN (**T12Fc**) was synthesized by the coupling of amino-terminated ODN with an activated ester of ferrocenecarboxylic acid according to our previous report.[1,4] A 16-mer ODN (**e16S**) which has five successive phosphorothioate units on its 5′-terminus was synthesized using Beaucage's reagent.[12]

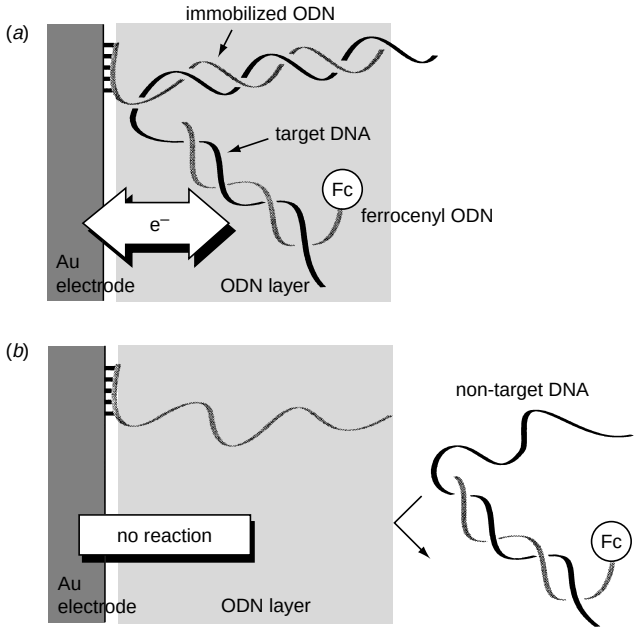
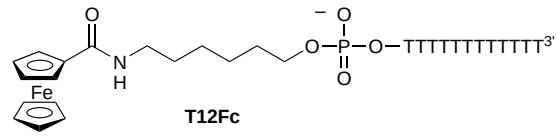



**Fig. 1** Schematic illustration of the electrochemical gene sensing system based on the formation of complementary sandwich-type complex. (*a*) Target DNA combines the ferrocenyl ODN with the ODN on electrode. Oxidation current due to the concentrated ferrocenyl units should reflect the concentration of the target. (*b*) Ferrocenyl units are not concentrated onto the electrode using non-target DNA.

**e16S** 5′TsTsTsTsTsTCTCATACATG3′
**e16** 5′TTTTTTCTCATACATG3′
**t19** 5′CATGTATAAAAAAAAAAAA3′
**m19** 5′CATCTATAAAAAAAAAAAA3′
**c19** 5′TTCCGCGAAAAAAAAAAAA3′




**T12Fc**

s = phosphorothioate linkage

The ODN was anchored on the gold electrode *via* chemisorption[13,14] in the following manner: a 10 μl droplet of a 50 μM aqueous solution of **e16S** (containing 100 mM KCl) was cast on well-polished gold disk electrodes (1.6 mm diameter, BAS). The electrodes were then washed with 100 mM KCl solution and stored at 5 °C before use.

Cyclic voltammetric (CV) measurements using a ferrocyanide/ferricyanide redox couple were carried out in order to confirm the ODN modification on the electrode.[13] While the electrode treated with **e16**, which does not have any sulfur atoms, gave the same voltammogram as the bare electrode, the peak current obtained for the **e16S**-modified electrode was significantly suppressed, indicating that the redox couple was excluded from the electrode surface due to electrostatic repulsion between the anionic redox species and the ODN polyanion anchored on the electrode. Heat-treatment of the **e16S**-modified electrode at 80 °C for 30 min in water made no difference to the voltammogram produced. It is likely that the multi-point anchoring of the DNA *via* the phosphorothioate moieties will give stable immobilization of DNA on the gold electrode. This method should be useful for fixation of synthetic DNA onto electrodes.

The electrode modified with **e16S** was immersed in a 50 μM aqueous solution of an equimolar mixture of **T12Fc** and **t19** [**T12Fc**–**t19**, the target containing 100 mM KCl, 5 mM Tris-HCl (pH 8.0)] for 24 h at 5 °C. The electrode was then rinsed with 100 mM KCl at 5 °C. In CV measurements in 100 mM KCl, the modified electrode gave reversible redox waves showing a peak separation of 50 mV. We estimated the amount of the bound probe (**T12Fc**) to be 22–55 pmol $cm^{-2}$ by integration of the charge under the anodic peak. Fig. 2 shows differential pulse voltammograms (DPVs) for the modified electrode. A significant anodic peak due to oxidation of the ferrocene moiety was observed for the electrode treated with the target DNA. On the other hand, only a slight peak was observed for the **e16S**-modified electrode which was treated similarly with a mixture of **T12Fc** and **m19** (**T12Fc**–**m19**, mismatch control) and **T12Fc** and **c19** (**T12Fc**–**c19**, control, data not shown).

The peak potential ($E_p$) of the DPV was +620 mV (*vs.* Ag/AgCl), which means the redox potential ($E_{1/2}$) of the ferrocenyl unit of **T12Fc** on the electrode was +645 mV [$E_{1/2} = E_p + (\Delta E/2)$]. This value is exceedingly positive compared with that in bulk solution; CV measurements of aqueous **T12Fc** showed a

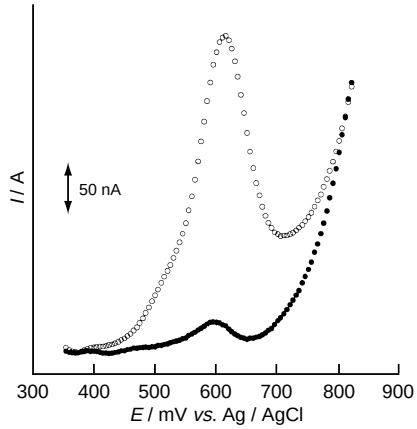



**Fig. 2** Differential pulse voltammograms of the ODN modified electrode treated with (○) **T12Fc–t19** (target) and (●) **T12Fc–m19** (mismatch control). The ODN electrode was sensitive only for the target **t19**. Electrodes: Pt plate, Ag/AgCl; pulse period: 200 ms; scan rate: 25 mV $s^{-1}$; pulse amplitude: 50 mV; pulse width: 50 ms, *T*: 5 °C.

redox potential of *ca.* +430 mV.[1] A similar positive shift was observed in Letsinger's study,[15] in which the ferrocenyl mononucleotide was confined on the electrode surface using sulfur (thiol group)–gold chemisorption.

While the peak for the target sample (**T12Fc–t19**) did not change at all after rinsing the electrode with 100 mM KCl at 5 and 10 °C, similar treatment at 20 °C reduced the peak current appreciably to *ca*. 25%, providing a comparable peak with those obtained for the control samples. On the other hand, the small peaks observed for the control sample (**T12Fc–c19**) and for the mismatch control sample (**T12Fc–m19**) scarcely changed after similar treatment at 20 °C. These results indicate that the binding of the target sample was temperature sensitive. That is, the target was recognized by means of complementary base-pairing with the ODN immobilized on the electrode. On the other hand, the slight current observed in the control and mismatch samples should be ascribed to the non-specific binding of **T12Fc–c19** and –**m19** to the ODN. Thus the detecting device proposed here should be a basis for a simple and highly selective sensing system. Optimization of the measurement conditions such as temperature, salt concentration and/or coexisting non-specific binding blocker (mRNA or sonicated calf thymus DNA) should be made to improve the sensitivity of this system. The electrode's durability also needs to be studied before practical application of this technique to gene diagnosis.

This work was partially supported by a Grant-in-Aid for Encouragement of Young Scientists (No. 08750941) and by a Grant-in-Aid for Scientific Research (B) (No. 08458290) from the Ministry of Education, Science, Sports, and Culture. The authors are also grateful to The Sagawa Foundation for Promotion of Frontier Science (T. I.) and to Terumo Life Science Foundation (M. M.).

## Footnote and References

† *Present address*: Department of Applied Chemistry and Biochemistry, Faculty of Engineering, Kumamoto University, Kurokami, Kumamoto 860, Japan. E-mail: toshi@chem.kumamoto-u.ac.jp

1 T. Ihara, Y. Maruo, S. Takenaka and M. Takagi, *Nucleic Acids Res.*, 1996, **24**, 4273.
2 S. Takenaka, T. Ihara and M. Takagi, *J. Chem. Soc., Chem. Commun.*, 1990, 1485.
3 S. Takenaka, H. Sato, T. Ihara and M. Takagi, *J. Heterocycl. Chem.*, 1997, **34**, 123.
4 S. Takenaka, Y. Uto, H. Kondo, T. Ihara and M. Takagi, *Anal. Biochem.*, 1994, **218**, 436.
5 X.-H. Xu and A. J. Bard, *J. Am. Chem. Soc.*, 1995, **117**, 2627.
6 S. R. Mikkelsen, *Electroanalysis*, 1996, **8**, 15.
7 B. Kolakowski, F. Battaglini, Y. S. Lee, G. Klironomos and S. R. Mikkelsen, *Anal. Chem.*, 1996, **68**, 1197.
8 K. Hashimoto, K. Ito and Y. Ishimori, *Anal. Chem.*, 1994, **66**, 3830.
9 X. Cai, G. Rivas, P. A. M. Farias, H. Shiraishi, J. Wang, M. Fojta and E. Palacek, *Bioelectrochem. Bioenerg.*, 1996, **40**, 41.
10 A. Lishanski, E. A. Ostrander and J. Rine, *Proc. Natl. Acad. Sci. USA*, 1994, **91**, 2674.
11 S. Palanti, G. Marrazza and M. Mascini, *Anal. Lett.*, 1996, **29**, 2309.
12 R. P. Iyer, W. Egan, J. B. Regan and S. L. Beaucage, *J. Am. Chem. Soc.*, 1990, **112**, 1253.
13 M. Maeda, Y. Mitsuhashi, K. Nakano and M. Takagi, *Anal. Sci.*, 1992, **8**, 83.
14 H. Taira, K. Nakano, M. Maeda and M. Takagi, *Anal. Sci.*, 1993, **9**, 199.
15 R. C. Mucic, M. K. Herrlein, C. A. Mirkin and R. L. Letsinger, *Chem. Commun.*, 1996, 555.

*Received in Cambridge, UK, 19th May 1997; 7/03401F*

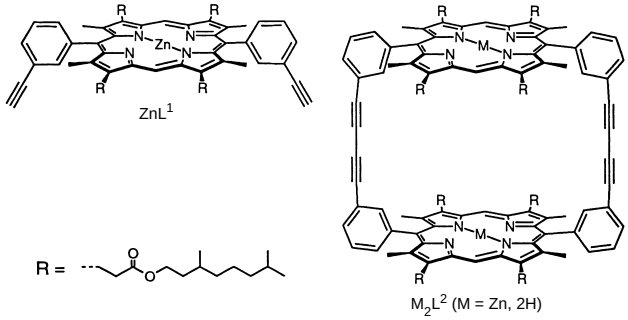
# Unexpectedly selective ligand binding within the cavity of a cyclic metalloporphyrin dimer

**R. Stephen Wylie, Esther G. Levy and Jeremy K. M. Sanders***

*Cambridge Centre for Molecular Recognition, University Chemical Laboratory, Lensfield Road, Cambridge, UK CB2 1EW*

**4-Substituted pyridines of an appropriate size show a remarkable preference for binding inside the cavity of a cofacial butadiyne-linked zinc porphyrin dimer; the origin of the effect is not entirely clear but may be related to solvent release or favourable host–guest contacts**

We report here that the binding of a pyridine ligand to a zinc porphyrin dimer can occur selectively on the inner face of a cavity rather than on the more accessible but otherwise apparently equivalent outer face.




Previous work in this laboratory had demonstrated that pyridine binds to monomers such as $ZnL^1$ and dimers such as $Zn_2L^2$ with essentially the same microscopic binding constant in $CH_2Cl_2$ solution;[1,2] each individual zinc porphyrin can form only a 1:1 complex with amines. For larger oligomers such as trimers, which have spacious cavities, we interpreted the results to indicate that binding of successive pyridines to different porphyrin subunits was independent and statistical; we also concluded that binding on the inside and outside occurred randomly and to the same extent. However, the small cavity associated with dimer $Zn_2L^2$ does not allow for the same independence of inner binding: ligation of a 4-substituted pyridine to the inner face of one porphyrin might tend to inhibit binding to the internal face of the other. We therefore expected that a careful study of the binding of pyridines to $Zn_2L^2$ [eqns. (1) and (2)] would demonstrate negative cooperativity: $K_1$

$$Zn_2L^2 + X \overset{K_1}{\rightleftharpoons} Zn_2L^2{\cdot}X \quad (1)$$

$$Zn_2L^2{\cdot}X + X \overset{K_2}{\rightleftharpoons} Zn_2L^2{\cdot}2X \quad (2)$$

should be twice as large as for binding to $ZnL^1$ ($K_{mon}$) due to the presence of two binding sites, each with the possibility of inner and outer binding, while $K_2$ should be less than half the size as inner binding of the second ligand would be hindered. The results for spectrophotometric titrations in toluene solution were very different from those expected. Pyridine itself has a $K_1/K_{mon}$ value (Table 1) of 3.2, which differs from the expected value of 2.0 by slightly more than the experimental error. The discrepancy is larger for 4-methylpyridine (4-Mepy), while the first 4-*tert*-butylpyridine (4-Bu$^t$py) binds some 50 times more strongly to the dimer than to the monomer.

**Table 1** Equilibrium constants (dm$^3$ mol$^{-1}$) for binding of ligands X to $ZnL^1$ and $Zn_2L^{2a}$ (X = $NC_5H_4R$)

| R | $Zn_2L^2$ ($K_1$) | $ZnL^2$ ($K_2$) | $ZnL^1$ ($K_{mon}$) | $K_1/K_{mon}$ | $K_2/K_{mon}$ |
|---|---|---|---|---|---|
| H | $1.6 \times 10^4$ | $2.9 \times 10^3$ | $5.0 \times 10^3$ | 3.2 | 0.6 |
| 4-Me | $6.2 \times 10^4$ | $1.1 \times 10^4$ | $1.1 \times 10^4$ | 5.6 | 1.0 |
| 4-Bu$^t$ | $7.3 \times 10^5$ | $3.0 \times 10^4$ | $1.4 \times 10^4$ | *ca.* 50 | 2.1 |

[a] In toluene at 25 °C using electronic spectroscopy;[2] estimated uncertainties 7–10%.

To rigorously exclude the possibility of problems that can easily arise from the analysis of multiple binding equilibria, the free-base dimer $H_4L^2$ was partially metallated, and the singly metallated $Zn(H_2L^2)$ species was isolated by chromatography. Now only a single ligand can be bound, and data analysis is simpler. Table 2 summarises the results for a wider range of ligands, the *f* value ( = $K_{dim}/K_{mon}$) giving a direct comparison of binding strength. The trends are similar to those seen for the doubly metallated host, the maximum effect of 25-fold being for *R* = 4-Bu$^t$ in toluene. Preferential binding is not restricted to alkyl substituents, as is apparent in the results for 4-hydroxymethylpyridine. Only when the substituent is so large that the ligand cannot comfortably fit inside the cavity is the *f* value less than 1. Similar trends were seen for titrations in dichloromethane (Table 2, results in italics), although the absolute size of the effect is smaller, and now pyridine itself is bound less well by the dimer than by the monomer.†

The larger *f* values for some ligands imply that binding occurs preferentially to one face of the porphyrin, presumably the intracavity one. One explanation for these results might be that molecules of solvent toluene are more strongly associated with the dimer cavity than with the open faces of the monomer,[3] and that binding of an appropriately sized ligand within the cavity would then lead to entropically favourable solvent release. Where one ligand releases more than one solvent molecule this can lead to entropy-driven binding.[4] However there is no

**Table 2** Equilibrium constants (dm$^3$ mol$^{-1}$) for binding of ligands X to $ZnL^1$ and $Zn(H_2L^2)^a$ (X = $NC_5H_4R$)

| R | $Zn(H_2L^2)$ ($K_{dim}$) | $ZnL^1$ ($K_{mon}$) | $f = K_{dim}/K_{mon}$ |
|---|---|---|---|
| H | $8.0 \times 10^3$ | $5.0 \times 10^3$ | 1.6 |
| | (*3.1* × *10$^3$*) | (*4.1* × *10$^3$*) | (*0.8*)[b] |
| 4-Me | $2.9 \times 10^4$ | $1.1 \times 10^4$ | 2.6 |
| 4-Pr$^i$ | $8.3 \times 10^4$ | $8.3 \times 10^3$ | 10 |
| 4-Bu$^t$ | $3.5 \times 10^5$ | $1.4 \times 10^4$ | 25 |
| | (*3.6* × *10$^4$*) | (*9.2* × *10$^3$*) | (*3.9*)[b] |
| 4-(1-Adamantyl) | $2.1 \times 10^4$ | $1.1 \times 10^4$ | 1.9 |
| 4-$CHBu_2$ | $3.8 \times 10^4$ | $8.3 \times 10^3$ | 4.6 |
| 4-Ph | $1.1 \times 10^4$ | $8.8 \times 10^3$ | 1.2 |
| 4-$CH_2OH$ | $1.0 \times 10^5$ | $9.5 \times 10^3$ | 11 |
| | (*2.0* × *10$^4$*) | (*5.4* × *10$^3$*) | (*3.7*)[b] |
| 3-Me, 5-Me | $9.5 \times 10^3$ | $6.3 \times 10^3$ | 1.5 |
| 4-Y[c] | $1.1 \times 10^4$ | $1.5 \times 10^4$ | 0.7 |

[a] In toluene at 25 °C using electronic spectroscopy; [2] estimated uncertainties 7–10%. [b] In $CH_2Cl_2$ at 25 °C. [c] Y = *trans*-(4-Pyridyl)ethenyl.

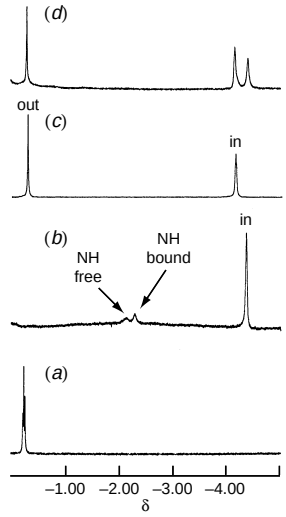



**Fig. 1** Partial 400 MHz $^1$H NMR spectra at −60 °C in [$^2H_8$]toluene of (*a*) $ZnL^1$ in the presence of 0.5 equiv. 4-Bu$^t$py, indicating that three complexes are formed (Fig. 2); (*b*) $Zn_2(H_2L^2)$ in the presence of 0.5 equiv. 4-Bu$^t$py, demonstrating exclusively inside cavity binding; (*c*) $Zn_2L^2{\cdot}2$(4-Bu$^t$py), showing inside and outside binding; and (*d*) $Zn_2L^2$ in the presence of 1.0 equiv. 4-Bu$^t$py showing the co-existence of 1 : 1 and 1 : 2 complexes

evidence for such an effect in this system: Van't Hoff plots (25–55 °C) for 4-Bu$^t$py binding in the temperature range 25–55 °C give very similar values for $-T\Delta S$ [24 kJ mol$^{-1}$ at 298 K for $ZnL^1$ and 23 kJ mol$^{-1}$ for $Zn(H_2L^2)$] in toluene. The major difference in driving force is in $-\Delta H$, which is 47 kJ mol$^{-1}$ for $ZnL^1$ and 54 kJ mol$^{-1}$ for $Zn(H_2L^2)$. Solvent-dependent binding within cavities has been reported in many other systems, but these can be usually be rationalised in terms of optimising host–guest or disrupting host–solvent interactions.[5]

To prove that preferential binding occurs within the cavity we turned to $^1$H NMR spectroscopy at a temperature low enough to ensure slow ligand exchange; the large ring current associated with the porphyrin π system leads to particularly marked shielding of ligands sandwiched inside the cavity of a dimer.[1, 2] At – 60 °C in [$^2H_8$]toluene, the Bu$^t$ resonance in the complex of 4-Bu$^t$py with $ZnL^1$ appears as three very close singlets at $\delta$ –0.2 [Fig. 1(*a*)], a shift of 1.2 ppm on binding; the three signals result from the slow exchange between three isomeric complexes (Fig. 2).[6] By contrast, when 0.5 equiv. 4-Bu$^t$py are added to $Zn(H_2L^2)$ at −60 °C in [$^2H_8$]toluene, a single Bu$^t$ resonance due to the complex of 4-Bu$^t$py appears at $\delta$ −4.3 [Fig. 1(*b*)], a binding shift of 5.3 ppm that is consistent only with the ligand being bound within the cavity as shown in Fig. 3(*a*); no externally bound ligand is seen. It is notable that the NH resonances of the free-base porphyrin are sensitive to the presence of the ligand within the cavity, shifting from $\delta$ −2.1 to −2.3 upon ligation of the other porphyrin unit. The $^1$H NMR spectrum of the $ZnL^2{\cdot}2$(4-Bu$^t$py) complex [Fig. 1(*c*)] contains

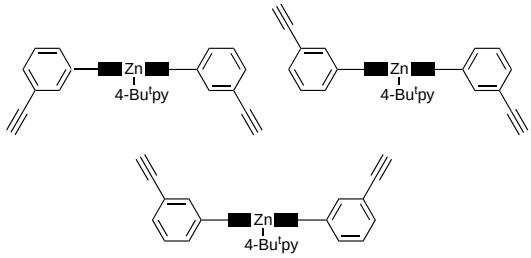



**Fig. 2** Three isomeric forms of the complexes of 4-Bu$^t$py with $ZnL^1$. The *trans*-atropisomer complex is statistically twice as abundant as either of the individual *cis*-atropisomer complexes.

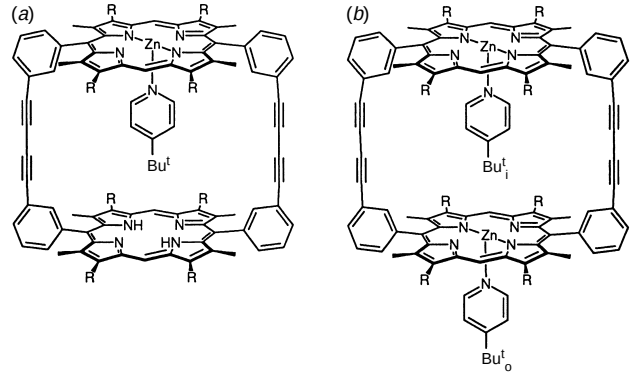



**Fig. 3** Geometries of (*a*) $Zn(H_2L^2){\cdot}$4-Bu$^t$py and (*b*) $Zn_2L^2{\cdot}2$(4-Bu$^t$-py)

two signals in a 1 : 1 intensity ratio and with shifts that show one ligand bound inside and one outside the cavity [Fig. 3(*b*)], while a deficiency of the ligand yields a mixture of the 1 : 2 complex with the inside-only 1 : 1 complex [Fig. 1(*d*)]. The results described here show that cavity effects can have unpredictable influences on the strength and position of binding. The dependence of the first binding constant on ligand size may reflect a direct van der Waals enthalpic contribution from ligand contact with the non-binding porphyrin,‡ but this explanation seems hard to reconcile with the similarity of effect between $Zn(H_2L^2)$ and $Zn_2L^2$, and between polar and non-polar substituents on the ligand. It seems more likely that the effect is an unpredictable outcome of the delicate changes in host and guest solvation that occur on complex formation. The corresponding cyclic porphyrin trimer in toluene displays small but measurable preferences for binding some ligands within its cavity, and this may influence the rate of host-catalysed reactions within the cavity. Details will be reported elsewhere.

We thank Dr Nick Bampos for the methyl ester analogue of $Zn(H_2L^2)$, NSERC Canada (R. S. W.), the Cambridge Commonwealth Trust and New Zealand Vice-Chancellors' Committee (E. G. L.) for financial support, and the EPSRC Mass Spectrometry Service for FAB spectra.

## Footnotes and References

* E-mail: jkms@cam.ac.uk

† Control experiments with the toluene-insoluble methyl ester analogues of $ZnL^1$ and $Zn(H_2L^2)$ (R = $CH_2CH_2CO_2Me$) in dichloromethane show no significant difference in binding behaviour, ruling out effects due to interaction with the long alkyl side-chains.

§ The small but probably real increase of $K_2$ for $Zn_2L^2$ with ligand size may reflect subtle geometry changes in the second porphyrin as the first ligand binds within the cavity and contacts the second porphyrin.

1 J. K. M. Sanders, *Comprehensive Supramolecular Chemistry*, ed. J. L. Atwood, J. E. D. Davies, D. D. Macnicol and F. Vögtle, 1996, vol. 9, pp. 131–164.
2 H. L. Anderson, S. Anderson and J. K. M. Sanders, *J. Chem. Soc., Perkin Trans. 1*, 1995, 2231 and following papers.
3 X. Xie, R. Bau and C. A. Reed, *Angew. Chem., Int. Ed. Engl.*, 1994, **33**, 2433.
4 R. Meissner, X. Garcias, S. Mecozzi and J. Rebek, *J. Am. Chem. Soc.*, 1997, **119**, 77.
5 K. T. Chapman and W. C. Still, *J. Am. Chem. Soc.*, 1989, **111**, 3075; J. Canceill, M. Cesario, A. Collet, J. Guilhem, L. Lacombe, B. Lozach and C. Pascard, *Angew. Chem., Int. Ed. Engl.*, 1989, **28**, 1246; D. B. Smithrud and F. Diederich, *J. Am. Chem. Soc.*, 1990, **112**, 339; R. P. Bonar-Law and J. K. M. Sanders, *J. Chem. Soc., Perkin Trans. 1*, 1995, 3085.
6 V. Marvaud, A. Vidal-Ferran, S. J. Webb and J. K. M. Sanders, *J. Chem. Soc., Dalton Trans.*, 1997, 985.

*Received in Basel, Switzerland, 28th April 1997; 7/02901B*

# New route to functionalized cyclohexenes from nitromethane and electrophilic alkenes without solvent under focused microwave irradiation

**David Michaud,[a] Sahar Abdallah-El Ayoubi,[a] Marie-Joëlle Dozias,[b] Loïc Toupet,[c] Françoise Texier-Boullet*[a] and Jack Hamelin[a]**

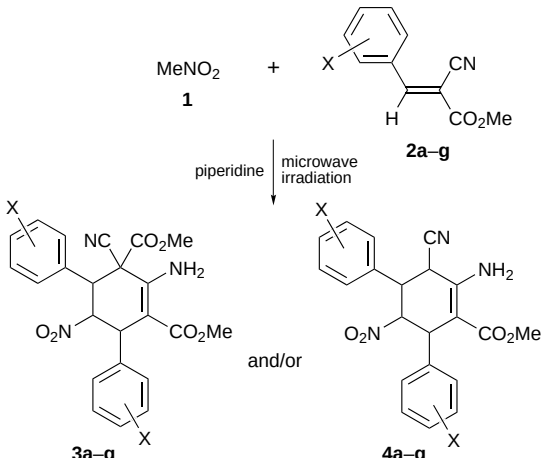
[a] *Synthèse et Electrosynthèse Organiques 3, UMR 6510, Université de Rennes I, Campus de Beaulieu, 35942 Rennes, France*
[b] *Prolabo, 54 Rue Roger Salengro, 94126 Fontenay sous Bois Cedex, France*
[c] *Groupe Matière Condensée et Matériaux, UMR C66-26, Université de Rennes I, Campus de Beaulieu, 35042 Rennes, France*

**Nitromethane reacts *via* a diastereoselective double Michael addition with electrophilic alkenes activated by cyano and methoxycarbonyl groups [$XC_6H_4CH{=}C(CN)CO_2Me$] in the presence of catalytic amounts of piperidine under solvent-free conditions coupled with focused microwave irradiation to afford new, highly functionalized cyclohexenes; no cyclopropane formation is observed.**

Organic synthesis in dry media coupled with microwave irradiation is currently a matter of increasing interest.[1–3] Microwave-assisted organic reactions in the presence or absence of solvents have recently been reviewed.[4] In the course of our studies related to the catalytic effect of piperidine towards condensations[5–7] under microwave irradiation (MWI), we report a novel reaction of nitromethane **1** with some electrophilic alkenes **2a–g**,† which leads to highly functionalized cyclohexenes **3a–g**‡ and/or **4a–g**‡ after demethoxycarbonylation of **3** (Scheme 1). Nitroalkanes and electrophilic alkenes are known to give cyclopropanes, although in the case of nitromethane, the yields are rather poor.[8–10]

The simple mixture of **1** and **2**, without solvent in the presence of adjusted amounts of piperidine, afforded **3** or **4** at room temperature (for example **3a** was obtained in 60% yield after 98 h, with 12 mol% piperidine with respect to the alkene) or in a few minutes under focused microwave irradiation in a Synthewave 402 Prolabo[11] at 90 °C (monitored temperature[12]) (see Tables 1 and 2). The reaction is highly diastereoselective: only two isomers were detected in the crude product by $^1H$ NMR spectroscopy. The relative configuration of the major isomer has been established by X-ray analysis (Fig. 1).[13] However, the relative configuration of the minor isomer has not yet been established.

In order to check the effect of the focused microwave irradiation, we performed the following experiments for the




**Scheme 1**

**Table 1** Microwave synthesis of **3a–g**

| | Irradiation time/min | Yield (%)[a] | Molecular formula |
|---|---|---|---|
| **3a** | 11 | 70 | $C_{23}H_{21}N_3O_6$ |
| **3b** | 15 | 73 | $C_{23}H_{19}N_3O_6Cl_2$ |
| **3c** | 25 | 70 | $C_{25}H_{25}N_3O_8$ |
| **3d** | 20 | 71 | $C_{23}H_{19}N_5O_{10}$ |
| **3e** | 15 | 75 | $C_{23}H_{19}N_3O_6F_2$ |
| **3f** | 15 | 75 | $C_{23}H_{19}N_3O_6F_2$ |
| **3g** | 15 | 75 | $C_{23}H_{19}N_3O_6Br_2$ |

[a] Pure isolated product after column chromatography on silica gel (eluent $CH_2Cl_2$) and then crystallization from diethyl ether.

**Table 2** Microwave synthesis of **4a–g**

| | Irradiation time/min | Yield (%)[a] | Molecular formula |
|---|---|---|---|
| **4a** | 11 | 75 | $C_{21}H_{19}N_3O_4$ |
| **4b** | 15 | 75 | $C_{21}H_{17}N_3O_4Cl_2$ |
| **4c** | 25 | 70 | $C_{23}H_{23}N_3O_6$ |
| **4e** | 15 | 72 | $C_{21}H_{17}N_3O_4F_2$ |
| **4f** | 15 | 70 | $C_{21}H_{17}N_3O_4F_2$ |
| **4g** | 15 | 75 | $C_{21}H_{17}N_3O_4Br_2$ |

[a] Pure isolated product after column chromatography on silica gel (eluent $CH_2Cl_2$) and then crystallization from diethyl ether.

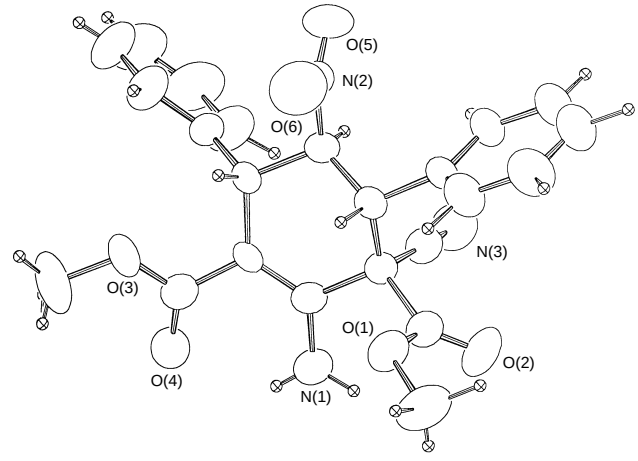
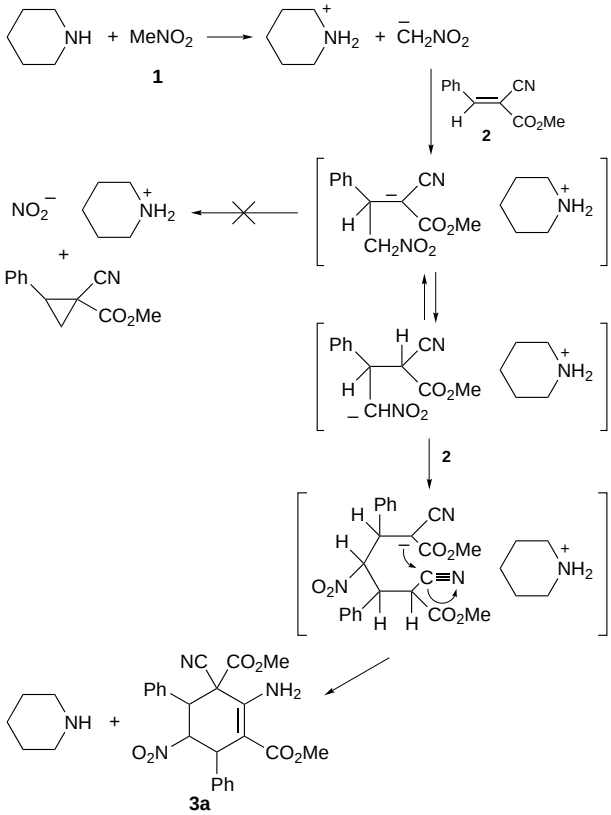



**Fig. 1** ORTEP diagram of **3a**



**Scheme 2**

synthesis of **3a**. (i) The reaction mixture was irradiated at 750 W in a domestic oven (Philips M602) for the same time (11 min, 97 °C measured at the end), and gave 5% of **3a** (estimated by $^1$H NMR spectroscopy). (ii) The same reaction mixture was placed in an oil bath at 90 °C for the same time (11 min), but the reaction only went to 60% completion; the low yield of **3a** (27%) is due to competition from the Michael monoadduct. After 20 min this yield remained unchanged.

Cyclohexene formation can be explained by the mechanism presented in Scheme 2. After a double Michael addition, the ring closure occurs *via* nucleophilic attack on the nitrile group by the carbanion and regeneration of piperidine in a catalytic cycle. A stoichiometric amount of piperidine promotes the demethoxycarbonylation of **3** to **4** by a mechanism already described by Carrié.[14]

This cyclohexene synthesis, previously unreported in the literature, is a simple, clean, economical and environmentally benign process which can be performed either at room temperature over a rather long reaction time or under focused microwave irradiation in a short time with better yields.

The extension of this reaction to other electrophilic alkenes (dicyano and cyano amide) is under investigation.

## Footnotes and References

* E-mail: Francoise.Texier@univ-rennes1.fr

† *Typical procedure*: A mixture of alkene (5 mmol), nitromethane (0.18 g, 3 mmol) and piperidine (20 μl, 0.2 mmol for **3a** and 250 μl, 2.5 mmol for **4a**) was placed in a quartz tube (diameter 37 mm) and introduced into a Synthewave 402 Prolabo microwave reactor (2.45 GHz) fitted with a rotational system, adjustable power within the range 20–300 W and a wave guide (monomode $T_{01}$) (ref. 11). Microwave irradiation was carried out at 90 °C (ref. 12) (obtained after 3 min and then maintained for 8 min). Other irradiation times are given in Tables 1 and 2. The mixture was cooled to room temperature and the crude residue was characterized by $^1$H NMR spectroscopy. Pure product was isolated after chromatography on silica gel (eluent $CH_2Cl_2$) and slow crystallization from diethyl ether.

‡ *Selected data* for **3a**: 70%; $\delta_H$ (300 MHz, $CDCl_3$) (major isomer) 3.36 (s, 3 H, $CO_2CH_3$), 3.72 (s, 3 H, $C{=}CCO_2CH_3$), 4.28 (d, 1 H, $C_5$-H, *J* 12.7), 4.52 (d, 1 H, $C^3$-H, *J* 9.6), 5.30 (dd, 1 H, $C^4$-H, *J* 12.7, 9.6), 6.26 (s, 2 H, $NH_2$), 7.15–7.34 (m, 10 H, $C_6H_5$); $\delta_C$ (75 MHz, $CDCl_3$) 47.65 (dm, $C^3$, *J* 135.3), 48.16 (dm, $C^5$, *J* 138.4), 51.16 (q, $CCO_2CH_3$, *J* 147.2), 54.81 (q, $C{=}CCO_2CH_3$, *J* 149.7), 55.90 (td, $C{=}CCO_2CH_3$), 91.55 (dt, $C^4$, *J* 151.7, 6.9), 97.44 (m, $C{=}CCO_2CH_3$), 115.16 (d, *C*N, *J* 9.9), 126.9–144 (m, 12 C arom), 145.35 (m, $CNH_2$), 164.89 (dq, $CCO_2CH_3$, *J* 4.1, 2.4), 168.37 (m, $C{=}CCO_2CH_3$); HRMS: Calc for [$M^{+\cdot} - HNO_2$]: 388.142. Found: 388.142. Found: C, 63.57; H, 4.88; N, 9.72. $C_{23}H_{21}N_3O_6$ requires C, 63.44; H, 4.86; N, 9.65%. For **4a**: 75%; $\delta_H$ (300 MHz, DMSO) (major isomer) 3.46 (s, 3 H,$OCH_3$), 3.71 (dd, 1 H, $C^5$-H, *J* 11.4, 12), 4.07 (dd, 1 H, $C^6$-H, *J* 11.4, 2.4), 4.24 (dd, 1 H, $C^3$-H, *J* 10.3, 2.4), 5.55 (dd, 1 H, $C^4$-H, *J* 10.3, 12), 6.22 (s, 2 H, $NH_2$), 7.19–7.38 (m, $C_6H_5$); $\delta_C$ (75 MHz, DMSO) 46.79 (dm, $C^3$, *J* 136), 47.41 (dm, $C^5$, *J* 133), 51.75 (dm, $C^6$, *J* 135), 52.4 (q, $OCH_3$, *J* 147.5), 74.75 (m, $CNH_2$), 91.67 (dt, $C^4$, *J* 156.5), 118.4 (s, CN), 127.23–139.61 (m, 12 C arom), 153.14 (m, $CCO_2CH_3$), 169.6 (m, $CO_2CH_3$); HRMS: Calc. for [$M^{+\cdot} - HNO_2$]: 330.1368. Found: 330.137. Found: C, 66.99; H, 5.17; N, 11.15. $C_{21}H_{19}N_3O_4$ requires C, 66.83; H, 5.07; N, 11.13%.

All products were fully characterized by $^1$H and $^{13}$C NMR and mass spectroscopy and elemental analysis.

§ *Crystal data* for **3a** (ref. 13): $C_{23}H_{21}N_3O_6$: *M* = 435.44, monoclinic, $P2_1/c$, *a* = 14.962(2), *b* = 10.028(2), *c* = 14.725(9) Å, $\beta$ = 91.96(3)°, *V* = 2208(2) Å$^{-3}$, *Z* = 4, $D_x$ = 1.310 Mg m$^{-3}$, $\lambda$(Mo-K$\alpha$) = 0.70926, $\mu$ = 0.899 cm$^{-1}$, *F*(000) = 912, *T* = 294 K, final *R* = 0.032 for 1812 observations and 373 parameters. Structure solved by direct methods and refined by the full-matrix least-squares technique to *R* = 0.032 for 1812 observations and 373 parameters. CCDC 182/536.


1 G. Bram, A. Loupy and D. Villemin, *Solid Supports and Catalysts*, in *Organic Synthesis*, ed. K. Smith, Ellis Horwood and Prentice Hall, 1992, vol. 12, pp. 302–325 and references cited therein.
2 A. Laurent, P. Jacquault, J. L. Di Martino and J. Hamelin, *J. Chem. Soc., Chem. Commun.*, 1995, 1101.
3 J. Hamelin, A. Loupy and D. Mathé, Microwave and High Frequency Heating 1995, St. John's College, Cambridge, UK, 17–21 September 1995; P. Jacquault, F. Texier-Boullet, J. P. Bazureau and J. Hamelin, PACIFICHEM 95, Honolulu, 17–22 December, 1995.
4 S. Caddick, *Tetrahedron*, 1995, **51**, 10 403.
5 S. Abdallah-El Ayoubi, F. Texier-Boullet and J. Hamelin, *Synthesis*, 1994, 258.
6 S. Jolivet, F. Texier-Boullet, P. Jacquault and J. Hamelin, *Heteroatom. Chem.*, 1995, **6**, 469.
7 S. Jolivet, S. Abdallah-El Ayoubi, D. Mathé, F. Texier-Boullet and J. Hamelin, *J. Chem. Res. (S)*, 1996, 300.
8 K. Annen, H. Hofmeister, H. Laurent, A. Seeger and R. Wiechert, *Chem. Ber.*, 1978, **111**, 3094.
9 N. Ono, T. Yanaï, I. Hamamoto, A. Kamimura and A. Kagi, *J. Org. Chem.*, 1985, **50**, 2807.
10 J. M. Melot, F. Texier-Boullet and A. Foucaud, *Synthesis*, 1987, 364.
11 R. Commarmot, R. Didenot and J. F. Gardais, Rhône-Poulenc/Prolabo, patent 84/03496, 27 October, 1986.
12 Prolabo, *Fr. Pat.* 62241/D, 14669 FR, 23 December, 1991.
13 C. K. Fair, MolEN, An Interactive Intelligent System for Crystal Structure Analysis, Enraf-Nonius, Delft, The Netherlands, 1990; *International Tables for X-Ray Crystallography, Part IV*, Kynoch Press, Birmingham, 1974; C. K. Johnson, ORTEP, Report ORNL-3794, Oak Ridge National Laboratory Tennessee, USA, 1974.
14 F. Texier, E. Marchand and R. Carrié, *Tetrahedron*, 1994, **30**, 3185.


*Received in Liverpool, UK, 25th February 1997; Revised manuscript received, 17th June 1997; 7/04241H*

# Oxidative trimerization of *o*-dialkoxybenzenes to hexaalkoxytriphenylenes: molybdenum(v) chloride as a novel reagent

**Sandeep Kumar* and M. Manickam**

*Centre for Liquid Crystal Research, P.O. Box 1329, Jalahalli, Bangalore 560 013, India*

**Symmetrically substituted hexaalkoxytriphenylenes are obtained from *o*-dialkoxybenzenes by oxidative trimerization with $MoCl_5$ in high yields; oxidative coupling of a 3,3′,4,4′-tetraalkoxybiphenyl and 1,2-dialkoxybenzenes yields unsymmetrically substituted derivatives of triphenylene and a direct coupling of a 3,3′,4,4′-tetraalkoxybiphenyl with alkoxyphenol produces the monofunctionalized triphenylenes.**

Hexasubstituted triphenylenes are the most widely synthesized and studied discotic mesogens.[1] Recently, these materials have been discussed as potential candidates for opto-electronic devices.[2,3] Several research groups are currently working on the synthesis of symmetrical, unsymmetrical and functionalized triphenylene discotic liquid crystals.[4–9] Here we report the synthesis of a variety of triphenylene derivatives using a novel reagent, molybdenum(v) chloride.

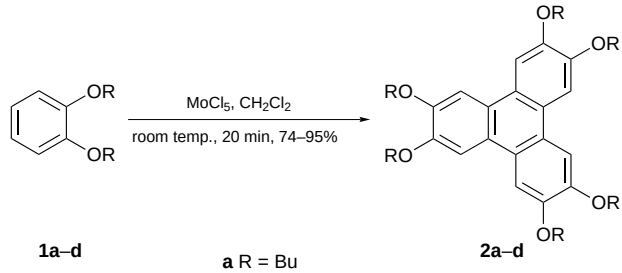
Synthesis of hexamethoxytriphenylene has been achieved previously by oxidative trimerisation of 1,2-dimethoxybenzene (veratrol) in $H_2SO_4$ using chloranil or iron chloride as oxidant.[10] The trimerization involves three consecutive Scholl reactions but surprisingly under normal Scholl conditions using aluminium chloride and nitrobenzene this does not work well.[10e] Triphenylene derivatives show mesomorphism only when the six peripheral alkoxy chains have a minimum of four carbon atoms, *i.e.* butoxy chains. The trimerization using chloranil is limited to the preparation of hexamethoxytriphenylene only and with higher homologues like 1,2-dihexyloxybenzene it gives only a poor yield of hexahexyloxytriphenylene with many side products.[4g] To prepare these long chain derivatives, the methyl groups of hexamethoxytriphenylene are dealkylated by $BBr_3$ or HBr and the resultant hexaphenol is realkylated with the appropriate alkyl halide to give different hexaalkoxytriphenylene discotics.

Hexamethoxytriphenylene can also be prepared by the cyclic anodic trimerization of dimethoxybenzene and, using a chemical or electrochemical reductive work-up, a moderate yield of the product can be obtained.[11] The method is not limited to dimethoxybenzene but can be extended to other dialkoxybenzenes to form directly hexaalkoxytriphenylene discotics, but this slow reaction is only applicable on a very small scale and, thus, limited in its use.

The use of $FeCl_3$ as oxidant was further explored by the Ringsdorf group, which reported the synthesis of hexahexyloxytriphenylene by the trimerization of 1,2-dihexyloxybenzene in 70% $H_2SO_4$ at 80 °C using iron chloride in 20% yield.[12] A further modification to this process was implemented by the Boden group, who used only a catalytic amount of $H_2SO_4$ (0.3%) in $CH_2Cl_2$ and reported yields of 55–86% for different alkoxytriphenylenes.[4g] Coupling of a tetraalkoxybiphenyl with the appropriate dialkoxybenzene under the same conditions gives unsymmetrical hexaalkoxytriphenylenes in 45–77% yield.[4f]

Well-defined synthesis of unsymmetrical and low degree substituted triphenylenes has been reported recently using organometallic chemistry and $FeCl_3$.[7,8] These sophisticated methods are useful for the preparation of low degree substituted triphenylenes but difficult to apply for a large scale production.

We have discovered that molybdenum(v) chloride is a novel reagent for the oxidative trimerization of 1,2-dialkoxybenzenes to hexaalkoxytriphenylenes in high yield. The reaction occurs under very mild conditions with or without acid catalyst and in a very short time at room temperature (Scheme 1). In a typical reaction, $MoCl_5$ (1.4 g, 0.0051 mol) was added to a solution of 1,2-dibutoxybenzene (1.1 g, 0.005 mol) in 10 ml of dry $CH_2Cl_2$. The reaction mixture was stirred at room temperature for 20 min under anhydrous conditions. It was then poured over cold MeOH (15 ml), diluted with water (20 ml) and extracted with hexane (4 × 20 ml). The combined extracts were washed with water and brine, dried over anhydrous sodium sulfate, the solvent was removed under vacuum and the crude product was purified by column chromatography over silica gel, yielding 1.04 g (95%) of hexabutoxytriphenylene. The product was characterized by its spectral data, phase behaviour and a direct comparison with an authentic sample. Yields of different hexaalkoxytriphenylenes are given in Table 1. As $MoCl_5$ is a 2 $e^-$ oxidant, only *ca.* 1 equiv. of the reagent is required to




**1a–d** **2a–d**

**a** R = Bu
**b** R = $C_6H_{13}$
**c** R = $C_{10}H_{21}$
**d** R = Me

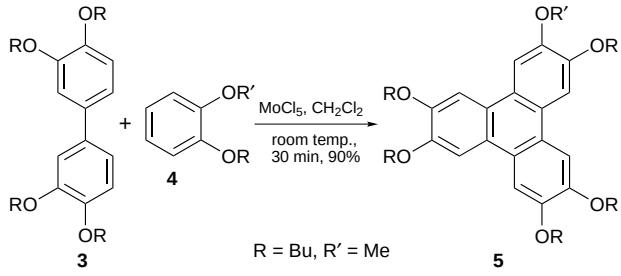
**Scheme 1**

**Table 1** Preparation of triphenylene derivatives using $MoCl_5$ in $CH_2Cl_2$ solution

| Starting Material | $H_2SO_4$ (%) | Product | Yield (%) |
|---|---|---|---|
| **1a** | 0.0 | **2a** | 95 |
| **1a** | 0.2 | **2a** | 92 |
| **1a** | 0.5 | **2a** + **7** | 78 + 5 |
| **1a** | 1.0 | **2a** + **7** | 41 + 25 |
| **1b** | 0.0 | **2b** | 94 |
| **1b** | 0.2 | **2b** | 90 |
| **1c** | 0.0 | **2c** | 80 |
| **1c** | 0.2 | **2c** | 78 |
| **1d** | 0.0 | **2d** | 74 |
| **1d** | 0.2 | **2d** | 74 |
| **3** + **4** | 0.0 | **5** | 90 |
| **3** + **4** | 0.2 | **5** | 75 |
| **3** + **6** | 0.0 | **7** | 44 |
| **3** + **6** | 0.2 | **7** | 47 |

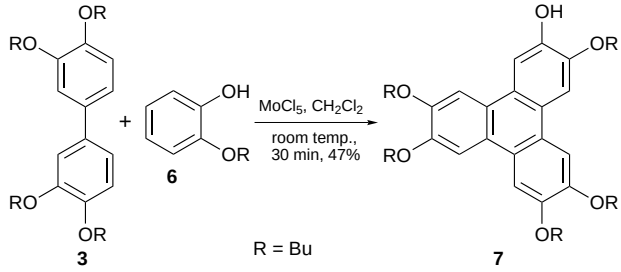
perform the reaction. The best yields of hexaalkoxytriphenylenes were obtained without using any acid and gave better yields than any of the known methods. We have also observed that on increasing the amount of $H_2SO_4$, partial dealkylation of hexaalkoxytriphenylenes occurs and variable amounts of monohydroxypentaalkoxytriphenylene can be isolated (Table 1). The work-up of the reaction is very simple; in most cases, on pouring the reaction mixture over MeOH, a white precipitate forms which can be filtered and recrystallized. Otherwise, addition of water followed by extraction with hexane gives a colourless product.

Synthesis of unsymmetrical and monofunctionalized triphenylenes was achieved by coupling a 3,3′,4,4′-tetraalkoxybiphenyl and appropriate 1,2-dialkoxybenzenes (Scheme 2) under similar reaction conditions. Thus, when 3,3′,4,4′-tetrabutoxybiphenyl **3**, prepared by classical Ullman coupling of dialkoxymonoiodobenzene, was coupled with 2-butoxyanisole **4**, 2-methoxy-3,6,7,10,11-butoxytriphenylene **5** was formed in 90% yield. Symmetrical and nonsymmetrical trimers of 1,2-dialkoxybenzenes were the two side products in this reaction.




**Scheme 2**

Monofunctionalized triphenylene, an extremely important precursor for the synthesis of discotic dimers, oligomers and polymers, can be prepared by direct coupling of a 3,3′,4,4′-tetraalkoxybiphenyl and monoalkoxyphenol. Thus, oxidative coupling of 3,3′,4,4′-tetrabutoxybiphenyl **3** and 2-butoxyphenol **6** using $MoCl_5$ under similar reaction conditions yielded 2-hydroxy-3,6,7,10,11-butoxytriphenylene **7** in 47% yield (Scheme 3).




**Scheme 3**

The potential of this new reagent is currently under investigation for the synthesis of different symmetrical, unsymmetrical and functionalized triphenylenes. The effects of different solvents, acids and concentrations are also under investigation and the results will be published in due course.

We are very grateful to Professor S. Chandrasekhar and Professor H. Ringsdorf for many helpful discussions.

## Footnote and References

* E-mail: uclcr@giasbg01.vsnl.net.in

1 For a brief review of discotics, see S. Chandrasekhar, *Liq. Cryst.*, 1993, **14**, 3. See also S. Chandrasekhar and S. Kumar, *Science Spectra*, 1997, **8**, 66.
2 N. Boden, R. Bissell, J. Clements and B. Movaghar, *Liquid Crystals Today*, 1996, **6**, 1.
3 S. Kumar, P. Schuhmacher, P. Henderson, J. Rego and H. Ringsdorf, *Mol. Cryst. Liq. Cryst.*, 1996, **288**, 211.
4 (*a*) N. Boden, R. J. Bushby, A. N. Cammidge, S. Duckworth and G. Headdoc *J. Mater. Chem.*, 1997, **7**, 601; (*b*) N. Boden, R. J. Bushby and A. N. Cammidge, *Mol. Cryst. Liq. Cryst.*, 1995, **260**, 307; (*c*) N. Boden, R. J. Bushby and A. N. Cammidge, *Liq. Cryst.*, 1995, **18**, 673; (*d*) N. Boden, R. J. Bushby, A. N. Cammidge and G. Headdock, *J. Mater. Chem.*, 1995, **5**, 2275; (*e*) N. Boden, R. J. Bushby, A. N. Cammidge and G. Headdock, *Synthesis*, 1995, 31; (*f*) N. Boden, R. J. Bushby and A. N. Cammidge, *J. Chem. Soc., Chem. Commun.*, 1994, 465; (*g*) N. Boden, R. C. Borner, R. J. Bushby, A. N. Cammidge and M. V. Jesudason, *Liq. Cryst.*, 1993, **15**, 851.
5 S. Kumar, *Mol. Cryst. Liq. Cryst.*, 1996, **289**, 247; S. Kumar and M. Manickam, *Mol. Cryst. Liq. Cryst.*, 1997, in the press.
6 J. A. Rego, S. Kumar and H. Ringsdorf, *Chem. Mater.*, 1996, **8**, 1402; J. A. Rego, S. Kumar, I. J. Dmochowski and H. Ringsdorf, *Chem. Commun.*, 1996, 1031; P. Henderson, S. Kumar, J. A. Rego, H. Ringsdorf and P. Schuhmacher, *J. Chem. Soc., Chem. Commun.*, 1995, 1059; F. Closs, L. Häussling, P. Henderson, H. Ringsdorf and P. Schuhmacher, *J. Chem. Soc., Perkin Trans. 1*, 1995, 829; P. Henderson, H. Ringsdorf and P. Schuhmacher, *Liq. Cryst.*, 1995, **18**, 191.
7 R. C. Borner and R. F. W. Jackson, *J. Chem. Soc., Chem. Commun.*, 1994, 845.
8 J. W. Goodby, M. Hird, K. J. Toyne and T. Watson, *J. Chem. Soc., Chem. Commun.*, 1994, 1701.
9 H. Naarmann, M. Hanack and R. Mattmer, *Synthesis*, 1994, 477.
10 (*a*) I. M. Matheson, O. C. Musgrave and C. J. Webster, *Chem. Commun.*, 1965, 278; (*b*) O. C. Musgrave and C. J. Webster, *J. Chem. Soc.*, 1971, 139; (*c*) M. Piatelli, E. Fattorusso, R. A. Nicolaus and S. Magno, *Tetrahedron*, 1965, **21**, 3229; (*d*) C. Destrade, M. C. Mondon and J. Malthete, *J. Phys. Colloq.*, 1979, **40**, C3; (*e*) O. C. Musgrave, *Chem. Rev.*, 1969, **69**, 499.
11 K. Bechgaard and V. D. Parker, *J. Am. Chem. Soc.*, 1972, **94**, 4749; V. Le Berre, L. Angely, N. Simonet-Gueguen and J. Simonet, *J. Chem. Soc., Chem. Commun.*, 1987, 984; V. Le Berre, J. Simonet and P. Batail, *J. Electroanal. Chem.*, 1984, **169**, 325; J. Chapuzet and J. Simonet, *Tetrahedron*, 1991, **47**, 791.
12 H. Bengs, O. Karthaus, H. Ringsdorf, C. Baehr, M. Ebert and J. M. Wendorff, *Liq. Cryst.*, 1991, **10**, 161.

*Received in Cambridge, UK, 13th June 1997; 7/04130F*

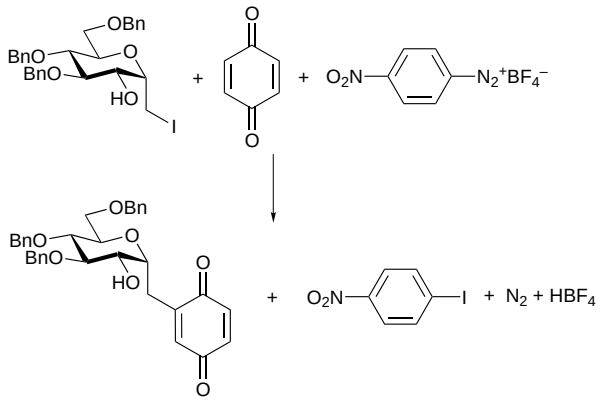
# *C*-Glucosyl quinones and related spacer-connected *C*-disaccharide

**Laura Cipolla,[a] Marco Guerrini,[b] Francesco Nicotra,*[a]† Giangiacomo Torri[b] and Elena Vismara*[c]**

[a] *Dipartimento di Chimica Organica e Industriale, Università degli Studi di Milano, Via Venezian 21, 20133 Milano, Italy*
[b] *Istituto di Chimica e Biochimica 'Giuliana Ronzoni', V. G. Colombo 81, 20133 Milano, Italy*
[c] *Dipartimento di Chimica, Politecnico di Milano, Via Mancinelli 7, 20131 Milano, Italy*

***C*-Glycosyl radicals obtained from iodide 1 react with benzo- and naphtho-quinone to afford, after deprotection, *C*-glycosyl quinones 4 and 6 which inhibit yeast α-glucosidase; employing a naphthoquinone linked to the non-reducing end of a sugar 7, a spacer-connected *C*-disaccharide 8 is obtained.**

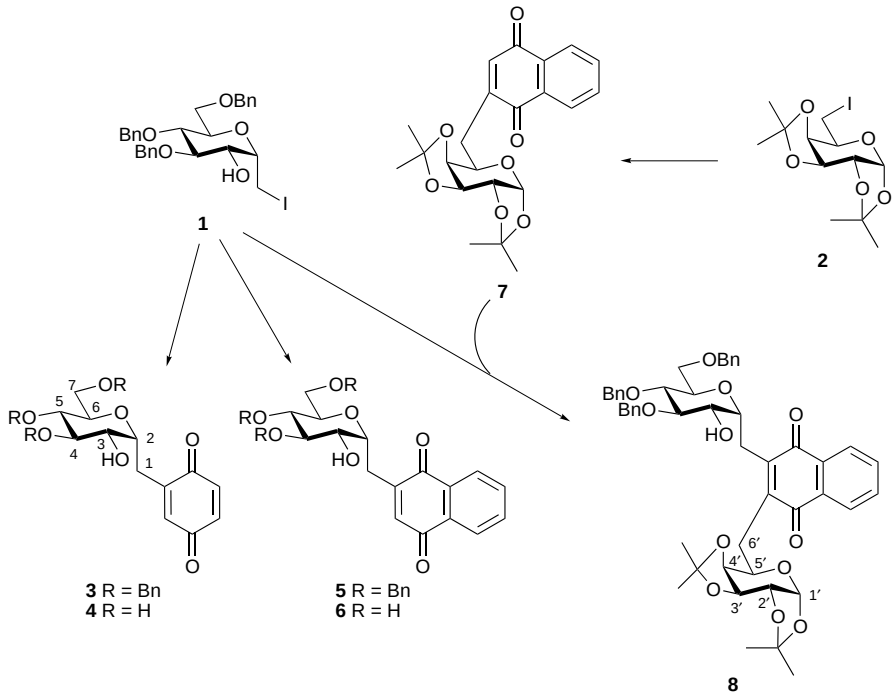
There is a growing interest in *C*-glycosides and *C*-disaccharides as potential inhibitors and regulators of carbohydrate processing enzymes and as stable mimics of saccharidic structures involved in recognition phenomena.[1] In this context, particular attention has been devoted to molecules that interfere in the biosynthesis of N-linked glycoproteins, so inhibiting pathologic processes such as HIV replication,[2] or tumour growth and metastasis formation.[3] The biosynthesis of N-linked glycoproteins involves a common asparagine-linked oligosaccharide intermediate which undergoes a trimming process, the first two trimming enzymes being α-glucosidases (I and II).[4] As a consequence α-glucoside mimics, among them α-*C*-glucosides, are potential inhibitors of N-linked glycoprotein biosynthesis.



**Scheme 1**

Many α-*C*-glucosides have been synthesised, among them aryl *C*-glucosides, in which the aromatic group is directly linked to the anomeric centre of the sugar.[5] Molecules of this kind, with quinones (especially flavonoids) directly linked to the anomeric centre of the sugar, are found in nature and are believed to form stable complexes with DNA. On the other hand, the presence of a naphthoquinone aglycon in *O*- and *S*-glycosides is responsible for antitumour[6] and antifungal[7] activity, and irreversible glycosidase inhibition.[8]

To mimic natural α-*O*-glucosides, and at the same time to produce a stable *C*-glycosidic linkage between the sugar and a quinone, we decided to synthesise α-*C*-glucosidic compounds in which the quinone is linked to the anomeric carbon through a methylene bridge. In the light of the fact that the conversion of this methylenic carbon into a nucleophile often gives rise to undesired elimination reactions or epimerization, we decided to use a radical approach. Quinones were in fact extensively studied as radical scavengers both from a mechanistic and a synthetic point of view.[9] In this context we decided to investigate the substitution by *C*-glycosyl radicals derived from



**Scheme 2**

*C*-glycosyl iodides and diazonium tetrafluoroborate according to Scheme 1. As this kind of quinone substitution is governed by enthalpic and, to a minor extent, steric effects, a radical at a methylenic carbon linked to the anomeric centre of a sugar appeared to be an attractive reagent.

An α-*C*-glucosyl radical can be obtained from the corresponding iodide provided that the hydroxy group at C-2 is not benzylated,[10] otherwise an abstraction of the benzylic hydrogen occurs with formation of the more stable benzyl radical. We synthesised (3,4,6-tri-*O*-benzyl-α-D-glucopyranosyl)iodomethane **2**, which lacks the benzyl protecting group at C-2, exploiting a vinylation–electrophilic cyclisation procedure[11] using 2,3,5-tri-*O*-benzyl-D-arabinose **1**.

In a typical experimental procedure (Scheme 2), a solution of 4-nitrobenzenediazonium tetrafluoroborate (2 mmol) in degassed DMSO (7 ml) was added dropwise to a solution of **1** (1 mmol), the quinone (1 mmol) and powdered $FeSO_4 \cdot 7H_2O$ (2 mmol) in degassed DMSO (15 ml). The solution was stirred until the evolution of nitrogen ceased. Usual work-up and chromatography afforded **3** {oil, $[\alpha]_D$ + 31.3 (*c* 1, $CHCl_3$)}‡ or **5** {oil, $[\alpha]_D$ + 47.6 (*c* 1, $CHCl_3$)}§ in 30–35% yield (80–85% yield based on converted **1**), and unreacted **1** was resubmitted to the reaction. Catalytic hydrogenation of **3** and **5** (Pd/C in EtOH) afforded **4** {oil, $[\alpha]_D$ − 9.7 (*c* 1, MeOH)} and **6** {mp 108–109 °C; $[\alpha]_D$ + 86.5 (*c* 1, acetone)}, respectively, in quantitative yield.

The biological activities of **4** and **6** as inhibitors of yeast α-glucosidase were tested according with the procedure reported by Wong.[12] Compound **4** is a poor competitive inhibitor ($K_i$ = 2.9 mM) but interestingly the presence of a further aromatic ring in **6** strongly enhances the inhibitory activity ($K_i$ = 0.17 mM).

The radical generated from **1** was also trapped (50% yield) by the sugar-substituted naphthoquinone **7**¶ (obtained from **2** *via* the procedure above). This reaction provided the naphthoquinone-connected *C*-disaccharide **8** {oil, [α] + 39.2 (*c* 1, $CHCl_3$); *m/z* 846}‖ in which two sugars are permanently linked through a naphthoquinone spacer. Recently, different saccharides connected with aliphatic[13] and aromatic[14] spacers have been synthesised to mimic biologically active natural oligosaccharides; this is the first example in which two saccharides are permanently connected *via* C–C linkages to a quinone spacer.

We gratefully thank MURST and CNR for financial support.

## Footnotes and References

† E-mail: nicotra@imiucca.csi.unimi.it

‡ *Selected data* for **3**: $^1$H NMR (500 MHz, $C_6D_6$, *J* values in Hz): δ 2.72 (dd, 1 H, *J* 15.1, 3.5, H-1a), 2.81 (dd, 1 H, *J* 15.1, 9.8, H-1b), 2.97 (d, 1 H, *J* 8.5, OH), 3.53 (t, 1 H, *J* 5.0, H-5), 3.57 (dd, 1 H, *J* 4.8, 10.3, H-7a), 3.64 (ddd, 1 H, *J* 8.5, 3.3, 5.0, H-3), 3.72 (t, 1 H, *J* 5.0, H-4), 3.77 (dd, 1 H, *J* 10.3, 6.2, H-7′a), 4.13 (br q, 1 H, *J* 5, H-6), 4.18 (dt, 1 H, *J* 9.8, 3.5, H-2), 4.25–4.42 (6 d, 6 H, OC$H_2$Ph), 6.03 (dd, 1 H, *J* 9.6, 3.0, =CH–C=O), 6.08 (d, 1 H, *J* 9.6, =CH–C=O), 6.63 (d, 1 H, *J* 3.0, =CH–C=O), 7.02–7.25 (m, 15 H, ArH).

§ *Selected data* for **5**: $^1$H NMR (500 MHz, $CDCl_3$): δ 2.85 (d, 2 H, *J* 6.7, H-1), 2.99 (d, 1 H, *J* 8.3, OH), 3.53 (m, 2 H, H-5, H-7a), 3.64 (ddd, 1 H, *J* 8.3, 5.5, 2.9, H-3), 3.71 (m, 2 H, H-4, H-7b), 4.03 (q, 1 H, *J* 5.0, H-6), 4.18 (dt, 1 H, *J* 6.7, 2.9 Hz, H-2), 4.37–4.60 (6 H, OC$H_2$Ph), 6.92 (s, 1 H, ArH, quinone), 7.12–7.27 (m, 15 H, $OCH_2C_6H_5$), 7.63 (2 H, Ar-H, quinone), 7.99 (2 H, Ar-H, quinone).

¶ *Selected data* for **7**: $^1$H NMR (300 MHz, $CDCl_3$): δ 1.30, 1.36, 1.48 (4 s, 12 H, $CH_3$), 2.84–2.89 (m, 2 H, H-6a, H-6b), 4.15 (m, 1 H, H-5), 4.22 (dd, 1 H, *J* 7.8, 1.8, H-4), 4.30 (dd, 1 H, *J* 5.4, 2.5, H-2), 4.63 (dd, 1 H, *J* 7.8, 2.5, H-3), 5.50 (d, 1 H, *J* 5.4, H-1), 7.02 (t, 1 H, *J* 1.2, =CH–C=O), 7.70–7.75 (m, 2 H, ArH), 8.04–8.11 (m, 2 H, ArH).

‖ *Selected data* for **8**: $^1$H NMR (500 MHz, $C_6D_6$, COSY): δ 0.92, 1.13, 1.41, 1.56 (4 s, 12 H, $CH_3$), 3.09 (dd, 1 H, *J* 13.6, 3.7, H-1a), 3.18 (d, 1 H, *J* 6.9, OH), 3.28 (dd, 1 H, *J* 13.5, 3.1, H-6′a), 3.49 (dd, 1 H, *J* 13.6, 10.3, H-1b), 3.71 (m, 1 H, H-5), 3.72 (m, 2 H, H-7a, H-6′b), 3.88 (m, 2 H, H-4, H-7b), 3.92 (m, 2 H, H-3, H-4′), 4.07 (dd, 1 H, *J* 2.4, 5.0, H-2′), 4.40 (m, 1 H, H-6), 4.45 (m, 2-H, H-2, H-3′), 4.57 (m, 1 H, H-5′), 4.24–4.60 (6 d, 6 H, OC$H_2$Ph), 5.31 (d, 1 H, *J* 5.0, H-1′), 6.95–7.20 (m, 15 H, $OCH_2C_6H_5$), 7.93 (d, 2 H, *J* 5.0, ArH), 8.03 (d, 2 H, *J* 5.0, ArH); $^{13}$C NMR (125.721 MHz, $C_6D_6$): δ 24.53, 24.89, 25.92, 26.41 ($CH_3$), 26.41 (C-6′), 29.48 (C-1), 67.35 (C-3′), 69.26 (C-7), 70.99 (C-2′), 71.22 (C-3), 71.65 (C-2), 73.20–73.85 ($OCH_2$Ph), 73.21 (C-4′), 73.38 (C-5′), 74.16 (C-6), 76.16 (C-5), 79.57 (C-4), 96.98 (C-1′), 108.51 (O–C–O), 109.34 (O–C–O), 126.02–148.23 (aromatic), 185.04 (C=O), 185.44 (C=O).

1 For a comprehensive description of *C*-glycosides, see M. H. D. Postema, *C-Glycoside Synthesis*, CRC Press, Boca Raton, 1995; D. E. Levy and C. Tang, *The Chemistry of C-Glycosides*, Tetrahedron Organic Chemistry Series, vol. 13, Pergamon, 1995.
2 See *inter alia* E. De Clercq, *J. Antimicrob. Chemother.*, 1989, **23**, 35.
3 See *inter alia* R. J. Bernacki, M. J. Niedbala and W. Korytnyk, *Cancer Metastasis Rev.*, 1985, **4**, 81.
4 U. Fuhrmann, E. Bause and H. Ploedh, *Biochim. Biophys. Acta*, 1985, **825**, 95.
5 C. Jaramillo and S. Knapp, *Synthesis*, 1994, 1.
6 M. M. de Oliveira, M. C. F. Linardi and M. R. P. Sampaio, *J. Pharm. Sci.*, 1978, **67**, 562.
7 S. G. Polinik, A. M. Tolkach, S. I. Stekhova, N. G. B. Shentsova and N. I. Uvarova, *Pharm. Chem. J.* (Engl. Transl.), 1992, **26**, 31.
8 M. Schnabelrauch, A. Vasella and S. G. Withers, *Helv. Chim. Acta*, 1994, **77**, 778.
9 F. Coppa, F. Fontana, F. Minisci, M. C. Nogueira Barbosa and E. Vismara, *Tetrahedron*, 1991, **47**, 7343 and references cited therein.
10 O. R. Martin, F. Xie, R. Kakarla and R. Benamza, *Synlett*, 1993, 165.
11 A. Boschetti, F. Nicotra, L. Penza and G. Russo, *J. Org. Chem.*, 1988, **53**, 4181.
12 K. K.-C. Liu, L. Chen, Z. Zhong, Y. Ichikawa and C.-H. Wong, *J. Org. Chem.*, 1991, **56**, 6280.
13 J. A. Ragan and K. Cooper, *Bioorg. Med. Chem. Lett.*, 1994, **4**, 2563; S. Hanessian and H. Prabhanjan, *Synlett*, 1994, 868; T. Uchiyama, T. J. Woltering, W. Wong, C.-C. Lin, T. Kajimoto, M. Takebayashi, G. Weitz-Schmidt, T. Asakura, M. Noda and C.-H. Wong, *Bioorg. Med. Chem.*, 1996, **4**, 1149.
14 N. Kaila, H.-A. Yu and Y. Xiang, *Tetrahedron Lett.*, 1995, **36**, 5503; J. C. Prodger, M. J. Bamford, M. I. Bird, P. M. Gore, D. S. Holmes, R. Priest and V. Saez, *Bioorg. Med. Chem.*, 1996, **4**, 793.

*Received in Cambridge, UK, 22nd May 1997; 7/03559D*

# Synthesis of a symmetric branched peptide. Assembly of a cyclic peptide on a small tetraacetate template

**Chuan-Fa Liu and James P. Tam***

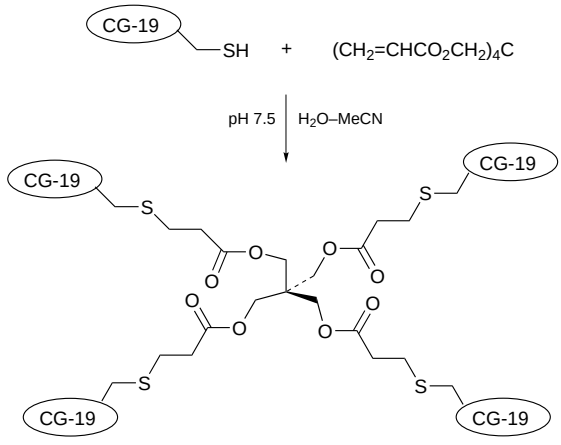
*Department of Microbiology and Immunology, Vanderbilt University, A5119 Medical Center North, Nashville, TN 37232-2363, USA*

**A method for the synthesis of a symmetric peptide dendrimer (MW 8685.0) by assembling four copies of an unprotected Cys-containing cyclic peptide *via* Michael addition onto a small organic template, pentaerythritol tetraacrylate, is described.**

Branched peptides in which peptides radiate from a central core are emerging as a new class of artificial proteins with many potential applications.[1–3] Notable examples include the cascade peptide dendrimers found in the design of Multiple Antigenic Peptides (MAPs), in which the core structures are peptidyl templates organized by geometric branching of a bivalent lysine,[2] and TASP, which contains a preorganized, linear lysyl peptide template.[3–5] More recently, small, rigid organic compounds,[6] such as cavitands[7] and Kemp's triacid,[8] have also been exploited as templates for branched peptides. These templates have the advantages that they are readily obtainable and form branched peptides that have pseudo-symmetry. We have report the use of a readily available small organic molecule, pentaerythritol tetraacrylate (PETA), as the tempalte to prepare a symmetrical branched peptide containing four copies of a large cyclic peptide *via* Michael addition of a cysteinyl thiol (Scheme 1).

Together with branched peptide design, efficient methods to accomplish their synthesis are also required. Thus, recent advances in the development of ligation methods using unprotected peptides as building blocks have greatly facilitated their preparation.[9–13] These methods are mainly dependent on either thiol or weak base–aldehyde chemistry.[2] Our scheme for synthesizing symmetric peptide dendrimers involves Michael addition of a cysteinyl thiol to the double bond of the acrylate moiety of PETA. In practice, a two-fold excess (8 equiv.) of peptide with respect to the tetravalent PETA† was found to be adequate to drive the reaction to completion in 45 min, even at a relatively dilute concentration of peptide (1–2 mM). The reaction was performed in $H_2O$ at pH 8 with MeCN (50%) as a cosolvent to increase the solubility of PETA. However, the assembly reaction could also be carried out in 4–6 M guanidine hydrochloride solutions with comparable reaction rates. The only detectable side reaction was the disulfide formation of CG-19, and which could be minimized when a trialkyl phosphine was present in the reaction medium.[12] In 15 min, > 80% of the four-branch peptide dendrimer was formed, together with < 15% of the two- and three-branch intermediates, as monitored by HPLC (Fig. 1). Both the three-branch and four-branch products were isolated from HPLC and analysed by MALDI-TOF MS, which gave expected mass units for both products: 6604.0 (calc. 6602.0) for three branch and 8685.7 (calc. 8685.0) for four-branch (Fig. 1). The tetravalent peptide dendrimer was stable at both acidic and basic pH, and no decomposed product was found after 24 h treatment at pH 2 or 8 as monitored by HPLC.

An advantage of our synthetic scheme is the regioselectivity of Michael addition by a thiol to the acrylate moiety in the presence of other amine nucleophiles. This selectivity permits the use of unprotected, cyclic peptide as the building block for the assemblage on the PETA template. Furthermore, such cyclic peptides with a pendant cysteinyl thiol side chain can be readily synthesized through the intramolecular orthogonal coupling methods developed recently in our laboratory.[16,17] the cyclic peptide CG-19, which is rich in amino side chains, is derived from the sequence of the V3 loop of the gp 120 protein of HIV-1 (III-B). The linear, unprotected peptide precursor was prepared by solid phase synthesis through Boc-benzyl chemistry on a thioester resin.[15] HF cleavage gave the unprotected peptide with an $N^{\alpha}$-Cys(Npys) and a thiocarboxylic acid at the C-terminus with all other side chains unprotected. Cyclization was achieved *in situ* immediately after HF cleavage in which the C-terminal CO–SH reacted with the N-terminal H-Cys(NPys) residue,




CG-19 = cyclo(CysAlaLysArgIleGlnArgGlyProGlyArgAlaPheValTheIleGly)

**Scheme 1**

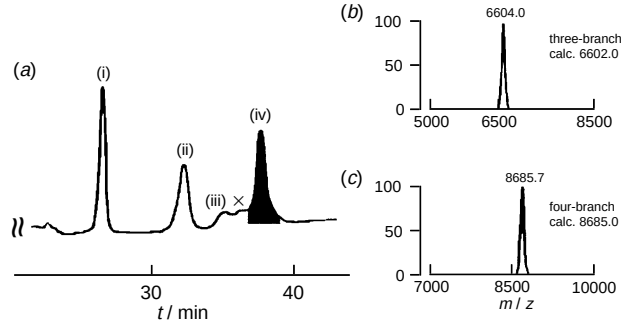



**Fig. 1** (*a*) HPLC monitoring of the Michael reaction of the thiol cyclic peptide CG-19 with PETA after 15 min. (*b*) MALDI MS of the 3-branch peptide dendrimer. (*c*) MALDI MS of the four-branch peptide dendrimer. Peaks are (i) cyclic peptide CG-19, (ii) cyclic peptide CG-9 disulfide, (iii) three-branch, (iv) four-branch (x = two-branch). HPLC analyses were run on a Shimadzu system with a Vydac analytical column (0.46 × 25 cm, $C_{18}$ reverse phase) at a flow rate of 1.5 ml $min^{-1}$, with UV detection at 225 nm and a linear gradient from 20 to 65% buffer B in buffer A in 45 min. Buffer A = $H_2O$ (0.045% TFA); Buffer B = 60% MeCN in $H_2O$ (0.04% TFA).

leading to the formation of an internal Gly–Cys peptide through proximity-driven acyl migration.[15] After purification, a cyclic peptide building block with unambiguous structure and composition was obtained for the subsequent assemblage on PETA. Michael addition of a thiol to the maleimido group has been extensively used for peptide–protein conjugates.[9] However, the hydrolysis of the maleimide at basic pH is a well recognized disadvantage.[9b] Thus, the use of PETA, which forms a more stable and non-maleimide product, is a significant advantage.

The method presented here provides a straightforward and practical approach to preparing branched peptide dendrimers that would be useful for the preparation of specific antibodies as well as for the development of synthetic vaccines. We anticipate that other types of artifical proteins might also be synthesized using this method.

This work was supported by US PHS grants CA 36544 and AI 37965.

## Footnote and References

† PETA was purchased directly from Aldrich and used after one HPLC purification.

1 J. P. Tam, *Proc. Natl. Acad. Sci. USA*, 1988, **85**, 54 099.
2 J. P. Tam and J. C. Spetzler, *Biomed. Pept. Proteins Nucleic Acids*, 1995, **1**, 123.
3 M. Mutter and S. Vuilleumier, *Angew. Chem., Int. Ed. Engl.*, 1989, **28**, 535.
4 M. Montal, M. S. Montal and J. M. Tomich, *Proc. Natl. Acad. Sci. USA*, 1990, **87**, 6929.
5 K. Sheldon, D. Liu, J. Ferguson and J. Gariepy, *Proc. Natl. Acad. Sci. USA*, 1995, **92**, 2056.
6 T. Sasaki and E. T. Kaiser, *J. Am. Chem. Soc.*, 1989, **111**, 380.
7 B. C. Gibb, A. R. Mezo and J. C. Sherman, *Tetrahedron Lett.*, 1995, **36**, 7587.
8 M. Goodman, Y. B. Feng, G. Melacini and J. P. Taulane, *J. Am. Chem. Soc.*, 1996, **118**, 5156.
9 (*a*) Y.-A. Lu, P. Clavijo, M. Galantino, Z.-Y. Shen, W. Liu and J. P. Tam, *Immunology*, 1991, **73**, 249; (*b*) T. Kitagawa and T. Aikawa, *J. Biochem.*, 1976, **79**, 233; (*c*) D. G. McCafferty, C. A. Slate, B. M. Nakhle, H. D. Graham, T. L. Austell, R. W. Vachet, B. H. Mulis and B. W. Erickson, *Tetrahedron*, 1995, **51**, 9859.
10 C. F. Liu and J. P. Tam, *J. Am. Chem. Soc.*, 1994, **116**, 4149; C. F. Liu and J. P. Tam, *J. Am. Chem. Soc.*, 1996, **118**, 307.
11 P. E. Dawson and S. B. H. Kent, *J. Am. Chem. Soc.*, 1994, **116**, 30.
12 J. P. Tam, Y.-A. Lu and J. Shao, *Proc. Natl. Acad. Sci. USA*, 1995, **92**, 12 485.
13 K. Rose, *J. Am. Chem. Soc.*, 1994, **116**, 30.
14 J. Shao, J. P. Tam, *J. Am. Chem. Soc.*, 1955, **117**, 3893.
15 C.-F. Liu, C. Rao and J. P. Tam, *Tetrahedron Lett.*, 1996, **37**, 933.
16 P. Botti, T. D. Pallin and J. P. Tam, *J. Am. Chem. Soc.*, 1966, **118**, 10 018.
17 L. Zhang and J. P. Tam, *J. Am. Chem. Soc.*, 1997, in the press.

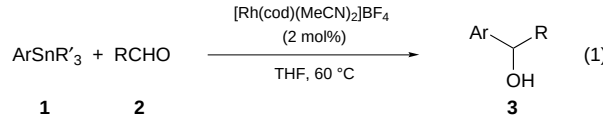
*Received in Corvallis, OR, USA, 27th March 1997; 7/02129A*

# Rhodium-catalysed arylation of aldehydes with arylstannanes

**Shuichi Oi,* Mitsutoshi Moro and Yoshio Inoue**

*Department of Materials Chemistry, Graduate School of Engineering, Tohoku University, Sendai 980-77, Japan*

**Aryltrimethylstannanes react with aldehydes in the presence of a catalytic amount of a cationic rhodium complex, [Rh(cod)(MeCN)$_2$]BF$_4$, affording the corresponding arylated secondary alcohols in good yields.**




The addition of organometallic reagents to aldehydes has been the general method for the synthesis of secondary alcohols. Among these reagents, organolithium and organomagnesium (Grignard reagent) compounds are recognized to be the most versatile. However, limitations to their use arise from the very nature of the reagents, namely, their extraordinary reactivity as nucleophiles and bases. This feature often gives rise to undesired reactions in the synthesis of multifunctional compounds such as natural products. In order to realize chemoselective addition to aldehydes, various organometallic reagents have been investigated. Nozaki and Hiyama[1] and Kishi[2] reported the addition of organochromium compounds to aldehydes in the presence of a nickel catalyst. Although this reaction is highly chemoselective and displays wide compatibility with the functional groups in both reaction partners, a large excess (200–1600 mol%) of chromium salt is required. The allylation of aldehydes with allylstannanes promoted by a Lewis acid is one of the most promising reactions and has been applied successfully in organic systhesis.[3] Recently, this allylation was reported to be also catalysed by transition metal complexes such as those of rhodium,[4] palladium and platinum.[5] There is, however, no report on the addition of other organostannanes to aldehydes except 1-carboranylstannane,[6] a very special agent. We wish to report here a novel, highly chemoselective arylation reaction of aldehydes with arylstannanes catalysed by a cationic rhodium complex [eqn. (1)].

The general procedure is as follows. A mixture of 1.2 mmol of arylstannane **1**, 1.0 mmol of aldehyde **2** and 0.02 mmol of [Rh(cod)(MeCN)$_2$]BF$_4$ (cod = cycloocta-1,5-diene) in 1 ml of dried THF was stirred at 60 °C for an appropriate period of time under $N_2$ atmosphere in a sealed Schlenk tube. The reaction was monitored by TLC. The reaction was quenched by adding a small amount of water and then stirred for 1 h. After the solvent was removed *in vacuo*, the product was isolated by silica gel column chromatography.

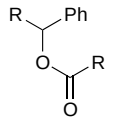
The results are summarized in Table 1. The arylation of benzaldehyde with trimethylphenylstannane proceeded smoothly in the presence of 2 mol% cationic rhodium complex [Rh(cod)(MeCN)$_2$]BF$_4$, affording diphenylmethanol in 85% isolated yield (entry 1). NMR examination of the reaction mixture prior to quenching the reaction by adding water indicated the formation of the corresponding stannyl ether. Therefore, the hydrolysis of the stannyl ether must take place during the work-up. Addition of phosphine ligands such as $PPh_3$ to [Rh(cod)(MeCN)$_2$]BF$_4$ inhibited the reaction. Neutral rhodium complexes such as RhCl($PPh_3$)$_3$ and [RhCl(cod)]$_2$ did not promote the reaction, nor did the traditional Lewis acids like $TiCl_4$ and $BF_3{\cdot}OEt_2$. The employment of tributylphenylstannane and tetraphenylstannane instead of trimethylphenylstannane gave diphenylmethanol in lower chemical yields of 65 and 17%, respectively (entries 2 and 3). The reaction of *p*-fluorophenyltrimethylstannane and *p*-methoxyphenyltrimethylstannane with benzaldehyde proceeded smoothly, affording the corresponding diarylmethanols in good

**Table 1** Arylation reaction of aldehydes with arylstannanes catalysed by [Rh(cod)(MeCN)$_2$]BF$_4$[a]

| | | | Reaction conditions | | |
|---|---|---|---|---|---|
| Entry | Arylstannane **1** | Aldehyde **2** | *T*/°C | *t*/h | Yield (%)[b] |
| 1 | $PhSnMe_3$ | PhCHO | 60 | 5 | 85 (87) |
| 2 | $PhSnBu_3$ | PhCHO | 60 | 5 | (65) |
| 3 | $Ph_4Sn$ | PhCHO | 60 | 20 | (17) |
| 4 | *p*-$FC_6H_4SnMe_3$ | PhCHO | 60 | 2 | 88 |
| 5 | *p*-$MeOC_6H_4SnMe_3$ | PhCHO | 60 | 2 | 91 |
| 6 | $PhSnMe_3$ | *p*-$MeOC_6H_4CHO$ | 60 | 24 | 85 |
| 7 | $PhSnMe_3$ | *p*-$MeC_6H_4CHO$ | 60 | 24 | 87 |
| 8 | $PhSnMe_3$ | *p*-$ClC_6H_4CHO$ | 60 | 5 | 91 |
| 9 | $PhSnMe_3$ | *p*-$MeC(O)C_6H_4CHO$ | 60 | 5 | 96 |
| 10 | $PhSnMe_3$ | *p*-$MeOC(O)C_6H_4CHO$ | 60 | 5 | 96 |
| 11 | $PhSnMe_3$ | *p*-$(NO_2)C_6H_4CHO$ | 60 | 5 | 94 |
| 12 | $PhSnMe_3$ | Furfural | 60 | 5 | 91 |
| 13 | $PhSnMe_3$ | $C_5H_{11}CHO$ | 60 | 20 | 34 (40)[c] |
| 14 | $PhSnMe_3$ | *c*-$C_6H_{11}CHO$ | 60 | 20 | 40[d] |
| 15 | $PhSnMe_3$ | *tert*-$C_4H_9CHO$ | 60 | 20 | 54[e] |
| 16 | $PhSnMe_3$ | Cyclohexanone | 60 | 24 | 29 |

[a] A mixture of **1** (1.2 mmol), **2** (1.0 mmol) and [Rh(cod)(MeCN)$_2$]BF$_4$ (0.02 mmol) in THF (1 ml) was stirred under $N_2$ atmosphere. [b] Isolated yield based on **2**. Values in parentheses were determined by GC. [c] Ester **4a** (28%) was formed concomitantly. [d] Ester **4b** (36%) was formed concomitantly. [e] Ester **4c** (8%) was formed concomitantly.

yields (entries 4 and 5). The reaction of trimethylphenylstannane with substituted benzaldehydes and furfural also proceeded smoothly, affording the corresponding diarylmethanol in good to excellent yields (entries 6 to 12). It is noted that the reaction was highly chemoselective, since other electrophilic functional groups in **2** such as the acetyl, methoxycarbonyl and nitro groups remained intact (entries 9, 10 and 11). The reactions of trimethylphenylstannane with aliphatic aldehydes, *i.e.* hexanal, cyclohexanecarboxaldehyde and trimethylacetaldehyde, afforded the corresponding alcohols in lower yields of 34, 40 and 54%, respectively (entries 13 to 15). In these cases, esters **4a**, **4b** and **4c** were formed as by-products

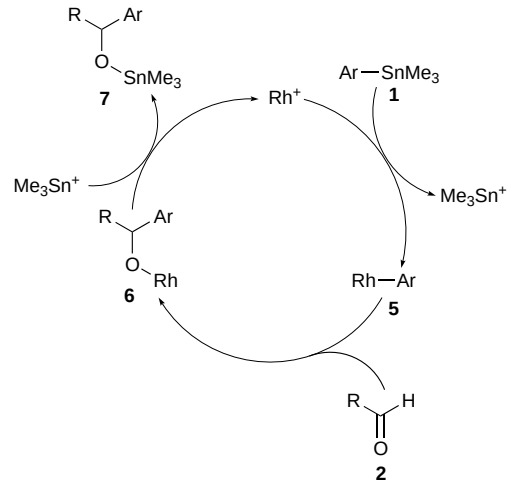


**4a** R = $C_5H_{11}$
**b** R = c-$C_6H_{11}$
**c** R = $Bu^t$

in 28 (0.14 mmol), 36 (0.18 mmol) and 8% (0.04 mmol) yield, respectively. On the contrary, the reactions of trimethylphenylstannane with ketones, *i.e.* acetophenone and heptan-2-one, did not take place at all under similar conditions. The reaction with cyclohexanone proceeded sluggishly, affording the corresponding alcohol in 29% yield (entry 16). To ensure the chemoselectivity of the reaction toward aldehyde and ketone, a competitive reaction of benzaldehyde (1 mmol) and cyclohexanone (1 mmol) with trimethylphenylstannane (1 mmol) was carried out at 60 °C for 5 h. The yield of diphenylmethanol was 79% and that of 1-phenylcyclohexanol was only 4%, indicating that the addition of trimethylphenylstannane to benzaldehyde occurred preferentially.

To gain information on the reaction mechanism, the reactivity of $[Rh(cod)(MeCN)_2]BF_4$ toward benzaldehyde was studied. However, the cationic rhodium complex did not show any indication of a reaction with an equimolar amount of benzaldehyde in THF. The interaction of the rhodium complex with trimethylphenylstannane **1a** was then investigated. When 0.1 mmol of $[Rh(cod)(MeCN)_2]BF_4$ was treated with 1.0 equiv. of **1a** in 5.0 ml of THF at 25 °C for 20 h followed by quenching the reaction with water, the stannane **1a** was consumed completely, affording benzene (44% yield) and a trace amount of biphenyl. On quenching the reaction with $D_2O$ instead of $H_2O$, the benzene formed was not deuteriated. On the other hand, 78% of the yielded benzene (62% yield) was deuteriated on carrying out the reaction in the presence of 1.0 mmol of $D_2O$. A control experiment confirmed that the stannane **1a** was inert to water. These results indicate the generation of a water-labile species from $[Rh(cod)(MeCN)_2]BF_4$ and the stannane **1a**, which we attribute to an unstable phenylrhodium species that should decompose rapidly to give benzene. Actually, the reaction of $[Rh(cod)(MeCN)_2]BF_4$ with 1.0 equiv. of **1a** in the presence of 2.0 equiv. of styrene gave *trans*-stilbene in 49% yield, which would be formed by a Heck-type reaction between the phenylrhodium species and the styrene.[7] We tried in vain to detect a peak corresponding to the species by $^1H$ and $^{13}C$ NMR measurement of the reaction performed in $[^2H_8]THF$. There are several reports on the transmetallation between transition metals and arylstannanes to give arylmetal species as are shown in the Stille coupling reaction.[8] It was also reported that a phenylrhodium complex, $RhPh(CO)(PPh_3)_2$, thermally decomposes into benzene,biphenyl and benzophenone.[9]

The presumed reaction pathway for the novel arylation reaction of aldehydes **2** with arylstannanes **1** is shown in



**Scheme 1**

Scheme 1. The transmetallation of the cationic rhodium complex with **1** would produce the arylrhodium intermediate **5**. Then, addition of **5** to an aldehyde would occur to afford a rhodium alkoxide complex **6**, which would afford the stannyl ether **7**. The presence of $PPh_3$ inhibited the reaction. This observation is in accord with that reported by Hegedus where alkyl- and aryl-rhodium(I) phosphine complexes prepared on the action of Grignard or organolithium reagents on the corresponding chlororhodium(I) complexes are unreactive to benzaldehyde.[10] Thus a phosphine-free phenylrhodium species is responsible for this reaction. The mechanism for the formation of the ester **4** would involve the insertion of another aldehyde **2** into the Rh–O bond of **6**. A similar mechanism was proposed by Slough in the Tishchenko-type disproportionation of aldehydes catalysed by rhodium complexes.[11]

The reaction reported herein represents a new method for highly chemoselective arylation of aldehydes with aryltrimethylstannanes under neutral conditions using a catalytic amount of a cationic rhodium complex. Further work is now in progress to investigate the full scope of this reaction.

## Footnote and References

* E-mail: oishu@aporg.che.tohoku.ac.jp


1 Y. Okude, S. Hirano, T. Hiyama and H. Nozaki, *J. Am. Chem. Soc.*, 1977, **99**, 3179; T. Hiyama, K. Kimura and H. Nozaki, *Tetrahedron Lett.*, 1981, **22**, 1037; K. Takai, K. Kimura, T. Kuroda, T. Hiyama and H. Nozaki, *Tetrahedron Lett.*, 1983, **24**, 5281; K. Takai, T. Kuroda, S. Nakatsukasa, K. Oshima and H. Nozaki, *Tetrahedron Lett.*, 1985, **26**, 5585; K. Takai, M. Tagashira, T. Kuroda, K. Oshima, K. Uchimoto and H. Nozaki, *J. Am. Chem. Soc.*, 1986, **108**, 6048.

2 H. Jin, J. Uenishi, W. J. Christ and Y. Kishi, *J. Am. Chem. Soc.*, 1986, **108**, 5644.

3 Review: Y. Yamamoto and N. Asao, *Chem. Rev.*, 1993, **93**, 2207.

4 J. M. Nuss and R. A. Rennels, *Chem. Lett.*, 1993, 197.

5 H. Nakamura, N. Asao and Y. Yamamoto, *J. Chem. Soc., Chem. Commun.*, 1995, 1273; H. Nakamura, H. Iwama and Y. Yamamoto, *J. Am. Chem. Soc.*, 1996, **118**, 6641.

6 H. Nakamura, N. Sadayori, M. Sekido and Y. Yamamoto, *J. Chem. Soc., Chem. Commun.*, 1994, 2581.

7 R. F. Heck, *J. Am. Chem. Soc.*, 1968, **90**, 5518.

8 J. K. Stille, *Angew. Chem., Int. Ed. Engl.*, 1986, **25**, 508.

9 W. Keim, *J. Organomet. Chem.*, 1969, **19**, 161.

10 L. S. Hegedus, P. M. Kendall, S. M. Lo and J. R. Sheats, *J. Am. Chem. Soc.*, 1975, **97**, 5448.

11 G. A. Slough, J. R. Ashbaugh and L. A. Zannoni, *Organometallics*, 1994, **13**, 3587.


*Received in Cambridge, UK, 12th June 1997; 7/04108J*

# Δ-*cis*-α-[Ru(*RR*-picchxnMe$_2$)(phen)]$^{2+}$ shows minor groove AT selectivity with oligonucleotides

**Emma M. Proudfoot,[a] Joel P. Mackay,[b] Robert S. Vagg,[a] Kymberley A. Vickery,[a] Peter A. Williams[c] and Peter Karuso*[a]**

[a] *School of Chemistry, Macquarie University, NSW, 2109, Australia*
[b] *School of Biochemistry, University of Sydney, NSW, 2006, Australia*
[c] *Department of Chemistry, University of Western Sydney, Nepean, NSW, 2747, Australia*

**NMR studies show that the ternary octahedral Δ-*cis*-α-[Ru(*RR*-picchxnMe$_2$)(phen)]$^{2+}$ cation binds with AT selectivity in the minor groove of [d(CGCGATCGCG)$_2$] and [d(ATATCGATAT)$_2$] duplexes through a non-intercalative interaction.**

The design of metal complexes for sequence-specific DNA-binding has attracted much attention recently,[1,2] and elucidation of the structural aspects of such binding is clearly a crucial step in the design process. Some measure of controversy exists over the general mode of interaction with DNA of complexes based on the ligand phen (1,10-phenanthroline). For example, on the basis of $^1$H NMR data, one study concluded that Δ-[Ru(phen)$_3$]$^{2+}$ binds intercalatively in the major groove of the [(GTGCAC)$_2$] duplex, while its Λ-isomer surface binds in the minor groove.[3] In contrast, a like study indicated minor groove non-intercalative binding for both Δ and Λ forms.[4] Furthermore, other studies employing a variety of experimental techniques and nucleotides arrive at different and often contradictory conclusions regarding the mode of binding of this complex.[5–7] Recent publications[4,8,9] have indicated that a similar debate exists over the binding site preferences of Δ- and Λ-[Ru(phen)$_2$(dppz)]$^{2+}$.

The interactions of potential intercalators with oligonucleotides may be probed using ternary complex compounds based on the [Ru(*R***R**-picchxnMe$_2$)(bidentate)]$^{2+}$ cation template.[2] In such complexes the tetradentate ligand *R***R**-picchxnMe$_2$ [(1*R**,2*R**)-*N*,*N*′-dimethyl-*N*,*N*′-di(2-picolyl)-1,2-diaminocyclohexane][10] determines the chirality of the cation and its overall shape, with the bidentate ligand serving as the putative intercalator.[2] In contrast to [Ru(bidentate)$_3$]$^{2+}$, ternary complexes of this type avoid complications due to averaging between the three possible bound states. Here we report the synthesis and preliminary NMR studies on the binding of the chiral Δ-*cis*-α-[Ru(*RR*-picchxnMe$_2$)(phen)]$^{2+}$ complex cation† (Fig. 1) to the self-complementary duplexes [d(CGCGATCGCG)$_2$] and [d(ATATCGATAT)$_2$]. The study is the first to allow a rigorous evaluation of sequence and groove selectivities for metalloprobes based on a single phen ligand.

Titration of the metal complex into a solution of duplex [d(CGCGATCGCG)$_2$], monitored by one-dimensional $^1$H NMR spectroscopy at 313 K (Fig. 2), shows considerable upfield shifts of all phen resonances ($-1.23 \geqslant \Delta\delta \geqslant -0.29$ ppm), consistent with significant shielding by the duplex. In contrast, the pyridyl and aliphatic protons of the picchxnMe$_2$ ligand are only slightly affected ($< \pm 0.2$ ppm). This titration also provides evidence for preferential binding at the central AT sequence of the oligonucleotide. At a 1 : 1 complex–duplex ratio, the A5H2 peak is observed to shift 0.29 ppm upfield, while each of the other DNA base protons move marginally downfield ($\leqslant 0.09$ ppm). The A5H2 upfield shift is consistent with the findings of a recent NMR study using the same oligonucleotide sequence and the Δ- and Λ-[Ru(phen)$_3$]$^{2+}$ complex enantiomers.[4]

While chemical shift changes alone are insufficient to deduce the nature of the binding interaction (for example, the AH2 proton has been noted for its sensitivity to the binding of small molecules in both the major and minor grooves[3]), our one-dimensional titration data are indicative of minor groove binding to the AT site. 2D NOESY spectra, recorded at both 303 and 273 K (1 : 1 complex–duplex ratio), provide evidence to support this conclusion. First, three NOE cross peaks are observed between A5H2 (which points into the minor groove) and the metal complex protons H3, H7 and H8 (Fig. 3). Secondly, both T6CH$_3$ and A5H8, which point directly towards the major groove and show a number of intramolecular NOEs, display no cross peaks with the protons of the cation. Thirdly, there is no measureable disruption in the intensities of the sequential H1′–H6/H8 NOE signals in the complex–duplex adduct, indicating that the regular B-form DNA helical structure is retained.[4]

In total, 25 intermolecular NOE signals have been unambiguously assigned at 303 K, all supporting a single binding site model for the ruthenium complex at the central AT sequence, and involving a non-intercalative minor groove binding mode. The NOESY spectrum recorded at 273 K reveals a number of weak intermolecular NOE signals involving cation protons and

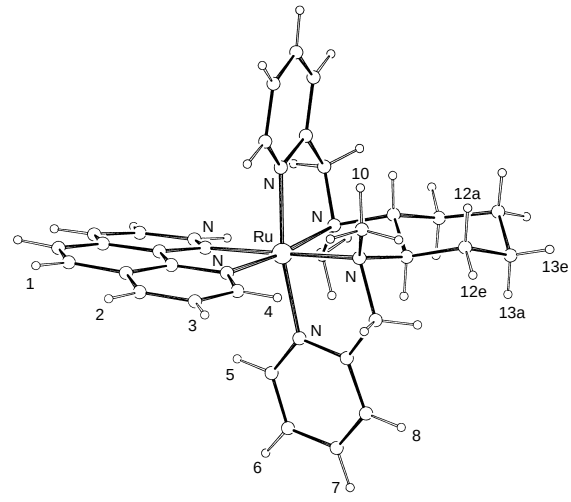



**Fig. 1** The structure of the Δ-*cis*-α-[Ru(*RR*-picchxnMe$_2$)(phen)]$^{2+}$ cation. The proton numbering system used in the text is indicated. The Δ absolute configuration of the cation was confirmed by NMR spectroscopy of the complex. In a compensated ROESY spectrum[12] ($\tau_m$ = 50 ms, 4 kHz spinlock), using the H13a–H13e cross peak intensity as a calibration (1.78 Å), the average distances for H10–H12a (2.64 Å) and H10–H12e (3.24 Å) were measured according to the formula $r_{ij}/r_{kl} = [\sigma_{kl}/\sigma_{ij}]^{1/6}$. (Due to differences in $\tau_c$ for individual protons, an error of 15% can be expected (ref. 13). These distances correspond well to those of the computed model of the Δ-isomer shown [H10$_{(av)}$–H12a = 2.75 Å; H10$_{(av)}$–H12e = 3.35 Å], but not to those of the Λ-isomer [H10$_{(av)}$–H12a = 3.89 Å; H10$_{(av)}$–H12e = 2.94 Å).

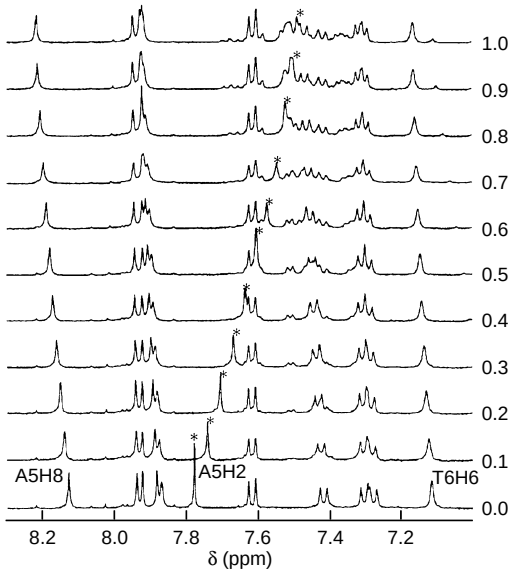



**Fig. 2** One-dimensional $^1$H NMR spectra of the nucleobase protons of [d(CGCGATCGCG)$_2$] at varying cation–duplex ratios (0.0–1.0) (313 K). Note that the resonances of A5H2 and A5H8 shift considerably with complex addition while the others are little affected.

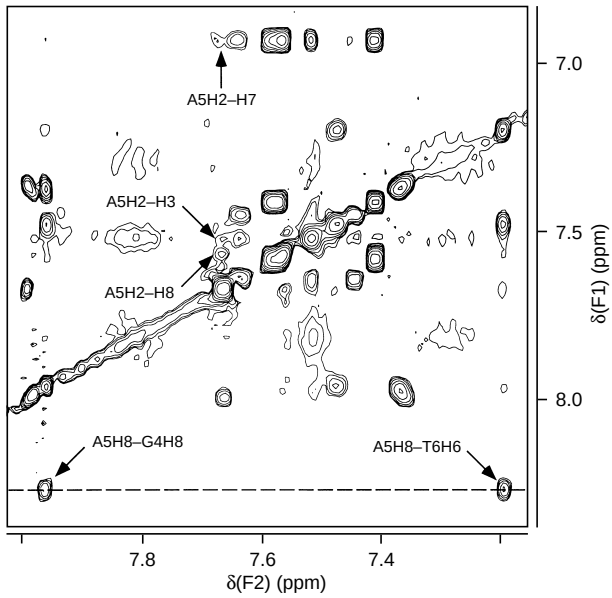



**Fig. 3** A $^1$H NOESY spectrum of the Δ-*cis*-α-[Ru(*RR*-picchxnMe$_2$)(phen)]$^{2+}$–[d(CGCGATCGCG)$_2$] adduct (1 : 1 ratio, 273 K) showing NOE cross peaks involving the complex protons H3, H7 and H8 and the A5H2 proton in the minor groove. The broken line indicates the positions at which any A5H8–complex cross peaks would be observed if present. These studies were carried out using Bruker AMX600/DMX600 and Varian XL400 NMR spectrometers ([oligonucleotide] = 1.25 mM in 100% $D_2O$ containing 10 mM $NaH_2PO_4$, 10 mM NaCl, 0.01% $NaN_3$, uncorrected pD 7.00). Proton assignments were made using DQF-COSY, TOCSY ($\tau_m$ = 80 ms) and NOESY ($\tau_m$ = 400 ms) spectra. Assignments for the free oligonucleotide were consistent with published data (ref. 14).

those on C1 and G10, suggesting that a secondary weaker binding mode exists at lower temperatures. This may involve aromatic stacking, which could occur at the termini of the duplex. None of these NOE signals are observed at 303 K, and there are no significant chemical shift changes for the C1H6 and G10H8 protons ($\Delta\delta \leqslant 0.01$ ppm), indicating that this interaction is weak.

A similar titration of the cation with a [d(ATATCGATAT)$_2$] duplex[11] was carried out at 298 K. On addition of the complex an immediate broadening of the A7H2, A7H8 and T4CH$_3$ resonances occurs, and at a 1 : 1 ratio significant broadening extends throughout the spectrum. 2D TOCSY and NOESY spectra at 313 K (1 : 1 complex–duplex ratio, $\tau_m$ = 400 ms) allowed the assignment of all resonances for the cation and nucleotide base, H1′, H2′, and H2″ protons (the A3-, A7- and A9-H2 resonances were not assignable due to severe line broadening even at higher temperatures). Ten weak intermolecular NOE cross peaks were observed, predominantly between the pyridyl protons of the cation and H1′ sugar protons of the T4, C5, A7, T8, A9 and T10 nucleobases. No NOE cross peaks were observed involving the major groove AH8 or TCH$_3$ protons. These results are consistent with binding occurring in the minor groove at the several AT sites available in this duplex. Thus it is clear that the preferential AT binding observed with the [d(CGCGATCGCG)$_2$] sequence is not due simply to the higher stability of the central part of that oligonucleotide, a potential problem with short DNA duplex sequences.

In conclusion, we have shown that Δ-*cis*-α-[Ru(*RR*-picchxnMe$_2$)(phen)]$^{2+}$ binds preferentially to AT sequences in duplex oligonucleotides, the predominant molecular binding component being the phen ligand. A range of chemical shift, line broadening and NOE evidence has been used to demonstrate that binding occurs non-intercalatively in the minor groove, thereby contributing significantly to the debate regarding the role of the phen ligand as a DNA-binding epitope. The present work provides a firm basis from which to evaluate the DNA binding properties of other ternary complexes incorporating known intercalating bidentate ligands and based on the [Ru(*R***R**-picchxnMe$_2$)(bidentate)]$^{2+}$ template.[2]

This research was supported by the Australian Research Council through an ARC large grant (to R. S. V., P. K. and P. A. W.), an ARC Mechanism C grant (to P. K. and others) for the purchase of the Bruker DMX600 600 MHz NMR spectrometer, and an ARC Research Fellowship (to J. P. M.). Δ-*cis*-α-[Ru(*RR*-picchxnMe$_2$)(phen)]$^{2+}$ was synthesised by K. Vickery. We gratefully acknowledge G. Ball and K. Tonkin for assistance with NMR measurements and W. Kett for assistance with HPLC.

## Footnotes and References

* E-mail: Peter.Karuso@mq.edu.au

† Isomeric mixtures containing both Δ-*cis*-α- and Δ-*cis*-β-[Ru(*RR*-picchxnMe$_2$)(phen)]$^{2+}$ are obtained by heating solutions containing stoichiometric quantities of *RR*-picchxnMe$_2$ (ref. 10) and $RuCl_3 \cdot nH_2O$ in propane-1,2-diol under reflux for *ca.* 1 h, followed by addition of a slight molar excess of phen. The isomeric forms of the product may be separated by cation exchange chromatography. In the present work, the complex was used in the chloride form.

1 T. W. Johann and J. K. Barton, *Philos. Trans. R. Soc. London A*, 1996, **354**, 299.
2 J. R. Aldrich-Wright, R. S. Vagg and P. A. Williams, *Coord. Chem. Rev.*, 1997, in the press.
3 J. P. Rehmann and J. K. Barton, *Biochemistry*, 1990, **29**, 1701.
4 M. Eriksson, M. Leijon, C. Hiort, B. Nordén and A. Gräslund, *Biochemistry*, 1994, **33**, 5031.
5 B. Nordén, N. Patel, C. Hiort, A. Gräslund and S. K. Kim, *Nucleosides and Nucleotides*, 1991, **10**, 195.
6 J. K. Barton, A. T. Danishefsky and J. M. Goldberg, *J. Am. Chem. Soc.*, 1984, **106**, 2172.
7 S. Satyanarayana, J. C. Dabrowiak and J. B. Chaires, *Biochemistry*, 1992, **31**, 9319.
8 E. Tuite, P. Lincoln and B. Nordén, *J. Am. Chem. Soc.*, 1997, **119**, 239.
9 C. M. Dupureur and J. K. Barton, *Inorg. Chem.*, 1997, **36**, 33.
10 R. R. Fenton, F. S. Stephens, R. S. Vagg and P. A. Williams, *Inorg. Chim. Acta*, 1991, **182**, 67.
11 J. Feigon, W. Leupin, W. A. Denny and D. R. Kearns, *Biochemistry*, 1983, **22**, 5943.
12 C. Griesinger and R. R. Ernst, *J. Magn. Reson.*, 1987, **75**, 261.
13 R. Abseher, S. Lüdemann, H. Schreiber and O. Steinhauser, *J. Am. Chem. Soc.*, 1994, **116**, 4006.
14 N. Patel, J. Bergman and A. Gräslund, *Eur. J. Biochem.*, 1991, **197**, 597.

*Received in Cambridge, UK, 9th June 1997; 7/04001F*

# Surface plasmon resonance analysis of glycopeptide antibiotic activity at a model membrane surface

**Matthew A. Cooper, Dudley H. Williams* and Younghoon R. Cho**

*Cambridge Centre for Molecular Recognition, Department of Chemistry, University of Cambridge, Lensfield Road, Cambridge, UK CB2 1EW*

**Affinity constants of glycopeptide antibiotics for peptides anchored in a lipid monolayer measured by surface plasmon resonance show a correlation with *in vitro* antimicrobial activity.**

The vancomycin group of glycopeptide antibiotics is active against a wide range of Gram-positive bacteria, particularly many *staphylococci* and *enterococci* responsible for post-surgical infections. Unfortunately resistance to vancomycin is now widespread,[1] and the accompanying increase in the number of deaths from bacterial infections has given new urgency to the search for novel antibiotics. The activity of the glycopeptide antibiotics arises from their ability to bind mucopeptide precursors terminating in the sequence –Lys-D-Ala-D-Ala (–KAA).[2,3] We have shown previously that with the exception of the teicoplanins, glycopeptide antibiotics dimerise in aqueous solution[4] and that dimerisation plays an important role in their biological activity.[5,6] We have employed sodium dodecyl sulfate micelles as model membranes to study the binding interactions between antibiotic and peptide ligands anchored to the lipid surface.[7,8] The small size of the micelles allows NMR analysis of antibiotic–ligand–micelle aggregates, but their high radius of curvature and surfactant properties make them a poor membrane model.

Biacore AB have recently commercialised a hydrophobic association chip for use in their surface plasmon resonance (SPR) instruments, which consists of a self assembled monolayer of alkanethiol on a gold film. Vesicles spontaneously absorb onto the alkane surface to form a supported lipid monolayer[9] which chemically and physically resembles the surface of a cell membrane. The phenomenon of surface plasmon resonance can then be exploited to study interactions with lipophilic ligands inserted into the monolayer. Changes in the measured refractive index at the interface, given in response units, are proportional to the amount of material in the immediate vicinity of the sensor surface.[10] Buffered solutions of an analyte are passed over the surface and the affinity of the binding event can be calculated from analysis of the resultant binding curve.

A phosphate buffered solution of phosphatidylcholine vesicles (0.5 mM) formed by extrusion through a 50 nm polycarbonate filter[11] was loaded on the chip at low flow rate (2 μl $min^{-1}$) immediately after an injection of octyl glucoside, a non-ionic detergent used to clean the alkanethiol surface (Fig. 1). Sodium hydroxide (10 mM) was then injected at high flow rate (to remove any multilamellar structures) which resulted in a stable baseline. Complete coverage of the chip surface with lipid was confirmed by the lack of non-specific binding of bovine serum albumin, which binds strongly to the hydrophobic self assembled monolayer alone. *N*-α-Docosanoyl-ε-acetyl-Lys-D-Ala-D-Ala (Doc-KAA) was then inserted into the lipid monolayer by direct injection across the surface as a dilute solution (data not shown). Antibiotics possessing some variation in measured binding affinities to di-*N*-acetyl-Lys-D-Ala-D-Ala (Ac-KAA) in free solution, but varying more in their propensity to dimerise (Table 1), were then exposed to the ligand–lipid monolayer (Fig. 2). Affinity constants were

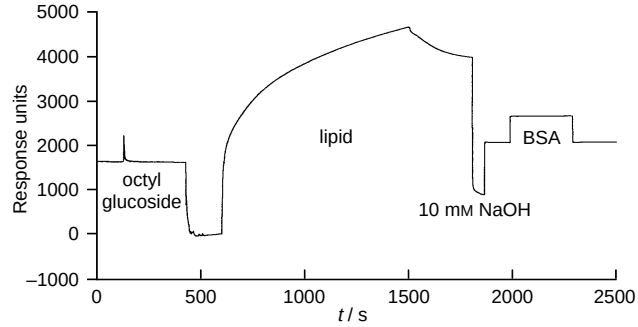



**Fig. 1** Loading of the chip with phosphatidylcholine vesicles formed by extrusion. (Note that dramatic changes in the measured response at the point of injection are due to bulk refractive index shifts between buffer and the injected solution.)

**Table 1** Minimum inhibitory concentrations, affinity constants ($K_A$) for Ac-KAA and Doc-KAA and dimerisation constants ($K_{dim}$) for various antibiotics

| Antibiotic | MIC[a] for *B. Subtilis*/ μg $ml^{-1}$ | $K_{dim}$/ $M^{-1}$[b] | $K_A/M^{-1}$[c] | |
|---|---|---|---|---|
| | | | Ac-KAA | Doc-KAA |
| $TA_3$-1 | 4 | — | $1.2 \times 10^6$ | $4.9 \times 10^5$ |
| Vancomycin | 0.25 | 700 | $2.4 \times 10^6$ | $1.4 \times 10^6$ |
| Ristocetin A | 1 | 300 | $5.9 \times 10^5$ | $6.3 \times 10^6$ |
| Eremomycin | 0.03 | $4.0 \times 10^5$ | $3.0 \times 10^4$ | $1.7 \times 10^7$ |
| CE | 0.03 | $1.6 \times 10^4$ | $1.0 \times 10^6$ | $2.1 \times 10^7$ |
| BCE | 0.008 | $2.0 \times 10^5$ | $5.9 \times 10^5$ | $1.4 \times 10^7$ |
| Teicoplanin | 0.5 | — | $1.6 \times 10^6$ | $1.0 \times 10^7$ |

[a] Minimum inhibitory concentration. [b] Ref. 12. [c] Refs. 4 and 17. [d] Refs. 13–16.

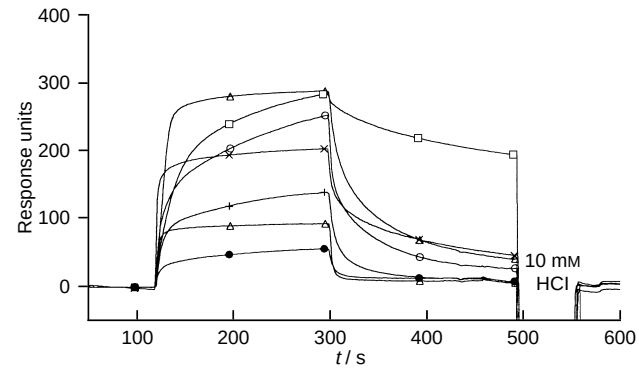



**Fig. 2** Binding of glycopeptide antibiotics at 2 μM to a Doc-KAA–lipid monolayer and removal of bound antibiotic with 10 mM HCl; (△ (ristocetin A, (□) BCE, (○) CE, (×) teicoplanin, (+) eremomycin, (△) $TA_3$-1 and (●) vancomycin

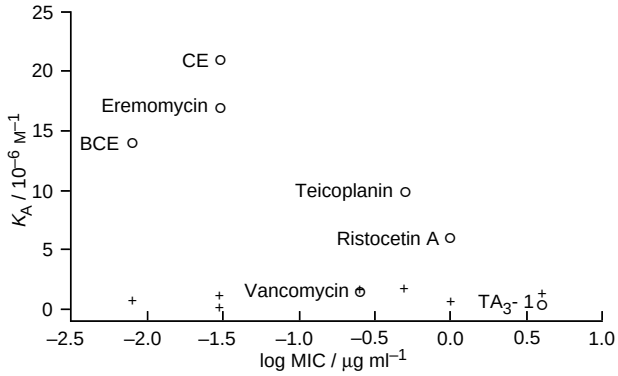



**Fig. 3** Correlation between surface affinity constants (○) of glycopeptide antibiotics to mucopeptide analogues and MIC values against *B. Subtilis*. Solution affinity constants (+) do not correlate with MIC values.

determined by Scatchard analysis of the equilibrium response levels at varying concentrations (kinetic analysis will be discussed in a full paper). Data from a flow cell containing the ligand–lipid monolayer were subtracted from data from a control flow cell containing lipid only. This control negates changes in the SPR signal due to unbound antibiotic in solution.

Affinity constants of antibiotics for Doc-KAA at the membrane-like surface determined by SPR showed a much better correlation with antimicrobial activity[12] than those measured to Ac-KAA[13–16] in solution by UV difference spectroscopy (Table 1, Fig. 3). Eremomycin, for example, has a low affinity constant to Ac-KAA in solution, but nevertheless has a low minimum inhibitory concentration (MIC) value (Table 1). This is because eremomycin dimerises strongly and is able to bind cooperatively[7] to a pair of ligands anchored to the surface. The initial binding of ligand to one half of the dimer is intermolecular, whereas binding to the other half of the dimer at the surface is effectively intramolecular and results in an affinity constant over 500-fold greater than that in solution (Table 1). In contrast the antibiotic $TA_3$-1, which has a high affinity for peptide in solution but is not known to dimerise,[16] has a relatively high MIC value. In this case there is no cooperative benefit to be gained from templated binding at a surface (Table 1) as the antibiotic can only bind as monomer. In general, strongly dimerising antibiotics[17] such as eremomycin and chloroeremomycin (CE, or LY264826)[18] have enhanced affinities for Doc-KAA at the surface, and weakly dimerising antibiotics such as ristocetin A[4] have correspondingly weaker enhancements. Teicoplanin is exceptional as it does not dimerise, yet has a higher affinity constant at the surface than in free solution. This is because teicoplanin possesses a $C_{11}$ acyl chain which functions as a membrane anchor to localise the antibiotic at the surface.[7] Binding to peptide in this case is cooperative as the antibiotic and peptide are attached to the same template and this event is effectively intramolecular as is the case with the dimerising antibiotics. Biphenylchloroeremomycin (BCE, or LY307599),[19] a semisynthetic derivative of CE that dimerises strongly and possesses a biphenyl substituent which can function as a membrane anchor,[8] also binds tightly to Doc-KAA at the surface. In accord with the hypothesis that dimerisation and membrane anchoring promote antibiotic activity, it has been shown that these features make the antagonism of antibiotic action by externally added Ac-KAA *in vitro* much more difficult.[6]

We have shown that SPR is well suited for the analysis of binding interactions at a model membrane surface and that the calculated binding affinities at the surface are more relevant to *in vitro* activity than corresponding values determined in free solution. We have shown that cooperativity in the binding of glycopeptides to bacterial cell wall analogues is promoted by dimerisation and membrane anchoring of the antibiotic. The joint operation of these two locating devices is crucial for the activity of semisynthetic antibiotics against vancomycin-resistant bacteria.[8,20]

We thank George Murray Foundation (M. A. C.), SmithKline Beecham (Y. R. C.), Association of Commonwealth Universities for a Commonwealth Scholarship (Y. R. C.), and NSERC Canada (Y. R. C.) for financial support, and Biacore AB, UK, for time on their BIAcore 2000 instrument.

## Footnote and References

* E-mail: dhw1@cam.ac.uk

1 P. Courvalin, *Antimicrob. Agents Chemother.*, 1990, **34**, 2291.
2 H. R. Perkins, *Biochem. J.*, 1969, **111**, 195.
3 J. C. J. Barna, D. H. Williams and M. P. Williamson, *J. Chem. Soc., Chem. Commun.*, 1985, 254.
4 U. Gerhard, J. P. Mackay, R. A. Maplestone and D. H. Williams, *J. Am. Chem. Soc.*, 1993, **115**, 232.
5 J. P. Mackay, U. Gerhard, D. A. Beauregard, M. S. Westwell, M. S. Searle and D. H. Williams, *J. Am. Chem. Soc.*, 1994, **116**, 4581.
6 D. A. Beauregard, D. H. Williams, M. N. Gwynn and D. J. C. Knowles, *Antimicrob. Agents Chemother.*, 1995, **39**, 781.
7 M. S. Westwell, B. Bardsley, R. J. Dancer, A. C. Try and D. H. Williams, *J. Chem. Soc., Chem. Commun.*, 1996, 589.
8 D. H. Williams, *Nat. Prod. Rep.*, 1996, **13**, 469.
9 S. Terrettaz, T. Stora, C. Duschl and H. Vogel, *Langmuir*, 1993, **9**, 1361.
10 E. Stenberg, B. Persson, H. Roos and C. Urbaniczky, *J. Colloid Interface Sci.*, 1991, **143**, 513.
11 R. C. Macdonald, R. I. Macdonald, B. P. M. Menco, K. Takeshita, N. K. Subbarao and L. R. Hu, *Biochim. Biophys. Acta*, 1991, **1061**, 297.
12 D. A. Beauregard, A. J. Maguire, D. H. Williams and P. E. Reynolds, *Antimicrob. Agents. Chemother.*, in the press.
13 A. Malabarba, A. Trani, G. Tarzia, P. Ferrari, R. Pallanza and M. Berti, *J. Med. Chem.*, 1989, **32**, 783.
14 M. Nieto and H. R. Perkins, *Biochem. J.*, 1971, **123**, 789.
15 V. M. Good, M. N. Gwynn and D. J. C. Knowles, *J. Antibiot.*, 1990, **43**, 550.
16 J. P. Mackay, U. Gerhard, D. A. Beauregard, R. A. Maplestone and D. H. Williams, *J. Am. Chem. Soc.*, 1994, **116**, 4573.
17 A. J. Maguire, *Ph.D. Thesis*, University of Cambridge, 1997.
18 K. V. I. Rolston, H. Nguyen and M. Messer, *Antimicrob. Agents Chemother.*, 1990, **34**, 2137.
19 T. I. Nicas, D. L. Mullen, J. E. Flokowitsch, D. A. Preston, N. J. Snyder, M. J. Zweifel, S. C. Wilkie, M. J. Rodriguez, R. C. Thompson and R. D. G. Cooper, *Antimicrob. Agents Chemother.*, 1996, **40**, 2194.
20 N. E. Allen, D. L. LeTourneau and J. N. Hobbs, *Antimicrob. Agents Chemother.*, 1997, **41**, 66.

*Received in Liverpool, UK, 4th June 1997; 7/03943C*

# Unexpected regiocontrol in the Pauson–Khand reaction due to 2-furyl substitution of the alkene component

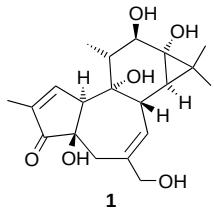
**Laurence M. Harwood*[a] and Lucía San Andrés Tejera[b]†**

[a] *Department of Chemistry, University of Reading, Whiteknights, Reading, UK RG6 6AD*
[b] *Dyson Perrins Laboratory, University of Oxford, South Parks Road, Oxford, UK OX1 3QY*

**2-Vinylfuran derivatives undergo regiocontrolled Pauson–Khand reaction, in which the furan exerts the dominant directing influence, to furnish 5-(2-furyl)cyclopent-2-enones, overwhelming the strong directing effects of a homoallylic thioether and appearing to inhibit intramolecular reaction in which bridging constraints are in opposition to the directing influence of the 2-furyl substituent.**

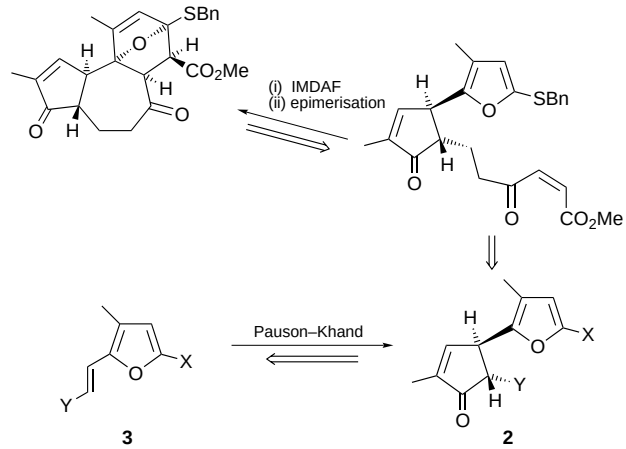
For sheer efficiency in construction of cyclopent-2-enones there is surely no match for the Pauson–Khand reaction, which links three components in a single process to furnish products in which the substitution pattern is often highly controlled and predictable.[1] Enantiocontrolled variants have been reported[2] and mild conditions developed in which amine oxides accelerate reaction.[3] The 2-methylcyclopent-2-enone motif is a recurrent sub–unit in many families of terpenoid natural products, such as the tiglianes,[4] and the Pauson–Khand reaction has proven its worth for synthetic approaches to such systems.[1]

In the course of our work towards the total synthesis of phorbol **1** and analogues, *via* an approach in which the lynchpin is the high pressure mediated intramolecular furan Diels–Alder reaction,[5] we required a flexible means of access to a range of 5–substituted 4-(2-furyl)-2-methylcyclopent-2-one intermediates of general structure **2**. We envisaged such structures might be accessible *via* Pauson–Khand reaction of the corresponding *(E)*-(2-furyl)prop–2–enyl derivatives **3** with μ-propynehexacarbonyldicobalt. Mechanistic considerations and literature precedent[6] made us hopeful of achieving the desired arrangement of the propyne-derived methyl substituent but we recognised the potential for regiochemical ambiguity of alkene incorporation during cyclisation (Scheme 1).




**1**

To investigate the outcome, substrates **7a**,**b** were prepared from the corresponding furan-2-carbaldehydes **4** by stereoselective Wittig olefination, reduction of the resultant esters **5** to the alcohols **6** and protection as the *tert*-butyldimethylsilyl ethers **7**.‡ Optimised Pauson–Khand reaction conditions [μ-propynehexacarbonyldicobalt (2 equiv.), $CH_2Cl_2$–MeOH (100 : 1), reflux, 10 days] led to a single cyclopentenone in both cases (**8a**: 67%, **8b**: 41%) uncontaminated by any diene side products (Scheme 2), in marked contrast to previous observations.[7] Attempts to accelerate reaction by addition of amine oxides to the reaction mixture had a detrimental effect. Unfortunately, analysis of NOE difference spectra and couplings in the two-dimensional $^1$H NMR spectra of the products

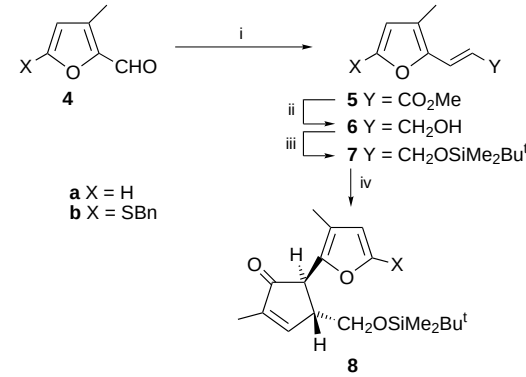



**Scheme 1**

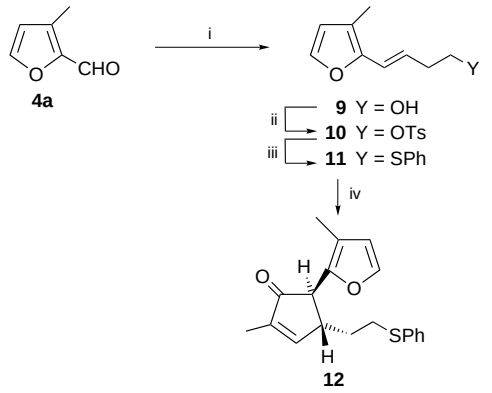
clearly showed that the undesired C-4/C-5 substitution had been selectively obtained in both cases.§

Reports that a homoallylic thioether on the alkene component accelerates and exerts good regiocontrol on its participation in the Pauson–Khand reaction[8] led us to synthesise **11** in an attempt to obtain the desired substitution pattern. This was achieved *via* reaction of **4a** with the ylide derived from 3-hydroxypropyl(triphenyl)phosphonium bromide to furnish **9**, followed by tosylation to form **10** and displacement with sodium phenylthiolate, giving the required substrate **11** (Scheme 3). Pauson–Khand reaction under previously optimised conditions again led to a single cycloadduct **12** (43%)§ in which the furyl group had apparently overwhelmed the directing influence of the homoallylic thioether to furnish the undesired regioisomer once more.

An attempt to force the regiocontrol led us to consider an intramolecular Pauson–Khand cyclisation; tethering the alkene

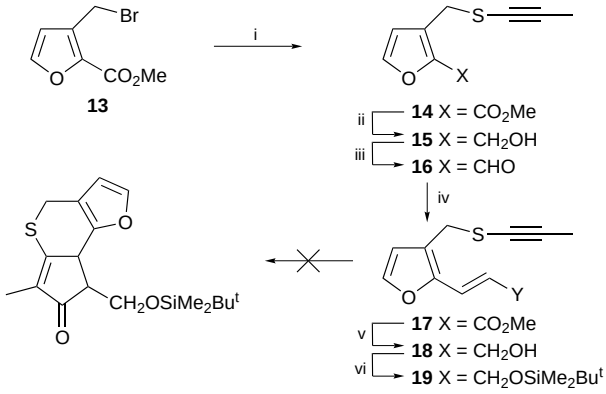



**Scheme 2** *Reagents and conditions*: i, $Ph_3P{=}CHCO_2Me$, $CH_2Cl_2$, reflux (**a** 74%, **b** 45%); ii, $Bu^i_2AlH$ (2 equiv.), toluene, −78 °C (**a** 93%, **b** 78%); iii, $Bu^tMe_2SiCl$, $Et_3N$, DMAP (cat.), $CH_2Cl_2$, 0 °C → room temp. (**a** 92%, **b** 78%); iv, $(HC{\equiv}CMe)Co_2(CO)_6$, $CH_2Cl_2$–MeOH (100 : 1), reflux, 10 days (**a** 67%, **b** 41%)




**Scheme 3** *Reagents and conditions*: i, $Ph_3P{=}CHCH_2CH_2O^-$ $Li^+$, THF, −78 °C → room temp., 58%; ii, TsCl, pyridine, 0 °C → room temp., 88%; iii, $PhS^-$ $Na^+$, THF, reflux, 57%; iv, $(HC{\equiv}CMe)Co_2(CO)_6$ (2 equiv.), $CH_2Cl_2$–MeOH (95 : 5), reflux, 10 days, 43%

and alkyne by a thioether which could be hydrogenolysed subsequent to directed cyclopentenylation. Methyl 3-methyl-2-furoate was converted *via* furylic bromination to **13**,[9] halide displacement with lithium propyne-1-thiolate to give **14** and two step conversion to furnish 3-(prop-1-ynylthiomethyl)furan-2-carbaldehyde **16** (Scheme 4). Subsequent elaboration as before gave the intramolecular Pauson–Khand reaction precursor **19** in three steps. However, despite extensive efforts, no conditions could be found which resulted in the isolation of any cyclopentenone, despite the fact that thioether bridges have been used successfully to direct such reactions in prop-2-ynylic systems.[10] From this we conclude that the influence of the 2-furyl substituent attached to the alkene plays a strong role in directing the Pauson–Khand cycloaddition to the extent that, in situations where regiochemical choice is not possible, reaction appears to be disfavoured.




**Scheme 4** *Reagents and conditions*: i, $Me{\equiv}CS^-Li^+$, $Et_2O$, −70 °C → room temp., 85%; ii, $NaBH_4$ (excess), EtOH, room temp., 79%; iii, $MnO_2$/C, $CH_2Cl_2$, room temp., 73%; iv, $Ph_3P{=}CHCO_2Me$, $CH_2Cl_2$, reflux, 87%; v, $Bu^i_2AlH$ (2 equiv.), toluene −70 °C, quant.; vi, $Bu^tMe_2SiCl$, $Et_3N$, DMAP (cat.), $CH_2Cl_2$, room temp., 98%

In conclusion, we present evidence that, for the intermolecular Pauson–Khand reaction, the presence of a 2-furyl substituent on the alkene component substrate exerts a powerful regiodirecting effect causing the furan unit to appear at C-5 of the resultant cyclopent-2-enone. Although rendering this approach inappropriate for our initial specific need, this unexpected regiocontrol has more general synthetic potential.

We thank the Gobierno Autònomo de Canarias, Spain, for a postdoctoral fellowship (to L. S. A. T.) and Dr W. J. Kerr of the Department of Pure and Applied Chemistry, University of Strathclyde, for valuable discussions.

## Footnotes and References

* E-mail: l.m.harwood@reading.ac.uk
† Current address: Instituto Universitario de Bio-Organica 'Antonio Gonzalez', Universidad de la Laguna, Carretera la Esperanza 2, 38206 La Laguna, Tenerife, Spain.

‡ All novel compounds isolated gave spectroscopic data in accordance with their assigned structures.

§ *Selected data* for **8a**: $\nu_{max}$(film)/cm$^{-1}$ 1718, 1255, 1110, 839; $\delta_H$ (500 MHz, $CDCl_3$) 0.46 (s, 6 H), 0.87 (s, 9 H), 1.84 (s, 3 H), 2.01 (s, 3 H), 3.14 (m, 1 H), 3.51 (d, *J* 3.3, 1 H), 3.70 (dd, $J_1$ 5.2, $J_2$ 10.0, 1 H), 3.79 (dd, $J_1$ 5.2, $J_2$ 10.0, 1 H), 6.20 (d, *J* 1.7, 1 H), 7.20 (d, *J* 1.7, 1 H), 7.31 (br s, 1 H); Selected NOE difference data: **7.31** → 3.65–3.85 (1.5%), 3.14 (4%), 1.84 (3%); *m/z* (CI, $NH_3$) 321 ($MH^+$); Calc. for $C_{18}H_{28}O_3Si$: C, 67.46, H, 8.80. Found: C, 67.24, H, 8.58%.

For **8b** $\nu_{max}$(film)/cm$^{-1}$ 1716, 1254, 1109, 837; $\delta_H$ (500 MHz, $C_6D_6$) 0.07 (s, 6 H), 0.86 (s, 9 H), 1.67 (s, 3 H), 1.79 (s, 3 H), 3.00–3.05 (m, 1 H), 3.33–3.41 (m, 2 H), 3.48 (d, *J* 3.5, 1 H), 3.59 (d, *J* 12.5, 1 H), 3.71 (d, *J* 12.5, 1 H), 6.09 (s, 1 H), 6.74 (br s, 1 H), 7.00–7.12 (m, 5 H); Selected NOE difference data: **6.74** → 3.00–3.05 (6%), 3.33–3.41 (3%), 1.67 (3.5%); *m/z* (CI, $NH_3$): 443 ($MH^+$), 91; Calc. for $C_{25}H_{34}O_3SiS$ : C, 67.83, H, 7.74; S. 7.24. Found: C, 68.03; H, 8.03; S, 7.43%.

For **12**: $\delta_{max}$(film)/cm$^{-1}$ 1713, 1481, 1439, 1149, 1088, 740; $\delta_H$ (200 MHz, $C_6D_6$) 1.45 (m, 2 H), 1.61 (s, 3 H), 1.81 (s, 3 H), 2.57 (m, 2 H), 2.93 (m, 1 H), 3.00 (d, *J* 3.3, 1 H), 5.98 (d, *J* 1.7, 1 H), 6.45 (s, 1 H), 6.91–7.23 (m, 6 H); *m/z* (CI, $NH_3$) 313 ($MH^+$); Calc. for $C_{19}H_{21}O_2S$: 313.12584. Found: 313.12623.

1 For reviews, see N. E. Schore, *Org. React*., 1991, **40**, 1; N. E. Schore, *Comprehensive Organic Synthesis*, ed. B. M. Trost, Pergamon Press, Oxford, 1991, vol. 5, pp. 1037–1064; P. L. Pauson, *Tetrahedron*, 1985, **41**, 5855.
2 For examples of chiral substrates, see C. Almansa, A. Moyano and F. Serratosa, *Tetrahedron*, 1988, **44**, 2657; S. Takano, K. Inomato and K. Ogasawana, *J. Chem. Soc., Chem. Commun*., 1992, 169; C. Johnstone, W. J. Kerr and U. Lange, *J. Chem. Soc., Chem. Commun*., 1995, 457; C. Mukai, M. Uchiyama, S. Sakamoto and M. Hanaoka, *Tetrahedron Lett.* 1995, **36**, 5761; H. B. Park, B. Y. Lee, Y. K. Cheng and Y. K. Chung, *Organometallics*, 1995, **14**, 3104; J. Tormo, X. Verdaguer, A. Moyano, M. A. Pericàs and A. Riera, *Tetrahedron*, 1996, **52**, 14 021. Chiral amine oxide promoted reaction: W. J. Kerr, G. G. Kirk and D. Middlemiss, *Synlett*, 1995, 1085. Chirally modified alkyne–cobalt complex: A. M. Hay, W. J. Kerr, G. G. Kirk and D. Middlemiss, *Organometallics*, 1995, **14**, 4986.
3 S. Shambayati, W. E. Crowe and S. L. Schreiber, *Tetrahedron Lett*., 1990, **31**, 5289; N. Jeong, Y. K. Chung, B. Lee, H. L. Lee and S-E. Yoo, *Synlett*, 1991, 204; A. R. Gordon, C. Johnstone and W. J. Kerr, *Synlett*, 1995, 1083; J. G. Donkervoort, A. R. Gordon, C. Johnstone, W. J. Kerr and U. Lange, *Tetrahedron*, 1996, **52**, 7391.
4 Naturally Occurring Phorbol Esters, ed. F. J. Evans, C.R.C. Press, Boca Raton, FL, 1986.
5 L. M. Harwood, T. Ishikawa, H. Philips and D. Watkin, *J. Chem. Soc., Chem. Commun*., 1991, 527 and references cited therein.
6 M. E. Krafft, R. H. Romero and I. L. Scott, *Synlett*, 1995, 577.
7 The diene is a common side product in this reaction, resulting from lack of insertion of carbon monoxide. It should be noted that aryl substituents on the alkene exert a similar regiodirecting influence to that observed for the 2-furyl group: I. U. Khand and P. L. Pauson, *J. Chem. Soc., Perkin Trans 1*, 1976, 30; I. U. Khand and P. L. Pauson, *J. Chem. Res.*, 1977, (*S*) 9; (*M*) 168; I. U. Khand, E. Murphy and P. L. Pauson, *J. Chem. Res.*, 1978, (*S*) 350; (*M*) 4434; I. U. Khand, C. A. L. Mahaffy and P. L. Pauson, *J. Chem. Res.*, 1978, (*S*) 352; (*M*) 4454.
8 M. E. Krafft, *J. Am. Chem. Soc.*, 1988, **110**, 968; M. E. Krafft, C. A. Juliano, I. L. Scott, C. Wright and M. D. McEachin, *J. Am. Chem. Soc.*, 1991, **113**, 1693; M. E. Krafft, I. L. Scott and R. H. Romero, *Tetrahedron Lett.*, 1992, **33**, 3829.
9 M.-C. Zaluski, M. Robba and M. Bonhomme, *Bull. Soc. Chim. Fr.*, 1970, 1445.
10 Others have also recently reported the use of this tether: A. Stumpf, N. Jeong and H. Sunghee, *Synlett*, 1997, 205.

*Received in Liverpool, UK, 30th May 1997; 7/03786D*

# Water-soluble calixarenes as new inverse phase-transfer catalysts. Nucleophilic substitution of alkyl and arylalkyl halides in aqueous media

**Shoichi Shimizu,* Katsuyuki Kito, Yasuyuki Sasaki and Choichiro Hirai**

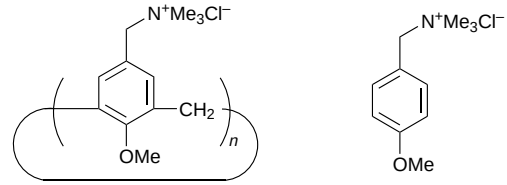
*Department of Industrial Chemistry, College of Industrial Technology, Nihon University, Narashino, Chiba 275, Japan*

**The water-soluble calix[*n*]arenes $\mathbf{1}_n$ (*n* = 4, 6 and 8) containing trimethylammoniomethyl groups act as efficient inverse phase-transfer catalysts in the nucleophilic substitution reaction of alkyl and arylalkyl halides with nucleophiles in water.**

Inverse phase-transfer catalysts facilitate reactions between two immiscible reactants *via* the transport of an organic substrate into an aqueous solution of a second reactant where reactions take place.[1,2] The use of inverse phase-transfer catalysis (IPTC) has two major advantages over that of normal phase-transfer catalysis (PTC): (i) the aqueous catalyst solution is easily separated and recycled, and (ii) no other organic solvent is necessary if organic reactants are liquid at the reaction temperature. However, in sharp contrast to the case of normal PTC, the understanding, development and applications of this method for conducting organic reactions have not expanded yet to the extent that it deserves. This is mainly due to the fact that only a limited number of inverse phase-transfer agents are known, *e.g.* cyclodextrins (CDs) and their derivatives, water-soluble metal complexes and pyridine *N*-oxides.[2]

We now report that water-soluble calix[n]arenes $\mathbf{1}_n$ (*n* = 4, 6 and 8) containing trimethylammoniomethyl groups can catalyse the nucleophilic substitution of alkyl and arylalkyl halides with simple nucleophiles in water, demonstrating the first example of the application of water-soluble calixarenes to organic reactions as efficient inverse phase-transfer catalysts.

During the past fifteen years, calixarenes have received increasing attention due to their utilization in supramolecular chemistry.[3] Some functionalized calixarenes have been developed as new phase-transfer agents for normal PTC reactions.[4] We thought that water-soluble calixarenes would serve as a new class of inverse phase-transfer catalysts *via* their ability to form inclusion complexes. In this work we have prepared the water-soluble calixarenes $\mathbf{1}_n$ (*n* = 4, 6 and 8)† and examined their catalytic ability using nucleophilic substitution reactions in water [eqn. (1)].‡ The results are summarized in Table 1.




$\mathbf{1}_n$ (*n* = 4, 6, 8) **2**

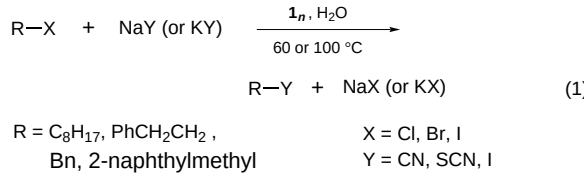



**Table 1** Nucleophilic substitution of alkyl and arylalkyl halides with simple nucleophiles[a]

| Entry | Catalyst | Substrate | Nucleophile | *T*/°C | *t*/h | Yield[b] (%) |
|---|---|---|---|---|---|---|
| 1 | none | $C_8H_{17}Br$ | NaCN | 100 | 6 | 6 |
| 2 | **2**[c] | $C_8H_{17}Br$ | NaCN | 100 | 6 | 3 |
| 3 | β-CD | $C_8H_{17}Br$ | NaCN | 100 | 6 | 20 |
| 4 | $\mathbf{1_4}$ | $C_8H_{17}Br$ | NaCN | 100 | 6 | 61 |
| 5 | $\mathbf{1_6}$ | $C_8H_{17}Br$ | NaCN | 100 | 6 | 83 |
| 6 | $\mathbf{1_8}$ | $C_8H_{17}Br$ | NaCN | 100 | 6 | 85 |
| 7 | $\mathbf{1_6}$ | $C_8H_{17}I$ | NaCN | 100 | 6 | 91 |
| 8 | none | $PhCH_2CH_2Br$ | NaCN | 100 | 6 | 24 |
| 9 | β-CD | $PhCH_2CH_2Br$ | NaCN | 100 | 6 | 45 |
| 10 | $\mathbf{1_4}$ | $PhCH_2CH_2Br$ | NaCN | 100 | 6 | 83 |
| 11 | none | BnBr | NaCN | 60 | 2 | 31 |
| 12 | β-CD | BnBr | NaCN | 60 | 2 | 55 |
| 13 | $\mathbf{1_6}$ | BnBr | NaCN | 60 | 2 | 85 |
| 14 | $\mathbf{1_6}$[d] | BnBr | NaCN | 60 | 2 | 72 |
| 15 | $\mathbf{1_6}$ | BnBr | KSCN | 60 | 2 | 88 |
| 16 | $\mathbf{1_6}$ | BnBr | KI | 60 | 2 | 78 |
| 17 | $\mathbf{1_4}$ | BnCl | NaCN | 60 | 12 | 67[e] |
| 18 | none | 2-Naphthyl$CH_2Br$ | NaCN | 60 | 2 | 0 |
| 19 | β-CD | 2-Naphthyl$CH_2Br$ | NaCN | 60 | 2 | 8 |
| 20 | $\mathbf{1_4}$ | 2-Naphthyl$CH_2Br$ | NaCN | 60 | 2 | 47 |
| 21 | $\mathbf{1_6}$ | 2-Naphthyl$CH_2Br$ | NaCN | 60 | 2 | 55 |
| 22 | $\mathbf{1_8}$ | 2-Naphthyl$CH_2Br$ | NaCN | 60 | 2 | 82 |

[a] Conditions: catalyst (0.5 mol%), substrate (4.6 mmol), nucleophile (10 mmol), water (5 ml), stirring speed 1300 rpm. In the reaction of 2-(bromomethyl)naphthalene, dipropyl ether (1 ml) was used (entries 18–22). [b] Based on substrate. Refers to GC yield (entries 1–7 and 11–17) or isolated yield (entries 8–10 and 18–22). [c] Catalyst: 3.0 mol% used. [d] Catalyst: 0.05 mol% used. [e] By-product: benzyl alcohol (8%).

Treatment of 1-bromooctane with NaCN in water for 6 h at 100 °C afforded 1-cyanooctane in 6% yield with 86% recovery of the starting material (entry 1). However, when we carried out the same reaction in the presence of the calixarene **1$_6$** (0.5 mol%), the yield of 1-cyanooctane increased to 83% (entry 5). To evaluate the ability of **1$_6$**, we examined the reactions with a conventional inverse phase-transfer catalyst, β-CD, and found that the calixarene **1$_6$** is more efficient than β-CD by a factor of 5.5 for cyanide substitution on 1-bromooctane, and 2.3 and 6.9 for benzyl bromide and 2-(bromomethyl)naphthalene, respectively (entries 13 and 21). Noteworthily, the use of as little as 0.05 mol% of **1$_6$** is sufficient, showing its remarkable catalytic activity (entry 14).

CDs function as inverse phase-transfer catalysts in aqueous–organic two-phase reactions of alkyl halides with nucleophiles owing to their ability to form host–guest complexes.[5–7] The water-soluble calixarenes may behave similarly to CDs, since they also have the ability to include organic guest molecules in their cavity. No acceleration effect is observed when (*p*-methoxybenzyl)trimethylammonium chloride **2** is added to the reaction mixture as a monomeric counterpart of **1$_6$** (entry 2). The distribution of **1$_6$** into the organic phase was negligible,§ indicating that the reaction catalysed by **1$_6$** takes place predominantly in the aqueous phase.

The efficiency of the calixarenes **1$_n$** varied depending on the size and/or shape of the substrate molecules. For example, no difference in the catalytic activities of **1$_n$** is detected in the reaction of benzyl bromide (**1$_4$** ≈ **1$_6$** ≈ **1$_8$**). On the other hand, their activities increase in the order of **1$_4$** < **1$_6$** ≈ **1$_8$** for 1-bromooctane and in the order of **1$_4$** ≤ **1$_6$** < **1$_8$** for 2-(bromomethyl)naphthalene. The size of the cavity of **1$_4$** is large enough for benzyl bromide, but **1$_8$** is required for bulkier 2-(bromomethyl)naphthalene. This result is consistently supported by the fact that *p*-sulfonatocalixarenes are capable of molecular recognition on the basis of the hole-size selectivity in an aqueous system.[8]

In conclusion, we have shown here that IPTC by water-soluble calixarenes **1$_n$** provides a simple and effective means for conducting nucleophilic substitution reactions of activated and unactivated organic halides, in which they exhibit much higher activity than CDs. This is the first example of the use of water-soluble calixarenes in organic reactions as inverse phase-transfer catalysts.

We thank Takashi Suzuki and Naoyuki Shinoda for their experimental assistance. The present work was partially supported by a General Individual Research Grant for 1995 from Nihon University.

## Footnotes and References

* E-mail: s5simizu@ccu.cit.nihon-u.ac.jp

† The water-soluble calix[*n*]arenes **1$_n$**·*n*H$_2$O (*n* = 4, 6 and 8) were prepared following literature methods (ref. 9) and identified by IR and NMR spectroscopy as well as elemental analysis.

‡ General procedure for the nucleophilic substitution reactions is as follows. A mixture of substrate (4.6 mmol), nucleophilic reagent (10 mmol), a catalytic amount (0.5 mol%) of **1$_n$**·*n*H$_2$O and water (5 ml) was heated to 60 or 100 °C and stirred with a magnetic stirring bar. The resulting mixture was extracted with $CHCl_3$. After the usual work-up, the crude product was purified by preparative GPC and its isolated yield was determined. For the reactions of 1-bromooctane and benzyl bromide with NaCN, the yield of product was determined by GC analysis of a mixture of $Et_2O$ extracts and an internal standard.

§ A mixture of **1$_6$**·6H$_2$O (0.157 g, 0.106 mmol) and water (25 ml) was extracted with $Et_2O$ (5 × 50 ml). The combined organic layer was dried over anhydrous $Na_2SO_4$, and concentrated under reduced pressure. No extract was detected by measurement of weight.

1 For the first report of IPTC, see L. J. Mathias and R. A. Vaidya, *J. Am. Chem. Soc*., 1986, **108**, 1093.
2 For reviews, see A. Harada, *J. Synth. Org. Chem. Jpn.*, 1990, **48**, 517; Y. Goldberg, *Phase Transfer Catalysis: Selected Problems and Applications*, Gordon, Berkshire, 1992, pp. 359–366; C. M. Starks, C. L. Liotta and M. Halpern, *Phase-Transfer Catalysis: Fundamentals, Applications, and Industrial Perspectives*, Chapman, London, 1994, pp. 179–183.
3 For representative reviews, see C. D. Gutsche, *Calixarenes*, *Monographs in Supramolecular Chemistry*, ed. J. F. Stoddart, The Royal Society of Chemistry, Cambridge, 1989; *Calixarenes: A Versatile Class of Macrocyclic Compounds*, ed. J. Vicens and J. Böhmer, Kluwer, Dordrecht, 1991; R. M. Izatt, H. S. Bradshaw, K. Pawlak, R. L. Bruening and B. Tarbet, *Chem. Rev.*, 1992, **92**, 1261; S. Shinkai, *Tetrahedron*, 1993, **49**, 8933; V. Böhmer, *Angew. Chem*., 1995, **107**, 785; *Angew. Chem., Int. Ed. Engl*., 1995, **34**, 713.
4 For the use of calixarenes as normal phase transfer-catalysts, see E. Nomura, H. Taniguchi, K. Kawaguchi and Y. Otsuji, *J. Org. Chem.*, 1993, **58**, 4709; K. Araki, A. Yanagi and S. Shinkai, *Tetrahedron*, 1993, **49**, 6763; E. Nomura, H. Taniguchi and Y. Otsuji, *Bull. Chem. Soc. Jpn.*, 1994, **67**, 309, 792; S. J. Harris, A. M. Kinahan, M. J. Meegan and R. C. Prendergast, *J. Chem. Res. (S)*, 1994, 342; Y. Okada, Y. Sugitani, Y. Kasai and J. Nishimura, *Bull. Chem. Soc. Jpn.*, 1994, **67**, 586; H. Taniguchi, Y. Otsuji and E. Nomura, *Bull. Chem. Soc. Jpn.*, 1995, **68**, 3563.
5 A. Z. Trifonov and T. T. Nikiforov, *J. Mol. Catal.*, 1984, **24**, 15.
6 N. Tanaka, A. Yamaguchi, Y. Araki and M. Araki, *Chem. Lett.*, **1987**, 715.
7 A. Deratani, G. Leliévre, T. Maraldo and B. Sébille, *Carbohydr. Res*., 1989, **192**, 215.
8 S. Shinkai, K. Araki and O. Manabe, *J. Chem. Soc., Chem. Commun.*, 1988, 187.
9 T. Arimura, T. Nagasaki, S. Shinkai and T. Matsuda, *J. Org. Chem.*, 1989, **54**, 3766; T. Nagasaki, K. Sisido, T. Arima and S. Shinkai, *Tetrahedron*, 1992, **48**, 797.

*Received in Cambridge, UK, 20th June 1997; 7/04347C*

# Reliable chiral transfer through thermodynamic equilibrium of the intramolecular Meerwein–Ponndorf–Verley reduction and Oppenauer oxidation

**Morifumi Fujita,*† Yoshihiro Takarada, Takashi Sugimura and Akira Tai***

*Faculty of Science, Himeji Institute of Technology, Kanaji, Kamigori, Ako-gun, Hyogo 678-12, Japan*

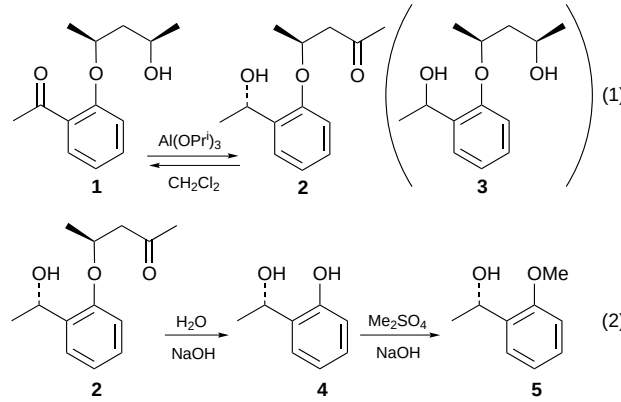
**Forward and reverse hydride transfer with rigorous diastereodifferentiation is attained using intramolecular Meerwein–Ponndorf–Verley reduction and Oppenauer oxidation of a 2-acetylphenyl ether containing an optically active 3-hydroxy-1-methylbutyl group.**

Meerwein–Ponndorf–Verley (MPV) reductions and Oppenauer oxidations have been revealed to proceed *via* reversible hydride transfer between carbonyl groups and alcohols.[1] Recently, intramolecular MPV reductions have been reported to proceed with high stereodifferentiation.[2–5] Reversible stereodifferentiating reactions, however, have the risk of lowering the stereochemical purity as well as chemical yield of products due to the reverse step, which does not always restore the formed product to the same stereoisomer as the initial reactant. Previous intramolecular stereocontrolled MPV reductions have succeeded as a result of the reaction being driven to completion under kinetic control.[2–5] In contrast, under thermodynamic equilibrium, both the forward and reverse steps must proceed with complete stereodifferentiation in order to prevent any decrease in optical purity of the reactant from the reverse step. Such stereodifferentiation reactions under thermodynamic equilibrium, however, have not yet been described for the intramolecular MPV–Oppenauer reaction.

We now report that the intramolecular hydride transfer of 2-acetylphenyl ether containing an optically active 3-hydroxy-1-methylbutyl group (**1**) proceeds with rigorous stereodifferentiation under thermodynamic equilibrium. The optically active 3-hydroxy-1-methylbutyl moiety acts as both the chiral auxiliary and hydride donor, and can easily be removed from the product **2** by alkaline hydrolysis as a result of the oxidation of the alcohol moiety to a ketone. Thus the multi-functional nature and simple structure of the optically active 3-hydroxy-1-methylbutyl moiety[4,6] provide an opportunity to construct a simple and reliable system for intramolecular chiral transfer *via* thermodynamic equilibration of the MPV–Oppenauer reaction.

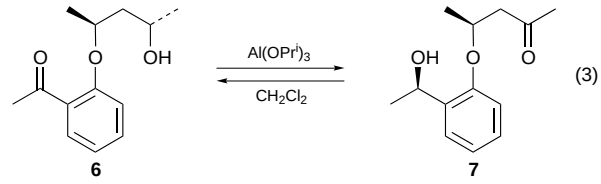
Evaluation of hydrogenation enthalpy data[1,7] for the conversion of ketones to the corresponding alcohols revealed that acetophenone is favorable to some extent as a hydride acceptor of intramolecular hydride transfer from the alcohol moiety, on the basis of the estimation that the enthalpy change ($\Delta H$) for reduction of acetophenone by propan-2-ol is $-3$ kJ mol$^{-1}$, from which the quilibrium constant ($K_{calc}$) is calculated to be 3.0 at 313 K. The reactant, (1′*S*,3′*R*)-2-(3′-hydroxy-1′-methylbutoxy)acetophenone **1**, was prepared in 66% yield *via* the Mitsunobu reaction[8] of (2*R*,4*R*)-pentane-2,4-diol with 2′-hydroxyacetophenone. The epimer of **1**, (1′*S*,3′*S*-)-2-(3′-hydroxy-1′-methylbutoxy)acetophenone **6**, was also obtained by inversion of the alcohol moiety of **1** in 78% yield *via* the Mitsunobu reaction of **1** with benzoic acid followed by hydrolysis.

Treatment of **1** with $Al(OPr^i)_3$ (2.0 equiv.) in $CH_2Cl_2$ at reflux for 20 h caused the intramolecular hydride transfer from the alcohol to the aromatic ketone to yield **2** as a single isomer in 68% yield [eqn. (1)]. It should be noted that no diol **3**, produced by intermolecular hydride transfer from isopropoxide or **1**, was obtained. The remaining 32% was recovered as the reactant **1**, with no epimer **6**.‡ The product **2** was readily hydrolysed under alkaline conditions to give 1-(2-hydroxyphenyl)ethanol **4**, which was isolated after conversion to 1-(2-methoxyphenyl)ethanol **5** [eqn. (2)]. From the negative



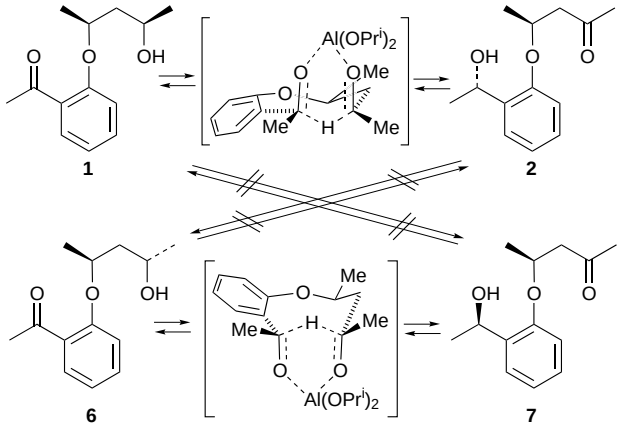

optical rotation of **5**, the absolute configuration of the α-position of **2** was determined to be *S*.[9]§

When **6** was treated with $Al(OPr^i)_3$ (2.0 equiv.) in $CH_2Cl_2$ at reflux for 20 h, the other diastereoisomer **7** was obtained at 67% yield [eqn. (3)] with the recovery of the reactant **6** in 33% yield.




These results indicate that the stereogenic centre at the hydroxy group, but at the ether, is responsible for that of the newly formed chiral centre.

The ratio of **1**:**2** remained constant at 1:2 and the epimerisation of **1** to **6** was also not observed even after extending the reaction period to 4 days. Increasing the quantity of $Al(OPr^i)_3$ to 4 equiv. also resulted in the same product distribution of **1**:**2**. The constant product ratio of **1**:**2** (1:2) which is independent of the reaction time and the amount of $Al(OPr^i)_3$ indicates that the intramolecular hydride transfer between **1** and **2** reaches an equilibrium with the equilibrium constant $K = 2.0$ The recovery of the initial reactant without empimerisation under the thermodynamic equilibrium implies the complete stereodifferentiation of the reverse step. Such rigorous stereodifferentiation in the reverse step as well as in the forward step may be a consequence of the restricted orientation of the carbonyl group and the alcohol in the transition state of




**Scheme 1**

the intramolecular MPV–Oppenauer reaction (Scheme 1). Preferential intramolecular coordination to aluminium also ensures from no formation of **3** generated by intermolecular MPV reduction is observed. Thus, the intramolecular hydride transfer proceeds without mixing the equilibrium between **1** and **2** with that between **6** and **7**.

In conclusion, a rigorous diastereodifferentiating hydride transfer has been achieved under a thermodynamic equilibrium, resulting from both the forward and reverse steps of the equilibrium proceeding diastereospecifically.

This work was partially supported by a Grant-in-Aid for Encouragement of Young Scientists No. 08750961 from the Ministry of Education, Science, Sports and Culture, Japan.

## Footnotes and References

† E-mail: fuji@sci.himeji-tech.ac.jp

‡ The epimers are distinguishable by use of $^1$H NMR (400 MHz, $CDCl_3$) spectroscopy. *Selected data* for **1**: $\delta$ 7.68 (d, *J* 7.8, 1 H), 7.41 (t, *J* 7.8, 1 H), 7.00 (d, *J* 7.8, 1 H), 6.95 (t, *J* 7.8, 1 H), 4.77–4.69 (m, 1 H), 4.03–3.98 (m, 1 H), 2.58 (s, 3 H), 2.56 (s, 1 H), 2.06–1.98 (m, 1 H), 1.74–1.68 (m, 1 H), 1.35 (d, *J* 5.9, 3 H), 1.23 (d, *J* 6.4, 3 H). For **2**: $\delta$ 7.33 (d, *J* 7.8, 1 H), 7.20 (t, *J* 7.8, 1 H), 6.93 (t, *J* 7.8, 1 H), 6.89 (d, *J* 7.8, 1 H), 5.07–5.01 (m, 1 H), 4.98–4.91 (m, 1 H), 2.96 (dd, *J* 5.9, 16.6, 1 H), 2.67 (dd, *J* 6.3, 16.6, 1 H), 2.50 (d, *J* 4.9, 1 H), 2.17 (s, 3 H), 1.45 (d, *J* 6.3, 3 H), 1.36 (d, *J* 5.9, 3 H). For **6**: $\delta$ 7.68 (d, *J* 7.8, 1 H), 7.41 (t, *J* 7.8, 1 H), 7.01 (d, *J* 7.8, 1 H), 6.95 (t, *J* 7.8, 1 H), 4.86–4.79 (m, 1 H), 4.12–4.04 (m, 1 H), 2.58 (s, 3 H), 2.04 (d, *J* 4.4, 1 H), 1.91–1.85 (m, 1 H), 1.79–1.72 (m, 1 H), 1.34 (d, *J* 6.4, 3 H), 1.23 (d, *J* 5.9, 3 H). For **7**: $\delta$ 7.32 (d, *J* 7.8, 1 H), 7.20 (t, *J* 7.8, 1 H) 6.93 (t, *J* 7.8, 1 H), 6.89 (d, *J* 7.8, 1 H), 5.07–5.02 (m, 1 H), 4.95–4.90 (m, 1 H), 2.96 (dd, *J* 6.3, 16.6, 1 H), 2.68 (dd, *J* 5.9, 16.6, 1 H), 2.17 (s, 3 H), 1.46 (d, *J* 6.3, 3 H), 1.35 (d, *J* 5.9, 3 H).

§ The enantiomeric purity of **5** was determined to be over 99% ee by GC analysis using a CHROMPACK-Chirasil-DEX CB (i.d. 0.25 mm × 25 m) column. The column temperature was maintained at 120 °C. The retention time of the *S* isomer **5** was 16.9 min and that of the *R* isomer was 19.0 min.

1 For recent review, see C. E. de Graauw, J. A. Peters, H. van Bekkum and J. Huskens, *Synthesis*, 1994, 1007.
2 K. Nishide, Y. Shigeta, K. Obata and M. Node, *J. Am. Chem. Soc.*, 1996, **118**, 13 103.
3 G. A. Molander and J. A. Mckie, *J. Am. Chem. Soc.*, 1993, **115**, 5821.
4 K. Ishihara, N. Hanaki and H. Yamamoto, *Synlett.*, 1993, 127; K. Ishihara, N. Hanaki and H. Yamamoto, *J. Am. Chem. Soc.*, 1993, **115**, 10 695; K. Ishihara, N. Hanaki and H. Yamamoto, *J. Am. Chem. Soc.*, 1991, **113**, 7074.
5 W. S. Zhou, X. M. Zhou and Y. Ni, *Acta Chim. Sinica*, 1984, **42**, 706; W. S. Zhou, Z. Q. Wang, H. Zhang, R. Y. Fei and Z. P. Zhuang, *Acta Chim. Sinica*, 1985, **43**, 168.
6 T. Sugimura, *J. Synth. Org. Chem. Jpn.*, 1997, **55**, 517.
7 J. B. Pedley, R. D. Naylor and S. P. Kirby, *Thermochemical Data of Organic Compounds*, Chapman and Hall, London, 1986.
8 T. Sugimura, H. Yamada, S. Inoue and A. Tai, *Tetrahedron: Asymmetry*, 1997, **8**, 649.
9 T. Hayashi, Y. Matsumoto and Y. Ito, *Tetrahedron: Asymmetry*, 1991, **2**, 601; P. V. Ramachandran, B. Gong and H. C. Brown, *Tetrahedron Lett.*, 1994, **35**, 2141.

*Received in Cambridge, UK, 20th June 1997; 7/04341D*

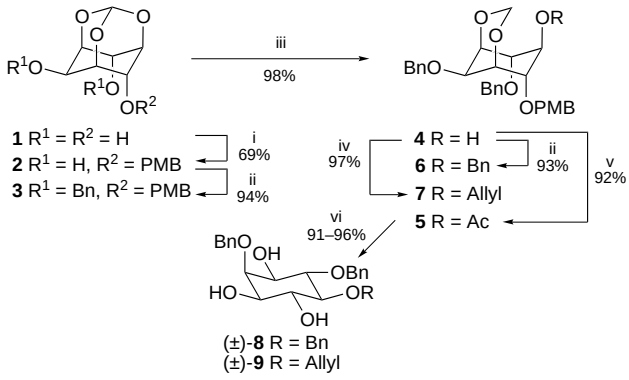
# Versatile synthesis of *myo*-inositol phospholipid precursors

**Simon J. A. Grove,[a] Ian H. Gilbert,[a] Andrew B. Holmes,*[a,b] Gavin F. Painter[a,b] and Malcolm L. Hill[c]**

[a] *Cambridge Centre for Molecular Recognition, Department of Chemistry, University of Cambridge, Lensfield Road, Cambridge, UK CB2 1EW*
[b] *Melville Laboratory for Polymer Synthesis, Department of Chemistry, University of Cambridge, Pembroke Street, Cambridge, UK CB2 3RA*
[c] *GlaxoWellcome, Medicines Research Centre, Gunnels Wood Road, Stevenage, UK SG1 2NY*

**Homochiral *myo*-inositol derivatives 16 and 20 and their corresponding enantiomers possessing either the natural or unnatural ring stereochemistry for inositol phospholipids are synthesised from *myo*-inositol derivatives 8 and 9 respectively using camphor dimethyl acetals in a resolution–protection sequence.**

The biological importance of various inositol phosphates and inositol phospholipids in cell signal transduction and related processes is well documented.[1] In most cases these compounds are not readily available in any quantity from natural sources owing to their low cellular concentrations.[2] Consequently their synthesis[3] has received extensive attention in recent years. Despite this effort many inositol derivatives are still not readily available, owing in part to the lack of availability of suitably protected homochiral *myo*-inositol derivatives.[4] Here we present concise routes to differentially protected ring enantiomers of *myo*-inositol compounds which are suitable starting materials for the synthesis of *myo*-inositol phospholipids.




**Scheme 1** *Reagents and conditions*: i, NaH, *p*-$MeOC_6H_4CH_2Cl$ (PMBCl), DMF, 0 °C to room temp.; ii, NaH, BnBr, DMF, 0 °C to room temp.; iii, DIBAL-H (2.5 equiv.), $CH_2Cl_2$–hexanes, 0 °C to room temp.; iv, NaH, allyl bromide, DMF, 0 °C to room temp.; v, $Ac_2O$, DMAP, pyridine, room temp.; vi, HCl, MeOH, reflux.



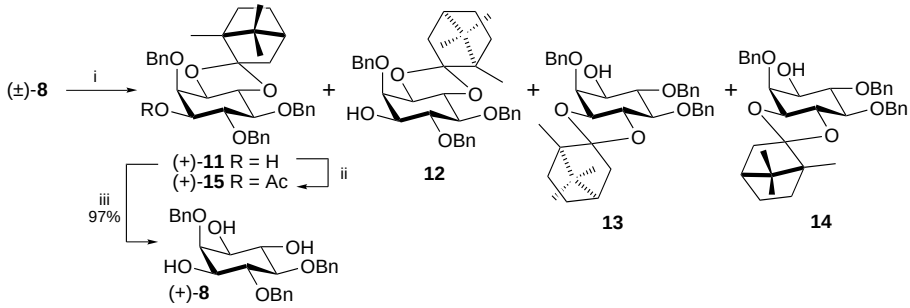

The readily available triol **1**[5] was chemoselectively *p*-methoxybenzylated[6] to give the diol **2** which was then benzylated to afford the fully protected derivative **3** (Scheme 1).† A regioselective DIBAL-H reduction[7,8] of the orthoformate **3** furnished the liberated alcohol **4** as a single isomer in high yield, the structure of which was confirmed by NMR experiments performed on the acetate **5**. Benzylation or allylation of the alcohol **4** afforded the required intermediates **6** and **7**, respectively. Acidic hydrolysis resulted in the simultaneous cleavage of the acetal and *p*-methoxybenzyl ether groups to give the racemic triols **8**[9] and **9** in overall yields of 58 and 56%, respectively, from the triol **1**.

Treatment[4] of **8** with (1*R*)-(+)-camphor dimethyl acetal **10** afforded a diastereoisomeric mixture of acetals **11**–**14** (Scheme 2). This procedure allowed simultaneous protection–resolution of (±)-**8**.

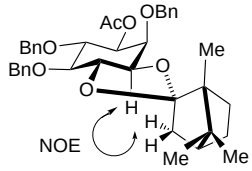
From this mixture the acetal (+)-**11** was isolated by flash chromatography in a yield of 31%, and the remaining acetals were obtained in a combined yield of 59%. The stereochemistry of the acetal (+)-**11** was determined by chemical correlation and NMR experiments. Mild acid hydrolysis (MeOH–AcCl) afforded the triol (+)-**8**,[10,11] which corresponds to the unnatural ring configuration for inositol phospholipids.

Acetylation of the hydroxy group of (+)-**11** gave the acetate (+)-**15** for which a positive NOE was observed between the signal due to the D-1-inositol ring proton and that of the camphor 3′-$H_{endo}$ methylene proton in the $^1H$ NMR spectrum. Since no enhancement of the methyl resonances was observed upon irradiation of the D-1-inositol ring proton, the stereochemistry of **15** was assigned as 1D-1-*O*-*endo*-6-*O*-*exo* (Fig. 1).

The chromatographically inseparable mixture of acetals enriched in **13** and **14** is also a source of (−)-**11** (Scheme 3).

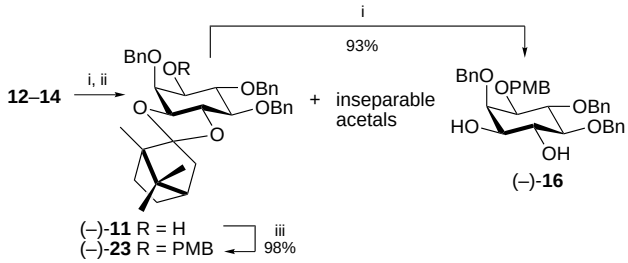



**Scheme 2** *Reagents and conditions*: i, (+)-**10** (2.3 equiv.), TsOH (cat.), $CH_2Cl_2$, reflux; ii, $Ac_2O$, DMAP, pyridine, room temp.; iii, AcCl, $CH_2Cl_2$–MeOH (2 : 1)




(+)-**15**

**Fig. 1** Assignment of relative stereochemistry of the acetal (+)-**15** by NOE measurement

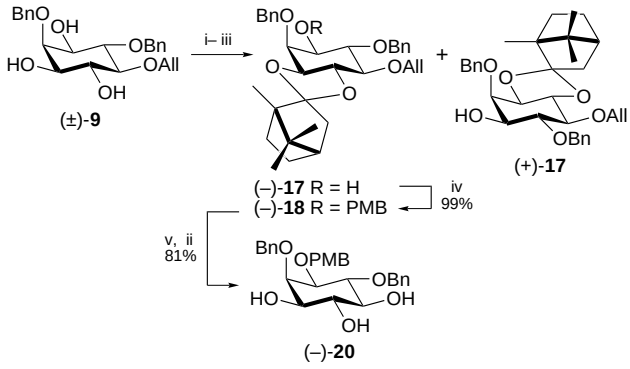



**Scheme 3** *Reagents and conditions*: i, AcCl, $CH_2Cl_2$–MeOH (2:1); ii, (−)-**10**, TsOH, $CH_2Cl_2$, reflux; iii, NaH, PMBCl, DMF

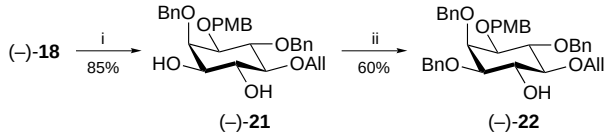
Hydrolysis of the mixture, followed by reacetalisation with the *enantiomeric* camphor dimethyl acetal (−)-**10** afforded after purification (−)-**11** in 40% yield (25% from racemic **8**). *p*-Methoxybenzylation of (−)-**11** gave the PMB ether (−)-**23** which yielded the diol (−)-**16**[10] on mild acidic hydrolysis. The diol (−)-**16** contains a suitable functional group array for elaboration to PtdIns(3,4)$P_2$.

In a similar protection–resolution sequence using the 5-allyloxy-1,3,4-triol **9**, the enantiomeric acetals (−)-**17** and (+)-**17** were obtained in 27 and 24% yield, respectively, (Scheme 4). *p*-Methoxybenzylation of the 1-hydroxy group of (−)-**17** gave (−)-**18**. Cleavage of the 5-allyloxy and 3,4-acetal groups gave (−)-**20**.[11] The triol **20** is a suitable precursor for elaboration to PtdIns(3,4,5)$P_3$.

Finally, mild acidic hydrolysis of the 3,4-acetal (−)-**18** afforded the diol (−)-**21** (Scheme 5). Monobenzylation of the 3-hydroxy group using Gigg's procedure[12] (dibutytin oxide, $Bu_4NBr$ and BnBr) furnished the 4-alcohol (−)-**22** in 60% yield. Cleavage of the 5-allyloxy ether would then lead to a suitable precursor for the preparation of PtdIns(4,5)$P_2$.




**Scheme 4** *Reagents and conditions*: i, (−)-**10**, TsOH, $CH_2Cl_2$, reflux, then separate; ii, AcCl, $CH_2Cl_2$–MeOH (2:1); iii, (+)-**10**, TsOH, $CH_2Cl_2$, reflux; iv, NaH, PMBCl, DMF; v, $(Ph_3P)_3RhCl$, DABCO, EtOH–toluene–$H_2O$ (7:3:1), reflux




**Scheme 5** *Reagents and conditions*: i, AcCl, $CH_2Cl_2$–MeOH (2:1); ii, $Bu_2SnO$, $Bu_4NBr$, BnBr, MeCN, reflux

In conclusion, the combination of a *meso* starting material, high yielding protection–deprotection sequences and especially a combined resolution–protection strategy, involving the camphor acetals **10**, provides ready access to a number of *myo*-inositol phospholipid precursors. In the accompanying communication we describe the reduction of this concept to practice.

We thank the EPSRC and BBSRC for financial support and provision of the Swansea Mass Spectrometry Service, Glaxo Wellcome and SmithKline Beecham Pharmaceuticals for CASE studentships (to S. J. A. G. and I. H. G. respectively), and Drs D. R. Marshall and R. Young for their interest in this work.

## Footnotes and References

* E-mail: abh1@cus.cam.ac.uk

† All new compounds exhibited satisfactory spectroscopic and analytical data. *Selected data* (*J* values in Hz) for (−)-**16**: mp 153–154 °C; $[\alpha]_D^{22}$ −14.9 (*c* 1.6 in $CHCl_3$); $\delta_H$(400 MHz; $CDCl_3$) 7.39–7.23 (17 H, m), 6.86–6.83 (2 H, m), 5.04 (1 H, d, *J* 11.5), 4.94 (1 H, d, *J* 10.7), 4.93 (1 H, d, *J* 11.2), 4.82 (1 H, d, *J* 10.8), 4.75 (1 H, d, *J* 11.5), 4.67–4.60 (3 H, m and 1 H, t, *J* 9.4), 3.98 (1 H, t, *J* 2.6), 3.82 (1 H, td, *J* 9.6, 2.0), 3.80 (3 H, s), 3.46 (1 H, dd, *J* 9.8, 2.4), 3.36 (1 H, ddd, *J* 9.7, 7.8, 3.8), 3.31 (1 H, t, *J* 9.2), 2.42 (1 H, d, *J* 2.1), 2.25 (1H, d, *J* 7.8). For (−)-**20**: mp 136 °C; $[\alpha]_D^{22}$ −5.9 (*c* 1.6 in $CHCl_3$); $\delta_H$(400 MHz; $CDCl_3$) 7.34–7.23 (12 H, m), 6.86–6.83 (2 H, m), 5.03 (1 H, d, *J* 11.5), 4.97 (1 H, d, *J* 11.2), 4.74 (1 H, d, *J* 11.2), 4.66 (1 H, d, *J* 11.5), 4.62 (2 H, s), 3.99 (1 H, t, *J* 2.6), 3.82 (1 H, t, *J* 9.4), 3.80 (3 H, s), 3.73 (1 H, br t, *J* 9.4), 3.44 (1 H, dd, *J* 9.7, 2.4), 3.38–3.33 (2 H, m), 2.95 (1 H, br s), 2.72 (1 H, br s), 2.46 (1 H, d, *J* 7.9).

1 M. J. Berridge and R. F. Irvine, *Nature*, 1989, **341**, 197; S. G. Rhee and K. D. Choi, *J. Biol. Chem.*, 1992, **267**, 12 393; L. A. Serunian, M. T. Haber, T. Fukui, J. W. Kim, S. G. Rhee, J. M. Lowenstein and L. C. Cantley, *J. Biol. Chem.*, 1989, **264**, 17 809; L. R. Stephens, T. R. Jackson and P. T. Hawkins, *Biochem. Biophys. Acta*, 1993, **1179**, 27.

2 P. W. Majerus, T. S. Ross, T. W. Cunningham, K. K. Caldwell, A. B. Jefferson and V. S. Vansel, *Cell*, 1990, **63**, 459.

3 D. C. Billington, *The Inositol Phosphates—Chemical Synthesis and Biological Significance*, VCH, Weinheim, 1993; A. Toker, M. Meyer, K. Reddy, J. R. Falck, R. Aneja, S. Aneja, A. Parra, D. J. Burns and L. C. Cantley, *J. Biol. Chem.*, 1994, **269**, 32 358; D. M. Gou and C. S. Chen, *J. Chem, Soc., Chem. Commun.*, 1994, 2125; K. K. Reddy, M. Saady, G. Whited and J. R. Falck, *J. Org. Chem.*, 1995, **60**, 3385; K. S. Bruzik and R. J. Kubiak, *Tetrahedron Lett.*, 1995, **36**, 2415; Y. Watanabe, M. Tamioka and S. Ozaki, *Tetrahedron*, 1995, **51**, 8969; S. G. Aneja, A. Parra, C. Stoenescu, W. Xia and R. Aneja, *Tetrahedron Lett.*, 1997, **38**, 803.

4 K. S. Bruzik and M. D. Tsai, *J. Am. Chem. Soc.*, 1992, **112**, 6361.

5 H. W. Lee and Y. Kishi, *J. Org. Chem.*, 1985, **50**, 4402.

6 D. C. Billington, R. Baker, J. J. Kulagowski, I. M. Mawer, J. P. Vacca, S. J. deSolms and J. R. Huff, *J. Chem. Soc., Perkin Trans. 1*, 1989, 1423.

7 I. H. Gilbert, A. B. Holmes and R. C. Young, *Tetrahedron Lett.*, 1990, **31**, 2633.

8 I. H. Gilbert, A. B. Holmes, R. C. Young and M. J. Pestchanker, *Carbohydr. Res.*, 1992, **234**, 117.

9 J. Gigg, R. Gigg, S. Payne and R. Conant, *J. Chem. Soc., Perkin Trans. 1*, 1987, 423.

10 T. Desai, J. Gigg, R. Gigg, S. Payne, S. Penades and H. G. Rogers, *Carbohydr. Res.*, 1992, **225**, 209.

11 A. M. Riley, R. Payne and B. V. L. Potter, *J. Med., Chem.*, 1994, **37**, 3918.

12 T. Desai, A. Fernandez-Mayoralas, J. Gigg, R. Gigg, C. Jaramillo, S. Payne, S. Penades and N. Schentz, in *Inositol Phosphates and Derivatives, Synthesis Biochemistry and Therapeutic Potential*, ed. A. B. Reitz, ACS Symp. Ser., American Chemical Society, 1991, vol. 463, p. 86.

*Received in Glasgow, UK, 6th May 1997; 7/03044D*

# Synthesis of dipalmitoyl phosphatidylinositol 3,4-bis(phosphate) and 3,4,5-tris(phosphate) and their enantiomers

**Simon J. A. Grove,[a] Andrew B. Holmes,*[a,b] Gavin F. Painter,[a,b] Phillip T. Hawkins[c] and Leonard R. Stephens[c]**

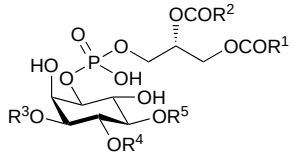
[a] *Cambridge Centre for Molecular Recognition, Department of Chemistry, University of Cambridge, Lensfield Road, Cambridge, UK CB2 1EW*

[b] *Melville Laboratory for Polymer Synthesis, Department of Chemistry, University of Cambridge, Pembroke Street, Cambridge, UK CB2 3RA*

[c] *Babraham Institute, Department of Signalling, Inositide Laboratory, Cambridge, UK CB2 4AT*

**The dipalmitoyl derivatives 4 and 5 of 3-phosphorylated *myo*-inositol phospholipids 2 and 3 and their enantiomers are synthesised from homochiral *myo*-inositol precursors 6 and 11; they serve as biological probes for cell signal transduction.**

The group of *myo*-inositol phospholipids PtdIns(3)P **1**, PtdIns(3,4)$P_2$ **2** and PtdIns(3,4,5)$P_3$ **3** are believed to have a role in the mechanisms by which cell surface receptors for antigens,



**1** $R^1 = C_{19}H_{31}$, $R^2 = C_{17}H_{35}$, $R^3 = P(O)(OH)_2$, $R^4 = R^5 = H$
**2** $R^1 = C_{19}H_{31}$, $R^2 = C_{17}H_{35}$, $R^3 = R^4 = P(O)(OH)_2$, $R^5 = H$
**3** $R^1 = C_{19}H_{31}$, $R^2 = C_{17}H_{35}$, $R^3 = R^4 = R^5 = P(O)(OH)_2$
**4** $R^1 = R^2 = C_{15}H_{31}$, $R^3 = R^4 = P(O)(OH)_2$, $R^5 = H$
**5** $R^1 = R^2 = C_{15}H_{31}$, $R^3 = R^4 = R^5 = P(O)(OH)_2$

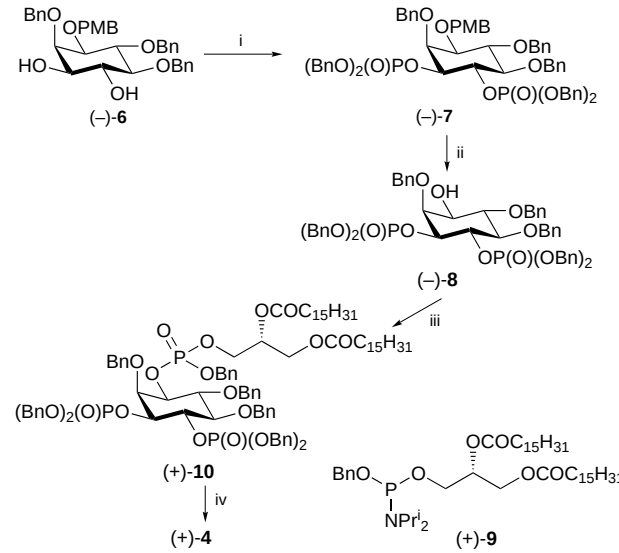
inflammatory stimuli and growth factors control a variety of cellular functions.[1–3] These lipids appear to be resistant to hydrolysis by phosphatidyl inositol-specific phospholipase C (PI-PLC),[4] implying an independent cell signalling pathway from that already established for PtdIns(4,5)$P_2$.[5] In order to probe the function of the phospholipids **2** and **3** in signal transduction we proposed to synthesise the functionally similar dipalmitoyl derivatives **4** and **5** and their enantiomers for use in biological assays. The synthetic work presented here utilises differentially protected homochiral *myo*-inositol derivatives **6** and **11** which were obtained efficiently from *myo*-inositol orthoformate.[6]

Dipalmitoyl PtdIns(3,4)$P_2$ **4** was prepared from (−)-**6** in four synthetic steps with an overall yield of 72% (Scheme 1). The 3,4-bisphosphorylated derivative (−)-**7** was prepared *via* phosphitylation of (−)-**6** with bis(benzyloxy)(*N*,*N*-diisopropylamino)phosphine[7] and 1*H*-tetrazole followed by *in situ* oxidation with MCPBA. After removal of the *p*-methoxybenzyl ether with ceric ammonium nitrate the 1-hydroxy group was coupled with the phosphoramidite (+)-**9**.[8,9] *In situ* oxidation of the phosphorus(III) species afforded the fully protected phospholipid (+)-**10**. Reductive debenzylation was readily effected using the conditions reported[10] by Kozikowski *et al.*, furnishing dipalmitoyl PtdIns(3,4)$P_2$ (+)-**4**.†

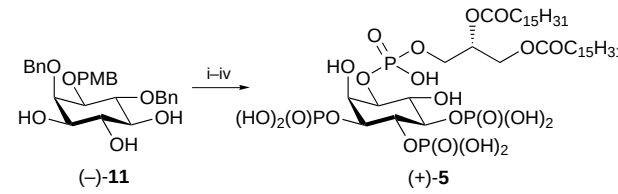
Elaboration of the antipodal diol (+)-**6** *via* the same reaction sequence as shown in Scheme 1 and coupling with (−)-**9**,‡ afforded (−)-4,† the enantiomer of dipalmitoyl PtdIns(3,4)$P_2$.

The use of similar reagents and reaction conditions as outlined for the synthesis of (+)-**4** afforded dipalmitoyl PtdIns(3,4,5)$P_3$ (+)-**5**† in 70% yield from the 3,4,5-triol (−)-**11** (Scheme 2). Similarly (−)-**5**† was synthesised from (+)-**11** and (−)-**9** by the route used in Scheme 2.

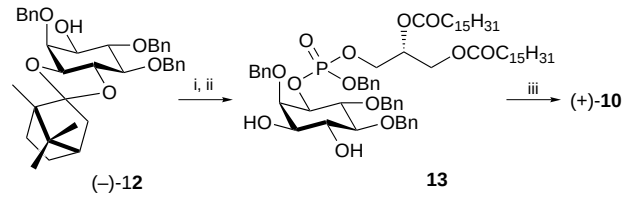
An alternative synthesis of dipalmitoyl PtdIns(3,4)$P_2$ (+)-**4** was also carried out from the 3,4-protected alcohol (−)-**12** (Scheme 3).[6] The alcohol was coupled directly with the



**Scheme 1** *Reagents and conditions*: $(BnO)_2PNPr^i_2$, 1*H*-tetrazole, $CH_2Cl_2$, then MCPBA; ii, $(NH_4)_2Ce(NO_3)_6$, MeCN–$H_2O$ (4:1); iii, (+)-**9**, 1*H*-tetrazole, $CH_2Cl_2$, then MCPBA; iv, $Pd(OH)_2$–C, $H_2$ (60 psi), $Bu^tOH$



**Scheme 2** *Reagents and conditions*: i, $(BnO)_2PNPr^i_2$, 1*H*-tetrazole, $CH_2Cl_2$, then MCPBA; ii, $(NH_4)_2Ce(NO_3)_6$, MeCN–$H_2O$ (4:1); iii, (+)-**9**, 1*H*-tetrazole, $CH_2Cl_2$, then MCPBA; iv, $Pd(OH)_2$–C, $H_2$ (60 psi), $Bu^tOH$



**Scheme 3** *Reagents and conditions*: i, (+)-**9**, 1*H*-tetrazole, $CH_2Cl_2$, then MCPBA; ii, AcCl, MeOH–$CH_2Cl_2$ (1:1); iii, $Pd(OH)_2$–C, $H_2$ (60 psi), $Bu^tOH$

phosphoramidite (+)-**9**, and the product was then cleaved at the 3,4-acetal with acid (AcCl–MeOH) to afford the 3,4-diol **13**. Phosphitylation of the free hydroxy groups with bis(benzyloxy)(*N*,*N*-diisopropylamino)phosphine and 1*H*-tetrazole, followed by *in situ* oxidation with MCPBA, afforded the common fully protected phospholipid (+)-**10**. This route required two fewer steps than the original procedure, as the *p*-methoxybenzyl protection and deprotection at the D-1-hydroxy are not required. The overall yield is slightly better than that of the original procedure.

In summary we have demonstrated a general synthesis of 3-phosphorylated *myo*-inositol phospholipids **4** and **5** from the homochiral precursors **6** and **11** which also allows the synthesis of enantiomeric derivatives containing the unnatural stereochemistry. These materials play an important rôle in evaluating the activation of protein kinase B.[11]

We thank the EPSRC and BBSRC for financial support and provision of the Swansea Mass Spectrometry Service, Glaxo-Wellcome for a CASE studentship (to S. J. A. G.), Drs D. R. Marshall and M. L. Hill for their interest in this work and Dr A. P. Kozikowski for experimental details of debenzylation procedures.

## Footnotes and References

E-mail: abh1@cus.cam.ac.uk

† All new compounds exhibited spectroscopic and analytical data in accord with the assigned structure (*J* values in Hz). *Selected data* for (+)-**4**, the dipalmitoyl analogue of PtdIns(3,4)$P_2$: $[\alpha]_D^{22}$ +0.65 [*c* 1.1 in $CHCl_3$–MeOH (1 : 1)]; $\delta_H$ (400 MHz, [$^2H_6$]DMSO) 5.18–5.11 (1 H, m), 4.35–4.28 (2 H, m), 4.14–4.02 (5 H, m), 3.90 (1 H, br t, *J* 9.1), 3.60 (1 H, t, *J* 9.3), 3.25 (1 H t, *J* 9.0), 2.33–2.24 (4 H, m), 1.55–1.44 (4 H, m), 1.28–1.19 (48 H, m), 0.85 (6 H, br t, *J* 6.7); $\delta_P$ (101 MHz, [$^2H_6$]DMSO) 1.64, 1.00, −0.16; Found (FAB MS): $(M + H + H)^+$, 972.4794. $C_{41}H_{83}O_{19}P_3$ requires $(M + H + H)^+$, 972.4741.

For (−)-**4**: $[\alpha]_D^{22}$ −0.75 [*c* 0.70 in $CHCl_3$–MeOH (1 : 1)].

For (+)-**5**, the dipalmitoyl analogue of PtdIns(3,4,5)$P_3$: $[\alpha]_D^{22}$ +1.85 [*c* 0.60 in $CHCl_3$–MeOH (1 : 1)]; $\delta_H$ (400 MHz, [$^2H_6$]DMSO) 5.19–5.11 (1 H, m), 4.47 (1 H, m), 4.31–3.99 (8 H, m), 3.75 (1 H, t, *J* 9.4), 2.33–2.22 (4 H, m), 1.54–1.45 (4 H, m), 1.29–1.19 (48 H, m), 0.85 (6 H, m); $\delta_P$ (101 MHz, [$^2H_6$]DMSO) 1.22, 0.98, 0.59, −0.20; Found (FAB): $(M + H)^+$, 1051.4350. $C_{41}H_{83}O_{22}P_4$ requires $(M + H)^+$, 1051.4326].

For (−)-**5**: $[\alpha]_D^{22}$ −1.75 [*c* 0.75 in $CHCl_3$–MeOH (1 : 1)].

‡ Compound (−)-**9** was synthesised in a similar manner to (+)-**9** starting from (*R*)-(−)-2,2-dimethyl-1,3-dioxolane-4-methanol (Aldrich).

1 A. Toker, M. Meyer, K. K. Reddy, J. R. Falck, R. Aneja, S. Aneja, A. Parra, D. J. Burns, L. M. Ballas and L. C. Cantley, *J. Biol. Chem.*, 1994, **269**, 32 358.
2 M. J. Berridge, *Nature*, 1993, **361**, 315.
3 L. R. Stephens, T. R. Jackson and P. T. Hawkins, *Biochem. Biophys. Acta*, 1993, **1179**, 27.
4 L. A. Serunian, M. T. Haber, T. Fukui, J. W. Kim, S. G. Rhee, J. M. Lowenstein and L. C. Cantley, *J. Biol. Chem.*, 1989, **264**, 17 809.
5 M. J. Berridge and R. F. Irvine, *Nature*, 1989, **341**, 197; S. G. Rhee and K. D. Choi, *J. Biol. Chem.*, 1992, **267**, 12 393.
6 S. J. A. Grove, I. H. Gilbert, A. B. Holmes, G. F. Painter and M. L. Hill, preceding communication.
7 K.-L. Yu and B. Fraser-Reid, *Tetrahedron Lett.*, 1988, **29**, 979.
8 J. C. Snowden and H. O. L. Fischer, *J. Am. Chem. Soc.*, 1941, **63**, 3244.
9 C. E. Dreef, C. J. J. Elie, P. Hoogerhout, G. A. van der Marel and J. H. van Boom, *Tetrahedron Lett.*, 1988, **29**, 6513.
10 A. P. Kozikowski, G. Powis and W. Tückmantel, *Angew. Chem., Int. Ed. Engl.*, 1992, **31**, 1379.
11 D. Stokoe, L. R. Stephens, T. Copeland, P. Gaffney, C. B. Reese, G. F. Painter, A. B. Holmes, F. McCormick and P. T. Hawkins, *Science*, 1997, in the press.

*Received in in Glasgow, UK, 6th May 1997; 7/03045B*

# Formation of 6,8-di-*tert*-butyl-3,4-dihydro-4,4-dimethyl-1-phosphanaphthalene by the reaction of 2,2-dibromo-1-(2,4,6-tri-*tert*-butylphenyl)-1-phosphaethene with butyllithium

**Shigekazu Ito,† Kozo Toyota and Masaaki Yoshifuji***

*Department of Chemistry, Graduate School of Science, Tohoku University, Aoba, Sendai 980-77, Japan*

**Sterically crowded 1-bromo-2-(2,4,6-tri-*tert*-butylphenyl)-2-phosphaethenyllithium gave 6,8-di-*tert*-butyl-3,4-dihydro-4,4-dimethyl-1-phosphanaphthalene by intramolecular insertion of an intermediary phosphinidene carbene species into one of the C–H bonds of the two *o*-*tert*-butyl groups.**

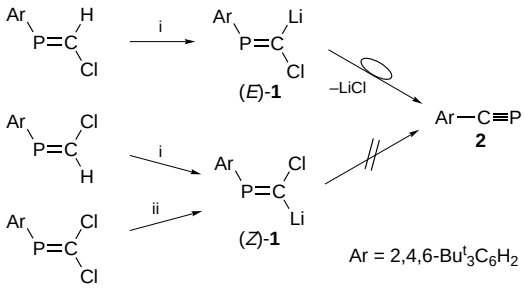
Compounds containing multiple bonds of heavier main group elements such as phosphorus are of current interest.[1] The 2,4,6-tri- *tert*-butylphenyl group (hereafter abbreviated to Ar) is one of the typical and powerful bulky protecting groups for such bonds and by utilizing this substituent we have prepared various types of low coordinated tervalent phosphorus compounds such as diphosphenes[2] and phosphacumulenes.[3]

Recently, we and others have reported on the conversion of (*E*)-1-chloro-2-(2,4,6-tri-*tert*-butylphenyl)-2-phosphaethenyllithium [(*E*)-**1**] to 2-(2,4,6-tri-*tert*-butylphenyl)-1-phosphaethyne **2** (Scheme 1),[4] as well as on the synthetic application of (*E*)- and (*Z*)-**1** as a building block having a phosphorus–carbon double bond.[5,6] Although formation and some reactions of the bromo analogue **3** have been described in the literature,[6,7] C–H insertion reactions involving the phosphinidene carbenoid have not been reported. We report here the formation of 6,8-di-*tert*-butyl-3,4-dihydro-4,4-dimethyl-1-phosphanaphthalene **4** *via* (2,4,6-tri-*tert*-butylphenyl)phosphinidene carbene **5**.

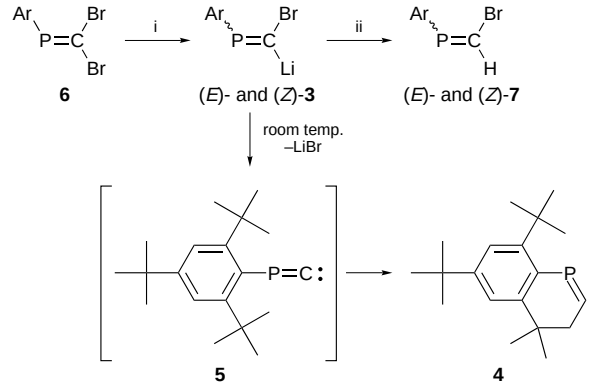
2,2-Dibromo-1-(2,4,6-tri-*tert*-butylphenyl)-1-phosphaethene[6,8] **6** was allowed to react with butyllithium in THF at −78 °C to give 1-bromo-2-(2,4,6-tri-*tert*-butylphenyl)-2-phosphaethenyllithium **3**.[8] Quenching of the resulting solution of **3** with MeOH at −78 °C gave (*E*)- and (*Z*)-2-bromo-1-phosphaethenes **7** in 2 and 58% yields, respectively, after column chromatographic treatment (Scheme 2). In a separate experiment, $^{31}$P NMR spectroscopy of the resulting solution at 210 K showed the formation of (*E*)- and (*Z*)-phosphaethenyllithiums in a 1 : 5 peak ratio [(*E*)-**3** : $\delta_P$ ([$^2H_8$]THF) 369.7; (*Z*)-**3** : $\delta_P$ 254.6].‡

When the mixed solution of (*E*)- and (*Z*)-**3** was warmed to room temperature, it turned violet, and the 3,4-dihydro-1-phosphanaphthalene derivative **4** was obtained in 17% yield after work up with silica-gel column chromatography.§ The formation of **4** is explicable by intramolecular insertion of an intermediary phosphinidene carbene **5** into one of the C–H bonds of the two *o*-*tert*-butyl groups, although attempts to trap the carbene with cyclohexene and tetracyanoethene failed. An analogous intramolecular C–H insertion reaction of alkylidene carbenoid has been reported by Köbrich in the reaction of 1-chloro-2,7-dimethylocta-1,6-diene with butyllithium to give 1-methyl-3-isobutenylcyclopent-1-ene.[9] Compound **4** was also obtained from the chloro congener (*Z*)-**1** in $Et_2O$ in a very low yield (1%), probably because of accompanying complicated reactions, although no formation of **4** was detected from (*Z*)-**1** in THF under similar conditions. In contrast to (*E*)-**1**, which gave the phosphaethyne **2** but not **4** as mentioned above, the 1-bromo-2-phosphaethenyllithium **3** did not afford **2**. These facts may indicate that the carbene **5** is smoothly generated from the bromo derivative **3**, because of the better leaving ability of bromide ion, to give **4** in a better yield, compared to either (*Z*)-**1** or (*E*)-**1**. Nevertheless, these results do not mean that phosphinidene carbenes should not isomerise to phosphaethynes. Competitive formation of phosphaethynes may accompany intra- and/or inter-molecular C–H insertion reactions if phosphinidene carbenes bear substituents which retard intramolecular C–H insertion reaction, since theoretical investigation (at the MP4/6-31G** level) has shown that the linear HPC and HCP isomers represent the transition state and the energy minimum, respectively, on the energy surface of the singlet ground state.[10]¶

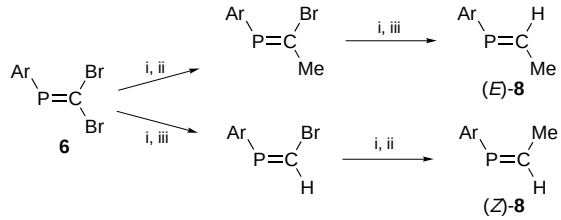
The UV spectrum of **4** was compared with those of 1-phosphapropenes (*E*)- and (*Z*)-**8**, which were prepared by the method shown in Scheme 3.‖ Although the three compounds exhibit absorption maxima at a similar wavelength of *ca.* 300 nm, the molar absorption coefficient of the dihydrophosphanaphthalene **4** is about ten times larger than those of (*E*)- and (*Z*)-**8**.§ This fact probably indicates that the phosphorus–carbon double bond in **4** is nearly coplanar with the aromatic ring (Ar) while the double bond systems in (*E*)- and (*Z*)-**8** are not coplanar with the Ar ring. In fact, X-ray crystallographic analysis of (*E*)- and (*Z*)-2-phenyl-1-(2,4,6-tri-*tert*-butylphenyl)-1-phosphaethenes, the phenyl analogues of



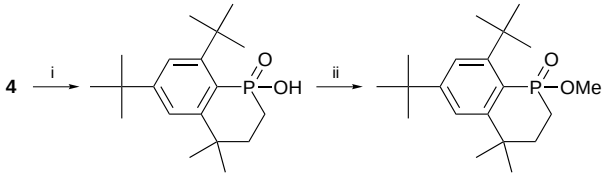

**Scheme 1** *Reagents and conditions*: i, Bu$^t$Li or Bu$^s$Li, THF, −78 °C; ii, Bu$^n$Li, THF, −78 °C




**Scheme 2** *Reagents and conditions*: i, Bu$^n$Li, THF, −78 °C; ii, MeOH, −78 °C



**Scheme 3** *Reagents and conditions*: i, Bu$^n$Li, THF, −78 °C; ii, MeI, −78 °C; iii, MeOH, –78 °C



**Scheme 4** *Reagents and conditions*: i, 1 M HCl aq., $Et_2O$–EtOH (5 : 1), air, room temp.; ii, $CH_2N_2$, $Et_2O$, room temp.

(*E*)- and (*Z*)-**8**, shows that the phosphorus–carbon double bonds for those are nearly perpendicular to the aromatic rings of the Ar groups to avoid steric congestion.[11] Attempted X-ray analyses of **4**, however, have been unsuccessful because of difficulties in obtaining a suitable single crystal.

When compound **4** was allowed to react with hydrochloric acid in $Et_2O$–EtOH, phosphinic acid **9** was obtained in 30% yield (Scheme 4),§ indicating that there is enough room around the phosphorus atom for the approach of water or oxygen.†† However, attempted reaction of **4** with $M(CO)_5$(thf) (M = Cr, W) in THF at room temperature resulted in the decomposition of **4**, which may indicate that the end-on coordination site in **4** is blocked by the *o*-*tert*-butyl groups. Furthermore, attempted reaction of **4** with either $PtCl_2(PPh_3)_2$ and $N_2H_4{\cdot}H_2O$ at 60 °C for side-on coordination or $Cr(CO)_6$ in refluxing dioxane for π-complex formation was not successful and resulted in the decomposition of **4**.

This work was supported in part by a Grant-in-Aid for Scientific Research (No. 08454193) from the Ministry of Education, Science, Sports and Culture, Japan.

## Footnotes and References

* E-mail: yoshifj@mail.cc.tohoku.ac.jp

† Recipient of a Japanese Junior Scientist Fellowship from the Japan Society for the Promotion of Science.

‡ Attempted selective generation of (*E*)-**3** by deprotonation of (*E*)-ArP=C(H)Br with butyllithium resulted in bromine–lithium exchange to give ArP=$CH_2$ after quenching with water.

§ *Selected spectroscopic data* for **4**: colourless crystals, mp 122–125 °C (decomp.); $\delta_H$ (600 MHz, $CDCl_3$) 1.34 (9 H, s, Bu$^t$), 1.35 (6 H, s, C*Me*$_2$), 1.63 (9 H, br s, Bu$^t$), 2.47 (2 H, dd, $^3J_{PH}$ 16.9, $^3J_{HH}$ 6.4, $CH_2$), 7.40 (1 H, d, $^4J_{HH}$ 2.0, arom.), 7.42 (1 H, dd, $^4J_{PH}$ 2.2, $^4J_{HH}$ 2.0, arom.), 8.03 (1 H, dt, $^2J_{PH}$ 36.7, $^3J_{HH}$ 6.4, P=CH); $\delta_C$ (150 MHz, $CDCl_3$) 28.8 (C*Me*$_2$), 31.2 (C*Me*$_3$), 33.2 (d, $J_{PC}$ 14.4, C*Me*$_3$), 35.2 (*C*Me$_3$), 35.9 (d, *J* 3.2, *C*Me$_2$), 37.7 (*C*Me$_3$), 41.8 (d, *J* 12.7, $CH_2$), 119.2 (arom., CH), 121.4 (d, *J* 7.2, arom., CH), 131.6 (d, *J* 53.9, arom., CP), 148.8 (d, *J* 4.3, arom.), 152.2 (d, *J* 2.9, arom.), 153.1 (d, *J* 16.5, arom.), 168.3 (d, *J* 34.1, P=C); $\delta_P$ (81 MHz, $CDCl_3$) 210.8 (dt, $^2J_{PH}$ 36.7, $^3J_{PH}$ 16.9); $\nu_{max}$(KBr)/cm$^{-1}$ 1597; $\lambda_{max}$(hexane)/nm (log ε) 240 (3.86), 301 (3.84); *m*/*z* (70 eV) 288 (M$^+$, 100), 273 (M$^+$ − Me, 25), 57 (Bu$^+$, 16); Found: 288.2011. Calc. for $C_{19}H_{29}P$: 288.2007. For (*E*)-**8**: colourless crystals, mp 62–65 °C; $\delta_H$ (200 MHz) 1.33 (9 H, s, *p*-Bu$^t$), 1.50 (18 H, d, $^5J_{PH}$ 0.6, *o*-Bu$^t$), 2.14 (3 H, dd, $^3J_{PH}$ 25.3, $^3J_{HH}$ 8.4, Me), 7.39 (2 H, d, $^4J_{PH}$ 1.2, *m*-Ar), 7.44 (1 H, dq, $^2J_{PH}$ 25.4, $^3J_{HH}$ 8.4, P=CH); $\delta_C$(50 MHz) 19.9 (d, *J* 30.8, Me), 31.4 (*p*-C*Me*$_3$), 32.5 (d, *J* 7.4, *o*-C*Me*$_3$), 34.9 (*p*-*C*Me$_3$), 38.2 (d, *J* 0.7, *o*-*C*Me$_3$), 121.5 (d, *J* 1.4, *m*-Ar), 139.9 (d, *J* 55.3, *i*-Ar), 149.2 (*p*-Ar), 153.5 (d, *J* 1.7, *o*-Ar), 175.1 (d, *J* 33.4, P=C); $\delta_P$ 250.3 (dq, $^2J_{PH}$ 25.4, $^3J_{PH}$ 25.3); $\lambda_{max}$ (hexane)/nm (log ε) 210 (4.40), 240 (4.18), 300 (3.07); *m*/*z* 304 (M$^+$, 100); Found: 304.2317. Calc. for $C_{20}H_{33}P$: 304.2320. For (*Z*)-**8**: colourless crystals, mp 37–39 °C; $\delta_H$ (200 MHz) 1.28 (3 H, dd, $^3J_{PH}$ 18.1, $^3J_{HH}$ 7.8, Me), 1.33 (9 H, s, *p*-Bu$^t$), 1.49 (18 H, d, $^5J_{PH}$ 0.6, *o*-Bu$^t$), 7.23 (1 H, dq, $^2J_{PH}$ 39.0, $^3J_{HH}$ 7.8, P=CH), 7.40 (2 H, d, $^4J_{PH}$ 1.0, *m*-Ar); $\delta_C$ (50 MHz) 19.7 (d, *J* 19.2, Me), 31.3 (*p*-C*Me*$_3$), 32.5 (d, *J* 7.5, *o*-C*Me*$_3$), 34.9 (*p*-*C*Me$_3$), 37.9 (d, *J* 1.1, *o*-*C*Me$_3$), 121.5 (d, *J* 1.0, *m*-Ar), 149.5 (*p*-Ar), 150.0 (d, *J* 62.6, *i*-Ar), 153.7 (d, *J* 1.6, *o*-Ar), 167.2 (d, *J* 41.3, P=C); $\delta_P$ 250.3 (dq, $^2J_{PH}$ 39.0, $^3J_{PH}$ 18.1); $\lambda_{max}$ (hexane)/nm (log ε) 213 (4.39), 240 (4.20), 300 (2.92). For **9**: colourless crystals, mp 280 °C (decomp.); $\delta_H$ (200 MHz) 1.31 (9 H, s, Bu$^t$), 1.39 (6 H, s, C*Me*$_2$), 1.64 (9 H, s, Bu$^t$), 2.0–2.3 (4 H, m, $CH_2CH_2$), 2.6–4.5 (OH),†† 7.34 (1 H, dd, $^4J_{PH}$ 5.2, $^4J_{HH}$ 2.0, arom.), 7.55 (1 H, dd, $^4J_{PH}$ 3.7, $^4J_{HH}$ 2.0, arom.); $\delta_P$ 44.6 [t, $J_{PH}$ 20.6 when $\delta_H$(OH) 4.5], 45.0 [br, when $\delta_H$(OH) 2.6];‡‡ $\nu_{max}$(KBr)/cm$^{-1}$ 1173 (P=O), 941 (P–O); *m*/*z* 322 (M$^+$, 43), 307 (M$^+$ − Me, 100). For **10**: colourless oil; $\delta_H$ (600 MHz) 1.30 (9 H, s, Bu$^t$), 1.36 (3 H, s, Me), 1.40 (3 H, s, Me), 1.61 (9 H, s, Bu$^t$), 1.90 (1 H, m, PCH), 2.05–2.21 (3 H, m, C*HH*$CH_2$), 3.70 (3 H, d, $^3J_{PH}$ 10.9, OMe), 7.35 (1 H, dd, $^4J_{PH}$ 5.0, $^4J_{HH}$ 1.9, arom.), 7.55 (1 H, dd, $^4J_{PH}$ 3.8, $^4J_{HH}$ 1.9, arom.); $\delta_C$ (150 MHz) 22.1 ($PCH_2$*C*$H_2$), 31.0 (C*Me*$_3$), 32.3 (Me), 32.8 (C*Me*$_3$), 33.3 (Me), 34.6 (d, *J* 5.6, $PCH_2$), 35.1 (*C*Me$_3$), 37.9 (d, *J* 7.3, C*Me*$_2$), 38.6 (d, *J* 3.2, *C*Me$_3$), 50.2 (d, *J* 6.4, OMe), 122.7 (d, *J* 58.0, arom., CP), 123.3 (d, *J* 12.0, arom., CH), 124.0 (d, *J* 11.5, arom., CH), 153.3 (d, *J* 12.1, arom.), 153.6 (arom.), 155.2 (d, *J* 6.3, arom.); $\delta_P$ 42.7; $\nu_{max}$ (KBr)/cm$^{-1}$ 1213 (P=O), 1032 (P–O); *m*/*z* 336 (M$^+$, 54), 307 (M$^+$ − Me, 100); Found: 336.2216. Calc. for $C_{20}H_{33}O_2P$: 336.2218.

¶ The conversion of (*E*)-**1** to **2** might proceed in a concerted fashion involving elimination of the chlorine atom accompanied with the migration of the Ar group.

‖ Compound **8** has already been described by Märkl and Bauer as a mixture of (*E*)- and (*Z*)-isomers (ref. 12).

†† Compound **9** was further converted to the corresponding methyl phosphinate **10** by the addition of a diazomethane–diethyl ether solution (91% yield).§

‡‡ Both $^{31}P$ and $^1H$ NMR chemical shifts vary depending on the moisture in the sample solution. In dry $CDCl_3$, $\delta_P$ 44.6 and $\delta_H$(OH) 4.5, whereas in wet $CDCl_3$, $\delta_P$ 45.0 and $\delta_H$(OH) 2.6.

1 M. Regitz and O. J. Scherer, *Multiple Bonds and Low Coordination in Phosphorus Chemistry*, Georg Thieme Verlag, Stuttgart, 1990.
2 M. Yoshifuji, I. Shima, N. Inamoto, K. Hirotsu and T. Higuchi, *J. Am. Chem. Soc.*, 1981, **103**, 4587; 1982, **104**, 6167.
3 M. Yoshifuji, K. Toyota, K. Shibayama and N. Inamoto, *Tetrahedron Lett.*, 1984, **25**, 1809; M. Yoshifuji, K. Toyota and N. Inamoto, *J. Chem. Soc., Chem. Commun.*, 1984, 689. See also: H. H. Karsch, F. H. Köhler and H.-U. Reisacher, *Tetrahedron Lett.*, 1984, **25**, 3687; R. Appel, P. Fölling, B. Josten, M. Siray, V. Winkhaus and F. Knoch, *Angew. Chem., Int. Ed. Engl.*, 1984, **23**, 619.
4 M. Yoshifuji, T. Niitsu and N. Inamoto, *Chem. Lett.*, 1988, 1733; M. Yoshifuji, H. Kawanami, Y. Kawai, K. Toyota, M. Yasunami, T. Niitsu and N. Inamoto, *Chem. Lett.*, 1992, 1053. See also: R. Appel and M. Immenkeppel, *Z. Anorg. Allg. Chem.*, 1987, **553**, 7.
5 M. Yoshifuji, S. Ito, K. Toyota and M. Yasunami, *Bull. Chem. Soc. Jpn.*, 1995, **68**, 1206; S. Ito, K. Toyota and M. Yoshifuji, *Chem. Lett.*, 1995, 747; M. van der Sluis, F. Bickelhaupt, N. Veldman, H. Kooijman, A. L. Spek, W. Eisfeld and M. Regitz, *Chem. Ber.*, 1995, **128**, 465.
6 R. Appel, C. Casser and M. Immenkeppel, *Tetrahedron Lett.*, 1985, **26**, 3551.
7 M. van der Sluis, J. B. M. Wit and F. Bickelhaupt, *Organometallics*, 1996, **15**, 174; H. Ramdane, H. Ranaivonjatovo, J. Escudié, S. Mathieu and N. Knouzi, *Organometallics*, 1996, **15**, 3070.
8 S. J. Goede and F. Bickelhaupt, *Chem. Ber.*, 1991, **124**, 2677.
9 R. H. Fischer, M. Baumann and G. Köbrich, *Tetrahedron Lett.*, 1974, 1207.
10 M. T. Nguyen and T.-K. Ha, *J. Mol. Struct: THEOCHEM*, 1986, **139**, 145.
11 M. Yoshifuji, K. Toyota, N. Inamoto, K. Hirotsu and T. Higuchi, *Tetrahedron Lett.*, 1985, **26**, 6443; M. Yoshifuji, K. Toyota, I. Matsuda, T. Niitsu, N. Inamoto, K. Hirotsu and T. Higuchi, *Tetrahedron*, 1988, **44**, 1363; R. Appel, J. Menzel, F. Knoch and P. Volz, *Z. Anorg. Allg. Chem.*, 1986, **534**, 100.
12 G. Märkl and W. Bauer, *Angew. Chem., Int. Ed. Engl.*, 1989, **28**, 1695.

*Received in Cambridge, UK, 22nd May 1997; 7/03554C*

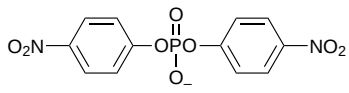
# Extraordinary acceleration of phosphodiester hydrolyses by thorium cations

**Robert A. Moss,* Jing Zhang and Kathryn Bracken**

*Department of Chemistry, Rutgers University, New Brunswick, New Jersey 08903, USA*

**$Th^{IV}$ cations in aqueous Brij micelles strongly promote the hydrolyses of several phosphodiester substrates; in the case of bis(*p*-nitrophenyl)phosphate 1, the observed rate constant (0.028 $s^{-1}$) represents an acceleration of *ca* 2.8 billion.**

Much attention is deservedly focused on the remarkable acceleration of phosphodiester hydrolyses educed by lanthanide (Ln) cations.[1] Acting as Lewis acids, they bind the substrate's P–$O^-$ and mitigate its negative charge, while simultaneously furnishing a metal-bound hydroxide nucleophile to attack the phosphodiester's phosphoryl group. Both Lewis acid strength and the acidity of the cation's water of hydration increase with increasing positive charge density, so that $Ce^{IV}$, the only lanthanide with a readily accessible +4 oxidation state, is of particular interest for the mediated hydrolysis of *e.g.* DNA.[2] Indeed, an excess of a 2 : 1 palmitate–$Ce^{IV}$ complex in aqueous Brij micelles at pH 7 and 37 °C cleaves the model phosphodiester substrate, bis(*p*-nitrophenyl)phosphate **1**, (BNPP), with



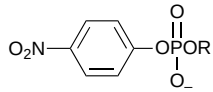
**1** (BNPP)

$k = 2.6 \times 10^{-2}$ $s^{-1}$,[3] representing a record enhancement of *ca.* $2 \times 10^9$ relative to the uncatalysed reaction at 25 °C.[1h]

Similarly, we examined hydrolyses mediated by the actinide uranyl cation.[4] Uranium offers a +6 oxidation state, but exists in water as $UO_2^{2+}$, which is less reactive than $Ce^{IV}$; *e.g.* $k = 9.5 \times 10^{-6}$ $s^{-1}$ for hydrolysis of BNPP by excess $UO_2^{2+}$–*N*-hexadecyl-*N*,*N*′,*N*′,- trimethylethylenediamine (HTMED, pH 4.9, 37 °C).[4] Although this is equivalent to a rate enhancement of at least $8.6 \times 10^5$ relative to the uncatalysed reaction, $UO_2^{2+}$ is inferior to $Ce^{IV}$ by a kinetic factor of *ca.* 1100 in the cleavage of BNPP.

The actinide thorium, however, affords a stable +4 oxidation state in aqueous solution with multiple coordinated water molecules.[5] The 'hard acid' $Th^{4+}$ readily coordinates with oxygen ligands (including phosphates),[5] so that we anticipate nonoxidative,[6] hydrolytic potency toward phosphodiesters. Indeed, $Th^{4+}$ accelerates the hydrolysis of plasmid DNA and nucleotides at pH 4 or 5, with rate constants approaching those of $Ce^{IV}$.[6]

In order to quantitatively evaluate $Th^{4+}$ relative to $UO_2^{2+}$ and various Ln promoters of phosphodiester cleavage, we have now determined the reactivity of $Th^{4+}$ toward BNPP and additional substrates **2**–**4**. We are pleased to report conditions under which



**2** R = $CH_2CH(OH)Me$
**3** R = $C_{16}H_{33}$
**4** R = Et

the reactivity of $Th^{4+}$ far exceeds that of $UO_2^{2+}$, is comparable to that of $Ce^{IV}$, and surpasses that of other metal cations.

Substrates **1**–**4** were hydrolysed readily in the presence of aqueous $Th(NO_3)_4$. Optimal conditions (see below) comprised 2 mM Brij-35, 10 mM HEPES buffer, pH 6.0 (10 mM KCl, 37 °C). We employed a 20-fold excess of $Th^{4+}$ (1 mM) over substrate (0.05 mM). Kinetics were followed spectrophotometrically, monitoring the disappearance of the substrate's *p*-nitrophenyl moiety (290 nm) and the concomitant appearance of *p*-nitrophenol (317 nm). Reactions were observed for more than eight half-lives and pseudo-first order rate constants were obtained as the means of triplicate runs with $r > 0.997$ and reproducibilities within ±5%.

Rate constants appear in Table 1, where $k$ for BNPP hydrolysis, 0.028 $s^{-1}$, represents an acceleration of *ca.* 2.8 *billion* relative to the uncatalysed reaction at pH 7,[1h] whilst the entry for the intramolecularly assisted cleavage of RNA model **2**, $k = 0.013$ $s^{-1}$, is *ca.* $3.9 \times 10^5$ greater than in the absence of metal cations at pH 7.[1a] These enhancements appear to be the largest reported to date for Ln or actinide cations with these commonly employed model substrates. We note, however, that the 20-fold excess of $Th^{4+}$ is necessary; $k_{obs}$ slows markedly as $[Th^{4+}]$ : [BNPP] is reduced below 15 : 1 at pH 6. Control experiments also reveal inhibition of the hydrolysis by (added) inorganic phosphate.

The hydrolysis of BNPP was examined in detail: pH was varied from 3.5–7.0 in water, aqueous HEPES buffer, or HEPES–micellar Brij; added ligands included *N*-octyl-D-glucamine.[3] In HEPES– Brij, $k_{obs}$ increased steadily from $9.3 \times 10^{-4}$ $s^{-1}$ at pH 3.5 to a maximum of $2.8 \times 10^{-2}$ $s^{-1}$ at pH 6.0, before declining slightly at pH 6.5 or 7.0. Above pH 7, precipitation of OH-bridged Th oligomers[5] was observed. A similar pH dependence was seen in water, with $k_{obs} = 5.2 \times 10^{-3}$ $s^{-1}$ at pH 3.5 and $2.2 \times 10^{-2}$ $s^{-1}$ at pH 6.0 (maximum). The $pK_a$ for water bound to $Th^{4+}$ varies from 2.4 to 5.0, depending on the exact conditions;[7] a recent report[6] gives $pK_{a1} = 3.89$ and $pK_{a2} = 4.20$. These data are consistent with our observation of a reactivity maximum around pH 6.

The $Th^{4+}$-mediated hydrolysis of BNPP occurs with release of both *p*-nitrophenyl groups. Kinetic experiments under the conditions of Table 1 reveal that $Th^{4+}$ hydrolysis of the presumptive intermediate, *p*-nitrophenylphosphate, is twice as fast ($k = 5.5 \times 10^{-2}$ $s^{-1}$) as that of BNPP. The reported rate constants therefore describe the hydrolysis of the first *p*-nitrophenyl group of BNPP, which is the rate-limiting step.

Brij micelles enhance the $Th^{4+}$ reactivity: $k_{obs}$ increases steadily at pH 6 in HEPES buffer from $5.5 \times 10^{-3}$ $s^{-1}$ in the absence of Brij, to a maximum of $2.8 \times 10^{-2}$ $s^{-1}$ at 2.0 mM Brij. Not only does micellar Brij potentiate the reactivity of $Th^{4+}$ (presumably by binding substrate molecules and cations), but its oxygen atoms appear to solubilize the $Th^{4+}$ cations or oligomers

**Table 1** Kinetics of $Th^{4+}$ mediated hydrolyses[a]

| Substrate | $k_{obs}/10^{-4}$ $s^{-1}$ |
|---|---|
| **1** | 282[b] |
| **2** | 132 |
| **3** | 11.9 |
| **4** | 8.54 |

[a] At pH 6.0, 37 °C; other conditions are detailed in the text. Rate constants are reported as means of three runs with $r > 0.997$ and reproducibilities within ±5%. [b] Both *p*-nitrophenyl groups were cleaved.

above pH 5. Brij-35 has been previously used to stabilize metal cation catalysts for phosphodiester hydrolysis.[4,8]

In contrast to $Ce^{IV}$, which requires both a complexing ligand and micellar Brij to remain in solution above pH 4–5, $Th^{IV}$ is stabilized by Brij alone; added ligands merely sap its reactivity. For example, $k_{obs} = 2.8 \times 10^{-2}$ s$^{-1}$ ($Th^{4+}$–BNPP in aqueous Brij at pH 6) is reduced to $1.4 \times 10^{-3}$ s$^{-1}$ upon the addition of 1 equiv. of *N*-octyl-D-glucamine, a ligand useful in the stabilization of $Ce^{IV}$.[3]

$Th^{4+}$ is much more reactive than $UO_2^{2+}$ toward substrates **1** or **2**. The rate constants of Table 1 can be compared with *k*(pH 4.9) = $9.5 \times 10^{-6}$ s$^{-1}$ for **1** ($UO_2^{2+}$–HTMED) or $2.2 \times 10^{-4}$ s$^{-1}$ ($UO_2^{2+}$) for **2**.† Using BNPP hydrolysis as a reactivity measure, $Th^{4+}$ is comparable to $Ce^{IV}$–palmitate in Brij ($k = 2.6 \times 10^{-2}$, pH 7),[3] but more reactive than $Eu^{3+}$ ($k = 1.7 \times 10^{-4}$ s$^{-1}$, pH 7, 50 °C),[1e,f] or various $Eu^{3+}$ complexes (2.0–6.7 $\times$ $10^{-4}$ s$^{-1}$, pH 7–7.4, 25–50 °C),[1f,9] $La^{3+}$ ($1.4 \times 10^{-7}$ s$^{-1}$)[1g] or $La^{3+}$–$H_2O_2$ ($4.8 \times 10^{-3}$ s$^{-1}$, both at pH 7, 25 °C),[1g] 1 : 1 $La^{3+}$–$Fe^{3+}$ ($2.8 \times 10^{-4}$ s$^{-1}$, pH 7, 50 °C),[10] or binuclear azamacrocyclic complexes of $Eu^{3+}$ ($1.4 \times 10^{-3}$ s$^{-1}$, pH 7, 50 °C) or $Pr^{3+}$ ($8.4 \times 10^{-4}$ s$^{-1}$, pH 7, 50 °C).[11]

It is clear from these comparisons that $Th^{IV}$ and $Ce^{IV}$ are the most reactive actinide or lanthanide cations yet reported for the acceleration of BNPP hydrolysis. A similar conclusion follows from the reactivity of $Th^{IV}$ toward substrate **2**. Indeed, $Th^{IV}$ and $Ce^{IV}$ appear to be more reactive toward BNPP or **2**[1c] than any other metal cations thus far described, including (complexes of) cobalt[12] and copper.[13]

Toward long-chain phosphodiester substrate **3**, comicellized with 2 mM Brij-35 (critical micelle concentration, 0.06–0.09 mM[8a]), excess $Th^{4+}$ affords $k_{obs} = 1.2 \times 10^{-3}$ s$^{-1}$. Comparisons are lacking except for $UO_2^{2+}$–HTMED where $k_{obs} = 1.1 \times 10^{-4}$ s$^{-1}$.[4] Perhaps a fairer comparison of $Th^{4+}$–Brij *vs.* $UO_2^{2+}$–HTMED is with the short-chain substrate **4**, where $Th^{4+}$ (Table 1) manifests a 500-fold rate advantage over $UO_2^{2+}$ ($k = 1.7 \times 10^{-6}$ s$^{-1}$).‡

In conclusion, $Th^{IV}$ cations are an extraordinarily reactive, readily employed promoter of the hydrolysis of a variety of model phosphodiester substrates. We are continuing to probe their application to challenging problems in this area.

We are grateful to the U.S. Army Research Office for financial support.

## Footnotes and References

† No attempt is made in the kinetic comparisons to correct for differing conditions or cation–substrate ratios. Rather, the maximum rate constants available in the literature are compared to those of $Th^{4+}$.

‡ The minimal rate advantage for $Th^{4+}$ cleavage of micellized substrate **3**, relative to nonmicellar analogue **4**, contrasts with rate enhancements of 50–70 previously observed with $Eu^{3+}$ or $UO_2^{2+}$ toward aggregated substrates (refs. 4, 14). The differing behaviour may be due to the Brij comicelles employed with $Th^{4+}$.


1 (*a*) R. Breslow and D. L. Huang, *Proc. Natl. Acad. Sci. USA*, 1991, **88**, 4080; (*b*) J. R. Morrow, L. A. Buttrey, V. M. Shelton and K. A. Berback, *J. Am. Chem. Soc.*, 1992, **114**, 1903; (*c*) J. R. Morrow, L. A. Buttrey and K. A. Berback, *Inorg. Chem.*, 1992, **31**, 16; (*d*) M. Komiyama, K. Matsumura and Y. Matsumoto, *J. Chem. Soc., Chem. Commun.*, 1992, 640; (*e*) H.-J. Schneider, J. Rammo and R. Hettich, *Angew. Chem., Int. Ed. Engl.*, 1993, **32**, 1716; (*f*) J. Rammo and H.-J. Schneider, *Liebigs Ann.*, 1996, 1757; (*g*) B. K. Takasaki and J. Chin, *J. Am. Chem. Soc.*, 1993, **115**, 9337; (*h*) B. K. Takasaki and J. Chin, *J. Am. Chem. Soc.*, 1995, **117**, 8582; (*i*) R. Breslow and B. Zhang, *J. Am. Chem. Soc.*, 1994, **116**, 7893.

2 B. K. Takasaki and J. Chin, *J. Am. Chem. Soc.*, 1994, **116**, 1121; M. Komiyama, T. Kodama, N. Takeda, J. Sumaoka, T. Shiiba, Y. Matsumoto and M. Yashiro, *J. Biochem.*, 1994, **115**, 809; M. Komiyama, T. Shiiba, T. Kodama, N. Takeda, J. Sumaoka and M. Yashiro, *Chem. Lett.*, 1994, 1025; J. Sumaoka, S. Miyama and M. Komiyama, *J. Chem. Soc., Chem. Commun.*, 1994, 1755; M. Komiyama, N. Takeda, Y. Takahashi, H. Uchida, T. Shiiba, T. Kodama and M. Yashiro, *J. Chem. Soc., Perkin Trans. 2*, 1995, 269.

3 K. Bracken, R. A. Moss and K. Ragunathan, unpublished work.

4 R. A. Moss, K. Bracken and J. Zhang, *Chem. Commun.*, 1997, 563.

5 S. Cotton, *Lanthanides and Actinides*, Oxford University press, New York, 1991, pp. 115–121.

6 T. Ihara, H. Shimura, K. Ohmori, H. Tsuji, J. Takeuchi and M. Takagi, *Chem. Lett.*, 1996, 687.

7 J. Burgess, *Metal Ions in Solution*, Halsted Press, New York, 1978, pp. 27–28.

8 (*a*) S. H. Gellman, R. Petter and R. Breslow, *J. Am. Chem. Soc.*, 1986, **108**, 2388; (*b*) J. G. J. Weijnen and J. F. J. Engbersen, *Recl. Trav. Chim. Pays-Bas*, 1993, **112**, 351.

9 J. R. Morrow, K. Aures and D. Epstein, *J. Chem. Soc., Chem. Commun.*, 1995, 2431.

10 N. Takeda, M. Irisawa and M. Komiyama, *J. Chem. Soc., Chem. Commun.*, 1994, 2773.

11 K. G. Ragunathan and H.-J. Schneider, *Angew. Chem., Int. Ed. Engl.*, 1996, **35**, 1219.

12 J. Chin, *Acc. Chem. Res.*, 1991, **24**, 145 and references cited therein.

13 E. Kövari and R. Krämer, *J. Am. Chem. Soc.*, 1996, **118**, 12 704; K. A. Deal and J. N. Burstyn, *Inorg. Chem.*, 1996, **35**, 2792.

14 R. A. Moss, B. D. Park, P. Scrimin and G. Ghirlanda, *J. Chem. Soc., Chem. Commun.*, 1995, 1627.


*Received in Corvallis, OR, USA, 22nd May 1997; 7/03568C*

# Reaction of phosphaacetylenes Bu$^t$C≡P and 1-AdC≡P with $(PhSe)_2$–$XeF_2$: first examples of vicinal bis-selenenylation (at P and C) to form novel phosphaalkenes

**Kenneth K. Laali,*[a] Wolfgang Fiedler[a,b] and Manfred Regitz[b]**

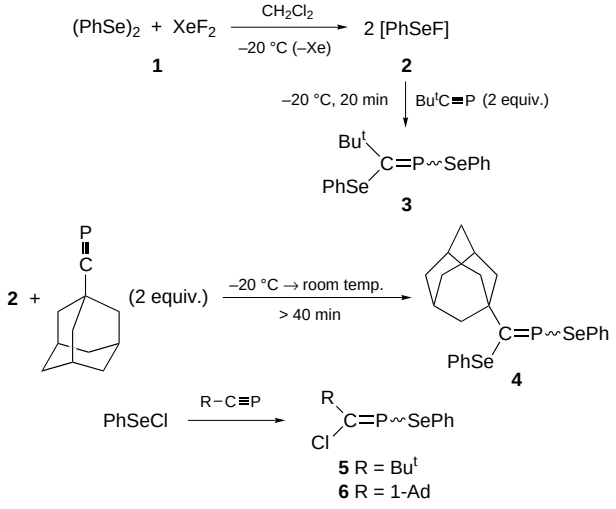
[a] *Department of Chemistry, Kent State University, Kent, OH 44242, USA*
[b] *Fachberich Chemie, Universität Kaiserslautern, Erwin-Schrödinger-Strasse, D-67663 Germany*

***tert*-Butyl- and 1-adamantyl-phosphaacetylenes (2 equiv.) react with $(PhSe)_2$–$XeF_2$ (→ 2 PhSeF) to give novel phosphaalkenes by vicinal bis-phenylselenenylation (at P and C), in contrast to acetylenes which undergo fluoroselenenylation.**

Whereas PhSeCl and PhSeBr are commercially available sources of selenenic electrophiles, PhSeF is too labile to be isolated. It was recently reported[1] that the system $(PhSe)_2$–$XeF_2$ **1** acts as an *in situ* source of PhSeF **2**, whose reaction with selected alkenes led to fluoroselenenylation (predominantly *E* alkenes). Subsequently, **1** was shown to be an efficient vicinal fluoroselenenylation reagent for alkynes.[2,3] The preferred *E* configuration of the alkene product (*trans* stereochemistry) may be traced to the intermediacy of the phenylselenirenium cation, a stable salt of which has been characterized.[4] In addition to **1**, PhSeBr·AgF in $CH_2Cl_2$ under sonication and PhSeCl·AgF in MeCN also serve as *in situ* sources of PhSeF for fluoroselenenylation of alkenes, alkynes and α-diazo ketones (α-diazo esters).[5]

In relation to our previous and ongoing studies of electrophilic chemistry of phosphaalkynes, ionization of phosphirenes (→ phosphirenylium cation) and electrophilic reactivity of the tetraphosphacubane skeleton,[6–9] we became interested in possible fluoroselenenylation of RC≡P, anticipating that, based on previous results on addition of protic and Lewis superacids,[6] 'PhSe$^+$' would attack at the P≡C carbon.

Under the conditions where **2** is expected to be present *via* system **1**,[2,3] Bu$^t$CP (2 equiv.) was added to the reaction mixture under argon in dry $CH_2Cl_2$ at −20 °C (rapid Xe loss) (Scheme 1); $^{31}$P NMR monitoring of the reaction mixture indicated that following 20 min at −20 °C, only traces of Bu$^t$CP remained unreacted. The solvent was removed *in vacuo* (room temp.), the residue was taken up in $CDCl_3$ and subjected to multinuclear NMR analysis (Fig. 1). The major product ( > 90% based on $^{31}$P NMR integral ratios)† gives rise to a phosphorus resonance at $\delta$ 351.9 with a one-bond P/Se coupling of 319.1 Hz and a two-




**Scheme 1**

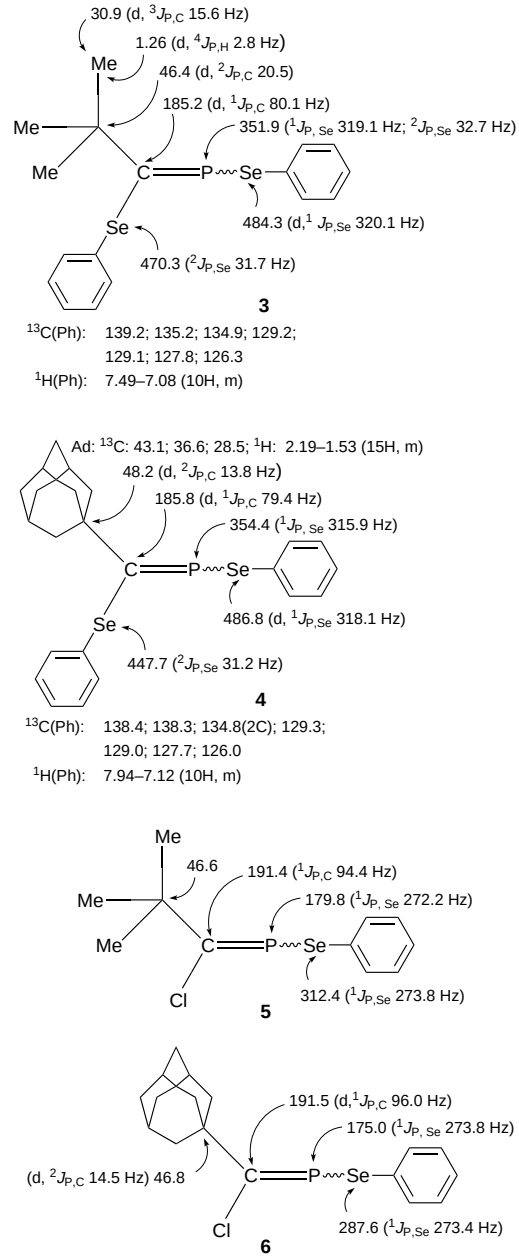



**Fig. 1** Multinuclear NMR data for **3**, **4**, **5** and **6**

bond P/Se coupling of 32.7 Hz. In the $^{77}$Se NMR spectrum, there are two resonances (1 : 1 ratio), one for the P–SePh moiety at $\delta$ 484.3 (one-bond P/Se coupling 320 Hz) and the other for C–SePh at $\delta$ 470.3 with a two-bond P/Se coupling of 31.7 Hz, supporting vicinal bis-selenenylation (→ **3**). Presence of an intact C=P moiety is apparant in the $^{13}$C NMR spectrum *via* a distinct doublet at $\delta$ 185.2 with a one-bond P/C coupling of 80.1 Hz typical of phosphaalkenes.[10] Both *tert*-butyl carbon resonances (at $\delta$ 46.4 and 30.9) appear as doublets due to phosphorus coupling. The SePh ring carbon resonances give rise to eight resonances between $\delta$ 139.2–126.3.

Phosphaalkene **3** has a limited life-time at room temp., and prolonged reaction times gave a complex mixture, as did attempted isolation. Additional proof of the structure came from the EI-MS spectrum of a freshly prepared sample, showing the $M^+$ at *m/z* 412 with the appropriate isotope pattern for two Se atoms.

Attempted Se-ethylation with one and two equivalents of EtOTf, to selectively form the derived mono- and di-selenonium cation salts,[3,11] led to complex mixtures ($^{31}$P NMR), probably by competing C=P ethylation.

Reaction of system **1** with the more sterically crowded 1-AdC≡P was slower. After the initial addition at −20 °C, the reaction was allowed to warm to room temperature under stirring. Following an additional 40 min stirring at room temp., **4** was formed (*ca*. 75% based on $^{31}$P NMR integrals; with *ca*. 25% of 1-AdC≡P remaining unreacted). Multinuclear NMR data on **4** (Fig. 1) fully agree with the suggested structure. The more shielded nature of the selenium centre (at C) in the more sterically crowded **4** as compared to **3** is noteworthy.

In the absence of $XeF_2$, vicinal bis-phenylselenenylation still occurs, albeit at a much slower rate. Thus $(PhSe)_2$ reacted slowly with Bu$^t$C≡P (1 equiv.) in dry $CH_2Cl_2$: $^{31}$P NMR monitoring showed that the initial product is **3**, but its slow formation and increase over time is accompanied by extensive decomposition at room temp. Similar observations were made in experiments where only *ca.* 0.1 equiv. of $XeF_2$ was used. Thus although fluoroselenenylation is not the final outcome, the presence of 1 equiv. of $XeF_2$ is needed. The presence of 2 equiv. of RC≡P is also required, since addition of 1 equiv. of Bu$^t$C≡P to **1** under similar conditions led only to traces of **3**. The need for a 1 : 1 PhSeF–RC≡P stoichiometry (as oppossed to 1 : 0.5) coupled to the absence of the additional equivalent of RC≡P in the $^{31}$P NMR is remarkable; it is tentatively rationalized by initial bis-fluoroselenenylation followed by 'elimination' (transfer fluorination of RC≡P and rapid polymerization of the resulting difluorophosphaalkene), somewhat similar to fluoroselenenylation of monosubstituted alkynes with *N*-phenylselenophthalimide–$Et_3N$–3HF forming vinylic diselenated compounds by HF loss.[12]

For comparison, we examined the reactions of Bu$^t$C≡P and 1-AdC≡P with PhSeCl (1 equiv.) in $CH_2Cl_2$ (Scheme 1). Dropwise addition of a solution of PhSeCl ($CH_2Cl_2$) to a cold solution of Bu$^t$C≡P ($CH_2Cl_2$) at dry ice–acetone temperature (over 30 min) followed by slow warming to room temp. and removal of solvent *in vacuo* gave the chloroselenenylation product **5** (70–80% in independent reactions). Under comparable conditions, chloroselenenylation of 1-AdC≡P was slower (→ **6**; *ca*. 60%). These reactions demonstrate that 'PhSe$^+$' attacks at phosphorus, not carbon.‡ Whereas the phosphorus and carbon environments in the phosphaalkene unit and the one-bond P/Se couplings are very similar for **5** and **6**, the selenium chemical shifts vary by almost 25 ppm. Observation of minor amounts of $(PhSe)_2$ ($\delta_{^{77}Se}$ 460.8) in both cases suggests possible intervention by a radical process.§

The observed bis-selenenylations with the $(PhSe)_2$–$XeF_2$ system points to a different addition mechanism for 'PhSeF' compared to PhSeCl towards the P≡C triple bond. Moreover, although PhSeCl effects chloroselenenylation, its regiochemistry is opposite to protonation and Lewis acid complexation reactions of RC≡P.[6]

The stereochemistry in **3** and **4** has not been unambiguously established, but the magnitude of $^2J_{C,P}$ is a good indicator of a synperiplanar relationship between the R group and the lone-pair at phosphorus (*syn* addition).[10,13]

We thank Dr S. Hollenstein for conducting some duplicate experiments. This material is based upon work supported by the US Army Research Office under grant number 35222-CH-II.

## Footnotes and References

* E-mail: klaali@kentvm.kent.edu

† Fluorinated minor products: $^{31}$P NMR: −30.2 (q, *J* 1014.3 Hz), −34.4 (quint, *J* 1013.4 Hz), −142.6 (quint, *J* 710.9 Hz); $^{19}$F NMR: −45.3 (dd, *J* 1013.5 and 9 Hz), −72.7 (d, *J* 713.5 Hz). In addition, there is a minor side-product (*ca.* 5%) in the phosphaalkene region; $^{31}$P NMR: 256.6 ($^1J_{P,Se}$ 227.3, $^1J_{P,Se}$ 280.4 Hz).

‡ A byproduct is present (10–30% in independent reactions); $^{31}$P NMR: $\delta$ 157.3 with two types of one-bond P/Se couplings at 317.7 and 195.6 Hz, with no indication of an intact P=C unit.

§ In the selenium NMR spectra, as well as $(PhSe)_2$ being present in both reactions ($\delta_{^{77}Se}$ 460.8), in the Bu$^t$CP reaction there is unreacted PhSeCl ($\delta_{^{77}Se}$ 446.5) and small peaks at $\delta_{^{77}Se}$ 449.8 and 451.4. In 1-AdC≡P reaction there are two peaks at $\delta_{^{77}Se}$ 426.7 and 424.9 (in 1 : 1 ratio with 100 Hz separation, a $^1J_{P,Se}$?)

1 K. Uneyama and M. Kanai, *Tetrahedron Lett.*, 1990, **31**, 3583.
2 H. Poleschner, M. Heydenreich, K. Spindler and G. Haufe, *Synthesis*, 1994, 1043.
3 H. Poleschner, M. Heydenreich and U. Schilde, *Leibigs. Ann.*, 1996, 1187.
4 G. H. Schmid and D. G. Garrett, *Tetrahedron Lett.*, 1975, 3991.
5 S. Tomoda and Y. Usuki, *Chem. Lett.*, 1989, 1235; Y. Usuki, M. Iwaoka and S. Tomoda, *Chem. Lett.*, 1992, 1507; Y. Usuki, M. Iwaoka and S. Tomoda, *J. Chem. Soc., Chem. Commun.*, 1992, 1148; J. R. McCarthy, D. P. Mathews and C. L. Barney, *Tetrahedron Lett.*, 1990, **31**, 973.
6 K. K. Laali, B. Geissler, M. Regitz and J. J. Houser, *J. Org. Chem.*, 1995, **60**, 6362.
7 K. K. Laali, B. Geissler, O. Wager, J. Hoffmann, R. Armbrust, W. Eisfeld and M. Regitz, *J. Am. Chem. Soc.*, 1994, **116**, 9407.
8 K. K. Laali, B. Geissler, M. Regitz and J. J. Houser, *J. Org. Chem.*, 1995, **60**, 47.
9 K. K. Laali, M. Regitz, M. Birkel, P. J. Stang and C. M. Crittell, *J. Org. Chem.*, 1993, **58**, 4105.
10 K. Karaghiosoff, in *Multiple Bonds and Low Coordination in Phosphorus Chemistry*, ed. M. Regitz and O. J. Scherer, Thieme, Stuttgart, 1990, p. 463f.
11 K. Laali, H. Y. Chen and R. J. Gerzina, *J. Org. Chem.*, 1987, **52**, 4126.
12 C. Saluzzo, G. Alvernhe and D. Anker, *Tetrahedron Lett.*, 1990, **31**, 2127.
13 T. W. Mackewitz, PhD Dissertation, Kaiserslautern, 1996.

*Received in Corvallis, OR, USA, 21st April 1997; 7/02737K*

# Synthesis and conformation of 3′-*O*,4′-*C*-methyleneribonucleosides, novel bicyclic nucleoside analogues for 2′,5′-linked oligonucleotide modification

**Satoshi Obika, Ken-ichiro Morio, Daishu Nanbu and Takeshi Imanishi***

*Faculty of Pharmaceutical Sciences, Osaka University, 1-6 Yamadaoka, Suita, Osaka 565, Japan*

**Novel bicyclic nucleoside analogues 3′-*O*,4′-*C*-methyleneribonucleosides 1 are conveniently prepared starting from uridine; the sugar puckering of 1 is found to be nearly in the *S*-conformation by means of PM3 calculations and $^1$H NMR studies.**

Non-genetic 2′,5′-linked oligonucleotides have been attracting much attention since the syntheses and properties of oligonucleotides with 2′,5′-linkages were reported in 1992.[1–3] Using NMR studies[4] and molecular modeling,[5] it was suggested that oligoribonucleotides containing 2′,5′-linkages (2′,5′-RNA) preferentially adopted the C2′-*endo* conformation (*S*-conformation), while 2′,5′-linked oligodeoxyribonucleotides (2′,5′-DNA) existed mainly with C3′-*endo* sugar puckering (*N*-conformation). Interestingly, these results are the opposite of what is observed with the corresponding 'genetic' 3′,5′-RNA and -DNA. There have been some reports concerning successful application of 2′,5′-linked oligonucleotides to antisense uses.[6–9] On the other hand, 2-5A (2′,5′-oligoadenylate 5′-triphosphate) is known to be formed in interferon-treated cells and to have antiviral activity with the aid of 2-5A dependent ribonuclease (RNase L),[10] and intensive studies on various 2-5A analogues have been reported.[11]

We have designed a bicyclic nucleoside analogue, 3′-*O*,4′-*C*-methyleneribonucleoside **1**,[12] which is a promising precursor for both novel types of therapeutic nucleoside derivatives and 2′,5′-linked oligonucleotide analogues. The sugar moiety in **1** consists of a 2,6-dioxabicyclo[3.2.0]heptane ring system, with the tetrahydrofuran part conformationally restricted by the fused oxetane ring. Here we describe a convenient first synthesis of **1** (B = U and C), and also discuss its conformation.

The synthetic route to the target molecule **1** (B = U) is shown in Scheme 1. A selective toluene-*p*-sulfonylation of the diastereotopic hydroxymethyl groups in 2′,3′-*O*-cyclohexylidene-4′-hydroxymethyluridine[13,14] **2** afforded monotosylate **3** (69%) along with its isomer **4** (12%). The stereochemistry at C4′ in **3** was confirmed by means of NOE measurements. Acidic hydrolysis of **3** gave triol **5** (94%) and then selective protection of the primary hydroxy group in **5** with a 4,4′-dimethoxytrityl (DMTr) group in the usual manner afforded **6** (56%).

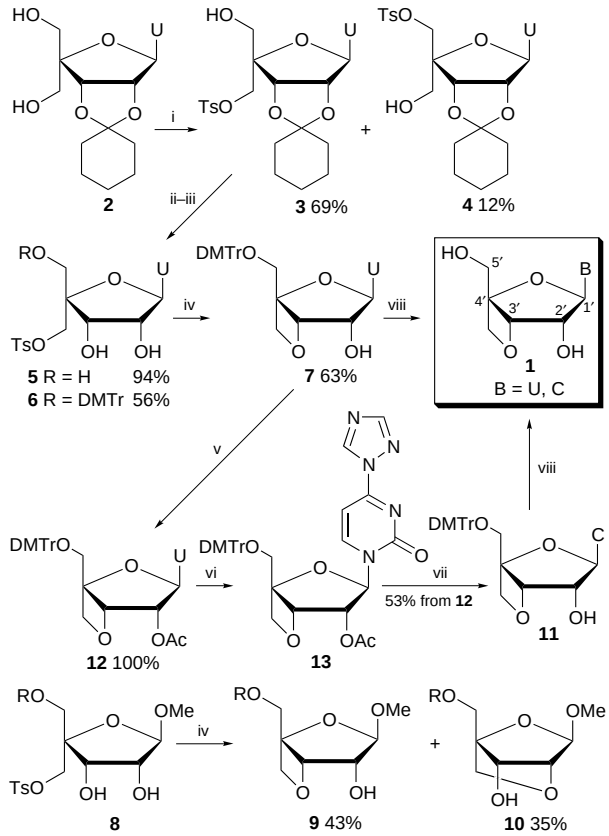
Oxetane ring formation from **6** was accomplished on treatment with a large excess of sodium hexamethyldisilazide in THF at room temperature, yielding the desired product **7**† (63%). The exclusive oxetane ring formation is attributable to the predominant *S*-conformation of the starting material **6**,‡ in which only the 3′-OH is thought to be located near the 4′-methylene carbon centre; the 2′-OH is too far away to attack the 4′-methylene carbon. In fact, 1′-methoxy congener **8**, which should exist mainly in the *N*-conformation due to the anomeric effect,‡ gives a *ca.* 1:1 mixture of 2′-*O*,4′-*C*-methylene derivative **9** and 3′-*O*,4′-*C*-methylene derivative **10** under the same conditions.[15]

Transformation of **7** into the cytidine derivative **11** by exchange of nucleobase was also undertaken as shown in Scheme 1. After 2′-*O*-acetylation of **7**, treatment of **12** with 1,2,4-triazole and 4-chlorophenyl phosphorodichloridate in pyridine[16] gave **13**, which was then subjected to ammonolysis to give **11**† (overall 53% yield from **7**). Acid catalysed detritylation of **7** and **11** gave the corresponding 2′,5′-diol compounds **1** (B = U)† and **1** (B = C)† quantitatively.

In general, the sugar moiety in natural and modified nucleosides exists in an equilibrium between *N*- and *S*-conformations. The conformation of nucleoside analogues in solution is easily obtainable from coupling constants between the ribose ring protons in the $^1$H NMR spectrum.[17] The simplest equation for calculation of percentage of *S* conformation is shown in eqn. (1). The calculation results for the obtained nucleoside

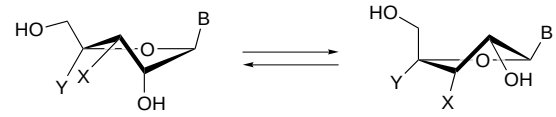
$$S(\%) = 100 \times (J_{1'2'} - 1)/6.9 \qquad (1)$$

analogues are summarized in Table 1, and show that all of the 3′-*O*,4-*C*-methyleneribonucleoside analogues have very large *S* values. A PM3 calculation[18]§ also indicates that an *S*-conformation (C1′-*exo*-C2′-*endo*) is the most stable conformation for the ribose ring in **1** (Fig. 1). It is very interesting and noteworthy that the oxetane ring fused nucleoside deriva-

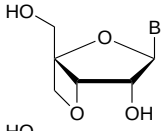
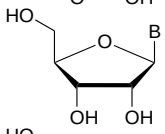
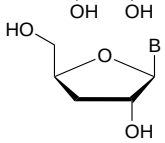



**Scheme 1** *Reagents and conditions*: i, TsCl (1.7 equiv.), 110 °C; ii, $CF_3CO_2H$–$H_2O$ (98:2), room temp.; iii, 4,4′-dimethoxytrityl chloride, DMAP, pyridine, room temp., iv, $(Me_3Si)_2NNa$ (10 equiv.), THF, 20 °C; v, $Ac_2O$, pyridine, room temp.; vi, 1,2,4-triazole, 4-chlorophenyl phosphorodichloridate, pyridine, room temp.; vii, aqueous $NH_3$, 1,4-dioxane, room temp.; viii, 3% $CCl_3CO_2H$ in $H_2O$, $CH_2Cl_2$, room temp.

**Table 1** Conformational analysis of nucleoside analogues using $^1$H NMR spectroscopy (in $CD_3OD$)




*N*-conformation ⇌ *S*-confirmation

| Nucleoside analogues | | $J_{1'2'}$/Hz | *S* (%)[a] |
|---|---|---|---|
|  | B = U | 7.5 | 94 |
| | B = C | 7.3 | 91 |
|  | B = U | 4.6 | 52 |
| | B = C | 2.8 | 26 |
|  | B = U | 1.2[b] | 3 |
| | B = C | 0[c] | 0 |

[a] Calculated from eqn. (1). [b] Ref. 19 (Measured in [$^2H_6$]DMSO). [c] Ref. 20.

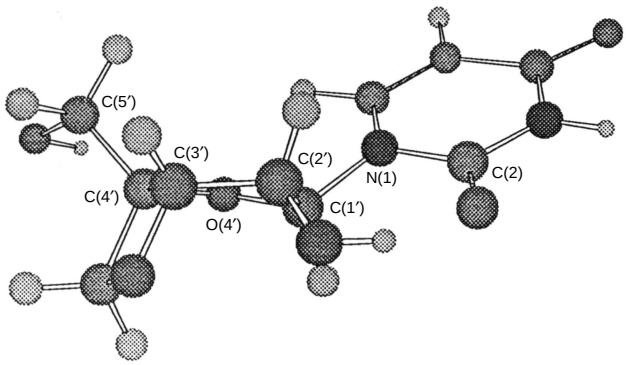



**Fig. 1** Computer-generated (PM3) representation of **1** (B = U)

tives **1** exist predominantly in an *S*-conformation, in contrast with the typical monocyclic nucleoside compounds (Table 1).[19,20]

Further chemical modification of **1** and its incorporation into oligonucleotides are now in progress.

## Footnotes and References

* E-mail address: imanishi@phs.osaka-u.ac.jp

† *Selected data* for **7**: mp 120–121 °C ($Et_2O$–hexane); $[\alpha]_D^{21}$ −37.7 (*c* 1.1, acetone); $^1$H NMR ([$^2H_6$]acetone): δ 2.92 (1 H, br s), 3.47, 3.51 (2 H, AB, *J* 10), 3.85 (6 H, s), 4.36 (1 H, dd, *J* 4, 4), 4.52, 4.83 (2 H, AB, *J* 8), 5.11 (1 H, d, *J* 4), 5.57 (1 H, d, *J* 8), 6.51 (1 H, d, *J* 8), 6.96 (4 H, d, *J* 9), 7.39–7.41 (7 H, m), 7.52 (2 H, d, *J* 5), 7.71 (1 H, d, *J* 9); *m*/*z* (EI) 558 ($M^+$). For **11**: mp 139–140 °C ($Et_2O$–hexane); $[\alpha]_D^{22}$ + 0.60 (*c* 0.34, MeOH); $^1$H NMR ($CD_3OD$): δ 3.40, 3.50 (2 H, AB, *J* 10), 3.76 (6 H, s), 4.14 (1 H, dd, *J* 4, 7), 4.48, 4.72 (2 H, AB, *J* 7), 4.98 (1 H, d, *J* 4), 5.79 (1 H, d, *J* 7), 6.56 (1 H, d, *J* 7), 6.85 (4 H, d, *J* 9), 7.21–7.42 (9 H, m), 7.67 (1 H, d, *J* 7); *m*/*z* (FAB) 558 $(M + H)^+$. For **1** (B = U): mp 215–216 °C (AcOEt); $[\alpha]_D^{17}$ −18.2 (*c* 1.2, acetone); $^1$H NMR ($CD_3OD$): δ 3.74, 3.82 (2 H, AB, *J* 12), 4.21 (1 H, dd, *J* 5, 8), 4.42, 4.82 (2 H, AB, *J* 8), 5.05 (1 H, d, *J* 5), 5.66 (1 H, d, *J* 9), 6.38 (1 H, d, *J* 8), 7.67 (1 H, d, *J* 9); Calc. for $C_{10}H_{12}N_2O_6 \cdot 1/2H_2O$; C, 45.29; H, 4.94; N, 10.56. Found C, 45.07; H, 4.82; N, 10.15%. For **1** (B = C): mp 224–225 °C ($Pr^iOH$); $[\alpha]_D^{25}$ +32.6 (*c* 0.49, $H_2O$); $^1$H NMR ($CD_3OD$): δ 3.73, 3.81 (2 H, AB, *J* 12), 4.16 (1 H, dd, *J* 5, 7), 4.52, 4.81 (2 H, AB, *J* 8), 5.04 (1 H, d, *J* 5), 5.94 (1 H, d, *J* 8), 6.41 (1 H, d, *J* 7), 7.68 (1 H, d, *J* 8); Calc. for $C_{10}H_{13}N_3O_5 \cdot 1/3H_2O$; C, 45.98; H, 5.27; N, 16.09. Found 46.04; H, 5.02; N, 15.82%.

‡ $J_{1'2'}$ Values (6.0 Hz for **6** and 0 Hz for **8**) provide the conformational information.

§ The MOPAC93 molecular orbital package (CS MOPAC Pro™, Cambridge Soft Corporation) utilizing the MNDO-PM3 Hamiltonian was used for the semi-empirical MO calculations. Geometry optimization was carried out with the use of the keyword MMOK implemented in MOPAC. All initial structures used for the MO calculation were generated by reference to the X-ray structures of natural nucleosides (ref. 21). Numerical calculations were performed on a Power Macintosh computer.

1 R. Kierzek, L. He and D. H. Turner, *Nucleic Acids Res.*, 1992, **20**, 1685.
2 J. P. Dougherty, C. J. Rizzo and R. Breslow, *J. Am. Chem. Soc.*, 1992, **114**, 6254.
3 H. Hashimoto and C. Switzer, *J. Am. Chem. Soc.*, 1992, **114**, 6255.
4 H. Robinson, K.-E. Jung, C. Switzer and A. H.-J. Wang, *J. Am. Chem. Soc.*, 1995, **117**, 837.
5 V. Lalitha and N. Yathindra, *Curr. Sci.*, 1995, **68**, 68.
6 P. A. Giannaris and M. J. Damha, *Nucleic Acids Res.*, 1993, **21**, 4742.
7 J. Seki, K. Kuroda, H. Ozaki and H. Sawai, *Nucleic Acids Symp. Ser.*, 1993, **29**, 71.
8 A. Maran, R. K. Maitra, A. Kumar, B. Dong, W. Xiao, G. Li, B. R. G. Williams, P. F. Torrence and R. H. Silverman, *Science*, 1995, **265**, 789.
9 E. R. Kanimalla, A. Manning, Q. Zhao, D. R. Shaw, R. A. Byrn, V. Sasisekharan and S. Agrawal, *Nucleic Acids Res.*, 1997, **25**, 370.
10 H. C. Schröder, R. J. Suhadolnik, W. Pfleiderer, R. Charubala and W. E. G. Muller, *Int. J. Biochem.*, 1992, **24**, 55; G. C. Sen and P. Lengyei, *J. Biol. Chem.*, 1992, **267**, 5017.
11 C. Horndler and W. Pfleiderer, *Helv. Chim. Acta*, 1996, **79**, 718 and references cited therein.
12 Some other bicyclic nucleoside analogues have appeared in the literature. For example, M. Tarkoy and C. Leumann, *Angew. Chem., Int. Ed. Engl.*, 1996, **35**, 1968; R. Zou and M. D. Matteucci, *Tetrahedron Lett.*, 1996, **37**, 941; K.-H. Altmann, R. Imwinkelried, R. Kesselring and G. Rihs, *Tetrahedron Lett.*, 1994, **35**, 7625.
13 S. L. Cook and J. A. Secrist, *J. Am. Chem. Soc.*, 1979, **101**, 1554.
14 G. H. Jones, M. Taniguchi, D. Tegg and J. G. Moffatt, *J. Org. Chem.*, 1979, **44**, 1309.
15 S. Obika, Y. Hari, K.-i. Morio, D. Nanbu and T. Imanishi, unpublished work.
16 T.-S. Lin, M.-Z. Luo, M.-C. Liu, Y.-L. Zhu, E. Gullen, G. E. Dutschman and Y.-C. Cheng, *J. Med. Chem.*, 1996, **39**, 693.
17 C. Altona and M. Sundaralingam, *J. Am. Chem. Soc.*, 1973, **95**, 2333; 1972, **94**, 8205.
18 J. J. P. Stewart, *J. Comput. Chem.*, 1989, **10**, 209, 221.
19 T.-S. Lin, J.-H. Yang, M.-C. Liu, Z.-Y. Shen, Y.-C. Cheng, W. H. Prusoff, G. I. Birnbaum, J. Giziewicz, I. Ghazzouli, V. Brankovan, J.-S. Feng and G.-D. Hsiung, *J. Med. Chem.*, 1991, **34**, 693.
20 T. L. Sheppard, A. T. Rosenblatt and R. Breslow, *J. Org. Chem.*, 1994, **59**, 7243.
21 S. Arnott and W. Hukins, *Biochem. J.*, 1972, **130**, 453.

*Received in Cambridge, UK, 23rd June 1997; 7/04376G*

# Ruthenium(II) ammine centres as efficient electron donor groups for quadratic non-linear optics

**Benjamin J. Coe,*[a] Jonathan P. Essex-Lopresti,[a] James A. Harris,[a] Stephan Houbrechts[a] and André Persoons[b,c]**

[a] *Department of Chemistry, University of Manchester, Oxford Road, Manchester, UK M13 9PL*
[b] *Laboratory of Chemical and Biological Dynamics, Center for Research on Molecular Electronics and Photonics, University of Leuven, Celestijnenlaan 200D, B-3001 Leuven, Belgium*
[c] *Optical Sciences Center, University of Arizona, Tucson, Arizona, AZ 85721, USA*

**Ruthenium(II) complex salts *trans*-$[Ru(NH_3)_4(L^D)(L^A)][PF_6]_3$ ($L^D$ = an N-donor ligand, $L^A$ = a 4,4′-bipyridinium ligand) exhibit large, tunable static first hyperpolarizabilities $\beta_0$ which are associated with intense, visible metal-to-ligand charge-transfer excitations.**

Organic materials possessing non-linear optical (NLO) properties are the focus of much current research activity directed towards applications in advanced electronics systems.[1] Within this field, transition-metal organometallic and coordination complexes have attracted limited attention,[2] but their great potential as novel NLO materials is yet to be fully explored.

Solution measurements of hyperpolarizability coefficients allow the correlation of NLO properties with molecular structure. This facilitates the rational design and synthesis of efficient NLO chromophores which may subsequently be incorporated into active materials. Extensive data concerning the first (quadratic) hyperpolarizability $\beta$ is now available for purely organic compounds,[1] but corresponding information for metal complexes is scarce.[2] This situation is gradually being rectified and $\beta$ values have been determined for selected complexes including bimetallic sesquifulvalenes,[3] Schiff-base derivatives,[4] and σ-acetylides.[5]

Recent reports show that ruthenium mixed-valence,[6] 2,2′-bipyridine (bipy),[7] and σ-acetylide[8] complexes can possess large $\beta$ values, although two-photon excited luminescence may explain these results for the bipy complexes.[9] Ruthenium(II) ammine complexes are promising candidates as high $\beta$ molecules due to the strong π-donor ability of the $d^6$ metal centres.[10] Such complexes are structurally versatile, and their readily accessible $Ru^{III/II}$ redox couples may permit reversible, molecular-level modulation of NLO properties.

A series of complex salts *trans*-$[Ru^{II}(NH_3)_4(L^D)(L^A)][PF_6]_3$ [Fig. 1; $L^D$ = $NH_3$, $L^A$ = *N*-methyl-4,4′-bipyridinium ($MeQ^+$) **1**, *N*-phenyl-4,4′-bipyridinium ($PhQ^+$) **2** or *N*-(2,4-dinitrophenyl)-4,4′-bipyridinium ($DNPhQ^+$) **3**; $L^D$ = 1-methylimidazole (mim), $L^A$ = $MeQ^+$ **4** or $PhQ^+$ **5**; $L^D$ = 4-dimethylaminopyridine (dmap), $L^A$ = $MeQ^+$ **6** or $PhQ^+$ **7**] have been synthesized by using established coordination chemistry based on $[Ru^{II}(NH_3)_5(H_2O)][PF_6]_2$ or *trans*-$[Ru^{II}Cl(NH_3)_4(SO_2)]Cl$;[11,12] **1**, **4** and **6** are known,[11,13] but the other salts are new. [$PhQ^+$]Cl and [$DNPhQ^+$]Cl were synthesized by using a modification of a literature report for *N*,*N*′-diphenyl-4,4′-bipyridinium dichloride.[14] All of the compounds have been fully characterized by using various techniques including UV–VIS spectroscopy and cyclic voltammetry,† and the first molecular hyperpolarizabilities $\beta$ of the complex salts have been determined *via* the hyper-Rayleigh scattering (HRS) technique.[15]

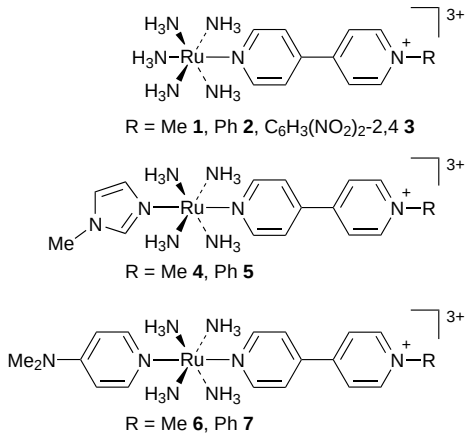



**Fig. 1** Structures of the complex cations in **1**–**7**

A common spectroscopic feature of low-valent ruthenium complexes of π-acceptor ligands are low-energy metal-to-ligand charge-transfer (MLCT) absorptions, the energies of which are governed by the electron-donor ability of the ruthenium centre and the ligand electron-acceptor capacity.[16] The exploitation of MLCT excited states as a basis for large $\beta$ values has often been suggested,[2] but only very recently demonstrated.[8] The $MeQ^+$ ligand is a particularly effective π acceptor due to conjugation between the pyridyl rings.[17]

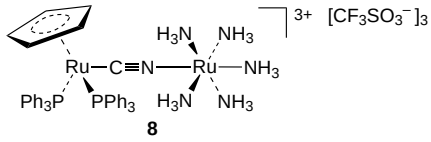
The complex salts show intense, broad $d_\pi(Ru^{II}) \rightarrow \pi^*(L^A)$ MLCT bands in the visible region (Table 1). For a given $L^D$, the MLCT energies decrease in the order $L^A$ = $MeQ^+$ > $PhQ^+$ > $DNPhQ^+$, with a red-shift of 70 nm going from **1** to **3**. This is because the electron acceptor strength of the ligand increases as the conjugation pathlength is extended. In keeping with this, the potentials for ligand-based reduction obtained *via* cyclic voltammetry (Table 1) show that the lowest unoccupied molecular orbital energy of $PhQ^+$ is lower than that of $MeQ^+$ by 140–160 mV. With $L^A$ fixed, the MLCT energies decrease in the order $L^D$ = $NH_3$ > mim > dmap, with a red-shift of 30 nm going from **2** to **7** reflecting the increasing basicity of $L^D$. The reversible $Ru^{III/II}$ oxidation waves are at constant potential, showing that the energy of the metal-based highest occupied molecular orbital is unaffected by the ligand changes. The MLCT bands are highly solvatochromic, with the maximum for **6** occurring at 604 nm in $MeNO_2$ and at 706 nm in HMPA. Such behaviour, which often accompanies large $\beta$ values in organic compounds,[18] confirms that the MLCT excitations are the primary contributors to $\beta$ in these complexes.

The HRS setup and the method for derivation of $\beta$ were as described in a recent report.[19] All samples were passed through a 0.45 mm filter, and were checked for fluorescence which can interfere with the HRS signal.[9,20] The $\beta$ values obtained are extremely large (Table 1), and similar to those reported for ruthenium organometallics.[8] A much smaller HRS $\beta_{1064}$ value of $78 \times 10^{-30}$ esu was found for the mixed-valence salt **8** (Fig. 2) in which the $\{Ru^{III}(NH_3)_5\}^{3+}$ centre acts as an electron acceptor.[9] Since salts **1**–**7** absorb in the region of the second harmonic at 532 nm (Table 1), their $\beta$ values are resonantly

**Table 1** Electrochemical, UV–VIS and non-linear optical data in acetonitrile for the salts *trans*-$[Ru(NH_3)_4(L^D)(L^A)][PF_6]_3$

| Salt | $L^D$ | $L^A$ | $E_{1/2}[Ru^{III/II}]$ ($\Delta E_p$)/$E_{1/2}[L^{A+/0}]$ ($\Delta E_p$) *V vs.* SCE/mV[a] | | $\lambda_{max}$[MLCT]/nm ($\varepsilon$/nm dm$^3$ mol$^{-1}$ cm$^{-1}$) | $\varepsilon_{532}$[b] (%) | $\beta_{1064}$ $10^{-30}$ esu | $\beta_0$ |
|---|---|---|---|---|---|---|---|---|
| **1** | $NH_3$ | $MeQ^+$ | 0.46 (75) | −0.91 (65) | 590 (15 800) | 61 | 750 | 123 |
| **2** | $NH_3$ | $PhQ^+$ | 0.46 (75) | −0.75 (70) | 628 (19 300) | 32 | 858 | 220 |
| **3** | $NH_3$ | $DNPhQ^+$ | 0.46[d] | −0.40[e] | 660 (16 900) | 23 | 871 | 289 |
| **4**[f] | mim | $MeQ^+$ | 0.47 (75) | −0.88 (70) | 602 (16 200) | 55 | 523 | 100 |
| **5** | mim | $PhQ^+$ | 0.46 (70) | −0.73 (70) | 648 (21 500) | 31 | 874 | 266 |
| **6**[f] | dmap | $MeQ^+$ | 0.46 (70) | −0.87 (65) | 614 (17 200) | 47 | 587 | 130 |
| **7** | dmap | $PhQ^+$ | 0.46 (75) | −0.73 (65) | 658 (20 000) | 28 | 794 | 260 |

[a] Measured in solution 0.1 M in $[NBu^n_4]PF_6$ at a Pt bead working electrode with a scan rate of 200 mV s$^{-1}$ (ferrocene internal reference $E_{1/2}$ = 0.40 V, $\Delta E_p$ = 65 mV). [b] Extinction at 532 nm as a percentage of that at the MLCT maximum. [c] $\beta_{1064}$ is the uncorrected first hyperpolarizability measured by using a 1064 nm Nd:YAG laser fundamental; $\beta_0$ is the static hyperpolarizability estimated by using the two-level model.[22] A relative error of ±15% is estimated for $\beta$ values. The quoted cgs units (esu) are converted into SI units (C$^3$ m$^3$ J$^{-2}$) by dividing by a factor of $2.693 \times 10^{20}$. [d] $E_{pa}$ for an irreversible oxidation process. [e] $E_{pc}$ for an irreversible reduction process. [f] Ref.13.




**8**

**Fig. 2** Structure of the diruthenium salt **8**

enhanced, to the greatest extent for **1** and to the least extent for **3**. Correlations between $\beta$ and the intramolecular charge-transfer (ICT) energy have been found for dipolar organics in which a single ICT absorption dominates $\beta$.[21] In similar fashion, $\beta$ for these complexes clearly increases as the MLCT band shifts to lower energy. This trend is evident despite the concomitant decreasing extent of resonance enhancement.

Static first hyperpolarizabilities $\beta_0$, which provide an estimate of the intrinsic molecular hyperpolarizability with resonance effects removed, were obtained by application of the two-level model.[22] The $\beta_0$ values are very large and are in excess of those for most NLO-active molecules. By way of contrast, the organic dye Brilliant Green has an ICT maximum at 632 nm and a $\beta_0$ value of $97 \times 10^{-30}$ esu derived from HRS in 5% MeOH–1,4-dioxane at 1064 nm.[23] A broad inverse correlation between $\beta_0$ and the MLCT energy is observed for **1**–**7**.

In conclusion, we have demonstrated that readily synthesized and structurally versatile ruthenium coordination complexes can exhibit very large $\beta$ and $\beta_0$ values which are associated with low-energy MLCT excitations. The MLCT energy is readily tuned by ligand modifications, which will allow the maximization of $\beta_0$ and the establishment of further structure–property correlations for this novel class of NLO molecules.

Support from The Royal Society, from the Belgian National Fund for Scientific Research (G.2103.93 and 9.0011.92), the Belgian government (IUAP-16) and the University of Leuven (GOA/1/95) is acknowledged. S. H. is a Research Assistant of the Belgian National Fund for Scientific Research. Johnson Matthey plc are thanked for a loan of ruthenium trichloride.

## Footnotes and References

* E-mail: b.coe@man.ac.uk

† The identity and purity of all of the ligands and complex salts were established by proton NMR spectroscopy and satisfactory elemental analyses.

1 *Nonlinear Optical Properties of Organic Molecules and Crystals*, ed. D. S. Chemla and J. Zyss, Academic Press, Orlando, 1987, vol. 1 and 2; *Molecular Nonlinear Optics*, ed. J. Zyss, Academic Press, New York, 1994.
2 S. R. Marder, in *Inorganic Materials*, ed. D. W. Bruce and D. O'Hare, Wiley, Chichester, 1992; N. J. Long, *Angew. Chem., Int. Ed. Engl.*, 1995, **34**, 21.
3 U. Behrens, H. Brussaard, U. Hagenau, J. Heck, E. Hendrickx, J. Körnich, J. G. M. van der Linden, A. Persoons, A. L. Spek, N. Veldman, B. Voss and H. Wong, *Chem. Eur. J.*, 1996, **2**, 98.
4 P. G. Lacroix, S. Di Bella and I. Ledoux, *Chem. Mater.*, 1996, **8**, 541.
5 P. Nguyen, G. Lesley, T. B. Marder, I. Ledoux and J. Zyss, *Chem. Mater.*, 1997, **9**, 406.
6 W. M. Laidlaw, R. G. Denning, T. Verbiest, E. Chauchard and A. Persoons, *Proc. SPIE, Int. Soc. Opt. Eng.*, 1994, **2143**, 14.
7 C. Dhenaut, I. Ledoux, I. D. W. Samuel, J. Zyss, M. Bourgault and H. Le Bozec, *Nature*, 1995, **374**, 339.
8 I. R. Whittall, M. G. Humphrey, A. Persoons and S. Houbrechts, *Organometallics*, 1966, **15**, 1935; S. Houbrechts, K. Clays, A. Persoons, V. Cadierno, M. P. Gamasa and J. Gimeno, *Organometallics*, 1996, **15**, 5266.
9 I. D. Morrison, R. G. Denning, W. M. Laidlaw and M. A. Stammers, *Rev. Sci. Instrum.*, 1996, **67**, 1445.
10 Y. K. Shin, B. S. Brunschwig, C. Creutz and N. Sutin, *J. Phys. Chem.*, 1996, **100**, 8157 and references therein.
11 J. C. Curtis, B. P. Sullivan and T. J. Meyer, *Inorg. Chem.*, 1983, **22**, 224.
12 E. Tfouni and P. C. Ford, *Inorg. Chem.*, 1980, **19**, 72.
13 B. J. Coe, M. C. Chamberlain, J. P. Essex-Lopresti, S. Gaines, J. C. Jeffery, S. Houbrechts and A. Persoons, *Inorg. Chem.*, 1997, in the press.
14 B. Emmert and N. Roh, *Ber.*, 1925, **58**, 503.
15 K. Clays and A. Persoons, *Phys. Rev. Lett.*, 1991, **66**, 2980; K. Clays and A. Persoons, *Rev. Sci. Instrum.*, 1992, **63**, 3285.
16 P. Ford, De F. P. Rudd, R. Gaunder and H. Taube, *J. Am. Chem. Soc.*, 1968, **90**, 1187; C. R. Johnson and R. E. Shepherd, *Inorg. Chem.*, 1983, **22**, 2439.
17 P. Chen, M. Curry and T. J. Meyer, *Inorg. Chem.*, 1989, **28**, 2271.
18 M. S. Paley and J. M. Harris, *J. Org. Chem.*, 1991, **56**, 568.
19 S. Houbrechts, K. Clays, A. Persoons, Z. Pikramenou and J.-M. Lehn, *Chem. Phys. Lett.*, 1996, **258**, 485.
20 E. Hendrickx, C. Dehu, K. Clays, J. L. Brédas and A. Persoons, *ACS Symp. Ser.*, 1995, **601**, 82; M. C. Flipse, R. de Jonge, R. H. Woudenberg, A. W. Marsman, C. A. van Walree and L. W. Jenneskens, *Chem. Phys. Lett.*, 1995, **245**, 297.
21 L.-T. Cheng, W. Tam, G. R. Meredith, G. Rikken and E. Meijer, *Proc. SPIE, Int. Soc. Opt. Eng.*, 1989, **1147**, 61; A. E. Stiegman, E. Graham, K. J. Perry, L. R. Khundkar, L.-T. Cheng and J. W. Perry, *J. Am. Chem. Soc.*, 1991, **113**, 7658.
22 J. L. Oudar and D. S. Chemla, *J. Chem. Phys.*, 1977, **66**, 2664; J. L. Oudar, *J. Chem. Phys.*, 1977, **67**, 446; J. Zyss and J. L. Oudar, *Phys. Rev. A*, 1982, **26**, 2016.
23 P. Kaatz and D. P. Shelton, *J. Chem. Phys.*, 1996, **105**, 3918.

*Received in Basel, Switzerland, 18th April 1997; 7/02681A*

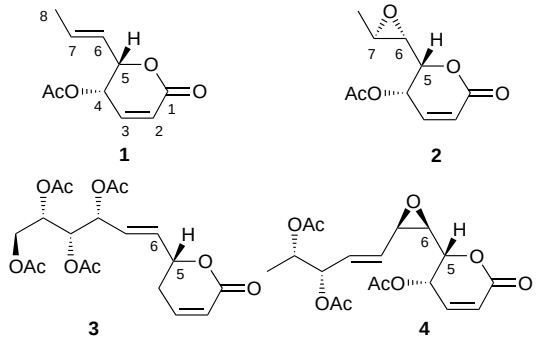
# A novel entry to naturally occurring 5-alkenyl α,β-unsaturated δ-lactones from D-glucose: syntheses of (+)-acetylphomalactone and (+)-asperlin

**Ana M. Gómez,* Beatriz López de Uralde, Serafín Valverde and J. Cristóbal López*†**

*Instituto de Química Orgánica General (CSIC), Juan de la Cierva 3, 28006 Madrid, Spain*

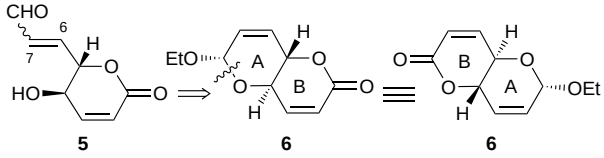
**A bicyclic pyranosidic glycoside 6, readily obtained from D-glucose, has been used as the key intermediate in enantioselective syntheses of (+)-acetylphomalactone and (+)-asperlin, in which the configuration at C-5 corresponds to that of the hexopyranosides in the L-sugar series.**

Naturally occurring 5-substituted α,β-unsaturated δ-lactones, *e.g.* **1**–**4**, represent an important class of products with a diverse range of biological activity.[1] They have been reported to be plant growth inhibitors, insect antifeedants and antifungal and antitumour agents.[1] They are widely distributed and have been isolated from both plants and fungi. Acetylphomalactone **1**[2] and asperlin **2**[3] are prominent members of this family. (+)-Acetylphomalactone **1** is an antimicrobial metabolite isolated from *Aspergillus caespitous*,[2] and (+)-Asperlin **2** was isolated from *Aspergillus nidulans* and possesses antitumour and antibacterial activity.[3] Among the more relevant structural characteristics of this family are: (i) the absolute configuration at C-5, and (ii) the presence of a chain at C-5, which normally presents a $\Delta^{6,7}$ unsaturation or an epoxide derived therefrom.[1] The design of a general, enantioselective approach to this family of lactones from currently available carbohydrates (D- series) is not obvious because the absolute configuration at C-5 correlates with that of a hexopyranoside of the L-series. Accordingly, D-sugars have been used in syntheses of unnatural isomers of asperlin **2**[4,5]‡ and anamarine **3**[6] as well as synthetic precursors for *ent*-olguine **4**.[7] Herein we report the first general approach to this family of lactones, starting from D-glucose, and its application to the syntheses of acetylphomalactone **1** and asperlin **2**.



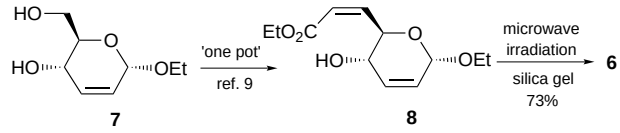
**1** **2** **3** **4**

Our strategy (Scheme 1) is based on the recognition that D-glucose-derived bicyclic glycoside **6** can be viewed as a 5-alkenyl α,β-unsaturated δ-lactone. Chemoselective cleavage of ring A on **6** leads to lactone **5**, which already fulfils the above-mentioned structural requirements.



**5** **6** **6**

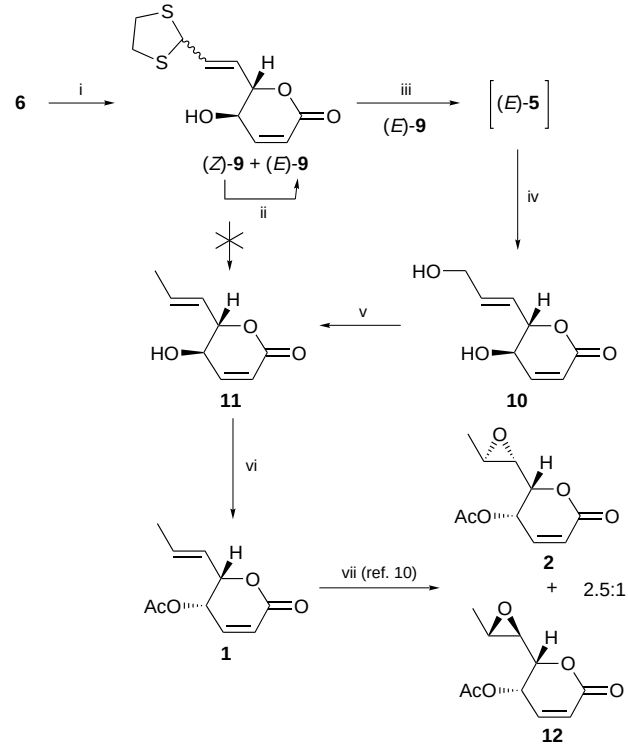
**Scheme 1**



**7** **8**

**Scheme 2**

Additionally, the feasibility of this approach greatly benefits from the facile preparation of **6** from readily available Ferrier's diol **7**[8] (Scheme 2). Thus, compound **7** is efficiently transformed, *via* a one pot operation, into hydroxy ester **8**,[9] and microwave-induced lactonization of the latter on silica gel gives rise to glycoside lactone **6** in fairly good yield (73%).§ The glycosidic moiety on **6** can be unravelled under acid catalysis in the presence of ethanedithiol to furnish a *ca.* 2 : 1 mixture of 5-alquenil lactones (*E*)-**9** and (*Z*)-**9**, which upon further treatment leads to (*E*)-**9** as a single isomer (83% overall) (Scheme 3). At this stage, direct desulfurization of (*E*)-**9** to yield **11** was attempted under a variety of conditions,¶ although in our hands this transformation still remains elusive. A less direct route to **11** was then designed which involves deprotection of



**Scheme 3** *Reagents and conditions*: i, $HSCH_2CH_2SH$, $BF_3{\cdot}OEt_2$, $CH_2Cl_2$, −20 °C; ii, $BF_3{\cdot}OEt_2$, $CH_2Cl_2$, 0 °C, 83% from **6**; iii, $CaCO_3$, MeI, MeCN–$H_2O$ (8 : 2), 60 °C; iv, $BH_3{\cdot}Me_2S$, THF, 0 °C, 66% from (*E*)-**9**; v, *N*-(phenylseleno)phthalimide, $PBu_3$, $CH_2Cl_2$, −20 °C, then $Bu_3SnH$, AIBN, PhMe, 80 °C, 41% from **10**; vi, $PPh_3$, AcOH, diisopropyl azodicarboxylate, THF, room temp., 61%; vii, MCPBA, $CH_2Cl_2$, 4 days, room temp.

the dithiane group followed by reduction of the resulting aldehyde function in **5**‖ to furnish diol **10** (66% overall). Sequential phenylselenation–tin mediated deselenation of the latter yielded **11** (41% overall). One additional isomer with a $\Delta^{7,8}$ unsaturation, resulting from the reduction of the allylic radical at C-6, was also observed (*ca*. 3.5 : 1 ratio). Mitsunobu inversion of **11** with acetic acid at C-4 led to **1**** (61%), which upon epoxidation gave raise to asperlin **2**,** along with its 6*R*,7*S*-diastereoisomer.[10]

In summary, we have developed an efficient synthetic approach to naturally occurring 5-alkyl and 5-alkenyl α,β-unsaturated δ-lactones[1] using D-glucose as the starting material. The approach illustrates the usefulness of bicyclic D-glycoside **6** as a key intermediate for biologically active lactones in which C-5 correlates with that of a hexopyranoside of the L-series. Further studies along this line for the preparation of other lactones are under way.

This research was supported by funds from the Dirección General de Investigación Científica y Técnica (grants PB96-0822 and PB94-0104). A. M. G. thanks the Consejo Superior de Investigaciones Científicas for financial support.

## Footnotes and References

† E-mail: clopez@cc.csic.es

‡Shing and Aloui prepared the 6*R*,7*S* diastereomer of **2** from D- glucose [refs. 4(*a*) and (*b*)]. Ramesh and Franck reported the synthesis of (+)-**2** from L-rhamnose (ref. 5).

§ Hydroxyester **8** (300 mg) was adsorbed on silica gel (4.5 g) and placed in a Pyrex vessel with an external bath of about 200 g of silica gel. Irradiation of the mixture in a commercial microwave oven (466 W, 6 min) afforded lactone **6**. A large number of different sets of conditions were investigated for this transformation but were not found to be synthetically useful because of low yields and/or long reaction times.

¶ Treatment of (*E*)-**9** with several kinds of Ni-Raney in different solvents and under different conditions, in our hands, did not result in the formation of **11**.

‖ Hydroxy aldehyde **5** is not a very stable compound. It dehydrates slowly at room temperature or upon purification on silica gel.

** Spectral data (300 MHz $^1$H NMR) for **1**,[2b] and **2**,[10a] are identical with those already reported for the natural compounds.

1 M. T. Davies-Coleman and D. E. A. Rivett, in *Progress in the Chemistry of Organic Natural Products*, ed. W. Herz, H. Grisebach, G. W. Kirby and Ch. Tamm, Springer-Verlag, Wien and New York, 1989, vol. 55, pp. 1–35.
2 (*a*) S. Mizuba, K. Lee and J. Jiu, *Can. J. Microbiol.*, 1975, **21**, 1781; (*b*) T. Honda, T. Kametani, K. Kanai, Y. Tatsuzaki and M. Tsubuki, *J. Chem. Soc., Perkin Trans. 1*, 1990, 1733.
3 A. D. Argoudelis and J. F. Zieserl, *Tetrahedron Lett.*, 1966, **7**, 1969.
4 (*a*) T. K. M. Shing and M. Aloui, *Can. J. Chem.*, 1990, **68**, 1035; (*b*) T. K. M. Shing and M. Aloui, *J. Chem. Soc., Chem. Commun.*, 1988, 1525; (*c*) S. Valverde, B. Herradón, R. M. Rabanal and M. Martin-Lomas, *Can. J. Chem.*, 1987, **65**, 339.
5 S. Ramesh and R. W. Franck, *Tetrahedron: Asymmetry*, 1990, **1**, 137.
6 S. Valverde, A. Hernández, B. Herradón, R. M. Rabanal and M. Martin-Lomas, *Tetrahedron*, 1987, **43**, 3499; F. W. Lichtenthaler, K. Lorenz and W-y. Ma, *Tetrahedron Lett.*, 1987, **28**, 47.
7 S. Valverde, B. Herradón, R. M. Rabanal and M. Martin-Lomas, *Can. J. Chem.*, 1987, **65**, 332; S. Valverde, M. Martin-Lomas and B. Herradón, *J. Carbohydr. Chem.*, 1987, **6**, 685; R. M. Rabanal, J. Escudero, M. Martin-Lomas and S. Valverde, *Carbohydr. Res.*, 1985, **141**, 49.
8 R. J. Ferrier and N. Prasad, *J. Chem. Soc. C*, 1969, 570.
9 A. M. Gómez, J. C. López and B. Fraser-Reid, *Synlett*, 1993, 557.
10 (*a*) T. Murayama, T. Sugiyama and K. Yamashita, *Agric. Biol. Chem.*, 1987, **51**, 2055; (*b*) H. Hiraoka, K. Furuta, N. Ikeda and H. Yamamoto, *Bull. Chem. Soc. Jpn.*, 1984, **57**, 2777.

*Received in Cambridge, UK, 22nd May 1997; 7/03561F*

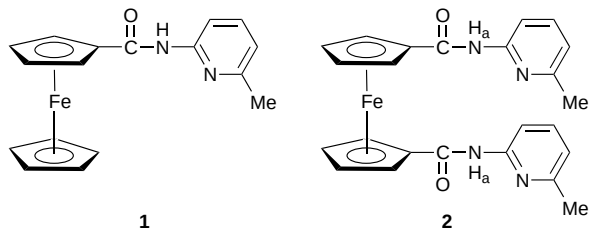
# Novel electrochemical sensors for neutral molecules

**Jonathan D. Carr,[a] Laurence Lambert,[a] David E. Hibbs,[b] Michael B. Hursthouse,[b] K. M. Abdul Malik[b] and James H. R. Tucker*[a]**

[a] *Department of Chemistry, University of Exeter, Stocker Road, Exeter, UK EX4 4QD*
[b] *Department of Chemistry, University of Wales Cardiff, PO Box 912, Cardiff, UK CF1 3TB*

**Two new ferrocene receptors bind to a series of neutral carboxylic acid guests *via* hydrogen bonding interactions; complexation induces a significant change in the electronic properties of the proximate ferrocene units, as evidenced by the recognition of these neutral guests by cyclic voltammetry.**

Supramolecular compounds that undergo a change in their redox properties upon complexation are relevant to the development of molecular sensing and switching devices.[1] So far, research in this area has focused almost exclusively on redox-active receptor molecules that bind and sense either cations[2] or anions.[3] However, although the chemistry of neutral molecule recognition is well-developed,[1,4] there are only a few reports of systems where the binding of neutral guest molecules in solution has been followed electrochemically.[5,6] The recent interest in hydrogen bonded supramolecular systems containing metal centres,[7] combined with evidence that hydrogen bonding contributes to the magnitude of redox potentials in metalloproteins,[8] suggest that effective electrochemical sensing of neutral molecules, *via* hydrogen bonding interactions, is within reach. Here we report two new receptor compounds containing ferrocene units and give preliminary results on their interaction with a range of neutral carboxylic acids.




Two simple redox-active ferrocene compounds **1** and **2**, containing a mono- and bis-amido pyridine moiety respectively, have been synthesised in good yield from the reaction of either chlorocarbonylferrocene or 1,1′-bis(chlorocarbonyl)ferrocene with 2-aminopicoline in $CH_2Cl_2$ in the presence of base.

Complex formation between receptors **1** and **2** and a series of monocarboxylic acids **3a**–**c** and a dicarboxylic acid, glutaric acid **4**, is evidenced by changes to the $^1$H NMR spectra of **1** and **2** in $CDCl_3$. For each receptor, the addition of excess substrate causes marked shifts in the signals corresponding to the amide and cyclopentadienyl protons. A complex of 1 : 1 stoichiometry between **2** and **4** is revealed by monitoring the downfield shift for the $H_a$ proton of **2** ([**2**] ≈ 1 mM) upon addition of aliquots of **4** (Fig. 1).† The large shift of *ca*. 1.9 ppm is strong evidence for a hydrogen bonding interaction.[7a,10]

Titrations of **1** and **2** (1 mM, $CDCl_3$) with monoacids **3a**–**c** give complexes of 1 : 1 and 1 : 2 (Fc : acid) stoichiometry respectively, whereas a titration of **1** with diacid **4** proceeds *via* a dimeric complex of 2 : 1 (Fc : acid) stoichiometry to give a 1 : 1 complex upon the addition of excess guest. In agreement with the solution studies, an X-ray structure of a crystal grown by slow evaporation of a $CDCl_3$–$Et_2O$ solution of **1** and excess **4** reveals a hydrogen bonded dimer (Fig. 2), consisting of two linked complexes of 1 : 1 stoichiometry [N(1)–H(1)–O(3) distance 2.92 Å, N(1)–H(1)–O(3) angle 166°; O(2)–H(2)–N(2) 2.65 Å, 171°; O(5)–H(5)–O(4) 2.63 Å, 167°].‡

This X-ray structure and the NMR studies suggest that the complex between **2** and **4** is likely to consist of an intermolecular four-point binding interaction, in which the guest is bridged between the two cyclopentadienyl rings. A similar geometry has been found by Hamilton[10] for related complexes between neutral terephthalate bis-amidopyridine derivatives and dicarboxylic acids.

Cyclic voltammetry studies in $CH_2Cl_2$ (1 mM) reveal that substrate complexation can be detected electrochemically (Table 1). The addition of excess monoacid (**3a**–**c**) to **1** causes small negative shifts ($\Delta E°$ = −20 to −25 mV) in the reversible redox wave of the receptor, whereas for receptor **2** the magnitude of the shift is approximately twice that amount ($\Delta E°$ = −55 to −60 mV). This indicates that the number of hydrogen bonds is approximately proportional to the shift in the redox potential. The shift of −20 mV found for **1** in the presence of excess **4** therefore denotes a 1 : 1 complex, which is in agreement with the NMR and X-ray studies. However, the significantly larger shift of −85 mV found for **2** with diacid **4** is likely to be a result of the effect of four strong hydrogen bonds, combined with the unique geometry of the complex. In this conformation the guest is bridged across the ferrocene unit, much closer to the redox-active iron centre.

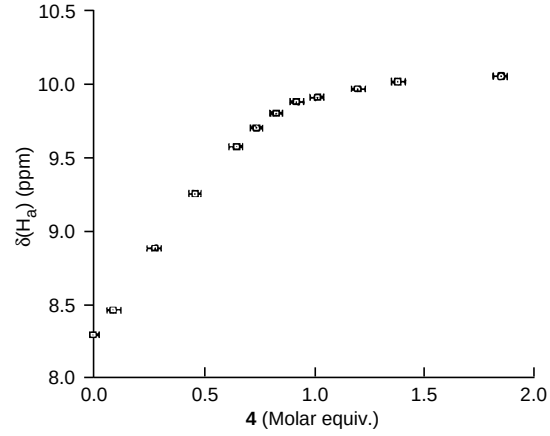



**Fig. 1** $^1$H NMR shift value of the $H_a$ proton of **2** in $CDCl_3$ as a function of molar equivalents of glutaric acid **4**

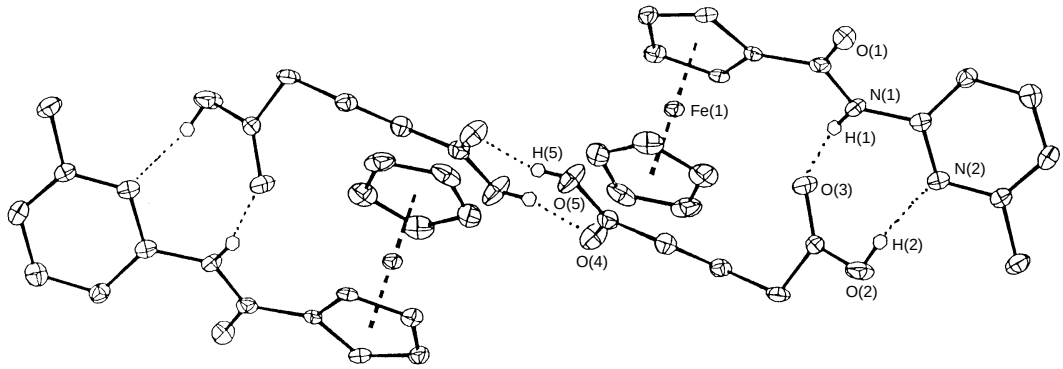



**Fig. 2** Crystal structure of [**1**·**4**]$_2$ (the dotted lines indicate strong hydrogen bonds between the two species and also between a pair of acid molecules

**Table 1** Electrochemical data[a] for compounds **1** and **2** in $CH_2Cl_2$ in the absence and presence of neutral guest substrates **3a**–**c** and **4**

| | | $\Delta E°$/V[c] | | | |
|---|---|---|---|---|---|
| Compound[b] | $E°$/V | **3a** | **3b** | **3c** | **4** |
| **1** | +0.24 | −20 | −20 | −25 | −20 |
| **2** | +0.44 | −60 | −55 | −55 | −85 |

[a] Cyclic voltammograms were carried out at a scan rate of 200 mV s$^{-1}$ in $CH_2Cl_2$ containing tetrabutylammonium perchlorate (TBAP) as supporting electrolyte (0.1 M), ferrocene as internal reference (*ca.* 1 mM) and the appropriate ferrocene receptor (1 mM) at room temp. The following electrode system was used: Pt wire working electrode, Pt wire counter electrode and Ag wire pseudo-reference electrode. [b] Redox potentials ($E°$) were referenced to ferrocene as an internal standard where $E° = 0.5 (E°_{pa} - E°_{pc})$. The confidence limit is ±10 mV. For each voltammogram, the reversibility of the redox wave matched that of the ferrocene internal reference ($\Delta E°_p$ = 70–100 mV). [c] The cathodic shift (mV) of the reversible redox couple of **1** or **2** upon addition of excess substrate.

In all cases, negative shifts in the redox waves of **1** and **2** are observed, which indicates that complexation increases the electron density at the iron centre. This is most likely a result of complexation delivering more electron density to the amide nitrogen. However, an attempt to monitor the change in the amide carbonyl stretch of 2 ($\nu_{C=O}$ 1668 cm$^{-1}$, KBr disc) using IR spectroscopy was hampered because of overlap by the carboxylic acid peaks of each guest. At any rate, there is no evidence of shifts being induced by protonation of the pyridine units, which would be the case if binding is of the zwitterionic form; addition of H$^+$ leads to large positive shifts in the redox waves of **1** and **2**.[9]

The $\Delta E°$ values reflect the difference in substrate binding strength between the two redox states of each complex.[11] In this case, the negative shifts indicate that each guest is bound more strongly once the ferrocene unit is oxidised. Such a trend is consistent with a positive charge on the ferrocene unit increasing the acidity of the amide N–H bond of the receptor.[12] However, recent quantitative studies on related systems[7b] show that the strength of hydrogen bonding may in fact increase or decrease upon the introduction of a postive charge at an adjacent metal centre. The direction and magnitude of this change appears to be strongly dependent upon the type of donor–acceptor system and the degree of conjugation between the metal centre and the binding site.

As far as we are aware, this system represents the most significant change in the redox properties of a supramolecular receptor compound that is induced by the complexation of a *neutral* guest. In other examples, the effect has either been smaller,[5] or has involved systems in which the guest, and not the host, is redox-active.[6] Studies are currently underway to fully explain the nature of this redox response in these and other related systems.

We thank the University of Exeter for the award of a University Research Studentship (J. D. C.) and the EC Erasmus Scheme.

## Footnotes and References

* E-mail: j.h.r.tucker@exeter.ac.uk

† The near complete complexation of **2** for a 1 : 1 molar ratio at millimolar concentrations suggests a stability constant between **2** and **4** of ⩾ $10^4$ M$^{-1}$. Comprehensive studies are now in progress to evaluate the stability constants between **1** and **2** and a range of carboxylic acid guests.[9]

‡ *Crystal data* for **1**·**4**: $C_{22}H_{24}FeN_2O_5$, orange crystals from $CDCl_3$–$Et_2O$, $M$ = 452.28, triclinic, $a$ = 7.4380(10), $b$ = 7.596(2), $c$ = 18.211(4) Å, $\alpha$ = 82.58(3), $\beta$ = 79.99(3), $\gamma$ = 86.10(3)°, $U$ = 1003.7(4) Å$^3$, space group $P\bar{1}$, $Z$ = 2, $D_c$ = 1.497 Mg m$^{-3}$, $\mu$(Mo-K$\alpha$) = 0.789 mm$^{-1}$, crystal size 0.14 × 0.12 × 0.10 mm. Final $R$ [ on 2194 $F > 4\sigma(F_o)$] = 0.0426 and $wR$ (on all $F^2$) = 0.1045. CCDC 182/546.

1 J. M. Lehn, *Supramolecular Chemistry–Concepts and perspectives*, VCH, Weinheim, 1995 and references cited therein.
2 P. D. Beer, *Chem. Soc. Rev.*, 1989, **18**, 409; T. Jørgensen, T. K. Hansen and J. Becher, *Chem. Soc. Rev.*, 1994, **23**, 41; P. D. Beer, *Adv. Mater.*, 1994, **6**, 607.
3 P. D. Beer, *Chem. Commun.*, 1996, 689.
4 M. Mascal, N. M. Hext, R. Warmuth, M. H. Moore and J. P. Turkenburg, *Angew. Chem., Int. Ed. Engl.*, 1996, **35**, 2204 and references cited therein; T. Koike, M. Takashige, E. Kimura, H. Fujioka and M. Shiro, *Chem. Eur. J.*, 1996, **2**, 617 and references cited therein; W. E. Allen, P. A. Gale, C. T. Brown, V. M. Lynch and J. L. Sessler, *J. Am. Chem. Soc.*, 1996, **118**, 12 471 and references cited therein.
5 J. H. R. Tucker, M. Shionoya, T. Koike and E. Kimura, *Bull. Chem. Soc. Jpn.*, 1995, **68**, 2465; P. D. Beer, P. A. Gale, Z. Chen and M. G. B. Drew, *Supramol. Chem.*, 1996, **7**, 241; A. R. van Doom, M. Bos, S. Harkema, J. van Eerden, W. Verboom and D. N. Reinhoudt, *J. Org. Chem.*, 1991, **56**, 2371; A. Ori and S. Shinkai,, *J. Chem. Soc., Chem. Commun.*, 1995, 1771.
6 P. A. Brooksby, C. A. Hunter, A. J. McQuillan, D. H. Purvis, A. E. Rowan, R. J. Shannon and R. Walsh, *Angew. Chem., Int. Ed. Engl.*, 1994, **33**, 2489; L. Zhang, A. Macias, T. Li, J. L. Gordon, G. W. Gokel and A. E. Kaifer, *J. Chem. Soc., Chem. Commun.*, 1993, 1017.
7 (*a*) M. S. Goodman, A. D. Hamilton and J. Weiss, *J. Am. Chem. Soc.*, 1995, **117**, 8447; (*b*) A. D. Burrows, C. W. Chan, M. M. Chowdhry, J. E. McGrady and D. M. P. Mingos, *Chem. Soc. Rev.*, 1995, **24**, 329; (*c*) C. Li, J. C. Medina, G. E. M. Maguire, E. Abel, J. L. Atwood and G. W. Gokel, *J. Am. Chem. Soc.*, 1997, **119**, 1609; (*d*) C. M. White, M. Fernandez Gonzalez, D. A. Bardwell, L. H. Rees, J. C. Jeffery, M. D. Ward, N. Armaroli, G. Calogero and F. Barigelletti, *J. Chem. Soc., Dalton Trans.*, 1997, 727 and references cited therein.
8 T. Okamura, N. Ueyama, A. Nakamura, E. W. Ainscough, A. M. Brodie and J. M. Waters, *J. Chem. Soc., Chem. Commun.*, 1993, 1658.
9 J. D. Carr and J. H. R. Tucker, unpublished work.
10 F. Garcia-Tellado, S. Goswami, S. K. Chang, S. J. Geib and A. D. Hamilton, *J. Am. Chem. Soc.*, 1990, **112**, 7393.
11 C. D. Hall, N. W. Sharpe, I. P. Danks and Y. P. Sang, *J. Chem. Soc., Chem. Commun.*, 1989, 419; J. C. Medina, T. T. Goodnow, S. Bott, J. L. Atwood, A. E. Kaifer and G. W. Gokel, *J. Chem. Soc., Chem. Commun.*, 1991, 290.
12 M. H. Abraham, *Chem. Soc. Rev.*, 1993, **22**, 73.

*Received in Liverpool, UK, 8th May 1997; 7/03183A*

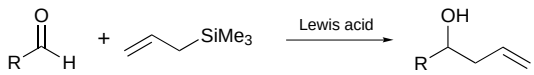
# $Yb(OTf)_3$ catalysed allylation of the hydrates of α-keto aldehydes and glyoxylates with allylsilane

**Yang Yang, Mingwen Wang and Dong Wang***

*Institute of Chemistry, Chinese Academy of Sciences, Beijing 100080, P. R. China*

**$Yb(OTf)_3$ catalysed allylation reactions of the hydrates of α-keto aldehydes and glyoxylates with allyltrimethylsilane at room temperature give α-keto and α-ester homoallylic alcohols in good yield.**

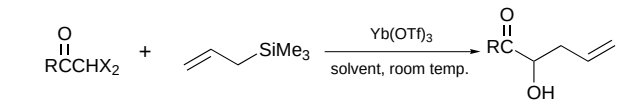
Recently, lanthanide trifluoromethanesulfonates [lanthanide triflates, $Ln(OTf)_3$] have attracted attention[1] because of their catalytic ability in various Lewis acid promoted carbon–carbon bond forming reactions, including Diels–Alder reactions,[2] Michael reactions[3] and allylation reactions of carbonyl compounds by allyl metals, for example allyltributylstannane and tetraallylgermane.[4] Kobayashi[5] also reported the $Ln(OTf)_3$ catalysed reaction of enol silyl ethers with carbonyl compounds (Mukaiyama aldol reaction) in aqueous media. Among the Lewis acid promoted C–C bond forming reactions, the allylation of carbonyl compounds with allylsilanes (Sakurai reaction,[6] Scheme 1) is one of the most important reactions in organic synthesis. However, stoichiometric amounts of Lewis acid must be employed due to the low nucleophilicity of allylsilane and the tight binding of the produced homoallylic alkoxide to the Lewis acid. The reaction can be performed using sub-stoichiometric amounts of silylating reagent [$Me_3SiOTf$, $Me_3SiI$ and $Me_3SiB(OTf)_4$],[7] while the $Ln(OTf)_3$ catalysed Sakurai reaction was not realized until quite recently.[8] Compared with typical Lewis acids such as $TiCl_4$, $SnCl_4$, $BF_3$ and $AlCl_3$, $Ln(OTf)_3$ possesses stronger Lewis acidity, and is water soluble or water-tolerant, air-stable and easy to handle, not requiring anhydrous treatment. On the basis of the tolerance of $Ln(OTf)_3$ to active protons, we examined the ytterbium trifluoromethanesulfonate [$Yb(OTf)_3$] catalysed allylation of α-keto aldehydes hydrates **2**–**4** and glyoxylate hydrates **5** and **6** with allyltrimethylsilane **1**. We also explored the extent of asymmetric induction in the allylation reactions of chiral glyoxylate hydrate **6** in the presence of catalyst $Yb(OTf)_3$.




**Scheme 1**

Oxidation of the substituted acetophenones with selenium dioxide gave the corresponding hydrates **2**–**4**, while the (−)-menthyl glyoxylate monohydrate **6** was prepared according to Kornblum's method,[9] starting from (−)-menthol. The allylation reactions (Scheme 2) were carried out following a standard procedure. To a solution of the hydrate (0.25 mmol) and $Yb(OTf)_3$ (0.025 mmol) in 2 ml of $CH_2Cl_2$, allyltrimethylsilane (0.3 mmol) was added, followed by stirring for a given time (Table 1) at room temperature. The reaction mixture was worked up with brine and extracted with $Et_2O$. The crude product was purified by flash chromatography. The experimental results are listed in Table 1.

Compounds with α-keto and α-ester homoallylic alcohol moieties have been used as precursors for a number of biologically active natural products such as antibiotics.[10] Among the procedures currently available for the preparation of these compounds, allylation of α-keto aldehydes and glyoxylates using allyltrimethylsilane promoted by Lewis acids is a convenient method. However, the α-keto aldehyde and glyoxylates are often moisture sensitive and easily hydrated and polymerized. In practice, although the hydrates are more stable to air and moisutre, it is necessary to transform them to the corresponding α-keto aldehydes and glyoxylates before carrying out the Lewis acid promoted reaction, in order to avoid interaction between the Lewis acid and the hydroxy group. Under conventional Lewis acid conditions, hydroxy




**2** R = Ph, X = OH
**3** R = *p*-$HOC_6H_4$, X = OH
**4** R = *p*-$MeOC_6H_4$, X = OH
**5** R = BuO, X = OH
**6** R = menthylO, X = OH
**7** R = BuO, $X_2$ = O
**8** R = Ph, $X_2$ = O

**1**

**9** R = Ph
**10** R = *p*-$HOC_6H_4$
**11** R = *p*-$MeOC_6H_4$
**12** R = BuO
**13** R = menthylO

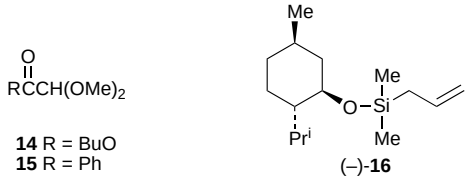
**Scheme 2**

**Table 1** $Yb(OTf)_3$ catalysed allylation of hydrates **2**–**6** and glyoxylates **7** and **8** at room temperature

| Entry | Substrate | Catalyst mol% | Solvent | *t*/h | Product | Yield[a] (%) | De (%) (Config.) |
|---|---|---|---|---|---|---|---|
| 1 | **2** | 10 | $CH_2Cl_2$ | 2 | **9** | 71 | |
| 2 | **3** | 10 | MeCN | 20 | **10** | 74 | |
| 3 | **4** | 10 | MeCN | 20 | **11** | 65 | |
| 4 | **5** | 10 | $CH_2Cl_2$ | 1.5 | **12** | 76 | |
| 5 | **6** | 10 | $CH_2Cl_2$ | 2 | **13** | 69 | 5 (*S*) |
| 6[b] | **6** | 10 | $CH_2Cl_2$ | 24 | **13** | 49 | 8 (*S*) |
| 7 | **6** | 10 | MeCN | 4 | **13** | 80 | 10 (*S*) |
| 8 | **6** | 10 | dioxane | 20 | **13** | 76 | 30 (*S*) |
| 9[c] | **6** | 10 | $CH_2Cl_2$ | 2 | **13** | 71 | 21 (*S*) |
| 10[c] | **6** | 10 | dioxane | 10 | **13** | 76 | 10 (*R*) |
| 11 | **7** | 5 | MeCN | 0.5 | **12** | 75 | |
| 12 | **8** | 5 | MeCN | 0.5 | **9** | 83 | |

[a] Isolated yield. [b] Performed at 0 °C. [c] Using (−)-**16** instead of **1**.

groups in the substrates need to be protected. In contrast, the results (entries 1–5) obtained here show that the catalytic capability of $Yb(OTf)_3$ appears not to be affected by hydroxy groups on the substrate, including the phenoxy group in **3**. The reactions proceeded smoothly with a catalytic amount of $Yb(OTf)_3$ (10 mol%), giving α-keto homoallylic alcohols **9**–**11** and α-ester homoallylic alcohols **12** and **13** in good yields (65–83%). The various substrates exhibited different reactivity, the glyoxylate hydrates **5** and **6** being more reactive than the α-keto aldehyde hydrates **2**–**4** (*cf.* entry 7 *vs.* entries 2 and 3). The solvents used strongly influenced the reaction rate, which is fast in $CH_2Cl_2$ but slow in 1,4-dioxane. For the hydrates **3** and **4**, MeCN is the solvent of choice becasue of the low solubility of the hydrates in $CH_2Cl_2$ and 1,4-dioxane. On reducing the reaction temperature to 0 °C, the reaction slowed down noticeably (*cf.* entry 5 *vs.* entry 6). While the aldehyde hydrates can be considered as equivalent to an aldehyde carbonyl function in these catalytic allylation reactions, the aldehyde carbonyl groups themselves are more reactive (entries 11 and 12 *vs.* entries 4 and 1). On the other hand, if the corresponding acetals **14** and **15** were used, $Yb(OTf)_3$ catalysed allylation with




**1** did not proceed at all, even in the presence of 20 mol% of catalyst.

When chiral glyoxylate hydrate **6** was employed, catalytic diastereoselective allylation occurred. The diastereoselectivity (de) of the reactions was low to moderate (5–30%), determined by the ratio of absorptions of diastereomeric protons in the $^1H$ NMR spectrum of the product **13**. The absolute configuration of the newly formed stereogenic centre was deduced through comparison with an authentic compound.[11] The de of the product strongly depended on the solvents used, with moderate de (30%) obtained in 1,4-dioxane, and rather poor de in $CH_2Cl_2$ and MeCN. Reducing the reaction temperature to 0 °C did not improve the de (entry 6). It is interesting to note that if (−)-allyldimethyl[(1*R*,2*S*,3*R*)-menthoxy]silane **16** was used, the de (*cf.* entry 5 *vs.* entry 9) increased noticeably (from 5 to 20%), but with 1,4-dioxane as the reaction solvent the absolute configuration of the new stereogenic centre was reversed. All these results indicated that the chiral group on the silicon participated in the stereocontrol of the allylation reaction. This is different from the conventional Lewis acid ($TiCl_4$, $AlCl_3$ and $BF_3$) promoted allylation of **6** with **16**, where the chiral group on the silicon did not affect the de of the product **13** to any significant extent.[11]

To our knowledge, these results are the first example of $Ln(OTf)_3$ catalysed allylation of aldehydes bearing unprotected hydroxy groups with allylsilane. $Ln(OTf)_3$ is therefore a novel mild catalyst for allylation with allylsilanes which is tolerant to substrates with active protons. It is expected that this $Ln(OTf)_3$ catalysed allylation reaction should also be effective in aqueous media.

We gratefully acknowledge financial support by the National Natural Science Foundation of China and the National Laboratory of Elemento-Organic Chemistry in Nankai University of China, and thank Professor T. H. Chan for helpful discussions.

## Footnote and References

* E-mail: dwang1@home.icm.ac.cn

1 R. W. Marshman, *Aldrichim. Acta*, 1995, **28**, 77 and references cited there.
2 S. Kobayashi, I. Hachiya, H. Ishitani and M. Araki, *Tetrahedron Lett.*, 1993, **34**, 4535.
3 S. Kobayashi, I. Hachiya, Y. Takahori, M. Araki and H. Ishitani, *Tetrahedron Lett.*, 1992, **33**, 6815.
4 T. Akiyama and J. Iwai, *Tetrahedron Lett.*, 1997, **38**, 853; H. C. Aspinall, A. F. Browning, N. Greeves and P. Ravenscroft, *Tetrahedron Lett.*, 1994, **35**, 4639.
5 S. Kobayashi and I. Hachiya, *J. Org. Chem.*, 1994, **59**, 3590.
6 H. Sakurai, *Pure Appl. Chem.*, 1982, 1; A. Hosomi and H. Sakurai, *Tetrahedron Lett.*, 1976, **17**, 1295.
7 T. Tsunoda, M. Suzuki and R. Noyori, *Tetrahedron Lett.*, 1980, **21**, 71; H. Sakurai, K. Sasaki and A. Hosomi, *Tetrahedron Lett.*, 1981, **22**, 745; A. P. Davis, and M. Jaspars, *Angew. Chem., Int. Ed. Engl.*, 1992, **31**, 470.
8 V. K. Aggrawal and G. P. Vennall, *Tetrahedron Lett.*, 1996, **37**, 3745.
9 N. Kornblum and H. W. Frazier, *J. Am. Chem. Soc.*, 1966, **88**, 365.
10 J. K. Whitesell, *Acc. Chem. Res.*, 1985, **18**, 280; P. Grossen, P. Herold, P. Mohr and C. Tamn, *Helv. Chim. Acta*, 1984, **67**, 1625; K. Mikami and T. Nakai, *J. Org. Chem.*, 1991, **56**, 2952.
11 Y. J. Chen, L. Huang, D. Wang and J. S. Li, *Chin. J. Chem.*, 1994, **12**, 440.

*Received in Cambridge, UK, 30th June 1997; 7/04560C*

# Preparation and X-ray crystallographic characterisation of the trititanate $[Ti_3O(\mu\text{-}OPr^i)_3(OPr^i)_4\{Me_2C(O)CH{=}C(O)CH_2C(O)Me_2\}]$, a reaction product of $[Ti(OPr^i)_4]$ and propan-2-one

**James V. Barkley, Jason C. Cannadine, Ian Hannaford, Marjorie M. Harding, Alexander Steiner, John Tallon and Robin Whyman***

*Department of Chemistry, University of Liverpool, PO Box 147, Liverpool, UK L69 7ZD*

**Reaction of $Ti(OPr^i)_4$ with propan-2-one, under initially anhydrous conditions, yields a colourless moisture-sensitive crystalline product which is structurally identified as the trinuclear oxoalkoxide $[Ti_3O\{\mu\text{-}OPr^i)_3(OPr^i)_4\{Me_2C(O)CH{=}C(O)CH_2C(O)Me_2\}]$ containing a coordinated $C_9$ ligand derived from the condensation of propan-2-one.**

There is considerable current interest in the identification and structural characterisation of titanium(IV) polyoxoalkoxides of the general formula $[Ti_xO_y(OR)_{4x-2y}]$ (where the value of $y/x$ is defined as the degree of condensation) which comprise intermediates in the condensation process between molecular $Ti(OR)_4$ entities and bulk $TiO_2$.[1] At present several structurally characterised titanium(IV) polyoxoalkoxides are known, with $y/x$ values in the range 0.57–1.33, as exemplified by $[Ti_{16}O_{16}(OEt)_{32}]$ and $[Ti_7O_4(OEt)_{20}]$. The lowest degree of polycondensation ($y/x$ = 0.33) to be found in these types of complexes is represented by a single example of a recently structurally characterised trinuclear oxoalkoxide $[Ti_3O(OMe)(OPr^i)_9]$, obtained from the reaction of $[Ti(OPr^i)_4]$ with water and methanol in isopropyl alcohol solution.[1] Titanium alkoxides are themselves widely used as catalysts for esterification, transesterification, and condensation reactions, and cross-linking of ester-containing resins and epoxides.[2] The reaction mechanisms involved in many of these transformations remain somewhat obscure although they are commonly interpreted in terms of the intermediacy of simple mononuclear titanium alkoxide complexes.[3,4]

Since the production of condensed titanium(IV) polyoxoalkoxides generally involves the controlled hydrolysis of the parent alkoxides, we reasoned that the ready ability of aldehydes and ketones to undergo condensation reactions of the aldol type,[4] with the co-production of water, might (*i*) facilitate such hydrolyses with a high degree of control and (*ii*) lead to the possible isolation and detection of coordinated intermediate fragments of aldol coupling. Consistent with this idea we have found that mixing $[Ti(OPr^i)_4]$ with freshly distilled dry propan-2-one and allowing to stand at room temp. under an atmosphere of dry dinitrogen leads to the deposition of a highly moisture-sensitive colourless crystalline product from a yellow solution.† X-Ray crystallographic analysis has shown this to represent the second example of a presumed family of low-nuclearity titanium polyoxoalkoxides based on a $Ti_3O_{11}$ core, which is formulated as

$[Ti_3O(\mu\text{-}OPr^i)_3(OPr^i)_4\{Me_2C(O)CH{=}C(O)CH_2C(O)Me_2\}]$ **1**

The molecular structure of **1**‡ (Fig. 1) contains a trinuclear $Ti_3O$ core supported by three doubly bridging [O(4), O(4a), O(4b)] and four monodentate isopropoxide groups. Three of the latter [O(5), O(5a), O(5b)] are located on one side of the $Ti_3$-triangular face within which the $\mu_3$-oxygen atom O(3) is situated, and the fourth $OPr^i$ group O(2″) is on the other side together with the tridentate $C_9$ ligand, which is the enolate form of a trimeric condensation product of propan-2-one, 2,6-dimethylhept-3-en-2,4,6-triol. The 2,6-oxygen atoms [O(2), O(2′)] of the enolate ligand are each coordinated in a monodentate manner to separate titanium atoms, while the central four-coordinate oxygen atom O(1) occupies a triply bridging position within interaction distance of all three titanium atoms, yielding a central $Ti_3O_{11}$ core which corresponds to the central arrangement of three distorted face sharing octahedra found in $[Ti_3O(OMe)(OPr^i)_9]$ (where a methoxide ligand provides the second $\mu_3$-O unit).

The space group symmetry $R\bar{3}$ m in the crystal structure of **1** implies a molecular $C_{3v}$ symmetry. Fig. 2 illustrates the resulting disorder at the $C_9$-ligand face to the $Ti_3$ triangle, which is generated by a crystallographic threefold axis and three associated mirror planes. Therefore both terminally arranged $Me_2CO$ units [O(2), C(3), C(4), C(5) and O(2)′, C(3′), C(4′), C(5′)] of the enolate ligand and the monodentate isopropoxide ligand [O(2″), C(3″), C(4″), C(5″)] occupy crystallographically identical positions. Beyond it the methyl groups are split over two positions. In the central ligand unit [–CH=C(O)–$CH_2$–] the oxygen atom O(1) is located on a fully occupied site (3 m), while C(1) in α position is symmetrically distributed over three and C(2) in β position over six sites, resulting in crystallographically identical positions for the $sp^2$ hybridised alkenic centre C(2) and the $sp^3$ hybridised methylene centre C(2′). However owing to the crystal symmetry, both central ligand bonds C(1)=C(2) [1.320(9) Å] and C(1)–C(2′) [1.620(9) Å] are

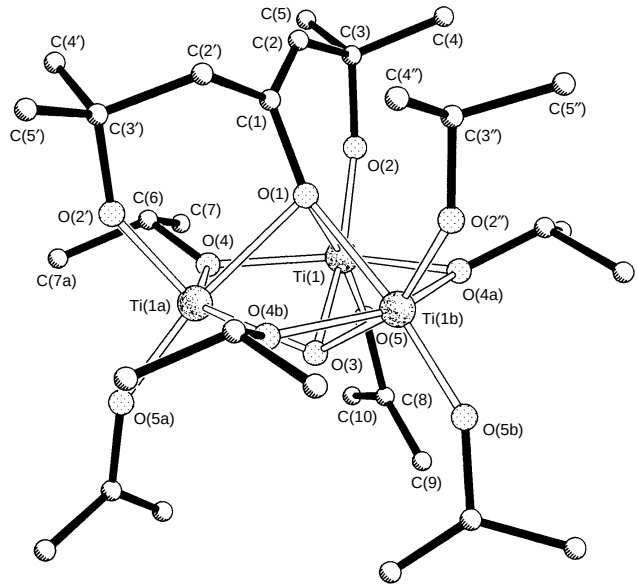



**Fig. 1** Molecular structure of **1**. Selected interatomic distances (Å) and angles (°): Ti(1)···Ti(1a) 2.962(2), Ti(1)–O(1) 2.205(4), Ti(1)–O(2) 1.803(3), Ti(1)–O(3) 1.969(4), Ti(1)–O(4) 2.024(3), Ti(1)–O(5) 1.780(4), O(1)–C(1) 1.47(2), C(1)–C(2) 1.32(2), C(1)–C(2′) 1.62(2), C(2)–C(3) 1.56(2), O(2)–C(3) 1.43(2); C(2)–C(1)–C(2′) 125(1), C(1)–C(2)–C(3) 111(1), C(1)–C(2′)–C(3′) 131(1).

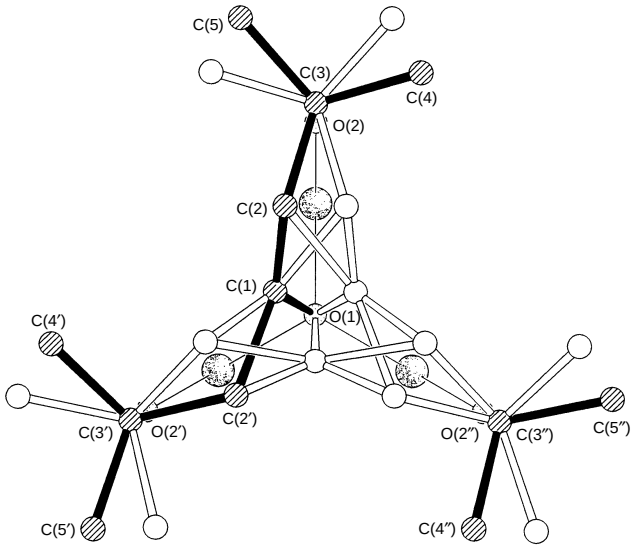
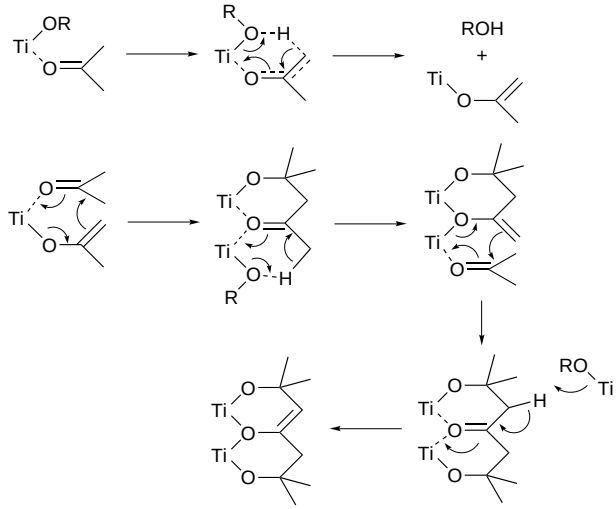



**Fig. 2** $C_9$-ligand face of $Ti_3$ unit illustrating the disorder along the crystallographic threefold axis. The six remaining $OPr^i$ ligands have been omitted for clarity.

chemically as well as crystallographically non-equivalent, because each one is generated by a different symmetry operation [relative to C(1)].

The very closely related structures of **1** and $[Ti_3O(OMe)(OPr^i)_9]$, where formally the tridentate $C_9$-ligand is substituted by one methoxide and two isopropoxide ligands illustrates a highly flexible ligand behaviour on a more or less rigid $Ti_3O_{11}$ core, which then can act as a template in the formation of the $C_9$-triolate ligand by a co-condensation reaction of three enolate moieties derived from propan-2-one.

Consistent with the structural observations relating to the identification and characterisation of the coordinated $C_9$ triolate ligand, GC–MS analysis of the mother-liquors from which the crystals were isolated confirms the presence of the common aldol condensation products of propan-2-one, namely, 4-methylpent-3-en-2-one (mesityl oxide) and 2,6-dimethylhepta-2,5-dien-4-one (phorone), together with propan-2-one and isopropyl alcohol. In addition, $^1$H NMR spectra of the reaction solutions show the appearance of new resonances at $\delta$ 1.87 and 6.09 which may be attributed to the presence of phorone and/or mesityl oxide and $\delta$ 3.56 which is consistent with the presence of hydroxyl protons present in, for example, diacetone alcohol. In view of the mild reaction conditions used in the preparative work, it is not unlikely that initially formed hydroxylated products of condensation are also present in the reacting solution but are dehydrated to, for example, mesityl oxide, within the injection ports of the gas chromatograph.




**Scheme 1**

The mechanism by which this unprecedented reaction product is formed is at present unclear. Notwithstanding an equilibrium constant (in water) of $2.5 \times 10^{-6}$ for the enolisation of propan-2-one[5] it seems most likely that the initial step in the reaction the involvement of coordination of propanone in the enolate form to the titanium centre, followed by the titanium alkoxide promoted oligomerisation reaction, as indicated in Scheme 1.§ Such reactions may prove, contrary to conventional wisdom,[3,4] the involvement of polynuclear rather than mononuclear reaction intermediates. Finally, it should be noted that the isolation and characterisation of **1** may also be of relevance to processes occurring during the initial stages of formation of polyketones.

The authors wish to thank Tioxide Specialties Ltd for supply of tetraisopropyltitanate, Mr J. Ridland (Tioxide) for helpful discussions, ICI Chemicals and Polymers Ltd for support (to J. C. C.) and Mr A. Mills (Liverpool) for the measurement of mass spectra.

## Footnotes and References

* E-mail: whyman@liverpool.ac.uk

† *Preparative details*: Mixtures of dried, freshly distilled propan-2-one and $[Ti(OPr^i)_4]$ in molar ratios ranging between 1 : 1 and 10 : 1 were allowed to stand under an atmosphere of dinitrogen. The solutions were initially colourless, became yellow over several hours following which large irregular three-dimensional colourless crystals deposited on standing for 2–3 days. These crystals continued to grow in needle-like columns if the solutions were allowed to stand for several weeks. The mother-liquors were decanted from the crystals which were washed several times with dry propan-2-one and subsequently dried under vacuum.

*Selected data for* **1**: IR(Nujol mull): $\nu$(C=C) of unsaturated coordinated triolate ligand, 1656 cm$^{-1}$. FABMS (3-noba): *m/z* 685 $[M^+ - 59\ (OPr^i)]$, 627 $[M^+ - 117\ (OPr^i + OC_3H_6)]$, 385 $[Ti_2(OPr^i)_2(C_9H_{15}O_3)]$ and 343 $[Ti_2(OH)(OPr^i)(C_9H_{15}O_3)]$, isotopic simulations consistent with these fragments, together with several sequences of higher masses at repeat intervals of 80 mass units which presumably correspond to the formation of poly-$TiO_2$ cluster ions within the mass spectrometer.

‡ *Crystal data* for **1**: $C_{30}H_{64}O_{11}Ti_3$, $M_w$ = 744.51, rhombohedral, space group $R\bar{3}m$, $a$ = 17.894(3), $c$ = 21.021(4) Å, $U$ = 5829(2) Å$^3$, $Z$ = 6, $\lambda$ = 0.71073 Å, $T$ = 153(2) K, $D_c$ = 1.273 Mg m$^{-3}$, $\mu$(Mo-K$\alpha$) = 0.651 mm$^{-1}$. Data were collected on a Rigaku AFC6S diffractometer using a crystal of dimensions 0.25 × 0.20 × 0.75 mm. Of a total of 2480 reflections ($2\theta_{max}$ = 50°), 1271 were independent ($R_{int}$ = 0.028). The structure was solved by direct methods (SHELXS-86) and refined by full-matrix least squares on $F^2$ using all data to final values of $R_1$ = 0.051 [$F > 4\sigma F$ (1014 reflections)], $wR_2$ = 0.139 (all data) (SHELXS-93). Largest features in the final difference map, 0.618 and −0.325 e Å$^{-3}$. All non-hydrogen positions have been refined anisotropically. Hydrogen positions have been set geometrically. In addition to the disorder of the $C_9$-ligand face at the central $Ti_3$ unit, which is described in the text, isopropoxide ligands at the opposite face of the metal plane are disordered and could be refined on two positions. No restraints have been applied at all in final refinement cycles. Refinements in the lower symmetry space groups $R\bar{3}$ and $R32$, respectively, gave either twinning or occupancy factors of 50% and led to higher $R$ factors in connection with considerable correlation between higher symmetry dependent parameters. CCDC 182/544.

§ The authors wish to acknowledge a referee for supporting the inclusion of a plausible reaction mechanism.

1 V. W. Day, T. A. Eberspacher, Y. Chen, J. Hao and W. Klemperer, *Inorg. Chim. Acta*, 1995, **229**, 391 and references therein.
2 C. S. Rondestvedt, *Kirk Othmer Encyclopaedia of Chemical Technology*, Wiley-Interscience, New York, 3rd edn., 1983, vol. 23, p. 176.
3 G. W. Parshall and S. D. Ittel, *Homogeneous Catalysis*, Wiley-Interscience, New York, 2nd edn., 1992, ch. 11.
4 R. Mahrwald and H. Schick, *Synthesis*, 1990, 592.
5 S. Forsen and M. Nilsson, *The Chemistry of the Carbonyl Group*, ed. J. Zabicky, Interscience, London, 1970, vol. 2, p. 163.

*Received in Cambridge, UK, 9th June 1997; 7/04000H*

# Synthesis, characterisation and reactivity of novel bis(tosyl)imidoruthenium(VI) porphyrin complexes; X-ray crystal structure of a tosylamidoruthenium(IV) porphyrin

**Sze-Man Au,[a] Wai-Hong Fung,[a] Ming-Chuan Cheng,[a] Chi-Ming Che*[a] and Shie-Ming Peng†[b]**

[a] *Department of Chemistry, The University of Hong Kong, Pokfulam Road, Hong Kong*
[b] *Department of Chemistry, National Taiwan University, Taipei, Taiwan*

**Bis(tosyl)imidoruthenium(VI) porphyrin complexes are prepared and characterised by spectroscopic means; [$Ru^{VI}$(tpp)$(NTs)_2$] can undergo imido group transfer reactions with alkenes to afford aziridines, as well as C–H bond oxidation of benzyl alcohol to give benzaldehyde; a tosylamido ruthenium(IV) complex is also isolated and characterised by X-ray diffraction.**

The transition metal catalysed aziridination of alkenes by PhINTs provides direct access to aziridines from alkenes. This reaction can be performed selectively and, in some cases, high enantioselectivity can be attained.[1–3] However, the mechanism of the reaction remains elusive, it becomes difficult to improve the catalysis in a rational manner. Although both the metal–imido species [M=NTs] and the Lewis-acid PhINTs adduct [M–N(Ts)(IPh)] have been proposed to be the reactive intermediates, neither has been isolated or spectroscopically characterised.[1] Reports on imidoruthenium complexes remain sparse, notable examples include [$Ru^{VI}$(tpp)$(NBu^t)$O],[4] *trans*-[$Ru^{IV}(NBu^t)_2(PMe_3)_4$][5] and [$Ru^{II}{\equiv}NC_6H_2Bu^t_3$-2,4,6)($\eta^6$-*p*-cymene)],[6] but none of them are known for imido group transfer reactions with alkenes. Indeed, there are few reports in the literature concerning alkene aziridination reactions using a well characterised metal–imido complex.[7] Herein we describe the synthesis, spectroscopic characterisation and reactivities of the bis(tosyl)imidoruthenium(VI) porphyrin complexes [$Ru^{VI}$(tpp)$(NTs)_2$] **1** and [$Ru^{VI}$(oep)$(NTs)_2$] **2** (tpp = dianion of 5,10,15,20-tetraphenylporphyrin, oep = dianion of 2,3,7,8,12,13,17,18-octaethylporphyrin, Ts = tosyl).

Complexes **1** and **2** were prepared by the treatment of the corresponding [$Ru^{II}$(por)(CO)(MeOH)] complexes[8] (por = dianion of porphyrin, 0.2 mmol) with PhINTs[9] (0.6 mmol) in dried $CH_2Cl_2$ (20 ml) for 5 min at room temp. under an inert atmosphere. Removal of the solvent followed by washing with MeOH afforded the desired products as red–violet solids. The complexes were further purified by chromatography on a short neutral alumina column with $CH_2Cl_2$ as the eluent (overall yield 60%†).

The imidoruthenium(VI) complexes **1** and **2** are stable in the solid state at −20 °C for days, whereas in purified $CH_2Cl_2$ the compounds can be kept for hours at room temp. without significant decomposition. Their UV–VIS absorption spectra highly resemble those of structurally related dioxoruthenium(VI) porphyrin complexes[10,11] (Fig. 1). The IR spectra of **1** and **2** exhibit intense $\nu_{as}$(Ru=NTs) stretching absorptions at 914 and 900 $cm^{-1}$ respectively, which are at lower wavenumbers than the $\nu_{as}$(Os=NTs) absorption at 924 $cm^{-1}$ found in [$Os^{VI}$(tpp)$(p\text{-}NC_6H_4NO_2)_2$].[12] It is important to note that the oxidation state markers for **1** and **2** appear at 1016 and 1018 $cm^{-1}$ respectively, which is in accordance with the formulation of the ruthenium(VI) oxidation state.[10a,11] The diamagnetic behaviour of the complexes, together with the above findings, strongly suggest a terminal $d^2$ metal–imido system. $^1$H NMR spectra reveal that **1** and **2** possess pseudo $D_{4h}$ symmetry, and the aromatic protons of the Ts groups (H′ and H″) appear as doublets at $\delta$ 6.45 and 4.87. The pyrrolic protons for **1** ($\delta$ 8.82) appear at higher field than that for [$Ru^{VI}$(tpp)$O_2$] ($\delta$ 9.1),[10] this coincides with the fact that the (tosyl)imido ligand is a stronger $\pi$ donor than the oxo ligand.[12]

At room temp., **1** reacts readily with alkenes to give aziridines in good yields (Table 1). With the addition of pyrazole (Hpz), apart from aziridines [$Ru^{IV}$(tpp)(NHTs)(pz)] **3** (NHTs = tosylamido) was also isolated and characterised.‡ The UV–VIS and IR absorption spectra of **3** (oxidation marker band at 1012 $cm^{-1}$) are very similar to those observed for [$Ru^{IV}$(tpp-$(OMe)_3$-3,4,5)$(NPh_2)_2$][tpp-$(OMe)_3$-3,4,5 = dianion of *meso*-tetrakis(3,4,5-trimethoxyphenyl)porphyrin].[13] Together with the magnetic susceptibility measurement [$\mu_{eff}$ = 3.20 $\mu_B$ (300 K), Evans method], the formulation as ruthenium(IV) with two unpaired electrons in the ground state is confirmed. The

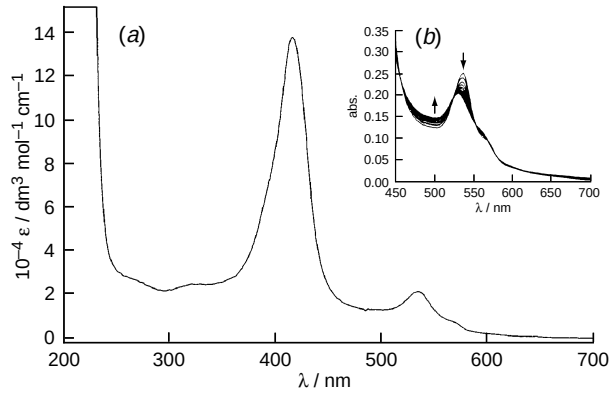



**Fig. 1** (*a*) UV–VIS spectrum of [$Ru^{VI}$(tpp)$(NTs)_2$] **1**; (*b*) UV–VIS spectral trace for the reaction of **1** with styrene in $CH_2Cl_2$ (2% pyrazole) (450–700 nm)

**Table 1** Stoichiometric alkene aziridination and C–H oxidation of benzyl alcohol by [$Ru^{VI}$(tpp)$(NTs)_2$]

| Entry | Substrate | Product | Yield[a] (%) |
|---|---|---|---|
| 1 | Ph | Ph, NTs | 75 |
| 2 | *p*-$MeC_6H_4$ | *p*-$MeC_6H_4$, NTs | 78 |
| 3 | *p*-$ClC_6H_4$ | *p*-$ClC_6H_4$, NTs | 71 |
| 4 | | NTs | 68 |
| 5 | Ph, OH | PhCHO | 95 |
| | | $TsNH_2$ | 100 |

[a] Isolated yield based on the amount of [$Ru^{VI}$(tpp)$(NTs)_2$].

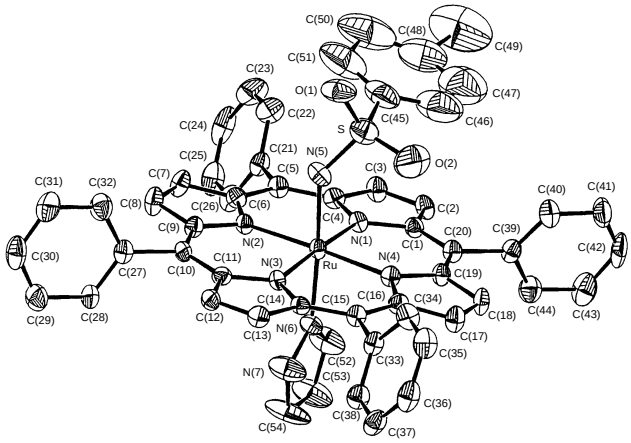



**Fig. 2** A perspective view of **3** with atom labelling scheme. Selected bond distances (Å) and angles (°): Ru–N(5) 2.025(11), Ru–N(6) 2.111(11), Ru–N(1) 2.041(8), Ru–N(2) 2.032(9), Ru–N(3) 2.033(8), Ru–N(4) 2.037(9); N(5)–Ru–N(6) 176.2(4), Ru–N(5)–S 136.4(7).

structure of **3** has been established by X-ray crystal analysis.‡ As shown in Fig. 2, the Ru–N(5) bond distance of 2.025(11) Å is comparable to the $Ru^{IV}$–N(amide) distances of 1.987–2.044(5) Å found in $[Ru^{IV}(chbae)(PPh_3)(py)]$ [chbae = 1,2-bis(3,5-dichloro-2-hydroxybenzamido)ethane tetraanion].[14] The Ru–N(5)–S(1) bond angle of 136.4(7)° is not unexpected for a coordinated amide ligand since a similar value of 138.4(6)° has been reported for $[Ru^{II}(Et_2dtc)(PPh_3)_2(CO)(NHSO_2C_6H_2Pr^i_3\text{-}2,4,6)]$ ($Et_2dtc$ = *N*,*N*'-diethyldithiocarbamate).[15]

The UV–VIS spectral trace for the reaction of **1** with excess styrene in $CH_2Cl_2$ containing pyrazole (2% m/m) exhibited clean isosbestic points [Fig. 1(*b*)]. The reactions of **1** with alkenes followed the second-order rate law, rate = $k_2[Ru^{VI}][alkene]$. The second-order rate constants $k_2$ measured at 298 K are $(9.7 \pm 0.3) \times 10^{-3}$ and $(1.1 \pm 0.1) \times 10^{-3}$ dm$^3$ mol$^{-1}$ s$^{-1}$for styrene and norbornene, respectively. The activation parameters for the styrene aziridination by **1** were determined to be $\Delta H^{\ddagger} = 4.7 \pm 0.1$ kcal mol$^{-1}$ and $\Delta S^{\ddagger} = -52.4 \pm 0.2$ cal K$^{-1}$ mol$^{-1}$ (1 cal = 4.184J). The negative value of $\Delta S^{\ddagger}$ is consistent with an associative mechanism. For the aziridination of various *para*-substituted styrenes (*p*-OMe, -Me, -F, -Cl, -$CF_3$) by **1**, the $k_2$ values were found to span a narrow range. The log $k_{rel}$ [$k_{rel} = k_2$(*p*-substituted styrene)/$k_2$(styrene)] values correlate linearly with the $\sigma^+$ values with a small magnitude of $\rho^+ = -1.1$ ($R = 0.98$); this indicates a minor development of positive charge in the transition state.

Stoichiometric oxidation of benzyl alcohol by **1** in dichloromethane containing pyrazole (2% m/m) gave benzaldehyde and tosyl amine quantitatively (Table 1), and **3** was formed as the product of the reduction of the imidoruthenium(VI) complex. The observed rate law for the reaction of benzyl alcohol with **1** was found to be: rate = $k_2[Ru^{VI}][PhCH_2OH]$, with the second-order rate constant of $(3.6 \pm 0.1) \times 10^{-1}$ dm$^3$ mol$^{-1}$ s$^{-1}$ at 298 K. It is noteworthy that a large primary kinetic isotope effect was observed using $PhCD_2OH$ ($k_H/k_D = 7.4$) indicating that the reaction should proceed *via* a hydrogen atom abstraction pathway.

We acknowledge support from The University of Hong Kong and the Hong Kong Research Grants Council.

## Footnotes and References

* E-mail: cmche@hkucc.hku.hk
† For correspondence regarding the crystallography.

‡ Satisfactory elemental analyses were obtained for all compounds. UV–VIS [$\lambda_{max}$/nm (log $\varepsilon_{max}$/dm$^3$mol$^{-1}$cm$^{-1}$)] ($CH_2Cl_2$): **1** 416 (5.14), 536 (4.18), 568 (3.77); **2** 406 (5.07), 520 (4.21), 551 (4.16); **3** 412 (5.07), 530 (3.96). $^1$H NMR (300 MHz, TMS, $CD_2Cl_2$): **1** $\delta_H$ 2.17(s, Me, 6H), 4.87(d, 4H), 6.45(d, 4H), 7.79(m, 12H), 8.18(m, 8H), 8.82(s, 8H); **2** $\delta_H$ 1.99(t, 24H), 2.29(s, 6H), 4.07(q, 16H), 4.63(d, 4H), 6.48(d, 4H), 10.0(s, 4H). IR (Nujol) **1** 914, 1016 cm$^{-1}$; **2** 900, 1018 cm$^{-1}$; **3** 1012 cm$^{-1}$.

§ *Crystal data* for **3**: $C_{54}H_{39}N_7O_2RuS$, $M = 951.09$, monoclinic, space group $P2_1/c$, $a = 13.308(2)$, $b = 14.473(5)$, $c = 25.678(6)$ Å, $\beta = 90.05(2)°$, $U = 4945.7(22)$ Å$^3$, $Z = 4$, $D_c = 1.277$ g cm$^{-3}$, $\mu = 33.162$ cm$^{-1}$, $F(000) = 1952$, crystal dimensions 0.03 × 0.10 × 0.50 mm. Intensity data were collected at 298 K on a Enraf-Nonius CAD4 diffractometer with graphite-monochromated Mo-Kα radiation ($\lambda = 1.5418$ Å). A total of 7540 unique reflections were measured and 4438 with $I > 2\sigma(I)$ were used as refinement; $R = 0.061$, $R_w = 0.087$, GOF = 1.43. The final Fourier difference map showed residual extrema in the range 1.36 to −0.650 e Å$^{-3}$. CCDC 182/535.

1 D. A. Evans, M. M. Faul and M. T. Bilodeau, *J. Am. Chem. Soc.*, 1994, **116**, 2742.
2 J. P. Mahy, G. Bedi, P. Battioni and D. Mansuy, *J. Chem. Soc., Perkin Trans. 2*, 1988, 1517.
3 R. Breslow and S. H. Gellman, *J. Chem. Soc., Chem. Commun.*, 1982, 1400.
4 J. S. Huang, C. M. Che and C. K. Poon, *J. Chem. Soc., Chem. Commun.*, 1992, 161.
5 A. A. Danopoulos, G. Wilkinson, B. Hussain-Bates and M. B. Hursthouse, *Polyhedron*, 1992, **11**, 2961.
6 A. K. Burrell and A. J. Steedman, *J. Chem. Soc., Chem. Commun.*, 1995, 2109.
7 J. T. Groves and T. Takahashi, *J. Am. Chem. Soc.*, 1983, **105**, 2073.
8 R. C. Young, J. K. Nagle, T. J. Meyer and P. G. Whitten, *J. Am. Chem. Soc.*, 1978, **100**, 4473.
9 Y. Yamada, T. Yamamoto and M. Okawara, *Chem. Lett.*, 1975, 361.
10 (*a*) W. H. Leung and C. M. Che, *J. Am. Chem. Soc.*, 1989, **111**, 8812; (*b*) C. Ho, W. H. Leung and C. M. Che, *J. Chem. Soc., Dalton Trans.*, 1991, 2933.
11 J. T. Groves and K. H. Ahn, *Inorg. Chem.*, 1987, **26**, 3831.
12 J. A. Smieja, K. M. Omberg and G. L. Breneman, *Inorg. Chem.*,1994, **33**, 614.
13 J. S. Huang, C. M. Che, Z. Y. Li and C. K. Poon, *Inorg. Chem.*,1992, **31**, 1315.
14 C. M. Che, W. K. Cheng, W. H. Leung and T. C. W. Mak, *J. Chem. Soc., Chem. Commun.*, 1987, 418.
15 W. H. Leung, M. C. Wu, J. L. C. Chim and W. T. Wong, *Inorg. Chem.*, 1996, **35**, 4801.

*Received in Cambridge, UK, 26th March 1997, 7/02093G*

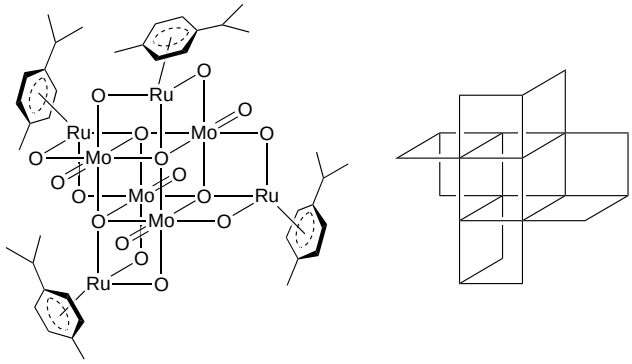
# $[(p\text{-}Pr^iC_6H_4Me)_4Ru_4Mo_4O_{16}]$: an amphiphilic organoruthenium oxomolybdenum cluster presenting a unique framework geometry

**Georg Süss-Fink,* Laurent Plasseraud, Vincent Ferrand and Helen Stoeckli-Evans**

*Institut de Chimie, Université de Neuchâtel, CH-2000 Neuchâtel, Switzerland*

**The amphiphilic title compound, easily accessible from (*p*-cymene)ruthenium dichloride dimer and sodium molybdate in aqueous solution, presents an unprecedented $Ru_4Mo_4O_{12}$ framework comprising a central $Mo_4O_4$ cube with four folded ORuO flaps resembling the sails of a windmill.**

The past two decades have witnessed a steadily growing interest in molecules containing both organometallic groups and oxometallic entities,[1] particularly since they provide molecular models for heterogeneous catalysts derived from organometallic complexes adsorbed at metal oxide surfaces.[2] Organometallic metaloxo clusters contain soft as well as hard metal centers, and hydrophobic as well as hydrophilic ligands. Since the discovery of the first species of this type, $[(C_5H_5)TiPW_{11}O_{39}]^{4-}$ in 1978,[3] this field has been pioneered mainly by the groups of Klemperer,[4] Isobe,[5] and Finke.[6] The combination of low- and high-valent transition metals and the amphiphilic character predispose these molecules also as homogeneous catalysts for oxidation reactions; the catalytic potential of these compounds has been reviewed recently.[7]



**1**

Here, we report the synthesis and structure of $[(p\text{-}Pr^iC_6H_4Me)_4Ru_4Mo_4O_{16}]$ **1**, a neutral organoruthenium oxomolybdenum cluster which presents an unprecedented geometry of the $Ru_4Mo_4O_{12}$ framework. Compound **1** is easily accessible from (*p*-cymene)ruthenium dichloride dimer and sodium molybdate in aqueous solution (Scheme 1).† Orange crystals of correct elemental composition are obtained by crystallization from dichloromethane–toluene. Compound **1** is amphiphilic, that is to say sparingly soluble in both water and aromatic hydrocarbons, and well soluble in polar organic solvents such as dichloromethane or methanol.

$$2\ [(p\text{-}Pr^iC_6H_4Me)_2Ru_2Cl_4] + 4\ Na_2MoO_4 \downarrow [(p\text{-}Pr^iC_6H_4Me)_4Ru_4Mo_4O_{16}] + 8\ NaCl$$

**Scheme 1**

The FAB mass spectrum of **1** shows the molecular ion at *m/z* 1581 presenting the expected $Ru_4Mo_4$ isotope pattern. In the $^1H$ NMR spectrum ($CD_2Cl_2$) of **1**, the four *p*-cymene ligands give rise to only one set of signals at $\delta$ 1.39 (d, 6, *J* 7 Hz), 2.27 (s, 3), 2.97 (spt, 1, *J* 7 Hz), 5.30 (d, 2, *J* 6 Hz) and 5.37 (d, 2, *J* 6 Hz), showing all ruthenium positions to be equivalent. In the IR spectrum (KBr) of **1**, the Mo=O stretching vibrations are observed at 921s and 874m $cm^{-1}$, while the Mo–O–Ru stretches are assigned to the absorptions at 785s, 739s, 642m and 602s $cm^{-1}$.

Single-crystal X-ray structure analysis§ of $\mathbf{1}\cdot 2C_6H_5Me$ (orange, rod-like crystals) revealed the molecule to contain a unique $Ru_4Mo_4O_{12}$ framework which can be described as a central $Mo_4O_4$ cube with four folded ORuO flaps resembling the sails of a windmill. The distortion [Mo(2)–O(2)–Mo(1) 106.04(12)°, O(12)–Mo(1)–O(2) 71.37(10)°] with respect to

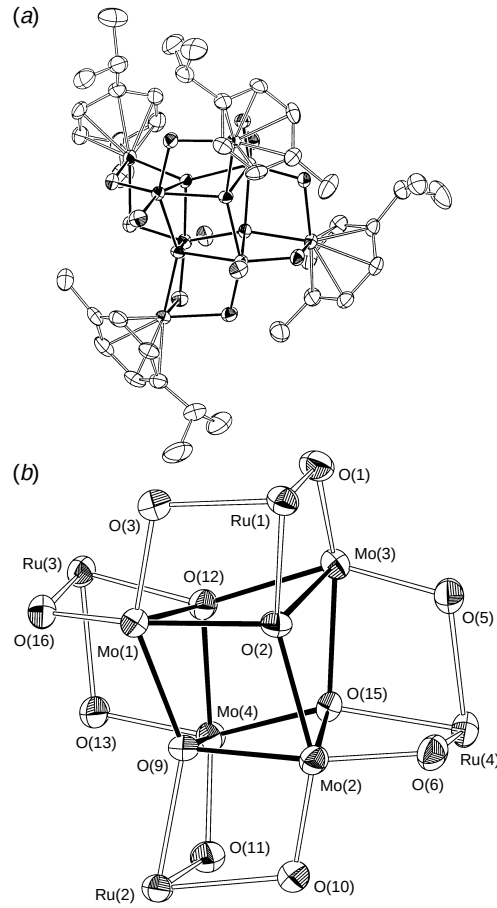
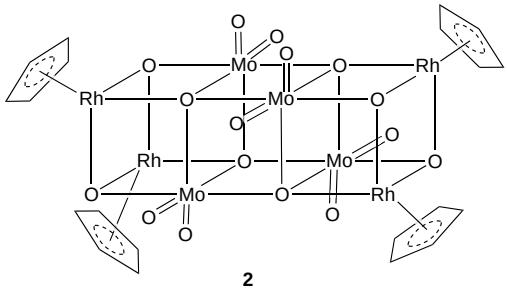



**Fig. 1** ORTEP[11] representation of the molecular structure of **1**. (*a*) Complete molecule, hydrogen atoms and two toluene molecules (in the crystal) omitted for clarity. (*b*) $Ru_4Mo_4O_{12}$ framework with labelling scheme. Selected bond distances and angles (°): Mo(1)–O(2) 2.122(3), Mo(1)–O(3) 1.804(3), Mo(1)–O(7) 1.706(3), Mo(1)–O(9) 2.073(3), Mo(1)–O(12) 2.365(3), Mo(1)–O(16) 1.798(3). Ru(1)–O(1) 2.088(3), Ru(1)–O(2) 2.089(3), Ru(1)–O(3) 2.094(3); O(12)–Mo(1)–O(9) 72.20(11), Mo(3)–O(12)–Mo(1) 105.31(11), O(7)–Mo(1)–O(16) 103.93(2). Ru(2)–O(9)–Mo(1) 145.40(2), O(10)–Ru(2)–O(11) 80.53(12).

the idealized cubic representation is due to the geometry of the oxygen atoms of the central cube which is more tetrahedral than octahedral (Fig. 1). Eight of the twelve framework oxygen atoms are doubly bridging, while four are quadruply bridging. Each ruthenium atom is coordinated to an $\eta^6$-*p*-cymene ligand [Ru(1)–$C_6$ ring centroid 1.627 Å], and each molybdenum atom carries a terminal oxo ligand [Mo(1)–O(7) 1.706(3) Å].

The cluster $[(C_5Me_5)_4Rh_4Mo_4O_{16}]$ **2**, reported by Isobe and coworkers,[5a] which is isoelectronic to **1**, has a completely different structure: the $Rh_4Mo_4O_{12}$ framework forms a triple cube which is more closed than the open windmill-like structure of **1**. As a consequence, each molybdenum atom carries two terminal oxo ligands, and four of the eight framework oxygen atoms are triply bridging, while the other four are quadruply bridging.




**2**

Another $Mo_4O_{16}$ unit, found in the solid phase $Cs_3Mo_4P_3O_{16}$, also contains a central $Mo_4O_{16}$ cube; however, the framework geometry is completely different: the $Mo_4O_{16}$ core must be considered as four $MoO_6$ octahedra each sharing three edges with three $MoO_6$ units giving an array with tetrahedral symmetry.[7]

Interestingly, with ruthenium the reaction seems to work only for the *p*-cymene derivative. Up to now it has not been possible to isolate the benzene and hexamethylbenzene analogues of **1**.

This work was supported by the Fonds National Suisse de la Recherche Scientifique (grant 20-46592.96). A generous loan of ruthenium trichloride hydrate from the Johnson Matthey Technology Centre is gratefully acknowledged.

## Footnotes and References

* E-mail: suess-fink@ich.unine.ch

† *Synthesis* of **1**: A suspension of $[(p\text{-}Pr^iC_6H_4Me)_2Ru_2Cl_4]$ (200 mg, $3.27 \times 10^{-4}$ mol) in 20 cm$^3$ of water was added dropwise to an aqueous solution (10 cm$^3$) of $Na_2MoO_4 \cdot 2H_2O$ (790 mg, $3.3 \times 10^{-3}$ mol). The mixture was stirred for 4 h at 25 °C. After evaporation of the water, the product was extracted with $CH_2Cl_2$ (20 cm$^3$) and crystallized from dichloromethane–toluene (1 : 1) to give, after drying *in vacuo*, analytically pure orange crystals (155 mg, 60%).

§ *Crystal structure data* for **1**: $C_{40}H_{56}Mo_4O_{16}Ru_4 \cdot 2C_7H_8$ (including two molecules of toluene per cluster), triclinic, space group, $P\bar{1}$, $a$ = 13.846(2), $b$ = 15.210(2), $c$ = 16.1038(14) Å, $\alpha$ = 88.124(11), $\beta$ = 78.938(10), $\gamma$ = 65.471(11)°, $U$ = 3023.7(6) Å$^3$, $Z$ = 2, $D_c$ = 1.939 g cm$^{-3}$, $T$ = 223 K, $\mu$(Mo-K$\alpha$) = 1.66 mm$^{-1}$. The data were measured using a Stoe-Siemens AED2 four-circle diffractometer with graphite-monochromated Mo-K$\alpha$ radiation ($\lambda$ = 0.710 73 Å). 11234 independent reflexions were measured by $\omega$–$2\theta$ scans in the range $2.0 < \theta < 25.5°$; 9939 were considered observed [$I > 2\,\sigma(I)$]. The structure was solved by Patterson and Fourier techniques using the program SHELXS-86[8] and refined by full-matrix least squares on $F^2$, using SHELXL-93.[9] Hydrogen atoms were included in calculated positions and treated as riding atoms using SHELXL-93 default parameters. An empirical absorption correction was applied using DIFABS[10] (transmission factors min., max. 0.722, 1.174). Refinement converged at $R_1$ = 0.0337 and $wR_2$ = 0.0757 (observed data). CCDC 182/532.

1 V. W. Day and W. G. Klemperer, *Science*, 1985, **228**, 533.
2 K. Isobe and A. Yagasaki, *Acc. Chem. Res.*, 1993, **26**, 524.
3 R. K. C. Ho and W. G. Klemperer, *J. Am. Chem. Soc.*, 1978, **100**, 6772.
4 H. K. Chae, W. G. Klemperer and V. W. Day, *Inorg. Chem*., 1989, **28**, 1424; H. K. Chae, W. G. Klemperer, D. E. Paez Loyo, V. W. Day and T. A. Ebersbacher, *Inorg. Chem*., 1991, **31**, 3187; H. K. Chae, W. G. Klemperer and T. A. Marquart, *Coord. Chem. Rev*., 1993, **128**, 209.
5 (*a*) Y. Hayashi, K. Toriumi and K. Isobe, *J. Am. Chem. Soc*., 1988, **110**, 3666; (*b*) Y. Do, X.-Z. You, C. Zhang, Y. Ozawa and K. Isobe, *J. Am. Chem. Soc*., 1991, **113**, 5892; (*c*) Y. Hayashi, Y. Ozawa and K. Isobe, *Inorg. Chem*., 1991, **30**, 1025; (*d*) J. T. Park, T. Nishioka, T. Suzuki and K. Isobe, *Bull. Chem. Soc. Jpn*., 1994, **67**, 1968.
6 Y. Lin, K. Nomiya and R. G. Finke, *Inorg. Chem*., 1993, **32**, 6040; A. Trovarelli and R. G. Finke, *Inorg. Chem*., 1993, **32**, 6034; M. Pohl and R. G Finke, *Organometallics*, 1993, **12**, 1453; B. M. Rapko, M. Pohl and R. G. Finke, *Inorg. Chem*., 1994, **33**, 3625; M. Pohl, D. K. Lyon, N. Mizuno, K. Nomiya and R. G. Finke, *Inorg. Chem*., 1995, **34**, 1413; K. Nomiya, Ch. Nozaki, M. Kaneko, R. G. Finke and M. Pohl, *J. Organomet. Chem*., 1995, **505**, 23; M. Pohl, Y. Lin, T. J. R. Weakley, K. Nomiya, M. Kaneko, H. Weiner and R. G. Finke, *Inorg. Chem*., 1995, **34**, 767.
7 C. L. Hill and C. M. Prosser-McCartha, *Coord. Chem. Rev*., 1995, **143**, 407.
8 G. M. Sheldrick, *Acta Crystallogr., Sect. A*, 1990, **46**, 467.
9 G. M. Sheldrick, Program for Crystal Structure Refinement, Universität Göttingen, 1993.
10 N. Walker and D. Stuart, *Acta Crystallogr., Sect. A*, 1990, **39**, 158.
11 C. K. Johnson, ORTEP, Oak Ridge National Laboratory, Oak Ridge TN, 1976; modified by L. Zolnai and H. Pritzkow, Universität Heidelberg, 1994.

*Received in Basel, Switzerland, 2nd May 1997; 7/03035E*

# A sulfur nitrogen triple, double and single bond in one ligand: synthesis and structure of $[Co\{N{\equiv}SF_2{-}N{=}S(O)F_2\}_4][AsF_6]_2{\cdot}SO_2$

**Reinhard Hoppenheit, Enno Lork, Jan Petersen and Rüdiger Mews***

*Institut für Anorganische und Physikalische Chemie der Universität Bremen, Leobener Strasse NW2, Postfach 330440, D-28334 Bremen, Germany*

**$NSF_2NS(O)F_2$ reacts quantitatively with $[Co(SO_2)_n][AsF_6]_2$ to give $[Co\{N{\equiv}SF_2{-}N{=}S(O)F_2\}_4][AsF_6]_2{\cdot}SO_2$; X-ray structure analysis confirms the presence of a triple, double and single bond in the same ligand.**

Sulfur nitrogen fluorine chemistry is one of the most fascinating fields in inorganic chemistry. Due to the possibilities of sulfur possessing different oxidation states and coordination numbers, forming single, double and triple bonds and being incorporated into acyclic and cyclic systems, an almost unprecedented variety of combination possibilities has been experimentally verified.[1] Although a large number of compounds have been reported, structural investigations on them are relatively rare. SN bond distances determined by electron diffraction on molecules in the gas phase range from 141.4 pm for $N{\equiv}SF_3$[2] to 169.8 pm in $SF_5{-}NF_2$[3] and in the solid state from 137–138 pm in coordination compounds of $NSF_3$ {*e.g.* $[M(NSF_3)_4(FAsF_5)_2]$,[4] $[Re(CO)_5(NSF_3)]^{+}$[5]} to 164–166 pm in $RSO_2{-}NR'_2$[6] and 169 pm in $SF_5N{=}CR_2$,[7] respectively, from X-ray structure determinations. The bond distances are dependent on the coordination number (hybridization) of sulfur and nitrogen[8] and on the oxidation state of sulfur. For $N{\equiv}SF_2{-}N{=}S(O)F_2$[9] the simple valence bond description suggests the presence of a triple, single and double bond between N and tetracoordinated $S^{VI}$ centres. Coordination of this ligand to the 'naked' $Co^{2+}$ centre[10] in pink $[Co(SO_2)_n][AsF_6]_2$[11] gives deep blue $[Co\{NSF_2NS(O)F_2\}_4][AsF_6]_2{\cdot}SO_2$ in quantitative yield.†

$$[Co(SO_2)_n][AsF_6]_2 \;+\; NSF_2NS(O)F_2\ (\text{excess}) \quad (\mathbf{1})$$

$$\downarrow$$

$$[Co\{NSF_2NS(O)F_2\}_4][AsF_6]_2{\bullet}SO_2 \quad (\mathbf{2})$$

At ambient temperature $SO_2$ is readily removed from **2** under dynamic vacuum. The structure of the cation of compound **2** is shown in Fig. 1.‡ The central $Co^{2+}$ is surrounded by a regular tetrahedron [N–Co–N 108.0(2)–110.4(2)°] the Co–N distances being in the range 195.4(4)–197.4(5) pm. The bond distances in the ligand justify the description as containing an NS triple, single and double bond between isocoordinated N and S centres in the same ligand.

$$[Co\{N \overset{138.9\ pm}{\equiv} SF_2 \overset{158.8\ pm}{-} N \overset{149.9\ pm}{=} S(O)F_2\}_4]^{2+}$$

So far, bond lengths for NS triple bonds have been documented only for coordination compounds of $NSF_3$[4,5] and $NSF_2NMe_2$[5] and lie in the range 137–139 pm, Exchange of one fluorine in $NSF_3$ by other substituents has little effect on the N≡S bond length. From 170 structure determinations of organic $-\overset{\|}{S}=$ N–systems reported in the CCDC an average of 154.4 pm for the NS double bond is found, while for $-\overset{\|}{S}-$N= single bonds

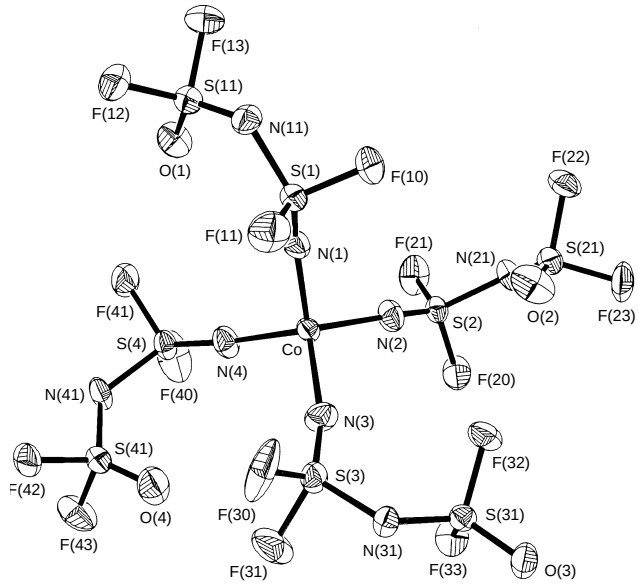



**Fig. 1** Structure of the cation of **2** with selected bond distances (pm) and angles (°): Co–N 195.4(4)–197.4(5) (av. 196.9), $N^1{\equiv}S^1$ 138.3(4)–139.3(5) (138.9), $S^1{-}F^1$ 151.8(4) 153.1(4) (152.5), $S^1{-}N^2$ 157.6(4)–159.5(4) (158.8), $N^2{=}S^2$ 149.4(4)–150.6(5) (149.9), $S^2{-}O$ 137.3(4)–138.8(4) (138.2), $S^2{-}F^2$ 149.0(4)–151.6(4) (151.0), $N^1{-}Co{-}N^2$ 108.0(2)–110.5(2) (109.5), Co–$N^1{\equiv}S^1$ 159.6(3)–171.6(3) (166.4), $N^1{\equiv}S^1{-}N^2$ 123.6(3)–127.1(3) (125.2), $S^1{-}N^2{=}S^2$ 121.4(3)–125.7(3) (123.5). $S^1$=S(1), S(2), S(3), S(4); $S^2$=S(11), S(21), S(31), S(41); $N^1$=N(1), N(2), N(3), N(4); $N^2$=N(11), N(21), N(31),N(41); $F^1$=F(10), F(11), F(20), F(21), F(30), F(31), F(40), F(41); $F^2$=F(12), F(13), F(22), F(23), F(32), F(33), F(42), F(43); O=O(1), O(2) O(3), O(4).

(334 examples) an average of 160.5 pm is reported.[12] The average N=S and N–S bond distances in **2** are significantly shorter than this as a result of orbital contraction owing to the highly electronegative substituents in our ligand system.

In the non-coordinating $SO_2$ molecule of **2** [S(10)–O(11) 138.4(5) pm, S(10)–O(12) 141.2(5) pm, O–S–O 119.9(4)°] the O–S–O angle is identical to that of $SO_2$ in the gas phase (O–S–O 119.3°, S–O 143.3 pm).[13] The difference in the S–O bond lengths in **2** is due to the differing thermal motions of the sulfur and both of the oxygen atoms, which may also be the cause of the shortened S–O bonds in **2** compared to free $SO_2$.

Support of the FNK (University of Bremen) and the Fonds der Chemischen Industrie is gratefully acknowledged.

## Footnotes and References

* E-mail: mews@chemie.uni-bremen.de

† *Preparation* of **2**: $SO_2$ (10 ml) was condensed onto $[Co(SO_2)_2][AsF_6]_2$ (1.01 g, 1.78 mmol)[4] at −196 °C in a thick-walled Schlenck vessel, and an excess of $NSF_2NS(O)F_2$ (1.8 g, 8.15 mmol) was added. On warming to room temp. the solution changed from pink to deep blue. The solvent and excess of ligand were removed at ambient temperature in dynamic vacuum to give 2.09 g of **2** (quantitative), IR (Nujol, Kel-F mull): 1660w (sh),

1560m, 1452m, 1435m, 1255m (sh) 1220s, 940 (sh) 920m, 831s, 815m, 759m, 700vs, 580m, 533m, 525m, 497m, 480m, 399vs $cm^{-1}$. Elemental analysis. Calc.: F, 45.3; N, 9.55. Found: F, 44.9; N, 9.2%.

‡ *Crystal data* for $As_2CoF_{28}N_8O_4S_8{\cdot}O_2S$: **2** crystallizes with one molecule of solvent per formula unit, monoclinic, space group $P2_1/c$, $a$ = 1712.6(3), $b$ = 1142.4(2), $c$ = 1844.1(4) pm; $\beta$ = 116.54(3)°, $U$ = 3.2277(11) nm, $Z$ = 4, $D_c$ = 2.546 g $cm^{-3}$, $\mu$ = 3.350 $mm^{-1}$, $F$(000) 2372, crystal dimensions 0.5 × 0.4 × 0.2 mm, 8191 reflections collected with 2.66 < $\theta$ < 27.51°, 5256 unique used in structural analysis. The data set was collected on a Siemens P4 diffractometer using Mo-K$\alpha$ radiation ($\lambda$ = 71.073 pm) at 173 K. The structure was solved by direct methods.[14] All atoms were refined anisotropically. An empirical absorption correction using $\psi$-scans was applied. The refinement (487 parameters) converged with $wR_2$ = 0.0779 ($R_1$ = 0.0398) and final difference electron density maxima and minimina of 455 and −602 e $nm^{-3}$. CCDC 182/539.


1 O. Glemser and R. Mews, *Angew. Chem., Int. Ed. Engl.*, 1980, **19**, 883.
2 W. H. Kirchhoff and E. B. Wilson Jr., *J. Am. Chem. Soc.*, 1962, **84**, 334.
3 J. Haase, H. Oberhammer, W. Zeil, O. Glemser and R. Mews, *Z. Naturforsch., Teil A*, 1971, **26**, 1333.
4 B. Buß, W. Clegg, G. Hartmann, P. G. Jones, R. Mews, M. Noltemeyer and G. M. Sheldrick, *J. Chem. Soc., Dalton Trans.*, 1981, **63**; U. Behrens, R. Hoppenheit, W. Isenberg, E. Lork, J. Petersen and R. Mews, *Z. Naturforsch., Teil B*, 1994, **49**, 238.
5 U. Behrens, E. Lork, J. Petersen, A. Waterfeld and R. Mews, *Z. Anorg. Allg. Chem.*, in the press.
6 Ž. Žack and A. Ružižka, *Z. Anorg. Allg. Chem.*, 1987, **549**, 67.
7 M. E. Sitzmann and R. D. Gilardi, *J. Fluorine Chem.*, 1993, **63**, 203.
8 H. W. Roesky, M. Diehl, H. Fuess and J. W. Bats, *Angew. Chem., Int. Ed. Engl.*, 1978, **17**, 58.
9 O. Glemser and R. Höfer, *Z. Naturforsch., Teil B*, 1974, **29**, 121.
10 J. Petersen, E. Lork and R. Mews, *Chem. Commun.*, 1996, 2593.
11 P. A. W. Dean, *J. Fluorine Chem.*, 1975, **5**, 499; C. D. Desjardins and J. Passmore, *J. Fluorine Chem.*, 1975, **6**, 279. In an $SO_2$ atmosphere $[Co(SO_2)_4(FAsF_5)_2]$ is isolated (E. Lork, J. Petersen and R. Mews, to be published), which readily loses $SO_2$ to give reasonably stable $[Co(SO_2)_2(AsF_6)_2]$ of unknown structure.
12 3D Search and Research Using the Cambridge Structural Database: F. H. Allen and O. Kennard, *Chem. Des. Automat. News*, 1993, **8**, 1; 31.
13 C. H. Holder Jr. and M. Fink, *J. Chem. Phys.*, 1981, **75**, 5323; Y. Morino, M. Tanimoto and S. Saito, *Acta Chem. Scand., Ser. A*, 1988, **42**, 346.
14 Structure solution and graphics, Siemens SHELXTL-Plus: G. M. Sheldrick, Release 4.0 for Siemens R3 Crystallographic Research Systems, Siemens Analytical X-Ray Instruments Inc., Madison, WI, 1989; Structure refinement, SHELXL-93, G.M. Sheldrick, University of Göttingen.



*Received in Cambridge, UK, 16th June 1997; 7/04174H*

# Porous clay heterostructures (PCH) as acid catalysts

**Anne Galarneau, Anis Barodawalla and Thomas J. Pinnavaia***

*Department of Chemistry and Center for Fundamental Materials Research, Michigan State University, East Lansing, MI 48824, USA*

**Porous clay heterostructures formed by surfactant assembly of open framework silica in the galleries of a smectite clay represent a new family of solid acid catalysts, as evidenced by the selective dehydration of 2-methylbut-3-yn-2-ol to 2-methylbut-3-yn-1-ene.**

Pillared interlayered clays have been extensively studied as promising solid-state alternatives to traditional acid catalysts, such as aluminium trichloride, sulfuric acid and hydrofluoric acid.[1,2] We recently reported a new type of clay intercalate with high surface area and a structural porosity substantially larger than pillared clays. These new derivatives, which we call porous clay heterostructures (PCH) are formed by surfactant-directed assembly of open-framework silica in the galleries of smectite clays with high charge density.[3] In contrast to microporous pillared clays with pore sizes typically below 10 Å, PCH materials exhibit regular porosity in the supermicropore to small mesopore range (15–25 Å).

PCH synthesis makes use of the micellar ordering of silicate species and surfactants in a manner not unlike the supramolecular ordering processes for mesoporous MCM-41 molecular sieves.[4,5] However, as shown in Fig. 1, PCH assembly differs from MCM-41 chemistry insofar as framework organization occurs in the restricted two-dimensional gallery region of the clay rather than in the three-dimensional bulk phase. Because PCH design combines the open framework structure of the gallery silica with the chemistry of the clay layer, new properties for selective heterogeneous catalysis may be anticipated. Using the dehydration of 2-methylbut-3-yn-2-ol (MBOH) as a probe reaction, we demonstrate in the present work the acid catalytic activity of PCH materials relative to alumina-pillared clays and related catalysts.

Cetyltrimethylammonium (CTMA) exchange cations and decylamine were used as co-surfactants to form a PCH with fluorohectorite as the clay host. Synthetic lithium fluorohectorite (Li-FH) with the unit cell composition $Li_{1.12}$-$[Li_{1.12}Mg_{4.88}](Si_8O_{20})F_4{\cdot}xH_2O$ (Corning, Inc.) was allowed to react at 50 °C with 0.3 M aqueous $[(C_{16}H_{33})NMe_3]Br$ in twofold excess of the clay cation exchange capacity. After a reaction time of 24 h, the product was washed with ethanol and water to remove the excess surfactant and air dried. The clay then was added to the decylamine in the molar ratio CTMA-FH : decylamine = 1 : 20, and the resulting suspension was stirred for 30 min. Sufficient tetraethylorthosilicate (TEOS) was added to achieve a final molar ratio of CTMA-FH : decylamine : TEOS = 1 : 20 : 150. After a reaction time of 4 h at room temp., the reaction product was recovered by centrifugation, air-dried and calcined at the desired temperature for 4 h using a temperature ramp rate of 2 °C $min^{-1}$. The calcined products were denoted FH-PCH-X where X is the calcination temperature in °C. Chemical analyses indicated the presence of 10.4 moles of gallery Si per fluorohectorite $O_{20}F_4$ unit cell.

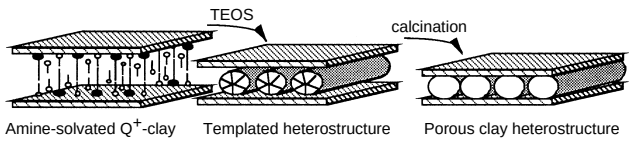



**Fig. 1** Schematic illustration of porous clay heterostructure (PCH) formation through surfactant-directed assembly of open framework silica in the galleries of a layered silicate co-intercalated by a quaternary ammonium ion surfactant (filled head groups) and a neutral amine co-surfactant (open head groups)

Table 1 provides the basal spacings, BET surface areas, and Horvath–Kowazoe pore sizes for FH-PCH samples calcined in the range 300–550 °C. Three orders of 00*l* X-ray reflection are observed in accord with a lamellar structure. Although the basal spacing decreases from 38.1 to 33.5 Å with increasing temperature, there is a general increase in the BET surface areas to a maximum value of 790 $m^2\ g^{-1}$ at 500 °C where the removal of gallery surfactant ( < 1 mass% C) and the dehydroxylation of the gallery silica become more complete. The lamellar structure is retained even at 700 °C, but the basal spacing begins to decrease more rapidly at this temperature. At 800 °C the PCH structure degrades substantially with the formation of quartz as a decomposition product. Clearly, the thermal stability of the PCH structure degrades substantially with the formation of quartz as a decomposition product. Clearly, the thermal stability of the PCH structure is sufficient to conduct a wide range of acid catalyzed conversions.

Table 1 also includes the results for the catalytic conversion of MBOH over calcined FH-PCH samples. This probe reaction is sensitive to the presence of acid-base sites on the catalyst surface.[6] Acidic sites result in the dehydration of MBOH to 2-methylbut-3-yn-1-ene (MByne), whereas basic sites cause cleavage to acetone and acetylene. As indicated by the high selectivity to MByne, particularly for FH-PCH-350, the surfaces of FH-PCH contain mainly acidic sites. In contrast, pristine $Li^+$ fluorohectorite is highly basic, affording primarily acetone and acetylene as reaction products. Thus, the intercalation of surfactant-assembled silica and the subsequent calcination of the heterostructure imparts acidic surface functionality.

The results given in Table 1 further show that FH-PCH-350 is a much more active acid catalyst than either mesoporous MCM-41 silica or microporous alumina pillared fluorohectorite (APF-350). The latter intercalate is an especially active alkylation catalyst among pillared clays.[7] The reactivity of FH-PCH-350 even approaches that of K-10 montmorillonite, a commercially available acid-restructured clay. This latter material, however, lacks framework porosity and is incapable of shape selective catalysis.

The FH-PCH materials reported here are hybrid structures of the smectite clay fluorohectorite, which is basic, and weakly acidic MCM-41 silica (*cf.* Table 1). Some Brønsted acidity is expected for PCH materials, however, because the initial gallery cations (*i.e.* $Li^+$) are replaced first by surfactant cations and then by protons upon destruction of the surfactant through calcination. Also, fluorohectorite is known[8] to undergo hydrolysis of lattice fluorine at temperatures above 250 °C. Proton dissociation from the resulting hydroxyl groups also can contribute to Brønsted acidity. In addition, the silicate layers of fluorohectorite can undergo local restructuring upon calcination at elevated temperatures, giving rise to Lewis-acid sites in the gallery region.[8]

**Table 1** Physical and acid catalytic properties of calcined FH-PCH derivatives and related solids

| Sample | $d_{001}$/Å | Surface area/ $m^2\ g^{-1}$ | HK pore size/Å | MBOH conv. (%) | MBOH product selectivity[a] | | |
|---|---|---|---|---|---|---|---|
| | | | | | Basic[b] | | Acidic MByne |
| | | | | | Acetylene | Acetone | |
| FH-PCH-300 | 38.1 | 575 | 18.9 | 47.0 | 0 | 0 | 100 |
| FH-PCH-350 | 38.7 | 555 | 19.6 | 52.7 | 0 | 0.1 | 99.9 |
| FH-PCH-450 | 37.1 | 630 | 22.3 | 32.9 | 0.2 | 0.2 | 99.6 |
| FH-PCH-500 | 35.3 | 790 | 22.6 | 23.6 | 0.4 | 0.8 | 98.9 |
| FH-PCH-550 | 33.5 | 750 | 21.7 | 19.0 | 2.9 | 3.4 | 93.8 |
| Li-FH | 10.5 | 50 | 0 | 5.0 | 36.2 | 46.5 | 17.3 |
| K-10[c] | — | 250 | 0 | 67.9 | 0 | 0.1 | 99.9 |
| APF-350[d] | 18.9 | 214 | < 10 | 16.4 | 3.6 | 3.6 | 92.9 |
| MCM-41[e] | — | 1100 | 22.0 | 11.0 | 8.0 | 7.0 | 85.0 |

[a] Reactions of MBOH were carried out over 150 mg quantities of catalyst at 180 °C in a packed-bed reactor linked to an on-line Perkin-Elmer 8500 gas chromatograph equipped with FID detection and a packed column of 3% SP-1500 on Carbopack B. The catalysts were activated at 200 °C for 2 h prior to testing under a helium flow of 20 ml $min^{-1}$. MBOH in the gas phase (0.35 mmol $h^{-1}$) was diluted to 2.5% in helium. [b] Basic active sites afford acetone and actylene as reaction products, whereas acid sites afford exclusively MByne. [c] A commercial acid-treated clay (Aldrich) calcined at 350 °C. [d] Alumina-pillared fluorohectorite, prepared according to ref. 8 and calcined at 350 °C. [e] Mesoporous silica molecular sieve assembled from cetyltrimethylammonium bromide according to ref. 4 and calcined at 350 °C.

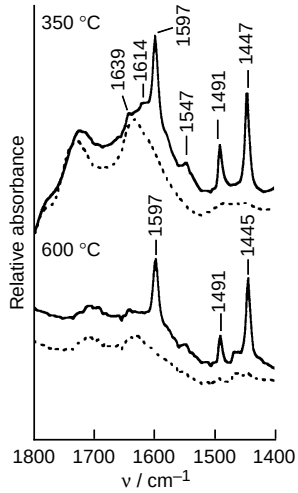



**Fig. 2** IR spectra of pyridine chemisorbed at 150 °C on FH-PCH samples calcined at 350 and 600 °C (solid lines). The dashed lines are spectra for the pristine FH-PCH samples prior to pyridine adsorption.

FTIR spectra for pyridine chemisorbed at 150 °C on FH-PCH-350 and -600 provide insights into the nature of the acid sites in PCH materials (Fig. 2). The C–C ring stretching frequencies near 1445 and 1547 $cm^{-1}$ are diagnostic of the bonding of pyridine to Lewis and Brønsted sites,[9] respectively. The relative intensities of these bands are very similar to those observed for APF. This similarity in acid functionality is somewhat surprising, because the Lewis acidity of alumina pillared clays normally is associated with the presence of coordinatively unsaturated sites on the alumina pillars. FH-PCH, however, contains no aluminium.

To better understand the origin of the observed acidity for FH-PCH materials and the relationship of the acidity to APF, we carried out $^{19}F$ and $^{29}Si$ MAS NMR studies for materials calcined to 550 °C. $^{19}F$ NMR showed that the fluorine sites associated with the negatively charged octahedral triads of the silicate layers ($\delta$ −16) diminish to *ca*. 25% of the initial intensity when calcined at 350 °C. This latter result is in accord with the previously observed hydrolysis chemistry of fluorohectorite (APF-350).[8] Also, $^{29}Si$ MAS NMR showed that the silicate layers in FH-PCH are locally restructured in a manner analogous to APF-350. Upon layer restructuring at calcination temperatures up to 350 °C, the $Q^3$ resonance of the clay broadens and shifts progressively from $\delta$ −93.3 to −96.6 signifying an increase in the Si–O–Si bond angle of the tetrahedral sheet. The $Q^3$ ($\delta$ −103) and $Q^4$ ($\delta$ −110) resonances of the assembled gallery silica, however, are not affected by calcination over this temperature range. Inversion and grafting of the clay tetrahedral sheet to the gallery silica, as evidenced by a new resonance at $\delta$ −99.7, does not occur until the FH-PCH is calcined in the range 450–550 °C. Such local restructuring of the silicate layer also occurs for APF over the same temperature range.

On the basis of the above FTIR and MAS NMR results we conclude that FH-PCH-350 and APF-350 share the same type of acid functionality and layered structural features. The important difference, of course, is that FH-PCH-350 is a surfactant-assembled supermicroporous to mesoporous intercalate, whereas APF-350 is exclusively a microporous pillared derivative. The enhanced access to the framework gallery sites in FH-PCH-350 most likely contributes greatly to the superior catalytic activity of this intercalate.

The partial support of this research by the National Science Foundation through CRG grants CHE-9224102 and -9633798 is gratefully acknowledged.

## Footnote and References

* E-mail: pinnavaia@cem.msu.edu

1 F. Figueras, *Catal. Rev.-Sci. Eng.*, 1988, **30**, 457.
2 Y. Izumi, K. Urabe and M. Onaka, *Zeolite, Clay, and Heteropoly Acid in Organic Reactions*, VCH Publishers, 1992, pp. 49–98.
3 A. Galarneau, A. Barodawalla and T. J. Pinnavaia, *Nature*, 1995, **374**, 529.
4 J. S.Beck, J. C. Vartuli, W. J. Roth, M. E. Leonowicz, C. T. Kresge, K. D. Schmitt, C. T.-W. Chu, D. H. Olson, E. W. Sheppard, S. B. McCullen, J. B. Higgins and J. L. Schlenker, *J. Am. Chem. Soc.*, 1992, **114**, 10 834.
5 C. T. Kresge, M. E. Leonowicz, W. J. Roth, J. C. Vartuli and J. S. Beck, *Nature*, 1992, **359**, 710.
6 H. Laron-Pernot, F. Luck and J. M. Popa, *Appl. Catal.*, 1991, **78**, 213.
7 J.-R.Butruille and T. J. Pinnavaia, *Catal. Today*, 1992, **14**, 141.
8 J.-R. Butruille, L. J. Michot and T. J. Pinnavaia, *J. Catal.*, 1993, **139**, 664.
9 E. P. Parry, *J. Catal.*, 1963, **2**, 371.

*Received in Columbia, MO, USA, 6th May 1997; 7/03101G*

# 2,6-Divinylation of phenols with ethyne

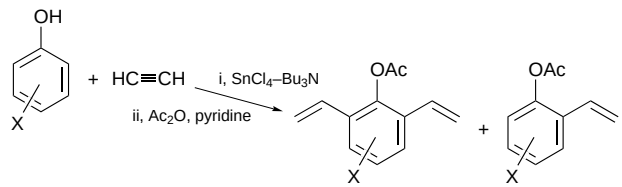
**Masahiko Yamaguchi,*[a] Mieko Arisawa,[b] Yoshiyuki Kido[a] and Masahiro Hirama[b]**

[a] *Faculty of Pharmaceutical Sciences, Tohoku University, Aoba, Sendai 980-77, Japan*
[b] *Department of Chemistry, Graduate School of Science, Tohoku University, Aoba, Sendai 980-77, Japan*

**Phenols are 2,6-divinylated by treatment with ethyne at 100 °C in chlorobenzene in the presence of $SnCl_4$–$Bu_3N$, the divinylation occurring predominantly to exclusively with phenol, alkylphenols and alkoxyphenols; an appropriate amount of the tin reagent and the correct reaction temperature are essential for the divinylation.**

Divinylbenzenes are an important class of chemicals possessing two reactive sites. They are popular cross-linking agents in polymer chemistry. Alternating copolymers have been synthesized by bis-addition reactions to divinylbenzenes, and use of the Heck reaction, amine addition reaction and olefin metathesis have been reported.[1] The Diels–Alder reaction of divinylbenzenes is a convenient method for the synthesis of polycyclic aromatic compounds.[2] In spite of their significance in polymer and organic synthesis, studies have been limited to the three isomers of divinylbenzene,[3] and very few functionalized derivatives are known. This is due to the lack of a straightforward method for their preparation, since the direct substitution of aromatic C–H bonds with C–CH=$CH_2$ groups has proved extremely problematic.[4] Divinylbenzenes have been synthesized by stepwise transformations from benzene *via* diethylbenzene, dihalobenzene, diformylbenzene *etc*.[5] Functionalized divinylbenzenes can be accessed only by multi-step syntheses if these methods are employed. Previously, we reported the direct *ortho*-vinylation of phenols with ethyne.[6] Described here is the direct 2,6-divinylation of phenols (Scheme 1). Two vinyl groups are introduced to the benzene nucleus at *meta*-positions in one step.

Ethyne was bubbled into a chlorobenzene solution of $SnCl_4$–$Bu_3N$ (5 equiv.) at −50 °C.† $SnCl_4$–$Bu_3N$ (2 equiv.) and *p-tert*-butylphenol (1 equiv.) were added, and the mixture was heated at 100 °C for 30–60 min. The reaction was quenched with 2 M NaOH and EtOH at reflux. After acetylation, 4-*tert*-butyl-2,6-divinylphenyl acetate and 4-(*tert*-butyl-2-vinylphenyl acetate were obtained in 71% combined yield in a ratio of 5 : 1 (by NMR spectroscopy). The divinylphenols were acetylated before isolation for the purpose of stabilization. When the reaction was conducted at 60 °C, monovinylphenol predominated. Serious decomposition took place at chlorobenzene reflux temperature (132 °C). Other aromatic solvents with high boiling points, such as toluene, *o*-xylene and 1,2-dichlorobenzene, could also be used. Treatment of isolated *o*-vinylphenol with ethyne under these conditions resulted in decomposition. Analogous to the monovinylation reaction of phenols,[6] the divinylation probably involves formation of alkynyltin and phenoxytin followed by the carbostannylation reaction between these species. The alkaline quench (2 M NaOH–EtOH at reflux) is essential for the effective protonation of the carbostannylated intermediate. The amount of tin reagent (5 + 2 equiv.) is also critical to obtain the divinylphenol predominantly. When it was changed, for example, to 2 + 2, 2 + 5, 5 + 5 or 5 + 0 equiv., 1 : 1 mixtures of monovinylated and divinylated products were formed. Employing a large excess of reagnet (12 + 0 equiv.) resulted in the monovinylation reaction dominating in a ratio of 6 : 1. The reaction mechanism of the divinylation therefore appears to be rather complex.




**Scheme 1**

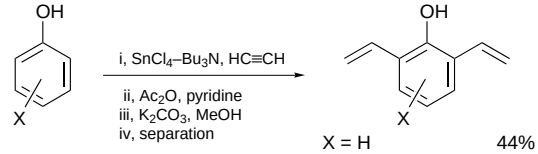
Several *para*- and *meta*-substituted phenols and phenol itself were treated with ethyne under the above conditions, and the results are summarized in Table 1. The reaction can be carried out on a 1 g scale. Alkoxy and alkyl derivatives gave divinylphenol predominantly or exclusively. *p*-Pivaloxyphenol and *p*-phenylphenol gave comparable amounts of monovinyl and divinyl derivatives. The divinylation is facilitated by electron-donating substitutents on the aromatic ring. Styrenes with oxygen functionalities at the *ortho*- and/or *para*-positions are known to be extremely sensitive to acids.[7] It is therefore notable that the present vinylation reaction can be applied to *m*-methoxyphenol and *m*-silyloxyphenols. Even 3,5-bis(silyloxy)phenol is divinylated giving a protected 2,6-divinylbenzene-1,3,5-triol. In order to avoid desilylation, the reactions of silyloxyphenols were quenched with either $K_2CO_3$ in MeOH or $K_2CO_3$ in THF–water at room temperature. The latter conditions were employed in the divinylation of *m*-silyloxyphenols. Alcohol addition to the reactive olefin took place when the protonation was conducted in the presence of MeOH.

Mixtures of di- and mono-vinylphenyl acetate were treated with $K_2CO_3$ in MeOH at room temperature to give 2,6-divinylphenol and 2-vinylphenol, which were readily separable by silica gel chromatography. Thus, divinylphenols are obtained from phenol, alkylphenols and alkoxyphenols in overall yields ranging from 40 to 60% (Scheme 2). The treatment of 4-(*tert*-butyldimethylsilyloxy)phenol with KF in MeOH gave 2,6-di-

**Table 1** 2,6-Divinylation of phenols with ethyne[a]

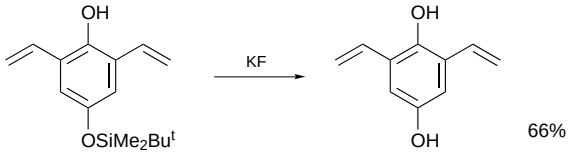
| X | Yield (%) | Divinyl : Monovinyl |
|---|---|---|
| H | 66 | 5 : 1 |
| 4-Me | 69 | 5 : 1 |
| 4-Bu$^t$ | 71 | 5 : 1 |
| 4-MeO | 77 | ⩾10 : 1 |
| 4-Bu$^t$$Me_2SiO$ | 73 | 6 : 1 |
| 4-Bu$^t$$Ph_2SiO$ | 72 | ⩾10 : 1 |
| 4-Ph | 80 | 1 : 1 |
| 4-Bu$^t$COO | 87 | 1 : 3 |
| 3-Me | 75 | 4 : 1[b] |
| 3-MeO | 25[c] | ⩾10 : 1 |
| 3-Bu$^t$$Me_2SiO$ | 48 | ⩾10 : 1 |
| 3-Bu$^t$$Ph_2SiO$ | 49 | ⩾10 : 1 |
| 3,5-(Bu$^t$$Me_2SiO)_2$ | 41 | 8 : 1 |

[a] Yields of acetates are shown. Ratios were determined by $^1$H NMR spectroscopy. [b] Monovinylated product is a 1 : 1 mixture of 2-vinyl-5-methylphenyl acetate and 2-vinyl-3-methylphenyl acetate. [c] The low yield is due to decomposition of the divinylphenol under the reaction conditions.




| | |
|---|---|
| X = H | 44% |
| X = 4-Me | 59% |
| X = 4-Bu$^t$ | 58% |
| X = 4-MeO | 48% |
| X = 4-Bu$^t$Me$_2$SiO | 48% |
| X = 4-Bu$^t$Ph$_2$SiO | 55% |
| X = 3-Me | 52% |

**Scheme 2**




66%

**Scheme 3**

vinylbenzene-1,4-diol (Scheme 3). mp 131–132 °C (toluene), which should be an interesting building block for redox polymers. In spite of their simple molecular structure, most of the divinylphenols formed, including the parent 2,6-divinylphenol itself, the new compounds.[8] These bifunctional and reactive substances should have various applications in polymer chemistry and organic chemistry.

We thank Mr Katsumi Kobayashi (Tohoku University) for his assistance in the present work. This work was supported by grants from JSPS (Research for the Future Program), the Ministry of Education, Science and Culture, Japan (No. 07554065 and 08404050) and a SUNBOR Grant.

## Footnotes and References

* E-mail: yama@mail.pharm.tohoku.ac.jp

† Typical experimental procedure: Ethyne was bubbled into chlorobenzene (170 ml) at −50 °C for 1 h. Bubbling was stopped, and $SnCl_4$ (5.9 ml, 50 mmol) and $Bu_3N$ (11.9 ml, 50 mmol) were added. The mixture was stirred at room temperature for 1 h under an argon atmosphere, and *p*-methoxyphenol (1.24 g, 10 mmol) in chlorobenzene (30 ml), $SnCl_4$ (2.3 ml, 20 mmol) and $Bu_3N$ (4.8 ml, 20 mmol) were added successively. After heated at 100 °C for 1 h, 2 M NaOH (400 ml) and ethanol (150 ml) were added, and heating was continued for another 2 h at 100 °C. The mixture was cooled, and acidified with 2 M HCl. The organic materials were extracted with diethyl ether, washed with brine, dried over $MgSO_4$ and filtered. After removal of the diethyl ether under reduced pressure, pyridine (8.1 ml) and acetic anhydride (4.7 ml) were added to the resulted chlorobenzene solution, and the products were acetylated by stirring at room temperature for 12 h. An aqueous work-up followed by flash chromatography (hexane–ethyl acetate 100 : 1) over silica gel gave 4-methoxy-2,6-divinylphenyl acetate (1.49 g, 77%), containing *ca.* 5% of 4-methoxy-2-vinylphenyl acetate as indicated by $^1$H NMR spectroscopy.

1 For example, M. Suzuki, J.-C. Lim and T. Saegusa, *Macromolecules*, 1990, **23**, 1574; A. Kumar and B. E. Eichinger, *Makromol. Chem., Rapid. Commun.*, 1992, **13**, 311; Y. Chujo, I. Tomita, Y. Kozawa and T. Saegusa, *Macromolecules*, 1993, **26**, 2643; E. Thorn-Csányi and K. P. Pflug, *J. Mol. Catal.*, 1994, **90**, 69.

2 For example, L. Liu and T. J. Katz, *Tetrahedron Lett.*, 1990, **31**, 3983; H. Hamana, K. Horiguchi, T. Hagiwara and T. Narita, *Bull. Chem. Soc. Jpn.*, 1990, **63**, 1884; A. B. Padias, T.-P. Tien and H. K. Hall, Jr., *J. Org. Chem.*, 1991, **56**, 5540; J. Nishimura, Y. Horikoshi, Y. Wada, H. Takahashi and M. Sato, *J. Am. Chem. Soc.*, 1991, **113**, 3485; T. Suzuki, T. Fukushima, Y. Yamashita and T. Miyashi, *J. Am. Chem. Soc.*, 1994, **116**, 2793.

3 Separation of isomeric divinylbenzenes: B. T. Storey, *J. Polym. Sci., Part A*, 1965, **3**, 265; R. H. Wiley, J. I. Jin and Y. Kamath, *J. Polym. Sci., Part A*, 1968, **6**, 1065.

4 M. Yamaguchi, Y. Kido, A. Hayashi and M. Hirama, *Angew. Chem., Int. Ed. Engl.* 1997, **36**, 1313 and references cited therein.

5 For example, H. W. Johnston and J. L. R. Williams, *J. Am. Chem. Soc.*, 1947, **69**, 2065; R. H. Mitchell, B. N. Ghose and M. E. Williams, *Can. J. Chem.*, 1977, **55**, 210; J. E. Plevyak and R. F. Heck, *J. Org. Chem.*, 1978, **43**, 2454; D. R. McKean, G. Parrinello, A. F. Renaldo and J. K. Stille, *J. Org. Chem.*, 1987, **52**, 422; O. Nuyken and F. Siebzehnrübl, *Makromol. Chem.*, 1988, **189**, 541.

6 M. Yamaguchi, A. Hayashi and M. Hirama, *J. Am. Chem. Soc.*, 1995, **117**, 1151.

7 C. G. Overberger, L. H. Arond, D. Tanner, J. J. Taylor and T. Alfrey, Jr., *J. Am. Chem. Soc.*, 1952, **74**, 4848; Y. Okamoto and H. C. Brown, *J. Org. Chem.*, 1957, **22**, 485; M. Mayen and E. Marechal, *Bull. Soc. Chim. Fr.*, 1972, 4662.

8 A patent for 4-methyl-2,6-divinylphenol has appeared: H. Kitano, *Jap. Pat.* 74 14 319, 1974 (*Chem. Abstr.*, 1975, **82**, 114031j).

*Received in Cambridge, UK, 23rd June 1997; 7/04379A*

# Hydrolysis of an iridium–methyl bond, formation of *trans*-[Ir(CO)(OH)$L_2$] from *trans*-[Ir(CO)Me$L_2$] [L = $PPh_2$(*m*-$C_6H_4SO_3Na$), $PPh_2$(*m*-$C_6H_4SO_3K$) or $P(C_6H_4SO_3Na)_3$] upon dissolving in water

**David P. Paterniti and Jim D. Atwood***

*Department of Chemistry, University at Buffalo, State University of New York, Buffalo, NY 14260-3000, USA*

**The synthesis, characterization and rapid hydrolysis of *trans*-[Ir(CO)Me$L_2$] (L = a water-soluble phosphine) to *trans*-[Ir(CO)(OH)$L_2$] and $CH_4$ are reported.**

There have been increasing reports on use of water-soluble organometallic complexes as catalysts for hydroformylation and hydrogenation of alkenes.[1,2] Such catalytic reactions involve, of necessity, formation of metal alkyls. Several alkyl complexes of $Cr^{III}$, $Co^{III}$ and $Pt^{III}$ have been studied in aqueous solution[2,3] with both homolytic and heterolytic decomposition pathways identified. However, alkyl complexes of lower valent organometallic centres have not been reported. In this manuscript we report the synthesis of the sodium and potassium salts of *trans*-[Ir(CO)Me(tppms)$_2$] [tppms = $PPh_2$(*m*-$C_6H_4SO_3^-$)], the attempted synthesis of *trans*-[Ir(CO)Me(tppts)$_2$] [tppts = P(*m*-$C_6H_4SO_3Na)_3$] and the rapid hydrolysis of the Ir–Me bond in water.

The methyl complexes of tppms were prepared by ligand exchange on *trans*-[Ir(CO)Me($PPh_3$)$_2$] [eqn. (1)].[4]†

$$trans\text{-}[Ir(CO)Me(PPh_3)_2] + 2tppms \xrightarrow{thf} trans\text{-}[Ir(CO)Me(tppms)_2](\downarrow) + 2PPh_3 \quad (1)$$

Both the $Na^+$ and $K^+$ salts precipitate from thf. The characterization data shown in Table 1 confirm the formulation as do the microanalytical data.‡

Dissolving *trans*-[Ir(CO)Me(tppmsNa)$_2$] in $H_2O$ (or $D_2O$) results in *trans*-[Ir(CO)(OH)(tppmsNa)$_2$][5] and $CH_4$ in seconds. The *trans*-[Ir(CO)(OH)(tppmsNa)$_2$] was indicated by the $^{31}P$ resonance at $\delta$ 28.4(s)[5] and the $CH_4$ by a sharp singlet at $\delta$ −0.07(s) in the $^1H$ NMR. No other resonances were observed in the $^{31}P$ or the $^1H$ NMR to higher field than $\delta$ 6.0. The NMR tube was opened and an IR spectrum recorded ($\nu_{CO}$ = 1953 $cm^{-1}$). To complete characterization of the iridium product the water was removed by vacuum and the residue dissolved in $(CD_3)_2SO$ and combined with 10 mg of *trans*-[Ir(CO)($CH_3$)(tppmsNa)$_2$] for NMR characterization. The $^1H$ and $^{31}P$ NMR spectra clearly showed equal quantities of *trans*-[Ir(CO)(OH)(tppmsNa)$_2$] {$^{31}P$ NMR [$(CD_3)_2SO$]}, $\delta$ 26.9(s); $^1H$ NMR [$(CD_3)_2SO$], $\delta$ 0.2 (t, $J_{PH}$ 6.5 Hz) and the methyl complex. Thus a rapid hydrolysis of the iridium–methyl bond occurred in water [eqn. (2), L = tppmsNa].

$$trans\text{-}[Ir(CO)MeL_2] + H_2O \rightarrow trans\text{-}[Ir(CO)(OH)L_2] + CH_4 \quad (2)$$

The reaction was sufficiently rapid that the methyl complex could not be observed in $H_2O$ by NMR.

Attempts to prepare *trans*-[Ir(CO)Me(tppts)$_2$] by biphasic exchange of tppts for $PPh_3$ always resulted in formation of *trans*-[Ir(CO)(OH)(tppts)$_2$]§ in a similar hydrolysis reaction.

The very rapid hydrolysis of iridium methyl complexes provides a caution for increasing use of water-soluble organometallic compounds as catalysts. Such hydrolyses, coupled with facile water–gas shift reactions, offer different mechanistic possibilities for organometallic complexes in water.

The authors are grateful to the Department of Energy, ER 13775, for support of this research.

**Table 1** IR and NMR characterization data for iridium complexes

| Complex | $\nu_{CO}$ ($Me_2SO$) | $\delta_P$ [$(CD_3)_2SO$] | $\delta_H$ [$(CD_3)_2SO$] ($J_{PH}$/Hz) |
|---|---|---|---|
| *trans*-[Ir(CO)Me($PPh_3$)$_2$] | 1935 | 31.2 | −0.4(t) (8.5) |
| *trans*-[Ir(CO)Me(tppmsK)$_2$] | 1937 | 31.5 | −0.4(t) (8.9) |
| *trans*-[Ir(CO)Me(tppmsNa)$_2$] | 1937 | 31.6 | −0.4(t) (8.5) |
| *trans*-[Ir(CO)(OH)(tppmsNa)$_2$] | 1953 | 26.9 | 0.2(t) (6.5) |

## Footnotes and References

* E-mail: jatwood@acsu.buffalo.edu

† In a glove box, *ca.* 100 mg of *trans*-[Ir(CO)($CH_3$)($PPh_3$)$_2$][4] was dissolved in 20 ml of thf and 90 mg of tppms added. The solution was stirred overnight and the canary yellow precipitate collected and washed with thf and with benzene. The yield of the $K^+$ salt was 87% (103 mg) and the yield of the $Na^+$ salt was 46% (54 mg).

‡ [Ir(CO)($CH_3$)(tppmsK)$_2$]. Found: C, 45.8; H, 3.7; P, 6.2; S, 6.3. Calc. C, 45.8; H, 3.1; P, 6.2; S, 6.4%. [Ir(CO)($CH_3$)(tppmsNa·$H_2O$)$_2$]. Found: C, 46.5; H, 3.7; S, 6.6. Calc.: C, 45.6; H, 3.5; S, 6.4%.

§ $\nu_{CO}(H_2O)$ = 1961; $^{31}P(D_2O)$ $\delta$ 28; $^1H$ [$(CD_3)_2SO$] $\delta$ 0.01 (t, $J_{PH}$ 7.6 Hz).

1 M. Beller, B. Cornils, C. D. Frohning and C. W. Kohlpaintner, *J. Mol. Catal. A*, 1995, **104**, 17; W. Herrmann and C. W. Kohlpaintner, *Angew. Chem., Int. Ed. Engl.*, 1993, **32**, 1524; P. Kalck and F. Monteil, *Adv. Organomet. Chem.*, 1992, **34**, 219; M. Barton and J. D. Atwood, *J. Coord. Chem.*, 1991, **24**, 43; F. Joó and Z. Toth, *J. Mol. Catal.*, 1980, **8**, 369.

2 D. M. Roundhill, *Adv. Organomet. Chem.*, 1995, **38**, 155.

3 J. H. Espenson, *Acc. Chem. Res.*, 1992, **25**, 222.

4 W. M. Rees, M. R. Churchill, Y. J. Li and J. D. Atwood, *Organometallics*, 1985, **4**, 1162.

5 P. J. Roman Jr. and D. P. Paterniti, see M. R. Churchill and J. D. Atwood, *Organometallics*, 1997, **16**, 1484.

*Received in Columbia, MO, USA, 1st April 1997; 7/02197F*

# Continuous hydrogenation of organic compounds in supercritical fluids

**Martin G. Hitzler and Martyn Poliakoff***

*Department of Chemistry, University of Nottingham, Nottingham, UK NG7 2RD*

**A small flow reactor (5 ml volume) is used for continuous hydrogenation in supercritical $CO_2$ or propane with polysiloxane-supported noble metal catalysts; a wide range of organic functionalities can be hydrogenated with good throughput (up to 1200 ml $h^{-1}$ in favourable cases) and the various parameters (temperature, pressure, concentration of $H_2$, *etc.*) can be controlled *independently* to optimise the selectivity for a particular product.**

Hydrogenation of organic compounds is a process of major chemical importance. Gaseous $H_2$ is an inexpensive and versatile reagent for hydrogenation but it can often be difficult to use in practice. Laboratory-scale hydrogenation is usually slow because $H_2$ is sparingly soluble in common solvents. By contrast, supercritical fluids are completely miscible[1] with $H_2$, but it is only recently that this miscibility has been exploited[2–9] for hydrogenation and related reactions, mostly as batch reactions in sealed autoclaves. However, the gas-like nature of supercritical fluids makes them particularly suitable for continuous flow reactors. For any reaction, a flow reactor can be smaller than the corresponding batch reactor needed to generate a comparable amount of product. This reduction in size is particularly attractive for supercritical fluid systems because it reduces both the cost and the safety problems of high pressure equipment. There is a very brief report[10] of an industrial supercritical hydrogenation process with a 250-fold reduction in the volume of the reactor, and more recently small-scale reactors have been used to hydrogenate fats and fatty esters in near-critical or supercritical $CO_2$ ($scCO_2$) and propane (scPropane).[11,12]

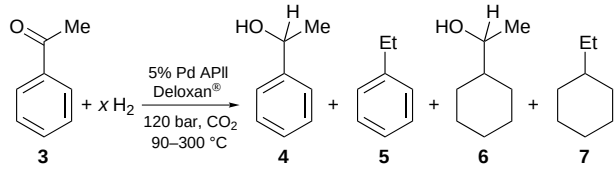
Here, we describe the use of a flow reactor system† for a wide range of continuous hydrogenation reactions. Although the reactor is larger than our previous flow reactors for the photochemical synthesis of organometallic dihydrogen compounds,[13] the entire apparatus can still be accommodated within a standard fume cupboard. The hydrogenation of cyclohexene **1** to cyclohexane **2** was used to establish the performance of the reactor. The reaction was extremely rapid in $scCO_2$ [$T_c$ = 31.1 °C, $P_c$ = 73.8 bar (10 bar = 1 MPa)] or scPropane ($T_c$ = 96.8 °C, $P_c$ = 42.6 bar) and could be initiated without any external heating of the reactor. Table 1 shows that the overall rate of conversion is extremely high, with up to 20 ml (0.2 mol) per minute of **1** hydrogenated in a reactor (5 ml volume) containing only 4 ml of catalyst.

The role of the supercritical fluid is almost certainly more complex than merely enhancing the concentration of $H_2$. The fluid reduces viscosity and increases diffusion rates compared to the liquid phase, so that transport to and from the catalyst surface is no longer a limiting factor. At flow rates > 1.5 ml $min^{-1}$ of substrate, we have measured temperatures > 300 °C in the catalyst bed, higher even than the critical temperature of cyclohexene itself ($T_c$ = 287.3 °C, $P_c$ = 43.4 bar). Indeed, at high throughput, we have found that once the temperature of the reactor has stabilised, only a very small flow of $scCO_2$ is required to sustain the reaction; the mixture is predominantly cyclohexene and $H_2$, which measurements in our laboratory have shown to be completely miscible under these conditions.‡ Experiments with a commercially significant derivative of cyclohexene indicate that hydrogenation in $scCO_2$ is more selective than the gas phase reaction and is quicker than the liquid phase, requiring *ca*. 35 times less catalyst.

The particular advantage of supercritical fluids is the ability to control conditions with great precision and, hence, to manipulate the selectivity of reactions. Thus, the hydrogenation of acetophenone **3** can lead to at least four possible products **4**–**7** (Scheme 1).

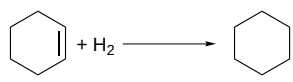
When the reactor is operated with $scCO_2$ at 90 °C, there is almost quantitative conversion of **3** to **4**. As the amount of $H_2$ and the temperature of the reactor are raised, there is a controllable shift towards the more hydrogenated products so that, by 300 °C, **7** is the major product (see Fig. 1).

However, the presence of a single phase within the reactor means that the various parameters (temperature, pressure, concentration of $H_2$, *etc.*) can be adjusted *independently*. Thus, reducing the ratio of $H_2$ : **3** from 4 : 1 to 2 : 1 (at $T$ = 200 °C and




**Scheme 1**

**Table 1** Hydrogenation of cyclohexene **1**




**1** **2**

| Catalyst | Fluid | Flow rate[a] of fluid/ l $min^{-1}$ | Flow of **1**/ ml $min^{-1}$ | Ratio of **1** : $H_2$ | $T_{wall}$/°C | Pressure/ bar | Yield of **2** (%)[b] |
|---|---|---|---|---|---|---|---|
| 5% Pd[c] | $scCO_2$ | 0.75–1.65 | 0.5–20.0 | 1 : 2–4 | 40–320 | 120 | 95–98 |
| 5% Pd[c] | scPropane | 0.75 | 0.5–2.0 | 1 : 2 | 100–170 | 60 | 96 |
| 5% Pt[d] | scPropane | 0.75 | 0.5–2.0 | 1 : 2 | 100–170 | 80 | 96 |

[a] Fluid flow rate measured at 1 atm and 20 °C as determined by bubble flow meter. [b] Analysis by GC using external standards. [c] APII 5% Pd Deloxan®, particle size: 0.3–0.8 mm. [d] APII 5% Pt Deloxan®, particle size: < 0.2 mm.

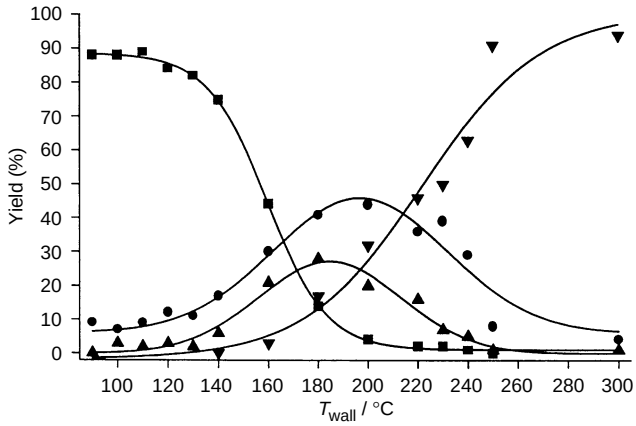
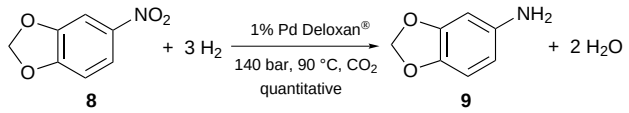



**Fig. 1** Dependence of product distribution on reactor wall temperature for the hydrogenation of acetophenone **3** in $scCO_2$ with 5% Pd APII Deloxan® catalyst: (■) **4**, (●) **5**, (▲) **6** and (▼) **7**. Reactions were run with flow rates of 0.5 ml $min^{-1}$ **3**, 1.0 ml $min^{-1}$ gaseous $CO_2$, and a ratio of $H_2$:**3** increasing from 2:1 to 6:1 at higher temperatures. The total pressure was held at 120 bar throughout. Product analysis by $^1H$ NMR spectroscopy ($CDCl_3$).

$p$ = 120 bar) increases the yield of **5** from 44 to 69% at the expense of **7**, or reducing the total pressure (at $T$ = 240 °C and with *constant* $H_2$:**3** = 4:1) from 120 to 40 bar (*i.e.* to the near-critical region) reduces the degree of hydrogenation, changing the ratio of products **5**:**7** from 1:2 to 2:1, presumably by reducing the residence time. Thus, without changing catalyst, one can tune conditions to maximise the yield of a particular product, and the reactor is then sufficiently stable to maintain those conditions.

The reactor is primarily designed to operate with reactants and products which are liquids at ambient temperature but it can also be used to hydrogenate solids, dissolved in an inert organic solvent. For example, 1,2-(methylenedioxy)-4-nitrobenzene§ **8** (mp 146–148 °C) was hydrogenated quantitatively to **9** in $scCO_2$ by pumping it through the reactor (*ca*. 8 g $h^{-1}$) in MeOH–THF (2:1 v/v) (Scheme 2).




**Scheme 2**

The flow reactor can be used to hydrogenate a substantial range of other organic functional groups. Epoxides, oximes, nitriles, alcohols and aromatic and aliphatic aldehydes and ketones have been successfully hydrogenated, most with conversions comparable to those described above and several with better selectivity than in non-supercritical hydrogenation. Most significantly, we have shown that compounds can be hydrogenated continuously on a relatively large scale using reactors of very small volume. Thus supercritical fluids can transform hydrogenation with gaseous $H_2$ into a viable, rapid and highly controllable laboratory technique for organic chemistry on a large preparative scale. At the same time, only modest scale-up will be required to generate compounds in quantities appropriate to the industrial production of some pharmaceuticals and fine chemicals.

We thank Thomas Swan & Co Ltd for fully funding this work and D. Campbell, S. K. Ross and J. C. Toler for their assistance. We are grateful to Degussa AG for donating the catalysts. We thank F. R. Smail, M. W. George, M. Guyler, S. M. Howdle, A. Kordikowski, K.-H. Pickel, K. Stanley, T. Tacke and S. Wieland for their help. M. P. thanks the EPSRC/Royal Academy of Engineering for a Fellowship.

## Footnotes and References

* E-mail: Martyn.Poliakoff@nottingham.ac.uk

† The substrate, supercritical fluid and $H_2$ are brought together in a heated mixer, passed through the reactor containing the catalyst, and then expanded to separate the product from the fluid and excess $H_2$. The reactor is assembled from commercially available units: $scCO_2$ and scPropane pump PM101, $H_2$ compressor CU105 and Expansion Module PE103 (all from NWA GmbH, Lörrach, Germany), a high pressure mixer (Medimix) and a Gilson 305 pump (for the organic substrate). **Safety note**: Flow reactors have a comparatively small volume under pressure. Nevertheless, equipment with the appropriate pressure and temperature rating should always be used for high pressure experiments.

‡ Although previous reports have shown that hydrogenation catalysts can be rather short-lived under supercritical conditions (ref. 11), we have found that the Deloxan® catalysts (S. Wieland and P. Panster, *Catalysis of Organic Reactions*, Marcel Dekker, New York, 1995, p. 383) have survived several hours under these harsh conditions and can even be used successfully up to 400 °C.

§ The hydrogenation of nitrobenzene itself over a 5% Pt APII Deloxan® catalyst in scPropane is particularly striking, with conversion of *ca*. 25% of the starting material to $NH_3$ and cyclohexane, a reaction which requires addition of no less than seven $H_2$ molecules to each molecule of nitrobenzene within a residence time of $< 5$ min in the reactor (200 °C, 80 bar). By contrast, a 1% Pd APII Deloxan® catalyst gives aniline in 100% yield under similar conditions.

1 C. Y. Tsang and W. B. Streett, *J. Eng. Sci.*, 1981, **36**, 993.
2 S. M. Howdle, M. A. Healy and M. Poliakoff, *J. Am. Chem. Soc.*, 1990, **112**, 4804.
3 J. W. Rathke, R. J. Klingler and T. R. Krause, *Organometallics*, 1991,**10**, 1350.
4 P. G. Jessop, T. Ikariya and R. Noyori, *Nature*, 1994, **368**, 231.
5 P. G. Jessop, Y. Hsiano, T. Ikariya and R. Noyori, *J. Am. Chem. Soc.*, 1996, **118**, 344.
6 M. J. Burk, S. Feng, M. F. Gross and W. Tumas, *J. Am. Chem. Soc.*, 1995, **117**, 8277.
7 B. Minder, T. Mallat, K.-H. Pickel, K. Steiner and A. Baiker, *Catal. Lett.*, 1995, **34**, 1.
8 O. Kröcher, R. A. Köppel and A. Baiker, *Chymia*, 1997, **51**, 48.
9 K.-H. Pickel and K. Steiner, *Proc. 3rd Int. Symp. Supercritical Fluids*, Strasbourg, 1994, **3**, 25.
10 *Roche Magazin*, 1992, **41**, 2.
11 T. Tacke, S. Wieland and P. Panster, *Process Technol. Proc.*, 1996, **12**, 17.
12 M. Härröd and P. Møller, *Process Technol. Proc.*, 1996, **12**, 43.
13 J. A. Banister, P. D. Lee and M. Poliakoff, *Organometallics*, 1995, **14**, 3876.

*Received in Liverpool, UK, 20th June 1997; 7/04371F*

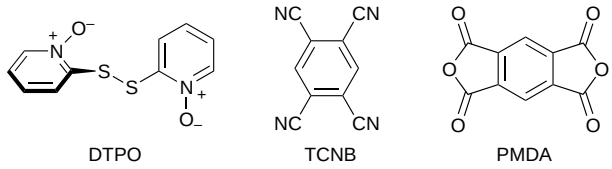
# Supramolecular networks *via* pyridine *N*-oxide CH···O hydrogen bonding in the crystal structures of 2,2′-dithiobis(pyridine *N*-oxide) and its complexes with 1,2,4,5-tetracyanobenzene and pyromellitic dianhydride

**Satish G. Bodige, Robin D. Rogers and Silas C. Blackstock***

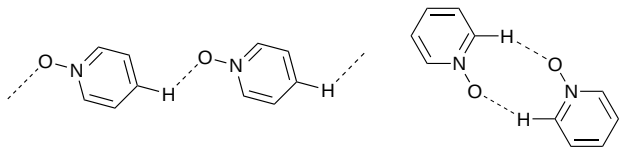
*Department of Chemistry, The University of Alabama, Tuscaloosa, Alabama 35487-0336, USA*

**CH··O hydrogen bonding in crystals of 2,2′-dithiobis(pyridine *N*-oxide) (DTPO) supports network formation.**

Crystal packing depends critically upon molecular geometry and directional intermolecular forces. Conventional hydrogen bonding (X–H··Y; X, Y = N or O) has been extensively employed to command supramolecular network formation in organic solids.[1,2] By comparison, the construction of networks *via* weak CH···O hydrogen bonding[3] is much less advanced, despite the widespread importance of these interactions.[4] Here, we present a set of new supramolecular networks constructed from pyridine *N*-oxide (PO) CH···O hydrogen bonds in the crystal structures of 2,2′-dithiobis(pyridine *N*-oxide) (DTPO) and its complexes with tetracyanobenzene (TCNB) and pyromellitic dianhydride (PMDA).




Precedence for PO self association *via* hydrogen bonding can be found in the Cambridge Structure Database (CSD).[5]† Both chain propagating (**X**) and chain termination (**Y**) modes of CH···O bonding occur, the former being much more common




than the latter. For DTPO, self-association in at least two dimensions *via* CH···O interactions should be possible if the conformational preference of aryl disulfides (twisted orientation of aryl rings) survives in the solid. Thus, we have investigated the CH···O network formation ability of DTPO in the solid state.

Crystals of DTPO **1** [mp 205 °C (decomp.)] were grown from nitromethane and analysed by X-ray diffraction.‡ The crystal structure is a three-dimensional CH···O bonded racemic supernetwork in which each DTPO molecule participates in eight (four unique) CH···O hydrogen bonds (see Fig. 1). By virtue of the disulfide conformational preference for a 90° C–S–S–C twist angle,[6] the DTPO molecule is axially dissymmetric. Both DTPO enantiomers are present in crystal **1**. We refer to the lattice as a supernetwork because it is composed of two interpenetrated three-dimensional homochiral DTPO networks which associate *via* two (of eight) CH···O hydrogen bonds per DTPO molecule.

The open network character of the homochiral fragments of **1** suggested that guest inclusion in a DTPO lattice might be possible. To test this possibility, DTPO was crystallized in the presence of electron-deficient additives TCNB and PMDA.[7]

Light yellow crystals of $(DTPO)_2TCNB(H_2O)_4$ **2** [mp 250 °C (decomp.)] were obtained from nitromethane,‡ Homochiral networks are not observed in **2**, but guest inclusion is observed. In this cocrystal, DTPO molecules self-assemble *via* **X** and **Y** mode CH···O bonding to yield a ladder host array clathrated by TCNB guests, as shown in Fig. 2. The ladder cavity dimensions are 8.4 × 6.5 Å, and the cavity contains π-stacked DTPO dimer donor and TCNB acceptor moieties with an inter-plane distance of *ca*. 3.25 Å, indicative of an attractive donor–acceptor (DA) interaction.[8] Two unique water molecules (not shown) also appear in the lattice between ladders and hydrogen bond to each other and to the DTPO oxygens of the ladder host. These water molecules fill space between the DTPO superstructures and, by OH···O hydrogen-bonding, effectively cross-link adjacent DTPO ladders which orient parallel to each other in the lattice.

In the presence of PMDA in MeCN, DTPO forms dark yellow plates of $(DTPO)_2PMDA$ **3** [mp 220 °C (decomp.)].‡ The crystal structure is shown in Fig. 3. The DTPO host network of **3** closely resembles that of **2**, yielding guest-occupied DTPO

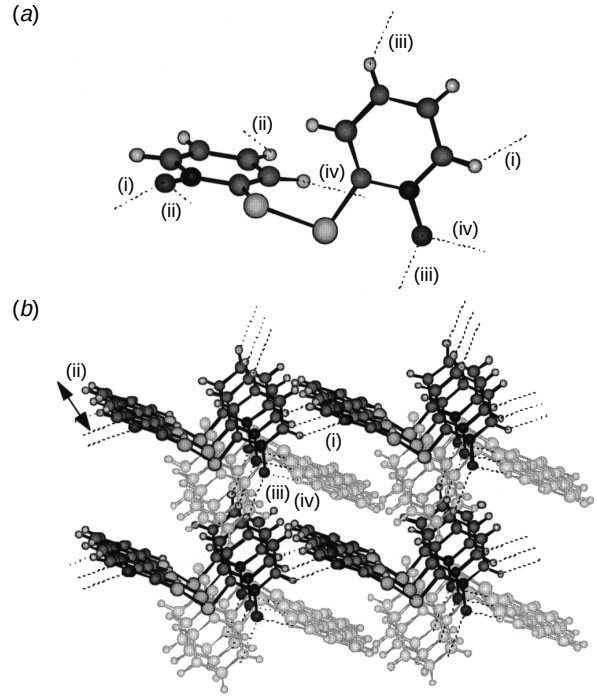



**Fig. 1** CH···O hydrogen bonding at DTPO in crystal **1**: (*a*) single DTPO molecule and (*b*) enantiomer-shaded racemic network; [H···O (Å), C(H)···O (Å), CH···O (°)]: (i) 2.36(2), 3.113(2), 137(2); (ii) 2.35(3), 3.170(3), 143(2); (iii) 2.41(2), 3.179(2), 146(2); (iv) 2.44(2), 3.346(2), 157(2)

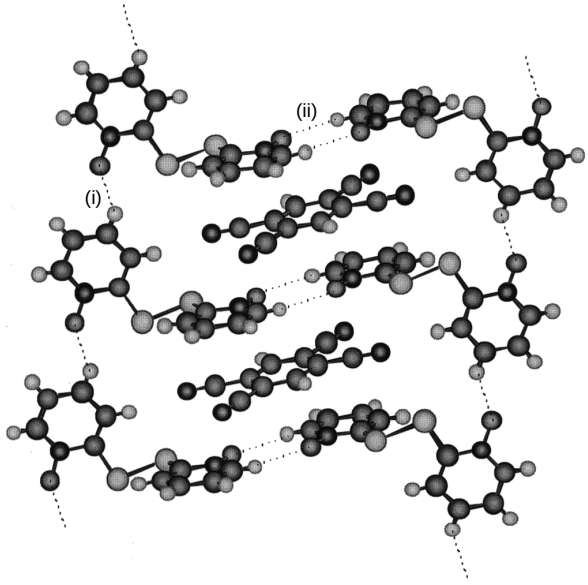



**Fig. 2** TCNB-occupied DTPO ladder host network of crystal **2**; [H···O (Å), C(H)···O (Å), CH···O (°)]: (i) 2.48(3), 3.252(3), 142(2); (ii) 2.38(3), 3.281(3), 169(3)

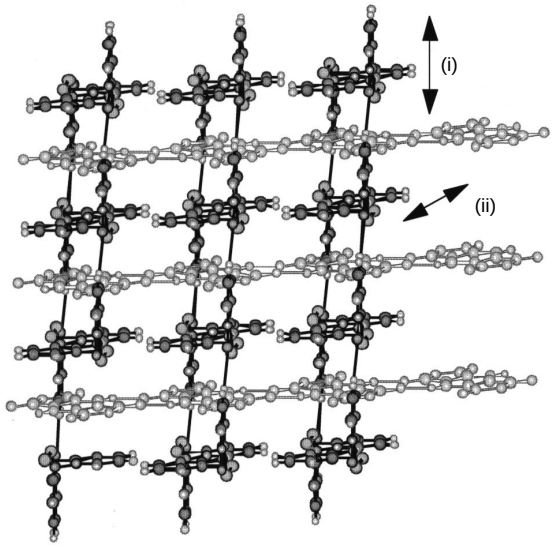
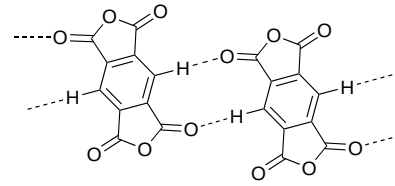



**Fig. 3** DTPO ladder host networks (dark) threaded by PMDA stands (light) in crystal **3**: [H···O (Å), C(H)···O (Å), CH···O (°)]: DTPO (i) 2.32(3), 3.130(3), 145(2); DTPO (ii) 2.35(3), 3.220(3), 172(3); PMDA 2.36(3), 3.257(3), 164(2)

ladders. An added feature of **3** is guest self-association. PMDA forms 10-membered rings as CH···O hydrogen bonded dimers,[9] giving PMDA tapes which thread the ladder host cavities to form a two-dimensional host–guest array with a novel supramolecular polypseudorotaxane architecture.[10] The plane-to-plane distance between DTPO and PMDA rings is *ca*. 3.3 Å. Adjacent DTPO ladders on different threads associate *via* a third (interladder) CH···O hydrogen bond‖ between DTPOs to complete three-dimensional ordering of the lattice. From a crystal engineering perspective, **3** is a novel solid in which three distinct supramolecular bonding schemes cooperate to effect three-dimensional molecular organization in the two-component solid.



In summary, the above structures illustrate the propensity of the pyridine *N*-oxide units of DTPO to form networks *via* CH···O bonding in the solid state. Knowledge of such interactions is important to crystal engineering with the POs whose strong molecular dipole makes them attractive substrates for optical or electronic materials preparation. Structures **2** and **3** display an interplay of CH···O and π DA interactions, culminating in three-dimensional host–guest arrays.

We acknowledge the NSF and donors of the Petroleum Research Foundation, administered by the ACS, for support and L. M. Rogers for technical assistance.

## Footnotes and References

* E-mail: sblackst@ua1vm.ua.edu

† Although CH···O hydrogen bonding of POs has not previously been exploited for crystal engineering, many previous examples can be found in the CSD. A PO substructure search (CSD, Dec. 1996) found 59 hits, all of which display CH···O close contacts.

‡ *Crystal data* was collected on a Siemons diffractometer ($\lambda$ = 0.71073 Å) with a SMART/CCD area detector. Hydrogens were positioned from difference Fourier maps and refined isotropically (SHELXL-93). Final full matrix least-squares refinement was done on $F^2$ with all data. CH··O geometries refer to normalized (1.08 Å) C–H distances. For **1**: $C_{10}H_8N_2O_2S_2$, triclinic, $P\bar{1}$, $a$ = 7.0793(2), $b$ = 7.0898(1), $c$ = 10.7979(3) Å, $\alpha$ = 86.800(1), $\beta$ = 73.725(2), $\gamma$ = 89.129(2)°, $V$ = 519.43(2) Å$^3$, $Z$ = 2, $D_c$ = 1.613 g cm$^{-3}$, $T$ = 173(2) K. Data collection (1.97 < $\theta$ < 27.92°) gave 2297 reflections with $I > 2\sigma(I)$ out of 3319 total unique reflections and refinement gave $R_1$ = 0.036, $wR_2$ = 0.080 and GOF = 1.019. For **2**: $C_{15}H_{13}N_4O_4S_2$, triclinic, $P\bar{1}$, $a$ = 7.1382(2), $b$ = 10.7477(3), $c$ = 11.3481(4) Å, $\alpha$ = 100.566(1), $\beta$ = 99.021(1), $\gamma$ = 91.340(1)°, $V$ = 844.05(4) Å$^3$, $Z$ = 2, $D_c$ = 1.485 g cm$^{-3}$, $T$ = 293(2) K. Data collection (1.85 < $\theta$ < 27.89°) gave 3752 reflections with $I > 2\sigma(I)$ and 5314 total unique reflections and refinement gave $R_1$ = 0.55, $wR_2$ = 0.107 and GOF = 1.163. For **3**: $C_{15}H_9N_2O_5S_2$, triclinic, $P\bar{1}$, $a$ = 6.9849(2), $b$ = 7.3531(2), $c$ = 15.3700(2) Å, $\alpha$ = 77.007(2), $\beta$ = 77.504(2), $\gamma$ = 81.529(2)°, $V$ = 746.93(3) Å$^3$, $Z$ = 2, $D_c$ = 1.607 g cm$^{-3}$, $T$ = 173(2) K. Data collection (1.38 < $\theta$ < 27.87°) gave 3307 reflections with $I > 2\sigma(I)$ and 4782 total unique reflections and refinement gave $R_1$ = 0.063, $wR_2$ = 0.109 and GOF = 1.038.

‖ The interaction occurs between a ladder rung DTPO CH *ortho* to the disulfide and the NO oxygen of an adjacent ladder rail with H···O 2.38(3), C(H)···O = 3.136(3) and CH···O = 139(2) Å.

1 For a review see: J.-M. Lehn, *Supramolecular Chemistry: Concepts and Perspectives*, VCH, Weinhiem, 1995 and references cited therein.
2 Y. Aoyama, K. Endo, T. Anzai, Y. Yamaguchi, T. Sawaki, K. Kobayashi, N. Kanehisa, H. Hashimoto, Y. Kai and H. Masuda, *J. Am. Chem. Soc.*, 1996, **118**, 5562 and references cited therein.
3 For a review, see G. R. Desiraju, *Acc. Chem. Res.*, 1996, **29**, 441.
4 R. Taylor and O. Kennard, *J. Am. Chem. Soc.*, 1982, **104**, 5063.
5 For an example see E. Buncel, S. R. Keum, M. Cygler, K. I. Varughese and G. I. Birnbaum, *Can. J. Chem.*, 1984, **62**, 1628.
6 *The Chemistry of Sulfur-Containing Functional Groups*, ed. S. Patai and Z. Rappoport, Wiley, New York, 1993.
7 For a report of guest inclusion to avoid network interpretation, see S. V. Kolotuchin, E. F. Fenlon, S. R. Wilson, C. J. Loweth and S. C. Zimmerman, *Angew. Chem., Int. Ed. Engl.*, 1995, **34**, 2654.
8 C. K. Prout and B. Kamenar, in *Molecular Complexes*, ed. R. Foster, Elek, London, 1973; R. Foster, *Organic Charge Transfer Complexes*, Academic Press, New York, 1969.
9 For a previous example of PMDA tape formation, see V. N. Baumer and V. A. Starodub, *Synth. Met.*, 1984, **9**, 467.
10 D. B. Ambilino and J. F. Stoddart, *Chem. Mater.*, 1994, **6**, 1159.

*Received in Columbia, MO, USA, 1st April 1997; 7/02199B*

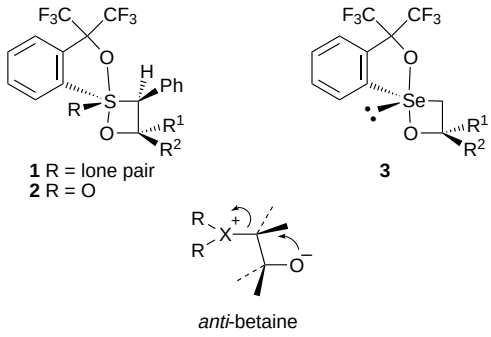
# Novel reactivity of tetracoordinate 1,2λ⁴-oxaselenetanes: oxirane formation reaction with retention of configuration

**Fumihiko Ohno, Takayuki Kawashima*† and Renji Okazaki***

*Department of Chemistry, Graduate School of Science, The University of Tokyo, 7-3-1 Hongo, Bunkyo-ku, Tokyo 113, Japan*

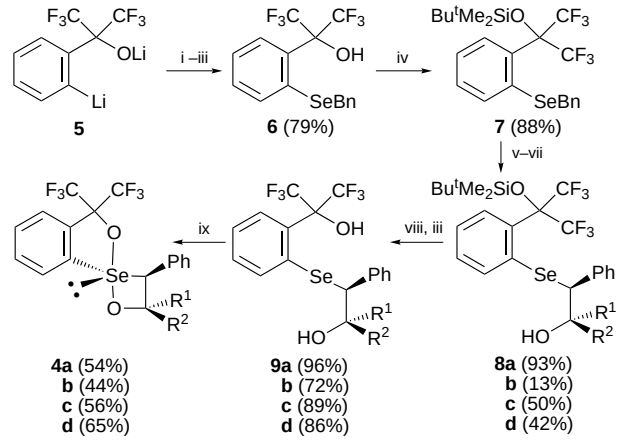
**Stable tetracoordinate 3-phenyl-1,2λ⁴-oxaselenetanes give the corresponding oxiranes upon thermolysis; in sharp contrast to Corey–Chaykovsky type reactions, oxirane formation proceeds with retention of configuration, and the reaction can be recognised as a new type of carbon–oxygen ligand coupling reaction of λ⁴-selenanes.**

The reactions of carbonyl compounds with phosphorus ylides (Wittig reaction) afford alkenes *via* 1,2λ⁵-oxaphosphetanes,[1] while those with group 16 element (S, Se, Te) ylides (Corey–Chaykovsky type reaction) give oxiranes.[2] The latter type of oxirane formation reaction has been proposed to involve the formation of an *anti*-betaine followed by a back side attack of an oxido anion on the β-carbon.[2,3] In the course of our study on oxetanes bearing a highly coordinate main group element at the position adjacent to the oxygen atom,[4] we have reported the syntheses and isolations of tetra- and penta-coordinate 1,2-oxathietanes **1** and **2**, and the oxirane formation reaction with




retention of configuration in the thermolysis of **2**.[5] This stereochemistry suggests another possible mechanism for the Corey–Chaykovsky reaction, *i.e.* the formation and carbon–oxygen ligand coupling reaction[6] of intermediary highly coordinate 1,2-oxathietanes, which prompted us to examine the reactivity of such a species on changing the central atom from sulfur to a heavier chalcogen. Although no oxirane formation was observed in the thermolysis of the first tetracoordinate 1,2λ⁴-oxaselenetanes **3** having no substituent at the 3-position,[7] 3-phenyl derivatives were expected to give the corresponding oxiranes in view of the reactivity of the sulfur analogues. We now report on the first example of oxirane formation from tetracoordinate 1,2λ⁴-oxaselenetanes and the stereochemistry of the reaction.

Tetracoordinate 3-phenyl-1,2-oxaselenetanes **4**‡ were synthesised from **5**[8] by the same method as that for the synthesis of sulfur analogues **1** (Scheme 1).[5]§ The $^{19}F$ and $^{1}H$ NMR spectra of the crude reaction mixtures showed the signals due to the diastereoisomers of **4** in which the phenyl group was *cis* to the lone pair. However, the *cis* isomers were less stable toward hydrolysis than **4** and gradually decomposed in the course of purification. All compounds **4** were stable colourless plates at room temperature in the air. The relative stereochemistry between the 3- and 4-positions of **4c** and **4d** was determined by differential NOE experiments; an NOE between the methine

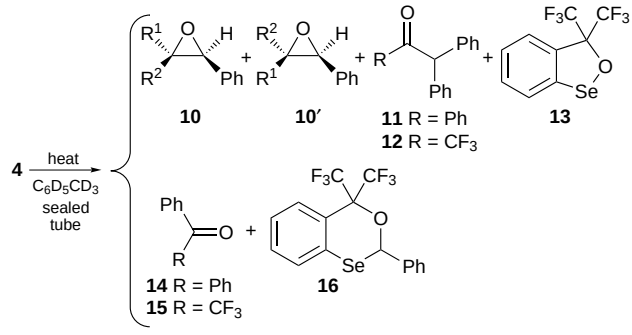



**Scheme 1** *Reagents and conditions*: i, Se, THF, 0 °C, then 25 °C, 12 h; ii, BnBr, 0 °C, then 25 °C, 2 h; iii, aq. $NH_4Cl$; iv, $Bu^tMe_2SiOSO_2CF_3$, $Et_3N$, $CH_2Cl_2$, 0 °C, then 40 °C, 1 d; v, LDA (2 equiv.), THF, −78 °C, 20 min; vi, $R^1R^2C{=}O$, THF, −78 °C, 30 min; vii, flash column chromatography (for **8c** and **8d**); viii, $Bu^n_4NF$ (2 equiv.), THF, 0 °C, 30 min; ix, $Et_3N$ (2 equiv.), $Br_2$ (1 equiv.), $CCl_4$, 0 °C, then 25 °C, 4 h.

proton of the 3-carbon and the *ortho*-protons of the phenyl group of the 4-carbon was observed for **4c** but not for **4d**.

The results of thermolysis ($C_6D_5CD_3$, in a degassed sealed tube) of **4** are summarised in Scheme 2 and Table 1. Although the yield of oxirane **10a** from the 3,4,4-triphenyl derivative **4a** was low because of concomitant phenyl-migrated ketone formation, **4b** gave oxirane **10b** almost quantitatively. Furthermore, thermolysis of **4c** and **4d** afforded the corresponding oxirane stereospecifically in high yield with retention of the relative stereochemistry of the starting oxaselenetanes, although a small amount (2%) of an inverted product was obtained from **4c**.

These results indicate that the stereochemistry of the oxirane formation from 1,2-oxaselenetanes **4** is the reverse of that

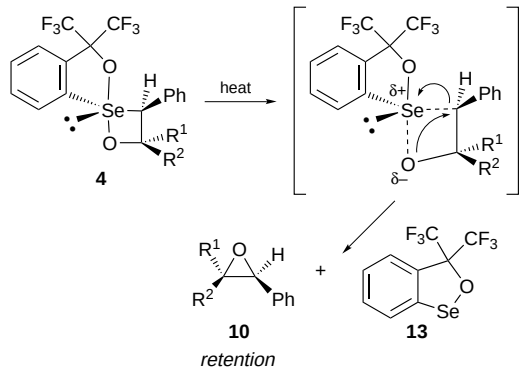



**Scheme 2**

**Table 1** Yields of products in the thermolysis of 1,2λ⁴-oxaselenetanes **4**

| | | | | | Yield (%)[a] | | | | | | | |
|---|---|---|---|---|---|---|---|---|---|---|---|---|
| | $R^1$ | $R^2$ | *T*/°C | *t* | **10** | **10′** | **11** | **12** | **13** | **14** | **15** | **16** |
| **4a** | Ph | Ph | 130 | 3 d | 43 | —[b] | 52 | — | 95 | —[c] | — | 5 |
| **4b** | $CF_3$ | $CF_3$ | 200 | 6 d | quant. | —[b] | — | — | quant. | — | — | — |
| **4c** | Ph | $CF_3$ | 200 | 30 h | 88 | 2 | — | 8 | 97 | — | 2 | 2 |
| **4d** | $CF_3$ | Ph | 200 | 5 h | quant. | — | — | — | quant. | — | — | — |

[a] Estimated by $^{19}F$ and $^1H$ NMR spectroscopy. [b] **10′** is equal to **10**. [c] Observed by GC–MS.




**Scheme 3**

expected from the back side attack of the oxido anion, and hence the reaction can be recognised as a carbon–oxygen ligand coupling reaction of λ⁴-selenanes (Scheme 3). In the thermolysis of **4**, migration of the phenyl group on the 4-carbon¶ and deprotonation from the 3-position by the oxido anion can be considered to be sterically inhibited by the phenyl group on the 3-position, which is absent in **3**. Moreover, it can be assumed that the phenyl group on the 3-carbon assists the Se–C bond cleavage by stabilising the anionic character of the 3-carbon induced in the transition state.

In the case of the sulfur analogues **1**,[5a,b] oxirane formation was observed to a minor extent, with fragmentation back to the starting ketone or isomerisation *via* a 1,3-proton shift being the major decomposition pathways; this made it difficult to elucidate the reaction mechanism although oxirane formation from **1** with retention of configuration was observed.[9] In sharp contrast, in the reaction of **4c** and **4d**, yields of oxirane were almost quantitative and the stereochemistry exhibited 96 and 100% retention of configuration, respectively. The present results and the stereochemistry of the thermolysis of **2**[5c] strongly suggest that such a concerted oxirane formation from highly coordinate oxachalcogenetanes generally proceeds regardless of the central atom or its coordination number.‖

This work was partially supported by a Grant-in-Aid for Scientific Research on Priority Area (No. 09239101) (T. K.) from the Ministry of Education, Science, Sports and Culture, Japan. F. O. is grateful for a Research Fellowship from the Japan Society for the Promotion of Science for Young Scientists. We thank Shin-etsu Chemicals, Central Glass and Tosoh Akzo Co. Ltd. for gifts of silyl chlorides, organofluorine compounds, and alkyllithiums, respectively.

## Footnotes and References

† E-mail: takayuki@chem.s.u-tokyo.ac.jp

‡ *Selected data* for **4c**: colourless plates (hexane–$Et_2O$); mp 192.4–194.0 °C (decomp.); $^1H$ NMR ($CDCl_3$, 500 MHz): δ 6.21 (s, 1 H, SeC*H*Ph), 7.32–7.41 (m, 3 H), 7.44–7.51 (m, 3 H), 7.54 (d, $^3J$ 7.6, 4 H), 7.64–7.68 (m, 2 H), 7.75–7.81 (m, 1 H), 8.57 (d, $^3J$ 7.9, 1 H); $^{77}Se$ NMR ($CDCl_3$, 95 MHz): δ 792.9 (q, $^4J_{SeF}$ 27). Calc. for $C_{24}H_{15}F_9O_2Se$: C, 49.25; H, 2.58. Found: C, 49.25; H, 2.64%.

For **4d**: colourless plates (hexane–$Et_2O$); mp 149.0–150.5 °C (decomp.); $^1H$ NMR ($CDCl_3$, 500 MHz): δ 6.46 (s, 1 H, SeC*H*Ph), 6.85 (d, $^3J$ 7.4, 2 H), 7.16–7.32 (m, 8 H), 7.74–7.79 (m, 2 H), 7.85–7.90 (m, 1 H), 8.57 (d, $^3J$ 8.0, 1 H); $^{77}Se$ NMR ($CDCl_3$, 51.5 MHz): δ 781.0 (s). Calc. for $C_{24}H_{15}F_9O_2Se$: C, 49.25; H, 2.58. Found: C, 49.39; H, 2.70%. Satisfactory $^{13}C$ and $^{19}F$ NMR spectra were obtained for both **4c** and **4d**.

§ In the synthesis of **8b**, other products formed by an electrophilic reaction of hexafluoroacetone at the *para*-position of the benzyl group were obtained.

¶ The phenyl migration in **4c** and **4d** was additionally retarded by the electronic effect of the adjacent trifluoromethyl group.

‖ Although the stereochemistry of the oxirane formation from 4,4-diaryl-3-phenyl derivatives has not been elucidated, it is unlikely that the trifluoromethyl group at the 4-position changed its stereochemistry completely, because the electron-withdrawing group of the position can electronically stabilise both the ground state and the transition state.

1 For reviews, see I. Gosney and A. G. Rowley, in *Organophosphorus Reagents in Organic Synthesis*, ed. J. I. G. Cadogan, Academic Press, New York, 1979, pp. 17–153; B. E. Maryanoff and A. B. Reitz, *Chem. Rev.*, 1989, **89**, 863.

2 For the Corey–Chaykovsky reaction, see J. Aubé, in *Comprehensive Organic Synthesis: Selectivity, Strategy, and Efficiency in Modern Synthetic Chemistry*, ed. B. M. Trost and I. Fleming, Pergamon, Oxford, 1991, vol. 1, pp. 822–825. For aminosulfoxonium ylides, see C. R. Johnson, *Acc. Chem. Res.*, 1973, **6**, 341. For selenonium ylides, see A. Krief, W. Dumont, D. Van Ende, S. Halazy, D. Labar, J.-L. Laboureur and T. Q. Lê, *Heterocycles*, 1989, **28**, 1203. For telluronium ylides, see A. Osuka and H. Suzuki, *Tetrahedron Lett.*, 1983, **24**, 5109; L.-L. Shi, Z.-L. Zhou and Y.-Z. Huang, *Tetrahedron Lett.*, 1990, **29**, 4173; Z.-L. Zhou, Y.-Z. Huang, L.-L. Shi and J. Hu, *J. Org. Chem.*, 1992, **57**, 6598.

3 C. R. Johnson and C. W. Schroeck, *J. Am. Chem. Soc.*, 1971, **93**, 5303; T. Durst, R. Viau, R. Van Den Elzen and C. H. Nguyen, *J. Chem. Soc., Chem. Commun.*, 1971, 1334; J. M. Townsend and K. B. Sharpless, *Tetrahedron Lett.*, 1972, 3313; T. Durst, C. R. Johnson, C. W. Schroeck and J. R. Shanklin, *J. Am. Chem. Soc.*, 1973, **95**, 5298.

4 T. Kawashima and R. Okazaki, *Synlett*, 1996, 600 and references cited therein.

5 (*a*) T. Kawashima, F. Ohno and R. Okazaki, *Angew. Chem., Int. Ed. Engl.*, 1994, **33**, 2094; (*b*) F. Ohno, T. Kawashima and R. Okazaki, *J. Am. Chem. Soc.*, 1996, **118**, 697; (*c*) T. Kawashima, F. Ohno, R. Okazaki, H. Ikeda and S. Inagaki, *J. Am. Chem. Soc.*, 1996, **118**, 12 455.

6 For a recent review, see S. Oae and Y. Uchida, *Acc. Chem. Res.*, 1991, **24**, 202. For a recent example, see S. Ogawa, S. Sato and N. Furukawa, *Tetrahedron Lett.*, 1992, **33**, 7925.

7 T. Kawashima, F. Ohno and R. Okazaki, *J. Am. Chem. Soc.*, 1993, **115**, 10 434.

8 E. F. Perozzi, R. S. Michalak, G. D. Figuly, W. H. Stevenson III, D. B. Dess, M. R. Ross and J. C. Martin, *J. Org. Chem.*, 1981, **46**, 1049.

9 F. Ohno, T. Kawashima and R. Okazaki, unpublished results.

*Received in Cambridge, UK, 18th June 1997; 7/04277I*

# The crystal packing of bis(2,2′-dipyridylamido)cobalt(II), $Co(dpa)_2$, is stabilized by C–H···N bonds: are there any real precedents?

**F. Albert Cotton,*[a] Lee M. Daniels,[a] Glenn T. Jordan IV[a] and Carlos A. Murillo*[a,b]**

[a] *Laboratory for Molecular Structure and Bonding, Department of Chemistry, Texas A&M University, College Station, TX 77843-3255, USA*

[b] *Department of Chemistry, University of Costa Rica, Ciudad Universitaria, Costa Rica*

**A crystallographic study of $Co(dpa)_2$ reveals that the pseudo-tetrahedral molecules stack together to form a one-dimensional ribbon with the molecules linked together through significant C–H···N interactions; the C···N separation is 3.41(3) Å and the angle at the hydrogen atom is 177(2)°.**

While studying the varied behavior of 2,2′-dipyridylamine, Hdpa, and its anion $dpa^-$, in cobalt complexes[1] we prepared† and structurally characterized‡ the pseudo-tetrahedral complex $Co(dpa)_2$, shown in Fig. 1. The two dpa anions are related by a crystallographic twofold axis and each is nearly planar; the dihedral angle between the two pyridyl rings within the ligand is only 3.6°. This feature is similar to that found for the copper analog.[2]

An analysis of the packing of the molecules in the crystal (Fig. 2) shows a prominent characteristic: the molecules stack in a way that gives an extended array with relatively short C(6)–H(6)···N(2B) contacts. The distances obtained from the X-ray diffraction studies are C(6)–H(6) 0.97(3) Å, H(6)···N(2B) 2.44(3) Å and C(6)···N(2B) 3.41(3) Å; the angle at the hydrogen atom is 177(2)°.

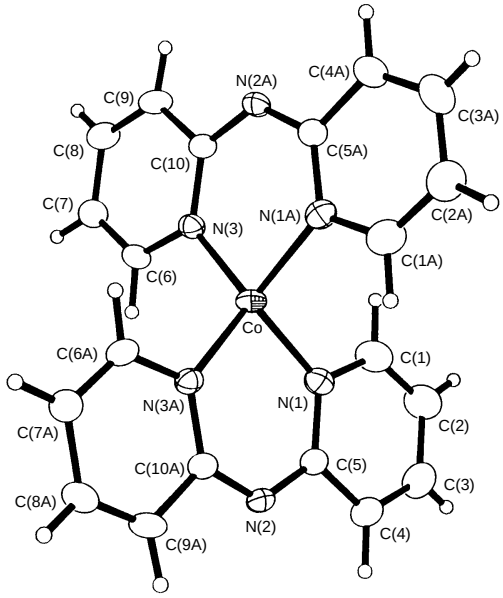



**Fig. 1** Molecular structure of $Co(dpa)_2$. Selected bond lengths (Å) and angles (°): Co–N(1) 1.972(2), Co–N(3) 1.963(2), N(1)–C(1) 1.364(4), N(1)–C(5) 1.367(4), N(2)–C(5) 1.346(4), N(2)–C(10A) 1.344(4), N(3)–C(6) 1.378(4), N(3)–C(10) 1.371(4); N(3)–Co–N(1) 120.66(9), N(3A)–Co–N(1) 94.5(1), C(10A)–N(2)–C(5) 128.2(2).

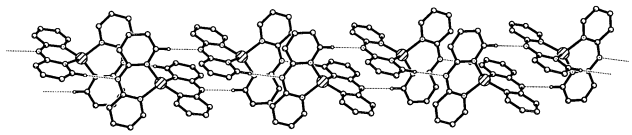


**Fig. 2** Packing diagram of $Co(dpa)_2$ viewed along the *a* axis showing the C–H···N bonds; C···N 3.41(3) Å, C–H 0.97(3) Å, N···H 2.44(3) Å, C–H···N 177(2)°

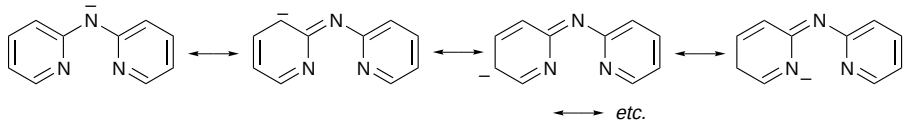
The questions that immediately arise are: how do these distances compare to those in other compounds with C–H···N interactions, and is it 'truly' a hydrogen bond? A superficial check of the literature quickly gives several references to 'C–H···N hydrogen bonds'.[3] However, as one starts to dig into the references to find the 'real examples' they are not easily found. Taylor and Kennard[4] give a few references to such bonds based on neutron diffraction studies. They assumed that C–H···N distances between 2.522 and 2.721 Å were indicative of hydrogen bonding. In their data, C–H···N angles varied from 157.3° to as low as 124.6°. Another system, which contains 1,3,5,7-tetrabromoadamantane, hexamethylenetetramine and $CBr_4$[5] is said to have a C–H···N bond when the C···N distance is 3.77 Å and the angle at the H atom is 151°.

Of course, the importance of hydrogen bonding is unquestionable in many aspects of chemistry,[6] particularly for so-called crystal engineering. As a result of the excitement in this field, the distinction between a simple classical van der Waals interaction and a hydrogen bond is being continuously blurred. A 'hydrogen bond' is regarded as 'any cohesive interaction X–H···Y, where H carries a positive and Y a negative (partial or full) charge',[7] where the angle at H can be anything > 90°, and consequently a 'very distorted geometry cannot be regarded as anomalous'.[8]

This type of very loose working definition has led to the proliferation of very questionable claims of 'hydrogen bonds' such as C–H···O in compounds where the C···O distance is 3.60 Å and the angle at H is 136°[9] or C···O of 3.82 Å and an angle of 154°.[10] Another recent example is the suggestion of 'intermolecular C–H···C interactions' in a complex which has a C···C distance of 3.83 Å and an angle at the H atom of 159°.[11]

It is clear that the field is getting muddier and muddier as the definition of a hydrogen bond is relaxed. What is not clear is why it is justified to continue to publish communications regarding this topic. We strongly disagree with the newer and more relaxed definitions that do not distinguish between a 'hydrogen bond' and what is nothing more than a classical van der Waals interaction.

In $Co(dpa)_2$, the linearity of the C–H···N moiety and the short N···H distance of 2.44 Å are possibly an indication of a relatively important hydrogen bonding interaction, especially when one takes into account that the C–H distance, as determined by X-ray crystallography, is roughly 0.10 Å shorter than the actual distance to the proton that would be determined by neutron diffraction.[12] Consequently, the probable N···H distance is about 2.33 Å. This value is among the shortest of the C–H···Y, Y = N or O distances.[13] A similar N···H interaction is also present in $Cu(dpa)_2$; the distance obtained from an X-ray crystallographic study is 2.52 Å. The reason why a short and possibly real C–H···N hydrogen occurs in $Co(dpa)_2$ is that the N atom doubtless bears a considerable amount of negative charge.




**Scheme 1**

From a valence bond resonance point of view, it appears that distribution of the negative charge on the dpa$^-$ ion away from the N atom from which the proton has been removed is not likely to be very complete, as shown in Scheme 1.

In the case of $Co(dpa)_2$ we believe that it is justified to invoke the existence of a C–H···N hydrogen bond. The sum of the van der Waals radii of H and N (1.2 + 1.5 = 2.7 Å) is significantly longer than the distance found (2.41 Å). Moreover, the C–H···N unit is very nearly linear. In most, if not all, of the previously claimed examples of C–H···N 'hydrogen bonds' the contact is little (or no) different from that expected for an ordinary, classical van der Waals contact and the angles at the H atom are well below (often far below) 180°. While the literature contains numerous allusions to C–H···N 'hydrogen bonds' there seems little if any reason to accept this description. Or, to invoke the parable of the emperor's new clothes, the question of why many people seem to find the emperor well dressed despite any persuasive evidence that he isn't naked, arises. In the packing of molecules containing both C–H bonds and N atoms, there seems to us to be no reason whatever to refer to perfectly normal van der Waals contacts between the two as 'hydrogen bonds'.

Support from the National Science Foundation and the University of Costa Rica is gratefully appreciated.

## Footnotes and References

* E-mail: cotton@tamu.edu; murillo@tamu.edu

† In a 100 ml round-bottom flask, 0.963 g (5.62 mmol) of Hdpa was dissolved in 30 ml of toluene. The solution was cooled to −78 °C and 4.1 ml of 1.4 M MeLi was added. The solution immediately turned milky white. The reaction mixture was warmed to near room temp. upon which 0.344 g (2.64 mmol) of anhydrous $CoCl_2$ was added from a solid addition tube. After several min of stirring, 20 ml of thf was added forming a dark red–brown solution. The reaction was stirred overnight at room temp. The majority of the product precipitates from solution as an orange powder. It was collected by filtration, washed twice with small amounts of thf, and dried under vacuum to yield 0.700 g (66.4%) of $Co(dpa)_2$. Crystals were obtained from work-up of the filtrate. The filtrate was evaporated to dryness and then dissolved in 25 ml of toluene to give a deep red-wine solution. This solution was filtered through Celite and layered with 40 ml of hexanes. Red crystals (0.0395 g, 3.75%) grew after two weeks of diffusion. IR (KBr, cm$^{-1}$): 3051w, 1609s, 1533s, 1440vs, 1250m, 1241m, 1146s, 1111w, 1095w, 1045w, 1006s, 894m, 849m, 786m, 767s, 733m, 726m, 656w, 553w. UV–VIS ($CH_2Cl_2$): $\lambda$ = 390, 355, 342 nm.

‡ *Crystal data* for $Co(dpa)_2$: crystal dimensions 0.18 × 0.15 × 0.13 mm, $C_{20}H_{16}CoN_6$, $M$ = 399.32, monoclinic, space group $I2/a$, $a$ = 12.325(1), $b$ = 10.689(5), $c$ = 14.229(1) Å, $\beta$ = 107.94(1)°, $U$ = 1783.4(9) Å$^3$, $Z$ = 4, $D_c$ = 1.487 g cm$^{-3}$, $\mu$(Mo-K$\alpha$) = 0.980 mm$^{-1}$. Data were obtained at 213(2) K on a Nonius FAST diffractometer. A total of 1164 unique reflections were collected using ellipsoid-mask fitting within a $2\theta$ range of 45.06°. The structure was solved by the Patterson method and refined by full-matrix least squares on $F^2$. All hydrogens were located from Fourier difference maps and their positional and thermal parameters were refined. The final refinement converged to $R_1$ = 0.038 and $wR_2$ = 0.079 (for 1164 data and 155 parameters). CCDC 182/500.

1 F. A. Cotton, L. M. Daniels, G. T. Jordan, IV and C. A. Murillo, *Polyhedron*, in the press.
2 O. R. Rodig, T. Brueckner, B. K. Hurlburt, R. K. Schlatzer, T. L. Venable and E. Sinn, *J. Chem. Soc., Dalton Trans.*, 1981, 196.
3 See for example: G. R. Desiraju, *Crystal Engineering The Design of Organic Solids*, Elsevier, Amsterdam, 1989, pp. 166–167; D. S. Reddy, D. C. Craig and G. R. Desiraju, *J. Am. Chem. Soc.*, 1996, **118**, 4090; J. Bernstein, R. E. Davis, L. Shimoni and N.-L. Chang, *Angew. Chem., Int. Ed. Engl.*, 1995, **34**, 1555; Z. Berkovitch-Yellin and L. Leiserowitz, *Acta Crystallogr., Sect. B*, 1984, **40**, 159; G. R. Desiraju, *Angew. Chem., Int. Ed. Engl.*, 1995, **34**, 2311.
4 R. Taylor and O. Kennard, *J. Am. Chem. Soc.*, 1982, **104**, 5063.
5 D. S. Reddy, D. C. Craig and G. R. Desiraju, *J. Chem. Soc., Chem Commun.*, 1994, 1457.
6 See for example: C. B. Aakeröy and K. R. Sneddon, *Chem. Soc. Rev.*, 1993, 397; G. M. Whitesides, E. E. Simanek, J. P. Mathias, C. T. Seto, D. N. Chin, M. Mammen and D. M. Gordon, *Acc. Chem. Res.*, 1995, **28**, 37; A. D. Burrows, C.-W. Chan, M. M. Chowdhry, J. E. McGrady and D. M. P. Mingos, *Chem. Soc. Rev.*, 1995, 329; Z. Gu, R. Zambrano and A. McDermott, *J. Am. Chem. Soc.*, 1994, **116**, 6368; J. A. Zerkowski, J. C. MacDonald, C. T. Setto, D. A. Wierda and G. M. Whitesides, *J. Am. Chem. Soc.*, 1994, **116**, 2382; D. Venkataraman, S. Lee, J. Zhang and J. S. Moore, *Nature*, 1994, **371**, 591.
7 T. Steiner and W. Saenger, *J. Am. Chem. Soc.*, 1993, **115**, 4540.
8 T. Steiner, J. A. Kanters and J. Kroon, *Chem. Commun.*, 1996, 1277.
9 D. A. Braden, G. L. Gard and T. J. R. Weakley, *Inorg. Chem.*, 1996, **35**, 1912.
10 V. R. Thalladi, K. Panneerselvam, C. J. Carrell, H. L. Carrell and G. R. Desiraju, *J. Chem. Soc., Chem. Commun.*, 1995, 341.
11 A. S. Batsanov, M. G. Davidson, J. A. K. Howard, S. Lamb and C. Lustig, *Chem. Commun.*, 1996, 1791.
12 See for example: F. A. Cotton, L. R. Falvello, C. A. Murillo and A. J. Schultz, *Eur. J. Solid State Inorg. Chem.*, 1992, **29**, 311; F. A. Cotton and R. L. Luck, *Inorg. Chem.*, 1989, **28**, 3210.
13 T. Steiner and W. Saenger, *J. Am. Chem. Soc.*, 1992, **114**, 10146; see also references 4 and 7.

*Received in Bloomington, IN, USA, 29th April 1997; 7/02948I*

# *In situ* ligand synthesis and construction of an unprecedented three-dimensional array with silver(I): a new approach to inorganic crystal engineering

**Alexander J. Blake, Neil R. Champness,* Simon S. M. Chung, Wan-Sheung Li and Martin Schröder***

*Department of Chemistry, The University of Nottingham, University Park, Nottingham, UK NG7 2RD*

**Reaction of 1,2-*trans*-(4-pyridyl)ethene with $AgBF_4$ results in the formation of a three-dimensional network based upon a cyclobutane-linked tetrapyridyl ligand, 1,2,3,4-tetrakis(4-pyridyl)cyclobutane, linked by $Ag^I$ ions; the *in situ* formation of the ligand represents a potential new direction for inorganic crystal engineering.**

Inorganic supramolecular chemistry and the construction of polymeric arrays is an area of great current interest.[1–5] The design of different network topologies *via* ligand design and the use of different transition-metal coordination numbers has resulted in a wide variety of structural motifs.[1–5] More subtle effects on network topology such as anion control[4] and the use of the π–π stacking have received growing attention.[5] During our research into polymeric arrays formed by silver(I) complexes of bipyridyl ligands we have observed a common structural motif of linear chains of alternating Ag ions and linking ligands.[2,4–6] In complexes where the ligand has significant π–π stacking ability, adjacent chains may tend to adopt an arrangement to maximise both π–π stacking and Ag–Ag interactions (Fig. 1).[4–6] However, the reaction of $AgBF_4$ with 1,2-*trans*-(4-pyridyl)ethene revealed an unexpected *in situ* cyclisation to yield the ligand 1,2,3,4-tetrakis(4- pyridyl)cyclobutane which is incorporated within a three-dimensional metal–complex polymeric array.

A crystalline sample from the reaction of $AgBF_4$ and 1,2-*trans*-(4-pyridyl)ethene was prepared in MeCN and $CH_2Cl_2$ in the presence of light. Colourless blocks, suitable for single-crystal X-ray analysis were grown following diffusion of the two solvents over the period of *ca.* one month.†

An X-ray structural determination‡ revealed that the ligand had undergone a [2 + 2] cyclisation to form a tetrapyridyl-substituted cyclobutane ring (Fig. 2). The complex exists as a three-dimensional cationic polymer in which each $Ag^I$ centre is coordinated in a tetrahedral geometry to four pyridyl groups [Ag–N 2.302(4), 2.360(4) Å] each from different 1,2,3,4-tetrakis(4-pyridyl)cyclobutane ligands. The lattice grows so that channels are generated which accommodate the $BF_4^-$ counter anions and MeCN solvent molecules (Fig. 3). These channels are intriguing in that the silver–pyridyl–cyclobutane–pyridyl–silver chain forms a helix which winds around the channel. The handedness of these helices alternates along adjacent channels providing the lattice with no overall chirality. Somewhat suprisingly and unusually for such three-dimensional networks, the lattice fills space efficiently without requiring inter-penetration of independent lattices. We believe that this non-interpenetrating lattice with helical channels is a previously unobserved network topology.

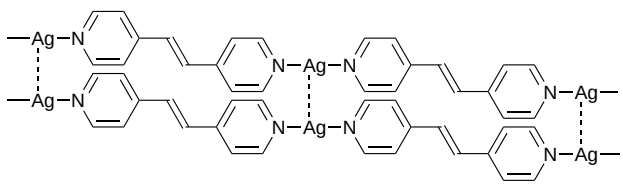



**Fig. 1** The common structural motif of linear chains observed for silver(I) bipyridyl complexes allowing Ag···Ag contacts and π–π interactions

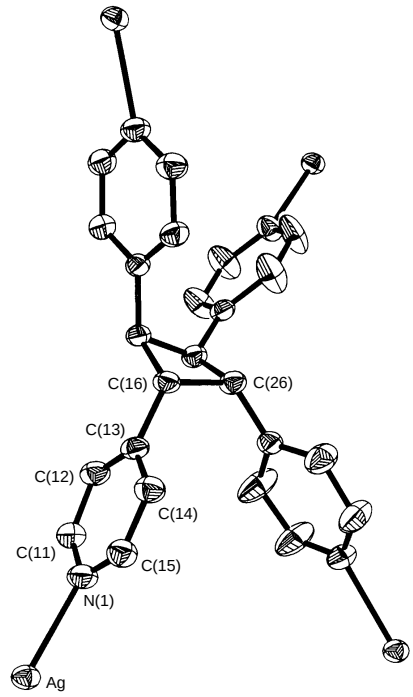



**Fig. 2** View of the structure of 1,2,3,4-tetrakis(4-pyridyl)cyclobutane with $Ag^I$ coordinated to each pyridyl group

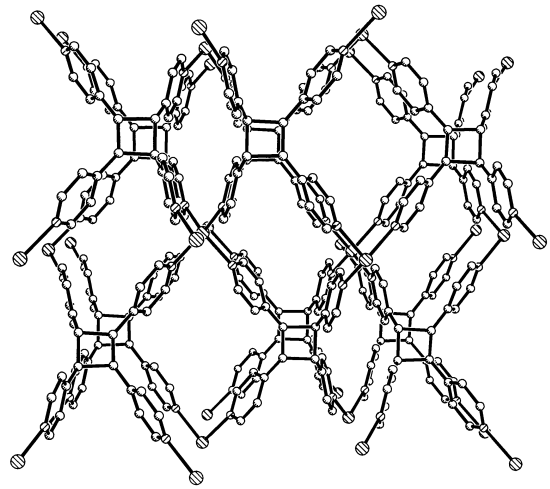


**Fig. 3** View of the polymeric array formed by [Ag{1,2,3,4-tetrakis(4-pyridyl)cyclobutane}]$^+$ illustrating the channels formed

Dimerisation of substituted alkenes is most commonly achieved by UV photolysis.[7,8] Interestingly, UV photolytic dimerisation of 1,2-*trans*-(4-pyridyl)ethene in MeOH or $C_6H_6$ affords two isomers of the ligand, but cyclisation does not occur in the absence of a UV source.[8] Furthermore, 1,2-*trans*-(4-pyridyl)ethene does not dimerise in the solid state, and this has been attributed to an unfavourable arrangement of the ligands within the crystalline lattice.[8] Interestingly, the reaction reported herein produces only a single isomer of the tetrapyridyl ligand (confirmed by NMR studies of the bulk product) consistent with the reaction proceeding in the solid state as outlined by Schmidt *et al.*,[7] and contrary to the reported UV photolytic dimerisation of 1,2-*trans*-(4-pyridyl)ethene in solution which would be expected to give two isomers of the cyclised ligand.[8] Significantly, no dimerisation product was observed in the reaction of $Ag^I$ with 1,2-*trans*-(4-pyridyl)ethene in the absence of light. This indicates a key role of the $Ag^I$ ions in the light-induced dimerisation process, but does not confirm whether the ligand cyclisation occurs in the solid state or in solution.

In conclusion, the reaction of $Ag^I$ with 1,2-*trans*-(4-pyridyl)-ethene represents the first example of the formation of an inorganic three-dimensional lattice *via* the *in situ* generation of a ligand, and the first structurally characterised network incorporating 1,2,3,4-tetrakis(4-pyridyl)cyclobutane. We are currently probing the mechanism of cyclodimerisation reactions and the wider applications of this approach to inorganic crystal engineering.

We thank the Nuffield Foundation (to S. S. M. C.) and EPSRC for funding.

## Footnotes and References

* E-mail: m.schroder@nott.ac.uk

† *Experimental*: {[Ag(1,2,3,4-tetrakis(4-pyridyl)cyclobutane]$BF_4$}$_\infty$. A solution of $AgBF_4$ (50 mg, 0.26 mmol) in MeCN (10 cm$^3$) was layered over a solution of 1,2-*trans*-(4-pyridyl)ethene (bpe) (95 mg, 0.52 mmol) in $CH_2Cl_2$ (10 cm$^3$). The two layers were allowed to diffuse and colourless block crystals were grown over a period of *ca.* one month. The sample was exposed to daylight throughout the experiment. Yield (63 mg, 44%). Satisfactory spectroscopic and analytical data were obtained.

‡ *Crystal data* for {[Ag(1,2,3,4-tetrakis(4-pyridyl)cyclobutane]$BF_4$·3MeCN}$_\infty$: $C_{30}H_{29}AgBF_4N_7$, $M$ = 682.28, orthorhombic, space group *Fddd* (no. 70), $a$ = 10.292(2), $b$ = 29.887(6), $c$ = 38.593(8) Å, $U$ = 11871(4) Å$^3$, $T$ = 150 K, $Z$ = 16, $F$(000) = 5536, $D_c$ = 1.527 g cm$^{-3}$, $\mu$(Mo-K$\alpha$) = 0.738 mm$^{-1}$. Colourless crystal (0.48 × 0.36 × 0.36 mm). Stoe Stadi-4 four-circle diffractometer, graphite-monochromated Mo-K$\alpha$ radiation, $\omega$–2$\theta$ scans, data collection range ($\theta_{max}$ = 25.0°). An absorption correction based upon $\psi$-scans was applied to the data ($T_{min}$ 0.645, $T_{max}$ 0.768), 2631 unique reflections, of which 2220 had $F_o > 4\sigma(F_o)$, were used in all calculations. The structure was solved using direct methods[9] and all non-H atoms were located using subsequent difference-Fourier methods.[10] The $BF_4^-$ counter anion was found to be disordered into two equally occupied sites. The two carbon atoms of one acetonitrile solvent molecule were found to be disordered over two equally occupied sites. Hydrogen atoms were placed in calculated positions and were allowed to ride on their parent atoms. All atoms except H, F, B and the disordered carbon atoms of a MeCN solvent molecule were refined with anisotropic thermal parameters. The weighting scheme {$w^{-1} = [\sigma^2(F_o^2) + (0.0756P)^2 + 175.39P]$, $P = [\max(F_o^2,0) + (2F_c^2)/3]$ was adopted. At final convergence[10] $R_1$ [$I > 2\sigma(I)$] = 0.054 $wR_2$ (all data) = 0.147 for 195 parameters, $S$ = 1.041, $(\Delta/\sigma)_{max}$ = −0.002, $\Delta\rho_{max}$ = 0.598 e Å$^{-3}$. CCDC 182/497.

1 R. Robson, B. F. Abrahams, S. R. Batten, R. W. Gable, B. F. Hoskins and J. Liu, *Supramolecular Architecture*, ACS, New York, 1992, ch. 19.
2 S. Subramanian and M. J. Zaworotko, *Angew. Chem.*, 1995, **107**, 2295; *Angew. Chem., Int. Ed. Engl.*, 1995, **34**, 2127; P. Losier and M. J. Zaworotko, *Angew. Chem.*, 1996, **108**, 2957; *Angew. Chem., Int. Ed. Engl.*, 1996, **35**, 2779; B. F. Abrahams, S. R. Batten, H. Hamit, B. F. Hoskins and R. Robson, *Angew. Chem.*, 1996, **108**, 1794; *Angew. Chem., Int. Ed. Engl.*, 1996, **35**, 1691; D. Venkataraman, S. Lee, J. S. Moore, P. Zhang, K. A. Hirsch, G. B. Gardner, A. C. Covey and C. L. Prentice, *Chem. Mater.*, 1996, **8**, 2030; O. M. Yaghi and H. Li, *J. Am. Chem. Soc.*, 1995, **117**, 10 401; D. M. L. Goodgame, S. Menzer, A. M. Smith and D. J. Williams, *Angew. Chem., Int. Ed. Engl.*, 1995, **34**, 574; P. C. M. Duncan, D. M. L. Goodgame, S. Menzer and D. J. Williams, *Chem. Commun.*, 1996, 2127; L. Carlucci, G. Ciani, D. W. v. Gudenberg, D. M. Proserpio and A. Sironi, *Chem. Commun.*, 1997, 631; B. B. Amabilino and J. F. Stoddart, *Chem. Rev.*, 1995, **95**, 2725.
3 A. J. Blake, N. R. Champness, S. S. M. Chung, W.-S. Li and M. Schröder, *Chem. Commun.*, 1997, 1005.
4 A. J. Blake, N. R. Champness, P. Hubberstey, M. Schröder and M. Withersby, *Angew. Chem.*, 1997, in the press.
5 A. J. Blake, N. R. Champness, A. N. Khlobystov, D. A. Lemenovskii, W.-S. Li and M. Schröder, *Chem. Commun.*, 1997, 1339.
6 A. J. Blake, N. R. Champness, S. S. M. Chung, A. N. Khlobystov, D. A. Lemenovski, W.-S. Li and M. Schröder, unpublished work.
7 M. D. Cohen and G. M. J. Schmidt, *J. Chem. Soc.*, 1964, 1996; M. D. Cohen, G. M. J. Schmidt and F. Sonntag, *J. Chem. Soc.*, 1964, 2000; G. M. J. Schmidt, *J. Chem. Soc.*, 1964, 2014.
8 J. Vansant, S. Toppet, G. Smets, J. P. Declercq, G. Germain and M. Van Meerssche, *J. Org. Chem.*, 1980, **45**, 1565; M. Horner and S. Hunig, *Liebigs Ann. Chem.*, 1982, 1183.
9 G. M. Sheldrick, SHELXS-86, *Acta Crystallogr., Sect. A*, 1990, **46**, 467.
10 G. M. Sheldrick, SHELXL-93, University of Göttingen, Germany, 1993.

*Received in Cambridge, UK, 10th May 1997; 7/02972A*

# Magnetically induced optical bi-stability of the molecular nanomagnet $Mn_{12}O_{12}(OOCMe)_{16}(H_2O)_4$ in an organic glass

**Myles R. Cheesman,[a] Vasili S. Oganesyan,[a] Roberta Sessoli,[b] Dante Gatteschi[b] and Andrew J. Thomson*[a]**

[a] *School of Chemical Sciences, University of East Anglia, Norwich, Norfolk, UK NR4 7TJ*
[b] *Department of Chemistry, University of Firenze, Firenze, Italy 50144*

**The magnetic hysteresis of the mixed-valence manganese cluster, $Mn_{12}O_{12}(OOCMe)_{16}(H_2O)_4$, ($Mn_{12}$),[1] a molecular superparamagnet,[2] can be optically detected in a dilute, frozen organic glass below the blocking temperature of 3.8 K by magnetic circular dichroism spectroscopy.**

The manganese ions of $Mn_{12}$ form a mixed valence cluster of overall tetragonal symmetry $S_4$, with four inner manganese(IV) ions each of spin $S = 3/2$, surrounded by eight manganese(III) ions of spin $S = 2$ (Fig. 1). Exchange interactions within the cluster result in a total cluster spin of $S = 10$. Anisotropy of uniaxial symmetry, due to the cluster crystalline field, separates the spins into a ladder of energy levels with $M_S = \pm 10$ being lowest in energy, about 60 K below the highest level with $M_S = 0$.[3,4] Thus the spins encounter a thermal barrier to re-orientation at ultra-low temperature and relaxation between sublevels $+S$ and $-S$ is extremely slow.[5,6] Consequently, at low temperatures, hysteresis is observed in the susceptibility as the magnetic field is cycled. Remarkably, hysteresis loops observed with single crystals of $Mn_{12}$, oriented with the unique molecular axis ($Z$) parallel to an applied field, show distinct stepped features at magnetic fields where the energies of different collective spin states of the manganese cluster coincide. This is interpreted as quantum mechanical tunnelling (QMT) of the electron spins through the thermal barrier.[5,6]

Although the absorption spectrum between 400 and 850 nm of an optically clear, organic glass of $Mn_{12}$ is almost featureless, the magnetic circular dichroism (MCD) spectrum[7] shows a series of broad bands of positive and negative signs, Fig. 1. At 1.7 K after application of a polarising field of ±5 T a circular dichroism signal remains at zero magnetic field with an intensity of 30% of the signal at magnetic saturation. The sign of this signal depends on the direction of the polarising magnetic field. Hence the MCD signal reports the previous magnetic history of the sample.

Measurement of the magnetic field dependence of the MCD intensity at a given wavelength at a temperatures below and above the blocking temperature of 3.8 K (Fig. 2) shows a marked hysteresis on cycling the field at 1.7 K but no hysteresis at 4.2 K. It is, at first sight, surprising that significant polarisation remains at zero field since there is no molecular orientation in the glass.

In the case of $Mn_{12}$ the optical selection rules for the cluster electronic states are $\Delta S = 0$ and $\Delta L = +1$ or $-1$ for the absorption of right or left circularly polarised light. It is expected that, in the wavelength region 400–800 nm, single-ion intra-d shell transitions will be present, arising from $^5E_g \rightarrow {}^5T_{2g}$ of $Mn^{III}$ and $^4A_{2g} \rightarrow {}^4T_{1g}$ and $^4T_{2g}$ of $Mn^{IV}$, under $O_h$, although the possibility of oxide to $Mn^{IV}$ charge transfer transitions cannot be excluded.[8,9] Exchange coupling of the $Mn^{III}$ and $Mn^{IV}$ imparts an overall cluster spin to these states. The orbital moments of the excited states dictate the selection rule $\Delta L = \pm 1$. Optical transitions arising from the ground-state spin manifolds $M_S = -S$ and $M_s = +S$ give rise to oppositely circularly polarised transitions whose intensity depends on the population differences between the $\pm S$ levels. Absorption of circularly polarised light requires that the optical transitions being excited have non-zero electric dipole components perpendicular to one another and to the applied field.[10] Hence $Mn_{12}$ cluster subpopulations with particular orientations will be selectively detected if either the Zeeman splitting is highly

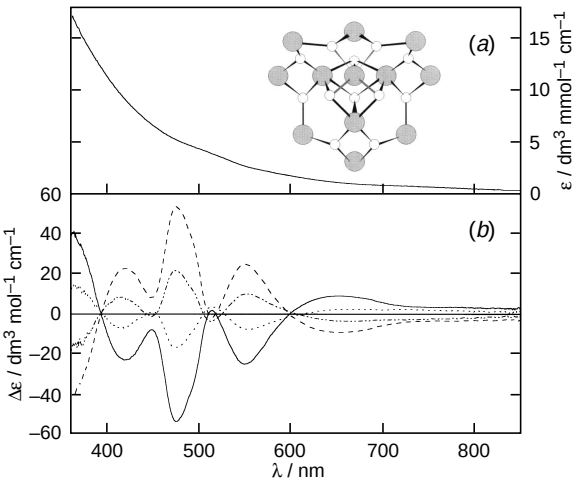



**Fig. 1** (*a*) Absorption spectrum of $Mn_{12}$ at room temperature; (*b*) MCD spectra of $Mn_{12}$ in a frozen organic glass (dmf–MeCN) at 1.70 K and magnetic fields of 5 T (——) followed by reduction of field to zero (·····) and then application of a field of − 5 T (– – –) followed by zero field (–·–·–). MCD spectra are measured as the differential absorption of left and right circularly polarised light, ($\Delta\varepsilon = \varepsilon_L - \varepsilon_R$), by applying a uniform magnetic field parallel to the direction of the light beam.[7]

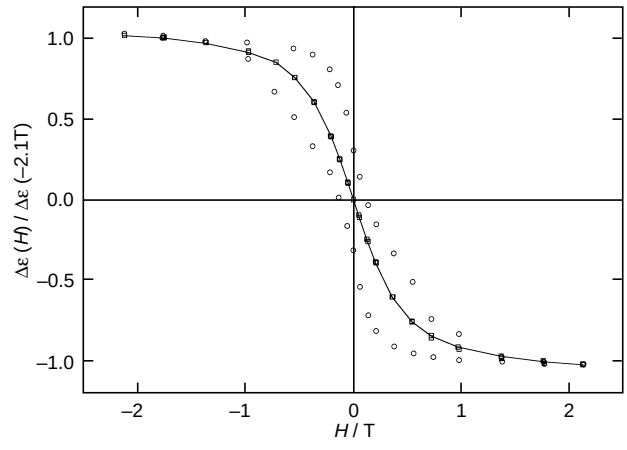



**Fig. 2** MCD magnetisation measured between −2.1 and +2.1 T at 474 nm and at temperatures of (□) 4.2. and (○) 1.70 K of a frozen glass of $Mn_{12}$: upper line, field swept from −2.1 to +2.1 T; lower line, field swept from +2.1 to −2.1 T. Each point was determined by changing the magnetic field to a new value in steps of 0.1–0.2 T and allowing the MCD signal to become static, a period of 20–30 s. No further change in the MCD signal was observed over a period of several minutes. The solid line is the simulated curve for a multi-step Orbach process with orientational averaging.

anisotropic or the optical transitions are strongly polarised. The field dependences of the MCD intensities, at temperatures above the blocking temperature, are sensitive to the linear polarisation of optical transitions, that is, whether they are polarised *XY* and *XZ* (or *YZ*).[11] The MCD magnetisation at 550 nm can be fit well to the case of a purely *XY* polarised transition whereas that of 475 nm component corresponds to an equal mixture of *XY* and *XZ* (or *YZ*) polarisation (data not shown). Thus MCD hysteresis can be detected *via* an optical transition which has mixed polarisation presumably because of the high *g*-value anisotropy, $g_{//} = 40$, $g_{\perp} = 0$, within the $M_S = \pm 10$ pair of ground levels.

Attempts have been made to simulate the MCD and susceptibility hysteresis curves using a model in which relaxation takes place between two potential wells *via* a multi-step Orbach process. In this model the system is excited from one spin level to the next, until it reaches the top of the anisotropy barrier, followed by decay to the bottom of the other well.[12] A phonon density distribution curve was used resulting in a single-parameter model giving a simulation of the effective rate which depends only on the spin–lattice relaxation rate. The simulation reproduces the overall form of the susceptibility curves, including the fields at which the polarisation falls to zero at three different temperatures, and the MCD curves at 4.2 K (Fig. 2). However, it fails to account adequately for the MCD hysteresis seen at 1.7 K. This is probably due to the importance of QMT effects at lower temperatures.[5,6,13–16]

In conclusion, we have shown that the MCD spectra of $Mn_{12}$ allow ground-state hysteresis effects to be measured even in randomly oriented molecular arrays. The MCD method offers a rapid method of surveying molecular paramagnets with potentially interesting properties. The shape of the curves suggests the need to include quantum tunnelling effects before the MCD hysteresis behaviour can be fully understood. But the feature of most significance reported here is that the resultant solutions are optically bi-stable and the effects can be induced or erased by application of a magnetic field. These properties suggest means of storing information in molecular magnetic devices with potential applications as quantum computers. Optical methods of addressing such molecules have the advantage of sensitivity and high speed combined with narrow band widths.

A. J. T. thanks the EPSRC/BBSRC for support of this work.

## Footnote and References

* E-mail: a.thomson@uea.ac.uk

1 T. Lis, *Acta Crystallogr., Sect. B*, 1980, 2042.
2 D. Gatteschi, A. Caneschi, L. Pardi and R. Sessoli, *Science*, 1994, **265**, 1054; R. Sessoli, D. Gatteschi, A. Caneschi and M. A. Novak, *Nature*, 1993, **365**,141.
3 R. Sessoli, H. L. Tsai, A. R. Schake, S. Wang, J. B. Vincent, K. Folting, D. Gatteschi, G. Christou and D. N. Hendrickson, *J. Am. Chem. Soc*., 1993, **115**, 1804.
4 J. R. Friedman, M. P. Sarachik, J. Tejada and R. Ziolo, *Phys. Rev. Lett.*, 1996, **76**, 3830.
5 A. Caneschi, D. Gatteschi, R. Sessoli, A. L. Barra, L C. Brunel and M. Guillot, *J. Am. Chem. Soc*., 1991, **113**, 5873.
6 L. Thomas, F. Lionti, R. Ballou, D. Gatteschi, R. Sessoli and R. Barbara, *Nature*, 1996, **383**, 145.
7 S. B. Piepho and P. N. Schatz, in *Group Theory with Applications to Magnetic Circular Dichroism*, Wiley-InterScience, New York, 1983.
8 A. B. P. Lever, *Inorganic Electronic Spectroscopy*, Elsevier, New York, 1984.
9 J. W. Wood, Ph. D. Thesis, University of East Anglia, 1968.
10 P. N. Schatz, R. L. Mowery and E. R. Krausz, *Mol. Phys*., 1978, **35**, 1537.
11 A. J. Thomson and M. K. Johnson, *Biochem. J.*, 1980**,** 191, 411.
12 J. Villain, F. Hartmann-Boutron, R. Sessoli and A. Rettori, *Europhys. Lett.*, 1994, **27**, 159.
13 P. Politi, A. Rettori F. Hartmann-Boutron and J. Villain, *Phys. Rev. Lett*., 1995, **75**, 537.
14 M. A. Novak and R. Sessoli, in *Quantum Tunnelling of the Magnetisation*, ed. L. Gunther and B. Barbara, NATO ASI Ser. E, 1995, vol. 301.
15 A. L. Burin, N. V. Prokofiev and P. C. E. Stamp, *Phys. Rev. Lett.* 1996, **76**, 3040.
16 P. C. E. Stamp, E. M. Chudnovsky and B. Barbara, *Int. J. Mod. Phys*.,1992, **136**,1355.

*Received in Bath, UK, 30th May 1997; 7/03839I*

# The first crystal structure determination of biphosphole–transition-metal complex: crystal structure of square-planer *meso*-[Pd(3,3′,4,4′-tetramethyl-1,1′-diphenyl-2,2′-biphosphole)$_2$][$BF_4$]$_2$

**Takahiko Kojima, Kaoru Saeki, Kazuhiro Ono, Masaaki Ohba and Yoshihisa Matsuda***

*Department of Chemistry, Faculty of Science, Kyushu University, Hakozaki, Higashi-Ku, Fukuoka 812-81, Japan*

**The first X-ray crystal structure determination of a biphosphole–transition-metal complex is reported; the square-planar palladium(II) complex has unique intramolecular π–π interaction between phenyl groups on chiral phosphorus atoms of two biphosphole ligands.**

Chelating phosphine ligands have contributed to the consstuction of a fertile background for organometallic chemistry and organometallic catalysis such as hydroformylation, hydrogenation, *etc*. Among these chelating phosphine ligands, we have focused on ligands in which the phosphorus atom is involved in conjugated π systems such as phosphorins (phosphabenzenes) and phospholes (phosphapyrroles) that have been synthesized by Mathey and coworkers.[1] These ligands are expected to give the metal center some intriguing properties which are different from those of usual tertiary phosphine–metal complexes. Therefore, we started our project to develop P-containing macrocyclic π-conjugation systems including phosphorus porphyrins and to investigate the properties and reactivity of those transition-metal complexes in low valence states. This is in sharp contrast to the fact that higher valent and hard metal ions are favored in metalloporphyrins.

As for transition-metal–phosphole complexes, only monodentate phosphole complexes have been synthesized and characterized.[2] However, there are no reports on metal complexes containing chelating phosphole ligands. Here, as an initial attempt toward the goal mentioned above, we describe the synthesis and characterization of a novel Pd complex containing a chelating biphosphole ligand, 3,3′,4,4′-tetramethyl-1,1′-diphenyl-2,2′-biphosphole (bidmpp).[3]

[Pd(bidmpp)$_2$][$BF_4$]$_2$ **1** was synthesized in moderate yield *via* ligand substitution between [Pd(MeCN)$_4$][$BF_4$]$_2$ and bidmpp in $CH_2Cl_2$.†

X-Ray crystallography of **1** showed a structure with an inversion center at palladium (Fig. 1);‡ the square-planar $Pd^{II}$ ion being surrounded by four phosphorus atoms [Fig. 1(*b*)]. The Pd–P bond lengths were all 2.343(3) Å and the bite angle of bidmpp [P(1)–Pd–P(2)] was 84.5(1)°, both of which were comparable to those found in homoleptic [Pd(dppe)$_2$]$^{2+}$ [dppe = 1,2-bis(diphenylphosphino)ethane].[4] The geometry around the phosphorus atoms of bidmpp was distorted tetrahedral [C(1)–P(1)–C(4) 92.4(6)°, Pd–P(1)–C(1) 133.1(4)°, C(13)–P(2)–C(16) 92.3(6)° and Pd–P(2)–C(16) 129.5(4)°]. The configuration of the chiral phosphorus atoms of bidmpp in **1** was (*S*),(*S*),(*R*),(*R*), for P(1), P(2), P(1*), P(2*), respectively; the structure determined by X-ray analysis was a *meso* form. The chirality of conformation of both chelate rings were λ for the (*S*,*S*)-bidmpp and δ for the counterpart. Owing to the steric hindrance of the methyl groups on the phosphole rings, bidmpp is compelled to be chiral and the conformation is rigid. As observed in the crystal structure, the interatomic distance between the two nearest methyl groups [C(6) and C(17)] was 3.87 Å and the dihedral angle between two phosphole rings was 126.6° so as to avoid repulsion. In this configuration, phenyl rings on the same side of the Pd coordination plane were cofacial as shown in Fig. 1(*b*) and exhibited an intramolecular π–π interaction [C(12)··C(20*) 3.41 Å, C(11)··C(21*) 3.65 Å]. This type of π–π interaction has not been reported previously even in similar complexes such as [Pd(dppe)$_2$]$^{2+}$ or [Ni(3,3′,4,4′-tetramethyl-1,1′-diphenyl-2,2′,5,5′-tetrahydro-2,2′-biphosphole)$_2$]$^{2+}$.[4,5]

$^1$H and $^{31}$P NMR studies revealed the existence of two species, *meso*- and *rac*-**1** (Fig. 2). In the $^1$H NMR spectrum in $CD_2Cl_2$, peaks assigned to methyl protons were observed at δ 2.22 (d, *J* 1 Hz) and 1.94 for *meso*-**1** and δ 2.36 (d, *J* 1 Hz) and 1.78 for *rac*-**1**. Even when the crystals of **1** were dissolved into

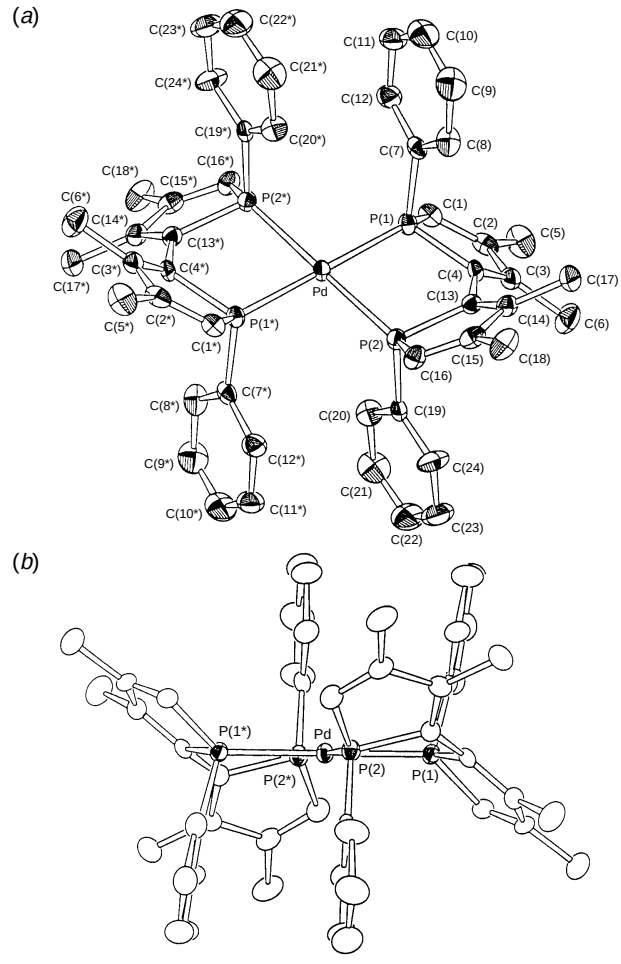



**Fig. 1** An ORTEP drawing of the dication of **1** (*a*) and a side view (*b*) with thermal ellipsoids at 30% probability level. Selected bond lengths (Å) and angles (°): Pd–P(1) 2.343(3), Pd–P(2) 2.343(3), P(1)–C(1) 1.78(1); P(1)–C(4) 1.79(1), P(1)–C(7) 1.82(1), C(1)–C(2) 1.34(2), C(2)–C(3) 1.49(2), C(3)–C(4) 1.34(2), C(2)–C(5) 1.49(2), C(3)–C(6) 1.50(2), C(4)–C(13) 1.46(2), P(1)–Pd–P(2) 84.5(2), P(1)–Pd–P(2*) 95.5(1), C(1)–P(1)–C(4) 92.4(6), C(1)–C(2)–C(3) 114(1), C(2)–C(3)–C(4) 113(1), C(3)–C(4)–C(5) 113(1), P(1)–C(4)–C(3) 109.8(9).

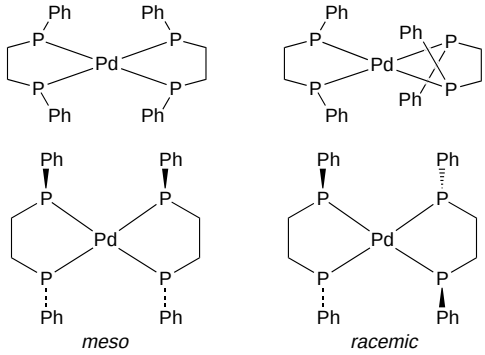



**Fig. 2** Possible isomers for $[Pd(bidmpp)_2]^{2+}$

$CD_2Cl_2$, two sets of peaks were observed, suggesting interconversion between the *meso* and *rac* forms. We distinguished them by their different solubility in $CHCl_3$ or $CH_2Cl_2$; the solubility of *meso*-**1** was much lower than that of *rac*-**1**. The ring proton signal of free bidmpp was observed at $\delta$ 6.41 as a multiplet in $CD_2Cl_2$ whereas those of the Pd-bound bidmpp showed downfield shifts from that of free bidmpp to overlap with phenyl proton resonances at $\delta$ *ca.* 7.3 and 7.7 for *meso*- and *rac*-**1**, respectively. We could detect the ring proton resonances by $^1$H–$^1$H COSY to observe cross peaks due to long-range coupling with methyl protons, however we were unable to determine the exact chemical shifts and the coupling constants because of overlap.

The $^{31}$P NMR spectrum of **1** in $CD_2Cl_2$ showed two singlets at $\delta$ 34.5 for *rac*-**1** and at $\delta$ 37.3 for *meso*-**1**. The assignments were made by comparing the integration of peaks in the $^{31}$P NMR spectrum with that in the $^1$H NMR spectrum. Both of the resonances were downfield shifted from free bidmpp ($\delta$ 17.6). Combined with the observation in $^1$H NMR spectroscopy, the bidmpp binds to the Pd center predominantly through σ-donation as observed in other tertiary phosphine complexes. The coordination shift of **1** in the $^{31}$P NMR spectrum is 17–20 ppm, which is much smaller than that of homoleptic $[Pd(dppe)_2]Cl_2$ in $CDCl_3$ ($\Delta\delta$ = 68.1 ppm).[6] Therefore, it is suggested that π-back bonding from the Pd center contributes to some extent to stabilize **1**, concomitant with σ-donation to the metal center.[2b]

We appreciate Professor F. Mathey (Ecole Polytechnique, France) for his helpful suggestion to synthesize bidmpp.

## Footnotes and References

* E-mail: matsuscc@mbox.nc.kyushu-u.ac.jp

† $[Pd(bidmpp)_2[BF_4]_2$ **1** was synthesized as follows: To a suspension of $[Pd(MeCN)_4][BF_4]_2$ (0.25 mmol) in $CH_2Cl_2$ (12 ml), was added a solution of bidmpp (200 mg, 0.53 mmol) in $CH_2Cl_2$ (3 ml) to give a reddish orange solution within 5 min. The solution was stirred for 30 min at room temp. and filtered through a Celite column. After removing the solvent, the residue was dissovled into a small volume of $CH_2Cl_2$ and then poured into hexane with stirring to obtain a reddish orange powder of **1** in 71% yield. Calc. for $C_{48}H_{48}B_2F_8P_4Pd$: C, 56.04; H, 4.70. Found: C, 55.67; H, 4.74%. FABMS: 941.2 ($[M - BF_4]^+$).

‡ A single crystal of **1** was obtained by recrystalization from $CH_2Cl_2$. *Crystal data*: $C_{48}H_{48}B_2F_8P_4Pd$, $M$ = 1028.81, orange prismatic (0.20 × 0.20 × 0.20 mm), trigonal, space group $R\bar{3}$, $a = b$ = 31.21(3), $c$ = 14.41(2) Å, $U$ = 12154(13) Å$^3$, $Z$ = 9, $D_c$ = 1.265 g cm$^{-3}$, $\mu$(Mo-Kα) = 5.19 cm$^{-1}$, $R$ = 0.055, $wR_2$ = 0.086 for 2492 refrections with $I > 3\sigma(I)$. Structural refinements and calculations were performed using the teXsan crystallographic software package. The structure was solved by direct methods and all non-hydrogen atoms were refined anisotropically. All hydrogen atoms were located at calculated positions but not refined. We could not determine the solvent molecules ($CH_2Cl_2$) of crystallization due to their partial dissipation and severe disorder; a differential Fourier map showed the $CH_2Cl_2$ molecules located at a special position on a threefold axis. CCDC 182/543.

1 F. Mathey and P. Le Floch, *Chem. Ber.*, 1996, **129**, 263 and references therein; F. Mathey, *Chem. Ber.*, 1988, **88**, 429 and references therein; E. Deschamps, L. Ricard and F. Mathey, *Angew. Chem., Int. Ed. Engl.*, 1994, **33**, 1158; E. Deschamps, L. Ricard and F. Mathey, *J. Chem. Soc., Chem. Commun.*, 1995, 1561.

2 (*a*) K. M. Chui and H. M. Powell, *J. Chem. Soc., Dalton Trans.*, 1974, 1879; (*b*) J. J. MacDougall, J. H. Nelson, F. Mathey and J. J. Mayerle, *Inorg. Chem.*, 1980, **19**, 709; (*c*) J. J. MacDougall, J. H. Nelson and F. Mathey, *Inorg. Chem.*, 1982, **21**, 2145; (*d*) F. Mathey, J. Fischer and J. H. Nelson, *Struct. Bonding* (*Berlin*), 1983, **55**, 153; (*e*) S. Attar, W. H. Bearden, N. W. Alcock, E. C. Alyea and J. H. Nelson, *Inorg. Chem.*, 1990, **29**, 425; (*f*) S. Attar, N. W. Alcock, G. A. Bowmaker, J. S. Frye, W. H. Bearden and J. H. Nelson, *Inorg. Chem.*, 1991, **30**, 4166; (*g*) S. Attar, G. A. Bowmaker, N. W. Alcock, J. S. Frye, W. H. Bearden and J. H. Nelson, *Inorg. Chem.*, 1991, **30**, 4743; (*h*) W. L. Wilson, J. Fischer, R. E. Wasylishen, K. Eichele, V. J. Catalano, J. H. Frederick and J. H. Nelson, *Inorg. Chem.*, 1996, **35**, 1486.

3 E. Deschamps and F. Mathey, *Bull. Soc. Chim. Fr.*, 1992, **129**, 486.

4 L. M. Engelhardt, J. M. Patrick, C. L. Raston, P. Twiss and A. H. White, *Aust. J. Chem.*, 1984, **37**, 2193.

5 L. Solujic, E. B. Milosavljevic, J. H. Nelson and J. Fischer, *Inorg. Chem.*, 1994, **33**, 5654.

6 C. H. Lindsay, L. S. Benner and A. L. Balch, *Inorg. Chem.*, 1980, **19**, 3503.

*Received in Cambridge, UK, 28th April 1997; 7/02864D*

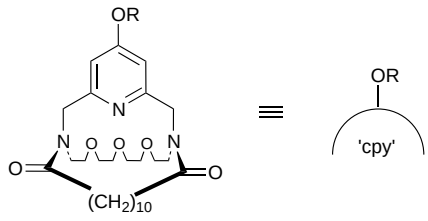
# Towards golf ball shaped reagents: dendrimer fixed concave pyridines

**Torsten Marquardt and Ulrich Lüning***

*Institut für Organische Chemie der Christian-Albrechts-Universität zu Kiel, Olshausenstraße 40, D-24098 Kiel, Germany*

**Two first generation dendrimers 5 and 7 carrying four and six concave pyridines on their surface have been synthesized by convergent synthesis; they have been applied as catalysts in selective acylations, and 7 can be separated from smaller molecules by nanofiltration.**

According to the concept of concave reagents,[1] a variety of bimacrocyclic concave acids and bases such as pyridines **1**, 1,10-phenanthrolines, carboxylic acids, sulfinic acids and bridged calixarenes have been synthesized by incorporation of an appropriate functional group into a concave environment.[2] The concave reagents have been investigated in a variety of model reactions and increases in selectivity by the use of these reagents have been achieved. As the synthesis is rather tedious and the recovery of these concave reagents has not yet been solved satisfactorily, larger scale application has not been realized up to now. The recovery problem can be avoided by using polymeric reagents.




**1a** R = Me
**b** R = $CH_2CH_2OH$
**c** R = $CH_2CH_2I$
**d** R = $CH_2CH_2$–Merrifield polymer
**e** R = $CH_2CH_2$–poly(vinylbenzyl chloride)

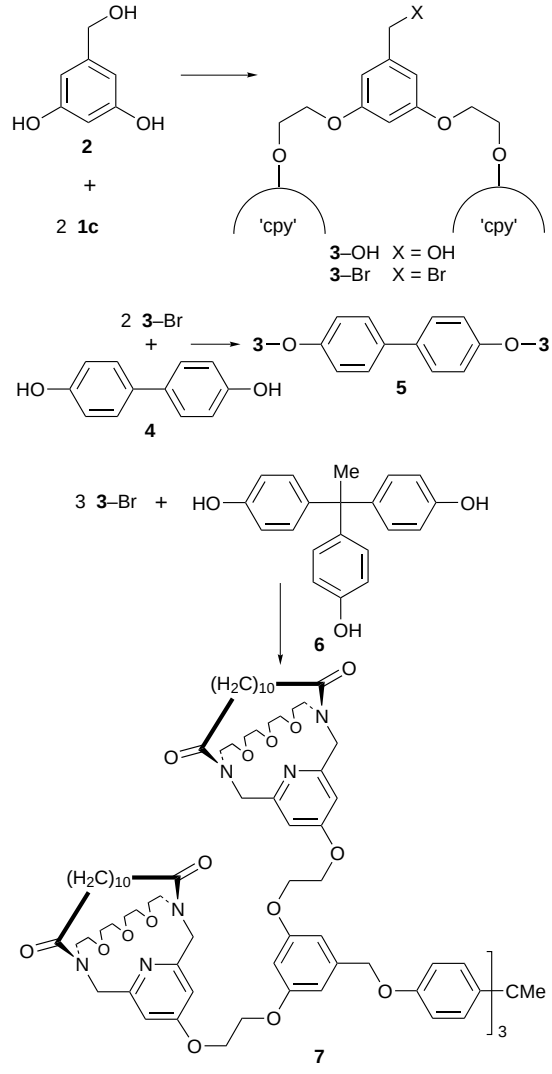
Here we describe the synthesis of the first generation of dendrimer fixed concave pyridines **1**. The fixation of a concave pyridine **1b** to a Merrifield polymer resin giving **1d** has been described.[3] Because of the insolubility of this functionalized resin, **1d** could only be used as a heterogeneous reagent or catalyst. Soluble polymers combine the advantages of common soluble reagents with attributes of solid phase reagents. Soluble polymers can be separated from the reaction products by ultrafiltration. In the case of linear polymers the problem of reptation through the semipermeable membrane must be overcome. It should be avoided by the use of soluble branched polymers.

These reflections consequently lead to dendrimer-fixed concave pyridines. Dendrimers are highly branched macromolecules with well-defined structures[4] which are rather easy to characterize because they possess a single molecular weight. We chose the poly(aryl alkyl ether) dendrimers developed by Frechet and Hawker[5] as the main frame, which are synthesized by a convergent route. The concave pyridine **1c** was fixed on the dendritic structure *via* its convex back side by a spacer.

In contrast to the polymers **1d** and **1e**, the fractional coverage of the dendrimers functionalized by concave pyridines (**5** and **7**) is 100% (83 wt%) [Merrifield polymer **1d**: 9% (20 wt%); linear soluble polymer **1e**: 29% (60 wt%)]. This guarantees the absence of other functional groups on the surface, and optimizes these fixed concave pyridines **5** and **7** for applications.[6]

The products **5** and **7**† were synthesised according to Scheme 1 and characterized by $^1$H NMR spectroscopy. Because of the large number of aliphatic protons in the side chains of the concave pyridines, the important portion of the spectra is between 4.5–8.5 ppm and contains the absorbtions of the aromatic and benzylic protons. The ratio between the aromatic pyridine protons and the aromatic phenyl protons, as well as the ratio between the aromatic (6.5–7.5 ppm) and benzylic protons (4.5–5.4 ppm), was diagnostic. These results and the $^{13}$C NMR spectra elucidated the structures of **5** and **7**.

The functionalized dendrimers **5** and **7** showed the same behaviour as the analogous unfixed concave pyridines **1a**, **1b** and **1c**. Three different amide conformers could be observed in the $^1$H NMR spectra of **5** and **7**, in the same ratio as it had been observed in solutions of the unfixed concave pyridines **1a**, **1b** and **1c**.[8] Because the dendrimer-fixed concave pyridines **5** and




**Scheme 1**

**Table 1** Selectivity increase in the base-catalysed acylation of primary, secondary and tertiary alcohols with diphenylketene[a]

| Catalyst | Selectivity | | |
|---|---|---|---|
| | EtOH | $Pr^iOH$ | $Bu^tOH$ |
| Pyridine | 4.7 | 1 | 0 |
| Lutidine | 7.1 | 1 | 0 |
| **1a** | 12.0 | 1 | 0 |
| **1e** | 9.5 | 1 | 0 |
| **1d** | 7.4 | 1 | 0 |
| **5** | 11.6 | 1 | 0 |
| **7** | 11.4 | 1 | 0 |

[a] Conditions have been described previously (ref. 6).

**7** showed the same conformer ratio, it might be expected that the selectivity increase in the model reaction would also be the same. This assumption was checked in the base catalysed acylation of primary, secondary and tertiary alcohols with diphenylketene in an intermolecular competition reaction.[6] As Table 1 shows, the selectivity increase was the same as found for the unfixed concave bases, such as **1a**, but better than the increase produced by the use of concave pyridines fixed on linear polymers **1e**, and much better than that produced by the use of concave pyridines fixed on the Merrifield polymer resin **1d**.

With **5** and **7**, the first two dendrimers loaded with concave reagents with molecular weights of 2557 (**5**) and 3863 (**7**), respectively, have been synthesized. Compound **7** is large enough to be filtered off by nanofiltration. Retention and permeation have been checked gravimetrically. It can be recovered in good yield (70–90%) from a $CH_2Cl_2$ solution using a nanofiltration membrane. Therefore dendrimer-fixed concave pyridines can be recycled from batch reaction mixtures by nanofiltration. For a continuous process, however, the retention needs to be optimized. This should be possible with higher generations of dendrimer-fixed concave pyridines. In these higher generations the coverage of the surface by concave reagents will increase, finally reaching an overall geometry which resembles a golf ball.

We thank Dr M. Felder and Dr U. Kragl at the Forschungszentrum Jülich for carrying out the nanofiltration experiments.

## Footnotes and References

* E-mail: noc03@rz.uni-kiel.d400.de

† *Synthesis:* The reaction of the concave pyridine **1c**[7] (2.1 equiv.) with 3,5-dihydroxybenzyl alcohol **2** (1 equiv.) in dry THF in the presence of $K_2CO_3$ (2.5 equiv.) and 18-crown-6 (0.4 equiv.) gave the first generation dendron **3**-OH as a colourless glassy solid with mp 105–108 °C in 76% yield. The conversion of the benzylic alcohol **3**-OH to the benzylic bromide **3**-Br succeeded with an excess of $CBr_3$ and $PPh_3$ in dry THF in 90% yield and gave a colourless glassy solid with mp 98–101 °C. This dendron **3**-Br (2.2 equiv.) reacted with the two-directional core **4** (1 equiv.) in the presence of $K_2CO_3$ (3 equiv.) and 18-crown-6 (0.4 equiv.) in dry THF yielding 67% of a colourless glassy solid **5** with mp 117–119 °C. The reaction of the three-directional core **6** (1 equiv.) with the dendron **3**-Br (3.3 equiv.) in the presence of $K_2CO_3$ (4 equiv.) and 18-crown-6 (0.4 equiv.) in dry acetone yielded 81% of a colourless glassy solid **7** with mp 118–120 °C.

1 U. Lüning, *Liebigs Ann. Chem.*, 1987, 949; Concave Reagents 23: H. Ross and U. Lüning, *Tetrahedron Lett.*, 1997, **38**, 4539.
2 U. Lüning, *Top. Curr. Chem.*, 1995, **175**, 57; U. Lüning, *J. Mater. Chem.*, 1997, **7**, 175.
3 U. Lüning and M. Gerst, *J. Prakt. Chem., Chem.-Ztg.*, 1992, **334**, 656.
4 D. A. Tomalia and H. D. Durst, *Top. Curr. Chem.*, 1993, **165**, 193; G. R. Newkome, C. N. Moorefield and F. Vögtle, *Dendritic Molecules*, VCH, Weinheim, 1996.
5 J. M. J. Frechet and C. Hawker, *J. Am. Chem. Soc.*, 1990, **112**, 7638; J. M. J. Frechet and C. Hawker, *J. Chem. Soc., Chem. Commun.*, 1990, 1010.
6 U. Lüning, W. Schyja and S. Petersen, *Liebigs Ann.*, 1996, 2099.
7 W. Hacker, Ph.D. Thesis, University of Freiburg, 1996.
8 U. Lüning, R. Baumstark, K. Peters and H. G. v. Schnering, *Liebigs Ann. Chem.*, 1990, 129; U. Lüning, R. Baumstark and M. Müller, *Liebigs Ann. Chem.*, 1991, 987.

*Received in Liverpool, UK, 7th May 1997; 7/03108D*

# Adsorption of ruthenadendrimers to silica–titania surfaces studied by optical waveguide lightmode spectroscopy (OWLS)

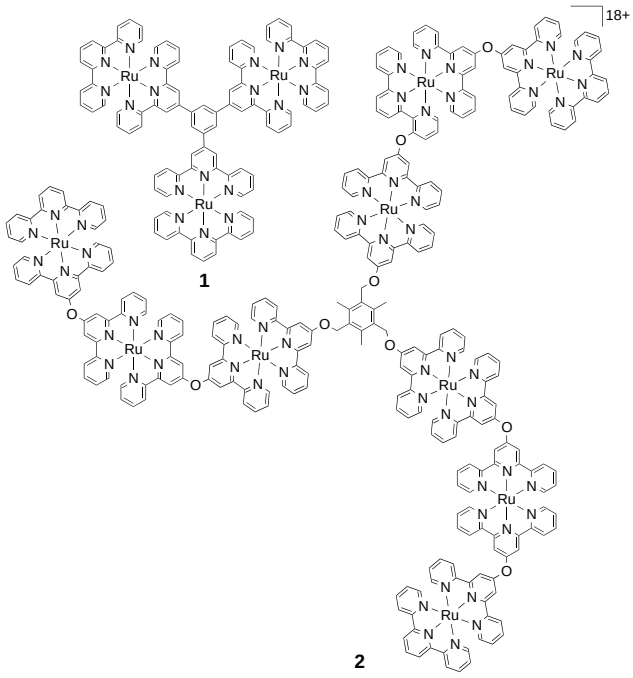
**Edwin C. Constable,[a] Peter Harverson[a] and Jeremy J. Ramsden*[b]**

[a] *Department of Inorganic Chemistry, University of Basel, Spitalstrasse 56, 4056 Basel, Switzerland*
[b] *Department of Biophysical Chemistry, University of Basel, Klingelbergstrasse 70, 4056 Basel, Switzerland*

**Kinetic analysis of the assembly of metallodendrimers at silica–titania surfaces shows that the deposition mode strongly depends on the bulk concentration.**

Metallodendrimers are potentially key components for future generations of ultraminiature computing, sensing and photoconversion devices. We are developing a methodology for the incorporation of metallodendrimers into nanostructured composites that relies on the assembly of mono- or multi-layers on substrate surfaces in contact with solutions of the desired component. Here we describe the use of optical waveguide lightmode spectroscopy (OWLS) for studying the assembly of surface layers of metallodendrimers on smooth silica–titania.

Our initial studies were made on the rigid triruthenium complex **1**[1] and the more flexible nonaruthenium compound **2**.[2] The measurements are based on the observation that the modes of an unclad waveguide shift their energies in response to




changes in the waveguide environment.[3,4] Planar optical waveguides are particularly convenient for probing surface deposition processes[4,5] not only because of their well defined geometry, but also because they can be fabricated from a wide variety of different materials. The mode spectrum can be very conveniently and accurately measured using a grating coupler.[6] In order to maximize the sensitivity of the measurements,[6] we used thin waveguides supporting only the zeroth order transverse magnetic (TM) and transverse electric (TE) modes. Measurement of the mode energies, expressed as effective refractive indices *N*, enabled the two optogeometric parameters characterizing the deposited layer, thickness $d_A$ and refractive index $n_A$, to be determined.[4,6] From these the surface density (Gibbs excess) $\Gamma$ in molecules per unit area can be calculated from:[4]

$$\Gamma = d_A(n_A - n_C)/(\mathrm{d}n/\mathrm{d}c) \quad (1)$$

where $n_C$ is the refractive index of the covering medium (in our case, acetonitrile), and d*n*/d*c* is the refractive index increment of the compound, determined using a Rayleigh interferometer (1.45 and 0.49 dm$^3$ mol$^{-1}$ for **1** and **2**, respectively). As substrates for adsorption, we used Si(Ti)$O_2$ planar optical waveguides. They were fabricated by oxidatively sputtering a Si/Ti target onto an optical glass support into which a shallow (*ca*. 10 nm) grating coupler (grating constant $\Lambda$ = 833.3 nm) had been photolithographically etched. Their surface composition was $Si_{0.76}Ti_{0.24}O_2$, measured using X-ray photoelectron spectroscopy, and their mean roughness was 0.12 ± 0.05 nm, measured using atomic force microscopy. A cylindrical cuvette (diameter = 9 mm) was sealed to the grating region of the waveguide using a 'Kalrez' o-ring and the mode spectrum measured at 632.8 nm. The baseline spectrum was recorded with pure acetonitrile (Baker spectroscopic grade) flowing through the cuvette. Flow was then switched to a solution (concentration $c_b$) of **1** or **2** in acetonitrile, while continuing to measure the mode spectrum. After an adsorption plateau appeared to have been attained, flow was switched back to pure acetonitrile. Desorption was negligible, except for the deposition of **2** at the largest bulk concentration tested (0.2 mM).

Transport to the surface is *via* convective diffusion and hence governed by a law of the type:

$$\mathrm{d}\Gamma/\mathrm{d}t = Dc_b/\delta \quad (2)$$

where $\delta$ is the thickness of the diffusion boundary layer[7] (*ca*. 80 μm in our experiments[8]), and *D* the diffusivity of the molecules in acetonitrile (estimated from the dimensions of the molecule as $8 \times 10^{-6}$ cm$^2$ s$^{-1}$).

Fig. 1 shows representative measurements of $\Gamma$ *vs. t*. The initial deposition rates d$\Gamma$/d*t* are much lower than predicted by eqn. (2), implying that energy barrier and/or orientational

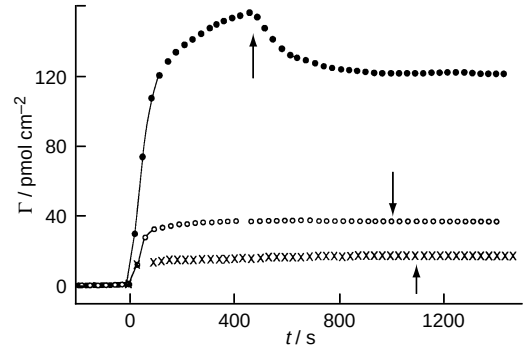



**Fig. 1** Representative experimental data: (×) **1**, $c_b$ = 4 μM; (○) **2**, $c_b$ = 2 μM; (●) **2**, $c_b$ = 200 μM. Bulk flow was switched to the ruthenadendrimer solution at $t$ = 0. The arrows denote when the flow reverted to pure buffer.

factors result in not every adsorption attempt being successful. Furthermore, the rate of deposition decreases with time, but since there is no desorption, this cannot be due to the establishment of an equilibrium, but rather to the progressive blockage of the adsorbing surface as molecules adsorb. Hence eqn. (2) must be modified to take these effects into account.

We do this by considering a layer of solution just above the plane of adsorption. Let the concentration of metallodendrimers in this plane be $c_1$. The rate of deposition is, per unit area $S$ of surface, $Sk_ac_1\phi$. The chemical rate constant $k_a$ is to a first approximation proportional to the product $\kappa\exp(-E_a)$, where $\kappa$ is the probability that the incoming molecule arrives in an orientation permitting incorporation into the surface adlayer, and $E_a$ is the energy barrier (electrostatic, *etc*.) hindering adsorption. $\phi$ is the fraction of the surface available for adsorption. Since the molecules are deposited at random onto a continuum, the dependence of $\phi$ on $\theta$, the fraction of the surface occupied ($\theta = \Gamma a$, $a$ being the area occupied per molecule) is not straightforword.[9,10] Analysis of the geometry of deposition, using the concept of exclusion zones, leads to the expression:[9]

$$\phi = \frac{(1-\tilde{\theta})^3}{1-0.812\tilde{\theta}+0.2336\tilde{\theta}^2+0.0845\tilde{\theta}^3}. \qquad (3)$$

Here $\tilde{\theta} = \theta/\theta_J$; $\theta_J$ (*ca*. 0.55 for disk-shaped objects[9]) is the jamming coverage, at which no spaces large enough to accept a further molecule exist on the surface.

Diffusion from the bulk to the layer above the surface follows the usual Fick–Smoluchowski kinetics, and hence

$$(V/S)(dc_1/dt) = (c_b - c_1)D/\delta - k_ac_1\phi \qquad (4)$$

where $V$ is unit volume. By letting the left hand side go to zero, an expression for $c_1$ is obtained, which is used to obtain a corrected rate law:

$$d\Gamma/dt = c_b/[\delta/D + 1/(k_a\phi)] \qquad (5)$$

This equation was fitted to the experimental data transformed by numerical differentiation into $d\Gamma/dt$ *vs*. $\Gamma$ plots, with $a$ and $k_a$ as free parameters. The results are given in Table 1. Also shown in the extreme right hand column is the product of the apparent plateau value of $\Gamma$ read off the experimental curves and the fitted $a$: the agreement with the expected jamming coverage $\theta_J$ of 0.55 is satisfactory. This is itself a strong indication that the random sequential adsorption (RSA) model[9,10] applies; further evidence is that eqn. (5), with $\phi$ given by eqn. (3), fitted all the transformed curves (except for compound **2** at $c_b$ = 20 nM, for which the $\Gamma$ *vs. t* plot consisted of two linear portions). There was no evidence for surface diffusion of the adsorbed molecules (which leads to $d\Gamma/dt$ decreasing linearly with $\Gamma$).[11]

**Table 1** Parameters derived from fitting eqn. (5) to the experimental data

| | $c_b$/μM | $a$/nm² | $k_a$/cm s$^{-1}$ | $\Gamma_\infty{}^a$/ pmol cm$^{-2}$ | $a\Gamma_\infty{}^b$ |
|---|---|---|---|---|---|
| **1** | 0.4 | 5.7 | $2.1 \times 10^{-3}$ | 16 | 0.61 |
| | 4 | 6.0 | $2.0 \times 10^{-3}$ | 17 | 0.56 |
| | 40 | 5.7 | $2.0 \times 10^{-3}$ | 17 | 0.58 |
| **2** | 0.02 | —[c] | $1.6 \times 10^{-4}$ [c] | 35 | —[c] |
| | 0.2 | 2.3 | $1.4 \times 10^{-1}$ [d] | 42 | 0.58 |
| | 2 | 2.4 | $7.0 \times 10^{-3}$ | 40 | 0.58 |
| | 20 | 1.8 | $2.0 \times 10^{-4}$ | 55 | 0.59 |
| | 200 | 0.51 | $4.3 \times 10^{-5}$ | 42 | 0.51 |

[a] The value of $\Gamma$ at saturation, estimated from the experimental curves. [b] *i.e.* $\theta_J$ (*cf.* the theoretial value of 0.55 for spheres/disks[9]). [c] Could not be determined since eqn. (5) did not fit the data. $\Gamma(t)$ consisted of two linear portions, with slope 3.2 fmol cm$^{-2}$ s$^{-1}$ initially, up to $\Gamma$ = 27 pmol cm$^{-2}$, *i.e.* $\theta \approx 0.4$, assuming $a \approx 2.4$ nm², and 0.3 fmol cm$^{-2}$ s$^{-1}$ thereafter, with no indication of exclusion effects. The given value of $k_a$ was obtained by dividing the initial rate by $c_b$. [d] Preceded by a linear portion up to $\Gamma$ = 34 pmol cm$^{-2}$ yielding $k_a = 4.6 \times 10^{-4}$ cm s$^{-1}$.

Compound **1** followed pure random sequential adsorption kinetics. The parameters were almost invariant with $c_b$ and consistent with the molecule lying flat on the surface.

Compound **2** behaved in a more complicated way, which differed qualitatively over the concentration range investigated. Since the molecule can adsorb to the surface in various conformations, the parameter $a$ must be interpreted as an average area. Surprisingly, even though **2** is much bigger than **1**, the area it occupies is much smaller. We interpret this as the molecule attaching itself to the surface with only one of its arms. At the highest bulk concentration (0.2 mM), the adsorption shows a qualitatively different pattern: the amounts adsorbed are much higher, and unlike the layers assembled from lower $c_b$, they desorb to a significant degree. This appears to indicate the formation of a second layer only weakly attached to the first and hence removable upon dilution of the cover solution, an inference supported by the mean thicknesses $d_A$ *ca*. 0.5 nm for $c_b \leqslant 20$ μM and 2.2 nm for $c_b \geqslant 0.2$ mM ('mean thickness' refers to the mean distance of the optically densest portion of the molecule from the adsorbing surface). The very small fitted $a$ for $c_b$ = 0.2 mM partly reflects the formation of the second layer, but it is in fact much less than half the value given by the lower $c_b$, and hence indicates that the molecules pack into a much more compact conformation within the layer. We propose that this is achieved *via* lateral interpenetration of the dendrimers: the RSA theory as developed hitherto[9,10,12] only considers smooth geometrical objects such as spheres, ellipsoids, *etc*.

These results demonstrate the primordial importance of bulk concentration in directing the self-assembly of complex molecules at surfaces.

E. C. C. thanks the Swiss National Science Foundation for support, and J. J. R. the Commission for Technology and Innovation, Berne.

## Footnote and References

* E-mail: ramsden@ubaclu.unibas.ch

1 E. C. Constable and A. M. W. Cargill Thompson, *J. Chem. Soc., Chem. Commun*., 1992, 617; *J. Chem. Soc., Dalton Trans*., 1992, 3467; *J. Chem. Soc., Dalton Trans*., 1995, 1615.
2 E. C. Constable, A. M. W. Cargill Thompson, P. Harverson, L. Macko and M. Zehnder, *Chem. Eur. J*., 1995, **1** 360; E. C. Constable and P. Harverson, *Chem. Commun*., 1996, 33; *Inorg. Chim. Acta*, 1996, **252**, 9.
3 P. K. Tien, *Rev. Mod. Phys*., 1977, **49**, 361.
4 J. J. Ramsden, *J. Statist. Phys*., 1993, **73**, 853.
5 J. J. Ramsden, D. J. Roush, D. S. Gill, R. G. Kurrat and R. C. Willson, *J. Am. Chem. Soc*., 1995, **117**, 8511.
6 K. Tiefenthaler and W. Lukosz, *J. Opt. Soc. Am. B*, 1989, **6**, 209.
7 V. G. Levich, *Physicochemical Hydrodynamics*, Prentice Hall, Englewood Cliffs, NJ, 1962.
8 R. Kurrat, J. J. Ramsden and J. E. Prenosil, *J. Chem. Soc., Faraday Trans*., 1994, **90**, 587.
9 P. Schaaf and J. Talbot, *J. Chem. Phys*., 1989, **91**, 4401.
10 G. Tarjus, P. Schaaf and J. Talbot, *J. Chem. Phys*., 1990, **93**, 8352.
11 J. J. Ramsden, G. I. Bachmanova and A. I. Archakov, *Phys. Rev. E*, 1994, **50**, 5072.
12 P. Viot, G. Tarjus, S. M. Ricci and J. Talbot, *J. Chem. Phys*., 1992, **97**, 5212.

*Received in Cambridge, UK, 18th December 1996; Revised manuscript received 1st July 1997; 7/04638C*

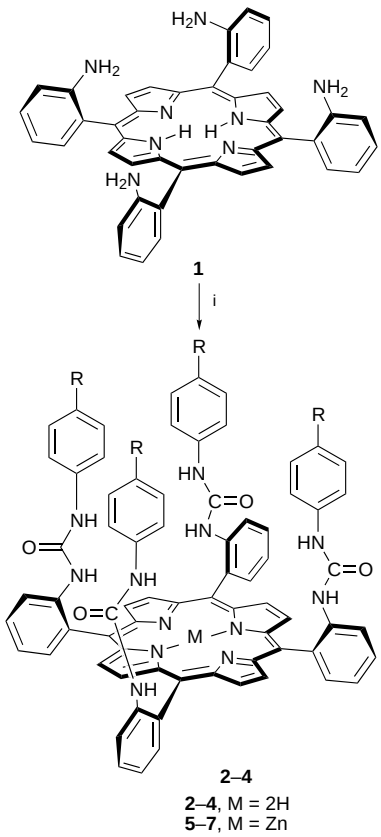
# (*cis*)-5,10,15,20-Tetrakis[2-(arylurea)phenyl]porphyrins: novel neutral ligands for remarkably selective and exceptionally strong chloride anion complexation in $(CD_3)_2SO$

**Raymond C. Jagessar and Dennis H. Burns***

*Department of Chemistry, Wichita State University Wichita, Kansas 67260-0051, USA*

**Urea appended free-base porphyrins 2–4 bind strongly ($K$ > $10^5$ dm$^3$ mol$^{-1}$) to spherical $Cl^-$ in $(CD_3)_2SO$ and exhibit significant binding selectivity since they complex with $Cl^-$ to a much greater extent ($10^3$–$10^2$ : 1) than with the trigonal $NO_3^-$ and tetrahedral $H_2PO_4^-$ anions.**

The importance of anion binding and transport in chemical and biochemical processes has been the impetus for the design and fabrication of supramolecular anion receptors.[1] We have begun a project to prepare neutral anion receptors that exhibit selective anion binding, ultimately for the development of sensors and transport mimics that function in an aqueous environment. Here, we report the synthesis (Scheme 1) of our initial receptors **2**–**7**, superstructured porphyrins functionalized with urea moieties. Owing to the different pocket size and orientation of urea groups on the porphyrin scaffolding, it was anticipated that **2**–**4** would exhibit different aptitudes and selectivities for anion complexation than those seen with the previously prepared urea appended receptors.[2–6] Furthermore, the addition of electronegative substituents (Cl, F) to the *para* position of the phenyl rings of **3** and **4**, as well as the porphyrin's ability to bind metals in its core, allow for the moderation of the strength and selectivity of anion binding for the supramolecule.




**Scheme 1**: *Reagents and conditions*: i, *p*-$RC_6H_4NCO$, $CHCl_3$, room temp.; R = H (**2**, **5**, **8**), Cl (**3, 6, 9**) or F (**4**, **7**, **10**)

These receptors are the first example of a class of neutral, free-base porphyrins† able to act as very selective anion receptors, with **2**–**4** binding $Cl^-$ greater than 1000 : 1 compared to $NO_3^-$ or 280 : 1 compared to $H_2PO_4^-$ (*vide infra*) ($Cl^-$ receptors are biologically relevant, for $Cl^-$ ion channels are involved in the facilitated exchange of $Cl^-$ for $HCO_3^-$ anions in erythrocytes, and, when not functioning properly, have been implicated in the genetic disease cystic fibrosis[7]). For comparison, the expanded porphyrin receptors can bind anions only when protonated, and thus exhibit modest anion selectivity due to nondirectional coulombic interactions[3] (for example, sapphyrin binds $H_2PO_4^-$ and $F^-$ ions with similar binding constants in methanol[1f]). Cobaltocene and ferrocene appended porphyrins have recently been reported.[8] The former is another example of a positively charged anion receptor, whereas the neutral ferrocene appended porphyrins do not bind anions unless metallated; both systems show little anion selectivity (no better than 4 : 1 binding selectivity between halides, nitrate and sulfate ions).

Porphyrins **2**–**4** were synthesized (Scheme 1) by the addition of 4 equiv. of the requisite isocyanate (**8**–**10**) to the *cis* isomer of $H_2TAPP$[9,10] **1** in $CHCl_3$ at room temp. and were obtained in yields of 70–85% after purification by silica-gel column chromatography and subsequent recrystallization from $CH_2Cl_2$–$C_6H_{14}$. The Zn complexes **5**–**7** were synthesized by stirring the free-base ligands with excess $Zn(OAc)_2{\cdot}2H_2O$ in $CH_2Cl_2$–MeOH (2 : 1, v/v) and were obtained in 90–95% yield. The model tetraphenylporphyrin was prepared using standard literature procedure.[11] The $^1$H NMR spectra of **2**–**4** recorded in $(CD_3)_2SO$ at ambient temperature revealed a singlet resonance for the β-pyrrole protons, indicative of the *cis* conformation of the molecules. In all cases, the urea NH protons were observed as two broad singlets, the one at high field presumably due to those in close proximity to the porphyrin ring, resulting from the shielding effect of the macrocycle. The proposed structures **2**–**4** were corroborated by HRFABMS.

UV–VIS spectral anion titration revealed anion binding through perturbation of the Soret and visible bands of **2**–**4** when the anions $Cl^-$, $NO_3^-$ and $H_2PO_4^-$ were added as their $NBu_4^+$ salts. Addition of $NO_3^-$ and $Cl^-$ anions produced a hypsochromic shift with concomitant decrease in intensity of the Soret band after the addition of 1 equiv. of anion. Further addition of anion resulted in an increase in intensity (Fig. 1). Titration of porphyrins **2**–**4** with $H_2PO_4^-$ produced a hypsochromic shift of the Soret band followed by a bathochromic shift and an increase in absorbance with the addition of >1 equiv. of anion. Furthermore, with porphyrins **3** and **4**, a broadened Soret band with the appearance of a shoulder was observed (Fig. 1). Changes in the Soret band combined with shifts of the porphyrin NH protons (*vide infra*) upon titration with the anions strongly suggests that the anions were bound within the porphyrin–urea pocket.

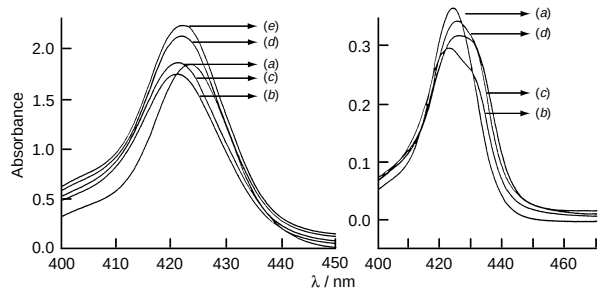



**Fig. 1** UV–VIS spectra of porphyrins **3** and **4** demonstrating the change in the Soret bands upon titration with anions in $CH_2Cl_2$. (Left) porphyrin **4** titrated with $NBu_4Cl$ in mol equiv.: (*a*) 0, (*b*) 1, (*c*) 2, (*d*) 5, (*e*) 10. (Right) porphyrin **3** titrated with $NBu_4H_2PO_4$ in mol equiv.: (*a*) 0, (*b*) 1, (*c*) 2, (*d*) 10.

Quantification of the association constants of neutral hosts **2**–**4** was accomplished by following the titrations of the anions by $^1$H NMR in the strongly solvating solvent $(CD_3)_2SO$. In all cases, proton shifts were observed for the receptor porphyrin-phenyl, β-pyrrole, porphyrin NH, and urea-phenyl protons. Larger shifts were observed for the urea NH protons, with the downfield urea proton the most perturbed. The larger shift of the urea NH proton was indicative of its essential role in the anion recognition process.[2,4] The association constants of **2**–**4** in $(CD_3)_2SO$ determined from their binding curves (Fig. 2) for the complexation of $Cl^-$ ion were calculated[12] to be $> 10^5$ dm$^3$ mol$^{-1}$ (Table 1),[13] so it was impossible to judge any selectivity in binding that might be occurring for these anions between the different porphyrins. However, binding constants for $Cl^- > 10^5$ dm$^3$ mol$^{-1}$ are significantly larger than those that have been previously reported for urea functionalized anion receptors.[1–6] The very strong binding of $Cl^-$ ion allowed the mole ratio method[14] to be used in the determination of the binding stoichiometry, which was found to be 1 : 1 for the three porphyrins.

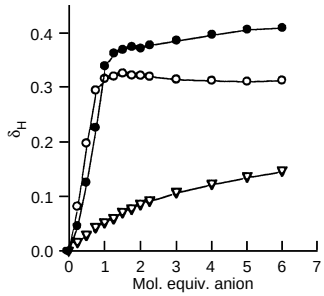



**Fig. 2** Binding curves for porphyrin **4** and $Cl^-$ (○), $H_2PO_4^-$ (●) and $NO_3^-$ (▽) ions in $(CD_3)_2SO$

The association constants of **2**–**4** in $(CD_3)_2SO$ for the binding of $H_2PO_4^-$ ion were 400, 300, and 1400 dm$^3$ mol$^{-1}$ (Table 1), respectively. Thus, there seemed to be some small selectivity between the *p*-fluorophenylurea porphyrin **4** and the other two porphyrins in their affinity for $H_2PO_4^-$. Presumably, the very electronegative *p*-F substituent produced a large enough increase in the acidity of the urea protons to strengthen their hydrogen bonding with the anion electrostatic field. Both Job's method of continuous variations[14] and the mole ratio method,[14] determined by UV–VIS spectrophotometry, showed the stoichiometry of binding was 1 : 1. The binding affinity of **2**–**4** for $NO_3^-$ was even weaker (Table 1).‡ The noteworthy selectivity in the binding of $Cl^-$ with **2**–**4** was presumably due to a less complementary fit of the trigonal $NO_3^-$ or tetrahedral $H_2PO_4^-$ than that of spherical $Cl^-$ within the urea binding pocket of the free-base porphyrins. Under analogous titration conditions, tetraphenylporphyrin exhibited negligible perturbation in its $^1$H NMR and UV–VIS spectra, indicating the changes observed with ligands **2**–**4** were truly caused by anion binding.

**Table 1** Binding constants ($K$/dm$^3$ mol$^{-1}$) for porphyrins **2**–**4** and $Cl^-$, $NO_3^-$ and $H_2PO_4^-$ anions in $(CD_3)_2SO$

| Porphyrin | $Cl^-$ | $NO_3^-$ | $H_2PO_4^-$ |
|---|---|---|---|
| **2** | $> 10^5$ | 90 | 400 |
| **3** | $> 10^5$ | 60 | 300 |
| **4** | $> 10^5$ | 55 | 1400 |

Future investigations will examine solvent systems where the association constants of **2**–**4** for the complexation of $Cl^-$ and other spherical anions are of the proper magnitude (*i.e.* $< 10^5$)[13] to allow for an accurate determination of their binding constants, and therefore the determination of possible selectivity trends with the different porphyrins. Future experiments will also examine if metallated receptors **5**–**7** will bind anions with the same selectivity trends as those observed with the free-base porphyrins.

We thank Dr Todd Williams for obtaining the FAB mass spectra. This research was supported by the National Science Foundation (EPS-9550487).

## Footnotes and References

* E-mail: burns@wsuhub.uc.twsu.edu

† Neutral *meso*-octaethylporphyrinogens have been shown to bind selectively to $F^-$ in $CD_2Cl_2$.[1a] However, the lack of macrocyclic aromaticity (*i.e.*, little useful UV–VIS, fluorescence, or electrochemical information) makes this system less attractive for sensor development.

‡ Although the complexation stoichiometries for porphyrins **2**–**4** and $NO_3^-$ have yet to determined by Job's method,[14] the calculated errors for the binding constants were small only when a 1 : 1 binding isotherm was utilized.

1 For reviews, see (*a*) R. M. Izatt, K. Pawlak and J. S. Bradshaw, *Chem. Rev.*, 1995, **95**, 2529; (*b*) B. Dietrich, *Pure Appl. Chem.*, 1993, **65**, 1457. For more recent examples (but by no means a comprehensive list), see (*c*) K. Kavallieratos, S. R. de Gala, D. J. Austin and R. H.. Crabtree, *J. Am. Chem. Soc.*, 1997, **119**, 2325; (*d*) A. P. Davis, J. J. Perry and R. P. Williams, *J. Am. Chem. Soc.*, 1997, **119**, 1793; (*e*) M. Berger and F. P. Schmidtchen, *J. Am. Chem. Soc.*, 1996, **118**, 8947; (*f*) V. Král, H. Furuta, K. Schreder, V. Lynch and J. L. Sessler, *J. Am. Chem. Soc.*, 1996, **118**, 1595; (*g*) P. A. Gale, J. L. Sessler, V. Král and V. Lynch, *J. Am. Chem. Soc.*, 1996, **118**, 5140.
2 J. Scheerder, J. F. J. Engbersen, A. Casnati, R. Ungaro and D. N. Reinhoudt, *J. Org. Chem.*, 1995, **60**, 6448.
3 P. Bühlmann, S. Nishizawa, K. P. Xiao and Y. Umezawa, *Tetrahedron*, 1997, **53**, 1647.
4 J. Scheerder, M. Fochi, J. F. J. Engbersen and D. N. Reinhoudt, *J. Org. Chem.*, 1994, **59**, 7815.
5 E. Fan, S. A. Van Arman, S. Kincaid and A. D. Hamilton, *J. Am. Chem. Soc.*, 1993, **115**, 369.
6 B. C. Hamann, N. R. Branda and J. Rebek, *Tetrahedron Lett.*, 1993, **34**, 6837.
7 L. Stryer, *Biochemistry*, W. H. Freeman, New York, 1988, pp. 963–964; J. W. Hanrahan, J. A. Tabcharani, F. Becq, C. J. Mathews, O. Augustinas, T. J. Jensen, X.-B. Chang and J. R. Riordan, in *Ion Channels and Genetic Diseases*, ed. D. C. Dawson and R. A. Frizzel, Rockefeller University Press, New York, 1995.
8 P. D. Beer, M. G. B. Drew, D. Hesek and R. Jagessar, *J. Chem. Soc., Chem. Commun.*, 1995, 1187; P. D. Beer, *Chem. Commun.*, 1996, 689; P. D. Beer, M. G. B. Drew and R. Jagessar, *J. Chem. Soc., Dalton Trans.*, 1997, 881.
9 T. N. Sorrell, *Inorg. Synth.*, 1980, **20**, 163.
10 J. S. Lindsey, *J. Org. Chem.*, 1980, **45**, 5215.
11 A. D. Adler, F. R. Longo, J. D. Finarelli, J. Goldmacher, J. Assour and L. Korsakoff, *J. Org. Chem.*, 1967, **32**, 476.
12 The computer program EQNMR was used to calculate binding constants: M. J. Hynes, *J. Chem. Soc., Dalton Trans.*, 1993, 311.
13 Binding constants greater than $10^5$ dm$^3$ mol$^{-1}$ cannot be determined accurately: T. Wang, J. S. Bradshaw and R. M. Izatt, *J. Heterocycl. Chem.*, 1994, **31**, 1097.
14 K. A. Connors, *Binding Constants*, Wiley, New York, 1987, pp. 24–28.

*Received in Columbia, MO, USA; 8th April 1997; 7/02389H*

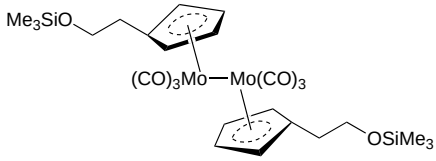
# Radical cage effects. Effect of radical mass and bond energies on cage recombination efficiencies for photochemical cage pair intermediates of $[Mo_2(CO)_6[(\eta^5\text{-}C_5H_4CH_2CH_2OSiMe_3)_2]$, $[Mo_2(CO)_6(\eta^5\text{-}C_5H_4Me)]$ and $[W_2(CO)_6(\eta^5\text{-}C_5H_4Me)]$

**Britt E. Lindfors, Jonathan L. Male, Katharine J. Covert and David R. Tyler***

*Department of Chemistry, University of Oregon, Eugene, Oregon 97403-1253, USA*

**The cage recombination efficiency of the $[(\eta^5\text{-}C_5H_4Me)(CO)_3W\cdot, \cdot W(CO)_3(\eta^5\text{-}C_5H_4Me)]$ radical cage pair in hydrocarbon solvent systems is higher than that of the analogous, but less massive, $[(\eta^5\text{-}C_5H_4Me)(CO)_3Mo\cdot, \cdot Mo(CO)_3(\eta^5\text{-}C_5H_4Me)]$ cage pair; the difference is shown to be attributable not to differences in the radical masses but to differences in the metal–metal bond energies or in the spin–orbit coupling.**

Radical cage effects[1–4] have an enormous impact on chemical reactivity in solution and they are necessary to explain some of the most fundamental physical reaction phenomena.[5–7] Despite the recognition that cage effects can be important, virtually nothing systematic or quantitative is known about how changes in radical mass affect the cage effect.‡ In a prior study, we showed that the cage effect for the photogenerated $[(\eta^5\text{-}C_5H_4Me)(CO)_3Mo\cdot, \cdot Mo(CO)_3(\eta^5\text{-}C_5\text{-}H_4Me)]$ radical pair was smaller than that for the similarly sized but more massive W analogue, $[(\eta^5\text{-}C_5H_4Me)(CO)_3W\cdot, \cdot W(CO)_3(\eta^5\text{-}C_5H_4Me)]$.[8] As tempting as it was to attribute the difference to a change in the mass of the radical fragments, the difference may instead be attributable to differences in the M–M bond energies or to differences in spin–orbit coupling.‡ In order to separate changes caused by differences in radical mass from changes caused by bond energies or spin orbit coupling, we synthesized and studied **1**.




**1**

This molecule was chosen because its constituent radicals have about the same mass (361.3) as the $W(CO)_3(\eta^5\text{-}C_5H_4Me)$ radicals (347.0), yet it has a Mo–Mo bond. A comparison of **1** with $[Mo_2(CO)_6(\eta^5\text{-}C_5H_4Me)_2]$ **2** (259.1 for the radical) will therefore allow us to eliminate the influence of different M–M bond energies. Here we report the results of our comparison of the cage effects in the $[(\eta^5\text{-}C_5H_4Me)(CO)_3M\cdot, \cdot M(CO)_3(\eta^5\text{-}C_5H_4Me)]$ (M = Mo, R = Me, $CH_2CH_2OSiMe_3$; M = W, R = Me) radical cage pairs.

Compound **1** was synthesized by the route shown in Scheme 1.§

$[Mo_2(CO)_6(\eta^5\text{-}C_5H_4CH_2CH_2OH)_2]$

↓ i, $Bu^nLi$, –80 °C, thf; ii, $Me_3SiCl$, –80 °C, thf

$[Mo_2(CO)_6(\eta^5\text{-}C_5H_4CH_2CH_2OSiMe_3)_2]$

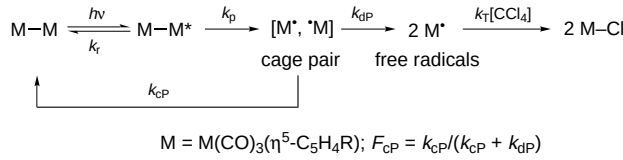
**Scheme 1**

The electronic spectra of **1** and **2** are virtually identical, a feature that suggests the Mo–Mo bond is not significantly perturbed by the changes in the side-chain and that therefore the Mo–Mo bond energies are essentially the same in each molecule.¶,‖

As previously reported,[8] the cage effect is measured by analyzing the quantum yields for disappearance of the dimer as a function of viscosity when the dimers are irradiated in the presence of a radical trap.** The radical trap used in these experiments was $CCl_4$ [eqn. (1), Scheme 2].[8]

$$[M_2(\eta^5\text{-}C_5H_4R)_2(CO)_6] \xrightarrow[CCl_4,\ \text{hexane–paraffin oil}]{h\nu\ (540\ \text{nm})} 2[M(\eta^5\text{-}C_5H_4R)(CO)_3Cl] \quad (1)$$

There is no back-reaction of the free radicals under the reaction conditions because the concentration of $CCl_4$ (2 M) is high enough to trap every free radical.†† The quantum yields for eqn. (1) were measured in hexane solution, and paraffin oil was used to increase the viscosity. (Paraffin oil was used to increase the viscosity since it is a straight-chain hydrocarbon; thus, we sought to avoid preferential solvation in the hexane solvent.[8]) Fig. 1 shows the quantum yields for the reactions of the two Mo dimers and $[W_2(CO)_6(\eta^5\text{-}C_5H_4Me)_2]$ **3** with $CCl_4$ as a function of viscosity.




M = $M(CO)_3(\eta^5\text{-}C_5H_4R)$; $F_{cP} = k_{cP}/(k_{cP} + k_{dP})$

**Scheme 2** Reaction scheme for metal–metal bond photolysis

Plots of the cage effect ($F_{cP}$) *vs*. viscosity for the three dimers are shown in Fig. 2. Note that at any viscosity, the cage effects increase in the order $Mo(CO)_3(\eta^5\text{-}C_5H_4Me) \approx Mo(CO)_3(\eta^5\text{-}C_5H_4CH_2CH_2OSiMe_3) << W(CO)_3(\eta^5\text{-}C_5H_4Me)$. The large difference in $F_{cP}$ between the $[(\eta^5\text{-}C_5H_4Me)(CO)_3W\cdot,$

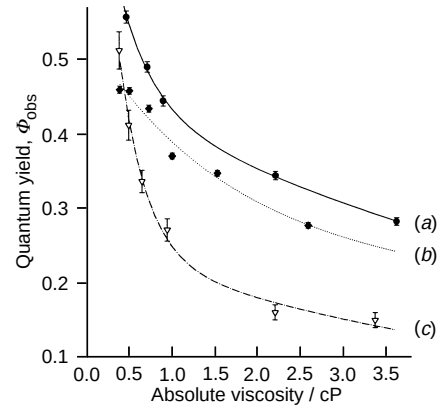



**Fig. 1** Plot of $\Phi_{obs}$ *vs*. viscosity for the photochemical reactions ($\lambda$ = 540 nm) of **1** (*a*), **2** (*b*) and **3** (*c*) with $CCl_4$ (2 M) in hexane–paraffin oil at 23 ± 1 °C. All error bars represent ±1$\sigma$.

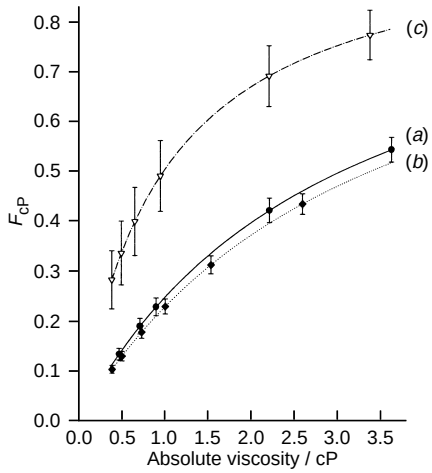



**Fig. 2** Plot of $F_{cP}$ *vs*. viscosity for **1** (*a*), **2** (*b*) and **3** (*c*) at 23 ± 1 °C in hexane–paraffin oil solutions. All error bars represent ±1$\sigma$.

·W(CO)$_3$($\eta^5$-C$_5$H$_4$Me)] and [($\eta^5$-C$_5$H$_4$CH$_2$CH$_2$OSiMe$_3$)(CO)$_3$Mo·, ·Mo(CO)$_3$($\eta^5$-C$_5$H$_4$CH$_2$CH$_2$OSiMe$_3$)] cage pairs (which have about the same mass) and the similarity in the cage effects for the Mo(CO)$_3$($\eta^5$-C$_5$H$_4$Me) and Mo(CO)$_3$($\eta^5$-C$_5$H$_4$CH$_2$CH$_2$OSiMe$_3$) cage pairs shows that a mass effect is not responsible for the difference reported earlier between [($\eta^5$-C$_5$H$_4$Me)(CO)$_3$Mo·, ·Mo(CO)$_3$($\eta^5$-C$_5$H$_4$Me)] and [($\eta^5$-C$_5$H$_4$Me)(CO)$_3$W·, ·W(CO)$_3$($\eta^5$-C$_5$H$_4$Me)]. The difference may be attributed to several factors. One possible factor is the smaller difference between the bond dissociation energy and the photochemical excitation energy for **2** compared to **3**.‡ The excess photonic energy for Mo may lead to an increase in translational energy in the photogenerated radicals and a consequent decrease in the cage effect. Alternatively, the larger cage effect for the W radical pair may reflect the increased driving force (and consequently lower activation barrier) for the recombination of the two W radicals compared to the Mo radicals. A third explanation is the increase in spin–orbit coupling for W compared to Mo. The increase will facilitate intersystem crossing, which may be important if there is a spin barrier to recombination of the cage pair.

It might be argued that the difference in cage effects between the W(CO)$_3$($\eta^5$-C$_5$H$_4$Me) and Mo(CO)$_3$($\eta^5$-C$_5$H$_4$MeCH$_2$-CH$_2$OSiMe$_3$) radical pairs depicted in Fig. 2 is attributable to a size effect.‡‡ This alternative explanation is unlikely for two reasons. First, in his mathematical description of the cage effect,[3] Noyes predicted that sterically larger radicals will have larger cage effects than smaller radical cage pairs. Second, our experiments with the $\eta^5$-C$_5$H$_4$CH$_2$CH$_2$OSiR$_3$ (R = Pr$^n$, Pr$^i$, *n*-C$_6$H$_{13}$) analogues of compound **1** show that, as the R group gets bigger, the cage effect increases.[11] Thus, our experiments confirm Noyes's prediction that bigger cage pairs will have larger cage effects. It is concluded therefore that the difference in cage effects between the W(CO)$_3$($\eta^5$-C$_5$H$_4$Me) and Mo(CO)$_3$($\eta^5$-C$_5$H$_4$CH$_2$CH$_2$OSiMe$_3$) radical pairs is not attributable to a size effect.

Two fundamental conclusions result from this study. First, the effects of radical mass on the cage effect are not nearly as pronounced as suggested by the previously reported data for the [($\eta^5$-C$_5$H$_4$Me)(CO)$_3$Mo·, ·Mo(CO)$_3$($\eta^5$-C$_5$H$_4$Me)] and [($\eta^5$-C$_5$H$_4$Me)(CO)$_3$W·, ·W(CO)$_3$($\eta^5$-C$_5$H$_4$Me)] cage pairs. Secondly, differences in bond energies may influence the cage effect, and it is important therefore to always compare systems with similar bond energies. We are continuing to investigate molecular parameters that influence the magnitude of the cage effect.

Acknowledgment is made to the National Science Foundation for the support of this work. B. E. L. was supported by a fellowship from the National Physical Science Consortium. Dr B. C. Taverner is thanked for a copy of Steric and his helpful assistance.

## Footnotes and References

* E-mail: dtyler@oregon.uoregon.edu

† Some incidental data are available, but no systematic studies have been done. See ref. 2(*a*), p. 174.

‡ $D_{W-W}$ ≈ 56 kcal mol$^{-1}$; $D_{Mo-Mo}$ ≈ 32 kcal mol$^{-1}$ [9] $h\nu$ = 52 kcal mol$^{-1}$.

§ The molecule was synthesized under nitrogen as follows: To a −80 °C (dry ice/acetone) solution of [Mo$_2$(CO)$_6$($\eta^5$-C$_5$H$_4$CH$_2$CH$_2$OH)$_2$] in thf was added 2.2 equiv. of Bu$^n$Li dropwise over 20 min. After 1 h of reaction time, a brick-red solid was allowed to settle. The supernatant was removed with a cannula and the solid was washed twice with thf at −80 °C (20 ml). Tetrahydrofuran (25 ml) was again added and the mixture was cooled to −80 °C. To the mixture was added 2 equiv. of Me$_3$SiCl. The reaction was allowed to proceed until the solution became clear and deep burgundy. After removal of thf *in vacuo*, hexanes were added and the resulting cloudy burgundy solution was filtered through a fine frit. The product was eluted with hexanes through a short, basic alumina column prior to crystallization from hexanes.

¶ The molecule has an intense band at 393 nm ($\varepsilon$ ≈ 20 000 dm$^3$ mol$^{-1}$ cm$^{-1}$), assigned to the σ→σ* transition, and a weaker band at 512 ($\varepsilon$ ≈ 2000), assigned to a $d_\pi$→σ* transition.

‖ By having a –CH$_2$CH$_2$– spacer, we also sought to minimize the difference in the electronic structures of the molecules. For an example of a similar strategy, see ref. 10.

** The cage effect is denoted by $F_{cP}$ and is defined as the ratio of the rate constant for cage recombination to the sum of the rate constants for all cage processes. The procedure for obtaining $F_{cP}$ is to plot $1/\Phi_{obs}$ *vs*. viscosity. The plots are linear with a *y* intercept equal to $1/\Phi_{pair}$, the quantum yield for the formation of the cage pair species. This value of $\Phi_{pair}$ is then used in the equation $1/\Phi_{obs} = [1/\Phi_{pair}][1 + k_{cP}/k_{dP}]$, and the value of $F_{cP}$ is calculated by rewriting $k_{cP}/k_{dP}$. Complete details are found in ref. 8 and 11. The $\Phi_{pair}$ values were: 0.51 ± 0.01 (**2**), 0.61 ± 0.02 (**1**), 0.58 ± 0.09 (**3**).

†† The quantum yields increased with increasing concentration of $CCl_4$ up to *ca*. 0.1 M, at which point saturation was achieved.

‡‡ The static molecular volumes of W(CO)$_3$($\eta^5$-C$_5$H$_4$Me) and Mo(CO)$_3$($\eta^5$-C$_5$H$_4$CH$_2$CH$_2$OSiMe$_3$) were calculated as 107 and 185 Å$^3$, respectively, by using the computer program Steric (written by B. Craig Taverner, Department of Chemistry, Witwatersrand, Private Bag 3, WITS 2050, Johannesburg, South Africa).

1 J. Franck and E. Rabinowitch, *Trans. Faraday Soc*., 1934, **30**, 120; E. Rabinowitch and W. C. Wood, *Trans. Faraday Soc*., 1936, **32**, 138l; E. Rabinowitch, *Trans. Faraday Soc*., 1937, **33**, 1225.

2 (*a*) T. Koenig and H. Fischer, in *Free Radicals*, ed. J. Kochi, Wiley, New York, 1973, vol. l, ch. 4; (*b*) T. Koenig, in *Organic Free Radicals*, ed. W. A. Pryor, ACS Symp. Ser. 69, 1978, ch. 3.

3 R. M. Noyes, *Prog. React. Kinet.*, 1961**, 1**, 129.

4 J. P. Lorand, *Prog. Inorg. Chem*., 1972, **17**, 207; S. A. Rice, *Comprehensive Chemical Kinetics*, Elsevier, Amsterdam, 1985, vol. 25.

5 N. J. Turro and B. Krautler, *Acc. Chem. Res*., 1980, **13**, 369.

6 T. Koenig, B. P. Hay and R. G. Finke, *Polyhedron*, 1988, **7**, 1499; T. Koenig and R. G. Finke, *J. Am. Chem. Soc*., 1988, **110**, 2657.

7 K. L. Brown and L. Zhou, *Inorg. Chem.*, 1996, **35**, 5032; C. D. Garr and R. G. Finke, *J. Am. Chem. Soc.*, 1992, **114**, 10 440; J. F. Endicott and T. L. Netzel, *J. Am. Chem. Soc.*, 1979, **101**, 4000; T. W. Scott and S. N. Liu, *J. Phys. Chem.*, 1989, **93**, 1393; A. I. Kruppa, M. B. Taraban, T. V. Leshina, E. Natarajan and C. B. Grissom, *Inorg. Chem.*, 1997, **36**, 758.

8 K. J. Covert, E. F. Askew, J. Grunkemeier, T. Koenig and D. R. Tyler, *J. Am. Chem. Soc*., 1992, **114**, 10 446.

9 J. R. Krause and D. R. Bininosti, *Can. J. Chem.*, 1975, **53**, 628; J. T. Landrum and C. D. Hoff, *J. Organomet. Chem.*, 1985, **282**, 215; S. Amer, G. Kramer and A. J. Poë, *J. Organomet. Chem.*, 1981, **209**, C28.

10 R. P. Hughes and H. A. Trujillo, *Organometallics*, 1996, **15**, 286.

11 B. E. Lindfors, J. L. Male, K. J. Covert and D. R. Tyler, manuscript in preparation.

*Received in Bloomington, IN, USA, 24th April 1997; 7/02819I*

# 5,10-Diphenyltripyrrane, a useful building block for the synthesis of *meso*-phenyl substituted expanded macrocycles

**Christian Brückner, Ethan D. Sternberg, Ross W. Boyle and David Dolphin***

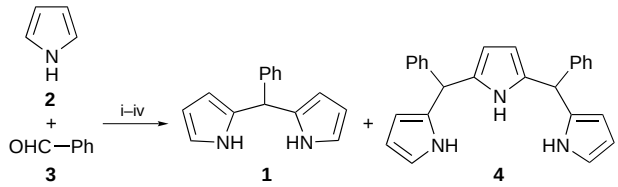
*Department of Chemistry, University of British Columbia, 2036 Main Mall, Vancouver, BC, V6T 1Z1, Canada*

**Pyrrole and benzaldehyde were condensed under acidic conditions to produce a mixture of 5-phenyldipyrromethane and 5,10-diphenyltripyrrane; the tripyrrane was utilized in syntheses of *meso*-phenylsapphyrins, *meso*-diphenylpentaphyrin and *meso*-hexaphenylhexaphyrin.**

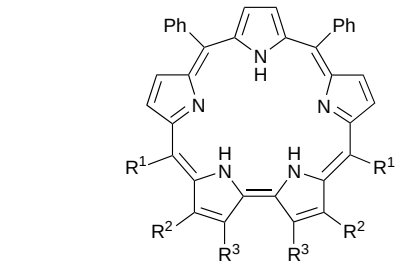
Expanded porphyrins[1] are a diverse class of pyrrolic compounds containing a larger macrocycle than that found in porphyrins. They are being utilized in fields such as photodynamic therapy (PDT),[2] neutral substrate binding, anion recognition[3] and annulene research.[4] Although β-unsubstituted *meso*-aryl substituted porphyrins are very prominent in the synthetic porphyrin field,[5] they are rarely found in expanded porphyrins.[6–8] This, perhaps, reflects the lack of a suitable building block as well as the reduced stability of some of these systems, as will be outlined below.

We report here the improved preparation of 5-phenyldipyrromethane, itself an important building block for *meso*-phenylporphyrinoids,[8] the one-step synthesis of the novel building block 5,10-diphenyltripyrrane and its use in 3 + 2- and 3 + 3-type syntheses to yield three *meso*-phenyl substituted sapphyrins varying in their β-substituents, a partially β-substituted pentaphyrin and a fully β-unsubstituted *meso*-hexaphenylhexaphyrin.

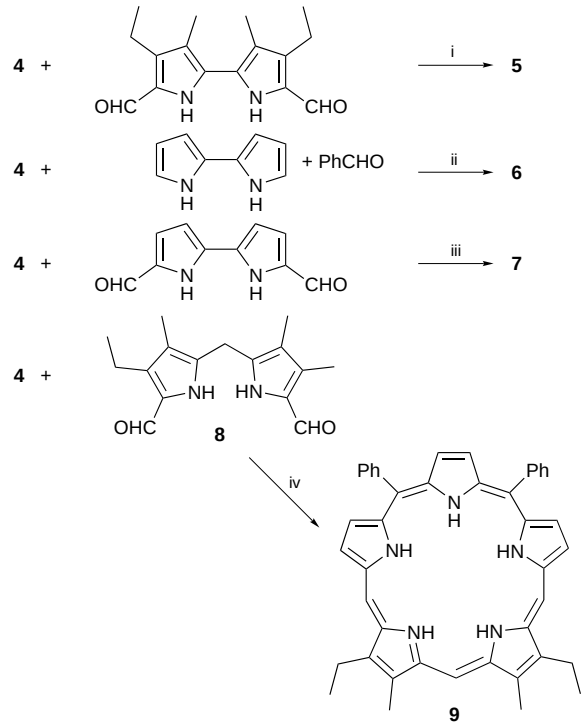
5-Phenyldipyrromethane **1** was synthesized by condensing excess pyrrole **2** and benzaldehyde **3** in the presence of an acid according to the procedures of Lee and Lindsey[9] or Carrel,[10] with the exception that generally 50% lower benzaldehyde to pyrrole ratios were used and, most importantly, work-up procedures were altered. The crude oils resulting from the condensation were, after pre-purification by column chromatography, transferred into a sublimation apparatus and heated under high vacuum (Scheme 1). Under these conditions, **1** sublimed as a white crystalline material of analytical purity. The reaction could be scaled up to provide up to 15 g (*ca.* 50% yield) of **1** per run. The residue left in the bottom of the sublimation apparatus hardened, upon cooling, into a red–orange glass. Analysis of this glass proved that it contained *ca.* 95% 5,10-diphenyltripyrrane **4**.† Lee and Lindsey[9] and Vigmond *et al.*[11] have previously reported the occurrence of a small amount of an unstable tailing component which, based on $^1$H NMR spectroscopy, was provisionally assigned structure **4**. In subsequent work, Lee and co-workers synthesized this tripyrrane in a multi-step procedure and utilized it in the formation of heteroporphyrins.[11] Tripyrrane **4** was obtained by us in yields ranging typically from 10–20%, and, even when ground into a powder, is stable in the solid form but could not, in our hands,




**Scheme 1** *Reagents and conditions*: i, pyrrole, PhCHO (1 : 10) (neat), TFA (5%), 1 h, under $N_2$, or pyrrole, PhCHO (1 : 8), PhMe, reflux, TsOH (cat.), under $N_2$; ii, evaporation of solvents *in vacuo*; iii, flash chromatography (silica gel, $CH_2Cl_2$); iv, sublimation at 130 °C at 1 torr, initial heating: 1 °C $min^{-1}$




**5** $R^1$ = H, $R^2$ = Et, $R^3$ = Me
**6** $R^1$ = Ph, $R^2$ = $R^3$ = H
**7** $R^1$ = $R^2$ = $R^3$ = H



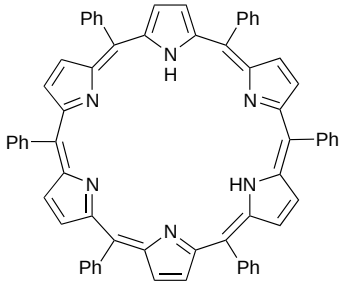

**Scheme 2** *Reagents and conditions*: i, abs. EtOH (1 mM), $O_2$ bubble, TsOH (4 equiv.); evaporation of solvents *in vacuo*; column chromatography (neutral alumina, activity I, 2.5% MeOH–$CH_2Cl_2$); ii, $CH_2Cl_2$, under $N_2$, $BF_3{\cdot}Et_2O$ (cat.), 1 h; chloranil, reflux, 30 min; evaporation of solvents *in vacuo*; column chromatography (neutral alumina, activity I, 2.5% MeOH–$CH_2Cl_2$); preparative TLC (alumina, 1 : 1 $CH_2Cl_2$–$CCl_4$); iii, abs. EtOH (1 mM), $O_2$ bubble, TsOH (4 equiv.); evaporation of solvents *in vacuo*; trituration with $CHCl_3$; preparative TLC (silica gel, 0.5% MeOH–$CH_2Cl_2$); iv, $CH_2Cl_2$, TFA (cat.), 48 h, room temp., neutralisation with $Et_3N$, then an additional 36 h; column chromatography (neutral alumina, 1–3% MeOH–$Ch_2Cl_2$); then preparative TLC (silica gel, $CH_2Cl_2$–20% EtOAc–1% $Et_3N$)

be further purified without retrieving it as an unstable oil. We attribute this, in part, to the presence of three stereoisomers in **4**. This route to tripyrrane **4** is comparatively simple given that the syntheses of β-alkyltripyrranes generally involve many reaction steps from starting materials which are not commercially available, unlike pyrrole and benzaldehyde. It is anticipated that the ease of preparation of **4** will encourage its use as a synthetic building block.

With the novel 5,10-diphenyltripyrrane **4** in hand, we had the opportunity to prepare *meso*-diphenyl substituted sapphyrins **5** and **7**‡ and, in a four-component Rothemund-type condensation, *meso*-tetraphenylsapphyrin **6** (Scheme 2). Recently, Sessler *et al.* published the synthesis of **5** *via* a multi-component condensation under Lindsey-type conditions[6] and Chmielewski *et al.* published the isolation of sapphyrin **6** as a side-product from a Rothemund synthesis of tetraphenylporphyrin.[7] Both procedures, however, produce the particular sapphyrins in low yields (*ca.* 10 and 1.1%, respectively) and both require extensive chromatographic work-up. The syntheses presented here using the preformed tripyrrolic precursor are short, produce up to 39% yield in the final sapphyrin condensation (for **5**) and, due to the absence of any other porphyrinic by-products, require only minimal chromatographic work-up. The inversion of one pyrrolic unit in **7** upon protonation–deprotonation as observable by NMR spectroscopy is analogous to that described before for **6**.[7] The *meso*-positions flanking the 'flipping' pyrrolic unit do not participate in this inversion.

A TFA catalysed 3 + 2-type condensation of tripyrrane **4** and dipyrromethane **8** in the presence of nitrogen, followed by treatment with base and then by chromatography, produced the orange *meso*-diphenyltetra-β-alkyl pentaphyrin **9** in 13% yield (Scheme 2). The pentaphyrin was characterized by 1H NMR spectroscopy, mass spectrometry and UV-VIS spectroscopy.§ Its optical properties are similar to those of previously reported β-alkyl pentaphyrins.[13] The strongly solvent-dependent $^1$H NMR spectrum can be rationalized in terms of inversions of pyrrolic units similar to those observed in sapphyrins. However, unlike the stable β-alkyl pentaphyrins, this macrocycle exhibited poor stability even in the solid state and decomposed when exposed to air, with a half-live of several days. It remains to be seen whether the macrocycle can be stabilized by metal complexation.[14]

On the other hand, a 3 + 3-type condensation reaction employing **4** and benzaldehyde **3** furnished, after oxidation with chloranil and chromatography, a blue product which could be identified by its mass and UV-VIS spectra as the *meso*-hexaphenylhexaphyrin **10**.¶ Its $^1$H NMR was complex and




**10**

largely depended on pH and the nature of the solvent. This may reflect its non-static conformation. Such flexibility of the macrocycle has also been observed for β-alkyl hexaphyrins. Further studies of this macrocycle were hampered by its instability.

The above examples prove the synthetic utility of **4**. It also emerges that the *meso*-phenyl substituted versions of the larger expanded macrocycles pentaphyrin and hexaphyrin exhibit a significantly decreased stability when compared with their β-alkyl analogues. This stability trend has been observed before,[8] and, if this is a general trend, may limit the extent to which *meso*-phenyl substituted analogues of other known expanded macrocycles can be made.

This work was supported by the Natural Sciences and Engineering Council of Canada.

## Footnotes and References

* E-mail: david@dolphin.chem.ubc.ca

† *Selected data* for **4**: $^1$H NMR (200 MHz, $CD_2Cl_2$): $\delta$ 5.35 (s, 2 H), 5.78 (d, $J$ = 4, 2 H), 5.89 (s, 2 H), 6.14 (m, 2 H), 6.66 (m, 2 H), 7.15–7.38 (m, 10 H), 7.75 (br s, 1 H), 7.88 (br s, 2 H); HRMS (EI, 200 °C) $C_{26}H_{23}N_3$ requires 377.1892. Found: 377.1881.

‡ *Selected data* for **7**: $^1$H NMR (400 MHz, $CDCl_3$): $\delta$ −1.52 (s, 2 H), −0.1 (br s, 1 H), 7.15–7.20 (m, 1 H), 7.25–7.30 (m, 1 H), 7.60 (t, $^3J$ 7, 2 H), 7.85 (t, $^3J$ 8, 4 H), 8.49 (br s, 4 H), 9.24 (d, $^3J$ 4.5, 2 H), 9.43 (d, $^3J$ 4.5, 2 H), 9.60 (d, $^3J$ 4.5, 2 H), 10.20 (d, $^3J$ 5.0, 2 H), 10.27 (s, 2 H); $\lambda_{max}$/nm ($CH_2Cl_2$–trace $Et_3N$) (log ε) 478 (4.86), 506 (4.71), 626 (3.67), 686 (3.97), 708 (sh), 786 (3.62); HRMS (EI, 180 °C) $C_{36}H_{25}N_5$ requires 527.21100. Found: 527.21015. For **7**·2HCl: $\lambda_{max}$/nm ($CH_2Cl_2$–trace HCl) (log ε) 482 (5.47), 656 (4.13), 682 (4.13), 724 (sh), 758 (4.70) nm.

§ *Selected data* for **9**: $^1$H NMR (400 MHz, $CDCl_3$–TFA): $\delta$ −3.6 (br s, 1 H), 2.9 (br s, 2 H), 2.12 (t, $^3J$ 8.2, 6 H), 4.08 (s, 6 H), 4.56 (br q, $^3J$ 8, 4 H), 7.5 (br m, 10 H), 8.1 (m, 4 H), 8.6 (br s, 2 H), 11.4 (s, obscured by TFA signal), 11.5 (s, obscured by TFA signal); $\lambda_{max}$/nm ($CH_2Cl_2$–TFA) (log ε) 492 (1.21), 682 (0.072), 742 (0.046); HRMS (LSIMS, thioglycerol) $C_{43}H_{40}N_5$ requires 626.32837. Found: 626.32756.

¶ *Selected data* for **10**: $\lambda_{max}$/nm ($CH_2Cl_2$) (rel. intensity) 385 (0.95), 466 (0.46), 520 (0.5) 636 (1.0); HRMS (EI, 350 °C) $C_{66}H_{44}N_6$ requires 920.36273. Found: 920.36550.

1 J. L. Sessler and S. J. Weghorn, *Expanded, Contracted, and Isomeric Porphyrins*, Pergamon, N.Y., 1997; A. Jasat and D. Dolphin, *Chem. Rev.*, 1997, in the press.
2 D. Dolphin, *Can. J. Chem.*, 1994, **72**, 1005; R. Bonnett, *Chem. Soc. Rev., 1995, 19.*
3 J. L. Sessler, M. Cyr, H. Furuta, V. Král, T. Mody, T. Morishima, M. Shionoya and S. Weghorn, *Pure Appl. Chem., 1993*, 65, 393; B. L. Iverson, K. Shreder, V. Kral, D. A. Smith, J. Smith, J. L. Sessler, *Pure Appl. Chem.*, 1994, **66**, 845.
4 D. O. Mártire, N. Jux, P. F. Aramedía, R. M. Negri, J. Lex, S. E. Braslavsky, K. Schaffner, and E. Vogel, *J. Am. Chem. Soc.*, 1992, **114**, 9969; E. Vogel, *Pure Appl. Chem.*, 1993, **65**, 143.
5 J. B. Kim, A. D. Adler and F. R. Longo, in *The Porphyrins*, ed. D. Dolphin, Academic Press, New York, 1978, vol. 1, pp. 85–100; J. S. Lindsey, S. Prathapan, T. E. Johnson and R. W. Wagner, *Tetrahedron*, 1994, **50**, 8941.
6 J. L. Sessler, L. Lisowski, K. A. Boudreaux, V. Lynch, J. Barry and T. J. Kodadek, *J. Org. Chem.*, 1995, **60**, 5975.
7 P. J. Chmielewski, L. Latos-Grazynski and K. Rachlewicz, *Eur. J. Chem.*, 1995, **1**, 68.
8 R. W. Boyle, L. Y. Xie and D. Dolphin, *Tetrahedron Lett.*, 1994, **35**, 5377; L. Y. Xie, R. W. Boyle and D. Dolphin, *J. Am. Chem. Soc*., 1996, **118**, 4853.
9 C.-H. Lee and J. S. Lindsey, *Tetrahedron*, 1994, **50**, 11427.
10 T. Carell, Ph.D. Thesis, Ruprechts-Karl-Universität, Germany, 1993. See footnotes of: G. Shipps, Jr. and J. Rebek, Jr., *Tetrahedron Lett.*, 1994, **35**, 6823.
11 S. J. Vigmond, M. C. Chang, K. M. R. Kallury and M. Thompson, *Tetrahedron Lett.*, 1994, **35**, 2455.
12 P.-Y. Heo, K. Shin and C.-H. Lee, *Tetrahedron Lett.*, 1996, **37**, 197; P. Y. Heo and C.-H. Lee, *Bull. Korean Chem. Soc.*, 1996, **17**, 515.
13 H. Rexhausen, and A. Gossauer, *J. Chem. Soc., Chem. Comm.*, 1983, 275; R. E. Dansodanquah, L. Y. Xie and D. Dolphin, *Heterocycles*, 1995, **41**, 2553.
14 A. K. Burrell, G. Hemmi, V. Lynch, and J. L. Sessler, *J. Am. Chem. Soc.*, 1991, **113**, 4690.

*Received in Corvallis, OR, USA, 26th February 1997; revised manuscript received, 26th June 1997; 7/04510G*

# Formation of a tetrahedral $Tl_4$ cluster directed by a novel homoscorpionate ligand

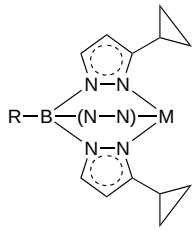
**Arnold L. Rheingold, Louise M. Liable-Sands and Swiatoslaw Trofimenko**

*Department of Chemistry and Biochemistry, University of Delaware, Newark, DE 19716, USA*

**The thallium complex of a novel ligand, hydrotris(3-cyclopropylpyrazol-1-yl)borate, forms a stable tetramer, $[Tl(Tp^{Cpr})]_4$, containing a perfect tetrahedron of Tl atoms, with each Tl in an octahedral environment.**

The formation of Tl···Tl bonds, or strong interactions between two Tl atoms, has been found or postulated in a number of thallium(I) compounds, although the exact nature of such bonding remained enigmatic.[1] Most of these examples featured two Tl atoms bridged by one, two, or three ligands enforcing a certain proximity between them, and leading to a Tl···Tl interaction. For instance, a Tl–Tl distance of 3.69 Å was found in a complex structure, containing a triangle consisting of two Tl atoms (further bonded to manganese carbonyl moieties) bridged by a $Mn(CO)_2$ link.[2] The Tl···Tl relationship was considered one of bonding interaction, being only 0.29 Å longer than the metal–metal distance in elemental Tl.[3] Other examples have also been reported,[4] and cited in a review devoted to this subject.[1] Some insight into the nature of the Tl–Tl interaction was elicited from an unbridged species, the quasi-dimer of $[Tl\{C_5(CH_2Ph)_5\}]$, formed about an inversion center, where the Tl···Tl distance is 3.63 Å.[5] It was proposed that bonding interaction results from the mixing of empty p levels into filled s combinations, with the desideratum expressed that 'further work is needed in finding more structures to develop a better understanding of this fascinating problem'.[1] Since that time, other examples appeared,[6] including a fairly unstable tetrameric cluster of the monoalkylthallium compound $[Tl\{C(SiMe_3)\}]_4$, containing Tl in a tetrahedral environment, within a distorted structure.[7] Earlier, similar group 13 analogue structures such as $[In\{C(SiMe_3)_3\}]_4$,[8] and $[Ga\{C(SiMe_3)_3\}]_4$,[9] containing tetrahedra of In and Ga, respectively, have been reported.

In the course of fine-tuning the coordinative behavior of homoscorpionate [hydrotris(pyrazol-1-yl)borate] ligands through modification of their 3-R substituents,[10] we had synthesized hydrotris(3-cyclopropylpyrazol-1-yl)borate ($Tp^{Cpr}$), isolated it as the stable, high-melting Tl salt,† and determined its structure by X-ray crystallography.‡




$[Tl(Tp^{Cpr})]$ R = H, M = Tl

–(N–N)– represents the third, hidden, 3-(cyclopropyl)pz

To our surprise, this thallium salt, $[Tl(Tp^{Cpr})]$, revealed a highly symmetrical tetrameric structure, containing a perfect tetrahedron of four Tl atoms, each capped by the three nitrogens of a $Tp^{Cpr}$ ligand, thus placing each Tl in an octahedral coordination environment, an unprecedented structure involving $Tl^{I}$–$Tl^{I}$ bonding. Previously, all structures of Tl salts of homoscorpionate ligands, including $[Tl(Tp^{But})]$,[11] $[Tl(Tp^{But,Me})]$,[12] $[Tl(Tp^{But2})]$,[13] $[Tl(Tp^{Menth})]$,[14] $[Tl(Tp^{Mementh})]$,[14] [Tl{tris(1,4-dihydroindeno[1,2-*c*]pyrazol-1-yl)borato}],[15] $[Tl(Tp^{Ant})]$,[16] [Tl{hydrotris(7-*tert*-butylindazol-2-yl)borate}][$Tl(Tp^{3Bo,7Me})$][17] and [Tl{HB(3,5-[*p*-$C_6H_4$-$But]_2pz)_3$}]],[18] [Tl{HB[pz$(CF_3)_2$-3,5]}]],[19] and $[Tl(Tp^{Tol})]$,[20] which have been determined by X-ray crystallography, are monomeric or in one case dimeric. In all these cases, Tl is coordinated to the three nitrogen atoms of the ligand, usually with retention of the ligand $C_{3v}$ symmetry, except for the very hindered $Tp^{But2}$ and $Tp^{Ant}$ derivatives which were distorted. The Tl–N bond lengths ranged from 2.50 to 2.68 Å, and the N–Tl–N angles from 76 to 78° with the exception of the distorted $Tp^{Ant}$, where the angle was 66°. The only thing resembling a Tl···Tl interaction was noted in the case of $[Tl(Tp^{Tol})]$, the structure of which showed two molecules in a face-to-face conformation, akin to that found in $[Tl\{C_5(CH_2Ph)_5\}]$, with the Tl atoms 3.86 Å apart. However, in contrast to $[Tl\{C_5(CH_2Ph)_5\}]$, which had a *trans*-bent geometry, the $[Tl(Tp^{Tol})]$ 'dimer' was not bent, but had a collinear B–Tl–Tl–B sequence.

The structure of $[Tl(Tp^{Cpr})]_4$ has the $Tl_4$ tetrahedron as its core (Fig. 1) with each Tl capped by a $Tp^{Cpr}$ ligand, and all Tl–Tl bonds equal at 3.6468(4) Å, with the Tl–Tl–Tl angles the expected 60°. Each $Tp^{Cpr}$ ligand is rotated by about 30° about its threefold axis with respect to a staggered relationship to the triangle of Tl atoms below. The crystals are face-centered cubic, and the unit cell consists of four discrete crystallographically perfect tetrameric tetrahedral thallium clusters (Fig. 2). The Tl–N bonds are 2.532(3) Å, which is close to the short end of the reported values, while the N–Tl–N angles are 76.58(12)°, and thus in the typical range for $[Tl(Tp^{x})]$ complexes. All the

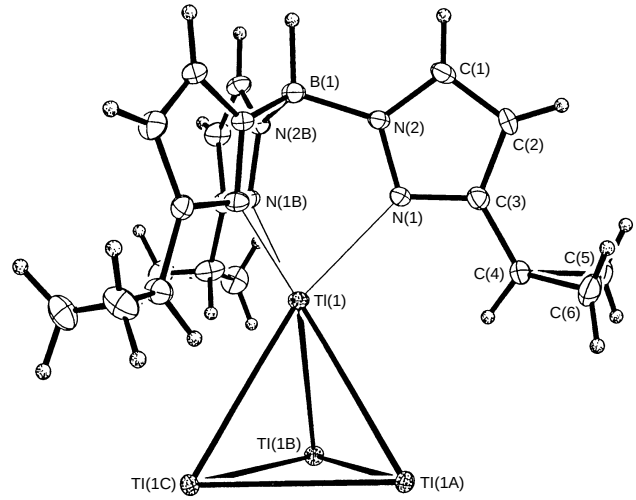



**Fig. 1** ORTEP diagram of $[Tl(Tp^{Cpr})]_4$ showing atom labelling scheme. Thermal ellipsoids at 30% probability. Hydrogen atoms and three of the $Tp^{Cpr}$ ligands have been omitted for clarity. Selected distances (Å) and angles (°): Tl(1)–Tl(2) 3.647; Tl(1)–N(1), 2.532; Tl(1)–Tl(2)–Tl(3) 60.0, N(1)–Tl(1)–N(2) 123.2.

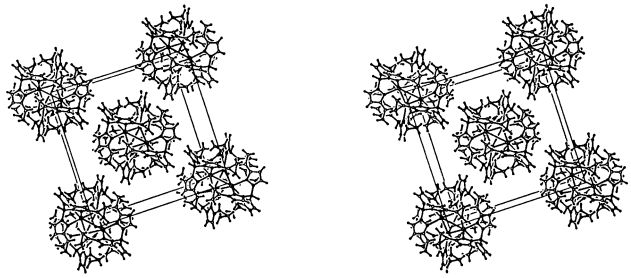


**Fig. 2** Stereoview of the unit cell showing discrete tetrameric tetrahedral thallium clusters

cyclopropyl groups are turned in such a way that only the tertiary hydrogen is pointed at the metal.

The reason why the $Tl_4$ cluster is formed with $Tp^{Cpr}$ but not with any of the other $Tp^x$ ligands cannot be simply a steric one, in the sense that the cyclopropyl group is smaller than any of the 3-R substituents in $[Tl(Tp^x)]$ complexes whose structures are known. We have determined the structure of [Tl(Tp)], the least hindered Tl homoscorpionate, with 3-R = H, and found only unassociated monomers in the crystal with the nearest Tl–Tl distance 4.8 Å, and thus definitely out of bonding range.[21] Since there is no steric hindrance to prevent formation of the $Tl_4$ cluster, what seems to be missing is an additional driving force for its formation, supplied by the 3-cyclopropyl substituent. Moreover, structures of the closely related $[Tl(Tp^x)]$ compounds with 3-R = $Pr^i$ or 3-R = *c*-$C_4H_9$ have also been determined and, again, found to be simple monomers.[21]

Looking at the space-filling model of the structure of $[Tl(Tp^{Cpr})]_4$, we see that the cyclopropyl groups from one ligand cross over past the Tl atom to which the ligand is bonded, and protrude over an adjacent Tl atom, creating an intimately interlocking network of 'rabbet joints', which involves all four ligands over the tetrahedral array of Tl atoms. This resembles somewhat the intermeshing of the R groups of $Tp^R$ ligands in octahedral $[M(Tp^R)_2]$ complexes, and makes the whole structure appear spherical (Fig. 2). However, in $[Tl(Tp^{Cpr})]_4$ each $Tp^{Cpr}$ ligand interlocks with three others, thus generating a rather rigid structure, with little rotational freedom for the cyclopropyl groups, or for twisting of the pz groups. It is this unstrained fit of all the components within $[Tl(Tp^{Cpr})]_4$ that seems to be the driving force for the formation of this supramolecular structure and, possibly, for the lowering of surface energy (cluster *vs*. four monomeric units) during crystallization of the monomeric species present in solution. The reported results are obviously unrelated to cases where individual Tp ligands are capping a corner in preformed metallic clusters, as for instance in $[Fe_4S_4]^{2+}$,[22] or in $[VFe_3S_4]^{2+}$.[23]

We have to conclude that the specific nature of the 3-R substituents in homoscorpionate ligands can exert a very subtle, and yet dominant, influence on their coordination chemistry, not always predictable *a priori*.[24]

## Footnotes and References

* E-mail: trofimen@udel.edu

† *Synthesis*: 3-cyclopropylpyrazole was synthesized in 58% yield from methyl cyclopropyl ketone by the method used for making 3-isopropylpyrazole.[25] Bp 122–124 °C (2.8 Torr.) $^1$H NMR: $\delta$ 12.45 (s, 1 H, NH), 7.46 (s, 1 H, H-5), 5.93 (d, 1 H, H-4), 1.97 (spt, 1 H, tertiary H), 0.93 (dt, 2 H, cyclopropyl) and 0.74 (dt, 2 H, cyclopropyl). $^{13}$C NMR: $\delta$ 7.89, 101.1, 134.0, 150.6 (the fifth peak is hidden under the $\delta$ 7.9 peak). Calc. for $C_6H_8N_2$: C, 66.7; H 7.41; N 25.9. Found: C, 66.9; H, 7.51; N, 25.7%.

$[Tl(Tp^{Cpr})]$ was prepared by heating 3-cyclopropylpyrazole with $KBH_4$ (3.6 : 1 mole ratio) until the theoretical amount of hydrogen was evolved. After distilling out excess 3-cyclopropylpyrazole *in vacuo*, the residue was dissolved in thf and converted to the Tl salt in 77% yield, by treatment with aqueous $TlNO_3$. Mp 144–146 °C. IR: BH 2438 cm$^{-1}$. $^1$H NMR: $\delta$ 7.50 (d,1 H, H-5), 5.74 (d, 1 H, H-4), 2.04 (m, 1 H, tertiary H), 0.93 (m, 2 H, cyclopropyl), 0.566 (m, 2 H, cyclopropyl). $^{13}$C NMR: $\delta$ 8.1, 9.0, 99.7, 135.9, 155.8. Calc. for $C_{18}H_{22}BN_6Tl$: C, 40.2; H, 4.10; N, 15.6. Found: C, 40.1; H, 4.18; N, 15.4%. $CDCl_3$ was used as NMR solvent in all cases. Molecular mass determination by the Signer method in chloroform gave a value of 556 (monomer 537).[26]

‡ *Crystal data* for $[Tl(Tp^{Cpr})]_4$: $C_{72}H_{88}B_4N_{24}Tl_4$: $M_w$ = 537.60, cubic, $F23$, $a$ = 20.5104(2) Å, $U$ = 8628.2(2) Å$^3$, $Z$ = 4, $T$ = 173(2), $D_c$ = 1.655 g cm$^{-1}$, $\mu$ = 75.00 cm$^{-1}$, $R(F)$ = 0.0217 and $R(wF^2)$ = 0.0627 for 1708 observed independent reflections ($3 \leqslant 2\theta \leqslant 56°$). CCDC 182/545.


1 C. Janiak and R. Hoffman, *J. Am. Chem. Soc.*, 1990, **112**, 5924.
2 M. Schollenberger, B. Nuber, M. L. Ziegler and E. Hey-Hawkins, *J. Organomet. Chem.*, 1993, **460**, 55.
3 A. F. Wells, *Structural Inorganic Chemistry*, Oxford University Press, London, 1975, 4th edn., p. 1013.
4 J. Beck and J. Strähle, *Z. Naturforsch., Teil B*, 1986, **41**, 1381; L. F. Dahl, G. L. Davis, D. L. Wampler and R. West, *J. Inorg. Nucl. Chem.*, 1962, **24**, 357; V. A. Maroni and T. G. Spiro, *Inorg. Chem.*, 1968, **7**, 193; M. Veith, A. Spaniol, J. Pohlmann, F. Gross and V. Huch, *Chem. Ber.*, 1993, **126**, 2625.
5 H. Schumann, C. Janiak, M. A. Khan and J. J. Zuckermann, *J. Organomet. Chem.*, 1988, **354**, 7.
6 K. W. Hellmann, L. H. Gade, R. Fleischer and D. Stalke, *Chem. Commun.*, 1997, 527; K. W. Hellmann, L. H. Gade, A. Steiner, D. Stalke and F. Möller, *Angew. Chem., Int. Ed. Engl.*, 1997, **36**, 160.
7 W. Uhl, S. U. Keimling, K. W. Klinkhammer and W. Schwartz, *Angew. Chem., Int. Ed. Engl.*, 1997, **36**, 64.
8 W. Uhl, R. Graupner, M. Layh and U. Schütz, *J. Organomet. Chem.*, 1995, **493**, C1.
9 W. Uhl, W. Hiller, M. Layh and W. Schwarz, *Angew. Chem., Int. Ed. Engl.*, 1992, **31**, 1364.
10 S. Trofimenko, *Chem. Rev.*, 1993, **93**, 943.
11 A. H. Cowley, R. L. Geerts, C. M. Nunn and S. Trofimenko, *J. Organomet. Chem.*, 1989, **365**, 19.
12 K. Yoon and G. Parkin, *Polyhedron*, 1995, **14**, 811.
13 C. Dowling, D. Leslie, M. H. Chisholm and G. Parkin, *Main Group Chem.*, 1995, **1**, 29.
14 D. D. Le Cloux, C. J. Tokar, M. Osawa, R. P. Houser, M. C. Keyes and W. B. Tolman, *Organometallics*, 1994, **13**, 2855.
15 A. L. Rheingold, R. L. Ostrander, B. S. Haggerty and S. Trofimenko, *Inorg. Chem.*, 1994, **33**, 3666.
16 R. Han, G. Parkin and S. Trofimenko, *Polyhedron*, 1995, **14**, 387.
17 A. L. Rheingold, L. M. Liable-Sands, G. P. A. Yap and S. Trofimenko, *Chem. Commun.*, 1996, 1233.
18 E. Libertini, K. Yoon and G. Parkin, *Polyhedron*, 1993, **12**, 2539.
19 O. Renn, L. M. Venanzi, A. Marteletti and V. Gramlich, *Helv. Chim. Acta*, 1995, **78**, 993.
20 G. Ferguson, M. C. Jennings, F. J. Lalor and C. Shanahan, *Acta Crystallogr., Sect. C*, 1991, **47**, 2079.
21 A. L. Rheingold, L. M. Liable-Sands and S. Trofimenko, unpublished work.
22 S. Ciurli, M. Carrié, J. A. Weigel, M. J. Carney, T. D. P. Stack, G. C. Papaefthymiou and R. H. Holm, *J. Am. Chem. Soc.*, 1990, **112**, 2654; J. A. Weigel and R. H. Holm, *J. Am. Chem. Soc.*, 1990, **112**, 4184.
23 S. Ciurli and R. H. Holm, *Inorg. Chem.*, 1989, **28**, 1685.
24 Efforts to study the $Tl_4$ cluster using density-functional methods and a variety of ersatz $Tp^{Cpr}$ replacements failed to reveal any evidence for a stable cluster arrangement. F. P. Arnold, Jr., personal communication.
25 S. Trofimenko, J. C. Calabrese, P. J. Domaille and J. S. Thompson, *Inorg. Chem.*, 1989, **28**, 1091.
26 R. Signer, *Ann.*, 1930, **478**, 246.


*Received in Bloomington, IN, USA; 14th May 1997; 7/03349D*



Typeset and printed by Black Bear Press Limited, Cambridge, England

ChemComm
FEATURE ARTICLE

# Assembly of the antifungal agent FR-900848 and the CETP inhibitor U-106305: studies on remarkable multicyclopropane natural products†

**Anthony G. M. Barrett,*[a] Wendel W. Doubleday,[b] Dieter Hamprecht,[a] Krista Kasdorf,[a] Gary J. Tustin,[a] Andrew J. P. White[a] and David J. Williams[a]**

[a] *Department of Chemistry, Imperial College of Science, Technology and Medicine, London, UK SW7 2AY*
[b] *Department of Chemistry, Colorado State University, Fort Collins, Colorado 80523, USA*

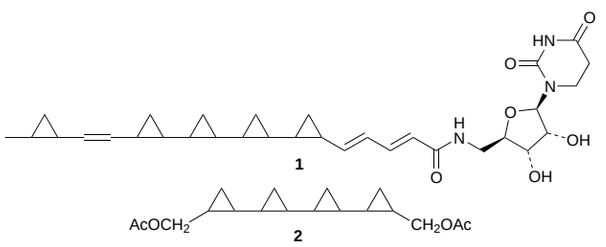
**The full structural elucidation of FR-900848, an antifungal pentacyclopropane nucleoside natural product from *Streptoverticillum fervens*, is reported. A series of model compounds are prepared using multiple asymmetric Simmons–Smith cyclopropanation reactions. Comparisons of spectroscopic data of synthetic 1,2-dicyclopropylethene, quatercyclopropane-2,2‴-dimethanol and 2-methylcyclopropanecarbaldehyde derivatives of defined absolute stereochemistry with FR-900848 and its degradation products are used to unequivocally establish the absolute stereochemistry of the natural product.**

**A $C_2$-symmetric quatercyclopropane-2,2‴-dimethanol is converted by a sequence of desymmetrisation, selective monocyclopropanation of a 5-(quatercyclopropyl)penta-2,4-dien-1-ol derivative, deoxygenation and Horner–Emmons homologation into the fatty acid side chain of FR-900848. Coupling of this carboxylic acid with 5′-amino-5′-deoxy-5,6-dihydrouridine gives synthetic FR-900848. The unusual helical structure of FR-900848 is discussed and compared with U-106305, a cholesteryl ester transfer protein inhibitor from the fermentation broth of *Streptomyces* sp. UC 11136. The full structure and stereochemistry of U-106305 is established by total synthesis using a bi-directional strategy closely following the route to FR-900848.**

## Introduction

There is very considerable alarm amongst the medical profession regarding fungal disease. Dermatophyte infections such as tinea pedis and candidiasis, although rarely fatal, are common and widespread throughout the world.[1] There are other fungal diseases that are far darker in reputation and significance. Pathogens such as *Candida albicans*, *Cryptococcus neoformans*, *Pneumocystis carinii* and *Aspergillus fumigatus* are the cause of considerable morbidity and mortality in immunocompromised patients. Current therapies for the treatment of serious systemic fungal infection are deficient. There is need for novel therapies for serious fungal disease and for the management of the legions of topical fungal infections. In consequence several pharmaceutical companies world-wide are seeking to develop superior fungicidal agents. Owing to evolutionary pressures of microbial antagonism, fermentation broths are rich sources of novel anti-infective agents, and natural product chemistry continues to play a major role in antibiotic discovery.

In 1990 Yoshida *et al*. in the Fujisawa laboratories in Tsukuba reported the partial structural elucidation of a remarkable natural product.[2]‡ Fractionation of the fermentation broth from *Streptoverticillium fervens* and extensive chromatography led to the isolation of a structurally unique nucleoside. The structure of the new isolate was established by extensive NMR spectroscopy and partial degradation. That the compound was a 5′-amino-5′-deoxy-5,6-dihydrouridine derivative was unusual but not especially exciting. However, the fact that FR-900848 **1**,




the unassuming Fujisawa file number for the new natural product, possessed an unusual fatty acid side chain was most noteworthy. This $C_{23}$ fatty acid residue is endowed with five cyclopropanes, four of which are contiguous. Although the initial degradation studies at Fujisawa determined the constitution of the molecule,[2] there remained eleven elements of ambiguity in the structure: the geometry of $\Delta^{18}$, the stereochemistry of the isolated cyclopropane and the stereochemistry of the quatercyclopropane unit. Tanaka and co-workers, however, did establish[3] that the central quatercyclopropane unit **2**, obtained by ozonolysis with a sodium borohydride work-up and acetylation, was $C_2$-symmetric. This partial structural assignment followed from the simplicity of the $^1$H NMR spectrum and the presence of only seven lines in the $^{13}$C NMR spectrum. In addition, the $[\alpha]_D$ for diester **2** was consistent with a $C_2$-structure rather than *meso* stereochemistry.

FR-900848 **1** shows potent, selective activity against filamentous fungi such as *Aspergillus niger*, *Mucor rouxianus*, *Aureobasidium pullulans*, various *Trichophyton* sp., *etc*. In contrast it is essentially inactive against non-filamentous fungi such as *Candida albicans* and Gram-positive and -negative bacteria. It shows activity *in vivo* and is not appreciably toxic.[2,4] Thus FR-900848 **1** represents a significant new lead for the design of nucleoside antifungal agents active against the major human pathogen *Aspergillus fumigatus*. It is certain that the fatty acid side chain of FR-900848 **1** is considerably conformationally restricted. The influence of this fact on bioactivity and mode of antifungal action is as yet undefined. The biosynthetic origin of FR-900848 **1** is not yet clear nor is it obvious as to what evolutionary advantage there is in endowing a fatty acid with five cyclopropane ring systems with the attendant strain energy of about 130 kcal mol$^{-1}$. Finally, FR-900848 **1** provides an intriguing model upon which to design a new class of materials: stereoregular poly(cyclopropene). Such compounds may well have unique and useful physical properties. All these factors underscore the potential importance of synthetic chemistry on FR-900848 **1** and related multicyclopropane arrays.

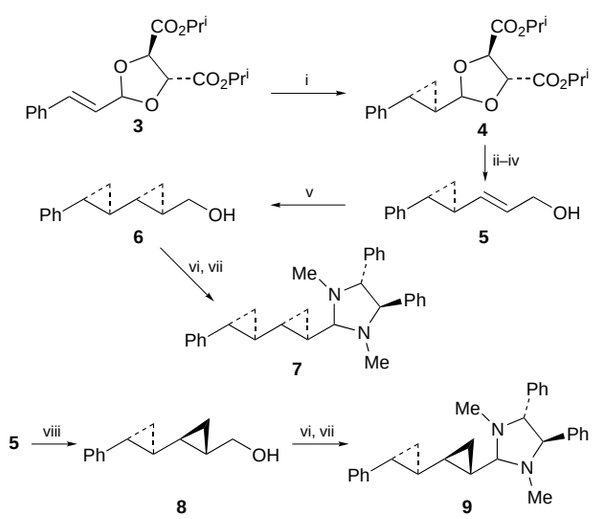
## Stereoselective synthesis of bicyclopropanes

There is an extensive literature on the synthesis and reactions of bicyclopropane arrays. For example, Buchert and Reissig[5] have reported the synthesis of highly substituted bicyclopropanes. In addition, Nijveldt and Vos have carried out an X-ray crystallographic study of bicyclopropane.[6] Prior to the discovery of FR-900848 **1**, little attention was paid to issues of stereochemistry in bicyclopropane chemistry. Recently, ourselves[7–9] and the Zercher[10,11] and Armstrong[12] groups have independently reported stereoselective methods for the preparation of bicyclopropane systems relevant to the total synthesis of FR-900848 **1**. All of these approaches have applied known asymmetric Simmons–Smith reactions to control all four stereocentres in the assembly of 2,2′-disubstituted bicyclopropanes.

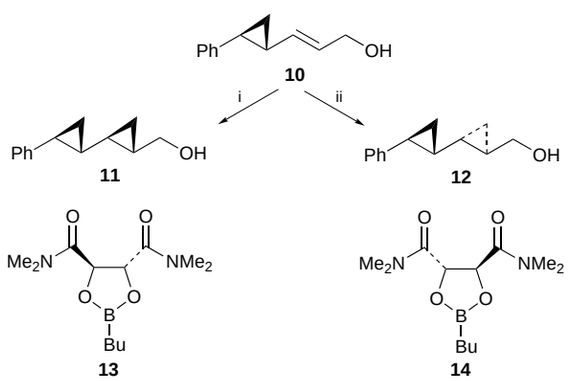
We have prepared both the *syn*- and *anti*-bicyclopropanes **6** and **8** stereoselectively using both Yamamoto[13,14] and Fujisawa[15] asymmetric cyclopropanation chemistry (Scheme 1). Thus Yamamoto cyclopropanation of the chiral acetal **3** gave cyclopropane **4**[13] as a single diastereoisomer following chromatographic purification. Subsequent acid hydrolysis, Horner–Emmons homologation and DIBAL-H reduction gave the enantiomerically pure allylic alcohol **5**. Reaction of alcohol **5** with diethylzinc and diiodomethane in the presence of L-(+)-diethyl tartrate or D-(−)-diethyl tartrate according to the Fujisawa protocol,[15] respectively gave the *syn*- and *anti*-bicyclopropane derivatives **6** (ds 6 : 1) and **8** (ds 6 : 1). Thus, *syn*- or *anti*-bicyclopropanes can be prepared *via* reagent control. In contrast, treatment of alcohol **5** with diethylzinc and diiodomethane with the absence of tartrate esters gave both bicyclopropanes **6** and **8** (*ca.* 1 : 1) in 82% yield. It is clear from these observations that the prexisting cyclopropane ring in alkene **5** has little influence on the stereochemistry of the second cyclopropanation reaction. Zercher has observed similar low stereoselectivity in the cyclopropanation of racemic alkene **5**.[10] The structures of the bicyclopropanes **6** and **8** were unambiguously established by oxidation and conversion[16,17] into the imidazolidines **7** and **9** respectively and an X-ray crystal structure analysis[7] of isomer **7**.

Zercher has utilised the excellent Charette asymmetric cyclopropanation reaction[18,19] for the highly stereoselective preparation of both *syn*- and *anti*-bicyclopropanemethanol derivatives.[10] These studies are exemplified by the chemistry in Scheme 2. Thus the allylic alcohol **10** was respectively converted into the bicyclopropanes **11** (67%) and **12** (72%) using the tartramide additives **13** and **14** to control absolute stereochemistry (ds > 12 : 1). In addition, the Zercher group has used double Charette asymmetric cyclopropanation chemistry and sulfur ylide methodologies to elaborate various bicyclopropanes with the *cis-trans*- and *cis-cis*-ring stereochemistries.[10,11] During these studies this group noted, in some cases, that the prexisting cyclopropane ring dramatically influenced the stereochemistry of the second cyclopropanation reaction. For example, this is underscored by the high *anti*-selectivity in the cyclopropanation of alkene **17** to provide bicyclopropane **18**, in contrast to the lower stereoselectivities observed on the cyclopropanation of alkenes **15** and **19** (Scheme 3). In general in these systems, except when substrate and reagent stereochemical biases are mismatched, Simmons–Smith cyclopropanation in the presence of the Charette additives **13** and **14** proceeds with good to excellent stereoselectivity. It is probable that the diastereoselectivity in the conversion of alkene **17** into the bicyclopropane **18** has its origin in steric approach control and the minimization of allylic 1,3-strain.[20] The use of the Charette chemistry[18,19] will feature repeatedly in this article and there is no doubt that the method represents a significant advance in enantioselective synthesis.

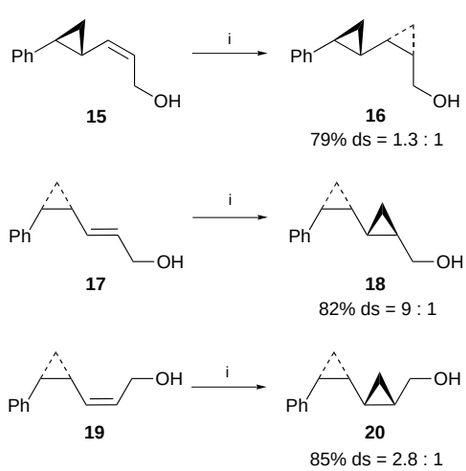
We have shown that 2,4-dienols **21** react with diethylzinc and diiodomethane in 1,2-dichloroethane at −20 °C to generate the corresponding racemic bicyclopropane derivatives **23** and **24** in good yield (68–80%) and with good diastereoselectivity (5 : 1 to > 95 : 5) favouring the *anti*-isomers **23** (Scheme 4).[8] It is reasonable to speculate that the reaction involves the intermediacy of the monocyclopropane **22** and stereoelectronic control of the second cyclopropanation step (see Fig. 1). In this analysis, overlap of the most electron-rich cyclopropane σ-bond



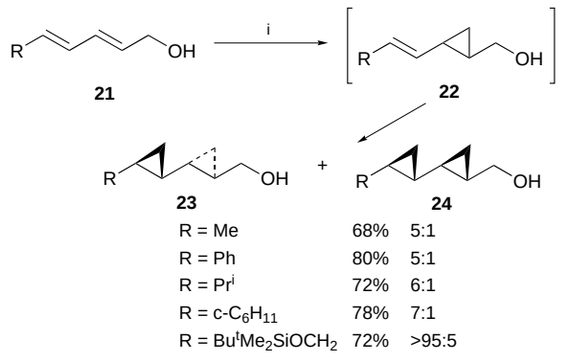

**Scheme 1** *Reagents and conditions*: i, $Et_2Zn$, $CH_2I_2$, PhMe, −20 °C, 91%; ii, TsOH, $H_2O$, THF, 60 °C, 93%; (iii) $(EtO)_2P(O)CH_2CO_2Et$, NaH, THF, 0 °C, 95%; iv, DIBAL-H, $CH_2Cl_2$, −78 °C, 89%; v, L-(+)-diethyl tartrate, $Et_2Zn$, $CH_2I_2$, $ClCH_2CH_2Cl$, −12 °C, 72%; vi, pyridinium chlorochromate, NaOAc, $SiO_2$, $CH_2Cl_2$, 0 °C; vii, (1*R*,2*R*)-*N*,*N*′-dimethyl-1,2-diphenylethanediamine, $Et_2O$, 4 Å molecular sieves, 25 °C; viii, D-(−)-diethyl tartrate, $Et_2Zn$, $CH_2I_2$, $ClCH_2CH_2Cl$, −12 °C, 84%




**Scheme 2** *Reagents and conditions*: i, $Et_2Zn$, $CH_2I_2$, **13**, 67%; ii, $Et_2Zn$, $CH_2I_2$, **14**, 72%




**Scheme 3** *Reagents and conditions*: i, $Et_2Zn$, $CH_2I_2$, 0 °C




**Scheme 4** *Reagents and conditions*: i, $Et_2Zn$, $CH_2I_2$, $(CH_2Cl)_2$, −20 °C

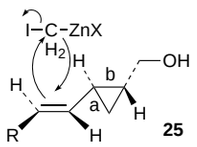
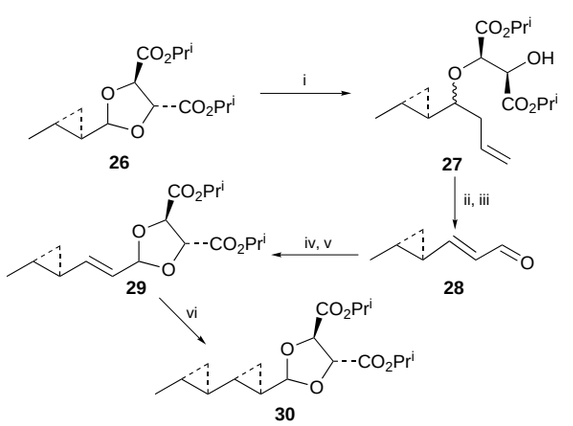


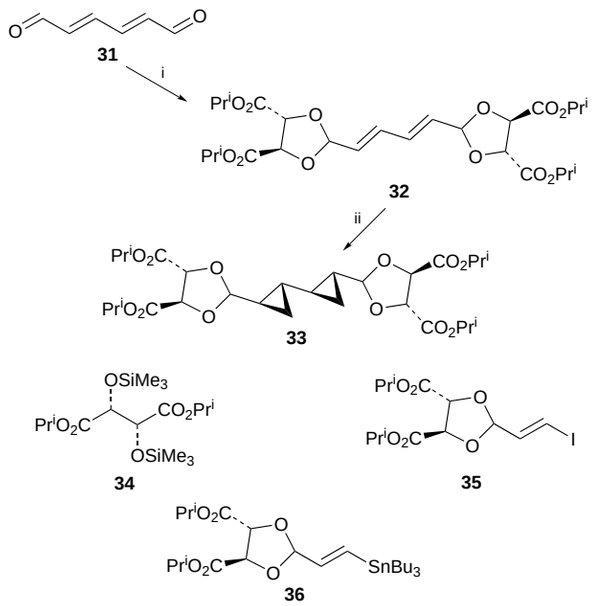

**Fig. 1**

(bond a, not bond b) with the alkene π-system should enhance its nucleophilicity and favour *anti*-delivery of the zinc carbenoid electrophile.

Armstrong has used both Yamamoto cyclopropanation[13] and allylsilane chemistry in the elaboration of a *syn*-bicyclopropane **30** (Scheme 5).[12] Thus sequential reaction of the acetal **26** with allylsilane in the presence of titanium(IV) chloride, ozone and triethylamine gave the enal **28**. Condensation with L-(+)-diisopropyl tartrate gave the corresponding acetal **29** and this was further cyclopropanated to produce the bicyclopropane **30** (65%, > 90% de). We have also used a double Yamamoto cyclopropanation strategy to produce a *syn*-bicyclopropane (Scheme 6).[9,21] Noyori acetalisation[22] of muconaldehyde[23] **31** or, alternatively, the Stille coupling[24] of vinyl iodide **35** with the vinyl stannane **36** gave the dienyl diacetal **32**. In turn, both alkenes **35** and **36** were prepared[21] from prop-2-ynyl alcohol *via* radical hydrostannylation, PCC oxidation and Noyori acetalisation.[22] Cyclopropanation of diene **32** according to the Yamamoto adaptation of the Simmons–Smith reaction[13] provided dicyclopropane **33** in good overall yield (56% from dial **31**) and essentially as a single diastereoisomer. A single crystal X-ray structure determination of bicyclopropane **33** was used to establish the relative and absolute stereochemistry of the four new chiral centres present in the molecule.[9] It is clear from this result that diene double cyclopropanation provides a simple




**Scheme 5** *Reagents and conditions*: i, $Me_3SiCH_2CH{=}CH_2$, $TiCl_4$, $CH_2Cl_2$, −78 °C, 59%; ii, $O_3$, then $Ph_3P$ work-up, 90%; iii, $Et_3N$, heat, 90%; iv, EtOH, pyridinium toluene-*p*-sulfonate, $HC(OEt)_3$; v, L-(+)-diisopropyl tartrate, EtOH, 35%; vi, $CH_2I_2$, $Et_2Zn$, 65%




**Scheme 6** *Reagents and conditions*: i, **34**, $Me_3SiOSO_2CF_3$ (cat), $MeC(OSiMe_3){=}NSiMe_3$, $CH_2Cl_2$, −78 to 25 °C, 73%; ii, $Et_2Zn$, $CH_2I_2$, $ClCH_2CH_2Cl$, −20 °C, 78%

entry to *syn*-bicyclopropane systems. Clearly, following the Yamamoto mechanistic model, each Lewis basic acetal oxygen should independently direct the Simmons–Smith zinc carbenoid to one face of the adjacent alkene.

## Stereoselective syntheses of quatercyclopropanes and the stereochemical elucidation of FR-900848 1

We have explored three strategies for the stereoselective construction of quatercyclopropane arrays: (i) a double Yamamoto cyclopropanation followed by a double Charette cyclopropanation,[9,25] (ii) a double Charette cyclopropanation followed by a second double Charette cyclopropanation,[26] and (iii) a tetraene tetracyclopropanation reaction.[21] In the first approach (Scheme 7), acid catalysed hydrolysis of the diacetal **33** gave the corresponding dialdehyde, which was directly homologated using a double Wittig reaction to provide a mixture of the *E*,*E*-diester **37** and the *E*,*Z*-diester **38** (3.7 : 1). DIBAL-H reduction of pure diester **37** gave the corresponding diol **39** in high yield (91%). Pre-mixing of diol **39** with dioxaborolane **14** followed by treatment with preformed bis(iodomethyl)zinc gave quatercyclopropane **40** (94%), essentially as a single diastereoisomer. Likewise, use of dioxaborolane **13** gave the quatercyclopropane **41** (100%). It was apparent from $^1H$ and $^{13}C$ NMR data that the quatercyclopropanes **40** and **41** were two different $C_2$-symmetric isomers, and we rigourously established structures by an X-ray crystallographic study[25] of the bis(4-bromobenzoate) ester derived from **40** (Fig. 2). Interestingly, the four cyclopropyl units that form the backbone of the molecule are arranged helically.

In addition, the quatercyclopropane **40** was prepared from mucondiol using two sequential double Charette cyclopropanation reactions.[26] Since this strategy was crucial in our total synthesis of FR-900848 **1**,[26] discussion of this approach is

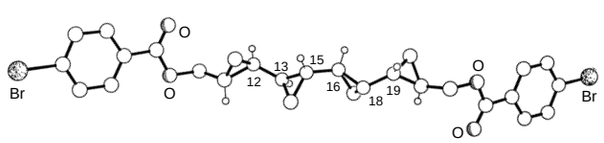
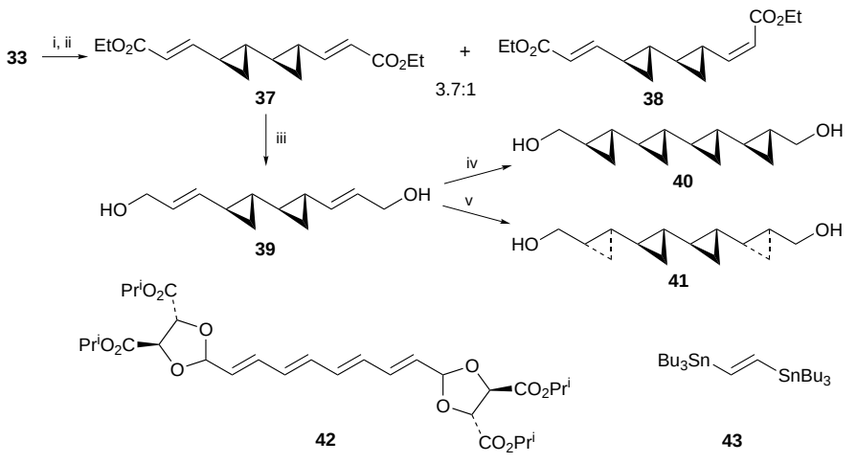


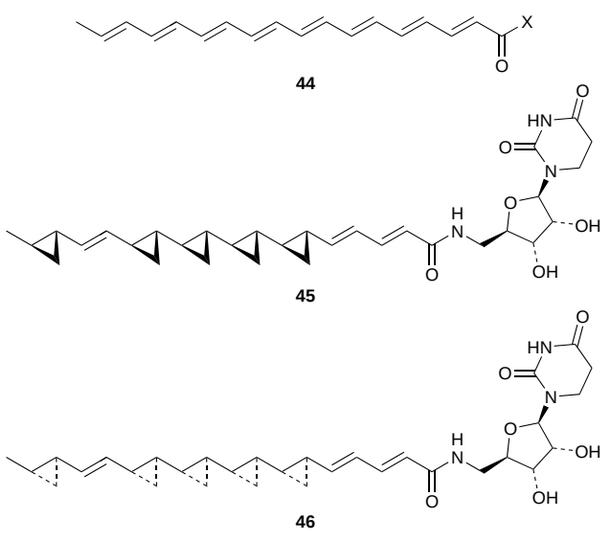

**Fig. 2** The molecular structure of the bis(4-bromobenzoate) ester of diol **40** showing the absolute stereochemistry



**Scheme 7** *Reagents and conditions*: i, TsOH, THF–$H_2O$, 55 °C; ii, $Ph_3P{=}CHCO_2Et$, $CH_2Cl_2$, 61% from **33**; iii, DIBAL-H, $CH_2Cl_2$, −78 °C, 91%; iv, **14**, $Zn(CH_2I)_2$, $CH_2Cl_2$, 0 °C to room temp. 94%; v, **13**, $Zn(CH_2I)_2$, $CH_2Cl_2$, 0 °C to room temp., 100%

delayed until the next section. Finally, we have briefly examined the preparation of a quatercyclopropane using the direct tetracyclopropanation of a tetraene. Thus tetraene **42** was prepared from the iodoalkene **35** and alkene **43** using a sequence of Stille coupling,[24] iododestannylation and a second Stille coupling. Although reaction of tetraene **42** with diiodomethane and diethylzinc gave a quatercyclopropane, the stereochemical identity of this substance has yet to be established.

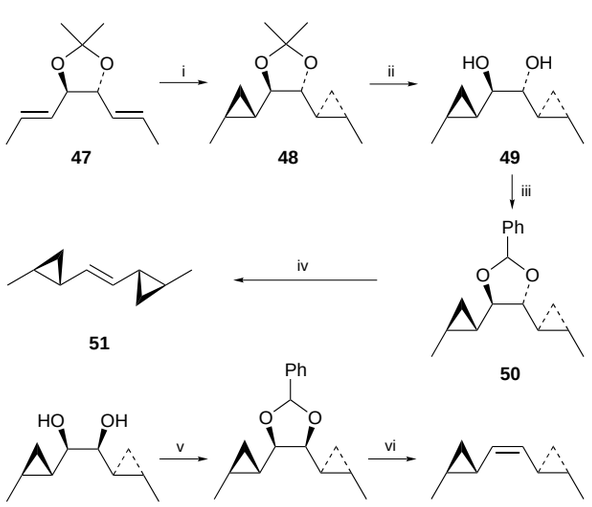
In our structural elucidation of FR-900848 **1** our planning was driven by speculation as to the biosynthetic origin of the natural product.[27] We considered that since the carbon count of **1** is odd at $C_{23}$, it is likely that all the cyclopropanes are introduced late from a polyenoic acid precusor. This precusor may be derived *via* a mixed acetate/propanoate biosynthetic origin and be already $C_{23}$ or, more likely, the precusor may be the $C_{18}$-polyene **44** in which the five cyclopropanes are



introduced from a $C_1$ source such as *S*-adenosyl methionine. If the $C_{18}$-polyene **44** is indeed a key biosynthetic intermediate then the geometry is most likely to be all *trans* since $\Delta^{2,4}$ are unequivocally *trans*. If these suppositions are true, FR-900848 **1** should be represented by either **45** or **46** since each enzymatic cyclopropanation should retain the alkene geometry and show the same absolute stereochemical bias. In addition, the geometry of $\Delta^{18}$ should be *trans* following the same biosynthetic speculation. In consequence of these considerations we sought to prepare model cyclopropane systems including quatercyclopropanes **40** and **41** to establish the sterochemistry of FR-900848 by correlation with key fragments from degradation. Falck[28] has also speculated as to the biosynthetic origin of the natural product and undertaken the synthesis of polycyclopropanated compounds as precursors to FR-900848 **1**.

Finally, Upjohn scientists have very recently reported on the isolation and biosynthesis of U-106305, a natural product related to FR-900848 **1**.[29] This substance has been shown to be biosynthetically derived from both acetate and methionine, but more of this later.

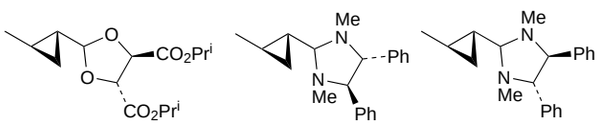
The isolated alkene unit of FR-900848 **1** was established to be *trans* by the following experiments (Scheme 8).[30–32] Double Simmons–Smith cyclopropanation of alkene **47** proceeded with excellent diastereoselectivity to provide only a single $C_2$-symmetric dicyclopropane **48** (89%). Sequential acid-mediated deprotection (63%) and condensation with benzaldehyde (64%) gave the benzylidene derivative **50**. Subsequent C-2 lithiation (1,3-dioxolane numbering) resulted in Whitham elimination[33] to provide the geometrically pure *E*-alkene **51** (60%). Alternatively, diol **52** was prepared from diol **49** *via* Swern oxidation[34] and sodium borohydride reduction. Whitham elimination of the derived acetal **53** gave the corresponding geometrically pure *Z*-alkene **54**. Comparison of the $^1H$ NMR



**Scheme 8** *Reagents and conditions*: i, $Et_2Zn$, $CH_2I_2$, $ClCH_2CH_2Cl$, −20 °C, 89%; ii, TsOH (cat), THF–$H_2O$ (5 : 1), 70 °C, 63%; iii, PhCHO, $H_2SO_4$ (cat), PhMe, 111 °C, 64%; iv, BuLi, pentane, 60%; v, PhCHO, camphorsulfonic acid, 96%; vi, BuLi, pentane

spectra of alkenes **51** and **54** with FR-900848 **1** was consistent with the assignment of the natural $\Delta^{18}$ geometry as *trans*. Clearly this stereochemical assignment is fragile unless the structures of the acetals **50** and **53** are secure. This insurance was underwritten by single crystal X-ray crystal structures[30,31] for both 3,5-dinitrobenzoate diesters derived from diols **49** and **52**.

The stereochemistry of the quatercyclopropane unit of FR-900848 **1** was determined[25,32] by comparison of the acetates prepared from the model diols **40** and **41** with the corresponding degradation product **2**[3] derived from the natural product. We were delighted to observe that quatercyclopropane **2** was identical in all respects, including the absolute stereochemistry, with the diacetate from diol **40**. Finally, two imidazolidine derivatives **56** and **57** were prepared from crotonaldehyde *via* acetal **55** using Yamamoto asymmetric cyclopropanation,[13,14]

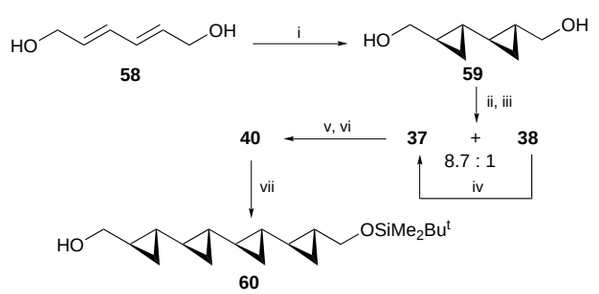



**55** **56** **57**

acid catalysed hydrolysis and condensation with the corresponding chiral diamines.[17] Ozonolysis of an authentic sample of FR-900848 **1** and subsequent reaction with (1*R*,2*R*)-*N*,*N*′-dimethyl-1,2-diphenylethanediamine gave an imidazolidene derivative which was identical with the synthetic adduct **56**. All these facts are consistent with the assignment of structure **45** to FR-900848.

### Total synthesis of FR-900848 45

We have recently reported the total synthesis of FR-900848 **45** using a sequence of Charette cyclopropanation reactions (Schemes 9, 10 and 11).[26] Mucondiol **58** was bicyclopropanated in the presence of the chiral auxillary **14**[18] to provide bicyclopropane **59** (89%) predominately as a single enantiomer (Scheme 9). PCC oxidation and subsequent direct homologation without purification of the intermediate dialdehyde provided a separable mixture of *E*,*E*-diester **37** and the *E*,*Z*-isomer **38** (8.7 : 1, 67% from **59**). The unwanted diester **38** was smoothly converted into diester **37** using $LiTi(OPr^i)_4(SPh)$, a reagent introduced by Hunter[35] for the *Z* to *E* isomerisation of α,β-unsaturated esters. DIBAL-H reduction of diester **37** (94%) and bicyclopropanation of the resultant diol under Charette conditions[18] provided diol **40** (93%), predominately as a single diastereoisomer. Subsequent mono-*tert*-butyldimethylsilylation, oxidation and Horner–Emmons homologation gave esters **61** and **62** (Scheme 10). Again, Hunter isomerisation[35] was crucial in converting the undesired isomer **62** into additional *E*,*E*-ester **61**. Finally, DIBAL-H reduction of *E*,*E*-ester **61** (91%) followed by a third Charette asymmetric cyclopropanation[19] gave the pentacyclopropane alcohol **63** in high yield (90%). Very recently, Charette has reported related monocyclopropanation reactions on related dienols.[36]



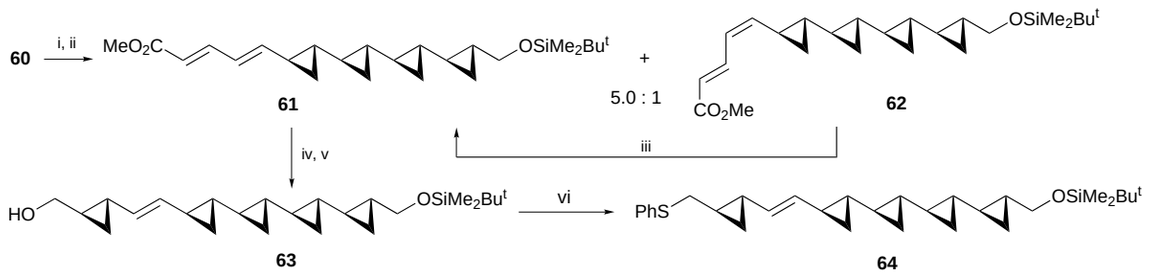

**Scheme 9** *Reagents and conditions*: i, **14**, $Et_2Zn$, $CH_2I_2$, $CH_2Cl_2$, 0 to 25 °C, 89%; ii, pyridinium chlorochromate, NaOAc, silica, $CH_2Cl_2$, 0 to 25 °C; iii, $Ph_3P{=}CHCO_2Et$, $CH_2Cl_2$, 67% from **59**; iv, PhSH, BuLi, $Ti(OPr^i)_4$, THF, 0 to 25 °C, 50%; v, DIBAL-H, $CH_2Cl_2$, −78 °C, 94%; vi, **14**, $Et_2Zn$, DME, $CH_2I_2$, $CH_2Cl_2$, −15 to 25 °C, 93%; vii, NaH, $Bu^tMe_2SiCl$, THF, 44%

In general we have been significantly frustrated in our attempts to effect substitution reactions on multiple cyclopropanemethanol derivatives *via* hydroxy activation and displacement. Although such approaches usually lead to extensive degradation, reaction of alcohol **63** with *N*-(phenylsulfenyl) succinimide and tributylphosphine[37] cleanly gave the sulfide **64** (89%). Treatment of sulfide **64** with Raney nickel followed by ammonium fluoride gave alcohol **65** without significant alkene hydrogenation or cyclopropane degradation (Scheme 11). Finally, PCC oxidation of alcohol **65**, Horner–Emmons homologation (with Hunter isomerisation[35] of the unwanted *E*,*Z*-ester **67**), potassium trimethylsilanolate[38] mediated hydrolysis and bis(2-oxo-3-oxazolidinyl)phosphinic chloride (BOP-Cl)[39] mediated coupling with the nucleoside amine **69**[40] gave FR-900848 **45**. Much to our delight the synthetic material was identical with an authentic sample of the natural product.

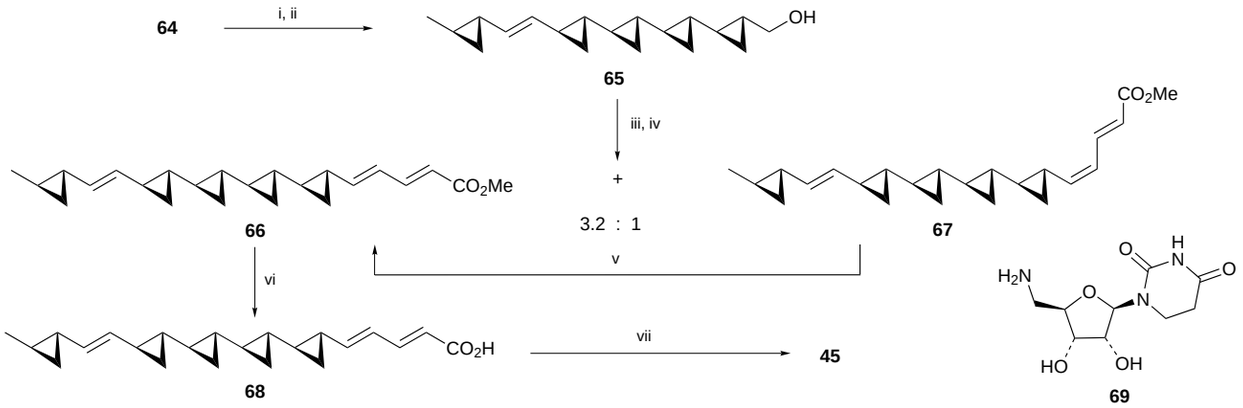
Falck *et al.* have also reported a total synthesis of FR-900848 **45** which elegantly underscores the value of Horeau amplification of absolute stereochemical purity (Scheme 12).[41] The vinylstannane **70** was converted into the corresponding cyclopropane **71** using Charette cyclopropanation[19] and protection. Tin to lithium to copper exchange and oxygenation gave the corresponding bicyclopropane **72**. This in turn was converted *via* the carboxylic acid **73**, Barton bromodecarboxylation[42] and a second dimerization reaction to reveal the quatercyclopropane **75**. These two oxidative dimerization reactions were accompanied by an enhancement in enantiomeric purity from 88–90% ee to > 99% ee in a process that is a variant of the Horeau amplification principle.[43] The diether **75** was converted into FR-900848 **45** using *inter alia* a Julia–Peterson olefination reaction, Horner–Emmons homologation and acylation *via* *p*-nitrophenyl ester activation.

### Total synthesis and structural elucidation of U-106305 80

In late 1995 Kuo *et al.* at Upjohn reported the isolation of U-106305 **80** from the fermentation broth of *Streptomyces* sp. UC 11136.[29] The authors determined that all the cyclopropanes are *trans*-disubstituted and that both alkenes are *E*, but the full structure was not determined. Their statement that 'U-106305 represents a structural class of compounds not

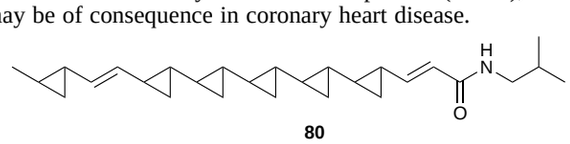



**Scheme 10** *Reagents and conditions*: i, pyridinium chlorochromate, NaOAc, silica, $CH_2Cl_2$, 0 to 25 °C; ii, (*E*)-$MeO_2CCH{=}CHCH_2P(O)(OMe)_2$, NaH, THF, 0 to 25 °C, 71% from **60**; iii, PhSH, BuLi, $Ti(OPr^i)_4$, THF, 0 to 25 °C, 63%; iv, DIBAL-H, $CH_2Cl_2$, −78 °C, 91%; v, **14**, $Et_2Zn$, DME, $CH_2I_2$, $CH_2Cl_2$, −40 °C, 90%; vi, *N*-(phenylsulfenyl)succinimide, $Bu_3P$, PhH, 89%

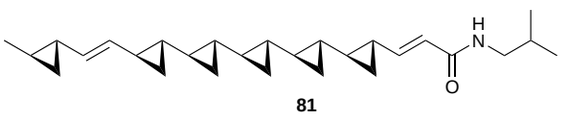



**Scheme 11** *Reagents and conditions*: i, Raney Ni, EtOH, −40 °C; ii, $NH_4F$, EtOH, 65 °C, 49% from **64**; iii, pyridinium chlorochromate, NaOAc, silica, $CH_2Cl_2$, 0 to 25 °C; iv, (*E*)-$MeO_2CCH{=}CHCH_2P(O)(OMe)_2$, NaH, THF, 0 to 25 °C, 63% from **65**; v, PhSH, BuLi, $Ti(OPr^i)_4$, THF, 0 to 25 °C, 51%; vi, $KOSiMe_3$, $CH_2Cl_2$, 85%; vii, **69**, BOP-Cl, $Et_3N$, DMA, 69%

previously reported from microbial fermentations' is inaccurate and both FR-900848 **45** and U-106305 **80** are clearly very closely related. It is therefore reasonable to speculate that U-106305 **80** has the same stereochemistry as **81**. It should be noted that U-106305 **80** is also biologically active. It is an inhibitor of cholesteryl ester transfer protein (CETP), which may be of consequence in coronary heart disease.

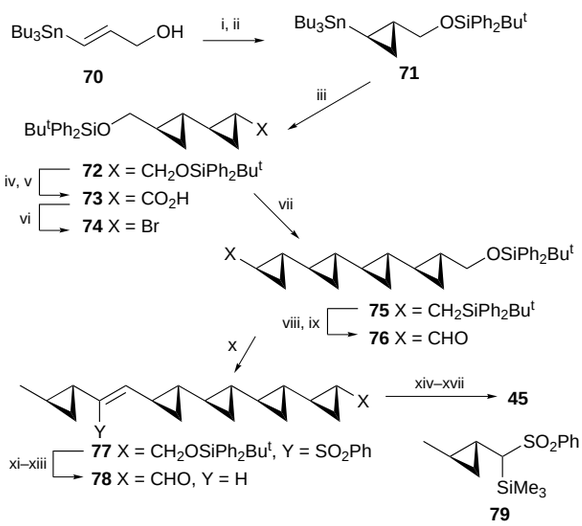



**80**




**81**

We have synthesized U-106305 **81** using a bi-directional approach to assemble the $C_2$-symmetrical quinquecyclopropane unit **87** using methodology as for FR-900848 **45** (Scheme 13).[44] Charette cyclopropanation[19] of diol **82** gave **83** in 89% ee. Dess–Martin oxidation[45] and Wittig olefination gave the diene diester **84**. Much to our delight, fractional recrystallization of **84** was especially efficient in enriching the material in the required enantiomer. Thus recrystallizaton from $Et_2O$–hexanes gave first racemic material and subsequently enantiomerically pure *E,E*-diester **84**. The structures for both the enantiomerically pure diester **84** and the corresponding racemic modification were confirmed by X-ray crystallography.[46] Diester **84** was converted onto the corresponding tercyclopropane and subsequently the quinquecyclopropane **87** using two sequential double Charette cyclopropanation reactions.[19] The structure of the near-helical quinquecyclopropane **87** was confirmed by X-ray analysis[44] and is shown in Fig. 3. This substance was




**Scheme 12** *Reagents and conditions*: i, **14**, $Et_2Zn$, $CH_2I_2$, $CH_2Cl_2$, 23 °C, 98%; ii, $Bu^tPh_2SiCl$, imidazole, DMF, 23 °C, 88%; iii, $Bu^sLi$, THF, −40 °C, then $[ICuPBu_3]_4$, −78 °C, then $O_2$, −78 °C, 73%; iv, $Bu_4NF$, THF, 23 °C, 72%; v, $RuCl_3$, $NaIO_4$, $CCl_4$, MeCN, $H_2O$, 23 °C, 91%; vi, *N*-hydroxypyridine-2-thione, DCC, DMAP, $BrCCl_3$, 23 °C; hν, 0 °C, 77%; vii, $Bu^tLi$, THF, −78 °C, then $[ICuPBu_3]_4$, −78 °C, then $O_2$, −78 °C, 75%; viii, $Bu_4NF$, THF, 23 °C, 72%; ix, $Pr_4NRuO_4$, NMO, 4 Å molecular sieves, $CH_2Cl_2$, 23 °C, 91%; x, **79**, BuLi, THF, −78 °C, 65%; xi, Li, naphthalene, THF, −78 °C, 70%; xii, $Bu_4NF$, THF, 23 °C, 95%; xiii, $Pr_4NRuO_4$, NMO, 4 Å molecular sieves, $CH_2Cl_2$, 23 °C, 91%; xiv, (*E*)-$EtO_2C$-$CH{=}CHCH_2P(O)(OEt)_2$, $LiN(SiMe_3)_2$, THF, −78 °C, 89%; xv, LiOH, MeOH, $H_2O$, 23 °C, 90%; xvi, 4-nitrophenol, DCC, DMAP, $CH_2Cl_2$, 23 °C, 73%; xvii, **69**, DMF, 23 °C, 76%

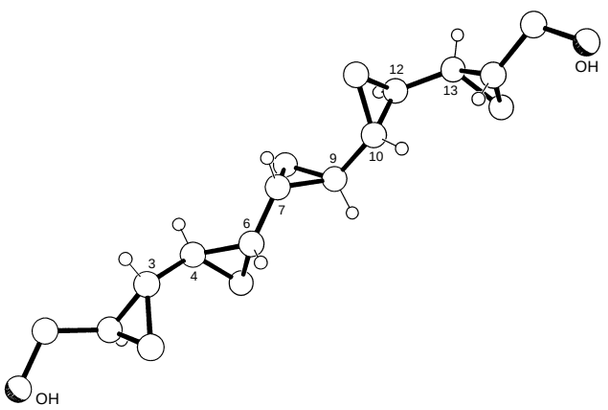
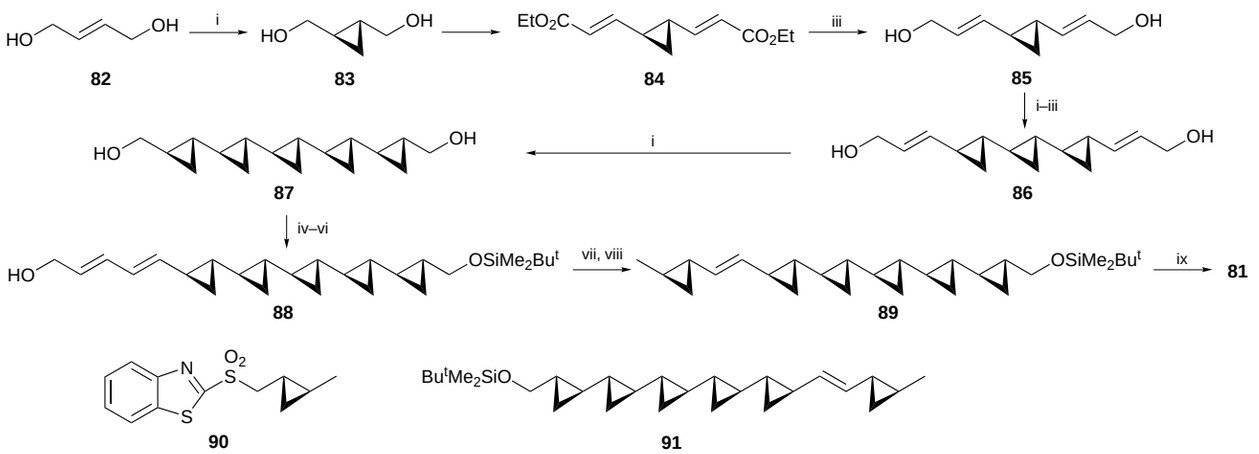



**Fig. 3** The molecular structure of the quinquecyclopropanedimethanol **87** showing the absolute stereochemistry

converted into U-106305 **81** using essentially the same strategy as in our synthesis of FR-900848 **45**. The synthetic material was identical in all respects with an authentic sample of U-106305. All these results clearly established the full structure and stereochemistry of U-106305 **81**. Charette and Lebel have also recently reported[47] a total synthesis of the antipode of U-106305 **81** using a bidirectional strategy that is closely related to our work. The synthesis differs in the later stages in the use of a Julia–Lythgo coupling[48] reaction to link the quinquecyclopropane and monocyclopropane units. The use of sulfone **90** provided the corresponding alkene **91** with 4 : 1 *E* : *Z* geometric selectivity.

## Future directions

Much remains to be done on the chemistry and biology of multiple cyclopropane arrays. It is clear from the Upjohn work that the biological effects mediated by multiple cyclopropane




**Scheme 13** *Reagents and conditions*: i, **14**, 4 Å molecular sieves, $Zn(CH_2I)_2$·DME, $CH_2Cl_2$, −40 to 25 °C, 83–91%; ii, Dess–Martin periodinane, pyridine, $CH_2Cl_2$ or DMSO, 25 °C, then $PPh_3$, *ca*. 10 °C, then $Ph_3P{=}CHCO_2Et$, 75–81%; iii, DIBAL-H, $CH_2Cl_2$, hexanes, −78 °C, 96–97%; iv, $Bu^tMe_2SiCl$, imidazole, $CH_2Cl_2$, 25 °C, 75% (calc.) at 78% conversion; v, Dess–Martin periodinane, pyridine, DMSO, 25 °C, then $PPh_3$, 25 °C, then $(E)$-$(MeO)_2P(O)CH_2CH{=}CHCO_2Me$, NaH, DBU, 25 °C, 88%; vi, DIBAL-H, $CH_2Cl_2$, hexanes, −78 °C, 95%; vii, **14**, 4 Å molecular sieves, $Zn(CH_2I)_2$·DME, $CH_2Cl_2$, −50 °C → −25 °C, 72%; viii, *N*-(phenylsulfenyl)succinimide, $PBu_3$, $C_6H_6$, 25 °C, 91%, then Raney nickel, THF, 25 °C, 44%; ix, $Bu_4NF$, THF, 25 °C, then DMSO, pyridine, 25 °C, Dess–Martin periodinane, 25 °C; then $PPh_3$, *ca*. 15 °C; then $Cl^-Ph_3P^+CH_2CONHCH_2Pr^i$, DBU, 25 °C, 91%

fatty amides should be much more general than anti-infective. Further aspects of the synthesis, reactions and properties of cyclopropene oligomers will be reported in due course.


## Acknowledgements

Dedicated to Professor Dieter Seebach on the occasion of his 60th Birthday, 31 October 1997.

We thank Glaxo Group Research Ltd. for the most generous endowment (to A. G. M. B.), the Wolfson Foundation for establishing the Wolfson Centre for Organic Chemistry in Medical Science at Imperial College, the Engineering and Physical Sciences Research Council, the U.S. Department of Education under the Graduate Assistance in Areas of National Need Program, the Overseas Research Students Program for fellowship support (to K. K.), the National Institutes of Health (AI-22252) for support when this work started in the U.S.A., the European Commission for a TMR Research Training Grant (to D. H.), the Fujisawa Pharmaceutical Company Ltd. for generous donations of samples of FR-900848 **1** and key spectroscopic data, Pharmacia & Upjohn, Inc. for a sample of U-106305 **80**, ChemGenics Pharmaceutical Inc. for support of our research on antifungal agents and G. D. Searle & Company for generous unrestricted support.


**Tony Barrett's research interests are concerned with the development of organic and organometallic methodology, the total synthesis of bioactive natural products, asymmetric synthesis and catalysis, polymer supported synthesis, and ligand design and coordination chemistry. He obtained his BSc and PhD degrees at Imperial College and was then appointed as Lecturer in that institute. In 1983 he was appointed a full professor of Chemistry at Northwestern University in Evanston, Illinois, USA and in 1990 he moved to Colorado State University. After nearly ten years research in the USA, he returned to his *alma mater*, Imperial College, as Glaxo Professor of Organic Chemistry, Director of the Wolfson Centre for Organic Chemistry in Medical Science and Head of the Organic Section. Professor Barrett has received several awards for his contributions to research including the 1980 Meldola Medal, the 1982 Harrison Medal, the 1986 Corday–Morgan Medal and the 1994 Tilden Lectureship from the Royal Society of Chemistry, a 1986 Arthur C. Cope Scholar Award from the American Chemical Society, a 1987 Teacher-Scholar Award from the Camille and Henry Dreyfus Foundation and a 1989 Fellowship from the Japan Society for the Promotion of Science.**

**Wendel Doubleday obtained his BS degree at Ursinus College in 1982 and his PhD degree with Professor Ted Cohen at the University of Pittsburgh (1991), and subsequently carried out postdoctoral work with Tony Barrett in Colorado State University. He is currently employed by Ligand Pharmaceuticals Inc. in San Diego, California.**

**Dieter Hamprecht studied chemistry at Würzburg and Munich. He obtained his diploma in 1992 and his PhD degree in 1995 with Professor Wolfgang Steglich at the University of Munich. Currently he is employed by SmithKline Beecham in Harlow, UK.**

**Krista Kasdorf obtained her BS degree at North Carolina State University in 1990. After working for a year at Research Triangle Institute she began her graduate studies at Colorado State University and in 1995 obtained her PhD degree at Imperial College. She is currently carrying out postdoctoral work with Professor Dennis Liotta in Emory University, Atlanta, Georgia.**

**Gary Tustin obtained his BSc degree at Warwick University in 1989 and his PhD degree with Sue Gibson at Imperial College (1992), and subsequently carried out postdoctoral work with Tony Barrett both at Colorado State University and Imperial College.**

**Andrew White obtained both his BSc (1990) and PhD degrees (1994 with Bill Grifith) at Imperial College, where he remains carrying out postdoctoral work with David Williams.**

**David Williams' principal research interests are in the area of supramolecular chemistry and the interpretation of the rôle non-covalent interactions play in determining short and long range molecular structure. He took his first degree in Physics and obtained a PhD in crystallography at Imperial College, where he has held the posts of Lecturer and Reader, and is currently Professor of Structural Chemistry in the Organic Section.**

## Footnotes and References


* E-mail: m.stow@ic.ac.uk


† This ChemComm is also available *via* the World Wide Web: http://chemistry.rsc.org/rsc/ccenha.htm

‡ For an earlier report of a natural product that may be identical with FR-900848, see B. C. Das, J. P. Cosson, E. Guittet, M. Hassani, T. Staron and

F. DeMaack, Book of Abstracts, 35 ASMS Conference on Mass Spectrometry and Allied Topics, Denver, Colorado, May 24–29, 1987, pp. 952–953.

1 J. K. Kwon-Chung and J. E. Bennett, *Medical Mycology*, Lee & Febiger, Philadelphia, 1992.
2 M. Yoshida, M. Ezaki, M. Hashimoto, M. Yamashita, N. Shigematsu, M. Okuhara, M. Kohsaka and K. Horikoshi, *J. Antibiot.* 1990, **43**, 748.
3 H. Tanaka, (Fujisawa Pharmaceutical Co. Ltd.), personal communication.
4 M. Yoshida and K. Horikoshi, *US Pat.*, 4 803 074, 1989.
5 M. Buchert and H. U. Reissig, *Chem. Ber.*, 1992, **125**, 2723.
6 D. Niveldt and A. Vos, *Acta Crystallogr., Sect. B: Struct. Sci.*, 1988, **44**, 281, 289, 296.
7 A. G. M. Barrett, W. W. Doubleday, G. J. Tustin, A. J. P. White and D. J. Williams, *J. Chem. Soc., Chem. Commun.*, 1994, 1783.
8 A. G. M. Barrett and G. J. Tustin, *J. Chem. Soc., Chem. Commun.*, 1995, 355.
9 A. G. M. Barrett, W. W. Doubleday, K. Kasdorf, G. J. Tustin, A. J. P. White and D. J. Williams, *J. Chem. Soc., Chem. Commun.*, 1995, 407.
10 C. R. Theberge and C. K. Zercher, *Tetrahedron Lett.*, 1994, **35**, 9181; 1995, **36**, 5495.
11 R. E. J. Cebula, M. R. Hanna, C. R. Theberge, C. A. Verbicky and C. K. Zercher, *Tetrahedron Lett.*, 1995, **36**, 5495; C. R. Theberge, C. A. Verbicky and C. K. Zercher, *J. Org. Chem.*, 1996, **61**, 8792.
12 R. W. Armstrong and K. W. Maurer, *Tetrahedron Lett.*, 1995, **36**, 357.
13 I. Arai, A. Mori and H. Yamamoto, *J. Am. Chem. Soc.*, 1985, **107**, 8524.
14 A. Mori, I. Arai and H. Yamamoto, *Tetrahedron*, 1986, **42**, 6447.
15 Y. Ukaji, M. Nishimura and T. Fujisawa, *Chem. Lett.*, 1992, 61.
16 P. Manganey, F. Grojea, A. Alexakis and J. R. Normant, *Tetrahedron Lett.*, 1988, **29**, 2675.
17 P. Manganey, F. Grojea, A. Alexakis and J. R. Normant, *Tetrahedron Lett.*, 1988, **29**, 2677.
18 A. B. Charette and H. Juteau, *J. Am. Chem. Soc.*, 1994, **116**, 2651.
19 A. B. Charette, S. Prescott and C. Brochu, *J. Org. Chem.*, 1995, **60**, 1081; A. B. Charette and J.-F. Marcoux, *Synlett*, 1995, 1197.
20 R. W. Hoffman, *Chem. Rev.*, 1989, **89**, 1841 and references cited therein.
21 A. G. M. Barrett, W. W. Doubleday and G. J. Tustin, unpublished observations.
22 T. Tsunoda, M. Suzuki and R. Noyori, *Tetrahedron Lett.*, 1980, **21**, 1357.
23 S. G. Davies and G. H. Whitham, *J. Chem. Soc., Perkin Trans. 1*, 1977, 1346.
24 J. K. Stille, *Angew. Chem., Int. Ed. Engl.*, 1986, **25**, 508.
25 A. G. M. Barrett, K. Kasdorf, G. J. Tustin and D. J. Williams, *J. Chem. Soc., Chem. Commun.*, 1995, 1143.
26 A. G. M. Barrett and K. Kasdorf, *Chem. Commun.*, 1996, 325; A. G. M. Barrett and K. Kasdorf, *J. Am. Chem. Soc.*, 1996, **118**, in the press.
27 A. G. M. Barrett, 6th International Kyoto Conference on New Aspects of Organic Chemistry, Kyoto, Japan, November 7–11, 1994.
28 J. R. Falck, B. Mekonnen and J. Yu, 209th American Chemical Society National Meeting, Anaheim, CA, April 2–6, 1995, Abstract 057.
29 M. S. Kuo, R. J. Zielinski, J. I. Cialdella, C. K. Marschke, M. Dupuis, G. P. Li, D. A. Kloosterman, C. H. Spilman and V. P. Marshall, *J. Am. Chem. Soc.*, 1995, **117**, 10 629.
30 A. G. M. Barrett, K. Kasdorf and D. J. Williams, *J. Chem. Soc., Chem. Commun.*, 1994, 1781.
31 A. G. M. Barrett, K. Kasdorf, A. J. P. White and D. J. Williams, *J. Chem. Soc., Chem. Commun.*, 1995, 649.
32 A. G. M. Barrett, W. W. Doubleday, K. Kasdorf and G. J. Tustin, *J. Org. Chem.*, 1996, **61**, 3280.
33 J. N. Hines, M.J. Peagram, E. J. Thomas and G. H. Whitham, *J. Chem. Soc., Perkin Trans. 1*, 1973, 2332.
34 M. G. Banwell and R. Onrust, *Tetrahedron Lett.*, 1985, **26**, 4543 and references cited therein.
35 R. Hunter, Frank Warren Conference, Orange Free State, South Africa, April 4–7, 1995; R. Clauss, W. Hinz and R. Hunter, *Synlett*, 1997, 57.
36 A. B. Charette, H. Juteau, H. Lebel and D. Deschênes, *Tetrahedron Lett.*, 1996, **37**, 7925.
37 K. A. M. Walker, *Tetrahedron. Lett.*, 1977, 4475.
38 E. D. Laganis and B. L. Chenard, *Tetrahedron Lett.*, 1984, **25**, 5831.
39 J. Cabre and A. L. Palomo, *Synthesis*, 1984, 413.
40 V. Skaric, D. Katalenic, D. Skaric and I. Salaj, *J. Chem. Soc., Perkin Trans. 1*, 1982, 2091.
41 J. R. Falck, B. Mekonnen, J. Yu and J.-Y. Lai, *J. Am. Chem. Soc.*, 1996, **118**, 6096.
42 D. H. R. Barton, D. C. Crich and W. B. Motherwell, *Tetrahedron Lett.*, 1983, **24**, 4979.
43 V. Rautenstrauch, *Bull. Soc. Chim. Fr.*, 1994, **131**, 515.
44 A. G. M. Barrett, D. Hamprecht, A. J. P. White and D. J. Williams, *J. Am. Chem. Soc.*, 1996, **118**, 7863.
45 D. B. Dess and J. C. Martin, *J. Am. Chem. Soc.*, 1991, **113**, 7277.
46 A. G. M. Barrett, D. Hamprecht, A. J. P. White and D. J. Williams, unpublished work.
47 A. B. Charette and H. Label, *J. Am. Chem. Soc.*, 1996, **118**, 10327.
48 J. B. Baudin, G. Hareau, S. A. Julia, R. Lorne and O. Ruel, *Bull. Chim. Soc. Fr.*, 1993, **130**, 856; N. D. Smith, P. J. Kocienski and S. D. A. Street, *Synthesis*, 1996, 652.

*7/00487G*

# Large variation of rates for platination of phosphorothioate-containing oligonucleotides: end effects and counter ion influence

**Johan Kjellström and Sofi K. C. Elmroth***

*Inorganic Chemistry 1, Chemical Center, Lund University, PO Box 124, S-221 00 Lund, Sweden*

**The rate of site-specific platination of short oligonucleotides can be varied up to 500 times by a change of the bulk composition and the molecular environment surrounding the binding site.**

Interactions between metal complexes and DNA are influenced by several factors. Some are related to the coordination environment and kinetic characteristics of the metal complex, others to the electrostatic and structural properties of the polymeric DNA. Improving our understanding of the mechanism for metal ion–DNA interactions is important, since DNA is believed to be the major target for many metal-based antitumour drugs.[1] In the case of biologically relevant intermediates of antitumour active *cis*-platinum complexes, several observations indicate that the location of their primary monofunctional adducts with DNA is likely to be controlled by kinetic rather than thermodynamic factors.[1–6] The aim of the present study was to further elucidate how general parameters such as location and molecular environment of a particular binding site as well as bulk composition may be utilized to obtain maximum kinetic separation between different types of adducts. The influence on reactivity originating from variations in the molecular structure surrounding the binding site was investigated by a comparison of the reactivity of $d(T_8p(S)T_8)$ with that of $d(Tp(S)T_{15})$ and d(Tp(S)T). Incorporation of a single phosphorothioate binding site has previously been shown to result in specific platination of the sulfur donor, both in the presence and absence of the naturally preferred G-N7 binding site.[2,3,7–9] The influence of bulk composition on the rate of platination of the oligonucleotides with *cis*-$[Pt(NH_3)(NH_2C_6H_{11})Cl(OH_2)]^+$ **1**, was studied at constant pH 4.2 by a variation of the concentration of inert monovalent bulk cations in the interval 1.5 mM–0.50 M. As previously discussed, the use of the monoaqua complex **1** simplifies the reaction mechanism to that of direct substitution of the labile $H_2O$ ligand by the nucleophilic sulfur atom of the phosphorothioate containing oligonucleotides.[3]

The cationic monoaqua complex **1** is a weak acid with p$K_a$ 6.4 ± 0.2, and its reactivity towards phosphorothioates has previously been shown to decrease with increasing bulk pH in the range 5–8.[3] This decrease in reactivity was rationalized in terms of an increase in concentration of the less reactive monohydroxo complex, *cis*-$[Pt(NH_3)(NH_2C_6H_{11})Cl(OH)]$ **2**. Such decrease has been observed also for other model systems for interactions of mono-aquated platinum complexes with DNA.[10,11] The use of binding sites located on a negatively charged oligonucleotide makes the mechanistic interpretation of rate variations as a function of pH more complicated in the present systems than in the case of reactions between small molecules, however. The non-selective electrostatic attraction of cations onto the surface of the polymer that can be expected to take place here,[12–14] implies that not only cationic reactants but also oxonium ions may accumulate in its vicinity.[15–17] In a situation where the distribution between **1** and **2** is sensitive towards small variations of pH, it may thus be possible that an observed difference in reactivity between adduct formation on the polymer and the corresponding reaction in absence of surrounding bases could, at least partially, be the result of a local pH change. The present study made at pH 4.2 minimizes such contributions since at this pH the equilibrium distribution between **1** and **2** is affected to a negligible extent by local changes of the oxonium ion concentration. The use of a diluted buffer allowed for pH control during the reaction with a minimum of interference from competitive reactions with buffer anions.[18]† The reactions of **1** with the oligonucleotides were studied under pseudo-first-order conditions with $Pt^{II}$ in *ca.* 10-fold excess compared to the concentration of oligomers by use of HPLC. The kinetic parameters were evaluated at 298 K from the time-dependent changes in integrated HPLC peak areas of unplatinated and platinated oligonucleotides, respectively (Supplementary data, Fig. S1).‡ Both the decay of reactants and formation of products were well described by single exponentials (Supplementary data, Fig. S2). The observed pseudo-first-order rate constants, $k_{obs}$, were linearly dependent on the total concentration of $Pt^{II}$ (Supplementary data, Table S1, and Fig. S3).

As shown in Fig. 1, the apparent second-order rate constants, $k_{2,app}$,§ for platination of the oligonucleotides exhibit a common trend for $[Na^+, K^+] \leqslant 0.3$ M with a monotonous increase in reactivity as a function of decreasing bulk cation concentration. In addition, a relative reactivity order of $k_{2,app}(d(T_8p(S)T_8)) > k_{2,app}(d(Tp(S)T_{15})) > k_{2,app}(d(Tp(S)T))$ is maintained throughout the whole concentration range investigated. There are striking differences in reactivity behaviour, however. First of all, the limiting rate constants obtained for $[Na^+, K^+] > 0.3$ M are significantly different for the three types of DNA: 5.7 ± 1.5, 0.87 ± 0.15 and 0.43 ± 0.05 $dm^3\ mol^{-1}\ s^{-1}$ for $d(T_8p(S)T_8)$, $d(Tp(S)T_{15})$ and d(Tp(S)T), respectively. Secondly, the response to decreasing salt concentration exhibits different characteristics with an increase in reactivity that is most pronounced, both in absolute and relative terms, for platination of $d(T_8p(S)T_8)$. The maximum second-order rate constant for the latter reaction was determined as 200 ± 40 $dm^3\ mol^{-1}\ s^{-1}$ at the lowest salt concentration investigated, $[Na^+, K^+]$ = 1.5 mM. At this concentration of bulk cations the rate constant for

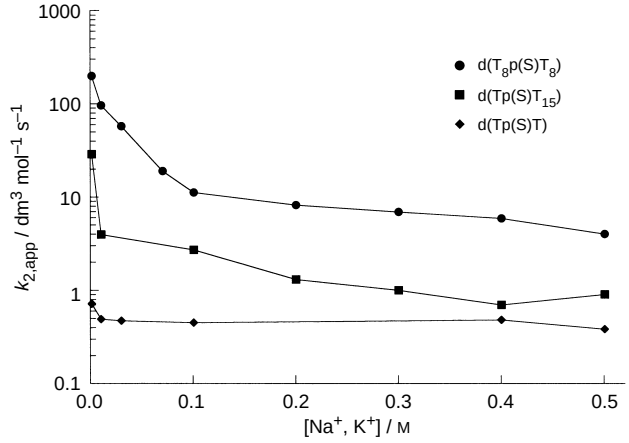



**Fig. 1** Semilogarithmic plot of the apparent second-order rate constant *vs.* the concentration of monovalent bulk cations for reaction of **1** with (●) $d(T_8p(S)T_8)$, (■) $d(Tp(S)T_{15})$ and (◆) d(Tp(S)T), at pH 4.2 and 25 °C

platination of d(Tp(S)$T_{15}$) was found to be 30 ± 10 $dm^3\ mol^{-1}\ s^{-1}$. With respect to the rate of platination of d(Tp(S)T), $k_{2,app}$ = 1.0 ± 0.5 $dm^3\ mol^{-1}\ s^{-1}$ at [$Na^+$, $K^+$] = 1.5 mM, these rate constants thus represent a 200- and 30-fold rate increase for d($T_8$p(S)$T_8$) and d(Tp(S)$T_{15}$), respectively.

These results clearly demonstrate that bulk conditions as well as the molecular environment of the phosphorothioate binding site have a large influence on the rate of platination also of short single-stranded oligonucleotides which lack the typical polyelectrolyte behaviour of extended DNA.[14,19–21] It is noteworthy, that although the absolute value of the rate constants may be changed by orders of magnitude by a variation of the concentration of monovalent cations in the bulk, such a variation does not affect the relative reactivity order for formation of the different types of adducts. Surprisingly, the rate of platination of d(Tp(S)$T_{15}$) exhibits reaction characteristics intermediate between those of d($T_8$p(S)$T_8$) and d(Tp(S)T). This observation suggests that association of the cationic metal complex with the polymer prior to adduct formation is of importance for the reaction mechanism also for platination of the end position where the polyelectrolyte effect can be expected to be reduced to a minimum.[19–21] The present study, in which pH effects can be excluded from contributing to the rate increase, indicates that rate accelerations similar to those observed for freely diffusing species[17] may be obtained also for reactions where the rate determining step involves formation of a covalent bond with donor atoms located on the charged phosphodiester backbone of the DNA. These findings thus give strong support for a previously suggested reaction mechanism for platination of oligonucleotides comprising preassociation of metal complex onto the oligomer followed by rapid diffusion along the contour length of the polymer to the kinetically preferred binding site.[3] In addition to the impact of this mechanism on biological systems, awareness of its large influence on reactivity, as exemplified here by a maximum variation of the platination rate between d($T_8$p(S)$T_8$) and d(Tp(S)T) by a factor of *ca.* 500, should also be of importance for antisense strategies using for example cross-linking reagents, as well as for synthetic chemistry.

Financial support from the Swedish Cancer Foundation (grant 961699, S. K. C. E.) is gratefully acknowledged. We also thank Ms Emma Svensson for preliminary experimental studies of the d(Tp(S)$T_{15}$) system and Mrs Bodil Eliasson for valuable technical assistance.

## Footnotes and References

* E-mail: Sofi.Elmroth@inorg.lu.se

† [$HC_8H_4O_4^-$] = 0.50 mM, pH = 4.2 adjusted with $HClO_4$.

‡ Available upon request from the authors.

§ Obtained as $k_{obs}/[Pt^{II}]_{tot}$.

1 See for example: *Metal Ions in Biological System*, ed. A. Sigel and H. Sigel, Marcel Dekker, New York, 1996, vol. 32.
2 S. K. C. Elmroth and S. J. Lippard, *J. Am. Chem. Soc.*, 1994, **116**, 3633.
3 S. K. C. Elmroth and S. J. Lippard, *Inorg. Chem.*, 1995, **34**, 5234.
4 F. Gonnet, F. Reeder, J. Kozelka and J.-C. Chottard, *Inorg. Chem.*, 1996, **35**, 1653.
5 F. Reeder, F. Gonnet, J. Kozelka and J.-C. Chottard, *Chem. Eur. J.*, 1996, **2**, 1068.
6 S. J. Berners-Price, K. J. Barnham, U. Frey and P. J. Sadler, *Chem. Eur. J.*, 1996, **2**, 1283.
7 K. G. Strothkamp and S. J. Lippard, *Proc. Natl. Acad. Sci. USA*, 1976, **73**, 2536.
8 D. J. Szalda, F. Eckstein, H. Sternbach and S. J. Lippard, *J. Inorg. Biochem.*, 1979, **11**, 279.
9 B. C. F. Chu and L. E. Orgel, *Nucl. Acids Res.*, 1990, **18**, 5163.
10 J. Arpalahti and P. Lehikoinen, *Inorg. Chem.*, 1990, **29**, 2564.
11 M. Mikola, P. Oksman and J. Arpalahti, *J. Chem. Soc., Dalton Trans.*, 1996, 3101.
12 G. S. Manning, *Quart. Rev. Biophys. II*, 1978, **2**, 179.
13 A. Pullman and B. Pullman, *Quart. Rev. Biophys.*, 1981, **14**, 289.
14 C. F. Anderson and M. T. Record, Jr., *Annu. Rev. Phys. Chem.*, 1995, **46**, 657.
15 G. Lamm and G. R. Pack, *Proc. Natl. Acad. Sci. USA*, 1990, **87**, 9033.
16 S. Hanlon, L. Wong and G. R. Pack, *Biophys. J.*, 1996, **72**, 291.
17 G. R. Pack and L. Wong, *Chem. Phys.*, 1996, **204**, 279.
18 J. E. Teggins, K. W. Lee, J. M. Baker and E. D. Smith, *J. Coord. Chem.*, 1971, **1**, 215.
19 M. C. Olmsted, C. F. Anderson and M. T. Record, Jr., *Proc. Natl. Acad. Sci. USA*, 1989, **86**, 7766.
20 M. O. Fenley, G. S. Manning and W. K. Olson, *Biopolymers*, 1990, **30**, 1191.
21 V. M. Stein, J. P. Bond, M. W. Capp, C. F. Anderson and M. T. Record, Jr., *Biophys. J.*, 1995, **68**, 1063.

*Received in Basel, Switzerland, 25th April 1997; 7/02845H*

# C–H··π interactions in ethynylbenzenes: the crystal structures of ethynylbenzene and 1,3,5-triethynylbenzene, and a redetermination of the structure of 1,4-diethynylbenzene

**Hans-Christoph Weiss,[a] Dieter Bläser,[a] Roland Boese,*[a] Brandon M. Doughan[b] and Michael M. Haley[b]**

[a] *Institut für Anorganische Chemie, Universität Essen, Universitätsstrasse 3-5, D-45117 Essen, Germany*
[b] *Department of Chemistry, University of Oregon, Eugene, Oregon 97403, USA*

**The crystal structures of 1,4-diethynylbenzene 1 and 1,3,5-triethynylbenzene 2 show similar packing principles with CH··π (triple bond)-zigzag networks; surprisingly, the packing motif of ethynylbenzene 3 is quite different.**

Recent work has shown that the π-electrons of a C≡C triple bond can act as a hydrogen bond acceptor.[1–6] In addition to the usual donor substituents, such as hydroxy and amino groups, it was shown that carbon-bonded hydrogen atoms can also display donor properties. Terminal alkynes represent one of the best CH··π hydrogen bond donors due to the acidity of the alkynyl hydrogen atom.[7] This functional group has the advantage of providing simultaneously donor and acceptor properties for CH··π hydrogen bridges. Whereas the expected geometry for this type of intermolecular interaction is T-shaped,[8] as in acetylene,[9] this idealized motif with a CH··π angle of (180 ± 10°) is rarely found in the solid state. We report herein the comparison of the CH··π interactions in the three title ethynylated aromatics.

Although already known,[10] the structure of 1,4-diethynylbenzene **1** was redetermined under the same conditions as for 1,3,5-triethynylbenzene **2** and ethynylbenzene **3** for a better comparison and higher accuracy (mainly for the positions of the hydrogen atoms).† In the solid state **1** has a layer structure; the arrangement within the layers is shown in Fig. 1.

The molecules are connected by CH··π hydrogen bridges in a zigzag pattern along a mirror glide plane similar to that known for other compounds with terminal ethynyl groups, *e.g.* DL-prop-2-ynylglycine,[7] but-3-ynoic acid[11] and 1,4-diethynylcubane.[12] Each molecule is fixed by four hydrogen bridges and the geometrical data indicate ideal conditions for relatively strong CH··X hydrogen bonds (Table 1). Between the layers there exist no herringbone interactions as in benzene, and only a staggering of the coplanar rings can be observed (plane–plane distance 353 pm). The CH··M contacts (M is the centre of the triple bond) are among the shortest contacts found in the Cambridge Structural Database.[13] The molecules are tilted by 25.0° to the 100 plane. Thus the major attractive forces which contribute to the lattice energy are the hydrogen bridges to the triple bonds, which form a two-dimensional network.

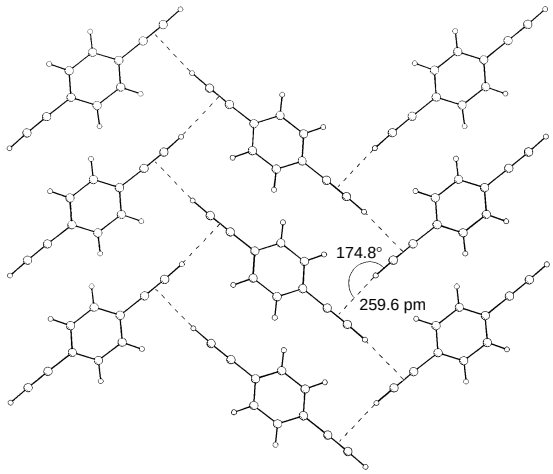



**Fig. 1** Section of the layer structure of **1** in the 100 direction

**Table 1** CH··π distances and angles for **1**–**3**

| Compound | Bond geometry[b] | H··M[a] distance/pm | CH··M[a] angle/° |
|---|---|---|---|
| **1** | trip | 259.6 | 174.8 |
| **2** | trip | 268.1 | 165.7 |
| | trip | 272.3 | 147.3 |
| | trip | 281.4 | 140.1 |
| **3** | ring | 260.2 | 143.6 |
| | ring | 268.3 | 160.5 |
| | trip | 257.7 | 174.3 |

[a] M = centre of the π-system. The positions of the hydrogen atoms were normalized to a C–H distance of 108 pm. [b] Ring = bond to π-system of the phenyl group; trip = bond to π-system of the triple bond.

A similar packing principle can be observed in the crystal structure of **2**; however, because of the different molecular geometry the packing is more complex and can be described as a folded layer structure. The main attractive forces between the molecules of **2** are also hydrogen bond bridges from the ethynyl hydrogen atoms to the π-electrons of the triple bonds. Each molecule acts three times as an acceptor and as a donor, making six contacts per molecule with three distinct distances (Fig. 2). The connections of each molecule to its environment, however, are not symmetrical: the first ethynyl group acts only as a donor, the second acts as a donor and an acceptor and the third acts as a donor and a double acceptor. All of the contacts are rather short and the angles $C_{ethynyl}H··M$ lie between 140 and 180° and compare well with those in **1**.

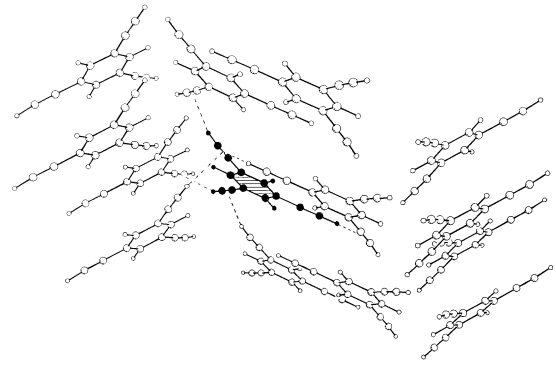


**Fig. 2** Folded layers of **2**; one highlighted molecule shows the six hydrogen bridges

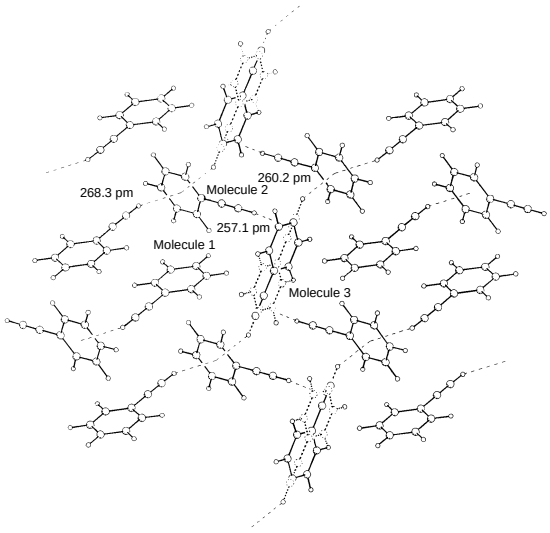



**Fig. 3** Packing of **3**; molecule 3 is disordered (additional dotted molecule)

Surprisingly, the parent ethynylated benzene derivative **3** exhibits a very different packing in the crystal lattice. Five molecules are found in the unit cell (space group $P\bar{1}$) with two and a half in the asymmetric unit; consequently the half molecule is disordered. One of the ethynyl hydrogen atoms points to a triple bond and the other two point to the π-systems of two surrounding phenyl rings.

In contrast to **1** and **2** the molecules in **3** show benzene-type edge-to- face interactions.[14,15] The angles between the planes of the rings lie between 80 and 90°, and the shortest CH···M contact is 282.2 pm (276.4 pm for benzene[14]). The crystal structure of **3** represents a compromise between the herringbone packing of benzene and the coplanar stacking, as found for **1**, with $CH\cdot\cdot\pi_{trip}$ interactions. The respective intermolecular distances and angles for **1**–**3** are summarized in Table 1.

Comparison of the physical properties of molecules **1**–**3** and benzene (Table 2) sheds light on the stability of the compromise packing of **3**. The melting point of **3** is abnormally low—over 50 °C lower than that of benzene. The calculated densities of the solids show a similar tendency: **1** and **2** have significantly higher densities than **3**. For **3** one would expect a higher density than for benzene, as its molecular mass is between those of benzene and **1**; however, the densities are approximately the same. These data clearly indicate that the lattice energy of **3** must be substantially less and that the compromise packing is not as efficient as that of benzene or of **1** and **2**.

**Table 2** Melting points and calculated densities[a] for **1**–**3** in the solid state

| Compound | mp/°C | $\rho_{calc}$/Mg m$^{-3}$ |
|---|---|---|
| Benzene[b] | 5.5[c] | 1.094 |
| **1** | 96.5[d] | 1.202 |
| **2** | 103–104[e] | 1.178 |
| **3** | −44.8[c] | 1.100 |

[a] Measured at −183 °C for benzene and −148 °C for **1**–**3**. [b] Ref. 14. [c] Ref. 16. [d] Ref. 17. [e] Ref. 18.

We gratefully acknowledge the DFG, the Fonds der Chemischen Industrie and the NSF for financial support of this work.

## Footnotes and References

* E-mail: boese@structchem.uni.essen.de

† *Crystal data* for **1** (ref. 17): $C_{10}H_6$, crystals obtained by sublimation (20 mbar, water cooled), space group $P2_1/c$, $a$ = 3.887(1), $b$ = 5.931(2), $c$ = 15.114(6) Å, $\beta$ = 90.84(3)°, $V$ = 348.4(2), $Z$ = 4, $D_c$ = 1.20 g cm$^{-3}$, 719 unique reflections, $F_o > 4\sigma(F_o)$, 58 parameters, $2\Theta_{max}$ = 60°, $R1$ = 0.054.

For **2** (ref. 18): $C_{12}H_6$, crystals obtained by sublimation (1 mbar, water cooled) space group $C2/c$, $a$ = 19.048(9), $b$ = 3.947(2), $c$ = 23.692(11) Å, $\beta$ = 108.04(3)°, $V$ = 1693.3(13), $Z$ = 8, $D_c$ = 1.18 g cm$^{-3}$, 665 unique reflections, $F_o > 4\sigma(F_o)$, 110 parameters, $2\Theta_{max}$ = 50°, $R$ = 0.058.

For **3**: $C_8H_6$ (Aldrich), crystallized *in situ* on the diffractometer (ref. 19), space group $P\bar{1}$, $a$ = 5.763(3), $b$ = 9.099(5), $c$ = 15.332(8) Å, $\alpha$ = 77.31(4), $\beta$ = 81.25(5), $\gamma$ = 80.62(4)°, $V$ = 768.1(7), $Z$ = 5, $D_c$ = 1.10 g cm$^{-3}$, 2541 unique reflections, $F_o > 4\sigma(F_o)$, 219 parameters, $2\Theta_{max}$ = 55°, $R1$ = 0.069.

All measurements were performed on a Nicolet R3m/V X-ray four circle diffractometer at −148 °C, using Mo-Kα X-rays ($\lambda$ = 0.71073), a graphite monochromator and the program SHELXTL (ref. 20); H-atom positions were refined isotropically. CCDC 182/560.

1 F. H. Allen, J. A. K. Howard, V. J. Hoy, G. R. Desiraju, D. S. Reddy and C. C. Wilson, *J. Am. Chem. Soc.*, 1996, **118**, 4081.
2 M. A. Viswamitra, R. Radhakrishnan, J Bandekar and G. R. Desiraju, *J. Am. Chem. Soc.*, 1993, **115**, 4868.
3 T. Steiner, M. Tamm, B. Lutz and J. van der Maas, *Chem. Commun.*, 1996, 1127.
4 T. E. Müller, D. M. P. Mingos and D. J. Williams, *J. Chem. Soc., Chem. Commun.*, 1994, 1787.
5 T. Steiner, E. B. Starikov, A. M. Amado and J. J. C. Teixeira-Dias, *J. Chem. Soc., Perkin Trans. 2*, 1995, 1321.
6 T. Steiner, M. Tamm, A. Grzegorzewski, N. Schulte, N. Veldman, A. M. M. Schreurs, J. A. Kanters, J. Kroon, J. van der Maas and B. Lutz, *J. Chem. Soc., Perkin Trans. 2*, 1996, 2441.
7 T. Steiner, *J. Chem. Soc., Chem. Commun.*, 1995, 95.
8 P. Hobza and R. Zahradnik, *Chem. Rev.*, 1988, **88**, 871.
9 R. K. McMullan and Å. Kvick, *Acta Crystallogr., Sect. B*, 1992, **48**, 726.
10 N. A. Ahmed, A. I. Kitaigorodskij and M. I. Sirota, *Acta Crystallogr. Sect. B*, 1972, **28**, 2875.
11 V. Benghiat and L. Leiserowitz, *J. Chem. Soc., Perkin Trans. 2*, 1972, 1772.
12 P. E. Eaton, E. Galoppini and R. Gilardi, *J. Am. Chem. Soc.*, 1994, **116**, 7588.
13 F. H. Allen, J. E. Davies, J. E. Galloy, J. J. Johnson, O. Kennard, C. F. Macrae, E. M. Mitchell, G. F. Mitchell, J. M. Smith and D. G. Watson, *J. Chem. Inf. Comput. Sci.*, 1991, **31**, 187.
14 G. E. Bacon, N. A. Curry and S. A. Wilson, *Proc. R. Soc. London, Ser. A*, 1964, **279**, 98.
15 C. A. Hunter, *Chem. Soc. Rev.*, 1994, 101.
16 *CRC Handbook of Chemistry and Physics*, CRC Press, Boca Raton, 77th edn.
17 A. S. Hay, *J. Org. Chem.*, 1960, **25**, 637.
18 E. Weber, M. Hecker, E. Koepp, W. Orlia, M. Czugler and I. Csöregh, *J. Chem. Soc., Perkin Trans. 2*, 1988, 1251.
19 R. Boese and M. Nussbaumer, *Organic Crystal Chemistry*, ed. D. W. Jones, Oxford University Press, Oxford, England, 1994, 20.
20 G. M. Sheldrick, SHELXTL93, Program for Crystal Structure Solution and Refinement, Universität Göttingen, 1993.

*Received in Liverpool, UK, 10th June 1997; 7/04070I*

# Efficient panchromatic sensitization of nanocrystalline $TiO_2$ films by a black dye based on a trithiocyanato–ruthenium complex

**Md. K. Nazeeruddin, P. Péchy and M. Grätzel***

*Institute of Photonics and Interfaces, Swiss Federal Institute of Technology, CH-1015 Lausanne, Switzerland*

**A black trithiocyanato–ruthenium(II) terpyridyl complex where the terpyridyl ligand is substituted by three carboxyl groups in 4,4′,4″-positions achieves very efficient panchromatic sensitization of nanocrystalline $TiO_2$ solar cells over the whole visible range extending into the near-IR region up to 920 nm.**

Dye-sensitized nanocrystalline $TiO_2$ solar cells are presently under intensive investigation.[1–3] So far, the best performing charge transfer sensitizer employed for such an application is a *cis*-dithiocyanato bis(4,4′-dicarboxy-2,2′-bipyridine)ruthenium(II) complex,[4] yielding solar to electric power conversion efficiency of 10% under standard AM 1.5 condition. To improve further the efficiency of such systems, an enhanced spectral response of the sensitizer in the red and near-IR region is required. The present study reports the synthesis and characterization of a new class of trithiocyanato–ruthenium(II) terpyridyl complex. Substitution of the terpyridyl ligand by three carboxyl groups in 4,4′,4″-positions yields a black dye displaying very efficient panchromatic sensitization over the whole visible range extending into the near-IR region up to 920 nm.

The oxidation of 4,4′,4″-trimethyl-2,2′:6′,2″-terpyridine[5,6] (0.32 g, 1.16 mmol) was carried out in sulfuric acid (4 ml), with chromium trioxide (1.05 g, 10.5 mmol) at 75 °C, yielding 4,4′,4″-tricarboxy-2,2′:6′,2″-terpyridine (0.15 g, 41%).†

4,4′,4″-Tricarboxy-2,2′:6′,2″-terpyridine (127 mg) was esterified by refluxing in methanol (15 ml) and sulfuric acid (70 mg) for 3 days. The white crystals were filtered, washed with methanol and diethyl ether successively, yielding 4,4′,4″-trimethoxycarbonyl-2,2′:6′,2″-terpyridine L (102 mg, 72%).‡

The $[RuLCl_3]$ complex was synthesized by adding a solution of 4,4′,4″-trimethoxycarbonyl-2,2′:6′,2″-terpyridine (40 mg), in dichloromethane (20 ml), to a solution of hydrated ruthenium trichloride (26 mg) in ethanol (30 ml). The reaction mixture was refluxed for 2 h and the solution was concentrated to 20 ml. The precipitated complex was collected and washed thoroughly with ethanol to remove any unreacted ruthenium trichloride (yield 48 mg, 79%).§

The complex $[NHEt_3][RuL(NCS)_3]$ **1** was obtained by refluxing $[RuLCl_3]$ (48 mg) and ammonium thiocyanate (100 mg) in dmf–water for 3.5 h at 120 °C, in the dark under an argon atmosphere. The ester groups of the terpyridine ligand were hydrolysed by further refluxing for 15 h in the presence of triethylamine (6 ml). The isolated solid was recrystallised from methanol–diethyl ether (yield 39 mg, 69%).¶

The UV–VIS absorption spectrum of **1** in ethanol shows an intense metal-to-ligand charge transfer band at 620 nm [Fig. 1(*a*)], with a molar absorption coefficient of 6500 $dm^3\ mol^{-1}\ cm^{-1}$. Bands at 291 and 329 nm with a distinct shoulder at 340 nm are assigned to the intraligand π–π* transition of the 4,4′,4″-tricarboxy-2,2′:6′,2″-terpyridine ligand. The interesting feature of complex **1** is the red-shifted MLCT absorption band in the visible region compared to the $[Ru(tpy)_2]^{2+}$ (tpy = 2,2′:6′,2″-terpyridine) family.[7] The three thiocyanato anionic ligands stabilize the excited states by electron donation to Ru causing a red shift in the MLCT bands. The electrochemical data of **1** suggest that the red shift in the MLCT is due to the decrease in the π* level of the 4,4′,4″-tricarboxy-2,2′:6′,2″-terpyridine ligand and an increase in the energy of the $t_{2g}$ metal orbital.

The MLCT and the π–π* bands of **1** were displaced to higher energy (590 nm) upon deprotonation of the carboxyl groups, which could be due to increase in the energy of the π* orbital of the 4,4′,4″-tricarboxy-2,2′:6′,2″-terpyridine ligand. When excited within the MLCT absorption band, **1** in ethanol solution at 298 K, exhibits a luminescence (measured as described in ref. 4) consisting of a single band with a maximum at 950 nm [Fig. 1(*b*)] and a lifetime of 18 ± 5 ns.

The cyclic voltammogram of **1** measured in dmf containing 0.1 M $[NBu_4][CF_3SO_3]$ shows one quasireversible wave at 0.6 V (*vs.* Ag/AgCl), which is attributed to the $[Ru^{II/III}L(NCS)_3]$ redox couple. In the negative potential range two irreversible waves at −1.1 and −1.2 V (*vs.* Ag/AgCl) are observed which are assigned to ligand reduction. A monolayer of complex **1** was adsorbed from a $2 \times 10^{-4}$ M solution in ethanol, containing 40 mM sodium taurodeoxycholate, as a co-adsorbent, onto a 12 nm thick nanocrystalline $TiO_2$ (anatase) film prepared on conducting glass as previously described.[4] The black film exhibited striking performance when tested in a photovoltaic cell in

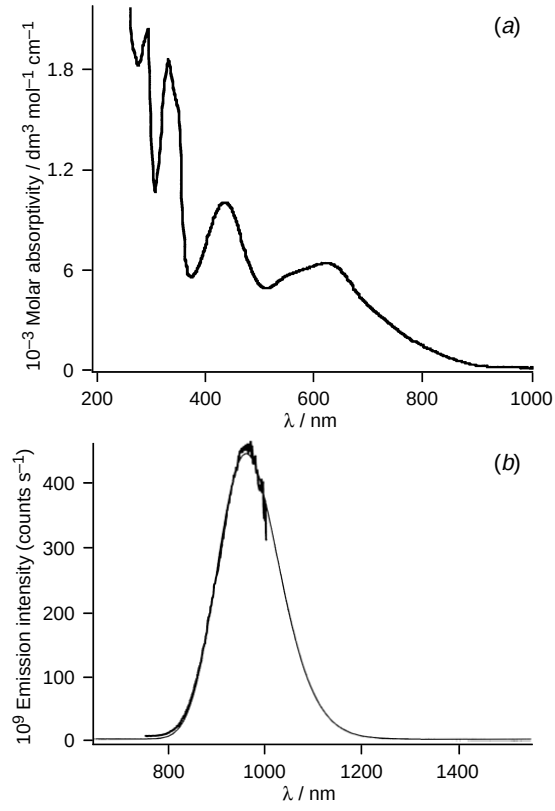



**Fig. 1** (*a*) Absorption spectrum of complex **1** in ethanol solution and (*b*) emission spectrum in ethanol solution at room temperature. The smoother curve corresponds to a Gaussian fit (instrument limit is 1000 nm).

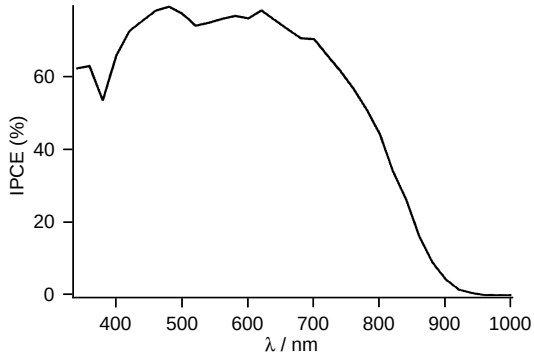



**Fig. 2** Photocurrent action spectrum obtained with a nanocrystalline $TiO_2$ film supported onto a conducting glass sheet and derivatized with complex **1**. The incident photon to current conversion efficiency is plotted as a function of wavelength. A sandwich type cell configuration was used to measure this spectrum.

conjunction with a redox electrolyte such as 0.9 M LiI and 0.1 M $LiI_3$ in propylene carbonate.

Fig. 2 shows the photocurrent action spectrum of such a cell where the incident photon to current conversion efficiency (IPCE) is plotted as a function of wavelength. Experimental details are described elsewhere.[4] The broad feature appears covering the entire visible spectrum and extending into the near-IR region up to 920 nm, the IPCE value in the plateau region being *ca.* 80%. Taking the light losses in the conducting glass into account the efficiency of electric current generation is practically 100% over a broad wavelength range extending from 400 to 700 nm. The overlap integral of this curve with the standard global AM 1.5 solar emission spectrum yields a photocurrent density of 20 mA $cm^{-2}$ and the first results obtained with these cells in the sun have confirmed these expectations. The discovery of this new black dye exhibiting enhanced light harvesting in the red and near-IR region opens up the way to improve significantly the overall efficiency of nanocrystalline photovoltaic devices.

This work was supported by grants from the Swiss Federal Institute for Energy (OFEN) and the Institut für Angewandte Photovoltaik (INAP, Germany). R. Humphrey-Baker assisted with the fluorescence work.

## Footnotes and References

* E-mail: michael.graetzel@icp.dc.epfl.ch

† MS (70 eV, CI, $NH_3$): *m/z* (rel. int.) 366 (12.2, M + 1), 365 (12.6, M), 322 (16.4), 321 (55.1, M − 44), 293 (4.1), 231 (1.3, M − 3 × 44 + 3), 79 (100). $^1$H NMR ($D_2O$–NaOH): $\delta$ 7.52 (2 H, d), 8.13 (2 H, s), 8.31 (2 H, s), 8.43 (2 H, d).

‡ Mp 238–239 °C (MeOH). Anal. for $C_{21}H_{17}N_3O_6$. Calc.: C, 61.92; H, 4.21; N, 10.31. Found: C, 61.90; H, 4.17; N, 10.30%. MS (thermospray, CI, $NH_4OAc$): *m/z* (rel. int.): 408 (100; M + 1). $^1$H NMR ($CDCl_3$): $\delta$ 4.04 (3 H, s), 4.05 (6 H, s), 7.94 (2 H, d), 8.90 (2 H, d), 9.03 (2 H, s), 9.13 (2 H, s). $^{13}$C NMR ($CDCl_3$): $\delta$ 165.7 (s), 165.6 (s), 156.5 (s), 156.1 (s), 150.1 (d), 139.9 (s), 138.6 (s), 123.27 (d), 121.1 (d), 120.8 (d), 52.8 (q), 52.7 (q).

§ Anal. for $C_{21}H_{17}Cl_3N_3O_6Ru$. Calc.: C, 41.02; H, 2.78; N 6.83. Found: C, 40.96; H, 2.75; N, 6.88%.

¶ Anal. for $C_{27}H_{31}N_7O_8RuS_3$. Calc.: C, 41.64; H, 4.01; N, 12.58. Found: C, 41.85; H, 4.05; N, 12.14%. $^1$H NMR ($D_2O$–NaOH): $\delta$ 9.09 (2 H, d), 8.76 (4 H, s), 8.14 (2 H, d), 3.18 (6 H, q), 1.28 (9 H, t).

1 M. Grätzel, *Platinum Met. Rev.*, 1994, **4**, 151.
2 K. Murakoshi, G. Kano, Y. Wada, S. Yanagida, H. Miyazaki, M. Matsumoto and S. Murasawa, *J. Electroanal. Chem.*, 1995, **396**, 27.
3 R. Argazzi, C. A. Bignozzi, T. A. Heimer and G. J. Meyer, *Inorg. Chem.*, 1997, **36**, 2.
4 M. K. Nazeeruddin, A. Kay, I. Rodicio, R. Humphry-Baker, E. Muller, P. Liska, N. Vlachopoulos and M. Grätzel, *J. Am. Chem. Soc.*, 1993, **115**, 6382.
5 P. E. Rosevear and W. H. F. Sasse, *J. Heterocycl. Chem.*, 1971, **8**, 483.
6 D. L. Feldheim, C. J. Baldy, P. Sebring, S. M. Hendrickson and C. M. Elliott, *J. Electrochem. Soc.*, 1995, **142**, 3366.
7 M. Maestri, N. Armaroli, V. Balzani, E. C. Constable and A. M. W. C. Thompson, *Inorg. Chem.*, 1995, **34**, 2759.

*Received in Basel, Switzerland, 12th May 1997; 7/03277C*

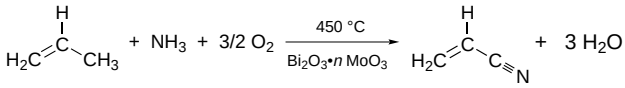
# Homogeneous modeling of ammoxidation chemistry: nitrile formation using a soluble analogue of $MoO_3$

**Thomas R. Mohs, Yuhua Du, Bruce Plashko and Eric A. Maatta***

*Department of Chemistry, Kansas State University, Manhattan, Kansas 66506, USA*

**The reaction of the soluble $MoO_3$ analogue $[Mo_6O_{19}]^{2-}$ with $Ph_3P{=}NCH_2Ph$ replicates key features of heterogeneous ammoxidation chemistry by producing moderate yields of PhC≡N through the proposed intermediacy of the benzylimido hexamolybdate complex $[Mo_6O_{18}(NCH_2Ph)]^{2-}$.**

The SOHIO/BP process for the heterogeneous oxidation of propene by $O_2$ in the presence of ammonia to yield acrylonitrile (*i.e.*, the 'ammoxidation' of propene) constitutes the largest volume example of an allylic oxidation in commercial practice.[1] A minimalistic representation of this remarkable transformation is provided in Scheme 1. It is now well established that the bismuth oxide component of the catalyst serves to abstract a hydrogen atom from propene, affording an allyl radical;[2] subsequent C–N bond formation and redox events occur at sites within the $MoO_3$ component.[3] Drawing on the extensive studies of Grasselli and Burrington,[4] key nitrogenous surface species proposed to be involved in this chemistry include imido {Mo≡NH}, allylamido {Mo=NHCH$_2$CH=CH$_2$}, allylimido {Mo≡NCH$_2$CH=CH$_2$}, and allylideneamido {Mo=N=CHCH=CH$_2$} fragments. Several groups have reproduced aspects of the proposed transformations in studies of various mononuclear systems.[5–7]




**Scheme 1**

In order to further refine these homogenous analogues of proposed ammoxidation events we sought to transfer this chemistry into a coordination environment which more closely resembles that provided by bulk $MoO_3$. As shown in Fig. 1, the soluble hexamolybdate cluster $[Mo_6O_{19}]^{2-}$ possesses an $MoO_6$ coordination sphere[8] which is conspicuously similar to that within $MoO_3$.[9] Realizing that a large number of organoimido-substituted hexamolybdates recently have been accessed through reactions of $[Mo_6O_{19}]^{2-}$ with various imido delivery reagents,[10] this structural correspondence suggested to us that allylimido- and benzylimido-hexamolybdates would provide the closest approximation yet available of purported ammoxidation surface species. We now report that the reaction of $[Mo_6O_{19}]^{2-}$ with the benzylimido delivery reagent $Ph_3P{=}NCH_2Ph$ affords benzonitrile in moderate yield (37%) thus replicating essential features of heterogeneous ammoxidation chemistry through the proposed intermediacy of an unstable benzylimido hexamolybdate system $[NBu_4]_2[Mo_6O_{18}(NCH_2Ph)]$, **1**.

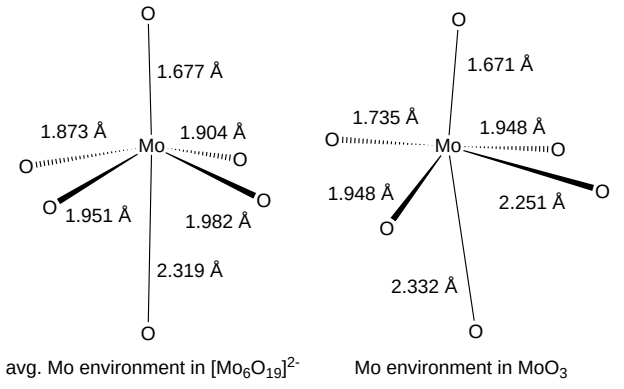
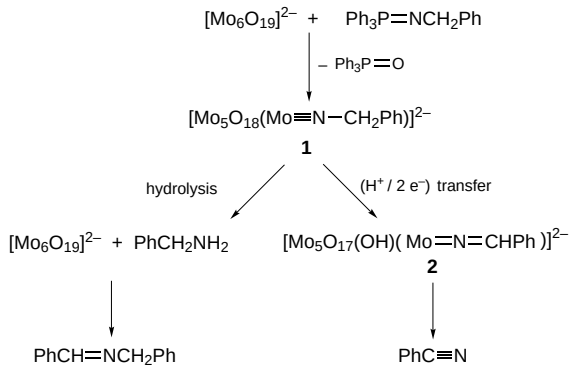



**Fig. 1** Comparison of the Mo environments in $[Mo_6O_{19}]^{2-}$[8] and in $MoO_3$[9]

The addition of 1.47 mmol of $Ph_3P{=}NCH_2Ph$ to an equimolar amount of $[NBu_4]_2[Mo_6O_{19}]$ in 30 ml MeCN at room temp. produces a brown coloration within 1 min of mixing. After this solution was heated at 82 °C under $N_2$ for 72 h, analysis by GC–MS techniques revealed the presence of benzonitrile (0.54 mmol, 37%) and *N*-benzylidenebenzylamine (0.25 mmol, 34%) along with quantitative production of triphenylphosphine oxide. Using an identical protocol, the thermolysis of $Ph_3P{=}NCH_2Ph$ in the absence of hexamolybdate produced only a trace of benzonitrile (0.009 mmol, 0.6%) and a modest amount of triphenylphosphine oxide (0.17 mmol, 11.7%); importantly, the latter product signals the presence of residual water in the acetonitrile solvent. $^1$H NMR monitoring throughout the reaction between $Ph_3P{=}NCH_2Ph$ and $[Mo_6O_{19}]^{2-}$ provided only broad and uninformative spectra, inferring the presence of paramagnetic species. In confirmation, aliquots withdrawn from the reaction solution were analyzed by EPR spectroscopy as frozen glasses and gave spectra identical to that published for the brown trianion $[Mo_6O_{19}]^{3-}$.[11]

In order to test whether $PhCH{=}NCH_2Ph$ is an intermediate in the formation of benzonitrile, a MeCN solution containing equimolar quantities of the imine and the hexamolybdate was treated and analyzed as above. No reaction occurred, suggesting that the imine is formed on a reaction pathway different from that leading to benzonitrile. Benzyl amine was suspected as the imine precursor since various polyoxometalates are known to effect this transformation.[12] Accordingly, the reaction of 1.47 mmol amounts of $PhCH_2NH_2$ and $[Mo_6O_{19}]^{2-}$ in MeCN was performed as described above and produced a brown solution immediately; subsequent GC–MS analysis revealed the production of $PhCH{=}NCH_2Ph$ (0.37 mmol, 46%) and only minor amounts of PhCN (0.029 mmol, 1.8%). It is important to note that the 0.25 mmol of $PhCH{=}NCH_2Ph$ produced in the reaction between $Ph_3P{=}NCH_2Ph$ and $[Mo_6O_{19}]^{2-}$ requires far more benzyl amine (0.50 mmol) than can be accounted for by hydrolytic decomposition of $Ph_3P{=}NCH_2Ph$ alone (0.17 mmol); this discrepancy can be accommodated by the reasonable assumption that the reaction between $Ph_3P{=}NCH_2Ph$ and $[Mo_6O_{19}]^{2-}$ affords an intermediate which is more sensitive than $Ph_3P{=}NCH_2Ph$ toward hydrolytic release of $PhCH_2NH_2$.

Since an initial redox reaction between $Ph_3P{=}CH_2Ph$ and the hexamolybdate is unlikely,† and given the demonstrations of forming complexes $[Mo_6O_{18}(NR)]^{2-}$ in reactions between the hexamolybdate and $Ph_3P{=}NR$ reagents,[10a,d] we propose that our observations are best accommodated by formation of an unstable benzylimido hexamolybdate $[Mo_6O_{18}(NCH_2Ph)]^{2-}$, **1**, which undergoes two modes of decomposition. In accord with observations on related d$^0$ benzylimido[13,14] (and allylimido[6]) complexes, **1** should be extremely moisture sensitive




**Scheme 2** Proposed decomposition pathways for **1**

and its hydrolysis (to produce benzyl amine and hexamolybdate) will initiate the reaction sequence leading to $PhCH{=}NCH_2Ph$ (Scheme 1).

The conversion $\{[Ph–CH_2–N]^{2-} \rightarrow Ph–C{\equiv}N\}$ requires the formal export of 2 $H^+$ and 4 $e^-$. Precedent suggests that the $\alpha$-$CH_2$ hydrogens within **1** should be acidic[6,13,14] while the oxo sites within **1** will display enhanced basicity[10*b*,*g*] as a result of the effective electron donation provided by the benzylimido ligand. These combined attributes suggest that the decomposition of **1** to produce benzonitrile is triggered by initial $H^+$ migration, probably in a pairwise[10*g*] fashion; an accompanying 2 $e^-$ reduction of its hexamolybdate cage will produce a reduced benzylideneamido dianion **2** (Scheme 2).[6,13] While further reduction of **2** is improbable, several species in the reaction solution should be capable of oxidizing **2** {the most potent of which is $[Mo_6O_{19}]^{2-}$}. Such an oxidation would increase the acidity of the remaining methine hydrogen atom, facilitating a second $H^+$–2 $e^-$ transfer process, allowing the release of benzonitrile. Efforts are underway to isolate complexes analogous to **1** and **2**.

We thank the Office of Basic Energy Sciences, Department of Energy (USA) for support of this work.

## Footnotes and References

* E-mail: eam@ksu.edu

† *p*-$CH_3C_6H_4N{=}PPh_3$ ($E_{pa}$ = 0.74 V *vs*. SCE) is easier to oxidize than is $PhCH_2N{=}PPh_3$ ($E_{pa}$ = 1.06 V *vs*. SCE), yet the former reacts with $[Mo_6O_{19}]^{2-}$ to give only metathesis without electron transfer.[10*a*]

1 R. K Grasselli, in *Heterogenous Catalysis*, ed. B. L. Shapiro, Texas A&M University Press, College Station, TX, 1984, p. 182.
2 J. D. Burrington, C. T. Kartisek and R. K. Grasselli, *J. Org. Chem.*, 1981, **46**, 1877; W. Martin and J. H. Lunsford, *J. Am. Chem. Soc.*, 1981, **103**, 3728.
3 J. Haber and B. Grzybowska, *J. Catal.*, 1973, **28**, 489; B. Grzybowska, J. Haber and J. Janas, *J. Catal.*, 1977, **49**, 150; J. D. Burrington and R. K. Grasselli, *J. Catal.*, 1979, **59**, 79; J. D. Burrington, C. T. Kartisek and R. K. Grasselli, *J. Catal.* 1983, **81**, 489.
4 R. K. Grasselli and J. D. Burrington, *Ind. Eng. Chem. Prod. Res. Dev.*, 1984, **23**, 394 and references therein.
5 D. M.-T. Chan and W. A. Nugent, *Inorg. Chem.*, 1985, **24**, 1422.
6 E. A. Maatta and Y. Du, *J. Am. Chem. Soc.*, 1988, **110**, 8249.
7 J. Belgacem, J. Kress and J. A. Osborn, *J. Mol. Catal.*, 1994, **86**, 267.
8 H. R. Allcock, E. C. Bissell and E. T. Shawl, *Inorg. Chem.*, 1973, **12**, 2963.
9 L. Kihlborg, *Ark. Kemi*, 1963, **21**, 357.
10 (*a*) Y. Du, A. L. Rheingold and E. A. Maatta, *J. Am. Chem. Soc.*, 1992, **114**, 345; (*b*) J. B. Strong, R. Ostrander, A. L. Rheingold and E. A. Maatta, *J. Am. Chem. Soc.*, 1994, **116**, 3601; (*c*) R. J. Errington, C. Lax, D. G. Richards, W. Clegg and K. A. Fraser, in *Polyoxometalates: From Platonic Solids to Anti-Retroviral Activity*, ed. M. T. Pope and A. Müller, Kluwer, Dordrecht, 1994, p. 105; (*d*) A. Proust, R. Thouvenot, M. Chaussade, F. Robert and P. Gouzerh, *Inorg. Chim. Acta*, 1994, **224**, 81; (*e*) W. Clegg, R. J. Errington, K. A. Fraser, S. A. Holmes and A. Schäfer, *J. Chem. Soc., Chem. Commun.*, 1995, 455; (*f*) J. L. Stark, A. L. Rheingold and E. A. Maatta, *J. Chem. Soc., Chem. Commun.*, 1995, 1165; (*g*) J. L. Stark, V. G. Young, Jr. and E. A. Maatta, *Angew. Chem., Int. Ed. Engl.*, 1995, **34**, 2547.
11 M. Che, M. Fournier and J. P. Launay, *J. Chem. Phys.*, 1979, **71**, 1954.
12 R. Neumann and M. Lissel, *J. Org. Chem.*, 1991, **56**, 5707; K. Nakayama, M. Hamamoto, Y. Nishiyama, and Y. Ishii, *Chem. Lett.*, 1993, 1699.
13 Y. Du, A. L. Rheingold and E. A. Maatta, *J. Chem. Soc., Chem. Commun.*, 1994, 2163.
14 Y. Du, Ph.D. Thesis, Kansas State University 1992.

*Received in Bloomington, IN, USA, 30th May 1997; 7/03790B*

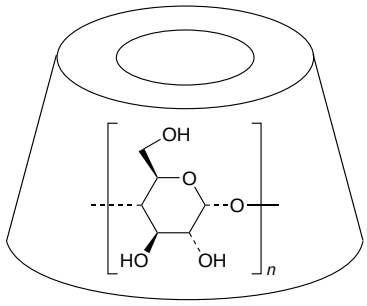
# Supramolecular control of the photochemistry of stilbenes by cyclodextrins

**Wolfgang Herrmann, Susanne Wehrle and Gerhard Wenz***

*Polymer-Institut der Universität Karlsruhe (TH), Hertzstrasse 16, D-76187 Karlsruhe, Germany*

**Upon UV irradiation in the presence of β-cyclodextrin, (*E*)-4,4′-bis(dimethylammoniomethyl)stilbene is transformed to the (*Z*)-isomer, but in the presence of γ-cyclodextrin only the [2 + 2]-cycloaddition products are obtained; the products are a molecular imprint of the cavity of the cyclodextrin.**

Supramolecular assemblies are formed by the self organisation of complementary molecules, *e.g.* host and guest molecules.[1] They may show a high degree of short range order which allows chemical reactions to be performed with high specificity. Photochemical reactions can be especially well-controlled by supramolecular assembly of the reactive molecules as the close vicinity of the molecules makes the selective transformation of highly energetic intermediates possible.[2] Processes like energy[3] or electron transfer,[4] dimerisations[5–7] and polymerisations[8] have been successfully performed in organised media.[9] Here we report on the control of the photochemistry of stilbenes by inclusion in cyclodextrins.




**1a** *n* = 6
**b** *n* = 7
**c** in = *8*

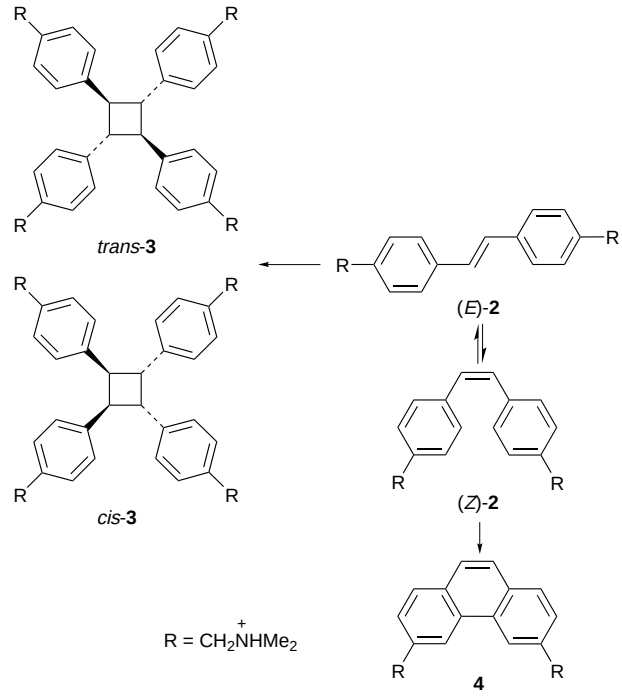
Cyclodextrins **1a**–**c** are torus shaped cyclic oligomers of glucose. They provide a hydrophobic cavity for the inclusion of hydrophobic guest molecules in aqueous solution.[10] The formation of ternary inclusion compounds of one cyclodextrin ring and two guests facilitates bimolecular reactions between the two guests:[11,12] the cyclodextrin ring acts like a molecular reaction vessel. Thus the photo-dimerisation of two anthracene,[13] acenaphthylene[14] or coumarin molecules[15] is accelerated by inclusion in **1c**. In contrast, the inclusion of stilbenes in **1b** leads to the prevention of the photo-dimerisation, as only one guest molecule is included.[16,17] Here the host **1b** seems to exert a shielding effect on the guest. We report on the influence of the ring size of a cyclodextrin on the photochemistry of the stilbene (*E*)-**2**. It is well suited for such investigations because of its high solubility in water.

The stilbene derivative[18] (*E*)-**2** was synthesised from 4,4-dimethylstilbene by bromination of the methyl groups and subsequent substitution with dimethylamine. UV irradiation† of an aqueous solution of [(*E*)-**2** afforded a mixture of products, mainly the (*Z*)-isomer (*Z*)-**2**, small amounts of the educt (*E*)-**2**, the tetraphenyl cyclobutanes *trans*-**3** and *cis*-**3** and phenanthrene **4**, as expected for stilbenes (Table 1 and Scheme 1).[19] The distribution of the products is dependent on the irradiation time (Fig. 1): the amount of the photo-stable products **3** and **4** increased with longer irradiation time.

**Table 1** Distribution of products after the irradiation of (*E*)-**2** in aqueous solution with UV light ($\lambda$ 312 nm) in the presence of cyclodextrins

| | | Content (%) | | | | |
|---|---|---|---|---|---|---|
| Cyclodextrin | *t*/h | (*E*)-**2** | (*Z*)-**2** | *trans*-**3** | *cis*-**3** | **4** |
| none | 24 | 10 | 62 | 7 | 2 | 19 |
| **1a** | 24 | 20 | 60 | 0 | 0 | 20 |
| **1b** | 24 | 16 | 83 | 0 | 0 | 1 |
| **1c** | 72 | 0 | 0 | 79 | 19 | 2 |

In the presence of hosts **1a** or **1b** the photo-dimerisation leading to cyclobutanes was totally restrained. Obviously, the stilbene moieties were shielded from each other by the formation of 1 : 1 inclusion compounds with **1a** or **1b**. Furthermore, inclusion in **1b** almost totally prevented the formation of phenanthrene **4**. Stilbenes **2** included in **1b** only show reversible photo-isomerisation with almost no side reactions. Consequently, **1b**–**2** is well suited for photo-switchable devices. In the presence of the larger host **1c**, the photo-dimerisation was found to be strongly favoured. After long irradiation times, high yields (up to 98%) of the cyclobutanes **3** were found (Table 1). For shorter times the (*Z*)-isomer (*Z*)-**2** of the educt appeared in the product mixture as an intermediate. Moreover, the presence of **1c** led to an increase of the rate of consumption of **2e**, *e.g.* after 1 h the product mixture contained 24% (44%) of (*E*)-**2** in the presence




**Scheme 1**

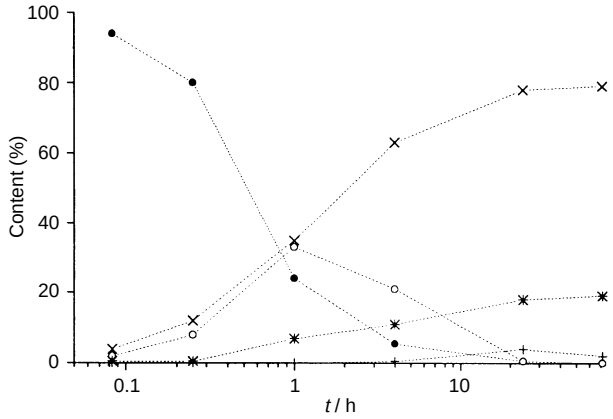



**Fig. 1** The time dependence of the product distribution after irradiation of (*E*)-**2** in the presence of **1c**: (●) (*E*)-**2**, (○) (*Z*)-**2**, (×) *trans*-**3**, (∗) *cis*-**3** and (+)-**4**

**Table 2** Thermodynamic parameters for the inclusion of the guests in cyclodextrins as determined by microcalorimetric titration (1 cal = 4.184 J)

| | $K_s$/ dm³ mol | $-\Delta G°_m'$/ kcal mol$^{-1}$ | $-\Delta H°_m'$/ kcal mol$^{-1}$ | $T\Delta S°_m'$/ kcal mol$^{-1}$ |
|---|---|---|---|---|
| **1a**–(*E*)-**2** | 1520 ± 50 | 4.3 | 6.4 ± 0.1 | −2.1 |
| **1a**–(*Z*)-**2** | 360 ± 110 | 3.5 | 1.9 ± 1.5 | 1.6 |
| **1b**–(*E*)-**2** | 705 ± 20 | 3.9 | 2.7 ± 0.1 | 1.2 |
| **1b**–(*Z*)-**2** | 540 ± 220 | 3.7 | 9.7 ± 8.4 | −6.0 |
| **1c**–(*E*)-**2** | 385 ± 10 | 3.5 | 1.1 ± 0.3 | 2.4 |
| **1c**–[(*E*)-**2**]$_2$ | 2730 ± 60 | 4.7 | 7.2 ± 0.1 | −2.5 |
| **1c**–*trans*-**3** | 18 000 ± 6600 | 5.8 | 7.1 ± 1.2 | −1.3 |
| **1c**–*cis*-**3** | 520 ± 700 | 3.7 | −5.4 ± 11.0 | 9.1 |

(absence) of host **1c**. The selective formation of cyclobutanes **3** upon addition of **1c** was attributed to the preceding formation of the ternary inclusion compound **1c**–**2**$_2$. The close proximity of the two included stilbenes should strongly favour the [2 + 2] addition.

To confirm this assumption we investigated‡ the formation of inclusion compounds of stilbenes **2** by microcalorimetric titration.[20] Indeed, host **1c** includes two molecules of **2**. The binding constant for the formation of **1c**–**2**$_2$ is relatively high compared to the literature values for other guest molecules (Table 2).[21] In contrast, we observed the formation of 1 : 1 inclusion compounds of **2** in hosts **1a** and **1b**. For the smallest host **1a**, the inclusion enthalpy is strongly negative for (*E*)-**2**, accompanied by a loss of entropy which is typical for a rather tight axial inclusion compounds **1a**–(*E*)-**2**.[22] On the other hand, the formation of inclusion compound **1b**–(*E*)-**2** has a low enthalpy gain but also some entropy gain. These findings are attributed to the formation of a loose complex as guest (*E*)-**2** is too slim to completely fill the cavity of **1b**. Turro drew the same conclusion from fluorescence lifetime measurements.[23] In contrast, isomer (*Z*)-**2** is tightly bound by **1b**, presumably in a non-axial arrangement, as Ramamurthy has postulated.[17]

Consequently, the photo-dimerisation of stilbenes **2** is hindered by a 1 : 1 inclusion in hosts **1a** and **1b** but enhanced by an 1 : 2 inclusion in host **1c**. An excited stilbene in **1c**–[(*E*)-**2**]$_2$ can react rapidly with its neighbour. Furthermore, we found that dimerisation products **3**, especially *trans*-**3**, form stable 1 : 1 inclusion compounds with **1c**. The inclusion of *trans*-**3** is accompanied by an enthalpy gain and an entropy loss, typical of a tight fit between host and guest. Consequently, in the presence of hosts **1b** and **1c** the formation of the photo-product with the highest affinity towards the host was favoured most. The main photo-product is therefore a molecular imprint (replica) of the host.[24] The principle might be further exploited for the targeted photochemical synthesis of other molecules. The photo-chemical synthesis of poly(rotaxane)s is the subject of our current research.

We thank the Deutsche Forschungsgemeinschaft (project We 1092/2-1) and Wacker-Chemie, Burghausen, for supporting this work.

## Footnotes and References

† A solution of (*E*)-**2**·(HCl)$_2$ (0.01 mol dm$^{-3}$; 10 cm³) was irradiated with UV light (λ 312 nm, source type D89008, 6 W, Bioblock Scientific, Illkirch Cedex, France) for 0.08, 0.25, 1.00, 5.00, 24.00 and 72 h. Afterwards, the solution was brought to pH 10 by addition of NaOH (2 mol dm$^{-3}$) and **2**–**4** were extracted with $CHCl_3$. The product distribution was determined by integration of the $^1$H NMR signals of the crude product in $CDCl_3$. *Selected data* for (*E*)-**2** $\delta_H$ ($CDCl_3$, 400 MHz) 2.26 (s, 12 H, $CH_3$), 3.44 (s, 4 H, $CH_2$), 7.10 (s, 2 H, =CH), 7.30 (d, *J* 8.4, 4 H, ArH), 7.47 (d, *J* 7.9, 4 H, ArH). For (*Z*)-**2**: $\delta_H$ 2.23 (s, 12 H, $CH_3$), 3.37 (s, 4 H, $CH_2$), 6.56 (s, 2 H, =CH), 7.15 (d, *J* 8.0, 4 H, ArH), 7.21 (d, *J* 8.0, 4 H, ArH). For *trans*-**3**: $\delta_H$ ($CDCl_3$, 400 MHz) 2.17 (s, 24 H, $CH_3$), 3.30 (s, 8 H), 4.42 (s, 4 H, CH), 7.04 (s, 16 H, ArH). For *cis*-**3**: $\delta_H$ ($CDCl_3$, 400 MHz) 2.26 (s, 24 H, $CH_3$), 3.40 (s, 8 H, $CH_2$), 3.63 (s, 4 H, CH), 7.23 (s, 16 H, ArH). For **4**: $\delta_H$ ($CDCl_3$, 400 MHz) 2.32 (s, 12 H, $CH_3$), 3.69 (s, 4 H, $CH_2$), 7.57 (d, *J* 7.9, 2 H, ArH), 7.70 (s, 2 H, ArH), 7.84 (d, *J* 7.9, 2 H, ArH), 8.62 (s, 2 H, ArH).

‡ The microcalorimetric titrations were carried out using a Microcal Omega Titration Calorimeter, MicroCal Inc., Northampton Massachusetts. A solution of cyclodextrin (0.002 mol dm$^{-3}$; 1.336 cm³) was titrated with 20 portions of guest (0.045 mol dm$^{-3}$; 5 μl) ammonium acetate buffer (pH 5.7; 0.1 mol dm$^{-3}$) at 25 °C. The interaction heat data were fitted to models for either 1 : 1 or stepwise 1 : 2 inclusion processes by the program Origin ITC, MicroCal Inc. The binding constants and enthalpies were obtained as fitting parameters. We could not isolate pure (*Z*)-**2**. Thus we used a mixture of (*Z*)-**2** (64%) and (*E*)-**2** (36%) for the inclusion experiment and the data were fitted to the model 'two sets of sites' of the program package Origin ITC. This procedure was also applied for the mixture of *trans*-**3** (79%) and *cis*-**3** (21%).

1 J.-M. Lehn, *Supramolecular Chemistry*, VCH, Weinheim, 1995.
2 V. Balzani, *Tetrahedron*, 1992, **48**, 10 443.
3 J. P. Cooper and P. J. Hagerman, *Biochemistry*, 1990, **29**, 9261.
4 A. M. Brun, S. J. Atherton, A. Harriman, V. Heitz and J. P. Sauvage, *J. Am. Chem. Soc.*, 1992, **114**, 4632.
5 G. H. J. Schmidt, in *Solid-State Photochemistry*, ed. D. Ginsburg, VCH, Weinheim, 1976, p. 2ff.
6 C. Mertesdorf, H. Ringsdorf and J. Stumpe, *Liq. Cryst.*, 1991, **9**, 337.
7 I. Cabrera, M. Engel, L. Häussling, C. Mertesdorf and H. Ringsdorf, in *Photoinduced structural changes in organized supramolecular systems*, ed. H.-J. Schneider and H. Dürr, VCH, Weinheim, 1991, p. 311ff.
8 *Polymerization in organized media*, ed. C. M. Paleos, Gordon and Breach Science Publishers, Philadelphia, 1992.
9 V. Ramamurthy, *Tetrahedron*, 1986, **42**, 5753.
10 G. Wenz, *Angew. Chem.*, 1994, **106**, 851; *Angew. Chem., Int. Ed. Engl.*, 1994, **33**, 803.
11 H.-J. Schneider and N.K. Sangwan, *Angew. Chem.*, 1987, **99**, 924; *Angew. Chem., Int. Ed. Engl.*, 1987, **26**, 896.
12 K. Takahashi and K. Hattori, *J. Inclusion Phenom.*, 1994, **17**, 1.
13 T. Tamaki, *Chem. Lett.*, 1984, 53.
14 Z. Tong and Z. Zhen, *Youji Huaxue*, 1986, 44; Chem. Abstr., 1986, **105**, 152330g.
15 J. N. Moorthy, K. Venkatesan and R. G. Weiss, *J. Org. Chem.*, 1992, **57**, 3292.
16 M. S. Syamala and V. Ramaurthy, *J. Org. Chem.*, 1986, **51**, 3712.
17 M. S. Syamala, S. Devanathan and V. Ramaurthy, *J. Photochem.*, 1986, **34**, 219.
18 G. Drehfahl and H. Lückert, *J. Prakt. Chem.*, 1959, **9**, 305.
19 H. Meier, *Angew. Chem.*, 1992, **104**, 1425; *Angew. Chem., Int. Ed. Engl.*, 1992, **31**, 1399.
20 T. Höfler and G. Wenz, *J. Inclusion Phenom.*, 1996, **25**, 81.
21 M. V. Rekharsky, R. N. Goldberg, F. P. Schwarz, Y. B. Tewari, P. D. Ross, Y. Yamashoji and Y. Inoue, *J. Am. Chem. Soc.*, 1995, **117**, 8830.
22 Y. Inoue, T. Hakushi, Y. Liu, L. Tong, B. Shen and D. Jin, *J. Am. Chem. Soc.*, 1993, **115**, 475.
23 G. L. Duveneck, E. V. Sitzmann, K. B. Eisenthal and N. J. Turro, *J. Phys. Chem.*, 1989, **93**, 7166.
24 G. Wulff, *Angew. Chem.*, 1995, **107**, 1958; *Angew. Chem., Int. Ed. Engl.*, 1995, **34**, 1812.

*Received in Liverpool, UK, 20th May 1997; 7/03485G*

# Iron complexes with an N/S chromophore relevant to the active site of the hydrolytic metalloenzyme nitrile hydratase†

**Alexandre L. Nivorozhkin,*[a]‡ Ali I. Uraev,[a] Gennadii I. Bondarenko,[a] Alla S. Antsyshkina,[b] Vasilii P. Kurbatov,[a] Alexandre D. Garnovskii,[a] Constantin I. Turta[c] and Nikolai D. Brashoveanu[c]**

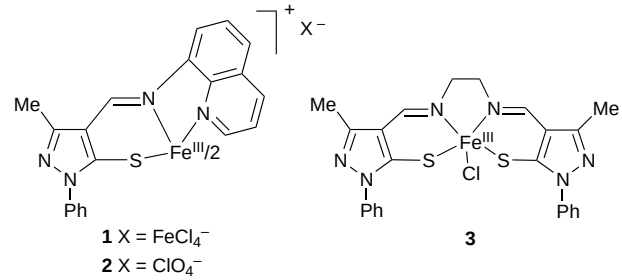
[a] *Institute of Physical Organic Chemistry, Rostov State University, pr. Stachki 194/2, 344104 Rostov on Don, Russia*
[b] *N. S. Kurnakov Institute of General and Inorganic Chemistry, Russian Academy of Sciences, Leninskii pr. 31, 117090 Moscow, Russia*
[c] *Institute of Chemistry, Moldavian Academy of Sciences, 277028 Kishinev, Moldova*

**Iron(III) complexes with a 3N/3S chromophore reproduce a mixed N/S heterocyclic ligand environment, metal–ligand bond lengths, and low-spin state ($S$ = 1/2) characteristic of the hydrolytic metalloenzyme nitrile hydratase; $Fe^{III}N_2S_2Cl$ species possesses a quantum mechanically admixed $S$ = 3/2, 5/2 state and able to form low-spin solvent adducts, possible analogues of the substrate-bound form of the enzyme.**

Iron–thiolate metal centers have until recently been considered mainly in the context of Fe–S cluster assemblies of metalloproteins and in relation to their role in electron-transfer processes. One of the emerging new non-redox functions of biological iron–thiolate centers is that associated with their Lewis-base activity in catalyzing hydration–dehydration reactions of organic substrates.[1,2] Even though most of these transformations are catalyzed by the metalloenzymes containing Fe–S clusters in their active site, *e.g.*, aconitase, certain others apparently lack cluster units. Another example of a metalloenzyme with an iron–thiolate active site that is not redox active and does not belong to the heme or Fe–S cluster families is bacterial nitrile hydratase, which catalyzes the conversion of nitriles to corresponding amides. Combined physicochemical results[3] provide solid evidence for the presence of a low-spin ($S$ = 1/2) $Fe^{III}N_3S_2$ chromophore with a sixth coordination site occupied by a water molecule or hydroxide ion, which is probably replaced by acetonitrile in the catalytic cycle. Synthetic iron(III) complexes with mixed N/S donor sets, common in coordination chemistry, can be useful models of the protein active site. However, there are only few examples[4] of such species owing to the often facile oxidation of thiolate ligand by $Fe^{III}$. Studying synthetic models of blue copper proteins, tetracoordinate bis-chelate copper(II)–thiolato complexes of Schiff-base ligands notorious for the same type of redox instability, we found[5] that the presence of the potentially supplementary coordinating group in the ligand structure leads to the stabilization of the higher metal oxidation states.

Following this strategy, we report novel stable iron(III) complexes **1** and **2** with a 3N/3S chromophore simulating the N/S ligand environment of the nitrile hydratase active site and some of its spectroscopic properties. Complex **3** contains a potentially labile terminal chloride ligand which may be substituted by solvent molecules involving acetonitrile. Possibilities for the ligand modifications in **1**–**3** provide an entry to an extended series of $Fe^{III}$–N/S complexes which might provide insight into intimate structural and electronic features of general interest and those relevant to the active site of metalloenzyme.

Reaction of the ligands $H_2L$ [*N*,*N*′-bis(5-mercapto-3-methyl-1-phenylpyrazol-4-ylmethylene)ethylenediamine] and HL [5-mercapto-1-phenyl-3-methyl-4-ylmethylene(8-amino)-quinoline] with $Fe(ClO_4)_3nH_2O$ or $FeCl_3{\cdot}6H_2O$ in ethanol affords in good yields complexes **1**–**3**.[6] The X-ray molecular structure§ of **1** is shown in Fig. 1 The iron center is octahedrally




**1** X = $FeCl_4^-$
**2** X = $ClO_4^-$
**3**

coordinated by the two azomethine, and two quinoline nitrogens and two thiolate sulfur atoms in *cis*-positions [S(1)–Fe–S(2) 95.15(8)°]. Three metal–ligand angles [S(1)–Fe–N(2) 175.1(2), S(2)–Fe–N(6) 173.2(2), N(1)–Fe–N(5) 176.5(2)°] are close to 180°, thus indicating a tendency for a cubic symmetry ligand arrangement. Iron–sulfur bond lengths, Fe(1)–S(1) 2.227(2) and Fe(1)–S(2) 2.230(2) Å, are similar to that reported for nitrile hydratase (2.21 Å from EXAFS data[3e] for a pH 7.3 form) and *ca*. 0.07 Å shorter than for a high-spin $FeN_2S_3$ complex.[4e] Iron–nitrogen bond lengths in **1**, Fe–$N_{av}$ 1.99 Å, are also identical to those in the enzyme.

The EPR spectra of **I** recorded in frozen $CHCl_3$ and dimethylformamide solutions display a very large signal at $g \approx$

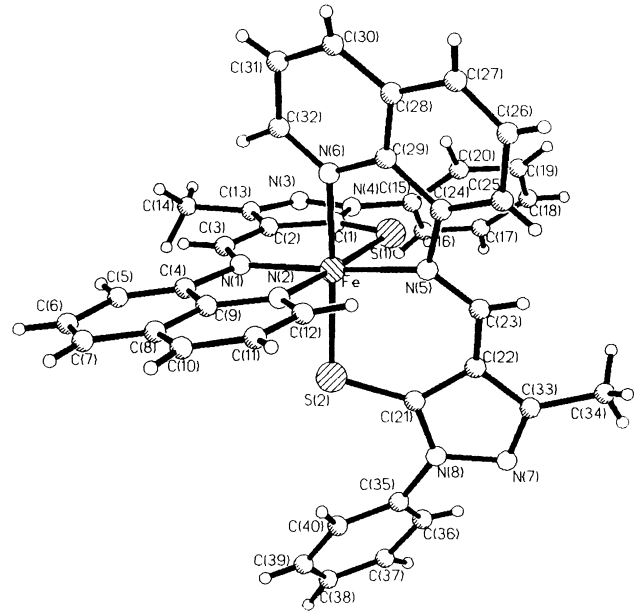



**Fig. 1** Molecular structure of **1**. Selected bond lengths (Å) and angles (°): Fe–S(1) 2.227(2), Fe–S(2) 2.230(2), Fe–N(1) 1.969(5), Fe–N(2) 2.005(6), Fe–N(5) 1.980(5), Fe–N(6) 2.004(6); S(1)–Fe–S(2) 95.15(8), S(1)–Fe–N(2) 175.1(2), S(1)–Fe–N(1) 99.7(2), S(1)–Fe–N(5) 81.5(2), S(2)–Fe–N(6) 173.2(2), N(1)–Fe–N(5) 176.5(2).

2, superimposed on which is a rhombic spectrum with the components $g$ = 2.19, 2.12 and 1.98, typical of a low-spin ($S$ = 1/2) iron(III) complex. Given a high-spin ($S$ = 5/2) nature of the anionic residue $FeCl_4^-$, low-spin features can be attributed to the $[FeL_2]^+$ species. Consistent with this assignment, complex **2** displays no broad component at $g$ = 2 but only a well resolved low-spin spectrum with $g$ = 2.193, 2.130 and 1.986.

Magnetic susceptibility measurements in the solid state reveal a low-spin ($S$ = 1/2) iron species **2** with $\mu_{eff}$ = 1.95 $\mu_B$, independent of temperature (77–300 K). Magnetic moments of **1**, containing $FeCl_4^-$ as a counter anion, are also temperature independent, 6.17 $\mu_B$ (per 2Fe) (4.44 $\mu_B$ per 1 Fe), which agrees well with presence of the contribution from the high-spin ($S$ = 5/2) center ($\mu_{eff}$ = 5.95 $\mu_B$).

The Mössbauer spectrum of **2** shows a symmetrical doublet with the following isomer shift and quadrupole splitting parameters at 77(300) K: $\delta$ = 0.15 (0.11) mm s$^{-1}$ (relative to Fe metal), $\Delta E_Q$ = 2.01 (1.99) mm s$^{-1}$. This situation corresponds to the $S$ = 1/2 iron complexes with an unpaired electron localized on the $d_{xy}$ orbital. Low values of the isomer shift indicate strong metal–ligand π interactions.[7a] For **1**, in addition to a similar doublet, $\delta$ = 0.25 (0.15) mm s$^{-1}$, $\Delta E_Q$ = 1.98 (2.08) mm s$^{-1}$ at 77(300) K there is another doublet with fairly small quadrupole splitting and isomer shift, $\delta$ = 0.29 (0.23) mm s$^{-1}$, $\Delta E_Q$ = 0.33(0.26) mm s$^{-1}$ which is typical for four-coordinate high-spin ($S$ = 5/2) iron(III) complexes and can be unequivocally assigned to the $FeCl_4^-$ anion.[7b]

Electronic spectra of **1** and **2** in $CHCl_3$ contain two bands in the IR region: $\lambda_{max}$/nm ($\varepsilon$/dm$^3$ mol$^{-1}$ cm$^{-1}$) 750 (600), 1005 (1410) (**1**) and 750 (535), 995 (1250) (**2**). Compared to nitrile hydratase [$\lambda_{max}$ = 715 nm ($\varepsilon$ = 1100 dm$^3$ mol$^{-1}$ cm$^{-1}$) at pH 7.3 and $\lambda_{max}$ = 690 ($\varepsilon$ = 1300) at pH 9], the 750 nm band may correspond to that observed in the enzyme and attributed to the Fe–S LMCT absorptions (with some contribution from an Fe–N chromophore) on the basis of a recent resonance-Raman study.[3d]

With respect to a specific low-spin nature of both substrate-free and bound nitrile hydratase, a significance of the particular ligand field strength may be to allow ligand substitution reactions to occur appropriately (at the early steps of nitrile binding) and also to activate a nitrile bond. To follow this line, we synthesized **3**, the complex with a potentially labile terminal ligand. Hydrolytic properties of the $Fe^{III}N_2S_2Cl$ species are implicated by the early results of Murray *et al.*,[4b] who failed to isolate a sulfur analogue of [Fe$^{III}$(salen)Cl] but only the complex with a partly hydrolyzed Schiff-base ligand, *N*-[(2-aminoethyl)thio]salicylideneamine. In contrast to the low-spin species **1** and high-spin [Fe$^{III}$(salen)Cl],[8] the magnetic moment of **3** in the solid state, $\mu_{eff}$ = 4.45 $\mu_B$ (300 K), indicates the less common intermediate-spin ($S$ = 3/2) state. This value drops to 3.84 $\mu_B$ at 77 K. The temperature dependence of the magnetic susceptibility for **3** suggests a contribution from the quantum mechanically admixtured $S$ = 5/2 spin state.[9] Consistently, the Mössbauer spectra of **3** display a single symmetrical doublet with similar parameters at 77(300) K: $\delta$ = 0.31(0.23) mm s$^{-1}$, $\Delta E_Q$ = 2.68 mm s$^{-1}$, typical of the mixed $S$ = 3/2, 5/2 state iron porphyrin complexes and also detected for $S$ = 3/2 iron species.[9b,10] In frozen solutions of **3**, we observed a low-spin species with spectral patterns similar to that for **2** in dmf ($g$ = 2.191, 2.159, 1.981), pyridine–DMF (1 : 1) ($g$ = 2.169, 1.979) and $CHCl_3$ ($g$ = 2.193, 2.162, 1.988) whereas in MeCN there is a low-spin spectrum ($g$ = 2.190, 2.161, 1.985) superimposed on the very broad signal. This result may be explained by formation of either a six-coordinate solvent adduct **3**·solv or a chloride-dissociated species with two axial solvent molecules.¶ The terminal ligand substitution reaction with a concomitant ground spin-state alteration are well established in porphyrin systems, although they usually occur with N-donor type ligands or strongly coordinating solvents.[9c] Complex **3** may be a suitable starting point to pursue an ultimate goal of nitrile hydrolysis[11] given the opportunities of ligand modifications, *e.g.*, conversion to corresponding aminothiol, variation of the bridging group and incorporation of the nitrile functionality into the ligand framework.

We are grateful to the Russian Fund of Fundamental Research (Grant No. 97-03-33479a) for a partial support of this work.

## Footnotes and References

* E-mail: alexniv@sanctuary.harvard.edu

† The results presented in this communication were reported in part in the lecture given by A. N. at the European Inorganic Chemistry Research Seminar, EICS-VI, *Biocoordination Chemistry, Inorganic Compounds with Framework Structures*, Karrebaeksminde, Denmark, September, 1996.

‡ Present address: Department of Chemistry and Chemical Biology, Harvard University, 12 Oxford St., Cambridge, MA 02138, USA.

§ *Crystal data* for **1**: $C_{40}H_{30}Cl_4Fe_2N_8S_2$, $M$ = 940.4, monoclinic, space group $P2_1/c$, $a$ = 11.485(2), $b$ = 17.489(30), $c$ = 20.574(5) Å, $\beta$ = 103.51(3)°, $U$ = 4018.2(5) Å$^3$, $Z$ = 4, $D_c$ = 1.55 g cm$^{-3}$, Mo-K$\alpha$ radiation (0.710 73 Å$^3$), SYNTEX P2$_1$ diffractometer, $T$ = 295 K. The structure was solved and the data reduced using the SHELX-93 program package. Hydrogen atoms were included at calculated positions with fixed isotropic thermal parameters ($U_H$ = 0.049 Å$^2$); $2\theta$ < 56°; 5100 unique reflections; 3732 observed reflections with $I > 3\sigma(I)$; number of the refined parameters 596; $R$ = 0.059 ($R_w$ = 0.081). The chlorine atoms of the $FeCl_4^-$ anion are disordered as can be judged from their large thermal displaced parameters ($U_{Cl}$ = 0.115 Å$^2$). CCDC 182/556.

¶ **3**: UV–VIS [$CHCl_3$, $\lambda_{max}$/nm ($\varepsilon$/dm$^3$ mol$^{-1}$ cm$^{-1}$)]: 420 (2960), 470(2715), 770(205)(sh). $^1$H NMR ($\delta$, 300 K): 10.2 (*m*-H, 4 H), 5.7 (*p*-H, 2 H) 2.7 (*o*-H 4 H), 1.4 (CH=N, 2 H), −0.55 ($CH_3$, 6 H) in $CDCl_3$; 9.8 (*m*-H), 6.4 (*p*-H), 3.4 (br), 2.7 (br), −0.5 ($CH_3$) in $CD_3CN$; 10.2 (*m*-H), 5.8 (*p*-H), 2.4 (br, CH=N, *o*-H) in $(CD_3)_2SO$; 8.65 (*m*-H), 6.25 (*p*-H) and 4.0 (br) in $(CD_3)_2SO$–[$^2H_5$]pyridine (1 : 1). Owing to poor solubility, it was possible to determine $\mu_{eff}$ for **3** by the Evans method only in $(CD_3)_2SO$ (2.04 $\mu_B$).

1 D. H. Flint and R. M. Allen, *Chem. Rev.*, 1996, **96**, 2315.
2 H. Beinert, M. C. Kennedy and C. D. Stout, *Chem. Rev.*, 1996, **96**, 2335.
3 (*a*) Y. Sugiura, J. Kuwahara, T. Nagasawa and H. Yamada, *J. Am. Chem. Soc.*, 1987, **109**, 5848; (*b*) M. J. Nelson, H. Jin, I. M. Turner, Jr., G. Grove, R. C. Scarrow, B. A. Brennan and L. Que, Jr., *J. Am.Chem. Soc.*, 1991, **113**, 7072; (*c*) H. Jin, I. M. Turner, Jr., M. J. Nelson, R. J. Gurbiel, P. E. Doan and B. M. Hoffman, *J. Am. Chem. Soc.*, 1993, **115**, 5290; (*d*) B. A. Brennan, J. G. Cummings, D. B. Chase, I. M. Turner and M. J. Nelson, *Biochemistry*, 1996, **35**, 10 068; (*e*) R. C. Scarrow, B. A. Brennan, J. G. Cummings, H. Jim, D. J. Duong, J. T. Kindt and M. J. Nelson, *Biochemistry*, 1996, **35**, 10 078.
4 (*a*) G. Fallon and B. M. Gatehouse, *J. Chem. Soc., Dalton Trans.*, 1975, 1344; (*b*) P. J. Marini, K. S. Murray and B. O. West, *J. Chem. Soc., Dalton Trans.*, 1983, 143; (*c*) T. Beissel, K. S. Bürger, G. Voigt, K. Weighardt, C. Butzlaff and A. X. Trautwein, *Inorg. Chem.*, 1993, **32**, 124; (*d*) S. C. Shoner, D. Barnhart and J. A. Kovacs, *Inorg. Chem.*, 1995, **34**, 4517; (*e*) N. Govindaswamy, D. A. Quarless, Jr. and S. A. Koch, *J. Am. Chem. Soc.*, 1995, **117**, 8468.
5 A. L. Nivorozhkin, G. I. Bondarenko, V. I. Nevodchikov, A. I. Uraev, I. S. Vasilchenko, A. S. Antsyshkina, L. E. Nivorozhkin, A. D. Garnovskii, in *Abstracts of the European Inorganic Chemistry Research Seminars, EICS-VI, Biocoordination Chemistry, Inorganic Compounds with Framework Structures*, Karrebaeksminde, Denmark, 1996, p. 64.
6 Yields 60–70%. Correct microanalyses. The ligands were prepared following literature procedures, A. I. Uraev and A. D. Garnovskii, *Russ. J. Koord. Khim.*, 1997, submitted; A. L. Nivorozhkin, H. Toftlund and M. Nielsen, *J. Chem. Soc., Dalton Trans.*, 1994, 361.
7 (*a*) S. Koch, S. C. Tang, R. H. Holm and R. B. Frankel, *J. Am. Chem. Soc.*, 1975, **97**, 914; (*b*) N. N. Greenwood and T. G. Gibb, *Mössbauer Spectroscopy*, Chapman & Hall, London, 1971, p. 154.
8 M. Gerloch and F. E. Mabbs, *J. Chem. Soc. A*, 1967, 1900.
9 (*a*) M. M. Maltempo, *J. Chem. Phys.*, 1974, **61**, 2540; (*b*) C. A. Reed, T. Mashiko, S. P. Bentley, M. E. Kastner, W. R. Sheidt, K. Spartalian and G. Lang, *J. Am. Chem. Soc.*, 1979, **101**, 2948; (*c*) W. R. Scheidt and C. A. Reed, *Chem. Rev.*, 1981, **81**, 543.
10 J. P. Fitzgerald, B. S. Haggerty, A. L. Rheingold, L. May and G. A. Brewer, *Inorg. Chem.*, 1992, **31**, 2067.
11 No synthetic iron–sulfur complexes able to hydrolyze nitriles are, as yet, reported. See for example, a recent review: R. A. Michelin, M. Mozzon and R. Bertani, *Coord. Chem. Rev.*, 1996, **147**, 299.

*Received in Bloomington, IN, USA; 8th July 1997; 7/04879C*

# Chemoenzymatic synthesis of a novel ligand for rhodium-catalysed asymmetric hydrogenation

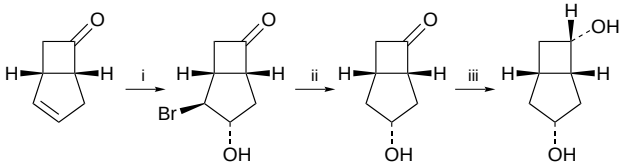
**Brian Adger,[a] Ulrich Berens,[a] Matthew J. Griffiths,[b] Michael J.Kelly,[c] Ray McCague,[a] John A. Miller,[c] Christopher F. Palmer,[a] Stanley M. Roberts,*[b] Rüdiger Selke,[d] Ute Vitinius[b] and Guy Ward[c]**

[a] *Chiroscience plc, Cambridge, UK CB4 4WE*
[b] *Department of Chemistry, University of Liverpool, Liverpool, UK L69 7ZD*
[c] *Department of Chemistry, University of Exeter, Exeter, UK EX4 4QD*
[d] *Max Planck-Gesellschaft Zur Förderung der Wissenschaften e.v., University of Rostock, D-18055 Rostock, Germany*

**The hydrogenation of alkenes 7a–g using a chiral rhodium catalyst 6 (based on a bicyclo[3.2.0]heptane framework) takes place to give the phenylalanine derivatives 8a–g with remarkably high stereoselectivity (59–92% ee).**

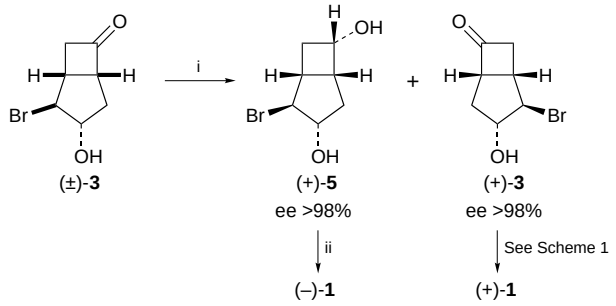
The relatively inflexible, angular shape of the bicyclo[3.2.0]heptane ring system means those substituents on the concave (*endo*) face of the molecule are positioned close together in space. Molecular modelling studies suggested that the hydroxy groups in bicyclo[3.2.0]heptan-3-*endo*, 6-*endo*-diol would be positioned in such a way that derivitization to form bis(diarylphosphinyl) groups may provide a novel chiral ligand for organorhodium-catalysed hydrogenation reactions.[1]

Optically pure diol **1** may be prepared from (−)-bicyclo[3.2.0]hept-2-en-6-one[2] **2** by the route described in Scheme 1. Thus, formation of the bromohydrin[3] **3**, hydrodebromination (furnishing **4**) and stereocontrolled reduction by delivery of hydride ion from the more exposed *exo*-face afforded the diol **1** in 50% overall yield.




**Scheme 1** *Reagents and conditions*: i, *N*-Bromosuccinimide, acetone, $H_2O$, 6 h, 80%; ii, $Bu_3SnH$, AIBN, toluene, heat, 82%; iii, $NaBH_4$, MeOH, −78 °C, 76%

However, since both enantiomers of the diol **1** were required as intermediates to the chiral ligands it seemed more sensible to perform a kinetic resolution further along the synthetic sequence. Kinetic resolution of the racemic alcohols **1** and **4** using lipase-catalysed acylation reactions were unsuccessful. The bromohydrin (±)-**3** was resolved by employing *Pseudomonas fluorescens* lipase in vinyl acetate[4] but a more satisfactory




**Scheme 2** *Reagents and conditions*: i, Yeast, $H_2O$, 6 h, 100% crude yield; ii, $Bu_3SnH$, AIBN, toluene, heat, 86%

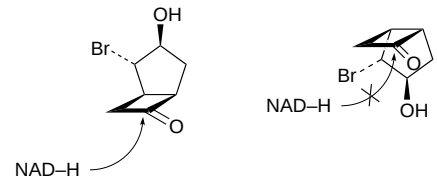


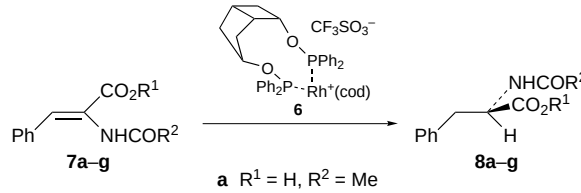
**Fig. 1** Delivery of hydride to **3**

and efficient biocatalytic method utilised a yeast-catalysed highly enantio- and stereo-selective reduction of racemic ketone **3** (Scheme 2).

It is noteworthy that reduction takes place to give only the (6*S*)-bromodiol **5**, unlike the corresponding non-enantioselective bioreduction on the parent compound **2** which gave (1*S*,5*R*,6*S*)-bicyclo[3.2.0]hept-2-en-6-*endo*-ol and (1*R*,5*S*,6*S*)-bicyclo[3.2.0]hept-2-en-6-*exo*-ol in almost equal quantities.[5] Presumably delivery of the hydride ion from the concave face of (+)-**3** is prohibited by unfavourable steric interactions within the active site of the dehydrogenase (Fig. 1).

The diol (−)-**1** was converted into the rhodium complex **6** using standard methodology, and this complex was used to catalyse the asymmetric hydrogenation of compounds **7a–g** to afford the (*R*)-phenylalanine derivatives **8a–g** in excellent yield and moderate to good enantiomeric excess (Table 1). Indeed,

**Table 1** Asymmetric hydrogenation of some enamide esters, **7a–g**




**a** $R^1$ = H, $R^2$ = Me
**b** $R^1$ = $R^2$ = Me
**c** $R^1$ = H, $R^2$ = Ph
**d** $R^1$ = Me, $R^2$ = Ph
**e** $R^1$ = Pr$^i$, $R^2$ = Ph
**f** $R^1$ = Bu$^t$, $R^2$ = Ph
**g** $R^1$ = Pr$^i$, $R^2$ = Me

| Starting material | Product | Enantiomeric excess[a] (%) | Yield (%) |
|---|---|---|---|
| **7a** | **8a** | 81 | > 95 |
| **7b** | **8b** | 73 | > 95 |
| **7c** | **8c** | 76 | > 95 |
| **7d** | **8d** | 59 | > 95 |
| **7e** | **8e** | 61 | > 95 |
| **7f** | **8f** | 66 | > 95 |
| **7g** | **8g** | 77 | > 95 |

[a] Estimation by HPLC using a Chirasil-Val column.

**Table 2** Asymmetric hydrogenation of enamide ester **7a**

| *T*/°C | Volume of solvent/ml | Enantiomeric excess of product (%) |
|---|---|---|
| 25 | 15 | 81 |
| 12 | 15 | 83.5 |
| 2 | 15 | 87.5 |
| 25 | 10 | 88 |
| 25 | 5 | 91.5 |
| 2 | 5 | 92.5 |

given the subtlety of the chirality of the bicyclo[3.2.0]heptane framework, the observed level of enantioselectivity is surprisingly high. The reaction rates were perfectly satisfactory (the reaction was completed in 2–10 min) using 1 mmol substrate and 0.01 mmol catalyst in MeOH (15 ml) under an atmosphere of hydrogen. Using similar conditions, itaconic acid was reduced to (2*S*)-methylsuccinate in quantitative yield and 80.5% ee.

The reaction conditions for the asymmetric reduction of substrate **7a** were investigated further. Lowering the temperature of the reaction and increasing the concentration of the reactants both proved to be beneficial, with a satisfactory 92.5% ee for product **8a** being obtained at low temperature and high concentration (Table 2).† The concentration effect may be explained by the effect on the rate of delivery of hydrogen to the catalyst, which will be slower in the reactions using small amounts of solvent. Thus, in the more concentrated solution the catalyst may experience a lower 'effective' hydrogen concentration.[6]

We thank the BBSRC for a Fellowship (to U. V.) and a CASE award (to M. J. G.), Chiroscience, and EPSRC and the University of Exeter for studentships (to J. M. and G. W.) and Donna Blackmond for enlightening discussions.

## Footnotes and References

* E-mail: sj11@liverpool.ac.uk

† Experimental procedure for the asymmetric hydrogenation of compound **7a**. A mixture of complex **6** (8 mg, 0.01 mmol) and α-acetamidocinnamic acid **7a** (205 mg, 1 mmol) was cooled (2 °C) under a nitrogen atmosphere. Dry, degassed MeOH (5 ml) was added to the mixture, which was stirred vigorously. The flask was evacuated, filled with hydrogen and stirred for 10 min. A 0.5 ml aliquot was removed from the reaction vessel and treated with $Me_3SiCHN_2$ (2.0 M solution in hexane) in order to convert the acid to the methyl ester. The solvent was evaporated and the residue was treated with diethyl ether; filtration and evaporation gave a crude residue (21 mg). The enantiomeric excess of the product **8a** was determined to be 92.5% by chiral gas chromatography, using a Chirasil-Val-III column.

1 Review: R. Noyori, *Asymmetric Catalysts in Organic Systhesis*, Wiley, New York, 1994, ch. 2; recent publications: G. Zhu, P. Cao, Q. Jiang and X. Zhang, *J. Am. Chem. Soc.*, 1997, **119**, 1799; R. Selke, M. Ohff and A. Riepe, *Tetrahedron*, 1996, **52**, 15079; M. J. Burk, Y. M. Wang and J. R. Lee, *J. Am. Chem. Soc.*, 1996, **118**, 5142; H.-J. Kreuzfeld, U. Schmidt, C. Döbler and H. W. Krause, *Tetrahedron: Asymmetry*, 1996, **7**, 1011; C. Dobler, H.-J. Kreuzfeld, M. Michalik and H. W. Krause, *Tetrahedron: Asymmetry*, 1996, **7**, 117; J. Albrechy and U. Nagel, *Angew. Chem., Int. Ed. Engl.*, 1996, **35**, 407.

2 K. Tanaka, O. Kakinoki and F. Toda, *Tetrahedron: Asymmetry*, 1992, **3**, 517.

3 Z. Grudzinski and S. M. Roberts, *J. Chem. Soc., Perkin Trans. 1*, 1975, 1767.

4 For enzymatic resolution of related bromohydrins, see I. C. Cotterill, A. G. Sutherland, S. M. Roberts, R. Grobbauer, J. Spreitz and K. Faber, *J. Chem. Soc., Perkin Trans. 1*, 1991, 1365; I. C. Cotterill and S. M. Roberts, *J. Chem. Soc., Perkin Trans. 1*, 1992, 2585.

5 R. F. Newton, J. Paton, D. P. Reynolds, S. Young and S. M. Roberts, *J. Chem. Soc., Chem. Commun.*, 1979, 908; J. Davies, S. M. Roberts, D. P. Reynolds and R. F. Newton, *J. Chem. Soc., Perkin Trans. 1*, 1981, 1317; See also G. Fantin, M. Fogagnolo, A. Medici, P. Pedrini, E. Marotta, M. Monti and R. Righi, *Tetrahedron: Asymmetry*, 1996, **7**, 277.

6 Y. Sun, R. N. Landau,J. Wang, C. LeBlond and D. G. Blackmond, *J. Am. Chem. Soc.*, 1996, **118**, 1348.

*Received in Cambridge, UK, 13th June 1997; 7/04136E*

# $[\{Mo^{VI}_8V^{IV}_4O_{36}(V^{V}O_4)(V^{IV}O)_2\}_n]^{7n-}$: capped α-Keggin fragments linked to a chain

**Achim Müller,* Michael Koop, Peter Schiffels and Hartmut Bögge**

*Fakultät für Chemie der Universität, D-33501 Bielefeld, Germany*

**The synthesis and single-crystal X-ray structure analysis of the unusual Mo/V polyoxometalate compound $Na_{0.5}K_{6.5}[Mo^{VI}_8V^{IV}_4O_{36}(V^{V}O_4)(V^{IV}O)_2]\cdot12.5H_2O$ which contains capped α-Keggin fragments linked to a chain is reported; this chain is an interesting object for magnetochemists and can be considered to consist of an assembly of electron storage units.**

Despite their ability to act as ligands, polyoxometalate clusters are generally reported as discrete entities, for instance as Keggin type anions or their derivatives.[1,2] Very few examples are known where polymers are built up (like chains) for instance by linking anionic polyoxometalate ligands with transition-metal centres[3–5] as in the case of $[\{(Co^{II}(H_2O)_4)_2(H_2W_{12}O_{42})\}_n]^{6n-}$. Only one compound has been reported in which a derivative of a lacunary $\{W_{11}\}$ type species (that means with an integrated low-valent metal atom) was linked to a chain,[6] but until now, no corresponding compound has been isolated in which chains are built up by a classical polyanion containing metal centres from only group 5 and 6. Here we report the synthesis and single-crystal X-ray structure analysis of the blue–violet mixed valent polyoxometalate compound $Na_{0.5}K_{6.5}[Mo^{VI}_8V^{IV}_4O_{36}(V^{V}O_4)(V^{IV}O)_2]\cdot12.5\ H_2O$ **1** containing capped, reduced α-Keggin type fragments which are linked to a chain.

Compound **1** was prepared by heating a solution of $VOCl_2$ (10 mmol), $Na_2MoO_4\cdot2H_2O$ (20 mmol) and KCl (93.9 mmol) in 60 ml degassed water (pH 6.2) for 5 days at 45–50 °C in an argon atmosphere. Blue–violet crystals of **1** which precipitated from the solution at 45 °C (46% yield based on Mo) were filtered and characterized by a single-crystal X-ray structure analysis (including bond valence sum calculations),† vibrational spectra‡ and redox titrations for the determination of the number of $V^{IV}$ centres. Compound **1** rapidly decomposes in solution in the presence of air, whereby a yellow colour is observed.

The crystal structure of **1** shows the abundance of chains built up by '*trans*-vanadium' capped α-Keggin type $\{Mo^{VI}_8V^{IV}_4O_{36}(V^{V}O_4)(V^{IV}O)_2\}$ units [Fig. 1(*a*)]. These are structurally similar to the two $\{Mo_8V_7O_{42}\}$ units which build up the discrete $[Mo^{VI}_{16}V^{IV}_{12}V^{V}_2O_{84}]^{14-}$ anion.[7] The structure of the basic (anionic) unit of **1** [Fig. 1(*b*)] can be described as follows: four $Mo^{VI}$ centres of an α-Keggin type $[Mo^{VI}_{12}O_{36}(V^{V}O_4)]^{3-}$ species are replaced by $V^{IV}$ centres resulting in a 'layered' type structure formed by the different metal atoms. The corresponding three layers are spanned by one $\{V_5\}$ set and two $\{Mo_4\}$ type sets, the latter being separated by 4.8 Å [Fig. 1(*a*)]. The $V^{IV}\cdots V^{V}$ distance between atoms within each layer is 5.1 Å and *ca.* 11 Å between layers in adjoining units. Therefore the compound is interesting for the study of exchange interactions by the magnetochemist. The rhombicuboctahedron spanned by 24 $\mu_3$-O atoms of the Keggin unit is capped at two parallel (100) planes by 2 $\{V^{IV}O\}$ [V(3)] groups (for details of the relevant topology see ref. 8). If all of the six equivalent planes were capped, a unit with a similar structure to the $\{V_{12}O_{36}(VO_4)(VO)_6\}$ type species[9] would result. Whereas the $Mo^{VI}$ and $V^{IV}$ centres Mo(1), Mo(2) and V(1) have, as expected, rather regular octahedral coordination environments, the two V(3) centres [Fig. 1(*b*)] possess a highly distorted octahedral coordination environment, bordering on the distorted trigonal-prismatic geometry described for the above mentioned discrete $[Mo^{VI}_{16}V^{IV}_{12}V^{V}_2O_{84}]^{14-}$ anion.[7] The Keggin fragments are linked by V(3)–O(11)$_2$–V(3) bridges forming chains along the *c* axis [V(3)–O(11) 1.88(1) Å; separation of adjacent V(3) centres 2.81(1) Å].

The formation of **1** is facilitated by the direct use of a solution containing $VO^{2+}$ ions. The relevant reaction using $V^{V}$ centres under similar reaction conditions at pH 4–6.5 yields the discrete $[Mo^{VI}_6V^{V}_2O_{26}(H_2O)_{16}]^{6-}$ anion.[10,11] In a previous investigation of the $V^{IV}/Mo^{VI}$ system[12,13] it was erroneously proposed that such solutions with relative concentration $Mo^{VI}/V^{IV} = 2$ yielded the salts $K_4H_2[V_2Mo_4O_{19}]\cdot9H_2O$ at pH 4.5 and $K_2H_4[V_2Mo_4O_{19}]$ at pH 3, whereby the authors assumed that these would contain Lindquist type anions. One can envisage the formation of the obtained chains *via* the initial formation of highly nucleophilic species such as $\{Mo^{VI}_8V_4{}^{IV}O_{36}(V^{V}O_4)\}^{11-}$ {whose structure may be analogous to the discrete $[Mo^{VI}_8V^{V}_4O_{40}(VO_4)]^{7-}$ anions[14]} and the subsequent interception of these by the $VO^{2+}$ nucleophiles present in solution. This deliberation corresponds to our general procedure to generate growth of species by increasing their negative charge and consequently their nucleophilicity, a procedure which facilitates the generation of increasingly larger molecular systems. In the

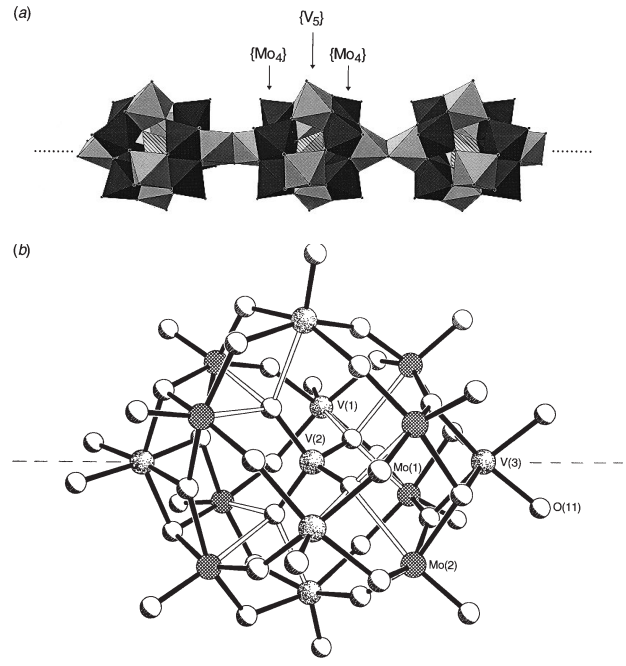



**Fig. 1** The structure of the polymeric anion in crystals of **1**: (*a*) polyhedral representation (darker polyhedra represent $Mo^{VI}O_6$ octahedra, hatched ones the $V^{V}O_4$ tetrahedra). The $Mo^{VI}$ and $V^{IV}$ atoms of the relevant polyhedra span $\{Mo^{VI}_4\}$ and $\{V^{IV}_4\}$ layers. (*b*) Ball-and-stick representation of the capped α-Keggin type unit with stoichiometry $\{Mo^{VI}_8V^{IV}_4O_{36}(V^{V}O_4)(V^{IV}O)_2\}$; V atoms dotted, Mo atoms cross hatched; V(2)–O 1.71(1) Å, V(3)–O(11) 1.88(1) Å, V(3)···V(3) 2.81(1) Å; O(11)–V(3)–O(11) 83.0(5)°.

present case, the increased nucleophilicity results from the simple replacement of metal centres with a high oxidation state ($Mo^{VI}$) by those with a lower one ($V^{IV}$). Groups containing the $V^{IV}$ centres are directly added to the reaction medium which is in contrast to an earlier investigation[15] where a solution containing $Mo^{VI}$ and $V^{V}$ centres was treated with a reducing agent, thus resulting in the reduction of the $V^{V}$, but also some of the $Mo^{VI}$. Additionally, it is important to note that in the present case, linking *via* $V^{IV}$–O–$V^{IV}$ bonds is preferred to linking *via* $Mo^{VI}$–O–$Mo^{VI}$ bonds as a consequence of the expected higher basicity of the O atom in M–O bonds containing M centres in lower oxidation states.

We thank Dr S. Dillinger, T. Heitkamp, K. Janiak and E. Krickemeyer for earlier contributions to the work and the Deutsche Forschungsgemeinschaft as well as the Fonds der Chemischen Industrie for their financial support.

## Footnotes and References

* E-mail: amueller@cheops.chemie.uni-bielefeld.de

† *Crystal data* for **1**: $H_{25}K_{6.5}Mo_8Na_{0.5}O_{54.5}V_7$, $M$ = 2286.95 g mol$^{-1}$, tetragonal, space group $I4/m$, $a$ = 14.941(2), $c$ = 22.124(5) Å, $U$ = 4938.8(15) Å$^3$, $D_c$ = 3.076 g cm$^{-3}$, $\mu$(Mo-Kα) = 3.89 mm$^{-1}$, $Z$ = 4, $T$ = 198 K, $R$ = 0.052 for 1428 reflections with $I_0 \geqslant 2\sigma(I_0)$, crystal dimensions: 0.1 × 0.1 × 0.2 mm; Siemens R3m/V diffractometer (Mo-Kα, graphite monochromator). A total of 2503 reflections were collected ($4 < 2\theta < 50°$). The structure was solved by direct methods[16] and refined[16] by full-matrix least-squares techniques. In the asymmetric unit two under-occupied sodium positions were found each at a distance of *ca*. 1.8 Å from two (also underoccupied) potassium positions. The occupancy factors of the disordered atoms were refined in agreement with the above given formula. $\Psi$-scan reflections for an empirical absorption correction were collected. As the absorption correction showed no significant effect, however, the uncorrected data were used in the final refinement process. The bond valence sum calculations indicate, as expected, the presence of only $Mo^{VI}$ and $V^{IV}$ centres in the shell, as well as one central $V^{V}$ atom. CCDC 182/547.

‡ *Characteristic spectroscopic data* for **1**: IR, $\nu$/cm$^{-1}$ (KBr pellet prepared under argon, 1100–400 cm$^{-1}$): $\nu$(V=O)/$\nu$(Mo=O) 976m, 952m; $\nu_{as}$(M–O–M′; M, M′ = Mo, V) 848s, 815m, 754m; Raman ($\lambda_e$ = 1064 nm): $\nu$(V=O)/$\nu$(Mo=O) 989w, 817s; VIS–NIR, $\lambda_{max}$ (KBr pellet): *ca.* 575 nm.

1 M. Pope and A. Müller, *Angew. Chem., Int. Ed. Engl.*, 1991, **30**, 34.
2 M. Pope, *Heteropoly and Isopoly Oxometalates, Inorganic Chemistry Concepts*, Springer, Berlin, 1983, vol. 8.
3 V. Molchanov, I. Tatjanina and E. Torchenkova, *J. Chem. Soc., Chem. Commun.*, 1981, 93.
4 T. Yamase and H. Naruke, *J. Chem. Soc. Dalton Trans.*, 1991, 285.
5 C. Giménez-Saiz, J. Galán-Mascarós, S. Triki, E. Coronado and L. Ouahab, *Inorg. Chem.*, 1995, **34**, 524.
6 J. Galán-Mascarós, C. Giménez-Saiz, S. Triki, C. Gómez-García, E. Coronado and L. Ouahab, *Angew. Chem., Int., Ed. Engl.*, 1995, **34**, 1460.
7 Y. Zhang, R. Haushalter and A. Clearfield, *J. Chem. Soc., Chem. Commun.*, 1995, 1149.
8 A. Müller, M. Penk and J. Döring, *Inorg. Chem.*, 1991, **30**, 4935.
9 A. Müller, J. Döring, H. Bögge and E. Krickemeyer, *Chimia*, 1988, **42**, 300.
10 A. Björnberg, *Acta Crystallogr., Sect. B*, 1979, **35**, 1995.
11 A. Bekturov, A. II'yasova and A. Amirbekova, *Zh. Neorg. Khim.*, 1970, **15**, 2781; *Russ. J. Inorg. Chem.*, 1970, **15**, 1446.
12 D. Labonnette and S. Ostrowetsky, *C. R. Acad. Sci. Ser. C*, 1976, **282**, 341.
13 D. Labonnette, *J. Chem. Res.*, 1979, (*S*) 252; (*M*) 2801.
14 A. Björnberg, *Acta Crystallogr., Sect. B*, 1980, **36**, 1530.
15 E. Krickemeyer, S. Dillinger, T. Heitkamp and K. Janiak, unpublished work.
16 SHELXS-86 and SHELXS-93, Programs for crystal structure solution and refinement, respectively, G. M. Sheldrick, University of Göttingen.

*Received in Basel, Switzerland, 2nd May 1997; 7/03036C*

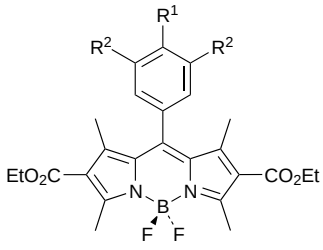
# Phenol/phenolate-dependent on/off switching of the luminescence of 4,4-difluoro-4-bora-3a,4a-diaza-*s*-indacenes

**Thomas Gareis,[a] Christian Huber,[b] Otto S. Wolfbeis*[b]† and Joerg Daub*[a]‡**

[a] *Institut für Organische Chemie der Universität Regensburg, Universitaetsstraße 31, D-93040 Regensburg, Germany*
[b] *Institut für Analytische Chemie, Chemo- and Biosensorik, Universitaetsstraße 31, D-93040 Regensburg, Germany*

**Boradiazaindacenes 1 and 2 bearing phenolic subunits show deprotonation/protonation dependent fluorescence off/on-switching; the lack of emission of the phenolate forms is attributed to photoinduced electron transfer (PET) between the phenolate and indacene subunits.**

There is still considerable need for novel molecular probes for fluorescent analysis and materials science chemistry. Difluoroboryldipyrromethene complexes are of high interest as fluorophores due to their favourable photophysical and opto-electronic properties.[1] Whilst the work on their syntheses,[2] photophysical properties[3] and application as fluorophoric probes is well established, their potential for sensing by optoelectronic switching has been only partially explored. Previously, we have demonstrated that reversible redox activation of boradiazaindacenes gives rise to efficient electrochemically generated luminescence[4,5a] (ECL). By using a non-fluorescent dimethylaminophenyl derivative, it could be shown that strong emission occurs on protonation.[5] The present study is directed towards shifting the on/off switching of luminescence to higher pH. Therefore, the phenol/phenolate couples **1** and **2** have been investigated.




**1** $R^1$ = OH, $R^2$ = H
**2** $R^1$ = OH, $R^2$ = $Bu^t$
**3** $R^1$ = $R^2$ = H

We synthesized the phenolic dyes **1** and **2**[4] according to previously applied procedure.[2] Owing to the presence of methyl groups at positions C-1 and C-7, the phenyl and boraindacene systems are twisted and conjugatively uncoupled. This follows from an X-ray analysis[5a] of a structurally similar compound and from the high-field NMR chemical shift of the methyl protons.[4] Both **1** and **2** are therefore representatives of orthogonal fluorophor–receptor systems.[6] A phenolate is formed by deprotonation, which may exhibit a PET-like quenching mechanism.[7]

The preliminary objective was to study the emissive properties of the phenol/phenolate equilibrium in organic solvents using an organic base for deprotonation. To avoid intermolecular charge transfer quenching, which is often observed in the presence of tertiary amines,[8] we used pyridine as the proton acceptor.

Fig. 1 shows the fluorescence titrations of **1** dissolved in $CHCl_3$ by successive addition of pyridine. The fluorescence signals of **1** and **2** significantly decrease, whereas the wavelength of emission remains unchanged. Reprotonation by addition of trifluoroacetic acid restores fluorescence. Switching between the fluorescent on/off states can be repeated without decomposition or formation of precipitates. To prove that the observed decrease in fluorescence intensity is due to the phenolic properties of **1** and **2**, the same titration experiments were performed with 8-phenylboradiazaindacene **3**.[2c] No base-dependent response could be observed. By fluorescence titration experiments in a MeOH–$H_2O$ mixture[9] (1 : 1), the p$K_a$ value of compound **1** was determined to be 10.4 ± 0.5 (see Fig. 2) which indicates the decoupling of the subunits.

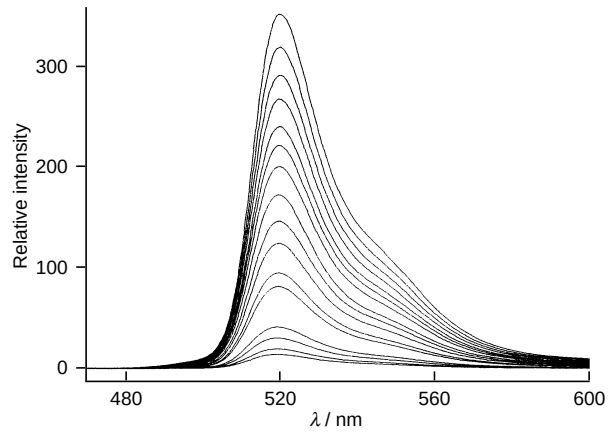



**Fig. 1** Decrease of fluorescence intensity during tiration of **1** on successive addition of pyridine (2.7 ml of dye; $2.1 \times 10^{-5}$ mol $l^{-1}$ in $CHCl_3$, excitation at 500 nm, end concentration of pyridine: $3.2 \times 10^{-1}$ mol $l^{-1}$)

The determination of p$K_a$ values for **2** failed due to its poor solubility in the aqueous solvent mixture. Compounds **1** and **2** also have been embedded into a hydrogel matrix, according to a previously published procedure,[9] with the aim of obtaining a material for use in sensors. Membranes were tested in a home-

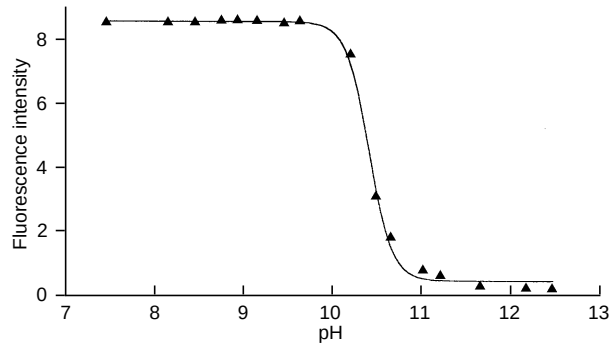



**Fig. 2** Fluorescence intensity–pH profiles of **1** (p$K_a$ 10.4) in a MeOH–$H_2O$ (1 : 1): (▲) measured values, (—) sigmoidal fit; ionic strength of 150 mmol $l^{-1}$ (NaCl) (dye concentration: $2 \times 10^{-6}$ mol $l^{-1}$; $I_{NaCl}$ = 150 mmol $l^{-1}$; $\lambda_{ex}$ = 490 nm; $\lambda_{em}$ = 506 nm)

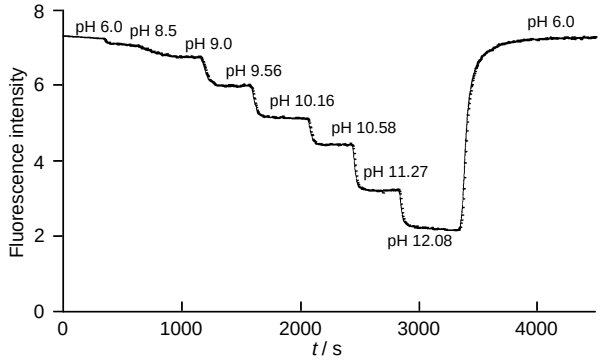



**Fig. 3** Relative signal change, response time and reversibility of **1** incorporated in a hydrogel matrix on exposure to a flow of buffers. The pH values are inserted in the graph. Ionic strength is kept constant at 150 mmol $l^{-1}$ (NaCl); concentration: 39 mmol per kg of matrix.

made flow-through cell with respect to the response of various pH values. To minimize effects of ionic strength, sodium chloride (150 mmol $l^{-1}$) was added. Again, the base form is only weakly fluorescent due to electron transfer from the phenolate group (the receptor) to the indacene fluorophore. The excitation/emission maxima of the membrane for **1** and **2** are at 504/515 nm and 502/508 nm, respectively. However, excitation was performed at 500 nm in order to minimize straylight. Fig. 3 shows the response behaviour and reversibility characteristics of **1** embedded in the matrix. The response times were faster (2 to 3 min) when going to lower pH than in the reverse direction (5 to 8 min).

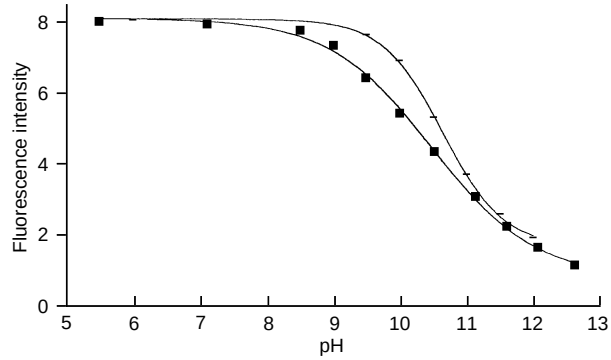



**Fig. 4** pH titration plot of **1** and **2** incorporated in a hydrogel matrix: (■) **1** (p$K_a$ 10.4) and (—) **2** (p$K_a$ 10.8)

The pH titration curves of sensors **1** and **2** exhibit the typical sigmoidal shape and are depicted in Fig. 4. The p$K_a$ values of the two membranes are 10.4 and 10.8, respectively.

## Footnotes and References

† E-mail: otto.wolfbeis@chemie.uni-regensburg.de
‡ E-mail: joerg.daub@chemie.uni-regensburg.de

1 I. D. Johnson, H. C. Kang and R. P. Haughland, *Anal. Biochem.*, 1991, **198**, 228; J. Karolin, L. B.-A. Johansson, L. Strandberg and T. Ny, *J. Am. Chem. Soc.*, 1994, **116**, 7801; T. G. Pavlopoulos, M. Shah and J. H. Boyer, *Apl. Opt.*, 1988, **27**, 4998; O. Driessen and J. Lugtenburg, *J. High Resolut. Chromatogr. Chromatogr. Commun.*, 1980, **3**, 405.
2 (*a*) A. Treibs and F.-H. Kreuzer, *Liebigs Ann. Chem.*, 1968, **718**, 208; (*b*) E. Vos de Wael, J. A. Pardoen, J. A. van Koeveringe and J. Lugtenburg, *Recl. Trav. Chim. Pays Bas*, 1977, **96**, 306; (*c*) H. Falk and G. Schoppel, *Monatsh. Chem.*, 1990, **121**, 67; (*d*) H. J. Wories, J. H. Koek, G. Lodder, J. Lugtenburg, R. Fokkens, O. Driessen and G. R. Mohn, *Recl. Trav. Chim. Pays Bas*, 1985, **104**, 288; (*e*) R. W. Wagner and J. S. Lindsey, *Pure Appl. Chem.*, 1996, **68**, 1373.
3 H. Falk and A. Leodolter, *Monatsh. Chem.*, 1978, **109**, 883; J. Karolin, L. B.-A. Johansson, L. Strandberg and T. Ny, *J. Am. Chem. Soc.*, 1994, **116**, 7801.
4 T. Gareis, Ph.D. Thesis, University of Regensburg, 1997; M. Kollmannsberger, Diploma Thesis, University of Regensburg, 1996.
5 (*a*) M. Kollmannsberger, T. Gareis, S. Heinl, J. Breu and J. Daub, *Angew. Chem.*, 1997, **109**, 1391; *Angew. Chem., Int. Ed. Engl.*, 1997, **36**, 1333; (*b*) T. Werner, C. Huber, S. Heinl, M. Kollmannsberger, J. Daub, O. S. Wolfbeis and Fresenius, *Z. Anal. Chem.*, in the press.
6 R. A. Bissel, A. P. de Silva, H. Q. N. Gunaratne, P. L. M. Lynch, G. E. M. Maguire and K. R. A. Samankumara Sandanayake, *Chem. Soc. Rev.*, 1992, **21**, 187.
7 For an introduction to photo induced electron transfer, see *Photoinduced Electron Transfer Part A-D*, ed. M. A. Fox and M. Chanon, Elsevier, Amsterdam, Oxford, 1988; A. P. de Silva and S. A. da Silva, *J. Chem. Soc., Chem. Commun.*, 1986, 1709; R. Grigg, J. M. Holmes, J. M. Jones and W. D. J. A. Norbert, *J. Chem. Soc., Chem. Commun.*, 1994, 185; J. P. Konopelski, F. Kotzyba-Hibert, J.-M. Lehn, J.-P. Desvergne, F. Fages, A. Castellan and H. Bouas-Laurent, *J. Chem. Soc., Chem. Commun.*, 1985, 433; M. E. Huston, K. W. Haider and A. W. Czarnik, *J. Am. Chem. Soc.*, 1988, **110**, 4460 and references cited therein.
8 Y.-P. Sun, C. Bunker and B. Ma, *J. Am. Chem. Soc.*, 1994, **116**, 9692 and references cited therein.
9 O. S. Wolfbeis, C. Huber and T. Werner, *Solid State Supramolecular Optical Sensors*, Proc. NATO Adv. Res. Workshop, *Chemosensors of Ion and Molecule Recongition*, ed. A. T. Czarnik and J. P. Desvergne, NATO Adv. Sci. Ser., part E, Kluwer, Dordrecht, Boston, London, 1997, in the press.

*Received in Liverpool, UK, 20th May 1997; 7/03536E*

# Synthesis and structure of $KIn(en)_2SnTe_4 \cdot 1.5en$ containing a mixed-metal one-dimensional chain

**Chwanchin Wang and Robert C. Haushalter*†**

*NEC Research Institute, 4 Independence Way, Princeton, NJ 08540, USA*

**The linkage of a coordination compound, *cis*-$[In(en)_2Te_2]$, and a Zintl anion, $[SnTe_4]$, into a one-dimensional chain by sharing Te atoms is observed for the first time in the title compound.**

Two decades ago, attempts to synthesize the low-dimensional transition-metal chalcogenide complexes that incorporated $[ME_4]^{n-}$ (M = transition or post-transition metal; E = S, Se) ligands and ethylenediamine (en) were conducted mainly to study the varied degree of the coordinating ability of the ligands and how these ligands affected the overall structure.[1,2] Based on these studies, it was proposed that these chalcogenide complexes might have low-dimensional structures. Recently, several ternary transition and post-transition metal sulfides and selenides, using, for example, $[As_xE_y]^{n-}$ (E = S, Se) as ligands in the construction of low-dimensional structures, were successfully synthesized, by using solventothermal synthesis, and structurally characterized.[3–5] The non-traditional solventothermal technique has been shown to be an efficient synthetic technique to obtain new materials with unusual structures which are not accessible by using more common synthetic methods. While the research has been mostly concentrated on the ternary sulfides and selenides, the ternary telluride systems are relatively unexplored. In the telluride system, an early study showed that the one-dimensional chain structures can also be built up by the incorporation of the $[ATe_4]^{4-}$ (A = Ge, Sn) building blocks in $K_2HgSnTe_4$, $(NEt_4)_2HgSnTe_4$ and $(PPh_4)InGeTe_4$.[6] The structures of these ternary tellurides are substitutional variants of the one-dimensonal chain compound $NaInTe_2$.[7] During our investigation of the ternary In–Sn–Te system using solventothermal synthesis in ethylenediamine, we have discovered a new compound, $KIn(en)_2SnTe_4 \cdot 1.5en$, which also uses $[SnTe_4]^{4-}$ as a building block to construct a new one-dimensional chain structure.

The telluride $KIn(en)_2SnTe_4 \cdot 1.5en$ was synthesized by mixing 0.3 g of $K_2Te$, SnTe, $In_2Te_3$ and Te in a mole ratio of 1 : 2 : 0.5 : 1.5 with 1 ml of ethylenediamine in an evacuated Pyrex tube (*ca.* 10 ml). The reaction tubes were heated to

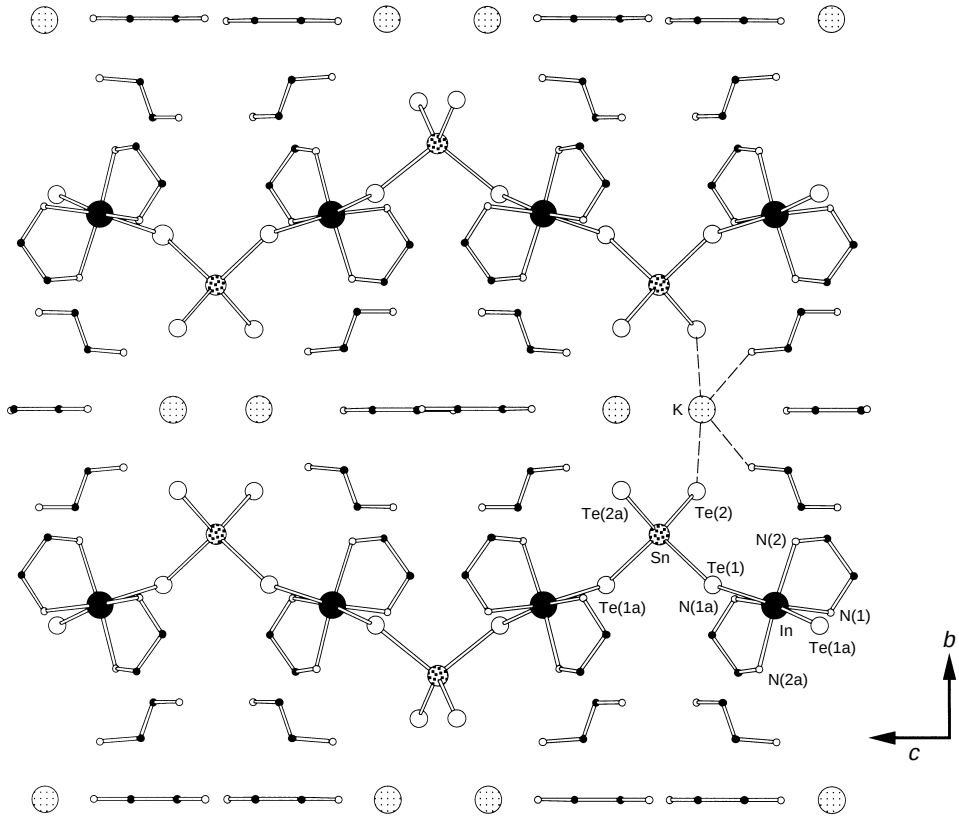



**Fig. 1** One-dimensional chain structure of the $[In(en)_2SnTe_4]^{1-}$ anion approximately projected onto the *bc* plane. The anionic chain consists of a corner-sharing of alternating *cis*-$[In(en)_2Te_2]$ octahedra and $[SnTe_4]$ tetrahedra. The close contacts between the K and both Te and N atoms are shown as dashed lines. Some selected bond distances (Å) and angles (°): Sn–Te(1)/Te(1a), 2.766(2), Sn–Te(2)/Te(2a), 2.691(2), In–Te(1)/Te(1a), 2.827(2), In–N(1)/N(1a), 2.35(1), In–N(2)/N(2a), 2.28(2), Te(1)–Sn–Te(1a), 104.89(9), Te(1)–Sn–Te(2), 110.64(5), Te(1)–Sn–Te(2a), 107.60(5), Te(2)–Sn–Te(2a), 115.0(1), Sn–Te(1)–In, 109.07(5), Te(1)–In–Te(1a), 85.32(7), Te(1)–In–N(1a), 94.2(4), Te(1)–In–N(1), 171.3(4), N(1)–In–N(1a), 87.6(7), N(1)–In–N(2), 75.5(5), N(1)–In–N(2a), 86.2(5), N(2)–In–N(2a), 154.6(8).

150 °C for 12 h and maintained at 150 °C for 3 days followed by cooling to room temp. at a rate of 10 °C $h^{-1}$. Dark red, cube-like crystals of $KIn(en)_2SnTe_4 \cdot 1.5en$ were isolated and separated from by-products in *ca*. 60% yield. Energy dispersive X-ray analysis on selected crystals gave an approximate ratio of 1 : 1 : 1 : 4.3 for K, In, Sn and Te atoms. $KIn(en)_2SnTe_4 \cdot 1.5en$ can also be successfully synthesized by using the extraction method on an alloy with an exact composition of $KInSnTe_4$, prepared from the fusion of KIn, Sn and Te in stoichiometric proportions. One gram of the alloy was extracted by dissolving it in 10 ml of ethylenediamine. After three weeks, $KIn(en)_2SnTe_4 \cdot 1.5en$ was obtained in the container which contained the $KInSnTe_4$ sludge, and the product of the red–brown extract turned out to be only $KInTe_2 \cdot 2en$.[8] These results also demonstrate one of the advantages of solventothermal synthesis in that it can accelerate the reaction toward the product formation.

While $(PPh_4)InGeTe_4$[6] adopts a one-dimensional chain structure which is composed of alternating $[InTe_4]$ and $[GeTe_4]$ tetrahedra, the structure‡ of $KIn(en)_2SnTe_4 \cdot 1.5en$, which is not isostructural with $(PPh_4)InGeTe_4$, is also built up from a one-dimensional chain with alternating $[In(en)_2Te_2]$ octahedra and $[SnTe_4]$ tetrahedra instead (Fig. 1). In the structure of $KIn(en)_2SnTe_4 \cdot 1.5en$, the In atom lies a twofold axis and is coordinated by two ethylenediamine and two Te atoms forming a distorted *cis*-$[In(en)_2Te_2]$ octahedron. The In–Te distances [2.827(2) Å] are comparable to those of the one-dimensional chain compound, $Na_5In_2Te_6$, (2.706–2.853 Å),[9] and are significantly longer than those in $(PPh_4)InGeTe_4$ [2.686(2) Å].[6] In the *cis*-$[In(en)_2Te_2]$ octahedron, the *trans* In–N(2) distances are slightly shorter than the *cis* In–N(1) distances, but neither is very different from those observed in the nitrogen-ligated complexes.[10] The Sn atom lies on a twofold axis and is bound to four Te atoms, forming a slightly distorted $[SnTe_4]$ tetrahedron which shares two Te atoms with the neighboring *cis*-$[In(en)_2Te_2]$ octahedra. The terminal Sn–Te bond distances [2.691(2) Å] are slightly shorter than those of the shared ones [2.766(2) Å] and are close to those observed in dimeric species, $(NMe_4)_4Sn_2Te_6$[11] and $Cs_4Sn_2Te_7$.[12] The *cis*-$[In(en)_2Te_2]$ octahedra and $[SnTe_4]$ tetrahedra then share two Te corners in the construction of the unusual one-dimensional $[In(en)_2SnTe_4]^-$ chain propagating along the *c* axis. There is only one crystallographically unique $K^+$ ion, located near the Te(2) atoms, that has close contact with four terminal Te(2) atoms (3.90–4.00 Å) and two N atoms [2.70(3) Å] from the ethylenediamine. A similar strong interaction between the K and the N atoms has been observed in $(PPh_4)_2[K_2Au_4Te_4(en)_4]$[13] and $K_6In_2Te_6 \cdot 4en$.[14] In Fig. 1, the unbound ethylenediamines are located in a large cavity (*ca*. 12 Å diameter across the $K^+$ ions), created by the surrounding $K^+$ ions, *cis*-$[In(en)_2Te_2]$ octahedra and $[SnTe_4]$ tetrahedra. Although the X-ray crystallography can not discern the difference between In and Sn atoms, the assignment of each atom in a specific position can be empirically confirmed by the use of bond valence sum calculations.[15] The bond valence sum calculation for $In^{3+}$ and $Sn^{4+}$ ions in $KIn(en)_2SnTe_4 \cdot 1.5en$, based on the structure mentioned above, results in the respective sums of 3.16 and 4.09.[16] When the In and Sn atoms are exchanged, the results are 3.62 and 3.53 for $In^{3+}$ and $Sn^{4+}$ ions, respectively. Thus, the results obtained from the bond valence sum calculation favor the assignment of the *cis*-$[In^{3+}(en)_2Te_2]$ octahedron and the $[Sn^{4+}Te_4]$ tetrahedron.

$KIn(en)_2SnTe_4 \cdot 1.5en$ represents the first example using both a Zintl anion, $[SnTe_4]$, and a coordination compound, *cis*-$[In(en)_2Te_2]$, in the construction of a one-dimensional chain compound. Recently, a similar strategy using the *cis*-octahedral units, incorporated with either tetrahedral or octahedral units, in the formation of the heteroatomic one-dimensional chain structures was reported in transition-metal hydroxo-complexes.[17] The investigation on the post-transition metal systems, based on this strategy, may lead to the discovery of new materials with unusual structures and properties.

## Footnotes and References

* E-mail: bobh@symyx.com
† Current address: Symyx Technologies, 3100 Central Expy., Santa Clara, CA 95051, USA.

‡ *Crystal data* for $KIn(en)_2SnTe_4 \cdot 1.5en$: orthorhombic, space group *Cmca* (no. 64), $a$ = 26.069(8), $b$ = 15.278(4), $c$ = 14.972(4) Å, $U$ = 5962(2) $Å^3$, $Z$ = 8, $D_c$ = 2.432 g $cm^{-3}$, $\mu$(Mo-K$\alpha$) = 56.04 $cm^{-1}$. 2922 unique reflections were collected at 273 K of which 1601 had $I \geqslant 3\sigma(I)$. An empirical absorption correction was applied. The structure was solved by direct methods and refined by the teXsan crystallographic software package of Molecular Structure Corporation to a final $R$ = 0.044 ($R_w$ = 0.060). All K, In, Sn and Te atoms were refined anisotropically. The carbon and nitrogen atoms of two ethylenediamines were refined isotropically while those of the third ethylenediamine, located on special positions, were fixed. The hydrogen atoms were calculated but not refined. Although the isotropic thermal parameter of $K^+$ ion is about four times larger than those of Te atoms, the refinement of a disordered model for splitting the $K^+$ ion was unsuccessful. However, the occupancy factor of the $K^+$ ion was refined and is close to unity. CCDC 182/540.

1 M. C. Chakravorti and A. Müller, *Inorg. Nucl. Chem. Lett.*, 1974, **10**, 63.
2 I. Gergen, R. Micu-Semeniuc and I. Haiduc, *Syn. React. Inorg. Met-Org. Chem.*, 1977, **7**, 183.
3 J.-H. Chou and M. G. Kanatzidis, *Inorg. Chem*, 1994, **33**, 1001.
4 J.-H. Chou and M. G. Kanatzidis, *J. Solid State Chem.*, 1996, **127**, 186.
5 J.-H. Chou and M. G. Kanatzidis, *Inorg. Chem.*, 1997, **36**, 4.
6 S. S. Dhingra and R. C. Haushalter, *Chem. Mater.*, 1994, **6**, 2376.
7 E. R. Franke and H. Schäfer, *Z. Naturforsch. Teil B*, 1972, **27**, 1308.
8 Yellow crystals of $KInTe_2 \cdot 2en$ crystallize in the tetragonal space group $P4_2/n$ (no. 86) with cell parameters $a$ = 19.814(7), $c$ = 7.215(3)Å, $U$ = 2832 $Å^3$, $Z$ = 8, and $D_c$ = 3.792 g $cm^{-3}$ with $R$ ($R_w$) = 0.091(0.093).
9 B. Eisenmann, A. Hofmann and R. Zagler, *Z. Naturforsch., Teil B*, 1990, **45**, 8.
10 *Encyclopedia of Inorganic Chemistry*, ed. R. B. King, Wiley, Chichester, 1994, pp. 1513–1531.
11 J. C. Huffman, J. P. Haushalter, A. M. Umarji, G. K. Shenoy and R. C. Haushalter, *Inorg. Chem.*, 1984, **23**, 2312.
12 C. Brinkmann, B. Eisenmann and H. Schäfer, *Mater. Res. Bull.*, 1985, **20**, 299.
13 R. C. Haushalter, *Angew. Chem., Int. Ed. Engl.*, 1985, **24**, 432.
14 C. Wang and R. C. Haushalter, *Inorg. Chem.*, in the press.
15 I. D. Brown and D. Altermatt, *Acta Crystallogr., Sect. B*, 1985, **41**, 244.
16 Supplementary material available upon request from the authors.
17 F. Rominger and U. Thewalt, *Z. Naturforsch., Teil B*, 1996, **51**, 1716.

*Received in Cambridge, UK, 23rd May 1997; 7/03585C*

# Synthesis and novel structure of the first crystallographically characterised chiral α-amino lithium alkoxide

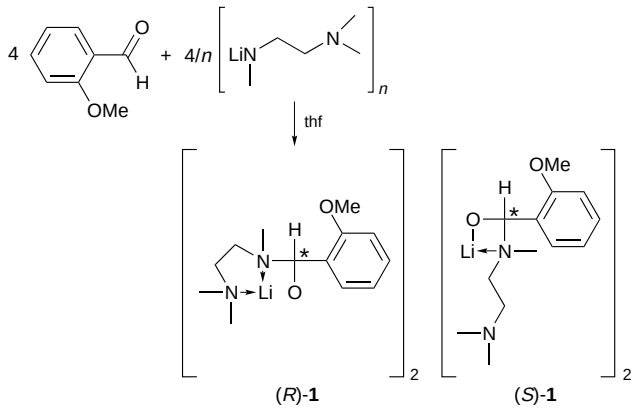
**John E. Davies, Paul R. Raithby, Ronald Snaith and Andrew E. H. Wheatley***

*Department of Chemistry, University of Cambridge, Lensfield Road, Cambridge, UK CB2 1EW*

**Lithium *N,N,N′*-trimethylethylenediamide, LiN(Me)$(CH_2)_2$NMe$_2$, reacts with *o*-anisaldehyde, *o*-MeOC$_6$H$_4$CHO, to afford a chiral α-amino lithium alkoxide 1, which in the solid state is a racemic tetramer with an 'open' pseudo-cubane core; the extent to which the *N,N,N′*-trimethylethylenediamido moieties internally solvate the Li centres varies with the chirality of the protected aldehyde groups.**

Directed metallations of aromatic systems have been the subject of intensive research.[1] In particular, various carbonyl-derived directing groups have been applied to the problem of regiospecifically metallating arylaldehydes.[2] It has been reported that *in situ* protection of benzaldehyde derivatives[2,3] and heterocyclic arylaldehydes[4] *via* reaction with lithium dialkylamides, so giving α-amino lithium alkoxides, can be followed by ring lithiation, affording a convenient one-pot route to *ortho*-substituted arylaldehydes. Typically, a lithium dialkylamide is reacted with 1 equiv. of arylaldehyde (see, *e.g.* Scheme 1), yielding the corresponding chiral α-amino lithium alkoxide which is capable not only of protecting the formyl functionality but also of directing subsequent lithiation, in the presence of excess Bu$^n$Li, to the *o*-ring position. It is surprising that the nature of chiral lithiated intermediates in general has gone largely unexplored, with only a few examples of solution studies,[5] solid-state structures[5a,b] and theoretical investigations reported.[6] It is this scarcity of data which prompted us to investigate chiral α-amino lithium alkoxides, in order to establish precisely how the Lewis-base N-centres of the added amino moieties might stabilise the metal centres and, thereby, how subsequent lithiation might be directed.

We report here the isolation and structural characterisation of the first lithium α-amino alkoxide, **1**. It is obtained by the 1 : 1 reaction of *o*-anisaldehyde with *in situ* generated lithium *N,N,N′*-trimethylethylenediamide in thf† at −78 °C (Scheme 1). Warming affords a yellow solution, the storage of which at room temp. for 24 h yields colourless crystals of **1**. X-Ray crystallography‡ shows that in the solid state **1** is a novel tetramer based on an 'open' pseudo-cubane core (Fig. 1). The molecule sits on a crystallographic twofold axis which passes through the Li(1)O(2)Li(1A)O(2A) and Li(2)O(4)Li(2A)O(4A) planes of the cube. The Li centres each demonstrate fourfold coordination, although the fashion in which this is achieved is linked to the chirality of the protected aldehyde carbon. The observed exclusion of thf from the product is due to intramolecular stabilisation of the metal centres. This could occur *via* coordination by the α-N- or the δ-N-centres, or by both. Although there are several examples of intact $(LiO)_4$ pseudo-cubanes demonstrating intramonomer N-stabilisation[5a,b,10,11] of the metal centres, including two diastereomeric aggregates,[5a,b] it is nevertheless intriguing that in **1** the amino moieties are mono- or bis-chelating depending upon whether they are associated with (*S*)- or (*R*)-ligands, respectively. Opening of one end of the pseudo-cubane, which results from bis-chelation by the (*R*)-ligands, necessarily incurs significant variations in core Li–O bond lengths. Viewing the tetramer as an aggregate in which a dimeric pair of (*R*)-ligands lie next to a dimeric pair of (*S*)-ligands (Fig. 1, right to left), the inter-dimer Li–O distances vary between 1.909(8) Å [Li(2)–O(2)] and 1.852(8) Å [Li(1A)–O(4)]. The four-membered $(LiO)_2$ ring which is associated with dimerisation of the two (*S*)-ligands and constitutes the closed face of the pseudo-cubane, is likewise composed of two Li–O bond types. Those between the two (*S*)-monomers [*e.g.* Li(1)–O(2) 1.903(8) Å] are rather shorter than those present in the




**Scheme 1**

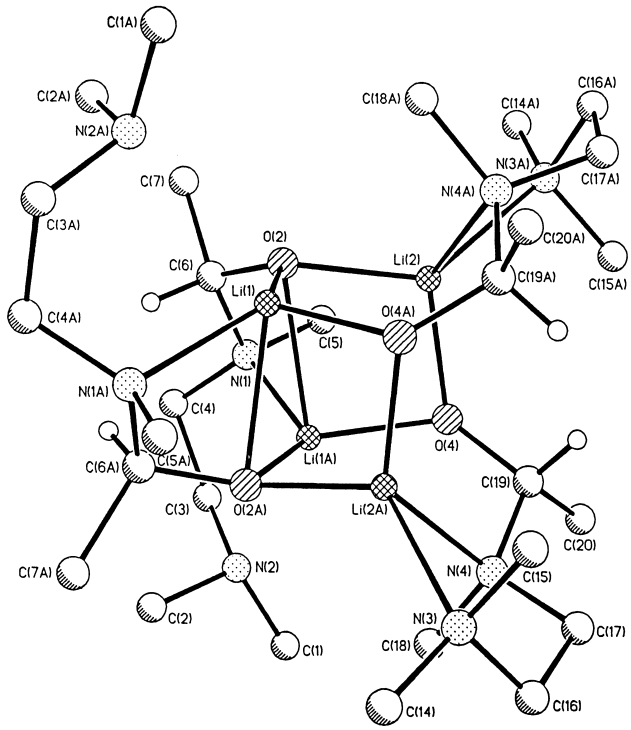



**Fig. 1** Structure of the $(LiO)_4$ 'open' pseudo-cubane core of **1**; hydrogen atoms (except the protected aldehyde hydrogens) have been omitted for clarity and only the *ipso*-carbon atoms of the aromatic rings are shown. The symmetry operation which relates original atoms to their 'A' equivalents is $1 - x, y, \frac{1}{2} - z$.

four-membered chelate rings [*e.g.* Li(1A)O(2)C(6)N(1), Li(1A)–O(2) 2.303(8) Å] which result from mono-chelation of the α-amino moieties and which demonstrate *anti*-geometrical isomerism about the C–N bond. At 2.101(8) Å, the Li(1A)–N(1) distance is consistent with distances found in related mono-chelates.[5a,b,10] The two (*R*)-ligands behave in a bis-chelating fashion with both α- and δ-N-centres stabilising the metal centres. Concomitantly, two eclipsed intramonomer Li–O bonds in the pseudo-cubane core have cleaved [*i.e.* Li(2)···O(4A)]. The result is that instead of each (*R*)-ligand incorporating a four-membered Li–O–C–N chelate ring, both (*R*)-ligands combine with two intact edges of the open pseudo-cubane, yielding an eight-membered $(Li–O–C–N)_2$ ring in a boat conformation, in which geometrical isomerism about the C–N bonds is once again of the *anti*-form. The intact Li–O bonds [Li(2)–O(4)], at only 1.872(8) Å, are rather shorter than those in the (presumably) strained four-membered mono-chelate rings associated with the (*S*)-isomers. While the α-N–Li [Li(2)–N(4A)] distance, at 2.118(8) Å, is essentially unchanged from the analogous interactions in the mono-chelated (*S*)-ligands, the δ-N–Li [Li(2)–N(3A)] bond length is somewhat longer, at 2.365(8) Å.

At 2.723(8) Å, the non-bonded Li(2)···O(4A) distance is relatively short compared with that of 3.14 Å in [PhOLi·thf]$_4$·PhOH, the only other known example of an 'open' $(LiO)_4$ pseudo-cubane.[12] However, unlike **1** this tetramer demonstrates opening of only one cubane bond, a phenomenon brought about by the inclusion of a non-lithiated phenol molecule whose hydroxyl group bridges one cubane edge. More extensive fragmentation, as seen in **1**, has been recorded in a lithium halide. Here, however, the fracture of intraaggregate bonds results from polymerisation,[13] $(LiBr·thf)_\infty$ representing the only previous example of an 'open' pseudo-cubane in which, as for **1**, two eclipsed Li–X bonds are absent.

Multinuclear NMR studies suggest the solution behaviour of **1** to be of a complicated nature. Firstly, $^7$Li NMR spectroscopy does not show two lithium environments in a 1 : 1 ratio. This suggests that the (*R*)- and (*S*)-monomers do not retain their solid-state differences in solution and that, therefore, either the tetramer is fluxional or it deaggregates. In fact, cryoscopy in benzene§ suggests that a monomer/dimer equilibrium is dominant in non-polar solution. Accordingly $^7$Li NMR spectroscopy shows two major features in a 3.8 : 1 ratio at ambient temperature in [$^2H_6$]benzene ($\delta$ −0.35, −0.47). Variable-temperature $^7$Li NMR spectroscopy in [$^2H_8$]toluene allows us to assign these as dimer and monomer respectively. The room-temp. spectrum shows peaks at $\delta$ −0.42 and −0.55 which are comparable to those observed in [$^2H_6$]benzene. However, at 193 K the high-field signal is absent, the low-field one having moved to $\delta$ −0.26.†

$^1$H NMR spectroscopy in [$^2H_6$]benzene at 298 K also reflects the complex behaviour of **1** in solution, showing as it does a dominant protected aldehyde signal at $\delta$ 6.48 along with five much smaller satellites in the range $\delta$ 6.12–6.01, all of which correlate with the protected aldehyde carbon centre at $\delta$ 88.60 (by HMQC spectroscopy).[14] Solution studies of **1** are on-going.

We thank the UK EPSRC (A. E. H. W.) and The Royal Society (J. E. D., P. R. R.) for financial support.

## Footnotes and References

* E-mail: cmc1006@cam.ac.uk

† Bu$^n$Li (1.88 ml, 1.6 M in hexanes, 3.0 mmol) was added to *N*,*N*,*N*′-trimethylethylenediamine (0.38 ml, 3.0 mmol) in thf (4 ml) at −78 °C under $N_2$. After stirring for 10 min, *o*-anisaldehyde (0.36 ml, 3.0 mmol) was added and the resultant colourless solution was stirred for a further 10 min at −78 °C. Warming to room temp. gave a white suspension, which afforded a yellow solution on gentle heating. Storage at room temp. for one day afforded colourless, rectangular crystals of **1**, mp, 160–161 °C, yield, 82%. $^1$H NMR (500.13 MHz, 298 K, $C_6D_6$), $\delta$ 8.14 (d, 1 H, Ar), 7.18 (d, 1 H, Ar), 7.14 (dd, 1 H, Ar), 6.78 (dd, 1 H, Ar), 6.48–6.01 [m, 1 H ArC(*H*)(O)$NR_2$], 3.72–3.31 (m, 3 H, $OCH_3$), 2.75–2.69, 2.32 (m, 2 H, $CH_2$), 2.68–2.21 (m, 3 H, $NCH_3$), 2.53–2.49 (m, 2 H, $CH_2$), 2.41–1.92 [m, 6 H, N′$(CH_3)_2$].$^{13}$C NMR (100.61 MHz, 298 K, $C_6D_6$), $\delta$ 157.03, 135.83, 130.61, 126.83, 119.91, 110.01 (Ar), 88.60 [Ar*C*(H)(O)$NR_2$], 59.02 ($CH_2$), 54.86 ($OCH_3$), 52.13 ($CH_2$), 46.66–45.54 [m, N′$(CH_3)_2$], 36.87–34.73 (m, $NCH_3$). $^7$Li NMR (155.51 MHz, 298 K, $C_6D_6$, ref. PhLi $\delta$ 0) $\delta$ −0.35 (s, 3.8 Li), −0.47 (s, 1 Li); (298 K, $C_6D_5CD_3$, ref. PhLi $\delta$ 0) $\delta$ −0.42 (s, 3.5 Li), −0.55 (s, 1 Li); (273 K) $\delta$ − 0.38 (s, 4.9 Li), −0.50 (s, 1 Li); (248 K) $\delta$ − 0.33 (s); (223 K) $\delta$ −0.29 (s); (193 K) $\delta$ −0.26 (s).

‡ *Crystal data* for **1**: $C_{52}H_{84}Li_4N_8O_8$, monoclinic, space group *C*2/*c*, $a$ = 21.795(6), $b$ = 12.828(4), $c$ = 20.754(7) Å, $\beta$ = 105.19(2)°, $M_r$ = 977.03, $Z$ = 4, $D_c$ = 1.159 Mg m$^{-3}$, $\mu$(Mo-Kα) = 0.077 mm$^{-1}$, $F$(000) = 2112. Data were collected by the $\omega$–2$\theta$ scan method on a Rigaku AFC5R four-circle diffractometer at 150(2) K using the 'oil drop mounting technique'.[7] Graphite-monochromated Mo-Kα radiation ($\lambda$ = 0.710 69 Å) was used in the range 5.12 < 2$\theta$ < 39.96°, ±$h$, ±$k$, +$l$; 2707 reflections of which 2604 were independent ($R_{int}$ = 0.0335) and used in all calculations. The structure was solved using direct methods[8] and subsequent Fourier-difference syntheses and refined[9] by full-matrix least squares on $F^2$ with anisotropic thermal parameters for all non-hydrogen atoms except Li. H-atoms were placed in geometrically idealised positions and refined using a riding model or as rigid methyl groups. Final $R(F)$ = 0.0536 for 2595 reflections with [$I > 2\sigma(I)$], $wR(F^2)$ = 0.1412 for all data; 316 parameters; goodness of fit = 1.045. Maximum peak and hole in final Fourier difference map 0.172 and −0.186 e Å$^{-3}$ respectively. CCDC 182/548.

§ Cryoscopy on **1** in benzene suggests that the average aggregation state varies from 1.3 to 1.5 (±0.1) in the concentration range 0.006–0.016 M (1.4–3.9 mg ml$^{-1}$). NMR spectroscopy used *ca.* 2 mg ml$^{-1}$ samples.

1 H. W. Gschwend and H. R. Rodriguez, *Org. React.*, 1979, **26**, 1; I. Omae, *Chem. Rev.*, 1979, **79**, 287; P. Beak and V. Snieckus, *Acc. Chem. Res.*, 1982, **15**, 306; N. S. Narasimhan and R. S. Mali, *Synthesis*, 1983, 957; N. S. Narasimhan and R. S. Mali, *Top. Curr. Chem.*, 1987, **138**, 63; V. Snieckus, *Chem. Rev.*, 1990, **90**, 879.
2 D. L. Comins and J. D. Brown, *J. Org. Chem.*, 1984, **49**, 1078 and references 2–10 therein.
3 D. L. Comins and J. D. Brown, *Tetrahedron Lett.*, 1981, **22**, 4213; D. L. Comins, J. D. Brown and N. B. Mantlo, *Tetrahedron Lett.*, 1982, **23**, 3979; D. L. Comins and J. D. Brown, *J. Org. Chem.*, 1989, **54**, 3730.
4 D. L. Comins and M. O. Killpack, *J. Org. Chem.*, 1987, **52**, 104.
5 (*a*) E. M. Arnett, M. A. Nichols and A. T. McPhail, *J. Am. Chem. Soc.*, 1990, **112**, 7059; (*b*) M. A. Nichols, A. T. McPhail and E. M. Arnett, *J. Am. Chem. Soc.*, 1991, **113**, 6222; (*c*) G. Hilmersson and Ö. Davidsson, *J. Organomet. Chem.*, 1995, **489**, 175; G. Hilmersson and Ö. Davidsson, *Organometallics*, 1995, **14**, 912; (*d*) G. Hilmersson and Ö. Davidsson, *J. Org. Chem.*, 1995, **60**, 7660; (*e*) H. J. Reich and K. J. Kulicke, *J. Am. Chem. Soc.*, 1995, **117**, 6621; (*f*) J. M. Saá, G. Martorelli and A. Frontera, *J. Org. Chem.*, 1996, **61**, 5194; (*g*) K. Sugasawa, M. Shindo, H. Noguchi and K. Koga, *Tetrahedron Lett.*, 1996, **37**, 7377.
6 A. Tatsukawa, K. Kawatake, S. Kanemasa and J. M. Rudzinski, *J. Chem. Soc., Perkin Trans. 2*, 1994, 2525; R. K. Dress, T. Rölle and R. W. Hoffmann, *Chem. Ber.*, 1995, **128**, 673; L. M. Pratt and I. M. Khan, *Tetrahedron Lett.*, 1995, **6**, 2165; G. Fraenkel, S. Subramanian and A. Chow, *J. Am. Chem. Soc.*, 1995, **117**, 6300.
7 T. Kottke and D. Stalke, *J. Appl. Crystallogr.*, 1993, **26**, 615.
8 G. M. Sheldrick, *Acta Crystallogr., Sect. C*, 1990, **A46**, 467.
9 G. M. Sheldrick, SHELXL-93, Program for Crystal Structure Refinement, University of Göttingen, 1993.
10 O. Graalmann, U. Klingebiel, W. Clegg, M. Haase and G. M. Sheldrick, *Angew. Chem.*, 1984, **96**, 904, *Angew. Chem., Int. Edn. Engl.*, 1984, **23**, 891; J. T. B. H. Jastrzebski, G. van Koten, M. J. N. Christophersen and C. H. Stam, *J. Organomet. Chem.*, 1985, **292**, 319; T. Maetzke and D. Seebach, *Organometallics*, 1990, **9**, 3032; S. C. Ball, I. Cragg-Hine, M. G. Davidson, R. P. Davies, M. I. Lopez-Solera, P. R. Raithby, D. Reed, R. Snaith and E. M. Vogl, *J. Chem. Soc., Chem. Commun.*, 1995, 2147.
11 G. W. Klumpp, *Rec. Trav. Chim. Pays-Bas*, 1986, **105**, 1.
12 M. Pink, G. Zahn and J. Sieler, *Z. Allorg. Allg. Chem.*, 1994, **620**, 749.
13 A. J. Edwards, M. A. Paver, P. R. Raithby, C. A. Russell and D. S. Wright, *J. Chem. Soc., Dalton Trans.*, 1993, 3265.
14 A. Bax, R. H. Griffey and B. L. Hawkins, *J. Magn. Reson.*, 1983, **55**, 301.

*Received in Cambridge, UK, 23rd May 1997; 7/03573J*

# Cuprophilicity? a rare example of a ligand-unsupported $Cu^{I}$–$Cu^{I}$ interaction

**Ulrich Siemeling,* Udo Vorfeld, Beate Neumann and Hans-Georg Stammler**

*Fakultät für Chemie, Universität Bielefeld, Universitätssraße 25, D-33615 Bielefeld, Germany*

**The reaction of 1,1′-bis(2-pyridyl)octamethylferrocene (L) with $[Cu(NCMe)_4]BF_4$ in $CH_2Cl_2$ affords $[CuL][CuCl_2]$, the structure of which is determined by a single-crystal X-ray diffraction study; this reveals a remarkably short ligand-unsupported $Cu^{I}$–$Cu^{I}$ contact of 281.0(2) pm.**

Attractive interactions between formally closed-shell metal centres ($s^2$ of $d^{10}$) are well documented.[1] The body of evidence is especially large in the case of gold(I). Here, the term 'aurophilicity' has been coined to describe this special kind of metal–metal bonding interaction,[2] which can be as strong as 11 kcal $mol^{-1}$ (1 cal = 4.184 J).[3] The question whether a similar metallophilicity[4] exists for the other two coinage metals, copper and silver, is still a matter of controversy. For example, the presence of such $d^{10}$–$d^{10}$ bonding interactions has been disputed on theoretical grounds for the dinuclear complexes $[M(MeC_6H_4NCHNC_6H_4Me)]_2$ in spite of short metal–metal distances [247.7(2)/270.5(1) pm for M = Cu/Ag], which were therefore attributed to the ligand architecture.[5] A most instructive case is that of the trinuclear copper complex $[Cu(MeC_6H_4N_5C_6H_4Me)]_3$, the metal centres of which have an average distance of only 235 pm.[6] The existence of a bonding interaction between them has both been supported[7] and refuted[8] at various levels of theory.

Metallophilic effects are easily blurred by the effects exerted by a bridging ligand architecture, and hence examples of ligand-unsupported metal–metal interactions are of great importance in this discussion. They are, however, notoriously scarce for silver[9] and especially for copper.[10] The first example of a copper complex exhibiting such an interaction appears to be the trinuclear species $[CuL']_3$ {HL′ = 2-[3(5)-pyrazolyl]pyridine}, which crystallises as a dimer showing two close metal–metal contacts between the two associated trinuclear units in the absence of any supportive bridging ligation [*d*(Cu–Cu) = 290.5(3) pm].[10]

We have obtained a species with an even shorter ligand-unsupported $Cu^{I}$–$Cu^{I}$ contact from the reaction of 1,1′-bis(2-pyridyl)octamethylferrocene[11] (L) with $[Cu(NCMe)_4]BF_4$ in dichloromethane, which yielded $[CuL][CuCl_2]$ **1**.† This species contains two copper(I) ions in an almost linear dicoordinate environment as shown by a single-crystal X-ray diffraction study (Figs. 1 and 2).‡ Whereas the $[CuCl_2]^-$ anion is very well known,[12] few structurally characterised examples of a copper(I) ion coordinated by just two N donors have been described to date.[13] The majority of the work published in this area was stimulated by the notion that complexes containing coordinatively unsaturated copper(I) ions and nitrogen heterocyclic ligands are of interest as possible models for deoxyhemocyanin.[14] An important feature of the structure of **1** is the short distance between the two copper centres of only 281.0(2) pm. The coordination axes of the anion and the cation, which are both slightly bent [N(1)–Cu(1)–N(2) 171.4(6), Cl(1)–Cu(2)–Cl(2) 176.9(3)°], are approximately perpendicular to each other [torsion angles: N(1)–Cu(1)–Cu(2)–Cl(1) 85.5, N(2)–Cu(1)–Cu(2)–Cl(2) 89.4°] (Fig. 3). There are no appreciable secondary interactions between the nitrogen-coordinated copper centre and the chlorine atoms of the anion, since both Cu–Cl distances [Cu(1)–Cl(1) 337, Cu(1)–Cl(2) 358 pm] are considerably larger than the sum of the van der Waals radii of Cu (140 pm) and Cl (175 pm).[15] There is no indication for intermolecular interactions of the Cl-coordinated Cu centre, its shortest intermolecular contact (Cu–C 398 pm) being that to the methyl group attached to C(1) of a neighbouring $[CuL]^+$ unit.

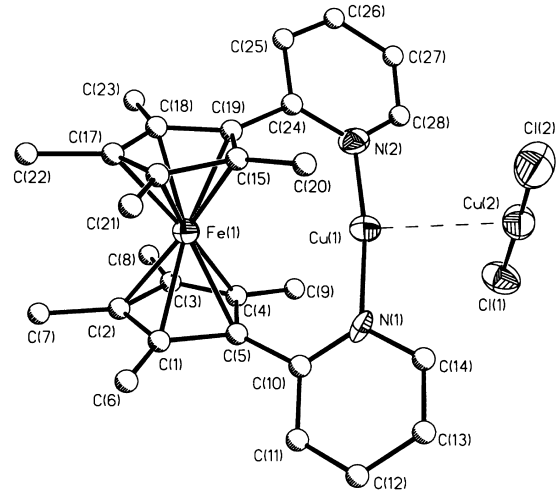



**Fig. 1** Molecular structure of **1**. Selected bond lengths (pm) and angles (°): Cu(1)–N(1) 195(2), Cu(1)–N(2) 190(2), Cu(2)–Cl(1) 212.3(7), Cu(2)–Cl(2) 206.6(7); N(1)–Cu(1)–Cu(2) 94.9(4), N(2)–Cu(1)–Cu(2) 93.6(5), Cl(1)–Cu(2)–Cu(1) 84.9(2), Cl(2)–Cu(2)–Cu(1) 93.2.

It has been noted in the chemistry of gold(I) that metallophilic energy minima can be rather shallow.[16] The same is assumed to be true for copper(I), so that crystal packing forces[17] may very well overrule weak cuprophilic interactions. In comparison, this appears to be the case for $[Cu(C_5H_2NMe_3\text{-}2,4,6)][CuCl_2]$,[13b,e] whose $Cu^{I}$–$Cu^{I}$ distance of 361.1(2) pm is *ca.* 80 pm longer than that in **1**, although the coordination parameters of the respective $Cu^{I}$ centres are quite similar for both complexes. Closer inspection reveals that the packing of the $[Cu(C_5H_2NMe_3\text{-}2,4,6)]^+$ units in the crystal, which involves stacking of

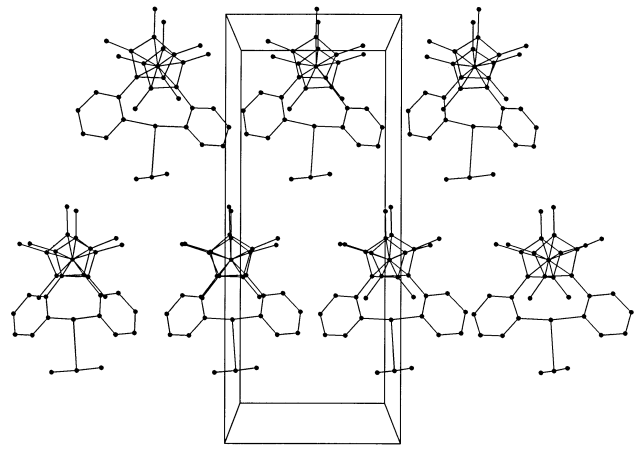


**Fig. 2** Packing diagram of **1** (viewed down the *c* axis of the unit cell)

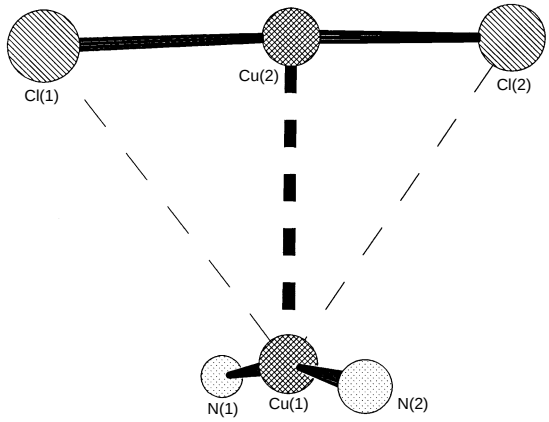



**Fig. 3** View of the coordination spheres of the copper centres in **1**

neighbouring collidine ligands with a closest inter-ring distance of 348 pm,§ prohibits a closer approach of the copper centres.

In summary, we have synthesised a rare example of a complex which exhibits a remarkably short ligand-unsupported $Cu^{I}$–$Cu^{I}$ contact, reflecting an interaction between the two formally closed-shell metal centres that may be due to a cuprophilic interaction between them.

We acknowledge financial support by the Deutsche Forschungsgemeinschaft, the Fonds der Chemischen Industrie and the University of Bielefeld. U. S. thanks Professor P. Pyykkö for making refs. 1(*a*) and 16 available to him prior to publication. We thank one of the referees for helpful comments.

## Footnotes and References

* E-mail: usie@hrz.uni-bielefeld.de

† *Preparation*: a solution of L (362 mg, 0.80 mmol) in dichloromethane (5 $cm^3$) was added at ambient temperature to a solution of $[Cu(NCMe)_4]BF_4$ (126 mg, 0.40 mmol) in $CH_2Cl_2$ (10 $cm^3$) with vigorous stirring. After 12 h volatile components were removed *in vacuo* leaving a viscous, brown–red oil, which was dissolved in a minimal amount of $CH_2Cl_2$. Vapour-phase diffusion of *n*-pentane into this solution afforded **1** {66 mg, 43% with respect to $[Cu(NCMe)_4]BF_4$} as red crystals (decomp. *ca.* 160 °C), which are insoluble in hydrocarbons and diethyl ether, very soluble in dichloromethane and moderately soluble in $CHCl_3$. The solvent obviously participated in the reaction, since it was the only source of Cl present. The reaction proved to be irreproducible. *Selected spectroscopic data*: FABMS *m*/*z* 515 ($[CuL]^+$, 100%), 453 ($[HL]^+$, 67%). $^1$H NMR ($CDCl_3$): $\delta$ 1.64, 1.86 (2 s, 24 H, Me), 7.25, 7.40, 7.74, 9.42 (4 br. s, 8 H, aromatic H). $^{13}C\{^1H\}$ NMR ($CDCl_3$) $\delta$ 9.7, 12.0 (Me), 80.2, 82.6, 85.6 (cyclopentadienyl ring C), 122.5, 127.7, 137.7, 151.9 (pyridyl CH), 158.7 (q pyridyl C).

‡ *Crystal data*: $C_{28}H_{32}Cl_2Cu_2FeN_2$, $M_r$ = 650.39; orthorhombic, space group $Pna2_1$, $a$ = 21.238(4), $b$ = 8.773(1), $c$ = 14.257(1) Å, $U$ = 2656.4(6) Å$^3$, $Z$ = 4, $D_c$ = 1.626 g cm$^{-3}$; $F$(000) = 1328, $\mu$(Mo-K$\alpha$) = 2.347 mm$^{-1}$, $\lambda$ = 0.71073 Å, $T$ = 173(2) K, crystal size 0.30 × 0.10 × 0.10 mm. A total of 2423 reflections all of which were unique were collected with a Siemens P2(1) four-circle diffractometer using ω scans with 1.92 < $\theta$ < 25.04°. The structure was solved by direct methods and developed routinely. Full-matrix least-squares refinement with 184 parameters was based on $F^2$. Hydrogen atoms were considered in calculated positions. Carbon atoms were refined isotropically and all other atoms anisotropically. The refinement converged at $R_1$ = 0.0688 and $wR_2$ = 0.1029 [for 1186 reflections with $I > 2\sigma(I)$] {$w = [\sigma^2(F_o^2) + (0.0319P)^2]^{-1}$ where $P = (F_o^2 + 2F_c^2)/3$}; final GOF = 1.039. The final difference map showed no peak > 0.6 and no hole < −0.5 e Å$^{-3}$. Programs used were Siemens SHELXTL plus and SHELXL-93. CCDC 182/531.

§ Calculated from the crystallographic data given in ref. 13(*e*).

1 See, for example: (*a*) P. Pyykkö, *Chem. Rev.*, 1997, **97**, 597; (*b*) *Unkonventionelle Wechselwirkungen in der Chemie metallischer Elemente*, ed. B. Krebs, VCH, Weinheim, 1992.
2 H. Schmidbaur, *Gold Bull.*, 1990, **23**, 11.
3 D. E. Harwell, M. D. Mortimer, C. B. Knobler, F. A. L. Anet and M. F. Hawthorne, *J. Am. Chem. Soc.*, 1996, **118**, 2679.
4 P. Pyykkö, J. Li and N. Runeberg, *Chem. Phys. Lett.*, 1994, **218**, 133.
5 F. A. Cotton, X. Feng, M. Makusz and R. Poli, *J. Am. Chem. Soc.*, 1988, **110**, 7077.
6 J. Beck and J. Strähle, *Angew. Chem.*, 1985, **97**, 419; *Angew. Chem., Int. Ed. Engl.*, 1985, **24**, 409.
7 K. M. Merz, Jr. and R. Hoffmann, *Inorg. Chem.*, 1988, **27**, 2120.
8 C. Kölmel and R. Ahlrichs, *J. Phys. Chem.*, 1990, **94**, 5536.
9 For three examples, see: T. Yamaguchi and O. Lindqvist, *Acta Chem. Scand. Ser. A*, 1983, **37**, 685; G. W. Eastland, M. M. Mazid, D. R. Russell and M. C. R. Symons, *J. Chem. Soc., Dalton Trans.*, 1980, 1682; P. W. R. Corfield and H. M. M. Shearer, *Acta Crystallogr.*, 1966, **20**, 502.
10 K. Singh, J. R. Long and P. Stavropoulos, *J. Am. Chem. Soc.*, 1997, **119**, 2942.
11 U. Siemeling, U. Vorfeld, B. Neumann and H.-G. Stammler, *Chem. Ber.*, 1995, **128**, 481.
12 B. J. Hathaway, in *Comprehensive Coordination Chemistry*, ed. G. Wilkinson, R. Gillard and J. A. McCleverty, Pergamon, Oxford, 1987, vol. 5, pp. 534–774.
13 See ref. 5 as well as (*a*) I. Sanyal, K. D. Karlin, R. W. Strange and N. J. Blackburn, *J. Am. Chem. Soc.*, 1993, **115**, 11 259; (*b*) A. Habiyakare, E. A. C. Lucken and G. Bernardinelli, *J. Chem. Soc., Dalton Trans.*, 1991, 2269; (*c*) G. O. Tan, K. O. Hodgson, B. Hedman, G. R. Clark, M. L. Garrity and T. N. Sorrell, *Acta Crystallogr., Sect. C*, 1991, **46**, 1773; (*d*) M. Munakata, S. Kitagawa, H. Shimono and H. Masuda, *Inorg. Chim. Acta*, 1989, **158**, 217; (*e*) P. C. Healy, J. D. Kildea, B. W. Skelton and A. H. White, *Aust. J. Chem.*, 1989, **42**, 115; (*f*) L. M. Engelhardt, C. Pakawatchai, A. H. White and P. C. Healy, *J. Chem. Soc., Dalton Trans.*, 1985, 117; (*g*) M. G. B. Drew, P. C. Yates, T.-C. Jadwiga, K. P. McKillop and S. M. Nelson, *J. Chem. Soc., Chem. Commun.*, 1985, 262; (*h*) T. N. Sorrell and D. L. Jameson, *J. Am. Chem. Soc.*, 1983, **105**, 6013; (*i*) M. J. Schilstra, P. J. M. W. L. Birker, G. C. Verschoor and J. Reedijk, *Inorg. Chem.*, 1982, **21**, 2637; (*j*) H. M. J. Hendriks, P. J. M. W. L. Birker, J. van Rijn, G. C. Verschoor and J. Reedijk, *J. Am. Chem. Soc.*, 1982, **104**, 3607; (*k*) T. N. Sorrell and D. L. Jameson, *J. Am. Chem. Soc.*, 1982, **104**, 2053; (*l*) P. J. W. M. L. Birker, H. M. J. Hendriks and J. Reedijk, *Inorg. Chim. Acta*, 1981, **55**, L17; (*m*) Y. Angus, R. Louis and R. Weiss, *J. Chem. Soc., Chem. Commun.*, 1980, 867; (*n*) J. E. O'Connor, G. A. Jansonius and E. R. Corey, *Chem. Commun.*, 1968, 445; (*o*) I. D. Brown and J. D. Dunitz, *Acta Crystallogr.*, 1961, **14**, 480.
14 For reviews, see: Z. Tyeklár and K. D. Karlin, *Acc. Chem. Res.*, 1989, **22**, 241; T. N. Sorrell, *Tetrahedron*, 1989, **45**, 3.
15 A. Bondi, *J. Phys. Chem.*, 1964, **68**, 441.
16 P. Pyykkö, W. Schneider, A. Bauer, A. Bayler and H. Schmidbaur, *Chem. Commun.*, 1997, 111.
17 See A. Martin and A. G. Orpen, *J. Am. Chem. Soc.*, 1996, **118**, 1464 and references therein.

*Received in Basel, Switzerland, 23rd April 1987; 7/02793A*

# What are the reacting species in the oxidation of bisulfite by hydrogen peroxide in water clusters?

**Mark A. Vincent, Ian H. Hillier* and Ian J. Palmer**

*Department of Chemistry, University of Manchester, Manchester, UK M13 9PL*

***Ab initio* calculations suggest that in the oxidation of $HSO_3^-$ to sulfuric acid by $H_2O_2$ under acid conditions, $SO_2$ and not $HSO_3^-$, is the reacting species, a result relevant to modelling the formation of acid rain.**

One of the most studied of the multiphase reactions in the troposphere is the oxidation of $SO_2$ to sulfuric acid in water droplets by oxidants such as $H_2O_2$.[1,2] The elucidation of the mechanism of this reaction is naturally central to modelling the formation of acid rain. It is usual to invoke the involvement of the bisulfite anion, $HSO_3^-$, in proposed reaction mechanisms.[3,4] However, the actual mechanism by which the proposed intermediate, the peroxymonosulfite ion, is produced, is unclear. Indeed many $S^{IV}$ species have been proposed to be involved along the reaction pathway.[3,4]

To provide further insight into this reaction we have studied the mechanism by employing high level *ab initio* electronic structure calculations. These were carried out using a 6-311+g** basis[5–7] and included electron correlation at the B3LYP level[8] *via* the Gaussian 94 suite of programs.[9] Two possible transition states for the reacting $H_2O_2$ and $HOSO_2^-$ species, leading to the proposed intermediate peroxymonosulfite ion,[3,4] have been determined. One of the transition states included two explicit water molecules and the other included no solvent (Fig. 1). A similar direct participation of additional water molecules has been invoked in the calculation of the reaction of $SO_3$ with $H_2O$ to form $H_2SO_4$.[10]

A common feature of both of these calculated transition states are the two very long S–O bond lengths (2.75–2.87 Å), and two others (1.47–1.48 Å) close to the value in $SO_2$ itself (1.46 Å). In addition, in both transition structures there is a well developed hydroxide group. Furthermore, if the unsolvated transition state is located without the $SO_2$ being present, the structure changes very little, and involves proton transfer between $HO^-$ and $H_2O_2$. Thus both transition states essentially correspond to the dissociation of the bisulfite ion to $SO_2$. However, it would be expected that in acid solution the developing negative charge on the OH group would be neutralized at an early stage to yield free $SO_2$.

Indeed there is evidence that in the absence of $H_2O_2$ protonation of aqueous bisulfite can lead to the formation of $SO_2$. NMR studies of aqueous bisulfite[11] have demonstrated exchange of the oxygen atoms associated with the sulfur atom, suggesting ease of formation of $SO_2$. Computationally we have previously found from *ab initio* calculations[12] that protonation of the OH oxygen atom of $HOSO_2^-$, in a small water cluster, also leads to the formation of $SO_2$ with little or no barrier, again suggesting the direct involvement of $SO_2$. This latter result is supported by the experimental[11] evidence that exchange of oxygen in the bisulfite ion is first order in both $H_3O^+$ and $HOSO_2^-$.

These results, both experimental and theoretical, suggest that under acid conditions the reacting species in water droplets containing bisulfite is probably $SO_2$. In view of this we have modelled the subsequent reaction of sulfur dioxide and $H_2O_2$. The corresponding transition state for the reaction leading to peroxymonosulfurous acid, and involving two explicit water molecules was located, and is shown in Fig. 2. This structure

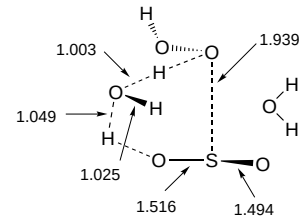



**Fig. 2** Transition state for the reaction of $SO_2$ and $H_2O_2$ involving two water molecules (bond lengths in Å)

involves somewhat greater perturbation of the $SO_2$ moiety than in the corresponding reaction of $HOSO_2^-$ (Fig. 1), with a well developed $H_3O^+$ entity acting as a proton shuttle between $H_2O_2$ and $SO_2$. Both this structure and the corresponding transition state for the reaction of $HOSO_2^-$ with $H_2O_2$ involve a six-membered ring, which is probably less strained than the cyclic transition state for the reaction without explicit solvation. When this structure is further solvated using a continuum approach[13] the barrier from the hydrogen bonded reactants is calculated to be 12.3 kcal mol$^{-1}$ (1 cal = 4.184 J). This value is somewhat larger than the experimental barrier[4] of 8.8 kcal mol$^{-1}$, for the formation of the peroxymonosulfite ion from $H_2O_2$ and $HOSO_2^-$ in acid solution.

There are thus compelling reasons to believe that the reactive species involved in the formation of acid rain, from bisulfite and hydrogen peroxide in acid solution, is $SO_2$.

We thank EPSRC for support of this research.

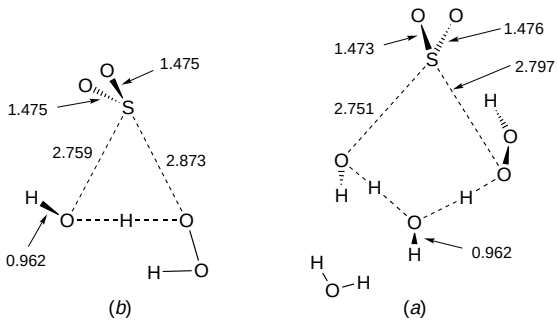



**Fig. 1** Transition states for the reaction of $HOSO_2^-$ and $H_2O_2$, (*a*) with and (*b*) without water (bond lengths in Å)

## Footnote and References

* E-mail: ian.hillier@man.ac.uk

1 G. P. Gervat, P. A. Clark, A. R. W. Marsh, I. Teasdale, A. S. Chandler, T. W. Choularton, M. J. Gay, M. K. Hill and T. A. Hill, *Nature*, 1988, **333**, 241.
2 A. S. Chandler, T. W. Choularton, G. J. Dollard, A. E. J. Eggleton, M. J. Gay, T. A. Hill, B. M. R. Jones, B. J. Tyler, B. J. Bandy and S. A. Penkett, *Nature*, 1988, **336**, 562.
3 M. R. Hoffmann and J. O. Edwards, *J. Phys. Chem.*, 1975, **79**, 2096.
4 J. V. McArdle and M. R. Hoffmann, *J. Phys. Chem.*, 1983, **87**, 5425.
5 A. D. McLean and G. S. Chandler, *J. Chem. Phys.*, 1980, **72**, 5639.

6 R. Krishnan, J. S. Binkley, R. Seeger and J. A. Pople, *J. Chem. Phys.*, 1980, **72**, 650.
7 T. Clarke, J. Chandrasekhar, G. W. Spitznagel and P. v. R. Schleyer, *J. Comput. Chem.*, 1983, **4**, 294.
8 A. D. Becke, *J. Chem. Phys.*, 1993, **98**, 5648.
9 M. J. Frisch, G. W. Trucks, H. B. Schlegel, P. M. W. Gill, B. G. Johnson, M. A. Robb, J. R. Cheeseman, T. A. Keith, G. A. Petersson, J. A. Montgomery, K. Raghavachari, M. A. Al-Laham, V. G. Zakrzewski, J. V. Ortiz, J. B. Foresman, J. Cioslowski, B. B. Stefanov, A. Nanayakkara, M. Challacombe, C. Y. Peng, P. Y. Ayala, W. Chen, M. W. Wong, J. L. Andres, E. S. Replogle, R. Gomperts, R. L. Martin, D. J. Fox, J. S. Binkley, D. J. Defrees, J. Baker, J. J. P. Stewart, M. Head-Gordon, C. Gonzalez and J. A. Pople, GAUSSIAN 94, Revision A.1, Gaussian, Inc., Pittsburgh, PA, 1995.
10 K. Morokuma and C. Muguruma, *J. Am. Chem. Soc.*, 1994, **116**, 10 316.
11 D. A. Horner and R. E. Connick, *Inorg. Chem.*, 1986, **25**, 2414.
12 M. A. Vincent, I. J. Palmer and I. H. Hillier, *J. Mol. Struct.*, (*THEOCHEM*), 1997, **394**, 1.
13 J. B. Foresman, T. A. Keith, K. B. Wiberg, J. Snoonian and M. J. Frisch, *J. Phys. Chem.*, 1996, **100**, 16 098.

*Received in Exeter, UK, 6th June 1997; 7/03949B*

# Intercalation of decamethylferrocenium cations in bimetallic oxalate-bridged two-dimensional magnets

**Miguel Clemente-León, Eugenio Coronado,* José-Ramón Galán-Mascarós and Carlos J. Gómez-García**

*Dpto. de Química Inorgánica. Univ. Valencia. Dr. Moliner 50, 46100 Burjasot, Spain*

**The structure and magnetic properties of novel hybrid molecule-based magnets formed by combination of two magnetically active sublattices, the bimetallic oxalato-bridged honeycomb net $[Mn^{II}M^{III}(ox)_3]$ ($M^{II}$ = Mn, Fe, Co, Cr, Ni, Cu; $M^{III}$ = Cr, Fe) and the organometallic cation decamethylferrocenium, are reported.**

Much interest has been shown in oxalate complexes in the search for new molecule-based magnets since the discovery at the beginning of the nineties of new polymeric bimetallic phases of variable dimensionality.[1] Especially interesting are the two-dimensional bimetallic phases $A[M^{II}M^{III}(ox)_3]$ ($M^{II}$ = Mn, Fe, Co, Cr, Ni, Cu; $M^{III}$ = Cr, Fe) because they behave as ferro-,[2] ferri-[3] or canted antiferro-magnets[4] with critical temperatures ranging from 5 up to 44 K. Their structure[5] consists of extended oxalate-bridged layers of the two metal atoms separated by $A^+$, an electronically 'innocent' counter ion of the type $[XR_4]^+$ (X = N, P; R = Ph, $Pr^n$, $Bu^n$), which may act as a template controlling the formation of the net structure and thus determining the interlayer separation.[4b] The change of this cation to an electroactive one could create new hybrid molecular materials with interesting properties or combinations of properties, depending on the nature of the cation and the possible interactions with the magnetic network. Very recently we reported an example of such hybrid materials: the $[TTF]_4\{M^{II}(H_2O)_2[M^{III}(ox)_3]_2\}\cdot nH_2O$ family,[6] in which the cation is the organic π-donor molecule tetrathiafulvalene (TTF), although instead of the extended two-dimensional network, a molecular layer of oxalato-bridged bimetallic trimeric clusters is formed.

Here we show that it is possible to combine the layered bimetallic oxalate complexes with the magnetically interesting organometallic cation $[Fe(Cp^*)_2]^+$ ($Cp^*$ = decamethylferrocenium), which has spin $S = 1/2$. It is to be noticed that other salts formed by decamethylmetallocenium cations and two-dimensional molecule-based magnets have been very recently reported, but the structure of these materials is unknown.[7]

The new family of organometallic–inorganic magnetic compounds has the formula $[Fe(Cp^*)_2][M^{II}M^{III}(ox)_3]$ ($M^{II}$ = Mn, Fe, Co, Ni, Cu, Zn; $M^{III}$ = Cr, Fe). They were obtained by the one-pot reaction of the tris(oxalato) complex $[M^{III}(ox)_3]^{3-}$ with the divalent metal ion $M^{II}$ and $[Fe(Cp^*)_2]^+$ cations in water. Crystals of good quality were obtained by diffusion, and the crystal structure was solved for the $Fe^{III}Mn^{II}$ derivative. The structure† consists of anionic layers of the well known honeycomb bimetallic oxalato-bridged network with decamethylferrocenium cations intercalated in between [Fig. 1(*a*)]. The bimetallic layers are eclipsed by each other creating hexagonal channels running along the *c* axis. The organometallic cations exhibit a staggered configuration (symmetry $D_{5d}$). They are ordered within the interlayer space. In fact, they are located at the center of the hexagonal channels forming a pseudo-hexagonal arrangement. These cations are tilted with respect to the layer by an angle of 32.6° (angle defined by the fivefold symmetry axis of the cation with the normal to the bimetallic plane) in such a way that the two pentamethylcyclopentadienyl molecules of each $[Fe(Cp^*)_2]^+$ cation are pointing towards the center of the hexagons of two adjacent layers [Fig. 1(*b*)]. The interlayer separation is 9.213 Å, similar to that found in previous compounds of two-dimensional phases,[5,4b] and there is no evidence of hydrogen-bond interactions between the cations and the layers (the minimum H···O distance is 2.584 Å). A distinctive feature of this structure with respect to the other structurally known two-dimensional phases is that now the cation does not penetrate into the honeycomb net (the minimum distance of the cation to this plane is 0.88 Å; distance from the mean plane defined by the metals to the closest hydrogen from a methyl group). A second difference deals with the stacking of the bimetallic layers. Thus, in contrast with the $[XR_4]^+$ derivatives, all the layers are of the same type so that the metals of one layer lie directly over those in the next layer.‡

All these compounds are magnets exhibiting spontaneous magnetization below $T_c$ and hysteresis loops. As in the $[XR_4]^+$ derivatives, the compounds of the $Cr^{III}M^{II}$ series behave as ferromagnets§ which have ferromagnetic interactions between $Cr^{III}$ and $M^{II}$ ions through the oxalate group, while in the $Fe^{III}M^{II}$ series this coupling is antiferromagnetic giving rise to ferrimagnets (for $M^{II}$ = Fe, Co) or canted antiferromagnets (for $Mn^{II}$ = Mn). We have performed ac susceptibility measure-

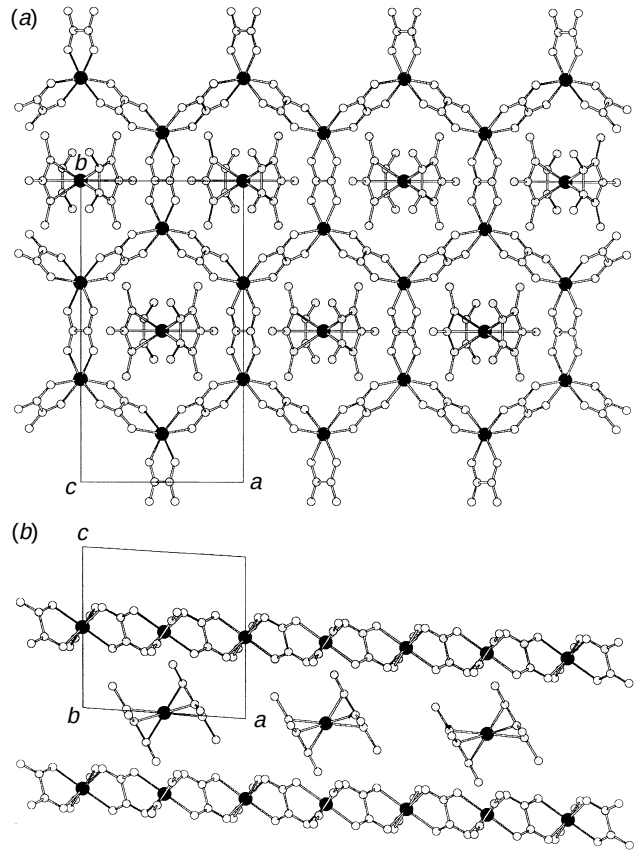



**Fig. 1** View of the structure in the *ab* plane showing the honeycomb magnetic layers (*a*) and in the *ac* plane (*b*)

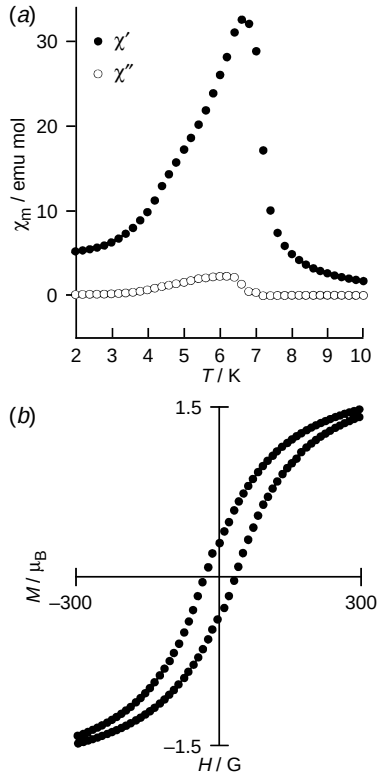



**Fig. 2** Magnetic properties of the $Cr^{III}Cu^{II}$ derivative: (*a*) ac susceptibility *vs.* temperature showing the out-of-phase signal ($\chi''$); (*b*) hysteresis loop at 5 K

ments in order to obtain accurate values of $T_c$. These data show a sharp peak in both the in-phase and the out-of-phase susceptibility signals at $t_c$ (Fig. 2). The relevant magnetic parameters (critical temperatures and coercive fields for the Cr–M ferromagnets and critical temperatures for the Fe–M ferrimagnets) are summarized in Table 1 and compared to those reported for the $[XR_4]^+$ derivatives. As we can see, the $[Fe(Cp^*)_2]^+$ salt of the $Fe^{III}Co^{II}$ derivative has no precedent among the $[XR_4]^+$ salts. This material undergoes ferrimagnetic ordering at $T_c$ = 19.5 K. As far as the magnetic ordering is concerned what becomes apparent from the above magnetic results is that the paramagnetic $[Fe(Cp^*)_2]^+$ cations are not

**Table 1** The series of compounds $[Fe(Cp^*)_2][M^{II}M^{III}(ox)_3]$. Critical temperatures and coercive fields (at 5 K) for $Cr^{III}M^{II}$ and critical temperatures for $Fe^{III}M^{II}$. Comparison with the $[XR_4]4^+$ salts

| | $T_c$/K | | $H_{coerc}$/G | |
|---|---|---|---|---|
| $M^{III}M^{II}$ | $[Fe(Cp^*)_2]^+$ | $[XR_4]^+$ | $[Fe(Cp^*)_2]^+$ | $[XR_4]^+$ |
| CrMn | 5.3 | 6 | 10 | 20 |
| CrFe | 13.0 | 12 | 320 | 320 |
| CrCo | 9.0 | 10 | 50 | 80 |
| CrNi | 14.5 | 14 | 250 | 160 |
| CrCu | 7.0 | 7 | 30 | 30 |
| FeMn | 28.4 | 25–29 | | |
| FeFe | 43.3 | 33–48 | | |
| FeCo | 19.5 | — | | |

directly involved in the long-range magnetic ordering, which is essentially controlled by the bimetallic layers. Thus, $T_c$ values are found to be roughly the same as those observed in the $[XR_4]^+$ derivatives. On the other hand, the coercive fields are also very similar. These results indicate that the two magnetic sublattices essentially behave independently, without a significant cation–layer electronic interaction, in agreement with the structural features. Unusual magnetic effects may arise from the coexistence of these two magnetic sublattices. For example, in the ordered state the magnetic layers are expected to polarize the spins of the metallocene layer and therefore a Zeeman splitting of the $S$ = 1/2 spins of the paramagnetic cations may be observed. Complete physical characterization of these and other molecular magnetic multilayers that can be obtained using the same methodology is now in progress.

This work is supported by the Spanish DGICYT (Grant PB94-0998). J. R. G. M. thanks the Generalitat Valenciana for a predoctoral fellowship.

## Footnotes and References

* E-mail: eugenio.coronado@uv.es

† *X-Ray crystal structure analyses*: Enraf-Nonius CAD4 diffractometer, Mo-K$\alpha$ radiation, $\lambda$ = 0.71069 Å, graphite monochromator, 295 K. Lorentz polarization and absorption corrections ($\psi$ scan). *Data collection, solution and refinement*: $\omega$–$2\theta$, direct methods using the SIR92 program, followed by Fourier synthesis, SHELXL-93 computer program. $[Fe(C_{10}H_{15})_2][MnFe(C_2O_4)_3]$ ($C_{26}H_{30}O_{12}Fe_2Mn$), monoclinic, space group $C2/m$, $a$ = 9.0645(8), $b$ = 17.143(3), $c$ = 9.215(4) Å, $\beta$ = 93.66(2)°, $U$ = 1429(1) Å$^3$, $Z$ = 2, $D_c$ = 1.630 g cm$^{-3}$, crystal size 0.2 × 0.05 × 0.05 mm. 1909 reflections measured in the range $4 < 2\theta < 64$, 1871 unique and 1434 assumed as observed with $I \geqslant 6\sigma(I)$. $R$ = 0.0348 and $wR_2$ 0.0937. CCDC 182/551.

‡ In the $[XR_4]^+$ derivatives a graphite-like stacking of the bimetallic layers has been found with a stacking order . . . ABAB . . . (for $NBu_4$), or . . . ABCABC . . . (for $PPh_4^+$).

§ The ferromagnetic ordering in the $Cr^{III}$–$M^{II}$ series is in agreement with the saturation magnetization values which roughly correspond to the total number of unpaired electrons per formula unit.

1 Z. J. Zhong, N. Matsumoto, H. Okawa and S. Kida, *Chem. Lett.*, 1990, 87; M. Ohba, H. Tamaki, N. Matsumoto, H. Okawa and S. Kida, *Chem. Lett.*, 1991, 1157; S. Decurtins, R. Pellaux, A. Hauser and M. E. von Arx, in *Magnetism: A Supramolecular Function*, ed. O. Kahn, NATO ASI Series, Kluwer, Dordrecht, 1996, vol. C484, p. 487 and references therein.

2 H. Tamaki, Z. J. Zhong, N. Matsumoto, S. Kida, M. Koikawa, N. Achiwa, Y. Hashimoto and H. Okawa, *J. Am. Chem. Soc.*, 1992, **114**, 6974.

3 H. Tamaki, M. Mitsumi, K. Nakamura, N. Matsumoto, S. Kida, H. Okawa and S. Iijima, *Chem. Lett.*, 1992, 1975; H. Okawa, N. Matsumoto, H. Tamaki and M. Ohba, *Mol. Cryst. Liq. Cryst.*, 1993, **233**, 257.

4 (*a*) C. Mathonière, S. G. Carling, D. Yusheng and P. Day, *J. Chem. Soc., Chem. Commun.*, 1994, 1551; (*b*) C. Mathonière, J. Nuttall, S. G. Carling and P. Day, *Inorg. Chem.*, 1996, **35**, 1201.

5 S. Decurtins, H. W. Schmalle, H. R. Oswald, A. Linden, J. Ensling, P. Gütlich and A. Hauser, *Inorg. Chim. Acta*, 1994, **216**, 65; (*b*) L. O. Atovmyan, G. V. Shilov, R. N. Lyubovskaya, E. I. Zhilyaeva, N. S. Ovanesyan, S. I. Pirumova and I. G. Gusakovskaya, *JETP Lett.*, 1993, **58**, 766.

6 E. Coronado, J. R. Galán-Mascarós, C. Gimenez-Saiz, C. J. Gómez-García, C. Ruiz-Perez and S. Triki, *Adv. Mater.*, 1996, **8**, 737.

7 Y. Pei, S. Turner, L. Founes, J. S. Miller and O. Kahn, *J. Mater. Chem.*, 1996, **6**, 1521.

*Received in Basel, Switzerland, 28th May 1997; 7/03712K*

# First synthesis of mesostructured thiogermanates

**Michael Fröba* and Nadine Oberender**

*Institute of Inorganic and Applied Chemistry, University of Hamburg, Martin-Luther-King-Platz 6, 20146 Hamburg, Germany*

**Two mesostructured thiogermanates are prepared and characterized by powder XRD, TEM and TG–DTA.**

Since the first synthesis of mesoporous M41S phases in 1992[1] numerous systems of mesoporous metal oxides have been reported.[2] The range of possible applications of mesoporous systems is broadened by the use of sulfides instead of oxides. Porous semiconductors are of interest owing to their special electronic and optical properties, such as luminescence. In the area of microporous sulfides promising results have already been achieved,[3] but there were only a few attempts to prepare mesostructure metal sulfides.[4–6]

In the present work we report the synthesis of different mesostructured thiogermanates dependent on pH, temperature and reaction time. We used amorphous germanium sulfide as the inorganic source and cetyltrimethylammonium bromide as the supramolecular template. The reactions were carried out under hydrothermal conditions.

There is a minimum temperature and, at lower temperatures, a minimum reaction time necessary to obtain mesostructured organic/inorganic composites (Fig. 1).

The powder diffraction pattern of the thiogermanates prepared at various pH values differ. Samples prepared at low pH (product 1) show generally one or two reflections with relatively low intensities indicating a lower crystallinity [Fig. 2(*a*)]. High pH values (product 2) lead to products with multiple, more intense reflections [Fig. 2(*b*)]. Both mesostructured thiogermanates have a lamellar structure whereas product 1 shows a higher degree of condensation between the inorganic building units.

In both cases all reflections can be indexed as 00*l* reflections whereas product 1 shows a larger *d* spacing (3.2 nm) for the 001 reflection than the corresponding *d* value of product 2 (2.8 nm).

For product 2 the TEM shows an ordered lamellar structure (Fig. 3). The distance between the layers is *ca.* 2.7 nm. In contrast product 1 is more disordered.

The results of thermochemical measurements also show significant differences between the two products. Fig. 4(*a*) and (*b*) show TG and DTA results of products 1 and 2, respectively. The former has a more simple mechanism of decomposition with three steps of mass loss whereas the latter shows a more complex course with at least five steps.

Calculations result in a much lower molar mass of *ca.* 230 for product 1 in contrast to 600 for product 2. These results suggest a much higher content of template in product 2 which is obvious because the degree of condensation is relatively low. At high pH charge-matching interactions between the surfactant cations

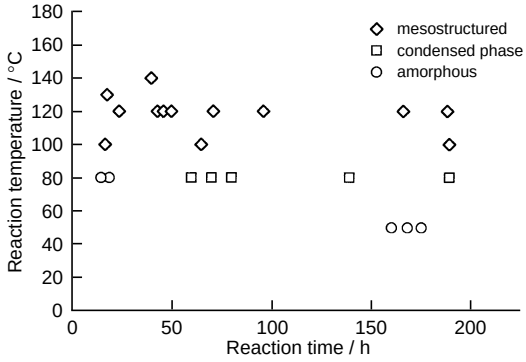



**Fig. 1** Correlation between reaction time, temperature and the products obtained

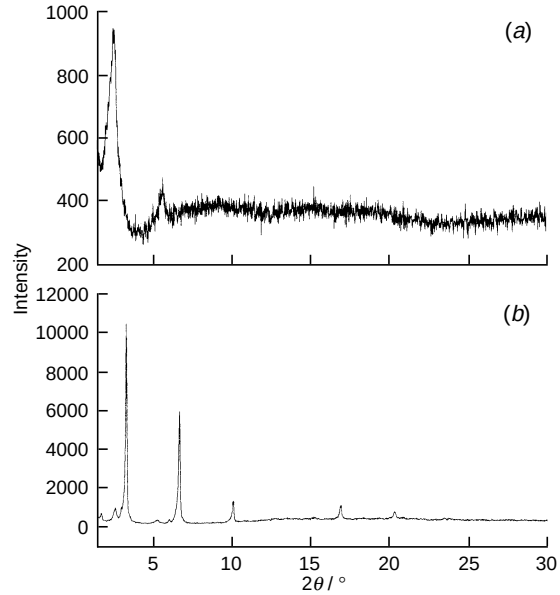



**Fig 2** X-Ray powder diffraction patterns of the mesostructured products 1 (*a*) and 2 (*b*)

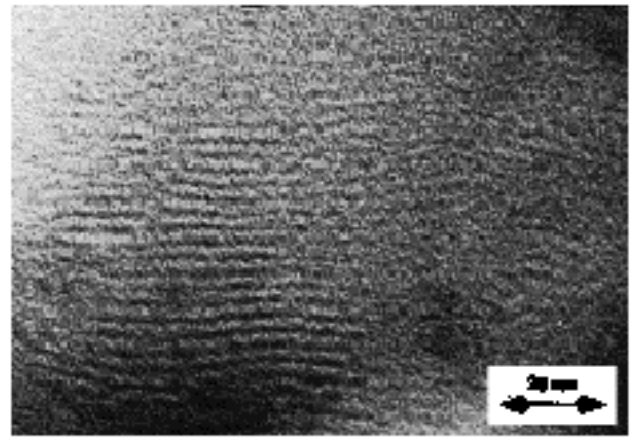


**Fig 3** Transmission electron micrograph of the mesostructured product 2

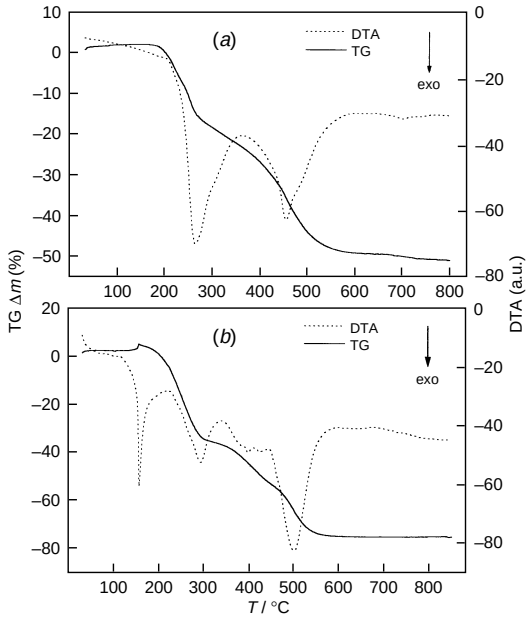



**Fig. 4** TG–DTA measurements of the mesostructured products 1 (*a*) and 2 (*b*) (atmosphere: oxygen, heating rate = 5 K $min^{-1}$)

and the smaller thiogermanate anions lead to a more crystalline saltlike structure [Fig. 2(*b*)] in order to attain electrical neutrality. At low pH additional condensation reactions take place and there is less charge per $Ge_xS_y$ as the units get larger. Elementary analysis data give the same results.

In conclusion, we were able to mesostructure thiogermanates and demonstrated the basic correlations between reaction time, temperature, pH and the corresponding structures of the products.

We thank Olaf Muth for carrying out the TEM measurements. Financial support by the University of Hamburg, the Swiss Federal Energy Office and the Deutsche Forschungsgemeinschaft is gratefully acknowledged.

## Footnote and References

* E-mail: froeba@chemie.uni-hamburg.de

1 C. T. Kresge, M. E. Leonowicz, W. J. Roth, J. C. Vartuli and J. S. Beck, *Nature*, 1992, **359**, 710.
2 Q. Huo, D. I. Margolese, U. Ciesla, P. Feng, T. E. Gier, P. Sieger, R. Leon, P. M. Petroff, F. Schüth and G. D. Stucky, *Nature*, 1994, **368**, 317.
3 R. L. Bedard, L. D. Vail, S. T. Wilson and E. M. Flanigan, *US Pat.*, 4 880 761, 1989 .
4 M. T. Anderson and P. Newcomer, *Mater. Res. Soc. Symp. Proc.*, 1995, **371**, 117.
5 P. V. Braun, P. Osenar and S. I. Stupp, *Nature*, 1996, **380**, 325.
6 J. Li, H. Kessler and L. Delmotte, *J. Chem. Soc., Faraday Trans.*, 1997, **93**, 665.

*Received in Bath, UK, 22nd May 1997; Com. 7/03634E*

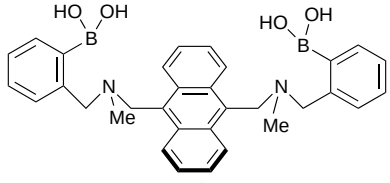
# Fluorescent sensing of uronic acids based on a cooperative action of boronic acid and metal chelate

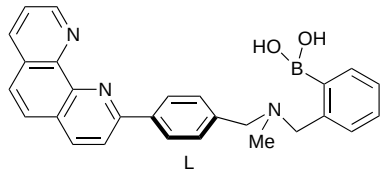
**Masayuki Takeuchi, Masashi Yamamoto and Seiji Shinkai***

*Department of Chemical Science & Technology, Faculty of Engineering, Kyushu University, Fukuoka 812, Japan*

**A new fluorescent molecular sensor for uronic acids is designed, which features two-point interactions of boronic acid–diol complexation and zinc(II)–carboxylate coordination.**

Saccharides are nature's conveyors of energy and play many crucial roles in metabolic cycles. Uronic acids are known to appear in the oxidation process of monosaccharides or in the biosynthetic process of L-ascorbic acid. The quantitative analysis of uronic acids has so far been accomplished by classical colorimetic methods such as naphthoresorcine–HCl[1] and carbazole–$H_2SO_4$.[2] Obviously, it seems very important to develop a new analytical method which is useful under physiological conditions and in addition, shows high selectivity and sensitivity towards uronic acids in the presence of concomitant neutral saccaharides. We have recently demonstrated the usefulness of the boronic acid function as a saccharide receptor in a saccharide recognition system.[3] Judging from the structure of uronic acids, molecular design including both a boronic acid moiety for diol binding and a metal chelate moiety for carboxylate binding within a molecule should lead to an excellent uronic acid receptor. To achieve high sensitivity it is desirable to combine this system with the concept of a photoinduced electron-transfer (PET) sensor.[4,5] We previously designed compound L′ which selectively binds 1,2- and 4,6-diols of glucose with two boronic acids and reports the binding event by a fluorescence change in the PET mechanism.[6] Here, we have rationally designed a molecular sensor L for uronic acids in which one boronic acid group in L′ is replaced by a metal chelation site. We have found that the zinc(II) complex of this new molecular sensor selectively responds to uronic acids in neutral aqueous solution.

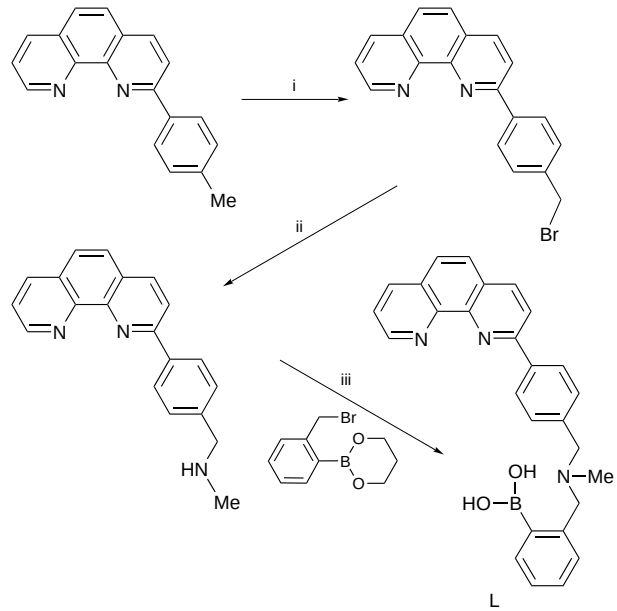


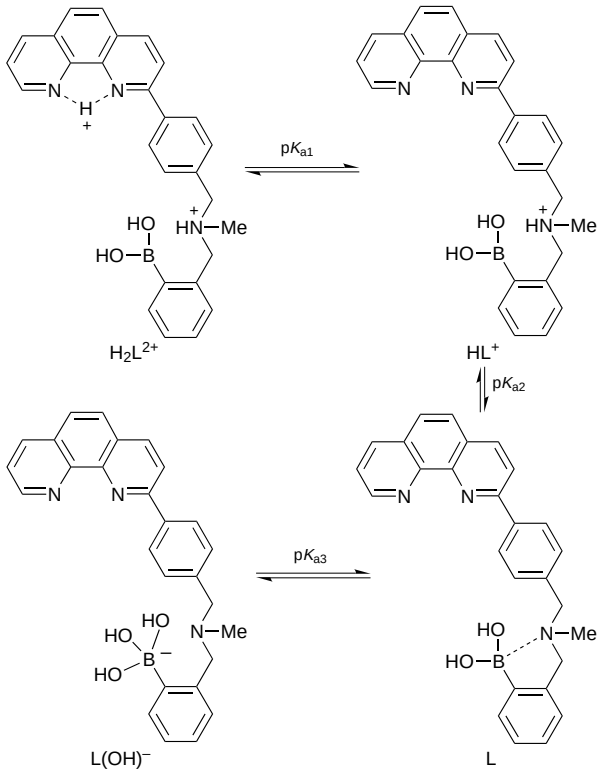

The synthesis of L was achieved from 2-(*p*-tolyl)-1,10-phenanthroline[7] by the route outlined in Scheme 1. The product (mp 166–169 °C) was identified by IR and $^1$H NMR spectroscopic evidence and elemental analysis.

Since the water solubility of L was not good, we used a mixed medium of water–MeOH (1 : 2 v/v) to avoid self-aggregation. The absorption maximum of L shifted from 301 to 290 nm upon a pH change from 2.0 to 7.5 with a tight isosbestic point (at 294 nm). This change corresponds to deprotonation of the chromophoric 1,10-phenanthroline moiety (p$K_{a1}$ 4.4, Scheme 2). The absorption spectra did not change further at higher pH. Using 294 nm as the excitation wavelength we measured the fluorescence spectra. Fig. 1 shows plots of the fluorescence intensity ($\lambda_{max}$ at 375 nm) *vs.* pH. In the absence of saccharide, the fluorescence intensity increase at pH 2–6 corresponds to deprotonation of the 1,10-phenanthroline moiety, which again gives p$K_{a1}$ 4.4. The fluorescence intensity decrease starting from pH 5.5 and pH 10 corresponds to deprotonation of the tertiary amine (p$K_{a2}$) and $OH^-$ adduct formation with the boronic acid group (p$K_{a3}$), respectively. Because of the overlap of the dissociation groups the p$K_{a2}$ could be only approximately estimated to be *ca.* 7, whereas the p$K_{a3}$ could not be determined accurately. In the presence of saccharide ([D-fructose] = 100 mmol dm$^{-3}$, Fig. 1), the fluorescence intensity is increased at pH 6–11. This is due to the B–N interaction intensified by complexation of saccharide with the boronic acid group.[6] The association constants ($K_{ass}$) in the absence of $Zn^{II}$ were estimated from plots of the fluorescence intensity against the saccharide concentration. The results are summarized in Table 1.

Addition of $Zn^{II}$ [added as $Zn(NO_3)_2 \cdot 6H_2O$] decreased the absorbance in the UV region of the absorption spectrum and the visible region of the fluorescence spectrum and the final spectra were very similar to those of $H_2L^{2+}$. The results suggest that $Zn^{II}$ is primarily associated with the phenanthroline moiety. Since the spectral changes were saturated at [$Zn^{II}$]/[L] = 4.0, we fixed the ratio to this value and then added saccharides. The fluorescence intensity increased with increasing saccharide concentration and was saturated at high concentration. From the




**Scheme 1** *Reagents and conditions* [yields]: i, NBS, AIBN, $CCl_4$, reflux; ii, $MeNH_2$, $CCl_4$ [30%, calculated from 2-(*p*-tolyl)-1,10-phenanthroline]; iii, $K_2CO_3$, MeCN, reflux [40%]




**Scheme 2**

analysis of the plots the $K_{ass}$ values in the presence of $Zn^{II}$ were determined and are summarized in Table 1.

Examination of Table 1 reveals that as expected,[6] D-fructose gives the largest $K_{ass}$ with L in the absence of $Zn^{II}$. On the other hand, uronic acids are scarcely bound to L (except D-galacturonic acid with $K_{ass}$ = 80 dm$^3$ mol$^{-1}$). In contrast, the $K_{ass}$ values for three uronic acids are remarkably improved in the presence of $Zn^{II}$ whereas those for three neutral monosaccharides are scarcely affected. The difference clearly supports the view that uronic acids are bound to $[Zn^{II}L]^{2+}$ by a cooperative action of boronic acid–diol complexation and zinc(II)–carboxylate coordination.

It is known that when saccharides interact with the receptor at two points to form a cyclic structure, the resultant complexes become CD-active.[6,8] In fact, D-glucuronic acid and D-galacturonic acid with large $K_{ass}$ values gave CD-active

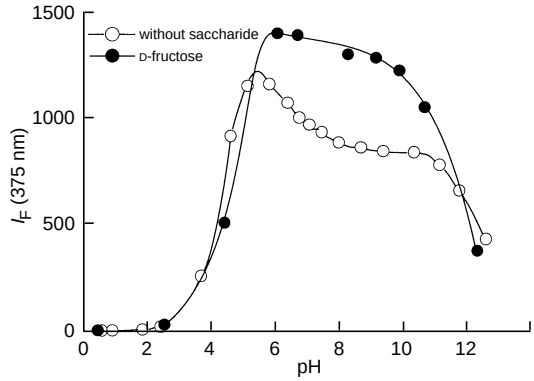



**Fig. 1** Fluorescence intensity *vs.* pH profile of L ($1.00 \times 10^{-5}$ mol dm$^{-3}$); 25 °C [D-fructose] = 0 or 100 mmol dm$^{-3}$, $\lambda_{ex}$ = 294 nm

**Table 1** Association constants (log $K_{ass}$)[a] for saccharides with L and $[Zn^{II}L]^{2+}$

| | Log $K_{ass}$ ($I_{max}/I_0$) | |
|---|---|---|
| Saccharide | L | $[Zn^{II}L]^{2+}$ |
| D-Glucuronic acid | —[b] | 3.4 (2.11) |
| D-Galacturonic acid | 1.9 (1.15) | 3.1 (3.69) |
| Sialic acid (*N*-Acetylneuraminic acid) | —[b] | 2.3 (1.83) |
| D-Glucose | —[b] | —[b] |
| D-Galactose | 1.7 (1.12) | 1.3 (1.50) |
| D-Fructose | 2.5 (1.33) | 2.4 (1.90) |

[a] pH = 8.0 (5.0 mmol dm$^{-3}$ MOPS buffer), water–MeOH (1 : 2 v/v). [b] Too small to determine (log $K_{ass}$ < 1).

complexes with $[Zn^{II}L]^{2+}$: $\lambda_{max}$ and $[\theta]$ = 305 nm and $4.0 \times 10^3$ ° cm$^{-2}$ dmol$^{-1}$ for D-glucuronic acid and 282 nm and $28.0 \times 10^3$ ° cm$^{-2}$ dmol$^{-1}$ for D-galacturonic acid. Job plots using the CD intensity provided a maximum at $[ZnL^{2+}]/([ZnL^{2+}] + [\text{uronic acid}]) = 0.50$, indicating that the stoichiometry of these complexes is 1 : 1.

In conclusion, the present study demonstrates a new saccharide receptor for uronic acids, which features two-point interactions of boronic acid–diol complexation and zinc(II)–carboxylate coordination. The receptor can discriminate well between uronic acids and neutral monosaccharides and the binding event can be sensitively read out by a fluorescence change. We believe that this is a new molecular design concept utilizing the cooperative action of boronic acid and the metal chelate. Further applications are continuing in this laboratory.

This work was supported by a Grant-in-Aid for COE Research 'Design and Control of Advanced Molecular Assembly Systems' from the Ministry of Education, Science and Culture, Japan (#08CE2005).

## Footnote and References

* E-mail: seijitcm@mbox.uc.kyushu-u.ac.jp

1 S. S. Cohen, *J. Biol. Chem*., 1953, **201**, 71 and references therein.
2 Z. Dische, *J. Biol. Chem*., 1953, **204**, 983 and references therein.
3 For comprehensive reviews see: T. D. James, P. Linnane and S. Shinkai, *Chem. Commun.*, 1996, 281; T. D. James, K. R. A. S. Sandanayake and S. Shinkai, *Angew. Chem., Int. Ed. Engl*., 1996, **35**, 1910.
4 A. P. de Silva, H. Q. N. Gunarathe and C. P. McCoy, *Chem. Commun*., 1996, 2399; A. P. de Silva, H. Q. N. Gunaratne, C. McVeigh, G. E. M. Maguine, P. R. S. Maxwell and E. Q'Hanlon, *Chem. Commun*., 1996, 2191; A. P. de Silva, H. Q. N. Gunaratne, T. Gunnlaugsson, C. P. McCoy, P. R. S. Maxwell, J. T. Rademacher and T. E. Rice, *Pure Appl. Chem.*, 1996, **68**, 1443.
5 A. W. Czarnik, *Acc. Chem. Res*., 1994, **27**, 302; *Fluorescent Chemosensors for Ion and Molecular Recognition*, ed. A. W. Czarnik, ACS Books, Washington, 1993.
6 T. D. James, K. R. A. S. Sandanayake and S. Shinkai, *Angew. Chem., Int. Ed. Engl*., 1994, **33**, 2207; T. D. James, K. R. A. S. Sandanayake, R. Iguchi and S. Shinkai, *J. Am. Chem. Soc*., 1995, **117**, 8982. Although the distance between the phenanthroline and the amino group is apparently farther than that in L′, the fluorescence change is as large as that in L′. Presumably the 2-phenyl group is included in the fluorophore.
7 M. S. Goodman, A. D. Hamilton and J. Weiss, *J. Am. Chem. Soc*., 1995, **117**, 8447.
8 T. Imada, H. Kijima, M. Takeuchi and S. Shinkai, *Tetrahedron Lett*., 1995, **36**, 2093; *Tetrahedron*, 1996, **52**, 2817.

*Received in Cambridge, UK, 20th May 1997; 7/03471G*

# The first double oxidative addition of $CH_2Cl_2$ to a metal complex: facile synthesis of $[Ru(CH_2)Cl_2\{P(C_6H_{11})_3\}_2]$

**Montserrat Oliván and Kenneth G. Caulton***

*Department of Chemistry, Indiana University, Bloomington, IN 47405-4001, USA*

**$[Ru(H)_2(H_2)_2L_2]$ [L = $P(C_6H_{11})_3$] serves as a formal source of zerovalent '$RuL_2$', and undergoes unprecedented oxidative addition of both C–Cl bonds of $CH_2Cl_2$ to a single metal center, providing a convenient synthesis of the alkene metathesis catalyst $[Ru(CH_2)Cl_2L_2]$.**

Ruthenium carbenes of the form $[Ru(CRR')Cl_2L_2]$ (L = phosphine) play a central role in alkene metathesis methodology in organic chemistry. The original form[1] of the ruthenium catalyst has now been simplified,[2] but access to carbene complexes remains less than rational: α-elimination from an alkyl complex or use of a diazoalkane reagent are the primary synthetic methodologies.

$$L_nM + X_2CRR' \rightarrow L_n(X)_2M{=}CRR' \qquad (1)$$

*gem*-Dihalogeno compounds are formally attractive as a source of a carbene ligand [eqn. (1)], but converting this idea into reality has been elusive. Eqn. (1) makes clear that $L_nM$ must be a 14-valence electron species, or its equivalent, and the scarcity of such species accounts for the rarity of eqn. (1). Eqn. (1) might be expected to proceed stepwise, with an X–M–CRR'X intermediate, and indeed, there are numerous examples of halogenomethyl ligands that have been formed from $CX_2RR'$.[3] However, a double oxidation addition of an $R_2CX_2$ $sp^3$ carbon is unprecedented. Set against this background, we report here the first oxidative addition of both C–Cl bonds of a *gem*-dihalide to a single metal center, where all constituents of $R_2CX_2$ become attached to a single metal in the product,[4] and an example where this occurs in high yield to produce the simplest of ruthenium alkene metathesis catalysts, $[Ru(CH_2)Cl_2L_2]$, with L = $P(C_6H_{11})_3$.

Reaction† of $[Ru(H)_2(H_2)_2L_2]$ [L = $P(C_6H_{11})_3$] with $CH_2Cl_2$ in pentane or benzene under argon occurs over 3 h at 25 °C (1 : 4 mol ratio) or 15 min at 60 °C (1 : 1.5 mole ratio) to give the known molecule $[RuCl_2(CH_2)L_2]$,[2b] characterized by $^1H$, $^{13}C$ and $^{31}P$ NMR spectroscopies. The $^1H$ NMR signal of the carbene ligand is the most unique spectroscopic feature, appearing at $\delta$ 19.4. If the reaction is carried out with $CD_2Cl_2$, $[RuCl_2(CD_2)L_2]$ is the only isotopomer produced ($^1H$ and $^2H$ NMR assay),‡ showing that there is no scrambling of the metal- and carbon-derived hydrogen. This reaction is remarkable because it involves a four-electron reduction of $CH_2Cl_2$ (to $Cl^-$ and what is formally $CH_2^{2-}$). It thus depends upon $[Ru(H)_2(H_2)_2L_2]$ being a formal source of uncharged $RuL_2$ (*i.e.* zerovalent Ru), by virtue of reductive elimination of hydride from $Ru^{II}$, as $H_2$. When this reaction is repeated in a closed NMR tube, we see ($^{31}P\{^1H\}$ NMR) no growth and decay of any intermediate. Since there is no evidence for production of $CH_3Cl$ or $CH_4$, this reaction is an unprecedented oxidative addition of both C–Cl bonds of $CH_2Cl_2$ to a single metal center. This reaction proceeds more slowly in an NMR tube under 1 atm argon, than in a well agitated, round-bottom flask with a considerable head-space, a fact we attribute to the accumulation of $H_2$, which shifts eqn. (2) to the left and thus decreases the amount of unsaturated $[Ru(H)_2(H_2)L_2]$, which is apparently the necessary reaction partner for $CH_2Cl_2$.[5]

$$[Ru(H)_2(H_2)_2L_2] \leftrightharpoons [Ru(H)_2(H_2)L_2] + H_2 \qquad (2)$$

This idea of competitive inhibition by $H_2$ is supported by the fact that, if $[Ru(H)_2(H_2)_2L_2]$ is stirred with $CH_2Cl_2$ (1 : 4) at 25 °C under 1 atm $H_2$ in pentane, there is no reaction over 3 h. The reaction is thus not outer-sphere electron transfer from $[Ru(H)_2(H_2)_2L_2]$, and a 16-electron complex is the reactive species.

Since $[RuH_3ClL_2]$[6] is also produced in < 15% yield in this reaction, we considered that HCl {which we independently verified could convert $[Ru(H)_2(H_2)_2L_2]$ to $[RuH_3(Cl)L_2]$} might participate in the reaction which forms the carbene complex. However, when the reaction of $[Ru(H)_2(H_2)_2L_2]$ with $CH_2Cl_2$ is executed in the presence of $NEt_3$ (1 : 4 : 2 mole ratio), the carbene product and yield are unchanged, as is (qualitatively) the rate. No $[NHEt_3]Cl$ precipitates. This gives support for the idea that $H_2$ is the fate of all metal-bound H, that $[RuH_3(Cl)L_2]$ is produced in a side reaction, and that a 'ClRuCH$_2$Cl' species mediates the reaction. However, any such species must react further to give carbene product faster than it reacts with $NEt_3$, to quaternize the amine (giving 'ClRuCH$_2$-$NEt_3^+$' and $Cl^-$); chloromethyl ligands readily react with nucleophiles.[3a]

The idea of multiple oxidative addition to $[Ru(H)_2(H_2)_2L_2]$, and the idea that facile multiple losses of $H_2$ from this molecule permits it to serve as a formal equivalent of zerovalent '$RuL_2$' deserves further exploration.

This work was supported by the NSF and by material support from Johnson-Matthey/Aesar. M. O. thanks the Spanish Ministerio de Educación y Cultura for a postdoctoral fellowship.

## Footnotes and References

* E-mail: caulton@indiana.edu

† $[RuCl_2(=CH_2)\{P(C_6H_{11})_3\}_2]$ (method A): To a suspension of $[RuH_2(H_2)_2\{P(C_6H_{11})_3\}_2]$[7] (100 mg, 0.15 mmol) in pentane (7 ml) was added $CH_2Cl_2$ (38 μl, 0.60 mmol) *via* a syringe. The resulting suspension was stirred at room temp. for 3 h. During this time, the suspension changed from white to brown–red. The red solid obtained by filtration was washed with pentane and dried *in vacuo*. Yield: 70 mg (63%). Alternatively (method B), the reaction could be carried out heating at 60 °C for 15 min, starting from $[RuH_2(H_2)_2\{P(C_6H_{11})_3\}_2]$ (100 mg, 0.15 mmol) and $CH_2Cl_2$ (14.4 μl, 0.22 mmol) in pentane (5 ml). Yield: 75 mg (67%). All the spectroscopic data are consistent with those reported previously.[2b] When the crude suspension was dried *in vacuo* and dissolved in $C_6D_6$, $^1H$ and $^{31}P$ NMR show the presence of $[RuH_3Cl\{P(C_6H_{11})_3\}_2]$,[6] in addition to $[RuCl_2(=CH_2)\{P(C_6H_{11})_3\}_2]$, in a yield of < 15%. This was shown independently to be formed by the action of $H_2$ on $[Ru(CH_2)Cl_2\{P(C_6H_{11})_3\}_2]$.

‡ $[RuCl_2(=CD_2)\{P(C_6H_{11})_3\}_2]$: this compound was prepared analogously as described for $[RuCl_2(=CH_2)\{P(C_6H_{11})_3\}_2]$ (method A) by starting from $[RuH_2(H_2)_2\{P(C_6H_{11})_3\}_2]$ (50 mg, 0.075 mmol) and $CD_2Cl_2$ (19 μl, 0.30 mmol). $^2H$ NMR (61 MHz, $C_6H_6$): $\delta$ 19.40 (s, Ru=$CD_2$).

1 S. D. Nguyen, L. K. Johnson, R. H. Grubbs and J. W. Ziller, *J. Am. Chem. Soc.*, 1992, **114**, 3974.

2 (*a*) P. Schwab, M. B. France, J. W. Ziller and R. H. Grubbs, *Angew. Chem., Int. Ed. Engl.*, 1995, **34**, 2039; (*b*) P. Schwab, R. H. Grubbs and J. W. Ziller, *J. Am. Chem. Soc.*, 1996, **118**, 100.

3 (*a*) H. B. Friedrich and J. R. Moss, *Adv. Organomet. Chem.*, 1991, **33**, 235; (*b*) H. Werner, *Angew. Chem., Int. Ed. Engl.*, 1983, **22**, 927;

(*c*) H. Haarman, J. M. Ernsting, M. Kranenburg, H. Kooijman, N. Veldman, A. L. Spek, P. W. N. M. van Leeuwen and K. Vrieze, *Organometallics*, 1997, **16**, 887; (*d*) M. Huser, M. Youinou and J. Osborn, *Angew. Chem., Int. Ed. Engl.*, 1989, **28**, 1386; (*e*) W. Herrmann, W. R. Thiel, C. Brossmer and K. Ofele, *J. Organomet. Chem.*, 1993, **461**, 51.

4 For examples of $M_2 + R_2CX_2 \rightarrow XM(\mu\text{-}CR_2)MX$, see; M. A. Ciriano, M. A. Tena and L. A. Oro, *J. Chem. Soc., Dalton Trans.*, 1992, 2123; G. E. Ball, W. R. Cullen, M. D. Fryzuk, B. R. James and S. J. Rettig, *Organometallics*, 1991, **10**, 3767; S. J. Young, B. Kellenberger, J. H. Reibenspies, S. E. Manning, O. P. Anderson and J. K. Stille, *J. Am. Chem. Soc.*, 1988, **110**, 5744.

5 Eqn. (2) is apparently the mechanism by which $N_2$ adds to $[Ru(H)_2(H_2)_2L_2]$ to give $[Ru(H)_2(N_2)_2L_2]$; S. Sabo-Etienne, M. Hernandez, G. Chung, B. Chaudret and A. Castel, *New J. Chem.*, 1994, **18**, 175; M. L. Christ, S. Sabo-Etienne, G. Chung and B. Chaudret, *Inorg. Chem.*, 1994, **33**, 5316.

6 B. Chaudret, G. Chung, O. Eisenstein, S. A. Jackson, F. J. Lahoz and J. A. López, *J. Am. Chem. Soc.*, 1991, **113**, 2314; M. L. Christ, S. Sabo-Etienne and B. Chaudret, *Organometallics*,, 1994, **13**, 3800.

7 B. Chaudret and R. Poilblanc, *Organometallics*, 1985, **4**, 1722.

*Received in Bloomington, IN, USA, 6th May 1997; 7/03097E*

# Photocontrol of the redox state of ruthenium–tris(bipyridine)-appended cytochrome $b_{562}$

**Itaru Hamachi,*[a] Shigeaki Tanaka,[a] Shinya Tsukiji,[a] Seiji Shinkai,[a] Masafumi Shimizu[b] and Teruyuki Nagamune[b]**

[a] *Department of Chemistry and Biochemistry, Graduate School of Engineering, Kyushu University, Hakozaki Fukuoka 812-81 Japan*

[b] *Department of Chemistry and Biotechnology, Graduate School of Engineering, The University of Tokyo, Hongo, Bunkyo-ku 113 Japan*

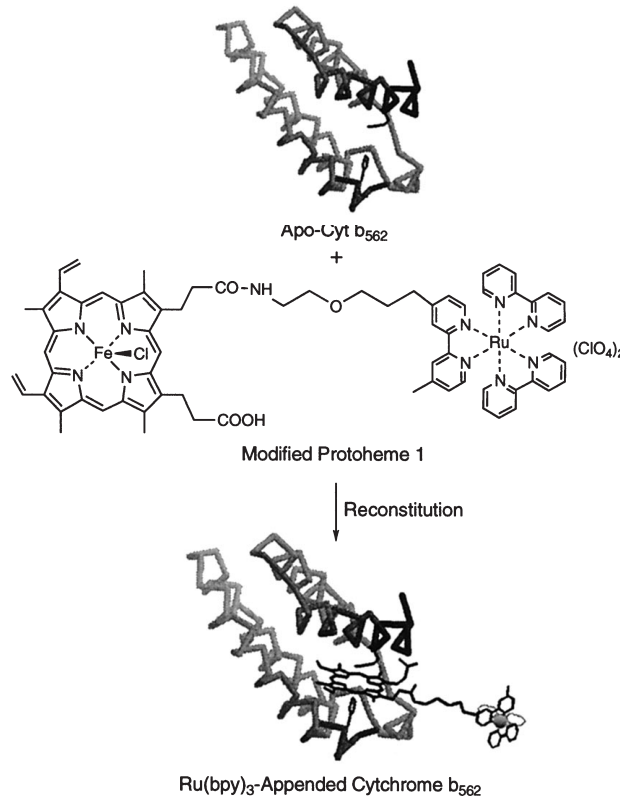
**Ruthenium–tris(bipyridine)-appended heme is successfully reconstituted with apo-cytochrome $b_{562}$ (Cyt-$b_{562}$); the redox state of the active site in the resultant semisynthetic Cyt-$b_{562}$ can be switched by visible light irradiation.**

Photocontrol of naturally occurring enzymes/proteins activity is one of the attractive targets in the recent protein engineering.[1] For the redox-active enzymes or proteins, it seems promising to modulate the redox state of the active site of the enzymes by photoelectron injection or abstraction.[2] We recently demonstrated that the dioxygen binding activity of myoglobin was successfully photoregulated by the covalent attachment of a ruthenium polypyridine complex to the heme site.[3] This approach is so convenient that it is desirable to establish the generality of our proposed method. In addition to myoglobin, we therefore applied the reconstitution method to another hemoprotein, cytochrome $b_{562}$, an electron-transporting hemoprotein, which possesses one protoheme in its active site.[4]

The soluble Cyt-$b_{562}$ was obtained and purified from *Escherichia coli* (strain TB-1 harboring pNS207 plasmid)[5] except that Cyt-$b_{562}$ was released from periplasmic space by treatment with chloroform.[6] The apoprotein was prepared at 4 °C using the butanone extraction method.[7] A synthetic heme **1** bearing ruthenium tris(2,2′-bipyridine) dissolved in dimethyl sulfoxide was added dropwise to the resultant apo-Cyt-$b_{562}$ solution (50% aqueous $Me_2SO$). After incubation at 4 °C for 1 h, the mixture was purified by gel-column chromatography [Sephadex G-50, 50 mM phosphate buffer (pH 7.0) eluent] to obtain a red solution. The UV–VIS spectrum of this solution showed a sharp absorption at 419 nm due to the Soret band and a weak band at 530 nm due to the Q band of the heme cofactor. Upon reduction with $Na_2S_2O_4$, the absorption maxima shifted to 427, 531 and 561 nm. These absorption maxima are identical to those of the oxidized $Fe^{III}$ and reduced $Fe^{II}$ state of native Cyt-$b_{562}$.[4] These results indicate that the synthetic heme **1** was successfully incorporated into the heme crevice of apo-Cyt-$b_{562}$ [Ru(bpy)$_3$–Cyt-$b_{562}$, Scheme 1].

Steady-state emission of Ru(bpy)$_3$ (emission at 610 nm, excitation at 450 nm) in an intermolecular mixture of Ru(bpy)$_3$ and native Cyt-$b_{562}$ was only slightly lowered (0.8-fold intensity), compared to that of the Ru(bpy)$_3$ itself. On the other hand, the emission intensity of Ru(bpy)$_3$ in Ru(bpy)$_3$–Cyt-$b_{562}$ was found to be markedly weaker than that of an intermolecular mixture (0.013-fold). This suggests that the intramolecular electron transfer quenching of the excited $Ru^{II}$ state by the heme in Ru(bpy)$_3$–Cyt-$b_{562}$ occurs more efficiently than in the intermolecular system under the present experimental conditions (protein concentration 0.3–10 μM).

Fig. 1 shows the absorption spectral change of Ru(bpy)$_3$–Cyt-$b_{562}$ during visible light irradiation (using a high-pressure Hg lamp, cut-off at $\lambda < 450$ nm) in the presence of *N*,*N*-dimethylaminobenzoate (NNDB), a sacrificial donor.[8] The absorbances at 419 and 530 nm gradually decrease and those at 430, 538 and 580 nm grow with six isosbestic points at 420, 444, 518, 538, 550 and 569 nm. These spectral changes clearly reveal the photoreduction of the oxidized Cyt-$b_{562}$ to the reduced form. The inset of Fig. 1 compares the photoreduction efficiency of Ru(bpy)$_3$–Cyt-$b_{562}$ to that for the intermolecular reaction system [*i.e.* a simple mixture of Ru(bpy)$_3$, native Cyt-$b_{562}$ (1 : 1 molar ratio) and NNDB]. Apparently, the intermolecular reaction proceeds very slowly. The initial reaction rate of the intramolecular Ru(bpy)$_3$–Cyt-$b_{562}$ (0.05 μM min$^{-1}$) is 28 times greater than the value of the intermolecular control experiment (0.0018 μM min$^{-1}$). The quantum yield ($\Phi$) of this photoreduction was determined to be 1.4–8.2 $\times$ $10^{-4}$ at protein concentrations of 0.7–7.6 μM. The activation efficiency is more than 10 times greater than that of the intermolecular system ($\Phi$ = 0.1–0.3 $\times$ $10^{-4}$).† This difference is in good agreement with the above-mentioned emission quenching efficiency; photoreduction does not take place in the absence of NNDB. The visible light on–off experiment showed that the visible light is essential for the reduction of the active center of Ru(bpy)$_3$–Cyt-




**Scheme 1** Reconstitution of ruthenium–tris(bipyridine)-appended heme to apo-cytochrome $b_{562}$

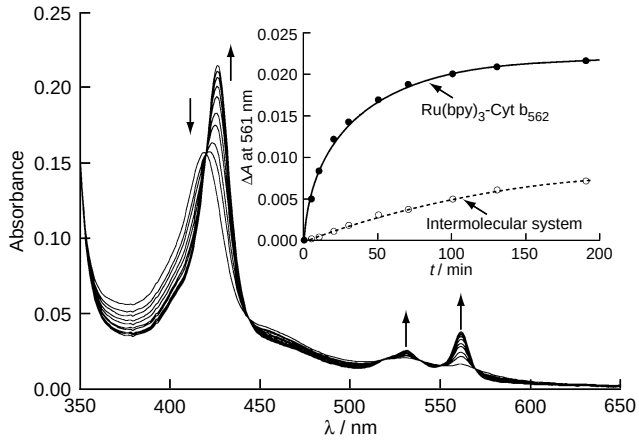



**Fig. 1** Absorption spectral changes of $Ru(bpy)_3$–Cyt-$b_{562}$ upon steady-state photoirradiation (wavelength cut-off below 450 nm, high-pressure Hg lamp) under anaerobic conditions: 1.5 μM $Ru(bpy)_3$–Cyt-$b_{562}$ and 10 mM NNDB in phosphate buffer (50 mM, pH 7.0) at 25 °C. The inset shows the time course of the photogeneration of red-Cyt-$b_{562}$ in the intramolecular [$Ru(bpy)_3$–Cyt-$b_{562}$] reaction system (——) and the intermolecular reaction system [$Ru(bpy)_3$ + native Cyt-$b_{562}$] (- - -).

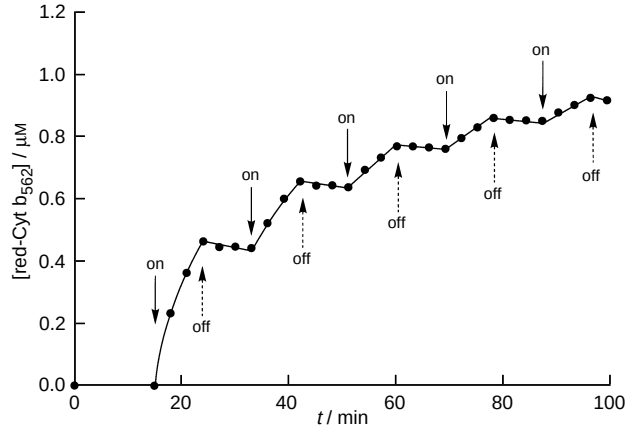



**Fig. 2** The light on–off experiment for $Ru(bpy)_3$–Cyt-$b_{562}$. The solid and dashed arrows indicate switching on and off, respectively: 1.5 μM $Ru(bpy)_3$–Cyt-$b_{562}$, 10 mM NNDB in phosphate buffer (50 mM, pH 7.0) at 25 °C.

$b_{562}$ in the present system. As shown in Fig. 2, the reduced form of $Ru(bpy)_3$–Cyt-$b_{562}$ is not generated in the absence of visible light. The reduction smoothly started upon light irradiation and completely stopped when the light was turned off. This process can be repeated by turning the light on and off.

Next, we conducted the tandem photoreduction of cytochromec (Cyt-c) using the semisynthetic $Ru(bpy)_3$–Cyt-$b_{562}$. When a mixed solution of Cyt-c and $Ru(bpy)_3$–Cyt-$b_{562}$ (5 : 1 mol : mol) was irradiated by visible light in the presence of NNDB, reduced Cyt-c was smoothly formed and $Ru(bpy)_3$-Cyt-$b_{562}$ catalytically cycled (turnover frequency = 0.33 $h^{-1}$) this reaction. We found that the present system was 3.5 times more efficient than the conventional intermolecular reaction [*i.e.* Cyt-c : Cyt-$b_{562}$ : $Ru(bpy)_3$ = 5 : 1 : 1].‡

In conclusion, with the aim of preparation of artificial photoenzymes, we successfully expanded the feasibility of the reconstitution method of the photosensitizer-appended cofactor to a hemoprotein other than myoglobin. It is suggested that the present semisynthetic $Ru(bpy)_3$–Cyt-$b_{562}$ has an interesting potential to regulate the activity of other proteins by photocoupling reactions. The detailed photocatalytic properties of $Ru(bpy)_3$–Cyt-$b_{562}$ are now being actively studied in our laboratory.

We are grateful to Professor S. Sligar for his kind gift of the TB-1 cells harboring the pNS207 plasmid. We thank Mr Hideki Horiuchi for his skilful preparation of a specially designed UV–VIS cell.

## Footnotes and References

* E-mail: itarutcm@mbox.nc.kyushu-u.ac.jp

† Quantum yields were determined using ferrioxalate actinometry under the following experimental conditions: protein concentration 0.7–7.6 μM, 10 mM NNDB, pH 7.0 at 25 °C under an Ar atmosphere.

‡ The reduction efficiency was estimated by subtracting the slightly overlapped autoreduction of Cyt-c from the apparent reduction rate.

1 I. Willner and S. Rubin, *Angew. Chem., Int. Ed. Engl.*, 1996, **35**, 367.
2 J. Berglund, T. Pascher, J. R. Winkler and H. B. Gray, *J. Am. Chem. Soc.*, 1997, **119**, 2464; E. Zahavy and I. Willner, *J. Am. Chem. Soc.*, 1996, **118**, 12 499.
3 I. Hamachi, S. Tanaka and S. Shinkai, *Chem. Lett.*, **1993**, 1417; *J. Am. Chem. Soc.*, 1993, **115**, 10 458; I. Hamachi, S. Tsukiji, S. Tanaka and S. Shinkai, *Chem. Lett.*, 1996, 751; I. Hamachi, T. Matsugi, S. Tanaka and S. Shinkai, *Bull. Chem. Soc. Jpn.*, 1996, **69**, 1657.
4 E. Itagaki and L. P. Hager, *J. Biol. Chem.*, 1966, **241**, 3687; E. Itagaki, G. Palmer and L. P. Hager, *J. Biol. Chem.*, 1967, **242**, 2272.
5 H. P. Nikkila, R. B. Gennis and S. G. Sligar, *Eur. J. Biochem.*, 1991, **202**, 309.
6 G. F.-L. Ames, C. Prody and S. Kustu, *J. Bacteriol.*, 1984, **160**, 1181
7 F. W. J. Teale, *J. Biochim. Biophys. Acta*, 1959, **35**, 543.
8 NNDB was reported to act as an oxidative quencher to $Ru(bpy)_3$, as well as a reductive quencher. L. P. Pan, M. Frame, B. Durham, D. Davis and F. Millett, *Biochemistry*, 1990, **29**, 3231.

*Received in Cambridge, UK, 28th April 1997; Revised manuscript received 4th July, 1997; 7/04767C (Formerly 7/02888A)*

# Intramolecular migration of $[Pt(dien)]^{2+}$ (dien = 1,5-diamino-3-azapentane) from sulfur to imidazole-$N^1$ in histidylmethionine (his-metH)

**Christian D. W. Fröhling and William S. Sheldrick***

*Lehrstuhl für Analytische Chemie, Ruhr-Universität Bochum, D-44780 Bochum, Germany*

**HPLC and NMR investigations of the kinetics of competitive binding by neighbouring side chains in his-metH demonstrate that at pH > 6 initial S coordination is followed by slow isomerization to an imidazole-$N^1$ bound complex through a dinuclear intermediate $[\{Pt(dien)\}_2$(his-metH-1κ$N^1$:2κ$S$)$]^{4+}$**

Pt binding by sulfur-containing bioligands such as L-methionine (Hmet) is believed to be responsible for the concentration-dependent nephrotoxicity of the widely used antitumor agent cisplatin, *cis*-$[PtCl_2(NH_3)_2]$.[1] Recent reports[2,3] of the replacement of a thioether S by guanine-$N^7$ in the square-planar coordination sphere of the model fragment $[Pt(dien)]^{2+}$ have also nourished the concept of a drug reservoir mechanism in which initial protein binding may provide a route to DNA platination.[4] Interestingly, whereas 5′-GMP selectively displaces Hmet in $[Pt(dien)(Hmet\text{-}\kappa S)]^{2+}$, no reaction is observed[3] between the likewise imidazole-containing amino acid L-histidine (Hhis) and this complex, even after 3 days. In contrast to this finding, we now report HPLC and NMR evidence for his-$N^1$ replacement of S-bound met, when both are neighbouring peptide residues.

Equimolar 0.8mM solutions of the three model dipeptides his-metH, met-hisH and *cyclo*-his-met with $[Pt(dien)(H_2O)]^{2+}$ in the range 3 < pH < 11 were incubated at 313 K for 14 days, after which the reaction products were separated by reversed-phase HPLC in the presence of 0.1% (v/v) pentafluoropropionic acid as an ion-pairing agent.[5,6] The distribution diagrams presented for the $[Pt(dien)(H_2O)]^{2+}$/his-metH system in Figs. 1–3 were calculated using peak areas of the separated species at the detection wavelength of 220nm and individual molar absorbance coefficients obtained from a least-squares fit for the chromatographic data collected over the full pH range. Products were characterized by FAB mass spectrometry and multinuclear ($^1$H,$^{195}$Pt) NMR spectroscopy.† Methionine κ$S$ coordination leads to a pronounced downfield shift for the thioether δ-$CH_3$ protons from $\delta$ 2.12 in the free dipeptide (pH* = 6.9) to $\delta$ 2.53 in $[Pt(dien)(his\text{-}metH\text{-}\kappa S)]^{2+}$ **1**, the dominant Pt complex in acid solution. At pH > 6.1, the $N^1$-bound complex, $[Pt(dien)(his\text{-}metH\text{-}\kappa N^1)]^{2+}$ **2**, provides the major species; **2** is characterized by its lack of a δ-$CH_3$ downfield shift, the equivalence of its $^3J(^1H\text{–}^{195}Pt)$ values (19 Hz) for the imidazole $H^2$ and $H^5$ resonances and its typical $^{195}$Pt NMR chemical shift (δ −2861) for a square-planar $N_4$ coordination sphere.[7] In contrast to Hhis itself with an $N^3/N^1$ binding ratio of 1.5 for $[Pt(dien)]^{2+}$ at pH* = 6.5,[8] the κ$N^3$ complex appears to play a minor role for his-metH in neutral aqueous solution, as is also the case for met-hisH and *cyclo*-his-met. These latter dipeptides exhibit respective crossover pH values of 5.9 and 3.8 for the change in their preferred binding mode from κ$S$ to κ$N^1$. Inspection of Fig. 1 indicates that a dinuclear complex $[\{Pt(dien)\}_2(his\text{-}metH\text{-}1\kappa N^1:2\kappa S)]^{4+}$ **3**, characterized by its FABMS base peak and two $^{195}$Pt resonances, reaches its maximum concentration at the crossover pH value and a similar state of affairs was established for met-hisH and *cyclo*-his-met.

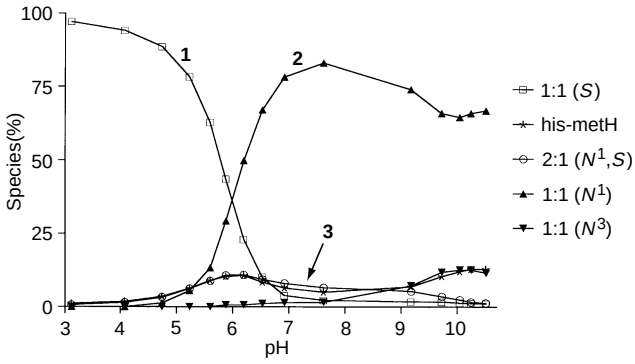



**Fig. 1** Species distribution for the 1 : 1 $[Pt(dien)(H_2O)]^{2+}$–his-metH reaction system as determined by HPLC for the range pH 3.0–10.5 ($T$ = 313 K, $t_{reaction}$ = 14 d). Two minor species are omitted for clarity.

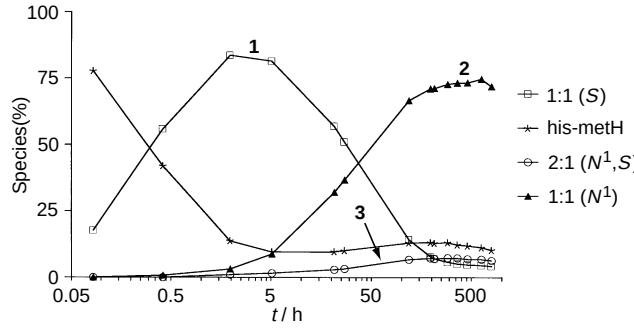



**Fig. 2** Time-course of the 1 : 1 reaction between $[Pt(dien)(H_2O)]^{2+}$ and his-metH at pH = 9.4 as monitored by reversed-phase HPLC ($T$ = 313 K). A minor species is omitted for clarity.

Time-dependent HPLC studies of the $[Pt(dien)(H_2O)]^{2+}$–his-metH reaction system at 313 K (Figs. 2 and 3) demonstrate that, as expected,[2–4,9] the kinetically favoured S-bound complex **1** is formed rapidly and reaches a maximum concentration within 2–3 h. At the pH values considered (6.5, 9.4), **1** then slowly isomerizes to the thermodynamically preferred κ$N^1$ complex **2** over a period of 500 h (Scheme 1). In Fig. 2, the dinuclear complex **3** appears in chromatograms together with **2** for the

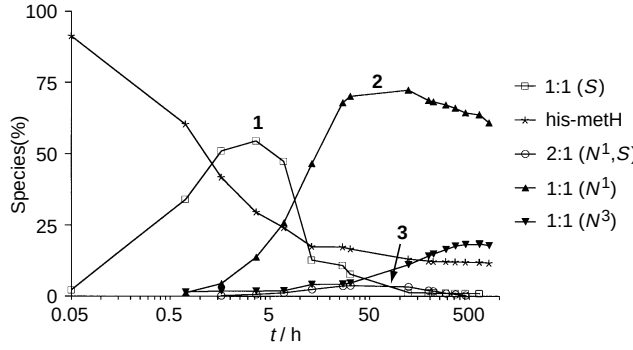
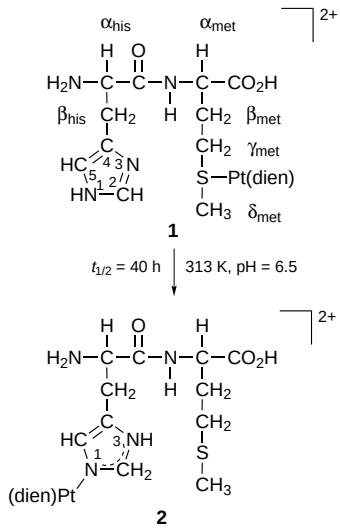



**Fig. 3** Time-course of the 1 : 1 reaction between $[Pt(dien)(H_2O)]^{2+}$ and his-metH at pH = 9.4 as monitored by reversed-phase HPLC ($T$ = 313 K). A minor species is omitted for clarity.




**Scheme 1** Isomerization **1** → **2**

first time after 2 h and exhibit a distribution curve with a time-dependence similar to that of the $N^1$-bound complex. Contrastingly, **2** reaches a maximum concentration after *ca*. 30 h at pH 9.4 (Fig. 3) and can no longer be detected after 500 h. In accordance with the findings of Sadler and coworkers,[3] we also confirmed[10] that the individual amino acid Hhis plays only a minor role in Pt binding when $[Pt(dien)(H_2O)]^{2+}$ is also allowed to react with an equimolar solution of Hmet and Hhis for 14 days at 313 K in the range $3 < pH < 11$. The S-bound complex $[Pt(dien)(Hmet\text{-}\kappa S)]^{2+}$ is present over the whole experimental range and exhibits a crossover pH (as dominant species) of 8.3 to a second N(amino)-bound Hmet complex. A two-step intramolecular route involving the dinuclear intermediate product **3**, which would contrast to a normal five-coordinate intermediate, can be discussed for the isomerization of **1** to **2**. Initial coordination of the kinetically favoured thioether S in **1** is the first step and blocks this binding site for further reactions. Subsequently a second $Pt(dien)^{2+}$ fragment is bound to the thermodynamically preferred imidazole-$N^1$ and the dinuclear complex **3** is formed. For an equimolar ratio of Pt to ligand, this complex dissociates to the mononuclear species **2** by cleavage of the less stable Pt–S bond (Fig. 3). This final step is favoured by the associated reduction in cation charge from +4 to +2. At the higher pH value (9.4), the required dinuclear intermediate **3** can no longer be detected after completion of the conversion **1** → **2**. In contrast, no intermediate could be established for the intramolecular migration of $Pt(dien)^{2+}$ from S to guanine-$N^7$ in S-guanosyl-L-homocysteine.[2,11] This isomerization is more rapid ($t_{\frac{1}{2}}$ = 10 h at 295 K, pH < 6.5) than for the conversion **1** → **2**, which exhibits a half-life ($t_{\frac{1}{2}}$ *ca.* 40 h at 313K, pH = 6.5) more comparable with that reported for the reaction of $[Pt(dien)(Hmet\text{-}\kappa S)]^{2+}$ with 5′-GMP ($t_{\frac{1}{2}}$ = 167 h at 300 K, pH* = 7.0).[3] Under pseudo-first-order conditions, the formation of the dinuclear complex **3** exhibits a reaction rate of $1 \times 10^{-4}$ $s^{-1}$, which is nearly an order of magnitude slower than that for **1** ($k = 9 \times 10^{-4}$ $s^{-1}$) but similar to the rate constant of **2** ($k = 8 \times 10^{-5}$ $s^{-1}$). Such values are, of course, not directly comparable with intramolecular competition conditions (1 : 1), because of pronounced changes in the final product distribution. The observed acceleration in formation of **2** at pH 9.4 (Fig. 3) could be due to faster coordination of a second $Pt(dien)^{2+}$ fragment to the now non-protonated imidazole ring. Temporary formation of **3** is then followed by disappearance of this dinuclear complex which is not thermodynamically stable under these conditions.

The present investigation provides evidence for intramolecular Pt migration from a kinetically favoured met residue to a thermodynamically preferred his side chain in peptides. Although the conversion is relatively slow, it should be remembered that Pt has an *in vivo* half-life of several days after administration of cisplatin.[12] The presence of spatially neighbouring his residues could, therefore, influence the reactivity of met-bound Pt in DNA-binding proteins and should be considered in discussions on the mechanism of action of Pt anticancer drugs.

## Footnotes and References

† $^1H$ and $^{195}Pt$ NMR data ($D_2O$) with chemical shifts ($\delta$) relative to respectively sodium 3-(trimethylsilyl)tetradeuteriopropionate (TSP, $\delta$ = 0.00) or sat. $K_2[PtCl_4]$–1mol $dm^{-3}$ NaCl (external, $\delta$ = −1628) at 295K. pH* values were not corrected for deuterium isotope effects.

his-metH: $^1H$, $\delta$ 8.06 ($H^2$), 7.17 ($H^5$), 4.29 ($\alpha_{met}$), 4.16 ($\alpha_{his}$), 3.24 ($\beta_{his}$), 2.52 ($\gamma_{met}$), 2.12 ($\delta_{met}$), 2.12, 1.98 ($\beta_{met}$) (pH* = 6.9). $[Pt(dien)(his\text{-}metH\text{-}\kappa S)]^{2+}$ **1**: FABMS, *m/z* 584 $M^+$; $^1H$, $\delta$ 8.68 ($H^2$), 7.47 ($H^5$), 4.61 ($\alpha_{his}$), 4.46 ($\alpha_{met}$), 3.56 ($\beta_{his}$), 2.53 ($\delta_{met}$), 2.4, 2.22 ($\beta_{met}$), 2.85–3.3 ($\gamma_{met}$, dien-$CH_2$), $^{195}Pt$, $\delta$ −3378 (pH* = 3.2). $[Pt(dien)(his\text{-}metH\text{-}\kappa N^1)]^{2+}$ **2**: FABMS, *m/z* 584 $M^+$; $^1H$, $\delta$ 7.88 [$H^2$, $^3J(^1H\text{–}^{195}Pt)$ 19 Hz], 6.88 [$H^5$, $^3J(^1H\text{–}^{195}Pt)$ 19 Hz], 4.26 ($\alpha_{his}$), 3.75 ($\alpha_{met}$), 3.29 ($\beta_{his}$), 2.5 ($\gamma_{met}$), 2.13 ($\delta_{met}$), 2.07, 1.94 ($\beta_{met}$), 2.85–3.3 (dien-$CH_2$); $^{195}Pt$, $\delta$ −2861 (pH* = 8.2). $[\{Pt(dien)\}_2(his\text{-}metH\text{-}1\kappa N^1 : 2\kappa S)]^{4+}$ **3**: FABMS, *m/z* 879 $M^+$; $^1H$, $\delta$ 7.94 [$H^2$, $^3J(^1H\text{–}^{195}Pt)$ 19 Hz], 6.99 [$H^5$, $^3J(^1H\text{–}^{195}Pt)$ 19Hz], 4.68 ($\alpha_{met}$), 4.28 ($\alpha_{his}$), 3.3 ($\beta_{his}$), 2.52 ($\delta_{met}$), 2.38, 2.18 ($\beta_{met}$), 2.8–3.3 ($\gamma_{met}$, dien-$CH_2$); $^{195}Pt$, $\delta$ −2861, −3380 (pH* = 1.0).


1 E. L. M. Lempers and J. Reedijk, *Adv. Inorg. Chem.*, 1991, **37**, 175.
2 S. S. G. E. van Boom and J. Reedijk, *J. Chem. Soc., Chem. Commun.*, 1993, 1397.
3 K. J. Barnham, M. I. Djuran, P. del Socorro Murdoch and P. J. Sadler, *J. Chem. Soc., Chem. Commun.*, 1994, 721.
4 K. J. Barnham, M. I. Djuran, P. del Socorro Murdoch, J. D. Ranford and P. J. Sadler, *J. Chem. Soc., Dalton Trans.*, 1995, 3721.
5 A. F. M. Siebert, C. D. W. Fröhling and W. S. Sheldrick, *J. Chromatogr. A*, 1997, **761**, 115.
6 A. F. M. Siebert and W. S. Sheldrick, *J. Chem. Soc., Dalton Trans.*, 1997, 385.
7 T. G. Appleton, J. W. Connor and J. R. Hall, *Inorg. Chem.*, 1988, **27**, 130.
8 T. G. Appleton, F. J. Pesch, M. Wienken, S. Menzer and B. Lippert, *Inorg. Chem.*, 1992, **31**, 4410.
9 T. G. Appleton, J. W. Connor, J. R. Hall and P. D. Prenzler, *Inorg. Chem.*, 1989, **28**, 2030.
10 D. A. Wolters, Diploma thesis, Ruhr-Universität, Bochum, 1995.
11 S. S. G. E. van Boom, Dissertation, University of Leiden, 1995.
12 A. W. Prestayko, in *Cisplatin, Current status and New Developments*, ed. A. W. Prestayko, S. T. Crooke and S. K. Carter, Academic Press, London, 1980, p. 2.


*Received in Basel, Switzerland, 28th April 1997; 7/02904G*

# Remarkable 'edge' ligation of a triphosphacyclopentenyl ring system. Synthesis, crystal and molecular structure of $[Ni(\eta^5\text{-}P_3C_2Bu^t_2)\{\eta^2\text{-}P_3C_2Bu^t_2CH(SiMe_3)_2Me\}]$

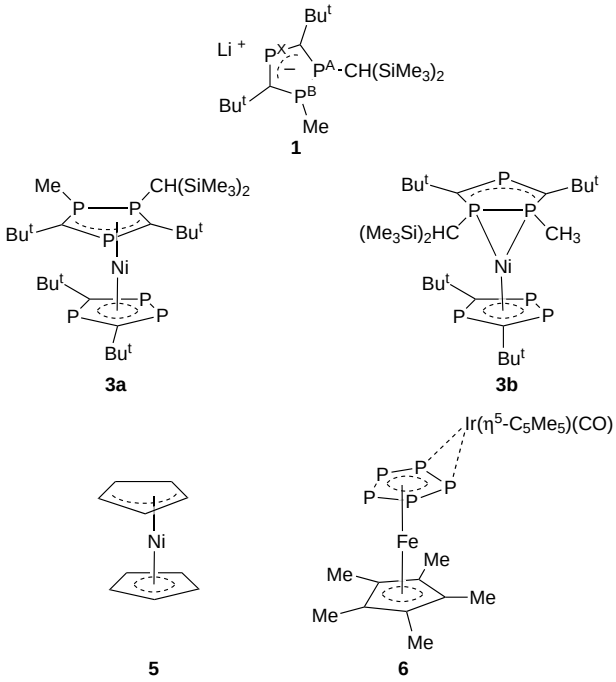
**Vinicius Caliman, Peter B. Hitchcock and John F. Nixon***

*School of Chemistry, Physics and Environmental Science, University of Sussex, Brighton, UK BN1 9QJ*

**In the nickel(II) complex $[Ni(\eta^5\text{-}P_3C_2Bu^t_2)(\eta^2\text{-}P_3C_2Bu^t_2CH(SiMe_3)_2Me)]$ the triphosphacyclopentenyl ring $P_3C_2Bu^t_2CH(SiMe_3)_2Me$ is unexpectedly coordinated to the metal exclusively *via* the two adjacent saturated ring phosphorus atoms, rather than *via* the 2-phosphaallyl fragment.**

Very recently[1] we reported the synthesis of the lithium triphosphacyclopentenyl salt $LiP_3C_2Bu^t_2RR'$ **1** [R = $(Me_3Si)_2$CH, R′ = Me] by treatment of the 1,2,4-triphosphole $P_3C_2Bu^t_2R$ **2**[2] with LiMe. The $^{31}P\{^1H\}$ NMR spectrum of **1** can be readily interpreted[1] in terms of the $\eta^3$-2-phosphaallylic structure [Fig. 1(*a*)]. Although several ligation modes of the triphosphacyclopentenyl ring anion in **1** towards transition metals can be envisaged, it was anticipated that $\eta^3$-ligation *via* the 2-phosphaallyl fragment would be most likely in complexes of nickel(II) halides, however, unexpectedly a completely different type of ligation of the ring to the metal centre occurs as discussed below.

Treatment of $Li[P_3C_2Bu^t_2CH(SiMe_3)_2Me]$ with 1 equiv. of $NiBr_2$ in diethyl ether at −78 °C affords a dark green solution which on further treatment with 1 equiv. of $Li[P_3C_2Bu^t_2]$ affords the purple complex $[Ni(\eta^5\text{-}P_3C_2Bu^t_2)\{P_3C_2Bu^t_2CH(SiMe_3)_2Me\}]$ **3**. Scheme 1 shows the likely steps of the synthesis of **3** *via* the postulated intermediate complex **4** which could not be isolated on account of its air- and moisture-sensitivity. Complex **3** was obtained in 45% yield after chromatography and was fully characterised by mass spectrometry, $^{31}P\{^1H\}$ and $^1H$ NMR spectroscopy.† Its structure, which was confirmed by a single-crystal X-ray diffraction study,‡ surprisingly proved not to involve the expected $\eta^5:\eta^3$ ligation of the two five-membered ring systems which is well known for the related cyclopentadienyl cyclopentenyl nickel(II) complex $[Ni(\eta^5\text{-}C_5H_5)(\eta^3\text{-}C_5H_7)]$ **5**.



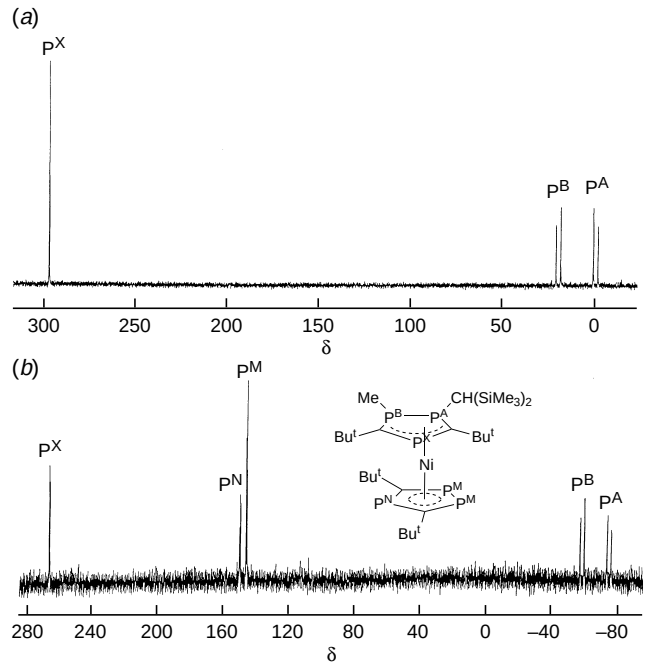
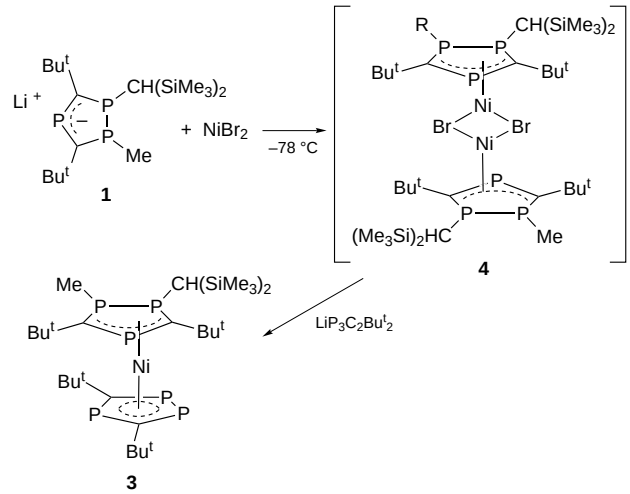




**Fig. 1** $^{31}P\{^1H\}$ NMR spectra of (*a*) **1** and (*b*) **3**




**Scheme 1**

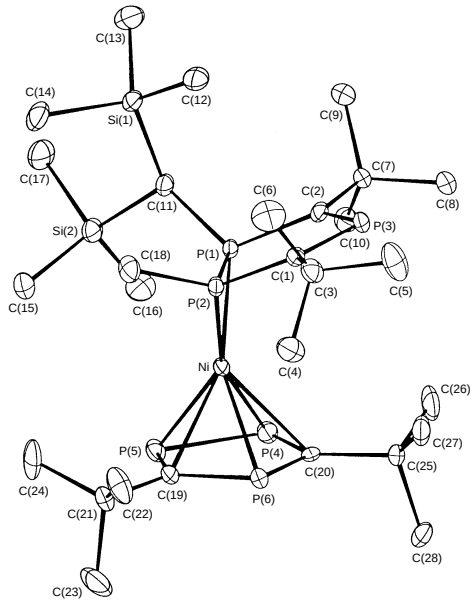



**Fig. 2** Molecular structure of **3** with atomic numbering scheme

The $^{31}P\{^{1}H\}$ NMR spectrum of **3** [Fig. 1(*b*)] exhibits a pattern of lines expected for an $[ABM_2NX]$ spin system. The $\eta^5$-$P_3C_2Bu^t_2$ ring gives rise to signals corresponding to $P^M$ and $P^N$ ($\delta$ 145.8 and 149.7, respectively) with the expected magnitude of the $^2J_{PP}$ coupling constant for this type of aromatic ring system.[3–6] The pattern of lines observed for the $P_3C_2Bu^t_2CH(SiMe_3)_2Me$ ring in **3** is similar to that exhibited for the free anion in **1**; the $P^A$ and $P^B$ resonances of the two $sp^3$-hydridised phosphorus showing characteristic high-field resonances ($\delta$ $P^A$ −74.5; $\delta$ $P^B$ −58.3) with a typically large one bond $^1J_{P^AP^B}$ coupling constants (251.3 Hz), whereas $P^X$ exhibits a typical chemical shift for an $sp^2$-hybridised phosphorus ($\delta$ $P^X$ 266.2), suggesting structure **3a**.

A single-crystal X-ray diffraction study on **3** unexpectedly revealed the remarkable molecular structure **3b** (Fig. 2), in which the 2-phosphaallylic fragment of the $P_3C_2Bu^t_2CH(SiMe_3)_2Me$ ring is not involved in bonding to the nickel, which is in fact solely ligated *via* the P(1) and P(2) lone pair electrons of the two saturated phosphorus centres. The two rings in **3** are both planar, with a dihedral angle of 18°, and structural data are summarised in Fig. 3. The $\eta^5$-ligated $P_3C_2Bu^t_2$ ring exhibits bond lengths and angles very similar to several related transition-metal complexes containing this triphospholyl anion.[3–6] The triphosphacyclopentenyl ring $P_3C_2Bu^t_2CH(SiMe_3)_2Me$ in **3** is attached to the $Ni^{II}$ *via* two P–Ni single bonds [P(1)–Ni 2.201(2), P(2)–Ni 2.155(2) Å] and the P(1)–Ni–P(2) bond angle is 58.64(5)°. The intracyclic bond lengths in the triphosphacyclopentenyl ring clearly confirm the partial double bond character expected for the two P–C bonds of the uncoordinated 2-phosphaallylic system [P(3)–C(1) 1.728(5), P(3)–C(2) 1.723(5) Å].

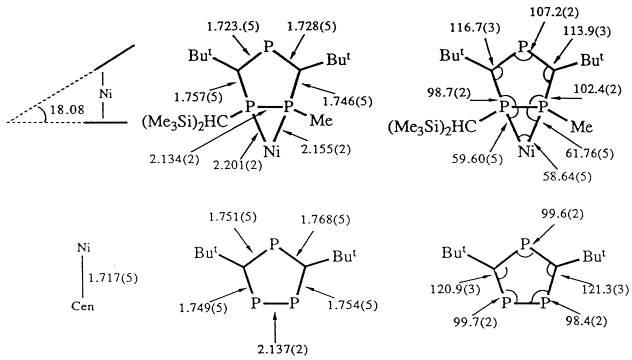



**Fig. 3** Important structural features from **3a**. Distances in (Å) and angles in (°).

To our knowledge, the bonding exhibited by the triphosphacyclopentenyl ring in **3** is unprecedented. Scherer and coworkers[7] recently reported the synthesis and molecular structure of the complex $[(\eta^5\text{-}C_5Me_5)Fe(\mu\text{-}\eta^5:\eta^2\text{-}P_5)Ir(\eta^5\text{-}C_5Me_5)(CO)]$ **6**, in which there is a $\eta^2$-'edge' coordination of the 16-electron $[Ir(CO)(\eta^5\text{-}C_5Me_5)]$ fragment to two adjacent phosphorus atoms in the pentaphospholyl ring. However, the $\eta^2$-coordination of the $P_5$ ring in **6** is completely different to that described for complex **3** above, since it involves an unsaturated P–P ring linkage. It is therefore 'alkene-like' in its ligating mode towards the $Ir^I$ centre, whereas in **3** the two saturated $sp^3$-hybridised phosphorus atoms must presumably utilise their lone pair electrons in bonding to $Ni^{II}$. These bonding differences are clearly reflected in the very different P–P bond lengths observed within the $\eta^5$-$P_5:\eta^2$-$P_5$ and $\eta^2$-$P_3C_2Bu^t_2CH(SiMe_3)_2Me$ rings in **3** and **6**. There is a significant lengthening (*ca.* 0.2 Å) of the P–P distance in **6** [P(1)–P(2) 2.359(2) Å], compared with that of the parent complex $[Fe(\eta^5\text{-}C_5Me_5)(\eta^5\text{-}P_5)]$,[7] whereas no such elongation results on $\eta^2$-coordination of the $P_3C_2Bu^t_2CH(SiMe_3)_2Me$ ring in **3**, and a normal P(1)–P(2) single bond distances [2.134(2) Å] is observed.

We thank CNPq (Brazil) for a studentship (for V. C.) and EPSRC for their continuing support for phosphaalkyne chemistry at Sussex.

## Footnotes and References

* E-mail: j.nixon@sussex.ac.uk

† Complex **3**. Satisfactory elemental analyses were obtained. $^{31}P\{^{1}H\}$ NMR (101.3 MHz, $C_6D_6$, 25 °C): $\delta$ 266.2 (dd, $P^X$, $^2J_{P^XP^A}$ 33.8, $^2J_{P^XP^B}$ 42.2 Hz), 149.7 (dd $P^N$, $^2J_{P^NP^M}$ 48.4, $^2J_{P^NP^A}$ 7.2 Hz), 145.8 (dt, $P^M$, $^2J_{P^MP^N}$ 48.4, $^2J_{P^MP^B}$ 9.2 Hz), −58.3 (ddd, $P^B$, $^1J_{P^BP^X}$ 251.3, $^2J_{P^BP^M}$ 42.2, $^2J_{P^BP^M}$ 9.2 Hz), −74.5 (ddd, $P^A$, $^1J_{P^AP^B}$ 251.3, $^2J_{P^AP^X}$ 33.8, $^2J_{P^AP^N}$ 7.2 Hz). $^1H$ NMR (250.2 MHz, $CDCl_3$, 25 °C): $\delta$ −0.16 [s, 9 H, $Si(CH_3)_3$], 0.44 [s, 9 H, $Si(CH_3)_3$], 0.83 (dt, 3 H, $PCH_3$, $^2J_{HP}$ 6.55, $^3J_{HP}$ 1.37 Hz), 1.10 [s, 9 H, $C(CH_3)_3$], 1.50 [d, 9 H, $C(CH_3)_3$, $^4J_{HP}$ 1.63 Hz], 1.52 [d, 9 H, $C(CH_3)_3$, $^4J_{HP}$ 1.48 Hz], 1.55 [s, 9 H, $C(CH_3)_3$], 2.02 (dd, 1 H, CH, $^2J_{HP}$ 10.54, $^3J_{HP}$ 5.65 Hz). Mass spectrum (EI) for **3**: *m/z*: 694 $[Ni(P_3C_2Bu^t_2)\{P_3C_2Bu^t_2CH(SiMe_3)_2Me\}]^+$ (22%), 535 $[Ni(P_3C_2Bu^t_2)(P_3C_2Bu^t_2Me)]^+$, 405 $[P_3C_2Bu^t_2)(P_3C_2Bu^t_2)]^+$, 73 $[SiMe_3]^+$.

‡ *Crystal data* for **3**: $C_{28}H_{58}NiP_6Si_2$, $M$ = 695.45, monoclinic, space group $P2_1/c$ (no. 14), $a$ = 10.782(3), $b$ = 19.243(4), $c$ = 19.319(7) Å, $\beta$ = 94.75(2)°, $U$ = 3995(2) Å$^3$, $Z$ = 4, $D_c$ = 1.16 g cm$^{-3}$, $F(000)$ = 1488. Monochromated Mo-Kα radiation $\lambda$ = 0.710 69 Å, $T$ = 173(2) K. Data were collected on an Enraf-Nonius CAD 4 diffractometer using a crystal of 0.40 × 0.40 × 0.20 mm. A total of 7010 unique reflections were measured for $2 < \theta < 25°$ of which 5120 had $I > 2\sigma(I)$. The structure was solved by direct methods using SHELXS-86 and refined on $F^2$ with all non-H atoms anisotropic using SHELXL-93. H atoms were included in riding mode with $U_{iso}$ = 1.2 $U_{eq}$(C) or 1.5 $U_{eq}$(C) for methyl groups. The final residuals were $R_1$ = 0.058 [for $I > 2\sigma(I)$] and $wR_2$ = 0.158 for all data. CCDC 182/553.

1 V. Caliman, P. B. Hitchcock, J. F. Nixon and N. Sakarya, *Bull. Soc. Chim. Belg.*, 1996, **105**, 675.
2 V. Caliman, P. B. Hitchcock and J. F. Nixon, *J. Chem. Soc., Chem. Commun.*, 1995, 1661.
3 R. Bartsch, P. B. Hitchcock and J. F. Nixon, *J. Chem. Soc., Chem. Commun.*, 1987, 1146.
4 J. F. Nixon, *Chem. Rev.*, 1988, **88**, 1327 and references therein.
5 J. F. Nixon, *Chem. Soc. Rev.*, 1995, 319 and references therein.
6 J. F. Nixon, *Coord. Chem. Rev.*, 1995, **145**, 201 and references therein.
7 M. Detzel, G. Friedrich, O. J. Scherer and G. Wolmershausen, *Angew. Chem., Int. Ed. Engl.*, 1995, **34**, 1321.

*Received in Cambridge, UK, 2nd June 1997; 7/03797J*

# Di-cyclopalladated Schiff's base liquid crystals: novel metallomesogens

**Donocadh P. Lydon and Jonathan P. Rourke***

*Department of Chemistry, Warwick University, Coventry, UK CV4 7AL*

**The double cyclopalladation of di-Schiff's bases and subsequent reaction with a β-diketone yields novel metallomesogens containing a dimetallated organometallic core: these compounds show nematic phases, and the use of simple alkyl substituted diketones has a very dramatic effect on both the melting and clearing points, bringing them down substantially.**

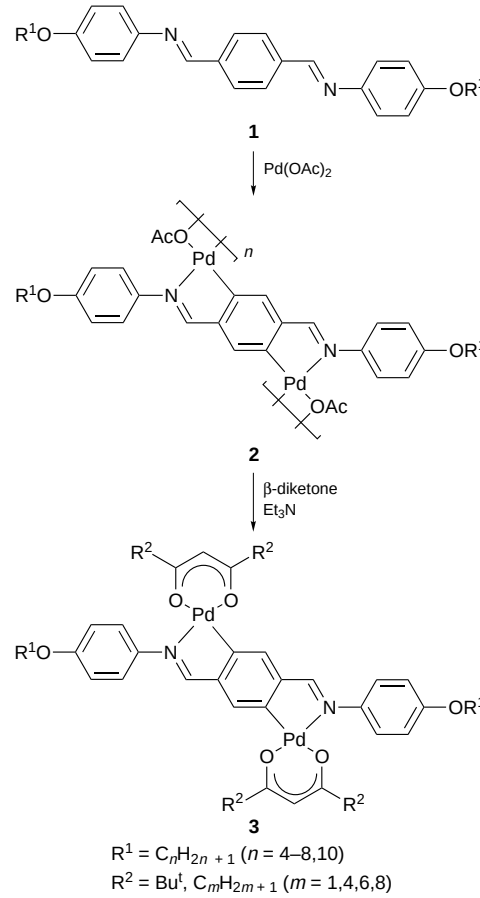
There is currently much interest in the synthesis of metal-containing liquid crystals (metallomesogens) due to the perceived advantages of combining the properties of liquid crystal systems with those of transition metals. The area has been well-reviewed recently,[1,2] with excellent new work appearing constantly.[3–7] Cyclopalladated compounds have proved to be a particularly fertile area of research, with many different examples from many different groups.[7–14]

Most recently, our own work has focused on the role of the co-ligand in a given mesogenic core.[14] Here we report the synthesis, characterisation and mesogenic behaviour of novel complexes that contain two metals cyclometallated to the central core. Although one co-ordination complex containing two metals has previously been reported[15] and two families of dimeric mesogens have been extensively investigated,[5,8,16–28] our new compounds represent the first examples of calamitic organometallic mesogens whose core contains two metals.

The synthesis of the new mesogens **3** is summarised in Scheme 1.† The complexes are based on a di-Schiff's base core[14] with two palladiums cyclometallated in a *trans* fashion to this core. The co-ligands on the palladium are diketonate derivatives. All the new compounds were analysed by $^1$H NMR spectroscopy and microanalysis.‡ Thus, compounds with alkyl chains of between four and ten carbons on the di-Schiff's base core were synthesised with a simple acetylacetonate co-ligand. In addition, with one Schiff's base core ($n$ = 8), the alkyl chain on the diketonate was systematically varied (R′ = Me, Bu, hexyl, octyl and Bu$^t$).

The thermal behaviour of the diketonate complexes **3** is detailed in Table 1 and summarised in Figs. 1 and 2. Thus nematic phases (identified on the basis of optical texture) were exhibited by all but three of the complexes. Confirmation of the mesomorphism was obtained by differential scanning calorimetry (DSC) measurements where possible (decomposition of some of the compounds obscured some of the transitions).

The simple acetylacetonate complexes (Fig. 1) exhibit nematic phases at relatively high temperatures (in most cases greater than 200 °C) and the transition from the nematic to the isotropic liquid was often accompanied by extensive decomposition. As one would expect, the melting and clearing points are brought down in temperature by the use of longer chains on the Schiff's base unit (*i.e.* increasing *n*). However, a more dramatic reduction in both the melting and clearing points (some 80 K) can be achieved by using short chain length alkyl diketones (Fig. 2). This effect is most marked for the $m$ = 4 case, *i.e.* R′ = Bu, where the mesophase is observed well below the decomposition point of the compound. In contrast, when Bu$^t$ groups are attached to the diketonate core, a high melting point is observed with no mesophase, even on rapid cooling. One way of viewing this behaviour is to consider the freely moving alkyl chains on the diketonate groups as disrupting the crystal




**Scheme 1**

**Table 1** Mesogenic behaviour of compounds **3**

| R$^1$ | R$^2$ | Transition | $T$/°C | $\Delta H$/J g$^{-1}$ |
|---|---|---|---|---|
| Bu | Me | K–D | 285[a] | — |
| Pentyl | Me | K–D | 280[a] | — |
| Hexyl | Me | K–N | 261 | — |
| | | N–I | 271[a] | — |
| Heptyl | Me | K–N | 238 | — |
| | | N–I | 253[a] | — |
| Octyl | Me | K–N | 203 | — |
| | | N–I | 255[a] | — |
| Decyl | Me | K–N | 187 | — |
| | | N–I | 246 | — |
| Octyl | Bu | K–N | 119 | 30.96 |
| | | N–I | 148 | 0.69 |
| Octyl | Hexyl | K–N | 133 | 29.25 |
| | | N–I | 142 | 0.46 |
| Octyl | Octyl | K–I | 140 | 25.59 |
| | | N–I | 129[b] | 0.53 |
| Octyl | Bu$^t$ | K–I | 262 | — |

[a] With decomposition. [b] Monotropic.

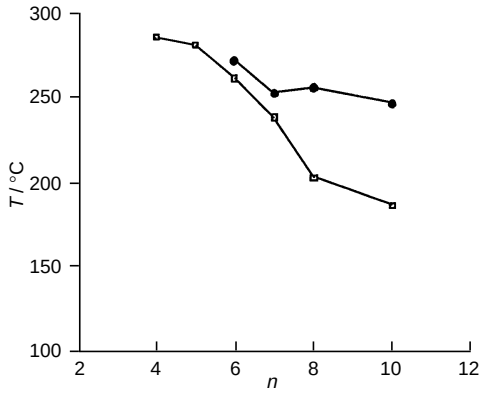



**Fig. 1** Phase behaviour of compounds **3** as a function of *n*; (□) K → N and (●) N → I

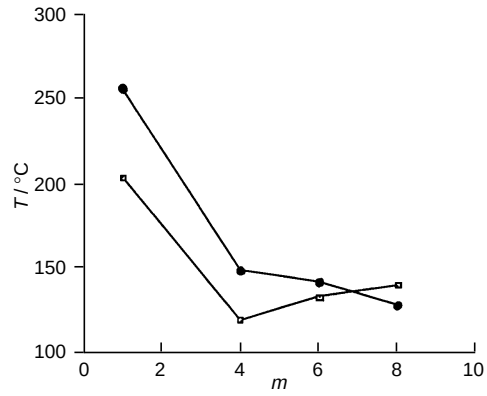



**Fig. 2** Phase behaviour of compounds **3** as a function of *m*; (□) K → N, I and (●) N → I

packing of the molecules and thus reducing the melting point. The Bu$^t$ group is a compact group that cannot move freely, and will not disrupt the packing forces, hence its much higher melting point.

It is perhaps surprising that compounds **3** show any mesogenic behaviour at all: others have suggested that at least four aromatic rings would be necessary to promote mesogenic behaviour in molecules with large metal groups pendant to the central core.[30,31] Here we have only three aromatic rings, and two pendant metal groups. If, however, we consider the core of the molecule to be the central benzene ring, the two cyclometallated units and the two diketonate groups with the alkoxyphenyl groups being the pendant moieties, we encounter a similar problem. Thus it appears that it would be best to consider all of the central Schiff's base unit, with both the alkoxyphenyl and Pd–diketonate groups, as the mesogenic core of the molecule.

In conclusion, we have synthesised a totally new family of metallomesogens with two metal groups in a *trans* fashion about the central ring, and are now working on the *cis* compounds, where both cyclopalladated groups are on the same side of the ring.

We thank the University of Warwick for financial support (D. P. L.), and Johnson-Matthey for the loan of chemicals.

## Footnotes and References

* E-mail: j.rourke@warwick.ac.uk

† Palladium acetate (0.150 g, 6.70 × $10^{-4}$ mol) was added to a solution of **1** (*n* = 10) (0.200 g, 3.35 × $10^{-4}$ mol) in acetic acid (200 ml) at 60 °C and stirred (24 h). The solvent was removed, and the product **2** (*n* = 10) used without further purification.

Compound **2** (*n* = 10) (0.180 g, 2.00 × $10^{-4}$ mol) and sodium acetylacetonate (0.073 g, 6.00 × $10^{-4}$ mol, 1.5 equiv.) were suspended in acetone (200 ml) and stirred (24 h). The solvent was removed and the crude product extracted with $CHCl_3$. The product was further purified by chromatography on silica (eluent: $CHCl_3$): yield 0.154 g (77%).

‡ *Selected data* for **3** (*n* = 10, R′ = Me) (all others are similar): $\delta_H$ 8.13 (2 H, s, imine), 7.56 (2 H, s, central ring), 7.39 (4 H, AA′XX′, aromatic), 6.88 (4 H, AA′XX′, aromatic), 5.34 (2 H, s, central acac), 3.99 (4 H, t, $^3J$ 6.5, $OCH_2$), 2.07 (6 H, s, acac Me), 1.89 (6 H, s, acac Me), 1.40 (28 H, m, chain), 0.89 (6 H, t, $^3J$ 6.5 chain $CH_3$). Good elemental analysis data were obtained for all compounds. Evidence for the *trans* arrangement of the palladium atoms about the central ring comes from preliminary single crystal X-ray studies (ref. 29).

1 J. L. Serrano, *Metallomesogens*, VCH, Weinheim, 1996.
2 D. W. Bruce, in *Inorganic Materials*, ed. D. W. Bruce and D. O'Hare, Wiley, Chichester, 2nd edn., 1996.
3 J. P. Rourke, D. W. Bruce and T. B. Marder, *J. Chem. Soc., Dalton Trans.*, 1995, 317.
4 H. Zheng, B. Xu and T. M. Swager, *Chem. Mater.*, 1996, **9**, 907.
5 M. J. Baena, P. Espinet, M. B. Ros and J. L. Serrano, *J. Mater. Chem.*, 1996, **6**, 1291.
6 F. Neve, M. Ghedini and A. Crispini, *Chem. Commun.*, 1996, 2463.
7 M. Ghedini, D. Pucci and F. Neve, *Chem. Commun.*, 1996, 137.
8 J. Barberá, P. Espinet, E. Lalinde, M. Marcos and J. L. Serrano, *Liq. Cryst.*, 1987, **2**, 833.
9 L. Zhang, D. Huang, N. Xiong, J. Yang, G. Li and N. Shu, *Mol. Cryst., Liq. Cryst.*, 1993, **237**, 285.
10 N. Hoshino, H. Hasegawa and Y. Matsunaga, *Liq. Cryst.*, 1991, **9**, 267.
11 M. Marcos, J. L. Serrano, T. Sierra and M. J. Giménez, *Chem. Mater.*, 1993, **5**, 1332.
12 K. Praefcke, S. Diele, J. Pickardt, B. Gündogan, U. Nütz and D. Singer, *Liq. Cryst.*, 1995, **18**, 857.
13 N. J. Thompson, R. Iglesias, J. L. Serrano, M. J. Baena and P. Espinet, *J. Mater. Chem.*, 1996, **6**, 1741.
14 D. P. Lydon, G. W. V. Cave and J. P. Rourke, *J. Mater. Chem.*, 1997, **7**, 403.
15 P. Berdagué, J. Courtieu and P. M. Maitlis, *J. Chem. Soc., Chem. Commun.*, 1994, 1313.
16 P. Espinet, J. Etxebarria, M. Marcos, J. Pérez, A. Remón and J. L. Serrano, *Angew. Chem., Int. Ed. Engl.*, 1989, **28**, 1065.
17 P. Espinet, E. Lalinde, M. Marcos, J. Pérez and J. L. Serrano, *Organometallics*, 1990, **9**, 555.
18 P. Espinet, J. Pérez, M. Marcos, M. B. Ros, J. L. Serrano, J. Barberá and A. M. Levelut, *Organometallics*, 1990, **9**, 2028.
19 M. J. Baena, P. Espinet, M. B. Ros and J. L. Serrano, *Angew. Chem., Int. Ed. Engl.*, 1991, **30**, 711.
20 M. J. Baena, J. Buey, P. Espinet, H.-S. Kitzerow and G. Heppke, *Angew. Chem., Int. Ed. Engl.*, 1993, **32**, 1201.
21 M. J. Baena, J. Barberá, P. Espinet, A. Ezcurra, M. B. Ros and J. L. Serrano, *J. Am. Chem. Soc.*, 1994, **116**, 1899.
22 J. Buey and P. Espinet, *J. Organomet. Chem.*, 1996, **507**, 137.
23 N. Usol'tseva, P. Espinet, J. Buey and J. L. Serrano, *J. Mater. Chem.*, 1997, **7**, 215.
24 M. Ghedini, S. Morrone, G. D. Munno and A. Crispini, *J. Organomet. Chem.*, 1991, **415**, 281.
25 M. Ghedini, D. Pucci, E. Cesarotti, P. Antogniazza, O. Francescangeli and R. Bartolino, *Chem. Mater.*, 1993, **5**, 883.
26 M. Ghedini, D. Pucci, R. Bartolino and O. Francescangeli, *Liq. Cryst.*, 1993, **13**, 255.
27 A. M. Levleut, M. Veber, O. Fracescangeli, S. Melone, M. Ghedini, F. Neve, F. P. Nicoletta and R. Bartolino, *Liq. Cryst.*, 1995, **19**, 241.
28 A. Crispini, M. Ghedini, S. Morrone, D. Pucci and O. Francescangeli, *Liq. Cryst.*, 1996, **20**, 67.
29 W. Errington, personal communication.
30 D. W. Bruce, *Adv. Mater.*, 1994, **6**, 699.
31 R. Deschenaux, J.-L. Marendaz and J. Santiago, *Helv. Chim. Acta*, 1993, **76**, 865.

*Received in Cambridge, UK, 12th June 1997; 7/04110A*

# First total synthesis of (±)-hyperolactone A

**Daisuke Ichinari,[a] Toshihiko Ueki,[a] Kazuo Yoshihara[b] and Takamasa Kinoshita*[a]**

[a] *Department of Chemistry, Faculty of Science, Osaka City University, Sugimoto-cho, Sumiyoshi-ku, Osaka 558, Japan*
[b] *Suntory Institute for Bioorganic Research, Shimamoto-cho, Osaka 618, Japan*

**The first total synthesis of (±)-hyperolactone A, isolated from *Hypericum chinense* L., is accomplished from 3-furoic acid and 2-methylbutanal.**

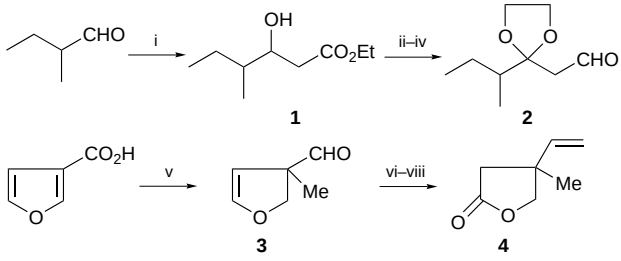
Hyperolactone A[1] is a unique spiro compound isolated from *Hypericum chinense* L., which has a 2-alkyl-9-methyl-9-vinyl-1,7-dioxaspiro[4,4]non-2-ene-4,6-dione skeleton, and is thus an interesting compound as a target for synthesis. The structure[1a] was deduced by spectroscopic experiments, chemical transformations and X-ray crystallography. We describe herein the first total synthesis of (±)-hyperolactone A **8a** by condensation of two fragments, aldehyde **2** and lactone **4**.

The aldol reaction of the lithium enolate of lactone **4**, derived from 3-furoic acid, with the aldehyde **2**, derived from 2-methylbutanal (Scheme 1), afforded **5**† in 81% yield (Scheme 2). The crude alcohol **5** was oxidized to furnish **6** (a mixture of four diastereoisomers‡) by the Swern method in 92% yield. Attempted oxidation of **6** with $MoO_5$·pyridine·HMPA (MoOPH)[3] was unsuccessful, giving the undesired **7b** only in 18% yield, while with Davis reagent[4] a separable isomeric mixture of **7a** and **7b**§ was obtained in 57% yield in a ratio of 2 : 3. A NOE was observed between the 9-methyl group and the OH for the minor isomer **7a**, but not for the major isomer.

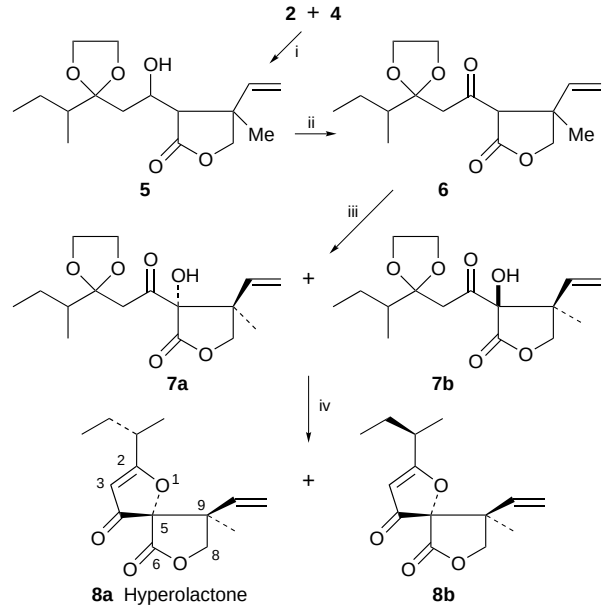
On treatment of **7a** with 3 M HCl in boiling THF to remove the ketal protecting group (which strongly resisted hydrolysis), a mixture of the final product **8a** and its isomer **8b** was obtained in 85% yield in a ratio of 1 : 1, which was separated to give (±)-hyperolactone **8a**¶ as an oil.

The advantages of this strategy are that it is short and efficient, and provides a one-step construction of the spirolactone by acid catalysis *via* deprotection, cyclization and elimination.

We are grateful to Professor M. Tada (Tokyo University of Agriculture and Technology) for kindly providing a reference spectra of Hyperolactone A and for useful comments.




**Scheme 1** *Reagents and conditions*: i, Zn, $BrCH_2CO_2Et$, $C_6H_6$, reflux, 1.5 h, 75%; ii, $CrO_3$, pyridine, $CH_2Cl_2$, room temp., 30 min, 83%; iii, $(CH_2OH)_2$, TsOH, PhMe, reflux, 7 h, 39%; iv, DIBAL-H, PhMe, −78 °C, 10 min, 98%; v, ref. 2; vi, $Ph_3MeP^+$ $Br^-$, BuLi, $Et_2O$, reflux, 12 h; vii, BuOH, TsOH, $CH_2Cl_2$; viii, $CrO_3$, $H_2SO_4$, acetone, 45% over three steps




**Scheme 2** *Reagents and conditions*: i, LDA, THF, −78 °C, 1 h, then −40 °C, 1.5 h, 81%; ii, DMSO, $(COCl)_2$, $CH_2Cl_2$, $Et_3N$, −78 °C, 10 min, 92%; iii, Davis reagent, 57%; iv, 6 M HCl, THF, reflux, 10 h, 85%

## Footnotes and References

* E-mail: takamasa@sci.osaka-cu.ac.jp

† Although a multitude of isomers are formed, in the light of the subsequent steps this does not matter.

‡ The relative proportion (2 : 2 : 2 : 1) was estimated from the carbonyl absorptions: $\delta_C$ 197.1, 198.8, 201.4 and 202.2.

§ The diastereoselectivity was not improved, even in the case of a less bulky electrophile such as the Davis reagent.

¶ *Selected data* [$\delta_H$ (400) MHz, $CDCl_3$)] for **8a**: 0.96 (3 H, t, *J* 7.3), 1.25 (3 H, d, *J* 7.3) 1.41 (3 H, s), 1.54–1.66 (1 H, m), 1.66–1.80 (1 H, m), 2.69 (1 H, tq, *J* 6.7), 4.04 (1 H, d, *J* 8.5), 4.89 (1 H, d, *J* 8.5), 5.24 (1 H, d, *J* 17.1), 5.28 (1 H, d, *J* 11.0), 5.37 (1 H, s), 5.93 (1 H, dd, *J* 11.0, 17.1). For **8b**: 0.98 (3 H, t, *J* 7.3), 1.27 (3 H, d, *J* 7.3), 1.41 (3 H, s), 1.50–1.60 (1 H, m), 1.62–1.80 (1 H, m), 2.66 (1 H, tq, *J* 6.7), 4.04 (1 H, d, *J* 8.5), 4.89 (1 H, d, *J* 8.5), 5.24 (1 H, d, *J* 17.1), 5.28 (1 H, d, *J* 11.0), 5.37 (1 H, s), 5.94 (1 H, dd, *J* 11.0, 17.1). The $^1$H NMR spectrum of (±)-**8a** thus obtained was identical with that of the natural product recorded by Tada *et al.* [ref. 1(*a*)].

1 (*a*) M. Tada, M. Nagai, C. Okumura, Y. Osano and T. Matsuzaki, *Chem. Lett.*, 1989, 683; (*b*) Y. Aramaki, K. Chiba and M. Tada, *Phytochemistry*, 1995, **38**, 1419.
2 T. Kinoshita, D. Ichinari and J. Sinya, *J. Heterocycl. Chem.*, 1996, **33**, 1313.
3 E. Vedejs and S. Larsen, *Org. Synth.*, 1990, **Coll. Vol. VII**, 277.
4 F. A. Davis and O. D. Stringer, *J. Org. Chem.*, 1982, **47**, 1774; F. A. Davis, L. C. Vishwakarma, J. M. Billmers and J. Finn, *J. Org. Chem.*, 1984, **49**, 3241.

*Received in Cambridge, UK, 16th June 1997; 7/04159D*

# Flash vacuum pyrolysis of trifluoromethylated diphenyldiazomethanes. Role of trifluoromethyl group in the arylcarbene rearrangement

**Hideo Tomioka* and Kohji Taketsuji**

*Chemistry Department for Materials, Faculty of Engineering, Mie University, Tsu, Mie 514, Japan*

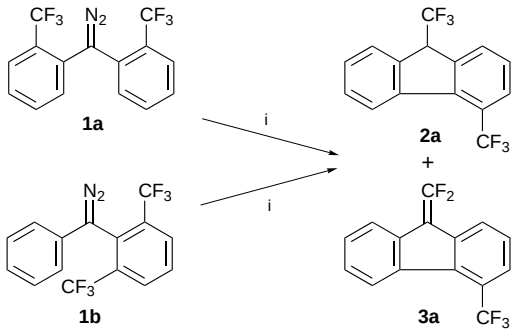
**Flash vacuum pyrolysis (350 °C/10$^{-4}$ Torr) of the title diazo compounds gives trifluoromethylated fluorenes, indicating that the C–F bonds are completely unreactive toward carbene even in the gas phase at high temperatures.**

Fluorinated molecules often display unique reactivity relative to their nonfluorinated analogues and have been the object of considerable interest for many years.[1] This is also true in the field of carbene chemistry.[2,3] The fluoro group is especially interesting in carbene chemistry because it can play key roles either intramolecularly or intermolecularly. On the other hand, C–F bonds are known to be almost the only type of bond unreactive toward carbenic centres. In spite of these unique characteristics, the influence of aryl $CF_3$ groups on the reactivity of arylcarbenes has been poorly characterized.[4] In this regard, we have examined the effect of $CF_3$ groups on the rearrangement of diarylcarbenes in the gas phase. The study not only reveals that $CF_3$ groups show a profound influence on the selectivity of the rearrangement, but also confirms that the C–F bond is completely unreactive toward carbenes, even in the gas phase at high temperature.

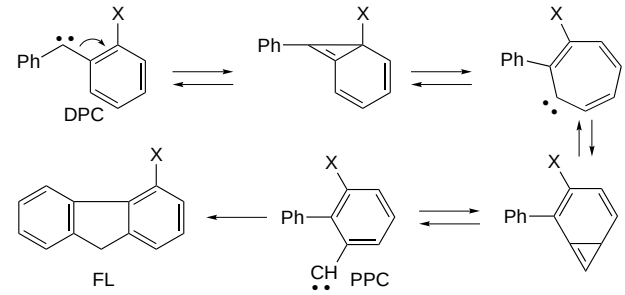
Flash vacuum pyrolysis (FVP)[5] of bis(2-trifluoromethylphenyl)diazomethane **1a**† at 350 °C/10$^{-4}$ Torr gave two fluorene derivatives **2a** (38%)‡ and **3a** (8%)‡ as volatile products (Scheme 1). Control experiments showed that FVP of **2a** under similar conditions gave **3a**, suggesting that **3a** can be produced by a secondary reaction of **2a** as a result of HF elimination.

It is well-documented that arylcarbenes undergo repeated rearrangement in the gas phase, where a divalent carbon is transmitted through a benzene ring to a position that is accessible for intramolecular reactions. Diphenylcarbene (DPC), for instance, rearranges to produce 2-phenylphenylcarbene (PPC), where the carbene centre is trapped by the 2-phenyl ring to form fluorene (FL) Scheme 2.

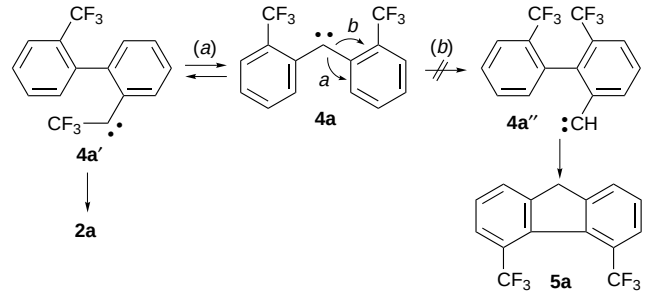
According to the mechanism, carbene **4a** generated from **1a** can undergo ring-expansion in two directions, one [path (*a*)] away from the $CF_3$ group and the other [path (*b*)] toward the substituent (Scheme 3). The former will produce carbene **4a′**, a precursor to **2a**, while the latter should generate **4a″** which should produce **5a**. Exclusive formation of **2a** suggests that the rearrangement of **4a** is highly selective with respect to the substituent. The fact that neither 1,2-F migration nor C–F bond insertion was observed indicates, on the other hand, that the C–F bond is unreactive toward carbenic centres even in the gas phase at this high temperature.




**Scheme 1** *Reagents and conditions*: i, 350 °C/10$^{-4}$ Torr

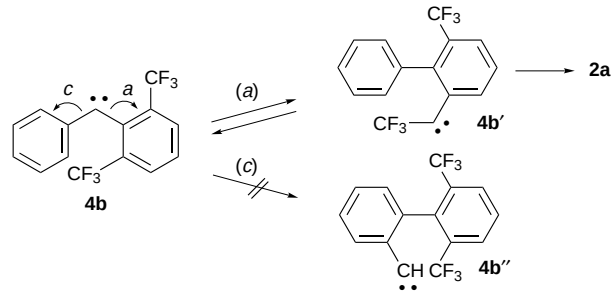



**Scheme 2**




**Scheme 3**

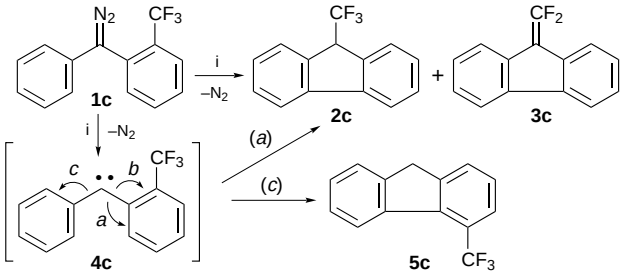
FVP of 2,6-bistrifluoromethylphenyl(phenyl)diazomethane **1b**,† a positional isomer of **1a**, under similar conditions gave essentially the same result, thus affording the same products, **2a** (48%) and **3a** (9%), in similar yields (Scheme 1). The results, although initially puzzling, can also be understood in terms of the carbene rearrangement (Scheme 4). Since the two rings in **4b** bear different substituents, regioselectivities in terms of ring arise in this case [*i.e.* path (*a*) and (*c*)], while there is no selection with respect to the ring substituents [*i.e.* Scheme 3, path (*a*) = path (*b*)]. The ring-expansion toward the substituted ring [path (*a*)] can generate carbene **4b′** responsible for the observed




**Scheme 4**

products, while the another movement [path (*c*)] should produce carbene **4b″**, which is not responsible for the product. The exclusive formation of **2a** might then indicate that the selectivity with respective to the rings is also very high in this case. It may be, however, that since the $CF_3$ group has been shown to be unreactive even under these conditions, the carbene **4b″** has no intramolecular reaction channels and hence regenerates **4b** which eventually produces **2a**.

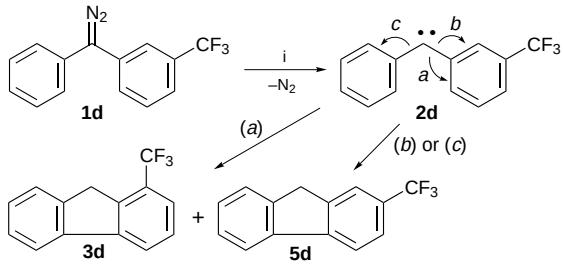
In order to check this possibility, we generated carbenes **4c** where the *ortho* C–H bonds are available for the carbenes from both types of rearrangement, *i.e.* **4c′** and **4c″**. FVP of **1c**† produced **2c**‡ (32%) and **3c**‡ (27%) again as the main products and only a very small amount of **5c**‡ (1%) was detected. The result shows that path (*a*) rearrangement is favoured over path (*c*), although not exclusively (Scheme 5).




**Scheme 5** *Reagents and conditions*: i, 350 °C/$10^{-4}$ Torr

Both types of regioselectivity are completely lost when the $CF_3$ group is introduced at the 3-position of diphenylcarbene. Thus, FVP of **1d**† afforded **2d**‡ (33%) and **5d**‡ (35%) in comparable yields (Scheme 6). Formation of **2d** is explicable in terms of type (*a*) rearrangement while **5d** might be produced by either type (*b*) or (*c*) rearrangement.

The regioselectivities of the rearrangement of diarylcarbenes carrying different substituents on the aryl rings can be interpreted in terms of a simple frontier MO analysis.[6] Thus, the occupied σ-orbital of carbene can interact with the LUMO of the aromatic ring in the ipso-position, while the vacant p orbital can interact with the aromatic HOMO in the *ortho*-position. The two interactions are synergetic. The σ-LUMO interaction is favoured by low-lying LUMOs possessing large coefficients in the *ipso* position and the p-HOMOs interactions is favoured by high-energy HOMOs with large coefficients in the *ortho*-positions. Phenyl(4-pyridyl)carbene, for instance, undergoes exclusive rearrangement involving the pyridine ring, since the pyridine LUMO has a large coefficient at positions 2 and 4. On the other hand, the rearrangement of phenyl(3-pyridyl)carbene does not involve the pyridine ring, since the LUMO coefficient at the 3-position is very small. Essentially the same explanation can be applied to the selectivities observed for the present system. Thus, a $CF_3$ group will lower the LUMO energy of the benzene ring, and trifluoromethylbenzene has large coefficients at positions 2 and 4. A high preference for the 2-trifluoromethylated phenyl ring will result in carbenes **4a**–**c**, while the regioselectivity is lost in **4d** where the LUMO coefficient of the aromatic ring in the *ipso*-position is small, and hence the p-HOMO interaction becomes competitive.




**Scheme 6** *Reagents and conditions*: i, 350 °C/$10^{-4}$ Torr

Regioselectivities with respect to the ring substituent are not well characterized. In the case of *ortho*-substituted phenylnitrenes, the nitrene nitrogen movement away from the substituent is preferred but is not exclusive and depends on other factors such as the nature of the reaction partner and electronic effects.[7] On the other hand, this issue has been examined extensively only for tolylcarbenes in the carbene rearrangement, where the methyl group is acting as a trap.[7,8] The 'away' selectivity is slightly favoured in this case. However, this again depends on the other factors such as the reaction conditions and precursors.[8]

Finally we wish to emphasize here that the present results reveal that trifluoromethylated diphenylcarbenes can be regarded as synthetically useful intermediates for trifluoromethylated fluorene derivatives which are otherwise not easily obtained. The method is specially advantageous since the $CF_3$ group is intact during the reaction, and its position in the resulting fluorene is predictable based on the regioselectivities shown above.

The authors are grateful to the Ministry of Education, Science and Culture of Japan for support of this work. We also thank Professor Curt Wentrup of the University of Queensland for helpful discussions.

## Footnotes and References

† All diazomethanes except **1b** employed in this study were prepared by the conventional hydrazonation–oxidation procedure and obtained as unstable red oils. 2,6-Bistrifluoromethylphenyl(phenyl)diazomethane **1b** was prepared by treating the corresponding *N*-nitrosocarbamate with KOBu$^t$.

‡ *Selected spectral properties* for **2a**: $\delta_H(CDCl_3)$ 4.61 (1 H, *J* 9.3 Hz), 7.41–7.56 (3 H, m), 7.74 (1 H, d, *J* 7.3 Hz), 7.79 (1 H, d, *J* 7.9 Hz), 7.93 (1 H, d, *J* 7.6 Hz), 8.12 (1 H, d, *J* 7.9 Hz); *m/z* 302 ($M^+$, 77%), 233 (100). For **3a**: $\delta_H(CDCl_3)$ 7.41–7.47 (3 H, m), 7.69–7.80 (2 H, m), 7.94 (1 H, d, *J* 7.6 Hz), 8.11–8.13 (1 H, m); *m/z* 282 ($M^+$, 100%). For **2c**: $\delta_H(CDCl_3)$ 4.59 (1 H, q, *J* 9.2 Hz), 7.30–7.50 (6 H, m), 7.58 (2 H, d, *J* 7.6 Hz), 7.77 (2 H, d, *J* 7.3 Hz); *m/z* 234 ($M^+$, 53%), 165 (100). For **3c**: $\delta_H(CDCl_3)$ 7.32–7.42 (4 H, m), 7.71–7.80 (4 H, m); *m/z* 214 ($M^+$, 100%). For **5c**: $\delta_H(CDCl_3)$ 4.11 (2 H, s), 7.41–7.45 (3 H, m), 7.66–7.78 (2 H, m), 7.92 (1 H, d, *J* 7.5 Hz), 8.10–8.12 (1 H, m); *m/z* 234 ($M^+$, 60%), 165 (100). For **2d**: $\delta_H(CDCl_3)$ 4.09 (2 H, s), 7.34–7.60 (6 H, m), 7.81 (1 H, d, *J* 6.6 Hz), 7.95 (1 H, d, *J* 7.3 Hz); *m/z* 234 ($M^+$, 66%), 165 (100). For **3d**: $\delta_H(CDCl_3)$ 3.96 (2 H, s), 7.36–7.65 (6 H, m), 7.83 (1 H, d, *J* 7.6 Hz), 8.01 (1 H, s); *m/z* 234 ($M^+$, 66%), 165 (100).

1 R. P. Chambers, *Fluorine in Organic Chemistry*, Wiley, New York, 1973; R. E. Banks, *Fluorocarbons and Their Derivatives*, Oldbourne Book Co. Ltd., London, England, 1964; B. E. Smart, in *The Chemistry of Functional Groups, Supplement D*, ed. S. Patai and Z. Rappoport, Wiley, Chichester, 1983, part 2, ch. 14, pp. 603–655; J. G. Riess and M. LeBlanc, *Angew. Chem., Int. Ed. Engl.*, 1978, **17**, 621.

2 H. Tomioka, K. Mizutani, K. Matsumoto and K. Hirai, *J. Org. Chem.*, 1993, **58**, 7128.

3 For a review on fluorinated carbenes, see D. L. S. Brahms and W. P. Dailey, *Chem. Rev.*, 1996, **96**, 1585.

4 For a general overview of the reactions of diarylcarbenes, see R. A. Moss and M. Jones, Jr., *Carbenes*, Wiley, New York, 1973, vol. 1, pp. 73–95; C. Wentrup, in *Mothoden der Organischen Chemic* (*Houben-Weyl*), ed. M. Regitz, thieme, Stuttgart, 1989, vol. E19, Wentrup, pp. 824–1021.

5 For details of FVP procedure, see H. Tomioka, N. Kobayashi, S. Murata and Y. Ohtawa, *J. Am. Chem. Soc.*, 1991, **113**, 8771.

6 C. Wentrup, *Reactive Molecules*, Wiley-Interscience, New York, 1984, pp. 215–217; C. Mayor and C. Wentrup, *J. Am. Chem. Soc.*, 1975, **97**, 7467.

7 R. Gleiter, W. Rettig and C. Wentrup, *Helv. Chim. Acta*, 1974, **57**, 2111 and references cited therein.

8 P. P. Gaspar, J.-P. Hsu, S. Chari and M. Jones, Jr., *Tetrahedron*, 1985, **41**, 1479.

*Received in Cambridge, UK, 3rd February 1997; 7/00779E*

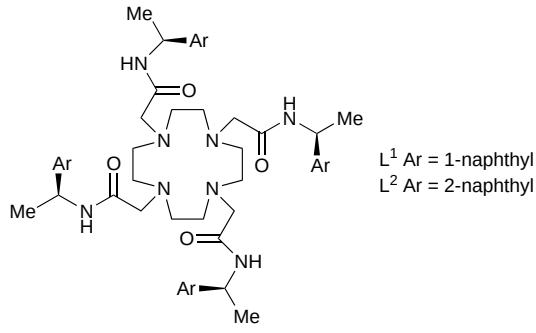
# Strong exciton coupling and circularly polarised luminescence in rigid complexes of chiral macrocyclic tetranaphthylamides

**Rachel S. Dickins,[a] Judith A. K. Howard,[a] Janet M. Moloney,[a] David Parker,*[a] Robert D. Peacock[b] and Giuliano Siligardi[c]**

[a] *Department of Chemistry, University of Durham, South Road, Durham, UK DH1 3LE*
[b] *Department of Chemistry, University of Glasgow, Glasgow, UK G12 8QQ*
[c] *Department of Pharmacy, King's College London, Manresa Road, London, UK SW3 6LX*

**Strong exciton coupling occurs between adjacent pairs of naphthyl chromophores in the chiral sodium and europium complexes of $L^1$; in the constitutionally isomeric complexes of $L^2$, intramolecular excimer formation is observed and both sets of Eu complexes give a well defined, metal-based circularly polarised emission.**

Recently we have been examining the luminescence behaviour of lanthanide complexes of N-substituted octadentate ligands derived from 1,4,7,10-tetraazacyclododecane (cyclen).[1–4] The chiral europium and terbium complexes of $L^3$ are conformationally rigid and stereochemically homogeneous in solution on the timescale of the metal-centred luminescence (*i.e.* ms), and the remote chiral centre at carbon in the N-substituent determines both the configuration of the macrocyclic ring and the helicity of the array of N-substituents.[1] With this model complex in mind, we have prepared the corresponding enantiomeric pairs of 1- and 2-naphthyl substituted ligands, $L^1$ and $L^2$ and their Eu complexes. A particular motivation for this work has been the consideration that strong exciton coupling between proximate chromophores may be a necessary condition in seeking the efficient population of the enantiomeric ($\pi$–$\pi^*$) excited states of these lanthanide complexes.




Reaction of (*S*)- or (*R*)-*N*-2-chloroethanoyl-1-(1′-naphthyl)-ethylamine with 1,4,7,10-tetraazacyclododecane (dmf, $K_2CO_3$, 60 °C) afforded the ligands (*S*)- or (*R*)-$L^1$ (mp 195 °C). The constitutionally isomeric ligand, $L^2$, based on 1-(2′-naphthyl)ethylamine was prepared analogously (mp 182 °C). Aqueous solutions of $[H_2L^2]^{2+}$, as the trifluoroacetate salt, gave rise to a structureless band in the emission spectrum at 400 nm whose intensity was independent of concentration in the range $10^{-4}$–$10^{-6}$ mol dm$^{-3}$. This band was not observed in MeOH or MeCN, so that intramolecular excimer formation[4] may be favoured by a particularly strong hydrophobic interaction involving expulsion of hydrogen-bonded water molecules from the solvated protonated ligand. In MeOH, the enantiomers of ligand $L^2$ gave mirror-image CD spectra. No exciton coupling features were observed for the CD bands at 280 and 310 nm, which were attributed to $^1L_a$ and $^1L_{1b}$ 2-naphthyl $\pi$–$\pi^*$ transitions.[5] In the far-UV region, the apparent bisignate CD spectrum was assigned to naphthyl $^1B_b$ (225 nm) and $^1C_b$ (210 nm) transitions, rather than exciton coupling.[5]† No sign of exciton coupling was evident from the mirror image CD spectra (MeOH) for the enantiomers of $L^1$, at room temp. (Fig. 1). The CD band at *ca.* 280 nm ($^1L_a$ $\pi$–$\pi^*$) appeared to mask the $^1L_b$ 1-naphthyl transition at 305 nm.[5] However, at −86 °C, a bisignate profile with crossover at 222 nm was observed for the free ligand (*R*)-$L^1$ and similar exciton coupling was observed at room temp. in the presence of 2 equiv. of $Na^+$, $K^+$, $Ca^{2+}$. The intensity of the bisignate profile was enhanced on lowering the temperature. Such behaviour is consistent with coupling of the electric dipole transition moments along the long axis of the naphthyl chromophores, and with positive chirality.

The crystal structure (Fig. 2) of the sodium complex of $L^1$‡ at 150 K revealed a twisted square-antiprismatic eight-coordinate geometry about the sodium ion [mean Na–O = 2.46(3) Å, Na–N = 2.72(4) Å, twist angle 28° from prismatic geometry]. All four naphthyl rings are steeply inclined to the $O_4$ coordination plane (angles ranging from 81 to 103°) and are in a near orthogonal relationship to each other. Given that the amplitude of exciton coupling is maximal when the dihedral angle between the two chromophores is *ca.* 70°, and tends to zero as the angle approaches 0 or 180°,[8] this arrangement of the naphthyl groups is consistent with the observed exciton

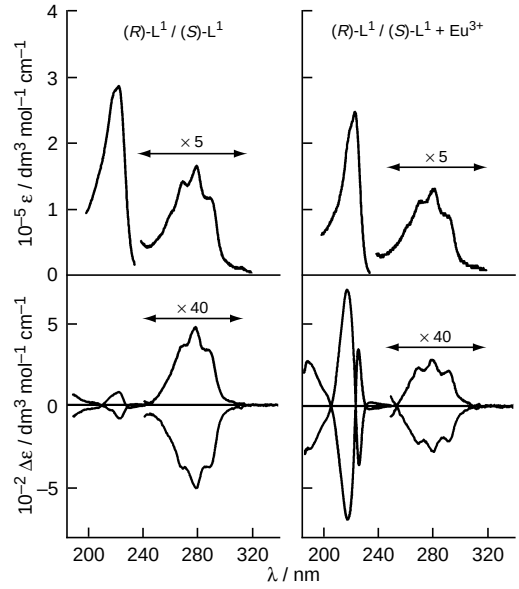



**Fig. 1** CD spectra of the enantiomers of $L^1$ and $[EuL^1][CF_3SO_3]_3$ in MeOH [293 K; (*R*)-enantiomer is upper trace] showing the bisignate profile in the metal complex associated with exciton coupling of the 1-naphthyl $^1B_b$ bands

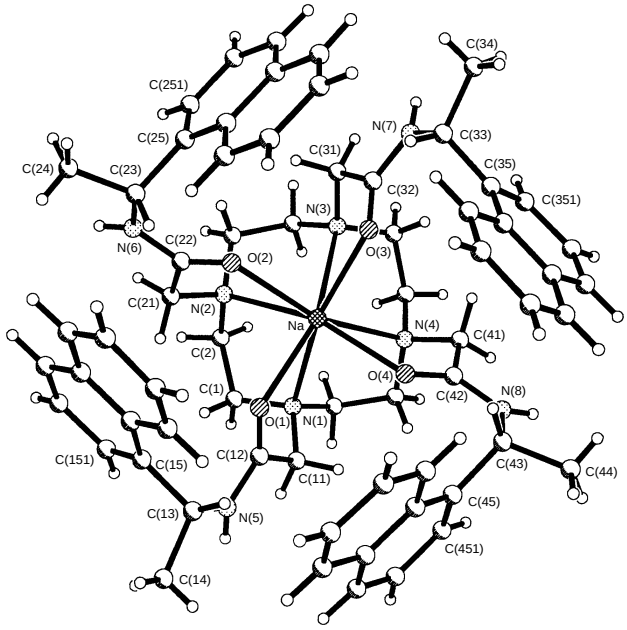



**Fig. 2** Structure of the complex $[NaL^1]CF_3CO_2$ in the crystal, showing the octadentate and twisted square-antiprismatic coordination about sodium

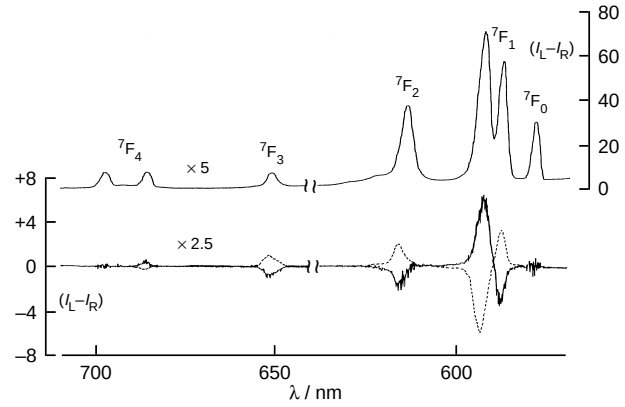



**Fig. 3** Total luminescence ($I_L + I_R$) and circularly polarised luminescence spectra ($I_L - I_R$) of $[Eu\{(R)\text{-}L^1\}]^{3+}$ (solid line) and $[Eu\{(S)\text{-}L^1\}]^{3+}$ (dashed line) [$\lambda_{exc}$ = 395 nm (Xe lamp), 293 K, MeOH, $2 \times 10^{-3}$ mol dm$^{-3}$]

coupling: for $[Na\{(R)\text{-}L^1\}]^+$: $\Delta\lambda$ = 10 nm; $g_{abs}$ (219) = $-2.2 \times 10^{-3}$, $g_{abs}$ (229) = $+1.4 \times 10^{-3}$. Methanolic solutions of (*S*)-L$^1$ in the presence of 2 equiv. of NaCl, NaOAc or $Na_2HPO_4$ gave rise to mirror-image CD spectra, with a bisignate profile typical of negative chirality, and independent of the anion.

Solution NMR studies in $CD_3OD$ of the Eu complexes of L$^1$ and L$^2$, indicated the presence of a single $C_4$-symmetric complex, that showed no evidence for exchange broadening in the range 200–320 K (400 MHz). With $[EuL^2]^{3+}$, there was no evidence for exciton coupling in the solution CD spectrum, and in the fluorescence emission spectrum, an excimer band was evident at 400 nm (40% of the monomer emission intensity) only if water was present. In 100% MeOH, no excimer was discerned, resembling the behaviour shown by the protonated ligand. Formation of an excimer requires the co-planarity of the two aryl groups and their close juxtaposition (3.5 Å): the absence of observed exciton coupling is consistent with this behaviour as the average interchromophoric dihedral angle must be near 0°. In the isomeric complex, [Eu L$^1$]$^{3+}$, the situation is reversed: no distinct excimer band was observed in the emission spectrum irrespective of the presence of water , and in the CD spectrum (Fig. 1) of $\{(R)\text{-}L^1\}[Eu]^{3+}$, positive chirality was exhibited with a bisignate profile associated with strong exciton coupling for which $g_{abs}$ (219) = $-6 \times 10^{-3}$ and $g_{abs}$ (229) = $+3 \times 10^{-3}$. Excimer emission between proximate naphthyl chromphores has been reported previously, *e.g.* in poly(1-naphthylmethylglutamate),[6] and in poly(1-naphthyl-Ala) no evidence for excimer formation was found whereas in the isomer, poly(2-naphthyl-Ala), a weak excimer emission was observed in degassed dmf solutions.[7]

Although these europium complexes are only weakly emissive in their metal-based luminescence spectra following sensitised excitation *via* the naphthyl antenna {[EuL$^1$]: $\lambda_{exc}$ = 280 nm, $\tau H_2O$ = 0.53, $\tau D_2O$ = 2.7 ms; [EuL$^2$]: $\tau H_2O$ = 0.55, $\tau D_2O$ = 2.1 ms} primarily because of competitive photoinduced charge transfer from the excited naphthyl singlet to the $Eu^{3+}$ ion,[15,16] both gave rise to well defined circularly polarised luminescence (CPL) spectra following excitation into the charge-transfer transition at 390 nm. The unpolarised luminescence is characteristic of Eu in a $C_4$ environment and the strength of the $^5D_0$–$^7F_0$ transition implies a large axial perturbation. The $^5D_0$–$^7F_0$ transition at 580 nm showed no CPL, but for the allowed transitions associated with a change in magnetic dipole, *e.g.* $^5D_0$–$^7F_1$, strong CPL was clearly observed (Fig. 3). For $\{(R)\text{-}L^1\}[Eu]$, the $g_{em}$ factors are −0.12(A) and +0.18(E) for $\Delta J$ = 1, −0.1 for $\Delta J$ = 2 (only the E is observed), −0.3 for $\Delta J$ = 3 and −0.11 and 0 for $\Delta J$ = 4. The enantiomeric Eu complexes gave rise to enantiomeric CPL spectra, and CPL spectra from $[EuL^2]^{3+}$ were very similar.

In summary, the Eu complex of L$^1$ gives rise to strong exciton coupling between adjacent pairs of naphthyl chromophores. In the isomeric 2-substituted Eu complex of L$^2$, the naphthyl chromophores are aligned almost parallel and excimer formation occurs.

We thank EPSRC, the BBSRC the National Chiroptical Service (King's, London) and the University of Durham for support.

## Footnotes and References

* E-mail: david.parker@durham.ac.uk

† Such assignments were confirmed by variable-temperature studies and by the appearance of true exciton coupling (negative chirality with a crossover at *ca*. 225 nm), on addition of 2 equiv. of KCl to (*R*)-L$^2$ (at room temperature) or $CaCl_2$ (revealed at −86 °C). In these latter two cases, the intensities of both bands of the bisignate profile increased as the temperature was lowered. No such behaviour was observed with the free ligand L$^2$.

‡ *Crystal data* for $C_{68}H_{75}F_3N_9NaO_6$, $M$ = 1194.36, orthorhombic, $P2_12_12_1$, $a$ = 15.022(1), $b$ = 17.136(1), $c$ = 23.900(1) Å, $U$ = 6152.1(8) Å$^3$, $D_c$ = 1.290 g cm$^{-3}$, $\lambda$(Mo-Kα) 0.710 73 Å, $Z$ = 4, $\mu$ = 0.96 mm$^{-1}$. Data were collected on a SMART at 150(2) K. Refinement of 745 parameters with SHELXL 93, using 7364 observations converged at $R$ = 0.071, $wR_2$ = 0.171 for 5660 reflections with $I > 2\sigma(I)$. CCDC 182/549.

1 R. S. Dickins, J. A. K. Howard, C. W. Lehmann, J. Moloney, D. Parker and R. D. Peacock, *Angew. Chem., Int. Ed. Engl.*, 1997, **36**, 521; S. Aime, M. Barge, M.Botta, D. Parker and A. S. de Sousa, *J. Am. Chem. Soc.*, 1997, **119**, 4767.
2 A. Beeby, R. S. Dickins, S. Faulkner, D. Parker and J. A. G. Williams, *Chem. Commun.*, 1997, 1401.
3 D. Parker and J. A. G. Williams, *J. Chem. Soc., Dalton Trans.*, 1996, 3613; A. Beeby, D. Parker and J. A. G. Williams, *J. Chem. Soc., Perkin Trans. 2*, 1996, 1565.
4 D. Parker and J. A. G. Williams, *J. Chem. Soc., Perkin Trans. 2*, 1995, 1355.
5 J. R. Platt, *J. Chem. Phys.*, 1949, **17**, 484.
6 A. Ueno, T. Ishigara, F. Toda, K. Uno and Y. Iwakura, *Biopolymers*, 1975, **14**, 353.
7 M. Sisido, S. Egusa, A. Okamoto and Y. Imanishi, *J. Am. Chem. Soc.*, 1983, **105**, 3351.

*Received in Liverpool, UK, 8th May 1997; 7/03182C*

# Synthesis, structure and cyclics content of hyperbranched polyesters

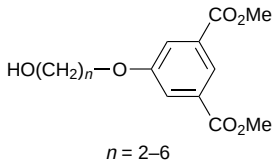
**W. James Feast, Angela J. Keeney, Alan M. Kenwright and David Parker**

*IRC in Polymer Science & Technology, University of Durham, Durham, UK DH1 3LE*

**Dimethyl 5-(hydroxyalkoxy)isophthalates undergo step growth condensation polymerisation to produce hyperbranched polymers with a degree of branching lower than statistically expected and with a high proportion of cyclic structures.**

The step-growth condensation polymerisation of $AB_x$ type monomers was described in a theoretical treatment by Flory, who predicted the formation of polydisperse polymers containing branched and linear segments.[1] It is often assumed that steric constraints preclude intramolecular reactions such as cyclisation, the absence of which is believed to be necessary for continued growth.[2,3]

Previously we have reported the single-step melt condensation polymerisation of dimethyl 5-(2-hydroxyethoxy)isophthalate.[4] As part of this continuing programme into the synthesis and properties of $AB_x$ hyperbranched polymers we have studied the step growth polymerisation of a series of dimethyl 5-(hydroxyalkoxy)isophthalates.




These $AB_2$ monomers underwent step growth polymerisation, eliminating methanol, on heating between 210 and 240 °C in a stream of dry nitrogen and in the presence of a transesterification catalyst which has found previous application in the commercial synthesis of linear polyesters. It utilises a combination of manganese(II) acetate and antimony trioxide, with triphenyl phosphate as a suppressant of thermal degradation.[5] The resulting $AB_2$ polyesters, unlike their linear analogues, were highly soluble in common organic solvents such as $CHCl_3$ and THF which allowed the determination of polystyrene equivalent molecular weights by size exclusion chromatography.

Variation of the alkylene chain length ($n$ = 2 to 6) had a marked effect upon the polymerisation characteristics. When $n$ = 2 both the molecular weight and polydispersity ($M_w/M_n$) of the polymer increased with increasing reaction time up to a weight average molecular weight of 107 000 and $M_w/M_n$ values of 15 after 24 h. This continuous increase in $M_w/M_n$ was as expected from Flory's predictions and has been observed in other hyperbranched systems.[6] However, on increasing the alkylene chain length ($n$ = 3 to 6) this steady increase in molecular weight and polydispersity with reaction conversion was no longer observed. The molecular weight in these instances was found to increase until a maximum was reached, after which it remained constant and no further growth was apparent. This phenomenon is consistent with deactivation or loss of the A functionality. Furthermore an 'odd/even effect' was observed, with alkylene chain lengths of 2, 4 and 6 methylene units yielding higher molecular weights than the corresponding 3 and 5 methylene chain polymers.

Copolymerisation of the $AB_2$ monomer, where $n$ = 2, with potential $B_2$ (dimethyl isophthalate) and $B_3$ (trimethyl benzene-1,3,5-tricarboxylate) core molecules afforded a method of molecular weight control for these systems. Increasing the core to monomer ratio resulted in a decrease in molecular weight and a narrowing of the polydispersity. In principle, an $AB_2$ condensation polymerisation can give rise to branched linear or terminal units (Fig. 1). A measure of the relative proportions of these structural units, the degree of branching (DB), is defined in eqn. (1), where $N_x$ is the number of type x units in the structure.

$$\mathrm{DB} = \frac{N_b + N_t}{N_b + N_l + N_t} \quad (1)$$

Quantitative $^{13}C$ NMR spectra of the polymers with $n$ = 2 at elevated temperature reveals fine structure attributable to the different types of repeat units in the polymers. These may be assigned to branched, linear and terminal contributions on the basis of their line-widths; the branched species are expected to be the least mobile and hence have the wider line-width, whilst the more mobile terminal species will have the narrower linewidth. Analysis of the $^{13}C$ NMR signals from the ester carbons (Fig. 2) gave a degree of branching of *ca* 0.5 which was independent of molecular weight. Analysis of the aromatic carbons in the structure confirm this DB. Purely statistical polymerisation would give a value of 0.66.

MALDI-TOF mass spectrometry (2,5-dihydroxybenzoic acid matrix + KCl, Kratos Kompact MALDI IV, linear mode) of polymers where $n$ = 2 or 3 showed a series of peaks corresponding to degrees of polymerisation in the range 3 to 16 (Figs. 3 and 4, for $n$ = 2). Ions were observed as their $[M + K]^+$ species. For low molecular weight polymers the main ion series corresponds to oligomers resulting from 3 to 16 simple condensation steps where the mass of an oligomer of $n$ units is [$n \times$ (monomer mass) $-$ ($n - 1$) $\times$ (mass of MeOH)]. A minor

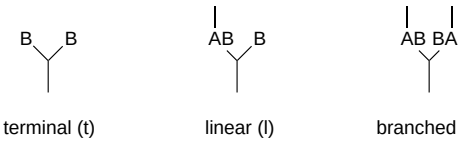



**Fig. 1** Structural sub-units of an $AB_2$ hyperbranched polymer

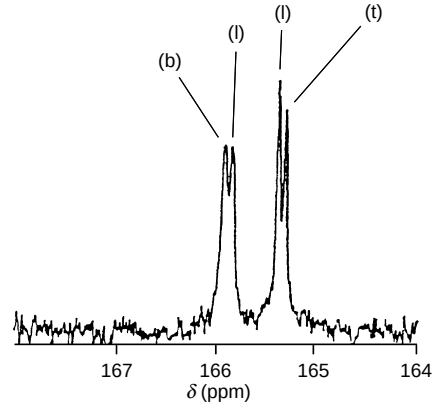



**Fig. 2** $^{13}C$ NMR peak assignments for ester carbonyls

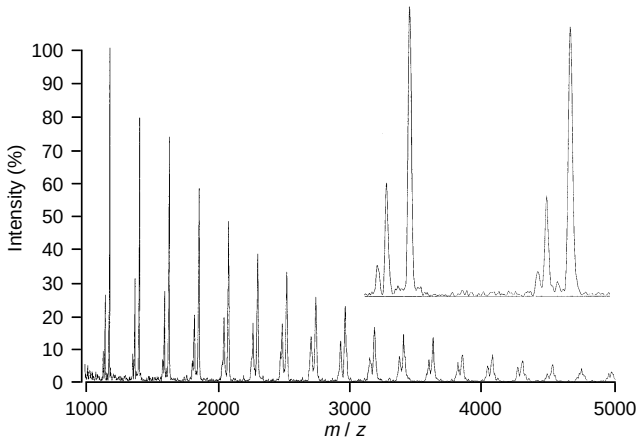



**Fig. 3** MALDI-TOF spectrum. Inset: region *m/z* 1340–1680

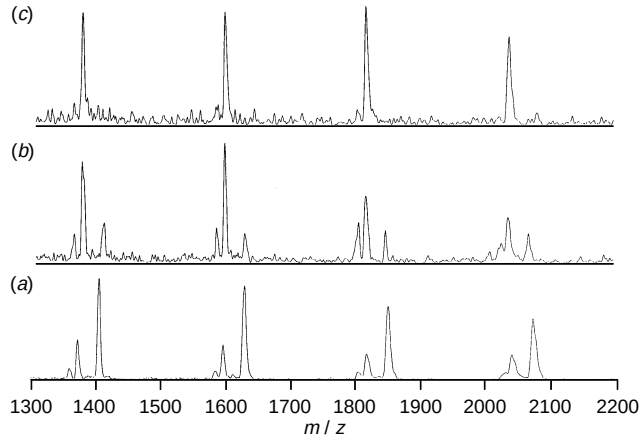



**Fig. 4** MALDI-TOF spectra for varying reaction times: (*a*) 1, (*b*) 2 and (*c*) 24 h

series of peaks is observed 32 mass units behind the main series. This is attributed to the loss of a further single methanol moiety to form a cyclic polymer. An alternative interpretation of this series would be hydrolysis of a single methyl ester unit; if this is occurring it seems reasonable to expect that, particularly for high mass species, more than one of the many methyl ester units in each molecule would undergo the reaction, but there is no evidence for the extra methanol losses required. The relative proportion of the cyclic oligomers increases with increasing oligomer size. For higher molecular weight polymers produced at longer reaction times *only* cyclic oligomers are observed. In the case of the $AB_2/B_x$ copolymers ($n = 2$, $x = 2$ or 3) two series of ions are observed attributable to polymer incorporating a core molecule and cyclic oligomers but no simple non-cyclic $AB_2$ oligomers. Cyclic structures predominate at low core to monomer ratios, whereas core terminated oligomers are more abundant at high core ratios.

This work clearly established that in $AB_2$ step growth polymerisations the outcome cannot be predicted by simple generalisations but is a sensitive function of monomer structure, reactions conditions and duration. In particular cyclisation, which can be growth terminating, occurs readily in the systems described here and becomes easier as the monomers become larger and more flexible. This observation is not unexpected but appears to have been overlooked previously.

We thank the Engineering and Physical Sciences Research Council for support through the IRC Special Grant and a Studentship (A. J. K.).

## Footnote and References

* E-mail: w.j.feast@durham.ac.uk

1 P. J. Flory, *J. Am. Chem. Soc.*, 1952, **74**, 2718.
2 E. Malmstrom and A. Hult, *Macromolecules*, 1996, **29**, 1222.
3 J. M. J. Frechet, *Comprehensive Polymer Science*, 2nd supplement, ed. S. L. Agarawal and S. Russo, Pergamon, Oxford, 1996, ch. 3.
4 W. J. Feast and N. M. Stainton, *J. Mater. Chem.*, 1995, **5**, 405.
5 B. Gumther and H. G. Zachmann, *Polymer*, 1983, **24**, 1008.
6 S. R. Turner, B. I. Voit and T. H. Mourey, *Macromolecules*, 1993, **26**, 4617.

*Received in Liverpool, UK, 23rd June 1997; 7/04464J*

# Unusual solvent-dependent behaviour of hydroxyiminophosphonamidates in the Beckmann reactions: choice between rearrangement or fragmentation to metaphosphonamidate species

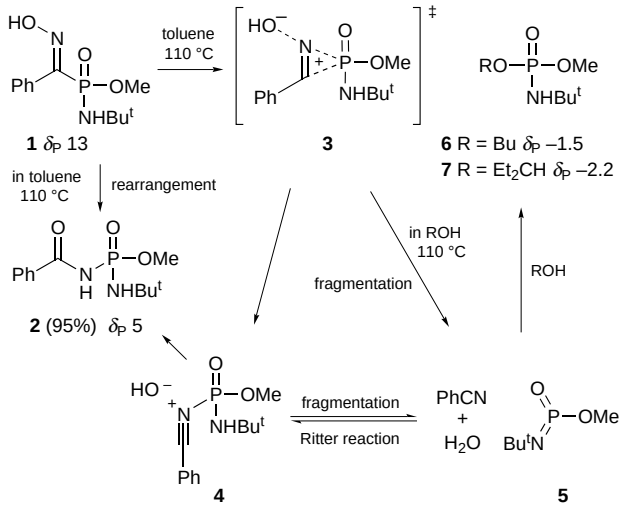
**Jan Kehler† and Eli Breuer***

*Department of Pharmaceutical Chemistry, The School of Pharmacy, The Hebrew University of Jerusalem, PO Box 12065, Jerusalem, 91120, Israel*

**Methyl α-hydroxyiminobenzyl-*N*-*tert*-butylphosphonamidate undergoes Beckmann rearrangement (BR) when heated in toluene, but fragmentation (*via* metaphosphonamidate) to a phosphoramidate and PhCN when heated in BuOH, supporting the assumption of a common intermediate for the BR and the Beckmann fragmentation; polar solvents retard the rearrangement.**

Recently it was reported from our laboratory that α-hydroxyiminobenzylphosphonamidates (*e.g.* **1**) rearrange easily ($t_{1/2}$ 92 min) in boiling toluene to *N*-benzoylphosphorodiamidates (*e.g.* **2**, Scheme 1).[1] Here we report that the behaviour of methyl *N*-*tert*-butyl α-hydroxyiminobenzylphosphonamidate **1** changes dramatically with a change in the solvent. While in aprotic solvents it undergoes cleanly Beckmann rearrangement (BR) to methyl *N*-benzoyl-*N*′-*tert*-butylphosphorodiamidate **2**, in alcohols it undergoes fragmentation to PhCN and a (mixed) dialkyl *N*-substituted phosphoramidate (*e.g.* **6** or **7**).

Although the mechanism of the Beckmann reactions is still not completely understood, according to the generally accepted view,[2] the BR and the Beckmann fragmentation reactions both involve the intermediacy of a nitrilium species (analogous to **4a**) formed by the concerted migration of the group *anti* to the departing hydroxy *via* a transition state such as **3**. Very recently it was calculated[3] that the first event in the classical BR is most likely protonation of the nitrogen, followed by a rate-determining 1,2 proton migration to the oxygen. Another result in this recent paper was the prediction of catalysis by solvents such as water, formaldehyde or formic acid, which were shown to play an important role in the transition state of the rate determining step. Once formed, the nitrilium species can undergo water addition to form the BR product or it can fragment in what is called the abnormal BR (considered a side reaction) to a nitrile and a carbocation or, as in our case, a metaphosphate species such as **5**. In the classical BR it has not been possible to control the ratio of rearrangement to fragmentation, however, it was found that the electronic properties of the migrating group played a crucial role. Thus, it was found that migrating groups capable of forming stable carbocations favour fragmentation.‡ The overall mechanistic picture is complicated by the fact that the nitrile and the electrophilic species can recombine in a Ritter reaction, reforming the nitrilium ion. Application of these mechanistic considerations to the Beckmann reaction of an α-hydroxyiminobenzylphosphonamidate is shown in Scheme 1.



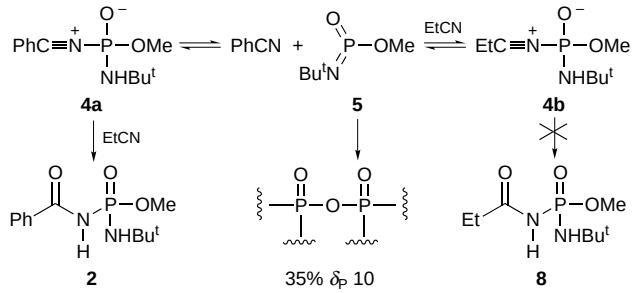

**Scheme 1**

Nitrilium species such as **4a** have been postulated as reversibly forming intermediates when metaphosphates were generated in MeCN.[4] Therefore, **4a** is conceivably a metaphosphonamidate (**5**) precursor. One of the commonly accepted diagnostic tests for metaphosphate-like species as reactive intermediates is the absence of any steric effect in the phosphorylation of hindered alcohols as compared to primary ones.[5] Consequently, in order to further investigate the present Beckmann fragmentation, we studied the thermal behaviour of methyl *N*-*tert*-butyl-α-hydroxyiminobenzylphosphonamidate **1** as a representative of this type of compounds in alcohols (butan-1-ol and pentan-3-ol) capable of trapping metaphosphates. The two alcohols were chosen as media for the thermal reactions of **1** for two reasons: (i) the closeness of their boiling points to that of toluene§ should allow easy comparison of reaction rates and (ii) their differing steric effects should shed light as to the nature of the reaction intermediates.[6] Monitoring by $^{31}$P NMR spectroscopy of a 0.18 M butan-1-ol solution of **1** kept at 110 °C revealed the relatively slow ($t_{1/2}$ 1829 min; first order kinetics) development of one new product ($\delta_P$ −1.5), along with concurrent consumption of the starting material ($\delta_P$ 13), in a clean reaction. The product was isolated and identified as butyl methyl *N*-*tert*-butylphosphoramidate **6**.¶ Similarly, heating a solution of **1** in pentan-3-ol at 110 °C gave methyl 1-ethylpropyl *N*-*tert*-butylphosphoramidate **7** ($\delta_P$ −2.5).‖ In addition, the presence of PhCN in both reaction mixtures was demonstrated by GC–MS and HPLC. Carrying out the reaction in a 1 : 1 (v/v) mixture of butan-1-ol and toluene gave the same result. When **1** was heated in a 1 : 1 (mol/mol) mixture of butan-1-ol and pentan-3-ol the formation of the two products **6** and **7** in 65 : 35 ratio was observed by $^{31}$P NMR spectroscopy.

The formation of the two phosphorodiamidates **6** and **7** in a 65 : 35 ratio in the thermolysis in the butan-1-ol–pentan-3-ol mixture is consistent with the formation of a reactive metaphosphonamidate intermediate **5** which is trapped by two alcohols with different steric requirements in an almost non-selective manner. If the alcohols were involved in the rate determining step of the reaction the ratio between the rates of formation of products should reflect the steric effects of the two alcohols[6] and therefore, the ratio of yields for **6** and **7** should be about 40 : 1.

Further considering the possible intermediacy of metaphosphate–nitrile addition species in the thermolytic reactions

of **1**, we reasoned that if species **4a** were involved, then carrying out the reaction in the presence of a large excess of another nitrile (*e.g.* EtCN) would cause the two nitriles to compete and lead to **4b** (Scheme 2), which in turn would give methyl *N*-propionyl-*N′*-*tert*-butylphosphorodiamidate. However, when **1** was heated in EtCN at 110 °C, it reacted ($t_{1/2}$ 225 min) to give two types of product only: (i) **2** (65%) by BR, and (ii) products (35%) having a group of signals at around $\delta_P$ −10,[7] consistent with oligomeric P–O–P type species; no methyl *N*-*tert*-butyl-*N′*-propionylposphorodiamidate was formed. In contrast, heating **1** in DMF at 100 °C, gave **2** cleanly in a slow ($t_{1/2}$ 5500 min) BR.




**Scheme 2**

Our system is unique in a number of ways. (i) In contrast to the normal BR, both the rearrangement and the fragmentation occur without acid catalysis. This makes it possible to isolate and to study the influence of further environmental and structural variations on the reactions and on the choice between them. (ii) In contrast to the predictions in ref. 3, in our case the BR is *retarded* by polar, basic solvents (DMF or EtCN) in comparison to toluene. This can be rationalized by assuming ground state stabilization of **1** by strong hydrogen bonding. In fact, **1** has a significantly lower solubility in toluene. Along with suppressing the rearrangement, the polar solvents DMF and alcohol (and to some extent EtCN) promote dissociation of intermediate **4a** by solvating the incipient metaphosphonamidate **5**, which can subsequently be trapped by the alcohols. The absence of steric effects observed in the reactions in alcohols is consistent with the formation of a reactive intermediate trapped nonselectively by alcohols of differing steric requirements. In EtCN the solvent forms an addition compound, thus stabilizing the metaphosphonamidate intermediate which polymerizes in the absence of an efficient trap, in addition to considerable proportion of the normal rearrangement product. (iii) The reactions described here proceed without acid catalysis, presumably because of the high migratory aptitude of the phosporus moiety. This seems to be a new manifestation of the 'β-effect' namely the ability of phosphorus functionalities to stabilize an electron deficient centre situated in β-relationship.[8]

In conclusion, our results show a new aspect of acylphosphonate and oxyiminophosphonate chemistry.[9] The versatility of this class of molecules, the countless ways they can be modified and the different types of reactions they can undergo so readily make them a focus of continuing interest and a source of models uniquely suitable for mechanistic studies.

Finally, our results seem to support the assumption that both the BR and the fragmentation proceed *via* a common intermediate. To the best of our knowledge, such a dramatic change in the reactions' course resulting from changing the solvent is unprecedented in this area.

## Footnotes and References

* E-mail: breuer@cc.huji.ac.il
† On leave from the Department of Organic Chemistry, University of Copenhagen.
‡ It should be noted that metaphosphates have certain features in common with carbocations: they are both frequently formed in dissociative-type reactions, they are both electrophilic and planar, and they both are intermediates leading to racemization.
§ Toluene: bp 111 °C; butan-1-ol: bp 118 °C; pentan-3-ol: bp 115 °C.
¶ *Selected data* for **6**: mp 87–88 °C; $\delta_P$ ($CDCl_3$) −1.5 (m); $\delta_H$ ($CDCl_3$) 8.40 (br s, 1 H, NH), 3.80 (dt, 2 H, $CH_2OP$), 3.50 (d, 3 H, *J* 10.5, $CH_3OP$), 1.60 (dt, 2 H, $CH_2$), 1.38 (s, 9 H, Bu$^t$), 1.38 (m, 2 H, $CH_2$), 0.89 (t, 3 H, *J* 7.2 Me); $\delta_C$ ($CDCl_3$) 63 (d, $J_{POC}$ 5.5, $CH_2OP$), 51 (d, $J_{POC}$ 5.5, $CH_3OP$), 49, 31 (d, $J_{PNC}$ 7.5, CNP), 26, 18, 12; *m/z* 223. Calc. ($C_9H_{22}NO_3P·H_2O$): C, 44.80; H, 10.03; N, 5.81. Found: C, 45.18; H, 10.03; N, 5.52%.
‖ *Selected data* for **7**: mp 134–136 °C; $\delta_P$ ($CDCl_3$) −2.2 (dquintet); $\delta_H$ ($CDCl_3$) 4.05 (m, 1 H, CHOP), 3.56 (d, 3 H, *J* 10.8, $CH_3OP$), 2.60 (br s, 1 H, NH), 1.60 (dq, 4 H, 2 × $CH_2$), 1.40 (s, 9 H, Bu$^t$), 0.39 (t, 6 H, *J* 7.5, 2 × $CH_3$); $\delta$C ($CDCl_3$) 78 (d, $J_{POC}$ 5.5, CHOP), 52 (d, $J_{POC}$ 5.5, $CH_3OP$), 51, 28, 27 (d, $J_{PNC}$ 7.5, CNP), 9; *m/z* 238. Calc. ($C_{10}H_{25}NO_3P·H_2O$): C, 46.67; H, 10.33; N, 5.46. Found: C, 46.60; H, 10.33; N, 5.46%.

1 E. Breuer, H. Zaher, Z. Tashma and D. Gibson, *Heteroatom Chem.*, 1996, **7**, 151.
2 R. E. Gawley, *Org. React.*, 1988, **35**, 1; other recent references to reviews of the Beckmann reactions are cited in ref. 3.
3 M. T. Nguyen, G. Raspoet and L. G. Vanquickenborne, *J. Am. Chem. Soc.*, 1997, **119**, 2552.
4 A. C. Satterthwait and F. H. Westheimer, *J. Am. Chem. Soc.*, 1978, **100**, 3197; J. M. Friedman, S. Freeman and J. R. Knowles, *J. Am. Chem. Soc.*, 1988, **110**, 1267.
5 F. Ramirez and J. F. Marecek, *Tetrahedron*, 1979, **35**, 1581; 1980, **36**, 3151; J. M. Friedman and J. R. Knowles, *J. Am. Chem. Soc.*, 1985, **107**, 6126; M. J. P. Harger and A. Smith, *J. Chem. Soc., Perkin Trans. 1*, 1990, 2507; M. P. Coogan and M. J. P. Harger, *J. Chem. Soc., Chem. Commun.*, 1990, 1745; S. Jankowski and L. D. Quin, *J. Am. Chem. Soc.*, 1991, **113**, 7011.
6 Taft has calculated a steric effect for pentan-3-ol, $E_s$ = −1.98, compared to $E_s$ = −0.39 for butan-1-ol: R. W. Taft, Jr., *J. Am. Chem. Soc.*, 1952, **74**, 3120.
7 Such species have been observed previously in the fragmentation of other metaphosphate precursors in aprotic solvents: F. Ramirez, J. F. Marecek and S. S. Yemul, *J. Am. Chem. Soc.*, 1982, **104**, 1345; E.Breuer, M. Mahajna, L. D. Quin and G. S. Quin, *J. Org. Chem.*, 1991, **56**, 4791; M. Mahajna and E. Breuer, *J. Org. Chem.*, 1993, **58**, 7822.
8 J. B. Lambert, R. W. Emblidge and Y. Zhao, *J. Org. Chem.*, 1994, **59**, 5397; J. B. Lambert and Y. Zhao, *J. Am. Chem. Soc.*, 1996, **118**, 3156; E.Breuer, A. Schlossman, M. Safadi, D. Gibson, M. Chorev and H. Leader, *J. Chem. Soc., Perkin Trans. 1*, 1990, 3263; E. Breuer, H. Zaher and Z. Tashma, *Tetrahedron Lett.*, 1992, **33**, 2067; E. Breuer and C. J. Solomon, *J. Org. Chem.*, 1997, **62**, 3858.
9 For a recent review on oxyiminophosphonates, see E.Breuer, in *The chemistry of organophosphorus compounds*, ed. F. R. Hartley, Wiley, New York, 1996, vol. 4, pp. 653–729.

*Received in Cambridge, UK, 7th July 1997; 7/04787H*

# A general synthesis of benzofuran-2-thiolates *via* intramolecular addition of phenolates to alkynethiolates

**Bart D'hooge, Stefan Smeets, Suzanne Toppet and Wim Dehaen***

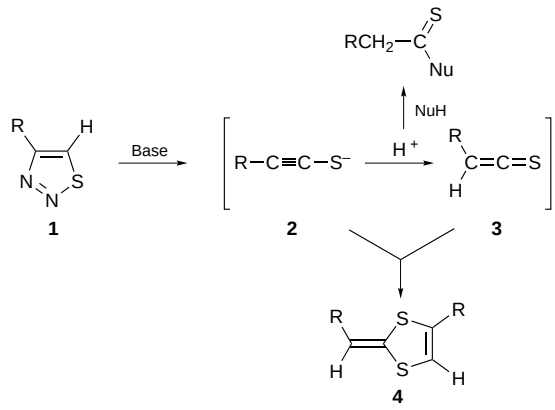
*Department of Chemistry, University of Leuven, Celestijnenlaan 200F, B-3001 Leuven (Heverlee), Belgium*

**4-(*ortho*-Hydroxyaryl)-1,2,3-thiadiazoles can be transformed into benzofuran-2-thiolates *via* an intramolecular cyclization.**

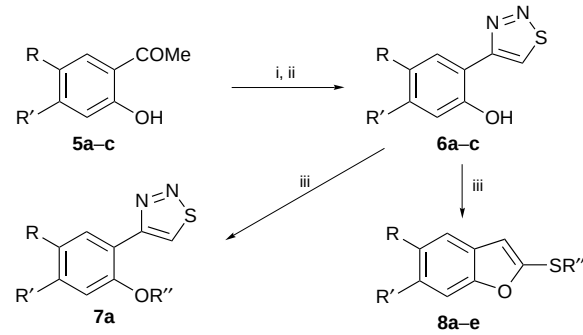
1,2,3-Thiadiazoles **1**, unsubstituted at the 5-position, are cleanly decomposed into alkynethiolates **2** under the influence of strong bases such as organolithium reagents, sodamide, sodium hydride and potassium *tert*-butoxide.[1] These alkynethiolates are interesting reagents which have been alkylated and acylated at sulfur, and converted with nucleophiles into derivatives of the thioketenes **3** which result from protonation at carbon of **2**.[1,2] Another possibility is the combination of alkynethiolate **2** with thioketene **3** to give a dithiafulvene **4**. The dimer **4**[2] will be formed in protic solvents or when no efficient nucleophile is present to trap the thioketene **3** (Scheme 1).

The method of Hurd and Mori[3] gives access to 5-unsubstituted 1,2,3-thiadiazoles **1**, and consists of reacting methyl ketones successively with ethyl carbazate (or tosylhydrazide) and thionyl chloride. This procedure was used to obtain 4-(orthohydroxyaryl)-1,2,3-thiadiazoles **6a**–**c** from the acetophenones **5a**–**c** in 37–74% overall yield.[4] We wanted to use the alkylation of phenol **6a** as a means to attach the 1,2,3-thiadiazole group to other molecules.[5] However, the thiadiazole **6a** proved to be susceptible to relatively weak bases, such as potassium carbonate, and in the presence of alkylating agents the unexpected thioethers **8a**–**c** were formed in high yields instead of the *O*-alkylated thiadiazoles **7**. Only with the very reactive methyl iodide is some *O*-alkylated product **7a** formed. The formation of **7a** can be suppressed by adding the alkylating agent after the decomposition is completed. (Scheme 2, Table 1).

The mechanism of this unusual reaction was elucidated by following the decomposition of **6a** by $^1$H NMR (400 MHz) spectroscopy. Thus, a solution of compound **6a** in $CD_3CN$ was treated with aqueous tetrabutylammonium hydroxide at room temperature. Initially, the phenolate **9** was present as indicated by the disappearance of the phenolic OH at $\delta_H$ 9.69 (as compared to the spectrum without base) and the downfield shift of the thiadiazole 5-H from $\delta_H$ 9.20 to 9.76. In addition, the




**Scheme 1**



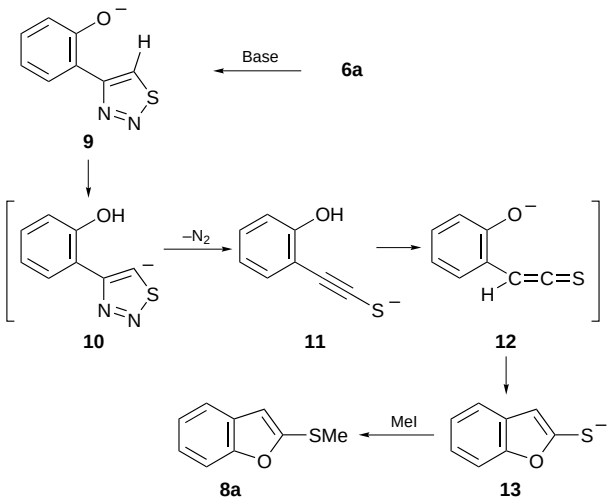

**Scheme 2** *Reagents and conditions*: i, $EtO_2CNHNH_2$; ii, $SOCl_2$; iii, base, R″X, acetone, reflux

phenyl protons at the 3, 4 and 5 positions moved upfield by 0.42, 0.34 and 0.64 ppm, respectively, whereas the 6-H was little affected ($\Delta\delta$ +0.17 ppm). Slow nitrogen evolution was observed, and after a period of 21 h the $^1$H NMR spectrum corresponded to a 1 : 1 mixture of compounds **9** and **13**. The 5-H of the 1,2,3-thiadiazole ring of **9** was partially deuterated under these conditions, proving the intermediacy of the 1,2,3-thiadiazol-5-yl anion **10**. After 93 h the reaction was completed and the NMR spectrum showed a clean absorption pattern of benzofuran-2-thiolate[7] with $\delta_H$ 5.98 (3-H), 6.81, 6.90 (5-H and 6-H) and 7.06 (4-H and 7-H), with no detectable impurities present. When the same reaction was followed by NMR spectroscopy in [$^2H_6$]DMSO, the alkynethiolate **11** (48%) was observed after 15 min, together with the phenolate **9** (35%) and benzofuran **13** (17%). Compound **11** showed peaks in the $^{13}$C NMR spectrum at $\delta$ 71.8 (d) and 101.2 (s) for the alkyne carbons (respectively $\beta$ and $\alpha$ to sulfur). After 3 h the phenolate **9** had disappeared and the spectrum showed a 1 : 1 mixture of **11** and **13**. The $^{13}$C NMR spectrum of thiolate **13** had peaks at 173.9 (d, $^2J_{CH}$ 9 Hz) and 99.1 (d, $^1J_{CH}$ 173 Hz) for the C-2 and C-3 carbons of the benzofuran, respectively. After one week, the transformation to benzofuranthiolate **13** was complete and the reaction could be treated with methyl iodide to give an immediate and quantitative reaction, affording the sulfide **8a**. From this it follows that an alternative pathway where, in the first step, the alkynethiolate **11** is alkylated, followed by

**Table 1** Products and yields from the reactions of **6a**–**c** with base and alkylating agents

| Starting material | R | R′ | R″X | Products | Yield (%)[a] 7 | 8 |
|---|---|---|---|---|---|---|
| **6a** | H | H | MeI | **7a** + **8a** | 43 | 56 |
| **6a** | H | H | BnCl | **8b** | 0 | 91 |
| **6a** | H | H | $C_{16}H_{33}Br$ | **8c** | 0 | 97 |
| **6b** | OH | H | $C_{16}H_{33}Br$ | **8d** | 0 | 92 |
| **6c** | H | OH | $C_{16}H_{33}Br$ | **8e** | 0 | 46 |

[a] Isolated yields after chromatographic separation.

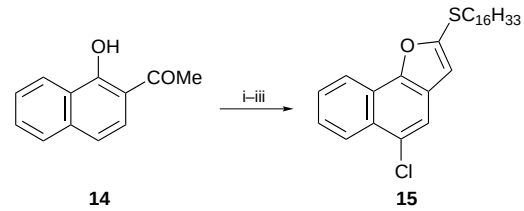



**Scheme 3**

intramolecular phenolate addition,[8] can be excluded (Scheme 3).

It is most unusual that a weak base such as phenolate would be capable of abstracting the 5-thiadiazole hydrogen. We found that the decomposition reaction to alkynethiolate **2** also occurs, although at a much slower rate (several days), when equal amounts of phenol and 4-phenyl-1,2,3-thiadiazole **1** are reacted in refluxing acetone in the presence of equivalent amounts of potassium carbonate and benzyl chloride. There is no observable reaction when only **1**, potassium carbonate and benzyl chloride are present, proving the intermediacy of the phenolate anion. Here, the major products are the known[2] dimeric dithiafulvalene **4** and benzyl phenyl ether. It is interesting to note that no dimers have been detected in the reactions starting from **6a**–**c**. Apparently, intramolecular phenolate addition is much more effective than the intermolecular dimerization process.

The generality of the reaction was investigated by reacting the 2,4-dihydroxyphenyl- and 2,5-dihydroxyphenyl-thiadiazoles **6b** and **6c** with hexadecyl bromide under the same reaction conditions. In the presence of one equivalent of alkylating agent, only the *S*-monoalkylated products **8d** and **8e**, respectively, were formed in fair to excellent yields (Scheme 1, Table 1). The chloronaphthofuran **15** was produced following a




**Scheme 4** *Reagents and conditions*: i, $EtO_2CNHNH_2$; ii, $SOCl_2$; iii, $K_2CO_3$, $C_{16}H_{33}Br$, acetone, reflux

similar strategy from 2-acetyl-1-naphthol **14**. The chlorine was introduced on the electron rich naphthol at the stage of the Hurd–Mori reaction (Scheme 4).[3]

Financial support from the University is gratefully acknowledged. B. D. thanks the I.W.T. for a predoctoral fellowship.

## Footnote and References

* E-mail: wim.dehaen@chem.kuleuven.ac.be

1 R. Raap and R. G. Micetich, *Can. J. Chem.*, 1968, **46**, 1057; G. L'abbé, W. Dehaen and B. Haelterman, *J. Chem. Soc., Perkin Trans. 1*, 1994, 2203.
2 R. Mayer, B. Hunger, R. Prousa and A. K. Müller, *J. Prakt. Chem.*, 1967, **35**, 294; A. Shafiee and I. Lalezari, *J. Heterocycl. Chem.*, 1973, **10**, 11.
3 C. D. Hurd and R. I. Mori, *J. Am. Chem. Soc.*, 1955, **77**, 5359; R. N. Butler and D. A. O'Donoghue, *J. Chem. Soc., Perkin Trans. 1*, 1982, 1223.
4 The synthesis of compound **6** has been reported before in a patent without experimental data: J. M. Muchowski and J. H. Fried, *US Pat*., 3 940 407, 1976; *Chem. Abstr.*, 1976, **85**, P63072a.
5 For instance, we used the isomeric 4-(4-hydroxyphenyl)-1,2,3-thiadiazole in a convergent synthesis of dendrimers: G. L'abbé, B. Haelterman and W. Dehaen, *Bull. Soc. Chim. Belg.*, 1996, **105**, 419.
6 The compounds **7a**, **8b**–**e** and **15** are new and were fully characterized by IR, mass, $^1$H NMR and $^{13}$C NMR spectroscopy. Benzofuran **8a** has been prepared before: B. Capon and S. Q. Lew, *Tetrahedron*, 1992, **48**, 7823.
7 P. C. Montevecchi and M. L. Navacchia, *J. Org. Chem.*, 1995, **60**, 6455; M. Wierzbich, G. Kirsch, D. Cagniant, M. Liebermann and T. W. Schafer, *Chim. Ther.*, 1977, **12**, 557.
8 F. Weselly and E. Zbiral, *Liebigs Ann. Chem.*, 1957, **605**, 98.

*Received in Liverpool, UK, 9th June 1997; 7/04025C*

# Stereoselective synthesis of a chiral synthon, 2,2,5-trisubstituted tetrahydropyran, based on simultaneous 1,3- and 1,6-asymmetric induction *via* nucleophilic acetal cleavage reaction of the bicyclic acetal: a total synthesis of (−)-malyngolide

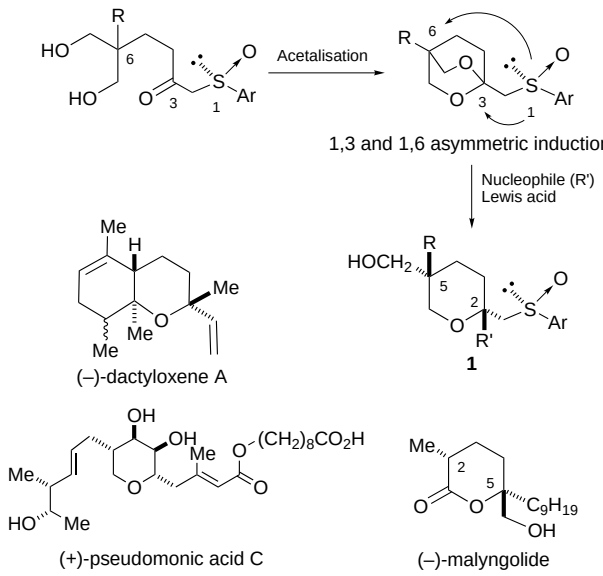
**Naoyoshi Maezaki,[a] Yûki Matsumori,[a] Takeshi Shogaki,[a] Motohiro Soejima,[a] Tetsuaki Tanaka,[a] Hirofumi Ohishi[b] and Chuzo Iwata*[a]**

[a] *Faculty of Pharmaceutical Sciences, Osaka University, 1-6 Yamadaoka, Suita, Osaka 565, Japan*
[b] *Osaka University of Pharmaceutical Sciences, 4-20-1 Nasahara, Takatsuki, Osaka 569-11, Japan*

**A chiral 2,2,5-trisubstituted tetrahydropyran is synthesised efficiently *via* facial and group selective nucleophilic acetal cleavage reaction of a bicyclic acetal, wherein simultaneous 1,3- and 1,6-asymmetric induction from a sulfinyl chirality is accomplished with high diastereoselectivity; this chiral synthon is successfully applied to a total synthesis of (−)-malyngolide.**

The development of a methodology for remote asymmetric induction is one of the most challenging problems in organic synthesis.[1,2] In addition, the simultaneous installation of chiral centres separated by more than two carbons is a very difficult task. We have previously reported a novel asymmetric desymmetrisation of a prochiral 1,3-diol *via* diastereoselective acetal cleavage reaction.[2] The results prompted us to develop a methodology for simultaneous 1,3- and 1,6-asymmetric induction *via* a nucleophilic acetal cleavage reaction,[3] wherein a chiral sulfinyl group controls both the diastereotopic C–O bond cleavage and diastereofacial nucleophilic addition, thereby yielding chiral 2,2,5-trisubstituted tetrahydropyrans with two chiral centres at the $C_2$ and $C_5$ positions (Scheme 1).† The resulting tetrahydropyran derivative **1** is considered as a useful chiral synthon for various natural products, *i.e.* (−)-dactyloxene A,[4] (+)-pseudomonic acid C[5] and (−)-malyngolide.[6]

Here we describe a novel method of synthesising 2,2,5-trisubstituted tetrahydropyran based on simultaneous 1,3- and 1,6-asymmetric induction with high diastereoselectivity *via* group and facial selective nucleophilic acetal cleavage reactions and apply this chiral synthon to a total synthesis of (−)-malyngolide.




**Scheme 1**

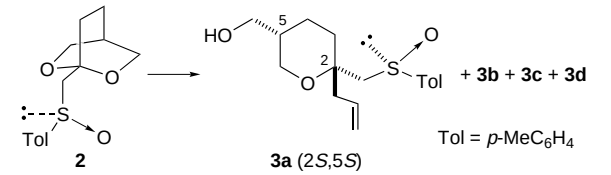
Upon treatment with a mixture of the bicyclic acetal **2**[2] and allyltrimethylsilane with $TiCl_4$, nucleophilic acetal cleavage reaction took place at −78 °C to produce allylated alcohol **3a** along with the three diastereomeric isomers **3b–d**‡ (67 : 10 : 17 : 6) (Table 1). Selectivity was increased by lowering the reaction temperature; $CH_2Cl_2$ was the most suitable solvent. The best result was obtained when $TiCl_4$ (5 equiv.) was added to a mixture of substrate and allyltrimethylsilane (10 equiv.) in $CH_2Cl_2$ at −100 °C. In this case, the ratio of **3a** and its three other isomers was 84 : 6 : 7 : 3.

The absolute configuration of the major product **3a** was inferred from the relative configuration determined by single crystal X-ray analysis of the p-nitrobenzoate§ and the known absolute configuration of the sulfoxide.¶

The reaction was rationalised as follows: $TiCl_4$ coordinates between the sulfinyl oxygen and one of the acetal oxygens to form the chelation intermediates **A** or **B**, in which the bulky tolyl group located at equatorial position (Fig. 1). The intermediate **A** is more favourable than **B**, since the electropositive sulfur atom is located between electronegative oxygens and is *anti* to the bulky 7-methylene group in the intermediate **A**.[7] The C–O bond coordinated by $TiCl_4$ is weakened or cleaved to produce transition state **C** or tight ion pair intermediate **D**, respectively. Allyltrimethylsilane reacts with the bicyclic acetal from the backside of the breaking C–O bond *via* an $S_N2$-type substitution (transition state **C**) or an $S_N1$-like mechanism (intermediate **D**)[8] to give the (2*S*,5*S*)-isomer **3a** diastereoselectively as a potential multifunctional chiral synthon.

We planned to apply this chiral synthon to the synthesis of a marine antibiotic, (−)-malyngolide.[6] Although various synthe-

**Table 1** Nucleophilic acetal cleavage reaction of the bicyclic acetal **2**




**2** **3a** (2*S*,5*S*)

| Conditons (equiv.) | Yield (%)[a] | Ratio[b] **3a** : **3b** : **3c** : **3d** |
|---|---|---|
| $TiCl_4$ (5), $Me_3Si$(allyl) (5), $CH_2Cl_2$, −20 °C | 91 | 19 : 26 : 48 : 7 |
| $TiCl_4$ (5), $Me_3Si$(allyl) (5), $CH_2Cl_2$, −78 °C | 93 | 67 : 10 : 17 : 6 |
| $TiCl_4$ (5), $Me_3Si$(allyl) (5), $CH_2Cl_2$, −100 °C | 92 | 79 : 6 : 9 : 6 |
| $TiCl_4$ (5), $Me_3Si$(allyl) (5), PhMe, −78 °C | 63 | 66 : 10 : 16 : 8 |
| $TiCl_4$ (5), $Me_3Si$(allyl) (5), THF, −78 °C | 0 | — |
| $TiCl_4$ (5), $Me_3Si$(allyl) (10), $CH_2Cl_2$, −100 °C | 90 | 84 : 6 : 7 : 3 |

[a] Isolated yield. [b] The ratio was determined by 500 MHz $^1$H NMR spectroscopic measurements.

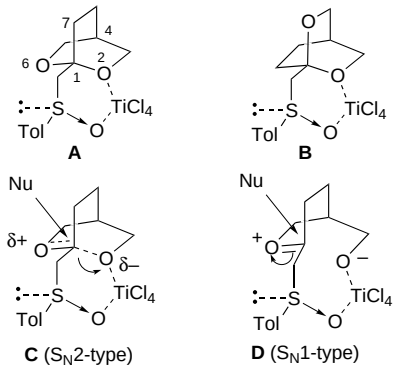
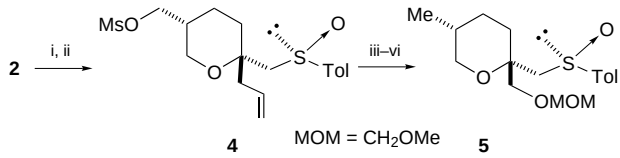


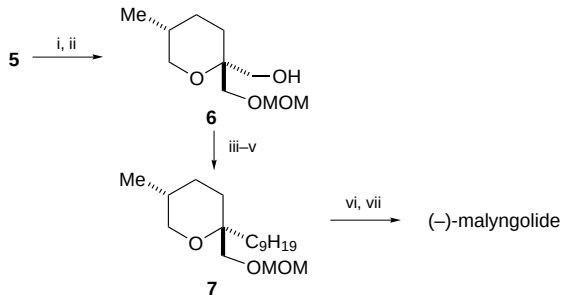

**Fig. 1**




**Scheme 2** *Reagents and conditions*: i, $TiCl_4$, allyltrimethylsilane, $CH_2Cl_2$, −100 °C; ii, MsCl, DMAP, $CH_2Cl_2$, 0 °C (73% in 2 steps); iii, $LiBEt_3H$, THF, room temp. (97%); iv, $PdCl_2(PhCN)_2$, benzene, 80 °C (60%, 90% based on recovery of material); v, $O_3$, MeOH, −78 °C then $NaBH_4$, room temp. (93%); vi, MOMCl, $Pr^i_2NEt$, $CH_2Cl_2$, room temp. (77%)

ses of malyngolide have been reported,[9] most of synthetic routes lack stereocontrol at the $C_2$ methyl group. A few methods overcome this problem by constructing the two chiralities one by one.[9a,c,e,f] After the nucleophilic acetal cleavage reaction of **2**, the major diastereomeric isomer **3a**, which possesses three appropriately installed side-chains for the synthesis of (−)-malyngolide, was isolated as a mesylate **4** (73% yield from **2**). After reduction of the mesylate moiety with Super Hydride®, a catalytic amount of $PdCl_2(PhCN)_2$ was used to isomerise the allyl group to a prop-1-enyl group.[10] Ozonisation was followed by a reductive work-up, and protection as a methoxymethyl (MOM) ether was undertaken to yield **5** (Scheme 2).

The *p*-tolylsulfinyl group was converted into the alcohol **6** *via* Pummerer rearrangement followed by reduction with $LiBH_4$. After Dess–Martin oxidation,[11] eight carbon elongation at the hindered position was successfully accomplished with a Wittig reagent followed by hydrogenation of the olefin to produce compound **7** in good yield. Finally, the tetrahydropyran ring was oxidised to the δ-lactone with $RuO_4$, and the MOM ether was removed with $Me_3SiBr$ to give (−)-malyngolide without epimerisation at the methyl group (Scheme 3). The spectroscopic data and specific rotation [$[\alpha]_D$ −12.5 ($CHCl_3$)] were consistent with the reported data [$[\alpha]_D$ −13.0 ($CHCl_3$)].[6]




**Scheme 3** *Reagents and conditions*: i, $Ac_2O$, AcONa, 130 °C (90%; 2 : 1 diastereomeric ratio); ii, $LiBH_4$, THF, room temp. (97%); iii, Dess–Martin periodinate, $CH_2Cl_2$, 0 °C (88%); iv, $Ph_3P^+(C_8H_{17})Br^-$, KHMDS, THF, 0 °C (94%); v, $H_2$, 10% Pd–C, MeOH, room temp. (86%); vi, $RuCl_3{\cdot}3H_2O$, $NaIO_4$, $CCl_4$–MeCN–$H_2O$ (57%, 80% based on recovery of material); vii, $Me_3SiBr$, $CH_2Cl_2$, −30 °C (85%)

In summary, we have synthesised 2,2,5-trisubstituted tetrahydropyran **1** as a multifunctional chiral synthon based on facial and group selective acetal cleavage reactions, in which highly diastereoselective 1,3- and 1,6-asymmetric induction was observed. The utility of this chiral synthon was demonstrated by its application to the total synthesis of (−)-malyngolide.

This work was supported by a Grant-in-Aid (No. 08772018) for Encouragement of Young Scientists from the Ministry of Education, Science, Sports and Culture, Japan.

## Footnotes and References

* E-mail: iwata@phs.osaka-u.ac.jp

† Relative and absolute configurations at the $C_2$ and the $C_5$ positions in the chiral synthon **1** can be controlled by the sulfinyl chirality. Furthermore, inversion of the stereochemistry at the $C_2$ position in **1** (R′ = allyl) is also possible, since both allyl and sulfinyl groups can be converted into variety of functional groups.

‡ The absolute configurations of **3b**–**d** were determined as (2*S*,5*R*), (2*R*,5*S*), and (2*R*,5*R*), respectively. Structural determination of these compounds will be reported elsewhere.

§ The X-ray crystal structure of compound **3a** confirms the relative configuration at $C_2$ and $C_5$ although the quality of the data is not adequate for publication. These assignments are supported by the conversion of **3a** into (−)-malyngolide.

¶ The absolute configuration of the sulfoxide moiety in **3a** was based on the optical rotation of the known methyl *p*-tolyl sulfoxide (ref. 12), from which **3a** was derived (ref. 2). Since all synthetic intermediates after introduction of the sulfinyl group (including **2** and **3a**) possess positve optical rotations, their absolute configurations on sulfur are assumed to be retained during the transformations [by the empirical rule (ref. 13)].

1 For selected recent references to 1, *n*-asymmetric induction ($n > 4$), see N. Magnus and P. Magnus, *Tetrahedron Lett.*, 1997, **38**, 3491 and references cited therein; H. Fujioka, H. Kitagawa, N. Matsunaga, Y. Nagatomi and Y. Kita, *Tetrahedron Lett.*, 1996, **37**, 2245; T. Sato, M. Kido and J. Otera, *Angew. Chem., Int. Ed. Engl.*, 1995, **34**, 2254; K. Mikami and A. Yoshida, *Tetrahedron Lett.*, 1994, **35**, 7793; H.-C. Zhang, M. J. Costanzo and B. E. Maryanoff, *Tetrahedron Lett.*, 1994, **35**, 4891; W. R. Roush and C. K. Wada, *J. Am. Chem. Soc.*, 1994, **116**, 2151; G. A. Molander and K. L. Bobbitt, *J. Am. Chem. Soc.*, 1993, **115**, 7517; R. J. Mears and A. Whiting, *Tetrahedron Lett.*, 1993, **34**, 8155.

2 N. Maezaki, M. Murakami, M. Soejima, T. Tanaka, T. Imanishi and C. Iwata, *Chem. Pharm. Bull.*, 1996, **44**, 1146; C. Iwata, N. Maezaki, M. Murakami, M. Soejima, T. Tanaka and T. Imanishi, *J. Chem. Soc., Chem. Commun.*, 1992, 516. Related work: N. Maezaki, A. Sakamoto, M. Soejima, I. Sakamoto, Y. X. Li, T. Tanaka, H. Ohishi, K. Sakaguchi and C. Iwata, *Tetrahedron: Asymmetry*, 1996, **7**, 2787 and references cited therein.

3 T. Harada and A. Oku, *Synlett*, 1994, 95; A. Alexakis and P. Mangeney, *Tetrahedron: Asymmetry*, 1990, **1**, 477.

4 F. J. Schmitz, F. J. McDonald and D. J. Vanderah, *J. Org. Chem.*, 1978, **43**, 4220.

5 D. R. Williams, J. L. Moore and M. Yamada, *J. Org. Chem.*, 1986, **51**, 3916; J. P. Clayton, P. J. O'Hanlon, N. H. Rogers and T. J. King, *J. Chem. Soc., Perkin Trans. 1*, 1982, 2827; J. P. Clayton, P. J. O'Hanlon and N. H. Rogers, *Tetrahedron Lett.*, 1980, **21**, 881.

6 J. H. Cardllina II and R. E. Moore, *J. Org. Chem.*, 1979, **44**, 4039.

7 E. Juaristi, in *Introduction to Stereochemistry and Conformational Analysis*, Wiley, New York, 1991, ch. 16, p. 271.

8 K. Ishihara, A. Mori and H. Yamamoto, *Tetrahedron*, 1990, **46**, 4595.

9 (*a*) D. Enders and M. Knopp, *Tetrahedron*, 1996, **52**, 5805 and references cited therein; (*b*) H. P. Zeng, J. Y. Su and L. M. Zeng, *Yaoxue Xuebao*, 1994, **29**, 680; (*c*) M. Asaoka, S. Hayashibe, S. Sonoda and H. Takei, *Tetrahedron*, 1991, **47**, 6967; (*d*) K. Machiya, I. Ichimoto, K. Tonari, M. Kirihara and H. Ueda, *Agric. Biol. Chem.*, 1985, **49**, 1767; (*e*) H. Hagiwara and H. Uda, *J. Chem. Soc., Perkin Trans. 1*, 1985, 1157; (*f*) T. Kogure and E. L. Eliel, *J. Org. Chem.*, 1984, **49**, 576.

10 J. K. Cha and R. J. Cooke, *Tetrahedron Lett.*, 1987, **28**, 5473; P. Golborn and F. Scheinmann, *J. Chem. Soc., Perkin Trans. 1*, 1973, 2870.

11 R. E. Ireland and L. Liu, *J. Org. Chem.*, 1993, **58**, 2899; D. B. Dess and J. C. Martin, *J. Am. Chem. Soc.*, 1991, **113**, 7277.

12 U. de la Camp and H. Hope, *Acta Crystallogr., Sect. B*, 1970, **26**, 846.

13 K. Mislow, M. M. Green, P. Laur, J. T. Melillo, T. Simmons and A. L. Ternay, Jr., *J. Am. Chem. Soc.*, 1965, **87**, 1958.

*Received in Cambridge, UK, 12th May 1997; 7/03242K*

# A versatile approach to pyrimidin-4-yl substituted α-amino acids from alkynyl ketones; the total synthesis of L-lathyrine

**Robert M. Adlington, Jack E. Baldwin,* David Catterick and Gareth J. Pritchard**

*The Dyson Perrins Laboratory, South Parks Road, Oxford, UK OX1 3QY*

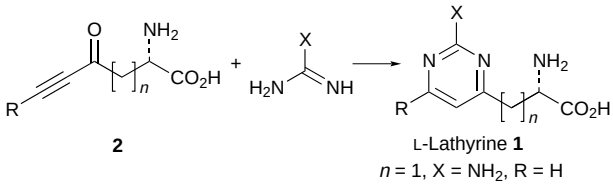
**A range of pyrimidin-4-yl substituted α-amino acids has been synthesised by the reaction of amidines with α-amino acid alkynyl ketones.**

The stereoselective synthesis of α-amino acids is an active field of research.[1] In particular heterocyclic substituted non-proteinogenic amino acids show a diverse range of biological activities. Examples of these include azatyrosine,[2] mimosine,[3] lathyrine **1**[4,5] and discadenine.[6] In view of the wide range of biological activities shown we wished to develop a versatile route to these types of compounds, which may also be applicable to parallel and/or combinatorial syntheses, thus providing families of related compounds.

Our initial target was to introduce alkynyl ketones as a versatile reactive group for the construction of heterocycles into the side chain of α-amino acids. Alkynyl ketones have been used in the synthesis of a range of heterocyclic systems[7] and very recently have been condensed with amidines to give pyrimidines.[8] As our approach offered the possibility of three different groups on the heterocyclic ring, one of which being an α-amino acid, a large range of structurally related families should be readily accessible (Scheme 1).

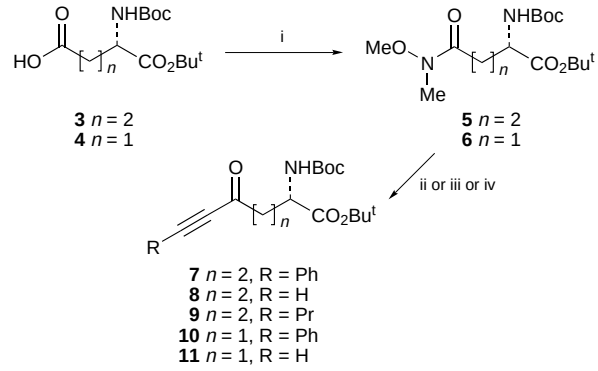
Glutamic acid and aspartic acid were considered as suitable precursors to **2**, where the side chain acid could be activated and reacted with a lithium acetylide. The activation chosen was the 'Weinreb' amide, which has been used to synthesise aryl ketone amino acids.[9,10] Thus α-*tert*-butyl *N*-*tert*-butoxycarbonyl-glutamate **3** was prepared following a five step procedure from L-glutamic acid,[11,12] which was then converted to the amide **5** by reaction of *N*,*O*-dimethylhydroxylamine *via* a mixed anhydride in satisfactory yield.[10] Subsequent reaction of the amide **5** with a five-fold excess of lithium phenylacetylide, ethynylmagnesium bromide or lithium propylacetylide at −78 °C in THF afforded the ethynyl ketones **7**, **8** and **9** in good yields (Scheme 2).

Trial cyclocondensations between **8** and benzamidine hydrochloride showed that optimal conditions for the formation of the desired pyrimidinyl substituted amino acid **12** were stirring an MeCN or EtOAc solution of the ethynyl ketone with benzamidine hydrochloride and solid $Na_2CO_3$ with a catalytic amount of water at reflux. Acetylenic ketones **7**, **8** and **9** containing aryl, hydrogen and alkyl functionalities respectively then underwent a series of cyclocondensations with a range of hetero, aryl, alkyl and hydrogen functionalised amidines to generate the pyrimidines **12**–**19** (Scheme 3 and Table 1). The enantiomeric purity of these compounds was determined by conversion of their N-deprotected forms (Boc deprotection carried out by azeotropic distillation with $TsOH·H_2O$–PhMe) to both (*R*)- and (*S*)-Mosher's amides and proved to be greater than 98% ee.[13]




**2** L-Lathyrine **1**
$n$ = 1, X = $NH_2$, R = H

**Scheme 1**

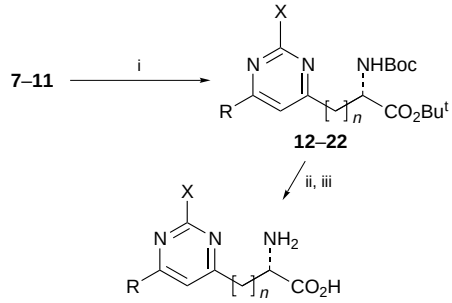



**3** $n$ = 2
**4** $n$ = 1
**5** $n$ = 2
**6** $n$ = 1
**7** $n$ = 2, R = Ph
**8** $n$ = 2, R = H
**9** $n$ = 2, R = Pr
**10** $n$ = 1, R = Ph
**11** $n$ = 1, R = H

**Scheme 2** *Reagents and conditions*: i, NMM,Bu$^i$OCOCl, THF, −15 °C; HN(OMe)Me·HCl, $NEt_3$, DMF, 74% (**5**), 76% (**6**); ii, PhCCLi (5 equiv.), THF, −78 °C, 79% (**7**), 62% (**10**); iii, HCCMgBr (5 equiv.), $Et_2O$, −78 °C, 61% (**8**), 78% (**11**); iv, PrCCLi (5 equiv.), THF, −78 °C, 95% (**9**)

Thus from a key precursor **5** a large family of diverse structures can be built up incorporating hydrogen, alkyl, aryl and hetero functionality. The amidine used allows control at the 2 position of the resulting pyrimidine whilst the choice of acetylide controls the 6 position.

To allow further variation in the substitution at the pyrimidine 4 position, the chemistry was expanded to L-aspartic acid. The α-*tert*-butyl *N*-*tert*-butoxycarbonylaspartate **4** was prepared and converted to the 'Weinreb' amide **6** as previously for **5**. The acetylenic ketones **10** and **11** were then formed by reaction of **6** with a five-fold excess of ethynylmagnesium bromide or lithium phenylacetylide respectively (Scheme 2). The ketones **10** and **11** underwent high yielding condensations to produce **20**, **21** and **22** (Scheme 3 and Table 1). Investigation




**30** $n$ = 2, R = Ph, X = Ph
**31** $n$ = 2, R = Ph, X = Me
**32** $n$ = 2, R = Ph, X = H
**33** $n$ = 2, R = Ph, X = SMe
**34** $n$ = 2, R = H, X = SMe
**35** $n$ = 2, R = H, X = $NH_2$
**36** $n$ = 2, R = Pr, X = SMe
**37** $n$ = 2, R = Pr, X = Me
**38** $n$ = 1, R = Ph, X = SMe
**39** $n$ = 1, R = Ph, X = 4-Cl$C_6H_4$
**40** $n$ = 1, R = H, X = SMe

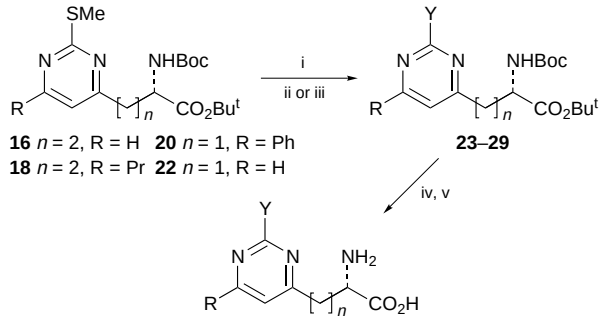
**Scheme 3** *Reagents and conditions*: i, HN(CX)$NH_2$·HCl or 0.5 $H_2SO_4$, EtOAc or MeCN, $Na_2CO_3$, $H_2O$ (cat.), reflux (or 40 °C for $n$ = 1); ii, TFA, anisole; iii, Dowex 50X8-100 ion-exchange resin

**Table 1** Pyrimidin-4-yl substituted protected α-amino acids from the cyclocondensations of ethynyl ketones with amidines

| Compound | *n* | R | X | Yield (%) |
|---|---|---|---|---|
| **12** | 2 | Ph | Ph | 87 |
| **13** | 2 | Ph | Me | 90 |
| **14** | 2 | Ph | H | 40 |
| **15** | 2 | Ph | SMe | 79 |
| **16** | 2 | H | SMe | 82 |
| **17** | 2 | H | $NH_2$ | 28 |
| **18** | 2 | Pr | SMe | 95 |
| **19** | 2 | Pr | Me | 83 |
| **20** | 1 | Ph | SMe | 91 |
| **21** | 1 | Ph | 4-$ClC_6H_4$ | 89 |
| **22** | 1 | H | SMe | 87 |

of the enantiomeric purity of these pyrimidines by Mosher's amide formation showed up to 5% racemisation when the cyclocondensations were carried out at reflux temperatures; however, this was reduced by carrying out the condensations at 40 °C affording enantiomeric purity greater than 98% ee.

One compound of note is pyrimidine **17**, which is a homologue of the naturally occurring amino acid L-lathyrine.[4] The condensation of **8** with guanidine to give **17** had, however, given a disappointingly low yield. In order to attempt the synthesis of L-lathyrine itself as well as other analogues and to further diversify the functionality at the pyrimidine 2 position it was decided to undertake nucleophilic aromatic substitutions of suitable leaving groups. It was expected that the existing thiomethyl functionality, derived from cyclisations of ethynyl ketones with 2-methyl-2-thiopseudourea, if oxidised to the corresponding sulfone, would be susceptible to substitution by nucleophiles.[14] Reaction of the pyrimidines **16**, **18**, **20** and **22** with 2 equiv. of MCPBA resulted in the corresponding sulfones **23**–**26**. Substitution of the methylsulfonyl group using liquid ammonia was then possible. Good yields of the corresponding pyrimidines **27**–**29** were thus achieved, **29** being protected L-lathyrine. When 1 M NaOH was used in the substitution reaction with **23**, followed by mild acidic work up ($KH_2PO_4$–$H_2O$) and purification by ion-exchange chromatography, pyrimidone **45** was obtained in 71% yield (Scheme 4 and Table 2).




**16** *n* = 2, R = H **20** *n* = 1, R = Ph
**18** *n* = 2, R = Pr **22** *n* = 1, R = H

**41** *n* = 2, R = H, Y = $SO_2Me$ **45** *n* = 2, R = H, Y = OH
**42** *n* = 2, R = Pr, Y = $SO_2Me$ **46** *n* = 2, R = Pr, Y = $NH_2$
**43** *n* = 1, R = Ph, Y = $SO_2Me$ **47** *n* = 1, R = Ph, Y = $NH_2$
**44** *n* = 1, R = H, Y = $SO_2Me$ **1** *n* = 1, R = H, Y = $NH_2$

**Scheme 4** *Reagents and conditions*: i, MCPBA (2 equiv.), $CH_2Cl_2$, room temp.; ii, 1,4-dioxane, 1 M NaOH, room temp.; iii,$NH_3$ (1), THF, room temp.; iv, TFA, anisole; v, Dowex 50X8-100 ion exchange resin

**Table 2** Results for oxidation of **16**, **18**, **20** and **22** and subsequent nucleophilic substitutions

| Compound | *n* | R | Y | Yield (%) |
|---|---|---|---|---|
| *Oxidation* | | | | |
| **23** | 2 | H | $SO_2Me$ | 86 |
| **24** | 2 | Pr | $SO_2Me$ | 88 |
| **25** | 1 | Ph | $SO_2Me$ | 76 |
| **26** | 1 | H | $SO_2Me$ | 100 |
| *Substitution* | | | | |
| **27** | 2 | Pr | $NH_2$ | 75 |
| **28** | 1 | Ph | $NH_2$ | 87 |
| **29** | 1 | H | $NH_2$ | 93 |

Deprotection of the protected pyrimidin-4-yl amino acids was achieved by dissolution in TFA–anisole. The free amino acids **30**–**32**, **34**–**38**, **40**–**47** and **1** were obtained by ion-exchange chromatography as solids in high yields (90–100%). A lower yield was observed for the deprotection/purification of **33** due to the low solubility of its TFA salt and **39** was preferentially isolated as its TFA salt (Schemes 3 and 4). The optical rotation of **1** (synthetic L-lathyrine) had a value of $[\alpha]_D^{21}$ −55.4 (*c* 1.2, $H_2O$), consistent with that reported for the naturally occurring amino acid [lit.,[5] −55.9 (*c* 1.2, $H_2O$)].

In conclusion we have developed a versatile approach, applicable to parallel synthesis, to a family of pyrimidin-4-yl substituted α-amino acids, the chemistry allowing diversification by control of the 2, 4 and 6 positions of the pyrimidine. This route allows the total synthesis of non-proteinogenic amino acids in approximately 20% overall yield from aspartic or glutamic acids. Further routes to other families of natural product derivatives will be reported in due course.

We thank the EPSRC for a studentship to D. C. and the EPSRC mass spectrometry service (Swansea) for high resolution mass spectra.

## Footnote and References

* E-mail: jack.baldwin@dpl.ox.ac.uk

1 For a recent review, see R. O. Duthaler, *Tetrahedron*, 1994, **50**, 1539.
2 For a recent synthesis, see A. G. Myers and J. L. Gleason, *J. Org. Chem.*, 1996, **61**, 813; and references cited therein.
3 G. A. Rosenthal, *Plant Nonprotein Amino and Imino Acids Biological, Biochemical and Toxicological Properties*, Academic Press, New York, 1982, p. 78.
4 G. A. Rosenthal, *Plant Nonprotein Amino and Imino Acids Biological, Biochemical and Toxicological Properties*, Academic Press, New York, 1982, p. 117.
5 E. A. Bell, *Biochim. Biophys. Acta*, 1961, **47**, 602.
6 J.-E. Son, K. Ramalingam and R. W. Woodard, *Synthesis*, 1988, 240.
7 K. Bowden and E. R. H. Jones, *J. Chem. Soc.*, 1946, 953.
8 D. Obrecht, C. Abrecht, A. Grieder and J. M. Vilalgordo, *Helv. Chim. Acta*, 1997, **80**, 65 and references cited therein.
9 S. Nahm and S. Weinreb, *Tetrahedron Lett.*, 1981, **22**, 3815.
10 T. L.Cupps, R. H.Boutin and H. Rapoport, *J. Org. Chem.*, 1985, **50**, 3972.
11 R. K. Olsen, K. Ramasamay and T. Emery, *J. Org. Chem.*, 1984, **49**, 3527.
12 R. L.Prestidge, D. R. K. Harding, J. E. Battersby and W. S. Handcock, *J. Org. Chem.*, 1975, **40**, 3287.
13 J. A. Dale, D. L. Dull and H. S. Mosher, *J. Org. Chem.*, 1969, **34**, 2543.
14 D. J. Brown and P. W. Ford, *J. Chem. Soc.* (*C*), 1967, 568.

*Received in Cambridge, 27th June 1997; 7/04526C*

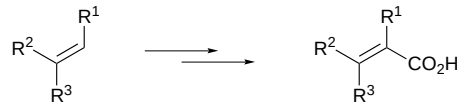
# The free-radical addition of phenyl trichloromethyl selenide to alkenes: a new method for the regioselective carboxylation of alkenes

**Thomas G. Back* and Kazimierz Minksztym**

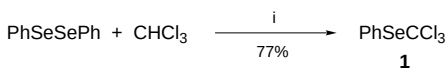
*Department of Chemistry, University of Calgary, Calgary, AB, Canada, T2N 1N4*

**The free-radical addition of phenyl trichloromethyl selenide to alkenes affords 2-phenylseleno-1-trichloromethylalkanes, which can be converted into α,β-unsaturated carboxylic acids or amides by base-promoted dehydrochlorination, followed by [2,3]sigmatropic rearrangement of the corresponding selenoxides in the presence of water or diethylamine, respectively.**

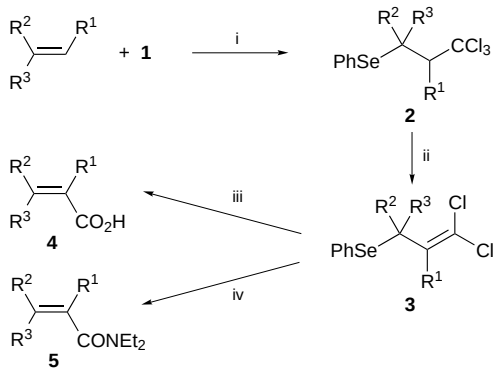
Free-radical 1,2-additions of selenium compounds of general structure PhSeX to alkenes and alkynes[1] provide a synthetically useful means for introducing the versatile phenylseleno group, as well as an additional functionality [*e.g.* X = $SO_2Ar$,[2] SePh,[3] C(=O)R,[4] SC(=O)Ph,[5] and $CHZ_2$,[6] where Z is an electron-withdrawing group] into the substrates. Free-radical additions of perhaloalkanes such as bromotrichloromethane are also well known.[7] Moreover, PhSe group transfers to alkyl radicals occur with rates comparable to those of bromine atom transfers,[8] suggesting that phenyl trichloromethyl selenide **1**[9] should undergo free-radical additions similar to those of bromotrichloromethane. We now report the novel photo-initiated or thermally initiated radical additions of **1** to alkenes, followed by some illustrative further transformations of the trichloromethyl and phenylseleno moieties that permit the overall conversion of the alkene into the corresponding α,β-unsaturated carboxylic acid (or amide), as shown in Scheme 1. Other methods for the carboxylation of alkenes generally require the presence of activating substituents to permit deprotonation of the alkene, or an existing functionality (*e.g.* halide, stannane) that provides a site for metallation, followed by reaction with carbon dioxide or



**Scheme 1**

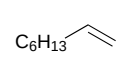
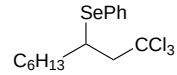
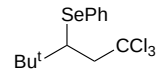
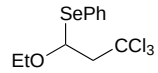
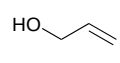
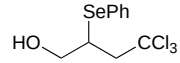
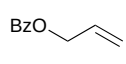
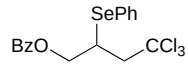
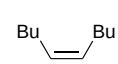
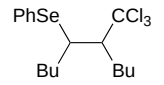
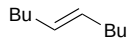
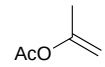
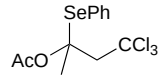
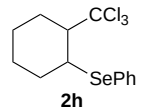
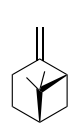
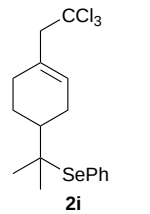


**Scheme 2** *Reagents and conditions*: i, 50% NaOH–$H_2O$, Adogen 464®, $O_2$, 15–20 °C



**Scheme 3** *Reagents and conditions*: i, *hν* or heat, AIBN; ii, $Bu^tOK$–THF, −30 or 10 °C; iii, 30% $H_2O_2$ $H_2O$, −30 °C; iv, MCPBA, $CH_2Cl_2$, −30 °C, then $Et_2NH$, room temp.

**Table 1** Addition of **1** to alkenes[a]

| Alkene | Product | Yield (%) | *t*/h |
|---|---|---|---|
|  |  **2a** | 88 | 12 |
| | | 62[b] | 60 |
| | | 78[c] | 25 |
|  |  **2b** | 75 | 13 |
|  |  **2c** | 81 | 5 |
|  |  **2d** | 65 | 13 |
|  |  **2e** | 69 | 12 |
|  |  **2f** | 60[d] | 19 |
|  | **2f** | 54[e] | 12 |
|  |  **2g** | 43 | 17 |
|  |  **2h** | 63[f] | 24 |
|  |  **2i** | 87 | 19 |

[a] All reactions were performed neat using photo-initiation and 5 equiv. of the alkene unless otherwise noted; isolated yields are reported. [b] Only 1.5 equiv. of the alkene was used. [c] Performed in benzene at 80 °C with 10 mol% of AIBN. [d] The diastereomeric ratio was 3.8 : 1, as determined by NMR integration. [e] The diastereomeric ratio was 4.2 : 1, as determined by NMR integration. [f] The *cis* : *trans* ratio was 1 : 1.8, as determined by NMR integration.

one of its synthetic equivalents.[10] The present method permits the use of unactivated olefins.

Selenide **1** was conveniently prepared by a new method from the base-catalysed reaction of diphenyl diselenide with $CHCl_3$ (Scheme 2). Thus, a mixture of the diselenide, a catalytic amount of Adogen 464® (methyltrialkylammonium chloride), 50% aqueous NaOH and $CHCl_3$ was stirred for 9 h at 15–20 °C, while air was bubbled through the reaction mixture to recycle the byproduct selenolate ($PhSe^-$). The product was isolated in 77% yield by flash chromatography.

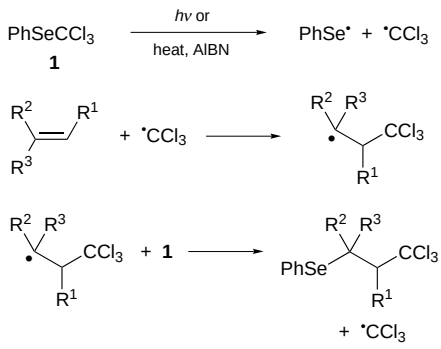
The free-radical 1,2-addition of **1** to various alkenes to give **2** was then effected as shown in Scheme 3 and Table 1. Monosubstituted alkenes afforded adducts **2a**–**e** with only traces ( < 5%) of their corresponding regioisomers, as indicated by NMR analysis. Both *cis*- and *trans*-dec-5-ene produced **2f** as the same *ca*. 4 : 1 mixture of diastereomers. Cyclohexene furnished a mixture of *cis* and *trans*-adducts **2h** in a ratio of 1 : 1.8. Thus, the additions are highly regioselective, but only moderately stereoselective. β-Pinene underwent ring-opening during the addition to afford the rearranged 1,6-adduct **2i**. In general, the reactions were performed by irradiation of the reaction mixture, either neat or in benzene solution, containing an excess (usually five-fold) of the alkene with a 300 W incandescent lamp. The use of a smaller excess of the alkene resulted in lower yields and required longer reaction times. The reaction was also performed in the case of **2a** in benzene at 80 °C in the presence of 10 mol% of the radical initiator AIBN. These results suggest a free-radical chain process in which cleavage of the Se–$CCl_3$ bond initiates the reaction, followed by addition of the trichloromethyl radical to the less substituted alkenic atom, and finally transfer of the PhSe group from **1** to the resulting 2-alkyl radical (Scheme 4).

Several of the adducts **2** were then transformed into allylic selenides **3** by dehydrochlorination with $KOBu^t$ in THF at −30 °C (except for **3f**, which required 6 h at 10 °C), and finally into α,β-unsaturated carboxylic acids **4** by oxidation and *in situ* [2,3]sigmatropic rearrangement (Scheme 3) of the resulting selenoxides.[11] Products **4a**, **4b** and **4f** were obtained as the *E*-isomers with high stereoselectivity. When $Et_2NH$ was present during the latter step, the corresponding diethylamides were obtained instead. These results are shown in Table 2. Presumably, the sigmatropic rearrangement produces **6** initially, which then hydrolyses to the carboxylic acid **4** (Scheme 5). On the other hand, **6** reacts preferentially by aminolysis in the presence of diethylamine to afford the amide **5** instead of **4** after aqueous workup.

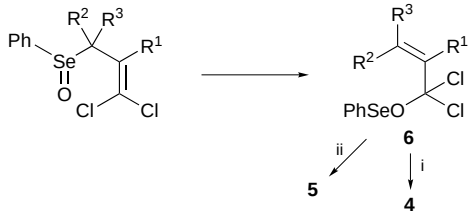
All new compounds reported here gave IR, $^1H$ NMR, $^{13}C$ NMR and low and high resolution mass spectra consistent with their structures.

These results demonstrate that the free-radical additions of readily available selenide **1** to alkenes occur efficiently and with high regioselectivity. Moreover, when the above process was used in conjunction with base-promoted dehydrochlorination and [2,3]sigmatropic rearrangement of the corresponding selenoxides, a novel method for the overall regioselective carboxylation of alkenes was achieved.

We thank the Natural Sciences and Engineering Research Council of Canada (NSERC) for financial support.



**Scheme 4**



**Scheme 5** *Reagents and conditions*: i, $H_2O$; ii, $Et_2NH$, then $H_2O$

**Table 2** Preparation of allylic selenides **3**, carboxylic acids **4** and amides **5** from **2**

| | | | | Isolated yields (%) | | |
|---|---|---|---|---|---|---|
| Adduct | $R^1$ | $R^2$ | $R^3$ | **3** | **4** | **5** |
| **2a** | H | $C_6H_{13}$ | H | 92 | 91 | 73 |
| **2b** | H | $Bu^t$ | H | 90 | 84 | 50 |
| **2f** | $Bu^n$ | $Bu^n$ | H | 92 | 81 | 59 |
| **2g** | –[$CH_2$]$_4$– | | H | 86 | 60 | 50 |

## Footnote and References

* E-mail: tgback@acs.ucalgary.ca

1 T. G. Back, in *Organoselenium Chemistry*, ed. D. Liotta, Wiley, New York, 1987, ch. 7; C. Paulmier, *Selenium Reagents and Intermediates in Organic Synthesis*, Pergamon, Oxford, 1986, pp. 214–218.
2 T. G. Back and S. Collins, *J. Org. Chem.*, 1981, **46**, 3249; T. G. Back, S. Collins and R. G. Kerr, *J. Org. Chem.*, 1983, **48**, 3077; R. A. Gancarz and J. L. Kice, *J. Org. Chem.*, 1981, **46**, 4899; T. Miura and M. Kobayashi, *J. Chem. Soc., Chem. Commun.*, 1982, 438.
3 T. G. Back and M. V. Krishna, *J. Org. Chem.*, 1988, **53**, 2533; A. Ogawa, H. Yokoyama, K.Yokoyama, T. Masawaki, N. Kambe and N. Sonoda, *J. Org. Chem.*, 1991, **56**, 5721.
4 D. L. Boger and R. J. Mathvink, *J. Org. Chem.*, 1989, **54**, 1777.
5 T. Toru, T. Seko, E. Maekawa and Y. Ueno, *J. Chem. Soc., Perkin Trans. 1*, 1988, 575.
6 J. H. Byers and G. C. Lane, *J. Org. Chem.*, 1993, **58**, 3355; J. H. Byers, J. G. Thissell and M. A. Thomas, *Tetrahedron Lett.*, 1995, **36**, 6403; D. P. Curran, E. Eichenberger, M. Collis, M. G. Roepel and G. Thoma, *J. Am. Chem. Soc.*, 1994, **116**, 4279; T. G. Back, P. L. Gladstone and M. Parvez, *J. Org. Chem.*, 1996, **61**, 3806; P. Renaud and S. Abazi, *Synthesis*, 1996, 253.
7 C. Walling and E. S. Huyser, *Org. React.*, 1963, **13**, 91.
8 D. P. Curran, A. A. Martin-Esker, S.-B. Ko and M. Newcomb, *J. Org. Chem.*, 1993, **58**, 4691.
9 D. H. R. Barton, T. Okano and S. I. Parekh, *Tetrahedron*, 1991, **47**, 1823; L. M. Yagupol'skii and N. V. Kondratenko, *Russ. J. Gen. Chem.*, 1967, **37**, 1686.
10 R. C. Larock, *Comprehensive Organic Transformations*, VCH, New York, 1989, pp. 185–188; R. P. A. Sneeden, in *The Chemistry of Carboxylic Acids and Esters*, ed. S. Patai, Wiley, London, 1969, ch. 4.
11 H. J. Reich, in *Organoselenium Chemistry*, ed. D. Liotta, Wiley, New York, 1987, ch. 8.

*Received in Corvallis, OR, USA, 13th June 1997; 7/04153E*

# First tetrathiolate-bridged dinuclear molybdacarbaboranes: scission and formation of the C–C cluster bond during oxidation processes

**Jae-Hak Kim, Mouad Lamrani, Jeong-Wook Hwang and Youngkyu Do***

*Department of Chemistry and Center for Molecular Science, Korea Advanced Institute of Science and Technology, Taejon 305-701, Korea*

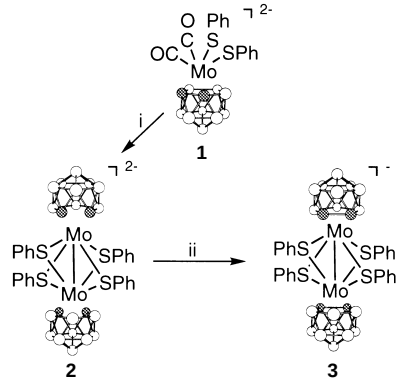
**Unprecedented tetrathiolate-bridged dinuclear ionic molybdacarbaboranes $[(C_2B_9H_{11})Mo(SPh)_2]_2^{n-}$ ($n$ = 2, 1) are prepared by successive oxidation of $[(C_2B_9H_{11})Mo^{II}(CO)_2(SPh)_2]^{2-}$ with diphenyl disulfide and iodosylbenzene: X-ray crystal structure determinations and NMR studies show unusual scission and reformation of the C–C carbaborane cage bond.**

We have recently demonstrated that the dicarbabollide anion [*nido*-7,8-$C_2B_9H_{11}]^{2-}$ is useful in synthesizing high oxidation state molybdenum oxo complexes.[1] In particular, the mononuclear thiolatomolybdacarbaborane $[(C_2B_9H_{11})Mo(CO)_2(SPh)_2]^{2-}$ **1**[1] coupled with iodosylbenzene as an oxygen-transfer agent was proven a convenient system in deriving oxometals, raising a possibility of using anion **1** as a synthon in preparing high oxidation state molybdenum thiolate complexes. To pursue this matter, the versatile oxidation reactivity of the synthon **1** has been exploited, leading to the first observation of tetrathiolate-bridged dinuclear molybdacarbaboranes $[(C_2B_9H_{11})Mo(\mu\text{-}SPh)_2]_2^{n-}$ ($n$ = 2 **2**, $n$ = 1 **3**) involving unusual scission and formation of the C–C bond of the unsubstituted carbaborane cage during oxidation processes.

Oxidation of a red solution of 0.5 mmol $[N(PPh_3)_2]_2$ **1** in 30 ml of MeCN with excess diphenyl disulfide (0.7 mmol) under refluxing for 24 h causes gradual precipitation of yellow product $[N(PPh_3)_2]_2$ **2**† (Scheme 1, path i) in 41% yield upon recrystallization from dmf–$Et_2O$. The dianionic **2** can be further oxidized to mixed-valence monoanionic **3** using PhIO [Scheme 1, path ii): treatment of a dmf solution (30 ml) of 0.1 mmol $[N(PPh_3]_2]_2$ **2** with six fold excess of PhIO at 100 °C for 24 h, filtration and addition of $Et_2O$ to the concentrated filtrate gave rise to a black precipitate. Recrystallization from dmf–$Et_2O$ yielded analytically† pure black crystalline $[N(PPh_3)_2]$ **3** in a yield of 74%. The use of $Br_2$ instead of PhIO also affords the monoanionic **3** in 66% yield.

The structures‡ of **2** (Fig. 1) and **3** (Fig. 2) are seen to be based on discrete dimers oriented about a crystallographic inversion center. In both compounds, four bridging thiolate groups are arranged such that two planar MoSMoS rhombi are perpendicular to each other, the MoS(1)Mo′S(1′) plane bisects the cage C···C vector and the overall symmetry lacks a mirror plane. The observation of two well resolved singlets at $\delta$ 3.63 and 3.92 for carbaboranyl protons in the $^1$H NMR spectrum of diamagnetic **2** in $(CD_3)_2SO$ at 23 °C is consistent with the expected magnetic inequivalency of two carboranyl CH protons. For **3**, similar observation was hampered by its paramagnetism ($\mu$ = 1.70 $\mu_B$). It is interesting to note that at elevated temperature **2** becomes fluxional and two carboranyl CH proton signals coalesce at 93 °C, suggesting that the free energy of activation associated with the fluxional motion of **2** is 74.2 kJ mol$^{-1}$ which is comparable to those of other thiolate bridged dimers $[Fe_2(CO)_6(\mu\text{-}SBu^t)_2]_2$[2] (77 kJ mol$^{-1}$) and $[W_2O_2Cl_4(\mu\text{-}Cl)(\mu\text{-}SBu^i)_2]^-$[3] (75 kJ mol$^{-1}$) where inversion[4] at the three-coordinate bridging sulfur atoms is operative.

The $C_2B_9Mo$ cage geometry in **2** is derived by the scission[5] of the C(1)–C(2) cage bond [C(1)···C(2), 2.55(6) Å] with concomitant movement of B(6) toward the molybdenum atom. The absence of the coupling peaks of carboranyl CH protons in the $^1$H–$^1$H COSY NMR spectra of **2** is in good agreement with the X-ray structure. On the other hand, the $C_2B_9Mo$ cage geometry in **3** is dictated by the formation of the C(1)–C(2) cage bond [1.65(2) Å]. The scission and the formation of the unsubstituted carbaborane C–C bond upon successive oxidation




**Scheme 1** Synthesis of $[N(PPh_3)_2]_2[(C_2B_9H_{11})Mo(SPh)_2]_2$ and $[N(PPh_3)_2][(C_2B_9H_{11})Mo(SPh)_2]_2$. *Reagents*: i, PhSSPh ; ii, 6PhIO.

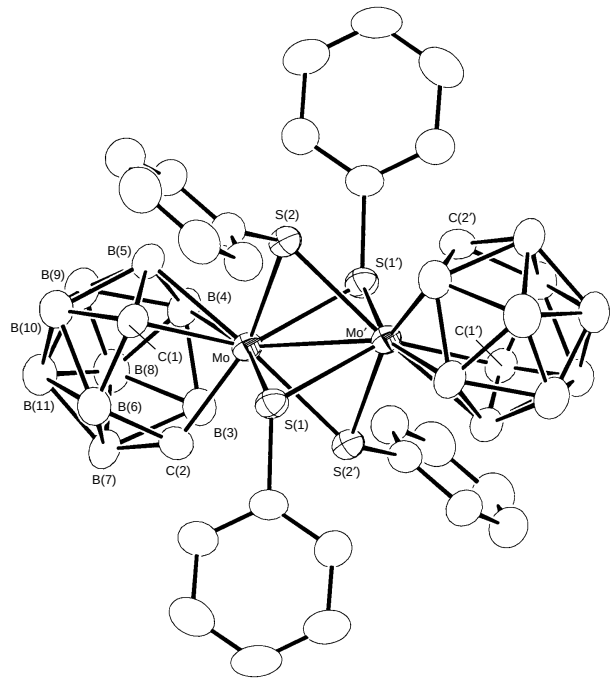



**Fig. 1** ORTEP drawing of the $[(C_2B_9H_{11})Mo(SPh)_2]_2^{2-}$ dianion **2**. Selected bond distances (Å) and angles (°): Mo–Mo′ 2.8124(7), C(1)···C(2) 2.55(6), Mo–C(1)2.174(4), Mo–C(2) 2.182(4), Mo–B(3) 2.377(5), Mo–B(4) 2.428(5), Mo–B(5) 2.371(5), Mo–B(6) 2.898, Mo–S(1) 2.5340(11), Mo–S(1′) 2.5098(11); C(1)–Mo-C(2) 72.8(2), S(1)–Mo–S(1′) 112.22(3), S(1)–Mo–Mo′ 55.70(3).

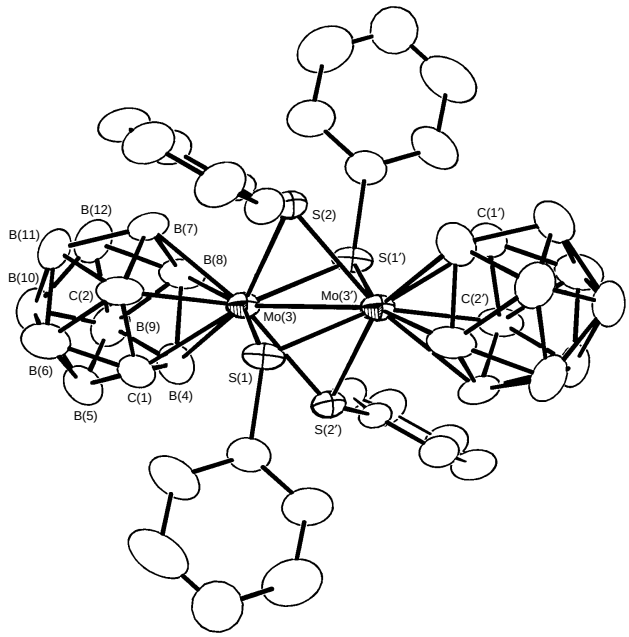



**Fig. 2** ORTEP drawing of the $[(C_2B_9H_{11})Mo(SPh)_2]_2^-$ monoanion. Selected bond distances (Å) and angles (°): Mo(3)–Mo(3′) 2.725(2), C(1)–C(2) 1.65(2), Mo(3)–C(1) 2.311(10), Mo(3)–C(2) 2.336(10), Mo(3)–B(4) 2.391(11), Mo(3)–B(6) 3.680, Mo(3)–B(7) 2.394(12), Mo(3)–B(8) 2.452(14), Mo(3)–S(1) 2.453(3), Mo(3)–S(1′) 2.485(3); C(1)–Mo(3)–C(2) 41.7(4), S(1)–Mo(3)–S(1′) 113.01(8), S(1)–Mo(3)–Mo(3′) 57.06(7).

processes, which constitutes the first example of its kind, are quite fascinating since it has often been surmised[5] that the presence of bulky and electron rich exo-cluster substituents at the cage carbon atoms induces the breaking of the C–C cage bond. It is interesting that the two-electron reduction of $[PtW(CO)_2(PEt_3)_2\{\eta^6\text{-}C_2B_9H_8(CH_2C_6H_4Me\text{-}4)Me_2\}]$,[6] where the carbaborane C atoms are both substituted, causes the $WC_2B_9$ framework change from open to closed geometry with an exopolyhedral B(3)–Pt σ–bond formation ($[PtW(\mu\text{-}H)\{\mu\text{-}\sigma,\eta^5\text{-}C_2B_9H_7(CH_2C_6H_4Me\text{-}4)Me_2\}(CO)_2(PMe_3)(PEt_3)_2]$). In our case, **2** was oxidized by a one-electron process and no rearrangement of the complex backbone has occurred. Additionally, the **2** and **3** are intriguing since no mixed metallacarbaboranes with bridged thiolate ligands have yet been reported in spite of the observation that the thiolate group bridging ligands have been previously shown to provide stable di- and poly-nuclear molybdenum compounds.[7–12]

The *closo* $MoC_2B_9$ icosahedal framework in the oxidized derivative **3** suggests that the $C_2B_9H_{11}$ cages in **3** behave as *nido* dianionic ligands. Therefore, the observed paramagnetism is consistent with the expected mixed $Mo^{III}Mo^{IV}$ valence for **3**. The closely interrelating features of the deltahedron nature[13] of the $MoC_2B_9$ cages and the oxidation states of the metal centers in **2** remain to be clarified. The straightforward availability of these stable compounds from the dicarbabollide and thiolate ligands may make similar classes of compounds accessible for further investigations, such as connecting the two carbon cage atoms by various bridging aliphatic groups [-$(CH_2)_n$-; $n$ = 3, 4] and in particular, tungsten homologue insertion reactions. We are currently investigating this possibility along with the XPS, electrochemical and electronic spectral studies on anions **2** and **3** to clarify the effects of electronic densities in these types of systems.

Support of this work by the Korea Science and Engineering Foundation is gratefully acknowledged.

## Footnotes and References

* E-mail: ykdo@single.kaist.ac.kr

† Elemental analysis: for **2**, $C_{100}H_{102}N_2B_{18}P_4S_4Mo_2$, C, 60.95; H, 5.22; N, 1.42. Found. C, 60.50; H, 5.28; N, 1.37. For **3**, $C_{64}H_{72}NB_{18}P_2S_4Mo_2$, C, 53.68; H, 5.07; N, 0.98. Found. C, 53.42; H, 5.15; N, 0.85% $^{11}B\{^1H\}$ NMR [$(CD_3)_2SO$, 373 K] for **2** [δ 16.34, 1.49, −3.01, −6.53, −20.76 (1 : 2 : 3 : 2 : 1).

§ *Crystal data*: for $[N(PPh_3)_2]_2$ **2**, $C_{100}H_{102}B_{18}Mo_2N_2P_4S_4$: $M_r$ = 1970.42, monoclinic, space group $P2_1/c$, $a$ = 12.7438(13), $b$ = 14.4567(14), $c$ = 26.508(5) Å, $\beta$ = 90.415(12)°, $U$ = 4883.5(11) Å$^3$, $Z$ = 2, $D_c$ = 1.340 g cm$^{-3}$, $F(000)$ = 2028, $\mu$(Mo-Kα) = 0.456 mm$^{-1}$, $R_1$ = 0.0501, $wR_2$ = 0.1439 for 6470 reflections [$|F_o| > 4.0\sigma(F_o)$].

For $[N(PPh_3)_2]$ **3**, $C_{64}H_{72}B_{18}Mo_2NP_2S_4$: $M_r$ = 1431.87, triclinic, space group $P\bar{1}$ {note both independent dimers are contained in the unit cell of the crystals of $[N(PPh_3)_2]$ **3** examined in this work}, $a$ = 13.060(2), $b$ = 13.061(2), $c$ = 21.782(4) Å, $\alpha$ = 74.645(15), $\beta$ = 74.575(15), $\gamma$ = 82.118(15)°, $U$ = 3444.9(11) Å$^3$, $Z$ = 2, $D_c$ = 1.380 g cm$^{-3}$, $F(000)$ = 1462, $\mu$(Mo-Kα) = 0.573 mm$^{-1}$, $R_1$ = 0.0704, $wR_2$ = 0.1887 for 5969 reflections [$|F_o| > 4.0\sigma(F_o)$].

Reflection data were collected on an Enraf-Nonius CAD4TSB diffractometer with graphite-monochromated Mo-Kα radition at 293 K. Accurate cell parameters and orientation matrices for **2** and **3** were determined from the least-square fit of 25 accurately centered reflections in the range of $20.48 \leqslant 2\theta \leqslant 28.64$ and $16.63 \leqslant 2\theta \leqslant 26.67$, respectively. All data were collected with the $\omega$–$2\theta$ scan mode and corrected for $L_p$ effects. ψ-Scan absorption correction was applied. The structure compounds was solved by Patterson's heavy-atom methods (SHELXS-86).[14] Non-hydrogen atoms were refined by full-matrix least-square techniques (SHELXL-93)[15] with anisotropic displacement parameters. The phenyl rings were refined as rigid groups with fixed bond lengths ($d_{CC}$ = 1.390 Å) and angles (120.0°). Phenyl hydrogen and carbaboranyl hydrogen atoms, except for two hydrogens bonded to carbon atoms of carbaboranyl groups in $[N(PPh_3)_2]_2$ **2**, were placed at their geometrically calculated positions ($d_{CH}$ = 0.930 Å for phenyl and $d_{BH}$ = 1.100 Å for carbaboranyl) and refined riding on the corresponding carbon atoms with isotropic thermal parameters [$U$ = 1.2 $U(C_{phenyl})$ and 1.2 $U(B_{carbaboranyl})$]. CCDC 182/552.

1 J. H. Kim, E. Hong, J. Kim and Y. Do, *Inorg. Chem.*, 1996, **35**, 5112.
2 G. Natile, L. Maesca and G. Bor, *Inorg. Chim. Acta*, 1977, **23**, 37.
3 V. D. Patel, P. M. Boorman, K. N. Kerr and K. J. Moynihan, *Inorg. Chem.*, 1982, **21**, 1383.
4 (*a*) P. C. Turley and P. Haake, *J. Am. Chem. Soc.*, 1967, **89**, 4617; (*b*) E. W. Abel, G. W. Farrow, K. G. Orrell and V. Sik, *J. Chem. Soc., Dalton Trans.*, 1977, 42.
5 (*a*) Z. G. Lewis and A. J. Welch, *J. Organomet. Chem.*, 1992, **430**, C45; (*b*) P. T. Brain, M. Bühl, J. Cowie, Z. G. Lewis and A. J. Welch, *J. Chem. Soc., Dalton Trans.*, 1996, 231; (*c*) A. J. Welch and A. S. Weller, *Inorg. Chem.*, 1996, **35**, 4548; (*d*) R. L. Thomas, G. M. Rosair and A. J. Welch, *Chem. Commun.*, 1996, 1327.
6 M. J. Attfield, J. A. K. Howard, A. N. de M. Jelfs, C. M. Nunn and F. G. A. Stone, *J. Chem. Soc., Chem., Commun.*, 1986, 918.
7 A. Müller, E. Diemann, R. Jostes and H. Bögge, *Angew. Chem., Int. Ed. Engl.*, 1981, **20**, 934.
8 S. Lincoln, S. L. Soong, S. A. Koch , M. Sato and J. H. Enemark, *Inorg. Chem.*, 1985, **24**, 1355.
9 G. J. Kubas, *Acc. Chem. Res.*, 1994, **27**, 183.
10 F. A. Cotton, R. L. Luck and C. S. Miertchin, *Inorg. Chem.*, 1991, **30**, 1155.
11 W. A. W. A. Bakar, J. L. Davidson, W. E. Lindsell, K. J. MaCullough and K. W. Muir, *J. Organomet. Chem.*, 1987, **322**, C1; W. A. W. A. Bakar, J. L. Davidson, W. E. Lindsell, K. J. MaCullough and K. W. Muir, *J. Chem. Soc., Dalton Trans.*, 1989, 991.
12 N. G. Connelly and L. F. Dahl, *J. Am. Chem. Soc.*, 1970, **92**, 7470.
13 B. Štíbr, J. D. Kennedy, E. Drdáková and M. Thornton-Pett, *J. Chem. Soc., Dalton Trans.*, 1994, 229.
14 G. M. Sheldrick, SHELXS-86 User Guides, Crystallographic Department, University of Göttingen, Germany, 1985.
15 G. M. Sheldrick, SHELXL-93 User Guides, Crystallographic Department, University of Göttingen, Germany, 1993.

*Received in Cambridge, UK, 16th June 1997; 7/04161F*

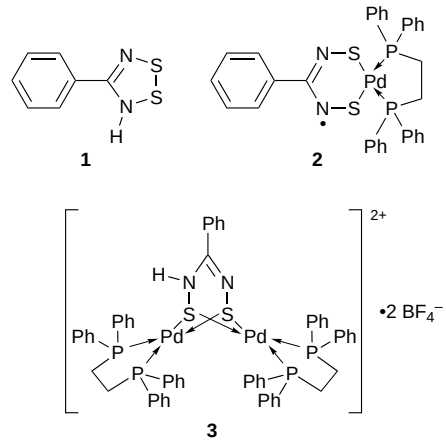
# Preparation and characterisation of a dithiadiazolyline complex: X-ray crystal structure of $[Pd_2\{\mu\text{-SNC(Ph)N(H)S-}S,S'\}(dppe)_2][BF_4]_2\cdot 3CDCl_3$

**Arthur J. Banister,[a] Judith A. K. Howard,[a] Iain May[a] and Jeremy M. Rawson*[b]**

[a] *Department of Chemistry, The University of Durham, South Road, Durham, UK DH1 3LE*
[b] *Department of Chemistry, The University of Cambridge, Lensfield Road, Cambridge, UK CB2 1EW*

**While the protonated dithiadiazolyl compound, PhCNSSNH 1 is unknown, oxidation of $[Pd(dppe)_2]$ with $[PhCNSSN]_2$ yields the monometallic complex [Pd{SNC(Ph)NS-*S*,*S*′}(dppe)] 2 which can be oxidized with $[NO][BF_4]$ in the presence of moisture to yield the dimetallic complex $[Pd_2\{\mu\text{-SNC(Ph)N(H)S-}S,S'\}(dppe)_2][BF_4]_2$ 3 which contains coordinated 1; the X-ray crystal structure of 3 is reported as its solvate $3\cdot 3CDCl_3$.**

Previously we have reported a series of dithiadiazolyl metal complexes[1–6] containing one, two or three metal centres. In the monometallic compounds, the dithiadiazolyl ligand ring-opens at the S–S bond and chelates the metal, *e.g.* $[Pt\{SNC(Ph)NS\text{-}S,S'\}(PPh_3)_2]$, whereas in the di- and tri-metallic complexes the dithiadiazolyl ligand bridges two metal centres, *e.g.* as in $[Ni_2(\eta\text{-}C_5H_5)_2\{\mu\text{-SNC(Ph)NS-}S,S'\}]$ and $[Pt_3\{\mu\text{-SNC(Ph)NS-}S,S'\}_2(PPh_3)_4]$. The versatility of this ligand is exemplified by the number of electrons which it can utilise for metal bonding; two to three electrons in the chelate mode and five or six electrons in the μ,μ-bridging mode. Recent NMR and IR studies (coupled with the absence of an EPR signal)[7,8] on the related complex $[Fe_2(CO)_6\{\mu\text{-SNC(Ph)NS-}S,S'\}]$ indicated that this complex had been protonated on the ring N and should be more correctly formulated as $[Fe_2(CO)_6\{\mu\text{-SNC(Ph)N(H)S-}S,S'\}]$. The free ligand, PhCNSSNH **1**, itself is unknown and we have been intrigued by the possibility of forming other complexes containing this species. We now report the synthesis of the first monometallic palladium dithiadiazolyl compound, [Pd{SNC(Ph)NS-*S*,*S*′}(dppe)] **2** in which the monometallic structure is stabilised through the presence of the chelating diphosphine dppe, and describe its reaction with $[NO][BF_4]$, in the presence of adventitious moisture, to yield the dimetallic palladium dithiadiazolyline complex, $[Pd_2\{\mu\text{-SNC(Ph)N(H)S-}S,S'\}(dppe)_2][BF_4]_2$ **3**.




Oxidative addition[3] of $(PhCNSSN)_2$ to $[M(PPh_3)_4]$ (M = Pt, Pd) yielded the trimetallic complexes, $[M_3\{\mu\text{-SNC(Ph)NS-}S,S'\}_2(PPh_3)_4]$. When M = Pt, this was shown to proceed *via* the monometallic complex $[M\{SNC(Ph)NS\text{-}S,S'\}(PPh_3)_2]$, but the analogous Pd complex could not be detected. We have now found that the chelating phosphine, dppe [1,2-bis(diphenylphosphino)ethane] stabilises the monometallic Pd complex and [Pd{SNC(Ph)NS-*S*,*S*′}(dppe)] **2** can be prepared† in excellent yield by direct reaction of $(PhCNSSN)_2$ with freshly prepared $[Pd(dppe)_2]$. The unpaired electron in **2** occupies an antibonding orbital based on the metalloheterocyclic framework, of the same symmetry[5] as $[Pt\{\mu\text{-SNC(Ph)NS}\}(PPh_3)_2]$ and the solution EPR spectrum of **2** (Fig. 1) exhibits hyperfine coupling to two equivalent N and two equivalent P nuclei, plus satellites for the low-abundance $^{105}Pd$ isotope (22%, $I$ = 5/2).

The antibonding character of the singly occupied molecular orbital,[5] and the electron-rich (16/17e$^-$) nature of the metal centre, indicated that one-electron oxidation of **2** should be facile. Preliminary electrochemical investigations on **2** showed three irreversible oxidations with half-wave potentials at −0.10, +0.30 and +1.12 V (referenced to the SSCE). Chemical oxidation‡ of **2** with 1 equiv. of $[NO][BF_4]$ in acetonitrile produced two products, by $^{31}P$ NMR, of which the major product [two doublets at $\delta$ 56.6 and $\delta$ 52.9 ($J_{PP}$ 28 Hz)] fortuitously crystallised from $CDCl_3$ and was found to be the dithiadiazolyline complex, $[Pd_2\{\mu\text{-SNC(Ph)N(H)S-}S,S'\}(dppe)_2][BF_4]_2$ **3**. Protonation at the heterocyclic nitrogen due to reaction with moisture renders the phosphorus environments inequivalent, resulting in a pair of doublets in the $^{31}P$ NMR

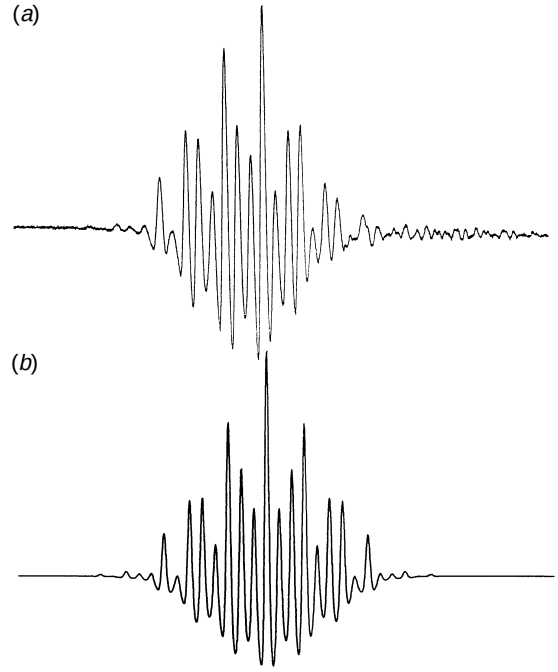



**Fig. 1** Solution EPR spectra of **2** in $CH_2Cl_2$ at room temp; (*a*) experimental, (*b*) simulation; $g$ = 2.031, $a_N$ = 5.7 G, $a_P$ = 3.8 G, $a_{Pd}$ = 37.2 G, $\Delta B_{PP}$ = 1.0 G

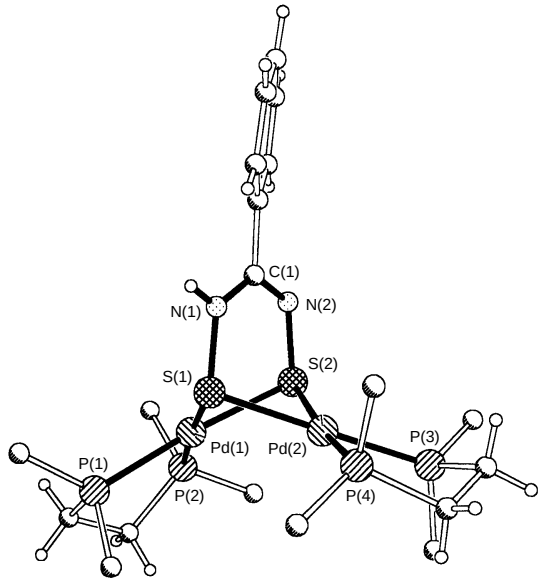



**Fig. 2** Structure of the dication in **3** (phosphine phenyl C atoms not bonded to P are removed for clarity). Further selected bond lengths (Å): Pd(1)–P(1) 2.305(2), Pd(1)–P(2) 2.283(2), Pd(2)–P(3) 2.283(2), Pd(2)–P(4) 2.297(2), Pd(1)–S(1) 2.351(2), Pd(1)–S(2) 2.352(2), Pd(2)–S(1) 2.354(2), Pd(2)–S(2) 2.384(2), N(1)–S(1) 1.690(6), N(2)–S(2) 1.683(6).

spectrum. The mass spectrum (FAB) shows a molecular ion peak at *m/z* 1191.6 consistent with ring-protonation {$[Pd_2\{\mu$-SNC(Ph)N(H)S-*S*,*S*′}$(dppe)_2]^{2+}$ has a formula mass of 1191.8}. Compound **3** gave satisfactory microanalytical data, an N–H absorption in the IR (3205 $cm^{-1}$) and was EPR inactive. The minor product, observed as a singlet at $\delta$ 59.6 in the $^{31}P$ NMR, has not been characterised.

The structure§ of the salt **3** was determined by X-ray crystallography and was found to crystallise as a $CDCl_3$ solvate, **3**·3$CDCl_3$. The structure of the dication in **3** is shown in Fig. 2. It consists of two approximately square-planar Pd atoms bridged by the two sulfur atoms of a protonated dithiadiazolyl ligand, with each Pd chelated by a dppe ligand. The bidentate nature of both $P_2$ and $S_2$ donor sets induces SPdS and PPdP bond angles to be less than the idealised 90° and the strain is accommodated by the Pd atoms which sit approximately 0.1 Å above the $P_2S_2$ mean plane. The Pd···Pd contact [3.0687(8) Å] is longer than the sum of the metallic radii (2.76 Å) and is unsurprising since no Pd–Pd bond is necessary to satisfy the bonding requirements of either metal (see below). Within the heterocyclic ring, the S–S bond is formally broken to accommodate the two metal ions [*cf.* 3.106(2) in **3** and 2.089(5) Å in the free ligand[9] $(PhC\overline{NSSN})_2$]. This ring-opening is accompanied by marked increases in the bond angles at C and N {128.8(7), 129.3(5) and 125.7(5)° at C(1), N(1) and N(2), respectively, *cf.* 121 and 116° for the free ligand $(PhC\overline{NSSN})_2$}. Although the location of the N–H proton could not be unambiguously determined from the X-ray data, an analysis of the heterocyclic bond lengths and angles clearly supports a more localised structure with protonation at N(1); within **3** the bond angle at N(1) is notably larger than that at N(2) and the C(1)–N(1) bond length is marginally (3 esds) longer than C(1)–N(2). In addition, the close approach of one of the $BF_4^-$ counter ions to N(1) [N(1)···F(21) at 2.82 Å] can be rationalised in terms of an N–H···F hydrogen bond.

The combined crystallographic and spectroscopic evidence, clearly support the presence of a protonated dithiadiazolyl ligand. Electronically, the protonated dithiadiazolyl ligand acts as a six-electron donor, each sulfur forming a σ bond to one Pd and a dative bond to the second Pd. Thus each Pd formally has a 16-electron configuration (ten valence electrons, four from the chelating phosphine, three from the dithiadiazolyline ligand, less one to accommodate the doubly positive charge on the ion) which is consistent with the observed square-planar geometry.

These results provide the first example of a monometallic Pd dithiadiazolyl complex (**2**) and also provide conclusive spectroscopic and structural evidence for the existence of dithiadiazolyline complexes. Compound **3** provides the first experimental evidence for a dimetallic intermediate in the formation of the trimetallic Pt and Pd complexes from the corresponding monometallic dithiadiazolyl derivatives. The exact source of protonation of the dithiadiazolyl ligand in **3** is presently unclear, although it is evident that the presence of adventitious moisture, as in the synthesis of $[Fe_2(CO)_6\{\mu$-SNC(Ph)NS-*S*,*S*$\}]$ could also play a role here. The $^{31}P$ NMR spectrum clearly indicates the protonation occurs readily at an early stage in the reaction and not during the slow recrystallisation process.

We would like to thank the EPSRC for a studentship (I. M.) and Dr R. C. B. Copley for able assistance with crystallographic data collection and Mr J. N. B. Smith for further characterisation of compound **3**.

## Footnotes and References

* E-mail: jmr31@cam.ac.uk

† Reaction of freshly prepared $[Pd(dppe)_2]$ [0.500 g, 0.55 mmol] with a slight excess of $(PhC\overline{NSSN})_2$ [0.11 g, 0.30 mmol] in toluene (20 ml) yielded an immediate deep green precipitate of [Pd{SNC(Ph)NS-*S*,*S*′}(dppe)] **2** under a light green solution. The product was filtered, washed with PhMe (3 × 10 ml) and dried *in vacuo*. Yield 0.37 g, 97%. Found: C, 58.0; H, 3.7; N, 4.4. Calc. for **2** C, 57.8; H, 4.08; N, 4.3%. Compound **2** slowly decomposes, even in the solid state, and was freshly prepared for all reactions.

‡ A solution of $[NO][BF_4]$ (0.039 g, 0.33 mmol) in MeCN was added dropwise to a suspension of **2** (0.228 g, 0.33 mmol) in MeCN. An immediate evolution of gas was observed and the solution turned red. After stirring for 3 h the resultant yellow solution was filtered and evaporated to yield crude **3** (0.17 g, 75%). Crystals suitable for X-ray diffraction were grown by slow evaporation of a $CDCl_3$ solution over 1 week. Found: C, 50.6; H, 3.8; N, 2.4; Calc. for **3**. C, 51.9; H, 4.0; N, 2.1%.

§ *Crystal data* for **3**·3$CDCl_3$: $C_{62}H_{57}B_2Cl_9F_8N_2P_4Pd_2S_2$, $M$ = 1723.57, monoclinic, space group $P2_1/c$, $a$ = 11.0729(7), $b$ = 23.3848(14), $c$ = 27.300(2) Å, $\beta$ = 94.718(1)°, $U$ = 7045.1(8) Å$^3$, $\mu$ = 1.064 $mm^{-1}$, $Z$ = 4, $D_c$ = 1.63 g $cm^{-3}$, $T$ = 150(2) K. A red crystal (0.48 × 0.34 × 0.18 mm) was examined on a Siemens SMART CCD three-circle diffractometer with graphite-monochromated Mo-Kα radiation ($\lambda$ = 0.710 73 Å). 29647 reflections were measured ($2.30 < 2\theta < 50.78°$) of which 11 549 were unique ($R_{int}$ = 0.449). The structure was solved by direct methods and refinement was carried out on $F^2$ values using SHELXTL software.[10] At convergence $R_1$ [$F > 2\sigma(F)$] = 0.070 and $wR_2$ (all data) = 0.148 with a goodness of fit of 1.25. Max. and min. residual electron densities were within ±1.8 e $A^{-3}$. All elements heavier than C were refined anisotropically except for the three disordered F atoms in one of the $BF_4^-$ anions. H atoms were added at calculated positions with a fixed thermal parameter. CCDC 182/562.

1 A. J. Banister, I. B. Gorrell, W. Clegg and K. A. Jørgensen, *J. Chem. Soc., Dalton Trans.*, 1989, 229.
2 A. J. Banister, I. B. Gorrell, W. Clegg and K. A. Jørgensen, *J. Chem. Soc., Dalton Trans.*, 1991, 1105.
3 A. J. Banister, I. B. Gorrell, S. E. Lawrence, C. W. Lehmann, I. May, G. Tate, A. J. Blake and J. M. Rawson, *J. Chem. Soc., Chem. Commun.*, 1994, 1779.
4 A. J. Banister and I. May, *Phosphorus, Sulfur, Silicon*, 1994, **93**–**94**, 447.
5 A. J. Banister, I. B. Gorrell, J. A. K. Howard, S. E. Lawrence, C. W. Lehmann, I. May, J. M. Rawson, B. K. Tanner, C. I. Gregory, A. J. Blake and S. P. Fricker, *J. Chem. Soc., Dalton Trans.*, 1997, 377.
6 A. J. Banister, I. May, J. M. Rawson and J. N. B. Smith, *J. Organomet. Chem.*, 1997, in the press.
7 V. Klassen, K. Preuss, K. H. Moock and R. T. Boeré, *Phosphorus, Sulfur, Silicon*, 1994, **93**–**94**, 449.
8 R. T. Boeré, K. H. Moock, V. Klassen, J. Weaver, D. Lentz and H. Michael-Schulz, K, *Can. J. Chem.*, 1995, **73**, 1444.
9 A. Vegas, A. Perez-Salazar, A. J. Banister and R. G. Hey, *J. Chem. Soc., Dalton Trans.*, 1979, 1812.
10 G. M. Sheldrick, SHELXTL, version 5.0, Siemens Analytical X-Ray Instruments Inc., Madison, WI, 1995.

*Received in Cambridge, UK, 16th June 1997; 7/03750C*

# Three procedures of reversible dissolution/deposition of gold using halogen-containing organic systems

**Yukimichi Nakao**

*National Institute of Materials and Chemical Research, 1-1 Higashi, Tsukuba, Ibaraki 305, Japan*

**Gold is reversibly and repeatedly dissolved and deposited under restricted conditions in a solution consisting of an elemental halogen, a halide and acetonitrile by a procedure involving one of three physical operations: addition of methanol, cooling, or evaporation to dryness.**

Most organic and inorganic substances are 'physically' dissolved in aqueous or organic media, and hence are often recovered from solution by means of physical operations such as (*i*) addition of non-solvent, (*ii*) cooling, or (*iii*) evaporation (to concentrated solutions or dryness), which results in deposition.[1,2] On the other hand, metals are 'chemically' dissolved as metal ions. Therefore, it has been believed that an appropriate reductive treatment is necessarily required to recover them in the metallic state.

We reported new organic solvent systems consisting of an elemental halogen ($X_2$), a halide ($X^-$), and an organic solvent (organic–X systems, X = Cl, Br, I), which dissolve a number of metals including noble metals.[3] It is found that metallic gold is deposited in solutions of some organic–X systems, which are previously saturated with gold, not by chemical treatment but by each of the physical operations (*i*)–(*iii*), and that gold is dissolved in solutions obtained from the resulting supernatants or residues. UV–VIS spectroscopy confirmed that such reversible dissolution/deposition of gold is, in most cases, a chemical process based on the following disproportionation equilibrium.[4]

$$3Au^+ \rightleftharpoons 2Au + Au^{3+} \quad (1)$$

Shifts to right and left in this equilibrium correspond to the deposition and dissolution of gold, respectively.

Three typical procedures of repeated dissolution/deposition of gold involving each of the operations were carried out in selected organic–X systems containing acetonitrile (AN). Dissolution of gold was performed using an excess amount of gold wire of 0.2 mm diameter under refluxing, and deposition of

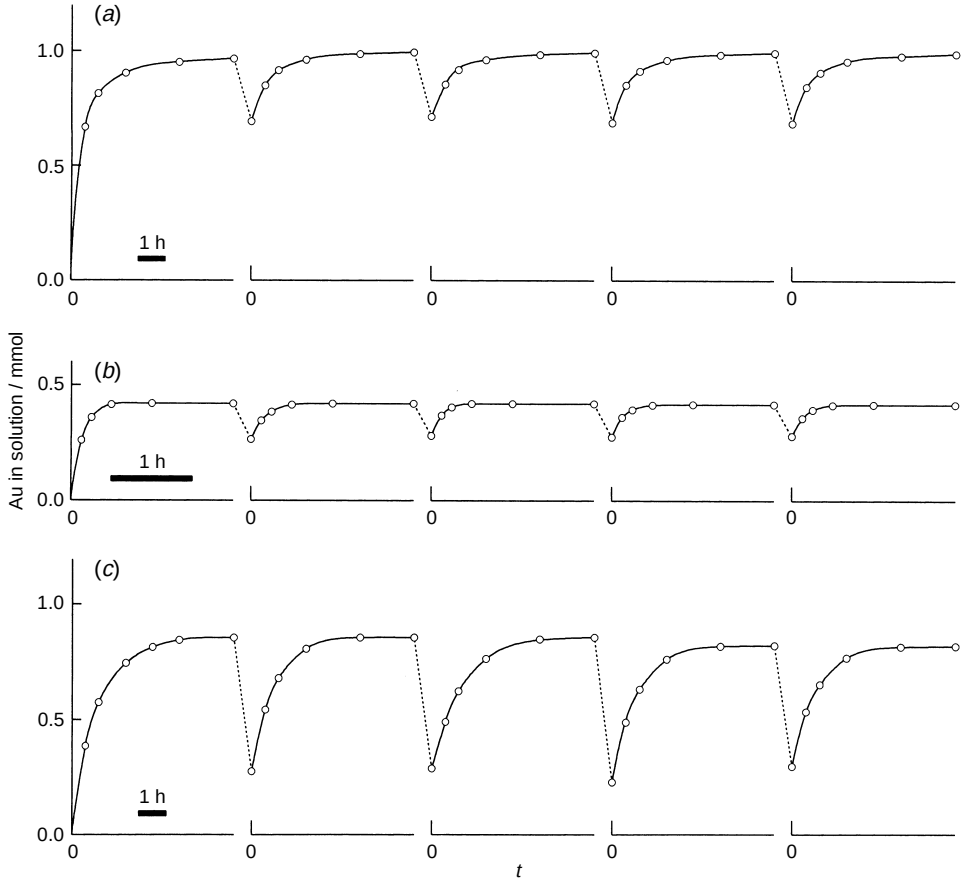



**Fig. 1** Time-course of gold content in the solutions during repeated dissolution/deposition of gold using (*a*) $Br_2$ (0.5 mmol)–[$NEt_4$]Br (1 mmol)–AN (2 g), (*b*) $I_2$ (1 mmol)–[$NEt_4$]I (1 mmol)–AN (10 g) and (*c*) $I_2$ (0.5 mmol)–NaI (1 mmol)–AN (2 g): dissolution of gold was carried out under refluxing at 82 °C. Each of the gold-saturated solutions was treated by (*a*) adding methanol (8 g), heating at 60 °C for 2 h, the supernatant was evaporated to dryness, and the residue was redissolved in An (2 g), (*b*) cooling to 20 °C and allowing to stand overnight or (*c*) evaporating to dryness, and the residue was redissolved in AN (2 g). The broken lines correspond to reduction in gold content in the solutions upon deposition of gold.

gold was carried out by adding methanol to the solution, cooling it, or evaporation to dryness. Amounts of gold in the solutions were determined by weighing the residual gold wire and the deposited gold. The contents of Au species in the solutions were evaluated by UV–VIS spectra which were measured using thin liquid films (8 or 200 μm thickness) on the basis of the characteristic bands of each species: $[AuBr_2]^-$ (192, 200, 212 nm), $[AuBr_4]^-$ (256, 395 nm), $[AuI_2]^-$ (217 nm) and $[AuI_4]^-$ (510, 670 nm).

First, deposition of gold was caused by adding methanol to gold-saturated solutions from organic–X systems in which the ratio $X_2/X^-$ was near to 0.5. The supernatant was then evaporated to dryness to give a residue, which was redissolved in AN, and the resulting solution, after separation from the deposited gold, was used for the next dissolution of gold. Fig. 1(*a*) shows a procedure of repeated dissolution/deposition of gold involving addition of methanol using an organic–Br system consisting of $Br_2$ (0.5 mmol), $[NEt_4]Br$ (1 mmol), and AN (2 g). The following equilibrium is proposed on the basis of UV–VIS spectra of the solutions before and after dissolution of gold.

$$3[NEt_4][AuBr_2] \rightleftharpoons 2Au + [NEt_4][AuBr_4] + 2[NEt_4]Br \quad (2)$$

A similar dissolution/deposition of gold occurred in gold saturated solutions of either organic–Cl systems or organic–I systems. In the latter, another equilibrium as given below seems to be involved, since the $Au^{3+}$ species was not detected.

$$2[NEt_4][AuI_2] \rightleftharpoons 2Au + [NEt_4]I_3 + [NEt_4]I \quad (3)$$

Although the methanol is apparently likely to act as non-solvent, it would actually shift the disproportionation equilibrium to the right as well as water.[4]

Second, as recently reported,[5] gold is deposited by cooling gold-saturated solutions of organic–I systems in which the $I_2/I^-$ ratio was $> 0.5$. Such deposition of gold was not observed in the solutions of either organic–Cl or organic–Br systems. The supernatants could be used for further dissolution of gold at elevated temperatures. Fig. 1(*b*) illustrates a procedure of repeated dissolution/deposition of gold using a system consisting of $I_2$ (1 mmol), $[NEt_4]I$ (1 mmol), and AN (10 g), which involves alternating heating and cooling. The following equilibrium has already been proposed for this process.[5]

$$3[NEt_4][AuI_2] + 2I_2 \rightleftharpoons 2Au + [NEt_4][AuI_4] + 2[NEt_4]I_3 \quad (4)$$

Third, gold was deposited in solutions from certain organic–I systems by concentrating the solution. It was reported that, when the ratio $I_2/I^-$ is 0.5 and the cation of the iodide is $[NEt_4]^+$, evaporation of the gold-saturated solution gives an $Au^+$ complex, $[NEt_4][AuI_2]$.[5] On the contrary, when the cation was an alkali-metal ion or an alkaline-earth metal ion, gold was deposited as the solution was concentrated by evaporation. After AN was completely removed, the resulting tarry residue was redissolved in AN, and the solution to be used again for dissolution of gold was separated from the deposited gold as quickly as possible. Fig. 1(*c*) shows a procedure using a system consisting of $I_2$ (0.5 mmol). NaI (1 mmol), and AN (2 g), involving deposition of gold by evaporation. In this case, the $Au^{3+}$ species, $[AuI_4]^-$, was confirmed to be formed with deposition of gold. Thus, the equilibrium for this process would be as follows.

$$3Na[AuI_2] \rightleftharpoons 2Au + Na[AuI_4] + 2NaI \quad (5)$$

Dissolution/deposition of gold in the procedures stated above were all reversible and the efficiency of dissolution of gold was maintained constant throughout although a definite amount of gold still remained dissolved in the solution after deposition of gold. These procedures can be expected to be applied to a completely closed gold-recovering process which is very useful for the extraction of gold from ores and wastes of electronics industries. The gold thus recovered should also be of higher purity.

## References


1 *Polymer Fractionation*, ed. M. J. R. Cantow, Academic Press, New York, 1967, pp. 43–66.
2 *An Introduction to Separation Science*, ed. B. L. Karger, L. R. Snyder and C. Horvath, Wiley, New York, 1973, pp. 303–336.
3 Y. Nakao, *J. Chem. Soc., Chem. Commun.*, 1992, 426.
4 R. J. Puddephatt, *The Chemistry of Gold*, Elsevier, Amsterdam, 1978, pp. 22; 65.
5 Y. Nakao and K. Sone, *Chem. Commun.*, 1996, 897.



*Received in Cambridge, UK, 16th June 1997; 7/04171C*

# First molecular and electronic structure determination of the dicationic salt of 1,11-(methanoselenomethano)-5*H*,7*H*-dibenzo[*b*,*g*][1.5]diselenocin by X-ray crystallographic analysis and *ab initio* calculation

**Tsukasa Nakahodo, Ohgi Takahashi, Ernst Horn and Naomichi Furukawa***

*Tsukuba Advanced Research Alliance Center, Department of Chemistry, University of Tsukuba, Tsukuba, Ibaraki 305, Japan*

**The X-ray crystallographic analysis of the dication salt of 1,11-(methanoselenomethano)-5*H*,7*H*-dibenzo[*b*,*g*][1,5]-diselenocin shows that the dication has a selenium atom in a trigonal-bipyramidal bonding environment; an *ab initio* calculation carried out for the dication revealed that the positive charge is exclusively carried by the three selenium atoms.**

Recently, we have reported the synthesis of a selenium-bridged diselenametacyclophane, 1,11-(methanoselenomethano)-5*H*,7*H*-dibenzo[*b*,*g*][1,5]diselenocin **1** and the isolation of its dicationic salt. We also reported the interconvertible redox structural changes resulting from the multicenter chalcogenide interaction between **1** and its dicationic salt as observed by NMR spectra.[1] However, until recently we could not obtain any structural data of the dicationic salt, because of the difficulty of obtaining suitable single crystals. After several recrystallization attempts using different counter anions, we obtained suitable crystals for a detailed X-ray structural analysis, and thus the structure of the dication was determined. Furthermore, the electronic structure of the dication was elucidated by an *ab initio* molecular orbital calculation.

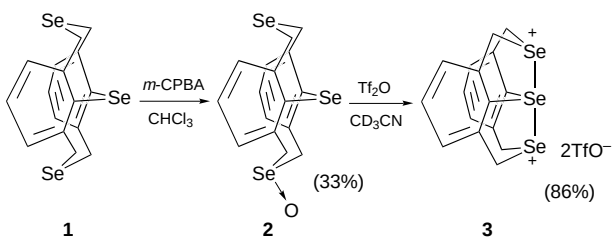
It is of particular interest that a conformational change of the selenoxide **2** occurred in the reaction of **2** with trifluoromethanesulfonic anhydride and triflic anhydride [$(CF_3SO_2)_2O$, $Tf_2O$]; *i.e.*, treatment of **2** with $Tf_2O$ (1 equiv.) in anhydrous $CHCl_3$ under an Ar atmosphere at room temp. resulted in the formation of the dicationic salt **3** (86%) (Scheme 1).†

The crystal structure of dicationic salt **3** was determined by single-crystal X-ray crystallographic analysis (Fig. 1).‡

The X-ray analysis clearly reveals that in the solid state the conformation of **3** is a distorted boat–boat form fixed by the three-center transannular bond between the three selenium atoms.

Although, normally in case of **1** and **2** the chair conformer has been shown to be more stable and rigid than the boat conformer.[1,2] The respective Se···Se distances, 2.645(2) and 2.556(2) Å for Se(1)···Se(2) and Se(2)···Se(3), are longer than the normal Se–Se single bond (2.34 Å) found in diselenides.[3] The Se(1)–Se(2)–Se(3) bond angle of 170.21 (6)° is almost linear, and the $C_{eq}$–Se(2)–$C_{eq}$ bond angle is 95.6(4)°. Thus, the bonding configuration about the seleniun atom is a distorted trigonal-bipyramidal structure with two apical Se–Se bonds, two equatorial Se–C bonds, and the lone-pair electrons occupying the third equatorial position. These structural features are consistent with a selenurane structure.[4]

In order to understand the electronic structure of the dication, we carried out an *ab initio* RHF calculation using the 3-21G(*) basis set.[5] The geometry was optimized with a $C_2$ symmetry constraint, and the optimized $C_2$ structure which is shown in Fig. 2 was confirmed to be a true minimum by a vibrational analysis. The calculated structure is in reasonably agreement with the X-ray determined structure.




**Scheme 1**

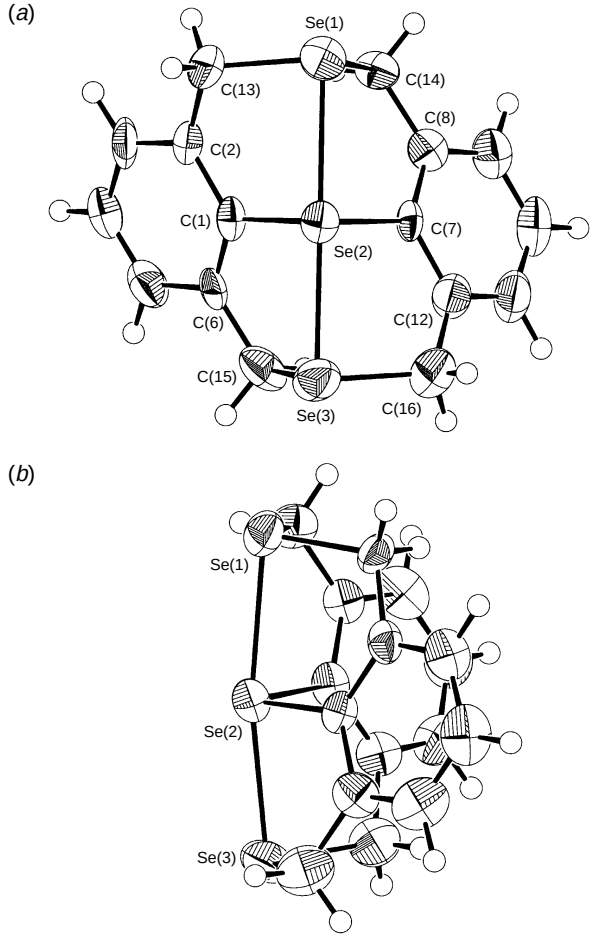



**Fig. 1** Crystal structure of dication **3**. (*a*) View from above. (*b*) Side-on view. For clarity, triflate anions are omitted. Selected bond lengths (Å) and angles (°) (X-ray): Se(1)–Se(2) 2.645(2), Se(2)–Se(3) 2.556(2), Se(1)–C(13) 1.96(1), Se(2)–C(1) 1.93(1), Se(2)–C(7) 1.962(10), Se(3)–C(15) 1.93(1), C(1)–C(2) 1.42(1), C(1)–C(6) 1.39(1), C(2)–C(13) 1.49(2), C(6)–C(15) 1.51(2); Se(1)–Se(2)–Se(3) 170.21(6), C(1)–Se(2)–C(7) 95.6(4), Se(1)–Se(2)–C(1) 86.5(3), Se(3)–Se(2)–C(1) 86.8(3), Se(2)–C(1)–C(2) 119.5(8), Se(2)–C(1)–C(6) 119.9(8), C(2)–C(1)–C(6) 120(1), C(1)–C(2)–C(13) 121.5(10), C(1)–C(6)–C(15) 122(1), Ce(1)–C(13)–C(2) 113.0(8), Se(3)–C(15)–C(6) 112.0(9).

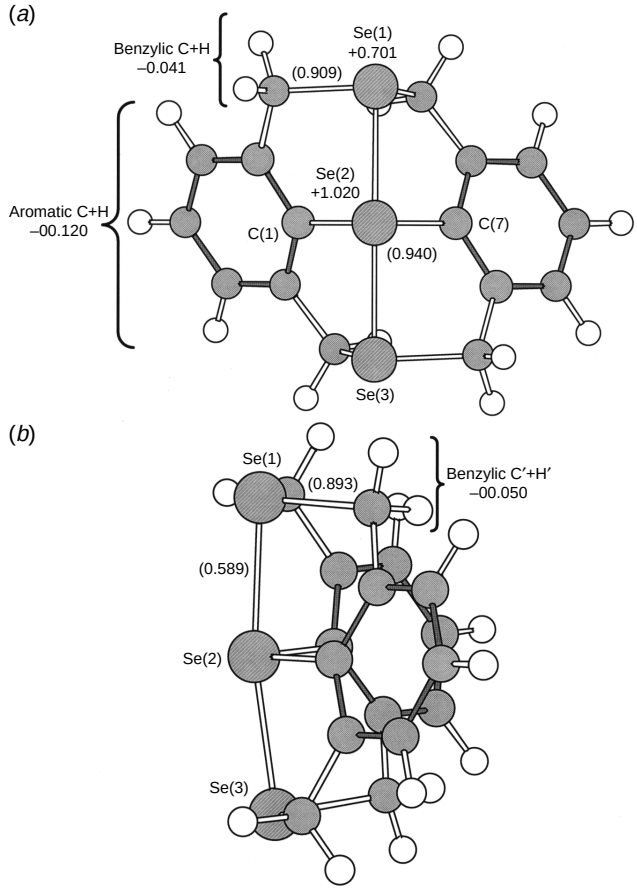



**Fig. 2** The RHF/3-21G(*) optimized structure ($C_2$) of the dication. (*a*) View from above. (*b*) Side-on view. Charge distribution and bond orders (in parentheses) are also shown. Selected bond lengths (Å) and angles (°): Se(1)–Se(2) 2.537, Se(2)–C(1) 1.931; Se(1)–Se(2)–Se(3) 170.2, C(1)–Se(2)–C(7) 98.0, Se(1)–Se(2)–C(1) 86.8, Se(3)–Se(2)–C(1) 86.8.

The charge distribution obtained by natural population analysis (NPA)[6] is shown in Fig. 2. The charge on the central Se atom is +1.020 and those of the apical Se atoms are +0.701, which indicates that the +2 charge is exclusively carried by the three Se atoms. It is surprising that the positive charge is not delocalized onto the benzene rings at all; the rings are slightly negatively charged. The Mulliken bond order of the Se–Se bonds was calculated to be 0.589, while that of the equatorial Se–C bonds was 0.940. The central Se atom carries a more positive charge than the two apical Se atoms, indicating that the two apical Se–Se bonds are highly polarized as in the neutral hypervalent molecules having a three-center-four-electron (3c–4e) bond. The 4d orbital population of the central Se atom is 0.039, which is small and comparable with those of the apical Se atoms (0.026). Thus, the 4d orbitals of the central Se atom are not significantly involved in the 3c–4e bond which is in accordance with the current view of hypervalent molecules.[7] In the 3c–4e model by Rundle[8] and Musher[9] the HOMO (−16.1 eV) and LUMO (−6.4 eV) correspond to the non-bonding and antibonding orbitals respectively, though the HOMO is largely delocalized onto the benzene rings as a result of an interaction between the Se–Se–Se non-bonding orbital and the HOMOs of the benzene rings.

Although the counter ions were not included in the *ab initio* calculation, the calculated structure is in good agreement with the X-ray structure. We think that the electrostatic factor is dominant in the dication–counter ions interaction. It should be noted that the positive charge is exclusively carried by the three Se atoms in the absence of the counter ions; a further accumulation of the positive charge induced by the counter ions is not expected.

We also calculated the two-center dication (boat–chair form). The optimized structure ($C_s$ symmetry) is 27.6 kcal mol$^{-1}$ (1 cal = 4.184 J) higher in energy than the three-center dication; the $Se^+$–$Se^+$ bond length were calculated to be 2.329 Å. The large energy gap between the two-center (boat–chair) and three-center (boat–boat) dications confirms that the dication always assumes a boat–boat form regardless of the environment in which it exists.

In summary, the hypervalent bonding structure of the dication salt of 1,11-(methanoselenomethano)-5*H*,7*H*-dibenzo[*b*,*g*][1,5]diselenocin **1** has been revealed by X-ray crystallographic analysis and *ab initio* calculation. Moreover, it has been shown that the positive charge is exclusively carried by the three Se atoms.

Further studies on related compounds are currently in progress.

This work was supported in part by the Ministry of Education, Science, Sports and Culture of Japan (Grant No. 07404035), and the Fund of Tsukuba Advanced Research Alliance (TARA) project (University of Tsukuba).

## Footnotes and References

* E-mail: fuwukawa@staff.chem.tsukuba.ac.jp

† *Physical and spectroscopic data* for **3**: mp 226–228 °C (decomp.); $^1$H NMR ($CD_3CN$) $\delta$ 4.60, 5.10 (ABq, $J$ 15.7 Hz, 8 H), 7.51 (d, $J$ 7.70 Hz, ArH, 2 H) and 7.75 (t, $J$ 7.70 Hz, ArH, 2 H); $^{13}$C NMR ($CD_3CN$) $\delta$ 39.7, 131.8, 132.5, 134.9 and 141.5; $^{77}$Se NMR $\delta$ 517.9 ($SeCH_2Ar$, 2 Se) and 837.8 (SeAr, 1 Se) (relative to $Me_2Se$); Anal. Calc. for $C_{18}H_{14}F_6O_6S_2Se_3$: C, 29.16; H, 1.90. Found: C, 29.11; H, 1.82%.

‡ *Crystal data* for the selenurane dication salt **3**: crystals of $C_{18}H_{14}F_6O_6S_2Se_3$ are monoclinic, space group $P2_1/c$ (no. 14), $a$ = 11.639(3), $b$ = 10.170(3), $c$ = 20.576(4) Å, $\beta$ = 105.87(2)°, $U$ = 2342.9(10) Å$^3$, $Z$ = 4, $D_c$ = 2.101 g cm$^{-3}$, Mo-K$\alpha$ radiation ($\lambda$ = 0.710 69 Å) from a Rigaku AFC7R diffractometer, 2166 reflections with $I > 2.00\sigma(I)$. The data were corrected for Lorentz and polarization effects, a linear decay (10.90%) and crystal absorption (DIFABS,[10] transmission factors ranging from 0.3275 to 1.0000). The structure was solved by direct methods and refined by a full-matrix least-squares method using the teXsan[11] crystallographic software package. The final residuals are $R$ = 0.049 and $R_w$ = 0.053. CCDC 182/542.

1 H. Fujihara, H. Mima, T. Erata and N. Furukawa, *J. Am. Chem. Soc.*, 1992, **114**, 3117.
2 H. Fujihara, N. Oi, R. Akaishi, T. Kawai and N. Furukawa, *Heterocycles*, 1989, **29**, 441.
3 *The Chemistry of Organic Selenium and Tellurium Compounds*, ed. S. Patai and Z. Rappoport, Wiley, New York, vol. 1 and 2, 1986 and 1988.
4 H. Fujihara, T. Nakahodo and N. Furukawa, *Chem. Commun.*, 1996, 311.
5 The calculation was carried out on a HP 735/125 workstation using Spartan 3. 1 (Wavefunction Inc.).
6 A. E. Reed, R. B. Weinstock and F. Weinhold, *J. Chem. Phys.*, 1985, **83**, 735.
7 A. E. Reed and P. v. R. Schleyer, *J. Am. Chem. Soc.*, 1990, **112**, 1434.
8 R. E. Rundle, *J. Am. Chem. Soc.*, 1963, **85**, 112.
9 J. I. Musher, *Angew. Chem., Int. Ed. Engl.*, 1969, **8**, 54.
10 DIFABS An empirical absorption correction program: N. Waker and D. Stuart, *Acta Crystallogr., Sect. A*, 1983, **39**, 158.
11 teXsan: Crystal Structure Analysis Package, Molecular structure Corp. The Woodlands, TX, 1985, 1992.

*Received in Cambridge, UK, 24th June 1997; 7/04431C*

# Synthesis and characterization of ordered organo–silica–surfactant mesophases with functionalized MCM-41-type architecture

**Christabel E. Fowler, Sandra L. Burkett and Stephen Mann***

*School of Chemistry, University of Bath, Bath, UK BA2 7AY*

**Ordered organo–silica–surfactant mesophases containing covalently linked functionalized moieties are prepared with MCM-41-type architectures by template-directed co-condensation of tetraethoxysilane and organotrialkoxysilanes $(RO)_3Si–R'$ [R = Me, Et; R′ = $(CH_2)_3SH$, $(CH_2)_3NH_2$, $(CH_2)_3OCH_2CH(O)CH_2$, $(CH_2)_3NCHNCH_2CH_2$ or $CH_2CHCH_2$].**

The synthesis of ordered mesoporous silica materials, MCM-41 (hexagonal symmetry) and MCM-48 (cubic symmetry), and related transition-metal oxide analogues, is a burgeoning field of materials chemistry (for recent reviews see refs. 1–4). Tailoring of these materials for specific applications requires both structural and compositional control. This can be achieved by chemical modification of the reaction constituents or *via* post-synthesis activation of the mesostructured product. In a recent paper,[5] we described a new route to the synthesis of MCM-41-type hybrid mesophases containing covalently linked phenyl or *n*-octyl groups. The basis of this approach was to couple the use of supramolecular surfactant templates with co-condensation reactions involving siloxane (tetraethoxysilane, TEOS) and organosiloxane precursors. TEOS was used as the primary silica source and as a reagent for the formation of fully saturated $Q^4$ linkages which are required to maintain structural integrity in the organo–silica–surfactant mesophase. Here we extend this approach to the direct synthesis of more complex organo–MCM-41-type materials containing covalently linked chemically reactive groups. We show that organosiloxanes containing thiol, amine, epoxide, imidazole or allyl functionalities can be incorporated into ordered hybrid mesophases by cooperative assembly of silicate and organosilicate species at the cationic headgroups of rod-like surfactant micelles.

Organo–silica–surfactant mesophases with MCM-41-type architectures were synthesized at room temp. from alkaline mixtures containing varying molar ratios of TEOS and a functionalized organotrialkoxysilane in the presence of the surfactant, hexadecyltrimethylammonium bromide ($C_{16}$TMABr) (molar composition = 0.12 $C_{16}$TMABr : 0.50 NaOH : 1.0 total siloxane : 130 $H_2O$).† The following functionalized organotrialkoxysilanes $(RO)_3Si–R'$ were used; 3-sulfanylpropyltrimethoxysilane [TTMS, R′ = $(CH_2)_3SH$], 3-aminopropyltriethoxysilane [ATES, R′ = $(CH_2)_3NH_2$], 3-(2,3-epoxypropoxy)propyltrimethoxysilane [EPTMS, R′ = $(CH_2)_3OCH_2CH(O)CH_2$], 3-imidazoletriethoxysilane [IMTES, R′ = $(CH_2)_3NCHNCH_2CH_2$], allyltrimethoxysilane (ALTMS, R′ = $CH_2CHCH_2$). Experiments with ATES and IMTES were repeated using a neutral surfactant, *n*-dodecylamine.[6] In each case, an acidic solvent extraction technique[7] was used to prepare functionalized mesoporous silicas by removal of the surfactant from the as-synthesized materials.

Small-angle X-ray powder diffraction (XRD) (Table 1) and transmission electron microscopy (Fig. 1) indicated that the as-synthesized materials were single phases with mesoscopic order. Samples were generally prepared with 20 mol% of the functionalized organotrialkoxysilane in the initial synthesis composition and gave a series of higher-order XRD peaks which were indexed to organo–silica–surfactant hexagonal mesophases with unit-cell parameters between 40 and 45 Å ($a = 2d_{100}/\sqrt{3}$). Materials prepared using $C_{16}$TMABr were more ordered than those synthesized in the presence of *n*-dodecylamine. Removal of the surfactant by acid extraction gave ordered organo-functionalized mesoporous silicas for the materials derivatized with amino and thiol moieties (Table 1). In each case, contractions in the lattice parameter and loss of the higher order reflections were observed. For the EPTMS, ALTMS and IMTES samples, surfactant extraction appeared to significantly disrupt the ordered mesostructure of the as-synthesized material.

The extent of organotrialkoxysilane incorporation into the mesostructured materials, and the local structure of the organosilica walls were determined by $^{29}$Si MAS NMR of the as-synthesized and post-synthesized materials. Distinct resonances were observed for the siloxane [$Q^n$ = $Si(OSi)_n(OH)_{4-n}$, $n$ = 2–4] and organosiloxane [$T^m$ = $RSi(OSi)_m(OH)_{3-m}$, $m$ = 1–3) units (Table 2). The data indicate that increasing amounts of the organo-functionalized moieties are condensed into the wall structures with increasing mol% in the synthesis composition, but that the yield of incorporation was often low (Table 2). The relative amounts of ($Q^4$ + $T^3$), ($Q^3$ + $T^2$) and ($Q^2$ + $T^1$) species were essentially constant and equal to the respective $Q^4$, $Q^3$ and $Q^2$ contents of a sample prepared from 100 mol% TEOS sample (data not shown), suggesting that the organosiloxane species are distributed uniformly throughout the silica network.

The nature of the organic functional groups incorporated into the ordered mesostructured silica framework was investigated by $^{13}$C CP MAS NMR. The data qualitatively indicated that functional groups such as amine, imidazole, allyl and thiol could be incorporated without significant modification after surfactant extraction (NMR data: ATES, $\delta$ 10.0, 21.3, 43.0; ALTES, $\delta$ 19.8, 115.3, 131.7; IMTES, $\delta$ 9.0, 20.0, 37.1, 45.6, 50.4, 159.3; TTMS, $\delta$ 11.2, 23.0, 41.4). In contrast, the epoxide moiety underwent a ring-opening reaction during the synthesis procedure. Under the highly alkaline conditions employed, the epoxide ring was transformed into a diol terminal group

**Table 1** XRD data for organo–silica–surfactant mesophases

| | XRD *d*-spacings/Å | | | |
|---|---|---|---|---|
| Sample | (100) | (110) | (200) | (210) |
| ATES 20% | 38.7 | 22.5 | 19.9 | 15.2 |
| ATES[a] 20% | 36.8 | 19.2 | — | — |
| | 35.7[b] | 18.9[b] | — | — |
| EPTMS 20% | 36.0 | 19.8 | — | — |
| IMTES 20% | 37.4 | 21.5 | 18.8 | 13.7 |
| IMTES[a] 20% | 35.1 | — | — | — |
| TTMS 20% | 35.1 | 20.0 | 17.9 | — |
| | 31.0[b] | — | — | — |
| ALTMS 10% | 37.9 | 21.7 | 18.5 | 14.0 |
| ALTMS 20% | 34.7 | — | — | — |
| ALTMS 40% | 36.5 | — | — | — |

[a] Samples prepared using *n*-dodecylamine surfactant. [b] Data from surfactant-extracted samples.

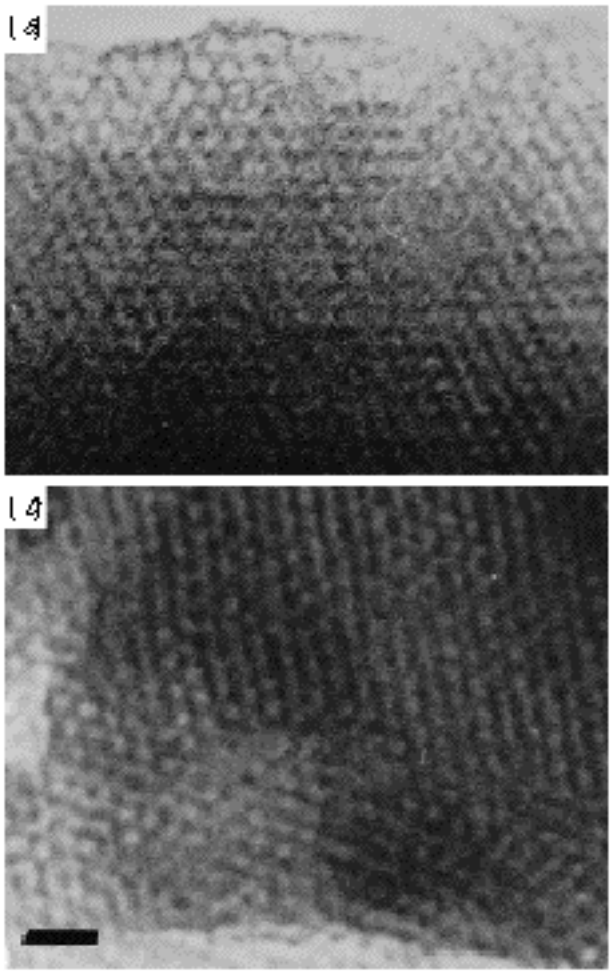


**Fig. 1** TEM micrographs of functionalized organo–silica–surfactant ordered mesophases containing covalently linked (*a*) amino and (*b*) thiol moieties; scale bar = 8 nm in both micrographs

(indicated by the broadening of the two resonances at $\delta$ 67 and 73 in the NMR spectrum of the as-synthesised material). The presence of hydrochloric acid in the surfactant extraction procedure led to further reaction and substitution of the beta hydroxyl group by chloride (NMR data: $\delta$ 46.8, 64.2).

Our results indicate that functionalized organotrialkoxysilanes can be covalently linked into ordered silica mesophases by co-condensation reactions in the presence of surfactant templates. Several different functional groups have been incorporated, suggesting that with appropriate modifications in the synthesis protocol, a wide range of ordered hybrid inorganic–organic frameworks could be prepared by this approach. A vinyl-functionalized MCM-41 has been reported recently.[8] The chemical reactivity of some of these materials is currently under investigation.

The authors would like to thank Dr David C. Apperley at the University of Durham, UK, for the solid-state NMR data, Christine G. Göltner and Ingrid Zenke at the Max Planck Institute of Colloids and Interfaces, Teltow, Germany, for small-angle XRD data, and the EPSRC and University of Bath for financial support.

**Table 2** $^{29}$Si NMR data for organo–silica–surfactant mesophases

| Sample | $\delta_{Si}$ [relative peak area] $T^2$ | $T^3$ | $Q^2$ | $Q^3$ | $Q^4$ | % Organic incorporation |
|---|---|---|---|---|---|---|
| ATES[a] | −58.2 | −66.6 | −90.9 | −100.6 | −110.2 | 11 |
| 20 mol% | [3.1] | [7.9] | [5.8] | [37.2] | [45.9] | |
| ATES | −56.0 | −65.9 | −91.3 | −100.8 | −110.0 | 13 |
| 20 mol% | [3.5] | [9.1] | [7.7] | [41.2] | [38.5] | |
| EPTMS | −55.7 | −64.2 | −91.9 | −100.7 | −109.4 | 14 |
| 20 mol% | [2.9] | [11.4] | [5.6] | [37.9] | [43.2] | |
| EPTMS | −56.9 | −64.8 | −92.1 | −100.6 | −108.9 | 27 |
| 50 mol% | [7.7] | [19.2] | [4.4] | [30.8] | [37.9] | |
| IMTES[a] | −57.6 | −66.5 | −91.0 | −100.5 | −109.4 | 11 |
| 20 mol% | [2.1] | [8.7] | [6.4] | [37.5] | [45.2] | |
| IMTES | −56.9 | −66.8 | −91.8 | −101.2 | −109.9 | 4 |
| 20 mol% | [0.7] | [3.1] | [5.2] | [40.3] | [50.7] | |
| TTMS | −57.2 | −65.4 | −91.2 | −100.5 | −108.9 | 20 |
| 20 mol% | [2.6] | [17.2] | [7.9] | [34.6] | [37.7] | |
| ALTMS | −61.6 | −70.9 | −90.1 | −99.0 | −108.6 | 11 |
| 10 mol% | [1.8] | [9.2] | [9.2] | [45.5] | [34.3] | |
| ALTMS | −60.9 | −69.7 | −91.7 | −100.6 | −109.4 | 25 |
| 20 mol% | [6.2] | [18.5] | [3.9] | [32.5] | [38.9] | |
| ALTMS | −60.5 | −70.6 | −90.7 | −100.7 | −109.1 | 38 |
| 40 mol% | [4.2] | [34.1] | [5.1] | [25.6] | [31.0] | |

[a] Samples prepared using *n*-dodecylamine surfactant.

## Footnotes and References

* E-mail: s.mann@bath.ac.uk

† In a typical preparation (20 mol% EPTMS), 0.40 g of $C_{16}$TMABr (Aldrich) was dissolved in 5.00 g of 1.0 mol dm$^{-3}$ NaOH and 17.55 g of distilled, deionized $H_2O$. 1.51 g of TEOS (Aldrich) and 0.43 g of EPTMS were added and the solution was stirred for 24 h at room temp. The solid product was filtered, washed with $H_2O$ and dried for 10 h at 100 °C *in vacuo*. ATES, EPTMS, IMTES and TTMS were obtained from Aldrich and ALTMS was obtained from Apollo Sci. Ltd. All compounds were used as received. Extraction of the surfactant was performed by stirring a suspension of the solid product (0.99 g dm$^{-3}$) in 1.0 mol dm$^{-3}$ HCl in EtOH at 75 °C for 24 h. The extracted material was filtered, washed with EtOH and dried for 10 h at 100 °C *in vacuo*. Extraction of the *n*-dodecylamine surfactant was carried out by stirring a suspension of the solid product (0.99 g dm$^{-3}$) in EtOH at 75 °C for 24 h. The extracted material was filtered, washed with EtOH and dried for 10 h at 100 °C *in vacuo*.

1 Q. H. Huo, D. I. Margolese and G. D. Stucky, *Chem. Mater.*, 1996, **8**, 1147.
2 J. S. Beck and J. C. Vartuli, *Curr. Opin. Solid State Mater. Sci.*, 1996, **1**, 76.
3 J. F. Ramsay, *Curr. Opin. Colloid Interface Sci.*, 1996, **1**, 208.
4 C. G. Göltner and M. Antonietti, *Adv. Mater.*, 1997, **9**, 431.
5 S. L. Burkett, S. D. Sims and S. Mann, *Chem. Commun.*, 1996, 1367.
6 P. T. Tanev and T. J. Pinnavaia, *Science*, 1995, **267**, 865.
7 C.-Y. Chen, H.-X. Li and M. E. Davis, *Microporous Mater.*, 1993, **2**, 17.
8 M. H. Lim, C. F. Blanford and A. Stein, *J. Am. Chem. Soc.*, 1997, **119**, 4090.

*Received in Cambridge, UK, 2nd July 1997; 7/04644H*

# Luminescent gold(I) supermolecules with trithiocyanuric acid. Crystal structure, spectroscopic and photophysical properties

**Biing-Chiau Tzeng,[a] Chi-Ming Che*[a] and Shie-Ming Peng[b]**

[a] *Department of Chemistry, The University of Hong Kong, Pokfulam Road, Hong Kong*
[b] *Department of Chemistry, Natonal Taiwan University, Taipei, Taiwan*

**The first example of an ordered array of $Au_6$ clusters with trithiocyanuric acid, $[(LAu)(AuPPhMe_2)_2]_2$ ($H_3L$ = trithiocyanuric acid), is prepared and characterized by X-ray crystallography; it has a two-dimensional structure *via* intermolecular $Au^I \cdots Au^I$ interactions and possesses photoluminescence properties; the ability of trithiocyanuric acid to act as a bridging ligand for molecular assembly of two-dimensional polymeric solids is demonstrated.**

Molecular materials composed of discrete metal clusters arranged in extended structures are useful model systems for understanding surface chemistry and catalysis, but the synthesis of such materials is usually serendipitous. Herein we show that $Au^I \cdots Au^I$ interactions can provide a driving force for self-assembly of such molecular solids,[1–6] as well as the first example of an ordered array of $Au_6$ clusters arranged in a two-dimensional structure *via* intermolecular $Au^I \cdots Au^I$ interactions. While examples of one-dimensional gold(I) chains are not uncommon in the literature,[1a,2b,4–6] gold(I) solids with two-dimensional structures are rare.[1b]

Complexes $L(AuPPh_3)_3$ **1** and $L(AuPPhMe_2)_3$ **2** were prepared by treating $AuCl(PPh_3)$ and $AuCl(PPhMe_2)$ respectively with a methanolic solution of $H_3L$ ($H_3L$ = trithiocyanuric acid) and NaOMe. Slow diffusion of diethyl ether into a $CH_2Cl_2$–MeOH solution of complex **2** gave $[(LAu)(AuPPhMe_2)_2]_2$ **3** with low solubility.†

Complexes **1** and **3** have been characterized by X-ray crystallography. The structure of complex **1** features a triazine with three bent S–Au–$PPh_3$ appendages pointing away from each other. This is similar to that of the reported $[\{CSAu(PPh_3)\}_6]$ supermolecule,[2c] whereas there is no intermolecular close contact of the gold(I) atoms in both complexes. Presumably, this is due to the steric hindrance provided by the $AuPPh_3^+$ units.

A perspective view of complex **3** and its extended two-dimensional structure are shown in Figs. 1 and 2, respectively. Complex **3** is a hexanuclear gold(I) supermolecule with a crystallographic centre of inversion at the centre of the 12-membered ring metallocycle. Four gold(I) centres are arranged in the form of a parallelogram with $Au^I \cdots Au^I$ distances of 2.964(2) and 2.987(2) Å, and a long transannular $Au^I \cdots Au^I$ separation of 3.347(3) Å. A similar arrangement of $Au_4$ has been found in $[\{Au_2(C_6H_4S_2\text{-}1,2)(PEt_3)\}_2]$[2d] and $[Au_4(\mu\text{-}S_2C_6H_3Me)_2(PEt_3)_2]$.[7] Notably, there is an intermolecular $Au^I \cdots Au^I$ close contact of 3.130(2) Å resulting in a novel two-dimensional structure with the $Au_6$ supermolecule as the repeating unit. One recent novel example is $[L'(AuCl)_4]_\infty$ [L′ = 1,4,8,11-tetrakis(diphenylphosphinomethyl)-1,4,8,11-tetraazacyclotetradecane].[1b] The intermolecular $Au^I \cdots Au^I$ separation in complex **3** is comparable to related values in one- and two-dimensional gold(I) solids such as 3.104(1) Å in $[L'(AuCl)_4]_\infty$,[1b] 3.174(1) Å in $[Au_2(C{\equiv}CPh)_2(\mu\text{-}C{\equiv}NBu^t{}_2C_6H_2N{\equiv}C]_\infty$[5a] and 3.200(1) Å in $[Au_2(p\text{-}tc)_2(dpppn)]_\infty$ [*p*-tc = *p*-thiocresol; dpppn = 1,5-bis(diphenylphosphino)pentane].[6b] Another important structural feature is coordination of $Au(PPhMe_2)^+$ units to one of the nitrogen atoms in each of the triazine rings, which is isolobal to a proton. A reaction scheme which rationalizes the formation of the $Au_6$ supermolecule is shown in Scheme 1.

Recently, the gold(I) complexes of two tridentate bridging ligands, 1,3,5-tris(diphenylphosphino)benzene[4b] and

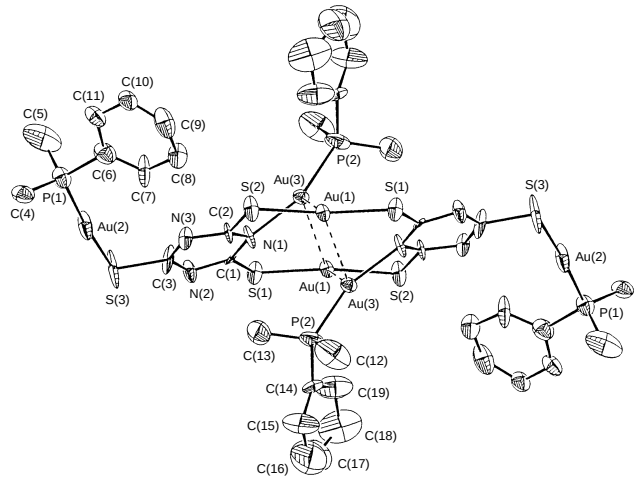



**Fig. 1** A perspective view of complex **3** (bond lengths in Å, angles in °): Au(1)···Au(3) 2.987(2), Au(1)···Au(3) 2.964(2), Au(3)···Au(3) 3.347(3), Au(1)–S(1) 2.279(9), Au(1)–S(2) 2.280(9), Au(2)–P(1) 2.234(10), Au(2)–S(3) 2.310(10), Au(3)–P(2) 2.210(11), Au(3)–N(1) 2.094(22); S(1)–Au(1)–S(2) 168.1(3), S(3)–Au(2)–P(1) 174.7(5), P(2)–Au(3)–N(1) 160.4(7)

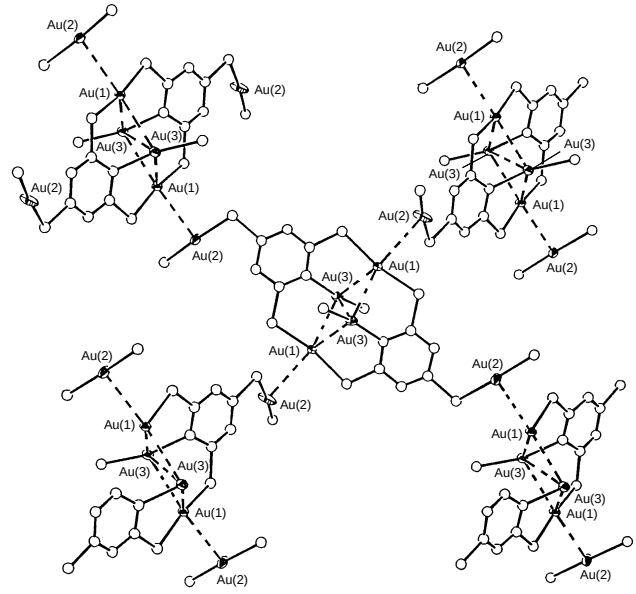
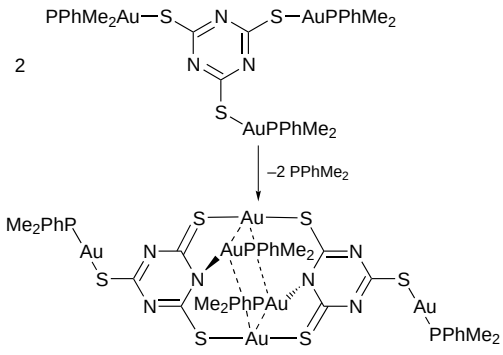



**Fig. 2** An extended two-dimensional structure of complex **3** with intermolecular Au···Au distances of 3.130(2) Å (the phenyl and methyl groups are omitted for clarity)




**Scheme 1**

$[C_6H_3(C{\equiv}C)_3]^{3-}$ [5b] are shown to form interesting one-dimensional polymeric solids *via* $Au^{I}\cdots Au^{I}$ interactions. Here, the trithiocyanuric acid demonstrates its ability to act as a bridging ligand for molecular assembly of two-dimensional polymeric solids.

The absorption spectra of complexes **1** and **2** measured in $CH_2Cl_2$ are very similar. As shown in Fig. 3 (insert), both complexes exhibit an intense absorption band at *ca*. 295 nm ($\varepsilon_{max}$ = 51 320 and 45 650 $dm^3\ mol^{-1}\ cm^{-1}$ for complexes **1** and **2**, respectively). However, complex **3** shows intense absorption at 320 nm ($\varepsilon_{max}$ = 44 870). This red shift in transition energy is not uncommon in $d^{10}$–$d^{10}$ systems and hence the 320 nm band in complex **3** is assigned to the $5d(d_{\sigma^*}) \rightarrow 6p(_{\sigma})$ tansition modified by $Au^{I}\cdots Au^{I}$ interactions.[8] As with most gold(I) complexes, complexes **1**–**3** are emissive both in solution and in the solid state, showing a broad emission at *ca*. 520–530 nm with long lifetimes (0.37, 0.34, 0.34 μs in degassed $CH_2Cl_2$; 3.7, 10.4, 11.6 μs in the solid state for complexes **1**, **2**, and **3**, respectively) upon photoexcitation at 300–400 nm (shown in Fig. 3), and these emissions are assigned to the $S \rightarrow Au$ excitation.[9]

This work highlights the application of $Au^{I}\cdots Au^{I}$ interactions as well as the judicious choice for bridging ligands in the formation of a two-dimensional array of luminescent metal clusters.

We acknowledge support from The University of Hong Kong, the Hong Kong Research Grants Council, and the Croucher Foundation.

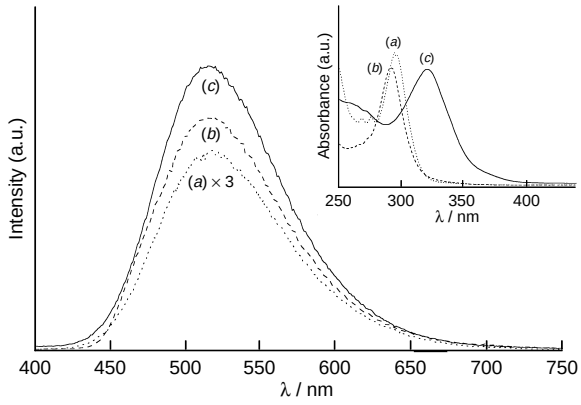



**Fig. 3** The emission spectra of complexes **1**–**3** measured in degassed $CH_2Cl_2$ at room temp. (insert is the absorption spectra of complexes **1**–**3** ($3.5 \times 10^{-5}$ M) in $CH_2Cl_2$); (*a*) **1** (*b*) **2**, (*c*) **3**

## Footnotes and References

* E-mail: cmche@hkucc.hku.hk

† $[L(AuPPh_3)_3]$ **1**: the reaction of $Na_3L$ [61 mg, obtained from $H_3L$ (44 mg) and NaOMe (41 mg) in MeOH (25 ml)] with $Au(PPh_3)Cl$ (148 mg) in $CH_2Cl_2$–MeOH (1 : 1, 50 ml) at room temp. for 4 h gave a pale-yellow solid which was recrystallized by diffusion of diethyl ether into $CH_2Cl_2$–dmf. Pale yellow crystals of $[L(AuPPh_3)_3]$ were obtained in *ca*. 80% yield. Its $^{31}P$ NMR spectrum recorded in $CDCl_3$ shows a singlet at $\delta$ 37.01. Anal. Calc.: C, 44.07; H, 2.90; N, 2.71. Found: C, 44.28; H, 2.74; N, 2.57%. FAB: $\{[L(AuPPh_3)_3]\}$, $m/z$ = 1552, 40%.

$[L(AuPPhMe_2)_3]$ **2**: It was similarly prepared to give a pale-yellow solid in *ca*. 75% yield, and its $^{31}P$ NMR spectrum recorded in $CDCl_3$ shows a singlet at $\delta$ 10.78. Anal. Calc.: C, 27.48; H, 2.80: N, 3.56. Found: C, 27.25; H, 2.64; N, 3.27% FAB: $\{[L(AuPPhMe_2)_3]\}$, $m/z$ = 1180, 80%.

$[(LAu)(AuPPhMe_2)_2]_2$ **3**: slow diffusion of diethyl ether into a $CH_2Cl_2$–dmf solution of complex **2** gave yellow crystals in *ca*. 40% yield. Anal. Calc.: C, 21.88; H, 2.11; N, 4.03. Found: C, 22.13; H, 2.34; N, 3.77% FAB: $\{[(LAu)(AuPPhMe_2)_2]_2\}$, $m/z$ = 2082, 15%.

*Crystal data*: **1**·$2C_3H_7NO$: $Au_3C_{63}H_{59}Au_3N_5O_2P_3S_3$, $M$ = 1698.18, monoclinic, space group $P2_1/n$, $a$ = 13.993(4), $b$ = 23.289(6), $c$ = 19.245(6) Å, $\beta$ = 92.07(3)°, $U$ = 6267(3) $Å^3$, $Z$ = 4, $D_c$ = 1.800 g $cm^{-3}$, $\mu$(Mo-Kα) = 71.90 $cm^{-1}$, $F$(000) = 3249. Intensity data were collected on Enraf-Nonius CAD4 diffractometer with graphite-monochromated Mo-Kα radiation ($\lambda$ = 0.7107 Å), 8173 unique reflection ($2\theta$ < 45°) were measured 4828 with $I > 2\sigma(I)$ were used in the refinement. Refinement of positional and anisotropic thermal parameters for all non-hydrogen atoms (713 variables) converged to $R$ = 0.047 and $R_w$ = 0.043. The final Fourier difference map showed residual extrema in the range of 1.57 to −2.07 e $Å^{-3}$.

**3**·2MeOH: $C_{40}H_{52}Au_6N_6O_2P_4S_6$, $M$ = 2146.93, monoclinic, space group $P2_1/c$, $a$ = 10.951(3), $b$ = 18.827(3), $c$ = 15.193(2) Å, $\beta$ = 105.90(2)°, $U$ = 3013(1) $Å^3$, $Z$ = 2, $D_c$ = 2.367 g $cm^{-3}$, $\mu$(Mo-Kα) = 149.15 $cm^{-1}$, $F$(000) = 1936. Intensity data were collected on Enraf-Nonius CAD4 diffractometer with graphite-monochromated Mo-Kα radiation ($\lambda$ = 0.7107 Å), 3926 unique reflection ($2\theta$ < 45°) were measured and 2206 with $I > 2\sigma(I)$ were used in the refinement. Refinement of positional and anisotropic thermal parameters for all non-hydrogen atoms (290 variables) converged to $R$ = 0.061 and $R_w$ = 0.054. The final Fourier difference map showed residual extrema in the range of 1.80 to −2.05 e $Å^{-3}$. CCDC 182/541.

1 (*a*) S.-J. Shieh, X. Hong, S.-M. Peng and C.-M. Che, *J. Chem. Soc., Dalton Trans.*, 1994, 3067; (*b*) B.-C. Tzeng, K.-K. Cheung and C.-M. Che, *Chem. Commun.*, 1996, 1681; (*c*) B.-C. Tzeng, C.-M. Che and S.-M. Peng, *J. Chem. Soc., Dalton Trans.*, 1996, 1769.

2 (*a*) H. Schmidbaur, *Chem. Soc. Rev.*, 1995, 391; (*b*) W. Schneider, A. Bauer and H. Schmidbaur, *Organometallics*, 1996, **15**, 5445; (*c*) H.-K. Yip, A. Schier, J. Riede and H. Schmidbaur, *J. Chem. Soc., Dalton Trans.*, 1994, 2333; (*d*) M. Nakamoto, A. Schier and H. Schmidbaur, *J. Chem. Soc., Dalton Trans.*, 1993, 1347.

3 D. M. P. Mingos, J. Yau, S. Menzer and D. J. Williams, *Angew. Chem., Int. Ed. Engl.*, 1995, **34**, 1894.

4 (*a*) P. M. V. Calcar, M. M. Olmstead and A. L. Balch, *J. Chem. Soc., Chem. Commun.*, 1995, 1773; (*b*) P. M. V. Calcar, M. M. Olmstead and A. L. Balch, *Chem. Commun.*, 1996, 2597.

5 (*a*) M. J. Irwin, G. Jia, N. C. Payne and R. J. Puddephatt, *Organometallics*, 1996, **15**, 51; (*b*) M. J. Irwin, L. M. Muir, K. W. Muir, R. J. Puddephatt and D. S. Yufit, *Chem. Commun.*, 1997, 219.

6 (*a*) M. Contel, J. Garrido, M. C. Gimeno, P. G. Jones, A. Laguna and M. Laguna, *Organometallics*, 1996, **15**, 4939; (*b*) R. Narayanaswamy, M. A. Young, E. Parkhurst, M. Ouellette, M. E. Kerr, D. M. Ho, R. C. Elder, A. E. Bruce and M. R. M. Bruce, *Inorg. Chem.*, 1993, **32**, 2506.

7 R. M. Dávila, A. Elduque, T. Grant, R. J. Staples and J. P. Fackler, Jr., *Inorg. Chem.*, 1993, **32**, 1749.

8 (*a*) C.-M. Che, H.-L. Kwong and C.-K. Poon, *J. Chem. Soc., Dalton Trans.*, 1990, 3215; (*b*) C.-M. Che, H.-L. Kwong, V. W.-W. Yam and K.-C. Cho, *J. Chem. Soc., Chem. Commun.*, 1989, 885; (*c*) C. King, J. C. Wang, M. N. I. Khan and J. P. Fackler, Jr., *Inorg. Chem.*, 1989, **28**, 2145.

9 W. B. Jones, J. Yuan, R. Narayanaswamy, M. A. Young, R. C. Elder, A. E. Bruce and M. R. M. Bruce, *Inorg. Chem.*, 1995, **34**, 1996.

*Received in Cambridge, UK, 4th June 1997; Com. 7/03891G*

# Solvothermal synthesis of $[Mn(en)_3]_2[Mn_4(en)_9(SbSe_4)_4]\cdot 2H_2O$: the first example of a selenoantimonate(v) acting as a ligand in a transition-metal complex

**Wolfgang Bensch,* Christian Näther and Michael Schur**

*Institut für Anorganische Chemie, Universität Kiel, Olshausenstr. 40, D-24098-Kiel, Germany*

**Reaction of elemental manganese, antimony and selenium under mild solvothermal conditions yields the complex anion $[Mn_4(en)_9(SbSe_4)_4]^{4-}$, the first example of a transition-metal complex with $SbSe_4^{3-}$ anions acting as ligands; the anions are coordinated in a terminal position as well as a bridging ligand.**

During recent years an increasing interest in new chalcogenide framework structures has been observed owing to their promising combination of 'zeotype' structures with new properties.[1] Application of mild solvothermal processes has led to a wealth of novel chalcogenides extending from unique thiometallate clusters to three-dimensional frameworks.[2,3] A special interest is focussed onto the combination of main-group and transition-metal chalcogenides, especially with respect to the incorporation of the latter into the 'open' frameworks of thio-germanates, -stannates or -antimonates.[4,5] Under mild solvothermal conditions we obtained new thioantimonate framework types,[6,7] thioantimonate polysulfides[8] and manganese-containing $Sb_xS_y$ frameworks.[9] Despite the expected new and unusual electronic properties the chemistry of the heavier chalcogenides is less developed. It is well documented that in aqueous solutions seleno- and telluro-metalates[3] undergo hydrolysis reactions and consequently non-aqueous reaction media are preferred for their syntheses. Nevertheless, the reaction of elemental antimony, selenium and manganese in an aqueous amine solution with addition of ethylenediamine (en) yielded the remarkable transition-metal complex $[Mn(en)_3]_2[Mn_4(en)_9(SbSe_4)_4]$.† The use of pure metals in the synthesis has attracted some attention in recent years including the insertion of transition metals into R–X bonds of alkyl- or phosphoryl-halogens[10] or the donor solvent mediated reaction of metals with sulfur to give polysulfido complexes.[11] The observation that the $SbSe_4^{3-}$ ligands in the title compound are formed using the elements as starting materials raises the question about the mechanism involved.

The crystal structure‡ of the title compound consists of isolated $Mn(en)_3^{2+}$ cations and the $[Mn_4(en)_9(SbSe_4)_4]^{4-}$ anions are probably stabilized by the large $Mn(en)_3^{2+}$ ions [Fig. 1(*a*) and (*b*)]. The anion is built up from two $SbSe_4$–$Mn(en)_2$–$SbSe_4$–$Mn(en)_2$ subunits, connected *via* a bridging ethylenediamine ligand, which is located around a center of inversion. The subunits contain two crystallographically independent manganese centers in distorted octahedral coordinations. The two different $SbSe_4^{3-}$ groups exhibit different binding modes. The $Se(1)_{br}$ (br = bridging) center of the $Sb(1)Se_4^{3-}$ unit joins the Mn(1) and Mn(2) atoms. Each Mn is chelated by two en ligands. The coordination sphere of Mn(2) is completed by $Se(5)_t$ (t = terminal) of the terminal $Sb(2)Se_4^{3-}$ ligand, leading to a *cis*-configuration of the distorted octahedral environment [Fig. 1(*a*)]. The Mn(1) centers are bridged by an en ligand, and therefore the Mn(1) is coordinated by five N atoms and one Se center.

The Sb–Se distances for both $SbSe_4^{3-}$ anions are in good agreement with those found in isolated $SbSe_4^{3-}$ anions[12,13] with the exception that $Sb(1)–Se(1)_{br}$ is elongated by *ca*. 0.04 Å. As expected the $Mn(2)–Se(5)_t$ distance of 2.673(2) Å is shorter than to the bridging $Se(1)_{br}$ atom. The Mn–Se distances to $Se(1)_{br}$ amount to 2.825(2) Å for Mn(1) and to 2.757(2) Å for Mn(2), a significant difference of 0.068(2) Å. This might be due to intramolecular hydrogen bonding between the $Se(2)_t$ center of the $Sb(1)Se_4^{3-}$ anion and an amino hydrogen of a chelate ligand bound to Mn(2). The Se(2)···H distance of 2.614(5) Å is significantly shorter than the sum of their van der Waals radii and the Se···H–N angle of 176.1(2)° is indicative of a hydrogen bond. There is an additional hydrogen bond between one amino hydrogen of a chelate ligand and the oxygen of a water molecule which is located in holes of the structure (Fig. 2). The O···H bond length is 2.39(2) Å and the O···H–N angle is 151.4(3)°.

The title compound is the first structurally characterized example of a transition-metal complex containing $SbSe_4^{3-}$ anions as ligands. Chalcogeno–antimonates(III) often crystallize as extended frameworks[14–16] whereas chalcogeno–antimonates(v) form isolated anions[12,13] or dense structures.[17,18] The

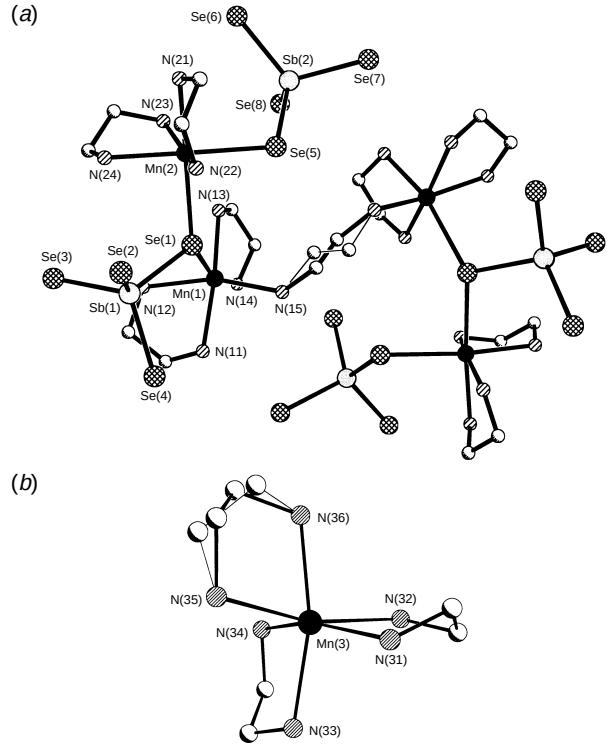



**Fig. 1** Crystal structure of $[Mn(en)_3]_2[Mn_4(en)_9Sb_4Se_{16}]$: (*a*) view of the anion $[Mn_4(en)_9Sb_4Se_{16}]^{2-}$ with numbering. Selected bond lengths (Å) and angles (°): Sb(1)–Se(2) 2.4550(8) Sb(1)–Se(4) 2.4690(7), Sb(1)–Se(3) 2.4713(8), Sb(1)–Se(1) 2.5111(7), Sb(2)–Se(8) 2.4439(10), Sb(2)–Se(6) 2.4738(8), Sb(2)–Se(7) 2.4787(8), Sb(2)–Se(5) 2.4812(8), Se(1)–Mn(2) 2.7573(11), Se(1)–Mn(1) 2.8251(12), Se(5)–Mn(2) 2.6728(12); Mn(2)–Se(1)–Mn(1) 128.32(4), Sb(2)–Se(5)–Mn(2) 110.88(3), Se(5)–Mn(2)–Se(1) 88.04(3); (*b*) note the disorder of one chelate ligand in the cation; hydrogen atoms are omitted for clarity

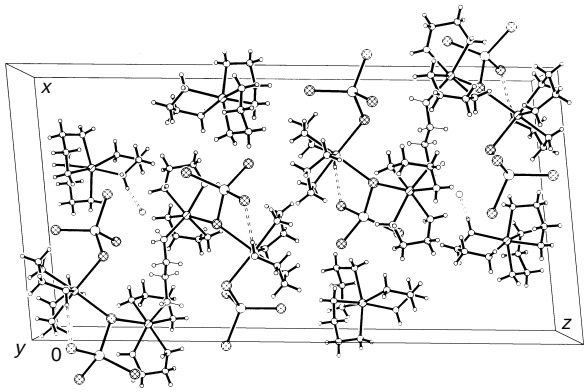



**Fig. 2** Packing of the molecules with view along the *b*-axis. For clarity, the disordered atoms of the ligands are omitted; hydrogen bonds are shown as broken lines.

combination of thio- and seleno-arsenates(III) with transition metals resulted in the preparation of a still growing number of low-dimensional structures.[19] However, the only examples of chalcogenopnictide(V) acting as ligands are $AsS_4^{3-}$ groups in nickel complexes as established by spectroscopical methods, but no structural data were reported.[20] It is noted that thiometallates of transition metals can be used as ligands.[21,22]

The complex anion in the crystal structure of the title compound may be regarded as a precursor for polymeric structures. Further studies are under way in order to enlarge the degree of condensation and to prepare extended structures.

This work was supported by the Hermann-Willkomm Stiftung, the Hermann-Schlosser Stiftung and the Hoechst AG.

## Footnotes and References

* E-mail: wbensch@ibmac.ac.uni-kiel.de

† *Synthesis*: The title compound was obtained by reacting stochiometric amounts of elemental manganese, antimony and selenium in an aqueous solution of 70 vol% ethylamine and 20 vol% ethylenediamine (en) (yield: *ca*. 95% based on Mn). The probe was heated to 130 °C for 6 days in a Teflon-lined steel vessel under autogenous pressure. The crystalline product was filtered, washed with dry ethanol and stored under vacuum. The crystals are dark red, moisture-sensitive prisms up to 5 mm long with excellent cleavage perpendicular to the needle axis. The compound could not be prepared in aqueous en solutions, whereas syntheses carried out in amine solutions without addition of en led to the rapid formation of $Sb_2Se_3$.

‡ *Crystal structure determination*: $[Mn(en)_3]_2[Mn_4(en)_9(SbSe_4)_4]\cdot 2H_2O$, $M$ = 3017.6 monoclinic, space group $P2/n$ (no. 13), $a$ = 16.519(2), $b$ = 8.248(1), $c$ = 32.599(3) Å, $\beta$ = 95.76(1)°, $U$ = 4419.1(9) Å$^3$, $T$ = 295 K, $Z$ = 2, STOE AED-II four-circle diffractometer (Mo-K$\alpha$ radiation, $\lambda$ = 0.7107 Å), $\mu$ = 8.664 mm$^{-1}$. 11 518 reflections collected in the range $3 \leqslant 2\theta \leqslant 53°$, 9180 unique reflections. Face-indexed absorption correction; structure solution with SHELXS-86; structure refinement against $F^2$ using SHELXL-93. 398 parameters, $R$ for 5968 reflections with $I > 2\sigma(I)$ = 0.0359, $wR_2$ for all 9180 data = 0.0990, GOF 1.013. Residual electron density: 1.525, −1.088 e Å$^{-3}$. The heavy atoms were refined anisotropically. The hydrogen atoms were positioned with idealized geometry and refined with individual isotropic displacement parameters using a riding model. The highest difference peak in the Fourier map according to a composition of $[Mn(en)_3]_2[Mn_4(en)_9(SbSe_4)_4]$ is located in the small cavity between the bridging and the terminal $SbSe_4$ ligands. It was assumed that this peak is due to incorporated solvent water molecules which was confirmed by IR spectroscopy showing a broad absorption band between 3600 and 3000 cm$^{-1}$. In space group $P2/n$ the two carbons of the bridging en ligand are around a center of inversion and hence they are disordered. This disorder is not observed in the non-centrosymmetric space group $Pn$. However, the detailed analysis of the refinements in $Pn$ and $P2/n$ clearly revealed the centrosymmetric arrangement of the remaining part of the structure. CCDC 182/557.

1 C. L. Bowes and G. A. Ozin, *Adv. Mater.*, 1996, **8**, 13.
2 B. Krebs, *Angew. Chem.*, 1983, **95**, 113.
3 W. S. Sheldrick and M. Wachhold, *Angew. Chem.*, 1997, **109**, 214.
4 L. Bedard, S. T. Wilson, L. D. Vail, J. M. Bennett and E. M. Flanigan, Elsevier, Amsterdam, 1989, p. 375.
5 H.-O. Stephan and M. G. Kanatzidis, *J. Am. Chem. Soc.*, 1996, **118**, 12226.
6 W. Bensch and M. Schur, *Z. Naturforsch., Teil B*, 1997, **52**, 405.
7 W. Bensch and M. Schur, *Eur. J. Solid State Inorg. Chem.*, submitted.
8 W. Bensch and M. Schur, *Z. Kristallogr.*, in the press.
9 W. Bensch and M. Schur, *Eur. J. Solid State Inorg. Chem.*, 1996, **33**, 1149.
10 B. Rosner and M. F. Rubner, *J. Chem. Soc., Chem. Commun.*, 1991, 1447; C. A. McAuliffe, S. M. Godfrey, A. G. Mackie and R. G. Pritchard, *J. Chem. Soc., Chem. Commun.*, 1992, 483; M. Godfrey, C. A. McAuliffe and R. G. Pritchard, *J. Chem. Soc., Dalton Trans.*, 1993, 371; 2229.
11 P. P. Paul, T. B. Rauchfuss and S. R. Wilson, *J. Am. Chem. Soc.*, 1993, **115**, 3316.
12 B. Eisenmann and R. Zagler, *Z. Naturforsch., Teil B*, 1989, **44**, 249.
13 M. Wachhold and W. S. Sheldrick, *Z. Naturforsch., Teil B*, 1996, **51**, 32.
14 G. Cordier and H. Schäfer, *Z. Naturforsch., Teil B*, 1979, **34**, 1053.
15 W. S. Sheldrick, *Z. Anorg. Allg. Chem.*, 1986, **536**, 114.
16 W. S. Sheldrick and H.-J. Häusler, *Z. Anorg. Allg. Chem.*, 1988, **557**, 98.
17 A. Pfitzner, *Z. Kristallogr.*, 1994, **209**, 685.
18 F. Pertlik, *J. Solid State Chem.*, 1994, **112**, 170.
19 G. A. Zank, T. B. Rauchfuss, S. R. Wilson and A. L. Rheingold, *J. Am. Chem. Soc.*, 1984, **106**, 7621; J.-H. Chou and M. G. Kanatzidis, *J. Solid State Chem.*, 1996, **123**, 115; J.-H. Chou, J. A. Hanko and M. G. Kanatzidis, *Inorg. Chem.*, 1997, **36**, 4.
20 I. Gergeu, R. Micu-Semeniuc and I. Haiduc, *Synth. Inorg. Metal. Org. Chem.*, 1977, **7**, 183.
21 A. Müller, *Angew. Chem.*, 1981, **93**, 957.
22 Q. Huang, X. Wang, T. Sheng and J. Lu, *Angew. Chem.*, 1996, **108**, 985; A. Müller, W. Jaegermann and W. Hellmann, *J. Mol. Struct.*, 1983, **100**, 559.

*Received in Basel, Switzerland, 25th April 1997; 7/02844J*

# SSZ-42: the first high-silica large pore zeolite with an undulating, one-dimensional channel system

**C. Y. Chen,[a] L. W. Finger,[b] R. C. Medrud,[a] P. A. Crozier,[c] I. Y. Chan,[a] T. V. Harris[a] and S. I. Zones*[a]**

[a] *Chevron Research & Technology Co., Richmond, CA 94802, USA*
[b] *Carnegie Institution of Washington, Geophysical Laboratory, Washington, D.C. 20015, USA*
[c] *Center for Solid State Science, Arizona State University, Tempe, AZ 85287, USA*

**The framework topology of the novel zeolite SSZ-42 is determined from single crystal data (15 × 15 × 35 μm) and refined from powder diffraction data; the crystalline architecture is characterized by an undulating, one-dimensional 12-membered ring channel system.**

In this report we describe the structure of a novel zeolite designated as SSZ-42. The zeolite is synthesized using *N*-benzyl-1,4-diazabicyclo[2.2.2]octane cation as the template molecule.[1] In one synthesis batch we were fortunate to find single crystals of uniform size (15 × 15 × 35 μm) which were optically of very high quality, and which extinguished uniformly under crossed polarizers.

The framework arrangement of SSZ-42 was solved from single-crystal data collected with a CCD camera in the applications laboratory of Siemens Energy and Automation, Inc. in Madison, WI, using a crystal that still contained the occluded template molecules. Although the measurable intensity was obtained on only about half of the available reflections in a three-dimensional set of data and most of those reflections were weak, the data from this very small SSZ-42 crystal were sufficient to locate the framework atoms by using direct methods in SHELXTL (version 5.03) to generate a very good trial model, but not precise enough to get good bond distances. The crystal system is monoclinic. The symmetry of the silica framework can be described in space group *C*2/*m*. There are four topologically distinct T-atoms and 10 O-atoms.

Full powder patterns for both as-synthesized and calcined samples (crystal size 1–2 μm) were collected at high-resolution beamline X7A of the National Synchrotron Light Source, Brookhaven National Laboratory.† The calcined sample used for the powder diffraction was prepared by heating the calcined material at 350 °C for several hours in a glass capillary under vacuum, to remove as much of the adsorbed species as possible, and then sealing. The unit-cell parameters from the powder data are shown in Table 1. The framework atom parameters from the single-crystal data were used as a starting model to refine the powder data from the calcined sample, which contains only the framework atoms. Convergence was accomplished without difficulty using the program GSAS.[2] Difference electron density slices through the channel cross-section show no residual electron density. The refinement led to residuals of $wR_p$ = 0.066, and $R_p$ = 0.050 and $R_{Bragg}$ = 0.061 with $\chi^2$ = 1.02. The Rietveld difference plot in Fig. 1 shows that the observed and calculated powder patterns of the calcined sample agree very well.

**Table 1** Unit-cell parameters for SSZ-42

| Sample | As-synthesized | Calcined |
|---|---|---|
| *a*/Å | 18.6309(9) | 18.4991(2) |
| *b*/Å | 13.3359(1) | 13.4078(1) |
| *c*/Å | 7.61731(3) | 7.57548(2) |
| *β*/° | 102.017(1) | 101.471(1) |
| *V*/Å$^3$ | 1851.12(1) | 1841.49(2) |

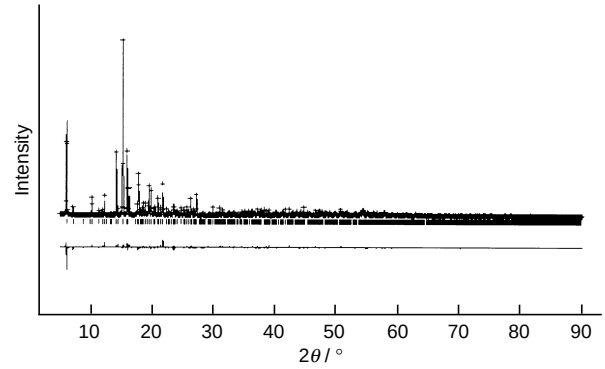



**Fig. 1** Results of Rietveld refinement of a calcined SSZ-42 sample

The framework structure, viewed along the 12-MR channel (Fig. 2), is characterized by an undulating, one-dimensional channel system with pores comprised of 12 T-atoms. The framework density is 17.4 T/1000 Å$^3$. The pore diameter at the narrowest point in the *XZ* projection is 6.4 Å. The cage at the widest point is *ca.* 10 Å. As shown by the *XZ* projection in Fig. 3, the channel exhibits 'side pockets' which are reminiscent of those in SSZ-33[3] and Beta[4] zeolites formed by the intersection of channels. In SSZ-42, however, there are no intersecting channels. In the perpendicular projection (*YZ*) there are no undulations and the pore diameter is 6.7 Å. It is apparent that the 12-membered ring is considerably distorted, giving the smaller than expected pore size.

The powder diffraction data from the as-synthesized sample displays considerable electron density in the channel. The template molecule must be disordered for the space group *C*2/*m*. Elemental analysis indicates two template molecules per unit cell. A possible location for the template molecule was generated by molecular modelling in the Insight computational environment (see Fig. 3).[5] The template molecule spans the

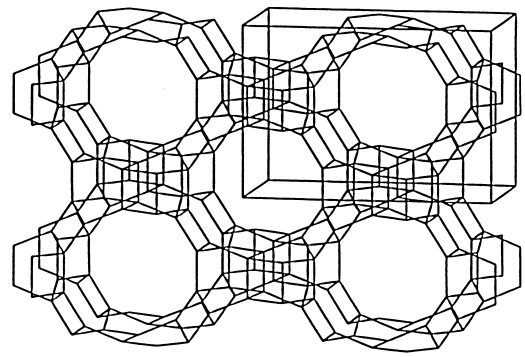


**Fig. 2** The SSZ-42 framework viewed along [001]

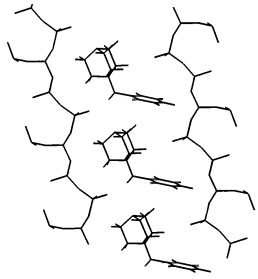


**Fig. 3** *XZ* projection of the SSZ-42 framework showing minimized location of template molecules

volume from one side pocket diagonally to the next. The details of further structure refinement based on the as-synthesized synchrotron powder XRD pattern will be discussed at a later date.[6] The atomic coordinates and selected bond distances and angles for the calcined form are listed in Tables 2 and 3, respectively. This structure does confirm once again the effective use of organocations as 'guest molecules' in developing the 'host' molecular sieve architecture.

Fig. 4 shows the experimental and simulated high-resolution electron micrograph (HREM) viewed along the [001] projection of SSZ-42. The experimental image is a spatially averaged image obtained with the low-dose method of Pan and Crozier.[7] Initial analysis of the circumference of the main channel led us to the preliminary proposal of a 10-MR channel system but we were unable to come up with a structure that would yield a good

**Table 2** Atomic coordinates for calcined SSZ-42

| | *x* | *y* | *z* | $10^2\ U_{iso}/Å^2$ |
|---|---|---|---|---|
| Si(1) | 0.9876(3) | 0.6151(4) | 0.6972(7) | 2.6(2) |
| Si(2) | 0.1471(3) | 0.6159(4) | 0.9006(7) | 3.0(2) |
| Si(3) | 0.7516(3) | 0.6122(4) | 0.3779(8) | 2.9(2) |
| Si(4) | 0.8393(3) | 0.7045(4) | 0.7280(8) | 3.2(2) |
| O(1) | 0.0625(8) | 0.6427(7) | 0.8284(15) | 3.9(4) |
| O(2) | 0.9241(6) | 0.6860(7) | 0.7350(13) | 1.9(3) |
| O(3) | 0.1769(6) | 0.6785(7) | 0.0793(14) | 2.6(4) |
| O(4) | 0 | 0.6250(14) | 0.5 | 6.5(7) |
| O(5) | 0.7902(6) | 0.6327(8) | 0.5818(16) | 4.1(4) |
| O(6) | 0.1944(6) | 0.6372(9) | 0.7491(15) | 6.3(5) |
| O(7) | 0.9689(8) | 0.5 | 0.7246(21) | 4.1(6) |
| O(8) | 0.6801(5) | 0.6819(7) | 0.3206(14) | 2.1(3) |
| O(9) | 0.1561(7) | 0.5 | 0.9579(21) | 5.8(7) |
| O(10) | 0.7219(7) | 0.5 | 0.3540(18) | 2.8(5) |

**Table 3** Selected bond distances (Å) and angles (°) for calcined SSZ-42

| | | | |
|---|---|---|---|
| Si(1)–O(1) | 1.582(8) | Si(3)–O(5) | 1.595(9) |
| –O(2) | 1.583(8) | –O(6) | 1.554(9) |
| –O(4) | 1.562(4) | –O(8) | 1.606(7) |
| –O(7) | 1.606(5) | –O(10) | 1.599(5) |
| Mean Si(1)–O | 1.583 | Mean Si(3)–O | 1.588 |
| Si(2)–O(1) | 1.593(8) | Si(4)–O(2) | 1.576(8) |
| –O(3) | 1.597(8) | –O(3) | 1.587(8) |
| –O(6) | 1.602(9) | –O(5) | 1.604(8) |
| –O(9) | 1.614(4) | –O(8) | 1.590(7) |
| Mean Si(2)–O | 1.602 | Mean Si(4)–O | 1.589 |
| | | | |
| Si(1)–O(1)–Si(2) | 147.1(5) | Si(2)–O(6)–Si(3) | 156.1(7) |
| Si(1)–O(2)–Si(4) | 149.1(6) | Si(1)–O(7)–Si(1) | 148.2(9) |
| Si(2)–O(3)–Si(4) | 143.0(6) | Si(3)–O(8)–Si(4) | 139.2(5) |
| Si(1)–O(4)–Si(1) | 170.3(13) | Si(2)–O(9)–Si(3) | 148.6(9) |
| Si(3)–O(5)–Si(4) | 148.7(6) | Si(3)–O(10)–Si(3) | 140.2(7) |

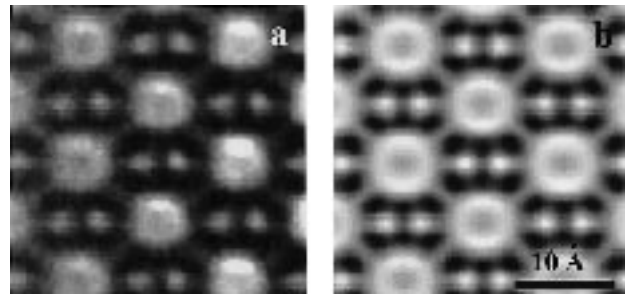



**Fig. 4** (*a*) Spatially averaged experimental HREM image from [001] projection of SSZ-42 acquired with a JEOL 4000 EX operating at 400 kV. The image (showing point-to-point resolution of 2.2 Å) was recorded from a wedge-shaped crystal resulting in a gradation of the image intensity from left to right. (*b*) Simulated image of proposed SSZ-42 structure in the [001] projection. The image was calculated using multi-slice techniques for a crystal 40 Å in thickness and the objective lens set to Scherzer defocus (−490 Å).

fit between the simulated image and the experimental image. However, if we use the atomic coordinates derived from the XRD data we obtain an excellent match between the simulated and experimental HREM data [see Fig. 4(*b*)]. In this case, the unusual geometry causes the 12-MR to appear as a 10-MR ring in [001] projection. However, the comparison between the experimental and simulated images is clearly a stringent test of the accuracy of the proposed structure model.

The existence of large pores was also experimentally confirmed by the adsorption of a series of molecules with varying dimensions. $N_2$, *n*-hexane, 2,2-dimethylbutane and cyclohexane have a high adsorption capacity of *ca.* 0.20 ml $g^{-1}$ in SSZ-42, which is closer to the adsorption data obtained in SSZ-33 and Beta, both possessing intersecting 10/12- or 12/12-MR channels. Based on these adsorption data, one could easily come to the incorrect conclusion that the framework architecture of this new material consists of an intersecting 10/12- or 12/12-MR channel system. In fact, the large adsorption capacity of SSZ-42 is due to large cages rather than to an intersecting channel system. The high adsorption capacity is exceptional for a large pore zeolite with a one-dimensional channel system.[6]

## Footnote and References

† Supported by the US Department of Energy, Division of Material Sciences and Division of Chemical Sciences. We thank D. E. Cox, G. Zhang and G. Mondo for assistance in collecting the synchrotron data. We thank Chevron Research and Technology Company for support of zeolite research in the catalyst area and especially D. J. O'Rear and C. M. Detz.

1 S. I. Zones and A. Rainis, *World Pat*., 95/908793, 1995.
2 A. C. Larson and R. B. Von Dreele, *GSAS—General Structure Analysis System*, Los Alamos National Laboratory Report LA-UR 86-748, 1986.
3 R. F. Lobo, M. Pan, I. Y., Chan, H. X. Li, R. C. Medrud, S. I. Zones, P. A. Crozier and M. E. Davis, *Science*, 1993, **262**, 1543.
4 J. M. Newsam, M. M. J., Treacy, W. T. Koetsier and C. B. deGruyter, *Proc. R. Soc. London, Ser. A*, 1988, **420**, 375.
5 Template docking studies were done with the CVFF forcefield using Solids_Docking and Discover modules of computer software distributed by the Catalysis and Sorption Consortium of Molecular Simulations, Inc., San Diego, CA.
6 C. Y. Chen, L. W. Finger, R. C. Medrud, P. A. Crozier, I. Y. Chan, T. V. Harris and S.I. Zones, in preparation.
7 M. Pan and P. A. Crozier, *Ultramicroscopy*, 1993, **48**, 332.

*Received in Columbia, MO, USA; 13th May 1997; 7/03323K*

# Luminescent chemosensors for pH, halide and hydroxide ions based on kinetically stable, macrocyclic europium–phenanthridinium conjugates†

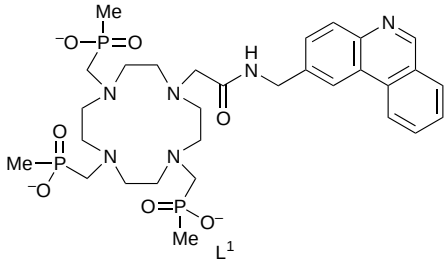
**David Parker,* Kanthi Senanayake and J. A. Gareth Williams**

*Department of Chemistry, University of Durham, South Road, Durham, UK DH1 3LE*

**The neutral europium complex [EuL$^1$] shows a pH dependent luminescence enhancement of over 500, while in the *N*-methylated analogue the metal-based luminescence is selectively quenched by chloride and (above pH 10) by hydroxide anions.**

Chemically robust, single-component luminescent sensors are needed not only for the analysis of the ionic composition of cells[1] but also in monitoring aqueous systems in the environment or during industrial processes. Fluorescent sensors have been devised for determining intracellular concentrations of species such as $Ca^{2+}$,[2] $Zn^{2+}$,[3] $H^+$ [4] and $Cl^-$.[5] Recently, the long-lived (ms range) luminescence of lanthanide complexes has been exploited in various bioassays with time-gating, permitting easy distinction from the shorter-lived (sub-μs) background fluorescence present in most biological systems.[6] Several of these sensors operate by ion-promoted suppression of photo-induced electron transfer (PET) from the ion receptor to the proximate lumophore. Examples include pH sensors incorporating a $Ru(bpy)_3^{2+}$ reporter (in $H_2O$–MeOH)[7] and a pentadentate terpyridyl ligand bearing aminomethyl substituents which in water forms a weak 1 : 1 complex with Tb.[8] The lanthanide luminescence is 'switched on' following amine protonation and luminescence enhancements of up to 16 were reported. The PET sensor principle is not the only means of allowing changes in ionic concentrations to be signalled: modulation of the spectral properties of the chromophore ($\varepsilon$, $\lambda_{abs}$) can be equally effective.

Following our recent work on the synthesis,[9] stereochemical analysis[10] and physicochemical properties[11] of kinetically stable macrocyclic lanthanide complexes in aqueous media, we have now prepared the charge-neutral europium complex of ligand L$^1$. Monoamide triphosphinate derivatives of



L$^1$

1,4,7,10-tetraazacyclododecane (cyclen) have been shown to form one predominant diastereomer in water following lanthanide binding[10] with partial hydration of the firmly bound lanthanide[12] ($\beta_{ML} \geqslant 10^{19}$). The phenanthridine chromophore was chosen because of its favourable absorption characteristics for excitation in biological media, its ease of N-alkylation allowing the study of halide induced quenching[5] of the derived phenanthridinium ion and because in its protonated or alkylated forms the phenanthridine moiety should serve as an effective 'antenna' for europium sensitisation minimising the ligand-to-metal charge-transfer process that often limits the overall luminescence efficiency of europium complexes in solution.[10]

Cyanation of 2-bromophenanthridine[13] (CuCN, dmf, 170 °C) followed by reduction with $BH_3$·thf afforded the aminomethyl derivative in 79% overall yield. Coupling with chloroacetic acid (EDC, HOBt, $CH_2Cl_2$) gave the corresponding α-haloamide (96%) which was used to monoalkylate the molybdenum-tricarbonyl complex of cyclen using established methodology.[9] Subsequent phosphinoxymethylation [$MeP(OEt)_2$, thf, $(CH_2O)_n$, 4 Å series] followed by base hydrolysis gave the octadentate ligand L$^1$ [$\delta_P$ (pD 6): 40.3] and reaction with $Eu(NO_3)_3$ in water followed by purification by alumina chromatography gave the neutral complex [EuL$^1$] [$\delta_P$ (pD 5.5): 101.1, 88.9, 70.3 with ⩾90% of this diastereoisomer]. Quaternisation of the phenanthridine N in [EuL$^1$] proceeded cleanly (MeI, MeCN, 40 °C), with the europium ion serving as a suitable protecting group for the ligand heteroatoms.

At pH 1.5 and 7, [EuL$^1$] possessed one bound water molecule ($\tau_{H_2O}$ = 0.71 ms, $\tau_{D_2O}$ = 1.92 ms). The phenanthridyl absorption and fluorescence excitation spectra were pH dependent and shifted to longer wavelength upon protonation with $CF_3CO_2H$. With excitation of the phenanthridyl antenna at 370 nm, luminescence from the Eu ion was 'switched on' following protonation (Figs. 1 and 2). The overall luminescence enhancement factor was at least 500 as can be seen by comparing the metal emission intensity at 594 nm ($\Delta J$ = 1) as a function of pH (Fig. 2). Indeed excitation at 380 nm (pH 7.4) gave rise to no measurable europium emission and acidification 'turns on' the red Eu europium luminescence, thereby creating a genuine pH switch. The p$K_a$ of [EuL$^1$] was calculated to be 4.45(8), and the same value was obtained from an analysis of the pH dependence of phenanthridyl fluorescence intensity ($\lambda_{em}$ = 405 nm, $\lambda_{exc}$ = 320 nm). Absolute quantum yields [relative to $Ru(bpy)_3^{2+}$, $\phi$ = 0.028][18] were measured for [EuL$^1$] (0.011 in $H_2O$, 0.034 in $D_2O$) and [Eu(HL$^1$)]$^+$ (0.030 in $H_2O$), and were independent of excitation wavelength above 300 nm. The PET process operative in this system evidently contributes little to the measured metal-based luminescence enhancement factors which are ascribed to the pH dependence ($\lambda_{abs}$, $\varepsilon$) of the sensitising antenna chromophore, (Fig. 1). Consistent with this analysis was the luminescence enhancement factor measured

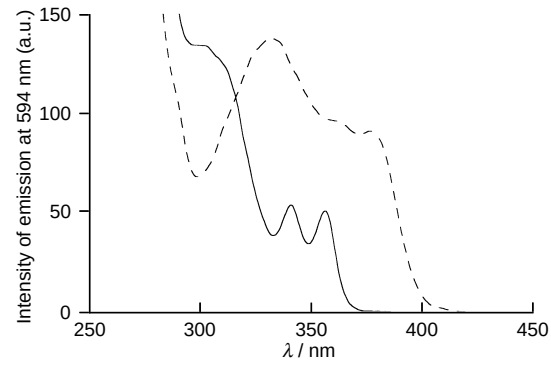



**Fig. 1** Metal luminescence excitation spectra ($\lambda_{em}$ = 594 nm, delay 0.1 ms) at pH 6.8 (solid line) and 1.5 (dashed)

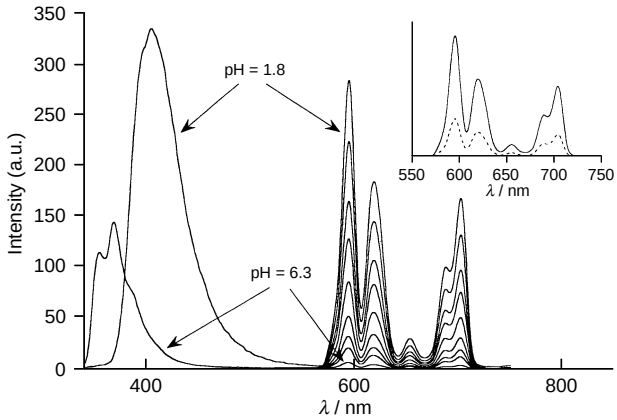


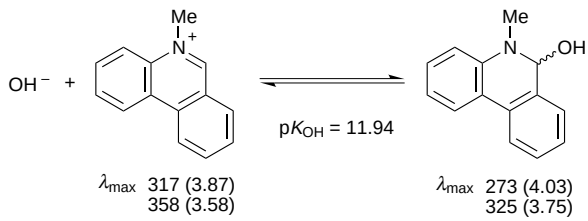

**Fig. 2** Effect of pH on phenanthridinium fluorescence (excitation at 320 nm) and on the intensity of europium luminescence ($\lambda_{exc}$ 370 nm, delay 0.1 ms, pH 1.88 to 6.33, $I$ = 0.1 M $NMe_4ClO_4$; spectra were acquired using a Perkin-Elmer LS 50B spectrofluorimeter). Insert shows the effect following excitation at the isosbestic point (solid line pH 1.8, dotted 6.3), where the difference in intensity reflects differences in the excited state behaviour only.

following excitation at the isosbestic point (315 nm): an enhancement of 3 was also seen (Fig. 2, insert).

N-Alkylated quinolinium and phenanthridinium ions possess a fluorescence which is quenched selectively by halide ions.[5] In complex [Eu(NMe)L1] [at pH 6.8, $\tau_{H_2O}$ = 0.73 ms, $\phi$ = 0.014 (as iodide salt with $\lambda_{exc}$ = 320 or 360 nm)], the europium luminescence was also quenched by addition of $Cl^-$, $Br^-$ or $I^-$ ions and an effective dissociation constant for $Cl^-$ binding of 45 mM was calculated. The observed luminescence quenching by $Cl^-$ was independent of pH (in the range 1.5–9), and was unaffected by the presence of added phosphate (5 mM), citrate (1 mM), lactate (5 mM) or bicarbonate (30 mM) auguring well for the development of such a sensory system for intracellular $Cl^-$ (typically 55–80 mM).

*N*-Methylphenanthridinium ions reversibly add hydroxide at the 6-position forming a pseudo-base (Scheme 1) and the equilibrium constant for the parent system is 11.94.[14] The concomitant change in the spectral characteristics of the aromatic chromophore (*e.g.* band at 358 nm disappears on adduct formation) suggested that the europium luminescence would be sensitive to the presence of $OH^-$ ions above pH 10. Addition of KOH to **1** caused a steep decrease in the sensitised europium luminescence, (Fig. 3), ($\lambda_{exc}$ = 360 nm, quenching factor ⩾200) and an effective binding constant of 12.2 (0.1) ($I$ = 0.1 M $NMe_4ClO_4$) was calculated in reasonable agreement with that measured for the parent system. Such behaviour, involving reversible C–O bond formation, constitutes an unusual method of assaying anionic species in solution, and has been observed previously in the quenching of N-methylacridinium fluorescence by $OH^-$, following attack at the 9-position.[14]

In summary, the europium complexes described constitute attractive new sensory systems for pH and for halide and hydroxide anions. Given the ease of modification of the heteroaromatic chromophore (and parallel quinolinium systems with p*K*as of *ca*. 5.8 have been recently prepared)[15] the facility of changing the Ln ion to Yb for near IR emission,[16] and the good selectivity of the halide sensor, practicable sensors for intracellular signalling based on such lanthanide probes (*e.g.* measuring the time-resolved emission intensity at 594 or 616 nm) may be expected. Furthermore the *N*-alkylphenanthridyl moieties are known to form relatively stable adducts with DNA and given that emissive enantiopure tetraamide complexes of Eu and Tb have been defined recently,[17,18] luminescent chiral lanthanide probes for DNA may also be feasible.




**Scheme 1**

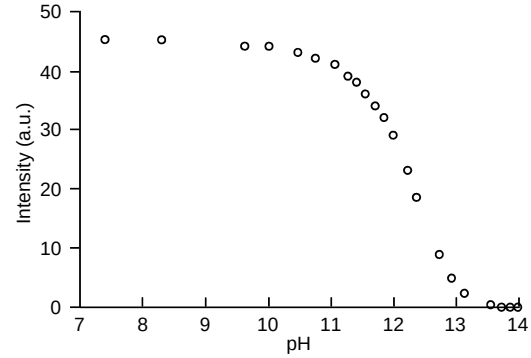



**Fig. 3** Effect of hydroxide ions on the intensity of the europium luminescence ($\lambda_{exc}$ = 380 nm, $\lambda_{em}$ = 594 nm, delay 0.1 ms; $I$ = 0.1 M $NMe_4ClO_4$)

We thank the EPSRC and BBSRC for grant support.

## Footnotes and References

* E-mail: david.parker@durham.ac.uk

† This ChemComm is also available in enhanced multi-media format *via* the World Wide Web: http://chemistry.rsc.org/rsc/cccenha.htm

1 A. W. Czarnik, *Acc. Chem. Res.*, 1994, **27**, 302; *Chem. Biol.*, 1995, **2**, 423.
2 G. Grynkiewicz, M. Poenie and R. Y. Tsien, *J. Biol. Chem.*, 1985, **260**, 3440.
3 H. A. Godwin and J. M. Berg, *J. Am. Chem. Soc.*, 1996, **118**, 6514; G. Walkup and B. Imperiali, *J. Am. Chem. Soc.*, 1997, **119**, 3443.
4 *Handbook of Fluorescent Probes and Research Chemicals*, ed. R. P. Haughland, Molecular Probes Inc., Eugene, OR, 1996; T. J. Rink, R. Y. Tsien and T. Pozzan, *J. Cell. Biol.*, 1982, **95**, 189.
5 S. S. C. Tom, P. C. Hauser, K. Wang, K. Fluri, K. Seiler, B. Rusterholz, G. Suter, M. Krüttli, U. E. Spichiger and W. Simon, *Anal. Chim. Acta*, 1991, **255**, 35; M. Vasseur, R. Frangne and F. Alvarado, *Am. J. Physiol.*, 1993, **264**, C27.
6 A. Mayer and S. Neuenhofer, *Angew. Chem., Int. Ed. Engl.*, 1994, **33**, 1044; E. F. G. Dickson, A. Pollak and E. P. Diamandis, *J. Photochem. Photobiol. B*, 1995, **27**, 3.
7 R. Grigg, J. M. Holmes, S. K. Jones and W. D. J. A. Norbert, *J. Chem. Soc., Chem. Commun.*, 1994, 185.
8 A. P. de Silva, H. Q. N. Gunaratne and T. E. Rice, *Angew. Chem., Int. Ed. Engl.*, 1996, **35**, 2116.
9 T. J. Norman, D. Parker, K. Pulukkody, L. Royle and C. J. Broan, *J. Chem. Soc., Perkin Trans. 2*, 1993, 605.
10 D. Parker and J. A. G. Williams, *J. Chem. Soc., Dalton Trans.*, 1996, 3613; S. Aime, M. Botta, D. Parker and J. A. G. Williams, *J. Chem. Soc., Dalton Trans.*, 1995, 2259.
11 S. Aime, A. Barge, M. Botta, D. Parker and A. S. deSousa, *J. Am. Chem. Soc.*, 1997, **119**, 4767.
12 S. Aime, M. Botta, D. Parker and J. A. G. Williams, *J. Chem. Soc., Dalton Trans.*, 1996, 17.
13 H. Gilman and J. Eisch, *J. Am. Chem. Soc.*, 1955, **77**, 6379.
14 J. W. Bunting and W. G. Meathrel, *Can. J. Chem.*, 1974, **52**, 981.
15 T. Gunnlaugsson and D. Parker, unpublished work.
16 A. Beeby, R. S. Dickins, S. Faulkner, D. Parker and J. A. G. Williams, *Chem. Commun.*, 1997, 1401.
17 R. S. Dickins, J. A. K. Howard, C. W. Lehmann, J. Moloney, D. Parker and R. D. Peacock, *Angew. Chem., Int. Ed. Engl.*, 1997, **36**, 521.
18 R. S. Dickins, J. A. K. Howard, J. Moloney, D. Parker and R. D. Peacock, *Chem. Commun.*, 1997, in press.

*Received in Liverpool, UK, 16th June 1997; 7/04318J*

# The role of back-bonding in the determination of classical *vs*. non-classical bonding in $EH_3^+$ and $EH_5^+$ minimum structures for E = C, Si and Ge

**Emma del Río, María I. Menéndez, Ramón López and Tomás L. Sordo***

*Departamento de Química Física y Analítica, Facultad de Química, Universidad de Oviedo, C/Julián Clavería, 8. 33006 Oviedo, Principado de Asturias, Spain*

**A rationalization of bonding in $EH_3^+$ and $EH_5^+$ classical and non-classical most stable minimum structures is proposed for E = C, Si and Ge by means of a back-bonding interaction which when present is clearly displayed by a configuration analysis and explains the lack of bridged hydrogens in the corresponding structure.**

Very recently there has been a strong interest in the study of the species $EH_3^+$ and $EH_5^+$ for E = C, Si and Ge.[1–8] For $CH_3^+$ high level computations have rendered no side-on $HC^+\cdots H_2$ complex the classical $D_{3h}$ symmetric structure being the most favored energetically. In contrast, for $SiH_3^+$ and $GeH_3^+$ two different minimum structures have been found: one of $D_{3h}$ symmetry and the other, a non-classical side-on complex, of $C_s$ symmetry.[1] On the other hand, for the $EH_5^+$ systems, the global minimum structures are non-classical $C_s$ structures characterized by a three-center–two-electron bond having a five-coordinate central atom and bridged hydrogens. No classical five-coordinate minimum structure have been found for these $EH_5^+$ systems.[2–8] It has been argued that this is so because the energy required to break the H–H bond is not compensated by the two newly formed E–H bonds[7] in contrast with the classical $EH_3^+$ structures where the $H_2$ cleavage seems to be adequately compensated.

In this work we propose a rationalization of bonding in the title $EH_3^+$ and $EH_5^+$ systems by using the back-bonding concept which when present is clearly displayed by a configuration analysis.

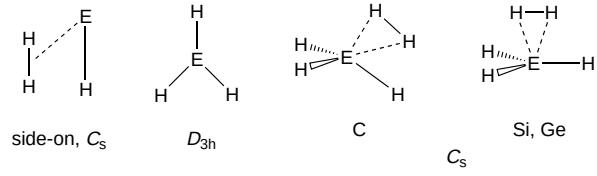
All structures were optimized at the Becke3LYP DTF level[9] with the standard 6-311++G(2d,2p) basis set using the Gaussian 94 program.[10] The nature of the stationary points was further characterized by frequency calculations which also gave the zero-point vibrational energy (ZPVE) correction. This theory level has previously proved to be adequate to study some of the title systems.[1] DFT wavefunctions were analyzed by means of a theoretical method developed by Fukui's group[11] using the ANACAL program.[12] This method is based on the expansion of the MOs of a complex system in terms of those of its fragments, and configuration analysis. This type of analysis has proved useful for understanding the chemical features of complex formation from chemically interacting systems.

Table 1 collects the Becke3LYP/6-311++G(2d,2p) total energies and ZPVE of the $EH_3^+$ and $EH_5^+$ (E = C, Si and Ge) minimum structures studied in this work: the classical $D_{3h}$ minimum structures of $CH_3^+$, $SiH_3^+$ and $GeH_3^+$, the side-on $C_s$ structures of $SiH_3^+$ and $GeH_3^+$, and the global minimum structures of $C_s$ symmetry of $CH_5^+$, $SiH_5^+$ and $GeH_5^+$. For $SiH_3^+$ and $GeH_3^+$ the $D_{3h}$ structures are the most stable ones by 28.4 and 11.1 kcal mol$^{-1}$, respectively (27.1 and 10.0 kcal mol$^{-1}$ when ZPVE is included).

Table 2 presents the most important changes in the electronic population of the Kohn–Sham MOs of $EH_3^+$ and $EH_5^+$ minimum structures. Table 3 displays the coefficients of the most important electronic configurations of fragments in the minimum structures studied in this work.

We see from Table 2 that in the $EH_3^+$ structures of $D_{3h}$ symmetry the HOMOs of both fragments and the NHOMO of the $EH^+$ fragment lose electronic population and the LUMO and the NLUMO of the $EH^+$ cationic fragment and the LUMO of $H_2$ become appreciably populated. Table 3 shows that this

**Table 1** Becke3LYP/6-311++G(2d,2p) total energy ($E_h$) and ZPVE [kcal mol$^{-1}$ (1 cal = 4.184 J)] of $EH_3^+$ and $EH_5^+$ minimum structures (E = C, Si, and Ge)




| Species | | Total energy | ZPVE |
|---|---|---|---|
| $CH_3^+$ | $D_{3h}$ | −39.49360 | 19.6 |
| $SiH_3^+$ | $D_{3h}$ | −290.96382 | 13.9 |
| | side-on, $C_s$ | −290.91861 | 12.6 |
| $GeH_3^+$ | $D_{3h}$ | −2078.46433 | 13.1 |
| | side-on, $C_s$ | −2078.44665 | 12.0 |
| $CH_5^+$ | $C_s$ | −40.74944 | 31.9 |
| $SiH_5^+$ | $C_s$ | −292.16795 | 23.8 |
| $GeH_5^+$ | $C_s$ | −2079.66377 | 22.7 |

**Table 2** Most important changes in the electronic population ($\Delta v$) of the Kohn–Sham MOs of $EH_3^+$ (A = $EH^+$; B = $H_2$) and $EH_5^+$ (A = $EH_3^+$; B = $H_2$) minimum structures (E = C, Si, Ge), net charge transfer (CT) from $H_2$ to the cation, and H–H distance (Å) where <1 Å

| | $CH_3^+$ | $SiH_3^+$ | | $GeH_3^+$ | | $CH_5^+$ | $SiH_5^+$ | $GeH_5$ |
|---|---|---|---|---|---|---|---|---|
| | $D_{3h}$ | $D_{3h}$ | side-on $C_s$ | $D_{3h}$ | side-on, $C_s$ | $C_s$ | $C_s$ | $C_s$ |
| A NLUMO | +0.09 | +0.03 | 0.0 | +0.75 | +0.19 | 0.0 | +0.03 | +0.01 |
| LUMO | +1.05 | +0.70 | +0.22 | +0.09 | 0.0 | +0.83 | +0.25 | +0.22 |
| HOMO | −0.61 | −0.70 | −0.05 | −0.61 | −0.03 | −0.24 | −0.03 | −0.02 |
| NHOMO | −0.14 | −0.17 | −0.01 | −0.18 | 0.0 | −0.03 | 0.0 | 0.0 |
| B LUMO | +0.72 | +1.08 | +0.04 | +1.08 | +0.03 | +0.15 | +0.02 | +0.02 |
| HOMO | −1.33 | −1.19 | −0.25 | −1.25 | −0.22 | −0.84 | −0.29 | −0.25 |
| CT | 0.41 | 0.01 | 0.18 | 0.07 | 0.17 | 0.52 | 0.24 | 0.20 |
| *d*(H–H) | | | 0.782 | | 0.773 | 0.988 | 0.777 | 0.772 |

**Table 3** Coefficients of the most important configurations of fragments in the $EH_3^+$ (A = $EH^+$; B = $H_2$) and $EH_5^+$ (A = $EH_3^+$; B = $H_2$) minimum structures (E = C, Si, Ge)

| Configuration | $CH_3^+$ $D_{3h}$ | $SiH_3^+$ $D_{3h}$ | $SiH_3^+$ side-on, $C_s$ | $GeH_3^+$ $D_{3h}$ | $GeH_3^+$ side-on, $C_s$ | $CH_5^+$ $C_s$ | $SiH_5^+$ $C_s$ | $GeH_5^+$ $C_s$ |
|---|---|---|---|---|---|---|---|---|
| AB | 0.0 | 0.0 | +0.7620 | 0.0 | +0.8017 | +0.3152 | +0.7480 | +0.7793 |
| $A^-B^+$(HO–LU) | 0.0 | 0.0 | +0.2515 | 0.0 | −0.0247 | +0.3691 | +0.2626 | +0.2513 |
| $A^-B^+$(HO–NLU) | 0.0 | 0.0 | 0.0 | 0.0 | +0.2366 | 0.0 | +0.0717 | +0.0500 |
| $A^{2-}B^{2+}$(HO–LU/HO–LU) | +0.1489 | +0.0753 | +0.0356 | 0.0 | 0.0 | +0.1514 | +0.0375 | +0.0341 |
| $A^{2-}B^{2+}$(HO–NLU/HO–NLU) | 0.0 | 0.0 | 0.0 | +0.0844 | +0.0307 | 0.0 | 0.0 | 0.0 |
| AB**(HO–LU/HO–LU) | +0.0844 | +0.1291 | 0.0 | +0.1415 | 0.0 | 0.0 | 0.0 | 0.0 |
| A*B*(HO–LU/HO–LU) | +0.1638 | +0.1808 | 0.0 | 0.0 | 0.0 | 0.0 | 0.0 | 0.0 |
| A*B*(HO–NLU/HO–LU) | 0.0 | 0.0 | 0.0 | +0.1660 | 0.0 | 0.0 | 0.0 | 0.0 |
| $A^{\pm}B^{\mp}$(HO–LU/HO–LU) | +0.1638 | +0.1808 | +0.0201 | 0.0 | 0.0 | +0.0916 | 0.0 | 0.0 |
| $A^{\pm}B^{\mp}$(HO–LU/HO–NLU) | 0.0 | 0.0 | 0.0 | +0.1660 | 0.0 | 0.0 | 0.0 | 0.0 |
| $A^-B^{+*}$(HO–LU/HO–LU) | +0.1865 | −0.1705 | 0.0 | −0.0546 | 0.0 | 0.0 | 0.0 | 0.0 |
| $A^-B^{+*}$(HO–NLU/HO–LU) | 0.0 | 0.0 | 0.0 | +0.1860 | 0.0 | 0.0 | 0.0 | 0.0 |
| $A^+B^{-*}$(HO-LU/HO–LU) | +0.0741 | −0.1368 | 0.0 | −0.1262 | 0.0 | 0.0 | 0.0 | 0.0 |
| $A^{*-}B^+$(HO–LU/HO–LU) | +0.1308 | −0.0799 | 0.0 | 0.0 | 0.0 | 0.0 | 0.0 | 0.0 |

electronic rearrangement is caused by two different interactions between the fragments: a charge transfer from the HOMO of $H_2$ to the LUMO or NLUMO of the $EH^+$ moiety, and a back-donation from the HOMO of the cationic fragment to the LUMO of $H_2$. In the side-on structures of $SiH_3^+$ and $GeH_3^+$ the spatial disposition of the fragments is compatible only with an interaction of dihydrogen with the vacant orbitals of $EH_3^+$. In effect, Table 2 shows that the LUMO or NLUMO of the $EH^+$ cationic fragment gain electronic population whereas the HOMO of $H_2$ becomes less populated. We see in Table 3 that this redistribution of electrons is due to an HOMO($H_2$)–LUMO ($SiH^+$) or HOMO($H_2$)–NLUMO ($GeH^+$) interaction. These are then donor–acceptor complexes between the dihydrogen ligand (donor) and $EH^+$ as already reported.[1] The reason why there is no side-on structure in the case of $CH_3^+$ is that the LUMOs of $CH^+$ are more stable (−0.55 eV) than the HOMO of $H_2$ (−0.43 eV). As a consequence, in a hypothetical side-on structure of $CH_3^+$ a very strong charge transfer would take place from $H_2$ to $CH^+$ in a first phase. The depopulation of the HOMO of $H_2$ produced by this charge transfer would cause an important elongation of the H–H bond and a stabilization of the LUMO of dihydrogen which would allow the interaction of $H_2$ with the HOMO of $CH^+$ through back-bonding and the formation of the $D_{3h}$ structure.

For the $EH_5^+$ systems the most stable structures have $C_s$ symmetry with the $H_2$ unit bound sideways to the $EH_3^+$ fragment. However, there is a significant difference between $CH_5^+$ and $SiH_5^+$ and $GeH_5^+$. In $SiH_5^+$ and $GeH_5^+$ the $H_2$ unit preserves its entity only slightly perturbed by the interaction with the $EH_3^+$ fragment whereas in $CH_5^+$ the $H_2$ unit presents a considerably elongated bond (see Table 2). This difference can be understood in terms of the electronic configurations of the fragments (see Table 3). In effect, for $SiH_5^+$ and $GeH_5^+$ the wavefunction is a mixture mainly of the zero configuration and the monotransference from the HOMO of $H_2$ to the LUMO of $EH_3^+$ whereas for $CH_5^+$ the wavefunction includes in addition the ditransference from the HOMO of $H_2$ to the LUMO of $EH_3^+$ and a small contribution from the cross transference from the HOMO of $H_2$ to the LUMO of $CH_3^+$, and from the HOMO of $CH_3^+$ to the LUMO of $H_2$. Accordingly, we see in Table 2 that the LUMO of the $EH_3^+$ fragment is considerably more populated and its HOMO loses more electronic density, and the HOMO of $H_2$ loses more electronic population and its LUMO becomes more populated in the case of $CH_5^+$ than in the other two cases. This can be explained again as a consequence of the fact that the LUMO of $CH_3^+$ (−0.49 eV) is more stable than the HOMO of $H_2$. This determines a very strong charge transference from the $H_2$ fragment to $CH_3^+$ which causes the elongation of the H–H bond making possible even a back donation from the HOMO of $CH_3^+$ to the LUMO of $H_2$. As a consequence, while in $SiH_5^+$ and $GeH_5^+$ the $H_2$ fragment interacts only with the $p_z$ orbital of the central atom whose three $sp^2$ hybrids form three E–H bonds, in $CH_5^+$ two of the $sp^2$ hybrids of the central atom form two C–H bonds and the NHOMO of the $CH_5^+$ is a linear combination of the third $sp^2$ hybrid, the 1s atomic orbital (AO) of the two H atoms of the $H_2$ moiety and the 1s AO of the remaining H atom. This difference is clearly appreciated in the geometry of the $EH_5^+$ systems. In the case of E = Si, Ge the $H_2$ fragment is symmetrically situated in front of the $p_z$ AO of the central atom parallel to the $sp^2$ plane whereas in $CH_5^+$ the $H_2$ fragment is placed between one of the $sp^2$ hybrids and the $p_z$ AO of C, the remaining H atom being displaced from the linear direction along the hybrid AO.

The authors are grateful to Professor Agustí Lledós for helpful comments and suggestions, and to DGICYT for financial support (PB94-1314-C03-01). E. del R. also thanks to the DGICYT (Spain) for a grant.

## References

1 J. Kapp, P. R. Schreiner and P. v. R. Schleyer, *J. Am. Chem. Soc.*, 1996, **118**, 12 154.
2 P. R. Schreiner, S.-J. Kim, H. F. Schaefer III and P. v. R. Schleyer, *J. Chem. Phys.*, 1993, **99**, 3716.
3 H. Müller, W. Kutzelnigg, J. Noga and W. Klopper, *J. Chem. Phys.*, 1997, **106**, 1863.
4 P. v. R. Schleyer, Y. Apeloig, D. Arad, B. T. Luke and J. A. Pople, *Chem. Phys. Lett.*, 1983, **95**, 477.
5 C. H. Hu, M. Shen and H. Schaefer III, *Chem. Phys. Lett.*, 1992, **190**, 543.
6 D. W. Boo and Y. T. Lee, *J. Chem. Phys.*, 1995, **103**, 514.
7 P. R. Schreiner, H. F. Schaefer III and P. v. R. Schleyer, *J. Chem. Phys.*, 1994, **101**, 2141.
8 E. F. Archibong and J. Leszczynski, *J. Phys. Chem.*, 1994, **98**, 10 084.
9 A. D. Becke, *Phys. Rev. A*, 1988, **38**, 3098; *J. Chem. Phys.*, 1993, **98**, 5648.
10 GAUSSIAN 94, M. J. Freisch, G. W. Trucks, H. B. Schlegel, P. M. W. Gill, B. G. Johnson, M. A. Robb, J. R. Cheesman, T. A. Keith, G. A. Petersson, J. A. Montgomery, K. Raghavachari, M. A. Al-Lahan, V. G. Zakrzewski, J. V. Ortiz, J. B. Foresman, J. Cioslowski, B. B. Stefanov, A. Nanayakkara, M. Challacombe, C. Y. Peng, P. Y. Ayala, W. Chen, M. W. Wong, J. L. Andres, E. S. Replogle, R. Gomperts, R. L. Martin, D. J. Fox, J. S. Binkley, D. J. Defrees, J. Baker, J. P. Stewart, M. Head-Gordon, C. Gonzalez and J. A. Pople, Gaussian Inc., Pittsburgh, PA, 1995.
11 H. Fujimoto, S. Kato, S. Yamabe and K. Fukui, *J. Chem. Phys.*, 1974, **60**, 572.
12 R. López, M. I. Menéndez, D. Suárez, T. L. Sordo and J. A. Sordo, *Comput. Phys. Commun.*, 1993, **76**, 235.

*Received in Exeter, UK, 10th June 1997; 7/04055E*

# Aminopropylated MCMs as base catalysts: a comparison with aminopropylated silica

**Duncan J. Macquarrie* and Dominic B. Jackson**

*Department of Chemistry, University of York, Heslington, York, UK YO1 5DD*

**Aminopropyl-functionalised MCMs, prepared *via* a one-pot method, are found to be effective base catalysts for the Knoevenagel reaction, with significant improvements in terms of turnover number and solvent dependence to the ostensibly similar aminopropylsilica.**

We, and others, recently reported a simple one-pot method for the preparation of surface-modified monodisperse MCM-type silica.[1,2] This method can be used to prepare organically modified materials in high yield, which have very high surface areas (650–1600 $m^2\ g^{-1}$) and are functionalised with a variety of organic groups. The pore size distribution of these materials is very narrow and in the mesoporous region (1.8–3.9 nm). Such properties would make these materials potentially very interesting as novel catalysts. We have recently reported that aminopropylated silica is an effective base catalyst, which is limited in its usefulness by an unusual solvent dependency, and which is poisoned by amide formation at the $NH_2$ groups.[3] We now wish to report our findings on aminopropylated MCMs, materials which display considerable differences in catalytic activity to the apparently similar aminopropylsilicas.

The aminopropylated MCMs were prepared according to known methods.[1] Three catalysts were prepared, whose structural and compositional characteristics are shown in Table 1. The ability to increase loading of these materials by changing the ratio of the two silanes [aminopropyl(trimethoxy)silane and tetraethoxysilane] used in their preparation makes this methodology more flexible than the post-modification of silica, where maximum loadings are in the region of 1 mmol $g^{-1}$. The surface area and pore size distributions are as expected for such materials, and their surface polarity, as measured using adsorption of Reichardts dye[4] is significantly higher than that of the corresponding silica-derived materials, and approaches that of underivatised silica [$E_N^T$ ($SiO_2$) = 0.89–0.96, depending on drying conditions. Similar values are obtained for unmodified MCMs]. This difference can be ascribed to the larger amount of exposed, unfunctionalised surface in the case of the MCM materials, and, in agreement with this, the 2.5 mmol $g^{-1}$ loading catalyst has a value lower than that of the 1.2 mmol $g^{-1}$ material. Such a difference might be expected to lead to different solvent dependency in reactions catalysed by the MCMs compared to the silica-derived catalysts, owing to different partitioning of reactants between the catalyst surface and the bulk solution.

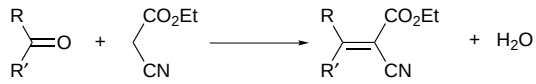
The catalysts were then evaluated in a series of reactions. Reactions used were the Knoevenagel condensation of aldehydes and ketones with ethyl cyanoacetate, a model reaction which has been studied in some detail.[3,5,6,7] The CH acid and the ketone (20 mmol of each) were added to a suspension of the catalyst (0.25 g) in the appropriate solvent (25 ml) at reflux. All reactions were run with continuous removal of water. Reactions were followed by GC using *n*-dodecane as internal standard, and products were isolated using conventional techniques. Results are shown in Table 2. Yields are generally high and compare favourable well with those in the literature.[3,5,6,8] As

**Table 1** Selected physical parameters of catalysts

| Catalyst | Pore diameter/nm | SSA/ $m^2\ g^{-1}$ | Loading/ mmol $g^{-1}$ | $E_N^T$ |
|---|---|---|---|---|
| **1** | 3.6 | 756 | 1.2 | 0.90 |
| **2** | 3.7 | 745 | 2.5 | 0.82 |
| **3** | 1.8 | 715 | 1.2 | 0.86 |
| AMPS[a] | 8.0 (br) | 254 | 0.95 | 0.56 |

[a] Aminopropyl-substituted silica.

**Table 2** Selected reaction data for reactions catalysed by aminopropyl-MCMs




| R | R′ | Catalyst | Solvent | *T*/°C | *t*/h | Yield (%)[a] | TON[b] |
|---|---|---|---|---|---|---|---|
| Ph | H | **1** | cyclohexane | 82 | 36 | 94 | |
| *n*-$C_7H_{15}$ | H | **1** | cyclohexane | 82 | 0.5 | 93 | >6000 |
| $cC_5H_{10}$ | | **1** | cyclohexane | 82 | 4 | 96 | 2450 (650) |
| $cC_5H_{10}$ | | **1** | cyclohexane | 82 | 12 | 70[c] | |
| $cC_5H_{10}$ | | **1** | toluene | 110 | 2 | 92 | |
| $cC_5H_{10}$ | | **1** | EtOAc | 78 | 4 | 11 | |
| $cC_5H_{10}$ | | **1** | $CHCl_3$ | 61 | 4 | 18 | |
| $cC_5H_{10}$ | | **1** | DCE[d] | 81 | 4 | 16 | |
| $cC_5H_{10}$ | | **3** | cyclohexane | 82 | 4 | 49 | |
| Et | Et | **1** | cyclohexane | 82 | 30 | 89 | 1127 (265) |
| Et | Et | **1** | toluene | 110 | 18 | 95 | |
| Et | Et | **2** | toluene | 110 | 4 | 97 | |
| Me | $Bu^n$ | **2** | toluene | 110 | 4 | 95 | 1244 |
| Me | Ph | **1** | toluene | 110 | 72 | 49 | 55 (250) |
| Me | Ph | **2** | toluene | 110 | 36 | 48 | 47 |

[a] GC yields with *n*-dodecane as internal standard. Isolated yields are 3–7% lower. [b] Number of moles product per mole of $NH_2$ groups. Figures in brackets are for reactions using 1.0 mmol $g^{-1}$ aminopropylsilica as catalyst. [c] Reaction carried out without removal of water. [d] 1,2-Dichloroethane.

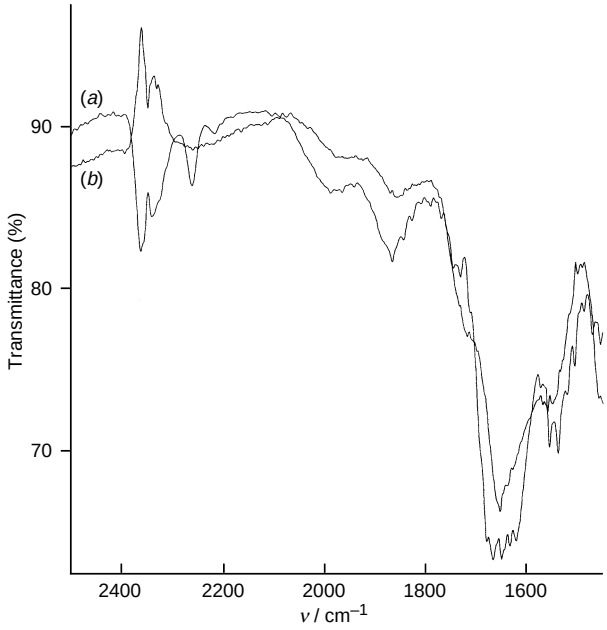



**Fig. 1** IR spectra of spent catalysts recovered from Knoevenagel reactions: (*a*) spent aminopropylsilica and (*b*) spent aminopropyl-MCM

can be seen, the overall reactivity bears some similarity to that of aminopropylated silica.[3,5] Aldehydes and ketones both react with ethyl cyanoacetate, chosen as a carbon acid of moderate activity and synthetic utility. Surprisingly, benzaldehyde reacts extremely sluggishly with the MCM catalysts, despite being a facile substrate with both the silica-derived catalysts and with homogeneous amines such as piperidine. Otherwise, the relative reactivity of ketones is typical of both aminopropyl-modified silica and of most homogeneous systems. For reactions of ketones, the rates of reaction in cyclohexane, the optimum solvent for the silica variant, are typically 20–30% slower with the catalysts described here. However, as will be discussed later, the MCM-type catalysts are less restricted by solvent than their amorphous silica equivalents. Immediately obvious is the generally increased turnover numbers (TONs), although the reactivity and TON of acetophenone is disappointingly low. This, coupled with the remarkably low activity of benzaldehyde, may suggest that the reduced electrophilicity of the aromatic carbonyl, relative to the aliphatic, plays an unusually significant role in reactions catalysed by these materials.

Other points of interest are that the small pore (1.8 nm) catalyst **3** gives a poor conversion compared to the larger pore analogue **1**. However, it is interesting to note that the rate of reaction caused by both catalysts is essentially identical, the difference being that **1** remains active for longer. Increasing the loading from 1.2 mmol $g^{-1}$ to 2.5 mmol $g^{-1}$ causes a corresponding increase in reaction rate. Such an increase in loading is readily achieved by altering the ratio of silanes in the preparation of the MCM catalysts, but is not possible with the post-functionalisation of silica, where 1.0 mmol $g^{-1}$ is the maximum loading achievable. In connection with TON, the mode of catalyst deactivation also differs between the two catalyst types. For the silica catalysts, there is clear evidence for a slow, irreversible formation of surface-bound amide groups, arising from the reaction of the surface-bound primary amine and the ester of the ethyl cyanoacetate [Fig. 1(*a*)]. In the case of the MCM catalysts, recovered spent catalyst does not display bands for nitrile or amide groups, but rather indicates the presence of some adsorbed organics [Fig. 1(*b*)]. The identity of the species responsible is currently the subject of investigation.

A further point of divergence between the two types of catalyst is their behaviour in different solvents. Whereas the silica-based catalyst has a very limited range of solvents in

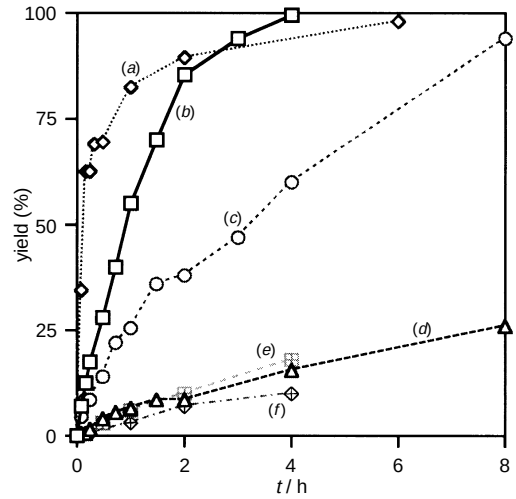



**Fig. 2** Effect of solvents on the rate of reaction with aminopropyl-MCM **1**: (*a*) toluene, (*b*) cyclohexane, (*c*) hexane, (*d*) 1,2-dichloroethane, (*e*) chloroform, (*f*) ethyl acetate

which it is effective,† the activity of the MCM catalyst seems to follow a simpler trend with respect to reflux temperature of the solvent. However, it is clear that more polar solvents are disadvantageous (Fig. 2). While the reasons for this behaviour are still under investigation, it may be the case that the rate of reaction is influenced by the partitioning of the (polar) reactants between the catalyst surface (polar) and the bulk medium (non-polar). The silica-based catalysts have a significantly lower polarity, as measured by the Reichardts dye method[4] (Table 1). This might mean that partitioning away from the catalyst is pronounced even in moderately polar solvents such as toluene, whereas the much more polar MCM catalysts can more effectively compete for the substrate, thus effectively extending the range of useful solvents, leading to reaction rates greater than those achievable with the silica-based materials.

In conclusion, the novel organofunctionalised MCM catalysts described here represent novel catalytic materials, differing significantly in many respects from their post-functionalised silica counterparts. Under optimum conditions they can outperform the silicas, in terms of both activity and catalyst turnover.

D. J. M. thanks the Royal Society for a University Research Fellowship.

## Footnotes and References

* E-mail: djm13@york.ac.uk

† The relative rates of reaction at reflux in various solvents are as follows: octane > heptane > cyclohexane > hexane > toluene > pentane ≫ chlorobenzene, 1,2-dichloroethane. Octane and heptane, however, lead to rapid deactivation of the catalyst. Initial rate studies with the alkane solvents indicate an Arrhenius-type behaviour, showing a simple temperature dependence of rate. More polar solvents such as toluene, PhCl and other chlorinated solvents show rates much reduced from those achieved in a hydrocarbon of similar boiling point.

1 D. J. Macquarrie, *Chem. Commun.*, 1996, 1961.
2 S. L. Burkett, S. D. Sims and S. Mann, *Chem. Commun.*, 1996, 1367.
3 D. J. Macquarrie, J. E. G. Mdoe, A. Priest, A. Lambert and J. H. Clark, *React. Funct. Polym.*, in the press.
4 S. J. Tavener, D. J. Macquarrie, G. Gray, P. A. Heath and J. H. Clark, *Chem. Commun.*, 1997, 1147.
5 E. Angeletti, C. Canepa, G. Martinetti and P. Venturello, *Tetrahedron Lett.*, 1988, **29**, 2261.
6 E. Angeletti, C. Canepa, G. Martinetti and P. Venturello, *J. Chem. Soc., Perkin Trans. 1*, 1989, 105.
7 G. Jones, *Org. React.*, 1967, **15**, 204 and references therein.
8 J. A. Cabello, J. M. Campelo, A. Garcia, D. Lisna and J. M. Marinas, *J. Org. Chem.*, 1984, **49**, 5195.

*Received in Cambridge, UK, 16th June 1997; 7/04156J*

# Triple-decker naphthalene complex of thulium(III); synthesis and molecular structure of [{Tm(dme)}$_2$($\eta^2$-$C_{10}H_8$)$_2$($\mu^2$-$\eta^4$ : $\eta^4$-$C_{10}H_8$)]

**M. N. Bochkarev,[a] I. L. Fedushkin,[a] A. A. Fagin,[a] H. Schumann[b] and J. Demtschuk[b]**

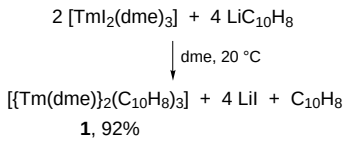
[a] *G. A. Razuvaev Institute of Organometallic Chemistry of Russian Academy of Sciences, Tropinina 49, 603600 Nizhny Novgorod GSP-445, Russian Federation*

[b] *Institut für Anorganische und Analytische Chemie der Technischen Universität Berlin, Straße des 17, Juni 135, D-10623 Berlin, Germany*

**The reaction of thulium(II) iodide with 2 equiv. of lithium naphthalenide in dme (dme = 1,2-dimethoxyethane) yields a binuclear thulium(III) complex with one bridging and two terminal dianions of naphthalene [{Tm(dme)}$_2$($\eta^2$-$C_{10}H_8$)$_2$($\eta^2$-$\eta^4$ : $\eta^4$-$C_{10}H_8$)] 1.**

Recently, the first molecular complex of divalent thulium, [$TmI_2$(dme)$_3$][1] was synthesized and characterized crystallographically. To develop the chemistry of divalent thulium further we studied its reaction with lithium naphthalenide. Previously, it had been shown that exchange reactions of the lanthanoid dihalides, [$LnI_2$(thf)$_2$] (Ln = Sm, Eu, Yb), and cyclopentadienyl lanthanoid dihalides, [Ln($\eta^5$-$C_5H_5$)$Cl_2$] (Ln = Y, Gd, Er, Tm, Lu), with alkali-metal naphthalenides in thf or dme resulted in the formation of naphthalene lanthanoid complexes of the type [Ln($C_{10}H_8$)(thf)$_2$][2] or [Ln($\eta^5$-$C_5H_5$)($C_{10}H_8$)(dme)].[3,4] While the latter complexes were fully characterized by structural and spectroscopic analyses, no structural information on the cyclopentadienyl-free complexes was obtained owing to difficulties in the preparation of crystalline samples suitable for X-ray analysis. In the case of lanthanoid triiodides, including [$TmI_3$(dme)$_3$], reactions with $LiC_{10}H_8$ in various molar ratios gave no products that could be identified. The only exception was the structurally characterized complex of lanthanum [{$LaI_2$(thf)$_3$}$_2$($C_{10}H_8$)] isolated from the reaction of equimolar amounts of [$LaI_3$(thf)$_3$], naphthalene and Li in dme.[5]

Here we report that the treatment of a [$TmI_2$(dme)$_3$] solution in dme with $LiC_{10}H_8$ in a 1 : 2 molar ratio leads to the formation of the binuclear naphthalene complex **1** in good yield (Scheme 1).




**Scheme 1**

The black crystals of **1** are sparingly soluble in dme and thf and insoluble in hydrocarbon solvents. They decompose slowly in solution at room temperature. In the solid state decomposition is observed above *ca*. 100 °C. The complex gave satisfactory elemental analysis for thulium (calc. 37.43; found 36.71%). Total elemental analysis could not be performed because of an extreme sensitivity of the complex to moisture and air. Careful oxidation of **1** in air leads to the formation of naphthalene in about 90% yield, in good agreement with the composition of the complex. The magnetic moment of **1** (6.59 $\mu_B$/Tm, 293 K) is somewhat lower than the value typical for thulium(III) derivatives (7.1–7.5 $\mu_B$).[6] That might be explained by the existence of an intramolecular antiferromagnetic Tm–Tm interaction. The observed magnetic moment is significantly different from the $\mu_{eff}$ of [$TmI_2$(dme)$_3$] (4.5 $\mu_B$)[1] confirming the oxidation of thulium during the course of the reaction. One can suggest that the reaction proceeds *via* the formation of [$Tm^{2+}$($C_{10}H_8$)$^{2-}$] a transient intermediate, which then reacts with free naphthalene, contained in the solution of $LiC_{10}H_8$, to give **1**. However, it should be noted, that in spite of the high reduction potential of $Tm^{II}$ (*ca*. −2.3 V),[7] [$TmI_2$(dme)$_3$] does not react with free naphthalene.

The IR spectrum† of **1** contains the absorption bands of the bridging (1500, 1400 $cm^{-1}$) and terminal naphthalene dianions (1250 $cm^{-1}$) which were observed previously in the complexes [{$LaI_2$(thf)$_3$}$_2$(μ-$C_{10}H_8$)][5] and [Lu($\eta^5$-$C_5H_5$)($C_{10}H_8$)(dme)].[3] An X-ray crystal structure analysis confirms this assignment.

Crystals formed directly in the reaction procedure were suitable for X-ray diffraction.‡ An ORTEP representation of the molecular structure of **1** is shown in Fig. 1. The molecule rests on the inversion centre located in between C(11) and C(11′), so only half of the molecule is unique. Both of the naphthalene rings of the bridging ligand are bent along the axis defined by the 1,4 naphthalene positions. The dihedral angle between the planes represented by C(12)C(13)C(14)C(15) and C(11)C(11′)C(15)C(12) is 19.28°. this value is somewhat higher than in the lanthanum(III) complex [{$LaI_2$(thf)$_3$}$_2$(μ-$C_{10}H_8$)] containing a bridging naphthalene dianion (15.2°).[5] The terminal naphthalene ligands display a different geometry: the naphthalene ring C(2)–C(4) remains flat, while the other ring is bent. The dihedral angle between the planes C(5)C(6)C(9)C(10) and C(6)C(7)C(8)C(9) (26.22°) is smaller than in complex [Lu($\eta^5$-$C_5H_5$)($C_{10}H_8$)(dme)] (30°).[3] The thulium–bridging naphthalene bonding mode is the same as that observed in the lanthanum complex mentioned above. Four Tm–C distances lie in a narrow range (2.59–2.62 Å) and are 0.2 Å shorter than in the lanthanum complex. This is in agreement with the difference in ionic radii between Tm and La.[8] The bonding mode of Tm with the terminal naphthalene ligand is quite different. The Tm–C(6) and Tm–C(9) distances are much

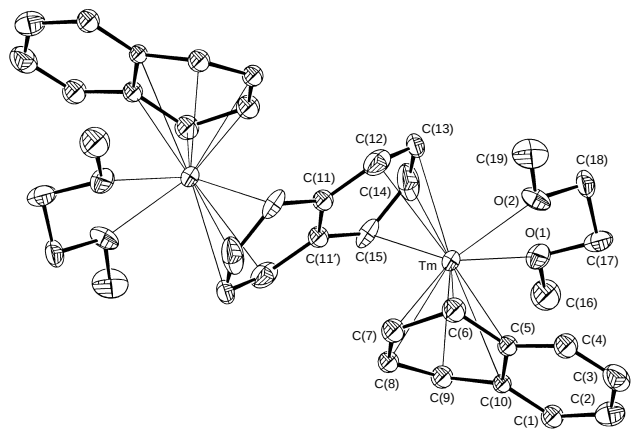



**Fig. 1** ORTEP representation of the molecular structure of **1**

shorter than Tm–C(7) and Tm–C(8) (2.41. 2.43, 2.54, 2.54 Å, respectively). The overall geometry of this fragment is almost identical to that observed in the complex [Lu($\eta^5$-$C_5H_5$)($C_{10}H_8$)(dme)]. The Tm–C(terminal $C_{10}H_8$) bond lengths are also close to Lu–C distances (2.406, 2.397, 2.579, 2.562 Å) owing to the nearly identical ionic radii of Tm and Lu (CN = 8: 0.994 and 0.977 Å, respectively).[8] Redistribution of C–C bond lengths in the naphthalene ligands and their non-planar shape reflect a dianionic nature of the ligands: the distances C(13)–C(14) and C(7)–C(8) become shorter (1.35, 1.31 Å) while all other C–C bonds are elongated compared to free naphthalene.[9] The naphthalene ring which is not coordinated to the Tm atom retains its aromaticity with similar C–C distances. Thus, the negative charge in the bridging naphthalene ligand is delocalized between all carbon atoms, but in the terminal naphthalene it is concentrated mainly on the C(6) and C(9) positions.

Previously we had shown that naphthalene complexes of the lanthanoids are very reactive towards organic and organometallic substances.[2,10,11] To illustrate the reactivity of **1** we carried out its reaction with cyclopentadiene. As might be anticipated the reaction proceeded smoothly at room temp. to give [Tm($\eta$-$C_5H_5$)$_3$] in good yield. We hope to use **1** for the synthesis of previously inaccessible complexes of thulium.

We thank the Russian Foundation for Basic Research (Grant No. 97-03-33112a) and the Volkswagen-Stiftung for financial support.

## Footnotes and References

* E-mail: schn0530@mailszrz.zrz.tu-berlin.de

† *Spectroscopic data*: IR(Nujol): 1330 1270s, 1250, 1200, 1185, 1160, 1130, 1100, 1060s, 1035, 1020s, 980, 870s, 790, 750, 730, 700s, 490, 450 cm$^{-1}$.

‡ *Crystal data* for **1**: $C_{38}H_{44}O_4Tm_2$, $M$ = 902.59, $T$ = 173(2) K, monoclinic, space group $P2_1/n$; $a$ = 7.722(2), $b$ = 15.687(5), $c$ = 13.605(04) Å, $\beta$ = 100.16(2)°, $U$ = 1622.2(8) Å, $Z$ = 2, $D_c$ = 1.848 g cm$^{-3}$, $\mu$ = 5.473 mm$^{-1}$, $F$(000) = 884, crystal size 0.09 × 0.09 × 0.03 mm. A total of 1932 unique reflections with $\theta$ = 2–20.9°, were collected. Reflections with $I > 2\sigma(I)$ 1706, $R$ [for $I > 2\sigma(I)$] = 0.0452. An Enraf-Nonius CAD4 diffractometer with monochromated Mo-K$\alpha$ radiation was used ($\lambda$ = 0.710 69 Å). Data were corrected for Lorenz, polarization and absorption effects. CCDC 182/559. Details of the crystal structure investigation are available on request from the Fachinformationszentrum Karlsruhe GmbH, D-76344 Eggenstein-Leopoldshafen (FRG), on quoting the depository number CSD-406861.

1 M. N. Bochkarev, I. L. Fedushkin, A. A. Fagin, T. V. Petrovskaya, J. W. Ziller, R. N. R. Broomhall-Dillard and W. J. Evans, *Angew. Chem.*, 1997, **109**, 123.
2 M. N. Bochkarev, A. A. Trifonov, E. A. Fedorova, N. S. Emelyanova, T. A. Basalgina, G. S. Kalinina and G. A. Razuvaev, *J. Organomet. Chem.*, 1989, **372**, 217.
3 A. V. Protchenko, L. N. Zakharov, M. N. Bochkarev and Yu. T. Struchkov, *J. Organomet. Chem.*, 1993, **447**, 209.
4 A. V. Protchenko, L. N. Zakharov, G. N. Fukin, Yu. T. Struchkov and M. N. Bochkarev, *Izv. Acad. Nauk Ser. Khim.*, 1996, 993 (in Russian).
5 I. L. Fedushkin, M. N. Bochkarev, H. Schumann, L. Esser and G. Kociok-Kohn, *J. Organomet. Chem.*, 1995, **489**, 145.
6 W. J. Evans and M. A. Hozbor, *J. Organomet. Chem.*, 1987, **326**, 299.
7 N. B. Mikheev, *Russ. J. Inorg. Chem.*, 1984, **29**, 258.
8 R. D. Shannon, *Acta Crystallogr., Sect. A*, 1976, **32**, 751.
9 C. P. Brock and J. D. Dunitz, *Acta Crystallogr., Sect. B*, 1982, **38**, 2218.
10 A. A. Trifonov, M. N. Bochkarev, H. Schumann and J. Löbel, *Angew. Chem., Int. Ed. Engl.*, 1991, **30**, 1149.
11 M. N. Bochkarev, I. L. Fedushkin, V. K. Cherkasov, V. I. Nevodchikov, H. Schumann and F. H. Görlitz, *Inorg. Chim. Acta*, 1992, **201**, 69.

*Received in Cambridge, UK, 27th May 1997; 7/03603E*

# Catalytic asymmetric cyclopropanation of electron deficient alkenes mediated by chiral sulfides

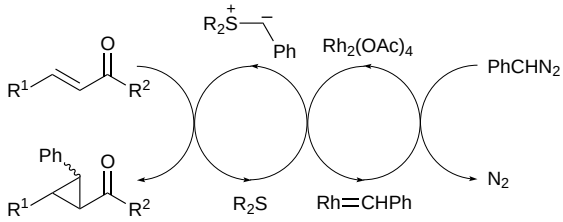
**Varinder K. Aggarwal,*[a] Helen W. Smith,[a] Ray V. H. Jones[b] and Robin Fieldhouse[b]**

[a] *Department of Chemistry, University of Sheffield, Brook Hill, Sheffield, UK S3 7HF*
[b] *Zeneca Process Technology Dept., Earls Road, Grangemouth, Stirlingshire, UK*

**Catalytic asymmetric cylopropanation of enones has been achieved using diazo compounds, catalytic quantities of a metal catalyst and a camphor-derived thioacetal; this sulfide shows exceptionally high levels of enantioselectivity.**

Cyclopropanes are common functional groups in biologically active molecules, the most notable examples being the pyrethroids which are a highly potent class of insecticides.[1] Much effort has therefore been expended in the synthesis of cyclopropanes in racemic and more recently, in asymmetric form.[2,3] High enantioselectivity has been achieved in the Simmons–Smith[4,5] cyclopropanation of allylic alcohols using chiral promoters.[6,7] High enantioselectivity has also been achieved in metal catalysed reactions of diazocarbonyl compounds with alkenes. The chirality may be linked to the metal in the form of a chiral ligand (*e.g.* bis-oxazolines[8]) or linked to both the metal and the diazo compound to enhance the enantioselectivity.[9,10] However, in all the above cases, the metal carbenoid only reacts efficiently with electron rich alkenes[11] and so methods are required for the cyclopropanation of electron deficient alkenes. Towards this end enantiomerically pure aminosulfoxonium ylides have been successfully employed in asymmetric cyclopropanation of electron deficient alkenes.[12,13] However, such reagents have to be employed in stoichiometric amounts, and cannot be recycled. Sulfur ylides are also known to react with electron deficient alkenes to furnish cyclopropanes, but there are no asymmetric examples and so we embarked on such a study. In addition, we sought to utilise our recently reported catalytic process for asymmetric epoxidation[14,15] and aziridination[16] so that catalytic quantities of sulfides could ultimately be employed (Scheme 1). Here we report our success in achieving these goals.

Reactions were carried out on enones with phenyldiazomethane (Table 1) and we initially used tetrahydrothiophene, in stoichiometric amounts, as a representive sulfide under the conditions previously employed for the epoxidation reaction.[15] However, only low yields of cyclopropanes were obtained (entries 1 and 2). We were surprised at the low yields obtained, as high yields were obtained in the related epoxidation and aziridination reactions. We suspected that the lower reactivity of enones compared to aldehydes† and imines could have been responsible for the lower yields observed, as the ylide will have a longer lifetime in reactions with enones. This in turn would mean that the ylide might have time to undergo competitive rearrangement reactions, such as the Stevens[17,18] or the Sommelet–Hauser rearrangement,[17,18] and indeed the Sommelet–Hauser product was observed.‡ Under standard reaction conditions an excess of the sulfonium salt[22] or the ylide is typically used to cyclopropanate alkenes, perhaps for this reason.

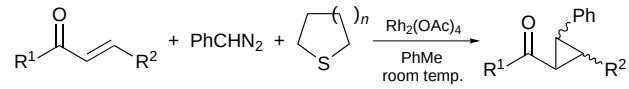



**Scheme 1** Catalytic process for cyclopropanation

To reduce the extent of this rearrangement the six membered analogue, pentamethylene sulfide, was employed and, gratifyingly, high yields of cyclopropanes were obtained (entries 3–6). Even using catalytic amounts of sulfide, cyclopropanes were formed in moderate to good yields (entries 7–10). The least reactive enone (entry 10) gave reduced yields as the rearrangement of the ylide was once again a significant competing side reaction.

We next explored asymmetric cyclopropanation (Table 2) and chose oxathiane **1** as this sulfide had previously given high enantioselectivity in epoxidation of carbonyl compounds[14] and aziridination of imines.[16] Furthermore, sulfide **1** is readily available, in either enantiomeric form, from camphorsulfonyl chloride in two steps.[14] We applied this sulfide to the 4-phenyl substituted enones (as this would give rise to a maximum of two diastereoisomers) and we were delighted to find that exceptionally high levels of enantioselectivity were obtained with both stoichiometric and catalytic amounts of sulfide.§ However, reduced yields were obtained when using catalytic compared to stoichiometric amounts of sulfide. This was also observed in the related epoxidation process[14,15] but the differences in yield are greater in cyclopropanation, presumably because of the lower reactivity of enones compared to aldehydes. The constant enantiomeric excess (no reduction observed) in reactions using catalytic quantities of sulfides indicates that no direct cyclopropanation occurs and that the sulfide reacts with the metal carbenoid (to give a sulfur ylide) at a significantly faster rate than the alkene (to give direct cyclopropanation). The major isomer of the cyclopropane is *tentatively* assigned as the *R,R*

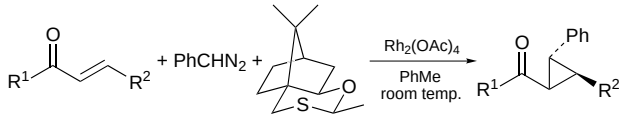
**Table 1** Cyclopropanation of enones using simple sulfides




| | Enone | | | Sulfide | | | |
|---|---|---|---|---|---|---|---|
| Entry | $R^1$ | $R^2$ | *t*/h[a] | *n* | Equiv. | Yield (%)[b] | Isomeric ratio[c] |
| 1 | Ph | Ph | 3 | 1 | 1.0 | 40 | 1 : 1 |
| 2 | Me | Ph | 3 | 1 | 1.0 | 41 | 1 : 1 |
| 3 | Ph | Ph | 3 | 2 | 1.0 | 92 | 4 : 1 |
| 4 | Me | Ph | 3 | 2 | 1.0 | 80 | 4 : 1 |
| 5 | Ph | Me | 12 | 2 | 1.0 | 65 | 1 : 1 : 1 |
| 6 | Me | Me | 12 | 2 | 1.0 | 55 | 1 : 1 : 1 |
| 7 | Ph | Ph | 12 | 2 | 0.2 | 70 | 4 : 1 |
| 8 | Me | Ph | 12 | 2 | 0.2 | 82 | 4 : 1 |
| 9 | Ph | Me | 12 | 2 | 0.2 | 50 | 1 : 1 : 1 |
| 10 | Me | Me | 12 | 2 | 0.2 | 30 | 1 : 1 : 1 |

[a] Addition of $PhCHN_2$ using syringe pump. [b] Yield of *cis* and *trans* isomers. [c] Ratios determined by NMR spectroscopy.

**Table 2** Cyclopropanation of enones using sulfide **1**




**1**

| Entry | Enone R1 | Enone R2 | t/h[a] | Sulfide (equiv.) | Yield (%)[b] | Isomeric ratio[c] | Ee (%)[d] | $[\alpha]_D^{25}$ [e] |
|---|---|---|---|---|---|---|---|---|
| 1 | Ph | Ph | 12 | 1.0 | 60 | 4 : 1 | 97[f] | −136 |
| 2 | Ph | Ph | 12 | 0.2 | 38 | 4 : 1 | 97[f] | −136 |
| 3 | Me | Ph | 12 | 1.0 | 55 | 4 : 1 | > 98[g] | − 65 |
| 4 | Me | Ph | 12 | 0.2 | 14 | 4 : 1 | > 98[g] | − 65 |

[a] Addition of $PhCHN_2$ using syringe pump. [b] Yield of *cis* and *trans* isomers. [c] Ratio determined by NMR spectroscopy. [d] Determined using HPLC (see footnote §). [e] Conditions: $c$ = 1, $CH_2Cl_2$. [f] Retention times: (*R*,*R*) enantiomer, 4.41 min; (*S*,*S*) enantiomer, 4.70 min. [g] Retention times: (*R*,*R*) enantiomer, 6.10 min; (*S*,*S*) enantiomer, 6.68 min.

isomer by analogy with the epoxidation[14] and the aziridination[16] processes. In these latter cases similarly high enantioselectivity was obtained (93–97% ee) for epoxides[14] and aziridines[16] and proof of their absolute stereochemistry (*R*,*R*) was obtained.

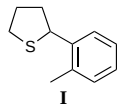
In conclusion we have developed a process for the catalytic asymmetric cylopropanation of enones, using a camphor-derived sulfur ylide which shows exceptionally high levels of enantioselectivity. We are currently extending the scope of this reaction.

## Footnotes and References

* E-mail: v.aggarwal@sheffield.ac.uk

† Competetive experiments between PhCHO, chalcone and substoichiometric amounts of ylide yielded epoxide only, indicating that aldehydes were much more reactive than enones towards benzylfulfonium ylide.

‡ Sulfide **I** was formed in 20% yield as a result of ylide equilibration and Sommelet–Hauser rearrangement from the reaction. Ylide equilibration and rearrangement has been reported (refs. 19–21).




**I**

§ A typical procedure for asymmetric cyclopropanation reaction: Chalcone (0.5 mmol), oxathiane **1** (0.5 mmol) and $Rh_2(OAc)_4$ (1 mol%) were dissolved in toluene (0.5 ml) under $N_2$. A solution of phenyldiazomethane in toluene (1.5 mmol) was added over 12 h *via* an inverted syringe pump. The crude mixture was purified by column chromatography to furnish the cyclopropane as a white solid (60%). The enantiomeric excess was determined by chiral HPLC on Hichrom column, stationary phase D-phenylglycine, using $Pr^iOH$–light petroleum (0.7 : 99.3) as eluent with a flow rate of 2 ml $min^{-1}$. The *R*,*R* enantiomer eluted at 265 s and the *S*,*S* enantiomer at 282 s.


1 H. N. C. Wong, M. Y. Hon, C. W. Tse, Y. C. Yip, J. Tanko and T. Hudlicky, *Chem. Rev.*, 1989, **89**, 165; T. Hudlicky and J. W. Reed, *Comprehensive Organic Synthesis*, ed. B. M. Trost and I. Fleming, Pergamon, Oxford, 1991, vol. 5, p. 899.
2 J. Salaun, *Chem. Rev*., 1989, **89**, 1247.
3 V. K. Singh, A. DattaGupta and G. Sekar, *Synthesis*, 1997, 137.
4 H. E. Simmons and R. D. Smith, *J. Am. Chem. Soc.*, 1958, **80**, 5323.
5 H. E. Simmons, T. L. Cairns, S. A. Vladuchick and C. M. Hoiness, *Org. React.*, 1973, **20**, 1.
6 A. B. Charette and H. Juteau, *J. Am. Chem. Soc.*, 1994, **116**, 2651.
7 A. B. Charette, S. Prescott and C. Brochu, *J. Org. Chem.*, 1995, **60**, 1081.
8 D. A. Evans, K. A. Woerpel, M. M. Hinman and M. M. Faul, *J. Am. Chem. Soc.*, 1991, **113**, 726.
9 H. M. L. Davies, N. J. S. Huby, W. R. Cantrell, Jr and J. L. Olive, *J. Am. Chem. Soc.*, 1993, **115**, 9468.
10 R. E. Lowenthal and S. Masumune, *Tetrahedron Lett.*, 1991, **32**, 7373.
11 For an example of metal carbenoid addition to an electron deficient alkene, see T. Hudlicky and R. P. Short, *J. Org. Chem.*, 1982, **47**, 1522. However, in this example the reaction is intramolecular, which no doubt facilitates the process. It was also noted in this example that marginally higher yields were obtained in the presence of sulfides, suggesting the intermediacy of a sulfur ylide. We thank one of the referees for bringing this paper to our attention.
12 C. R. Johnson and C. W. Schroek, *J. Am. Chem. Soc.*, 1973, **95**, 7418.
13 S. G. Pyne, Z. Dong, B. W. Skelton and A. H. White, *J. Org. Chem.*, 1997, **62**, 2337.
14 V. K. Aggarwal, J. G. Ford, A. Thompson, R. V. H. Jones and M. Standen, *J. Am. Chem. Soc*., 1996, **118**, 7004.
15 V. K. Aggarwal, H. Abdel-Rahman, F. Li, R. V. H. Jones and M. C. H. Standen, *Chem. Eur. J*., 1996, **2**, 1024.
16 V. K. Aggarwal, A. Thompson, R. V. H. Jones and M. C. H. Standen, *J. Org. Chem.*, 1996, **61**, 8368.
17 E. Block, *The Chemistry of the Sulphonium Group*, ed. C. J. M. Stirling and S. Patai, Wiley, New York, 1981, p. 673.
18 I. E. Markó, *Comprehensive Organic Synthesis*, ed. B. M. Trost and I. Fleming, Pergamon, Oxford, 1991, vol. 3, p. 913.
19 W. Ando, M. Yamada, E. Matsuzaki and T. Migita, *J. Org. Chem.*, 1972, **37**, 3791.
20 N. A. Nesmayanov and V. A. Kalyavin, *Org. Soedin. Sery*, 1980, **2**, 330 *Chem. Abstr.*, 1981, **94**, 192 063.
21 M. Yoshimine and M. J. Hatch, *J. Am. Chem. Soc.*, 1967, **89**, 5831.
22 M. Hetschko and J. Gossleck, *Chem. Ber.*, 1973, **106**, 996.


*Received in Liverpool, UK, 16th June 1997; 7/04214K*

# The efficient and regioselective synthesis of the naphthoquinone core of streptovaricin U

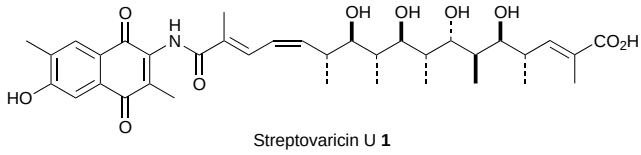
**Masaaki Miyashita,*[a] Takahiro Yamasaki,[b] Tomonori Shiratani,[b] Susumi Hatakeyama,[b] Masahiro Miyazawa[a] and Hiroshi Irie[b]**

[a] *Division of Chemistry, Graduate School of Science, Hokkaido University, Hokkaido 060, Japan*
[b] *Faculty of Pharmaceutical Sciences, Nagasaki University, Nagasaki 852, Japan*

**The efficient and regioselective synthesis of the naphthoquinone core of streptovaricin U 1 *via* the Diels–Alder reaction of 1-methoxy-2-methyl-3-trimethylsilyloxybuta-1,3-diene 5 with the 2,6-dibromo-3-methyl-1,4-benzoquinone 6 is described.**

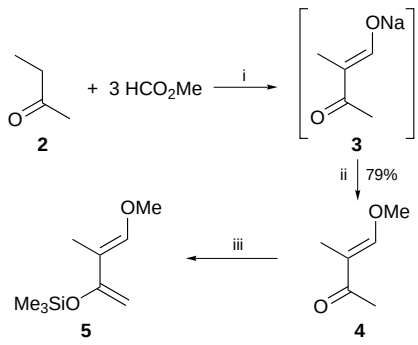
The streptovaricin family are representative ansamycin antibiotics as well as rifamycins and have been used clinically as an important class of antibiotics.[1] So far more than fifteen congeners have been isolated from *Streptomyces spectabilis* and all consist of a unique naphthoquinone core and a polypropionate ansa chain composed of nine contiguous chiral centres.[1] The unique structures and important biological activity of the streptovaricins have elicited considerable attention from synthetic chemists.[2]

Recently we reported the highly stereoselective synthesis of the ansa chain segment of streptovaricin U **1** and protostreptovaricins including nine contiguous chiral centres[3] by the use of the stereospecific methylation of γ,δ-epoxy acrylates with trimethylaluminium.[4] Streptovaricin U **1** is a unique open-chain ansamycin from the streptovaricin family and shows inhibitory activity against RAUSCHER leukemia virus RNA-dependent DNA polymerase.[5] We now report the highly efficient synthesis of the naphthoquinone core of streptovaricin U **1** *via* the Diels–Alder reaction of the silyloxy diene **5** with the dibromoquinone **6**.



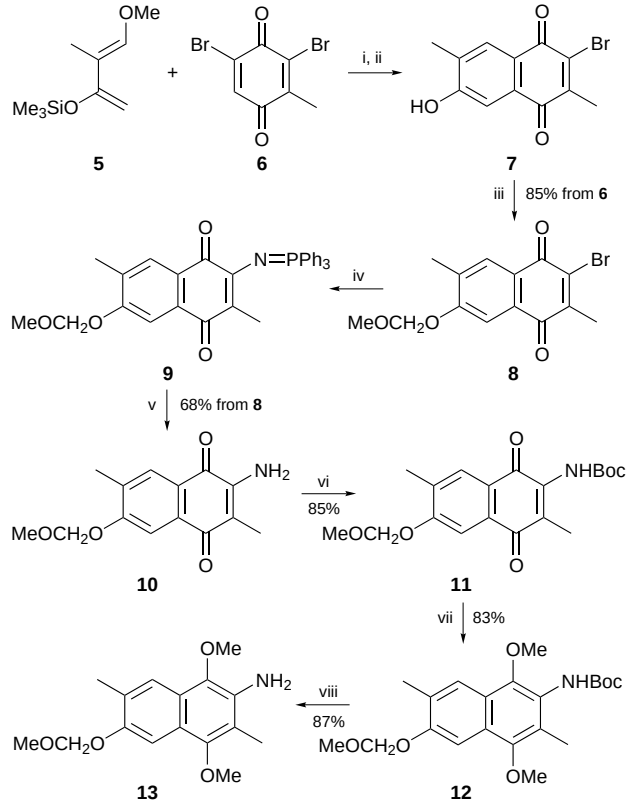
Streptovaricin U **1**

Although 1-methoxy-2-methyl-3-trimethylsilyloxybuta-1,3-diene **5** is a known compound and has often been used in Diels–Alder reactions,[6] we prepared it by the modified procedure shown in Scheme 1 for improved yield and synthetic convenience. Thus butan-2-one **2** was treated with NaH and $HCO_2Me$ in THF at 0 °C to give the sodium enolate **3**, which was treated, after the solvent was replaced from THF to DMF, with dimethyl sulfate to give *trans*-4-methoxy-3-methylbut-3-en-2-one **4**[7] in 79% yield.† The butenone **4** was quantitatively transformed into the silyloxy diene **5** by treatment with LDA in THF followed by addition of $Me_3SiCl$. The crude diene **5** thus obtained was used directly for the Diels–Alder reaction. On the other hand, 2,6-dibromo-3-methyl-1,4-benzoquinone **6**, the dienophile for the Diels–Alder reaction, was synthesized according to the protocol of Trost and Pearson[8] in two steps; (i) bromination of *m*-cresol with $Br_2$ in AcOH; (ii) oxidation of the resulting tribromide with chromium(III) oxide in AcOH (90% yield for the two steps).




**Scheme 1** *Reagents and conditions*: i, NaH (1.5 equiv.), THF, 0 °C, 1 h; ii, $(MeO)_2SO_2$ (2 equiv.), DMF, 0 °C, 1 h, then 1 M aq. $K_2CO_3$, MeOH; iii, LDA, THF, −78 °C, then $Me_3SiCl$, −78 °C to room temp.

The key Diels–Alder reaction was performed by heating a mixture of the diene **5** (4.1 mmol) and the dibromoquinone **6** (3.2 mmol) in benzene (20 ml) at 90 °C for 2 h in a sealed tube (Scheme 2). After cooling, the solvent was evaporated under




**Scheme 2** *Reagents and conditions*: i, $C_6H_6$, sealed tube, 90 °C, 2 h; ii, 2% HCl, DME, 12 h; iii, $MeOCH_2Cl$, $Pr^i_2NEt$, $CH_2Cl_2$, 3.5 h; iv, $NaN_3$, $PPh_3$, DMSO, 3 h; v, aq. HCHO, THF, 2 d; vi, $H_2$, $PtO_2$, $Boc_2O$ (5 equiv.), EtOH, 3 h, then $O_2$, 12 h; vii, $H_2$, $PtO_2$, EtOH, 1 h, then $(MeO)_2SO_2$ (10 equiv.), 1 M NaOH, 2 h; viii, $Ph_2O$, 185 °C, sealed tube, 12 h

reduced pressure and the residue was treated with 2% HCl in DME, giving rise to the adduct **7**. The crude product **7** was subsequently treated with $ClCH_2OMe$ and $Pr^i_2NEt$ in $CH_2Cl_2$ to afford the protected bromoquinone **8** as light yellow crystals (mp 169–172 °C) in 85% overall yield. Subsequent conversion of **8** to the aminonaphthoquinone **10** was accomplished by the reaction of **8** with $NaN_3$ and $PPh_3$ in DMSO followed by treatment of the resulting iminophosphorane **9** with aqueous formaldehyde in THF. Thus the desired aminonaphthoquinone **10** was obtained as red crystals (mp 177–179 °C) in 68% yield. Although compound **10** is itself the naphthoquinone core of streptovaricin U **1**, it is necessary to further transform it into the naphthalene derivative **13** for the coupling reaction with the ansa chain segment, since the amino group on a naphthoquinone ring such as **10** is not sufficiently basic for further transformation. The conversion of **10** into the target molecule **13** was, however, unexpectedly troublesome and required ingenuity. Eventually the desired transformation was overcome by the following reaction sequence. Hydrogenation of **10** over Adams' catalyst in EtOH in the presence of di-*tert*-butyl dicarbonate ($Boc_2O$) followed by treatment with oxygen gave rise to the *N*-Boc-aminonaphthoquinone **11** as light yellow crystals (mp 141–143 °C) in 85% yield. The product **11** was subsequently converted to the naphthalene dimethyl ether **12** (mp 104–106 °C) by hydrogenation over Adams' catalyst in EtOH followed by treatment of the resulting dihydroquinone with dimethyl sulfate and 1 M NaOH in 83% yield. The synthesis of the fully functionalized aromatic core **13** of streptovaricin U **1** was accomplished by removal of the Boc group in **12** by thermolysis in $Ph_2O$ at 185 °C (sealed tube), resulting in formation of **13** in 87% yield.

Thus an efficient and regioselective synthesis of the naphthoquinone core of streptovaricin U **1** has been established. The overall yield of **13** from the dibromoquinone **6** was 35%. The manipulations employed in the conversion of **10** into **13** may be widely applicable to the synthesis of various aminonaphthoquinones. The coupling reaction of the aromatic core **13** with the ansa chain segment toward the total synthesis of **1** is now in progress.

This work was also supported by a Grant-in-Aid for Scientific Research on Priority Areas (No. 08245101) and a Grant-in-Aid for Scientific Research (No. 09874149) from the Ministry of Education, Science, Sports, and Culture of Japan.

## Footnotes and References

* E-mail: miyasita@schem.ec.hokudai.ac.jp

† All new compounds exhibited satisfactory spectra ($^1H$ and $^{13}C$ NMR, IR) and elemental analyses.

1 K. L. Reinhart, Jr. and L. S. Shield, *Fortschr. Chem. Org. Naturst.*, 1976, **33**, 231; P. V. Desshmukh, K. Kakinuma, J. J. Ameel, K. L. Reinhart, Jr., P. F. Wiley and L. H. Li, *J. Am. Chem. Soc.*, 1976, **98**, 870; K. L. Reinhart, Jr., F. J. Antosz, P. V. Desshmukh, K. Kakinuma, P. K. Martin, B. I. Milavetz, K. Sasaki, T. R. Willy, L. H. Li and F. Reusser, *Antibiotics*, 1976, **29**, 201.

2 P. A. McCarthy, *Tetrahedron Lett.*, 1982, **23**, 4199; B. M. Trost and W. H. Pearson, *Tetrahedron Lett.*, 1983, **24**, 269; B. Fraser-Reid, L. Magdzinski, B. F. Molino and D. R. Mootoo, *J. Org. Chem.*, 1987, **52**, 4495; B. Fraser-Reid, B. F. Molino, L. Magdzinski and D. R. Mootoo, *ibid.*, 1987, **52**, 4505; D. R. Mootoo and B. Fraser-Reid, *ibid.*, 1987, **52**, 4511; P. A. McCarthy and M. Kageyama, *ibid.*, 1987, **52**, 4681; W. R. Roush and A. D. Palkowitz, *ibid.*, 1989, **54**, 3009; D. R. Mootoo and B. Fraser-Reid, *ibid.*, 1989, **54**, 5548; Z. Wang and S. L. Schreiber, *Tetrahedron Lett.*, 1990, **31**, 31; D. R. Mootoo and B. Fraser-Reid, *J. Chem. Soc., Perkin Trans. 1*, 1990, 739; *Tetrahedron*, 1990, **46**, 185; W. R. Roush and D. J. Madar, *Tetrahedron Lett.*, 1993, **34**, 1553.

3 M. Miyashita, T. Shiratani, K. Kawamine, S. Hatakeyama and H. Irie, *Chem. Commun.*, 1996, 1027.

4 M. Miyashita, M. Hoshino and A. Yoshikoshi, *J. Org. Chem.*, 1991, **56**, 6483.

5 W. M. J. Knoll, K. L. Rinehart, Jr., P. F. Wiley and L. H. Li, *J. Antibiot.*, 1980, **33**, 249.

6 S. Danishefsky, C.-F. Yan, R. K. Singh, R. B. Gammill, P. M. McCurry, Jr., N. Fritsch and J. Clardy, *J. Am. Chem. Soc.*, 1979, **101**, 7001; A. P. Kozikowski and K. Sugiyama, *Tetrahedron Lett.*, 1980, **21**, 3257.

7 S. Sugasawa, S. I. Yamada and M. Harahashi, *J. Pharm. Soc. Jpn.*, 1951, **71**, 1345.

8 B. M. Trost and W. H. Pearson, *Tetrahedron Lett.*, 1983, **24**, 269.

*Received in Cambridge, UK, 1st July 1997; 7/04596D*

# Highly diastereoselective radical addition to glyoxylic oxime ether: asymmetric synthesis of α-amino acids

**Hideto Miyabe, Chikage Ushiro and Takeaki Naito***

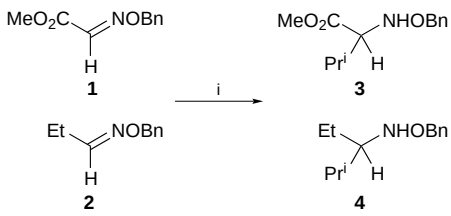
*Kobe Pharmaceutical University, Motoyamakita, Higashinada, Kobe 658, Japan*

**A high degree of stereocontrol in radical addition to the Oppolzer's camphor sultam derivative of glyoxylic oxime ether was achieved, providing a convenient method for preparing a variety of enantiomerically pure α-amino acids.**

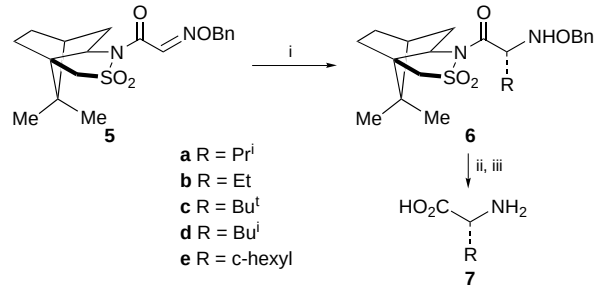
Asymmetric induction in free radical-mediated reactions of acyclic systems is a subject of current interest.[1] Oxime ethers are well known to be excellent radical acceptors because of the extra stabilisation of the intermediate aminyl radical provided by the lone pair on the adjacent oxygen atom.[2] We now describe the first example of an efficient and diastereoselective carbon radical addition to acyclic oxime ethers which was successfully applied to the novel asymmetric synthesis of α-amino acids.

Studies on the radical reaction of oxime ethers have concentrated on radical cyclisation,[3] except for a few outstanding examples of intermolecular radical reaction.[4] Therefore, stereocontrol in intermolecular radical addition to oxime ethers is a challenging problem. Prior to exploring diastereoselective radical addition to acyclic oxime ethers, we first investigated competitive reactions using two types of oxime ether in order to survey the intermolecular reactivity of oxime ethers with carbon radicals. Treatment of a 1 : 1 mixture of glyoxylic oxime ether **1** and aldoxime ether **2** with isopropyl radical, generated from $Pr^iI$, $Bu_3SnH$ and $Et_3B$ as a radical initiator, at −78 °C for 30 min gave the isopropylated product **3** in 78% yield with no detection of the other adduct **4** (Scheme 1). As expected, the addition of an isopropyl radical to **2** under the same reaction conditions did not take place and 90% of the starting compound **2** was recovered. These results suggest that the carbon radical does not add to the aldoxime ether **2**, but does add to glyoxylic oxime ether **1** even at −78 °C.

We then extended the carbon radical addition to the Oppolzer's camphor sultam derivative of glyoxylic oxime ether **5**[5] which would allow access to a wide range of enantiomerically pure natural and unnatural α-amino acids (Scheme 2). The reaction of **5** with $Pr^iI$, $Bu_3SnH$ and $Et_3B$ in $CH_2Cl_2$ at 20 °C proceeded smoothly to give a 86 : 14 diastereomeric mixture of the desired isopropylated product **6a** accompanying by a small amount of the ethylated product **6b**, which would be formed by a competitive reaction with ethyl radical generated from $Et_3B$ and $O_2$ (Table 1, entry 1). In the absence of $Pr^iI$, treatment of **5** with $Bu_3SnH$ and $Et_3B$ afforded exclusively the corresponding ethylated product **6b** as the result of a similar stereoselective radical reaction. In order to optimise the reaction conditions, we then investigated the reaction by varying the




**Scheme 1** *Reagents and conditions*: i, $Pr^iI$ (1.1 equiv.), $Bu_3SnH$ (1.1 equiv.), $Et_3B$ (1.1 equiv.), $CH_2Cl_2$, −78 °C, 30 min




**Scheme 2** *Reagents and conditions*: i, RI, $Bu_3SnH$, $Et_3B$, 30 min; ii, $Mo(CO)_6$; iii, LiOH

reaction temperature, solvent and Lewis acid. The stereoselectivity for **6a** was shown to be dependent on the reaction temperature, thus changing the temperature from 20 to −78 °C led to an effective increase in the diastereoselectivity to 94 : 6 (entry 2). The replacement of $CH_2Cl_2$ with $Et_2O$ as solvent led to higher selectivity, comparable to or better than that obtained by the known addition of organometallic reagents to the oxime ethers (entry 4).[5,6] Although the addition of Lewis acids as an additive did not dramatically influence the degree of stereoselectivity, the presence of $BF_3{\cdot}OEt_2$ in $CH_2Cl_2$ was found to be useful for asymmetric induction (entry 5). The absolute configuration at the newly formed stereocentre of the major product was determined to be *R* by converting the adduct **6a** into authentic D-valine **7a**. The reductive cleavage of the nitrogen–oxygen bond of **6a** by treatment with $Mo(CO)_6$[7] and subsequent removal of the sultam auxiliary by standard hydrolysis[8] afforded the enantiomerically pure D-valine **7a** without any loss

**Table 1** Radical addition to the oxime ether **5**[a]

| Entry | RI[b] | Lewis acid[c] | Solvent | Yield[d] (%) | Selectivity[e] |
|---|---|---|---|---|---|
| 1 | $Pr^iI$ | none | $CH_2Cl_2$ | 76[f] | 86 : 14 |
| 2 | $Pr^iI$ | none | $CH_2Cl_2$ | 73[f] | 94 : 6 |
| 3 | $Pr^iI$ | none | toluene | 74[f] | 93 : 7 |
| 4 | $Pr^iI$ | none | $Et_2O$ | 71[f] | 96 : 4 |
| 5 | $Pr^iI$ | $BF_3{\cdot}OEt_2$ | $CH_2Cl_2$ | 80[f] | 96 : 4 |
| 6 | $Pr^iI$ | $Et_2AlCl$ | $CH_2Cl_2$ | 57[f] | 90 : 10 |
| 7 | $Pr^iI$ | $Zn(OTf)_2$ | $CH_2Cl_2$ | 81[f] | 94 : 6 |
| 8 | $Pr^iI$ | $Yb(OTf)_3$ | $CH_2Cl_2$ | 74[f] | 92 : 8 |
| 9 | EtI | none | $Et_2O$ | 54 | 96 : 4 |
| 10 | EtI | $BF_3{\cdot}OEt_2$ | $CH_2Cl_2$ | 80 | 95 : 5 |
| 11 | $Bu^tI$ | none | $Et_2O$ | 25[f] | > 98 : 2 |
| 12 | $Bu^tI$ | $BF_3{\cdot}OEt_2$ | $CH_2Cl_2$ | 83[f] | > 98 : 2 |
| 13 | $Bu^iI$ | none | $Et_2O$ | 39[f] | 97 : 3 |
| 14 | $Bu^iI$ | $BF_3OEt_2$ | $CH_2Cl_2$ | 83[f] | 97 : 3 |
| 15 | c-HexylI | none | $Et_2O$ | 74[f] | 96 : 4 |
| 16 | c-HexylI | $BF_3{\cdot}OEt_2$ | $CH_2Cl_2$ | 86[f] | 96 : 4 |

[a] Reaction was carried out with $Bu_3SnH$ (2.5 equiv.) and $Et_3B$ in hexane (5 equiv.) under $N_2$ at 20 °C (entry 1). Other reactions were carried out at −78 °C (entries 2–16). [b] 5 equiv. of RI was used. [c] 2 equiv. of Lewis acid was used. [d] Isolated yields of major diastereomer **6a**–**f**. [e] Diastereoselectivities were determined by $^1H$ NMR analysis. [f] The ethylated product **6b** was obtained in 3–22% yield.

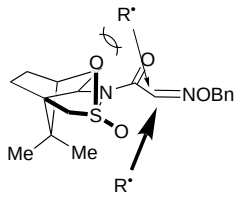



**Figure 1**

of stereochemical purity. High chemical yield and diastereoselectivity were also observed in radical additions using different radical precursors such as ethyl, *tert*-butyl, isobutyl and cyclohexyl iodides (entries 9–16).

The stereochemical features of this reaction can be rationalised in terms of steric control in the conformationally restricted sultam derivative **5**. The s-*cis* conformation of **5** would be preferred due to repulsion between the oxime ether and sulfonyl groups, thus alkyl radical addition takes place predominantly from the less hindered π-face of the oxime derivative **5**, as indicated (Fig. 1).

The traditional addition of anionic carbon nucleophiles to oxime ethers has been widely investigated as a carbon–carbon bond forming reaction with excellent stereoselectivity, although the addition is frequently plagued by the abstraction of α-protons adjacent to the carbon–nitrogen double bond, the lability of the nitrogen–oxygen bond, and the poor electrophilicity of the oxime ether group.[9] We suggest that many of these fundamental problems would be solved by the newly found mild addition of strictly neutral species such as uncharged free radicals.

Acknowledgement is made to the Ministry of Education, Science, Sports and Culture of Japan and the Science Research Promotion Fund of the Japan Private School Promotion Foundation for research grants.

## Footnote and References

* E-mail: taknaito@kobepharma-u.ac.jp

1 D. P. Curran, N. A. Porter and B. Giese, *Stereochemistry of Radical Reactions*, VCH, Weinheim, 1996. For recent reviews: W. Smadja, *Synlett*, 1994, 1; N. A. Porter, B. Giese and D. P. Curran, *Acc. Chem. Res.*, 1991, **24**, 296.

2 S. E. Booth, P. R. Jenkins, C. J. Swain and J. B. Sweeney, *J. Chem. Soc., Perkin Trans. 1*, 1994, 3499.

3 For some recent examples: D. L. J. Clive and J. Zhang, *Chem. Commun.*, 1997, 549; J. Marco-Contelles, G. Balme, D. Bouyssi, C. Destabel, C. D. Henriet-Bernard, J. Grimaldi and J. M. Hatem, *J. Org. Chem.*, 1997, **62**, 1202; G. E. Keck and T. T. Wager, *J. Org. Chem.*, 1996, **61**, 8366; G. J. Hollingworth, G. Pattenden and D. J. Schulz, *Aust. J. Chem.*, 1995, **48**, 381; J. L. Chiara, J. Marco-Contelles, N. Khiar, P. Gallego, C. Destabel and M. Bernabé, *J. Org. Chem.*, 1995, **60**, 6010; M. Santagostino and J. D. Kilburn, *Tetrahedron Lett.*, 1995, **36**, 1365; J. W. Grissom and D. Klingberg, *J. Org. Chem.*, 1994, **59**, 7876; K. A. Parker and D. Fokas, *J. Org. Chem.*, 1994, **59**, 3927; T. Naito, K. Tajiri, T. Harimoto, I. Ninomiya and T. Kiguchi, *Tetrahedron Lett.*, 1994, **35**, 2205; E. W. Della and A. M. Knill, *Aust. J. Chem.*, 1994, **47**, 1833.

4 B. Bhat, E. E. Swayze, P. Wheeler, S. Dimock, M. Perbost and Y. S. Sanghvi, *J. Org. Chem.*, 1996, **61**, 8186; S. Kim, I. Y. Lee, J.-Y. Yoon and D. H. Oh, *J. Am. Chem. Soc.*, 1996, **118**, 5138; D. J. Hart and F. L. Seely, *J. Am. Chem. Soc.*, 1988, **110**, 1631.

5 S. Hanessian and R.-Y. Yang, *Tetrahedron Lett.*, 1996, **37**, 5273.

6 Y. Yamamoto and W. Ito, *Tetrahedron*, 1988, **44**, 5415; J.-C. Fiaud and H. B. Kagan, *Tetrahedron Lett.*, 1970, 1813.

7 S. Cicchi, A. Goti, A. Brandi, A. Guarna and F. De Sarlo, *Tetrahedron Lett.*, 1990, **31**, 3351; M. Nitta and T. Kobayashi, *J. Chem. Soc., Perkin Trans. 1*, 1985, 1401.

8 W. Oppolzer, O. Tamura and J. Deerberg, *Helv. Chim. Acta*, 1992, **75**, 1965.

9 N. Risch and M. Arend, *Stereoselective Synthesis*, ed. G. Helmchen, R. W. Hoffmann, J. Mulzer and E. Schaumann, Thieme, Stuttugart, New York 1966, vol. 3, p. 1876; R. A. Volkmann, *Comprehensive Organic Synthesis*, ed. B. M. Trost, Pergamon Press, Oxford 1991, vol. 1, p. 355.

*Received in Cambridge, UK, 30th June 1997; 7/04562J*

# Mechanism of photobleaching of Ethyl Violet non-covalently bound to bovine serum albumin

**Mauricio Baptista and Guilherme Indig***

*School of Pharmacy, University of Wisconsin, Madison, WI53706, USA*

**Upon laser excitation of Ethyl Violet non-covalently bound to bovine serum albumin, leuco-Ethyl Violet and 4,4'-bis(diethylamino)benzophenone are formed as reaction photoproducts**

Photodynamic Therapy (PDT)[1] has recently been approved by regulatory agencies of several countries as a new modality of cancer treatment. The current enthusiasm for this general technique has fomented the search for new photosensitizers tailored for specific therapeutical applications.[1b,c] The development of new drugs for PDT requires the comprehension of the mechanisms of action of promising dyes, or families of dyes, under conditions that closely parallel those observed *in vivo*. This report describes a study on the mechanisms of photoreaction of a triarylmethane dye (Ethyl Violet, EV) non-covalently bound to a model biological host (bovine serum albumin, BSA). Triarylmethanes (TAM) are known to efficiently bind to anionic polyelectrolytes in solution,[2] and are among the families of dyes presently under intense evaluation as potential photosensitizers for employment in PDT.

The fluorescence lifetime of triarylmethane dyes in low viscosity environments is typically in the picosecond range as a consequence of fast relaxation processes that occur *via* rotational motions of their aromatic rings.[3] Accordingly, TAM dyes show poor photoreactivity in aqueous solutions. In more viscous media, or in microenvironments that render steric hindrance to rotational relaxation processes, fluorescence and intersystem crossing become more competitive events, and photoreactivity tends to increase.[2c] The effect of BSA on EV fluorescence in 0.01 M phosphate buffer pH 7.3 at 20 °C is shown in Fig. 1. The increase in EV fluorescence as a function of BSA concentration indicates that the BSA binding sites are very effective in preventing 'free rotor' motions in the dye moiety. This reduces the efficiency of radiationless deactivation of EV, a process that involves a low-lying twisted intramolecular charge transfer state (TICT),[3c] and leads to an enhancement in its fluorescence quantum yield from $9.6 \times 10^{-5}$ (free) to $1.7 \times 10^{-2}$ (protein-bound), as measured using corrected fluorescence spectra and quinine sulfate[4] as fluorescence standard. The fluorescence decay of EV bound to BSA (a typical multiple-binding-site carrier[5]) follows double exponential functions. The global analysis of three independent determinations yielded fluorescence lifetimes of 392 ± 42 ps and 2.95 ± 0.19 ns ($\chi^2$ = 1.032). These are remarkably high values if compared with the lifetime of EV free in low viscosity media (5 to 10 ps[3b,d]), and suggest the existence of two dominant ground state conformers of EV in the BSA environment (bound to different types of binding sites[5b,c]). Upon photoexcitation, the population of EV molecules displaying conformation closer to that of the TICT state is the one which relaxes faster.[3b] The Scatchard analysis[5b] of our fluorescence data confirmed the existence of two distinct types of BSA binding sites capable of accommodating EV molecules. The amino acid composition of these macromolecular domains may also affect the fluorescence lifetime of bound EV molecules (see below).

The observed increase in EV fluorescence lifetime and quantum yield suggests that the efficiency of intersystem crossing ($\phi_{ISC}$) might also undergo expressive increase as a consequence of binding. The bleaching of BSA-bound EV upon laser excitation at 532 nm is shown in Fig. 2. Under photolysis conditions essentially all dye molecules are bound to BSA (plateau region of the binding isotherm; large [protein] : [dye] ratio), therefore experiencing loss of rotational degrees of

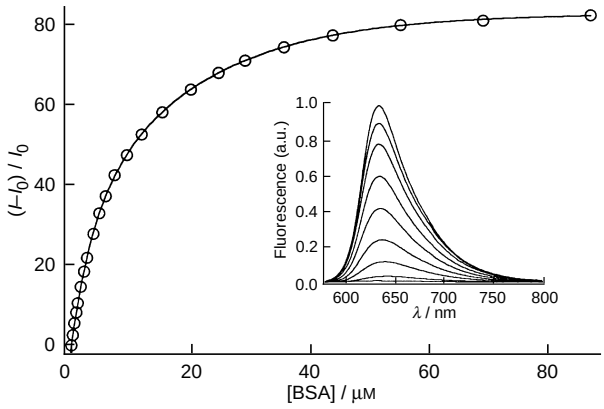



**Fig. 1** Effect of BSA concentration on the integrated fluorescence of EV. Inset: representative spectra employed in the construction of the binding isotherm. For visual clarity only one third of the data set is shown. From the bottom, in order of increasing fluorescence intensity at 634 nm, the BSA concentrations were 0.0, 0.27, 1.06, 2.64, 5.76, 11.8, 24.7, 44.0 and 87.4 μM. Excitation at 520 nm; [EV] = 10 μM; phosphate buffer (0.01 M) pH 7.3; $T$ = 20 °C.

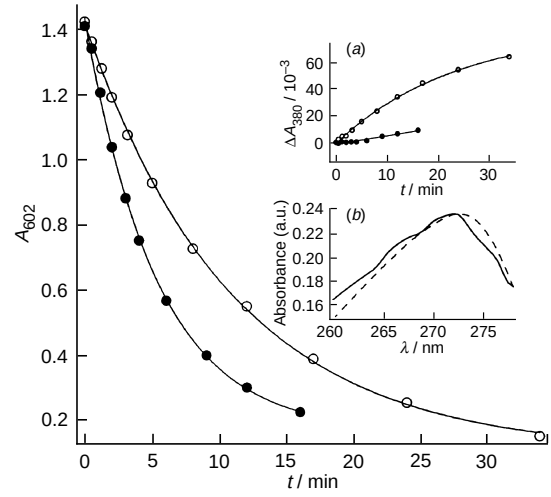
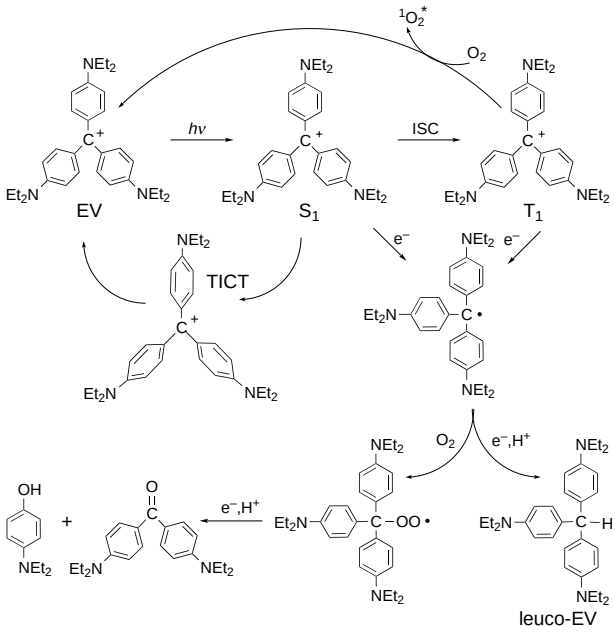



**Fig. 2** Effect of photolysis time on the maximum absorption of the BSA–EV complex (602 nm); (●) nitrogen-purged samples and (○) air-equilibrated samples. Excitation at 532 nm, 87 mJ pulse$^{-1}$, 10 Hz. Inset (*a*): respective changes in absorption at 380 nm, the region in which 4,4-bis(diethylamino)-benzophenone absorbs. Inset (*b*): differential spectrum (—) obtained after 16 min of photolysis of the nitrogen-purged sample, *i.e.* the spectrum recorded at $t$ = 16 min minus the spectrum recorded at $t$ = 0, and the absorption spectrum of leuco-EV in EtOH (---).




**Scheme 1**

freedom. The quantum efficiency of photobleaching was found to be two fold higher in nitrogen-purged than in air-equilibrated samples. The increased bleaching efficiency in nitrogen-purged as compared to air-equilibrated samples is direct evidence of the involvement of the first excited triplet state of the dye in the bleaching process. The comparison between the photobleaching efficiency of EV free in solution and protein-bound is more prominent. A 13-fold increase is observed as a consequence of binding (air-equilibrated samples). Using Methylene Blue[2c] as a laser flash photolysis standard we have estimated $\phi_{ISC}$ as 0.03 for BSA-bound EV. For the case of the dye free in solution we were unable to detect any transient signal (ns–μs range) following ns laser excitation at 560 nm.

The analysis of reaction products was performed by extraction of photolysed samples with EtOAc and characterization of the extracted compounds by thin-layer chromatography (silica gel; 2 : 1 hexanes–EtOAc). 4,4′-Bis(diethylamino)benzophenone and leuco-EV were identified as photoproducts. The former was more prominent in air-equilibrated samples, the latter in nitrogen-purged samples. The reaction mechanism shown in Scheme 1 accommodates the results observed. The reductive formation of leuco-EV from EV is a two electron process (formally $2e^- + H^+$ or $H + e^-$), initiated in this case by a photoinduced electron or hydrogen atom transfer from the protein to the dye moiety. 78 out of the 583 BSA amino acid residues are readily susceptible of photosensitized oxidation[2a] (2 Trp, 4 Met, 17 His, 20 Tyr and 35 Cys).[6] After initiation the semi-reduced dye radical can either react with dissolved molecular oxygen to produce 4,4′-bis(diethylamino)benzophenone or accommodate a second electron to form leuco- EV (Scheme 1). The intermediate dye radical can also transfer one electron back to the protein or to molecular oxygen to regenerate EV. Because the electronic excitation of the dye moiety occurs within a ground state protein-dye complex, the first excited singlet state of EV is born physically attached to the protein. Therefore, it is conceivable that not only the dye's triplet, but also the relatively short lived excited singlet populations, engage in the initial electron transfer process that leads to the formation of the semi-reduced dye radical (no diffusion needed for the reaction to occur). The competitive reaction pathways demonstrated by the characterization of reaction products in air-equilibrated and nitrogen-purged samples is also made evident through absorption spectroscopy measurements. Fig. 2 [inset (*a*)] shows that upon laser excitation of BSA-bound EV in nitrogen-purged solution the photoproduct that absorbs in the 380 nm region, 4,4′-bis(diethylamino)benzophenone, is not formed in significant amounts, but the differential absorption spectrum in the 250–280 nm region clearly indicates the formation of the dye's reduced (leuco) form as photoproduct [Fig. 2, inset (*b*)]. Under aerobic conditions a parallel route of formation of 4,4-bis(diethylamino)benzophenone is possible. The singlet oxygen generated by triplet–triplet energy transfer from triplet EV to ground state oxygen might, in principle, add to EV to generate an unstable dioxetane intermediate, whose thermal cleavage would produce 4,4′-bis(diethylamino)benzophenone. This last mechanistic path is, however, unlikely to be playing a significant role here.[7]

Another mechanistic possibility of interest, and presently under investigation, is the formation of heteroadducts through the covalent linkage of the semi-reduced dye radical with BSA. Independently of the bleaching path that is dominant under anaerobic conditions (sequential two-electron abstraction from the protein *or* one-electron abstraction followed by covalent-linking), upon laser excitation of protein-bound EV the photoinduced transformation of the host protein occurs *via* a free radical process that does not require molecular oxygen. This peculiar reaction course is well suited for the treatment of hypoxic or poorly perfused tumour areas. Our preliminary investigations have demonstrated that the photobleaching of Malachite Green and Crystal Violet proceed *via* equivalent paths, suggesting that this novel oxygen-independent mechanism may be rather common when considering the photochemistry of cationic photosensitizers non-covalently bound to biopolymers. Based on the relative values of photodecomposition quantum efficiency for a larger series of TAM dyes bound to BSA and other model proteins, and the extent to which the mechanistic details are conserved among the series, a better understanding of the structure–photoreactivity relationship for TAM dyes will be achieved, allowing the development of more effective photosensitizers.

Aided by grant number IRG-35-37-3 from the American Cancer Society.

## Footnote and References

* E-mail: glindig@falstaff.wisc.edu

1 (*a*) T. J. Dougherty, *Photochem. Photobiol.*, 1993, **58**, 895; (*b*) J. J. Schuitmaker, P. Bass, H. L. L. M. Vanleengoed, F. W. Vandermeulen, W. M. Star and N. Vanzandwijk, *J. Photochem. Photobiol. B: Biol.*, 1996, **34**, 3; (*c*) G. Jori, *J. Photochem. Photobiol. B: Biol.*, 1996, **36**, 87.

2 (*a*) J. S. Bellin and C. A. Yankus, *Arch. Biochem. Biophys.*, 1968, **123**, 18; (*b*) S. Yariv, D. K. Ghosh and L. G. Hepler, *J. Chem. Soc., Faraday Trans.*, 1991, **87**, 1201; (*c*) G. Jones II, C. Oh and K. Goswami, *J. Photochem. Photobiol. A: Chem.*, 1991, **57**, 65; (*d*) M. K. Paul and J. K. Ghosh, *Spectrochim. Acta*, 1994, **50**, 119.

3 (*a*) P. Wirth, S. Schneider and F. Dörr, *Ber. Bursenges Phys. Chem.*, 1977, **81**, 1127; (*b*) V. Sundström, T. Gillbro and H. Bergström, *Chem. Phys.*, 1982, **73**, 439; (*c*) M. Vogel and W. Rettig, *Ber. Bursenges Phys. Chem.*, 1985, **89**, 962; (*d*) M. M. Martin, P. Plaza and Y. H. Meyer, *Chem. Phys.*, 1991, **153**, 297.

4 S. R. Meech and D. Phillips, *J. Photochem.*, 1983, **23**, 193; C. G. Morgan, Y. Hua, A. C. Mitchell, J. C. Murray and A. D. Boardman, *Rev. Sci. Instrum.*, 1996, **67**, 41.

5 (*a*) M. L. Klotz and D. L. Huston, *Trends Pharmacol. Sci.*, 1988, **4**, 253; (*b*) R. Das, S. Mitra, D. Nath and S. Mukherjee, *J. Phys. Chem.*, 1996, **100**, 14 514; (*c*) K. A. Koeplinger and Z. Y. Zhao, *Anal. Biochem.*, 1996, **243**, 66.

6 N. Hirayama, S. Akashi, M. Furuya and K. Fukuhara, *Biochem. Biophys. Res. Commun.*, 1990, **173**, 639.

7 N. Kuramoto and T. Kitao, *Dyes Pigm.*, 1982, **3**, 49; S. Denman, S. Jameel, J. Hay and J. K. Sugden, *Dyes Pigm.*, 1996, **30**, 67.

*Received in Corvallis, OR, USA, 16th May 1997; 7/03400H*

# Chiroselective transcription of the sugar structure to Δ- or Λ-$[Co^{III}(bpy)_3]^{3+}$ using a boronic acid–sugar template interaction

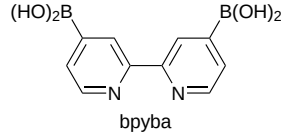
**Toshihisa Mizuno,[a] Masayuki Takeuchi,[a] Itaru Hamachi,[a] Kazuaki Nakashima[b] and Seiji Shinkai*[a]**

[a] *Department of Chemical Science and Technology, Faculty of Engineering, Kyushu University, Fukuoka 812, Japan*
[b] *Chemical and Textile Industry Research Institute, Fukuoka Industrial Technology Center, 332-1 Kamikoga, Chikushino, Fukuoka 818, Japan*

**In order to apply boronic acid–saccharide interactions to the chiroselective synthesis of Δ- and Λ-$[Co^{III}(bpy)_3]^{3+}$ a saccharide-binding ligand, 2,2′-bipyridine-4,4′-diboronic acid (bpyba) is newly synthesized; the enantiomeric excess under the optimum reaction conditions reached 79% ee!**

The recognition of biologically important molecular species by synthetic molecular receptors has gained momentum. Since the chemistry of saccharides plays a significant role in the metabolic pathways of living organisms, the detection of biologically important saccharides is necessary in a variety of medical and industrial contexts. Although hydrogen-bonding interactions play a central role in most reported synthetic receptors,[1] it has recently been shown that boronic acid–saccharide covalent interactions which readily and reversibly form in aqueous media represent an important alternative binding force in the recognition of saccharides and related molecular species.[2–7] Stable boronic acid-based saccharide receptors offer the possibility of designing saccharide sensors which are selective and sensitive for the specific saccharide.[6] Through these studies we have noticed that boronic acid–saccharide interactions create a variety of supramolecular structures which are founded on the absolute configuration of each saccharide.[8–10] This implies that saccharides are very useful as chiral building blocks to create oriented supramolecular assemblies or as chiral auxiliaries for asymmetric syntheses. This viewpoint has escaped attention for a long time, even though nature gifts us with a variety of saccharides with chiral structures. Tris[2,2′-bipyridine(bpy)]–metal complexes have inherent Δ *vs.* Λ chirality. It occurred to us that two pyridine rings may be asymmetrically oriented by a boronic acid–saccharide interaction[11] and the metal complexes thus formed may contain an excess amount of either Δ- or Λ-isomer over the other.[12]

With this object in mind we synthesized 2,2′-bipyridine-4,4′-diboronic acid (bpyba),[13] expecting that the saccharide-induced chiral orientation of this ligand eventually leads to the enantiomeric excess of either Δ- or Λ-isomer in the resultant metal complexes.



bpyba

To test the above working hypothesis we contrived the following reaction scheme. First, bpyba (6.37 mg, $1.69 \times 10^{-5}$ mol) and a saccharide ($3.38 \times 10^{-5}$ mol) were dissolved in a water (pH 7.4 with 50 mM MOPS buffer–methanol (1 : 1 v/v) solution (1.0 ml), and then the solution was mixed with a water–methanol (1 : 1 v/v) solution (1.0 ml) containing $Co(OAc)_2$ (1.00 mg, $5.65 \times 10^{-6}$ mol) at the appropriate temperature. The reaction mixture was stirred at this temperature for 2 days under a nitrogen atmosphere. As $[Co^{II}(bpy)_3]^{2+}$ is known to isomerize between Δ- and Λ-isomer (*i.e.* substitution active),[14] the $[Co^{II}(bpyba)_3]^{4-}$–saccharide complex should reach some Δ *vs.* Λ equilibrium under the influence of added saccharides. Then, the $[Co^{II}(bpyba)_3]^{4-}$–saccharide complex was oxidized to the $[Co^{III}(bpyba)_3]^{3-}$–saccharide complex by bubbling $O_2$ into this solution for 48 h. The completion of this oxidation process was confirmed by the following observations: (*i*) the absorption spectrum of the resultant complex is the same as the authentic $[Co^{III}(bpyba)_3]^{3-}$ complex prepared from $[Co^{III}Cl(NH_3)_5]^{2+}$ and bpyba, (*ii*) the absorption spectrum is unaffected by further oxidation with $H_2O_2$, (*iii*) the complex is EPR silent and (*iv*) the $^1H$ NMR spectrum does not show any indication that the complex is paramagnetic (*e.g.* line-broadening, unusual chemical shift, *etc.*). As $[Co^{III}(bpyba)_3]^{3-}$ is substitution-inactive,[14] the Δ *vs.* Λ ratio has been fixed at this step.

The CD spectrum of the $[Co^{III}(bpyba)_3]^{3-}$–saccharide complex obtained at 4 °C in the presence of D-glucose (sample A) is shown in Fig. 1(*a*). We also prepared a complex (sample B) in which D-glucose was added after $[Co^{II}(bpyba)_3]^{4-}$ is oxidized to $[Co^{III}(bpyba)_3]^{3-}$ [Fig. 1(*b*)]. Although both samples are CD active, one must consider that the CD band arising from Δ *vs.* Λ chirality overlaps with the saccharide-induced ICD band. In fact, a mixture of racemic $[Co^{III}(bpyba)_3]^{3-}$ and D-glucose resulted in a CD spectrum similar to Fig. 1(*b*). To estimate whether the CD spectra truly contain the CD band arising from Δ *vs.* Λ chirality we added an excess amount of optically inactive *cis*-cyclopentane-1,2-diol (*cis*-CPD): this compound shows the high affinity with boronic acids and can competitively substitute D-glucose bound to the boronic acid groups in $[Co^{III}(bpyba)_3]^{3-}$.[3–15] As shown in Fig. 1(*b*), the CD band of sample B decreased with increasing *cis*-CPD concentration and almost disappeared at [*cis*-CPD]/[D-glucose] = 25. In contrast, the CD band of sample A also decreased with increasing *cis*-CPD concentration but remained still CD active with $[\theta]_{460}$ =

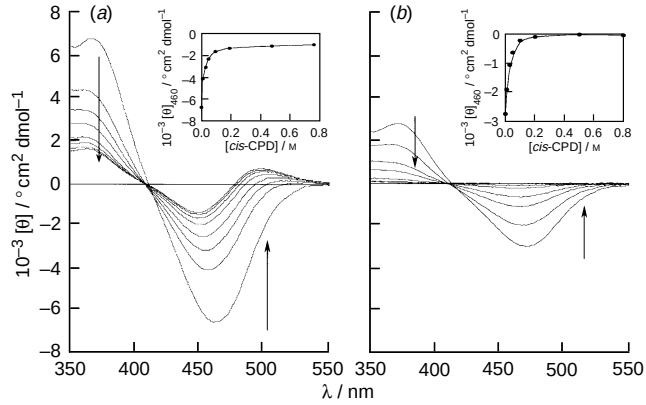



**Fig. 1** CD spectra of $[Co^{III}(bpyba)_3]^{3-}$ ($5.56 \times 10^{-4}$ M) and the influence of added *cis*-CPD at 25 °C: (*a*) sample A, [D-glucose] = 3.38 mM, [*cis*-CPD] = 0, 10, 30, 50, 100, 200, 500, 800 mM (from bottom to top at 460 nm); (*b*) sample B, [D-glucose] = 3.38 mM, [*cis*-CPD] = 0, 10, 30, 50, 100, 200, 500, 800 mM (from bottom to top at 460 nm)

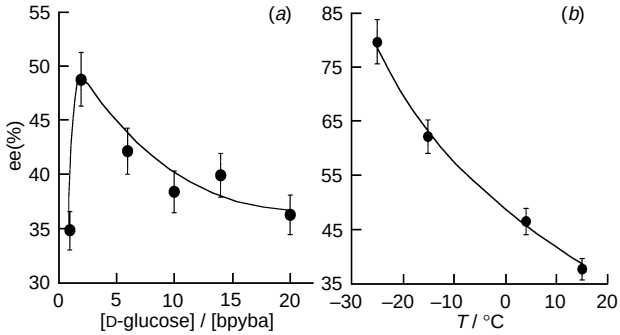



**Fig. 2** Influence of the D-glucose concentration (*a*) and the reaction temperature (*b*) on the ee of $[Co^{III}(bpy)_3]^{3+}$

1100° cm² dmol$^{-1}$ even in the presence of excess *cis*-CPD. The results clearly indicate that sample B consists of a 1 : 1 racemic mixture of Δ- and Λ-isomers whereas in sample A one isomer exists in excess over the other.

To estimate the enantiomeric excess (ee) of the $[Co^{III}(bpyba)_3]^{3-}$–saccharide complexes we applied a HPLC method with chiral-packed columns and a $^1$H NMR spectroscopic method with chiral shift reagents but failed. It is known that a boronic acid group in phenylboronic acid can be eliminated by treatment with $AgNO_3$.[16] We applied this method to the $[Co^{III}(bpyba)_3]^{3-}$–saccharide complexes and tried to determine the ee by comparison with authentic Δ- and Λ-$[Co^{III}(bpy)_3]^{3+}$.[17] Thus, $AgNO_3$ (500 mg, 2.9 mmol) was added to the sample A solution and the mixture was stirred at room temperature. The progress of the reaction was monitored by HPLC [Zorbax ODS, water–methanol (1 : 4 v/v)]. It showed that $[Co^{III}(bpyba)_3]^{3-}$ is quantitatively converted to $[Co^{III}(bpy)_3]^{3+}$ after one day.[18] After membrane filtration (Millipore LCR 13-LH), the filtrate was purified using gel filtration [Toyopearl HW-40, water–methanol (1 : 1 v/v)]. The yield of recovered $[Co^{III}(bpy)_3]^{3+}$ after gel filtration was 80%. The CD spectrum of $[Co^{III}(bpy)_3]^{3+}$ was thus obtained. By comparison with the CD spectrum of optically pure Δ-$[Co^{III}(bpy)_3]^{3+}$[17] the optical purity of this sample could be determined to be 47% ee (Δ excess). We repeated the sample preparation in the presence of various saccharides and obtained the following results: 47% ee (Λ excess) for L-glucose, 2% ee (Δ excess) for D-ribose, 10% ee (Δ excess) for D-mannose, 2% ee (Λ excess) for D-talose, 6% ee (Λ excess) for D-xylose, 12% ee (Δ excess) for D-maltose, and 3% ee (Δ excess) for D-cellobiose. Further examination was carried out with D-glucose which gave the highest ee among saccharides tested herein.

Fig. 2(*a*) shows the influence of the D-glucose concentration (in feed) on the ee of Δ-$[Co^{III}(bpy)_3]^{3+}$. The maximal ee (47%) appeared at [D-glucose] = $5.66 \times 10^{-3}$ M, which corresponds to [D-glucose]/[bpyba] = 2.0. This ratio indicates that the ee of Δ-$[Co^{III}(bpy)_3]^{3+}$ becomes maximal when one boronic acid group binds one D-glucose molecule. Fig. 2(*b*) shows the influence of the reaction temperature on the ee of Δ-$[Co^{III}(bpy)_3]^{3+}$. It is seen from Fig. 2(*b*) that the ee increases with lowering the reaction temperature and at −25 °C it even reaches 79%. Under the similar conditions in the presence of L-glucose we could obtain Λ-$[Co^{III}(bpy)_3]^{3+}$ in 79% ee.

The foregoing results clearly establish that the saccharide-templated synthesis is useful as a new concept for the preparation of chiral tris(2,2′-bipyridine)–metal complexes. Furthermore, the Δ *vs.* Λ equilibrium can be shifted in either direction by the selection of saccharide enantiomers. The chemistry of chiral tris(2,2′-bipyridine)–metal complexes has become a very active area of endeavour in relation to asymmetric synthesis, asymmetric memory transduction, non-linear optics, photoinduced electron or energy transfer, *etc.*[19–21] However, these fields have always been hampered by difficulty in the preparation of the chiral metal complexes. We believe that the present method provides an important breakthrough for these advanced fields of science.

We thank Dr Tony D. James (University of Birmingham) for helpful discussions.

## Footnote and References

* E-mail: seijtcm@mbox.nc.kyushu-u.ac.jp

1 For comprehensive reviews on hydrogen-bond-based synthetic receptors, see: J. Rebek, Jr., *Angew. Chem., Int. Ed. Engl.*, 1990, **29**, 245; A. D. Hamilton, *Bioorg. Chem. Front.*, 1991, **2**, 115; J.-H. Fuhrhop and J. Köning, *Membranes and Molecular Assemblies: The Synkinetic Approach*, ed. J. F. Stoddart, Royal Society of Chemistry, Cambridge, 1994; G. M. Whitesides, E. E. Simanek, J. P. Mathias, T. S. Christopher, N. C. Donovan, M. Mathai and M. G. Dana, *Acc. Chem. Res.*, 1995, **28**, 37.
2 J. Yoon and A. W. Czarnik, *J. Am. Chem. Soc.*, 1992, **114**, 5874; L. K. Mohler and A. W. Czarnik, *J. Am. Chem. Soc.*, 1993, **115**, 2998.
3 P. R. Westmark and B. D. Smith, *J. Am. Chem. Soc.*, 1994, **116**, 9343 and references therein.
4 Y. Nagai, K. Kobayashi, H. Toi and Y. Aoyama, *Bull. Chem. Soc. Jpn.*, 1993, **66**, 2965.
5 G. Wulff, S. Krieger, B. Kubneweg and A. Steigel, *J. Am. Chem. Soc.*, 1994, **116**, 409 and references therein.
6 K. Tsukagoshi and S. Shinkai, *J. Org. Chem.*, 1991, **56**, 4089; Y. Shiomi, M. Saisho, K. Tsukagoshi and S. Shinkai, *J. Chem. Soc., Perkin Trans. 1*, 1993, 2111; J. C. Norrild and H. Eggert, *J. Am. Chem. Soc.*, 1995, **117**, 1479.
7 For comprehensive reviews on boronic-acid-based saccharide receptors, see: T. D. James, K. R. A. S. Sandanayake and S. Shinkai, *Supramol. Chem.*, 1995, **6**, 141; T. D. James, P. Linnane and S. Shinkai, *Chem. Commun.*, 1996, 281; T. D. James, K. R. A. S. Sandanayake and S. Shinkai, *Angew. Chem., Int. Ed. Engl.*, 1996, **35**, 1911.
8 M. Mikami and S. Shinkai, *J. Chem. Soc., Chem. Commun.*, 1995, 153; *Chem. Lett.*, 1995, 603; M. Takeuchi, T. Imada and S. Shinkai, *J. Am. Chem. Soc.*, 1996, **118**, 10658.
9 S. Arimori, M. Takeuchi and S. Shinkai, *J. Am. Chem. Soc.*, 1996, **118**, 245; L. D. Sarson, K. Ueda, M. Takeuchi and S. Shinkai, *Chem. Commun.*, 1996, 619; M. Takeuchi, Y. Chin, T. Imada and S. Shinkai, *Chem. Commun.*, 1996, 1867.
10 H. Yamashita, K. Amano, S. Shimada and K. Narasaka, *Chem. Lett.*, 1996, 537; H. Yamashita and S. Narasaka, *Chem. Lett.*, 1996, 539.
11 This prospect is supported by our previous finding that the two planes of biphenyl-3,3′-boronic acid can be asymmetrically immobilized by added saccharides: K. Kondo, Y. Shiomi, M. Saisho, T. Harada and S. Shinkai, *Tetrahedron*, 1992, **48**, 8239.
12 In 1964 Liu *et al.* reported that the asymmetric synthesis of $[Ru^{II}(bpy)_3]^{2+}$ is achieved (although in low ee) by the reaction of $Ru^{2+}$ and 2,2′-bipyridine in the presence of sodium D-tartrate or sucrose: C. F. Liu, N. C. Liu and X. Bailar, Jr., *Inorg. Chem.*, 1964, **3**, 1085. Conceivable, this chirality is induced when D-tartarate or sucrose coordinated to $Ru^{2+}$ is substituted with 2,2′-bipyridine and the concept is entirely different from the present system.
13 K. Nakashima and S. Shinkai, *Chem. Lett.*, 1994, 1267.
14 D. F. Shriver, P. W. Atkins and C. H. Langfold, *Inorganic Chemistry*, Oxford, 2nd edn., 1994, p. 266.
15 T. Kimura, S. Arimori, M. Takeuchi, T. Nagasaki and S. Shinkai, *J. Chem. Soc., Perkin Trans. 2*, 1995, 1889; M. Takeuchi, T. Mizuno, M. Shinmori, M. Nakashima and S. Shinkai, *Tetrahedron*, 1996, **52**, 1195.
16 K. Torssell, *Ark. Kemi.*, 1957, **10**, 473.
17 S. F. Mason and B. J. Deart, *J. Chem. Soc., Dalton Trans.*, 1973, 949.
18 F. H. Burstall and R. S. Nyholm, *J. Chem. Soc.*, 1952, 3570.
19 K. Ohkubo, H. Ishida, T. Hamada and T. Inaoka, *Chem. Lett.*, 1989, 1545; H. Ishida, T. Hamada, Y. Fujishima, Y. Saito and K. Ohkubo, *Bull. Chem. Soc. Jpn.*, 1993, **66**, 714.
20 A. Tatehara and A. Muraida, *Chem. Lett.*, 1996, 461.
21 C. Dhenaut, I. Ledoux, I. D. W. Samuel, J. Zyss, M. Bourgault and H. L. Bozec, *Nature*, 1995, **374**, 339.

*Received in Cambridge, UK, 10th June 1997; 7/04041E*

# Induction of metal-centered chirality by planar chirality in [Fe{η-$C_5H_2Me(R^1)(CO_2R^2)$}(COR)(CO)($PR_3$)] complexes

**Yasushi Morimoto, Katsuhiro Ando, Mitsunari Uno and Shigetoshi Takahashi***

*The Institute of Scientific and Industrial Research, Osaka University, 8-1 Mihogaoka, Ibaraki, Osaka 567, Japan*

**The reaction of planar-chiral (alkyl)(cyclopentadienyl)dicarbonyliron complexes with triphenylphosphine gives [Fe{η-$C_5H_2Me(R^1)(CO_2R^2)$}(CO)(COR)($PPh_3$)] with a high diastereoselectivity ( > 90%) for the induction of metal-centered chirality.**

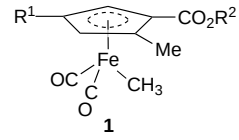
Optically active organometallic complexes have increasingly become useful in application to organic syntheses and mechanistic studies. Among the complexes, optically active cyclopentadienyl–metal complexes such as planar-chiral and chiral-at-metal cyclopentadienyl complexes have received recent interest.[1] Several asymmetric reactions using the latter complexes including [Fe(η-$C_5H_5$)(COR)(CO)($PR_3$)],[2] [Re(η-$C_5H_5$)(NO)($PPh_3$)(ArCHO)][$PF_6$][3] and [Rh(η-$C_9H_6$-1-$(CH_2)_m PR_2$)(COR)I][4] have appeared in the literature, whereas successful examples, in which a stereocontrol reaction occurring at a metal center is effectively governed by a planar chirality, are scarce. Information about the stereochemistry controlled by a certain chirality source is of prime importance in new applications to asymmetric reactions.

We previously showed a new method for the synthesis of planar chiral cyclopentadienyl–cobalt,[5] –rhodium[6] and –ruthenium[7] complexes using a chiral trisubstituted cyclopentadiene and isolated them in an enantiomerically pure form. Here we have applied this method to the preparation of planar chiral (alkyl)(cyclopentadienyl)dicarbonyliron complexes and found that they undergo asymmetric induction of metal-centered chirality controlled by the planar chirality [eqn. (1)].

$$[Fe\{\eta\text{-}C_5H_2Me(R^1)(CO_2R^2)\}(CO)_2R] + L \rightarrow [Fe^*\{\eta\text{-}C_5H_2Me(R^1)(CO_2R^2)\}(COR)(CO)L] \quad (1)$$

It is well known that cyclopentadienyliron–alkyl complexes, [Fe(η-$C_5H_5$)$(CO)_2$R], undergo a migratory insertion of carbon monoxide on treatment with phosphorus compounds such as phosphines and phosphites, and afford three-legged piano-stool iron-acyl complexes, [Fe(η-$C_5H_5$)(CO)($PR_3$)(COR)], which show chirality at the metal center.[8] Several reports have appeared on the induction of iron-centered chirality,[9] however only a modest diastereoselectivity of the asymmetric induction has been attained using chiral cyclopentadienyl ligands.[9b] Here we report the effective induction of metal-centered chirality in the reaction of planar-chiral (alkyl)(trisubstitutedcyclopentadienyl)dicarbonyliron complexes with phosphines.

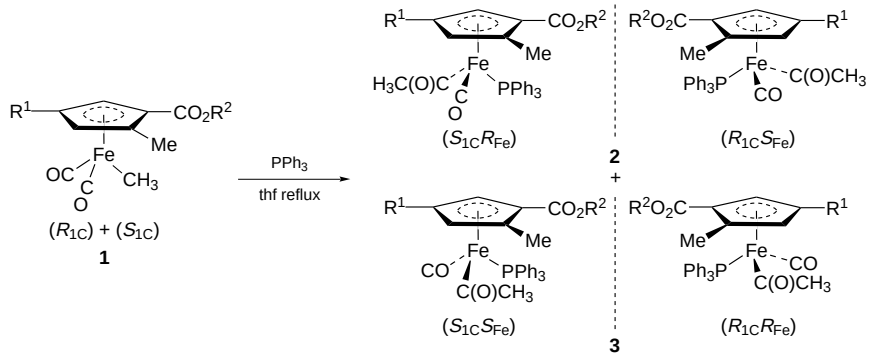
We synthesized the planar-chiral iron–alkyl complexes **1** by a literature method starting from trisubstituted cyclopentadienes.[10]




**1**

**1a** $R^1 = R^2 = Me$
**b** $R^1 = Ph$; $R^2 = Me$
**c** $R^1 = Me$; $R^2 = Et$
**d** $R^1 = Ph$; $R^2 = Et$

We investigated the influence of the planar chirality on the stereochemistry of a reaction occurring at the iron center in the reaction with phosphines giving acetyl iron complexes. Thus racemic iron–methyl complexes **1** ($R_{1c}$ + $S_{1c}$) were heated with 5 equiv. of triphenylphosphine in thf for 48 h and acetyl complexes were obtained as a stereoisomeric mixture (Scheme 1), which were purified by column chromatography on alumina and identified by $^1$H and $^{31}$P NMR and IR spectroscopy. The resulting acetyl complexes possess two chiral centers, *i.e.* metal-centered chirality and planar chirality, and hence may exist as a mixture of two diastereomerically related pairs of enantiomers **2**(*SR,RS*) and **3**(*SS,RR*). The ratio of **2** to **3** has been determined by $^1$H NMR† and HPLC‡ using a chiral column. The diastereoselectivities found in the above reactions are summarized in Table 1 along with chemical yields. The planar chirality effectively induces iron-centered chirality, and the size of a range of substituents $R^1$ on the cyclopentadienyl ligand strongly affects the diastereoselectivity of the reaction. A methyl group on the cyclopentadienyl ring gives a modest diastereoselectivity of *ca.* 75 : 25 while a larger phenyl group results in an increased diastereoselectivity up to *ca.* 95 : 5. It has already been reported that planar-chiral [Fe(η-$C_5H_3$Me-1-Ph-3)$(CO)_2$Me] did not exhibit any diastereoselectivities upon reaction with triphenylphosphine[9a] and even a diastereomeric analog bearing a chiral (*S*)-binaphthyl group on the cylopentadienyl ring showed only a modest diastereoselectivity of 40%.[9b] The high diastereoselectivity (*ca.* 90% de) observed in the




**Scheme 1**

**Table 1** Asymmetric induction of planar-chiral [Fe{η-$C_5H_2Me(R^1)$-$(CO_2R^2)$}$(CO)_2$Me] complexes on treatment with $PPh_3$

| Product | $R^1$ | $R^2$ | Yield (%) | **2** : **3**[a] |
|---|---|---|---|---|
| **2a**, **3a** | Me | Me | 80 | 74 : 26 |
| **2b**, **3b** | Ph | Me | 58[b] | 96 : 4 |
| **2c**, **3c** | Me | Et | 85 | 75 : 25 |
| **2d**, **3d** | Ph | Et | 52[b] | 95 : 5 |

[a] Determined by HPLC using Chiralcel OD and $^1$H NMR analyses. [b] Some decomposition of **1** was observed during the reaction, but the crude and purified products showed the same ratio of **2** to **3**.

present work may be attributed to an effective asymmetrical environment constructed by three suitable substituents, *i.e.* small, moderate and large groups, on the cyclopentadienyl ring.

A diastereomeric mixture of acetyl complexes was separated into two diastereomerically related pairs of enantiomers, **2** and **3**, by fractional crystallization from hexane–benzene. X-Ray crystallographic analysis has been performed for the major isomer **2c** (Fig. 1) and revealed that the absolute configuration is a pair of (*SR*) and (*RS*) configurational isomers, indicating that planar chirality $S_{1c}$ induces metal-centered chirality $R_{Fe}$ in the reaction of **2** with $PPh_3$.§,¶ In addition, the diastereoselectivity in the present reaction has been found to be thermodynamically controlled since a separate experiment showed that pure diastereomer **2c** was converted to a mixture of **2c** and **3c** with a diastereoisomer ratio of 75 : 25 when heated in thf for 48 h which is the same diastereoisomeric ratio as observed in the reaction of **1c** with triphenylphosphine under the same reaction conditions.

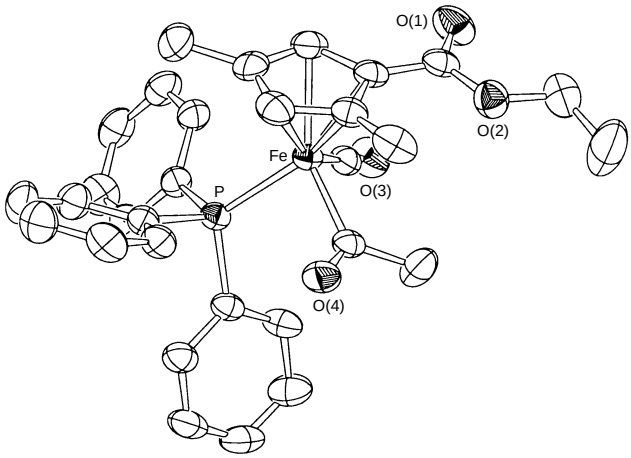



**Fig. 1** Molecular structure of **2c** with hydrogen atoms omitted for clarity

## Footnotes and References

* E-mail: takahashi@sanken.osaka-u.ac.jp

† *Selected data*: **2c**: reddish orange crystal. IR(Nujol) 1930, 1720, 1610 $cm^{-1}$. $^1$H NMR (270 MHz, $C_6D_6$): $\delta$ 4.86 (d, 1 H), 4.42–4.35 (q, 2 H), 3.98 (t, 1 H), 2.40 (s, 3 H), 1.62 (s, 3 H), 1.51 (s, 3 H), 1.21 (t, 3 H). $^{31}$P NMR ($C_6D_6$, $PPh_3$): $\delta$ 73.12. **3c**: yellow orange crystal. IR(Nujol) 1930, 1720, 1610 $cm^{-1}$. $^1$H NMR (270 MHz, $C_6D_6$): $\delta$ 4.60 (d, 1 H), 4.16–4.03 (q, 2 H), 3.86 (t, 1 H), 2.60 (s, 3 H), 2.37 (s, 3 H), 1.33 (s, 3 H), 0.94 (t, 3 H), $^{31}$P NMR ($C_6D_6$, $PPh_3$): $\delta$ 71.55.

‡ The HPLC analyses were carried on a chiral stationary phase HPLC (Daicel Chiralcel OD).

§ *Crystal data* for **2c**: $C_{31}H_{31}FeO_4P$, $M$ = 554.40, triclinic, space group $P\bar{1}$, $a$ = 10.651(2), $b$ = 13.604(2), $c$ = 9.611(2) Å, $\alpha$ = 95.10(1), $\beta$ = 103.51(1), $\gamma$ = 83.01(1)°, $U$ = 1341.3(4) Å$^3$, $Z$ = 2, $D_c$ = 1.37 g $cm^{-3}$, $\mu$ = 6.53 $cm^{-1}$, $T$ = 293 K. 8276 measured reflections, 7883 unique reflections, $R$ = 0.051, $R_w$ = 0.063. The data were collected on a Rigaku AFC5R four-circle diffractometer with graphite-monochromated Mo-Kα radiation ($\lambda$ = 0.71069 Å) by the $\omega$–2$\theta$ scan method to $2\theta_{max}$ = 60.1°.

The structure was solved by heavy-atom Patterson methods. Hydrogen atoms were placed in appropriate trigonal or tetrahedral positions. All calculations were performed using the teXan crystallographic software package from the Molecular Structure Corporation. CCDC 182/554.

¶ T. Tanaka and M. Sawada, Materials Analytical Center, The Institute of Scientific and Industrial Research, Osaka University.

1 R. L. Halterman, *Chem. Rev.*, 1992, **92**, 965 and references therein.
2 S. G. Davies, *Organotransition Metal Chemistry: Applications to Organic Synthesis*, Pergamon, Oxford, 1982.
3 J. A. Gladysz, *J. Chem. Soc., Chem. Commun.*, 1995, 279.
4 K. Tani, *42nd. Symposium on Organometallic Chemistry*, 1995, abstr. PA216.
5 M. Uno, K. Ando, N. Komatsuzaki and S. Takahashi, *J. Chem. Soc., Chem. Commun.*, 1992, 964.
6 M. Uno, K. Ando, N. Komatsuzaki, T. Tsuda, T. Tanaka, M. Sawada and S. Takahashi, *J. Organomet. Chem.*, 1994, **473**, 303.
7 N. Komatsuzaki, M. Uno, K. Shirai, Y. Takai, T. Tanaka, M. Sawada and S. Takahashi, *Bull. Chem. Soc. Jpn.*, 1996, **69**, 17.
8 H. Brunner and E. Schmidt, *Angew. Chem., Int. Ed. Engl.*, 1969, **8**, 616.
9 (*a*) T. G. Attig and A. Wojcicki, *J. Organomet. Chem.*, 1974, **82**, 397; (*b*) S. L. Colletti and R. L. Haltermann, *Organometallics*, 1992, **11**, 980.
10 R. B. King, *Organomet. Synth.*, 1965, **1**, 93; Y. Morimoto and S. Takahashi, *Chem. Lett.*, 1996, **10**, 887.

*Received in Cambridge, UK, 5th June 1997; 7/03917D*

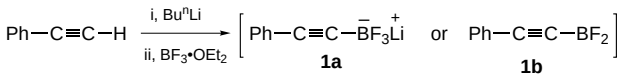
# Reaction of an alkynyllithium reagent with boron trifluoride: the structure of a likely intermediate in alkynyl anion chemistry

**John E. Davies, Paul R. Raithby, Ronald Snaith and Andrew E. H. Wheatley***

*Department of Chemistry, University of Cambridge, Lensfield Road, Cambridge, UK CB2 1EW*

**Lithium phenylacetylide reacts with 1 equiv. of $BF_3{\cdot}OEt_2$ in thf–toluene to yield both a thf adduct of tris(phenylacetylido)borane 2, which is probably the true intermediate in RC≡CLi/$BF_3$-promoted alkynyl anion chemistry, and $LiBF_4$, products which are considered to form *via* sequential LiF elimination from previously proposed acetylidoborate intermediates; complex 2 is the first structurally characterised tris(alkynyl)borane and in the solid state it forms an unusual hydrogen-bonded dimer.**

The value of organometallic nucleophilic addition to imines[1] has been limited in the past by the poor reactivity of the latter as acceptors,[2] and by their propensity for enolisation in the presence of, for example, organolithium species.[3] While initial attempts at activating imines towards nucleophilic addition of organometallic reagents involved the use of organocopper–boron trifluoride complexes[4] it was subsequently reported that supposed *in situ* generation of alkynylborane/borate species[5] led to β-aminoacetylenes from aldimines.[6] More recent work has incorporated the use of similar *in situ* boron-containing intermediates in the synthesis of allenes from *N*-aziridinylimines.[7] In each case, however, the existence of the alkynylborane/borate intermediate was assumed, the presumption being that lithium phenylacetylide[8] reacted with 1 equiv. of $BF_3{\cdot}OEt_2$ to yield either the monophenylacetylidoborate, **1a**, or, following the elimination of lithium fluoride, the monophenylacetylidoborane, **1b** (Scheme 1). An unexplained anomaly was that the subsequent nucleophilic addition reactions gave higher yields in the presence of 2 or, better, 3 equiv. of **1a**/**b**.




**Scheme 1**

We have investigated and now report on the actual species obtained from reacting a 1 : 1 mixture of a lithium acetylide with $BF_3{\cdot}OEt_2$. They are not the intermediates **1a**/**b** suggested previously (Scheme 1). They do, however, explain the preference for excess intermediate to be present during subsequent reaction with amide,[5] aldimine,[6] or *N*-aziridinylimine.[7] Thus, reaction of *in situ* generated lithium phenylacetylide with just 1 equiv. of $BF_3{\cdot}OEt_2$ in thf–toluene affords, as one of the products, an air-stable mono-thf adduct of tris(phenylacetylido)borane **2**,† the X-ray crystal structure of which has been determined.‡ A search of the Cambridge Crystallographic Database shows that **2** is not only the first structurally characterised tris(acetylido)borane, but that it is also the first acetylidoborane structure to incorporate an O-donor molecule. It exists as a hydrogen-bonded dimer in the solid state (Fig. 1), the boron centres having distorted tetrahedral geometries, with the fourth coordination site being occupied by the oxygen of the thf [mean C–B–C 114.2(2)°, mean O–B–C 104.1(2)°]. Unsurprisingly, at 1.633(3) Å, the observed B–O distance is rather longer than any previously observed in three-coordinate monoacetylidoborane structures containing direct B–O linkages.[11] Both the B–C [mean 1.580(4) Å] and C≡C [mean 1.209(3) Å] distances show close agreement with those in other (*i.e.* mono and bis) acetylidoboranes. Dimerisation *via* hydrogen bonding is seemingly a new feature in the solid state for acetylidoborane structures. The relevant interaction is between the adduct O-centre and the *m*-aromatic proton on a phenylacetylide ligand in an adjacent borane monomer. This results in the formation of a 16-membered ring, incorporating an O···C hydrogen bonding distance[12] of 3.46(1) Å.

Notwithstanding the structure of **2**, obtained from the 1 : 1 reaction of Ph–C≡C–Li and $BF_3{\cdot}OEt_2$ in thf, NMR studies show that the bulk product is a co-crystalline mixture. While $^1$H and $^{13}$C NMR spectra of the product were consistent with the observed structure of **2**, $^{11}$B NMR spectroscopy in $Me_2SO$ yielded only a first-order quintet at $\delta$ −0.75. At 1.1 Hz, coupling was identical to that demonstrated by the quartet observed in the $^{19}$F spectrum at $\delta$ −147.59 and accorded with previously observed $^1J_{^{11}BF}$ coupling for the tetrafluoroborate anion.[13] Confirmation that $LiBF_4$, **3**, was present in the isolated crystals came from the observation of a very sharp singlet at $\delta$ −0.11 in the $^7$Li spectrum in $Me_2SO$, suggesting the presence of $[Li(Me_2SO)_4]^+$.

At room temperature, $^{11}$B NMR spectroscopy of the bulk product in $Me_2SO$ failed to yield any signal attributable to **2**. Studies were therefore undertaken in alternative media. Whereas treatment of the co-crystalline product (**2**/**3**) with $Me_2SO$ yielded a solution, $^{11}$B NMR spectroscopy demonstrated that the necessity to filter the suspension afforded in [$^2H_6$]benzene prior to spectral analysis reflected the complete failure of the tetrafluoroborate component to dissolve. Accordingly, the $^{11}$B NMR spectrum at room temp. now showed no quintet, but rather a broad signal attributable to **2** ($\delta$ *ca.* 0.03, $\Delta\nu_{1/2}$ = 450 Hz). Complete dissolution of **2**/**3** was afforded by [$^2H_8$]thf, yielding both the tetrafluoroborate quintet ($\delta$ −1.18) with a slightly expanded $^1J_{BF}$ coupling (1.8 Hz), and a broad, high-field signal ($\delta$ *ca.* −7.32, $\Delta\nu_{1/2}$ = 340 Hz), the relative integrations suggesting a 1.25 : 1 ratio of **2** to **3**.

Spectroscopic evidence points, therefore, not only to the elimination of LiF from **1a**, yielding **1b** in the first instance, but also to the subsequent addition of LiF to an unreacted boron

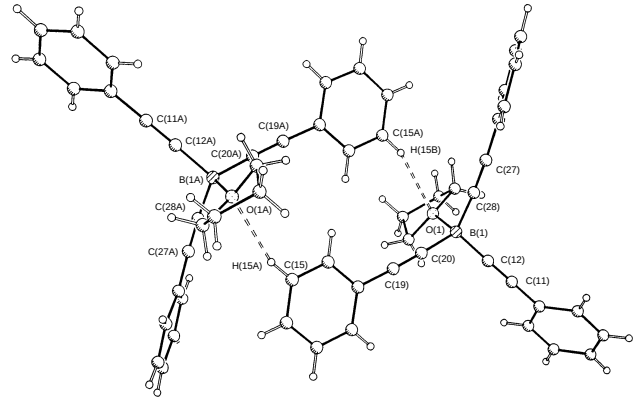
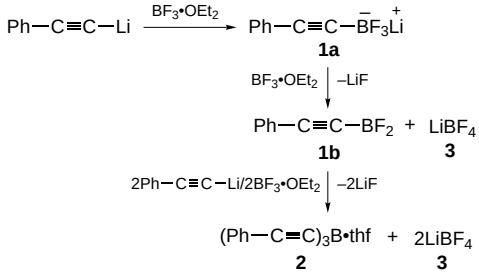
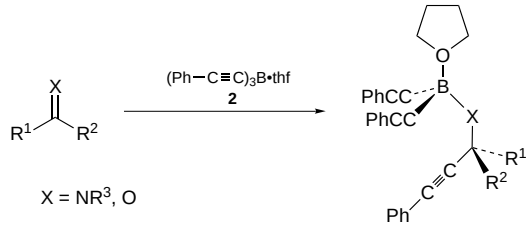



**Fig. 1** Dimeric structure of **2**; hydrogen bonding between thf and a *m*-aromatic proton yields a 16-membered ring




**Scheme 2**

trifluoride molecule, generating **3**. Furthermore, it appears that **1b** is attacked by 2 further equiv. of lithium phenylacetylide, eliminating LiF each time and ultimately giving **2** (Scheme 2). It is also apparent that an explanation of the favourability of utilising 2 or 3 equiv. of the supposed acetylidoborate/borane intermediate (**1a**,**b**) in subsequent nucleophilic addition chemistry is then at hand. Thus, the true alkynyl anion intermediate, **2**, contains not one, but three phenylacetylido-ligands. The implication is that one phenylacetylido-ligand is relatively active with respect to subsequent nucleophilic behaviour while the other two are largely inactive. This can be rationalised in terms of the sterically congested intermediate species resulting from the addition of **2** across just one carbonyl,[5] imine[6] or *N*-aziridinylimine (Scheme 3).[7]




**Scheme 3**

In conclusion, formation of **2**, the first example of a structurally characterised tris(acetylidoborane), is probably *via* the sequential elimination of LiF from acetylidoborate precursors (*e.g.* **1a**). Addition of the eliminated LiF to unreacted boron trifluoride means that formation of **2** is concomitant with that of $LiBF_4$, **3**, as evidenced by multinuclear NMR spectroscopy. Finally, the fact that **2** is the true intermediate in RC≡CLi/$BF_3$-promoted alkynyl anion chemistry, rather than **1a** or **1b**, helps to explain the stoichiometries required for efficient subsequent nucleophilic addition reactions.

We thank the UK EPSRC (A. E. H. W) and The Royal Society (J. E. D., P. R. R.) for financial support.

## Footnotes and References

* E-mail: cmc1006@cam.ac.uk

† $Bu^nLi$ (1.88 ml, 1.6 M in hexanes, 3.0 mmol) was added to phenylacetylene (0.33 ml, 3.0 mmol) in thf–toluene (5 : 1 ml) at −78 °C under nitrogen. After stirring for 10 min, $BF_3{\cdot}OEt_2$ (0.37 ml, 3.0 mmol) was added and the resultant yellow solution was stirred for a further 10 min at −78 °C. Warming to room temp. gave a white suspension, which afforded a colourless solution on gentle heating. Storage at +5 °C for three days afforded a colourless co-crystalline mixture of **2** and **3**. Yield (based on $^{11}B$ NMR spectroscopy and Scheme 2), 61% (**2**) and 16% (**3**), mp 163–164 °C. $^1H$ NMR [250 MHz, 25 °C, $(CD_3)_2SO$], $\delta$ 7.45–7.35 (m, 15 H, Ph), 3.59 (m, 4 H, thf), 1.76 (m, 4 H, thf). $^{13}C$ NMR (400 MHz, 25 °C, $Me_2SO$), $\delta$ 131.1, 128.5 (*o*-,*m*-Ph), 127.5 (*p*-Ph), 124.7 (*ipso*-C-Ph), 95.3 (≡C–Ph), 67.1, 25.2 (thf). $^{19}F$ NMR (235.361 MHz, 25 °C, $Me_2SO$, $CCl_3F$ $\delta$ = 0), $\delta$ −147.59 (q, $^{11}BF_4^-$, $^1J_{^{11}BF}$ 1.1 Hz), −147.53 (br m, $^{10}BF_4^-$). $^7Li$ NMR (155.508 MHz, 25 °C, $Me_2SO$, PhLi $\delta$ = 0), $\delta$ −0.11 [s, $Li(Me_2SO)_4^+$]. $^{11}B$ NMR (128.379 MHz, 25 °C, $Me_2SO$ $BF_3{\cdot}OEt_2$ $\delta$ = 0), $\delta$ −0.75 (qnt., $BF_4^-$, $^1J_{BF}$ 1.1 Hz); ($C_6D_6$, $BF_3{\cdot}OEt_2$ $\delta$ = 0), **d** *ca.* 0.03 (br s, $\Delta\nu_{1/2}$ 450 Hz); ([$^2H_8$]thf, $BF_3{\cdot}OEt_2$ $\delta$ = 0), $\delta$ −1.18 (qut., 1B, $^1J_{BF}$ 1.8 Hz), *ca.* −7.32 (br s, 1.25B, $\Delta\nu_{1/2}$ = 340 Hz).

‡ *Crystal data* for **2**: $C_{28}H_{23}BO$, monoclinic, space group $P2_1/n$, $a$ = 10.188(4), $b$ = 15.159(3), $c$ = 14.5899(11) Å, $\beta$ = 104.385(9)°, $U$ = 2182.6(9) Å$^3$, $M_r$ = 386.27, $Z$ = 4, $D_c$ = 1.176 Mg m$^{-3}$, $\mu$(Mo-K$\alpha$) = 0.069 mm$^{-1}$, $F$(000) = 816. Data were collected by the ω–2θ scan method on a Rigaku AKC5R four-circle diffractometer at 153(2) K using graphite-monochromated Mo-*K*K$\alpha$ radiation ($\lambda$ = 0.710 69 Å) in the range $5.16 < 2\theta < 45.00°$, $+h$, $+k$, $\pm l$; 3045 reflections of which 2857 were independent ($R_{int}$ = 0.0222) and used in all calculations. The structure was solved using direct methods[9] and subsequent Fourier difference syntheses and refined[10] by full-matrix least squares on $F^2$ with anisotropic thermal parameters for all non-hydrogen atoms. Hydrogen atoms were placed in geometrically idealised positions and refined using a riding model. In the final cycles of refinement a weighting scheme of the form $w^{-1} = [\sigma^2(F_o^2) + (0.0745P)^2 + 1.58P]$, where $P = (F_o^2 + 2F_c^2)/3$, was employed which produced a flat analysis of variance. Final $R(F)$ = 0.0452 for 2084 reflections with [$I > 2\sigma(I)$], $wR(F^2)$ = 0.2247 for all data; 271 parameters; goodness of fit = 1.039. Maximum peak and hole in final Fourier difference map 0.238 and −0.197 e Å$^{-3}$ respectively. CCDC 182/562.

1 R. A. Volkmann, in *Comprehensive Organic Synthesis*, ed. B. M. Trost and I. Fleming, Pergamon, New York, 1991, vol. 1, ch. 1.12.
2 R. W. Layer, *Chem. Rev*., 1963, **63**, 489; R. A. Volkmann, J. T. Davis and C. N. Meltz, *J. Am. Chem. Soc*., 1983, **105**, 5946.
3 A. I. Meyers, D. R. Williams and M. Druelinger, *J. Am. Chem. Soc.*, 1976, **98**, 3032.
4 M. Wada, Y. Sakurai and K. Akiba, *Tetrahedron Lett*., 1984, **25**, 1079.
5 M. Yamaguchi, T. Waseda and I. Hirao, *Chem. Lett*., 1983, 35.
6 M. Wada, Y. Sakurai and K. Akiba, *Tetrahedron Lett.*, 1984, **25**, 1083.
7 S. Kim, C. M. Cho and J.-Y. Yoon, *J. Org. Chem.*, 1996, **61**, 6018.
8 B. Schubert and E. Weiss, *Angew. Chem.*, 1983, **95**, 499; *Angew. Chem., Int. Ed. Engl.*, 1983, **22**, 496; B. Schubert and E. Weiss, *Chem. Ber.*, 1983, **116**, 3212.
9 G. M. Sheldrick, *Acta Crystallogr., Sect. C*, 1990, **A46**, 467.
10 G. M. Sheldrick, SHELXL-93, Program for Crystal Structure Refinement, University of Göttingen, 1993.
11 A. Meller, W. Maringgele, G. Elter, D. Bromm, M. Noltemeyer and G. M. Sheldrick, *Chem. Ber.*, 1987, **120**, 1437; W. Maringgele, H. Knop, D. Bromm, A. Meller, S. Dielkus, R. Herbst-Irmer and G. M. Sheldrick *Chem. Ber.*, 1992, **125**, 1807; H. Schulz, G. Gabbert, H. Pritzkow and W. Siebert, *Chem. Ber.*, 1993, **126**, 1593.
12 Hydrogen-bonding interactions are generally regarded as having C···O interactive distances of 3.0–4.0 Å. Analysis of 868 $R_3CH{\cdots}O$ systems gives a mean of 3.59 Å; R. Taylor and O. Kennard, *J. Am. Chem. Soc.*, 1982, **104**, 5063.
13 For $NBu^n_4BF_4$ in $CH_2Cl_2$, $^1J_{^{11}BF}$ 1.0 Hz at −80 °C; J. S. Hartmann and G. J. Schrobilgen, *Inorg. Chem.*, 1972, **11**, 940.

*Received in Cambridge, UK, 16th June 1997; 7/04185C*

# Synthesis of the first amine–dicarboxyboranes and their derivatives

**Zoltán Berente and Béla Györi***

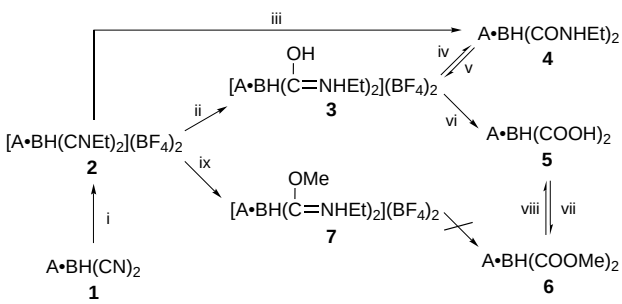
*Department of Inorganic and Analytical Chemistry, Lajos Kossuth University, Debrecen, H-4010, Pf. 21., Hungary*

**The first amine–dicarboxyboranes and their dimethyl esters are synthesized from amine–dicyanoboranes *via* [amine–bis(ethylnitrilium)hydroboron(2+)] tetrafluoroborates, [amine–bis(*C*-hydroxy-*N*-ethyliminium)hydroboron(2+)] cations and amine–bis(*N*-ethylcarbamoyl)boranes; *C*-methoxy-*N*-ethyliminium groups adjacent to boron undergo unusual hydrolysis.**

Amine–carboxyboranes have been known for two decades,[1] and their biological and pharmaceutical activities have been extensively studied.[2] Amine–carboxyboranes and related compounds have shown anticancer,[3] antiosteoporotic,[4] anti-inflammatory[5] and hypolipidemic[6] properties. Since the preparation of the first representative of amine–carboxyboranes they have been generally considered to be the boron analogues of the protonated amino acids,[7] based on the isoelectronic relation between C–$N^+$ and B–N bonds. On the other hand, amine–carboxyboranes can be regarded as analogues of aliphatic carboxylic acids, since the B–N bond is not only isoelectronic but also isosteric to the C–C bond, according to Langmuir's definition.[8] In contrast to amino acids, amine–carboxyboranes do not form chelates with transition metal ions and their p$K_a$ values are approximately 6 units larger than those of amino acids.[9] These facts, along with many qualitative observations, suggest that the $R_3N$–B group has a marked electron-donating effect towards its substituents.[10]

Here we report the synthesis of the first amine–dicarboxyboranes, the boron analogues of geminal dicarboxylic acids. Our long-term project, directed towards the synthesis of boron-substituted amine–carboxyboranes,[11] was initiated for two reasons. First, the introduction of new functional groups (here a second carboxylic group) offers potential biological activity. Second, the substitution of a hydrogen for an electron-withdrawing substituent on the boron is expected to increase the stability of the B–H bond, and brings the electron distribution of the carboxylic group closer to that in aliphatic carboxylic acids.

The synthetic sequence is outlined in Scheme 1.† The amine–dicyanoboranes **1a**–**d** were readily synthesized by base exchange (Table 1). The reaction between **1a**–**c** and $Et_3OBF_4$ in refluxing $CH_2Cl_2$ afforded the [amine–bis(*N*-ethylnitrilium)hydroboron(2+)] tetrafluoroborates **2a**–**c**. Owing to their low solubility in $CH_2Cl_2$, pure **2a** and **2c** could be isolated from the reaction mixtures in 80–88% yields. However, **2b** could not be separated from the excess $Et_3OBF_4$, but it did not cause the formation of byproducts in the subsequent reactions. **2d** could not be obtained at all, though both mono- and di-ethylated products were formed in the initial stage, but later they decomposed when a significant amount of starting material was still present. NMR monitoring of the ethylation reactions showed significant amounts of **1** and/or **2** besides the intermediate [amine–cyanoethylnitriliumhydroboron(1+)] cations during the whole reaction period even when only 1 mol equiv. of $Et_3OBF_4$ was employed. Consequently, there is only a surprisingly small difference between the rates of the consecutive steps, and preparation of the pure intermediates does not seem feasible.




**Scheme 1** (**a** A = quinuclidine; **b** A = $Me_3N$; **c** A = pyridine; **d** A = DMAP; **e** A = piperidine). *Reagents and conditions:* i, 2.5 mol equiv. $Et_3OBF_4$, $CH_2Cl_2$, reflux, 6–10 h; ii, $H_2O$, room temp. 50–70 min; iii–iv, 1 M NaOH, room temp. immediate; v, $HBF_4$, $H_2O$ room temp., immediate; vi, 1 M HCl, 120 °C, 1.5 atm, 10 min; vii, 7.5 mM HBr–MeOH, room temp., 5–10 min; viii, 0.05 M HCl, 60 °C, 15 min; ix, MeOH, room temp. 5–10 min.

Water readily adds to **2a**–**c** in 50–70 min in water or in 1 M HCl at room temp. affording [amine–bis(*C*-hydroxy-*N*-ethyliminium)hydroboron(2+)] tetrafluoroborates **3a**–**c**. **3a** could be prepared and characterized as a solid,‡ since it precipitated from water. Such stability of protonated aliphatic amides in aqueous medium is quite unusual,[12] and is probably due to the strong electron-releasing effect of the $R_3N$–B group. Water addition also takes place when **2a**–**c** are exposed to moisture.

In 1 M NaOH **2a**–**c** were transformed to the corresponding amine–bis(*N*-ethylcarbamoyl)boranes **4a**–**c** within 5 min, and the pure products were obtained from the $CH_2Cl_2$ extracts of the alkaline solutions. **4d** and **e** were synthesized from **4a** or **b** employing base exchange reactions (Table 1). Protonation of **4** leads to **3**: addition of 50% $HBF_4$ to a concentrated aqueous solution of **4a** resulted in the precipitation of **3a**.

In contrast to amine–*N*-ethylcarbamoylboranes, the acidic hydrolysis of amine–bis(*N*-ethylcarbamoyl)boranes **4**, presumably *via* **3** cations formed *in situ*, required vigorous conditions, probably owing to the much larger steric hindrance of the acyl carbons.[14] **4a** and **e** could be transformed into the amine–dicarboxyboranes **5a**§ and **e**. Best yields (60%) were achieved

**Table 1** Syntheses employing base exchange

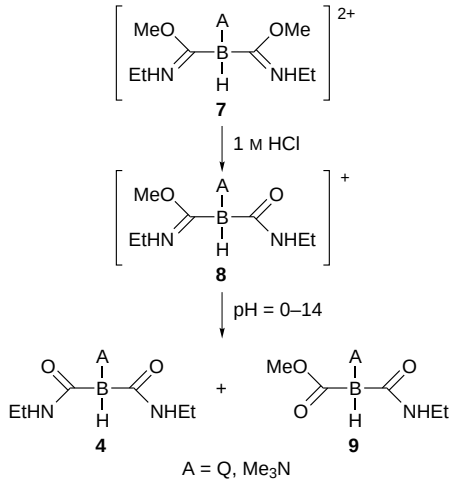
$$A{\cdot}BHX_2 \xrightarrow{MeCN} A'{\cdot}BHX_2$$

| Product | A | A′ | A : A′ | X | *t*/min | *T*/°C | Yield[a] (%) |
|---|---|---|---|---|---|---|---|
| **1a** | 4-CN-py[b] | Q[c] | 1 : 1.03 | CN | 5 | 25 | 96 |
| **1b** | 4-CN-py[b] | $Me_3N_{(g)}$ | — | CN | 15 | 25 | 97 |
| **1d** | 4-CN-py[b] | DMAP | 1 : 1.03 | CN | 5 | 25 | 100 |
| **4d** | $Me_3N$ | DMAP | 1 : 1 | CONHEt | 240 | 80 | 88 |
| | Q[c] | DMAP | 1 : 10 | CONHEt | 180 | 80 | 67 |
| **4e** | $Me_3N$ | Piperidine | 1 : 100[d] | CONHEt | 300 | 80 | 93 |
| | Q[c] | Piperidine | 1 : 30[d] | CONHEt | 600 | 80 | 81 |
| **5d** | Q[c] | DMAP | 1 : 10 | COOH | 360 | 80 | 83[e] |
| **5e** | Q[c] | Piperidine | 1.25[d] | COOH | 60 | 80 | 30[e] |
| **6e** | Q[c] | Piperidine | 1.25[d] | COOMe | 180 | 80 | 50 |

[a] Yields are not optimized. [b] For preparation see ref. 13. [c] Q = quinuclidine. [d] The reaction was run in piperidine. [e] The crude product was a mixture of **5** and its salt formed with the corresponding base. Pure **5d**, **e** were obtained from the suspension of the crude products in 0.1 M HCl.

for **5a** in 1 M HCl, at 120 °C. **4b**–**d** completely decomposed at even lower temperatures and/or less acidic solutions to the corresponding amine hydrochlorides. The lower hydrolytic stability of **4b** and **c** may be due to the relatively weak B–N bond in these complexes. On the other hand, the B–N bond in both **4d** and **5d** is presumably stronger than in **4a** and **5a**, since **4d** and **5d** could be prepared *via* a base exchange reaction (Table 1) from **4a** and **5a**. In accordance with our expectations, preliminary observations (salt formation during base exchange, –COOH chemical shifts) suggest that amine–dicarboxyboranes are stronger acids than amine–carboxyboranes. Decomposition during the hydrolysis of **4d** in acidic medium may be the consequence of the strong electron-donating property of DMAP (4-dimethylaminopyridine), which increases the hydridic character of the hydrogen attached to the boron. Such phenomena have been reported in the case of amine–(alkyl)carbamoylboranes.[15]

Similarly to amine–carboxyboranes,[16] all amine–dicarboxyboranes **5a**, **d**, **e** can be conveniently esterified in methanol in the presence of a catalytic amount (3 mol% relative to carboxyl groups) of HBr. Hydrolysis of the resulting amine–bis(methoxycarbonyl)boranes **6a**, **d**, **e** yielded the corresponding amine–dicarboxyboranes in minutes at 50 °C at pH ≈ 1. The latter reaction might offer a different, mild route to amine–dicarboxyboranes, so we attempted to synthesize **5** through the path **2** → **7** → **6** → **5**, since the acidic hydrolysis of alkylimidate salts $[RC(OR')=NR''R''']^+$ typically yields the corresponding esters $RC(O)OR'$.[17] [Amine–bis(*C*-methoxy-*N*-ethyliminium)hydroboron(2+)] tetrafluoroborates **7a**–**c** were readily obtained in minutes after dissolving **2a**–**c** in methanol. Unexpectedly, the hydrolysis of **7a**–**c** does not result in the formation of **6a**–**c** even in 1 M HCl (Scheme 2). Instead, NMR studies of the hydrolysis of **7a**, **b** showed release of methanol, and the resulting [amine–*N*-ethylcarbamoyl-(*C*-methoxy-*N*-ethyliminium)hydroboron-(+1)] tetrafluoroborates **8a**, **b** could be isolated.¶ Further hydrolysis of **8a** leads to a mixture of **4a** and quinuclidine–*N*-ethylcarbamoylmethoxycarbonylborane **9a** in both 1 M HCl and 1 M NaOH, producing more **4a** in alkaline medium. Hydrolysis of **8b** follows a similar pattern, but yields other products as well. **7c** undergoes no reaction in 1 M HCl at 25–80 °C, but it slowly decomposes to give boric acid and pyridinium chloride at 100 °C. Our results for **7c** are in agreement with those observed in the acidic hydrolysis of pyridine–(*C*-methoxy-*N*-ethylimino)borane.[18]




**Scheme 2**

In conclusion, we have investigated three different synthetic methods for the preparation of amine–dicarboxyboranes, boron analogues of geminal dicarboxylic acids. Based upon our findings three amine–dicarboxyboranes and their derivatives have been prepared and several more compounds of this type may be synthesized in the future.

The support of the Hungarian Science Foundation (OTKA T014985/1995) is appreciated.

## Footnotes and References

* E-mail: bgyori@tigris.klte.hu

† General comments: all manipulations, except those involving aqueous solutions, were performed using general Schlenk techniques under dried and $O_2$-free nitrogen atmosphere. All solvents were absolutized before use. All new compounds were characterized by analytical and spectroscopic methods.

‡ *Selected data* for **3a**: $\nu_{max}$ (KBr)/cm$^{-1}$ 3353 (OH), 2468 (BH), 1618 (C=N); $^1$H NMR (360 MHz; [$^2H_6$]acetone): $\delta$ 1.20 (6 H, t), 1.89 (6 H, dt), 2.04 (1 H, spt), 3.24 (6 H, br t), 3.45 (4 H, m); $^{11}$B NMR (64.2 MHz; acetone; $BF_3{\cdot}OEt_2$): $\delta$ −5.8 (s), −10.8 (d, *J* 105 Hz).

§ *Selected data* for **5a**: $\nu_{max}$ (KBr)/cm$^{-1}$ 2448 (BH), 1655, 1635 (C=O); $^1$H NMR [360 MHz; $(CD_3)_2SO$]: $\delta$ 1.72 (m), 1.93 (spt), 3.28 (dt), 10.7 (br s); $^{11}$B NMR (64.2 MHz; $Me_2SO$; $BF_3{\cdot}OEt_2$): $\delta$ −10.4 (br d).

¶ *Selected data* for **8a**: $\nu_{max}$ (KBr)/cm$^{-1}$ 3398, 3237 (NH), 2460 (BH), 1637, 1576, 1535, 1487, 1465 (amide bands); $^1$H NMR (360 MHz; $CDCl_3$): $\delta$ 1.16 (3 H, t), 1.30 (3 H, t), 1.87 (6 H, dt), 2.07 (1 H, spt), 3.04–3.19 and 3.28–3.42 (6 H, m), 3.28 (2 H, m), 3.53 (2 H, m), 4.37 (3 H, s), 7.05 (1 H, br s), 11.2 (1 H, br s); $^{11}$B NMR (64.2 MHz; $CHCl_3$; $BF_3{\cdot}OEt_2$): $\delta$ −1.2 (s), −12.4 (br d).

1 B. F. Spielvogel, L. Wojnowich, M. K. Das, A. T. McPhail and K. D. Hargrave, *J. Am. Chem. Soc.*, 1976, **98**, 5702.
2 See for example: I. H. Hall, C. O. Starnes, A. T. McPhail, P. Wisian-Neilson, M. K. Das and L. Wojnowich, *J. Pharm. Sci.*, 1979, **68**, 685; A. Sood, C. K. Sood, B. F. Spielvogel and I. H. Hall, *Eur. J. Med. Chem.*, 1990, **25**, 301; M. E. Murphy, R. P. Shrewsbury, A. Sood, B. F. Spielvogel and I. H. Hall, *Met.-Based Drugs*, 1995, **2**, 257; S. Y. Chen, B. S. Burnham, B. F. Spielvogel, A. Sood, S. D. Wyrick and I. H. Hall, *Appl. Organomet. Chem.*, 1996, **10**, 279.
3 See for example: C. K. Sood, A. Sood, B. F. Spielvogel, J. A. Yousef, B. Burnham and I. H. Hall, *J. Pharm. Sci.*, 1991, **80**, 1133; S. Karthikeyan, A. Sood, J. Tomasz, B. F. Spielvogel and I. H. Hall, *Amino Acids*, 1995, **8**, 323.
4 K. G. Rajendran, S. Y. Chen, A. Sood, B. F. Spielvogel and I. H. Hall, *Biomed. Pharmacother.*, 1995, **49**, 131; K. G. Rajendran, A. Sood, B. F. Spielvogel, I. H. Hall, V. M. Norwood, III and K. W. Morse, *Appl. Organomet. Chem.*, 1995, **9**, 111.
5 See for example: I. H. Hall, K. G. Rajendran, S. Y. Chen, O. T. Wong, A. Sood and B. F. Spielvogel, *Arch. Pharm.* (*Weinheim*), 1995, **328**, 39.
6 See for example: I. H. Hall, B. F. Spielvogel, A. Sood, K. W. Morse, V. M. Norwood, III and O. T. Wong, *Met.-Based Drugs*, 1994, **1**, 329.
7 C. Morin, *Tetrahedron*, 1994, **50**, 12 521, and references therein.
8 I. Langmuir, *J. Am. Chem. Soc.*, 1919, **41**, 1543.
9 K. H. Scheller, R. B. Martin, B. F. Spielvogel and A. T. McPhail, *Inorg. Chim. Acta*, 1982, **57**, 227; V. M. Norwood, III and K. W. Morse, *Inorg. Chem.*, 1986, **25**, 3690.
10 B. Györi, Z. Kovács and Z. Berente, in preparation.
11 B. Györi, Z. Kovács, J. Emri and Z. Berente, *J. Organomet. Chem.*, 1994, **484**, 225.
12 B. C. Challis and J. A. Challis, in *Comprehensive Organic Chemistry*, ed. D. Barton and W. D. Ollis, Pergamon Press, Oxford, 1979, vol. 2, p. 995.
13 B. Györi, J. Emri and I. Fehér, *J. Organomet. Chem.*, 1983, **255**, 17.
14 B. C. Challis and J. A. Challis, in *Comprehensive Organic Chemistry*, ed. D. Barton and W. D. Ollis, Pergamon Press, Oxford, 1979, vol. 2, p. 1007.
15 A. Sood and B. F. Spielvogel, *Main Group Met. Chem.*, 1989, **12**, 143; C. H. Sutton, M. W. Baize and L. J. Todd, *Inorg. Chem.*, 1992, **31**, 4911; 1994, **33**, 4221.
16 B. Györi, Z. Berente, J. Emri and I. Lázár, *Synthesis*, 1995, 191.
17 D. G. Neilson, in *The Chemistry of Amidines and Imidates*, ed. S. Patai, Wiley, London, 1975, p. 422.
18 M. Mittakanti and K. W. Morse, *Inorg. Chem.*, 1990, **29**, 554.

*Received in Basel, Switzerland, 25th April 1997; 7/02843A*

# Cycles frustrating fractal formation in an $AB_2$ step growth polymerization

**Colin Cameron,[a] Allan H. Fawcett,*[b] Cecil R. Hetherington,[b] Richard A. W. Mee[b] and Frederick V. McBride[c]**

[a] *Courtaulds Coatings, Stoneygate Lane, Felling, Gateshead, UK NE10 0JY*
[b] *School of Chemistry, The Queen's University of Belfast, UK BT9 5AG*
[c] *Institute of Computer-Based Learning, The Queen's University of Belfast, UK BT9 5AG*

**The step growth of a flexible $AB_2$ monomer, normally considered to produce dendrimers or fractal molecules, as they are themselves self-similar to their branches, is frustrated by the formation of one cycle within each molecule, according to a Monte Carlo lattice study of the evolution of the topological trees that are embedded in three-dimensional space; the number of cycles of $m$ residues is well fitted by the relationship $R_m = K_0 p_a^m m^{-e}$, $p_a$ being the extent of reaction of the A groups; at the end of a polymerization of $N_0$ monomers the total number of cycles, and of molecules, is given by the product of $K_0$ and the Euler–Riemann function $\xi(e)$ so there is a simple relationship between these quantities and the mean number average degree of polymerization at infinite time: $N_0 = K_0 < x >_{n,\infty} \xi(e)$.**

The step growth of an $AB_2$ monomer, the next more elaborate after the AB system, is usually considered to follow the classical branching pattern of polymerization of Flory,[1,2] the molecules evolving in the forms of Cayley trees,[3] each being rooted upon an A group. At each step the A group of one molecule reacts with a B group of another. A and B groups might form, for example, ester links. The growth has a fractal characteristic, for at each step molecules and branches are self-similar.[4] The assumption that intramolecular reactions do not take place, or the neglect of them in the treatment, means that molecules tend towards an infinitely high molecular mass with one A group each.[1] This common[5] assumption is inherently unrealistic, unless some special stiffness factor applies, such as the presence of *p*-substituted aromatic rings.[6] We envisage intramolecular reactions in molecules that have several flexible bonds between the functional groups, each bond being subject to simple rotational isomeric state considerations,[7] as when developing step-growth chemistry of difunctional monomers did Carothers, who recognised the formation of small rings as competing with linear growth.[8] To tackle such issues in a manner that allows the proper competition in three-dimensional space between fractal growth to yield trees and their cyclisation to yield graphs[3,9] we have embedded them upon a lattice of a type that we have devised to minimise any effect from its particular structure,[10] and explore it with the Monte Carlo method to establish the involved and elusive pattern of behaviour.[11,12] Our three-dimensional lattice model for step growth[10] resembles the two-dimensional fluctuating bond model used for other purposes:[13] components of the structures are linked through bonds that lie on the lattice spacings, $l$, on the in-plane diagonals, $\sqrt{2}l$, and on the through-space diagonals, $\sqrt{3}l$. (One such bond corresponds to several covalent bonds in a real molecule.[10,13]) Here we represent the monomer on four lattice sites as $A–N(B)_2$, the A group and the two B groups attached directly to the node *N*. This allows the explicit representation as a three-membered ring of the loop, the pendent structure that forms from an A group and a B group on the same node. 10% of the lattice sites were left vacant to represent free volume to facilitate movement throughout the polymerization.

We show a single monomer and a dimer placed upon the lattice in two dimensions in Fig. 1(*a*) in the form of Cayley trees. In Fig. 1(*b*) is the structure obtained by a B group movement, and the product after that dimer reacts to form a loop. In Fig. 1(*c*) is a hexamer with two possible internal reactions of the A group, and one is performed. Though this is rather confined, it does show that, as the lattice-represented molecule grows in size, the A group may become surrounded by an increasing number of B groups within the same molecule, and the chance of an intramolecular reaction may well increase. A group reactions will take place quite readily for there is always an excess of B groups. A simple consideration will recognise that eventually all the free A groups, located throughout at the root of a tree,[3] if not used in a step growth to enhance the degree of polymerization, will be so consumed, and then growth within the system will cease. This may have happened with a tetrafunctional siloxane alkene system,[14] for it was reported that the molecular mass was not increased by extra time or catalyst.

Initially the molecules were placed in random orientations within layers, and then were moved to randomise their configurations and positions. A,B pairs adjacent upon the lattice were randomly joined by a new bond, and simultaneously units moved upon the lattice by exchanging bead sites within the constraints of the molecular framework to randomise configurations.[15,16] We have tested that movements cause no bond or unit to pass through another: topological requirements are respected.[15] Five attempts at movement were performed each time a reaction was with success rates ( > 70%) higher than for a single chain on a simple cubic lattice.[17] The competing processes of chain branching and cycle formation thus take place in a manner that faithfully reflects the considerations of space, topology and configurations, as the A groups react with the excess of B groups present. (This competition is also present in gel formation.[18,19]) For the system of $60^3$ lattice sites, we used 5M CHOICE[11] or time cycles, when only 0.003% of the A groups remained.

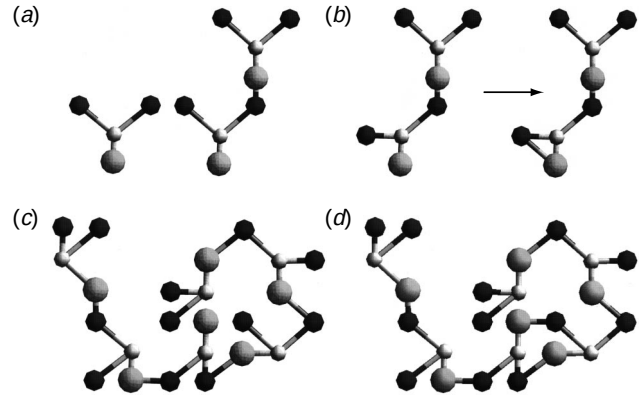



**Fig. 1** (*a*) $AB_2$ monomer and dimer displayed as trees, (*b*) dimer after a B group movement that facilitates the reaction whose product is shown, (*c*) a representative hexamer: note how the A end group is adjacent to two B groups on the same molecule, (*d*) the structure formed by an intramolecular reaction: a two-residue ($m$ = 2) cycle with two two-residue tails. The products in (*b*) and (*d*) lack A groups. These illustrations are drawn in two dimensions; the simulations were performed in three dimensions.

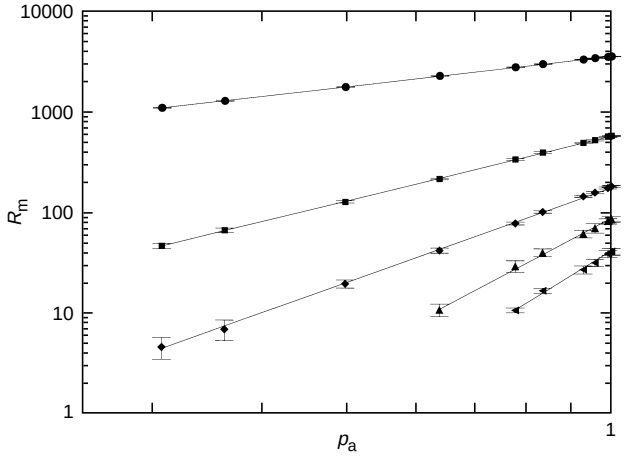



**Fig. 2** Logarithmic plots of $R_m$, the number of rings of size $m$ found in the system, against the extent of reaction, $p_a$. The lines fall in the order $m$ = 1,2, . . 5, and have integer slopes.

We obtained from the records $R_m$, the number of cycles involving $m$ residues, at several values of $p_a$. From nine simulations we plot the mean data for loops ($m$ = 1) and cycles up to $m$ = 5 on the log $R_m$–log $p_a$ plots of Fig. 2, where it may be seen that the points fall onto good straight lines: the slopes of these lines are well given by the integers, $m$, within a standard error or so [*e.g.* for the cycles with $m$ = 5 the exponent obtained by non-linear least-squares fitting[20] is 5.13 (±0.14)]. Thus $R_m = C_m p_a^m$. It is not difficult to envisage such integer power relationships as a limiting behaviour at low $p_a$ and when $m$ is small, for example the formation of a loop ($m$ = 1) will have a finite probability at the very start, and once a dimer has formed with a chance proportional to $p_a$ its cyclization will have the same proportionality to $p_a$. But this clearly persists to the end of the reaction and at higher $m$, where it expresses the structural results of a complex set of serial and parallel chemical reactions within a variety of configurations and structural isomers of an increasingly large range of oligomers.

If we examine the data as a function of $m$, we find that at each value of $p_a$ they are well fitted by $R_m = A_p m^\gamma$, the values of $\gamma$ falling linearly with $p_a$ as usual during the reaction.[10] It appears that $\gamma$ at the end of the polymerization is 2.714 (±0.0005), which is not significantly different from e. These two power relationships may be combined to yield:

$$R_m = K_0 p_a^m m^{-e} \quad (1)$$

the incidence of rings of size $m$ within the system at any $p_a$, when growth is kinetically controlled ($K_0 = A_1 = C_1$).

When $p_a$ = 1, the total number of rings is the product of $K_0$ and the Euler–Riemann $\xi$ function,[21] $K_0\,\xi(e) = K_0\,(1 + 2^{-e} + 3^{-e} + \ldots)$, a finite number as e > 1. Since the number of rings and the number of molecules is then identical, for each molecule contains one cycle, we have the relationship between the initial number of molecules, $N_0$ the number average degree of polymerization finally achieved, $\langle x \rangle_{n,\infty}$:

$$N_0 = K_0 \langle x \rangle_{n,\infty}\, \xi(e) \quad (2)$$

Taking our value of $C_1 = 3564 \pm 3 = K_0$, we find $\langle x \rangle_{n,\infty}$ to be 10.75 ± 0.01 model residues, a number which compares well with the ratio of the number of molecules present at the start to that at the end, 10.78 ± 0.07. A real $AB_2$ molecule may have a different propensity to form loops from the 78.2% predicted in this calculation, depending upon the configurations it might adopt and the possibilities of ring strain,[7] so cycle numbers may deviate from eqn. (1). (There might be too few bonds to allow a reaction between the A and B functional groups to form loops: then rings of size $m$ = 2 might assume the main role for limiting the formation of high molecular mass material.[16]) We note a second study using a different lattice representation of the flexible $AB_2$ monomer found essentially the same behaviour:[22] the forms of eqns. (1) and (2) are not dependent upon the monomer representation. As well as first utilising e,[23] Euler also introduced the $\xi$-function with real arguments when developing number theory.[21] Here e appears unusually as an exponent of the integers $m$ in this account of the formation of single cycle graphs from Cayley trees when both are embedded and growing from $AB_2$ monomers within three-dimensional space.

This $AB_2$ step growth follows a complicated pattern of two competing processes, the development of highly branched structures resplendent with functional groups and simultaneous cyclizations to give a range of ring sizes. Though cyclization consumes only a small proportion of the A functional groups, the proportion being 1 in $\langle x \rangle_{n,\infty}$, it does eventually terminate the polymerization. Fractal formation by a flexible $AB_2$ monomer is frustrated by the formation of cycles.

C. R. H. thanks DENI for a CAST Studentship, supported by Courtaulds Coatings and R. A. W. M. thanks the EPSRC for a Fellowship.

## References

1 P. J. Flory, *Principles of Polymer Chemistry*, Cornell University Press, Ithaca, New York, 1953, ch. 9.
2 P. J. Flory, *J. Phys. Chem.*, 1942, **42**, 132.
3 R. J. Wilson, *Introduction to Graph Theory*, Longman, Harlow, 4th edn., 1996.
4 B. B. Mandelbrot, *The Fractal Geometry of Nature*, Freeman, Oxford, 1982.
5 E. Malmstrom and A. Hult, *Macromolecules*, 1996, **29**, 1222.
6 R. H. Jin and Y. Andou, *Macromolecules*, 1996, **29**, 8010.
7 P. J. Flory, *Statistical Mechanics of Chain Molecules*, Interscience, New York, 1969.
8 *Collected Papers of Wallace H. Carothers on Polymerization*, ed. H. Mark and C. S. Whitby, Interscience, New York, 1940.
9 K. Dusek, *Recl. Trav. Chim. Pays-Bas*, 1991, **110**, 507.
10 A. H. Fawcett, R. A. W. Mee and F. V. McBride, *Macromolecules*, 1995, **28**, 481.
11 *Monte Carlo Methods in Statistical Physics*, ed. K. Binder, Springer Verlag, Berlin, 1979.
12 A. H. Fawcett, in *Macromolecular Chemistry, Specialist Periodical Reports*, ed. A. D. Jenkins and J. F. Kennedy, Royal Society of Chemistry, 1984, vol. 3.
13 I. Carmesin and K. Kremer, *Macromolecules*, 1988, **21**, 2819.
14 L. J. Mathias, T. W. Carothers and R. Bozen, *ACS Polym. Prep.*, 1991, **32**, 82.
15 A. H. Fawcett, R. A. W. Mee and F. V. McBride, *J. Chem. Phys.*, 1996, **104**, 1743.
16 A. H. Fawcett, F. V. McBride, D. McKay and R. A. W. Mee, work in progress.
17 P. Romiszowski and W. H. Stockmayer, *J. Chem. Phys.*, 1984, **80**, 485.
18 M. Gordon and S. B. Ross-Murphy, *Pure Appl. Chem.*, 1975, **43**, 1.
19 C. R. Hetherington, PhD Thesis, Queen's University of Belfast.
20 J. J. Volberg, *Prediction Analysis*, Van Nostrand, London, 1967.
21 *Encyclopedia of Mathematics*, ed. I. M. Kinogradov, Reidel, Lancaster, 1988, vol. 1A–B.
22 C. Cameron, A. H. Fawcett, C. R. Hetherington, R. A. W. Mee and F. V. McBride, submitted.
23 C. B. Boyer and U. C. Merzbach, *A History of Mathematics*, Wiley, Chichester, 2nd edn., 1989.

*Received in Cambridge, UK, 22nd May 1997; 7/03567E*

# Unique silane modified perfluorosulfonic acids as versatile reagents for new solid acid catalysts

**Mark A. Harmer,* Qun Sun, Michael J. Michalczyk and Zhenyu Yang**

*Central Research and Development, The DuPont Company, Wilmington, Delaware 19880-0356, USA*

**A new versatile reagent, a perfluorosulfonate/trisilanol [$(OH)_3Si(CH_2)_3(CF_2)_2O(CF_2)_2SO_3^-M^+$], is synthesized and a series of surface bound strong solid acid catalysts developed which are active for catalyzing a range of reactions, for example alkene isomerization, alkylations and acylations.**

Over recent years there has been considerable interest in the development of solid acid catalysts[1–6] as environmentally benign replacements for their homogeneous counterparts such as HF. The importance of this area of research has been highlighted by a number of reviews where the use of strong solid acids such as sulfated zirconia,[1] heteropolyacids,[2] zeolites,[3] aluminosilicates,[4] perfluorinated resinsulfonic acids[5] and the weaker polystyrene-based sulfonic acid resins with low thermal stability[6] has been described. In the case of perfluorinated sulfonic acid resins, access to the acid sites can be restricted giving rise to low activity for reactions in non-polar solvents or in the gas phase. The high acid strength and chemical and thermal stability of perfluorosulfonic acids is well known[5] and the ability to heterogenize these functional groups, at the same time maintaining ready accessibility, would be a major step forward.

In this paper we describe the synthesis of $[(OEt)_3Si(CH_2)_3(CF_2)_2O(CF_2)_2SO_2F]$ **1** *via* the direct hydrosilylation of $CH_2{=}CHCH_2(CF_2)_2O(CF_2)_2SO_2F$ with $HSi(OEt)_3$ using a platinum catalyst which produces exclusively **1** in 85% yield.† This can be hydrolyzed to $[(OH)_3Si(CH_2)_3(CF_2)_2O(CF_2)_2SO_3^-M^+]$ **2**. This new reagent can be surface attached to yield a new type of strong solid acid catalyst.

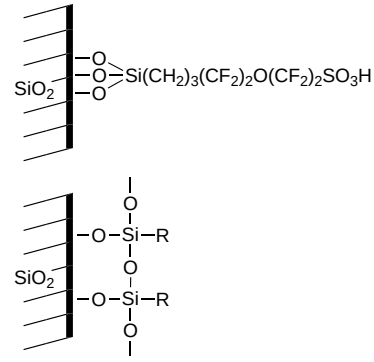
The triethoxysilyl perfluorosulfonyl fluoride, **1**, can be hydrolyzed by the reaction of **1** in a mixture of distilled water, dimethyl sulfoxide and potassium hydroxide (58% water–30% $Me_2SO$–12% KOH). Typically compound **1** is left to react at 90 °C for 18 h in water and basic $Me_2SO$ solution, after which time the sulfonyl fluoride is completely hydrolyzed giving a stable, clear solution. The loss of the sulfonyl fluoride peak at 47 ppm can be monitored using $^{19}F$ NMR spectroscopy. After hydrolysis only signals at −77.2 ($–OCF^*_2CF_2SO_2F$), −83 ($–CH_2CF_2CF^*_2O–$), −112 ($–CH_2CF^*_2CF_2–$) and −112.3 ($–CF_2CF^*_2SO_2F$) ppm are observed in the $^{19}F$ NMR spectrum. The $^{29}Si$ NMR spectrum with a peak at −46.3 ppm, shows the silicon alkoxides are hydrolyzed to $–Si(OH)_3$ (or ion-dissociated forms), having less than 10% forming –SiOSi– bonds. The new compound, which can be described as $[(OH)_3Si(CH_2)_3(CF_2)_2O(CF_2)_2SO_3^-M^+]$ **2**, has been used to synthesize a series of surface-bound strong solid acid catalysts.

Solid acid catalysts formed from **2** can be made by surface modification and attachment to an existing support or, alternatively, materials can be synthesized using an *in situ* sol–gel technique. Using both of these approaches a covalently bonded perfluorosulfonic acid is attached to the surface (see Scheme 1, the two structures denote low to high loadings). We have found the acid functionality to be readily accessible, stable on the surface and very active for a range of catalytic reactions.

Using an *in situ* sol–gel approach, tetralkoxysilanes are hydrolyzed and co-condensed in the presence of **2** to yield very high surface area materials with pendent sulfonic acid groups. The formation of silica networks and organically modified silica networks[8,9] has been described in detail previously. A typical procedure for these new materials is outlined below. Compound **2** (from heating **1**, 2.6 g in 40 ml of the water–$Me_2SO$–KOH mixture, overnight at 90 °C), was cooled and the pH was adjusted to 6 (4 M HCl). A solution of hydrolyzed tetramethoxysilane was then added (68 g TMOS, 10.9 g water and 1 g of 0.04 M HCl, stirred for 30 min). Gellation occurs in *ca*. 30 s. The dried modified silica network is then re-acidified by washing with 4 M nitric acid. The final materials (*ca*. 0.5–2 mm in size) are hard, glass-like, with high surface areas. The surface area (determined by BET), pore volume, and pore diameter are found to be 550 $m^2\ g^{-1}$, 0.75 $cm^3\ g^{-1}$ and 55 Å respectively. Successful incorporation of **2** is shown using solid-state $^{19}F$ NMR spectroscopy, chemical analysis, thermogravimetry (TG) coupled with measurements of the acid equivalents. The number of acid equivalents (for a material which contains 6 mass% organics from TG in the range 300–500 °C) is 0.18 mequiv. $g^{-1}$ (determined *via* titration), with F and S contents of 2.77 and 0.69 mass% respectively from pendent $–(CH_2)_3(CF_2)_2O(CF_2)_2SO_3H$ functionalities. The solid-state $^{19}F$ NMR spectrum has strong peaks at −84.5 and −122.5 ppm (close to the parent **2**). We estimate *ca*. 90% incorporation of **2** within the silica network. Higher loadings (up to 25 mass% of **2**) have also been developed.

Compound **2** has also been attached to a range of pre-formed supports. The chemistry strongly parallels that of silane coupling chemistry to surfaces (using trialkoxysilanes) which is well documented.[10] A solution of **2** was added to a high surface area silica support (CS-1020E, PQ corporation; *ca*. 400 $m^2\ g^{-1}$) and the support and surface modifier were treated with acid to neutrality. The material was then dried and re-acidified. The materials are very stable to leaching; for example, when left overnight in 4 M nitric acid at 90 °C no significant leaching occurred.

These materials are catalytically active for a number of acid catalyzed reactions. In some cases the activity of these materials (based upon acid equivalents) compared to Amberlyst resins are orders of magnitude higher reflecting the increased acid strength due to the perfluorosulfonic acid group. In Table 1, we




Surface attached perfluorosulfonic acid

**Scheme 1**

**Table 1** Catalytic conversions (mol%) shown for reactions over the solid acid catalysts

| | Catalyst | | |
|---|---|---|---|
| | Surface/$Si(CH_2)_3$-$(CF_2)_2O(CF_2)_2$-$SO_3H$ | NR50 | Amberlyst-15 |
| Acid capacity/ (mequiv $H^+$) $g_{cat}^{-1}$ | 0.2 | 0.9 | 4.6 |
| Linear alkylbenzene (LAB)[a] | 43 | 3 | 5 |
| Toluene alkylation with hept-1-ene[b] | 99 | 5 | 13 |
| But-1-ene isomerization[c] | 95 | 14 | 47 |
| *m*-Xylene acylation[d] | 89 | 99 | —[e] |

[a] Reaction conditions: 1 g catalyst, 21.5 g benzene, 10 g of dodec-1-ene, reacted at 80 °C for 1 h. Dodec-1-ene conversion measured using GC. [b] 1 g catalyst, 8.4 g heptene, 15.6 g of toluene, reacted at 100 °C for 2 h, conversion is based on hept-1-ene. [c] Conversion of but-1-ene to *cis–trans* isomers of but-2-ene over 5 g catalyst under ambient pressure with flow rates of He = but-1-ene = 38 ml $min^{-1}$, MHSV of but-1-ene = 1 $h^{-1}$ at 50 °C. [d] 1 g catalyst, 14 g benzoyl chloride and 21.2 g *m*-xylene reacted at 140 °C for 6 h, conversion is based on benzoyl chloride, the reaction rates are 76 and 300 mM (mequiv $H^+)^{-1}$ $h^{-1}$ for NR50 and the surface modified catalyst, respectively. [e] Reaction temperature too high for Amberlyst-15 catalyst.

show the catalytic activity of this material for three types of reactions, electrophilic aromatic alkylations, alkene isomerizations and Friedel–Crafts acylation. For comparison we also show the activity of a perfluorinated resinsulfonic acid (Nafion resin NR50) which in non-swelling solvents is known to have limited access to all the acid sites,[11] and that of Amberlyst-15. Both the surface modified materials and the *in situ* formed materials show the same kind of activity. The results demonstrate the utility of these new materials as solid acid catalysts. Notice that the acid capacities of Amberlyst-15 and NR50 are significantly higher than that of the surface modified catalyst. The differences of reaction rates based on the same amount of acids in the catalysts are much more pronounced than the conversions. Linear alkylbenzenes (LAB) which are made in large quantities (using HF) are widely used in the manufacture of detergents. The new catalyst was found to be very effective as the alkylation catalyst. Conversion of > 99% was obtained with 2 g of catalyst and after 6 h. Similar activity patterns (the optimum being the surface attached fluorosulfonic acid) were observed for the isomerization of longer chain α-alkenes (> $C_{12}$) which are important for use as lubricants. The higher activity of these materials, compared to the polymer Nafion NR50 resin, indicates that most of the acid sites, which are exclusively on the surface, are readily accessible in contrast to the gel type NR50 where most of the acids are buried inside the polymer particles. Data in Table 1 indicated that the surface modified catalyst and NR50 are very effective heterogeneous catalysts for Friedel–Crafts acylation. This is routinely carried out using Lewis acids such as $AlCl_3$, which produces large amounts of waste streams, for use in the fine chemical and other industries. NR50 is more efficient for this reaction mainly due to the higher temperature and polar reagent employed that swells the framework of Nafion resin which enhances the acid sites accessibilities.

A quantitative kinetic study of the dimerization of α-methylstyrene (AMS) catalyzed by sulfonic acid resins was also investigated. A detailed kinetic study has been reported previously.[6,12] The first order rate constants for the surface attached **2**, Nafion NR 50 and Amberlyst-15 (AMS, 6 g in 54 g of cumene as solvent, using 1 g of catalyst, at 50 °C) was found to be 1000, 0.1 and 0.6 [(mequiv. $H^+)^{-1}$ $h^{-1}$], respectively. Supported Nafion also shows low activity. The higher activity, > 1000-fold, is striking.

## Footnotes and References

* E-mail: mark.a.harmer@usa.dupont.com

† The perfluoroiodide (213 g), $ICF_2CF_2OCF_2CF_2SO_2F$,[7] was stirred under nitrogen with allyl acetate (57 g) and heated to 100 °C. Benzoyl peroxide (4 g) was added over 4 h. The solution was distilled to yield 200 g of pure product $CH_3COOCH_2CHICH_2(CF_2)_2O(CF_2)_2SO_2F$, bp 87 °C at 0.1 mmHg. $^{19}F$ NMR: δ +45.1 (m, 1F), −82.7 (m, 2F), −87.9 (dt, *J* 142.4 13.0 Hz, 1F), −88.8 (dt, *J* 142.4, 12.8 Hz, 1F), −112.7 (m, 2F), −117.3 (ddd, *J* 262.3, 26, 10.2, Hz, 1F), −118.6 (ddd, *J* 262, 24 Hz, 1F). The product was added to 35 ml isopropyl alcohol, 42 ml acetic acid and 54.4 g zinc powder (90 °C). The mixture was left for a further 4 h. The residue was washed with water and aqueous sodium hydrogencarbonate solution. Distillation gave 108 g of pure $CH_2{=}CHCH_2(CF_2)_2O(CF_2)_2SO_2$ (85% yield), bp 134–135°, $^{19}F$ NMR: δ +45.0 (m, 1F), −82.6 (m, 2F), −87.3 (m, 2F), −112.6 (m, 2F), −117.4 (t, *J* 17.6 Hz, 2F). See G. Caiyun and C. Qingyun, *Huaxue Xuebao*, 1984, 592. $(OEt)_3Si(CH_2)_3(CF_2)_2O(CF_2)_2SO_2F$: $^1H$ NMR ($C_6D_6$) δ 0.51 (t, 2 H, $CH_2Si$), 1.13 (t, 9 H, $CH_3$), 1.66–2.01 (m, 4 H, $CH_2CH_2$), 3.71 (q, 6 H, $CH_2O$).[13] C NMR ($C_6D_6$) δ 10.86 ($SiCH_2$), 15.05 ($CH_2$), 18.18 ($CH_3$), 33.54 [t, $CH_2CF_2$, $^2J$(CF) 21.6 Hz], 58.94 ($OCH_2$), 108–123. (m, $CF_2$). MS (EI) *m/z* 503 ($M^+ - H$), 489 ($M^+ - CH_3$), 459 ($M^+ - OCH_2CH_3$); exact mass for $M^+ - H$ fragment, $C_{13}H_{20}SO_6FSi$, calc. *m/z* 503.06061803, found *m/z* 503.060178. Anal. Calc. for $C_{13}H_{21}SF_9SiO_6$: C, 30.95; H, 4.19; S, 6.36. Found: C, 30.44; H, 3.89; S, 6.46%.


1 X. Song and A. Sayari, *Catal. Rev. Sci. Eng.*, 1996, **38**, 329.
2 I. V. Kozhievnikov, *Catal. Rev. Sci. Eng.*, 1995, **37**, 311.
3 P. B. Venuto, *Microporous Mater.*, 1994, **2**, 297.
4 A. Corma, *Chem. Rev.*, 1995, **95**, 559.
5 G. A. Olah, in *Acidity and Basicity of Solids, Theory, Assessment and Utility*, ed. J. Fraissard and L. Petrakis, 1994, Nato ASI Ser., Kluwer Academic, Dordrecht, 1994, vol. 444, pp. 305–334.
6 A. Chakrabarta and M. M. Sharma, *React. Polym.*, 1993, **20**, 1.
7 $ICF_2CF_2OCF_2CF_2SO_2F$, available from the Shanghai Institute of Organic Chemistry, Academica Sinica, Shanghai, PR China.
8 C. J. Brinker and G. W. Scherer, *Sol–Gel Science*, Academic Press, New York, 1990.
9 J. Wen and G. L. Wilks, *Chem. Mater.*, 1996, **8**, 1667.
10 *Silane and Other Coupling Agents*, ed. K. L. Mitall, VSP, Netherlands, 1992.
11 M. A. Harmer, Q. Sun and W. E. Farneth, *J. Am. Chem. Soc.*, 1996, **118**, 7708.
12 Q. Sun, M. A. Harmer and W. E. Farneth, *J. Catal.*, 1996, **164**, 62.


*Received in Bloomington, IN, USA, 19th June 1997; 7/04320A*

# Controlled aggregation of supramolecular boxes

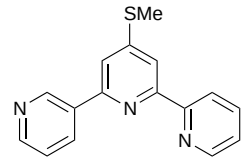
**Michael J. Hannon,* Claire L. Painting and William Errington**

*Department of Chemistry, University of Warwick, Gibbet Hill Road, Coventry, UK CV4 7AL*

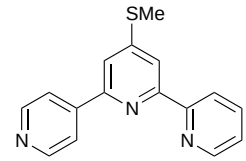
**Supramolecular boxes are prepared and their aggregation controlled by self-assembly; the crystal structure of a polymeric assembly of silver(I) cage units of 4-thiomethyl-6-(4-pyridyl)-2,2′-bipyridine is reported.**

The controlled design of complex molecular architectures represents a considerable synthetic challenge. The supramolecular synthetic approach has been used to assemble large molecular aggregates[1–3] and extension to polymeric systems has impacted on the field of crystal engineering.[4,5] Sophisticated macromolecular targets will require the ability to assemble small supramolecular units which may be further aggregated in a controlled fashion. To achieve this we are targeting metallosupramolecular species which contain binding sites on their exterior. Recently, we reported the construction of metallosupramolecular cage species by interacting metal ions with simple dinucleating ligands.[2] These cyclophane analogues were prepared in a single-step assembly process without the need for ancillary ligands which block coordination sites on the metal centre. The metal centres incorporated into the box framework did not use all of their coordination sites in the construction process and we reasoned that these unused coordination sites (which are filled with solvent molecules) might be used to aggregate the box structures. To achieve our sophisticated assemblies, an additional ligating site must be incorporated within the system in such a way that it does not interfere with the box assembly process. Our cage design utilises dinucleating ligands which contain bipyridyl and pyridyl binding sites. Thiomethyl substituents may readily be introduced onto the outside of such ligands.[6] Although thiomethyl groups on the back of oligopyridyl units have not previously been observed to coordinate to metal ions, the chemistry of thioether ligands is well established.[7] Indeed Reid and coworkers recently reported a polymeric 3D coordination array generated by ligating silver(I) to a ligand containing two monodentate thioether sites.[8] The thiomethyl unit is a less effective donor than the pyridine groups and therefore should not compete with or disrupt the box formation while the hard/soft principle might allow the problem of controlled and selective aggregation to be addressed.

The ligand 4-thiomethyl-6-(3″-pyridyl)-2,2′-bipyridine (bpy-3-py) forms discrete box structures with copper(I) and cadmium(II) and thioether coordination is not observed with these metals.[2] Switching to the softer silver(I) ion might allow access to this bonding mode. Reaction of the ligand with silver(I) salts gives colourless solutions from which salts of formula $\{Ag(bpy\text{-}3\text{-}py)X\}_n$ may be isolated (X = counter-ion). Unfortunately we have so far been unable to obtain material suitable for X-ray structural characteristation from this reaction.



bpy-3-py



bpy-4-py

Modelling indicated that the related ligand 4-thiomethyl-6-(4″-pyridyl)-2,2′-bipyridine (bpy-4-py) should give analogous box structures and so we have examined the ligation of silver(I) to this ligand. The ligand was prepared in good yield (72%) in a one-pot Potts[6] reaction of 3,3-bis(methylthio)-1-(2′-pyridinyl)prop-2-en-1-one with the potassium enolate of 4-acetylpyridine, followed by ring closure with ammonium acetate.

Warming methanolic solutions of the ligand with 1 equiv. of silver(I) salts leads to the rapid formation of colourless solutions from which white salts of formula $[Ag_2(bpy\text{-}4\text{-}py)_2][PF_6]_2$ were isolated on the addition of methanolic ammonium hexafluorophosphate. Mass spectrometric analysis (FAB) showed the presence of dinuclear $M_2L_2$ and $M_2L_2X$ peaks consistent with this formulation. Recrystallisation of the salt from acetonitrile solution by the slow diffusion of diethyl ether afforded colourless crystals, the structure of which has been determined† and which is shown in Fig. 1.

As anticipated the bpy-4-py ligand bridges between metal centres. Each silver(I) centre is bound to a bipyridyl unit from one ligand and a pyridyl from the other, resulting in the formation of a dimeric $M_2L_2$ box species. The metal–ligand bond lengths and angles are unremarkable and the intermetallic Ag···Ag distance is 6.686(2) Å. The pyridyl and bipyridyl binding domains are twisted with respect to each other [dihedral

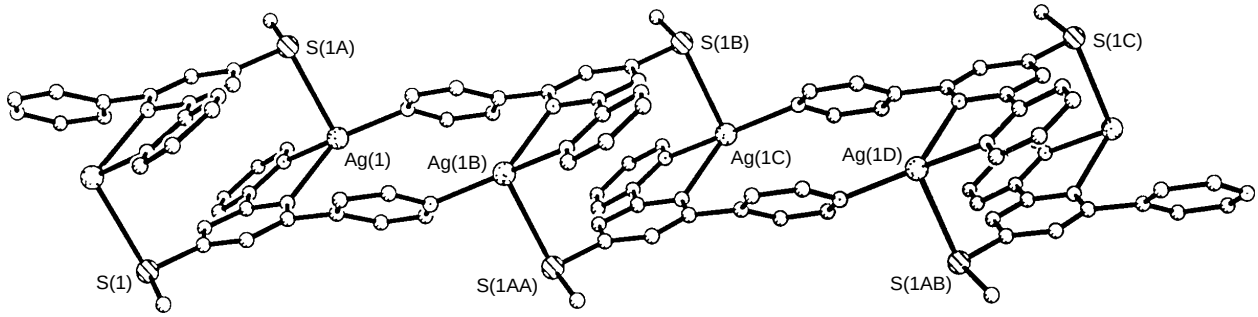



**Fig. 1** Crystal and molecular structure of the cation $[Ag_2(bpy\text{-}4\text{-}py)_2]_n^{2n+}$

angle 47.4(4)°] and a cavity between the pyridyl units of the two ligands results. This twisting is anticipated and is similar to that observed in the box complexes of bpy-3-py. The twisting results in the aromatic rings defining an aryl-lined cavity. The centroid–centroid distance between the two monodentate pyridyl rings, which define the cavity, is 4.00 Å. The box structure is, as would be anticipated from the ligand connectivity, slightly flatter than those formed with bpy-3-py.[2]

Each silver(I) ion is four coordinate and its coordination sphere is completed by coordination to a thioether unit from an adjacent box. This interaction links the boxes together into a polymeric array. The elongated Ag–S bonds [2.940(3) and 2.961(3) Å] are approximately 0.3 Å longer than those observed in other thioether silver(I) complexes.[8] The coordination of the thioether groups brings the aryl rings of adjacent boxes into close contact. The central pyridyl rings, bearing the thiomethyl substituents, are coplanar and offset, with a centroid–centroid distance of 3.86 Å. This may represent a weak π-stacking contribution to the aggregation process.

This form of supramolecular architecture may be contrasted with the elegant solid-state cavity-containing arrays of Robson and coworkers and Fujita *et al*.[5] In their approach they allow the repeat cavity unit to propagate through the stucture with each cavity sharing a corner and/or side with the adjacent units. Our structure is somewhat different. The repeat cavity unit is assembled independently and the units are then linked *via* sulfur bridges. The cavities share neither edges nor corners with their adjacent neighbours.

While the crystallographic study confirms the aggregation in the solid state this is not the case in solution. The $^1$H NMR spectra of $CD_3CN$ solutions of the salts showed the expected eight resonances in the aromatic region and the presence of a single thiomethyl resonance. The thiomethyl resonance appears at a similar chemical shift in both the complex ($\delta$ 2.69) and the free ligand ($\delta$ 2.66), indicating that the aggregation process is not occurring in acetonitrile solution. This is unsurprising as the donor solvent is expected to compete effectively with the weakly coordinating thiomethyl group.

We are grateful to the EPSRC for a studentship (C. L. P.) and the EPSRC and Siemens for grants enabling the purchase of the diffractometer.

## Footnotes and References

* E-mail: m.j.hannon@csv.warwick.ac.uk

† *Crystal data* for $[Ag_2(bpy\text{-}4\text{-}py)_2][PF_6]_2\cdot MeCN$: $C_{34}H_{29}Ag_2F_{12}N_7P_2S_2$, $M$ = 1105.44, triclinic, space group $P\bar{1}$, $a$ = 10.9196(2), $b$ = 14.3306(3), $c$ = 15.0364(3) Å, $\alpha$ = 113.967(1), $\beta$ = 104.25(1), $\gamma$ = 100.635(1)°, $U$ = 1973.47(7) Å$^3$, $Z$ = 2, $T$ = 230(2) K, $\mu$ = 1.274 mm$^{-1}$; final $R1$, $wR2$ and $S$ are 0.071, 0.169 and 1.167 for 532 parameters. Data were collected using a Siemens SMART CCD area-detector diffractometer. Refinement was by full-matrix least squares on $F^2$ for all data using SHELXL-96.[9] CCDC 182/571.

1 J.-M. Lehn, *Supramolecular Chemistry–Concepts and Perspectives*, VCH, Weinheim, 1995; D. Philp and J. F. Stoddart, *Angew. Chem., Int. Ed. Engl.*, 1996, **35**, 1155.
2 M. J. Hannon, C. L. Painting and W. Errington, *Chem. Commun.*, 1997, 307.
3 D. P. Funeri, J.-M. Lehn, G. Baum and D. Fenske, *Chem. Eur. J.*, 1997, **3**, 99; P. N. W. Baxter, J.-M. Lehn, J. Fischer and M.-T. Youinou, *Angew. Chem., Int. Ed. Engl.*, 1994, **33**, 2284.
4 B. F. Robson, in *Comprehensive Supramolecular Chemistry*, ed. J. L. Atwood, J. E. D. Davies, D. D. MacNicol, F. Vogtle and J.-M. Lehn, Pergamon, Oxford, 1997, vol. 6; M. J. Zarorotko, *Chem. Soc. Rev.*, 1994, **23**, 284.
5 B. F. Abrahams, S. R. Batten, H. Hamit, B. F. Hoskins, D. M. Michail and R. Robson, *Angew. Chem., Int. Ed. Engl.*, 1996, **35**, 1690; B. F. Abrahams, B. F. Hoskins, D. M. Michail and R. Robson, *Nature*, 1994, **369**, 727; M. Fujita, Y. J. Kwon, S. Washizu and K. Ogura, *J. Am. Chem. Soc.*, 1994, **116**, 1151.
6 K. T. Potts, M. J. Cipullo, P. Ralli and G. Theodoridis, *J. Org. Chem.*, 1982, **47**, 3027; E. C. Constable, *Prog. Inorg. Chem.*, 1994, **42**, 67.
7 *Comprehensive Coordination Chemistry*, ed. G. Wilkinson, R. D. Gillard and J. A. McCleverty, Pergamon, Oxford, 1987.
8 J. R. Black, N. R. Champness, W. Levason and G. Reid, *J. Chem. Soc., Chem. Commun.*, 1995, 1277.
9 G. M. Sheldrick, SHELXL-96, Program for Crystal Structure Refinement, University of Göttingen, Germany, 1996.

*Received in Basel, Switzerland, 27th May 1997; 7/03646I*

# An inexpensive approach to supramolecular architecture

**Michael J. Hannon,* Claire L. Painting, Alexander Jackson, Jacqueline Hamblin and William Errington**

*Department of Chemistry, University of Warwick, Gibbet Hill Road, Coventry, UK CV4 7AL*

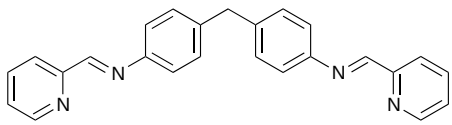
**A new approach to generating supramolecular architectures, based on inexpensive and easy-to-prepare imine ligands, is described together with its application to the self-assembly of supramolecular triple-helicates.**

There is considerable current interest in the supramolecular synthetic approach and its application to the quest to control molecular architecture.[1] The application of metal–ligand interactions has proved particularly fruitful and complex molecular architectures such as helicates,[2–4] knots,[5] grids,[3] catenanes,[5] cylinders[3] and boxes[6] have all been assembled. Indeed in a recent report, Lehn and co-workers have described a supramolecular system in which a number of different structural motifs are possible.[7]

A disadvantage to this metallo-supramolecular approach has been the almost exclusive use of ligand systems constructed from polypyridyl,[2,3] benzimidazole[4] and catechol binding sites.[4] These systems require time-consuming multi-step syntheses from relatively expensive starting materials. If supramolecular chemistry is to achieve its full potential then it is highly desirable that new, inexpensive and easy-to-prepare systems be developed. Not only should the development of an inexpensive system enable wider access to and application of this field, but creating systems which are easy to prepare and readily modified should enhance the rate at which novel molecular architectures are developed. For these reasons we are targeting inexpensive approaches to supramolecular architecture and communicate here both our approach and the preliminary results of our studies.

As an alternative donor set we have selected imine-based ligands. Imines are formed in high yield by simply mixing aldehydes and amines, a large number of which are available commercially at very competitive prices. Moreover multinucleating imine ligands may be prepared by simple iterative reactions.[8] The stability of the imine bond towards hydrolysis is greatly enhanced by conjugation with an aryl ring and the coordination chemistry of such donor units is well established. One of us has recently used copper(I) pyridylimine compounds to control atom transfer radical polymerisation processes.[9] An earlier report of an imine based double helix has appeared and recent work has identified double-helical twists in imine based macrocyclic complexes.[10]

To date, helices represent the best developed and most investigated supramolecular architectures.[1–4] To establish our approach we chose to address the challenge of creating the triple-helical architecture[4] using an inexpensive system. To achieve this we have prepared the ligand L. Our ligand design




L

incorporates two pyridylimine binding sites separated by a spacer. The chosen spacer incorporates phenylene groups that sterically prevent the two metal binding sites from coordinating to a single metal centre. The central methylene unit introduces enhanced flexibility into the ligand backbone. This enhanced flexibility permits the ligand to support triple-helical ligand arrays. Importantly, the ligand is not sufficiently flexible to give the bridging non-helical arrangement observed by others.[11] Thus, octahedral metal ions, which require three didentate pyridylimine units to satisfy their coordination requirements, should induce the formation of the triple-helical architecture.

The ligand is prepared by simply mixing ethanolic solutions of pyridine-2-carbaldehyde and 4,4′-methylenedianiline. On stirring at room temperature, the ligand precipitates from the reaction mixture in high yield (80% after 8 h) and may be isolated by filtration. The ease of synthesis and the high yield in a single-step reaction from commercial, inexpensive reagents makes this an extremely attractive ligand system.

Warming methanol solutions containing 3 equiv. of ligand and 2 equiv. of nickel(II) salts at reflux for 4 h leads to the formation of red solutions from which salts of formulation $[Ni_2L_3][X]_4$ are isolated in high ( > 80%) yield on addition of methanolic $[NH_4][X]$ (X = $PF_6$ or $BF_4$). Mass spectrometric analysis (ESI) shows the presence of peaks corresponding to $\{M_2L_3X_3\}^+$, $\{M_2L_3X_2\}^{2+}$, $\{M_2L_3X\}^{3+}$ and $\{M_2L_3\}^{4+}$ consistent with this formulation. Modelling indicates that this formulation is consistent only with a triple-helical structure. Recrystallisation of the tetrafluoroborate complex salt from methanol afforded crystals suitable for X-ray analysis.† The structure of one of the two enantiomers of the cation is shown in Fig. 1 and confirms the formation of the triple-helical structure. Each nickel(II) centre is bound to three pyridylimine binding units to attain a pseudo-octahedral coordination geometry. Coordination to the metal centre forces interannular twisting between the phenylene ring and the pyridylimine unit and the logical consequence is the formation of a triple-helical array. The bond lengths and angles are unremarkable and the two nickel(II) centres are separated by 11.576(1) Å. The ligand twists through a half-turn around the metal–metal axis leading to a helical pitch of about 27 Å. This compares with pitches of around 18 Å for Williams' cobalt triple helicates[4] and 41 Å for Lehn's nickel triple helix.[3] The twisting of the phenylene units results in a chiral aryl-lined cavity at the centre of the helix with the shortest carbon–centroid distance *ca.* 2.8 Å, giving a 'hole' with the potential to trap small molecules. No face–face π-stacking interactions are observed.

Reaction of methanol solutions of 3 equiv. of the ligand with 2 equiv. of iron(II) salts leads to the instantaneous formation of

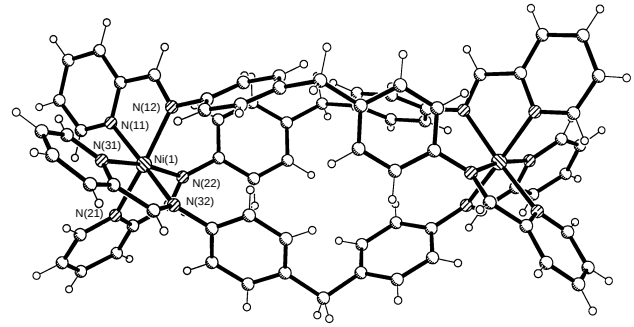



**Fig. 1** Crystal and molecular structure of the cation $[Ni_2L_3]^{4+}$

purple solutions. Heating at reflux for 3 h followed by treatment with $[NH_4][X]$ gives similar $[Fe_2L_3][X]_4$ salts. The purple colour ($\lambda_{max}$ = 572 nm, $\varepsilon$ = 15 000 dm$^3$ mol$^{-1}$ cm$^{-1}$) is characteristic of iron(II) trispyridylimine compounds. Mass spectrometric analysis (ESI) is consistent with this formulation and a preliminary crystallographic study has confirmed the triple-helical nature of the cation. The 250 MHz $^1$H NMR spectrum of this diamagnetic compound in $CD_3CN$ reveals, as anticipated, the presence of one aliphatic and seven aromatic proton resonances. The phenylene rings in the spacer rotate freely at room temperature and the four protons give rise to two resonances. As the temperature is decreased to 243 K, the rate of rotation decreases and the peaks split to give four resonances.

Reacting the ligand with tetrahedral metal ions such as copper(I) and silver(I) gives rise to dimeric $[M_2L_2]^{2+}$ cations. Whilst modelling indicates a unique triple-helical structure when the ligand complexes to octahedral metal ions, the flexibility of the ligand is such that for the dimeric $[M_2L_2]^{2+}$ species two conformations are possible: a double-helical structure or a non-helical bridging cage-like structure. At low temperature, the $^1$H NMR spectra of $CD_3CN$ solutions of the salts show the presence of two species, one of which is present only in small amounts. Similar behaviour in potentially double-helical systems has been reported by Harding and Sauvage.[12] This is the subject of further investigation.

We have established a novel ligand system which is prepared simply by mixing inexpensive commercial reagents and which allows us to generate a complex triple-helical molecular architecture. This inexpensive system makes the triple-helical architecture readily accessible for the first time. We are currently investigating the possibililty of binding small molecules in the chiral helical cavity and we are also developing our approach further to create related ligands with which we will address a variety of alternative architectures.

We are grateful to the Nuffield Foundation for an Award to Newly Appointed Science Lecturers (M. J. H.) and an Undergraduate Research Bursary (NUF-URB96; A. J.), the EPSRC for a studentship (C. L. P.) and the Swansea National Mass Spectrometry Centre for recording the mass spectra.

## Footnotes and References

* E-mail: m.j.hannon@csv.warwick.ac.uk

† *Crystal data* for $[Ni_2L_3][BF_4]_4$·2MeOH; $C_{77}H_{67}O_2N_{12}B_4F_{16}Ni_2$, $M$ = 1657.09, monoclinic, space group $C2/c$, $a$ = 29.037(2), $b$ = 10.4395(10), $c$ = 24.446(3) Å, $\beta$ = 93.025(3)°, $U$ = 7400.1(11) Å$^3$, $Z$ = 4, $T$ = 180(2) K, $\mu$ = 0.606 mm$^{-1}$. Goodness-of-fit on $F^2$ was 1.008, $R1$ [for $I > 2\sigma(I)$] = 0.056, $wR2$ = 0.142 for 551 parameters. Largest diff. peak and hole 0.715 and −0.367 e Å$^{-3}$. Data were collected using a Siemens SMART CCD area-detector diffractometer; a multiscan absorption correction was applied using SADABS[14] and gave $T_{max,min}$ = 0.94, 0.79. The structure was solved by direct methods using SHELXTL-PC[15] and refined by full matrix least-squares on $F^2$ for all data using SHELXL-96.[13] CCDC 182/570.

1 *Comprehensive Supramolecular Chemistry*, ed. J.-M. Lehn, Pergamon, Oxford, 1996; D. Philp and J. F. Stoddart, *Angew. Chem., Int. Ed. Engl.*, 1996, **35**, 1155.
2 E. C. Constable, *Prog. Inorg. Chem.*, 1994, **42**, 67; E. C. Constable, A. J. Edwards, M. J. Hannon and P. R. Raithby, *J. Chem. Soc., Chem. Commun.*, 1994, 1991; E. C. Constable, S. M. Elder, M. J. Hannon, A. Martin, P. R. Raithby and D. A. Tocher, *J. Chem. Soc., Dalton Trans.*, 1996, 2423; E. C. Constable, M. J. Hannon, A. J. Edwards and P. R. Raithby, *J. Chem. Soc., Dalton Trans.*, 1994, 2669.
3 J.-M. Lehn, *Supramolecular Chemistry—Concepts and Perspectives*, VCH, Weinheim, 1995.
4 A. F. Williams, *Pure Appl. Chem.*, 1996, **68**, 1285; C. Piguet, G. Bernardinelli, B. Bocquet, A. Quattropani and A. F. Williams, *J. Am. Chem. Soc.*, 1992, **114**, 7440; M. Albrecht and R. Frohlich, *J. Am. Chem. Soc.*, 1997, **119**, 1656; E. J. Enemark and T. D. P. Stack, *Angew. Chem., Int. Ed. Engl.*, 1995, **34**, 996; B. Kersting, M. Meyer, R. E. Powers and K. N. Raymond, *J. Am. Chem. Soc.*, 1996, **118**, 7221.
5 J. C. Chambron, C. O. Dietrich-Buckecker, V. Heitz, J. J. Nierengarten, J. P. Sauvage, C. Pascard and J. Guilheim, *Pure Appl. Chem.*, 1995, **67**, 233 and references therein.
6 M. J. Hannon, C. L. Painting and W. Errington, *Chem. Commun.*, 1997, 307; M. Fujita and K. Ogura, *Bull. Chem. Soc. Jpn.*, 1995, **69**, 1471; P. J. Stang and K. Chen, *J. Am. Chem. Soc.*, 1995, **117**, 1667 and references therein.
7 B. Hasenknopf, J.-M. Lehn, B. O. Kneisel, G. Baum and D. Fenske, *Angew. Chem., Int. Ed. Engl.*, 1996, **35**, 1838.
8 E. C. Kesslen and W. B. Euler, *Tetrahedron Lett.*, 1995, **36**, 4725; M. J. Hannon, A. Jackson and L. J. Clemo, unpublished results.
9 D. M. Haddleton, C. B. Jasieczek, M. J. Hannon and A. J. Shooter, *Macromolecules*, 1997, **30**, 2190.
10 G. C. van Stein, G. van Koten, K. Vriez, C. Brevard and A. L. Spek, *J. Am. Chem. Soc.*, 1984, **106**, 4486; D. E. Fenton, R. W. Matthews, M. McPartlin, B. P. Murphy, I. J. Scowen and P. A. Tasker, *J. Chem. Soc., Chem. Commun.*, 1994, 1391; P. Comba, A. Fath, T. W. Hambley and D. T. Richens, *Angew. Chem., Int. Ed. Engl.*, 1995, **34**, 1883.
11 B. R. Serr, K. A. Andersen, C. M. Elliott and O. P. Anderson, *Inorg. Chem.*, 1988, **27**, 4499.
12 A. Bilyk, M. M. Harding, P. Turner and T. W. Hambley, *J. Chem. Soc., Dalton Trans.*, 1994, 2783; C. O. Dietrich-Buchecker, J. F. Nierengarten, J. P. Sauvage, N. Armaroli, V. Balzani and L. DeCola, *J. Am. Chem. Soc.*, 1993, **115**, 11 237.
13 G. M. Sheldrick, SHELXL-96, Program for Crystal Structure Refinement, University of Göttingen, Germany, 1996.
14 G. M. Sheldrick, SADABS, Empirical Absorption Corrections Program, University of Göttingen, Germany, 1997.
15 Siemens, SHELXTL-PC Version 5.0 Reference Manual, Siemens Industrial Autom., Inc., Analytical Instrumentation, Madison, WI, USA, 1994.

*Received in Basel, Switzerland, 28th May 1997; 7/03713I*

# A cage ligand with three convergent pyridine donors†

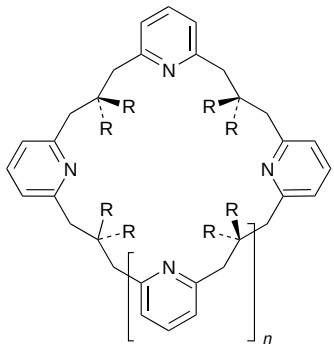
**Fritz Vögtle,*[a] Stefan Ibach,[a] Martin Nieger,[b] Christine Chartroux,[c] Torsten Krüger,[c] Holger Stephan[c] and Karsten Gloe[c]**

[a] *Kekulé-Institut für Organische Chemie und Biochemie, Universität Bonn, Gerhard-Domagk-Str. 1, 53121 Bonn, Germany*
[b] *Anorganisch Chemisches Institut der Universität Bonn, Gerhard-Domagk-Str. 1, 53121 Bonn, Germany*
[c] *Institut für Anorganische Chemie, Technische Universität Dresden, 01062 Dresden, Germany*

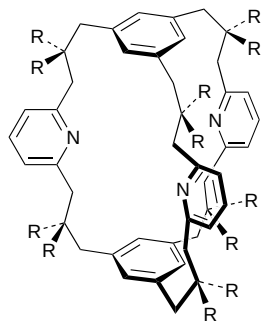
**A macrocyclic malonic ester condensation with pyridine building blocks leads to the new bicyclic host molecule 1 with defined cavity size, the X-ray structure analysis of which reveals three convergent nitrogen donor centres; in radiotracer phase-transfer measurements 1 turns out to be remarkably selective for $Ag^{I}$ cations while discriminating against $Cu^{I}$ and $Cu^{II}$ cations.**

Owing to their interesting complexation behaviour, pyridine subunits play an important role as donor sites for selective complexation of cations.[1,2] In this context Newkome's Cryptanal,[3] the bipyridine cryptands[4] synthesised by Lehn and coworkers, aza-bridged cage ligands[5] and homocalixpyridines[6] are characteristic examples.

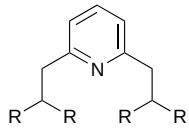
A few years ago we reported about macromonocyclic ligands containing pyridine subunits of the metacyclophane type **I**,



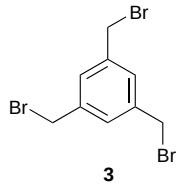
**I** R = $CO_2Et$



**1** R = $CO_2Et$



**2** R = $CO_2Et$



**3**

which could be obtained with different ring sizes by a malonic ester condensation-like pathway.[7] Now we are able to extend this method into the third dimension and to obtain the macrobicyclic tris(pyridine) cage ligand **1**. Because of the convergent (*endo*) orientation of the pyridine nitrogens in **1**, a cooperative binding of guest ions and incorporation in the cavity should be possible. In addition, the overall 12 peripheral ethyl ester groups guarantee good solubility in organic solvents like $CHCl_3$, $CH_2Cl_2$, THF and acetone.

The synthesis of **1** was achieved as follows: the tetraethyl ester[7] **2** and 1,3,5-tris(bromomethyl)benzene[8] **3** were added dropwise and simultaneously under dilution conditions to a stirred suspension of NaH in refluxing 1,4-dioxane, and stirred for 48 h. The reaction mixture was then concentrated *in vacuo*, and the oily residue recovered was dissolved in $CH_2Cl_2$, washed with diluted HCl and water and dried over $Na_2SO_4$ to give a brown oil upon removal of the solvent. After chromatographic separation of the crude product, **1**‡ was isolated as colourless crystals (mp 203 °C, EtOH–$CHCl_3$) in 4% yield.§ The rather poor yield is due to the fact that five components must approach each other to close six σ-bonds and is in accordance with the literature.[1a,9] The optimisation of the yield by stepwise synthesis[1b] or metal ion template strategy (*e.g.* caesium or silver) is currently being investigated.

Indeed, the X-ray structure of **1** shows an *endo* orientation of the pyridine units with a distance of 475 pm between two pyridine nitrogen atoms [N(1), N(2)], while the third pyridine nitrogen N(3) has distances of 771 and 749 pm, respectively, from these two atoms [Fig. 1]. The two benzene rings are not exactly parallel to each other, and the distance between their centres is 454 pm. The deviation from the parallel orientation amounts to 36°. Thus, the cavity of the free ligand is slightly contracted.¶

Molecular modeling calculations revealed almost the same conformation [*cf.* Fig. 1]. The calculated minimum energy conformation of the ligand (PM3) is in very good accordance with the X-ray results (RMS deviation 0.13 Å).

The ligand **1** therefore seems to be suitable for the complex formation with metal ions preferring a linear coordination ($Cu^{I}$, $Ag^{I}$) between the two adjacent pyridine donor atoms. Starting from the minimum energy conformation, a silver complex of **1** was calculated (ZINDO/1). The conformation of the complexed ligand is only a little changed compared to the free ligand. The silver ion is arranged in the middle of N(1) and N(2), both Ag–N bonds being 251 pm long. Additional interaction with N(3) or with benzene rings seems unlikely considering the steric situation.

The complexation behaviour of **1** has been studied experimentally by liquid–liquid extraction[10]‖ measurements: as designed, the pyridine-containing cage ligand **1** shows evidence for $Ag^{I}$ selectivity in extraction. Under experimentally chosen conditions 19.5% of the silver were transferred into the organic phase. In contrast to this, the other metal ions investigated ($Na^{I}$, $Tl^{I}$, $Cu^{I}$, $Ca^{II}$, $Cu^{II}$, $Zn^{II}$, $Hg^{II}$) remained in the aqueous phase (> 99.9%). The high selectivity for $Ag^{I}$ over $Cu^{I}$, $Cu^{II}$ and $Hg^{II}$

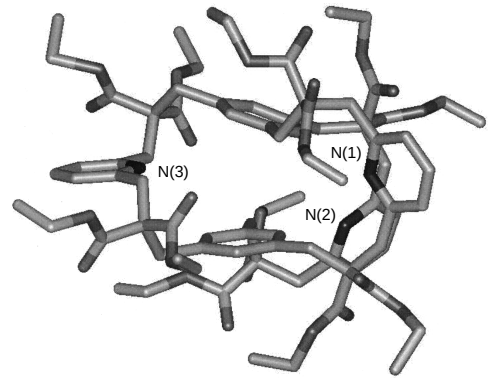
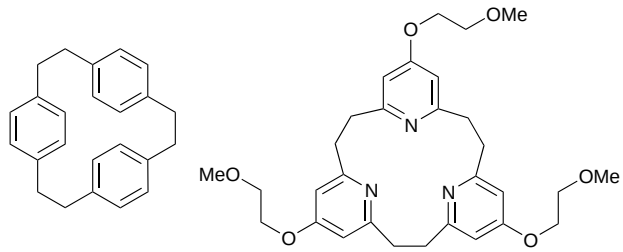



**Fig. 1** X-Ray structure of **1** (side view)

is particularly remarkable. Measuring the distribution ratio $D_{Ag}$ as a function of the ligand concentration in the organic phase, the data obtained with a slope of 1 from the Log $D_{Ag}$ *vs.* Log $c_L$ diagram indicate that 1 : 1 complexes are formed both in picrate (Log $K_{Ex,1}$ = 4.35) and nitrate (Log $K$ = 1.33) containing solution.

Compound **1** turns out to be a more efficient silver extracting reagent than silver-selective concave hydrocarbons[11] and the hydrocarbon [2.2.2]paracyclophane (**4**, picrate system, Log




**4** **5**

$K$ = 3.62) while remaining very selective [Fig. 2]. The interaction of the pyridine nitrogen with the silver ion is apparently stronger than that of π-donors. When a third pyridine nitrogen donor atom is introduced into a ligand molecule (at a suitable distance), the silver affinity is further raised. This is the case for the *all*-homocalix[3](2,6) pyridine (**5**, nitrate system, Log $K_{Ex,1}$ = 5.00)[12,6] with a much more coplanar orientation of the pyridine rings compared to **1**. However, it is at the expense of the separation selectivity; in the case of **5**, mercury(II) and copper(II) ions are extracted as well [Fig. 2].

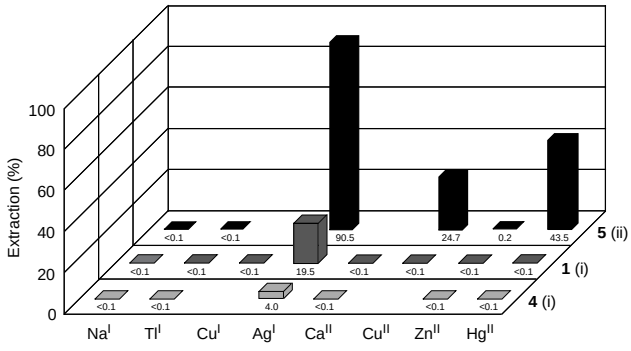



**Fig. 2** Extraction of different metal ions using compounds **1**, **4** and **5**. *Experimental conditions*: (i) [$AgNO_3$] = 1 × $10^{-4}$ M, [picric acid] = 1 × $10^{-2}$ M, [ligand] = 5 × $10^{-4}$ to 5 × $10^{-2}$ M, $CHCl_3$; (ii) [$AgNO_3$] = 1 × $10^{-4}$ M, [$KNO_3$] = 1 × $10^{-1}$ M, pH 6.3 (MES–NaOH buffer, 5 × $10^{-2}$ M), [ligand] = 5 × $10^{-4}$ to 4 × $10^{-3}$ M, $CHCl_3$.

The MALDI-TOF mass spectrum of ligand **1** revealed the molecule peak $[M]^+$ and the species $[Na\cdot\mathbf{1}]^+$ (*m/z* 1519.8) and $[K\cdot\mathbf{1}]^+$ (*m/z* 1535.7). The addition of $CF_3SO_3Ag$ to the sample solution totally suppresses $[Na\cdot\mathbf{1}]^+$ and $[K\cdot\mathbf{1}]^+$ and is accompanied by the formation of $[Ag\cdot\mathbf{1}]^+$ (*m/z* 1607.4).

Because of its ability to form stable complexes due to its novel molecular architecture and its well balanced lipophilicity, **1** is a highly selective phase-transfer host for silver ions. Replacing the ethyl ester groups by long chain aliphatic ones will lead to (ion selective) membrane insertable $Ag^I$ ligands.[13] Similar novel host molecules with larger cavities having more pyridine donor sites should be accessible for the selective complexation of biological relevant guests such as carbohydrates, amino acids, purine and pyrimidine bases.[1b]

We thank the Deutsche Forschungsgemeinschaft for partial support of this work (Vo 145/46-1, GI 183/3-1), and Professor Dr G. R. Newkome, University of South Florida, for providing unpublished results regarding Cryptanal.

## Footnotes and References

* E-mail: voegtle@uni-bonn.de

† A part of this work has been presented as poster contribution at the Symposium on Bioorganic and Bioinorganic Chemistry, Münster, Germany, December 1996.

‡ IUPAC name of **1**: 5,5,13,13,21,21,29,29,34,34,42,42-dodekakis(ethoxycarbonyl)-45,47,48-triazaheptacyclo-[15.15.11.1$^{3,31}$.1$^{7,11}$.1$^{15,19}$.1$^{23,27}$.-1$^{36,40}$]octatetraconta-1,3(44),7(45),8,10,15(46),16,18,23(47),24,26,31,-36(48),37,39-pentadecaene.

§ **1** was fully characterised by $^1$H and $^{13}$C NMR spectroscopy and MALDI-TOF-MS. Elemental analysis: Calc. for $C_{81}H_{99}N_3O_{24}\cdot 2H_2O$: C, 63.35; H, 6.83; N, 2.74; O, 27.09. Found: C, 63.43; H, 6.60; N, 2.76%; sample was recrystallized for X-ray analysis.

¶ *Crystal data* for **1**: $C_{81}H_{99}N_3O_{24}$, $M_r$ = 1498.63, triclinic, space group $P\bar{1}$ (no. 2), $a$ = 13.131(1), $b$ = 13.554(1), $c$ = 22.520(1) Å, $\alpha$ = 88.24(1), $\beta$ = 86.82(1), $\gamma$ = 89.64(1)°, $V$ = 3997.0(5) Å$^3$, $Z$ = 2, $\mu$(Cu-Kα) = 0.759 mm$^{-1}$, $F$(000) = 1596, $T$ = 293(2) K, residual electron density 0.41 and −0.46 e Å$^{-3}$, 12 395 intensity data ($2\Theta_{max}$ = 120°) were collected, 11 809 unique data were used for the structure solution (direct methods) and refinement (full-matrix least-squares on $F^2$, 959 parameters, 16 restraints) to $wR2$ = 0.184 [$R_1$ = 0.062 for $I > 2\sigma(I)$]. CCDC 182/563.

‖ Liquid–liquid extraction investigations were performed according to ref. 11. Screening tests were made in the system metal nitrate (1 × $10^{-4}$ M)–picric acid (1 × $10^{-2}$ M), ligand **1** (1 × $10^{-3}$ M) in $CHCl_3$, without buffer for $Na^I$, $Tl^I$, $Ag^I$, $Ca^{II}$, $Cu^{II}$, $Zn^{II}$, $Hg^{II}$ and copper nitrate (1 × $10^{-4}$ M), and hydroxylammonium sulfate (5 × $10^{-3}$ M)–$KNO_3$ (1 × $10^{-2}$ M) in MES–NaOH buffer (pH 5.3) for $Cu^I$, respectively. After a shaking time of 30 min the equilibrium was reached. Control experiments were performed for each metal ion over a 24 h period.

1 (*a*) For an overview, see *Comprehensive Supramolecular Chemistry*, ed. J. L. Atwood, J. E. D. Davies, D. D. MacNicol and F. Vögtle, Pergamon, Oxford, 1996, Vol. 1; (*b*) F. Vögtle, C. Seel and P.-M. Windscheif, *ibid.*, vol. 2, p. 211; (*c*) A. v. Zelewsky, *Stereochemistry of coordination compounds*, Wiley, Chichester, New York, 1996; (*d*) E. C. Constable, *Metals and ligand reactivity*, VCH, Weinheim, New York, Basel, Cambridge, Tokyo, 1995.

2 T. W. Bell and S. K. Sahni, *Inclusion Compounds*, ed. J. L. Atwood, J. E. D. Davies and D. D. MacNicol, Oxford University Press, Oxford, New York, Tokyo, 1991, vol. 4, p. 325; G. R. Newkome and V. K. Majestic, *Top. Curr. Chem.*, 1982, **106**, 79.

3 G. R. Newkome, V. K. Majestic and F. R. Fronczek, *J. Am. Chem. Soc.*, 1979, **101**, 1047; G. R. Newkome, V. K. Majestic and F. R. Fronczek, *Tetrahedron Lett.*, 1981, **22**, 3035.

4 J. M. Lehn, *Supramolecular Chemistry*, VCH, Weinheim, New York, Basel, Cambridge, Tokyo 1995; J. de Mendoza, E. Mesa, J.-C. Rodriguez-Ubis, P. Vázquez, F. Vögtle, P.-M. Windscheif, K. Rissanen, J.-M. Lehn, D. Lilienbaum and R. Ziessel, *Angew. Chem., Int. Ed. Engl.*, 1991, **30**, 1331.

5 H. Takemura, N. Kon, K. Tani, K. Takehara, J. Kimoto, T. Shinmyozu and T. Inazu, *J. Chem. Soc., Perkin Trans. 1*, 1997, 239; I. M. Atkinson, A. M. Groth, L. F. Lindoy, O. A. Matthews and G. V. Meehan, *Pure Appl. Chem.*, 1996, **68**, 1231; L. F. Lindoy, *2nd International Symposium on Macrocyclic Chemistry*, Program and Abstracts, Seoul, Korea, 1997, p. 22.

6 F. Vögtle, G. Brodesser, M. Nieger and K. Rissanen, *Recl. Trav. Chim. Pays-Bas*, 1993, **112**, 325.

7 C. Meiners, M. Nieger and F. Vögtle, *Liebigs Ann. Chem.*, 1996, 297; see also M. Zuber and F. Vögtle, *Synthesis*, 1972, 543; T. Shinmyozu, T. Inazu and T. Yoshino, *Chem. Lett.*, 1976, 1405.

8 N. L. Allinger, M. A. DaRooge and R. B. Herman, *J. Am. Chem. Soc.*, 1964, **83**, 6878; F. Vögtle, M. Zuber and G. Lichtenthaler, *Chem. Ber.*, 1973, **106**, 717.

9 B. Dietrich, P. Viout and J.-M. Lehn, *Macrocyclic Chemistry*, VCH, Weinheim, New York, Basel, Cambridge, Tokyo, 1993, p. 241.

10 K. Gloe and P. Mühl, *Isotopenpraxis*, 1979, **15**, 236; 1983, **19**, 257.

11 J. Groß, G. Harder, A. Siepen, J. Harren, F. Vögtle, H. Stephan, K. Gloe, B. Ahlers, K. Cammann and K. Rissanen, *Chem. Eur. J.*, 1996, **2**, 1585.

12 H. Stephan, T. Krüger, K. Gloe, G. Brodesser, F. Vögtle, W. Hasse, B. Ahlers, K. Cammann and K. Rissanen, unpublished work.

13 In cooperation with Professor K. Cammann, ICB Münster, Germany; see for reference: K. Cammann, *Das Arbeiten mit Ionenselektiven Electroden*, Springer, Berlin, Heidelberg, New York, 1966.

*Received in Liverpool, UK, 28th May 1997; 7/03715E*

# Synthesis of fluorinated block copolymers and their application as novel polymerisation surfactants in supercritical carbon dioxide

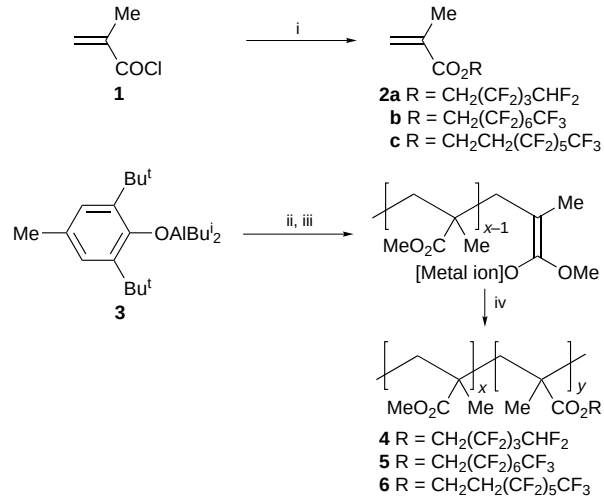
**Tuck-Mun Yong,[a] William P. Hems,[b] Johanna L. M. van Nunen,[b] Andrew B. Holmes,*[a,b] Joachim H. G. Steinke,[b] Philip L. Taylor,[c] John A. Segal[d] and David A. Griffin[e]**

[a] *Department of Chemistry, University of Cambridge, Lensfield Road, Cambridge, UK CB2 1EW*
[b] *Melville Laboratory for Polymer Synthesis, Department of Chemistry, University of Cambridge, Pembroke Street, Cambridge, UK CB2 3RA*
[c] *ICI Paints, Decorative Research, Wexham Road, Slough, UK SL2 5DS*
[d] *ICI Acrylics, PO Box 90, Wilton Middlesbrough, Cleveland, UK TS90 8JE*
[e] *Zeneca Agrochemicals, Jealott's Hill Research Station, Bracknell, UK RG12 6EY*

**Screened anionic copolymerisation of methyl methacrylate with the perfluoroalkyl methacrylates 2 affords well-defined AB block copolymers 4–6, which serve as effective surfactants in the dispersion polymerisation of methyl methacrylate in supercritical carbon dioxide.**

Fluorinated polymers possess interesting properties such as low surface energy, toughness, good chemical resistance and high temperature stability.[1–3] It is consequently expected that AB block copolymers consisting of a flexible poly(methyl methacrylate) (PMMA) block and a more rigid poly(perfluoroalkyl methacrylate) (PFMA) block will also exhibit interesting properties, and that they may have potential uses in specialist applications. The 'screened' anionic polymerisation (SAP) method has been developed to obtain well-defined block copolymers of methyl methacrylate (MMA) derivatives with narrow molecular weight distribution.[4] The key advantage of this methodology is the ability to operate at temperatures close to 0 °C while maintaining a controlled polymerisation, which results from the 'shielding' of the propagating terminus from unwanted side reactions by a bulky lithium–aluminium alkyl complex at the enolate chain-end. We report the use of a modified SAP methodology for the synthesis of AB block copolymers, consisting of a PMMA block and a PFMA block, as well as their application as novel surfactants in the dispersion polymerisation of methyl methacrylate in supercritical carbon dioxide ($scCO_2$).[5]

The syntheses of three AB block copolymers **4**, **5** and **6** with different lengths of perfluoroalkyl side chains in the PFMA block are shown in Scheme 1. The fluorinated monomers **2** were synthesised by esterification of methacryloyl chloride **1** with the corresponding fluorinated alcohols in the presence of triethylamine. Table 1 summarises the polymerisation results. The SAP initiator was prepared by mixing *tert*-butyllithium with (2,6-di-*tert*-butyl-4-methylphenoxy)diisobutylaluminium [Al(BHT)-$Bu^i_2$] **3** in toluene at 0 °C. A toluene solution of methyl methacrylate (MMA) was added dropwise to the initiator and polymerisation took place within minutes. Directly afterwards, a toluene solution of fluorinated monomer **2** was added to the reaction mixture. This resulted in ill-defined block copolymers for some examples (*e.g.* entry 3) where the proportion of **2b** incorporated into the PFMA block was less than expected, as indicated by the yield and $^1$H NMR analysis. Gel permeation chromatography (GPC) against polystyrene standards revealed that the sample contained a copolymer with broad molecular weight distribution, whereas a sample of the PMMA block obtained before addition of **2b** revealed a polymer composition of low polydispersity ($Mw/Mn \leqslant 1.3$). This indicated that loss of control occurred after addition of **2b**, which is probably a result




**Scheme 1** *Reagents and conditions*: i, ROH, $Et_3N$, THF, 69–79%; ii, $Bu^tLi$, PhMe, 0 °C; iii, MMA, PhMe; iv, **2**, PhMe, 1,3-bis(trifluoromethyl)benzene, −10 °C

**Table 1** Synthesis of AB block copolymers **4**, **5** and **6**[a]

| Entry | **2** (mmol) | Solvent[b] | Polymer | PMMA : PFMA[c] | Yield[d] (%) | $M_n$[e]/$10^{-3}$ | $M_w/M_n$[e] |
|---|---|---|---|---|---|---|---|
| 1 | **2a** (5.9) | 1 : 0 | **4′** | 1.0 : 2.1 | 76 | 20.0 | 1.2 |
| 2 | **2a** (5.8) | 3 : 1 | **4″** | 1.0 : 2.3 | 83 | 19.0 | 1.2 |
| 3 | **2b** (1.9) | 1 : 0 | **5′** | 1.0 : 0.3 | 45 | *f* | *f* |
| 4 | **2b** (1.9) | 4 : 3 | **5″** | 1.0 : 0.6 | 86 | 217 | 1.1 |
| 5 | **2c** (2.5) | 1 : 3 | **6′** | 1.0 : 1.1 | 81 | 17 | 1.5 |
| 6 | **2c** (3.5) | 1 : 15 | **6″** | 1.0 : 1.3 | 72 | 197 | 1.3 |

[a] To initiate the polymerisation a mixture of *tert*-butyllithium (0.17 mmol) and Al(BHT)$Bu^i_2$ (0.7 mmol) was used. In each experiment 2.8 mmol of MMA were used except entry 5 (2.5 mmol). [b] Ratio (v/v) toluene : 1,3-bis(trifluoromethyl)benzene. [c] Determined from $^1$H NMR spectroscopy. [d] Yields quoted after two reprecipitations in hexane. [e] From GPC analysis ($CHCl_3$, polystyrene standards). [f] GPC assay revealed two peaks: (i) $M_n$ 16 400 $M_w/M_n$ 1.3, (ii) $M_n$ 245 000 $M_w/M_n$ 2.0.

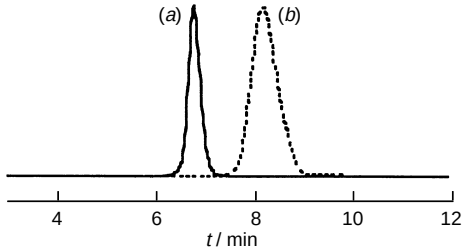
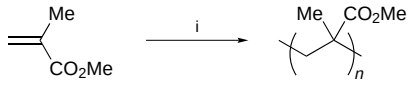



**Fig. 1** GPC trace (polystyrene standards, $CHCl_3$) of a sample of (*a*) **5″** ($M_n$ 218 000, $M_w/M_n$ 1.1) and (*b*) the PMMA block before addition of **2b** ($M_n$ 9300, $M_w/M_n$ 1.3)

of the insolubility of the propagating fluorinated block. In the case of the copolymer **4′** with a shorter perfluoroalkyl side chain, this solubility problem was less apparent. Good yields of **4′** were obtained, and the polydispersity was relatively narrow, even for samples with a high proportion of PFMA in relation to the PMMA block (entry 1). The solubility problem could be overcome by the use 1,3-bis(trifluoromethyl)benzene as a co-solvent with toluene, which enabled the preparation of block copolymer **5″** with a high proportion of PFMA block (entry 4). The GPC chromatogram of copolymer **5″** is shown in Fig. 1. The chromatogram of a sample of PMMA obtained before addition of **2b** is also shown. Both unimodal traces with narrow polydispersity reveal that a controlled polymerisation is maintained throughout the reaction.†

Block copolymers can exhibit micelle-like aggregation if they are dissolved in a solvent which is more selective towards one of the blocks.[6] Fluorinated homopolymers have been known to be very soluble in both liquid $CO_2$ and $scCO_2$.[7] In the case of the AB block copolymers described above, the PFMA block will have a much higher solubility in $scCO_2$ compared with the PMMA block, and may thus be employed as a stabiliser or surfactant in a dispersion polymerisation.[7] In preliminary studies we have polymerised MMA under free radical conditions in $scCO_2$ using copolymers **4** and **6** as surfactants (Scheme 2).[8] These results demonstrate that these surfactants play an important rôle in stabilising a dispersion of the growing PMMA chain in $scCO_2$. In the presence of **4″** (Table 2, entry 2), both the yield and molecular weight ($M_n$) of the polymer are significantly higher than observed in the control experiment without surfactant (Table 2, entry 1). However, elongation of the fluorinated side-chain improved these results even more (Table 2, entry 3). The effect of the molecular weight of the surfactant, where there is an increase of the length of the different blocks, is illustrated by comparing the surfactant **6′** with **6″**. In the latter case (Table 2, entry 4) we were able to obtain PMMA as a free flowing powder together with further increase in molar mass.

In summary, we have developed a highly controlled synthesis of fluorinated AB block copolymers. The ability to vary the side chain as well as to 'tune' the length of the different blocks in these block copolymers, according to specific requirements, is an advantage of the synthetic route described. Moreover, the improved stabilising efficiency of block copolymer **6″**, compared with block copolymer **4″**, in the dispersion polymerisation of MMA in $scCO_2$ demonstrates the applicability of this synthetic methodology. We shall describe the power of the tunability of the surfactant in a forthcoming publication.




**Scheme 2** *Reagents and conditions*: i, AIBN, $scCO_2$, 285 bar, 70 °C, 5 h, **4** or **6**

**Table 2** Radical polymerisation of MMA (1.2 M) with AIBN (2 wt%) as initiator in $scCO_2$ with and without block copolymers as surfactant

| Entry | Surfactant (1 wt%) | Yield[a] (%) | $M_n$[b]/$10^{-3}$ | $M_w/M_n$[b] |
|---|---|---|---|---|
| 1 | — | 22 | 12.0 | 2.0 |
| 2 | **4″** | 56 | 38.0 | 2.2 |
| 3 | **6′** | 69 | 77.4 | 3.0 |
| 4 | **6″** | 72[c] | 81.9 | 2.3 |

[a] Yields quoted after two reprecipitations in hexane. [b] GPC analysis ($CHCl_3$, polystyrene standards) confirmed by multiple angle light scattering analysis in THF. [c] Yield quoted without reprecipitation; free-flowing powder obtained.

We thank EPSRC for support of this work and provision of the Swansea Mass Spectroscopy Service, ICI for a Strategic Research Fund award (T. M. Y.), the UK Committee of Vice-Chancellors and Principals for an ORS award, the Cambridge Commonwealth Trust for a bursary, Clare College for a Research Fellowship (T. M. Y.) and Zeneca Agrochemicals for a CASE award (W. P. H.). We acknowledge with gratitude the extensive advice received from Professor M. Poliakoff and Dr S. Howdle (Nottingham).

## Footnotes and References

* E-mail: abh1@cus.cam.ac.uk

† It is possible that the molecular weight obtained for **4**, **5** and **6** is overestimated, owing to the rigidity of the PFMA block compared with the flexible polystyrene reference standards used.

1 H. F. Mark, N. M. Bikales and C. G. Overberger, *Encyclopaedia of Polymer Science*, ed. J. I. Kroschwitz, Wiley, New York, 2nd edn., 1987, vol. 7, p. 256.
2 P. E. Cassidy, T. M. Aminabhavi and J. M. Faraday, *J. Macromol. Sci. Rev. Macromol. Chem. Phys.*, 1989, **C29**, 365.
3 *Contact Angle, Wettability and Adhesion, Advances in Chemistry Series*, ed. W. A. Zisman, ACS Symposium, Washington, 1964, vol. 43.
4 D. G. H. Ballard, R. J. Bowles, D. M. Haddleton, S. N. Richards, R. Sellens and D. L. Twose, *Macromolecules*, 1992, **25**, 590.
5 For the use of fluorinated homopolymers as surfactants, see Z. Guan and J. M. DeSimone, *Macromolecules*, 1994, **27**, 5527; J. M. DeSimone, E. E. Maury, Y. Z. Menceloglu, J. B. McClain, T. J. Romack and J. R. Combes, *Science*, 1994, **265**, 356.
6 L. J. Vagberg, K. A. Cogan and A. P. Gast, *Macromolecules*, 1991, **24**, 1670 and references cited therein.
7 J. M. DeSimone, Z. Guan and C. S. Elsbernd, *Science*, 1992, **257**, 945.
8 During the course of our study the use of fluorinated block copolymers in the dispersion polymerisation of styrene (see D. A. Canelas, D. E. Betts, J. M. DeSimone, *Macromolecules*, 1996, **29**, 2818) as well as the use of fluorinated graft copolymers in the dispersion polymerisation of MMA in $scCO_2$ was reported (see C. Lepilleur and E. J. Beckman, *Macromolecules*, 1997, **30**, 745).

*Received in Cambridge, UK. 6th May 1997; 7/05399A*

# Novel dimanganese(II) complexes with ($\mu$-$H_2O$)($\mu$-OAc)$_2$ bridges. Models for dimanganese enzymes

**Bao-Hui Ye, Toby Mak, Ian D. Williams and Xiao-yuan Li***

*Department of Chemistry, The Hong Kong University of Science and Technology, Clear Water Bay, Kowloon, Hong Kong*

**We describe the syntheses and characterization of two new complexes, $Mn_2(\mu\text{-}H_2O)(\mu\text{-}OAc)_2(L)_4(OAc)_2$ 1 (L = imidazole) and 2 (L = benzimidazole), which display some novel structural features, and may have implications for the hydrolytic activity of arginase.**

The cooperative action of closely coupled dinuclear or multinuclear centers is required for several manganese enzymes to carry out their biological functions.[1,2] In arginase[3] and the ribonuclease H domain of HIV-1 reverse transcriptase,[4] the coupled di-$Mn^{II}$ center is required for the hydrolysis of substrate through activation of a water molecule. In redox-type Mn enzymes such as Mn catalase,[2,5] bacterial ribonucleotide reductase[6] and photosynthetic water oxidase,[2,7] Mn ions were also found or estimated to be assembled in very close proximity by the protein's coordinating side chains such as carboxylate groups from glutamates and/or aspartates.[1] Therefore, carboxylate bridged di- or poly-manganese centers have been attracting growing interest in both synthetic modelling and physical characterization.[8,9] Three di-$Mn^{II}$† model complexes with $[Mn_2(\mu\text{-}H_2O)(\mu\text{-}O_2CR)_2]^{2+}$ cores have been reported to date.[9] One of them is based on all-oxygen coordination spheres,[9a] while the other two are based on $N_2O_4$ coordination spheres around each Mn ion but with synthetic bidentate N-donor ligands.[9b] Our goal has been to synthesize aqua and carboxylate bridged dimetallic complexes employing monodentate N-donor ligands such as imidazole (Im) and benzimidazole (Bzim) which are truly good mimics of the histidine side chain. We chose Im and Bzim as the N-donor ligands not only to avoid the steric strains in most of the bidentate or multidentate ligands but also for utilization of the non-coordinating NH groups which can form hydrogen bonds with neighbouring molecules. Such hydrogen bonding is believed to play a very crucial role in the structural assembly and/or the function of many biological systems.[10] Here we report the syntheses, crystal structures and magnetic properties of two new di-$Mn^{II}$ complexes with a ($\mu$-aqua)bis($\mu$-carboxylate) unit, $[Mn_2(\mu\text{-}H_2O)(\mu\text{-}OAc)_2(L)_4(OAc)_2]$ (L = Im **1**, Bzim **2**), which are very good structural models for the active sites of di-$Mn^{II}$ enzymes such as arginase and manganese catalase. Certain novel structural features in **1** and **2** provide some insight into the possible mode of enzyme action for arginase.[3a]

Complexes **1** and **2** were synthesized by mixing Im or Bzim with $Mn(OAc)_2{\cdot}4H_2O$ in 2.4 : 1 ratio, in absolute ethanol under nitrogen at room temperature. Prism-shaped, pale tan single crystals of **1** and **2** were grown from mixed solvents of absolute ethanol and diethyl ether. Their molecular structures were determined by single-crystal X-ray diffraction.‡ Both complexes are of similar structure and contain a di-$Mn^{II}$ core bridged by an aqua and two bidentate acetates. Each of the $Mn^{II}$ ions is further coordinated by one additional monodentate carboxylate and two N-donor ligands, forming two equivalent but slightly distorted $MnN_2O_4$ octahedra joined at their shared vertex by the oxygen atom of the bridging aqua ligand in a face-to-face fashion (see Fig. 1). The molecules lie on a crystallographically imposed twofold axis passing through the bridging aqua oxygen O(1). The hydrogen atoms of the bridging aqua were revealed as the highest residual electron density peak after all other atoms were included in X-ray structure elucidation. The bridging aquas were identified on the basis of the Mn–O(1) distances in **1** [2.246(2) Å] and in **2** [2.227(2) Å] which are significantly longer than those in $\mu$-O–$Mn^{III}_2$ complexes (1.78–1.81 Å)[8] and those in $\mu$-OH–$Mn^{II}_2$ complexes (2.05–2.09 Å).[8] The Mn···Mn distances in **1** [3.777(1) Å] and **2** [3.756(1) Å] are longer than those in **4** [3.5950(9) Å][9b] and **5** [3.621(2) Å],[9b] but very similar to that in **3** [3.739(2) Å].[9a] This is attributable to the opening up of the Mn–O($H_2$)–Mn angles from *ca*. 110° in **4** and **5** to *ca*. 114° in **1**, **2** and **3**, and the elongation of Mn–O(aqua) distances from 2.182(3) Å in **4** and 2.215(5) Å in **5** to 2.228(7) Å in **3**, 2.227(2) Å in **2** and 2.246(2) Å in **1**. The N–Mn–N angles in **1** (92.6°) and **2** (92.9°) are significantly

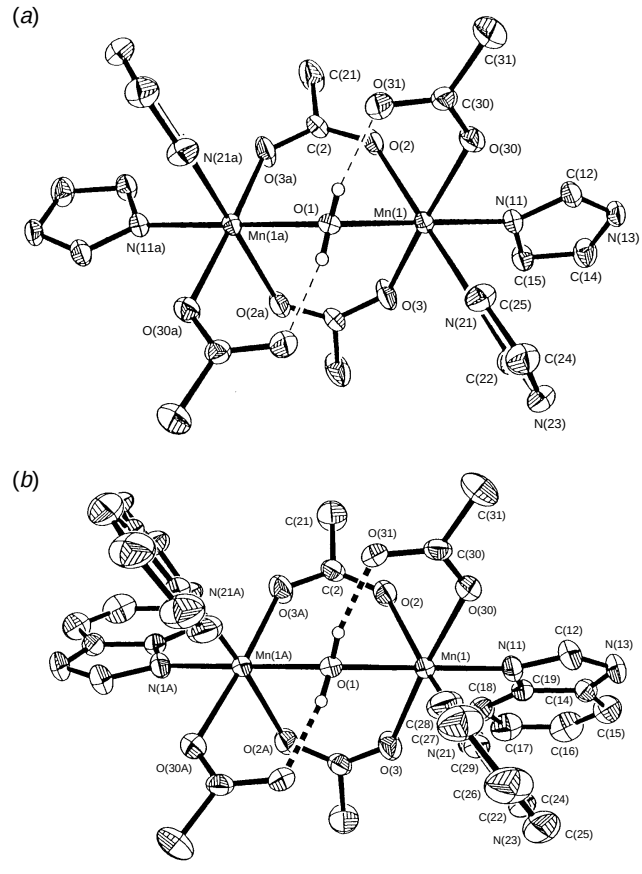



**Fig. 1** Structures of **1** (*a*) and **2** (*b*), showing 40% probability thermal ellipsoids and the atom-labelling scheme. Important interatomic distances (Å) and angles (°) of **1** and **2** [in brackets] are as follows: Mn(1)···Mn(1a) 3.777(1) [3.756(1)], O(1)···O(31) 2.631(5) [2.621(3)], N(23)···O(31b) 2.741(6) [2.737(4)], N(13)···O(2c) 2.775(6) [2.808(4)], Mn(1)–O(1) 2.246(2) [2.227(2)], Mn(1)–O(2) 2.212(3) [2.206(2)], Mn(1)–O(3) 2.109(3) [2.138(2)], Mn(1)–O(30) 2.171(3) [2.183(2)], Mn(1)–N(11) 2.212(3) [2.248(2)], Mn(1)–N(21) 2.249(3) [2.269(3)], Mn(1a)–O(1) 2.246(2) [2.227(2)], C(2)–O(2) 1.252(4) [1.254(4)], C(2)–O(3a) 1.247(4) [1.242(4)], C(30)–O(30) 1.242(4) [1.252(4)], C(30)–O(31) 1.258(4) [1.262(4)]; Mn(1)-O(1)–Mn(1a) 114.4(2) [114.97(14)], O(1)–H(1)–O(31) 164.9(5) [160.6(6)].

larger than those in **4** (72°) and **5** (78°), resulting apparently from the replacement of the bidentate N-donor ligands in the latter by the two monodentate N-donor ligands. The Mn···Mn distances observed in $[Mn^{II}_2(\mu\text{-}H_2O)(\mu\text{-}O_2CR)_2]^{2+}$ cores (3.595–3.777 Å ) are between those observed in the $[Mn^{II}_2(\mu\text{-}OAc)_3]^+$ core [4.034(2) Å][8] and the $[Mn^{II}_2(\mu\text{-}OH)(\mu\text{-}OAc)_2]^+$ core [3.351(3)Å].[8]

Several quite interesting structural features are noticeable in **1** and **2**. First and most important, the terminal monodentate acetate groups display an unexpected geometry. The distances of C–O(free) in **1**, 1.258(4) Å and **2**, 1.262(4) Å, are actually longer than those of their respective C–O(binding) in **1**, 1.242(4) Å and in **2**, 1.252(4) Å. Although this is only just of statistical significance based on the bond length standard deviation, this observation is contrary to the classical geometry of the terminal monodentate binding mode of a carboxylate group. Examination of over 40 related transition-metal carboxylates in the Cambridge Structural Database§ showed that the distance of C–O(free) is typically 0.03Å shorter than that of C–O(binding).[11] The reversal of C–O bond lengths is rare but has been seen, for example, in $M(CO)_5(O_2CCF_3)$ anions (M = Mo, Cr).[12] A careful examination of the structures led us to believe that the elongated C–O(free) distance may be a consequence of two hydrogen bonds, an intramolecular one with the bridging aqua ligand [O(free)···O(1) distance in **1**, 2.631(5) Å and in **2**, 2.621(3) Å] and an intermolecular one with the non-coordinating NH group from an adjacent molecule [O(free)···N in**1**, 2.741(6) Å and in **2**, 2.737(4) Å], giving rise to what may be regarded as a 'pseudo-bridging' arrangement in the terminal acetate groups.[13] The second interesting observation is that the bidentate acetate bridges are markedly asymmetric which can be attributed in part to an additional intermolecular H-bond formed between one oxygen atom of the acetate bridge and the NH group from an adjacent molecule [O(2)···N(13c) distances in**1**, 2.775(6) Å and in **2**, 2.808(4) Å], and in part to the structural *trans* effect. The significance of the observed framework of H-bonds in the formation and stabilization of **1** and **2** can therefore be envisioned. The aqua molecule bridging between two metals is stabilized by intramolecular H-bonds formed with the terminal carboxylates. This typical H-bond plays a crucial role in fixing and activating the bridging aqua or hydroxide in the process of arginine hydrolysis by arginase.[3a] Indeed, search of the CSD§ revealed *ca*. 25 other μ-aqua transition-metal complexes and in almost all cases the μ-aqua ligand was stabilized by H-bonds.

Magnetic susceptibility data for a powder sample of **1** were collected in the temperature range 5–285 K. The molar paramagnetic susceptibility increases with decreasing temperature and reaches a maximum at *ca.* 9 K with $\chi_m T = 2.129$ cm$^3$ mol$^{-1}$ K, below which the susceptibility starts to decrease, indicative of antiferromagnetic coupling between the two $Mn^{II}$ ions. A least-squares fit of the molar susceptibility by the general isotropic exchange Hamiltonian, $H = -2JS_1S_2$, $S_1 = S_2 = 5/2$, produced the best fit with $J = -1.26$ cm$^{-1}$ and $g = 1.97$. The very small negative exchange coupling constant $J$ in **1** is consistent with the relatively large Mn···Mn separation and the weak superexchange provided by the aqua bridge.[9a] The $J$ value found for **1** is comparable with that deduced from EPR measurements for arginase from rat liver ($J = -2.0 \pm 0.5$ cm$^{-1}$),[3b] and that of **4** ($J = -2.73$ cm$^{-1}$) and **5** ($J = -2.952$ cm$^{-1}$).[9b] We also made variable temperature EPR mesurements on **1** and found the same $J$ value as obtained from variable temperature magnetic measurements.

In summary, we have reported the syntheses, the structures and the magnetic properties of two new di-$Mn^{II}$ complexes with (μ-aqua)bis(μ-carboxylate) bridging cores and with monodentate N-donor Im or Bzim ligands in each of the two joint $MnN_2O_4$ coordination spheres. This is the first symmetric di-$Mn^{II}$ complex built up entirely with true mimics of amino acid side chains. The terminal monodentate carboxylates bind to Mn with a distinctive geometry in **1** and **2**, suggesting the possible existence of tautomeric forms of carboxylate in its coordination chemistry. Finally, we believe that the formation of strong H-bonds between the bridging aqua and the ancillary carboxylate groups in **1** and **2** provides a good mimic for arginase in which the terminal carboxylate Asp128 stabilizes and activates the bridging aqua or hydroxide, generating the basic $Mn^{II}_2(\mu\text{-}OH)^{3+}$ or superbasic $Mn^{II}_2(\mu\text{-}O)^{2+}$ by H-bond-guided proton transfer.[3a] The study of the reactivity of the title compounds and related synthetic models are currently in progress.

This work was supported by the Research Grant Council of Hong Kong, the Croucher Foundation and Hong Kong University of Science and Technology.

## Footnotes and References

* E-mail: chxyli@usthk.ust.hk

† $[Mn_2(\mu\text{-}H_2O)(\mu\text{-}O_2CC_2F_5)_2(L)_2(O_2CC_2F_5)_2(H_2O)_2]$ **3**, L = 2-ethyl-4,4,5,5-tetramethyl-3-oxo-4,5-dihydro-1H-imidazolyl-1-oxyl; $[Mn_2(\mu\text{-}H_2O)(\mu\text{-pivalate})_2(L)_2(\text{pivalate})_2]$ **4**, L = 4,4′-dimethyl-2,2′-bipyridine; $[Mn_2(\mu\text{-}H_2O)(\mu\text{-}OAc)_2(L)_2(OAc)_2]$ **5**, L = *N*,*N*,*N*′,*N*′-tetramethylethylenediamine.

‡ *Crystal data* for **1** and **2** [in brackets]: $C_{20}H_{30}Mn_2N_8O_9$ [$C_{36}H_{38}Mn_2N_8O_9$], $M$ = 636.4 [836.6], orthorhombic [orthorhombic], space group *Aba*2 [*Aba*2], $a$ = 8.671(2) [19.043(2)], $b$ = 19.273(2) [8.9010(10)], $c$ = 16.789(2) [22.924(2)] Å, $U$ = 2805.7(8) [3885.7(7)] Å$^3$, $Z$ = 4 [4], $D_c$ = 1.497 [1.430] g cm$^{-3}$, $F$(000) = 1312 [1728], $\lambda$(Mo-Kα) = 0.710 73 Å. Scan method: $\theta$–2$\theta$, 2$\theta$ range: 3.0 ⩽ 2$\theta$ ⩽ 55 [3 ⩽ 2$\theta$ ⩽ 60]°, μ = 0.954 [0.713] mm$^{-1}$, $T$ = 198 [228] K. 1857 [2900] independent reflections were used in the refinement of which 1609 [2895] were observed. $F \geqslant 4\sigma(F)$. The final $R$ = 0.0282 [0.0336] and $R_w$ = 0.0322 [$wR_2$ = 0.0830] [$2\sigma(I) = 4\sigma(F)$]. The absolute configurations for both **1** and 2 were confirmed from anomalous scattering. CCDC 182/568.

§ Cambridge Structural Database, CCDC, Cambridge, April, 1995.

1 R. H. Holm, P. Kennepohl and E. I. Solomon, *Chem. Rev*., 1996, **96**, 2239; N. Sträter, W. N. Lipscomb, T. Klabunde and B. Krebs, *Angew. Chem., Int. Ed. Engl.*, 1996, **35**, 2024.
2 G. C. Dismukes, *Chem. Rev*., 1996, **96**, 2909.
3 (*a*) Z. F. Kanyo, L. R. Scolnick, D. E. Ash and D. W. Christianson, *Nature*, 1996, **383**, 554; (*b*) S. V. Khangulov, P. J. Pessiki, V. V. Barynin, D. E. Ash and G. C. Dismukes, *Biochemistry*, 1995, **34**, 2015.
4 J. F. Davies, Z. Hostomska, Z. Hostomsky, S. R. Jordan and D. A. Matthews, *Science*, 1991, **252**, 88; M. Atta, P. Nordlund, A. Aberg, H. Eklund and M. Fontecave, *J. Biol. Chem.*, 1992, **267**, 20682.
5 S. V. Khangulov, V. V. Barynin, N. V. Voevodskaya and A. I. Grebenko, *Biochim. Biophys. Acta* , 1990, **1020**, 305.
6 A. Willing, H. Follmann and G. Auling, *Eur. J. Biochem.*, 1988, **170**, 603.
7 R. J. Debus, *Biochim. Biophys. Acta*, 1992, **1102,** 269 and references therein.
8 For recent reviews, see: V. L. Pecoraro, M. J. Baldwin and A. Gelasso, *Chem. Rev.*, 1994, **94**, 807; L. Que, Jr. and A. E. Trye, *Prog. Inorg. Chem.*, 1990, **38**, 97; K. Wieghardt, *Angew. Chem., Int. Ed. Engl.*, 1989, **28**, 1153.
9 (*a*) A. Caneschi, F. Ferraro, D. Gatteschi, M. C. Melandui, P. Rey and R. Sessoli, *Angew. Chem., Int. Ed. Engl.*, 1989, **28**, 1365; (*b*) S.-B. Yu, S. J. Lippard, I. Shweky and A. Bino, *Inorg. Chem.*, 1992, **31**, 3502.
10 See for example: D. W. Christianson and C. A. Fierke, *Acc. Chem. Res*., 1996, **29**, 331; D. W. Christianson, *Adv. Protein Chem*., 1991, **42**, 281; W. W. Cleland and M. M. Kreevoy, *Science*, 1994, **264**, 1887; A. Warshel, A. Papazyan and P. A. Kollman, *Science*, 1995, **269**, 102.
11 C. Oldham, in *Comphrehensive Coordination Chemistry*, ed. G. Wilkinson, R. D. Gillard and J. A. McCleverty, Pergamon, Oxford, 1987, vol. 2, p. 435.
12 F. A. Cotton, D. J. Darensbourg and B. W. S. Kolthammer, *J. Am. Chem. Soc*., 1981, **103**, 398.
13 G. B. Deacon and R. J. Phillips, *Coord. Chem. Rev*., 1980, **33**, 227.

*Received in Cambridge, UK, 28th May 1997; 7/03684A*

ChemComm
FEATURE ARTICLE

# Solid-state chemistry of lithium power sources†

**Peter G. Bruce***

*School of Chemistry, University of St. Andrews, St. Andrews, Fife, UK KY16 9ST*

**This article describes the solid-state chemistry of intercalation compounds that underpins a revolutionary new rechargeable lithium battery which has recently achieved phenomenal commercial success. The battery can store more than twice the energy compared with conventional alternatives of the same size and mass and holds the key to the future improvement of consumer electronic products (*e.g.* mobile telephones), electric vehicles and implantable medical devices (*e.g.* the artificial heart). Attention is focused on those lithium intercalation compounds that are useful as positive electrodes in rechargeable lithium batteries. The basic operation of the cell is summarised briefly and the structure/property relationships are developed that are important for the solid-state chemist when attempting to design and synthesise new lithium intercalation compounds capable of operating as positive electrodes. Finally, the structure, electronic structure and intercalation chemistry of several important positive intercalation electrodes are discussed including some which show considerable promise for applications in future generations of rechargeable lithium batteries.**

## Introduction

Why should chemists be interested in rechargeable lithium batteries? For better or worse, chemical research must now find expression in its benefit to industrial competitiveness or the quality of life. This is not necessarily in conflict with its more timeless *raison d'être, i.e.* the advancement of knowledge. In many areas of chemistry it is possible, although often hard, to be interesting and useful at the same time. Some of the most exciting fundamental scientific developments in solid-state chemistry within the last decade, *e.g.* zeolites for catalysis, have occurred against a background of attempting to advance technology and reduce energy costs.

The overwhelming need for lightweight and compact sources of portable electricity has resulted in a massive international effort into the development of radically new rechargeable batteries. This has led recently to the first successful commercialisation of a rechargeable lithium battery.[1,2] The device is a triumph of solid-state chemistry and electrochemistry; the relevance of electrochemistry to lithium batteries is obvious, however if it were not for crucial advances in the solid-state chemistry of intercalation solids, rechargeable lithium batteries would not have achieved the success that they have. In this article I aim to highlight the key challenge presented to the solid-state chemist, namely, the development of new intercalation compounds as positive electrodes for rechargeable lithium batteries.

## Rechargeable lithium batteries

The considerable technological impetus in this area comes from three main sources, consumer electronics (*e.g.* mobile telephones), electric vehicles and implantable medical devices (*e.g.* the artificial heart).

The introduction by Sony in 1990 of the world's first commercially successful rechargeable lithium battery represented a revolution in the power source industry.[1–3] It has been likened by some to the semiconductor revolution which saw the replacement of the valve by the transistor in the 1940s and 50s. The new cell can store more than twice the energy compared with conventional rechargeable batteries of the same size and mass, an achievement which is remarkable in an industry that traditionally measures improvements in a few percentage points. The Sony cell represents but a first step on the road to greatly improved sources of portable electrical power, there is much scope and indeed need for further development.[2]

The essential elements of the Sony cell are shown schematically in Fig. 1(*a*). The cell is constructed in the discharged state and consists of a positive electrode composed of a thin layer of powdered $LiCoO_2$ mounted on aluminium foil, a negative electrode formed from a thin layer of powdered graphite, or certain other carbons, mounted on a copper foil. The two electrodes are separated by a porous plastic film soaked typically in $LiPF_6$ dissolved in a mixture of dimethyl carbonate and ethylene carbonate. Charging the cell involves diffusion of lithium ions within the $LiCoO_2$ particles towards their interface with the electrolyte, the lithium ions then cross the electrolyte and are intercalated between the carbon layers in the graphite electrode. Charge balance requires that the equivalent number of electrons must pass around the external circuit. Discharge reverses the process moving lithium out of the graphite and reforming $LiCoO_2$. This cell may be contrasted with earlier designs which employed lithium metal rather than graphite as the negative electrode, Fig. 1(*b*). The reactivity of lithium metal and the difficulty of plating and stripping it with high efficiency, have resulted in concerns over safety and the performance of this design. The Sony cell, which is known variously as a rocking-chair, swing or LION cell, to distinguish it from the lithium metal design, is a true expression of solid-state intercalation chemistry involving, as it does, the flow of lithium

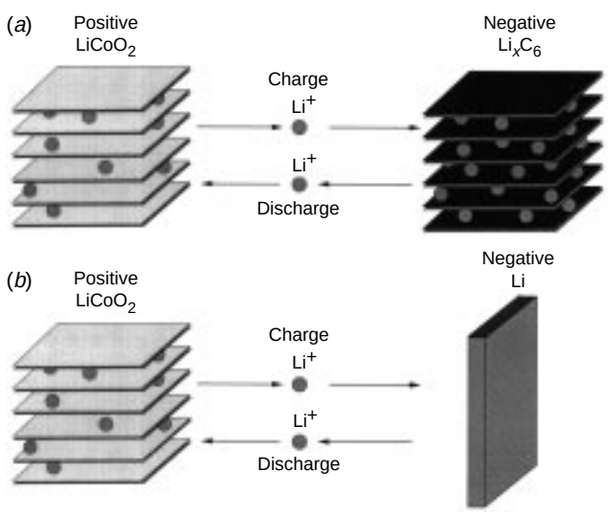



**Fig. 1** Schematic representation of (*a*) the Sony rocking-chair cell and (*b*) a rechargeable lithium cell with a lithium metal negative electrode. The maximum lithium content in ordered graphite is $LiC_6$.

ions between two intercalation hosts. The performance advantage over more conventional rechargeable batteries such as nickel–cadmium lies largely in the voltage. The Sony cell has an average potential of 3.6 V which is almost three times that of nickel–cadmium so that three conventional cells can be replaced by only one lithium cell![1,3]

A number of reviews have appeared which deal with rechargeable lithium batteries including graphite and other carbon-based negative electrodes.[4–7] Although the Sony cell currently uses a liquid electrolyte, the future will see replacement of this by a solid polymer leading to all-solid-state rechargeable lithium batteries.[8]

## Relating solid-state chemistry to positive intercalation electrodes

For our purposes, intercalation or insertion solids may be defined as hosts into which atoms (or more commonly ions + electrons) may be inserted or removed without a major disruption of the structure.[9–12] Molecular intercalation has been reviewed by O'Hare.[13]

In order to use our knowledge of solid-state chemistry to design and synthesise new intercalation compounds that will exhibit improved performance as positive electrodes for new generations of rechargeable lithium batteries, we must first understand what properties the intercalation solid should possess and how this relates to the structure and composition of the solid. The key structure/property relationships are listed in Table 1. As can be seen, a single compound must possess fourteen, often quite distinct, attributes and this serves to illustrate how challenging it is to develop solids which will be technologically competitive! Let us consider some of these attributes and their relationship to the solid-state chemistry in more detail.

Firstly, positive electrodes must be intercalation compounds; only such compounds avoid the large kinetic barriers of defect diffusion and nucleation and growth associated with the majority of solid-state reactions. Also, as prepared, they should contain lithium, *i.e.* be in the fully discharged state since rocking chair cells are assembled in this state.

The voltage of the cell is a crucial parameter and this should be large. If we consider a rocking-chair cell, such as graphite/$LiCoO_2$, then the voltage between the two electrodes is related to the work the cell can deliver on transferring electrons around an external circuit and to the free energy change on transferring lithium from one intercalation electrode to the other. The free energy change associated with the transfer of one mole of lithium between the two intercalation electrodes is equivalent to the difference in the chemical potential of lithium in the two electrodes [eqn. (1)],[14,15]

$$V = -\frac{(\mu_{Li}^{int} - \mu_{Li}^{graph})}{nF} \quad (1)$$

where $V$ is the open circuit voltage of the cell, $\mu_{Li}^{int}$ and $\mu_{Li}^{graph}$ the chemical potentials of lithium in the positive intercalation and graphite electrodes respectively, $n = 1$ (since one $e^-$ is transferred for each lithium) and $F$ is Faraday's constant. On discharge, lithium is transferred from a state of high $\mu_{Li}^{graph}$ (high energy) in the negative graphite electrode to one of low $\mu_{Li}^{int}$ (low energy) in the positive intercalation electrode; as a result work can be done by the cell. According to eqn. (1), in order to ensure a large cell voltage we must select positive intercalation electrodes which possess a low $\mu_{Li}^{int}$. On discharging a rocking-chair cell the lithium content and hence chemical potential and voltage, will change in each electrode ($\mu_{Li} = \mu_{Li}^{o} + RT\ln a$, where $a$ is the activity of lithium). It is convenient and normal practice therefore to measure the potential of a positive intercalation electrode against lithium metal (which has an invariant $\mu_{Li}$) and to use the latter's chemical potential as the standard state for lithium in the positive electrode. Lithium is rarely in the form of Li atoms in the intercalation compounds of interest here but instead exists as $Li^+$ ions along with their charge-compensating electrons, the latter located in the d levels of the transition-metal ion. As a result, it is helpful when considering structure–property relationships to separate $\mu_{Li}^{int}$ according to eqn. (2)

$$\mu_{Li}^{int} = \mu_{Li^+}^{int} + \mu_{e^-}^{int} \quad (2)$$

where $\mu_{Li^+}^{int}$ and $\mu_{e^-}^{nt}$ represent respectively the chemical potentials of $Li^+$ ions and electrons.‡ The ion and electron chemical potentials include both energy and entropy terms. In developing the gross structure–property relationships the entropy terms may be neglected since over most of the composition range they are small, vary little and make a similar contribution to each intercalation compound. The entropy of electrons in a band is negligible.

This torrid trip through some simple thermodynamics has brought us to the conclusion, important for the solid-state chemist, that the potential of a positive intercalation electrode, and hence the voltage of the cell, will depend on the energy of the electrons and the $Li^+$ ions in the host. On inserting electrons into an intercalation host they will enter at the Fermi level, $E_F$ and this is the electron energy of importance [eqn. (3)].§¶

$$E_F = \mu_e \quad (3)$$

The site energy for $Li^+$ is the major factor determining the ion contribution to the overall energy. Mutual repulsion between the $Li^+$ ions is usually of secondary importance. Hence maximising the positive electrode potential reduces to designing intercalation compounds with a low Fermi level and a high stability (low energy) for $Li^+$ in its sites. It is important to note that the electrode potential of graphite or other carbon electrodes is some +10 to +800 mV *vs*. lithium, therefore for rocking chair cells we must select intercalation electrodes with somewhat larger positive potentials (*i.e.* lower Li chemical potentials) than is necessary for cells with lithium metal electrodes.

Let us consider further the problem of engineering a low Fermi level. The lowest Fermi level which can be achieved for an intercalation compound is determined by the energy corresponding to the top of the valence band. In oxides the valence band is largely of oxygen 2p parentage and lies significantly below the top of the 3p valence band in the corresponding sulphides. As a result, Fermi levels in oxides can be more than 2 eV lower, resulting in potentials of between 4 and 5 V *vs*. the $Li^+$/Li couple. Therefore, the focus is on oxides rather than chalcogenides. For any given transition-metal oxide the Fermi level is set by the position of the cation d levels. The lowest d levels are associated with those ions from the centre or right of the first transition series, *i.e.* Cr, Fe, Mn, Co, Ni; these all exhibit +4 oxidation states corresponding to d levels which lie close to (usually just above) the top of the oxygen valence

**Table 1** Criteria for intercalation compounds as positive electrodes

| | |
|---|---|
| 1 | Must be an intercalation host for lithium |
| 2 | Low Fermi level and $Li^+$ site energy → high open-circuit voltage |
| 3 | Electrode potential varies little with lithium content → cell voltage varies little with state of charge |
| 4 | Capable of accommodating large quantities of lithium per formula unit → high capacity |
| 5 | Low formula mass → high gravimetric energy density |
| 6 | Low molar volume → high volumetric energy density |
| 7 | Sustain high rates of lithium intercalation and deintercalation → high cell discharge/charge rates |
| 8 | Highly reversible lithium intercalation → many charge–discharge cycles |
| 9 | Avoid co-intercalation of solvent |
| 10 | Stable in contact with candidate electrolytes |
| 11 | Adequate electronic conductivity |
| 12 | Low cost |
| 13 | Easily fabricated into electrode |
| 14 | Evironmentally friendly |

band. $Li_{1-x}Cr_2O_4$, for example, when combined with a lithium negative electrode gives an open circuit potential of 5 V associated with the $Cr^{4+/3+}$ mixed-valence state.[17]

As lithium is inserted into the intercalation host forming a continuous range of solid solutions, the electrons fill up the band while the mutual repulsions between the $Li^+$ ions rises. The net effect is that the potential will decrease somewhat with increasing Li content; whereas in many systems it turns out that this can be rationalised entirely by considering only the ion repulsions,[14] in some cases both ion and electron interactions are important.[18] If, on the other hand, intercalation induces the formation of a new phase and both phases have fixed composition then insertion is simply accompanied by the conversion of one phase to the other. This in turn is associated with a constant change of chemical potential and therefore a constant voltage as a function of the degree of intercalation (state-of-charge).

Before leaving the topic of electrode potentials it is worth noting that the relationship between the cell voltage and the lithium chemical potentials in the electrodes can be derived in another way which serves to highlight a frequently misunderstood fact. It is often stated that the voltage of a cell is determined by the difference between the Fermi levels of the two electrodes, this is incorrect. The voltage is equal to the difference in the Fermi levels between the electrodes only when they are in a cell *i.e.* in mutual contact with an electrolyte. Such Fermi levels are not those of the isolated electrodes. Selecting a lithium intercalation electrode based on its Fermi level will not yield the desired cell voltage.‖

One of the most important factors governing the performance of a cell is the energy which can be stored per unit weight and volume, *i.e.* the gravimetric and volumetric energy density. For electric vehicles, batteries are required which provide a high gravimetric energy density whereas for implantable medical devices volumetric energy is more important. Since energy is stored in the form of lithium in the intercalation electrodes the gravimetric and volumetric energy density of the positive electrode is of great importance and is given by eqn. (4),

$$E = V_e Q \quad (4)$$

where $E$ is the volumetric or gravimetric energy density, $V_e$ is the electrode potential and $Q$ is the charge stored per unit mass or volume of the intercalation compound. Energy densities are conventionally expressed in terms of W h $kg^{-1}$ or W h $l^{-1}$ whereas $Q$ is expressed in terms of mA h $g^{-1}$ or A h $l^{-1}$. The energy density depends therefore on two separate factors, the electrode potential and the charge. Potential has been dealt with above. The charge stored is equivalent to the amount of lithium that can be accommodated within the intercalation host. It is important for the solid-state chemist to design intercalation hosts which can reversibly insert a large amount of lithium per formula unit. If the capacity to store lithium is high, then a high gravimetric energy density will be assured provided the molar mass of the intercalation host is small. A high volumetric energy density will be obtained provided the molar volume is small. We see again that oxides will be preferable to chalcogenides in order to achieve a high gravimetric energy density and that we wish to choose intercalation hosts that contain the active redox couple and little else. Considering both $V_e$ and $Q$, a metal oxide of the formula $LiMO_2$ from which all the lithium may be reversibly deintercalated and in which M is a light element, in a high oxidation state ($M^{4+/3+}$ couple) and with a close-packed structure would seem to be optimal. It is no coincidence that the positive electrode in the Sony cell is $LiCoO_2$.

The rate at which a cell can be discharged or charged is an important parameter and is limited by the rate of lithium intercalation or deintercalation. Electroneutrality demands that the magnitude of the flux of $Li^+$ ions and their charge compensating electrons into and out from the host must be the same. It is the coupled diffusion of $Li^+$ and electrons down a concentration gradient that is important, rather than the individual diffusivities (mobilities) of the ions and electrons alone. A coupled diffusion coefficient may be defined, it is generally known as the chemical diffusion coefficient, $\tilde{D}_{Li}$, and is a measure of the intrinsic rate capability of the electrode.

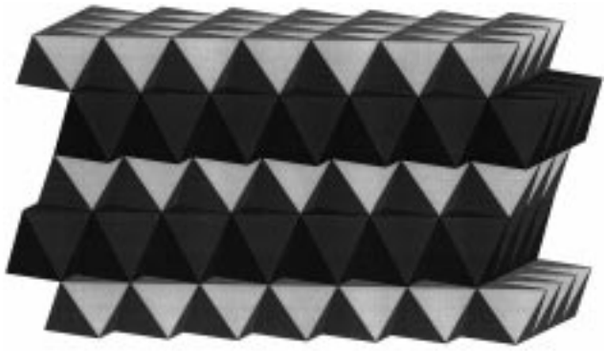


**Fig. 2** The crystal structure of $LiCoO_2$ or $LiNiO_2$. Dark and light octahedra represent respectively the sites for the transition-metal and lithium ions.

Several other factors are also of crucial importance. The chosen electrode must be stable in contact with the electrolyte of the cell. The surfaces of transition-metal oxides provide an ideal environment for catalytic decomposition of many electrolytes and this can present problems. Indeed metal oxide electrodes are frequently used for electrocatalysis in other applications! The starting materials used to prepare the intercalation electrode should be of low cost as should the preparation method. However, above all, the intercalation electrode must be environmentally benign.

## Intercalation electrodes

Many intercalation compounds have been studied as possible positive electrodes for rechargeable lithium batteries. Limitations of space demands that attention is concentrated on the three compounds of main interest. The author apologises to those whose work could not be included.

### *$LiCoO_2$ and $LiNiO_2$*[19–21]

The structures of $LiCoO_2$ and $LiNiO_2$ are identical and shown in Fig. 2. The oxide ions adopt a cubic close-packed arrangement with $Co^{3+}$ or $Ni^{3+}$ ions occupying octahedral sites between adjacent oxide ion layers. Only alternate sheets of octahedral sites are occupied by the transition metal ions with the remaining sheets being occupied by $Li^+$. The structure is slightly distorted giving rise to rhombohedral symmetry, space group $R\bar{3}m$.

The electronic structure of intercalation electrodes is an important factor which as we have seen has a strong influence on the voltage and can also induce structured distortions. Too little attention has been paid to the rôle of electronic structure in the past. The electronic structure of $LiCoO_2$ may be derived as follows. $Co^{3+}$ ($3d^6$) adopts a low-spin configuration ($t_{2g}{}^6e_g{}^0$) in an octahedral oxygen environment. The $t_{2g}$ orbitals are energetically close to the oxygen 2p orbitals and those 2p orbitals of $\pi$ symmetry will overlap strongly with the Co $t_{2g}$ orbitals. As a result there is considerable covalent mixing and consequently a high degree of delocalisation over the $CoO_6$ octahedra. The Co–O–Co angle is close to 90° and hence neighbouring cobalt ions overlap with mutually orthogonal 2p orbitals on the bridging oxygens. This inhibits long-range Co–O–Co interactions, thus attenuating band formation due to metal–oxygen interactions. Spectroscopic data suggests that the electronic structure of $LiCoO_2$ more closely approximates to a localised Co($3d^6$) electronic configuration than to a band. Full occupancy of the $t_{2g}$ $\pi^*$ orbitals which are separated energetically from the $e_g$ $\sigma^*$ orbitals ensures semiconductor behaviour for $LiCoO_2$. The extraction of lithium from between the oxide ion layers is facile and a chemical diffusion coefficient for the

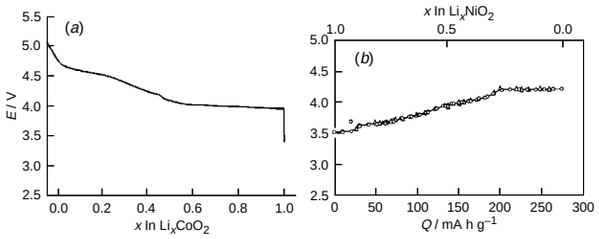



**Fig. 3** Open-circuit voltage *vs*. $Li^+/Li$ couple as a function of lithium content in (*a*) $Li_xCoO_2$, reproduced from ref. 28 and (*b*) $Li_xNiO_2$, based on a figure presented in ref. 29. With the permission of The Electrochemical Society.

coupled ($Li^+ + e^-$) diffusion of $5 \times 10^{-8}$ $cm^2$ $s^{-1}$ at $Li_{0.65}CoO_2$ has been measured.[22] Such extraction is accompanied by oxidation of $Co^{3+}$ to $Co^{4+}$ (low-spin $d^5$). The associated contraction of the *a* axis of the unit cell (which lies in the oxide layers) signals a shorter Co···Co distance, reduced from 2.83 Å in the case of $LiCoO_2$ to 2.81 Å for $Li_{0.9}CoO_2$. The strongly covalent Co–O interactions, will, due to the nephaluxetic effect, produce expanded antibonding d orbitals. Together the orbital expansion and shorter Co···Co distance conspire to make possible direct overlap of cobalt $t_{2g}$ orbitals across a shared octahedral edge resulting in a narrow d band and hole conduction in the mixed valence $Co^{4+/3+}$ system. The critical Co···Co distance for direct $t_{2g}$–$t_{2g}$ interactions is 2.82 Å, consistent with the switch from insulator to metallic behaviour on extracting a relatively small amount (10%) of lithium from $LiCoO_2$. Experimental evidence verifies that extraction of small quantities of lithium from $LiCoO_2$ does indeed induce metallic behaviour.[23] Of course we cannot rule out the possibility of $Co^{4+}$ d levels being located just below the top of the oxygen 2p band and introducing holes in it which would also lead to metallic behaviour; further studies are required to resolve this. In any case the low lying $Co^{4+/3+}$ couple gives rise to a high potential of $>4$ V *vs*. the $Li^+/Li$ couple, Fig. 3.

$LiNiO_2$ adopts a low-spin $d^7$ configuration with fully occupied $t_{2g}$ levels and one electron in the $e_g$ orbitals. Full occupancy of the $t_{2g}$ levels implies that we must focus our attention on the single electron in the $e_g$ orbitals to understand the conduction process. The $e_g$ orbitals will overlap with oxygen 2p orbitals of σ symmetry giving rise to strong interactions but again neighbouring nickel ions form a 90° Ni–O–Ni geometry and therefore overlap is with mutually orthogonal 2p orbitals on the bridging oxygen. This inhibits delocalisation extending beyond the $NiO_6$ octahedron and again attenuates band formation. As a result the $e_g$ electron remains in a localised atomic orbital on nickel although these are strongly antibonding associated with significant Ni–O covalency. A localised low-spin $d^7$ configuration is Jahn–Teller active. There is some evidence for a dynamic Jahn–Teller distortion from EXAFS studies but no cooperative, static, distortion of the structure has been detected.[24] Deintercalation is again facile with the chemical diffusion coefficient for Li reaching a maximum of $2 \times 10^{-7}$ $cm^2$ $s^{-1}$, amongst the highest observed in such materials.[25] Extraction of lithium is associated with oxidation of $Ni^{3+}$ to $Ni^{4+}$. Since the $e_g$ orbitals point towards the coordinating oxygens there is little opportunity for direct nickel–nickel interaction in contrast to the situation with the $t_{2g}$ orbitals in the cobalt compound. As a result, measurements of electronic transport on $Li_xNiO_2$ exhibit a small but definable activation energy for electronic transport associated with small polaron hopping in the mixed-valence $Ni^{4+/3+}$ state.[26] The location of the Fermi level in the higher energy $e_g$ orbitals, compared with the lower energy $t_{2g}$ orbitals in the analagous cobalt compound, results in an average voltage several hundred mV lower for $Li_xNiO_2$, Fig. 3(*b*).[19,27,28]

Considering now the structural changes that accompany lithium deintercalation from $LiCoO_2$ in more detail; this process does not correspond to a simple continuous solid solution as was first believed, instead several minor structural transformations occur.[28] Within the composition range $0.9 < x < 1$ in $Li_xCoO_2$, a single hexagonal phase exists, whereas within the range $0.78 < x < 0.9$, two hexagonal phases coexist giving way to a region, $0.51 < x < 0.78$, within which the second hexagonal phase exists alone. On further removal of lithium a monoclinic distortion of this second phase is observed for compositions in the narrow range $0.46 < x < 0.51$. Extraction of lithium from $x = 1$ to $x = 0.5$ is accompanied by an expansion in the *c* lattice parameter from approximately 14.1 to 14.5 Å. The loss of lithium from between the otherwise weakly van der Waals' bonded oxide layers is the origin of this expansion. Decrease in the *a* lattice parameter associated with oxidation of $Co^{3+}$ to the smaller $Co^{4+}$ has been highlighted above. Further deintercalation below $x = 0.46$ results in reversion to a hexagonal phase until the composition $Li_{0.22}CoO_2$ is reached whereupon a second monoclinic phase appears coexisting with the hexagonal phase until the composition $Li_{0.18}CoO_2$ is obtained, at which point the monoclinic phase exists alone. Below $x = 0.15$ another hexagonal phase appears corresponding to the fully delithiated $CoO_2$.[28] The monoclinic distortion at around $x = 0.5$ has been ascribed to lithium ordering,[27] however a complete rationale for the structural phase changes which occur on deintercalation has not yet been presented; nevertheless, there is no doubting the complexity of the structural chemistry. Until the recent studies by Amatucci, Tarascon and Klein,[28] it had been generally believed that the weak van der Waals' bonding exhibited by adjacent oxide ion layers would result in instability for a layered $CoO_2$ compound. These authors have shown this to be incorrect and have demonstrated that the structure of $CoO_2$ is not based on cubic close-packing but hexagonal close-packing ($CdI_2$ structure). This is the same structure commonly adopted by the layered chalogenides, *e.g.* $TiS_2$.[28] Two factors may play a rôle in stabilising $CoO_2$ with adjacent oxide layers. First, the low-lying $d^5$ configuration of $Co^{4+}$ ensures very significant covalent mixing with the neighbouring oxygen 2p orbitals resulting in a high degree of delocalisation. It is not therefore realistic to view the compound as possessing adjacent $O^{2-}$ layers. Second, as proposed before, a cooperative displacement of the $Co^{4+}$ ions results in a ferroelectric distortion establishing dipoles which will oppose the repulsive interactions between the oxide ion layers thus assisting stabilisation of the structure.[22]

The structural chemistry of $Li_xNiO_2$ is also complex.[27,29,30] Solid solutions with rhombohedral symmetry exist within the composition ranges $0.85 < x < 1$ and $0.32 < x < 0.43$. Between $x = 0.50$ and 0.75 a single monoclinic phase is observed. Over the range $x = 0$–$0.32$ a mixture of two rhombohedral phases is evident, one of these being $NiO_2$. Two-phase mixtures are also observed between each of the other single-phase ranges. The monoclinic distortion is believed to be associated with a superlattice arising from the ordering of lithium ions.[24,27,29] Arguments similar to those used for $CoO_2$ may be employed to explain the stability of $NiO_2$ particularly the high degree of Ni–O covalency. It is interesting to note that $NiO_2$ retains the cubic close packed structure of $LiNiO_2$ (*i.e.* the $CdCl_2$ structure type).[29]

In contrast to $LiCoO_2$, $LiNiO_2$ has proved impossible to prepare as a stoichiometric material. Instead compounds with the formula $Li_{1-\delta}Ni_{1+\delta}O_2$ are obtained. The closest approach to stoichiometry that has been possible so far corresponds to a δ of approximately 0.02 and may be prepared by reacting $Li_2O_2$ with NiO in oxygen at 700 °C.[31] Non-stoichiometry is associated with lithium deficiency and the presence of $Ni^{2+}$ ions in the lithium layers. These nickel ions serve to pin the oxide layers together reducing the mobility of the lithium ions, however compounds approaching the stoichiometric composition do exhibit a similar *c* lattice expansion on deintercalation to that observed for $LiCoO_2$. There is evidence that at high degrees of deintercalation further nickel ions may migrate from the Ni to the Li layers. Work by Delmas *et al.* has shown that the quantity

of lithium extracted on first charging lithium nickel oxide cannot be reinserted.[24] In fact these authors claim that the capacity loss on the first cycle is a more significant factor than any loss of capacity due to continuous disordering of nickel on extended cycling. Even for relatively stoichiometric materials, reintercalation up to the composition $Li_{0.85}NiO_2$ is easy but beyond this limit proves very difficult. The mechanism they propose to explain this capacity loss is based on oxidation of the nickel ions in the lithium layers at high degrees of deintercalation, subsequent structural collapse around the $Ni^{3+}$ ions and the relatively high charge of these ions mitigates against $Li^+$ ions reoccupying the sites around nickel. The best electrochemical performance is obtained from materials that are as close as possible to the stoichiometric composition.

Comparing the properties of the $LiCoO_2$ and $LiNiO_2$ compounds as positive electrodes for rechargeable lithium batteries, both exhibit high voltages and facile lithium diffusion rates despite the complex structural changes. The fact that these structural changes are small and in some cases, at least, only associated with lithum ordering, explains the preservation of fast cycling kinetics. Complete removal of lithium from $LiNiO_2$ corresponds to a charge storage capacity of 275 mA h $g^{-1}$. In practical cells based on liquid electrolytes cycling can occur over the approximate composition range $0.3 < x < 0.9$ corresponding to 150–160 mA h $g^{-1}$ depending on the rate of charge/discharge. In the case of $LiCoO_2$, deintercalation to $Li_{0.5}CoO_2$ is possible with almost complete reinsertion of lithium, corresponding to a more modest 130 mA h $g^{-1}$ but at a slightly higher potential than the nickel electrode. As we now know the limits of deintercalation for this compound are not imposed by structural collapse *per se* but by the instability of the highly charged, and therefore high voltage, oxide in contact with the liquid electrolytes used in the commercial cells.[21] It is the somewhat more modest voltage of $LiNiO_2$ which gives rise to the greater capacity. $LiNiO_2$ is also attractive because it is cheaper than the cobalt alternative. However, $LiCoO_2$ has the significant advantage that it is easier to synthesise as a highly stoichiometric material and its structure is robust with respect to cycling, at least over the limited composition range stated above, with no evidence for cobalt disordering into the lithium layers. It is this that led to its selection by Sony for the first generation rechargeable lithium batteries.

### *Li(NiAl)$O_2$ and Li(NiCo)$O_2$*

In an attempt to improve on the properties of $LiNiO_2$ and take advantage of the lower cost of this material, partial substitution of nickel by other ions has been investigated. The work of Ohzuku *et al*. has shown that $LiAl_{0.25}Ni_{0.75}O_2$ can deliver a capacity of *ca*. 150 mA h $g^{-1}$ and with excellent capacity retention on cycling.[32] A complete range of solid solutions $Li(Ni_{1-y}Co_y)O_2$ may be prepared. It has been shown that partial replacement of Ni by Co yields a material which is cheaper than $LiCoO_2$ but with many of its advantages.[33] This solid solution will be used in future commercial rocking chair cells.

### *$LiMn_2O_4$ and related spinels*

Manganese is approximately 1% of the cost of cobalt and significantly more environmentally benign than either cobalt or nickel. These are major advantages and explain the intense interest in developing manganese oxide based positive electrodes. The use of $LiMn_2O_4$ spinels as positive electrode materials was first reported in 1983.[34–36] The attractive features of $LiMn_2O_4$ led in 1996 to the announcement by Nippon Moli, Japan of the first commercial rechargeable lithium battery in which $LiCoO_2$ is replaced by the lithium manganese oxide spinel.[37]

$LiMn_2O_4$ is quite distinct from the layered oxides mentioned above in that it is a three-dimensional host. The spinel structure (space group $Fd\bar{3}m$) consists of cubic close-packed oxide ions

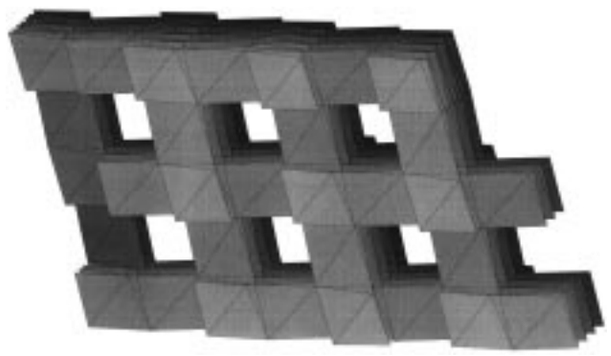


**Fig. 4** The $Mn_2O_4$ framework of the $LiMn_2O_4$ spinel consisting of a three-dimensional network of $MnO_6$ octahedra

with Mn ions in one half of the octahedral sites and $Li^+$ in one eighth of the tetrahedral sights within the cubic close-packed oxide array.[34,36] The $Mn_2O_4$ framework of the spinel structure is highly stable, Fig. 4, and defines a series of tunnels formed by the face-sharing of tetrahedral lithium (8a) and empty octahedral (16c) sites. These tunnels intersect in three dimensions and support rapid lithium diffusion, but unlike the layered compounds the spinels, because of their greater structural rigidity, are selective for lithium ions over solvent molecules or other larger cations (*i.e.* deleterious effects of solvent co-intercalation are avoided). Half of the octahedrally coordinated manganese ions are $Mn^{3+}$ (high-spin $3d^4$, $t_{2g}^3e_g^1$) and half $Mn^{4+}$ ($3d^3$, $t_{2g}^3$). Neighbouring Mn ions form 90° Mn–O–Mn interactions ensuring that the $t_{2g}$ and $e_g$ orbitals on adjacent Mn ions interact with mutually orthogonal oxygen 2p orbitals on the bridging oxygens, inhibiting band formation. The $t_{2g}$ orbitals are too contracted to overlap directly across a shared octahedral edge. As a result the d electrons are localised. Half the Mn sites are occupied by the Jahn–Teller active $Mn^{3+}$ ions and this is insufficient to promote a cooperative Jahn–Teller distortion until just below room temperature, the crystal structure at and above room temperature remains cubic. Electronic transport will occur by thermally activated small polaron hopping of the $e_g$ electron between neighbouring $Mn^{3+}/Mn^{4+}$ ions, the polaron is magnified by a dynamic Jahn–Teller distortion which must follow the electron. $LiMn_2O_4$ is a remarkable material. Li may be extracted yielding, when fully deintercalated, a polymorph of $MnO_2$($MnO_2$-λ) which cannot be prepared by other means. This is an excellent example of the rational synthesis of a target compound by *chimie douce* (soft chemistry).[38] Such deintercalation is associated with a potential of 4 V *vs*. $Li^+$/Li, Fig. 5. Lithium may also be intercalated into $LiMn_2O_4$ up to a maximum composition $Li_2Mn_2O_4$.[34,36] This is associated with the insertion of lithium into the octahedral (16c) sites and a potential of 3 V *vs*. $Li^+$/Li. The origin of this large voltage difference between lithium removal and insertion is believed to be related to the difference in the site energy of $Li^+$ in the tetrahedral (8a) and octahedral (16c) positions and its influence on the $\mu_{Li^+}^{int}$ and hence the potential [eqns. (1) and (2)]. In both cases the redox couple is $Mn^{4+/3+}$.

Let us consider the important intercalation chemistry of $LiMn_2O_4$ in more detail beginning with $Li_xMn_2O_4$ where $1 < x < 2$. Although this is a 3 V process and of limited interest in the context of rocking-chair cells it is of considerable importance for cells employing lithium metal negative electrodes. The gravimetric energy density of lithium is 3860 mA h $g^{-1}$, more than ten times that of graphite (372 mA h $g^{-1}$). For this reason, particularly in the context of developing batteries for electric vehicles, lithium metal systems continue to be intensively studied, although key problems connected with lithium cycling and safety remain to be solved. On inserting lithium into the octahedral (16c) sites of $Li_xMn_2O_4$ ($x = 1$), the $Mn^{4+}$ ions are reduced to $Mn^{3+}$ and a continuous solid solution is obtained up

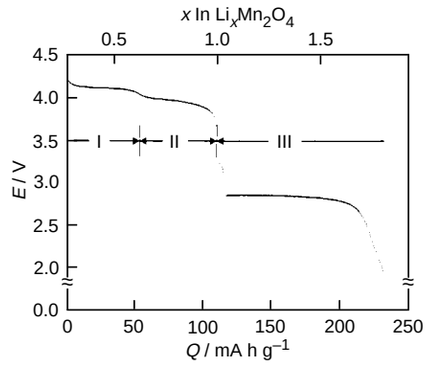



**Fig. 5** Open-circuit voltage *vs*. $Li^+/Li$ couple as a function of lithium content in $Li_xMn_2O_4$. Reproduced with permission from Ohzuku, Kitagowa and Hiral, *J. Electrochem. Soc.*, 1990, **17**, 769.

to $x = 1.1$. At this composition the Jahn–Teller active $Mn^{3+}$ ions are present in sufficient concentration to promote a cooperative distortion of the octahedral sites to tetragonal symmetry. Associated with this the cubic crystal symmetry of $LiMn_2O_4$ is lowered to tetragonal.[34,36] For $1.1 < x < 2$ a mixture of the cubic and tetragonal spinels coexist and intercalation involves the continuous conversion, within each particle, of the former phase to the latter. As a result the voltage does not vary with the lithium content in this composition range. Although the phase change is displacive and appears to be quite facile as judged by the rate of lithium insertion and removal, the abrupt change in unit-cell volume (6.5%) which accompanies the cubic-to-tetragonal phase transition in the spinel has a deleterious effect on the cyclability. Only tetragonal $Li_2Mn_2O_4$ should be present at the end of each discharge; however we have shown by X-ray diffraction carried out as a function of cycling that cubic $LiMn_2O_4$ accumulates at the end of discharge and that this is the primary cause of the significant loss of capacity to store lithium observed on cycling the spinel electrodes, Fig. 6.[39,40] The capacity loss arises because the particles contract on deintercalation resulting in a loss of mutual contact. Some particles may become isolated from the rest of the electrode and hence unable to act as host for lithium insertion on subsequent discharge. The $LiMn_2O_4$ compounds used in early studies were prepared by the solid-state reaction between lithium carbonate and $Mn_2O_3$ at 850 °C in air. Alternative synthesis routes to the spinel have been reported which possess the common factor that they employ low firing temperatures and this significantly improves the capacity retention on cycling.[41–43] Our solution-based synthesis may be carried out in air and involves the reaction between $Li_2CO_3$ and $Mn(MeCO_2)_2$ in aqueous solution followed by firing at the exceptionally low temperature of 200 °C.[40,42,43] This route gives a marked improvement in the cycling performance compared with the original spinel materials. X-Ray data have shown a significant reduction in the amount of cubic (unintercalated) $LiMn_2O_4$ phase present at the end of discharge on extended cycling.[39] We have also found that by adding < 1 mass% of carbon black to the aqueous solution before firing, a dramatic improvement in the capacity retention of up to 50% after 300 cycles and at high cycling rates (currents of 1 mA $cm^{-2}$ of the electrode area), can be obtained.[42,43] Powder X-ray diffraction has demonstrated that there is a further marked drop in the accumulation of cubic material at the end of discharge when synthesised with carbon.[40] The low-temperature routes yield material of lower crystallinity as is evident from the broad peaks in the powder X-ray diffraction patterns but the particle size remains in the micron range. It may be that there is an extensive mosaic structure of small coherent crystalline regions within each particle that is better able to accommodate the volume change. Alternatively the carbon black may act as a flexible electronic contact between particles facilitating the cubic to tetragonal conversion. As well as

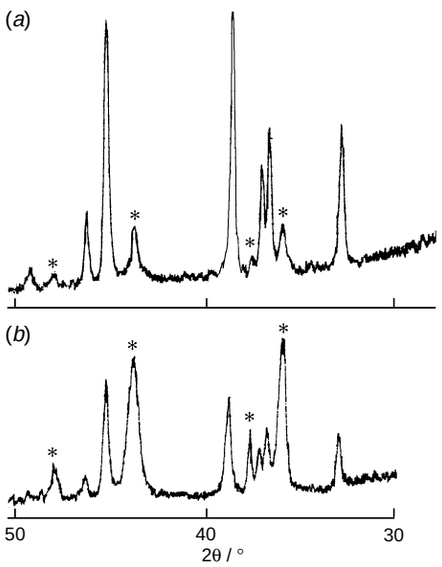



**Fig. 6** Powder X-ray diffraction patterns of electrodes constructed from $LiMn_2O_4$ prepared by solid-state reaction at 850 °C, (*a*) at the end of discharge after two cycles, (*b*) at the end of discharge after 50 cycles. In both cases peaks from residual cubic phase (denoted by *) are present and this phase accumulates with cycling. Cells were cycled at 0.5 mA $cm^{-2}$ between 3.7 and 2.0 V *vs*. $Li^+/Li$.

improving capacity retention on cycling, the low-temperature synthesis yields material which depart from the stoichiometric $LiMn_2O_4$ composition, for example our low-temperature solution route yields, after firing at 200 °C, a composition $LiMn_2O_{4.1}$. These compounds are in fact cation deficient with two possible extreme cation distributions, $Li_{0.98}[Mn_{1.95}\square_{0.05}]_{oct}O_4$ (where □ represents a vacant cation site) or $Li_{0.93}[Mn_{1.95}Li_{0.05}]_{oct}O_4$. $LiMn_2O_{4.1}$ contains 60% $Mn^{4+}$ and this implies an increase in the theoretical capacity to accept lithium from 148 to 178 mA h $g^{-1}$, *i.e.* 20% more than the stoichiometric spinel. To accommodate this, lithium ions must simultaneously occupy face-sharing octahedral (16c) and tetrahedral (8a) sites. The fact that improved overall capacity, in addition to the improved capacity retention on cycling, can be obtained from these low-temperature materials transformed the lithium manganese oxide spinels from materials with little practical interest, despite their other attributes, to compounds that are competitive for applications, Fig. 7.

Turning now to the performance of the spinel in the 4 V regime within which lithium is extracted from the 8a sites, this appears to occur over a continuous range of solid solutions for $0.5 < x < 1$.[35,44] At *x ca.* 0.5 it has been suggested that lithium ion ordering occurs involving occupancy of one half of the tetrahedral 8a sites and that deintercalation below this composition is an event in which two cubic spinel phases of approximate composition $x = 0$ and 0.5 coexist (note that the precise composition range over which the two phases are observed is still controversial). A small step of around 100 mV between two essentially flat voltage profiles is observed at *x ca.* 0.5. Again, the original materials prepared by high-temperature solid-state reaction at 850 °C gave disappointing cycling performance, although significantly better than that in the 3 V region. Several reasons have been advanced for this.

(*i*) The two-phase nature of the process in the range $0 < x < 0.5$ leading to a cell volume change and loss of particle contact.[45] (*ii*) Dissolution of $Mn^{2+}$ in the electrolyte as a result of the disproportionation reaction $2Mn^{3+} \rightarrow Mn^{2+} + Mn^{4+}$.[46,47] (*iii*) Electrolyte decomposition at a high degree of deintercalation *i.e.* high voltage.[48]

Probably all these factors play a role in the capacity fade of the spinel material. It has however been shown that by careful control of the composition a dramatic improvement in the

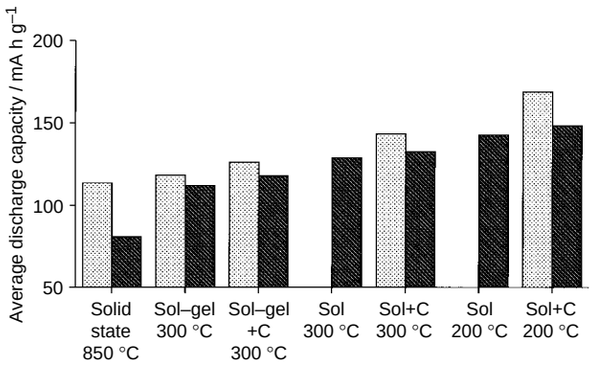



**Fig. 7** Histogram plot comparing the performance of several 3 V electrodes containing lithium manganese oxide spinels prepared under different conditions. The electrodes and cycling conditions are identical in all cases, the only difference being the active material. The discharge capacities on the *y*-axis are an average taken over the first four cycles. The cycling current densities are 0.5 mA cm$^{-2}$ (left) and 1 mA cm$^{-2}$ (right). The temperatures used to fire the spinels are shown. C refers to the addition of 1 mass% carbon black during the synthesis, 'sol–gel' refers to the use of the synthesis method described in ref. 41 and 'sol' indicates use of our own synthesis described in the text. The material prepared from the solid-state reaction was obtained by firing $Li_2CO_3$ and $Mn_2O_3$ in air.

cycling performance may be achieved.[46,49,50] Excellent cyclability can be obtained by replacing a small amount of the manganese on the 16d octahedral sites by lithium, $Li_{1+\delta}Mn_{2-\delta}O_4$ ($\delta$ = 0.1).[30,47,51] Other divalent ions *e.g.* Zn, Mg, *etc*. have also been used,[47] however lithium is attractive since it introduces no new cations into the system and a small amount of this monovalent ion corresponds to a significant increase in the average manganese valence above $Mn^{3.5+}$. This seems to be the key factor responsible for improved capacity retention on cycling. It should be noted however that such solid solutions will reduce the capacity associated with the 4 V plateau, since there is less $Mn^{3+}$ available for oxidation. It has also been shown that such solid solutions reduce dissolution of Mn and promote a single phase composition over the range $0 < x < 1$.[45] The synthesis of a spinel modified to yield an oxidation state slightly greater than $Mn^{3.5+}$ may be easily carried out by firing an aqueous mixture of $Li_2CO_3$ and $Mn(MeCO_2)_2$, first at 200 °C (*i.e.* the same conditions used to prepare a spinel for use at 3 V) and then heating at 650 °C, thus forming the non-stoichiometric spinel $LiMn_2O_{4.02}$ which is marginally cation deficient.[43,52,53] Our compound shows excellent capacity retention on cycling even at high current rates, Fig. 8. Many other solid solutions have been formed based on replacing Mn by, for example, Co, Ni, Cu, Be, Ga, Cr, *etc.*[54,55] and some of these also demonstrate improved performance. It is evident that the performance of the spinels, in contrast to $LiCoO_2$, is very sensitive to the preparative conditions.

## Future prospects

### *Layered $LiMnO_2$*[40,56]

Despite strenuous effects by a number of groups over the past few years the synthesis of $LiMnO_2$ with the $LiCoO_2$ structure had proved elusive until recently. Layered $LiMnO_2$ is potentially attractive since it combines the proven performance of the $LiCoO_2$ structure with the low cost and low toxicity of manganese. Furthermore, $MnO_2$ is more stable than $CoO_2$ in liquid solvents offering the possibility of obtaining the full capacity to deliver lithium compared with only half a lithium in the case of $LiCoO_2$. The difficulty is that Li–Mn–O compositions do not readily form layered structures. Very recently we have succeeded in synthesising layered $LiMnO_2$ with the structure of $LiCoO_2$ using an ion-exchange route.[40,56] Neutron powder diffraction has confirmed the layered structure. All of the lithium may be removed chemically or electrochemically

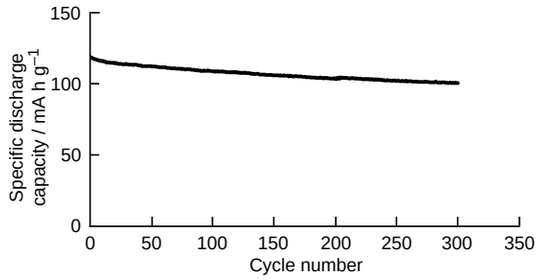



**Fig. 8** Capacity to store charge in the spinel at 4 V *vs*. number of charge–discharge cycles. Cycling was carried out between 4.3 and 3.6 V at 30 °C and at charge and discharge currents of 0.5 mA cm$^{-2}$. The electrolyte was a 1 molar solution of $LiPF_6$ dissolved in a 1 : 1 mixture of dimethyl carbonate and ethylene carbonate.

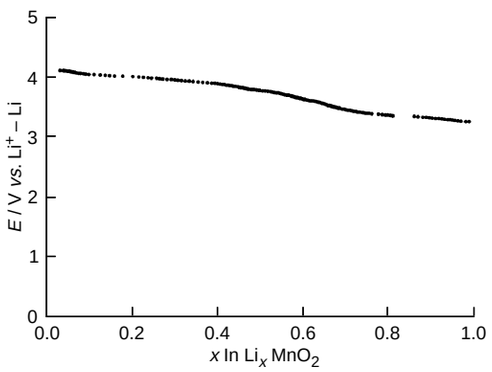



**Fig. 9** Variation of the voltage with lithium content in layered $Li_xMnO_2$ on charging at a low current (10 μA cm$^{-2}$)

yielding a total capacity of 270 mA h g$^{-1}$, Fig. 9.[40,56] Despite the high capacity, the cycling performance of these early materials is not satisfactory.[56,57] It is important to recall that the early $LiMn_2O_4$ spinels, although attractive in many ways, did not demonstrate sufficient capacity retention on cycling, however minor modification of their composition has resulted in their commercial success. The importance of layered $LiMnO_2$ may be that it opens a new avenue of exploration that will lead to optimised materials.

### *Iron Oxides*

An interesting recent development is the use of iron(III) sulfates as hosts for lithium intercalation.[58] Up to two lithiums may be reversibly inserted into $Fe_2(SO_4)_3$ accompanied by the reduction of $Fe^{3+}$ to $Fe^{2+}$. The host consists of $FeO_6$ octahedra linked by corner-sharing through $SO_4$ tetrahedra. Lithium intercalation is associated with a potential of 3.6 V *vs*. $Li^+/Li$ which is much higher than the potential associated with the same $Fe^{3+/2+}$ couple in a simple oxide. Replacement of $O^{2-}$ by $SO_4$ groups polarises the oxygens reducing the covalency of the Fe–O interactions and lowering the energy of the antibonding d levels. As a result the voltage is higher. The fact that more modest oxidation states of the first-row transition-metal ions can achieve higher voltages in these more complex framework compounds is something which deserves further exploration and may lead to a range of possibilities for the synthesis of new intercalation hosts as positive electrodes in rechargeable lithium batteries in the future.

There can be no doubt that significant advances in the performance of rechargeable lithium batteries will be achieved over the next 10 years. As was the case with the success of the first-generation systems, future development will rely heavily on the ability of solid-state chemists to rise to the challenge of designing new intercalation compounds for lithium which optimise the many different properties that are important for a positive electrode in a rechargeable lithium battery.

## Acknowledgements

P. G. B. is indebted to the EPSRC, NEDO and the EU for financial support.

**Peter Bruce was born and educated in Scotland. He was awarded a BSc and PhD from the University of Aberdeen and after periods spent at Oxford and Heriot-Watt Universities he moved to St. Andrews where he is currently Professor of Chemistry and Head of Department. He has held a Pickering Fellowship from The Royal Society and a further research Fellowship from The Royal Society of Edinburgh. He was elected a Fellow of the Royal Society of Edinburgh in 1995.**

## Footnotes

* E-mail: p.g.bruce@st-and.ac.uk

† This ChemComm is also available in enhanced multi-media format *via* the World Wide Web: http://chemistry.rsc.org/rsc/cccenha.htm

‡ It should be recalled that this separation does not imply independence of these terms since ion–electron interactions must be present, only $\mu_{Li}^{int}$ has a rigorous thermodynamic meaning.

§ Strictly $E_F$ equates to the electrochemical potential of the electron which can include a, usually small, contribution from electric fields due to dipoles on the surface of the solid, even for an otherwise uncharged solid.[16] We shall neglect this perturbation.

¶ Note that the ion–electron interactions (including those between the $Li^+$ ions and the electrons) together with the electron–electron interactions and the one-electron energy of the $e^-$ all contribute to the Fermi energy of the electron.

‖ A derivation which demonstrates that the cell voltage depends on the Fermi level difference between the two electrodes but only when they are in the cell, can be found in the enhanced version of this article on the WWW.

## References

1 T. Nagaura, Paper presented at *4th Int. Rechargeable Battery Seminar*, Deerfield Beach, FL, 1990; T. Nagaura and K. Tazawa, *Prog. Batteries Col. Cells*, 1990, **9**, 20.
2 P. G. Bruce, *Philos. Trans. R. Soc. Lond. A*, 1996, **354**, 1577.
3 K. Ozawa, *Solid State Ionics*, 1994, **69**, 212.
4 *Lithium Batteries. New Materials, Developments and Perspectives*, ed. G. Pistoia, Elsevier Science B.V., Amsterdam, 1994.
5 Recent Advances in Rechargeable Li Batteries, *Solid State Ionics*, 1994, **69**, no. 3, p. 4.
6 Materials for Electrochemical Power Systems, *Philos. Trans. R. Soc. London A*, 1996, **354**, 1513.
7 *Handbook of Solid State Batteries and Capacitors*, ed. M. Z. A. Munshi, World Scientific, 1995.
8 P. G. Bruce, *Philos. Trans. R. Soc. London A*, 1996, **354**, 415.
9 *Solid State Electrochemistry*, ed. P. G. Bruce, Cambridge University Press, Cambridge, 1995.
10 *Intercalation Chemistry*, ed. A. J. Jacobson and M. S. Whittingham, Academic Press, New York, 1982.
11 A. M. Chippindale, P. G. Dickens and A. V. Powell, *Prog. Solid State Chem.*, 1991, **21**, 133.
12 W. Weppner, *Solid State Electrochemistry*, ed. P. G. Bruce, Cambridge University Press, Cambridge, 1995, 199.
13 D. O'Hare, in *Inorganic Materials*, ed. D. W. Bruce and D. O'Hare, Wiley, New York, 1995.
14 W. R. McKinnon, *Solid State Electrochemistry*, ed. P. G. Bruce, Cambridge University Press, Cambridge, 1995, p. 163.
15 H. Rickert, *Electrochemistry of Solids: An Introduction*, Springer-Verlag, Berlin, 1982.
16 J. Goodisman, *Electrochemistry: Theoretical Foundations*, Wiley, New York, 1987.
17 C. Sigala, D. Guyomard, A. Verbaere, Y. Piffard and M. Tournoux, *Solid State Ionics*, 1995, **81**, 167.
18 P. G. Bruce and M. Y. Saidi, *Electrochim. Acta*, 1991, **36**, 569.
19 K. Mizushima, P. C. Jones, P. J. Wiseman and J. B. Goodenough, *Mater. Res. Bull.*, 1980, **15**, 783.
20 J. B. Goodenough, K. Mizushima and T. Takeda, in *Proceedings of the 4th Int. Conference on Ternary and Multinary Compounds*, Tokyo, 1980.
21 M. G. S. R. Thomas, P. G. Bruce and J. B. Goodenough, *J. Electrochem. Soc.*, 1985, **132**, 1521.
22 M. G. S. R. Thomas, P. G. Bruce and J. B. Goodenough, *Solid State Ionics*, 1985, **17**, 13.
23 M. Shibuya, T. Nishina, T. Matsue and I. Uchida, *J. Electrochem. Soc.*, 1996, **143**, 3157.
24 C. Delmas, J. P. Peres, A. Rougier, A. Demourgues, F. Weill, A. Chadwick, M. Broussely, F. Perton, Ph. Biensan and P. Willmann, Presented at the *8th Int. Meeting on Lithium Batteries*, Nagoya, Japan, 1996.
25 P. G. Bruce, A. Lisowska-Oleksiak, M. Y. Saidi and C. A. Vincent, *Solid State Ionics*, 1992, **57**, 353.
26 G. Dutta, A. Manthiram, J. B. Goodenough and J.-C. Grenier, *J. Solid State Chem.*, 1992, **96**, 123.
27 W. Li, J. N. Reimers and J. R. Dahn, *Solid State Ionics*, 1993, **67**, 123.
28 G. G. Amatucci, J. M. Tarascon and L. C. Klein, *J. Electrochem. Soc.*, 1996, **143**, 1114.
29 T. Ohzuku, A. Ueda and M. Nagayama, *J. Electrochem. Soc.*, 1993, **140**, 1862.
30 M. M. Thackeray, *J. Electrochem. Soc.*, 1995, **142**, 2558.
31 R. Kanno, T. Shirane, Y. Kawamoto, Y. Takeda, M. Takano, M. Ohashi and Y. Yamaguchi, *J. Electrochem. Soc.*, 1996, **143**, 2435.
32 T. Ohzuku, A. Ueda and M. Kouguchi, *J. Electrochem. Soc.*, 1995, **142**, 4033.
33 (*a*) C. Delmas, I. Saadoune and A. Rougier, *J. Power Sources*, 1993, **43**/**44**, 595; (*b*) C. Delmas, *Lithium Batteries. New Materials, Developments and Perspectives*, ed. G. Pistoia, Elsevier Science B.V., Amsterdam, 1994.
34 M. M. Thackeray, W. I. F. David, P. G. Bruce and J. B. Goodenough, *Mater. Res. Bull.*, 1983, **18**, 461.
35 M. M. Thackeray, P. J. Johnson, L. A. de Picciotto, W. I. F. David, P. G. Bruce and J. B. Goodenough, *Mater. Res. Bull.*, 1984, **19**, 179.
36 J. B. Goodenough, M. M. Thackeray, W. I. F. David and P. G. Bruce, *Rev. Chim. Minér.*, 1984, **21**, 435.
37 Japan Electronics, March 6th, 1996.
38 J. C. Hunter, *J. Solid State Chem.*, 1981, **39**, 142.
39 H. Huang, Ph.D. Thesis, University of St. Andrews, 1997.
40 P. G. Bruce, A. R. Armstrong and H.Huang, *J. Power Sources*, in the press.
41 P. Barboux, J. M. Tarascon and F. K. Shokoohi, *J. Solid State Chem.*, 1991, **94**, 185.
42 H. Huang and P. G. Bruce, *J. Electrochem. Soc.*, 1994, **141**, L76.
43 H. Huang and P. G. Bruce, *J. Power Sources*, 1995, **54**, 52.
44 T. Ohzuku, M. Kitagawa and T. Hirai, *J. Electrochem. Soc.*, 1990, **137**, 769.
45 Y. Xia and M. Yoshio, *J. Electrochem. Soc.*, 1996, **143**, 825.
46 J. M. Tarascon, F. Coowar, G. Amatuci, F. K. Shokoohi and D. G. Guyomard, *J. Power Sources*, 1995, **54**, 103.
47 R. J. Gummow, A. de Kock and M. M. Thackerary, *Solid State Ionics*, 1994, **69**, 59.
48 (*a*) G. Pistoia, A. Antonni, R. Rosati and D. Zane, *Electrochim. Acta*, 1996, **41**, 2683; (*b*) G. Pistoia, D. Zane and Y. Zhang, *J. Electrochem. Soc.*, 1995, **142**, 2551.
49 J. M. Tarascon, W. R. McKinnon, F. Coowar, T. N. Bowmer, G. Amatucci and D. Guyomard, *J. Electrochem. Soc.*, 1994, **141**, 1421.
50 V. Manev, B. Banov, A. Momchilov and A. Nassalevska, *J. Power Sources*, 1995, **57**, 99.
51 Y. Gao and J. R. Dahn, *J. Electrochem. Soc.*, 1996, **143**, 100.
52 H. Huang and P. G. Bruce, *J. Electrochem. Soc.*, 1994, **141**, L106.
53 H. Huang and P. G. Bruce, in *Proceedings of the Int. Workshop of Advanced Batteries*, Osaka, Japan, Feb. 1995.
54 L. Guohua, H. Ikita, T. Uchida and M. Wakihara, *J. Electrochem. Soc.*, 1996, **143**, 178.
55 Q. Zhong, A. Bonakdarpour, M. Zhang, Y. Gao and J. R. Dahn, *J. Electrochem. Soc.*, 1997, **144**, 205.
56 A. R. Armstrong and P. G. Bruce, *Nature*, 1996, **381**, 499.
57 C. Delmas and F. Capitaine, Presented at the *8th Int. Meeting on Lithium Batteries*, Nagoya, Japan, 1996.
58 K. S. Nanjundaswamy, A. K. Padhi, J. B. Goodenough, S. Okada, H. Ohtsuka, H. Arai and J. Yamaki, *Solid State Ionics*, 1996, **92**, 47.

*6/08551B*

# Positive and negative ionochromism and UV sensor properties of oxygen-containing polysilanes

**Chien-Hua Yuan and Robert West***

*Department of Chemistry, University of Wisconsin, Madison, WI 53706-1396, USA*

**Addition of lithium trifluoromethanesulfonate (LiOTf) to poly[(4-ethoxyethoxybutyl)octylsilylene] (PEBOS) prevents the normal thermochromic transition to longer wavelength (negative ionochromism), whereas addition LiOTf to poly-[bis(5-ethoxyethoxypentyl)silylene] (PEEPS) induces a thermochromic transition (positive ionochromism); the latter effect is reversed in the presence of water or THF vapour, so that LiOTf-doped PEEPS serves as a UV sensor for $H_2O$ or THF.**

Recently, polythiophenes having oligoether ($OCH_2CH_2O$) sidechains have been shown to undergo chromotropic changes in the presence of alkali metal cations.[1] The cations are presumed to bind to the oligoether oxygens and alter the chain conformation, resulting in a strong blue shift of the absorption bands; this type of change we will term 'negative ionochromism.'†

Polysilane polymers generally display strong electronic absorption bands in the near ultraviolet region, assigned to $\sigma \rightarrow \sigma^*$ transitions.[3] The energy of this transition depends on the conformation of the polymer chain.[4] Many polysilanes show chromotropic behavior, associated with changes in the backbone conformation which after the σ-conjugation. Thermochromism is especially common, but in selected polysilanes electrochromism,[5] piezochromism[6] and solvatochromism[7] have also been reported.

We have now synthesized several polysilanes containing oxygen atoms in the organic side chains,[8] and examined the effect of added cations.‡ The UV spectrum of a thin film of PEBOS as a function of temperature is shown in Fig. 1(*a*). As the polymer is cooled, the absorption band at 320 nm disappears and is replaced by one at 354 nm; the midpoint of the transition is at *ca.* −32 °C. This sort of thermochromic transition, reflecting a change from a coiled to an all-*trans* conformation, is found for many polysilanes.[3,4]

The effect of adding lithium trifluoromethanesulfonate to PEBOS is shown in Fig. 1(*b*)–1(*d*). With 12.5 and 25.0 mol% LiOTf, the thermochromic transition is progressively inhibited. At 50 mol% LiOTf, no change in the UV spectrum is observed upon cooling, even at −70 °C [Fig. 1(*d*)]. The lithium-complexed PEBOS thus exhibits negative ionochromism, perhaps because the lithium ions freeze the polymer into a coiled conformation.

The UV spectrum for PEEPS is shown in Fig. 2(*a*). Like PEBOS, this polymer also undergoes a thermochromic transition from 320 to 352 nm, with a midpoint at *ca.* −38 °C. The effect of added lithium triflate is, however, entirely different. As shown in Fig. 2(*b*), with 0.75 mol% LiOTf, PEEPS exhibits a thermochromic transition centred at *ca.* 35 °C. Thus in this polymer, lithium complexing causes the bathochromic shift, providing an example of positive ionochromism; the lithium cations apparently serve to lock the polymer into an extended conformation.

For both polymers, these changes in optical absorption upon LiOTf complexing were reflected in the thermal properties. In

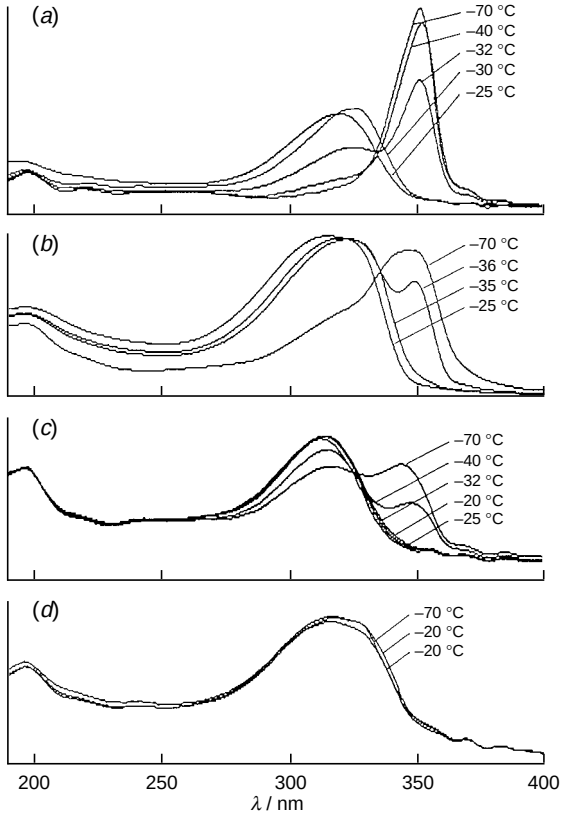



**Fig. 1** Thermochromism of PEBOS complexes with LiOTf: Li/Si = (*a*) 0, (*b*) 12.5, (*c*) 25 and (*d*) 50 mol%

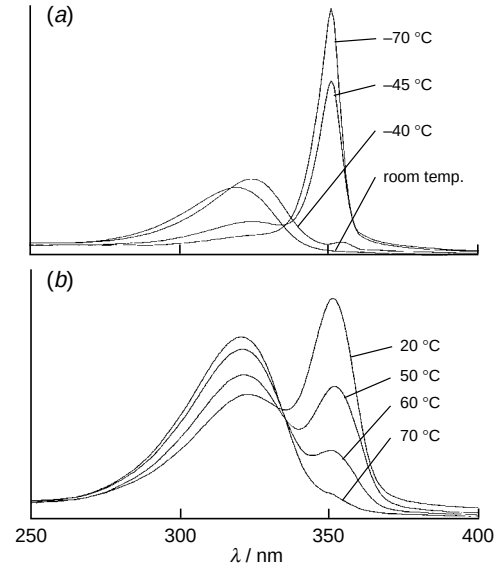



**Fig. 2** Thermochromism of (*a*) a thin film of PEEPS compared to (*b*) a thin film of PEEPS–$LiSO_3CF_3$ complex (Li/Si = 75 mol%)

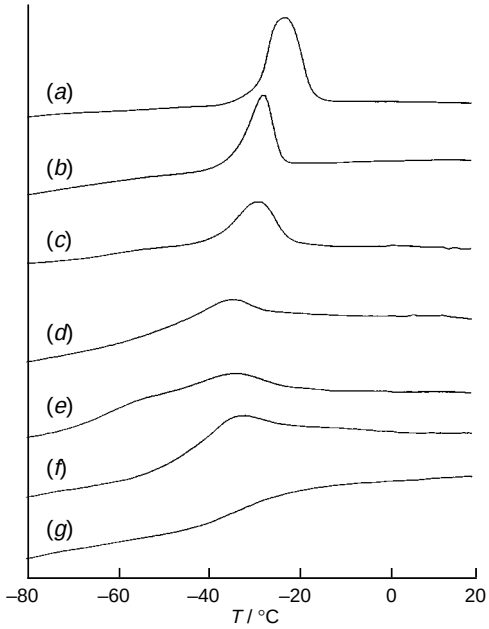



**Fig. 3** DSC thermogram of PEBOS–$LiSO_3CF_3$ complexes. Li/Si = (*a*) 0, (*b*) 12.5, (*c*) 25, (*d*) 40, (*e*) 50, (*f*) 60 and (*g*) 80 mol.

the differential scanning calorimetry (DSC) thermogram for PEBOS, shown in Fig. 3(*a*) a first order transition is found at a temperature near that of the thermochromic change.§ As LiOTf is added, the thermal transition weakens and moves to lower temperature [Fig. 3(*b*)–(*d*)]; with 50 mol% LiOTf, only a second-order transition is seen. For PEEPS, a thermal transition is found at −35 °C (Fig. 4). As LiOTf is added this transition weakens and a new thermal transition appears above 0 °C. With 75 mol% LiOTf, the thermogram is dominated by a transition at 35 °C, corresponding to the UV thermochromic transition.

PEEPS exhibits yet another unexpected phenomenon involving a new type of chromotropic behavior. The spectra in Fig. 2 were determined in a cryostat, out of contact with the atmosphere. If the cryostat is opened to admit moist air (at 25 °C) the long wavelength band at 352 nm disapears and is replaced by the higher energy, 320 nm absorption. This change is reversible; pumping on the sample to remove moisture regenerates the long wavelength band. Exposure to THF vapour likewise reversibly shifts the absorption band from 352 to 320 nm. Thus PEEPS behaves as an ultraviolet sensor for small basic molecules. We theorize that water and THF compete with the oxygen atoms in the PEEPS sidechains for the lithium cations,[10] allowing the polymer to relax into the coiled form which it normally adopts at room temperature. The effect is quite structure-specific, since diethyl ether vapour does not induce the hypsochromic shift.

Similar, but much weaker, effects were observed when salts of $Na^+$ or $K^+$ were added to PEBOS and PEEPS. The reason for the striking difference in behaviour between these two polymers is not clear; we are now synthesizing other ($OCH_2CH_2O$)-containing polysilanes to explore the effect of structural variability on these novel chromotropic effects.

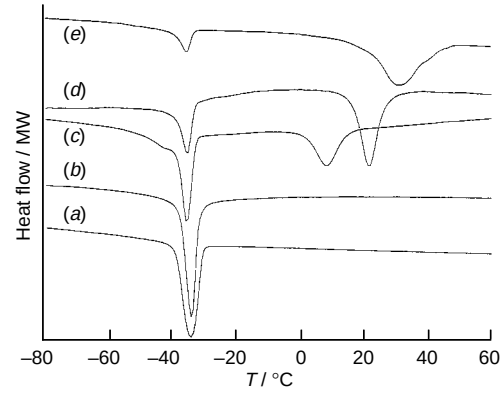



**Fig. 4** DSC curve of PEEPS–$LiSO_3CF_3$ complexes. Li/Si = (*a*) 0, (*b*) 25, (*c*) 50, (*d*) 75 and (*e*) 100 mol%.

This work was supported by a grant from the U.S. Office of Naval Research.

## Footnotes and References

* E-mail: west@chem.wisc.edu

† Positive ionochromism has been observed for polythiophenes having calixarene substituents with $Na^+$ ion (ref. 2).

‡ The prepartion of PEBOS and PEEPS was carried out by sodium condensation of diorganodichlorosilanes, as described in an earlier paper (ref. 9). PEBOS was precipitated from PhMe solution with MeOH, and PEEPS was precipitated from PhMe with MeCN–$H_2O$ (1 : 2). The structures of the polymers were confirmed by $^1H$, $^{13}C$ and $^{29}Si$ NMR spectroscopy. Gel permeation chromatography indicated a bimodal *M*w distribution for PEBOS (*M*w $1.4 \times 10^6$ and $2 \times 10^4$ *vs.* polystyrene standard) and a monomodal distribution for PEEPS (*M*w $1.6 \times 10^6$).

§ Differential scanning calorimetry thermograms were determined at a heating and cooling rate of 10 °C $min^{-1}$ under a dry helium atmosphere over the temperature range from 100 to −100 °C.

1 I. Levesque and M. Leclerc, *J. Chem. Soc., Chem. Commun.*, 1995, 2293; *Chem. Mater.*, 1995, **8**, 2843; *cf.* R. D. McCullough and S. P. Williams, *Chem. Mater.*, 1995, **7**, 2001.
2 M. J. Marsella, R. J. Newland, P. J. Carroll and T. M. Swager, *J. Am. Chem. Soc.*, 1995, **117**, 9842.
3 R. West, in *Comprehensive Organometallic Chemistry II*, ed. E. W. Abel, F. G. A. Stone and G. Wilkinson, Pergamon, Oxford, 1995, vol. 2, pp. 77–109; R. D. Miller and J. Michl, *Chem. Rev.*, 1989, **89**, 1359; R. West, in J. E. Mark, H. R. Allcock and R. West, *Inorganic Polymers*, Prentice Hall, Englewood Cliffs, NJ, 1992, ch. 5, pp. 186–23.
4 S. S. Bukalov, L. A. Leites, R. West and T. Asuke, *Macromolecules*, 1996, **29**, 907; K. S. Schweitzer, *J. Chem. Phys.*, 1986, **85**, 1156, 1176.
5 M. Fujino, T. Hiaki and N. Matsumoto, *Macromolecules*, 1995, **28**, 5017.
6 K. Song, H. Kuzmany, G. M. Wallraff, R. D. Miller and J. F. Rabolt, *Macromolecules*, 1990, **23**, 3870.
7 K. Oka, N. Fujiue, T. Dohmaru, C.-H. Yuan and R. West, *J. Am. Chem. Soc.*, 1997, **119**, 4074.
8 K. Oka, N. Fujiue, S. Nakanishi, T. Takata, T. Dohmaru, C.-H. Yuan and R. West, *Chem. Lett.*, 1995, 875.
9 C.-H. Yuan and R. West, *Macromolecules*, 1993, **26**, 2645.
10 A. Wendsjø, J. O. Thomas and J. Lindgren, *Polymer*, 1993, **34**, 2243.

*Received in Cambridge, UK, 19th June 1997; 7/04294I*

# Synthesis of 1,3-dioxolan-4-one from trioxane and carbon monoxide on HZSM-5 zeolite

**Tsuneji Sano,*[a] Takashi Sekine,[a] Zhengbao Wang,[a] Kazuo Soga,[a] Ikuo Takahashi[b] and Takashi Masuda[c]**

[a] *School of Materials Science, Japan Advanced Institute of Science and Technology, Tatsunokuchi, Ishikawa 923-12, Japan*
[b] *Daicel Chemical Industries Ltd., Himeji, Hyougo 671-12, Japan*
[c] *National Institute of Materials and Chemical Research, Tsukuba, Ibaraki 305, Japan*

**Cabonylation of formaldehyde with carbon monoxide has been carried out on HZSM-5 zeolite; from spectroscopic analysis of the products obtained, the formation of 1,3-dioxolan-4-one on the Brønsted acid sites of HZSM-5 zeolite has been demonstrated.**

Carbonylation with carbon monoxide (CO) is one of the most important reactions for fundamental and industrial applications, and various kinds of homogeneous and heterogeneous catalysts are used.[1,2] Recently, carbonylation on zeolite catalysts has received considerable attention. It has been shown that CO and $H_2O$ can react with small alkenes on HZSM-5 zeolite to form carboxylic acids[3,4] and that, under anhydrous conditions, ethene, isobutene and oct-1-ene react to form ketones instead of carboxylic acids.[5] The formation of benzoic acid on HY zeolite from the carbonylation of benzene with CO has also been reported.[6] However, no report is available of the synthesis of lactones. Here we report the formation of 1,3-dioxolan-4-one (1,3-DOX-4) *via* carbonylation of formaldehyde with CO on HZSM-5.

HZSM-5 zeolites and silicalite were prepared following the previously described procedure.[7] The $SiO_2/Al_2O_3$ ratios (53, 101, 191 and 3300) were determined by X-ray fluorescence. Prior to the experiments, the zeolite was activated by heating at 400 °C for 8 h. Trioxane was used as the source of formaldehyde, and was purified by crystallization from $CH_2Cl_2$ and dried *in vacuo* at room temperature for 1 h. $CH_2Cl_2$ (research grade) was used as solvent. When the residual moisture in the $CH_2Cl_2$ was greater than 1000 ppm, the carbonylation of formaldehyde with CO did not occur and paraformaldehyde was mainly obtained. Therefore, dehydration of the $CH_2Cl_2$ was required using 4 Å molecular sieves, the residual moisture, measured by the Karl Fischer method, was less than 30 ppm.

The carbonylation of formaldehyde with CO was carried out using a 100 ml autoclave as follows. Trioxane (10 g), $CH_2Cl_2$ (40 ml) and zeolite (1 g) were placed in the autoclave under a nitrogen atmosphere, and CO ( > 99.95%) was introduced. The initial CO pressure at room temperature was varied in the range of 15 to 75 MPa. The reaction temperature (40–180 °C) was reached within 1 h. After 2–50 h of reaction, the zeolite and the solid product were filtered off. The filtrate was distilled under reduced pressure several times. The product (a colourless liquid) obtained by distillation at 85 °C and 60 mmHg was analysed by GC–MS, as well as IR and $^1$H and $^{13}$C NMR spectroscopy. The yield of 1,3-DOX-4 obtained was calculated by GC using sulfolane as an internal standard. GC analyses were carried out on a Shimadzu GC-15A gas chromatograph (FID) equipped with a 25 m × 0.22 mm ID HiCap-CBP1 Shimadzu capillary column. $^1$H and $^{13}$C NMR spectra were recorded on a Varian Gemini 300 spectrometer (300 MHz for $^1$H, 75.4 MHz for $^{13}$C).

In the $^1$H NMR spectrum of the product obtained by distillation, two intense signals were observed at $\delta$ 5.5 and 4.2. These signals were assigned to the $OCH_2O$ and $OC(=)CH_2O$ methylene groups, respectively. In the $^{13}$C NMR spectrum, three signals were observed at $\delta$ 171.3, 96.1 and 62.4. These signals were assigned to the $CO_2$ carboxyl carbon and the methylene carbons of the $OCH_2O$ and $OC(=O)CH_2O$ groups, respectively. Characteristic bands were also observed in the IR spectrum. The 1798 $cm^{-1}$ band is characteristic of the stretching vibration of C=O ester groups and the band at about 1210 $cm^{-1}$ is characteristic of stretching of C–O ester groups. These results strongly indicate the selective formation of 1,3-DOX-4 on the HZSM-5 zeolite catalyst. The formation of 1,3-DOX-4 (*m/z* 88, 87 and 44) was also confirmed by GC–MS. Although it has already been reported that glycolic acid[8] and the polymer polyglycolide[9,10] can be synthesized from formaldehyde and CO using various acid catalysts, the preferential formation of 1,3-DOX-4 has never been reported.

To obtain more information related to carbonylation on HZSM-5 zeolite, the catalytic performance of HZSM-5 zeolite was examined under various reaction conditions. At first, to clarify the active site of the formation of 1,3-DOX-4, the carbonylation was conducted on various HZSM-5 zeolites with different $SiO_2/Al_2O_3$ ratios. As shown in Table 1, the yield of 1,3-DOX-4 decreased with an increase in the $SiO_2/Al_2O_3$ ratio (entries 1–4). In the case of silicalite, which has almost no Brønsted acid sites, 1,3-DOX-4 was not obtained. This indicates that the carbonylation is promoted on the acid sites of HZSM-5 zeolite. Next, the influence of the reaction temperature and CO pressure on the 1,3-DOX-4 yield was studied. 1,3-DOX-4 was obtained in very low yields at 40 and 80 °C (entries 5 and 6). At reaction temperatures higher than 80 °C, the yield increased with the reaction temperature and then decreased after reaching a maximum yield at 160 °C (entries 7–9). The yield of 1,3-DOX-4 was dependent on the initial CO pressure (entries 8, 10–12). The yield increased with the initial CO pressure and a

**Table 1** Synthesis of 1,3-DOX-4 from trioxane and CO on zeolite catalysts[a]

| | | Reaction conditions | | | |
|---|---|---|---|---|---|
| Entry | Zeolite ($SiO_2/Al_2O_3$) | *T*/°C | $P_{CO}$/MPa[b] | *t*/h | Yield/mmol (%) |
| 1 | HZSM-5 (53) | 120 | 35 | 2 | 101 (60.7) |
| 2 | HZSM-5 (101) | 120 | 35 | 2 | 51 (30.6) |
| 3 | HZSM-5 (191) | 120 | 35 | 2 | 46 (27.6) |
| 4 | Silicalite (3300) | 120 | 35 | 2 | 0 (0) |
| 5 | HZSM-5 (191) | 40 | 35 | 5 | 0 (0) |
| 6 | HZSM-5 (191) | 80 | 35 | 5 | 2 (1.2) |
| 7 | HZSM-5 (191) | 120 | 35 | 5 | 93 (55.9) |
| 8 | HZSM-5 (191) | 160 | 35 | 5 | 102 (61.3) |
| 9 | HZSM-5 (191) | 180 | 35 | 5 | 83 (49.8) |
| 10 | HZSM-5 (191) | 160 | 15 | 5 | 60 (36.0) |
| 11 | HZSM-5 (191) | 160 | 55 | 5 | 114 (68.5) |
| 12 | HZSM-5 (191) | 160 | 75 | 5 | 89 (53.5) |
| 13 | HZSM-5 (191) | 160 | 35 | 2 | 71 (42.6) |
| 14 | HZSM-5 (191) | 160 | 35 | 13 | 61 (36.6) |
| 15 | HZSM-5 (191) | 160 | 35 | 50 | 6 (3.6) |

[a] Reaction conditions: trioxane (10 g, 111 mmol), $CH_2Cl_2$ (40 ml), zeolite (1 g). [b] Initial CO pressure at room temperature.

maximum yield of 114 mmol was obtained at a CO pressure of 55 MPa. As the maximum yield of 1,3-DOX-4 calculated from the amount of trioxane (111 mmol) used is 166.5 mmol, this indicates the preferential formation of 1,3-DOX-4. The time dependence of the 1,3-DOX-4 yield was also studied. The yield increased with the reaction time, and then decreased markedly after the maximum yield was reached at a reaction time of *ca*. 5 h (entries 8, 13–15). Taking into account the fact that the yield of solid product increased with an increase in the reaction time, this seems to indicate that 1,3-DOX-4 is the initial product and that the decrease in the yield is attributable to the later ring opening polymerization of 1,3-DOX-4 to form polyglycolide, probably inside the zeolite crystals.[9,10]

From the above results, it has been shown that 1,3-DOX-4 is selectively synthesized from trioxane and CO, although the CO pressure needed for the synthesis is higher than 15 MPa. Although the detailed reaction mechanism has not been clarified at the present time due to limited data, the preferential formation of 1,3-DOX-4 appears to be due to the supression of formation of polymers because the active sites (Brønsted acid sites) are in zeolitic pores.

## Footnote and References

* E-mail: t-sano@jaist.ac.jp

1 J. Falbe, *New Synthesis with Carbon Monoxide*, Springer-Verlag, Berlin, 1980.
2 W. Keim, *Catalysis in $C_1$-Chemistry*, Reidel, Dordrecht, 1983.
3 W. Hölderich, J. Reuvers, R. Kummer and L. Hupfer, EP 249 976, 1987.
4 A. G. Stepanov, M. V. Luzgin, V. N. Romannikov and K. I. Zamaraev, *J. Am. Chem. Soc.*, 1995, **117**, 3615.
5 M. V. Luzgin, V. N. Romannikov, A. G. Stepanov and K. I. Zamaraev, *J. Am. Chem. Soc.*, 1996, **118**, 10 890.
6 T. H. Clingenpeel and A. I. Biaglow, *J. Am. Chem. Soc.*, 1997, **119**, 5077.
7 T. Sano, N. Yamashita, Y. Iwami, K. Takeda and Y. Kawakami, *Zeolites*, 1996, **16**, 258.
8 D. L. Loder, USP 2 152 852, 1939.
9 M. Ragazzini, M. Modena, E. Gallinella and G. Cevidalli, *J. Polym. Sci., A*, 1964, **2**, 5203.
10 T. Masuda, K. Kagami, K. Murata, A. Matsuda and Y. Takami, *Nippon Kagaku Kaishi*, 1982, 257.

*Received in Cambridge, UK, 11th July 1997; 7/04972B*

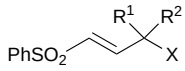
# Conjugate addition of allylic and prop-2-ynylic alcohols to 3-halogeno-1-phenylsulfonylprop-1-enes; synthesis and radical induced cyclization of 2-alkenyloxy-3-halogenopropylphenyl sulfones

**Riccardo Giovannini and Marino Petrini***

*Dipartimento di Scienze Chimiche, Università di Camerino, via S. Agostino, 1 I-62032 Camerino, Italy*

**Allylic and prop-2-ynylic alcohols add in a conjugate fashion to 3-halogeno-1-phenylsulfonylprop-1-enes in the presence of KF–basic alumina and the resulting halogenoallyl sulfones can be efficiently cyclized using tributyltin hydride under various conditions.**

The ability of vinyl sulfones to act as two carbon acceptors in Michael additions is the basis of their widespread use in synthesis.[1] In this context, 3-halogeno-1-alkenyl sulfones **1**



**1a** X = Br, $R^1$ = $R^2$ = H
**b** X = Cl, $R^1$ = $R^2$ = H
**c** X = Br, $R^1$ = H, $R^2$ = Me
**d** X = Br, $R^1$ = $R^2$ = Me

possess two electrophilic adjacent carbon atoms in their structure and therefore conjugate additions would compete with direct $S_N2$ displacements of the halogen atom. Allylic and aryl Grignard reagents are able to attack the double bond of **1a** and ultimately lead to substituted cyclopropanes *via* a subsequent nucleophilic displacement of the bromide anion.[2] On the contrary, sodium enolates afford direct substitution products when reacted with **1a**.[3]

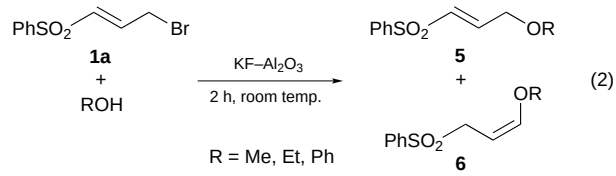
The behaviour of these systems towards different nucleophiles has been studied in great detail by Bordwell and coworkers.[4] They showed that weakly basic nucleophiles react with primary halogeno derivatives **1a**,**b** giving exclusively direct substitution products arising from an $S_N2$ process. Michael adducts are obtained only when tertiary halogeno derivative **1d**, which is almost unreactive towards $S_N2$ substitutions, reacts with sodium methoxide in MeOH.[4b]

We report here that allylic, prop-2-ynylic and benzylic alcohols efficiently add to the double bond of vinyl sulfones **1a**,**b** in the presence of KF–basic alumina [eqn. (1)].[5] The

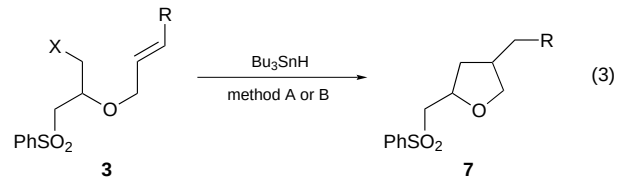



reaction is carried out under heterogeneous conditions by simply mixing the vinyl sulfone **1** with the appropriate alcohol and adding the solid base at room temperature.† The corresponding adducts are usually obtained in satisfactory yields upon extraction with $CH_2Cl_2$ and purification by column chromatography (Table 1).‡ The yields of these adducts obtained starting from bromide **1a** are generally comparable with those attained using chloride **1b**, especially when simple allylic and prop-2-ynylic alcohols are used (Table 1, entries 1–4). Chloride **1b** displays enhanced reactivity towards substituted allylic alcohols (Table 1, entries 8–11) which react poorly with the bromide derivative **1a**. No solvent is required for this procedure, and the presence of solvents as THF, $CH_2Cl_2$ and $Et_2O$ gives rise to complex product mixtures and prolonged reaction times. Steric crowding around the reaction centre also has a deleterious effect on reactivity. Every attempt to obtain addition products from vinyl sulfone **1c** results in a fast, base-assisted dehydrobromination that produces (*E*)-1-phenylsulfonylbuta-1,3-diene **4** in 40% yield.

A completely different result is observed when short chain alcohol such as methanol, ethanol or phenol are used. In this instance an ordinary direct nucleophilic displacement of the halogen atom occurs, followed by a partial regioisomerisation of the double bond with consequent formation of products **5** and **6** [eqn. (2)].[6]




The allylic ethers **3** prepared by this procedure were recognized immediately as ideal candidates for the synthesis of a tetrahydrofuran moiety *via* a radical cyclization route [eqn. (3)].[7] Ring closure of compound **3** under standard conditions

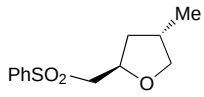
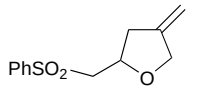
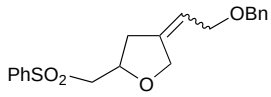
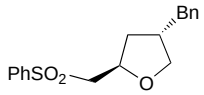
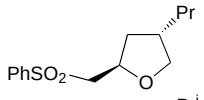
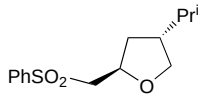



($Bu_3SnH$, AIBN catalytic, benzene at reflux)§ gives the corresponding 2,4-disubstituted tetrahydrofuran derivatives **7**

**Table 1** Products and yields of the reaction between vinyl sulfones **1** and alcohols **2** in the presence of KF–basic alumina without solvent at room temperature

| Entry | Vinyl sulfone | Alcohol **2** | Product | Yield (%) |
|---|---|---|---|---|
| 1 | **1a** | $CH_2$=$CHCH_2OH$ | **3a** | 80 |
| 2 | **1b** | $CH_2$=$CHCH_2OH$ | **3b** | 75 |
| 3 | **1a** | CH≡$CCH_2OH$ | **3c** | 78 |
| 4 | **1b** | CH≡$CCH_2OH$ | **3d** | 73 |
| 5 | **1a** | $BnOCH_2C$≡$CCH_2OH$ | **3e** | 55 |
| 6 | **1b** | $BnOCH_2C$≡$CCH_2OH$ | **3f** | 71 |
| 7 | **1a** | BnOH | **3g** | 77 |
| 8 | **1b** | PhCH=$CHCH_2OH$ | **3h** | 70 |
| 9 | **1b** | EtCH=$CHCH_2OH$ | **3i** | 80 |
| 10 | **1b** | 2-(furyl)$CH_2OH$ | **3j** | 83 |
| 11 | **1b** | $Me_2C$=$CHCH_2OH$ | **3k** | 65 |

**Table 2** Products and yields of the radical cyclization of unsaturated sulfones **3** in the presence of $Bu_3SnH$

| Entry | Sulfone | Tetrahydrofuran **7** | *trans*:*cis* ratio (method)[a] | Yield (%) |
|---|---|---|---|---|
| 1 | **3a** |  | 68:32 (A)<br>86:14 (B)[b] | 92<br>88 |
| 2 | **3c** |  | (A) | 88 |
| 3 | **3e** |  | 55:45 (A)[c]<br>60:40 (B)[b,c] | 50<br>83 |
| 4 | **3h** |  | 85:15 (A)<br>90:10 (B)[b,d] | 75<br>78 |
| 5 | **3i** |  | 73:27 (A)<br>80:20 (B)[b] | 83<br>90 |
| 6 | **3k** |  | 66:34 (A)<br>77:23 (B)[b] | 85<br>88 |

[a] Method A: $Bu_3SnH$, AIBN, benzene at reflux. Method B: $Bu_3SnH$, $Et_3B$, $O_2$, −78 °C. [b] Cyclization is conducted on the iodide obtained by refluxing the corresponding halide with sodium iodide in acetone. [c] This ratio refers to the *E*/*Z* stereoisomers. [d] Reaction conducted at room temperature.

as a diastereoisomeric mixture, usually in good yields (Table 2, method A).‡ These diastereoisomers are inseparable by standard chromatographic techniques, but a survey of available literature data on similar compounds allowed us to assign the *trans* configuration to the major component of the mixture.[8] It is known that radical cyclizations of monohalogeno derivatives of type **7** proceed following a chair-like transition state in which the phenylsulfonylmethyl group and the alkene prefer an equatorial orientation **8** (Scheme 1) that produces the *trans* isomer.[9] The diastereoselectivity obtainable in refluxing benzene is, however, rather poor as witnessed for the cyclization of compound **3a** (Table 2, entry 1, method A, *trans*:*cis* 68:32). Better results are achieved using $BEt_3$ initiator ($Bu_3SnH$, $BEt_3$, $O_2$, $CH_2Cl_2$, method B),§ which permits rapid cyclization even at very low temperatures (−78 °C).[10] In this way the diastereoisomeric ratio can be substantially improved for ring closure of **3a** (Table 2, entry 1, method B, *trans*:*cis* 86:14), although in other entries (Table 2, entries 4–6) this gain in diastereoselectivity is rather small, as the isomeric ratio is already quite satisfactory even with method A. The cyclization of alkyne derivative **3e** proceeds with a low degree of stereoselectivity (Table 2, entry 3). This is not surprising since the stereochemistry of compound **7e** is governed by the topicity of the hydrogen abstraction, in which the intermediate alkenyl radical is involved.[11]

In conclusion, a chemoselective conjugate addition of unsaturated alcohols to 3-halogenovinyl sulfones has been accomplished using KF–basic alumina as the basic medium. The resulting adducts can be stereoselectively cyclized by a radical process, affording functionalized 2,4-disubstituted tetrahydrofurans that are suitable for further transformations.



**8** **8a**

**Scheme 1**

The authors thank the University of Camerino for financial assistance.

## Footnotes and References

* E-mail: petrini@camserv.unicam.it

† *Typical experimental procedure for Michael addition*: Vinyl sulfone **1** (5 mmol) was mixed with the appropriate alcohol **2** (15 mmol) and cooled to 0 °C. KF–basic alumina (1 g) was added, the mixture was shaken vigorously for 5 min and then left to stand for 2 h at room temperature. After this time, the mixture was washed with $CH_2Cl_2$ (5 × 10 ml) and, after evaporation of the solvent at reduced pressure, the crude product was purified by column chromatography.

‡ *Selected data* for **3b**: oil, $\nu_{max}$/cm$^{-1}$ 3060, 1600, 1290, 1130; $\delta_H$ (300 MHz, $CDCl_3$) 3.47 (2 H, dd, *J* 1.5, 6.3), 3.66 (2 H, dd, *J* 1.4, 4.5), 3.94–4.05 (2 H, m), 4.12–4.20 (1 H, m), 5.11–5.20 (2 H, m), 5.62–5.78 (1 H, m), 7.52–7.67 (3 H, m), 7.91–7.95 (2 H, m); *m*/*z* 181, 141, 77, 75. For **3c**: oil, $\nu_{max}$/cm$^{-1}$ 3260, 2100, 1290, 1140; $\delta_H$ 2.46 (1 H, t, *J* 2.4), 3.49 (2 H, d, *J* 5.1), 3.60 (2 H, d, *J* 4.8), 4.17 (2 H, d, *J* 2.4), 4.32–4.37 (1 H, m), 7.53–7.68 (3 H, m), 7.91–7.96 (2 H, m); *m*/*z* 317 ($M^+$), 223, 141, 125, 77, 51, 39. For **7a**: mp 39 °C; $\nu_{max}$/cm$^{-1}$ 3050, 1580, 1290, 1130; $\delta_H$ 1.00 (3 H, d, *J* 6.8), 1.73–1.90 (2 H, m), 2.28–2.31 (1 H, m), 3.21–3.45 (3 H, m), 3.94–3.92 (1 H, m), 4.35–4.41 (1 H, m), 7.51–7.65 (3 H, m), 7.89–7.92 (m, 2 H); $\delta_C$ 17.75, 18.04, 33.38, 33.64, 40.07, 41.38, 61.88, 62.17, 72.98, 73.93. 75.14, 75.48, 128.55, 129.66, 134.17, 140.41; *m*/*z* 240 ($M^+$), 98, 85, 77.

§ *Typical experimental procedure for ring closure of compounds* **3**: Method A: $Bu_3SnH$ (1.5 mmol) and AIBN (0.15 mmol) were added to a benzene solution (0.06 M) of compound **3** (1 mmol). The mixture was refluxed for 1 h and then the solvent was evaporated at reduced pressure. The oily residue was taken up in $Et_2O$ (40 ml) and washed with aqueous 10% KF. Usual work up gave the crude product, which is purified by column chromatography.

Method B: $Bu_3SnH$ (1.5 mmol) and $BEt_3$ (0.3 mmol) were added to a $CH_2Cl_2$ solution (0.05 M) of compound **3**. The mixture was cooled to −78 °C and then $O_2$ (8 ml) was slowly (45 min) bubbled through the mixture *via* a syringe. After 1 h the mixture was warmed, the solvent was evaporated and the residue was worked up as described in method A.


1 N. S. Simpkins, *Sulphones in Organic Synthesis*, Pergamon, Oxford, 1993; N. S. Simpkins, *Tetrahedron*, 1990, **46**, 6951; P. L. Fuchs and T. F. Braish, *Chem. Rev.*, 1986, **86**, 903.

2 J. J. Eisch and J. E. Galle, *J. Org. Chem.*, 1979, **44**, 3277.

3 Y. Masuyama, K. Yamada, H. Tanaka and Y. Kusuru, *Synth. Commun.*, 1987, **17**, 1525.

4 (*a*) F. G. Bordwell and T. G. Mecca, *J. Am. Chem. Soc.*, 1972, **94**, 5829; (*b*) F. G. Bordwell and G. A. Pagani, *J. Am. Chem. Soc.*, 1975, **97**, 118.

5 KF–basic alumina was prepared according to: D. E. Bergbreiter and J. J. Lalonde, *J. Org. Chem.*, 1987, **52**, 1601; Review: G. W. Kabalka and R. M. Pagni, *Tetrahedron*, 1997, **53**, 7999.

6 B. M. Trost and M. R. Ghadiri, *Bull. Soc. Chim. Fr.*, 1993, **130**, 433.

7 D. P. Curran, N. A. Porter and B. Giese, *Stereochemistry of Radical Reactions: Concepts, Guidelines and Synthetic Applications*, VCH, Weinheim, 1996; D. P. Curran, in *Comprehensive Organic Synthesis*, ed. B. M. Trost, I. Fleming and M. F. Semmelhack, Pergamon, Oxford, 1991, p. 799; B. Giese, *Radicals in Organic Synthesis: Formation of Carbon–Carbon Bonds*, Pergamon, Oxford, 1986.

8 E. Montaudon, X. Lubeight and B. Maillard, *J. Chem. Soc., Perkin Trans 1*, 1991, 1531.

9 A. L. J. Beckwith, C. J. Easton, T. Lawrence and A. K. Serelis, *Aust. J. Chem.*, 1983, **36**, 545; D. C. Spellmeyer and K. N. Houk, *J. Org. Chem.*, 1987, **52**, 959; Y. Watanabe and T. Endo, *Tetrahedron Lett.*, 1988, **29**, 321; V. H. Rawal, S. P. Singh, C. Dufour and C. Michoud, *J. Org. Chem.*, 1993, **58**, 7718.

10 K. Miura, Y. Ichinose, K. Nozaki, K. Fugami, K. Oshima and K. Utimoto, *Bull. Chem. Soc. Jpn.*, 1989, **42**, 143.

11 T. Ooi, Y. Hokke and K. Maruoka, *Angew. Chem., Int. Ed. Engl.*, 1997, **36**, 1181; B. Giese, J. A. Gonzalez-Gomez, S. Lachhein and J. O. Metzger, *Angew. Chem., Int. Ed. Engl.*, 1987, **26**, 479.


*Received in Cambridge, UK, 21st July 1997; 7/05180H*

# Studies towards a new one-pot heterocyclization: Bu$^t$OK-promoted oxa- and aza-Michael addition–intramolecular carbocyclization of prop-2-ynyl alcohols and amines with α,β-disubstituted nitroalkenes

**Estelle Dumez, Jean Rodriguez and Jean-Pierre Dulcère**

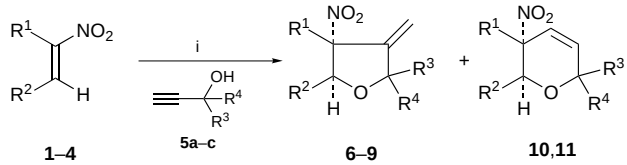
*RéSo, Réactivité en Synthèse organique, Faculté des Sciences et Techniques Centre de St Jérôme, UMR 6516, av. Esc. Normandie-Niemen, Boîte D 12, F-13397 Marseille Cedex 20, France*

**Bu$^t$OK-promoted reaction of prop-2-ynyl alcohols 5 or *N*-methylprop-2-ynylamine 12 with nitroalkenes 1–4 affords 3-methylenetetrahydrofurans 6–9 and 3,4-dihydropyrans 10 and 11 or 3-methylenepyrrolidines 13–16, respectively, in moderate to good yields, with total allylic 1,3-strain-controlled diastereoselectivity.**

Five-membered heterocycles are among the most common structures in bioactive compounds.[1] Moreover, the presence of an unsaturated bond available for further elaboration, particularly in α-methylene γ-butyrolactones,[2] has for many years stimulated interest in synthetic routes to 3-methylenetetrahydrofurans.[2,3] Finally, the pyrrolidine ring is an extensively studied heterocyclic system,[4] as a consequence of the interesting biological activity exhibited by several polysubstituted pyrrolidines.[5] This paper describes a new one-pot access to these heterocyclic compounds from readily available α,β-disubstituted nitroalkenes **1**–**4**.

While the oxa-Michael addition of prop-2-ynyl alcohols to β-monosubstituted α-nitroalkenes in the presence of sodium or potassium hydride led to β-nitroprop-2-ynyl ethers,[6] to the best of our knowledge, only few recent preparation of five- or six-membered heterocycles involve intramolecular addition of carbon nucleophiles to alkynes;[7]† among them, Bu$^t$OK-promoted double Michael addition of 4-hydroxybut-2-ynoates[8] and tandem oxa-Michael $S_N2'$ substitution of 4-chlorobut-2-yn-1-ol[9] with α,β-disubstituted nitroalkenes generate a nitro-stabilized carbon nucleophile, which adds to the activated alkyne moiety to provide unsaturated tetrahydrofurans or pyrans.‡ Also of interest is the two-step synthesis of α-methylene γ-lactams from 1-nitrocyclohexene, involving the formation of β-nitroamides, which then undergo a Triton B-promoted carbanion addition to an unactivated terminal alkyne.[10] These results enhance the crucial effect of both the nitroalkene substitution pattern and the nature of the base on the reaction process.

Therefore, we investigated the base-promoted Michael addition of prop-2-ynyl alcohols **5a**–**c** to α,β-disubstituted




**1**,**6**,**10** $R^1$–$R^2$ = –$(CH_2)_4$–
**2**,**7** $R^1$–$R^2$ = –$(CH_2)_3$–
**3**,**8**,**11** $R^1$ = Me, $R^2$ = $C_5H_{11}$
**4**,**9** $R^1$ = Me, $R^2$ = Ph

**a** $R^3$ = $R^4$ = H
**b** $R^3$ = H, $R^4$ = Me
**c** $R^3$ = $R^4$ = Me

**Scheme 1**

**Table 1** Heterocyclization of nitroalkenes **1**–**4**

| Nitroalkene | Prop-2-ynyl alcohol **5** | Yield (%)[a] | Products | Ratio 5-*exo*/6-*endo* |
|---|---|---|---|---|
| **1** | **a** | 78 | **6a** + **10a** | 1.7 : 1 |
| **1** | **b** | 47 | **6b** + **10b** | 3 : 1 |
| **1** | **c** | 31 | **6c** + **10c** | 8 : 1 |
| **2** | **a** | 84 | **7a**[b] | |
| **2** | **b** | 80 | **7b**[b] | |
| **2** | **c** | 78 | **7c**[b] | |
| **3** | **a** | 57 | **8a** + **11a** | 20 : 1 |
| **3** | **b** | 20 | **8b** + **11b** | 10 : 1 |
| **3** | **c** | 25 | **8c** + **11c** | 16 : 1 |
| **4** | **a** | 73 | **9a**[b] | |
| **4** | **b** | 31 | **9b**[b] | |
| **4** | **c** | 58 | **9c**[b] | |

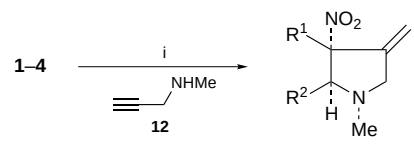
[a] Isolated total yields of chromatographically homogeneous, spectroscopically pure products are reported. [b] 6-*endo* adducts were not detected by $^1$H NMR in the crude reaction mixture.

α-nitroalkenes **1**–**4**, since this route should afford 3-methylenetetrahydrofurans, provided a nucleophilic addition of the resulting nitronate on the triple bond occurs.

Best results were obtained when nitroalkenes **1**–**4** were added slowly to a solution of prop-2-ynyl alcohols **5** in THF containing Bu$^t$OK (Scheme 1). Other bases such as BuLi, KH, or $K_2CO_3$ were ineffective; for instance, the reaction of **1** with **5a** in the presence of BuLi produced a complex reaction mixture,§ while changing the base for KH delivered β-nitroprop-2-ynyl ethers.[6]

Although the reaction proceeded with total diastereoselectivity due to allylic 1,3-strain,[9,11] unexpected regioselectivity was observed (Table 1). Indeed, 5-*exo* adducts **6**–**9** were isolated, along with **10** and **11**¶‖ resulting from 6-*endo* cyclization mode when the reaction was performed on nitroalkenes **1** and **3** (ratio 5-*exo*/6-*endo* 1.7–20 : 1). Heterocycles **6b**–**9b** and **10b** and **11b** provided by reaction with secondary alcohol **5b** were obtained as a 0.7–0.9/1 mixture of diastereomers.

Interestingly, aza-Michael addition of *N*-methylprop-2-ynylamine **12** on nitroalkenes **1**–**4** also proceeded with intramolecular nucleophilic addition to provide, regio- and diastereo-selectively, 3-methylenepyrrolidines **13**–**16**¶‖ (Scheme 2).




**Scheme 2**

Factors that govern the regioselectivity of this new one-pot heterocyclisation are currently under investigation.

## Footnotes and References

* E-mail: jean-pierre.dulcere@reso.u-3mrs.fr

† To the best of our knowledge, the construction of carbocycles by either intramolecular addition of alkyllithiums to non-terminal alkynes (ref. 12) or Pd-mediated cyclization of acetylenic compounds bearing a nucleophilic functionality (ref. 13) have never been extended to heterocycles.

‡ For other related intramolecular additions of stabilized carbon nucleophiles to activated alkynes, see ref. 14.

§ Prop-2-ynyloxycyclohexanone, resulting from Nef reaction of the β-nitroprop-2-ynyl ether intermediate, could be isolated from the reaction mixture (20% yield).

¶ Bicyclic adducts are *cis* ring fused.

‖ Satisfactory analytical and spectral data were obtained for all compounds. *Selected data* for **6a**: $\delta_H$ (400 MHz, $CDCl_3$) 1.45 (m, 3 H), 1.6 (m 2 H), 1.85 (m, 1 H), 2.15 (m, 1 H), 2.4 (m, 1 H), 4.45 (dt, *J* 13.6, 2.1, 1 H), 4.52 (dt, *J* 13.6, 2.6, 1 H), 4.54 (t, *J* 5.8, 1 H), 5.25 (td, *J* 2.1, 1.1, 1 H), 5.35 (td, *J* 2.6, 1.1, 1 H); $\delta_C$ (100.61 MHz, $CDCl_3$) 145.2, 109.5, 94.5, 80.0, 69.1, 31.2, 26.8, 21.8, 20.8. For **10a**: $\delta_H$ (400 MHz, $CDCl_3$) 1.45 (m, 3 H), 1.6 (m, 2 H), 1.85 (m, 1 H), 2.0 (m, 1 H), 2.3 (m, 1 H), 4.17 (dt, *J* 18.4, 2.6, 1 H), 4.22 (dt, *J* 18.4, 2.4, 1 H), 4.41 (dd, *J* 6.5, 4.7, 1 H), 5.84 (dt, *J* 10.2, 2.3, 1 H), 6.00 (dt, *J* 10.2, 2.5, 1 H); $\delta_C$ (100.61 MHz, $CDCl_3$) 131.0, 125.3, 88.2, 72.6, 63.3, 34.6, 26.9, 21.5, 21.2. For **13**: $\delta_H$ (400 MHz, $CDCl_3$) 1.75–1.27 (m, 6 H), 2.04–1.89 (m, 1 H), 2.28 (s, 3 H), 2.51–2.40 (m, 1 H), 3.17 (dt, *J* 13.9, 2.8, 1 H), 3.29 (m, 1 H), 3.59 (d, *J* 13.9, 1 H), 5.06 (ddd, *J* 2.3, 1.8, 0.5, 1 H), 5.19 (ddd, *J* 2.8, 2.1, 0.5, 1 H); $\delta_C$ (100.61 MHz, $CDCl_3$) 146.4, 107.9, 94.4, 66.8, 59.2, 39.1, 33.1, 22.3 (2C), 19.7; $\nu_{max}/cm^{-1}$ 2958, 1669, 1536, 1090, 1019, 798; *m*/*z* 196 ($M^+$, 12%), 163 (58), 150 (63), 149 (100), 148 (35).


1 M. H. D. Postema, *Tetrahedron*, 1992, **48**, 8545; W. Westle, *Polyether Antibiotics: Naturally Occuring Acid Ionophores*, Marcel Dekker, New York, 1982, vols. 1 and 2; T. L. B. Boivin, *Tetrahedron*, 1987, **43**, 3309; A. Padwa, H. Nimmesgern and G. S. K. Wong, *J. Org. Chem.*, 1985, **50**, 5620.

2 M. Okabe, M. Abe and M. Tada, *J. Org. Chem.*, 1982, **47**, 1775; J.-P. Dulcère, M. N. Mihoubi and J. Rodriguez, *J. Org. Chem.*, 1993, **58**, 5709.

3 B. M. Trost and P. J. Bonk, *J. Am. Chem. Soc.*, 1985, **107**, 1778; J. Van der Louw, J. L. Van der Baan, H. Stichter, G. J. J. Out, F. J. J. de Kanter, F. Bickelhaupt and G. W. Klumpp, *Tetrahedron*, 1992, **48**, 9877; G. Pandey, K. S. S. Poleswara Rao and K. V. Nageshwar Rao, *J. Org. Chem.*, 1996, **61**, 6799; L. Engman and V. Gupta, *J. Org. Chem.*, 1997, **62**, 157; A. Krief and W. Dumont, *Tetrahedron Lett.*, 1997, **38**, 657.

4 J. Steele, *Contemp. Org. Synth.*, 1994, **1**, 95; M. Mori, N. Uesaka, F. Saitoh and M. Shibasaki, *J. Org. Chem.*, 1994, **59**, 5643.

5 A. R. Pinder, in *The Alkaloids*, ed. M. F. Grundon, Chemical Society, London, 1982, vol. 12.

6 J. L. Duffy, J. A. Kurth and M. J. Kurth, *Tetrahedron Lett.*, 1993, **34**, 1259.

7 M. Yoshimatsu, K. Machida, T. Fuseya, H. Shimizu and T. Kataoka, *J. Chem. Soc., Perkin Trans. 1*, 1996, 1839.

8 T. Yakura, T. Tsuda, Y. Matsumura, S. Yamada and M. Ikeda, *Synlett*, 1996, 985.

9 J.-P. Dulcère and E. Dumez, *Chem. Commun.*, 1997, 971.

10 R. Patra, S. B. Maiti and A. Chatterjee, *Tetrahedron Lett.*, 1991, **32**, 1363.

11 R. W. Hoffmann, *Chem. Rev.*, 1989, **89**, 1841.

12 W. F. Bailey, T. V. Ovaska and T. K. Leipert, *Tetrahedron Lett.*, 1989, **30**, 3901; W. F. Bailey and T. V. Ovaska, *Tetrahedron Lett.*, 1990, **31**, 627; G. Wu, F. E. Cederbaum and E. Negishi, *Tetrahedron Lett.*, 1990, **31**, 493; W. F. Bailey and T. V. Ovaska, *J. Am. Chem. Soc.*, 1993, **115**, 3080; W. F. Bailey and P. H. Aspris, *J. Org. Chem.*, 1995, **60**, 754; T. V. Ovaska, R. R. Warren, C. E. Lewis, N. Wachter-Jurcsak and W. F. Bailey, *J. Org. Chem.*, 1994, **59**, 5868.

13 G. Fournet, G. Balme and J. Goré, *Tetrahedron*, 1991, **47**, 6293.

14 S. H. Rosenberg and H. Rapoport, *J. Org. Chem.*, 1985, **50**, 3979; J. F. Lavallée, G. Berthiaume and P. Deslongchamps, *Tetrahedron Lett.*, 1986, **27**, 5455; E. J. Corey and W. Su, *Tetrahedron Lett.*, 1988, **29**, 3423; W. D. Rudorf and R. Schwartz, *Z. Chem.*, 1988, **28**, 101.


*Received in Cambridge, UK, 14th July 1997; 7/05016J*

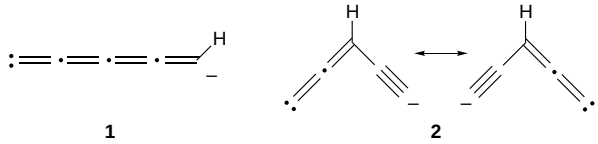
# The synthesis and structure of the symmetrical isomer of $C_5H^-$

**Stephen J. Blanksby, Suresh Dua, John H. Bowie* and John C. Sheldon**

*Department of Chemistry, The University of Adelaide, Adelaide, South Australia 5005, Australia*

**The ion $(C_2CHC_2)^-$ is formed in the gas phase by the process $^-C{\equiv}C–CH(OCOR)–C{\equiv}CD \rightarrow (C_2CHC_2)^- + (\text{'}RDCO_2\text{'})$ [R = H, Me or Et]; the ground state structure is a singlet, with $C_{2v}$ symmetry.**

Unusual organic molecules have been detected in circumstellar gas and dust envelopes which surround red giant stars.[1] These include $C_3$, $C_5$ and the hydrocarbons $C_nH$ ($n$ = 2–6), which have been identified around the bright carbon-rich star IRC + 10216.[1–3] The high electron affinities of these neutrals suggest the possibility that the corresponding anions may co-occur with the neutrals in circumstellar envelopes,[4,5] and it is of interest in this context that negative ions are present in the coma of comet Halley.[6] We have reported the syntheses of $C_3H^-$,[7] $C_5^{-\cdot}$,[8] and linear $C_5H^{-\cdot}$[8] (and their conversion through the appropriate neutral to decomposing positive ions) in the ion source of a VG ZAB 2HF mass spectrometer. *Ab initio* calculations [at CISD/6-311G (d,p) level] indicate that linear $C_5H^-$ has both singlet and triplet states, with triplet **1** being the ground state, and that the corresponding neutral has an electron affinity of 2.4 eV.[8]



**1** **2**

*Ab initio* calculations [GAUSSIAN 94[9] at CISD/6-311G (d,p) level] indicate further that (i) there is a stable symmetrical isomer $C_2CHC_2^-$, and that this isomer (like linear $C_5H^-$) also has stable singlet and triplet forms, and (ii) there is no energy and stable species $C_3CHC^-$. *Ab initio* data for $C_2CHC_2^-$ are summarised in Tables 1 and 2. In this case the singlet is significantly more stable than the triplet. The geometry of the central carbon of the ground-state singlet approximates to trigonal planar (the $C_2$–$C_3$–$C_4$ angle is close to 130°), and the $C_1$–$C_2$ and $C_2$–$C_3$ bonds have significant triple and double bond character respectively (see Table 2). The structure is depicted (in valence bond form) as **2**. Isomer **2** is less stable than isomer **1** by 170 kJ mol$^{-1}$ at the level of theory indicated. The electron affinity of the neutral corresponding to **2** is calculated to be 4.2 eV.

**Table 1** *Ab initio* calculations for $C_2CHC_2^-$ [a]

| State | Singlet | Triplet |
|---|---|---|
| Symmetry | $C_{2v}$ | $C_{2v}$ |
| HF/6-311G (d,p) | −189.74150 | −189.67132 |
| Zero point vibrational energy | 0.03188 | 0.02767 |
| Total thermal energy | 0.03685 | 0.03282 |
| CISD/6-311G (d,p) | −190.286804 | −190.20186 |

[a] *Ab initio* optimization used the Berny procedure (ref. 12) at HF/6-311G (d,p), GAUSSIAN 94 (ref. 9). The correctness of the geometries was confirmed by the lack of negative analytical computed harmonic vibration frequencies. The post Hartree–Fock energies (CISD) were calculated at the Hartree–Fock geometries. All energies are recorded in hartrees.

We initially attempted to form the elusive **2** in the ion source of the VG 2HF mass spectrometer by a number of methods related to that shown in eqn. (1):

$$^-(C{\equiv}C)–CH(OMe)–C{\equiv}CD \rightarrow [(:C{=}C{=}CH–C{\equiv}CD)\ ^-OMe] \rightarrow C_5D^- + MeOH \quad (1)$$

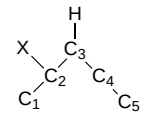
$$^-(C{\equiv}C)–CH(OCOR)–C{\equiv}CD \rightarrow (C_2CHC_2)^- + [RCDO_2] \quad (2)$$

$$^-(C{\equiv}C)–CD(OCOR)–C{\equiv}CH \rightarrow (C_2CDC_2)^- + [RCHO_2] \quad (3)$$

unfortunately, the base deprotonates exclusively at the central position to yield linear $C_5D^-$ (*cf.* **1**) rather than remove $D^+$ to form $C_2CHC_2^-$. However the energised precursor anions shown in eqns (2) and (3) (R = H, Me, Et) [formed by the reaction of $HO^-$ with DC≡C–CH(OCOR)–C≡CD and HC≡C–CD(OCOR)–C≡CH] decompose to yield $(C_2CHC_2)^-$ and $(C_2CDC_2)^-$ respectively and exclusively. We are not sure whether this process involves incipient $R^-$ deprotonating at the terminal position (to yield $CO_2$ and RH as neutral products) or whether the acetylenic H transfers to oxygen to yield $RCO_2H$ as the neutral products.

When source formed $(C_2CHC_2)^-$ ions are fired through a collision cell containing Ar (at $2 \times 10^{-7}$ Torr; 1 Torr = *ca.* 133 Pa) the resultant tandem negative ion mass spectrum exhibits only loss of H$^\cdot$ to form $C_5^{-\cdot}$ (*cf.* ref. 8). Under the same experimental conditions, charge stripping of $(C_2CHC_2)^-$ ions yields energised parent cations $C_5H^+$, whose resultant spectrum [the charge reversal spectrum[10,11] of $(C_2CHC_2)^-$] is *m/z* (composition relative abundance) 61 ($C_5H^+$, 35), 60 ($C_5^{+\cdot}$, 100), 49 ($C_4H^+$, 77), 48 ($C_4^{+\cdot}$, 62), 37 ($C_3H^+$, 81), 36 ($C_3^{+\cdot}$, 69), 25 ($C_2H^+$, 4), 24 ($C_2^{+\cdot}$, 21), 12 ($C^{+\cdot}$, 0.2). Although this spectrum shows the same peaks as those observed in the corresponding spectrum of isomer **1** (*cf.* ref. 8), the peak abundances in the two spectra are significantly and reproducibly different. In particular, the abundances of *m/z* 61 ($C_5H^+$) and 60 ($C_5^{+\cdot}$) are 35 and 100 for **2**, and 100 and 76 for **1**. Since the two charge reversal spectra are different, we conclude that isomers **1** and **2** are stable. However, the data cannot exclude the possibility of

**Table 2** Bond lengths and angles for $C_2CHC_2^-$ taken from *ab initio* calculations



| | Singlet | Triplet |
|---|---|---|
| *Bond length*/Å | | |
| $C_1$–$C_2$ | 1.2425 | 1.2746 |
| $C_2$–$C_3$ | 1.3679 | 1.3636 |
| $C_3$–H | 1.0843 | 1.1048 |
| *Bond angle* (°) | | |
| $C_1$–$C_2$–X | 85.3 | 80.0 |
| X–$C_2$–$C_3$ | 90.0 | 90.0 |
| $C_2$–$C_3$–H | 115.3 | 107.2 |

minor interconversion of **2** to **1** under the experimental conditions.

The neutral analogue of **1** has already been detected in the interstellar environment:[1–3] it would be of interest to search for anions **1**, **2** and the neutral corresponding to **2**.

We thank the Australian Research Council for the financial support of this project.

## Footnote and References

* E-mail: jbowie@chemistry.adelaide.edu.au

1 H. Olofsson, *Molecular Abundances in the Envelopes around Evolved Stars*, in *Molecules in the Stellar Environment, Lecture Notes in Physics*, ed. O. G. Jorgenson, Springer, Heidelberg, 1994, pp. 114–133 and references cited therein.
2 P. F. Bernath, K. H. Hinkle and J. J. Keady, *Science*, 1989, **244**, 562; K. H. Hinkle, *Infrared Spectroscopy of Molecules in Circumstellar Envelopes*, in *Molecules in the Stellar Environment, Lecture Notes in Physics*, ed. O. G. Jorgensen, Springer, Heidelberg, 1994, pp. 99–114 and references cited therein.
3 A. Omont, *Polyyenes and Polycyclic Aromatic Molecules in C-rich Circumstellar Envelopes*, in *Molecules in the Stellar Environment, Lecture Notes in Physics*. ed. O. G. Jorgenson, Springer, Heidelberg, 1994, pp. 135–148 and references cited therein.
4 J. Natterer, W. Koch, D. Schröder, N. Goldberg and H. Schwarz, *Chem. Phys. Lett.*, 1994, **229**, 429.
5 S. Petrie, *Mon. Not. R. Astron. Soc.*, 1996, **281**, 137.
6 P. Chaizy, H. Rème, J. A. Sauvaud, C. d'Uston, R. P. Lin, D. E. Larson, D. L. Mitchell, K. A. Anderson, C. W. Carlson, A. Korth and D. A. Mendis, *Nature*, 1991, **349**, 393.
7 S. Dua, J. H. Bowie and J. C. Sheldon, *J. Chem. Soc., Perkin Trans. 2*, 1994, 543.
8 S. Dua, J. C. Sheldon and J. H. Bowie, *J. Chem. Soc., Chem. Commun.*, 1995, 1067.
9 GAUSSIAN 94, Revision C3, M. J. Frish, G. W. Trucks, H. B. Schlegel, P. M. W. Gill, B. G. Johnson, M. A. Robb, J. R. Cheeseman, T. Keith, G. A. Petersson, J. A. Montgomery, K. Raghavavhari, M. A. Al-Latham, V. G. Zakrzewski, J. V. Ortiz, J. B. Foresman, J. Cioslowski, B. B. Stefanov, A. Nanayakkara, M. Challacombe, C. Y. Peng, P. V. Ayala, W. Chen, M. W. Wong, J. L. Andres, E. S. Replogle, R. Gomperts, R. L. Martin, D. J. Fox, J. S. Binkley, D. J. Defrees, J. Baker, J. P. Stewart, M. Head-Gordon, C. Gonzalez and J. A. Pople, Gaussian Inc., Pittsburgh, PA, 1995.
10 J. H. Bowie and T. Blumenthal, *J. Am. Chem. Soc.*, 1975, **97**, 2959; J. E. Szulejko, J. H. Bowie, I. Howe and J. H. Beynon, *Int. J. Mass Spectrom. Ion Phys.*, 1980, **13**, 76.
11 R. Clair, J. L. Holmes, A. A. Mommers and P. C. Burgers, *Org. Mass Spectrom.*, 1985, **20**, 207; W. DeLange and N. M. M. Nibbering, *Int. J. Mass Spectrom Ion Processes*, 1986, **68**, 111.
12 C. Peng, P. Y. Ayala, H. B. Schlegel and M. J. Frisch, *J. Comput. Chem.*, 1996, **17**, 49.

*Received in Cambridge, UK, 20th May 1997; 7/03475J*

# A highly efficient catalyst precursor for ethanoic acid production: $[RhCl(CO)(PEt_3)_2]$; X-ray crystal and molecular structure of carbonyldiiodo(methyl)bis(triethylphosphine)rhodium(III)

**Joanne Rankin,[a] Andrew D. Poole,[b] Attila C. Benyei[a]† and David J. Cole-Hamilton*[a]**

[a] *School of Chemistry, University of St Andrews, Fife, Scotland, UK KY16 9ST*
[b] *B.P. Chemicals Ltd, Hull Research and Technology Centre, Saltend, Hull, UK HU12 8DS*

**Under mild conditions, $[RhI(CO)(PEt_3)_2]$, is more active for the carbonylation of methanol to ethanoic acid than $[Rh(CO)_2I_2]^-$, which is widely used industrially; intermediates in the catalytic cycle have been identified and characterised.**

The $[Rh(CO)_2I_2]^-$ catalysed carbonylation of methanol is the most widely used commercial route to ethanoic acid.[1] The rate determining step for the catalytic cycle[2] is oxidative addition of iodomethane to $[Rh(CO)_2I_2]^-$, so that increasing the electron density on the metal centre should increase the rate of oxidative addition and hence the overall rate of production of ethanoic acid. There have been attempts to modify $[Rh(CO)_2I_2]^-$ by using electron donating ligands.[3–6] For instance, Baker *et al.*[3] used $[RhI(CO)(Ph_2PCH_2P(S)Ph_2)]$ to enhance the rate of carbonylation at 185 °C. Cavell and coworkers[4] prepared complexes of the form, $[RhCl(CO)(PPh_2CH_2PPh_2NR)]$, where R is a substituted phenyl group. Wegman *et al.*[5] compared the methanol carbonylation rate at 80 °C using $[Rh(CO)_2I_2]^-$ and $[RhCl(CO)_2(Ph_2P(CH_2)_2P(O)Ph_2)]$ and noted an 80-fold increase with the latter. Dilworth *et al.*[6] used rhodium(I) carbonyl complexes containing phosphinothiolate and thioether ligands to promote the rate of carbonylation of methanol under the relatively forcing conditions of 70 bar and 185 °C. To our knowledge, the use of trialkylphosphines as promoters for rhodium based carbonylation catalysts has not been investigated, despite the fact that they are strongly electron donating. We now report the results of such a study.

Complexes of the form $[RhX(CO)(PEt_3)_2]$ (X = Cl, Br or I) have $\nu_{CO}$ at *ca.* 1960 $cm^{-1}$ compared with 1988 and 2059 $cm^{-1}$ for $[Rh(CO)_2I_2]^-$, suggesting that the rhodium centre is more electron rich in the triethylphosphine complexes. We have shown that these complexes are active for the double carbonylation of $CH_2I_2$[7] and of allylic halides[8] and so have attempted to increase the rate of carbonylation of methanol by using these complexes and have found that $[RhCl(CO)(PEt_3)_2]$ is an extremely active catalyst precursor for ethanoic acid production. We report the first direct comparison of $[Rh(CO)_2I_2]^-$ with a rhodium phosphine complex under the conditions of 120–150 °C and 27 bar carbon monoxide pressure. The initial carbonylation rates using $[RhCl(CO)(PEt_3)_2]$ and $[Rh(CO)_2Cl]_2$ as sources of rhodium at 120 and 150 °C in the presence of differing water concentrations are shown in Table 1.

The results of Table 1 show that, in the presence of 17.1% m/m $H_2O$ under the mild conditions of 120 or 150 °C and 27 bar pressure (runs 1–4), $[RhI(CO)(PEt_3)_2]$ catalyses the carbonylation of methanol at a rate nearly double that of $[Rh(CO)_2I_2]^-$. Water acts to maintain the catalyst in its active form[9] *i.e.* as a rhodium(I) complex and decreases the formation of inactive rhodium(III) complexes such as $[Rh(CO)_2I_4]^-$ or $[RhI_3(CO)(PEt_3)_2]$. Thus, as shown in Table 1, the rate of carbonylation is dramatically enhanced in the presence of a significant concentration of water. Under lower water conditions (runs 5 and 6), no appreciable benefit is obtained by using $[RhCl(CO)(PEt_3)_2]$ over $[Rh(CO)_2Cl]_2$ as catalyst precursors.

The mechanistic cycle has been studied using high pressure and variable temperature NMR and high pressure IR spectroscopies[10] as well as stoichiometric reactions. Thus, addition of methyl iodide to $[RhI(CO)(PEt_3)_2]$ in $CH_2Cl_2$ leads smoothly to the formation of $[RhMeI_2(CO)(PEt_3)_2]$, which has been fully characterised spectroscopically‡ and by single crystal X-ray diffraction§ (Fig. 1). The methyl group is *cis* to the carbon monoxide, as required for migratory insertion. There have been no previously published crystallographic analyses of complexes of the type $[RhX_2Me(CO)(PR_3)_2]$. However, there are examples of crystal structures of other six-coordinate rhodium phosphine complexes where methyl iodide has been oxidatively added.[11–13] Most have iodide and methyl ligands in mutually *trans* positions.

The isolation of the methyl complex for a catalytically active system is rather unusual since, generally, the insertion of carbon monoxide into the Rh–C bond is extremely rapid. For $[Rh(CO)_2I_2]^-$, the methyl complex has a very short lifetime and has only been detected as a transient by IR spectroscopy in neat methyl iodide,[14] whilst for the related $[RhCl(CO)(PPh_3)_2]$, oxidative addition of methyl iodide gives the six-coordinate $[RhMeClI(CO)(PPh_3)_2]$, but this is in equilibrium with the five-coordinate insertion product, $[RhClI(MeCO)(PPh_3)_2]$.[15] Presumably the high electron density on the metal in $[RhMeI_2(CO)(PEt_3)_2]$ is responsible for the less facile methyl migration in this case. Despite the stability of the methylrhodium(III) complex, preliminary kinetic studies suggest that oxidative addition of MeI is still rate determining. The catalytic reaction

**Table 1** Results of carbonylation experiments[a]

| Run | *T*/°C | Rhodium source | Initial water (% m/m) | Initial rate/ mol $dm^{-3}$ $h^{-1}$ |
|---|---|---|---|---|
| 1 | 120 | $[RhCl(CO)(PEt_3)_2]$[b] | 17.1 | 1.6 |
| 2 | 120 | $[Rh(CO)_2Cl]_2$[c] | 17.1 | 0.9 |
| 3 | 150 | $[RhCl(CO)(PEt_3)_2]$[b] | 17.1 | 9.2 |
| 4 | 150 | $[Rh(CO)_2Cl]_2$[c] | 17.1 | 5.0 |
| 5 | 120 | $[RhCl(CO)(PEt_3)_2]$[b] | 3.2 | 0.6 |
| 6 | 120 | $[Rh(CO)_2Cl]_2$[c] | 3.2 | 0.6 |

[a] Experiments were carried out in a 300 $cm^3$ Hastelloy B2 autoclave equipped with a ballast vessel, Magnedrive stirrer, liquid injection facility and cooling coils. For reactions requiring 17.1% $H_2O$ m/m, a solution of MeCOOH (987 mmol), MeOAc (474 mmol), $H_2O$ (1.82 mol) and MeI (396 mmol) was charged to the vessel. Similarly for reactions requiring 3.2% $H_2O$ m/m, a solution of MeCOOH (1.75 mol), MeOAc (286 mmol), $H_2O$ (354 mmol) and MeI (396 mmol) was charged to the vessel. The reaction vessel was heated to the required temperature whilst stirring under *ca.* 5 bar CO pressure. Once the desired temperature had been reached, the rhodium source, dissolved in MeOAc (13.5 mmol) and $MeCO_2H$ (117 mmol), was injected into the autoclave to initiate the reaction. The autoclave was pressurised to 27 bar and stirred at 600 rpm. The rate of carbonylation was monitored by recording the rate of carbon monoxide uptake from a ballast vessel every 2 s. [b] Assumed to form $[RhI(CO)(PEt_3)_2]$ rapidly under the reaction conditions. [c] Forms $[Rh(CO)_2I_2]^-$ under the reaction conditions.

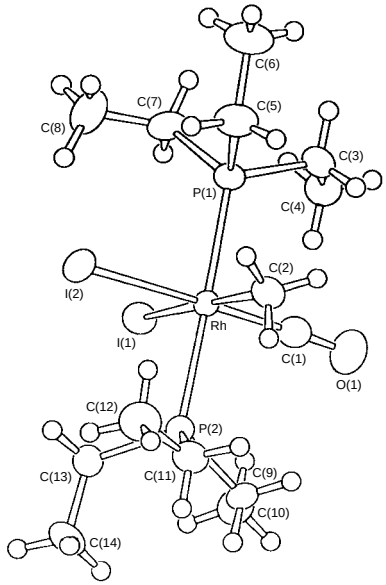



**Fig. 1** X-Ray crystal structure and numbering scheme for [$RhMeI_2$-$(CO)(PEt_3)_2$]

is zero order in $p_{CO}$ and first order in [MeI]. However, we have found that at 298 K the rate of oxidative addition of MeI for $[RhI(CO)(PEt_3)_2]$ ($1.37 \times 10^{-3}$ dm$^3$ mol$^{-1}$ s$^{-1}$) is 57 times faster than that for $[Rh(CO)_2I_2]^-$ ($2.39 \times 10^{-5}$ dm$^3$ mol$^{-1}$ s$^{-1}$); this compares with 120 times faster[16] for $[Ir(CO)_2I_2]^-$ relative to $[Rh(CO)_2I_2]^-$.

Migratory insertion of carbon monoxide occurs under CO pressure (27 bar) to form $[RhI_2(MeCO)(CO)(PEt_3)_2]$ which has been fully spectroscopically characterised.‡ The rate of the insertion reaction at room temperature and 27 bar is 38 times slower than for $[RhMe(CO)_2I_3]^-$,¶ but this slowing is not sufficient to make the migratory insertion step rate determining at 150 °C (shifts to 1740 cm$^{-1}$, MeOAc, on addition of MeOH). In contrast, for $[Ir(CO)_2I_2]^-$, the insertion reaction is slowed by $10^5$–$10^6$ times[16] compared to $[Rh(CO)_2I_2]^-$ and becomes rate determining.

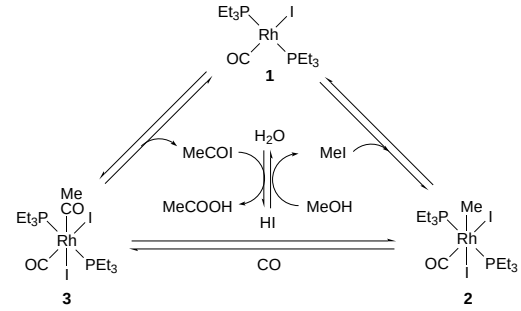
Heating a solution of $[RhI_2(MeCO)(CO)(PEt_3)_2]$ to 75 °C in the presence of excess methyl iodide and 40 bar carbon monoxide produces a product with a large absorption at 1799 cm$^{-1}$ arising from ethanoyl iodide.[17] This reductive elimination step completes the catalytic cycle. It has been shown that the usual mechanism for the formation of ethanoic acid or methyl ethanoate involves reductive elimination of ethanoyl iodide followed by reaction with water or methanol;[2,18] however, it is unusual to observe ethanoyl iodide. The high electron density on the rhodium centre caused by the electron donating system would be expected to favour the $Rh^{III}$ complex, $[RhI_2(MeCO)(CO)PEt_3)_2]$, over $[RhI(CO)(PEt_3)_2]$ and MeCOI. However, the way in which the reaction is performed allows the catalytic production of MeCOI because the $Rh^{I}$ complex can be trapped by addition of methyl iodide when this is in excess. The overall catalytic cycle for the carbonylation of methanol in the presence of $[RhI(CO)(PEt_3)_2]$, for which each complex has been characterised, is shown in Scheme 1.

At 150 °C the catalyst loses activity over *ca*. 10 min with the formation of $Et_3PO$ and $[Rh(CO)_2I_2]^-$. Current studies are aimed at stabilising the catalyst towards phosphine loss.

We thank Dr Anthony Haynes for useful discussions. We thank B.P. Chemicals Ltd and the EPSRC for a studentship (J. R.) and the European Commission for support under a TEMPUS programme (A. C. B.).

## Footnotes and References

* E-mail: djc@st-and.ac.uk
† Current address: Chemistry Department, Kossuth Lajos University, Debrecen, Hungary.




**Scheme 1** Proposed cycle for the carbonylation of methanol catalysed by $[RhI(CO)(PEt_3)_2]$

‡ *Selected spectroscopic data*: all NMR spectra were recorded in $CD_2Cl_2$ unless otherwise stated. For **1**: $^{31}P\{^1H\}$: $\delta$ 20.2 (d, $^1J_{RhP}$ 111 Hz); $^{13}C\{^1H\}$: $\delta$(CO) 186.0 (dt, $^1J_{RhC}$ 79 Hz, $^2J_{PC}$ 16 Hz); $\nu_{CO}$/cm$^{-1}$ ($CH_2Cl_2$) 1961. For **2**: $^{31}P\{^1H\}$: $\delta$ 2.4 (d, $^1J_{RhP}$ 85 Hz); $^{13}C\{^1H\}$: $\delta$(CO) 183.3 (dt, $^1J_{RhC}$ 64 Hz, $^2J_{PC}$ 10 Hz), $\delta(CH_3)$ −3.1 (dt, $^1J_{RhC}$ 19 Hz, $^2J_{PC}$ 4 Hz); $\nu_{CO}$/cm$^{-1}$ ($CH_2Cl_2$) 2043. For **3**: $^{31}P\{^1H\}$: $\delta$ 2.1 (d, $^1J_{RhP}$ 88 Hz); $^{13}C\{^1H\}$ ($C_6D_6$): $\delta$(CO) 179.3 (dt, $^1J_{RhC}$ 69 Hz, $^2J_{PC}$ 8 Hz), $\delta(COCH_3)$ 226 (dt, $^1J_{RhC}$ 25 Hz, $^2J_{PC}$ 5 Hz), $\delta(COCH_3)$ 47.6 (d, $^2J_{RhC}$ 3 Hz); $\nu_{CO}$/cm$^{-1}$ ($CH_2Cl_2$) 2065, 1665.

§ *Crystal data* for **2**, $[RhMeI_2(CO)(PEt_3)_2]$, $C_{14}H_{33}I_2OP_2Rh$, $M_r$ = 636.08, monoclinic, space group *Pn* (no. 7), $a$ = 7.402(5), $b$ = 11.785(5), $c$ = 12.520(4) Å, $\beta$ = 96.01(4)°, $U$ = 1086.2(9) Å$^3$, $Z$ = 2, $D_c$ = 1.95 g cm$^{-3}$, $F(000)$ = 612, $\mu$(Mo-K$\alpha$) = 37.7 cm$^{-1}$, $\lambda$ = 0.71069 Å, $T$ = 220 K. Crystal size, 0.5 × 0.4 × 0.4 mm. Of the 2787 reflections which where collected ($3 < 2\theta < 50°$) on a Rigaku AFC7S diffractometer, 2598 were unique and 2453 were observed. Structure solved by direct methods and expanded using Fourier techniques. The non-hydrogen atoms were refined anisotropically. The maximum and minimum residual electron densities are 1.29 and −1.19 e Å$^{-3}$. $R$ = 0.026, $R_w$ = 0.027. CCDC 182/566.

Important dimensions: bond lengths (Å): Rh–P(1) 2.387(2), Rh–P(2) 2.390(2), Rh–C(1) 1.836(9), Rh–C(2) 2.109(9), Rh–I(1) 2.7823(7), Rh–I(2) 2.721(1), C(1)–O(1) 1.113(10); bond angles (°) I(1)–Rh–I(2) 94.18(4), I(1)–Rh–P(2) 91.36(5), I(1)–Rh–C(2) 173.8(2), I(2)–Rh–P(2) 88.22(5), I(2)–Rh–C(2) 91.8(2), P(1)–Rh–C(1) 92.2(3), P(2)–Rh–C(1) 90.0(3), C(1)–Rh–C(2), 85.0(3), I(1)–Rh–P(1) 90.34(5), I(1)–Rh–C(1) 89.0(2), I(2)–Rh–P(1) 89.48(5), I(2)–Rh–C(1) 176.3(2), P(1)–Rh–P(2) 177.24(7), P(1)–Rh–C(2) 88.1(2), P(2)–Rh–C(2) 90.4(2).

¶ For $[RhMe(CO)_2I_3]^-$ this insertion reaction is independent of carbon monoxide pressure whilst for $[RhMeI_2(CO)(PEt_3)_2]$ a first order dependence on carbon monoxide is observed.

1 M. J. Howard, M. D. Jones, M. S. Roberts and S. A. Taylor, *Catal. Today*, 1993, **18**, 325.
2 D. Forster, *Adv. Organomet. Chem.*, 1979, **17**, 255.
3 M. J. Baker, M. F. Giles, A. G. Orpen, M. J. Taylor and R. J. Watt, *J. Chem. Soc., Chem. Commun.*, 1995, 197.
4 K. V. Katti, B. D. Santarsiero, A. A. Pinkerton and R. G. Cavell, *Inorg. Chem.*, 1993, **32**, 5919.
5 R. W. Wegman, *Eur. Pat.*, 171804, 1986; *Chem. Abstr.*, 1986, **105**, 78526g.
6 J. R. Dilworth, J. R. Miller, N. Wheatley, M. J. Baker and J. G. Sunley, *J. Chem. Soc., Chem. Commun.*, 1995, 1579.
7 W. S. Weston, R. C. Gash and D. J. Cole-Hamilton, *J. Chem. Soc., Chem. Commun.*, 1994, 745.
8 M. C. Simpson, M. J. Payne and D. J. Cole-Hamilton, *J. Chem. Soc., Dalton Trans.*, 1994, 2899.
9 E. C. Baker, D. E. Hendriksen and R. Eisenberg, *J. Am. Chem. Soc.*, 1980, **102**, 1020.
10 W. R. Moser, J. E. Cnossen, A. W. Wang and S. A. Krouse, *J. Catal.*, 1985, **95**, 21.
11 T. G. Schenck, C. R. C. Milne, J. F. Sawyer and B. Bosnich, *Inorg. Chem.*, 1985, **24**, 2338.
12 G. J. Lamprecht, G. J. Van Zyl and J. G. Leipoldt, *Inorg. Chim. Acta*, 1989, **164**, 69.
13 M. J. Menu, P. Desrosiers, M. Darguenave and Y. Dartiguenave, *Organometallics*, 1987, **6**, 1822.
14 A. Haynes, B. E. Mann, G. E. Morris and P. M. Maitlis, *J. Am. Chem. Soc.*, 1993, **115**, 4093.
15 I. C. Douek and G. Wilkinson, *J. Chem. Soc. A*, 1969, 2604.
16 M. Bassetti, D. Monti, A. Haynes, J. M. Pearson, I. A. Stanbridge and P. M. Maitlis, *Gazz. Chim. Ital.*, 1992, **122**, 391.
17 J. Ramsey and J. Ladd, *J. Chem. Soc. B*, 1968, 188.
18 P. M. Maitlis, A. Haynes, G. J. Sunley and M. J. Howard, *J. Chem. Soc., Dalton Trans.*, 1996, 2187.

*Received in Cambridge, UK, 4th June 1997; 7/03895J*

# Mono- and bis-silylated tellurium reagents in silver–telluride cluster synthesis: characterisation of $Ag_{30}Te_{21}$ and $Ag_{46}Te_{29}$ complexes

**John F. Corrigan and Dieter Fenske***

*Institut für Anorganische Chemie der Universität, Engesserstrasse, Geb. Nr. 30.45, D-76128 Karlsruhe, Germany*

**AgCl, dissolved in ether solvents with tertiary phosphine ligands, reacts with a combination of the silylated reagents $Te(SiMe_3)_2$ and $Te(R')SiMe_3$ (R′ = Ph, mes) to yield the cluster complexes $[Ag_{30}(TePh)_{12}Te_9(PEt_2R)_{12}]$ (R = Et 1a, Ph 1b) and $[Ag_{46}\{Te(mes)\}_{12}Te_{17}(PEt_3)_{16}]$ 2 in good yields; the molecular structures of 1a and 2 are described.**

The synthesis of mono-disperse, high-nuclearity metal–chalcogenide nanocluster particles represents a formidable challenge. Recent efforts in this area have lead to the isolation and structural characterisation of zinc– and cadmium–sulfide complexes whose molecular structures may be viewed as fragments of the bulk semi-conducting solid materials.[1] Reports detailing the synthesis of high-nuclearity metal–chalcogenide clusters of the heavier congeners Se and Te are, however, still relatively rare.[2] Our efforts in this area have focussed on low-temperature reactions using the bis-silylated reagents $E(SiMe_3)_2$ (E = S, Se, Te) with copper(I) salts in the presence of solubilising and (kinetically) stabilising phosphine ligands.[3] Controlled reaction conditions are essential in ensuring crystalline cluster formation *vs.* the precipitation of amorphous, bulk phase solids and it has thus been possible to isolate and characterise a variety of copper–chalcogenide clusters. Efforts to extend this chemistry to related silver–chalcogenides using a similar synthetic strategy have however proven unsuccessful to date as the phosphine ligands are unable to sufficiently stabilise the Ag–E molecular cores. We,[4a,b] and others,[4c,d] have however shown that silver–chalcogenolate $[Ag_x(ER)_x$, R = alkyl, aryl] polynuclear complexes are accessible. Using sterically demanding or functionalised chalcogenolato ligands, it has been possible to isolate homoleptic polynuclear complexes.[4c,d] We set out to exploit the utility of both phosphine ligands and tellurium bonded alkyl/aryl chains in order to stabilise various AgTe cores. The synthesis of these complexes offers a rich and varied structural chemistry by modification of the $PR_3$ and TeR centres.[4a,b] We reasoned that the incorporation of additional Te sites within the cluster cores should be possible with the reagent $Te(SiMe_3)_2$ leading to even larger molecular frameworks. Herein we present the initial results of our findings, detailing the synthesis and molecular structures of $[Ag_{30}(\mu_3\text{-}TePh)_{10}(\mu_4\text{-}TePh)_2Te_9(PREt_2)_{12}]$ **1** (R = Et **1a**, Ph **1b**) and $[Ag_{46}\{\mu_3\text{-}Te(mes)\}_{12}Te_{17}(PEt_3)_{16}]$ **2** (mes = $C_6H_2Me_3$).

The preparations of **1** and **2**† are summarised in Scheme 1. Thus when a AgCl–$PR_3$ (1 : 2) solution is treated with 0.5 equiv. of $Te(Ph)SiMe_3$ and 0.25 equiv. $Te(SiMe_3)_2$ at −40 °C, a dark red, homogeneous solution is produced from which crystals of **1** form within a few days at −30 °C (yield: **1a** = 20%; **1b** = 95%). The molecular structures of both **1a** and **1b** are essentially identical, and, owing to the better quality of the X-ray data set of the former, only it will be used in discussing the structural parameters.‡ The cluster core is comprised of 12 tellurolate [$Te(Ph)^-$, Te(1)–Te(12)] and 9 telluride [$Te^{2-}$, Te(13)–Te(21)] ligands in addition to the 30 silver atoms (Fig. 1).[5] The order of addition of the silylated reagents does not affect the yield of product produced. The tellurolate ligands in **1a** adopt both $\mu_3$ [Te(1)–Te(9), Te(11)] and $\mu_4$ [Te(10)–Te(12)] bonding modes. The former exhibit an unsymmetrical pattern of one 'shorter' [2.717(3)–2.826(3) Å], one longer [2.842(3)–2.981(3) Å] and one intermediate Ag–Te bonding distances with Te(9) and Te(11) showing the least deviation [Ag–Te 2.817(3)–2.853(3), 2.790(3)–2.842(3) Å, respectively]. On average, the difference in length between the longest and shortest Ag–Te contacts is 0.14 Å. The $\mu_4$-Te(Ph)–Ag bond lengths in **1** are noticeably longer [2.933(8) Å av.] than their $\mu_3$ counterparts. The nine $Te^{2-}$ ligands [Te(13)–Te(21)] are each six coordinate [Ag–Te 2.703(3)–3.185(3) Å] and atoms Te(14) and Te(16) also exhibit a longer contact to a seventh metal site [3.260(3), 3.229(3) Å, respectively]. A +1 oxidation state can be assigned to the silver atoms and the Ag···Ag contacts [2.849(3)–3.351(3) Å] preclude any strong bonding interactions between them. Of the twelve phosphine bonded silver sites, all exhibit tetrahedral coordination with the exception of Ag(1) and Ag(2) which are trigonal planar. Of the phosphine free silver atoms, Ag(18) and Ag(19) form but two bonds each [Te–Ag–Te 153.1(1) and 153.22(9)°, respectively], whereas atoms Ag(3), Ag(6), Ag(11), Ag(12), Ag(17), Ag(20), Ag(25) and Ag(26) are three coordinate and Ag(9), Ag(10), Ag(13), Ag(14), and Ag(21)–Ag(24) display tetrahedral coordination geometries. This varied coordination about silver contrasts with the solid state structure of the mineral




**Scheme 1**

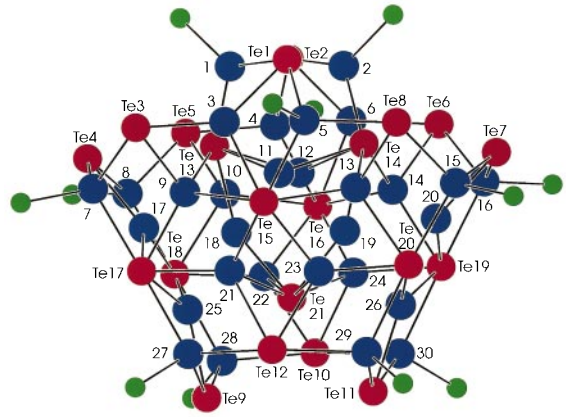



**Fig. 1** Molecular structure of $[Ag_{30}(TePh)_{12}Te_9(PEt_3)_{12}]$ **1a** (carbon atoms omitted; red: Te; blue: Ag; green: P). Silver atoms are labelled with numbers only for clarity. Tellurium atoms labelled Te(1)–Te(12) are the tellurolate ligands. Selected bond lengths (Å): Te–C: 2.13(1)–2.18(2), $\mu_3$-Te(Ph)–Ag 2.717(3)–2.981(3); $\mu_4$-Te(Ph)–Ag 2.878(3)–3.013(3); $\mu_{6/7}$-Te–Ag 2.703(3)–3.229(2), Ag···Ag 2.849(3)–3.351(3).

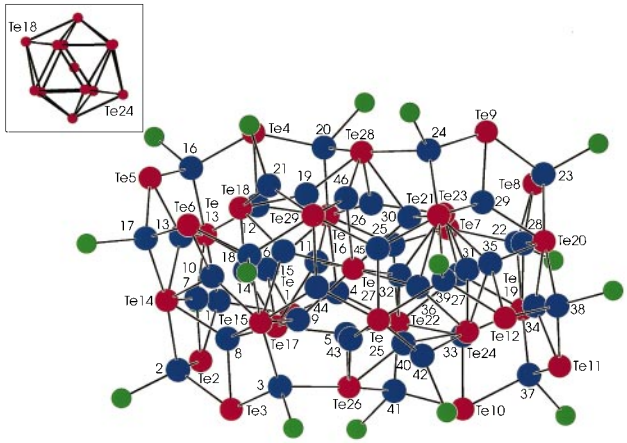



**Fig. 2** The molecular structure of $[Ag_{46}\{Te(mes)\}_{12}Te_{17}(PEt_3)_{16}]$ **2** (carbon atoms omitted; red: Te; blue: Ag; green: P). Tellurium atoms Te(1)–Te(12) are the tellurolate ligands. Selected bond lengths (Å): Te–C 2.139(13)–2.179(11), $\mu_3$-Te(mes)–Ag 2.732(2)–2.947(2), $\mu_6$-Te–Ag 2.688(2)–3.338(2), $\mu_7$-Te–Ag 2.676(2)–3.304(2), $\mu_8$-Te–Ag 2.785(2)–3.294(2), Ag···Ag 2.748(9)–3.377(4).

hessite ($Ag_2Te$) in which all Ag atoms are in tetrahedral sites.[6]

The Ag–Te framework in **1** is less spherical in nature than those observed in related CuTe systems.[7] The latter crystallise with parallel $Cu_nTe_m$ layers yielding a rather close packed arrangement. In **1**, the AgTe planes defined by Te(4)Te(18)-Te(9)Te(17)/Ag(7)Ag(8)Ag(27)Ag(28) and Te(7)Te(19)-Te(11)Te(20)/Ag(15)Ag(16)Ag(29)Ag(30) lie at an angle of 56° to one another.

An analogous reaction as for **1** with the bulkier reagent $Te(mes)SiMe_3$ (Scheme 1) leads to the exclusive formation of $[Ag_{46}Te_{17}(Temes)_{12}(PEt_3)_{16}]$ **2** as dark red–black crystals (yield 85%, Fig. 2). As in **1**, cluster **2** contains a mixture of telluride and tellurolate ligands. There is a pseudo, non-crystallographic twofold rotation axis which bisects the central $Te^{2-}$ [Te(27)] approximately perpendicular to the plane defined by the page (the projection is slightly rotated for clarity). About the central telluride can be found an additional 12 $Te^{2-}$ [Te(15)–Te(18), Te(21)–Te(26), Te(28), Te(29)] arranged to form a slightly distorted [non-bonded, Te···Te 4.523(2)–5.288(2) Å] centered icosahedron (Fig. 2, insert). Eight silver metal atoms are bonded to Te(27) [2.814(2)–3.198(2) Å] and are found within the icosahedral frame with six additional Ag atoms [Ag(4), Ag(5), Ag(25), Ag(26), Ag(44), Ag(45)] lying within its deltahedral faces. Twenty of the thirty $Te_2$ edges of the icosahedron are spanned by Ag atoms. This central $Ag_{36}Te_{13}$ unit is surrounded by 16 tellurium [12 × $Te(mes)^-$, 4 × $Te^{2-}$] and 12 Ag centres. As observed in **1**, the coordination number about the silver centres varies from two to four.

As in **1**, the metal core is stabilised with $PR_3$ ligands and aromatic groups bonded to the outer tellurium atoms. Indeed, there is a close structural relationship between the outer fragments found in **1** and **2**. The relative arrangement in **1** of atoms Te(3)–Te(5), Te(9), Te(10), Te(12) and Te(13) and the silver atoms bonded to them is also repeated in cluster **2**. Two such fragments share a common 'edge' in **1** whereas in **2** they are separated by the larger inner core. This perhaps reflects the better shielding ability of the bulkier mesityl groups and the additional coordinated $PR_3$ ligands.

The synthetic strategy outlined herein opens the doorway to accessing a variety of silver–chalcogenide clusters. We are currently actively pursuing the generation and characterisation of new and even larger molecular species.

We are grateful to the Deutsche Forschungsgemeinschaft (SFB 195), to the Fonds der Chemischen Industrie and the EU through the HCM program for support of this work. J. F. C. thanks the Natural Sciences and Engineering Research Council (Canada) for a postdoctoral fellowship.

## Footnotes and References

* E-mail: john@achibm6.chemie.uni-karlsruhe.de

† *Preparation of* **1**: a 0.16 g (1.12 mmol) sample of AgCl was dissolved in 36 ml of dried ether–thf (3 : 1) with 2.2 mmol of $PEt_2R$ (R = Et **1a**, Ph, **1b**) and the clear, colourless solution cooled to −40 °C. 0.13 ml $Te(Ph)SiMe_3$ (0.6 mmol) was added followed by 0.06 ml $Te(SiMe_3)_2$ resulting in a homogeneous yellow reaction solution. The solution was stirred for 1 h while warming to −30 °C gradually darkening in colour to deep red. Crystals of **1** grew within several days at this temperature. Yield: **1a**, 20%; **1b**, 95%. A similar procedure using $PEt_3$ and $Te(mes)(SiMe_3)$ in ether yielded red–black crystals of **2** in 85% yield.

‡ *Crystal data*: for **1a**: $C_{144}H_{240}Ag_{30}P_{12}Te_{21}{\cdot}OC_4H_{10}$, red plate fragment, 0.15 × 0.19 × 0.23 mm, $M$ = 8332.8, monoclinic, space group $P2_1/n$, $a$ = 28.614(6), $b$ = 28.163(6), $c$ = 29.296(6) Å, $\beta$ = 93.56(3)°, $U$ = 23580(8) Å$^3$, at 200 K, $Z$ = 4, $D_c$ = 2.347 g cm$^{-3}$, $\mu$ = 5.089 mm$^{-1}$, $2\theta_{max}$ = 52.2°, 40888 independent reflections measured ($R_{int}$ = 0.1266) on a STOE IPDS diffractometer. The structure was solved by direct methods and refined on $F^2$ using SHELXTL software. All P, Ag and Te atoms were refined anisotropically, all C atoms isotropically to yield $R$ = 0.0900, $wR_2$ = 0.2345, GOF = 1.073 for 18883 data [$F_o > 4\sigma F_o$]. Phenyl rings were refined as rigid groups, the bond distances of the solvent molecule and the P–C distances about P(1) and P(2) were each refined with common values.

**1b**: $C_{192}H_{240}Ag_{30}P_{12}Te_{21}$, red plate fragment, 0.06×0.15×0.20 mm, $M$ = 835.2, monoclinic, space group $P2_1/n$, $a$ = 24.052(5), $b$ = 31.045(6), $c$ = 37.611(8) Å, $\beta$ = 103.33(3)°, $U$ = 27327(9) Å$^3$, at 180 K, $Z$ = 4, $D_c$ = 2.147 g cm$^{-3}$, $\mu$ = 4.398 mm$^{-1}$, $2\theta_{max}$ = 44.5°, 18826 independent reflections measured ($R_{int}$ = 0.1544) on a STOE IPDS diffractometer. The structure was solved by direct methods and refined as for **1a** to yield $R$ = 0.1392, $wR_2$ = 0.3698, GOF = 1.050 for 12081 data [$F_o > 4\sigma F_o$]. Phenyl rings were refined as rigid groups and not all C atoms could be located in the difference Fourier map.

**2**: $C_{204}H_{372}Ag_{46}P_{16}Te_{29}{\cdot}3OC_4H_{10}$, dark red block, 0.7 × 0.7 × 0.7 mm, $M$ = 12205.3, triclinic, space group $P\bar{1}$, $a$ = 19.894(4), $b$ = 25.672(3), $c$ = 37.771(3) Å, $\alpha$ = 72.94(1), $\beta$ = 81.17(2), $\gamma$ = 68.37(2)°, $U$ = 17121(4) Å$^3$, at 180 K, $Z$ = 2, $D_c$ = 2.368 g cm$^{-3}$, $\mu$ = 5.093 mm$^{-1}$, $2\theta_{max}$ = 44.5°, 42728 independent reflections measured ($R_{int}$ = 0.0905) on a STOE IPDS diffractometer. The structure was solved by direct methods and refined as for **1** to yield $R$ = 0.0663, $wR_2$ = 0.1771, GOF = 1.057 for 33664 data [$F_o > 4\sigma F_o$]. Atoms Ag(21) and Ag(42) were disordered over two sites and each refined satisfactorally with 70 : 30 and 65 : 35 relative occupancies, respectively. CCDC 182/558.

1 M. D. Nyman, M. J. Hampden-Smith and E. N. Duesler, *Inorg. Chem.*, 1996, **35**, 802; T. Vossmeyer, G. Reck, L. Katsikas, E. T. K. Haupt, B. Schulz and H. Weller, *Science*, 1995, **267**, 1476; T. Vossmeyer, G. Reck, B. Schulz, L. Katsikas and H. Weller, *J. Am. Chem. Soc.*, 1995, **117**, 12881; N. Herron, J. C. Calabrese, W. E. Farneth and Y. Wang, *Science*, 1993, **259**, 1426.

2 S. Behrens, M. Bettenhausen, A. Eichoeffer, D. Fenkse, A. Lohde and W. Woggon, *Angew. Chem., Int. Ed. Engl.*, 1996, **35**, 2215; I. Dance and K. Fisher, *Prog. Inorg. Chem.*, 1994, **41**, 637.

3 S. Dehnen and D. Fenske, *Chem. Eur. J.*, 1996, **2**, 1407; S. Dehnen, A. Schäfer, R. Ahlrichs and D. Fenske, *Chem. Eur. J.*, 1996, **2**, 429; S. Dehnen and D. Fenske, *Angew. Chem., Int. Ed. Engl.*, 1994, **33**, 2287; H. Krautscheid, D. Fenske, G. Baum and M. Semmelmann, *Angew. Chem., Int. Ed. Engl.*, 1993, **32**, 1303.

4 (*a*) J. F. Corrigan and D. Fenske, *Chem. Commun.*, 1996, 943; (*b*) J. F. Corrigan, D. Fenske and W. P. Power, *Angew. Chem.*, 1997, **109**, 1224; (*c*) P. J. Bonasia, G. P. Mitchell, F. J. Hollander and J. Arnold, *Inorg. Chem.*, 1994, **33**, 1797; (*d*) J. Zhao, D. Adcock, W. T. Pennington and J. Kolis, *Inorg. Chem.*, 1990, **29**, 4360.

5 E. Keller, SCHAKAL 92, A Computer Program for the Graphic Representation of Molecular and Crystallographic Models, Universität Freiburg, 1992.

6 A. J. Frueh, Jr., *Am. Mineral.*, 1961, **46**, 655; *Z. Kristallogr.*, 1959, **112**, 44.

7 D. Fenske and J.-C. Steck, *Angew. Chem., Int. Ed. Engl.*, 1993, **32**, 238.

*Received in Basel, Switzerland, 13th June 1997; 7/04132B*

# Solution volume studies of a deep cavity inclusion complex of $C_{60}$: [*p*-benzylcalix[5]arene ⊂ $C_{60}$]

**Neil S. Isaacs,*[a] Peter J. Nichols,[b] Colin L. Raston,*[b] Christian A. Sandova[b] and David J. Young*[c]**

[a] *Department of Chemistry, University of Reading, PO Box 224, Reading, UK RG6 2AD*
[b] *Department of Chemistry, Monash University, Clayton, Melbourne, Victoria 3168, Australia*
[c] *Faculty of Science and Technology, Griffith University, Nathan, Brisbane, Queensland 4111, Australia*

**Molecular complexation of $C_{60}$ with *p*-benzylcalix[5]arene in toluene is associated with a partial molar volume change of +195 cm$^3$ mol$^{-1}$ which is consistent with the displacement of two toluene molecules from the cavity of the calixarene.**

Inclusion of fullerenes in container molecules is of interest in the direct purifying of fullerenes from fullerite, and the opportunities that such host–guest complexes have as nanometer size components in building up novel supramolecular arrays.[1–17] Further developments require gaining control over inherently weak host–guest interactions which are in competition with fullerene–fullerene, solvent–host and guest–solvent interactions, and is compounded by the essentially spherical, non-polarised nature of $C_{60}$.[10,15] Container molecules which form discrete complexes with $C_{60}$ and/or $C_{70}$ include calix[6,8]arenes,[5–13] cyclotriveratrylene (CTV),[14,15] γ-cyclodextrin,[16] and azacrown ethers.[17] Only three of these complexes have been structurally authenticated, a bis-mixed *p*-methyl/iodo-substituted calix[5]arene complex with $C_{60}$,[13] and two complexes of CTV with $C_{60}$ of composition $(C_{60})_n$(CTV), ($n$ = 1, 1.5). The latter structures are based on 'ball-and-socket' local host–guest supermolecules with the gross structures dominated by fullerene–fullerene interactions. The solid-state structure of another complex, the 1:1 complex of *p*-Bu$^t$-calix[8]arene with $C_{60}$ has been predicted as containing a micelle-like triangular aggregate of three fullerenes shrouded by three host molecules, each in a double cone conformation.[10] Similar micelle-like species are formed in the confines of a mesoporous silica with mean pores size diameter of 5.4 nm.[12]

In solution there is some evidence for the formation of solvated host–guest supermolecules[13,15] which can lead to micelle-like species.[15] We now further explore host–guest chemistry in solution for $C_{60}$ in the presence of *p*-benzylcalix[5]arene **1** using high-precision densitometry to measure the change in partial molar volume ($\Delta\bar{V}$) on complexation. This technique has been recently employed to measure the partial molar volume of $C_{60}$ in different organic solvents[18] but has not been used previously for studying supramolecular assemblies in

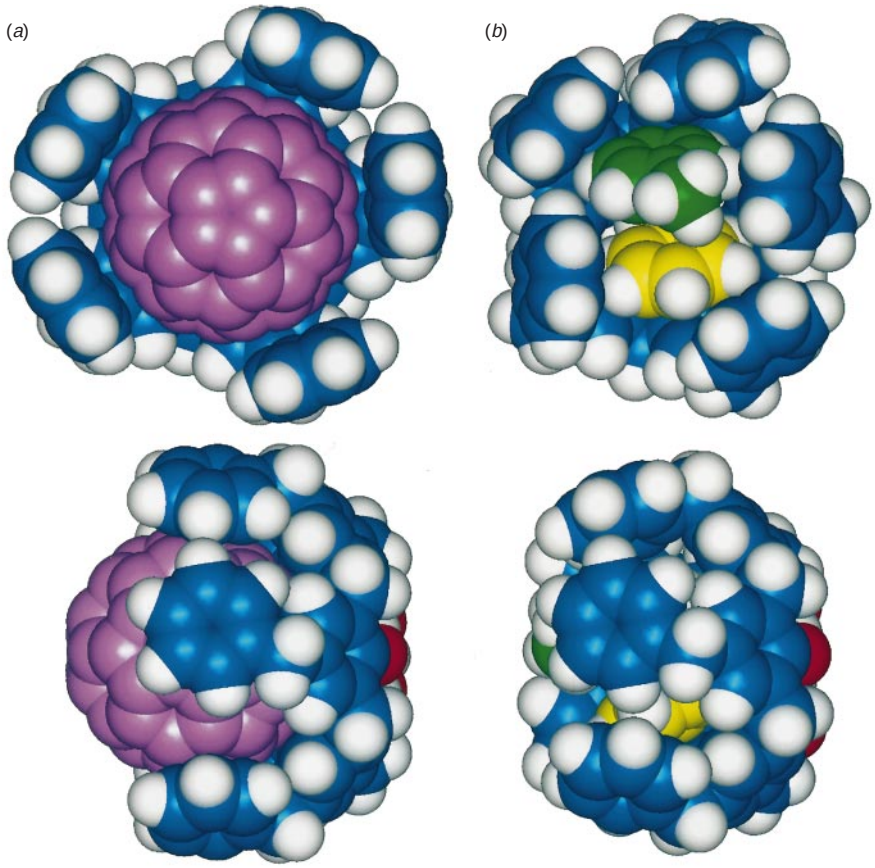
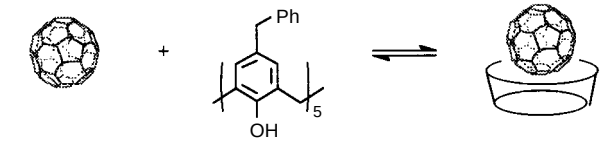



**Fig. 1** Space filling molecular mechanics structures of (*a*) [*p*-benzylcalix[5]arene ⊂ $C_{60}$] and (*b*) [*p*-benzylcalix[5]arene ⊂ $(toluene)_2$] [Insight II/Discover with standard CVFF forcefields; structure minimised using the conjugate gradients algorithm with a convergence criterion of the average derivative being < 0.001 kcal mol$^{-1}$ (1 cal = 4.184 J]




$C_{60}$ **1** **2**

$\bar{V}$ = 366 ±20 cm$^3$ mol$^{-1}$ $\bar{V}$ = 789 ±5 cm$^3$ mol$^{-1}$ $\bar{V}$ = 1350 ±50 cm$^3$ mol$^{-1}$

**Scheme 1**

solution. Choice of calixarene **1** was based on the availability of a deep cavity with a large internal surface area offering π-cloud overlap with the electron deficient fullerene. Furthermore, this overlap is optimised by the matching of the $C_5$ symmetry of the calixarene cavity with a $C_5$ symmetry axis of the fullerene.

*p*-Benzylcalix[5]arene, **1**, was prepared by a variation of a published procedure.[19] On heating a toluene solution of **1** with $C_{60}$ (1 : 1) the characteristic magenta colour of $C_{60}$ in solution changed to red and crystals slowly precipitated on cooling, albeit as the 2 : 1 calixarene to $C_{60}$ complex.† However, titration of $C_{60}$ with **1** in toluene revealed the appearance of a shoulder in the visible spectrum around 450 nm which was unchanged for concentrations of **1** in excess of 1.0 equiv., indicating 1 : 1 stoichiometry of the complex in solution. This is consistent with a recent finding that a *p*-methyl/iodo-substituted calixarene forms a 1 : 1 complex in solution,[13] while a 2 : 1 complex precipitates from solution. $^1$H and $^{13}$C NMR analysis of solutions of **1** and $C_{60}$ (1 : 1) revealed little change on complexation other than a small downfield shift (0.2 ppm) in the $^1$H resonance for the phenolic protons which is consistent with proximity of the O centres to the electron deficient $C_{60}$ and a commensurate upfield shift (0.3 ppm) in the $^{13}$C resonance for $C_{60}$.[13]

Molecular modelling of the 1 : 1 complex (Fig. 1) shows that while much of the fullerene is in the cavity of the calixarene an area is exposed for intimate contact with a fullerene of another supermolecule. In solution, the absence of an interfullerene resonant band at 460 nm[15] rules this out and the spectrum is similar to that obtained on mixing $C_{60}$ in toluene with a toluene solution of an allyl substituted CTV where there is formation of solvated host–guest species.[15] Interestingly, this CTV is like *p*-benzylcalix[5]arene in having extended arms. When a toluene solution of **1** is added to a mesoporous silica containing pre-mobilised $C_{60}$, a broad band at 460 nm appears which is assigned as an interfullerene resonant transition.[12] Thus in the confines of the mesopores there is some association of the supermolecules *via* fullerene–fullerene interactions, but not so in solution, and also in the solid state where the fullerene is most likely completely shrouded by two calixarenes.

The partial molar volumes of $C_{60}$, calixarene **1** and the 1 : 1 complex **2** in toluene at infinite dilution (Scheme 1) were determined using a Parr high-precision, vibrating-tube density meter at 25.35 ± 0.05 °C. At least three density measurements were made at three–six concentrations over the range 6.5 × 10$^{-4}$ –2.0 × 10$^{-3}$ M and extrapolated to $c$ = 0. The partial molar volume measured for $C_{60}$ in toluene was in good agreement with the range given by Ruelle *et al.* (358.3–364.4 cm$^3$ mol$^{-1}$).[18] The partial molar volume of **2** was calculated assuming a negligible dissociation to $C_{60}$ and calixarene as indicated by the UV spectrum. The uncertainties in the volume measurements for $C_{60}$ and **2** are perhaps somewhat larger than usual (5% for $C_{60}$, 4% for **2**) owing to the sparing solubility of these compounds in toluene which precludes density measurements over a wider concentration range.

The reaction volume ($\Delta\bar{V}_{c\rightarrow 0}$) on complex formation is, therefore, +195 cm$^3$ mol$^{-1}$ which is equivalent to the partial molar volume of *ca*. 1.8 toluene molecules.[18] This value can be interpreted in terms of the displacement of two toluene molecules from the cavity of the calixarene by $C_{60}$. This interpretation is supported by molecular mechanics using BIOSYM software.[20] Several minimised conformations for toluene molecules within the *p*-benzylcalix[5]arene cone were found. In particular, the toluene molecules with the same orientation (either both methyl groups orientated towards or away from the O rim) or reverse orientations (as shown in Fig. 1) gave rise to similar system energies. The minimised complex [*p*-benzylcalix[5]arene ⊂ $C_{60}$] and two free toluene molecules is favoured energetically by approximately 28 kcal mol$^{-1}$ over the minimised complex comprising [{*p*-benzylcalix[5]arene} ⊂ (toluene)$_2$] and free $C_{60}$.

One practical implication of this positive reaction volume is that elevated pressures would, perhaps unexpectedly, disfavour complex formation.

We gratefully acknowledge the Australian Research Council and the Commonwealth Department of Industry, Science and Tourism for financial support.

## Footnotes and References

*E-mail: colin.raston@sci-monash.edu.au

† *p*-Benzylcalix[5]arene (7.5 mg, 7.6 μmol) in toluene (1 ml) and $C_{60}$ (5.5 mg, 7.6 μmol) in toluene (1 ml) were filtered into a common vessel and heated to 80 °C for 30 min. On cooling dark red crystals were obtained which were washed with hexane, yield 80–90%, and analysed as (**1**)$_2$ $C_{60}$·8$C_6H_5$Me.

1 M. M. Olmstead, A. S. Ginwalla, B. C. Noll, D. S. Tinti and A. L. Balch, *J. Am. Chem. Soc.*, 1996, **118**, 7737 and references therein.
2 D. M. Eichhorn, S. Yang, W. Jarrell, T. F. Baumann, L. S. Beall, A. P. J. White, D. J. William, G. M. Barrett and B. M. Hoffman, *J. Chem. Soc., Chem. Commun.*, 1995, 1703; L. Y. Chaing, J. W. Swirczewski, K. Liang and J. Millar, *Chem. Lett.*, 1994, 981.
3 C. L. Raston, *Complexation of Fullerenes, in Comprehensive Supramolecular Chemistry*, ed. G. W. Gokel, 1996, vol. 1, p. 777.
4 O. Ermer, *Helv. Chim. Acta*, 1991, **74**, 1339; O. Ermer and C. Robke, *J. Am. Chem. Soc.*, 1993, **115**, 10 077.
5 J. L. Atwood, G. A. Koutsantonis and C. L. Raston, *Nature*, 1994, **368**, 229.
6 T. Suzuki, K. Nakashima and S. Shinkai, *Chem. Lett.*, 1994, 699.
7 R. M. Williams, J. M. Zwier, G. H. Nachtegaal and A. P. M. Kentgens, *J. Am. Chem. Soc.*, 1994, **116**, 6965.
8 T. Suzuki, K. Nakashima and S. Shinkai, *Tetrahedron Lett.*, 1995, **36**, 249.
9 W. M. Williams and J. W. Verhoeven, *Recl. Trav. Chim. Pays-Bas*, 1992, **111**, 531.
10 C. L. Raston, J. L. Atwood, P. J. Nichols and I. B. N. Sudria, *Chem. Commun.*, 1996, 2615.
11 K. Araki, K. Akao, A. Ikeda, T. Suzuki and S. Shinkai, *Tetrahedron Lett.*, 1996, **37**, 73.
12 A. Drijaca, C. Kepert, C. L. Raston, C. A. Sandoval, L. Spiccia and T. D. Smith, *Chem. Commun.*, 1997, 195.
13 T. Haino, M. Yanase and Y. Fukazawa, *Angew. Chem., Int. Ed. Engl.*, 1997, **36**, 259.
14 J. L. Atwood, M. J. Barnes, R. S. Burkhalter, P. C. Junk, J. W. Steed and C. L. Raston, *J. Am. Chem. Soc.*, 1994, **116**, 10346.
15 J. L. Atwood, M. J. Barnes, M. G. Gardiner and C. L. Raston, *Chem. Commun.*, 1996, 1449.
16 T. Anderson, G. Westman, G. Stenhagen, M. Sundahi and O. Wennerstrom, *Tetrahedron Lett.*, 1995, **36**, 597 and references therein.
17 F. Diederich, J. Effing, U. Jonas, L. Jullien, T. Plesnivy, H. Ringsdorf, C. Thilgen and D. Weinstien, *Angew. Chem., Int. Ed. Engl.*, 1993, **31**, 1599.
18 P. Ruelle, A. Farina-Cuendet and U. W. Kesselring, *J. Am. Chem. Soc.*, 1996, **118**, 1777.
19 B. Souley, Z. Asfari and J. Vicens, *Polish J. Chem.*, 1992, **66**, 959.
20 Insight II (0.3.0.0), MSI, San Diego, CA, USA.

*Received in Columbia, MO, USA; 1st April 1997; 7/02200J*

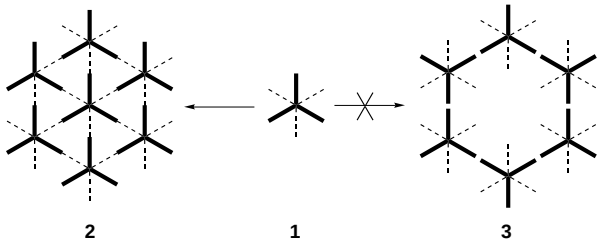
# Engineering of an octupolar non-linear optical crystal: tribenzyl isocyanurate

**Venkat R. Thalladi,[a] Sophie Brasselet,[b] Dieter Bläser,[c] Roland Boese,*[c] Joseph Zyss,*[b] Ashwini Nangia*[a] and Gautam R. Desiraju*[a]†**

[a] *School of Chemistry, University of Hyderabad, Hyderabad 500 046, India*
[b] *France Télécom CNET, Laboratoire de Bagneux, Département d'Electronique Quantique Moléculaire, 196, avenue Henri Ravera, 92225 Bagneux, France*
[c] *Institüt für Anorganische Chemie, FB 8, Universität-GH Essen, Universitätsstrasse 5-7, D-45177 Essen, Germany*

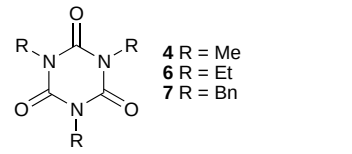
**The title compound has a C–H··O hydrogen bond-mediated trigonal network structure that leads to octupolar NLO behaviour in the solid state.**

Crystal engineering,[1] or solid state supramolecular synthesis,[2] is increasingly turning towards the design of functionalised materials.[3] Non-linear optical (NLO) properties, with such applications as second harmonic generation (SHG) or electrooptic (EO) modulation have attracted interest.[4] Traditional crystal engineering strategies towards SHG-active materials have been based on preventing the crystallisation of molecules with large dipole moments in an antiparallel and therefore centrosymmetric arrangement. These dipolar molecules suffer from other disadvantages.[1,5] Recently, a new class of SHG-active substances, octupolar molecules, have been proposed and been shown to display significant NLO behaviour at the molecular level.[6] The engineering problem at the crystalline or supramolecular level amounts to steering the structure of an appropriately substituted trigonal molecule **1** towards the trigonal, non-centrosymmetric network structure **2** characterised by specific interactions between unlike groups in the molecular skeleton, rather than towards the hexagonal, centrosymmetric network **3** characterised by close approaches between like groups.[7] Of course, the majority of trigonal molecules **1** adopt neither structure **2** nor **3** and instead adopt a trivial close-packed structure, and this renders the engineering problem more challenging.

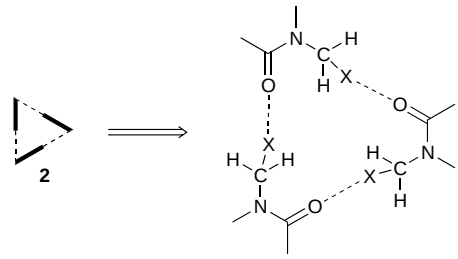


**2** **1** **3**

Some of us have reported the crystal structure of the 1 : 1 complex of trimethyl isocyanurate **4** and 1,3,5-trinitrobenzene wherein the respective components are in distinct layers, each possessing the trigonal symmetry of **2**.[8] Specifically, the molecules of **4** are linked *via* C–H··O mediated supramolecular synthon **5** that may be readily identified in network **2**.[2b] In general, single component crystals are preferred to molecular complexes for NLO applications because of issues connected with material purification, crystal growth and optical characterisation in both solution and the solid state. Therefore we turned our attention to the symmetrical isocyanurates, all of which have alternating C–H··O donors and acceptors in the molecular structure. Such an alternation is a prerequisite for the formation of network **2**. In pure **4**, the structure consists of a complicated three-dimensional networking of C–H··O hydrogen bonds.[9,10] In triethyl isocyanurate **6**, however, the trigonal network **2** is not



**4** R = Me
**6** R = Et
**7** R = Bn



**2**

**5** X = H
**8** X =

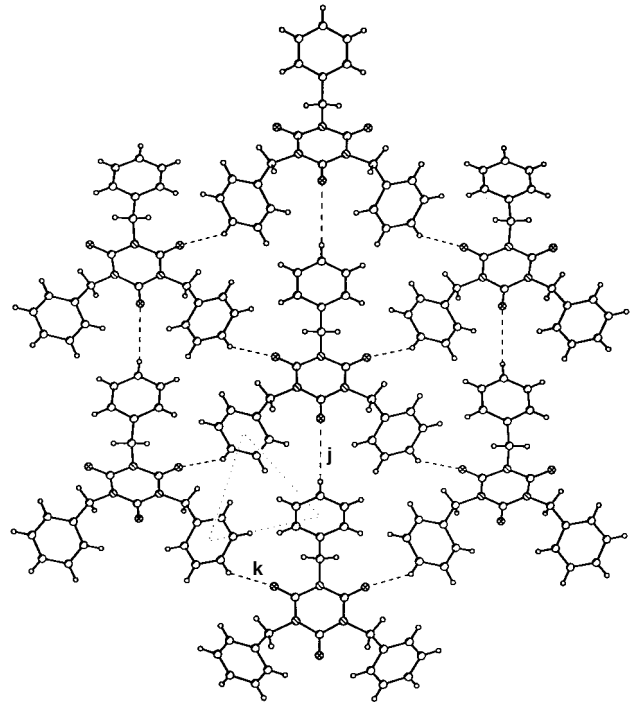



**Fig. 1** A view of the crystal structure of tribenzyl isocyanurate **7** down [010] to show the trigonal network structure. C–H··O hydrogen bonds are indicated as **j** and **k**, while herringbone interactions are indicated as dotted lines. Notice the occurrence of supramolecular synthon **8** and the overall non-centrosymemtry of the network.

found;[10] the very low acidity of the C–H groups probably leads to non-adoption of the desired structure, based as it is on C–H··O hydrogen bonds.

Keeping such carbon acidity considerations in mind,[11] tribenzyl isocyanurate **7** was examined. The crystal structure (Fig. 1) shows that the desired non-centrosymmetric trigonal network has been obtained.‡ The structure is characterised by synthon **8**, which is the tris-phenylogous extension of synthon **5**. Fig. 2 shows that **7** is far from planar. With respect to the central heterocyclic ring, two benzyl groups point in one direction whilst the third points in the other, leading to an overall 'chair'-shape. The layer structure in **7** is corrugated as shown in Fig. 3, with two distinct intralayer C–H··O hydrogen bonds. Molecules translated along [001] are connected by the interaction designated **j** in Fig. 1 (*D*, 3.91 Å; *d*, 2.97 Å; $\theta$, 145°) to form chains. Adjacent chains are *n*-glide related and connected by interaction **k** (*D*, 3.43 Å; *d*, 2.51 Å; $\theta$, 142°). The chains are additionally interconnected by herringbone interactions (dotted lines in Fig. 1). The corrugated layers are stacked along [010] and weak C–H··π interactions (*D*, 3.51, 3.63 Å; *d*, 2.73, 3.32 Å; $\theta$, 139, 150°) complete the structure.

The non-centrosymmetric nature of crystalline **7** was confirmed by a visible SHG powder signal at 1.064 μm of the order of 0.1 × urea. The nonlinear characterisation of **7** at the molecular level was performed by harmonic light scattering (HLS) measurements in solution.[5,12,13] The nonlinear $\beta = \sqrt{\langle\beta^2\rangle}$ HLS coefficient measured at 1.064 μm in $CHCl_3$ is (10 ± 2) × $10^{-30}$ esu, which is comparable to that of the classical dipolar PNA molecule under the same measurement conditions. We note that **7** is completely transparent in the visible region. The weak second harmonic signal of **7** can be ascribed to poor charge transfer, the methylene groups preventing conjugation between the peripheral and central rings. The octupolar structure of **7** was confirmed by a HLS depolarisation measurement and the depolarisation ratio[14] $D = 0.65$ is close to the theoretical value of 2/3 for purely octupolar molecular structures.[14] In the context of planar octupolar structures, the orientational isotropic averaging relation[5] $\langle\beta\rangle = 8/21\beta_{\gamma\gamma\gamma}$ leads to a predominant molecular nonlinear coefficient $\beta_{\gamma\gamma\gamma} = 16.2 \times 10^{-30}$ esu. The theoretical crystalline nonlinear coefficient was inferred from the molecular hyperpolarisability using the oriented gas model. From the geometry of the unit cell, the overall norm of the macroscopic coefficient is 96 × $10^{-9}$ esu.

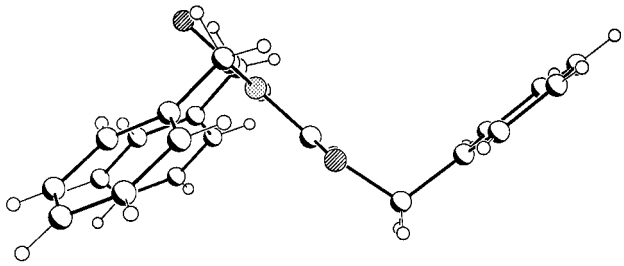


**Fig. 2** View of an individual molecule of **7** to show its non-planar character. Nitrogen and oxygen atoms are shown as dotted and hatched circles.

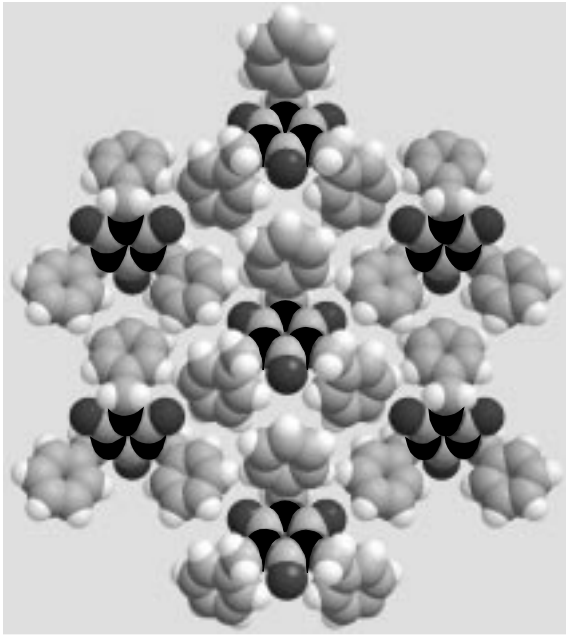


**Fig. 3** Space-filling view of the network structure shown in Fig. 1. Notice the corrugation in the layer structure.

This work describes a successful application of the supramolecular retrosynthetic strategy for the design of an octupolar nonlinear crystal and shows that network structures can be developed with the supposedly weak C–H··O interactions. Further molecular engineering that seeks to optimise the electronic charge transfer is necessary, but such manipulations must keep the favourable crystal packing intact and this is not a trivial exercise, involving as it does a carry-over of molecular symmetry into crystal symmetry or pseudosymmetry.

G. R. D. and A. N. acknowledge financial support from the Department of Science and Technology, Government of India (Grant SP/S1/G19/94). R. B. thanks the Fonds der Chemischen Industrie for support. V. R. T. thanks the Department of Atomic Energy, Government of India, for fellowship support and the Heinrich Hertz-Stiftung des Landes Nordrhein-Westfalen for travel assistance.

## Footnotes and References

† E-mail: grdch@uohyd.ernet.in

‡ *Crystal structure determination* of tribenzyl isocyanurate **7**: $C_{24}H_{21}N_3O_3$, $M = 399.44$, orthorhombic, $Pmn2_1$, $a = 18.986(3)$, $b = 4.574(1)$, $c = 11.421(2)$ Å, $V = 991.8(3)$ Å$^3$, $Z = 2$, $F(000) = 420$, $D_c = 1.338$ Mg m$^{-3}$, $\mu$(MoK$\alpha$) = 0.90 cm$^{-1}$, $T = 293$ K, 1442 non-zero (4 $\sigma$) reflections out of 1889 collected with $4.16 < 2\theta < 50.84$, number of parameters 156, solution SHELXS-86, refinement SHELXL-93 on $F^2$, $R_1$(observed) = 0.053, $R_1$ (all data) = 0.064, $wR_2$ (observed) = 0.133, $wR_2$ (all data) = 0.156; C, N, O anisotropic, H isotropic. Space group *Pmnm* which is also compatible with the crystal symmetry and systematic absences was evaluated and discarded. This was validated by the subsequent SHG measurements. Full-matrix least-squares refinement in $Pmn2_1$ proceeded satisfactorily with no correlations due to any pseudosymmetry. CCDC 182/575.

1 G. R. Desiraju, *Crystal Engineering: The Design of Organic Solids*, Elsevier, Amsterdam, 1989.
2 (*a*) D. Philp and J. F. Stoddart, *Angew. Chem., Int. Ed. Engl.*, 1996, **35**, 1154; (*b*) G. R. Desiraju, *Angew. Chem., Int. Ed. Engl.*, 1995, **34**, 2311; (*c*) J. A. Zerkowski, C. T. Seto and G. M. Whitesides, *J. Am. Chem. Soc.*, 1992, **114**, 5473.
3 A. Gavezzotti, *Curr. Opin. Solid State Mater. Sci.*, 1996, **1**(4), 501; G. R. Desiraju, *Curr. Opin. Solid State Mater. Sci.*, 1997, **2**(4), 451.
4 I. Ledoux and J. Zyss, in *Novel Optical Materials and Applications*, ed. I. C. Khao, F. Simoni and C. Umeton, Wiley, Chichester, 1997, pp. 1–48.
5 J. Zyss and I. Ledoux, *Chem. Rev.*, 1994, **94**, 77.
6 C. Dhenaut, I. Ledoux, I. D. W. Samuel, J. Zyss, M. Bourgault and H. L. Bozec, *Nature*, 1995, **374**, 339.
7 I. Ledoux, J. Zyss, J. Siegel, J. Brienne and J.-M. Lehn, *Chem. Phys. Lett.*, 1990, **172**, 440.
8 V. R. Thalladi, K. Panneerselvam, C. J. Carrell, H. L. Carrell and G. R. Desiraju, *J. Chem. Soc., Chem. Commun.*, 1995, 341.
9 F. Belaj and E. Nachbaur, *Montasch. Chem.*, 1987, **118**, 1077.
10 V. R. Thalladi, A. K. Katz, H. L. Carrell, A. Nangia and G. R. Desiraju, unpublished work.
11 V. R. Pedireddi and G. R. Desiraju, *J. Chem. Soc., Chem. Commun.*, 1992, 988.
12 D. Maker, *Phys. Rev. A*, 1970, **1**, 923.
13 J. Zyss, *J. Chem. Phys.*, 1993, **98**, 6583.
14 S. Brasselet and J. Zyss, *J. Nonlinear Phys. Mater.*, 1996, **5**, 4.

*Received in Cambridge, UK, 4th July 1997; 7/04737A*

# Synthesis of direct templated aligned mesoporous silica coatings within capillaries

**Maria E. Raimondi,[a] Thomas Maschmeyer,[b] Richard H. Templer[a] and John M. Seddon*[a]**

[a] *Department of Chemistry, Imperial College, London, UK SW7 2AY*
[b] *Davy Faraday Laboratories, The Royal Institution of Great Britain, 21 Albemarle Street, London, UK WX1 4BS*

**Mesoporous liquid-crystal templated silica forms intact coatings with channels adopting a curious alignment, when synthesised within thin capillaries.**

The design of tailor-made mesoporous structures, templated by assemblies of surfactant molecules, has attracted a great deal of interest from materials scientists and chemists alike. The synthesis and structural characterisation of one particular family of silica-based mesoporous materials, denoted M41S, is now well documented.[1,2] These materials are templated under alkaline conditions, at elevated temperatures, in the presence of cationic quaternary ammonium surfactants. Several other synthetic procedures employing different surfactant templates, silica precursors and/or reaction conditions to prepare similar mesoporous products, have been described in the literature.[3–6] Most of the synthetic procedures use low surfactant concentration regimes, and rely on a co-precipitation process whereby the surfactant micelles are trapped within the silica, providing a structure-directing environment for the mesostructured solid.

By contrast, in our work gels containing relatively high concentrations of a non-ionic polyoxyethylene surfactant are used as a 'direct' templating medium for the formation of hexagonal mesoporous silica. The synthetic method was first described by Attard *et al.*,[7] and is termed true liquid crystal templating (TLCT). Their calcined products, templated using octaethylene glycol monododecyl ether ($C_{12}EO_8$) consisted of hexagonal arrays of 28 Å diameter channels, as seen by transmission electron microscopy, with a *d*-spacing of 34 Å (seen by powder X-ray diffraction). The arrays of pores in the TLCT materials strongly resembled those seen for MCM-41, the hexagonal M41S analogue. $N_2$ BET adsorption measurements showed that the calcined mesoporous silica had a specific surface area of 1400 $m^2\ g^{-1}$. Our synthetic mixtures were closely analogous to those used by Attard *et al.*,[7] consisting of an *n*-alkyl, octaoxyethylene surfactant template in an acidic TLCT system with tetramethylorthosilicate (TMOS) as the silica precursor. Two different surfactants were used as templates: octaethylene glycol monododecyl ether ($C_{12}EO_8$) and octaethylene glycol monodecyl ether ($C_{10}EO_8$). The weight ratio of the components in both synthetic mixtures was 1 $C_nEO_8$ : 1 $H_2O$ (pH 2) : 2.11 TMOS ($n$ = 10 or 12), and the hydrolysis/polymerization reaction was carried out overnight under vacuum at room temperature. The mesoporous product obtained from these mixtures was transparent, with the same characteristic optical texture under the polarising microscope as previously observed by Attard *et al.*[7]

The synthesis of a single, monolithic mesoporous structure, containing aligned pores, is a particularly exciting goal. A material of this kind would have potential applications in nanoscale engineering, separation technology, microelectronics, biomaterials engineering and catalysis. In biological systems, control of hierarchical ordering in biomineralization processes is achieved by the use of organic templates and confinement by surfaces such as membranes. Various attempts at aligning MCM-41 type materials with a view to producing monoliths (monodomain samples) have been described in the literature; such work could lead to an extension of the applications of the powder-like products usually obtained.[8–11] The alignment of these mesoporous films relied on heterogeneous nucleation of the surfactant/inorganic precursor onto the aligning surface being favoured over precipitation (homogeneous nucleation) within the bulk solution.

To produce alignment of the TLCT material, we inserted the synthesis gel into a 0.5 mm (internal diameter) glass or quartz capillary by capillary action. The capillary was left with one end dipping into the synthesis gel and the assembly was placed under vacuum overnight, coating the inside walls of the capillary with birefringent mesoporous material which was stable to removal of the template by calcination at 500 °C. Polarising microscopy on the calcined quartz capillary gave similar optical textures to the as-synthesized material, with enhanced colours. A void in the centre of the capillary was clearly visible and the coating was continuous. No discernible difference between coatings on glass and quartz walls was observed, indicating that the precise atomic arrangement of the silica within the capillary walls does not influence the alignment.

Very well aligned six-spot patterns were systematically obtained by X-ray diffraction, employing an image intensified CCD-based X-ray detector of our own design,[12] when the beam was passed at right angles to the capillary axis through the top or bottom edges of the coated capillary before calcination. The orientation of the reciprocal lattice shows that in real space the channels are arranged on a hexagonal lattice, one face of which is parallel to the capillary wall [Fig. 1(*a*)]. After calcination these six-fold spots [corresponding to the (10) reflections] were more intense, and two higher orders [the (11) and the (20) reflections] of the hexagonal diffraction pattern became visible. This implies that calcination results in increased local ordering of the mesoporous product. Both the X-ray diffraction and the polarising microscopy results suggest that the channels of the as-synthesised and calcined products are arranged in rings, or a tight coil, as depicted in Fig. 1(*a*).

When the X-ray beam was passed through the capillary at positions marginally closer to its centre, the diagonal spots in the six-fold pattern spread into arcs, suggesting that the hexagonally packed channels twist and/or bend within their coiled arrangement, *cf.* Fig. 1(*b*). When the beam was passed centrally through the capillary, no diffraction spots were observed. The alignment experiment was found to be reproducible using both $C_{10}$ and $C_{12}$ POE surfactant systems. The *d*-spacings of the materials were 40 and 45 Å before calcination, and 35 and 38 Å after calcination, respectively, for the two chain lengths. The corresponding lattice parameters for the two templated materials were respectively 46 and 52 Å before calcination, and 40.5 and 44 Å after calcination.

For both as-synthesised and calcined products, a slight distortion away from hexagonal symmetry, presumably induced by the surface alignment interactions, was observed. A similar distortion has recently been observed for films of mesoporous silica aligned on mica and graphite surfaces.[9] The fact that the coating remained intact after calcination suggests that the channels in the coating must have outlets through which the organic phase can escape, without disturbing the structure. We

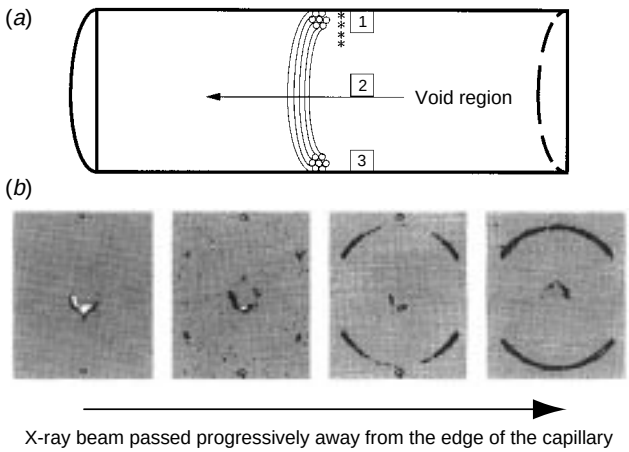



**Fig. 1** (*a*) Schematic longitudinal section of a coated capillary showing hexagonally packed channels of mesoporous $SiO_2/C_nEO_8$ product lining the capillary walls ($n$ = 10 or 12). Six-spot patterns were obtained when the X-ray beam was passed perpendicularly through the capillary at positions (1) and (3); no diffraction pattern was obtained when the X-ray beam was passed through the centre of the capillary (2). (*b*) Sequence of X-ray diffraction patterns obtained for the aligned $SiO_2/C_{10}EO_8$ composite coating when the X-ray beam crossed the capillary at positions shown by asterisks in (*a*). (*c*) Pattern obtained for the calcined sample when the X-ray beam was passed through the edge of the capillary.

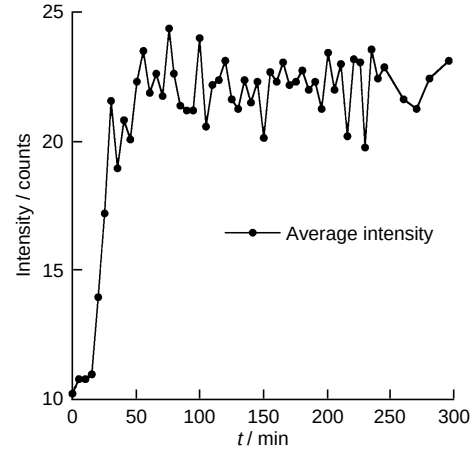



**Fig. 2** Plot of average diffraction spot intensity *versus* time for an *in situ* X-ray diffraction experiment to probe the kinetics of the alignment process

propose that the channels are in fact spiralling in tight coils from one end of the coating to the other, with an outlet at either end, rather than consisting of individual closed rings.

When the alignment experiment was carried out using capillaries treated with phenyltrimethoxysilane (to render the surfaces hydrophobic), both polarising microscopy and X-ray diffraction suggest that the alignment of the product was severely disturbed. The nature of the supporting surface is therefore important for successful alignment. However, it should be noted that the alignment effect is not observed when the synthesis mixtures were spread in a thin layer on a flat piece of glass or quartz and allowed to react under vacuum, under identical conditions to those used for the capillary alignment experiments. This indicates that the alignment is predominantly due to confinement within the capillaries.

The kinetics of self-assembly were followed using *in situ* X-ray diffraction. The intensity of the X-ray diffraction *versus* time is plotted in Fig. 2 for one of the six spots of the aligned pattern (obtained when passing the beam through the edge of the capillary). An exposure was taken every five minutes over a period of 3 h, and a 'box integration' was made on the same area of each pattern (containing the diffraction spot) to obtain the intensity data. The data show that the self-assembly occurs over a period of about 15 min. Interestingly, there were no patterns other than the aligned six-fold spot pattern observable throughout the experiment, indicating the observed alignment to be both the kinetically and thermodynamically favoured arrangement.

In this work, TLCT has been found to be a suitable method for producing aligned mesoporous siliceous materials. The results obtained show that macroscopically aligned coatings can be made from TLCT systems, simply by confining the synthesis mixtures in a capillary. The coatings, which are systematically and reproducibly obtained, contain coils of aligned mesopores, lining the walls of the capillary. The aligned coatings of composite product are stable to calcination (removal of the organic template) at 500 °C. The kinetic investigations of the system show that there are no detectable intermediate structures between gel hydrolysis and the final aligned coating.

M. E. R. thanks the EPSRC for a studentship and T. M. thanks the EU for a TMR Fellowship. Helpful discussions with Professor C. R. A. Catlow are gratefully acknowledged.

## Footnotes and References

* E-mail: j.seddon@ic.ac.uk

1 J. S. Beck, J. C. Vartuli, W. J. Roth, M. E. Leonowicz, C. T. Kresge, K. D. Schmitt and C. T.-W. Chu, *J. Am. Chem. Soc.*, 1992, **114**, 10 834.
2 J. S. Beck and J. C. Vartuli, *Curr. Opin. Solid State Mater. Sci.*, 1996, **1**, 76.
3 Q. Huo, D. L. Margolese, U. Ciesla, P. Feng, T. E. Gier, P. Sleger, R. Leon, P. M. Petroff, F. Schüth and G. D. Stucky, *Nature*, 1994, **368**, 317.
4 D. Khushalani, A. Kuperman, N. Coombs and G. A. Ozin, *Chem. Mater.*, 1996, **8**, 2188.
5 S. A. Bagshaw, E. Prozet and T. J. Pinnavaia, *Science*, 1995, **269**, 1242.
6 P. T. Tanev and T. J. Pinnavaia, *Chem. Mater.*, 1996, **8**, 2068.
7 G. S. Attard, J. C. Glyde and C. G. Göltner, *Nature*, 1995, **378**, 366.
8 H. Yang, A. Kuperman, N. Coombs, S. Mamich-Afara and G. A. Ozin, *Nature*, 1996, **379**, 703.
9 I. A. Aksay, M. Trau, S. Manne, I. Honma, N. Yao, L. Zhou, P. Fenter, P. M. Elsenberger and S. M. Gruner, *Science*, 1996, **273**, 892.
10 H. Yang, N. Coombs, I. Sokolov and G. A. Ozin, *Nature*, 1996, **381**, 589.
11 S. Schacht, Q. Huo, I. G. Voigt-Martin, G. D. Stucky and F. Schüth, *Science*, 1996, **273**, 768.
12 R. H. Templer, S. M. Gruner and E. F. Eikenberry, *Adv. Electron Phys.*, 1988, **74**, 275.

*Received in Bath, UK, 3rd June 1997; 7/03964F*

# Synthesis and characterisation of the first stable, heteroleptic silylstannylenes†

**Christian Drost, Barbara Gehrhus, Peter B. Hitchcock and Michael F. Lappert***

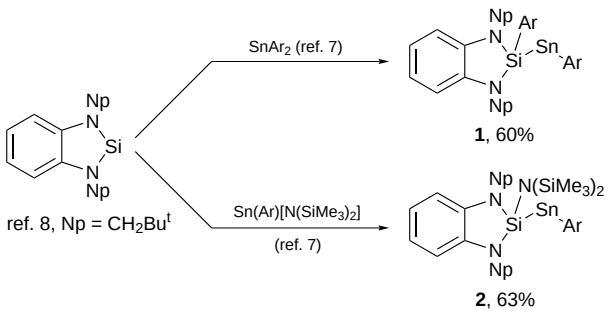
*The Chemistry Laboratory, University of Sussex, Brighton, UK BN1 9QJ*

**Treatment of the silylene Si[$C_6H_4$($NCH_2Bu^t$)$_2$-1,2] with $SnAr_2$ or SnAr[$N(SiMe_3)_2$] yields the thermally stable (silyl)stannylene SnAr[Si{$C_6H_4$($NCH_2Bu^t$)$_2$-1,2}X] [X = Ar 1 or $N(SiMe_3)_2$ 2], having $\delta$ [$^{119}$Sn{$^1$H}] 412 [$^1J$($^{29}$Si–$^{117/119}$Sn) 715/749 Hz] (1) and $\delta$ 621 (2); crystalline 1 has a V-shaped Si–Sn–C skeleton, $l$(Sn–Si) = 2.636(2) Å and two remote Sn···N contacts, av. 2.75 Å (to one $NMe_2$ group of each of the aryl groups).**

Homoleptic heavier group 14 metal(II) (M = Ge, Sn or Pb) compounds in which M is bound to a more electropositive element than carbon (*e.g.*, Si, Ge or a metal) are rare. Two types of group 6 metal complexes are known, [Pb{Mo($\eta^5$-$C_5Me_5$)-$(CO)_3$}$_2$(thf)][1a] [and $\eta^5$-$C_5H_5$ or $\eta^5$-$C_5H_3(SiMe_3)_2$-1,3 analogues] and [Ge{$C_6H_3$($C_6H_2Me_3$-2′,4′,6′)$_2$-2,6}{Mo($\eta^5$-$C_5H_5$)$(CO)_2$}],[1b] as well as some tin(II) phosphides[2a,b] and arsenides,[2b,c] but especially relevant to the present work are three silyl derivatives: [Sn{$Si(SiMe_3)_3$}$_2$]$_2$,[3] [Sn{$Si(SiMe_3)_3$}$_2$($\mu$-Cl)Li(thf)$_3$][4] and Pb[$Si(SiMe_3)_3$]$_2$[3] (thf = $OC_4H_8$). Each of these five X-ray characterised compounds was prepared by a metathetical exchange reaction, using an alkali metal salt of the appropriate ligand and M′$Cl_2$ (M′ = Ge or Pb) or[3] M′[$N(SiMe_3)_2$]$_2$ (M′ = Sn or Pb). Two transient heterobinuclear complexes have been identified spectroscopically or by trapping experiments, Ge($C_6H_2Me_3$-2,4,6)$_2$M′$X_2$ [M′$X_2$ = Si($C_6H_2Me_3$-2,4,6)$_2$[5] or Sn($C_6H_2Pr^i_3$-2,4,6)$_2$],[6] each obtained from tetravalent precursors.

Thermally stable mononuclear heavier group 14 metal(II) compounds $MX_2$ (M = Ge, Sn or Pb and $X^-$ is a mono- or bidentate ligand) are highly reactive, but insertion reactions into M–X bonds leading to new $M^{II}$ complexes MX′$_2$ or M(X)X′ have not previously been reported. The latter (heteroleptic) type is in any event rare.[7]

We now describe the synthesis (Scheme 1) and characterisation of the first heteroleptic (silyl)stannylenes, the crystalline, yellow–orange, diamagnetic SnAr[Si{$C_6H_4$($NCH_2Bu^t$)$_2$-1,2}Ar] **1** and the red–brown SnAr[Si{$C_6H_4$($NCH_2Bu^t$)$_2$-1,2}{$N(SiMe_3)_2$}] **2** [Ar = $C_6H_3(NMe_2)_2$-2,6]. They were obtained by treatment of the yellow silylene Si[$C_6H_4$($NCH_2Bu^t$)$_2$-1,2][8] with for **1** the yellow $SnAr_2$[7] in *n*-hexane at ambient temperature in a slow reaction, or for **2** with the yellow SnAr[$N(SiMe_3)_2$][7] under the same conditions but in a faster reaction.

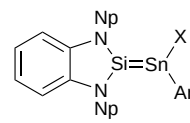



**Scheme 1** Synthesis of the silylstannylenes **1** and **2** [Ar = $C_6H_3(NMe_2)_2$-2,6]; yields refer to crystalline products (from $Et_2O$ for **1** or *n*-$C_6H_{14}$ for **2**)

The crystalline aryl(silyl)stannylenes **1** and **2** were thermally robust, decomposing before melting only at *ca.* 120 °C. The orange (**1**) and orange–red (**2**) hexane solutions were more labile (**1** > **2**), the former slowly (days) depositing tin at ambient temperature. Their stability may, in part, be due to close contacts between tin and one or more *o*-nitrogen atoms of the $Ar^-$ ligand(s), *cf.* ref. 7. Each of **1** and **2** gave satisfactory microanalytical results, as well as multinuclear NMR spectra.‡ The EI (70 eV) mass spectra showed the parent molecular ion in 2% intensity for **1** and 9% for **2**, as the highest *m/z* peak; the most intense fragment ion was [Si{$C_6H_4$($NCH_2Bu^t$)$_2$-1,2}Ar]$^+$ for **1** and [Si{$C_6H_4$($NCH_2Bu^t$)$_2$-1,2}{$N(SiMe_3)_2$}]$^+$ for **2**. Single crystal X-ray diffraction data established the molecular structure of **1**.§

The $^1$H NMR spectrum of **1** in $C_6D_6$ at 298 K showed separate signals for each of the two $CH_2C\mathit{Me}_3$ groups and several for the eight NMe groups of the two Ar moieties.‡ The corresponding spectrum of **2** in [$^2H_8$]toluene at 298 K revealed two signals for the $SiMe_3$ groups but only one for the two $CH_2C\mathit{Me}_3$ groups and a broad feature for the $NMe_2$ protons. The latter split into two separate signals at 238 K. This indicates that at the higher temperature there is a rapid N → Sn exchange process involving the Sn···NMe-2⇌Sn···NMe-6 fragments, while at the lower temperature only one of the two $NMe_2$ groups is bound to tin, as also found in the solid state for **1**, *vide infra*. This interpretation is consistent (at least for **1**) with the values found for the $^{119}$Sn{$^1$H} NMR spectral chemical shifts: $\delta$ 412 (**1**) and $\delta$ 621 (**2**) in PhMe–$C_6D_6$ at 298 K, which may be compared with $\delta$ 442 for $SnAr_2$ and 422 for SnAr[$N(SiMe_3)_2$] having four- and three-coordinate tin, respectively.[7] A comparison of these results with the two existing (silyl)tin(II) compounds is not possible; since attempts to detect $^{119}$Sn or $^{29}$Si NMR spectral signals in the range −60 to +30 °C for [Sn{$Si(SiMe_3)_3$}$_2$]$_2$ were unsuccessful,[3] while for [Sn{$Si(SiMe_3)_3$}$_2$($\mu$-Cl)Li(thf)$_3$] only the $^{29}$Si chemical shifts were recorded, $\delta$ −6.23 for *Si*($SiMe_3$)$_3$ and $\delta$ −22.14 for Si(*Si*$Me_3$)$_3$.[4] The SiSn $^{29}$Si{$^1$H} NMR spectral chemical shifts in PhMe–$C_6D_6$ at 298 K were found at $\delta$ 48.8 for **1** and $\delta$ −27.8 for **2**. The former signal, unlike the latter, showed readily discernible coupling to tin: $^1J$($^{29}$Si–$^{117}$Sn) 715 Hz and $^1J$($^{29}$Si–$^{119}$Sn) 749 Hz; these values may be compared with $^1J$($^{29}$Si–$^{119}$Sn) of 580 Hz for Sn($SiMe_3$)$Me_3$[9] and 515 Hz for $(SnPh_3)_2SiPh_2$.[10] The $^{29}$Si–Sn coupling in **2** may have been obscured by coupling to the $^{14}$N nucleus of the $N(SiMe_3)_2$ group.

The pathway leading to **1** or **2** may have implicated an initial transient heterodinuclear tin–silicon 'double-bonded' complex **3**, which was rapidly isomerised by a 1,2-shift of X [X = Ar or $N(SiMe_3)_2$] from tin to silicon. Evidence for **3** rests on the




**3a** X = Ar
**3b** X = $N(SiMe_3)_2$

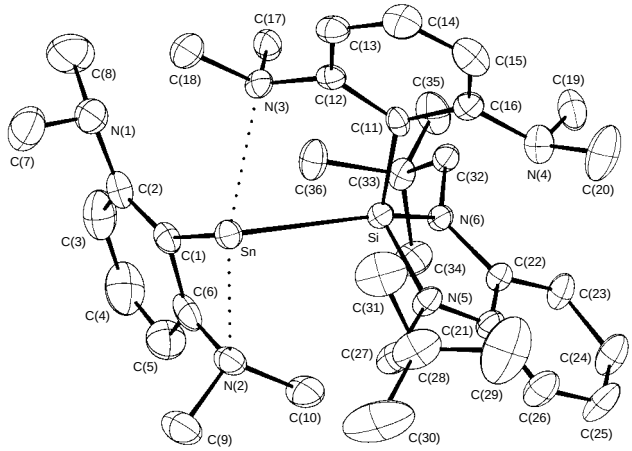



**Fig. 1** CAMERON[16] representation (50% thermal vibration ellipsoids) of the molecular structure of SnAr[Si{$C_6H_4$($NCH_2Bu^t$)$_2$-1,2}Ar] **1** [Ar = $C_6H_3(NMe_2)_2$-2,6]. Selected bond lengths (Å) and angles (°): Sn–C(1) 2.210(8), Sn–Si 2.636(2), Sn···N(3) 2.569(6), Sn···N(2) 2.580(6), Si–C(11) 1.904(8); C(1)–Sn–Si 107.0(2), N(5)–Si–N(6) 91.0(3), C(6)–C(1)–Sn 102.5(6), C(2)–C(1)–Sn 140.0(6).

existence of related kinetically inert homonuclear complexes such as [Sn{$CH(SiMe_3)_2$}$_2$]$_2$,[11] [Sn{$Si(SiMe_3)_3$}$_2$]$_2$[3] and X″$_2$SnSnCl$_2$ [X″ = $CH(SiMe_3)C_9H_6$N-8][12] and the labile heterodinuclear analogue X′$_2$SiGeX′$_2$ (X′ = $C_6H_2Me_3$-2,4,6) **4**.[5] Precedents for a 1,2-aryl shift in group 14 element chemistry include Wagner–Meerwein rearrangements, the photolytic scrambling between $Si_2X'_4$ and $Si_2X'''_4$ (X‴ = $C_6H_3Me_2$-2,6),[13] and the trapping of **4** with Si(H)$Et_3$ generating GeH($SiEt_3$)-($SiX'_3$)X′ with GeX′($SiX'_3$) as the presumed intermediate.[5]

The molecular structure of the crystalline aryl(arylsilyl)-stannylene **1**, illustrated in Fig. 1, shows it to be mononuclear with a V-shaped Si–Sn–C(1) skeleton but with Sn having further remote contacts to N(2) and N(3) (from an $NMe_2$ of each aryl group). The tin bonding environment may thus be regarded as approximating to a distorted trigonal bipyramid, N(2) and N(3) being axial and Si, C(1) and the lone pair in equatorial sites. The Si–Sn–C(1) angle of 107.0(2)° is similar to the 105.6(2)° in $SnAr_2$,[7] and the Sn–C(1) distance of 2.108(2) Å in **1** is likewise close to the av. of 2.214 Å in $SnAr_2$.[7] The Sn–Si bond length of 2.636(2) Å is comparable to the av. 2.672 Å in [Sn{$Si(SiMe_3)_3$}$_2$]$_2$[3] and the 2.681(2) Å in [Sn{Si-($SiMe_3$)$_3$}$_2$(μ-Cl)Li(thf)$_3$].[4] The Sn···N(2) and Sn···N(3) contacts in **1**, av. 2.75 Å, are slightly more remote than in $SnAr_2$ (av. 2.64 Å)[7] or Sn[$C_6H_3$($CH_2NMe_2$)($CH_2NMe_2$)-2,6]Cl (2.56 Å).[14] The aromatic ring containing C(1) is strongly tilted about the Sn–C(1) vector so as to allow N(2) to approach Sn, as evident from the significant deviations from the sp$^2$ values of the C(6)–C(1)–Sn [102.5(6)°] and C(2)–C(1)–Sn [140.0(6)°] angles; these are close to those found in $SnAr_2$, 104.0 and 138.2°.[7] The Sn···N(3) contact from the SiAr group does not involve strain, as shown by the more typical sp$^2$ values for the C(12)–C(11)–Si [118.3(6)°] and C(16)–C(11)–Si [123.5(6)°] angles.

The reactions shown in Scheme 1 provide the first examples of insertion of (i) an unsaturated reagent into an M–Z bond of a carbene or a heavier group 14 element analogue $MZ_2$ generating a new metallene and (ii) a silylene into a metal–aryl or metal–amide bond. As to (ii), the reaction leading to **2** demonstrates that the migratory aptitude of N($SiMe_3$)$_2$ is greater than that of Ar, as also evident from the faster rate of formation of **2** than **1**. Such reactions are likely to be antecedents of a wider series; for example involving the silylene and M[N($SiMe_3$)$_2$]$_2$ (M = Ge, Sn or Pb).[15]

We thank the European Comission for providing fellowships for C. D. and B. G. (category 30), Drs A. G. Avent (NMR) and A. Abdul-Sada (MS) for data and the EPSRC for other support.

## Footnotes and References

* E-mail: m.f.lappert@sussex.ac.uk

† No reprints available.

‡ *NMR spectroscopic data* [$^1$H NMR at 250.0 MHz in $C_6D_6$ for **1** or at 300.0 MHz in [$^2H_8$]toluene for **2**; $^{13}$C{$^1$H} NMR at 75.47 MHz in $C_6D_6$, $^{29}$Si{$^1$H} NMR at 99.33 MHz and $^{119}$Sn{$^1$H} NMR at 93.2 MHz, all in PhMe with $C_6D_6$; at 298 K unless otherwise stated]. **1**: $^1$H $\delta$ 0.78 and 1.02 (2s, 18 H, $CMe_3$), 2.39, 2.49 and 2.63 (3s, 18 H, $NMe_2$), 2.98 and 3.26 (2s, 6 H, $NMe_2$), 2.97–3.61 (AB-type, part. hidden, $CH_2$), 6.52–7.18 (m, 10 H, phenyl); $^{13}$C $\delta$ 29.41 and 29.84 (C$Me_3$), 34.25 and 34.89 ($CMe_3$), 44.98, 46.56, 47.89 (broad, $NMe_2$), 57.04 and 59.77 ($CH_2$), 109.06, 109.50, 111.88, 114.61, 116.11, 116.46, 116.80, 131.76, 135.30, 144.92. 146.43, 151.97, 159.44, 161.03, 162.34 and 163.46 (arom. C); $^{29}$Si $\delta$ 48.8 [$^1J$($^{29}$Si–$^{117/119}$Sn) 715, 749 Hz]; $^{119}$Sn $\delta$ 412. **2**: $^1$H (238 K) $\delta$ 0.1 and 0.45 (2s, 18 H, $SiMe_3$), 0.95 and 1.11 (2s, 18 H, $CMe_3$), 2.17 and 2.61 (2s, 12 H, $NMe_2$), 2.28, 2.48, 2.52, 3.04, 3.09, 3.51 and 3.56 (AB-type, one signal hidden, broad signals, 4 H, $CH_2$), 5.95, 5.98, 6.52–7.07 (m, phenyl); $^{13}$C $\delta$ 5.16 and 5.67 ($SiMe_3$), 30.09 (C$Me_3$), 33.78 ($CMe_3$), 45 (vbr, $NMe_2$), 56.44 ($CH_2$), 109.24, 117.18, 119.44, 128.47, 144.06, 146.15 and 159.88 (arom. C); $^{29}$Si $\delta$ 1.28 ($SiMe_3$), −27.65 (Si–Sn); $^{119}$Sn $\delta$ 620.94.

§ *Crystal data*: **1**, $C_{36}H_{56}N_6SiSn$, $M$ = 719.6, monoclinic, space group $P2_1/n$ (non-standard no. 14), $a$ = 16.118(5), $b$ = 11.124(3), $c$ = 21.526(5) Å, $\beta$ = 101.71(2)°, $U$ = 3779(2) Å$^3$, $F$(000) = 1512; $Z$ = 4, $D_c$ = 1.26 g cm$^{-3}$, $\mu$(Mo-Kα) = 7.4 cm$^{-1}$, specimen 0.2 × 0.2 × 0.06 mm, 4802 reflections collected for 2 < $\theta$ < 22°, 4614 independent reflections [$R$(int) = 0.057], $R1$ = 0.049 for 2872 reflections with $I > 2\sigma(I)$, $wR2$ = 0.123 (for all data).

Intensities were measured on an Enraf-Nonius CAD4-diffractometer [$T$ = 293(2) K] using monochromated Mo-Kα radiation ($\lambda$ = 0.71073 Å); no crystal decay. Full-matrix least squares on all $F^2$ refinement with SHELXL-93, H atoms in riding mode and all non-H atoms anisotropic. CCDC 182/572.

1 (*a*) P. B. Hitchcock, M. F. Lappert and M. J. Michalczyk, *J. Chem. Soc., Dalton Trans.*, 1987, 2635; (*b*) R. S. Simons and P. P. Power, *J. Am. Chem. Soc.*, 1996, **118**, 11966.
2 (*a*) P. B. Hitchcock, M. F. Lappert, P. P. Power and S. J. Smith, *J. Chem. Soc., Chem. Commun.*, 1984, 1669; (*b*) M. Driess, R. Janoschek, H. Pritzkow, S. Rell and U. Winkler, *Angew. Chem., Int. Ed. Engl.*, 1995, **34**, 1614; (*c*) P. B. Hitchcock, M. F. Lappert and S. J. Smith, *J. Organomet. Chem.*, 1987, **320**, C27.
3 K. W. Klinkhammer and W. Schwarz, *Angew. Chem., Int. Ed. Engl.*, 1995, **34**, 1334.
4 A. M. Arif, A. H. Cowley and T. M. Elkins, *J. Organomet. Chem.*, 1987, **325**, C11.
5 K. M. Baines, J. A. Cooke, C. E. Dixon, H. W. Liu and M. R. Netherton, *Organometallics*, 1994, **13**, 631.
6 M.-A. Chaubon, J. Escudié, H. Ranaivonjatovo and J. Satgé, *Chem. Commun.*, 1996, 2621.
7 C. Drost, P. B. Hitchcock, M. F. Lappert and L. J.-M. Pierssens, *Chem. Commun.*, 1997, 1141.
8 B. Gehrhus, P. B. Hitchcock, M. F. Lappert, J. Heinicke, R. Boese and D. Bläser, *J. Organomet. Chem.*, 1996, **521**, 211.
9 B. Wrackmeyer, *$^{119}$Sn-NMR Parameters*, *Annu. Rep. NMR Spectrosc.*, 1985, **16**, 73.
10 S. Adams and M. Dräger, *J. Organomet. Chem.*, 1987, **323**, 11.
11 D. E. Goldberg, P. B. Hitchcock, M. F. Lappert, K. M. Thomas, A. J. Thorne, T. Fjeldberg, A. Haaland and B. E. R. Schilling, *J. Chem. Soc., Dalton Trans.*, 1986, 2387.
12 W.-P. Leung, W.-H. Kwok, F. Xue and T. C. W. Mak, *J. Am. Chem. Soc.*, 1997, **119**, 1145.
13 H. B. Yokelson, D. A. Siegel, A. J. Millevolte, J. Maxha and R. West, *Organometallics*., 1990, **9**, 1005.
14 J. T. B. H. Jastrzebski, P. A. van der Schaaf, J. Boersma, G. van Koten, M. C. Zoutberg and D. Heijdenrijk, *Organometallics*, 1989, **8**, 1373.
15 B. Gehrhus, P. B. Hitchcock and M. F. Lappert, unpublished work.
16 D. J. Watkin and L. J. Pearce, CAMERON, an interactive graphics editor, University of Oxford, 1993.

*Received in Basel, Switzerland, 9th June 1997; 7/03971I*

# Modelling the active sites of heterogeneous titanium-centred epoxidation catalysts with soluble silsesquioxane analogues

**Thomas Maschmeyer,*[a,b] Marek C. Klunduk,[a] Caroline M. Martin,[a] Douglas S. Shephard,[a] John Meurig Thomas[b] and Brian F. G. Johnson*[a]**

[a] *The University Chemical Laboratories, The University of Cambridge, Lensfield Road, Cambridge, UK CB2 1EW*
[b] *Davy Faraday Research Laboratories, The Royal Institution of Great Britain, 21 Albemarle Street, London, UK W1X 4BS*

**By synthesising and structurally characterising new soluble titanosilsesquioxanes, and by following the dynamics of epoxidation of cyclohexene in their presence, the tripodally anchored $Ti^{IV}$ active sites in Ti–$SiO_2$ heterogeneous catalysts are modelled structurally and catalytically.**

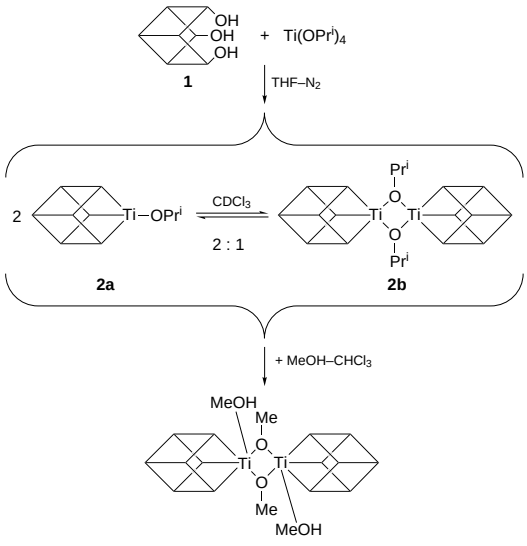
There is a growing family of titanosilicates (*e.g.* titano-zeolite β,[1] TS-1,[2] TS-2,[3] ETS-10,[4] JDF-L1[5] and Ti-MCM41[6–8]) which are particularly good catalysts for the selective oxidation of organic molecules. Of these, Ti ↑ MCM41 (in which isolated, accessible $Ti^{IV}$ ions are grafted to the inner surface of the mesoporous silica MCM41 using titanocene dichloride as precursor) exhibits high performance in the epoxidation of alkenes under mild conditions.[9,10]

As direct studies of the active site in heterogeneous systems are difficult, modelling studies, by either chemical or computational methods,[11] are essential in any attempts to elucidate the full characteristics of the active site(s). It is therefore desirable to prepare soluble molecular titanosilicates, especially since previously a similar strategy has proved helpful in the elucidation of the nature of the active site in Os- and Cr-containing silicas.[12]

We extend earlier modelling studies[13,14] by going beyond the simulation of just the first step of anchoring titanocene dichloride to the silica surface; the coordination environment after removal of the cyclopentadienyl ligand is modelled by reacting the well characterised cubic trisilanols [(c-pentyl)$_7$-$Si_7O_9(OH)_3$], **1a**, and [(c-hexyl)$_7Si_7O_9(OH)_3$], **1b**, with titanium tetra(isopropoxide) in tetrahydrofuran (THF) (Scheme 1).†

Three of the four titanium isopropoxide ligands of the trisilanols were substituted yielding titanosilsesquioxane **2** of formula [(c-pentyl)$_7Si_7O_9Ti(OPr^i)]_n$·THF with loosely coordinated THF molecules. On extraction in hexane and recrystallisation from chloroform it is possible to displace the THF molecules and obtain pure **2**.‡ Studies of the $^{13}C$ NMR spectrum of this compound in $CDCl_3$ show an equilibrium between the four-coordinate monomer **2a** and five-coordinate dimer **2b**. A related dimeric $Ti^{III}$ silsesquioxane without additional alkoxide ligands has been observed previously.[15] These monomeric and dimeric forms are easily identified on the basis of their cycloalkyl *ipso*-carbon resonances.[16] In addition, bridging[17] and terminal[18] isopropoxide ligands have been identified, by both $^1H$ and $^{13}C$ NMR spectroscopy, the relative ratios of which indicate a monomer–dimer ratio of *ca.* 2 : 1 in $CDCl_3$ at room temp.[17]

Addition of methanol to a solution of **2** in $CDCl_3$ leads to fast ligand exchange and the almost exclusive formation of the six-coordinate dimer, titanosilsesquioxane **3**. Interestingly, no monomeric species could be observed in solution by NMR spectroscopy.[17] By switching from trisilanol **1a** to **1b** it has been possible to isolate a single crystal of **3** suitable for X-ray diffractive analysis and to establish its molecular structure (Fig. 1).§




**Scheme 1**

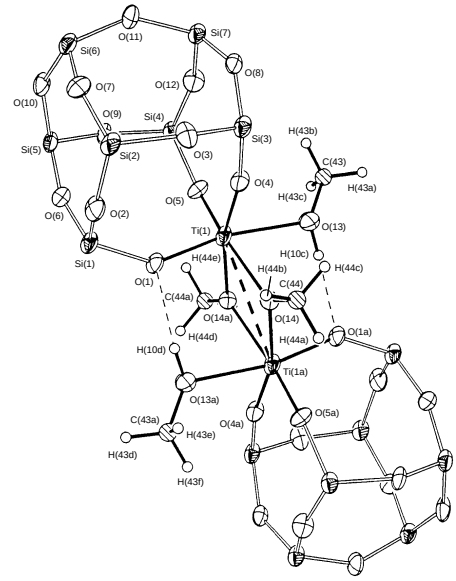



**Fig. 1** Molecular structure of **3**, showing the atomic labelling scheme and H-bonding interactions in the dimer. Principal bond distances (Å) and angles (°): Ti(1)–O(1) 1.837(7), Ti(1)–O(13) 2.210(7), Ti(1)–O(14) 2.004(7), Ti(1)–O(14a) 2.022(7), Ti(1)···Ti(1a) 3.253(4), mean Si–O 1.619(8); O(1)–Ti(1)–O(4) 98.4(3), O(1)–Ti(1)–O(5) 100.6(3), O(1)–Ti(1)–O(13) 168.8(3); H(10d)–O(1) 1.985 Å shows directionality w.r.t the O(1) lone pair, O(13a)-H(10d)-O(1) 147.6, $C_6H_{11}$ groups are omitted for clarity. Symmetry operation: $-x, -y, -z$.

The molecule is composed of two quasi-cubic silsesquioxanes related by a centre of inversion which lies between the two titanium atoms. These in turn are linked by two bridging methoxy groups with a mean Ti–O bond distance of 2.014(7) Å. The sixth position in the coordination sphere around the titanium is occupied by a datively bonded methanol group. The mean Ti–O silsesquioxane bond distance of 1.826(7) Å corresponds closely to that of grafted Ti ↑ MCM41 determined by EXAFS spectroscopy and calculational studies (1.81 Å and 1.82 Å, respectively).[9,11] The Ti–O distance of the datively coordinated methanol group [2.213(7) Å] corresponds closely to that observed for the Ti–substrate interaction (2.25 Å), observed for Ti ↑ MCM41 in its reactive state. This suggests a similar dative bonding of the substrate (most likely the peroxide, *cf*. Ti–O bonding distance of 2.26 Å in a *tert*-butylperoxotitanium complex[19]) to the titanium centre of the heterogeneous catalyst.

Dimer **2b** provides one free coordination site per titanium centre and the monomer **2a** two, allowing interactions with substrate molecules. Reactions with various peroxides showed that yellow peroxide complexes were readily formed, $\lambda_{max}$ = 320 nm, indicative of $\eta^2$-coordinated peroxide.[20]

Monomer **2a**, with its readily available second free coordination site on the same titanium centre, makes this a close model for the postulated tripodally surface-anchored titanium monohydroxide proposed for grafted Ti ↑ MCM41.

Model compound **2** displays catalytic activity which compares well with earlier studies† in that after 1 h at 50 °C, 48% conversion was achieved for the epoxidation of cyclohexene with tetrabutylperoxyhydroxide (TBPH) in $CDCl_3$ using a catalyst–substrate ratio of 1 : 70 : 70 with 98% selectivity towards the epoxide. When comparing its turnover frequency (TOF) with that of the actual grafted Ti ↑ MCM41 catalyst (3 mmol cyclohexene g $cat^{-1}$ $min^{-1}$) under identical conditions,¶ a TOF of 0.7 mmol g $cat^{-1}$ $min^{-1}$ was observed, resulting in 13% conversion after 1 h. Interestingly, the titanosilsesquioxane **3** exhibited a much higher TOF (4.8 mmol cyclohexene g $cat^{-1}$ $min^{-1}$) resulting in 93% conversion after 1 h. Importantly, the catalytic conversion of cyclohexene to the epoxide is highly selective (98%) for both catalysts.

The lower performance of titanosilsesquioxane **2** relative to **3** runs counter to simple expectation as **3** is coordinatively saturated and the dimer–monomer equilibrium established for **2** shows it has free coordination sites. This result might be taken to imply a synergistic effect of the two titanium centres being in close proximity. However, such an effect has not been claimed for the Sharpless catalyst $[Ti(tartrate)(OR)_2]_2$ which is structurally related to **3**,[21] nor is there any evidence for it in heterogeneous catalysts, where it is well established that the TOF per titanium centre increases with their increased dispersion and isolation

Therefore, we have also prepared a series of titanosilsesquioxanes, encompassing methoxy, butoxy and isopropoxy groups at the fourth coordination site and find that the reactivity of these catalysts is indeed dependent upon the nature of the alkoxy group (in the order of decreasing activity : MeO > $OBu^t$ ≫ $OPr^i$). The longer, but linear, butoxy group allows better access to the titanium centre than the shorter, but non-linear, isopropoxy group, further suggesting that accessibility to the tetrahedral $Ti^{IV}$ centre is the main parameter controlling reactivity.

We are grateful for the support of the EPSRC, the EU and ICI.

## Footnotes and References

* E-mail: tm212@cus.cam.ac.uk or thomas@ri.ac.uk

† Typical yield over 90% based on the silsesquioxane.

‡ *Selected spectroscopic data* for **2** (mixture of **2a** and **2b**): $^1$H NMR ($CDCl_3$, 400 MHz, 295 K) $\delta$ 0.97 (m, 7 H, *ipso*-H), 1.21 [d, 4.3 H, terminal $OCH(CH_3)_2$], 1.18 [d, 2.1 H, bridging $OCH(CH_3)_2$], 1.52 (m, 36 H), 1.73 (m, 20 H), 4.00 [m, $OCH(CH_3)_2$] 3.93 [m, $OCH(CH_3)_2$]; $^{13}C\{^1H\}$ NMR ($CDCl_3$, 400 MHz, 295 K) $\delta$ 21.98, 22.08, 22.20 [s, 1 : 3 : 3, CH, *ipso*-C (monomer)], 21.52, 22.54, 22.62, 22.65, 22.67; [1 : 2 : 1 : 2 : 1, s, CH, *ipso*-C(dimer)], 25.30 [s, $CH_3$, bridging $OCH(CH_3)_2$], 25.71 [s, $CH_3$, terminal $OCH(CH_3)_2$], 26.59, 26.81, 26.83, 26.87, 26.94, 26.97, 27.03, 27.09, 27.16, 27.20, 27.27, 27.29, 27.33, 27.34, 27.36 (s, $CH_2$, unassignable), 72.20 [s, CH, terminal $OCH(CH_3)_2$]; *m/z* ($FAB^+$): 919 (M − $OPr^i$), 876 [(M + $2H_2O)^+ - 2C_5H_9$], 858 [(M + $2H_2O)^+ - 2C_5H_9$], 840 ($M^+ - 2C_5H_9$); UV–VIS (THF) $\lambda$/nm ($\lambda_{max}$/nm): 210–340 (260) (2 only), 210–500 (260, 320) (pre-catalysis), 210–370 (260) (post-catalysis).

For **3**: $^1$H NMR ($CDCl_3$, 400 MHz, 295 K) $\delta$ 0.63, 0.73 (br m, 13 H, *ipso*-H), 1.19, 1.20 (br m, 71 H, cyclohexyl $CH_2$), 1.63, 1.69, 1.72 (br m, 73 H, cyclohexyl $CH_2$ and $HOCH_3$), 3.48 (br s, 6.3 H, $HOCH_3$), 4.05 (br s, 3.3 H, bridging $OCH_3$); $^{13}C\{^1H\}$ NMR ($CDCl_3$, 400 MHz, 295 K) $\delta$ 23.22, 23.49 (br s, 5 : 2, *ipso*-C), 26.67, 26.76, 26.90, 26.97, 27.55, 27.67 (s, cyclohexyl $CH_2$, unassignable), 51.2 (br s, bridging $OCH_3$). Satisfactory elemental analyses obtained.

§ *Crystal data* for **3**: $C_{88}H_{168}O_{28}Si_{14}Ti_2$, 0.40 × 0.30 × 0.12 mm, $T$ = 150 K, $M$ = 2163.28, triclinic, space group $P\bar{1}$ (no. 2), $a$ = 15.748(5), $b$ = 16.911(7), $c$ = 11.742(2) Å, $\alpha$ = 106.88(2), $\beta$ = 96.78(2), $\gamma$ = 101.40(3)°, $U$ = 2882(2) Å$^3$, $Z$ = 1, $D_c$ = 1.247 Mg m$^{-3}$, $\lambda$ = 0.71069 Å, $F(000)$ = 1160, $R_1$ = 0.0826 [3029 reflections with $I > 2\sigma(I)$], $wR_2$ = 0.2235 for 5354 independent reflections corrected for adsorption [$\mu$(Mo-K$\alpha$) = 0.350 mm$^{-1}$] and 370 parameters [Ti, Si and O atoms anisotropic, except O(14)]. Structure solved by direct methods.[22] Refinement and all other calculations performed using SHELXL 93.[23] CCDC 182/569.

¶ The catalytic oxidation reactions of cyclohexene with tetrabutylperoxyhydroxide (TBPH) were performed analogously to the procedure outlined in ref. 9, *i.e.* under argon following standard procedures, at 40 °C with a ratio of 1 : 12 cyclohexene–TBPH and a cyclohexene–catalyst ratio of 1 : 0.05 by mass, using an 8% solution of cyclohexene in dry chloroform.

1 D. H. Olson and W. M. Meier, *Zeolites*, 1996, **17**, 1.
2 M. Taramasso, G. Perego and B. Notari, *US Pat.*, 4410501, 1983.
3 B. Notari, *Adv. Catal.*, 1996, **41**, 253.
4 M. W. Anderson, O. Terasaki, T. Ohsuna, A. Philipou, S. P. MacKay, A. Ferreira, J. Rocha and S. Lindin, *Nature*, 1994, **367**, 347.
5 M. A. Roberts, G. Sankar, J. M. Thomas, R. H. Jones, H. Du, J. Chen, W. Pang and R. Xu, *Nature*, 1996, **381**, 410.
6 A. Corma, M. T. Navarro and J. Pérez-Periente, *J. Chem. Soc., Chem. Commun.*, 1994, 147.
7 P. T. Tanev, M. Chibwe and T. J. Pinnavaia, *Nature*, 1994, **368**, 321.
8 G. Sankar, F. Rey, J. M. Thomas, G. N. Greaves, A. Corma, B. R. Dobson and A. J. Dent, *J. Chem. Soc., Chem. Commun.*, 1994, 2279; J. M. Thomas, *Nature*, 1994, **368**, 289.
9 T. Maschmeyer, F. Rey, G. Sankar and J. M. Thomas, *Nature*, 1995, **378**, 159.
10 R. D. Oldroyd, P. A. MacFaul, T. Maschmeyer, J. M. Thomas, D. W. Snelgrove, K. U. Ingold and D. D. M. Wayner, *Angew. Chem., Int. Ed. Engl.*, 1996, **35**, 2787.
11 P. Sinclair, G. Sankar, C. R. A. Catlow, J. M. Thomas and T. Maschmeyer, *J. Phys. Chem.*, 1997, **101**, 4232; F. J. Feher and R. L. Blanski, *J. Chem. Soc., Chem. Commun.*, 1990, 1614; T. Maschmeyer, PhD Thesis, The University of Sydney, 1994.
12 T. Maschmeyer, J. M. Thomas and A. F. Masters, *NATO ASI Ser., New Trends in Materials Chemistry*, in the press.
13 T. Maschmeyer, C. M. Lindall, A. F. Masters and L. D. Field, *Aust. J. Chem.*, 1994, **47**, 1127; T. Maschmeyer, A. F. Masters, I. Buys, T. W. Hambley and A. K. Smith, *J. Mol. Catal.*, 1994, **86**, 309; T. Maschmeyer, C. M. Lindall, A. F. Masters, L. D. Field, T. W. Hambley and A. K. Smith, *Chem. Aust.*, 1993, **7**, 333.
14 H. Abbenhuis, S. Krijnen and R. van Santen, *Chem. Commun.*, 1997, 331.
15 F. J. Feher, S. L. Gonzales and J. W. Ziller, *Inorg. Chem.*, 1988, **27**, 3440.
16 F. J. Feher, T. A. Budzichowski, R. L. Blanski, K. J. Weller and J. W. Ziller, *Organometallics*, 1991, **10**, 2526.
17 A. R. Siedle and J. C. Huffman, *Inorg. Chem.*, 1990, **29**, 3131.
18 T. J. Boyle, D. L. Barnes, J. A. Heppert, L. Morales and F. Takusagawa, *Organometallics*, 1992, **11**, 1112.
19 G. Boche, K. Möbus, K. Harms and M. Marsch, *J. Am. Chem. Soc.*, 1996, **118**, 2770.
20 R. Guilard, J.-M. Latour, C. Lecomte, J.-C. Marchon, J. Protas and D. Ripoll, *Inorg. Chem.*, 1978, **17**, 1228.
21 M. G. Finn and K. B. Sharpless, *J. Am. Chem. Soc.*, 1991, **113**, 113.
22 G. M. Sheldrick, SHELXS 86, Program for crystal structure solution, *Acta Crystallogr., Sect. A*, 1990, **46**, 467.
23 G. M. Sheldrick, SHELXL 93, Program for crystal structure refinement, University of Göttingen, Germany, 1993.

*Received in Basel, Switzerland, 27th May 1997, 7/03642F*

# Co-ZSM-5 and Mn-ZSM-5 synthesised directly from aqueous fluoride gels

**Catherine I. Round, Craig D. Williams* and Catherine V. A. Duke**

*University of Wolverhampton, School of Applied Sciences, Wulfruna Street, Wolverhampton, UK WV1 1SB*

**Isomorphously substituted zeolite ZSM-5 is synthesised using an aqueous, slightly acidic, fluoride medium incorporating tetrahalometallate compounds of cobalt and manganese; final products were characterised using XRD, SEM, XRF, FTIR, TG–DTA, and evidence of metal incorporation into the zeolite framework is given.**

Zeolite ZSM-5 is a catalyst of great industrial importance owing to its reactant, product and transition-state selectivity.[1] Modification to acid site strengths and density by isomorphic substitution of transition-metal elements can enhance catalytic activity, stability and selectivity. For example methane is generally regarded as a non-selective reducing agent, yet a cobalt or manganese exchanged HZSM-5 has proved to be an effective catalysts for the selective catalytic reduction of $NO_x$ by methane, with excess oxygen.[2–4]

Zeolite gels are normally prepared from solutions of silicates and aluminates at high pH. The as-synthesised material is then calcined and ion-exchanged with acid or ammonium salts to produce the Brønsted- and Lewis-acid sites necessary for catalytic activity. Metals are exchanged into the zeolite matrix by such complex secondary synthesis methods as cation exchange using metal nitrate solutions[5] and impregnation by metal carbonyl vapour.[6] The metal either inserts into lattice defect sites, or it acts as a charge balancing species which can then migrate and agglomerate at the external surface.[7,8]

This work reports the synthesis of Co-ZSM-5 and Mn-ZSM-5 by primary synthesis methods, employing a non-alkaline aqueous fluoride medium. Synthesis in a fluoride medium, replacing $OH^-$ with $F^-$ as a mineralising agent has been extensively studied in recent years.[9,10] It allows controlled nucleation and slower growth rates resulting in larger crystals with fewer lattice defects.[10]

Pure silica ZSM-5 was synthesised from a gel with molar composition $0.25HF : 0.75NaF : 0.25NaCl : 1.25TPABr : 10SiO_2 : 330H_2O$.[11] CAB-O-SIL M5 fumed silica (BDH 98%) was dispersed in deionised water, NaF (Fluka Chemika 99%) and HF (Fluka Chemika, puriss 40%) were added to the silica slurry, NaCl (General purpose reagent) and TPABr (Aldrich 98+%) added last and stirred by hand to homogeneity. Gels were heated to 170 °C in Teflon-lined reaction vessels. Samples were removed at regular intervals, quenched, filtered and dried at 40 °C. X-Ray powder diffraction (XRD) analysis confirmed highly crystalline ZSM-5 had been synthesised (Fig. 1). Scanning electron microscopy (SEM) analysis showed elongated prismatic crystals, typical of ZSM-5[12] 490–570 μm long.

$[NEt_4]_2[CoCl_4]$ and $[NPr_4]_2[MnBr_4]$ were crystallised as salts of large organic cations.[13] These tetrahedral tetrahalometallates have been used successfully in the synthesis of a number of highly substituted aluminophosphate zeotypes[14] but are unstable in basic conditions. The reaction gels for the metal substituted zeolites had a molar composition of $0.25HF : 0.75NaF : 0.25NaCl : 1.25\ (1 - x)$ TPABr : $x[NR_4]_2[MX_4] : 10SiO_2 : 330H_2O$ where $x$ is in the range 0–0.5, and $[NR_4]_2[MX_4]$ represents $[NEt_4]_2[CoCl_4]$ or $[NPr_4]_2$-$[MnBr_4]$. Molar compositions of the various reaction gels, and the products formed are listed in Table 1.

XRD analysis showed the products to be crystalline with the orthorhombic space group *Pnma* (Fig. 1). The volume of the unit cell, given in Table 2, increases with the levels of gel substitution.

SEMs of the substituted systems showed a change in crystal morphology. The 0.1 mole fraction cobalt system produced smaller crystals *ca*. 80–100 μm in length with irregular facets. This system showed a decreasing level of crystallinity inversely proportional to the level of substitution, which could be attributed to the increasing mole fraction of the associated $TEA^+$. The manganese system at 0.1 mole fraction showed an average crystal length of *ca.* 165 μm with the appearance of raised faces along the crystallographic *c* axis. The 0.2 Mn

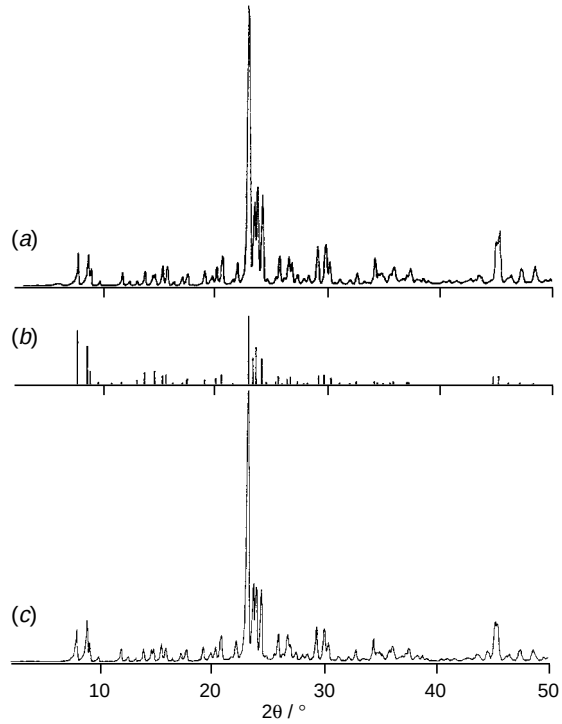



**Fig. 1** (*a*) XRD pattern of protonated pure silica ZSM-5, (*b*) JCPDS pattern 37-359 and (*c*) XRD pattern of Mn : Si substituted at 0.2 mole fraction

**Table 1** Molar compositions of reaction gels

| TPABr | $TEA_2CoCl_4$ | $TPA_2MnBr_4$ | Start pH | Final pH | Product[a] |
|---|---|---|---|---|---|
| 1.25 | | | 6.3 | 5.5 | 37-359 ZSM-5 |
| 1.05 | 0.1 | | 6.0 | 4.5 | 37-359 |
| 0.85 | 0.2 | | 6.2 | 5.3 | 37-359 |
| 0.65 | 0.3 | | 5.4 | 3.5 | 37-359[b] |
| 1.05 | | 0.1 | 5.9 | 5.3 | 37-359 |
| 0.85 | | 0.2 | 6.1 | 5.4 | 37-359 |
| 0.65 | | 0.3 | 5.5 | 5.2 | 37-359 |
| 0.25 | | 0.5 | 5.0 | 4.8 | Amorphous |

[a] With reference to XRD (JCPDS) on-line analysis standard reference patterns. [b] Poorly crystalline material.

**Table 2** Chemical analysis and unit-cell parameters

| M mol | Chemical formulation[a] | LOI[b] (%) | $U^c$/Å$^3$ |
|---|---|---|---|
| —[d]— | $Si_{95.2}Zn_{0.7}Na_{0.1}O_{192}\cdot 12.3H_2O$ | 11.8 | 5306[e] |
| Co 0.05 | $Si_{95.6}Co_{0.18}Zn_{0.2}Na_{0.12}O_{192}\cdot 12H_2O$ | 13.2 | 5310 |
| Co 0.1 | $Si_{95.2}Co_{0.7}Zn_{0.1}Na_{0.2}O_{192}\cdot 11.8H_2O$ | 11.2 | 5354 |
| Co 0.15 | $Si_{94.9}Co_{0.7}Zn_{0.4}O_{192}\cdot 12.4H_2O$ | 10.4 | 5370 |
| Co 0.2 | $Si_{94.5}Co_{1.2}Zn_{0.3}O_{192}\cdot 12.6H_2O$ | 11.2 | 5455 |
| Co 0.3 | $Si_{92.9}Co_{2.9}Zn_{0.1}O_{192}\cdot 12H_2O$ | 6.87 | 5071 |
| Mn 0.05 | $Si_{95.5}Mn_{0.1}Zn_{0.3}Na_{0.2}O_{192}\cdot 12H_2O$ | 12.2 | 5371 |
| Mn 0.1 | $Si_{95.3}Mn_{0.3}Zn_{0.3}Na_{0.1}O_{192}\cdot 10.9H_2O$ | 12.1 | 5110 |
| Mn 0.15 | $Si_{95.3}Mn_{0.5}Zn_{0.1}Na_{0.2}O_{192}\cdot 11.4H_2O$ | 14.1 | 5305 |
| Mn 0.2 | $Si_{94.9}Mn_{0.7}Zn_{0.4}Na_{0.1}O_{192}\cdot 12.3H_2O$ | 12.1 | 5360 |
| Mn 0.3 | $Si_{95.2}Mn_{0.6}Zn_{0.3}Na_{0.1}O_{192}\cdot 12.2H_2O$ | 10.7 | 5381 |
| Mn 0.5 | —[f]— | 11.4 | —[g]— |

[a] X-Ray fluorescence. [b] Loss on ignition determined by TG. [c] Unit-cell volume. [d] Pure Si form. [e] Lit. value for ZSM-5 = 5332 Å.[16] [f] Not obtained, poorly crystalline. [g] Not obtained.

system had smaller crystals, *ca.* 60 μm and there was crystal twinning along both *b* and *c* crystallographic axes with raised faces still evident (see graphical abstract). The reduction in crystal sizes is similar to that observed by Dwyer *et al.*,[15] and the raised faces indicates that crystallisation has occurred in a less supersaturated medium.[10]

TG losses on ignition (LOI) for the most crystalline samples compare well with the literature value[11] of 12%. The manganese substituted series has one type of templating species, $TPA^+$, and shows a two stage mass loss above 300 °C. The DTA trace shows a regular increase in the second stage mass loss, at the higher temperature, with increasing levels of substitution. The small mass losses, below 300 °C, in both the cobalt and the manganese systems are attributed to the water content, or to the two types of template cations either on the crystal surface or associated to anionic surface species ($F^-$ or $CoO_2^{2-}$).

The DTA trace in the cobalt system, also shows a two-stage mass loss above 300 °C. This system contains two types of templating species, $TPA^+$ and $TEA^+$ as the levels of substitution are increased. However, according to Szostak,[16] a two-stage mass loss is due to two types of $TPA^+$ species. The first type is occluded in the zeolite channels, it is less strongly bound and is lost at a lower temperature. The second type is a more strongly bound counter ion species and is lost at a higher temperature. The counter ions could be associated with an occluded fluoride anion or to a negatively charged $MO_4^{2-}$ coordinated into the silica framework. The fluoride in the gel has remained constant at 1 mole fraction, the increase in the template loss therefore could be due to those cations associated with the increased mole fraction of heteroatoms.

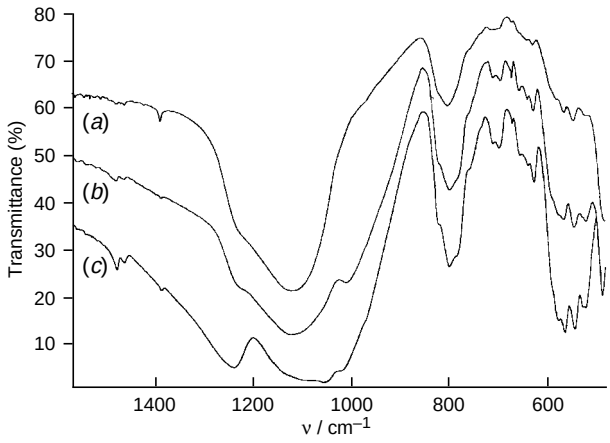



**Fig. 2** FTIR transmission spectra of (*a*) pure silica ZSM-5, (*b*) cobalt 1.5 mole fraction and (*c*) manganese 1.5 mole fraction

FTIR transmission spectra of the pure silica ZSM-5 closely matched literature spectra.[17] Substitution of cobalt and manganese into ZSM-5 resulted in a broadening in the T–O–T asymmetric stretching region, ranging from 1230 to 1085 $cm^{-1}$ (Fig. 2), which indicates heteroatom substitution.

It is clear from the analytical data that there are changes in the substituted materials compared with the pure silica form. This work represents levels of substitution comparable to levels currently reported but with the advantage of using a simple primary synthesis procedure. The materials produced in a fluoride medium do not require complex ion-exchange procedures to obtain the protonated form necessary for catalytic activity.

## Footnote and References

* E-mail: c.williams@wlv.ac.uk

1 R. M. Barrer and J. Klinowski, *Philos. Trans. R. Soc. London Ser. A*, 1977, **285**, 637.
2 Y. Li and N. J. Armor, *Appl. Catal. Lett. B: Environ.*, 1993, **2**, 239.
3 Y. Li and N. J. Armor, *Appl. Catal. Lett. B: Environ.*, 1992, **1**, L31.
4 T. Sun, L. M. Trudeau and J. Y. Ying, *J. Phys. Chem.*, 1996, **100**, 13662.
5 J. M. Stencel, V. U. S. Rao, J. R. Diehl, K. H. Rhee, A. G. Dhere and R. J. DeAngelis, *J. Catal.*, 1983, **84**, 109.
6 A. G. Dhere and R. J. DeAngelis, *J. Catal.*, 1985, **92**, 145.
7 J. A. Rossin, C. Saldarriaga and M. E. Davis, *Zeolites*, 1987, **7**, 295.
8 T. Inui, J. Kim and T. Takeguchi, *Zeolites*, 1996, **17**, 354.
9 J. L. Guth, H. Kessler, P. Caullet, J. Hazm, A. Merrouche and J. Patarin, *Proceedings of the 9th International Zeolite Conference Montreal*, ed. R. Von Ballmoos, Butterworth Heinemann Press, 1993, p. 215.
10 H. Kessler, J. Patarin and C. Schott Darie, *Stud. Surf. Sci. Catal.*, 1995, **85**, 75.
11 A. Tavolaro, R. Mostowicz, F. Crea, A. Nastro, R. Aiello and J. B. Nagy, *Zeolites*, 1992, **12**, 756.
12 Zhao Daquing, Qui Shilun and Pang Wenqin, *Proceedings of the 9th International Zeolite Conference Montreal*, ed. R. Von Ballmoos, Butterworth Heinemann Press, 1993, pp. 337–344.
13 N. S. Gill and F. B. Taylor, *Inorg. Synth.*, 1969, **8**, 136.
14 C. V. A. Duke, S. J. Hill and C. D. Williams, *Zeolites*, 1995, **15**, 413.
15 J. Dwyer, J. Zhao and D. Rawlence, *Proceedings of the 9th International Zeolite Conference Montreal*, ed. R. Von Ballmoos, Butterworth Heinemann Press, 1992, pp. 155–160.
16 R. Szostak, *Handbook of Molecular Sieves*, Van Nostrand Reinhold, New York, 1992, pp. 518–528.
17 A. Miecznikowski and J. Hanuza, *Zeolites*, 1987, **12**, 249.

*Received in Cambridge, UK, 13th June 1997; 7/04148I*

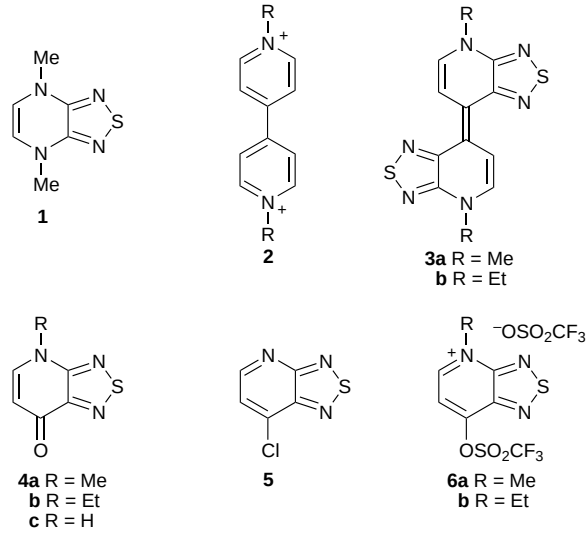
# Synthesis and characterization of new electron donors containing 1,2,5-thiadiazole and 1,1′-dihydro-4,4′-bi(pyridylidene) units

**Yoshiro Yamashita,* Katsuhiko Ono, Masaaki Tomura and Kenichi Imaeda**

*Institute for Molecular Science, Myodaiji, Okazaki 444, Japan*

**Novel electron donors composed of the title heterocycles are highly polarized and afford cation radical salts and charge transfer complexes with interesting crystal structures.**

Molecules containing 1,2,5-thiadiazole rings have been used as components of organic conductors.[1] Introduction of this electron-withdrawing heterocycle to strong electron-donating skeletons leads to novel highly-polarized electron donors.[2–4] In some cases, interesting molecular networks are formed by intermolecular interactions between the heteroatoms of the thiadiazoles. For example, 4,7-dimethyl-4,7-dihydro-




[1,2,5]thiadiazolo[3,4-*b*]pyrazine **1** is a highly-polarized strong electron donor which forms a sheet-like network in the crystal.[2] On the other hand, viologens **2** are widely used as electron-transfer reagents since they are easily prepared and show well-defined redox processes.[5] Although viologens are stable in air, their cation radical and neutral states are unstable toward oxygen due to their very low oxidation potentials. We have now fused 1,2,5-thiadiazole rings to the dihydrobipyridine skeleton in order to enhance the stability of the neutral state of viologens. The compounds **3** are expected to be highly polarized and form a tape-like network with short S···N contacts, as are found in the related bis[1,2,5]thiadiazole derivatives.[6] We report here the preparation and properties of **3** and its cation radical salts and charge-transfer complexes.

Thiadiazolopyridone derivative **4a** was obtained from chloropyridine derivative **5**.[4] The ethyl derivative **4b** was prepared by ethylation of **4c**, which was obtained by hydrolysis of **5** with hydrochloric acid. Reaction of **4a**,**b** with trifluoromethanesulfonic anhydride afforded pyridinium compounds **6a**,**b**. The bi(pyridothiadiazolylidene)s **3a**,**b** were obtained by reduction of **6a**,**b** with zinc in acetone. The yields of **3** from **4** were 20–40% over two steps. The donors **3a**,**b** are stable in air, in contrast to the unstable neutral viologens. They have absorption maxima in the long wavelength region (**3a**: 623, **3b**: 627 nm in $CH_2Cl_2$), which are regarded as the intramolecular charge-transfer bands. Their cyclic voltammograms showed reversible two-stage one-electron oxidation waves (**3a**: 0.27, 0.57 V, **3b**: 0.26, 0.56 V).† Their oxidation potentials are higher than those of methylviologen (−0.40, −0.81 V),[5] leading to the stability of **3**. This is attributed to the electron-withdrawing properties of the thiadiazole ring. However, the values are lower than those of tetrathiafulvalene (TTF) (0.46, 0.87 V) measured under the same conditions, indicating that they are stronger electron donors than TTF. The difference between the first and second oxidation potential in **3** (0.30 V) is smaller than that in TTF (0.41 V), methylviologen (0.41 V) and **1** (0.80 V),[2] indicating that the on-site Coulomb repulsion in **3** is decreased due to extended π-conjugation.

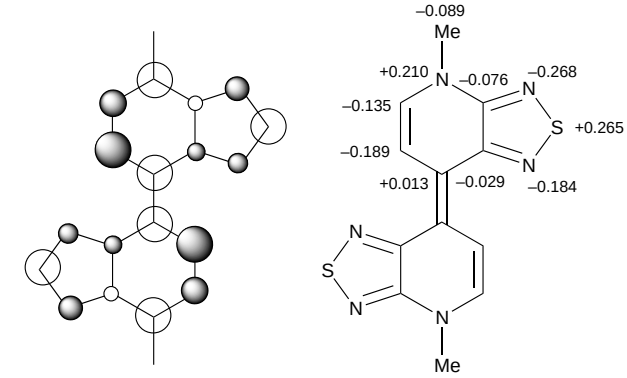



**Fig. 1** HOMO and net atomic charges of **3a** calculated by the PM3 method

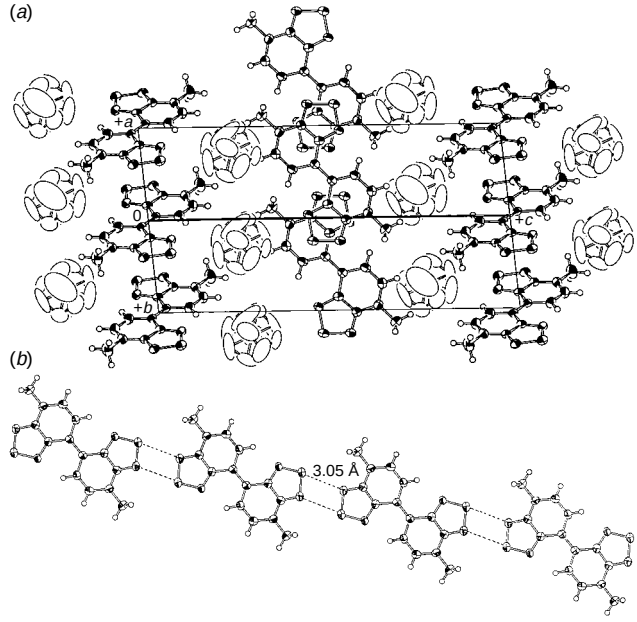



**Fig. 2** (*a*) Crystal structure of **3a**–$PF_6$; (*b*) tape-like network

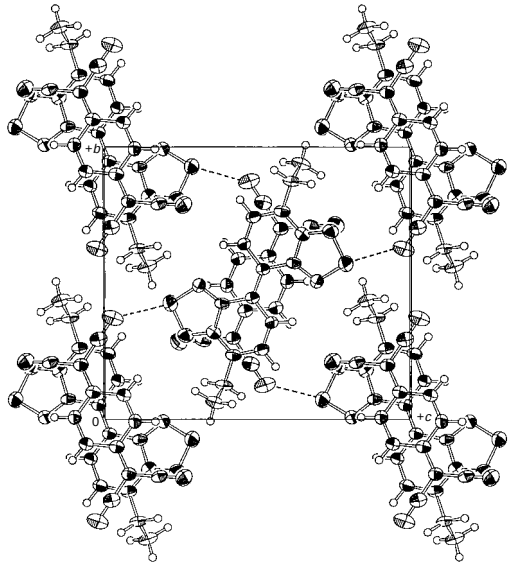



**Fig. 3** Crystal structure of **3b**–TCNQ

The HOMO and net atomic charges of **3a** calculated by the PM3 method[7] are shown in Fig. 1. The charge distribution indicates that the sulfur atom is positively charged and the nitrogen atoms of the thiadiazoles are negatively charged. For this polarized structure, short S···N contacts between the thiadiazole rings are expected to give a molecular network. There may be an electronic interaction through the S···N contacts in the cation radical state since these atoms have fairly large coefficients in the HOMO.

The donor **3a** gave $PF_6$ and $AsF_6$ salts of the cation radical upon electrochemical oxidation in $CH_2Cl_2$. They are 1 : 1 salts and show low conductivities (**3a**–$PF_6$: $8 \times 10^{-5}$ S cm$^{-1}$ as a compressed pellet, **3a**–$AsF_6$: $5 \times 10^{-4}$ S cm$^{-1}$ as a single crystal). The temperature dependence of the conductivity of the $AsF_6$ salt showed semiconductive behaviour, with an activation energy of 0.27 eV. The structures of the salts are isomorphous.‡ The crystal structure of the $PF_6$ salt is shown in Fig. 2. The planar donor molecules are stacked in an interesting mode where one donor molecule bridges two other molecules. Another interesting feature is that a tape-like network of the donor molecules is formed by short S···N contacts (3.05 Å) as expected. The counter anions exist between the molecular tapes which are arranged in two difference directions.

The donors **3a**,**b** afforded 1 : 1 charge-transfer complexes with tetracyanoquinodimethane (TCNQ). They showed moderate conductivities (**3a**–TCNQ: $1.6 \times 10^{-2}$ S cm$^{-1}$, **3b**–TCNQ: $4.9 \times 10^{-3}$ S cm$^{-1}$ as compressed pellets). We succeeded in preparing a single crystal of **3b**–TCNQ and carried out an X-ray crystal analysis.‡ The structure is shown in Fig. 3. The donor and TCNQ molecules form a mixed stack. The C–C bond length of the dicyanomethylene of the TCNQ molecule (1.416 Å) is comparable to that of TCNQ anion,[8] indicating that almost complete charge transfer occurs in the complex. An interesting feature is that short S···N contacts (3.15 Å) exist between the sulfur of the thiadiazole ring and the nitrogen of the cyano group, forming a two-dimensional network. This finding suggests that the inter-heteroatom interactions can be used for controlling the structures of charge transfer complexes.

This work was supported by a Grant-in-Aid for Scientific Research from the Ministry of Education, Science, Sports and Culture, Japan.

## Footnotes and References

* E-mail: yoshiro@ims.ac.jp

† *Conditions*: $Bu_4NBF_4$ (0.1 mol dm$^{-3}$) in PhCN, Pt electrode, scan rate 100 mV s$^{-1}$, V *vs.* saturated calomel electrode (SCE).

‡ *Crystal data* for **3a**–$PF_6$: $C_{12}H_{10}N_6S_2 \cdot PF_6$, $M$ = 447.35, monoclinic, space group $C2/c$, $Z$ = 4, $a$ = 11.7998(7), $b$ = 6.3967(5), $c$ = 22.030(2) Å, $\beta$ = 101.474(6)°, $V$ = 1629.6(2) Å$^3$, $D_c$ = 1.823 g cm$^{-3}$. The final $R$ value was 0.061 for 1663 reflections with $I > 2\sigma(I)$. For **3a**–$AsF_6$: $C_{12}H_{10}N_6S_2 \cdot AsF_6$, $M$ = 491.30, monoclinic, space group $C2/c$, $Z$ = 4, $a$ = 11.8546(3), $b$ = 6.3851(6), $c$ = 22.429(1) Å, $\beta$ = 101.51(3)°, $V$ = 1663.6(2) Å$^3$, $D_c$ = 1.962 g cm$^{-3}$. The final $R$ value was 0.088 for 1693 reflections with $I > 2\sigma(I)$. For **3b**–TCNQ: $C_{26}H_{18}N_{10}S_2$, $M$ = 534.62, monoclinic, space group $P2_1/n$, $Z$ = 2, $a$ = 7.1926(4), $b$ = 12.3259(9), $c$ = 14.1518(7) Å, $\beta$ = 104.575(4)°, $V$ = 1214.3(1) Å$^3$, $D_c$ = 1.46 g cm$^{-3}$. The final $R$ value was 0.049 for 1029 reflections with $I > 3\sigma(I)$. CCDC 182/565.

1 T. Naito, H. Kobayashi, A. Kobayashi and A. E. Underhill, *Chem. Commun.*, 1996, 521; Y. Yamashita, M. Tomura and K. Imaeda, *Chem. Commun.*, 1996, 2021.
2 Y. Yamashita, J. Eguchi, T. Suzuki, C. Kabuto, T. Miyashi and S. Tanaka, *Angew. Chem., Int. Ed. Engl.*, 1990, **29**, 643.
3 Y. Yamashita, S. Tanaka, K. Imaeda, H. Inokuchi and M. Sano, *Chem. Lett.*, 1992, 419.
4 K. Ono, S. Tanaka, K. Imaeda and Y. Yamashita, *J. Chem. Soc., Chem. Commun.*, 1994, 899.
5 T. M. Bockman and J. K. Kochi, *J. Org. Chem.*, 1990, **55**, 4127.
6 K. Ono, S. Tanaka and Y. Yamashita, *Angew. Chem., Int. Ed. Engl.*, 1994, **33**, 1977; Y. Yamashita, K. Ono, M. Tomura and S. Tanaka, *Tetrahedron*, 1997, **53**, 10 169.
7 J. J. P. Stewart, *J. Comput. Chem.*, 1989, **10**, 209, 221.
8 T. J. Kistenmacher, T. J. Emge, A. N. Bloch and D. O. Cowan, *Acta Crystallogr., Sect. B*, 1982, **38**, 1193.

*Received in Cambridge, UK, 23rd June 1997; 7/04375I*

# Optical nonlinearity of an open-shell and degenerate π-conjugated polymer: poly(4-oxyphenyl-1,2-phenylenevinylene) radical

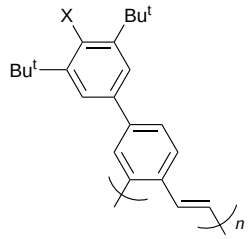
**Masahiro Takahashi,[a] Shinji Yamada,[b] Hiro Matsuda,*[b] Hachiro Nakanishi,[c] Eishun Tsuchida[a] and Hiroyuki Nishide*[a]**

[a] *Department of Polymer Chemistry, Waseda University, Tokyo 169, Japan*
[b] *National Institute of Materials and Chemical Research, Tsukuba 305, Japan*
[c] *Institute for Chemical Reaction Science, Tohoku University, Sendai 980-77, Japan*

**Third-order nonlinear optical susceptibility is enhanced by three orders of magnitude for the degenerate and high-spin ground state conjugated polymer, poly(4-oxyphenyl-1,2-phenylenevinylene), as compared with a precursor conjugated polymer with a closed-shell configuration, in a z-scan measurement.**

A great deal of research has been done on π-conjugated backbone polymers in regards to achieving sufficient third-order nonlinearity to produce optical devices.[1] Typical examples exhibiting this type of third-order nonlinear optical susceptibility ($\chi^{(3)}$) are poly(diacetylene)s[2] and poly(phenylenevinylene)s.[3] The authors at the National Institute in Tsukuba studied the optical nonlinearity of poly(diacetylene) derivatives that have π-conjugated side-chain groups,[4] and also recently measured $\chi^{(3)}$ values of their polymers with the z-scan method using a picosecond laser.[5]

On the other hand, much effort has been expended in synthesizing purely organic π-conjugated polyradicals which are in a high-spin or multiplet ground state and display molecular-based magnetism.[6] Some of the π-conjugated and alternant but non-Kekulé-type polymers that were substituted with polyradical groups satisfied the formulation based on MO or VB theory and yielded a stable radical or open-shell configuration and a degenerate high-spin ground state. Recently, the authors at Waseda University have for the first time succeeded in realizing this type of high-spin polymer, by synthesizing poly(1,2-phenylenevinylene) that is 4-substituted with a 3,5-di-*tert*-butyl-4-oxyphenyl group (**1a**).[7] The π-conjugated polyradical is characterized by the degenerate and delocalized single occupied molecular orbitals (SOMOs) on the poly(phenylenevinylene) backbone which overlap each other. The effective overlap integral of the SOMOs provides a spin-exchanging interaction sufficient to realize the high-spin ground state. This characteristic of the open-shell π-conjugated linear polymer bearing side-chain radical groups is in contrast to the electron configuration of open-shell but cross-conjugated polyradicals or radicals formed on the main chain,[8] where the SOMOs are localized in their diradial repeating unit.




**1a** X = O•
**b** X = OH

There has been only one research paper about the optical nonlinearity of a π-conjugated open-shell radical dye molecule. Zyss[9] studied 2-(4-nitrophenyl)-4,4,5,5-tetramethyl-4,5-dihydro-1*H*-imidazolyl-1-oxy 3-oxide which exhibits ferromagnetic behaviour below 0.9 K,[10] by the electric-field-induced second-harmonic generation method, but they could not find any differences in the nonlinear optical responses of the radical dye molecule. This is probably because the spin interaction in the radical molecules is caused by a through-space or intermolecular interaction between the radical, low-molecular-weight molecule and does not involve any overlapping of SOMOs.

π-Conjugated polymers with extensively delocalized electrons have highly nonlinear optical responses and numerous conjugated polymers with high third-order nonlinearities have been reported to try and understand their structure–property relationship and to provide a strategy for the synthesis of materials with large optical nonlinearities.[1,11] Here we have examined the possibility of a high-spin organic radical (open-shell) polymer, which possesses delocalized and degenerate SOMOs in its π-conjugated structure, as a nonlinear optical material.

The polyradical, poly[4-(3,5-di-*tert*-butyl-4-oxyphenyl-1,2-phenylenevinylene)] **1a**, was prepared *via* the oxidation of our precursor polymer **1b**.[7] The resulting brown–green powder with a molecular weight of 5100 and a spin (radical) concentration of 0.6 spin unit$^{-1}$ was soluble in common solvents such as $CHCl_3$, benzene and THF. The half-life of the polyradical in $CHCl_3$ solution was 3.4 days at room temperature. The UV–VIS absorption spectrum of the porlyradical **1a** (Fig. 1) involves π—π* absorption at $\lambda_{max}$ = 420 nm and broad absorption at *ca.* 680 nm. The former, which is based on the poly(1,2-phenylenevinylene) backbone, shifted bathochromically in comparison with that of **1b** ($\lambda_{max}$ = 350 nm), which can be ascribed to the development of π-conjugation or a

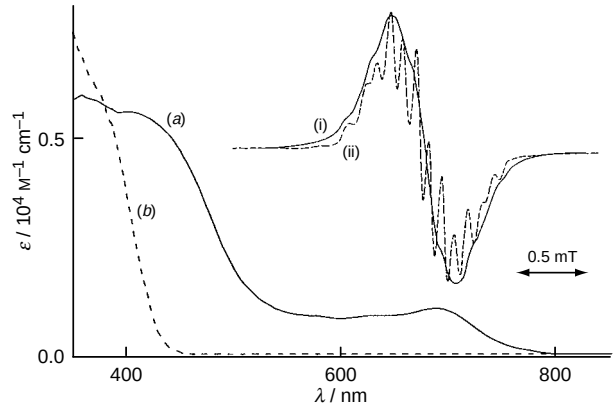



**Fig. 1** UV–VIS spectra of (*a*) polyradical 1a and (*b*) precursor polymer **1b**. Inset: solution EPR spectra of the radicals: (i) the polyradical **1a** at a low spin concentration, and (ii) 1-(3,5-di-tert-butyl-4-oxyphenyl)-3,4-di-styrylbenzene.

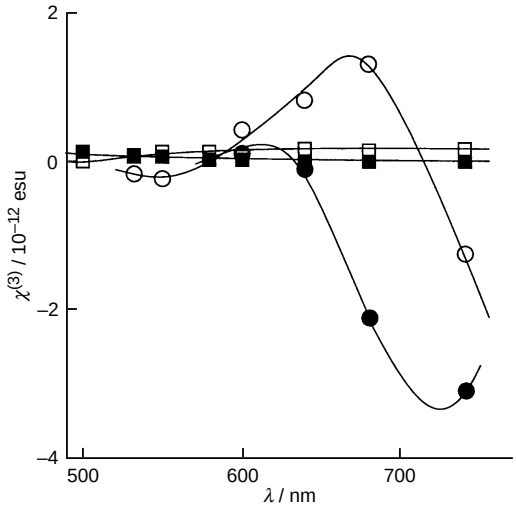



**Fig. 2** Wavelength dependency of Re$\chi^{(3)}$ and Im$\chi^{(3)}$ for a 0.091 wt% $CHCl_3$ solution of the polyradical **1a** [(○) Re$\chi^{(3)}$ and (●) Im$\chi^{(3)}$] and a 1.8 wt% $CHCl_3$ solution of the precursor **1b** [(□) Re$\chi^{(3)}$ and (■) Im$\chi^{(3)}$

narrowing of the band gap that was caused by radical SOMO generation between the HOMO and LUMO. The latter absorption is a n–π* forbidden transition which is similar to that of 2,4,6-tri-*tert*-butylphenoxyl.

The formation of the polyradical was recognized by a strong EPR signal (inset in Fig. 1). The EPR spectrum of **1a** at low spin concentration gave a broadened hyperfine structure at $g$ = 2.0043 due to an unresolved coupling of 5–7 protons of the phenyl ring and the phenylenevinylene backbone. The spin density distribution over the whole π-conjugation of **1a** was supported by the clear hyperfine structure (the dashed line in the inset in Fig. 1) of the repeating unit analogue, 1-(3,5-di-*tert*-butyl-4-oxyphenyl)-3,4-di-styrylbenzene,† which was ascribed to the coupling of 7–9 protons of the phenyl ring and two vinylenes. Static magnetic susceptibility and magnetization of **1a** were mesured with a SQUID magnetometer.‡ The former gave a spin concentration of 0.6, and the latter indicated quintet spin multiplicity at ground state.

The $\chi^{(3)}$ of the polyradical was measured with a z-scan laser setup.[5]§ The z-scan method has the following two advantages: (i) it can estimate both real and imaginary parts of $\chi^{(3)}$, Re$\chi^{(3)}$ and Im$\chi^{(3)}$, respectively, including positive or negative signs, and (iii) can elongate the interaction time with the sample. The nonlinear refractive index and the nonlinear absorption coefficient were calculated from the z-scan signals using a procedure that was developed by Sheik-Bahae *et al.*,[12] which gave the Re$\chi^{(3)}$ and Im$\chi^{(3)}$ values in Fig. 2, respectively.¶ There was no damage to the sample, as was confirmed by a scan from the opposite direction on the z-axis which gave an identical result. Sample damage or degradation of the polyradical was also ruled out by UV–VIS and NMR spectroscopy after the laser-irradiated measurements.

Both Re$\chi^{(3)}$ and Im$\chi^{(3)}$ for a 1.8 wt% $CHCl_3$ solution of the precursor **1b** were quite small ($10^{-13}$ esu) at over 500 nm in the nonresonant region, and could not be distinguished from the nonlinearity of the $CHCl_3$ solvent. On the other hand, the wavelength dependence of the nonlinearity for the polyradical **1a** was clearly observed in the region between 500 and 740 nm. The maximum values of Re$\chi^{(3)}$ and Im$\chi^{(3)}$ for a 0.091 wt% $CHCl_3$ solution of the polyradical **1a**, obtained at 740 nm, were $-2.4 \times 10^{-12}$ esu and $-3.1 \times 10^{-12}$ esu, respectively. Converting these results with respect to the polymer concentration, gave a third-order optical nonlinearity for the polyradical **1a** of *ca.* $10^{-9}$ esu, an enhancement of more than three orders of magnitude.‖ Re$\chi^{(3)}$ and Im$\chi^{(3)}$ swiched from positive to a negative at *ca.* 700 and 650 nm, respectively, which corresponds to a band gap narrowing due to SOMO generation and/or a resonant effect *via* the degenerate SOMOs.

This work was partially supported by a Grant-in-Aid for Scientific Research (Nos. 267/08236231 and 09305060) from the Ministry of Education, Science and Culture, Japan, and the Shorai Foundation for Science and Technology.

## Footnotes and References

† 1-(3,5-Di-*tert*-butyl-4-hydroxyphenyl)-3,4-distyrylbenzene was synthesized *via* sequential Heck coupling reactions of 4-(3,5-di-*tert*-butyl-4-acetoxyphenyl)-2-bromostyrene with iodobenzene and styrene, and the deprotection of the acetyl group. $\delta_H$ ($CDCl_3$, 500 MHz) 1.51 (s, 18 H, $C(CH_3)_3$], 5.28 (s, 1 H, OH), 7.01–7.76 (m, 19 H, phenyl); *m/s* 486 ($M^+$), calc. for M, 486.

‡ Magnetization and static magnetic susceptibility were mesured with a Quantum Design MPMS-7 SQUID magnetometer from 2 to 300 K in a field from 0.5 to 7 T.

§ An LBO-based OPG/OPA output (420–1800 nm), which was pumped by a third-harmonic from Nd:YAG laser, was used as a light sourse. The pulse width was *ca.* 20 ps and the repetition rate was 10 Hz. The Gaussian beam was extracted by a spatial filter using a diamond pin-hole (100 μm) in an evacuated chamber. Transmittance of the samples with and without a finite aperature in the far field was measered as the sample was scanned through the focal plane along the propagation direction z. At each z position, 15 laser shots were averaged in order to remove noise.

¶ For the calculation, the refractive index of $CHCl_3$ ($n_D$ = 1.446) was used for sample solutions in which there is no wavelength dispersion in the measuring region.

‖ For the conversion from $\chi^{(3)}$ of the solution to that of the neat sample, the density of the polymers was assumed to be unitiy. This enhancement of Re$\chi^{(3)}$ was, however, accompanied with increase in the linear absorption. As the sign of Im$\chi^{(3)}$ was negative, the strong absorption saturation should be effective for applications for optical devices without loss of light intensity.

1 P. N. Prasad and D. J. Williams, *Introduction to Nonlinear Optical Effects in Molecules and Polymers*, Wiley, New York, 1991; J. L. Bredas, C. Adant, P. Tackx and A. Persoons, *Chem. Rev*., 1994, **94**, 243.
2 C. Sauteret, J.-P. Herman, R. Frey, F. Pradere, J. Ducuing, R. H. Baughman and R. R. Chance, Phys. Rev. Lett., 1976, **36**, 956.
3 T. Kaino, H. Kobayashi, K. Kubodera, T. Kurihara, S. Saito, T. Tsutsui and S. Tokito, *Appl. Phys. Lett.*, 1989, **54**, 1619; J. Swiatkiewicz and P. N. Prasad, *Appl. Phys. Lett.*, 1990, **56**, 892.
4 H. Matsuda, H. Nakanishi, T. Hosomi and M. Kato, *Macromolecules*, 1988, **21**, 1238.
5 H. Matsuda, S. Yamada, E. V. Keuren, H. Katagi, H. Kasai, S. Okada, H. Oikawa, H. Nakanishi, E. C. Smith, A. K. Kar and B. S. Wherrett, *SPIE Annu. Tech. Symp. Proc.*, 1997, **2998**, 241.
6 J. S. Miller and A. J. Epstein, *Angew. Chem., Int. Ed. Engl.*, 1994, **33**, 385; A. Rajca, Chem. Rev., 1994, 94, 871
7 H. Nishide, T. Kaneko, T. Nii, K. Katoh, E. Tsuchida and K. Yamaguchi, *J. Am. Chem. Soc.*, 1995, **117**, 548; H. Nishide, T. Kaneko, T. Nii, K. Katoh, E. Tsuchida and P. M. Lahti, *J. Am. Chem. Soc.*, 1996, **118**, 9695.
8 Y. Teki, T. Takui, H. Yagi and K. Itoh, *J. Chem. Phys.*, 1985, **83**, 539; A. Rajca and S. Rajca, *J. Am. Chem. Soc.*, 1995, **117**, 806.
9 G. Puccetti, I. Ledoux and J. Zyss, *Chem. Phys. Lett.*, 1990, **175**, 257.
10 K. Awaga and Y. Maruyama, *Chem. Phys. Lett.*, 1989, **158**, 556: K. Awaga and Y. Maruyama, *J. Chem. Phys.*, 1989, **91**, 2743.
11 J. P. Hermann and J. Ducuing, *J. Appl. Phys.*, 1974, **45**, 5199; A. Mathy, K. Ueberhofen, R. Schenk, H. Gregorius, R. Garay, K. Müllen and C. Bubeck, *Phys. Rev. B*, 1996, **53**, 4367.
12 M. Sheik-Bahae, A. A. Said, T.-H. Wei, D. J. Hagan and E. W. Van Stryland, *IEEE J. Quantum Electron.*, 1990, **26**, 760.

*Received in Cambridge, UK, 14th July 1997; 7/05028C*

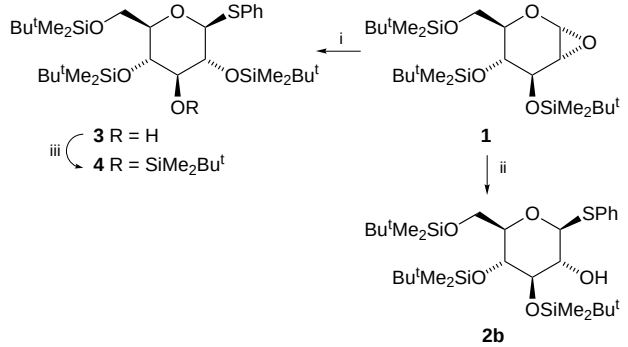
# Reaction of thiophenol with glucal epoxides: X-ray structure of 3,4,6-tri-*O*-*tert*-butyldimethylsilyl-1-*S*-phenyl-1-thio-α-D-glucopyranoside

**Caroline Walford, Richard F. W. Jackson,* Nicholas H. Rees, William Clegg and Sarah L. Heath**

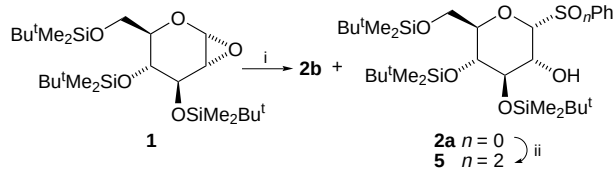
*Department of Chemistry, Bedson Building, The University of Newcastle, Newcastle upon Tyne, UK NE1 7RU*

**The reaction of the *tert*-butyldimethylsilyl protected glucal epoxide 1 with thiophenol under a variety of conditions gives three distinct adducts, including the α-phenylthioglycoside 2a, which exists both in solution and in the solid state in a $^1C_4$ conformation in which the C-2, C-3, C-4 and C-5 substituents are all axial.**

1-Phenylthioglucosides have been widely used in glycosylation reactions. In the context of a project to develop nucleophilic glycosyl donors, we were interested in the development of effective routes to protected α- and β-phenylthioglucosides **2a** and **2b**. Our planned approach involved the reaction of the epoxide **1** (prepared by oxidation of the readily available glucal with dimethyldioxirane)[1] with phenylthiolate, a reaction which had been previously reported on the corresponding tribenzyl protected derivative by Spilling (using NaSPh)[2] and Danishefsky (using $Bu_4NSPh$).[3] Spilling obtained a low yield, and Danishefsky obtained a mixture of both α- and β-phenylthioglucosides. When the epoxide **1** was treated with lithium phenylthiolate (Scheme 1), the adduct **3** was cleanly obtained (72%), in which the initial product of ring-opening had undergone a silyl shift. However, treatment of the epoxide **1** with thiophenol in the presence of triethylamine did give the expected sulfide **2b** (85%). The structures of the two products were assigned on the basis of extensive two-dimensional NMR studies, including the preparation of acetylated derivatives. While conversion of the sulfide **2b** into the *tetra*-silylated derivative **4** (*tert*-butyldimethylsilyl trifluoromethanesulfonate, 2,6-lutidine, −78 °C to room temp., 16 h) proceeded reasonably efficiently (58%), the analogous reaction on **3** was very slow, and gave **4** in very poor yield (12%), testifying to the hindered nature of the C-3 hydroxy group.[4] We believe that the best explanation for these results is that the presence of two bulky protecting groups at C-3 and C-4 is unfavourable, and it is the relief of steric hindrance which is the driving force in the silyl migration.[5] In the ring-opening reaction in the presence of triethylamine, the triethylammonium cation presumably acts as a proton source, thus neutralising the C-2 alkoxide and thereby preventing silyl migration.




**Scheme 1** *Reagents and conditions*: i, PhSLi (from PhSH and BuLi), 0 °C to room temp., THF, 16 h; ii, PhSH, $NEt_3$, 0 °C to room temp., 16 h, THF; iii, $Bu^tMe_2SiOSO_2CF_3$, 2,6-lutidine, $CH_2Cl_2$, −78 °C to room temp., 16 h




**Scheme 2** *Reagents and conditions*: i, PhSH, 0 °C to room temp., THF, 16 h; ii, MCPBA, $NaHCO_3$, $CH_2Cl_2$, 0 °C, 1.5 h

In order to explore this reaction further, we also examined the reaction of the epoxide **1** with thiophenol itself (Scheme 2). The major product from this reaction was the α-phenylthioglycoside **2a** (36%), together with a minor amount of the β-phenylthioglycoside **2b** (28%), already identified. Although the yields are not very high, the process has not been optimised, especially with respect to solvent. In this case, the reaction probably proceeds through the intermediacy of an oxonium ion, formed by ring opening of the epoxide, which is then selectively trapped from the α-face.

The adduct **2a** was crystalline, and we were able to confirm its structure by X-ray diffraction, as indicated in Fig. 1.† We were surprised to discover a $^1C_4$ conformation in the crystalline state, in which the four substituents at C-2, C-3, C-4 and C-5 are in axial positions, with the phenylthio group equatorial. The other notable feature is that there is a hydrogen bond between the C-2 hydroxy proton and O-1, which may help to stabilise the $^1C_4$ conformation. The $^1C_4$ conformation does appear to be very rare, although it has been observed in the case of a bis(*tert*-butyldiphenylsilyl) α-aryl *C*-olivoside, in which three substituents, rather than four, are in an axial position.[6] Analysis of the $^1H$ NMR spectrum of **2a** suggested that, in $CDCl_3$ at least, the solution conformation was very similar to that in the solid

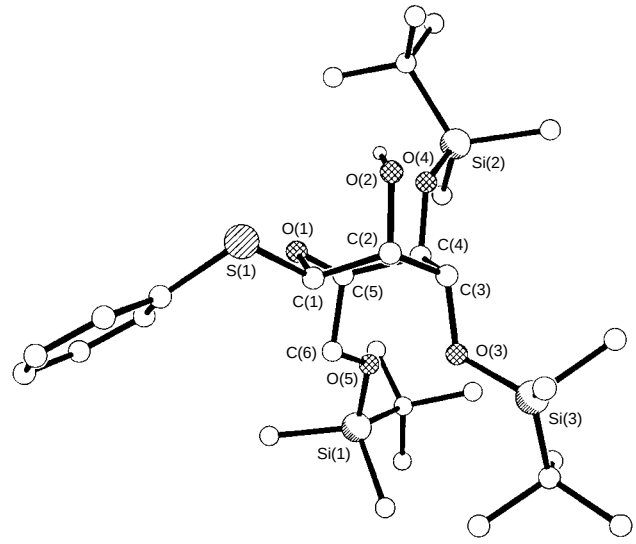



**Fig. 1** The conformation of **2a** in the crystal structure. Hydrogen atoms, other than the hydroxy proton, and minor disorder components are omitted for clarity.

state, with very small vicinal coupling constants around the ring, and significant long-range (*W*) coupling between H-2 and H-4, and between H-3 and H-5 (indicating that each of these protons was in an equatorial position). The corresponding sulfone **5**, prepared by oxidation of the sulfide **2a**, exhibited almost identical coupling constants and is therefore probably also in the same conformation in solution.

The '*A* value' of the phenylthio group (4.60–5.19 kJ $mol^{-1}$)[7] is not sufficiently large to force the other substituents axial, so the most obvious explanation is that the adjacent *tert*-butyldimethylsilyloxy groups at C-3 and C-4 are more sterically encumbered when they are diequatorial than when they are diaxial.‡ Eliel's important report on the '*A* values' of silyloxy groups, which clearly showed (rather counter-intuitively) that a *tert*-butyldimethylsilyloxy group had a *smaller* '*A* value' than a trimethylsilyloxy group,[8] provides strong support for this idea. The ease with which the *tert*-butyldimethylsilyl group at C-3 of **2b** migrates to C-2 is probably another manifestation of this same phenomenon.

It is clear that the pronounced conformational effects of *tert*-butyldimethylsilyl ethers may have useful consequences in control of reaction stereoselectivity.

We thank the EPSRC for a CASE award (C. L. W.) and for equipment grants, Rhône-Poulenc Rorer for support and Drs B. Porter, A. J. Ratcliffe and M. Podmore (RPR) for helpful discussions. R. F. W. J. also thanks the Nuffield Foundation for a One Year Science Research Fellowship.

## Footnotes and References

* E-mail: r.f.w.jackson@newcastle.ac.uk

† *Crystal data* for **2a**: $C_{30}H_{58}O_5SSi_3$, $M_r$ = 615.1, orthorhombic, $P2_12_12_1$, $a$ = 27.1719(17), $b$ = 10.9754(7), $c$ = 12.3479(8) Å, $V$ = 3682.4(4) Å$^3$, $Z$ = 4, $D_c$ = 1.109 g cm $^{-3}$, $\mu$ = 0.22 mm$^{-1}$ (Mo-K$\alpha$, $\lambda$ = 0.71073 Å), $T$ = 160 K. Measurements were made on a Siemens SMART CCD area detector diffractometer. Data were collected by narrow-frame $\omega$ rotation. 19 575 reflections, $2\theta \leqslant 50°$, 6467 unique reflections, $R_{int}$ = 0.091, semi-empirical absorption correction, transmission 0.84–0.97. Structure solution was by direct methods, refinement on $F^2$ for all data, with anisotropic displacement parameters, riding H atoms (with rotational freedom for methyl and hydroxy hydrogen atoms), and two-fold disorder for one silyl group. $R_w = [\Sigma w(F_o^2 - F_c^2)/\Sigma w(F_o^2)^2]^{\frac{1}{2}} = 0.223$ for all data, conventional $R = 0.101$ for $F$ values of 5551 reflections with $F_o^2 > 2\sigma(F_o^2)$, goodness of fit 1.129, absolute configuration indicated by refinement of enantiopole parameter (ref. 9) to −0.3(2), residual electron density within ± 0.61 e Å$^{-3}$. The indicated absolute configuration was consistent with the known absolute configuration of the starting material. The quality of data collection and structure refinement are limited by the deformed nature of the crystals (apparently slightly bent, giving distorted reflections) and the structural disorder. Programs were standard Siemens control and integration software, Siemens SHELXTL, and local programs. CCDC 182/580.

‡ This suggestion was first made by Suzuki (ref. 6). This type of behaviour has been noted before in the case of glycals (ref. 10), and in β-lactams derived from glycals by cycloaddition (ref. 11). It has also been suggested as an influence on reactivity, but without direct evidence (ref. 4.).

1 R. L. Halcomb and S. J. Danishefsky, *J. Am. Chem. Soc.*, 1989, **111**, 6661.
2 C. H. Marzabadi and C. D. Spilling, *J. Org. Chem.*, 1993, **58**, 3761.
3 D. M. Gordon and S. J. Danishefsky, *Carbohydr. Res.*, 1990, **206**, 361.
4 For a related observation, see: T. Iimori, H. Takahashi and S. Ikegami, *Tetrahedron Lett.*, 1996, **37**, 649.
5 A closely related migration of a *tert*-butyldimethylsilyl group has been reported: R. W. Friesen and A. K. Daljeet, *Tetrahedron Lett.*, 1990, **31**, 6133. For an analogous migration of a trimethylsilyl group, see V. Pedretti, A. Veyrières and P. Sinäy, *Tetrahedron*, 1990, **46**, 77.
6 T. Hosoya, Y. Ohashi, T. Matsumoto and K. Suzuki, *Tetrahedron Lett.*, 1996, **37**, 663.
7 O. A. Subbotin, V. A. Palyulin, S. I. Kozhushkov and N. S. Zefirov, *J. Org. Chem. USSR* (*Engl. Transl.*), 1978, **14**, 196.
8 E. L. Eliel and H. Satici, *J. Org. Chem.*, 1994, **59**, 688.
9 H. D. Flack, *Acta Crystallogr., Sect. A*, 1983, **39**, 876.
10 D. Horton, W. Priebe and O. Varela, *Int. Carbohydr. Symp. XIIth, Utrecht*, July 1–7, 1984, Abstr. D8.35, p. 519.
11 M. Chmielewski, Z. Kaluza, H. Dodziuk, K. Suwinska, D. Rosenbaum, H. Duddeck, P. D. Magnus and J. C. Huffmann, *Carbohydr. Res.*, 1990, **203**, 183.

*Received in Liverpool, UK, 27th June 1997; 7/04534D*

# A study of asymmetric protonation with chiral β-hydroxy sulfoxides. Asymmetric synthesis of (−)-epibatidine

**Hiroshi Kosugi,* Makito Abe, Ryota Hatsuda, Hisashi Uda and Michiharu Kato**

*Institute for Chemical Reaction Science, Tohoku University, Katahira, Aoba-ku, Sendai 980-77, Japan*

**The asymmetric synthesis of (−)-epibatidine 1, employing as the key step the asymmetric protonation of the achiral lithum enolate of cyclohexanone derivative 5 with chiral β-hydroxy sulfoxide 3b, is described.**

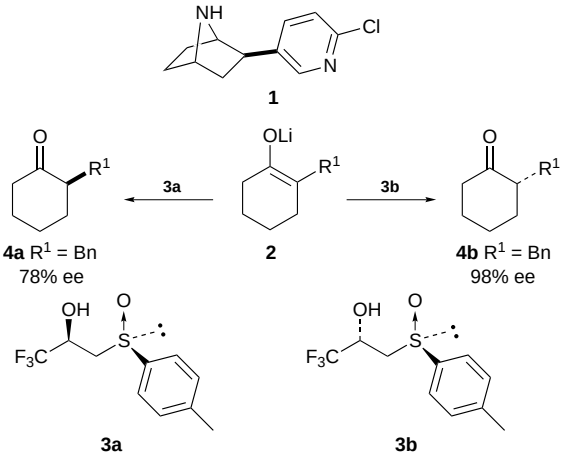
Epibatidine **1** was isolated from the poisonous Ecuadoran frog *Epipedobates tricolor*, and was found to be a novel potent antinociceptive agent that acts through nicotinic receptors.[1] Because of the scarcity of **1** in nature, the determination of its absolute stereochemistry was extremely difficult. In 1994, Fletcher *et al*. reported the absolute stereochemistry of **1** to be 1*R*,2*R*,4*S* by the HPLC comparison of synthetic specimens with natural **1**.[2f] Owing to interest in this novel biological activity and its intriguing chemical structure, many synthetic routes to **1** have been reported.[2] The synthetic approaches to optically active **1** are somewhat limited and involve an optical resolution of either a product at some stage of the synthesis or the final product **1**. [2g,3] Here we report the asymmetric synthesis of (−)-**1** based on the asymmetric protonation of achiral lithium enolates derived from cyclohexanone derivatives with chiral β-hydroxy sulfoxides.

We have recently developed, using enantiomerically pure β-hydroxy sulfoxides **3a** or **3b** as protonating reagents, the effective asymmetric protonation of achiral lithium enolates of 2-substituted cyclohexanones **2** to give enantiomers **4a** and **4b**, respectively, with high enantiopurity (Scheme 1).[4] Extension of the methodology to other substituted cyclohexanones, especially 4,4-ethylenedioxycyclohexanone derivatives, would be useful for procurement of chiral synthetic intermediates for natural product synthesis. For example, as shown in Scheme 2, when the asymmetric protonation is applied to the cyclohexanone acetal bearing a 4-chloropyridinyl moiety at the C(2) position, the compound (*R*)-**5** obtained might be readily converted to **6**, which has been employed as the common synthetic intermediate for the construction of the 7-azabicyclo-[2.2.1]heptane system of epibatidine, in the synthesis originally developed by Broka.[2a]

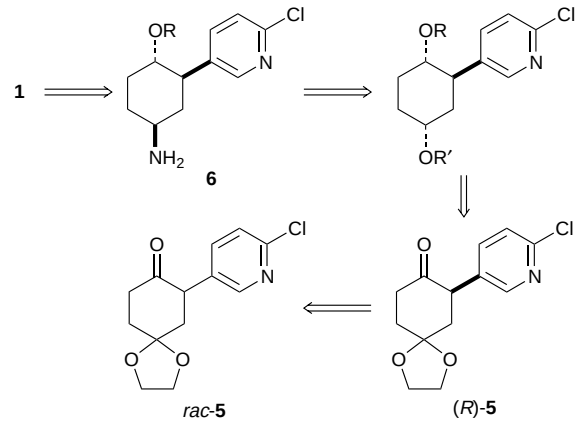
The starting cyclohexanone derivative *rac*-**5** was synthesized from 4-*tert*-butyldimethylsilyloxycyclohex-2-en-1-one[5] by a sequence of conventional reactions: (i) conjugate addition of 4-lithio-2-chloropyridine in the presence of lithium thienylcyanocuprate according to a reported procedure,[2i] and (ii) acetalisation and deprotection of the silyloxy group, followed by Swern oxidation to give *rac*-**5** (Scheme 3).

Regioselective enol acetate formation was accomplished by treatment of *rac*-**5** with Bu$^t$OK, followed by addition of $Ac_2O$ to give enol acetate **7** in 99% yield. The asymmetric protonation was performed as follows. The lithium enolate generated from **7** by treatment with MeLi (2 equiv.) in $Et_2O$ was protonated by adding **3b**[6] (2.5 equiv.) in $CH_2Cl_2$ at −90 °C for 1.5 h, during which time the reaction temperature rose to −60 °C. The product (*R*)-**5** [63% yield, $[\alpha]_D^{25}$ + 18.3 (*c* 0.316, $CHCl_3$)] obtained was found to have an enantiomeric excess of 82% by HPLC (Daicel AD chiralcel column). The chiral **5** was reduced with $NaBH_4$ in MeOH to the *trans*-alcohol **8** (77%) accompanied by some of the *cis*-alcohol (18%). It is worthwhile to mention that, at this stage, optical purification to obtain the enantiomerically pure **8a** was achieved using achiral silica gel chromatography.† The absolute stereochemistry was determined to be 3*R*,4*S* by applying the exciton coupled circular dichroic (CD) method[6] to the benzoate **8b** [UV (MeOH) $\lambda_{max}$ 218 nm ($\varepsilon$ 16 700); CD (MeOH) $\lambda_{ext}$ 227.4 nm ($\Delta\varepsilon$ +12.9), 215.4 (−1.04)] derived from **8a**. Consequently, the absolute structure of (+)-**5** is suggested to be 3*R*, as depicted in Scheme 3. It should be noted that the sense of the enantiofacial recognition of cyclohexanone derivatives bearing an acetal moiety at the C(4) position is the reverse of that of simple 2-substituted cyclohexanones in the asymmetric protonation with **3b**.[4]

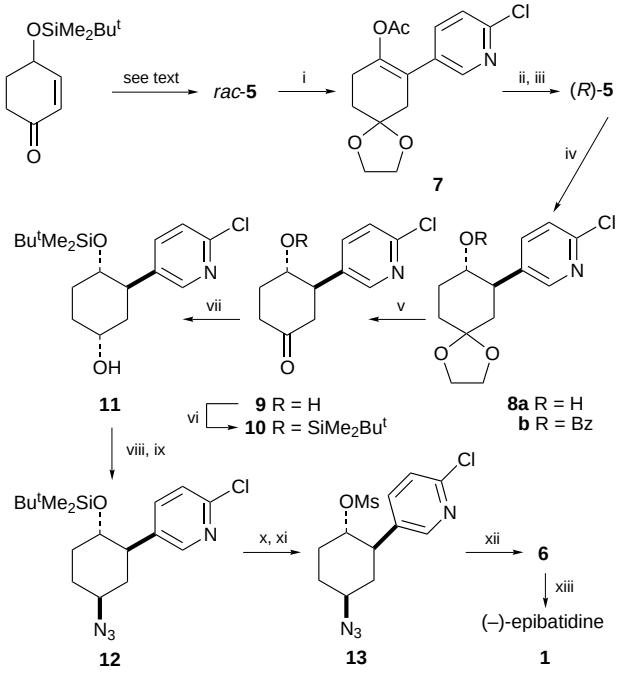
Conversion of the enantiomerically pure alcohol **8a** to epibatidine **1** was straightforward, employing the slightly modified procedure of Broka.[2a] Deprotection of the carbonyl group, followed by protection of the hydroxy group as the Bu$^t$Me$_2$Si ether afforded **10** in 81% overall yield from **8**. The carbonyl reduction of **10** with LiBBu$^s_3$H (L-selectride) in THF




**Scheme 1**




**Scheme 2**




**Scheme 3** *Reagents and conditions*: i, Bu$^t$OK, $Ac_2O$, THF; ii, MeLi (2 equiv.), $Et_2O$, 0 °C, 15 min; iii, **3b**, $CH_2Cl_2$, (2.5 equiv.), −90 to −60 °C; iv, $NaBH_4$, MeOH; v, 80% aq. AcOH; vi, Bu$^t$Me$_2$SiCl, Pr$^i_2$NEt, DMF; vii, LiBBu$^s_3$H, THF; viii, MsCl, $Et_3N$, $CH_2Cl_2$; ix, $NaN_3$, DMF; x, $Bu_4NF$, THF; xi, MsCl, $Et_3N$, $CH_2Cl_2$; xii, $SnCl_2·2H_2O$, MeOH–THF; xiii, $CHCl_3$, reflux

afforded the axial alcohol **11** (63%). Conversion of the hydroxy group to azide was performed *via* a two-step procedure to give **12** in 76% yield from **11**. Deprotection of the silyl ether, followed by mesylation ($MeSO_2Cl$, $Et_3N$, $CH_2Cl_2$) gave the mesylate **13** in 95% yield. Finally, the mild reduction of the azide function with $SnCl_2$ and ring closure of the resulting amine **6** in refluxing $CHCl_3$ for 3 d gave enantiomerically pure (−)-**1** {$[\alpha]^{25}_D$ −6.99 (*c* 0.229, $CHCl_3$): mp 62–62.5 °C, 69% yield from **13**} which was identical in all respects with the reported physical data.[2f]

In conclusion, the synthetic utility of asymmetric protonation of prochiral lithium enolates with chiral β-hydroxy sulfoxides has been demonstrated by the asymmetric synthesis of enantiomerically pure (−)-epibatidine. Further studies on the scope and limitations of the present asymmetric protonation are in progress.

We are grateful to Professor Nobuyuki Harada of this Institute for a helpful discussion of the CD spectroscopic analysis. This work was supported in part by a Grant-in-Aid for Scientific Research from the Ministry of Education, Science, and Culture of Japan.

## Footnotes and References

* E-mail: hkosugi@icrs.tohoku.ac.jp

† There have been a few examples of the chromatographic separation of partially enantio-enriched compounds under achiral conditions (ref. 8). When a sample of the hydroxy acetal **8a** (80% ee) was loaded on a silica gel column [MPLC: Kusano pre-packed silica gel column Si-10; eluted with 3 : 1 hexane–EtOAc; UV (254 nm) and RI detectors], enantiomerically pure **8a** was first eluted, followed by *rac*-**8a** as a shoulder. We have examined the separation of some partially enantio-enriched (23–80% ee) homologues such as *trans*-3-substituted 4-hydroxycyclohex-1-enone ethylene ketals {*e.g.* 3-benzyl and 3-[(*E*)-3-phenylprop-2-enyl] derivatives} as well as their *cis*-isomers by achiral silica gel column chromatography, and found that the chromatographic behaviour is quite general. The results will be reported elsewhere.

1 T. F. Spande, H. M. Garraffo, M. W. Edwards, H. J. C. Yeh, L. Pannell and J. W. Daly, *J. Am. Chem. Soc.*, 1992, **114**, 3475.
2 (*a*) C. A. Broka, *Tetrahedron Lett.*, 1993, **34**, 3251; (*b*) D. F. Huang and T. Y. Shen, *Tetrahedron Lett.*, 1993, **34**, 4477; (*c*) S. R. Fletcher, R. Baker, M. S. Chambers, S. C. Hobbs and P. J. Mitchell, *J. Chem. Soc., Chem. Commun.*, 1993, 1216; (*d*) S. C. Clayton and A. C. Regan, *Tetrahedron Lett.*, 1993, **34**, 7493; (*e*) E. J. Corey, T.-P. Loh, S. AchyuthaRao, D. C. Daley and S. Sarshar, *J. Org. Chem.*, 1993, **58**, 5600; (*f*) S. R. Fletcher, R. Baker, M. S. Chambers, R. H. Herbert, S. C. Hobbs, S. R. Thomas, H. M. Verrier, A. P. Watt and R. B. Ball, *J. Org. Chem.*, 1994, **59**, 1771; (*g*) C. Sztántay, Z. Kardos-Balogh, I. Moldvai, C. Sztántay, Jr., E. Majar-Temesváry and G. Blaskó, *Tetrahedron Lett.*, 1994, **35**, 3171; (*h*) K. Senokuchi, H. Nakai, M. Kawamura, N. Katsube, S. Nonaka, H. Sawaragi and N. Hamanaka, *Synlett*, 1994, 343; (*i*) K. Sestanj, E. Melenski and L. Jirkovsky, *Tetrahedron Lett.*, 1994, **35**, 5417; (*j*) S. Y. Ko, J. Lerpiniere, I. D. Linney and R. Wrigglesworth, *J. Chem. Soc., Chem. Commun.*, 1994, 1775; (*k*) E. Albertini, A. Barco, S. Benetti, C. D. Risi, G. P. Pollini, R. Romagnoli and V. Zanirato, *Tetrahedron Lett.*, 1994, **35**, 9297; (*l*) P. L. Koitan and F. I. Carroll, *Synth. Commun.*, 1995, **25**, 63; (*m*) R. Xu, G. Chu and D. Bai, *Tetrahedron Lett.*, 1996, **37**, 1463; (*n*) C. Zhang and M. L. Trudell, *J. Org. Chem.*, 1996, **61**, 7189.
3 Asymmetric synthesis: B. M. Trost and G. R. Cook, *Tetrahedron Lett.*, 1996, **37**, 7485.
4 H. Kosugi, K. Hoshino and H. Uda, presented in part at the 16th International Symposium on the Organic Chemistry of Sulfur (ISOCS), Merseburg, 1994; the abstract appeared in the Proceedings, which have been published: *Phosphorus Sulfur Silicon*, 1994, **95**–**96**, 401; H. Kosugi, K. Hoshino and H. Uda, *Tetrahedron Lett.*, in the press.
5 R. K. Boeckman and M. Ramaiah, *J. Org. Chem.*, 1977, **42**, 1581.
6 F. Bravo, E. Piovosi and G. Resnati, *Synthesis*, 1986, 579; T. Yamazaki, N. Ishikawa, H. Iwatsubo and T. Kitazume, *J. Chem. Soc., Chem. Commun.*, 1987, 1340; P. Bravo, M. Frigerio and G. Resnati, *Synthesis*, 1988, 955.
7 N. Harada and K. Nakanishi, *Circular Dichroic Spectroscopy-Exciton Coupling in Organic Stereochemistry*, University Science Books, Mill Valley, 1983.
8 K. C. Cundy and P. A. Crooks, *J. Chromatogr.*, 1983, **281**, 17; R. Charles and E. Gil-Av, *J. Chromatogr.*, 1984, **298**, 516; A. Dobashi, Y. Motoyama, K. Kinoshita, S. Hara and N. Fukusaku, *Anal. Chem.*, 1987, **59**, 2209; W. L. Tsai, K. Hermann, E. Hug, B. Rhode and A. S. Dreiding, *Helv. Chim. Acta*, 1985, **68**, 2238; R. Matusch and C. Coors, *Angew. Chem., Int. Ed. Engl.*, 1989, **28**, 626; P. Diter, S. Taudien, O. Samuel and H. B. Kagan, *J. Org. Chem.*, 1994, **59**, 370.

*Received in Cambridge, UK, 7th July 1997; 7/04779G*

# Stereospecific synthesis of 1,9-bis(β-D-glycosyl)adenines: a chemical route to stable analogues of cyclic-ADP ribose (cADPR)

**Edward J. Hutchinson, Brian F. Taylor and G. Michael Blackburn***

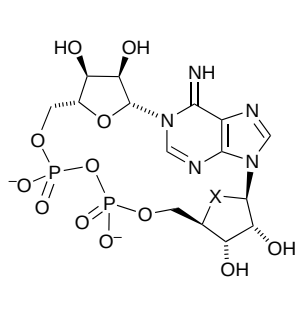
*Krebs Institute for Biomolecular Science, Department of Chemistry, University of Sheffield, Sheffield, UK S3 7HF*

**Stereospecific syntheses of two hydrolysis-resistant analogues of the 1,9-bis(β-D-ribosyl)adenine moiety of cyclic-ADP ribose are described.**

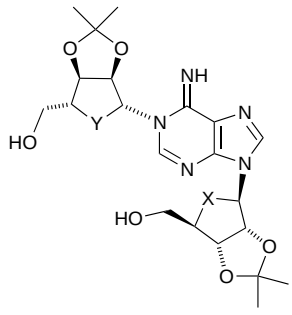
Cyclic-ADP Ribose, cADPR **1**, is a naturally occurring metabolite of $NAD^+$ and is deemed to be a secondary messenger involved in intracellular calcium mobilisation.[1] The precise role of this compound and the mechanism by which it acts at receptor sites other than those activated by inositol-1,4,5-triphosphate[2] remain unclear. cADPR is formed through the action of ADP-ribosyl cyclase, an enzyme found in many mammalian and invertebrate tissues, which brings about displacement of the nicotinamide group of $NAD^+$ by $N^1$ of its own adenine residue with overall retention of configuration.[3] The labile $C^{1''}$–$N^1$ glycosylic bond formed in this process is easily hydrolysed to give adenosine diphosphate ribose, ADPR **2**, by either enzymatic or spontaneous hydrolysis, thus accounting for the extremely low concentrations (sub-micromolar) of cADPR observed in cells.

As part of an ongoing investigation of the detailed function of cADPR, we are seeking to make novel analogues of cADPR for use in competitive enzyme inhibition studies as well as in investigations of agonist/antagonist action at the ryanodine receptor.[4] In a recent report,[5] we described the synthesis of a carbocyclic $NAD^+$ analogue containing a stable methylenebisphosphonate linkage which is designed to inhibit the formation of cADPR and thus can be employed in structural studies in a binary complex with the enzyme.

Hitherto, analogues of cADPR have generally been formed by enzymatic cyclisation[6] of an analogue of $NAD^+$, though Sekine has described a chemical procedure which gave the α-configuration at $N^1$ for a cADPR derivative.[7] Both Lee[8] and Potter[9] have described antagonist activity from 8-substituted cADPR derivatives whilst Sih[10] has used a part enzyme, part chemical synthesis to generate cADPR species with changes in the pyrophosphate linkage. Potter[11] has employed aristeromycin to prepare a longer-acting cADPR analogue **3** with a carbaribose moiety at $N^9$ though necessarily retaining a ribofuranose moiety at $N^1$.



**1** X = O, cADPR
**3** X = $CH_2$

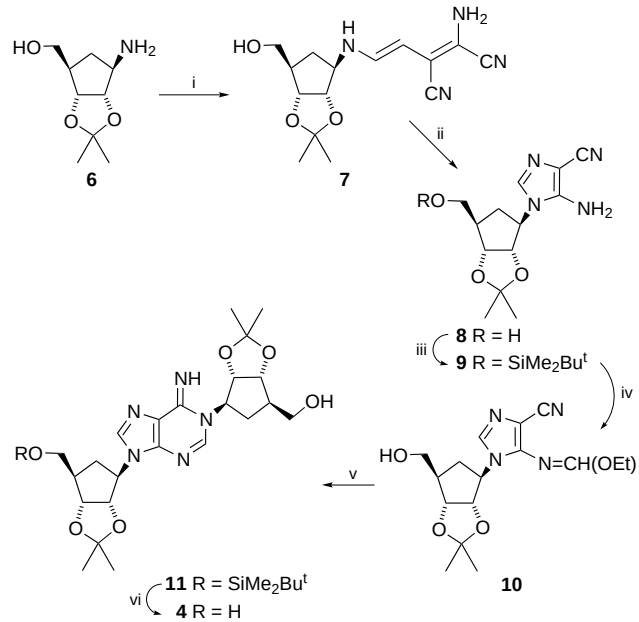


**4** X = $CH_2$, Y = $CH_2$
**5** X = O, Y = $CH_2$

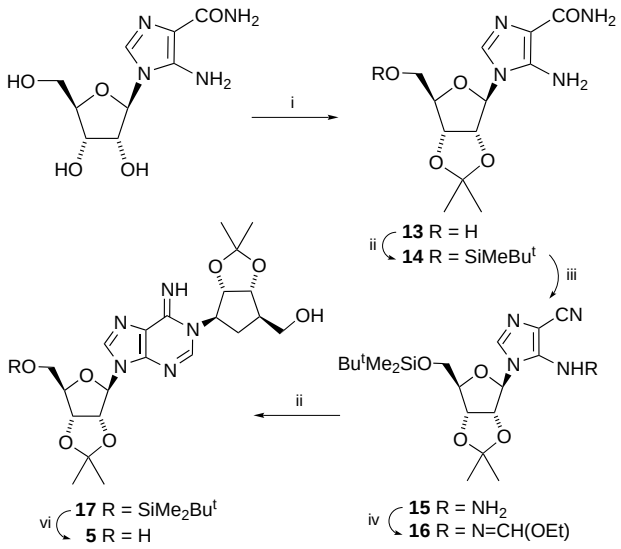
No group has as yet sought directly to address the inherent instability of the labile (O)$C^{1''}$–$N^1$ glycosylic bond. Carbocyclic sugars have been employed in many nucleoside analogues to achieve stability of the glycosylic linkage,[12] and the incorporation of a carbaribose at $N^1$ in cADPR seemed a logical target for this application. Because we predicted† that a nicotinamide carbocyclic riboside $NAD^+$ derivative would have insufficient reactivity at the glycosylic position to be a substrate for enzymatic cyclisation, the choice of a chemical route to carbaribose analogues of cADPR became unavoidable.

We here report the stereospecific synthesis of the nucleoside framework of two analogues of cADPR, both having a carbocyclic sugar moiety at the $N^{1'}$ position, namely the derivative **4** and the 1-β-D-carbaribosyl-9-β-D-ribofuranosyladenine derivative **5**. This route can also be employed to prepare the parent 1,9-bis(β-D-ribofuranosyl)adenine. We are currently developing both of these carbocyclic species *via* 5′,5″-bisphosphorylation and 5′,5″-methylenebisphosphorylation to generate novel, hydrolytically-stable analogues of cADPR.

The synthetic scheme is built around the repeated use of the cyclopentylamine **6** of defined β-configuration at $C^1$ (Scheme 1). Amine **6** is obtained in five high-yielding steps from commercially available (−)-2-azabicyclo[2.2.1]hept-5-en-3-one as outlined in a previous report.[5] Imidazole **9** was prepared *via* amidine **7** using diaminomaleonitrile as described by Booth,[13] which proved much superior to alternative reagents explored. Intermediate **7** was purified by silica gel chromatography, although prolonged exposure to air and light resulted in extensive darkening and decomposition. The required amino



**Scheme 1** *Reagents and conditions*: i, diaminomaleonitrile, $PhNH_3^+Cl^-$ (cat), EtOAc, room temp., dark, 18 h, 65%; ii, DBU (2 equiv.), $H_2O$, room temp., 2 h, 100%; iii, $Bu^tMe_2SiCl$, imidazole, DMF, room temp., 18 h, 92%; iv, $HC(OEt)_3$, heat, 4 h, 94%; v, **6**, EtOH, $EtO^-$ (cat), 50 °C, 40%; vi, $Bu_4NF$, THF, room temp., 18 h, 96%




**Scheme 2** *Reagents and conditions*: i, acetone, HC(OEt)$_3$, TsOH, room temp., 2 h, 78%; ii, Bu$^t$Me$_2$SiCl, imidazole, DMF, room temp., 18 h, 84%; iii, TsCl, pyridine, room temp., 3 h, 83%; iv, HC(OEt)$_3$, heat, 4 h, 100%; v, **6**, EtOH, EtO$^-$ (cat), 50 °C, 40%; vi, Bu$_4$NF, THF, room temp., 18 h, 94%

imidazole **8** was duly formed by base-induced cyclisation with excess DBU and followed by silyl protection with Bu$^t$Me$_2$SiCl to give imidazole **9**. Reaction of **9** with neat triethyl orthoformate resulted in near quantitative conversion into imidate **10**, the key precursor for cyclisation. Addition of amine **6** to an ethanolic solution of imidate **10** in the presence of catalytic sodium ethoxide for 48 h at 50 °C provided 1,9-bis(carbaribosyl)adenine **11** in 40% yield. Deprotection of the 5′-hydroxy group with Bu$_4$NF gave the required diol **4** in an overall yield of 14% after twelve synthetic steps.

Attempts to prepare the corresponding imidazole **15** using this procedure with commercially available 2,3-*O*-isopropylidene-1-β-D-ribofuranosylamine were unsuccessful. It appeared that the intermediate amidine is considerably more labile than its carbocyclic counterpart **7** and only degradation fragments were obtained. In an alternative synthesis (Scheme 2), commercially available AICAR **12** was protected as its 2′,3′-*O*-isopropylidene derivative using acetone–triethyl orthoformate–TsOH to give **13** in 78% yield. Following silylation of the 5′-hydroxy group, dehydration of the amide to nitrile **15** was achieved using TsCl in pyridine in 84% yield. Refluxing **15** in triethyl orthoformate produced imidate **16** which was condensed with carbocyclic amine **6** and cyclised as before. Removal of the 5′-*O*-SiMe$_2$Bu$^t$ protecting group with Bu$_4$NF gave the required 1-β-D-carbaribosyl-9-β-D-ribofuranosyladenine derivative **5** in 21% overall yield.

The 1,9-dialkyladenine structure for the analogues rests not only on synthesis but is confirmed by their p$K_a$ and spectroscopic characteristic. The p$K_a$ values of 8.36 for the 1,9-bis(β-D-carbaribosyl)adenine derivative **4** and 7.93 for the 1-β-D-carbaribosyl-9-β-D-ribosyladenine derivative **5** are close to p$K_a$ 8.30 for cADPR[3] and differ greatly from the p$K_a$s for 6,9-dialkyladenines,[3,16] which lie in the range 3.5–4. The UV absorption spectra for analogues **4** and **5** exhibit the strong shoulder at 300 nm characteristic of both cADPR and of 1,9-dialkyl adenines and absent in 6,9-dialkyl adenines.[15] Compounds **4** and **5** and the related intermediates described have been fully characterised by UV,‡ NMR and mass spectral analysis.§ In both analogues, the N$^1$–C$^{1''}$ bond appears to have the desired level of stability to hydrolysis, with no cleavage of the N$^1$–C$^{1'}$ bond over a week in aqueous solution under ambient conditions. In fact, the slow transformations of **4** and **5** observed at higher pH appear to result from isomerisation by a Dimroth rearrangement to give *N*$^6$,*N*$^9$-disubstituted adenines, as characterised by markedly changed UV spectral properties.[15] Such rearrangements have been shown[16] to be accelerated by a β-D-ribofuranosyl group at the 9-position. This process appears to be very slow in the case of analogues **4** and **5** (half life ⩾1 day at pH 9) and is the subject of further investigations.

We thank the EPSRC for financial support (GR/J39120).

## Footnotes and References

* E-mail: g.m.blackburn@sheffield.ac.uk

† Recent results using NAD$^+$ cyclase and a synthetic methylenebisphosphonate carbaNAD$^+$ analogue (ref. 5) have confirmed this prediction.

‡ p$K_a$ Determinations: For both analogues **4** and **5**, optical density at 300 nm was recorded at 25.0 °C at various pH values in the range 5.5–11.5 using a range of buffers (0.05 M buffer + 0.1 M NaCl where buffer = MES, EPPS, CHES, of CAPS). Absorbance values were plotted against the corresponding pH values and the p$K_a$ for each analogue was determined using a Kaleidagraph™ curve-fit analysis.

§ *Selected data* for **4**: mp 110–112 °C; $\lambda_{max}$/nm (3t) 260 (11 230), 300 (sh) (2458) ($H_2O$); FAB$^+$ [M + H]$^+$, 476.2506. $C_{23}H_{33}N_5O_6$ requires [M + H], 476.2509; $\delta_H$($CDCl_3$) 7.85 (1 H, br s), 7.72 (1 H, s), 5.31 (1 H, dd, *J* 5.5 and 5.5), 4.85 (1 H, dd, *J* 6.5 and 6), 4.76 (1 H, dd, *J* 6 and 2), 4.75–4.69 (1 H, m), 4.67 (1 H, dd, *J* 6.5 and 4 Hz), 4.65–4.55 (1 H, m), 3.84 (1 H, dd, *J* 10.8 and 6), 3.82 (1 H, dd, *J* 10.6 and 7.5), 3.79 (1 H, dd, *J* 10.6 and 5), 3.72 (1 H, dd, *J* 10.8 and 2.5), 2.62–2.42 (5 H, m), 2.32 (1 H, m), 1.60 (6 H, s), 1.31 (3 H, s), 1.30 (3 H, s). For **5**: mp 98–100 °C. For **17**: $\lambda_{max}$/nm ($\varepsilon$) 260 (11 570), 300 (sh) (3475) (MeOH); FAB$^+$ [M + H]$^+$, 478.2259. $C_{22}H_{31}N_5O_7$ requires [M + H], 478.2301; $\delta_H$($CDCl_3$) 7.78 (1 H, br s), 7.76 (1 H, s), 5.81 (1 H, d, *J* 4.5), 5.27 (1 H, dd, *J* 5.7), 5.03 (1 H, dd, *J* 6 and 1.5), 4.99 (1 H, dd, *J* 6 and 4.5), 4.73 (1 H, dd, *J* 6 and 2.4), 4.67–4.58 (1 H, br m), 4.48 (1 H, ddd, *J* 1.6, 1.6 and 1.6), 3.92 (1 H, dd, *J* 12.5 and 1.6), 3.81 (1 H, dd, *J* 11 and 3) 3.75 (1 H, dd, *J* 12.5 and 1.6), 3.72 (1 H, dd, *J* 11 and 3), 2.61–2.53 (2 H, br m), 2.52–2.47 (1 H, br m), 1.62 (3 H, s,), 1.55 (3 H, s), 1.36 (3 H, s), 1.30 (3 H, s).

1 H. C. Lee, R. M. Graeff and T. F. Walseth, *Biochimie*, 1995, **77**, 345; R. Aarhus, R. M. Graeff, D. M. Dickey, T. F. Walseth and H. C. Lee, *J. Biol. Chem.*, 1995, **270**, 30 327.
2 M. J. Berridge, *Nature*, 1993, **361**, 315.
3 H. Kim, E. L. Jacobson and M. K. Jacobson, *Science*, 1993, **261**, 1330; H. Kim, E. L. Jacobson and M. K. Jacobson, *Biochem. Biophys. Res. Commun.*, 1993, **194**, 1143.
4 S. Takasawa, K. Nata, H. Yonekura and H. Okamoto, *Science*, 1993, **259**, 370.
5 E. J. Hutchinson, B. F. Taylor and G. M. Blackburn, *Chem. Commun.*, 1996, 2765.
6 Q.-M. Gu and C. J. Sih, *J. Am. Chem. Soc.*, 1994, **116**, 7481.
7 K. Aritomo, C. Urashima, T. Wada and M. Sekine, *Nucleic Acid Symp. Ser.*, 1994, No. 31, 7.
8 T. F. Walseth and H. C. Lee, *Biochim. Biophys. Acta*, 1993, **1178**, 235.
9 G. A. Ashamu, A. Galione and B. V. L. Potter, *J. Chem. Soc., Chem. Commun.*, 1995, 1359.
10 Q.-M. Gu and C. J. Sih, *Bioorg. Med. Chem. Lett.*, 1996, **6**, 1203.
11 V. C. Bailey, S. M. Fortt, R. J. Summerhill, A. Galione and B. V. L. Potter, *FEBS Lett.*, 1996, **379**, 227.
12 A. D. Borthwick and K. Biggadike, *Tetrahedron*, 1992, **48**, 571 and references cited therein.
13 M. J. Alves, B. L. Booth and M. F. J. R. P. Proenç, *J. Chem. Soc., Perkin Trans 1*, 1990, 1705; B. L. Booth and P. R. Eastwood, *Tetrahedron Lett.*, 1993, **34**, 5503.
14 H. G. Windmueller and N. O. Kaplan, *J. Biol. Chem.*, 1961, **236**, 2716.
15 N. J. Leonard, K. L. Carraway and J. P. Helgeson, *J. Heterocycl. Chem.*, 1965, **2**, 291.
16 T. Fuji and T. Saito, *Chem. Pharm. Bull.*, 1985, **33**, 3635.

*Received in Glasgow, UK, 27th June 1997; 7/04533F*

# Chemoenzymatic synthesis of nucleopeptides

**Herbert Waldmann* and Stefanie Gabold**

*Universität Karlsruhe, Institut für Organische Chemie, Richard-Willstätter-Allee 2, D-76128 Karlsruhe, Germany*

**Acid- and base-labile multifunctional nucleopeptides have been selectively constructed under mild conditions by means of enzymatic protecting group techniques.**

Nucleoproteins are naturally occuring biopolymers in which the hydroxy group of a serine, a threonine or a tyrosine is linked *via* a phosphodiester group to the 3′- or 5′-end of DNA or RNA.[1] These protein conjugates play decisive roles in important biological processes; in particular, they may hold a central position in the process of viral replication *via* nucleoprotein-primed elongation of the oligonucleotide strand.[2] For the study of the biological phenomena in which nucleoproteins are involved, nucleopeptides embodying the characteristic linkage between the peptide chain and the oligonucleotide of their parent nucleoproteins may serve as powerful tools. In particular, the possibility of delineating the details of the above-mentioned mechanism of viral replication and developing a new class of antiviral agents based thereupon calls for the development of efficient methods for the construction of these peptide conjugates. However, their synthesis poses two major challenges: (i) the multifunctionality of the peptide-nucleotide conjugates makes the application of a variety of orthogonally stable amino, carboxy-, phosphate- and hydroxy-blocking groups necessary, and (ii) fully protected serine/threonine nucleopeptides are acid-labile (under acidic conditions the purine nucleotides may be depurinated[3]) and base-labile (under basic conditions, *i.e.* pH ⩾ 8, the entire oligonucleotide part may be split off *via* β-elimination[4]).

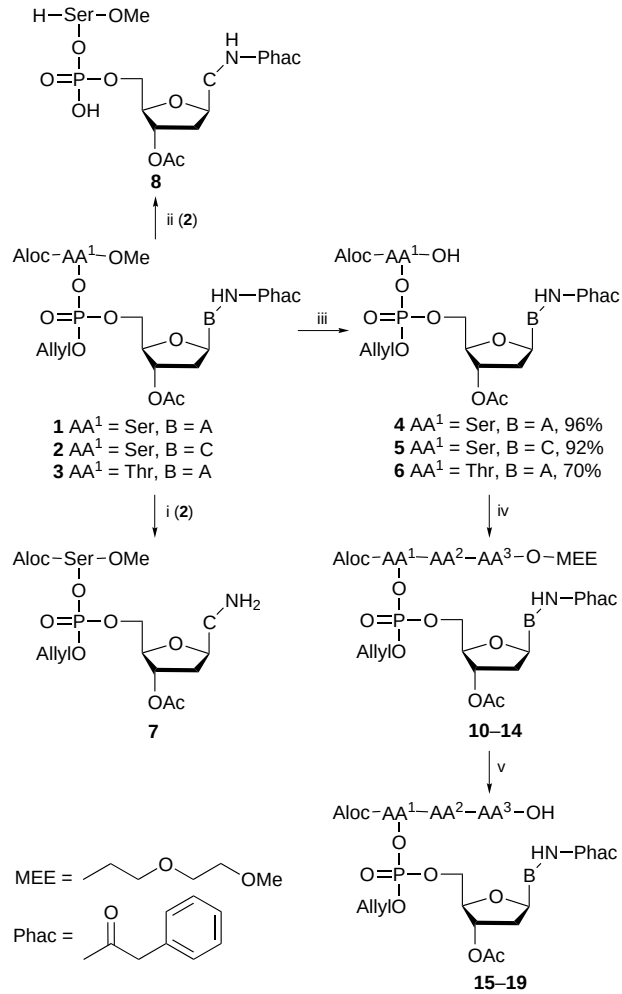
Consequently, in nucleopeptide chemistry not only is a variety of orthogonally stable blocking functions needed, they all must be removable selectively under mild, preferably neutral conditions. In the light of these seemingly contradictory demands it is not surprising that only a few reports on the successful construction of nucleopeptides have appeared.[4,5]

We have now found that enzymatic protecting group techniques[6] are efficient methods for the selective deprotection of the carboxylic acids and nucleobases of nucleopeptides.

In order to develop an enzymatic protecting group strategy for nucleopeptide synthesis, the protected nucleoamino acids **1**–**3** were constructed by means of established methods of oligonucleotide chemistry.† In these compounds, the nucleobases were masked with enzyme-labile phenylacetamide groups[7] and the carboxy groups of the amino acids were protected as methyl esters.

From the nucleoamino acid esters **1**–**3** the C-terminal protecting groups could be selectively removed by saponifying the methyl esters with the protease papain from *Carica papaya* at pH 6.6 and 37 °C (Scheme 1).[8] The conditions of the enzymatic transformations were so mild that the selectively unmasked nucleoamino acids **4**–**6** were obtained in high yield and without any undesired side reactions, *i.e.* the acid labile purine nucleosides remained intact and a β-elimination of the nucleotide, which readily takes place under weakly basic conditions (*vide supra*), was not observed. The protease did not attack the *O*-acetates. On the other hand, the nucleobase of *e.g.* **2** could be selectively N-deprotected by means of penicillin acylase-catalysed removal of the phenylacetamido base protecting group[7] at pH 7 and room temp. in 77% isolated yield (Scheme 1). In addition, the allyl-type blocking groups present in **2** were cleaved off without undesired side reaction by $Pd^0$-mediated allyl transfer to $PhSiH_3$ as accepting nucleophile[9] at room temp. in 89% isolated yield (Scheme 1).

Whereas the protease papain could advantageously be used to unmask the amino acid esters **1**–**3** its application to the deprotection of nucleopeptides might result in an undesired attack of the enzyme on the formed peptide bonds.[10] Therefore, for the selective C-terminal deprotection of nucleopeptides the lipase-mediated cleavage of the 2-(2-methoxyethoxy)ethyl (MEE) esters[11] was investigated, since lipases do not display any protease activity. To this end, the selectively deprotected nucleoamino acids **4**–**6** were coupled with different amino acid or dipeptide MEE esters **9** to give the fully masked nucleopeptides **10**–**14** in high yields (Scheme 1, Table 1). Upon treatment of the nucleopeptide acid MEE esters **10**–**14** with lipase from




**Scheme 1** *Reagents and conditions*: i, Penicillin acylae, phosphate buffer pH 7)–MeOH, 80 : 20; ii, $Pd(PPh_3)_4$, $PhSiH_3$; iii, papain from *Carica papaya*, cysteine buffer, pH 6.6; iv, H–$AA^2$–$AA^3$–OMEE **9**, 1-(3-dimethylaminopropyl)-3-ethylcarbodiimide hydrochloride, 1-hydroxybenzotriazole; v, lipase from *Aspergillus niger*, phosphate buffer (pH 7)–acetone, 90 : 10

**Table 1** Synthesis of the nucleopeptide esters **8**–**12** and their selective deprotection with lipase from *Aspergillus niger* (AA = amino acid, B = nucleobase)

| | | | | | Coupling | | Deprotection | |
|---|---|---|---|---|---|---|---|---|
| Entry | AA[1] | AA[2] | AA[3] | B | Yield (%) | | Yield (%) | |
| 1 | Ser | Gly | Asp (All) | C | **10** | 61 | **15** | 70 |
| 2 | Ser | Glu (All) | — | C | **11** | 62 | **16** | 58 |
| 3 | Ser | Phe | — | C | **12** | 75 | **17** | 70 |
| 4 | Ser | Val | Phe | C | **13** | 69 | **18** | 59 |
| 5 | Thr | Phe | — | A | **14** | 71 | **19** | 63 |

*Aspergillus niger* at pH 7 and 37 °C the C-terminal carboxylic acid was smoothly deprotected (Scheme 1, Table 1). In the case of these multifunctional, complex peptide conjugates, too, the enzymatic transformations occured without any undesired side reaction, *i.e.* neither the acetate, N-terminal urethane, allyl phosphate, phenylacetamide and peptide bonds, nor the acid-labile purine nucleoside and the extremely base-labile serine phosphates were attacked. The biocatalyst again tolerated the presence of purine and pyrimidine bases and different amino acids and amino acid sequences in the nucleopeptides. Its substrate specificity guaranteed that the allyl esters which were employed for masking of the amino acid side chain functions in **10** and **11** were not removed either. By means of this enzymatic protecting group technique the desired selectively unmasked nucleopeptides **15**–**19** were obtained in high yield. Nucleopeptide **15** represents the characteristic linkage region of the nucleoprotein of adenovirus 2,[12] and **16** is derived from the nucleoprotein of bacteriophage Ø 29.[13]

Overall, the enzymatic protecting group strategy and the set of orthogonally stable blocking groups described here open a route to the construction of complex and sensitive nucleopeptides by means of a flexible building block strategy. The ready accessibility of these multifunctional peptide conjugates may serve to develop new tools for research at the interface between chemistry and biology.

This work was supported by the Bundesministerium für Bildung und Forschung, the Boehringer Mannheim GmbH and the Fonds der Chemischen Industrie.

## Footnote and References

† Synthesis of **1**–**3**: i, $Me_3SiCl$ (6 equiv.), pyridine, room temp., then $PhCH_2COCl$ (3 equiv.), 1-hydroxybenzotriazole (2 equiv.), MeCN–pyridine (2 : 1), room temp., then conc. $NH_3$, 0 °C, 87–92%; ii, 4,4′-dimethoxytrityl chloride (1.2 equiv.), pyridine, room temp., then $Ac_2O$ (6 equiv.), DMAP, 81–89%; iii, $ZnBr_2$, $MeNO_2$, room temp., 10 min, 71–74%; iv, *N*-allyloxycarbonyl amino acid methyl ester phosphoroamidate, tetrazole, room temp., then $Bu^tOOH$, 0 °C, 68–82%.

1 B. A. Juodka, *Nucleosides Nucleotides*, 1984, **3**, 445; J. C. Wang, *Annu. Rev. Biochem.*, 1985, **54**, 665; A. B. Vartapetian and A. A. Bogdanov, *Progress Nucleic Acids Res. Mol. Biol.*, 1987, **34**, 209; T. J. Kelly, M. S. Wold and J. Li, *Adv. Virus Res.*, 1988, **34**, 1.
2 Review: M. Salas, *Annu. Rev. Biochem.*, 1991, **160**, 39; L. Blanco, J. M. Lázaro, M. de Vega, A. Bonnin and M. Salas, *Proc. Natl. Acad. Sci. USA*, 1994, **91**, 12 198.
3 For a recent review on the synthesis of nucleotides which also adresses the problems encountered in the removal of the blocking functions, see S. L. Beaucage and R. P. Iyer, *Tetrahedron*, 1992, **48**, 2223.
4 B. Juodka, V. Kirveliene and P. Povilionis, *Nucleosides Nucleotides*, 1982, **1**, 497; E. Kuyl-Yeheskiely, P. A. M. van der Klein, G. M. Visser, G. A. van der Marel and J. H. van Boom, *Recl. Trav. Chim. Pays-Bas*, 1986, **105**, 69.
5 E. Kuyl-Yeheskiely, C. M. Tromp, A. W. M. Lefeber, G. A. van der Marel and J. H. van Boom, *Tetrahedron*, 1988, **44**, 6515; E. Kuyl-Yeheskiely, C. M. Dreef-Tromp, A. Geluk, G. A. van der Marel and J. H. van Boom, *Nucleic Acids Res.*, 1989, **17**, 2897; C. M. Dreef-Tromp, J. C. M. van der Marel, H. van den Elst, G. A. van der Marel and J. H. van Boom, *Nucleic Acids Res.*, 1992, **20**, 4015; Y. Ueno, R. Saito and T. Hata, *Nucleic Acids Res.*, 1993, **21**, 4451; J. Robles, E. Pedroso and A. Grandas, *Tetrahedron Lett.*, 1994, **35**, 4449; J. Robles, E. Pedroso and A. Grandas, *J. Org. Chem.*, 1994, **59**, 2482; J. Robles, E. Pedroso and A. Grandas, *Nucleic Acids Res.*, 1995, **23**, 4151.
6 Reviews: (*a*) H. Waldmann and M. Schelhaas, *Angew. Chem.*, 1996, **108**, 2192; *Angew. Chem., Int. Ed. Engl.*, 1996, **35**, 2056; (*b*) H. Waldmann and D. Sebastian, *Chem. Rev.*, 1994, **94**, 911; (*c*) T. Kappes and H. Waldmann, *Liebigs Ann. Recl.*, 1997, 803.
7 H. Waldmann and A. Reidel, *Angew. Chem.*, 1997, **109**, 642; *Angew. Chem., Int. Ed. Engl.*, 1997, **36**, 647; H. Waldmann, A. Heuser and A. Reidel, *Synlett* 1994, 65-67.
8 For the enzymatic removal of methyl esters from glycosylated amino acids, see D. Cantacuzene, S. Attal and S. Bay, *Bioorg. Med. Chem. Lett.*, 1991, **1**, 197; S. Attal, S. Bay and D. Cantacuzene, *Tetrahedron*, 1992, **48**, 9251; H. Ishii, K. Unabashi, Y. Mimura and Y. Inoue, *Bull. Chem. Soc. Jpn.*, 1990, **63**, 3042.
9 M. Dessolin, M.-G. Guillerez, N. Thieriet, F. Guibé and A. Loffet, *Tetrahedron Lett.*, 1995, **36**, 5741.
10 For the undesired attack of proteases on peptide bonds in the course of enzymatic removals of blocking functions from peptides see the references given in ref. 6(*b*), in particular: E. Walton, J. O. Rodin, C. H. Stammer and F. W. Holly, *J. Org. Chem.*, 1962, **27**, 2255; G. Kloss and E. Schröder, *Hoppe-Seylers Z. Physiol. Chem.*, 1964, **336**, 248.
11 For the enzymatic removal of MEE esters from glycosylated amino acids and glycopeptides, see J. Eberling, P. Braun, D. Kowalczyk, M. Schultz and H. Kunz, *J. Org. Chem.*, 1996, **61**, 2638.
12 J. E. Smart and B. W. Stillmann, *J. Biol. Chem.*, 1982, **257**, 13 499.
13 J. M. Hermoso and M. Salas, *Proc. Natl. Acad. Sci. USA*, 1980, **77**, 6425; J. M. Hermoso, E. Mendez, F. Soriano and M. Salas, *Nucleic Acids Res.*, 1985, 13, 7715.

*Received in Glasgow, UK, 16th June 1997; 7/04215I*

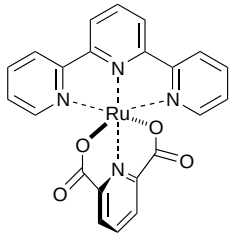
# Novel ruthenium–pyridinedicarboxylate complexes of terpyridine and chiral bis(oxazolinyl)pyridine: a new catalytic system for alkene epoxidation with [bis(acetoxy)iodo]benzene as an oxygen donor

**Hisao Nishiyama,* Tomoo Shimada, Hirofumi Itoh, Hirotaka Sugiyama and Yukihiro Motoyama**

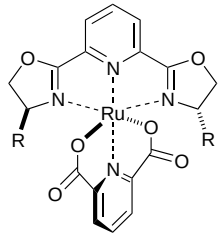
*School of Materials Science, Toyohashi University of Technology, Tempaku-cho, Toyohashi 441, Japan*

**Ruthenium–pyridine-2,6-dicarboxylate (pydic) complexes 1–3 of terpyridine and chiral bis(oxazolinyl)pyridines (pybox-*ip* and pybox-*ph*), which can be synthesized from [Ru(*p*-cymene)$Cl_2$]$_2$ and the corresponding ligands, exhibit catalytic activity for epoxidation of *trans*-stilbene in combination with [bis(acetoxy)iodo]benzene: asymmetric induction with 2 was observed in 74% ee for *trans*-stilbene.**

Ruthenium complexes with nitrogen-based ligands have been intensively investigated in order to develop catalysts for organic oxidation processes and to simulate the mechanism of bio-organic oxidation. This is because ruthenium complexes act as oxidation catalysts, often *via* ruthenium-oxo species, oxidizing alcohols or alkanes and epoxidizing alkenes.[1,2] We are especially interested in Balavoine's alkene epoxidation using $RuCl_3$–bipyridine–$NaIO_4$, in which addition of bipyridine can efficiently minimize cleavage of the alkene, even in the presence of $NaIO_4$.[3] In connection of our studies of transition-metal catalysis with terdentate bis(oxazolinyl)pyridine (Pybox) ligands,[4] we have been studying an applicaton of Ru–bisoxazoline catalysts for catalytic epoxidation of alkenes accompanied by asymmetric induction.[5] In this respect, Waegell reported an asymmetric alkene epoxidation with Ru–oxazoline catalysts with low asymmetric induction,[6] and Che described an asymmetric and stoichiometric oxygen transfer from a chiral ruthenium complex to styrene; 56% ee for 4-chlorostyrene.[7] As a new catalyst design, we adopted the introduction of dual closed meridional stereotopes around an active metal and consequently chose pyridine-2,6-dicarboxylate (pydic) as the counterpart. Here we disclose a synthesis of Ru(pydic)(terpy) (terpy = 2,2′:6′,2″-terpyridine) **1** as a non-



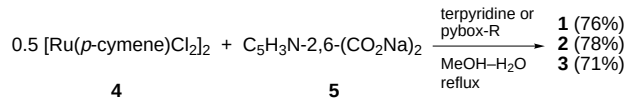
**1**



**2** R = Pr$^i$
**3** R = Ph

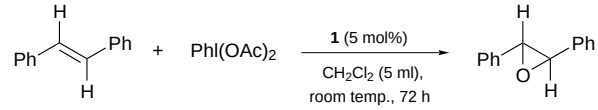
chiral catalyst and Ru(pydic)(pybox-R) **2** (R = Pr$^i$) and **3** (R = Ph) as chiral catalysts, and their catalytic activity for alkene epoxidation is also demonstrated.

A mixture of [Ru(*p*-cymene)$Cl_2$]$_2$ **4**, disodium pyridine-2,6-dicarboxylate **5**, and 2,2′:6′,2″-terpyridine was treated in MeOH–$H_2O$ at reflux for 1 h under argon atmosphere. After cooling the reaction mixture, Ru(pydic)(terpy) **1** was obtained in 78% yield as a dark violet precipitate by filtration (Scheme 1).† Complex **1**, which is stable in air, is slightly soluble in MeOH (*ca*. 10 mg in 25 ml), but almost insoluble in $CH_2Cl_2$ and $CHCl_3$ (*ca*. < 10 mg in 200 ml). Chiral complexes **2** and **3** were also prepared by the same procedure as shown in Scheme 1.‡




**Scheme 1**

We first examined epoxidation of *trans*-stilbene **6** (0.5 mmol) with iodosobenzene (PhIO) (1.5 mmol) in $CH_2Cl_2$ (5 ml) in the presence of **1** (5 mol%) (Scheme 2) (Table 1, run 1) *trans*-Stilbene oxide **8** was obtained in good to excellent yield (67%) with a small amount of benzaldehyde (8%), and some **6** (5%) was recovered. After screening of several oxidants, we found that [bis(acetoxy)iodo]benzene **7** [PhI(OAc)$_2$]§ served as an efficient oxygen donor assisted by complex **1**; PhI(OAc)$_2$ has better solubility in $CH_2Cl_2$. When **7** (1.0 mmol) was added to a suspension of complex **1** (14 mg, 5 mol%) in a $CH_2Cl_2$ (5 ml) solution of **6** (0.5 mmol), complex **1** spontaneously reacted, dissolved and gave a dark brown solution. The catalytic epoxidation proceeded slowly at room temperature for 72 h to give *trans*-stilbene oxide in excellent yield (92%) (run 3). However, use of $NaIO_4$ resulted in exclusive cleavage of the alkene (run 5). Epoxidation under aerobic epoxidation with Bu$^t$CHO/$O_2$ (1 atm). (run 6) and use of Bu$^t$OOH (run 7) resulted in yields of 86 and 81%, respectively.




**Scheme 2**

We then examined asymmetric epoxidation of *trans*-stilbene **6** with Ru(pydic)(pybox-*ip*) **2** (5 mol%), which also exhibited catalytic activity with PhIO (3 equiv.) and PhI(OAc)$_2$ (3 equiv.)

**Table 1** Catalytic epoxidation of *trans*-stilbene with Ru(pydic)(terpy) **1**[a]

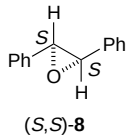
| Run | Oxidant | Oxidant : *trans*-stilbene/mmol | *t*/h | Yield (%) | Recovered alkene (%) |
|---|---|---|---|---|---|
| 1 | PhIO | 1.5 : 0.5 | 72 | 67 | 5 |
| 2 | PhI(OAc)$_2$ | 0.5 : 0.5 | 96 | 49 | 39 |
| 3 | PhI(OAc)$_2$ | 1.0 : 0.5 | 72 | 92 | 0 |
| 4 | PhI(OAc)$_2$[b] | 1.0 : 0.5 | 96 | 90 | 5 |
| 5 | $NaIO_4$[c] | 2.5 : 0.5 | 96 | 0 | 0[d] |
| 6 | $O_2$/Bu$^t$CHO[e] | 2.5 : 0.5 | 48 | 86 | 1 |
| 7 | Bu$^t$OOH | 2.0 : 0.5 | 24 | 81 | 1 |

[a] Catalyst **1** (0.025 mmol, 5 mol% of *trans*-stilbene), $CH_2Cl_2$ (5 ml), at room temperature. The yields are based on 0.5 mmol of *trans*-stilbene. Benzaldehyde was obtained in the range 2–10%. [b] Acetone (5 ml) was used as a solvent. [c] $NaIO_4$ (3.5 mmol), $H_2O$ (2.5 ml), room temp. [d] Benzaldehyde (27%) was obtained. [e] Bu$^t$CHO (2.5 mmol), $O_2$ (1 atm).

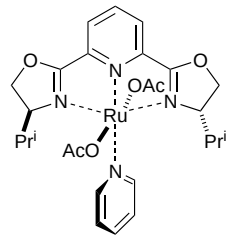
**Table 2** Asymmetric catalytic epoxidation of *trans*-stilbene with Ru(pydic)(pybox-*ip*) **2**[a]

| Run | Oxidant | Oxidant : *trans*-stilbene/mmol | Solvent | *T* °C | *t*/h | *trans*-Stilbene oxide Yield (%) | *trans*-Stilbene oxide Ee (%) | Recovered alkene (%) |
|---|---|---|---|---|---|---|---|---|
| 1 | PhIO | 1.5 : 0.5 | PhMe | 25 | 96 | 67 | 24 | 9 |
| 2 | $PhI(OAc)_2$ | 1.5 : 0.5 | PhMe | 25 | 96 | 80 | 63 | 3 |
| 3 | $PhI(OAc)_2$ | 1.5 : 0.5 | PhMe | 0 | 96 | 63 | 74 | 18 |
| 4 | $PhI(OAc)_2$ | 1.5 : 0.5 | $C_6H_6$ | 25 | 96 | 43 | 52 | 22 |
| 5 | $PhI(OAc)_2$ | 1.5 : 0.5 | $CH_2Cl_2$ | 25 | 96 | 40 | 36 | 27 |
| 6 | $NaIO_4$[b] | 2.5 : 0.5 | PhMe | 5 | 96 | trace | — | trace |
| 7 | $O_2$/Bu$^t$CHO[c] | 2.5 : 0.5 | PhMe | 25 | 96 | 67 | 5 | 3 |
| 8 | Bu$^t$OOH | 2.0 : 0.5 | $CH_2Cl_2$ | 25 | 72 | 38 | 16 | 38 |

[a] Catalyst **2** (0.025 mmol, 5 mol% of *trans*-stilbene), solvent (10 ml). The yields are based on 0.5 mmol of *trans*-stilbene. Benzaldehyde was obtained in the range 2–14%. The ees were determined by chiral LC (Daicel Chiralcel OD). All epoxides had (1*S*,2*S*) configuration. [b] $NaIO_4$ (3.5 mmol), $H_2O$ (2.5 ml). [c] Bu$^t$CHO (2.5 mmol), $O_2$ (1 atm).




(*S*,*S*)-**8**




**9**

to give 67 and 80% yields of (1*S*,2*S*)-*trans* stilbene oxide (*S*,*S*)-**8** (24 and 63% ee), respectively (Table 2, runs 1 and 2). The best result for this catalytic system was obtained at 0 °C (74% ee, run 3). When performed in toluene rather than $CH_2Cl_2$ or $C_6H_6$, epoxidation using complex **2** (5 mol%) and $PhI(OAc)_2$ (3 equiv.) gave higher yields (runs 2, 4 and 5). Aerobic oxidation and oxidation with Bu$^t$OOH proceeded but gave relatively low yields and enantiomeric excesses (runs 7 and 8).

The Ru(pydic)(pybox-*ph*) complex **3** gave slightly lower enantioselectivities than **2**; oxidation of *trans*-stilbene under the same conditions as in run 2 of Table 2 gave the epoxide in 84% yield (58% ee).

In comparison, *trans*-$(AcO)_2$Ru(pybox-*ip*)(pyridine) **9**, prepared by reaction of $[Ru(p\text{-cymene})(OAc)_2]_2$,[8] pybox-*ip* and pyridine, was examined as an oxidation catalyst with $PhI(OAc)_2$. The complex **9** (5 mol%) similarly catalysed the epoxidation of **6** under the same conditions as in run 2 of Table 2 to give racemic *trans*-stilbene oxide in 49% yield; 15% of the alkene was recovered. This finding implies that the meridional tridentate connected structure of pydic on **2** and **3** must be rigid enough during the catalysis to help pybox maintain the chiral environment, inducing the enantioselection.

Thus, we have found a new alkene epoxidation methodology utilizing ruthenium(II) complexes having the dual meridional system of pydic with terpyridine and pybox, in combination with $PhI(OAc)_2$ as the oxygen donor. Our studies are now focused on the scope and limitations of this alkene epoxidation and its mechanism.

## Footnotes and References

* E-mail: hnishi@tutms.tut.ac.jp

† Synthesis of Ru(pydic)(terpy) **1**. To a solution of $[Ru(p\text{-cymene})Cl_2]_2$ **4** (150 mg, 0.24 mmol) and 2,2′ : 6′,2″-terpyridine (144 mg, 0.48 mmol) in MeOH (8 ml) was added a solution of disodium pyridine-2,6-dicarboxylate **5** (0.48 mmol) in MeOH–$H_2O$ (2 : 1, 7.2 ml) under argon atomosphere. The mixture was stirred at 60 °C for 1 h. The dark violet precipitate was collected by filtration to give **1** (183 mg, 0.37 mmol) in 76% yield. Calc. for $C_{22}H_{14}N_4O_4Ru(H_2O)$: C, 49.35; H, 3.39; N, 10.46. Found: C, 49.11; H, 3.52; N, 10.65%; $\nu_{max}$(KBr)/cm$^{-1}$ 1650, 1620.

‡ Synthesis of Ru(pydic)(pybox-*ip*) **2**. To a solution of $[Ru(p\text{-cymene})Cl_2]_2$ **4** (306 mg, 0.5 mmol) and pybox-*ip* (301 mg, 1.0 mmol) in MeOH (7 ml) was added a solution of disodium pyridine-2,6-dicarboxylate **5** (1.0 mmol) in MeOH–$H_2O$ (2 : 1, 15 ml) under argon atmosphere. The mixture was stirred at 60 °C for 1 h. The mixture was extracted with $CH_2Cl_2$ (40 ml). The combined organic layers were concentrated and the residue was purified by silica gel column chromatography with $CH_2Cl_2$–MeOH (50 : 1) to give **2** as a dark violet solid (444 mg, 0.78 mmol) in 78% yield; mp > 240 °C (decomp.) $\delta_H$ (270 MHz, $CDCl_3$, $Me_4Si$) 0.48 (d, *J* 6.8, 6 H), 0.62 (d, *J* 6.8, 6 H), 1.09 (m, 2 H), 3.71 (m, 2 H), 4.61 (dd, 2 H), 4.70 (dd, 2 H), 7.64 (t, 1 H), 7.88 (d, 2 H), 8.11 (t, 1 H), 8.34 (d, 2 H). Calc. for $C_{24}H_{26}N_4O_6Ru$: C, 50.79; H, 4.62. Found: C, 50.59; H, 4.72%.

§ $PhI(OAc)_2$ was purchased from ACROS. See *Encyclopedia of Reagents for Organic Synthesis*, ed. L. A. Paquette, Wiley, New York, 1995, vol. 2, p. 1479.

1 For review, see G. A. Barf and R. A. Sheldon, *J. Mol. Catal. A: Chem.*, 1995, **102**, 23 and references cited therein; C.-M. Che, *Pure Appl. Chem.*, 1995, **67**, 225; T. Mukaiyama and T. Yamada, *Bull. Chem. Soc. Jpn.*, 1995, **68**, 17; K. A. Jörgensen, *Chem. Rev.*, 1989, **89**, 431; S. I. Murahashi, *Angew. Chem., Int. Ed. Engl.*, 1995, **34**, 2443.

2 For example: G. A. Barf, D. van den Hoek and D. Sheldon, *Tetrahedron*, 1996, **52**, 12 971; A. M. J. Jorna, A. E. M. Boerrijk and H. J. Hoorn, *React. Funct. Polym.*, 1996, **29**, 10; H. Aneetha, J. Padmaja and P. S. Zacharias, *Polyhedron*, 1996, **15**, 2445; M. H. Robbins and R. S. Drago, *J. Chem. Soc., Dalton Trans.*, 1996, 105; W.-Y. Ru, W.-C. Cheng and C.-M. Che, *Polyhedron*, 1994, **13**, 2963.

3 G. Balavoine, C. Eskenazi, F. Meunier and H. Rivière, *Tetrahedron Lett.*, 1984, **25**, 3187; C. Eskénazi, G. Balavione, F. Meuneir and H. Rivière, *J. Chem. Soc., Chem. Commun.*, 1985, 1111.

4 H. Nishiyama, Y. Itoh, Y. Sugawara, H. Matsumoto, K. Aoki and K. Itoh, *Bull. Chem. Soc. Jpn.*, 1995, **68**, 1247 and references cited therein.

5 H. Nishiyama, S.-B. Park, M. Haga, K. Aoki and K. Itoh, *Chem. Lett.*, 1994, 1111.

6 C. Augier, L. Malara, V. Lazzeri and B. Waegell, *Tetrahedron Lett.*, 1995, **36**, 8775 and references for ruthenium-catalysed oxidation cited therein. For a review, see G. A. Barf and R. A. Sheldon, *J. Mol. Catal. A: Chem.*, 1995, **102**, 23.

7 W.-H. Fung, W.-C. Cheng, W.-Y. Yu, C.-M. Che and T. C. W. Mak, *J. Chem. Soc., Chem. Commun.*, 1995, 2007.

8 D. A. Tocher, R. O. Gould and T. A. Stephenson, *J. Chem. Soc., Chem. Commun.*, 1983, 1571.

*Received in Cambridge, UK, 17th July 1997; 7/05109C*

# Solvent effects on thermodynamic parameters for porphyrin–quinone interaction through multiple hydrogen bonding

**Takashi Hayashi,*† Takashi Miyahara, Norihiro Koide and Hisanobu Ogoshi*‡**

*Department of Synthetic Chemistry and Biological Chemistry, Graduate School of Engineering, Kyoto University, Sakyo-ku, Kyoto 606-01, Japan*

**The enthalpy–entropy compensation plots for noncovalently linked porphyrin–quinone complexation exhibit a non-linear hook-shaped relationship between $\Delta H°$ and $T\Delta S°$ at various polarities in a toluene–ethanol binary solvent.**

In general, water disrupts the formation of host–guest complexes linked by hydrogen bonding and complicates the binding mode in biological systems.[1,2] Thus, a simple host–guest model system would be very useful for evaluation of the effect of water on the thermodynamic parameters of the binding process. Recently, we have examined hydrogen-bonded porphyrin–quinone complexation,[3] in which ethanol was used as a co-solvent to simulate the behaviour of traces of water in a hydrophobic binding pocket in an enzyme. Here we report the solvent effects on the enthalpy and entropy changes upon binding between *meso*-α,α,α,α-tetrakis(2-hydroxy-1-naphthyl)porphyrin **1** and 2,3,5,6-tetramethoxy-*p*-benzoquinone **2** in a toluene–ethanol or toluene–butan-2-one binary solvent system (Fig. 1).[4,5]

Upon addition of ethanol or butan-2-one to the toluene solution, the affinity of **2** for **1** decreased with the increasing polarity of solvent.[6]§ Thermodynamic parameters ($\Delta H°$ and $\Delta S°$) for **1·2** complexation at various polarities were determined from van't Hoff plots obtained by UV–VIS titrimetric measurement. The van't Hoff plots show linearity in pure toluene and at > 5.2 mol% of ethanol in toluene, whereas the plots at 0.36–3.5 mol% of ethanol in toluene gave a curved line, suggesting that $\Delta H°$ is a temperature-dependent parameter with non-zero heat capacity changes.¶ In contrast, a linear relationship was observed for the toluene–butan-2-one binary solvent system.

It is known that enthalpy–entropy diagrams for host–guest complexation generally display a linear relationship in a solvent system of varying polarity.[7] However, in this work, the $\Delta H°$ *vs.* $T\Delta S°$ compensation plots for **1·2** complexation in a toluene–ethanol binary system exhibit a unique hook-shaped line as shown in Fig. 2(*a*), with a turning point at approximately 3.5 mol% ethanol in toluene. One plausible interpretation is given in Fig. 3. In the presence of a polar solvent such as ethanol, we observe only the overall complexation comprised of solvent free complex **1·2** and various states of solvated complex **1·2**. Assuming that the affinity of ethanol molecules for complex free **1** and **2** is larger than that for complex **1·2**, $-\Delta H°$ drastically decreases upon addition of ethanol, since the functional sites of complex free **1** and **2** are saturated and stabilized by ethanol co-solvent even at low concentrations of ethanol ($|\Delta H°_a| > |\Delta H°_b|$ in Fig. 3). In contrast, the solvation of complex **1·2** gradually increases with the increasing number of ethanol molecules, and $\Delta H°$ becomes more negative in the presence of sufficient interactive ethanol to complex **1·2** ($|\Delta H°_b| < |\Delta H°_c|$ in Fig. 3). On the other hand, the entropy changes seem to depend on the behaviour of the ethanol molecules. At lower concentrations of ethanol, the desolvation of functional groups in **1** and **2** upon complexation contributes to entropy gain, whereas at higher concentrations of ethanol, the ethanol solvation of complex **1·2** and the formation of aggregated cluster of excess ethanol itself in apolar toluene

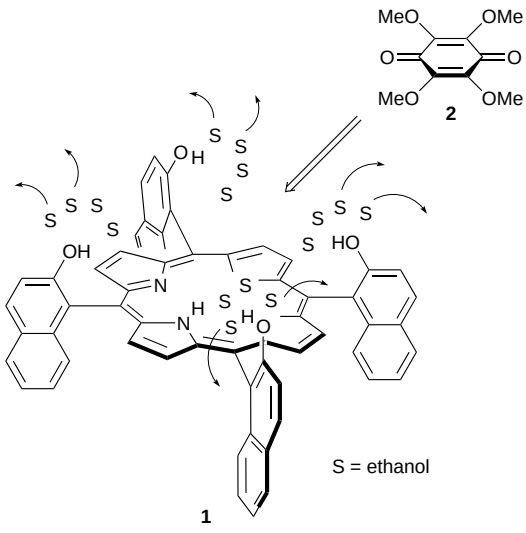



**Fig. 1**

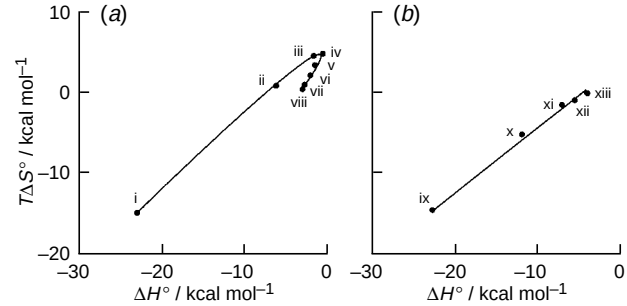



**Fig. 2** Plots of the apparent $\Delta H°$ *vs.* $T\Delta S°$ for the binding of quinone **2** to porphyrin **1** at 298 K in (*a*) toluene–ethanol and (*b*) toluene–butan-2-one mixtures: (i) 0, (ii) 0.9, (iii) 1.8, (iv) 3.5, (v) 5.2, (vi) 8.3, (vii) 13 and (viii) 15 mol% EtOH in toluene, and (ix) 0, (x) 3.4, (xi) 11, (xii) 19 and (xiii) 28 mol% butan-2-one in toluene

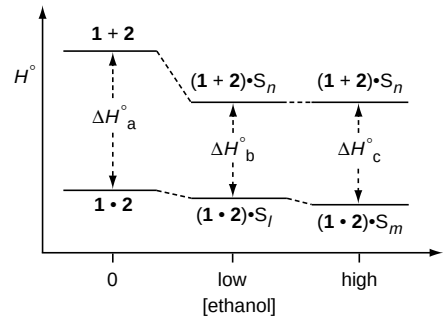



**Fig. 3** Variation of $H°$ with concentration of EtOH; (**1** + **2**)·S = solvated **1** and **2**, (**1·2**)·S = solvated complex of **1·2**, S = ethanol molecule(s), *l*, *m* and *n* represent the number of ethanol molecules

gives rise to entropy loss.[8] In contrast, the same compensation plots in the toluene–butan-2-one binary solvent system show a linear relationship [Fig. 2(*b*)], suggesting that the solvation of functional groups in **1** and **2** in toluene–butan-2-one is weaker than that in the toluene–ethanol binary solvent system.

To the best of our knowledge, this is the first example of a hook-shaped $\Delta H°$ *vs.* $\Delta S°$ relationship in host–guest complexation *via* hydrogen-bonding interaction. Eftink has reported the simulation of the hook-shaped enthalpy–entropy relationship due to the protonation of a protein–ligand complex in a variety of pH conditions.[9,10]‖ Thus, our present results derived from the solvation of recognition sites at a variety of polarities is consistent with previous results from the literature that focused on the protonation of each component in protein–ligand binding.

In conclusion, this work indicates that the enthalpy and entropy changes for binding processes *via* hydrogen-bonding recognition are strongly influenced by solvation in a compensating manner.

T. M. is grateful for a Research Fellowship from the Japan Society for the Promotion of Science for Young Scientists.

## Footnotes and References

† E-mail: hayashi@sbchem.kyoto-u.ac.jp
‡ Current address: Fukui National College of Technology, Sabae, Fukui 916, Japan.

§ In the $^1$H NMR spectrum of **1**, the OH proton at δ 4.97 in pure toluene was shifted downfield with increasing concentration of ethanol or butan-2-one. The downfield shift in toluene–ethanol is approximately twice that in toluene–butan-2-one.

¶ The discussion of heat capacity changes has been previously reported [ref. 3(*c*)]. We calculated the thermodynamic parameters from non-linear van't Hoff plots by use of following equation:

$$R\ln K(T) = -[\Delta H°(T)/T] + \Delta S°(T)$$
$$= -[\Delta H°(T_0) + (T - T_0)\Delta C_p°]/T + \Delta C_p°\ln(T/T_o) + \Delta S°(T_0)$$

where $K(T)$, $\Delta H°(T)$ and $\Delta S°(T)$ are temperature-dependent parameters and $\Delta H°(T_0)$ and $\Delta S°(T_0)$ are constants with $T = T_0$.

‖ It has been suggested that hook-shaped $\Delta H°$ *vs.* $\Delta S°$ compensation plots in ligand binding could be caused by a change in pH, ionic strength, solvent composition or macromolecule concentration (ref. 10).

1 R. Lumry and S. Rajender, *Biopolymers*, 1970, **9**, 1125.
2 M. Eftink and R. Biltonen, in *Biological Microcalorimetry*, ed. A. E. Beezer, Academic Press, New York, 1980, pp. 343–412.
3 (*a*) T. Hayashi, T. Miyahara, N. Hashizume and H. Ogoshi, *J. Am. Chem. Soc.*, 1993, **115**, 2049; (*b*) T. Hayashi, T. Miyahara, Y. Aoyama, M. Kobayashi and H. Ogoshi, *Pure Appl. Chem.*, 1994, **66**, 797; (*c*) T. Hayashi, T. Miyahara, N. Koide, Y. Kato, H. Masuda and H. Ogoshi, *J. Am. Chem. Soc.*, 1997, **119**, 7281.
4 J. C. Adrian, Jr. and C. S. Wilcox, *J. Am. Chem. Soc.*, 1992, **114**, 1398; R. P. Bonar-Law and J. K. M. Sanders, *J. Am. Chem. Soc.*, 1995, **117**, 259.
5 Recently, there have been several model studies focusing on the solvent effect using a cyclophane–substrate complex linked by hydrophobic contacts in polar solvent: J. C. Harrison and M. R. Eftink, *Biopolymers*, 1982, **21**, 1153; D. A. Stauffer, R. E. Barrans, Jr. and D. A. Dougherty, *J. Org. Chem.*, 1990, **55**, 2762; F. Diederich, D. B. Smithrud, E. M. Sanford, T. B. Wyman, S. B. Ferguson, D. R. Carcanague, I. Chao and K. N. Houk, *Acta Chem. Scand.*, 1992, **46**, 205; B. Zhang and R. Breslow, *J. Am. Chem. Soc.*, 1993, **115**, 9353.
6 D. B. Smithrud and F. Diederich, *J. Am. Chem. Soc.*, 1990, **112**, 339.
7 D. B. Smithrud, T. B. Wyman and F. Diederich, *J. Am. Chem. Soc.*, 1991, **113**, 5420.
8 P. Nagy and R. Herzfeld, *Acta Phys. Chim.*, 1985, **31**, 736; B. B. Swain, *Curr. Sci.*, 1985, **54**, 504.
9 M. R. Eftink, A. C. Anusiem and R. Biltonen, *Biochemistry*, 1983, **22**, 3884.
10 A. C. Anusiem, J. G. Beetlestone and D. H. Irvine, *J. Chem. Soc. A*, 1966, 357; A. C. Anusiem, J. G. Beetlestone and D. H. Irvine, *J. Chem. Soc. A*, 1968, 960.

*Received in Cambridge, UK, 12th June 1997; 7/04107A*

# Synthesis of a bifunctional cannabinoid ligand

**Marcus A. Tius,* Jakob Busch-Petersen and Andrew R. Marris**

*Department of Chemistry, University of Hawaii, 2545 The Mall, Honolulu, Hawaii 96822, USA*

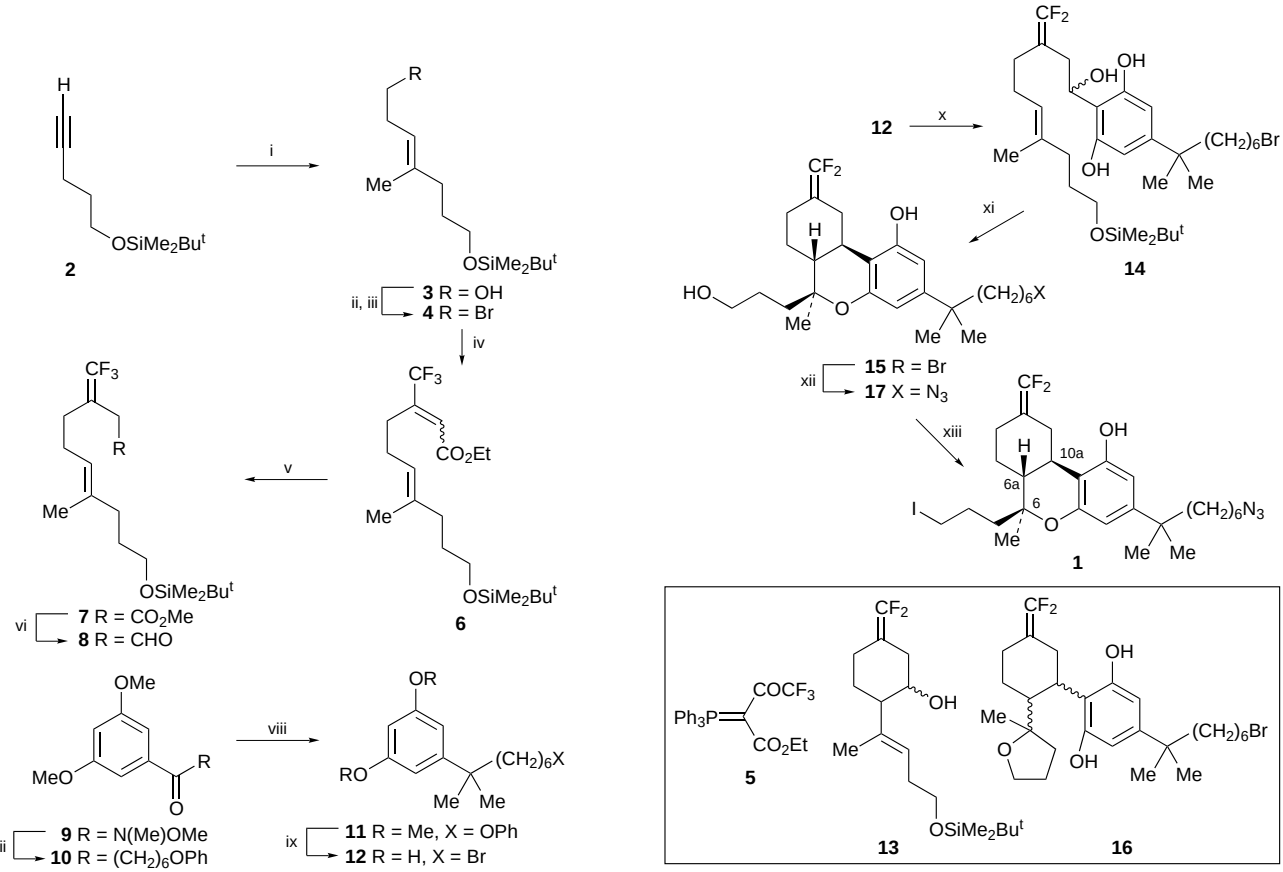
**A novel bifunctional classical-nonclassical hybrid cannabinoid has been prepared expeditiously through the Diels–Alder reaction of an *ortho*-quinomethane.**

The identification of two distinct cannabinoid receptors[1] has led to a resurgence of interest in this area. Rational design of new materials for pharmaceutical development requires a detailed understanding of receptor–ligand interactions at the molecular level. The availability of cloned cannabinoid CB1 receptor and our identification of a class of high-affinity ligands suggested an experiment in which irreversible covalent binding[2] of the ligand to the receptor at two sites would take place. Partial digestion of the receptor–ligand covalent complex, followed by analysis of the fragments, would serve to locate the ligand within the active site.

A convergent synthesis of the racemate of classical-nonclassical cannabinoid **1** (Scheme 1) is described. The C7′ azido group in **1** can be activated photochemically, whereas the iodo group is expected to react with proximal nucleophilic residues within the active site. In earlier work we have shown that the β-3-iodopropyl group at C6 confers improved binding properties of ligands to the CB1 receptor.[3]

The aliphatic portion of **1** was prepared from the *tert*-butyldimethylsilyl ether of pent-4-yn-1-ol **2** *via* a carboalumination–alkylation process (Scheme 1).[4] Published procedures call for evaporation of the halogenated solvent and its replacement by $Et_2O$ prior to the formation of the alanate. This works well, but is inconvenient on a large scale. We have determined that solvent replacement is unnecessary. Slow addition of a precooled solution of *n*-butyllithium in hexane to the intermediate alane derived from **2** in either $ClCH_2CH_2Cl$ or $CH_2Cl_2$ at −78 °C produced the alanate.[5] Quenching with ethylene oxide gave alcohol **3** in 88% yield. This represents a significant improvement for the process.

Bromide **4** was obtained from **3** *via* the toluene-*p*-sulfonate following treatment with LiBr. Metal–halogen exchange, addition of the lithio species to phosphorane **5**[6] and treatment with acetic acid gave α,β-unsaturated ester **6**. Exposure of **6** to




**Scheme 1** *Reagents and conditions*: i, $Cp_2ZrCl_2$, $AlMe_3$, $CH_2Cl_2$, 0 °C, 16 h; $Bu^nLi$, −45 °C, 0.5 h; ethylene oxide, −30 to 0 °C, 4 h, 88%; ii, TsCl, pyridine, 0 °C; iii, LiBr, acetone, room temp., 82% from **2**; iv, $Bu^tLi$, $Et_2O$, −78 °C; **5**, THF, −78 to −14 °C, 16 h; AcOH, 0 °C, 0.5 h, 74%; v, Mg, MeOH, room temp., 16 h; vi, DIBAL-H, $Et_2O$, −78 °C, 3 h; EtOH, −78 °C, 91% from **6**; vii, $Li(CH_2)_6OPh$, THF, −78 °C, 62%; viii, $TiCl_4$, $ZnMe_2$, $CH_2Cl_2$, −30 °C to room temp., 4 h; ix, $BBr_3$, $CH_2Cl_2$, −78 °C to room temp., 84% from **10**; x, MeMgBr, $Et_2O$, 0 °C, 1 h; $MgBr_2$, **8**, $CH_2Cl_2$, −78 °C to room temp.; xi, $Tf_2NH$, $ZnCl_2$, toluene, reflux, 4 h; $Tf_2NH$, $ZnCl_2$, MeOH, reflux, 4 h, 38% from **8**; xii, $TMGN_3$, $MeNO_2$, 50 °C, 3 h; xiii, $I_2$, $PPh_3$, imidazole, PhH, 35 °C, 0.75 h, 69% from **15**

Mg in MeOH led to difluoromethylene compound **7**, the desired product of fluoride elimination from a β-anionic intermediate. Small amounts (5–7%) of the saturated, β-trifluoromethyl ester were also obtained. Reduction of **7** with DIBAL-H led to aldehyde **8**.

The aromatic portion of **1** was prepared from the Weinreb amide **9** of 3,5-dimethoxybenzoic acid. Reaction of **9** with 6-phenoxyhexyllithium gave phenone **10**. Treatment of **10** with $TiCl_4$ and $ZnMe_2$ introduced the benzylic *gem*-dimethyl grouping in nearly quantitative yield.[7] Subsequent exposure of **11** to $BBr_3$ in $CH_2Cl_2$ cleaved all three ether groups and introduced the C7′ bromide of **12**. The overall yield of **12** from **10** was 84%. This protocol represents a significant improvement in terms of total number of steps and convenience over the established synthesis of the 5-(1′,1′-dimethylheptyl)resorcinol moiety.[8,9]

The coupling of **12** to **8** was challenging. Attempts to effect the reaction under Lewis acid catalysis led primarily to **13**, from the intramolecular ene reaction of **8**. Success was realized when resorcinol **12** was first converted to the monobromomagnesium salt, and then treated with a deficiency of aldehyde **8** in the presence of catalytic $MgBr_2$ to produce the coupled material **14** in 53% yield.[10] Unreacted **12** was recycled. Exposure of **14** to toluene-sulfonic acid (TsOH) in MeOH at reflux[11] gave a modest yield of dihydrobenzopyran **15** accompanied by larger amounts of tetrahydrofuran **16**.† The tetrahydrofuran probably results from a stepwise, ionic process.

The cyclization to **15** took place upon treatment of **14** with bis(trifluoromethylsulfonyl)amine[12] and $ZnCl_2$, first in toluene and then in MeOH. The relative stereochemistry at C6, C6a and C10a was determined by NOE experiments in conjunction with HMQC and HMBC experiments. The observed stereochemistry could not have been predicted with confidence from the outset. Cyclization to form the C9 methyl cannabinoid skeleton is known from precedent[11] to produce the C6a–C10a *trans* stereoisomer. Our own work[13] has shown that cyclization to form the $\Delta^9$ unsaturated series produces the unnatural C6a–C10a *cis* stereoisomer as the exclusive product, therefore the stereochemical outcome of the cyclization is easily perturbed by minor structural changes in the *seco* precursor (*cf.* **14**).

The conversion of **14** to **15** is also noteworthy because it provides the strongest support to date for the mechanism, which is postulated to involve formation of a transient *ortho*-quinomethane which undergoes intramolecular hetero-Diels–Alder cycloaddition. Product **15** provides the first example of a Diels–Alder cyclization to a cannabinoid with a stereogenic C6 carbon atom. The fact that only the β-3-hydroxypropyl isomer was formed is consistent with a concerted cycloaddition proceeding through an *exo* transition state. A stepwise ionic process would have led to diastereoisomers at C6.[14] All earlier examples of this reaction led to cannabinoids with a *gem*-dimethyl group at C6.

The conversion of **15** to C7′ azido derivative **17** was effected with tetramethylguanidinium azide ($TMGN_3$).[15] Treatment of the crude reaction product with $PPh_3$–$I_2$ complex in the presence of imidazole[16] gave **1** in 69% overall yield from **15**.‡ It is critical that an excess (*ca.* 20 mol%) of $I_2$ over $PPh_3$ be used so as to suppress the Staudinger reaction of the phosphine with the azide. It is significant that no protecting groups were used during the execution of these steps. The enantiomers of **1** were easily separated by chiral HPLC.

The methodology which has been outlined in Scheme 1 is currently being applied to the synthesis of a series of cannabinoid ligands. Full experimental details of this work, as well as the receptor binding properties of the products, will be reported in due course.

Acknowledgement is made to NIDA (DA 09158 and DA 07215) for their generous support of this work.

## Footnotes and References

* E-mail: tius@gold.chem.hawaii.edu

† The stereochemistry of **16** was not determined.

‡ *Selected data* for (−)-**1**: $[\alpha]_D$ −14 (*c* 3.0, $CHCl_3$); $\delta_H$ ($CDCl_3$, 500 MHz) 6.32 (d, *J* 1.9, 1 H), 6.19 (d, *J* 1.9, 1 H), 4.77 (br s, 1 H), 3.93 (br d, 1 H), 3.32–3.21 (m, 2 H), 3.22 (t, *J* 6.9, 2 H), 2.61 (br d, *J* 13.1, 1 H), 2.50 (td, *J* 11.4, 3.2, 1 H), 2.14–2.06 (m, 1 H), 2.05–1.97 (m, 1 H), 1.91–1.86 (m, 2 H), 1.78–1.73 (m, 2 H), 1.60 (td, *J* 11.4, 2.2, 1 H), 1.56–1.48 (m, 4 H), 1.38–1.28 (m, 3 H), 1.25–1.20 (m, 3 H), 1.20 (s, 6 H), 1.14–1.04 (m, 2 H), 1.06 (s, 3 H); $\delta_C$ ($CDCl_3$, 125 MHz) 154.65, 154.42, 151.33 (t, *J* 280), 150.21, 108.52, 107.89, 105.38, 87.12 (t, *J* 18), 77.59, 51.49, 45.69, 44.14, 40.69, 37.30, 35.08 (t, *J* 3), 29.70, 28.77, 28.69, 28.67, 28.22 (t, *J* 2), 27.08 (t, *J* 2), 27.00, 26.52, 24.41, 24.17 (t, *J* 2), 18.38, 7.60; $\delta_F$ ($CDCl_3$, 376 MHz) −97.71 (part of AB quartet, *J* 58), −97.87 (part of AB quartet, *J* 58); $\nu_{max}$ (neat)/$cm^{-1}$ 3650–3100 (broad), 2960, 2920, 2100, 1760, 1625, 1575, 1415, 1260, 1050; *m*/*z* 601 ($M^+$, 37%), 476 (100), 456 (30), 128 (39), 127 (26). Calc. for $C_{27}H_{38}F_2IN_3O_3$: 601.1977. Found: 601.1988. Chiral HPLC (1 × 25 cm, Chiracel OD column; 5% $Pr^iOH$ in hexane; 1.75 ml $min^{-1}$; UV detection at 254 nm) retention time: 29.9 min. Retention time for (+)-**1**: 33.7 min.

1 J. Busch-Petersen, W. A. Hill, P. Fan, A. Khanolkar, X.-Q. Xie, M. A. Tius and A. Makriyannis, *J. Med. Chem.*, 1996, **39**, 3790 and references cited therein.
2 A. Charalambous, G. Yan, D. B. Houston, A. C. Howlett, D. R. Compton, B. R. Martin and A. Makriyannis, *J. Med. Chem.*, 1992, **35**, 3076.
3 D. J. Drake, P. Fan, W. A. G. Hill, M. A. Tius and A. Makriyannis, *J. Med. Chem.*, in the press.
4 M. Kobayashi, L. F. Valente and E. Negishi, *Synthesis*, 1980, 1034.
5 For previous examples of alkyllithium reactions in chlorinated solvent see: K. Maruoka, I. Shimada, H. Imoto and H. Yamamoto, *Synlett*, 1994, 519.
6 Y. Shen, S. Gao, *J. Chem. Soc., Perkin Trans. 1*, 1994, 1473.
7 M. T. Reetz, J. Westermann, and S.-H. Kyung, *Chem. Ber.*, 1985, **118**, 1050.
8 S. J. Dominianni, C. W. Ryan and C. W. DeArmitt, *J. Org. Chem.*, 1977, **42**, 344.
9 R. A. Archer, W. B. Blanchard, W. A. Day, D. W. Johnson, E. R. Lavagnino, C. W. Ryan and J. E. Baldwin, *J. Org. Chem.*, 1977, **42**, 2277.
10 G. Casiraghi, M. Cornia, G. Casnati, G. Gasparri Fava, M. Ferrari Belicchi and L. Zetta, *J. Chem. Soc., Chem. Commun.*, 1987, 794.
11 Z. G. Lu, N. Sato, S. Inoue and K. Sato, *Chem. Lett.*, 1992, 1237.
12 K. Ishihara, M. Kubota and H. Yamamoto, *Synlett*, 1996, 1045.
13 M. A. Tius and X.-Q. Gu, *J. Chem. Soc., Chem. Commun.*, 1989, 1171.
14 M. A. Tius, A. M. Makriyannis, X. L. Zou and V. Abadji, *Tetrahedron*, 1994, **50**, 2671.
15 A. J. Papa, *J. Org. Chem.*, 1966, **31**, 1426.
16 P. J. Garegg and B. Samuelsson, *J. Chem. Soc., Perkin Trans. 1*, 1980, 2866.

*Received in Corvallis, OR, USA, 8th July 1997; 7/04889K*

# 7-Deazaisoguanine quartets: self-assembled oligonucleotides lacking the Hoogsteen motif

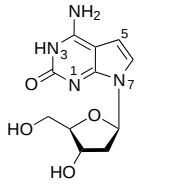
**Frank Seela* and Changfu Wei**

*Laboratorium für Organische und Bioorganische Chemie, Institut für Chemie, Universität Osnabrück, Barbarastr. 7, D-49069 Osnabrück, Germany*

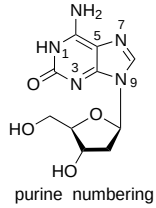
**Oligonucleotides containing consecutive 7-deazaisoguanine residues form self-assembled quartets, indicating that the purine nitrogen-7 of isoguanine is not participating in the hydrogen bonding pattern.**

Oligodeoxyribonucleotides with consecutive isoguanine residues, *e.g.* d($T_4$isoG$_4T_4$),† form self-assembled structures.[1,2] Such aggregates have also been observed in the case of the homopolyribonucleotide poly(isoguanylic acid)[3] and the monomeric ribonucleoside isoguanosine.[4] Like the G-quartet the aggregate of isoguanine has properties of an ionophore.[5] The stability of the metal complexes depend on the size of the particular ion.[6] Ion-exchange HPLC experiments showed that the aggregate of d($T_4$isoG$_4T_4$) has the same number of negative phosphate charges as that of d($T_4G_4T_4$). Due to this observation a tetrameric structure was also proposed for d($T_4$isoG$_4T_4$).[2] The stoichiometry of this complex was established using isoguanine-containing oligonucleotides with different dT-tails at the 3′- and 5′-termini.[7] So far, the isoguanine-quartet shows behaviour similar to that of guanine. Although the tetrameric assembly of isoguanine has been verified, several structural motifs have been proposed for the quartet structure.[2–4]

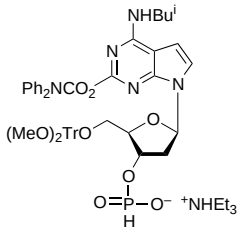
Base-modified nucleosides are useful tools to probe the structure of such high-molecular assemblies, in particular those which are held together by hydrogen bonds. Regarding this it has already been shown that the base pairing pattern can be restricted to the Watson–Crick motif when 7-deazaguanine is replacing guanine.[8] As a result, Hoogsteen quartets cannot be formed and the oligonucleotides are unable to form aggregates.[9] Based on this principle, 7-deaza-2′-deoxyisoguanosine **1** ($c^7iG_d$) has been employed to probe the oligonucleotide quartet structure formed by 2′-deoxyisoguanosine **2** (isoG$_d$). New oligonucleotide quartets should be accessible when the purine nitrogen-7 does not participate in the hydrogen bonding pattern. For this purpose the oligonucleotide building blocks **3** and **4** were synthesised. Oligonucleotides with consecutive 7-deaza-isoguanine residues were prepared and their ability to form self-assembled aggregates was studied.



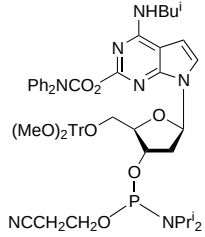

**1**



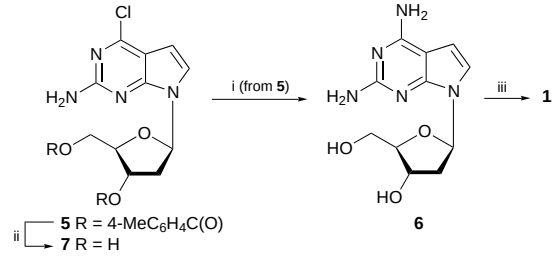

**2**




**3**




**4**



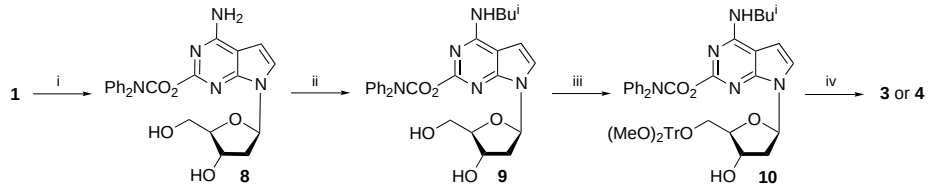

**Scheme 1** *Reagents and conditions*: i, 25% $NH_3$–dioxane (1:1 v/v), 120 °C, 3 d, 88%; ii, 25% $NH_3$–dioxane (1:1 v/v), 60 °C, 3 d, 80%; iii, $NaNO_2$, 20% aq. AcOH, 67%

7-Deaza-2′-deoxyisoguanosine **1** has already been prepared (i) by convergent nucleoside synthesis[10] or (ii) by photosubstitution on 2-chloro-7-deaza-2′-deoxyadenosine.[11] Now, a more efficient route has been employed using glycosylation of the 2-amino-4-chloro-7*H*-pyrrolo[2,3-*d*]pyrimidine anion[12] with 2-deoxy-3,5-di-*O*-(4-methylbenzoyl)-α-D-*erythro*-pentofuranosyl chloride. The resulting nucleoside **5** was treated with conc. $NH_3$–dioxane (autoclave, 120 °C, 3 d) to give 2-amino-7-deaza-2′-deoxyadenosine **6**.[13] The deprotected compound **7** was also obtained (60 °C, conc. $NH_3$–dioxane, 3 d). Selective deamination of **6** ($NaNO_2$ in aq. AcOH) furnished the nucleoside **1** (Scheme 1). It is stable in acidic solution whereas 2′-deoxyisoguanosine **2** is an extremely labile nucleoside.[1]

For the preparation of **3** and **4**, compound **1** was blocked on the 2-oxo function with a $Ph_2NC(O)$ group ($Ph_2NCOCl$, $Pr^i_2NEt$–pyridine, room temp.) to give derivative **8**. The isobutyryl residue was then introduced to protect the amino group, yielding compound **9**. Standard conditions were employed to block the 5′-hydroxy group with a DMT residue† (**9** → **10**).‡ The phosphonate **3** as well as the phosphoramidite **4** were prepared from **10** according to known procedures (Scheme 2).

As discussed above, DNA quartets have been constructed from oligonucleotides containing short runs of isoguanine, *e.g.* d($T_4$isoG$_4T_4$).[1,2] These self-assembled structures were identified by HPLC ion exchange chromatography [Fig. 1(*a*)].[2] Their chromatographic behaviour was almost identical to that observed for d($T_4G_4T_4$). The chromatogram shows two peaks, a fast migrating peak for the monomeric oligonucleotide and a slow migrating peak for the tetramer (Fig. 1). The same experiment was then performed with oligonucleotides containing consecutive 7-deazaisoguanine residues.§ For this purpose, the oligomers 5′-d($T_4c^7iG_4T_4$) **11** and 5′-d($T_2c^7iG_6T_4$) **12** were prepared by solid-phase synthesis.

The oligomer 5′-d($T_4c^7iG_4T_4$) **11** gives only one peak when chromatographed on an ion exchange HPLC column under the conditions described for d($T_4$isoG$_4T_4$) [Fig. 1(*b*)].[2] This fast migrating peak contains only the single-stranded oligomer. However, when the number of consecutive $c^7iG_d$-residues is increased from four to six by replacing another two dT-residues as in the oligomer d($T_2c^7iG_6T_4$) **12**, a slow migrating zone



**Scheme 2** *Reagents and conditions*: i, $Ph_2NCOCl$, 80%; ii, $Me_3SiCl$, $Bu^iCl$, 80%; iii, DMTCl, 51%; iv (for **3**) $PCl_3$, *N*-methylmorpholine, 1*H*-1,2,4-triazole, 93%; (for **4**) $(NCCH_2CH_2O)(Pr^i_2N)PCl$, $EtNPr^i_2$, 85%

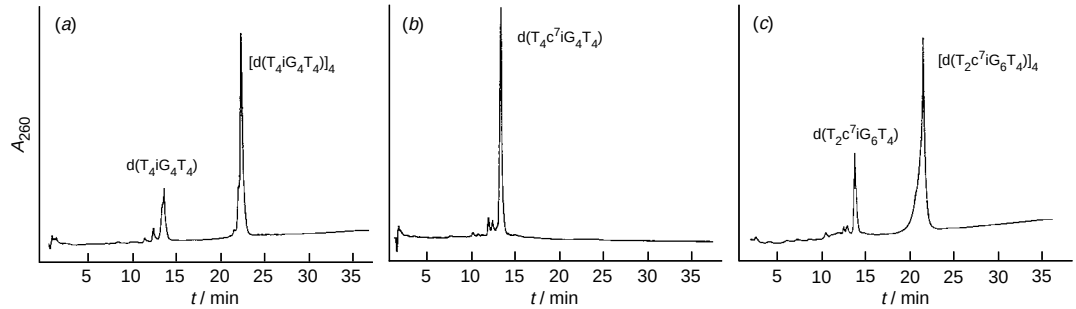



**Fig. 1** Ion exchange HPLC profiles of (*a*) 5′-d($T_4$iso$G_4T_4$), (*b*) 5′-d($T_4c^7iG_4T_4$) and (*c*) 5′-d($T_2c^7iG_6T_4$) at 25 °C. Solvent systems: A = 25 mM Tris-HCl (containing 1 mM EDTA buffer, pH 8.0)–MeCN, 90 : 10; B = A containing 1.0 M NaCl. Gradient: $t$ = 0–30 min, 20 → 80% B in A; $t$ = 30–35 min, 80% B in A.

($t_R$ = 22 min) appeared along with the fast migrating peak ($t_R$ = 14 min) [Fig. 1(*c*)]. The latter contains the single-stranded oligomer, while the slow migrating peak represents the aggregate. Consequently, the aggregate of d($T_2c^7iG_6T_4$) **12** reflects a self-assembled structure. The almost identical mobilities of compounds d($T_4$iso$G_4T_4$) and d($T_2c^7iG_6T_4$) on ion-exchange HPLC indicate that both aggregates are formed by assembly of four strands. This is the result of an identical number of negative phosphate charges, which are responsible for the chromatographic mobility.

From model building it is obvious that the structure of the isoguanine quartet has to be different from that of guanine. The structure of the two bases differs with regard to the position of the purine substituents, thereby changing their donor–acceptor pattern. Various aggregate motifs have been suggested for the polyribonucleotide poly(isoG),[3] for the monomeric isoguanosine,[4] and also for oligodeoxyribonucleotides.[2,14] Some structures do not use the purine nitrogen-7 to form the supramolecular assembly. Among them the most probable structure for the quartet of **12** is **A** (Fig. 2). It follows a motif which has been proposed for a monomeric isoguanosine derivative.[4]

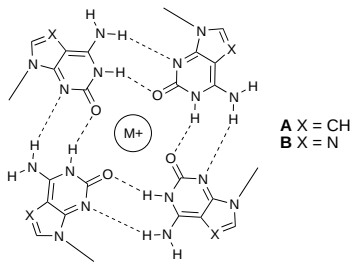



**Fig. 2**

The experiments described suggest that oligonucleotides containing either 7-deazaisoguanine or isoguanine form similar supramolecular structures with an identical hydrogen bonding pattern (**A** or **B**). Nevertheless, due to the structural changes of the heterocyclic base—a purine system is replaced by a pyrrolo[2,3-*d*]pyrimidine heterocycle—the strength of the hydrogen bonding array results in somewhat lower stability for the 7-deazaisoguanine quartet **A** compared to that formed by isoguanine (**B**). Unlike 2′-deoxyisoguanosine, which is very sensitive to acidic conditions (glycosylic bond hydrolysis), 7-deaza-2′-deoxyisoguanosine is very stable. This makes it a good candidate to form ionophors with good chemical stability.

## Footnotes and References

* E-mail: fraseela@rz.uni-osnabrueck.de

† *Abbreviations*: $isoG_d$ or d(isoG), 2′-deoxyisoguanosine; $c^7iG_d$ or d($c^7$iG), 7-deaza-2′-deoxyisoguanosine; DMT or $(MeO)_2Tr$, 4,4′-dimethoxytriphenylmethyl.

‡ *Selected data* for **10** (systematic numbering): $\lambda_{max}$(MeOH)/nm ($\varepsilon$) 274 (9800), 294 (7600); $\delta_H$ ([$^2H_6$]DMSO) 1.13, 1.14 (2 s, 2 $CH_3$), 2.30 [m, H-C(2′)], 2.88 (m, CH), 3.16 [m, 2 H-C(5′)], 3.72 (s, 2 $CH_3O$), 3.95 [m, H-C(4′)], 4.38 [m, H-C(3′)], 5.37 [br s, HO-C(3′)], 6.58 [m, H-C(1′)], 6.83 [d, *J* 7.6, H-C(5)], 7.22–7.46 [m, H-C(6) and 23 arom. H]; calc. for $C_{49}H_{47}N_5O_8$ (833.95): C, 70.57; H, 5.68; N, 8.40; found: C, 70.29; H, 5.65; N, 8.33%.

§ *General procedure*. The samples for ion exchange HPLC were prepared by preheating to 90 °C for 2 min, cooling to room temperature for 10 min, and storing at −20 °C for 30 min. The sample was then brought to room temperature and injected onto a NucleoPac PA-100 column. Elution was performed with Tris-HCl buffer, pH 8.0, by increasing the NaCl concentration from 0.2 to 0.8 M (ref. 2).

1 F. Seela and C. Wei, *Helv. Chim. Acta*, 1997, **80**, 73.
2 F. Seela, C. Wei and A. Melenewski, *Nucleic Acids Res.*, 1996, **24**, 4940.
3 T. Golas, M. Fikus, Z. Kazimierczuk and D. Shugar, *Eur. J. Biochem.*, 1976, **65**, 183.
4 J. T. Davis, S. Tirumala, J. R. Jenssen, E. Radler and D. Fabris, *J. Org. Chem.*, 1995, **60**, 4167.
5 S. Tirumala and J. T. Davis, *J. Am. Chem. Soc.*, 1997, **119**, 2769.
6 F. Seela, C. Wei and A. Melenewski, unpublished work.
7 F. Seela, C. Wei and A. Melenewski, *Origins Life Evol. Biosphere*, 1997, in the press.
8 F. Seela, Q.-H. Tran-Thi and D. Franzen, *Biochemistry*, 1982, **21**, 4338.
9 F. Seela and K. Mersmann, *Helv. Chim. Acta*, 1993, **76**, 1435.
10 F. Seela, S. Menkhoff and S. Behrendt, *J. Chem. Soc. Perkin Trans. 2*, 1986, 525.
11 Z. Kazimierczuk, R. Mertens, W. Kawczynski and F. Seela, *Helv. Chim. Acta*, 1991, **74**, 1742.
12 F. Seela, A. Kehne and H.-D. Winkeler, *Liebigs Ann. Chem.*, 1983, 137.
13 F. Seela, H. Steker, H. Driller and U. Bindig, *Liebigs Ann. Chem.*, 1987, 15.
14 R. Krishnamurthy, S. Pitsch, M. Minton, C. Miculka, N. Windhab and A. Eschenmoser, *Angew. Chem.*, 1996, **108**, 1619.

*Received in Glasgow, UK, 8th July 1997; 7/04866A*

# Synthesis of a D-lactosyl cluster–nucleoside conjugate†

**Andrew R. Vaino,[a] William T. Depew[b] and Walter A. Szarek*[a]**

[a] *Department of Chemistry, Queen's University, Kingston, Ontario, Canada K7L 3N6*
[b] *Department of Medicine, Queen's University, Kingston, Ontario Canada K7L 3N6*

**The synthesis of a nucleoside–oligolactoside conjugate, expected to provide site-specific drug delivery to the human liver, is described.**

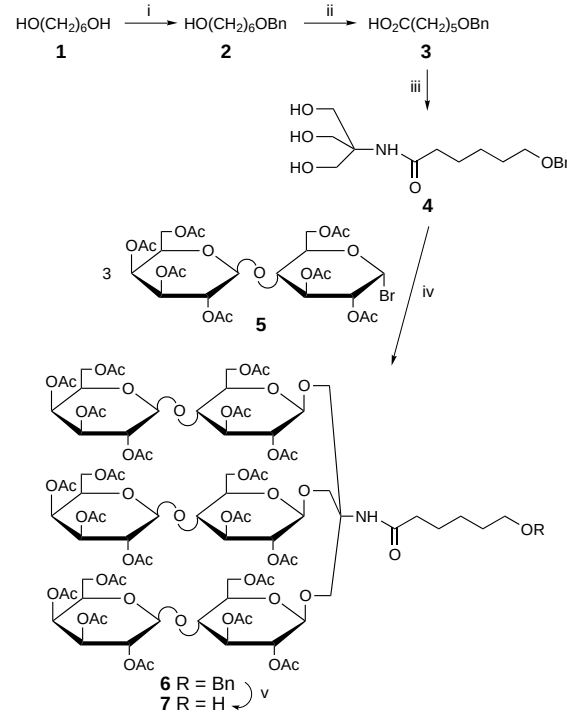
The hepatitis B virus (HBV) represents a major health concern, afflicting 350 million people worldwide.[1] While the virus itself is debilitating, it is not always fatal. However, liver cancer, which often arises from HBV infection, is responsible for upwards of 1 million deaths annually.[2] The mode of action of the HBV is thought to be similar to that of the HIV virus, in that it involves reverse transcription in the cytoplasm.[3] Thus, many nucleosides known to inhibit HBV reverse transcriptase, with their unwanted side-effects, have been examined as a means of controlling this deadly affliction.

The mammalian hepatocyte plasma membrane expresses the asialoglycoprotein receptor (ASGP-R),[4] a unique integral membrane receptor exhibiting specificity for terminal, nonreducing, β-D-galactopyranosyl or 2-acetamido-2-deoxy-β-D-galactopyranosyl residues. This specific binding to liver cells has been examined with a variety of oligogalactosides[5] and oligolactosides.[6] The biological evaluation of the binding of a host of molecules containing various numbers of terminal D-galactopyranosyl residues has demonstrated that, as the number of these residues increased, so did binding.[5b,6] Previous studies in this laboratory have involved adding one, two or three D-lactose units to a glycerol backbone.[7] Thus, attempts were made to extend this type of molecule, with its *hepatophilicity*, by the addition of an extra functional group, through which a hepatotoxic nucleoside could be appended. Ideally, by directing such a nucleoside directly to the liver, the devastating side-effects of HBV treatment would be obviated.

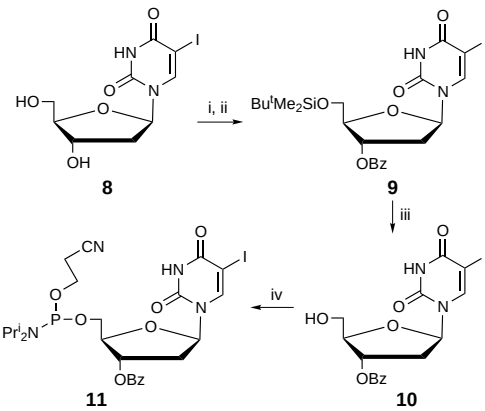
Previous work with D-galactose has utilized the well-known buffer tris(hydroxymethyl)methylamine (TRIS) as a backbone.[5] In the present work TRIS was modified such that, after addition of three D-lactose units, a cytotoxic nucleoside could be readily introduced. The nucleoside chosen was 2′-deoxy-5-iodouridine (dIU), known to inhibit HBV.[8]

To synthesize the acetylated *delivery vehicle* **7** (Scheme 1), a suitably modified backbone was required. Beginning with hexane-1,6-diol, a single benzyl group was introduced, followed by oxidation of the remaining hydroxy group to the corresponding carboxylic acid. Addition to the amino group of TRIS was performed using the well-known peptide-coupling agent 2-ethoxy-1-ethoxycarbonyl-1,2-dihydroquinoline (EEDQ).[9] Glycosylation of the three primary hydroxy groups of **7** with 2,3,6,2′,3′,4′,6′-hepta-*O*-acetyl-α-D-lactosyl bromide, prepared by the method of Kartha and Jennings,[10] was achieved in 69% yield using the Helferich modification[11] of the Königs–Knorr reaction. Removal of the benzyl group was readily accomplished in 85% yield by catalytic hydrogenolysis. The confirmation of the structure of this oligolactoside was accomplished using Fourier-transform, proton chemical-shift correlation spectroscopy (COSY)[12] and heteronuclear correlation spectroscopy (HETCOR).[13] The β-D configuration for the glycosidic linkage between the lactose units and the backbone was revealed by the observation of a characteristic coupling constant[14] ($J_{1,2}$ 7.9 Hz). It should be noted, however, that identification of trace amounts of material having α-D linkages would have been precluded by the detection limit of the NMR experiment.

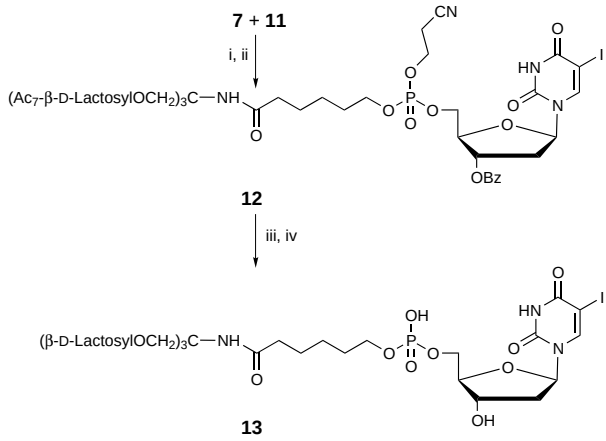
The nucleoside selected, namely dIU, required protection of the hydroxy group at C-3′ prior to attachment to the delivery moiety. Thus, the selectivity of the $Bu^tMe_2Si$ group for primary hydroxy groups[15] allowed for an efficient two-step, one-pot procedure to form **9** (Scheme 2) in a high yield. The $Bu^tMe_3Si$




**Scheme 1** *Reagents*: i, BnBr (0.7 equiv.), NaH, THF; ii, Jones reagent; iii, $(HOCH_2)_3CNH_2$, EEDQ, EtOH; iv, **5** (3 equiv.), $Hg(CN)_2$, 1 : 1 $MeNO_2$–$C_6H_6$; v, $H_2$, 10% Pd/C, $HCO_2H$, MeOH




**Scheme 2** *Reagents and conditions*: $Bu^tMe_2SiCl$, pyridine, room temp.; ii, BzCl, 0 °C, pyridine; iii, 1% $I_2$ in MeOH; iv, β-CDCP, $Pr^i_2NEt$, MeCN, 0 °C




**Scheme 3** *Reagents*: i, 1*H*-tetrazole, MeCN; ii, $I_2$, THF, $H_2O$, pyridine; iii, LiOH, MeOH; iv, Amberlite IR-120 ($H^+$)

group was readily removed by treatment with a solution of $I_2$ in MeOH at reflux temperature[16] to afford **10**, ready for coupling.

Many possibilities exist for the joining of the nucleoside and the carrier molecule, however, most of these were quickly discounted on the basis of possible reactivity *in vivo*; the use of a phosphoric monoester was selected. A well-established modification of the standard phosphite assembly method[17] was employed, with the reagent β-cyanoethyl *N*,*N*-diisopropylchlorophosphoramidite (β-CDCP)[18] as the coupling agent. Compound **10** afforded an unstable intermediate, presumably **11**, which, on coupling to the carrier molecule **7** in the presence of 1*H*-tetrazole followed by oxidation of the product with iodine, afforded **12** (Scheme 3) in 12% yield.‡ Simultaneous cleavage of the acetic and benzoic esters, along with elimination of the β-cyanoethyl group, afforded the desired conjugate **13**.§

To conclude, we have demonstrated the synthesis of an easily prepared vehicle for the targeting of drugs directly to the mammalian liver. The advantages of site-specific, drug delivery are clear. Thus, the potential for conjugates such as **13**, in which a vehicle known to have a high specificity for hepatocytes is coupled to a hepatotoxic nucleoside, is tremendous. Full experimental details of this and related compounds, along with biological evaluation of the binding of these compounds to the ASGP-R and inhibition studies with HBV, will be reported in due course.

The authors thank the Natural Sciences and Engineering Research Council Canada for financial support of this research.

## Footnotes and References

* E-mail: szarekw@chem.queensu.ca

† Synthesis and binding of D-galactose-terminated ligands to human and rabbit asialoglycoprotein receptor. Part VII. For Part VI, see ref. 6.

‡ Subsequent couplings with other nucleosides have been achieved in yields approaching 80%.

§ All products were identified by $^1H$, $^{13}C$, and, where applicable, $^{31}P$ NMR spectroscopy, as well as mass spectrometry (except for **9** and **10**). Also, novel compounds **3**, **4**, **6**, **7**, **9** and **13** gave satisfactory elemental analyses.

1 P. Tiollais, C. Pourcel and A. Dejean, *Nature*, 1985, **317**, 489.
2 R. P. Beasley, *Cancer*, 1988, **61**, 1942.
3 J. Summers and W. S. Mason, *Cell*, 1982, **29**, 403; R. H. Miller, P. L. Marion and W. S. Robinson, *Virology*, 1984, **139**, 64.
4 G. Ashwell and J. Harford, *Annu. Rev. Biochem.*, 1982, **51**, 531; M. Spiess, *Biochemistry*, 1990, **29**, 10 009.
5 (*a*) Y. C. Lee, *Carbohydr. Res.*, 1978, **67**, 509; (*b*) R. T. Lee, P. Lin and Y. C. Lee, *Biochemistry*, 1984, **23**, 4255; (*c*) H. J. M. Kempen, C. Hoes, J. H. van Boom, H. H. Spanjer, J. de Lange, A. Langendoen and T. J. C. van Berkel, *J. Med. Chem.*, 1984, **27**, 1306; (*d*) M. G. Peter, P. C. Boldt, Y. Niederstein and J. Peter-Katalinic, *Liebigs Ann. Chem.*, 1990, 863; (*e*) E. A. L. Biesen, D. M. Beuting, H. C. P. F. Roelen, G. A. van de Marel, J. H. van Boom and T. J. C.van Berkel, *J. Med. Chem.*, 1995, **38**, 1538.
6 A. Krebs, W. T. Depew, W. A. Szarek, G. W. Hay and L. J. J. Hronowski, *Carbohydr. Res.*, 1994, **254**, 257.
7 L. J. J. Hronowski, W. A. Szarek, G. W. Hay, A. Krebs and W. T. Depew, *Carbohydr. Res.*, 1989, **190**, 203; L. J. J. Hronowski, W. A. Szarek, G. W. Hay, A. Krebs and W. T. Depew, *Carbohydr. Res.*, 1991, **219**, 33.
8 E. Matthes, M. von Janta-Lipinski, H. Will, H. C. Shröder, H. Merz, R. Steffen and W. E. G. Müller, *Biochem. Phamacol.*, 1992, **43**, 1571; P. C. N. Rensen, M. C. M. van Dijk, E. C. Havenaar, M. K. Bijsterbosch, J. K. Fruijt and T. J. C. van Berkel, *Nature Medicine*, 1995, **1**, 221.
9 B. Belleau, R. Martel, G. Lacasse, M. Ménard, N. L. Weinberg and Y. G. Perron, *J. Am. Chem. Soc.*, 1968, **90**, 823; B. Belleau and G. Malek, *J. Am. Chem. Soc.*, 1968, **90**, 1651.
10 K. P. R. Kartha and H. J. Jennings, *J. Carbohydr. Chem.*, 1990, **9**, 777.
11 B. Helferich and K. Weis, *Chem. Ber.*, 1956, **89**, 314.
12 A. Bax, R. Freeman and G. Morris, *J. Magn. Reson.*, 1981, **42**, 164; R. Benn and H. Günther, *Angew. Chem., Int. Ed. Engl.*, 1983, **22**, 350.
13 A. A. Mandsley and R. R. Ernst, *Chem. Phys. Lett.*, 1977, **50**, 368; G. Bodenhaussen and R. Freeman, *J. Magn. Reson.*, 1977, **28**, 471.
14 A. Bax, W. Egan and P. Kovác, *J. Carbohydr. Chem.*, 1984, **3**, 593; L. D. Hall, *Adv. Carbohydr. Chem. Biochem.*, 1974, **29**, 11.
15 K. K. Ogilvie, S. L. Beaucage, A. L. Schifman, N. Y. Theriault and K. L. Sadana, *Can. J. Chem.*, 1978, **56**, 2768; K. K. Ogilvie, A. L. Schifman and C. L. Penney, *Can. J. Chem.*, 1979, **57**, 2230.
16 A. R. Vaino and W. A. Szarek, *Chem. Commun.*, 1996, 2351.
17 R. L. Letsinger and W. B. Lunsford, *J. Am. Chem. Soc.*, 1976, **98**, 3655.
18 N. D. Sinha, J. Biernat and H. Köster, *Tetrahedron Lett.*, 1983, **24**, 5843.

*Received in Cambridge, UK, 24th April 1997; 7/02809A*

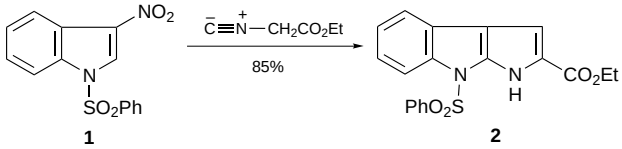
# One-step syntheses of the pyrrolo[3,4-*b*]indole and pyrrolo[2,3-*b*]indole ring systems from 3-nitroindoles

**Erin T. Pelkey and Gordon W. Gribble***

*Department of Chemistry, Dartmouth College, Hanover, NH 03755, USA*

**The reaction of 1-ethoxycarbonyl-3-nitroindole with ethyl isocyanoacetate in the presence of DBU gives ethyl 4-ethoxycarbonyl-2,4-dihydropyrrolo[3,4-*b*]indole-3-carboxylate, averting a novel rearrangement that we previously reported with 3-nitro-1-phenylsulfonylindole that yielded ethyl 8-phenylsulfonyl-1,8-dihydropyrrolo[2,3-*b*]indole-2-carboxylate.**

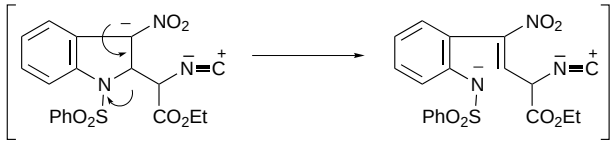
We recently reported a remarkable rearrangement which led to an expeditious synthesis of the pyrrolo[2,3-*b*]indole ring system.[1] Thus, treatment of 3-nitro-1-phenylsulfonylindole **1** with ethyl isocyanoacetate[2] and DBU gave pyrrolo[2,3-*b*]indole **2** in 85% yield (Scheme 1).[1] We anticipated that this application of the Barton–Zard pyrrole synthesis[3] would give a pyrrolo[3,4-*b*]indole[4–7] which could be utilized as a fused stable analogue of indole-2,3-quinodimethane,[8] in continuation of our interest in a related fused ring system, the furo[3,4-*b*]indoles.[9]



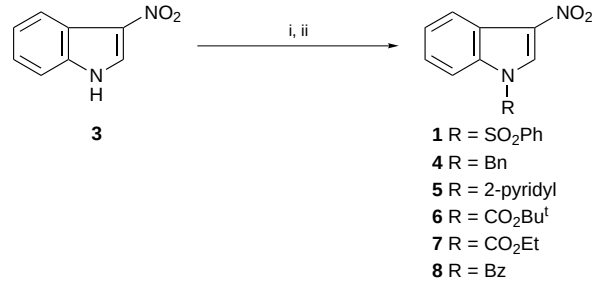

**Scheme 1** *Reagents and conditions*: i, DBU, THF, room temp., 20 h, 85%

To explain the outcome of this abnormal Barton–Zard reaction leading to the rearranged product **2**, we proposed a mechanism which involved a fragmentation of the indole ring system (Scheme 2),[1] which can be rationalized by the presence of a good leaving group, the aryl sulfonamide anion [*N*-(phenylsulfonyl)benzenesulfonamide has a p$K_a$ of 11.8[10]].

To circumvent this fragmentation and subsequent rearrangement in order to develop a succinct route to the pyrrolo[3,4-*b*]indole ring system, which was our original goal, we have investigated this reaction with 3-nitroindole substrates containing *N*-protecting groups that are less electron-withdrawing than *N*-phenylsulfonyl but which will still activate the indole double bond to the initial C-2 Michael addition. The requisite protected 3-nitroindoles were synthesized from 3-nitroindole **3**[11] utilizing sodium hydride as the base in DMF. For example, treatment of **3** with sodium hydride in DMF followed by benzenesulfonyl chloride gave **1**[12] in 86% yield. Likewise, 3-nitroindoles **4**–**8** were synthesized in variable yields utilizing benzyl bromide (79% yield), 2-fluoropyridine (19% yield),[13] *tert*-butyl phenyl carbonate (40% yield),[14] ethyl chloroformate (50% yield)[15] and benzoyl chloride (31% yield),[15] respectively (Scheme 3).



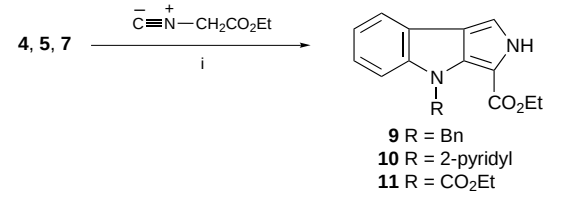

**Scheme 2**



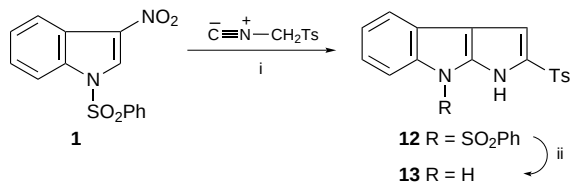

**Scheme 3** *Reagents and conditions*: i, NaH, DMF, 0 °C, 0.5–2 h; ii, (for **1**) $PhSO_2Cl$, 86%; (for **4**) $PhCH_2Br$ (79%); (for **5**) 2-fluoropyridine, 100 °C, 10 h, 19%; (for **6**) $PhOCO_2Bu^t$, 40%; (for **7**) $ClCO_2Et$, 50%; (for **8**) BzCl, 31%

The abatement of the rearrangement was first observed when *N*-benzylindole **4** was subjected to the Barton–Zard pyrrole synthesis conditions (Scheme 4). In the event, treatment of **4** with ethyl isocyanoacetate and DBU in THF at room temperature resulted in no reaction, but after being heated at reflux for 9 h, pyrrolo[3,4-*b*]indole **9**† was obtained in 30% yield. The low yield is most likely due to the decreased degree of electrophilicity associated with **4** as compared to **1**. To confirm the structure of this product, we synthesized the corresponding known isomer, ethyl 8-benzyl-1,8-dihydropyrrolo[2,3-*b*]indole-2-carboxylate,[16] which was clearly different from **9** in all respects (IR, TLC, UV, and $^1$H NMR). An increase in yield utilizing milder reaction conditions was observed with the more electrophilic *N*-(2-pyridyl)indole **5**, which, upon treatment with ethyl isocyanoacetate and DBU in THF at room temperature, gave pyrrolo[3,4-*b*]indole **10** in 72% yield. A simple and reliable method for determining the regiochemistry of these Barton–Zard reactions is to determine the pyrrole ring C-1 proton–NH coupling constant. For the pyrrolo[2,3-*b*]indole systems, the resulting four bond coupling is usually 1.5 Hz, while for pyrrolo[3,4-*b*]indole systems the resulting three bond coupling is usually 3.0 Hz. Indeed, the coupling constant observed for the pyrrole ring proton of **10** is 3.3 Hz.

Although the synthesis of **10** in good yield accomplished the initial goal of precluding the rearrangement, a more practical protecting group was sought which could provide a similar result. Treatment of *N*-benzoylindole **8** under the usual conditions resulted in deprotection, and similar treatment of *N*-butoxycarbonylindole **6** resulted in no reaction even after prolonged reflux. Finally, to our delight, treatment of




**Scheme 4** *Reagents and conditions*: i, (for **9**) DBU, THF, reflux, 9 h, 30%; (for **10**) DBU, THF, room temp., 12 h, 72%; (for **11**) DBU, THF, room temp., 18 h, 91%

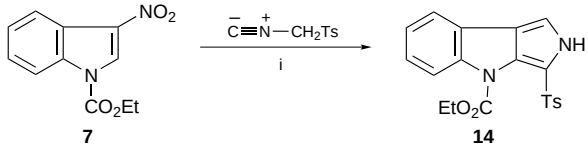



**Scheme 5** *Reagents and conditions*: i, DBU, THF, room temp., 22 h, 63%; ii, 6% Na/Hg, THF, MeOH, −40 °C, 73%

*N*-ethoxycarbonylindole **7** with ethyl isocyanoacetate in DBU at room temperature gave the desired pyrrolo[3,4-*b*]indole **11**† in 91% yield.

We have also found that the fragmentation–rearrangement pathway occurs with tosylmethyl isocyanide (TsMIC).[17] Treatment of **1** with TsMIC and DBU in THF gave pyrrolo[2,3-*b*]indole **12**† in 63% yield, which was subsequently deprotected with sodium amalgam[18] to afford pyrrolo[2,3-*b*]indole **13** in 73% yield (Scheme 5). In accord with the structural assignment, the coupling constants for the pyrrole ring protons of **12** and **13** are 1.8 and 1.5 Hz, respectively.

In contrast, treatment of **7** under the same conditions gave the corresponding pyrrolo[3,4-*b*]indole **14**† in 41% yield (Scheme 6). Support for the structural assignment of **14** can again be found with the observed pyrrole ring proton coupling constant of 3.3 Hz.




**Scheme 6** *Reagents and conditions*: i, DBU, THF, room temp., 20 h, 41%

In conclusion, we have shown that both pyrrolo[2,3-*b*]indoles and pyrrolo[3,4-*b*]indoles can be synthesized from 3-nitroindole substrates depending on the *N*-indole protecting group in one step *via* the Barton–Zard pyrrole synthesis.

The authors acknowledge the Donors of the Petroleum Research Fund, administered by the American Chemical Society, Pfizer, and Wyeth-Ayerst for partial support of this work, and Louis Chang for the preparation and some initial studies of **4**. Mass spectral data for **11**, **12** and **14** were provided by the Boston University School of Medicine Mass Spectrometry Resource, which is supported by NIH/NCRR Grant No. P41-RR10888 (to C. E. Costello).

## Footnotes and References

* E-mail: grib@dartmouth.edu

† *Selected data* for **9**: mp 202–204 °C; $\nu$(KBr)/cm$^{-1}$ 3250, 1658; $\lambda_{max}$(EtOH)/nm 210, 238, 278, 302, 330; $\delta_H$ (300 MHz, [$^2H_6$]DMSO) 11.80 (br s, 1 H), 7.75 (d, 1 H, *J* 7.5), 7.46 (d, 1 H, *J* 3.6), 7.13–7.32 (m, 7 H), 7.05 (m, 1 H), 5.83 (s, 2 H), 4.22 (q, 2 H, *J* 7.2), 1.19 (t, 3 H, *J* 7.2); $\delta_C$ ([$^2H_6$]DMSO) (one quaternary carbon missing) 159.8, 144.7, 139.0, 128.3, 126.8, 126.5, 123.5, 120.1, 120.0, 119.0, 116.2, 113.6, 109.9, 99.6, 59.2, 47.6, 14.4; *m/z* 319 ($M^+$ + 1), 273, 246, 195, 155, 119; Calc. for $C_{20}H_{18}N_2O_2$ ($M^+$); 318.1638. Found: 318.1637. For **11**: mp 143–145 °C; $\delta_H$ (300 MHz, $CDCl_3$) 9.34 (br s, 1 H), 8.20 (d, 1 H, *J* 8.4), 7.67 (m, 1 H), 7.35 (m, 1 H), 7.27 (m, 1 H), 7.19 (d, 1 H, *J* 3.0), 4.50 (q, 2 H, *J* 6.9), 4.38 (q, 2 H, *J* 7.2), 1.43 (t, 3 H, *J* 6.9), 1.40 (t, 3 H, *J* 7.2); $\delta_C$ ($CDCl_3$) 159.9, 151.9, 143.7, 132.7, 125.5, 123.5, 123.0, 120.2, 119.6, 116.3, 110.8, 106.4, 63.3, 60.7, 14.8, 14.6; *m/z* 323.1 (M + $Na^+$); Calc. for $C_{16}H_{16}N_2O_4$: C, 63.99; H, 5.37; N, 9.33. Found: C, 63.73; H, 5.38; N, 9.31%. For **12**: mp 236–238 °C (decomp.); $\nu$(KBr)/cm$^{-1}$ 3256; $\lambda_{max}$(EtOH)/nm 210, 274 (sh), 300, 346 (sh); $\delta_H$ (300 MHz, $CDCl_3$) 9.78 (br s, 1 H), 7.89 (m, 3 H), 7.76 (m, 2 H), 7.52 (m, 2 H), 7.37 (m, 4 H), 7.26 (m, 2 H), 7.11 (d, 1 H, *J* 1.8), 2.41 (s, 3 H); $\delta_C$ ($CDCl_3$) 144.3, 139.6, 138.5, 137.6, 136.4, 134.8, 130.2, 129.6, 128.8, 127.2, 126.9, 125.0, 124.6, 124.3, 120.1, 114.8, 113.4, 107.6, 21.8; *m/z* 473.1 (M + $Na^+$); Calc. for $C_{23}H_{18}N_2O_4S_2$: C, 61.32; H, 4.03; N, 6.22; S, 14.23. Found: C, 61.35; H, 4.04; N, 6.23; S, 14.23%. For **14**: mp 121–123 °C (decomp.); $\delta_H$ (300 MHz, $CDCl_3$) 9.97 (br s, 1 H), 8.17 (d, 1 H, *J* 7.8), 7.66–7.73 (m, 3 H), 7.33 (d, 1 H, *J* 3.3), 7.24–7.37 (m, 4 H), 4.27 (q, 2 H, *J* 7.2), 2.39 (s, 3 H), 1.17 (t, 3 H, *J* 7.2); $\delta_C$ ($CDCl_3$) 150.9, 143.4, 142.0, 141.3, 130.1, 129.5, 126.2, 126.0, 123.7, 122.4, 120.3, 120.2, 116.6, 111.7, 108.5, 63.2, 21.7, 14.4; *m/z* 405.0 (M + $Na^+$).

1 E. T. Pelkey, L. Chang and G. W. Gribble, *Chem. Commun.*, 1996, 1909.
2 G. D. Hartmann and L. M. Weinstock, *Org. Synth.*, 1988, **Coll. Vol. VI**, 620.
3 D. H. R. Barton and S. Z. Zard, *J. Chem. Soc., Chem. Commun.*, 1985, 1098; D. H. R. Barton, J. Kervagoret and S. Z. Zard, *Tetrahedron*, 1990, **46**, 7587.
4 W. M. Welch, *J. Org. Chem.*, 1976, **41**, 2031.
5 C.-K. Sha, K.-S. Chuang and J.-J. Young, *J. Chem. Soc., Chem. Commun.*, 1984, 1552; C.-K. Sha, K.-S. Chuang and S.-J. Wey, *J. Chem. Soc., Perkin Trans. 1*, 1987, 977; C.-K. Sha and J.-F. Yang, *Tetrahedron*, 1992, **48**, 10 645.
6 R. P. Kreher and G. Dyker, *Z. Naturforsch. Teil B: Chem. Sci.*, 1987, **42**, 473; G. Dyker and R. P. Kreher, *Chem.-Ztg.*, 1988, **112**, 235.
7 A. Jeevendam and P. C. Srinivasan, *J. Chem. Soc., Perkin Trans. 1*, 1995, 2663.
8 U. Pindur and H. Erfanian-Abdoust, *Chem. Rev.*, 1989, **89**, 1681.
9 M. G. Saulnier and G. W. Gribble, *Tetrahedron Lett.*, 1983, **24**, 5435; G. W. Gribble, M. G. Saulnier, M. P. Sibi and J. A. Obaza-Nutaitis, *J. Org. Chem.*, 1984, **49**, 4518; D. A. Davis and G. W. Gribble, *Tetrahedron Lett.*, 1990, **31**, 1081; G. W. Gribble, *Adv. Heterocycl. Nat. Prod. Synth.*, 1990, **1**, 43; G. W. Gribble, *Synlett*, 1991, 289; G. W. Gribble, D. J. Keavy, D. A. Davis, M. G. Saulnier, B. Pelcman, T. C. Barden, M. P. Sibi, E. R. Olson and J. J. BelBruno, *J. Org. Chem.*, 1992, **57**, 5878.
10 F. G. Bordwell, *Acc. Chem. Res.*, 1988, **21**, 456 and references cited therein.
11 G. Berti, A. D. Settimo and E. Nannipieri, *J. Chem. Soc. C*, 1968, 2145.
12 E. Wenkert, P. D. R. Moeller and S. R. Piettre, *J. Am. Chem. Soc.*, 1988, **110**, 7188.
13 K. Seki, K. Ohkura, M. Terashima and Y. Kanaoka, *Heterocycles*, 1994, **37**, 993.
14 D. Dhanak and C. B. Reese, *J. Chem. Soc., Perkin Trans. 1*, 1986, 2181.
15 T. Itahara, *Synthesis*, 1979, 151.
16 C. J. Moody and J. G. Ward, *J. Chem. Soc., Perkin Trans. 1*, 1984, 2903.
17 A. M. van Leusen, H. Siderius, B. E. Hoogenboom and D. van Leusen, *Tetrahedron Lett.*, 1972, **13**, 5337.
18 G. W. Gribble, T. C. Barden and D. A. Johnson, *Tetrahedron*, 1988, **44**, 3195.

*Received in Corvallis, OR, USA, 16th June 1997; 7/04217E*

# An enantioselective synthesis of 2-alkyl-3-phenyltropanes by an asymmetric 1,3-dipolar cycloaddition reaction

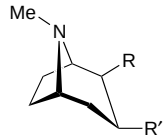
**Gian Luca Araldi,[a] K. R. C. Prakash,[a] Clifford George[b] and Alan P. Kozikowski*[a]**

[a] *Drug Discovery Laboratory, Georgetown University Medical Center, Institute for Cognitive and Computational Sciences, 3970 Reservoir Road NW, Washington, DC 20007-2197, USA*

[b] *Laboratory for the Structure of Matter, Code 6030, Naval Research Laboratory, 4555 Overlook Avenue SW, Washington, DC 20375-5000, USA*

**A method for gaining access to 2-alkyl-3-phenyl-substituted tropanes using the chiral dipolarophile (*R*)-*p*-tolyl vinyl sulfoxide in the asymmetric 1,3-dipolar cycloaddition reaction with the oxidopyridinium betaine 4 is described.**

(*R*)-Cocaine[1] **1** is a plant alkaloid purified from the leaves of *Erythroxylum coca*; its abuse is one of the greatest concerns of the American public today, and it is clear that immediate therapies are needed for the treatment of individuals who have become addicted to this powerful reinforcing drug.[2] In order to discover agents for use in the treatment of cocaine abuse, we believe that it will be valuable to identify molecules that can act as cocaine antagonists or partial agonists. Previously, we have shown that cocaine's C-2 ester group can be replaced by alkyl and alkenyl groups as in **3** with no loss in activity,[3] while other workers have shown that replacement of the C-3 benzoate by phenyl leads to compounds **2** of higher potency (these phenyl-bearing structures are often referred to as the WIN series compounds).[4] In order to more quickly identify those structural changes that may lead to altered functional activity, we required a chemical approach to diversely substituted 2-alkyl-3-phenyltropanes. We recently reported[5] a pyridinium betaine-based dipolar cycloaddition route to racemic tropane derivatives **3**.




**1** R = $CO_2$Me, R′ = OBz
**2** R = $CO_2$Me, R′ = Ph
**3** R = alkyl or alkenyl, R′ = Ph

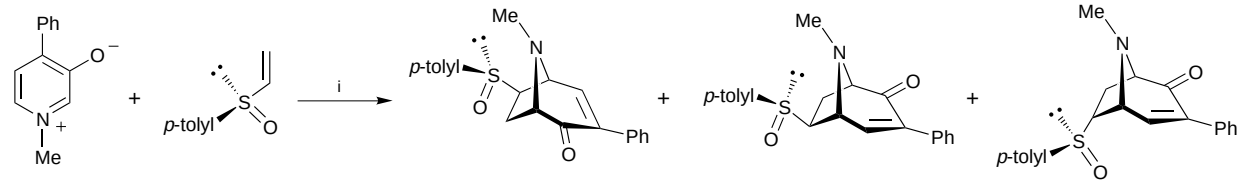
Asymmetric 1,3-dipolar cycloaddition reactions using chiral dipolarophiles are well documented.[6] Herein we report the cycloaddition reaction of the sulfoxide **5**[6a] and the oxidopyridinium betaine **4**[5] to afford the tropenone intermediates **6**–**8** with good diastereoselectivity and complete regioselectivity (Scheme 1). The reaction was performed in dioxane at reflux for 20 h to give a mixture of both *exo* and *endo* cycloadducts (70 : 30). Silica gel flash column chromatography of the crude mixture led to the separation of the *exo* products (4 : 1 mixture of the diastereomers **6** and **7**; 55% overall yield) from the *endo* product **8** (22% yield). The major *exo* diastereomer **6** was obtained by crystallization from EtOAc of the above 4 : 1 mixture and had $[\alpha]_D^{25}$ −51 (*c* 0.5, acetone), $R_f$ 0.6 (EtOAc), and mp 166 °C. The *endo* product **8** had $[\alpha]_D^{25}$ +73 (*c* 0.5, acetone), $R_f$ 0.3 (EtOAc), and mp 98–104 °C. The absolute configurations of **6** and **8** were determined by X-ray diffraction studies.†

The major *exo* product **6** was converted to the 2β-alkyl-3β-phenyltropane derivatives **11a** and **11b** as shown in Scheme 2. Thus, ketone **6** underwent exclusive 1,2-reduction using the Luche protocol[7] to provide the allylic alcohol intermediate as a mixture of the α- and β-stereoisomers. These alcohols were converted to their acetates followed by reduction of the sulfoxide with $PCl_3$ in DMF at 0 °C.[6b] The resulting sulfide **9** (3 : 1 mixture of the α- and β-acetates) underwent a CuCN-catalysed cross coupling reaction using RMgBr (R = $Pr^n$ or $Bu^n$) as the nucleophile[8] to afford the alkene intermediates **10a** and **10b**. As previously reported,[5] this reaction is completely regioselective (only γ-alkylation products are observed), and the final stereochemistry of the alkyl-bearing centre is independent of that of the acetate intermediate (*i.e.* only β-diastereoisomers are observed).

The alkenes **10a** and **10b** were subjected in turn to a one-step desulfurization and hydrogenation reaction using Raney-nickel (W2) in EtOH to yield the 2β,3β-isomers **11a** and **11b** (12–13%) together with the 2β,3α-isomers **12a** and **12b** (40–43%) derived from β-face hydrogenation. These mixtures were separated by preparative TLC (hexane–EtOAc–$Et_3N$ 9 : 0.8 : 0.2) on silica gel. The 2β-*n*-propyl-3β-phenyltropane **11a** had $[\alpha]_D^{25}$ −49 (*c* 0.25, $CH_2Cl_2$); the corresponding 2β,3α-isomer **12a** had $[\alpha]_D^{25}$ −50 (*c* 1.0, $CH_2Cl_2$). The *n*-butyl derivatives **11b** and **12b** had $[\alpha]_D^{25}$ −64 (*c* 0.2, $CH_2Cl_2$) and −43 (*c* 0.5, $CH_2Cl_2$), respectively.

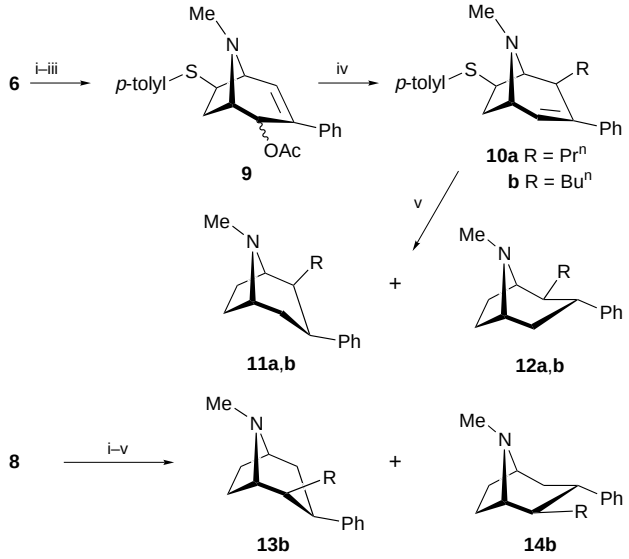
Compound **8** was subjected to the same sequence of reactions as presented in Scheme 2 for the intermediate **6** using $Bu^n$MgBr as Grignard reagent. Two products were obtained after complete reduction of the intermediate alkene: 2β-*n*-butyl-3β-phenyltropane **13b** with $[\alpha]_D^{25}$ +62 (*c* 0.2, $CH_2Cl_2$) and the corresponding 2β,3α isomer **14b** with $[\alpha]_D^{25}$ +41 (*c* 0.5, $CH_2Cl_2$).

The structures and stereochemical assignments for these compounds were determined using $^1$H NMR, $^{13}$C NMR,




**4** **5** (1*S*, 5*S*, 6*R*, $R_S$)-**6** (44%) (1*R*, 5*R*, 6*S*, $R_S$)-**7** (11%) (1*R*, 5*R*, 6*R*, $R_S$)-**8** (22%)

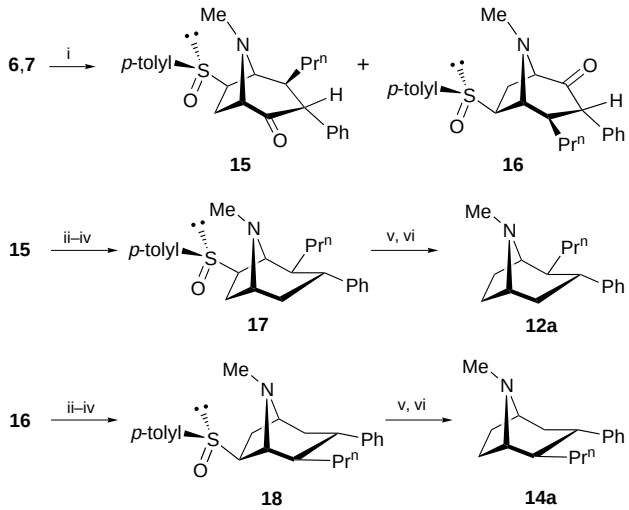
**Scheme 1** *Reagents and conditions*: i, 1,4-dioxane, reflux, 24 h




**Scheme 2** *Reagents and conditions*: i, $NaBH_4$, $CeCl_3$, MeOH, room temp.; ii, $Ac_2O$, pyridine, room temp.; iii, $PCl_3$, DMF, 0 °C, 88%; iv, RMgBr, CuCN, $Et_2O$, room temp., 77%; v, Raney-Ni (W2), EtOH, reflux

HETCOR and 2D COSY experiments. Because the stereochemical assignment of the final compounds **11** and **12** is problematic due to the complexity of their $^1$H NMR spectra, we synthesized the chair-like compounds **11a**,**b** from natural (−)-cocaine by the procedure previously reported.[3] Our synthetic samples proved to be identical in all respects with the samples obtained from natural (−)-cocaine.

Additionally using the mixture of diastereoisomers **6** and **7**, we developed another route that would unequivocally afford only the 2β,3α-tropane derivatives **12a** and **14a** (Scheme 3). This mixture readily underwent the copper(I)-catalysed conjugate addition reaction of $Pr^nMgBr$ in the presence of $Me_3SiCl$ and HMPA[9] to afford the two alkylated derivatives **15** and **16**, which were separated by flash chromatography on silica gel. The relative stereochemistry of the C-3 and C-4 substituents in these two derivatives was assigned by the observation of $J_{3,4}$ = 8.1 and 7.5 Hz for compounds **15** and **16**, respectively. These coupling constants are comparable with those reported




**Scheme 3** *Reagents and conditions*: i, $Pr^nMgBr$, CuBr.$Me_2S$, HMPA, $Me_3SiCl$, THF, −78 °C; ii, $LiAlH_4$, THF, room temp.; iii, LDA, ClC(S)OPh, THF, −78 °C; iv, $Bu_3SnH$, AlBN, toluene, 90 °C; v, $PCl_3$, DMF, 0 °C; vi, Raney-Ni, EtOH, reflux

earlier in the literature[5] wherein the stereochemistry of these compounds was confirmed by X-ray analysis.

The ketone **15** was reduced with $LiAlH_4$ to afford the 2α-alcohol in 56% yield as a single isomer. Next, this alcohol was treated with LDA followed by *O*-phenyl chlorothioformate in THF to provide the thiocarbonate intermediate, which was deoxygenated with $Bu^n_3SnH$ and AIBN[10] to give the tropane **17** in an overall yield of 34%. Reduction of the sulfoxide with $PCl_3$ followed by desulfurization with Raney-nickel in EtOH at reflux yielded the tropane **12a**. The $^1$H NMR spectrum and optical rotation of this sample were identical to those of the sample obtained by the methods of Scheme 2; this result accordingly further supports the assignment of the stereochemistry of compounds **11** and **12**.

Using the same methodology of Scheme 3, **16** was converted to the *trans* derivative **14a** that had $[\alpha]_D^{25}$ +53 (*c* 1.0, $CH_2Cl_2$).

In conclusion, the use of (*R*)-*p*-tolyl vinyl sulfoxide in the 1,3-dipolar cycloaddition reaction affords access to the non-racemic alkyltropanes **11** and **12**. This synthetic approach is particularly useful for the asymmetric synthesis of compounds of the general formula **3** bearing a substituent in position 6 of the tropane ring. The versatility of this method may be further enhanced through chemical modification of the *p*-tolyl sulfoxide moiety other than by reduction. Furthermore, using the method described in Scheme 3, we are able to selectively synthesize either enantiomer of the 2β,3α-tropane derivatives in optically pure form. These analogues are important since they are more selective for the dopamine transporter relative to the 5-HT transporter than the 2β,3β-isomers.[11]

We are indebted to NIH/NIDA (grant No. DA 10458) for support of this work.

## Footnotes and References

* E-mail: kozikowa@GICCS.GEORGETOWN.EDU

† *Crystal data* for **6**: $C_{21}H_{21}NO_2S$, *M* = 351.45, orthorhombic, $P2_12_12_1$, *a* = 8.0505(6), *b* = 13.5650(11), *c* = 16.7466(9) Å, *V* = 1828.8(2) Å$^3$, *Z* = 4, *T* = 293(2) K, μ = 1.674, 1882 reflections, 1637 observed, *R* = 0.0376, *wR* = 0.0957. For **8**·0.4 EtOAc: $C_{21}H_{21}NO_2S·0.4(C_4H_8O_2)$, *M* = 386.69, monoclinic, $P2_1$, *a* = 12.9389(10), *b* = 6.1551(5), *c* = 14.340(2) Å, *V* = 1041.6(2) Å$^3$, *Z* = 2, *T* = 293(2) K, μ = 1.544, 1909 reflections, 1645 observed, *R* = 0.0486, *wR* = 0.1195. CCDC 182/581.

1 M. Lounasmaa, *The Alkaloids*, 1988, **33**, 1.
2 W. L. Woolverton and K. M. Johnson, *Trends Pharmacol. Sci.*, 1992, **13**, 193; W. L. Woolverton and M. S. Kleven, *NIDA Research Monograph*, 1988, **88**, 160.
3 A. P. Kozikowski, M. K. Eddine Saiah, K. M. Johnson and J. S. Bergmann, *J. Med. Chem.*, 1995, **38**, 3086.
4 R. L. Clarke, S. J. Daum, A. J. Gambino, M. D. Aceto, J. Pearl, M. Levitt, W. R. Cumiskey and E. F. Bogado, *J. Med. Chem.*, 1973, **16**, 1260; F. I. Carroll, Y. Gao, M. A. Rahman, P. Abraham, K. Parham, A. H. Lewin, J. W. Boja and M. J. Kuhar, *J. Med. Chem.*, 1991, **34**, 2719; F. I. Carroll, A. H. Lewin, J. W. Boja and M. J. Kuhar, in *Drug Design for Neuroscience*, ed. A. P. Kozikowski, Raven Press, New York, 1993, pp. 149–166.
5 A. P. Kozikowski, G. L. Araldi and R. G. Ball, *J. Org. Chem.*, 1997, **62**, 503.
6 (*a*) B. Ronan and H. B. Kagan, *Tetrahedron: Asymmetry*, 1992, **3**, 115; (*b*) T. Takahashi, A. Fujii, J. Sugita, T. Hagi, K. Kitano, Y. Arai and T. Koizumi, *Tetrahedron: Asymmetry*, 1991, **2**, 1379; (*c*) T. Koizumi, H. Hirai and E. Yoshii, *J. Org. Chem.*, 1982, **47**, 4005.
7 J. L. Luche, *J. Am. Chem. Soc.*, 1978, **100**, 2226.
8 C. C. Tseng, S. D. Paisley and H. L. Goering, *J. Org. Chem.*, 1986, **51**, 2884.
9 Y. Horiguchi, S. Matsuzawa, E. Nakamura and I. Kuwajima, *Tetrahedron Lett.*, 1986, **27**, 4025.
10 D. B. Berkowitz, M. J. Eggen, Q. Shen and R. K. Shoemaker, *J. Org. Chem.*, 1996, **61**, 4666.
11 C. R. Holmquist, K. I. Keverline-Frantz, P. Abraham, J. W. Boja, M. J. Kuhar and F. I. Carroll, *J. Med. Chem.*, 1996, **39**, 4139.

*Received in Corvallis, OR, USA, 16th June 1997; 7/04216G*

# A simple 'one pot' route to the hyperbranched analogues of Tomalia's poly(amidoamine) dendrimers

**Lois J.Hobson, Alan M. Kenwright and W. James Feast***

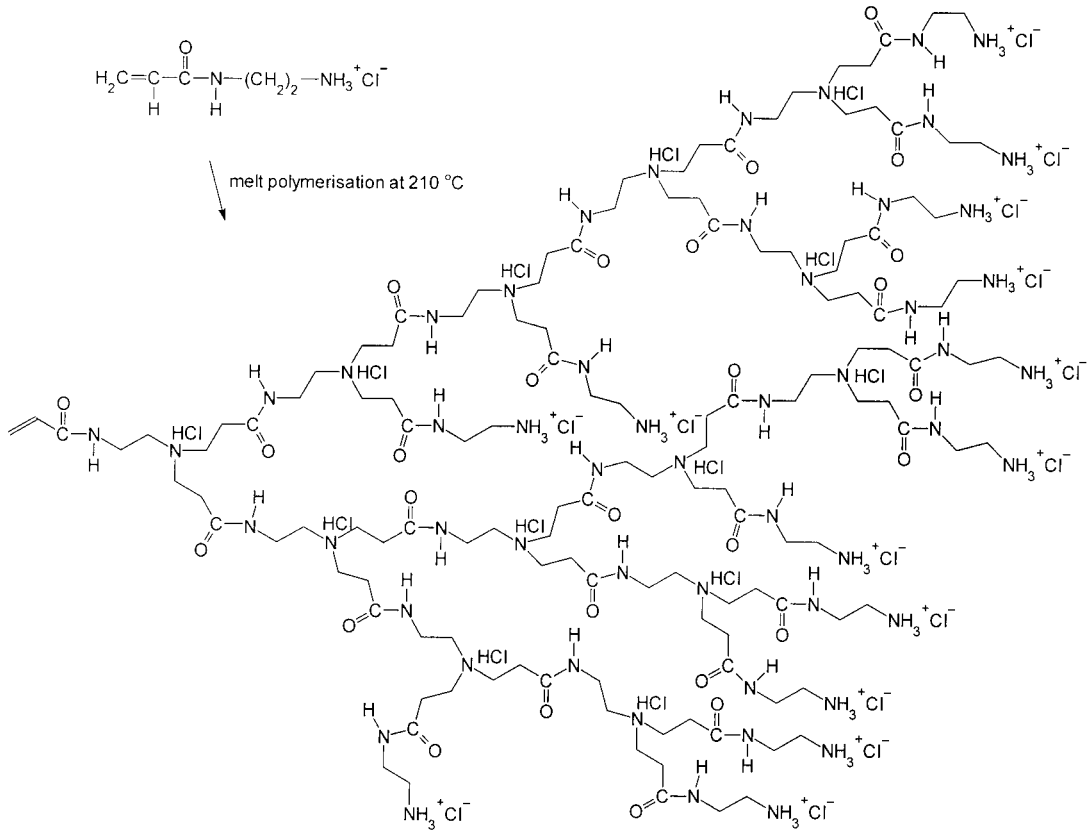
*I.R.C. in Polymer Science and Technology, University of Durham, Durham, UK DH1 3LE*

**Melt polymerisation of *N*-acryloyl-1,2-diaminoethane hydrochloride gives the hyperbranched hydrochloride salt analogues of Tomalia's poly(amidoamine) dendrimers, for which spectroscopic analysis establishes a branching ratio close to one.**

Scientific and technological interest in dendrimers grew rapidly following Tomalia's stimulating review,[1] but bulk applications remain inhibited by the labour intensive syntheses involved. A characterising feature of dendritic polymers is that, past a critical point, their intrinsic viscosity decreases with increasing molecular weight.[2] This contrasts with linear and lightly branched polymers and has potential technological implications. It would be attractive to mimic this unusual molecular weight–viscosity behaviour in more readily accessible materials.

As part of a programme of research into the synthesis and properties of $AB_n$ hyperbranched polymers we have studied the melt polymerisation of *N*-acryloyl-α,ω-diaminoalkane hydrochlorides, $H_2C{=}CHCONH(CH_2)_nNH_3^+Cl^-$, ($n$ = 2–7). The monomers, produced by a straightforward protection/deprotection strategy,[3] polymerised, *via* a Michael addition process, on heating at 210 °C under nitrogen. The products, water soluble polyelectrolytes, had the same elemental analysis as the monomers. Variation of the polymethylene spacer length ($n$ = 2–7) had a marked effect on both monomer reactivity (*e.g.* $n$ = 2 reacts much faster than $n$ = 6) and the structure and properties of the polymer. The process is summarised in Scheme 1 for the case where $n$ = 2.

$^1$H and $^{13}$C NMR spectroscopy unambiguously demonstrated the loss of the acrylamide vinyl unit and generation of new methylene units during polymerisation, and allowed an estimation of the number average molecular weight ($M$n) based on end group counting, The $M$n values obtained would be overestimates if significant cyclisation through the focal acrylate group had occurred. Aqueous gel permeation chromatography of these polyelectrolytes was uninformative, but MALDI-TOF mass spectrometry (2,5-dihydroxybenzoic acid matrix, Kratos Kompact MALDI IV in linear detection mode) showed a series of ions corresponding to degrees of polymerisation (dp) in the range 2 to 38. In the spectrum reproduced in Fig. 1, recorded for the polymer derived from *N*-acryloyl-1,6-diaminohexane hydrochloride ($n$ = 6), the major ion sequence corresponds to the simple multiple addition products detected as mono-protonated oligomers of the free base. The minor series, 55 mass units behind the parent ions, corresponds to loss of the focal




**Scheme 1**

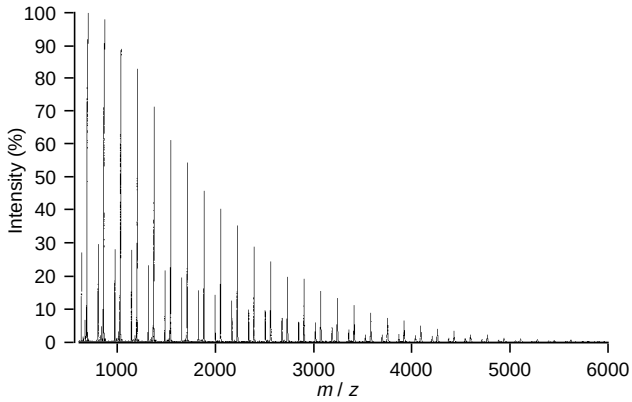



**Fig. 1** MALDI-TOF mass spectrum of the polymer prepared from *N*-acryloyl-1,6-diaminohexane hydrochloride ($n$ = 6) recorded using MALDI 4 with pulsed extraction

$CH_2$=CHCO unit or to one part of a process of random amide link fragmentation. The comparative intensity of this minor series increases with increasing laser power. However, the absence of the other fragment expected from a random cleavage at amide links leads us to favour the first postulate. In further support of this view we observe that under conditions which favour fragmentation, both of the expected series of ions from random fragmentation at amide bonds can be seen.

Analysis of this spectrum using the Kompact software gave a value of 1500 for *M*n of the free base, which compared well with the value of 1570 calculated from the $^1$H NMR spectrum. The intensity distribution of peaks in Fig. 1 qualitatively resembles the distribution predicted by Flory,[4] but careful quantitative analysis shows that in these cases the MALDI-TOF technique fails to provide a representative picture of the whole sample, this is particularly evident when considering materials of broader polydispersity and produced at higher degrees of conversion.[5]

Michael addition polymerisation of these monomers can, in principle, yield secondary or tertiary amines corresponding to linear or branched sub-units. Thus amide and primary (terminal, T), secondary (linear, L) and tertiary (branched, B) amine nitrogen environments are possible. The frequency of the branched and terminal groups is connected, T = B + 1. $^{15}$N NMR spectroscopy, recorded quantitatively in natural abundance, revealed three signals; the amide and primary amine nitrogens are readily identified on the basis of chemical shift (relative to liquid ammonia) and literature assignments of related compounds,[6] but the signals for amine nitrogens in linear and branched units overlap; however, integration allows an assignment of the extent of branching.

Thus, for polymers derived from *N*-acryloyl-α,ω-diaminoalkane hydrochlorides, each repeat unit contributes one amide and one amine nitrogen species. Three signals are observed in the spectra, which we assigned as one amide and two amine salt signals. Where $n$ = 2, (Fig. 2) the two amine salt signals are of approximately equal intensity and must represent terminal and branched units since, if the polymer was composed entirely of linear units, the terminal contributions would be negligible (only one signal per chain) and the linear salt signal would be equal in intensity to the amide signal.

In fact the sum of the relative intensities of the terminal and branched signals equals that of the amide signal within the limits of experimental error, an observation consistent with

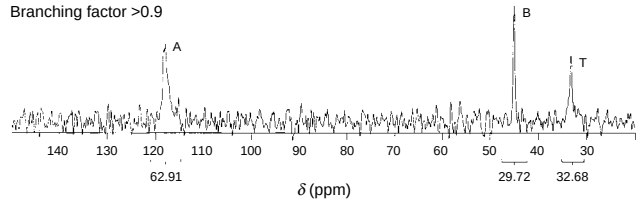



**Fig. 2** Quantitative $^{15}$N NMR spectrum ($D_2O$) of the polymer prepared from *N*-acryloyl-1,2-diaminoethane hydrochloride (pH 1)

virtually complete branching. For this system the relationship between the degree of branching[7] and the terminal (T), branched (B) and amide (A) contributions can be expressed as: branching factor = (B + T)/A. It can therefore be concluded that the polymer is highly branched with few or no linear units, and within the limits of the experiment a degree of branching greater than 0.9 can be assigned. Only monomers with $n$ = 2 give rise to such highly branched polymers. Increasing the internal $CH_2$ chain length of the monomer decreases the degree of branching; for example, the polymers where $n$ = 4, display a branching factor of *ca*. 0.7, much closer to the statistical value proposed by Flory.[4]

These poly(amidoamine) hydrochlorides exhibit classic polyelectrolyte viscosity–concentration behaviour, which can be suppressed by the addition of 1% lithium chloride to allow an experimental value for intrinsic viscosity to be obtained. For these polymers we observe a trend of decreasing intrinsic viscosity with increasing molecular weight, a property more associated with dendritic than with linear structure.

As their hydrochloride salts these $AB_2$ poly(amidoamine) hyperbranched wedges are readily soluble in both water and MeOH, but are insoluble in all common organic solvents as their free bases. However, further work has revealed that core terminated systems, prepared through $AB_2/B_n$ copolymerisations using the $AB_2$ monomer *N*-acryloyl-1,2-diaminoethane hydrochloride, retain their solubility as free bases. Consequently this work provides a simple route to hyperbranched polymers with a degree of branching approaching one and some of the structural features and properties of materials with perfect dendritic architecture.

We thank Kratos Analytical for recording the spectrum reproduced as Fig. 1.

## Footnote and References

* E-mail: w.j.feast@durham.ac.uk

1 D. A. Tomalia, A. N. Naylor and A. Goddard, *Angew. Chem., Int. Ed. Engl.*, 1990, **29**, 138.
2 T. H. Mourey, S. R. Turner, M. Rubinstein, J. M. J. Fréchet, C. J. Hawker and K. L. Wooley, *Macromolecules*, 1992, **25**, 2401.
3 G. L. Stahl, R. Walter and C. W. Smith, *J. Org. Chem.*, 1978, **43**, 2285.
4 P. J. Flory, *J. Am. Chem. Soc.*, 1952, **74**, 2718.
5 K. Martin, J. Spickermann, H. J. Rader and K. Mullen, *Rapid Commun. Mass Spectrom.*, 1996, **10**, 1471.
6 P. H. B. Van genderen, M. W. P L. Baars, C. Elissen-Roman, E. M. M. de Brabander-van den Berg and E. W. Meijer, *Polym. Mater. Sci. Eng.*, 1995, **73**, 336.
7 C. J. Hawker, R. Lee and J. M. J. Fréchet, *J. Am. Chem. Soc.*, 1991, **113**, 4583.

*Received in Liverpool, UK, 9th June 1997; 7/04023G*

# Stoichiometric assembly of $[Sb(PCy)_3]_2Li_6{\cdot}6HNMe_2{\cdot}2C_6H_5Me$; a highly fluxional antimony(III) phosphinidine complex containing $Me_2NH$ ligation of lithium†

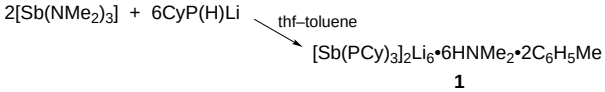
**Michael A. Beswick,* Jonathan M. Goodman, Christopher N. Harmer, Alexander D. Hopkins, Michael A. Paver, Paul R. Raithby, Andrew E. H. Wheatley and Dominic S. Wright***

*Department of Chemistry, University of Cambridge, Lensfield Road, Cambridge, UK CB2 1EW*

**All of the $Me_2NH$ produced by the reaction of $[Sb(NMe_2)_3]$ with CyP(H)Li (Cy = $C_6H_{11}$) coordinates the $Li^+$ cations of the product $[Sb(PCy)_3]_2Li_6{\cdot}6HNMe_2{\cdot}2C_6H_5Me$ 1; the complex contains the first example of a group 15 metal phosphinidine anion $\{[Sb(PR)_3]^{3-}\}$.**

Although group 13 metal imido ($RN^{2-}$) and phosphinidine ($RP^{2-}$) compounds are now comparatively common,[1] far fewer imido complexes are known for the heaviest (most metallic) group 14 (Sn, Pb) and 15 (Sb, Bi) elements. We have recently investigated the use of the stepwise metallation of primary amines with organolithiums and $[Sb(NMe_2)_3]$ as a general strategy to a range of polyimido antimony anions, *e.g.* the $[Sb(NR)_3]^{3-}$ trianion of the cage complex $[\{Sb(NCH_2CH_2Ph)_3\}_2Li_6{\cdot}2thf]$.[2,3] These species have an extensive coordination chemistry towards alkali, transition and p-block metals, where they act as surprisingly robust multidentate ligands.[4] A related methodology, involving the transmetallation reactions of lithiated primary amines and phosphines with imido tin(II) cubanes,[5] provides an approach to the metallacyclic phosphinidine complex $[Sn(\mu\text{-}PCy)_2(\mu\text{-}PCy)]_2(Li{\cdot}thf)_4$.[6]

We report here the stoichiometric assembly of the complex $[Sb(PCy)_3]_2Li_6{\cdot}6HNMe_2{\cdot}2C_6H_5Me$ **1** from the reaction of $[Sb(NMe_2)_3]$ with CyP(H)Li (Scheme 1).‡ The cage arrangement of **1** is similar to that occurring in the imido antimony(III) complex $[\{Sb(NCH_2CH_2Ph)_3\}_2Li_6{\cdot}2thf]$[3] and in a few unsolvated group 14 cages of $Si^{IV}$ and $Ge^{IV}$.[7] However, this complex contains the first phosphinidine anion of a group 15 element (As–Bi). Although solvation of alkali-metal cations by $NH_3$ has been well documented for solutions of the metals in liquid ammonia,[8] the incorporation of a small protic ligand such as $Me_2NH$ (a gas above 7 °C) in a reaction involving conventional organic solvents is a surprising structural feature of **1**.




**Scheme 1**

A low-temperature X-ray crystallographic study of **1**§ shows it to be a mixed-metal cage complex, $[Sb(PCy)_3]_2Li_6{\cdot}6HNMe_2{\cdot}2C_6H_5Me$, consisting of a 14-membered $\{Sb_2P_6Li_6\}$ core (Fig. 1). In addition there are two lattice-bound toluene molecules per molecule of **1**. The structure, which arises from the association of two $[Sb(PCy)_3]^{3-}$ trianions by six $Li^+$ cations, can be described as a hexameric phosphido-lithium 'stack' capped at the open $Li_3P_3$ faces by two Sb atoms. However, direct evidence of the integrity of the $[Sb(PCy)_3]^{3-}$ trianions of **1**, and the fact that these units dominate the bonding pattern of the core,[9] is given in the $^7Li$ NMR spectrum in which a binomial septet ($^1J_{^{31}P^{7}Li}$ 14 Hz) occurs as a result of the coupling of all the $Li^+$ cations to the P atoms of two intact trianions (203–298 K) (Fig. 2). Preliminary semi-empirical PM3 calculations¶ indicate that interchange of the six $Li^+$ cations occurs by a

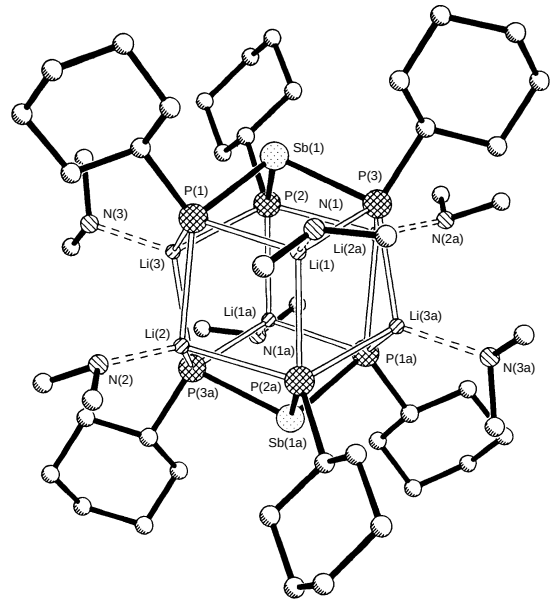



**Fig. 1** The molecular structure of $[Sb(PCy)_3]_2Li_6{\cdot}6HNMe_2{\cdot}2C_6H_5Me$ **1** showing the atom numbering scheme. The $C_6H_5Me_3$ lattice solvation and hydrogen atoms have been omitted for clarity. Selected bond lengths (Å) and angles (°): Sb(1)–P(1) 2.519(6), Sb(1)–P(2) 2.517(5), Sb(1)–P(3) 2.516(5), Li(1)–P(3) 2.59(3), P(1)–Li(3) 2.56(3), Li(1)–P(1) 2.55(3), Li(3)–P(2) 2.62(3), P(1)–Li(2) 2.62(3), N(3)–Li(3) 2.08(3), N(2)–Li(2) 1.96(4), N(1)–Li(1) 2.10(4); P(3)–Sb(1)–P(2) 101.3(2), P(2)–Sb(1)–P(1) 103.4(2), P(3)–Sb(1)–P(1) 100.3(2).

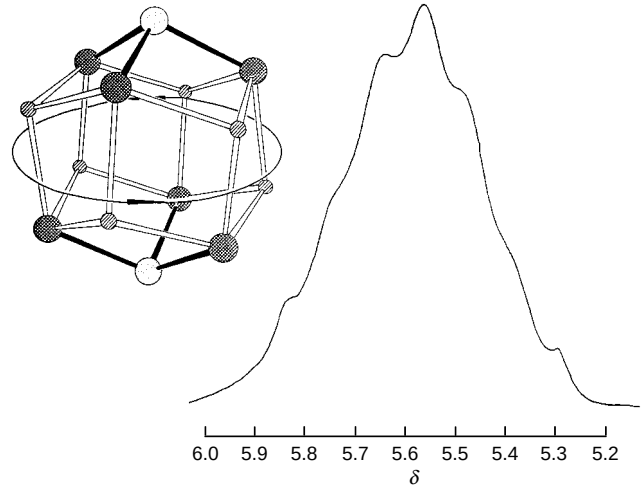



**Fig. 2** Dynamic 'carousel' process and the $^7Li$ NMR spectrum of **1**

dynamic ('carousel') process, analogous to that observed for $[Me_2Si(NSiMe_3)_2]_2InLi$ in solution,[10] in which the $Sb^{III}$ centres are not involved. The $^{31}P$ NMR chemical shift ($\delta$ −263.5) is vastly different to that observed for $[(2,4,6\text{-}Bu^t_3C_6H_2)P{=}Sb\{CH(SiMe_3)_2\}]$ ($\delta$ 600),[11] reflecting the development of negative charge on the P centres of **1**.

In the polymeric ladder structure of the monolithiated cyclohexyl phosphine precursor to **1** $(CyPHLi\cdot thf)_\infty$,[12] the P–Li bonds (av. 2.61 Å) are similar to those found in **1** [range 2.55(3)–2.66(3) Å]. The Sb–P bonds in **1** (av. 2.52 Å) are close to those observed in $[SbP(2,4,6\text{-}Bu^t_3C_6H_2)]_2$ [range 2.561(2)–2.583(1) Å] (the only other Sb or Bi phosphinidine complex to be structurally characterised).[13] An interesting structural feature of complex **1** is that the P–Sb–P angles (av. 101.6°) are significantly larger than the N–Sb–N angles (av. 94.5°) found in the related imido complex $[\{Sb(NCH_2CH_2Ph)_3\}_2Li_6\cdot 2thf]$.[3] Although the flattening of the $[Sb(PCy)_3]^{3-}$ trianion may partially reflect the differences in the extents of Lewis-base solvation of the cores {two thf in $[\{Sb(NCH_2CH_2Ph)_3\}_2Li_6\cdot 2thf]$ and six $Me_2NH$ in **1**}, it is likely that the major reason for this is the lower electronegativity difference between Sb and P (*ca*. 0.2 on the Pauling scale; *cf*. 1.1 between Sb and N).

A particularly novel structural feature of **1** is the complexation of the six $Li^+$ cations of the core by $Me_2NH$. This is a gas above 7 °C and its formation can be envisaged as normally providing the thermodynamic driving force in the reactions of $[Sb(NMe_2)_3]$ with organic acids. However, the stoichiometric inclusion into **1** of all the $Me_2NH$ formed in this reaction is surprising since it not only competes for $Li^+$ coordination with thf but exists as a gas under normal conditions. $^1H$ NMR spectroscopic studies and elemental analysis of **1** illustrate that, although the $Me_2NH$ ligation is almost completely removed by placing the complex under vacuum (0.1 atm, 15 min), this solvation is comparatively robust and is largely retained in fresh samples not subjected to reduced pressure. Recent *ab initio* calculations[14] on the deprotonation of organic acids (RH) with lithium amides ($R'_2NLi$)[15] suggest that complexation of the amine produced ($R'_2NH$) to the $Li^+$ cation {in $[(R'_2NH)LiR]$} may contribute significantly to the thermodynamics of these reactions. The formation of **1** provides the first direct evidence in favour of this proposition and that even for gaseous amines $Li^+$ ligation is likely to play a role.

The incorporation of a phosphorus donor functionality in the $[Sb(PCy)_3]^{3-}$ trianion creates a softer ligand set and a greater ligand bite than the imido congeners and may allow the stabilisation of low oxidation state transition-metal centres.

We thank the EPSRC (M. A. B., D. S. W., P. R. R., C. N. H., A. E. H. W.), Electron Tubes, Ruislip, UK (A. D. H.) and Jesus College for a Fellowship (M. A. P.) for financial support. We also thank Oxford Molecular for the gift of VAMP 5.6.

## Footnotes and References

* E-mail: dsw1000@cam.ac.uk

† This ChemComm is also available in enhanced multi-media format *via* the World Wide Web: http://chemistry.rsc.org/rsc/cccenha.htm

‡ *Synthesis of* **1**: to a stirred and chilled suspension of $[LiP(H)Cy]_n$ (7.53 mmol of monomer) in toluene (5 ml) was added a solution of $[Sb(NMe_2)_3]$ (2.51 mmol, 1.36 $cm^3$, 1.84 mol $dm^{-3}$ in toluene). The suspension was stirred and gradually allowed to warm towards 0 °C at which stage a yellow precipitate was observed. This was dissolved by the addition of chilled toluene (8 $cm^3$) and thf (1 $cm^3$). The red solution produced was stored at −35 °C for 48 h over which period crystals suitable for X-ray diffraction studies grew. The complex loses $Me_2NH$ of solvation gradually at 25 °C and this is almost completely removed by placing **1** under vacuum (15 min, 0.1 atm). However, if isolated without exposure to vacuum the $Me_2NH$ is largely retained. The following data refer to this material: yield 1.02 g (57%); decomp. 170 °C; IR (Nujol), major bands at 1257m, 1178s, 1051s, 992.5m, 897s, 846s, 730m, 694w $cm^{-1}$; $^1H$ NMR (400.16 MHz, +25 °C, $C_6D_5CD_3$), $\delta$ 7.0 (5 H, m, aryl C–H, $C_6H_5CH_3$), 3.94 (13 H, s, Me, $Me_2NH$), 2.5–1.2 [33 H, overlapping m, Cy and $C_6H_5CH_3$ (2.10)]; $^7Li$ NMR (1.55.513 MHz, +25 °C, $C_6D_5CD_3$), $\delta$ 5.57 (binomial spt, $^1J_{31P^7Li}$ 14 Hz) (rel. to LiCl–$D_2O$) ($\delta$ 7.14 rel. to PhLi–$C_6D_5CD_3$); $^{31}P$ NMR (162.000 MHz, +25 °C, $C_6D_5CD_3$), $\delta$ −263.5 [rel. to neat $(MeO)_3P$; br s, width at half-height 1130 Hz]; Analysis Calc. C, 52.3; H, 8.7; N, 5.6. Found: C, 52.0; H, 8.4; N, 4.4 (no N remains after 15 min at 0.1 atm).

§ *Crystal data* for **1**; $C_{31}H_{62}Li_3N_3P_3Sb$, $M$ = 712.32, monoclinic, space group $P2_1/c$, $a$ = 13.460(3), $b$ = 18.123(3), $c$ = 16.589(4) Å, $\beta$ = 99.83(2)°, $U$ = 3987(2) Å$^3$, $Z$ = 4, $D_c$ = 1.187 Mg m$^{-3}$, $T$ = 150(2) K, $\mu$(Mo-K$\alpha$) = 0.834 mm$^{-1}$, $F$(000) = 1496. Yellow cubes, crystal dimensions 0.30 × 0.25 × 0.20 mm. 3717 reflections ($2\theta$ < 45.0°) were collected on a Siemens R3mV diffractometer using Mo-K$\alpha$ radiation ($\lambda$ = 0.710 73 Å), graphite monochromator and $\omega$–$2\theta$ scans ($2.57 \leqslant \theta \leqslant 19.99°$). 3717 independent reflections ($R_{int}$ = 0.021) after a semiempirical absorption correction was applied. The structure was solved using direct methods and refined by full-matrix least squares based on $F^2$ (SHELXL93),[16] with all non-hydrogen atoms assigned anisotropic displacement parameters; cyclohexyl, toluene and amine H atoms were fixed in idealised positions and allowed to ride on the relevant C or N atoms. The refinement converged to $R_1$ = 0.0748 for data $I > 2\sigma(I)$ and $wR_2$ = 0.2722 for all data, goodness of fit = 1.013, and weighting scheme $w = 1/[\sigma^2(F_o^2) + (0.0597P)^2 + 18.32P]$, where $P = (F_o^2 + 2F_c^2)/3$. Largest peak and hole in the final difference map; 0.913, −0.689 e Å$^{-3}$. Crystals of **1** were weakly diffracting. Restraints were applied for the lattice-bound toluene which is disordered over two (50 : 50) sites about a twofold axis. CCDC 182/564.

¶ Calculations were carried out using VAMP 5.6 (Oxford Molecular) (J. J. P. Stewart, *J. Comput. Chem.*, 1989, **10**, 209) on a Silicon Graphics R4400 workstation.

1 M. A. Paver, C. A. Russell and D. S. Wright, *Comprehensive Organometallic Chemistry*, 1995, vol. 1, ch. 5.
2 A. J. Edwards, M. A. Paver, P. R. Raithby, M.-A. Rennie and D. S. Wright, *Angew. Chem.*, 1994, **106**, 1334; *Angew. Chem., Int. Ed. Engl.*, 1994, **33**, 1277.
3 R. A. Alton, D. Barr, A. J. Edwards, M. A. Paver, P. R. Raithby, M.-A. Rennie, C. A. Russell and D. S. Wright, *J. Chem. Soc., Chem. Commun.*, 1994, 1481.
4 M. A. Beswick, C. N. Harmer, M. A. Paver, P. R. Raithby, A. Steiner, D. S. Wright, *Inorg. Chem.*, 1997, **36**, 1740; D. Barr, A. J. Edwards, S. Pullen, M. A. Paver, P. R. Raithby, M.-A. Rennie, C. A. Russell and D. S. Wright, *Angew. Chem.*, 1994, **106**, 1960; *Angew. Chem., Int. Ed. Engl.*, 1994, **33**, 1875.
5 R. E. Allan, M. A. Beswick, A. J. Edwards, M. A. Paver, M.-A. Rennie, P. R. Raithby and D. S. Wright, *J. Chem. Soc., Dalton Trans.*, 1995, 1991.
6 R. E. Allan, M. A. Beswick, N. L. Cromhout, M. A. Paver, P. R. Raithby, A. Steiner, M. Trevithick and D. S. Wright, *Chem. Commun.*, 1996, 1501.
7 L. Zsolnai, G. Huttner and M. Dreiss, *Angew. Chem.*, 1993, **105**, 1549; *Angew. Chem., Int. Ed. Engl.*, 1993, **32**, 1439; M. Dreiss, G. Huttner, N. Knopf, H. Pritzkow and L. Zsolnai, *Angew. Chem.*, 1995, **107**, 354; *Angew. Chem., Int. Ed. Engl.*, 1995, **34**, 316; D. J. Brauer, H. Burger, G. L. Liewald and J. Wilke, *J. Organomet. Chem.*, 1985, **287**, 305; D. J. Brauer, H. Burger and G. L. Liewald, *J. Organomet. Chem.*, 1986, **308**, 119; M. Veith, A. Spaniol, J. Pôhlmann, F. Gross and V. Huch, *Chem. Ber.*, 1993, **126**, 2625.
8 *Non-aqueous Solvent Systems*, ed. T. C. Waddington, Academic Press, London, 1965, ch. 1, pp. 1–45 (W. L. Jolly and C. J. Hallada, *Liquid Ammonia*).
9 N. D. R. Barnett, W. Clegg, L. Horsburgh, D. M. Lindsay, Q.-Y. Liu, F. M. Mackenzie, R. E. Mulvey and P. G. Williard, *Chem. Commun.*, 1996, 2321.
10 M. Veith, M. Zimmer and S. Müller-Becker, *Angew. Chem.*, 1993, **105**, 1771; *Angew. Chem., Int. Ed. Engl.*, 1993, **32**, 1733.
11 A. H. Cowley, J. G. Lasch, N. C. Norman, M. Pakulski and B. R. Whitlesey, *J. Chem. Soc., Chem. Commun.*, 1983, 881.
12 E. Hey-Hawkins and S. Kurz, *Phosphorus, Sulfur, Silicon*, 1994, **90**, 281.
13 P. Jutzi, U. Meyer, S. Opiela, M. M. Olmstead and P. P. Power, *Organometallics*, 1991, **9** 1459.
14 D. R. Armstrong, M. G. Davidson, R. P. Davies, H. J. Mitchell, R. M. Oakley, P. R. Raithby, R. Snaith and S. Warren, *Angew. Chem., Int. Ed. Engl.*, 1996, **17**, 1942.
15 B. J. Wakefield, *Organolithium Methods*, Academic Press, New York, 1988; P. G. Williard, *Comprehensive Organic Synthesis*, ed. B. M. Trost and I. Fleming, Pergamon, New York, 1991, vol. 1; L. Maier, *Organic Phosphorus Compounds*, ed. G. M. Kosolapoff and M. Maier, Wiley, New York, 1972, vol. 1.
16 G. M. Sheldrick, SHELXL 93, University of Göttingen, 1993.

*Received in Cambridge, UK, 9th June 1997; 7/03979D*

# On the formation of titanyl (Ti=O) groups in mesoporous and microporous titanosilicate catalysts: a computational study

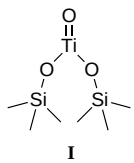
**Phillip E. Sinclair* and C. Richard A. Catlow***

*The Davy Faraday Research Laboratory, The Royal Institution of Great Britain, 21 Albemarle Street, London, UK W1X 4BS*

**Density functional theory calculations are reported which suggests that titanyl groups, $Ti^{IV}$=O, can form by relatively low energy pathways in titanium(IV) silicate catalysts, thereby providing a possible route to the active oxygen donating site responsible for partial oxidation reactions in these materials.**

Knowledge of the structure and chemical properties of the active site in any catalytic reaction is critical to the understanding of the detailed reaction mechanisms. Industrially important examples are provided by the partial oxidation processes over titanium(IV) framework silicates[1] exemplified by TS-1, TS-2[2] and Ti-MCM-41.[3–5] These reactions occur essentially in the liquid phase involving reactant, solvent, sacrificial oxidant such as $H_2O_2$ or $Bu^tOOH$, and the titanium(IV) substituted heterogeneous catalyst. Use of $Ti^{IV}$ embedded in some manner into a silicate framework produces a catalyst with the desirable qualities of guest molecule shape selectivity and one in which oxidation is effected with very high turnover rates and selectivities with respect to both the reactant and the sacrificial oxidant.[5–9] Although it is becoming increasingly evident[5,8] that $Ti^{IV}OH$ centres tripodally attached by O to Si are the major sites for catalytic activity in these systems, a number of questions concerning intermediate titanates still remain. This work reports first principles quantum chemical calculations in order to derive possible models for titanium containing species that could occur on the reaction coordinate to formation of the active oxygen donating species in these systems.

One of the earliest suggestions for the nature of these titanium containing species (originally with respect to $Ti^{IV}$ incorporated into amorphous silicates) was that of a titanyl group stabilised by the silicate host (species **I**, Fig. 1).[10,11] It has been suggested that this titanyl species is responsible for the very high oxidation capacity of titanium(IV) silicates. Titanyl groups have not, however, been observed in TS-1 or similar catalysts unlike its unambiguous characterisation (albeit in a state of five coordination) in the mineral fresnoite[12] and the synthetic layered titanosilicate JDFL-1.[13] Indeed, the lack of UV–VIS absorption corresponding to species **I**[14] has been taken by many to indicate that this species is not present in these materials. Species **I** can, however, account for a number of experimental observations such as the catalyst's IR and NMR responses and its behaviour in $^{18}O$ labelling experiments.[15] Many workers, however, favour the model of $Ti^{IV}$ in four-coordinate sites within the framework, (Fig. 2, species **II**), or grafted onto the surface of a silicate material, (Fig. 2, species **III** and **IV**).[5,7,16,17] Species **III** and species **IV** illustrate the hydroxide forms of the $Ti^{IV}$ sites.




**I**

**Fig. 1** Schematic representation of a titanyl (Ti=O) group, a species suggested as a possible titanium(IV) oxygenate in titanium(IV) silicate catalysts

Organic derivatives have also been prepared[18] and it is noted that these catalysts may behave differently. It is also noted that Fig. 2 represents the state of the $Ti^{IV}$ centres in a dehydrated system. Expansion of the $Ti^{IV}$ coordination shell on addition of coordinating solvents such as water has now been well characterised both experimentally[1,16] and computationally.[19] The partial hydrolysis of the Ti–OSi bonds in the absence of coordinated water can also be described in terms of species **II**, **III** and **IV** (see the reaction at the bottom of Fig. 2).[17]

Recently, we have reported first principles, density functional theory cluster calculations of the processes shown in Fig. 2,[19] *i.e.* over the hydroxide forms of the catalyst. Using a $H_3SiOH$ fragment to model the silanol species produced during the hydrolysis and calculating the energy differences at infinite separation of the silanol and the hydrolysed $Ti^{IV}$ fragment, the internal energies, $\Delta E_1$ and $\Delta E_2$, were calculated to be 20 and 22 kJ $mol^{-1}$, respectively. However, given that in an actual silicate system the hydrolysed titanium(IV) hydroxide complex and the resulting silanols would be in hydrogen-bonding distance, and that typical hydrogen-bond energies are of the order of 20 kJ $mol^{-1}$, it is expected that a mixture of species **II**, **III** and **IV** would be present in systems where $Ti^{IV}$ is isomorphously substituted into the silicate framework, *e.g.* TS-1;[17] and a mixture of species **III** and **IV** would be present in systems where $Ti^{IV}$ is grafted onto a silicate surface, *e.g.* the titanium(IV) hydroxide form of surface grafted Ti-MCM-41.[5] We also showed that within the cluster approximation and in the absence of any adsorbates the formation of species **I** from **III** was energetically unfavourable (requiring 110 kJ $mol^{-1}$). We now report on new computational evidence suggesting that species **I** is energetically accessible from the hydroxide form of titanium(IV) silicates, species **III** and **IV**, in the presence of water and/or other protic solvents.

Fig. 3 shows the calculated reaction profile for formation of species **I** from **III**, unsolvated and in the presence of one molecule of water. The geometries and energies were optimised using the Becke–Perdew'86 gradient corrected density functional included self-consistently in all stages of the calculation as implemented in the Cray Research code DGauss 3.0[20] (a 'fine' integration grid was also employed). A valence double-zeta basis set with polarisation functions on non-hydrogen atoms (DZVP) was used throughout. This method has now been used for a number of problems in the field of silicate chemistry and is known to give reliable geometries and binding ener-

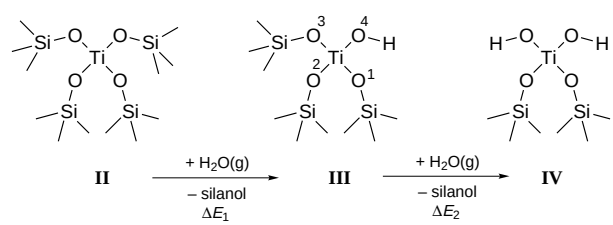



**Fig. 2** Schematic representation of possible four-coordinate titanium(IV) oxygenates in titanium(IV) silicate catalysts. The process shown at the bottom of the figure illustrates the hydrolysis of these species in the presence of a single molecule of water.

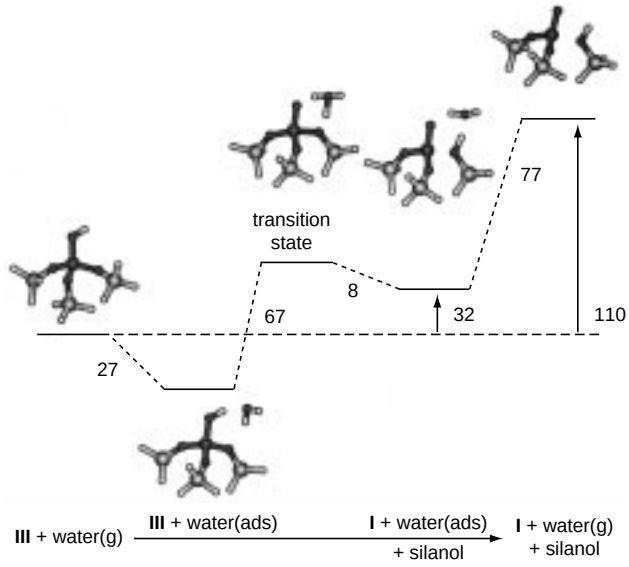



**Fig. 3** DFT optimised reaction path for the formation of a titanyl group (species **I**), modelled by $(H_3SiO)_2Ti{=}O{\cdot}HOSiH_3$, from a silicate embedded titanium hydroxide (species **III**), modelled by $(H_3SiO)_3TiOH$, in the presence of a single molecule of water. Energies are in kJ mol$^{-1}$.

gies.[21,19,22] Activation barriers are more problematic and are generally accepted to be underestimates.[23] The cluster model for the hydroxide species **III**, $(H_3SiO)_3TiOH$, was fully optimised with respect to all atomic degrees of freedom. All other clusters models were then optimised under the constraint that the Si coordinates were fixed at the values obtained from the cluster model of species **III**. These constraints were enforced to prevent unrealistic relaxation of the cluster. This does however introduce an unknown error into the calculated energy changes for the hydrolysis reaction due to structural strain. The strain is difficult to estimate without resorting to computationally prohibitive clusters, for example, 'closed' cubic silasesquioxanes. The error will however be system- and site-dependent although it is likely that the constraints imposed in the current calculations will lead to the energy changes being upper bounds; the silanols formed during the reaction being unable to relax (under the constraints imposed by the silicate host).

Clearly the process shown in Fig. 3 is essentially one of proton transfer from $O^4$ to one on the other oxygens $O^1$ to $O^3$ (Fig. 2) and is thus dependent on one of the hydroxide forms of $Ti^{IV}$ being present. It is also clear that, as described above, unsolvated species **III** is much more stable than species **I**. In the presence of a single molecule of water however, titanyl species **I** can be formed with a true activation barrier of 67 kJ mol$^{-1}$ or an effective barrier of 40 kJ mol$^{-1}$ with respect to the original reactants. Furthermore, in the presence of a single water molecule, species **I** is only 32 kJ mol$^{-1}$ less stable than the separated titanium(IV) hydroxide (species **III**) and water, a change of 77 kJ mol$^{-1}$ with respect to the unsolvated case. Despite the hydrophobic nature of TS-1 and similar silicates, small amounts of water and/or other protic solvents (generated, for example, during oxidation reactions) will be present enhancing the probability of forming titanyl species **I** from any accessible titanium(IV) hydroxide groups.

At present, no account of the environment of the $Ti^{IV}$ site has been included within the calculations. However, if we examine the calculated change in the dipole moment ($\mu$) of the complexes leading to the transition state for formation of titanyl species **I**, we note that activation results in an increase in $\mu$ [3.23–4.21 D (1 D $\approx 3.336 \times 10^{-30}$ C m)]. We expect therefore that the environment provided by a partial ionic silicate framework would stabilise the transition state more than the solvated titanium(IV) hydroxide (species **III**) and that the calculated activation barrier shown in Fig. 3 would therefore be an overestimate. It is also expected that the real barrier would be strongly correlated with the topological position of the titanium(IV) complex within the host framework as well as with the chemical composition of that framework.

In conclusion, we have employed density functional theory methods to show that titanyl groups, *i.e.* species **I**, can be formed with relative ease from the hydroxide forms of four-coordinate titanium(IV) silicates in the presence of even small amounts (in this case one molecule) of water and probably other protic solvents. Their formation is likely to be correlated with the precise nature of the $Ti^{IV}$ environment. However, given that the limiting case of aqueous $TiO^{2+}$ is known to be a very labile species (oxygen exchange rate estimated at 16 000 ± 5000 s$^{-1}$ at 298 K)[24] and that no Ti=O UV–VIS absorption has been measured in silicates, titanyl species are probably very short-lived species in dynamic equilibrium with the hydroxide species **III** and/or species **IV**. We suggest however, on the basis of the current calculations, that they could be present in sufficient concentration to provide a route to the active oxygen-donating species for partial oxidation catalysis in hydroxide forms of titanium(IV) silicates.

The authors would like to thank Professor Sir J. M. Thomas, Dr Sankar and Dr Oldroyd both of the Royal Institution of Great Britain for useful discussions and collaboration. P. E. S. would also like to thank EPSRC for financial support and computer resources.

## Footnote and References

* E-mail: phillip@ri.ac.uk, richard@ri.ac.uk

1 B. Notari, *Adv. Catal.*, 1996, **41**, 253.
2 M. Taramasso, G. Perego and B. Notari, *US Pat.*, 4 410 501, 1983.
3 P. T. Tanev, M. Chibwe and T. J. Pinnavaia, *Nature*, 1994, **368**, 321.
4 A. Corma, M. T. Navarro and J. Perez-Pariente, *J. Chem. Soc., Chem. Commun.*, 1994, 147.
5 T. Maschmeyer, F. Rey, G. Sankar and J. M. Thomas, *Nature*, 1995, **378**, 159.
6 R. D. Oldroyd, J. M. Thomas, T. Maschmeyer, P. A. MacFaul, D. W. Snelgrove, K. U. Ingold and D. D. M. Wayner, *Angew. Chem., Int. Ed. Engl.*, 1996, **35**, 2787.
7 T. Blasco, A. Corma, M. T. Navarro and J. P. Pariente, *J. Catal.*, 1995, **156**, 65.
8 J. M. Thomas, *Faraday Discuss.*, 1997, **105**, 1.
9 J. M. Thomas, *Philos. Trans. R. Soc. London A*, 1990, **333**, 17.
10 R. A. Sheldon and J. A. van Doorn, *J. Catal.*, 1973, **31**, 427.
11 R. A. Sheldon, *J. Mol. Catal.*, 1980, **7**, 107.
12 S. A. Markgraf, A. Halliyal, A. S. Bhalla, R. E. Newnham and C. T. Prewitt, *Ferroelectrics*, 1985, **62**, 17.
13 M. A. Roberts, G. Sankar, J. M. Thomas, R.H. Jones, H. Du, J. Chen, W. Pang and R. Xu, *Nature*, 1996, **381**, 401.
14 M. R. Boccuti, K. M. Rao, A. Zeccina, G. Leofanti and G. Petrini, *Stud. Surf. Sci. Catal.*, 1989, **48**, 133.
15 G. Bellussi, A. Carati, M. G. Clerici, G. Maddinelli and R. Millini, *J. Catal.*, 1992, **133**, 220.
16 S. Bordiga, S. Coluccia, C. Lamberti, L. Marchese, A. Zecchina, F. Boscherini, F. Buffa, F. Genoni, G. Leofanti, G. Petrini and G. Vlaic, *J. Phys. Chem.*, 1994, **98**, 4125.
17 F. Geobaldo, S. Bordiga, A. Zecchina, E. Giamello, G. Leofanti and G. Petrini, *Catal. Lett.*, 1992, **16**, 109.
18 T. Maschmeyer, personal communication.
19 P. E. Sinclair, G. Sankar, C. R. A. Catlow, J. M. Thomas and T. Maschmeyer, *J. Phys. Chem.*, 1007, **101**, 4232.
20 DGauss 3.0, Cray Research Inc., 1995, J. Andzelm and E. Wimmer, *J. Chem. Phys.*, 1992, **96**, 1280.
21 M. Neurock and L. E. Manzer, *Chem. Commun.*, 1996, 1133.
22 P. E. Sinclair and C. R. A. Catlow, *J. Chem. Soc., Faraday Trans.*, 1997, **93**, 333.
23 J. Andzelm, J. Baker, A. Scheiner and M. Wrinn, *Int. J. Quantum Chem.*, 1995, **56**, 733.
24 P. Comba and A. Merbach, *Inorg. Chem.*, 1987, **26**, 1315.

*Received in Cambridge, UK, 30th June 1997; 7/04567K*

# Synthesis of $Fe_4(CO)_8(\mu\text{-}PPh_2)_2(\mu_4\text{-}\eta^1,\eta^1,\eta^2,\eta^2\text{-}C_2Ph)_2$ *via* coupling of acetylides at a binuclear centre: a molecule with through-the-cluster carbon–carbon bonding?

**Arthur J. Carty,*[a] Graeme Hogarth,[a,b] Gary Enright[a] and Gilles Frapper[a]**

[a] *Steacie Institute for Molecular Sciences, National Research Council of Canada, 100 Sussex Drive, Ottawa, K1A 0R6, Canada*
[b] *Department of Chemistry, University College London, 20 Gordon Street, London, UK WC1H 0AJ*

**Thermolysis of $Fe_2(CO)_6(\mu\text{-}PPh_2)(\mu\text{-}\eta^1,\eta^2\text{-}C_2Ph)$ affords the rectangular cluster $Fe_4(CO)_8(\mu\text{-}PPh_2)_2(\mu_4\text{-}\eta^1,\eta^1,\eta^2,\eta^2\text{-}C_2Ph)_2$ with two face-capping acetylides linked through the $Fe_4$ face by a short carbon–carbon contact: reaction with CO leads to $Fe_3(CO)_8\{\mu\text{-}Ph_2PC(CPh)\text{=}C(CPh)PPh_2\}$ as a result of C–C and C–P bond-forming processes.**

The acetylide group (–C≡CR) is an extremely versatile ligand capable of binding to one or more metal centres in a variety of coordination modes, donating up to 5 electrons to a cluster centre.[1] In fact, metal acetylides and polyacetylides have recently emerged as promising molecules and precursors for advanced materials and there is now intense interest in both carbon-rich polyacetylide complexes and multimetallic systems where the π-electrons of the polyunsaturated fragment are used for additional coordination. One strategy for the synthesis of polymetallic arrays is to effect the coupling of multi-site bound acetylides and we have recently described the generation of a series of new tetraruthenium clusters from bimetallic precursors.[2] Herein we describe the high yield synthesis of the symmetrical rectangular tetrairon cluster $Fe_4(CO)_8(\mu\text{-}PPh_2)_2(\mu_4\text{-}\eta^1,\eta^1,\eta^2,\eta^2\text{-}C_2Ph)_2$ **2** *via* dimerisation and CO loss on thermolysis of $Fe_2(CO)_6(\mu\text{-}PPh_2)(\mu\text{-}\eta^1,\eta^2\text{-}C_2Ph)$ **1**. The molecule **2** has two face-capping acetylides with a short 'through-the-cluster' $C_\alpha$–$C_\alpha$ distance such that the two acetylides resemble a $PhC_4Ph$ diyne. Complex **2** undergoes a further facile conversion to $Fe_3(CO)_8\{\mu\text{-}\eta^2,\eta^4,\eta^2\text{-}Ph_2PC(CPh)C(CPh)PPh_2\}$ *via* acetylide–phosphido coupling.

Heating a toluene solution of $Fe_2(CO)_6(\mu\text{-}PPh_2)(\mu\text{-}\eta^1,\eta^2\text{-}C_2Ph)$[3] **1** at 140 °C for 2 h results in a darkening of the solution and the appearance of new ν(CO) bands at 2004 and 1976 $cm^{-1}$ in the IR spectrum. After removal of solvent and washing with hexane, $Fe_4(CO)_8(\mu\text{-}PPh_2)_2(\mu_4\text{-}\eta^1,\eta^1,\eta^2,\eta^2\text{-}C_2Ph)_2$ **2** was isolated as a dark red solid in 90% yield.† The simplicity of the IR spectrum and the presence of a single resonance in the $^{31}P\{^1H\}$ NMR spectrum at δ 252.2 were suggestive of high symmetry. The precise nature of **2** was established by a crystallographic study (Fig. 1).‡

The molecule is centrosymmetric and consists of a rectangle of iron atoms characterised by Fe–Fe distances of 2.5282(4) [Fe(1)–Fe(2)] and 2.8652(5) Å [Fe(1a)–Fe(2)], short edges being bridged symmetrically by phosphido ligands [Fe(1)–P(1) 2.1996(7); Fe(2)–P(1) 2.2010(7) Å]. Each face of the rectangle is capped by an acetylide ligand which is σ-bonded to two metal atoms [Fe(1)–C(5a) 1.992(2); Fe(2)–C(5a) 2.002(2) Å] and π-bonded to the other two [Fe(1)–C(5) 2.143(2); Fe(2)–C(5) 2.141(2); Fe(1)–C(6) 2.030(2); Fe(2)–C(6) 2.001(2) Å]. Although several clusters with $\mu_4$-acetylides on $M_4$ faces are known,[4] we are unaware of any examples where two such moieties are bound on opposite faces of an $M_4$ rectangle. Within each acetylide ligand the $C_\alpha$–$C_\beta$ distance [C(5)–C(6) 1.383(3) Å] is similar to that found in $Ru_5(CO)_{13}(\mu\text{-}PPh_2)(\mu_4\text{-}\eta^1,\eta^1,\eta^2,\eta^2\text{-}C_2Ph)$ [1.342(11) Å] where the acetylide is also coordinated on an $M_4$ face.[5] The most noteworthy feature of **2** is the C(5)–C(5a) distance of 1.596(4) Å, indicative of a direct through-space interaction between the two $C_\alpha$ carbon atoms. Indeed this distance could be interpreted as indicative of a C–C single bond elongated somewhat *via* interactions of C(5) and C(5a) with the iron atoms. The metallic valence electron count (MVEC) of **2** is 62 or 64 electrons depending on whether the hydrocarbyl ligands $(C_2Ph)_2$ are acting as one 8-electron donor diyne or as two 5-electron donor acetylides. Extended Hückel computations show that the LUMO for **2** lies 1.99 eV above the HOMO, ensuring the stability of **2** for an MVEC of 64 electrons. This model for the electronic structure of **2**, with the acetylides contributing 10 electrons to the MVEC, does not require any through-space C···C bonding. Nevertheless, a strongly positive $C_\alpha$-$C_\alpha$ overlap population (+0.66) is computed, reflecting a significant attractive interaction between the $C_\alpha$ atoms capping the metallic core. Both size and electronic factors contribute to the short C···C contact in**2**. A smaller P···P overlap population of 0.226, indicative of a P···P interaction across the cluster face in $Fe_4(CO)_{12}(\mu_4\text{-}PH)_2$ has been calculated by Halet and coworkers.[6] The EHMO calculations on **2** also revealed that the negative charge on $C_\beta$ was significantly higher than that on $C_\alpha$ (−0.21 *vs.* + 0.20). Consistent with this, in the $^{13}C\{^1H\}$ NMR spectrum of **2**, $C_\alpha$ [$\delta$ 143.23(d); $J_{P-C}$ 23.0 Hz] is much more deshielded than $C_\beta$ [$\delta$ 95.21(s)].

In light of the interaction between $C_\alpha$ atoms in **2** we investigated whether formal coupling of the two acetylides to a diyne could be induced. While **2** is stable to prolonged reflux at 160 °C, bubbling CO through a toluene solution at 100 °C leads

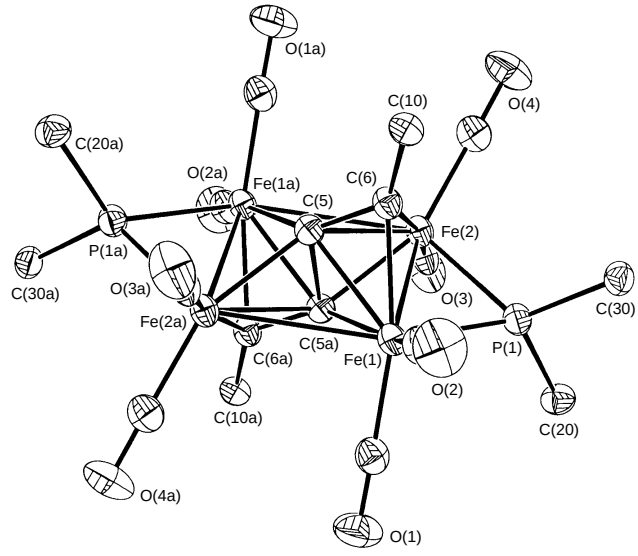



**Fig. 1** Molecular structure of **2** with selected bond lengths (Å) and angles (°): Fe(1)–Fe(2) 2.5282(4), Fe(1)–Fe(2a) 2.8652(5), Fe(1)–P(1) 2.1996(7), Fe(2)–P(1) 2.2010(7), Fe(1)–C(5a) 1.9916(22), Fe(2)–C(5a) 2.0018(23), Fe(1)–C(5) 2.1429(22), Fe(2)–C(5) 2.1407(22), Fe(1)–C(6) 2.0296(22), Fe(2)–C(6) 2.0008(23), C(5)–C(6) 1.383(3), C(5)–C(5a) 1.596(4); Fe(1)–P(1)–Fe(2) 70.130(22), C(5)–C(6)–C(10) 130.77(21)

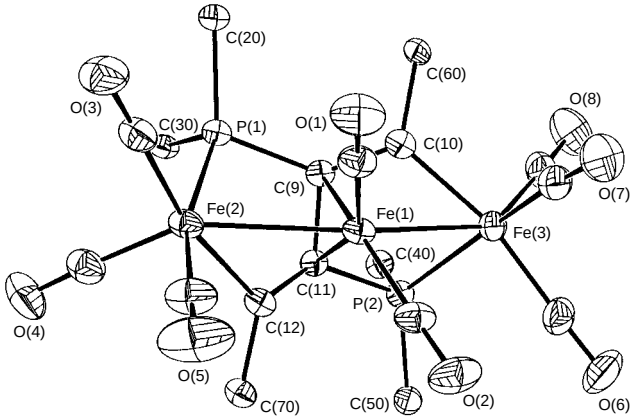
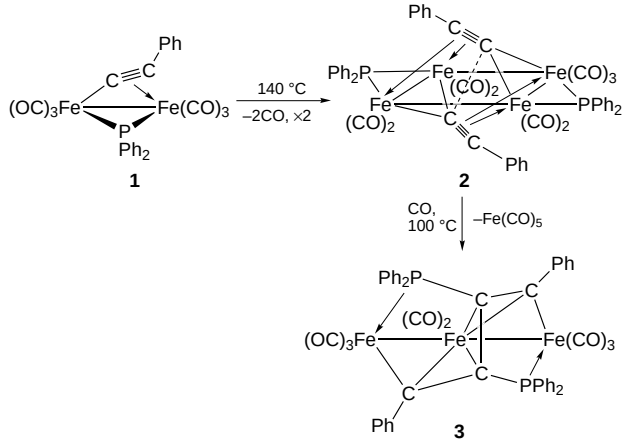



**Fig. 2** Molecular structure of **3** with selected bond lengths (Å) and angles (°): Fe(1)–Fe(2) 2.6327(15), Fe(1)–Fe(3) 2.6506(15), Fe(2)–P(1) 2.247(2), Fe(3)–P(2) 2.258(2), Fe(1)–C(9) 2.037(6), Fe(1)–C(10) 2.104(7), Fe(1)–C(11) 2.038(6), Fe(3)–C(10) 2.004(7), Fe(1)–C(12) 2.108(6), Fe(2)–C(12) 2.029(6), C(9)–C(10) 1.422(9), C(11)–C(12) 1.418(9), C(9)–C(11) 1.485(9), P(1)–C(9) 1.821(6), P(2)– C(11) 1.821(6); Fe(2)–Fe(1)–Fe(3) 153.37(5)

to the rapid appearance of new IR bands and the isolation after workup of $Fe_3(CO)_8\{\mu\text{-}Ph_2PC(CPh)=C(CPh)PPh_2\}$ **3** in 65% yield as a cherry-red solid.§ The $^{31}P$ NMR spectrum showed only a single resonance ($\delta$ 67.1) well upfield of **2**, suggesting that P–C coupling had occurred. An X-ray analysis revealed the molecular structure shown in Fig. 2.‡

The molecule consists of a near linear triiron backbone [Fe(2)–Fe(1)–Fe(3), 153.37(5)°] with the two outer atoms carrying three carbonyls and the central iron atom carrying two. This metal core [Fe(1)–Fe(2) 2.6327(15), Fe(1)–Fe(3) 2.6506(15) Å] is spanned by an unusual bis-2,3-diphenylphosphinodiyne which has resulted from the coupling of both of the phosphido bridges and the two acetylide ligands. To our knowledge, this diphosphine has not previously been synthesised. The coupling of the acetylides is through the two α-carbon atoms as might be expected from their close proximity in **2**. The phosphido groups also couple to the α-carbons and each is coordinated to a single outer iron centre. This new bridging ligand acts as 10-electron donor to the cluster, which then has the expected 50-electron count for a linear trimetallic complex. A closer look at the bond lengths within the diphosphine ligand reveals that the C(9)–C(11) distance of 1.485(9) Å is only 0.11 Å shorter than the corresponding $C_\alpha$-$C_\alpha$ distance found in **2**, while the C(9)–C(10) and C(11)–C(12) lengths of 1.422(9) and 1.418(9) Å are somewhat longer than those in the precursor. It is interesting to note that binuclear **1**[3] results from the reaction of $Fe_3(CO)_{12}$ with the phosphinoalkyne, $Ph_2PC_2Ph$, and thus the overall transformation of this ligand *via* **1** and **2** to give **3** (Scheme 1) represents the metal-mediated $C_\alpha$–$C_\alpha$ coupling of two phosphinoalkynes.




**Scheme 1**

We are currently exploring both the mechanism of formation of **2** and the broader implication of acetylide coupling at polynuclear centres for the synthesis of new polyyne clusters.

We are grateful to the Natural Sciences and Engineering Research Council of Canada and the National Research Council for financial support of this work.

## Footnotes and References

* E-mail: Arthur.Carty@NRC.CA

† Spectroscopic data for **2**: IR ($CH_2Cl_2$) $\nu$(CO) 2004s, 1976m $cm^{-1}$; $^1H$ NMR ($CDCl_3$): $\delta$ 8.4–6.5 (m, Ph); $^{31}P$ NMR ($CDCl_3$): $\delta$ 252.2 (s) (85% $H_3PO_4$); $^{13}C$ NMR ($CDCl_3$): $\delta$ 213.36 (d, *J* 4.7, CO), 211.05 (d, *J* 10.7, CO), 143.23 (d, *J* 23.0, $C_\alpha$), 136–125 (m, Ph), 95.21 (s, $C_ß$): MS(FAB+) *m*/*z* 1020; Anal. Calc. for $Fe_4C_{48}H_{30}P_2O_8$. C, 56.47, H, 2.94. Found: C, 55.43, H, 2.76%.

‡ *Crystal data* for **2**: X-ray intensity data were collected on a Siemens CCD diffractometer using Mo-Kα radiation and the $\omega$-scan mode; T = 293 K $Fe_4C_{48}H_{30}P_2O_8$, $M_r$ = 1020.09, triclinic, space group $P\bar{1}$, $a$ = 9.3789(10), $b$ = 11.2897(10), $c$ = 12.1423(10) Å, $\alpha$ = 104.14(1), $\beta$ = 101.70(1), $\gamma$ = 114.35(1)°, $D_c$ = 1.588 g $cm^{-3}$, $F$(000) = 517, $Z$ = 1, $\mu$ = 1.46 $mm^{-1}$, $2\theta$(max) = 48°, $R$ ($R_w$) = 2.8% (4.0%) for 2930 reflections [$I > 2.5\sigma(I)$] and 323 parameters. For **3**: intensity data: Siemens CCD diffractometer using Mo-Ka radiation and $\omega$-scan mode; T = 293 K $Fe_3C_{48}H_{32}P_2O_8$, $M_r$ = 982.23, triclinic, space group $P\bar{1}$, $a$ = 11.1911(10), $b$ = 11.6675(15), $c$ = 16.9642(12) Å, $\alpha$ = 97.960(10), $\beta$ = 93.137(10), $\gamma$ = 94.407(10)°, $F$(000) = 1003, $D_c$ = 1.495 g $cm^{-3}$, $Z$ = 2, $\mu$ = 1.11 $mm^{-1}$, $2\theta$(max) = 49°, $R$ ($R_w$) = 5.59% (6.70%) for 6857 reflections [$I > 2\sigma(I)$] and 567 parameters. CCDC 182/567.

§ Spectroscopic data for **3**; IR($CH_2Cl_2$) ν(CO) 2049m, 2025s, 1979m, 1968m(sh), 1911w $cm^{-1}$; $^1H$ NMR ($CDCl_3$): δ 7.8–6.5 (m, Ph); $^{31}P$ NMR ($CDCl_3$): 67.08 (s) ppm (85% $H_3PO_4$): MS(FAB+) m/z 964; Anal.Calcd. for $Fe_3C_{48}H_{30}P_2O_8.H_2O$, C, 58.66, H, 3.05; Found, C, 58.20, H, 3.13 %.

1 R. Nast, *Coord. Chem. Rev.*, 1982, **47**, 89; A. J. Carty, *Pure Appl. Chem.*, 1982, **54**, 113; E. Sappa, A. Tiripicchio and P. Braunstein, *Coord. Chem. Rev.*, 1985, **65**, 219. P. R. Raithby and M. J. Rosales, *Adv. Inorg. Chem. Radiochem.*, 1986, **29**, 169.
2 Y. Chi, A. J. Carty, P. Blenkiron, E. Delgado, G. D. Enright, W. Wang, S. Pend and G. Lee, *Organometallics*, 1996, **15**, 5269.
3 G. N. Mott and A. J. Carty, *Inorg. Chem.*, 1983, **22**, 2726.
4 C. Weatherell, N. J. Taylor, A. J. Carty, E. Sappa and A. Tiripicchio, *J. Organomet. Chem.*, 1985, **291**, C9; S. A. MacLaughlin, N. J. Taylor and A. J. Carty, *Organometallics*, 1983, **2**, 1194; M. Lanfranchi, A. Tiripicchio, E. Sappa, S. A. MacLaughlin and A. J. Carty, *J. Chem. Soc., Chem. Commun.*, 1982, 538.
5 A. J. Carty, S. A. MacLaughlin and N. J. Taylor, *J. Am. Chem. Soc.*, 1981, **103**, 2456.
6 J.-F. Halet, R. Hoffmann and J.-Y. Saillard, *Inorg. Chem.*, 1985, **24**, 1695; J.-F. Halet and J.-Y. Saillard, *Nouv. J. Chim.*, 1987, **11**, 315.

*Received in Bloomington, IN, USA, 11th June 1997; 7/04074A*

# Chemical and biochemical properties of 2-hydroxypentadienoic acid, a homologue of enolpyruvic acid

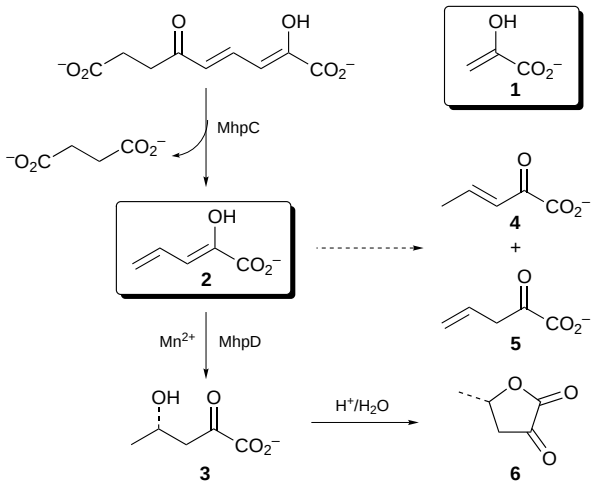
**John R. Pollard,† Ian M. J. Henderson and Timothy D. H. Bugg***

*Department of Chemistry, University of Southampton, Highfield, Southampton, UK SO17 1BJ*

**2-Hydroxypentadienoic acid is shown to be a biochemical intermediate on the phenylpropionate catabolic pathway of *Escherichia coli*; its stability and ketonisation behaviour are compared with those of its homologue, enolpyruvate.**

The enol tautomer of pyruvic acid, enolpyruvate **1**, has been implicated as an intermediate in several enzymatic reactions.[1,2] The buffer- and enzyme-catalysed ketonisation of **1** have been studied in detail.[1–4] Its extended homologue 2-hydroxypentadienoic acid **2** has been proposed as an intermediate in a number of bacterial *meta*-cleavage pathways,[5–8] however very little is known about its chemical and biochemical properties. We have previously verified using $^1$H NMR spectroscopy that **2** is the product of the reaction catalysed by C–C hydrolase MhpC, on the phenylpropionate catabolic pathway in *Escherichia coli* (see Scheme 1).[6] However, there is uncertainty over whether the dienol tautomer of **2** or one of two possible keto tautomers **4** or **5** is the substrate for the subsequent enzymatic hydration reaction to give 4-hydroxy-2-oxopentanoic acid **3**.[8–10] Here we analyse some chemical properties of 2-hydroxypentadienoic acid **2**, compare them with those of its homologue enolpyruvate, and confirm the biochemical intermediacy of **2**.

2-Hydroxypentadienoic acid **2** was generated by the reaction of C–C hydrolase MhpC, as previously described.[6] The appearance of **2** was monitored by UV spectroscopy ($\lambda_{max}$ 270 nm) and organic acids HPLC.‡ Production of **2** was followed by a first-order decay in $A_{270}$ over a 1–10 min time period (see Fig. 1), correlating with the disappearance of the HPLC peak, thus corresponding to the decomposition of **2**. The appearance and disappearance of **2** could be fitted accurately to a double exponential curve, allowing determination of the rate constants for production and decomposition of **2**. By extrapolation of the first-order decay of **2** to zero time, starting from a known concentration of the MhpC substrate ($\varepsilon_{394}$ 15 600 M$^{-1}$ cm$^{-1}$), the extinction coefficient for **2** was determined as $\varepsilon_{270}$ = 19 200 M$^{-1}$ cm$^{-1}$ at pH 5.0 in 50 mM NaOAc. This value was found to remain fairly constant over the pH range 5–10, and is somewhat higher than the value of 9600 M$^{-1}$ cm$^{-1}$ reported for enolpyruvate,[2] as expected for a more conjugated system.




**Scheme 1** The substrate for MhpC is the extradiol ring fission product of 2,3-dihydroxyphenylpropionic acid, whose structure has been verified previously (ref. 6).

The observed decomposition of **2** was thought to correspond to the ketonisation of its dienol functional group, which could take place either at C-3 (α-protonation) or C-5 (γ-protonation). A sample of **2** generated by MhpC was allowed to decompose, and after lyophilisation was analysed by $^1$H NMR spectroscopy. The product contained 90% 2-oxopent-3-enoic acid **4**, 10% 2-oxopent-4-enoic acid **5** and a small amount (< 5%) of dienol **2**,§ verifying that decomposition was due to ketonisation, and indicating a 9 : 1 ratio of γ-protonation to α-protonation.

By carrying out the MhpC conversion in various buffers, it was possible to determine the rate of ketonisation ($k_{obs}$) *versus* pH and buffer type. Compound **2** was found to be more than five-fold more stable in phosphate or acetate buffers than in citrate, Mes or Tris buffers. $k_{obs}$ was found to increase with pH [see Figs. 1 and 2(*a*)], as observed for enolpyruvate,[4] implying that the ketonisation of **2** is base-catalysed. In 50 mM NaOAc pH 5.0 a $k_{obs}$ value of 0.026 min$^{-1}$ was measured, corresponding to a half-life of 27 min. The half-life of enolpyruvate in $H_2O$ at pH 5.0 is approximately 30 s,[3] thus **2** is more than 50-fold more stable than enolpyruvate in aqueous solution. Generation of **2** in 50 mM NaOAc (pH 5.0) in the presence of 5 mM $MnCl_2$ gave a 2.4-fold increased $k_{obs}$, indicating that the ketonisation of **2** is catalysed by divalent metal ions, as found for enolpyruvate.[3]

It was also found that $k_{obs}$ increased when larger amounts of MhpC were used for its generation [see Fig. 2(*b*)], thus the ketonisation of **2** is also catalysed by MhpC. At normal assay concentrations of MhpC (0.05–0.1 u ml$^{-1}$), < 20% of the observed decomposition is enzyme-catalysed, but at concentrations of 1 u ml$^{-1}$ approximately 75% of $k_{obs}$ is due to enzyme-catalysed ketonisation. This behaviour can be rationalised mechanistically, since the first step of the MhpC-catalysed reaction is thought to be the ketonisation of a structurally similar dienol precursor at C-5.[6] From the gradient

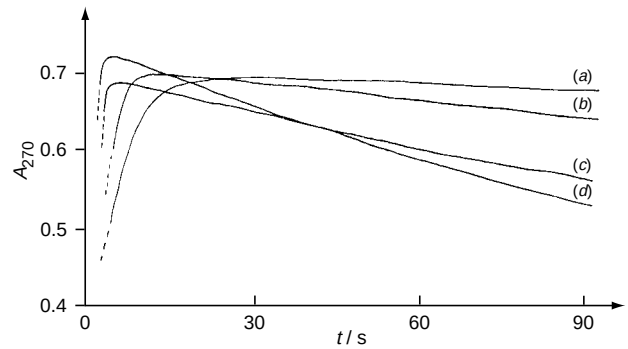



**Fig. 1** Production of **2** by the reaction catalysed by hydrolase MhpC, and the subsequent decomposition of **2** at (*a*) pH 5, (*b*) pH 6, (*c*) pH 7 and (*d*) pH 8, as observed by UV spectroscopy. Assays contained 40 μM ring fission product, 0.1 u ml$^{-1}$ MhpC and 50 mM buffer (NaOAc at pH 5, $KH_2PO_4$ at pH 6, 7 and 8), and were carried out at 20 °C.

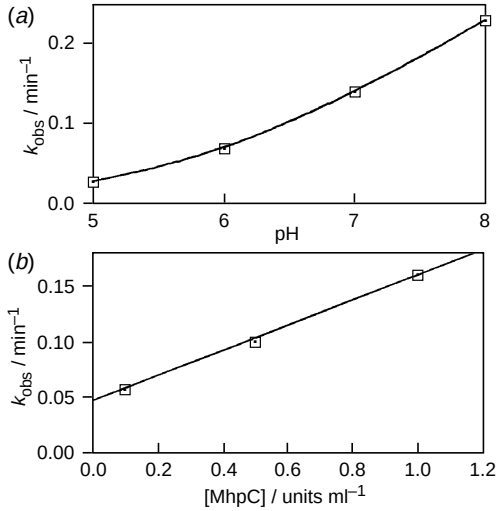



**Fig. 2** Deduced first-order rate constants ($k_{obs}$) for ketonisation of **2**. (*a*) Variation of $k_{obs}$ *versus* pH. Assays contained either 50 mM sodium acetate (pH 5) or 50 mM potassium phosphate (pH 6, 7 and 8). (*b*) Variation of $k_{obs}$ *versus* concentration of the producing enzyme MhpC (measured in units MhpC per ml assay mixture). Specific activity of MhpC is 75 u mg$^{-1}$, $M_r$ 29 kDa, substrate concentration, 58 μM.

of the plot in Fig. 2(*b*) the rate of MhpC-catalysed ketonisation of **2** can be calculated at 18 min$^{-1}$, 1.5% of $k_{cat}$ for the MhpC-catalysed production of **2**. The ketonisation of enolpyruvate is also catalysed by an enzyme, pyruvate kinase (see Table 1).[2]

Is the dienol tautomer of **2** the substrate for the ensuing hydratase enzyme MhpD? Addition of *E. coli* extract containing MhpD enzyme activity to a solution of freshly-generated **2** gave rise to a rapid decrease in $A_{270}$. The rate of the enzyme-dependent decomposition of **2** was proportional to enzyme concentration, and samples of protein containing no MhpD showed no effect on **2**. This assay has been used to purify hydratase enzyme MhpD, as described elsewhere, and the pure enzyme shows the same effect by UV spectroscopy.[11] The conversion of **2** to 4-hydroxy-2-oxopentanoic acid **3** by MhpD has been confirmed by the lactonisation of **3** under acidic conditions, to give a sample of 2-oxo-4-methyl-γ-butyrolactone **6** which shows identical analytical data to synthetic samples of **6**.[12] Enzymatic processing of dienol **2** at rates considerably in excess of $k_{obs}$ for ketonisation of **2** implies that the dienol tautomer is used as a substrate for MhpD-catalysed hydration. Studies to elucidate the mechanism of the MhpD-catalysed hydration are discussed elsewhere.[11] The $Mn^{2+}$- and MhpC-catalysed decomposition of **2** lead to low yields for large scale substrate conversions of **2** by hydratase MhpD, which requires $Mn^{2+}$ for activity.[11]

**Table 1** Comparison of the properties of **2** with its homologue enolpyruvate **1**

| | Enolpyruvate **1** | 2-Hydroxypentadienoic acid **2** |
|---|---|---|
| $\lambda_{max}$/nm | 225 | 270 |
| $\varepsilon_{max}$/M$^{-1}$ cm$^{-1}$ | 9600[a] | 19 200 |
| $k_{obs}$ (pH 5)/min$^{-1}$ | 1.32[b] | 0.026 |
| $t_{1/2}$ (pH 5)/min | 0.5 | 27 |
| Non-enzymatic catalysis | $OH^-$, $M^{2+}$ [b] | $OH^-$, $M^{2+}$ |
| Enzymatic catalysis ($k_{cat}$/min$^{-1}$) | pyruvate kinase (50)[a] | MhpC (18) |

[a] Data from ref. 2. [b] Data from ref. 3. Measured in 20mM NaOAc (pH 5), 0.2 mM $MnCl_2$.

On the catechol *meta*-cleavage pathway of *Pseudomonas putida*, **2** is generated by a decarboxylase enzyme which forms a 1 : 1 complex with the ensuing hydratase enzyme.[10] It has been proposed that the formation of such a complex favours the processing of the unstable intermediate **2**.[10] We have no evidence of any association between hydrolase MhpC and hydratase MhpD, however it is noteworthy that the catalytic efficiency of purified MhpD is very high ($k_{cat}/K_m$ = 1.1 × 10$^7$ M$^{-1}$ s$^{-1}$).[11] In conclusion, 2-hydroxypentadienoic acid shows similar chemical properties but enhanced kinetic stability with respect to its homologue enolpyruvate, and represents a further example of a biologically important enol.

This work was supported by an Earmarked studentship (J. R. P.) and a research grant (B04835) from the BBSRC. We thank Sarah Fleming for assistance with NMR spectroscopy, and Dr Jonathan Percy (University of Birmingham) for helpful comments.

## Footnotes and References

* E-mail: tdb@soton.ac.uk
† Present address: Department of Chemistry, University of St. Andrews, Fife, Scotland, UK KY16 9ST.

‡ HPLC analysis of **2**: retention time, 42 min ($\lambda_{max}$ 270 nm) on Bio-Rad HPX-87H Organic acids column, eluent 0.005 M $H_2SO_4$, flow rate 0.6 ml min$^{-1}$.

§ *Selected data* for **4**: $\delta_H$ (270 MHz, $D_2O$) 1.95 (3 H, dd, *J* 1.8, 7.2, H-5), 6.16 (1 H, dq, *J* 16.2, 1.5, H-3), 7.04 (1 H, dq, *J* 16.2, 7.0, H-4). For **5**: $\delta_H$ 3.47 (2 H, dt, *J* 7.0, 1.4, H-3), 5.1–5.2 (2 H, m, H-5), 5.85 (1 H, m, H-4).

1 I. A. Rose, *Methods Enzymol.*, 1982, **87**, 84.
2 D. J. Kuo, E. L. O'Connell and I. A. Rose, *J. Am. Chem. Soc.*, 1979, **101**, 5025.
3 B. A. Miller and D. L. Leussing, *J. Am. Chem. Soc.*, 1985, **107**, 7146.
4 J. A. Peliska and M. H. O'Leary, *J. Am. Chem. Soc.*, 1991, **113**, 1841.
5 S. Dagley, *Essays Biochem.*, 1975, **11**, 81.
6 W. W. Y. Lam and T. D. H. Bugg, *J. Chem. Soc., Chem. Commun.*, 1994, 1163.
7 F. Junker, J. A. Field, F. Bangerter, K. Ramsteiner, H. P. Kohler, C. L. Joannou, J. R. Mason, T. Leisinger and A. M. Cook, *Biochem. J.*, 1994, **300**, 429.
8 H. Lian and C. P. Whitman, *J. Am. Chem. Soc.*, 1994, **116**, 10403.
9 W. L. Collinsworth, P. J. Chapman and S. Dagley, *J. Bacteriol.*, 1973, **113**, 922.
10 S. Harayama, M. Rekik, K. Ngai and L. N. Ornston, *J. Bacteriol.*, 1989, **171**, 6251.
11 J. R. Pollard and T. D. H. Bugg, unpublished work.
12 A. Rossini and H. Schinz, *Helv. Chim. Acta*, 1948, **31**, 473. HPLC retention time for lactone **6**: 35 min (see footnote ‡ for conditions).

*Received in Glasgow, UK, 1st July 1997; 7/04635I*

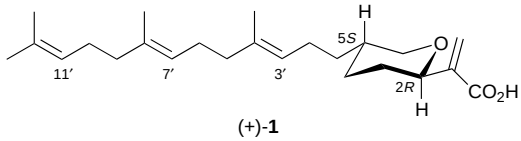
# Synthesis of norsesterterpene *rac*- and *ent*-rhopaloic acid A

**Ryukichi Takagi, Asami Sasaoka, Satoshi Kojima and Katsuo Ohkata***

*Department of Chemistry, Faculty of Science, Hiroshima University, 1-3-1 Kagamiyama, Higashi-Hiroshima 739, Japan*

**The stereoselective synthesis of *rac*- and *ent*-rhopaloic acid A 1 has been accomplished, *via* successive homologation of (2*E*,6*E*)-farnesol 2 and cyclization to form a tetrahydropyran ring, together with final introduction of an α-methylene group; the asymmetric synthesis was achieved *via* an Evans' asymmetric alkylation using (*S*)-4-benzyloxazolidin-2-one as a chiral auxiliary; the synthetic rhopaloic acid A, with a predicted absolute configuration of (2*S*,5*R*), had a specific rotation of opposite sign to that of the natural product, and therefore the configuration of natural rhopaloic acid A should be assigned as (2*R*,5*S*).**

(+)-Rhopaloic acid A (+)-**1**, a potent cytotoxic agent, was isolated from the marine sponge *Rhopaloeides* sp.[1] The interesting biological activity of the compound may be attributed to the structurally unique feature of having a hydrophilic pyranylacrylic acid moiety connected to a hydrophobic isoprenoid part.[2] The acrylic acid moiety is also found in compounds such as conconadine[3a] and gerin,[3b] and the related 2-methylene-γ-lactone group is found in many bioactive natural products. The potential of (+)-**1** and its analogues as biological probes provided the incentive for this synthetic undertaking. Here the total syntheis of racemic rhopaloic acid A *rac*-**1** and the nonnatural enantiomer *ent*-rhopaloic acid A (−)-*ent*-**1** is described.



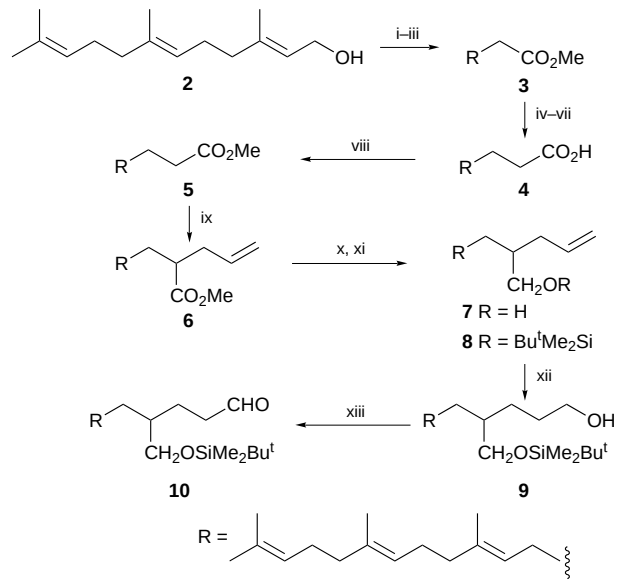

(+)-**1**

Our synthetic strategy consists of successive homologations of (2*E*,6*E*)-farnesol **2** and cyclization to form a tetrahydropyran ring, together with the final introduction of an α-methylene group.

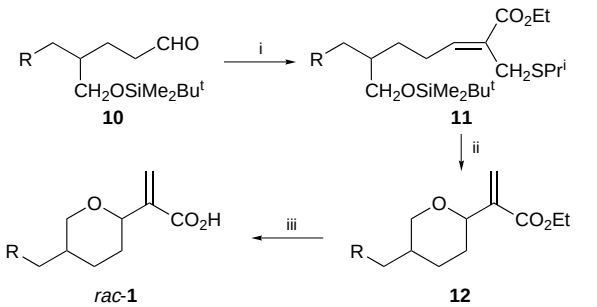
The two-carbon homologation exploited malonic esterification starting from (2*E*,6*E*)-farnesol **2** (Scheme 1). Treatment of farnesol with $PPh_3$–$CBr_4$ at 0 °C afforded farnesyl bromide.[4] The bromide contained less than 5% of the (2*Z*,6*E*)-isomer and was used for the following reaction without further purification. Treatment of the bromide with dimethyl malonate (5 equiv.) in the presence of NaH (1 equiv.) gave the dimethyl ester in 80% yield.[5] Demethoxycarbonylation of the dimethyl ester under neutral conditions (NaCl in moist DMF) afforded monomethyl ester **3** in 87% yield. Reduction of **3** with $LiAlH_4$ afforded the alcohol in quantitative yield. Treatment of the alcohol with $Ph_3P$–$CBr_4$ gave the bromide in 86% yield. Cyanation of the bromide with NaCN in DMF afforded the nitrile in quantitative yield. Hydrolysis of the nitrile under basic conditions afforded carboxylic acid **4** and esterification of **4** with MeI–$K_2CO_3$[6] gave methyl ester **5** in 76% yield over two steps.

Treatment of **5** with LDA followed by allyl bromide gave allylated methyl ester **6** in 83% yield. Reduction of **6** with $LiAlH_4$ afforded alcohol **7** in 88% yield. Protection of **7** with *tert*-butyldimethylsilyl chloride followed by hydroboration–oxidation with 9-BBN–$H_2O_2$ gave primary alcohol **9** (79%). Swern oxidation of **9** afforded aldehyde **10** (80%).

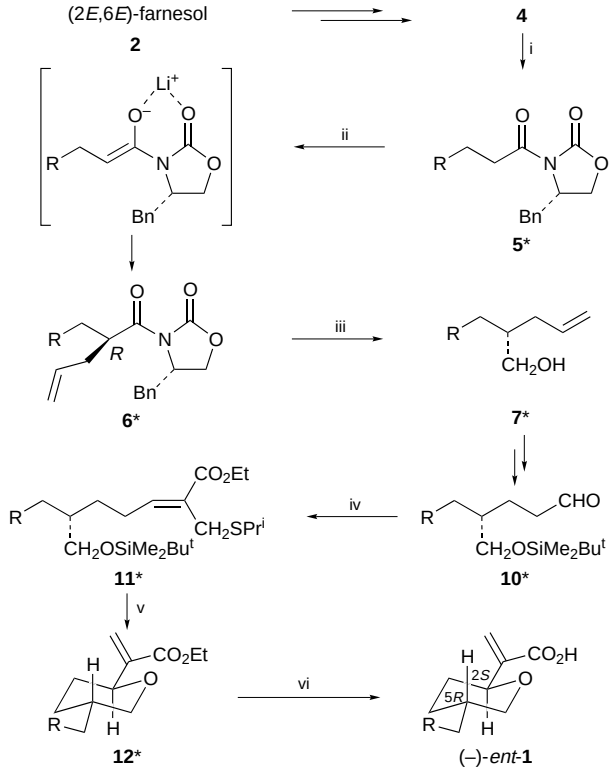
The modified Wittig–Horner–Emmons reaction of **10** with $(EtO)_2P(O)C(=CH_2)CO_2Et$ in the presence of $NaSCHMe_2$ furnished **11** with only *Z* geometry in 57% yield as a single isomer (Scheme 2).[8]† Exposure of **11** to methylation reagent MeI–$AgBF_4$ followed by desilylation with $Bu_4NF$ afforded ethyl pyranylacrylate derivative **12** in 32% yield as the *trans* isomer.[9]‡ The ester **12** contained less than 10% of the *cis* isomer. Hydrolysis of **12** with aq. KOH afforded *rac*-**1** with




**Scheme 1** *Reagents and conditions*: i, $PPh_3$ (1.2 equiv.), $CBr_4$ (1.3 equiv.), $CH_2Cl_2$, 0 °C, 3 h; ii, NaH (1 equiv.), $CH_2(CO_2Me)_2$ (5 equiv.), DMF, 0–25 °C, overnight, 80% over two steps; iii, NaCl (2 equiv.), $H_2O$ (2 equiv.), DMF, reflux, 20 h, 87%; iv, $LiAlH_4$ (1.3 equiv.), THF, 0 °C, 1 h, 96%; v, $Ph_3P$ (1.2 equiv.), $CBr_4$ (1.5 equiv.), $CH_2Cl_2$, 0 °C, 1 h, 86%; vi, NaCN (2.5 equiv.), DMF, 25 °C, 1 h, 99%; vii, KOH (10 equiv.), $H_2O$, EtOH, reflux, 30 h, 78%; viii, MeI (2 equiv.), $K_2CO_3$ (2 equiv.), 25 °C, 3 h, 98%; ix, LDA (1.1 equiv.), THF, −78 °C, 30 min, then allyl bromide (4 equiv.), −78 to 25 °C, overnight, 83%; x, $LiAlH_4$ (1.5 equiv.), THF, 0 °C, 3 h, 88%; xi, $Bu^tMe_2SiCl$ (1.1 equiv.), imidazole (2 equiv.), DMF, 3 h, 87%; xii, 9-BBN (1.5 equiv.), THF, 0 to 25 °C, overnight, then aq. NaOH (4 equiv.), 30% aq. $H_2O_2$ (4 equiv.), overnight, 79%; xiii, DMSO (2 equiv.), $(COCl)_2$ (1.1 equiv.), $Et_3N$ (5 equiv.), $CH_2Cl_2$, −60 °C, 5 h, 80%




**Scheme 2** *Reagents and conditions*: i, NaH (1 equiv.), $Me_2CHSH$ (1 equiv.), $(EtO)_2P(O)C(=CH_2)CO_2Et$ (1 equiv.), THF, 0 °C, 10 min, then **10**, 25 °C, overnight, 57% (*Z* isomer only); ii, MeI (3 equiv.), $AgBF_4$ (1 equiv.), $CH_2Cl_2$, 2 h, then $Bu_4NF$ (3 equiv.), THF, 16 h, 32%; iii, aq. KOH (excess), reflux, 14 h, 34%




**Scheme 3** *Reagents and conditions*: i, $Et_3N$ (1.2 equiv.), pivaloyl chloride (1.2 equiv.), THF, then *N*-lithiooxazolidin-2-one, THF, −78 °C, 15 h, 66%; ii, LDA (1.1 equiv.), THF, −78 °C, 30 min, then allyl bromide (4 equiv.), −20 to −10 °C, 6 h, 44%; iii, $LiAlH_4$ (3 equiv.), THF, 0 °C, 15 h, 92% iv, NaH (1 equiv.), $Me_2CHSH$ (1 equiv.), $(EtO)_2P(O)(=CH_2)CO_2Et$, THF, 0 °C, 10 min, then **10***, 25 °C, 28 h, 46% (*Z* isomer only); v, MeI (3 equiv.), $AgBF_4$ (1 equiv.), $CH_2Cl_2$, 5 h then $Bu_4NF$ (3 equiv.), THF, 25 °C, 13 h, 35%; vi, aq. KOH (excess), reflux, 18 h, 56%

retained stereochemistry in 34% yield.§ The $^1H$ and $^{13}C$ NMR and mass spectra of the carboxylic acid *rac*-**1** and the ethyl ester **12** were identical with those recorded for authentic samples of (+)-rhopaloic acid A (+)-**1** and its ethyl ester derivative, respectively.

Asymmetric synthesis of *ent*-rhopaloic acid A was carried out by way of the Evans' asymmetric alkylation as shown in Scheme 3. The auxiliary moiety, (*S*)-4-benzyloxazolidin-2-one, was introduced into **4** (66%) to give **5***. The lithium enolate of **5*** was treated with allyl bromide at −20 to −10 °C to give **6*** as the pure diastereoisomer (44% yield, 99% de).[7,10]¶ Consideration of the chelation model of the enolate intermediate predicted the stereochemistry at the C2 position of **6*** to be 2*R*.[10] Following removal of the chiral auxiliary by $LiAlH_4$ reduction (92%) and protection (79%) of the alcohol **7*** with a *tert*-butyldimethylsilyl group, silyl ether **8*** was subjected to regioselective hydroboration with 9-BBN followed by oxidation with $H_2O_2$ to give **9*** (68%). Swern oxidation of **9*** gave **10*** in 80% yield. The modified Wittig–Horner–Emmons reaction of **10*** afforded α,β-unsaturated ester **11*** (46%), which was cyclized into **12*** (35%). Hydrolysis of **12*** gave the optically pure (2*S*,5*R*)-*ent*-**1**‖ in 9% overall yield from **10***. The specific rotation of *ent*-**1** was $[\alpha]_D^{25}$ −37.6 (*c* 0.315, $CHCl_3$), which was of opposite sign to that of the natural product (+)-**1**. Therefore, it is presumed that the configuration of natural rhopaloic acid A {$[\alpha]_D^{25}$ + 40 (*c* 0.47, $CHCl_3$)}[1] is 2*R*,5*S*.

In order to investigate the structure–bioactivity relationship of **1** and other biomechanistic problems, an alternative synthesis of **1** and related compounds is now progress.[11]

Spectra of an authentic sample were kindly provided by Dr S. Ohta (Hiroshima University). The authors thank Shiono Koryo Kaisha, Ltd. and Kurare Co. for the gift of farnesol. NMR and mass spectra and optical rotations were measured at the Instrument Center for Chemical Analysis, Hiroshima University.

## Footnotes and References

* E-mail: ohkata@sci.hiroshima-u.ac.jp

† The product ratio changed with the reaction conditions. Only the *Z* isomer, the thermodynamically stable product, was obtained when the reaction mixture was stirred overnight at 25 °C. A ratio of *Z*:*E* = 2.4:1.0 was obtained when the reaction mixture was stirred at 0 °C for 3 h. The relative configuration of the product was determined with difference NOE experiments: when 3-H of the *E* isomer was irradiated, the intensity of the 2-$CH_2$S signal was enhanced by 8.2%.

‡ For **12**, the assigned relative stereochemistry was confirmed by intensity enhancement of 2-H by 10.9% upon irradiation of 6-$H_{ax}$. The assignment of 6-$H_{ax}$ was determined by measurement of coupling constants: $J_{5,6\text{-ax}}$ = 11.2 Hz, $J_{5,6\text{-eq}}$ = 3.9 Hz.

§ The relative stereochemistry of *rac*-**1** was assigned using the same considerations as for **12** ($J_{5,6\text{-ax}}$ = 11.2 Hz, $J_{5,6\text{-eq}}$ = 3.9 Hz); when 6-$H_{ax}$ was irradiated, an intensity enhancement of 2-H by 6.9% was observed.

¶ The diastereoselectivity of the allylation was evaluated by conversion of the optical active alcohol **7*** into its benzoate ester, followed by analysis with a DAICEL CHIRALCEL-OD column (hexane–AcOEt 400:1).

‖ *Selected data* for (2*S*,5*R*)-**1**: colourless oil; $[\alpha]_D^{25}$ −38 (*c* 0.315, $CHCl_3$); $\delta_H$ (270 MHz, $CDCl_3$) 1.1–1.3 (m, 4 H, 1′-H, 3-$H_{ax}$, 4-$H_{ax}$), 1.3–1.6 (m, 1 H, 5-$H_{ax}$), 1.60 (s, 9 H, vinyl-Me), 1.68 (s, 3 H, vinyl-Me), 1.9–2.1 (m, 12 H, 3-$H_{eq}$, 4-$H_{eq}$, 2′-H, 5′-H, 6′-H, 9′-H, 10′-H), 3.18 (t, *J* 11, 1 H, 6-$H_{ax}$), 4.07 (ddd, *J* 12, 4, 2, 1 H, 6-$H_{aq}$), 4.12 (d, *J* 12, 1 H, 2-H), 5.89 (s, 1 H, α-methylene), 6.36 (br s, 1 H, α-methylene); $\delta_C$ (125 MHz, $CDCl_3$) 16.0, 17.7, 24.9, 25.7, 26.6, 26.8, 30.2, 31.8, 32.4, 35.2, 39.7, 74.0, 76.4, 124.0, 124.2, 124.4, 126.7, 131.3, 135.0, 135.5, 140.7, 168.6; $\nu_{max}$(neat)/cm$^{-1}$ 3500–3000, 2900, 2850, 1680, 1620, 1430, 1370, 1280, 1160, 1140, 1080, 950, 830; Calc. for $C_{24}H_{38}O_3$ 374.2821. Found: 374.2830.

1 S. Ohta, M. Uno, M. Yoshimura, Y. Hiraga and S. Ikegami, *Tetrahedron Lett.*, 1996, **37**, 2265.
2 R. L. Letsinger, S. K. Chaturvedi, F. Farooqui and M. Salunkhe, *J. Am. Chem. Soc.*, 1993, **115**, 7535; W. Ding and G. A. Ellestad, *J. Am. Chem. Soc.*, 1991, **113**, 6617; U. S. Singh, R. T. Scannell, H. Au, B. J. Carter and S. M. Hecht, *J. Am. Chem. Soc.*, 1995, **117**, 12 691; S. B. Singh, D. L. Zink, J. M. Liesch, M. A. Goetz, R. G. Jenkins, M. Nallin-Omstead, K. C. Silverman, G. F. Bills, R. T. Mosley, J. B. Gibbs, G. Albers-Schonberg and R. B. Lingham, *Tetrahedron*, 1993, **49**, 5917.
3 J. M. Muller, H. Fuhrer and J. Gruner, *Helv. Chim. Acta*, 1976, 2506; E. Rodriguez, B. Sanchez, P. A. Grieco, G. Majetich and T. Oguri, *Phytochemistry*, 1979, **18**, 1741.
4 J. P. Schaefer and J. Higgins, *J. Org. Chem.*, 1967, **32**, 1607.
5 M. J. Kates and J. H. Schauble, *J. Org. Chem.*, 1996, **61**, 4164.
6 Y. Harada, M. Shibata, T. Sugiura, S. Kato and T. Shioiri, *J. Org. Chem.*, 1987, **52**, 1252.
7 W. He, E. Pinard and L. A. Paquette, *Helv. Chim. Acta*, 1995, **78**, 391.
8 M. F. Semmelhack, J. C. Tomesch, M. Czany and S. Boettger, *J. Org. Chem.*, 1978, **43**, 1259; M. F. Semmelhack, A. Yamashita, J. C. Tomesch and K. Hirotsu, *J. Am. Chem. Soc.*, 1978, **100**, 5565.
9 N. D. Smith, P. J. Kocienski and S. D. A. Street, *Synthesis*, 1996, 652; A. T. F. Edmunds and W. Trueb, *Tetrahedron Lett.*, 1997, **38**, 1009.
10 D. A. Evans, T. C. Briton, J. A. Ellman and R. L. Dorow, *J. Am. Chem. Soc.*, 1990, **112**, 4011; P. P. Waid, G. A. Flynn, E. W. Huber and J. S. Saabol, *Tetrahedron Lett.*, 1996, **37**, 4091.
11 M. Tokumasu, A. Sasaoka, R. Takagi, Y. Hiraga and K. Ohkata, *Chem. Commun.*, 1997, 875.

*Received in Cambridge, UK, 30th June 1997; 7/04563H*

# Tandem annulations: a one operation construction of bicyclo[3.3.0]octan-1-ol and bicyclo[3.2.1]octan-1-ol skeletons by a three-component coupling reaction of alk-4-enyl iodides with CO and alkenes in the presence of zinc

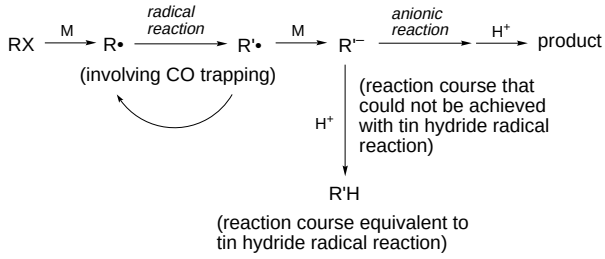
**Shinji Tsunoi,[a] Ilhyong Ryu,*[b]† Sumiaki Yamasaki,[b] Minoru Tanaka,[a] Noboru Sonoda*[b]‡ and Mitsuo Komatsu[b]**

[a] *Research Center for Environmental Preservation, Osaka University, Suita, Osaka 565, Japan*
[b] *Department of Applied Chemistry, Faculty of Engineering, Osaka University, Suita, Osaka 565, Japan*

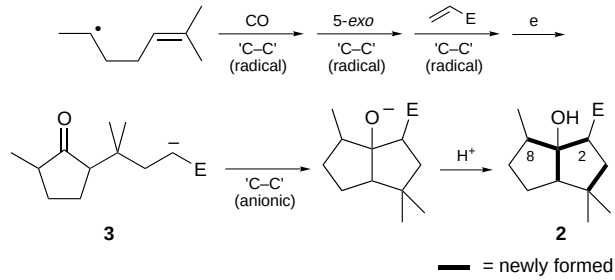
**Under a one-electron reduction system composed of zinc and an aprotic solvent, alk-4-enyl iodides react with CO and alkenes to give bicyclo[3.3.0]octan-1-ols and bicyclo[3.2.1]octan-1-ols *via* radical/anionic dual annulations.**

Tin radical mediated C1 chemistry has the potential to play an increasingly important role in the synthesis of a variety of carbonyl compounds.[1] In a previous paper, we have shown that a one-electron reduction system composed of zinc and a protic solvent can replace some of the useful transformations developed for tin hydride mediated radical carbonylation reactions.[2] An attractive feature of metal mediated one-electron reduction chemistry is its applicability to the design of unique tandem reaction systems, in which two different species, radicals and anions, can be subtly combined in synthetically useful reactions (Scheme 1).[3] Recent reports provide a useful reminder of the effectiveness and importance of this concept.[4] Here we report a three-component coupling reaction of alk-4-enyl iodides, CO and alkenes in the presence of zinc that delivers bicyclo-[3.3.0]octanols[5] and bicyclo[3.2.1]octanols, providing the first demonstration that radical carbonylation can be successfully sequenced by consecutive radical/anionic reactions.

In radical carbonylation using a reductive metal/protic solvent system, after an acyl radical cyclization and addition to a C–C double bond, the newly formed radical is reduced to an anion, which is subsequently protonated.[2] In aprotic solvents, however, the anionic species could conceivably undergo nucleophilic addition to the newly formed internal carbonyl group rather than undergoing protonation.[6] To test this hypothesis, we conducted the reaction of 6-iodo-2-methylhept-2-ene **1** with zinc under CO pressures in aprotic solvents to determine if a bicyclic compound is produced *via* a pathway outlined in Scheme 2. After several experiments, we found that when the usual zinc powder[7] was used in THF or MeCN solvent, the desired reaction took place. In a stainless steel autoclave, a THF solution of **1** (476 mg, 2 mmol, 0.1 M), acrylonitrile (53 mg, 1 mmol) and zinc (197 mg, 3 mmol) was sitrred under CO pressure (60 atm) at 60 °C. After 10 h, the anticipated 2-cyano-4,4,8-trimethylbicyclo[3.3.0]octan-1-ol **2** (137 mg, 71% yield, 60 : 40) was obtained after isolation by flash chromatography on silica gel (Table 1, entry 1). Only two of the four possible diastereoisomers were produced, as judged by both $^1$H and $^{13}$C NMR spectroscopy. A separation of the diastereoisomers was performed by careful chromatography on silica gel, and the absolute structures were confirmed to be *exo* at the CN group and either *endo* or *exo* at the Me group by NOE experiments.§ The major isomer was identified as 8-*exo*-Me, and the minor as 8-*endo*-Me. The consecutive radical/anionic reactions shown in Scheme 2 account for the formation of **2**: (i) an alkyl radical, formed by a one-electron reduction of the starting iodide, adds to CO; (ii) the resulting acyl radical cyclizes in the 5-*exo* mode to give a tertiary alkyl radical; (iii) this radical adds to acrylonitrile; (iv) the resulting α-cyano radical is reduced to an α-cyano anion **3**; (v) anion **3** adds to an internal carbonyl group, (vi) protonation during the work-up leads to bicyclo[3.3.0]octan-1-ol **2**. The observed diastereoselectivities with respect to the *exo*-orientation of the CN group may be rationalized on the basis of steric effects in the anionic cyclization step: the transition state giving the *endo*-CN product is disfavoured, due to steric repulsion between the CN group and the cyclopentanone ring (Fig. 1).[8]




**Scheme 1**




**Scheme 2**

Similarly, carbonylation of **1** in the presence of methyl acrylate and zinc gave the corresponding bicyclo[3.3.0]octanol **4** in 50% yield (entry 2). Again, only two of the four possible diastereoisomers were produced. With diethyl fumarate, a mixture of four isomers of bicyclo[3.3.0]octanol **5** was obtained in 52% yield (entry 3).

We demonstrated cases where the initial acyl radical cyclization takes place in the 5-*exo* mode. An extension of the present strategy, which uses a system that favours 6-*endo*

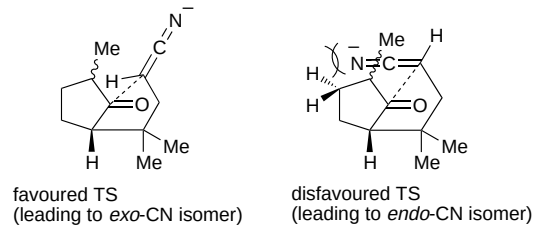
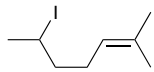
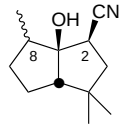
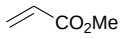
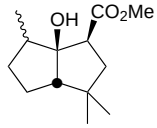
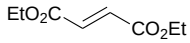
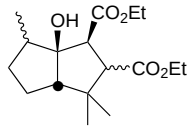
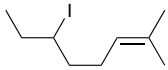
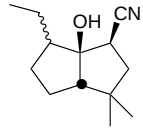
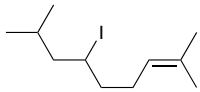
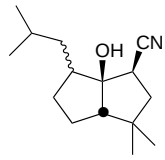
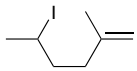
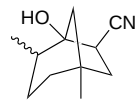
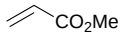
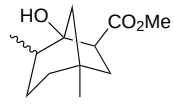



**Fig. 1**

**Table 1** Synthesis of bicyclic octanols[a]

| Entry | Alk-4-enyl iodide | Alkene | Product (% yield,[b] *exo*/*endo* ratio[c]) |
|---|---|---|---|
| 1 |  **1** |  |  **2** (71, 60:40) |
| 2 | **1** |  |  **4** (50, 52:48) |
| 3 | **1** |  |  **5** (52, 32:31:20:17)[d] |
| 4 |  **6** |  |  **7** (63, 61:39) |
| 5 |  **8** |  |  **9** (64, 59:41) |
| 6 |  **10** |  |  **11** (51, 57:43) |
| 7 | **10** |  |  **12** (43, 50:50) |

[a] Conditions: alk-4-enyl iodide (2 mmol), alkene (1 mmol), Zn (3 mmol), CO (60 atm), THF (10–20 ml), 60 °C, 10–22 h. [b] Isolated yields (based on the alkene used) by column chromatography for the *endo*/*exo* mixture. [c] Determined by $^1$H NMR spectroscopy (except for entry 3: GC). [d] Stereochemistry was not determined.

cyclization[9] rather than 5-*exo* cyclization to the construction of bicyclo[3.2.1]octanol skeletons was also successful. Thus, we examined 5-iodo-2-methylhex-1-ene **10**, a substrate having a methyl group at an internal position on the alkene. As expected, the reaction of **10** with CO and acrylonitrile in the presence of zinc led to bicyclo[3.2.1]octanol **11** in 51% isolated yield (entry 6). Similarly, reaction with methyl acrylate yielded the corresponding bicyclo[3.2.1]octanol **12** in 43% yield (entry 7).

This study demonstrates that radical carbonylation can be successfully combined with a sequential radical/anionic reaction system,[10] which is of great synthetic potential. The reaction reported here provides a convenient route to bicyclo[3.3.0]octanols and bicyclo[3.2.1]octanols from easily accessible starting compounds, such as alk-4-enyl iodides, CO and electron deficient alkenes. It is also noteworthy that the former reactions involve [4 + 1](radical)/[3 + 2](anionic) dual annulations, and the latter reactions involve [5 + 1](radical)/[3 + 2](anionic) dual annulations. We believe that the concepts outlined in this study have wide applicability for numerous synthetically useful processes.

This work was supported by a Grant-in-Aid for Scientific Research from the Ministry of Education, Science and Culture, Japan. We are grateful to Professor Kazuhiko Takai for stimulating discussions.

## Footnotes and References

† E-mail: ryu@chem.eng.osaka-u.ac.jp
‡ Present address: Department of Applied Chemistry, Faculty of Engineering, Kansai University, Suita, Osaka 564, Japan.

§ Preparative HPLC (GPC columns, $CHCl_3$ as the eluent) is also available to separate the *endo*/*exo* isomers of **2**. Absolute structures were confirmed to be the *endo*/*exo* isomers at the 8-position by NOE experiments (8-*exo*-**2**: 5%, 2-H *vs.* 8-H-*endo*-**2**: 10% 2-H *vs.* 8-Me).

*Selected data* for 8-*exo*-**2**: colourless liquid, $\delta_H$($CDCl_3$, 600 MHz) 0.88 (s, 3 H), 1.11 (d, 3 H, *J* 6.63), 1.13 (s, 3 H), 1.13–1.18 (m, 1 H), 1.48 (ddt-like, 1 H, *J ca.* 6.6, 13.7, 2.0), 1.62–1.71 (m, 1 H), 1.83 (m, 1 H), 1.88 (dd, 1 H, *J* 6.19, 12.16), 1.95–2.03 (m, 1 H), 2.10–2.36 (m, 2 H) 2.62 (dd, 1 H, *J* 6.19, 12.83), 2.66 (br s, 1 H); $\delta_C$ ($CDCl_3$, 150 MHz) 13.30 (q), 23.02 (q), 25.53 (t), 31.06 (q), 34.37 (t), 34.59 (d), 40.39 (s), 44.87 (t), 45.00 (d), 61.39 (d), 93.27 (s), 120.06 (s).

*Selected data* for 8-*endo*-**2**: colourless liquid; $\delta_H$($CDCl_3$, 600 MHz) 0.89 (s, 3 H), 1.06 (d, 3 H, *J* 6.85), 1.15 (s, 3 H), 1.26–1.34 (m, 1 H), 1.53–1.61 (m, 1 H), 1.62–1.73 (m, 2 H), 1.85 (q, 1 H, *J* 5.72), 1.96 (dd, 1 H, *J* 6.60, 12.50), 2.11 (br s, 1 H), 2.14 (t-like, 1 H, *J ca.* 9.10 Hz), 2.20 (t-like, 1 H, *J ca.* 11.74), 2.71 (dd, 1 H, *J* 6.45, 11.15); $\delta_C$ ($CDCl_3$, 150 MHz) 12.53 (q), 24.00 (q), 24.12 (t), 30.16 (q), 35.72 (t), 38.95 (s), 39.17 (d), 45.50 (d), 46.75 (t), 63.55 (d), 91.14 (s), 120.06 (s).

1 I. Ryu, N. Sonoda and D. P. Curran, *Chem. Rev.*, 1996, **96**, 177; I. Ryu and N. Sonoda, *Angew. Chem., Int. Ed. Engl.*, 1996, **35**, 1050.
2 S. Tsunoi, I. Ryu, H. Fukushima, M. Tanaka, M. Komatsu and N. Sonoda, *Synlett*, 1995, 1249.
3 For reviews, see G. A. Molander, *Chem. Rev.*, 1992, **92**, 29; D. P. Curran, T. L. Fevig, C. P. Jasperse and M. J. Totleben, *Synlett*, 1992, 943; J. Iqbal, B. Bhatia and N. K. Nayyar, *Chem. Rev.*, 1994, **59**, 519; P. I. Dalko, *Tetrahedron*, 1995, **51**, 7579; G. A. Molander and C. R. Harris, *Chem. Rev.*, 1996, **96**, 307.
4 G. A. Molander and C. R. Harris, *J. Am. Chem. Soc.*, 1996, **118**, 4059; K. Takai, T. Ueda, N. Ikeda and T. Moriwake, *J. Org. Chem.*, 1996, **61**, 7990.
5 These skeletons are frequently found in Silphinene and related compounds; see F. Saitoh, M. Mori, K. Okamura and T. Date, *Tetrahedron*, 1995, **51**, 4439; M. Franck-Neumann, M. Miesch and L. Gross, *Tetrahedron Lett.*, 1991, **32**, 2135; H.-Y. Lee, D.-I. Kim and S. Kim, *Chem. Commun.*, 1996, 1539.
6 T. Shono, I. Nishiguchi and M. Sasaki, *J. Am. Chem. Soc.*, 1978, **100**, 4314.
7 Zinc was purchased from Nacalai Tesque Inc, and was used without activation: *cf.* K. Takai, T. Kakiuchi, Y. Kataoka and K. Utimoto, *J. Org. Chem.*, 1994, **59**, 2668; K. Takai, T. Kakiuchi and K. Utimoto, *J. Org. Chem.*, 1994, **59**, 2671.
8 Alternatively, the thermodynamically stable *exo*-CN isomer may be formed *via* isomerization. For related *exo*-selectivity, see W. Flitsch and P. Russkamp, *Liebigs Ann. Chem.*, 1985, 1398.
9 D. L. Boger and R. J. Mathvink, *J. Org. Chem.*, 1992, **57**, 1429; L. Chen, G. B. Gill and G. Pattenden, *Tetrahdedron Lett.*, 1994, **35**, 2593; L. Chen, G. B. Gill, G. Pattenden and H. Simonian, *J. Chem. Soc., Perkin Trans. 1*, 1996, 31; A. Batsanov, L. Chen, G. B. Gill and G. Pattenden, *J. Chem. Soc., Perkin Trans. 1*, 1996, 45.
10 *cf.* For radical/cationic reactions involving carbonylation, see I. Ryu and H. Alper, *J. Am. Chem. Soc.*, 1993, **115**, 7543; S. Tsunoi, I. Ryu and N. Sonoda, *J. Am. Chem. Soc.*, 1994, **116**, 5473; K. Okuro and H. Alper, *J. Org. Chem.*, 1996, **61**, 5312.

*Received in Cambridge, UK, 10th July 1997; 7/04934J*

# Switching 'on' the luminescence of one metal ion with another: selectivity characteristics with respect to the emitting and triggering metal

**A. Prasanna de Silva, H. Q. Nimal Gunaratne, Terence E. Rice and Siobhan Stewart**

*School of Chemistry, Queen's University, Belfast, UK BT9 5AG*

**Complexes 1a·Eu$^{III}$ and 1b·Eu$^{III}$, but not 1a·Tb$^{III}$ and 1b·Tb$^{III}$, display strong 'off–on' switching of delayed luminescence with alkali cations; the switching efficiency of 1b·Eu$^{III}$ is stronger with K$^+$ rather than Na$^+$.**

Light emission of many organic molecules[1] and supermolecules[2] can be triggered by metal ions. This forms the basis of fluorescent sensors for metal ions.[3] Conversely, metal-centred emission can be induced by non-metal guests in a few carefully designed instances.[4] The third combination, that of organic molecular emission arising from the complexation of organic species, is also being developed in several laboratories.[5] The final combination of this quartet, that of metal ion-triggered metal-centred emission, is currently unavailable according to the best of our knowledge.[6] Metal-containing, but not metal-centred, emissive systems have been switched 'on' or 'off' by various species including metal ions.[7] We now fill this gap with examples of europium(III) complexes whose luminescence is switched 'on' with alkali metal ions.[8] We also note an interesting selectivity aspect in that the corresponding terbium(III) complexes are relatively immune to alkali cation-induced switching. Following this proof of principle, it will be possible to design delayed luminescent[9] sensors for metal ions of medical and environmental interest which operate in aqueous solution. Many suitable metal ion receptors[10] and lanthanide lumophores[11] are available[6] for incorporation into this design.

The following systems are designed as delayed luminescent versions of fluorescent PET (photoinduced electron transfer) sensors[2b,3a] for alkali cations.[12] Ligands **1a**,**b** were synthesized from the known compound 4,4″-bis(*p*-tolyl)-6,6″-bis-(methoxycarbonyl)-2,2′:6′,2″-terpyridine[13] **1c** by bromination with *N*-bromosuccinimide and amination with the appropriate monoazacrown ether.† The binding of **1a**,**b** with Tb$^{III}$ or Eu$^{III}$, when monitored by UV absorption spectroscopy, fits a 1:1 binding isotherm.[14] The conformational locking of the terpyridyl diester by the lanthanide ion leads to the growth of long-wavelength bands upto 340 nm. Monitoring of the complexation process in **1c** by $^1$H NMR spectroscopy shows Eu$^{III}$-induced upfield displacement of the methoxycarbonyl signal by 0.6 ppm as well as displacements of the other signals by upto 1.0 ppm. Much higher lanthanide ion concentrations than those employed here are needed before they bind to the azacrown moieties of **1a**,**b**.[10b] Binding of alkali cations to the azacrown units of **1a**·Eu$^{III}$ and analogues leads to small but measurable hypsochromic shifts in their UV absorption spectra. These allow determination of the binding constants $\beta_{Na}$ and $\beta_K$, which are in close agreement with literature values for the binding of alkali cations to unsubstituted monoazacrown ethers.[10b]

Most importantly, the delayed luminescence of **1a**·Eu$^{III}$ and **b**·Eu$^{III}$ is enhanced by over an order of magnitude when the azacrown units are bound by alkali cations (Fig. 1). Luminescence quantum yields reach values as high as 0.47 (for **1a**·Eu$^{III}$–K$^+$ in MeOH). Such switching 'on' of luminescence arises from the alkali cation-induced suppression of PET from the azacrown nitrogen to the lumophore.[12] Eu$^{III}$ complexes are known to participate in PET processes.[15] It is notable that K$^+$ produces the larger luminescence enhancement (LE) with **1b**·Eu$^{III}$ in spite of its lower charge density than Na$^+$. This is probably because the loosely fitting Na$^+$ moves away from the soft nitrogen towards the harder oxygens, thus lessening the PET suppression. Analysis of these luminescence intensity ($I_{Lum}$) – $(M)_{total}$ profiles (M = Na or K) gives $\beta_{Na}$ and $\beta_K$ values which are gratifyingly close to the values determined absorptiometrically. The average number of lanthanide-bound MeOH molecules[16] ($q$), determined by comparison of luminescence lifetimes ($\tau$) in MeOH and MeOD, is two. This suggests that the usual minimum coordination number of nine[17] is made up by two counterions, which is reasonable given the substantial ion-pairing in the moderately dielectric medium and the tripositive nature of **1a**·Eu$^{III}$ and analogues.

The immeasurably weak delayed luminescence of complexes **1a**·Tb$^{III}$ and **b**·Tb$^{III}$ is not noticeably enhanced by Na$^+$ or K$^+$ ions. However protons, the strongest PET suppressants of all,

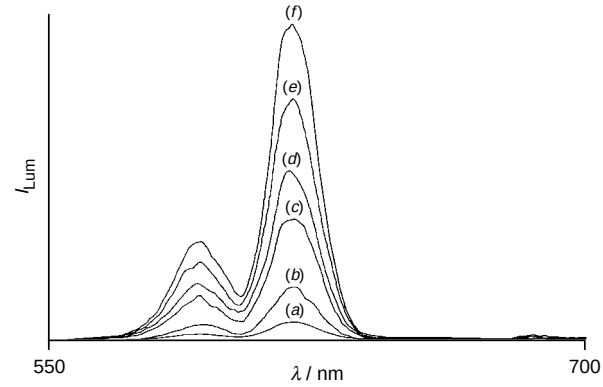
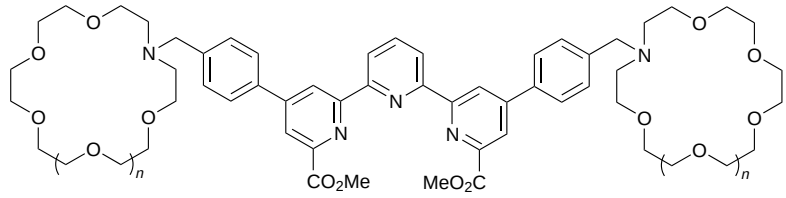



**Fig. 1** Delayed luminescence emission spectra of **1b**·Eu$^{III}$ upon addition of K$^+$. The spectra are uncorrected for the wavelength response of the detector which degrades rapidly at wavelengths longer than 650 nm. p$K_{total}$ = (*a*) ∞, (*b*) 5.0, (*c*) 4.4, (*d*) 4.2, (*e*) 4.0 and (*f*) 3.4.




**1a** $n$ = 0
**b** $n$ = 1

**Table 1** Optical and ion-binding parameters[a]

| Parameter | **1a**·$Eu^{III}$ | **1b**·$Eu^{III}$ | **1a**·$Tb^{III}$ | **1b**·$Tb^{III}$ |
|---|---|---|---|---|
| $\lambda_{Abs}$/nm (log $\varepsilon$)[b] | 294 (4.88) | 294 (5.02) | 294 (4.94) | 294 (5.03) |
| | 333 (4.59) | 333 (4.80) | 333 (4.66) | 333 (4.76) |
| | 345 (4.58) | 345 (4.77) | 345 (4.76) | 345 (4.73) |
| log $\beta$[c] | 4.9 | 4.8 | 4.7 | 4.9 |
| $\phi_{Lum}$[d] | 0.027 | 0.026 | < 0.001 | < 0.001 |
| log $\beta_{Na}$[c] | 2.5,[e] 2.3[f] | 2.9,[e] 2.6[f] | —,[e,g] 2.4[f] | —,[e,g] 2.4[f] |
| log $\beta_{K}$[c] | 2.2,[e] 2.3[f] | 4.3,[e] 4.6[f] | —,[e,g] 2.5[f] | —,[e,g] 4.3[f] |
| $\phi_{Lum\cdot Na}$ ($LE_{Na}$)[h] | 0.32 (12) | 0.23 (9) | < 0.001 (—)[g] | < 0.001 (—)[g] |
| $\phi_{Lum\cdot K}$ ($LE_{K}$)[h] | 0.20 (7) | 0.47 (18) | < 0.001 (—)[g] | < 0.001 (—)[g] |
| $\phi_{Lum\cdot H}$ ($LE_{H}$)[h] | 0.47 (17) | 0.46 (18) | 0.016 ( > 16) | 0.014 ( > 14) |
| $\tau$/ms[i] | 0.67 | 0.66 | 0.32 | 0.33 |
| $q$[j] | 2.0 | 1.9 | 2.3 | 2.0 |

[a] **1a** or **1b** $10^{-6}$ M in MeOH with $TbCl_3^{III}$ or $EuCl_3^{III}$ ($3 \times 10^{-5}$ M) and 1,8-diazabicyclo[5.4.0]undec-7-ene (DBU) ($10^{-4}$ M) as proton scavenger, except when $\phi_{Lum\cdot H}$ ($LE_H$) values are being determined. $Na^+$ and $K^+$ added as acetates. $H^+$ added as trifluoroacetate. The $\lambda_{Abs}$ (log $\varepsilon$) values for **1a** and **1b** are 240 (5.05), 276sh (4.86) and 324sh (4.07), and 240 (5.14), 276sh (5.03) and 324sh (4.32) nm, respectively. Lanthanide luminescence emission spectra were obtained by excitation at the isosbestic wavelength of 340 nm, with a delay time of 0.1 ms and a gate time of 1.5 ms for all four lanthanide complexes. [b] Extinction coefficient $\varepsilon$ in units of $M^{-1}\,cm^{-1}$. [c] The binding constant for the **1**–lanthanide (Ln) interaction was obtained by analysing absorbance ($A$) − (Ln) profiles according to: $\log[(A - A_{min})/(A_{max} - A)] = \log[(Ln)_{total} - (\mathbf{1})_{total}(A - A_{min})/(A_{min})/(A_{max} - A)] + \log\beta$ (ref. 14). Log $\beta_{Na\ or\ K}$ values for the **1**·Ln–Na or **1**·Ln–K interaction were similarly determined by analysing absorbance − $(M)_{total}$ profiles according to: $\log[(A - A_{min})/(A_{max} - A)] = \log[(M)_{total} - (\mathbf{1}\cdot Ln)_{total}(A - A_{min})/(A_{max} - A)] + \log\beta_{Na\ or\ K}$. M = $Na^+$ or $K^+$. Luminescence intensity can be used instead of absorbance as the dependent variable for determining log $\beta_{Na\ or\ K}$. [d] Luminescence quantum yields obtained by comparison with the $Eu^{III}$ complex of the carboxylate form of **1c** (ref. 13) and the $Tb^{III}$ complex with EDTA and sulfosalicyclic acid (ref. 19). [e] Luminescence measurements. [f] Absorbance measurements. [g] Spectroscopic change is too small to permit measurement. [h] Ion ($Na^+$, $K^+$ or $H^+$) induced luminescence enhancement factor, *e.g.* $LE_{Na} = \phi_{Lum\cdot Na}/\phi_{Lum}$. [i] Determined by the first-order decay expression for luminescence intensity. $\tau$ values are given as an average (±0.01 ms) in the presence of $Na^+$, $K^+$ or $H^+$ for $Eu^{III}$ complexes. Only the value in the presence of $H^+$ is accessible for $Tb^{III}$ complexes. [j] $q$ values are given as an average (±0.1) in the presence of $Na^+$, $K^+$ or $H^+$ for $Eu^{III}$ complexes. Only the value in the presence of $H^+$ is accessible for $Tb^{III}$ complexes.

produce measurable, but still small, luminescent quantum yields of 0.016 and 0.014, respectively. The weakness of this emission is probably due to an additional deactivation channel of the $Tb^{III}$ $^5D_4$ emissive state. The triplet level of the complexed ligand, as measured from the 77 K phosphorescence maximum of **1c**·$Gd^{III}$, lies only 4.1 kcal $mol^{-1}$ (1 kcal = 1 kJ) above the $Tb^{III}$ $^5D_4$ state, which means that rapid back energy transfer occurs under ambient conditions.[18] This leads to the complexed ligand triplet and subsequent de-excitation *via* the ligand state manifold. Such back energy transfer is absent in **1a**·$Eu^{III}$ and **1b**·$Eu^{III}$ owing to the much larger triplet $Eu^{III}$ $^5D_0$ state energy gap of 13.2 kcal $mol^{-1}$.

In conclusion, metal-triggered metal-centred emission has been demonstrated. The selectivity determinants are (i) the ability of the triggering metal to block PET from an azacrown nitrogen and (ii) the energy separation of the ligand triplet and the metal emitting state.

We thank the SERC/EPSRC and DENI for support.

## Footnotes and References

* E-mail: a.desilva@qub.ac.uk

† *Selected data* for **1a**; *m/z* 963;4625 ($C_{53}H_{65}N_5O_{12}$ requires 963.4630); $\delta_H$ 2.84 (t, 8 H, $NCH_2CH_2O$), 3.57–3.69 (m, 32 H, $CH_2O$), 3.76 (s, 4 H, $ArCH_2$), 4.10 (s, 6 H, $CO_2CH_3$), 7.51–8.98 (m, 15 H, Ar*H*). For **1b**: *m/z* 1051.51492 ($C_{57}H_{73}N_5O_{14}$ requires 1051.51540); $\delta_H$ 2.82 (t, 8 H, $NCH_2CH_2O$), 3.60–3.72 (m, 40 H, $CH_2O$), 3.75 (s, 4 H, $ArCH_2$), 4.10 (s, 6 H, $CO_2CH_3$), 7.53–8.99 (m, 15 H, Ar*H*).


1 A. Fernandez-Gutierrez and A. Munoz de la Pena, in *Molecular Luminescence Spectroscopy Methods and Applications. Part 1*, ed. S. G. Schulman, Wiley, New York, 1985, p. 371.

2 (*a*) V. Balzani and F. Scandola, *Supramolecular Photochemistry*, Ellis-Horwood, Chichester, 1991; (*b*) R. A. Bissell, A. P. de Silva, H. Q. N. Gunaratne, P. L. M. Lynch, G. E. M. Maguire and K. R. A. S. Sandanayake, *Chem. Soc. Rev.*, 1992, **21**, 187; (*c*) J.-M. Lehn, *Supramolecular Chemistry*, VCH, Weinheim, 1995.

3 (*a*) R. A. Bissell, A. P. de Silva, H. Q. N. Gunaratne, P. L. M. Lynch, G. E. M. Maguire, C. P. McCoy and K. R. A. S. Sandanayake, *Top. Curr. Chem.*, 1993, **168**, 223; (*b*) A. W. Czarnik, *Acc. Chem. Res.*, 1994, **27**, 302; (*c*) B. Valeur, in *Probe Design and Chemical Sensing. Topics in Fluorescence Spectroscopy*, ed. J. R. Lackowicz, Plenum, New York, 1994, p. 21; (*d*) L. Fabbrizzi and A. Poggi, *Chem. Soc. Rev.*, 1995, **24**, 197; (*e*) *Chemosensors for Ion and Molecule Recognition*, ed. J.-P. Desvergne and A. W. Czarnik, Kluwer, Dordrecht, 1997.

4 Z. Pikramenou, K. M. Johnson and D. G. Nocera, *Tetrahedron Lett.*, 1993, **34**, 3581; M. A. Mortellaro and D. G. Nocera, *J. Am. Chem. Soc.*, 1996, **118**, 7414; S. T. Mullins, P. G. Sammes, R. M. West and G. Yahioglu, *J. Chem. Soc., Perkin Trans. 1*, 1996, 75; H. Matsumoto, A. Ori, F. Inokuchi and S. Shinkai, *Chem. Lett.*, 1996, 301; A. P. de Silva, H. Q. N. Gunaratne and T. E. Rice, *Angew. Chem., Int. Ed. Engl.*, 1996, **35**, 2116.

5 A. Ueno, *Adv. Mater.*, 1993, **5**, 132; W. K. Hartmann, M. H. B. Gray, A. Ponce, D. G. Nocera and P. A. Wong, *Inorg. Chim. Acta*, 1996, **243**, 239; A. P. de Silva, H. Q. N. Gunaratne, C. McVeigh, G. E. M. Maguire, P. R. S. Maxwell and E. O'Hanlon, *Chem. Commun.*, 1996, 2191; T. D.James, K. R. A. S. Sandanayake and S. Shinkai, *Angew. Chem., Int. Ed. Engl.*, 1996, **35**, 1910.

6 A. P. de Silva, H. Q. N. Gunaratne, T. Gunnlaugsson, A. J. M. Huxley, C. P. McCoy, J. T. Rademacher and T. R. Rice, *Chem. Rev.*, 1997, **97**, 1515.

7 R. Grigg, J. M. Holmes, S. K. Jones and W. D. J. A. Norbert, *J. Chem. Soc., Chem. Commun.*, 1994, 185; S. C. Rawle, P. Moore and N. W. Alcock, *J. Chem. Soc., Chem. Commun.*, 1994, 684; P. D. Beer, *Chem. Commun.*, 1996, 689; F. Szemes, D. Hesek, Z. Chen, S. W. Dent, M. G. B. Drew, A. J. Goulden, A. R. Graydon, R. Grieve, R. J. Mortimer, T. Wear, J. S. Weightman and P. D. Beer, *Inorg. Chem.*, 1996, **35**, 5868; Y. B. Shen and B. P. Sullivan, *J. Chem. Ed.*, 1997, **74**, 685.

8 C. Piguet, J. C. G.Bunzli, G. Bernardinelli, G. Hopfgartner, S. Petoud and O. Schaad, *J. Am. Chem. Soc.*, 1996, **118**, 6681. This article describes a luminescent mixed complex containing europium and zinc ions, but not its switching.

9 A. Mayer and S. Neuenhofer, *Angew. Chem., Int. Ed. Engl.*, 1994, **33**, 1044; D. Parker and J. A. G. Williams, *J. Chem. Soc., Dalton Trans.*, 1996, 3613.

10 (*a*) R. D. Hancock and A. E. Martell, *Chem. Rev.*, 1989, **89**, 1875; (*b*) R. M. Izatt, K. Pawlak, J. S. Bradshaw and R. L. Bruening, *Chem. Rev.*, 1991, **91**, 1721.

11 C. O. Paul-Roth, J.-M. Lehn, J. Guilhem and C. Pascard, *Helv. Chim. Acta*, 1995, **78**, 1895; M. Li and P. R. Selvin, *J. Am. Chem. Soc.*, 1996, **118**, 1565; A. Beeby, D. Parker and J. A. G. Williams, *J. Chem. Soc., Perkin Trans. 2*, 1996, 1565.

12 A. P. de Silva, H. Q. N. Gunaratne and T. Gunnlaugsson, *Chem. Commun.*, 1996, 1967.

13 J. L. Toner, *US Pat.*, 4 837 169, 1989.

14 K. Connors, *Binding Constants: The Measurement of Molecular Complex Stability*, Wiley, New York, 1987.

15 A. Abu-Saleh and C. F. Meares, *Photochem. Photobiol.*, 1984, **39**, 763.

16 R. C. Holz, C. A. Chang and W. DeW. Horrocks, *Inorg. Chem.*, 1991, **30**, 3270. For lanthanide-bound water, see W. DeW. Horrocks and D. R. Sudnick, *Acc. Chem. Res.*, 1981, **14**, 384; *c.f.* L. Prodi, M. Maestri, R. Ziessel and V. Balzani, *Inorg. Chem.*, 1991, **30**, 3798; I. Hemmila, V.-M. Mukkala and H. Takalo, *J. Fluoresc.*, 1995, **5**, 159; R. S. Dickins, D. Parker, A. S. de Sousa and J. A. G. Williams, *Chem. Commun.*, 1996, 697.

17 V. Alexander, *Chem. Rev.*, 1995, **95**, 273.

18 N. Sabbatini, M. Guardigli and J.-M. Lehn, *Coord. Chem. Rev.*, 1993, **123**, 201.

19 R. G. Charles and E. P. Riedel, *J. Inorg. Nucl. Chem.*, 1966, **28**, 527.


*Received in Cambridge, UK, 29th July 1997; 7/05478E*

# A novel synthesis of α- and β-morpholino enones by electron transfer sensitized photooxidation of 2-morpholinocyclopropanols

**Wilfried Weigel* and Hans-Georg Henning**

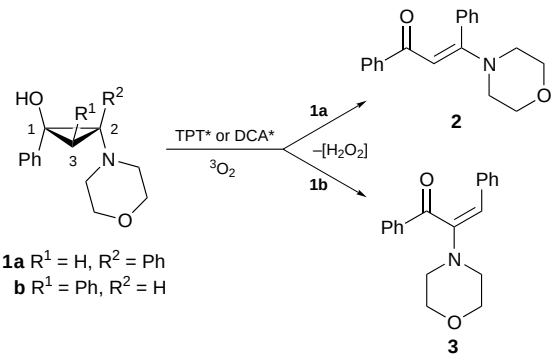
*Department of Chemistry, Humboldt-University of Berlin, Hessische Str. 1-2, D-10115 Berlin, Germany*

**An electron transfer mechanism is proposed to account for the photooxidation of 2-morpholinocyclopropanols 1 to the amino enone derivatives 2 and 3 in the presence of 9,10-dicyanoanthracene or triphenylpyrylium tetrafluoroborate and triplet oxygen.**

Photoinduced electron transfer (ET) *cis–trans* isomerization and oxidative ring opening of cyclopropanes have been the subject of numerous investigations.[1,2] Dioxolane derivatives and, in some cases, hydroperoxides and chalcones are formed by electron transfer photooxidation of aryl substituted cyclopropanes. Several mechanisms involving the superoxide anion radical, a chain reaction with triplet oxygen, or reaction of triplet oxygen with a 1,3-biradical formed by back electron transfer to the cyclopropane cation radical have been discussed.[3–5] Recently we reported that the irradiation of β-(*N*,*N*-dialkylamino)propiophenones gives 2-aminocyclopropanols that undergo oxidative ring opening to β-amino enones.[6a] Due to the electron donor properties of amino groups, 2-morpholino-1,2-diphenylcyclopropanol **1a** and 2-morpholino-1,3-diphenylcyclopropanol **1b** appeared to be excellent candidates for electron transfer studies. They were synthesized by photocyclization[6] and used as model compounds to investigate the possibility of oxidative ring opening in presence of the photoexcited electron acceptors 9,10-dicyanoanthracene (DCA) or triphenylpyrylium tetrafluoroborate (TPT).

Irradiation ($\lambda_{irr}$ > 395 nm) of aerated solutions of **1a** ($2 \times 10^{-4}$ M) in the presence of catalytic amounts (0.1 equiv.) of DCA in MeCN or TPT in $CH_2Cl_2$ gave the β-morpholino-β-phenylvinyl phenyl ketone **2** in 36 ($t_{irr}$ = 0.5 min) and 41% ($t_{irr}$ = 5.2 min) yield, respectively. Photolysis of a mixture of **1b** and DCA or TPT under the same conditions gave the α-morpholino chalcone **3** in 28 and 26% yield, respectively (Scheme 1). Continuous irradiation leads to the decomposition of **2** and **3**. The reported yields are the maximum values observed during the photolysis.† The formation of **2** and **3** was confirmed by HPLC analysis with authentic reference compounds.‡

The oxidation potentials $E(D/D^+)$ of **1a** and **1b** together with the $\Delta G$ values for photoinduced ET are given in Table 1. The free energy changes ($\Delta G$) for the one-electron transfer process




**1a** $R^1$ = H, $R^2$ = Ph
**b** $R^1$ = Ph, $R^2$ = H

**Scheme 1**

**Table 1** Oxidation potentials and calculated $\Delta G$ values for ET from **1** to $^{1/3}$TPT* and $^1$DCA*

| | | $\Delta G$/kcal mol$^{-1}$ | | |
|---|---|---|---|---|
| Compound | $E(D/D^+)/V^{a,b}$ | $^1$TPT*[c] | $^3$TPT*[c] | $^1$DCA*[d] |
| **1a** | 1.44 | −25.11 | −13.11 | −12.27 |
| **1b** | 1.37 | −26.72 | −14.72 | −13.88 |

[a] Pt electrode/SCE, 0.1 M $Et_4NClO_4$ in MeCN. [b] **2**: $E(D/D^+)$ = 1.53 V. [c] $E(A^-/A)$ = −0.29 V, $E(^1A^*)$ = 65 kcal mol$^{-1}$, $E(^3A^*)$ = 53 kcal mol$^{-1}$ (ref. 13). [d] $E(A^-/A)$ = −0.89 V, $E(^1A^*)$ = 66 kcal mol$^{-1}$ (ref. 13).

from the cyclopropane derivatives to photoexcited $^1$TPT* or $^1$DCA* were estimated by application of the Rehm–Weller equation [eqn. (1)].[8] The Coulombic term ($e^2/\varepsilon a$) was neglected

$$\Delta G = E(D/D^+) - E(A^-/A) - E(A^*) - e^2/\varepsilon a \qquad (1)$$

due to the lack of charge separation in case of TPT and the small estimated value of 0.06 eV[9] in MeCN for DCA as photosensitizer. Involvement of $^3$TPT* in photoinduced ET processes, especially at low donor concentrations (*ca.* $10^{-4}$ M), has been reported and cannot be ruled out in the case of **1**.[10,11]

Fluorescence quenching experiments of $^1$TPT* by **1a** and **1b** ($0.4 \times 10^{-3}$–6 x $10^{-3}$ M) were performed in aerated $CH_2Cl_2$ solutions.§ The fluorescence was quenched at almost diffusion controlled rates (**1a**: $k_q = 2.1 \times 10^{10}$ M$^{-1}$ s$^{-1}$; **1b**: $k_q = 2.0 \times 10^{10}$ M$^{-1}$ s$^{-1}$), calculated from the slopes of the Stern–Volmer plots (**1a**: $k_q\tau$ = 61 M$^{-1}$; **1b**: $k_q\tau$ = 58 M$^{-1}$) and a singlet lifetime of TPT of 2.9 ns.[12] As expected, the formation of **2** in the DCA-sensitized photolysis of **1a** was completely quenched by the addition of an equimolar amount of triethylamine, whose oxidation potential [$E(D/D^+)$ = 0.76 V, SCE, MeCN][13] is lower than that of **1a**. The DCA anion radical was detected by EPR measurements in the DCA-sensitized photoreaction of **1a** and **1b** in oxygen free MeCN.¶ No signals could be detected for the cation radical of **1**. The formation of the DCA anion radical was also observed by DCA-sensitized photolysis of the β-amino enone **2**.

The values of the oxidation potentials of **1** (Table 1) are lower than those of the *trans* and *cis* isomers of 1,2-diphenylcyclopropane, [$E(D/D^+)$ = 1.51 and 1.75 V].‖ Even though the measured oxidation potentials of **1a,b** are unexpectedly high compared to those for tertiary amines [*N*-methylmorpholine: $E(D/D^+)$ = 1.1 V, Ag/AgCl, MeCN][9] for reasons that are not clear, they reflect the good electron donor ability of **1**. The negative $\Delta G$ values for single electron transfer from **1a** and **1b** to $^{1/3}$TPT* and $^1$DCA*, the fluorescence quenching of $^1$TPT* at a diffusion controlled rate and the detection of $DCA^{-\cdot}$ by EPR spectroscopy strongly suggest that the formation of the radical cation of **1** by photoinduced ET is the primary process in the photooxidation of **1**. The cation radical of **1** could undergo reaction with triplet oxygen to give **1**–$O_2^{+\cdot}$. Back ET gives **1**–$O_2$ or the ground state reactants. Hydroperoxides formed from **1**–$O_2$ by internal hydrogen transfer are assumed to be intermediates which form **2** or **3** by elimination of hydrogen peroxide. In contrast to TPT, the DCA-sensitized photooxida-

$$\mathbf{1} + TP^{+*} / DCA^{*} \rightarrow \mathbf{1}^{+\bullet} + TP^{\bullet} / DCA^{-\bullet}$$

$$\mathbf{1}^{+\bullet} + {}^3O_2 \rightarrow \mathbf{1}\text{–}O_2^{+\bullet}$$

$$\mathbf{1}\text{–}O_2^{+\bullet} + TP^{\bullet} / DCA^{-\bullet} \rightarrow \mathbf{1}\text{–}O_2 + TP^{+} / DCA$$

$$DCA^{-\bullet} + {}^3O_2 \rightarrow DCA + {}^3O_2^{-\bullet}$$

$$\mathbf{1}^{+\bullet} + {}^3O_2^{-\bullet} \rightarrow \mathbf{1}\text{–}O_2$$

$$\mathbf{1}\text{–}O_2 \rightarrow \mathbf{2} \text{ or } \mathbf{3} + H_2O_2$$

**Scheme 2**

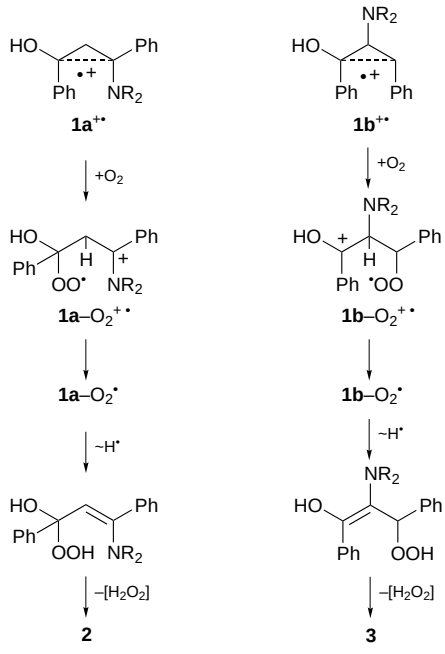
tion could lead to the formation of a superoxide anion radical by reaction of triplet oxygen with $DCA^{-\bullet}$ and would provide a second pathway to generate **1**–$O_2$.[10] A simplified mechanism for photoinduced ET oxidation of **1** is summarized in Scheme 2.

Possible pathways for the formation of **2** and **3** by reaction of the cation radicals of **1a** and **1b** with oxygen are given in Scheme 3. Obviously, the regioselectivity of ring opening is determined by the position of the phenyl groups. C(1)–C(3) ring cleavage of **1b** excludes resonance stabilization of the radical cation by the electron releasing morpholino group. However, the almost bisected conformation of the C(3)-phenyl group and the cyclopropane ring of **1b** should allow a strong interaction between their orbitals, in contrast to the morpholino group, which is the better electron donor but is arranged in a perpendicular fashion.[6a]**

High quantum yields for consumption of **1a** in the presence of TPT* ($8 \times 10^{-5}$ M) in $CH_2Cl_2$ were found.†† The values show considerable dependence on the concentration of the donor **1a** and amount to 11 ([**1a**] = $4.1 \times 10^{-4}$ M), 20 ([**1a**] = $6.0 \times 10^{-4}$ M) and 27 ([**1a**] = $1.6 \times 10^{-3}$ M). The high values indicate that a chain reaction occurs with generation of $\mathbf{1a}^{+\bullet}$ by hole transfer from **1a**–$O_2^{+\bullet}$ to **1a**. Quantum yields > 1 were reported for ET sensitized oxygenations and ring opening of several cyclopropanol derivatives and small strained ring systems.[3,16] An alternative pathway for the photooxidation could involve singlet oxygen generated by energy transfer from photoexcited TPT and DCA. However, the cyclopropanol **1a** was completely recovered after photolysis ($\lambda_{irr}$ > 395 nm) in MeCN in the presence of Methylene Blue as photosensitizer for singlet oxygen.

In summary, the novel synthesis of α- and β-morpholinoenones by DCA- or TPT-sensitized photooxidation of 2-morpholinocyclopropanols described herein increases the synthetic utility of the photochemical reactivity of cyclopropane derivatives.

We thank Professor Dr H. Kurreck at the Free University of Berlin for use of his EPR spectrometer. Helpful discussions with Professor Dr W. Abraham at the Humboldt University of Berlin are gratefully acknowledged.




**Scheme 3**

## Footnotes and References

* E-mail: weigel@chemie.fu-berlin.de

† Consumption of **1** > 85%; **2** and **3** are formed in the *E* configuration, assigned from $\lambda_{max}$ = 350 (**2**) and 282 nm (**3**); **2** and **3** were isolated by column chromatography from irradiations in $CH_2Cl_2$ of **1a** or **1b** ($4 \times 10^{-3}$ M) in the presence of TPT ($4 \times 10^{-4}$ M) and identified by their NMR spectra.

‡ Reference compounds **2** and **3** were prepared according to literature procedures (ref. 7).

§ [TPT] = $3.6 \times 10^{-5}$ M in $CH_2Cl_2$, excitation at 410 nm, fluorescence intensity measured at 460 nm.

¶ Hyperfine coupling constants for $DCA^{-\bullet}$ at 245 K generated by > 395 nm irradiation of **1** ($5 \times 10^{-3}$ M) and DCA ($2 \times 10^{-3}$ M) in MeCN recorded on a X Band Spectrometer Bruker ER 220D: **1a**/DCA, 0.238, 0.132, 0.114 mT; **1b**/DCA, 0.242, 0.125, 0.111 mT; *cf.* ref. (14).

‖ Oxidation potentials ($Ag/AgNO_3$, MeCN) from ref. (1), 0.34 V added for SCE as reference electrode.

** It should be noted that formation of **2** and **3** indicates the cleavage of the respective longest cyclopropane bond of **1a**, C(1)–C(2) = 1.54, C(1)–C(3) = 1.51, C(2)–C(3) = 1.50 Å and of **1b**, C(1)–C(3) = 1.52, C(1)–C(2) = 1.50, C(2)–C(3) = 1.49 Å, see X-ray structures of **1a** and **1b** in ref. 6(a).

†† Consumption of **1a** < 10%; $\lambda_{irr}$ = 405 nm by combination of a band pass filter WG 305 and a metall interference filter UV-SKIF 405 nm (Carl Zeiss Jena); actinometer potassium ferri oxalate (ref. 15).

1 P. C. Wong and D. R. Arnold, *Tetrahedron Lett.*, 1979, **23**, 2101; S. B. Karki, J. P. Dinnocenzo, S. Farid, J. L. Goodman, I. R. Gould and T. A. Zona, *J. Am. Chem. Soc.*, 1997, **119**, 431.
2 T. Tamai, K. Mizuno, I. Hashida and Y. Otsuji, *J. Org. Chem.*, 1992, **57**, 5338 and references cited therein.
3 K. Mizuno, N. Kamiyama, N. Ichinose and Y. Otsuji, *Tetrahedron*, 1985, **41**, 2207.
4 K. Gollnick and U. Paulmann, *J. Org. Chem.*, 1990, **55**, 5954; K. Gollnick, X.-L. Xiao and U. Paulmann, *J. Org. Chem.*, 1990, **55**, 5945.
5 F. Algarra, M. V. Baldovi, H. Garcia, M. A. Miranda and J. Primo, *Tetrahedron*, 1993, **47**, 10 897.
6 (*a*) W. Weigel, G. Reck, S. Schiller and H.-G. Henning, *Tetrahedron Lett.*, 1993, **34**, 6737; (*b*) W. Weigel, S. Schiller and H.-G. Henning, *Tetrahedron*, 1997, **53**, 7855; (*c*) W. Weigel and P. J. Wagner, *J. Am. Chem. Soc.*, 1996, **118**, 12 858.
7 N. H. Cromwell, *J. Am. Chem. Soc.*, 1940, **62**, 2897; F. Felluga, P. Nitta, G. Pitacco and E. Valentin, *J. Chem. Soc., Perkin Trans. 1*, 1971, 1648.
8 D. Rehm and A. Weller, *Ber. Bunsenges. Phys. Chem.*, 1969, **73**, 834.
9 P. E. Correa, G. Hardy and D. P. Riley, *J. Org. Chem.*, 1988, **53**, 1695.
10 M. A. Miranda and H. Garcia, *Chem. Rev.*, 1994, **94**, 1063.
11 R. Akaba, H. Sakuragi and K. Tokumaru, *Chem. Phys. Lett.*, 1990, **174**, 80.
12 G. Haucke, P. Czerney and F. Cebulla, *Ber. Bunsenges. Phys. Chem.*, 1992, **96**, 880.
13 G. J. Kavarnos and N. J. Turro, *Chem. Rev.*, 1986, **86**, 401.
14 E. Brunner, *Ber. Bunsenges. Phys. Chem.*, 1968, **68**, 468; A. P. Schaap, K. A. Kaklika and L. Kaskar, *J. Am. Chem. Soc.*, 1980, **102**, 389.
15 H. J. Kuhn, S. E. Braslavsky and R. Schmidt, *Pure Appl. Chem.*, 1989, **2**, 187.
16 K. Mizuno, N. Ichinose and Y. Otsuji, *J. Org. Chem.*, 1992, **57**, 1855; K. Okada, K. Hisamitsu and T. Mukai, *Tetrahedron Lett.*, 1981, **22**, 1251.

*Received in Liverpool, UK, 9th June 1997; 7/04024E*

# Photoreaction of halomethyl substituted benzocyclic ketones with amines: radical cyclization and ring expansion reactions promoted through photoinduced electron transfer processes

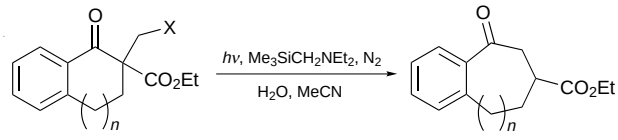
**Eietsu Hasegawa,* Yukinobu Tamura and Emi Tosaka**

*Department of Chemistry, Faculty of Science, Niigata University, Ikarashi, Niigata 950-21, Japan*

**Photoreaction of ethyl 2-bromomethyl-1-oxo-1,2,3,4-tetrahydronaphthalene-2-carboxylate 1a or other related compounds 1b–d with $Me_3SiCH_2NEt_2$ in aqueous MeCN afforded ethyl 5-oxo-6,7,8,9-tetrahydrobenzocycloheptene-7-carboxylate 2a or corresponding ring expansion products 2a–d respectively.**

Irradiation of carbonyl compounds in the presence of electron donors such as amines produces carbonyl anion radicals and donor cation radicals.[1] Apparently proton transfer from donor cation radicals to carbonyl anion radicals is a feasible process. On the other hand, it is also reasonable to expect that carbonyl anion radicals must act as single electron donors. Therefore, generation of carbonyl anion radicals would irreversibly reduce distant carbon–halogen bonds in the same molecules through intramolecular electron transfer.[2] Although photoreactions of a few carbonyl compounds categorized in this group have been explored in the presence of electron donors, the substrates studied were limited to enones and dienones.[3] In this context, photoinduced electron transfer (PET) reaction of haloalkylated benzocycloalkanones such as **1** must be interesting since reductive carbon–halogen bond cleavage should generate carbon radicals followed by radical cyclization and ring expansion pathways.[4] Moreover, the literature observation that the yields of ring expansion products from **1** (X = Br) were relatively low under ordinary free radical conditions[5] also prompted us to explore photoreaction of **1** with electron donors. We report here the first example of PET promoted radical cyclization and ring expansion reactions of ethyl 2-bromomethyl-1-oxo-1,2,3,4-tetrahydronaphthalene-2-carboxylate **1a** and other related compounds **1b–d** (Scheme 1).

When a $N_2$ pre-purged MeCN solution (10 ml) of **1a** ($\lambda$ = 295 nm, $\varepsilon$820; 0.64 mmol) and $Me_3SiCH_2NEt_2$ (5 equiv.)[6] was irradiated for 1 h with a 500 W Xe-Hg lamp through Pyrex, 50% of the desired benzocycloheptanone **2a**, 10% of the reduced product **3a** and 21% of unexpected dimeric compound **4a** (as a mixture of two diastereomers $\mathbf{4a_1}:\mathbf{4a_2}$ = 55 : 45) was isolated together with 35% of unreacted **1a** after chromatographic separation (the product yields are reported on the basis of the conversion of **1a**).† Stirring of a similar solution for 2 h in the dark resulted in quantitative recovery of **1a**. Upon irradiation of **1a** for 2 h in the absence of $Me_3SiCH_2NEt_2$, 92% of **1a** was recovered without formation of **2a**. These control experiments clearly suggest that **2a** is produced through the interaction between the photoexcited **1a** and $Me_3SiCH_2NEt_2$.



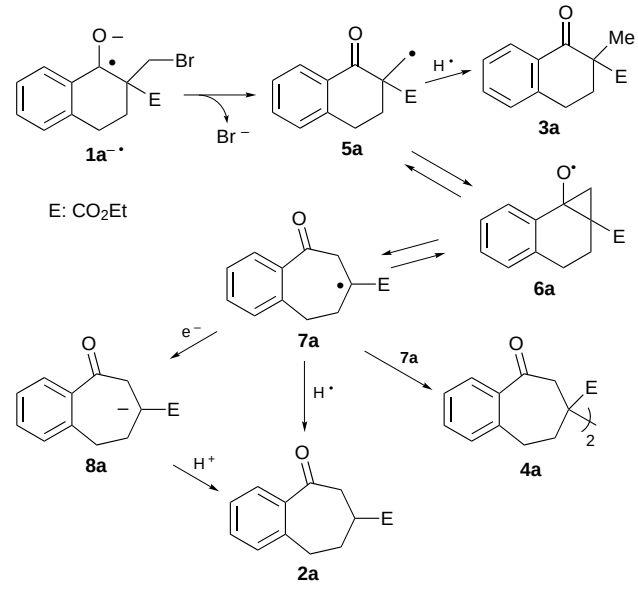

**1a** X = Br, *n* = 1
**b** X = I, *n* = 1
**c** X = Br, *n* = 2
**d** X = Br, *n* = 0

**2a** *n* = 1
**c** *n* = 2
**d** *n* = 0

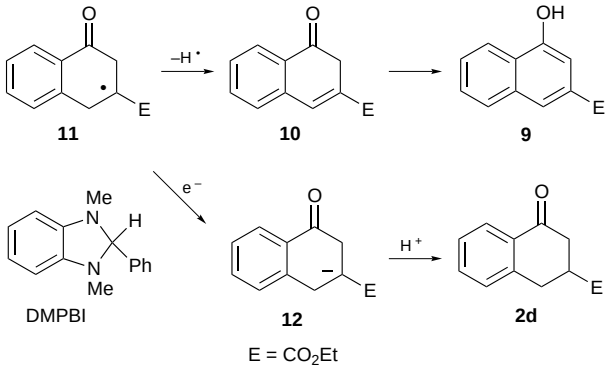
**Scheme 1**

It was also found that water significantly affects the product ratio when the reactions were conducted for 1 h in MeCN containing various amounts of water: 61% of **2a**, 10% of **3a**, 20% of **4a** and 24% of **1a** in 5% aq. MeCN; 68, 7, 16 and 25% in 10% aq. MeCN; 75, 6, 10 and 25% in 30% aq. MeCN. While addition of water increased the yield of **2a** and decreased the yields of **3a** and **4a**, the total yield of the products remained almost constant at about 90%. This would suggest that the observed products are formed through common intermediates. In order to obtain information on the nature of the intermediates, a deuterium labeling experiment was performed. Thus, when irradiation of **1a** for 2 h were conducted in 5% $D_2O$ as well as 5% $H_2O$ containing MeCN solutions, similar conversions (90 and 90%) as well as product yields (**2a**: 60 and 59%; **3a**: 7 and 7%) were observed, respectively. NMR analyses of the isolated products revealed that *ca.* 82% of hydrogen at $C_3$ in **2a** was substituted by deuterium and no deuterium was incorporated in **3a**. Therefore, **2a** is mainly formed through an ionic route in which its precursor is protonated. On the other hand, **3a** is formed through hydrogen abstraction by the radical intermediate.

On the basis of the above results, the reaction mechanism in Scheme 2 is proposed. Single electron transfer to the photoexcited state of **1a** from $Me_3SiCH_2NEt_2$ produces the anion radical of **1a** and the cation radical of $Me_3SiCH_2NEt_2$.‡ The resulting anion radical of **1a** rapidly reacts,§ undergoing carbon–bromine bond cleavage through intramolecular electron transfer to give the carbon radical **5a**. The radical **5a** abstracts hydrogen to produce **3a**, which is consistent with the deuterium labeling experiment. On the other hand, **5a** cyclizes to give the oxy radical **6a** followed by the ring opening to the ethoxy




**Scheme 2**




**Scheme 3**

carbonyl substituted carbon radical **7a**. Apparently, **7a** has a long enough lifetime to dimerize, giving **4a**. Cyclization of the carbon radical on the carbonyl group and ring opening would be a reversible process (**5a** → **6a** → **7a**).[7] If **7a** abstracts hydrogen, **2a** should be formed. However, the deuterium labeling experiment suggests that this is a minor route, even though it exists. Instead, **7a** is reduced to its anion **8a** followed by protonation to give the formation of **2a**.

In the proposed reaction mechanism, the most plausible candidate for the reducing agent of **7a** must be the α-amino radical formed through desilylation of the cation radical of $Me_3SiCH_2NEt_2$. Thus, effective formation of the α-amino radical is required for the formation of **2a**. Indeed, when **1a** was irradiated with 1,4-diazabicyclo[2.2.2]octane (DABCO) for 5 h in MeCN, no formation of **2a** was observed. Although DABCO is a strong enough electron donor,‡ its cation radical is known to be stable, so that the efficient formation of the α-amino radical by deprotonation cannot be expected.[8] In the reaction system of **1a** and $Me_3SiCH_2NEt_2$, water would act as a silophile to generate the α-amino radical by desilylation of the cation radical of $Me_3SiCH_2NEt_2$.[9] On the other hand, water would not be a strong enough base for α-deprotonation of an amine cation radical.[10] This was confirmed by the observation that photoreactions of **1a** with triethylamine‡ in dry as well as wet MeCN reveal no significant water effect on the product ratio. Another notable observation was made when the reactions were conducted for 1 h with addition of various quantities of $Me_3SiCH_2NEt_2$ in 10% aq. MeCN: 56% of **2a**, 7% of **3a**, 24% of **4a** and 39% of **1a** with 1.5 equiv. of $Me_3SiCH_2NEt_2$; 68, 7, 16 and 25 with 5 equiv.; 73, 10, 12 and 27 with 10 equiv. Increasing the quantity of $Me_3SiCH_2NEt_2$ increased the yield of **2a** as well as **3a** and decreased that of **4a**, which would suggest that excess $Me_3SiCH_2NEt_2$ donates a hydrogen to the radical intermediates, leading to the formation of **2a** and **3a**, and eventually decreasing the yield of **4a**.

In order to determine the generality of this PET reaction, photoreactions of other halo ketones **1b**–**d** were briefly conducted (product yields were not optimized). Irradiation of the iodide **1b** with $Me_3SiCH_2NEt_2$ produced 46% of **2a**. The moderate yield of **2c** (41%) from **1c** is still encouraging since thermal reaction of **1c** with tributyltin hydride produced **2c** only as a minor product.[5] More interestingly, it turned out that the major product from **1d** was ethyl 1-hydroxynaphthalene-3-carboxylate **9** (52%) instead of **2d**, which was isolated in 14% yield in the photoreaction of **1d** with $Me_3SiCH_2NEt_2$. As shown in Scheme 3, naphthol **9** is considered to be an enol form of ketone **10**, which is probably formed *via* hydrogen abstraction from the ethoxy carbonyl substituted carbon radical **11**. If so, the relative yield of **2d** *vs.* **9** should increase under the conditions in which **11** is efficiently reduced to its anion **12**. This was actually the case when $Me_3SiCH_2NEt_2$ was replaced by 1,3-dimethyl-2-phenylbenzimidazoline (DMPBI),[11] which gave 47% of **2d** and 11% of **9**.¶ Since the α-amino radical derived from the cation radical of DMPBI is readily oxidized to a stable imidazolium ion, it would act as a stronger reductant than that from the cation radical of $Me_3SiCH_2NEt_2$.

As described above, we have discovered that a PET process can promote the conversion of certain halomethyl substituted benzocyclic ketones to ring expanded ketones. Further studies focused on designing substrates as well as electron donors are now in progress, with the aim of providing a thorough mechanistic understanding and an expansion of the synthetic versatility of this unique PET reaction.

This work was partly supported by a Grant-in-Aid for Scientific Research (No. 08640676) from the Ministry of Education, Science, Sports and Culture of Japan. We thank Professors Yasutake Takahashi and Tsutomu Miyashi (Tohoku University) for performing the pulsed laser photolyses and their useful comments. We thank Professor Masaki Kamata (Faculty of Education) for his assistance in measuring redox potentials. We thank Professors Yoshiki Okamoto and Takaaki Horaguchi (Faculty of Science) for their generous support.

## Footnotes and References

* E-mail: ehase@sc.niigata-u.ac.jp

† Ring expansion products **2a**,**c** and the reduced product **3a** are known compounds (ref. 5). The structure of unknown **2d** was determined by direct comparison of its spectral data with that of the compound independently prepared by reaction of **1d** with tributyltin hydride. Compounds **4a** and **9** were satisfactorily characterized by their NMR and IR spectroscopic data.

‡ Free energy changes ($\Delta G$) for single electron transfer between the triplet excited state of **1a** and amines were estimated (D. Rehm and A. Weller, *Isr. J. Chem.*, 1970, **8**, 259) from the triplet energy of 1,2,3,4-tetrahydronaphthalen-1-one (72.7 kcal $mol^{-1}$: S. L. Murov, *Handbook of Photochemistry*, Marcel Dekker, New York, 1973) and the redox potentials of **1a** (−1.85 V *vs.* SCE) and amines[3] (−19 kcal $mol^{-1}$ for $Me_3SiCH_2NEt_2$, −15 kcal $mol^{-1}$ for DABCO, −11 kcal $mol^{-1}$ for $NEt_3$).

§ Pulsed laser photolysis (355 nm) of **1a** in nitrogen-saturated MeCN resulted in a transient absorption around 370 nm which was assigned as the T–T absorption. In the presence of $Me_3SiCH_2NEt_2$, the T–T absorption was replaced by a new shoulder absorption ranging from 400 to 500 nm, which decayed with a rate constant of *ca.* $3 \times 10^6$ $s^{-1}$. A plausible explanation for these observations is that the triplet excited state of **1a** is quenched by $Me_3SiCH_2NEt_2$ to generate the anion radical of **1a**, which decays rapidly owing to its high intramolecular reactivity. The cyclic voltammetric behaviour of **1a** is also consistent with the above explanation: the redox process of **1a** is totally irreversible (100 mV $s^{-1}$ in MeCN).

¶ An alternative explanation for this phenomenon would be the occurrence of direct hydrogen transfer from the cation radical of DMPBI or its neutral form to the radical **11** to give **2d** (Note added in proof).

1 *Photoinduced Electron Transfer, Part C*, ed. M. A. Fox and M. Chanon, Elsevier, Amsterdam, 1988; U. C. Yoon, P. S. Mariano, R. S. Givens and B. W. Atwater III, in *Advances in Electron Transfer Chemistry*, ed. P. S. Mariano, JAI, Greenwich, 1994, vol. 4, pp. 117–205.
2 N. Kimura and S. Takamuku, *J. Am. Chem. Soc.*, 1994, **116**, 4087.
3 R. S. Givens and B. W. Atwater III, *J. Am. Chem. Soc.*, 1986, **108**, 5028; E. Hasegawa, Y. Tamura, T. Horaguchi, K. Isogai and T. Suzuki, *Tetrahedron Lett.*, 1994, **35**, 8643.
4 P. Dowd and Z. Wei, *Chem. Rev.*, 1993, **93**, 2091.
5 W. R. Bowman and P. J. Westlake, *Tetrahedron*, 1992, **48**, 4027.
6 E. Hasegawa, W. Xu, P. S. Mariano, U. C. Yoon and J. U. Kim, *J. Am. Chem. Soc.*, 1988, **110** 8099.
7 D. P. Curran, in *Comprehensive Organic Synthesis*; ed. B. M. Trost and I. Fleming, Pergamon, Oxford, 1991, vol. 4, pp. 779–831.
8 Y. L. Chow, W. C. Danen, S. F. Nelsen and D. H. Rosenblatt, *Chem. Rev.*, 1978, **78**, 243.
9 X. Zhang, S. R. Ye, M. Freccero, A. Albini, D. E. Falvey and P. S. Mariano, *J. Am. Chem. Soc.*, 1994, **116** 4211.
10 S. Das and C. von Sonntag, *Z. Naturforsh.*, 1986, **416**, 505.
11 E. Hasegawa, T. Kato, T. Kitazume, K. Yanagi, K. Hasegawa and T. Horaguichi, *Tetrahedron Lett.*, 1996, **37**, 7079 and references cited therein.

*Received in Cambridge, UK, 9th June 1997; 7/03974C*

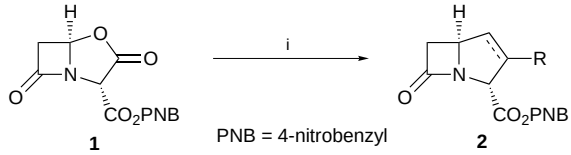
# The azomethine ylide strategy for β-lactam synthesis: the structure of the key 1,3-dipolar intermediate

**Sarah R. Martel,[a] Denis Planchenault,[a] Richard Wisedale,[a] Timothy Gallagher*[a]† and Neil J. Hales*[b]**

[a] *School of Chemistry, University of Bristol, Bristol, UK BS8 1TS*
[b] *Zeneca Pharmaceuticals, Mereside, Alderley Park, Macclesfield, UK SK10 4TG*

**The thermolysis of the β-lactam-based oxazolidinone 1 leads to the formation of cycloadducts 2 and evidence is presented for the participation of the carboxylated azomethine ylide 4, rather than 3 (the more conventional product of oxazolidinone fragmentation), as the key 1,3-dipolar intermediate in this process.**

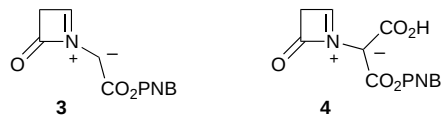
Recently, we disclosed a new and highly convergent cycloaddition strategy for the synthesis of bicyclic β-lactams **2**, encompassing carbapenems and $\Delta^1$-carbapenems (Scheme 1),[1] as well as the sulfur-based penams and penems.[2] A critical step in this sequence involves the fragmentation of a β-lactam-based oxazolidinone **1** to release a reactive 1,3-dipole (a stabilised azomethine ylide); evidence for the structure of this key reaction intermediate is presented here.




**1** **2**

**Scheme 1** *Reagents and conditions*: i, $RCH{=}CH_2$ or $RC{\equiv}CH$, MeCN, 80 or 100 °C

Simpler oxazolidinones are known[3] to undergo a concerted and irreversible decarboxylation to produce azomethine ylides and this reaction has contributed significantly to the utility of 1,3-dipolar cycloaddition reactions within heterocyclic chemistry.[4,5] Extrapolating this established mechanism to the process shown in Scheme 1 points, in the first instance, towards participation of the ester-stabilised azomethine ylide **3** formed *via* direct decarboxylation of **1**. While production of cycloadducts **2** (which is usually the major regioisomer observed with monosubstituted alkenes/alkynes) can obviously be formulated in terms of the simple azomethine ylide **3**, we can now provide evidence that, under our usual reaction conditions, fragmentation of the β-lactam-based oxazolidinone **1** leads to the carboxylated azomethine ylide **4** as the key intermediate involved in the conversion of **1** to cycloadducts **2**.




**3** **4**

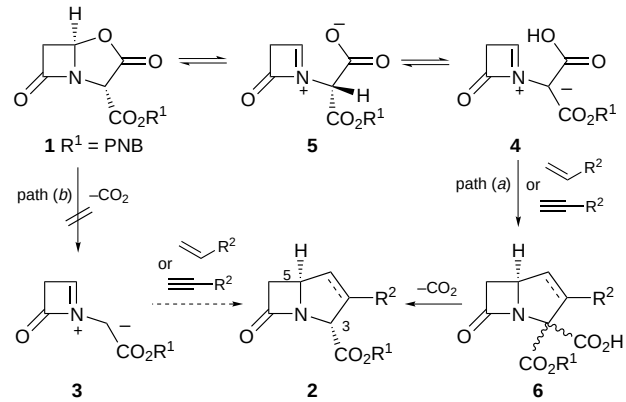
Thermolysis of the enantiomerically-pure oxazolidinone **1**[6] in the presence of an alkene or an alkyne provides the racemic carbapenams and $\Delta^1$-carbapenems respectively. The rate of formation of cycloadducts **2** shows a significant dependence on the reactivity of the dipolarophile and, although this observation in of itself is not inconsistent with the 'concerted decarboxylation' pathway,[7] this would require participation of a relatively stable dipolar intermediate which has never been detected.‡ The more general fate of oxazolidinone **1** cannot, however, be reconciled with the established ('concerted decarboxylation') mechanism.[3] When oxazolidinone **1** was heated (as a 0.033 M solution in MeCN at 80 °C for 17 h) in the *absence* of a dipolarophile, decomposition (decarboxylation) of **1** was *not observed*. Moreover, the starting oxazolidinone **1**, which was recovered cleanly after this period of time, had undergone *complete racemisation* under these conditions, which correspond to those employed in the cycloaddition process shown in Scheme 1.§

A mechanistic rationale for the formation of cycloadducts **2**, which is consistent with our experimental observations and does not require involvement of the azomethine ylide **3**, is presented in Scheme 2.

We suggest that oxazolidinone **1** undergoes an initial fragmentation to generate the iminium intermediate **5** and this step is then followed by tautomerisation of the now highly activated malonyl proton to provide azomethine ylide **4**, a carboxylated variant of **3**. Azomethine ylide **4** is then the reactive species involved in the subsequent cycloaddition step but in the absence of a trap, collapse of **4** back to oxazolidinone **1** is facile and this provides an explanation for the observed thermal racemisation of **1**. The equilibrating steps linking **1** and **4** can, however, be intercepted by a dipolarophile (alkene or alkyne, or thiocarbonyl), displacing the equilibrium and leading, in what is likely to be the rate determining event, to cycloadduct **6** [path (*a*)]. Finally, decarboxylation of **6** serves to set the thermodynamically more stable relative *cis* configuration[9] between C(3) and C(5) of the bicyclic β-lactam product **2**.

The principal difference between path (*a*) (Scheme 2) and that normally associated[3] with the generation of azomethine ylides from oxazolidinones [path (*b*) *via* **3**] is that the decarboxylation step *follows, rather than precedes*, the cycloaddition event, although studies are still needed to establish all the details of this mechanism.

While no details are available for the positions of the two pre-cycloaddition equilibria shown in Scheme 2, displacing either of these to the right should increase the concentration of azomethine ylide **4** and accelerate the overall cycloaddition process. This acceleration has been achieved using LiBr as a

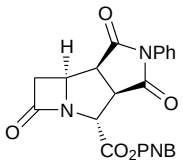



**1** $R^1$ = PNB **5** **4**

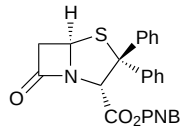
**3** **2** **6**

**Scheme 2**

mild Lewis acid¶ and thermolysis of **1** in the presence of *N*-phenylmaleimide (NPM) (0.040 M of **1**, 1.1 equiv. of NPM and 1.1 equiv. of LiBr in MeCN at 80 °C) led to complete consumption of **1** in 4 h and cycloadduct **7**[1] was isolated in 42% yield. This compares to a reaction time of 25 h (and 49% yield of **7**) when the same reaction was carried out in the absence of LiBr. Using thiobenzophenone as the dipolarophile, reaction time was cut (from 80 h to 1.5 h) using 1.1 equiv. of LiBr, although the yield of cycloadduct **8**[2] did decrease (30 *vs.* 51% without LiBr). The role played by the Lewis acid is not yet clear but it would be premature to exclude the intermediacy of an alternative dipolar component, for example **3**, under these modified conditions.




**7**




**8**

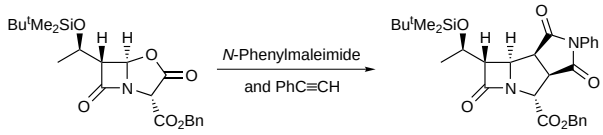
The mechanism shown in Scheme 2 does not require any reassessment of the 1,3-dipolar cycloreversion mechanism which characterises the concerted fragmentation of simpler oxazolidinones.[3] When compared to the more usually encountered oxazolidinones, β-lactam derivatives such as **1** are different in a number of important respects that may favour the formation of azomethine ylide **4**: **1** is an *N*-acyl-, rather than an *N*-alkyl-oxazolidinone, which also incorporates a significant degree of strain and contains an unusual malonate moiety.‖ Nevertheless, we have uncovered an alternative pathway for expressing azomethine ylide reactivity from an oxazolidinone precursor and this unexpected pathway provides a method for generating cycloadducts carrying new and varied substitution patterns. These mechanistic concepts are currently being evaluated for a range of bicyclic oxazolidinones other than those based on a β-lactam, both to define the more general applicability and also to establish further details of this alternative 'cycloaddition-decarboxylation' sequence outlined in Scheme 2.

We thank The Royal Society, The Swiss National Science Foundation, the EPSRC and Zeneca Pharmaceuticals for financial support.

## Footnotes and References

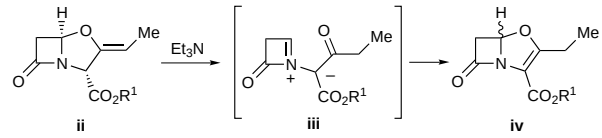
† E-mail: t.gallagher@bristol.ac.uk

‡ Qualitative rate differences have been observed for the reaction of **1** with a variety of dipolarophiles and more detailed kinetic studies are underway. In addition, direct competition experiments have been carried using *N*-phenylmaleimide and PhC≡CH with a limiting quantity of the C(6) substituted β-lactam oxazolidinone **i** and only the maleimide cycloadduct (ref. 1), which is enantiomerically pure, was observed.




**i** only adduct observed

§ The racemisation of **1** was followed by both optical rotation and $^1$H NMR spectroscopy using Eu(hfc)$_3$ and was shown to be a first order process ($t_{\frac{1}{2}}$ = 2.5 h, MeCN at 80 °C). After more prolonged heating (48 h), decomposition of **1** was observed. Workers at Glaxo (ref. 8) have reported that desoxyclavulanic acid **ii** undergoes both C=C bond isomerisation *and* racemisation to give (±)-**iv** when treated with $Et_3N$. The intermediacy of the stabilised azomethine ylide **iii**, which is structurally related to **4**, has been implicated in this study.




**ii** **iii** **iv**

¶ A wide variety of other, more conventional Lewis acids have been evaluated [*e.g.* AgOAc, $AgNO_3$, $ZnBr_2$, $Sc(OTf)_2$, $Ti(OPr^i)_4$] but all led to decomposition of oxazolidinone **1**.

‖ The strain associated with **1** may play an important activating role in the specific case of the β-lactam-based system and, for this reason, a stepwise cycloaddition pathway may intervene. Alkenes (dimethyl maleate and dimethyl fumarate) do undergo stereospecific cycloaddition (ref. 1), but the possibility that, for example, the iminium component of **5** is trapped by a direct nucleophilic addition (as the first step of a cycloaddition process) cannot be excluded, especially when more highly polarisable dipolarophiles, such as thiocarbonyls, are involved. Solvent effects are also apparent and the rate of formation of cycloadducts **2** is faster in MeCN than in toluene at comparable temperatures.

1 S. R. Martel, R. Wisedale, T. Gallagher, L. D. Hall, M. F. Mahon, R. H. Bradbury and N. J. Hales, *J. Am. Chem. Soc.*, 1997, **119**, 2309.

2 D. Planchenault, R.Wisedale, T. Gallagher and N. J. Hales, *J. Org. Chem.*, 1997, **62**, 3438.

3 For the key mechanistic work in this area, see R. Grigg, S. Surendrakumar, S. Thianpatanagul and D. Vipond, *J. Chem. Soc., Perkin Trans. 1*, 1988, 2693; R. Grigg, J. Idle, P. McMeekin, S. Surendrakumar and D. Vipond, *J. Chem. Soc., Perkin Trans. 1*, 1988, 2703.

4 For other examples of the use of oxazolidinones as precursors to azomethine ylides, see: G. P. Rizzi, *J. Org. Chem.*, 1970, **35**, 2069; A. Eschenmoser, *Chem. Soc. Rev.*, 1976, **5**, 377; K. Burger, A. Meffert and S. Bauer, *J. Fluorine Chem.*, 1977, **10**, 57; O. Tsuge, S. Kanemasa, M. Ohe, K. Yorozu, S. Takenaka and K. Ueno, *Bull. Chem. Soc. Jpn.*, 1987, **60**, 4067.

5 J. W. Lown, *1,3-Dipolar Cycloaddition Chemistry*, ed. A. Padwa, Wiley, New York, 1984, vol. 1, p. 653; R. Grigg, *Chem. Soc. Rev.*, 1987, **16**, 89; W. H. Pearson, *Studies in Natural Products Chemistry*, ed. Atta-ur-Rahman, Elsevier, Amsterdam, 1988, vol. 1; O. Tsuge and S. Kanemasa, *Advances in Heterocyclic Chemistry*, ed. A. R. Katritzky, Academic Press, San Diego, 1989, vol. 45, p. 231.

6 A. G. Brown, D. F. Corbett, J. Goodacre, J. B. Habridge, T. T. Howarth, R. J. Ponsford, I. Stirling and T. J. King, *J. Chem. Soc., Perkin Trans. 1*, 1984, 635; T. T. Howarth and I. Stirling, *Ger. Offen.*, 2,655,675 (*Chem. Abstr.*, 1977, **87**, 102 313).

7 S. Kanemasa, K. Sakamoto and O. Tsuge, *Bull. Chem. Soc. Jpn.*, 1989, **62**, 1960.

8 P. C. Cherry, C. E. Newall and N. S. Watson, *J. Chem. Soc., Chem. Commun.*, 1978, 469; P. C. Cherry, C. E. Newall and N. S. Watson, *J. Chem. Soc., Chem. Commun.*, 1979, 663; C. E. Newall, *Recent Advances in the Chemistry of β-Lactam Antibiotics*, ed. G. I. Gregory, Royal Society of Chemistry, London, 1981, ch. 13, p. 151.

9 T. C. Smale and R. Southgate, *J. Chem. Soc., Perkin Trans. 1*, 1985, 2235; S. Wolfe and R. Z. Sterzycki, *Can. J. Chem.*, 1987, **65**, 26; A. G. M. Barrett and S. Sakadarat, *J. Org. Chem.*, 1990, **55**, 5110.

*Received in Liverpool, UK, 11th June 1997; 7/04099G*

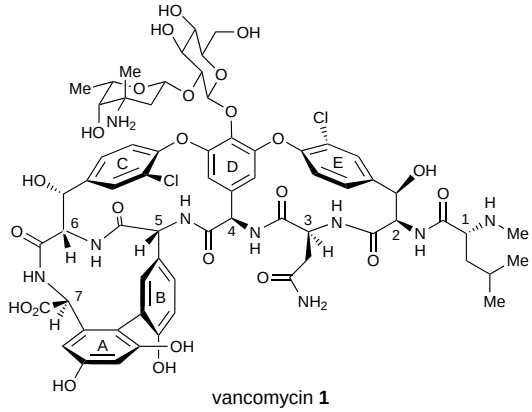
# A Suzuki coupling–macrolactamization approach to the *AB-COD* bicyclic system of vancomycin

**K. C. Nicolaou,* Joshi M. Ramanjulu, Swaminathan Natarajan, Stefan Bräse, Hui Li, Christopher N. C. Boddy and Frank Rübsam**

*Department of Chemistry and The Skaggs Institute for Chemical Biology, The Scripps Research Institute, 10550 North Torrey Pines Road, La Jolla, California 92037, USA* and *Department of Chemistry and Biochemistry, University of California, San Diego, 9500 Gilman Drive, La Jolla, California 92093, USA*

**The effectiveness of the Suzuki coupling reaction in the formation of the *AB* biaryl moiety and the beneficial role of a preexisting *COD* ring system in a lactamization approach to the *AB-COD* ring system of vancomycin is demonstrated.**

Vancomycin **1** is a polycyclic glycopeptide antibiotic effective against drug-resistant bacterial strains.[1] The daunting synthetic challenge posed by its structure[2,3] is largely due to the strained nature of the 12-membered biaryl framework (*AB* ring system) and the two 16-membered biaryl ethers (*COD* and *DOE* ring systems). While several approaches for the construction of the biaryl ether rings have been reported,[4–6] only two methods so far exist for the synthesis of the *AB* biaryl ring system.[7,8] Here we report a macrolactamization strategy to this system that has the potential of contributing to vancomycin's total synthesis.



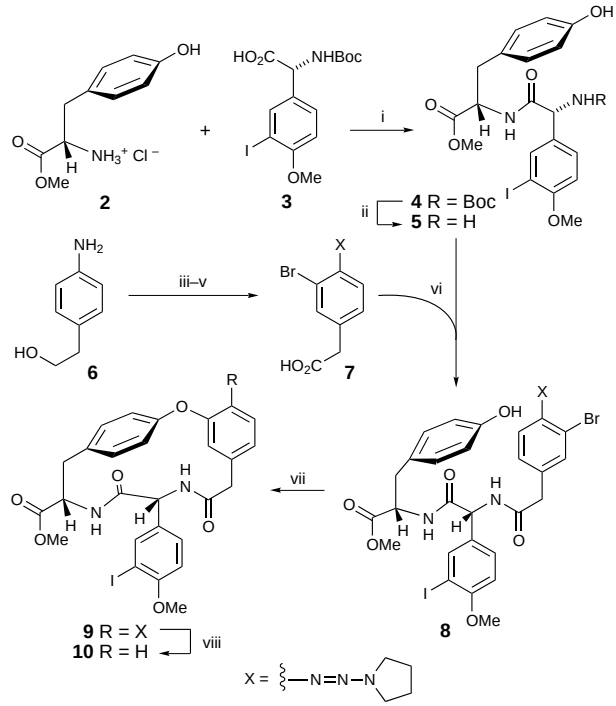
vancomycin **1**

Since attempts to form the *AB* framework of vancomycin as a single system by a lactamization approach were unsuccessful,[9] we reasoned that an attached *COD* structure might facilitate the process by preorganization, in much the same way as occurred in the elegant synthesis of a similar *AB-COD* framework by the Evans group, who employed a vanadium catalyst.[7] A Suzuki coupling reaction was chosen for the construction of the biaryl system which, of course, is potentially capable of atropisomerism.

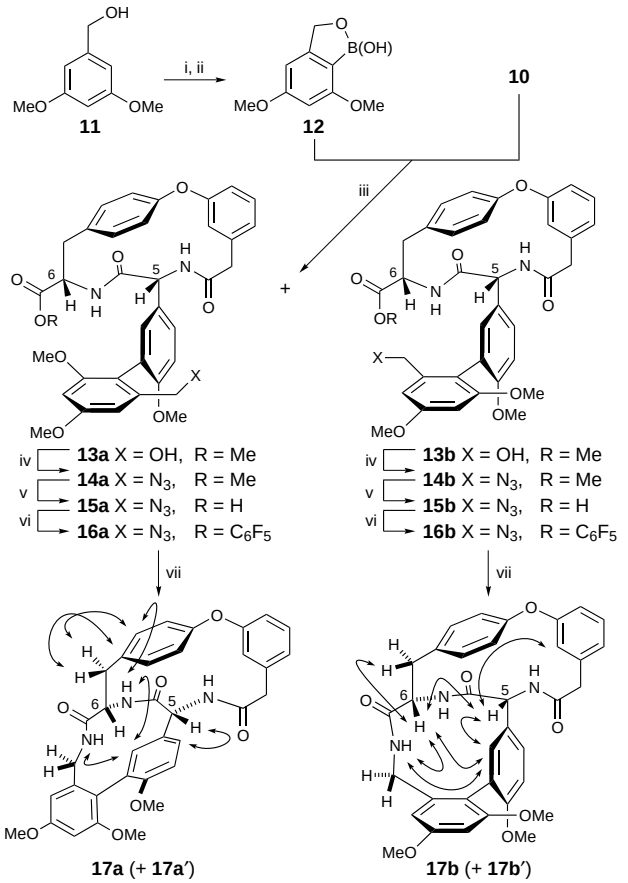
Scheme 1 summarizes the construction of the requisite *COD* model system **10**. Thus, (*S*)-tyrosine methyl ester **2** was coupled with (*R*)-4-methoxy-3-iodophenylglycine derivative **3**[8] in the presence of 2-(1*H*-benzotriazol-1-yl)-1,1,3,3-tetramethyluronium hexafluorophosphate (HBTU) and $Et_3N$ to afford dipeptide **4**† in 80% yield.

Removal of the Boc group from **4** with TFA gave, in quantitative yield, amine **5**, which was coupled with triazene carboxylic acid **7** [prepared from **6** by monobromination (62%), triazene formation (83%) and 2,2,6,6-tetramethyl-1-piperidyloxy (TEMPO) oxidation (86%)] as described above for **2** and **3**, leading to tripeptide **8** (90% yield). Cyclization[5] of **8** in the presence of $K_2CO_3$–CuBr·$SMe_2$ in refluxing MeCN furnished triazene **9** in 67% yield, along with 10% recovered starting material and 6% of the arylglycine epimer of **9**. Chromatographic purification of **9** was followed by reductive removal of the triazene moiety with TFA–$Cu_2O$[10] at reflux to give the desired *COD* intermediate **10** (90% yield).

The elaboration of the *COD* building block **10** to the vancomycin bicyclic systems is shown in Scheme 2. Thus, 2,5-dimethoxybenzyl alcohol **11** was converted to boronic acid **12** by *N*-iodosuccinimide (NIS) iodination followed by reaction with BuLi and $B(OMe)_3$ in 27% overall yield (unoptimized). Suzuki coupling of iodide **10** with **12** was facilitated by $Pd(Ph_3P)_4$ catalyst and $Na_2CO_3$ to afford a 1 : 1 mixture of the two atropisomers **13a** and **13b** in 80% combined yield.[9,11] Suzuki coupling of the parent boronic acid corresponding to **12** (without the methoxy groups) with iodide **10** (Scheme 2) led to



**Scheme 1** *Reagents and conditions*: i, HBTU (1.2 equiv.), $Et_3N$ (3 equiv.), DMF 0 → 25 °C, 3 h, 90%; ii, TFA–$CH_2Cl_2$ (1 : 1), 0 °C, 1 h, 100%; iii, NBS (1.2 equiv.), DMF, 62%; iv, conc. HCl (1.2 equiv.), $NaNO_2$ (1 equiv.), 25 ml of 1 M NaOH, $K_2CO_3$ (2 equiv.), pyrrolidine (10 equiv.), 83%; v, TEMPO (1 equiv.), KBr (0.1 equiv.), NaOCl (1.3 equiv.), acetone–5% $NaHCO_3$ (1 : 1), 86%; vi, HBTU (1.2 equiv.), $Et_3N$ (3 equiv.), DMF, 0 → 25 °C, 3 h, 90%; vii, CuBr·$SMe_2$ (2.9 equiv.), $K_2CO_3$ (2.4 equiv.), pyridine, (3 equiv.), MeCN, reflux, 36 h, 67%; viii, TFA (2.2 equiv.), $Cu_2O$ (5 equiv.), MeCN–THF–$H_2O$ (1 : 1 : 0.5), reflux, 1 h, 90%




**Scheme 2** *Reagents and conditions*: i, NIS (1.2 equiv.), DMF, 25 °C, 12 h, 89%; ii, BuLi (2.1 equiv.), $B(OMe)_3$ (3 equiv.), THF, −40 → 25 °C, 3 h, dil. HCl, 30%; iii, $Pd(PPh_3)_4$ (10 mol%), $Na_2CO_3$ (1 equiv.), MeOH–toluene–$H_2O$, 90 °C, 2 h, 80%; iv, $HN_3$ (5 equiv.), DEAD (5 equiv.), $PPh_3$ (5 equiv.), THF, 0 → 25 °C, 1 h, 69%; v, LiOH (1.5 equiv.), THF–$H_2O$ (1 : 1), 0 °C, 0.5 h, 100%; vi, $C_6F_5OH$ (2 equiv.), DCC (1.2 equiv.), DMAP (0.2 equiv.), $CH_2Cl_2$, 25 °C, 1 h; vii, 4-pyrrolidinopyrridine (3 equiv.), 10% Pd/C (30 mol%), dioxane–EtOH–cyclohexene (90 : 8 : 2), high dilution, 90 °C, 5 h, 30% from **15a**

a single compound by TLC and $^1$H NMR spectroscopy, supporting the atropisomeric relationship of isomers **13a** and **13b** (no epimerization at C5 and C6). In contrast to the simpler coupling product, isomers **13a** and **13b** did not interconvert, even at 333 K. The two isomers were chromatographically separated and individually elaborated further. Thus, the more polar compound **13a** ($R_f$ = 0.20, silica, 80% EtOAc in hexanes) was treated with $HN_3$–diethyl azodicarboxylate (DEAD)–$PPh_3$[9] (**CAUTION**: hydrazoic acid is toxic and explosive!) to afford azide **14a** (69% yield) which was saponified (LiOH, THF–$H_2O$, 0 °C) and converted to the corresponding pentafluorophenyl ester **16a** *via* carboxylic acid **15a**. Slow addition of a dioxane–cyclohexene solution of crude **16a** to a mixture of 10% Pd/C and pyrrolidinopyridine in dioxane and EtOH at 90 °C led to the formation of two cyclic products, **17a** and **17a′** epimeric at C-6 (*ca.* 1 : 2 ratio) in 30% combined yield overall from acid **15a**. The less polar atropisomer **13b** ($R_f$ = 0.30, silica, 80% EtOAc in hexanes) was subjected to the same sequence of reactions, leading to **17b**‡ and **17b′** in similar yields. The observed epimerization at C-6, which is presumed to occur in the final step of the sequence, may not be an issue when the entire *AB-COD-DOE* framework of vancomycin is in place, particularly if thermodynamics favour the desired stereoisomer.

The stereochemical assignments of the four bicyclic systems **17a**, **17a′**, **17b** and **17b′** were based on $^1$H–$^1$H NOESY experiments, which revealed the NOEs for **17a** and **17b** shown in Scheme 2.

In summary, we have demonstrated the power of the Suzuki coupling reaction in the formation of the fully substituted *AB* biaryl moiety[9,11] and the beneficial effect of a preexisting *COD* ring system in a lactamization approach to the *AB* ring system of vancomycin. The asymmetric version of the Suzuki reaction and its application in an intramolecular sense may offer further opportunities in this area of synthesis.

This work was financially supported by the National Institutes of Health (USA) and the Skaggs Institute for Chemical Biology.

J. M. R. acknowledges the NIH, S. B. the NATO/DAAD, and F. R. the Alexander von Humboldt-Stiftung for post-doctoral fellowships. Dedicated to Professor Madeleine Joullié on the occasion of her 70th birthday.

## Footnotes and References

* E-mail: kcn@scripps.edu

† All new compounds exhibited satisfactory spectral and exact mass data.

‡ *Selected data* for **17b**: $R_f$ = 0.31 [silica, 5% MeOH in $CHCl_3$]; $[\alpha]_D^{25}$ −31.5 (*c* 0.20 in $CHCl_3$); $\nu_{max}$(film)/cm$^{-1}$ 2919, 2848, 1725, 1640, 1605, 1504, 1459, 1228, 1152, 1092; $\delta_H$(600 MHz, $CDCl_3$, 323 K) 2.47 (dd, *J* 12.0, 13.2, 1 H, $CH_2$), 3.47 (s, 3 H, $OCH_3$), 3.45, 3.57 (AB system, $J_{AB}$ 15.0, 2 H, $CH_2$), 3.65 (s, 3 H, $OCH_3$), 3.81 (s, 3 H, $OCH_3$), 3.72 (dd, *J* 2.7, 12.0, 1 H, $CH_2$), 3.74 (dd, *J* 5.9, 14.9, 1 H, $CH_2$), 4.16 (ddd, *J* 2.7, 11.4, 13.2, 1 H, CH), 4.2–4.3 (m, 1 H, $CH_2$), 5.04 (d, *J* 5.8, 1 H, CH), 5.12 (br d, 1 H, NH), 5.63 (br dd, 1 H, NH), 5.78 (br s, 1 H, Ar-H), 6.32 (br s, 1 H, Ar-H), 6.48 (d, *J* 2.0, 1 H, Ar-H), 6.57 (d, *J* 2.0, 1 H, Ar-H), 6.78 (d, *J* 7.2, 1 H, Ar-H), 6.94 (d, *J* 8.7 Hz, 1 H, Ar-H), 6.81 (dd, *J* 2.4, 8.1, 1 H, Ar-H), 7.03–7.05 (m, 3 H, Ar-H), 7.08 (d, *J* 8.1, 1 H, Ar-H), 7.20 (dd, *J* 2.3, 8.8, 1 H, Ar-H), 7.22 (d, *J* 6.3, 1 H, Ar-H), 7.29 (dd, *J* 2.0, 8.1, 1 H, Ar-H); $\delta_C$(150.84 MHz, $CDCl_3$, 323 K) 35.0, 43.4, 43.6, 49.2, 55.1, 56.1, 56.6, 56.8, 99.23, 108.23, 111.9, 112.4, 114.1, 116.9, 119.7, 121.1, 122.1, 123.4, 125.6, 129.1, 130.0, 130.5, 132.9, 134.4, 135.5, 136.6, 137.7, 154.1, 156.9, 158.1, 160.0, 160.9, 169.1, 170.7, 171.3; HRMS (FAB): calc. for $C_{35}H_{33}N_3O_7$ (M + $Cs^+$), 740.1373. Found, 740.1398.

1 *Glycopeptide Antibiotics*, ed. R. Nagarajan, Dekker, New York, 1994.
2 G. M. Sheldrick, P. G. Jones, O. Kennard, D. H. Williams and G. A. Smith, *Nature*, 1978, **271**, 223; P. J. Loll, A. E. Bevivino, B. D. Korty and P. H. Axelson, *J. Am. Chem. Soc.*, 1997, **119**, 1516.
3 M. H. McCormick, W. M. Stark, R. C. Pittenger and G. M. McGuire, *Antibiot. Ann.*, 1955–1956, 606.
4 D. A. Evans, J. C. Barrow, P. S. Watson, A. M. Ratz, C. J. Dinsmore, D. A. Evrard, K. M. DeVries, J. A. Ellman, S. D. Rychnovsky and J. Lacour, *J. Am. Chem. Soc.*, 1997, **119**, 3419; M. Boischoussy, L. Neuville, R. Beugelmans and J. P. Zhu, *J. Org. Chem.*, 1996, **61**, 9309; D. L. Boger, R. M. Borzilleri and S. Nukui, *J. Org. Chem.*, 1996, **61**, 3561; H. Konishi, T. Okuno, S. Nishiyama, S. Yamamura, K. Koyasu and Y. Terada, *Tetrahedron Lett.*, 1996, **37**, 8791; A. J. Pearson, G. Bignan, P. Zhang and M. Celliah, *J. Org. Chem.*, 1996, **61**, 3940; T. Inoue, T. Sasaki, H. Takayanagi, Y. Harigaya, O. Hoshino, H. Hara and T. Inaba, *J. Org. Chem.*, 1996, **61**, 3936.
5 K. C. Nicolaou, C. N. C. Boddy, S. Natarajan, T. Y. Yue, H. Li, S. Bräse and J. M. Ramanjulu, *J. Am. Chem. Soc.*, 1997, **119**, 3421.
6 For recent reviews for the synthesis of glycopeptides, see A. V. R. Rao, M. K. Gurjar, K. L. Reddy and A. S. Rao, *Chem. Rev.*, 1995, **95**, 2135; J. P. Zhu, *Synlett*, 1997, 133 and references cited therein.
7 D. A. Evans and C. J. Dinsmore, *Tetrahedron Lett.*, 1993, **34**, 6029; D. A. Evans, C. J. Dinsmore, A. M. Ratz, D. A. Evrard and J. C. Barrow, *J. Am. Chem. Soc.*, 1997, **119**, 3417.
8 K. C. Nicolaou, X.-J. Chu, J. M. Ramanjulu, S. Natarajan, S. Bräse, F. Rübsam and C. N. C. Boddy, *Angew. Chem.*, 1997, **109**, 1518; *Angew. Chem., Int. Ed. Engl.*, 1997, **36**, 1539.
9 A. G. Brown, M. J. Crimmin and P. D. Edwards, *J. Chem. Soc., Perkin Trans. 1*, 1992, 123.
10 T. Cohen, A. G. Dietz, Jr. and J. R. Miser, *J. Org. Chem.*, 1977, **42**, 2053.
11 M. K. Gurjar and N. K. Tripathy, *Tetrahedron Lett.*, 1997, **38**, 2163.

*Received in Corvallis, OR, USA, 14th July 1997; 7/05050J*

# Surface plasmon enhanced non-linear optical response of gold nanoparticles at the air/toluene interface

**Rodolphe Antoine,[a] Pierre F. Brevet,[a] Hubert H. Girault,*[a] Donald Bethell[b] and David J. Schiffrin[b]**

[a] *Laboratoire d'Electrochimie, Ecole Polytechnique Fédérale de Lausanne, CH-1015 Lausanne, Switzerland*
[b] *Department of Chemistry, The University of Liverpool, Liverpool, UK L69 3BX*

**Colloidal gold nanoparticles in toluene solution, synthesised using a two-phase liquid/liquid system, display second harmonic generation, wavelength analysis of which indicates the narrow frequency band of the gold surface plasmon for nanoparticles present at the air/toluene interface.**

There is a great deal of interest in the preparation of simple thiol derivatised gold metal clusters of nanometre dimensions[1–4] and more recently, in the synthesis of a new family of well defined compounds in which clusters of metal atoms are stabilised by groups carrying organic functionalities.[5–7] Two aspects are of current interest, the chemistry of the stabilising groups and the electronic properties of the metal core, the size of which can be altered by the preparation conditions. The control of these properties is essential for the use of these compounds in the preparation of superlattices[8] and other applications where the linking of nanoparticles can lead to complex structures with unusual electronic properties. Potential applications are in many fields such as chemical catalysis, molecular electronics or biosensors.[9] Here, we report the use of surface second harmonic generation (SSHG)[10,11] as a new technique for the characterisation of the noble-metal nanoparticles at air/liquid interfaces where the technique has been shown to be powerful, even in the non-resonant case.[12] This non-linear technique is highly sensitive to resonant plasmon excitation, which is observed for the first time for gold nanoparticles adsorbed at the air/toluene interface.

Colloidal gold nanoparticles were prepared using a two-phase (water/toluene) reduction of $AuCl_4^-$ by sodium tetrahydroborate.[13] The solution was stored in the dark at room temp. and the colloid did not show any signs of precipitation after several months. High-resolution TEM photographs of similar preparations gave an average particle diameter of 6 mm.[13] The UV–VIS absorption spectrum of the Au solution presents a strong absorption band at $\lambda_{max}$ *ca.* 530 nm. This prominent optical feature is attributed to plasmon oscillation modes of conduction electrons in the colloidal nanoparticles which are coupled to the applied electromagnetic field. Both the physical nature of this plasmon mode and its dependence on particle size and shape is well understood.[14,15]

Second harmonic generation experiments were carried out at the air/toluene interface for the gold nanoparticles in toluene. Wavelength analysis of the second harmonic response from the gold particles adsorbed at the interface was performed with a nanosecond $Nd^{3+}$–YAG system pumping an optical parametric oscillator (Spectra-Physics, GCR170-10 pumping a MOPO 710) delivering pulses in the wavelength range 800–1200 nm, at a frequency of 10 Hz and of 5 ns duration. Pulse energy was kept below 1.5 mJ to avoid surface damage. The incident beam was collimated by a telescope and directed onto the air/toluene interface. The reflected SSHG signal generated in the visible range at each exciting wavelength was collected with a lens. It was then passed through IR filters to reject residual fundamental radiation, focused onto a monochromator and detected with a gated photon counter (recording of 50 s duration). The frequency of the exciting laser was changed in steps between 800 and 1200 nm.

Fig. 1 shows the intensity of the second harmonic response as a function of the SSHG wavelength for a solution of gold nanoparticles. Toluene shows no absorbance between 800 and 1200 nm and as expected, negligible SSHG signal was observed from a pure toluene/air interface. In the presence of colloidal gold, the SSHG spectrum displays a strong resonance in the range 450–600 nm of the harmonic wavelength with a maximum of the SSHG resonance at 520 nm. The bandwidth and the maximum of the SSHG response are very similar to those observed in the absorption spectrum and hence, the SSHG spectrum clearly shows the narrow frequency band of the plasmon excitations caused by the Au nanoparticles adsorbed at the air/toluene interface. This enhancement arises from the coupling, through the surface, between the resonant local field of the incident light wave with the conduction electrons of the metal colloid.

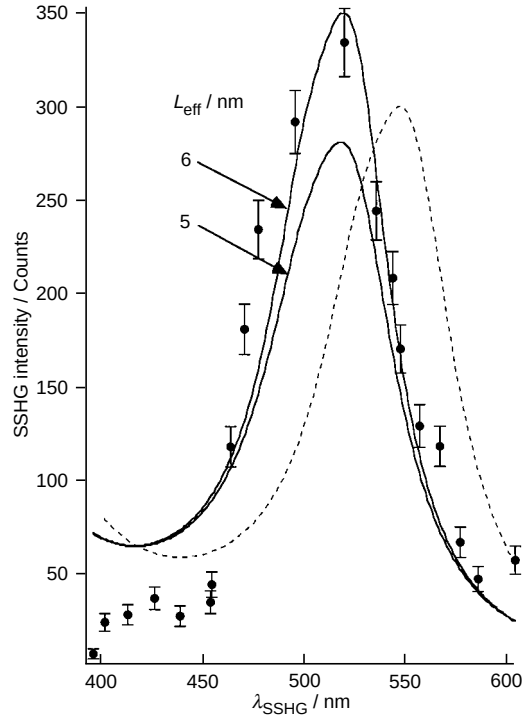



**Fig. 1** SSHG spectrum for the underivatised gold nanoparticles at the air/toluene interface (circles). The adsorption band corresponds to surface plasmon excitations and has a maximum at 520 nm. The solid line represents the calculated SSHG spectrum, using eqn. (1) (term in brackets multiplied by $\omega^2$) for gold nanoparticles in toluene taking size effects into account ($L_{eff}$ = 6 and 5 nm). The solid line is for $\lambda_p$ = 138.5 nm, corresponding to bulk gold; the dotted line is for a material with a free electron concentration 10% lower than that of bulk gold, for $\lambda_p'$ = 146 nm and $v_f'$ = 1.342 × $10^6$ m $s^{-1}$ (and $L_{eff}$ = 6 nm).

The theory of second harmonic signal generation for metal spheres in the Mie approximation has been developed by Agarwal and Jha.[16] At the plasmon resonance frequency, the term attributed to the surface non-linear polarization contribution dominates over the volume contribution, with a net enhancement compared to the non-resonant case. The output second harmonic power for spherical particles in vacuum is given by eqn. (1):[16]

$$S = \frac{3ce^2|E^{(i)}|^4}{m_e^2}\left(\frac{2R}{c}\right)^6 \omega^2 \left\{\left|\frac{1-\varepsilon(2\omega)}{[\varepsilon(\omega)+2][\varepsilon(2\omega)+2]}\right|^2 + \frac{36}{5}\left|\frac{\varepsilon(\omega)-1}{[\varepsilon(\omega)+2]^2[2\varepsilon(2\omega)+3]}\right|^2\right\} \quad (1)$$

where $E^{(i)}$ is the intensity of the electric field at the surface, $\varepsilon$ is the complex dielectric function of the particles, $\omega$ is the frequency of the exciting radiation, $2\omega$ is the second harmonic frequency, $m_e$ is the effective mass of the electron, $R$ is the particle radius, $c$ is the velocity of light and $e$ is the electronic charge. For particles in a medium of relative permittivity $\varepsilon_m$, the dielectric function to be used in eqn. (1) is the permittivity relative to that of the medium, $\varepsilon_{rel} = \varepsilon/\varepsilon_m$.

In order to show qualitatively that the SSHG signal observed does correspond to the presence of colloidal gold at the interface, the dielectric function for particles of radius $R$ was calculated following well established procedures.[17] When the interband contribution is small compared with that due to core and free electrons, the complex dielectric function is given by eqn. (2):[18]

$$\varepsilon = \varepsilon_\infty - \frac{\omega_p^2}{\omega^2 - i\omega\left(\frac{1}{\tau_{bulk}} + \frac{v_f}{L_{eff}}\right)} \quad (2)$$

where $\omega_p$ is the bulk plasma frequency, $\varepsilon_\infty$ is the dielectric contribution due to the atomic core polarizability, $\tau_{bulk}$ is the electron relaxation time in the bulk metal, $v_f$ is the electron velocity at the Fermi level and $L_{eff}$ is the effective electronic mean free path. Values of $\omega_p = 1.36 \times 10^{16}$ s$^{-1}$ ($\lambda_p = 138.5$ mm), $v_f = 1.4 \times 10^6$ m s$^{-1}$ and $\tau_{bulk} = 9.1 \times 10^{-15}$ s were used in the calculations,[18] $\varepsilon_m$ for pure toluene was taken as 2.23. The dielectric function of gold employed was calculated from eqn. (2) taking a value of $\varepsilon_\infty$ of 9.9 based on the data from Innes and Sambles.[18] The data from Johnston and Christy[19] leads to a value of 12.0. However, the differences between these and other values in the literature for the dielectric function of Au are due to the nature of the thin films used in the measurements, since other effects related to film thickness, crystallographic orientation and imperfections come into operation. Different values of $\varepsilon_\infty$ lead to a shift in the position of the maximum in the SSHG signal but do not alter the features of the calculated wavelength dependence. The calculated second harmonic intensity functions, using eqn. (1) (term in brackets multiplied by $\omega^2$), for gold nanoparticles in toluene, with 6 and 5 nm of effective electronic mean free path, are presented in Fig. 1. The agreement between experimental data and calculation for $L_{eff} = 6$ nm is very good. Fig. 1 also shows the effect of a decrease of 10% in the concentration of free electrons, highlighting the sensitivity of the technique to the electronic properties of the nanoparticles. For the calculation, we only consider that the change of the free electron density alters the bulk plasma frequency and the Fermi velocity ($\omega_p' = 1.29 \times 10^{16}$ s$^{-1}$, $v_f' = 1.342 \times 10^6$ m s$^{-1}$).[20] Changing the free electron density may probably affect $\varepsilon_\infty$ and $\tau_{bulk}$, but since there is no straightforward relation with the free electron density, we use the same value already mentioned (*i.e.* $\varepsilon_\infty = 9.9$ and $\tau_{bulk} = 9.1 \times 10^{-15}$ s). Although the sample is not monodisperse, from the point of view of a preliminary analysis of the experimental observations, the results shown in Fig. 1 represent a strong confirmation of the non-linear optical properties of Au nanoparticles present at the air/toluene interface.

To our knowledge, this is the first example of a SSHG resonance observed for solutions of nanosized metal particles. Previous SSHG work on colloidal metal particles was carried out by Efrima and coworkers.[21] In this work silver metal liquid-like films were formed at the interface of immiscible liquids from large individual colloidal silver particles stabilised by detergents and shown to exhibit second harmonic signals. Gold nanoparticles are easily derivatised with functional ligands for the subsequent attachment of chromophores, redox labels or biomolecules.[5,6] The optical SSHG technique described is a powerful method to investigate specific interfacial adsorption, and the electronic properties of chemically functionalised metal nanoclusters. The latter is of importance owing to the rapid advances in synthetic nanoparticles chemistry.[6]

This work is supported by the European Community Training and Mobility of Researchers Programme (TMR) through the Network on Organization, Dynamics and Reactivity at Electrified Liquid–Liquid Interface (ODRELLI), European Community Contract No. FRMX-CT96-0078. Useful comments by Dr Jha, Tata Institute of Fundamental Research, Mumbai, India, on the second harmonic response from small metal particles, are gratefully acknowledged.

## Footnote and References

* E-mail: antoine@igcsun3.epfl.ch

1 M. Brust, M. Walker, D. Bethell, D. J. Schiffrin and R. Whyman, *J. Chem. Soc., Chem. Commun.*, 1994, 801.
2 R. H. Terrill, T. A. Postlethwaite, C. H. Chen, C. D. Poon, A. Terzis, A. Chen, J. E. Hutchison, M. R. Clark, G. Wignall, J. D. Londono, R. Superfine, M. Falvo, C. S. Johnson, E. T. Samulski and R. W. Murray, *J. Am. Chem. Soc.*, 1995, **117**, 12 537.
3 A. Badia, L. Cuccia, L. Demers, F. Morin and R. B. Lennox, *J. Am. Chem. Soc.*, 1997, **119**, 2682.
4 D. V. Leff, L. Brandt and J. R. Heath, *Langmuir*, 1996, **12**, 4723.
5 M. Brust, J. Fink, D. Bethell, D. J. Schiffrin and C. Kiely, *J. Chem. Soc., Chem. Commun.*, 1995, 1655.
6 M. J. Hostetler, S. J. Green, J. J. Stokes and R. W. Murray, *J. Am. Chem. Soc.*, 1996, **118**, 4212.
7 S. R. Johnson, S. D. Evans, S. W. Mahonand and A. Ulman, *Langmuir*, 1997, **13**, 51.
8 R. L. Whetten, J. T. Khoury, M. M. Alvarez, S. Murthy, I. Vezmar, Z. L. Wang, P. W. Stephens, C. L. Cleveland, W. D. Luedtke and U. Landman, *Adv. Mater.*, 1996, **8**, 428.
9 M. Brust, D. Bethell, D. J. Schiffrin and C. Kiely, *Adv. Mater.*, 1995, **7**, 795.
10 Y. R. Shen, *The Principles of Nonlinear Optics*, Wiley, New York, 1984.
11 P. F. Brevet, *Surface Second Harmonic Generation*, Presses Polytechniques et Universitaires Romandes, Lausanne, 1997.
12 A. A. Tamburello-Luca, Ph. Hébert, P. F. Brevet and H. H. Girault, *J. Chem. Soc., Faraday Trans.*, 1995, **91**, 1763.
13 D. Bethell, M. Brust, D. J. Schiffrin and C. Kiely, *J. Electroanal. Chem.*, 1996, **409**, 137.
14 C. F. Bohren and D. R. Huffman, *Absorption and Scattering of Light by Small Particles*, Wiley, New York, 1983.
15 U. Kreibig and L. Genzel, *Surf. Sci.*, 1985, **156**, 678.
16 G. S. Agarwal and S. S. Jha, *Solid State Commun.*, 1982, **41**, 499.
17 P. Mulvaney, *Langmuir*, 1996, **12**, 788.
18 R. A. Innes and J. R. Sambles, *J. Phys. F*, 1987, **17**, 277.
19 P. B. Johnston and R. W. Christy, *Phys. Rev. B*, 1972, **8**, 4370.
20 N. W. Aschcroft and N. D. Mermin, *Solid State Physics*, Holt-Saunders International Editions, New York, 1976.
21 R. Bavli, D. Yogev, S. Efrima and G. Berkovic, *J. Phys. Chem.*, 1992, **95**, 7422.

*Received in Exeter, UK, 8th July 1997; 7/04846G*

# Hydrogen atoms location in $[Re_4(\mu_3\text{-}H)_4(CO)_{12}]$ by joint X-ray single-crystal and neutron powder diffraction analysis

**Norberto Masciocchi,[a] Giuseppe D'Alfonso,[b] Winfried Kockelmann,[c] Wolfgang Schäfer[c] and Angelo Sironi*[a]**

[a] *Dipartimento di Chimica Strutturale e Stereochimica Inorganica, Università di Milano, via Venezian 21, 20133 Milano, Italy*
[b] *Dipartimento di Chimica Inorganica, Metallorganica ed Analitica, Università di Milano, via Venezian 21, 20133 Milano, Italy*
[c] *Mineralogisch-Petrologisches Institut der Universität Bonn, Außenstelle für Neutronenbeugung im Forschungszentrum Jülich, 52425 Jülich, Germany and ISIS Facility, Rutherford Appleton Laboratory, Chilton, Didcot, Oxfordshire, UK OX11 0QX*

**The hydrogen atom locations in $[Re_4(\mu_3\text{-}H)_4(CO)_{12}]$ are accurately determined by joint X-ray single-crystal and time-of-flight neutron powder diffraction analysis; this new methodology does not require large crystals of several mm dimensions but only a sizeable amount of monophasic microcrystalline sample.**

A number of different methodologies are available to solve structural problems, whatever the aggregation state of the sample.[1] Surely single-crystal (SC) X-ray (X) diffraction is the easiest, quickest and most definitive method. However, when (*i*) suitable crystals are unavailable or (*ii*) the relative atomic scattering powers in the sample are too different (hampering, for instance, the location of hydrogens in the presence of heavy atoms) or (*iii*) too similar (inhibiting the distinction of neighbouring elements), the power of XSC weakens and other techniques are better suited. While it has been known for a long time that neutron (N) diffraction on relatively large SCs offers an elegant, although expensive, solution to point (*ii*), only recently powder (P) diffraction has been shown to overcome point (*i*) (at least for moderately complex structures).[2] As large SCs needed for neutron diffraction are often not available, we propose, to tackle point (*ii*) [and (*iii*)], a joint XSC, NP approach which relies, for the burden of the structure determination, on XSC data, while subtle structural details are essentially rescued from NP measurements, the final model being validated by simultaneous refinements on both data sets. A similar approach has been used in studying the cation distribution in doped $KTiOPO_4$[3] and the incommensurately modulated structure of $Bi_2Sr_2CaCu_2O_{8+y}$.[4]

The combined use of different radiations as well as of different spectroscopic and computational methods, under the assumption that 'different' biases may cancel out, likely affords results of higher quality than those obtainable from the individual techniques, allowing to refine more complex structures. This approach has been pioneered, within the crystallographic community, by the combined use of X–N data (from either two SC datasets[5] or two P diffraction experiments[6]), by the introduction of steric energy contributions into protein structure refinements[7] or, more frequently, by the sagacious use of stereochemical knowledge (by imposing geometrical restraints) in complex refinements. Combined EXAFS and powder diffraction analyses have been recently reported.[8] The proposed methodology differs from other more conventional complementary X–N studies, in which juxtaposition of individual results leads to a unitary interpretation; moreover, even if it can be exemplified on a high symmetry crystal phase, it may not necessarily require simple systems (like other powder diffraction methods), since XSC data should grant superior convergence properties to the joint least-squares refinement.

Despite the relevance of transition-metal hydrides in modern inorganic chemistry, the ubiquitous hydrido ligand is still the most poorly structurally characterised. Even if its coordination behaviour and/or classical/non-classical nature can be qualitatively retrieved from a number of experimental techniques (X-ray diffraction, IR, NMR, inelastic neutron scattering), the only definitive technique is neutron diffraction. Compounds containing face-bridging ($\mu_3$) hydrides are much less common than those with edge-bridging ($\mu$) or terminal hydrides, with only five NSC crystal structures reported in the literature, $[FeHCo_3(CO)_9\{P(OMe)_3\}_3]$,[9] $[Ni_4H_3(C_5H_5)_4]$,[10] $[Rh_4H_4(C_5Me_5)_4][BF_4]_2$,[11] $[HCu\{P(p\text{-}C_6H_4Me)_3\}]_6$[12] and $[Cr_4(\mu\text{-}H)_5(\mu_3\text{-}H)_2(C_5R_5)_4]$,[13] none of them regarding third-row transition elements. $[Re_4(\mu_3\text{-}H)_4(CO)_{12}]$ **1** is unusual among metal cluster compounds, being one of the few known 'unsaturated' carbonyl clusters (56 *vs.* 60 CVEs); its XSC structure has been previously reported and the $\mu_3$-H character inferred from local stereochemical considerations and an 'image enhanced' (*i.e.* symmetry averaged) difference Fourier map (estimated average Re–H 1.77 Å).[14] Here we present the complete structural characterisation, from XSC and TOF NP diffraction data,† of the new $\mathbf{1}\cdot 2C_6D_6$ crystal phase which is the major product of the standard synthetic approach to **1**,‡ but has never been recognized before. The availability of sizeable amounts of this phase (but not of large SC) and our experience with XP on coordination and organometallic systems[15] prompted us to attempt the viability of the above mentioned method.

TOF neutron scattering measurements (Fig. 1) easily afford powder patterns with good counting statistics (if compared to the constant wavelength mode); however, their analysis in conjunction with conventional laboratory X-ray diffraction data needs some extra care. Since the very same structural model (coordinates and $U_{ij}$ values) is being refined simultaneously on X and N diffraction data, but there are intrinsic differences in physical interactions, size of the samples and experimental geometries, one must ensure that systematic errors have been properly corrected. In particular, since absorption effects may lead to fake, incongruent thermal parameters, a $\theta$-dependent

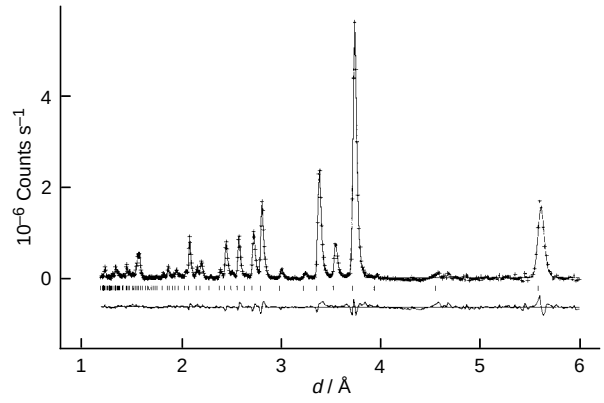



**Fig. 1** Final Rietveld refinement plot for TOF neutron data, in the range 1.2 < $d$ < 6.0 Å. Peak markers and difference plot at the bottom. For sake of clarity, the high $d$-values section (6.0 < $d$ < 9.0 Å, with only two reflections) has been omitted from the plot.

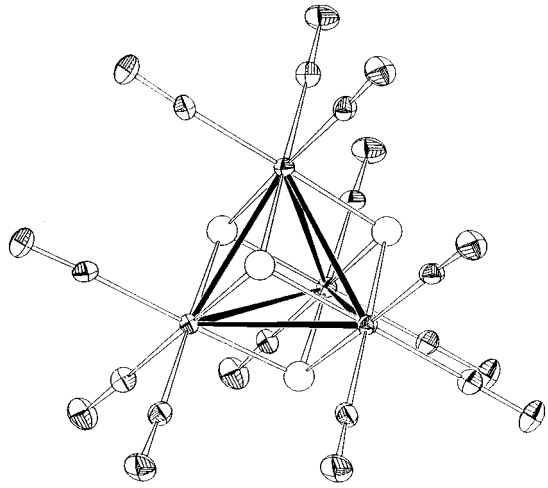


**Fig. 2** An ORTEP drawing of the $[Re_4H_4(CO)_{12}]$ molecule, showing the $H_n$ atom position at 1.99(2) Å from the rhenium atoms. Selected bond distances (Å) and angles (°): Re–Re 2.924(2), Re–C 1.912(8), C–O 1.14(1), Re–$H_x$ 1.88(12), Re–$H_n$ 1.99(2); Re–C–O 178(1), C–Re–C 86.9(4), $H_n$–Re–$H_n$ 85.(1), C–Re–$H_n$ 93.8(6) and 179.0(9), Re–$H_n$–Re 94.(1), Re–Re–C 92.2(3) and 136.5(2).

(spherical—on top of $\psi$-scans, XSC) and a *d*-dependent (NP) corrections have been carefully applied. In addition, in order to deal with the different interactions of X and N beams (with electrons and nuclei, respectively) and the off-centre polarisation of H-valence electron(s) due to the metal–H bond(s), a split-atom H refinement has been performed, defining two pseudoelements [$H_x$ and $H_n$] with null contribution to the N and X structure factors, respectively. This makes, *inter alia*, the $H_n$ location substantially insensitive to the intrinsic 'overweightness' of the X data set (in terms of quality and, perhaps, number of observations).

Our results show that $[Re_4(\mu_3\text{-}H)_4(CO)_{12}]$ in **1**·$2C_6D_6$ has a crystallographically imposed $T_d$ symmetry (see Fig. 2), with a $Re_4(CO)_{12}$ core virtually identical to that found in **1**, and confirm the $\mu_3$-nature of the hydrido ligands as originally proposed by Wilson and Bau;[14] however, significant differences are observed in the H-bonding parameters [Re–$H_x$ 1.88(12) *vs.* 1.77 Å, Re–$H_n$ 1.993(17) Å]. As for the precision of our results, our study shows that the (room temp.) esd values related to the $H_n$ atoms are about three to five times poorer than those from conventional NSC data (mostly collected at temperatures below 90 K), but one order of magnitude smaller than those concerning $H_x$. Unfortunately, in assessing the accuracy of this work we lack the internal consistency check with the C–D distance because the clathrated $C_6D_6$ molecules are rotationally disordered; however, since the observed $\Delta$(Re–$H_x$, Re–$H_n$) value (0.11 Å) is within the range found in most structural comparisons between X- and N-SC results, we think that the actual Re–$H_n$ bond distance should not be affected by severe systematic errors. The observed M–H value might look slightly longer than that in $[Rh_4H_4(C_5Me_5)_4][BF_4]_2$[11] (58 CVEs, av. Rh–H and Rh–Rh 1.86 and 2.76 Å, respectively); however, a much larger apparent metal radius [Re–Re 2.924(2) Å] partially accounts for the observed difference.

## Footnotes and References

* E-mail: angelo@csmtbo.mi.cnr.it

† *Crystal data* for **1**·$2C_6H_6$: $C_{24}H_{16}O_{12}Re_4$, $M$ = 1241.2, cubic, *Pn*-3*m*, $a$ = 11.1774(5) Å, $U$ = 1396.4(1) Å$^3$, $Z$ = 2, $D_c$ = 2.951 g cm$^{-3}$. XSC data were collected on a 0.15 × 0.15 × 0.15 mm crystal with Mo-Kα radiation on an Enraf-Nonius CAD4 diffractometer ($6 < 2\theta < 54°$); 316 unique data [230 with $F_o^2 > 3\sigma(F_o^2)$], corrected for Lorentz, polarisation and absorption effects ($\psi$-scan + spherical corrections, $\mu R$ = 2.0, min. max. transmission factors = 0.061, 0.093); NPD data ($1.0 < d < 10$ Å) were collected on the TOF neutron diffractometer ROTAX at the spallation source ISIS at the RAL (UK). 600 mg of finely ground sample, containing 100% perdeuteriated benzene (as checked by $^1$H NMR of dissolved material), were enclosed in a vanadium can with a drop of $C_6D_6$ (to ensure crystal stability) under an $N_2$ atmosphere. Structure solution was performed by Patterson, difference Fourier and least-squares techniques using the XSC dataset. The combined use of X-ray and neutron data and the Fourier routines for powder diffraction data implemented in GSAS[16] allowed unambiguous location of the hydrogen atom of the organometallic cluster and of the deuterium atom bound to the benzene molecules clathrated in the crystal lattice. Fig. 1 shows the final Rietveld refinement plot for TOF data; final agreement factors: (XSC) $R_w(F^2)$ 0.048; $R(F^2)$ 0.042; $R(F)$ 0.023; (NP) $R_{wp}$ 0.040, $R_p$ 0.028. The $C_6D_6$ molecule was found to be disordered in two in-plane orientations [30° off, with refined populations of 0.65(2) : 0.35(2)]; its refinement required the use of geometrical restraints, making any internal accuracy assessment on the C–D distance meaningless. CCDC 182/584.

‡ $[Re_4H_4(CO)_{12}]$ was prepared by hydrogenation of $[Re_2(CO)_{10}]$ (1.214 g) at 165 °C in decalin and isolated as a deep red solid by addition of benzene to the solution, according to a literature method.[17] In the original paper, the presence of solvated decalin was reported, while the solid we have obtained in this way contained benzene (as indicated by $^1$H NMR and X-ray analyses). Four cycles of dissolution in $CH_2Cl_2$ and evaporation to dryness enabled complete elimination of benzene. $[Re_4H_4(CO)_{12}]\cdot 2C_6D_6$ (615 mg) was obtained by slow precipitation with $C_6D_6$ (3 ml) from a $CH_2Cl_2$ solution (150 ml).


1 E. A. V. Ebsworth, D. W. H. Rankin and S. Cradock, *Structural Methods in Inorganic Chemistry*, Blackwell Scientific Publications, Oxford, 1987.
2 For recent review papers, see: K. D. Harris and M. Tremayne, *Chem. Mater.*, 1996, **8**, 2554; N. Masciocchi and A. Sironi, *J. Chem. Soc., Dalton Trans.*, 1997, in press.
3 S. J. Crenell, J. J. Owen, C. P. Grey, A. K. Cheetham, J. A. Kaduk and R. H. Jarman, *J. Mater. Chem.*, 1991, **1**, 113.
4 Y. Gao, P. Coppens, D. E. Cox and A. R. Moodenbaugh, *Acta Crystallogr., Sect. A*, 1993, **49**, 141.
5 F. A. Cotton, L. F. Chen and A. J. Schultz, *C. R. Acad. Sci., Ser. II*, 1996, **323**, 539; A. G. Orpen, A. V. Rivera, E. G. Bryan, D. Pippard, G. M. Sheldrick and K. D. Rouse, *J. Chem. Soc., Chem. Commun*., 1978, 723.
6 R. E. Morris, W. T. A. Harrison, J. M. Nicol, A. P. Wilkinson and A. K. Cheetham, *Nature*, 1992, **359**, 519.
7 A. Jack and M. Levitt, *Acta Crystallogr., Sect. A*, 1978, **34**, 931.
8 N. Binsted, M. T. Weller and J. Evans, *Physica B*, 1995, **208**/**209**, 129; N. Binsted, M. J. Pack, M. T. Weller and J. Evans, *J. Am. Chem. Soc.*, 1996, **118**, 10200.
9 R. G. Teller, D. D. Wilson, R. K. McMullan, T. F. Koetzle and R. Bau, *J. Am. Chem. Soc.*, 1978, **100**, 3071.
10 T. F. Koetzle, J. Muller, D. L. Tripton, D. W. Hart and R. Bau, *J. Am. Chem. Soc.*, 1979, **101**, 5631.
11 J. S. Ricci, T. F. Koetzle, R. J. Goodfellow, P. Espinet and P. M. Maitlis, *Inorg. Chem.*, 1984, **23**, 1828.
12 R. C. Stevens, M. R. McLean, R. Bau and T. F. Koetzle, *J. Am. Chem. Soc.*, 1989, **111**, 3472.
13 R. A. Heintz, T. F. Koetzle, R. L. Ostrander, A. L. Rheingold, K. H. Theopold and P. Wu, *Nature*, 1995, **378**, 359.
14 R. D. Wilson and R. Bau, *J. Am. Chem. Soc.*, 1976, **98**, 4687.
15 N. Masciocchi, M. Moret, P. Cairati, A. Sironi, G. A. Ardizzoia and G. La Monica, *J. Am. Chem. Soc.*, 1994, **116**, 7768; N. Masciocchi, G. A. Ardizzoia, G. La Monica, M. Moret and A. Sironi, *Inorg. Chem.*, 1997, **36**, 449; N. Masciocchi, P. Cairati, F. Ragaini and A. Sironi, *Organometallics*, 1993, **12**, 4499; N. Masciocchi, M. Moret, P. Cairati, F. Ragaini and A. Sironi, *J. Chem. Soc., Dalton Trans.*, 1993, 471.
16 A. C. Larson and R. B. Von Dreele, LANSCE, MS-H805, Los Alamos Laboratory, Los Alamos, NM, 1994.
17 J. R. Johnson and H. D. Kaesz, *Inorg. Synth.*, 1978, **18**, 60.


*Received in Cambridge, UK, 21st July 1997; 7/05240E*

# EXAFS analysis of a chiral alkene polymerisation catalyst incorporated in the mesoporous silicate MCM-41

**Stephen O'Brien,[a] Jonathan Tudor,[a] Thomas Maschmeyer[b] and Dermot O'Hare*†**

[a] *Inorganic Chemistry Laboratory, University of Oxford, South Parks Road, Oxford, UK OX1 3QR*
[b] *The University Chemical Laboratories, University of Cambridge, Lensfield Road, Cambridge, UK CP2 1EW*

**The chiral metallocene *rac*-ethylenebis(1-indenyl)zirconium dichloride, when immobilised on the surface of methylalumoxane-modified mesoporous silica MCM-41, is an effective catalyst for the production of highly isotactic polypropene with a unique spherulite morphology; Zr K-edge EXAFS studies of the organometallic–inorganic composite reveal not only an intact indenyl ligand framework after the immobilisation, but also the presence of a short Zr–C bond and the absence of the chloride ligands.**

We have recently reported that the modification of the mesoporous silicate MCM-41 with an excess of methylalumoxane (MAO) effectively removes the protic sites on the surface silanol groups, yielding a high surface area material (although the surface area is reduced from on average 900 to 400 $m^2\ g^{-1}$).[1] Subsequent treatment with saturated solutions of (EBI)$ZrCl_2$ [EBI = *rac*-ethylenebis(1-indenyl)zirconium dichloride] in toluene produces a hybrid organometallic–inorganic composite material in which the organometallic moiety has been grafted onto the surface of the MCM-41. This hybrid organometallic–inorganic material is active in the stereoselective polymerisation of propylene to yield highly isotactic polypropylene. The as produced polymer exhibits a higher melting point and has a distinct spherulite morphology atypical of polymers produced from an analogous homogeneous system. We suggest that the heterogeneous catalyst is effective due to the adsorptive capacity of the mesoporous silica support, and whilst not being homogeneous in nature, it allows a great deal of contact between the catalytic centres and propene. We believe that the spherulite polymer morphology is formed as a result of the channels inherent to MCM-41, as it has been observed that a similar catalyst on ordinary amorphous silica does not produce the same morphology. X-Ray powder diffraction indicates that the hexagonal framework of the mesoporous material is retained after reaction with both MAO and the organometallic catalyst precursor, but provides no information regarding the nature of the local atomic environment of the organometallic metal centre. We have recently used EXAFS to verify the status of organometallic molecules successfully grafted onto the walls of MCM-41,[2] and one of us (T. M.) used both XANES (X-ray absorption near edge structure) and EXAFS to determine the local structure around titanium centres incorporated into MCM-41.[3]

In order to study the local coordination around the zirconium catalyst, X-ray absorption spectroscopy was used to measure the Zr K-edge EXAFS. Data was collected on Station 9.2 at the SRS, Daresbury Laboratory, UK.‡ Data analysis of the EXAFS was performed using the XFIT(WIN95) suite of programs[5] employing both single and multiple scattering techniques.

The observed EXAFS data and the corresponding Fourier transform, together with the calculated fits are shown in Fig. 1. The EXAFS structural model parameters resulting from multiple scattering treatments are shown in Table 1. Initially, a broad range of model structures was examined, however, when varying atom types and refining structural parameters using single scattering techniques a clear trend became apparent, pointing towards retention of both indenyl ligands and an absence of the chloride ligands. The single scattering calculations, although providing sensible model parameters, were unable to account for some contributions in the Fourier transform at $R > 2.5$ Å (not phase shift corrected). These might be due to multiple scattering effects. Multiple scattering paths involving the $C_5$ 'cyclopentadienyl' fragment of the indenyl rings correspond to a distance comparable to that of the outer ligand framework, and when this is incorporated into the refinement the second envelope might be modelled more fully. Hence, by using a three-dimensional model based on the simplified crystal structure of the starting material it was possible to obtain very good agreement between theory and experiment.

The first shell of the final model corresponds to radius of 2.12 Å which is a short distance for a Zr–$CH_3$ bond. There are crystal structures for a cationic zirconocene derivative based upon the EBI ligand, in which the Zr–C bond length was found to be 2.18

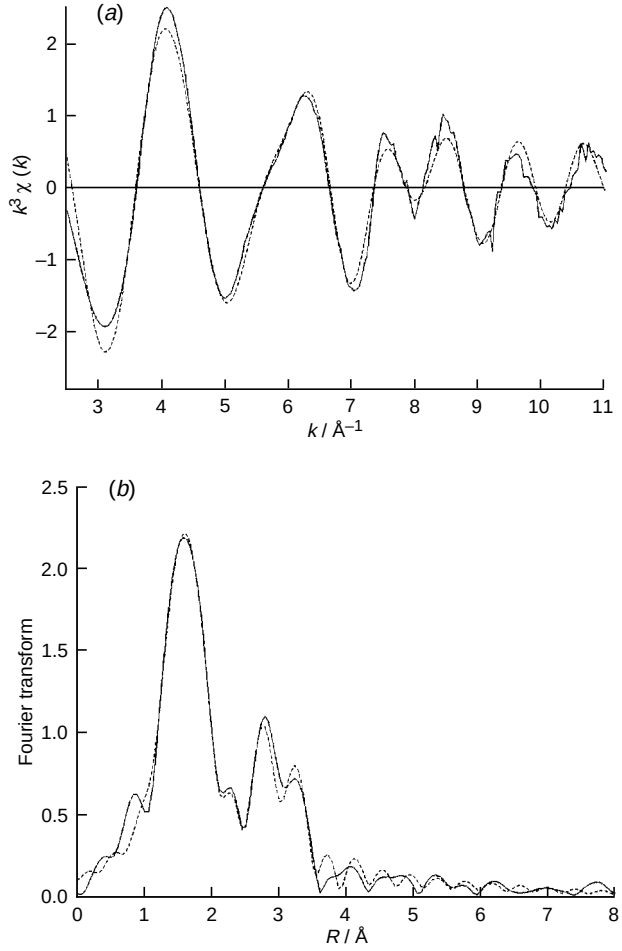



**Fig. 1** (*a*) Zr K-edge $k^3$ weighted EXAFS and (*b*) Fourier transform data for the (EBI)$ZrCl_2$/MAO/MCM-41 material [(—) experimental and (---) theoretical]

**Table 1** Structural parameters of multiple scattering model for Zr K-edge EXAFS of (EBI)$ZrCl_2$/MAO/MCM41[a]

| Shell | Scattering atom | *N* | *r*/Å | $\sigma^2$/Å$^2$ | Assignment |
|---|---|---|---|---|---|
| 1 | C | 1.3 | 2.12 | 0.008 | methyl C |
| 2 | C | 5.1[b] | 2.60 | 0.008 | $C_5$ indenyl C |
| 3 | C | 5.1[b] | 2.78 | 0.007 | $C_5$ indenyl C |
| 4 | C | 1.8 | 3.32 | 0.010 | methylene bridge |
| 5 | C | 3.6 | 3.47 | 0.011 | $C_6$ indenyl C |
| 6 | C | 2.5 | 4.24 | 0.012 | $C_6$ indenyl C |

*N* = coordination number, *r* = interatomic distance, $\sigma^2$ = root mean-square deviation of the interatomic distance about *r*. [b] Restrained to keep rings co-planar and equal number of atoms.

Å.[6] The EXAFS data does not show any evidence for a Zr–Cl bond, or the presence of a Cl scatterer beyond normal bond lengths. The chloride anion need not necessarily reside in close proximity to the central Zr atom; if the Zr species becomes highly polarised or cationic in nature, then the associated chloride anion can be dissipated in the MAO oligomeric cage away from the metal centre. The second and third shells have been assigned to the carbon atoms of the two $C_5$ rings of the bridging indenyl ligand, and correspond to average bond lengths for similar Zr–C bonds in *rac*-(EBI)$ZrCl_2$. It should be noted that the two $C_5$ rings were modelled with two slightly different distances (*i.e.* 2.60 and 2.78 Å), indicating that the rings may be tilted. The fourth shell at 3.32 Å contains contributions from C atoms from both the $C_6$ rings of the indenyl system and the ethylene bridge. The fifth (3.47 Å) and sixth (4.24 Å) shells are due to the remaining C atoms on the $C_6$ rings of the indenyl system.

Our assignments for each shell are based upon the known crystallographic information for *rac*-(EBI)$ZrCl_2$,[7] and are consistent with the previously proposed general mechanism for the interaction of MAO with group 4 metallocene dichlorides, which assumes the metal chloride bonds are first methylated, and a cationic monoalkylated species is formed as the active catalyst.[8,9] The preservation of the ligand framework is also supported in the literature.[10] Based upon this model of a highly electropositive zirconium centre, one could anticipate a shorter Zr–$CH_3$ distance for the species bound to the mesopore.

In conclusion, X-ray absorption spectroscopy has proved to be a powerful technique in the structural characterisation of *rac*-(EBI)$ZrCl_2$ bound to the surface of MAO modified MCM-41. The ability to use three-dimensional models as inputs for the multiple scattering calculations in XFIT(WIN95) has been essential in deriving a good fit between theory and experiment. EXAFS data analysis of the hybrid organometallic–inorganic material indicates that the carbon framework has remained essentially intact around the central Zr. The Fourier transform also reveals a short Zr–C bond, indicative of the increased charge at the metal centre as a result of the interaction between the metal chloride and the MAO-MCM-41 support.

We would like to thank J. F. W. Mosselmans and G. E. Van Dorssen (Daresbury Laboratory) for discussions and advice, and Shell UK for financial support.

## Footnotes and References

* E-mail: dermot.ohare@icl.ox.ac.uk
† D. O'Hare is the Royal Society of Chemistry Sir Edward Frankland Fellow.
‡ K-edge transmission EXAFS of the Zr compound were performed at room temp. on Station 9.2 at the CLRC Radiation Source, Daresbury, operating in multi-bunch mode, 2 GeV, with typical currents of 180–250 mA. A double crystal monochromator in non-dispersive configuration equipped with flat (220) Si crystals was used. Calibration was done on Zr foil of 50 μm thickness. Samples of *rac*-(EBI)$ZrCl_2$/MAO/MCM-41 were diluted in dry MgO (5 : 1), compressed into a pellet of minimal thickness (*ca.* 1 mm) and then sealed in an inert polyimide wallet under $N_2$.

1 J. Tudor and D. O'Hare, *Chem. Commun.*, 1996, 603.
2 S. O'Brien, J. Tudor, S. Barlow, M. J. Drewitt, S. J. Heyes and D. O'Hare, *Chem. Commun.*, 1997, 641.
3 T. Maschmeyer, F. Rey, G. Sankar and J. M. Thomas, *Nature*, 1995, **378**, 159.
4 N. Binstead, J. W. Cambell, S. J. Gurman and P. Stephenson, EXCURV92-Program, SERC Daresbury Labs., 1992.
5 P. J. Ellis and H. C. Freeman, *J. Synchrotron Rad.*, 1995, **2**, 190; Australian Synchrotron Research Program Inc., c/- ANSTO, Private Mail Bag 1, Menai, NSW, 2234, Australia.
6 A. D. Horton and A. G. Orpen, *Organometallics*, 1991, **10**, 3910.
7 F. Piemontesi, I. Camurati, L. Resconi, D. Balboni, A. Sironi, M. Moret, R. Zeigler and N. Piccolrovazzi, *Organometallics*, 1995, **14**, 1256.
8 D. Cam and U. Giannini, *Makromol. Chem.*, 1992, **193**, 1049.
9 W. Kaminsky and R. Steiger, *Polyhedron*, 1988, **7**, 2375.
10 P. G. Gassman and M. R. Callstrom, *J. Am. Chem. Soc.*, 1987, **109**, 7875.

*Received in Cambridge, UK, 26th June 1997; 7/04499B*

# Addition of alcohols and pyrroles to *trans*-$[RuCl_2\{(Ph_2P)_2C{=}CH_2\}_2]$. A polypyrrole bearing a covalently bound metal–diphosphine complex†

**Simon J. Higgins,* Heather L. Jones, Mark K. McCart and Thomas J. Pounds**

*Department of Chemistry, University of Liverpool, Chemistry Buildings, Crown Street, Liverpool, UK L69 7ZD*

**Alcohols and pyrroles undergo base-catalysed addition to *trans*-$[RuCl_2\{(Ph_2P)_2C{=}CH_2\}_2]$ to afford *trans*-$[RuCl_2\{(Ph_2P)_2CHCH_2Z\}_2]$ (Z = $-OCH_2Ph$ 2a, $-OCH_2CH_2C_4H_3S$-3 2b, $-NC_4H_4$ 3a, $-NC_4H_3C_6H_{13}$-3 3b); complexes 2b and 3b are suitable for electropolymerization to give heterocyclic conducting polymers, and 3b is copolymerized with *N*-methylpyrrole to afford a polypyrrole incorporating a functionalized metal–diphosphine complex, for the first time.**

There is much interest in electrodes modified with polymers containing redox-active metal complexes, since these have potential applications in sensing, in electrocatalysis and in electrochromic displays.[1,2] The electrochemical polymerization of complexes bearing pendant *N*-pyrroles, by oxidation of the pyrrole moieties, is often employed to prepare such modified electrodes.[3,4] The complexes used have normally been classical redox-active and potentially electrocatalytic species, for example porphyrins[4] or complexes of 2,2′-bipyridine (bpy) derivatives;[1,5] the latter have the advantage that the synthesis of pyrrole-functionalized derivatives is straightforward. In spite of the interest in fixing them to surfaces for catalysis, metal–phosphine complexes (apart from a few examples with bpy derivatives as coligands[5]) have not so far been incorporated into conducting polymers, and have rarely been investigated for electrode modification.[6]

Although the synthesis of chelating phosphine ligands bearing pendant heterocycles, suitable for electropolymerization, might be expected to be problematic, nucleophilic addition to coordinated dppen [dppen = $(Ph_2P)_2C{=}CH_2$] offers a route to functionalized diphosphine complexes in one step and in high yield.[7,8] We have shown that prolonged treatment of *trans*-$[RuCl_2(dppen)_2]$ **1** with a large excess of $RNH_2$ affords functionalized, redox-active diphosphine complexes *trans*-$[RuCl_2\{(Ph_2P)_2CHCH_2NHR\}_2]$, and that one example {R = $-(CH_2)_3Si[OEt]_3$} could be used to modify oxide surfaces with a ruthenium(II)–diphosphine complex monolayer.[6] Amine addition is inappropriate for the preparation of derivatives bearing pendant thiophenes or pyrroles for oxidative electropolymerization; the linkage between the heterocycle and metal centre must be non-basic.[9] Although the reactivity of **1** towards nucleophiles is limited compared with platinum(II) and palladium(II) complexes of dppen,[10] we were gratified to find that treatment of **1** in $CH_2Cl_2$ with a large (≥ 10-fold) excess of a primary alcohol, in the presence of catalytic amounts of $KOBu^t$ and 18-crown-6, generated the hoped-for adducts $[RuCl_2\{(Ph_2P)_2CHCH_2Z\}_2]$ (Z = $-OCH_2Ph$ **2**, $-OCH_2CH_2C_4H_3S$-3 **2b**) in acceptable yield.‡ These were characterized by $^{31}P\{^1H\}$ and $^1H$ NMR spectroscopy, microanalytical data and FAB mass spectrometry.§ Their spectroscopic properties are similar to those of the primary amine adducts described earlier.[6,10] The addition of other primary alcohols (EtOH, $n$-$C_6H_{13}OH$) to **1** also proceeds in solution, as monitored by $^{31}P\{^1H\}$ NMR spectroscopy, but we did not isolate the products. The adduct **2b** has been the subject of an X-ray crystal structure determination; details will be reported later. Complex **2b** is in principle suitable for incorporation, by electropolymerization, into polythiophenes.

Pyrrole NH groups have p$K_a$s similar to alcohol OH groups.[11] Earlier, we found that the very reactive complex $[Pd(OAc)_2(dppen)]$ reacted with pyrrole *via* electrophilic aromatic substitution, to give a mixture of (after metathesis) $[PdI_2\{(Ph_2P)_2CHCH_2C_4H_3NH\text{-}x\}]$ ($x$ = 2, major isomer; $x$ = 3; minor isomer).[8] Interestingly, on treatment with an excess of pyrrole in chlorobenzene in the presence of catalytic amounts of $KOBu^t$ and 18-crown-6, **1** gave, exclusively and in high yield, *trans*-$[RuCl_2\{(Ph_2P)_2CHCH_2NC_4H_4\}_2]$ **3a**, also fully characterized; the pyrrole proton resonances (AA′XX′ spin system) in the $^1H$ NMR spectrum were particularly diagnostic.¶ Complex **3a** was insufficiently soluble for electrochemical study, and we therefore added 3-*n*-hexylpyrrole[12] to **1** to give *trans*-$[RuCl_2\{(Ph_2P)_2CHCH_2NC_4H_3R\}_2]$ (R = *n*-hexyl, **3b**), which was much more soluble in $CH_2Cl_2$.‖

The cyclic voltammogram** of **3b** in $CH_2Cl_2$–0.2 M $NBu_4BF_4$ showed a reversible one-electron oxidation wave at +0.11 V owing to the $Ru^{II}$–$Ru^{III}$ couple, and a further irreversible oxidation wave commencing at *ca.* + 0.87 V owing to the oxidation of the pendant pyrrole units; this high value for a pyrrole is likely a consequence of the fact that it is both N- and 3-substituted, and is in a sterically crowded environment. No polymer film formed, even when we used a 10 mM solution of **3b**. Since N-functionalized pyrroles have significantly higher oxidation potentials than pyrrole itself, we therefore chose to co-polymerize **3b** (10 mM) with *N*-methylpyrrole (20 mM). Once grown, the copolymer-modified electrodes were washed, and transferred to MeCN–0.2 M $NEt_4BF_4$ media for redox-cycling experiments.

Fig. 1 compares the cyclic voltammogram (CV) of a poly(*N*-methylpyrrole) film grown using a 30 mM monomer solution, from 0.2 M $NBu_4BF_4$–$CH_2Cl_2$ (*i.e.* conditions as similar as possible to those used for copolymer formation), and the CV of the copolymer. The poly(*N*-methylpyrrole) CV closely resembles those of films grown using more conventional media (*e.g.* $NEt_4BF_4$–MeCN);[13] use of $CH_2Cl_2$–$NBu^n_4BF_4$ as the electrolyte for film growth does not appear to have a detrimental effect on the voltammetry of the polymer. It can be seen that, at 10 mV $s^{-1}$ scan rate, a $Ru^{II}$–$Ru^{III}$ wave is superimposed upon the broad redox wave due to the poly(*N*-methylpyrrole) backbone for the copolymer film. It occurs at a potential *ca.* 0.05 V more positive than that for **3b** in solution in $CH_2Cl_2$. This

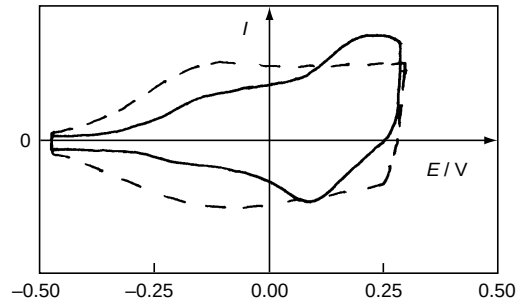



**Fig. 1** Cyclic voltammograms of (dashed line) poly(*N*-methylpyrrole) (30 mV $s^{-1}$) and (full line) a copolymer of *N*-methylpyrrole and **3b** (10 mV $s^{-1}$). Pt disk electrode, 0.30 $cm^2$ area.

is excellent evidence that the copolymerization strategy has worked and we have prepared a polypyrrole bearing a covalently bound metal–diphosphine complex, the first time that this has been demonstrated. Moreover, the electroactivity of the conducting polymer backbone has been preserved. For a surface-localised redox process, there should be no peak separation between anodic and cathodic processes. This is clearly not the case for the $Ru^{II}$–$Ru^{III}$ wave in the copolymer, but there are likely to be kinetic limitations due to the necessity for ion ingress/egress from the polymer film.

In summary, we have used base catalysis to add alcohols and pyrroles, weak nucleophiles, to **1**, and this affords a convenient route to thiophene- and pyrrole-functionalized ruthenium(II)–diphosphine complexes. We have successfully electrocopolymerized the pyrrole derivative **3b**, immobilising a redox-active ruthenium(II)–diphosphine complex in a polypyrrole matrix for the first time. This chemistry offers the opportunity of coating conducting surfaces with a polymer layer containing defined platinum metal–diphosphine complexes, providing that the latter are stable at the positive potentials needed to electropolymerize the heterocycles.

We thank the EPSRC for 'Earmarked' (T. J. P.) and Quota (M. K. M.) studentships, the Royal Society for a grant (ref. 18038), the EPSRC National Mass Spectrometry Service (Swansea) for FAB mass spectra, Dr Richard Batchelor (Pilkington Group Research, Lathom) for ITO-coated glass electrodes and Johnson-Matthey for a loan of $RuCl_3{\cdot}nH_2O$.

## Footnotes and References

* E-mail: shiggins@liv.ac.uk

† *Note added in proof:* The synthesis of a derivative of the adduct $H_3B{\cdot}Ph_2PCH_2CH_2PPh_2{\cdot}BH_3$ bearing a pendant *N*-alkylpyrrole function, its electropolymerization to afford a diphosphine-functionalized polypyrrole, and the reaction of this with $Pd(OAc_2)_2$, have recently been described (O. Stéphan, N. Riegel and S. Jugé, *J. Electroanal. Chem.*, 1997, **421**, 5). We became aware of this paper after our manuscript had been submitted.

‡ **1** (0.1 g) was dissolved in dry $CH_2Cl_2$ (50 $cm^3$). To this was added $PhCH_2OH$ **2a** or 2-(3-thienyl)ethanol **2b** (0.5 $cm^3$), $KOBu^t$ (*ca.* 20 mg) and 18-crown-6 (*ca.* 20 mg). The mixture was set aside at room temp., and examined periodically using $^{31}P$ NMR spectroscopy (10 mm tube; 5 mm coaxial tube containing $CDCl_3$ as lock) until the reaction was > 95% complete (*ca.* 5–7 days). The solvent was removed *in vacuo*, the dark brown oil was triturated with MeOH and the resulting yellow solid was filtered off and dried. The crude product was recrystallised from $CH_2Cl_2$–MeOH. Yields 62–65%.

§ *Data*: **2a**: Anal. Calc. for $C_{66}H_{60}Cl_2P_4O_2Ru{\cdot}H_2O{\cdot}CH_2Cl_2$: C, 62.67; H, 5.02. Found: C, 62.20; H, 5.19%. FABMS: *m*/*z* 1182 (100) $M^+$; 1147 (82) $[M - Cl]^+$; 1109 (20) $[M - Cl - HCl]^+$; 1074 (55) $[M - ROH]^+$; 1039 (39) $[M - ROH - Cl]^+$. $^{31}P$ NMR (101 MHz, $CDCl_3$), $\delta$ 8.06 (s). Selected $^1H$ NMR data (200 MHz, $CDCl_3$) $\delta$ 7.59 (8 H, m, Ph), 5.71 (2 H, complex m, $P_2CHCH_2$), 3.72 (4 H, complex m, $P_2CHCH_2$), 3.27 (4 H, s, $PhCH_2O$). **2b**: Anal. Calc. for $C_{64}H_{60}Cl_2P_4O_2Ru{\cdot}0.5CH_2Cl_2$: C, 61.31; H, 4.87. Found: C, 61.33; H, 4.98%. FABMS: *m*/*z* 1222 (100) $M^+$; 1187 (43) $[M - Cl]^+$; 1092 (19) $[M - ROH]^+$; 1057 (7) $[M - ROH - Cl]^+$. $^{31}P$ NMR (101 MHz; $CDCl_3$) $\delta$ 7.99 (s). Selected $^1H$ NMR data (200 MHz, $CDCl_3$) $\delta$ 7.55, 7.37 (m, Ph), 6.89, 6.68, 6.66 (6 H, overlapping multiplets, $SC_4H_3R$-3), 5.55 (2 H, complex m, $P_2CHCH_2$), 3.58 (4 H, complex m, $P_2CHCH_2$), 3.28 (4 H, t, $J_{HH}$ 6.3 Hz, $OCH_2CH_2C_4H_3S$), 2.68 (4 H, t, $OCH_2CH_2C_4H_3S$).

¶ To **1** (0.15 g, 0.16 mmol) in chlorobenzene (25 $cm^3$) under a nitrogen atmosphere was added pyrrole (0.5 $cm^3$), 18-crown-6 (0.02 g) and $KOBu^t$ (0.02 g). The mixture was stirred for 16 h, whereupon a yellow precipitate of **3a** appeared. This was filtered off, washed with MeOH and dried *in vacuo*. Yield 0.14 g, 81%. Anal. Calcd. for $C_{60}H_{54}Cl_2N_2P_4Ru$: C, 65.58; H, 4.95; N, 2.55. Found: C, 65.30; H, 4.87; N, 2.54%. FAB MS: *m*/*z* 1098 (100) $M^+$; 1063 (21) $[M - Cl]^+$. $^{31}P$ NMR ($CH_2Cl_2$–$CDCl_3$) $\delta$ 8.89 (s). Selected $^1H$ NMR data ($CD_2Cl_2$) $\delta$ 6.07, 6.02 (8 H, AA′BB′, $|J_{AB} + J_{AB'}|$ 4.1 Hz, N-subst. pyrrole), 5.35 (2 H, complex m, $P_2CHCH_2$), 4.42 (4 H, complex m, $P_2CHCH_2$).

‖ To **1** (0.40 g, 0.415 mmol) in chlorobenzene (50 $cm^3$) under a nitrogen atmosphere was added freshly prepared 3-(*n*-hexyl)pyrrole (0.5 $cm^3$),[12] 18-crown-6 (0.02 g) and $KOBu^t$ (0.02 g). The mixture was stirred for 64 h. Solvent was removed *in vacuo*, and the oily product was triturated with MeOH, whereupon a yellow solid (**3b**) formed. This was filtered off, washed with a little diethyl ether and dried *in vacuo*. Yield 0.46 g, 88%. Anal. Calc. for $C_{72}H_{78}Cl_2N_2P_4Ru{\cdot}0.25CH_2Cl_2$: C, 67.35; H, 6.14; N, 2.17. Found: C, 67.47; H, 6.14; N, 2.16%. FABMS: *m*/*z* 1267 (100) $M^+$; 1232 (21) $[M - Cl]^+$. $^{31}P$ NMR, $\delta$ 8.01 (s). Selected $^1H$ NMR data, $\delta$ 5.88, 5.78, 5.74 (6 H, m, pyrrole CH), 5.61 (2 H, complex m, $P_2CHCH_2$, app. $J_{PH}$ 6 Hz), 4.06 (4 H, complex m, $P_2CHCH_2$, app. $J_{PH}$ 5 Hz), 2.24 (4 H, t, $J_{HH}$ 7.4 Hz, $NC_4H_3CH_2R$), 1.47, 1.30, 1.20 (16 H, m, other hexyl $CH_2$), 0.80 (6 H, t, $J_{HH}$ 6.5 Hz, hexyl $CH_3$).

** All potentials quoted in this paper are with respect to the ferrocene–ferrocenium redox couple, which was routinely monitored after electrochemical experiments. Conducting polymer films were grown by repetitive cyclic voltammetric scans from *ca.* −0.5 V, to a potential *ca.* 0.1 V beyond the potential at which heterocycle oxidation commenced, using Pt disk or indium-doped tin oxide (ITO)-coated glass working electrodes. The films were removed from the cell with the film in the neutral (reduced) state, washed thoroughly with $CH_2Cl_2$ to ensure that any Ru complex within the film is covalently anchored, dried and stored. Subsequent voltammetric experiments were conducted in 0.2 M $NEt_4BF_4$–MeCN. Other details of electrochemical methodology were as previously described.[6]

1 S. J. Higgins, *Chem. Soc. Rev.*, 1997, in the press.
2 R. W. Murray, *Molecular Design of Electrode Surfaces*, Wiley, New York, 1992.
3 D. Curran, J. Grimshaw and S. D. Perera, *Chem. Soc. Rev.*, 1992, **20**, 391.
4 F. Bedioui, J. Devynck and C. Bied-Charreton, *Acc. Chem. Res.*, 1995, **28**, 30.
5 H. C. Y. Bettega, J. C. Moutet and S. Tingry, *J. Electroanal. Chem.*, 1995, **391**, 51.
6 S. J. Higgins, M. K. McCart, M. McElhinney, D. C. Nugent and T. J. Pounds, *J. Chem. Soc., Chem. Commun.*, 1995, 2129.
7 F. S. M. Hassan, S. J. Higgins, G. B. Jacobsen, B. L. Shaw and M. Thornton-Pett, *J. Chem. Soc., Dalton Trans.*, 1988, 3011.
8 G. King, S. J. Higgins and A. Hopton, *J. Chem. Soc., Dalton Trans.*, 1992, 3403.
9 P. N. Bartlett, L.-Y. Chung and P. Moore, *Electrochim. Acta*, 1990, **35**, 1051.
10 J. Barkley, S. J. Higgins, M. K. McCart and T. J. Pounds, *Inorg. Chem.*, 1997, submitted.
11 A. R. Katritzky and C. W. Rees, *Comprehensive Heterocyclic Chemistry*, Pergamon, New York, 1984.
12 B. L. Bray, P. H. Mathies, R. Naef, D. R. Solas, T. T. Tidwell, D. R. Artis and J. M. Muchowski, *J. Org. Chem.*, 1990, **55**, 6317.
13 A. F. Diaz, J. I. Castillo, J. A. Logan and W. Y. Lee, *J. Electroanal. Chem., Interfacial Electrochem.*, 1981, **129**, 115.

*Received in Cambridge, UK; 2nd July 1997; 7/04677D*

# Irreversible dinitrogen adsorption on Cu-ZSM-5 catalysts and *in situ* IR identification of the NO decomposition sites

**Sandro Recchia,*[a] Carlo Dossi,[a] Achille Fusi,[a] Rinaldo Psaro,[b] Renato Ugo[a] and Giuliano Moretti[c]**

[a] *Dipartimento di Chimica Inorganica, Metallorganica e Analitica, Università di Milano, Via Venezian 21, 20133-Milano, Italy*
[b] *Centro di Studio CNR 'SSCMTBSO', Università di Milano, Via Venezian 21, 20133-Milano, Italy*
[c] *Centro di Studio CNR 'SACSO', Dipartimento di Chimica, Università 'La Sapienza', Piazzale Aldo Moro 5, 00185-Roma, Italy*

**Dinitrogen chemisorbs on two neighbouring copper atoms of Cu-ZSM-5 catalysts that are demonstrated to be the active sites for NO decomposition.**

Dinitrogen chemisorption at room temperature on supported metal particles has been reported for rhodium on aluminium-rich zeolites and on titania.[1,2] On Cu/mordenite (Cu/NaM)[3–5] and $Cu^{I}$-ZSM-5[6] systems, IR evidence supports a simple physisorption of $N_2$ while the presence of a small amount of strongly adsorbed $N_2$ on Cu sites is only claimed.

We now report adsorption data and direct IR evidence of $N_2$ chemisorption on different Cu/zeolites systems, with correlation to their catalytic activity for NO decomposition to $N_2$ + $O_2$.

NaY (Si/Al = 2.4) and H-ZSM-5 (Si/Al = 17) zeolites were ion-exchanged at room temp. with dilute solutions of copper acetate. Dinitrogen adsorption isotherms were determined by a conventional volumetric apparatus at 273 K in the range 0–100 Torr. Samples were pretreated at $10^{-5}$ Torr for (*a*) 1 h at 788 K before the first $N_2$ adsorption and (*b*) 0.5 h at 273 K before the second $N_2$ adsorption. The $N_2$ adsorptions were calculated from the intercepts at $P = 0$ Torr of the straight lines in the high-pressure range of the first and the second isotherm, respectively.

With NaY, H-ZSM-5 and Cu/NaY the same behaviour reported for NaM[3–5] was observed: the intercepts of the straight lines are zero, corresponding only to $N_2$ physisorption. Moreover, the turnover frequency for NO decomposition on Cu/NaY is very low and quite insensitive of the copper loading.[7,8] The Cu-ZSM-5 systems, catalytically very active, show instead an irreversible $N_2$ coverage [0.03, 0.04, 0.12 mol $N_2$ (mol Cu)$^{-1}$ at 25, 65, 117% Cu exchange, respectively]. The adsorption process was also investigated in a flow cell by diffuse reflectance infrared FT spectroscopy (DRIFTS), in order to retain the working conditions of the catalyst and to avoid the diffusional limitations often encountered when the sample is a self-supporting wafer.

DRIFTS measurements were carried out at room temperature on Cu-ZSM-5 (98% Cu exchange), activated in flowing Ar [Fig. 1(*a*)]. A weak band at 2130 cm$^{-1}$ [Fig. 1(*b*)] appears in $N_2$ flow and does not change its intensity even after 12 h of Ar purging at room temp. The observed stretching frequency is much lower than the $\nu_{N-N}$ vibrations at 2299 and at 2295 cm$^{-1}$ attributed to physisorbed $N_2$ on Cu/NaM (150% Cu exchange)[3–5] and $Cu^{I}$-ZSM-5,[6] respectively, or the vibrations at 2334 and 2352 cm$^{-1}$ due to physisorbed $N_2$ on Brønsted- and Lewis-acid sites of H-ZSM-5.[9]

According to the reported relationship between $\nu_{N-N}$ and the N–N bond lengths,[10] the red shift of 201 cm$^{-1}$ with respect to the gaseous $N_2$ molecule (bond length = 1.098 Å) suggests a chemisorbed $N_2$ with a bond length of *ca*. 1.12 Å. Such a value is similar to those reported for the N–N bond distances in many $N_2$-dinuclear transition-metal complexes of [M–N≡N–M] type[10] and is in accord with an 'end-on' bridging coordination with the nitrogen molecule bonded to two different copper centers. The arrangement of two copper ions bridged by extra framework OH species was found by static atomistic simulation techniques to be particularly stable in ZSM-5 zeolite,[11] moreover, such binuclear species were independently proposed as the active sites for NO decomposition.[12,13]

Information about the nature of the sites responsible for this kind of $N_2$ chemisorption was gained through competitive adsorption of $N_2$ and CO experiments.

The spectrum in Fig. 1(*c*), obtained after carbonylation, shows a strong band at 2154 cm$^{-1}$ with a shoulder at 2138 cm$^{-1}$ and a weak band at 2107 cm$^{-1}$, all being commonly assigned to linearly chemisorbed CO on different $Cu^{+}$ intrazeolitic sites.[14]

Fig. 1(*d*) depicts the changes brought about by flowing $N_2$. The appearance of a new weak band at 2130 cm$^{-1}$ due to chemisorbed $N_2$ (partially overlapping the CO band at 2138 cm$^{-1}$), together with the marked decrease of the CO band at 2154 cm$^{-1}$, indicates an unexpected ability of $N_2$ to displace CO from that specific site. The driving force of this ligand-exchange reaction may be accounted for by the proposed bridging coordination of $N_2$ on two neighbouring copper sites.

Fig. 2 shows how the pattern of the 2154 cm$^{-1}$ carbonyl band intensity closely matches that of the catalytic activity at 773 K *vs*. % Cu exchange.[7] A direct correlation between the number of NO decomposition sites and the intensity of the 2154 cm$^{-1}$ CO band emerges from the comparison of these two profiles; as a consequence of such a correlation, the adsorption of $N_2$ is proved to occur only on these catalytically active sites.

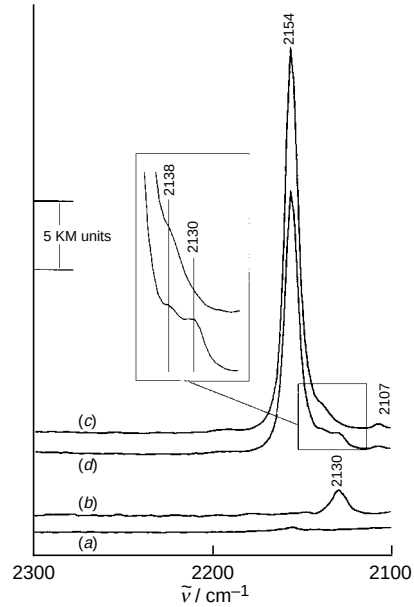



**Fig. 1** DRIFT spectra recorded at 293 K of 98% Cu exchanged Cu-ZSM-5 system: (*a*) after activation in flowing Ar from 293 K to 703 K for 1 h (ramp 3 K min$^{-1}$), (*b*) (*a*) after 3 h in flowing $N_2$ at 293 K, (*c*) activation as in (*a*) followed by 12 h in flowing CO at 293 K and subsequent Ar degassing, (*d*) (*c*) after 3 h in flowing $N_2$ at 293 K

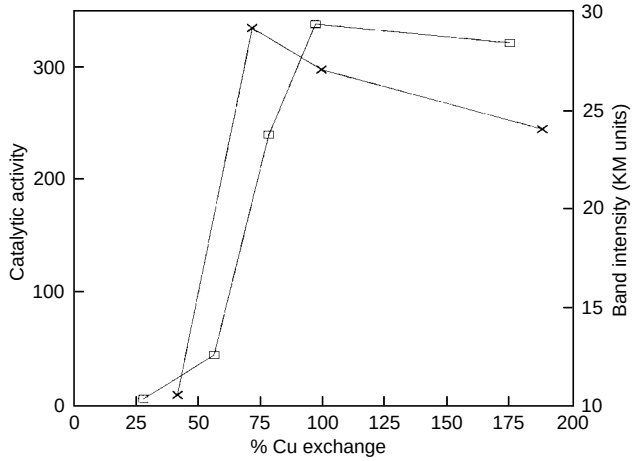



**Fig. 2** (×) Intensity of the CO band at 2154 $cm^{-1}$ of four Cu-ZSM-5 catalysts *vs*. % Cu exchange: spectra recorded in Ar after the same sequence reported in Fig. 1(*c*). (□) Catalytic activity at 773 K *vs*. % Cu exchange (ref. 6): the catalytic activity is expressed as $10^{-16}$ *x* (number of NO molecules converted to $N_2$) (g catalyst s)$^{-1}$.

The unique role of the ZSM-5 framework in the unusual catalytic activity of Cu-ZSM-5 systems can be therefore accounted for by its ability to provide the correct geometrical arrangement of dual copper sites for N≡N bond formation from two NO molecules.

We thank the Ministry of University and Scientific and Technological Research (MURST) for financial support.

## Footnote and References

* E-mail: sandy@csmtbo.mi.cnr.it

1 H. Miessner, *J. Chem. Soc., Chem. Commun.*, 1994, 927.
2 V. Vishwanathan, *J. Chem. Soc., Chem. Commun.*, 1989, 848.
3 Y. Kuroda, H. Maeda, Y. Yoshikawa, R. Kumashiro and M. Nagao, *J. Phys. Chem. B*, 1997, **101**, 1312.
4 Y. Kuroda, S. Konno, K. Morimoto and Y. Yoshikawa, *J. Chem. Soc., Chem. Commun.*, 1993, 18.
5 Y. Kuroda, Y. Yoshikawa, S. Konno, H.Hamano, H. Maeda, R. Kumashiro and M. Nagao, *J. Phys. Chem.*, 1995, **99**, 10 621.
6 C. Lamberti, S. Bordiga, M. Salvalaggio, G. Spoto, A. Zecchina, F. Geobaldo, G. Vlaic and M. Bellatreccia, *J. Phys. Chem. B*, 1997, **101**, 344.
7 M. C. Campa, V. Indovina, G. Minelli, G. Moretti, I. Pettiti, P. Porta and A. Riccio, *Catal. Lett.*, 1994, **23**, 141.
8 Y. Li and W. K. Hall, *J. Catal.*, 1991, **129**, 202.
9 F. Wakabayashi, J. N. Kondo, K. Domen and C. Hirose, *J. Phys. Chem.*, 1996, **100**, 4154.
10 J. D. Cohen, M. Mylvaganam, M. D. Fryzuk and T. M. Loehr, *J. Am. Chem. Soc.*, 1994, **116**, 9534.
11 D. C. Sayle, C. R. A. Catlow, J. D. Gale, M. A. Perrin and P. Nortier, *J. Phys. Chem. A*, 1997, **101**, 3331.
12 M. Iwamoto, H. Yahiro, N. Mizuno, W.-X. Zhang, Y. Mine, H. Furukawa and S. Kagawa, *J. Phys. Chem.*, 1992, **96**, 9360.
13 G. Moretti, *Catal. Lett.*, 1994, **28**, 143.
14 K. I. Hadjiivanov, M. M. Kantcheva and D. G. Klissurski, *J. Chem. Soc., Faraday Trans.*, 1996, **92**, 4595.

*Received in Cambridge, UK, 16th June 1997; 7/04218C*

# Differing degrees of five-coordination for similar tin atoms in the polymetallic complex $[(OC)_3Fe(\mu\text{-}Ph_2Ppy)(SnPh_2)(\mu\text{-}Cl)(SnClPh_2)]$

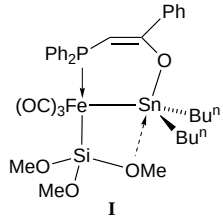
**Pierre Braunstein,*[a] Chantal Charles,[a] Guido Kickelbick[b] and Ulrich Schubert[b]**

[a] *Laboratoire de Chimie de Coordination, URA 416 CNRS, Université Louis Pasteur, 4 rue Blaise Pascal, F-67070 Strasbourg Cedex, France*

[b] *Institut für Anorganische Chemie, Technische Universität Wien, Getreidemarkt 9/153, A-1060 Wien, Austria*

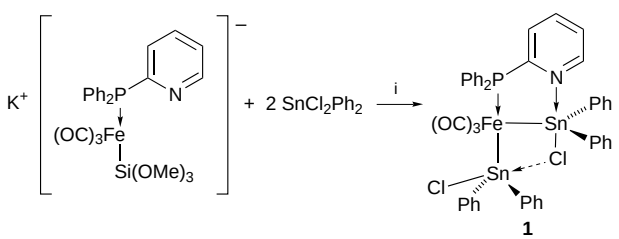
**The unusual iron–bistin complex, $[(OC)_3Fe(\mu\text{-}Ph_2Ppy)(SnPh_2)(\mu\text{-}Cl(SnClPh_2)]$, obtained by silicon–tin exchange from a Si–Fe–Sn precursor, contains two tin atoms showing different degrees of five-coordination, a unique feature of relevance to hypercoordination of main-group elements.**

The structural chemistry of tin in its complexes is diversified and the preferred geometries are tetrahedral, trigonal bipyramidal or octahedral.[1] Structural deformations encountered in crystallographically characterized molecules may often be analysed as representing snap-shots along the reaction coordinates of nucleophilic displacements at the tin centre.[2] It is also known that hypercoordination of a main-group element strongly influences its reactivity and may be used to promote catalytic behaviour. In transition-metal tin compounds M–Sn–R (R = alkyl or aryl), the bond angles decrease in the order M–Sn–R > R–Sn–R as there is more s character in the metal–tin bond.[3] Following our report of the structure of an unusual phosphinoenolate-bridged Si–Fe–Sn complex **I** in which the coordination at the tin centre was distorted tetrahedral, toward trigonal bipyramidal, with the oxygen donor ligands being *trans* to each other,[4] we have now observed that varying the nature of the assembling ligand led *via* a silicon–tin exchange reaction to a $FeSn_2$ complex in which the tin centres display different degrees of hypercoordination. This feature is of particular interest since it occurs in the same molecule, with tin ions in the same formal oxidation state.




**I**

The reaction of the iron metalate $K[Fe(CO)_3\{Si(OMe)_3\}(Ph_2Ppy\text{-}P)]$[5] [$Ph_2Ppy$ = 2-(diphenylphosphino)-pyridine] with $[SnCl_2Ph_2]$ (Scheme 1) required 2 equiv. to reach completion.† The product **1** was characterised by three $\nu$(CO) absorptions (2041m, 2001m, 1969s $cm^{-1}$) consistent with a *mer*-arrangement of the carbonyl ligands. Its $^{31}P\{^1H\}$ NMR spectrum contains a singlet at $\delta$ 77.9 attributed to the iron-bound P atom, coupled to two sets of $^{117,119}Sn$ isotopes with $^2J(P^{117,119}Sn)$ 161.7 and 217.6 Hz. This is consistent with the presence of two different tin atoms in the molecule, *cis* and *trans* to the P → Fe bond, respectively.[6a]




**1**

**Scheme 1** *Reagents and conditions*: i, thf, room temp., 30 min, − $SiCl(OMe)_3$, −KCl

A perspective view of the molecular structure of this complex is shown in Fig. 1.‡ The iron atom has a slightly distorted octahedral environment with three meridional carbonyl ligands, two *cis* tin atoms and the P atom of the bridging phosphinopyridine ligand. The nitrogen atom is coordinated to Sn(1) which has a trigonal-bipyramidal environment with the phenyl groups and the Fe atom in the equatorial plane, the sum of the corresponding bond angles being 359.2°. The Sn(1)–Cl(1) bond length of 2.557(2) Å is slightly longer than the average value for this bond.[7] This is probably due to the presence of a rather

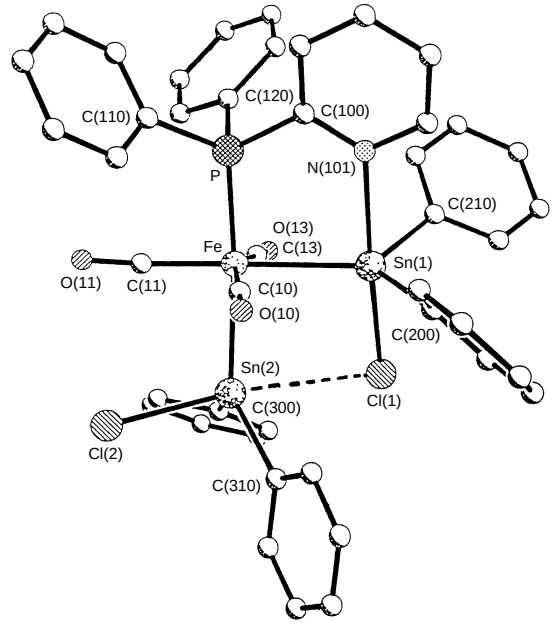



**Fig. 1** View of one molecule of **1**. Selected bond distances (Å) and angles (°): Fe–C(10) 1.796(9), Fe–C(11) 1.785(9), Fe–C(13) 1.799(9), Fe–P 2.241(2), Fe–Sn(1) 2.6111(12), Fe–Sn(2) 2.6026(12), P–C(100) 1.831(8), Sn(1)–Cl(1) 2.557(2), Sn(1)–C(200) 2.163(8), Sn(1)–C(210) 2.156(8), Sn(1)–N(101) 2.499(7), Sn(2)–Cl(2) 2.485(2), Sn(2)–C(300) 2.149(9), Sn(2)–C(310) 2.150(8), Sn(2)–Cl(1) 3.076(2); C(10)–Fe–C(11) 100.5(4), C(11)–Fe–C(13) 96.3(4), C(10)–Fe–C(13) 159.5(4), P–Fe–Sn(1) 92.73(6), P–Fe–Sn(2) 175.12(7), Sn(1)–Fe–Sn(2) 91.74(4), C(200)–Sn(1)–Fe 122.4(2), C(210)–Sn(1)–Fe 124.7(2), N(101)–Sn(1)–Fe 87.3(2), Cl(1)–Sn(1)–Fe 95.31(6), N(101)–Sn(1)–Cl(1) 176.4(2), C(200)–Sn(1)–C(210) 112.1(3), C(200)–Sn(1)–N(101) 88.2(3), C(210)–Sn(1)–N(101) 85.6(3), C(200)–Sn(1)–Cl(1) 92.6(2), C(210)–Sn(1)–Cl(1) 90.9(2), C(300)–Sn(2)–Fe 114.8(2), C(310)–Sn(2)–Fe 126.0(2), Cl(2)–Sn(2)–Fe 102.08(7), Cl(1)–Sn(2)–Cl(2) 171.6(3), Cl(2)–Sn(2)–Fe 102.08(7), Cl(2)–Sn(2)–C(300) 95.7(3), Cl(2)–Sn(2)–C(310) 92.5(2), C(300)–Sn(2)–C(310) 115.1(3).

strong N–Sn(1) bond [2.499(7) Å][7b,8] *trans* to it and to an intramolecular coordination of Cl(1) to Sn(2). Although the Sn(2)–Cl(1) separation of 3.076(2) Å is relatively long, it is only 0.04 Å longer than in the five-coordinated tin complex $[SnCl_2Me_3]^-$.[9] The bond angles around Sn(2) are consistent with a distorted trigonal-bipyramidal geometry, the Cl(1)–Sn(2)–Cl(2) angle of 171.6(3)° and the sum of the interligand angles involving Fe, C(200) and C(210) of 355.9(2)° being close to the ideal values for a trigonal bipyramid. The angles between Cl(2) and the three equatorial substituents [Fe, C(300), C(310)] [between 92.5(2) and 102.08(7)°] are again consistent with a distortion of the tetrahedral geometry around Sn(2) towards trigonal bipyramidal as a result of the Sn(2)–Cl(1) interaction. The value of the Cl(1)–Sn(2)–Cl(2) angle illustrates the view of this structure representing a snap-shot along the reaction coordinates of an intramolecular nucleophilic substitution at the Sn(2) centre.[2] Accordingly, the Sn(2)–Cl(2) distance of 2.485(2) Å is longer than in tetrahedral tin complexes. Complex **1** represents therefore a unique example where in the same molecule, two hypercoordinated tin atoms displaying different degrees of Sn–Cl interactions are present. It is also interesting that although the Fe–Sn(1) bond is supported by an assembling ligand in contrast to the Fe–Sn(2) bond, their lengths of 2.6111(12) and 2.6026(12) Å are only marginally different and compare well with those in relevant molecules.[6]

The reactivity of the Fe–Si bond, *trans* to P in the iron metalate, is dependent on the nature of the assembling ligand, as shown by the differences observed when $Ph_2Ppy$ (this work), dppm[6a] or $Ph_2PCH_2C(O)Ph$ are used. In the former cases, $FeSn_2$ complexes are formed whereas in the latter, spontaneous deprotonation of the Fe-coordinated ketophosphine ligand occurred to give a phosphino enolate bridging ligand.[4]

We are grateful to Dr J. Rocha (Aveiro, Portugal) for the solid-state NMR data, to the Ministère de l'Enseignement Supérieur et de la Recherche for a Ph. D. Grant for C. C. and to the Centre National de la Recherche Scientifique (Paris) and the Commission of the European Communities (contract ERBCHRXCT93 277) for financial support.

## Acknowledgements

Dedicated to Professor R. B. King (Athens, GA) on the occasion of his 60th birthday.

## Footnotes and References

* E-mail: braunst@chimie.u-strasbg.fr

† All reactions were performed under purified nitrogen, using carefully dried solvents.

*Synthesis of mer*-$[Fe(CO)_3\{SnClPh_2\}_2(Ph_2Ppy)]$ **1**: to a stirred solution of $K[Fe(CO)_3\{Si(OMe)_3\}(Ph_2Ppy\text{-}P)]$ prepared *in situ* from the corresponding hydride (0.525 g, 1.0 mmol) and a slight excess of KH (0.05 g) in thf, was added $[SnCl_2Ph_2]$ (0.688 g, 2.0 mmol). Rapid formation of a white precipitate occurred. The solution was stirred for 30 min, slowly concentrated and filtered through Celite to eliminate KCl. The product was precipitated by addition of hexane and washed with hexane and a small amount of diethyl ether. Crystals were obtained by slow diffusion of hexane into a $CH_2Cl_2$ solution of **1**. Yield: 79%. IR $\nu$(C≡O) ($CH_2Cl_2$): 2041m, 2001w, 1969s cm$^{-1}$; (KBr): 2037m, 1994w, 1967s cm$^{-1}$. $^1$H NMR ($CDCl_3$): $\delta$ 6.90–8.35 (m, 34 H, aromatics), 8.85 [d, 1 H, $H_{ortho}$(py), $^2J$(HH) 4.7 Hz]. $^{31}$P{$^1$H} NMR ($CDCl_3$): $\delta$ 77.9 [s, P(Fe), $^2J$(P$^{119,117}$Sn) 161.7, $^2J$(P$^{119,117}$Sn) 217.6 Hz]. $^{31}$P NMR (solid state, CP MAS, 15 kHz) : $\delta$ 74.1. $^{119}$Sn NMR (solid state, CP MAS, 15 kHz): $\delta$ 2 and −65. Mass spectrum (FAB$^+$): 984 ($M^+$ − Cl, 84), 947 ($M^+$ − 2Cl, 32), 919 ($M^+$ − 2Cl − CO, 18), 891 ($M^+$ − 2Cl − 2CO, 15%).

‡ *Crystal data* for **1** (pale orange crystals, 0.24 × 0.20 × 0.14 mm): $C_{44}H_{34}Cl_2FeNO_3PSn_2\cdot CH_2Cl_2$, $M$ = 1104.75. The crystals were mounted on a Siemens SMART CCD area detector diffractometer. Mo-K$\alpha$ radiation was used for the measurement ($\lambda$ = 0.710 73 Å, graphite monochromated). Monoclinic, space group $P2_1/c$, $a$ = 11.4534(2), $b$ = 11.6281(3), $c$ = 34.1379(6) Å, $\beta$ = 97.643(1), $U$ = 4506 Å$^3$, $Z$ = 4, $D_c$ = 1.628 g cm$^{-3}$. The cell dimensions were refined with all unique reflections. The data collection at 293(2) K covered a hemisphere of the reciprocal space, by a combination of three sets of exposures. Each set had a different $\phi$ angle for the crystal and each exposure took 20 s and covered 0.3° in $\omega$. The collected data range was $1.20 \leqslant \theta \leqslant 25.00°$ ($-13 \leqslant h \leqslant 16$, $-16 \leqslant k \leqslant 15$, $-48 \leqslant l \leqslant 48$) by a crystal-to-detector distance of 3.85 cm. 25 359 reflections were collected and 7942 unique reflections ($R_{int}$ = 0.057) were obtained after correction of polarization and Lorentz effects and an empirical absorption correction (program SADABS, $\mu$ = 1.73 mm$^{-1}$).[10] The structure was solved by direct methods (SHELXS86). Refinement was performed by the full-matrix least-squares method based on $F^2$ (SHELXL93). All non-hydrogen atoms were refined with anisotropic thermal parameters. The hydrogen atoms were added in idealized positions and were refined with a riding model. The carbon atom of the solvent molecule was refined with constrained C–Cl distances. $R$ = 0.071, $R_w$ = 0.145 for 6395 reflections with $I$ = 2.0 $\sigma(I)$; $w = 1/[\sigma^2(F_o^2) + (0.1402P)^2 + 28.94P]$ [$P = (F_o^2 + 2F_c^2)/3$]. The largest residual electron density was 1.5 e Å$^{-3}$ at Sn(1) and Sn(2). CCDC 182/587.

1 A. G. Davies, in *Comprehensive Organometallic Chemistry II*, ed. E. W. Abel, F. G. A. Stone and G. Wilkinson, vol 2, p. 217.
2 H. B. Bürgi and J. D. Dunitz, *Acc. Chem. Res.*, 1983, **16**, 153; *Structure Correlations*, ed. H. B. Bürgi and J. D. Dunitz, VCH, Weinheim, 1994.
3 M. S. Holt, W. L. Wilson and J. H. Nelson, *Chem. Rev.*, 1989, **89**, 11; J. A. Zubieta and J. J. Zuckerman, *Prog. Inorg. Chem.*, 1978, **24**, 251.
4 P. Braunstein, C. Charles, A. Tiripicchio and F. Ugozzoli, *J. Chem. Soc., Dalton Trans.*, 1996, 4365.
5 G. Reinhard, B. Hirle, U. Schubert, M. Knorr, P. Braunstein, A. DeCian and J. Fischer, *Inorg. Chem.*, 1993, **32**, 1656.
6 (*a*) P. Braunstein, M. Knorr, M. Strampfer, A. DeCian and J. Fischer, *J. Chem. Soc., Dalton Trans.*, 1994, 117; (*b*) M. Knorr, H. Piana, S. Gilbert and U. Schubert, *J. Organomet. Chem.*, 1990, **388**, 327; (*c*) P. Braunstein, C. Charles, R. D. Adams and R. Layland, *J. Cluster Sci.*, 1995, **7**, 145; (*d*) F. W. B. Einstein and R. Restivo, *Inorg. Chim. Acta*, 1971, **5**, 501.
7 (*a*) W. Clegg, C. M. J. Grievson and K. Wade, *J. Chem. Soc., Chem. Commun.*, 1987, 969; (*b*) J. Vicente, M. T. Chicote, M. C. Ramirez-de-Arellano, G. Pelizzi and F. Vitali, *J. Chem. Soc., Dalton Trans.*, 1990, 279; (*c*) A. L. Balch, H. Hope and F. E. Wood, *J. Am. Chem. Soc.*, 1985, **107**, 6936; (*d*) H. Weichmann, J. Meunier-Piret and M. van Meerssche, *J. Organomet. Chem.*, 1986, **309**, 267.
8 J. T. B. H. Jastrzebski, G. van Koten, C. T. Knaap, A. M. M. Schreurs, J. Kroon and A. L. Spek, *Organometallics*, 1986, **5**, 1551; J. T. B. H. Jastrzebski, J Boersma, P. M. Esch and G. van Koten, *Organometallics*, 1991, **10**, 930; (*c*) J. T. B. H. Jastrzebski, E. Wehman, J. Boersma, G. van Koten, K. Goubitz and D. Heijdenrijk, *J. Organomet. Chem.*, 1991, **409**, 157; (*d*) S. K. Lee and B. K. Nicholson, *J. Organomet. Chem.*, 1986, **309**, 257.
9 S. E. Johnson, K. Polborn and H. Nöth, *Inorg. Chem.*, 1991, **30**, 1410.
10 SADABS, Program for empirical absorption correction for Siemens area detectors; G. M. Sheldrick, University of Göttingen, 1996.

*Received in Cambridge, UK, 4th July 1997; 7/04749E*

# 2-Aminopurine peptide nucleic acids (2-*ap*PNA): intrinsic fluorescent PNA analogues for probing PNA–DNA interaction dynamics

**Bargur P. Gangamani, Vaijayanti A. Kumar* and Krishna N. Ganesh*†**

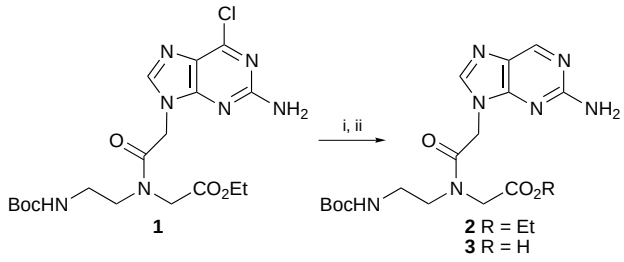
*Organic Chemistry Synthesis Division, National Chemical Laboratory, Pune 411008, India*

**Peptide nucleic acids, containing intrinsically fluorescent 2-aminopurine in place of non-fluorescent adenine, are useful as fluorescent probes to study PNA–DNA interaction dynamics.**

Peptide nucleic acids (PNA) are DNA analogues in which the sugar–phosphate backbone is replaced by a peptide amide bond backbone.[1] PNAs exhibit unique properties that set them apart from other traditional DNA analogues. These properties are: (i) unprecedented strong binding to complementary, mixed DNA/RNA sequences to form duplexes, (ii) high specificity in discrimination of mismatched base pairs and (iii) 'strand invasion' at polypurine/pyrimidine stretches on a DNA duplex to form a $PNA_2$·DNA triplex.[2] This fact, coupled with their resistance to proteases and nucleases and chemical stability over a wide pH range, has led to the development of novel applications that cannot be satisfactorily executed with other DNA analogues. Such applications include blocking and activation of gene expression *via* D-loop complexes, identification of point mutations by PNA-directed PCR clamping, using fluorophore conjugated PNA as probes to locate individual genes in a DNA map and antisense drug development.[2,3]

Most of the structural changes to improve PNA properties so far have centred on backbone modifications to introduce conformational constrain and chirality.[1–4] Herein we report on a novel type of PNA analogue which has intrinsic fluorescence due to the presence of 2-aminopurine (2-*ap*),[5] an isomer of non-fluorescent adenine (6-aminopurine). The base 2-*ap* can be selectively excited in the presence of normal bases, making it an ideal real-time spectroscopic probe to study the dynamics and local environmental changes due to DNA binding with other molecules.[6] Incorporation of this into versatile PNA would therefore add a new dimension to the existing repertoire of PNA properties and potential applications. This is the first report of the synthesis of a PNA analogue which is intrinsically fluorescent, and also examines PNA–DNA complexation *via* fluorescence changes.

The desired PNA monomer **3** carrying a 2-aminopurine moiety was synthesised in two steps (Scheme 1) starting from the previously known compound ethyl *N*-(2-amino-6-chloropurin-9-ylacetyl)-*N*-(2-butoxycarbonylaminoethyl)glycinate **1**.[7] The 6-chloro group in **1** was first removed by hydrogenation over Pd–C to afford **2**, which was followed by hydrolysis of the ester with aq. NaOH to give the corresponding carboxylic acid **3**.‡ This monomer was used directly for incorporation into PNA oligomer **5** without protecting the 2-amino function, since it is inactive for normal peptide coupling conditions. The assembly of the PNA oligomers **4** and **5** was performed manually on Merrifield resin prior functionalised with β-alanine (0.3 equiv. $g^{-1}$) by standard solid phase peptide synthesis.[7] For the oligomer **5**, the 2-*ap* monomer **3** was used in place of A monomer in the indicated position (*A*). At the end of the synthesis, the oligomers were cleaved from the resin using $CF_3SO_3H$–TFA and the products assessed by reverse phase HPLC.§ The complementary oligonucleotides **6** and **7** designed for parallel and antiparallel PNA·DNA duplexes were synthesised on an automated DNA synthesiser.




**Scheme 1** *Reagents*: i, $H_2$/Pd–C; ii, aq. NaOH

**4** PNA $H_2N$–T A T T A T T A T T–$CONHCH_2CH_2CO_2H$

**5** 2-*ap*PNA $H_2N$–T A T T ***A*** T T A T T–$CONHCH_2CH_2CO_2H$

**6** DNA 5' A T A A T A A T A A 3'

**7** 3' A T A A T A A T A A 5'

**8** 3' A A A A A A A A A A 5'

***A*** = 2-aminopurine

The fluorescence spectra¶ of the monomer **3** was similar to that of the 2-aminopurine base, with emission at 367 nm upon excitation at 308 nm; the fluorescence intensity changed negligibly with increasing temperature in the range 10–60 °C. The fluorescent observables ($\lambda_{ex}$, $\lambda_{em}$) from 2-*ap*PNA **5** were similar to those of the monomer, but the fluorescence yield of 2-*ap* in PNA was significantly lower than that of the free base. The PNA oligomer **5** exhibited an increase in intensity as a function of temperature upto 40 °C (total 25%), after which a slight decrease in intensity was observed (Fig. 1). No meaningful changes in $\lambda_{ex}$/$\lambda_{em}$ (±1 nm) were seen with changes in temperature. However, the measurement of fluorescence anisostropy at different temperatures (15 °C, 0.073; 25 °C, 0.060; 35 °C, 0.040; 50 °C, 0.040) showed an appreciable decrease with increasing temperature until *ca*. 40 °C and remained constant thereafter. This behaviour indicates that 2-*ap*PNA, like PNA, is considerably self-organized at low temperatures and melts at higher temperature. Thus, the 2-*ap* residue in **5** senses the local changes in conformation/environment accompanying the self-melting of

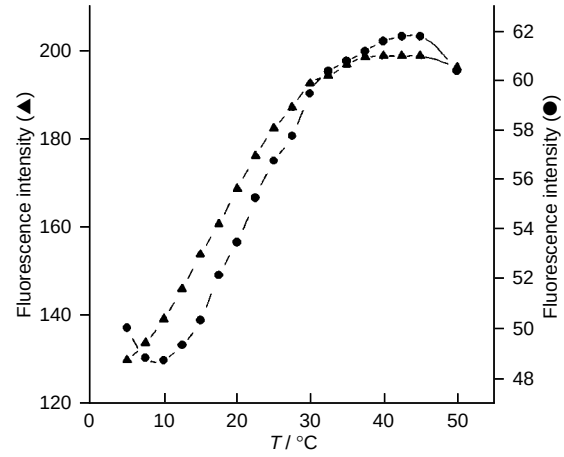



**Fig. 1** Fluorescence ($\lambda_{em}$ 365 nm) melting profiles of (●) 2-*ap*PNA **5** and (▲) 2-*ap*·DNA duplex **5·7**

PNA from an ordered chain to a random coil, a process that also reorients the fluorophore.

The mixed sequence PNAs form both parallel and antiparallel duplexes with appropriate complementary DNA sequences, with antiparallel duplexes being more stable than parallel duplexes.[2] The effect of incorporating 2*ap* in place of A on the thermal stability of duplexes is seen from the UV absorbance–temperature data for PNA·DNA duplexes ($T_m$; **5·6**, 25.5 °C; **5·7**, 25.0 °C; **4·6**, 28.0 °C; **4·7**, 28.5 °C). The single replacement of A by 2*ap* caused a lowering of $T_m$ by 2–3 °C for both parallel (N/5′, **5·6**) and antiparallel (N/3′, **5·7**) 2*ap*-PNA·DNA duplexes as compared to the corresponding unmodified control duplexes **4·6** and **4·7** respectively. The data indicate a relatively large increase in fluorescence intensity (60%) of 2 *ap* in duplex with temperature as compared to that in 2*ap*PNA alone (25%). Further, a slight blue shift in emission maxima (2 nm) was noticed at 50 °C compared to that at 5 °C, indicating a more hydrophilic environment for 2*ap* after melting. The fluorescence intensity showed a small decrease beyond 40 °C, similar to 2*ap*-PNA (Fig. 1). The parallel PNA·DNA duplex (**5·6**) gave temperature dependent fluorescence spectra (not shown) similar to those of the antiparallel (**5·7**) duplex. Surprisingly, the decrease in fluorescence anisotropy (10%) of the 2*ap* moiety in PNA upon PNA·DNA melting was less than that seen with 2-*ap*PNA alone (45%).

The fluorescence $T_m$ obtained from the data in Fig. 1 for 2*ap*-PNA·DNA melting (**5·7**, 27.5 °C) was less by 5 °C than the $T_m$ for self-melting of 2*ap*-PNA (**5**, 32.5 °C), consistent with the general observation that the thermal stability of the PNA·DNA duplex is lower than that of PNA.[2] It is interesting, but not unprecedented,[6a] to note that the fluorescence $T_m$ of the duplexes (**5·6**, 27.5 °C; **5·7**, 27.0 °C) were *ca*. 2.5 °C higher than the $T_m$ of the corresponding duplexes derived from UV absorbance changes. This difference may arise from the fact that the UV equilibrium melting curves monitor the global duplex dissociation while the fluorescent melting curve monitors local duplex perturbations in the vicinity of the fluorophore.[6] The temperature dependent fluorescence data is also influenced by transient kinetic states that are not reflected in equilibrium data.

The kinetics of the PNA·DNA hybridization process were examined by monitoring the fluorescence emission decay at 367 nm as a function of time after mixing of 2*ap*-PNA **5** with the complementary antiparallel DNA **7** (Fig. 2). The emission intensity decreased exponentially over a period of 6 min [Fig. 2, curve (*c*)] and thereafter remained constant. In contrast, either 2*ap*PNA **5** alone or its mixture with DNA $dA_{10}$, **8** having three mismatches with PNA, did not exhibit any effect on the PNA fluorescence [Fig. 2, curves (*a*) and (*b*)]. The time-dependent decrease in fluorescence of **5** immediately upon mixing with **7** may therefore be attributed to specific formation of a 2*ap*PNA·DNA hybrid (**5·7**). Similar kinetic behaviour has been previously observed for PNA·PNA hybrid by monitoring the evolution of a circular dichroism signal arising from helical propagation in a 10-mer lys-PNA upon mixing with a complementary PNA sequence[8] where signal saturation occurred at around 6 min. The decay profile observed could be fitted to a double exponential function with time constants of 46 and 290 s, indicating that the fluorescent base 2-*ap* in PNA monitors at least two types of local events, a fast duplex formation by complementary hydrogen bonding followed by a slow reorganization of the helix after duplex formation.

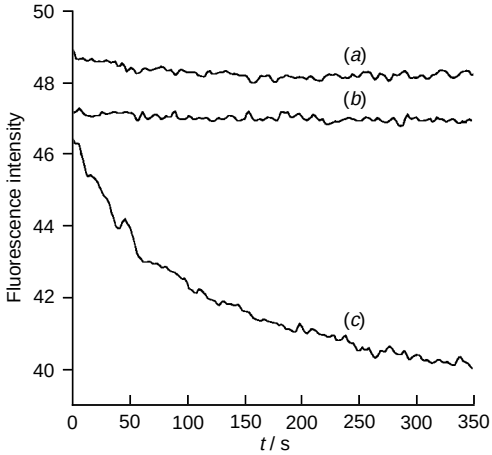



**Fig. 2** Fluorescence decay kinetics at 15 °C monitored by emission at 365 nm: (*a*) **5**, (*b*) **5·8** and (*c*) **5·7**

Structural studies of DNA/PNA using fluorescence are best performed without perturbing their structures, which is possible only with the use of intrinsic fluorescence from the base. In this context, 2*ap* is an ideal fluoroprobe since it senses both steady state and dynamic conformational changes. The present results clearly demonstrate that 2-*ap* is easily accommodated in a PNA chain and the intrinsic fluorescence can be employed to monitor PNA self-melting and PNA·DNA duplex transitions. The anisotropy changes suggest that the 2-*ap* residue in a PNA chain is more ordered than its environment in a PNA·DNA duplex. Since 2-*ap* can be placed at any point in a PNA·DNA helix to monitor local events, the type of probes reported here have potential for studying the consequences of backbone modifications on the PNA self-structure and on PNA·DNA duplex. Apart from their utility in diagnostics, these PNA probes may be applicable to other areas, such as the study of cellular uptake and intracellular distribution of PNA by employing fluorescence microscopy, and as sequence specific DNA biosensors.[9]

## Footnotes and References

† E-mail: kng@ems.ncl.res.in

‡ *Selected data* for **2**: $\delta_H$ ($CDCl_3$) 8.65 (s, 1 H, AH8), 7.93–7.90 (s, 1 H, AH6), 5.80 (br s, 1 H, NH), 5.40 (br s, 1 H), 5.00–4.85 (s, 2 H, $glyCH_2$), 4.17–4.05 (s, 2 H, N–$CH_2$), 4.25 (m, 2 H), 3.67–3.56 (m, 2 H), 3.40–3.32 (m, 2 H), 1.45 (s, 9 H), 1.25 (m, 3 H); $\delta_C$($CDCl_3$) 169.6–169.3 ($CO_2$Et), 167.3–166.9 (CONH), 159.9 (C2), 156.2 (BocOCON), 153.4 (C8), 148.6 (C6), 143.7 (C4), 126.8 (C5), 79.7 ($Me_3CO$), 62.1, 61.5, 48.4, 38.6, 28.3 (all $CH_2$), 13.9 ($Me_3C$). For **3**: $\delta_H$($D_2O$) 8.7 (s, 1 H), 8.33 (s, 1 H), 5.31 and 5.12 (s, 2 H), 4.17 and 4.07 (s, 2 H), 3.7 (t, 2 H), 3.58 (t, 2 H), 3.4 (t, 2 H), 3.23 (t, 2 H), 1.42 and 1.43 (s, 9 H); $\delta_C$($CDCl_3$) 171.6–171.07 ($CO_2$Et), 167.7–167.2 (CONH), 161.0 (C2), 156.3 (BocOCON), 153.9 (C6), 149.3 (C8), 143.9 (C4), 126.9 (C5), 78.7 ($Me_3CO$), 50.2, 48.9, 47.6, 43.6, 28.7 (all $CH_2$), 13.9 ($Me_3C$).

§ RP 18 column; buffer A: 0.1% TFA in water, buffer B: 0.1% TFA in MeCN gradient 0–40% B in A in 30 min. *R*: **4**, 12.28 min; **5**, 12.26 min.

¶ Fluorescence spectra were recorded on a Perkin-Elmer LS 50B spectrometer, equipped with a flow cell and attached to a Julabo water circulator for variable temperature measurements, using a slit width of 5 nm. The PNA·DNA duplexes were constituted by mixing equimolar amounts of each strand (4 μM) in 10 mM phosphate buffer (pH 7.0, 2 ml) followed by heating at 80 °C for 3 min, cooling to ambient temperature and storage at 4 °C overnight.

1 P. E. Nielsen, *Annu. Rev. Biophys. Biomol. struct.*, 1995, **24**, 167.
2 B. Hyrup and P. E. Nielsen, *Bioorg. Med. Chem. Lett.*, 1996, **4**, 5.
3 D. R. Corey, *Trends Biotechnol.*, 1997, **15**, 224.
4 G. Haaima, A. Lohse, O. Buchardt and P. E. Nielsen, *Angew. Chem., Int. Ed. Engl.*, 1996, **35**, 1939; B. P. Gangamani, V. A. Kumar and K. N. Ganesh, *Tetrahedron*, 1996, **52**, 15 017.
5 D. C. Ward, E. Reich and L. Stryer, *J. Biol. Chem.*, 1969, **244**, 1228.
6 (*a*) D. Xu, K. O. Evans and T. M. Nordlund, *Biochemistry*, 1994, **33**, 9592; (*b*) S. M. Law, R. Eritja, M. F. Goodman and K. J. Breslauer, *Biochemistry*, 1996, **35**, 12 329; (*c*) D. P. Millar, *Curr. Opin. Struct. Biol.*, 1996, **6**, 322; (*d*) R. A. Hochstrasser, T. E. Carver, L. C. Sowers and D. P. Millar, *Biochemistry*, 1994, **33**, 11 971; (*e*) M. W. Frey, L. C. Sowers, D. P. Millar and S. J. Benkovic, *Biochemistry*, 1995, **34**, 9185.
7 P. C. Meltzer, A. Y. Liang and P. Matsudaira, *J. Org. Chem.*, 1995, **60**, 4305.
8 P. Wittung, M. Eriksson, R. Lyang, P. E. Nielsen and B. Norden, *J. Am. Chem. Soc.*, 1995, **117**, 10 167.
9 J. Wang, E. Palecek, P. E. Nielsen, G. Rivas, X. Cai, H. Shiraish, N. Dontha, D. Lere and P. A. M. Farias, *J. Am. Chem. Soc.*, 1996, **118**, 7667.

*Received in Cambridge, UK, 31st July 1997 (NCL Communication No. 6397); 7/05539K*

# Methyltrioxorhenium supported on silica tethered with polyethers as catalyst for the epoxidation of alkenes with hydrogen peroxide

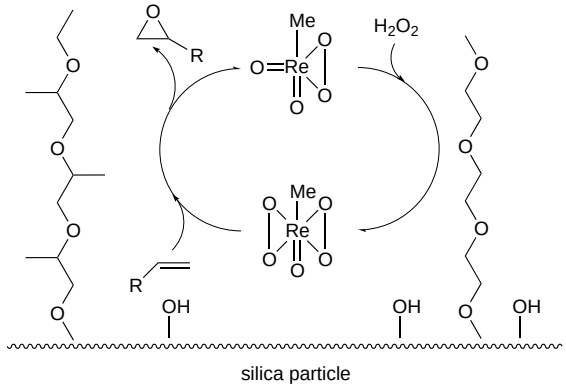
**Ronny Neumann* and Tie-Jun Wang**

*Casali Institute of Applied Chemistry, Graduate School of Applied Science, The Hebrew University of Jerusalem, Jerusalem, Israel 91904*

**Methyltrioxorhenium has been supported on silica functionalized with polyether tethers; in the absence of an organic solvent, this catalytic assembly catalysed the epoxidation of alkenes with 30% aqueous $H_2O_2$ in high selectivity compared to the ring opening products observed in homogeneous media.**

Simplification of catalyst recovery procedures by immobilizing selective and highly active homogeneous catalysts on a insoluble support is an ongoing endeavour designed to increase the use of catalysis in industrial settings.[1] The most common method of covalent attachment of a catalyst to an insoluble support usually yields a catalytic assembly of reduced selectivity and activity. The method of supported liquid or aqueous phase catalysis, where a film of solvent containing the catalyst is adsorbed on an insoluble particle such as silica, is an important improvement because reactions occur at a liquid–liquid interface, somewhat reducing the mass transfer limitations.[2] However, leaching of the solvent and thus catalyst still remains an important concern in such systems. We recently improved this technique of supported liquid phase catalysis by covalently attaching polyethers to a silicate particle using sol-gel procedures.[3] The attached polyether phase acted as the solvent for the catalyst (polyoxometalate) and allowed contact with one or more substrate phases.

Here we extend this concept on the use of silica with polyether tethers to a different catalytic oxidation reaction, the supported methyltrioxorhenium (MTO) catalysed epoxidation of alkenes with 30% aqueous $H_2O_2$. MTO has been shown to be an excellent epoxidation catalyst, with the shortcoming that the use of the necessary protic solvent leads to ring-opened products rather than epoxides.[4] Here we show that the use of methyltrioxorhenium supported on silica tethered with polyethers gives epoxides in high yields by tailoring the hydrophilic–hydrophobic balance of the polyether phase. As represented in the schematic drawing, (Scheme 1), the hydrophobic poly(propylene oxide) (PPO) units may increase the solubility of the alkene substrate in the solvent anchored phase, whereas the poly(ethylene oxide) (PEO) units serve to dissolve the aqueous hydrogen peroxide oxidant and stabilize the peroxo intermediate responsible for catalytic activity.[5]




**Scheme 1**

The silica particles with tethered polyether units were prepared in two steps. First, the relevant trialkoxysilanes **1**, with the appropriate polyethers groups, $(MeO)_3SiC_6H_4$-$CH_2O(CH_2CHRO)_nMe$ (R = H, Me), were prepared.† Second, the funtionalized xerogels were prepared by copolymerizing the appropriate amount of the monomer **1** and the non-functionalized monomer, $Si(OEt)_4$.‡ Typical epoxidation reactions were carried out by mixing functionalized silica, 30% $H_2O_2$ and MTO in small magnetically stirred vials. After stirring vigorously for about 5 min, the alkene substrates were added. The reactions were quenched by adding either $CH_2Cl_2$ or $Et_2O$ to extract the substrate and products for GC and GC–MS analysis.

In order to probe the effect of the polyether tethers in the heterogeneous assembly, cyclohexene (which is known[4] to give *trans*-cyclohexane-1,2-diol as product in the homogenous aqueous–*tert*-butyl alcohol solvent system) was selected as model substrate in the current catalytic system. The results as presented in Table 1 show that MTO supported on non-functionalized silica demonstrated essentially no catalytic activity. MTO immobilized on polyether tethered silica showed several trends. Functionalization with only PEO showed increased conversion as a function of the amount of PEO, but low selectivities to epoxide. The low selectivity can be explained by the highly hydrophilic nature of the only-PEO assembly, which is similar to the homogeneous system. Use of only small amounts of PPO gave high yields but only moderate selectivities. Increased amounts of PPO without PEO reduced the conversion considerably, apparently due to the lower accessibility of the oxidant to the catalytic site. A balanced amount of both PEO and PPO gave the best results with almost quantitative (99.9%) conversion and high (86.4%) epoxide selectivity. The PPO is clearly shown to contribute to the

**Table 1** Epoxidation of cyclohexene catalysed by methyltrioxorhenium supported on polyether tethered silica[a]

| Polyether tether[b] | Conversion (mol%) | Selectivity (mol%)[c] |
|---|---|---|
| 0%[d] | 0.8 | — |
| 5% PEO | 10.3 | 12.0 |
| 10% PEO | 69.9 | 0 |
| 20% PEO | 78.9 | 8.6 |
| 10% PEO, 5% PPO | 81.6 | 57.2 |
| 10% PEO, 10% PPO | 99.9 | 86.4 |
| 10% PEO, 20% PPO | 33.1 | 84.9 |
| 4% PPO | 92.4 | 55.9 |
| 10% PPO | 19.6 | 64.4 |
| 20% PPO | 1.0 | — |

[a] Reaction conditions: cyclohexene (1 mmol), 30% $H_2O_2$ (2 mmol), MTO (0.02 mmol) and polyether tethered silica (100 mg), room temp. 3 h. [b] The amount of polyether is the mol% of the relevant monomer used in the preparation of the silica, as described in footnote.‡ [c] Selectivity to the epoxide product; the only other product was *trans*-cyclohexane-1,2-diol. [d] Non-functionalized silica prepared by the sol-gel method.

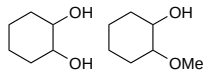
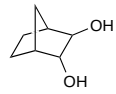
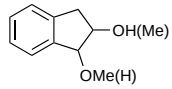
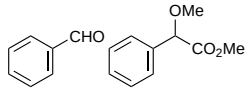
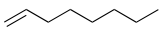
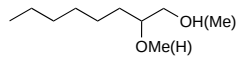
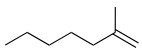
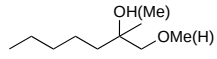
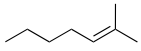
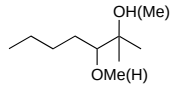
selectivity of the reaction whereas the PEO contributes to the conversion and thus a careful balance of hydrophobic–hydrophilic characteristics§ of a silica particle can be uniquely used to maximize both the activity and selectivity of a supported catalyst. Although the effect of the polyether composition on activity and selectivity clearly indicated that the reaction was occuring in the polyether phase, additional verification showing that MTO was not dissolved in either of the reactants was possible by mixing 10% PEO, 10% PPO-$SiO_2$, 30% $H_2O_2$ and MTO for 10 min. After filtration, the filtrate (30% $H_2O_2$) showed no catalytic activity upon addition of cyclohexene. Similarly, mixing 10% PEO, 10% PPO-$SiO_2$, cyclohexene and MTO for 10 min, followed by filtration and addition of 30% $H_2O_2$ to the filtrate, showed no cyclohexene conversion.

In order to demonstrate the generality of this reaction, the oxidation of various other alkenes using the optimal heterogeneous system (MTO on 10% PEO–10% PPO-$SiO_2$) was compared to a typical homogeneous reaction using MeOH as solvent, (Table 2). Compared to the homogeneous standard, where quantitative conversions were the norm, the polyether tethered silica support showed somewhat lower activity even with more oxidant (three-fold excess) but very considerable selectivity to the epoxide, even in the case of indene whose epoxide is believed unstable under acidic conditions.[6] Oxidation of styrene also yielded benzaldehyde, the product of carbon–carbon bond cleavage. The homogeneous reaction system gave almost exclusively the ring opened products which were identified by GC–MS, except in the case of norbornene where epoxide was also observed. Finally, initial experiments were carried out to test the possibility of catalyst recycling. At the end of each reaction period the catalytic assembly was filtered under vacuum and washed with 1 ml of cold $Et_2O$, followed by addition of more substrate and oxidant. For four cycles the catalytic activity (85 ± 7 mol% conversion) and selectivity (89 ± 6 mol% epoxide) remained high, although there were rather considerable fluctuations. From the fifth cycle onward, both conversion and selectivity dropped considerably. Analysis by GC–MS of the reaction mixture after each cycle showed some polyether remnants, indicating that deactivation was by polyether detachment from the silica particle.

MTO supported on silica particles with polyether tethers is an effective catalytic assembly for the epoxidation of alkenes with $H_2O_2$ under environmentally benign conditions, *i.e.* no organic solvent. The ability to design and control the hydrophobic–hydrophilic balance of the attached polyether phase holds much promise for the development of new heterogeneous catalytic systems, especially where reactants are immiscible.

This research was supported by grant No. 95-00076 from the United States-Israel Binational Science Foundation (BSF), Jerusalem, Israel.

**Table 2** Comparative oxidation of alkenes catalysed by methyltrioxorhenium supported on 10% PEO–10% PPO-$SiO_2$ *vs.* a homogeneous reaction[a]

| Substrate | Conversion (mol%)[b] | Selectivity (mol%)[c] | Other products (mol%) |
|---|---|---|---|
|  | 99.9 (100) | 86.4 (0) |  13.6 (7.9) 0 (92.1) |
|  | 94.2 (100) | 71.0 (28.0) |  24.2 (64.4) |
|  | 88.5 (100) | 94.3 (0) |  5.7 (100) |
|  | 83.8 (100) | 33.8 (0) |  66.2 (0) 0 (100) |
|  | 62.7 (100) | 100 (62.9) |  0 (37.1) |
|  | 80.2 (100) | 79.4 (0) |  20.6 (100) |
|  | 72.8 (100) | 93.2 (0) |  6.8 (100) |

[a] Reaction conditions (heterogeneous): alkene (1 mmol), 30% $H_2O_2$ (3 mmol), MTO (0.02 mmol) on 10% PEO–10% PPO-$SiO_2$ (100 mg); (homogeneous): alkene (1 mmol), 30% $H_2O_2$ (2 mmol), MTO (0.02 mmol), MeOH (1 ml); 25 °C, 3 h. Values given in parentheses are for the homogeneous reaction. [b] Alkene conversion. [c] Selectivity to the epoxide product.

## Footnotes and References

* E-mail: ronny@vms.huji.ac.il

† $(MeO)_3SiC_6H_4CH_2Cl$ (50 mmol) was reacted with poly(ethylene glycol) monomethyl ether (PEGME, MW = 350) (50 mmol) or poly(propylene glycol) monomethyl ether (PPGME, MW = 200) (50 mmol) in acetone (200 ml) in the presence of solid $K_2CO_3$ (250 mmol) at reflux for 18 h to form $(MeO)_3SiC_6H_4CH_2O(CH_2CHRO)Me$ **1a** (R = H) and **1b** (R = Me).

‡ A mixture of **1** and $Si(OEt)_4$ (total 10 mmol), water (100 mmol) and dibutyltin dilaurate (0.1 mmol) (polymerization catalyst) in acetone (40 ml) were heated at 60 °C for 3 h. The solution was kept in a beaker and the volatile organics were left to slowly evaporate over a period of two days at ambient temperature. The functionalized silica was then carefully washed twice with water and EtOH and dried *in vacuo*. Polymerization was quantitative (> 99%) as determined by microanalysis. The polymerization technique used is generally assumed to lead to a random (mixed) polymer (ref. 7). A detailed kinetic investigation of the rates of hydrolysis and self- and cross-condensation of **1** and $Si(OEt)_4$ would be required to verify this assumption and to exclude the formation of PEO and/or PPO enriched domains.

§ A wetting angle of 55° was measured for a 10% PEO–10% PPO-$SiO_2$ film. This wetting angle is indeed intermediate between hydrophilic (15–25°) and hydrophobic (80–100°).

1 F. R. Hartley, *Supported Metal Complexes*, Reidal, Dordrecht, 1985; R. A. Sheldon, *Curr. Opin. Solid State Mater. Sci.*, 1996, **1**, 101.
2 P. E. Rony, *J. Mol. Catal.*, 1975, **1**, 13; M. E. Davis, *Chemtech*, 1992, 498; K. T. Wan and M. E. Davis, *Nature*, 1994, **370**, 449.
3 R. Neumann and M. Cohen, *Angew. Chem., Int. Ed. Engl.*, 1997, in the press.
4 W. A. Herrmann, R. W. Fisher, M. U. Rauch and W. Schere, *J. Mol. Catal.*, 1994, **86**, 243; A. M. Al-Ajlouni and J. H. Espenson, *J. Am. Chem. Soc.*, 1995, **117**, 9243.
5 W. A. Herrmann, R. W. Fisher, W. Schere and M. U. Rauch, *Angew. Chem. Int. Ed. Engl.*, 1993, **32**, 1157.
6 F. Fringuelli, F. Pizzo, R. Germani and G. Savelli, *Org. Prep. Proced. Int.*, 1989, **21**, 757.
7 C. J. Brinker, *Sol-Gel Science*, Academic Press, 1990.

*Received in Cambridge, UK, 26th June 1997; 7/04496H*

# Acyl transfer reactions in dipolar aprotic medium: desolvated phosphate ion as acyl acceptor in the formation of energy-rich phosphate compounds

**Vanderlei Gageiro Machado and Faruk Nome***

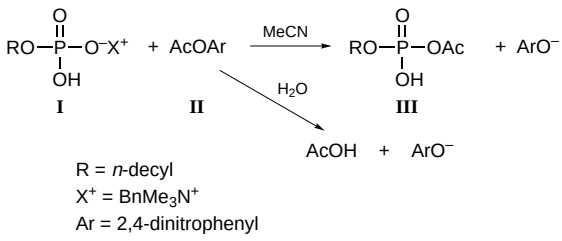
*Departamento de Química, Universidade Federal de Santa Catarina, Florianópolis, SC, 88040-900, Brazil*

**The reaction between an acetate ester and *n*-decylphosphate ions in dipolar aprotic medium provides a system which allows the facile formation of acetyl phosphate derivatives, by means of restricting the quantities of water available in the reacting system; the role of water is explained in terms of the inhibition of the nucleophilic attack of the phosphate group, which is disfavoured by its presence.**

In order to promote the interconversion of different forms of energy, cells use phosphate compounds such as ATP and acetyl phosphate as the currency of energy exchange.[1] The synthesis and the hydrolysis of these compounds are catalysed by enzymes able to perform energy transduction. During the last two decades, different laboratories have dedicated their efforts to the elucidation of this fascinating puzzle.[2–5] Lehn and co-workers[4] have demonstrated that a variety of macrocyclic polyamines mediate the phosphorylation of phosphate ion, *via* an energy-rich intermediate phosphoramidate, generating energy-rich compounds such as ATP and pyrophosphate. This model system was successful as a 'mimick' of enzymes responsible for the phosphorylation of many compounds. In all cases, the enzymatic models needed, in order to make the phosphoryl transfer, an energy-rich compound to phosphorylate the macrocycle.

Here we show that a dipolar aprotic medium allows the easy reaction of organic phosphate ions with an acetate ester to generate the corresponding energy-rich acetyl phosphate compound. Specifically, we found that addition of benzyltrimethylammonium *n*-decylphosphate **I**, in anhydrous MeCN, enables its facile reaction with 2,4-dinitrophenyl acetate **II** by nucleophilic addition to the carbonyl group. Compound **I** was used in order to increase the solubility of the organic phosphate to concentrations adequate for the acquisition of kinetic and spectroscopic data. In our experiment, the solubility limit of the salt in MeCN was *ca.* $1.2 \times 10^{-3}$ M. Acetyl *n*-decylphosphate **III** is then produced, and 2,4-dinitrophenolate is liberated. In aqueous solution the hydrolysis reaction is dominant, forming acetate and 2,4-dinitrophenolate ions as products (see Scheme 1).

The rate of acetyl transfer was determined at 40 °C by monitoring the formation of the 2,4-dinitrophenolate at 363 nm. The reaction is first-order in each of the reactants and proceeds quantitatively. The linear dependence of rate constants *vs.* the concentration of *n*-decylphosphate ions is maintained up to the solubility limit of the salt **I** in MeCN or MeCN–water mixtures (*ca.* $2 \times 10^{-3}$ M in MeCN containing 1% water). The second-order rate constant in anhydrous MeCN is $k_2 = 13.2$ l mol$^{-1}$ s$^{-1}$. The formation of **III** was followed by observation of the carbonyl region in the infrared spectra in MeCN, using a NaCl cell with a path length of 0.5 mm. While the peak corresponding to the ester carbonyl at 1786 cm$^{-1}$ disappears, a new band appears at 1754 cm$^{-1}$, a reasonable position for the carbonyl stretching vibration of **III**.[6] The product could be also trapped and quantified by an adaptation of the method of Lipmann and Tuttle.[7]†




R = *n*-decyl
$X^+ = BnMe_3N^+$
Ar = 2,4-dinitrophenyl

**Scheme 1**

The rate of the reaction under consideration shows a dramatic dependence on the water content of the aprotic solvent (Fig. 1). We observe a decrease of 68 times the value of the rate constant for the reaction when 6% of water is added to anhydrous MeCN ($[H_2O] = 2.65$ M), with a corresponding increase in the half-life of the reaction from 46 to 3136 s. Surprisingly, addition of 10% water in dry MeCN provokes a 660-fold inhibition. These results clearly show the primordial role of water in this particular acyl transfer reaction.

To verify the influence of water in the course of the reaction between the ester and the *n*-decylphosphate, the yields of the different products described in Scheme 1 were determined (Fig. 2). The data clearly demonstrates the strong influence of water in the course of the reaction under investigation. A reduction in yield of 50% of the acetyl phosphate is triggered by addition of 5% water to MeCN. Upon addition of 30% water, acetyl phosphate production could not be detected either by IR spectroscopy or by the adaptation of Lipmann's method.[7]† In this particular case, the only products are those resulting from ester hydrolysis. Clearly, for a mild, rapid and high yielding synthesis of energy-rich compounds such as **III**, an anhydrous microenvironment is needed.

Recently, de Meis has suggested[5] that energy-rich phosphate compounds can be synthesized on the enzymatic surface without the need of energy at a hydrophobic enzyme site. Indeed, the binding-change mechanism that is extensively used to describe ATP synthesis by ATP synthases[2] indicates that

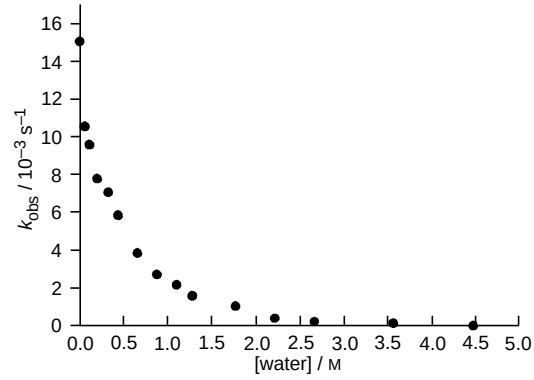



**Fig. 1** Effect of water on the first order rate constant for the reaction of 2,4-dinitrophenyl acetate ($3.0 \times 10^{-5}$ M) with benzyltrimethylammonium *n*-decylphosphate ($1.57 \times 10^{-3}$ M) in MeCN. The value corresponding to anhydrous MeCN was calculated using the experimental second-order rate constant.

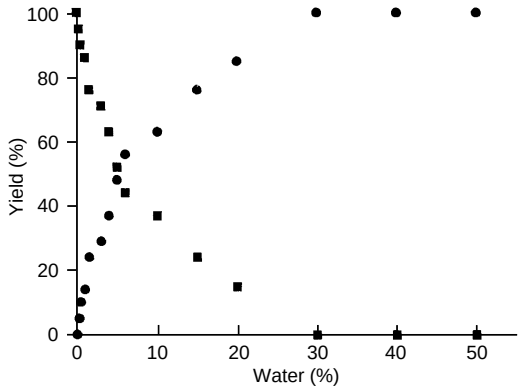



**Fig. 2** Effect of water on the yields of (■) acetyl phosphate and (●) hydrolysed ester for the reaction between 2,4-dinitrophenyl acetate and benzyltrimethylammonium *n*-decylphosphate in MeCN

ATP synthesis occurs spontaneously at the catalytic sites, and energy is needed only to release the ATP produced.

Analysis of the experimental results described above, although for a model system, is relevant in terms of the chemistry of living systems. The fundamental reason why water promotes the inhibition of the acyl transfer reaction is probably the fact that solvation of the phosphate anion decreases the nucleophilicity of this compound, allowing the simultaneous appearance of the ability of this compound to act as a general base in hydrolytic reactions.[8,9] An alternative explanation involving slow nucleophilic attack followed by relatively fast hydrolysis of the acyl phosphate was experimentally excluded, since **III** was stable under our experimental conditions. Indeed, the hydrolysis of acyl phosphates has been proven to be independent of solvent composition in water–MeCN mixtures, with a rate constant of *ca.* $7.3 \times 10^{-5}$ $s^{-1}$.[10] Thus, the predominance of the hydrolysis, or the formation, of a particular energy-rich compound is intrinsically related to the environment in which the reaction is taking place. Accordingly, the reversibility of these particular reactions should be achievable in normal solutions, under appropriate conditions, such as those described in this work. By analogy, if we are allowed to extrapolate these conclusions to enzyme catalysed reactions, a hydrolytic reaction which is spontaneous in aqueous media may well not be so on the surface of the enzyme (*e.g.* in a hydrophobic pocket).

The experimental fact that the reaction in anhydrous MeCN differs significantly from that in the presence of even small amounts of water, and completely from that observed in aqueous systems, shows, in our understanding, that the study of reactions of biochemical importance in purely aqueous systems may not adequately contribute to the understanding of enzyme catalysis. For reactions occurring in the hydrophobic pocket of a particular enzyme, water is certainly not an adequate standard state for the comparison of equilibrium and/or rate constants.[6] A typical example of this is that ionic intermediates are sometimes favoured in reactions occurring in polar solvents, but are considered to be of high energy in non-polar systems.[8,11] It may well be that this handling of the equilibrium thermodynamics of reactions is one of the factors that enzymes and nature use to promote the synthesis of energy-rich compounds.

In conclusion, we believe that the role of water, and particularly of its absence, in biochemically important events is a question still little explored. The present model represents, to the best of our knowledge, the first organic system that resulted in the facile formation of energy-rich compounds and, we hope, this fact will shed some light on the operational mode of some of the enzymes responsible for energy transduction. It provides an example that allows us to rationalize how water (or its absence) in the microenvironment of the active-site of an enzyme can determine both rate accelerations and changes in equilibrium constants.

The authors are grateful to CNPq and PADCT/FINEP for financial support of this work.

## Footnotes and References

* E-mail: faruk@reitoria.ufsc.br

† The yield of acetyl phosphate was determined by mixing compound **I** (46.8 μmol) with 2,4-dinitrophenyl acetate (11.7 μmol) in MeCN (25 ml), with a known water concentration. The reaction mixture was then stirred at 25 °C in a stoppered flask until completion of the reaction. The solvent was removed and water (1 ml) was added to the residue. This aqueous solution was added to a mixture of aqueous hydroxylamine (1 ml) [all solutions were identical with those originally described by Lipmann and Tuttle (ref. 7)] and acetate buffer (1 ml), and the mixture was left to stand for 10 min. Then aqueous HCl (1 ml) and aqueous ferric chloride (1 ml) was added. The solution was filtered and the UV–VIS spectrum of the purple solution, caused by complexation of the quantitatively formed hydroxamic acid with $Fe^{3+}$, was determined at 500 nm ($\varepsilon$ = 925 $cm^{-1}$ $M^{-1}$).

1 F. Lipmann, *Adv. Enzymol.*, 1941, **1**, 99.
2 H. S. Penefsky and R. L. Cross, *Adv. Enzymol. Relat. Areas Mol. Biol.*, 1991, **64**, 173; P. D. Boyer, *Biochim. Biophys. Acta*, 1993, **1140**, 215; R. L. Cross, *Nature*, 1994, **370**, 594.
3 J. P. Abrahams, A. G. W. Leslie, R. Lutter and J. E. Walker, *Nature*, 1994, **370**, 621.
4 J.-M. Lehn, *Angew. Chem., Int. Ed. Engl.*, 1988, **27**, 89; M. W. Hosseini and J.-M. Lehn, *J. Chem. Soc., Chem. Commun.*, 1991, 451; H. Fenniri and J.-M. Lehn, *J. Chem. Soc., Chem. Commun.*, 1993, 1819.
5 L. de Meis, *Biochim. Biophys. Acta*, 1989, **973**, 333; L. de Meis, *Arch. Biochem. Biophys.*, 1993, **306**, 287.
6 G. Wallerberg and P. Haake, *J. Org. Chem.*, 1981, **46**, 43; J. Hajdu and G. M. Smith, *J. Am. Chem. Soc.*, 1981, **103**, 6192.
7 F. Lipmann and L. C. Tuttle, *J. Biol. Chem.*, 1945, **159**, 21.
8 W. P. Jencks, *Chem. Rev.*, 1972, **72**, 705.
9 F. M. Menger, in *Nucleophilicity*, ed. J. M. Harris and S. P. McManus, American Chemical Society, Washington, 1987, p. 209; M. J. S. Dewar and D. M. Storch, *J. Chem. Soc., Chem. Commun.*, 1985, 94; J. Chandrasekhar, S. F. Smith and W. L. Jorgensen, *J. Am. Chem. Soc.*, 1985, **107**, 154.
10 G. Di Sabato and W. P. Jencks, *J. Am. Chem. Soc.*, 1961, **83**, 4400.
11 J. Druzian, C. Zucco, M. C. Rezende and F. Nome, *J. Org. Chem.*, 1989, **54**, 4767.

*Received in Corvallis, OR, USA, 12th June 1997; 7/04128D*

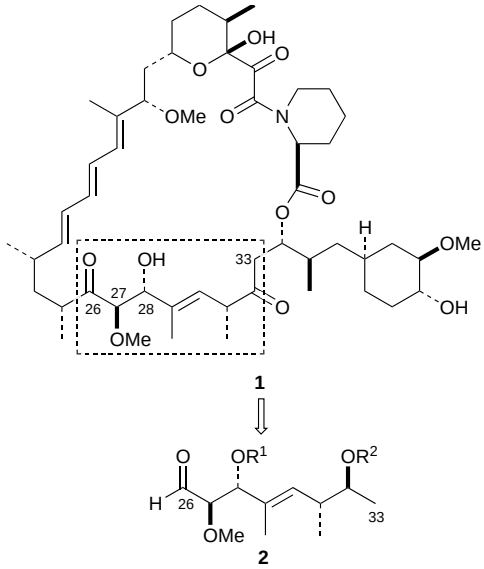
# Enhanced reactivity and *anti* selectivity in the asymmetric Lewis acid-mediated Mukaiyama aldol reaction of α-alkoxythiolketene acetals with α,β-disubstituted enals: synthesis of the C26–C33 segment of rapamycin

**James D. White* and Jörg Deerberg**

*Department of Chemistry, Oregon State University, Corvallis, OR 97331-4003, USA*

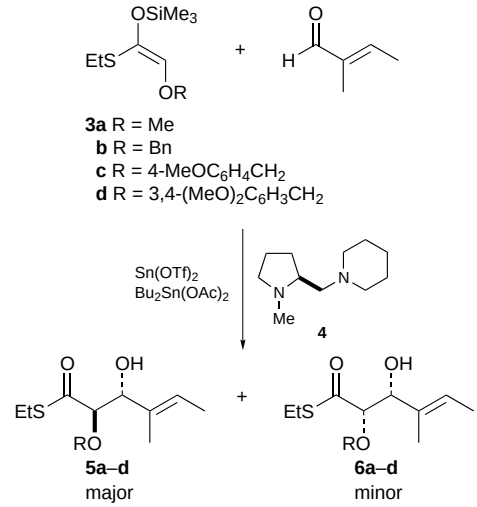
**The tin(II)-mediated reaction of α-alkoxythiolketene acetals 3a–d with *trans*-2-methylbut-2-enal and aldehyde 10 was found to give enhanced reactivity and high *anti* selectivity in the glycolate product when an α-benzyloxy substituent was present in 3, a finding which was applied to the synthesis of a segment (C26–C33) of the immunosuppressant rapamycin.**

In the course of our studies directed towards a total synthesis of the immunosuppressive agent rapamycin **1**,[1] a subunit was




required which contained functionality suitable for its incorporation as the C26–C33 segment of the macrolide. A difficulty associated with preparing such a fragment resides in controlling relative and absolute configuration of the vicinal *anti* diol moiety at C27–C28. In an attempt to solve this problem in the context of synthesis of a segment **2** required for rapamycin, we were attracted by the chiral Lewis acid-mediated *anti* glycolate aldolization methodology of Mukaiyama[2] and Fukuyama,[3] in which α-alkoxythiolketene acetals were reacted with aldehydes in the presence of tin(II) trifluoromethanesulfonate (triflate) and a proline-derived diamine ligand.[4] We now report that this methodology is readily extended to sterically demanding α,β-disubstituted enals, that both the reactivity and diastereoselectivity of the aldol process are controlled by the ketene acetal α-alkoxy substituent, and that appropriate selection of the *O*-protecting group of the ketene acetal allows differentiation of the adjacent oxygen functions in the aldol product.

Our initial studies were carried out with *trans*-2-methylbut-2-enal and the four α-alkoxythiolketene acetals **3a–d** (Scheme 1). The latter were synthesized from the corresponding thiol esters† by low temperature silylation [lithium tetramethylpiperidine (LTMP), −100 °C, $Me_3SiCl$] and were obtained predominantly as the (*Z*) isomer in each case. The reaction of ketene




**Scheme 1**

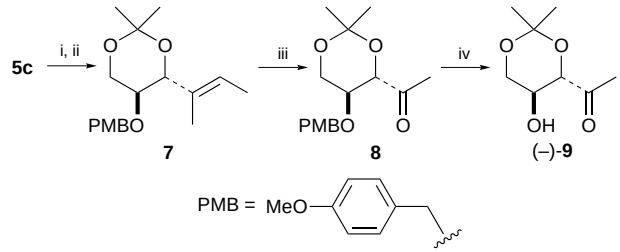
acetals **3a–d** with *trans*-2-methylbut-2-enal in the presence of (*S*)-1-methyl-2-[(1-piperidyl)methyl]pyrrolidine **4** under the conditions specified by Mukaiyama[2] gave aldol adducts **5** and **6** as a mixture of diastereoisomers‡ (Table 1). The *anti* adducts **5a–d** were found to be the major stereoisomers in each case;§ their optical purity was determined by chiral HPLC analysis¶ and by comparison with diastereoisomerically pure racemates synthesized independently. Absolute configuration was assigned in the case of **5c** by correlation with a substance of known stereochemistry (Scheme 2). Thus, reduction of thiol ester **5c** to the corresponding 1,3-diol, followed by acetonide formation, yielded **7** which after ozonolysis gave ketone **8**. Removal of the *p*-methoxybenzyl ether afforded (−)-**9** [$[\alpha]_D^{23}$ −24.8 (*c* 1.0, $CH_2Cl_2$)] which exhibited spectral data and analytical properties identical to those of its antipode (+)-**9** [$[\alpha]_D^{23}$ +23.6 (*c* 1.0, $CH_2Cl_2$)‖ prepared from D-glucose.[5]

The results in Table 1 indicate that an increase in both chemical yield *and* diastereoselectivity is observed in the aldol reaction of Scheme 1 when an electron-releasing α-alkoxy

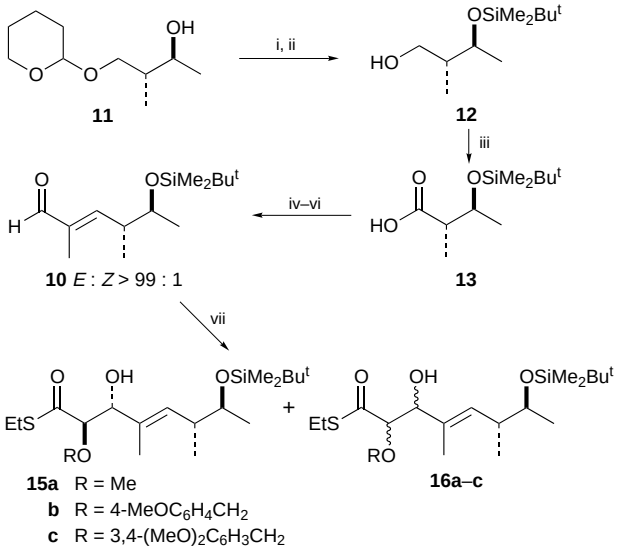
**Table 1** Asymmetric Lewis acid-catalysed reaction of *trans*-2-methylbut-2-enal with α-alkoxythiolketene acetals[a]

| Ketene acetal (*Z*:*E*) | Aldol products (**5** and **6**) R | Yield (%)[b] | *Anti* (**5**): *syn* (**6**)[c] | Ee of **5** (%)[d] |
|---|---|---|---|---|
| **3a** (4:1) | Me | 32 | 70:30 | 87 |
| **3b** (12:1)[e] | Bn | 82[f] | 85:15 | 93 |
| **3c** (10:1) | 4-$MeOC_6H_4CH_2$ | 74 | 90:10 | 96 |
| **3d** (6:1) | 3,4-$(MeO)_2C_6H_3CH_2$ | 80 | 95:5 | 92 |

[a] Reactions were carried out in $CH_2Cl_2$ at −78 °C for 30–36 h except where specified. [b] Isolated yield of **5** + **6**, except where specified. [c] See footnote §. [d] See footnote ¶. [e] Experiment carried out at −50 °C. [f] Isolated yield of **5**.




**Scheme 2** *Reagents and conditions*: i, $LiAlH_4$, THF, 0 °C → room temp., 3 h; ii, $Me_2C(OMe)_2$, TsOH, room temp., 2 h, 80%; iii, $O_3$, MeOH–pyridine (cat), −78 °C, 4 min, then $Me_2S$, 95%; iv, 2,3-dichloro-5,6-dicyano-1,4-benzoquinone (DDQ): $CH_2Cl_2$–$H_2O$, 48%




**Scheme 3** *Reagents and conditions*: i, $Bu^tMe_2SiCl$, imidazole, $CH_2Cl_2$, room temp., 12 h; ii, $MgBr_2{\cdot}OEt_2$ (excess), $Et_2O$, 4 h, 93%; iii, $Pr_4NRuO_4$ (cat), 4-methylmorpholine *N*-oxide, $CH_2Cl_2$, room temp., 15 min, *ca*. 100%; iv, LDA, $Bu^tN{=}CHCH(Me)SiMe_3$ **14**, THF, −78 °C; v, $(HO_2C)_2$, $H_2O$; vi, $I_2$ (cat), $Bu^tNH_2$, hexane, 50 °C, 12 h, 62% from **13**; vii, **4**, $Sn(OTf)_2$, $Bu_2Sn(OAc)_2$, **3a**,**c**,**d**, $CH_2Cl_2$, −78 °C, 30–36 h

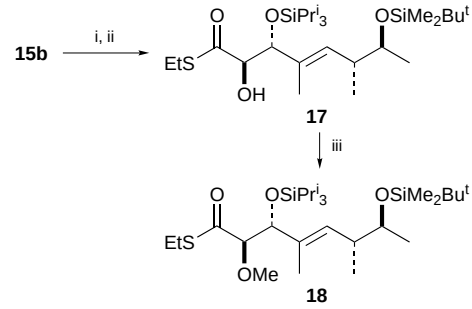
substituent such as 4-methoxybenzyl (PMB) or 3,4-dimethoxybenzyl (DMB) is present in the thiolketene acetal. Best results were obtained with DMB, whereas an α-methoxy substituent resulted in low diastereoselectivity and poor yield.

With this information in hand, our efforts focused upon α,β-unsaturated aldehyde **10** needed for synthesis of subunit **2**. Alcohol **11**, obtained from methyl (*R*)-3-hydroxy-2-methylpropionate,[6] was transformed to **12**[7] which was oxidized to aldehyde **13** with perruthenate.[8] Conversion of this labile substance to α,β-unsaturated aldehyde **10** was accomplished by the procedure of Corey *et al*.[9] in which condensation of **13** with the α-lithio derivative of imine **14** was followed by mild, acid-catalysed Peterson olefination. The initial *ca*. 2 : 1 mixture of (*E*) and (*Z*) isomers of enals was smoothly equilibrated to a > 99 : 1 ratio favouring (*E*) isomer **10** upon exposure to a catalytic quantity of iodine in warm hexane containing a trace (6 mol%) of *tert*-butylamine (Scheme 3).

**Table 2** Asymmetric Lewis acid-catalysed aldol reaction of **10** with α-alkoxythiolketene acetals

| Ketene acetal | Aldol Products (**15** and **16**) R | Yield (%) | *Anti* (**15**) : *syn*(**16**)[a] |
|---|---|---|---|
| **3a** | Me | 7 | 75 : 25 |
| **3c** | 4-$MeOC_6H_4CH_2$ | 54 | 90 : 10 |
| **3d** | 3,4-$(MeO)_2C_6H_3CH_2$ | 80 | 92 : 8 |

[a] See footnote §.




**Scheme 4** *Reagents and conditions*: i, $Pr^i_3SiOTf$, 2,6-lutidine, $CH_2Cl_2$, −40 → °C; ii, DDQ, $CH_2Cl_2$–$H_2O$, room temp., 1.5 h, 85% from **15b**; iii, $CH_2N_2$, $BF_3{\cdot}OEt_2$ (1 equiv.), $CH_2Cl_2$, 94%

The reaction of **10** with α-alkoxythiolketene acetals **3a**,**c**,**d** under the conditions employed with *trans*-2-methylout-2-enal yielded *anti* aldol products **15a**–**c** as the major diastereoisomers (Table 2). Again, PMB- and DMB-substituted ketene acetals **3c** and **3d** showed superior stereoselectivity, whereas α-methoxy derivative **3a** was virtually unreactive with **10**. Protection of **15b** as its triisopropylsilyl ether, followed by oxidative cleavage of the PMB ether,[10] gave **17** (Scheme 4), and treatment of the liberated alcohol with $CH_2N_2$ in $CH_2Cl_2$ containing $BF_3{\cdot}OEt_2$ furnished methyl ether **18**. This material now stands ready in conveniently protected form for connection at each terminus to other subunits required for the synthesis of **1**.

One of us (J. D.) is grateful to the Swiss National Science Foundation for a Postdoctoral Fellowship (Fellowship No. 81GE-41174). This work was assisted financially by the National Institutes of Health through grant GM50574.

## Footnotes and References

* E-mail: whitej@ccmail.orst.edu

† Thiol esters were prepared either by reaction of the corresponding acyl chloride with EtSH or from the corresponding benzylglycolic acid by treatment with DCC, catalytic DMAP and EtSH (ref. 11). 4-Methoxybenzylglycolic acid and 3,4-dimethoxybenzylglycolic acid were obtained in 91 and 87% yield, respectively, by ether synthesis from chloroacetic acid and the corresponding sodium benzylates (NaH, toluene, reflux).

‡ In the case of **3b**, adducts were separated by flash chromatography.

§ Diastereoselectivities were determined by $^1H$ NMR analysis of crude reaction mixtures after workup.

¶ Chiral HPLC column: DAICEL ChiralPak AD, 350 × 4 mm.

‖ This value is in conflict with that reported by David *et al*.[5] for (+)-**9** [$[\alpha]_D^{20}$ +40.5 (*c* 7, $CH_2Cl_2$)], which is shown to be in error by this work.

1 J. D. White and S. C. Jeffrey, *J. Org. Chem.*, 1996, **61**, 2600.
2 T. Mukaiyama, *Aldrichim. Acta*, 1996, **29**, 59; T. Mukaiyama, I. Shiina, K. Sakata, T. Emura, K. Seto and M. Saitoh, *Chem. Lett.*, 1995, 179; T. Mukaiyama, I. Shiina, H. Uchiro and S. Kobayashi, *Bull. Chem. Soc. Jpn.*, 1994, **67**, 1708.
3 Y. Kanda and T. Fukuyama, *J. Am. Chem. Soc.*, 1993, **115**, 8451.
4 T. Mukaiyama, N. Iwasawa, R. W. Stevens and T. Haga, *Tetrahedron*, 1984, **40**, 1381.
5 S. David, B. Estramereix, J.-C. Fischer and M. Thérisod, *J. Chem. Soc., Perkin Trans. 1*, 1982, 2131.
6 R. Baker, R. H. Boyes, D. M. P. Broom, M. J. O'Mahony and C. J. Swain, *J. Chem. Soc., Perkin Trans. 1*, 1987, 1613.
7 K. Mori and M. Itou, *Liebigs Ann. Chem.*, 1992, 87.
8 L. A. Paquette, C. F. Sturino, X. Wang, J. C. Prodger and D. Koh, *J. Am. Chem. Soc.*, 1996, **118**, 5620.
9 E. J. Corey, D. Enders and M. G. Bock, *Tetrahedron Lett.*, 1976, 7.
10 K. Horita, T. Yoshioka, T. Tanaka, Y. Oikawa and O. Yonemitsu, *Tetrahedron*, 1986, **42**, 3021.
11 B. Neises and W. Steglich, *Angew. Chem., Int. Ed. Engl.*, 1978, **17**, 522.

*Received in Cambridge, UK, 29th July 1997; 7/05481E*

# Functional selectivity in Friedel–Crafts alkylations with allylic halides promoted by solid composite lead fluoride reagent

**Junko Ichihara***

*Institute of Scientific and Industrial Research, Osaka University, Mihogaoka, Ibaraki, Osaka 567, Japan*

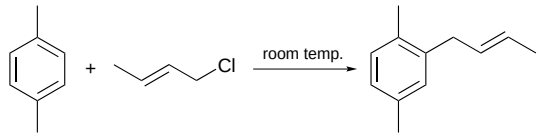
**The composite lead fluoride reagent prepared from $PbF_2$ and NaBr is a nonhygroscopic and efficient solid reagent for promoting Friedel–Crafts type reaction of aromatic compounds with allylic halides selectively to afford the monoallylated compounds.**

Friedel–Crafts type allylation of aromatic compounds using allylic alcohols or halides and Lewis acid catalysts has proved unsatisfactory, because the reaction occurs both at the double bond and at the allylic carbon to yield polyaryl-substituted alkanes.[1] The reactions with allylic halides liberates hydrogen halide, which further attacks the double bond of the products to induce the second reaction. Recently Kodomari *et al.* have reported successful selective monoallylation by using a combination of a solid acid and a solid base, $ZnCl_2$–$SiO_2$ and $K_2CO_3$–$Al_2O_3$.[2] The solid base operates as a scavenger of hydrogen halide liberated during the reaction and does not influence the catalytic activity of the solid Lewis acid because of the distance between both solid supported reagents. Solid acids such as acidic zeolites and clays has been applied to achieve functionally selective allylations with allylic alcohols.[3,4]

We have studied the use of synergistic interactions between diverse inorganic solid reagents for enhancing solid–liquid heterogeneous reactions with organic compounds dissolved in organic solvents. Recently we have observed that a combination of lead fluoride and a small amount of sodium bromide accelerates the fluorination of allylic and benzylic halides.[5,6] It was found that a new inorganic lead compound was formed from the solid reagents during the fluorination of organic halides, and that its formation process is associated with activation of the alkyl halides. This prompted us to examine it as a promoter for Friedel–Crafts alkylation reactions. Here we report that the composite lead fluoride reagent is a mild and efficient solid reagent for promotion of selective Friedel–Crafts type monoallylation when used in stoichiometric amounts.[7]

A composite lead fluoride reagent **A** ($Pb_3BrF_5$) was easily prepared by mixing aqueous NaBr and $PbF_2$ powder (3 equiv.).†

**Table 1** Friedel–Crafts allylation of *p*-xylene and 1-chlorobut-2-ene

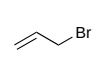
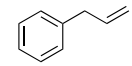
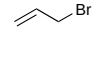
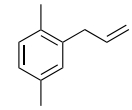
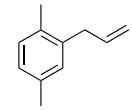
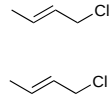
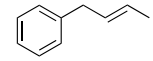
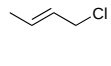
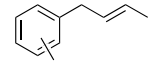
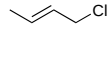
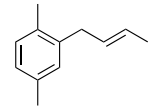
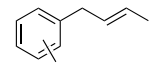
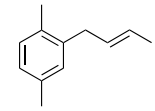
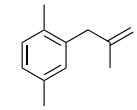
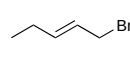
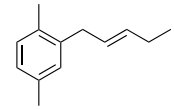
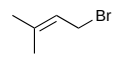
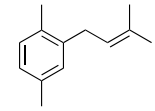



| Run | Reagent | GC Yield of **ArR** (%) (*t*/h)[a] | |
|---|---|---|---|
| 1 | Reagent **A** ($Pb_3BrF_5$) | 43 (1) | 86 (2) |
| 2 | Reagent **B** ($Pb_3ClF_5$) | 27 (1) | 80 (2) |
| 3 | NaBr–$PbF_2$ | 36 (1) | 48 (2) |
| 4 | $PbF_2$ | 0 (1) | 0 (2) |
| 5 | $TiCl_4$ (10 mol%) at 3–4 °C | 65 (1)[b] | |
| 6 | $ZnCl_2$–K10 (10 mol%) | 63 (0.5)[b] | |

[a] 1-Chlorobut-2-ene : *p*-Xylene: Reagent = 1 : *ca.* 20 : 0.6. [b] By-products were observed by GC.

Using the solid reagent **A**, an electrophilic substitution of *p*-xylene with 1-chlorobut-2-ene proceeded at room temp. to give the corresponding monosubstituted products (**ArR**) in 86% yield after 2 h (Table 1). The composite lead fluoride reagent **B**, prepared from NaCl and $PbF_2$, also showed high reactivity. Under the same reaction conditions, $PbF_2$ showed no reactivity, but a mixture of NaBr and $PbF_2$ promoted the reaction.

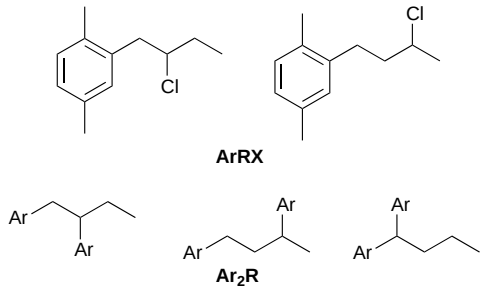
**Table 2** Friedel–Crafts allylation using $Pb_3BrF_5$ solid reagent[a]

| Allylic Halides | Aromatics | *T*/°C | *t*/h | Products | Yield (%) |
|---|---|---|---|---|---|
|  | Benzene | 60 | 2 |  | 94 |
|  | *p*-Xylene | 60 | 2 |  | 91 |
|  | *p*-Xylene | 60 | 10 |  | 91 |
|  | Benzene | room temp. | 3 |  | 45[b] |
|  | Toluene | room temp. | 2 |  | 99[c,d] |
|  | *p*-Xylene | room temp. | 2 |  | 77 |
|  | Toluene | room temp. | 2 |  | 85[d] |
|  | *p*-Xylene | room temp. | 2 |  | 77 |
|  | *p*-Xylene | room temp. | 48 |  | 87[c] |
|  | *p*-Xylene | room temp. | 2 |  | 93[c] |
|  | *p*-Xylene | room temp. | 1 |  | 70[b,c] |

[a] Alkyl halide : aromatic $Pb_3BrF_5$ = 1 : *ca.* 20 : 0.5. [b] Alkyl halide : aromatic : $Pb_3BrF_5$ = 1 : 140 : 1. [c] Isolated yields. The others are GC yields. [d] *opm*-isomer ratio = 1 : 1 : 0.1, determined by $^1H$ NMR spectroscopy.

Accordingly, in the latter case the reagent **A** or **B**, formed in the course of the reaction, was considered to participate in the reaction.

Catalytic activities of $TiCl_4$ and $ZnCl_2$–Montmollironite K-10 ($ZnCl_2$–K-10), well-known as mild Lewis acid catalysts, were compared with those of the lead reagents in the reaction.[8,9]‡ These catalysts showed higher reactivities but gave considerable amounts of by-products. In the presence of 10 mol% of $ZnCl_2$–K-10, a 63% yield of the monoallylated product **ArR** and a 24% yield of its hydrogen chloride adduct (**ArRX**) were formed as major products, with a 2% yield of diaryl substituted alkanes ($\mathbf{Ar_2R}$). Kodomari *et al.* have reported that **ArRX**- and $\mathbf{Ar_2R}$-type products are mainly formed in the reaction of benzene and allyl chloride with silica-supported $ZnCl_2$. On the contrary, in the case of our reagent **A** such by-products were scarcely detected by GC, and the desired product **ArR** was selectively formed and maintained intact in the reaction mixture even after prelonged. Thus, the reagent was found to have functional selectivity, in that it operates on the allylic carbon rather than on the double bond. The selective allylation occurs because the reagent behaves as both the Lewis acidic catalyst and a trap for the liberated halide, *via* exchange with fluoride.




The reaction required at least stoichiometric amounts of the reagent. It was shown by powder X-ray diffraction analysis that the reagent **A** is converted to PbClF during the reaction.

Table 2 shows typical examples for some allylic halides. In all cases the heterogeneous reaction of aromatic compounds and allylic halides using the $Pb_3BrF_5$ solid reagent proceeded smoothly under mild reaction conditions and the corresponding monoallylated compounds were obtained in good to excellent yields. The allylation of *p*-xylene by the more reactive 1-chloro-3-methylbut-2-ene was also performed without consecutive cyclization at C–C double bond. Further, our allylation method can be performed under the atmosphere, and requires simple isolation procedures, since the solid reagent is nonhygroscopic and easy to handle.

In conclusion, composite lead fluoride reagents were found to promote Friedel–Crafts allylation selectively and efficiently, thus demonstrating that they are a new and unique type of solid reagent exhibiting mild Lewis acidity and halide capture abilities.

## Footnotes and References

* E-mail: ichihara@sanken.osaka-u.ac.jp

† Powder X-ray diffraction analysis of the reagent **A** showed not a mixture of the known lead compounds $PbF_2$, PbBrF or $PbBr_2$, but the formation of a new lead compound. It was determined by X-ray fluorescence analysis that the reagent was composed of Pb, Br and F in 1.0 : 0.3 : 1.8 molar ratio. Therefore, the reagent **A** has the formula $Pb_3BrF_5$.

‡ $ZnCl_2$–K10 purchased from Fluka was used.

1 R. Koncos and B. S. Friedmann, *Friedel–Crafts and Related Reactions*, ed. G. H. Olah, Interscience, New York, 1964, vol. II, part 1, pp. 289–412.
2 M. Kodomari, S. Nawa and T. Miyoshi, *J. Chem. Soc., Chem. Commun.*, 1995, 1895.
3 P. H. Espeel, B. Janssens and P. A. Jacobs, *J. Org. Chem.*, 1993, **58**, 7688.
4 K. Smith and G. M. Pollaud, *J. Chem. Soc., Perkin Trans 1*, 1994, 3519.
5 J. Ichihara, T. Hanafusa, Y. Takai and Y. Ito, *Chem. Lett.*, 1992, 1161.
6 J. Ichihara, Y. Takai, T. Hanafusa and K. Tomioka, *J. Fluorine Chem.*, 1995, **71**, 131.
7 J. Ichihara, T. Hanafusa, Y. Ito and K. Tomioka, *Jpn. Kokai Tokkyo Koho, Jap. Pat.*, 95-51 250, 1995.
8 P. Laszlo and A. Mathy, *Helv. Chim. Acta*, 1987, **70**, 577.
9 J. H. Clark, A. P. Kybett, D. J. Macquarrie, S. J. Barlow and P. Landon, *J. Chem. Soc., Chem. Commun.*, 1989, 1353.

*Received in Cambridge, UK, 1st July 1997; 7/04606E*

# Unprecedented electrophilic behaviour of tetrathiafulvalenium salts

**Owen Callaghan, Xavier Franck and John A. Murphy***

*Department of Pure and Applied Chemistry, The University of Strathclyde, 295 Cathedral Street, Glasgow, UK G1 1XL*

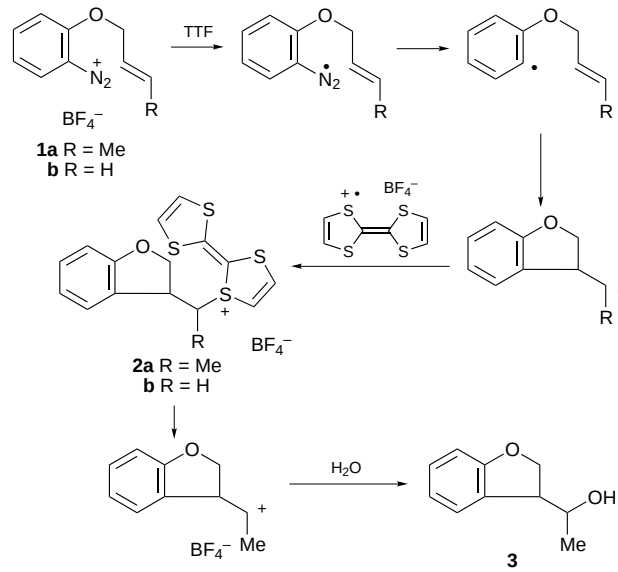
**Primary tetrathiafulvalenium salts display a diverse and unprecedented reactivity towards nucleophiles.**

Tetrathiafulvalene (TTF) and its derivatives have attracted widespread interest in the preparation of novel materials.[1] Recently, the synthetic value of TTF has become apparent as a result of its catalysis of 'radical-polar crossover[2] chemistry'. This leads to the formation of tetrathiafulvalenium salts **2** (Scheme 1) which have been isolated. In appropriate cases, *e.g.* **2a**, these compounds undergo facile $S_N1$ substitution at room temperature by such nucleophiles as water, alcohols and MeCN. Since this happens *in situ*, TTF is regenerated and so functions as a catalyst. The catalyst is effective down to a concentration of *ca*. 5 mol% but, below this level incomplete conversions are seen. It is clear that the catalyst is slowly destroyed during such reactions.

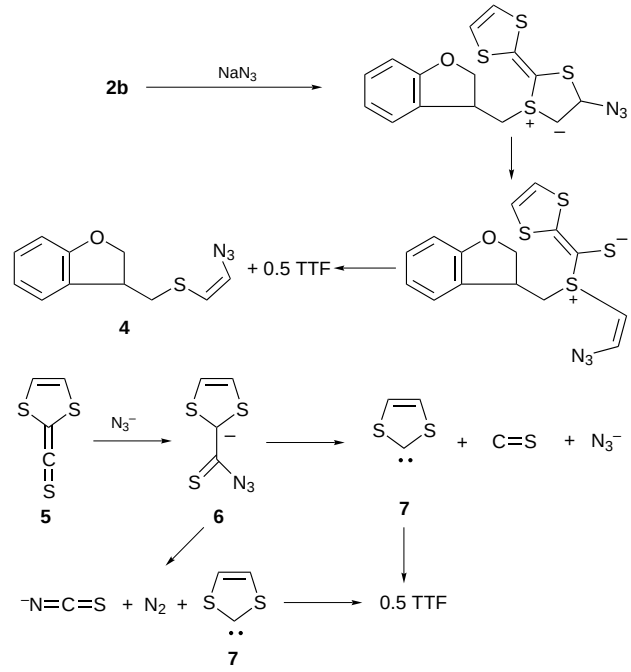
One of the goals for the future of this research is to develop catalysts with greater efficiency, *i.e.* with greater turnover numbers. To achieve this, it is necessary to develop an understanding of what processes other than substitution can occur with TTF salts. In the case of salts such as **2a**, these processes can only compete poorly with the substitution chemistry. This means that side-products are formed in very small amounts in such cases, and hence it is difficult to determine the nature of the side-reactions which ultimately limit the catalytic life of TTF.

A logical way to determine the nature of side-reactions would be to study TTF salts where $S_N1$ substitution reactions are inhibited. Alternative reactions observed under such conditions then provide useful information on potential side-reactions in normal radical-polar reactions. We have previously described[1] that when the TTF moiety is attached to a primary carbon, as in **2b**, no substitution was observed. It is totally reasonable that substrates such as **2b** should not undergo $S_N1$ substitution, and we assumed that the mildness of the nucleophiles rendered any alternative reactions too slow to observe. We now report the results of exposing primary tetrathiafulvalenium salts to various nucleophiles.

The salt **2b** was subjected to attack by sodium azide in acetone (Scheme 2). The principal products from this reaction were tetrathiafulvalene (45%) and the vinyl azide **4** (46%). Although the appearance of tetrathiafulvalene initially suggested that an $S_N2$ substitution had occurred, this is clearly not the case. To explain the formation of these products, we propose the sequence of steps depicted in Scheme 2. The thioketene **5** has not been detected, but could suffer attack by azide, which in turn would lead to fragmentation to afford the stabilised carbene **7** together with either carbon monosulfide and azide ion or thiocyanate ion plus nitrogen gas. The carbene **7** is an established synthetic precursor of TTF in other contexts.[3]

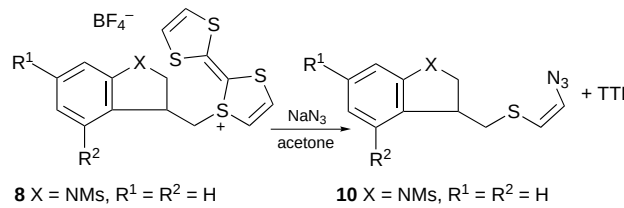



**Scheme 1**




**Scheme 2**

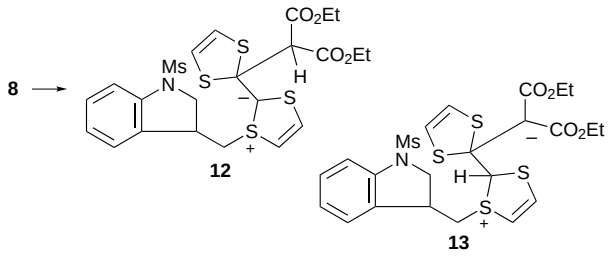
To determine the generality of this process, two further primary tetrathiafulvalenium salts **8** and **9** were prepared and treated with sodium azide in acetone, producing the vinyl azides **10** (36%) and **11** (41%) respectively (Scheme 3). In both cases,




**8** X = NMs, $R^1 = R^2 = H$ **10** X = NMs, $R^1 = R^2 = H$

**9** X = O, $R^1 = CH_2OH$, $R^2 = OMe$ **11** X = O, $R^1 = CH_2OH$, $R^2 = OMe$

**Scheme 3**



**Scheme 4**

TTF was also produced (49 and 21%, respectively). Compound **11** was converted into its crystalline 3,5-dinitrobenzoate ester. However, attempts to produce a suitable crystal for X-ray structure determination were not successful.

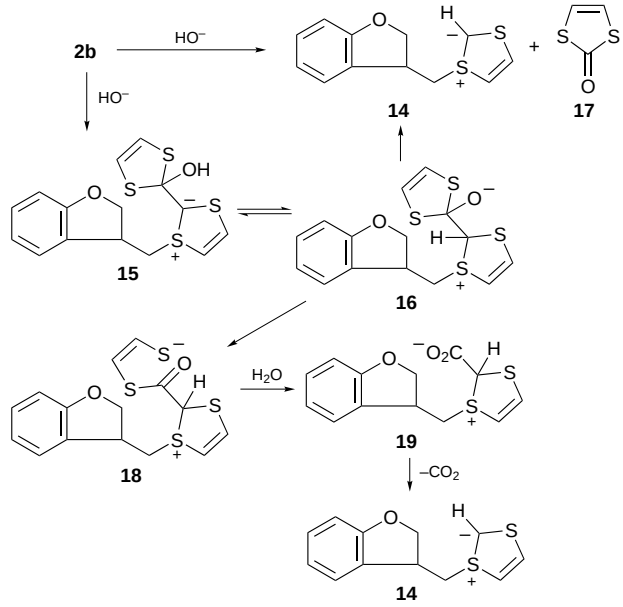
The fragmentations seen above represent a previously unseen reaction of TTF salts. However, a completely different mode of reaction was seen when **2b** was treated with the anion of diethyl malonate (Scheme 4). In this case, the product **12** (38%) resulted from reaction at the central carbon–carbon double bond of the salt. The structure **12** rather than **13** is suggested for the product, since the $^1$H NMR spectrum exhibits a one-proton singlet at δ 3.1; this is in the expected region for a malonate proton but is considerably upfield of the expected shift for the proton in **13**. In this reaction, no attack on the peripheral double bonds of the TTF salt was observed. The reason for the complete change in selectivity for azide and malonate as nucleophiles is unknown.

Finally, the salt **2b** was treated with potassium hydroxide as base under different conditions (KOH in methanol, KOH in DMSO, KOH in acetone). In these cases, an alternative but very clean fragmentation to **14** (79% NMR yield, 66% isolated yield) was seen. Possible mechanisms for this reaction are proposed in Scheme 5. The base-sensitive dithiocarbonate **17** has not been detected, even when only 1 equiv. of base was used.

The ylide proton in **14** appeared as a singlet at $\delta$ 3.1, and this correlated with a methine carbon at $\delta_C$ 84. The chemical shift of both the carbon and the proton indicate that this structure is best viewed as an ylide *i.e.* featuring $^{-}$C–S$^{+}$ rather than a C=S π-bond. However, one interesting feature is that the $^1$H and $^{13}$C NMR spectra of **14** show no indications of the presence of diastereoisomers. This contrasts with **2b**, where signals due to diastereoisomers are clearly seen. This may indicate that inversion at the sulfonium sulfur in **14** occurs rapidly on the NMR timescale.[4]

In conclusion, primary tetrathiafulvalenium salts exhibit a rich and complex chemistry. The design of improved radical-polar crossover catalysts should take into account the observed nucleophilic attack on both the periphery and the internal alkene of these TTF salts.

These studies may also prove useful in materials chemistry.[1] A vast number of salts with intriguing electrical conductivity properties are known. These salts result from electron transfer from TTF to appropriate acceptor molecules, and hence the salts formally involve the TTF radical-cation, TTF$^{+\cdot}$. Although these



**Scheme 5**

cations are different from the alkylated TTF cations discussed here, it is clear that quenching of the conducting properties of these compounds could arise by attack by nucleophiles on the TTF nucleus.

We thank the EPSRC and Merck Ltd. for funding and the EPSRC National Mass Spectrometry Service Centre, Swansea, for mass spectra. We thank Dr Richard Hartley, University of Glasgow, for helpful discussions.

## Footnote and References

* E-mail: john.murphy@strath.ac.uk

1 M. R. Bryce, *J. Mat. Chem.*, 1995, **5**, 1481; S. Horiuchi, H. Yamochi, G. Saito, K. Sakaguchi and M. Kusunoki, *J. Am. Chem. Soc.*, 1996, **118**, 8604; A. Charlton, A. E. Underhill, G. Williams, M. Kalaji, P. J. Murphy, K. M. A. Malik and M. B. Hursthouse, *J. Org. Chem.*, 1997, **62**, 3098.

2 C. Lampard, J. A. Murphy and N. Lewis, *J. Chem. Soc., Chem. Commun.*, 1993, 295; C. Lampard, J. A. Murphy, F. Rasheed, N. Lewis, M. B. Hursthouse and D. E. Hibbs, *Tetrahedron Lett.*, 1994, **35**, 8675; M. J. Begley, J. A. Murphy and S. J. Roome, *Tetrahedron Lett.*, 1994, **35**, 8679; R. J. Fletcher, C. Lampard, J. A. Murphy and N. Lewis, *J. Chem. Soc., Perkin Trans 1*, 1995, 1349; N. Lewis, J. A. Murphy, F. Rasheed and S. J. Roome, *Chem. Commun.*, 1996, 737; R. J. Fletcher, D. E. Hibbs, M. B. Hursthouse, C. Lampard, J. A. Murphy and S. J. Roome, *Chem. Commun.*, 1996, 739; M. Kizil, C. Lampard and J. A. Murphy, *Tetrahedron Lett.*, 1996, **37**, 2511.

3 See for example: A. J. Moore and M. R. Bryce, *Synthesis*, 1997, 407.

4 For rapid inversion at sulfur in a sulfur ylide, see: H. Nozaki, M. Takaku and K. Kondo, *Tetrahedron*, 1966, **22**, 2145.

*Received in Cambridge, UK, 3rd July 1997; 7/04690A*

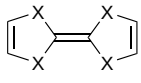
# New hybrid tetrachalcogenofulvalenes: diselenaditellurafulvalene and its dimethyl derivative

**Kazuo Takimiya, Atsushi Morikami, Yoshio Aso and Tetsuo Otsubo***

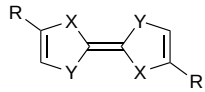
*Department of Applied Chemistry, Faculty of Engineering, Hiroshima University, Kagamiyama, Higashi-Hiroshima 739, Japan*

**A simple two-stage synthesis of hybrid tetrachalcogenofulvalenes containing two tellurium and two selenium atoms and the properties of their highly conductive TCNQ complexes are described.**

Since the discovery of the metallic conductivity of the TTF–TCNQ complex,[1] much effort has been devoted to the development of novel TTF-type electron donor molecules.[2] One of the successful structural modifications of TTF is to replace the skeletal sulfur atoms by selenium or tellurium atoms with large polalizabilities.[3] Thus the TCNQ complexes of tetra-



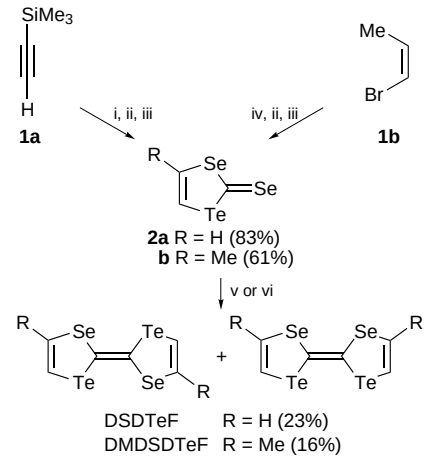
TTF X = S
TSF X = Se
TTeF X = Te



DSDTF X = S, Y = Se, R = H
DSDTeF X = Se, Y = Te, R = H
DMDSTeF X = Se, Y = Te, R = Me

selenafulvalene (TSF)[4] and tetratellurafulvalene (TTeF)[5] showed much higher conductivities (800 and 2200 S $cm^{-1}$, respectively) than TTF–TCNQ (500 S $cm^{-1}$). Of them, TTeF has attracted more attention, not only in that the complex has an extraordinarily high conductivity, but also in that it remains metallic down to a measurable low temperature (2 K). In contrast, the TTF–TCNQ and TSF–TCNQ complexes demonstrate a metal–insulator transition (Peierls transition) at 59 and 40 K, respectively, characteristic of a one-dimensional organic metal. In the TTeF–TCNQ complex, strong nonbonded tellurium–tellurium interactions are responsible for the suppression of the Peierls transition. Compared to TTF and TSF, a disadvantage of TTeF is its poor accessibility,[6] and the fact that only a limited number of its derivatives have been prepared.[7] Although a hybrid of TTF and TSF, diselenadithiafulvalene (DSDTF), has long been known,[8,9] no analogous tellurium-hybrid tetrachalcogenofulvalenes have been studied. Such hybrid compounds are expected not only to offer additional examples of tellurium-containing conductive complexes, but also to provide useful information on the contribution of the tellurium atoms to the design of organic metals. Here we describe the simple two-stage synthesis and properties of diselenaditellurafulvalene (DSDTeF) and its dimethyl derivative (DMDSDTeF) as the first tellurium-hybrid tetrachalcogenofulvalenes.

All the preceding TTeF donors were synthesized by a three-component reaction of 1,2-ditellurolate anion and tetrachloroethene. On the other hand, DSDTeF was obtained by the simple two-stage route as shown in Scheme 1, previously used for the syntheses of TSF[4] and DSDTF.[9] The precursor, 1,3-selenatellurole-2-selone **2a** was readily obtained in 83% yield by metallation of commercially available trimethylsilylacetylene **1a** with 1 equiv. of BuLi in THF at −78 °C followed by successive *in situ* treatment with 1 equiv. tellurium powder at −78 °C and then with 1 equiv. carbon diselenide at −90 °C, and finally quenching with water.[10] Subsequent triethyl phosphite-promoted homocoupling reaction of **2a** in refluxing toluene




**Scheme 1** *Reagent and conditions*: i, BuLi (1 equiv.), $Me_2NC_2H_4NMe_2$, THF, −78 °C, 0.5 h; ii, Te powder (1 equiv.), −78 °C then room temp., 3 h; iii, $CSe_2$ (1 equiv.), −90 °C, 3 min., then $H_2O$–THF (1 : 1, v/v); iv, BuLi (2 equiv.), THF, −78 °C, 2 h; v, excess $P(OEt)_3$, toluene, reflux, 2 h (for DSDTeF); vi, excess $P(OEt)_3$, benzene, reflux, 10 h (for DMDSDTeF)

afforded DSDTeF in 23% yield.† Similarly, 5-methyl-1,3-selenatellurole-2-selone **2b** was prepared in 61% yield from lithium 1-propynide, *in situ* generated by dehydrobromination of 1-bromopropene **1b** with BuLi, and subjected to a similar homocoupling reaction, producing DMDSDTeF in 16% yield.

The $^1H$ NMR spectrum of DSDTeF contains two sets of AB multiplets in a ratio of 4 : 6, indicating that it consists of a mixture of the *cis*- and *trans*- (*E* and *Z*) isomers, as seen in the case of DSDTF.[8,9] These geometrical isomers could not be separated by conventional purification methods. DMDSDTeF was also obtained as an isomeric mixture (3 : 7 ratio), but its recrystallization from benzene precipitated the pure main isomer. The cyclic voltammetry of DSDTeF showed two reversible one-electron oxidation waves at +0.43 and +0.73 V *vs.* Ag/AgCl; thus DSDTeF is a somewhat stronger electron donor than TSF ($E_{1/2}$ +0.49 and +0.78 V). Furthermore, DMDSDTeF has slightly lower oxidation potentials, as expected from the substituent effect of the methyl groups ($E_{1/2}$ +0.41 and +0.71 V).

Upon equimolar reaction of DSDTeF with TCNQ and $TCNQF_2$ in MeCN, crystalline 1 : 1 charge-transfer complexes were formed.‡ The room temperature conductivity of the DSDTeF–TCNQ complex measured on a single needle crystal was very high (1400 ± 300 S $cm^{-1}$, 10 samples), as was that of the DSDTeF–$TCNQF_2$ complex (900 ± 200 S $cm^{-1}$, 5 samples). DMDSDTeF also formed a conductive 1 : 1 complex with TCNQ ($\sigma_{rt}$ = 37 S $cm^{-1}$ measured on a compressed pellet). The conductivity of DSDTeF–TCNQ is just in between those of TSF–TCNQ and TTeF–TCNQ. In addition, variable temperature measurements demonstrate that, as shown in Fig. 1, the conductivity steadily increases to 2.5 times this value as the temperature drops to 4 K, and there is no metal-insulator transition as seen for TTeF–TCNQ.[5] These results clearly indicate that the two tellurium atoms of DSDTeF serve to

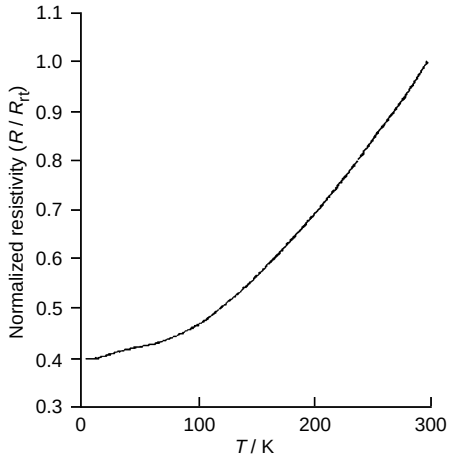



**Fig. 1** Electrical resistance of **1**–TCNQ

enhance intermolecular interactions enough not only to induce the high conduction of its charge-transfer complexes but also to suppress the Peierls transition. On considering their ready accessibility as compared to TTeF, the present tellurium-hybrid tetrachalcogenofulvalenes are electron donors of choice to study tellurium-containing organic metals.

This work was partially supported by Grants-in-Aid for Scientific Research from the Ministry of Education, Science, Sports and Culture of Japan.

## Footnotes and References

* E-mail: otsubo@ipc.hiroshima-u.ac.jp

† New compounds were characterized by elemental analysis and NMR and mass spectroscopy. *Selected data* for DSDTeF: black prisms from benzene, mp 139.0–140.0 °C; $\delta_H$ ($CDCl_3$, 400 MHz) (major isomer) 7.60 (d, *J* 8.23) and 8.15 (d, *J* 8.23); (minor isomer) 7.76 (d, *J* 8.23) and 8.08 (d, *J* 8.23); *m/z* 492 ($M^+$) with an isotopic pattern containing two selenium and two tellurium atoms. Calc. for $C_6H_4Se_2Te_2$: C, 14.73; H, 0.82. Found: C, 14.96; H, 0.87%. For DMDSDTeF: black crystals from benzene (major isomer); mp 189.0–190.0 °C (decomp.); $\delta_H$ ($CDCl_3$, 400 MHz) 2.23 (d, *J* 1.46, 6 H) and 7.50 (q, *J* 1.46, 2 H); *m/z* 520 ($M^+$) with an isotopic pattern containing two selenium and two tellurium atoms. Calc. for $C_8H_8Se_2Te_2$: C, 18.58; H, 1.56. Found: C, 18.60; H, 1.47%. Minor isomer: $\delta_H$ ($CDCl_3$, 400 MHz) 2.22 (d, *J* 1.46, 6 H) and 7.44 (q, *J* 1.46, 2 H). For **2a**: black plate from chlorobenzene; mp 128 °C (decomp. without melting); $\delta_H$ ($CDCl_3$, 400 MHz) 8.27 (d, *J* 8.46) and 8.80 (d, *J* 8.46); $\nu_{max}$ (KBr)/$cm^{-1}$ 845 (C=Se); *m/z* 326 ($M^+$) with an isotopic pattern containing two selenium and one tellurium atoms. Calc. for $C_3H_2Se_2Te$: C, 11.14; H, 0.62. Found: C, 11.27; H, 0.60%. For **2b**: black prisms from chlorobenzene; mp 115.5–116.0 °C; $\delta_H$ ($CDCl_3$, 400 MHz) 2.53 (d, *J* 1.32, 3 H) and 8.23 (q, *J* 1.32, 1 H). $\nu_{max}$(KBr)/$cm^{-1}$ 851 (C=Se); *m/z* 340 ($M^+$) with an isotopic pattern containing two selenium and one tellurium atoms. Calc. for $C_4H_4Se_2Te$: C, 14.23; H, 1.19. Found: C, 14.22; H, 1.15%.

‡ The ratio of donor to acceptor was determined as 1 : 1 based on elemental analyses.

1 J. Ferraris, D. O. Cowan, V. Walatka Jr. and J. H. Perlstein, *J. Am. Chem. Soc.*, 1973, **95**, 948.
2 For a recent review, see J. M. Williams, J. R. Ferraro, R. J. Thorn, K. D. Carlson, U. Geiser, H. H. Wang, A. M. Kini and M.-H. Whangbo, *Organic Superconductors* (*Including Fullerenes*)*: Synthesis, Structure, Properties, and Theory*, Prentice Hall, New Jersey, 1992.
3 D. Cowan and A. Kini, in *The Chemistry of Organic Selenium and Tellurium Compounds*, ed. S. Patai, Wiley, New York, 1987, vol. 2, ch. 12.
4 E. M. Engler and V. V. Patel, *J. Am. Chem. Soc.*, 1974, **96**, 7376; S. Etemad, T. Penney, E. M. Engler, B. A. Scott and P. E. Seiden, *Phys. Rev. Lett.*, 1975, **34**, 741; E. M. Engler, B. A. Scott, S. Etemad, T. Penney and V. V. Patel, *J. Am. Chem. Soc.*, 1977, **99**, 5909.
5 R. D. McCullough, G. B. Kok, K. A. Lerstrup and D. O. Cowan, *J. Am. Chem. Soc.*, 1987, **109**, 4115; M. D. Mays, R. D. McCullough, D. O. Cowan, T. O. Poehler, W. A. Bryden and T. J. Kistenmacher, *Solid State Commun.*, 1988, **65**, 1089; M. D. Mays, R. D. McCullough, A. B. Bailey, D. O. Cowan, W. A. Bryden, T. O. Poehler and T. J. Kistenmacher, *Synth. Met.*, 1988, **27**, B493; D. O. Cowan, M. D. Mays, T. J. Kistenmacher, T. O. Poehler, M. A. Beno, A. M. Kini, J. M. Williams, Y. Kwok, K. D. Carlson, L. Xiao, J. J. Novoa and M.-H. Whangbo, *Mol. Cryst. Liq. Cryst.*, 1990, **181**, 43; D. O. Cowan, R. McCullough, A. Bailey, K. Lerstrup, D. Talham, D. Herr and M. Mays, *Phosphorous Sulfur Silicon*, 1992, **67**, 277.
6 D. E. Herr, M. D. Mays, R. D. McCullough, A. B. Bailey and D. O. Cowan, *J. Org. Chem.*, 1996, **61**, 7006.
7 K. Lerstrup, D. Talham, A. Bloch, T. Poehler and D. Cowan, *J. Chem. Soc., Chem. Commun.*, 1982, 336; F. Wudl and E. Aharon-Shalom, *J. Am. Chem. Soc.*, 1982, **104**, 1154; K. Lerstrup, D. O. Cowan and T. J. Kistenmacher, *J. Am. Chem. Soc.*, 1984, **106**, 8303; K. Lerstrup, A. Bailey, R. McCullough, M. Mays, D. Cowan and T. Kistenmacher, *Synth. Met.*, 1987, **19**, 647.
8 M. V. Lakshmikantham, M. P. Cava and A. F. Garito, *J. Chem. Soc., Chem. Commun.*, 1975, 383; M. V. Lakshmikantham and M. P. Cava, *J. Org. Chem.*, 1980, **45**, 2632.
9 E. M. Engler and V. V. Patel, *J. Chem. Soc., Chem. Commun.*, 1975, 671; E. M. Engler, F. B. Kaufman, D. C. Green, C. E. Klots and R. N. Compton, *J. Am. Chem. Soc.*, 1975, **97**, 2921.
10 A similar convenient preparation of 1,3-dithiole-2-thiones and 1,3-diselenole-2-thiones was recently reported; K. Takimiya, A. Morikami and T. Otsubo, *Synlett*, 1997, 319.

*Received in Cambridge, 11th July 1997; 7/04974I*

# Electron transfer properties of active aldehydes derived from thiamin coenzyme analogues

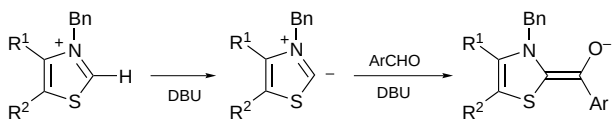
**Ikuo Nakanishi, Shinobu Itoh, Tomoyoshi Suenobu and Shunichi Fukuzumi***

*Department of Applied Chemistry, Faculty of Engineering, Osaka University, 2-1 Yamada-oka, Suita, Osaka 565, Japan*

**The rate constants and reorganization energies of electron transfer reactions between active aldehydes, derived from thiamin coenzyme analogues, and the corresponding one-electron oxidized radical species have been determined to demonstrate the efficient electron transfer properties of the active aldehydes.**

The conjugate base of 2-(α-hydroxyethyl)thiamin, a so called 'active aldehyde', derived from thiamin diphosphate coenzyme and pyruvate in the presence of a base is known to act as an efficient electron transfer catalyst which can mediate electron transport from pyruvate to various physiological electron acceptors. These include the lipoamide in pyruvate dehydrogenase multienzyme complex,[1] flavin adenine dinucleotide (FAD) in pyruvate oxidase[2] and the $Fe_4S_4$ cluster in pyruvate-ferredoxin oxidoreductase.[3] However, very little is known about the redox behaviour of active aldehydes because of their instability and tendency to undergo acyloin condensation with a second pyruvate molecule in the absence of oxidizing agents.[4] We report herein that active aldehyde **2**$^-$ derived from thiazolium salts **1a**–**c** and *o*-tolualdehyde in the presence of a strong base (Scheme 1) can be stabilized by the steric bulk of an *o*-methyl group and that the radical species produced by the one-electron oxidation of stabilized active aldehydes can be readily detected by EPR spectroscopy. The important electron transfer properties of the active aldehydes, such as reorganization energies of electron transfer reactions between the active aldehydes and the corresponding one-electron oxidized radical species, are determined by analysing linewidth variations in the EPR spectra.

The active aldehyde **2a**$^-$ ($\lambda_{max}$ = 380 nm)[5] was prepared by the addition of 1,8-diazabicyclo[5.4.0]undec-7-ene (DBU) to an MeCN solution of **1a** and *o*-tolualdehyde, keeping the ratio of the components constant (**1a** : *o*-tolualdehyde : DBU = 1 : 50 : 2). Then, the solution was partially electrolysed at −0.70 V *vs*. SCE, which is between the redox potentials for the **2a**$^-$/**2a**$^{\cdot}$ (−0.96 V *vs*. SCE in MeCN) and **2a**$^{\cdot}$/**2a**$^+$ couples (−0.52 V *vs*. SCE in MeCN),[6] to give the corresponding radical species **2a**$^{\cdot}$. EPR spectra for **2a**$^{\cdot}$ were obtained at different concentrations of **2a**$^-$, as shown in Fig. 1. The spectra of the radical species were persistent for several hours after the electrolysing potential had been switched off. The hyperfine splitting constants shown in Table 1 and the maximum slope linewidths ($\Delta H_{msl}$) were determined from a computer simulation of the EPR spectra (Fig. 1). The $\Delta H_{msl}$ value thus determined increases linearly with an increase in the concentration of **2a**$^-$, as shown in Fig. 2. Such linewidth variations of the EPR spectra can be used to investigate the rate processes involving the radical species.[7] The rate constants ($k_{et}$) of the electron transfer reactions between **2a**$^-$ and **2a**$^{\cdot}$ [eqn. (1)] were




**1a** $R^1$ = Me, $R^2$ = H
**b** $R^1$ = $R^2$ = Me
**c** $R^1$ = $R^2$ = H

Ar = *o*-$MeC_6H_4$

**2**$^-$

**Scheme 1**

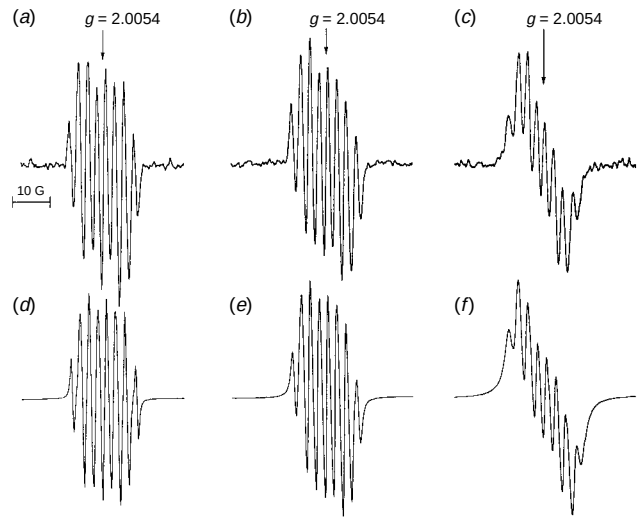
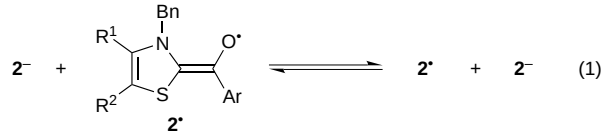



**Fig. 1** EPR spectra (X-band) of **2a**$^{\cdot}$ observed in the presence of different concentrations of **2a**$^-$: (*a*) 1.5 × $10^{-3}$, (*b*) 6.5 × $10^{-3}$ and (*c*) 3.0 × $10^{-2}$ M (in MeCN at 298 K, microwave frequency 9.21 GHz; modulation frequency 100 kHz; modulation amplitude 2.5 × $10^{-3}$ G; microwave power 10 mW; scan rate 19 G $min^{-1}$), and the corresponding computer simulation spectra using the hyperfine splitting values shown in Table 1 and linewidths of (*d*) 0.50, (*e*) 0.70 and (*f*) 1.55 G



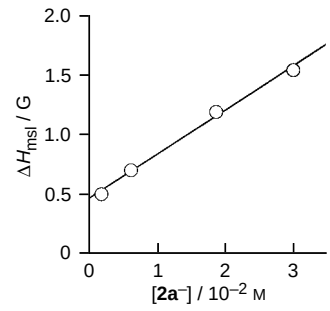




**Fig. 2** Plot of [**2a**$^-$] *vs*. $\Delta H_{msl}$ for EPR spectra of **2a**$^{\cdot}$ in MeCN at 298 K

determined using eqn. (2), where $\Delta H_{msl}$ and $\Delta H^0_{msl}$ are the

$$k_{et} = \frac{1.57 \times 10^7 (\Delta H_{msl} - \Delta H^0_{msl}}{(1 - P_i)[\mathbf{2}^-]} \quad (2)$$

maximum slope linewidth of the EPR spectra in the presence and absence of $\mathbf{2}^-$, respectively, and $P_i$ is a statistical factor which can be taken as nearly zero. The $k_{et}$ values for other active aldehydes $\mathbf{2b}^-$ and $\mathbf{2c}^-$ were determined in a similar manner and are listed in Table 1. The reorganization energies (λ) of the electron transfer reactions are obtained from the $k_{et}$ values using eqn. (3) ($Z = 10^{11}$ M$^{-1}$ s$^{-1}$),[8] and the λ values are also listed in

$$k_{et} = Z \exp(-\lambda/4kT) \quad (3)$$

Table 1. No prominent change in the $k_{et}$ or λ values is observed depending on the presence of methyl substituents on the thiazolium rings. The λ values are as small as those of fast electron transfer exchange systems such as *p*-benzoquinone/semiquinone radical anion (55 kJ mol$^{-1}$ in DMF) and naphthalene/radical anion of naphthalene (50 kJ mol$^{-1}$ in DMF) systems.[9]

The largely negative oxidation potentials of the active aldehydes derived from thiamin coenzyme analogues and the small reorganization energies for the electron transfer reactions indicate that the active aldehydes have strong electron donor abilities and that they are suitable for fast electron transfer systems where they can act as efficient electron transfer catalysts in electron transfer from pyruvate to physiological electron acceptors in enzymatic systems.

**Table 1** Hyperfine splitting values for $\mathbf{2}^{\cdot}$ produced by the one-electron oxidation of $\mathbf{2}^-$ and the observed rate constants ($k_{et}$) and the reorganization energies (λ) of the electron transfer reactions between $\mathbf{2}^-$ and $\mathbf{2}^{\cdot}$ in MeCN at 298 K[a]

| | Hyperfine splitting/G | | | | |
|---|---|---|---|---|---|
| Active aldehyde | $a_{N-}$ (N) | $a_{H-}$ (N–$CH_2$) | $a_{H-}$ (C–5) | $k_{et}/10^8$ M$^{-1}$ s$^{-1}$[b] | λ/kJ mol$^{-1}$[b] |
| $\mathbf{2a}^-$ | 4.71 | 2.35 | 2.89 | 5.6 | 52 |
| $\mathbf{2b}^-$ | 4.75 | 2.07 | 2.64 | 6.6 | 50 |
| $\mathbf{2c}^-$ | 4.89 | 2.66 | 2.66 | 4.5 | 54 |

[a] ±0.5 K. [b] Experimental error = ±5%.

## Footnote and References

* E-mail: fukuzumi@chem.eng.osaka-u.ac.jp

1 L. J. Reed, *Acc. Chem. Res.*, 1974, **7**, 40.
2 L. P. Hager, *J. Biol. Chem.*, 1957, **229**, 251.
3 K. Uyeda and J. C. Rabinowitz, *J. Biol. Chem.*, 1971, **246**, 3120; L. Kerscher, S. Nowitzki and D. Oesterhelt, *Eur. J. Biochem.*, 1982, **128**, 223.
4 R. Breslow, *J. Am. Chem. Soc.*, 1958, **80**, 3719; L. O. Krampitz, *Annu. Rev. Biochem.*, 1969, **38**, 213; R. Kluger, *Chem. Rev.*, 1987, **87**, 863; W. Tagaki and H. Hara, *J. Chem. Soc., Chem. Commun.*, 1973, 891; F. Diederich, and H.-D. Lutter, *J. Am. Chem. Soc.*, 1989, **111**, 8438; Y.-T. Chen, G. L. Barletta, K. Haghjoo, J. T. Cheng and F. Jordan, *J. Org. Chem.*, 1994, **59**, 7714.
5 G. Barletta, W. P. Huskey and F. Jordan, *J. Am. Chem. Soc.*, 1992, **114**, 7607; C. C. Chiu, K. Pan and F. Jordan, *J. Am. Chem. Soc.*, 1995, **117**, 7027; G. L. Barletta, Y. Zou, W. P. Huskey and F. Jordan, *J. Am. Chem. Soc.*, 1997, **119**, 2356.
6 I. Nakanishi, S. Itoh, T. Suenobu, H. Inoue and S. Fukuzumi, *Chem. Lett.*, 1997, 707.
7 R. Chang, *J. Chem. Ed.*, 1970, **47**, 563; K. S. Cheng and N. Hirota, in *Investigation of Rates and Mechanisms of Reactions*, ed. G. G. Hammes, Wiley-Interscience, New York, 1974, vol. VI, p. 565.
8 R. A. Marcus, *Annu. Rev. Phys. Chem.*, 1964, **15**, 155.
9 L. Eberson, *Adv. Phys. Org. Chem.*, 1982, **18**, 79 and references cited therein.

*Received in Cambridge, UK, 30th June 1997; 7/04559J*

# On the mechanism of remote induction using (5-alkoxypent-2-enyl)stannanes: trapping the intermediate allyltin trihalides by phenyllithium and the X-ray crystal structure of [(2*SR*,3*RS*)-1-(4-bromobenzoyloxy)-2-methylpent-3-yl]-(triphenyl)stannane

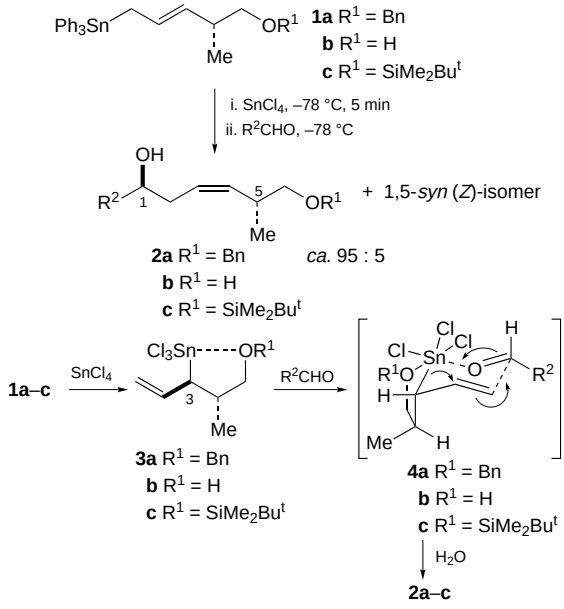
**Roy L. Beddoes, Lindsay A. Hobson and Eric J. Thomas***

*The Department of Chemistry, The University of Manchester, Manchester, UK M13 9PL*

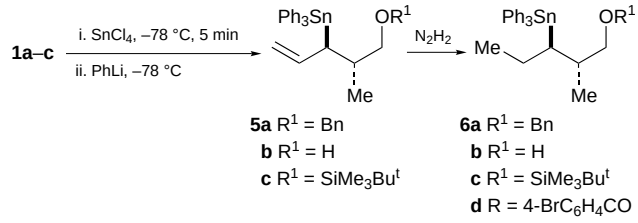
**Allyltin trihalides, intermediates in tin(IV) halide promoted reactions of 5-alkoxy-4-methylpent-2-enyl(triphenyl)-stannanes with aldehydes which proceed with 1,5-induction, have been trapped by phenyllithium to give [(3*RS*,4*SR*)-5-alkoxy-4-methylpent-1-en-3-yl](triphenyl)stannanes.**

Useful levels of 1,5-, 1,6- and 1,7-asymmetric induction have been found in reactions of (alkoxyalk-2-enyl)stannanes with aldehydes promoted by tin(IV) halides.[1] For example, treatment of [(4*R*)-5-benzyloxy-4-methylpent-2-enyl](triphenyl)stannane **1a** with tin(IV) chloride followed by addition of an aldehyde gives the 1,5-*anti* (*Z*)-alkenol **2a** (1,5-*anti* : 1,5-*syn* = 95 : 5) (Scheme 1).[2] To explain the stereo- and regio-selectivity of this reaction, it was suggested that transmetallation of the allylstannane **1a** is stereoselective and generates the allyltin trichloride **3a** in which the methyl and vinyl groups are *trans*-disposed about the oxastannane ring formed by coordination of the electron deficient tin by the oxygen of the benzyloxy group. This allytin trichloride then reacts with the aldehyde *via* the cyclic, chair-like transition structure **4a** in which the axial preference of the group next to tin determines the facial selectivity of the reaction with the aldehyde and introduces the double-bond into the product with (*Z*)-geometry.[1,3] Similar results were obtained using the 5-hydroxy- and 5-(*tert*-butyldimethylsilyloxy)-pent-2-enylstannanes **1b** and **1c** (1,5-*anti* : 1,5-*syn* = 80 : 20).[4] We now report evidence for the participation of allyltin trichlorides **3** in these reactions.

It was decided to attempt the conversion of the allyltin trichlorides into isolable products using a reaction which would




**Scheme 1**




**Scheme 2**

retain their C(3)–Sn bonds. It was found that addition of an excess of phenyllithium to the reaction mixture formed by treatment of the racemic pentylstannanes **1a**–**c** with tin(IV) chloride for 5 min gave the pent-2-en-3-yl(triphenyl)stannanes **5a**–**c** with excellent stereoselectivity (*ca*. 95 : 5) (Scheme 2). These allylstannanes were isolated and characterised, and reduced using diimide to give the pentan-3-ylstannanes **6a**–**c** to avoid problems associated with 1,3-migration of the tin.[5]

The structure of the (hydroxypentan-3-yl)stannane **6b** was established by an X-ray crystal structure of its 4-bromobenzoate **6d**.† Fig. 1 shows a projection of a molecule of the 4-bromobenzoate which illustrates its stereochemistry. Benzylation and silylation of **6b** gave the benzyloxy- and silyloxypentan-3-ylstannanes **6a** and **6c**, confirming their structures.

The formation of the [(3*RS*,4*SR*)-pentenyl](triphenyl)stannanes **5a**–**c** in these reactions is consistent with stereoselective formation of the allyltin trichlorides **3a**–**c**, which are trapped by phenyllithium.‡§ To probe the mechanism of transmetallation, the [(3*RS*,4*SR*)-5-benzyloxypent-2-en-3-yl]stannane **5a** was treated with tin(IV) chloride followed by the addition of an aldehyde (Scheme 3). The 1,5-*syn* diastereoisomers **7a**–**c** were the major products from these reactions if 2 min was allowed between the addition of the tin(IV) chloride and addition of the aldehyde, although the yields were modest and the stereoselectivity varied with the aldehyde. The stereoselectivity was also dependent upon the time allowed between the addition of the tin(IV) chloride and addition of the aldehyde, *e.g.* with

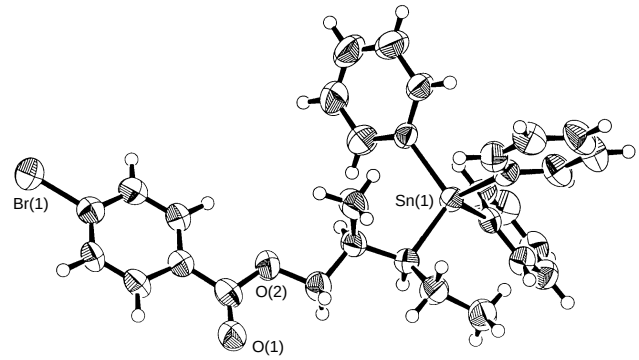
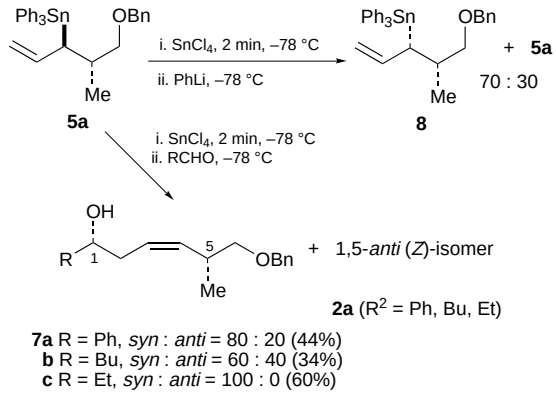


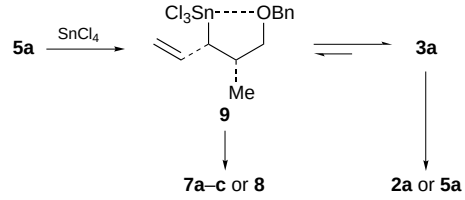

**Fig. 1** Projection of a molecule of the 4-bromobenzoate **6d** as determined by X-ray crystallography




**Scheme 3**

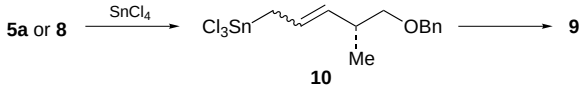
benzaldehyde the stereoselectivity of 80 : 20 in favour of the 1,5-*syn* product **7a** was reduced to 60 : 40 if 5 min was left before addition of the aldehyde, and reversed to 80 : 20 in favour of the 1,5-*anti* product **2a** ($R^2$ = Ph; 40%) if the mixture was left for 10 min before the addition of the aldehyde. Addition of phenyllithium to the allyltin trichloride generated by transmetallation of the 5-benzyloxypentenylstannane **5a** for 2 min gave the (3*RS*,4*RS*)-5-benzyloxypentenylstannane **8** as the major product together with its (3*RS*,4*SR*)-isomer **5a** (ratio 70 : 30).¶

It would appear that the (3*RS*,4*RS*)-allyltin trichloride **9** is the major, kinetically-formed intermediate from transmetallation of the allylstannane **5a** (Scheme 4) and leads to the formation of the 1,5-*syn* products **7a**–**c** and the (3*RS*,4*RS*)-allylstannane **8** if 2 min only is allowed before addition of the aldehyde or phenyllithium. If, however, the addition of the aldehyde or phenyllithium is delayed, equilibration of **9** to **3a** takes place, leading to increased amounts of the 1,5-*anti* products **2a**.

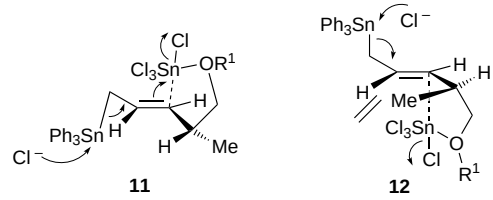



**Scheme 4**

The formation of the (3*RS*,4*RS*)-allyltin trichloride **9** from the allylstannane **5a** corresponds to an electrophilic substitution with inversion of configuration at the more substituted end of an allylstannane when an SE′ process might have been expected. However, treatment of the (3*RS*,4*RS*)-allylstannane **8** with tin(IV) chloride for 3 min followed by addition of benzaldehyde also gives the 1,5-*syn* alcohol **7a** as the major product (1,5-*syn* : 1,5-*anti* = 73 : 27, 60% combined yield), and trapping the intermediate allyltin trichloride with phenyllithium returns the (3*RS*,4*RS*)-allylstannane **8** together with its epimer **5a** (ratio 70 : 30). The (3*RS*,4*RS*)-allyltin trichloride **9** is therefore involved in reactions of both allylstannanes **5a** and **8**. Perhaps transmetallation of the allylstannanes **5a** and **8** proceeds *via* formation of the terminal allyltin trichloride **10** (Scheme 5), in which, for the (*Z*)-isomer, the electron deficient tin would be coordinated by the alkoxy group, followed by rapid isomerisation to the (3*RS*,4*RS*)-allyltin trichloride **9**. This is then trapped by the aldehyde or phenyllithium or isomerises to the (3*RS*,4*SR*)-allyltin trichloride **3a** on standing.




**Scheme 5**




**Scheme 6**

The high stereoselectivities in reactions of allylstannanes **1a**–**c** promoted by tin(IV) chloride would appear primarily to be due to kinetic control of the transmetallation. Perhaps the tin(IV) chloride is delivered by the oxygen of the 5-substituent to the allylstannane at C(3) with transition structure **11** being preferred over the alternative transition structure **12** (Scheme 6) because of increased steric interaction between the terminal methyl group and H(2) in **12**.

We thank the University of Manchester and SmithKline Beecham for support (to L. A. H.) under the CASE Scheme, Dr M. Fedouloff of SmithKline Beecham for helpful discussions and Dr M. Helliwell for preparing the X-ray data for publication.

## Footnotes and References

* E-mail: e.j.thomas@man.ac.uk

† *X-Ray crystal data* for **6d**: $C_{31}H_{31}BrO_2Sn$, $M$ = 634.18, triclinic, space group $P\bar{1}$, $a$ = 10.390(2), $b$ = 17.643(3), $c$ = 8.429(2) Å, $\alpha$ = 92.81(2), $\beta$ = 113.88(1), $\gamma$ = 90.83(1)°, $U$ = 1410.2(4) Å$^3$ (by least-squares refinement on diffractometer angles of 25 automatically centred reflections), $\lambda$ = 0.71069 Å, $Z$ = 2, $D_c$ = 1.493 g cm$^{-3}$, $\mu$ = 23.51 cm$^{-1}$, $F(000)$ = 636.00, colourless prism, crystal dimensions 0.2 × 0.2 × 0.25 mm. Data were collected at 293 K using a Rigaku AFC-5R diffractometer with graphite monochromated Mo-Kα radiation and a rotating anode generator. A total of 5290 reflections were measured in the $\omega$–2$\theta$ scan mode to a $2\theta_{max}$ of 50.1°, which gave 4987 independent reflections ($R_{int}$ = 0.024). A semi-empirical absorption correction was applied, based on the azimuthal scans of several reflections (transmission factors: 0.8958–1.00). A decay correction was also applied (3.16% decline). 3413 reflections had $I > 3\sigma(I)$. The structure was solved by Patterson methods using DIRDIF92 PATTY (ref. 6) and refined using full-matrix least-squares refinement using TEXSAN (ref. 7). All non-hydrogen atoms were refined anisotropically and hydrogen atoms were included in calculated positions. Refinement of the 316 variables converged with $R$ = 0.040, $R_w$ = 0.038 based on the 3413 reflections with $I > 3\sigma(I)$ and where $w = 1/[\sigma^2|F_o| + 0.00005|F_o|^2]$. Max/min peaks in the final difference map: 0.70/−0.38 eA$^{-3}$. CCDC 182/557.

‡ [(4*R*)-5-Benzyloxy-4-methylpent-2-enyl](tributyl)stannane also gave the triphenylstannane **5a** after transmetallation by tin(IV) chloride and addition of phenyllithium, so confirming that the phenyl substituents in **5a** are derived from the phenyllithium and not from the starting material **1a**. Trapping the allyltin trichloride **3a** with methyllithium also gave the trimethylstannyl analogue of **5a** (40%).

§ An alternative explanation would be that a mixture of rapidly equilibrating isomeric allyltin trichlorides is present after transmetallation of the pentenylstannanes **1a**–**c** but that the (2*SR*,3*RS*)-isomers are the most reactive. However this explanation is inconsistent with the formation of different products from the allyltin trichlorides **3a** and **9**.

¶ The isolation of both of the triphenylpentenylstannanes **5a** and **8** during this work meant that we knew we were able to distinguish them.

1 E. J. Thomas, *Chem. Commun.*, 1997, 411.
2 J. S. Carey and E. J. Thomas, *Synlett*, 1992, 585.
3 A. H. McNeill and E. J. Thomas, *Tetrahedron Lett.*, 1990, **31**, 6239; V. J. Jephcote, A. J. Pratt and E. J. Thomas, *J. Chem. Soc., Perkin Trans. 1*, 1989, 1521.
4 J. S. Carey, T. S. Coulter and E. J. Thomas, *Tetrahedron Lett.*, 1993, **34**, 3933.
5 V. J. Jephcote and E. J. Thomas, *J. Chem. Soc., Perkin Trans. 1*, 1991, 429.
6 P. T. Beurskens, G. Admiraal, G. Beurskens, W. P. Bosman, S. Garcia-Granda, R. O. Gould, J. M. M. Smits and C. Smykalla, The DIRDIF Program System, 1992, Technical Report of the Crystallography Laboratory, University of Nijmegen, The Netherlands.
7 TEXSAN: Crystal Structure Analysis Package, Molecular Structure Corporation, 1985 and 1992.

*Received in Liverpool, UK, 18th June 1997; 7/04293K*

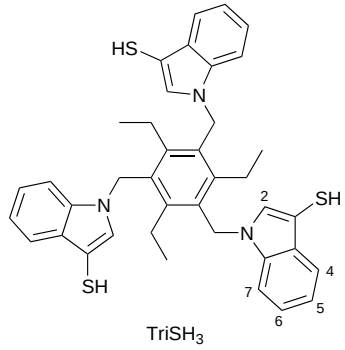
# A preorganised doubly tripodal hexathiol: syntheses and crystal structures of complexes with two 3 : 1 subsite-differentiated $Fe_4S_4$ clusters

**Christian Walsdorff,* Wolfgang Saak, Detlev Haase and the late Siegfried Pohl**

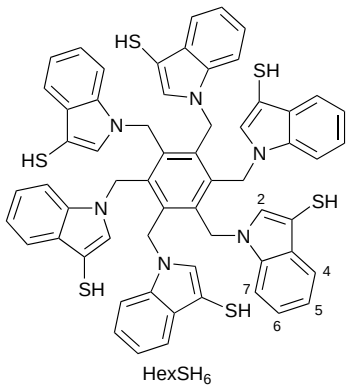
*Fachbereich Chemie der Carl von Ossietzky Universität, Postfach 2503, 26111 Oldenburg, Germany*

**Hexakis(3-sulfanylindolyl[1]methyl)benzene is highly preorganised to embed upon deprotonation two $Fe_4S_4$ clusters at a rigid separation of 12.8 Å.**

We have recently reported the convenient synthesis of 1,3,5-tris(3-sulfanylindolyl[1]methyl)-2,4,6-triethylbenzene ($TriSH_3$) from 1,3,5-tris(bromomethyl)-2,4,6-triethylbenzene.[1] This trithiol is highly preorganised to coordinate in the deprotonated form $TriS^{3-}$ to three iron subsites of $Fe_4S_4$ cluster cores thereby affording 3 : 1 subsite differentiated clusters. A key feature in the preorganisation of the molecular framework is the central hexasubstituted benzene ring that enforces a predominant *ababab*-conformation.† A detailed account of the design, underlying principles, synthesis and coordination properties has been given along with concise bibliographical reference.[1] Replacing 1,3,5-tris(bromomethyl)-2,4,6-triethylbenzene[2] with hexakis(bromomethyl)benzene[3] we have adapted the synthesis of $TriSH_3$ to obtain the novel ligand hexakis(3-sulfanylindolyl[1]methyl)benzene ($HexSH_6$), a doubly tripodal hexathiol that is preorganised to provide upon deprotonation two tripodal coordination spheres that are suitable to embed a single cluster core each.‡




$TriSH_3$




$HexSH_6$

Single crystals of $HexSH_6$ for X-ray structure analysis have not been obtained. By analogy with $TriSH_3$ rough $S_6$ or $D_{3d}$ symmetry should be expected for $HexSH_6$ in that the 3-sulfanylindolyl moieties point alternately above and below the plane of the central arene ring and the bulky annelated benzo groups are directed towards the periphery in order to avoid steric pressure while the HS groups in turn are all directed inward to provide two tripodal coordination spheres. This conformation is reflected in the $^1H$ NMR spectrum shown in Fig. 1. The indolyl $H^2$ protons are highfield shifted in the spectra of both $TriSH_3$ and $HexSH_6$ owing to shielding by the central arene ring. A similar shielding of the indolyl $H^7$ protons in $HexSH_6$ may be expected, since these protons are sandwiched between the neighbouring indolyl groups and should experience a shielding influence from them. Indeed a significant highfield shift is observed with one of the two pseudo-doublets whereas the other one appears in the normal range. This allows the unequivocal assignment of these signals that had remained ambiguous in the spectrum of $TriSH_3$. The sharp lines in the spectrum of $HexSH_6$ (actually dd were resolved instead of mere pseudo-doublets) further illuminate both the predominance and rigidity of the expected conformation.

The preorganisation of $HexSH_6$ is mirrored by the smooth reaction with $Fe_4S_4$ clusters to afford discrete double clusters. This has been established by X-ray structure analysis of the compounds $[PPh_4]_4[(Br)Fe_4S_4(HexS)Fe_4S_4(Br)]$ **1** and $[PPh_4]_4[(PhS)Fe_4S_4(HexS)Fe_4S_4(SPh)]$ **2**.§ Fig. 2 depicts the representative double cluster anion from **2**. Crystal inversion symmetry is imposed on the anion that renders both cluster cores equivalent. Coordination of the cluster cores closely resembles that in $[PPh_4]_2[Fe_4S_4(TriS)(SPh)]$,[1] *e.g.* the ligand deviates from trigonal symmetry, as can be seen from the non-equal thiolate-S···thiolate-S distances, to allow the slight tetragonal distortion that is typical of $Fe_4S_4$ clusters.[1] The cluster centroids are 12.83 Å apart, similar to the value of *ca*. 12 Å found by protein crystallography of *Peptococcuc aerogenes*,

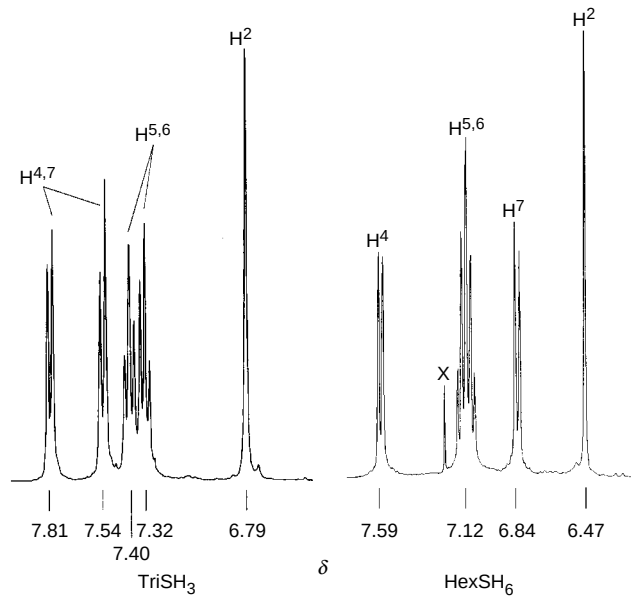



**Fig. 1** The range of aromatic protons in the $^1H$ NMR spectra ($CDCl_3$) of $TriSH_3$ and $HexSH_6$ (X = $CHCl_3$)

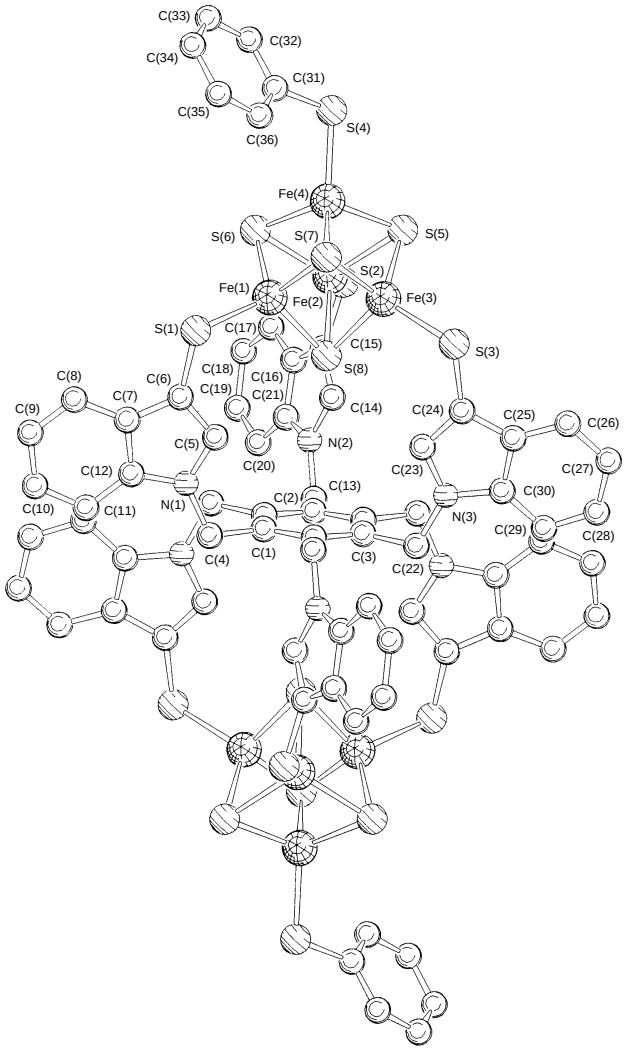



**Fig. 2** The double cluster anion from the structure of **2**·4dmf·2Et$_2$O (H atoms omitted for clarity). Selected interatomic distances (pm): Fe(1)–S(6) 229.7(2), Fe(1)–S(7) 230.1(2), Fe(1)–S(8) 226.9(2), Fe(2)–S(5) 229.8(2), Fe(2)–S(6) 226.9(2), Fe(2)–S(8) 229.1(2), Fe(3)–S(5) 230.2(2), Fe(3)–S(7) 227.3(2), Fe(3)–S(8) 229.7(2), Fe(4)–S(5) 226.3(2), Fe(4)–S(6) 229.6(3), Fe(4)–S(7) 228.4(2), S(1)···S(2) 685.0, S(1)···S(3) 631.4, S(2)···S(3) 650.3. The structure of the anion from **1**·6dmf is very similar. Selected interatomic distances (pm): Fe(1)–S(4) 229.8(3), Fe(1)–S(6) 229.9(3), Fe(1)–S(7) 225.6(3), Fe(2)–S(4) 226.5(3), Fe(2)–S(5) 230.3(3), Fe(2)–S(7) 229.5(2), Fe(3)–S(5) 230.0(3), Fe(3)–S(6) 226.9(3), Fe(3)–S(7) 229.2(3), Fe(4)–S(4) 229.1(3), Fe(4)–S(5) 225.9(3), Fe(4)–S(6) 230.0(3), Fe(4)–Br 236.6(2), S(1)···S(2) 634.8, S(1)···S(3) 666.5, S(2)···S(3) 654.0.

a ferredoxin with two separate $Fe_4S_4$ clusters.[4] A series of model compounds for such two-cluster enzymes that employ bidentate thiolate ligands to link the cluster cores have been reported.[5] However, separation and relative orientation of the cluster cores are poorly defined in these compounds owing to the flexible bridging. On the contrary the rigid polydentate ligand $HexS^{6-}$ may be reasonably expected to control the relative arrangement of the cluster cores in solution, too. This very property makes us believe that the ligand as a prototype for further ligands of a similiar design deserves considerable interest also in various fields beyond iron–sulfur chemistry.

## Footnotes and References

* New address: Inorganic Chemistry Laboratories, Pohang University of Science and Technology, San 31, Hyojadong, Pohang 790-784, S Korea.

† The '*ab*' terminology was introduced by MacNicol *et al.*[5] According to force-field calculations for the closely related hexaethylbenzene and hexa(*n*-propyl)benzene the ground-state *ababab* conformation lies some 15–19 kJ mol$^{-1}$ below the conformers that are next higher in energy.[7]

‡ Typical synthetic procedures, purification of solvents and experimental techniques have been described elsewhere.[1] Yields are given for isolated, crystalline and $^1$H NMR spectroscopically pure compounds.

Hexakis(3-methoxymethylthioindolyl[1]methyl)benzene: (88%); $\delta_H$ ($CDCl_3$, 300 MHz) 3.43 (18 H, s, $OCH_3$), 4.70 (12 H, s, $SCH_2$), 5.27 (12 H, s, $NCH_2$), 6.79 (6 H, s, indolyl H$^2$), 6.90 (6 H, d, indolyl H$^7$), 7.21 (12 H, m, indolyl H$^{5,6}$), 7.76 (6 H, d, indolyl H$^4$); $\delta_C$ ($CDCl_3$, 75 MHz) 44.16, 56.06, 79.63, 106.64, 109.63, 120.05, 121.32, 123.36, 129.26, 130.23, 136.62, 138.75.

$HexSH_6$·0.5Et$_2$O: (20%); $\delta_H$ ($CDCl_3$, 300 MHz) 2.78 (6 H, d, *J* 1.3 Hz, SH), 5.25 (12 H, s, $NCH_2$), 6.47 (6 H, d, *J* 1.3 Hz, indolyl H$^2$), 6.84 (6 H, dd, $J_{12}$ 6.6 Hz; $J_{13}$ 1.5 Hz, indolyl H$^7$), 7.12 (12 H, m, indolyl H$^{5,6}$), 7.59 (6 H, dd, $J_{12}$ 6.8 Hz; $J_{13}$ 1.7 Hz, indolyl H$^4$); $\delta_C$ ($CDCl_3$, 75 MHz) 44.27, 98.49, 109.02, 119.77, 121.02, 123.22, 128.73, 130.44, 136.04, 138.58.

The electrochemical reduction of **2** was investigated by cyclic voltammetry (dmf, Pt electrodes *vs.* SCE, 100 mV s$^{-1}$, 0.1 M [$NBu_4$]$ClO_4$) in the range −460 to −1660 mV. The reduction is chemically reversible (no loss of current in successive cycles), but the reduction wave is broadened ($E_{pc}$ = −1000; $E_{pa}$ = −1210) owing to disproportionation equlibria in the two-electron process. Nevertheless no splitting into two separate potentials is observed, that might be caused by a strong electrochemical interdependence of the two cluster cores. However such a splitting should not be expected with two $Fe_4S_4$ clusters that far apart.[5]

§ Single crystals were grown by vapour diffusion of diethyl ether into the reaction solution (dmf). Suitable specimens were sealed in glass capilaries under an atmosphere of dinitrogen and mounted on a Siemens-Stoe AED 2 four-circle diffractometer. Intensity data collections were performed 296(2) K using Mo-K$\alpha$ radiation ($\lambda$ = 71.073 pm), a graphite monochromator and $\omega$ scan techniques. Both structures were solved (direct methods) and refined on $F^2$ using the SHELXTL package.[8] The anion of **2** has been drawn with the program SCHAKAL 92.[9]

*Crystal data*: **1**·6dmf, $C_{174}H_{164}Br_2Fe_8N_{12}O_6P_4S_{14}$, black plates, crystal size 0.49 × 0.34 × 0.15 mm, $M$ = 3698.51, triclinic, space group $P\bar{1}$, $a$ = 1679.8(2), $b$ = 1686.0(2), $c$ = 1712.6(2) pm, $\alpha$ = 68.82(1), $\beta$ = 73.54(1), $\gamma$ = 88.53(2)°, $U$ = 4.3213(9) pm$^3$, $Z$ = 1, $D_c$ = 1.421 Mg m$^{-3}$, $\mu$ = 1.378 mm$^{-1}$. 9241 independent reflections ($\theta_{max}$ = 20.98°) of which 6686 were observed [$I > 2\sigma(I)$]. A semi-empirical absorption correction from $\psi$ scans was applied. H atoms were refined on fixed positions. The phenyl groups of the cations and the dmf molecules were refined with idealized geometry. The dmf molecules and one cation phenyl group were disordered and refined on split positions with occupancy factors of 0.5 : 0.5. All other atoms were refined anisotropically. Refinement converged with GOF = 1.199 for 838 parameters, $R_1$ = 0.0652 and $wR_2$ = 0.1400 [$I > 2\sigma(I)$], $R_1$ = 0.1037 and $wR_2$ = 0.1820 (all data), $e_{max}$, $e_{min}$ = 762, = −687 e nm$^{-3}$.

**2**·4dmf·2Et$_2$O, $C_{188}H_{180}Fe_8N_{10}O_6P_4S_{16}$, black needles, crystal size 2.58 × 0.27 × 0.08 mm, $M$ = 3759.06, triclinic, space group $P\bar{1}$, $a$ = 1513.9(2), $b$ = 1752.1(3), $c$ = 1939.1(2) pm, $\alpha$ = 100.67(1), $\beta$ = 101.73(2), $\gamma$ = 110.94(1)°, $U$ = 4.5127(11) nm$^3$, $Z$ = 1, $D_c$ = 1.383 Mg m$^{-3}$, $\mu$ = 0.903 mm$^{-1}$. 11 043 independent reflections ($\theta_{max}$ = 22.02°) of which 8183 were observed [$I > 2\sigma(I)$]. A volume correction for a long needle was applied. H-atoms were refined on fixed positions. The phenyl groups of the cations and the solvent molecules were refined with idealized geometry. The solvent molecules were disordered and refined on split positions with occupancy factors of 0.5 : 0.5 but one dmf molecule (0.65 : 0.35). All other atoms were refined anisotropically. Refinement converged with GOF = 1.159 for 895 parameters, $R_1$ = 0.0659 and $wR_2$ = 0.1509 [$I > 2\sigma(I)$], $R_1$ = 0.0994 and $wR_2$ = 0.1936 (all data), $e_{max}$, $e_{min}$ = 831, = −680 e nm$^{-3}$. CCDC 182/574.

1 C. Walsdorff, W. Saak and S. Pohl, *J. Chem. Soc., Dalton Trans.*, 1997, 1857.
2 C. Walsdorff, W. Saak and S. Pohl, *J. Chem Res.* (*M*), 1996, 1601.
3 J. Závada, M. Pánková, P. Holý and M. Tichý, *Synthesis*, 1994, 1132.
4 E. T. Adman, L. C. Sieker and L. H. Jensen, *J. Biol. Chem.*, 1973, **248**, 3987.
5 T. D. P. Stack, M. J. Carney and R. H. Holm, *J. Am. Chem. Soc.*, 1989, **111**, 1670.
6 D. D. MacNicol, P. R Mallinson and C. D. Robertson, *J. Chem. Soc., Chem. Commun.*, 1985, 1649.
7 D. J. Iverson, G. Hunter, J. F. Blount, J. R. Damewood and K. Mislow, *J. Am. Chem. Soc.*, 1981, **103**, 6073; G. Hunter, T. J. R. Weakley and W. Weissensteiner, *J. Chem. Soc., Perkin Trans. 2*, 1987, 1633.
8 G. M. Sheldrick, Universität Göttingen, 1990 and 1993.
9 E. Keller, Kristallographisches Institut der Universität Freiburg, 1993.

*Received in Basel, Switzerland, 30th June 1997; 7/04555G*



Typeset and printed by Black Bear Press Limited, Cambridge, England

ChemComm
FEATURE ARTICLE

# Enzymatic cleavage and formation of cyanohydrins: a reaction of biological and synthetic relevance

**Herfried Griengl,*[a] Andrea Hickel,[a] Dean V. Johnson,[a] Christoph Kratky,[b] Michael Schmidt[a] and Helmut Schwab[c]**

[a] *Specialforschungsbereich Biokatalyse am Institut für Organische Chemie, Technische Universität Graz, Stremayrgasse 16, A-8010 Graz, Austria*
[b] *Institut für Physikalishce Chemie, Karl Franzens Universität Graz, Heinrichstrasse 28, A-8010 Graz, Austria*
[c] *Institut für Biotechnologie, Technische Universität Graz, Petersgasse 12, A-8010 Graz, Austria*

**Hydroxynitrile lyases (Hnls) catalyse enantioselectively both the cleavage and formation of cyanohydrins. Besides the well known (*R*)-selective enzyme from almonds, (*S*)-Hnls have recently become available in larger quantities by cloning and over-expression. The first three-dimensional structure of a Hnl has been established for the enzyme from *Hevea brasiliensis*. These results are the basis for a still broader application of Hnls for biocatalytic asymmetric syntheses on a preparative scale.**

## Introduction

Hydroxynitrile lyases (Hnls, EC 4.1.2.10, EC 4.1.2.11, EC 4.1.2.37, EC 4.1.2.39) are enzymes which catalyse the cleavage and formation of cyanohydrins.[1] Early work concentrated on the enzyme which is isolated easily from almond meal,[2] and which gives (*R*)-configured cyanohydrins from aromatic and aliphatic aldehydes. Although (*S*)-Hnls are also known (see below) their application for enantioselective biocatalytic syntheses has been hindered by the difficulty of obtaining sufficient amounts for larger scale preparations. Recently, the genes for the (*S*)-Hnls from *H. brasiliensis* and *Manihot esculenta* were cloned and over-expressed[3,4] and the first X-ray structure of a Hnl, the (*S*)-Hnl from *H. brasiliensis*, was elucidated.[5] Therefore, on the basis of suggestions on the mechanism of the enzyme catalysed cyanohydrin reaction (deduced from knowledge of the three-dimensional structure) and due to the availability of both (*R*)- and (*S*)-Hnls, the field now seems open to still broader synthetic applications. For this reason it is appropriate to summarise recent developments here. Although special emphasis is given to the Hnl from *H. brasiliensis* developed in this laboratory, a more general view is intended.

## Natural function and biochemical characterization of hydroxynitrile lyases

Cyanogenesis, the release of hydrogen cyanide (HCN) from the tissue of plants or other organisms which occurs upon tissue damage, has been extensively described to date. This source of HCN has been identified in over 2000 plants as being cyanogenic glycosides or cyanolipids. One group of enzymes involved in this catabolism are the hydroxynitrile lyases. Their natural function is the catalysis of cyanohydrin cleavage from cyanogenic glycosides to give HCN and the corresponding aldehydes or ketones.

Cyanogenic glycosides have been found to possess two main functions in nature. (i) Plant defence. If the subcellular structures are destroyed by herbivoral, fungal or mechanical means, the catabolic enzymes can act on the cyanogenic glycosides. The catabolism is initiated by cleavage of the carbohydrate moiety by one or more β-glycosidases. After cleavage of the carbohydrate moiety the intermediates (cyanohydrins) may decompose either spontaneously or enzymatically, in the presence of a hydroxynitrile lyase, which considerably accelerates the reaction velocity. (ii) Nitrogen source. Cyanogenic glycosides may also be catabolised without release of hydrogen cyanide. HCN is refixed by the enzyme β-cyanoalanine synthetase and forms β-cyanoalanine with L-cysteine. β-Cyanoalanine is then hydrolysed by β-cyanoalanine hydrolase to L-asparagine. Consequently, HCN can also be considered as a nitrogen source for amino acid synthesis.

Eleven different Hnls from six different plant families have been isolated to date.[1] Interesting preparative applications in organic synthesis have been described only for four enzymes: (*R*)-hydroxynitrile lyase from *Prunus amygdalus* and (*S*)-hydroxynitrile lyases from *Sorghum bicolor*, *H. brasiliensis* and *M. esculenta* (Table 1). The differences between these four enzymes lies not only in their biochemical characteristics and enantiospecificities, but also in their substrate specificities. The Hnl of *P. amygdalus* (Pa-Hnl) accepts aromatic as well as aliphatic, unsaturated and heterocyclic aldehydes.[2] The Hnl of *S. bicolor* (Sb-Hnl) accepts only aromatic and heterocyclic aldehydes.[6] On the contrary, the Hnl of *H. brasiliensis* (Hb-Hnl) catalyses the formation of cyanohydrins from aliphatic, aromatic and heterocyclic aldehydes.[7] The Hnl of *M. esculenta* (Me-Hnl) is very similar to the *H. brasiliensis* enzyme, and therefore a very similar substrate specificity is to be expected.

## Molecular cloning, characterization and overexpression of the *hnl*-gene from *Hevea brasiliensis*

Based on polyclonal antibodies and partial sequence information obtained from the Hnl which was purified to homogeneity from plant material,[11,12] the gene encoding for the Hb-Hnl enzyme could be cloned by antibody screening of a cDNA library prepared from leaves of the rubber tree.[4] Sequencing of the cDNA relevaed an open reading frame encoding for a polypeptide of 257 amino acids with a predicted molecular mass of 29 227 kDa (Fig. 1). This was in good agreement with the molecular weight of 30 kDa found for the natural Hnl, as determined by SDS polyacrylamide gel electrophoresis.

Detailed sequence homology studies were performed and revealed that Hb-Hnl is highly homologous to Hnl of cassava (*M. esculenta*)[10] but shows no significant homology to the (*R*)-hydroxynitrile lyase from *P. serotina*[13] or to the (*S*)-hydroxynitrile lyase from *S. bicolor*.[9a] Identification of distant relationships and homologies at the secondary structure level indicated that Hb-Hnl is a new member of the α/β-hydrolase fold family of enzymes.[14] The involvement of $Ser_{80}$ and $His_{235}$ in the catalytic action was clearly confirmed by replacing these amino acid residues of the predicted catalytic triad by site-specific mutagenesis. Both the $Ser_{80} \rightarrow Ala$ and the $His_{235} \rightarrow Ala$ mutant proteins were completely inactive.

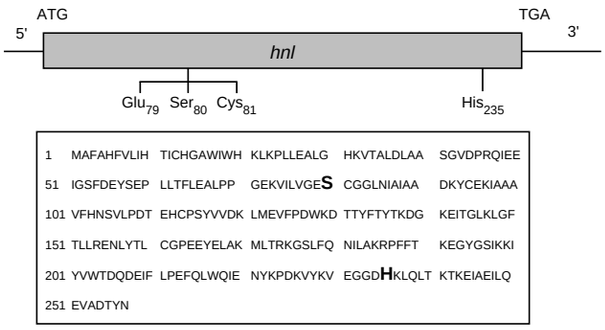



**Fig. 1** The *hnl* gene from *Hevea brasiliensis* and deduced amino acid sequence of the Hnl polypeptide. The active site $Ser_{80}$ and the $His_{235}$ of the catalytic triade are highlighted in the sequence by bold letters.

Replacing the residues adjacent to the active site, $Ser_{80}$, $Glu_{79}$ and $Cys_{81}$, resulted in low levels (1 and 3%) of the remaining specific Hnl activity of the mutant proteins $Glu_{79} \rightarrow$ Ala and $Cys_{81} \rightarrow$ Ser, which indicates that these residues may play an important role in enzyme function.[14]

The Hnl-encoding cDNA was used to construct expression vectors for overexpression of the *hnl* gene in different microorganisms. Overexpression in the bacterium *Escherichia coli* K12 resulted in efficient production of heterologous Hnl protein, however, the protein was intracellularly accumulated as insoluble inclusion bodies. Extraction of solubilized active Hnl enzyme was generally possible but resulted in low levels of specific activity. In contrast, expression in *Saccharomyces cerevisiae* resulted in efficient intracellular expression of soluble and highly active Hnl enzyme.[4] the specific activity of purified Hnl obtained by heterologous expression in *S. cerevisiae* (22 U $mg^{-1}$) was even slightly higher than the value of 18 U $mg^{-1}$ found for the Hnl enzyme purified from plant leaves. The most successful heterologous expression could be achieved by the methanol-inducible *Pichia pastoris* (methylotrophic yeast) expression system. High levels (up to about 60% of total cellular proteins) of intracellularly produced soluble Hnl protein, exhibiting specific activity of around 40 U $mg^{-1}$ (about twice the value found with the purified natural enzyme), were obtained. This expression system is also well developed for high cell density cultivation and yields more than 20 g of pure Hnl protein per litre of culture volume.[15] This high expression level represents an excellent basis for the establishment of efficient industrial processes for the production of recombinant *H. brasiliensis* Hnl enzyme.

## Three-dimensional structure of the Hnl from *Hevea brasiliensis*

Knowledge of the three-dimensional structure is a prerequisite for understanding the enzyme mechanism as well as for any attempt to alter enzyme properties by chemical or genetic means. Therefore, efforts to crystallize Hnls with the goal of determining their three-dimensional structures by X-ray crystallography have been undertaken.[16] These efforts have recently led to the successful conclusion of the structure analysis of Hb-Hnl, yielding the first three-dimensional structure of an enzyme with hydroxynitrile lyase activity.[5] Preliminary suggestions pertaining to the reaction mechanism could be derived from these recent results, which also form the basis for continued mutagenesis experiments.

### *The Hnl from* H. brasiliensis *belongs to the* α/β*-hydrolase fold family*

This is evident from the topology diagram [Fig. 2(*a*)] and from the three-dimensional structure [Fig. 2(*b*)]. The α/β-hydrolase fold is characterized by a well-conserved, large central β-sheet surrounded by α-helices in a less-well conserved arrangement, plus a variable 'cap' region. Other known members of this class of enzyme superfamily[17] have esterase, carboxypeptidase, dehalogenase and oxidoreductase activities, with somewhat related enzymatic mechanisms. Apart from their overall architecture, they also share a number of structurally conserved features in the vicinity of the active site, which can be used to identify the location of the active site as well as some of the residues involved in enzyme catalysis.

The active site is deeply buried inside the protein and connected to the surface by a narrow channel, as shown in Fig.3. This is consistent with the previously suggested ordered uni-bi mechanism[11,18] of hydroxynitrile lyases, which implies that substrates or products, depending on the reaction direction, access the active site in a sequential fashion. In the crystal structure, residual electron density interpreted as originating from a histidine molecule (presumably carried through from the buffer during enzyme purification) was observed within the active site region.

### *A (presumably) catalytic triad*

A triad consisting of residues $Ser_{80}$, $His_{235}$ and $Asp_{207}$ was identified by sequence and structure comparison with other α/β-hydrolase fold enzymes, and its catalytic relevance was assessed by mutagenesis studies.[4,14] Other characteristic features of α/β-hydrolases were identified ('nucleophile elbow') or at least tentatively assigned ('oxyanion hole') by structural

**Table 1** Biochemical characteristics of the hydroxynitrile lyases used for organic synthesis

| Plants, Plant Family and Parts | Stereo-selectivity | Molecular weight/kDa | | Optimum pH (co-enzyme) | Natural substrate (cyanogenic glycoside) |
|---|---|---|---|---|---|
| *Prunus amygdalus* Rosaceae almonds[a] | *R* | native:<br>SDS-Page: | 72 ± 2<br>72 ± 2 | 5–6 (FAD) | (*R*)-mandelonitrile (amygdalin, prunasin) |
| *Sorghum bicolor* Graminae seedlings | *S* | native:<br>SDS-Page:<br>reduced: | 108 ± 3<br>55 ± 2<br>33 ± 1 (α)<br>23 ± 1(β) | n.d.[c] (none) | (*S*)-4-hydroxymandelonitrile (dhurrin) |
| *Manihot esculenta* Euphorbiaceae leaves[d] | *S* | native:<br>SDS-Page: | 92–124<br>28.5–30 | 5.4 (none) | acetone cyanohydrin, (*S*)-butan-2-one cyanohydrin, (linamarin, lotaustralin) |
| *Hevea brasiliensis* Euphorbiaceae leaves[e] | *S* | native:<br>SDS-Page: | 58<br>30 ± 1 | 5.5–6.0 (none) | acetone cyanohydrin (linamarin) |

[a] Ref. 8. [b] Ref. 9. [c] n.d. = not determined. [d] Refs. 3 and 10. [e] Ref. 11.

comparison with other enzymes of the superfamily, most notably acetyl cholineesterase.[19] Each of the structurally conserved features of α/β-hydrolases is likely to play a similar function in the catalytic mechanism of the corresponding enzyme. Thus, the terminal residue of the catalytic triad ($Ser_{80}$ in Hnl) is believed to act as an activated nucleophile, which typically attacks a carbonyl carbon atom (*e.g.* in serine carboxypeptidases[20]). The resulting negative charge on the oxygen of the thus formed tetrahedral intermediate is stabilized by accommodating this oxygen within what is frequently called the 'oxyanion hole'. The structural conservation of the catalytic triad in Hnl suggests a similar function. Therefore, it was proposed[5] that the catalytic cycle of Hnl also involves a tetrahedral intermediate formed by nucleophilic attack of the (activated) $Ser_{80}$ oxygen on the carbonyl group of the cyanohydrin. For the natural substrate (acetone cyanohydrin) of the Hb-Hnl, the structure of the tentative intermediate (filled into the Hnl crystal structure by molecular modelling) is shown in Fig. 4. The $Cys_{81}$ residue was proposed to be involved in proton transfer to and from cyanide[5] as deduced from the reduced catalytic activity of the $Cys_{81} \rightarrow$ Ser mutant.

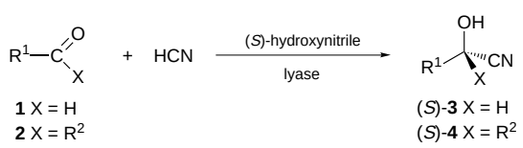
## Enzyme catalysed synthesis of cyanohydrins

For preparative purposes, the (*R*)-Hnl from *P. amygdalus* can be easily isolated in sufficient quantities.[8] Its high stability made it possible to investigate its properties and substrate range. It was shown that aliphatic, aromatic and heteroaromatic aldehydes[21] as well as ketones[22] could be converted to the corresponding cyanohydrins in good yield and selectivity.

The first (*S*)-hydroxynitrile lyase employed for the synthesis of chiral cyanohydrins was isolated from four to eight day old shoots of *S. bicolor*.[6] For reactions on a larger scale this preparation is rather laborious. Broad application of this Hnl is not possible as only aromatic carbonyl compounds are accepted as substrates. In contrast to this, the hydroxynitrile lyase from *H. brasiliensis* was reported to be the first (*S*)-Hnl which also accepts aliphatic aldehydes as substrates.[7] This enzyme could be prepared in large quantities by over-expression in the yeast *P. pastoris*.[4] Recently, an (*S*)-Hnl has been isolated from *M. esculenta*,[10,23] which shows similar properties[24] to the enzyme from *H. brasiliensis*.[7,25] Regarding the (*S*)-cyanohydrins, the most thoroughly studied enzyme is Hb-Hnl. Therefore its use in organic synthesis will be concentrated on.

The hydrogen cyanide required for the cyanohydrin formation (Scheme 1) can be added directly into an organic reaction medium or created *in situ* by the addition of acid to an aqueous solution of alkali cyanide. Alternatively the method of transhydrocyanation can be employed.[7a,26,27] Here, HCN is set free from acetone cyanohydrin in a preequilibrium step. To obtain chiral cyanohydrins in good enantiomeric purity a fundamental prerequisite is the suppression of the spontaneous addition of HCN to the carbonyl group. The extent of this non-enzymatic reaction strongly depends on the conditions. An aqueous reaction medium is only suitable if pH values below 4.0 are employed.[28] It is also possible to suppress the non-enzymatic addition of hydrogen cyanide by the use of an organic solvent. This reaction system has the additional advantage that the isolated yields of the corresponding cyanohydrins are in general higher than in aqueous medium. The first results were obtained mainly with aliphatic aldehydes[7] and ketones employing an aqueous, buffered reaction medium at pH 3.75 to 4.0 (Table 2). The majority of the substrates investigated can be converted into the corresponding cyanohydrins with good to excellent enantiomeric excess. By this means (*S*)-cyanohydrins of aryl-substituted aliphatic aldehydes became enzymatically accessible for the first time using hydroxynitrile lyases.[25] Also the excellent selectivity of this Hnl for thiophene and furane aldehydes in comparison to hydroxynitrile lyases from other plant sources is remarkable.

Using an aqueous reaction system, the isolated yields of the cyanohydrins are only moderate, probably due in part to the low solubility of several substrates in water. This can be circumvented by employing an organic solvent. It is not necessary to immobilise the enzyme. One can also apply a crude, concentrated aqueous enzyme solution together with an organic solvent as a second phase. Solvents of choice are ethyl acetate and some ethers. After performing the reaction, the aqueous phase containing the enzyme can be reisolated by a simple phase separation step. The activity of the enzyme used is unchanged.




**Scheme 1**

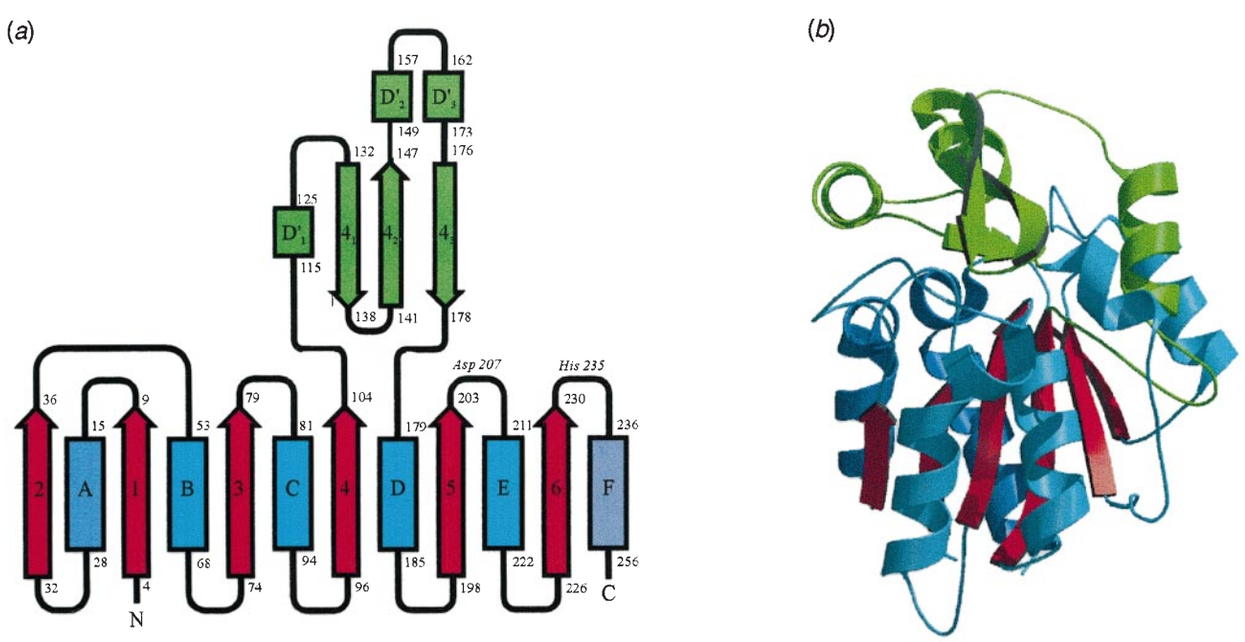



**Fig. 2** (*a*) Topology diagram and (*b*) three-dimensional and structure of the hydroxynitrile lyase from *Hevea brasiliensis*. The 'cap' region is colour-coded in green, helices are blue and β-strands are red.

Therefore, the same batch of enzyme can be reused several times without significant reduction in the isolated yield and the enantiomeric excess of the product. This fact is of importance with respect to industrial applications in order to enhance the productivity of the desired process. The pH value of the reaction mixture can be adapted to a certain substrate by adding an aqueous buffer solution to the aqueous enzyme solution. In order to obtain high yields of the corresponding cyanohydrins in short reaction times, concentrated solutions of the starting material (1 to 1.5 M) in the desired organic solvent can be employed. Furthermore, the temperature has a great influence on the course of the reaction. The reaction rate of the spontaneous addition of HCN, which will reduce the enantiomeric purity of the product, can be suppressed with respect to the enzymatic reaction if the reaction temperature is kept below 5 °C. At this temperature, the stability of the enzyme against denaturation is also enhanced. In almost all cases a reaction time of approximately 1 h at 0–5 °C was sufficient to obtain the corresponding chiral cyanohydrin in good yield and enantiomeric purity (see Table 3).

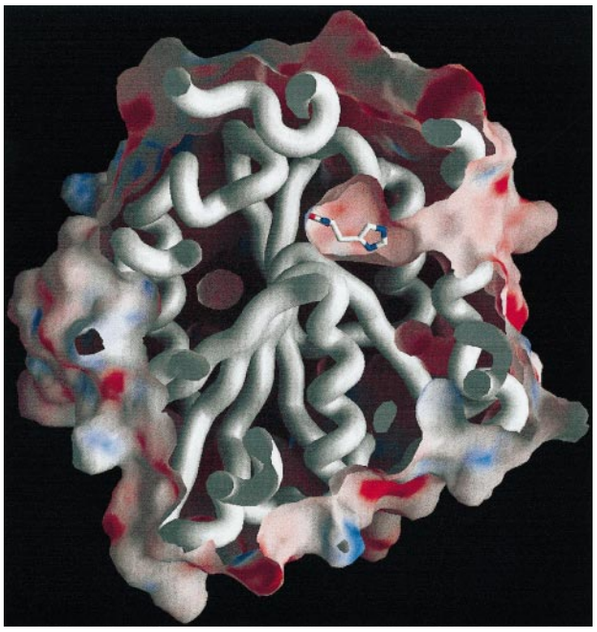


**Fig. 3** Section through a surface representation of the Hnl crystal structure. The colour coding is according to the electrostatic potential. The section passes through the active site cavity and the tunnel connecting it with the surrounding solvent. Also shown is a histidine molecule observed within the active site.

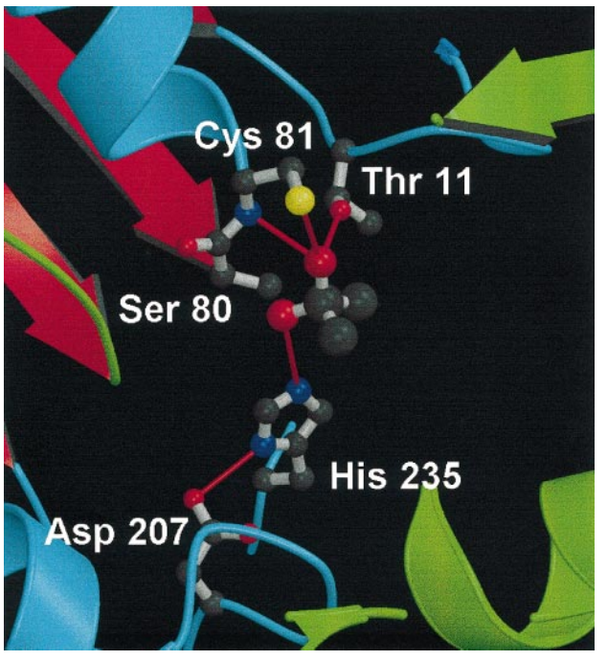



**Fig. 4** Structure of the tentative tetrahedral intermediate formed by nucleophilic attack of the $Ser_{80}$ oxygen on the carbonyl carbon of acetone. The structure of this intermediate was deduced by molecular modelling.

## Synthetic transformations of chiral cyanohydrins

Cyanohydrins, in particular those derived from aldehydes, are functionalised chiral units that possess broad synthetic utility. Scheme 2 summarizes some recent developments. Several synthetic routes are shown, each of which describes an alternative transformation of either the hydroxy or cyano moiety. Thus following route A, it can be seen that conversion of the hydroxy functionality to the silyloxy ether allows for a range of amino alcohols and hydroxy ketones to be generated, *via* nucleophilic addition of a Grignard reagent (*e.g.* methylmagnesium iodide) to the nitrile followed by reduction[29] or acidic hydrolysis[30] of the intermediate imine. This addition reaction has been further exploited by developing a transimination reaction[31] which yields an *N*-derivatized amino alcohol. When the hydroxy group is suitably protected (usually a silyloxy ether), the cyanohydrin can be converted to an

**Table 2** Preparation of (*S*)-cyanohydrins $R^1R^2CH(OH)CN$ in aqueous buffer using the (*S*)-Hnl from *H. brasiliensis*

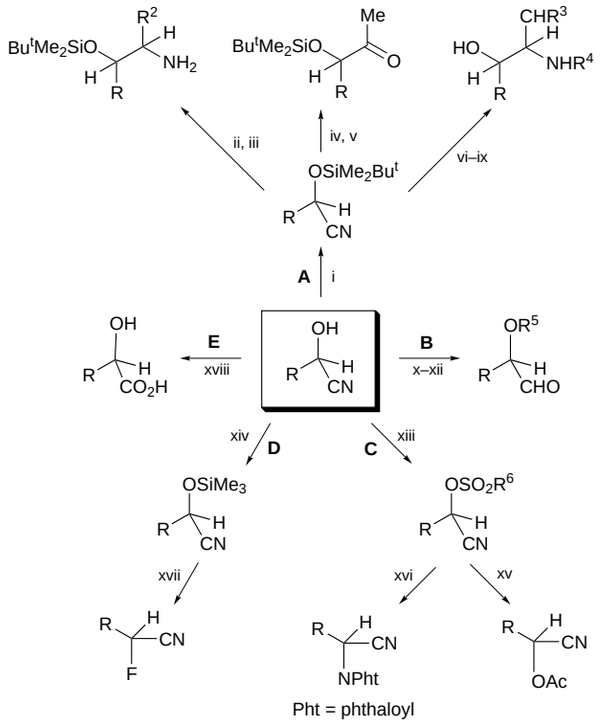
| $R^1$ | $R^2$ | Yield (%) | Ee (%) |
|---|---|---|---|
| Ph | H | 67 | 99 |
| Bn | H | 44 | 99 |
| $Ph(CH_2)_2$ | H | 88 | 93 |
| (*E*)-PhCH=CH | H | 50 | 95 |
| 2-$MeOC_6H_4$ | H | 61 | 77 |
| 3-$MeOC_6H_4$ | H | 80 | 99 |
| 4-$MeOC_6H_4$ | H | 49 | 95 |
| 3-$PhOC_6H_4$ | H | 9 | 99 |
| $PhOCH_2$ | H | n.d.[a] | 0 |
| $CH_2$=CH | H | 38 | 94 |
| PrC≡C | H | 43 | 80 |
| Cyclohex-3-enyl | H | 87 | 99 |
| 2-furyl | H | 55 | 98 |
| 3-furyl | H | 61 | 99 |
| 2-thienyl | H | 52 | 99 |
| 3-thienyl | H | 49 | 99 |
| $Pr^i$ | Me | 23 | 52 |
| $Pr^i$ | Me | 38 | 88 |
| Pr | Me | 51 | 75 |
| $Bu^t$ | Me | 49 | 78 |
| Bn | Me | 74 | 95 |

[a] n.d. = not determined.

**Table 3** Comparison of selected examples of conversions of aldehydes ($R^1CHO$) in $Pr^i_2O$ and results obtained in aqueous reaction medium

| | Aqueous buffer, pH 4.5 | | $Pr^i_2O$ | |
|---|---|---|---|---|
| $R^1$ | Yield (%) | Ee (%) | Yield (%) | Ee (%) |
| Ph | 67 | 99 | 96 | 99 |
| (*E*)-PhCH=CH | 50 | 95 | 77 | 92 |
| 3-$PhOC_6H_4$ | 9 | 99 | 98 | 99 |
| $BnOCH_2$ | n.d.[a] | 0 | 92 | 12 |
| Cyclohexyl | 94 | 99 | 95 | 99 |
| 2-furyl | 55 | 98 | 95 | 94 |
| 3-furyl | 61 | 99 | 96 | 97 |
| $C_5H_{11}$ | n.d.[a] | 84 | 81 | 96 |
| (*E*)-$Me(CH_2)$CH=CH | 62 | 99 | 96 | 99 |

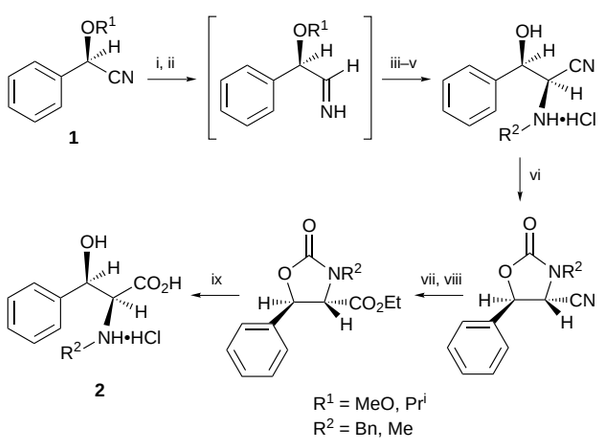
[a] n.d. = not determined.




**Scheme 2** *Reagents*: i, $Bu^tMe_2SiCl$, imidazole; ii, $R^2MgBr$; iii, $NaBH_4$; iv, MeMgI; v, $H_3O^+$; vi, $R^3CH_2MgBr$; vii, $R^4NH_2$; viii, $NaBH_4$; ix, $LiAlH_4$; x, $R^5X$; xi, DIBAL-H; xii, $H_3O^+$; xiii, $R^6SO_2Cl$, pyridine; xiv, $Me_3SiCl$, pyridine; xv; KOAc, DMF; xvi, potassium phthalimide, DMF; xvii, $Et_2NSF_3$; xviii, conc. HCl

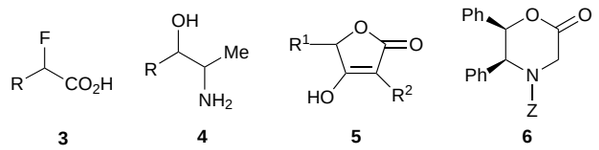
α-hydroxy aldehyde by treatment with excess diisobutylaluminium hydride followed by mild acidic hydrolysis (route B).[32] Alternatively, conversion of the hydroxy functionality into a suitable leaving group followed by nucleophilic displacement with various nucleophiles (*e.g.* acetate,[33] phthalimide[34] or fluoride[35]) introduces a new alternative functionality at the chiral centre with stereochemical inversion. The free cyanohydrins are particularly stable under anhydrous, strongly acidic conditions (*e.g.* dry hydrogen chloride), but treatment with an aqueous strong acid yields α-hydroxy acids.[6a] A more detailed coverage of the reactions presented in this scheme is given in recent reviews.[32,36]

A representative example of the synthetic potential of Hnls is shown in Scheme 3, where the cyanohydrin **1** (prepared from benzaldehyde) is elaborated[37] to the β-hydroxy-α-amino acid **2**,




**Scheme 3** *Reagents*: i, DIBAL-H; ii, $NH_4Br$, MeOH; iii, $R^2NH_2$; iv, HCN; v, HCl; vi, 1,1′-carbonylbis(1*H*-imidazole); vii, $K_2CO_3$, EtOH; viii, HCl; ix, 2 M KOH

which has the structural features of the amino acid side chain of Taxol. Therefore, in the chiral cyanohydrins the provision of a single asymmetric centre with at least two different functionalities is of significant practical synthetic value for differential and selective chemical elaboration to bioactive compounds and natural products. These products include α-fluoro carboxylic acids (**3**),[35] ethanol amines (**4**),[29] tetronic acids (**5**)[38] and the Williams glycine template (**6**).[39]




*Unsaturated cyanohydrins from aldehydes*

The synthetic utility of the chiral cyanohydrins can be extended by employing unsaturated aldehydes as substrates. The subsequent unsaturated cyanohydrins represent enzymatic products from enzyme catalysed reactions with an enhanced synthetic potential. Such opportunities include oxidative cleavage or epoxidation of the unsaturated functionality, nucleophilic substitution at the hydroxy centre and metal assisted addition to, or reduction of, the nitrile functionality (Fig. 5). This versatility makes them an important tool for organic chemists.

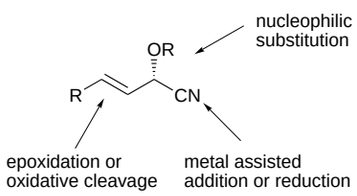


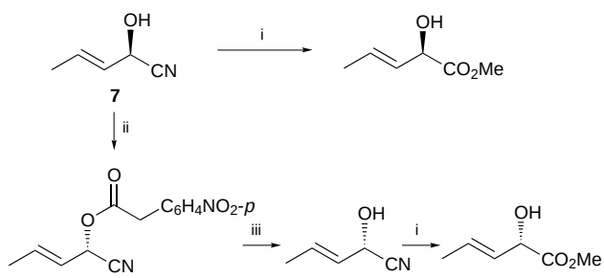

**Fig. 5** Opportunities for further transformation of unsaturated *O*-protected cyanohydrins

*Unsaturated hydroxy esters*[40]

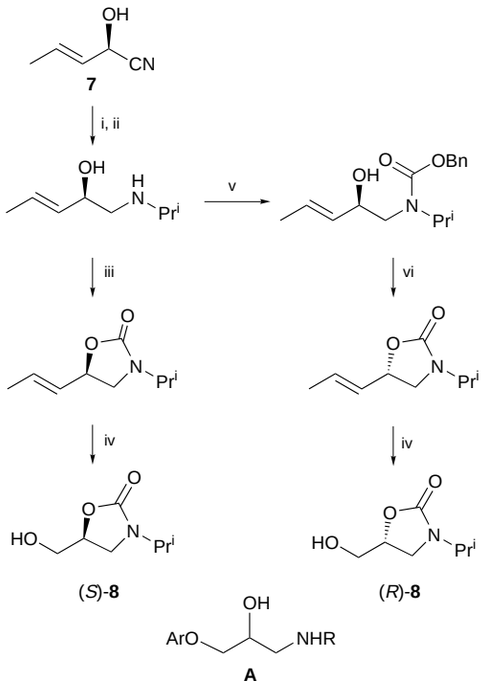
On treatment with MeOH–$HCl_{(g)}$, the unsaturated cyanohydrins (*e.g.* **7**) are easily converted into the corresponding esters (Scheme 4). These compounds are the multifunctional chiral starting materials for a number of organic transformations. Inherent in their structures are the properties of an allylic alcohol combined with those of α-hydroxy esters and β,γ-unsaturated carboxylic esters. The hydroxy group facilities directed epoxidation whilst the unsaturated ester (or carboxylic acid) may be applied to a variety of addition reactions. The enantiomeric counterpart of **7** can also be prepared by inversion of the chiral hydroxy group, under Mitsunobu conditions, followed by acidic hydrolysis of the *p*-nitrophenyl acetate and application of the Pinner reaction once more (Scheme 4).

*Oxidative cleavage*[41]

(*R*,*E*)-(−)-2-hydroxypent-3-enenitrile **7** has proven to be particularly useful in a synthesis in which, at an appropriate juncture,



**Scheme 4** *Reagents*: i, HCl, MeOH–$Et_2O$, then $H_2O$, then $H_2O$; ii, $EtO_2CN{=}NCO_2Et$, $PPh_3$, *p*-nitrophenylacetic aicd; iii, MsOH, MeOH

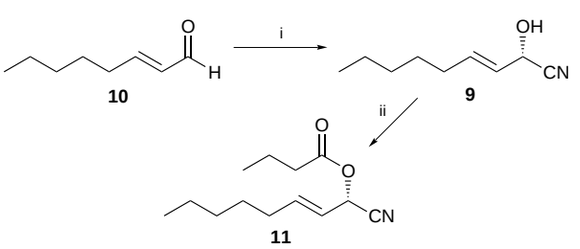


**Scheme 5** *Reagents*: i, 2-methoxypropene; ii, DIBAI-H, then MeOH, $NH_4Br$, $Pr^iNH_2$; iii, 1,1′-carbonylbis(1*H*-imidazole); iv, $O_3$, then $NaBH_4$; v, benzyl chloroformate; vi, $SOCl_2$

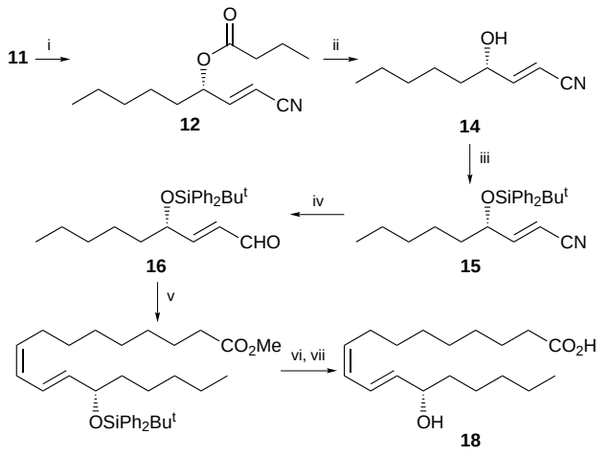
the carbon–carbon double bond is broken *via* oxidative cleavage. The (*R*)-cyanohydrin **7** was converted into both enantiomers of oxazolidinone **8**, which is a key intermediate in the synthesis of β-blockers of the general structure A (Scheme 5).

*Synthesis of (*9E,11E,13S*)*-13-*hydroxyoctadeca*-9,11-*dienoic acid by chirality transfer*[42,43]

The stereoselective addition of HCN to unsaturated aldehydes to yield unsaturated (*S*)-cyanohydrins using the hydroxynitrile lyase from *H. brasiliensis* was first reported here in Graz in 1995.[7b] This work showed that the enantiomeric excess of the subsequent cyanohydrin increased with the chain length of the aldehyde. With this in mind, the synthesis of a natural product, (9*Z*,11*E*,13*S*)-13-hydroxyoctadeca-9,11-dienoic acid, was established[42] in which the key chiral synthon **9** (Scheme 6) is generated from the Hnl catalysed addition of HCN to octenal **10**. The cyanohydrin product **9** was derivatized to the butyrate **11** which was shown to possess an enantiomeric excess of 99%. The butyrate was then easily converted into the unsaturated nitrile **12** using a [3,3]-sigmatropic rearrangement catalysed by bis(acetonitrile)dichloropalladium **13** (Scheme 7). This rearrangement proceeded, as previously described,[44,45] in a stereospecific manner with complete retention of configuration and enantiomeric excess. Hydrolysis of the butyrate yielded the alcohol **14**, which was then protected with the *tert*-butyldiphenylsilyloxy functionality to yield the nitrile **15**. Chiral analysis



**Scheme 6** *Reagents*: i, Hnl from *Hevea brasiliensis*, HCN; ii, butyric anhydride, pyridine



**Scheme 7** *Reagents*: i, $Pd(MeCN)_2Cl_2$, **13**, THF; ii, $K_2CO_3$, MeOH; iii, $Bu^tPh_2SiCl$, imidazole, DMF; iv, DIBAL-H, then $H_3O^+$; v, $Ph_3P^+Br^-(CH_2)_8CO_2Me$, **17**, $(Me_3Si)_2NLi$, THF, HMPA, −78 °C; vi, $Bu_4NF$, THF; vii, LiOH, $H_2O$–$Pr^iOH$, then acidification to pH 7

(high performance liquid chromatography) revealed that the nitrile **15** possessed an enantiomeric excess of 99%. The synthesis was then completed in a straightforward fashion. Reduction of **15** with DIBAL-H followed by acidic workup gave the unsaturated aldehyde **16**, which was coupled with the phosphonium salt **17** using a Wittig reaction. Deprotection of the hydroxy group and hydrolysis of the methyl ester then followed, which yielded the desired compound **18** (Scheme 7).

## Conclusions and outlook

On the basis of the studies presented in this article it is expected that the enzyme catalysed cyanohydrin reaction will be further established as a versatile method to obtain enantiopure chiral intermediates. Investigations on the three-dimensional structure of Hnls from different source are in progress, together with genetic studies. The scope and limitations of the reaction are being clarified and the synthetic transformation of the enantiopure cyanohydrins to target structures of both scientific and industrial interest is in progress in several laboratories.

Taking into consideration the synthetic importance of enantiopure cyanohydrins, it is not surprising that methods other than the ones described above have been investigated to achieve this goal. With regard to enzymatic methods other than the use of hydroxynitrile lyases, the resolution of esters of racemic cyanohydrins has also been investigated.[46–48] Another approach uses cyclic dipeptides for asymmetric cyanohydrin synthesis,[36,49,50] or applies chiral Lewis acids.[36,50,51] However, regarding chemical yield, enantiopurity and substrate range accepted, the application of hydroxynitrile lyases at present seems to be the optimum choice.


## Acknowledgments

The names of colleagues and co-workers, other than the authors, engaged in research in the area of hydroxynitrile lyases are given in the respective references. We are deeply obliged to them for their enthusiasm, cooperation and support. Funding by the Austrian Science Foundation, Forschungsförderungsfonds der Gewerblichen Wirtschaft and DSM-Chemie Linz is gratefully acknowledged.



**Herfried Griengl received his chemical education in Graz, Heidelberg and Munich. He was a research fellow with Paul D. Bartlett at Harvard University (1968–1969) and is now Professor of Organic Chemistry at the Technical University, Graz. His main research area is biocatalysis.**

**Christoph Kratky was born in Graz, Austria, on December 25, 1946. He studied Chemistry at the Eidgenössischen Technische Hochschule in Zürich (Switzerland), where he also obtained his PhD under the supervision of J. D. Dunitz in the field of chemical crystallography. Following a post-doctoral year at Harvard University in the group of M. Karplus, he joined the University of Graz in 1977, where he now holds the position of Professor in Physical Chemistry. His research is mainly concerned with biophysics and the structure analysis of biological molecules with X-ray diffraction.**

**Dean V. Johnson was born in Welwyn Garden City, England on December 15, 1967, and received his batchelors degree (1989) followed by his doctoral degree (1992) in Chemistry from Exeter University. He was a research fellow with Carl Johnson at Wayne State University (Detroit), then with Irving Wainer at McGill University (Canada). He is currently a research associate at the Technical University, Graz.**

**Andrea Hickel was born in Graz, Austria, on September 6, 1967. She studied chemistry at the Technical University, Graz, where she received her doctoral degree under the supervision of Herfried Griengl in 1996. A post-doctoral research stay in the group of H. W. Blanch in Berkeley will follow.**

**Michael Schmidt was born in Graz, Austria, on November 26, 1964. In 1991 he received the degree of a Diplomingenieur at the Technical University, Graz. After several years in industry he returned to the Technical University, where he is currently working at his doctoral thesis, dealing with chiral syntheses.**

**Helmut Schwab was born in Feldbach, Austria in 1950. He studied biochemistry/biotechnology and received his doctoral degree at the Technial University, Graz, in 1980. After a post-doctoral period in industry, he returned to the Technical University, Graz, and is now heding the Genetics group at the Institute of Biotechnology. His interests are focussed on molecular biotechnology and include gene expression in industrial microorganisms, genetic stability, molecular enzymology and enzyme engineering.**

## Footnote and References

* E-mail: sekretariat@orgc.tu-graz.ac.at


1 For a recent review, see A. Hickel, M. Hasslacher and H. Griengl, *Physiol. Plant.*, 1996, **98**, 891.
2 F. Effenberger, T. Ziegler and S. Förster, *Angew. Chem.*, 1987, **99**, 491; *Angew. Chem., Int. Ed. Engl.*, 1987, **26**, 458; T. Ziegler and F. Effenberger, *Synthesis*, 1990, 575.
3 H. Wajant, S. Förster, H. Böttinger, D. Selmar, F. Effenberger and K. Pfizenmaier, *Plant. Physiol.*, 1995, **109**, 1231.
4 M. Hasslacher, M. Schall, M. Hayn, H. Griengl, S. D. Kohlwein and H. Schwab, *J. Biol. Chem.*, 1996, **271**, 5884.
5 U. G. Wagner, M. Hasslacher, H. Griengl, H. Schwab and C. Kratky, *Structure*, 1996, **4**, 811.
6 (*a*) F. Effenberger, B. Hörsch, S. Förster and T. Ziegler, *Tetrahedron Lett.*, 1990, **31**, 1249; (*b*) U. Niedermeyer and M.-R. Kula, *Angew. Chem.*, **102**, 1990, 423; *Angew. Chem., Int. Ed. Engl.*, 1990, **29**, 386.
7 (*a*) N. Klempier, H. Griengl and M. Hayn, *Tetrahedron Lett.*, 1993, **34**, 4769. (*b*) N. Klempier, U. Pichler and H. Griengl, *Tetrahedron: Asymmetry*, 1995, **6**, 845.
8 W. Becker, U. Benthin, E. Eschenhof and E. Pfeil, *Biochem. Z.*, 1963, **337**, 156; G. J. M. van Scharrenburg, J. B. Sloothaak, C. G. Kruse, E. Smitskamp-Wilms and J. Brussee, *Ind. J. Chem.*, 1993, **32B**, 16; H.-J. Aschoff and E. Pfeil, *Hoppe-Seyler's Z. Physiol. Chem.*, 1970, **351**, 818; W. Becker and E. Pfeil, *Biochem. Z.*, 1966, **346**, 301; I. Jansen, R. Woker and M.-R. Kula, *Biotechnol. Appl. Biochem.*, 1992, **15**, 90; M. K. Seely, R. S. Criddle and E. E. Conn, *J. Biol. Chem.*, 1966, **241**, 4457; E. Smitskamp-Wilms, J. Brussee, A. van der Gen, G. J. M. van Scharrenburg and J. B. Sloothaak, *Recl. Trav. Chim. Pays-Bas*, 1991, **110**, 209.
9 (*a*) H. Wajant, D. Riedel, S. Benz and K.-W. Mundry, *Plant Sci.*, 1994, **103**, 145; (*b*) H. Wajant, K.-W. Mundry and K. Pfizenmaier, *Plant Mol. Biol.*, 1994, **26**, 735; (*c*) H. Wajant and K.-W. Mundry, *Plant. Sci.*, 1993, **89**, 127; (*d*) H. Wajant, H. Böttinger and K.-W. Mundry, *Biotechnol. Appl. Biochem.*, 1993, **18**, 75; (*e*) G. J. M. van Scharrenburg, J. B. Sloothaak, C. G. Kruse, E. Smitskamp-Wilms and J. Brussee, *Ind. J. Chem.*, 1993, **32B**, 16; (*f*) E. Smitskamp-Wilms, J. Brussee, A. van der Gen, G. J. M. van Scharrenburg and J. B. Sloothaak, *Recl. Trav. Chim. Pays-Bas*, 1991, **110**, 209.
10 J. Hughes, F. J. P. De Carvalho and M. A. Hughes, *Arch. Biochem. Biophys.*, 1994, **311**, 496.
11 M. Schall, Ph.D. Thesis, University Graz, Austria, 1996.
12 H. Wajant, and S. Föster, *Plant. Sci.*, 1996, **115**, 25.
13 L. P. Cheng, and J. E. Poulton, *Plant. Cell Physiol.*, 1993, **34**, 1139.
14 M. Hasslacher, C. Kratky, H. Griengl, H. Schwab and S. D. Kohlwein, *Proteins*, 1997, **27**, 1.
15 M. Hasslacher, S. D. Kohlwein, H. Griengl and H. Schwab, unpublished work.
16 H. Lauble, K. Muller, H. Schindelin, S. Föster and F. Effenberger, *Proteins: Struct. Funct. Genet.*, 1964, **19**, 343; U. G. Wagner and C. Kratky, *Acta Crystallogr., Sect. D*, 1996, **52**, 591.
17 D. L. Ollis, E. Cheah, M. Cygler, B. Dijkstra, F. Frolow, S. M. Franken, M. Harel, S. J. Remington, I. Silman, J. Schrag, J. L. Sussman, K. H. G. Verschueren and A. Goldman, *Protein Eng.*, 1992, **5**, 197; M. Cygler, J. D. Schrag, J. L. Sussman, M. Harel, I. Silman, M. K. Gentry and B. P. Doctor, *Protein Sci.*, 1993, **2**, 366.
18 J. S. Jorns, *J. Biol. Chem.*, 1979, **254**, 12145; L. C. Smith, F. Faustinella and L. Chan, *Curr. Opin. Struct. Biol.*, 1992, **2**, 490.
19 J. L. Sussman, M. Harel, F. Frolow, C. Oefner, A. Goldman, L. Toker and I. Silman, *Science*, 1991, **253**, 872.
20 J. Kraut, *Annu. Rev. Biochem.*, 1977, **46**, 331.
21 W. Becker and E. Pfeil, *J. Am. Chem. Soc.*, 1966, **88**, 4299.
22 F. Effenberger, B. Hörsch, F. Weigart and S. Kühner, *Tetrahedron Lett.*, 1991, **32**, 2605.
23 H. Wajant, S. Förster, H. Böttinger, F. Effenberger and K. Pfizenmaier, *Plant Sci.*, 1995, **108**, 1.
24 S. Förster, J. Roos, F. Effenberger, H. Wajant and A. Sprauer, *Angew. Chem.*, 1996, **108**, 493; *Angew. Chem., Int. Ed. Engl.*, 1996, **35**, 437.
25 M. Schmidt, S. Hervé, N. Klempier and H. Griengl, *Tetrahedron*, 1966, **52**, 7833.
26 V. I. Ognyanov, V. K. Datacheva and K. S. Kyler, *J. Am. Chem. Soc.*, 1991, **113**, 6992.
27 A. Hickel, G. Gradnig, H. Griengl, M. Schall and H. Sterk, *Spectrochim. Acta, Part A*, 1996, **52**, 93.
28 U. Kragl, U. Niedermeyer, M. R. Kula and C. Wandrey, *Ann. N.Y. Acad. Sci.*, 1990, **613**, 167.
29 J. Brussee, F. Dofferhoff, C. G. Kruse and A. van der Gen, *Tetrahedron*, 1960, **46**, 5, 1653.
30 J. Brussee, E. C. Roos and A. van der Gen, *Tetrahedron Lett.*, 1988, **35**, 29, 4485.
31 J. Brussee and A. van der Gen, *Recl. Trav. Chim. Pays-Bas*, 1991, **110**, 25.
32 C. G. Kruse, in *Chirality in Industry*, ed. A. N. Collins, G. N. Sheldrake and J. Crosby, Wiley, London, 1192, 279.
33 F. Effenberger and U. Stelzer, *Chem. Ber.*, 1993, **126**, 779.
34 F. Effenberger and U. Stelzer, *Angew. Chem.*, 1991, **103**, 866; *Angew. Chem., Int. Ed. Engl.*, 1991, **30**, 873.
35 U. Stelzer and F. Effenberger, *Tetrahedron: Asymmetry*, 1993, **4**, 161.
36 F. Effenberger, *Angew. Chem.*, 1994, **106**, 1609; *Angew. Chem., Int. Ed. Engl.*, 1994, **33**, 1555.
37 P. Zanderberger, J. Brussee, A. van der Gen and C. G. Kruse, *Tetrahedron: Asymmetry*, 1994, **3**, 769.
38 J. J. Duffield and A. C. Regan, *Tetrahedron: Asymmetry*, 1996, **7**, 663.
39 A. M. C. H. van der Niewendijk, E. G. J. C. Wamerdam, J. Brussee and A. van der Gen, *Tetrahedron: Asymmetry*, 1995, **6**, 801.
40 E. G. J. C. Wamerdam, A. M. C. H. van der Niewendijk, C. G. Kruse, J. Brussee and A. van der Gen, *Recl. Trav. Chim. Pays-Bas*, 1996, **115**, 20.
41 E. G. J. C. Warmerdam, J. Brussee, A. van der Gen and C. G. Kruse, *Helv. Chim. Acta*, 1994, **77**, 252.
42 D. V. Johnson and H. Griengl, *Tetrahedron*, 1997, **53**, 617.
43 G. A. Blondin, *Ann. N.Y. Acad. Sci.*, 1975, **264**, 98.
44 A. C. Oehlschlager, P. Mishra and D. Dhami, *Can. J. Chem.*, 1984, **62**, 791.
45 A. Abe, H. Nitta, A. Mori and S. Inoue, *Chem. Lett.*, 1992, 2443.
46 N. Matsuo and N. Ohno, *Tetrahedron Lett.*, 1985, **26**, 5533; A. von Almsick, J. Buddrus, P. Hönicke-Schmidt, K. Laumen and M. P. Schneider, *J. Chem. Soc., Chem. Commun.*, 1989, 1391.
47 H. Ohta, Y. Miyamae and G. Tsuchihashi, *Agric. Biol. Chem.*, 1986, **50**, 3181.

48 F. Effenberger, B. Gutterer, T. Ziegler, E. Eckhardt and R. Aichholz, *Liebigs Ann. Chem.*, 1991, 47.
49 J. Oku, N. Ito and S. Inoue, *Makromol. Chem.*, 1979, **180**, 1089.
50 M. North, *Synlett*, 1993, 807.
51 J. D. Elliott, V. M. F. Choi and W. S. Johnson, *J. Org. Chem.*, 1983, **48**, 2294.

*7/00907K*

# A new type of alumoxane obtained by controlled hydrolysis of *N,N*-dialkylcarbamato complexes of aluminium; crystal and molecular structure of $[Al_4(\mu_3\text{-}O)_2(O_2CNPr^i{}_2)_8]$

**Ulrich Abram,[a] Daniela Belli Dell'Amico,[b] Fausto Calderazzo,*[b] Stefan Kaskel,[a] Luca Labella,[b] Fabio Marchetti,[b] Riccardo Rovai[b] and Joachim Strähle*[a]**

[a] *Institut für Anorganische Chemie der Universität Tübingen, Auf der Morgenstelle 18, D-72076 Tübingen, Germany*
[b] *Università di Pisa, Dipartimento di Chimica e Chimica Industriale, Via Risorgimento 35, I-56126 Pisa, Italy*

**The aluminium(III) *N,N*-diisopropylcarbamato derivative $[Al_2(O_2CNPr^i{}_2)_6]$ undergoes hydrolysis with a stoichiometric amount of water giving the $\mu_3$-oxo derivative $[Al_4(\mu_3\text{-}O)_2(O_2CNPr^i{}_2)_8]$, which is analytically, spectroscopically and structurally characterized.**

Hydrolysis of aluminium derivatives is an area of considerable interest, the ultimate goal being a better understanding of the processes leading to aluminium oxides[1] or aluminosilicates[2] from appropriate precursors. In this connection, halo-,[3] alkoxo,[1a,2] and alkyl derivatives[1d,4] of aluminium have been studied extensively. Some alkylalumoxanes[4] have been characterized crystallographically by Barron and coworkers, who obtained them by partial hydrolysis of aluminium alkyls; thus, hydrolysis of $AlBu^i{}_3$ gave[4b,c] the tetranuclear $[Al_4(\mu_3\text{-}O)_2Bu^i{}_8]$ together with the octanuclear $[Al_8(\mu_3\text{-}O)_8Bu^i{}_8]$.

Our earlier work on homoleptic *N,N*-dialkylcarbamato complexes of aluminium[5] prompted us to study the hydrolysis of these compounds, and to verify their aptitude as alumoxane precursors. This paper reports the first case of a hydrolytic process involving an aluminium-bonded *N,N*-dialkylcarbamato group, and the first member of a new type of alumoxane.

The dinuclear[5] *N,N*-diisopropylcarbamato derivative $[Al_2(O_2CNPr^i{}_2)_6]$ undergoes hydrolysis with a stoichiometric amount of water [eqn. (1)] giving the $\mu_3$-oxo derivative $[Al_4(\mu_3\text{-}O)_2(O_2CNPr^i{}_2)_8]$.† An alternative, less satisfactory preparative procedure, consists of treating anhydrous $AlCl_3$ and $AlCl_3{\cdot}6H_2O$ in the appropriate molar ratio, with $Pr^i{}_2NH$–$CO_2$, [eqn. (2)].

$$2[Al_2(O_2CNPr^i{}_2)_6] + 2H_2O \rightarrow [Al_4(\mu_3\text{-}O)_2(O_2CNPr^i{}_2)_8] + 4Pr^i{}_2NH + 4CO_2 \quad (1)$$

$$11\ AlCl_3 + AlCl_3{\cdot}6H_2O + 24\ CO_2 + 60\ Pr^i{}_2NH \rightarrow 3[Al_4(\mu_3\text{-}O)_2(O_2CNPr^i{}_2)_8] + 36\ [NH_2Pr^i{}_2]\ Cl \quad (2)$$

In the latter case, the toluene soluble μ-oxo derivative is separated by filtration from the substantially insoluble dialkylammonium chloride. X-Ray diffraction‡ has established the molecular structure of the title compound, as the heptane solvated product, to consist of a tetranuclear assembly of aluminium atoms joined together by $\mu_3$-oxo ligands and by carbamato bridges (Fig. 1). The structure contains two $Al_2(\mu_3\text{-}O)(O_2CNPr^i{}_2)_4$ fragments with the Al(1)–O(1)–Al(2) and the Al(3)–O(2)–Al(4) sequences joined together by bridging carbamato groups and by the third coordination site of the $\mu_3$-oxo ligand. Bridging carbamato groups have also been found in the homoleptic dinuclear precursor $[Al_2(O_2CNPr^i{}_2)_6]$[5] and in the recently reported alkylcarbamato complexes $[(Me_2Al)_2\{\mu\text{-}O_2CNPr^i{}_2\}_2]$ and $[(Me_2Al)_2\{(\mu\text{-}O_2CNPr^i{}_2)_2\}_2Mg]$.[8] The present molecule contains five- [Al(1), Al(3)] and six-coordinate [Al(2), Al(4)] aluminium atoms with distorted trigonal-bipyramidal and octahedral geometries, respectively. It is worth noting that five-coordination to oxygen-containing ligands is uncommon for aluminium; known cases are found in andalusite, $Al_2SiO_5$[9a] and in an aluminium–barium glycolate.[9b] Drying *in vacuo* at room temp. converts the heptane solvated tetranuclear substance into the desolvated species, through a presumably topotactic process[9c,d] which maintains an elevated degree of crystallinity, as shown by X-ray powder diagrams.§

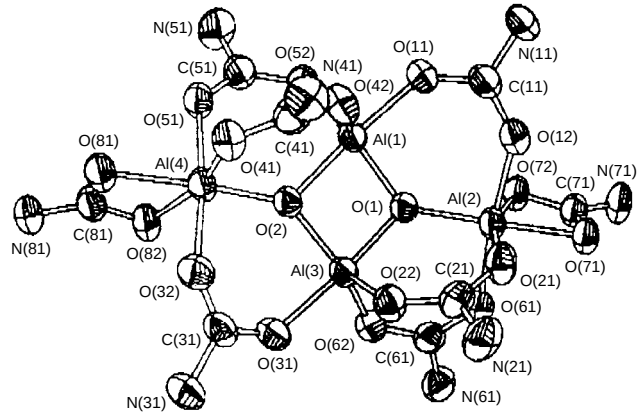
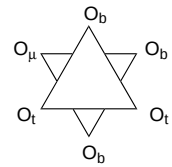



**Fig. 1** ZORTEP drawing of $[Al_4(\mu_3\text{-}O)_2(O_2CNPr^i{}_2)_8]{\cdot}0.5C_7H_{16}$ with the atom numbering scheme. Ellipsoids are at 50% probability, dialkyl groups and solvent are omitted for clarity. Relevant bond distances (Å) and angles (°). Five-coordinate aluminium: Al(1)–O(11) 1.863(2), Al(1)–O(42) 1.836(2), Al(1)–O(52) 1.811(2), Al(1)–O(1) 1.781(2) Al(1)–O(2) 1.832(2), O(42)–Al(1)–O(52) 106.4(1), O(1)–Al(1)–O(42) 119.3(9), O(1)–Al(1)–O(52), 134.3(1). Six-coordinate aluminium: Al(2)–O(12) 1.899(2), Al(2)–O(61) 1.935(2), Al(2)–O(72) 1.958(2), Al(2)–O(71) 1.937(2), Al(2)–O(1) 1.775(2); O(12)–Al(2)–O(72) 89.9(9), O(61)–Al(2)–O(72) 88.1(1), O(21)–Al(2)–O(61) 89.9(1), O(12)–Al(2)–O(21) 90.2(1), O(1)–Al(2)–O(71) 171.3(1). $\mu_3$-Oxygen; Al(1)–O(1)–Al(2) 134.0(1), Al(1)–O(1)–Al(3) 97.2(1), Al(2)–O(1)–Al(3) 120.9(1), Al(1)–O(2)–Al(3) 97.7(1), Al(1)–O(2)–Al(4) 120.9(1), Al(3)–O(2)–Al(4) 134.3(1).

To a first approximation, the six-coordinate aluminium can be regarded as asymmetric, as shown below in a view along two opposite triangular faces of the octahedron [$O_b$, $O_t$ and $O_\mu$ are the oxygen atoms belonging to bridging and terminal carbamato groups, and to the triply bridging oxo group, respectively]. As the tetranuclear aluminium compound crystallizes in the centrosymmetric space group $P\bar{1}$, the two enantiomers in the crystal are related by an inversion centre.




The spectroscopic data are consistent with the literature data for μ-oxo derivatives.[10–12] An intense IR band at 772 $cm^{-1}$ is attributed to the $(\mu_3\text{-}O)Al_3$ system. The presence of a single Al–

O stretching vibration in the tetranuclear aluminium compound suggests either accidental degeneracy or an almost planar ($\mu_3$-O)$Al_3$ system; the latter hypothesis is consistent with the solid-state data showing that the triply bridging oxides O(1) and O(2) are 0.28 and 0.27 Å, respectively, away from the plane of the three aluminium atoms to which they are connected. On the other hand, the $Al_4(\mu_4\text{-O})_2$ system is also almost planar, the dihedral angle between the Al(1)–Al(2)–Al(3) and Al(1)–Al(3)–Al(4) planes being only 8°. The $Al_4O_2$ frame closely resembles the tetranuclear alkylalumoxane $[Al_4(\mu_3\text{-O})_2Bu^i_8]$ with two $\mu_3$-oxo ligands and a substantially planar $Al_4O_2$ core. The $Al_4O_2$ frame is also known in a few cases, namely the anionic $[Al_4O_2Me_{10}]^{2-}$ [4a] and $[Al_4O_2Cl_{10}]^{2-}$ [3c] or the alkylalumoxane $[Al_4(\mu_3\text{-O})_2Bu^i_8]$.[4b] The $Al_3(\mu_3\text{-O})$ moieties in $[Al_5(Bu^t)_5(\mu_3\text{-O})_2(\mu_3\text{-OH})_2(\mu\text{-OH})_2(\mu\text{-O}_2CPh)_2]\cdot MeCN$,[1d] containing five-coordinate aluminium, show Al–O distances in the range 1.785(4)–1.827(3) Å, similar to those observed in our case; the Al–O–Al angles are 106.1(2), 107.1(2) and 130.0(2)°, corresponding to a greater deviation from planarity.

Despite the low symmetry of the aluminium environment, the NMR data are relatively simple. The broad $^{27}$Al NMR resonance at $\delta$ 4.0 with a shoulder at $\delta$ *ca*. 50 is suggestive of non-equivalent aluminium centres[13a] broadened by the large quadrupole moment of the metal.[13b] The $^{13}$C NMR spectrum shows three main $O_2CNR_2$ resonances due to non-equivalent carbamato groups. The $^1$H NMR spectra indicate the presence of non-equivalent alkyl groups within the tetranuclear compound; fast rotation around the C–N bond, on the NMR timescale, is further suggested by the observation of two main CH (multiplets) and four main $CH_3$ (doublets) resonances.

This work was supported by the Consiglio Nazionale delle Ricerche, Progetto Strategico 'Metodologie Chimiche Innovative', the Deutsche Forschungsgemeinschaft, and the Fonds der Chemischen Industrie. We are also grateful to the European Community for a grant to R. R. for a period of study at the University of Tübingen, within the framework of the Erasmus Programme, and to the Deutsche Forschungsgemeinschaft for a Heisenberg fellowship to U. A.

## Footnotes and References

* E-mail: facal@dcci.unipi.it

† Anhydrous $AlCl_3$ (7.65 g, 57.37 mmol) was added to a toluene solution (400 ml) of diisopropylamine (60.3 ml, 430 mmol) presaturated with $CO_2$. The mixture was stirred for 3 d under carbon dioxide at room temp. The dialkylammonium chloride was filtered off and washed with toluene (3 × 50 ml) and the colourless filtrate was hydrolyzed under a dinitrogen atmosphere by dropwise addition of water (0.5 ml, 27.78 mmol) dissolved in thf (350 ml), corresponding to a Al/$H_2O$ molar ratio of 2.07. Vacuum–dinitrogen cycles were repeated several times during the hydrolysis. The volatiles were then removed *in vacuo*; the solid residue was dried for 6 h at 50 °C and heptane (250 ml) was then added. The resulting suspension was filtered and the colourless μ-oxo derivative was dried *in vacuo* at room temp. for several hours. Yield 12.29 g, 66%. Anal. Calc. for $C_{56}H_{112}Al_4N_8O_{18}$: Al, 8.3; $CO_2$, 27.2. Found: Al, 8.0; $CO_2$, 26.7%. Samples of the vacuum-dried polycrystalline substance gave an X-ray diffraction diagram (dry argon, Siemens D5000 diffractometer) with the following parameters [spacings *d*/Å, intensities (%) in parentheses]: 14.091(21), 13.156(3), 12.079(75), 11.842(100), 10.659(44), 9.240(4), 8.634(12), 8.085(6), 7.352(3), 7.011(12), 6.429(9), 6.239(3), 5.894(6), 5.581(10), 5.412(8), 5.300(17), 5.143(8), 4.634(9), 4.530(4), 4.395(6), 4.316(5), 4.191(3), 4.040(4), 3.948(3), 3.790(3), 3.659(4), 3.605(3), 3.531(3), 3.119(3). *Selected spectroscopic data*, NMR (benzene, $\delta$); $^1$H: 1.09 (d), 1.27 (d), 1.34 (d), 1.45 (d), 3.86 (m), 4.40 (m); $^{27}$Al: 3.5 (s), *ca*. 50(sh), with respect to $[Al(H_2O)_6]Cl_3$; $^{13}$C: 160.2, 161.4, 167.1 ($O_2CNR_2$). IR (cm$^{-1}$, Nujol, PCTFE): 1613s, 1580s (br), 1520s (br), 1460s, 1391s, 1380s, 1361s, 1319m, 1262w, 1216s, 1164s, 1136s, 1075s, 1062m, 1038m, 922m, 902m, 873m, 817m, 805s, 772s ($\mu_3$-O)$_3$, 689m, 629s, 564s, 540m, 514m, 476s, 438m.

‡ X-Ray quality single crystals of the heptane-solvated substance were obtained from hot dry heptane by slow cooling to room temp.; the crystals were not subjected to drying *in vacuo* in order to prevent loss of heptane and formation of the microcrystalline unsolvated product (*vide infra*). *Crystal data* for $[Al_4(\mu_3\text{-O})_2(O_2CNPr^i_2)_8]\cdot 0.5C_7H_{16}$: $C_{59.5}H_{120}Al_4N_8O_{18}$, $M$ = 1343.6, triclinic, space group $P\bar{1}$, $a$ = 14.937(3), $b$ = 16.534(3), $c$ = 18.039(4) Å; $\alpha$ = 89.23(1); $\beta$ = 71.83(2); $\gamma$ = 82.39(1)°; $Z$ = 2; $U$ = 4193(2) Å$^3$; $D_c$ = 1.064 g cm$^{-3}$; Cu-K$\alpha$ radiation ($\lambda$ = 1.541 84 Å). Colourless blocks, 0.8 × 0.5 × 0.5 mm, $T$ = 203 K, 15576 reflections collected, $\theta$ range 5.12–65.05°, 13 868 independent reflections, 11639 observed [$I \geqslant 2\sigma(I)$], $\omega$-scans. Structure calculation: data reduction SDP,[7a] solution SHELXS86,[7b] refinement SHELXL93[7c] molecular graphics ZORTEP,[7d] 1215 parameters, $R_1$ = 0.064, $wR_2$ = 0.209 for all independent reflections, GOF = 1.060, $\mu$ = 1.009 mm$^{-1}$, absorption correction: $\psi$-scans ($T_{min}$ = 0.970, $T_{max}$ = 1.000). CCDC 182/555. Further details of the crystal structure investigations may be obtained from Fachinformationszentrum Karlsruhe, D-76344 Eggenstein-Leopoldshafen, Germany, by quoting the depository number CSD 406324.

§ A single crystal of the solvated product, after drying *in vacuo* at room temp. was converted to the polycrystalline solid, and gave the following X-ray powder diagram [Debye–Scherrer camera, spacings *d*/Å, intensities (%) in parentheses]: 13.9(78), 12.1(86), 11.7(61), 10.4(100), 8.52(53), 6.97(61), 6.33(46), 6.26(25), 5.86(3.6), 5.55(43), 5.39(21), 5.27(82), 4.78(3.6), 4.66(39), 4.56(14), 4.434(18), 4.318(32), 4.186(7). The diagram is consistent with that reported above for the unsolvated product, and different from that calculated[6] on the basis of the single-crystal parameters.

1 (*a*) S. Rezgui, B. C. Gates, S. I. Burkett and M. E. Davis, *Chem. Mater.*, 1994, **6**, 2390; (*b*) Y. Kimura, S. Sugaya, T. Ichimura and I. Taniguchi, *Macromolecules*, 1987, **20**, 2329; (*c*) Y. Kimura, M. Furukawa, H. Yamane and T. Kitao, *Macromolecules*, 1989, **22**, 79; (*d*) Y. Koide and A. R. Barron, *Organometallics*, 1995, **14**, 4026.

2 F. Chaput, A. Lecomte, A. Dauger and J. P. Boilot, *Chem. Mater.*, 1989, **1**, 199.

3 (*a*) T. A. Zawodzinski, Jr. and R. A. Osteryoung, *Inorg. Chem.*, 1990, **29**, 2842; (*b*) P. Sobota, M. O. Mustafa, J. Utko and T. Lis, *J. Chem. Soc., Dalton Trans.*, 1990, 1809; (*c*) U. Thewalt and F. Stollmaier, *Angew. Chem. Suppl.*, 1982, 209.

4 (*a*) J. L. Atwood and M. J. Zaworotko, *J. Chem. Soc., Chem. Commun.*, 1983, 302; (*b*) M. R. Mason, J. M. Smith, S. G. Bott and A. R. Barron, *J. Am. Chem. Soc.*, 1993, **115**, 4971; (*c*) C. J. Harlan, M. R. Mason and A. R. Barron, *Organometallics*, 1994, **13**, 2957.

5 D. Belli Dell' Amico, F. Calderazzo, M. Dell' Innocenti, B. Güldenpfennig, S. Ianelli, G. Pelizzi and P. Robino, *Gazz. Chim. Ital.*, 1993, **123**, 283.

6 W. Kraus and G. Nolze, POWDER CELL, program for manipulation and visualisation of crystal structures of polycrystalline samples, *J. Appl. Crystallogr.*, 1996, **29**, 301.

7 (*a*) B. A. Frenz, Enraf-Nonius structure determination package, SDP users guide, Enraf-Nonius, Delft, 1983; (*b*) G. M. Sheldrick, SHELXS86, a FORTRAN program for the solution of X-ray structures, University of Göttingen, 1986; (*c*) G. M. Sheldrick, SHELXL93, a FORTRAN program for the refinement of X-ray structures, University of Göttingen, 1993; (*d*) L. Zsolnai, ZORTEP, a program for the ellipsoid representation of crystal structures.

8 C.-C. Chang, B. Srinivas, M.-L. Wu, W.-H. Chiang, M. Y. Chiang and C.-S. Hsiung, *Organometallics*, 1995, **14**, 5150.

9 (*a*) R. L. Ralph, L. W. Finger, R. M. Hazen and S. Ghose, *Am. Miner.*, 1984, **69**, 513; (*b*) M. C. Cruickshank and L. S. Dent Glasser, *J. Chem. Soc., Chem. Commun.*, 1985, 84; (*c*) L. S. Dent Glasser, F. P. Glasser and H. F. W. Taylor, *Quart. Rev.*, 1962, **16**, 343; (*d*) A. Deschanvers and B. Raveau, *Rev. Chim. Minéral.*, 1968, **5**, 201.

10 K. Nakamoto, *Infrared Spectra of Inorganic and Coordination Compounds*, Wiley, New York, 1963.

11 B. N. Figgis and G. B. Robertson, *Nature*, 1965, **205**, 694; S. C. Chang, G. A. Jeffrey, *Acta Crystallogr., Sect. B*, 1970, **26**, 673; M. K. Johnson, D. B. Powell and R. D. Cannon, *Spectrochim. Acta, Part A*, 1981, **37**, 995.

12 Y. Kushi and Q. Fernando, *Chem. Commun.*, 1969, 555.

13 (*a*) R. Benn, A. Rufinska, H. Lehmkuhl, E. Janssen and C. Krüger, *Angew. Chem., Int. Ed. Engl.*, 1983, **22**, 779; (*b*) J. F. Hinton and R. W. Briggs, *NMR of the Periodic Table*, ed. R. K. Harris and B. E. Mann, Academic, London, 1978, p. 297.

*Received in Basel, Switzerland, 12th May 1997; 7/03278A*

# Thioether macrocycles as spacers for crystal engineering: synthesis and crystal structures of $[Ag_2([24]aneS_8)(CF_3SO_3)_2(MeCN)_2]_\infty$ and $[Ag([16]aneS_4)(BF_4)]_\infty$ ([24]aneS$_8$ = 1,4,7,10,13,16,19,22-octathiacyclotetracosane; [16]aneS$_4$ = 1,5,9,13-tetrathiacyclohexadecane)

**Alexander J. Blake, Wan-Sheung Li, Vito Lippolis and Martin Schröder***

*Department of Chemistry, The University of Nottingham, University Park, Nottingham, UK NG7 2RD*

**The polymeric complexes $[Ag_2([24]aneS_8)(CF_3SO_3)_2(MeCN)_2]_\infty$ and $[Ag([16]aneS_4)(BF_4)]_\infty$ show infinite ladder and layered structures respectively, with the thioether crown controlling the multi-dimensional architecture.**

The coordination chemistry of crown thioethers has been of great interest over the past decade.[1] Most studies have been focused on the coordination chemistry of these ligands to transition metal ions,[1–4] although very little information is available on $Ag^I$ complexes with crown thioethers containing four or eight S-donor atoms.[5] Parallel to this, the design of solid-state architectures has become an area of increasing interest,[6–9] with attention focused predominantly upon the use of supramolecular contacts (particularly hydrogen bonding) between suitable organic molecules to generate multi-dimensional arrays and networks.[6–9] In comparison, the design of inorganic networks,[10–12] particularly polymeric metal complexes, is less well developed[13] with most of the examples being based upon linear bridging ligands bound to tetrahedral metal ions such as $Cu^I$ and $Ag^I$.[11,12,14] Few polymeric structures for thioether crown complexes have been reported, dimensional control being achieved mainly by variation of the counter-anion.[2,5] We report herein two new polymeric thioether crown complexes of $Ag^I$ whose multi-dimensional architecture is controlled by the thioether crowns building blocks.

Reaction of [24]aneS$_8$ with 2 equiv. of $AgCF_3SO_3$ in $CH_2Cl_2$–$CH_3CN$ affords a white solid which can be recrystallised from $CH_3CN$–$Et_2O$.† A single crystal X-ray structure determination‡ confirms the product to be a one-dimensional polymer, $[Ag_2([24]aneS_8)(CF_3SO_3)_2(MeCN)_2]_\infty$, in which each $Ag^I$ ion is coordinated to four S-donors in a distorted tetrahedral geometry with S–Ag–S angles ranging from 85.83(5) to 127.36(5)° and Ag–S bond distances from 2.5400(14) to 2.627(2) Å. The four S-donors come from two different ligand molecules to generate an infinite ladder polymer along the *b* axis (Fig. 1). Within the ladder, pairs of symmetry-related $Ag^I$ ions are coordinated between two macrocyclic ligands, so that all eight S-donors of each [24]aneS$_8$ molecule are engaged in coordination. Each metal ion is also a spiro centre, being the common atom of two almost perpendicular $AgS_2C_2$ rings. The macrocycle adopts a unique pattern of alternate *endo*- and *exo*-orientated S-donors, with 9 out of 12 torsion angles less than 90° and all the S–C–C–S torsion angles having a *gauche* arrangement. Stacks of $CF_3SO_3^-$ ions and acetonitrile molecules are observed between the polymeric chains. Significantly, the use of $NO_3^-$ as counter-anion leaves the structure of the polymeric $Ag^I$ complex unchanged in $[Ag_2([24]aneS_8)(NO_3)_2(H_2O)]_\infty$.

Reaction of [16]aneS$_4$ with $AgBF_4$ in 1 : 1 molar ratio in $CH_3CN$–$CH_2Cl_2$ affords a white powder which can be recrystallised from hot dmf.† A single crystal X-ray structure determination‡ confirms the product to be a three-dimensional polymer, $[Ag([16]aneS_4)(BF_4)]_\infty$. Each $Ag^I$ ion occupies a crystallographic $\bar{4}$ ($S_4$) site and is coordinated by four symmetry-equivalent S-donor atoms in a tetrahedral geometry with S–Ag–S angles of 119.44(2) and 90.98(3)° and Ag–S bond distances of 2.6121(7) Å. The donor atoms are derived from four symmetry-related [16]aneS$_4$ molecules, each of which is bound to four different $Ag^I$ ions (Fig. 2). The mcrocycle adopts a [4444] conformation with all the sulfur atoms *exo*-oriented. The [16]aneS$_4$ molecules lie in sheets perpendicular to the *c* axis, within which 24-membered rings can be recognised: these comprise four $Ag^I$ ions and one S–C–C–C–S edge from four different thioether ligands (Fig. 2). Successive layers are stacked offset along *c* so that the [16]aneS$_4$ molecules and the 24-membered rings alternate, giving rise to channels within which the $BF_4^-$ anions lie at the centres of the larger rings. This compound represents the first structurally characterized complex of $Ag^I$ with an unfunctionalised tetradentate thioether

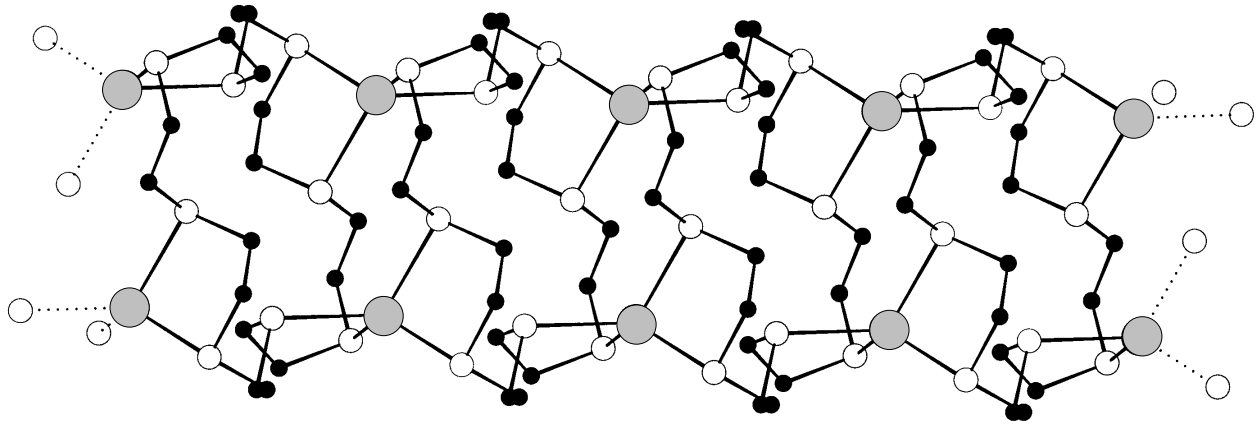


**Fig. 1** Packing diagram for the $\{[Ag_2([24]aneS_8)]^{2+}\}_\infty$ polymeric chain. Counter-anion omitted for clarity. Carbon, small black circles, sulfur, white circles; silver, large grey circles.

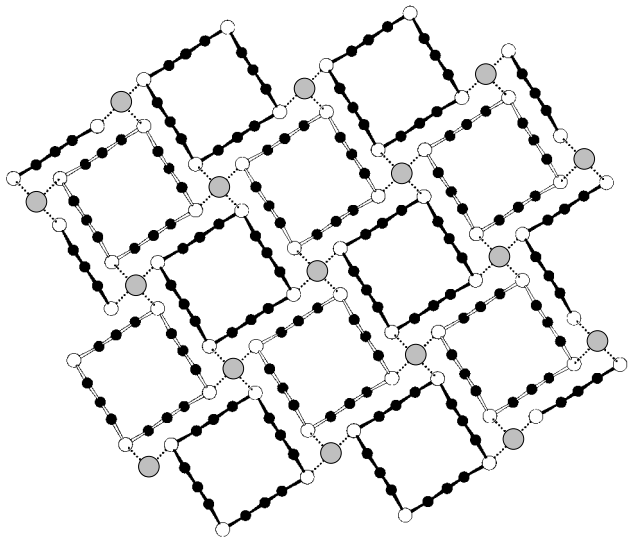


**Fig. 2** View of the packing diagram for the $\{[Ag([16]aneS_4)]^+\}_\infty$ polymeric complex along the *c* axis. Counter-anion omitted for clarity. Atoms shaded as in Fig. 1.

crown, although a polymeric structure has been reported with the ligand $(OH)_2$-[16]aneS$_4$[5] in which the OH groups play a major role in the crystal packing through extensive hydrogen bonding.

This work illustrates the potential of thioether crowns as building blocks for the synthesis of inorganic architectures using their *exo*-orientated S-donors. We are currently investigating how we may fine-tune the multi-dimensional architectures of polymeric Ag$^I$ complexes with tetradentate thioether crowns.

We thank the EPSRC for financial support.

## Footnotes and References

* E-mail: M.schroder@nott.ac.uk

† $[Ag_2([24]aneS_8)(CF_3SO_3)_2(MeCN)_2]_\infty$. To a well stirred solution of [24]aneS$_8$ (50 mg, 0.104 mmol) in $CH_2Cl_2$–$CH_3CN$ (20 ml, 1 : 1 v/v) was added a solution of $AgCF_3SO_3$ (53.44 mg, 0.208 mmol) in $CH_3CN$ (5 ml). The mixture was stirred at room temp. for 1 h. The white solid formed was filtered off and dried under reduced pressure (70 mg, 62.5% yield). Single crystals were obtained by recrystallization from $CH_3CN$–$Et_2O$.

$[Ag([16]aneS_4)(BF_4)]_\infty$. To a well stirred solution of [16]aneS$_4$ (35.44 mg, 0.1195 mmol) in $CH_2Cl_2$–$CH_3CN$ (15 ml, 1 : 1 v/v) was added a solution of $AgBF_4$ (23.26 mg, 0.1195 mmol) in $CH_3CN$ (5 ml). The mixture was stirred at room temp. for 24 h. The white solid formed was filtered off and dried under reduced pressure (30 mg, 51.0% yield). Single crystals were obtained by recrystallization from hot dmf. Satisfactory elemental analyses were obtained for both compounds.

‡ Stoe Stadi-4 four-circle diffractometer, graphite-monochromated Mo-K$\alpha$ radiation, $\omega$–$\theta$ scans, $\theta_{max}$ = 25°. Both structures were solved using direct methods[15] and all non-H atoms were located using subsequent difference Fourier methods.[16] Hydrogen atoms were placed in calculated positions and thereafter allowed to ride on their parent atoms.

*Crystal data* for $[Ag_2([24]aneS_8)(CF_3SO_3)_2(MeCN)_2]_\infty$: $C_{22}H_{38}Ag_2F_6N_2O_6S_{10}$, $M$ = 1076.88, monoclinic, space group $P2_1/c$ (no. 14), $a$ = 13.285(2), $b$ = 6.3340(10), $c$ = 22.547(3) Å, $\beta$ = 91.721(14)°, $U$ = 1890.7(3) Å$^3$, $Z$ = 2, $F(000)$ = 1080, $D_c$ = 1.892 g cm$^{-3}$, $\mu$(Mo-K$\alpha$) = 1.66 mm$^{-1}$. Colourless plate (0.07 × 0.21 × 0.25 mm), $\psi$-scan absorption corrections ($T_{min}$ = 0.61, $T_{max}$ = 0.81), 3344 unique reflections, of which 2255 had $I \geqslant 2\sigma(I)$. The weighting scheme $w^{-1} = [\sigma^2(F_o^2) + (0.0252P)^2 + 0.40P]$, $P = [\max(F_o^2, 0) + 2F_c^2]$, was applied. At final convergence $R_1$ [$I \geqslant 2\sigma(I)$] = 0.0431, $wR_2$ (all data) = 0.0874 for 218 refined parameters, $S$ = 1.03, $(\Delta/\sigma)_{max}$ = −0.001, $\Delta\rho_{max}$ = 0.55 e Å$^{-3}$.

*Crystal data* for $[Ag([16]aneS_4(BF_4)]_\infty$: $C_{12}H_{24}AgBF_4S_4$, $M$ = 491.23, tetragonal, space group $I\bar{4}$ (no. 82), $a$ = 10.3955(14), $c$ = 8.227(2) Å, $U$ = 889.1(2) Å$^3$, $Z$ = 2, $F(000)$ = 496, $D_c$ = 1.835 g cm$^{-3}$, $\mu$(Mo-K$\alpha$) = 1.632 mm$^{-1}$. Colourless tablet (0.15 × 0.27 × 0.29 mm), $\psi$-scan absorption corrections ($T_{min}$ = 0.614, $T_{max}$ = 0.709), 778 unique reflections ($R_{int}$ = 0.040), of which 767 had $I \geqslant 2\sigma(I)$. The weighting scheme $w^{-1} = [\sigma^2(F_o^2) + (0.0272P)^2 + 0.51P]$, $P = [\max(F_o^2, 0) + 2F_c^2]$ was adopted. At final convergence $R_1$ [$I \geqslant 2\sigma(I)$] = 0.0176, $wR_2$ (all data) = 0.0471 for 51 refined parameters, $S$ = 1.07, $(\Delta/\sigma)_{max}$ = 0.001, $\Delta\rho_{max}$ = 0.38 e Å$^{-3}$. CCDC 182/573.


1 A. J. Blake and M. Schröder, *Adv. Inorg. Chem.*, 1990, **35**, 1; S. C. Rawle and S. R. Cooper, *Struct. Bonding*, 1991, **72**, 1.
2 A. J. Blake, D. Collison, R. O. Gould, G. Reid and M. Schröder, *J. Chem. Soc., Dalton Trans.*, 1993, 521.
3 H. J. Küppers, K. Wieghardt, Y. H. Tsay, C. Krüger, B. Nuber and J. Weiss, *Angew. Chem., Int. Ed. Engl.*, 1987, **26**, 575.
4 R. Alberto, W. Nef, A. Smith, T. A. Kaden, M. Neuburger, M. Zehender, A. Frey, U. Abram and P. A. Schubiger, *Inorg. Chem.*, 1996, **35**, 3420.
5 M. Munakata, L. P. Wu, M. Yamamoto, T. Kuroda-Sowa and M. Maekawa, *J. Chem. Soc., Dalton Trans.*, 1995, 3215.
6 G. R. Desiraju, in *Crystal Engineering: Design of Organic Solids*, Elsevier, Amsterdam, 1989.
7 *The Crystal as a Supramolecular Entity*, ed. G. R. Desiraju, Wiley, Chichester, 1995.
8 G. R. Desiraju, *Angew. Chem., Int. Ed. Engl.*, 1995, **34**, 2311.
9 R. Robson, B. F. Abrahams, S. R. Batten, R. W. Gable, B. F. Hoskins and J. Liu, *Supramolecular Architecture*, ACS, Washington DC, 1992, ch. 19.
10 L. Carlucci, G. Ciani, D. M. Proserpio and A. Sironi, *J. Chem. Soc., Chem., Commun.*, 1994, 2755.
11 S. B. Copp, K. T. Holman, J. O. S. Sangster, S. Subramaniam and M. J. Zaworotko, *J. Chem. Soc., Dalton Trans.*, 1995, 223 and references therein.
12 B. F. Abrahams, S. R. Batten, H. Hamit, B. F. Hoskins and R. Robson, *Angew. Chem., Int. Ed. Engl.*, 1996, **35**, 4432; L. Carlucci, G. Ciani, D. M. Proserpio and A. Sironi, *J. Am. Chem. Soc.*, 1995, **117**, 4562; O. M. Yaghi and H. Li, *J. Am. Chem. Soc.*, 1995, **117**, 10 401; B. F. Abrahams, S. R. Batten, H. Hamit, B. F. Hoskins and R. Robson, *Chem. Commun.*, 1996, 1313; L. Carlucci, G. Ciani, D. M. Proserpio and A. Sironi, *Chem. Commun.*, 1996, 1393.
13 M. Munakata, T. Kuroda-Sowa, M. Maekawa, A. Hirota and S. Kitagawa, *Inorg. Chem.*, 1995, **34**, 2705; M. Munakata, T. Kuroda-Sowa, M. Maekawa, A. Honda and S. Kitagawa, *J. Chem. Soc., Dalton Trans.*, 1994, 2771; J. R. Black, N. R. Champness, W. Levason and G. Reid, *Inorg. Chem.*, 1996, **35**, 4432.
14 A. J. Blake, N. R. Champness, S. S. M. Chung, W.-S. Li and M. Schröder, *Chem. Commun.*, 1997, 1005; A. J. Blake, N. R. Champness, A. N. Khlabystov, D. A. Lemenovskii, W.-S. Li and M. Schröder, *Chem. Commun.*, 1997, 1339; A. J. Blake, N. R. Champness, S. S. M. Chung, W.-S. Li and M. Schröder, *Chem. Commun.*, 1997, 1675.
15 G. M. Sheldrick, SHELXS-86, *Acta Crystallogr., Sect. A*, 1990, **46**, 467.
16 G. M. Sheldrick, SHELXL-93, Universität Göttingen, 1993.


*Received in Cambridge, UK, 7th July 1997, 7/04796G*

# Realumination of dealuminated HZSM-5 zeolites by acid treatment

**Tsuneji Sano,* Rie Tadenuma, Zhengbao Wang and Kazuo Soga**

*School of Materials Science, Japan Advanced Institute of Science and Technology, Tatsunokuchi, Ishikawa 923-12, Japan*

**$^{27}$Al MAS NMR and FTIR spectroscopy shows that part of non-framework aluminiums in dealuminated HZSM-5 zeolites are reinserted into the framework upon treatment with aqueous hydrochloric acid.**

Physicochemical properties of zeolites such as catalytic, sorptive and ion-exchange abilities are strongly dependent on their framework (tetrahedrally coordinated) aluminiums in the zeolite structure. Dealumination from zeolite framework has been widely studied to alter the $SiO_2/Al_2O_3$ ratio of the framework. We have kinetically investigated the dealumination behavior of ZSM-5 zeolite and metallosilicate by thermal and hydrothermal treatments, and already reported that the dealumination rate by hydrothermal treatment has an apparent third-order dependence on the number of framework aluminiums.[1–3] As the framework aluminium atoms are isolated from each other in the case of highly siliceous zeolites such as ZSM-5, this indicates that the dealumination *via* hydrolysis of Si–O–Al bonds in the zeolite framework is catalyzed by acid (protons) which move freely in the zeolite pores. Realumination, the reverse reaction of hydrolysis of the Si–O–Al bond, as well as dealumination of zeolites has received considerable attention from the standpoint of regeneration of zeolite catalysts. There are several papers concerning the realumination of dealuminated zeolite by treatment with aqueous alkali solution, suggesting the reinsertion of non-framework aluminium into the framework (a decrease in the framework $SiO_2/Al_2O_3$ ratio).[4–10] However, no study of realumination by acid treatment has been reported in the literature. Here, the realumination of dealuminated HZSM-5 zeolites by treatment with aqueous HCl was investigated.

HZSM-5 zeolite was prepared following the procedure previously described.[1] A $SiO_2/Al_2O_3$ ratio of 71 was determined by X-ray fluorescence (XRF, Philips PW-2400) while a framework $SiO_2/Al_2O_3$ ratio of 78 was determined by $^{27}$Al MAS NMR spectroscopy (Varian VXP-400) using a calibration curve, which was produced by measuring $^{27}$Al MAS NMR spectra of HZSM-5 zeolites with various $SiO_2/Al_2O_3$ ratios.[2,3] Dealumination of the HZSM-5 zeolite was carried out by thermal and hydrothermal treatments at 600 °C using a muffle furnace and a quartz reactor tube. The water vapor pressure in the hydrothermal treatment was 10 kPa, generated using nitrogen as the diluent gas. HCl treatment (realumination) was carried out as follows: 1 g of dealuminated HZSM-5 zeolite was treated with 100 ml of aqueous 2 M HCl at 100 °C, stirring for a given time. The product was filtered off, washed thoroughly with deionized water, dried at 100 °C and calcined at 380 °C for 8 h. Characterization of dealuminated and realuminated HZSM-5 zeolites was achieved by $^{27}$Al MAS NMR spectroscopy, diffuse reflectance FTIR (JEOL JIR-7000), and nitrogen adsorption (Bel Japan Belsorp 28SA).

X-Ray diffraction diagrams of realuminated HZSM-5 zeolites after HCl solution treatment show no peaks other than those corresponding to ZSM-5 zeolite. The intensities of the peaks observed were almost the same as those of the dealuminated zeolite, indicating no structural degradation. This was also confirmed by the fact that no difference in the micropore volume $W_0(N_2)$ of 0.18 $cm^3$ (liquid) $g^{-1}$ obtained by the Dubinin–Raushkevich (DR) plot of the nitrogen adsorption isotherm was observed between dealuminated and realuminated zeolites. Fig. 1 shows FTIR spectra of the parent HZSM-5 (total $SiO_2/Al_2O_3$ ratio 71), the dealuminated HZSM-5 prepared by thermal treatment at 600 °C for 48 h (total $SiO_2/Al_2O_3$ ratio 72) and the realuminated HZSM-5 after HCl treatment (total $SiO_2/Al_2O_3$ ratio 78). The decrease in the peak at 3605 $cm^{-1}$ assigned to an acidic bridged OH of Si(OH)Al was observed in the spectrum of dealuminated HZSM-5 zeolite, while a clear increase in the peak intensity was observed in the spectrum of realuminated zeolite. This result suggests the reinsertion of non-framework aluminiums in the dealuminated zeolite into the framework.

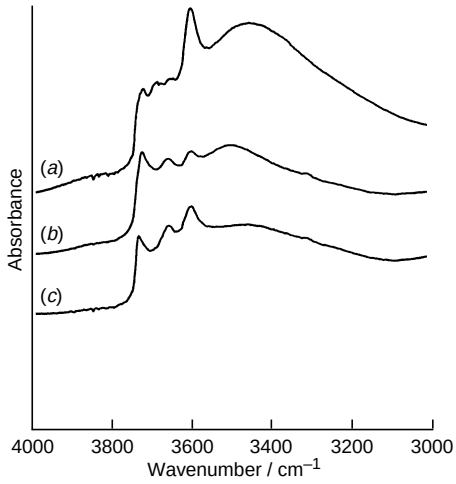



**Fig. 1** FTIR spectra of HZSM-5 zeolites of (*a*) parent, (*b*) after thermal dealumination at 600 °C for 48 h and (*c*) after realumination of (*b*) with 2 M HCl at 100 °C for 120 h

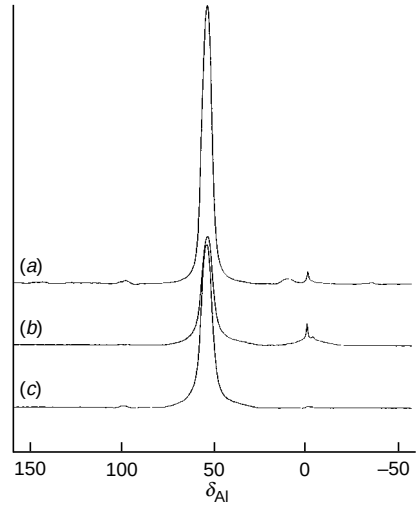



**Fig. 2** $^{27}$Al MAS NMR spectra of HZSM-5 zeolites of (*a*) parent, (*b*) after thermal dealumination at 600 °C for 48 h and (*c*) after realumination of (*b*) with 2 M HCl at 100 °C for 120 h

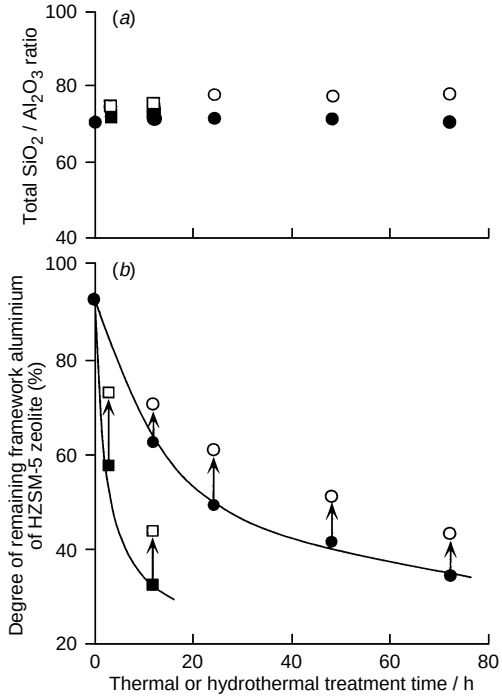



**Fig. 3** Total $SiO_2/Al_2O_3$ ratios and degrees of remaining framework aluminium of dealuminated and realuminated HZSM-5 zeolites. (●), HZSM-5 dealuminated by thermal treatment at 600 °C; (○), after treatment with 2 M HCl at 100 °C for 120 h; (■), HZSM-5 dealuminated by hydrothermal treatment at 600 °C and $P_{H_2O}$ of 10 kPa; (□), after treatment with 2 M HCl at 100 °C for 120 h.

To clarify this possibility of reinsertion, the $^{27}$Al MAS NMR spectra of these samples were measured. The normalized intensity of the peak at $\delta$ 53 assigned to framework aluminium of HZSM-5 zeolite was based on 1 g of zeolite. As shown in Fig. 2, the peak intensity of the dealuminated HZSM-5 zeolite definitely increased upon treatment with HCl. The calculated framework $SiO_2/Al_2O_3$ ratios of the dealuminated and the realuminated HZSM-5 zeolite were 173 and 140, respectively. As the total $SiO_2/Al_2O_3$ ratio of the realuminated zeolite was 78, dissolution of non-framework aluminium occurred during treatment with HCl; this indicates that some of the non-framework aluminium in dealuminated HZSM-5 zeolite is reinserted into the framework.

However, there is another possible explanation for the increase in the peak intensities of $^{27}$Al MAS NMR and FTIR spectra, namely that the increase is attributable to the removal of the framework silicon atoms.[12,13] To clarify this, therefore, silicon and aluminium concentrations in the liquid phase after HCl treatment were analyzed by inductively coupled argon emission spectroscopy (Seiko SPS7700). The degrees of elution of silicon and aluminium atoms from the dealuminated zeolite during the HCl treatment were 0.99 and 9.3%, respectively, indicating that the removal of framework silicon atoms scarcely takes place during this process. This is consistent with the result reported by Kooyman *et al.*[14] Therefore, we can conclude that realumination of dealuminated zeolite occurs during acid treatment.

To gain more information about the realumination, the realumination of several dealuminated HZSM-5 zeolites with different framework $SiO_2/Al_2O_3$ ratios was carried out at 100 °C for 120 h using 2 M HCl. Dealuminated HZSM-5 zeolites with different degrees of dealumination were prepared by varying the thermal treatment time. Fig. 3 shows the total $SiO_2/Al_2O_3$ ratios and the degree of remaining framework aluminium of dealuminated and the corresponding realuminated HZSM-5 zeolites. The total $SiO_2/Al_2O_3$ ratios of realuminated HZSM-5 zeolites were slightly higher than those of dealuminated zeolites. All framework aluminium ion concentrations of dealuminated HZSM-5 zeolite increased upon HCl treatment. Dealuminated HZSM-5 zeolites were also prepared by hydrothermal treatment at 600 °C under a water vapor pressure of 10 kPa and then treated with HCl and the result is also illustrated in Fig. 3 with reinsertion of non-framework aluminium into the framework also being observed.

From the above results, it is concluded that some of the non-framework aluminium in dealuminated HZSM-5 zeolite is reinserted into the framework in the presence of an aqueous solution of hydrochloric acid although the detailed mechanism of the realumination is not clear. As it is well known that non-framework aluminium is not uniform and exists in different states,[15] we primarily speculate that realumination proceeds mainly through reinsertion of non-framework aluminium species where the aluminium atom is connected to the zeolite framework by only one or two chemical bonds.

## Footnote and References

E-mail: t-sano@jaist.ac.jp

1 T. Sano, N. Yamashita, Y. Iwami, K. Takeda and Y. Kawakami, *Zeolites*, 1996, **16**, 258.
2 K. Takeda, T. Sano and Y. Kawakami, *Nippon Kagaku Kaishi*, 1996, 680.
3 T. Sano, H. Ikeya, T. Kasuno, Z. B. Wang, Y. Kawakami and K. Soga, *Zeolites*, in the press.
4 D. W. Breck and G. W. Skeels, *Proc. 5th Int. Conf. on Zeolites*, ed. L. V. C. Rees and B. E. Heyden, London, 1980, p. 335.
5 X. Lin, J. Klinowski and J. M. Thomas, *J. Chem. Soc., Chem. Commun.*, 1986, 582.
6 H. Hamdan, B. Sulikowski and J. Klinowski, *J. Phys. Chem.*, 1989, **93**, 350.
7 Z. Zhang, X. Liu, Y. Xu and R. Xu, *Zeolites*, 1991, **11**, 232.
8 H. Ishida and Y. Fukuoka, *Nippon Kagaku Kaishi*, 1994, 690.
9 D. Lin, S. Bao and Q. Xu, *Zeolites*, 1997, **18**, 162.
10 N. Y. Chen, *J. Phys. Chem.*, 1976, **80**, 60.
11 D. H. Olson, W. O. Haag and R. M. Lao, *J. Catal.*, 1980, **61**, 390.
12 G. Engelhardt and U. Lohse, *J. Catal.*, 1984, **88**, 513.
13 L. Aouali, J. Jeanjean, A. Dereign, P. Tougne and D. Delafosse, *Zeolites*, 1988, **8**, 517.
14 P. J. Kooyman, P. van der Waal and H. van Bekkum, *Zeolites*, 1997, **18**, 50.
15 E. Loeffler, U. Lohse, Ch. Peuker, G. Oehlmann, L. M. Kustov, V. L. Zholobenko and V. B. Kazansky, *Zeolites*, 1990, **10**, 266.

*Received in Cambridge, UK, 21st July 1997; 7/05192A*

# ‘Soft–soft’ halogen–halogen interactions in solid ion pairs of solvent-free $Pr^i_3PCl_2$ and $CH_2Cl_2$-solvated $Pr^i_3PBr_2$: structural features of chloro- and bromo-triisopropylphosphonium salts

**Frank Ruthe, Wolf-W. du Mont* and Peter G. Jones**

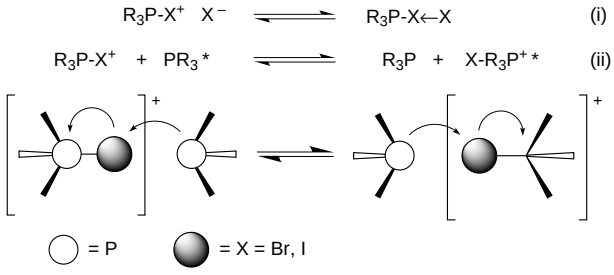
*Institut für Anorganische und Analytische Chemie, Technische Universität Braunschweig, Postfach 3329, D 38023, Braunschweig, Germany*

**An X-ray crystallographic study of solvent-free $Pr^i_3PCl_2$ and dichloromethane-solvated $Pr^i_3PBr_2$ reveals that both halogenophosphonium halides exist as monomeric ion pairs $Pr^i_3P^+$–X···$X^-$; elongations of P–Cl and P–Br bonds are associated with Cl···Cl and Br···Br interactions.**

Iodine atoms and bromine atoms adjacent to phosphonium centers behave as soft electrophiles. Nucleophilic attack by tertiary phosphanes $R_3P$ at I (of $R_3PI^+$) or Br (of $R_3PBr^+$) leads to rapid $I^+$ or $Br^+$ transfer in solution (‘fluxional $P^{III}$–$P^V$ systems’), as detected by $^{31}P$ and $^1H$ NMR spectroscopy[1–3] (Scheme 1). In the solid state, I···I interactions of iodophosphonium ions $R_nPI_{4-n}^+$ with iodide counter ions lead, depending on the number of iodine atoms adjacent to phosphorus, to ‘spoke’ structures with approximately linear P–I···I units ($n$ = 3; $R_3PI_2$)[3–7] to rings, helices and zigzag chains ($n$ = 2, $R_2PI_3$),[8–11] or to interpenetrating puckered layers and three-dimensional networks ($n$ = 1, $RPI_4$).[12]

Evidence for related structures with Br···Br or even Cl···Cl interactions is still extremely scarce. McAuliffe *et al.* found that $Ph_3PBr_2$ also exists (as do $Ph_3PI_2$[4] and $Ph_3PIBr$[13]) as a ‘molecular charge-transfer-like spoke’;[14] dichloromethane-solvated $Ph_3PCl_2$, however, contains $[Ph_3PCl{\cdots}Cl{\cdots}ClPPh_3]^+$ cations that are well separated from $Cl^-$ anions.[15] Is there a general difference between the solid state structures of compounds $R_3PCl_2$ compared with $R_3PI{\cdots}I$ and $R_3PBr{\cdots}Br$, or is the structure of dichloromethane-solvated $Ph_3PCl_2$ an exceptional case? To determine whether ion–dipole interactions of the anion with dichloromethane or other effects contribute to the latter ‘exceptional’ structure, it was desirable to solve the structure of a related solvent-free species $R_3PCl_2$ and of a solvated species $R_3PBr_2$ (R = alkyl). Fortuitously, the crystallisation behaviour of triisopropylphosphane derivatives $Pr^i_3PX_2$ (X = Cl **1**,[17] X = Br **2**[16]) was found to meet just the above requirements.

Crystallisation from dichloromethane provided solvent-free **1**, which is, to the best of our knowledge, the first crystallographically characterised solvent-free compound of stoichiometry $R_3PCl_2$. **2**, however, gave crystals containing 0.5 equiv. of $CH_2Cl_2$ under comparable conditions. Both solid compounds contain $R_3P^+$–X···$X^-$ ion pairs with approximately linear P–X···X units;[3,4] the bromide ions of two such ion pairs of **2** are ‘bridged’ by a $CH_2Cl_2$ molecule (Figs. 1 and 2). We have




**Scheme 1** The positions of equilibria i and ii depend on R

since found that the corresponding P–I compound $[(Pr^i_3PI_2)_2{\cdot}CH_2Cl_2]$[18] is isostructural. The $Br^-{\cdots}H$–C–H···Br contacts can be understood as bromide solvation by ion–dipole interactions.

The Cl···Cl distance within ion pairs of **1** [3.234(1) Å] is slightly shorter than those of $Ph_3PCl{\cdots}Cl{\cdots}ClPPh_3]^+$ [3.279(6) Å];[15] the degree of interaction by (valence-shell expanding) $Cl \rightarrow Cl\ n \rightarrow \sigma^*$ overlap is obviously not very dependent on the coordination number of the donating chloride ion. Packing and anion solvation effects might both contribute to the structural difference between $Ph_3PCl_2{\cdot}CH_2Cl_2$[15] and **1**. A reinvestigation of the structure of $[Pr^i_3PCl]^+[N(SO_2CH_3)_2]^-{\cdot}CH_2Cl_2$[19] **3** reveals that here chlorine atoms of a well ordered $CH_2Cl_2$ approach the Cl atom of the $[Pr^i_3PCl]^+$ cation [3.407(2) Å] to satisfy its Lewis-acidic needs, which apparently cannot be met by the $[N(SO_2Me)_2]^-$ counter ion.

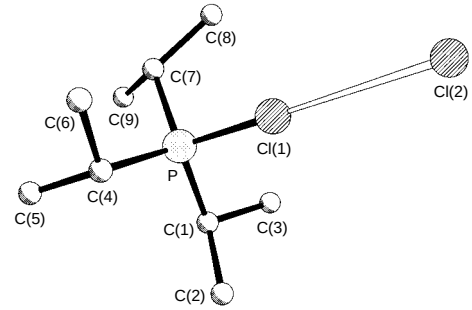



**Fig. 1** Molecular structure of **1**. H atoms have been omitted for clarity. Selected bond lengths (Å) and angles (°): P–Cl(1) 2.002(1), Cl(1)···Cl(2) 3.234(1); P–Cl(1)···Cl(2) 177.5(1).

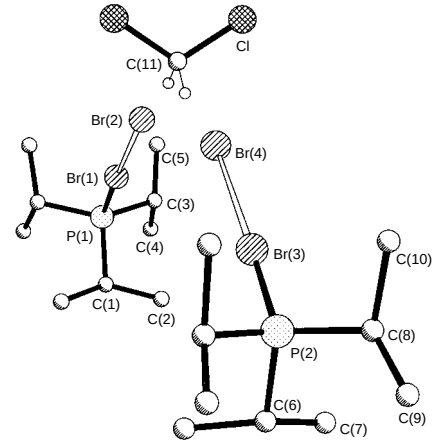



**Fig. 2** Molecular structure of **2**. H atoms have been omitted for clarity. Selected bond lengths (Å) and angles (°): P(1)–Br(1) 2.185(3), Br(1)···Br(2) 3.369(2), P(2)–Br(3) 2.174(3), Br(3)···Br(4) 3.315(2); P(1)–Br(1)···Br(2) 175.0(1), P(2)–Br(3)···Br(4) 176.5(1).

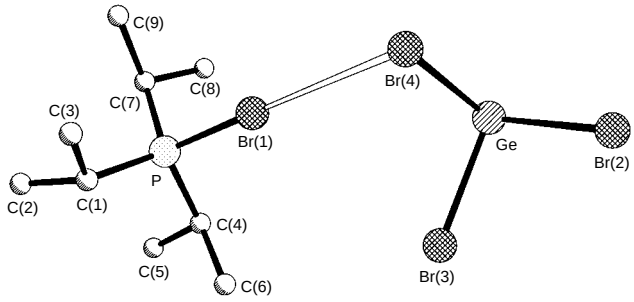



**Fig. 3** Molecular structure of **4**. H atoms have been omitted for clarity. Selected bond lengths (Å) and angles (°): P–Br(1) 2.155(2), Br(1)···Br(4) 3.415(1), Ge–Br(4) 2.556(1), Ge–Br(2) 2.481(1), Ge–Br(3) 2.480(1); P–Br(1)···Br(4) 177.8(1).

Bromotrialkylphosphonium tribromogermanates(II) and tribromostannates(II) have been identified spectroscopically as the products from reactions of bulky phosphanes with germanium and tin tetrabromides;[2] structural evidence by X-ray methods, however, has not yet been provided. In salts $[R_3PBr]^+[MBr_3]^-$ (M = $Ge^{II}$, $Sn^{II}$), cation–anion interactions might occur *via* Br···$M^I$ or Br···Br contacts. In the latter case, the Br···Br contacts would provide an interesting comparison with those of compound **2**. We therefore reacted $Pr^i_3P$ with $GeBr_4$: the new compound $Pr^i_3PBr^+GeBr_3^-$ **4**, formed in high yield, provides the first crystallographic characterisation of a product from a germanium or tin tetrahalide/tertiary phosphane redox reaction.[2,20,21] Consistent with the lower donor ability of the Br atoms of the $GeBr_3^-$ anion, cation–anion Br···Br contacts in **4** [3.415(1) Å] are slightly longer and the P–Br bond in **4** [2.155(2) Å] is slightly shorter than those in **2** (Fig. 2) or in $Ph_3PBr_2$ {*d*(Br–Br) 3.123(2), *d*(P–Br) 2.181(3) Å} (Fig. 3).[14]

P–I bonds of iodophosphonium ions are affected by $n \rightarrow \sigma^*$ overlap from nucleophiles attacking the I atoms. P–Br bond lengths [**2**, 2.185(3), 2.174(3) Å; **4**, 2.155(2) Å] are less affected by cation–nucleophile interactions than P–I bond lengths and the related impact on P–Cl bond lengths [**1**, 2.002(1) Å; **3**, 1.994(2) Å;[19] $Me_3PCl^+SbCl_6^-$, 1.986(2) Å[22]] is even smaller.

In contrast to the above-mentioned rapid $I^+$ or $Br^+$ transfer between phosphanes,[1,2] which is also observed in mixtures of **2** and $Pr^i_3P$ in $CH_2Cl_2$ solution at room temperature (1 : 1 mixture: $\delta_P$ 57), comparable $R_3PCl^+$–$R_3P$ systems do not give averaged $P^{III}$–$P^V$ NMR signals, indicating that transition states $[R_3P–X–PR_3]^+$ are of higher energy when X = Cl. $^{31}$P NMR shifts of the cations of **1**–**4** are only slightly anion dependent ($\delta_P$ in $CH_2Cl_2$ solution: **1**, 120.1; **2**, 114.9; **3**, 119.8;[19] **4**, 114.3).

In conclusion, phosphoranes with one I or Br atom bonded to pentacoordinated phosphorus are known;[23,24] however all as yet structurally characterised solid halogenophosphonium halides $R_3PX_2$ (X = Cl, Br, I) do not contain pentacoordinated phosphorus, but are ionic and exhibit similar types of cation–anion halogen–halogen interactions. The increasing significance of X···X interactions, the increasing extent of P–X bond lengthening and the increasing accessibility of $[R_3P···X···PR_3]^+$ transition states (Cl ≪ Br < I) associated with 'soft–soft' ($n \rightarrow \sigma^*$) interactions are all consistent with the known range of increasing electrophilicity and polarisability of the heavier halogens.

## Footnotes and References

* E-mail: dumont@mac1.anchem.nat.tu-bs.de

† *Crystal data*: **1**: $C_9H_{21}Cl_2P$; *M* = 231.13, orthorhombic, space group $P2_12_12_1$, *a* = 9.437(2), *b* = 10.101(2), *c* = 13.262(2) Å, *U* = 1264.1(4) Å$^3$, *Z* = 4, $D_c$ = 1.214 Mg m$^{-3}$, $\mu$ = 0.596 mm$^{-1}$, *F*(000) = 496, 2629 independent reflections to 2$\theta$ max. 55°, *T* = 173 K, *S* = 1.027, *R*[*F*, > 4$\sigma$(*F*)] = 0.0394, *wR*($F^2$) = 0.0902, 45 restraints and 116 parameters, highest peak 0.471 and deepest hole −0.196 e Å$^{-3}$, absolute structure parameter *x* = 0.06(11).

**2**: $C_{9.5}H_{22}Br_2ClP$; *M* = 362.51, orthorhombic, space group *Pnma*, *a* = 15.576(2), *b* = 10.594(2), *c* = 18.219(2) Å, *U* = 3006.4(8) Å$^3$, *Z* = 8, $D_c$ = 1.602 Mg m$^{-3}$, $\mu$ = 5.644 mm$^{-1}$, *F*(000) = 1448, 2766 independent reflections to 2$\theta$ max. 50°, *T* = 173 K, *S* = 0.958, *R*[*F*, > 4$\sigma$(*F*)] = 0.599, *wR*($F^2$) = 0.1518, 44 restraints and 142 parameters, highest peak 1.357 and deepest hole −0.765 e Å$^{-3}$. The displacement parameters of some isopropyl C atoms are slightly higher than expected for low-temperature structures (*ca.* 0.15 Å$^2$), which may be due to slight disorder.

**4**: $C_9H_{21}Br_4GeP$; *M* = 552.46, monoclinic, space group $P2_1/n$, *a* = 10.717(3), *b* = 8.285(3), *c* = 18.765(4) Å, $\beta$ = 91.80(3)°, *U* = 1665.3(8) Å$^3$, *Z* = 4, $D_c$ = 2.203 Mg m$^{-3}$, $\mu$ = 11.507 mm$^{-1}$, *F*(000) = 1048, 2930 independent reflections to 2$\theta$ max. 50°, *T* = 143 K, *S* = 1.107, *R*[*F*, > 4$\sigma$(*F*)] = 0.0443, *wR*($F^2$) = 0.1156, 143 parameters, highest peak 1.058 and deepest hole −0.894 e Å$^{-3}$.

All X-ray datasets were collected with monochromated Mo-K$\alpha$ radiation ($\lambda$ = 0.710 73 Å) on a Siemens P4 (**1**, **2**) or a Stoe STADI-4 (**4**) four-circle diffractometer. Absorption corrections were based on $\psi$-scans. The structures were solved by direct (**1**, **4**) or heavy-atom methods (**2**) and refined anisotropically by full-matrix least squares on $F^2$. H atoms were included using a riding model for all non-methyl group protons. Methyls were refined as rigid groups except C(10) in **2** (riding). CCDC 182/576.

‡ $^{31}$P NMR data (300 K $CH_2Cl_2$–$C_6D_6$): **1**, $\delta$ 120.1; **2**, $\delta$ 114.9; **4**, $\delta$ 114.3.

1 W.-W. du Mont and H. J. Kroth, *J. Organomet. Chem.*, 1976, **113**, C35.
2 W.-W. du Mont, *Z. Anorg. Allg. Chem.*, 1979, **458**, 85.
3 W.-W. du Mont, M. Bätcher, S. Pohl and W. Saak, *Angew. Chem.*, 1987, **99**, 945; *Angew. Chem., Int. Ed. Engl.*, 1987, **26**, 912.
4 S. M. Godfrey, D. G. Kelly, C. A. McAuliffe, A. G. Mackie, R. G. Pritchard and S. M. Watson, *J. Chem. Soc., Chem. Commun.*, 1991, 1163.
5 N. Bricklebank, S. M. Godfrey, A. G. Mackie, C. A. McAuliffe, R. G. Pritchard and S. M. Watson, *J. Chem. Soc., Dalton Trans.*, 1993, 101.
6 N. Bricklebank, S. M. Godfrey, H. P. Lane, C. A. McAuliffe, R. G. Pritchard and J. M. Moreno, *J. Chem. Soc., Dalton Trans.*, 1995, 2421.
7 P. Deplano, S. M. Godfrey, C. A. McAuliffe, M. L. Mercuri and E. F. Trogu, *Chem. Ber.*, 1997, **130**, 299.
8 M. Bätcher, W.-W. du Mont, S. Pohl and W. Saak, *XI Int. Conf. on Phosphorus Chemistry, Tallinn*, 1989, Abstr. 1–23, *Phosphorus Sulfur Silicon*, 1990, **49**/**50**, 147.
9 V. Stenzel, J. Jeske, W.-W. du Mont and P. G. Jones, *Inorg. Chem.*, 1995, **34**, 5166.
10 V. Stenzel, J. Jeske, W.-W. du Mont and P. G. Jones, *Inorg. Chem.*, 1997, **36**, 443.
11 R. Binnewies and S. Kopitzky, unpublished work; S. Kopitzky, PhD thesis, Universität Hannover, 1996.
12 W.-W. du Mont, V. Stenzel, J. Jeske, P. G. Jones, A. Sebald, S. Pohl, W. Saak and M. Bätcher, *Inorg. Chem.*, 1994, **33**, 1502.
13 N. Bricklebank, S. M. Godfrey, C. A. McAuliffe and R. G. Pritchard, *J. Chem. Soc., Dalton Trans.*, 1993, 2261.
14 N. Bricklebank, S. M. Godfrey, C. A. McAuliffe, A. G. Mackie and R. G. Pritchard, *J. Chem. Soc., Chem. Commun.*, 1992, 355.
15 S. M. Godfrey, C. A. McAuliffe, R. G. Pritchard and J. M. Sheffield, *Chem. Commun.*, 1996, 2521.
16 R. Bartsch, O. Stelzer and R. Schmutzler, *Z. Naturforsch., Teil B*, 1981, **36**, 1349.
17 B. V. Timokhin, V. P. Feshin, V. I. Dmitriev, V. I. Glukhikh, G. V. Dolgushin and M. G. Voronkov, *Dokl. Akad. Nauk SSSR*, 1977, **230**, 933.
18 W.-W. du Mont, F. Ruthe, M. Bätcher, P. G. Jones, P. Deplano and M. L. Mercuri, unpublished work.
19 A. Blaschette, P. G. Jones, M. Näveke and E. Schulte-Körne, *Phosporus Sulfur Silicon*, 1991, **61**, 211.
20 W.-W. du Mont, H.-J. Kroth and H. Schumann, *Chem. Ber.*, 1976, **109**, 3017.
21 O. J. Scherer and G. Schnabl, *Z. Naturforsch., Teil B*, 1976, **31**, 1462.
22 R. Minkwitz, G. Medger and H. Preut, *Z. Anorg. Allg. Chem.*, 1992, **614**, 102.
23 R. Schmutzler, J. Breker, P. G. Jones and D. Stalke, *Angew. Chem.*, 1988, **100**, 1620.
24 J. Breker, P. G. Jones, R. Schmutzler and D. Schomburg, *Phosphorus Sulfur Silicon*, 1991, **62**, 139.

*Received in Basel, Switzerland, 3rd July 1997; 7/04684G*

# Cyclisation/cleavage of macrocycles by ring-closing metathesis on solid support—conformational studies

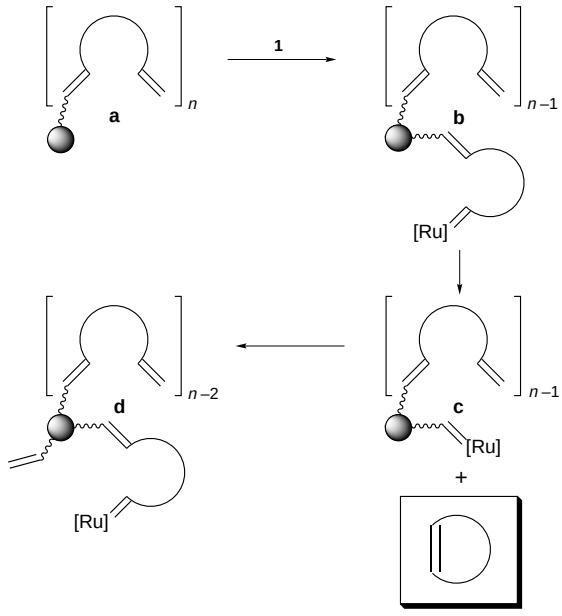
**Josef Pernerstorfer, Matthias Schuster and Siegfried Blechert***

*Institut für Organische Chemie, Sekr. C3, Technische Universität Berlin, Strasse des 17. Juni 135, D-10623 Berlin, Germany*

**Grubbs' ruthenium metathesis catalyst 1 was used to investigate the catalytic cyclisation/cleavage of tetrapeptide-derived macrocycles from a solid support; the rate dependence on substrate conformation has been studied.**

Recent developments in the field of alkene metathesis[1] were initiated by the introduction of catalysts[2] with unprecedented activities even in the presence of polar functional groups. In particular, ring-closing metathesis (RCM) has emerged as a powerful tool for the synthesis of different ring systems from five-membered rings to macrocycles.[3,4] Usually, cyclisations to large rings are performed in diluted solutions to supress competing acyclic diene metathesis (ADMET). RCM is also applicable to polymer-supported substrates.[5] In addition to ring closure, metathesis catalysts have been employed to facilitate catalytic binding[6] of alkenes to polystyrene-based resins as well as their catalytic cleavage.[7] A most interesting approach combines both RCM and the liberation of the cyclic alkene.[8]

Herein, we report investigations into the cyclisation/cleavage of macrocycles from solid support. Metatheses were performed using the well-established Grubbs' ruthenium initiator $Cl_2(PCy_3)_2Ru{=}CHPh$ **1** (Cy = cyclohexyl).[2] According to our concept (Scheme 1), **1** is expected to selectively attack a terminal double bond for steric reasons. This initial step (**a** → **b**) is followed by a RCM resulting in the liberation of one equivalent of the macrocycle and in the formation of polymer-bound metal–carbene complex **c**. Assuming sufficient flexibility, a transfer of the metal complex on the polymer surface (**c** → **d**) should take place, thus, enabling further catalytic cleavage cycles.[9] Byproducts resulting from quasi-intermolecular crossed metatheses of terminal double bonds remain bound to the resin during the entire process.

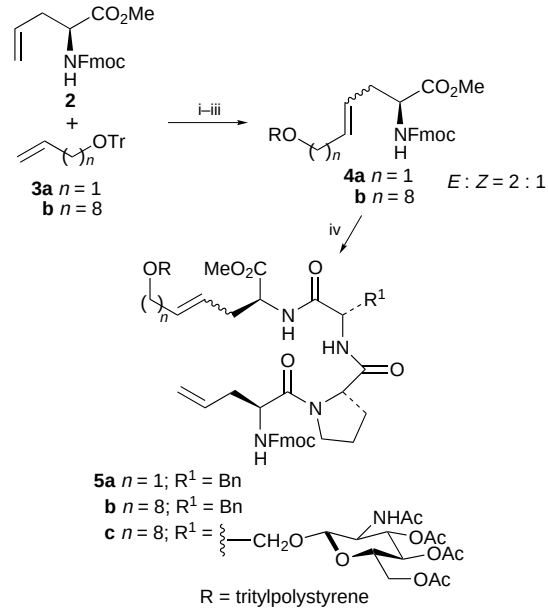



**Scheme 1**

We choose to perform our studies on peptide structures, since the sequence-dependence of their conformations is empirically well described.[10] Chlorotritylpolystyrene was used as the solid support, since solid-phase-bound reaction byproducts are easily monitored after cleaving the acid-labile trityl ether bond. Polymer-supported dialkenic tetrapeptides were obtained by standard Fmoc peptide chemistry using L-Fmoc-amino acids.

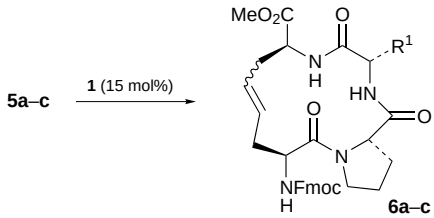
Under catalysis of **1** the side chain of Fmoc-allylglycine methyl ester **2** was selectively cross-coupled with *O*-trityl-protected hydroxy alkenes **3a,b** of different chain length.† To date, few comparable examples for synthetic applications of catalytic crossed metatheses have been described.[11] After deprotection, metathesis products were reacted with chlorotritylpolystyrene resin to give resin-linked, Fmoc-protected *C*-allylglycines **4** serving as starting materials for the solid phase synthesis of dialkenic tetrapeptides **5a–c** (Scheme 2). The terminal double bond was introduced by coupling Fmoc-*C*-allylglycine as the N-terminal amino acid. All resins described herein contained approximately 0.5 mmol $g^{-1}$ of tetrapeptide. The tetrapeptide motif of **5a** and **5b**, respectively, is closely related to disulfide bridge-stabilized β-turns found in redox-active proteins[12] and is, therefore, well suited for cyclisation as demonstrated by Miller *et al.* recently.[13] Results for ruthenium-catalysed cyclisations are given in Table 1.‡

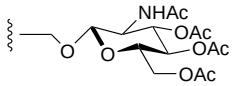
Remarkably, **5b** cyclised smoothly despite the high loading of 0.5 mmol $g^{-1}$. Comparison with the conversion of **5a** reveals that the extent of cyclisation/cleavage depends strongly on spacer length and, thus, mobility of the polymer-supported intermediates. Subsequent work was therefore carried out using the long spacer. Cyclisation of **5c** to cyclic glycopeptide **6c** with




**Scheme 2** *Reagents and conditions*: i, **1** (4 mol%); ii, TFA; iii, RCl; iv, piperidine–DMF, Fmoc-amino acid, PyBOP (iteratively) (PyBOP = benzotriazol-1-yloxytripyrrolidinophosphonium hexafluorophosphate)

**Table 1** Results of cyclisation/cleavage of acyclic **5** to macrocycles **6**




| Product | $R^1$ | *n* | Yield (%) | Purity (%) |
|---|---|---|---|---|
| **6a** | Bn | 1 | 30 | 65 |
| **6b** | Bn | 8 | 70 | 85 |
| **6c** |  | 8 | 30 | 85 |

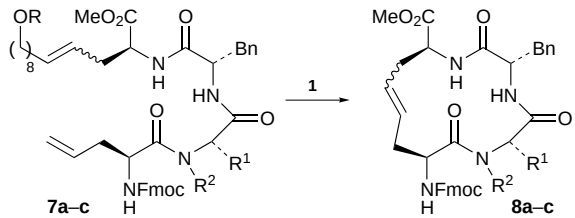


good product purity demonstrates that highly functionalized dienes are also tolerated by our reaction system.

Since cleavage rates were expected to depend on the conformations of the acyclic precursors, we attempted to correlate the relative cyclisation/cleavage rates of different precursor dienes with their probability to form β-turn-like structures. Rate experiments are easily performed, since most byproducts formed during the metathesis reaction remain bound to the polymer. In **5a**–**c** a β-turn-like structure is induced by the proline residue. Consequently, the proline in **5b** was exchanged by alanine, sarcosine and glycine, respectively, all representing minimal structural analogues of proline. The resulting polymer-supported tetrapeptides **7a**–**c** are less likely to exhibit β-turn-like structures and are, therefore, expected to cyclise significantly slower than **5b** itself. To test this assumption, **5b**, **7a**, **7b** or **7c** were mixed with an equal amount of **5c** serving as an internal standard and reacted with **1**.§ The amounts of cyclic tetrapeptides formed relative to **6c** were determined by HPLC analysis. Relative rates are given in Table 2.

As expected, **7a**–**c** all exhibit significantly decreased cleavage rates as compared to **5b**. The higher rate of sarcosine-containing **7a** compared to **7c** may be explained by the *N*-methyl group expanding the conformational space by abolishing the partial double bond character of the X–Gly peptide bond. To characterize the reaction system polymer-bound byproducts formed during the cyclisation of **5b** (very fast) and **7c** (very slow) were analysed after acidic cleavage from the trityl resin. In case of **5b**, 25% of $\Delta^9$-octadecene-1,18-diol, resulting from dimerisation of the spacer after cleavage of the macrocycle, as well as negligible amounts of acyclic products were isolated. No starting material could be detected. In the case of **9**, besides open-chain byproducts (36%), 40% of the starting material also remained bound to the resin after cyclisation.¶ This latter finding suggests that intermolecular reaction of two terminal double bonds on the resin surface proceeds significantly slower than the cyclisation/cleavage.

**Table 2** Relative cyclisation/cleavage rates of polymer-supported tetrapeptides with different residues in the (*i* + 1)-position (R = tritylpolystyrene)




| Substrate | $R^1$ | $R^2$ | Cyclisation rate relative to **5c** |
|---|---|---|---|
| **5b** | | | 1.36 |
| **7a** | H | Me | 0.15 |
| **7b** | Me | H | 0.11 |
| **7c** | H | H | < 0.02 |

In summary, polymer-bound substrates cyclise rapidly when exhibiting favourable conformations. Macrocycles cleaved at lower rates are obtained in good purity, since byproducts remain bound to the polymer.

## Footnotes and References

* E-mail: sibl@wap0105.chem.tu-berlin.de

† Selective cross-metathesis: **2** (0.6 g, 17 mmol) was combined with **3** (34 mmol) in $CH_2Cl_2$ (10 ml) and reacted with **1** (50 mg, 0.062 mmol) at reflux for 12 h with exclusion of moisture and air. Cross-metathesis products were purified by flash chromatography and isolated in 75% yield each.

‡ Cyclisation/cleavage: polymer (200 mg) was suspended in $CH_2Cl_2$ (1.5 ml) and refluxed after addition of **1** (9 mg, 0.011 mmol). After 17 h the resin was filtered off and washed twice with $CH_2Cl_2$. The contents of the filtrate were analysed by analytical HPLC. A SEDEX 55 (ERC, Germany) Evaporative-Light-Scattering Detector (ELSD) was employed to ensure comparable mass responses for different analytes. Cyclic products were purified by semi-preparative HPLC and characterized by $^1$H NMR spectroscopy and HRMS. They were formed as *E*/*Z* mixtures, as indicated by HPLC and $^1$H NMR spectroscopy.

§ Competition experiments: **5c** and the diene to be tested (**5b**, **7a**, **b** or **c**) (30 mg of each) were suspended in $CH_2Cl_2$ and heated to reflux for 2 h after addition of **1** (2.5 mg, 0.003 mmol). Product mixtures were filtered and dried. The relative amounts of cyclic products formed were determined by HPLC. For product characterisation, cyclisation/cleavage of the tested diene was performed on a preparative scale using the procedure given above.

¶ Acyclic byproducts were unambigiously identified as cross-metathesis products between the double bonds of two tetrapeptide molecules or tetrapeptide and spacer arm.


1 A. Stephen and K. Hashmi, *J. Prakt. Chem.*, 1997, **339**, 195.
2 Ruthenium catalysts: P. Schwab, M. B. France, J. W. Ziller and R. H. Grubbs, *Angew. Chem.*, 1995, **107**, 2179; *Angew. Chem., Int. Ed. Engl.*, 1995, **34**, 2039.
3 Review on RCM: R. H. Grubbs, S. J. Miller and G. C. Fu, *Acc. Chem. Res.*, 1995, **28**, 446.
4 Natural product synthesis: Z. Xu, C. W. Johannes, S. S. Salman and A. H. Hoveyda, *J. Am. Chem. Soc.*, 1996, **118**, 10 926; Z. Yang, Y. He, D. Vourloumis, H. Vallberg and K. C. Nicolaou, *Angew. Chem.*, 1997, **109**, 170; *Angew. Chem., Int. Ed. Engl.*, 1997, **36**, 166; D. Schinzer, A. Limberg, A. Bauer, O. M. Böhm and M. Cordes, *Angew. Chem.*, 1997, **109**, 543; *Angew. Chem., Int. Ed. Engl.*, 1997, **36**, 523.
5 M. Schuster, J. Pernerstorfer and S. Blechert, *Angew. Chem.*, 1996, **108**, 2111; *Angew. Chem., Int. Ed. Engl.*, 1996, **35**, 1979.
6 M. Schuster, N. Lucas and S. Blechert, *Chem. Commun.*, 1997, 823.
7 J. Peters and S. Blechert, *Synlett*, 1997, 348.
8 A comparable strategy was applied to the synthesis of seven-membered rings: J. H. van Maarseveen, J. A. J. den Hartog, V. Engelen, E. Finner, G. Visser and C. G. Kruse, *Tetrahedron Lett.*, 1996, **37**, 8249.
9 Metathesis cleavage of a macrocycle from Merrifield resin at a loading of 0.1 mmol $g^{-1}$ using **1** in almost stoichiometric amount has most recently been reported: K. C. Nicolaou, N. Wissinger, J. Pastor, S. Nincovic, F. Sarabia, Y. He, D. Vourloumis, Z. Yang, T. Li, P. Giannakakou and E. Hamel, *Nature*, 1997, **387**, 268.
10 P. Y. Chou and G. D. Fasman, *Biochemistry*, 1974, **13**, 222.
11 O. Brümmer, A. Rückert and S. Blechert, *Chem. Eur. J.*, 1997, **3**, 207; A. G. M. Barrett, J. C. Beall, V. C. Gibson, M. R. Giles and G. L. P. Walker, *Chem. Commun.*, 1996, 2229; A. G. M. Barrett, S. P. D. Baugh, V. C. Gibson, M. R. Giles, E. L. Marshall and P. A. Procopiou, *Chem. Commun.*, 1997, 155.
12 H.-J. Musiol, F. Siedler, D. Quarzago and L. Moroder, *Biopolymers*, 1994, **34**, 1553; F. Siedler, D. Quarzago, S. Rudolph-Bohner and L. Moroder, *Biopolymers*, 1994, **34**, 1563.
13 S. Miller, H. E. Blackwell and R. H. Grubbs, *J. Am. Chem. Soc.*, 1996, **118**, 9606.


*Received in Cambridge, UK, 11th July 1997; 7/04976E*

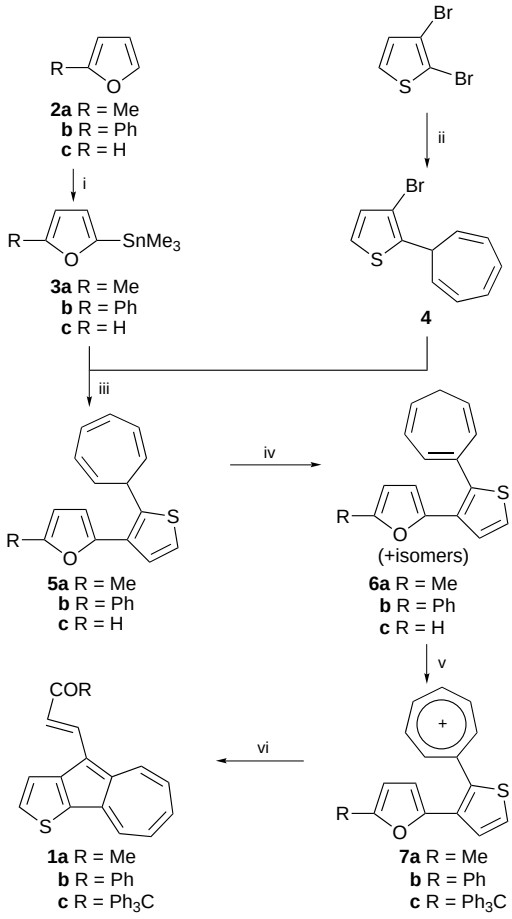
# A facile synthesis of β-(4-azuleno[1,2-*b*]thienyl) α,β-unsaturated ketones

**Naoki Kusuhara,[a] Yuka Sugano,[a] Hideki Takagi,[a] Hideyoshi Miyake[b] and Kimiaki Yamamura*[a]**

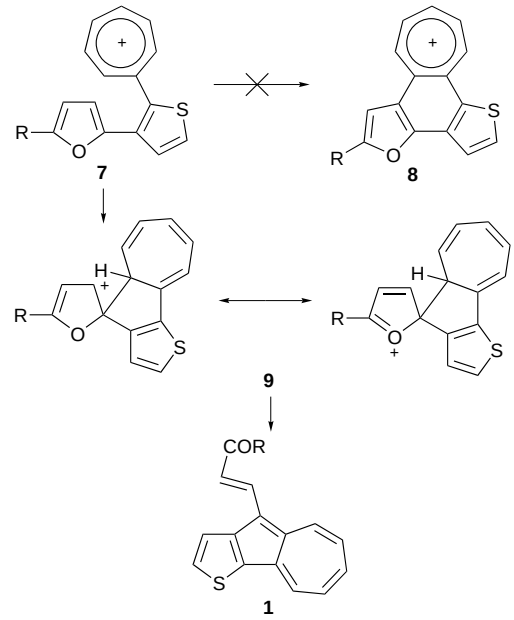
[a] *Department of Chemistry, Faculty of Science, Kobe University, Nada, Kobe 657, Japan*
[b] *Department of Biofunctional Chemistry, Faculty of Agriculture, Kobe University, Nada, Kobe 657, Japan*

**The facile and novel synthesis of β-(4-azuleno[1,2-*b*]thienyl) α,β-unsaturated ketones 1 from 2-tropylio-3-(2-furyl)thiophenes 7 is reported; a mechanism involving a novel ring cyclization by intramolecular attack of the tropylium ion at the 2-position of the furan ring is postulated.**

The azulenoid heterocyclic aromatic compounds which consist of the azulene ring condensed with heterocyclic aromatic nuclei are of interest not only for their physical and chemical properties, but also their pharmaceutical and physiological activity. Several azulene derivatives condensed with heteroaromatics such as thiophene, furan, pyrrole and pyridine rings are known.[1] Most of them were prepared by the heteroaromatization of the azulene derivatives, and were restricted to the parent compounds and alkyl-, aryl- or alkoxycarbonyl-substituted derivatives. Herein we disclose a novel and facile synthesis of azuleno[1,2-*b*]thiophenes having an α,β-unsaturated ketone group from the corresponding 2-tropylio-3-(2-furyl)thiophenes **7**.




**Scheme 1** *Reagents and conditions*: i, BuLi, $Me_3SnCl$, THF, −78 °C; ii, BuLi, $C_7H_7^+$, THF, −78 °C to room temp; iii, $PdCl_2(Ph_3P)_2$, THF, reflux; iv, xylene, reflux; v, $Ph_3C^+BF_4^-$, $CH_2Cl_2$, room temp; vi, $CH_2Cl_2$ or $CH_2ClCH_2Cl$




**Scheme 2**

The synthetic sequence leading to **1** from the readily available 2-substituted furans **2** is depicted in Scheme 1.† 2-Cycloheptatrienyl-3-(2-furyl)thiophenes **5** were prepared by the palladium(II)-catalysed Stille reaction[2] of 2-trimethylstannylfurans **3** with 2-cycloheptatrienyl-3-bromothiophene **4**. Thermal sigmatropic rearrangement of **5** to **6** and subsequent hydride abstraction using triphenylmethyl tetrafluoroborate gave 2-tropylio-3-(2-furyl)thiophenes **7** in 65–85% yields.‡ It might be expected that the intramolecular electrophilic substitution reaction of the tropylium moiety with the furan ring would afford the tetracyclic carbocations **8**, which are isoelectronic with triphenylene.[3] However, when a $CH_2Cl_2$ solution of **7a**§ was refluxed for 7 h, neutral red–black prisms were obtained instead of the expected carbocations **8a**. The structure of these prisms was confirmed to be 4-(4-azuleno[1,2-*b*]thienyl)but-3-ene-2-one **1a** *via* its spectral data,[5] together with elemental analysis. In the same manner, the chalcone-type compound **1b** and triphenylmethyl derivative **1c** were obtained as green–black needles (43%) and black needles (36%), respectively, from the corresponding tropylio derivatives **7b** and **7c**.

A possible mechanism for the formation of β-(4-azuleno-[1,2-*b*]thienyl) α,β-unsaturated ketones **1** from the corresponding 2-tropylio-3-(2-furyl)thiophenes **7** is illustrated in Scheme 2. The intramolecular electrophilic attack of the tropylium ion on the 2-poisition of the furan ring gives the spiro-type intermediate **9**, which can be converted to **1** by a ring-opening reaction. Although it is well-known that the 2-position of the furan ring is much more reactive towards electrophiles than the 3-position and that furans are readily ring-opened under acidic conditions,[4] this is to the best of our knowledge the first

tropylium ion-mediated furan ring-opening reaction to yield α,β-unsaturated carbonyl derivatives of azuleno[1,2-*b*]thiophene compounds. Since 2-substituted furans **2** are readily available and the procedure is simple and easy, it is considered that this is a valuable general synthetic route to various β-(4-azuleno[1,2-*b*]thienyl) α,β-unsaturated ketones.

The authors thank Miss Masuko Nishinaka for elemental analyses. The present work was supported in part by Grant-in-Aid for Scientific Research (C) (No. 08640685) from the Ministry of Education, Science, Sports and Culture, Japan.

## Footnotes and References

* E-mail: kyama@kobe-u.ac.jp

† All new compounds were fully characterized by mass and $^1$H NMR spectroscopy and elemental analysis.

‡ With **6c**, triphenylmethyl tetrafluoroborate acts as both a hydride abstraction reagent and an electrophile, and triphenylmethyl-substituted tropylium ion derivative **7c** was obtained.

§ *Selected data* for **7a**: ($\delta_H$ $CD_2Cl_2$, 250 MHz) 2.22 (3 H, s, $CH_3$), 6.20 (1 H, d, furan-H), 6.75 (1 H, d, furan-H), 7.43 (1 H, d, thiophene-H), 7.95 (1 H, d, thiophene-H), 8.68–8.83 (4 H, m, tropylium-H), 8.93–9.00 (2 H, m, tropylium-H). For **1a**: $\delta_H$ ($CD_3Cl$, 250 MHz) 2.46 (3 H, s, $CH_3$), 6.90 (1 H, d, olefinic-H), 7.26 (2 H, dd, seven-membered ring-H), 7.62 (1 H, dd, seven-membered ring-H), 7.73 (1 H, d, thiophene-H), 7.89 (1 H, d, thiophene-H), 8.28 (1 H, d, olefinic H), 8.29 (1 H, d, seven-membered ring-H), 8.49 (1 H, d, seven-membered ring-H), $\delta_C$ ($CD_3Cl$, 75 MHz) 198.2 (C=O), 150.1 (quaternary), 143.6 (quaternary), 137.3, 135.7 (quaternary), 134.8, 134.0, 133.7, 133.1 (quaternary), 131.9, 126.4, 125.4, 123.3, 119.8, 116.4 (quaternary), 27.8 ($CH_3$). Calc. for $C_{16}H_{12}SO$: C, 76.16; H, 4.79. Found: C, 76.30; H, 4.63%.

1 K. Matsui and T. Nozoe, *Chem. Ind.*, 1960, 1302; T. Nozoe, S. Seto and S. Matsumura, *Chem. Ind.*, 1961, 1715; T. Nozoe and K. Kikuchi, *Bull. Chem. Soc. Jpn.*, 1963, **36**, 633; S. Hayashi, S. Kurokawa, M. Okano and T. Matsuura, *Tetrahedron Lett.*, 1967, 3443; L. L. Replogle, K. Katsumoto and H. L. Ammon, *J. Am. Chem. Soc.*, 1968, **90**, 1086; T. Nozoe, K. Takase, T. Nakazawa, S. Sugita and M. Saito, *Bull. Chem. Soc. Jpn.*, 1974, **47**, 1750; K. Kohara, H. Tachibana, Y. Masuyama and Y. Otani, *Bull. Chem. Soc. Jpn.*, 1979, **52**, 1549; K. Yamane, K. Fujimori and T. Takeuchi, *Bull. Chem. Soc. Jpn.*, 1981, **54**, 2537; T. Morita, T. Nakadate and K. Takase, *Heterocycles*, 1981, **15**, 835; K. Fujimori, T. Fujita, K. Yamane, M. Yasunami and K. Takase, *Chem. Lett.*, 1983, 1721.

2 J. K. Stille, *Angew. Chem., Int. Ed. Engl.*, 1986, **25**, 508; T. R. Bailey, *Tetrahedron Lett.*, 1986, **27**, 4407; A. Dondoni, A. R. Mastellari, A. Medict, E. Negrini and P. Pedrini, *Synthesis*, 1986, 757; V. N. Kalinin, *Synthesis*, 1992, 413; T. N. Mitchell, *Synthesis*, 1992, 803.

3 K. Yamamura, H. Miyake, S.Nakatsuji and I. Murata, *Chem. Lett.*, 1992, 1213.

4 M. V. Sargent and T. M. Cresp, *Comprehensive Organic Chemistry*, Pergamon, Oxford, 1979, vol. 4, p. 693.

*Received in Cambridge, UK, 30th June 1997; 7/004583B*

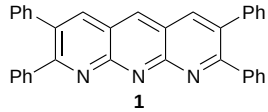
# Evidence for the characterisation of the C–H··π interaction as a weak hydrogen bond: toluene and chlorobenzene solvates of 2,3,7,8-tetraphenyl-1,9,10-anthyridine

**N. N. Laxmi Madhavi,[a] Amy K. Katz,[b] H. L. Carrell,[b] Ashwini Nangia*[a] and Gautam R. Desiraju*[a]†**

[a] *School of Chemistry, University of Hyderabad, Hyderabad 500 046, India*
[b] *Fox Chase Cancer Center, 7701 Burholme Avenue, Philadelphia 19111, USA*

**The crystal structures of the toluene and chlorobenzene solvates of 2,3,7,8-tetraphenyl-1,9,10-anthyridine are nearly identical save for differences in the mode of solvent inclusion; these differences have an important bearing on the nature of the C–H··π interactions in these structures.**

During the synthesis[1] and purification of 2,3,7,8-tetraphenyl-1,9,10-anthyridine **1**‡ it was noticed that the compound failed to yield crystals for X-ray analysis from several solvents such as anisole, benzene, chloroform, ethyl acetate, mesitylene, nitrobenzene, pyridine and xylene, ill-defined powders being obtained in every case. Curiously, well-formed bright yellow crystals were obtained easily from toluene and analysis showed that they correspond to the 1 : 1 solvate **2**. Noting that the methyl




**1**

**2** = **1**•toluene
**3** = **1**•chlorobenzene

group is replaceable by the chloro group without a change in crystal structure (the so-called 'chloro–methyl exchange rule')[2] recrystallisation was attempted from chlorobenzene and we were not surprised to find that in this case too diffraction-quality crystals, now of the corresponding 1 : 1 solvate **3**, were obtained. The crystal structures of the toluene and chlorobenzene sovlates, **2** and **3**, were then determined at low temperature and to good precision.§ While the structures are very similar, with nearly the same unit cell dimensions and space group symmetry, there are small differences with respect to the positioning of the solvent molecules. Although small, these differences are significant and show that the C–H··π interactions found in these structures have the characteristics of weak hydrogen bonds.

Figs. 1 and 2 show the crystal structures of solvates **2** and **3**. The positioning of the heterocyclic molecule in the two unit cells is identical and so are the gross packing features.¶ Fig. 1 shows that the ordered toluene molecule in **2** is situated in a pocket formed by three molecules of **1**. Inspection of Fig. 2 shows that the ordered chlorobenzene molecule in **3** is situated in a nearly identical pocket. However, the Me and Cl substituents point in almost opposite directions in the two cases. This is unusual. When chloro–methyl exchange is obtained, the two substituents behave in an isosteric fashion with only shape and size factors controlling the packing.[2] The switching around of the substituent Me and Cl groups in **2** and **3** is indicative of the fact that electronic factors are involved in stabilisation of the solvent molecule in one or both cases.

A very short C–H··π interaction of 2.54(2) Å (all H-atom positions normalised in this and subsequently discussed contacts) in **2** (**a** in Fig. 1) is noteworthy. This interaction is clearly of the H··ring centroid type ($\theta$ = 151°),[3] the distances from the H-atom to the six ring atoms of the toluene molecule lying in the range 2.73–3.05 Å. Such H··centroid distances have been reported previously[3,4] but are definitely at the short end of the accepted distance range for this contact.[5] Accompanying contact **a** is a much longer contact of 3.01 Å ($\theta$ = 126°, **b** in Fig. 1) so that the toluene molecule may be said to be positioned at unequal distances from adjacent glide-related molecules of anthyridine **1**. In contrast, let us consider the two corresponding contacts, **g** [2.61(2) Å, $\theta$ = 143°] and **h** [2.62(2) Å, $\theta$ = 147°] in **3** (Fig. 2). These are formed by C–H groups that are chemically equivalent and therefore of the same acidity as the C–H group that forms contact **a** in **2**. However, contacts **g** and

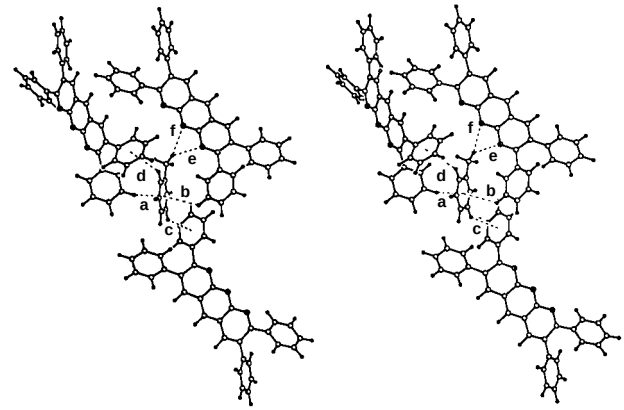



**Fig. 1** Stereoview of the crystal structure of solvate **2** approximately down [010], showing the binding of the toluene molecule. The anthyridine molecules are inversion- and glide-related. Interactions **a**–**f** are indicated. Notice the cooperative scheme of C–H··π hydrogen bonds and the positioning of the methyl H-atom between the two heterocyclic N-atoms. Interaction **a** is unusually short.

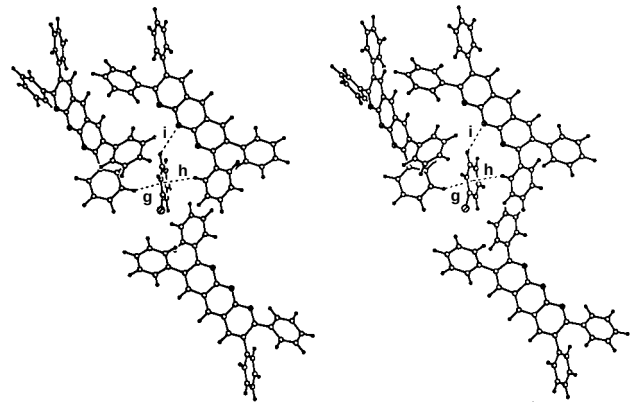



**Fig. 2** Stereoview of the crystal structure of solvate **3** showing the binding of the chlorobenzene molecule. Interactions **g**–**i** are indicated. Contrast this with Fig. 1. Notice that the Cl-atom is not involved in any specific intermolecular contact.

**h** are significantly longer than contact **a**. Unlike the toluene molecule in **2**, the chlorobenzene molecule in **3** may therefore be considered as being disposed at nearly equal distances to the adjacent molecules of **1**.

In general, short intermolecular distances such as **a** in **2** are taken as evidence of crystal stabilisation but it should be noted that shortness alone does not constitute proof of an attractive interaction. It is always possible that a short contact is repulsive and that it arises from the overall balance of interactions in a crystal structure.[6] However, when as in this case, the shortness of **a** with respect to **g** and **h** also correlates with the electron-rich character of the aromatic ring in toluene *vis-a-vis* chlorobenzene, and also given that there would be little steric problem were the toluene molecule to be placed symmetrically between the two approaching C–H groups, one may state with confidence that the C–H··π interaction **a** is stabilised by the electron rich aromatic ring in toluene. Hydrogen bonds of all types are fortified by increasing acidities and basicities of donor and acceptor groups, respectively,[7,8] and our observations here adduce evidence that the C–H··π interaction has structural properties of weak hydrogen bonds, similar to O–H··π and N–H··π interactions.[9] Because of its weakness, however, it is difficult in general to obtain clear evidence for the existence of this type of hydrogen bond. It is possible to do so in this case because structures **2** and **3** are similar in just about every respect except the interaction of interest.

Hydrogen bonds formed by carbon acids and π-bases are soft and this in turn can lead to the cooperative patterns of interactions.[10–13] Again, the structure of **2** is revealing. It would seem that the weak hydrogen bond **a** is able to activate the C–H groups in the toluene molecule at least to the extent that the long contacts **c**–**f** are possible. Interactions **c** (2.90 Å, $\theta$ = 140°) and **d** (3.01 Å, $\theta$ = 140°) formed by the aromatic C–H groups are the C–H··π type while interactions **e** (2.76 Å, $\theta$ = 146°) and **f** (2.83 Å, $\theta$ = 161°) formed by the methyl C–H groups are of the C–H··N type. Although long, these contacts are within the accepted distance ranges.[5,11] In contrast, there is just one extra interaction of the C–H··N type in the unactivated structure **3** (**i**; 2.87 Å, $\theta$ = 139°). All these interactions may make only small contributions to the crystal binding energy but they help in defining the structures of the solvates. For example, it is possible that these secondary interactions are the causes for the opposite orientations of the toluene and chlorobenzene molecules referred to above and also to the fact that the solvent molecules are ordered in **2** and **3**. It is pertinent to state here that of the 1171 toluene and 75 chlorobenzene solvates in the Cambridge Structural Database (CSD, April 1997, version 6.2, 167 797 entries) for which coordinates are available, the solvent is ordered in only 413 and 35 structures, respectively.‖ Although the binding of chlorobenzene in the anthyridine pocket is poorer than that of toluene, it is still not just shape-controlled; compound **1** failed to form diffraction-quality crystals with either fluorobenzene or bromobenzene. In this regard, the formation of solvates **2** and **3** is reminiscent of guest-induced host crystallisation of the type encountered in the benzene solvate of the mono-enol form of cyclohexane-1,3-dione.[14]

Since the pioneering work of Nishio, who first postulated the existence of the C–H··π interaction,[15] much work has been done in this area. With the current interest in crystal engineering and supramolecular chemistry, there is now a new appreciation for this form of intermolecular association. The hydrogen bond is an attractive, directional interaction which, though predominantly electrostatic, also has polarisation and charge transfer characteristics. While it has always been recognised that C–H··π interactions in highly activated systems such as terminal acetylenes are of the hydrogen bond type, the present work shows that even moderately activated systems such as tolyl rings participate in interactions that may be considered to be weak hydrogen bonds formed by soft acids and soft bases. In this regard, it could be stated that the grey area between the weak hydrogen bond and the herringbone interaction is gradually diminishing.

A. N. and G. R. D. thank the DST (SP/S1/G-19/94) and CSIR (1(1431)/96/EMR-II) for financial support. A. K. K. and H. L. C. acknowledge support from the NIH (Grant No. CA-10925). N. N. L. M. is the recipient of an SRF from the CSIR.

## Footnotes and References

† E-mail: grdch@uohyd.ernet.in

‡ *Synthesis* of **1**: as described in ref. 1 *via* the Friedländer condensation of 2,6-diaminopyridine-3,5-dicarbaldehyde with deoxybenzoin.

§ *Crystal data* for **2**: 2,3,7,8-tetraphenyl-1,9,10-anthyridine–toluene 1 : 1 solvate ($C_{35}H_{23}N_3{\cdot}C_7H_8$, $M$ = 577.70). Monoclinic, space group $P2_1/c$; $a$ = 17.543(5), $b$ = 9.308(4), $c$ = 18.972(4) Å, $\beta$ = 98.58(1)°, $V$ = 3063(2) Å$^3$, $Z$ = 4, $D_c$ = 1.25 g cm$^{-3}$, Enraf Nonius FAST area detector, $T$ = 120 K, Mo-Kα, $\omega$–$\theta$ scan mode, 6891 unique reflections, 5155 with $F^2 > 2\theta(F^2)$, no absorption corrections. Structure solution and refinement with standard methods (SHELXS86 and SHELXL93); H-atoms refined isotropically. Final $R$ = 0.050 (observed), 0.066 (all), $wR(F^2)$ = 0.130 (observed), 0.152 (all).

For **3**: 2,3,7,8-tetraphenyl-1,9,10-anthyridine–chlorobenzene 1 : 1 solvate ($C_{35}H_{23}N_3{\cdot}C_6H_5Cl$, $M$ = 598.11). Monoclinic, space group $P2_1/c$; $a$ = 17.646(4), $b$ = 9.319(3), $c$ = 18.807(2) Å, $\beta$ = 100.48(1)°, $V$ = 3041.1(12) Å$^3$, $Z$ = 4, $D_c$ = 1.31 g cm$^{-3}$, Enraf Nonius FAST area detector, $T$ = 120 K, Mo-Kα, $\omega$–2$\theta$ scan mode, 6802 unique reflections, 4121 with $F^2 > 2\sigma(F^2)$, no absorption corrections. Structure solution and refinement with SHELXS86 and SHELXL93; H-atoms refined isotropically. Final $R$ = 0.046 (observed), 0.082 (all); $wR(F^2)$ = 0.113 (observed), 0.214 (all). CCDC 182/598.

¶ The near identity of the packing of the anthyridine molecules in the two structures was also quantified with an inspection of the NIPMAT plots for the two structures. For a description of the NIPMAT procedure, see ref. 11. We thank Dr S. R. Rowland for making available a copy of this program.

‖ However, we found only two pairs of isostructural toluene and chlorobenzene solvates (KERREE, KERROO; KERRII, KERRUU) in these CSD searches.

1 P. Caluwe and T. G. Majewicz, *J. Org. Chem.*, 1977, **42**, 3410.
2 G. R. Desiraju and J. A. R. P. Sarma, *Proc. Ind. Acad. Sci. (Chem. Sci.)*, 1986, **96**, 599.
3 T. Steiner, E. B. Starikov and M. Tamm, *J. Chem. Soc., Perkin Trans. 2*, 1996, 67.
4 D. B. Amabilino, P. R. Ashton, J. F. Stoddart, S. Maenzer and D. J. Williams, *J. Chem. Soc., Chem. Commun.*, 1994, 2475.
5 T. Steiner, E. B. Starikov, A. M. Amado and J. J. C. Teixeira-Dias, *J. Chem. Soc., Perkin Trans. 2*, 1995, 1321.
6 P. Seiler, L. Isaacs and F. Diederich, *Helv. Chim. Acta*, 1996, **79**, 1047.
7 V. R. Pedireddi and G. R. Desiraju, *J. Chem. Soc., Chem. Commun.*, 1992, 988.
8 T. Steiner, *J. Chem. Soc., Chem. Commun.*, 1994, 2341.
9 M. A. Viswamitra, R. Radhakrishnan, J. Bandekar and G. R. Desiraju, *J. Am. Chem. Soc.*, 1993, **115**, 4869.
10 T. Fujimoto, R. Yanagihara, K. Kobayashi and Y. Aoyama, *Bull. Chem. Soc. Jpn.*, 1995, **68**, 2113.
11 G. R. Desiraju, *Acc. Chem. Res.*, 1996, **29**, 441.
12 T. Steiner, *J. Chem. Soc., Chem. Commun.*, 1995, 95.
13 T. Steiner, M. Tamm, A. Grzegorzewski, N. Schulte, N. Veldman, A. M. M. Schreuers, J. A. Kanters, J. Kroon, J. van der Maas and B. Lutz, *J. Chem. Soc., Perkin Trans 2*, 1996, 2441.
14 M. C. Etter, Z. Urbánczyk-Lipkowska and D. Jahn, *J. Am. Chem. Soc.*, 1986, **108**, 5871.
15 M. Nishio, *Kagaku No Ryoiki*, 1977, **31**, 998; M. Nishio and M. Hirota, *Tetrahedron*, 1989, **45**, 7201; M. Nishio, Y. Umezawa, M. Hirota and Y. Takeuchi, *Tetrahedron*, 1995, **51**, 8665.

*Received in Cambridge, UK, 11th August 1997; 7/05836E*

# Dissecting the effects of cooperativity on the stabilisation of a *de novo* designed three stranded anti-parallel β-sheet

**Gary J. Sharman and Mark S. Searle***

*Department of Chemistry, University of Nottingham, University Park, Nottingham, UK NG7 2RD.*

**Cooperative effects between two sets of weak interactions at different hydrogen bonded interfaces are shown to stabilise a *de novo* designed three-stranded anti-parallel β-sheet: NMR and CD (circular dichroism) spectroscopy have been used to compare and contrast the stability of the β-sheet (residues 1–24) and the isolated C-terminal β-hairpin (residues 9–24).**

Molecular recognition phenomena, including host–guest interactions in chemical systems and the processes by which complex structures self-assemble in biology, are fundamentally dependent on large numbers of weak, non-covalent interactions and their cooperative interplay.[1,2] Cooperativity frequently complicates attempts at quantitative analysis of such interactions because ligand binding constants are seldom only a measure of the interactions occurring at one particular molecular interface but reflect some property of the whole set of linked weak interactions within the ligand complex.[1–7] Here we describe a peptide system that has enabled us to investigate the interplay between two sets of weak interactions that occur at two different hydrogen bonded interfaces within a *de novo* designed anti-parallel three stranded β-sheet (Fig. 1). To dissect-out possible cooperative interactions we have synthesised two peptides. The first peptide (9–24) of 16 residues was designed to form a β-hairpin. The second peptide (1–24) ends with the same 16 residues but has a preceding 8 amino acid sequence designed to form a second β-turn and the third strand (S3) of the anti-parallel β-sheet. The first strand (S1 in Fig. 1) is in the same environment in both folded structures and undergoes the same changes in backbone solvation and hydrophobic interactions when it interacts with S2. Thus, the indirect influence of the third strand on the stability of the interaction between S1 and S2 can be assessed in this system. We report here evidence from CD and NMR studies that 1–24 folds into a three stranded sheet in which the C-terminal hairpin is cooperatively stabilised with respect to the isolated hairpin (9–24). There is much current interest in the autonomous folding of β-hairpin peptides for probing the sequence-dependent factors important in their stabilisation.[8]

In aqueous solution, the two peptides showed limited evidence of folding. Qualitative analysis of CD (circular dichroism) spectra suggested that substantial populations of random coil conformations persist with both peptides showing very similar molar ellipticity values (per residue) at 198 nm. Addition of methanol (in the range 0–50% v/v) to the aqueous peptide solutions was found to promote secondary structure formation. In 50% aqueous methanol peptide 1–24 showed only a small negative ellipticity at 198 nm, but a pronounced minimum around 216 nm, characteristic of a substantial population of β-sheet and β-turn conformation.[9,10] In contrast, the changes in molar ellipticity (per residue) on addition of methanol are less marked for the shorter peptide (9–24), with residual random coil structure still evident.

Both peptides were subsequently investigated under identical conditions by $^1$H NMR spectroscopy. $H_\alpha$ chemical shift deviations from random coil values have been shown to be an excellent probe of protein secondary structure.[11] In the mixed solvent system [50% $CD_3OD$–50% $D_2O$ (or 50% $H_2O$) solution at pH 3.9 and 2 mM concentration], $H_\alpha$ shifts for peptide 1–24 (Fig. 2) were indicative of three β-strands (downfield shifts of up to 0.7 ppm) separated by two β-turns (upfield shifts of $< 0.3$ ppm).[12] These structural features were confirmed by the pattern and intensity of NOEs: strong inter-residue and weak intra-residue $H_\alpha$–NH NOEs were observed within the strands, whereas these were of similar intensity within the turn regions. Also, the only significant sequential NH–NH NOEs were observed between residues 9–10 and 17–18, again characteristic of the two β-turns. The observation of long range NOEs provided the most conclusive evidence for the formation of folded structure in solution, consistent with the alignment of the peptide chain shown in Fig. 1(*a*). These included many of the

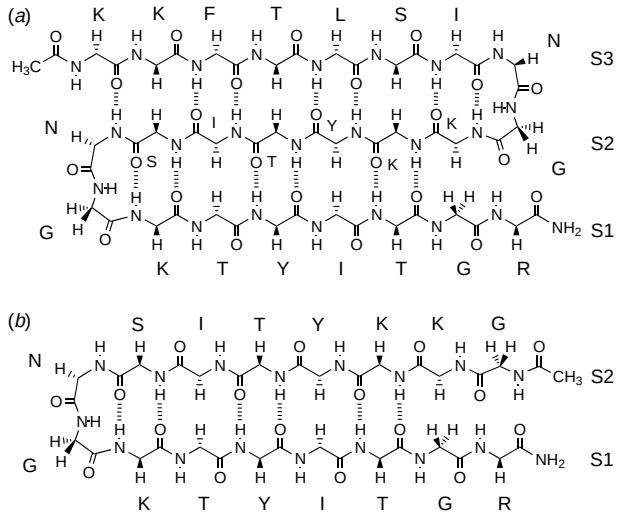



**Fig. 1** Structures and sequences of (*a*) the designed three-stranded β-sheet (residues 1–24) and (*b*) β-hairpin (residues 9–24). The first strand (S1) is in an identical environment in both folded structures.

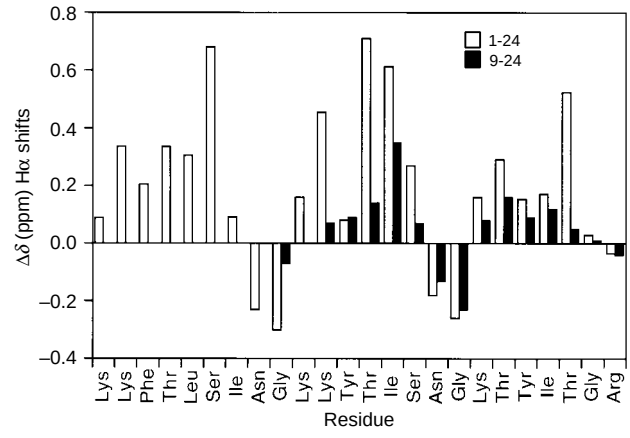



**Fig. 2** $H_\alpha$ chemical shift deviations from random coil values for sheet (1–24) and hairpin (9–24) in 50% v/v aq. methanol, 2 mM peptide, pH 3.9, 283 K

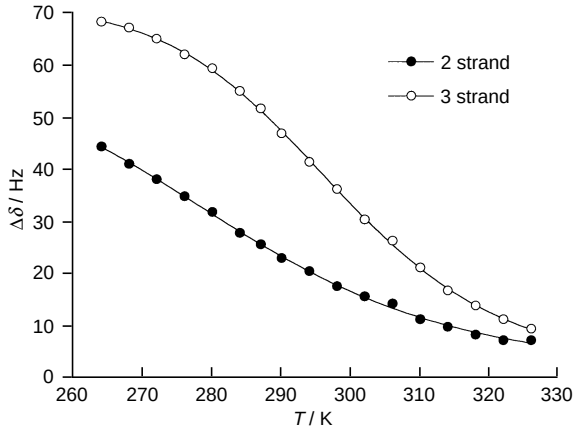



**Fig. 3** Melting curves for 1–24 and 9–24 determined from the temperature-dependence of the chemical shift difference ($\Delta\delta$/Hz) between the $H_\varepsilon$ resonances of Y12 and Y20. Data were fitted to a two-state model and the limiting values for $\Delta\delta$ determined iteratively. In both cases correlation coefficients ($R$) were > 0.99. At 298 K, peptide 1–24 was estimated to be 50% folded, while peptide 9–24 was only 25% folded.

expected cross-strand $H_\alpha$–$H_\alpha$ NOEs (K2→S15, T4→T13, S6→K11, K10→G23, I14→T19), NH–NH NOEs (F3→I14, I7→K10, T13→Y20, S15→K18) and interactions between side chains in close proximity (F3→I14 and L5→Y12→I21).

The shorter peptide (9–24) (Fig. 1) showed evidence of a rather less folded structure. Much less pronounced downfield shifts are observed for $H_\alpha$ resonances of residues within the strands (Fig. 2). NOE intensity measurements indicate a less ordered more dynamic structure than observed for the same residues in the three stranded sheet. In contrast to the large number of long range interstrand NOEs identified for peptide 1–24, no long range $H_\alpha$–$H_\alpha$ or NH–NH NOEs were detected, although the side chain interaction between Y12 and I21 was still apparent, suggesting a small population of a less well-ordered β-hairpin. Despite the apparently weak interaction between the two proposed β-strands, the observation of a strong NH–NH NOE between residues G17–K18, and similar shift perturbations for G17 $H_\alpha$ and K18 NH in both peptides, suggests that the β-turns may be populated to similar extents in the two structures.

To illustrate further the cooperative nature of the interactions, we have measured the temperature-dependence of the stability of both peptides (Fig. 3). The folded population in each case was conveniently monitored by measuring the chemical shifts of the aromatic protons of the two tyrosine residues (Y12 and Y20) which are common to both the hairpin and sheet, and whose chemical shifts diverge as the temperature is lowered. Sigmoidal melting curves are observed for both peptides indicative of a cooperative unfolding process. However, a sharper transition is evident for the three-stranded sheet, together with a higher mid-point transition temperature (298 *versus* 278 K). Thus, the larger number of hydrogen bonding interactions within the sheet gives rise to a greater degree of cooperativity.[2] The data are reminiscent of DNA melting curves where the transition also becomes sharper as the number of base pairs (interacting units) increases.[2]

The above data lead us to conclude that the stability of the C-terminal hairpin is cooperatively enhanced by interaction with the N-terminal portion of the sequence. This may in part be due to a chelate-like effect, in that the first strand can be envisaged to fold against a pre-ordered hairpin, such that the entropic cost of folding is reduced. In addition, this pre-organisation could lead to stronger hydrogen bonds through a restriction of backbone motions allowing shorter range interactions.[13,14] A further possibility is that electrostatic effects, mediated through the extended hydrogen bonding network, might further strengthen the interactions at the second interface through polarisation of amide bonds. Such a mechanism is supported by *ab initio* calculations on solvated hydrogen bonded amide dimers.[15] The effect of organic solvents in promoting intramolecular hydrogen bonding is generally regarded to have an electrostatic origin by weakening competing interactions between solute and solvent.[16–19] The experimental conditions described have proved ideal for monitoring this cooperative effect between the strands of a designed β-sheet; both the hairpin and sheet structures have only marginal stability, allowing even small perturbations to conformational equilibria between folded and unfolded states to be readily detected by measurable changes in NMR and CD parameters.

We thank the BBSRC for providing support to G. J. S. and gratefully acknowledge grants from The Nuffield Foundation and The Royal Society, and the support of The Department of Chemistry of the University of Nottingham. We are grateful to John Keyte for solid phase peptide synthesis and access to HPLC facilities in the Biochemistry Department, University of Nottingham.

## Footnote and References

* E-mail: mark.searle@nottingham.ac.uk

1 D. H. Williams and M. S. Westwell, *Chem. Biol.*, 1996, **3**, 695.
2 M. S. Westwell, M. S. Searle and D. H. Williams, *J. Mol. Recognit.*, 1996, **9**, 88.
3 D. H. Williams, M. S. Searle, M. S. Westwell, J. P. Mackay, P. Groves and D. A. Beauregard, *Chemtracts*, 1994, **7**, 133.
4 J. P. Mackay, U. Gerhard, D. A. Beauregard, M. S. Westwell, M. S. Searle and D. H. Williams, *J. Am. Chem. Soc.*, 1994, **116**, 4581.
5 M. F. Perutz, *Proc. R. Soc. London, Ser. B*, 1980, **208**, 135.
6 Q. X. Hua, W. H. Jia, B. H. Frank and M. A. Weiss, *J. Mol. Biol.*, 1993, **230**, 387.
7 J. Monod, J. Wyman and J. P. Changeux, *J. Mol. Biol.*, 1965, **12**, 88.
8 F. J. Blanco, G. Rivas and L. Serrano, *Nat. Struct. Biol.*, 1994, **1**, 584; F. J. Blanco, M. A. Jimenez, J. Herranz, M. Rico, J. Santoro and J. L. Nieto, *J. Am. Chem. Soc.*, 1993, **115**, 5887; M. S. Searle, D. H. Williams and L. C. Packman, *Nat. Struct. Biol.*, 1995, **2**, 999; E. de Alba, M. A. Jimenez M. Rico and J. L. Nieto, *Folding Des.*, 1996, **1**, 133; E. de Alba, M. A. Jimenez and M. Rico, *J. Am. Chem. Soc.*, 1997, **119**, 175; T. S. Haque and S. H. Gellman, *J. Am. Chem. Soc.*, 1997, **119**, 2303; A. J. Maynard and M. S. Searle, *Chem. Commun.*, 1997, 1297.
9 W. C. Johnson, *Annu. Rev. Biophys. Biophys. Chem.*, 1988, **17**, 145.
10 J. T. Yang, C. C. Wu and H. M. Martinez, *Methods Enzymol.*, 1986, **130**, 208.
11 D. S. Wishart, B. D. Sykes and F. M. Richards, *J. Mol. Biol.*, 1991, **222**, 311.
12 NMR chemical shifts and line widths were shown to be independent of concentration in the range 5 mM to 50 μM.
13 M. S. Searle, M. S. Westwell and D. H. Williams, *J. Chem. Soc., Perkin Trans. 2*, 1995, 141.
14 M. S. Searle, G. J. Sharman, P. Groves, B. Benhamu, D. A. Beauregard, M. S. Westwell, R. J. Dancer, A. J. Maguire, A. C. Try and D. H. Williams, *J. Chem. Soc., Perkin Trans. 1*, 1996, **23**, 2781.
15 H. Guo and M. Karplus, *J. Phys. Chem.*, 1994, **98**, 7104.
16 T. Arakawa, and D. Goddette, *Arch. Biochem. Biophys.*, 1985, **240**, 21.
17 J. W. Nelson and N. R. Kallenbach, *Proteins*, 1986, **1**, 211.
18 F. D. Sonnichsen, J. E. Van Eyk, R. S. Hodges and B. D. Sykes, *Biochemistry*, 1992, **31**, 8790.
19 R. W. Storrs, D. Truckses and D. E. Wemmer, *Biopolymers*, 1992, **32**, 1695.

*Received in Cambridge, UK, 25th July 1997; 7/05376B*

# Antibody-catalysed glycosyl transfer reactions from *in vitro* immunization

**Jaehoon Yu,*[a] So Young Choi,[a] Sungsoo Lee,[a] Hyun Joo Yoon,[b] Sunjoo Jeong,[c] Hansuh Mun,[a] Hokoon Park[a] and Peter G. Schultz*[d]**

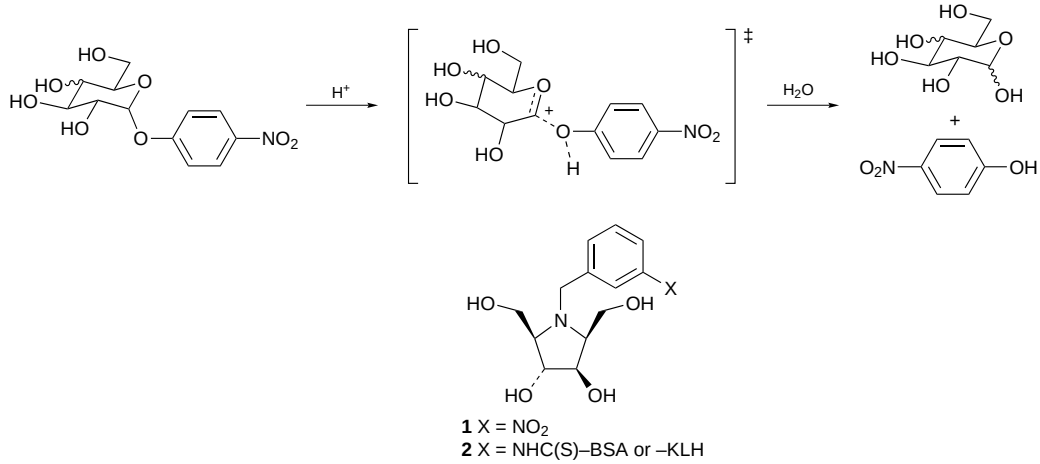
[a] *Division of Applied Science, Korea Institute of Science and Technology, PO Box 131, Cheongryang, Seoul 131-179, Korea*
[b] *Department of Microbiology, College of Natural Sciences, Inje University, Kimhae 621-749, Korea*
[c] *Department of Molecular Biology, College of Natural Sciences, Dankook University, Seoul140-714, Korea*
[d] *Howard Hughes Medical Institute, Department of Chemistry, University of California, Berkeley, USA*

***In vitro* immunization using a 5-membered ring iminocyclitol afforded antibodies that catalyse the hydrolysis of *p*-nitrophenyl glucopyranoside and *p*-nitrophenyl galactopyranoside with rate enhancements ($k_{cat}/k_{uncat}$) of greater than $10^4$.**

The generation and characterization of antibodies that catalyse glycosyl transfer reactions should provide insights into the mechanisms of naturally occuring glycosidases, and may lead to the development of glycosidases with novel specificities.[1–3] Previous efforts to generate antibodies with glycosidase activity made use of cyclic acetals as model substrates and antibodies generated against charged and conformationally restricted analogues of the oxocarbonium ion intermediate.[1–3] Rate accelerations of the order of $10^2$–$10^3$-fold were reported for these catalytic antibodies. More recently, an antibody that catalyses the hydrolysis of *p*-nitrophenyl galactopyranoside with a rate enhancement ($k_{cat}/k_{uncat}$) of $7 \times 10^4$ was isolated by screening a library of antibodies specific for a five-membered ring iminocyclitol using a suicide substrate.[4] We have independently used a similar positively-charged twist boat hapten to directly generate an antibody that catalyses the cleavage of *p*-nitrophenyl-β-D-glucopyranoside **3** with a rate enhancement ($k_{cat}/k_{uncat}$) of *ca.* $2 \times 10^4$. Antibodies were produced by *in vitro* immunization with free hapten, suggesting this might be a general method for generating catalytic antibodies, especially for unstable or toxic immunogens.[5]

The pyranoside ring is known to have a half-chair or twist-boat conformation in the transition state for glycosidic bond cleavage.[6] Another distinctive feature of the transition state is the development of partial positive charge at the anomeric position. Based on these structural and electronic characteristics, hapten **1** was used as a transition state analogue[7] to elicit antibodies that catalyse the cleavage of the β-glucosidic bond of *p*-nitrophenyl-β-D-glucopyranoside (Scheme 1). Hapten **1** was synthesized from 5-keto-D-fructose and benzhydrylamine in three steps.† The $NaBH_4$ dependent reductive amination of 5-keto-D-fructose with benzhydrylamine[8] afforded, after recrystallization, the indicated diastereoisomer (Scheme 1) of the corresponding *N*-benzhydryl azasugar. Removal of the protecting group by catalytic hydrogenation, and alkylation of the resulting secondary amine with 3-nitrobenzyl bromide, yielded hapten **1**. The nitro group was then reduced with $H_2$ using Lindlar catalyst, converted to the isothiocyanate and coupled to the carrier proteins keyhole limpet hemocyanin (KLH) and bovine serum albumin (BSA).[9] Sixteen hybridomas antibody specific for hapten **1** were generated by standard methods[10] and ascites from each cell line were generated. Antibodies were purified using Protein-A affinity chromatography[11] followed by ion-exchange chromatography using a mono S column,‡ and were tested using the following substrates: *p*-nitrophenyl-α- and -β-D-glucopyranosides, *p*-nitrophenyl-α- and -β-D- galactopyranosides and *p*-nitrophenyl-α- and β-mannopyranosides. HPLC analysis of the reaction products indicated that none of the antibodies showed any hydrolytic activity under a range of buffer conditions.‡

However, encouraged by recent progress in immunization methods, we decided to generate antibodies by *in vitro* immunization, wherein carrier free hapten is mixed directly with spleen cells in culture.[11] Using this method, fourteen hybridoma cell lines secreting antibodies specific for hapten **1** were identified by enzyme-linked immunosorbent assay and ascites were generated. The ascites were purified and assayed as described above. Two antibodies were found to be catalytic: Ab24 and AB21 catalysed the hydrolysis of *p*-nitrophenyl-β-D-glucopyranoside **3** and *p*-nitrophenyl-β-D-galactopyranoside **4**, respectively. These antibodies displayed saturation kinetics and their Michaelis constants were determined in 10 mM 2-(4-mor-




**1** X = $NO_2$
**2** X = NHC(S)–BSA or –KLH

**Scheme 1**

pholino)ethanesulfonic acid (MES), 100 mM NaCl, 0.02% $NaN_3$ buffer, pH 4.5, at 37 °C; rate constants for the uncatalysed reaction were determined under the same conditions.‡ Antibody Ab21 catalysed the hydrolysis of *p*-nitrophenyl-β-D-galactopyranoside **4** (and not **3**) with a $k_{cat}$ of 0.035 $h^{-1}$ and $K_m$ of 310 μM ($k_{cat}/k_{uncat}$ = 2.5 × $10^4$); antibody Ab24 catalysed the hydrolysis of *p*-nitrophenyl-β-D-glucopyranoside **3** (and not **4**) with a $k_{cat}$ of 0.02 $h^{-1}$ and $K_m$ of 160 μM ($k_{cat}/k_{uncat}$ = 2.2 × $10^4$). Antibodies purified from different preparations of ascites showed the same specific activities. Moreover, the catalytic activity could be stoichiometrically titrated by absorbing antibodies on increasing amounts of protein A agarose and analysing the activity of the filtrate *versus* the amount of bound antibody. The isolation of two antibodies, one specific for substrate **3** and the other for substrate **4**, also argues against enzymic contamination.

The antibodies were inhibited by hapten **1** with a $K_i$ value of 60 μM for the Ab21-catalysed hydrolysis of glucopyranoside **3**, and a $K_i$ value of 380 μM for the Ab24-catalysed hydrolysis of galactopyranoside **4**.[12] For both antibodies the rate acceleration does not correlate with the relative affinities of the antibody for substrate and hapten **1**. This behaviour suggests that a structural feature of the hapten (*i.e.* an amino or hydroxy group) results in the presence of a catalytic group, such as aspartic or glutamic acid, in the antibody combining site which can function as a general acid in catalysis but does not contribute substantially to the overall binding energy for the hapten. Indeed, diazoacetamide treatment of antibody Ab21 led to a 97% reduction in catalytic activity; 60% of the catalytic activity was retained when modification was carried out in the presence of 2 mM hapten **1**.[13] The relatively low affinities of the antibodies for hapten **1** resulting from the *in vitro* immunization likely reflect the absence of affinity maturation that normally occurs during an immune response.[14] In addition, antibodies generated against carbohydrates typically show relatively low affinities. It is of interest that both β-glucosidase and β-galacosidase activities were generated using hapten **1**. The five-membered ring in hapten **1** is flattened, mimicking a boat or twist-boat conformation of the pyranoside ring in the transition state. Either hapten **1** has some conformational flexibility or its geometry must map onto the critical recognition elements for both substrates and/or transition states.

Finally, Lerner[4] reported that direct immunization of a related hapten afforded catalytic antibodies with only 100-fold rate enhancements; we isolated no catalytic antibodies from direct immunization. This suggests that *in vitro* immunization, like antibody phage display methods, may complement conventional approaches for producing catalytic antibodies.

This work was partially supported by the Korea Institute of Science (Grant No E14100-1996) and the Ministry of Health and Welfare of Korea (Grant No HMP-96-D-1-1024). This work was also supported by the Director, Office of Energy Research, Office of Basic Energy Sciences, Division of Materials Sciences, and also by the Division of Energy Biosciences of the U.S. Department of Energy under Contract No. DE-AC03-76SF00098. P. G. S. is a Howard Hughes Medical Institute Investigator and a W. M. Keck Foundation Investigator.

## Footnotes and References

† 5-Keto-D-fructose was synthesized by incubating D-fructose with *Gluconobactor cerinus* (ATCC catalogue number IFO 3267). Hapten **1** was purified on silica gel using $CH_2Cl_2$–MeOH (9 : 1 v/v) as eluent ($R_f$ = 0.37); $\delta_H$ (300 MHz, $CDCl_3$) 8.1 (s, 1 H), 8.0 (d, 1 H, *J* 3), 7.6 (d, 1 H, *J* 8), 7.45 (dd, 1 H, *J* 8, 3), 4.0–3.8 (m, 4 H), 3.6–3.3 (m, 8 H including 4H from 4 OHs), 3.1 (m, 1 H), 2.7 (m, 1 H); $\delta_C$ (75 MHz, [$^2H_6$]DMSO) 147.6 (3′ phenyl), 143.4 (1′ phenyl), 135.3 (6′ phenyl), 129.3 (4′ phenyl), 122.9 (2′ phenyl), 121.6 (4′ phenyl), 77.0, 76.1 (C3 and C4), 72.6 (C benzyl), 67.4, 62.0 (C2 and C5), 60.3, 57.4 (C1 and C6); *m/z* 299 ($MH^+$).

‡ Antibodies were purified using a SP-Separose® (HiLoad™ 16/10) column (Pharmacia). For the mobile phase, buffer A (50 mM MES, pH 5.5) and buffer B (50 mM MES, 1.0 M NaCl, pH 5.5) were co-eluted with a linear gradient of 0–50% B over 40 min and a flow rate of 2 ml $min^{-1}$. Assays were carried out by mixing 90 μl of antibody (2–3 mg $ml^{-1}$) and 10 μl of substrate (20 mM), each in reaction buffer, and then incubating at 37 °C for 3 days. The reaction was analysed by HPLC using a C18 microsorb column (4.6 mm × 15 cm, 5 μm), eluting with 50% aqueous MeOH at 0.8 ml $min^{-1}$ and monitoring a 315 nm. The rate was determined when less than 1% of the substrate was converted to product. The data were fitted directly to the Michaelis–Menten equation, $v = (V_{max}[S])/([S] + K_m)$, using the nonlinear curve fitting program from the Kaleidagraph software suite. The second order rate constants for the $H^+$, $OH^-$ and AcOH catalysed reactions and the psuedo-first order rate constant for the reaction in water are: $k_{H^+}$ = 1.1 × $10^{-3}$ $M^{-1}$ $h^{-1}$, $k_{OH^-}$ = 0.29 $M^{-1}$ $h^{-1}$, $k_{AcOH}$ = 1.2 × $10^{-6}$ $M^{-1}$ $h^{-1}$, and $k'_{H_2O}$ = 8.0 × $10^{-7}$ $h^{-1}$ for substrate **3**; $k_{H^+}$ = 3.8 × $10^{-3}$ $M^{-1}$ $h^{-1}$, $k_{OH^-}$ = 0.58 $M^{-1}$ $h^{-1}$, $k_{AcOH}$ = 2.0 × $10^{-6}$ $M^{-1}$ $h^{-1}$ and $k'_{H_2O}$ = 1.6 × $10^{-6}$ $h^{-1}$ for substrate **4**.

1 J.-L. Reymond, K. D. Janda and R. A. Lerner, *Angew. Chem., Int. Ed. Engl.*, 1991, **30**, 1711.
2 H. Suga, N. Tanimoto, A. J. Sinskey and S. Masamune, *J. Am. Chem. Soc.*, 1994, **116**, 11197.
3 J. Yu, L. C. Hsieh, L. Kochersperger, S. Yonkovich, J. C. Stephans, M. A. Gallop and P. G. Schultz, *Angew. Chem., Int. Ed. Engl.*, 1994, **33**, 339.
4 K. Janda, L.-C. Lo, M.-M. Shin, R. Wang, C.-H. Wong and R. A. Lerner, *Science*, 1997, **275**, 945.
5 M. Stahl, B. Goldie, S. P. Bourne and N. R. Thomas, *J. Am. Chem. Soc.*, 1995, **117**, 5164.
6 M. L. Sinnott, *Chem. Rev.*, 1990, **90**, 1171; S. Rosenberg and J. F. Kirsch, *Biochemistry*, 1981, **20**, 3196; L. E. H. Smith, L. H. Mohr and M. A. Raftery, *J. Am. Chem. Soc.*, 1973, **95**, 7497; B. A. Malcolm, S. Rosenberg, M. J. Corey, J. S. Allen, A. de Baetselier and J. F. Kirsch, *Proc. Natl. Acad. Sci. USA*, 1989, **86**, 133; R. Kuroki, L. H. Weaver and B. W. Matthews, *Science*, 1993, **262**, 2030; T. L. Amyes and W. P. Jencks, *J. Am. Chem. Soc.*, 1989, **111**, 7888; S. G. Withers and I. P. Street, *J. Am. Chem. Soc.*, 1988, **110**, 8551; V. L. Schramm, B. A. Horenstein and P. C. Kline, *J. Biol. Chem.*, 1994, **269**, 18259.
7 K.-C. Liu, *J. Org. Chem.*, 1991, **56**, 6280.
8 A. B. Reitz and E. W. Baxter, *Tetrahedron Lett.*, 1990, **31**, 6777.
9 A. C. Braisted and P. G. Schultz, *J. Am. Chem. Soc.* 1994, **116**, 2211.
10 E. Harlow and D. Lane, *Antibodies: A Laboratory Manual*, Cold Spring Harbor Press, New York, 1988.
11 U. B. Fredriksson, L. G. Fagerstam, A. W. G. Cole and T. Lundgreb, *Protein A-Sepharose C1-4B Affinity Purification of Ig G Monoclonal Antibodies*, Pharmacia AB, Uppsala, Sweden, 1986.
12 I. H. Segel, *Enzyme Kinetics*, Wiley, New York, 1975.
13 A. L. Grossberg and D. Pressman, *J. Am. Chem. Soc.*, 1960, **82**, 5478.
14 C. A. Borrebaeck, *Trends Biotechnol.*, 1986, **4**, 147 and references cited therein.

*Received in Corvallis, OR, USA, 7th July 1997; 7/04885H*

# Liquid–liquid extractions using poly(propylene imine) dendrimers with an apolar periphery

**Maurice W. P. L. Baars,[a] Peter E. Froehling[b] and E. W. Meijer*[a]**

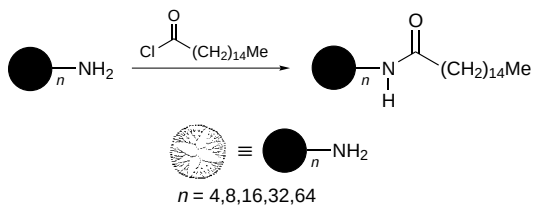
[a] *Laboratory of Organic Chemistry, Eindhoven University of Technology, PO Box 512, NL-5600 MB Eindhoven, The Netherlands*
[b] *DSM Research, PO Box 18, NL-6160 MD Geleen, The Netherlands*

**The modification of poly(propylene imine) dendrimers with apolar endgroups yields effective and highly selective basic extractants of anionic dye molecules from water to solvents, like dichloromethane and toluene.**

Liquid–liquid extraction is a well known technique in the field of (preparative) organic, inorganic and analytical chemistry.[1a,b] The technique is based upon the transfer of a substance (solute) from one liquid (*e.g.* aqueous phase) to a second liquid (*e.g.* organic phase), the latter being reasonably immiscible with the first one. Extractants can influence the distribution of the solute molecules between the two phases to a large extent. It is well known that acidic extractants, like alkylphosphoric acids and alkylcarboxylic acids can extract positively charged (metal) ions[1a,b] while basic extractants are capable of extracting anionic species from water to the organic phase. Primary, secondary and tertiary amines are interesting extractants because of their organophilic nature (high solubility in organic solvents) and their basicity.[2a–c]

Recently, we have been investigating the endgroup modification of polar poly(propylene imine) ASTRAMOL™ dendrimers[3] with apolar endgroups, *e.g.* linear alkyl chains and adamantane.[4] These and other dendrimers are interesting molecules to study host–guest properties.[5a–g] In this paper we describe generations 1–5 (number of endgroups $n$ = 4–64) of the poly(propylene imine) dendrimers modified with palmitoyl chloride[6] yielding 'inverted unimolecular dendritic micellar' structures with a polar interior of tertiary amines and an apolar periphery (Scheme 1). The extraction properties of the dendritic structures were investigated, using different anionic xanthene dyes as solute molecules (**I** Fluorescein, **II** 4,5,6,7-tetrachlorofluorescein, **III** Erythrosin B, **IV** Rose Bengal).

The extraction yield,† using a fifth-generation palmitoyl dendrimer as a function of the pH of the aqueous solution (Fig. 1) indicated that at low pH all four solute molecules, as a 1 : 1 mol ratio of dye and dendrimer could be transferred to the organic layer, whereas at higher pH no extraction is possible, except for Rose Bengal. The sensitive and abrupt pH-dependent extraction yield describes the distribution ratio of the solute between the two phases. Differences in p$K_a$ and hydrophobicity of the solutes are likely to account for the different inflection points of the 'titration' curves. The (large) hydrophobicity of Rose Bengal seems a reasonable explanation for extraction of this probe by clathration even at high pH (pH > 12). From the fact that cationic probes, like Ethidium Bromide can not be extracted into the organic phase, we conclude that the interaction between solute and dendritic structure is mainly determined by their acid–base properties and that the dendritic structures behave as basic extractants.




**Scheme 1** Modification of poly(propylene imine) dendrimers

Under different pH conditions the relative absorption in UV–VIS of Rose Bengal in the aqueous layer was determined as a function of the dendrimer to dye ratio (Fig. 2). At pH = 7 the interaction between solute and dendrimer is much stronger than at pH = 11 and 14. From the inset in Fig. 2 (pH = 7) we can determine the dendrimer to dye ratio of the complex that is initially formed in the organic phase. It is concluded that approximately 50 (!) dye molecules ($M_{dye}$ = 1 × 10³) are

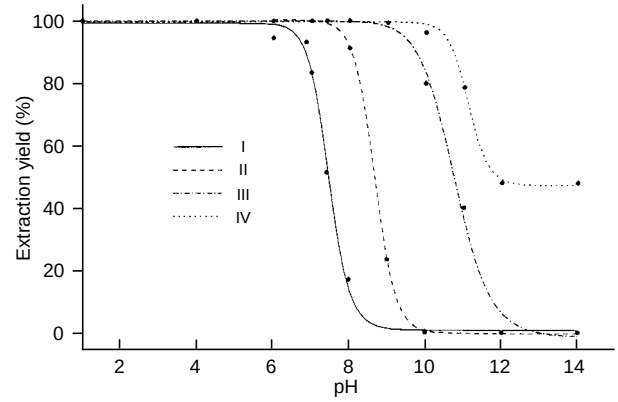



**Fig. 1** Extraction yield of fifth-generation palmitoyl dendrimer as a function of pH for different dye molecules **I**–**IV**. Dendrimer : dye ratio is 1 : 1 (mol/mol); [dendrimer] = 2.5 × 10⁻⁵ M. Equal volumes of both phases are used.

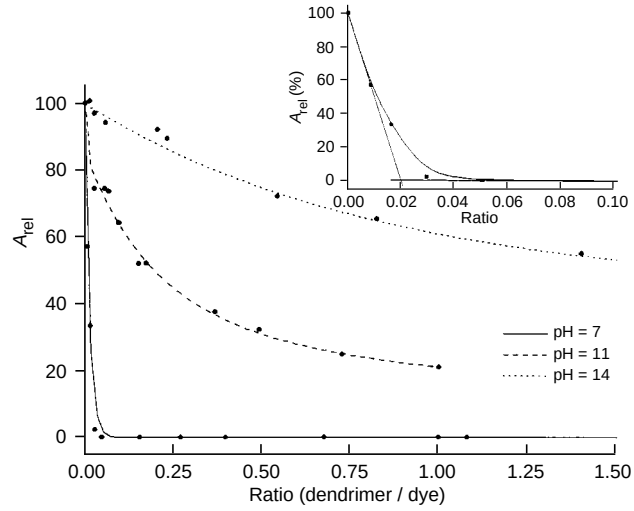



**Fig. 2** Relative absorbance of Rose Bengal **IV** in the aqueous layer as a function of the dendrimer to dye ratio. Fifth-generation palmitoyl dendrimer was used as dendritic extractant. Dye concentration was kept constant during measurement (2.5 × 10⁻⁵ M). Inset shows cut-off at a ratio ≈ 0.020, *i.e.* 50 dye molecules per dendrimer.

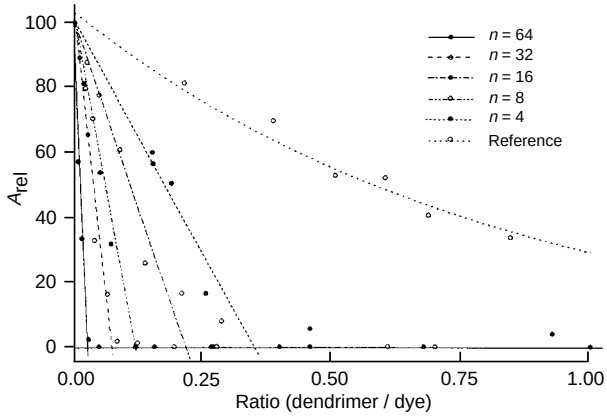



**Fig. 3** Relative absorbance of Rose Bengal **IV** in the aqueous layer as a function of the dendrimer to dye ratio for different generations of palmitoyl dendrimers ($n$ = 4, 8, 16, 32, 64). Tri-*n*-octylamine was used as reference compound. The concentration of extractant was kept constant [$2.5 \times 10^{-5}$ M] for all measurements.

extracted per fifth generation dendrimer ($M_{dendr} = 2.3 \times 10^4$). At pH = 7 all solute molecules can be extracted whereas at higher pH (pH > 10) there is an equilibrium and the dye is distributed over both layers. Even at higher ratios the extraction is not complete. The higher the extraction yield at a specific pH (Fig. 1), the faster is the (exponential) decrease in the absorption of the aqueous layer (Fig. 2).

Comparing all the generations of the palmitoyl dendrimers, we can conclude that the extraction is directly related to the number of tertiary amines in the dendritic interior (Fig. 3). The higher the generation of the dendrimer and the larger the number of tertiary amines in the interior, the more dye molecules can be extracted per dendrimer. Reference compound tri-*n*-octylamine (one tertiary amine) follows the same trend under these conditions as the dendritic extractants, but the extraction strength is less.

The dendritic extractant shows (almost) no difference in extraction yield of Fluorescein and Rose Bengal if the organic phase is changed from dichloromethane into toluene. Only in the case of Rose Bengal and high pH, is toluene less effective than dichloromethane. The extraction yield of tri-*n*-octylamine however deviates substantially when changing the organic phase; whereas in dichloromethane it is still possible to extract Fluorescein and Rose Bengal, Fluorescein can not be extracted into toluene using tri-*n*-octylamine. Rose Bengal still can be extracted, but the effectiveness is much smaller as is demonstrated by the inflection point that is several pH units lower. The results of tri-*n*-octylamine demonstrate that the strength of solvation decreases in the order dichloromethane > toluene, which is in full agreement with literature data.[26] Dendritic extractants, however, are not influenced by a change in solvent, probably due to their micellar character that shields the interior from the solvent.

The pH-dependent extraction behavior of the dendritic extractants (Fig. 1) enables us to perform back-extraction of the solute molecules. Fluorescein can be extracted into the organic phase at pH = 7 with a high extraction yield (*ca.* 90%). All Fluorescein in the organic phase can be recovered (extracted back) if an aqueous solution is used with pH = 10. In Fig. 1 it was already demonstrated that at pH = 10 no Fluorescein can be detected in the organic phase. Rose Bengal and Fluorescein show a pH region (pH *ca.* 8–10) in which there is maximum difference in extraction yield (Fig. 1). By adding Fluorescein and Rose Bengal in different ratios in the aqueous layer and determining the absorption of both layers, it was demonstrated that even in a 10 000 : 1 ratio, Rose Bengal could be selectively extracted into the organic layer. This high selectivity is only possible due to the specific topology of the dendritic extractant in the liquid–liquid extraction process.

In summary, we conclude that the extraction of anionic solutes by modified poly(propylene imine) dendrimers is related to their tertiary amine interior. As a consequence the behaviour of these dendrimers is that of acting as long chain tertiary amines. The dendritic molecules, however, are solvent-independent extractants, while the high local concentration of tertiary amines in the dendritic interior, typical for the poly(propylene imine) dendrimers, creates a high selectivity in the extraction of solutes with different p$K_a$ and hydrophobicity. As a consequence dendritic extractants might be very useful in the selective purification of anionic compounds.

This work has been supported by the Netherlands Foundation for Chemical Research (SON) with financial aid from the Netherlands Organisation for Scientific Research (NWO). We thank Marcel van Genderen, Albert Schenning and Bas de Waal for stimulating discussions and valuable assistance. Jørn Cristensen is gratefully acknowledged for synthetic input. Manon Muré-Mak and Ellen de Brabander-van den Berg are acknowledged for providing the poly(propylene imine) dendrimers.

## Footnotes and References

* E-mail: tgtobm@chem.tue.nl

† The extraction yield is defined as the relative extraction of the solute into the organic phase and is determined by measuring the decrease and increase in absorption of the aqueous and organic layer, respectively in UV–VIS. The absorption is determined at $\lambda_{max}$ in both solvents for all dyes, where a small solvatochromic shift of $\lambda_{max}$ in organic solvents is observed. In all cases a decrease in absorption of the aqueous layer simultaneously gives a complementary increase in absorption of the organic layer. If no extractant is dissolved in the organic layer, the solute (dye molecule) shows no detectable distribution into the organic layer.

1 (*a*) T. Sekine and Y. Hasegawa, *Solvent Extraction Chemistry. Fundamentals and Applications*, 1997, Marcel Dekker, New York; (*b*) Y. Marcus and A. S. Kertes, *Ion Exchange and Solvent Extraction of Metal Complexes*, 1969, Wiley, London.

2 (*a*) A. M. Eyal and R. Canari, *Ind. Eng. Chem. Res.*, 1995, **34**, 1789; (*b*) A. M. Eyal, E. Bressler, R. Bloch and B. Hazan, *Ind. Chem. Res. Eng.*, 1994, **33**, 1067; (*c*) J. A. Tamada, S. A. Kertes and C. J. King, *Ind. Chem. Res. Eng.*, 1990, **29**, 1319.

3 E. M. M. de Brabander-van den Berg and E. W. Meijer, *Angew. Chem., Int. Ed. Engl.*, 1993, **32**, 1308, *Angew. Chem.*, 1993, **105**, 1370; ASTRAMOL™ is a registered trademark (DSM Research) descriptor of poly(propylene imine) dendrimers.

4 M. W. P. L. Baars and E. W. Meijer, *Polym. Mater. Sci. Eng.*, 1997, in press.

5 (*a*) G. R. Newkome, C. N. Moorefield and F. Vögtle, *Dendritic Molecules Concepts, Syntheses, Perspectives*, VCH, New York, 1996 and references therein; (*b*) J. M. J. Frechèt, *Science*, 1994, **263**, 1710; (*c*) D. A. Tomalia, A. M. Naylor and W. A. Goddard III, *Angew. Chem., Int. Ed. Engl.*, 1990, **29**, 138; (*d*) G. R. Newkome and X. Lin, *Macromolecules*, 1991, **24**, 1443; (*e*) J. F. G. A. Jansen, E. M. M. de Brabander-van den Berg and E. W. Meijer, *Science*, 1994, **226**, 1226; (*f*) D. Seebach, J.-M. Lapierre, C. Skobridis and G. Greiveldinger, *Angew. Chem.*, 1994, **106**, 457; (*g*) P. Walliman, P. Seiler and F. Diederich, *Helv. Chim. Acta*, 1996, **79**, 779.

6 S. Stevelmans, J. C. M. van Hest, J. F. G. A. Jansen, D. A. F. J. van Boxtel, E. M. M. de Brabander-van den Berg and E. W. Meijer, *J. Am. Chem. Soc.*, 1996, **118**, 7398.

*Received in Bath, UK, 17th July 1997; 7/05126C*

# The first structurally characterised solvent-free σ-bonded diorganocalcium, $Ca[C(SiMe_3)_3]_2$

**Colin Eaborn,* Simon A. Hawkes, Peter B. Hitchcock and J. David Smith***

*School of Chemistry, Physics and Environmental Science, University of Sussex, Brighton, UK BN1 9QJ*

**The monomeric solvent-free compound $CaR_2$ 1 [R = $C(SiMe_3)_3$] is obtained as colourless air- and moisture-sensitive crystals from the reaction between KR and $CaI_2$; in the solid the C–Ca–C axis is bent with Ca–C 2.459(9) Å and C–Ca–C 149.7(6)°; reactions of 1 with ethers ROEt give RH, ethene and $Ca(OEt)_2$.**

The structures of several bis(cyclopentadienyl) derivatives of the heavier group 2 elements have been determined[1] but to our knowledge the only structural determination of a σ-bonded diorgano derivative is that of bis[bis(trimethylsilyl)methyl] calcium which was characterised as a 1,4-dioxane adduct $Ca[CH(SiMe_3)_2]_2{\cdot}2C_4H_8O_2$.[2] Other σ-bonded dialkyls and diaryls have been characterised by the products of their reactions with electrophiles such as $CO_2$, carbonyl compounds, nitriles, or terminal alkynes.[3,4] We recently showed that the readily available reagent KR [R = $C(SiMe_3)_3$] reacts with $LnI_2$ (Ln = Yb, Eu) in benzene[5] or Sm in thf–heptane[6] (thf = tetrahydrofuran), to give solvent-free dialkyls $LnR_2$. Here we report a similar reaction with $CaI_2$ to give solvent-free bis[tris(trimethylsilyl)methyl]calcium, $Ca\{C(SiMe_3)_3\}_2$ **1** which was isolated as a colourless air- and moisture-sensitive solid.†

The structure of **1** (Fig. 1) was determined by an X-ray diffraction study‡ on a very thin plate that separated from heptane–benzene. Although the molecules lie across a crystallographic inversion centre there are three independent sites for the calcium atom, which is disordered over positions related by an approximate $\bar{3}$ axis. This indicates that the equilibrium structure in the solid is bent. (Refinement with a linear C–Ca–C skeleton led to unacceptably large anisotropic displacement parameters with electron density away from the molecular axis.) Although the atoms of the alkyl group R appear to be well defined, their positions must be an average of closely related sites corresponding to the various Ca positions. However, the values for the Ca–C distance, the C–Ca–C angle and probably the mean C–Si distances are reliable. The Ca–C distance, 2.459(9) Å, is similar to those in the adduct $Ca[CH(SiMe_3)_2]_2{\cdot}2C_4H_8O_2$ [2.483(5) Å], in which the Ca is four-coordinate.[2] It is significantly shorter than the Ca–C distances in cyclopentadienyl derivatives (*ca.* 2.65 Å), in the 2,3-dimethyl-1,4-diphenylbutadiene adduct Ca(PhCH=C-MeCMe=CHPh)$(thf)_4$ [2.588(7)–2.777(7) Å], in which the Ca is six-coordinate,[8] and in the electron-deficient methyl-bridged compound $[(C_5Me_5)_2CaAlMe_3(thf)]_2$ [2.948(7), 2.999(7) Å].[9] In **1** there are three Ca···Me contacts of *ca.* 3.08 Å for each position of the Ca atom [from Ca to C(4), C(7′), and C(9), *cf.* Ca···Me 2.98 Å in $Ca(C_5Me_5)_2$ **2**]. The most important feature of the structure is the C–Ca–C angle [149.7(6)°], which is almost the same as those (147 and 154°, respectively) in crystalline[10] and gaseous[11] **2**, a little smaller than that (162°) in the exceedingly crowded $Ca(C_5HPr^i_4)_2$[12] and similar to that (148°) reported for gaseous $CaI_2$.[13] (though the value for $CaI_2$ may be affected by the presence of dimers and shrinkage effects associated with the $\nu_2$ bending vibration[14]). Simple electron repulsion rules predict that the monomeric calcium compounds $CaX_2$ (X = halogen, alkyl, *etc.*) should be linear but bent structures have been suggested by recent modifications to the original theory.[15,17] High level *ab initio* calculations also indicate that many calcium compounds, including $CaMe_2$, are quasilinear, *i.e.* the plot of potential energy *vs.* bending angle is almost flat, at least out to 160°;[18,19] angles of 131 and 116°, respectively, are predicted for $SrMe_2$ and $BaMe_2$. For compound **1** in the crystalline state the bending could possibly be attributed to crystal packing forces influenced by the intramolecular Ca···Me interactions but, in contrast to the situation in **2**, there are no significant intermolecular interactions. It is noteworthy and perhaps important that the C–Ca–C angles in compounds **1**, **2** and gaseous $CaI_2$ are all in the range 148–154°. In the compound $Yb[C(SiMe_3)_3]_2$ **3** and the Eu analogue **4** the C–M–C angles are 136–137° but the Mg compound **5** is linear.[20]

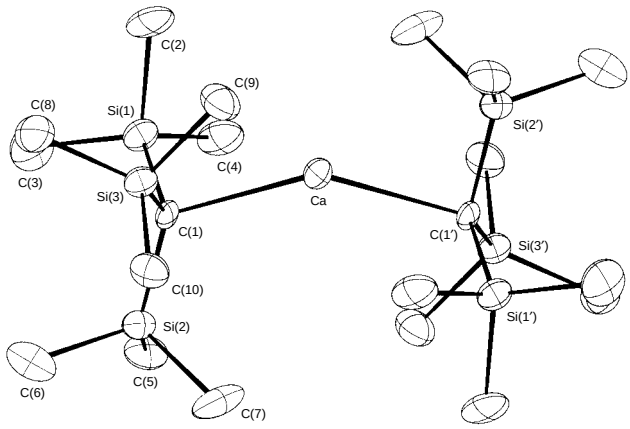



**Fig. 1** The molecular structure of **1**. Selected bond distances (Å) and angles (°): Ca–C 2.459(9), mean C(1)–Si 1.83(1), mean Si–Me 1.87(2); C–Ca–C 149.7(6), mean Si–C(1)–Si 114.8(6), mean Me–Si–Me 104.8(6).

The inner Si–C bond length in **1** is similar to those in **3** and **4** but shorter than that in **5**, suggesting that the metal–carbon bonds in the Ca, Yb and Eu derivatives are more ionic than those in the Mg compound.

We showed previously[5] that **3** reacted with diethyl ether to give the alkyl alkoxy compound $Yb[C(SiMe_3)_3](OEt)$, characterised by others as the diethyl etherate.[21] NMR-tube experiments showed that the analogous reaction of **1** with an excess of $Et_2O$ yielded RH [R = $C(SiMe_3)_3$], quantitatively, ethene, identified by its signal at $\delta_H$ 5.26, and insoluble $Ca(OEt)_2$ [eqn. (1)].

$$CaR_2 + 2Et_2O \rightarrow 2RH + 2C_2H_4 + Ca(OEt)_2 \qquad (1)$$

With 1 equiv. of $Et_2O$ only half of the $CaR_2$ was consumed, showing that the intermediate $Ca[C(SiMe_3)_3](OEt)$ reacts faster with $Et_2O$ than the dialkyl. Reactions with other ethers ROEt (R = $Bu^t$, Ph) proceeded in the same way but more slowly. No reaction was detected with PhOMe or $Pr^i_2O$. Compound **1** reacted rapidly with thf to give what appeared to be polymeric material (this was surprising since there are reports that organocalcium compounds are formed in much higher yield in thf than in $Et_2O$[4]). The reaction of **1** (1.99 mmol) with an excess of MeI gave RH (0.47 mmol), RI (0.96 mmol) and RMe (0.56 mmol), behaviour analogous to that of the ytterbium compound

**3** but different from that of $Mg[C(SiMe_3)_3]_2$ **5** which does not react with MeI under similar conditions.[20] The higher reactivity of **1** than of **4** is probably due in part to the structural differences. In **4** the Mg–C bond is short [2.116(2) Å], and the methyl groups interlock tightly round the linear C–Mg–C axis to protect the central atom.[20] In contrast the metal–carbon bond in **1** is longer, the skeleton is bent, and both the metal and the carbanionic centres are more exposed to attack.

The authors thank the EPSRC for financial support.

## Footnotes and References

* E-mail: j.d.smith@sussex.ac.uk

† A solution of $KC(SiMe_3)_3$ (2.5 g, 9.23 mmol) in benzene (20 $cm^3$) was added to a suspension of $CaI_2$[7] (1.45 g, 4.93 mmol) in benzene (20 $cm^3$) and the mixture was stirred for 48 h. The solvent was removed under vacuum and the residue was extracted with light petroleum (bp 40–60 °C, 60 $cm^3$). The extract was filtered through Celite and the solvent pumped away. The residue was recrystallised from heptane–benzene (3 : 1) to give **1** (2.03 g, 87%), mp 244–246 °C. Anal. Calc. for $C_{20}H_{54}CaSi_6$: C, 47.7, H, 10.7. Found: C, 41.7; H, 9.5%. $\delta_H$ (300 MHz, $C_6D_6$) 0.24 (s, $SiMe_3$); $\delta_C$ 7.2 ($SiMe_3$), 20.3 [$J$(SiC) 39.6 Hz, $CSi_3$]; $\delta_{Si}$ 12.1. EIMS *m/z* 502 (1% M), 487.220 (8%, M − Me, $C_{19}H_{51}CaSi_6$ requires *m/z* 487.223), 271, 100%.

‡ *Crystal data* for **1**: $M$ = 503.3; triclinic, space group $P\bar{1}$; $a$ = 8.948(2), $b$ = 9.104(2), $c$ = 12.067(2) Å, $\alpha$ = 95.53(2), $\beta$ = 104.79(2), $\gamma$ = 119.05(2)°, $U$ = 802.1(3) Å$^3$; $D_c$ = 1.04 Mg m$^{-3}$, $Z$ = 1, $F$(000) = 278, Mo-K$\alpha$ radiation, $\lambda$ = 0.710 73 Å, crystal size 0.40 × 0.40 × 0.05 mm, $\mu$(Mo-K$\alpha$) = 0.43 mm$^{-1}$, $T$ = 225(2) K. CAD4 diffractometer, $\theta$–2$\theta$ scan mode, 2 < $\theta$ < 22°, 1961 independent reflections. Structure solution by direct methods (SHELXS-86) and full-matrix least-squares refinement (SHELXL-93) with all non-H atoms anisotropic and H atoms in riding mode with $U_{iso}$ = 1.5 $U_{eq}$(C). The Ca–C(1) distances for the three alternative sites were loosely restrained to a single value. Final $R_1$ 0.102 for 1013 reflections with $I > 2\sigma(I)$, $wR_2$ 0.326 (all data). CCDC 182/585.


1 T. P. Hanusa, *Polyhedron*, 1990, **9**, 1345; *Chem. Rev.*, 1993, **93**, 1023.
2 F. G. N. Cloke, P. B. Hitchcock, M. F. Lappert, G. A. Lawless and B. Royo, *J. Chem. Soc., Chem. Commun.*, 1991, 724.
3 H. Gilman and L. A. Woods, *J. Am. Chem. Soc.*, 1945, **67**, 520.
4 K. A. Kocheshkov, I. E. Paleeva, N. I. Sheverdina and M. A. Zemlyanichenko, *Izv. Akad. Nauk SSSR, Ser. Khim.*, 1970, 1921; M. A. Zemlyanichenko, N. I. Sheverdina, V. A. Chernoplekova and K. A. Kocheshkov, *Zh. Obshch. Khim.*, 1972, **42**, 841.
5 C. Eaborn, P. B. Hitchcock, K. Izod and J. D. Smith, *J. Am. Chem. Soc.*, 1994, **116**, 12 071; C. Eaborn, P. B. Hitchcock, K. Izod, Z.-R. Lu and J. D. Smith, *Organometallics*, 1996, **15**, 4783.
6 S. K. Gupta, personal communication.
7 C. Hadenfeldt, *Z. Naturforsch, Teil B*, 1975, **30**, 165.
8 K. Mashima, H. Sugiyama, N. Kanehisa, Y. Kai, H. Yasuda and A. Nakamura, *J. Am. Chem. Soc.*, 1994, **116**, 6977.
9 P. S. Tanner, R. A. Williams and T. P. Hanusa, *Inorg. Chem.*, 1993, **32**, 2234.
10 R. A. Williams, T. P. Hanusa and J. C. Huffman, *Organometallics*, 1990, **9**, 1128.
11 R. A. Andersen, R. Blom, J. M. Boncella, C. J. Burns and H. V. Volden, *Acta Chem. Scand. Ser. A*, 1987, **41**, 24.
12 R. A. Williams, K. F. Tesh and T. P. Hanusa, *J. Am. Chem. Soc.*, 1991, **113**, 4843.
13 V. V. Kasparov, Yu. S. Ezhov and N. G. Rambidi, *J. Struct. Chem.* (*Engl. Transl.*), 1979, **20**, 285.
14 E. Vajda, M. Hargittai, I. Hargittai, J. Tremmel and J. Brunvoll, *Inorg. Chem.*, 1987, **26**, 1171.
15 R. J. Gillespie and I. Hargittai, *The VSEPR Model of Molecular Geometry*, Allyn and Bacon, Boston, MA, 1991, pp. 99.
16 I. Bytheway, R. J. Gillespie, T.-H. Tang and R. F. W. Bader, *Inorg. Chem.*, 1995, **34**, 2407.
17 R. J. Gillespie and E. A. Robinson, *Angew. Chem., Int. Ed. Engl.*, 1996, **35**, 495.
18 M. Kaupp and P. v. R. Schleyer, *J. Am. Chem. Soc.*, 1992, **114**, 491; M. Kaupp, P. v. R. Schleyer, M. Dolg and H. Stoll, *J. Am. Chem. Soc.*, 8202.
19 L. Seijo, Z. Barandiarián and S. Huzinaga, *J. Chem. Phys.*, 1991, **94**, 3762.
20 S. S. Al-Juaid, C. Eaborn, P. B. Hitchcock, K. Kundu, C. A. McGeary and J. D. Smith, *J. Organomet. Chem.*, 1994, **480**, 199.
21 P. B. Hitchcock, S. A. Holmes, M. F. Lappert and S. Tian, *J. Chem. Soc., Chem. Commun.*, 1994, 2691.


*Received in Basel, Switzerland, 9th June 1997; 7/03972G*

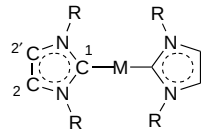
# An experimental and theoretical investigation of the electronic structure of Pd and Pt bis(carbene) complexes

**Jennifer C. Green,*[a] Robert G. Scurr,[a] Polly L. Arnold[b] and F. Geoffrey N. Cloke[b]**

[a] *Inorganic Chemistry Laboratory, South Parks Road, Oxford, UK OX1 3QR*
[b] *School of Chemistry, Physics and Environmental Science, University of Sussex, Brighton, UK BN1 9QJ*

**Photoelectron spectra and density functional calculations are reported for $M(CN_2R_2C_2H_2)_2$ (M = Pd, Pt); bonding occurs predominantly through σ donation from the carbene lone pairs into a metal ($d_{z^2}$ + s) hybrid; the corresponding ($d_{z^2}$ − s) is destabilised with respect to the other metal orbitals; there is little evidence for π bonding and the carbene π orbitals are essentially unperturbed on complexation.**

Isolation by Arduengo of stable carbenes by deprotonation of imidazolium salts[1] has opened up new routes to the synthesis of transition-metal carbene compounds.[2–6] The bis(carbenes) of the group 10 metals, Ni, Pd and Pt, are particularly striking being examples of stable neutral two-coordinate complexes. Together with the isoelectronic complexes of the group 11 metal ions, $Cu^+$, $Ag^+$ and $Au^+$, they show linear coordination,[5,6] which is common for $d^{10}$ metal ions. Though the bonding in the case of the monocations is likely to be predominantly σ donation from the nucleophilic carbene carbons, with the group 10 metals the question arises as to the degree of π-back donation from the metal to the carbene.



**1** M = Pd, R = Bu$^t$ **3** M = Pd, R = H
**2** M = Pt, R = Bu$^t$ **4** M = Pt, R = H

Crystal structure determinations on $M(CN_2Bu^t_2C_2H_2)_2$ (M = Pd **1**, Pt **2**) show the molecular framework to approximate to $D_{2d}$ symmetry with the two rings orthogonal to one another.[7] We consequently classify the molecular orbitals (MO) in this point group. It is also helpful to define their symmetry with respect to the local symmetry at the metal, $D_{\infty h}$. The primary bonding orbital ($a_1$ or $\sigma_g$) is expected to be a linear combination of the carbene lone pairs and a metal ($d_{z^2}$ + s) hybrid directed towards the ligands [Fig. 1(*a*)]. Interaction of the out-of-phase lone pair combination ($b_2$ or $\sigma_u$) with the metal $p_z$ orbital is expected to be less favourable on both energy and overlap grounds [Fig. 1(*b*)]. The metal orbitals which are possible candidates for π-back donation to the ligands are the $d_{xz}$ and $d_{yz}$ orbitals (e or $\pi_g$). They can interact with ligand $\pi_1$, $\pi_3$ or $\pi_5$ orbitals. The ligand $\pi_2$ and $\pi_4$ orbitals give linear combinations $b_1$ and $a_2$ in symmetry (δ and φ respectively). The remaining d orbitals which are δ in symmetry ($d_{xy}$ $b_2$ and $d_{x^2-y^2}$ $b_1$) are expected to have minimal interaction with the ligands. The ten metal electrons will occupy four metal d orbitals and a $d_{z^2}$ − s hybrid [Fig. 1(*c*)].

We have investigated the bonding in these compounds by a combination of photoelectron (PE) spectroscopy and calculations using density functional theory (DFT).

He I and II PE spectra were obtained for **1** and **2**.† The Ni compound was insufficiently volatile for PE spectroscopy. The spectra are shown in Fig. 2 and vertical ionisation energies ($E_i$) are given in Table 1 together with those of ($CN_2Bu^t_2C_2H_2$).[8]

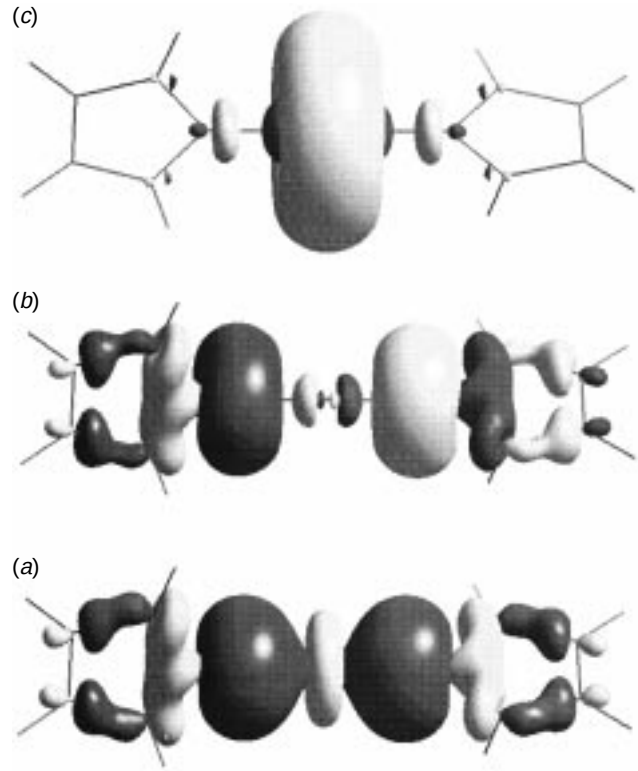



**Fig. 1** The principal σ orbitals of **3** and **4**: (*a*) $\sigma_g$ bonding orbital (*b*) $\sigma_u$ bonding orbital (*c*) s–$d_{z^2}$ hybrid (surfaces were generated using the Cerius2 package of MSI)

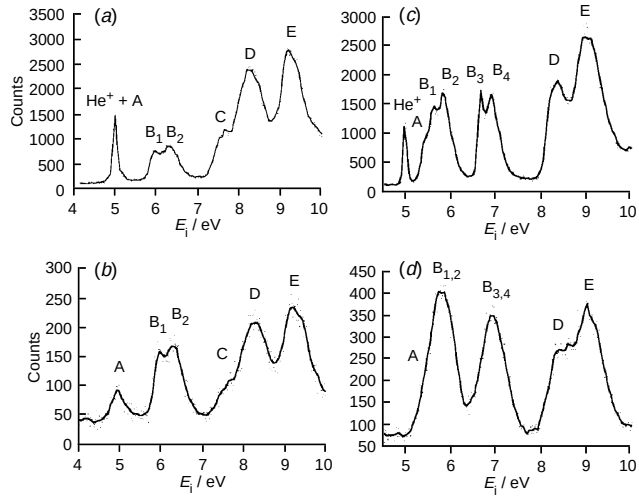



**Fig. 2** He I (*a*) and He II (*b*) PE spectra of **1** and He I (*c*) and He II (*d*) PE spectra of **2**

**Table 1** Experimental $E_i$s for **1** and **2** and free ligand **5**, calculated $E_i$s for **3** and **4** and ion state assignments

| Band | $E_i$ **1** | Calc $E_i$ **3** | Assignment | | Orbital type[a] | | $E_i$ **2** | Calc $E_i$ **4** | Assignment | | Orbital type[a] | | $E_i$ **5** | Assignment |
|---|---|---|---|---|---|---|---|---|---|---|---|---|---|---|
| A | 5.00 | 6.4 | $^2A_1$ | $\sigma_g$ | $z^2 - s$ | nb | 5.5 | 6.8 | $^2A_1$ | $\sigma_g$ | $z^2 - s$ | nb | | |
| $B_1$ | 5.96 | 7.3 | $^2E$ | $\pi$ | *xz*, *yz* | nb | 5.64 | 7.2 | $J = 5/2$ | $\delta$ | $x^2 - y^2$, *xy* | nb | | |
| $B_2$ | 6.36 | 7.5 | $^2B_1$, $^2B_2$ | $\delta$ | $x^2 - y^2$, *xy* | nb | 5.84 | 7.2 | $J = 3/2$ | $\pi$ | *xz*, *yz* | nb | | |
| $B_3$ | | | | | | | 6.67 | 7.2 | $J = 1/2$ | $\pi$ | *xz*, *yz* | nb | | |
| $B_4$ | | | | | | | 6.93 | 7.2 | $J = 3/2$ | $\delta$ | $x^2 - y^2$, *xy* | nb | | |
| C | 7.36 | 9.5 | $^2B_2$ | $\sigma_u$ | lig. $\sigma$ | b | | | | | lig. $\sigma$ | b | 7.68 | $\sigma$ |
| D | 8.25 | 8.8 | $^2E$ | $\pi$ | lig. $\pi_3$ | nb | 8.34 | 8.9 | $^2E$ | $\pi$ | lig. $\pi_3$ | nb | 8.22 | $\pi_3$ |
| E | 9.17 | 10.3 | $^2A_2$, $^2B_1$ | $\delta$ | lig $\pi_2$ | nb | 8.98 | 9.8 | $^2B_2$ | $\sigma_u$ | lig. $\pi_2$ | nb | 9.24 | $\pi_2$ |
| | | | | | | | | 10.3 | $^2A_2$, $^2B_1$ | $\delta$ | | | | |
| | | 11.7 | $^2A_1$ | $\sigma_g$ | $z^2 + s +$ lig. $\sigma$ | b | | 13.0 | $^2A_1$ | $\sigma_g$ | $z^2 + s +$ lig. $\sigma$ | b | | |

[a] nb = non-bonding, b = bonding, lig. = ligand.

The spectrum of **1** shows one low lying ionisation band, A; in the He I spectrum, the first band lies under the sharp He self-ionisation band (He ionised by He II radiation) but is readily apparent in the He II spectrum. This is followed by a more complex band structure B. Intensity changes between the He I and He II spectra indicate that bands A and B arise from ionisation of metal localised electrons. Band A is assigned ionisation from the $d_{z^2} - s$ hybrid and band B to ionisation from the four Pd d orbitals. Bands C, D and E correspond closely in position to the first three ionisation bands of the free carbene (Table 1).[8] The band profile, however, differs in that band C is lower in intensity in the complex and bands D and E are less resolved. In the free carbene the first PE band is associated with ionisation of the carbene lone pair. The change in band profile on complexing is consistent with stabilisation of the $\sigma_g$ linear combination of the lone pairs in the complex. Band C in the Pd complex is assigned to ionisation of the $\sigma_u$ orbital. The lack of shift or apparent splitting of bands D and E suggest negligible metal–ligand $\pi$ interaction. From the spectrum there is no direct evidence of the location of the $\sigma_g$ ionisation band.

The PE spectrum of **2** is assigned by comparison with that of **1**. The first band A, the $\sigma_g$ ionisation lies at higher energy. Band B, assigned to the d ionisations, shows a significantly greater spread of $E_i$. Given an effective linear potential at Pt, the splitting is attributable to spin–orbit (SO) coupling, that of the $\delta$ orbitals, giving $J = 5/2$ and 3/2, being twice that of the $\pi$ orbitals, giving $J = 3/2$ and 1/2. In the absence of SO coupling the $\pi$ and $\delta$ $E_i$s would be *ca*. 6.2 eV, closely similar to those found for Pd. This suggests that the larger $E_i$ for band A is due to the relativistic stabilisation of the Pt 6s orbital. Band C of the Pd spectrum has no analogue in the spectrum of **2**. We infer that the $\sigma_u$ orbital is more tightly bound compared with the $\pi$ ligand bands which again give rise to bands D and E with similar $E_i$s to the free ligand. There is no direct evidence for the $\sigma_u$ and $\sigma_g$ ionisation bands but the changed intensities of bands D and E compared with the Pd spectrum suggests that the $\sigma_u$ ionisation may lie under band E.

DFT calculations have been carried out for $M(CN_2H_2C_2H_2)_2$ (M = Pd **3**, Pt **4**), assuming $D_{2d}$ symmetry.‡ The geometries were optimised for the ground-state molecules. The distances and angles thus found are compared with those from the crystal structures of **1** and **2**.§ Ionisation energies were calculated both by Slater's transition-state method[14] and by carrying out calculations for the molecular ions $\mathbf{3}^+$ and $\mathbf{4}^+$ in the ion ground state and the first eight excited states using the optimised geometry for the molecule. Though both methods gave a similar $E_i$ pattern the values by the former method were more satisfactory. They are compared with the $E_i$s measured for **1** and **2** in Table 1. The presence of the *tert*-butyl groups in the measured compounds means that precise agreement with theory is not anticipated; alkyl substitution is expected to lower the $E_i$ of a molecule. Good agreement between the pattern of calculated and experimental $E_i$ confirms the assignment of bands given above. Comparing **3** with **1** suggests that the calculation overestimates the ionisation energy of the $\sigma_u$ orbital. The calculations also suggest that for both **1** and **2** the $\sigma_g$ bonding ionisation lies under the main band which commences at 10 eV, and that for **2** the $\sigma_u$ ionisation lies in the envelope of bands D and E.

The combined weight of the experimental and theoretical evidence suggests that the bis(carbenes) of Pd and Pt have metal–ligand $\sigma$ bonds and $\pi$ bonding is minimal.

## Footnotes and References

* E-mail. jennifer.green@icl.ox.ac.uk

† PE spectra were measured using a PES Laboratories 0078 spectrometer and calibrated with He, Xe and $N_2$

‡ Calculations were performed using the density functional methods of the Amsterdam Density Functional (ADF) code Version 2.0.1.[9] The basis set used triple-$\zeta$ accuracy sets of Slater orbitals with a single polarisation function added to main group atoms, 2p on H, 3d on C and N. Cores of the atoms were frozen (C, 1s; N, 1s; Pd, 4p; Pt, 5p), those of Pd and Pt being relativistic. Vosko, Wilk and Nusair's local exchange correlation potential[10] was employed with non-local exchange corrections by Becke[11] and non-local correlation corrections by Perdew.[12,13]

§ Experimental bond lengths for **1** and **2** and calculated bond lengths for **3** and **4** (Å)

| | **1** | **2** | **3** | **4** |
|---|---|---|---|---|
| M–C(1) | 2.041(6) | 1.965(12) | 2.08 | 2.00 |
| C(1)–N | 1.361(6) | 1.384(11) | 1.39 | 1.40 |
| N–C(2) | 1.374(9) | 1.397(13) | 1.41 | 1.41 |
| C(2)–C(2′) | 1.36(2) | 1.31(2) | 1.37 | 1.37 |


1 A. J. Arduengo III, R. R. Harlow and M. Kline, *J. Am. Chem. Soc.*, 1991, **113**, 361.
2 M. Regitz, *Angew. Chem., Int. Ed. Engl.*, 1996, **35**, 725.
3 N. Kuhn, T. Kratz, R. Boese and R. Blaeser, *J. Organomet. Chem.*, 1994, **470**, C8.
4 K. Öfele, W. A. Herrmann, D. Mihalios, M. Elison, E. Herdweck, W. Scherer and J. Mink, *J. Organomet. Chem.*, 1993, **459**, 177.
5 A. J. Arduengo III, S. G. Gamper, J. C. Calabrese and F. Davidson, *J. Am. Chem. Soc.*, 1994, **116**, 4391.
6 A. J. Arduengo III, H. V. Raisaka Dias, J. C. Calabrese and F. Davidson, *Organometallics*, 1993, **12**, 3405.
7 P. L. Arnold, F. G. N. Cloke, T. Geldbach and P. B. Hitchcock, manuscript in preparation.
8 A. J. Arduengo III, H. Bock, H. Chen, M. Denk, D. A. Dixon, J. C. Green, W. A. Herrmann, N. Jones, M. Wagner and R. West, *J. Am. Chem. Soc.*, 1994, **116**, 6641.
9 B. te Velde and E. J. Baerends, *J. Comput. Phys.*, 1992, **99**, 84.
10 S. H. Vosko, L. Wilk and M. Nusair, *Can. J. Phys.*, 1980, **58**, 1200.
11 A. D. Becke, *Phys. Rev. A*, 1988, **38**, 2398.
12 J. P. Perdew, *Phys. Rev. B*, 1986, **33**, 8822.
13 J. P. Perdew, *Phys. Rev. B*, 1986, **34**, 7046.
14 J. S. Slater, *The Calculation of Molecular Orbitals*, Wiley, New York, 1979.


*Received in Cambridge, UK, 18th July 1997; 7/05157C*

# Square-prismatic *vs.* square-antiprismatic coordination in complexes of lead(II) with a simple bidentate chelating ligand; effects of intermolecular hydrogen bonding

**Elefteria Psillakis, John C. Jeffery,* Jon A. McCleverty and Michael D. Ward***

*School of Chemistry, University of Bristol, Cantock's Close, Bristol, UK BS8 1TS*

**Whereas the eight-coordinate complex cation of $[PbL_4][(MeO)_2PO_2]\cdot 2H_2O$ [L = 3-(2-pyridyl)pyrazole] has square prismatic geometry stabilised by hydrogen bonding between the pyrazolyl NH groups and the dimethylphosphate anion, the complex cation of $[PbL_4][PF_6]_2$, in which there are no significant hydrogen-bonding interactions, has a structure distorted towards square antiprismatic with a 22° twist between the planes.**

Eight-coordination in metal complexes is largely confined to two common geometries : square antiprismatic ($D_{4d}$) and dodecahedral ($D_{2h}$). Rather rarer, but also well represented, are other geometries such as bicapped trigonal prismatic and hexagonal bipyramidal.[1–3] In contrast, the simple cubic (or square prismatic, $D_{4h}$) geometries are very rare in discrete metal complexes, although well known in ionic solids with the CsCl or $CaF_2$ structures.

Regular cubic coordination requires monodentate ligands, as in $Na_3[MF_8]$ (M = Pa, U, Np)[4] and $[NEt_4]_4[M(NCS)_8]$ (M = U,[5] Th[6]). In the latter examples crystal packing forces are significant in imposing the cubic geometry on the complex anion, as $[U(NCS)_8]^{4-}$ is square-antiprismatic both in solution[7] and in crystals with $Cs^+$ as the cation.[8] $[NEt_4]_4[M(SCN)_7(H_2O)]$ (M = various lanthanoid ions) are also cubic.[9] In contrast, the bite-angle limitations of bidentate chelating ligands mean that regular cubic geometry is not possible. Instead, compressed square-prismatic structures arise with the bidentate chelating ligands lying along the four shorter edges, linking the two square planes.[10–13] Most of these examples have a lanthanide or actinide ion as the central metal, consistent with the requirement for f-orbital participation.[3]

We describe here two eight-coordinate complexes of lead(II) with the bidentate chelating ligand 3-(2-pyridyl)pyrazole (L), of which one is square prismatic and the other is skewed towards a square-antiprismatic geometry. This pair of structures is of interest for two reasons: firstly, they provide a very rare example of square-prismatic geometry outside of the f-block elements, and secondly, they show how intermolecular hydrogen-bonding interactions can overcome the steric problems associated with a square prismatic structure.

We recently reported the synthesis and crystal structure of $[PbL^1{}_2]\cdot H_2O$, containing the potentially tetradentate ligand bis[3-(2-pyridyl)pyrazol-1-yl]phosphinate ($L^1$).[14] On recrystallising a batch of this material from MeOH we found that it had been converted to $[PbL_4][(MeO)_2PO_2]\cdot 2H_2O$, *via* solvolysis of the phosphinate group.† The crystal structure of the centrosymmetric complex is shown in Fig. 1.‡ The four bidentate ligands L form a square-prismatic array about the $Pb^{II}$ centre with each ligand spanning one of the short edges of the square prism, as in $[U(bipy)_4]$.[10] The sides of each 'square' [N(21), N(41), N(11A), N(31A)] are all between 3.30 and 3.50 Å in length, with the distance between the parallel planes [*i.e.* N(11)–N(21) and N(31)–N(41)] being 2.78 Å. The angles within the square prism described by the eight N atoms all lie between 87.5 and 92.3°.

The disposition of the four asymmetric chelating ligands is 'up–up–down–down', such that each end of the complex has two *cis*-related pyridyl donors and two *cis*-related pyrazolyl donors. This allows the two pyrazolyl NH groups at each side of the complex to form an NH···O hydrogen-bonding interaction with O(3) of the dimethylphosphate anion, with the non-bonded O(3)···N(32) and O(3)···N(12) distances being 2.81 and 2.96 Å respectively. This hydrogen-bonding interaction is a significant factor in the adoption of square-prismatic geometry, since the two pyrazolyl NH groups need to be held close enough together to be able to hydrogen bond to the same oxygen atom; the non-bonded N(12)···N(32) separation is 3.73 Å.

To test this theory we prepared the complex cation $[PbL_4]^{2+}$ as its hexafluorophosphate salt.† The crystal structure of $[PbL_4][PF_6]_2$ is in Fig. 2.‡ There are three significant differences between this structure and that of $[PbL_4][(MeO)_2PO_2]\cdot 2H_2O$. Firstly, the four ligands all have the same 'head-to-tail' orientation such that all four pyridyl groups are at one end

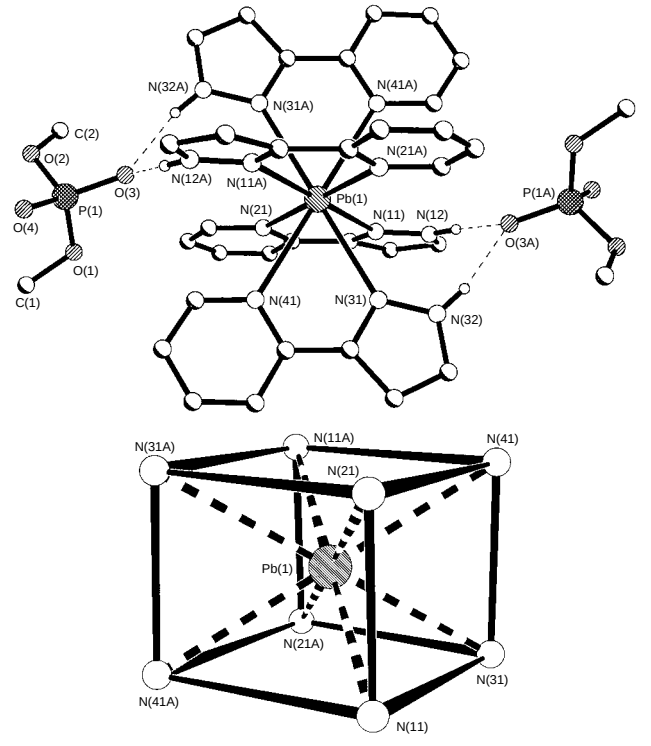



**Fig. 1** Crystal structure of $[PbL_4][(MeO)_2PO_2]\cdot 2H_2O$, showing (top) the complex cation and the hydrogen-bonded anions, and (bottom) the coordination geometry. Selected bond lengths (Å) and angles (°): Pb(1)–N(11) 2.765(6), Pb–N(21) 2.718(6), Pb–N(31) 2.760(6), Pb(1)–N(41) 2.794(6); N(11)–Pb(1)–N(21) 60.3(2), N(31)–Pb(1)–N(41) 59.9(2). Non-bonded N···N separations within the square prism (Å): N(11)···N(31) 3.37, N(31)···N(21A) 3.31, N(21)···N(41) 3.50, N(11)···N(41A) 3.34, N(11)···N(21) 2.78, N(31)···N(41) 2.78.

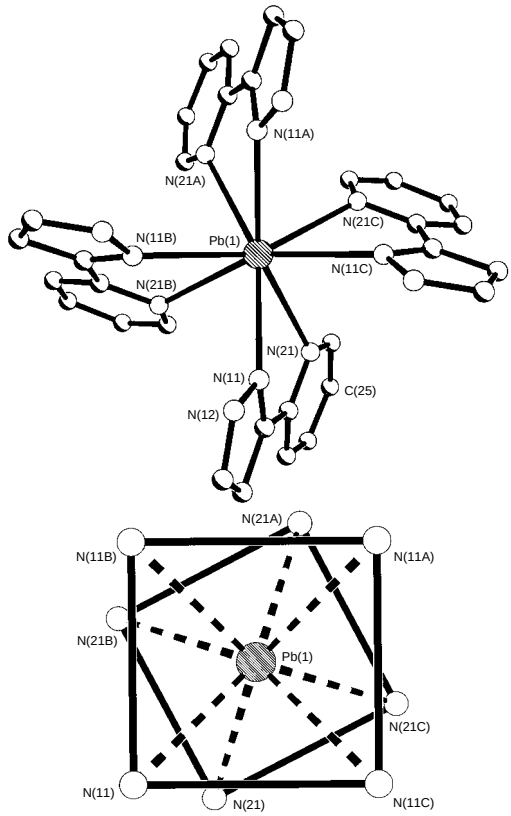



**Fig. 2** Crystal structure of $[PbL_4][PF_6]_2$, showing (top) the complex cation, and (bottom) the coordination geometry. Selected bond lengths (Å) and angles (°): Pb(1)–N(11) 2.702(4), Pb–N(21) 2.775(4); N(11)–Pb(1)–N(21) 60.80(13), N(11)–Pb(1)–N(11B) 80.23(7), N(21)–Pb(1)–N(21B) 75.07(7). Non-bonded N···N separations within the coordination polyhedron (Å): N(11)···N(11C) 3.48 Å, N(21)···N(21B) 3.38 Å, N(11)···N(21) 2.77 Å.

of the complex and the four pyrazolyl groups are at the other end. The complex has crystallographic $C_4$ symmetry with all four ligands equivalent. Secondly, the geometry is no longer square prismatic: the two mean planes are skewed with respect to one another by 22°, and the complex is therefore about half way between square prismatic and square antiprismatic. This twist brings the parallel planes closer together (2.52 Å, compared to 2.78 Å in the previous structure). This illustrates an important steric factor that does not occur in complexes with eight monodentate ligands, where the adoption of square-antiprismatic geometry to relieve the steric strain of an eclipsed prismatic structure does not have the unfavourable side-effect of also bringing the planes together. With four bidentate ligands of fixed length spanning the two planes this effect is inevitable and may explain why the offset of the two planes is only 22 rather than 45°. Thirdly, there are no significant hydrogen-bonding interactions between the complex cation and the hexafluorophosphate anions. An additional consequence of the 'skew' is that the adjacent pyrazolyl NH groups can move further apart; the separations between them [*e.g.* N(12)···N(12B)] have increased to 4.20 Å, as these groups are no longer held in proximity by forming hydrogen bonds to a common atom. The $N_4$ planes are perfect squares, with the square described by the four pyridyl groups (edge length 3.38 Å) being slightly smaller than that described by the four pyrazolyl groups (edge length 3.48 Å).

Crystal packing effects are known to be able to overcome the steric barrier to adoption of cubic geometries, as shown by comparison of $[NEt_4]_4[U(NCS)_8]$ and $Cs_4[U(NCS)_8]$.[5,8] We should be cautious in making comparisons between these two new structures. It does look however as if the hydrogen bonding in $[PbL_4][(MeO)_2PO_2]\cdot 2H_2O$ is partly responsible for the adoption of the very rare square-prismatic geometry, the first example of which we are aware for a main-group molecular species.

## Footnotes and References

* E-mail: mike.ward@bristol.ac.uk

† *Preparations*. $[PbL_4][(MeO)_2PO_2]\cdot 2H_2O$: A sample of $[Pb(L^1)_2]$ (ref. 14) was dissolved in MeOH and allowed to crystallise by slow evaporation over several days, to give X-ray quality crystals of $[PbL_4][(MeO)_2PO_2]\cdot 2H_2O$ in 67% yield. $[PbL_4][PF_6]_2$: A mixture of L (ref. 15) (0.290 g, 2 mmol) and $Pb(ClO_4)_2\cdot 3H_2O$ (0.203 g, 0.5 mmol) in MeCN (15 $cm^3$) was vigorously agitated in an ultrasound cleaning bath for 30 min. To the resulting solution was added aqueous $NH_4PF_6$, resulting in precipitation of the product as a white powder in 43% yield. X-Ray quality crystals were grown by slow evaporation of a methanol solution. Both complexes gave satisfactory elemental analyses and FAB mass spectra.

‡ *Crystallographic data*. $[PbL_4][(MeO)_2PO_2]\cdot 2H_2O$: $C_{36}H_{48}N_{12}O_{10}P_2Pb$, $M$ = 1073.96, colourless blocks, crystal size 0.25 × 0.15 × 0.10 $mm^3$, triclinic, space group $P\bar{1}$, $a$ = 8.9120(13), $b$ = 9.462(2), $c$ = 13.394(2) Å, $\alpha$ = 102.17(2), $\beta$ = 101.508(14), $\gamma$ = 92.83(2)°, $U$ = 1076.9(3) $Å^3$, $Z$ = 1, $D_c$ = 1.656 g $cm^{-3}$, $F(000)$ = 536, $\mu$(Mo-K$\alpha$) = 4.060 $mm^{-1}$. 4995 data were collected with $2\theta_{max}$ = 46.5° at −100 °C, and merged to give 3079 unique data ($R_{int}$ = 0.0485). Refinement of 284 parameters converged at $R_1$ [selected data with $I \geqslant 2\sigma(I)$] = 0.041, $wR_2$ (all data) = 0.103. The Pb atom lies on an inversion centre.

$[PbL_4][PF_6]_2$: $C_{32}H_{28}N_{12}F_{12}P_2Pb$, $M$ = 1077.79, colourless blocks, crystal size 0.30 × 0.20 × 0.05 $mm^3$, tetragonal, space group $P4/ncc$, $a$ = 13.136(2), $c$ = 21.667(3) Å, $U$ = 3738.8(9) $Å^3$, $Z$ = 4, $D_c$ = 1.915 g $cm^{-3}$, $F(000)$ = 2096, $\mu$(Mo-K$\alpha$) = 4.703 $mm^{-1}$. 21236 data were collected with $2\theta_{max}$ = 55° at −100 °C, and merged to give 2145 unique data ($R_{int}$ = 0.0532). Refinement of 123 parameters converged at $R_1$ [selected data with $I \geqslant 2\sigma(I)$] = 0.032, $wR_2$ (all data) = 0.080. The Pb atom lies on a $C_4$ axis.

Both data sets were collected on a Siemens SMART diffractometer with an area detector. See refs. 15 and 16 for experimental details and software used. CCDC 182/586.

1 C. W. Haigh, *Polyhedron*, 1996, **15**, 4; C. W. Haigh, *Polyhedron*, 1995, **14**, 2871.
2 D. L. Kepert, in *Comprehensive Coordination Chemistry*, ed. G. Wilkinson, R. D. Gillard and J. A. McCleverty, Pergamon, Oxford, 1987, vol. 1, p. 31.
3 S. J. Lippard, *Prog. Inorg. Chem.*, 1967, **8**, 109; S. F. A. Kettle and A. J. Smith, *J. Chem. Soc. A*, 1967, 688.
4 D. Brown, J. F. Easey and C. E. F. Rickard, *J. Chem. Soc. A*, 1969, 1161.
5 R. Countryman and W. S. McDonald, *J. Inorg. Nucl. Chem.*, 1971, **33**, 2213.
6 P. Charpin, M. Lance and A. Navaza, *Acta Crystallogr., Sect. C*, 1983, **39**, 190.
7 W. P. Griffith and M. J. Mockford, *J. Chem. Soc., Dalton Trans.*, 1996, 1057.
8 G. Bombieri, P. T. Moseley and D. Brown, *J. Chem. Soc., Dalton Trans.*, 1975, 1520.
9 Y. Tateyama, Y. Kuniyasu, Y. Suzuki and A. Ouchi, *Bull. Chem. Soc. Jpn.*, 1988, **61**, 2805.
10 G. Del Piero, G. Perego, A. Zazzetta and G. Brandi, *Cryst. Struct. Commun.*, 1975, **4**, 521.
11 A. R. A. Karaghouli, R. O. Day and J. S. Wood, *Inorg. Chem.*, 1978, **17**, 3702.
12 W. L. Smith and K. N. Raymond, *J. Am. Chem. Soc.*, 1981, **103**, 3341.
13 K. S. Hagen, *Angew. Chem., Int. Ed. Engl.*, 1992, **31**, 764.
14 E. Psillakis, J. C. Jeffery, J. A. McCleverty and M. D. Ward, *J. Chem. Soc., Dalton Trans.*, 1997, 1645.
15 P. L. Jones, A. J. Amoroso, J. C. Jeffery, J. A. McCleverty, E. Psillakis, L. H. Rees and M. D. Ward, *Inorg. Chem.*, 1997, **36**, 10.
16 SHELXTL 5.03 program system; Siemens Analytical X-Ray Instruments, Madison, WI, USA, 1995; Software package for use with the SMART diffractometer; Siemens Analytical X-Ray Instruments, Madison, WI, USA, 1995.

*Received in Basel, Switzerland, 27th May 1997; 7/03643D*

# Synthesis and structure of a $Mn^{III}$(OH) complex generated from dioxygen

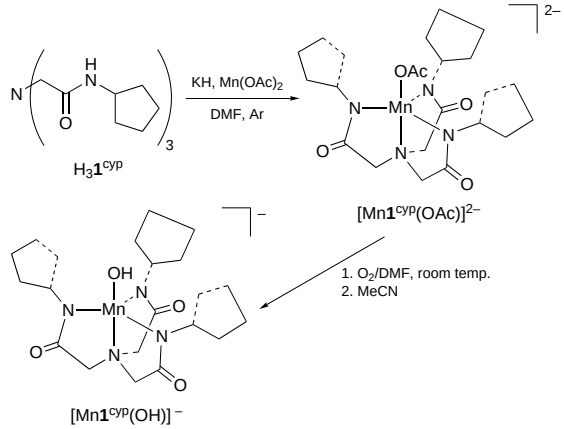
**Zahida Shirin,[a] Victor G. Young, Jr.[b] and A. S. Borovik*[a]**

[a] *Department of Chemistry, University of Kansas, Lawrence, KS 66045, USA*
[b] *Department of Chemistry, University of Minnesota, Minneapolis, MN 55455, USA*

**Dioxygen activation at room temperature by a new $Mn^{II}$ complex having a cavity motif yields a monomeric $Mn^{III}$ complex with a terminally bonded hydroxo ligand whose oxygen atom is derived from $O_2$.**

The interactions of manganese ions with dioxygen are involved in a number of biological and synthetic processes.[1] In synthetic manganese complexes, dioxygen activation often leads to the isolation of multinuclear μ-oxo (hydroxo) bridged species having Mn–Mn separation of < 3.5 Å.[2,3] We recently developed a new class of tripodal ligands based on tris(*N*-alkylcarbamoylmethyl)amine that, when coordinated to a metal ion, create cavities that can regulate subsequent ligand binding.[4] Modeling studies (CPK) suggested that appending cyclopentyl groups from the amidate nitrogen ($H_3$**1**$^{cyp}$)[5] would afford a cavity that has space for binding only one exogenous donor to the metal, in addition to preventing the formation of multinuclear metal complexes with metal–metal distances of < 3.5 Å. Thus, while the binding and activation of dioxygen by $Mn^{II}$ complexes of [**1**$^{cyp}$]$^{3-}$ is possible, the formation of oxo(hydroxo)-bridge manganese complexes should be hindered, allowing us to study the formation of a new manganese complex derived from dioxygen.[6] Here, we report the room-temperature $O_2$ activation by a $Mn^{II}$ complex of [**1**$^{cyp}$]$^{3-}$ that produces a monomeric $Mn^{III}$ complex with a terminally bonded hydroxo ligand whose oxygen atom is derived from dioxygen. Preliminary mechanistic studies suggest a reaction pathway that involves C–H bond cleavage from solvent to form the hydroxo ligand.[7]

Treating an anhydrous dmf solution of $K_2$[Mn**1**$^{cyp}$(OAc)]† with 1 equiv. of dry $O_2$ at room temp. results in the formation of blue K[Mn**1**$^{cyp}$(OH)]‡ in 63% yield after washing with MeCN (Scheme 1). K[Mn**1**$^{cyp}$(OH)]18-crown-6 can be isolated in 90% yield when the reaction is carried out at room temp. in anhydrous MeCN. Initial assignment of the product as a monomeric $Mn^{III}$(OH) species is based on its room-temp. solid-state magnetic moment of 4.96 $\mu_B$ which is typical of a high-spin $Mn^{III}$ ion,[8] and its FTIR spectrum containing a sharp peak at 3643 $cm^{-1}$, within the range found for known M–OH complexes.[9]




**Scheme 1**

The presence of a monomeric $Mn^{III}$(OH) moiety in K[Mn**1**$^{cyp}$-(OH)] was confirmed by an X-ray diffraction study.¶ The solid-state molecular structure of [Mn**1**$^{cyp}$(OH)]$^-$ shows the Mn ion having a trigonal-bipyramidal coordination geometry (Fig. 1). The three amidate nitrogens of [**1**$^{cyp}$]$^{3-}$ bind in the trigonal plane with an average Mn–$N_{amide}$ distance of 2.069(2) Å and $N_{amide}$–Mn–$N_{amide}$ angle of 117.07(7)°. These Mn–$N_{amide}$ distances are significantly longer than those observed in the only other structurally characterized $Mn^{III}$ amidate complex where the amidate nitrogens coordinate in a square-planar arrangement [av. M–$N_{amide}$ 1.913(3) Å].[3] The Mn ion sits 0.355 Å out of the trigonal plane toward the hydroxo ligand. The hydroxo oxygen O(4) is positioned nearly *trans* to the apical nitrogen N(1) [N(1)–Mn–(O4) 177.7(2)°] with Mn–N(1) and Mn–O(4) distances of 2.036(2) and 1.816(4) Å. The Mn–O(4) distance observed in [Mn**1**$^{cyp}$(OH)]$^-$ is comparable to that reported for the only other known monomeric $Mn^{III}$(OH) complex {[Mn**1**(OH)];[5] Mn–O, 1.827(3) Å}.[10] The $OH^-$ is located in a cavity formed by the three cyclopentyl substituents which are oriented such that the methine hydrogens on each ring are positioned outside the cavity toward the amide carbonyl groups. This conformation of cyclopentyl groups leads to a cavity structure that enshrouds the $Mn^{III}$(OH) motif, preventing the OH ligand from binding to another Mn complex.

Complexes containing Mn(OH) moieties are rare: only four other structurally characterized synthetic complexes have been reported.[10,11] Of these four, only one contains a monomeric $Mn^{III}$(OH) unit which is obtained by treating [Mn**1**Cl] with NaOH to yield the six-coordinate complex [Mn**1**(OH)].[10] The structure most closely associated with that found in [Mn**1**$^{cyp}$-(OH)]$^-$ is the active site of the manganese superoxide dismutase (MnSOD) isolated from *Thermus thermophilus*; this site contains a trigonal-bipyramidal geometry around a $Mn^{III}$ center with an axially coordinated hydroxo ligand.[12] The hydroxo ligand in MnSOD, like those found in synthetic Mn(OH) complexes, is derived from a source other than dioxygen (*e.g.*, $OH^-$ or $H_2O$). Although $Mn^{III}$(OH) complexes have been proposed as either intermediates or products in several reactions involving $O_2$ and Mn ions there are no examples,[1,13] to our knowledge, where structural proof verifies the identity of these species.

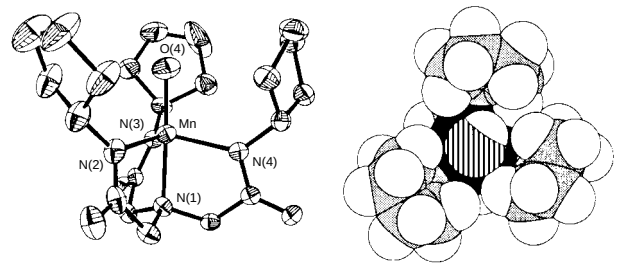



**Fig. 1** Thermal ellipsoid diagram of [Mn**1**$^{cyp}$(OH)]$^-$ and a space-filling representation of the complex. The ellipsoids are drawn at the 50% probability level and hydrogens are removed for clarity. Selected bond distances (Å) and angles (°): Mn–N(1) 2.036(3), Mn–N(2) 2.061(3), Mn–N(3) 2.053(3), Mn–N(4) 2.094(3), Mn–O(4) 1.816(4), N(2)–Mn–N(3) 125.43(1), N(2)–Mn–N(4) 113.5(1), N(3)–Mn–N(4) 112.3(1), N(1)–Mn–O(4) 177.7(2).

In [Mn**1**$^{cyp}$(OH)]$^{-}$ the oxygen atom of the hydroxo group originates from $O_2$: this was confirmed by treating $K_2$[Mn**1**$^{cyp}$(OAc)] with $^{18}O_2$ in MeCN to afford [Mn**1**$^{cyp}$($^{18}$OH)]$^{-}$ [FTIR; $\nu$($^{18}$OH) 3630 cm$^{-1}$, $\nu$($^{16}$OH)/$\nu$($^{18}$OH) = 1.004; calc. 1.003]. In addition, the stoichiometry of the $O_2$ reaction, as determined by manometry, gives Mn complex : $O_2$ = 2 : 1. In the presence of $PPh_3$P (1 equiv.), the oxidation of [Mn**1**$^{cyp}$(OAc)]$^{2-}$ with $O_2$ produces [Mn**1**$^{cyp}$(OH)]$^{-}$ and $Ph_3PO$ which is observed in 33% yield. Moreover, when the reaction is carried in $CD_3CN$ (99.5% D) the product is exclusively [Mn**1**$^{cyp}$(OD)]$^{-}$ [FTIR; $\nu$(OD) 2687 cm$^{-1}$, $\nu$(OH)/$\nu$(OD) = 1.356; calc. 1.374], demonstrating that solvent can serve as the source of the hydrogen (or deuterium) in the Mn$^{III}$[OH(D)] moiety. Similar results were obtained when the oxidation reaction was performed in [$^2H_8$]thf.

These observations are consistent with the formation of a dinuclear peroxo-bridge species during the reaction. A 1,2-μ-peroxo bridge species is postulated because the steric constraints of the cyclopentyl cavity prevents other modes of peroxide coordination.[14] Homolysis of the O–O bond can produce a Mn oxo intermediate whose oxo moiety is sufficiently buried inside the cavity that it is unable to react with other hindered Mn centers to form oxo-bridged clusters. With this pathway eliminated, the Mn oxo species is competent to react with solvent to form [Mn**1**$^{cyp}${OH(D)}]$^{-}$, a process that most likely occurs *via* a H atom abstraction. Support for an oxo intermediate comes from the observed oxygenation of $PPh_3$ to $Ph_3PO$: such oxo-transfer reactions have been proposed to be promoted by high-valent oxo species.[15] Further studies into the mechanism and oxo-transfer properties of this system are in progress.[16]

The $O_2$ reactivity exhibited by [Mn**1**$^{cyp}$(OAc)]$^{2-}$ is the first Mn complex of which we are aware that mediates the formation of a terminally bonded hydroxo ligand directly from $O_2$. In fact, this type of reactivity is rare for transition-metal complexes[17] and usually only occurs for reactions done at low temperatures (*e.g.*, Fe$^{II}$ porphyrins).[6*a*] The room-temperature activation process observed for [Mn**1**$^{cyp}$(OAc)]$^{2-}$ is controlled, in part, by the cavity motif provided by [**1**$^{cyp}$]$^{3-}$ that surrounds the $O_2$ binding site. This result contrasts with that reported by Floriani and coworkers for the room-temp. $O_2$ reactivity of a non-cavity containing Mn$^{II}$ Schiff-base complex.[18] In that system, a μ-OH bridged Mn$^{III}$ polymer is formed after $O_2$ activation with concomitant oxidation of the Schiff-base ligand where an imino group is converted to an amidato. We have not detected[19] any products that indicate modification of [**1**$^{cyp}$]$^{3-}$ during $O_2$ activation. A possible explanation for the lack of ligand oxidation in our system is the positioning of the methine C–H bonds of the cyclopentyl groups outside the cavity, away from the metal centers,[20] which protects these reactive sites from interacting with the activated (di)oxygen–Mn center(s).

Finally, Mn$^{III}$(OH) moieties have been recently proposed as key intermediates in the pathway for $O_2$ production from the oxygen evolving complex of photosynthesis.[21] Now that [Mn**1**$^{cyp}$(OH)]$^{-}$ is well characterized, reactivity studies will allow us to further evaluate the feasibility of this model,[22] efforts for which are underway.

We thank the NIH (GM50781 to A. S. B.) and the University of Kansas for financial support of this research, and Drs Charlie Riordan, Dan Stack, Eric Maatta and Tom Sorrell for helpful discussions.

## Footnotes and References

* E-mail: aborovik@caco3.chem.ukansas.edu

† *Selected data* for $K_2$[Mn**1**$^{cyp}$(OAc)]: $\mu_{eff}$ = 6.02 $\mu_B$ (solid, 298 K). FTIR (Nujol, cm$^{-1}$), $\nu$(CO) 1661 (dmf, s); 1558 (amide, s); 1581 and 1343 (acetate, s, $\Delta\nu$ = 238 cm$^{-1}$); and $\nu$(CN) 2150 (MeCN, m); $\Delta\nu$ observed for the two acetate bands in $K_2$[Mn**1**$^{cyp}$(OAc)] is consistent with monodentate acetato coordination.[9]

‡ *Selected data* for K[Mn**1**$^{cyp}$(OH)]: $\mu_{eff}$ = 4.96 $\mu_B$ (solid, 298 K). FTIR (Nujol, cm$^{-1}$), $\nu$(OH) 3643, $\nu$(CO) 1606 and 1584; $\lambda_{max}$/nm (dmf) 433 (285 dm$^3$ mol$^{-1}$), 673 (460); $E_{pa}$ = 0.48 V *vs.* SCE; $E_{pc}$ = −1.29 V *vs.* SCE.

§ $E_{pa}$ = 0.48 V *vs.* SCE; $E_{pc}$ = −1.29 V *vs.* SCE.

¶ *Crystal data* for K[Mn**1**$^{cyp}$(OH)]$C_3H_7NO$: triclinic, space group $P\bar{1}$, $a$ = 9.1855(5), $b$ = 10.3085(5), $c$ = 15.9444(8) Å, $\alpha$ = 90.182(1), $\beta$ = 94.849(1), $\gamma$ = 112.600(1)°; $V$ = 1397.79(12) Å$^3$, $Z$ = 2. Of 7341 reflections collected [Mo-K$\alpha$, 1.28 ⩽ $\theta$ ⩽ 25.05°; 173(2) K] 4752 were unique data ($R_{int}$ = 0.0399) and 3962 with $F_o^2 > \sigma F_o^2$; $R_1$ = 0.0540 and $wR_2$ = 0.12137 with a GOF ($F^2$) = 1.083. CCDC 182/593.

1 W. M. Coleman and L. T. Taylor, *Coord. Chem. Rev.*, 1980, **32**, 1; V. L. Pecoraro, M. J. Baldwin and A. Gelasco, *Chem Rev.*, 1994, **94**, 807 and refs. therein; R. Hage, *Recl. Trav. Chem. Pays-Bas*, 1996, **115**, 385.

2 Recent reports: K. Wieghardt, *Angew. Chem., Int. Ed. Engl.*, 1989, **28**, 1153; C. A. Kipke, M. J. Scott, J. W. Gohdes and W. H. Armstrong, *Inorg. Chem.*, 1990, **29**, 2193; J. W. Gohdes and W. H. Armstrong, *Inorg. Chem.*, 1992, **31**, 369; E. Larson, M. S. Lah, X. Li, J. A. Bonadies and V. L. Pecoraro, *Inorg. Chem.*, 1992, **31**, 373; C. P. Horwitz, P. J. Winslow, J. T. Warden and C. A. Lisek, *Inorg. Chem.*, 1993, **32**, 82.

3 Notable exception: F. M. MacDonnell, N. L. P. Fackler, C. Stern and T. V. O'Halloran, *J. Am. Chem. Soc.*, 1994, **116**, 7431.

4 M. Ray, G. P. A. Yap, A. Rheingold and A. S. Borovik, *J. Chem. Soc., Chem. Commun*., 1995, 1777; M. Ray, A. P. Golombek, M. P. Hendrich, V. G. Young Jr. and A. S. Borovik, *J. Am. Chem. Soc.*, 1996, **118**, 6084; B. H. Hammes, D. Ramos- Maldonado, G. P. A. Yap, L. Liable-Sands, A. L. Rheingold, V. G. Young Jr. and A. S. Borovik, *Inorg. Chem.*, 1997, **36**, 3210.

5 Abbreviations: $H_3$**1**$^{cyp}$ = tris(*N*-cyclopentylcarbamoylmethyl)amine; **1** = bis(2-hydroxy-5-nitrobenzyliminopropyl)methylamine.

6 For the use of this concept in probing Fe$^{II}$ and Ru$^{II}$ porphyrin $O_2$ interactions see: A. L. Balch, Y.-W. Chan, R.-J. Cheng, G. N. La Mar, L. Latos-Grazynski and M. W. Renner, *J. Am. Chem. Soc.*, 1984, **106**, 7779; J. T. Groves and R. Quinn, *J. Am. Chem. Soc.*, 1985, **107**, 5790.

7 An example where intramolecular C–H cleavage occurs subsequent to dioxygen activation has been reported: N. Kitajima, M. Osawa, M.Tanaka and Y. Moro-oka, *J. Am. Chem. Soc.*, 1991, **113**, 8952.

8 R. Drago, *Physical Methods in Inorganic Chemistry*, Saunders, Philadelphia, 1977, ch. 11.

9 K. Nakomoto, *Infrared and Raman Spectra of Inorganic and Coordination Compounds*, 3rd edn., Wiley, New York, 1978.

10 D. M. Eichhorn and W. H. Armstrong, *J. Chem. Soc., Chem. Commun.*, 1992, 85.

11 K. Wieghardt, U. Bossek, B. Nuber, J. Weiss, J. Bonvoisin, M. Corbella, S. E. Vitols and J. J. Girerd, *J. Am. Chem. Soc.*, 1988, **110**, 7398; S. Pal and W. H. Armstrong, *Inorg. Chem.*, 1992, **31**, 5417; S. Pal, M. K. Chan and W. H. Armstrong, *J. Am. Chem. Soc.*, 1992, **114**, 6398.

12 M. L. Ludwig, A. L. Metzger, K. A. Pattridge and W. C. Stallings, *J. Mol. Biol.*, 1991, **219**, 335.

13 W. M.Coleman and L. T. Taylor, *Inorg. Chem.*, 1977, **16**, 1114; U. Bossek, T. Weyhermüller, K. Wieghardt, B. Nuber and J. Weiss, *J. Am. Chem. Soc.*, 1990, **112**, 6387.

14 R. R. Jacobsen, Z. Tyeklár, A. Farooq, K. D. Karlin, S. Liu and J. Zubieta, *J. Am. Chem. Soc.* 1988, **110**, 3690; O. M. Reinaud, G. P. A. Yap, A. L. Rheingold and K. H. Theopold, *Angew. Chem., Int. Ed. Engl.*, 1995, **34**, 2051; K. Kim and S. Lippard, *J. Am. Chem. Soc.*, 1996, **118**, 4914.

15 R. H. Holm, *Chem. Rev.*, 1987, **87**, 1401 and references therein.

16 Anaerobic oxidation of [Mn**1**$^{cyp}$(OAc)]$^{2-}$ with ferrocenium yielded a brown species that does not contain a Mn$^{III}$OH moiety.

17 Conversion of Os and Ru hydrides to their corresponding hydroxide complexes *via* $O_2$ has been reported: K. R. Grundy, K. R. Laing and W. R. Roper, *Chem. Commun.*, 1970, 1500.

18 E. Gallo, E. Solari, N. Re, C. Floriani, A. Chiesi-Villa and C. Rizzoli, *Angew. Chem., Int. Ed. Engl.*, 1996, **35**, 1981.

19 $H_3$**1**$^{cyp}$ was recovered quantitatively after dioxygen activation and analyzed by GCMS and NMR spectroscopy.

20 Similar comformations of cyclopentyl (and isopropyl) groups have been observed in other transition-metal complexes of this type of tripodal ligand, unpublished work.[3]

21 C. W. Hoganson, N. lydakis-Simantris, X. Tang, C. Tommos, K. Warncke, G. T. Babcock, B. A. Diner, J. McCracken and S. Styring, *Photosynth. Res.*, 1995, **35**, 15080.

22 Studies on synthetic systems to evaluate this theory have been reported: M. T. Caudle and V. L. Pecoraro, *J. Am. Chem. Soc.*, 1997, **119**, 3415.

*Received in Bloomington, IN, USA; 16th May 1997; 7/03395H*

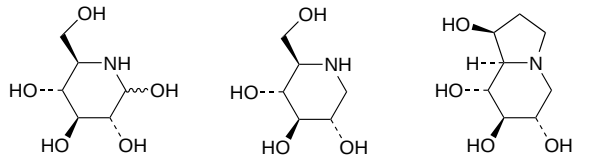
# *N*-Thiocarbonyl azasugars: a new family of carbohydrate mimics with controlled anomeric configuration

**José L. Jiménez Blanco,[a] Víctor M. Díaz Pérez,[a] Carmen Ortiz Mellet,*[a]† J. Fuentes,[a] José M. García Fernández,*[b]‡ Juan C. Díaz Arribas[c] and Francisco J. Cañada[c]**

[a] *Departamento de Química Orgánica, Facultad de Química, Universidad de Sevilla, Apartado 553, E-41071 Sevilla, Spain*
[b] *Instituto de Investigaciones Químicas, CSIC, Américo Vespucio s/n, Isla de la Cartuja, E-41092 Sevilla, Spain*
[c] *Instituto de Química Orgánica General, CSIC, Juan de la Cierva 3, E-28006 Madrid, Spain*

**Bicyclic azasugar glycomimetics structurally related to the polyhydroxy-indolizine and -piperidine series incorporating a stereoelectronically controlled pseudoanomeric axial hydroxy group have been prepared by tautomeric rearrangement of cyclic thiocarbamate precursors; preliminary enzyme inhibition tests show an increased selectivity towards yeast α-glucosidase for the α-D-glucopyranose analogue as compared with castanospermine or nojirimicin.**

Nitrogen-in-the-ring carbohydrate mimics (azasugars) represent an important group of tight-binding glycosyl hydrolase inhibitors useful for studies on glycoconjugate function, targeting and turnover.[1] An additional stimulus of great impact on the synthesis and use of these compounds comes from their application as chemotherapeutic agents for the treatment of several diseases such as diabetes, cancer, inflammation or viral replication, including the human immunodeficiency virus (HIV).[2] Although many potent azasugar glycosidase inhibitors are now available, they generally suffer from lack of specificity. Thus, nojirimycin **1**, a polyhydroxypiperidine derivative having an hydroxylation pattern of spatial similarity to that of D-glucose, and its 1-deoxy analogue **2** are good inhibitors of various α- as well as β-glycosidases. A higher enzyme specificity is observed for the configurationally related indolizidine alkaloid castanospermine **3**, which has been ascribed to the rigidity of the bicyclic structure that locks the homologous bond to C-5–C-6 in hexopyranoses.

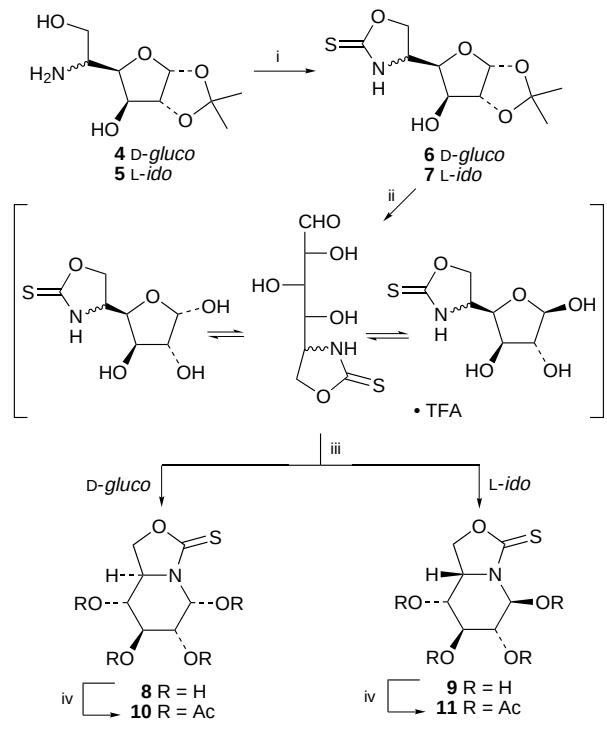


nojirimycin **1** 1-deoxynojirimycin **2** castanospermine **3**

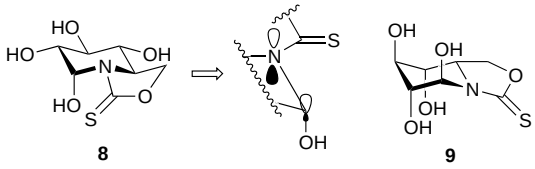
Neither of the above mentioned naturally occurring azasugars, nor virtually all the reported synthetic analogues, possess a defined configuration at the pseudoanomeric centre in aqueous solution. An ideal glycosidase ligand should, however, account for the stereocomplementarity of the leaving aglyconic oxygen atom with the key bilateral carboxylic acid and carboxylate groups in the active site of the enzyme, which is probably responsible for the α- or β-linkage specificity shown by many glycosidases.[3] Although the hydroxy group would be a universal surrogate for the natural glycosidic bond of the putative substrates, its hemiacetalic character results in rapid epimerization and low stability (*e.g.* **1**). In fact, indolizidine azasugars bearing a pseudoanomeric hydroxy substituent are unknown.[4]

We have previously shown that thioamide moieties in six-membered ring systems exert a definitive influence in the orientational properties of vicinal hydroxy groups.[5] Exclusively axial OH dispositions are allowed, probably due to a very efficient delocalization interaction between the π-type lone-pair orbital of the $sp^2$-hybridized N-atom in the ground state of *N*-thiocarbonyl functionalities and the σ* antibonding orbital of the contiguous C–O bond. We have now extended this concept to the preparation of carbohydrate mimics endowed with the favourable structural features of polyhydroxyindolizidines and incorporating a configurationally anchored pseudoanomeric hydroxy group.[6]

The synthetic strategy relies on the ability of the ambident *N*-thiocarbonyl group to act as a nitrogen nucleophile in coupling reactions with carbonyl compounds.[7] Thiocarbonylation of 5-amino-5-deoxy-1,2-*O*-isopropylidene-α-D-glucofuranose **4**, available in eight steps from commercial D-glucofuranurono-3,6-lactone,[8] with carbon disulfide–DCC afforded the five-membered cyclic thiocarbamate **6** in excellent yield.§ Hydrolysis of the acetal protecting group under acidic conditions led to a mixture of the protonated α- and β-furanoses, as seen from a $^{13}C$ NMR spectrum of the crude reaction mixture, which after neutralisation rearranged to the fused bicyclic



**Scheme 1** *Reagents and conditions*: i, $CS_2$, DCC, −10 °C, 6 h, 80–85%; ii, 9 : 1 TFA–$H_2O$, room temp., 2 h; iii, coevaporation with water, then IR 45 ($OH^-$) ion exchange resin, GPC (Sephadex G-10, 1 : 1 MeOH–$H_2O$), 75–90%; iv, 1 : 1 $Ac_2O$–pyridine, room temp., 16 h, quant.




**8** **9**

**Fig. 1** Ring conformation of compounds **8** and **9** showing the OH orientational pattern. The π-electron stabilization interaction responsible of the strong anomeric effect is also represented for the pseudo $^4C_1$ chair conformation of the six-membered ring (*e.g.* **8**).

azasugar **8** by intramolecular nucleophilic addition of the thiocarbamate *N*-atom to the masked aldehydo group of the monosaccharide (Scheme 1).

The $^1$H and $^{13}$C NMR spectra of **8** in $D_2O$ showed the presence of a single tautomeric form having the *R* configuration at the pseudoanomeric centre, *i.e.* a molecular framework analogous to that of α-D-glucopyranose (Fig. 1). No traces of the *S*-epimer or furanoid tautomers were detected even after conventional acetylation (→ **10**), corroborating the total stereoelectronic control induced by the vicinal thiocarbamate segment. The potential of this approach to design glycomimetics bearing a pseudoanomeric oxygen atom with defined configurational and conformational properties is further illustrated by the preparation of the L-*ido* derivative **9** from the corresponding C-5 epimeric amino sugar[8] **5** following a similar reaction sequence (Scheme 1). The all-OH-axial bicyclic tautomer with *S* configuration at the pseudoanomeric centre (Fig. 1) was exclusively detected in $D_2O$ solution or after acetylation (→ **11**).¶ Both the vicinal $^3J_{H,H}$ coupling constants and computational calculations‖ support a rigid conformation for the bicyclic skeleton of **8** close to that of castanospermine **3**. Preliminary glycosyl hydrolase inhibition tests showed, however, a totally different scenario. Considering the most widely used glycosyl hydrolases, sweet almond β-glucosidase and yeast α-glucosidase, the inhibition constants for **8** (150 000 and 90 μmol dm$^{-3}$, respectively)** indicated a reverse linkage specificity as compared to **3** (1.5 and > 1500 μmol dm$^{-3}$) or **1** (0.89 and 6.3 μmol dm$^{-3}$).[1a] Although the latter is a one order of magnitude stronger inhibitor of yeast α-glucosidase than **8**, the selectivity ratio for **8** is above $10^4$-fold higher.

We thank the Dirección General de Investigación Científica y Técnica for financial support (grant no. PB 94/1440-CO2-01 and PB 93/0127-CO2-01) and the Junta de Andalucía for a doctoral fellowship (J. L. J. B.).

## Footnotes and References

† E-mail: mellet@cica.es
‡ E-mail: jogarcia@cica.es

§ The use of thiophosgene or *N*,*N*′-thiocarbonyldiimidazole as thiocarbonylation reagents resulted in lower yields of **6** due to formation of thiocarbamate and thiocarbonate derivatives involving the remaining unprotected OH-3. For previous reports on the reactivity of unprotected amino sugars towards thiocarbonylation reagents see ref. 9.

¶ All new compounds gave satisfactory microanalytical, NMR ($^1$H and $^{13}$C) and mass spectral data in accord with the proposed structures. *Selected data* for **8**: $[\alpha]_D$ +0.8 (*c* 0.8, $H_2O$); $\delta_H$(500 MHz, $D_2O$, *J*/Hz) 5.78 (1 H, d, $J_{1,2}$ 4.0, H-1), 4.77 (1 H, t, $J_{5,6b} = J_{6a,6b}$ = 9.2, H-6a), 4.56 (1 H, dd, $J_{2,3}$ 9.6, H-2), 4.48 (1 H, dd, $J_{5,6b}$ 7.3, H-6b), 4.12 (1 H, ddd, $J_{4,5}$ 9.6, H-5), 3.70 (1 H, t, $J_{3,4}$ 9.6, H-3), 3.50 (1 H, t, H-4). For **9**: $[\alpha]_D$ +64 (*c* 0.8, $H_2O$); $\delta_H$(500 MHz, $D_2O$, *J*/Hz) 5.48 (1 H, d, $J_{1,2}$ 1.4, H-1), 4.62 (1 H, dd, $J_{5,6b}$ 9.4, $J_{6a,6b}$ 7.9, H-6a), 4.50 (1 H, td, $J_{4,5}$ 6.0, $J_{5,6b}$ 7.9, H-5), 4.44 (1 H, t, H-6b), 3.77 (1 H, t, $J_{2,3} = J_{3,4}$ = 3.4, H-3), 3.72 (1 H, dd, H-2), 3.61 (1 H, t, H-4). For clarity of presentation, the notation of atoms for NMR data has been kept consistent with the parent monosaccharides.

‖ Molecular mechanics calculations were performed using MM2* as integrated in MACROMODEL 5.5, using the GB/SA continuum solvent model for $H_2O$.

** β-Glucosidase from almonds and α-glucosidase from yeast were purchased from Aldrich. The inhibition constants were determined spectrophotometrically (410 nm) at 37 °C at pH 5 and 7, respectively. The Michaelis constants $K_M$ obtained for the corresponding *p*-nitrophenyl β- and α-glucosides were 3.5 and 0.25 mmol dm$^{-3}$, respectively.

1 For reviews see: (*a*) G. Legler, *Adv. Carbohydr. Chem. Biochem.*, 1990, **48**, 319; (*b*) M. L. Sinnott, *Chem. Rev.*, 1990, **90**, 1171; (*c*) G. P. Kaushal and A. D. Elbein, *Methods Enzymol.*, 1994, **230**, 316; (*d*) C.-H. Wong, R. L. Halcomb, Y. Ichikawa and T. Kajimoto, *Angew. Chem., Int. Ed. Engl.*, 1995, **34**, 521; (*e*) B. Ganem, *Acc. Chem. Res.*, 1996, **29**, 340.
2 N. Asano, K. Oseki, H. Kizu and K. Matsui, *J. Med. Chem.*, 1994, **37**, 3701; A. D. Elbein, *Semin. Cell Biol.*, 1991, **2**, 309; A. D. Elbein, *Annu. Rev. Biochem.*, 1987, **56**, 497.
3 G. Legler and M.-T. Finken, *Carbohydr. Res.*, 1996, **292**, 103.
4 J. Cossy and P. Vogel, in *Studies in Natural Product Chemistry*, ed. Atta-ur-Rahman, Elsevier, 1993, vol. 12, pp. 275–363.
5 J. L. Jiménez Blanco, C. Oritz Mellet, J. Fuentes and J. M. García Fernández, *Chem. Commun.*, 1996, 2077.
6 J. M. García Fernández, C. Ortiz Mellet, J. L. Jiménez Blanco, V. M. Díaz Pérez, J. M. Benito and J. Fuentes, preliminary results presented at the 9th European Carbohydrate Symposium, Utrecht, Netherlands, 1997, abstract A38.
7 J. M. García Fernández and C. Ortiz Mellet, *Sulfur Rep.*, 1996, **19**, 61.
8 K. Dax, B. Gaigg, V. Grassberger, B. Köblinger and A. E. Stütz, *J. Carbohydr. Chem.*, 1990, **9**, 479.
9 J. M. García Fernández, C. Ortiz Mellet, J. L. Jiménez Blanco and J. Fuentes, *J. Org. Chem.*, 1994, **59**, 5565; J. M. García Fernández, C. Ortiz Mellet and J. Fuentes, *J. Org. Chem.*, 1993, **58**, 5192.

*Received in Glasgow, UK, 6th August 1997; 7/05755E*

# Molecularly imprinted polymer of β-cyclodextrin for the efficient recognition of cholesterol

**Hiroyuki Asanuma, Masaya Kakazu, Masahiko Shibata, Takayuki Hishiya and Makoto Komiyama***

*Department of Chemistry and Biotechnology, Graduate School of Engineering, The University of Tokyo, Hongo, Tokyo 113, Japan*

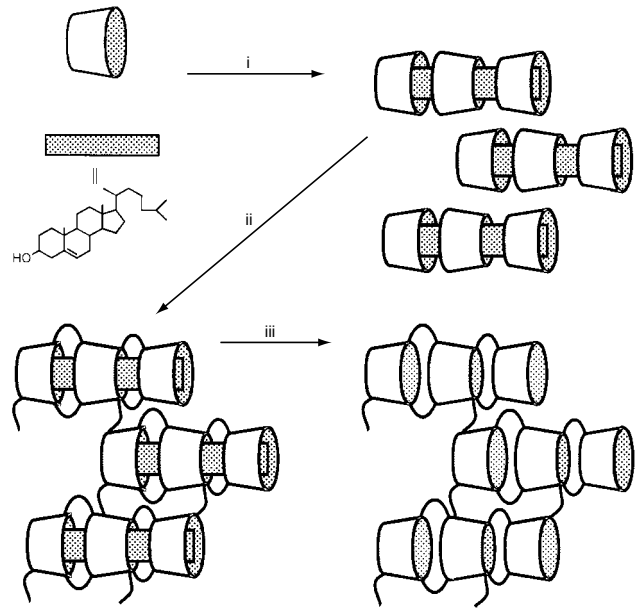
**Polymeric receptors for cholesterol have been prepared by crosslinking β-cyclodextrin with diisocyanates in dimethyl sulfoxide in the presence of cholesterol as template.**

To date, a number of organic receptors which recognize small guest molecules have been synthesized.[1–3] Highly selective guest-binding was successfully achieved by placing appropriate functional residues at the required sites. Furthermore, a molecular imprinting method was developed to prepare tailor-made artificial receptors.[4–10] In this technique, the adducts between a guest and functionalized monomer(s) are polymerized, and hence the positions and orientations of the functional residues of the monomers in the adducts, which fit the physicochemical properties of the guest, are immobilized in the polymers. The studies on the recognition of small guest molecules have been so fruitful that the current interest is gradually focusing on receptors for still larger guests, such as steroids, oligopeptides, oligosaccharides, *etc*. Whitcombe *et al.* prepared a receptor for cholesterol by polymerizing a cholesterol-attached monomer, followed by the removal of the steroid residue.[11] Another promising strategy for the preparation of these receptors is to build up several host molecules, each of which binds a part of the large guest molecule, so that the resultant assembly of the hosts as a whole recognizes the guest.[12] However, the methodology for the construction of these ordered assemblies has not yet been established.

Recently, Breslow and Zhang[13] showed that cholesterol can be bound by a receptor in which two molecules of β-cyclodextrin (β-CyD: a cyclic oligomer of seven glucose units)[14–16] are connected to each other by an appropriate linker. These two β-CyD residues are precisely placed to bind cholesterol, which is too large to be accommodated in the cavity of a single β-CyD residue (free β-CyD forms a 3 : 1 complex with cholesterol).[17] Here we prepare polymeric receptors for cholesterol by crosslinking β-CyD molecules. The mutual orientations of the β-CyD residues are regulated by using the molecular imprinting technique. The crucial importance of the choice of both the crosslinking agent and the solvent for the templating is evidenced.

The templated β-CyD polymers were prepared as depicted in Scheme 1.† In dimethyl sulfoxide (DMSO), the β-CyD–cholesterol complex was treated with either hexamethylene diisocyanate (HMDI) or toluene 2,4-diisocyanate (TDI). After the crosslinking reaction, the cholesterol (used as the template) was removed from the polymer by treatment with acetone, THF and hot EtOH, and this was confirmed from $^{13}$C-CP/MAS NMR spectroscopy. These polymers were then dried and used for the adsorption experiments.

The templated β-CyD polymer, prepared using HMDI as the crosslinking agent (abbreviated as HMDI-Imp), efficiently adsorbed cholesterol, which was present in a water–THF mixture (5 : 6 v/v).‡ The adsorption reaction was completed within 5 min. By this simple procedure, 15% of the cholesterol was removed from the liquid phase (Table 1). The amount of adsorbed cholesterol was proportional to the amount of the polymer. Stigmasterol, a derivative of cholesterol, was also adsorbed by the polymeric receptor in a similar amount (10%). In contrast, non-templated β-CyD polymer (synthesized in the absence of the cholesterol template: HMDI-Non) did not adsorb cholesterol to a measurable extent. Thus, the 'templating' is essential to prepare the polymeric receptor which notably binds cholesterol. The templated polymer TDI-Imp showed an even greater adsorbing activity (70% of the cholesterol was adsorbed). This was probably due to the molecular rigidity of TDI being able to regulate the positions of β-CyD residues more precisely.




**Scheme 1** *Reagents and conditions*: i, hexane–$H_2O$; ii, diisocyanate in DMSO; iii, acetone, $H_2O$, THF, EtOH

All the adsorbed cholesterol was easily removed from the polymeric receptors by treating the polymer–cholesterol adducts with boiling EtOH. On the next run, both the rate of cholesterol adsorption and the adsorbing capacity were identical to those in the foregoing adsorption. Thus, the adsorption described here is totally reversible. The potential applicability

**Table 1** Adsorption of cholesterol from the water–THF mixture by crosslinked β-CyD polymers

| Crosslinking agent | Adsorbing activity[a] | | Templating effect[b] |
|---|---|---|---|
| | Templated | Non-templated | |
| HMDI | 0.15 | < 0.01 | > 15 |
| | (0.05)[c] | (0.05)[c] | (1.0)[c] |
| TDI | 0.70 | 0.19 | 3.7 |
| Epichlorohydrin | < 0.01 | < 0.01 | — |

[a] The ratio of the decrease in cholesterol concentration in the liquid phase to the initial concentration, under the adsorption conditions presented in footnote ‡. [b] The ratio of the adsorbing activity of the templated polymer to that of non-templated polymer. [c] Phenol is used as the guest, in place of cholesterol.

of these adsorbents to practical removal of cholesterol has been indicated.[18]

It is noteworthy that the β-CyD polymers, prepared by crosslinking with epichlorohydrin,[19]§ did not adsorb cholesterol (Table 1; a similar result was reported by Breslow and Zhang).[13] The templated polymer synthesized from the β-CyD–cholesterol complex (in place of free β-CyD) was also inactive. The use of DMSO is advantageous for the 'templating', since the β-CyD inclusion complexes are satisfactorily formed in this solvent.[14,15,20]¶ The formation of well-defined complexes under mild conditions is presumably responsible for the selectivity. The crosslinking of β-CyD by epichlorohydrin is achieved under highly alkaline conditions, where the β-CyD–cholesterol complexes mostly dissociate.

These arguments are further supported by the fact that the adsorbing activity of the HMDI-Imp on phenol was identical with the value of the HMDI-Non (see the numbers in parentheses in Table 1).[14,15]‖ The present finding indicates that artificial polymeric receptors for varieties of large guest molecules can be prepared by using the molecular imprinting technique for the immobilizaton of β-CyD.

This work was partially supported by a Grant-in-Aid for Scientific Research from The Ministry of Education, Science and Culture, Japan. The support by the Kawakami Memorial Foundation (for H. A.) is also acknowledged.

## Footnotes and References

* E-mail: mkomi@chembio.t.u-tokyo.ac.jp

† The 3 : 1 β-CyD–cholesterol complex was prepared according to ref. 17, and was reacted with the diisocyanate agents in dry DMSO at 65 °C for a few hours ([diisocyanate]/[β-CyD] = 4.2). All the reactants (β-CyD, cholesterol and the diisocyanates) were satisfactorily soluble in DMSO. The polymer, obtained by pouring the mixture into acetone, was ground with a mortar and pestle, and then sufficiently washed with hot water, THF and hot EtOH to remove the cholesterol and free β-CyD completely. The ratios of the diisocyanate residue to β-CyD in the polymers were 3.4 for both HMDI and TDI, as estimated by elemental analysis. Non-templated β-CyD polymers were similarly prepared in the absence of the cholesterol template.

‡ The adsorption experiment was carried out by incubating the polymeric receptor (0.5 mmol of β-CyD residue) in 11 ml water–THF (5 : 6 v/v) containing 0.05 mmol of cholesterol. After being magnetically stirred at 25 °C, the mixture was centrifuged and the liquid phase was analysed by gas chromatography. The water–THF mixture was used as the solvent, since the solubility of cholesterol in water is too small and the addition of THF was required to provide homogeneous solutions.

§ The epichlorohydrin-immobilized β-CyD was prepared by reacting β-CyD (25 g) with the crosslinking agent (20 g) at 50 °C in 50 wt% of aqueous NaOH solution, according to ref. 19. The ratio of the crosslinking residue to β-CyD residue in the polymer was 3.6.

¶ The complex formation between β-CyD and cholesterol in DMSO was confirmed by $^1$H NMR spectroscopy using 3-(trimethylsilyl)[2,2,3,3-$^2H_4$]propionic acid as the internal standard. When β-CyD (30 mM) was added to a DMSO solution of cholesterol (2 mM) at 25 °C, the 18 methyl protons of cholesterol, for example, showed upfield shift (0.046 ppm) with respect to the value in the absence of β-CyD. The remarkable 'templating' efficiency is partially associated with the fact that, due to a proximity effect, the β-CyD residues in the cholesterol complex are crosslinked by the diisocyanates more quickly than are free β-CyD molecules in the solutions.

‖ In order to shed light on the role of the cavity of β-CyD in the present cholesterol binding, dextran was crosslinked by HMDI under the conditions employed for the immobilization of β-CyD. The resultant dextran polymer did not adsorb phenol at all. The possibility that phenol is simply adsorbed to either the outside of β-CyD or the crosslinking residue is unlikely. The complex formation between phenol and the templated polymer was further confirmed by solid-state $^{13}$C-NMR: C1 of β-CyD showed a downfield shift of 0.4 ppm on the complex formation, whereas the shift of C4 was marginal. The C2, C3 and C5 carbon atoms could not be sufficiently resolved under the conditions.

1 Y. Kato, M. M. Conn and J. Rebek, Jr., *Proc. Natl. Acad. Sci. USA*, 1995, **92**, 1208.
2 E. Fan, S. A. V. Arman, S. Kincaid and A. D. Hamilton, *J. Am. Chem. Soc.*, 1993, **115**, 369.
3 R. P. Bonar-Law and J. K. M. Sanders, *J. Am. Chem. Soc.*, 1995, **117**, 259.
4 B. Sellergren, M. Lepisto and K. Mosbach, *J. Am. Chem. Soc.*, 1988, **110**, 5853.
5 G. Wulff and S. Schauhoff, *J. Org. Chem.*, 1991, **56**, 395.
6 K. J. Shea, D. A. Spivak and B. Sellergren, *J. Am. Chem. Soc.*, 1993, **115**, 3368.
7 J. Matsui, Y. Miyoshi, O. Doblhoff-Dier and T. Takeuchi, *Anal. Chem.*, 1995, **67**, 4404.
8 J. Matsui, O. Doblhoff-Dier and T. Takeuchi, *Chem. Lett.*, 1995, 489.
9 J. Matsui, Y. Miyoshi, R. Matsui and T. Takeuchi, *Anal. Sci.*, 1995, **11**, 1017.
10 G. Wulff, *Angew. Chem., Int. Ed. Engl.*, 1995, **34**, 1812.
11 M. J. Whitcombe, M. E. Rodriguez, P. Villar and E. N. Vulfson, *J. Am. Chem. Soc.*, 1995, **117**, 7105.
12 (*a*) F. Vögtle, *Supramolecular Chemistry: An Introduction*, 1989, John Wiley, Chichester; (*b*) D. B. Amabilino, P.-L. Anelli, P. R. Ashton, G. R. Brown, E. Córdova, L. A. Godínez, W. Hayes, A. E. Kaifer, D. Philp, A. M. Z. Slawin, N. Spencer, J. F. Stoddart, M. S. Tolley and D. J. Williams, *J. Am. Chem. Soc.*, 1995, **117**, 11 142.
13 R. Breslow and B. Zhang, *J. Am. Chem. Soc.*, 1996, **118**, 8495.
14 M. L. Bender and M. Komiyama, *Cyclodextrin Chemistry*, 1978, Springer-Verlag, Berlin.
15 J. Szèjtlí, *Cyclodextrin Technology*, 1988, Kluwer Academic Publishers, Budapest.
16 Molecular tubes from CyD rotaxanes have been elegantly synthesized by immobilizing the CyDs with epichlorohydrin: (*a*) A. Harada, J. Li and M. Kamachi, *Nature*, 1993, **364**, 516; (*b*) G. Wenz and B. Keller, *Angew. Chem., Int. Ed. Engl.*, 1992, **31**, 197.
17 P. Claudy, J. M. Letoffe, P. Germain, J. P. Bastide, A. Bayol, S. Blasquez, R. C. Rao and B. Gonzalez, *J. Thermal Anal.*, 1991, **37**, 2497.
18 D. G. Oakenfull, R. J. Pearce and G. S. Sidhu, *Aust. J. Dairy Technol.*, 1991, **46**, 110.
19 J. L. Hoffman, *J. Macromol. Sci. Chem.*, 1973, **7**, 1147.
20 B. Siegel and R. Breslow, *J. Am. Chem. Soc.*, 1975, **97**, 6869.

*Received in Cambridge, UK, 16th June, 1997; 7/04176D*

# Photospecific cleavage of one of the cyclopropyl σ-bonds of vinylnorcaradienes

**Shigeo Kohmoto,* Hisao Yajima, Shin-ichi Takami, Keiki Kishikawa, Makoto Yamamoto and Kazutoshi Yamada**

*Department of Materials Science, Faculty of Engineering, Chiba University, Yayoi-cho, Inage-ku, Chiba 263, Japan*

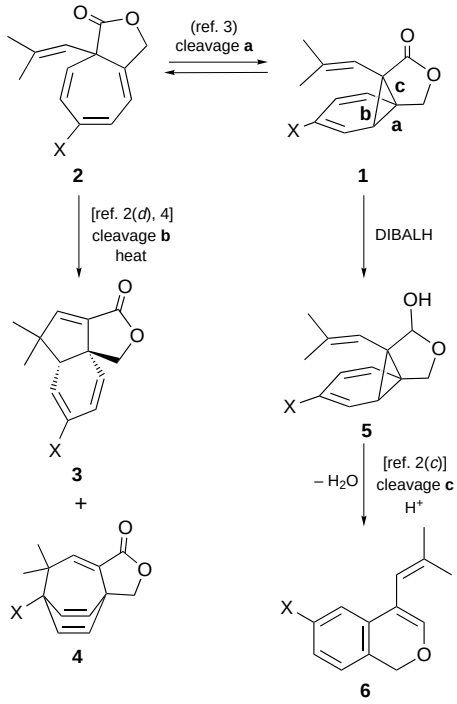
**The benzophenone sensitised photochemical reaction of vinylnorcaradiene derivatives 1, 5-(2-methylprop-1-enyl)-3-oxatricyclo[4.4.0.0$^{1,5}$]deca-7,9-dien-4-ones, resulted in the regioselective cleavage of one of the cyclopropyl σ-bonds to afford the isochroman-3-one derivatives 7.**

With the release of the large ring strain as a powerful driving force, the cleavage and ring expansion of the cyclopropyl ring has been intensively studied and demonstrated to be a useful synthetic tool.[1] The selective cleavage of one of the three cyclopropyl σ-bonds is an interesting subject from both mechanistic and synthetic view points. If the cleavage is perfectly controlled, then one of the three modes of rearrangement can be utilised at choice starting from the same compound. To the best of our knowledge, such a control has never been cited.

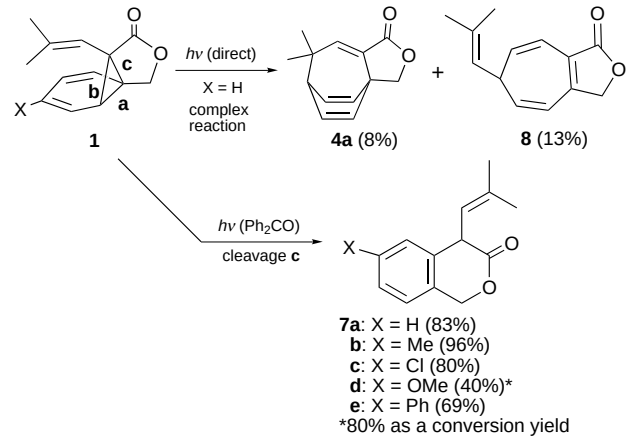
In our study of stable tricyclic vinylnorcaradienes **1**,[2] we have been interested in the photo- and thermo-specific, and regioselective cleavage of the cyclopropyl σ-bonds in the norcaradiene structure. The following three types of cleavage are possible (Scheme 1). The cleavage of bond **a** results in the formation of cycloheptatriene **2**, which corresponds to the norcaradiene–cycloheptatriene equilibrium.[3] The cleavage of the bond **b** has been reported in the thermal rearrangements of vinylnorcaradienes to afford vinylcyclopropane–cyclopentene and Cope rearrangement products, **3** and **4**, respectively.[4] The third type of cleavage, the cleavage of bond **c**, has been shown in the acid-catalysed dehydrative aromatisation of lactols **5** derived from the reduction of **1** to afford **6**.[2c] Here we report on cleavage **c** of **1** which results in the formation of **7** directly.

Since the thermal reaction of **1** led to the cleavage of the cyclopropyl σ-bond **b**,[2d,4] we have investigated the photochemical reaction. In order to survey which part of the molecule, the diene or the carbonyl moiety, would act as the chromophore and be responsible for the photochemical reaction, a PM3 calculation of **1a** was carried out. The calculation showed that the lobe of the 1,3-diene moiety was much larger than the rest of the molecule in the LUMO of **1a**. The carbonyl moiety contributed to the excited state of **1a** in its next LUMO. The energy difference between the two states, the LUMO and the next LUMO, was large (0.94 eV). Therefore, the photochemical reaction of **1a** could possibly be initiated from the excited state of the 1,3-diene moiety.

Direct irradiation of a benzene solution of **1a** (X = H, $2.5 \times 10^{-2}$ M) in a Pyrex test-tube cooled in a water bath was carried out externally with a 400 W high pressure mercury lamp for 5 h through a Pyrex filter under argon bubbling. The photoreaction was complex and two products, **4a**[2d] (X = H, 8%) and **8** (13%) (Scheme 2),† were isolated in low yields by preparative HPLC purification together with 35% recovery of **1a**. The Cope rearrangement product **4a** was the result of the cleavage of bond **b** and **8a** was derived from the 1,5-shift of vinyl group from cycloheptatriene **2a**. The Cope rearrangement product **4a** can also be obtained thermally, however its formation requires heating at over 130 °C.[2d] Therefore, **4a** is almost certainly the photochemical product in the present case. No product corresponding to the rearrangement *via* the cleavage of bond **c** was found. However, when the reaction of **1a** (X = H, 0.12 mmol) was sensitised by the addition of benzophenone (1 equiv.) in benzene (10 ml) and irradiated with a 400 W high pressure mercury lamp for 70 min, **7a** (X = H) was obtained in 83% yield as a sole product.† The triplet excited state of the 1,3-diene moiety is probably responsible for the photorearrangement. This benzophone sensitised photorearrangement also worked well for other vinylnorcaradienes **1b** (X = Me), **1c** (X = Cl), **1d** (X = OMe) and **1e** (X = Ph) to give the




**Scheme 1**




**Scheme 2**

corresponding rearrangement products **7b**–**7e** in 96, 80, 40 (80% as a conversion yield) and 69% yields with irradiation times of 70, 80, 75, 60 and 720 min, respectively.† The reason for the relatively low photoreactivity of **1e** compared to the others is unclear. The phenyl substituent on the diene lowers the energy of the LUMO, from −0.31 eV for **1a** to −0.66 eV for **1e** as calculated by PM3, which might be responsible for inefficient energy transfer. The multiplicity dependent photochemical reaction of cyclohexa-1,3-diene derivatives has been reported.[5] In the present work, the selective cleavage of the cyclopropyl σ-bond **c** requires such a multiplicity dependent reaction of a cyclohexa-1,3-diene chromophore.

The results show a nice contrast to that of the reported thermolysis (cleavage of bond **b**) and provide useful information on the photochemistry of cyclopropane derivatives.[6]

## Footnotes and References

* E-mail: komoto@tcom.tech.chiba-u.ac.jp

† All photo-products gave satisfactory spectral data. *Selected data* for compound **7a**: mp 78.5–79.5 °C; $\nu_{max}$(KBr)/cm$^{-1}$ 1730; $\delta_H$(270 MHz, $CDCl_3$) 1.76 (3 H, d, *J* 1.4 Hz), 1.93, (3 H, d, *J* 1.4 Hz), 4.41 (1 H, d, *J* 8.9 Hz), 5.31 (1 H, d, *J* 13.9 Hz), 5.38 (1 H, d, *J* 13.9 Hz), 5.45 (1 H, qqd, *J* 1.4, 1.4 and 8.9 Hz), 7.39–7.18 (m, 4 H); $\delta_C$(22.4 MHz, $CDCl_3$) 18.29 (q), 25.74 (q), 44.66 (d), 69.21 (t), 116.95 (d), 124.68 (d), 125.90 (d), 127.12 (d), 128.70 (d), 131.57 (s), 134.49 (s), 138.34 (s), 171.97 (s) [Found: $MH^+$, 203.1065. $C_{13}H_{15}O_2$ ($MH^+$) requires 203.1072].

1 B. M. Trost, *Top. Curr. Chem.*, 1986, **133**, 3.
2 (*a*) S. Kohmoto, T. Kawatsuji, K. Ogata, M. Yamamoto and K. Yamada, *J. Am. Chem. Soc.*, 1991, **113**, 5476; (*b*) S. Kohmoto, T. Funabashi, N. Nakayama, T. Nishio, I. Iida, K. Kishikawa, M. Yamamoto and K. Yamada, *J. Org. Chem.*, 1993, **58**, 4764; (*c*) S. Kohmoto, I. Koyano, T. Funabashi, K. Kishikawa, M. Yamamoto and K. Yamada, *Tetrahedron Lett.*, 1995, **36**, 553; (*d*) S. Kohmoto, N. Nakayama, S. Takami, K. Kishikawa, M. Yamamoto and K. Yamada, *Tetrahedron Lett.*, 1996, **37**, 7761; (*e*) S. Kohmoto, I. Koyano, T. Kawatsuji, H. Kasimura, K. Kishikawa, M. Yamamoto and K. Yamada, *Bull. Chem. Soc. Jpn.*, 1996, **69**, 3261.
3 H. Ledon, H. G. Cannic, G. Linstrumelle and S. Julia, *Tetrahedron Lett.*, 1970, 3971; H. Ledon, G. Linstrumelle and S. Julia, *Tetrahedron*, 1973, **29**, 3609; A. Saba, *Tetrahedron Lett.*, 1990, **31**, 4657; M. Kennedy and M. A. McKervey, *J. Chem. Soc., Perkin Trans. 1*, 1991, 2565.
4 P. J. Battye, D. W. Jones and H. P. Tucker, *J. Chem. Soc., Chem. Commun.*, 1988, 495; H. M. L. Davies, D. Smith, B. Hu, S. M. Klenzak and F. J. Hegner, *J. Org. Chem.*, 1992, **57**, 6900.
5 J. S. Swenton, A. R. Crumrine and T. J. Walker, *J. Am. Chem. Soc.*, 1970, **92**, 1406; H. E. Zimmerman and G. A. Epling, *J. Am. Chem. Soc.*, 1970, **92**, 1411.
6 A. Padwa, *Org. Photochem.*, 1979, **4**, 261.

*Received in Cambridge, UK, 21st July 1997; 7/05199I*

# Synthesis and structure of $[Sn(mit)_6Cu_4]$; a $[SnCu_4]$ cage supported by Sn–Cu cluster bonding [mit = $(\overline{CH)_2N(Me)C(=S)=N}$]

**Robert E. Allan,[a] Alan Bashall,[b] Julie S. Palmer,[a] Mary McPartlin,[b] Marta E. G. Mosquera,[a] Jeremy M. Rawson,[a] Andrew E. H. Wheatley[a] and Dominic S. Wright*[a]**

[a] *Chemistry Department, University of Cambridge, Lensfield Road, Cambridge, UK CB2 1EW*
[b] *School of Applied Chemistry, University of North London, Holloway Road, London, UK N7 8DB*

**The reaction of $[Sn(mit)_2]_n$ with CuCl gives the heterobimetallic complex [{$Sn(mit)_6Cu_4$] 1, in which the *hypho*-hexagonal-bipyramidal $[SnCu_4]$ core is stabilised by $Sn^{II}$–$Cu^{I}$ cluster bonding between the *endo* lone pair of the Sn centre and the tetrahedral $Cu_4$ fragment.**

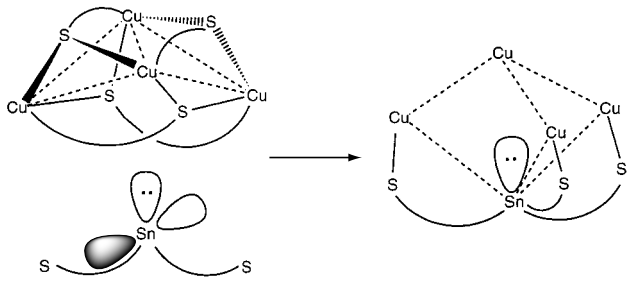
Much of our recent research has focused on the applications of a range of neutral and anionic p-block metal based ligands in the preparation of mixed-metal complexes.[1,2] The organometallic anions of group 14 metals ($[R_3E]^-$; E = Ge–Pb)[2b,3] and their metallo-organic relatives ($[\{RY\}_3E]^-$; Y = O, S, N, P)[1a,4] are a readily prepared and extensive class of ligands. Unfunctionalised tri(organo) metal anions have been employed as metal-centred monodentate ligands to a variety of main-group[3] and transition metals,[5] giving heterobimetallic complexes containing metal–metal bonds. In contrast, the metallo-organic derivatives [*e.g.* tris(alkoxy) and tris(amido) stannates] generally act as bidentate or tridentate ligands, utilising the heteroatoms in their coordination to metal ions.[4,6] However, the ability of these species to behave as multifunctional (metal- and heteroatom-centred) ligands has been utilised in the construction of mixed-metal complexes such as [{$(CO)_5MSn(\mu$-$OBu^t)_3In\{Mo(CO)_5\}$] (M = Cr, Mo).[7]

We report here that the addition of [CuCl] to a suspension of $[Sn(mit)_2]_n$[8] [mit = $(\overline{CH)_2N(Me)C(=S)=N}$] in thf gives the novel heterobimetallic cage complex $[Sn(mit)_6Cu_4]$ **1**.† The complex contains an unprecedented $SnCu_4$ cage arrangement in which a tris(amido) stannate unit supports the cluster by a combination of heteroatom and metal-centred donation. The synthesis of **1** can be conceived as occurring *via* the initial formation of $[Cu(mit)]_4$[9e] which is then complexed by a $[Sn(mit)_2]$ monomer (Scheme 1). The latter can be described as a synergic complexation reaction (*i.e.* resulting from a combination of N donation to Sn and lone pair donation from Sn to Cu).

A low-temperature (173 K) crystallographic study of **1**‡ shows it to be the heterobimetallic $Cu^{I}Sn^{II}$ complex $[Sn(mit)_6Cu_4]$ (Fig. 1), which has crystallised with four molecules of thf. The cage molecules of **1** are constructed from a $C_{3v}$ symmetric *hypho*-hexagonal $[SnCu_4]$ metal core linked together by a combination of N,S- and N,μ-S-chelating mit ligands.[9] The $Sn^{II}$ atom of **1**, which is bonded to the N centres of three mit ligands [Sn(1)–N(5a) 2.202(6) Å], adopts a typical-pyramidal geometry [N(5a)–Sn–N(5aa) 90.0(2)°] which is symptomatic of the presence of a stereochemically active *endo* lone pair, which is directed along the major axis of the $[SnCu_4]$ core, toward Cu(3). Three symmetry related mit ligands form bridges between the Sn atom and each of the equatorial Cu atoms of the core [S(7a)–Cu(2) 2.266(2) Å], with the remaining mit ligands N,μ-S-chelating the three available $Cu_3$ faces of the $Cu_4$ pyramid. The arrangement of the mit ligands in **1** results in identical trigonal planar geometries for the equatorial Cu centres and in a pyramidal coordination geometry for the apical Cu atom [S(7b)–Cu(3)–S(7ba) 113.78(5)°]. The remaining vacant coordination site of the latter corresponds to the shortest Sn···Cu contact made with the $Sn^{II}$ lone pair [Sn(1)···Cu(3) 2.727(2) Å being close to the sum of the metallic radii 2.69 Å,[10] Sn(1)···Cu(3)–S(7b) 104.72(7)°]. In addition, the Sn centre also has longer interactions with the equatorial Cu atoms of the $Cu_4$ fragment [Sn(1)···Cu(2) 2.902(1) Å].

Although no Ge–, Sn– or Pb–$Cu^{I}$ bonded complexes have been structurally characterised, bonds between the heavier group 14 elements and $Au^{I}$ have been observed in a number of simple σ-bonded complexes.[11] The presence of relatively short Sn···Cu contacts in **1** and the geometries of Cu(3) and Sn(1) strongly indicate that Cu–Sn bonding supports the core. In addition, the involvement of the Sn centre results in a large rearrangement in the $Cu_4$ core from the folded-square arrangement present in $[Cu(mit)]_4$ {Cu···Cu range 2.671(2)–3.132(2) Å in $[Cu(mit)]_4$;[9e] Cu(2)···Cu(3) 2.683(1) in **1**; *cf.* 2.56 Å in Cu metal}.[10]

In order to assess the extent to which Sn···Cu and Cu···Cu interactions support the cage of **1**, an extended Hückel molecular orbital (EHMO)[12] calculation was performed on its $[SnCu_4]^{6+}$ metal core.§ The lowest lying metal–metal bonding




**Scheme 1**

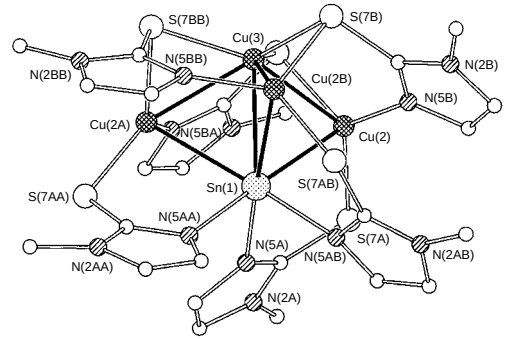



**Fig. 1** Cage structure of **1**, showing the $SnCu_4$ arrangement. Key bond lengths (Å) and angles (°); Sn(1)···Cu(2) 2.902(1), Sn(1)···Cu(3) 2.727(2), Cu(2)···Cu(3) 2.683(1), Sn(1)–N(5a) 2.202(6), Cu(2)–S(7a) 2.266(2), Cu(2)–S(7ba) 2.300(2), Cu(3)–S(7a) 2.315(2), Cu(2)–N(5b) 1.967(6), C(6a)–S(7a) 1.731(7), C(6a)–N(5a) 1.335(9), C(6b)–S(7b) 1.736(8), C(6b)–N(5b) 1.34(1); S(7b)–Cu(3)–S(7ba) 113.78(5), Sn(1)···Cu(3)–S(7b) 104.72(7), N(5a)–Sn–N(5aa) 90.0(2).

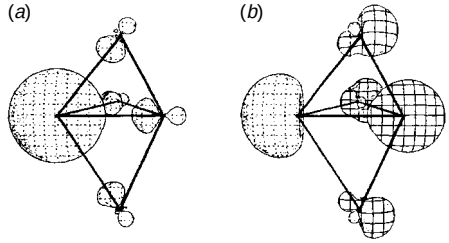



**Fig. 2** Extended Hückel molecular orbital calculation (EHMO) of $[SnCu_4]^{6+}$; (*a*) lowest metal-metal bonding MO, (*b*) the out-of-phase combination (LUMO)

orbital involves the totally in-phase interaction of the $Sn^{II}$ lone pair with all four Cu centres [Fig. 2(*a*)], with the corresponding out-of-phase interaction forming the LUMO [Fig. 2(*b*)]. The bonding between the metal centres is predominantly of s or s/p character, with less than 10% d character being contributed from the Cu centres. The strongest bonding interaction occurs between Sn and the apical Cu centre (overlap population 0.15), with weaker bonding occurring between the Sn and equatorial Cu atoms (overlap population 0.10) and with Cu···Cu interactions only being present between the apical and equatorial Cu ions (overlap population 0.07). The formation of the $[SnCu_4]^{6+}$ cluster is accompanied by the donation of charge from $Sn^{II}$ approximately equally to the $Cu^{I}$ centres (total 0.35 e). The magnitudes of the Cu···Cu interactions in **1** are similar to those calculated by Hoffman for naked $[Cu]_4^{4+}$ using the same EHMO parameters.[13] The small attraction between the Cu centres in the latter arises from mixing of the s and p orbitals with the d orbitals.[13] The cluster MO of **1** corresponds to a similar combination of Cu atomic orbitals as in $[Cu]_n^{n+}$ with the s orbital of Sn. Clearly, the geometric constraints and bonding preferences of the ligands are likely to have the largest effect on the metal core geometry of **1**. However, the structural and calculational findings support the view that weak Sn···Cu metal–metal cluster bonding reinforces the cage arrangement.

We gratefully acknowledge the EPSRC (R. E. A., M. M., J. S. P.), the Royal Society (D. S. W.), the Leverhulme Trust (M. A. B.) and the Spanish Government (M. E. G. M) for financial support.

## Footnotes and References

† *Synthesis of* **1**; [$Bu^tNH_2$] (0.26 ml, 2.5 mmol) was added to a solution of [$Sn(NMe_2)_2$] (0.52 g, 2.5 mmol) in toluene (20 ml). After bringing briefly to reflux, a yellow solution of $[SnNBu^t]_4$ was produced to which was added Hmit (0.28 g, 2.5 mmol). Stirring at room temp. (10 min) gave a white precipitate {later confirmed by elemental analysis and $^1$H NMR to be $[Sn(mit)_2]_n{\cdot}xC_6H_5Me$ ($x$ = 0.4–0.5)} The solvent was removed under vacuum and thf was added (20 ml). CuCl (0.125 g, 1.25 mmol) was added and, after stirring the mixture at reflux (5 min), a clear yellow solution was produced. Removal of *ca.* 10 ml of solvent under vacuum and subsequent storage at room temp. (2 d) gave colourless cubic crystals of **1** (0.17 g, 52% with respect to CuCl supplied). Decomp. *ca.* 200 °C with final melting at *ca.* 320 °C; IR (Nujol), $\nu_{max}$/cm$^{-1}$ 1541w, 1524m (C≒C and C≒N str), 1294s, 1280s, 1143s, 1124s, 1063s, 743s, 716s, 697s, 679s; $^1$H NMR [250 Mz, $(CD_3)_2SO$, +25 °C], $\delta$ 6.89 (s, CH of mit), 3.58 (m, thf), 3.43 (s, Me of mit), 1.78 (m, thf); $^{119}$Sn [149.1 MHz, $(CD_3)_2SO$, +25 °C, relative to $SnCl_2$–$D_2O$], $\delta$ 317.3 (s); analytical results indicate that only *ca.* 1.5 thf molecules are retained in the lattice when **1** is isolated under vacuum (0.1 atm, 10 min). Found C, 31.2; H, 3.7; N, 14.2. Calc. for $[Sn(mit)_6Cu_4]{\cdot}1.5$thf: C, 31.1; H, 3.6; N, 14.5%.

‡ *Crystal data* for **1**·4thf: $C_{40}H_{72}Cu_4N_{12}O_4S_6Sn$, $M$ = 1340.23, rhombohedral, space group $R\bar{3}$, $a$ = 16.0538(6), $c$ = 39.001(3) Å, $U$ = 8704.8(8) Å$^3$, $Z$ = 6, $D_c$ = 1.552 Mg m$^{-3}$, $\lambda$ = 0.710 73 Å, $T$ = 173(2) K, $\mu$(Mo-K$\alpha$) = 2.15 mm$^{-1}$, $F$(000) = 4080. Data were collected on a Siemens P4 diffractometer using an oil-coated rapidly cooled crystal[14] of dimensions 0.32 × 0.30 × 0.28 mm by the $\theta$–2$\omega$ method (1.55 ≤ $\theta$ ≤ 24.92°). Of a total of 4144 collected reflections, 3363 were independent ($R_{int}$ = 0.0791). The structure was solved by direct methods and refined by full-matrix least-squares on $F^2$ to final values of $R_1[F > 4\sigma(F)]$ = 0.062 and $wR_2$ = 0.192 (all data);[15,16] largest peak and hole in the final difference map 1.299 and −1.318 e Å$^{-3}$. Three symmetry related molecules of thf had slight configurational disorder and a fourth thf molecule was equally disordered over two sites of $C_3$ symmetry. CCDC 182/583.

§ Calculations were carried out using the same arrangement as found in the solid-state structure of **1**. Parameters utilised- Sn, $\zeta_s$ 2.120, $H_s$ −16.16, $\zeta_p$ 1.820, $H_p$ −8.32; Cu $\zeta_s$ 2.200, $H_s$ −11.40, $\zeta_p$ 2.200, $H_p$ −6.06, $\zeta_{d1}$ 5.950, $H_d$ −14.00, $c_1$ 0.5933, $\zeta_{d2}$ 2.300, $c_2$ 0.5744.

1 M. A. Paver, C. A. Russell and D. S. Wright, *Angew. Chem.*, 1995, **107**, 1077; *Angew. Chem., Int. Ed. Engl*., 1995, **34**, 1545; M. A. Beswick, C. N. Harmer, M. A. Paver, P. R. Raithby, A. Steiner and D. S. Wright, *Inorg. Chem.*, 1997, 36, 1740; D. Barr, A. J. Edwards, S. Pullen, M. A. Paver, P. R. Raithby, M.-A. Rennie, C. A. Russell and D. S. Wright, *Angew. Chem.*, 1994, **106**, 1960; *Angew. Chem., Int. Ed. Engl*., 1994, **33**, 1875; A. J. Edwards, M. A. Paver, M.-A. Rennie, C. A. Russell, P. R. Raithby and D. S. Wright, *Angew. Chem.*, 1995, **107**, 1088; *Angew. Chem., Int. Ed. Engl*., 1995, **34**, 1012.

2 (*a*) C. Belle, M. A. Beswick, M. K. Davies, P. R. Raithby, A. Steiner and D. S. Wright, *Chem. Commun.*, 1996, 2619; (*b*) M. A. Beswick, M. K. Davies, P. R. Raithby, A. Steiner and D. S. Wright, *Organometallics*, 1997, **16**, 1109.

3 D. Reed, D. Stalke and D. S. Wright, *Angew. Chem.*, 1991, **103**, 1539; *Angew. Chem., Int. Ed. Engl.*, 1991, **30**. 1459; P. B. Hitchcock, M. F. Lappert, G. A. Lawless and B. Royo, *J. Chem. Soc., Chem. Commun.*, 1993, 554; D. R. Armstrong, M. G. Davidson, D. Moncrieff, D. Stalke and D. S. Wright, *J. Chem. Soc., Chem. Commun.*, 1992, 1413.

4 M. Veith, *Coord. Chem. Rev.*, 1990, **90**, 3 and references therein.

5 See for example: F. Calderazzo, F. Pampaloni, G. Pelizzi and F. Vitali, *Polyhedron*, 1988, **7**, 2039; B. Crociani, M. Nicolini, D. A. Clemente and G. Bandoli, *J. Organomet. Chem.*, 1973, **49**, 249.

6 See for example: A. Steiner and D. Stalke, *J. Chem. Soc., Chem. Commun.*, 1993, 1702; M. Veith and R. Rösler, *Angew. Chem.*, 1988, **94**, 867; *Angew. Chem., Int. Ed. Engl.*, 1988, **27**, 1381.

7 M. Veith and K. Kunze, *Angew. Chem.*, 1991, **30**, 92; *Angew. Chem., Int. Ed. Engl.*, 1991, **103**, 95.

8 Several mixed-metal complexes have been prepared by the reactions of early main-group metal thiolato complexes with transition-metal salts, for examples, see M. G. Davidson, P. R. Raithby, R. Snaith, D. Stalke and D. S. Wright, *Angew. Chem.*, 1991, **103**, 1696; *Angew. Chem., Int. Ed. Engl.*, 1991, **30**, 1648; M. G. Davidson, S. C. Llewellyn, M.-I. Lopez-Solera. P. R. Raithby, R. Snaith and D. S. Wright, *J. Chem. Soc., Chem. Commun.*, 1992, 573.

9 For other complexes of $Cu^{I}$ containing *N*,*S*-bridged organic groups, see: (*a*) E. S. Raper, *Coord. Chem. Rev*., 1985, **61**, 115; (*b*) P. Karagiannidas, P. Aslamidis, S. Papastefanon, D. Mentzafos, H. Hountas and A. Tergis, *Inorg. Chim. Acta*, 1989, **156**, 265; (*c*) R. Uson, A. Laguna, J. Jimenez, M. P. Gomez, A. Sainz and P. G. Joner, *J. Chem. Soc., Dalton Trans.*, 1990, 3457; (*d*) E. W. Ainscough, B. F. Anderson, E. N. Baker, A. G. Bingham, M. L. Brader, A. M. Brodie and G. J. Gainsford, *Inorg. Chim. Acta*, 1985, **105**, L5; (*e*) E. S. Raper, J. R. Creighton and W. Clegg, *Inorg. Chim. Acta*, 1991, **183**, 179; (*f*) J. P. Fackler Jr., C. A. Lopez, R. L. Staples, S. Wang, R. E. P. Winpenny and R. P. Lattimer, *J. Chem. Soc., Chem. Commun.*, 1992, 146; (*h*) M. A. Beswick, C. Brasse, M. A. Halcrow, P. R. Raithby, C. A. Russell, A. Steiner, R. Snaith and D. S. Wright, *J. Chem. Soc., Dalton Trans.*, 1996, 3793.

10 M. L. McGlashan, *Chemistry Data Book*, ed. J. G. Stark and H. G. Wallace, John Murray, London, 1976 and references therein.

11 (*a*) W. Clegg, *Acta Crystallogr. Sect. B*, 1978, **34**, 278; (*b*) Z. Demidowicz, R. L. Johnson, J. C. Machell, D. M. P. Mingos and J. D. Williams, *J. Chem. Soc., Dalton Trans.*, 1988, 1751; (*c*) S. Wang, G. Garson, C. King, J.-C. Wang and J. P. Fackler Jr., *Inorg. Chem.*, 1989, **28**, 4623; (*d*) D. M. P. Mingos, H. R. Powell and T. L. Stolbert, *Transition Met. Chem.*, 1992, **17**, 334; (*e*) A. Bauer and H. Schmidbauer, *J. Am. Chem. Soc.*, 1996, **118**, 5324; (*f*) M. Contel, K. W. Hellmann, L. H. Gade, I. J. Scowen, M. McPartlin and M. Laguna, *Inorg. Chem.*, 1996, **35**, 3713.

12 C. Mealli and D. M. Proserpio, *J. Chem. Educ.*, 1990, **67**, 399 (PC version 4.0, 1994).

13 P. K. Mehrotra and A. Hoffman, *Inorg. Chem.*, 1978, **17**, 2187.

14 D. Stalke and T. Kottke, *J. Appl. Crystallogr.*, 1993, **26**, 615.

15 SHELXTL PC version 5.03, Siemens Analytical Instruments, Madison, WI, 1994.

16 G. M. Sheldrick, SHELXA, University of Göttingen, 1990.

*Received in Cambridge, UK, 21st July 1997; 7/05220K*

# Covalent surface confinement of osmium–terpyridine complexes: a UV–VIS and XPS study

**Mai Zhou, J. Mickey Laux, Kimberly D. Edwards, John C. Hemminger and Bo Hong***

*Department of Chemistry, University of California, Irvine, CA 92612, USA*

**Well defined monolayers of $–Si(CH_2)_4Ph–tpy–OsCl_3$, $–Si(CH_2)_4Ph–tpy–Os(tpy)$ and $–Si(CH_2)_4Ph–tpyOsCl–(PPh_2)_2C=C=C(PPh_2)_2–Os(bpy)_2$ (tpy = 2,2′:6′,2″-terpyridine, bpy = 2,2′-bipyridine) on polycrystalline quartz surfaces are prepared and studied by UV–VIS and X-ray photoelectron spectroscopy.**

Well defined monolayers and multilayers containing chromophores and redox-active centers are important owing to their diverse applications in photocatalysis, light-harvesting, nonlinear optical materials, and sensor technology.[1–5] We report here the preparation of monolayers and multilayers containing covalently confined osmium–terpyridine chromophores and the subsequent characterization using electronic absorption and X-ray photoelectron spectroscopy. Osmium–terpyridine complexes are known to be photostable and have well known solution-state absorption, luminescence, and redox properties.[6] Upon incorporation into the self-assembled organosilane monolayer structures *via* covalent linkage, surface-confined osmium–terpyridine units, in combination with other building block modifications, may allow the expedient assembly of robust monolayer and multilayer structures.

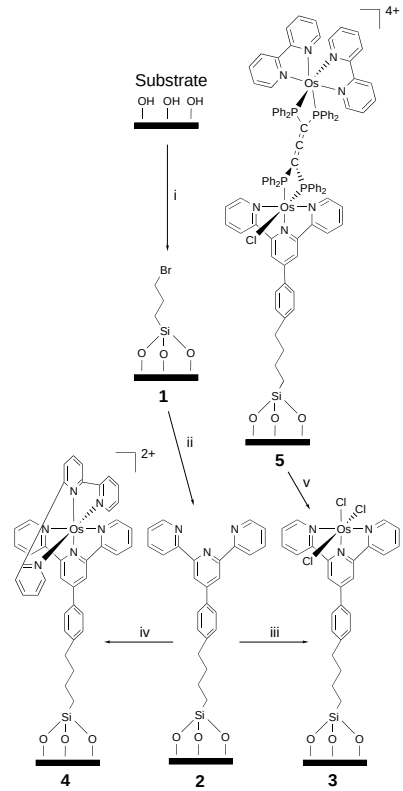
Scheme 1 illustrates the present approach to Os-containing monolayers and multilayers on polycrystalline quartz surfaces. It involves the initial direct reaction of a carbanion derived from a methyl-substituted terpyridine ligand with a preformed bromoalkylsilane surface,[4,5] giving a hydrocarbon tether to the quartz surface (Scheme 1, steps i and ii). The subsequent attachment of $OsCl_3$ to the modified surface was obtained by refluxing in aqueous ethanolic solution of $OsCl_3·3H_2O$ for 3 h. The surface treatment with $Os(tpy)Cl_3$ (tpy = 2,2′:6′,2″-terpyridine), in the presence of $NH_4PF_6$, step iv, was carried out in a similar way but with much longer refluxing time (up to 3 d) to ensure the completion of surface attachment. This results in the monolayer **4** with terminal –tpy–Os–tpy units.

Also shown in Scheme 1, the terminal $OsCl_3$ units in monolayer **3** can be used as structural motifs in the further construction of multilayer structures, since Cl ligands can be replaced by σ or π ligands such as phosphine or polypyridine units in other molecular building blocks. Step v shows a representative reaction of surface confined $–OsCl_3$ units with a monometallic building block $[Os(bpy)_2\{(PPh_2)_2C=C=C(PPh_2)_2\}][PF_6]_2$† (bpy = 2,2′-bipyridine) in refluxing thf for 24 h,[7] giving the bilayer thin film **5**.

Spectrophotometric changes are monitored during the surface treatment using UV–VIS spectroscopy. Polycrystalline quartz has no significant absorption above 250 nm. Upon surface modification, typically we observe a weak increase of absorption after attachment of $–Si(CH_2)_4Ph–tpy$. Broad absorption bands at about 280 and 320 nm are observed upon addition of Os centers. The intensity of these two peaks increases as a function of reaction time and reaches maximum after three days. No significant increase or decrease in absorbance is observed after 3 d, indicating that a stable monolayer with terminal $–CH_2Ph–tpy–Os–tpy$ units is obtained.

The UV–VIS spectrum of the solution sample of $Os(ttp)(tpy)(PF_6)_2$‡ (ttp = $CH_3Ph–tpy$) has absorption bands at 275 nm ($\varepsilon$ = 28 430 dm$^3$ mol$^{-1}$ cm$^{-1}$), 315 (43 100), 485 (11 490) and 665 (2840). When compared with the solution sample, the observed transition bands of the surface bound $–CH_2Ph–tpy–Os–tpy$ units in sample **4** are relatively broad and slightly shifted (shift *ca.* 5 nm towards longer wavelength), and tailed into 500 nm. However, no significant $^3$MLCT band in the range 500–700 nm is observed for the surface samples with attached Os centers owing to the much lower absorption coefficient of the band at 665 nm.§

The calculation of surface coverage, using UV–VIS spectroscopy, has also been carried out. The solution $\varepsilon_{max}$ values were assumed to be invariant in order to provide an approximation to the two-dimensional surface absorption coefficients ($\varepsilon_s$) in the calculations.[4,5] Using the lowest energy π–π* transition at 280 nm, the estimated values of monolayer surface coverages for modified surfaces with terminal $–CH_2Ph–tpy–Os–tpy$ ($\varepsilon_{s,280}$ = 2.8 × 10$^7$ cm$^2$ mol$^{-1}$) and $–CH_2Ph–tpy–OsCl_3$ ($\varepsilon_{s,280}$ = 1.2 × 10$^7$ cm$^2$ mol$^{-1}$) units are 2.0 × 10$^{-10}$ and 3.6 × 10$^{-10}$ mol cm$^{-2}$, respectively. These values are comparable with the reported values (typically, 1 × 10$^{-10}$ mol cm$^{-2}$) of the surface coverages for monolayers with complexes of Fe, Ru or Re.[4,5] The estimated surface coverage for bilayer with $–CH_2Ph–tpy–$




**Scheme 1** *Reagents and conditions*: i, $Br(CH_2)_3SiCl_3$, thf, ambient temp.; ii, 4′-tolyl-2,2′:6′,2″-terpyridine and LDA, thf, ambient temp.; iii, $OsCl_3·3H_2O$, EtOH–$H_2O$ (1:1), reflux 3 h; iv, $[Os(tpy)Cl_3]$, $NH_4PF_6$, EtOH–$H_2O$ (1:1), reflux for up to 3 d; v, $[Os(bpy)_2\{(PPh_2)_2C=C=C(PPh_2)_2\}][PF_6]_2$, thf, reflux 24 h

**Table 1** X-Ray photoelectron spectroscopic analysis of modified surfaces

| Surface-confined units[a] | Binding energy/eV | | | | | | | |
|---|---|---|---|---|---|---|---|---|
| | Si 2p | O 1s | C 1s | Br 3d | N 1s | Os 4f | Cl 2p | P 2p |
| –$Si(CH_2)_3$–Br **1** | 107.15 | 536.40 | 288.40 | 74.60 | | | | |
| –$Si(CH_2)_3$–ttp **2** | 106.20 | 535.80 | 287.85 | | 402.40 | | | |
| –$Si(CH_2)_3$–ttp–$OsCl_3$ **3** | 106.20 | 535.80 | 287.85 | | 402.40 | 53.85<br>56.45 | 200.00 | |
| –$Si(CH_2)_3$–ttp–Os–tpy **4** | 105.80 | 535.95 | 287.60 | | 402.75 | 53.80<br>56.40 | | |
| –$Si(CH_2)_3$–ttp–OsCl–$P_4C_3$–$Os(bpy)_2$ **5** | 106.00 | 535.50 | 287.85 | | 402.40 | 53.30<br>55.90 | —[b] | —[b] |

[a] $P_4C_3$ = $(PPh_2)_2C{=}C{=}C(PPh_2)_2$; ttp represents a –$CH_2$Ph–tpy unit. [b] Not observed; P peak position overlaps with Si.

$OsCl[(PPh_2)_2C{=}C{=}C(PPh_2)_2]Os(bpy)_2$ ($\varepsilon_{s,280}$ = $4.4 \times 10^7$ $cm^2$ $mol^{-1}$) units is $2.7 \times 10^{-11}$ mol $cm^{-2}$.

We have monitored each surface modification step by studying the modified surfaces by XPS (Fig. 1).[8] The elements involved in our modification procedures have their characteristic binding energies which can be clearly identified. Representative XPS data observed in each modification step are included in Table 1. Specifically, the successful modification of quartz surfaces by 3-bromopropyltrichlorosilane (step i) was verified by observation of Br 3d XPS (74.60 eV) in addition to Si 2p (107.15 eV), O 1s (536.40 eV) and C 1s (288.40 eV). Upon further reaction of terminal Br group with lithiated ttp ligand, step ii, N 1s (402.40 eV) is observed, while no significant Br 3d peak is found. After step iii or iv, XPS analysis gives Os 4f at 53.85 eV ($4f_{7/2}$) and 56.45 eV ($4f_{5/2}$) for sample **3** as well as 53.80 eV ($4f_{7/2}$) and 56.40 eV ($4f_{5/2}$) for sample **4**, all of which are characteristic of the Os 4f peaks.[9] Upon further addition of the $Os(bpy)_2[(PPh_2)_2C{=}C{=}C(PPh_2)_2]$ unit, the observed Os 4f peaks in sample **5** shifted to slightly lower energies, with 53.30 and 55.90 eV for $4f_{7/2}$ and $4f_{5/2}$, respectively. Since there are both $Os^{III}$ and $Os^{II}$ centers in **5** and the reported energies of 4f peaks of $Os^{II}$ are slightly lower than those of $Os^{III}$ {*i.e.*, with the same types of ligands, $4f_{7/2}$ is *ca.* 50.2–50.8 eV in $[Os^{II}Cl_2(PhPMe_2)_4]$ and *ca.* 51.4–52.0 eV in $[Os^{III}Cl_3(PhPMe_2)_3]$[9]}, the small shift of Os 4f peaks in **5** towards the lower energy region may be, partly, due to the overlapping Os 4f peaks of both $Os^{II}$ and $Os^{III}$ centers. No XPS peak corresponding to P can be unambiguously identified owing to the overlap of its peak with that of Si. Efforts have also been made to identify the peak corresponding to the inner Cl ligand on the $Os^{III}$ center in **5**, but no significant peak is observed.

A control experiment has been carried out in order to verify whether Os-based units could, instead of a covalent linkage, adsorb on quartz surfaces. After we refluxed $OsCl_3$ or $[Os(tpy)(ttp)(PF_6)_2]$ with clean quartz slides (no modification steps i–ii used) in EtOH–$H_2O$ for 3 d and followed the same cleaning procedures, no significant change was observed in either UV–VIS or XPS analysis of treated surfaces when compared with that of clean quartz surface. This indicates that without the modification steps i and ii, Os-based units cannot be attached to quartz surfaces.

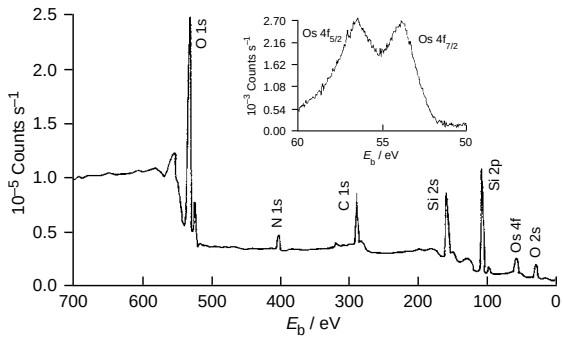



**Fig. 1** XPS spectra of modified surface with attached –$Si(CH_2)_4$Ph–tpy–Os–tpy after 3 d reaction (inset: high-resolution scan of the Os 4f region)

This work is supported by the startup funds of UCI and Faculty Research Grant from UCI Academic Senate Committee on Research. Acknowledgment is made to the donors of The Petroleum Research Fund, administrated by the ACS, for partial support of this research. B.H. also gratefully acknowledges support from UCI Faculty Career Development Award.

## Footnotes and References

* E-mail: bhong@uci.edu

† Preparation of $Os(bpy)_2[(PPh_2)_2C{=}C{=}C(PPh_2)](PF_6)_2$. $(PPh)_2C{=}C{=}C(PPh_2)$[10] (296 mg, 0.38 mmol) in 15 ml thf was heated to reflux under $N_2$, and $[Os(bpy)_2Cl_2]\cdot 2H_2O$ (100 mg, 0.16 mmol) in ethylene glycol was added dropwise. The resulting solution was refluxed for 2 h, and excess $NH_4PF_6$ was added. The solution mixture was then refluxed for 60 h. Upon removal of thf, the solution was added dropwise to 100 ml of saturated aqueous $KPF_6$ solution. The precipitate thus formed was collected by vacuum filtration. Yield: 89%. $^{31}P\{^1H\}$ NMR ($CD_3CN$, 202 MHz, 22 °C): $\delta$ −30.49, −37.37. FABMS: *m/z* 1425 $(M - PF_6)^+$.

‡ *Preparation of* $[Os(tpy)(ttp)(PF_6)_2]$: $[Os(tpy)(H_2O)_3][PF_6]_3$ (50 mg, 0.09 mmol) and ttp (50 mg, 0.15 mmol) were heated at *ca.* 150 °C in ethylene glycol for 1 h. The resulting solution was added dropwise to 100 ml of saturated aqueous $KPF_6$ solution to induce precipitation. The brown product was collected *via* vacuum filtration and washed with distilled water (3 × 20 ml). FABMS: *m/z* 893 $(M - PF_6)^+$. $^1H$ NMR ($CD_3CN$): $\delta$ 2.56 (s, 3 H, $CH_3$), 7.06–9.01 (25 H, m, Ar-H).

§ For surface-confined Os(tpy)(ttp) units, $\varepsilon$ at 665 nm is only *ca.* 6–10% of the values at 275 or 315 nm. Hence, the expected absorbance would be a much lower value (*ca.* 0.0005–0.001) at 665 nm.

1 A. J. Bard, *Integrated Chemical Systems: A Chemical Approach to Nanotechnology*, Wiley, New York, 1994.
2 M. O. Wolf and M. A. Fox, *J. Am. Chem. Soc.*, 1995, **117**, 1845.
3 S. Yitzchaik and T. J. Marks, *Acc. Chem. Res.*, 1996, **29**, 197.
4 Y. Liang and R. H. Schemehl, *J. Chem. Soc.*, 1995, 1007.
5 S. Paulson; K. Morris and B. P. Sullivan, *J. Chem. Soc., Chem. Commun.*, 1992, 1615.
6 J.-P. Sauvage, J.-P. Collin, J.-C. Chambron, S. Guillerez, C. Coudret, V. Balzani, F. Barigelletti, L. De Cola and L. Flamigni, *Chem. Rev.*, 1994, **94**, 993; V. Balzani, A. Juris, M. Venturi, S. Campagna and S. Serroni, *Chem. Rev.*, 1996, **96**, 759.
7 The preparation of this compound is included elsewhere: B. Hong, S. R. Woodcock and S. M. Saito, *Inorg. Chem.*, 1997, submitted.
8 J. Huang and J. C. Hemminger, *J. Am. Chem. Soc.*, 1993, **115**, 3342; M. R. Linford, P. Fenter, P. M. Eisenberger and C. E. D. Chidsey, *J. Am. Chem. Soc.*, 1995, **117**, 3145; M. J. Tarlov, D. R. Burgess, Jr. and G. Gillen, *J. Am. Chem. Soc.*, 1993, **115**, 5305.
9 J. F. Moulder, W. F. Stickle, P. E. Sobol, K. D. Bomben and J. Chastain, *Handbook of X-ray Photoelectron Spectroscopy*, Perkin-Elmer Corporation, 1992.
10 This ligand was prepared according to the procedures reported in the following references: H. Schmidbaur and T. Pollok, *Angew. Chem., Int. Ed. Engl.*, 1986, **25**, 348; H. Schmidbaur, S. Manhart, A. Schier, *Chem. Ber.*, 1993, **126**, 2389.

*Received in Bloomington, IN, USA, 9th June 1997; 7/03970K*

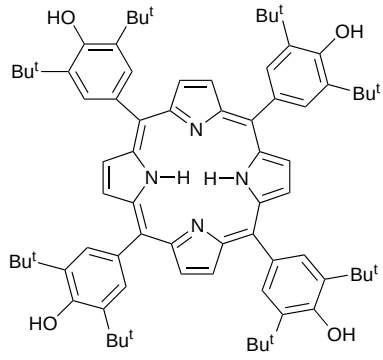
# Synthesis of a phthalocyanine derivative containing easily oxidised sterically-hindered phenolic substituents

**Guy J. Clarkson, Paul Humberstone and Neil B. McKeown***

*Department of Chemistry, University of Manchester, Manchester, UK M13 9PL*

**A novel phthalocyanine containing four redox-active 3,5-di-*tert*-butyl-4-hydroxyphenyl substituents is readily oxidised in aerated, basified solution to give a complex product mixture; the oxidation is apparently localised on the phenolic moieties without disturbing the structure of the phthalocyanine core.**

Phthalocyanines (Pcs) are of continuing interest as organic materials which possess interesting electronic and optical properties.[1] Recent synthetic work has sought to modify the electronic behaviour of the Pc macrocycle by the attachment of redox-active moieties based on ferrocene,[2] fullerene[3] and tetrathiafulvalene.[4] Sterically hindered phenols are readily oxidised to stable radical species (*e.g.* the galvinoxyl radical) and are used as radical scavengers for the stabilisation of monomers, polymers and solvents. They may also undergo further oxidation to form quinones. Previous studies concerning *meso*-tetrakis(3,5-di-*tert*-butyl-4-hydroxyphenyl)porphyrin **1** reveal that cooperative quinone formation occurs rapidly across the porphyrin ring system on addition of base to an aerated solution.[5] This process results in a dramatic distortion of the porphyrin ring system and loss of aromaticity.[6] It is of interest to establish whether similar cooperative processes may occur *via* the related Pc macrocycle. This communication describes the synthesis of a novel Pc derivative containing four 3,5-di-*tert*-butyl-4-hydroxyphenyl (DTBHP) substituents and the results of a preliminary examination of its behaviour under oxidative conditions.




**1**

Aromatic nucleophilic substitution of the nitro group of commercially available 4-nitrophthalonitrile **2**, using oxygen, nitrogen or sulfur nucleophiles, is a well established method of preparing phthalonitrile precursors to tetra-substituted Pc derivatives with enhanced solubility.[7] This is exemplified by the reaction between **2** and the anion of 3,5 di-*tert*-butylphenol **3** in DMF which gives 4-(3,5-di-*tert*-butylphenoxy)phthalonitrile **5** in 70–80% yield (Scheme 1). Several previous studies have illustrated the ability of the anion of 2,6-di-*tert*-butylphenol **4** to behave as a carbon nucleophile in the preparation of biphenyl derivatives *via* aromatic nucleophilic substitution.[8] Encouragingly, we found that the anion of **4** reacts with **2** as a carbon nucleophile efficiently displacing the nitro group to give the novel 4-(3,5-di-*tert*-butyl-4-hydroxyphenyl)phthalonitrile **6** in 75–85% yield. The structure of **6** was assigned using $^1$H NMR and IR spectroscopy and by a strong bathochromic shift from 345 to 505 nm in the $\lambda_{max}$ of its UV–VIS absorption spectrum on addition of base, which is characteristic of the formation of a conjugated phenolic anion.† In addition, its biphenyl structure was confirmed by a single crystal X-ray diffraction study. Cyclotetramerisation of phthalonitriles **5** or **6** is catalysed by lithium pentanolate in refluxing pentanol to give Pcs **7** and **8**, respectively, in 10–30% yield. These two isomeric Pcs are each composed of four inseparable regioisomers and give $^1$H NMR, UV–VIS absorption, IR, fast atom bombardment (FAB) mass spectra and elemental analyses which are consistent with their proposed structures.†

The cyclic voltammetry (CV) of deaerated solutions of Pcs **7** and **8** in $CH_2Cl_2$ give very similar results consistent with previous CV studies of soluble metal-free Pcs.[9] However, on the addition of excess tetrabutylammonium hydroxide (TBAH), Pc **8** exhibits a strong reversible redox transition ($E_{1/2}$ = 50 mV *vs.* $Ag^+/Ag$) of an intensity consistent with a four-electron oxidative process to give the tetra-phenolic radical species.

The UV–VIS absorption spectra of $CH_2Cl_2$ solutions of Pc **7** ($\lambda$ = 701 and 667 nm) and **8** ($\lambda$ = 715 and 683 nm) both exhibit the characteristic split Q-band of metal-free Pc [Fig. 1(*a*)]. On the addition of an excess of TBAH the Q-band of Pc **7** changes appearance to give a single sharp band at 690 nm [similar to Fig. 1(*c*)] consistent with the formation of a $Pc^{2-}$ anion due to the loss of the two protons from the central cavity. No change in this spectrum is seen over an extended period of time. However, the Q-band of Pc **8** exhibits an initial strong bathochromic shift to 796 nm on addition of the base [Fig. 1(*b*)]. This dramatic shift demonstrates that the deprotonated DBTHP substituents interacts strongly with the Pc macrocycle resulting in a Q-band position which is similar to that shown by naphthalocyanines, of interest as IR-absorbing dyes. If left to stand in aerated conditions the bathochromic shift gradually reduces until, after

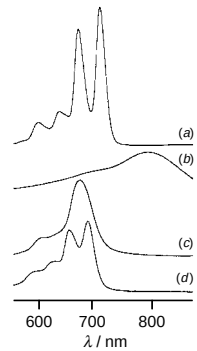
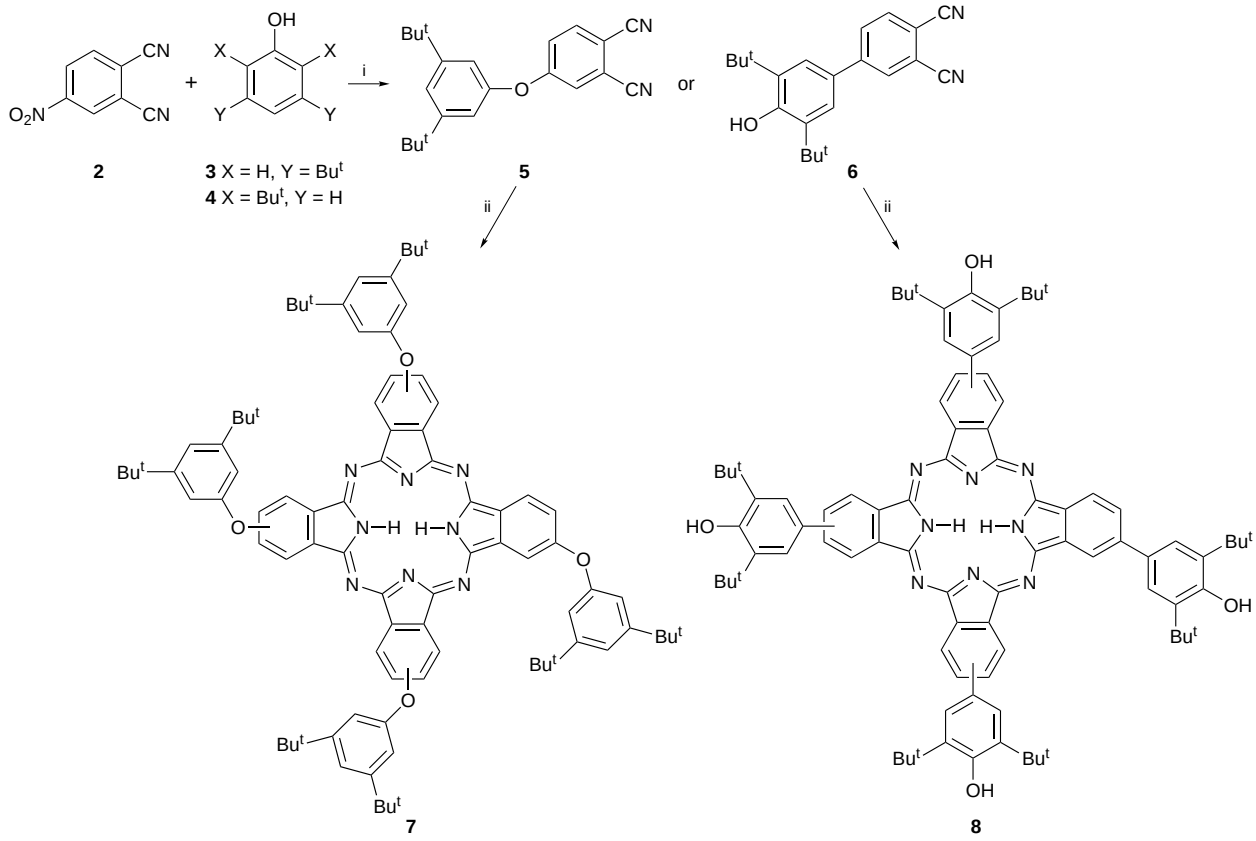



**Fig. 1** UV–VIS absorption spectra of Pc **8** in aerated $CH_2Cl_2$ (*a*) under neutral conditions; (*b*) immediately after the addition of excess TBAH; (*c*) after leaving the solution for 72 h; (*d*) upon addition of excess acetic acid




**Scheme 1** *Reagents and conditions*: i, anhydrous $K_2CO_3$, DMF, 40 °C; ii, $C_5H_{11}OLi$, $C_5H_{11}OH$, 135 °C

a period of 2–3 days, a characteristic $Pc^{2-}$ visible absorption spectrum [Fig. 1(*c*)] is obtained ($\lambda$ = 680 nm) similar to that observed for the $Pc^{2-}$ anion of **7**. On neutralisation with acetic acid, the familiar split Q-band of a metal-free Pc is regained [Fig. 1(*d*)], although slightly blue-shifted ($\lambda$ = 700 and 665 nm) relative to the original Q-band position of **8**. We conclude from these observations that, in contrast to the simple, rapid and cooperative oxidative process observed for porphyrin **1**, the structural integrity of the planar Pc macrocycle is retained and that oxidation is localised on the DTBHP subunits.

TLC and $^1$H NMR analysis of Pc **8** subsequent to the oxidation process suggests the formation of a highly complex product mixture from which no discrete compounds could be isolated by chromatography. FAB MS analysis of the product mixture was unhelpful due to the lack of ions with mass greater than 500 Da. However, the IR analysis (KBr disc) of the oxidised material indicates the presence of quinone type functionality ($\nu$ = 1640 and 1670 cm$^{-1}$). Elemental analyses, although irreproducible between different batches of oxidised **8**, indicate the presence of additional oxygen. It is highly likely that the DTBHP substituents undergo the various complex, but well understood, transformations of 4-aryl-2,6-di-*tert*-butylphenols in aerated basic solution.[10] These include the formation of 4-aryl-2,6-di-*tert*-butyl-4,5-epoxy-6-hydroxycyclohex-2-enones, 4-aryl-2,6-di-*tert*-butyl-5,6-epoxy-4-hydroxycyclohex-2-enones and 3-aryl-2,5-di-*tert*-butylcyclopenta-2,4-dienones *via* subsequent decomposition of the initially formed 2- and 4-hydroperoxycyclohexadienone anions. Each resulting Pc molecule would possess a combination of oxidised DTBHP fragments, hence the complex nature of the product mixture.

It is clear from this initial study that the synthesis of novel phthalonitrile precursor **6** allows the preparation of DTBHP containing metal-free or metal ion containing Pc derivatives, with symmetrical or unsymmetrical substitution.[11] Studies of the synthesis and redox properties of these Pcs under deaerated conditions are in progress.

## Footnotes and References

* E-mail: neil.mckeown@man.ac.uk

† *Selected spectroscopic data* for **5**: $\nu$(KBr)/cm$^{-1}$ 2233 (CN); *m/z* (EI) 332 (M$^+$); $\delta_H$($CDCl_3$, 200 MHz) 1.33 (18 H, s), 6.89 (2 H, s), 7.21–7.30 (3 H, m), 7.72 (1 H, d). For **6**: $\nu$(KBr)/cm$^{-1}$ 3416 (OH), 2231 (CN); *m/z* (EI) 332 (M$^+$); $\delta_H$($CDCl_3$, 200 MHz) 1.51 (18 H, s), 5.55 (1 H, s), 7.39 (2 H, s), 7.75–8.00 (3 H, m). For **7**: $\lambda$($CH_2Cl_2$)/nm 701, 667, 639, 607, 342; $\nu$(KBr)/cm$^{-1}$ 3290 (NH); *m/z* (FAB) 1334; $\delta_H$($C_6D_6$, 500 MHz) 1.45 (72 H, br s), 7.50–8.05 (16 H, br m), 8.81 (8 H, br m). For **8**: $\lambda$($CH_2Cl_2$)/nm 715, 683, 652, 620, 344; $\nu$(KBr)/cm$^{-1}$ 3289 (NH), 3641 (OH); *m/z* (FAB) 1334; $\delta_H$($C_6D_6$, 500 MHz) 1.8 (72 H, br s), 5.25 (4 H, s), 8.17–8.60 (12 H, br m), 9.1–10.0 (12 H, br m).

1 N. B. McKeown, *Phthalocyanine Materials: Synthesis, Structure and Function*, Cambridge University Press, Cambridge, in the press.
2 Z. Jin, K. Nolan, C. R. McArthur, A. B. P. Lever and C. C. Leznoff, *J. Organomet. Chem.*, 1994, **468**, 205.
3 T. G. Linßen, K. Durr, M. Hanack and A. Hirsch, *J. Chem. Soc., Chem. Commun.*, 1995, 103.
4 M. J. Cook, G. Cooke and A. Jafarifini, *Chem. Commun.*, 1996, 1925.
5 T. G. Traylor, K. B. Kolan, R. Hildreth and T. A. Evans, *J. Am. Chem. Soc.*, 1983, **105**, 6149; L. R. Milgrom, *Tetrahedron*, 1983, **39**, 3895.
6 A. J. Golder, L. R. Milgrom, K. B. Nolan and D. C. Povey, *J. Chem. Soc., Chem. Commun.*, 1989, 1751.
7 W. O. Siegl, *J. Heterocycl. Chem.*, 1981, **18**, 1613; S. A. Mikhalenko, V. M. Derkacheva and E. A. Luk'yanets, *Zh. Obshch. Khim.*, 1981, **51**, 1650; I. Guerol, V. Ahsen and O. Bekaroghi, *J. Chem. Soc., Dalton Trans.*, 1994, 497.
8 I. N. Chechulina, E. R. Milaeva, A. I. Prokofev and Y. G. Bundel, *Zh. Obshch. Khim.*, 1988, **58**, 1075; J. Wright and E. C. Jorgensen, *J. Org. Chem.*, 1968, **33**, 1245; G. P. Stahly, *J. Org. Chem.*, 1985, **50**, 3091.
9 C. C. Leznoff, S. Greenburg, S. M. Marcuccio, P. C. Minor, P. Seymour and A. B. P. Lever, *Inorg. Chim. Acta*, 1984, **89**, L35.
10 A. Nishinaga, T. Itahara and T. Matsuura, *J. Am. Chem. Soc.*, 1978, **100**, 1826; A. Nishinaga, T. Shimizu and T. Matsuura *J. Org. Chem.*, 1979, **44**, 2983.
11 P. Humberstone, G. J. Clarkson, N. B. McKeown and K. E. Treacher, *J. Mater. Chem.*, 1996, **6**, 315.

*Received in Cambridge, UK, 11th August 1997; 7/05840C*

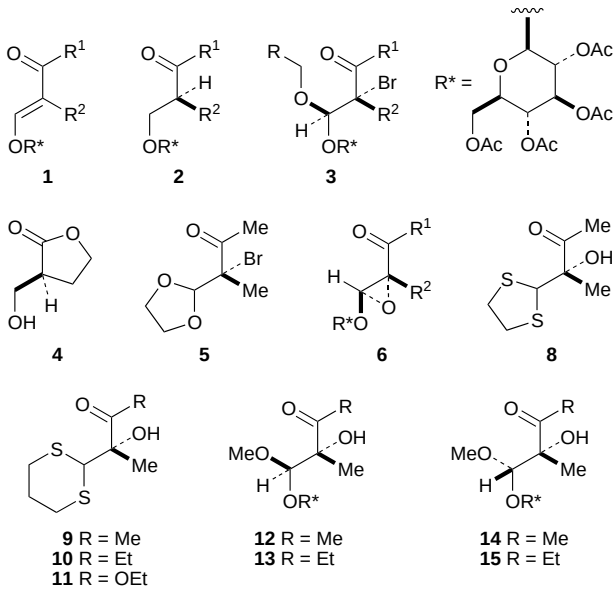
# Stereoselective epoxidations of vinylogous esters/carbonates directed by the 2,3,4,6-tetra-*O*-acetyl-β-D-glucopyranosyl auxiliary: a route to near stereopure tertiary alcohols bearing functional arms

**Gurpreet S. Bhatia, Richard F. Lowe, Robin G. Pritchard and Richard J. Stoodley***

*Department of Chemistry, UMIST, PO Box 88, Manchester, UK M60 1QD*

**The 2,3,4,6-tetra-*O*-acetyl-β-D-glucopyranosyl auxiliary is effective in directing the epoxidation of vinylogous esters/carbonates with dimethyldioxirane; the derived epoxides are convertible into a versatile class of 1,2,3-trifunctional chirons.**

As part of a programme to develop the 2,3,4,6-tetra-*O*-acetyl-β-D-glucopyranosyl unit as an auxiliary in asymmetric synthesis, we have embarked on a study of vinylogous esters/carbonates of type **1**.[1,2] To date, we have established that such systems undergo stereoselective catalytic hydrogenations (to give mainly dihydro derivatives of type **2**) and regio- and stereoselective bromoalkoxylations (to furnish bromoalkoxy adducts of type **3** preferentially). Whilst the diastereomeric ratios were not high (generally, around 85 : 15), it was possible to isolate many of the major adducts in stereopure states and in acceptable yields simply by fractional crystallisation. Moreover, in selected cases, it was possible to remove the auxiliary under mildly acidic conditions to give chirons featuring tertiary stereogenic centres, *e.g.* **4** and **5**. Recognising the potential synthetic versatility of epoxides of type **6**, we have sought to prepare such compounds and to study their reactivity. Our findings are the subject of this communication.



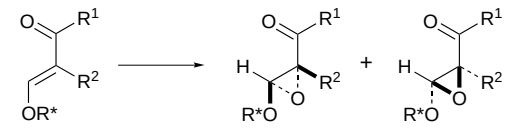

After screening a variety of epoxidising agents, dimethyldioxirane (DMDO)[3,4] was found to be extremely effective in promoting the oxidation of vinylogous esters/carbonates† of type **1**. Table 1 summarises the outcome of the reactions. From the results, it is clear that better stereoselectivities are observed with the reactants **1a**,[1,5] **1b**,[2,6] **1c**,[1] **1e**[1] and **1f**[1] (*i.e.* $R^2$ = alkyl group) than with the reactants **1d**[7] and **1g**‡§ (*i.e.* $R^2$ = H). Moreover, in the former examples, the major epoxides **6a**§ {mp 126–127 °C, $[\alpha]_D$ −8.3 (*c* 0.5, $CH_2Cl_2$)}, **6b**§¶ (mp 106–107 °C), **6c**§ {mp 93–94 °C, $[\alpha]_D$ −40 (*c* 0.3, $CH_2Cl_2$)}, **6e**§ {mp 108 °C, $[\alpha]_D$ −33 (*c* 0.5, $CH_2Cl_2$)} and **6f**§ {mp 171–172 °C, $[\alpha]_D$ −46 (*c* 0.7, $CH_2Cl_2$)} could be isolated‖ in stereopure states and in reasonable yields simply by fractional crystallisation.

That the major epoxide arising from the reaction of the vinylogous ester **1a** with DMDO possessed the stereostructure **6a** was established by X-ray crystallography** (Fig. 1).

Seeking to detach the auxiliary and generate the dithiolane **8**, the epoxide **6a** was treated with ethane-1,2-dithiol under a range of acidic conditions. The best yield of the desired product (56% after chromatography) was achieved by heating the epoxide **6a** with the dithiol (120 mol%) and toluene-*p*-sulfonic acid monohydrate (*p*-TsOH·$H_2O$) (100 mol%) in toluene (*ca.* 72 °C, 3 h); however, the dithiolane **8**,§ $[\alpha]_D$ +35 (*c* 0.6, MeOH), was found to possess an ee of only 66% by HPLC analysis.†† Under similar conditions (1.5 h), the epoxide **6a** reacted with propane-1,3-dithiol to give the dithiane **9**§¶ (54% yield after chromatography), mp 80 °C, with an ee of 82%.†† Clearly, the dithioacetalisation reactions were accompanied by partial racemisation.

When subjected to methanolysis conditions [MeOH–$CH_2Cl_2$ (4 : 1), *p*-TsOH·$H_2O$ (cat.), 19 h], the epoxide **6a** was converted essentially quantitatively into a 90 : 10 mixture of the alcohols **12** and **14** (tentative stereostructures); crystallisation of the mixture provided the major diastereomer **12**,§ mp 112 °C, $[\alpha]_D$ −46 (*c* 0.3, $CH_2Cl_2$), in 58% yield. The mixture of the alcohols **12** and **14** reacted with propane-1,3-dithiol [$CHCl_3$, *p*-TsOH·$H_2O$ (100 mol%), $CF_3SO_3H$ (cat.), 21 h] to give the dithiane **9**¶ (55% yield based on **6a**), mp 102–103 °C, with an ee of 98%. Under the acidic conditions mentioned earlier

**Table 1** Epoxidation of vinylogous esters/carbonates of type **1** with DMDO[a]




| Reactant **1** | $R^1$ | $R^2$ | Products | Ratio[b] | Yield (%)[c] |
|---|---|---|---|---|---|
| **a** | Me | Me | **6a**,**7a** | 90 : 10 | 73 |
| **b** | Et | Me | **6b**,**7b** | 90 : 10 | 52 |
| **c** | $-CH_2CH_2CH_2-$ | | **6c**,**7b** | 91 : 9 | 64 |
| **d** | Me | H | **6d**,**7d** | 69 : 31 | — |
| **e** | OEt | Me | **6e**,**7e** | 91 : 9 | 74 |
| **f** | $-OCH_2CH_2-$ | | **6f**,**7f** | 86 : 14 | 70 |
| **g** | OEt | H | **6g**,**7g** | 67 : 33 | — |

[a] The oxidations were carried out using a distilled solution of DMDO in acetone (*ca.* 0.08 mol $dm^{-3}$). [b] The product ratio was determined by NMR spectroscopic and/or HPLC analysis. [c] The yield refers to the major epoxide isolated in a stereopure state after crystallisation.

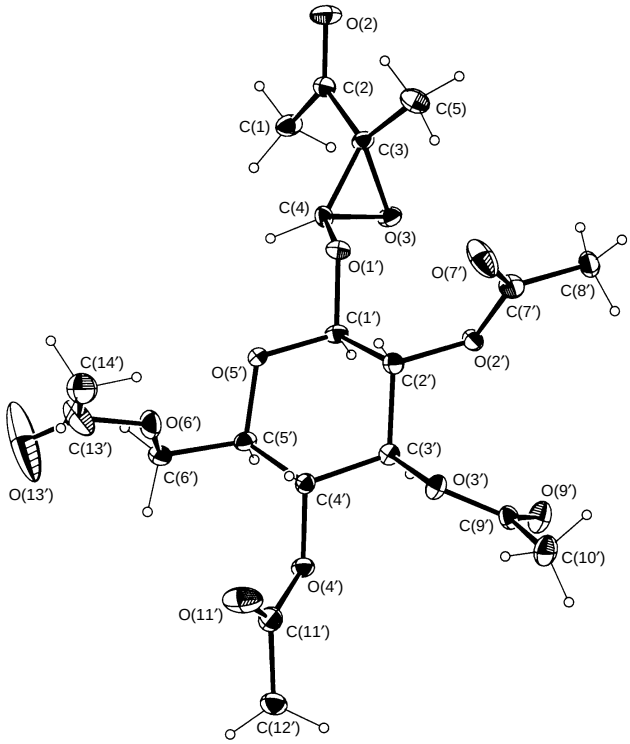



**Fig. 1** Molecular structure of compound **6a**

[PhMe, *p*-TsOH·$H_2O$ (100 mol%), *ca.* 72 °C, 4 h], the dithiane **9** underwent significant racemisation (98% → 29% ee). Presumably, the partial racemisations noted in the **6a** → **8** and **6a** → **9** transformations were the results of acid-induced α-ketol rearrangements[8] of the products **8** and **9**.

Conversion of the epoxide **6b**, by way of a 89 : 11 mixture of the alcohols **13** and **15**, into the dithiane **10**§ (48% yield), $[\alpha]_D$ +2.2 (*c* 0.5, MeOH), with an ee of 93%,†† was similarly effected.

Under the conditions used to effect the direct **6a** → **9** transformation, the epoxide **6e** was converted into the dithiane **11**§¶ (83% yield), mp 61–62 °C, with an ee of 98%.†† The lack of any significant racemisation in this process supports the notion that α-ketol rearrangements are implicated in the partial racemisation of compounds **8** and **9**.

The afore-cited findings are of note in several respects. They extend further the role of the 2,3,4,6-tetra-*O*-acetyl-β-D-glucopyranosyl unit as an auxiliary in asymmetric synthesis. They reveal that the model used to explain the diastereofacial reactivity of vinylogous esters/carbonates of type **1** in catalytic hydrogenations[1] and bromoalkoxylations[2] is also applicable to epoxidation reactions. They illuminate a reactivity feature of vinylogous esters/carbonates that hitherto has not been exploited. Finally, compounds **6a**–**c**, **6e**–**f**, **8**–**11** and **12** are representatives of new classes of trifunctional chirons with notable synthetic potential.

We thank the EPSRC for a research grant (GR/J/65464), the Isle of Man Government for a research studentship (to R. F. L.), Dr C. M. Raynor for performing the HPLC analyses and Dr J. A. Whatley (Roche Products Ltd.) for help in devising the conditions used for the HPLC analyses.

## Footnotes and References

* E-mail: richard.stoodley@umist.ac.uk

† There appear to be relatively few studies of epoxidations of vinylogous esters/carbonates using DMDO (see ref. 9).

‡ The vinylogous carbonate **1g**, mp 116–118 °C, $[\alpha]_D$ −13 (*c* 1.1, $CHCl_3$), was prepared (53% yield after crystallisation) by the Wittig condensation of ethoxycarbonylmethylenetriphenylphosphorane with 1-*O*-formyl-2,3,4,6-tetra-*O*-acetyl-β-D-glucopyranose (see ref. 6).

§ This compound displayed analytical and spectral properties that supported its assigned structure.

¶ This compound possessed no significant optical rotation in a range of solvents.

‖ The thermal stability of epoxides of type **6** is striking. In general, epoxides derived from vinylogous esters/carbonates tend to decompose at ambient temperature (see ref. 9).

** *Crystal data* for **6a**: $C_{19}H_{26}O_{12}$, $M$ = 446.4, monoclinic, space group $P2_1$ (no. 4), $a$ = 11.621(3), $b$ = 7.500(2), $c$ = 12.855(3) Å, $\beta$ = 98.53(2)°, $Z$ = 2, $D_c$ = 1.338 g cm$^{-3}$, $F$(000) = 472, $\mu$(Mo-Kα) = 1.05 cm$^{-1}$, crystal size 0.40 × 0.25 × 0.25 mm. A total of 2022 reflections were measured, 1893 unique ($R_{int}$ = 0.0336), on a Siemens R3m/V diffractometer using the $\omega/2\theta$ scan method ($\lambda$ = 0.71069 Å) at 23 °C. The structure was solved by direct methods and refined by full-matrix least-squares based on $F^2$, with all non-hydrogen atoms anisotropic and hydrogen atoms constrained in calculated positions. The final cycle converged to $R$ = 0.053 and $wR^2$ = 0.115. CCDC 182/589.

†† The enantiomers were separated on a Chiralpak AD column, using hexanes–propan-2-ol (9 : 1) as eluent (flow rate: 1 cm$^3$ min$^{-1}$) in the cases of **8**/*ent*-**8** and **9**/*ent*-**9** and hexanes–ethanol (9 : 1) as eluent (flow rate: 1 cm$^3$ min$^{-1}$) in the case of **10**/*ent*-**10**.

1 D. S. Larsen, A. Schofield, R. J. Stoodley and P. D. Tiffin, *J. Chem. Soc., Perkin Trans. 1*, 1996, 2487.
2 M. S. Idris, D. S. Larsen, A. Schofield, R. J. Stoodley and P. D. Tiffin, *Tetrahedron Lett.*, 1995, **36**, 3251.
3 W. Adam, J. Bialas and L. Hadjiarapoglou, *Chem. Ber.*, 1991, **124**, 2377.
4 R. W. Murray, *Chem. Rev.*, 1989, **89**, 1187; W. Adam, R. Curci and J. O. Edwards, *Acc. Chem. Res.*, 1989, **22**, 205; W. Adam and L. Hadjiarapoglou, *Top. Curr. Chem.*, 1993, **164**, 45; R. Curci, A. Dinoi and M. F. Rubino, *Pure Appl. Chem.*, 1995, **67**, 811.
5 R. C. Gupta, D. S. Larsen, R. J. Stoodley, A. M. Z. Slawin and D. J. Williams, *J. Chem. Soc., Perkin Trans. 1*, 1989, 739.
6 D. S. Larsen and R. J. Stoodley, *J. Chem. Soc., Perkin Trans. 1*, 1989, 1841.
7 R. C. Gupta, P. A. Harland and R. J. Stoodley, *Tetrahedron*, 1984, **40**, 4657.
8 D. J. Coveney, in *Comprehensive Organic Synthesis*, ed. B. M. Trost and I. Fleming, Pergamon, Oxford, 1991, vol. 3 (ed. G. Pattenden), p 791.
9 W. Adam and L. Hadjiarapoglou, *Chem. Ber.*, 1990, **123**, 2077; W. Adam, D. Golsch, L. Hadjiarapoglou and T. Patonay, *Tetrahedron Lett.*, 1991, **32**, 1041; *J. Org. Chem.*, 1991, **56**, 7292; D. Yang, M.-K. Wong and Y.-C. Yip, *J. Org. Chem.*, 1995, **60**, 3887.

*Received in Liverpool, UK, 29th July 1997; 7/05498J*

# Ruthenium-catalysed conversion of triynes to benzene derivatives—a novel metathesis cascade

**Jens-Uwe Peters and Siegfried Blechert***

*Institut für Organische Chemie der Technischen Universität, Strasse des 17. Juni 135, D-10623 Berlin, Germany*

**In a novel application of [$PhCH_2$=$Ru(PCy_3)_2Cl_2$] 1, triynes are isomerised to benzene derivatives; a cascade of four metathesis reactions is proposed as a mechanistic explanation.**

Cyclotrimerisation of acetylenes is catalysed by a variety of transition metal catalysts[1] and provides easy access to highly substituted benzene derivatives.[2] Cobalt[3] and rhodium[4] catalysts have been used to make this reaction the key step in a number of elegant natural product syntheses. Metallacyclooligoolefins are believed to be pivotal intermediates in the acetylene trimerisation catalytic cycle.[5] An exception is the palladium-catalysed reaction *via* vinylpalladium intermediates.[6]

Another approach to transform acetylenes into benzene derivatives is the metathesis of mono-[7] or bis-acetylenic[8] compounds with stoichiometric amounts of transition metal carbonyl carbene complexes with subsequent CO insertion. These methodologies have also found ample application in efficient constructions of structurally complex synthetic targets.[9]

Mechanistically interesting is the conversion of an alkylidyne complex to a benzylidene complex with 3 equiv. of an acetylene by a metathesis cascade.[10]

However, a catalytic metathesis process for the isomerisation of triynes to benzene derivatives has not yet been described.

In several instances, it has been shown that ruthenium carbene complexes derived from Grubbs' metathesis catalyst **1**[11] insert intramolecular C≡C triple bonds regioselectively, with metallacyclobutenes as likely intermediates.[12] Recent work shows that intermolecular additions of such carbene complexes to C≡C triple bonds also proceed regioselectively.[13]

Ring-closing olefin metathesis employing **1** is a well established reaction.[14] In general, ruthenium-catalysed ring-closing olefin metatheses are initiated by the *in situ* transformation of the stable benzylidene complex **1** into a reactive methylidene complex as the active catalytic species.[15] However, far less reactive[15] ruthenium benzylidene complexes similar to **1** were also involved as catalytic species in ring-closing olefin metatheses.[16]

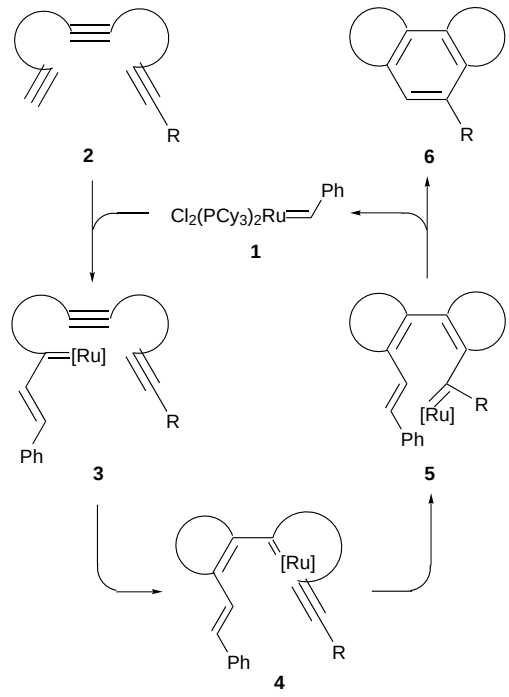
Metathesis catalytic cycles usually commence with a regioselective addition of the catalytic species to the substrate's least hindered site as is suggested by the outcome of conversions of substrates with differently substituted C≡C and C=C bonds.[17]

Based on these findings, we projected a metathesis cascade process for the isomerisation of acyclic triynes to benzene derivatives by **1** (Scheme 1).

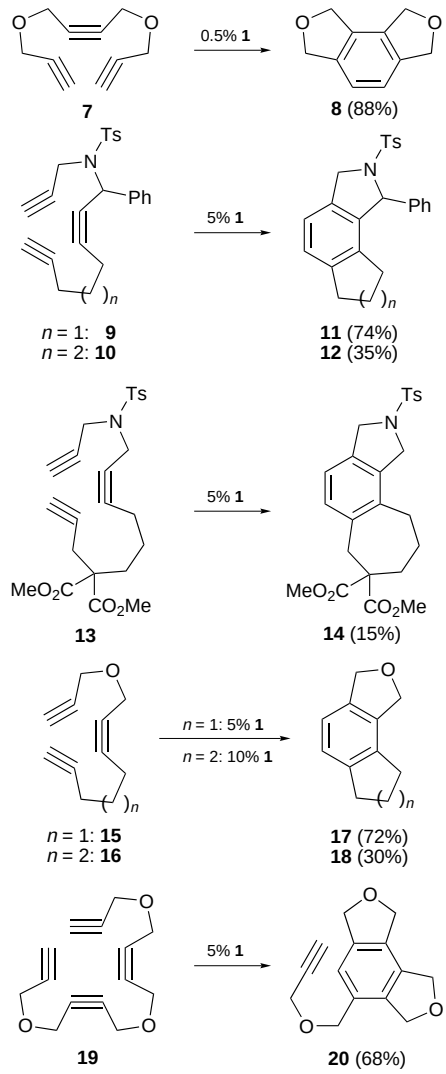
In an initial intermolecular reaction, ruthenium benzylidene complex **1** adds to the least hindered triple bond of triyne **2**. The resulting vinyl carbene complex **3** undergoes an intramolecular metathesis reaction *via* **4** to produce a conjugated carbene complex **5**, with two of the newly formed double bonds embedded in ring structures and thus forced to be *Z*. This is a prerequisite for the final ring-closing olefin metathesis step which releases benzylidene complex **1**, thus making the entire process catalytic. The formation of an aromatic system **6** should provide a strong driving force for the overall reaction cascade.

To test our concept, we treated the easily accessible triyne **7**[18] as a 2 M solution in $CH_2Cl_2$ with 5 mol% of **1** (Scheme 2). The desired tetrasubstituted benzene derivative **8** was obtained in excellent yield after only seconds of vigorous reaction. Optimisation revealed that as little as 0.5 mol% of **1** is sufficient to convert all starting material of **7** as a 1 M solution in $CH_2Cl_2$ in an exothermic reaction within 2 h.† The small amount of catalyst necessary for this supposedly four-fold metathesis cascade is remarkable since most applications of catalyst **1** require several mol%;[14] *e.g.* 20 mol% of **1** has been used in macrocycle syntheses.[19]

To explore the scope of this novel acetylene oligomerisation to see which ring sizes might be accessible, acyclic triynes **9**, **10** and **13** were treated with **1** (Scheme 2). Compared to the formation of **8** from **7**, larger amounts of **1** and longer reaction times were required in all cases for complete conversion. Whereas indane derivative **11** was obtained in good yield from its acyclic precursor **9** after 12 h, the structurally similar **10** gave an only moderate yield of the tetralin **12**. Compound **13** was isomerised in poor yield to benzene derivative **14** with an annulated seven-membered ring. In the latter cases, the desired conversions proceeded slowly (2 d) and the competing formation of obviously polymeric byproducts explains the diminished yields. A similar trend was observed in the formation of indane derivative **17** and tetralin derivative **18** from their respective precursors **15** and **16**. Again, the indane




**Scheme 1** Cy = cyclohexyl




**Scheme 2** Ts = *p*-$MeC_6H_4SO_2$

derivative was obtained in good yield after 12 h, whereas the tetralin derivative was formed in a moderate yield along with polymeric byproducts in a sluggish reaction (2 d). We assume that benzene derivatives with two annulated five-membered rings are generally formed in good yields from acetylenic precursors by reaction with **1**. This was confirmed by further investigations with triynes similar to **7** (yields of 67% or higher).

The tetraacetylenic **19** could potentially be converted to either a cyclooctatetraene or a pentasubstituted benzene **20**. However, when **19** was treated with **1**, **20** was found to be the exclusive product. The long reaction time of 2 d for this conversion can be rationalised by the known susceptibility of the reactivity of ruthenium carbene complexes to steric hindrance;[15] in contrast to all other examples shown in Scheme 2, the final ring-closing olefin metathesis step of the catalytic cycle (Scheme 1) starts from a disubstituted carbene complex **5** (R ≠ H). Only a few examples of ring-closing olefin metatheses involving such ruthenium intermediates are known.[17] A sterically demanding and thus less reactive carbene complex **5** should make this final step slow and rate determining. Despite the slow reaction, **20** was isolated in good yield.

In conclusion, this novel application of **1** expands the scope of the versatile synthetic tool of acetylene cyclooligomerisation by employment of a catalyst which is commercially available and tolerates a wide range of functionalities.

## Footnotes and References

* E-mail: sibl@wap0105.chem.tu-berlin.de

† Synthesis of **8**: **7**[18] (80 mg; 0.49 mmol) was dissolved in $CH_2Cl_2$ (0.25 ml). After addition of **1** (0.25 ml of a solution of 8 mg of **1** in 1 ml of $CH_2Cl_2$; 2.5 μmol; 0.5 mol%), the colour of the mixture turned from red to brown within seconds. The reaction was complete after 2 h at ambient temperature (GC and TLC). Evaporation of the solvent and column chromatography of the residue (hexane–*tert*-butyl methyl ether, 9 : 1) gave **8** (70 mg; 88%). Spectroscopic data were consistent with the literature.[18]

1 C. W. Bird, *Transition Metal Intermediates in Organic Synthesis*, Logos Press, London, 1967.
2 For a review on synthetic applications of transition-metal catalysed acetylene cyclisation see: K. P. C. Vollhardt, *Acc. Chem. Res.*, 1977, **10**, 1.
3 K. P. C. Vollhardt, *Angew. Chem.*, 1984, **96**, 525; *Angew. Chem., Int. Ed. Engl.*, 1084, **23**, 53.
4 S. J. Neeson and P. J. Stevenson, *Tetrahedron Lett.*, 1988, **29**, 813.
5 J. P. Colman and L. S. Hegedus, *Principles and Applications of Organotransition Metal Chemistry*, University Science Books, Menlo Park, CA, 1980.
6 E. Negishi, L. S. Harring, Z. Owczarczyk, M. M. Mohamud and M. Ay, *Tetrahedron Lett.*, 1992, **33**, 3253.
7 For a review see: K. H. Dötz, *Angew. Chem.*, 1984, **96**, 573; *Angew. Chem., Int. Ed. Engl.*, 1984, **23**, 587.
8 J. Bao, W. D. Wulff, V. Dragisich, S. Wenglowsky and R. G. Ball, *J. Am. Chem. Soc.*, 1994, **116**, 7616.
9 D. F. Harvey and D. M. Sigano, *Chem. Rev.*, 1996, **96**, 271.
10 H. Strutz, J. C. Dewan and R. R. Schrock, *J. Am. Chem. Soc.*, 1985, **107**, 5999.
11 P. Schwab, M. B. France, J. W. Ziller and R. H. Grubbs, *Angew. Chem.*, 1995, **107**, 2179; *Angew. Chem., Int. Ed. Engl.*, 1995, **34**, 2039.
12 A. Kinoshita and M. Mori, *Synlett*, 1994, 1020; S.-H- Kim, W. J. Zuercher, N. B. Bowden and R. H. Grubbs, *J. Org. Chem.*, 1996, **61**, 1073; A. Kinoshita and M. Mori, *J. Org. Chem.*, 1996, **61**, 8356.
13 R. Stragies, M. Schuster and S. Blechert, in the press.
14 For a review, see: A. S. K. Hashmi, *J. Prakt. Chem.*, 1997, **339**, 195.
15 P. Schwab, R. H. Grubbs and J. W. Ziller, *J. Am. Chem. Soc.*, 1996, **118**, 100.
16 J.-U. Peters and S. Blechert, *Synlett*, 1997, 348.
17 S.-H. Kim, N. Bowden and R. H. Grubbs, *J. Am. Chem. Soc.*, 1994, **116**, 10801.
18 R. Grigg, R. Scott and P. Stevenson, *J. Chem. Soc., Perkin Trans. 1*, 1988, 1357.
19 T. D. Clark and M. R. Ghadiri, *J. Am. Chem. Soc.*, 1995, **117**, 12364; S. J. Miller, H. E. Blackwell and R. H. Grubbs, *J. Am. Chem. Soc.*, 1996, **118**, 9606.

*Received in Liverpool, UK, 4th August 1997; 7/05718K*

# A calixarene-based extractant with selectivity for $Am^{III}$ over $Ln^{III}$

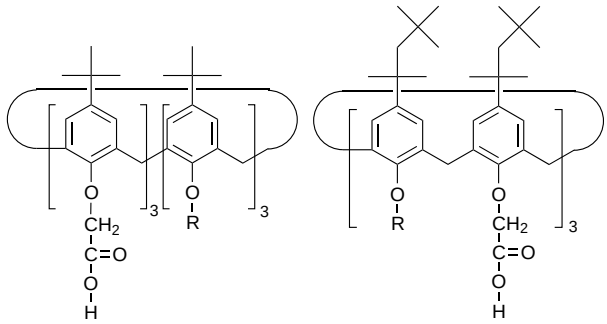
**Rainer Ludwig,*[a] Kenji Kunogi,[a]† Nguyen Dung[a]‡ and Shoichi Tachimori[b]**

[a] *Institute for Inorganic and Analytical Chemistry, Radiochemical Division, Freie Universität Berlin, Fabeckstr. 34-36, 14195 Berlin, Germany*

[b] *Department of Chemistry and Fuel Research, Japan Atomic Energy Research Institute, Tokai-mura, Ibaraki 319-11, Japan*

**Calix[6]arene-based extractant 4 shows high selectivity and extractability for $Am^{III}$ from weakly acidic solutions due to the cooperativity of different ligating groups.**

Among the [1$_n$]metacyclophane-based ligands[1,2] tested as extractants for metal ions, calix[4]arenes and, to a smaller extent, calix[6]arenes are two of the most popular to date.[3] While calix[4]arenes with ester, amide, carboxylic acid or other monodentate groups can extract alkaline, alkaline earth, several transition and noble metal ions selectively, the larger calix[6]-arenes often display a lower selectivity. We previously observed in the case of noble metal extraction that the selectivity can be greatly influenced by the presence of different donor groups, such as $CO_2H$ and amide in a calix[4]arene.[4] Although the mutual separation of lanthanides by calix[4]arenes bearing $CO_2H$ groups is improved by co-extracted sodium ions,[5,6] those ligands have a lower overall extractability towards lanthanides[4] and actinides, such as $Am^{III}$,[7] compared with calix[6]arenes. On the other hand, calix[6]arenes such as ligand **1a**, which serves as a reference compound in the communication, perform as good extractants for $Ln^{III}$ and $Am^{III}$, but with poor group and mutual separation factors. Conventional extractants such as liquid anion exchangers utilize the concurrent complexation by anions for achieving Ln/Am separation. We now report on the progress in achieving selectivity in the cation exchange-based extraction due to the introduction of mixed monodentate functional groups into calix[6]arenes. The emphasis will be on the relationship between ligand structure and complex formation–extraction.



**1a** R = $CH_2CO_2H$
**3** R = Me

**1b** R = $CH_2CO_2H$
**2** R = Me
**4** R = $CH_2C(O)NEt_2$

The distribution ratios $D$ ($D = c_{metal,\,org.}/c_{metal,\,aq.}$) of six selected lanthanide ions $Ln^{3+}$ (Nd, Eu, Tb, Dy, Er, Yb) in the competitive extraction from aqueous into $CHCl_3$ solutions containing ligand **1a** are shown in Fig. 1 on a logarithmic scale as a function of the equilibrium pH. The distribution ratio of $Am^{3+}$ (single element, trace amounts) with ligand **1a** is plotted in the same figure. There is no significant difference in the extractability between $Ln^{III}$ and $Am^{III}$ in these reference systems.

As a first step on the way to improve extractability as well as solubility, we changed *tert*-butyl to *tert*-octyl in the calix[6]arenes.[8] These highly branched ligands are very soluble in low polar organic solvents even without a modifier. The distribution ratios of $Am^{III}$ increase slightly with **1b**, compared with **1a** (Fig. 1). The slope of the plot log $D$ *vs*. pH is 3.0 in accordance to the metal ion charge.

Next, three carboxylic acid groups were introduced alternating with methoxy groups and the extraction into $CHCl_3$ by ligand **2** at 3 mM concentration was studied.§ The extractability decreased significantly [$pH_{0.5}$(Am) = 3.3, $pH_{0.5}$(Ln) > 4.5] due to the smaller number of carbonyl oxygen donor atoms and a less shielded ionophoric cavity, while the selectivity of $Am^{III}$ over $Ln^{III}$ improved, compared with **1b**. The calculated distribution ratios follow the order Am ⩾ Eu, Nd > Tb > Dy > Yb > Er. The slopes of the plots log $D$ *vs*. pH are lower than 3.0 which may be caused by the co-extraction of an anion in the metal ion coordination sphere.

At this point, we tested the influence of ligand geometry on the selectivity and extractability under the same conditions by using ligand **3**.¶ The extractability was low, with $pH_{0.5}$ being 3.5 for Am, Eu and Nd. The selectivity of Am over Ln at pH ⩾ 3, where more than 10% of Am is extracted, was low due to different slopes of the plots log $D$ *vs*. pH. It thus became clear that the geometrical arrangement of functional groups on the calixarene backbone is a key factor for the separation in the present system.

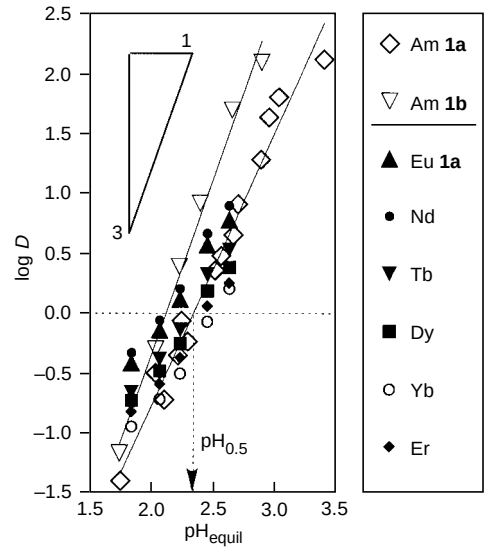



**Fig. 1** Distribution coefficients $D$ of trivalent Am and Ln in the extraction from aqueous to $CHCl_3$ solutions at 298 K by ligands **1a** and **1b**. Aq. phase (Am series): $^{241}Am^{III}$ activity 1 kBq ml$^{-1}$ ($3.3 \times 10^{-8}$ M), $HNO_3$ (various conc.); organic phase (Am series): 5 mM (◇, ▽) ligand, series (◇) contains 2% octan-1-ol as modifier, analysis by liquid scintillation counting of the aq. phase after extraction; aq. phase (Ln series): 0.6 mM $Ln(ClO_4)_3$ (Ln = Nd + Eu + Tb + Dy + Yb + Er, 0.1 mM each), $HClO_4$ (various conc.); organic Phase (Ln series): 3 mM ligand **1a**, 4% octan-1-ol, analysis by ICP-AES of aq. and back-extracted phase (stripping by titriplexIII, mass balance >99%).

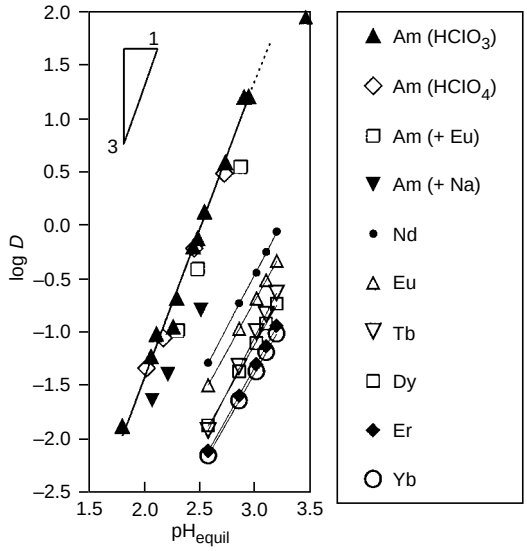



**Fig. 2** Distribution coefficients of trivalent Am and Ln for ligand **3**. Aq. phase (Am series): $^{241}Am^{III}$ (1 kBq ml$^{-1}$), $HNO_3$ (▲, ▼) or $HClO_4$ (◇, □), additional 0.3 mM $Eu(ClO_4)_3$ or 0.01 M $NaNO_3$ as indicated; aq. phase (Ln series) see Fig. 1; organic phase: $CHCl_3$ containing 3 mM ligand **4**.

In order to improve the extractability (expressed as log *D*), while keeping a good group separation, three amide groups were introduced alternating with three carboxylic acid groups and ligand **4** was obtained, thus avoiding an undesirable excess of ionizable groups over the metal ion charge, but having a sufficient number of carbonyl oxygen donor atoms.‖ The results are shown in Fig. 2. The extractability of $Am^{III}$ was high, thereby achieving high selectivity over $Ln^{III}$. A similar improvement in extraction was previously observed for $Pd^{II}$ and $Au^{III}$ upon substituting excessive $CO_2H$ groups by amide groups.[4] The proposed stoichiometry of the extracted complex is 1 : 1 (Am : **4**). The extractability of $Am^{III}$ is still high, when $Eu^{III}$ at a $10^4$ times higher or $Na^+$ at a $3 \times 10^5$ times higher concentration is present in the aqueous phase.

In conclusion, ligand **4** has an only slightly higher $pH_{0.5}$ value of 2.5 compared with reference ligand **1a** (2.35), but a much higher selectivity over trivalent lanthanides. The separation factors at pH = 3.0 are 66 (Am/Nd) and 118 (Am/Eu). Further studies will deal with competitive extraction of actinides at higher concentrations.

The authors appreciate the suggestions of Professor Y. Hasegawa (Science University of Tokyo). Financial support by Deutsche Forschungsgemeinschaft is gratefully acknowledged.

## Footnotes and References

* E-mail: rludwig@ki1.chemie.fu-berlin.de
† Present address: Department of Chemistry, Saga University, Saga 840, Japan.
‡ Permanent address: Analytical Centre, Vietnam Atomic Energy Commission, 59 Ly Thuong Kiet, Hanoi, Vietnam.

§ *Synthesis* of **2**: *p-tert*-Octylcalix[6]arenehexaol was treated with $K_2CO_3$ (3.3 equiv.)–MeI (20 equiv.) in boiling acetone for 20 h. The trimethoxy derivative [$^1$H NMR ($CDCl_3$): 0.58 (s, 27 H), 0.66 (s, 27 H), 1.18 (s, 18 H), 1.27 (s, 18 H), 1.52 (s, 6 H), 1.63 (s, 6 H), 3.46 (s, 9 H, OMe), 3.86 (s, 12 H, $ArCH_2$), 6.78 (s, 3 H, OH), 6.93 (s, 6 H, $H_{Ar}$), 6.97 (s, 6 H, $H_{Ar}$)] was separated over silica gel 60 with $CH_2Cl_2$ ($R_f$ = 0.35, yield 15% after workup) from the tetramethoxy by-product, treated with ethyl bromoacetate (13.5 equiv.)–NaH (9 equiv.) in hot THF for 12 h to substitute OH by $OCH_2CO_2OEt$ in **2b** [MS (EI): 1568; $^1$H NMR ($CDCl_3$): 0.63 (s, 36 H), 0.73 (s, 9 H), 0.87 (s, 27 H), 1.34 (t, 9 H, Me ester), 1.43 (s, 24 H), 1.85 (s, 6 H, $CH_2$), 2.34 (s, 9 H, OMe), 3.46 (d, 6 H, $ArCH_2$), 4.30 (m, 6 H, C*H*Me), 4.53 (d, 6 H, $ArCH_2$), 4.69 (s, $OCH_2$), 6.64 (s, 6 H, $H_{Ar}$), 7.24 (s, 6 H, $H_{Ar}$); conformation: *cone*.] This was then finally hydrolysed with $NMe_4OH$ in boiling THF to give **2** [$^{13}$C NMR ($CD_3OD$; 295 K): 172.03, 155.15, 151.76, 146.09, 145.75, 133.88, 129.27, 125.73, 69.87, 61.04, 57.32, 57.1, 38.61, 38.53, 32.91, 32.67, 32.55, 32.16, 31.06, 30.57; $^1$H NMR: 0.66, 0.86, 1.39, 1.41, 1.5, 1.84, 2.62 (br s), 3.5–4.5 (br), 4.5 (br s), 6.75, 7.24].

¶ *Synthesis* of **3**: *p-tert*-Butylcalix[6]arenehexaol was treated with $Cs_2CO_3$ (3 equiv.)–MeI (8 equiv.) in boiling acetone for 8 h. The product mixture was reacted with ethyl bromoacetate–NaH, recrystallized and separated by prep. HPLC [71Si4A, $CH_2Cl_2$–EtOAc (5%)–MeOH (0.5%)], to give the trimethoxy tris(ethoxycarbonyl)methoxy precursor **3a** [44.7% yield; MS (EI): 1273; TLC ($CH_2Cl_2$–ethyl acetate 95 : 5, silica gel 60): $R_f$ = 0.93; $^1$H NMR ($CDCl_3$): 0.96(s) and 1.07 (s + m) (27 H), 1.25–1.33 (m, 24 H), 1.39 (s, 12 H), 2.1 (br s, 3 H), 2.83 (s, 2 H), 3.44 (s, 2 H), 3.4–4.22 (br m, 22 H), 4.44 (br s, 4 H), 6.68 (s, 2 H), 6.91–7.01 (m, 6 H), 7.2 (d, 4 H)]. **3a** was then hydrolysed by $NMe_4OH$ in boiling THF to **3** [$^1$H NMR ($CDCl_3$–$CD_3OD$ 1 : 1): 1.12 (s, 45 H), 1.2 (s, 9 H), 3.52 (br s, 15 H, Ar-$CH_2$ and OMe), 4.0 (br s) and 4.5 (br m) (10 H, $ArCH_2$ and $OCH_2$), 6.91 (s, 2 H), 6.96 (s, 4 H), 7.02 (s, 4 H), 7.08 (s, 2 H), 8.5 (s, 3 H, OH)].

‖ *Synthesis* of **4**: Removal of the protective methyl groups in the $NaClO_4$ complex of precursor **2b** with $Me_3SiI$ (6.7 equiv.) in boiling $CHCl_3$ for 20 h gives intermediate **4b** after workup [TLC, ($CHCl_3$–MeOH 5 : 1): $R_f$ = 0.91; MS (EI): 1568 (no higher masses); $^1$H and $^{13}$C NMR ($CDCl_3$): disappeared 2.34 and 60.4 (OMe), $H_{Ar}$: 6.99–7.10 (4 s)]. Treatment of **4b** with *N*,*N*-diethylchloroacetamide–NaI–$K_2CO_3$ (12 equiv. each) in boiling acetone for 20 h yields **4c** [72% yield after workup; MS (EI): 1907; TLC ($CHCl_3$–MeOH 5 : 1): $R_f$ = 0.87; $^{13}$C NMR ($CDCl_3$): new 41.2, 40.2, 12.9 [$N(C_2H_5)_2$]. Selective hydrolysis of the ester groups with $NMe_4OH$ in boiling THF then gives **4** [$^{13}$C NMR ($CDCl_3$): 170.8, 167.94, 153.28, 151.88, 145.88, 145.31, 132.9, 131.9, 129.19, 124.16, 71.97, 69.74, 56.59, 41.59, 40.16, 37.99, 37.82, 37.73, 32.25–30.0, 13.98, 12.43; proposed conformation: *cone*; TLC ($CHCl_3$–MeOH 5 : 1): $R_f$ = 0.44].

1 *Calixarenes. A Versatile Class of Macrocyclic Compounds*, ed. J. Vicens and V. Böhmer, Kluwer, Dortrecht, 1990.
2 V. Böhmer, *Angew. Chem.*, 1995, **107**, 785.
3 R. Ludwig, *JAERI-Review 95-022*, Japan Atomic Energy Research Institute, 1995.
4 R. Ludwig and S. Tachimori, *Solvent Extr. Res. Dev., Jpn.*, 1996, **3**, 244.
5 K. Ohto, M. Yano, K. Inoue, T. Nagasaki, M. Goto, F. Nakashio and S. Shinkai, *Polyhedron*, 1997, **16**, 1655.
6 R. Ludwig, K. Inoue and T. Yamato, *Solv. Extr. Ion Exch.*, 1993, **11**, 311.
7 R. Ludwig, S. Tachimori and T. Yamato, *Nukleonika*, 1997, in the press.
8 K. Ohto, M. Yano, K. Inoue, T. Yamamoto, M. Goto, F. Nakashio, S. Shinkai and T. Nagasaki, *Anal. Sci*., 1995, **11**, 893; J. W. Cornforth, P. D'Arcy Hart, G. A. Nicholls, R. J. W. Rees and J. A. Stock, *Br. J. Pharmacol*., 1955, **10**, 73.

*Received in Liverpool, UK, 8th July 1997; 7/04868H*

# Asymmetric synthesis of keto-substituted *P*-chiral phosphines by means of an unusual *exo*/*endo*-stereochemically controlled Diels–Alder reaction

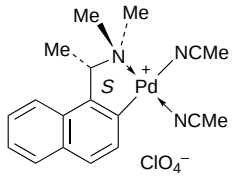
**Pak-Hing Leung,*[a]† Soh-Kheang Loh,[a] Jagadese J. Vittal,[a] Andrew J. P. White[b] and David J. Williams[b]**

[a] *Department of Chemistry, National University of Singapore, Kent Ridge 119260, Singapore*
[b] *Department of Chemistry, Imperial College, London, UK SW7 2AY*

**An asymmetric Diels–Alder reaction between 1-phenyl-3,4-dimethylphosphole and ethyl vinyl ketone promoted by a chiral organopalladium complex gives the corresponding keto-substituted phosphine ligands in which the keto group can be stereospecifically located in the *endo*- or *exo*-positions of the phosphanorbornene skeleton.**

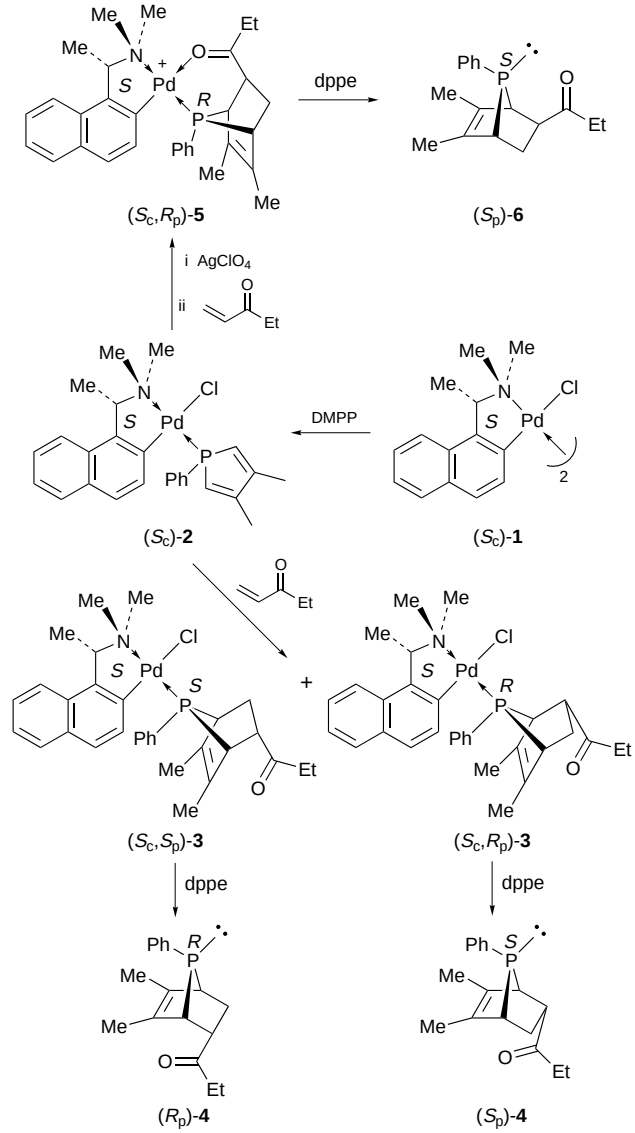
Asymmetric Diels–Alder reactions undoubtedly provide one of the most efficient and elegant methods for the synthesis of chiral 6-membered rings.[1] Since its discovery in 1928, this methodology has been used frequently in the synthesis of important chiral natural products such as antibiotics and prostaglandins. Using this method for carbon–carbon bond formation, we herein report the first asymmetric synthesis of keto-substituted *P*-chiral phosphines. Although ketophosphines are relatively common and their distinct chemistry as well as their synthetic applications are well established,[2] the number of such optically active P–O ligands is surprisingly low.[3] Certainly, no enantiomerically pure ketophosphines containing resolved tertiary phosphorus stereocentres have been reported hitherto.

Uncoordinated 1-phenyl-3,4-dimethylphosphole (DMPP) shows no reaction with ethyl vinyl ketone. The coordination of



($S_c$)-**7**

the phosphine ligand to the chiral reaction template ($S_c$)-**1**,[4] however, activates the cyclic diene towards [4 + 2] cycloaddition reactions (Scheme 1). Hence, treatment of the neutral complex ($S_c$)-**2** with ethyl vinyl ketone in $CH_2Cl_2$ at room temperature for 6 d gave a 1 : 2.5 diastereomeric mixture of the two *endo*-cycloaddition products, ($S_c$,$R_p$)-**3** and ($S_c$,$S_p$)-**3**, in quantitative yield. Prior to crystallization, the 202 MHz $^{31}$P NMR spectrum of the crude product in $CDCl_3$ exhibited two sharp singlets at $\delta_P$ 125.5 (major) and 126.6 (minor). The major isomer was subsequently crystallized from $CH_2Cl_2$–$Et_2O$ as pale yellow needles (70%), mp 135–136 °C, $[\alpha]_D$ +31.8 (*c* 1, $CH_2Cl_2$). An X-ray structural analysis revealed that this major isomer is ($S_c$,$S_p$)-**3** and the absolute configurations of the four new chiral centres at P, C(22), C(25) and C(27) are *S*, *R*, *S* and *R*, respectively (Fig. 1).‡ Treatment of ($S_c$,$S_p$)-**3** with 1,2-bis(diphenylphosphino)ethane (dppe) in $CH_2Cl_2$ liberated the optically pure ketophosphine, ($R_p$)-**4**, from the chiral metal template as an air-sensitive colourless oil in 85% yield, $[\alpha]_D$ −30.0 (*c* 1, $CHCl_3$), $\delta_P$ 109.0 (s). Stereospecific displacement of the ketophosphine was confirmed by the quantitative re-preparation of ($S_c$,$S_p$)-**3** from liberated ($R_p$)-**4** and ($S_c$)-**1**: the 202 MHz $^{31}$P NMR spectrum of the crude product indicated the diastereomer ($S_cS_p$)-**3** only. In a further test of optical purity, the diastereomer ($R_c$,$S_p$)-**3** was prepared from ($R_p$)-**4** and the equally accessible ($R_c$)-**1**: only one sharp singlet was observed at $\delta_P$ 126.6. Partially resolved ($S_p$)-**4** was liberated similarly from ($S_c$,$R_p$)-**3** by treatment with dppe. The free ligand was purified by re-coordination to ($R_c$)-**1** forming the highly crystalline complex ($R_c$,$R_p$)-**3** from which pure ($S_p$)-**4** was liberated. It is noteworthy that the intermolecular cycloaddition process could be completed in 16 h by heating the reaction mixture at 70 °C in 1,2-dichloroethane. Under these more vigorous reaction conditions, however, the product formation became non-selective and a 1 : 1 mixture of the two diastereomeric complexes was obtained.



**Scheme 1**

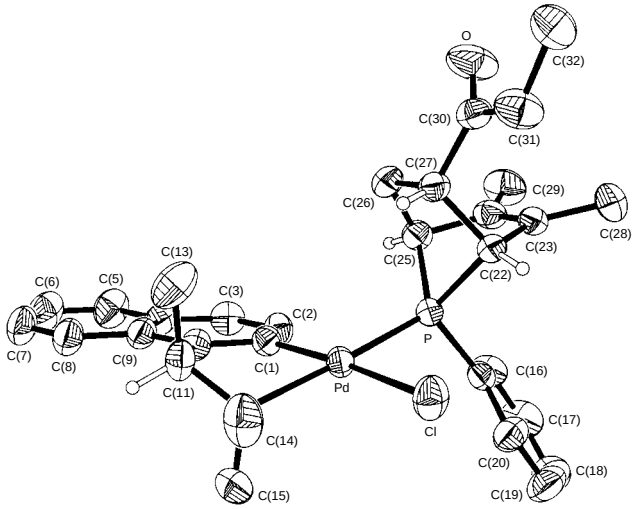



**Fig. 1** Molecular structure and absolute stereochemistry of complex ($S_c$,$S_p$)-**3**. Selected bond lengths (Å) and angles (°); Pd–P 2.241(0), Pd–Cl 2.411(1), Pd–C(1) 2.014(2), Pd–N(12) 2.151(1), P–C(22) 1.860(2), P–C(25) 1.858(2), O–C(30) 1.201(2), C(22)–C(27) 1.582(2), C(27)–C(30) 1.530(2), C(23)–C(24) 1.336(3); C(1)–Pd–N(12) 80.7(1), C(22)–P–C(25) 81.0(1), P–C(22)–C(27) 98.8(1), C(22)–C(27)–C(30) 110.3(1), C(27)–C(30)–O 121.3(2).

Interestingly, the removal of the chloro ligand in ($S_c$)-**2** clearly decelerates the cycloaddition process. Thus, when a $CH_2Cl_2$ solution of ($S_c$)-**2** was stirred with a stoichiometric quantity of $AgClO_4$, filtered, and then treated directly with ethyl vinyl ketone at room temperature, the corresponding cycloaddition reaction required 9 d for completion. Furthermore, the $^{31}P$ NMR spectrum of a $CDCl_3$ solution of the crude product obtained from this slow reaction indicated that both ($S_c$,$R_p$)-**3** and ($S_c$,$S_p$)-**3** were not formed. The spectrum included only a singlet at $\delta_P$ 107.3. This new product was crystallized from $CH_2Cl_2$–$Et_2O$ as yellow prisms (85%), mp 197–198 °C, $[\alpha]_D$ + 232.7 (*c* 1, $CH_2Cl_2$). An X-ray structural analysis confirmed that it is ($S_c$,$R_p$)-**5** and the absolute configurations of its four chiral centres at P, C(22), C(25) and C(27) are *R*, *S*, *R* and *R*, respectively (Fig. 2).‡ It is noted that, interestingly, the C=O bond distance [1.218(6) Å] in this cationic complex is longer than its counterpart [1.201(2) Å] in ($S_c$,$S_p$)-**3**. The lengthening

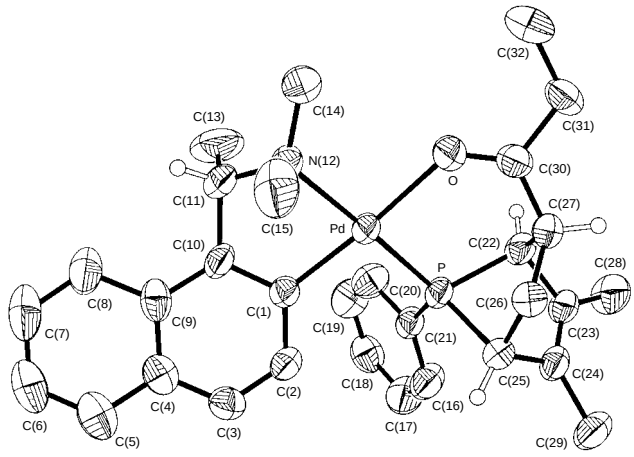



**Fig. 2** Molecular structure and absolute stereochemistry of the cation in ($S_c$,$R_p$)-**5**. Selected bond lengths (Å) and angles (°); Pd–P 2.226(1), Pd–O 2.156(4), Pd–C(1) 1.980(5), Pd–N(12) 2.134(4), P–C(22) 1.840(5), P–C(25) 1.853(5), O–C(30) 1.218(6), C(22)–C(27) 1.571(8), C(27)–C(30) 1.503(7), C(23)–C(24) 1.312(9); P–Pd–O 91.2(1), P–Pd–C(1) 95.7(1), P–Pd–N(12) 177.0(2), O–Pd–C(1) 172.4(2), O–Pd–N(12) 91.0(2), C(1)–Pd–N(12) 82.3(2), Pd–P–C(22) 112.1(2), Pd–P–C(25) 115.6(2), C(22)–P–C(25) 81.4(2), P–C(22)–C(27) 100.2(3), C(22)–C(27)–C(30) 109.1(4), C(27)–C(30)–O 123.1(5), C(30)–O–Pd 128.9(4).

of the C=O bond in the *O*-bonded complex is perhaps an indication of the weakening of the double bond character *via* coordination. Treatment of ($S_c$,$R_p$)-**5** with dppe liberated the optically pure ($S_p$)-**6** from the chiral metal template as an air-sensitive colourless oil in 73% yield, $[\alpha]_D$ −17.2 (*c* 1, $CH_2Cl_2$), $\delta_P$ 94.5 (s). The optical purity of ($S_p$)-**6** was confirmed by the quantitative re-preparation of ($S_c$,$R_p$)-**5** from the liberated ligand and ($S_c$)-**7**:[5] the 202 MHz $^{31}P$ NMR spectrum of the crude product indicated diastereomer ($S_c$,$R_p$)-**5** only. Consistent with this, the diastereomeric complex ($R_c$,$R_p$)-**5**, prepared from ($S_p$)-**6** and ($R_c$)-**7**, showed a sharp singlet at a clearly different $^{31}P$ chemical shift, *i.e.* at $\delta_P$ 110.0.

From a mechanistic standpoint, the transition state involved in the formation of ($S_c$,$R_p$)-**5** requires both the diene and the dienophile to be coordinated simultaneously on the cationic palladium template during the course of the intramolecular cycloaddition reaction. Such an intramolecular mechanism, however, is not involved in the synthesis of *endo*-diastereomers **3** which are clearly produced by an intermolecular cycloaddition reaction. Furthermore, we believe that the coordinated DMPP is electronically activated by the neutral palladium template throughout the intermolecular *endo*-cycloaddition process. Owing to the electron deficiency in the cationic transition state of the *exo*-cycloaddition reaction, the coordinated DMPP is less activated and hence a longer reaction time is required for the intramolecular process. Indeed, such a low activation prohibits the potential competing intermolecular cycloaddition reaction and hence the *exo*-cycloadduct is formed exclusively. Furthermore, as the diene and the dienophile of the *exo*-cycloaddition reaction are coordinated on the chiral template, their stereochemical orientations in the transition state are being controlled simultaneously by the naphthylamine auxilliary. Accordingly the slower *exo*-cycloaddition shows a much higher degree of stereoselectivity than the corresponding faster *endo*-process.

## Footnotes and References

† E-mail: chmlph@nus.sg

‡ *Crystal data* for ($S_c$,$S_p$)-**3**: $[C_{31}H_{37}ClNOPPd]\cdot Et_2O$, $M$ = 686.56, orthorhombic, space group $P2_12_12_1$, $a$ = 11.8359(2), $b$ = 14.0404(2), $c$ = 20.7878(3) Å, $V$ = 3454.53(9) Å$^3$, $Z$ = 4, $D_c$ = 1.320 g cm$^{-3}$, $\mu$(Mo-Kα) = 6.91 cm$^{-1}$, $F(000)$ = 1432. A colourless block with dimensions 0.50 × 0.38 × 0.28 mm was used for diffraction studies, 8315 ($R$ = 0.0152) independent reflections were measured on a Siemens SMART CCD diffractometer with Mo-Kα radiation using $\omega$-scans. All the non-hydrogen atoms were refined anisotropically. Full-matrix least-squares refinement based on $F^2$ with absorption corrected data gave $R_1$ = 0.0198, $wR_2$ = 0.0483 for 7844 independent observed reflections [$|F_o| > 4\sigma(|F_o|)$, $2\theta \leqslant 58.20°$] and 379 parameters.

*Crystal data* for ($S_c$,$R_p$)-**5**: $[C_{31}H_{37}NOPPd][ClO_4]$, $M$ = 676.4, monoclinic, space group $P2_1$, $a$ = 7.625(1), $b$ = 16.814(2), $c$ = 12.400(1) Å, $\beta$ = 104.82(1)°, $V$ = 1536.9(3) Å$^3$, $Z$ = 2, $D_c$ = 1.46 g cm$^{-3}$, $\mu$(Mo-Kα) = 7.82 cm$^{-1}$, $F(000)$ = 696. A pale yellow prism of dimensions 0.53 × 0.38 × 0.15 mm was used. 3639 independent reflections were measured on a Siemens P4/PC diffractometer with Mo-Kα radiation using $\omega$-scans. All the non-hydrogen atoms were refined anisotropically. In the full-matrix least-squares refinement on $F^2$ the model converged at $R_1$ = 0.035, $wR_2$ = 0.088 for 3351 independent observed reflections [$|F_o| > 4\sigma(|F_o|)$, $2\theta \leqslant 55°$] and 349 parameters. CCDC 182/597.

1 W. Oppolzer, in *Comprehensive Organic Synthesis*, ed. B. M. Trost, Pergamon, Oxford, New York, Seoul, Tokyo, 1991, vol. 5, ch. 4.
2 A. Bader and E. Lindner, *Coord. Chem. Rev.*, 1991, **108**, 27; J. Andrieu, P. Braunstein, Y. Dusausoy and N. E. Ghermani, *Inorg. Chem.*, 1996, **35**, 7174.
3 D. A. Knight, D. J. Cole-Hamilton, D. C. Cupertino, M. Harman and M. B. Hursthouse, *Polyhedron*, 1992, **11**, 1987.
4 D. G. Allen, G. M. McLaughlin, G. B. Robertson, W. L. Steffen, G. Salem and S. B. Wild, *Inorg. Chem.*, 1982, **21**, 1007.
5 S. Y. M. Chooi, S. Y. Siah, P. H. Leung and K. F. Mok, *Inorg. Chem.*, 1993, **32**, 4812.

*Received in Cambridge, UK, 11th August 1997; 7/05830F*

# Reductive etherification of substituted cyclohexanones with secondary alcohols catalysed by zeolite H-MCM-22

**Michel J. Verhoef, Edward J. Creyghton, Joop A. Peters and Herman van Bekkum***

*Laboratory of Organic Chemistry and Catalysis, Delft University of Technology, Julianalaan 136, 2628 BL Delft, The Netherlands*

**Zeolite MCM-22 is an active and regenerable catalyst for a remarkably shape selective reductive etherification of cyclohexanones with bulky substituents at the 4-position, employing secondary alcohols as reductants.**

Zeolite MCM-22 has recently been introduced as a unique biporous zeolite.[1] It has been shown that it contains two independent pore systems,[2,3] one defined by sinusoidal 10-membered ring channels extended in two dimensions, and the other by large 12-membered ring supercages (7.1 × 7.1 × 18.1 Å) connected by 10-membered ring channels. The material has a high thermal stability, a BET surface area of $> 400$ m$^2$ g$^{-1}$ and a sorption capacity of 0.16 ml g$^{-1}$,[4,5] which make it very interesting for catalysis. MCM-22 in its acidic form has already been claimed to be active in, for example, the conversion of lower alkenes to heavier hydrocarbons, and of aliphatic hydrocarbons to aromatics, the disproportionation of toluene and the alkylation of benzene.[6]

Here we report on the use of H-MCM-22 as a bifunctional catalyst in the reductive etherification of cyclohexanones having bulky substituents at the 4-position, using secondary alcohols as reductants. The zeolite appears to be active for both acid-catalysed conversion of the ketones to (hemi)acetals and consecutive Meerwein–Ponndorf–Verley (MPV)-type hydride transfer to yield ethers. Until now two catalysts were always required to achieve this, *i.e.* a strong acid for the acetalisation and a transition metal for the reduction step.[7,8] Various solid catalysts including zeolites have been applied in acid-catalysed acetal fomation[9] and the MPV reaction.[10,11] However, the combination of both properties in a single zeolite, enabling the direct synthesis of ethers from ketones, is novel.

MCM-22 with a Si/Al ratio of 15 was synthesized following a literature procedure,[12] dried at 60 °C *in vacuo* and subsequently calcined in a flow of air at 540 °C for 12 h. The acidic form was obtained by four-fold ion-exchange with 1 M aqueous ammonium nitrate at 80 °C for 12 h, followed by calcination as described above. X-Ray diffraction studies and the NMR ($^{29}$Si and $^{27}$Al) spectra of the resulting material were in agreement with literature data.[13] The $^{27}$Al NMR spectra indicated the presence of some extra-framework aluminium ($\delta$ −1.0). Transmission electron microscopy measurements showed the material to consist of small disk-like particles (130 × 130 × 15 nm), in agreement with scanning electron microscopy data.[2]

Reactions were conducted by refluxing ketone (9 mmol), catalyst (1 g) and 1,3,5-tri-*tert*-butylbenzene (1.6 mmol) as internal standard in Pr$^i$OH or Bu$^s$OH (70 ml). The reactions were monitored by GC (CP wax 52 CB column).

H-MCM-22 proved to be active and selective in the reductive etherification of 4-*tert*-butylcyclohexanone with the above mentioned alcohols, giving the corresponding ethers with a *cis* : *trans* ratio of 60 : 40 ( Table 1). Only trace amounts ( < 5%) of 4-*tert*-butylcyclohexanol, formed by direct MPV reduction, were observed. Continuous removal of water from the reflux by a bed of zeolite Na-A significantly increased both the conversion and the selectivity to the ether (Table 1). The catalyst could be re-used, following regeneration at 450 °C for 12 h in air, without any loss in activity or crystallinity.

The size and the shape of the ketone substrate appears to be decisive for the course of the reaction. For example, 4-phenylcyclohexanone and 4-methylcyclohexanone could be etherified, although with poor conversions and selectivity. On the other hand, 4-trimethylsilylcyclohexanone, with a similar size and shape to 4-*tert*-butylcyclohexanone, reacted smoothly.

Secondary alcohols are found to be required as hydride donors. With MeOH only acetal formation occurred. Acid sites appear to be essential, since with Na-MCM-22 as catalyst in the etherification of 4-*tert*-butylcyclohexanone only a 5% yield was obtained after 24 h. The reductive etherification is irreversible. Starting from the ether, water and acetone in Pr$^i$OH in the presence of zeolite H-MCM-22, no reaction occurred.

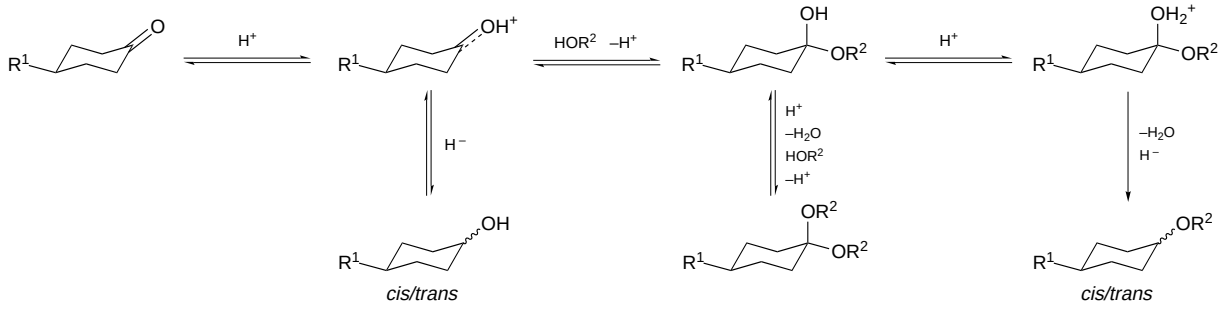
Some zeolites, especially zeolite Beta, perform well in MPV reductions.[14] However, a mechanism involving MPV reduction of the cyclohexanone, followed by acid-catalysed etherification by the solvent, can be excluded, since no reaction occurred on starting from 4-*tert*-butylcyclohexanol under similar reaction conditions. It seems more likely that the reaction proceeds *via* Brønsted acid-catalysed formation of a hemiacetal followed by a Lewis acid-catalysed, MPV-like hydride transfer to yield the ether (see Scheme 1).

The involvement of (hemi)acetals is supported by the fact that when the reaction of 4-*tert*-butylcyclohexanone was performed with a mixture of MeOH and Pr$^i$OH (1 : 1 mixture) both the dimethyl and the mixed methyl isopropyl acetals were formed almost instantaneously. These acetals were slowly converted into the isopropyl and methyl ethers. With 4-phenyl- and 4-methyl-cyclohexanones, dissolved in a 1 : 1 mixture of MeOH and Pr$^i$OH in the presence of zeolite H-MCM-22, acetal formation also occurred; however, only trace amounts of ether were formed together with some cyclohexene derivatives. The

**Table 1** Reductive etherification of various 4-substituted cyclohexanones with secondary alcohols and H-MCM-22 as the catalyts[a]

| Substrate | Conversion (%) | Selectivity (%) Ether | Alcohol | TON[b] |
|---|---|---|---|---|
| 4-*tert*-butylcyclohexanone[c] | 22 | 19 | 35 | 1.6 |
| 4-*tert*-butylcyclohexanone | 100 | 78 | 6 | 7.3 |
| 4-*tert*-butylcyclohexanone[d] | 96 | 93 | 6 | 7.0 |
| 4-*tert*-butylcyclohexanone[e] | 98 | 87 | 9 | 8.2 |
| 4-*tert*-butylcyclohexanone[f] | 6 | 65 | 29 | 0.3 |
| 4-phenylcyclohexanone[g] | 15 | 20 | 0 | 1.1 |
| 4-phenylcyclohexanone[d,g] | 15 | 20 | 0 | 1.2 |
| 4-methylcyclohexanone[g] | 15 | 0 | 0 | 1.5 |
| 4-methylcyclohexanone[d,g] | 12 | 60 | 0 | 1.3 |
| 4-trimethylsilylcyclohexanone | > 95 | 60 | < 5 | 4.8 |

[a] Reaction conditions: ketone (9 mmol), catalyst (1 g) and 1,3,5-tri-*tert*-butylbenzene (1.6 mmol) as an internal standard, in Pr$^i$OH (70 ml) under reflux and stirring. Water abstraction from the vapour phase by a Soxhlet apparatus filled with zeolite NaA. [b] Based on the total number of aluminium sites present in 1 g of catalyst. [c] Without removal of water. [d] Reaction with Bu$^s$OH. [e] Regenerated catalyst. [f] Reaction with Na-MCM-22 as catalyst. [g] Conversions are corrected for the amount of substrate in the vapour phase and the amount adsorbed by the catalyst.




$R^1$ = $Bu^t$, Ph, Me, $SiMe_3$
$R^2$ = $Pr^i$, $Bu^s$
$H^+$ = zeolite OH
$H^-$ = activated H of Al-coordinated secondary alcohol

**Scheme 1**

diisopropyl acetal was not observed in any reaction although this acetal can easily be prepared homogeneously.[9] Steric strain might prevent its formation. It cannot be excluded, however, that formation of the diisopropyl acetal occurs in the zeolite supercages, from where it cannot escape.

The role of $Pr^iOH$ as hydride donor was demonstrated by a reaction in $Pr^iOD$ (25% labelling). GC–MS and $^2H$ NMR of the reaction product showed that the C(1)-position of the cyclohexane ring and the secondary carbon of the isopropoxy group were 25% deuterated.

It remains unclear why H-MCM-22 shows this unusual behaviour, while various other solid acids yield only the MPV reduction products.[14] Possibly the number of Brønsted acid sites in H-MCM- 22 greatly exceeds the number of sites capable of catalysing the MPV reduction, resulting in the fast formation of (hemi)acetals followed by a slow conversion to the ethers. An explanation for the remarkable shape selectivity of the reaction may be that it takes place in the zeolite supercages (see Fig. 1).

The aluminium site in MCM-22, required for the hydride transfer, is assumed to be located mostly at the positions marked with an arrow.[15] When 4-*tert*-butyl- (and 4-trimethylsilyl)-cyclohexanone is adsorbed into the zeolite cage, it is forced into an orientation which brings the carbonyl group into close proximity to that site. In this tentative mechanism the aluminium atom plays a three-fold role: activation of the ketone, hydride transfer and stabilisation of the carbocation intermediate formed after water elimination. In contrast, the 4-methyl- and 4-phenyl-cyclohexanones are not forced to adopt this specific orientation.

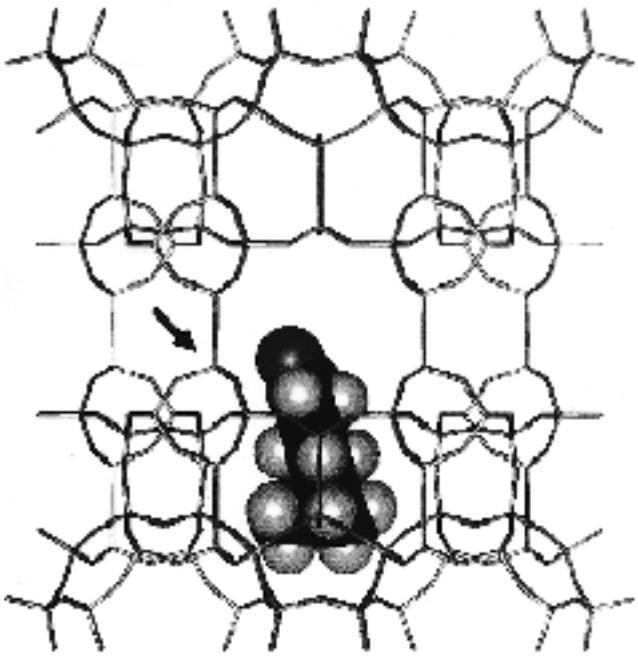


**Fig. 1** 4-*tert*-Butylcyclohexanone in an MCM-22 supercage

In conclusion, H-MCM-22 is an active catalyst in the reductive etherification of substituted cyclohexanones. The mechanism is proposed to proceed *via* the formation of a hemiacetal followed by an MPV-like reduction.

The authors thank Dr P. J. Kooyman of the National Centre for High Resolution Electron Microscopy, Delft University of Technology, Delft, The Netherlands, for performing the electron microscopy investigations and Ms S. L. Njo for her help with Fig. 1. The IOP Catalysis (Innovation Oriented Research Programmes) is gratefully acknowledged for financial support.

## Footnote and References

* E-mail: secretariat-ock@stm.tudelft.nl

1 M. K. Rubin and P. Chu, *US Pat.*, 4 954 325, 1990.
2 M. E. Leonowicz, J. A. Lawton, S. L. Lawton and M. K. Rubin, *Science*, 1994, **264**, 1910.
3 W. Souverijns, W. Verrelst, G. Vanbutsele, J. A. Martens and P. A. Jacobs, *J. Chem. Soc., Chem. Commun.*, 1994, 1671.
4 W. Kolodziejski, C. Zicovich-Wilson, C. Corell, J. Pérez-Pariente and A. Corma, *J. Phys. Chem.*, 1995, **99**, 7002.
5 A. Corma, C. Corell, J. Pérez-Pariente, J. M. Guil, R. Guil- Lopez, S. Nicolopoulos, J. Gonzales Calbet and M. Vallet-Regi, *Zeolites*, 1996, **16**, 7.
6 C. T-W. Chu, *US Pat.*, 4 956 514, 1990; C. T-W. Chu, T. F. Degnan and B. K. Huh, *US Pat.*, 4 982 033, 1991; R. P. L. Absil, S. Han, D. O. Marler and D. S. Shihabi, *US Pat.*, 4 962 257, 1990.
7 M. Verzele, M. Acke and M. Anteunis, *J. Chem. Soc.*, 1963, 5598.
8 Y. M. Y. Haddad, H. B. Henbest, J. Husbands, T. R. B. Mitchell and J. Trocha-Grimshaw, *J. Chem. Soc., Perkin Trans. 1*, 1974, 596.
9 D. P. Roelofsen and H. van Bekkum, *Synthesis*, 1972, **8**, 419.
10 For a review see: C. F. de Graauw, J. A. Peters, H. van Bekkum and J. Huskens, *Synthesis*, 1994, 1007.
11 E. J. Creyghton, J. Huskens, J. C. van der Waal and H. van Bekkum, *Stud. Surf. Sci. Catal.*, 1997, **108**, 531.
12 Unverricht, M. Hunger, S. Ernst, H. G. Karge and J. Weitkamp, *Stud. Surf. Sci. Catal.*, 1994, **84**, 37.
13 A. Corma, C. Corell, V. Fornés, W. Kolodziejski and J. Pérez- Pariente, *Zeolites*, 1995, **15**, 576.
14 E. J. Creyghton, S. D. Ganeshie, R. S. Downing and H. van Bekkum, *J. Chem. Soc., Chem. Commun.*, 1995, 1859; E. J. Creyghton, S. D. Ganeshie, R. S. Downing and H. van Bekkum, *J. Mol. Catal. A*, 1997, **115**, 457.
15 S. L. Lawton, A. S. Fung, G. J. Kennedy, L. B. Alemany, C. D. Chang, G. H. Hatzikos, D. N. Lissy, M. K. Rubin, H-K. C. Timken, S. Steuernagel and D. E. Woessner, *J. Phys. Chem.*, 1996, **100**, 3788.

*Received in Cambridge, UK, 21st July 1997; 7/05196D*

# Structural influence of hydrotalcite on Pd dispersion and phenol hydrogenation

**S. Narayanan* and K. Krishna**

*Catalysis Division, Indian Institute of Chemical Technology, Hyderabad 500 007, India*

**An interesting structure dispersion relationship of Pd/hydrotalcite is studied by changing the calcination temperature of hydrotalcite support and evaluated for phenol hydrogenation.**

Efforts are being directed towards searching for new and efficient supports for dispersing noble metals. Hydrotalcites (HTs) have brucite-like positively charged layers of magnesium and aluminium octahedra sharing edges and have interstitial carbonate anions.[1] Supported metal hydrotalcites have created much scientific interest because of their interesting properties in catalytic reforming.[2,3] However, not much attention has been paid to the characterization of hydrotalcite supported metals. We have investigated the high phenol hydrogenation activity of Pd/HT to cyclohexanone,[4] which is an important raw material for the production of caprolactam. Here we discuss, for the first time, the interesting changes in properties of the HT support with calcination and its influence on metal dispersion and hydrogenation activity.

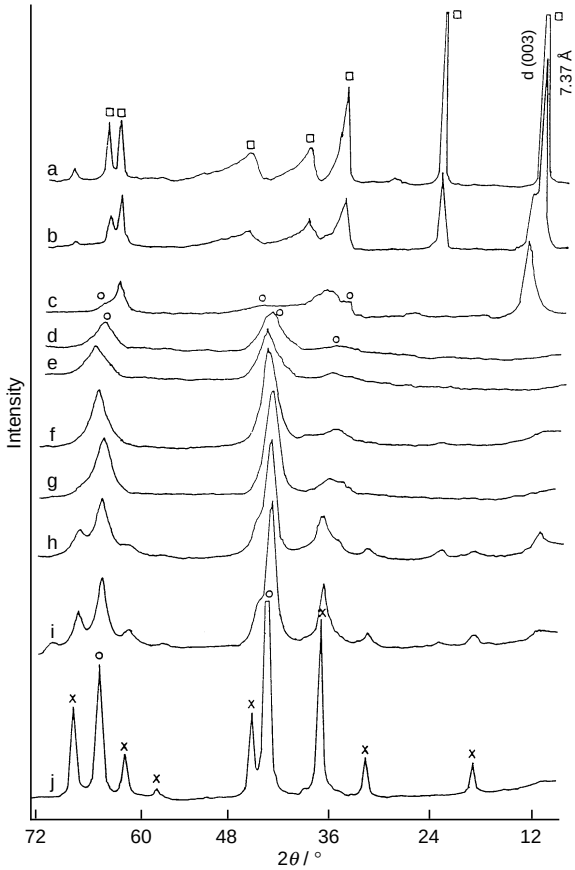



**Fig. 1** XRD patterns of the hydrotalcites calcined at different temperatures (K): (a) 373, (b) 473, (c) 573, (d) 673, (e) 773, (f) 873, (g) 973, (h) 1073, (i) 1173 and (j) 1273. (□) HT, (○) MgO, (×) $MgAl_2O_4$.

HT was prepared according to the method described by Reichle *et al.*[5] HT was calcined in air for 4 h in the temperature range 473–1273 K and XRD patterns were recorded in air. Apart from calcined HTs, γ-$Al_2O_3$ and $MgAl_2O_4$ were also used as supports for loading 1 mass% of Pd. Impregnation was done with a standard $PdCl_2$ solution acidified with HCl. Surface area of the support and CO chemisorption on 1 mass% Pd/HT were measured. Phenol hydrogenation was carried out at 453 K over *ca.* 0.2 g of the catalyst at a phenol WHSV of 0.037 mol $g^{-1}$ $h^{-1}$. The experimental details are given elsewhere.[4]

Fig. 1 shows XRD patterns of calcined HTs. The sample dried at room temperature (not shown) and 373 K showed the same diffraction patterns and $d_{(003)}$ basal spacing (7.37 A°) indicating retention of interlayer water. At 473 K, owing to the loss of gallery water, the basal spacing decreased by 0.56 Å. The patterns showed both anhydrous and hydrated HT, the latter might have formed owing to fast rehydration of HT.[6] The sample calcined at 573 K showed a basal spacing of 6.6 Å indicating dehydrated HT of low crystallinity along with MgO peaks. Between 373 and 573 K, the intensity of $d_{(003)}$ peak decreased, broadened and shifted towards higher $2\theta$ values indicating the progressive destruction of the layered structure. Beyond 573 K, broad and diffuse peaks corresponding to mixed oxides of MgO are observed. With increase in calcination temperature the MgO peaks intensify and at 1073 K HT showed peaks representing a mixture of crystalline MgO and spinel $MgAl_2O_4$. At 1273 K mainly $MgAl_2O_4$ along with crystalline MgO are formed.

The surface area remained almost the same (Fig. 2) up to a calcination temperature of 573 K, indicating that the layered structure of HT is predominantly present. Beyond 573 K and up to 773 K, there is an increase in surface area. This is due to the loss of water and $CO_2$ which creates craters in the metal oxide sheet.[5] Above 773 K, there is a progressive decrease in surface area as the crystallinity of the material increases.

Fig. 2 shows the effect of calcination temperature of HT on dispersion and catalytic activity of Pd. Two maxima in dispersion (*ca.* 60%) and conversion (≥90%) can be seen when

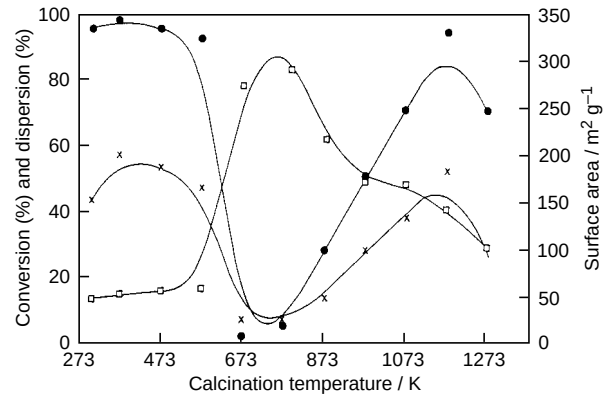



**Fig. 2** Effect of calcination on surface area of HT, metal dispersion and activity of 1 mass% Pd/HT. (□) Surface area, (●) conversion (%), (×) dispersion (%).

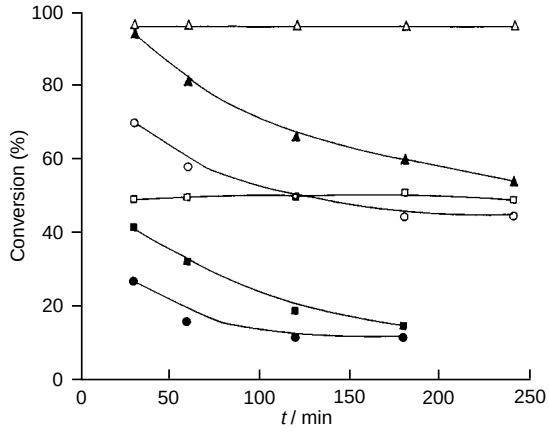



**Fig. 3** Effect of time on stream over 1 mass% Pd/support. HT support calcined at different temperatures (K): (△) 373, (□) 973, (○) 1073 and (▲) 1173, (●) 1 mass% $Pd/Al_2O_3$, (■) 1 mass% $Pd/MgAl_2O_4$.

the support is calcined in the region of room temp. to 573 K and at 973–1173 K. The dispersion of Pd slightly increases when the support is dried at 373 K and calcined at 473 K compared to the support dried at room temp. and calcined at 573 K. There is an abrupt decrease in CO uptake when the support is calcined between 673 and 773 K, and CO uptake progressively increases up to a calcination temperature of 1173 K and again decreases thereafter. Despite a large surface area of HT having the MgO phase, the dispersion of Pd is low on these supports. There is no direct relationship between surface area of the support, which exists in different phases, and Pd dispersion indicating that the structural properties are playing a major role in metal dispersion. Phenol conversion follows the same trend as that of dispersion and metal area. The selectivity towards cyclohexanone is ⩾95%.

Acidification of $PdCl_2$ leads to $PdCl_4^{2-}$ anion which on impregnation replaces the carbonate anion at the external edge surface of the non-porous HTs. This interaction results in a fine dispersion of palladium precursor which on reduction gives highly dispersed palladium. The replacement of carbonate anion in the internal surface sites can be ruled out as there is no change in the basal spacing of the palladium-loaded HT (XRD not shown). The physically adsorbed water in room-temperature dried HT inhibits $CO_3^{2-}$ access to $PdCl_4^{2-}$; therefore the deposition of the precursor is relatively more on the surface. This results in less dispersion of palladium compared to the sample dried at 373 K. The dispersion over HT dried at 373 K and calcined at 473 K is almost the same. This indicates that the structural water did not alter the dispersion as the precursor is mostly deposited by ion-exchange of $CO_3^{2-}$ on the external edge surface. The dispersion is less over HT which is partially decarbonated and dehydroxylated and includes both the phases of MgO and HT. Even though aluminium is distributed uniformly throughout the HT layer, on calcination, alumina segregates out to the surface and as the calcination temperature increases the concentration of alumina on the surface increases. The increase in crystallinity of MgO and the segregation of $Al_2O_3$ to the surface with increase in calcination temperature in the range 673–973 K, improves the dispersion of Pd though the role of these two phases is not very clear. The dispersion of Pd on HT calcined in the range 1073–1273 K increases with the increase in $MgAl_2O_4$ phase and decreases over the support containing a large amount of crystalline MgO and $MgAl_2O_4$. The decrease in dispersion could be due to sintering of Pd on this highly crystalline phase. From Fig. 1 and 2 it is observed that there exists a correlation between dispersion of Pd and $MgO/MgAl_2O_4$ ratio with a maximum dispersion at an optimum ratio.

Fig. 3 shows time on stream over Pd/HT, $Pd/Al_2O_3$ and $Pd/MgAl_2O_4$. $Pd/Al_2O_3$, $Pd/MgAl_2O_4$ deactivate due to the formation of coke by the acid sites of alumina.[7] Pd/HT in which the support was calcined upto to 973 K did not show any appreciable deactivation. Spectroscopic techniques show that, on calcination of HT, a small portion of octahedral Al is converted to tetrahedral Al possibly residing on the surface and the amount increases with calcination temperature.[8] This alumina is in a local oxidic environment that does not favor the acid-catalysed reaction that typically occurs over alumina.[9] The stability of the catalyst, in which the HT is calcined up to 973 K, against coke formation could be explained based on the above observation. The role of impurities which may surface during calcination in preventing the catalyst from deactivation can not be ruled out. Above calcination at 973 K the HT shows a spinel $MgAl_2O_4$ phase and there is appreciable deactivation. The rate of deactivation increases with increase in spinel phase in the support.

Some interesting observations have been made in this study. Pd dispersion depends on the HT structure. Palladium is highly dispersed over HT having a layered structure with carbonate interlayer anions and also on a mixture of crystalline MgO and $MgAl_2O_4$ spinel. In spite of partial segregation of alumina to the surface during calcination it did not show appreciable deactivation in phenol hydrogenation which is a problem with acidic alumina. In summary HTs are attractive alternative supports for noble metals.

K. K. thanks CSIR, New Delhi for the award of Senior Research Fellowship.

## Footnote and References

* E-mail: root@csiict.ren.nic.in

1 F. Cavani, F. Trifiro and A. Vaccari, *Catal. Today*, 1990, **11**, 173.
2 R. J. Davis and E. G. Derouane, *Nature*, 1991, **349**, 313.
3 I. I. Ivanova, A. Pasau-Claerbout, M. Seirvert, N. Blum and E. G. Derouane, *J. Catal*., 1996, **158**, 512.
4 S. Narayanan and K. Krishna, *Appl. Catal.*, 1997, **147**, L253.
5 W. T. Reichle, S. Y. Kang and D. S. Everhardt, *J. Catal*., 1986, **101**, 352.
6 V. R. L. Constantion and T. J. Pinnavaia, *Inorg. Chem*., 1995, **34**, 883.
7 G. Neri, A. M. Visco, A. Donato, C. Milone, M. Malentacchi and G. Gubitosa, *Appl. Catal.*, 1994, **110**, 49.
8 F. Rey, V. Fornes and J. M. Rojo, *J. Chem. Soc., Faraday Trans.*, 1992, **88**, 2233.
9 A. L. McKenzie, C. J. Fishel and R. J. Davis, *J. Catal.*, 1992, **138**, 547.

*Received in Cambridge, UK, 1st July 1997; 7/04599I*

# A nucleophilic niobium(v) nitride prepared by isocyanate decarbonylation

**Michael G. Fickes, Aaron L. Odom and Christopher C. Cummins*†**

*Department of Chemistry, 2-227, Massachusetts Institute of Technology, 77 Massachusetts Avenue, Cambridge, MA 02139-4307, USA*

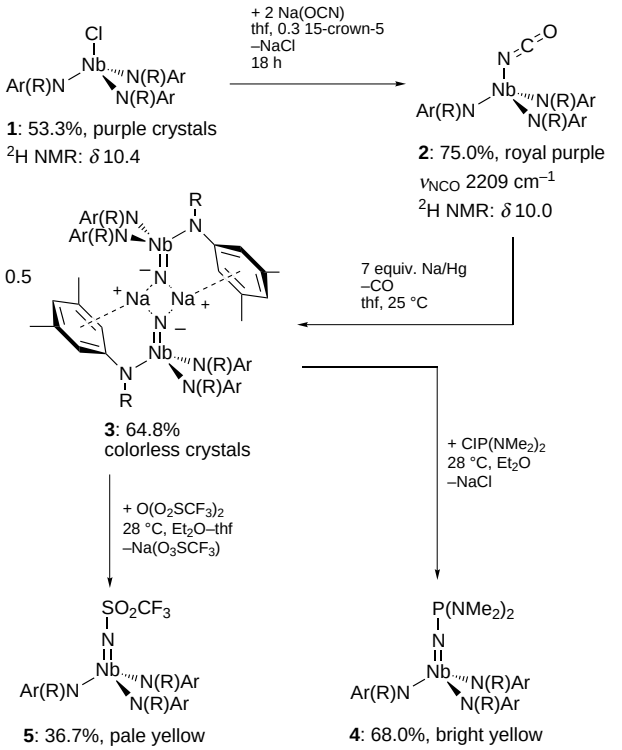
**Carbon monoxide is lost upon sodium amalgam reduction of [(OCN)Nb{N(R)Ar}$_3$] [R = C(CD$_3$)$_2$CH$_3$, Ar = C$_6$H$_3$Me$_2$-3,5] to give crystallographically characterized [Na{NNb-[N(R)Ar]$_3$}]$_2$, a nucleophilic niobium(v) nitride which reacts with ClP(NMe$_2$)$_2$ and O(SO$_2$CF$_3$)$_2$ to give P- and S-substituted imido complexes, respectively.**

New synthetic routes to d$^0$ transition-metal complexes containing the terminal nitride functionality have emerged in recent years.[1] Various small molecules or ions, including $N_2$,[2,3] $N_2O$,[4] NO,[5] $N_3^-$,[6] and organic nitriles,[7] have been identified as N-atom sources for metal–nitrogen triple bond formation. This work describes the finding that cyanate ion $NCO^-$ can be added to the foregoing list in the context of niobium chemistry.

A handful of niobium complexes bearing sterically demanding amido ligands such as NPh$_2$,[8,9] N(SiMe$_3$)$_2$,[8,10] and N(c-C$_6$H$_{11}$)$_2$,[11] have been described in recent years. Given the demonstrated effectiveness of the N(R)Ar [R = C(CD$_3$)$_2$CH$_3$, Ar = C$_6$H$_3$Me$_2$-3,5) ligand in molybdenum chemistry,[2,4,12] and the convenience of the $^2$H NMR spectroscopic handle afforded by it,[13] this ligand was selected for our investigation of niobium isocyanate chemistry.‡ Accordingly, treatment of [NbCl$_4$(thf)$_2$] with 3 equiv. of Li[N(R)Ar](OEt$_2$) in hexane led to formation of purple [ClNb{N(R)Ar}$_3$] **1**, which was obtained in 53% yield as a hydrocarbon- and diethyl ether-soluble crystalline solid (Scheme 1). Toluene solutions of compound **1** exhibit an EPR signal ($g_{iso}$ = 1.966, $a_{iso}$ = 105.1 G) characteristic of a d$^1$ niobium ($^{93}$Nb, $I$ = 9/2) center, along with a single $^2$H NMR signal ($\delta$ 10.4, $\Delta\nu_{1/2}$ 116 Hz); the compound exhibits a $\mu_{eff}$ of 2.1 $\mu_B$ ([$^2$H$_6$]benzene).[14] The pseudotetrahedral monomeric nature of **1** has been confirmed in preliminary fashion by an X-ray diffraction study showing that **1** is isostructural with the related compound [SMo{N(R)Ar}$_3$],[15] with which **1** is isoelectronic.

Displacement of chloride by isocyanate was effected by treating, for 18 h, a 28 °C thf solution of **1** with an excess of sodium cyanate (2 equiv.) in the presence of 15-crown-5 (0.30 equiv). Compound **2** [(OCN)Nb{N(R)Ar}$_3$], was obtained subsequently as dark purple needles in 75% yield by recrystallization from pentane; the compound exhibits a $\mu_{eff}$ of 2.2 $\mu_B$ ([$^2$H$_6$]benzene). A strong band at 2209 cm$^{-1}$ in the IR spectrum of **2** is attributable to $\nu_{NCO}$,[16] consistent with the proposal of an N-bound, $\eta^1$ mode of ligation for the $NCO^-$ ion. The decarbonylation chemistry of **2** (see below) likewise is suggestive of its isocyanate character.

Decarbonylation occurred upon treatment of **2** with an excess of 0.5% sodium amalgam (7 equiv. Na, unoptimized) in thf for 18 h at 28 °C. Trapping experiments to be described in detail elsewhere confirmed that a substantial fraction of the carbon monoxide lost is evolved as free CO. The anionic niobium(v) nitride [Na{NNb[N(R)Ar]$_3$}]$_2$, **3**, was obtained as a thf-free, benzene-soluble, colorless solid in 65% yield subsequent to trituration with hexane and recrystallization from ether. Compound **3** was found by X-ray crystallography to adopt a dimeric structure in the solid state (Fig. 1),§ the dimer possessing a center of inversion about a central $Na_2N_2$ square core. The environment about sodium involves two nitrido nitrogens and $\eta^6$-aryl complexation, with Na–C$_{aryl}$ distances averaging 2.94 Å. Interaction of alkali-metal cations with benzene-like organic $\pi$ systems is a well documented phenomenon,[17] and in the present case this interaction serves to explain the ready isolation of **3** in thf-free form. NMR spectra of diamagnetic **3** are




**Scheme 1**

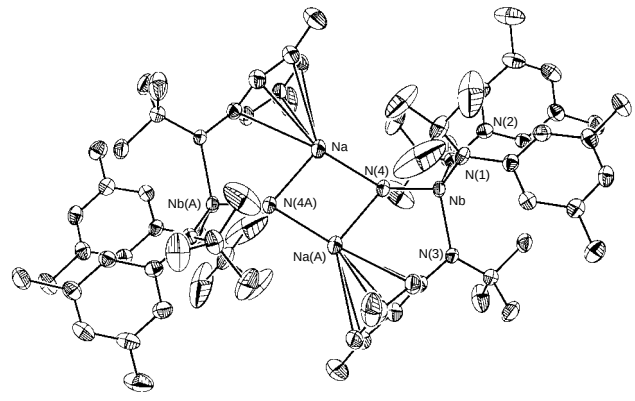



**Fig. 1** Structural drawing of **3** with thermal ellipsoids at the 35% probability level. Selected bond lengths (Å) and angles (°): Nb–N(4) 1.718(3), Nb–N(1) 2.041(3), Nb–N(2) 2.074(3), Nb–N(3) 2.089(3), N(4)–Na 2.351(4), N(4)–Na(A) 2.336(4); Nb–N(4)–Na 129.0(2), Nb–N(4)–Na(A) 148.5(2), N(4)–Na–N(4A) 96.62(12), N(4)–Nb–N(1) 104.3(2), N(4)–Nb–N(2) 105.7(2), N(4)–Nb–N(3) 101.3(2), N(1)–Nb–N(2) 115.61(14), N(1)–Nb–N(3) 113.40(13), N(2)–Nb–N(3) 114.42(13).

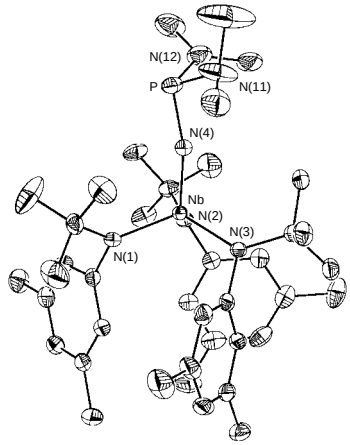



**Fig. 2** Structural drawing of **4** with thermal ellipsoids at the 35% probability level. Selected bond lengths (Å) and angles (°): Nb–N(4) 1.796(3), Nb–N(1) 2.010(3), Nb–N(2) 2.018(4), Nb–N(3) 2.021(3), N(4)–P 1.687(4), P–N(11) 1.744(5), P–N(12) 1.658(4); Nb–N(4)–P 166.5(2), N(4)–Nb–N(1) 108.0(2), N(4)–Nb–N(2) 109.5(2), N(4)–Nb–N(3) 108.0(2), N(4)–P–N(11) 99.4(2), N(4)–P–N(12) 106.5(2), N(11)–P–N(12) 99.0(3).

consistent with its solid-state structure if a fluxional process is invoked to explain the observed equivalence of the N(R)Ar ligands on the NMR timescale at 25 °C. The enthalpic driving force for the decarbonylation producing **3** is understandable in terms of formation of a very strong Nb–N multiple bond, free carbon monoxide, and solvated sodium ion. Despite its evident favorability the latter transformation appears to be unique in isocyanate coordination chemistry. The reverse reaction, isocyanate formation by intramolecular coupling of N and CO ligands, has been described in at least one report.[18]

The utility of **3** stems from its nucleophilic character as evinced by its reactions with chlorobis(dimethylamino)phosphine and triflic anhydride, producing the unusual imido derivatives **4** and **5**, respectively. (A related nucleophilic vanadium nitride anion, $[NV(NPh_2)_3]^-$, was reported recently.[9]) Compound **4**, $[(Me_2N)_2PNNb\{N(R)Ar\}_3]$, was obtained in 68% yield as a bright yellow lipophilic crystalline solid. Diamagnetic **4** exhibits a single broad $^{31}P$ NMR signal at $\delta$ 135.0 ($\Delta\nu$ 101 Hz), the breadth of which is attributable to $^{93}Nb$ coupling. X-Ray crystallography confirmed that **4** is a pseudotetrahedral monomer (Fig. 2) with a relatively linear Nb–N–P linkage (166.5°) and a Nb–$N_{imido}$ distance [1.796(3) Å] that is short by comparison with the Nb–$N_{amido}$ distances [av. 2.016(3) Å].§

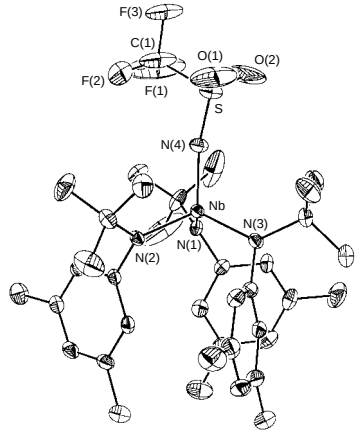



**Fig. 3** Structural drawing of **5** with thermal ellipsoids at the 35% probability level. Selected bond lengths (Å) and angles (°): Nb–N(4) 1.853(5), Nb–N(1) 1.978(5), Nb–N(2) 1.988(5), Nb–N(3) 1.983(5), N(4)–S 1.550(5), S–O(1) 1.415(7), S–O(2) 1.398(7), S–C(1) 1.807(12); Nb–N(4)–S 167.0(4), N(4)–Nb–N(1) 109.8(2), N(4)–Nb–N(2) 110.5(2), N(4)–Nb–N(3) 110.2(2), N(4)–S–O(1) 113.5(4), N(4)–S–O(2) 113.2(4), N(4)–S–C(1) 104.2(4), O(1)–S–O(2) 117.7(7), O(1)–S–C(1) 102.3(5), O(2)–S–C(1) 103.7(7).

'Triflimide' **5**, $[(CF_3SO_2)NNb\{N(R)Ar\}_3]$, was also characterized by X-ray diffraction (Fig. 3).§ The compound exhibits a relatively long Nb–$N_{imido}$ distance [1.853(5) Å] reflective of the highly electron-withdrawing nature of the trifluoromethanesulfonyl substituent. Interestingly, compound **5** appears to be the first example of a triflimide transition-metal complex. Although the formation of **5** appears to proceed smoothly according to the $^1H$ NMR spectrum of the crude reaction mixture, the compound, a pale yellow solid, was obtained in moderate (37%) yield after a diethyl ether wash.

For funding this work we thank the Packard Foundation, the Alfred P. Sloan Foundation, the National Science Foundation (CAREER Award CHE-9501992), 3M, DuPont, and Union Carbide. C. C. C. also wishes to thank Sandro Gambarotta for stimulating discussions.

## Footnotes and References

* E-mail: ccummins@mit.edu
† Alfred P. Sloan Fellow, 1997–2000.

‡ All manipulations were carried out under an atmosphere of dry nitrogen using solvents purified by standard methods. The new compounds **1**–**5** gave satisfactory elemental analyses (C, H, and N).

§ *Crystallographic data*: **3**: monoclinic, space group $P2_1/c$, $a$ = 18.149(4), $b$ = 13.682(2), $c$ = 16.306(2) Å, $\beta$ = 113.009(8)°, $U$ = 3727.0(11) Å$^3$, $Z$ = 4, $T$ = 183 K, $\mu$(Mo-K$\alpha$) = 0.362 mm$^{-1}$, no. of unique reflections = 5146, data/parameter ratio = 14, $R_1$ = 0.0432, $wR_2$ = 0.1288, GOF = 1.111, residuals based on $I > 2\sigma(I)$.

**4**: orthorhombic, space group $P2_12_12_1$, $a$ = 12.336(2), $b$ = 13.182(2), $c$ = 25.894(3) Å, $U$ = 4210.9(10) Å$^3$, $Z$ = 4, $T$ = 183 K, $\mu$(Mo-K$\alpha$) = 0.357 mm$^{-1}$, no. of unique reflections = 6042, data/parameter ratio = 14, $R_1$ = 0.0372, $wR_2$ = 0.0800, GOF = 0.913, residuals based on $I > 2\sigma(I)$.

**5**: monoclinic, space group $C2/c$, $a$ = 30.0096(7), $b$ = 10.6464(3), $c$ = 24.3461(7) Å, $\beta$ = 93.8780(10)°, $U$ = 7760.6(4) Å$^3$, $Z$ = 8, $T$ = 183 K, $\mu$(Mo-K$\alpha$) = 0.414 mm$^{-1}$, no. of unique reflections = 5562, data/parameter ratio = 13, $R_1$ = 0.0714, $wR_2$ = 0.1372, GOF = 1.277, residuals based on $I > 2\sigma(I)$. CCDC 182/595.

1 K. Dehnicke and J. Strähle, *Angew. Chem., Int. Ed. Engl.*, 1992, **31**, 955.
2 C. E. Laplaza, M. J. A. Johnson, J. C. Peters, A. L. Odom, E. Kim, C. C. Cummins, G. N. George and I. J. Pickering, *J. Am. Chem. Soc.*, 1996, **118**, 8623.
3 C. E. Laplaza and C. C. Cummins, *Science*, 1995, **268**, 861.
4 C. E. Laplaza, A. L. Odom, W. M. Davis, C. C. Cummins and J. D. Protasiewicz, *J. Am. Chem. Soc.*, 1995, **117**, 4999.
5 A. L. Odom, C. C. Cummins and J. D. Protasiewicz, *J. Am. Chem. Soc.*, 1995, **117**, 6613.
6 D. M.-T. Chan, M. H. Chisholm, K. Folting, J. C. Huffman and N. S. Marchant, *Inorg. Chem.*, 1986, **25**, 4170.
7 R. R. Schrock, M. L. Listemann and L. G. Sturgeoff, *J. Am. Chem. Soc.*, 1982, **104**, 4291.
8 S. G. Bott, D. M. Hoffman and S. P. Rangarajan, *Inorg. Chem.*, 1995, **34**, 4305.
9 J.-I. Song and S. Gambarotta, *Chem. Eur. J.*, 1996, **2**, 1258.
10 L. G.Hubert-Pfalzgraf, M. Tsunoda and G. Le Borgne, *J. Chem. Soc., Dalton Trans.*, 1988, 533.
11 P. Berno and S. Gambarotta, *Organometallics*, 1995, **14**, 2159.
12 C. E. Laplaza, W. M. Davis and C. C. Cummins, *Angew. Chem., Int. Ed. Engl.*, 1995, **34**, 2042.
13 G. N. La Mar, W. D. Horrocks Jr. and R. H. Holm, *NMR of Paramagnetic Molecules*, Academic Press, New York, 1973.
14 S. K. Sur, *J. Magn. Reson.*, 1989, **82**, 169.
15 A. R. Johnson, W. M. Davis, C. C. Cummins, S. Serron, S. P. Nolan, D. G. Musaev and K. Morokuma, *J. Am. Chem. Soc.*, 1997, **119**, submitted.
16 A. H. Norbury, *Adv. Inorg. Chem. Radiochem.*, 1975, **17**, 231.
17 E. Weiss, *Angew. Chem., Int. Ed. Engl.*, 1993, **32**, 1501.
18 R. B. Hitam, A. J. Rest, M. Herberhold and W. Kremnitz, *J. Chem. Soc., Chem. Commun.*, 1984, 471.

*Received in Bloomington, IN, USA, 17th June 1997; 7/04253A*

# A terminal molybdenum carbide prepared by methylidyne deprotonation

**Jonas C. Peters, Aaron L. Odom and Christopher C. Cummins*†**

*Department of Chemistry, Massachusetts Institute of Technology, 77 Massachusetts Avenue, Cambridge, MA 02139, USA*

**The carbide anion $[CMo\{N(R)Ar\}_3]^-$ [R = $C(CD_3)_2CH_3$, Ar = $C_6H_3Me_2$-3,5], is obtained by deprotonation of the corresponding methylidyne compound, $[HCMo\{N(R)Ar\}_3]$, and is characterized by X-ray diffraction as its $\{K(benzo\text{-}15\text{-}crown\text{-}5)_2\}^+$ salt, thereby providing precedent for the carbon atom as a terminal substituent in transition-metal chemistry.**

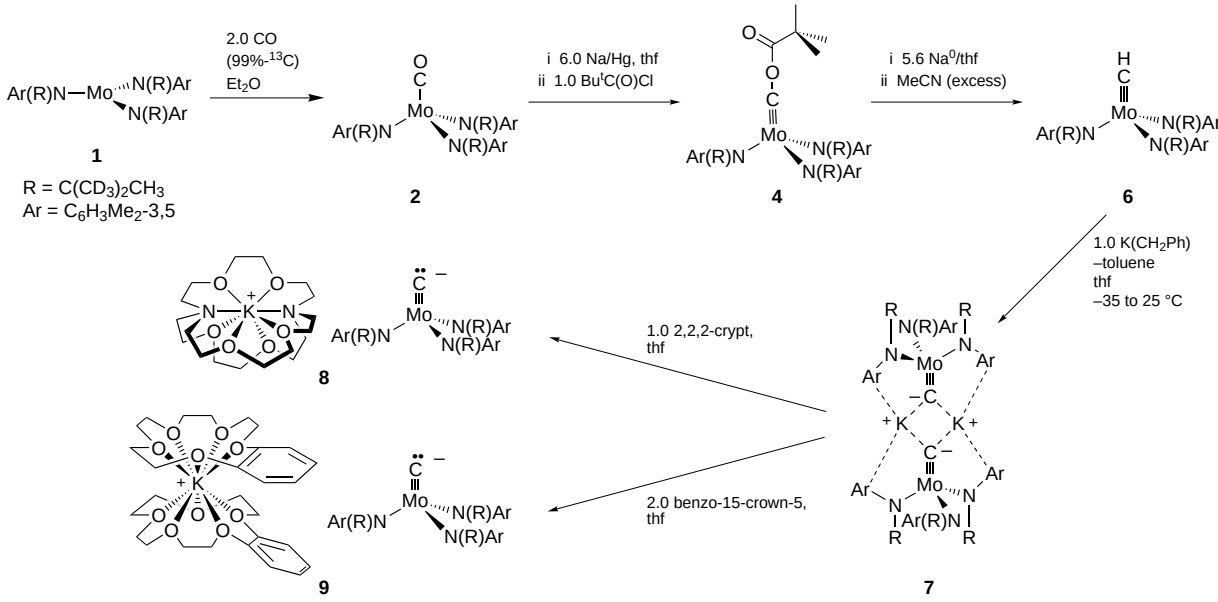
Recent work has shown that the molybdenum–nitrogen multiple bond in the nitride species $[NMo\{N(R)Ar\}_3]$ [R = $C(CD_3)_2CH_3$, Ar = $C_6H_3Me_2$-3,5] is exceedingly strong, and that this complex is quite robust.[1,2] Recognizing that the anionic carbide $[CMo\{N(R)Ar\}_3]^-$ would be isoelectronic with $[NMo\{N(R)Ar\}_3]$, we set out to synthesize it. As described herein, a successful synthesis was accomplished *via* deprotonation of the $d^0$ methylidyne complex $[HCMo\{N(R)Ar\}_3]$. Previously reported molecular carbide complexes feature carbon atoms with at least two nearest neighbors.[3–10]

Three-coordinate $[Mo\{N(R)Ar\}_3]$ **1** was treated with 99% $^{13}C$ carbon monoxide to give the paramagnetic ($\mu_{eff}$ = 1.73 $\mu_B$) carbonyl complex $[(O^{13}C)Mo\{N(R)Ar\}_3]$ **2** ($\nu_{CO}$ 1797 $cm^{-1}$) as a brown solid in 88% yield.‡§ One-electron reduction of **2** was effected with sodium amalgam in tetrahydrofuran (thf) giving $[(NaO^{13}C)Mo\{N(R)Ar\}_3]_2$ **3** [$\delta(^{13}C)$ 243.0] in essentially quantitative yield. **3** was obtained either as a solvent-free dimer or as an ether or thf solvate. *In situ* generated **3** was found to be sufficiently pure for synthetic purposes. Reaction of **3** with pivaloyl chloride[11] provided the 'carbido pivalate' complex $[Bu^tC(O)O(^{13}C)Mo\{N(R)Ar\}_3]$ **4** [$\delta(^{13}C)$ 217.2] in 82% yield as a beige crystalline solid.¶ Removal of the pivalate moiety in **4** was effected by treatment with sodium in thf giving, according to $^{13}C$ NMR analysis, a mixture of 'sodium carbide' $[Na(^{13}C\text{-})Mo\{N(R)Ar\}_3]_2$ **5** [$\delta(^{13}C)$ 474.2], methylidyne $[H(^{13}C)Mo\{N(R)Ar\}_3]$ **6** [$\delta(^{13}C)$ 287.5, $^1J_{CH}$ 157 Hz] and **3**. Treatment of the mixture with an excess of acetonitrile converted **5** to **6**, solubilized **3** and precipitated **6** in essentially pure form. Methylidyne **6**, an off-white solid, was isolated by this procedure in 53% yield from **2**.‖ Several other routes to the terminal methylidyne functionality have been documented.[12–17]

Deprotonation of **6** was effected by benzylpotassium in thf,[18] giving the potassium–molybdenum carbido complex $[K(^{13}C)Mo\{N(R)Ar\}_3]_2$ **7** [$\delta(^{13}C)$ 494.5][19,20] in 69% yield after recrystallization from pentane–thf.** In thf solution **7** presumably exists as a thf solvate, but the indicated thf-free, benzene-soluble dimer stabilized by intramolecular $K^+$–arene interactions[21] is readily obtained. Dimer **7** has been shown by X-ray crystallography to possess a central $K_2(carbide)_2$ square array situated about a crystallograpic inversion center.[22,23]

Treatment in thf of the potassium–molybdenum carbide **7** with 2,2,2-crypt[24] led to formation of the thf-soluble, benzene-insoluble salt $[K(2,2,2\text{-crypt})][^{13}CMo\{N(R)Ar\}_3]$ **8** [$\delta(^{13}C)$ 482.8].†† The $^1H$ NMR spectrum of **8** in $[^2H_8]$thf showed the expected four sharp resonances for the threefold-symmetric anion, along with the three signals characteristic of the $[K(2,2,2\text{-crypt})]^+$ cation. The curious fact that the $^{13}C$ NMR signal for the carbido carbon in **8** is broad ($[^2H_8]$thf, $\Delta\nu_{1/2}$ 1400 Hz) contrasts with the situation for **7**, which (in $C_6D_6$) exhibits a sharp signal.

A salt of the $[CMo\{N(R)Ar\}_3]^-$ anion amenable to X-ray crystallography, **9**, was obtained upon treatment of **7** with 2 equiv. (per K) of benzo-15-crown-5.[25] Crystals of salt **9**, which exhibited solubility characteristics similar to **8**, were obtained from thf–pentane.‡‡ The X-ray diffraction study of **9** revealed discrete and separate $[CMo\{N(R)Ar\}_3]^-$ anions and $[K(benzo\text{-}15\text{-}crown\text{-}5)_2]^+$ cations (Fig. 1).§§ The molybdenum–carbon distance in **9** was found to be 1.713(9) Å, at the low end of the known range for Mo–C multiple bonds.[26] The three N(R)Ar




**Scheme 1**

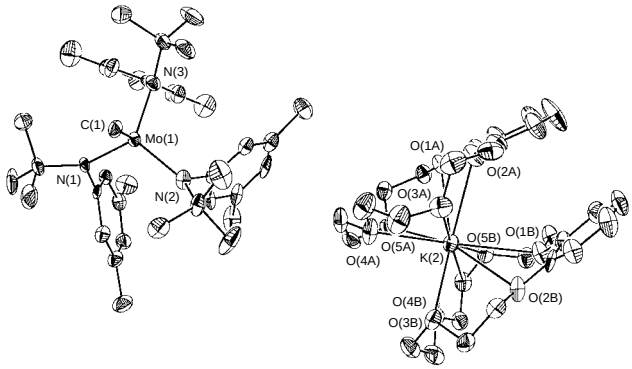



**Fig. 1** Structural representation of [K(benzo-15-crown-5)$_2$][CMo{N-(R)Ar}$_3$] **9** with thermal ellipsoids at the 35% probability level. Selected bond lengths (Å) and angles (°): Mo(1)–C(1) 1.713(9), Mo(1)–N(1) 2.008(6), Mo(1)–N(2) 2.010(7), Mo(1)–N(3) 2.013(6); C(1)–Mo(1)–N(1) 102.7(3), C(1)–Mo(1)–N(2) 103.9(3), N(1)–Mo(1)–N(2) 114.7(3), C(1)–Mo(1)–N(3) 103.8(3), N(1)–Mo(1)–N(3) 116.9(3), N(2)–Mo(1)–N(3) 112.6(3).

ligands in [CMo{N(R)Ar}$_3$]$^-$ adopt a propeller motif with the aryl rings π stacked[27] on one side of the molecule and the *tert*-butyl groups on the other side forming a protective 'pocket' about the Mo–C multiple bond. The gross structural and conformational features of [CMo{N(R)Ar}$_3$]$^-$ were anticipated based on structures of the related nitrido and phosphido derivatives [NMo{N(Bu$^t$)Ph}$_3$][1] and [PMo{N(R)Ar}$_3$].[28]

For funding this work we thank the Packard foundation, the Alfred P. Sloan Foundation, the National Science Foundation (CAREER Award CHE = 9501992), 3M, DuPont, and Union Carbide. J. C. P. is grateful for a Department of Defense Graduate Research Fellowship. This work is dedicated to the memory of Professor Jeremy K. Burdett.

## Footnotes and References

* E-mail: ccummins@mit.edu
† Alfred P. Sloan Fellow, 1997–2000.

‡ All manipulations were carried out under an atmosphere of dry nitrogen using solvents purified by standard methods.

§ *Other data* for **2**: $^2$H NMR (46 MHz, pentane, 25 °C); δ 8.0 [s, Δν$_{1/2}$ 14 Hz, C(CD$_3$)$_2$]; $\mu_{eff}$ (300 MHz, 25 °C, C$_6$D$_6$) = 2.2 $\mu_B$. FTIR (heptane, KBr); ν ($^{13}$CO) 1797 cm$^{-1}$. Anal. Calc. for $C_{37}H_{36}D_{18}MoN_3O$: C, 66.24; H, 8.11; N, 6.26. Found: C, 65.85; H, 8.44; N, 6.19%.

¶ The reaction to produce **4** was carried out using 6.5 mmol of **2**. *Other data* for **4**: $^1$H NMR (300 MHz, C$_6$D$_6$, 25 °C); δ 6.67 (s, 3 H, C$_6H_3$Me$_2$, *p*-H), 6.09 (s, 6 H, C$_6H_3$Me$_2$ *o*-H), 2.10 (s, 18 H, C$_6$H$_3$*Me*$_2$), 1.50 [s, 9 H, C(CD$_3$)$_2$C*H*$_3$], 1.22 [s, 9 H, C(C*H*$_3$)$_3$]. Anal. Calc. for $C_{42}H_{45}D_{18}MoN_3O_2$: C, 66.73; H, 8.40; N, 5.56. Found: C, 66.64; H, 8.24; N, 5.79%.

‖ The reaction to produce **6** was carried out using 2.66 mmol of **4**. *Other data* for **6**: $^1$H NMR (300 MHz, C$_6$D$_6$, 25 °C); δ 6.64 (s, 3 H, C$_6H_3$Me$_2$, *p*-H), 6.00 (s, 6 H, C$_6H_3$Me$_2$, *o*-H), 5.66 [d, 1 H, Mo(CH), $^1J_{CH}$ 157 Hz], 2.07 (s, 18 H, C$_6$H$_3$*Me*$_2$), 1.49 [s, 9 H, C(CD$_3$)$_2$C*H*$_3$]. Anal. Calc. for $C_{37}H_{37}D_{18}MoN_3$: C, 67.75; H, 8.45; N, 6.41. Found: C, 67.61; H, 8.29; N, 6.72%.

** The reaction to produce **7** was carried out using 1.164 mmol of **6**. *Other data* for **7**: $^1$H NMR (300 MHz, C$_6$D$_6$, 25 °C); δ 6.86 (s, 6 H, C$_6H_3$Me$_2$, *o*-H), 6.60 (s, 3 H, C$_6H_3$Me$_2$, *p*-H), 2.22 (s, 18 H, C$_6$H$_3$*Me*$_2$), 1.48 [s, 9 H, C(CD$_3$)$_2$C*H*$_3$] $^1$H NMR (300 MHz, [$^2$H$_8$]thf, 25 °C); δ 6.38 (sh s, 3 H, C$_6H_3$Me$_2$, *p*-H), 6.25 (vbr s, 6 H, C$_6H_3$Me$_2$, *o*-H), 2.04 (sh s, 18 H, C$_6$H$_3$*Me*$_2$), 1.31 [br s, 9 H, C(CD$_3$)$_2$C*H*$_3$]. Anal. Calc. for $C_{37}H_{36}D_{18}KN_3Mo$: C, 64.04; H, 7.84; N, 6.05. Found: C, 64.71; H, 7.59; N, 5.85%.

†† The reaction to produce **8** was carried out using 0.05 mmol of **7**. *Other data* for **8**: $^1$H NMR (300 MHz, [$^2$H$_8$]thf, 25 °C); δ 6.26 (s, 3 H, C$_6H_3$Me$_2$, *p*-H), 5.71 (vbr s, 6 H, C$_6H_3$Me$_2$, *o*-H), 3.58 (m, 12 H, crypt), 3.53 (m, 12 H, crypt), 2.53 (m, 12 H, crypt), 1.92 (s, 18 H, C$_6$H$_3$*Me*$_2$), 1.50 [s, 9 H, C(CD$_3$)$_2$C*H*$_3$].

‡‡ The reaction to produce **9** was carried out using 0.21 mmol of **7**. *Other data* for **9**: $^1$H NMR (300 MHz, [$^2$H$_8$]thf, 25 °C); δ 6.85 (m, 8 H, crown aryl), 6.60 (s, 3 H, C$_6H_3$Me$_2$, *p*-H), 5.81 (br s, 6 H, C$_6H_3$Me$_2$, *o*-H), 3.5–4.1 (m, 16 H, crown methylene), 2.06 (s, 18 H, C$_6$H$_3$*Me*$_2$), 1.36 [s, 9 H, C(CD$_3$)$_2$(C*H*$_3$)]. Anal. Calc. for $C_{65}H_{52}D_{18}KMoN_3O_{10}$: C, 63.44; H, 7.70; N 3.42. Found: C, 62.83; H, 7.72; N, 3.36%.

§§ Details of the X-ray diffraction study of **9**: monoclinic, space group $P2_1/n$, $a$ = 14.094(4), $b$ = 31.815(8), $c$ = 17.589(7) Å, $\beta$ = 97.60(2)°, $U$ = 7818(4) Å$^3$, $Z$ = 4; data/parameter ratio = 10.1, $R_1$ = 0.0829, $wR_2$ = 0.1650, GOF on $F^2$ = 1.083; residuals based on $I > 2\sigma(I)$. CCDC 182/596.

1 C. E. Laplaza, M. J. A. Johnson, J. C. Peters, A. L. Odom, E. Kim, C. C. Cummins, G. N. George and I. J. Pickering, *J. Am. Chem. Soc.*, 1996, **118**, 8623.
2 C. E. Laplaza and C. C. Cummins, *Science*, 1995, **268**, 861.
3 M. H. Chisholm, C. E. Hammond, V. J. Johnston, W. E. Streib and J. C. Huffman, *J. Am. Chem. Soc.*, 1992, **114**, 7056.
4 K. G. Caulton, R. H. Cayton, M. H. Chisholm, J. C. Huffman, E. B. Lobkovsky and Z. Xue, *Organometallics*, 1992, **11**, 321.
5 R. L. Miller, P. T. Wolczanski and A. L. Rheingold, *J. Am. Chem. Soc.*, 1993, **115**, 10 422.
6 D. R. Neithamer, R. E. LaPointe, R. A. Wheeler, D. S. Richeson, G. D. Van Duyne and P. T. Wolczanski, *J. Am. Chem. Soc.*, 1989, **111**, 9056.
7 D. Mansuy, J.-P. Lecomte, J.-C. Chottard and J.-F. Bartoli, *Inorg. Chem.*, 1981, **20**, 3119.
8 V. L. Goedkin, M. R. Deakin and L. A. Bottomley, *J. Chem. Soc., Chem. Commun.*, 1982, 607.
9 S. L. Latesky and J. P. Selegue, *J. Am. Chem. Soc.*, 1987, **109**, 4731.
10 M. Etienne, P. S. White and J. L. Templeton, *J. Am. Chem. Soc.*, 1991, **113**, 2324.
11 E. M. Carnahan, J. D. Protasiewicz and S. J. Lippard, *Acc. Chem. Res.*, 1993, **26**, 90.
12 G. M. Jamison, A. E. Bruce, P. S. White and J. L. Templeton, *J. Am. Chem. Soc.*, 1991, **113**, 5057.
13 M. R. Churchill, A. L. Rheingold and H. J. Wasserman, *Inorg. Chem.*, 1981, **20**, 3392.
14 K.-Y. Shih, K. Totland, S. Seidel and R. R. Schrock, *J. Am. Chem. Soc.*, 1994, **116**, 12 103.
15 J. Manna, R. J. Kuk, R. F. Dallinger and M. D. Hopkins, *J. Am. Chem. Soc.*, 1994, **116**, 9793.
16 P. R. Sharp, S. J. Holmes, R. R. Schrock, M. R. Churchill and H. J. Wasserman, *J. Am. Chem. Soc.*, 1981, **103**, 965.
17 M. H. Chisholm, K. Folting, D. M. Hoffman and J. C. Huffman, *J. Am. Chem. Soc.*, 1984, **106**, 6794.
18 R. R. Schlosser and J. Hartmann, *Angew. Chem., Int. Ed. Engl.*, 1973, **12**, 508.
19 C. P. Casey, M. W. Meszaros, P. J. Fagan, R. K. Bly, S. R. Marder and E. A. Austin, *J. Am. Chem. Soc.*, 1986, **108**, 4043; see this reference and ref. 20 for a $^{13}$C NMR shift of *ca*. 500 ppm.
20 C. P. Casey, M. A. Gohdes and M. W. Meszaros, *Organometallics*, 1986, **5**, 196.
21 E. Weiss, *Angew. Chem., Int. Ed. Engl.*, 1993, **32**, 1501.
22 J. C. Peters, A. L. Odom and C. C. Cummins, unpublished work.
23 M. G. Fickes, A. L. Odom and C. C. Cummins, *Chem. Commun.*, 1997, this issue; see this paper for structural data pertaining to [Na{NNb[N-(R)Ar]$_3$}]$_2$, which is analogous structurally to [K{CMo[N(R)Ar]$_3$}]$_2$.
24 L. F. Lindoy, *The Chemistry of Macrocyclic Ligand Complexes*, Cambridge University Press, Cambridge, 1989.
25 *Comprehensive Supramolecular Chemistry*, ed. G. W. Gokel, Pergamon, New York, 1996.
26 W. A. Nugent and J. M. Mayer, *Metal–Ligand Multiple Bonds*, Wiley, New York, 1988.
27 C. A. Hunter and J. K. M. Sanders, *J. Am. Chem. Soc.*, 1990, **112**, 5525.
28 C. E. Laplaza, W. M. Davis and C. C. Cummins, *Angew. Chem., Int. Ed. Engl.*, 1995, **34**, 2042.

*Received in Bloomington, IN, USA, 17th June 1997; 7/04251E*

# Reversible oxidation of $[Mo_nW_{3-n}(\eta^5\text{-}C_5H_5)_3(CO)_6(\mu_3\text{-}P)]$ ($n$ = 0–3) by sulfur; synthesis and characterisation of $[Mo_nW_{3-n}(\eta^5\text{-}C_5H_5)_3(CO)_6(\mu_3\text{-}PS)]$ ($n$ = 0–3)

**John E. Davies, Martin J. Mays,* Elizabeth J. Pook, Paul R. Raithby and Peter K. Tompkin**

*Department of Chemistry, Cambridge University, Lensfield Road, Cambridge, UK CB2 1EW*

**The trimetallic tetrahedrane complexes $[Mo_nW_{3-n}(\eta^5\text{-}C_5H_5)_3(CO)_6(\mu_3\text{-}P)]$ ($n$ = 0–3) are oxidised in carbon disulfide solution by elemental sulfur to the corresponding $\mu_3$-PS complexes $[Mo_nW_{3-n}(\eta^5\text{-}C_5H_5)_3(CO)_6(\mu_3\text{-}PS)]$; the new complexes lose the sulfur atom upon standing in solution at room temp. to regenerate $[Mo_nW_{3-n}(\eta^5\text{-}C_5H_5)(CO)_6(\mu_3\text{-}P)]$; the X-ray crystal structure of $[W_3(\eta^5\text{-}C_5H_5)_3(CO)_6(\mu_3\text{-}PS)]$ is determined.**

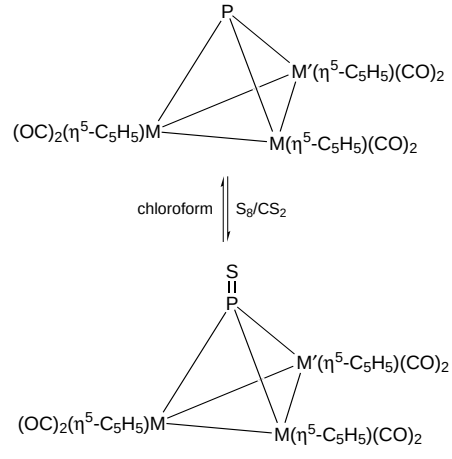
The synthesis of complexes containing naked group 15 ligands has been the subject of much research over recent years.[1] The reported chemistry of such complexes is, however, rather sparse, being limited in the main to the further coordination of 16-electron organometallic fragments to lone pairs present on the group 15 atom.[2] We recently reported that the trimetallic complexes $[Mo_nW_{3-n}(\eta^5\text{-}C_5H_5)_3(CO)_6(\mu_3\text{-}P)]$ ($n$ = 0–3) could be oxidised to the respective $\mu_3$-PO complexes by standing in air,[3] although attempts to prepare the $\mu_3$-PS complexes by oxidation with sulfur using toluene as the solvent were unsuccessful. Complexes featuring the phosphorus sulfide ligand are extremely uncommon; to the best of our knowledge there exist only three previous examples with the PS ligand coordinated through phosphorus in the $\mu_3$ mode,[4–7] two examples in which it adopts the $\mu,\eta^2$ mode of coordination[6–8] and one example where the ligand is terminally coordinated through phosphorus.[9] We now report that the trimetallic species complexes $[Mo_nW_{3-n}(\eta^5\text{-}C_5H_5)_3(CO)_6(\mu_3\text{-}P)]$ ($n$ = 0–3) can be oxidised by sulfur in $CS_2$ solution to the complexes $[Mo_nW_{3-n}(\eta^5\text{-}C_5H_5)_3(CO)_6(\mu_3\text{-}PS)]$ ($n$ = 0–3) and that this oxidation may be reversed simply by dissolution in organic solvents in the absence of excess dissolved sulfur. None of the previously prepared PS complexes have been reported to undergo such a spontaneous self-reduction.

Reaction of elemental sulfur with carbon disulfide solutions of the phosphorus capped trimetallics $[Mo_nW_{3-n}(\eta^5\text{-}C_5H_5)_3(CO)_6(\mu_3\text{-}P)]$ ($n$ = 3 **1**, $n$ = 2 **2**, $n$ = 1 **3**, $n$ = 0 **4**)[3] affords in good yield the unstable trimetallic complexes $[Mo_nW_{3-n}(\eta^5\text{-}C_5H_5)_3(CO)_6(\mu_3\text{-}PS)]$ ($n$ = 3 **5**, $n$ = 2 **6**, $n$ = 1 **7**; $n$ = 0 **8**), featuring a capping phosphorus monosulfide ligand (Scheme 1).

All four $\mu_3$-PS complexes lose sulfur on standing in solution in common organic solvents in the absence of excess sulfur to give the corresponding $\mu_3$-P complex. The rate of this reverse reaction increases with an increasing number of molybdenum atoms in the complexes. Time-lapse $^1$H NMR studies on $[W_3(\eta^5\text{-}C_5H_5)_3(CO)_6(\mu_3\text{-}PS)]$ **8** revealed the formation of $[W_3(\eta^5\text{-}C_5H_5)_3(CO)_6(\mu_3\text{-}P)]$ **4** as the only significant cyclopentadienyl-containing product. The stabilities of the PS capped complexes in solution decrease in the order **8** > **7** > **6** > **5**. A study of the kinetics of this decomposition is being undertaken and will be the subject of a later paper. The oxidation of naked phosphorus ligands by sulfur has previously been reported both for ligands consisting of a single phosphorus atom[5,9] and for the $P_2$ ligand, this latter oxidation giving $P_2S_2$ coordinated to a tetrairon core.[10]

The spectroscopic data for the new complexes† are in accord with the proposed structures. All the complexes exhibit a similar IR absorption pattern in the carbonyl region, with the frequencies being similar to those observed for the corresponding phosphorus monoxide complexes.[3] The $^{31}$P NMR spectra of **5**–**8** show more positive chemical shifts and smaller $^1J_{PW}$ coupling constants as the number of tungsten atoms is decreased, as was also observed for the $\mu_3$-PO complexes.[3]

The molecular structure of $[W_3(\eta^5\text{-}C_5H_5)_3(CO)_6(\mu_3\text{-}PS)]$ **8** has been determined by X-ray diffraction,‡ and is shown in Fig. 1 along with selected bond lengths and angles. The complex crystallises along with 1 equiv. of $CH_2Cl_2$ in the space group $P2_12_12_1$, whereas $[Mo_3(\eta^5\text{-}C_5H_5)_3(CO)_6(\mu_3\text{-}PO)]\cdot CH_2Cl_2$ crystallises in space group $Pna2_1$.[3] Each $W(\eta^5\text{-}C_5H_5)(CO)_2$ fragment is distinct in the solid state on account of the differing relative geometry of the $\eta^5$-$C_5H_5$ and CO ligands with respect to the PS capping ligand, as also observed for $[Mo_3(\eta^5\text{-}C_5H_5)_3(CO)_6(\mu_3\text{-}PO)]$.[3] Only one cyclopentadienyl signal is observed in the $^1$H NMR spectrum of **8**, indicating a fluxional process in solution. The P=S bond is essentially perpendicular to the plane defined by the three tungsten atoms. The P=S separation of 1.992(7) Å is at the long end of the range for phosphorus–sulfur double bonds, these being typically observed to fall in the range 1.85–1.95 Å for alkyl and aryl phosphine sulfides,[11] and is in agreement with the observed weakness of this bond. As compared to the alkyl and aryl phosphine sulfides, back-donation from the filled metal d orbitals to vacant d orbitals on phosphorus is likely to reduce the effectiveness of the S → P π component of the PS bond. The W–W and W–P distances correspond to the presence of single bonds, as requires by simple electron counting schemes.




**5** M = M′ = Mo
**6** M = Mo, M′ = W
**7** M = W, M′ = Mo
**8** M = M′ = W

**Scheme 1**

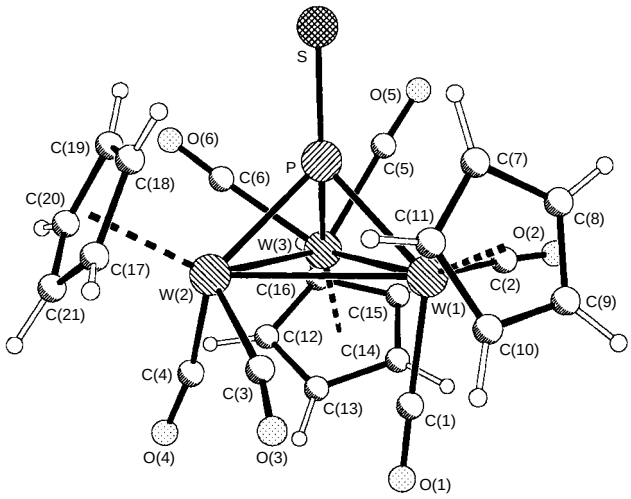



**Fig. 1.** Molecular structure of **8**, showing the atom labelling scheme adopted. Selected bond lengths (Å) and angles (°): P–S 1.992(7), P–W(1) 2.377(5), P–W(2) 2.403(5), P–W(3) 2.441(5), W(1)–W(2) 3.153(2), W(1)–W(3) 3.122(2), W(2)–W(3) 3.109(2); W(1)–W(2)–W(3) 59.79(3), W(1)–W(3)–W(2) 60.80(4), W(2)–W(1)–W(3) 59.41(3), W(1)–P–W(2) 82.5(2), W(1)–P–W(3) 80.7(2), W(2)–P–W(3) 79.9(2), P–W(1)–W(2) 49.09(13), P–W(1)–W(3) 50.52(13), P–W(2)–W(1) 48.38(12), P–W(2)–W(3) 50.60(13), P–W(3)–W(1) 48.74(12), P–W(3)–W(2) 49.54(12), W(1)P–S 132.0(3), W(2)–P–S 128.7(3), W(3)–P–S 133.3(3).

We thank the EPSRC for funding the X-ray diffractometer and for financial support to J. E. D. and P. K. T, and the Cambridge Crystallographic Data Centre for support to J. E. D.

## Footnotes and References

* E-mail: mjm14@cam.ac.uk

† Selected spectroscopic data [IR($\nu_{CO}$/cm$^{-1}$) recorded in $CH_2Cl_2$ solution; $^1$H and $^{31}$P NMR shifts recorded in $CDCl_3$ solution; $^{31}$P NMR shifts recorded relative to $P(OMe)_3$ at $\delta$ 0.0 with upfield shifts negative (add 140.2 ppm to convert reference to 85% $H_3PO_4$) ; $J$ in Hz]. **5**: $\nu_{CO}$ 1995m, 1959vs, 1938s, 1903m ; $^1$H NMR, $\delta$ 5.17 (d, $^3J_{HP}$ 0.5); $^{31}$P NMR, $\delta$ +308.2 (s); FABMS, *m/z* 714 ($M^+$). **6**: $\nu_{CO}$ 1995m, 1957vs, 1935s, 1900m ; $^1$H NMR, $\delta$ 5.20 [s, 5 H, $(C_5H_5)$W], 5.18 [d, 10 H, $^3J_{HP}$ 0.6, $(C_5H_5)$Mo]; $^{31}$P NMR, $\delta$ +273.6 (s, $^1J_{PW}$ 534); FABMS *m/z* 803 ($M^+$ + 1). **7**: $\nu_{CO}$ 1993m, 1956vs, 1932s, 1896m ; $^1$H NMR, $\delta$ 5.23 [d, 10 H, $^3J_{HP}$ 0.8, $(C_5H_5)$W], 5.19 [d, 5 H, $^3J_{HP}$, 0.8, $(C_5H_5)$Mo]; $^{31}$P NMR, $\delta$ +237.3 (s, $^1J_{PW}$ 471); FABMS, *m/z* 891 ($M^+$ + 1). **8**: $\nu_{CO}$ 1991m, 1955vs, 1932s, 1893m ; $^1$H NMR, $\delta$ 5.23 (d, $^3J_{HP}$ 0.6, $(C_5H_5)$); $^{31}$P NMR, $\delta$ +200.7, $^1J_{PW}$ 415; FABMS, *m/z* 979 ($M^+$ + 1).

‡ *Crystal structure determination* of **8**·$CH_2Cl_2$. $C_{21}H_{15}O_6PSW_3 \cdot CH_2Cl_2$, $M_r$ = 1062.84, orthorhombic, space group $P2_12_12_1$, $a$ = 13.476(5), $b$ = 18.114(11), $c$ = 10.447(6) Å, $U$ = 2550(2) Å$^3$ (by least-squares refinement on diffractometer angles from 25 centred reflections, 15 < 2$\theta$ < 20°), $Z$ = 4, $D_c$ = 2.768 Mg m$^{-3}$, $\mu$(Mo-K$\alpha$) = 13.890 mm$^{-1}$, semi-empirical absorption correction based on $\psi$-scans,[12,13] relative transmission factors 0.593–1.000, $F$(000) = 1936, dark green–brown block with dimensions 0.15 × 0.15 × 0.10 mm. Data were collected by the $\omega$–2$\theta$ scan method on a Rigaku AFC5R four-circle diffractometer at 150(2) K using graphite-monochromated Mo-K$\alpha$ radiation ($\lambda$ = 0.710 73 Å) in the range 5.42 < 2$\theta$ < 50.0°, +$h$, +$k$, +$l$; three standard reflections showed no significant variation in intensity; 2775 reflections of which 2743 were independent ($R_{int}$ = 0.025) and used in all calculations. Structure was solved using direct methods[14] and subsequent Fourier difference syntheses and refined by full-matrix least-squares on $F^2$[15] with anisotropic thermal parameters for W, P, S and Cl atoms. Hydrogen atoms were placed geometrically in idealised positions and refined using a riding model. In the final cycles of refinement a weighting scheme of the form $w^{-1}$ = [$\sigma^2(F_o^2)$ + (0.0283$P$)$^2$ +24.032$P$], where $P$ = ($F_o^2$ + 2$F_c^2$)/3, was employed which produced a flat analysis of variance. Final $R(F)$ = 0.0404, $wR(F^2)$ = 0.0912 for 2260 observed reflections [$I$ > 2$\sigma(I)$], $R(F)$ = 0.0739, $wR(F^2)$ = 0.2048 for all data; 176 parameters; GOF = 1.041, maximum $\Delta/\sigma$ = 0.08. Maximum peak and hole in final difference electron density 2.21 and −1.81 e Å$^{-3}$, respectively. CCDC 186/590.

1 O. J. Scherer, *Angew. Chem., Int. Ed. Engl.*, 1990, 1104.
2 For examples of activation of co-ordinated phosphorus ligands see: J. E. Davies, M. J. Mays, P. R. Raithby, G. P. Shields and P. K. Tompkin, *Chem. Commun.*, 1997, 361; J. E. Davies, M. J. Mays, P. R. Raithby, G. P. Shields and P. K. Tompkin, *Chem. Commun.*, 1996, 2051.
3 J. E. Davies, M. C. Klunduk, M. J. Mays, P. R. Raithby, G. P. Shields and P. K. Tompkin, *J. Chem. Soc., Dalton Trans.*, 1997, 715.
4 A. Visi-Orosz, G. Pályi and L. Markò, *J. Organomet. Chem.*, 1973, **60**, C25.
5 J. Foerstner, F. Olbrich and H. Butenschön, *Angew. Chem., Int. Ed. Engl.*, 1996, **35**, 1234.
6 O. J. Scherer, C. Vondung and G. Wolmerhäuser, *Angew. Chem., Int. Ed. Engl.*, 1997, **36**, 1303.
7 I.-P. Lorenz, W. Pohl and K. Polborn, *Chem. Ber.*, 1996, **129**, 11.
8 H. Brunner, U. Klement, W. Meier, J. Wachter, O. Serhadle and M. L. Ziegler, *J. Organomet. Chem.*, 1987, **335**, 339.
9 C. E. Laplaza, W. M. Davis and C. C. Cummins, *Angew. Chem., Int. Ed. Engl.*, 1995, **34**, 2042.
10 O. J. Scherer, G. Kemeny and G. Wolmershäuser, *Chem. Ber.*, 1995, **128**, 1145.
11 See for example: W. Dreissig, K. Plieth and P. Zaske, *Acta Crystallogr., Sect. B.*, 1972, **28**, 3473; A. J. Blake, R. A. Howie and G. P. McQuillan, *Acta Crystallogr., Sect. B.*, 1981, **37**, 1959; A. E. Shalamov, A. I. Yanovskii, Yu. T. Struchkov, A. P. Loganov, Yu. G. Bosyakov and O. V. Agashin, *Zh. Struckt. Khim.*, 1985, **26**, 140; C. Piccinni-Leopardi, J. Reisse, G. Germain, J. P. Declercq, M. Van Meerssche, K. Jurkschet, C. Mugge, A. Zschunke, J.-P. Dutasta and J.-B. Robert, *J. Chem. Soc., Perkin Trans. 2*, 1986, 85; A. E. Shalamov, A. I. Yankovskii, Yu. T. Struchkov, O. V. Agashin, G. P. Revenko, A. P. Logunov and Yu. G. Bosyakov, *Izv. Akad. Nauk. Kaz. SSR, Ser. Khim.*, 1986, 69; B. F. Hoskins and E. R. T. Tiekink, *Aust. J. Chem.*, 1988, **41**, 405.
12 TeXsan, Version 1.7-1, Molecular Structure Corporation, The Woodlands, TX, USA, 1985, 1992, 1995.
13 A. C. T. North, D. C. Phillips and F. S. Mathews, *Acta Crystallogr., Sect. A*, 1968, **24**, 351.
14 A. Altomare, G. Cascarano, C. Giacavazzo, A. Guagliardi, M. C. Burla, G. Polidori and M. Camalli, *J. Appl. Crysallogr.*, 1994, **27**, 435.
15 G. M. Sheldrick, SHELXL-93, University of Göttingen, 1993.

*Received in Basel, Switzerland, 12th June 1997; 7/04124A*

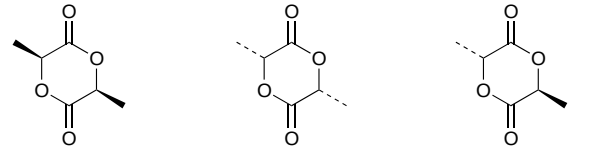
# Concerning the stereochemistry of poly(lactide), PLA. Previous assignments are shown to be incorrect and a new assignment is proposed

**Malcolm H. Chisholm*, Suri S. Iyer, Michael E. Matison, David G. McCollum and Marty Pagel**

*Department of Chemistry, Indiana University, Bloomington, IN 47405, USA*

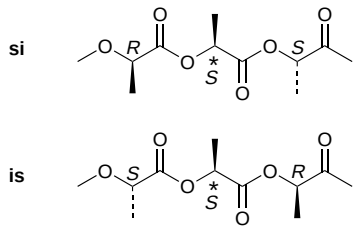
**HETCOR NMR spectra reveal that previous assignments of the stereochemistry of poly(lactide) derived from *rac* and *meso*-lactide are incorrect; an alternative assignment is made at the tetrad level of resolution.**

Poly(lactide), PLA,[1] and its co-[2] and ter-polymers[3] provide an important class of biodegradable and biocompatible polymers with wide ranging applications from bulk commodity materials (Ecochem®)[4] to specialty medicinal products such as sutures, staples, fibers and rods (Dexon® and Vicryl®),[4] drug delivery agents (Leupron Depot® and Zoladex®)[5] and artificial tissue matrices.[6] The specific properties of these polymers relate directly to their microstructure and the latter is thus of considerable importance.[7] PLA is typically produced by ring-opening polymerization of the lactide cyclic dimers shown below by catalyst precursors such as tin octoate,[8] $Bu_3SnOMe$[9]

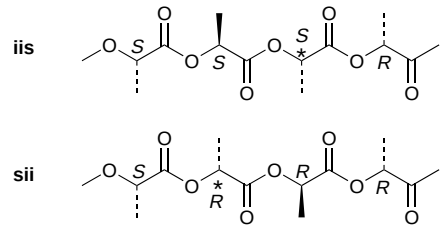



and $Al(acac)_3$[10] which allow for little kinetic selectivity in the ring-opening process. Attempts to establish the stereochemical microstructure of PLA have been based on NMR studies and Bernoullian statistics.[1a,2,10,11] Work has proceeded to infer stereochemical preferences in polymerization processes and by going to higher magnetic field strengths assignments of $^1H$ and $^{13}C\{^1H\}$ chemical shifts have been extended from the tetrad to the hexad level.[12] It is the purpose of this work to correct an error in the assignment of the microstructure and therefore to halt the propagation of errors relating to continuing studies of this polymer and assumptions and claims concerning stereo-preferential polymerizations.[11c,12,13]

In considering this polymer it is important to recognize that the ring opening of either an L- or D-lactide unit will generate an isotactic junction whereas opening a *meso*-lactide unit forms a syndiotactic unit. Thus at the triad level poly(L-lactide) and poly(D-lactide) will be denoted **ii** but polymerization of either racemic (50 : 50 D and L lactide) or *meso*-lactide will, in addition, contain both **si** and **is** units and unlike a poly(α-alkene) or poly(vinyl acetate) these two are not equivalent as shown below.†




At the tetrad level of assignment of PLA we are faced with the situation that the chemical shift of a given carbon or proton must be influenced by the stereochemistry of the polymer as read two to the left and one to the right, or two to the right and one to the left. There will always be ambiguity over the assignment **iis**/**sii**, shown below, because Bernoullian statistics renders them equivalent.




All previous assignments of PLA have followed from the work of Kriechldorf *et al.*[11a] based on (1) the homodecoupled methine proton and carbon resonances of polymers derived from the polymerization of *rac*- and *meso*-lactide and various mixtures thereof and (2) the assumption of Bernoullian statistics in polymer formation.[11b,c] These assignments of poly(*rac*-lactide) and poly(*meso*-lactide) are shown schematically in Fig. 1. In the absence of epimerization, which is effected by strong bases such as $KOBu^t$, poly(*rac*) will contain only **iii**, **iis**, **sii**, **sis** and **isi** tetrads whereas poly(*meso*) will be comprised of **sss**, **ssi**, **iss**, **sis** and **isi**. Thus common to both polymers are tetrad units **sis** and **isi**.

The assignments of **iii**, which can be identified independently from polymerization of either pure L-or pure D-lactide, and **sss**, which is favored statistically by polymerization of *meso*-lactide are correct but as shown by the HETCOR NMR spectra in Figs. 2 and 3 others are incorrect. The HETCOR spectra

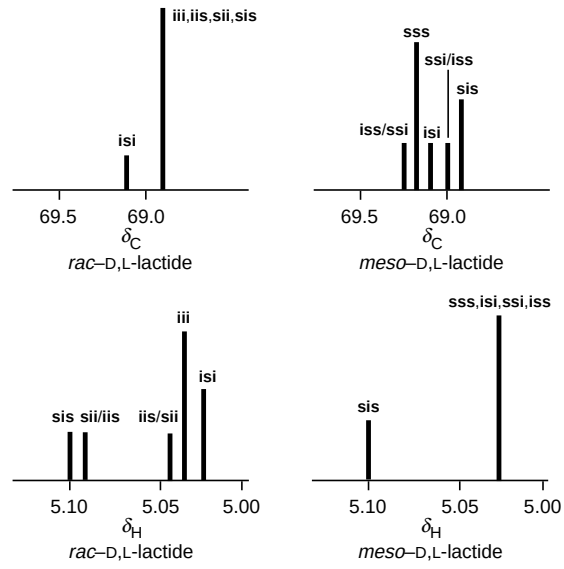



**Fig. 1** Schematic representation of the currently accepted assignments (CH) for PLA at the tetrad level following from ref. 11(*a*)

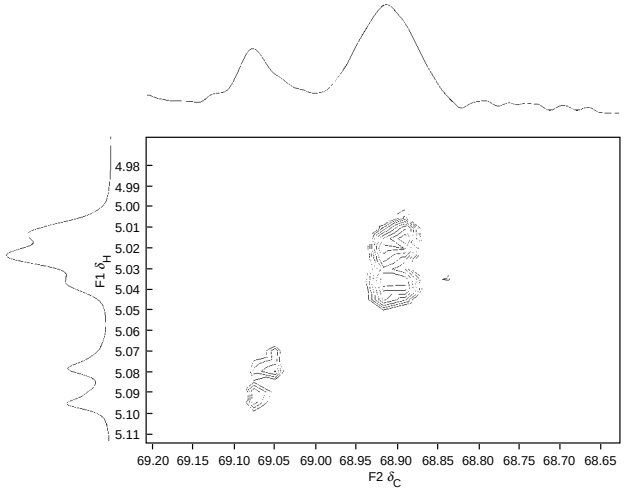



**Fig. 2** HETCOR spectrum showing the correlation of the homodecoupled methine protons with the methine carbon signals, $^{13}C\{^1H\}$, of poly(*rac*-lactide) in $CDCl_3$, 27 °C, recorded on a Brüker AM 500

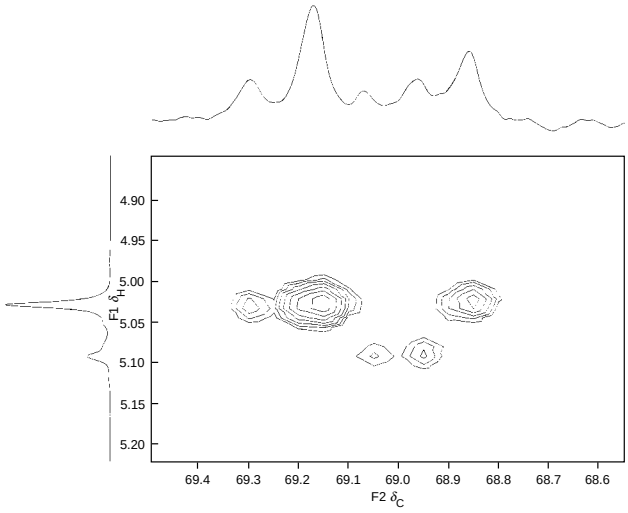



**Fig. 3** HETCOR spectrum showing the correlation of the homodecoupled methine protons with the methine carbon, $^{13}C\{^1H\}$, signals of poly(*meso*-lactide) in $CDCl_3$, 27 °C, recorded on a Varian I 400

correlate the homodecoupled methine protons with the methine carbons. We propose the alternate assignments shown in Fig. 4.

We have worked at field strengths of 400, 500, 600 and 750 MHz ($^1H$) and also employed long range HETCOR experiments. As other workers[12] have pointed out with higher magnetic field strengths resolution at the hexad level becomes possible but only when the correct assignment at the tetrad level is made will this be meaningful and useful in terms of microstructural analysis and in stereochemical preference in polymer formation, *i.e.* kinetic resolution of propagating steps. Work is in progress to elucidate further the microstructure of this polymer and to introduce stereospecificity into the polymer by use of chiral catalysts.

We thank the Department of Energy, Office of Basic Research, Chemical Sciences Division and the Petroleum Research Fund for support and Cargill Co., Minnesota for a gift of a sample of 93 : 7 *meso* : *rac* lactide.

## Footnotes and References

* E-mail: chisholm@indiana.edu

† While the normal representation of m and r can be used in the polylactide system, the authors would like to spare the reader of the possible confusion arising from this nomenclature as the monomers used are also m(eso) and r(acemic). For this reason we choose to use **i** (isotactic) and **s** (syndiotactic).

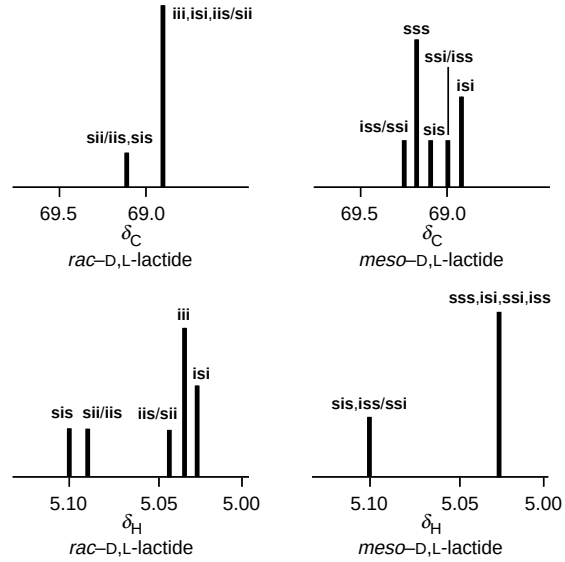



**Fig. 4** Proposed assignments for PLA at the tetrad level based on the HETCOR NMR spectra shown in Figs. 2 and 3

1 (*a*) H. R. Kricheldorf, I. Kreiser-Saunders, C. Jurgens and D. Wolter, *Macromol. Symp.*, 1996, **103**, 85; (*b*) N. B. Graham, M. E. McNeill and A. Rashid, in *Advances in Drug Delivery Systems*, ed. M. J. Anderson and S. W. Kim, Elsevier Science Publishers, Amsterdam, 1986, p. 231; (*c*) N. B. Graham, M. E. McNeill and M. Zulfiqar, *Polymer Prep.*, 1980, **21**, 104; (*d*) N. B. Graham and M. E. McNeill, *Biomaterials*, 1984, **5**, 27.

2 X. D. Feng, C. X. Song and W. Y. Chen, *J. Polym. Sci., Polym. Lett. Ed.*, 1981, **21**, 593; C. X. Song and X. D. Feng, *Macromolecules*, 1984, **17**, 2764; H. R. Kricheldorf, T. Mang and J. M. Jonte, *Macromolecules*, 1984, **17**, 2173; J. M. Vion, R. Jerome, P. Teyssie, M. Aubin and R. E. Prud'homme, *Macromolecules*, 1986, **21**, 1828.

3 A. S. Sawhney and J. A. Hubbell, *J. Biomed. Mater. Res.*, 1990, **24**, 1397.

4 Ecochem® is a polylactide based packaging material developed by DuPont ConAgra.

5 Dexon®, Vicryl®, Leupron Depot® and Zoladex® are products of Davis & Geek Corporation, Wayne, New Jersey; Ethicon, Inc., Somerville, NJ; Takeda Chemical Industries, Ltd., Japan, and Zeneca Pharmaceuticals, respectively. The first two are biodegradable sutures and Leupron Depot® is a drug delivery system.

6 J. A. Hubbell and R. Langer, *Chem. Eng. News*, Mar. 1995, p. 42; R. Langer and J. P. Vacanti, *Science*, 1993, **220**, 920.

7 A. Joshi and K. J. Himmelstein, *J. Control Rel.*, 1991, 15, 95; R. T. Macdonald, S. P. McCarthy and R. A. Gross, *Macromolecules*, 1996, **29**, 7356; K. A. M. Thakur, R. T. Kean, J. M. Zupfer, N. U. Buehler, M. A. Doscotch and E. J. Munson, *Macromolecules*, 1996, **29**, 8844.

8 A. J. Nijenhuis, D. W. Grijpma and A. J. Pennings, *Macromolecules*, 1992, **25**, 6419.

9 S. Sakai, Y. Kiyohara, M. Ogura and Y. Ishii, *J. Organomet. Chem.*, 1994, **72**, 93; Y. Hori, Y. Takahashi, A. Yamagushi and T. Nishishita, *Macromolecules*, 1993, **26**, 4388.

10 M. Bero, J. Kasperczyk and G. Adamus, *Makromol. Chem.*, 1993, **194**, 907.

11 (*a*) H. A. Kricheldorf, C. Boettcher and K. U. Tonnes, *Polymer*, 1992, **33**, 2817; (*b*) M. Bero, J. Kasperczyk and Z. Jedlinski, *J. Makromol. Chem.*, 1990, **191**, 2287; (*c*) T. E. Kasperczyk, *Macromolecules*, 1995, **28**, 3937.

12 K. A. M. Thakur, R. T. Kean, E. S. Hall, J. J. Kolstad, T. A. Londgren, M. A. Doscotch, J. I. Siepmann and E. J. Munson, *Macromolecules*, 1997, **30**, 2422.

13 N. Spassky, M. Wisniewski, C. Pluta and A. Le Borgne, *Macromol. Chem. Phys.*, 1996, **28**, 2627; A. Schlinder and K. D. Gaetano, *J. Polym. Sci., Part C, Polym. Lett.*, 1988, **26**, 47.

*Received in Cambridge, UK, 28th May 1997; 7/03676K*

# The reduction of $Nb_2Cl_6(tmeda)_2$ by $R_2NLi$. Formation of a diamagnetic niobium(II) cluster with short Nb–Nb triple bond and amide C–N bond cleavage

**Maryam Tayebani, Aparna Kasani, Khalil Feghali, Sandro Gambarotta* and Corinne Bensimon**

*Department of Chemistry, University of Ottawa, Ottawa, Ontario, Canada K1N 6N5*

**Reduction of trivalent $Nb_2Cl_6(tmeda)_2$ with either lithium diisopropylamide or *n*-butyllithium yields a novel $Nb^{II}$ cluster which performs oxidative addition into the amide C–N bond.**

Halide complexes of divalent Nb and Ta are particularly rare and limited to a few di- and poly-nuclear structures of halide derivatives mainly bridged by tetrahydrothiophene (THT) ligands.[1] The M–M triple bonds in these species are surprisingly long and thus to evaluate their properties it is important to prepare a variety of multiply bonded systems with the greatest possible diversity of ligand environments.

This work was prompted by the simple idea that low-valent niobium and tantalum amides may be able to form polymetallic structures with or without bridging ligands. The choice of these anions as supporting ligands was advised by their well established ability to stabilize highly reactive medium valent early transition metals.[2] With the dual purpose of bypassing the difficulties arising from the treatment of $MCl_5$ (M = Nb, Ta) starting materials with anionic amides[3] and possible complications arising from their subsequent reduction, and in an attempt to gain some insight into the stability of trivalent Nb and Ta amide, we have now reacted the dinuclear $[MCl_3(tmeda)]_2$ (M = Nb, Ta; tmeda = *N*,*N*,*N*′,*N*′-tetramethylethylenediamine)[4] with $R_2NLi$ derivatives. Herein we describe our preliminary findings.

A stoichiometric 1 : 3 ratio of Nb to amide, as well as an extended reflux in thf, was always necessary to complete the reactions of $[NbCl_3(tmeda)]_2$ with RR′NM′ [RR′NM′ = $Ph_2NNa$, $Pr^i_2NLi$, $(C_6H_3Me_2$-3,5)(Ad)NLi (Ad = adamantyl)] and to avoid the presence of unreacted starting materials in the reaction mixtures. However, in the particular case of LDA (lithium diisopropylamide) the reaction was completed in a few hours at room temp. After suitable work-up, well formed, dark-brown, and air-sensitive crystals of a new diamagnetic product were isolated in poor yield. The IR and the NMR of the crystalline product clearly indicated that the complex contained two non-equivalent tmeda ligands. The presence of lithium, suggested by qualitative flame tests, was confirmed by $^7$Li NMR spectroscopy. Combustion analysis data were in agreement with the formulation $(tmeda)_3Nb_2Cl_5Li$ **1**. An X-ray structure confirmed the formula and elucidated the molecular connectivity (Fig. 1).†

The crystal structure of **1** provides a rare example of a dinuclear niobium(II) complex. The diamagnetism and the very short Nb–Nb distance [Nb–Nb 2.4001(5) Å], suggest the

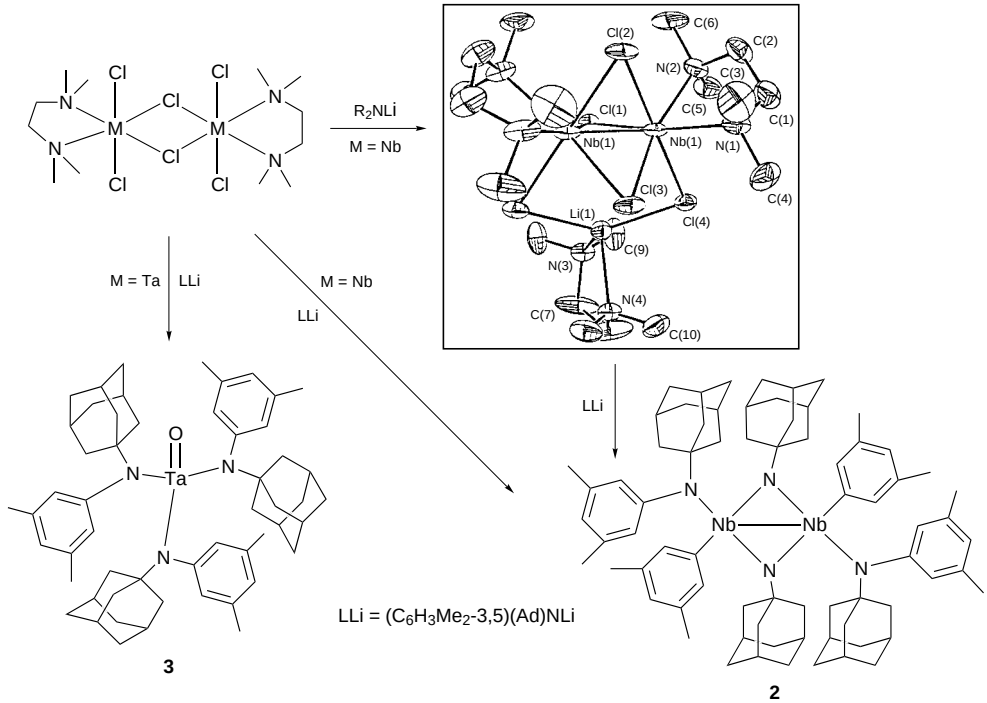



**Fig. 1** Selected bond distances (Å) and angles (°) for complex **1**: Nb(1)–Nb(1a) 2.4001(5), Nb(1)···Li(1) 3.217(8), Nb(1)–Cl(1) 2.5712(9), Nb(1)–Cl(2) 2.579(1), Nb(1)–Cl(3) 2.569(1), Nb(1)–Cl(4) 2.5583(9), Nb(1)–N(1) 2.390(2), Nb(1)–N(2) 2.366(3), Li(1)–Cl(4) 2.489(3), Li(1)···Cl(3) 2.840(8), Li(1)···Cl(1) 3.031(9), Li(1)–N(3) 2.199(9), Li(1)–N(4) 2.162(9), Cl(1)–Nb(1)–Cl(2) 95.90(3), Cl(1)–Nb(1)–Cl(3) 108.13(3), Cl(1)–Nb(1)–Cl(4) 84.39(3), Cl(1)–Nb(1)–N(1) 165.65(8), Cl(1)–Nb(1)–N(2) 85.83(7), Cl(2)–Nb(1)–Cl(3) 95.28(4), Cl(2)–Nb(1)–Cl(4) 84.16(3), Cl(2)–Nb(1)–N(1) 86.24(8), Cl(2)–Nb(1)–N(2) 85.45(8), Cl(3)–Nb(1)–Cl(4) 84.16(3), Cl(3)–Nb(1)–N(1) 85.73(8), Cl(3)–Nb(1)–N(2) 165.82(7), Cl(4)–Nb(1)–N(1) 93.60(8), Cl(4)–Nb(1)–N(2) 95.06(8), N(1)–Nb(1)–N(2) 80.2(1).

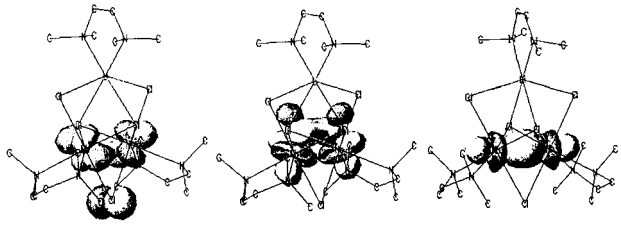



**Fig. 2** Pictorial view of the frontier orbitals of **1**

presence of a Nb–Nb triple bond.[5] However, the shortness of the intermetallic distance contrasts with those of the few previously reported divalent diniobium or ditantalum THF bridged complexes,[1] whose unusually long M–M distances were ascribed to an intrinsic weakness of the metal–metal bonds.[1b] Theoretical calculations carried out on the atomic crystallographic coordinates of **1** show that the three highest occupied molecular orbitals are mainly Nb–Nb centered with a metal atom contribution of predominantly d-orbital character and a minor but significant contribution from the p orbitals of the bridging chlorine atoms. The HOMO–LUMO gap (0.53 eV) is rather small yet sufficient to account for the observed diamagnetism in solution. The three MOs are formed by the overlap of hybrid atomic orbitals of the two niobium atoms. The shape of the HOMO (Fig. 2) is reminiscent of a M–M δ bond while the LUMO (−10.32 eV) is the corresponding out-of-phase combination. The next occupied molecular orbital, located at −11.24 eV is also M–M centered and has some π-bond character, while the third next orbital (−12.17 eV) is a regular σ bond lying symmetrically on the intermetallic vector. At this stage is not clear which factor (electronic or steric) is responsible for the short Nb–Nb distance. Certainly, we cannot rule out the possibility that the lithium cation may ultimately determine the intermetallic distance by bringing together the two vertices of the two octahedra.

The reduction of the metal center to the divalent state by LDA implies that the amide acted as a strong reductant.[6] Thus, it was possible to prepare **1** in higher yield by simply reacting $[NbCl_3(tmeda)]_2$ with 2 equiv. of $Bu^nLi$ in ether and in the presence of a small excess of tmeda. Even though the ability of amides to act as reductants is documented in the literature,[7] the fact that the same reaction with $Ph_2NNa$ (instead of LDA) gave the tetravalent derivative $(Ph_2N)_4Nb$ (45%)[8] suggests that the reduction of the metal center during the formation of **1** might occur through the disproportionation of an unstable niobium(III) intermediate. In addition, the reaction of $[NbCl_3(tmeda)]_2$ with $(C_6H_3Me_2$-3,5)(Ad)NLi yielded the tetravalent, dinuclear and diamagnetic $[C_6H_3Me_2$-3,5(Ad)N]Nb(3,5-$Me_2Ph)\}_2(\mu$-NAd)$_2\cdot 2Et_2O$ **2** (Fig. 1).† However, this product is likely to be originated by the further reaction of **1** with the lithium amide (the reaction requires reflux in thf for several hours in this case) to form a transient $[(C_6H_3Me_2$-3,5)(Ad)N]$_2$Nb species which generates **2** *via* oxidative addition into the C–N bond of the amide function.[9] Accordingly, direct reaction of **1** with 2 equiv. of $(C_6H_3Me_2$-3,5)(Ad)NLi also gave complex **2** in crystalline form.

The reaction of $[TaCl_3(tmeda)]_2$ with amides took a different pathway. While the majority of these reactions led to intractable materials, in the case of the reaction with $(C_6H_3Me_2$-3,5)(Ad)NLi the pentavalent $[(C_6H_3Me_2$-3,5)(Ad)N]$_3$Ta(O) **3** was isolated and characterized.‡ The complex is likely to be originated by the reaction of the initially formed $[(C_6H_3Me_2$-3,5)(Ad)N]$_3$Ta species with thf since reactions carried out in different solvent led to different results. This hypothetical intermediate obviously possesses a greater stability with respect to the niobium analogue and performs a two-electron reduction of thf. Accordingly, significant amounts of $CH_4$ and $CH_3CH_3$ (27 and 31%, respectively based on Ta) were recovered from the reaction mixture (Toepler pump and GC combined experiments).

This work was supported by the Natural Sciences and Engineering Council of Canada (NSERC).

## Footnotes and References

* E-mail: sgambaro@oreo.uottowa.ca

† *Crystal data*: $C_{18}H_{48}LiCl_5N_6Nb_2$ **1**, $M$ = 718.64, orthorhombic, space group *Cmc*21, $a$ = 15.2097(2), $b$ = 16.8896(2), $c$ = 12.0285(1) Å, $U$ = 3089.95(6) Å$^3$, $Z$ = 4, $D_c$ = 1.545 g cm$^{-3}$, $F$(000) = 1471.49, $\mu$ = 11.9 cm$^{-1}$, $T$ = −145 °C, $R$ = 0.026, $R_w$ = 0.031, GOF = 1.01 for 196 parameters and 2972 reflections out of 3508 unique collected with a Siemens CCD diffractometer. $C_{40}H_{58}N_2NbO$ **2**, $M$ = 675.81, monoclinic, space group $P2_1/c$, $a$ = 12.5969(2), $b$ = 14.3835(1), $c$ = 20.3103(3) Å, $\beta$ = 104.223(1)°, $U$ = 3567.17(8) Å$^3$, $Z$ = 4, $D_c$ = 1.258 g cm$^{-3}$, $F$(000) = 1436.34, $\mu$ = 3.7 cm$^{-1}$, $T$ = −145 °C, $R$ = 0.045, $R_w$ = 0.057, GOF = 1.05 for 397 parameters and 6960 reflections out of 9089 unique collected with a Siemens CCD diffractometer. $C_{64}H_{95}N_3O_2Ta$ **3**, $M$ = 1119.41, monoclinic, space group $P2_1/n$, $a$ = 14.2622(2), $b$ = 25.3107(1), $c$ = 16.1753(2) Å, $\beta$ = 101.706(3), $U$ = 5717.6(1) Å$^3$, $Z$ = 4, $D_c$ = 1.300 g cm$^{-3}$, $F$(000) = 2355.36, $\mu$ = 1.96 cm$^{-1}$, $T$ = −165 °C, $R$ = 0.033, $R_w$ = 0.041, GOF = 1.41 for 641 parameters and 11 040 reflections out of 14 513 unique collected with a Siemens CCD diffractometer. CCDC/602.

1 (*a*) F. A. Cotton, M. P. Diebold and W. J. Roth, *J. Am. Chem. Soc.*, 1987, **109**, 5506; (*b*) F. A. Cotton, M. P. Diebold and W. J. Roth, *J. Am. Chem. Soc.*, 1986, **108**, 3538; (*c*) J. Kohler and A. Simon, *Angew. Chem., Int. Ed. Engl.*, 1986, **25**, 996; (*d*) D. M. Curtis and J. Real, *Organometallics*, 1985, **4**, 940; (*e*) F. Calderazzo, G. Pampaloni, L. Ricchi, J. Strahle and K. Wurst, *J. Organomet. Chem.*, 1991, **413**, 91; (*f*) F. A. Cotton, J. H. Matonic and C. A. Murillo, *J. Am. Chem. Soc.*, 1997, **119**, 7889.

2 C.-E. Laplaza and C.-C. Cummins, *Science*, 1995, **268**, 861; J. S. Frendlich, R. R. Schrock, C. C. Cummins and W. M. Davis, *J. Am. Chem. Soc.*, 1994, **116**, 6476; M. Moore, S. Gambarotta, G. Yap, L. M. Liable-Sands and A. Rheingold, *Chem. Commun.*, 1997, 645; P. Berno, S. Hao, R. Minhas and S. Gambarotta, *J. Am. Chem. Soc.*, 1994, **116**, 7417; P. Berno and S. Gambarotta, *Organometallics*, 1994, **13**, 2569.

3 *Ad hoc* synthetic procedures have been developed for niobium and tantalum(v) amides: D. M. Hoffman and S. P. Rangarajan, *Polyhedron*, 1993, **12**, 2899; Y. W. Chao, S. Polson and D. E. Wigley, *Polyhedron*, 1990, **9**, 2709; Y. W. Chao, P. A. Wexler and D. E. Wigley, *Inorg. Chem.*, 1989, **28**, 3860; D. C. Bradley, M. B. Hursthouse, A. J. Howes, A. N. M. Jelfs, J. D. Runnacles and M. Thornton-Pett, *J. Chem. Soc., Dalton Trans.*, 1991, 841; W. A. Nugent and R. L. Harlow, *J. Chem. Soc., Chem. Commun.*, 1978, 579; F. Guerin, D. H. McConville and J. J. Vittal, *Organometallics*, 1995, **14**, 3154; F. P. O'Flaherty, R. A. Henderson and D. L. Hughes, *J. Chem. Soc., Dalton Trans.*, 1990, 1087.

4 J. A. M. Canich and F. A. Cotton, *Inorg. Chem.*, 1987, **26**, 4236.

5 R. H. Sommerville and R. Hoffmann, *J. Am. Chem. Soc.*, 1979, **101**, 3821; J. L. Templeton, W. C. Dorman, J. C. Clardy and R. E. McCarley, *Inorg. Chem.*, 1978, **17**, 1263; B. E. Bursten, F. A. Cotton and A. Fang, *Inorg. Chem.*, 1983, **22**, 2127.

6 Typically, strong reducing agents such as alkali metals, amalgams or potassium graphite are necessary for obtaining divalent niobium. See for example: M. A. Araya, F. A. Cotton, J. H. Matonic and C. A. Murillo, *Inorg. Chem.*, 1995, **34**, 5424; E. Guggloz, M. L. Ziegler, H. Biersack and W. A. Herrmann, *J. Organomet. Chem.*, 1980, **194**, 317; M. L. Luetkens, J. C. Huffman and A. P. Sattelberger, *J. Am. Chem. Soc.*, 1983, **105**, 4474; T. W. Coffindaffer, I. P. Rothwell, K. Folting, J. C. Huffman and W. E. Streib, *J. Chem. Soc., Chem. Commun.*, 1985, 1519.

7 See for example: M. H. Chisholm, F. A. Cotton, B. A. Frenz, W. W. Reichert, L. W. Shive and B. R. Stults, *J. Am. Chem. Soc.*, 1976, **98**, 4469; M. H. Chisholm and W. W. Reichert, *J. Am. Chem. Soc.*, 1974, **96**, 1249; D. C. Bradley and M. H. Chisholm, *J. Chem. Soc. A*, 1971, 1511; M. H. Chisholm, F. A. Cotton, B. A. Frenz, L. W. Shive and B. R. Stults, *J. Chem. Soc., Chem. Commun.*, 1974, 480; J. R. Dilworth, S. J. Harrison, R. A. Henderson and D. R. M. Walton, *J. Chem. Soc., Chem. Commun.*, 1984, 176.

8 Identified by comparison of the cell parameters and analytical data with those of an analytically pure sample: S. G. Bott, D. M. Hoffman and S. P. Rangarajan, *Inorg. Chem.*, 1995, **34**, 4305 and references therein.

*Received in Bloomington, IN, USA; 12th May 1997; 7/03280C*

# Extraction and HPLC purification of Li@$C_{60/70}$

**Andrei Gromov,[a] Wolfgang Krätschmer,[a] Nela Krawez,[b] Ralf Tellgmann[b] and Eleanor E. B. Campbell*[b]**

[a] *Max-Planck-Institut für Kernphysik, Postfach 103980, D-69029 Heidelberg, Germany*
[b] *Max-Born-Institut für Nichtlineare Optik und Kurzzeitspektroskopie, Postfach 1107, D-12474 Berlin, Germany*

**Thin films containing up to 30% endohedral Li@$C_{60/70}$ are dissolved in $CS_2$ and the purified endohedral material is isolated by HPLC.**

We have recently reported a new, general method for producing endohedral metal fullerenes using low-energy ion bombardment of fullerene films. The method has the advantage of limiting the endohedral species to one particular product, determined by the deposited fullerene film (in our case $C_{60}$ or $C_{70}$) and the ion used for the bombardment. We have shown that it is possible to produce films of a few hundred nanometres thickness which contain *ca.* 30% Li@$C_{60}$, as determined by laser desorption mass spectrometry (LD-TOF).[1,2] The efficiency of the method drops for larger alkali metals but the films still contain of the order of a few percent endohedrals.[2] The Li@$C_{60}$ films have been characterised by LD-TOF,[1,2] IR[1,3] and Raman spectroscopy[3] which all give convincing evidence for the endohedral nature of the product.

Here we show that it is possible to dissolve these endohedral films and to chromatographically purify the material. This will enable a full characterisation of the electronic and optical properties of these new materials to be carried out.

The method by which the thin films containing Li@$C_{60/70}$ are produced has been described in detail before.[2] Films of 400 nm thickness and surface areas of *ca.* 4 $cm^2$ were produced by successively depositing monolayers of fullerenes and ions on a conducting substrate. The ion energy was 30 eV which has been shown previously to produce the maximum amount of endohedral fullerenes.[2] Films were produced either with a Li : fullerene ratio of 6 : 1 which converts *ca.* 25–30% of the fullerenes in the film to endohedrals, or a ratio of 1 : 1 which converts *ca.* 4–6%, as determined by LD-TOF.[2]

We investigated many solvents for dissolving the films containing endohedral species and found $CS_2$ to yield the best results. The films could also be partly dissolved using pyridine and aniline. In both cases, in contrast to the results with $CS_2$, the endohedral species were more dominant than the empty $C_{60}$ in the solutions.

Once the films have been initially dissolved in $CS_2$ the dissolved material can be redissolved in a wide range of typical fullerene solvents.

The standard procedure used to dissolve the films was to place them in $CS_2$ and treat them with ultrasonic irradiation for 3 h. The $CS_2$ extract obtained was filtered through a 0.45 μm membrane. According to LD-TOF data the filtered solution contained only $C_{60}$ and Li@$C_{60}$. Analysis showed that up to 25% of the film material was dissolved in the $CS_2$ for the films produced with an ion to fullerene ratio of 6 : 1 increasing to over 90% for the films produced with a 1 : 1 ratio. The remaining non-dissolved material contained relatively more endohedral species with respect to empty fullerenes than the initial film and the resulting solution.

The HPLC separation of the $CS_2$ solutions was carried out using either a Cosmosil 5PBB analytical column or a Buckyprep column. Fig. 1 shows the chromatogram obtained from a 6 : 1 film with detection set at 405 nm, $CS_2$ eluent and a flow rate of 1.0 ml $min^{-1}$. Three well defined peaks (denoted as fractions **1**, **2** and **3**, respectively) can be clearly seen. The separated fractions were analyzed by LD-TOF (Brucker Biflex mass spectrometer with a 337 nm $N_2$ laser, detection of positive ions). As can be seen in the LD-TOF mass spectrum shown at the top of Fig. 2, the chromatographic fraction **1**, with the retention time of 4.5 min, corresponds to $C_{60}$, whereas the fractions **2** and **3**, with retention times peaking at *ca.* 5.8 and 7.9 min, respectively, can both be assigned to species comprised of Li@$C_{60}$. The latter fractions show small $C_{60}$ peaks in the mass spectra accompanied by very strong signals due to the endohedral Li@$C_{60}$. We have investigated the dependence of the relative intensity of peaks **2** and **3** on the amount of endohedral material in our sample. Fig. 1 was produced under conditions where we obtain the maximum yield of endohedral Li@$C_{60}$ (*ca.* 30% of the fullerenes in the film containing Li).[1] This corresponds to an ion energy of 30 eV and a ratio of $Li^+ : C_{60}$ of 6 : 1. If we reduce this ratio we obtain a smaller percentage of endohedral compounds in our films but better solubility. Practically all of the 'empty' fullerenes and a large proportion of the endohedral compounds could be dissolved from the films produced with $Li^+ : C_{60}$ = 1 : 1. We have carried out experiments for a range of $Li^+ : C_{60}$ ratios and been able to show that the relative intensity of peak **2** to peak **3** correlates very clearly with the percentage of endohedral compounds in the films. Fraction **3** is, however, less stable in solution over a timescale of a few days and its concentration decreases with respect to that of fraction **2**. The mass spectra obtained from the 1 : 1 fractions are very similar to those in Fig. 2 but have relatively more 'empty' $C_{60}$ (*ca.* 1 : 2 $C_{60}$ : Li@$C_{60}$). This may be due to the tail of the much larger $C_{60}$ fraction.

With $C_{70}$ we see only one clearly separated fraction which contains endohedral species. The HPLC retention time for this fraction as well as its LD-TOF mass spectrum and its long-time stability in solution are consistent with the $C_{60}$ results for fraction **3**.

The material was further purified by passing the separated fractions through a Buckyprep column with toluene–DCB eluent (11 : 1) which gives a better resolution of the peaks. The results are shown in Fig. 3. It should be noted that these chromatograms were obtained with a different wavelength (340

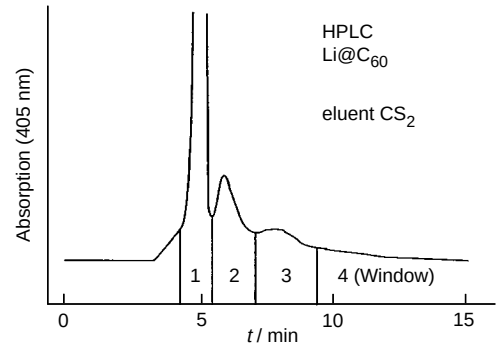



**Fig. 1** HPLC peak profiles of the $CS_2$ extract from the thin film containing Li@$C_{60}$. Obtained using a Cosmosil 5PBB analytical column, $CS_2$ eluent, 405 nm detection, 1.0 ml $min^{-1}$ flow rate. Thin film produced with $Li^+ : C_{60}$ = 6 : 1.

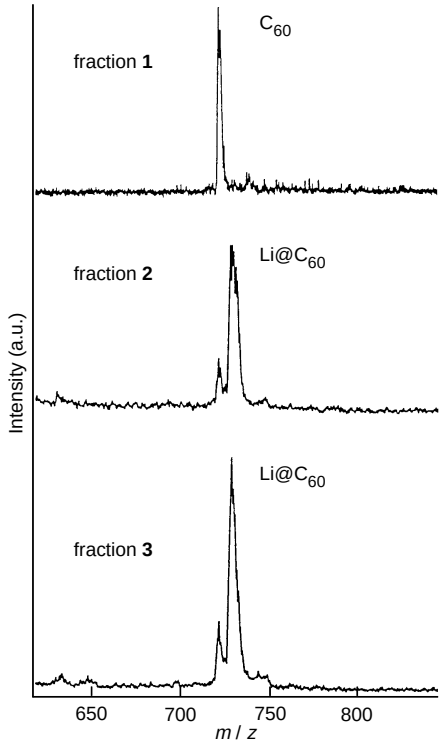



**Fig. 2** LD-TOF mass spectra of fractions **1**, **2** and **3** shown in Fig. 1

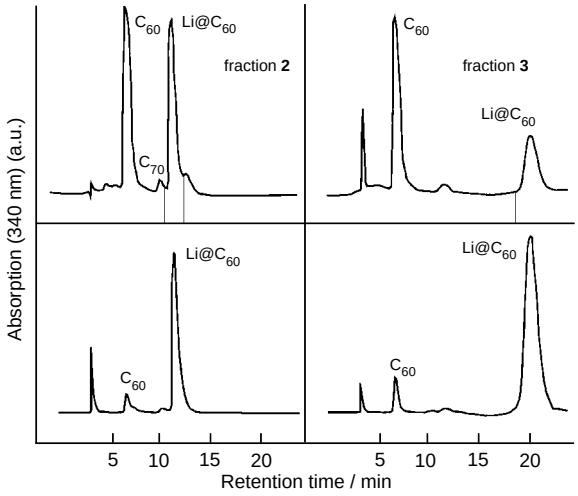



**Fig. 3** HPLC peak profiles of fractions **2** (left hand side) and **3** (right hand side) obtained from the PBB column with $CS_2$ eluent separated in a second stage with a Buckyclutcher column and toluene–DCB eluent (upper part). The endohedral fractions were again collected and separated once more with the Buckyclutcher column and toluene–DCB eluent yielding highly purified compounds (lower part).

nm instead of 405 nm in Figs. 1 and 3) which gives a much larger signal for $C_{60}$ than for the endohedral fractions as can be seen from the UV–VIS spectra of toluene solutions of the three different fractions in Fig. 4. The chromatograms of the endohedral fractions first separated by the PBB column (top half of Fig. 3) both show a fairly large $C_{60}$ peak, however, taking the higher detection efficiency into account, this is in keeping with the mass spectra of fractions **2** and **3** from films produced with a 1 : 1 ratio. Taking the endohedral fractions and

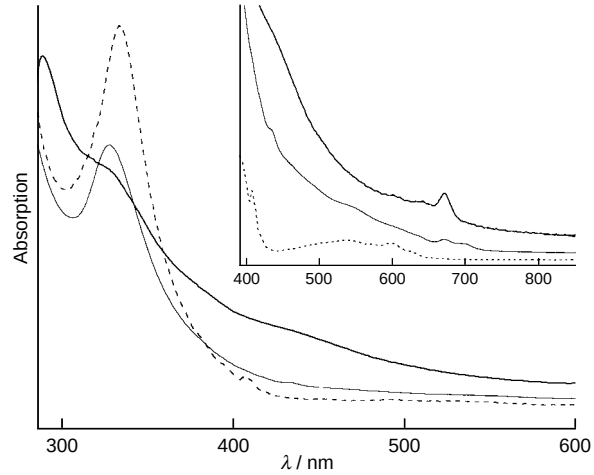



**Fig. 4** UV–VIS spectra of fractions **1**, **2** and **3** dissolved in toluene. Dashed line: fraction **1** ($C_{60}$); thin line: fraction **2**; thick line: fraction **3**.

again passing them through the Buckyprep column with the toluene–DCB eluent yields the two chromatograms shown in the bottom half of Fig. 3. In this way it is possible to almost completely isolate the Li@$C_{60}$ endohedral fraction.

The reason for having two separable endohedral fractions is not yet clear. Close inspection of the mass spectra reveals that fraction **2** has a considerably broader mass peak indicating the attachment of some H atoms to the fullerene cage. This fraction is also more dominant from films produced with large amounts of Li which also contain a range of interstitial reaction products of the intercalated Li with air. We also have reason to believe that the endohedral molecules show a strong propensity for forming oligomers and it is possible that fraction **2** is a dimer and fraction **3** the isolated monomer species. This is the subject of further work. The UV–VIS spectrum of fraction **2** is consistent with the dimer hypothesis.[4] The optical bands are broadened, reduced in peak intensity and shifted with respect to $C_{60}$. In addition, the typical $C_{60}$ features between 400 and 700 nm are lost and the absorption onset for both endohedral containing fractions lies much further in the IR. It is certainly the case that fractions **2** and **3** are two different chemical species since they have significantly different UV–VIS spectra, as clearly seen in Fig. 4, and also different solubilities and stability in solution. Fraction **2** dissolves more readily than fraction **3** and is stable in solution over a timescale of many days whereas fraction **3** decreases significantly in intensity.

Financial support from the BMBF (13N6652/7) for the MBI group and from the EU through the HCM network 'Formation, stability and photophysics of fullerenes' is gratefully acknowledged. We would also like to thank Prof. I.V. Hertel for his interest in and encouragement of this project.

## Footnote and References

* E-mail: campbell@mbi.fta-berlin.de

1 R. Tellgmann, N. Krawez, S.-H. Lin, E. E. B. Campbell and I. V. Hertel, *Nature*, 1996, **382**, 407.
2 E. E. B. Campbell, R. Tellgmann, N. Krawez and I. V. Hertel, *J. Phys. Chem. Solids*, in the press.
3 H. Jantoljak, N. Krawez, I. Loa, R. Tellgmann, E. E. B. Campbell, A. P. Litvinchuk and C. Thomsen, *Z. Phys. Chem.*, 1997, **200**, 157.
4 G.-W. Wang, K. Komatsu, Y. Murata and M. Shiro, *Nature*, 1997, **387**, 583.

*Received in Exeter, UK, 1st July 1997; 7/04609J*

# 4-[2,4-Dimethoxyphenyl(*N*-fluoren-9-ylmethoxycarbonyl-*N*-alkylaminooxy)-methyl]phenoxymethyl polystyrene: a multiple solid-phase approach to *N*-alkylhydroxamic acids

**Sarah L. Mellor and Weng C. Chan***

*Department of Pharmaceutical Sciences, University of Nottingham, University Park, Nottingham, UK NG7 2RD*

***N*-Fluoren-9-ylmethoxycarbonyl-*N*-alkylhydroxylamines, prepared *via* $K_2CO_3$-catalysed *N*-alkylation of *N*,*O*-bis(*tert*-butoxycarbonyl)hydroxylamine, undergo a highly efficient condensation with 4-[2,4-dimethoxyphenyl(chloro)methyl]-phenoxymethyl polystyrene (PS) to afford 4-[2,4-dimethoxyphenyl(*N*-fluoren-9-ylmethoxycarbonyl-*N*-alkylaminooxy)methyl]phenoxymethyl PS, which is used for the facile synthesis of structurally diverse *N*-substituted hydroxamic acids.**

Peptide hydroxamic acids, *e.g.* actinonin, foroxymithine and matlystatin B, isolated from microorganisms are known to be potent and selective inhibitors of many important metalloproteases.[1] The ability of the hydroxamic acid functionality to form a bidentate chelate with the zinc atom in the enzyme's active site is considered to be an important functional feature.[1] Recently, exploitation of this concept has led to the design and synthesis of α-alkylmalonyl and 2-phenyloxazoline hydroxamic acids as potent inhibitors of endothelin-converting enzyme and *E. coli* uridine 5′-diphosphate-3-*O*[3*R*)-3-hydroxymyristoyl]-*N*-acetyl-glucosamine deacetylase, respectively.[2]

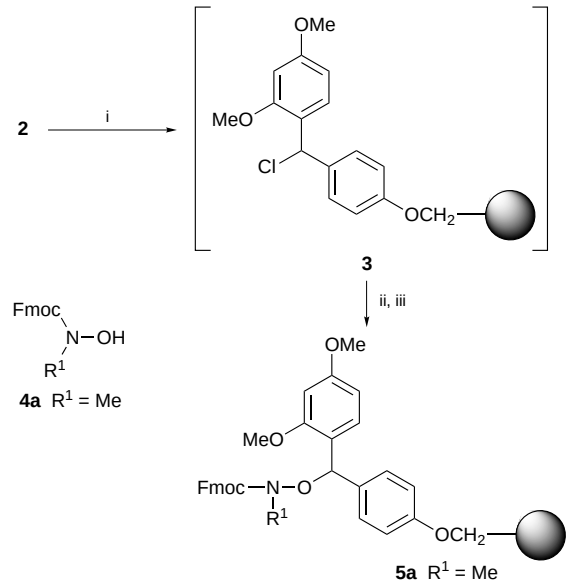
The implication of combinatorial chemistry for high throughput generation of structurally diverse hydroxamic acids is self evident. Recently, several solid phase approaches for the synthesis of hydroxamic acids have been reported.[3,4] For example, we outlined a facile solid phase procedure using the high-loading resin, *N*-fluoren-9-ylmethoxycarbonylaminooxy-2-chlorotrityl polystyrene **1**.[3] However, these strategies are evidently not applicable for the synthesis of *N*-alkyl hydroxamic acids, which is necessary in order to provide a further dimension in chemical diversity, in a manner analogous to our previously reported[5] peptidyl *N*-alkyl amides. We report herein a novel parallel solid phase strategy to *N*-alkyl hydroxamic acids. The key feature of our strategy is the multiple synthesis of *N*-fluoren-9-ylmethoxycarbonyl-*N*-alkyl hydroxylamines **4**, followed by *O*-alkylation by the unique 4-[2,4-dimethoxyphenyl(chloro)methyl]phenoxymethyl PS **3** to afford 4-[2,4-dimethoxyphenyl(*N*-fluoren-9-ylmethoxycarbonyl-*N*-alkyl-aminooxy)methyl]phenoxymethyl PS **5**.

Preliminary investigations suggested that existing solid phase strategies[3,4] could not be adapted for the synthesis of *N*-alkyl hydroxamic acids for two reasons: (i) inefficient (65–80%) reduction was observed with *O*-benzylhydroxylamine-derived oximes using either $NaBH_3CN$ in 30–50% AcOH in MeOH–THF or $BH_3$·THF in THF, and (ii) negligible acylation ( < 5%) of NH(Me)O-2-chlorotrityl PS[3] was achieved as a result of considerable steric effect. In view of these results, we focused our efforts in the development of a new linker resin.

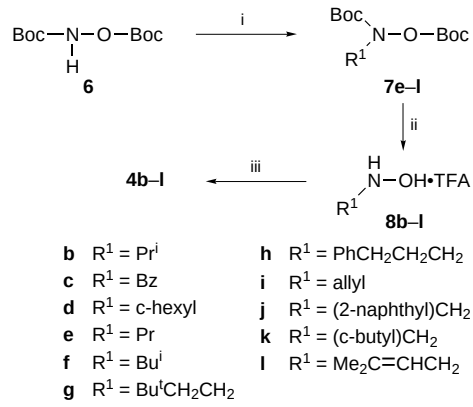
The acidolysis of 4-[2,4-dimethoxyphenyl(hydroxy)methyl]-phenoxymethyl PS **2** and its esters is well documented,[6] and since the linker group in **2** has significantly less steric hindrance than 2-chlorotrityl, we have established a facile solid phase procedure to the new linker resin **5** starting with commercially available **2**† (Scheme 1). Following evaluation of a series of chlorinating reagents and conditions, the conversion of **2** to the chloride **3** is best achieved by a simple $S_N1$ approach. Thus, treatment of **2** with 1% HCl in $CH_2Cl_2$–THF under continuous flow conditions gave **3** with typically *ca.* 70% efficiency.‡ In initial model experiments, the condensation of **3** with FmocN-(Me)OH[3] **4a** proceeded smoothly to afford **5a** with *ca.* 95% efficiency (0.38 mmol $g^{-1}$).† Any remaining reactive sites on the linker resin were 'eliminated' by treatment with MeOH and $Ac_2O$. We were then able to successfully acylate the Fmoc-deprotected **5a** with Fmoc-Phe-OH, carboxy-activated using HATU-based[7] method, with 89% efficiency, which on treatment with 1–5% TFA in $CH_2Cl_2$ yielded within 5 min the desired hydroxamic acid, Fmoc-Phe-N(Me)OH, in excellent purity ( > 95%).§

Furthermore, using commercially available **8b**–**d**·HCl, the Fmoc-derivatives **4b**–**d** were synthesized (Scheme 2) using our previously reported procedure[3] in excellent yields (71–86%), which on condensation with **3** yielded **5b**–**d** with good efficiencies (58–92%, 0.20–0.37 mmol $g^{-1}$). As expected, **4b** and **4d** were observed to react with lower efficiencies (58 and 73%, respectively) due to steric hindrance.

In order that the above strategy could be used as a generic solid phase approach to *N*-substituted hydroxamic acids, we went on to investigate synthetic methodology to chemically diverse Fmoc-N($R^1$)OH **4**. Following a systematic study, we have established a facile method to compounds **4** *via* *N*-alkylation of *N*,*O*-bis(*tert*-butoxycarbonyl) hydroxylamine[8,9] **6** in predominantly good overall yields (Scheme 2).¶ The alkylation of **6** was accomplished using the appropriate bromides in the presence of $K_2CO_3$ to furnish **7e**–**l** in typically 78–90% yields. In addition, we have also achieved alkylation of **6** using 3 equiv.



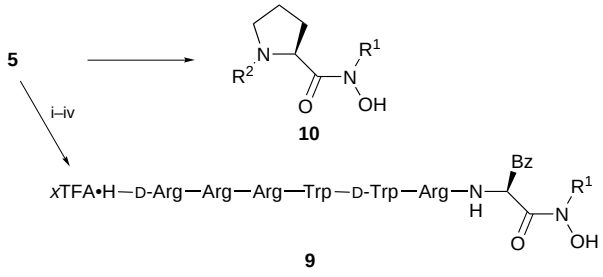

**Scheme 1** *Reagents and conditions*: i, 1% w/v HCl in $CH_2Cl_2$–THF; ii, **4** (1.5 equiv.), $Pr^i_2EtN$ (1.5 equiv.), $CH_2Cl_2$, 18 h; iii, MeOH–$CH_2Cl_2$, 30 min, then $Ac_2O$, $Pr^i_2EtN$, DMF, 4 h




**Scheme 2** *Reagents and conditions*: i, R′Br, $K_2CO_3$, DMF, 18 h; ii, 30% v/v TFA in $CH_2Cl_2$; iii, FmocCl, aq. $NaHCO_3$, 4 h

of a chloride, $Me_3C(CH_2)_2Cl$ in the presence of $K_2CO_3$ (1.25 equiv.) in DMF at 55 °C for 72 h, to give **7g** in 68% yield. The key building blocks **4e**–**l** were then readily obtained by, firstly, deprotection of **7e**–**l** with 30% v/v TFA–$CH_2Cl_2$, followed by introduction of the *N*-Fmoc protecting group using FmocCl to yield crystalline **4e**–**l** (65–81%).¶ In all cases, we observed high reaction efficiencies (78–97%) between **4e**–**l** and **3** to afford our key linker resins **5e**–**l** (0.26–0.30 mmol $g^{-1}$; 0.23 mmol $g^{-1}$ for **5j**.† In addition, the Fmoc-deprotected **5e**–**l** were readily acylated with HATU-activated Fmoc-Phe-OH (18 h) to yield the resin-bound Fmoc-Phe-(Fmoc-deprotected) **5e**–**l** in typically 93–100% yield, upon which 5% TFA-mediated cleavage afforded exclusively the desired hydroxamic acids Fmoc-Phe-N($R^1$)OH (> 95% purity judged by RP-HPLC§).

The utility of **5** was further illustrated by the synthesis of the model heptapeptidyl *N*-alkyl hydroxamic acids **9** (Scheme 3), using standard solid phase peptide chemistry.[10] The assembled peptidyl-(Fmoc-deprotected) **5e**–**l** following a two-step TFA treatment yielded **9e**–**l** in excellent purity and yield (80–90%).§ In addition, **5** was used for the solid phase synthesis of a biased 'small molecule' library comprising the generic template $N^1$-alkyl/acyl imino acyl *N*-alkyl hydroxamic acids, *e.g.* **10**; the $N^1$-alkylation step was typically accomplished using 4 equiv. of an alkyl bromide in the presence of 1 equiv. of DBU.




**Scheme 3** *Reagents and conditions*: i, 20% piperidine–DMF; ii, Fmoc-Phe-OH–HATU–HOAt–$Pr^i_2EtN$ (1 : 1 : 1 : 2, 10 equiv., *ca*. 0.3 M in DMF], 18 h; iii, standard Fmoc/$Bu^t$ solid-phase procedures (2.5 h acylation); iv, TFA–$Et_3SiH$–$CH_2Cl_2$ (5 : 1 : 94), 5 min, then TFA–$Pr^i_3SiH$–$HSCH_2CH_2SH$–$H_2O$ (90 : 1 : 4 : 5), 4 h, 30 °C

In summary, we have outlined a facile solid phase approach to *N*-substituted hydroxamic acids *via* the new linker resin **5** prepared from readily accessible building blocks **4**. The strategy allows the cleavage of target molecules from the solid support under exceptionally mild acidic conditions. The synthesized compounds **9** and **10** are currently being evaluated for biological activity.

We acknowledge Nottingham University for a research studentship award to S. L. M.

## Footnotes and References

* E-mail: weng.chan@nottingham.ac.uk

† Compound **2** has a chemically reactive hydroxy loading of either 0.54 or 0.64 mmol $g^{-1}$. The derivatised resin loading is based on spectrophotometric determination of the Fmoc-derived chromophore liberated upon treatment with 20% piperidine–DMF using $\varepsilon_{290}$ = 5253 $M^{-1}$ $cm^{-1}$.

‡ The following reaction was performed using oven-dried glasswares. A solution of *ca*. 1% w/v HCl was prepared by the addition of $SOCl_2$ (2.50 ml) to THF–$CH_2Cl_2$(1 : 3, 100 ml) followed by MeOH (1.25 ml). The resin **2** (0.5 mmol), suspended in $CH_2Cl_2$ in a glass column (15 × 150 mm), was treated with the 1% w/v HCl solution (100 ml) at *ca*. 4 ml $min^{-1}$ and washed with $CH_2Cl_2$ (20 ml), THF–$CH_2Cl_2$ (5 ml) and $CH_2Cl_2$ (20 ml) to afford **3**, which was used immediately. To the suspension of **3** in $CH_2Cl_2$ (*ca*. 6 ml) was added **4** (0.75 mmol) followed by $Pr^i_2EtN$ (0.13 ml, 0.75 mmol), and the resultant mixture was gently stirred at ambient temperature overnight to yield **5**. MeOH (0.2 ml) was added to the reaction mixture, stirred for 30 min and the resin was then washed with DMF (30 ml). The resin, now suspended in DMF, was treated with $Ac_2O$ (5 mmol)–$Pr^i_2EtN$ (0.5 mmol) for 4 h, after which the resin was washed with DMF, filtered off, washed repeatedly with $CH_2Cl_2$ and MeOH, and dried *in vacuo*. The chloride loading in **3** was determined using an acid–base back-titration procedure.

§ Crude hydroxamic acids **9** and **10** were analysed by RP-HPLC on a Hypersil Pep $C_{18}$ columnn (4.6 × 150 mm). All purified synthetic compounds gave the expected ES-MS, *e.g.* **9d**: calc. $M^+$ 1259.52, found 1258.38; **9g**: calc. 1261.54, found 1261.34; **9h**: calc. 1295.54, found 1294.95; **10f** ($R^2$ = $CH_2CH_2CH_2Ph$): calc. $MH^+$ 305.43, found 305.3; **10k** [$R^2$ = $CH_2$(2-naphthyl)]: calc. $MH^+$ 339.44, found 339.5.

¶ A typical procedure for the synthesis of *N*-fluoren-9-ylmethoxycarbonyl-*N*-alkyl hydroxylamine FmocN(Php)OH **4h**: To a solution of **6** (5 mmol) in DMF (10 ml) was added $K_2CO_3$ (6.25 mmol) followed by portionwise addition of 1-bromo-3-phenylpropane (5.2 mmol), and the resultant mixture was vigorously stirred at room temperature overnight. Following a standard work-up procedure trituration with ice-cold pentane yielded **7h** (1.58 g, 90%) as a white crystalline solid [mp 75–76 °C; > 95% purity when analysed by RP-HPLC; ES-MS : $MH^+$ calc. 352.45, found 352.3].

A solution of **7h** (4 mmol) in TFA–$CH_2Cl_2$ (3 : 7, 10 ml) was left at ambient temperature for 3–4 h, and then evaporated to dryness to yield **8h** (1.05 g, 99%; mp 67–69 °C), which was dried *in vacuo* over KOH pellets and used without further purification.

Compound **4h** was obtained by treating a solution of **8h** in EtOAc–aq. $NaHCO_3$ (2.2 equiv.) with FmocCl (1.1 equiv.) using the procedure previously outlined (ref. 3) in 67% yield [mp 84–86 °C; $\delta_H$($CDCl_3$, 250 MHz) 1.98 (2 H, m, Php $CH_2CH_2CH_2N$), 2.64 (2 H, t, *J* 7.8, Php $CH_2CH_2CH_2N$), 3.59 (2 H, t, *J* 7.0, Php $CH_2CH_2CH_2N$), 4.26 (2 H, t, *J* 6.7, Fmoc C*H*), 4.50 (2 H, d, *J* 6.7, Fmoc $CH_2$), 7.12–7.47, 7.56, 7.81 (13 H, Fmoc and Ph ArH); ES-MS : $MH^+$ calc. 374.45, found 374.4].

1 H. Umezawa, T. Aoyagi, T. Tanaka, H. Suda, A. Okuyama, H. Naganawa, M. Hamada and T. Takeuchi, *J. Antibiot.*, 1985, **38**, 1629; H. Umezawa, T. Aoyagi, K. Ogawa, T. Obata, H. Iinuma, H. Naganawa, M.Hamada and T. Takeuchi, *J. Antibiot.*, 1985, **38**, 1813; K. Tamaki, T. Ogita, K. Tanzawa and Y. Sugimura, *Tetrahedron Lett.*, 1993, **28**, 683.
2 R. Bihovsky, B. L. Levison, R. C. Loewi, P. W. Erhardt and M. A. Polokoff, *J. Med. Chem.*, 1995, **38**, 2119; H. R. Onishi, B. A. Pelak, L. S. Gerkens, L. L. Silver, F. M. Kahan, M.-H. Chen, A. A. Patchett, S. M. Galloway, S. A. Hyland, M. S. Anderson and C. R. H. Raetz, *Science*, 1996, **274**, 980.
3 S. L. Mellor, C. McGuire and W. C. Chan, *Tetrahedron Lett.*, 1997, **38**, 3311.
4 C. D. Floyd, C. N. Lewis, S. R. Patel and M. Whittaker, *Tetrahedron Lett.*, 1996, **37**, 8045; L. S. Richter and M. C. Desai, *Tetrahedron Lett.*, 1997, **38**, 321.
5 W. C. Chan and S. L. Mellor, *J. Chem. Soc., Chem. Commun.*, 1995, 1475.
6 H. Rink, *Tetrahedron Lett.*, 1987, **28**, 3787.
7 L. A. Carpino, A. El-Faham, C. A. Minor and F. Albericio, *J. Chem. Soc., Chem. Commun.*, 1994, 201.
8 M. A. Staszak and C. W. Coecke, *Tetrahedron Lett.*, 1993, **34**, 7043.
9 For a comprehensive review on the use of bis-protected hydroxylamines, see J. L. Romine, *Org. Prep. Proced. Int.*, 1996, **28**, 249.
10 G. B. Fields and R. L. Noble, *Int. J. Peptide Protein Res.*, 1990, **35**, 161.

*Received in Cambridge, UK, 5th August 1997; 7/05683D*

# First observation of non-bridging thiolates or tetrahedral geometries within thiolate-containing Schiff-base macrocycles: $[Zn_2L][CF_3SO_3]_2$

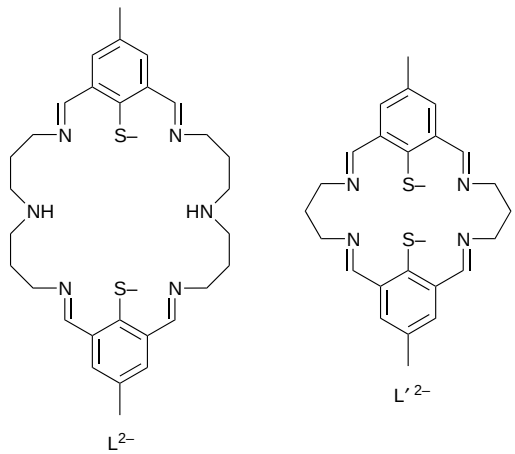
**Sally Brooker* and Tony C. Davidson**

*Department of Chemistry, University of Otago, PO Box 56, Dunedin, New Zealand*

**The structure determination of $[Zn_2L][CF_3SO_3]_2$ 1 reveals the first example of non-bridging thiolates within a thiolate-containing Schiff-base macrocyclic complex: the flexibility of such macrocycles is also clearly demonstrated as this is the first example of the provision of distorted tetrahedral metal ion binding sites.**

Thiolate-containing complexes are currently of great interest as model complexes for a number of metalloprotein active sites such as Fe–S clusters,[1] Ni–Fe hydrogenase,[2] $Cu_A$ site of cytochrome c oxidase[3] and Zn fingers.[4] The complexes are also of interest in their own right as they exhibit very different properties to those of complexes with other, more common donors such as oxygen or nitrogen. We have therefore incorporated the 'head unit' *S*-(2,6-diformyl-4-methylphenyl)dimethylthiocarbamate, which contains a masked thiolate, into a series of Schiff-base macrocycles:[5–7] the thiolate donor is best generated from the masked 'head unit' by base hydrolysis prior to the cyclisation reaction.[6] To date, the reported di- and tetra-nuclear Schiff-base macrocyclic complexes formed from this unmasked thiolate have exhibited a wide range of geometries, albeit predominantly square-based ones: from square planar, square pyramidal and octahedral through to one example of trigonal bipyramidal.[5–9] In all of the examples to date the thiolate donors bridge the two metal ions. Here we describe the synthesis and structure of a new dinuclear Schiff-base macrocyclic complex which exhibits very different features.

Hydrolysis of *S*-(2,6-diformyl-4-methylphenyl)dimethylthiocarbamate with NaOH, followed by reaction with *N*-(3-aminopropyl)-1,3-propanediamine in the presence of zinc(II) template ions, yields a yellow powder, $[Zn_2L][CF_3SO_3]_2$ **1**, in 85% yield (Scheme 1).† The IR spectrum of **1** was consistent with the presence of a Schiff-base macrocycle; an imine band was present at 1633 $cm^{-1}$ and there were no primary amine or carbonyl bands. Based on the geometry we observed for the zinc ions in a related macrocyclic complex $[Zn_2L'(H_2O)_2]^{2+}$ **2** (Scheme 1) we expected that the zinc ions in this new complex might also be trigonal bipyramidal, but that now *all* of the donors could be supplied by the macrocycle.[6] To test this proposal a structure determination was carried out on **1**.




**Scheme 1** Ligands $L^{2-}$ and $L'^{2-}$

Yellow single crystals were obtained by diethyl ether diffusion into an acetonitrile solution of **1**.‡ The X-ray structure determination revealed, in contrast to the predicted trigonal-bipyramidal geometry, the first example of a thiolate-containing Schiff-base macrocyclic complex containing metal ions with a distorted tetrahedral geometry (Fig. 1). Each of the two zinc atoms is bound to a single thiolate donor, two imine nitrogen donors and an amine nitrogen donor, and has adopted an approximately tetrahedral geometry. Tetrahedral coordination of zinc ions in mixed thiolate/nitrogen coordination environments is not uncommon[10] and presumably a trigonal-bipyramidal geometry is not observed in this case due to an unfavourable spatial arrangement of the required donors, due to the constraint of them all coming from a single polydentate macrocyclic ligand.[11] Another unique feature of this structure is that the thiolate donors do not bridge the two metal ions. This is in stark contrast with all of the related macrocyclic complexes prepared to date,[5–9,12] and with the well known ability of thiolates to bridge metal ions, a feature of thiolate chemistry which has often resulted in the uncontrolled (and usually undesired) formation of polymers.[13] We have found that the use of thiolate-containing macrocycles has allowed us to control this aspect of thiolate coordination chemistry (as well as a number of other common problems)[6,13] and has thus facilitated the formation of discrete complexes where the thiolate donors only bridge between the metal ions incorporated in the macrocycle.[5–7] However, in this new macrocyclic complex there is no thiolate bridging whatsoever.

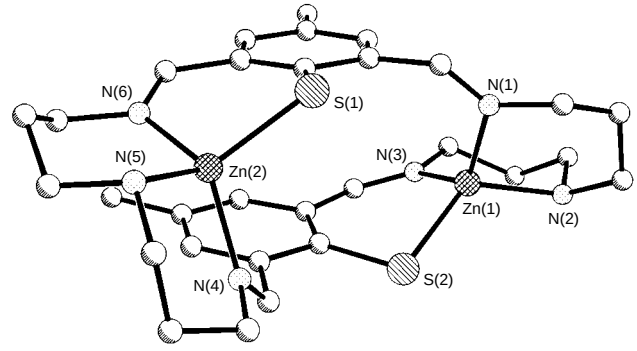



**Fig. 1** Perspective diagram of the cation of **1**, $[Zn_2L]^{2+}$. Selected bond lengths (Å) and angles (°): Zn(1)–N(3) 2.007(7), Zn(1)–N(1) 2.024(8), Zn(1)–N(2) 2.031(8), Zn(1)–S(2) 2.254(3), Zn(2)–N(6) 2.001(7), Zn(2)–N(4) 2.032(7), Zn(2)–N(5) 2.036(8), Zn(2)–S(1) 2.253(2), S(1)···S(2) 4.516(3), Zn(1)···Zn(2) 6.077(2); N(3)–Zn(1)–N(1) 126.1(3), N(3)–Zn(1)–N(2) 100.3(3), N(1)–Zn(1)–N(2) 98.6(3), N(3)–Zn(1)–S(2) 100.2(2), N(1)–Zn(1)–S(2) 108.5(2), N(2)–Zn(1)–S(2) 125.5(3), N(6)–Zn(2)–N(4) 123.9(3), N(6)–Zn(2)–N(5) 100.6(3), N(4)–Zn(2)–N(5) 98.6(3), N(6)–Zn(2)–S(1) 100.3(2), N(4)–Zn(2)–S(1) 110.5(2), N(5)–Zn(2)–S(1) 124.7(2), C(1)–S(1)–Zn(2) 99.7(3), C(16)–S(2)–Zn(1) 99.6(3).

The macrocycle has clearly adopted a very different conformation to those observed previously and in so doing reveals considerable flexibility. The use of an aromatic thiolate 'head unit' has allowed the formation of π–π interactions to influence the overall structure.[14] Specifically, favorable π–π interactions exist between the two aromatic rings within the macrocyclic unit: the two aromatic ring planes intersect at 6.8° and are 3.32–3.62 Å apart. Intermolecular π–π interactions are also observed and lead to the molecules packing together in chains. The two monodentate thiolate donors are relatively exposed but intermolecular bridging does not occur. The two triflate anions hydrogen bond to the two secondary amines (O···N 2.85, 2.89 Å), and destroy the otherwise approximate twofold symmetry of the complex.

Molar conductance measurements show that **1** is a 2:1 electrolyte in dimethylformamide (dmf) indicating that the cation $[Zn_2L]^{2+}$ is present in solution. $^1H$ and $^{13}C$ NMR spectra were obtained in both $[^2H_7]$dmf and $CD_3CN$. In each case the imine, aromatic and methylene resonances are chemically inequivalent which is consistent with the maintenance of the solid-state structure in solution. Preliminary cyclic voltammetry studies in MeCN show that **1** undergoes an irreversible, approximately two-electron, oxidation at $E_{pa}$ = +1.03 V *vs.* 0.01 M $AgNO_3$/Ag. This behaviour is very similar to that of complex **2** and is currently under further investigation.[6,7]

In summary, we have prepared a new thiolate-containing macrocyclic ligand, as a dizinc(II) complex, and it has very different characteristics from previous thiolate-containing Schiff-base macrocycles. Transmetallations and attempts to induce the thiolates to bridge to introduced metal ion complexes are underway. Further development of this and related systems will provide excellent opportunities to manipulate both the bridging tendency of the incorporated thiolates and the geometries adopted by the incorporated metal ions, giving us, in a controlled way, access to complexes of our own design.[7]

This work was supported by grants from the University of Otago. We thank Professor W. T. Robinson (University of Canterbury) for the X-ray data collection. S. B. thanks the University of Otago for the granting of study leave which has facilitated the writing of this paper, and gratefully acknowledges her host Professor K. Wieghardt and the financial support of the Alexander von Humboldt Stiftung.

## Footnotes and References

* sbrooker@alkali.otago.ac.nz

† Satisfactory C,H,N,S analysis was obtained for **1**.

‡ *Crystal data* for **1**: $C_{32}H_{40}F_6N_6O_6S_4Zn_2$, pale yellow block, crystal dimensions 0.80 × 0.26 × 0.18 mm, monoclinic, space group $P2_1/c$, $a$ = 14.830(2), $b$ = 21.422(3), $c$ = 14.148(2) Å, $\beta$ = 114.723(9)°, $U$ = 4083(1) Å$^3$, $\mu$ = 1.456 mm$^{-1}$. Data were collected at 170 K on a Siemens P4 four-circle diffractometer using graphite-monochromated Mo-Kα radiation ($\lambda$ = 0.71073 Å). 6963 Reflections were collected in the range $4 < 2\theta < 48°$ and the 6336 independent reflections were used in the structural analysis after a semi-empirical absorption correction had been applied. The structure was solved by direct methods (SHELXS-86)[15] and refined against all $F^2$ data (SHELXL-93)[16] to $R_1$ = 0.071 [for 4028 $F > 4\sigma(F)$; $wR_2$ = 0.204 and goodness of fit = 1.04 for all 6336 $F^2$; 517 parameters; all non-hydrogen atoms anisotropic, $CF_3$ groups disordered]. CCDC 182/600.

1 See for example: R. H. Holm, S. Ciurli and J. A. Weigel, *Prog. Inorg. Chem.*, 1990, **38**, 1.
2 See for example: A. F. Kolodziej, *Prog. Inorg. Chem.*, 1994, **41**, 493; M. A. Halcrow and G. Christou, *Chem. Rev.*, 1994, **94**, 2421; A. Volbeda, E. Garcin, C. Piras, A. L. De Lacey, V. M. Fernandez, E. C. Hatchikian, M. Frey and J. C. Fontecilla-Camps, *J. Am. Chem. Soc.*, 1996, **118**, 2989.
3 See for example: S. Iwata, C. Ostermeier, B. Ludwig and H. Michel, *Nature*, 1995, **376**, 660; H. Bertagnolli and W. Kaim, *Angew. Chem., Int. Ed. Engl.*, 1995, **34**, 771.
4 See for example: B. L. Vallee and D. S. Auld, *Acc. Chem. Res.*, 1993, **26**, 543; J. M. Berg, *Science*, 1996, **271**, 1081.
5 S. Brooker and P. D. Croucher, *J. Chem. Soc., Chem. Commun.*, 1995, 1493; 2075; *Chem. Commun.*, 1997, 459.
6 S. Brooker, P. D. Croucher and F. M. Roxburgh, *J. Chem. Soc., Dalton Trans.*, 1996, 3031.
7 S. Brooker, P. D. Croucher, T. C. Davidson, G. S. Dunbar, P. D. Smith, S. P. Cramer, C. Y. Ralston, A. McAuley and S. Subramanian, unpublished work.
8 A. J. Atkins, A. J. Blake and M. Schröder, *J. Chem. Soc., Chem. Commun.*, 1993, 1662; A. J. Atkins, D. Black, A. J. Blake, A. Marin-Becerra, S. Parsons, L. Ruiz-Ramirez and M. Schröder, *Chem. Commun.*, 1996, 457; N. D. J. Branscombe, A. J. Blake, A. Marin-Becerra, W-S. Li, S. Parsons, L. Ruiz-Ramirez and M. Schröder, *Chem. Commun.*, 1996, 2573.
9 P. E. Kruger and V. McKee, *Chem. Commun.*, 1997, 1341.
10 See for example: J. Castro, J. Romero, J. A. García-Vázquez, M. L. Durán, A. Castiñeiras, A. Sousa and D. E. Fenton, *J. Chem. Soc., Dalton Trans.*, 1990, 3255; C. Zhang, R. Chadha, H. K. Reddy and G. N. Schrauzer, *Inorg. Chem.*, 1991, **30**, 3865; R. Baggio, M. T. Garland and M. Perec, *J. Chem. Soc., Dalton Trans.*, 1993, 3367; J. J. Wilker and S. J. Lippard, *J. Am. Chem. Soc.*, 1995, **117**, 8682; U. Brand, R. Burth and H. Vahrenkamp, *Inorg. Chem.*, 1996, **35**, 1083.
11 V. McKee, *Adv. Inorg. Chem.*, 1993, **40**, 323.
12 G. A. Lawrance, M. Maeda, T. M. Manning, M. A. O'Leary, B. W. Skelton and A. H. White, *J. Chem. Soc., Dalton Trans.*, 1990, 2491.
13 See for example: I. G. Dance, *Polyhedron*, 1986, **5**, 1037; J. R. Dilworth and J. Hu, *Adv. Inorg. Chem.*, 1993, **40**, 411.
14 See for example: C. A. Hunter and J. K. M. Sanders, *J. Am. Chem. Soc.*, 1990, **112**, 5525; P. R. Ashton, P. T. Glink, M. V. Martinez-Diaz, J. F. Stoddart, A. J. P. White and D. J. Williams, *Angew. Chem., Int. Ed. Engl.*, 1996, **35**, 1930; H. Adams, F. J. Carver, C. A. Hunter, J. C. Morales and E. M. Seward, *Angew. Chem., Int. Ed. Engl.*, 1996, **35**, 1542; I. Dance and M. Scudder, *Chem. Eur. J.*, 1996, 481.
15 G. M. Sheldrick, *Acta Crystallogr., Sect. A*, 1990, **46**, 467.
16 G. M. Sheldrick, *J. Appl. Crystallogr.*, 1997, manuscript in preparation.

*Received in Cambridge, UK, 28th July 1997; 7/05415G*

# High-nuclearity mixed-metal carbonyl clusters of osmium and palladium; molecular structures of $[Os_5Pd_6(CO)_{13}(\mu\text{-}CO)_5(\mu\text{-}H)_2(\mu\text{-}dppm)_2]\cdot 2CH_2Cl_2\cdot C_6H_{14}$ and $[Os_5Pd_6(CO)_{13}(\mu\text{-}CO)_6(\mu\text{-}dppm)_2]$

**Janesse Wing-Sze Hui and Wing-Tak Wong***

*Department of Chemistry, The University of Hong Kong, Pokfulam Road, Hong Kong, PR China*

**The high-nuclearity mixed-metal carbonyl clusters $[Os_5Pd_6(CO)_{13}(\mu\text{-}CO)_5(\mu\text{-}H)_2(\mu\text{-}dppm)_2]$ 1 and $[Os_5Pd_6(CO)_{13}(\mu\text{-}CO)_6(\mu\text{-}dppm)_2]$ 2 are synthesized from the reaction of $[Os_3(CO)_{10}(\mu\text{-}H)_2]$ with $[Pd_2(\mu\text{-}dppm)_2Cl_2]$; their molecular structures are determined by X-ray analysis.**

High-nuclearity mixed-metal clusters have attracted considerable interest due to their novel structural features and interesting chemical and physical properties.[1] Most of these mixed-metal clusters are the combination of late transition metals. For examples, Fe/Pd,[2] Fe/Pt,[3] Fe/Cu,[4] Ru/Pt,[5] Ru/Cu,[6] Os/Pt,[7] Os/Hg,[8] Co/Hg,[9] Rh/Ni,[10] Rh/Pt,[11] Ni/Pt[12] are well established. However, mixed-metal clusters of osmium and palladium are relatively rare.[13] We recently established some reliable synthetic routes to osmium and palladium mixed-metal clusters. These systems are all osmium rich. Herein we report the synthesis and structural characterization of two novel high-nuclearity Os/Pd mixed-metal carbonyl clusters containing an essentially, identical metal core.

The reaction of $[Os_3(CO)_{10}(\mu\text{-}H)_2]$ with a slight excess of $[Pd_2(\mu\text{-}dppm)_2Cl_2]$ in $CH_2Cl_2$ at room temp for 6 h affords two new osmium–palladium clusters: dark green $[Os_5Pd_6(CO)_{13}(\mu\text{-}CO)_5(\mu\text{-}H)_2(\mu\text{-}dppm)_2]$ **1** and brownish–green $[Os_5Pd_6(CO)_{13}(\mu\text{-}CO)_6(\mu\text{-}dppm)_2]$ **2** in 5 and 10% yields respectively. The major products isolated from this system are phosphine containing clusters $[Os_3(CO)_8(\mu\text{-}dppm)]$ (23%) and $[Os_4(CO)_{10}(\mu\text{-}dppm)]$ (18%) (confirmed by IR and $^1$H NMR spectroscopy). Both clusters **1** and **2** were isolated as air-stable solids upon thin layer chromatographic separation on silica. Spectroscopic† and analytical data are consistent with their formulations. In order to establish their molecular structures, X-ray analyses have been carried out on single crystals of **1** and **2**.‡ Suitable crystals of **1** and **2** were obtained as dark green prisms **1** and brownish–green blocks **2**, using $CH_2Cl_2$–*n*-hexane mixture at 0 °C for a period of 2 weeks, respectively. Clusters **1** and **2** were found to have an essentially identical metal core, see Fig. 1. Their full structures are depicted in Fig. 2 and Fig. 3 together with some important bond parameters. The cluster core geometry of **1** and **2** may be viewed as an 'inner' $Pd_6$ bicapped tetrahedron with several triangular faces asymmetrically capped by Os(1), Os(2), Os(4) and Os(5) on Pd(1)Pd(2)Pd(3), Pd(2)Pd(3)Pd(5), Pd(3)Pd(4)Pd(5) and Pd(4)Pd(5)Pd(6) respectively. In addition, the Os(3) capped onto Os(2)Pd(2)Pd(5) so that the cluster cores become asymmetric or otherwise a twofold axis is possible. The only significant Os–Os interaction is observed between Os(2) and Os(3) [3.0074(7) Å in **1** and 2.8861(9) Å in **2**]. This metal framework can be viewed as a distorted fragment of three close-packed layers of metal atoms and is unprecedented in both homo- and hetero-metallic clusters containing osmium. Of the 18 carbonyl groups in cluster **1**, 13 are terminally bonded and 5 are bridging the Os–Pd bonds. In **2**, the CO distributions are almost identical to that observed in **1**, except for an extra bridging C(10)–O(10) across Os(3)–Pd(5). In **1**, there are two hydride ligands. This was as evident from the $^1$H NMR spectroscopy. However, their positions cannot be determined by X-ray analysis directly. Detailed examination of the CO disposition on the ligand envelope and metal–metal bond distances suggested that one may bridge across the Os(2)–Pd(2) edge while the other one may bridge across Os(2)–Os(3). Both of these metal–metal distances are significantly longer than those observed in **2** where no hydride ligands are present.

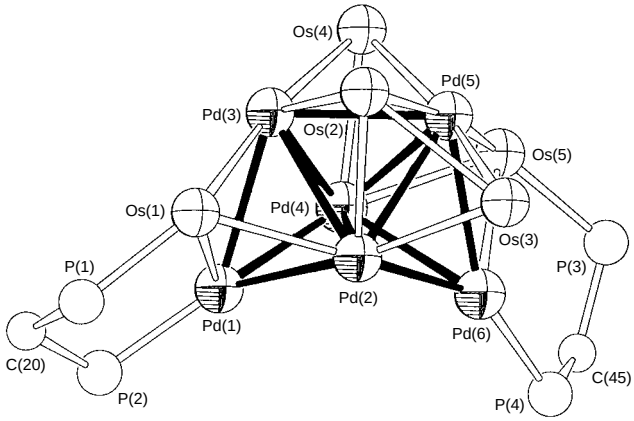



**Fig. 1** The metal core geometry of **1** and **2**

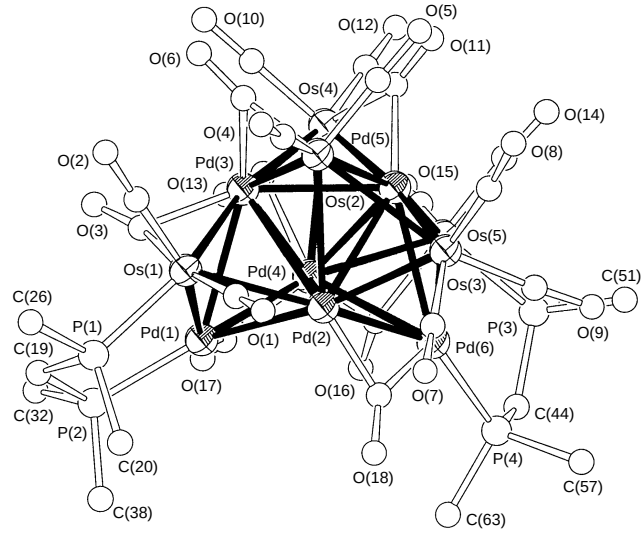



**Fig. 2** The molecular structure of **1** showing the atom numbering scheme (phenyl rings are omitted for clarity). Selected bond lengths (Å): Os(1)–Pd(1) 2.935(1), Os(1)–Pd(2) 2.833(1), Os(1)–Pd(3) 2.834(1), Os(2)–Os(3) 3.0074(7), Os(2)–Pd(2) 3.024(1), Os(2)–Pd(3) 2.725(1), Os(2)–Pd(5) 2.779(1), Os(3)–Pd(2) 2.774(1), Os(3)–Pd(5) 2.831(1), Os(4)–Pd(3) 2.890(1), Os(4)–Pd(4) 2.852(1), Os(4)–Pd(5) 2.730(1), Os(5)–Pd(4) 2.791(1), Os(5)–Pd(5) 3.030(1), Os(5)–Pd(6) 3.116(1), Pd(1)–Pd(2) 2.893(2), Pd(1)–Pd(3) 2.943(2), Pd(1)–Pd(4) 2.707(2), Pd(2)–Pd(3) 2.918(1), Pd(2)–Pd(4) 3.097(2), Pd(2)–Pd(5) 2.877(2), Pd(2)–Pd(6) 2.683(1), Pd(3)–Pd(4) 2.759(1), Pd(3)–Pd(5) 2.853(2), Pd(4)–Pd(5) 2.923(2), Pd(4)–Pd(6) 3.013(2), Pd(5)–Pd(6) 2.988(1).

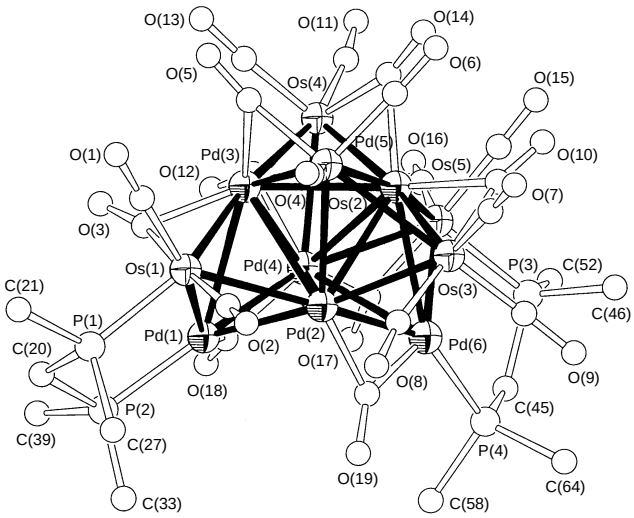



**Fig. 3** The molecular structure of **2** showing the atom numbering scheme (phenyl rings are omitted for clarity). Selected bond lengths (Å): Os(1)–Pd(1) 2.963(2), Os(1)–Pd(2) 2.868(1), Os(1)–Pd(3) 2.819(1), Os(2)–Os(3) 2.8861(9), Os(2)–Pd(2) 2.913(1), Os(2)–Pd(3) 2.716(1), Os(2)–Pd(5) 2.768(1), Os(3)–Pd(2) 2.756(1), Os(3)–Pd(5) 2.787(1), Os(4)–Pd(3) 2.841(1), Os(4)–Pd(4) 2.839(2), Os(4)–Pd(5) 2.747(1), Os(5)–Pd(4) 2.837(1), Os(5)–Pd(5) 3.016(1), Os(5)–Pd(6) 3.180(2), Pd(1)–Pd(2) 2.828(2), Pd(1)–Pd(3) 3.004(2), Pd(1)–Pd(4) 2.722(2), Pd(2)–Pd(3) 2.881(2), Pd(2)–Pd(4) 3.162(2), Pd(2)–Pd(5) 2.914(2), Pd(2)–Pd(6) 2.706(2), Pd(3)–Pd(4) 2.786(1), Pd(3)–Pd(5) 2.867(2), Pd(4)–Pd(5) 2.939(2), Pd(4)–Pd(6) 2.935(2), Pd(5)–Pd(6) 2.948(2).

It is a common observation that the metal–metal bond elongates as it is bridged by hydride.[14] Although the solid-state structure of **1** revealed two hydride environment, in solution some dynamic processes may be possible and a broad $^1$H NMR singlet is observed. Both **1** and **2** possess 146 CVE. However, their structures can not be rationalized by common electron counting rules.[15] This is not entirely unexpected as many Os/Pd or Os/Pt mixed–metal clusters do not obey simple electron counting rules owing to an alternative stable 16-electron configuration of Pd and Pt.

Our present results establish new examples of the high-nuclearity Os/Pd clusters. Although the yields are quite low, the syntheses under these experimental conditions are reproducible. At this stage, we do not detect any interconversion between **1** and **2** even though their molecular structures are very similar. Further studies would screen the experimental conditions and stoichiometry of the reactants to improve the yield of these novel species so that their chemical reactivities can be investigated.

W.-T. W. acknowledges the financial support from the Croucher Foundation and the University of Hong Kong. J. W.-S. H. thanks the receipt of a postgraduate studentship administered by the University of Hong Kong and the Sir Edward Youde Memorial Fellowship (1996–1997) administrated by the Sir Edward Youde Memorial Fund Council.

## Footnotes and References

* E-mail: wtwong@hkucc.hku.hk

† *Spectroscopic data*: **1**: IR [$\nu$(CO), $CH_2Cl_2$] 2076w, 2046s, 2034vs, 2019m, 1992m, 1968w cm$^{-1}$; Negative FAB mass spectrum: *m*/*z* = 2861 (2863 calc.); $^1$H NMR($CD_2Cl_2$) $\delta$ −14.93 (s, br, 2 H), 5.35 [t, *J*(HP) 1.04 Hz, 4 H], 7.45–7.59 (m, 40 H); $^{31}$P{$^1$H} NMR ($CD_2Cl_2$) $\delta$ 24.5 [d, $^2J$(PP) 88.7 Hz], 11.0 [d, $^2J$(PP) 88.7 Hz], −1.9 [d, $^2J$(PP) 84.4 Hz], −5.3 [d, $^2J$(PP) 84.4 Hz].

**2**: IR [$\nu$(CO), $CH_2Cl_2$] 2074w, 2053s, 2034vs, 2015m, 1992m, 1968w cm$^{-1}$; Negative FAB mass spectrum: *m*/*z* = 2886 (2890 calc.); $^1$H NMR ($CD_2Cl_2$) $\delta$ 5.22 [t, *J*(HP) 1.04 Hz, 4 H], 7.48–7.62 (m, 40 H); $^{31}$P{$^1$H} NMR ($CD_2Cl_2$) $\delta$ 30.4 [d, $^2J$(PP) 88.6 Hz], 9.2 [d, $^2J$(PP) 88.6 Hz], 1.3 [d, $^2J$(PP) 83.2 Hz], −3.5 [d, $^2J$(PP) 83.6 Hz].

‡ *Crystal data*: **1**: $C_{76}H_{64}Cl_4O_{18}Os_5P_4Pd_6$, *M* = 3118.42, primitive monoclinic, space group $P2_1/c$ (no. 14), *a* = 14.348(1), *b* = 21.721(2), *c* = 28.797(2) Å, $\beta$ = 97.48(2)°, *U* = 8898(1) Å$^3$, *Z* = 4, $D_c$ = 2.328 g cm$^{-3}$, *F*(000) = 5784, Mo-K$\alpha$ radiation ($\lambda$ = 0.71073 Å), $\mu$(Mo-K$\alpha$) = 85.38 cm$^{-1}$, dimensions 0.19 × 0.21 × 0.25 mm. MAR research image plate scanner. 69022 reflections were collected and merged to give 9312 ($R_{int}$ = 0.04) observed data [$I > 3.00\sigma(I)$]. Structure solved by direct methods (SIR88)[17] and Fourier-difference techniques, refined by full-matrix least-squares analysis to $R$ = 0.040, $R'$ = 0.037.

**2**: $C_{69}H_{44}O_{19}Os_5P_4Pd_6$, *M* = 2890.39, trigonal *R*-centered, space group $R\bar{3}$ (no. 148), *a* = 47.060(2), *c* = 20.568(1) Å, *U* = 39448(2) Å$^3$, *Z* = 18, $D_c$ = 2.190 g cm$^{-3}$, *F*(000) = 23868, Mo-K$\alpha$ radiation ($\lambda$ = 0.710 73 Å), $\mu$(Mo-K$\alpha$) = 85.40 cm$^{-1}$, dimensions 0.18 × 0.19 × 0.23 mm. MAR research image plate scanner. 102482 reflections were collected and merged to give 9044 ($R_{int}$ = 0.04) observed data [$I > 3.00\sigma(I)$]. Structure solved and refined as for **1** to $R$ = 0.049, $R'$ = 0.057. CCDC 182/604.

1 *Clusters and Colloids From Theory to Applications*, ed. G. Schmid, VCH, New York, 1994.
2 G. Longoni, M. Manassero and M. Sansoni, *J. Am. Chem. Soc.*, 1980, **102**, 3242.
3 G. Longoni, M. Manassero and M. Sansoni, *J. Am. Chem. Soc.*, 1980, **102**, 7973.
4 G. Doyle, K. A. Ericksen and D. van Engen, *J. Am. Chem. Soc.*, 1985, **107**, 7914; 1986, **108**, 445.
5 M. I. Bruce, G. Shaw and F. G. A. Stone, *Chem. Commun.*, 1971, 1288; M. I. Bruce, G. Shaw and F. G. A. Stone, *J. Chem. Soc., Dalton. Trans.*, 1972, 1781.
6 M. A. Beswick, J. Lewis, P. R. Raithby and M. C. R. Arellano, *Angew. Chem., Int. Ed. Engl.*, 1997, **3**, 291.
7 R. D. Adams, J. C. Lii and W. Wu, *Inorg. Chem.*, 1992, **31**, 2556.
8 Y. K. Au and W.-T. Wong, *Inorg. Chem.*, 1997, **36**, 2062; M. Charalambous, L. H. Gade, B. F. G. Johnson, T. Kotch, A. J. Lees, J. Lewis and M. McPartlin, *Angew. Chem., Int. Ed. Engl.*, 1990, **10**, 1137; L. H. Gade, B. F. G. Johnson, J. Lewis, M. McPartlin, T. Kotch and A. J. Lees, *J. Am. Chem. Soc.*, 1991, **113**, 8698.
9 J. M. Ragosta and J. M. Burlitch, *Organometallics*, 1988, **7**, 1469.
10 D. Nagaki, J. V. Badding, A. M. Stacy and L. F. Dahl, *J. Am. Chem. Soc.*, 1986, **108**, 3825.
11 A. Fumagalli, S. Martinengo and G. Ciani, *J. Chem. Soc., Chem. Commun.*, 1983, 1381; A. Fumagalli, S. Martinengo, G. Ciani, N. Masciocchi and A. Sironi, *Inorg. Chem.*, 1992, **31**, 336.
12 A. Ceriotti, F. Demartin, G. Longoni, M. Manassero, G. Piva, G. Piro, M. Sansoni and B. T. Heaton, *J. Organomet. Chem.*, 1986, **301**, C5; A. Ceriotti, F. Demartin, G. Longoni, M. Manassero, M. Marchionna, G. Piva and M. Sansoni, *Angew. Chem., Int. Ed. Engl.*, 1985, **24**, 697.
13 S. Chan and W.-T. Wong, *J. Chem. Soc., Dalton. Trans.*, 1994, 1605; S. Chan and W.-T. Wong, *J. Chem. Soc., Dalton. Trans.*, 1995, 3987; S. Chan and W.-T. Wong, *J. Organomet. Chem.*, 1995, **489**, C78; S. Chan, S.-M. Lee, Z. Lin and W.-T. Wong, *J. Organomet. Chem.*, 1996, **510**, 219; J. W.-S. Hui and W.-T. Wong, *J. Chem. Soc., Dalton Trans.*, 1996, 2887; J. W.-S. Hui and W.-T. Wong, *J. Chem. Soc., Dalton Trans.*, 1997, 1515.
14 M. R. Churchill, in *Transition Metal Hydrides*, Adv. Chem. Ser. No. 167; American Chemical Society, Washington, DC, 1978.
15 D. M. P. Mingos, *Acc. Chem. Res.*, 1984, **17**, 311; *J. Chem. Soc., Chem. Commun.*, 1983, 706.
16 D. M. P. Mingos and A. S. May, in *The Chemistry of Metal Cluster Complexes*, ed. D. F. Shriver, H. D. Kaesz and R. D. Adams, VCH, New York, 1990, ch. 2; C. Couture and D. H. Farrar, *J. Chem. Soc., Dalton Trans.*, 1987, 2253; R. D. Adams and T. S. A. Hor, *Inorg. Chem.*, 1984, **23**, 4723.
17 M. C. Burla, M. Camalli, G. Cascarano, C. Giacovazzo, G. Polidori, R. Spagna and D. Viterbo, *J. Appl. Crystallogr.*, 1989, **22**, 389.

*Received in Cambridge, UK, 24th July 1997; 7/05348G*

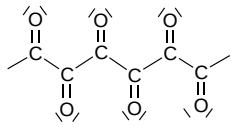
# Can carbon monoxide polymerize? A theoretical investigation of polyketone

**Gilles Frapper,[a,b,c]† Chang-Xing Cu,[a,d] Jean-François Halet,[b] Jean-Yves Saillard[b] and Miklos Kertesz[a]‡**

[a] *Steacie Institute for Molecular Sciences, National Research Council of Canada, Ottawa, Ontario K1A OR9, Canada*
[b] *LCSIM-UMR 6511, Université de Rennes 1, 35042 Rennes Cedex, France*
[c] *Department of Chemistry, Georgetown University, Washington, DC 20057-1227, USA*
[d] *Allied-Signal Inc., Research and Technology, Morriston, NJ 07962, USA*

**State of the art *ab initio* calculations on R(CO)$_n$R (R = H, Me; $n$ = 1–11) indicate that the hypothetical polymer of carbon monoxide, poly-CO, would be energetically less stable than the molecular form only by a few kcal mol$^{-1}$, making it a plausible stable allotropic form of CO.**

Predictive quantum chemistry offers the opportunity to design new polymers with potentially interesting physical or structural properties. One can design these new materials by linking building blocks which sometimes can exist alternatively as stable monomers, dimers or even larger finite aggregates.[1–3] Our contribution in this field concerns the investigation of a hypothetical polymer of carbon monoxide by means of *ab initio* and density functional calculations. This polymer **1**, named

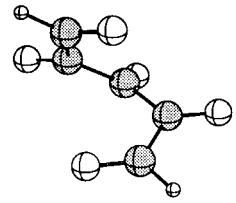


**1**

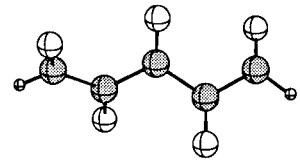
poly-CO throughout this paper, has the unusual property of having a repeat unit that is isoelectronic, albeit not isodesmic, to molecular CO: the [C=O] repeat units are linked together through C(sp$^2$)–C(sp$^2$) single bonds. Standard bond energy calculations[4] indicate that CO polymerization should be roughly thermoneutral, suggesting that poly-CO should be thermodynamically stable. Moreover, vicinal oligoketones, R(CO)$_n$R ($n$ < 6), have been shown to exist,[5] as well as one-dimensional (BC)$^{3-}$ chains, isoelectronic to poly-CO, which are encountered in several MBC (M = rare earth metal) solid state phases.[6] Previous semi-empirical calculations by some of us[7] and by Hoffmann[8] on poly-CO suggest that it should have an helical conformation.

We have evaluated the poly-CO total energy per repeat unit from calculations on a series of linear R(CO)$_n$R (R = H, Me) oligomers by using the finite difference method.[9] Assuming that, for a given $n$ value, $E_n$ is the total energy of the most stable conformer of R(CO)$_n$R, the difference function $\Delta E_n = E_{n+1} - E_n$ is expected to tend to the poly-CO energy per CO unit when $n$ becomes large enough. We have performed *ab initio* and DFT calculations§ on R(CO)$_n$R (R = H, Me) oligoketones, up to $n$ = 11.¶ The corresponding $\Delta E_n - E$(CO) energy values are shown in Fig. 1.

The potential energy surface was fully explored up to $n$ = 5 for R = H. In this case, for example, seven conformational isomers were identified, all differing from the relative rotational orientation of their CO groups. All these conformers lie in an energy range of *ca.* 8 kcal mol$^{-1}$, the four lowest in energy differing by less than 3 kcal mol$^{-1}$. It is worth noting that for R(CO)$_5$R (R = H, Me) the lowest energy corresponds to the helical form, **2a**, a conformation experimentally observed for Ph(CO)$_n$Bu$^t$.[5d,e] The second lowest in energy corresponds to the all-*trans* conformation **2b** lying above **2a** by less than 1.5 kcal mol$^{-1}$‖ From these results it is clear that the potential



**2a**, TCCT



**2b**, TTTT

energy surface associated with the conformational fluxionality of oligoketones is particularly soft.** For larger oligomers, the number of conformations becomes too large to allow a full structural investigation, and we restricted our research to isomers having the $C_2$ symmetry. It turns out that for $n$ > 2, all the optimized conformers are non-planar and typical C–C and C=O bond lengths are computed. The carbon atoms always maintain their expected (locally planar) sp$^2$ hybridization. Therefore, the conformation of the oligoketones can simply be described by the series of the dihedral angles ($\alpha$) between adjacent CO units, which are reported in supplementary material.‖

From Fig. 1, one may see that the $\Delta E_n$ variations computed at the HF and B3LYP geometries behave similarly, showing that optimized HF geometries can be used, allowing the study of longer H(CO)$_n$H chains up to $n$ = 11. Furthermore, the calculations performed with R = Me for smaller $n$ values provide evidence that no special end effect is present in the calculations with R = H. It is clear that for $n$ = 9 the parity oscillations due to the small-size effect are damped, as well as the asymptotic value of $\Delta E_n$ is nearly reached. When ZPVE corrections are included,§ poly-CO is computed to be less stable

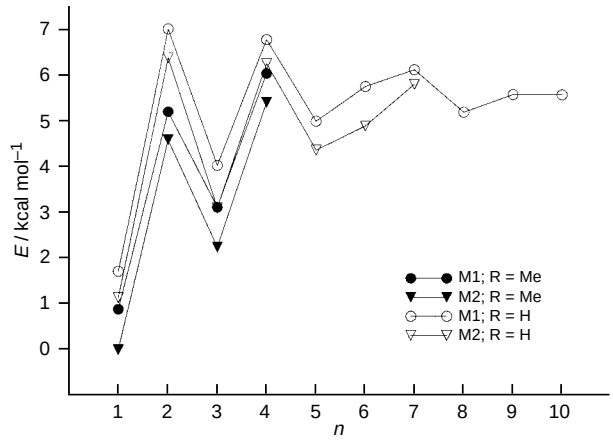



**Fig. 1** Plots of $E$[R(CO)$_n$R] − $E$[R(CO)$_n$R] − $E$[CO] (R = H, Me) with respect to $n$. Calculations are made at the B3LYP/6-311 + G**//HF/6-31G** (M1) and B3LYP/6-311 + G**//B3LYP/6-31G** (M2) levels, including ZPVE corrections. Filled and empty symbols are for (Me)-(CO)$_n$(Me) and H(CO)$_n$H oligomers, respectively.

than free CO monomer by only 5.5 kcal mol$^{-1}$. However, ZPVE terms are obtained assuming isolated molecules, while the hypothetical polymer is expected to exist as a solid in which the vibrational energy could be different. Discarding ZPVE corrections leads to an even smaller energy difference (3.5 kcal mol$^{-1}$). Dipole–dipole and van der Waals interactions, present in the solid-state phase of the polymer, are not taken into account in this study. They may reduce this energy difference or even perhaps change its sign. Moreover, as the potential energy surfaces of the studied oligoketones is particularly flat, the conformation of poly-CO in the hypothetical condensed phase (as under high pressure) may be different from the calculated gas phase helical conformation.[7] In any case, these calculations strongly suggest that poly-CO is a stable allotropic variation of carbon monoxide. The crucial point for its synthesis would be to overcome kinetic problems.

G. F. gratefully acknowledges financial support from the Région Bretagne (1991–96) and the National Research Council of Canada (1996–1997).

## Footnotes and References

† Present address: LACCO-UMR 6503, Faculté des Sciences, Université de Poitiers, 86022 Poitiers Cedex, France.
‡ E-mail: frapper@ss3.univ-poitiers.fr; saillard@univ-rennes1.fr; kertesz-@guvav.acc.georgetown.edu
§ Geometry optimisations were carried out with the use of the GAUSSIAN 94 package[10] at the HF, MP2 and B3LYP levels, using the 6-31G** basis set. Harmonic vibrational frequencies and zero-point vibrational energies (ZPVE) were computed at HF level for all systems and in some cases, at the MP2 and B3LYP levels. Single point B3LYP calculations using the larger 6-311 + G** basis set were also performed on the optimised geometries. Since the three levels of calculations lead to similar qualitative conclusions, only single-point B3LYP/6-311 + G** energies on the optimised geometries [HF (M1) and B3LYP/6-31G** (M2)] are discussed here.
¶ The stability of finite oligomers, such as $C_2O_2$ or cyclic $C_nO_n$ molecules, has been discussed.[5a,11] Our preliminary calculations on these cyclic species indicate that they are significantly less stable than free CO, at least for $n < 9$ (to be published).
‖ Tables which summarize the main energetic and conformational data of the most stable $R(CO)_nR$ conformers can be requested from the authors.
** A critical factor related to the energy of these species in their planarity or non-planarity. Conjugation, *i.e.* $\pi$–$\pi^*$ mixing, tends to favor planarity. On the other hand, a second-order Peierls distortion away from planarity, associated to $\sigma_n$–$\pi$ mixing is expected for poly-CO. O··O lone pair repulsions also disfavour planar conformations. Finally, non-bonding interactions involving the terminal R groups can also play some role in the conformational choice, by forming weak intramolecular hydrogen bonds.[5,7,12]

1 M. N. Glukhovtsev, H. Jiao and P. von Ragué Schelyer, *Inorg. Chem.*, 1996, **35**, 7124 and references cited therein.
2 H. Genin and R. Hoffmann, *J. Am. Chem. Soc.*, 1995, **117**, 12 328; C. Kollmar and R. Hoffmann, *J. Am. Chem. Soc.*, 1990, **112**, 8230.
3 M. Haser, U. Schneider and R. Ahlrichs, *J. Am. Chem. Soc.*, 1992, **114**, 9551.
4 L. Pauling, *The Nature of the Chemical Bond*, Cornell University Press, Ithaca, 3rd edn., 1960.
5 (*a*) M. B. Rubin, *Chem. Rev.*, 1975, **75**, 177; (*b*) M. Kaftory and M. B. Rubin *J. Chem. Soc., Perkin Trans. 2*, 1983, 149; (*c*) G. Schultz, I. Hargittai, T. Doerner and R. Gleiter, *Chem. Ber.*, 1991, **124**, 1411; (*d*) R. Gleiter, G. Krenrich and M. Langer, *Angew. Chem., Int. Ed. Engl.*, 1986, **25**, 999; (*e*) R. Gleiter, E. Litterst, T. Oerser and H. Irngartinger, *Angew. Chem., Int. Ed. Engl.*, 1990, **29**, 1048.
6 F. Wiitkar, S. Kahlal, J.-F. Halet, J.-Y. Saillard, J. Bauer and P. Rogl, *Inorg. Chem.*, 1995, **34**, 1248.
7 C. X. Cui and M. Kertesz, *Chem. Phys. Lett.*, 1990, **169**, 445.
8 R. Hoffmann, *Vestn. Mosk. Univ., Ser. 3 Fiz. Astron.*, 1962, **69**, 69 (in Russian).
9 A. Karpfen, J. Ladik, R. Rusegger, P. Schuster and S. Suhai, *Theor. Chim. Acta*, 1974, **34**, 115; C. X. Cui, M. Kertesz and Y. Jiang, *J. Phys. Chem.*, 1990, **94**, 5172.
10 GAUSSIAN 94, Revision B.1, M. J. Frisch *et al.*, Gaussian Inc., Pittsburgh, PA, 1995.
11 A. A. Korkin, A. Baklova, R. J. Bartlett, R. J. Boyds and P. von Ragué Schleyer, *J. Phys. Chem.*, 1996, **100**, 5702 and references cited therein; R. Gleiter, I. Hyla-Kryspin and K.-H. Pfeifer, *J. Org. Chem.*, 1995, **60**, 5878; G. Frenking, *Angew. Chem., Int. Ed. Engl.*, 1990, **29**, 2410.
12 S. L. Henke, C. M. Hadad, K. M. Morgan, K. B. Wiberg and H. H. Wasserman, *J. Org. Chem.*, 1993, **58**, 2830.

*Received in Cambridge, UK, 5th August 1997; 7/05721K*

# Ammoxidation of ethane to acetonitrile over Co-beta zeolite

**Yuejin Li and John N. Armor***

*Air Products and Chemicals, Inc., 7201 Hamilton Boulevard, Allentown, PA 18195-1501, USA*

**Co-beta zeolite selectively catalyzes the ammoxidation of ethane to acetonitrile with a rate that is 1–2 orders of magnitude higher than those over typical metal oxide catalysts.**

There is considerable interest in converting light alkanes directly to higher value organic chemicals because of the low cost and abundance of the alkanes. On the other hand, alkanes are chemically stable, which poses a tremendous challenge to achieve a high selectivity in their conversions. A commercially successful example of alkane activation is the manufacture of maleic anhydride by selective oxidation of butane[1] using V–P–O based catalyst. Another example is the recently announced production of acrylonitrile by reacting propane with $NH_3$ and $O_2$ (ammoxidation) over an Sb–V–Al mixed oxide catalyst.[2] In spite of these commercial advances, limited progress has been made for conversion of other alkanes. There were a few attempts to apply the propane ammoxidation catalysis on ethane to make acetonitrile. However, the propane ammoxidation catalyst, V–Sb–Al, was found ineffective for the ethane ammoxidation to acetonitrile. As postulated by Catani and Centi,[3] different mechanistic pathways are required for these two reactions because of the fundamental difference between propene, an intermediate for propane ammoxidation, and ethene, an intermediate for ethane ammoxidation.

Using $Al_2O_3$ supported Nb–Sb oxides, Catani and Centi investigated ethane ammoxidation between 480 and 540 °C with a contact time of 2.6 s.[3] They obtained ethane to acetonitrile selectivity of 50%, CO selectivity of > 20% and variable selectivities for $CO_2$ formation. HCN was also formed during this reaction with a constant selectivity of 5%. Earlier, a USSR patent[4] disclosed that ethane was converted to acetonitrile with a maximum yield of 10% over a Cr–Nb–Mo oxide catalyst at 350–500 °C with a contact time of 19 s. By-products of this reaction were not specified. Here, we report our recent discovery[5] using a metal exchanged zeolite as a superior catalyst for ethane ammoxidation with a very high reaction rate and selectivity to acetonitrile.

Some metal exchanged zeolites are known to activate small alkanes for selective reduction of $NO_x$.[6] In the case of $NO_x$ reduction with methane over Co-zeolites, $CH_4$ was activated by abstracting a proton with a $NO_2$ species which was adsorbed on $Co^{2+}$ sites.[7] Metal cations exchanged in zeolites are atomically dispersed on the coordinately unsaturated sites to balance the negative changes of the zeolite framework. These cations provide unique catalytic centers, as Lewis-acid sites, with a high site density which is usually not achievable by bulk or supported metal oxides.[8] We sought to utilize the unusual properties of metal-zeolite systems to activate ethane for its ammoxidation reaction [eqn. (1)].

$$C_2H_6 + NH_3 + 3/2O_2 \rightarrow CH_3CN + 3H_2O \qquad (1)$$

$NH_4$-beta zeolite (Si/Al = 14) (20 g) was exchanged with a 2 l, 0.02 M cobalt acetate aqueous solution at 70–80 °C for 24 h. After washing with 1 l of deionized water, the zeolite was dried overnight at 110 °C. Elemental analysis showed that the Co/Al atomic ratio was 0.35 (70% of the cation exchange capacity) or 2.2% Co by mass. The reactions were conducted in a microreactor system operating in a steady-state plug-flow mode at atmospheric pressure. The reactor is a U-shaped quartz tube with 0.25 in od at the inlet section and 0.375 in od at the outlet section. The catalyst was located in the outlet section at the center of the electrical furnace which surrounds the reactor tube. Quartz wool plugs were used to support and secure the catalyst bed. A typical feed consisted of 5% $C_2H_6$, 10% $NH_3$ and 6.5% $O_2$ in He with a total flow rate of 100 $cm^3\ mol^{-1}$. A 0.2 g catalyst sample sieved between 20/40 mesh was used for each run, which renders a GHSV of 15000 or a contact time of 0.24 s. The reactor effluent was analyzed by two on-line gas chromatograghs in series, each equipped with a thermal conductivity detector.

As shown in Fig. 1, $C_2H_6$ was selectively converted to acetonitrile over a Co-beta catalyst with a selectivity as high as 76%. The selectivity moderately decreased with increasing temperature. Major by-products for the ethane conversion are $CO_2$ and $C_2H_4$. The selectivity of $CO_2$ was *ca.* 20%, and the selectivity of $C_2H_4$ was generally low but increased linearly with increasing temperature. The conversion of $C_2H_6$ was strongly dependent on the reaction temperature and the availability of $O_2$. The highest conversion was 47% obtained at 475 °C.

An interesting observation for this reaction is that the total $C_2$ selectivity ($C_2H_4$ + $CH_3CN$) is relatively constant, 73 ± 3%. The mutually compensating effect between the formations of $C_2H_4$ and $CH_3CN$ suggests that $C_2H_4$ is the primary product of this reaction. Indeed, a reference reaction with $C_2H_4$–$NH_3$–$O_2$ under similar conditions tripled the nitrile yield. We believe that $C_2H_6$ is first converted to $C_2H_4$ *via* oxidative dehydrogenation on $NH_3$ moderated $Co^{2+}$ sites. Ammonia is strongly adsorbed on most of the $Co^{2+}$ sites as a Lewis base. The ethene molecule then adds on top of the adsorbed $NH_3$ forming an adsorbed

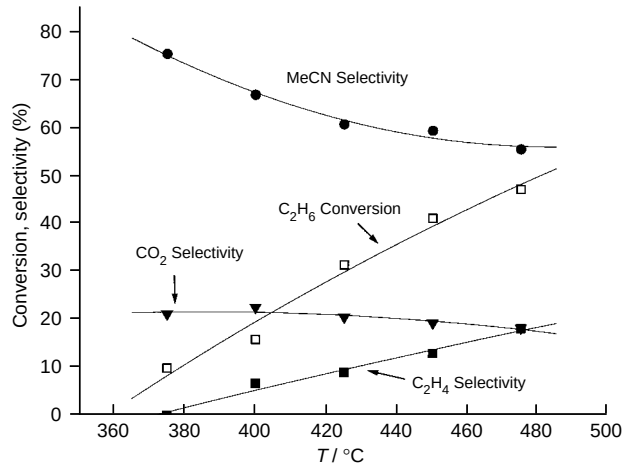



**Fig. 1** Ethane ammoxidation to acetonitrile over Co-beta catalyst as a function of temperature

**Table 1** Comparison between Co-beta and metal oxides for ethane $CH_3CN$ ammoxidation[a]

| Catalyst | Catalyst composition | Ref. | Catalyst mass/g | $CH_3CN$ yield (%) | $10^4$ $CH_3CN$ production rate/ mol $g^{-1}$ $h^{-1}$ |
|---|---|---|---|---|---|
| Co-beta | Si/Al = 14, Co/Al = 0.35 | This work | 0.2 | 26.4 | 160 |
| VPO | P/V = 0.10 (atomic ratio) | 9 | 0.2 | 0.2 | 1.2 |
| $SbVO_4$ | Sb/V = 1.0 (atomic ratio) | 2 | 0.2 | 0.06 | 0.4 |
| Nb–Sb oxides/$Al_2O_3$ | 70 mass% $Al_2O_3$ Nb/Sb = 1 : 5 | 3 | 0.5 | 1.2 | 3.0 |
| Cr–Zr–Mo oxides | Cr : Zr : Mo = 18.1 : 1 : 31.2 | 4 | 0.5 | 2.6 | 6.4 |

[a] All catalysts were tested at 500 °C, except for Co-beta (475 °C), under conditions described within the text.

ethylamine molecule, which is readily dehydrogenated to $CH_3CN$ in the presence of $O_2$.

The Co-beta catalyst was compared with a variety of metal oxide catalysts for the ethane ammoxidation reaction. As shown in Table 1, the $CH_3CN$ formation rate over Co-beta (at 475 °C) is 1–2 orders of magnitude higher than those over metal oxide catalysts (at 500 °C). Nb–Sb–Al and Cr–Zr–Mo were reported to be active for this reaction.[3,4] However, they were active only with a much longer contact time, 3–19 s. With a shorter contact time ($< 1$ s), the amount of $CH_3CN$ produced was barely detectable. It is obvious that Co-beta, a non-traditional selective ammoxidation catalyst, is superior in terms of reaction rate and selectivity to nitrile. In addition, our Co-zeolite catalysts were tested on stream for 100 h without significant deactivation.

In summary, we have found that Co-beta was a very good catalyst for converting ethane to acetonitrile with high rate and selectivity. We believe this to be a positive step towards utilizing ethane to make valuable chemicals.

## Footnote and References

* E-mail: armorjn@apci.com

1 G. Emig and F. Martin, *Catal. Today*, 1987, **1**, 477.
2 A. T. Guttmann, R. K. Grasselli and J. F. Brazdil, *US Pat.*, 4,746,641, 1988.
3 R. Catani and G. Centi, *J. Chem. Soc., Chem. Commun*., 1991, 1081.
4 S. M. Aliev, V. D. Sokolovskii and G. B. Boreskov, *USSR Pat.*, SU-738 657, 1980.
5 Y. Li and J. N. Armor, *Eur. Pat. Appl.*, EP 0761 654 A2, 1997.
6 Y. Li and J. N. Armor, *Appl. Catal. B*, 1993, **2**, 239.
7 Y. Li, T. L. Slager and J. N. Armor, *J. Catal*., 1994, **150**, 388.
8 J. N. Armor, in *Science and Technology in Catalysis 1994*, Kodansha Press, Tokyo, 1995, p. 51.
9 P. M. Michalakos, M. C. Kung, I. Jahan and H. H. Kung, *J. Catal*., 1993, **140**, 226.

*Received in Bloomington, IN, USA, 30th May 1997, 7/03788K*



Typeset and printed by Black Bear Press Limited, Cambridge, England

ChemComm
FEATURE ARTICLE

# β-Peptides: a surprise at every turn

**Dieter Seebach* and Jennifer L. Matthews**

*Laboratorium für Organische Chemie, ETH-Zentrum, Universitätstrasse 16, CH-8092 Zürich, Switzerland*

**β-Peptides, *i.e.* oligomers of β-amino acids, containing as few as six residues may form surprisingly stable helices, with half-lives for the H/D exchange of the central NH protons of up to several days. Furthermore, these β-peptides (carrying the side chains of familiar α-amino acids such as Ala, Val, Leu, Phe, Lys in the 2- and/or 3-position of their 3-amino carboxylic moieties) have been shown to be stable to common peptidases for at least two days. In this article, a brief account of the results obtained since we started work in this area in early 1995 is given. The synthesis of enantiopure β-amino acids can be achieved by homologation of α-amino acids. The greater structural variability of β-amino acids leads to an even greater multitude of possible β-peptide primary and secondary structures. Circular dichroism, NMR and X-ray investigations have unveiled helical, pleated-sheet and tubular arrangements of linear and cyclic β-peptides composed of up to twelve β-amino acids. The prospects for the use of β-peptides as drugs, the construction of large, enzymatically-active β-proteins and their interaction with the natural, α-peptidic counterparts are discussed.**

Polymers derived from β-amino acids (so-called Nylon-3 derivatives[1]) have been the subject of many investigations in the past few decades. In particular, those[2] derived from aspartic acid (the only proteinogenic β-amino acid) have attracted much attention. There has also been some—rather speculative—conjecture concerning the possibility that β-peptides might form secondary structures.[3] Even given this, three years ago, whenever we succeeded in eliciting an opinion from specialists, they were convinced that the extra carbon atom and hence, the additional 'freely-rotating' C–C σ-bond in the β-amino acid building blocks would result in β-peptides having a lower tendency to form highly ordered structures than the analogous natural α-peptides.

This question had been frequently asked because, at the start of 1995, we began to tackle a project that we had been contemplating for a long time—namely, replacing the oxygens in the chain of oligo-(*R*)-3-hydroxybutanoates[4] (oligo-HB) by NH groups in the hope that we would see whether the helical substructures found[5] in the crystalline oligolides of HB [Fig. 1(*a*)] would be stabilised by hydrogen bonds. Since then, it has turned out that the first of the β-hexapeptides we prepared[6] (from homologated valine, alanine and leucine) formed a helix when dissolved in MeOH [Fig. 1(*b*)]. Furthermore, it was found[6,7] to be stable against the peptidase pepsin. The results of the last two years have sparked off a flurry of activity and reports have now appeared with titles such as

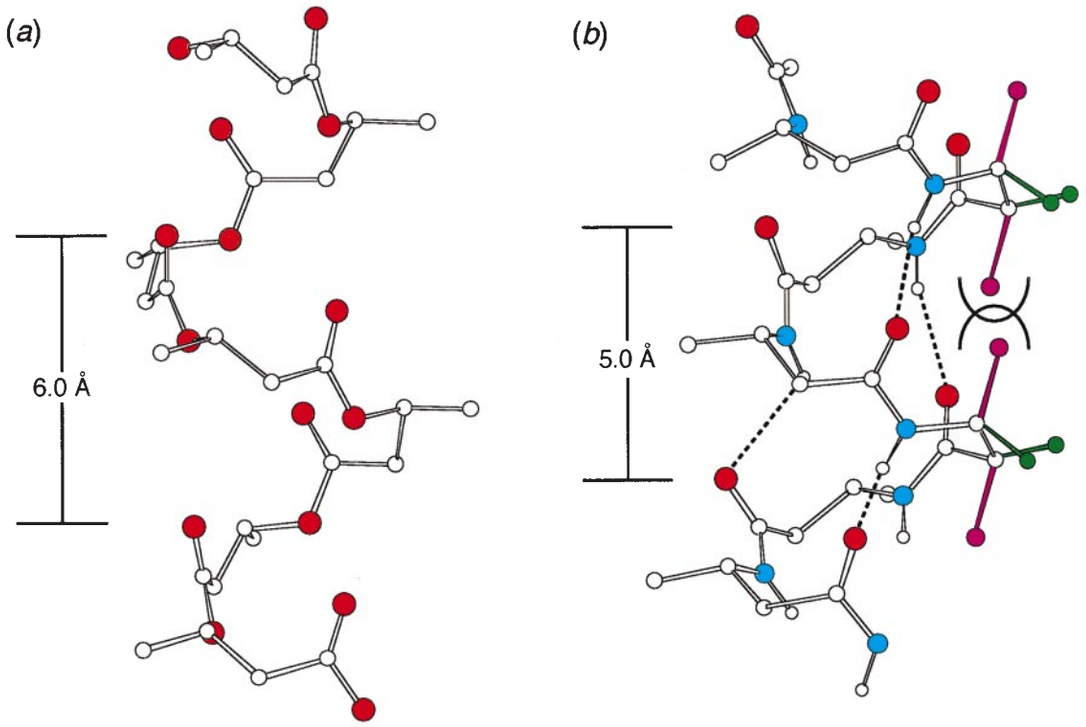



**Fig. 1** (*a*) Left handed or (*M*) $3_1$ helix of (*S*)-3-hydroxybutanoate (HB), modelled using X-ray structural parameters obtained from HB oligolides. The C=O bonds are approximately parallel to the helix axis and their oxygen atoms are close to the backbone oxygens. Top: O terminus, bottom: C terminus. (*b*) Idealised (*M*) $3_1$ helix (crystallographic nomenclature) or $3_{14}$ helix (peptide nomenclature) of a β-peptide; top: N terminus, bottom: C terminus. Lateral substitution (substituents coloured green) does not break up the helix; axial substitution (purple substituents) prevents helix formation. (Taken with permission from ref. 6.)

'Betas are brought into the fold', 'β-Peptides: Novel secondary structures take shape', 'β-Peptides: nature improved?' and 'Molecules without life: the search for artificial proteins'.[8]

In the following sections, we will first discuss the preparation of the β-amino acids and the β-peptides constructed from them. The subsequent sections will compare and contrast the properties and structures of β-peptides investigated to date with those of α-peptides (peptides consisting of natural and unnatural α-amino acids).

## β-Amino acid preparation

A glance through the eyes of a synthetic chemist at the formulae of an α- and β-amino acid immediately tells you that there is a much wider variety of possible strategies for the synthesis of the latter (Fig. 2). Furthermore, as you move from an α- to a β-amino acid (Fig. 3), the incorporation of an additional carbon atom between the carboxy and the amino groups results in an enormous increase in the number of possible constitutional and configurational isomers. A recently published book[9] reviews the methods available for the synthesis of β-amino acids and one of the chapters[10] deals with the method that we have made the most use of, namely, the Arndt–Eistert homologation [Scheme 1, route (*a*)]. Clearly, the big advantage of this reaction sequence is that the enantiomerically pure β-amino acid derivatives are readily prepared from the appropriate α-amino acid (for instance, with peptidic side chains[7]). Furthermore, reaction of the resulting β-amino acid derivatives leads[11] easily to the α,β-disubstituted compounds [Scheme 1, route (*b*)]. For the preparation of β-amino acids with the side chain in the α-carbonyl position [Scheme 1, route (*c*)], we turned to Evans' chiral auxiliary methodology.[12,13] Enantiomerically pure cyclic derivatives, such as *trans*-2-aminocyclopentanecarboxylic acid and *trans*-2-aminocyclohexanecarboxylic acid, have been prepared by other methods and also subsequently used in the construction of β-peptides.[14,15]

Before proceeding any further, we must first mention the nomenclature we have adopted for the description of β-amino acids and β-peptides. The derivatives with 'natural' side chains in the 2- or 3-position are described as H-β$^2$-Xxx-OH and H-β$^3$-Xxx-OH, respectively. β-Peptides built exclusively from one of these two types of β-amino acids are defined as β$^2$- or β$^3$-peptides, respectively [Fig. 4(*b*) and (*c*)].

## β-Peptide preparation

In our own work we have, in the main, incorporated the sequence β-HVal-β-HAla-β-HLeu into the β-peptides. This is due to the fact that α-peptides with the analogous sequence Val-Ala-Leu have been the subject of numerous structural investigations (above all, those[16] of Karle *et al.*). We also hoped that this approach would facilitate the best possible comparison between the two types of peptides without reference to the distorted picture that would result from a restriction of conformational freedom.[14,15]

We have used[6,7,17–20] the well-established methods of peptide synthesis for the coupling of the β-amino acids, making use of Z-, Boc- or Fmoc-protected amino groups, methyl or benzyl esters for the acid terminus and, usually, carbodiimide methods for the coupling step. We have principally performed

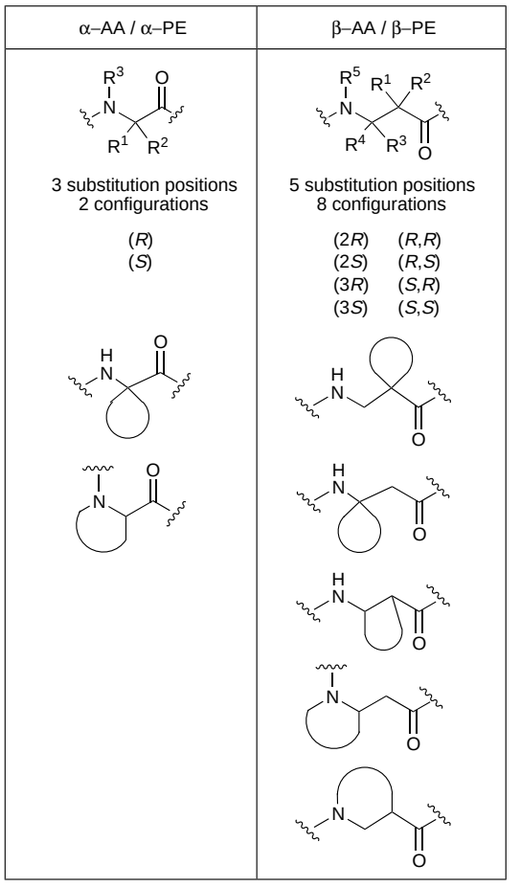
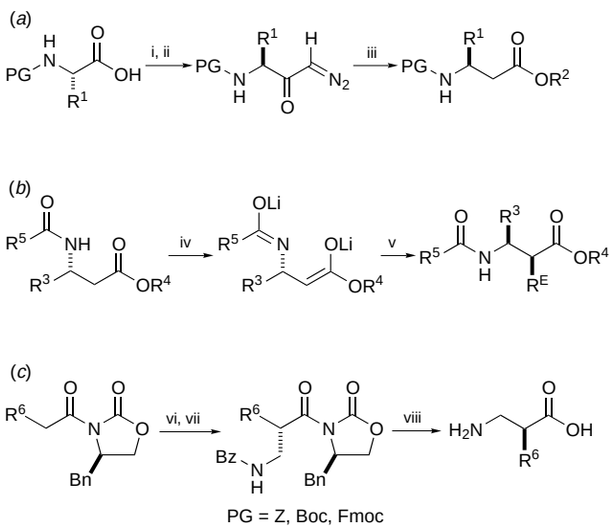



**Fig. 3** Contrasting substitution patterns and configurations of α- and β-amino acid residues in peptides




**Scheme 1** *Reagents and conditions*: i, $ClCO_2Et$, $NEt_3$, THF; ii, $CH_2N_2$, $Et_2O$; iii, $Ag^+$, $NEt_3$, $R^2OH$; iv, $LiNR_2$, LiCl; v, electrophile ($R^EX$); vi, $TiCl_4$, $NEt_3$; vii, $BzNHCH_2Cl$; viii, hydrolysis

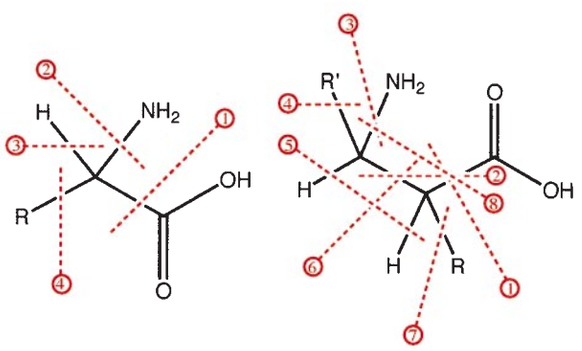


**Fig. 2** Retrosynthetic analysis of an α- and a β-amino acid. The numbers ①–⑧ indicate the bond(s) made in the corresponding synthesis. For literature on α- and β-amino acid syntheses, see textbooks, monographs and a book (ref. 9), which has appeared recently.

these procedures in solution but have recently begun to investigate the use of solid phase techniques.[21] The yields of the coupling steps are excellent; racemisation or epimerisation is not possible for the β³-amino acids and we only occasionally observe a loss of configurational purity with the β²-amino acids. The products have been purified by preparative HPLC and their composition has been determined by both mass spectrometry and degradation of the component amino acids. To date, β-oligopeptides built from up to twelve amino acids have been prepared (the different types are shown in Fig. 4) including the β-peptides **1**–**14**, which are the objects of discussion in the following sections.

### CD spectra of β-peptides

Circular dichroism is a powerful tool for the detection and determination of the secondary structures of α-peptides. Thus the most common, so-called α-helix of α-peptides[22] [a right handed or (*P*) $3.6_1$ helix with a pitch of 5.6 Å containing 13-membered hydrogen bonded rings] gives rise to CD minima at *ca*. 208 and 222 nm. A chain of at least 15 amino acid residues is required for this helix to be observed in protic solvents such as water or MeOH. Most helical substructures of proteins and enzymes consist of 10–15 amino acids. In contrast, and to everybody's great surprise, β³- and β²-oligopeptides (*e.g.* **1** and **9**, respectively) built of only six or seven (*S*)-β-amino acids† show[6,13,17,21] an intense CD minimum at *ca*. 215 nm, followed by a maximum at *ca*. 200 nm in MeOH [Fig. 5(*a*)], a pattern which is independent of the presence or absence of terminal protecting groups and of the concentration (0.02 to 1 mM). Within this series, the most intense CD absorptions were observed[23] with the β²,³-hexapeptide **3** consisting of β-amino acids with methyl groups in the 2-position and the side chains Val, Ala and Leu in the 3-position‡ [(*S*,*S*)-β³-HXxx(2-Me)] [Fig. 5(*a*)]. Yet another surprise came when we measured[20,25] the CD spectra of mixed β-peptides **4**–**8** containing β²- and β³-amino acid moieties: depending upon the sequence of these isomeric building blocks in the chain and upon the presence or absence of terminal protecting groups, the corresponding peptides showed either the familiar 215/200 nm extrema or a

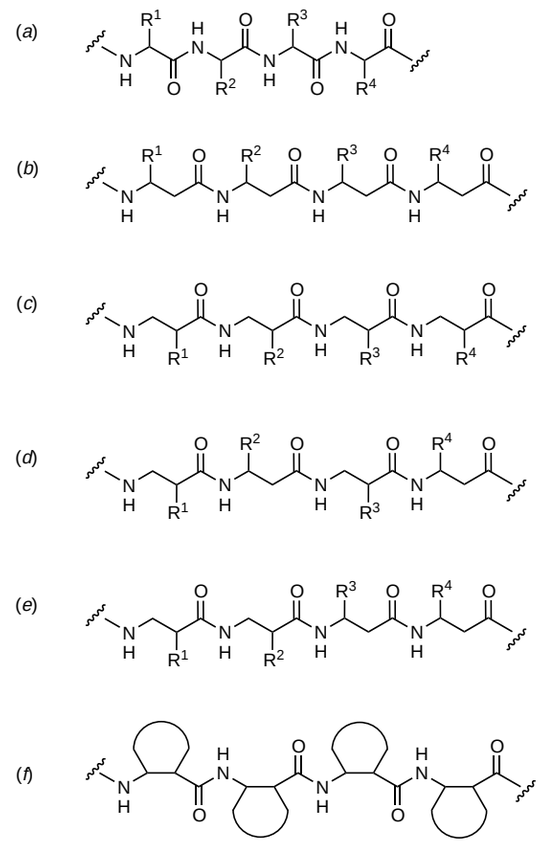
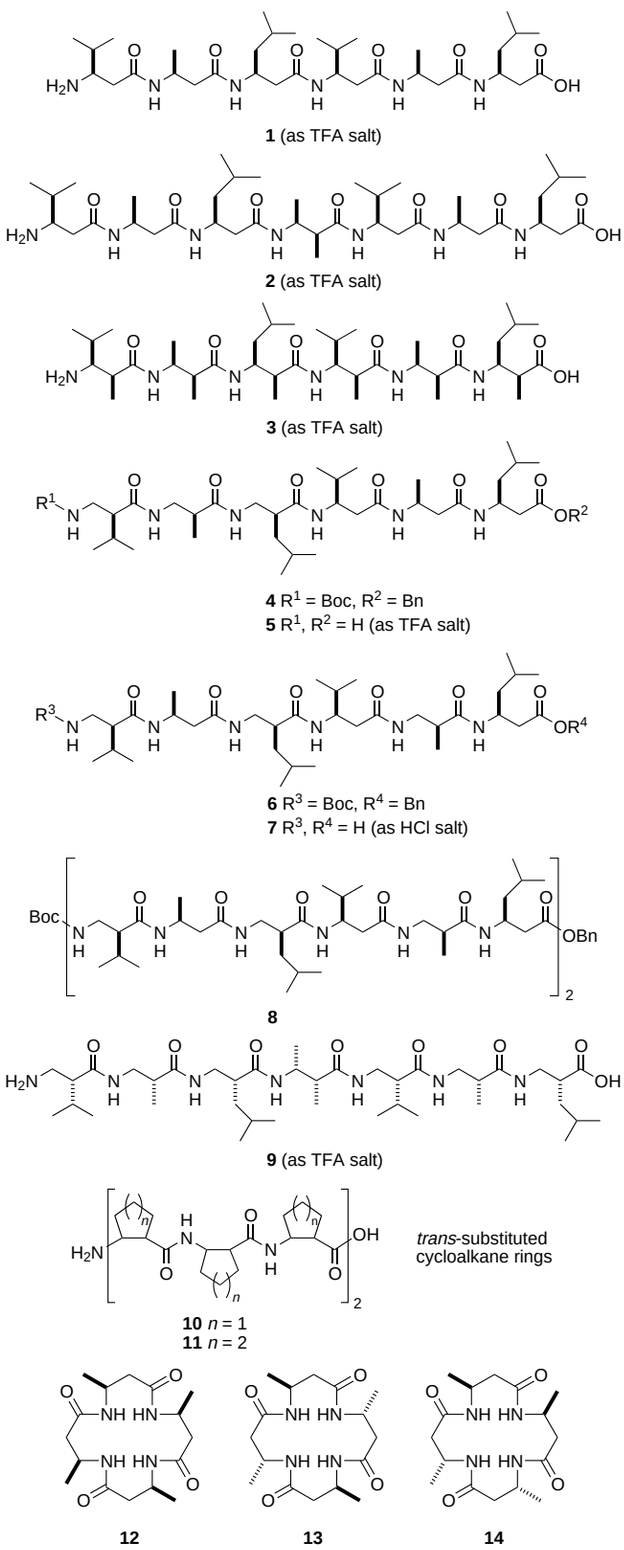



**Fig. 4** (*a*) An α-peptide. (*b*) A β³-peptide: a β-peptide consisting of β-substituted β-amino acids. (*c*) A β²-peptide: a β-peptide consisting of α-substituted β-amino acids. (*d*) A β-peptide consisting of alternating β²- and β³-amino acids. (*e*) A β-peptide consisting of block-coupled β²- and β³-amino acids. (*f*) A β-peptide consisting of aminocycloalkanecarboxylic acids.



single intense maximum at *ca*. 205 nm [Fig. 5(*b*) and (*c*)], which is again essentially concentration independent. From NMR investigations, we can conclude that the former CD pattern is caused by a left-handed helix and the latter one by an as yet unknown, different secondary structure (see following section). The CD spectrum of an oligomer **10** built from (*R*,*R*)-2-aminocyclopentanecarboxylic acid shows a concentration independent minimum at *ca*. 221 nm and a maximum at 204 nm.[15]

### Solution structures of β-peptides determined by NMR spectroscopy

Full NMR analyses (COSY, TOCSY, HSQC, HMBC, ROESY, NOE restrained modelling) have been performed[6,15,17,23,25] on the β$^3$-hexapeptides **1** and **2**, the β$^{2,3}$-hexapeptide **3**, the mixed β-hexapeptide **7**, the β$^2$-heptapeptide **9** and the derivative **10** containing cyclopentane rings. The result is that those β-peptides containing no ring and having identical configuration and substitution pattern of the amino acids adopt a $3_1$-helical conformation in both [$^2H_5$]pyridine or $CD_3OH$ solution [Fig. 6(*a*)]. These are left-handed or (*M*) helices for peptides containing amino acid residues with stereocentres of (*S*) configuration (*e.g.* **1**) and right-handed or (*P*) helices with amino acids of (*R*) configuration (*e.g.* **9**). The helix has a 5 Å pitch with the substituents in the 2- and 3-positions of the component amino acids and the hydrogens occupying lateral and axial positions, respectively [see Fig. 1(*b*)]. Lateral substituents at the *i* and (*i* + 3) position are directly aligned with a 5 Å distance between them and, if a substituent is forced into adopting an axial position, the $3_1$ helix breaks up.[17]

Molecular dynamics calculations (GROMOS96 program package) on the β-heptapeptide **2** in MeOH produced[26] a remarkable result: after a sudden temperature increase from 298 to 350 K, the $3_1$ helix unwinds. However, as the temperature is held at a constant 350 K, the helix is spontaneously restored within 400 ps and, even more amazingly, it is still stable after 2000 ps in this computational experiment which was performed without NOE restrictions. Such behaviour has never been observed with α-peptides.

In line with their different CD spectra, and most astonishingly for us, the mixed β-hexapeptides constructed from β$^2$- and β$^3$-amino acid building blocks (*e.g.* **6**–**8**, with β$^2$,β$^3$,β$^2$,β$^3$,β$^2$,β$^3$ sequences) form a different secondary structure. The NMR analysis shows strong NOEs between corresponding hydrogens of amino acids *i* and *i* + 2, rather than *i* and *i* + 3 as for the $3_1$ helix. This finding[20,25] caught us by surprise because these molecules could have formed the $3_1$ helix with all substituents in lateral positions. As Gellman has found,[15] the β-hexapeptide from *trans*-2-aminocyclopentanecarboxylic acid is present as a helix, but not a $3_1$ helix, when dissolved in both MeOH and pyridine [Fig. 6(*b*)]. It may be that the secondary structures of our mixed β$^2$,β$^3$-peptides **6**–**8** are similar to the helix shown in Fig. 6(*b*); however, at the time of writing, the NMR analysis is not conclusive.

Thus, in contrast to the analogous α-peptides, the short-chain β-oligopeptides are able to form helical secondary structures and, indeed, it has now been experimentally proven that they are able to form at least two different helices which result from rather subtle changes in structure. Investigations and calculations on compounds of the general formula, H[NHCH($CO_2$R)$CH_2$CO]$_n$OH (derived from aspartic acid) have revealed[2] that there might be additional stable β-peptide helices.

### Solid state structures of β-peptides from X-ray scattering

While we have, so far, not succeeded in crystallising any of the helix-forming β-peptides bearing the side chains of natural amino acids, the β-oligopeptides derived from *l*-2-aminocyclopentane- and *l*-2-aminocyclohexane-carboxylic acid§ gave crystals of sufficient quality for X-ray analysis.[14,15] In both cases, the structures found in solution were confirmed to be also present in the solid state: the cyclohexane derivative folds to a $3_1$ helix which is essentially superimposable with the NMR structures (the cyclohexane ring bonds occupy the two lateral positions). The $2.5_1$ helix of the cyclopentane derivative has an average NH–C–C–CO dihedral angle of 86° (with a spread of 75° to 109°) which compares with 55° in the crystal of the cyclohexane analogue acid.[14]

A pleated-sheet arrangement of a β-peptide fragment was found in the crystal structure of Boc-β$^3$-HVal-β$^3$-HAla-β$^3$-HLeu-OMe (Fig. 7), with intermolecular hydrogen bonding in 14-membered rings.

Finally, the steroisomeric cyclo-β-tetrapeptides **12**, **13** and **14** [with (*S*,*S*,*S*,*S*), (*R*,*S*,*R*,*S*) and (*R*,*R*,*S*,*S*) configuration, respectively] were found[28] to form tube-like, hydrogen-bonded stacks in the solid state (Fig. 8).

### Comparison of β-peptides with α-peptides—are they orthogonal to each other?

While the Gellman group approached the field of β-peptides from a supramolecular chemistry perspective[29] and hence made

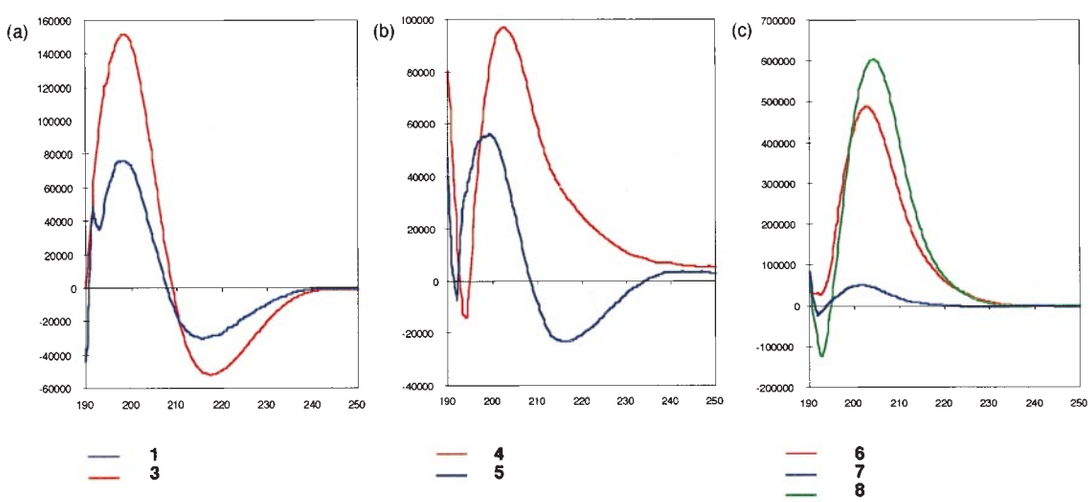



**Fig. 5** Circular dichroism (CD) spectra of β-peptides **1**,**3**–**8** in MeOH (0.2 mM). The typical CD pattern assigned to a left-handed $3_1$ helix [*cf*. Figs. 1(*b*) and 6(*a*)] is shown in (*a*) and the blue curve in (*b*). The characteristic CD pattern of a secondary structure which is, as yet, unassigned is shown in (*c*) and the red curve in (*b*). The most intensive Cotton effects were measured with disubstituted β-amino acid moieties [**3**, red in (*a*)], with a (β$^2$)$_3$(β$^3$)$_3$ (protected) sequence [**4**, red in (*b*)] and with the protected (β$^2$,β$^3$)$_6$ dodecapeptide [**8**, green in (*c*)].

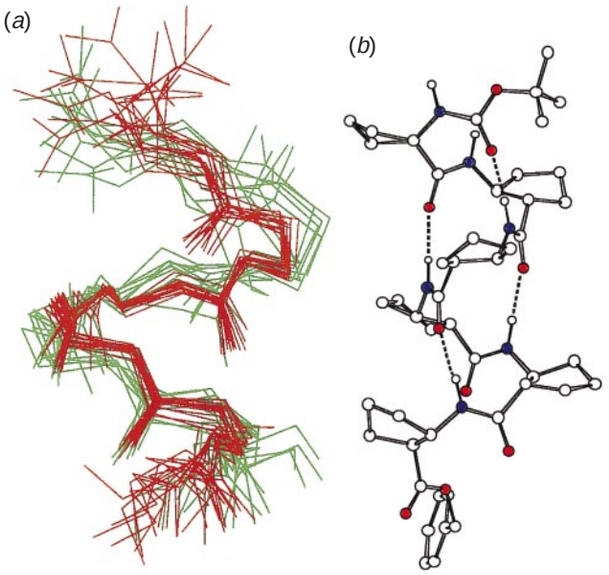



**Fig. 6** NMR structural determination. (*a*) The $3_{14}$ (peptide nomenclature) helical conformations of **1** in MeOH (green) and in pyridine (red) (taken with permission from ref. 17); (*b*) MacMoMo presentation of the $2.5_{12}$ helical conformation of a hexa-β-peptide **10** derived from (*S*,*S*)-2-amino-cyclopentanecarboxylic acid. The NMR structure determination of **10** was carried out on the (*R*,*R*)-isomer; the coordinates were inverted for the presentation shown here to allow a better comparison with other known β-peptide structures.

cycloalkane derivatives (which, as far as the side chains are concerned, bear no resemblance to natural peptidic structures), our entry was triggered by research on the biopolymer[4] poly(hydroxybutanoate) (PHB) and on peptide backbone modifications[30–32] (*e.g.* in cyclosporine), so that we actually prepared β-peptides from α-amino acids. This now puts us in a

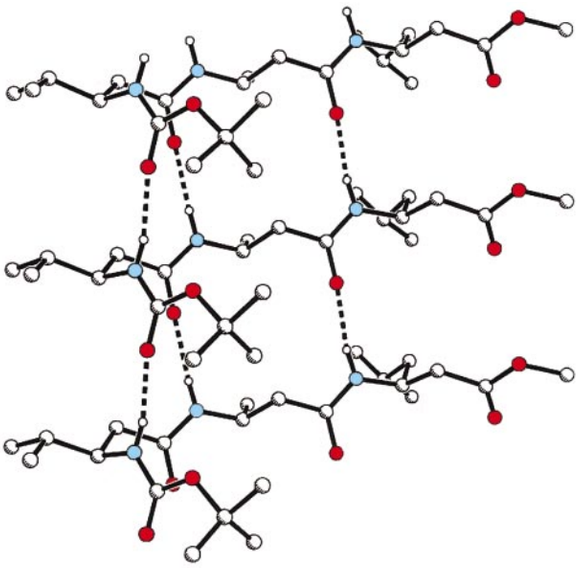


**Fig. 7** Section of the crystal structure of Boc-β$^3$-HVal-β$^3$-HAla-β$^3$-HLeu-OMe with the pleated-sheet type arrangement of two parallel β-peptide fragments

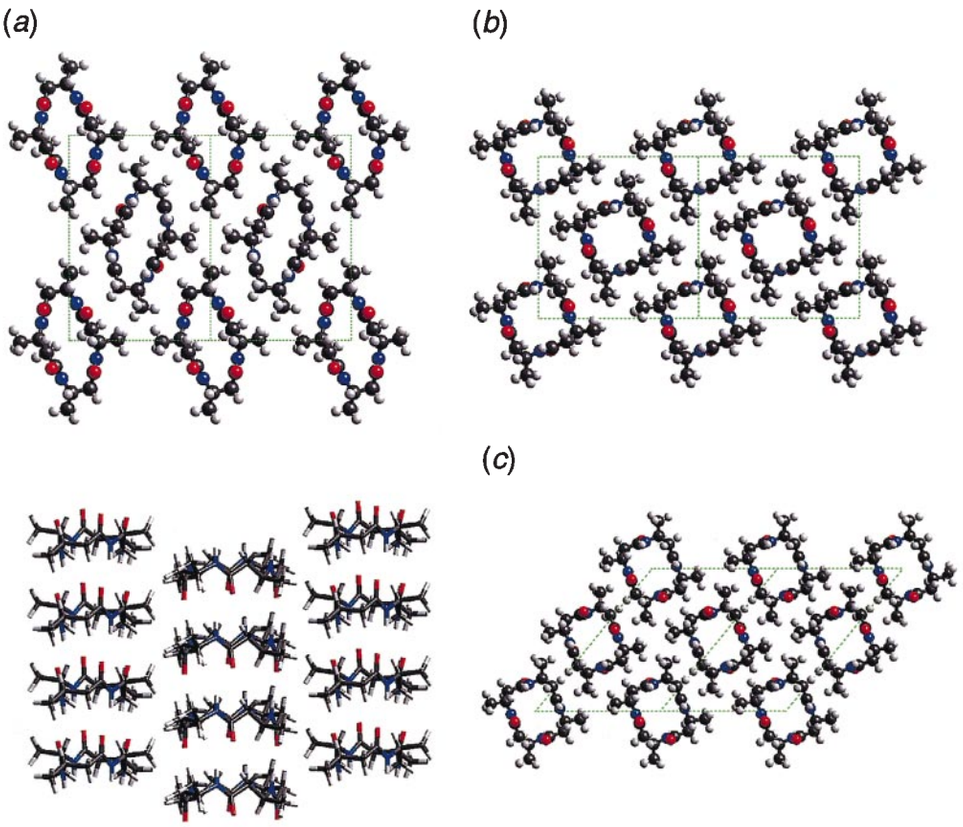



**Fig. 8** Tubular stacking of cyclo-β-tetrapeptides in the solid state (from powder diffraction data). (*a*) **12** [(*S*,*S*,*S*,*S*); top view (above), side view (below)]; (*b*) **13** [(*R*,*S*,*R*,*S*)], top view; (*c*) **14** [(*R*,*R*,*S*,*S*)], top view. In **12**, the ring adopts a rhomboidal shape, in **13**, a square and in **14**, a rectangular shape. All four C=O and N–H bonds are unidirectional in (*a*), two C=O and two N–H bonds point up and down on opposite faces in (*b*) and on adjacent faces in (*c*). (Taken with permission from ref. 28.)

position where we can closely compare related α- and β-peptides and learn something about the hydrogen bonding along the backbones, side chain interactions and possible interactions between α- and β-peptidic structures.

The comparative structural analysis of an α-peptidic $3.6_1$ helix with the $3_1$ and $2.5_1$ helices of β-peptides in Fig. 9 reveals the following points: (i) the helices have different polarities with respect to their C and N-termini; (ii) their shapes and sizes differ drastically; (iii) the $3_1$ β-peptide helix can exist only when its residues are homochiral or have 2,3-*l* relative configuration,§ and not with geminal disubstitution (in contrast, the α-helix is stabilised[33] by incorporation of geminally disubstituted α-amino acids such as Aib or Iva); (iv) the helices are stabilised by hydrophobic interactions between side chains, a contribution which may be responsible for the difference between $\beta^2$- and $\beta^3$-peptides ($3_1$ helix) on the one hand and the mixed $\beta^2/\beta^3$-peptides on the other hand.

From the crystal structure shown in Fig. 7, we are able to make a comparison of pleated sheets of α- and β-peptides (Fig. 10) and they differ in the following features: (i) the amide planes in an extended conformation are separated by one and two tetrahedral carbons, respectively; (ii) these planes are thus arranged in a zig-zag and in a parallel-displaced fashion; (iii) the C=O and N–H bonds are pointing up and down (approximately perpendicular to the chain) in the α-peptidic sheet, with O,O and O,H distances of 6.5, 3.6 and 2.8 Å, while they are unidirectional (all C=O up, all N–H down) in the β-peptidic case (O,O and H,H distances 4.9 Å); (iv) the antiparallel and the less common parallel pleated sheet of an α-peptide carry the side chains pointing perpendicular, above and below, the average plane of the sheet, while the sheet of a β-peptide built from homochiral§ (*all*-$\beta^2$ or *all*-$\beta^3$) components is obscured on only one face by the side chains; (v) while α-peptides containing the twenty proteinogenic amino acids may show a certain *tendency* for forming either a helix or a β-sheet (the Chou–Fasman algorithm[34]), the chain of a β-peptide can be *prevented* from forming a $3_1$ helix and *forced* to adopt an extended conformation, for instance, by constructing it from 2,3-disubstituted 3-amino acids of *u* configuration§¶ [$R^1$, $R^2 \neq$ H in Fig. 10(*b*)].

The additional versatility of β-peptides is further demonstrated by the cyclo-β-peptides: cyclic α-peptides are able to adopt a wide variety of conformations, but in order to exhibit regular tubular crystal packing each ring must be constructed from alternating (*R*)- and (*S*)-amino acid residues such that C=O and N–H bonds point alternately up and down and are parallel to the stacking direction[35] [Fig. 11(*d*)]. However, for cyclic β-peptides the extra $CH_2$ units remove these restrictions and more isomers are able to adopt a conformation suitable for the formation of tubular stacks [Fig. 11(*a*)–(*c*)].

Conformations other than extended chains, helices and circular stacks of β-peptides are yet to be found (*e.g.* turns or random coils); it will be interesting to see which conformation a β-peptide consisting of alternating (*R*)-$\beta^2$/(*S*)-$\beta^2$ or (*R*)-$\beta^3$/(*S*)-$\beta^3$ units[23] (sequences which should not be able to form either a $3_1$ helix or a pleated sheet) adopts. In this context, a couple of unusual CD curves of β-heptapeptides and analogues wait to be interpreted on the basis of NMR analyses.

The structural differences between α- and β-peptides, as outlined in the previous sections, suggest that they cannot exhibit supramolecular back-bone interactions with each other—something that is a prerequisite, for instance, for peptides to be accepted by peptidases as substrates. Thus, we have subjected six different β-tetra-, β-hexa- and β-heptapeptides to the action of the same number of various peptidases (20 different combinations): There was no indication of cleavage after two days but the peptidases had maintained activity towards their standard substrates.[7] The α- and β-peptidic structures in this experiment do not appear to interact in a way which would lead to the cleavage of peptide bonds. Furthermore, preliminary results of animal experiments with a water-soluble β-heptapeptide indicate that, in contrast to a common α-peptide, the β-peptide has an unusually long half-life in the blood serum of a rodent.

## Conclusion and outlook

At the outset of our work on β-peptides, the expectation of many a colleague and protein specialist was that insertion of a $CH_2$ group into each residue in a peptide backbone would lead to conformational chaos. Although we are convinced that we have by no means uncovered all secondary structures of β-peptides, we think that it is now justified to state that they have a much

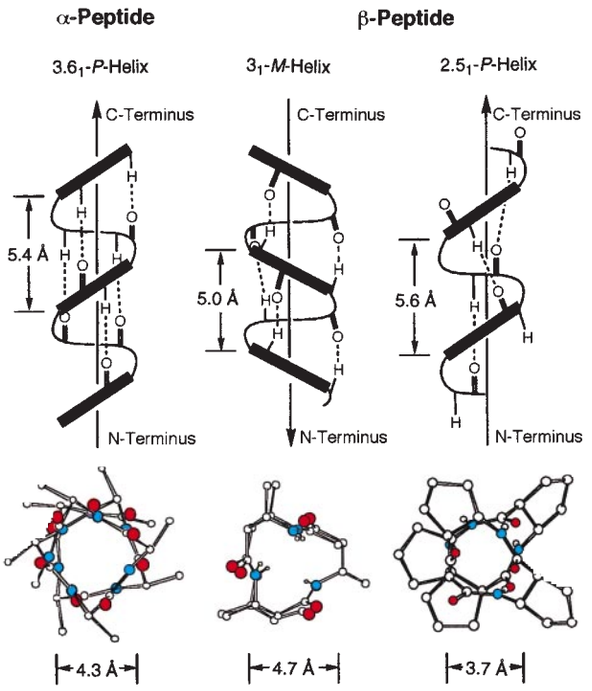



**Fig. 9** Polarities, pitches, diameters and positioning of the side chain in α- and β-peptide helices. (*a*) Schematic presentation of the three helices from (*S*)-α-, (*S*)-β- and (*S*,*S*)-β-amino acids. (*b*) View along the helix axes of the $3.6_{13}$, $3_{14}$ and $2.5_{12}$ helices (peptide nomenclature) as extracted from crystal or NMR structural data.

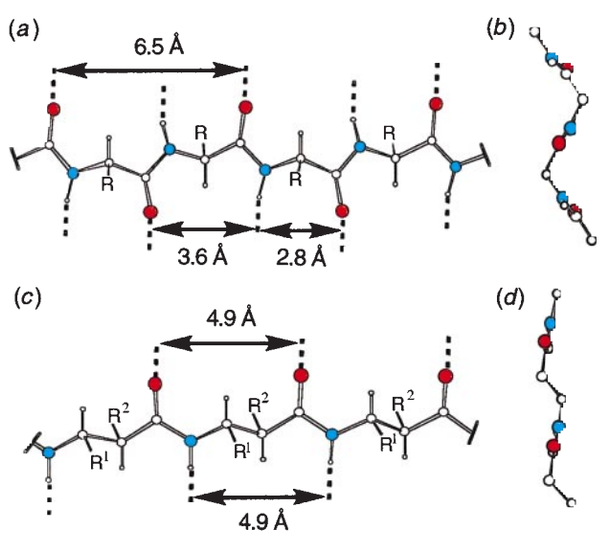



**Fig. 10** Models of the extended conformation of (*a*) an α-peptide and (*b*) a β-peptide which would permit pleated sheet formation. Geminal disubstitution is helix-breaking in both cases. The two types of peptides cannot possibly form 'mixed' sheets. (Taken with permission from ref. 7.)

richer conformational energy surface, with more stable secondary structures, than their α-peptide counterparts. The biological stability of β-peptides suggests that compounds of this type, with recognition-specific side chains attached to the backbone in the right geometry, will be able to bind to an α-peptidic receptor. Combined with their stability towards cleavage by peptidases, this could mean that β-peptides are candidates for useful drugs. Large β-peptides will probably be immunogenic, and it will be exciting to see how an α-peptidic globular protein such as an antibody copes with the challenge of specifically binding (recognising!) a β-peptide. Finally, with various secondary and tertiary β-peptidic structural building blocks in our arsenal (there will be more possible combinations than with conventional amino acid residues) we hope to be able to construct large, complex, protein-like molecules from β-amino acids, with properly arranged functional groups, to create active sites and generate enzymatic properties. The results of research in this area will undoubtedly lead to insights about natural proteins and it will be amusing to discuss the question 'why did nature use α- and not β-amino acids for the construction of the molecules central to life on earth?'‖


## Acknowledgements

It is a pleasure for us to acknowledge the efforts of our co-workers past and present—without them, many of the results described in this article would never have been realised and this article would never have taken shape. The help of Professor M. Dobler (crystallographic nomenclature), Karl Gademann (NMR structure figures), Beat Rheiner (X-ray crystal structure figures) and Paul Comina (proof-reading) is also greatly appreciated. We thank the many collaborators [B. Jaun, L. B. McCusker, C. Baerlocher, W. F. van Gunsteren (all ETH-Zürich), R. Amstutz and H. Widmer (Novartis Pharma, Basle) and all their respective co-workers] for their contributions to and interest in this work. Professor S. H. Gellman (Wisconsin-Madison) and Professor C. Alemán (Barcelona) are thanked for providing us with the coordinates resulting from their groups' work on β-peptides. Awards from the Royal Society, Great Britain (to J. L. M.), the Swiss National Science Foundation (Grant No. 21-40659.94) and the continuing support of Novartis Pharma AG, Basle, are appreciated.

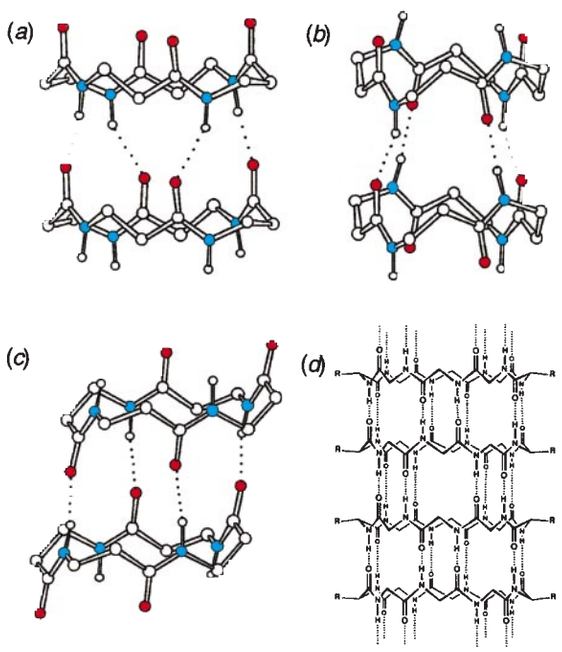




**Fig. 11** Arrangement of the cyclo-β-tetrapeptides (*a*) **12**, (*b*) **13** and (*c*) **14** as found in the solid state (*cf.* Fig. 8). All hydrogen-bonded rings are 14-membered with (7 + 7) and (8 + 6) combinations of the participating fragments. Me substituents and hydrogen atoms bound to carbon are omitted for clarity. For comparison, the stacking of a cyclo-α-octapeptide with alternating configuration of the residues is shown in (*d*). [Taken with permission from refs. 28 and 35(*c*).]


**Dieter Seebach was born in Karlsruhe, Germany, in 1937. He studied chemistry at the University of Karlsruhe and completed his PhD thesis on small rings and peroxides under the supervision of R. Criegee in 1964. After spending two years at Harvard University as postdoctoral co-worker (with E. J. Corey) and lecturer, he returned to Karlsruhe and, in 1969, completed his habilitation on the topic of S- and Se-stabilised carbanion and carbene derivatives. In 1971, he moved to the University of Giessen as a full professor and then in 1977 to the Eidgenössische Technische Hochschule in Zürich. He has received many prizes and titled lectureships, including the first Fluka Prize for Reagent of the Year (1987), the RSC Centenary Lectureship (1991) and the ACS Award for Creative Work in Organic Synthesis (1992), and he was the most recent Baker Lecturer at Cornell University (1997). His research has been directed towards the development of new synthetic methods and involves mechanistic studies and determination of structures. His attention is now focused on further developments of TADDOLs, on the short-chain oligomers of 3-hydroxybutanoic acid and the biopolymer PHB, on chiral dendrimers and on peptide modification.**

**Jennifer Matthews was born in Enfield, Middlesex in 1970. She studied chemistry at the University of Durham and after obtaining a BSc degree in 1991, remained there to complete a PhD on the preparation of asymmetric organosilicon compounds in 1994 under the supervision of Dr Patrick G. Steel. In January 1995, she joined Professor Seebach's group having obtained a Royal Society European Science Exchange Programme Fellowship. Throughout her stay in Zürich, her work has been in the β-peptide field. She has recently returned to the UK and is now a Royal Society Dorothy Hodgkin Research Fellow and Lecturer in Chemistry at the University of Glasgow.**


## Footnotes and References


* E-mail: seebach@org.chem.ethz.ch


† Due to a reversal of CIP priorities, H-β$^3$-HVal-OH has (*R*) configuration.

‡ β-Peptides built from identical 2,3-disubstituted β-amino acids (2-allyl-3-aminobutanoic acids of *like* configuration) have also been prepared *via* a stereocontrolled free radical allylation reaction by Hanessian and co-workers. Molecular modelling studies have suggested that a related β-hexapeptide might adopt a helical conformation (ref. 24).

§ For stereochemical definitions, see Helmchen's glossary (ref. 27).

¶ In fact, a β-tripeptide prepared from the amino acids (2*R*,3*S*)-Pr$^i$-CH($NH_2$)-CH(Me)-$CO_2$H, (2*R*,3*S*)-Pr$^i$-$CH_2$-CH($NH_2$)-CH(Me)-$CO_2$H and (2*R*,3*S*)-Me-CH($NH_2$)-CH(Me)-$CO_2$H was so insoluble that we were unable to add a fourth such amino acid or to perform a fragment coupling to yield a hexamer (ref. 23).

‖ *Cf.* 'Why pentose and not hexose nucleic acids?' (ref. 36).


1 S. Muñoz-Guerra, F. López-Carrasquero, J. M. Fernández-Santin and J. A. Subirana, in *Polymeric Materials Encyclopedia*, ed. J. C. Salomone, CRC Press, Boca Raton, FL, 1996, vol. 6, pp. 4694–4700.

2 C. Alemán, J. J. Navas and S. Muñoz-Guerra, *Biopolymers*, 1997, **41**, 721; M. García-Alvarez, A. Martínez de Ilarduya, S. León, C. Alemán and S. Muñoz-Guerra, *J. Phys. Chem. A*, 1997, **101**, 4215 and references cited therein.

3 G. P. Dado and S. H. Gellman, *J. Am. Chem. Soc.*, 1994, **116**, 1054.

4 D. Seebach, A. Brunner, B. M. Bachmann, T. Hoffmann, F. N. M. Kühnle and U. D. Lengweiler, *Biopolymers and oligomers of* (R)-*3-Hydroxyalkanoic Acids—Contributions of Synthetic Organic Chemists*, Ernst Schering Research Foundation, Berlin, 1995, vol. 28, pp. 1–105.

5 D. Seebach, T. Hoffmann, F. N. M. Kühnle and U. D. Lengweiler, *Helv. Chim. Acta*, 1994, **77**, 2007.

6 D. Seebach, M. Overhand, F. N. M. Kühnle, B. Martinoni, L. Oberer, U. Hommel and H. Widmer, *Helv. Chim. Acta*, 1996, **79**, 913.

7 T. Hintermann and D. Seebach, *Chimia*, 1997, **51**, 244.
8 B. L. Iverson, *Nature* (*London*), 1997, **385**, 113; U. Koert, *Angew. Chem., Int. Ed. Engl.*, 1997, **36**, 1836; S. Borman, *Chem. Eng. News*, June 16, 1997, 32; D. Bradley, *The Alchemist*, 1997, http://www.chemweb.com
9 *Enantioselective Synthesis of β-Amino Acids*, ed. E. Juaristi, Wiley-VCH, New York, 1997.
10 J. L. Matthews, C. Braun, C. Guibourdenche, M. Overhand and D. Seebach, *Preparation of Enantiopure β-Amino Acids from α-Amino Acids Using the Arndt–Eistert Homologation*, in *Enantioselective Synthesis of β-Amino Acids*, ed. E. Juaristi, Wiley-VCH, New York, 1997, pp. 105–126.
11 D. Seebach and H. Estermann, *Tetrahedron Lett.*, 1987, **28**, 3103; H. Estermann and D. Seebach, *Helv. Chim. Acta*, 1988, **71**, 1824.
12 D. A. Evans, F. Urpi, T. C. Somers, J. S. Clark and M. T. Bilodeau, *J. Am. Chem. Soc.*, 1990, **112**, 8215.
13 T. Hintermann and D. Seebach, *Synlett*, 1997, 437.
14 D. H. Apella, L. A. Christianson, I. L. Karle, D. R. Powell and S. H. Gellman, *J. Am. Chem. Soc.*, 1996, **118**, 13 071.
15 D. H. Apella, L. A. Christianson, D. A. Klein, D. R. Powell, S. Huang, J. J. Barchi and S. H. Gellman, *Nature* (*London*), 1997, **387**, 381.
16 I. L. Karle, J. L. Flippen-Anderson, M. Sukumar, K. Uma and P. Balaram, *J. Am. Chem. Soc.*, 1991, **113**, 3952 and references cited therein.
17 D. Seebach, P. E. Ciceri, M. Overhand, B. Jaun, D. Rigo, L. Oberer, U. Hommel, R. Amstutz and H. Widmer, *Helv. Chim. Acta*, 1996, **79**, 2043.
18 J. L. Matthews, M. Overhand, F. N. M. Kühnle, P. E. Ciceri and D. Seebach, *Liebigs Ann.*, 1997, 1371.
19 K. Gademann, Diplomarbeit (Master's Thesis), ETH Zürich, 1996.
20 J. V. Schreiber, Diplomarbeit (Master's Thesis), ETH Zürich, 1997.
21 G. Guichard and D. Seebach, *Chimia*, 1997, **51**, 315.
22 G. Quinkert, E. Egert and C. Griesinger, *Aspects of Organic Chemistry: Structure*, VCHA, Basel and VCH, Weinheim, 1996; *Peptides: Synthesis, Structures, and Applications*, ed. B. Gutte, Academic Press, San Diego, 1995.
23 S. Abele and D. Seebach, unpublished results. Part of the projected PhD Thesis of S. Abele, ETH Zürich.
24 S. Hanessian, H. Yang and R. Schaum, *J. Am. Chem. Soc.*, 1996, **118**, 2507; S. Hanessian, personal communication.
25 D. Seebach, K. Gademann, J. V. Schreiber, J. L. Matthews, T. Hintermann, B. Jaun, U. Hommel, L. Oberer and H. Widmer, *Helv. Chim. Acta*, 1997, **80**, November issue.
26 X. Daura, W. F. van Gunsteren, D. Rigo, B. Jaun and D. Seebach, *Chem. Eur. J.*, 1997, 1410.
27 G. Helmchen, in *Houben Weyl—Stereoselective Synthesis*, 4th edn., ed. G. Helmchen, R. W. Hoffmann, J. Mulzer and E. Schaumann, Thieme, Stuttgart, 1996, vol. 1, pp. 1–74.
28 D. Seebach, J. L. Matthews, A. Meden, T. Wessels, C. Baerlocher and L. B. McCusker, *Helv. Chim. Acta*, 1997, **80**, 173.
29 G. P. Dado, J. M. Desper, S. K. Holmgren, C. J. Rito and S. H. Gellman, *J. Am. Chem. Soc.*, 1992, **114**, 4834.
30 D. Seebach, *How I became a Peptide Chemist*, Lonza Brochure, Lonza Ltd., Basel, 1990.
31 D. Seebach, *Aldrichimica Acta*, 1992, **25**, 59.
32 D. Seebach, A. K. Beck and A. Studer, *Some Effects of Lithium Salts, of Strong Bases, and of the Cosolvent DMPU in Peptide Chemistry, and Elsewhere*, in *Modern Synthetic Methods 1995*, ed. B. Ernst and C. Leumann, VCHA, Basel, and VCH, Weinheim, 1995, vol. 7, pp. 1–178.
33 I. L. Karle and P. Balaram, *Biochemistry*, 1990, **29**, 6747; B. Jaun, M. Tanaka, P. Seiler, F. N. M. Kühnle, C. Braun and D. Seebach, *Liebigs Ann.*, 1997, 1697 and references cited therein.
34 P. Prevelige and G. D. Fasman, in *Prediction of Protein Structure and the Principles of Protein Conformation*, ed. G. D. Fasman, Plenum Press, New York, 1989, pp. 391–416.
35 (*a*) X. Sun and G. P. Lorenzi, *Helv. Chim. Acta*, 1994, **77**, 1520; (*b*) J. D. Hartgerink, J. R. Granja, R. A. Milligan and M. R. Ghadiri, *J. Am. Chem. Soc.*, 1996, **118**, 43; (*c*) M. R. Ghadiri, J. R. Granja, R. A. Milligan, D. E. McRee, N. Khazanovich, *Nature* (*London*), 1993, **366**, 324.
36 S. Pitsch, S. Wendeborn, B. Jaun and A. Eschenmoser, *Helv. Chim. Acta*, 1993, **76**, 2161; G. Otting, M. Billeter, K. Wüthrich, H.-J. Roth, C. Leumann and A. Eschenmoser, *Helv. Chim. Acta*, 1993, **76**, 2701.

*7/04933A*

# Hydrogen bonding in DNA—a return to the *status quo*

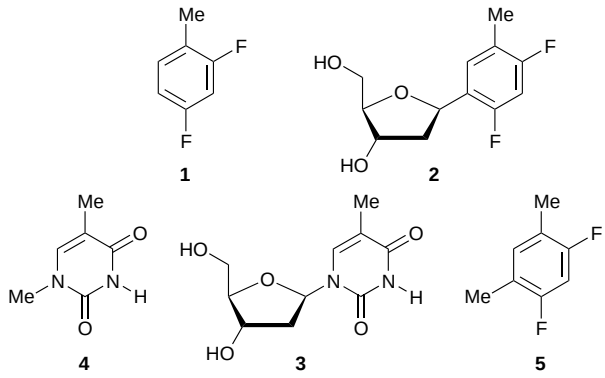
**Timothy A. Evans and Kenneth R. Seddon***

*School of Chemistry, The Queen's University of Belfast, Stranmillis Road, Belfast, Northern Ireland, UK BT9 5AG*

**Recent claims that 'conventional hydrogen bonds may not be necessary for high efficiency and fidelity in DNA synthesis' and that 'DNA polymerase can exert high fidelity even when a base pair completely lacks conventional hydrogen bonds' are shown to be in error.**

Both Watson and Crick's original *Nature* paper,[1] and Watson's subsequent account of the discovery of the structure of DNA,[2] focus upon the central role of hydrogen bonds between base pairs in defining the formation of the double helix—a view which has become a paradigm, and has remained effectively unchallenged until the appearance this year of a communication (preannounced by Bradley)[3] from Kool,[4] in which the rôle of the hydrogen bond is questioned. Since such doubts as to the importance of hydrogen bonding to molecular recognition undermine not only many of the basic theories of biochemistry, but also the foundations of supramolecular chemistry[5] and crystal engineering,[6–8] it is particularly important that the basis for these radical criticisms be established beyond reasonable doubt. We describe here the reasons why we believe, despite its synthetic elegance, the work of Moran *et al.*[4] is flawed.

At the heart of the communication[4] is the contention that 2,4-difluorotoluene **1** is nonpolar, and incapable of forming hydrogen bonds: if this tenet of their approach is incorrect, the basis for their argument is fallacious. We demonstrate here that they have misunderstood the hydrogen bonding capabilities of such a molecule, that their basic experimental approach is thus flawed, and that there is no reason to change our fundamental understanding of the rôle of hydrogen bonding in the formation of the DNA double helix.




In the title of the paper ('Difluorotoluene, a Nonpolar Isostere for Thymine, Codes Specifically and Efficiently for Adenine in DNA Replication') and in the text it is stated that **1** is nonpolar.[4] However, AM1 calculations† give a dipole moment of 1.86 D (*cf.* AM1 calculations on 1,3-difluorobenzene give a dipole moment of 1.55 D; the experimental value is 1.58 D[9]), a value greater than that for water (1.82 D).[10] Thus, **1** is demonstrably polar, as is the derivative nucleoside **2** which is specifically mentioned[4] as 'a nonpolar shape mimic for natural thymidine' **3**. Furthermore, it is stated[4] that **2** 'would serve as a good test for the importance of thymidine's hydrogen bonding groups on fidelity, because [it] lacks the strongly localized charges but retains nearly the exact steric shape of the natural molecule'. Fig. 1 illustrates the charge distributions of 1-methylthymine **4**, an analogue of **3**, and **5**, an analogue of **2**, as obtained by *ab initio* calculations at the 6-31G** level (essentially similar results were produced by AM1). The pattern and relative magnitude of the localized charges in both molecules are essentially identical, and thus **1** or **2** should not be used for the test described.

The authors state[4] that **2** has a 'non-polar, non-hydrogen-bonding nature', and that their work provides evidence 'that a DNA polymerase can exert high fidelity even when a base pair completely lacks hydrogen bonds'. These statements apparently originate with their belief that the C–F··H–N hydrogen bond is 'unconventional' [*sic*],[4] and that C–H··N hydrogen bonds are not possible upon the observation that 'difluorotoluene is a highly hydrophobic species which does not pair with adenine even in chloroform'.[4] This latter statement is based upon an inconclusive experiment (9-ethyladenine has a very limited solubility in $CHCl_3$), in with 9-ethyladenine was titrated against a dilute (millimolar) solution of **2** in $CDCl_3$, and the N[4]–*H* resonance was monitored on the 9-ethyladenine:[11] the C–*H* resonances of the difluorotoluene do not appear to have been

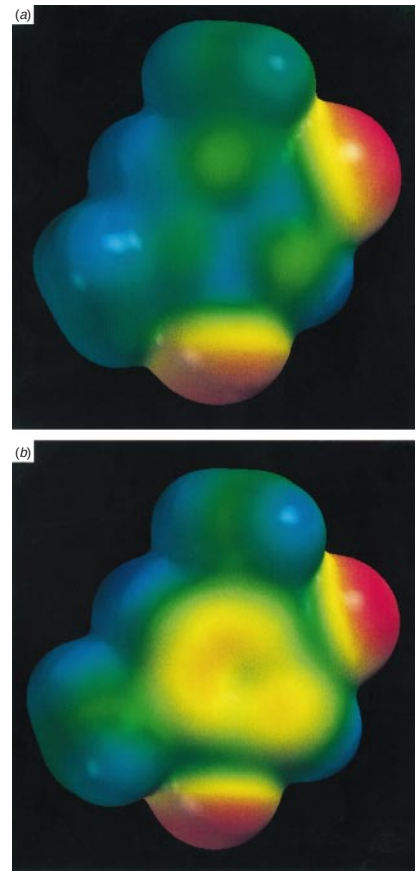



**Fig. 1** The total electron density isosurfaces for (*a*) **4** and (*b*) **5**, each being encoded with the value of its electrostatic potential (red = most negative, blue = most positive), calculated at the 6–31G** level. Both show essentially the same relative charge distribution, although the absolute values are smaller for **4** than for **5**. Calculations on **2** and **3** also reveal similar relative charge distributions.

examined. In our hands, even the simple bases pyridine (p$K_a$ 5.18)[12] and 3-chloropyridine (p$K_a$ 2.84),[13] which are respectively stronger and weaker bases than adenine (p$K_a$ 4.20),[14] are capable of forming hydrogen bonds with **1**. Both pyridine and 3-chloropyridine are hydrogen-bond acceptors and, in both cases, the C–*H*$^3$ proton of **1** exhibits concentration dependent downfield shifts (see Fig. 2), both with respect to an internal reference ($SiMe_4$), and with respect to the methyl protons of **1**. Indeed, the AA′MXY spin system is converted, in the hydrogen-bonded base pair, into an ABMXY system. This is behaviour characteristic of hydrogen-bond formation in solution,[15–17] and provides hard evidence in direct contradiction of the recent claims.[4] Moreover, the phenomenon of C–H···X hydrogen bonds is well established,[8,18–22] and is no longer considered either controversial or 'unconventional'. In addition, in a study of hydrogen bonds formed by fluorinated hydrocarbons, Howard *et al.*[23] report (on the basis of exhaustive searching of the Cambridge Structural Database and high level *ab initio* calculations) that 'Encouraging for the bio-organic chemist is that substrate/protein interactions may offer an environment for optimal F···H bonding. [...] the F···H–X interaction may contribute to the overall binding energy, up to half of the strength of the original hydrogen bond to oxygen'. Our own gas-phase calculations (AM1, PM3 and 6-31G*) on the stabilization of base pairs between **4** or **5** and 9-methyladenine confirm this view, all resulting in the same fully-optimized co-planar structures **6** and **7**, respectively. Both these base pair structures have hydrogen-bonding motifs which encode identically as $N_1 = R_2^2(8)$ using Etter's topological analytical method for the comparison of hydrogen-bonding networks,[24,25] The calculated NH···F bond in **7** is only about 0.1 Å longer than the calculated NH···O bond in **6**, reflecting the smaller charges in **5** than in **4**, but representing significant hydrogen bonding. The CH···N bond in **7** is, as expected, significantly longer (0.4 Å) than the NH···N bond in **6**, but still represents a significant weak interaction. The difference in binding energies between the two structures represents a 60% decrease in substituting **5** for **4**. This energy difference is entirely in accord with the reported empirical measurements.[11,26,27] The existence of CH···N and NH···F hydrogen bonds in **7** explains the observed surprisingly high efficiency and fidelity in DNA synthesis: the choice of **2** as a replacement for **3** was inspired—it mimicked not only its shape, but also its relative charge distribution and hydrogen-bonding patterns.

In conclusion, the arguments presented elsewhere[4] are flawed: we have demonstrated here that 2,4-difluorotoluene is both polar and capable of acting as a hydrogen-bond donor and acceptor. It has been stated that 'conventional hydrogen bonds may not be necessary for high efficiency and fidelity in DNA synthesis' and that 'DNA polymerase can exert high fidelity even when a base pair completely lacks conventional hydrogen bonds'. These views contradict 'most if not all current models for replication fidelity'.[4] Using the well-established philosophical principle of Occam's Razor,[28] it is clear that these workers[4] have reported no results which disturb the *status quo*. Indeed, in

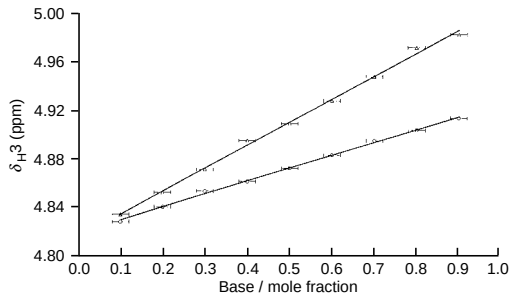
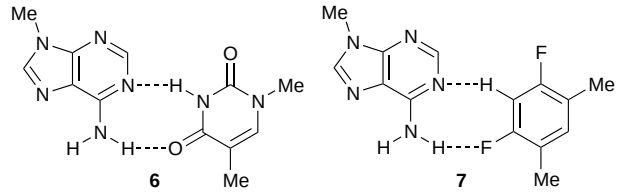



**Fig. 2** The chemical shift of the H$^3$ proton of **1** measured with respect to the methyl resonance, and plotted as a function of the mole fraction of added base, for the addition of (Δ) pyridine and (○) 3-chloropyridine




view of the expected hydrogen bonding ability of **2**, they may well have underlined the validity of the conventional model.

We are indebted to the EPSRC and Royal Academy of Engineering for the award of a Clean Technology Fellowship (to K. R. S.), to the EPSRC for the award of a ROPA grant, and to Richard Murphy, Mark Nieuwenhuyzen, and Drs John Holbrey, Martyn Earle, Yasmin Patell and John Wilson for their assistance and advice. We would particularly like to acknowledge a suggestion from a referee which prompted our use of 3-chloropyridine.

## Footnotes and References

* E-mail: k.seddon@qub.ac.uk

† All the calculations reported here were performed using the Spartan 4.1.1 suite of software. The results cited correspond to the Hamiltonians quoted in the text, and all results represent fully optimized geometries with no applied constraints. In all cases, calculations were performed at the AM1, PM3, STO-3G, 6-31G* and 6-31G** levels, and full details of these calculations will be reported in a future manuscript. Inclusion of an aqueous solvation sheath in $AM1_{aq}$ calculations does not significantly perturb the conclusions.

1 J. D. Watson and F. H. C. Crick, *Nature*, 1953, **171**, 737.
2 J. D. Watson, *The Double Helix: A Personal Account of the Discovery of the Structure of DNA*, Atheneum, New York, 1968.
3 D. Bradley, *New Scientist*, 22nd February 1977, **153**, 19.
4 S. Moran, R. X.-F. Ren, S. Rumney IV and E. T. Kool, *J. Am. Chem. Soc.*, 1997, **119**, 2056.
5 J.-M. Lehn, *Supramolecular Chemistry: Concepts and Perspectives*, VCH, Weinheim, 1995.
6 G. R. Desiraju, *Crystal Engineering: The Design of Organic Solids*, Elsevier, Amsterdam, 1989.
7 *The Crystal as a Supramolecular Entity*, ed. G. R. Desiraju, Wiley, Chichester, 1996, vol. 2.
8 C. B. Askeröy and K. R. Seddon, *Chem. Soc. Rev.*, 1993, **22**, 397.
9 E. M. Moore and M. E. Hobbs, *J. Am. Chem. Soc.*, 1949, **71**, 411.
10 A. L. McClellan, *Tables of Experimental Dipole Moments*, W. H. Freeman and Company, San Francisco, 1963.
11 B. A. Schweitzer and E. T. Kool, *J. Am. Chem. Soc.*, 1995, **117**, 1863.
12 R. K. Murmann and F. Basolo, *J. Am. Chem. Soc.*, 1955, **77**, 3484.
13 H. C. Brown and D. H. McDaniel, *J. Am. Chem. Soc.*, 1955, **77**, 3752.
14 R. M. Izatt and J. J. Christensen, *J. Phys. Chem.*, 1962, **66**, 359.
15 M. Nakano, N. I. Nakano and T. Higuchi, *J. Phys. Chem.*, 1967, **71**, 3954.
16 J. W. Akitt, *N.M.R. and Chemistry: An Introduction to the Fourier Transform–Multinuclear Era*, Chapman and Hall, London, 2nd edn., 1983.
17 A. G. Avent, P. A. Chaloner, M. P. Day, K. R. Seddon and T. Welton, *J. Chem. Soc., Dalton Trans.*, 1994, 3405.
18 G. R. Desiraju, *J. Chem. Soc., Chem. Commun.*, 1989, 179.
19 G. R. Desiraju, *Acc. Chem. Res.*, 1991, **24**, 290.
20 G. R. Desiraju, *Mol. Cryst. Liq. Cryst.*, 1992, **211**, 63.
21 G. R. Desiraju, *Angew. Chem., Int. Ed. En.*, 1995, **34**, 2311.
22 C. B. Aakeröy and K. R. Seddon, *Z. Naturforsch., Teil B*, 1993, **48**, 1023.
23 J. A. K. Howard, V. J. Hoy, D. O'Hagan and G. T. Smith, *Tetrahedron*, 1996, **52**, 12613.
24 M. C. Etter, *Acc. Chem. Res.*, 1990, **23**, 120.
25 M. C. Etter, J. C. Macdonald and J. Bernstein, *Acta Crystallogr., Sect. B*, 1990, **46**, 256.
26 J. Pranata, S. G. Wierschke and W. L. Jorgensen, *J. Am. Chem. Soc.*, 1991, **113**, 2810.
27 I. K. Yanson, A. B. Teplitsky and L. F. Sukhodub, *Biopolymers*, 1979, **18**, 1149.
28 B. Russell, *History of Western Philosophy*, George Allen & Unwin, London, 2nd edn., 1961.

*Received in Cambridge, UK, 27th March 1997; Revised version received, 31st July 1997; 7/05239A*

# Engineering an atomically well defined active site for the catalytic epoxidation of alkenes

**Richard D. Oldroyd, John Meurig Thomas* and Gopinathan Sankar**

*Davy–Faraday Research Laboratory, The Royal Institution of Great Britain, 21 Albermarle Street, London, UK W1X 4BS*

**The improvement effected by replacing one of the three O–Si≡ groups to which a $Ti^{IV}$ ion is anchored (to a mesoporous silica support) by a O–Ge≡ group is described, as is the detailed structure retrieved by *in situ* X-ray absorption spectroscopy of the created active site.**

The immediate atomic environment of a catalytically active metallic ion may be determined by X-ray absorption spectroscopy.[1–3] Using this technique we find that, in the case of $Ti^{IV}$ ions anchored onto the walls of a high-area, crystalline mesoporous silica[4] (Ti ↑ MCM41) by condensing titanocene dichloride and pendant ≡Si–OH groups in a manner previously described,[5,6] the coordination numbers and spatially averaged bond distances for the epoxidation catalyst (see Fig. 1) are as shown in Table 1. It has hitherto been established[6,7] that this epoxidation catalyst functions in a radical-free fashion, and that it epoxidises cyclohexene with a selectivity as high as 95% and turnover numbers of *ca.* 35 $h^{-1}$ (under the conditions used in the cited study) with alkyl hydroperoxide oxidants. This performance is a good deal superior to that of the catalyst produced by incorporation of $Ti^{IV}$ ions into the interior of the walls during the synthesis of the MCM41 mesoporous silica from the parent gel (Ti→MCM41).[8–10]

Titanium and germanium K-edge extended X-ray absorption fine structure (EXAFS) spectroscopy, supplemented by FTIR spectroscopy and spatially resolved elemental analysis (using scanning transmission electron microscopy), show that the exposed active sties in the Ti ↑ MCM41 catalyst (Si : Ti = 44.7 : 1) are $Ti^{IV}$ centres tripodally attached to the support *via* three Ti–O–Si≡ linkages (Fig. 1). We have grafted $Ge^{IV}$ centres onto the MCM41 surface using a procedure similar to that of Nédez *et al.*[11] to which the catalytically active $Ti^{IV}$ centres have been subsequently attached. The synthesis entails exposing the dehydrated mesoporous silica (surface area = 1020 ± 10 $m^2\ g^{-1}$) to tetrabutylgermanium at 180 °C and then, after washing, calcining and dehydrating the resulting sample, introducing the $TiCp_2Cl_2$ in an analogous fashion to the procedure used for unmodified MCM41. The resulting atomic ratios are Si : Ge : Ti = 44.9 : 0.07 : 1 and 44.7 : 0 : 1 for the germanium-modified and Ti ↑ MCM41 catalysts, respectively. Full preparative and analytical details are to be given elsewhere.[12]

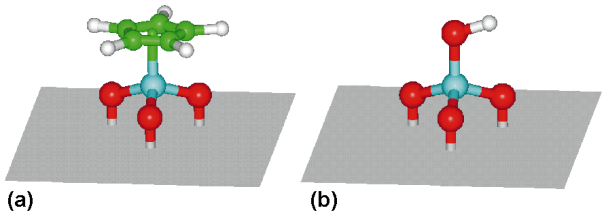



**Fig. 1** Illustration of the Ti environment in Ti ↑ MCM41 before (*a*) and after (*b*) removal of the Cp moiety by calcination. (Ti = cyan, C = green, O = red, H = white). For clarity, the $SiO_2$ background of the mesoporous support is not shown in atomic detail.

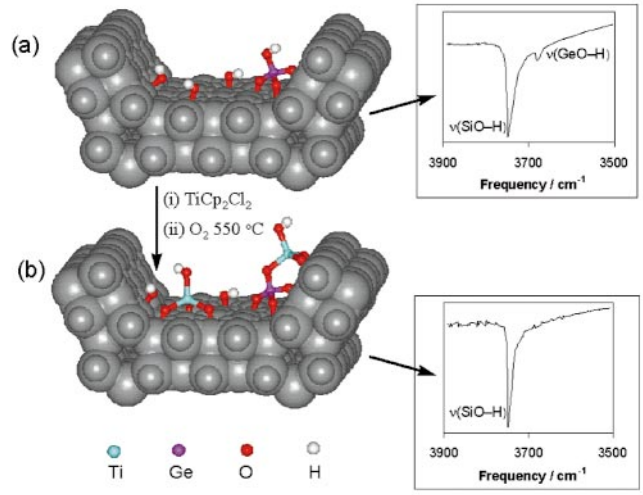



**Fig. 2** Representation of the derived structures of calcined Ge ↑ MCM41 (*a*) and Ti ↑ Ge ↑ MCM41 (*b*). The insets show the respective FTIR spectra. Most of the surface silanol groups have been omitted for clarity. (Note that the ratio of the different active sites shown here are not the same as in the real catalyst, but are purely illustrative.)

**Table 1** Bond distances and angles derived from analysis of Ti and Ge K-edge EXAFS data

| Material | Edge | Atom type | Occupancy | Distance/Å | $2\sigma^2$/Å$^2$ | Angle/° |
|---|---|---|---|---|---|---|
| Ti ↑ MCM41 (calcined) | Ti | O | 4.1 | 1.82 | 0.005 | Ti–O–Si(A) : 138 |
| | | Si(A)[a] | 2.3 | 3.19 | 0.006 | Ti–O–Si(B) : 160 |
| | | Si(B) | 0.8 | 3.37 | 0.006 | |
| Ge ↑ MCM41 (calcined) | Ge | O | 3.9 | 1.73 | 0.004 | Ge–O–Si : 132 |
| | | Si | 2.7 | 3.04 | 0.005 | |
| Ti ↑ Ge ↑ MCM41(calcined) | Ti | O | 3.8 | 1.81 | 0.002 | Ti–O–Si(A) : 139 |
| | | Si(A)[a] | 1.7 | 3.19 | 0.004 | Ti–O–Si(B) : 158 |
| | | Si(B) | 1.1 | 3.34 | 0.004 | |
| | Ge | O | 4.1 | 1.72 | 0.004 | Ge–O–Si : 136 |
| | | Ti | 0.8 | 2.80 | 0.003 | Ge–O–Ti : 106 |
| | | Si | 3.3 | 3.10 | 0.003 | |

[a] Self-consistent results pertaining to coordination numbers and bond lengths are best achieved by recognising two distinct Si shells.

The resulting so-called Ti ↑ Ge ↑ MCM41 catalyst was investigated by scanning transmission electron microscopy, X-ray absorption spectroscopy and also by IR spectroscopy. The salient results are given in Table 1, from which the representation of the created active sites (Fig. 2) is derived. It is evident that titanium attaches to the germanium centres (as well as unmodified regions of the MCM41 surface) from the disappearance of the $\nu$(GeO–H)[13] band at 3680 $cm^{-1}$ in the IR spectrum and the appearance of a Ge···Ti shell from the Ge K-edge EXAFS spectrum.

The difference in catalytic activity between the two catalysts is quite dramatic. Although the germanium loading on the MCM41 surface is low (only *ca.* 0.15 mass%) there is a substantial improvement in catalytic activity of as much as 18%. It can be calculated that for those titanium centres that are surrounded tripodally by two O–Si≡ and one O–Ge≡ there is a 140% increase in turnover frequency with *tert*-butyl hydroperoxide (TBHP) and some 80% increase with cumene hydroperoxide (CuHP) as oxidants at 30 °C compared to titanium centres bound to three O–Si≡ moieties. Turnover frequencies towards the epoxide were 33.8 and 39.8 $h^{-1}$ for Ti ↑ MCM41 and Ti ↑ Ge ↑ MCM41 respectively in the presence of TBHP, and 31.2 and 34.9 $h^{-1}$ using CuHP. In each case the selectivity towards cyclohexene oxide was > 75%, the remaining products being cyclohexenol and cyclohexan-1,2-diol.

Attempts to modify the active site with Sn (using $SnBu_4$ in place of $GeBu_4$)[14] prior to anchoring the titanium were not successful since there was a strong tendency for Sn–O–Sn linkages to form, and hence crystallites of extraframework $SnO_2$, which significantly inhibited catalysis. A detailed account of this work will be submitted elsewhere.[12]

We are grateful to the EPSRC for a rolling grant (to J. M. T.) and a ROPA award (to R. D. O.) and the staff at the Daresbury Laboratory for provision of facilities for the XAS experiments. We also acknowledge the efforts of Dr D. Lewis for preparing the figures.

## Footnote and References

* E-mail: richie@ri.ac.uk

1 J. W. Couves, J. M. Thomas, D. Waller, R. H. Jones, A. J. Dent, G. E. Derbyshire and G. N. Greaves, *Nature*, 1991, **354**, 465.
2 J. M. Thomas and G. N. Greaves, *Science*, 1994, **265**, 1675.
3 J. M. Thomas, G. N. Greaves, G. Sankar, P. A. Wright, J. S. Chen, A. J. Dent and L. Marchese, *Angew. Chem., Int. Ed. Engl.*, 1994, **33**, 1871.
4 C. T. Kresge, M. E. Leonowicz, W. J. Roth, J. C. Vartuli and J. S. Beck, *Nature*, 1992, **359**, 710.
5 T. Maschmeyer, F. Rey, G. Sankar and J. M. Thomas, *Nature*, 1995, **378**, 159.
6 R. D. Oldroyd, J. M. Thomas, T. Maschmeyer, P. A. MacFaul, D. W. Snelgrove, K. U. Ingold and D. D. M. Wayner, *Angew. Chem., Int. Ed. Engl.*, 1996, **35**, 2787.
7 R. A. Sheldon, *J. Mol. Catal.*, 1980, **7**, 106.
8 H. C. L. Abbenhius, S. Krijnen and R. A. van Santen, *Chem. Commun.*, 1997, 331.
9 G. Sankar, F. Rey, J. M. Thomas, G. N. Greaves, A. Corma, B. R. Dobson and A. J. Dent, *J. Chem. Soc., Chem. Commun.*, 1994, 2279.
10 P. Tanev, M. Chibwe and T. J. Pinnavaia, *Nature*, 1994, **368**, 197.
11 C. Nédez, A. Choplin and J. M. Basset, *Inorg. Chem.*, 1994, **33**, 1094.
12 R. D. Oldroyd, G. Sankar, J. M. Thomas and D. Özkaya, *J. Phys. Chem.*, in press.
13 H. Kosslick, V. A. Tuan and R. Fricke, *Ber. Bunsen-Ges. Phys. Chem.*, 1992, **96**, 1761.
14 C. Nédez, A. Theolier, F. Lefebvre, A. Choplin, J. M. Basset and J. F. Joly, *J. Am. Chem. Soc.*, 1993, **115**, 722.

*Received in Basel, Switzerland, 3rd April 1997; Revised manuscript accepted 8th August 1997; 7/06387C*

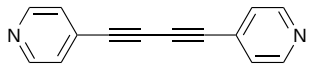
# Polycatenated copper(I) molecular ladders: a new structural motif in inorganic coordination polymers

**Alexander J. Blake,[a] Neil R. Champness,*[a] Andrei Khlobystov,[a,b] Dmitri A. Lemenovskii,[b] Wan-Sheung Li[a] and Martin Schröder*[a]**

[a] *Department of Chemistry, The University of Nottingham, University Park, Nottingham, UK NG7 2RD*
[b] *Department of Chemistry, Moscow State University, 119899 Moscow, Russia*

**The complex $\{[Cu_2(MeCN)_2L_3](PF_6)_2\}_\infty$ [L = 1,4-bis(4-pyridyl)butadiyne] is prepared and characterised by X-ray diffraction studies which show an undulating polycatenated molecular ladder structure involving fully interwoven two-dimensional sheets.**

The study of inorganic coordination polymers and their use in constructing solid-state architectures has become an area of increasing interest.[1] Although the design of inorganic networks is less well developed than corresponding hydrogen-bonded systems,[2] recent examples have helped to extend the understanding of this rapidly expanding area.[1,3–8] Of particular interest in inorganic co-ordination polymers is the degree and nature of interpenetration or polycatenation[3] and to this end we have been investigating the effect of ligand functionality upon the construction of two- and three-dimensional arrays, and in particular adamantoid or super-diamondoid networks based upon copper(I) complexes.[4,5] We have established recently a degree of control over the assembly of these copper(I) adamantoid networks showing that the degree of interpenetration of independent networks can be increased or decreased by variation of the length[4] and steric bulk[5] of the linking ligand. During further investigations into such systems we have isolated a remarkable new structural motif for inorganic coordination polymers, a polycatenated undulating molecular ladder.




L

The reaction of $[Cu(MeCN)_4]PF_6$ with 1,4-bis(4-pyridyl)-butadiyne (L) in $MeCN–CH_2Cl_2$ yields a deep red solution from which red crystals of composition $\{[Cu_2(MeCN)_2L_3](PF_6)_2\}_\infty$ were isolated by layering with $Et_2O$.† The same product is isolated even in the presence of a large excess of ligand, with metal : ligand ratios of up to 1 : 4. X-Ray diffraction studies‡ of these crystals show that the compound exists as a network of molecular ladders in which the two independent $Cu^I$ centres are each coordinated in a tetrahedral geometry to three ligands L, Cu–N 1.993(9)–2.114(10) Å, and one MeCN ligand, Cu–N 1.980(13), 1.997(12) Å, (Fig. 1). The ladder structure is generated *via* the 1,4-bis(4-pyridyl)butadiyne ligands which each bridge two $Cu^I$ centres. This structure is particularly surprising as insoluble adamantoid networks have been previously observed from this type of reaction.[4–6] Molecular ladders have been observed for relatively few related systems although in all previous cases the metal junction of the ladder has been a pseudo-octahedral[7] or octahedral[8] centre generating what may be termed a flat ladder with all linking ligands coplanar.[7,8] In the case reported here the tetrahedral $Cu^I$ centres allow the ladder to undulate. The large cavities between the rungs of the ladder encourage the inclusion of discrete symmetry-related ladders. Examples of molecular ladders based upon cobalt(II)-bipyridyl complexes exhibit no interpenetration.[8] Interpenetration of symmetry-related ladders has been observed although this interpenetration was found to be perpendicular to the orientation of the original ladder, generating a three-dimensional polycatenated structure.[7] In the example reported here the ladders are polycatenated to give a remarkable two-dimensional layer structure involving undulating ladders which interweave in a parallel fashion (Fig. 2). These two-dimensional layers are flattened by a distortion of the N(1)–Cu(1)–N(5) and N(1′)–Cu(2)–N(4) angles from tetrahedral to 128.4(4) and 124.9(4)°, respectively, allowing a significant flattening of each ladder. Each ladder is polycatenated by a further four ladders which weave through the first ladder so as to fill the spaces between the ladders' rungs giving a fully polycatenated sheet (Fig. 3). Potential π–π interactions between adjacent, symmetry-related ladders at a distance of 3.484 Å may presumably contribute to the stability of the observed structural motif. The two-dimensional sheets of interwoven ladders are separated by $PF_6^-$ counter-anions and solvent molecules with the co-ordinated MeCN molecules pointing towards the next sheet in the crystal.

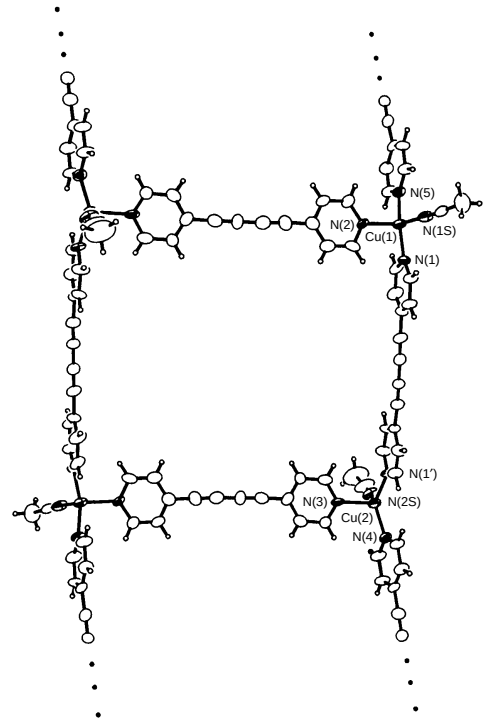



**Fig. 1** A view of part of one infinite undulating ladder. Cu(1)–N(1S) 1.997(12), Cu(1)–N(1) 1.997(9), Cu(1)–N(5) 1.998(9), Cu(1)–N(2) 2.087(9), Cu(2)–N(2S) 1.980(13), Cu(2)–N(4) 1.993(9), Cu(2)–N(1′) 2.032(9), Cu(2)–N(3) 2.114(10) Å.

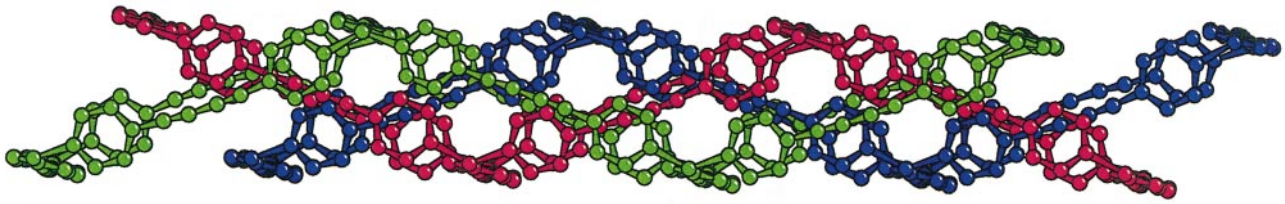


**Fig. 2** A lateral view of three undulating ladders distinguished by colour showing their interweaving. The $PF_6^-$ anions, solvent molecules and coordinated MeCN are omitted for clarity.

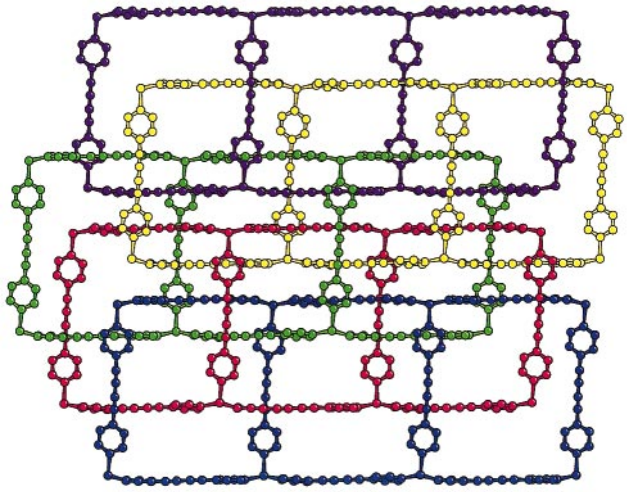


**Fig. 3** An orthogonal view whose central area shows the interpenetration of five ladders, which are distinguished by colour. The $PF_6^-$ anions, solvent molecules and coordinated MeCN are omitted for clarity.

In conclusion we have isolated a unique polycatenated undulating molecular ladder which forms interwoven two-dimensional sheets. We are currently investigating the factors that effect the formation of molecular ladders instead of the more common adamantoid networks in copper(I) bipyridyl arrays.

We thank the Nuffield Foundation and EPSRC for support.

## Footnotes and References

* E-mail: m.schroder@nott.ac.uk

† *Experimental*: $\{[Cu_2(MeCN)_2\{1,4\text{-bis(4-pyridyl)butadiyne}\}_3](PF_6)_2\}_\infty$. A solution of 1,4-bis(4-pyridyl)butadiyne (32 mg, 0.16 mmol) in MeCN (10 $cm^3$) was layered over a solution of $[Cu(MeCN)_4]PF_6$ (16 mg, 0.04 mmol) in $CH_2Cl_2$ (10 $cm^3$). Diffusion between the two phases over a period of days gave a homogeneous red solution. Diethyl ether was then diffused into the solution to give deep red crystals.

‡ *Crystal data* for $\{[Cu_2(MeCN)_2\{1,4\text{-bis(4-pyridyl)butadiyne}\}_3](PF_6)_2\}_\infty \cdot 0.5MeCN \cdot 0.5Et_2O$: $C_{49}H_{35}Cu_2F_{12}N_{8.5}O_{0.5}P_2$, $M$ = 1167.88, triclinic, space group $P\bar{1}$ (no. 2), $a$ = 12.789(6), $b$ = 15.139(6), $c$ = 16.192(8) Å, $\alpha$ = 110.59(5), $\beta$ = 91.36(4), $\gamma$ = 107.43(4)°. $U$ = 2771(2) Å$^3$, $Z$ = 2, $F(000)$ = 1177, $D_c$ = 1.400 g cm$^{-3}$, $\mu$(Mo-K$\alpha$) = 0.907 mm$^{-1}$. A red tabular crystal (0.30 × 0.16 × 0.15 mm) was used for data collection on a Stoe Stadi-4 four-circle diffractometer (graphite-monochromated Mo-K$\alpha$ radiation, $\omega$–$\theta$ scans, $\theta_{max}$ = 22.5°). No absorption correction was applied, 7210 unique reflections [$R_{int}$ = 0.0676], of which 4256 had $I \geqslant 2\sigma(I)$, were used in all calculations. A correction for crystal decay (37%) was applied during data reduction. The structure was solved using direct methods[9] and all non-H atoms were located using subsequent difference-Fourier methods.[10] Both $PF_6^-$ anions were found to be disordered, the first with each F atom split over two sites of occupancy 0.75 and 0.25, the second with the whole $PF_6^-$ disordered over two equally occupied sites. The MeCN and $Et_2O$ molecules were both found to have a half occupancy in their respective sites. Hydrogen atoms were placed in calculated positions and were allowed to ride on their parent atoms. The weighting scheme $w^{-1} = [\sigma^2(F_o^2) + (0.2P)^2]$, $P = [\text{max.}\ (F_o^2,0) + 2F_c^2]/3$ was adopted. At final convergence[10] $R_1$ [$I > 2\sigma(I)$] = 0.1232, $wR_2$ (all data) = 0.3699 for 649 parameters, $S$ = 1.219, $(\Delta/\sigma)_{max}$ = 0.008, $\Delta\rho_{max}$ = 0.94 e Å$^{-3}$. The high value for $R_1$ is attributed to the effects of crystal decay. CCDC 182/608.


1 R. Robson, B. F. Abrahams, S. R. Batten, R. W. Gable, B. F. Hoskins and J. Liu, *Supramolecular Architecture*, ACS publications, 1992, ch. 19; S. R. Batten, B. F. Hoskins and R. Robson, *Angew. Chem.*, 1997, **109**, 652; *Angew. Chem., Int. Ed. Engl.*, 1997, **36**, 636; B. F. Hoskins, R. Robson and D. A. Slizys, *J. Am. Chem. Soc.*, 1997, **119**, 2952; L. Carlucci, G. Ciani, D. M. Proserpio and A. Sironi, *J. Chem. Soc., Chem. Commun.*, 1994, 2755; S. Subramanian and M. J. Zaworotko, *Angew. Chem.*, 1995, **107**, 2295; *Angew. Chem., Int. Ed. Engl.*, 1995, **34**, 2127; B. F. Abrahams, S. R. Batten, H. Hamit, B. F. Hoskins and R. Robson, *Angew. Chem.*, 1996, **108**, 1794; *Angew. Chem., Int. Ed. Engl.*, 1996, **35**, 1691; D. Venkataraman, S. Lee, J. S. Moore, P. Zhang, K. A. Hirsch, G. B. Gardner, A. C. Covey and C. L. Prentice, *Chem. Mater.*, 1996, **8**, 2030; M. A. Withersby, A. J. Blake, N. R. Champness, P. Hubberstey, W.-S. Li and M. Schröder, *Angew. Chem., Int. Ed. Engl.*, 1997, in the press; A. J. Blake, N. R. Champness, S. S. M. Chung, W.-S. Li and M. Schröder, *Chem. Commun.*, 1997, 1675.

2 G. R. Desiraju in *Crystal Engineering: Design of Organic Solids*, Elsevier, Amsterdam, 1989; *The Crystal as a Supramolecular Entity*, ed. G. R. Desiraju, Wiley, 1995; G. R. Desiraju, *Angew. Chem., Int. Ed. Engl.*, 1995, **34**, 2311.

3 D. B. Amabilino and J. F. Stoddart, *Chem. Rev.*, 1995, **95**, 2725.

4 A. J. Blake, N. R. Champness, S. S. M. Chung, W.-S. Li and M. Schröder, *Chem. Commun.*, 1997, 1005.

5 A. J. Blake, N. R. Champness, A. Khlobystov, D. A. Lemenovskii, W.-S. Li and M. Schröder, *Chem. Commun.*, 1997, 1339.

6 L. R. MacGillivary, S. Subramanian and M. J. Zaworotko, *J. Chem. Soc., Chem. Commun.*, 1994, 1325.

7 M. Fujita, Y. J. Kwon, O. Sasaki, K. Yamaguchi and K. Ogura, *J. Am. Chem. Soc.*, 1995, **117**, 7287.

8 P. Losier and M. J. Zaworotko, *Angew. Chem.*, 1996, **108**, 2957; *Angew. Chem., Int. Ed. Engl.*, 1996, **35**, 2779; T. L. Hennigar, D. C. Macquarrie, P. Losier, R. D. Rogers and M. J. Zaworotko, *Angew. Chem.*, 1997, **109**, 1044; *Angew. Chem., Int. Ed. Engl.*, 1996, **36**, 972.

9 G. M. Sheldrick, SHELXS-86, *Acta Crystallogr., Sect. A*, 1990, **46**, 467.

10 G. M. Sheldrick, SHELXL-93, University of Göttingen, Germany, 1993.


*Received in Cambridge, UK, 11th August 1997; 7/05853E*

# Stabilization of aragonite on thiol-modified gold surfaces: effect of temperature

**Jörg Küther and Wolfgang Tremel***

*Institut für anorganische und analytische Chemie, Johannes Gutenberg-Universität Mainz, J. J. Becherweg 24, D-55099 Mainz, Germany*

**While the slow crystallization of calcium carbonate at 22 °C on self-assembled ω-substituted alkylthiol surfaces yields in most cases, depending on the surface, the vaterite and calcite modifications, elevating the temperature to 45 °C allows the stabilization of the aragonite modification as well.**

The number of minerals known to be formed in biological systems has increased considerably during the past few years. The majority of these minerals contain Ca, and the precision by which these minerals are replicated in terms of structure, morphology and distribution indicates that the mechanisms of nucleation, growth and organization are specific for any biological system. Interest in the controlled crystallization of calcium carbonate is twofold. First, there is the geological and biological ubiquity of the various mineral modifications of $CaCO_3$, *viz*., calcite, vaterite and aragonite. Secondly these are interesting model systems for heterogeneous nucleation at organic–inorganic boundaries, such as those involved in natural biomineralization processes.[1] Extensive studies on $CaCO_3$ crystals grown under Langmuir films and in the presence of additives have been reported.[2,3] The crystallization of the calcite modification on self-assembled monolayers (SAMs) of substituted alkyl silanes on Si(001) has also been described.[4] We have been interested in the factors that determine why one modification is preferred over another, as well as crystal habit and how it can be controlled. To this end, we have studied the slow crystallization of $CaCO_3$ on well characterized SAMs of ω-substituted alkylthiols of different chain lengths, which build up highly ordered surfaces.[5] Depending on the ω-substituent, we are able to obtain calcite and vaterite phases at 22 °C either in pure form or as mixtures, with the actual proportions being determined by the Rietveld refinement of the powder X-ray profiles. In one case, to be described later, aragonite is also obtained. The focus of this work is our finding that by elevating the temperature at which the crystallization is carried out to 45 °C, we observe the stabilization of the aragonite modification as well. On certain surfaces, notably $HS(CH_2)_3SO_3Na$-modified Au, aragonite is the principal phase. This is of some importance since previous reports of aragonite crystallization under mild conditions have been carried out only in the presence of extraneous molecules or cations such as $Mg^{2+}$ or $Li^+$,[6,7] with the exception of a recent report on the template-directed synthesis of aragonite under Langmuir films of 5-hexadecyloxyisophthalic acid.[8] Here, we discuss the growth of $CaCO_3$ on a few surfaces, comparing the results of crystallization carried out at 45 °C with the results obtained on the same surfaces when the crystallization is carried out at 22 °C. We thus attempt to find factors that favour the formation of aragonite under these relatively mild conditions.

The glass/Cr/Au substrates used for crystallization were prepared by vacuum evaporation with film thickness being monitored using a quartz crystal oscillator. The SAMs were grown from ethanol solutions. Surface plasmon spectroscopy, contact angle measurements and reflectance FTIR spectroscopy were used to characterize the SAMs. Calcium carbonate crystallization was performed in a closed desiccator using solid $(NH_4)_2CO_3$ to raise, by diffusion,[9] the $CO_3^{2-}$ concentration of $CaCl_2$ solution.† The substrates were held downwards in solution to prevent gravitational precipitation. The whole apparatus was placed in an oven to control the temperature. Crystallization times were typically 48 h. The formation of crystals was followed by SEM (Zeiss DSM 962) and by PXRD (Siemens D5000) in transmission geometry with the crystals transferred from the substrates to Scotch™ tape. Fig. 1(*a*) shows an SEM micrograph of $CaCO_3$ crystals on the $HS(CH_2)_{15}CO_2H$-modified Au surface on which they have been grown. The three different crystal modifications are clearly seen, being small platelets of vaterite in the middle left, small well formed rhombs of calcite, and preponderantly, running diagonally across are clusters of aragonite needles.

Fig. 1(*b*) shows one such cluster of aragonite needles at higher magnification. The morphology is familiar from previous work, with the growth (needle) axis being in the *c* direction of the unit cell. Nucleation of the clusters take place along a line, as seen from panel (*a*) of this figure, and this

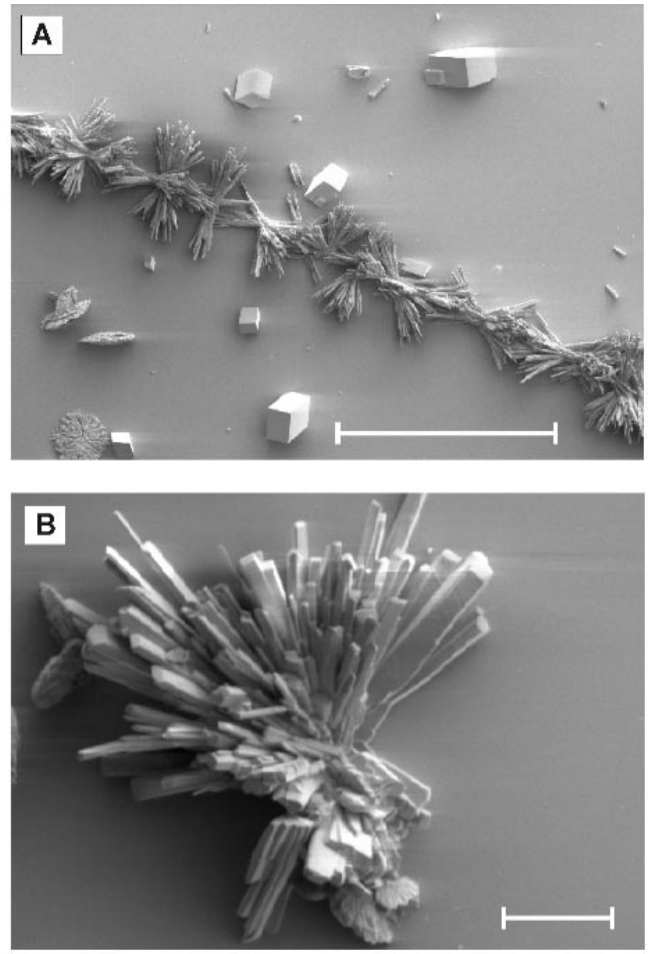



**Fig. 1** Scanning electron micrographs of calcium carbonate crystals on a $HS(CH_2)_{15}CO_2H$-modified Au surfaces. (*a*) Low magnification (bar = 200 μm), (*b*) high magnification (bar = 20 μm) of a cluster of aragonite needles.

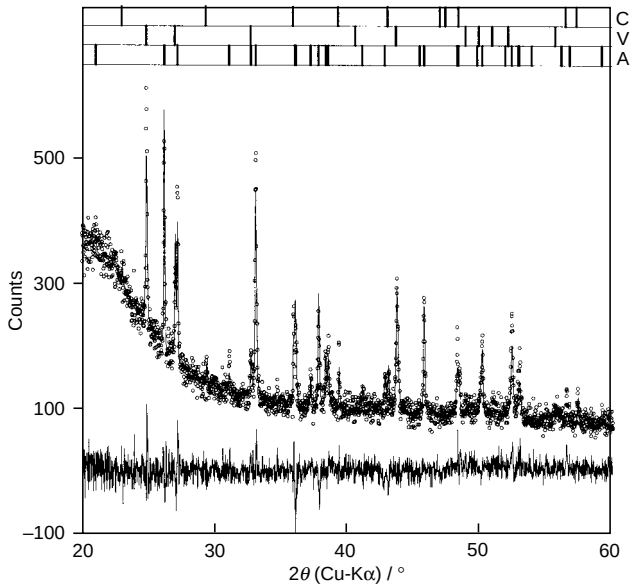



**Fig. 2** Powder X-ray data (points), Rietveld profile fits(lines) and difference profiles of $CaCO_3$ crystals grown on a $HS(CH_2)_3SO_3Na$-modified surface at 45 °C. The horizontal lines mark expected reflection positions for calcite (C), vaterite (V) and aragonite (A).

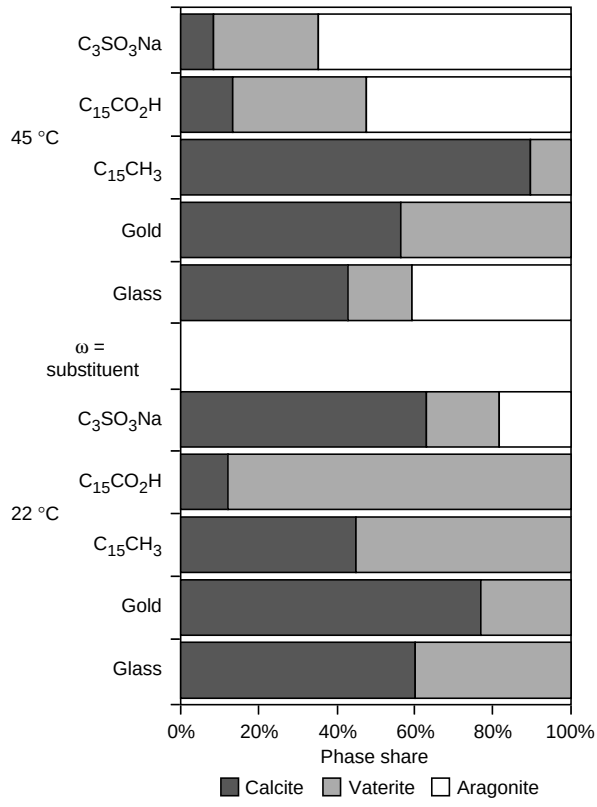



**Fig. 3** Histogram of phase composition obtained from Rietveld refinements of powder X-ray profiles from crystals of $CaCO_3$ grown at 22 and 45 °C on different substrates (indicated) $C_{15}CH_3$ refers to $HS(CH_2)_{15}CH_3$, ($C_{15}CO_2H$) to $HS(CH_2)_{15}CO_2H$ and $C_3SO_3Na$ to $HS(CH_2)_3SO_3Na$. We estimate the absolute errors to be < 10%.

provides some clues to factors that favour aragonite formation as discussed presently.

To improve quantification, we have acquired powder X-ray profiles and analyzed them using the Rietveld method[10] incorporated in the XND program.[11] Scale factors, lattice and profile parameters, including preferred orientations were refined. The structures were taken from the literature.[12–14] Actual mass fractions were estimated from the scale factors using the procedures discussed in ref. 15. Since estimating volumes of the crystallites is difficult in the present case, Brindley corrections were not applied.[16] These and other factors such as disparate crystallite sizes and poor powder averaging (due to the sub-milligram quantities used) are expected to decrease the reliability of such estimates. Fig. 2 shows a typical Rietveld profile fit for $CaCO_3$ grown on a $HS(CH_2)_3SO_3Na$-modified Au surface. Using this Rietveld procedure we illustrate in Fig. 3 histograms of the quantities of the different modifications of $CaCO_3$ grown on five different surfaces, clean glass, clean gold, and SAMs of $HS(CH_2)_{15}CO_2H$, $HS(CH_2)_3SO_3Na$ and $HS(CH_2)_{15}CH_3$, at 22 and at 45 °C. It is interesting that a small temperature difference can result in such large changes in the preference of one modification over others.

We now attempt to identify the factors that might favour aragonite growth. We note that aragonite formation in solution is generally favoured at higher temperatures.[17] Clearly, the fact that aragonite grows on clean glass disallows templating being invoked as the only responsible parameter in the present case. Since clean gold and the long chain alkyl terminated thiol do not show up any aragonite even at 45 °C, we believe that aragonite is not favoured on highly ordered surfaces. Polar, short-chain (and hence less ordered) SAMs on the other hand, seem to favour aragonite. Indeed of the ten or more surfaces examined, the SAM of $HS(CH_2)_3SO_3Na$ is the only one which is able to induce aragonite crystallization even at 22 °C. Going back to Fig. 1(*a*), we see that the nucleation in this case takes place along a line which is probably a step or a terrace boundary on the surface, where the local roughness might be high. The present observation of aragonite on certain surfaces and not on others at 45 °C thus is likely to be due to the combined effects of promotion on the one hand as well as inhibition on the surfaces where it is not observed.

We thank Professor W. Knoll (Max-Planck-Institut für Polymerforschung) for help and encouragement and Dr R. Seshadri for assistance with the Rietveld refinements and the Fonds der chemischen Industrie for financial support.

## Footnotes and References

* E-mail: tremel@indigotrem1.chemie.uni-mainz.de

† Crystals of calcium carbonate were grown on gold-coated (50 nm thick) glass substrates in a 10 mM solution of $CaCl_2 \cdot 4H_2O$ (Merck, Suprapur™) in pure water (Barnstead Easypure UV, $\rho$ > 18.3 MΩ cm); the pH was adjusted to 10 with 0.1 M NaOH. Temperatures for crystallization were 22 ± 3 and 45 ± 2 °C.

1 H. A. Lowenstam and S. Weiner, in *On Biomineralisation*, Oxford University Press, New York, 1989.
2 S. Mann, F. C. Meldrum, B. R. Heywood, D. D. Archibald, J. M. Didymus and V. J. Wade, *MRS Bull.*, 1992, 32.
3 L. Leiserowitz, D. Jacquemain, S. G. Wolf, F. Leveiller, M. Deutsch, K. Kjaer, J. Als-Nielsen and M. Lahav, *Angew. Chem.*, 1992, **104**, 134.
4 D. D. Archibald, S. B. Quadri and B. P. Gaber, *Langmuir*, 1996, **12**, 538.
5 A. Ulman, *Chem. Rev.*, 1996, **96**, 1533.
6 S. Mann and B. R. Heywood, *Chem. Mater.*, 1994, **6**, 311.
7 S. Mann, S. D. Sims and J. M. DIdymus, *J. Chem. Soc., Chem. Commun.*, 1995, 1031.
8 S. Mann, A. L. Litvin, S. Valiyaveettil and D. L. Kaplan, *Adv. Mater.*, 1997, **9**, 124.
9 S. Weiner, S. Albeck and L. Addadi, *Chem. Eur. J.*, 1996, **2**, 278.
10 H. M. Rietveld, *J. Appl. Crystallogr.*, 1969, **2**, 65.
11 J. F. Berar and P. Garnier, in *Accuracy in Powder Diffraction, Proc. II, Intl. Conf. Gaithersburg*, 1992, *NIST Special Publ.*, 1992, **846**, 212.
12 R. Wartchow, *Z. Kristallogr.*, 1989, **186**, 300.
13 S. R. Kamhi, *Acta Crystallogr.*, 1963, **16**, 770.
14 J. P. R. de Villiers, *Am. Mineral.*, 1971, **56**, 758.
15 J. Rodriguez-Carvajal, manual of the FullProf Rietveld program; Collected Abstracts of Powder Diffraction Meeting, Toulouse, France; 1990, p. 127.
16 G. W. Brindley, *Philos. Mag.*, 1945, **36**, 347.
17 J. L. Wray and F. Daniels, *J. Am. Chem. Soc.*, 1957, **79**, 2031.

*Received in Basel, Switzerland, 30th May 1997; 7/03775I*

# Visualisation of axial chirality using $^2$H-{$^1$H} NMR in poly(γ-benzyl L-glutamate), a chiral liquid crystal solvent

**William Smadja,[a]† Sandie Auffret,[a] Philippe Berdagué,[a] Denis Merlet,[a] Cécile Canlet,[a] Jacques Courtieu,*[a]‡ Jean-Yves Legros,[b] André Boutros[b] and Jean-Claude Fiaud[b]**

[a] *Laboratoire de Chimie Structurale Organique, URA-CNRS 1384, Institut de Chimie Moléculaire Organique Bâtiment 410, Université de Parix XI, 91405 Orsay, France*
[b] *Laboratoire des Réactions Organiques Sélectives, URA-CNRS 1497, Institut de Chimie Moléculaire Organique Bâtiment 420, Université de Parix XI, 91405 Orsay, France*

**Disubstituted, racemic, axially chiral compounds with true and isotopic chiralities have been discriminated through the differential ordering effect of enantiomers when dissolved in a chiral liquid crystal solvent made of organic solutions of poly(γ-benzyl L-glutamate).**

As a result of the widespread interest in the axial chirality found in allenes[1–4] and alkylidenecyclohexanes,[5] it is important to develop a general, reliable and precise method for the measurement of their enantiomeric excesses (ees).[1] It is already known that, for some disubstituted allenes, the use of $^1$H NMR chiral lanthanide shift reagents (CLSR)[1,6a–c] and $^{195}$Pt[1] and $^{31}$P[6d] NMR chiral derivatising agents (CDA), give good results. Recently, ees of trisubstituted allenes and bromoallenes were determined by $^1$H NMR[6e] using as a permethylated β-cyclodextrin a chiral solvating agent (CSA).

A direct and very efficient technique has been recently developed in our laboratory, using deuterium NMR in a chiral liquid crystal medium made of organic solutions of poly(γ-benzyl L-glutamate) (PBLG).[7a–c] This technique appears to be much more sensitive and more general than those previously described in which only the variation of a chemical shift is utilised. In our anisotropic environment, enantiomers have different averaged orientations towards the PBLG α-helix which results in a difference in the order-sensitive NMR interactions, noticeably the deuterium quadrupolar splitting ($\Delta\nu_Q$). Thus the proton-decoupled deuterium NMR [$^2$H-{$^1$H} NMR] spectrum of a chiral deuteriated substrate in a PBLG–organic solvent medium is evident and appears as two quadrupolar doublets, one for each enantiomer. A schematic illustration is given for a 50% ee mixture (Fig. 1).

The differential ordering effect[8] of enantiomers may be defined as the difference between the quadrupolar splittings of the *R* and *S* molecules: DOE = $|\Delta\nu_Q^R - \Delta\nu_Q^S|$. More conveniently the DOE value relative to the average splitting is used; eqn. (1). The NDOE may be seen as an enantiomeric discrimination measurement.

$$\text{NDOE} = (|\Delta\nu_Q^R - \Delta\nu_Q^S|)/[\tfrac{1}{2}(|\Delta\nu_Q^R| + |\Delta\nu_Q^S|)] \qquad (1)$$

This communication describes the application of the PBLG method to visualise axially chiral racemic compounds **1**–**4**§

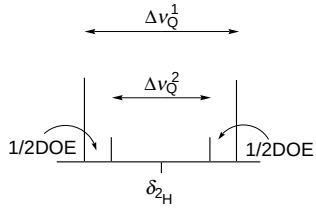
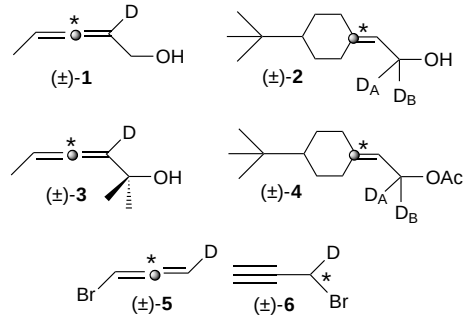



**Fig. 1** Enantiomer visualisation using $^2$H-{$^1$H} NMR in PBLG. When the enantiomers are not assigned, the superscripts *R* and *S* in eqn. (1) are replaced by 1 and 2.




bearing *polar* substituents. The $^2$H-{$^1$H} NMR spectra in PBLG–organic solvent media of products **1**–**4** have been recorded. For all of them the discrimination between enantiomers is large enough to allow an accurate ee measurement (Fig. 2). The enantiomers of primary alcohols **1** and **2** appeared as one and two pairs of doublets respectively. The deuterium of

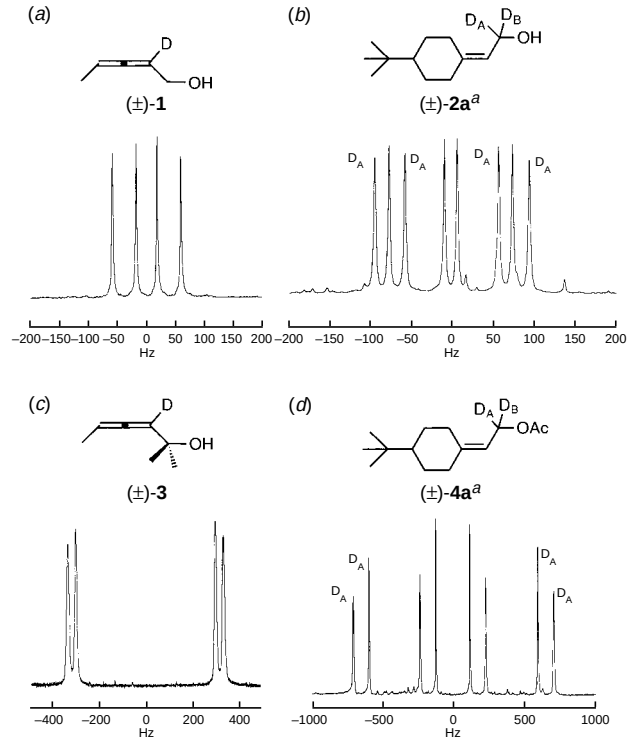



**Fig. 2** Visualisation of axial chiralities in compounds (±)-**1**–(±)-**4** using $^2$H-{$^1$H} NMR (64.1 MHz) in PBLG–organic solvent mixture. [a] For clarity, only diastereotopic deuteriums $D_A$ are quoted, the remaining signals belong to $D_B$.

**Table 1** Enantiomeric discrimination of racemic axially chiral compounds (±)-**1**–(±)-**5** using $^2$H-{$^1$H} NMR (64.1 MHz at 300 K) in PBLG–organic solvent

| Entry/ compound no. | Solvent | PBLG (%) | $\Delta\nu_Q^1$/ Hz[a] | $\Delta\nu_Q^2$/ Hz[a] | NDOE |
|---|---|---|---|---|---|
| **1** | $CH_2Cl_2$ | 14 | 118 | 36 | 1.06 |
| | | | 164 | 96 | 0.52 ($D_A$) |
| **2** | $CH_2Cl_2$ | 14 | | | |
| | | | 141 | 19 | 1.51 ($D_B$) |
| **3** | DMF | 30 | 664 | 595 | 0.11 |
| | | | 1413 | 1190 | 0.17 ($D_A$) |
| **4**[b] | DMF | 30 | | | |
| | | | 462 | 239 | 0.63 ($D_B$) |
| **5** | $CHCl_3$ | 19 | 231 | 174 | 0.28 |
| **6** | $CHCl_3$ | 19 | 951 | 631 | 0.40 |

[a] For racemic compounds (±)-**1**–(±)-**6**, quadrupolar splittings of the *R* and *S* enantiomers are not known at this stage, therefore, in the formula (see text) superscripts *R* and *S* are replaced by 1 and 2 [eqn. (1)]. [b] At 320 K.

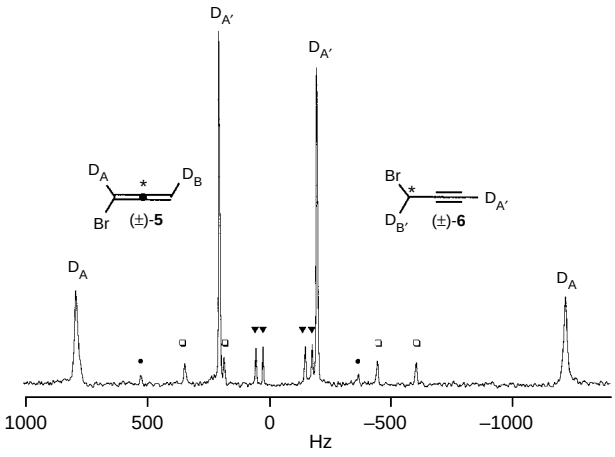



**Fig. 3** Visualisation of allenic and prop-2-ynylic isotopic chiralities in compounds (±)-**5** and (±)-**6** using $^2$H-{$^1$H} NMR (64.1 MHz) in PBLG, $CHCl_3$ at 300 K; (●) $CDCl_3$, (▼) $D_B$ in (±)-**5** and (□) $D_{B'}$ in (±)-**6**

allene **1** is split with an NDOE value of 1.06 (entry 1, Table 1) [Fig. 2(*a*)], whereas the $D_A$ and $D_B$ diastereotopic deuteriums of methylenecyclohexane **2**, are split with NDOEs of 0.52 and 1.51 respectively (entry 2, Table 1) [Fig. 2(*b*)]. The excellent visualisation of the enantiomers of alcohols **1** and **2** is probably due to a hydrogen-bond interaction between their primary hydroxy groups and the PBLG in $CH_2Cl_2$. Indeed, in this solvent, low or even no discrimination was observed with the corresponding tertiary alcohol **3** and primary acetate **4** respectively, which are known to give poor hydrogen-bonding associations. The enantiomers of **3** and **4**, are well-differentiated only when $CH_2Cl_2$ is replaced by DMF, together with a PBLG concentration increasing from 14 to 30%. Again, two and four doublets were observed for **3** and **4**, with NDOEs of 0.11, 0.17 and 0.63 respectively (entries 3 and 4, Table 1) [Fig. 2(*c*) and (*d*)]. In the methylenecyclohexanes **2** and **4**, the differentiation of diastereotopic deuteriums with no-discrimination through their chemical shifts ($\delta_A$ and $\delta_B$), mainly arises from a different orientation of the C–$D_A$ and C–$D_B$ bonds towards the magnetic field [Fig. 2(*b*) and (*d*)].

The efficiency of the PBLG technique may be emphasised by the result obtained with the allenic bromide **5**§ which is chiral only by virtue of an isotopic substitution. It is worth noting that the enantiomers of this compound, now, identically orientated but with an axis of isotopic chirality, are discriminated with an NDOE of up to 0.28 (entry 5, Table 1) (Fig. 3). Furthermore and as expected, enantiomers of an acetylenic counterpart **6**§ with a centro-symmetric isotopic chirality[7c] are also discriminated (entry 6, Table 1) (Fig. 3).

In conclusion, the $^2$H-{$^1$H} NMR spectra in PBLG successfully discriminate enantiomers with the axis of true chirality found in allenes **1**, **3** and methylenecyclohexanes **2**, **4** bearing *polar* substituents, whether or not the substituents interact strongly through hydrogen-bonding with PBLG. Whereas, enantiomers of bromoallene **5** with an axis of isotopic chirality are clearly visualised by our method.

## Footnotes and References

† E-mail: wismadja@icmo.u-psud.fr
‡ E-mail: courtieu@icmo.u-psud.fr

§ Compounds **1**–**6** gave satisfactory mass and/or $^1$H, $^2$H and $^{13}$C NMR data. Allenols **1** and **3** were synthesised by the Landor method[2] ($LiAlD_4$ reduction of mono-THP-ether of prop-2-ynylic glycol followed by elimination of OTHP). Bromides **5** and **6** were obtained as a mixture by the Elsevier method[3] (bromination of prop-2-ynylic tosylate followed by a prop-2-ynylic–allenic rearangement). Finally, **2** and **4** were obtained by Wittig–Horner reaction of 4-*tert*-butyl cyclohexanone[5] followed by $LiAlD_4$ reduction and subsequent esterification using $Ac_2O$, DMAP and $Et_3N$.

1 For ee determination by NMR, see D. Parker, *Chem. Rev.*, 1991, **91**, 1441. Ee determination of α-deuteriated primary chiral molecules (acids, alcohols and amines) using $^2$H NMR of CDAs, have previously been described, see D. Parker, *J. Chem. Soc., Perkin Trans. 2*, 1983, 83.
2 For synthesis of α-allenols, see: (*a*) J. S. Cowie, P. D. Landor and S. R. Landor, *J. Chem. Soc., Chem. Commun.*, 1969, 541; (*b*) L.-I. Olsson and A. Claesson, *Acta Chem. Scand., Ser. B*, 1977, **31**, 614; see also (*c*) H. F. Schuster and G. M. Coppola, *Allenes in Organic Chemistry*, Wiley, New York 1984, p. 132–45.
3 For synthesis of bromoallenes, see ref. 2(*c*) pp. 272–280.
4 For a review on stereoselective reactions on allenes see W. Smadja, *Chem. Rev.*, 1983, **83**, 263.
5 M. Duraisamy and H.M. Walborsky, *J. Am. Chem. Soc.*, 1983, **105**, 3252.
6 For ee determination for allenes using CLSRs see (*a*) A. Claesson, L.-I. Olsson, G. R. Sullivan and H. S. Mosher, *J. Am. Chem. Soc.*, 1975, **97**, 2919; (*b*) see ref. 2(*b*); CDAs: (*c*) P. Salvadori, G. Uccello-Baretta, R. Lazzaroni and A. M. Caporusso, *J. Chem. Soc., Chem. Commun.*, 1990, 1121; (*d*) D. Parker and R. J. Taylor, *Tetrahedron*, 1988, **44**, 2241; see also A. Alexakis, J. C. Frutos, S. Mutti and P. Mangeney, *J. Org. Chem.*, 1994, **59**, 3326; CSAs; (*e*) G.Uccello-Baretta, F. Balzano, A. M. Caporusso and P. Salvadori, *J. Org. Chem.*, 1994, **59**, 836. Enantiomers of trisubstituted bromoallenes have been visualised with $\Delta\delta$ = 1.8 Hz on a 300 MHz machine.
7 For ee determination using $^2$H-{$^1$H} NMR in PBLG, see (*a*) J. P. Bayle, J. Courtieu, E. Gabetty, A. Lowenstein and J.-M. Péchiné, *New J. Chem.*, 1992, **16**, 1837; (*b*) A. Meddour, I. Canet, A. Lowenstein, J.-M. Péchiné and J. Courtieu, *J. Am. Chem. Soc.*, 1994, **116**, 9652; (*c*) I. Canet, J. Courtieu, A. Lowenstein, A. Meddour and J.-M. Péchiné, *J. Am. Chem. Soc.*, 1995, **117**, 6520.
8 For the DOE and NDOE concepts, see P. Lesot, Y. Gounelle, D. Merlet, A. Lowenstein and J. Courtieu, *J. Phys. Chem.*, 1995, **99**, 14871.

*Received in Liverpool, UK, 14th July 1997; 7/05036D*

# On the Diels–Alder reactivity of β,β-difluorinated dienophiles

**P. J. Crowley,[b] J. M. Percy*[a] and K. Stansfield[a]†**

[a] *School of Chemistry, University of Birmingham, Edgbaston, Birmingham, UK B15 2TT*
[b] *Zeneca Agrochemicals, Jealotts Hill Research Station, Bracknell, Berkshire, UK RG12 6EY*

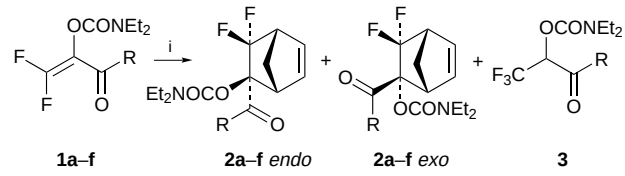
**A range of substituted β,β-difluoroenones and a β,β-difluoroalkenoate underwent [4 + 2] cycloadditions with cyclopentadiene, and other dienes, under thermal and Lewis acid-catalysed conditions.**

In the burgeoning area of the chemistry of fluorinated building blocks,[1] there are few concise ways of building ring systems that contain a fluorinated or difluorinated carbon atom. Diels–Alder cycloadditions of activated fluorinated dienophiles would therefore be extremely useful, but there are very few relevant reports. One tantalising example was provided by Leroy *et al.*[2] who described the [4 + 2] cycloaddition reaction between methyl 2,2-difluoropropenoate and furan in an approach to fluorinated analogues of shikimic acids. While the dienophile could be prepared *via* a reasonably short sequence, the cycloaddition and the manipulation of the cycloadducts were problematic and there do not appear to be any subsequent examples of applications of this chemistry.

Difluoroalkenyl compounds that contain electron-withdrawing groups undergo conjugate addition/elimination reactions which lead to loss of fluoride ion. Concomitant overall hydrofluorination follows, presenting a serious obstacle to the development of new chemistry. However, the presence of an *N*,*N*-diethylcarbamoyloxy group at the α-position in a β,β-difluoro dienophile offers some stabilisation against the side reaction.[3,4] Recently, we described some vinylcopper chemistry that allowed access to β,β-difluoroenones **1a**–**f**.[5] Heating the enones in sealed tubes in the presence of excess cyclopentadiene afforded inseparable mixtures of cycloadducts **2a**–**f** in moderate to good yields (Scheme 1, Table 1).‡ Stereoselectivities were low,[6] favouring the stereoisomer in which the π-acceptor group occupied the *exo* orientation. The *exo* : *endo* ratio increased as the ketonic alkyl group increased in size, while the yields of cycloadducts and hydrofluorination product **3** decreased and increased respectively. The stereoisomer ratios were determined by integrating $^{19}$F NMR spectra. Structural correlation was achieved by dihydroxylation[7] of the crude *exo*–*endo* mixture followed by separation and crystallisation of the major diol product; the crystal structure data will be reported elsewhere.

Thermal reactions with all other dienes failed and **3** was isolated as the sole product. In an attempt to achieve cycloaddition at lower temperatures, we examined the effect of added trimethylsilyl trifluoromethanesulfonate ($Me_3SiOTf$) on the reaction and found that cycloaddition occurred between −78 °C and ambient temperature, and that the reaction became highly stereoselective (*exo* : *endo* = 8 : 1). Although the yield of isolated cycloadduct was lower, the reaction was more efficient in diene, requiring only 1 equiv. under the catalytic conditions. Nevertheless, other dienes still failed to react and the formation of **3** predominated. Other Lewis acids [such as $TiCl_4$, $Sc(OTf)_3$, $Yb(OTf)_3$, $ZnI_2$] were ineffective promoters and **3** was formed instead.[8]

Palladium-catalysed coupling§ of our vinylcopper reagent with ethyl chloroformate[9] afforded **4**, a considerably more robust and (one order of magnitude) less reactive compound, which has undergone (to date) a limited number of Diels–Alder reactions affording cycloadducts with cyclopentadiene (**5a**, **5b**




**1a–f** **2a–f** *endo* **2a–f** *exo* **3**

**Scheme 1** *Reagents and conditions*: i, cyclopentadiene, sealed tube, 100 °C, hydroquinone

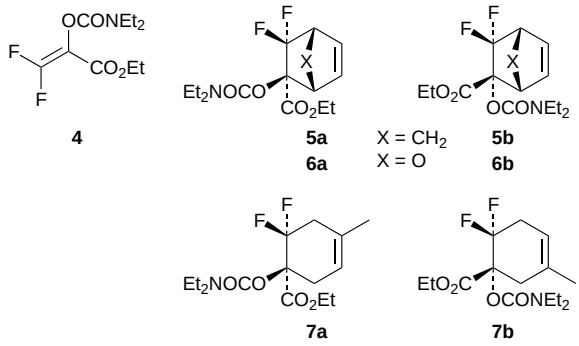
**Table 1**




**A** **B** **C**

| Diene | Dienophile | R | Conditions[a] | Cycloadduct | Yield (%)[b] | Ratio (*exo* : *endo*)[c] | **3** (%)[c] |
|---|---|---|---|---|---|---|---|
| **A** | **1a** | Ph | A | **2a** | 64 | 1 : 1 | 10 |
| **A** | **1b** | Et | A | **2b** | 81 | 1.5 : 1 | 0 |
| **A** | **1b** | Et | B | **2b** | 54 | 8 : 1 | 0 |
| **A** | **1c** | Bu$^n$ | A | **2c** | 54 | 1.5 : 1 | 0 |
| **A** | **1d** | Bu$^i$ | A | **2d** | 67 | 1.5 : 1 | 5 |
| **A** | **1e** | Pr$^i$ | A | **2e** | 64 | 2.5 : 1 | 5 |
| **A** | **1f** | Bu$^t$ | A | **2f** | 17 | 3 : 1 | 34 |
| **A** | **4** | — | C | **5** | 74 | 1.5 : 1 | — |
| **B** | **4** | — | D | **6** | 5[d] | 1.5 : 1 | — |
| **B** | **4** | — | E | **6** | 20 | 1.5 : 1 | — |
| **C** | **4** | — | D | **7** | 67[d,f] | — | — |

[a] Conditions: A, neat cyclopentadiene (20 equiv.), 100 °C, 4 h, sealed tube; B, cyclopentadiene (1.0 equiv.), $Me_3SiOTf$ (0.1 equiv.), $CH_2Cl_2$, −78 °C to room temp.; C, neat cyclopentadiene (20 equiv.), 100 °C, 40 h, sealed tube; D, neat diene (20 equiv.), 100 °C, 72 h, sealed tube; E, neat furan (20 equiv.), $ZnI_2$ (0.5 equiv.), 80 °C, 48 h. [b] Isolated yields after chromatography are reported. [c] Determined by $^{19}$F NMR spectroscopy. [d] Starting material **4** was also recovered. [e] Ratio based on isolated yields after chromatographic separation of stereoisomers. [f] A 1 : 1 mixture of regioisomeric products was isolated.




74%), furan (**6a**, **6b** 20%, zinc iodide catalysis) and isoprene (**7**, 67%). Importantly, the alkenoate could be recovered from each reaction suggesting that considerable scope exists for the development of efficient catalytic conditions and thus, mild general syntheses of highly functionalised difluorinated cyclohexene derivatives. We should emphasise that the lower reactivity is acceptable because the problematic hydrofluorination reaction appears to be considerably slower in the case of **4**. We now wish to explore the effects exerted by the *N*,*N*-dialkylcarbamoyloxy group upon the stereoselectivity and reactivity of these transformations.

## Footnotes and References

* E-mail: jmpercy@chemistry.bham.ac.uk
† Current address: Noguchi Institute, 1-8-1, Kaga, Itabashi-Ku, Tokyo 173, Japan.

‡ *Typical procedure* for **2b** *exo*/*endo*: Enone **1b** (0.24 g, 1 mmol) was dissolved in freshly-cracked cyclopentadiene (1.32 ml, 20 mmol) together with a crystal of hydroquinone. The mixture was degassed and sealed in a ACE pressure tube which was immersed in an oil bath (100 °C). After 4 h, the tube was removed from the bath, cooled and opened. Purification of the residue by flash column chromatography (10% ethyl acetate–hexane, $R_f$ = 0.18) afforded adducts *exo* and *endo* **2b** as a clear oil (0.24 g, 81%).

*Exo*: $\delta_H$(300 MHz; $CDCl_3$) 6.26–6.18 (2 H, m), 3.72–3.60 (1 H, m), 3.50–3.18 (4 H, m), 3.12–3.00 (1 H, m), 2.44 (2 H, q, $^2J_{H\text{-}H}$ 7.0), 2.20–2.10 (1 H, m), 1.95–1.85 (1 H, m), 1.30–1.10 (9 H, m); $\delta_F$(284 MHz; $CDCl_3$) −101.7 (1 F, d, $^2J_{F\text{-}F}$ 226.8), −106.4 (1 F, d, $^2J_{F\text{-}F}$ 226.8); $\delta_C$(75 MHz; $CDCl_3$) 204.5, 153.7, 138.1, 133.7 (d, $^3J_{C\text{-}F}$ 6.2), 127.9 (dd, $^1J_{C\text{-}F}$ 276.6, 277.1), 87.5 (dd, $^2J_{C\text{-}F}$ 30.2, 30.9), 49.4 (dd, $^2J_{C\text{-}F}$ 24.1, 20.7), 48.3, 44.3 (d, $^3J_{C\text{-}F}$ 5.3), 42.2, 42.0, 32.2, 14.2, 13.6, 7.7.

*Endo*: $\delta_H$(300 MHz; $CDCl_3$) 6.68–6.62 (1 H, m), 5.96–5.90 (1 H, m), 3.72–3.60 (1 H, m), 3.50–3.18 (4 H, m), 3.10–3.00 (1 H, m), 2.44 (2 H, q, $^2J_{H\text{-}H}$ 7.0), 2.12–2.04 (1 H, m), 1.90–1.80 (1 H, m), 1.30–1.10 (9 H, m); $\delta_F$(270 MHz; $CDCl_3$) −100.5 (1 F, d, $^2J_{F\text{-}F}$ 223.9), −104.7 (1 F, d, $^2J_{F\text{-}F}$ 223.9); $\delta_C$(75 MHz; $CDCl_3$) 203.0, 153.9, 138.9, 129.2 (d, $^3J_{C\text{-}F}$ 6.2), 127.4 (dd, $^1J_{C\text{-}F}$ 276.6, 277.1), 89.6 (dd, $^2J_{C\text{-}F}$ 27.5, 27.5), 49.4 (dd, $^2J_{C\text{-}F}$ 24.1, 20.7), 48.6, 44.3 (d, $^3J_{C\text{-}F}$ 5.3), 42.8, 42.3, 32.1, 14.4, 13.4, 7.5; *m/z* (CI) 302, (100%, $[M + H]^+$), 100 (20, $[CONEt_2]^+$); HRMS calc. for $C_{15}H_{22}NO_3F_2$: 302.15687; found: 302.15563.

§ A solution of 1-(diethylcarbamoyloxy)-2,2-difluoroethenylcopper[5] (1.37 mmol) was cooled to −78 °C and $Pd_2(dba)_3$ (0.025 g, 0.03 mmol) was added followed by ethyl chloroformate (0.35 ml, 3.24 mmol). The reaction was warmed to room temperature over 30 min then stirred for 24 h. The reaction was quenched with 10% aqueous ammonium chloride and the products extracted with $Et_2O$, then the combined organic extracts were dried ($MgSO_4$), and concentrated *in vacuo*. Flash column chromatography (10% ethyl acetate–hexane, $R_f$ = 0.14) afforded **4** as a colourless oil. (0.42 g, 67%); $\delta_H$(300 MHz; $CDCl_3$) 4.25 (2 H, q, $^3J_{H\text{-}H}$ 7.0), 3.30 (4 H, q, $^3J_{H\text{-}H}$ 7.0), 1.40–1.10 (9 H, m); $\delta_F$(284 MHz; $CDCl_3$) −81.4. (d, $^2J_{F\text{-}F}$ 9.0), −84.6 (d $^2J_{F\text{-}F}$ 9.0); $\delta_C$(75 MHz; $CDCl_3$); 163.6, 155.7 (t, $^1J_{C\text{-}F}$ 300.2), 151.6, 101.4 (t, $^2J_{C\text{-}F}$ 25.0), 61.7, 42.7, 42.2, 14.0, 13.0, 13.2; *m/z* (CI) 252 (100%, $[M + H]^+$, 100, (70 $[CONEt_2]^+$). HRMS calc. for $C_{10}H_{16}NO_4F_2N$: 252.10485; found: 252.10447.

1 J. M. Percy, *Contemp. Org. Synth.*, 1995, **4**, 251.
2 J. Leroy, H. Molines and C. Wakselman, *J. Org. Chem.*, 1987, **52**, 290.
3 P. J. Crowley, J. M. Percy and K. Stansfield, *Tetrahedron Lett.*, 1996, **37**, 8233.
4 G. Q. Shi and Z. Y. Cao, *J. Chem. Soc., Chem. Commun.*, 1995, 1969.
5 P. J. Crowley, J. A. Howarth, W. M. Owton, J. M. Percy and K. Stansfield, *Tetrahedron Lett.*, 1996, **37**, 5975.
6 O. G. Dealba, J. Chanona, F. Delgado, G. Zepeda, F. Labarrios, R. W. Bates, S. Bott, E. Juaristi and J. Tamariz, *An. Quim.*, 1996, **92**, 108 and references cited therein. Extensive studies of enones substituted at the α-position described similar low and variable stereoselectivities which are very substrate- and Lewis acid-sensitive. Arguments based upon steric and dipolar effects have been advanced as rationalisations for the experimental results.
7 V. VanRheenen, R. C. Kelly and D. Y. Cha, *Tetrahedron Lett.*, 1976, 1973.
8 J. Ichikawa, S. Miyazaki, M. Fujiwara and T. Minami, *J. Org. Chem.*, 1995, **60**, 2320.
9 J. Ichikawa, S. Hamada, T. Sonoda and H. Kobayashi, *Tetrahedron Lett.*, 1992, **33**, 337. Oxidative dimerisation of the vinylcopper reagent occurred exclusively in the absence of the palladium catalyst, in contrast to the behaviour reported by the Kyushu group.

*Received in Liverpool, UK, 3rd July 1997; 7/04717G*

# COPE elimination reaction observed in the biodegradation of quaternary ammonium surfactants

**Shaun F. Clancy,*[a]† Michael Thies[b,c] and Henrich Paradies*[b,c]‡**

[a] *Safety, Health and Environmental Affairs, Witco Corporation, One American Lane, Greenwich, CT 06831-2559, USA*
[b] *Märkische Fachhochschule, Biotechnology and Physical Chemistry, D-58590 Iserlohn, PO Box 2061, Germany*
[c] *Universität Paderborn, Fachbereich Chemie, Institut für Physikalische Chemie and Chemietechnik, D-33095 Paderborn, Germany*

**The biodegradation of dialkyldimethylammonium compounds in aqueous solutions indicates that part of the degradation pathway includes the Cope elimination reaction, which does not occur under mild conditions in the absence of microorganisms.**

This report details the first report of the Cope reaction mediated by microorganisms and starting with long-chained quaternary ammonium compounds. This reaction appears to be a key step in the biodegradation of quaternary ammonium compounds ('quats'). The quats which are the subject of this study are either dialkylethoxymethylammonium, dialkylamidoammonium or dialkylmethylimidazolinium quats.

Long-chained quaternary ammonium compounds have found use in a variety of products and sometimes end their life-cycle by disposal into wastewater or surface waters. Thus the biodegradation of these compounds has been the subject of many studies. It has been found that a wide variety of microorganisms can utilise quats as energy sources. It is also known that many microorganisms can utilise alkylamines as a substrate and use an inducible monooxygenase (EC 1.14.13.8) which is capable of oxidising the substrate to the corresponding *N*-oxide.[1] We have discovered that a key step in the biodegradation of these quats is the formation of an *N*-oxide which is formed once the quats have first degraded to an alkyldimethylamine. During our investigations of the biodegradation of dialkydimethylammonium salts (DADMA X; X = F, Cl, Br, I, OH), and subsequent determination of the metabolic pathway by fermentation of these compounds, we isolated the corresponding *N*-oxides and cleavage products of these *N*-oxides, *e.g.* the $C_{18}$ alkene and the corresponding hydroxylamine. The *N*-oxide is converted to the corresponding trialkylamine and formaldehyde (which are mineralised to $CO_2$ and $H_2O$) by an amine *N*-oxide aldolase (EC 4.1.2-) functioning as a demethylase.[2] The degradation of the quats was done using acclimated bacterial strains, fungi and yeasts for fermentation, typical of those known to be present in the environment.

The Cope reaction is the cleavage of dialkylamine *N*-oxides to produce alkenes and hydroxylamines.[3] Mild conditions are used to reduce side reactions, and the generated olefins do not normally rearrange. In this report we show the transformation of dialkyldimethylammonium salts to *N*-oxides, followed by cleavage of the *N*-oxides to the corresponding alkenes in a Cope-like process using a crude enzymatic preparation from microorganisms of environmental origin. We also show an enhancement of the kinetics of olefin formation due to the presence of the DADMA X micelles (primarily for X = OH).

Fermentation was performed with 12 strains of microorganism§ known to be present in soil and aquatic systems, including waste treatment (*Xanthomonas compestis*, salt regulative #33951, *Bacillus subtilis vulgatus* #6984, *Torulopsis* spp. #34356, together with aerobic and faculative anaerobic bacterial genera *e.g. Actinobacter, Agrobacterium, Alcaligenes, Nocardia, Arthrobacter, Cellulomonas, Mycobacterium* and *Candida albicans*). The cells were harvested, centrifuged, washed with 0.1 M $KH_2PO_4$–$K_2HPO_4$, pH 7.5 and stored at −10 °C. The intracellular contents were purified by $(NH_4)_2SO_4$ fractionation (25–65% of a saturated solution at 5 °C). The portions containing the monooxygenase activity were found in the fractions collected in 48–60% saturated $(NH_4)_2SO_4$ solutions. These fractions were used to prepare the S-100 supernatant at 5 °C. The supernatant was used as a crude enzyme preparation and stored in 10% (v/v) glycerol in the presence of 0.01 M $KH_2PO_4$–$K_2HPO_4$, 5 mM $MgCl_2$ and 1 mM β-mercaptoethanol (pH 7.8, 20 °C). The S-100 fraction containing 10–15 mg $ml^{-1}$ protein was used in the enzymatic experiments in the presence of glycerol¶ and the distearyldimethylammonium salt (DSDMA OH; 5 mM) at pH 7.8 (37–40 °C) for studying enzyme mediated olefin formation, eqn. (1), where R = $C_nH_{2n+1}$ and $n$ = 8, 10, 12, 14, 16

$$(R)_2N^+CH_3{\rightarrow}O \longrightarrow (R)CH_3NOH + CH_2{=}CH(CH_2)_{15}CH_3 \quad (1)$$

or, as in the example given here, 18. The formation of the $(R)_2N(CH_3){\rightarrow}O$ compounds have also been studied at pH 6.0 in 0.01 M borate buffer at a protein concentration of 1 mg $ml^{-1}$, in the presence of 5 mM $NADH_2^+$ (or 3.5 mM $NAD^+$), and a $NADH_2^+$ ($NAD^+$) regenerating system at 37 °C.‖ Formation of the olefins has not been observed in the absence of the crude, enzymatic mixture at 37 °C under the same conditions. However, by refluxing the *N*-oxides in xylene in the presence of 1 mM NaOH for two hours the corresponding olefin can be obtained in an almost quantitative yield. Since the formation of *N*-oxides operates only at pH 6.0–6.5 (37 °C) and the olefin formation is seen mainly in the presence of 10% (v/v) glycerol and pH 7.5–8.0, both pathways can be studied separately. The *N*-oxides studied have also been prepared chemically by reacting the appropriate amine with 30% hydrogen peroxide at 0 °C for 10 min and characterised using standard methods. The *N*-oxides obtained from the enzymatic reactions were characterised in the same fashion.

Fig. 1 shows the yields of the olefin $CH_2{=}CHC_{16}H_{33}$ generated from distearylmethylamine *N*-oxide (10 mg $ml^{-1}$) using the crude enzymatic fraction in the presence of 5 mM DSDMA X (X = OH, F, Cl, Br, I) (pH 7.8, 37 °C) and 10% (v/v) glycerol. The most effective yield is obtained in the presence of 5 mM DSDMA OH [10% (v/v) glycerol], whereas at pH 6.5 the yield is very low as it was for the Br. Furthermore, addition of 1–10 mM NaCl to the reaction medium reveals inhibition of olefin generation ($C_i$ = 6 mM NaCl, 50% inhibition). The influence of NaCl can be related to: (i) the salt induced change of the colloidal state of DSDMA OH from vesicle to micelle,[4,5] and (ii) the shifting of the equilibrium of DSDMA OH + $Cl^-$ ⟷ DSDMA Cl + $OH^-$, toward the insoluble DSDMA Cl and colloidal state of both the hydroxide and chloride.

The biotransformation of DADMA X is strongly dependent on the critical micelle concentration (CMC) pH, temperature and ionic strength.[6] The initial rate constants for the anion exchange step where DSDMA X ⟶ DSDMA OH (X = Cl,

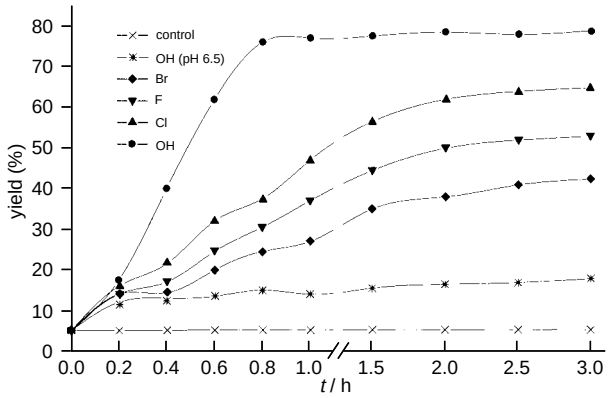



**Fig. 1** Olefin generation ($CH_2$=$CHC_{16}H_{33}$) from distearylmethylamine *N*-oxide in the presence of 5 mM DSDMA X (X = OH, F, Cl, Br) at pH 7.5, 37 °C in 0.01 M $K_2HPO_4$, 5 mM $MgCl_2$, containing 10 mg $ml^{-1}$ protein. Aliquots from the reaction vessel (10 ml) were taken after 15 min, analysed for remaining *N*-oxide and $CH_2$=$CHC_{16}H_{33}$ by GC–MS techniques.

Br) are strongly pH dependent, *e.g.* for DSDMA Cl at pH 5.0: $k^*_{app}$ = 20.1 × $10^3$ $M^{-2}$ $s^{-1}$ and at pH 8.0: $k^*_{app}$ = 0.105 $M^{-2}$ $s^{-1}$. Measurements below the CMC revealed a rate constant of $k$ = 6.79 × $10^9$ l $mol^{-1}$ $s^{-1}$ for $Cl^-$ ($OH^-$) and $k$ = 6.25 × $10^9$ l $mol^{-1}$ $s^{-1}$ for $Br^-$. These values are typical for a diffusion limited rate process between ions. Furthermore, a plot of log $k$ *vs.* $I^{1/2}$ reveals the influence of DSDMA Cl (Br) + $OH^-$ on the ionic strength, and is linear with a slope of 1.03 at pH 7.5–8.0 below the CMC, and 0.35 above the CMC. Furthermore, the fraction of exchange of $Cl^-$ ($\alpha$) by $OH^-$ at pH 6.0 (25 °C) at equilibrium is 1.56%, and at pH 7.5 it is 30.6%. So the second rate constant for exchange is $k_q\alpha$, which is the rate for forming the ternary complex (DSDMA Cl + $OH^-$ ⟷ DSDMA OH + $Cl^-$) times the fraction of that complex leading to exchange, *e.g.* at pH 6.0 (25 °C) to 318.6 $M^{-2}$ $s^{-1}$ and at pH 8.0 to 0.379 $M^{-2}$ $s^{-1}$, respectively.

Long chain ammonium salts having two different chain lengths and two methyl groups, *e.g.* $(C_{12}H_{25})(C_{18}H_{37})N^+(CH_3)_2$ $X^-$, particularly for X = OH, have also been studied. For these materials *N*-oxidation by this enzymatic transformation could yield the chiral (*S*)-(−)- and (*R*)-(+)-*N*-oxides. Chiral analysis




of the products** shows that the amounts of the two kinds of enantiomers are dependent on the chain length. Keeping $C_{18}$ and choosing the other chain length as between $C_8$ and $C_{16}$, the enantiomeric excesses (ees) were found to be of the order 60% (*R*) and 40% (*S*). When the second chain length was between $C_4$ to $C_6$, the ees changed to 40% (*R*) and 60% (*S*). In addition, when the *N*-oxides were reacted according to eqn. (1), it was found that the olefins produced were generated from the shorter chain length residue where the chiral *N*-oxide has the (*S*)-(−) conformatioin (80%), whereas the (*R*)-(+)-*N*-oxide generated only 10–15% alkene for $R^1$ = $C_{18}$, $R^2$ = $C_{12}$. Changing the chirality of the *N*-oxide from (*S*) to (*R*) for $R^1$ = $C_{18}$ and $R^2$ = $C_4$–$C_6$, the generated olefins are of the order of 80%. Racemic $R^1R^2$ *N*-oxides generated in the average 40–45% of the corresponding alkenes.

## Footnotes and References

† E-mail: Shaunc2@aol.com
‡ E-mail: HParadies@aol.com

§ The fermentation broth consisted of 10 g glucose, 2.5 g $KH_2PO_4$, 0.05 g peptone, 0.01 g urea and 10 mM DSDMA OH in 2.5 l HPLC grade water (pH 7.5, 20 °C). The broth was aerated and the $pO_2$ and $pCO_2$ were also computer controlled (100 Hz).

¶ The monooxygenase activity was measured through an $NADPH_2$ regenerating system, comprised of 10 mM NADP, 1.5 M glucose-6-phosphate and 75 mM of glucose-6-phosphate dehydrogenase (6-GPD)–10 ml 0.01 M $K_2HPO_4$ buffer, pH 7.8 (37 °C). The 6-GPD (EC 1,1,1,49) was from Baker's yeast and Torula (100 units). The activities for monooxygenase of the crude enzyme preparation were found to be of 14.2 ± 1.2 nmol $mg^{-1}$ for ethylmorphine *N*-dimethylase, 40.1 ± 4.2 nmol $mg^{-1}$ $min^{-1}$ for aminopyridine *N*-dimethylase and 45 nmol $mg^{-1}$ $min^{-1}$ for aniline hydroxylase, respectively, applying the Hantzsch reaction.

‖ Glucose dehydrogenase (GDH) from *B. cereus* was used for the cofactor regeneration (Sigma, St Louis, MO) since this enzyme can use glucose as a substrate and accepts either $NAD^+$ or $NADP^+$ as a cofactor. The regeneration of $NADH_2^+$ ($NADPH_2^+$) or synthesis of olefin can be maintained (37 °C) in a 10 ml solution containing glucose (0.35 M), 5 mM bromomercaptoethanol, GDH (700 units) in 0.01 M sodium borate buffer, pH 6.0, containing 0.05 M $MgCl_2$, 0.05 M NaCl and 0.05 M $CaCl_2$.

** The concentrations of (*S*)- and (*R*)-enantiomers of the *N*-oxides were measured by HPLC and NMR, using a Regis-DNB-phenylglycine Pirkle column, monitoring the change of the refractive index at 500 nm. Enantiomeric excess (ee) is defined as: ee = ([*R*]-[*S*])/([*R*] + [*S*]) × 100%. The NMR method used the derivatization of the protonated *N*-oxides with (*R*)-(+)-2-methoxy-2-trifluoromethylphenylacetic acid in pyridine.

1 J. Higgins, D. Scott and R. G. Hammond, in *Microbial Degradation of Organic Compounds*, ed. D. T. Gibson, Marcel Dekker, New York, 1984, pp. 43–87; D. Hampton and L. J. Zatman, *J. Biochem. Soc. Trans.*, 1983, **1**, 667; J. Colby and L. J. Zatman, *Biochem. J.*, 1973, **132**, 101; P.J. Larje, C. A. Boulton and M. G. C. Crabbe, *Biochem. J.*, 1972, **128**, 1879.
2 P. J. Larje, *FEBS Lett.*, 1971, **18**, 297; J. Colby and L. J. Zatman, *Biochem. J.*, 1975, **148**, 513; L. E. Zajic, B. Volesky and A. Wellman, *Can. J. Microbiol.*, 1985, **15**, 122; C. A. Boulton, J. C. Crabbe and P. J. Larje, *Biochem. J.*, 1974, **140**, 253.
3 A. C. Cope and E. R. Trumbull, *Org. React.*, 1960, **11**, 317; A. C. Cope, N. A. Le Bel and W. R. Moore, *J. Am. Chem. Soc.*, 1961, **83**, 3861; A. C. Cope and N. A. Le Bel, *J. Am. Chem. Soc.*, 1960, **82**, 4656; A. C. Cope, E. Ciganek, C. F. Howell and E. E. Schwerter, *J. Am. Chem. Soc.*, 1960, **82**, 4663.
4 H. H. Paradies, *J. Phys. Chem.*, 1986, **90**, 5956; H. H. Paradies, *Medicinale*, 1984, **14**, 1.
5 S. F. Clancy, P. H. Steiger, D. A. Tanner, M. Thies and H. H. Paradies, *J. Phys. Chem.*, 1994, **98**, 11 143.
6 M. Thies, S. F. Clancy and H. H. Paradies, *J. Phys. Chem.*, 1996, **100**, 9881.

*Received in Cambridge, UK, 14th July 1997; 7/05002J*

# Evidence for a trigonal bipyramidal intermediate during nucleophilic substitution at a sulfonyl centre and for a sulfonylium cation in the acid catalysed reaction

**Nicholas J. Baxter, Andrew P. Laws, Laurent Rigoreau and Michael I. Page***

*Department of Chemical and Biological Sciences, The University of Huddersfield, Queensgate, Huddersfield, UK HD1 3DH*

**The rate of alkaline hydrolysis of a substituted β-sultam shows a dominant term second-order in hydroxide ion, clearly indicating the reversible formation of a monoanionic trigonal bipyramidal intermediate; substituent effects and kinetic parameters for the acid catalysed hydrolysis are indicative of the formation of a sulfonylium ion intermediate.**

Direct substitution at sulfonyl sulfur is thought to occur with inversion of configuration.[1] Although this indicates that the geometry of the displacement probably involves one in which the entering and leaving groups occupy the two apical positions of a trigonal bipyramid, it does not distinguish between an $S_N2$ type transition state and an intermediate with a real life-time. In fact, unlike substitution at phosphonyl centres[2] there is no real good evidence for the formation of trigonal bipyramidal intermediates for reactions at sulfonyl sulfur.[3]

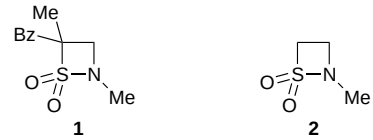
One of the most convincing pieces of evidence for the formation of tetrahedral intermediates during the hydrolysis of carboxylic acid amides is that terms second order in hydroxide ion have been observed for the hydrolysis of some anilides[4] and acetylpyrroles.[5] Important factors in determining the pathway of breakdown of tetrahedral intermediates are the basicity of the amine nitrogen leaving group and the acidity of the hydroxy group formed from the attacking nucleophilic hydroxide ion.[5]

We have studied the reactivity of β-sultams as potential mimics of the β-lactam antibiotics and shown that they undergo base-catalysed hydrolysis at a rate which is over $10^7$-fold faster than that of an analogous acyclic sulfonamide, but by a pathway which is first order in hydroxide ion.[6] We reasoned that β-sultams with electron-withdrawing groups α to the sulfonyl centre may generate a trigonal bipyramidal intermediate which requires a second hydroxide-ion to facilitate its breakdown.

The pseudo-first order rate constants ($k_{obs}$) for the alkaline hydrolysis of the β-sultam **1** are clearly second-order in hydroxide ion (Fig. 1) and a plot of $k_{obs}$/[OH$^-$] against [OH$^-$] (Fig. 2) shows that this is the dominant term in the rate law, equation (1). The values of $k_{OH1}$ and $k_{OH2}$ are $8.98 \times 10^{-3}$

$$k_{obs} = k_{OH1}[OH^-] + k_{OH2}[OH^-]^2 \quad (1)$$

dm$^3$ mol$^{-1}$ s$^{-1}$ and $3.87 \times 10^{-2}$ dm$^6$ mol$^{-2}$ s$^{-1}$ respectively at 30 °C and $I$ = 1.0 M (KCl).




The second-order term in hydroxide ion is strong evidence for the formation of a trigonal bipyramidal intermediate (TBPI) with a hypervalent sulfur. Initial but *reversible* attack of hydroxide ion on the β-sultam **1** generates a monoanionic TBPI$^-$, which requires deprotonation by a second hydroxide ion before the intermediate can collapse to products (Scheme 1). The third order rate constant $k_{OH2}$ would then be determined by eqn. (2), with $k_{-1} \gg k_2[OH^-]$.

$$k_{OH2} = (k_1k_2[OH^-]^2)/(k_{-1} + k_2[OH^-]) \quad (2)$$

Not only is the observation of the term second-order in hydroxide ion evidence for the formation of a TBPI, it

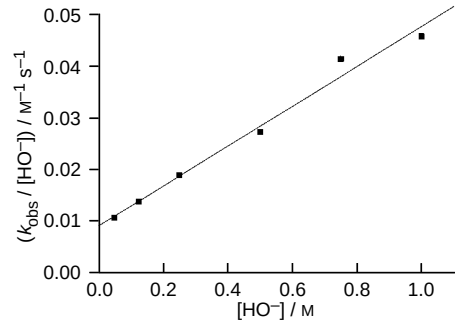



**Fig. 2** Plot of the apparent second order rate constants, $k_{obs}$/[OH$^-$], for the hydrolysis of the β-sultam, **1**, against hydroxide ion concentration at 30 °C, $I$ = 1.0 M (KCl)

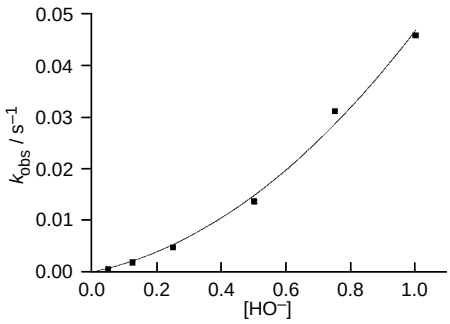
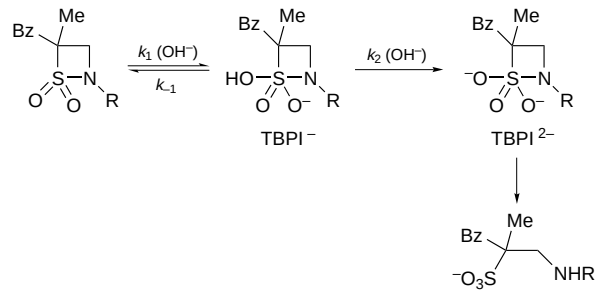
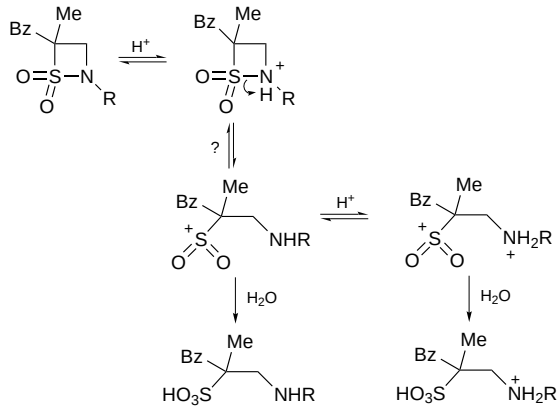



**Fig. 1** Plot of the observed pseudo-first order rate constant, $k_{obs}$, for the hydrolysis of β-sultam, **1**, against the hydroxide ion concentration at 30 °C, $I$ = 1.0 M (KCl)




**Scheme 1**



**Scheme 2**

demonstrates that $k_{-1}$, the rate constant for expulsion of hydroxide ion to regenerate starting material, is greater than ring opening of the strained four-membered β-sultam. It is a surprising fact that β-lactams do not undergo ring opening at a rate predicted by the release of strain energy in the four-membered ring.[7] It now appears that this is also the case for β-sultams. The rate limiting step for the alkaline hydrolysis of the β-sultam **1** could be either diffusion controlled deprotonation of the monoanionic TBPI$^-$, the subsequent breakdown of the dianionic TBPI$^{2-}$ or a concerted process involving both these steps. The solvent kinetic isotope effect for the term first order in hydroxide in $k_{OH1}^{H_2O}/k_{OD1}^{D_2O}$ is 0.49 whereas that for the term second order in hydroxide ion $k_{OH2}^{H_2O}/k_{OD2}^{D_2O}$ is 0.35. The latter is consistent with a stepwise process for product formation. For any process involving a proton in flight in the transition state the solvent kinetic isotope effect would be greater than unity. If formation of the dianionic TBPI$^{2-}$ is rate limiting this would be determined by the rate of the diffusion controlled encounter of hydroxide ion with the monoanionic trigonal bipyramidal intermediate TBPI$^-$. Alternatively, breakdown of the dianionic TBPI$^{2-}$ could be rate limiting. The entropy of activation for the third order rate constant $k_{OH2}$ is $-131$ J K$^{-1}$ mol$^{-1}$ which is similar to that for the second order rate constant, $k_{OH1}$, of $-121$ J K$^{-1}$ mol$^{-1}$ and is again indicative of a stepwise mechanism for the subsequent reaction of TBPI$^-$ rather than a concerted process.

The second-order rate constant for the *acid* catalysed hydrolysis of the β-sultam **1** is $1.90 \times 10^{-3}$ dm$^3$ mol$^{-1}$ s$^{-1}$ which is $1.5 \times 10^3$-fold less than that for the derivative lacking the α-benzoyl group **2**. This enormous rate retardation by electron-withdrawing substituents generates an apparent Hammett $\rho_I$ value for α-substitution of $-10$. By contrast, the effect of acyl substituents upon the rate of acid catalysed hydrolysis of amides is small, with electron-withdrawing substituents producing either a small increase or decrease in rate.[8] Although only based on a single substituent, this effect indicates a unimolecular A1-type process in which the N-conjugate acid of the β-sultam undergoes rate-limiting ring opening to form an electron-deficient sulfonylium ion which is then trapped by water to give the product β-amino sulfonic acid (Scheme 2).

Although sulfonylium ions are much more difficult to form than acylium ions[9] and there are no well established cases for their formation during substitution at sulfonyl centres,[3] the present case is compatible with the similar acylium ion mechanism suggested for the acid catalysed hydrolysis of β-lactams.[10]

We thank EPSRC for financial support.

## Footnote and References

* E-mail: m.i.page@hud.ac.uk

1 M. A. Sabol and K. K. Anderson, *J. Am. Chem. Soc*., 1969, **91**, 3603; E. U. Jonsson and C. R. H. Johnson, *J. Am. Chem. Soc.*, 1971, **93**, 5308; A. J. Buglass and J. G. Tillett, in *The Chemistry of Sulfonic Acids, Esters and their Derivatives*, ed. S. Patai and Z. Rappoport, Wiley Chichester, 1991, ch. 19.
2 G. R. J. Thatcher and R. Kluger, *Adv. Phys. Org. Chem.*, 1989, **25**, 99.
3 J. L. Kice, *Adv. Phys. Org. Chem.*, 1980, **17**, 65; I. M. Gordon, H. Maskill and M.-F. Ruasse, *Chem. Soc. Rev.*, 1989, **18**, 123.
4 R. H. DeWolfe and R. C. Newcomb, *J. Org. Chem.*, 1971, **36**, 3870; S. O. Eriksson, *Acta. Chem. Scand.*, 1968, **22**, 892; J. K. Young, S. Pazhanisamy and R. L. Schowen, *J. Org. Chem.*, 1984, **49**, 4148.
5 F. M. Menger and J. A. Donohue, *J. Am. Chem. Soc.*, 1973, **95**, 432; R. S. Brown, A. J. Bennet and H. Slebocka-Tilk, *Acc. Chem. Res.*, 1992, **25**, 481.
6 N. J. Baxter, A. P. Laws, L. Rigoreau and M. I. Page, *J. Chem. Soc., Perkin Trans. 2*, 1996, 2245.
7 P. Webster, L. Ghosez and M. I. Page, *J. Chem. Soc., Perkin Trans. 2*, 1990, 805; M. I. Page, *Adv. Phys. Org. Chem.*, 1987, **23**, 165; M. I. Page, *Phil. Trans. R. Soc. London, Ser. B,* 1991, **332**, 149.
8 A. Bruylants and F. Kezdy, *Rec. Chem. Prog*., 1960, **21**, 213; P. D. Bolton and G. L. Jackson, *Aust. J. Chem*., 1969, **22**, 257.
9 G. A. Olah, S. Kobayashi and J. Nishimura, *J. Am. Chem. Soc.*, 1973, **93**, 564.
10 P. Proctor, N. P. Gensmantel and M. I. Page, *J. Chem. Soc., Perkin Trans. 2*, 1982, 1185; M. I. Page, in *The Chemistry of β-Lactams*, ed. M. I. Page, Blackie London, 1992, pp. 79–100.

*Received in Cambridge, UK, 28th July 1997; 7/05416E*

# Samarium(II) iodide promoted carbon–carbon bond fragmentation: a facile route to bridged eight membered rings and 1,3-disubstituted cyclopentanes

**Azizul Haque and Subrata Ghosh***

*Department of Organic Chemistry, Indian Association for the Cultivation of Science, Jadavpur, Calcutta-700032, India*

**Samarium(II) iodide has been found to induce carbon–carbon bond cleavage in a number of bicyclo[2.2.1]heptane derivatives having a 1,4-dicarbonyl moiety under conditions at which the 1,4-dicarbonyl moiety undergoes intramolecular pinacol coupling.**

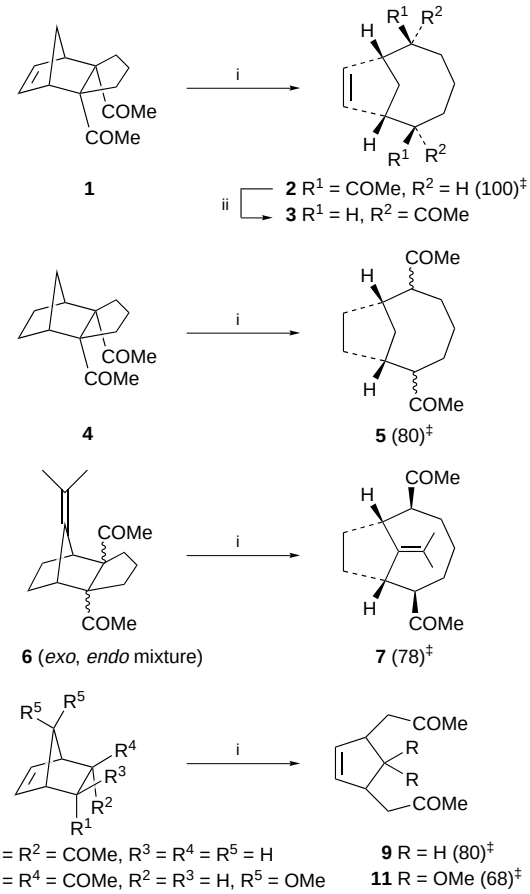
The development of reactions promoted by samarium(II) iodide is of continued interest in organic synthesis. After its introduction as a powerful single electron transfer agent, it has been extensively used in C–C bond formation reactions.[1] Reactions involving fragmentation of carbon–heteroatom bonds[2] like dehalogenation, deoxygenation and deamination utilising samarium(II) iodide have also been widely investigated. However, little attention has been focused on fragmentation of C–C bonds. In 1982, Magnus and co-workers[3] reported a $SmI_2$-promoted reductive cleavage of a C–C bond of a six membered ring in a steroidal system. Subsequently C–C bond cleavage induced by $SmI_2$ has been observed in cyclopropanes[4] and cyclopentanes.[5] However, in the latter case, reduction was found to compete favourably with ring cleavage. To date these are the only rings reported to undergo cleavage promoted by $SmI_2$.

Hoffmann and co-workers[6] have recently demonstrated that 1,4-diketones undergo smooth pinacol coupling with $SmI_2$ to produce cyclobutane-1,2-diols. Even pinacol formation was found to be facile to produce cyclobutane-1,2-diols incorporated in highly strained ring systems. In connection with our interest in the synthesis of propellanes[7] of various ring sizes from the diketone **1**, we anticipated that its intramolecular pinacol coupling, according to Hoffmann *et al.*, would proceed smoothly to provide an easy access to [3.3.2]propellanes. Herein, we report our findings on attempted pinacol coupling of the 1,4-diketone embodied in norbornane derivatives leading to facile C–C bond cleavage.

Treatment of a solution of the diketone **1** (Scheme 1) in THF–HMPA (8 : 1) containing a catalytic amount of Bu$^t$OH at room temperature with 2.5 equiv. of $SmI_2$ (0.1 M in THF) afforded a liquid in quantitative yield. Surprisingly the product was found to contain carbonyl groups as evidenced by an IR absorption at 1700 $cm^{-1}$, and a COMe singlet at $\delta$ 2.15 integrating for six protons and a carbonyl carbon at $\delta$ 210.5 by $^1H$ and $^{13}C$ NMR spectra,† respectively. All these data indicated that the reaction did not follow the usual course of intramolecular pinacol coupling. Careful analysis of the $^1H$ and $^{13}C$ NMR spectra of the product revealed its structure to be that of **2**. The presence of two sets of methine carbons at $\delta$ 43.8 and 55.1 in the $^{13}C$ NMR spectrum of the product instead of only one set of methine carbons at $\delta$ 52.7 in the starting diketone **1** was a clear indication of the cleavage of the 2,6-bond. Conclusive evidence of the ring cleavage was obtained when the product epimerised on refluxing with NaOMe–MeOH to produce a mixture of the epimeric diketones **2** and **3** with the latter predominating. The stereochemical assignment of the ring cleaved product **2** was made by comparing the chemical shift of its bridgehead protons with that of the epimerised product. The bridgehead protons *syn* to the COMe group as in **2** must experience a deshielding effect of the carbonyl group. Thus, the diketone with the bridgehead protons appearing at $\delta$ 3.36 was assigned the structure **2** and the major component of the epimerised product with bridgehead protons at $\delta$ 3.06 was assigned the structure **3**.

The cleavage of the C–C bond in **1** having a 1,4-dicarbonyl functionality suitably oriented for intramolecular pinacol type coupling is remarkable. Pinacol reaction of the diketone **1** would probably involve an enormous increase in strain energy of the strained norbornene system. Hence the initially formed diketyl radical, instead of coupling, undergoes homolysis of the C–C bond to produce a relatively less strained system.

However, reduction of the strain of the parent system by structural modification left the reaction course unaltered. For example, the saturated diketone **4** underwent smooth ring cleavage under the same conditions. Similarly, a mixture of the *endo* and *exo* diketones **6** produced a single ring cleaved product **7** in excellent yield. Even the simple norbornene diketone **8** produced exclusively the ring cleaved product **9**. Finally, the diketone **10** in which the carbonyl groups are oriented *anti* to each other also underwent ring cleavage to produce the highly functionalised cyclopentane derivative **11**.




**Scheme 1** *Reagents and conditions*: i, $SmI_2$, THF, HMPA, Bu$^t$OH, room temp., 2–3 min, then 0.1 M HCl; ii, 2% NaOMe, MeOH, reflux, 7 h

The samarium(II) iodide promoted cleavage of C–C bonds in norbornene derivatives may be useful for application in organic synthesis. For example, the cleavage of the diketones **1**, **4** and **6** to provide the bridged eight membered ring derivatives **2**, **5** and **7**, respectively, may provide a convenient route for entry into taxanes.[8] The 1,3-disubstituted cyclopentenes have previously served as precursors[9] to cyclopentanoid natural products.

We are grateful to the Council of Scientific and Industrial Research, New Delhi, for financial support.

## Footnotes and References

* E-mail: ocsg@iacs.ernet.in

† All new compounds gave satisfactory microanalytical data. *Selected NMR spectral data* for **2**, $^1$H (300 MHz) $\delta$ 1.37–1.57 (m, 6 H), 2.15 (s, 6 H), 2.17–2.26 (m, 2 H), 2.65 (d, *J* 3.3 Hz, 2 H), 3.36 (dd, *J* 3.9, 10.5 Hz, 2 H), 5.75 (s, 2 H); $^{13}$C (75 MHz) $\delta$ 19.6 ($CH_2$), 28.4 ($CH_2$), 28.5 ($CH_3$), 28.8 ($CH_2$), 43.8 (CH), 55.1 (CH), 134.8 (CH), 210.5 (CO). For **3**, $^1$H (300 MHz) $\delta$ 1.42–1.67 (m, 6 H), 1.83–2.00 (m, 2 H), 2.17 (s, 6 H), 2.65–2.81 (m, 2 H), 3.06 (d, *J* 10.8, 2 H), 5.77 (s, 2 H); $^{13}$C (75 MHz) $\delta$ 22.4 ($CH_2$), 28.3 ($CH_2$), 29 ($CH_3$), 29.2 ($CH_2$), 43.8 (CH), 59.6 (CH), 134.3 (CH), 210 (CO). For **9**, $^1$H (300 MHz) $\delta$ 1.35 (d, *J* 4.8 Hz, 2 H), 2.12 (s, 6 H), 2.42 (dd, *J* 8.1, 16.2 Hz, 2 H), 2.55 (dd, *J* 6.3, 16.6 Hz, 2 H), 3.03–3.12 (m, 2 H), 5.62 (s, 2 H); $^{13}$C (75 MHz) $\delta$ 30.1 ($CH_3$), 37.1 ($CH_2$), 40.8 (CH), 50.4 ($CH_2$), 134.3 (CH), 207 (CO). For **11**, $^1$H (300 MHz) $\delta$ 2.17 (s, 6 H), 2.76 (dd, *J* 7.8, 18.5 Hz, 2 H), 2.98 (dd, *J* 3.9, 18.5 Hz, 2 H), 3.13 (s, 3 H), 3.20 (s, 3 H), 3.23–3.34 (m, 2 H), 6.03 (s, 2 H); $^{13}$C (75 MHz) $\delta$ 30 ($CH_3$), 43.8 ($CH_2$), 48.2 (CH), 52.2 ($OCH_3$), 57 ($OCH_3$), 92.9, 131.8 (CH), 206.1 (CO).

‡ Figures in parentheses represent yields of pure products isolated by column chromatography.

1 G. A. Molander and C. R. Haris, *Chem. Rev.*, 1996, **96**, 307.
2 For a comprehensive account of carbon–heteroatom bond cleavage see: G. A. Molander, *Chem. Rev*., 1992, **92**, 29; For some recent work see: G. A. Molander and P. J. Stengel, *J. Org. Chem.*, 1995, **60**, 6660; E. J. Enholm and J. A. Schreier, *J. Org. Chem.*, 1995, **60**, 1110.
3 T. P. Ananthanarayan, T. Gallagher and P. Magnus, *J. Chem. Soc., Chem. Commun.*, 1982, 709.
4 G. A. Molander and J. A. Mckie, *J. Org. Chem.*, 1991, **56**, 4112; R. A. Batey and W. B. Motherwell, *Tetrahedron Lett.*, 1991, **32**, 6649; R. Beerli, E. J. Bruner and H. J. Broschberg, *Tetrahedron Lett.*, 1992, **33**, 6449.
5 T. Honda, K. Naito, S. Yamane and Y. Suzuki, *J. Chem. Soc., Chem. Commun.*, 1992, 1218.
6 H. M. R. Hoffmann, I. Munnich, O. Nowitzki, H. Stucke and D. J. Williams, *Tetrahedron*, 1996, **52**, 11783; O. Nowitzki, I. Munnich, H. Stucke and H. M. R. Hoffmann, *Tetrahedron*, 1996, **52**, 11 799.
7 S. Ghosh, S. Saha Roy and A. Bhattacharya, *Synth. Commun.*, 1989, **19**, 3191.
8 K. C. Nicolaou, W. Dai and R. K. Guy, *Angew. Chem., Int. Ed. Engl.*, 1994, **33**, 15; A. N. Boa, P. R. Jenkins and N. J. Lawrence, *Contemp. Org. Synth.*, 1994, 47.
9 D. P. Curran and M. Chen, *Tetrahedron Lett.*, 1985, **26**, 4991.

*Received in Cambridge, UK, 11th August 1997; 7/05843H*

# First metal-encapsulating star polysulfoxide incorporating 2-amino-1,3,4-thiadiazole

**Chi Yang,*[a,b] Xiao-Ming Chen,*[b] Xiao-Quan Lu,[b] Qin-Hai Zhou[a] and Yan-Sheng Yang*[b]**

[a] *Department of Chemical Engineering, Guangdong University of Technology, 729 Dongfeng Road East, Guangzhou 510090, China*

[b] *Department of Chemistry, Zhongshan University, Guangzhou 510275, China*

**The first star polysulfoxide 2 is synthesized by selective oxidation of a new hexaaminohexathioether 1, which gives a novel binuclear bis-tripodant species by encapsulating a pair of $Cu^{II}$ ions.**

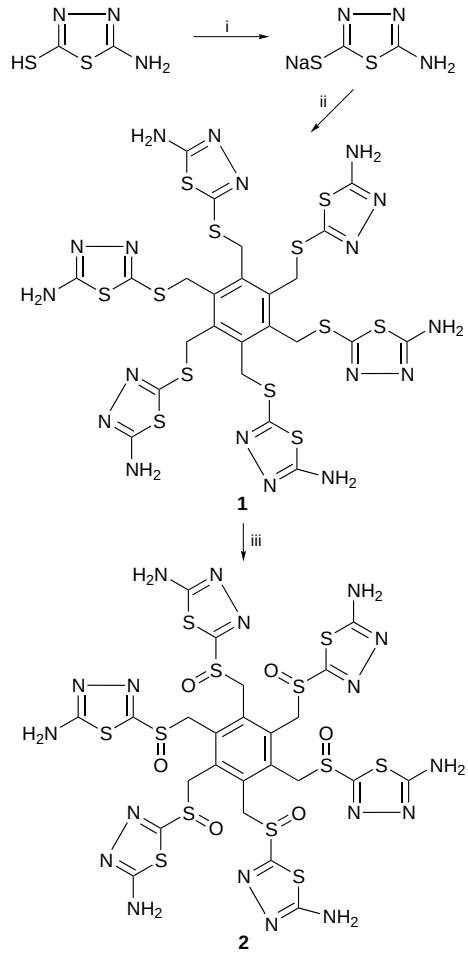
Suitably hexa-substituted benzene derivatives as new hosts and complex-forming ligands with a great underlying potential have received considerable attention in recent years.[1] A series of such macromolecules with specific enclathration properties have been uncovered, which are related to octopus,[2] hexa-host,[3] hexa-pedals,[4] aromatic propeller[5] and star polymers.[6] In particular, octopus polythioethers fitted with numerous donor atoms show unusual complexing tendency to metal cations owing to their conformational mobility being impeded by spatial crowding.[7] The binding of $Cu^{II}$ to polythioethers has led to a great understanding of Cu–S interactions in copper enzymes.[8] However, no report has yet appeared on the synthesis of octopus polysulfoxide or solid metal complexes of octopus ligands. We now report the synthesis and properties of novel $Cu^{II}$ complexes with a novel octopus polythioether **1** and the first star polysulfoxide **2**.

Synthesis of **1** was both straightforward and high yielding. Refluxing of hexakis(bromomethyl)benzene with the sodium salt of 2-amino-5-sulfanyl-1,3,4-thiadiazole gave **1** in > 93% yield.† Mild and selective oxidation of **1** with an excess of dilute hydrogen peroxide in dilute HCl solution at ambient temperature for 18 h afforded **2** in high yield ( > 90%),† with amino groups preserved and no over oxidation (see Scheme 1). Octopus compounds **1** and **2** can form inclusion compounds with DMF and $Me_2SO$ with host : guest = 1 : 1 and 1 : 2, respectively.

The hexasubstituted benzene octopus may form two possible types of metal complexes directed by suitable metal ions based on their preferential conformations: (*a*) a mononuclear species with the six arms of an octopus encapsulating a metal ion; (*b*) a binuclear bis-tripodant species with three arms of an octopus at 1,3,5-positions located above the phenyl plane encapsulating a metal ion, and the remaining three arms at 2,4,6-positions located below the plane encapsulating another metal ion. Copper(II) complexes of **1** and **2** were prepared in hot HCl solution in quantitative yield, giving a mononuclear species of **1**·$CuCl_2$ **3**,† and a binuclear species **2**·$Cu_2Cl_4$ **4**.† The $FAB^+$ mass spectrum of **3** which exhibits a peak at *m/z* 1011 ($[Cu\mathbf{1}]^{2+}$) is clearly indicative of the formation of a 1 : 1 complex. The presence of the characteristic molecular peak at *m/z* ($FAB^+$ MS) 1171 ($[Cu_2\mathbf{2}]^{4+}$) unambiguously shows complexation of two $Cu^{II}$ ions per molecule of **2** in **4**. The IR spectra suggest that the amino groups and exocyclic sulfur do not coordinate to the metal ions, only the 1,3,4-thiadiazole rings participate in coordination.[9] Thus, it is highly possible that in **3** one $Cu^{II}$ ion is encapsulated by six arms of **1**, and in **4**, two $Cu^{II}$ ions are each encapsulated by three arms of **2**.

Mononuclear complex **3** shows broad $^1H$ NMR peaks as usual for paramagnetic copper(II) complexes. In contrast, binuclear complex **4** produces very narrow $^1H$ NMR peaks, such an observation is similar to those found for some magnetically coupled dimeric copper(II) complexes.[10] The anisotropic X-band EPR spectrum of polycrystalline **3** at 100 K ($g_\perp$ = 2.263, $g_\parallel$ = 2.061) exhibits the usual line shape for mononuclear copper(II) complexes with a $d_{x^2-y^2}$ ground state. The EPR spectrum of **4** shows a unique quasi-isotropic, broad absorption centered at $g$ = 2.072 (100 K) with a half-weight width of *ca*. 300 G; the broadness of this EPR signal is typical of weak metal–metal interaction, and hence implies a dimeric structure.[11] Thermogravimetry of **4** shows a total mass loss of 87.1%, which correlates well with the expected loss of 87.9% for a metal : ligand molar ratio of 2 : 1.

There is no redox peaks observed for **1**, while cyclic voltammetry (CV) (Fig. 1) of **2** shows three quasi-reversible redox waves at $E_{1/2}$ = 0.052, −0.46 and −0.425 V *vs*. SCE, corresponding to the successive reduction waves of the three 2-amino-5-sulfinyl-1,3,4-thiadiazole arms located at the same side of the benzene plane (*i.e.* the groups at 1,3,5-positions),




**Scheme 1** *Reagents and conditions*: i, Na, EtOH, room temp.; ii, EtOH, 80 °C, Ar, 22 h; iii, $H_2O_2$, HCl–$H_2O$, room temp., 18 h

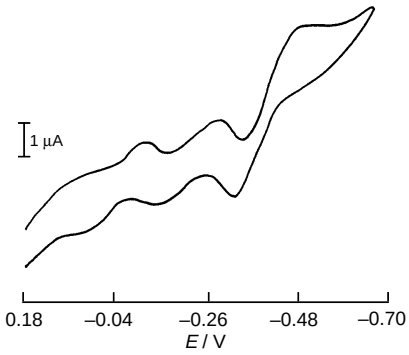



**Fig. 1** Cyclic voltammetry of **2** ($5 \times 10^{-5}$ M) on a carbon-glass electrode with $NBu_4Cl$ ($10^{-3}$ M) in HCl (3 M). Sweep rate: 100 mV $s^{-1}$.

leading to the overall formation of a hexa-anion. The shapes of the waves are in accordance with a six-electron transfer and each wave behaving as a two-electron wave, similar to those of cryptates.[12] These results indicate that the redox process of **2** is mainly ascribed to the presence of redox-active sulfinyl groups. CV studies of **3** and **4** show two similar quasi-reversible cathodic waves at $E_{1/2} = -0.121$ and $-0.225$ V, and at $E_{1/2} = 0.21$ and 0.295 V (*vs.* 10 mM $Ag^I/AgCl$), respectively, corresponding to the following reduction:[13]

$$[Cu^{II}\mathbf{1}]^{2+} \leftrightarrow [Cu^{I}\mathbf{1}]^{+} \leftrightarrow [Cu^{0}\mathbf{1}]^{0}$$

$$[Cu^{II}Cu^{II}\mathbf{2}]^{4+} \leftrightarrow [Cu^{II}Cu^{I}\mathbf{2}]^{3+} \leftrightarrow [Cu^{II}Cu^{0}\mathbf{2}]^{2+}$$

A possible reason for the observed behaviour of the binuclear species **4** is that only one $Cu^{II}$ ion, surrounded by three arms, can approach and be adsorbed by the electrode surface at a given time, resulting in similar behaviour to that observed for **3**.

We thank the State Commission of Science and Technology of China for financial support.

## Footnotes and References

* E-mail: cedc03@zsu.edu.cn

† *Selected data*: **1**·3HCl: Anal. Calc. for $C_{24}H_{27}Cl_3N_{18}S_{12}$: C, 27.32; H, 2.56; N, 23.91; Cl, 10.12. Found: C, 27.39; H, 2.57; N, 24.03; Cl, 10.21%; UV ($\lambda_{max}$/nm): 286; FABMS: *m/z* 949; IR (KBr): 1630, 1496, 1032, 800, 744, 702, 610 $cm^{-1}$; $^1H$ NMR [300 MHz, $(CD_3)_2SO$, 25 °C]: $\delta$ 4.51 (br, 12 H, $NH_2$), 4.76 (br, 12 H, $CH_2$).

**2**·HCl: Anal. Calc. for $C_{24}H_{25}ClN_{18}O_6S_{12}$: C, 26.65; H, 2.31; N, 23.32; Cl, 3.29%. Found: C, 26.57; H, 2.33; N, 23.51; Cl, 3.31%. FABMS: *m/z* 1045; IR (KBr): 1609, 1496, 1321, 1124, 1039, 786, 463 $cm^{-1}$; $^1H$ NMR [400 MHz, $(CD_3)_2SO$, 25 °C]: $\delta$ 5.10 (br, 12 H, $NH_2$), 8.14 (br, 12 H, $CH_2$).

**3**: Anal. Calc. for $C_{24}H_{26}CuN_{18}O_2S_{12}$: C, 27.53; H, 2.49; N, 24.20; Cu, 6.22; S, 36.74%. Found: C, 27.42; H, 2.50; N, 24.25; Cu, 6.16; S, 36.70%. FABMS: *m/z* 1011. IR(KBr): 1623, 1496, 1039, 744, 695 $cm^{-1}$; $^1H$ NMR [400 MHz, $(CD_3)_2SO$, 25 °C]: $\delta$ 3.68 (br, 12 H, $NH_2$), 4.46 (br, 12 H, $CH_2$).

**4**: Anal. Calc. for $C_{24}H_{24}Cl_4Cu_2N_{18}O_6S_{12}$: C, 21.93; H, 1.84; N, 19.18; S, 29.27; Cu, 9.67%. Found: C, 21.82; H, 1.85; N, 18.97; Cu, 9.69%. FABMS: *m/z* 1172. IR (KBr): 1609, 1496, 1046, 463 $cm^{-1}$; $^1H$ NMR [400 MHz, $(CD_3)_2SO$, 25 °C]: $\delta$ 5.40 (s, 12 H, $NH_2$), 7.88 (s, 12 H, $CH_2$).

1 C. M. Hartshorn and P. J. Stell, *Angew. Chem., Int. Ed. Engl.*, 1996, **35**, 2655.
2 F. Vögtle and E. Weber, *J. Inclusion Phenom. Mol. Recognit. Chem.*, 1992, **12**, 75.
3 D. D. MacNicol, *Inclusion Compounds*, ed. J. L. Atwood, J. E. Davies and D. D. MacNicol, Academic Press, London, 1985, vol. 2, p. 123.
4 S. A. Bourne, K. L. G. Nash and F. Toda, *J. Chem. Soc., Perkin Trans. 2*, 1996, 2145;
5 C. Foces-Foces, A. L. Llamas-Saiz, R. M. Claramunt, N. Jagerovic, M. L. Jimeno and J. Elguero, *J. Chem. Soc., Perkin Trans. 2*, 1995, 1395.
6 E. Cloutet, J.-L. Fillaut, Y. Gnanou and D. Astruc, *Chem. Commun.*, 1996, 2047; H.-W. Marx, F. Moulines, T. Wagner and D. Astruc, *Angew. Chem., Int. Ed. Engl.*, 1996, **35**, 1701.
7 *Top. Curr. Chem.*, 1988, **140**; 1989, **149**.
8 C. Beguin, P. Chautemps, A. El Marzouki, J. L. Pierre, S. M. Refaif, G. Serratrice, E. Saint-Aman and P. Rey, *J. Chem. Soc., Dalton Trans.*, 1995, 1939; A. J. Blake and M. Schröder, *Adv. Inorg. Chem.*, 1990, **35**, 1.
9 D. Lin-Vien, N. B. Colthup, W. G. Fateley and J. G. Grasselli, *The Handbook of Infrared and Raman Characteristic Frequencies of Organic Molecules*, Academic Press, New York, 1991; K. Makamoto, *Infrared and Raman Spectra of Inorganic and Coordiation Compounds*, Wiley, Chichester, 3rd edn., 1978.
10 J. H. Satcher and A. L. Balch, *Inorg. Chem.*, 1995, **34**, 3371.
11 I. Sanyal, P. Ghosh and K. D. Karlin, *Inorg. Chem.*, 1995, **34**, 3050; X.-M. Chen, Y.-X. Tong, Z.-T. Xu and T. C. W. Mak, *J. Chem. Soc., Dalton Trans.*, 1995, 4001.
12 L. Echegoyen, E. P. Cordero, C. Roth and J.-M. Lehn, *Inorg. Chem.*, 1993, **32**, 572 and references therein.
13 *Bioinorganic Chemistry of Copper*, ed. K. D. Karlin and Z. Teklar, Chapman and Hall, New York, 1993.

*Received in Cambridge, UK, 28th May 1997; 7/03677I*

# Diastereoselective formation of disilver(I) double helicates with chiral 2,2′ : 6′,2″ : 6″,2‴-quaterpyridines

**Gerhard Baum,[b] Edwin C. Constable,*[a] Dieter Fenske[b] and Torsten Kulke[a]**

[a] *Institut für Anorganische Chemie, Spitalstrasse 51, CH-4056 Basel, Switzerland*
[b] *Institut für Anorganische Chemie, Universität Karlsruhe (TH), Engesserstraße, Geb. Nr. 30.45, 76128 Karlsruhe, Germany*

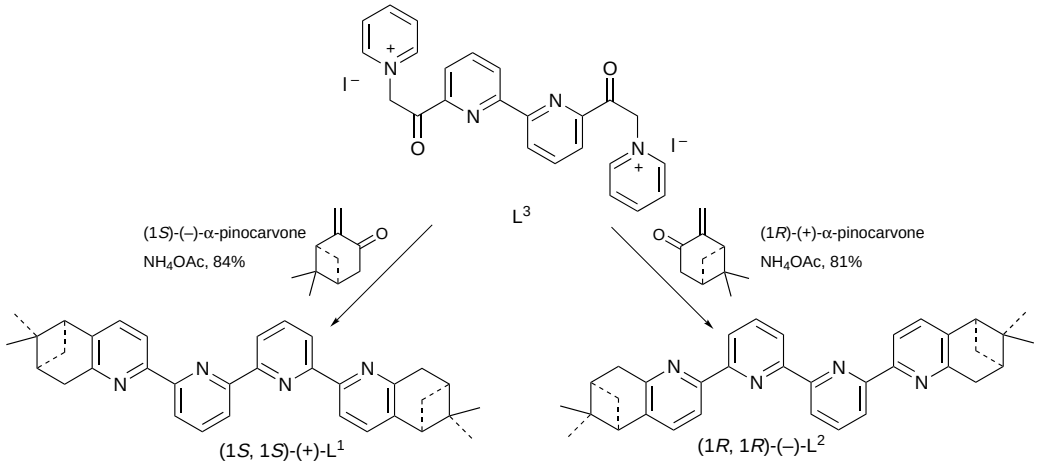
**Chiral 2,2′:6′,2″ : 6″,2‴-quaterpyridines bearing fused chiral groups in the 5,6- and 5‴,6‴-positions are prepared; these ligands preferentially form *P* or *M* dinuclear double helicates upon coordination to silver(I), one of which has been structurally characterised.**

Oligopyridines and oligopyridine metal-binding domains are a recurrent feature in metallosupramolecular chemistry[1] and it is now well established that the higher oligopyridines can give multiple-helical transition-metal complexes.[2] Although pre-organised chiral ligands bearing multiple oligopyridine domains have been previously studied[3,4] we have recently shown that the right- or left-handed chirality of the helix may also be controlled in true self-assembly processes by the use of chiral oligopyridines and have demonstrated that modest diastereomeric excesses (de, 75%) of the *P* or *M* double helicates are formed upon reaction of enantiomerically pure chiral 2,2′:6′,2″-terpyridines with copper(I).[5] Here, we show that acceptably high de values may be obtained by (*i*) varying the metal, (*ii*) increasing the number of donor atoms and (*iii*) increasing the number of chiral sites in the ligands.

2,2′ : 6′,2″:6″,2‴-Quaterpyridines react with silver(I) salts to give dinuclear double helicates.[6,7] A pair of enantiomeric 2,2′:6′,2″:6″,2‴-quaterpyridines (1*S*, 1*S*)-(+)-$L^1$ and (1*R*, 1*R*)-(−)-$L^2$ were prepared enantioselectively from (1*S*)-(−) or (1*R*)-(+) pinocarvone[8] by reaction with salt $L^3$ (ref. 9) and ammonium acetate in a mixture of acetic acid and acetic anhydride in near quantitative yield as white crystalline solids (Scheme 1).† The ligands were fully characterised and exhibited spectroscopic properties closely resembling those of analogous lower homologues first reported by von Zelewsky and co-workers.[10]

The reaction of $L^1$ or $L^2$ with silver(I) acetate in methanol followed by precipitation with ammonium hexafluorophosphate gave cream coloured precipitates of $[Ag_2L^1{}_2][PF_6]_2$ or $[Ag_2L^2{}_2][PF_6]_2$ as established by elemental analysis and mass spectrometry [*m*/*z* 1358 ($M^+ - PF_6$)] in 85–90% yield.‡ In principle, each ligand could give a pair of diastereomeric double helicates, for example $L^1$ could give *P*-$[Ag_2\{(1S, 1S)\text{-}L^1\}_2]^{2+}$ or *M*-$[Ag_2\{(1S, 1S)\text{-}L^1\}_2]^{2+}$. Unlike the case investigated earlier[5] the use of the symmetrically substituted ligands $L^1$ and $L^2$ eliminates any additional complications from head–tail isomerism. The $^1$H NMR spectrum of $CD_3CN$ solutions of the crude precipitates revealed a 0.024 : 1.00 ratio of diastereomers in each case [Fig. 1(*a*)]. This corresponds to a 95.3% de of one of the two diastereomers. A single recrystallisation from acetonitrile yielded good quality crystals which $^1$H NMR spectroscopy revealed to contain only the major diastereomer. Circular dichroism spectroscopy confirmed that the compounds prepared from $L^1$ and $L^2$ possessed equal and opposite chiroptical properties [Fig. 1(*b*)] as expected for an enantiomeric pair of (*S**,*S**,*S**,*S**)-P* and (*R**,*R**,*R**,*R**)-*M** helicates. After a single recrystallisation, a de of 100% has been obtained. The only question remaining was to determine which of the two helical conformations (*P* or *M*) was favoured in each case. In related systems, a large positive CD absorption at *ca.* 320 nm is characteristic of a *P* helicate, whereas a negative mode is seen for *M*-helicates.[10] On this basis, we propose *P*-$[Ag_2\{(1S, 1S)\text{-}L^1\}_2]^{2+}$ and *M*-$[Ag_2\{(1R, 1R)\text{-}L^2\}_2]^{2+}$ structures. Molecular modelling gave equivocal results and we have determined the X-ray structure of $[Ag_2\{(1S, 1S)\text{-}L^1\}_2]\text{-}[PF_6]_2$.§

Initial attempts to determine the structure revealed a very large unit cell [$U$ = 49 245(9) Å$^3$] and the structure was only solved using data from an area detector. The structure of the cation present in $[Ag_2\{(1S, 1S)\text{-}L^1\}_2][PF_6]_2$ is presented in Fig. 2(*a*). The double-helical geometry is confirmed and the double helix is revealed unambiguously to possess a *P* conformation [most easily seen in the space-filling representation in Fig. 2(*b*)]. The Ag–N distances [2.245(6), 2.343(6) Å] are unremarkable and closely resemble those in the parent 2,2′:6′,2″ : 6″,2‴-quaterpyridine complex (2.223–2.409 Å).[6,7] The Ag···Ag distance within the cation of 3.230(2) Å is slightly longer than observed in the parent 2,2′ : 6′,2″ : 6″,2‴-quaterpyr-




**Scheme 1**

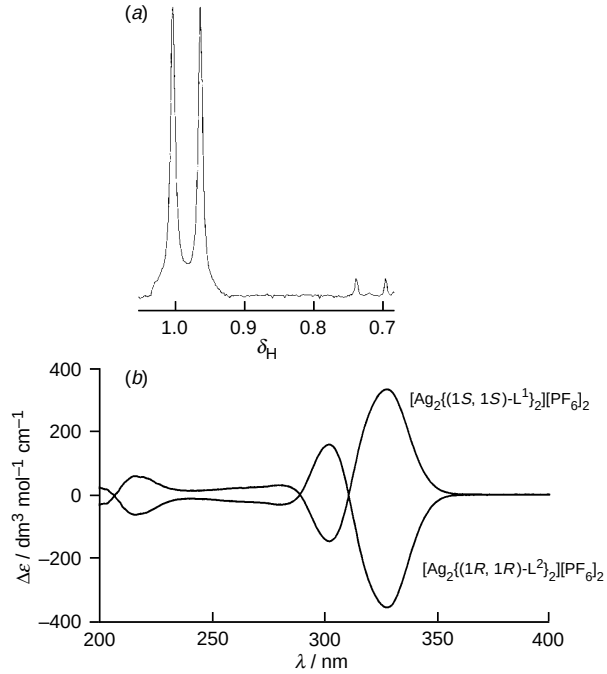



**Fig. 1** (*a*) Part of the $^1$H NMR spectrum of a $CD_3CN$ solution showing $H^{7PB}$ of the crude product [Ag$_2${(1*R*, 1*R*)-L$^2$}$_2$][PF$_6$]$_2$ showing the 95% de of one of the two diastereomers and (*b*) the CD spectra of the diastereomerically pure products obtained from the recrystallisation of [Ag$_2${(1*S*, 1*S*)-L$^1$}$_2$][PF$_6$]$_2$ and [Ag$_2${(1*R*, 1*R*)-L$^2$}$_2$][PF$_6$]$_2$

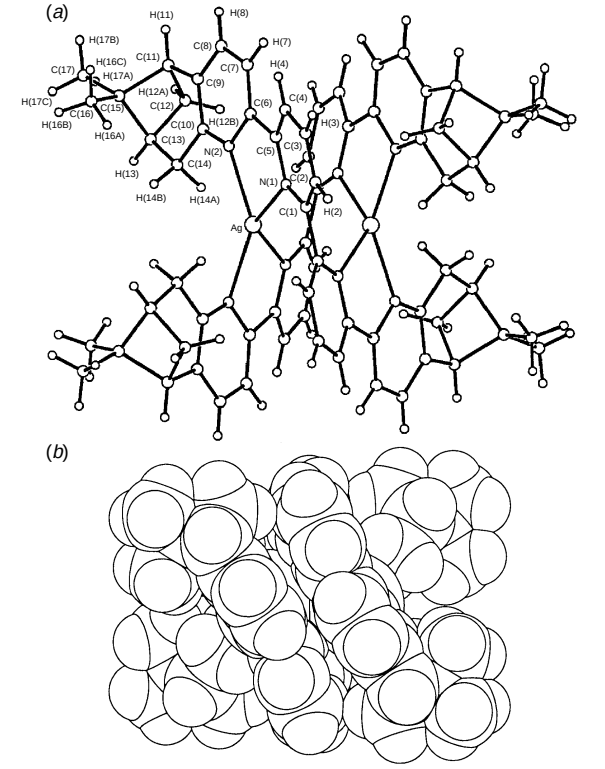



**Fig. 2** Crystal and molecular structures of (*a*) the double-helical cation with *P* chirality in the lattice of *P*-[Ag$_2${(1*S*, 1*S*)-**1**}$_2$][PF$_6$]$_2$ showing the numbering scheme and adopted and (*b*) a space-filling representation of the same cation

idine complex [3.107(2) Å][6,7] which presumably represents the repulsion between the fused chiral substituents. The principal twisting within the ligand occurs between the two central rings (41.4°) although a significant twist of 17.4° occurs between the outer rings (*cf.* 45–47 and 13.0–13.5° in the 2,2′:6′,2″:6″,2‴-quaterpyridine complex).[6,7] Interestingly, the (*S*,*S*,*S*,*S*)-*P* and (*R*,*R*,*R*,*R*)-*M* preference that is shown is opposite to the (*S*,*S*)-*M* and (*R*,*R*)-*P* preferences shown with monofunctionalised 2,2′:6′,2″-terpyridines.

In conclusion, we have demonstrated that 2,2′:6′,2″:6″,2‴-quaterpyridines bearing two fused chiral substituents give high diastereomeric excesses of *P* or *M* helicates upon reaction with silver(I). We are currently probing the origin of the diastereoselectivity and attempting to increase the selectivity further.

We should like to thank the Schweizerischer Nationalfonds zur Förderung der wissenschaftlichen Forschung and the University of Basel (E. C. C., T. K.) for support. We should also like to thank Professor A. von Zelewsky for helpful discussions and for access to unpublished data.

## Footnotes and References

* E-mail: constable@ubaclu.unibas.ch

† *Selected data* for **1** and **2**: mp. > 250 °C. MS (MALDI TOF): *m*/*z* 499 ($M^+$). IR (KBr): $\nu$/cm$^{-1}$ 2919, 1563, 1431, 1421, 807. [$\alpha$]$^D_{21}$ +66.8° (**1**), −63.0° (**2**). $^1$H NMR ($CDCl_3$): $\delta$ 0.69 (3 H, s, $H^{6PA}$), 1.33 (2 H, d, *J* 9.3 Hz, $H^{7PB}$), 1.43 (3 H, s, $H^{6PB}$), 2.41 (2 H, m, $H^{5P}$), 2.72 (2 H, m, $H^{7PA}$), 2.83 (2 H, t, *J* 5.9, 5.4 Hz, $H^{1P}$), 3.21 (4 H, d, *J* 2.4 Hz, $H^{4P}$), 7.38 (2 H, d, *J* 7.8 Hz, $H^4$), 8.42 (2 H, dd, *J* 7.8, 1.0 Hz, $H^{3\prime}$), 7.94 (2 H, t, *J* 7.8 Hz, $H^{4\prime}$), 8.31 (2 H, 2, *J* 7.8 Hz, $H^3$), 8.62 (2 H, dd, *J* 7.8, 1.0 Hz, $H^{5\prime}$):$^{13}$C NMR ($CDCl_3$): $\delta$ 21.35, 26.09, 31.98, 36.74, 39.58, 40.29, 46.54, 117.97, 120.40, 120.64, 133.75, 137.61, 142.27, 153.71, 155.46, 155.88, 156.35.

‡ *Selected spectroscopic data* for the major diastereomer of [Ag$_2$L$^1_2$][PF$_6$]$_2$ or [Ag$_2$L$^2_2$][PF$_6$]$_2$: mp. > 250 °C, MALDI TOF mass spectrum: *m*/*z* 1358 ($M^+ - PF_6$), 1105 ([AgL$^2$]$^+$), 606 ([AgL]$^+$), 499 (L$^+$). IR (KBr): $\nu$/cm$^{-1}$ 2926, 1564, 1432, 1422, 833, 560. [$\alpha$]$^D_{21}$ +1128.3° (**1**), −1132.4° (**2**). $^1$H NMR ($CDCl_3$): $\delta$ 0.36 (3 H, s, $H^{6PA}$), 0.98 (2 H, d, *J* 9.8 Hz, $H^{7PB}$), 1.30 (3 H, s, $H^{6PB}$), 1.65 (2 H, dd, *J* 2.9, 17.6 Hz, $H^{4PB}$), 1.94 (2 H, m, $H^{5P}$), 2.63 (2 H, dd, *J* 2.0, 17.6 Hz, $H^{4PA}$), 2.66 (2 H, m, $H^{7PA}$), 2.85 (2 H, t, *J* 5.9, 5.4 Hz, $H^{1P}$), 7.47 (2 H, d, *J* 7.8 Hz, $H^4$), 7.7 (2 H, d, *J* 7.3, 1.0 Hz, $H^{3\prime}$), 7.96 (2 H, t, *J* 7.8 Hz, $H^{4\prime}$), 7.66 (2 H, 2, *J* 7.8 Hz, $H^3$), 8.06 (2 H, d, *J* 7.4 Hz, $H^{5\prime}$).

§ *Crystal data* for [Ag$_2$L$^1_2$][PF$_6$]$_2$·0.33$H_2O$: colourless crystal, $C_{68}H_{62}Ag_2F_{12}N_8O_{0.33}P_2$, *M* = 1502.27, cubic, space group *F*432, *a* = 36.654(4) Å, *U* = 49 245 (9) Å$^3$, *Z* = 24, $D_c$ = 1.216 g cm$^{-3}$, *F*(000) = 18 256, $\lambda$ = 0.71073 Å, $\mu$(Mo-K$\alpha$) 0.582 mm$^{-1}$. Intensity data were collected on a Stoe IPDS diffractometer (1.84 < $\theta$ < 125.10°) at 200 K; of 40 542 reflections measured, 3672 independent reflections were used in the structure solution. The structure was solved by direct methods using SHELXS-86[11] and refined using SHELXL-93[12] to give final *R* and $wR_2$ values of 0.0713 and 0.2169 for 2577 observed reflections with $I \geqslant 2\sigma(I)$ respectively (all data values: *R* 0.0956 and $wR_2$ 0.2403). The absolute structure parameter was 0.01(9). CCDC 182/582.

1 E. C. Constable, *Prog. Inorg. Chem.*, 1994, **42**, 67; *Tetrahedron*, 1992, **48**, 10 013.
2 E. C. Constable, in *Comprehensive Supramolecular Chemistry*, ed. J. L. Atwood, J. E. D. Davies, D. D. MacNicol, F. Vögtle, J.-P. Sauvage and M. W. Hosseini, Pergamon, Oxford, 1996, vol. 9. p. 213.
3 C. R. Woods, M. Benaglia, F. Cozzi and J. S. Siegel, *Angew. Chem., Int. Ed. Engl.*, 1996, **35**, 1830; W. Zarges, J. Hall, J.-M. Lehn and C. Bolm, *Helv. Chim. Acta*, 1991, **74**, 1843.
4 E. C. Constable, T. Kulke, M. Neuburger and M. Zehnder, *Chem. Commun.*, 1997, 489.
5 E. C. Constable, T. Kulke, M. Neuburger and M. Zehnder, *Chem. Commun*., 1997, 489.
6 E. C. Constable, M. J. Hannon, A. Martin, P. R. Raithby and D. A. Tocher, *Polyhedron*, 1992, **11**, 2967.
7 E. C. Constable, S. M. Elder, M. J. Hannon, A. Martin, P. R. Raithby and D. A. Tocher, *J. Chem. Soc., Dalton Trans*., 1996, 2423.
8 E. D. Mihelich and D. J. Eickhoff, *J. Org. Chem.*, 1983, **48**, 4135.
9 M. D. Ward, Ph.D. Thesis, Cambridge, 1990
10 M. Ziegler and A. von Zelewsky, personal communication; P. Hayoz and A. von Zelewsky, *Tetrahedron Lett.*, 1992, **33**, 5165; P. Hayoz, A. von Zelewsky and H. Stoeckli-Evans, *J. Am. Chem. Soc.*, 1993, **113**, 5111; M. Gianini and A. von Zelewsky, *Synthesis*, 1996, **6**, 703; N. C. Fletcher, F. R. Keene, M. Ziegler, H. Stoeckli-Evans, H. Viebrock and A. von Zelewsky, *Helv. Chim. Acta*, 1996, **79**, 1192; N. C. Fletcher, F. R. Keene, H. Viebrock and A. von Zelewsky, *Inorg. Chem*., 1997, **36**, 1113.
11 G. M. Sheldrick, SHELXS-86. Program for the solution of crystal structures, 1986, University of Göttingen, Germany.
12 G. M. Sheldrick, SHELXL-93. Program for the refinement of crystal structures, 1993, University of Göttingen, Germany.

*Received in Cambridge, UK, 17th July 1997; 7/05130A*

# Application of triple-channel $^{13}C\{^{1}H,^{19}F\}$ NMR techniques to probe structural properties of disordered solids

**Alison Nordon,[a] Robin K. Harris,*[a] Lily Yeo[b] and Kenneth D. M. Harris*[b]**

[a] *Department of Chemistry, University of Durham, South Road, Durham, UK DH1 3LE*
[b] *School of Chemistry, University of Birmingham, Edgbaston, Birmingham, UK B15 2TT*

**Triple-channel $^{13}C$ MAS NMR experiments are carried out to characterize intermolecular interactions in disordered molecular solids containing fluorinated *n*-alkanes; an approach involving a combination of $^{1}H \rightarrow {}^{13}C$ and $^{19}F \rightarrow {}^{13}C$ cross-polarization experiments, with both single-channel ($^{1}H$) and double-channel ($^{1}H$,$^{19}F$) decoupling is developed to assign resonances for a given type of $^{13}C$ nucleus in different intermolecular environments.**

In molecular crystals, structural disorder often arises when the molecules are able to take up more than one orientation (not necessarily with equal energy) within the space available to them. Fundamentally, such disorder raises important issues concerning the intermolecular interactions within the crystal. Although the space- and time-averaged crystal structure, as determined by diffraction-based techniques, can generally indicate the existence of disorder, it is often unable to provide information at a sufficiently detailed level. Techniques that can be used to study local structural and/or dynamic properties of solids must then come to the fore, and in this regard solid-state NMR spectroscopy proves to be a versatile and powerful approach. As described here, the application of triple-resonance techniques[1,2] can enhance considerably the scope and potential of solid-state NMR in this field. In particular, this paper reports solid-state $^{13}C$ NMR studies carried out to characterize intermolecular interactions in disordered molecular solids containing organofluorine compounds. Selective cross-polarization from $^{1}H$ or $^{19}F$, together with decoupling of $^{1}H$ and/or $^{19}F$, have been exploited to probe the local structure around organic functional groups that are disordered between local intermolecular environments that either contain fluorine or do not contain fluorine. The approach is applied to orientational disorder of 1-fluorotetradecane [$FH_2C(CH_2)_{12}CH_3$] 'guest' the molecules within the crystalline urea tunnel structure[3] in 1-fluorotetradecane–urea inclusion compound.

Carbon-13 CP MAS spectra recorded for the 1-fluorotetradecane–urea inclusion compound are shown in Fig. 1. An initial assignment of the resonances in the $^{1}H \rightarrow {}^{13}C$ CP MAS spectrum [Fig. 1(*a*)], acquired using $^{1}H$ and $^{19}F$ double-decoupling, was made, in part, on the basis of a previous study of alkane–urea inclusion compounds.[4] There are two resonances for $CH_2F$ ($\delta$ 84.1, 83.9) and two for $CH_3$ ($\delta$ 14.7, 14.4), whereas all other $^{13}C$ positions within the molecule give rise to only one distinguishable resonance (note that an italic letter is used to specify the assignment of resonances). As first proposed and demonstrated by Hollingsworth *et al.*[5,6] (see also ref. 3), such chemical shift differences for the end-groups of unsymmetric guest molecules $X(CH_2)_nY$ (abbreviated to X–Y) in urea inclusion compounds can arise from the existence of the different end-group interactions X···X, X···Y and Y···Y (rather than other possible sources such as conformational disorder). On this basis, the observation of two resonances for $CH_2F$ in 1-fluorotetradecane–urea may be attributed tentatively to the $CH_2F\cdots FH_2C$ and $CH_2F\cdots H_3C$ end-group environments and the observation of two resonances for $CH_3$ may be similarly assigned to the $CH_3\cdots H_3C$ and $CH_3\cdots FH_2C$ end-group environments. Previously, assignments of such resonances to the different end-group situations have been made by comparing the spectrum for the urea inclusion compound containing X–Y guest molecules with: (*a*) spectra for urea inclusion compounds containing the corresponding symmetric guest molecules X–X and/or Y–Y; and/or (*b*) spectra for urea inclusion compounds containing mixtures of the guest molecules X–Y and X–X, and/or mixtures of the guest molecules X–Y and Y–Y.

In the approach devised here, the two resonances for $CH_3$ carbons in the 1-fluorotetradecane–urea inclusion compound can be assigned using two complementary experiments which exploit the $^{13}C$–$^{19}F$ dipole–dipole interaction. First, we consider a $^{19}F \rightarrow {}^{13}C$ CP MAS experiment with the spectrum [see Fig. 1(*b*)] acquired using both $^{1}H$ and $^{19}F$ decoupling; clearly, $^{19}F \rightarrow {}^{13}C$ CP gives rise to signals only from $^{13}C$ nuclei that have a dipolar interaction with (and therefore proximity to) $^{19}F$. Second, we discuss a $^{1}H \rightarrow {}^{13}C$ CP MAS experiment with the spectrum [see Fig. 1(*c*)] acquired using only $^{1}H$ decoupling; although all $^{13}C$ nuclei will cross-polarize from $^{1}H$, resonances arising from $^{13}C$ nuclei that experience $^{13}C$–$^{19}F$ dipole–dipole interactions will be broadened significantly in this experiment (note the absence of $^{19}F$ decoupling). In Fig. 1(*b*), the resonance at $\delta$ 14.4 is present, whereas the resonance at $\delta$ 14.7 is absent. In Fig. 1(*c*), the resonance at $\delta$ 14.4 is broadened severely, whereas the resonance at $\delta$ 14.7 is a narrow peak. These observations imply that the resonance at $\delta$ 14.4 arises from $CH_3\cdots FH_2C$ end-group environments, whereas the resonance at $\delta$ 14.7 arises from $CH_3\cdots H_3C$ end-group environments.

Clearly, the resonances for $CH_2F$ cannot be assigned using the above experiments, as the $^{13}C$ nucleus of interest is directly bonded to $^{19}F$. Instead, the classic approaches[5,6] may be used. Thus, $^{1}H \rightarrow {}^{13}C$ CP MAS spectra, acquired using both $^{1}H$ and $^{19}F$ decoupling, for the 1,10-difluorodecane–urea and 1,12-di-

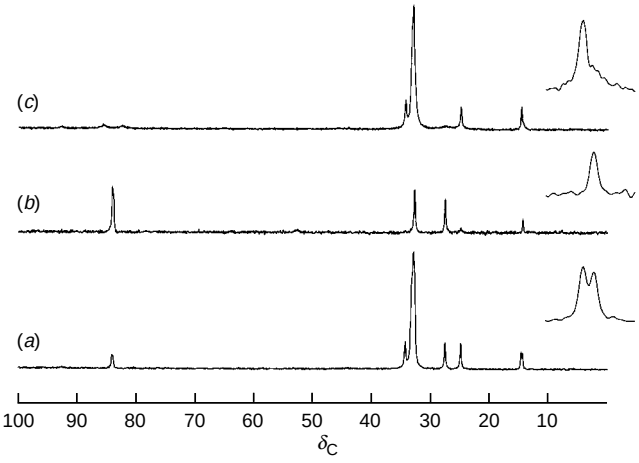



**Fig. 1** Carbon-13 CP MAS spectra (guest region only) of the 1-fluorotetradecane–urea inclusion compound: (*a*) $^{1}H \rightarrow {}^{13}C$ cross-polarization spectrum acquired with $\{^{1}H,^{19}F\}$ double-decoupling; (*b*) $^{19}F \rightarrow {}^{13}C$ cross-polarization spectrum acquired with $\{^{1}H,^{19}F\}$ double-decoupling; (*c*) $^{1}H \rightarrow {}^{13}C$ cross-polarization spectrum acquired with only $^{1}H$ decoupling. In each case the inset shows the $CH_3$ signals on expanded scale.

**Table 1** Carbon-13 chemical shifts and assignments for the 1-fluorotetradecane–urea inclusion compounds

| $\delta_C$ | Assignment |
|---|---|
| 14.4 | $CH_3\cdots FH_2C$ |
| 14.7 | $CH_3\cdots H_3C$ |
| 25.0 | $CH_2CH_3$ |
| 27.6 | $CH_2CH_2CH_2F$ |
| 32.8 | $CH_2CH_2F$ |
| 33.0 | 'inner' $CH_2$ |
| 34.3 | $CH_2CH_2CH_3$ |
| 83.9 | $CH_2F\cdots H_3C$ |
| 84.1 | $CH_2F\cdots FH_2C$ |

fluorododecane–urea inclusion compounds have single resonances due to $CH_2F$ at $\delta$ 84.1 for 1,10-difluorodecane–urea and at $\delta$ 84.2 for 1,12-difluorododecane–urea (in these inclusion compounds, all end-group interactions are of the type $CH_2F\cdots FH_2C$). This suggests that the resonance at $\delta$ 84.1 for 1-fluorotetradecane–urea arises from $CH_2F\cdots FH_2C$ end-group interactions. This assignment has been corroborated by considering the change in relative intensities of the two resonances in $^1H \rightarrow {}^{13}C$ CP MAS spectra for a urea inclusion system containing a mixture of 1-fluorotetradecane and tetradecane (for which the relative proportion of $CH_2F\cdots H_3C$ end-group environments should be higher than that in the 1-fluorotetradecane–urea inclusion compound).

All our assignments of isotropic chemical shifts for 1-fluorotetradecane in the urea tunnel structure are summarized in Table 1.

Although $^{19}F$ NMR has several advantages over $^{13}C$ NMR (including substantially greater sensitivity), it is noteworthy that we have been unable to distinguish different intermolecular environments for $^{19}F$ in the 1-fluorotetradecane–urea inclusion compound using $^{19}F$ MAS NMR (with $^1H$ decoupling). Presumably the $^{19}F$ chemical shift difference between the $CH_2F\cdots H_3C$ and $CH_2F\cdots FH_2C$ end-group environments is too small to be resolved, which in turn probably arises because $^{13}C$ linewidths are significantly smaller ($\Delta\nu_{\frac{1}{2}}$ *ca.* 12 Hz) than $^{19}F$ widths ($\Delta\nu_{\frac{1}{2}}$ *ca.* 125 Hz) for these systems.

The research described here has demonstrated that selective cross-polarization experiments in solid-state $^{13}C$ NMR can provide local structural information on intermolecular arrangements in disordered solids. This shows how triple-resonance solid-state NMR techniques may be exploited to extend our understanding of fundamental structural properties of solids.

Carbon-13 MAS NMR spectra were recorded on a Chemagnetics CMX200 NMR spectrometer operating at 50.33 MHz for $^{13}C$, 200.13 MHz for $^1H$ and 188.27 MHz for $^{19}F$. A Chemagnetics HFX triple-resonance probe was used, with the sample contained in zirconia rotors (7.5 mm outer diameter) fitted with boron nitride spacers and a Kel-F drive tip and end-cap. For $^{13}C$ CP MAS experiments, typical spectral conditions were: $\pi/2$ pulse duration, 4.5 μs; contact times, 1.0 ms ($^1H \rightarrow {}^{13}C$ CP) and 3.0–12.0 ms ($^{19}F \rightarrow {}^{13}C$ CP); spectral width, 20 kHz; recycle delay, 5–10 s; acquisition time, 102.4–153.6 ms; $^1H$ and $^{19}F$ decoupler powers, 56 kHz; MAS frequencies, 1.0–3.0 kHz. Chemical shifts were referenced externally, by rotor replacement, to the high-frequency resonance of adamantane ($\delta$ 38.4 with respect to the signal for tetramethylsilane). All urea inclusion compounds were prepared by slow cooling of solutions containing the guest molecules and urea in either methanol or a mixture of methanol and *tert*-amyl alcohol.

We thank EPSRC for the award of a studentship and ICI for a scholarship to A. N. and EPSRC also for financial support under research grant L02906. Ciba Specialty Chemicals Ltd and the University of Birmingham are thanked for the award of studentships to L. Y. We are grateful to Dr Paul Coe for synthesis of the 1,10-difluorodecane and 1,12-difluorododecane samples used in this work.

## Footnotes and References

* E-mail: r.k.harris@durham.ac.uk; k.d.m.harris@bham.ac.uk

1 C. H. M. Papavoine, W. E. J. R. Maas, W. S. Veeman, G. H. W. Buning and J. M. J. Vankan, *Macromolecules*, 1993, **26**, 6611.
2 S. C. Campbell, R. K. Harris, M. J. Hardy, D. C. Lee and D. J. Busby, *J. Chem. Soc., Perkin Trans. 2*, in the press.
3 M. D. Hollingsworth and K. D. M. Harris, *Comprehensive Supramolecular Chemistry*, ed. D. D. MacNicol, F. Toda and R. Bishop, Pergamon, Oxford, 1996, vol. 6, ch. 7, *Urea, Thiourea and Selenourea*, pp. 177–237.
4 F. Imashiro, T. Maeda, T. Nakai, A. Saika and T. Terao, *J. Phys. Chem.*, 1986, **90**, 5498.
5 M. D. Hollingsworth and N. Cyr, *Mol. Cryst. Liq. Cryst.*, 1990, **187**, 135.
6 M. D. Hollingsworth and A. R. Palmer, *J. Am. Chem. Soc.*, 1993, **115**, 5881.

*Received in Cambridge, UK, 15th July 1997; 7/05053D*

# $CS_2$ insertion into a gold–carbon bond. First syntheses and characterization of 2,2-diacetylethylene-1,1-dithiolato complexes. Crystal structure of $[N(PPh_3)_2][Au\{\eta^2\text{-}S_2C{=}C(COMe)_2\}_2]$†

**José Vicente,*[a]‡ María Teresa Chicote,*[a] Pablo González-Herrero[a] and Peter G. Jones*[b]§**

[a] *Grupo de Química Organometálica,¶ Departamento de Química Inorgánica, Facultad de Química, Universidad de Murcia, Aptdo. 4021, E-30071 Murcia, Spain*

[b] *Institut für Anorganische und Analytische Chemie, Technische Universität Braunschweig, Postfach 3329, 38023 Braunschweig, Germany*

**The reaction of $[N(PPh_3)_2][Au(acac)_2]$ (acac = acetylacetonate) with $CS_2$ gives $[N(PPh_3)_2]_2[Au_2\{\mu^2:\eta^2\text{-}S_2C{=}C(COMe)_2\}_2]$, which reacts with $PhICl_2$ to give $[N(PPh_3)_2][Au\{\eta^2\text{-}S_2C{=}C(COMe)_2\}_2]$, for which the crystal structure is determined; these are the first characterized 2,2-diacetylethylene-1,1-dithiolato complexes of any element.**

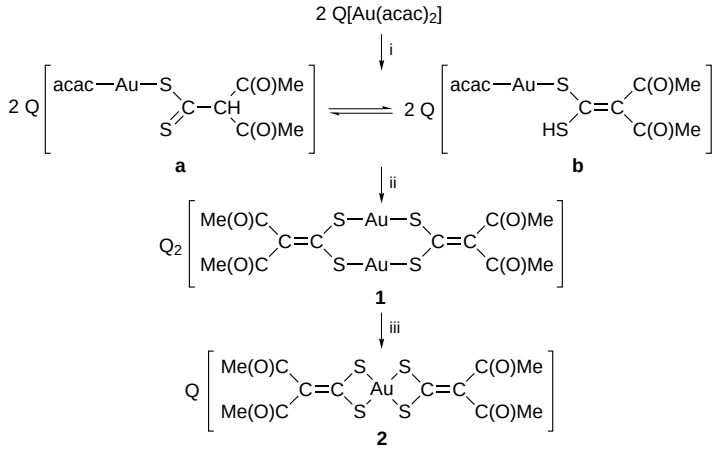
Interest in gold complexes containing S-bonded ligands stems from their potential application in the glass and ceramic industries[1] and, more importantly, in medicine (chrysotherapy).[2] Thiolatogold(I) complexes such as the commercial Myocrisin, Allochrysine, Solganol, or Auranofin, are among the most efficient antiarthritic drugs.[2] In addition, Solganol and Auranofin show *in vitro* inhibitory effects on Human Immunodeficiency Virus 1,[3] high cytotoxicity to tumor cells[4] and activity against i.p. P388 leukaemia.[5]

We have found that $CS_2$ reacts with $[N(PPh_3)_2][Au(acac)_2]$[6] to give $[N(PPh_3)_2]_2[Au_2\{\mu^2:\eta^2\text{-}S_2C{=}C(COMe)_2\}_2]$ **1** (Scheme 1). As far as we are aware, this is the first fully characterized 2,2-diacetylethylene-1,1-dithiolato complex of any element.

In the absence of any mechanistic data, we assume that the $CS_2$ inserts into one of the gold–carbon bonds to produce a dithiocarboxylato complex **a** (see Scheme 1), likely to be in tautomeric equilibrium with the ethylene-1,1-dithiolato form **b**, the remaining acac ligand being responsible for intermolecular deprotonation and subsequent dimerization to give **1** with concomitant formation of acetylacetone.

Insertion reactions of $CS_2$ into transition-metal–H, –C, –N, –P, –S, or –Cl bonds are known to produce dithioformiato, dithiocarboxylato, dithiocarbamato, phosphinodithiocarboxylato, trithio- or perthio-carbonato, or chlorodithioformiato complexes, respectively.[7] However, in the case of gold these reactions have scarcely been studied and thus only two other $CS_2$ insertion reactions have been described so far, namely those into the Au–C bond in $[Au\{\eta^1\text{-}C_5Me_5\}(PR_3)]$ complexes to give dithiocarboxylato complexes $[Au\{\eta^1\text{-}S_2CC_5Me_5\}(PR_3)_n]$ (R = Ph, *n* = 2; R = Pr$^i$, *n* = 3)[8] or into an Au–Cl bond of $[Au_2Cl_6]$ to give the chlorodithioformate complex $[AuCl_2(\eta^2\text{-}S_2CCl)]$.[9] We have ourselves described the insertion of $CS_2$ into an Au–S (or S–H) bond in $[N(PPh_3)_2][Au(SH)_2]$ to produce the first trithiocarbonatogold complex.[10] In the reaction of $CS_2$ with $[Au(C_6F_5)(PPh_2CHPPh_2Me)]$ the complex $[Au^{III}\{PPh_2C(PPh_2Me)CS_2\}_2][Au^I(C_6F_5)_2]$, resulting from a carbon–carbon coupling reaction, is obtained.[11]

The reaction of methylene active compounds with $CS_2$ and $LiNR_2$, NaH,[12] or $K_2CO_3$,[13] led to the synthesis of the corresponding 2,2-disubstituted ethylene-1,1-dithiolate salts, which were treated *in situ* with MeI to give ketene dithioacetals. In this context acetylacetone has been used to prepare the 2-acetyl-2-oxopropylidene-*S*,*S*-acetal $[(MeS)_2C{=}C\{C(O)Me\}_2]$.[13–15] Our synthetic method is, therefore, unprecedented. Ketene dithioacetals are of current interest because the double carbon–carbon bond they present is amenable to both nucleophilic and electrophilic attack.[14] Indeed, they are very versatile starting materials for the synthesis of a wide variety of fused heterocycles,[13,16] polysubstituted pyridines,[17] pyrazoles,[18] *etc.* On the other hand, the interest in ketene dithioacetals with electron-withdrawing substituents stems from some of their physical properties as push–pull polarized ethylenes. Thus, the effect of chiral substituents or hydrogen bonding on second-order non-linearity,[19] the free energy of activation for rotation around the carbon–carbon double




**Scheme 1** Q = $[N(PPh_3)_2]$, acac = acetylacetonate. *Reagents and conditions*: i, $CS_2$ (excess) in acetone, 1 h, room temp; ii, −2 Hacac; iii, + $Cl_2IPh$ − PhI − $Q[AuCl_2]$, $CH_2Cl_2$, 45 min, room temp.

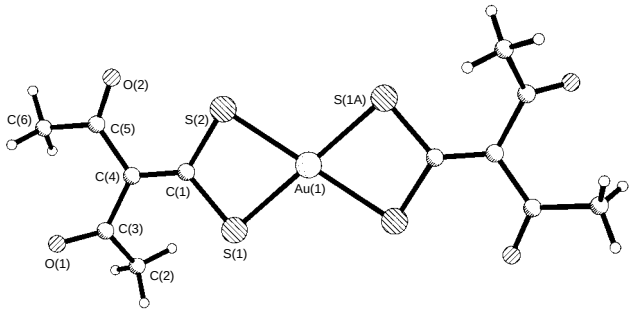



**Fig. 1** Structure of one of the two independent anions of **2**. Selected bond lengths (Å) and angles (°): Au(1)–S(1) 2.3234(13), 2.3375(13), Au(1)–S(2) 2.3479(12), 2.3217(12), C(1)–S(1) 1.758(4), 1.748(4), C(1)–S(2) 1.744(4), 1.755(4), C(1)–C(4) 1.353(6), 1.365(6); S(1)–Au(1)–S(2) 74.16(4), 74.46(4), S(2)–Au(1)–S(1A) 105.84(4), 105.54(4), S(1)–C(1)–S(2) 107.0(2), 107.2(2), S(1)–C(1)–C(4) 125.8(3), 126.1(3), S(2)–C(1)–C(4) 127.2(3), 126.8(4).

bond,[15,20] or the influence of the double bond twisting on the position of the IR $\nu_{C=C}$ stretching band[21] or on the photoionization energy[22] have been studied. Our synthesis opens a new access for such studies. The only 2,2-diacetylethylene-1,1-dithiolato complexes (of $Mn^{II}$, $Co^{II}$, $Ni^{II}$, $Cu^{II}$ and $Zn^{II}$) mentioned in the literature were prepared from the corresponding sodium salt of the ligand and their composition was only established by elemental analysis, while amperometric and potentiometric titrations were unsuccessful.[23]

Many dinuclear gold(I) complexes are known to undergo oxidative addition reactions with halogens, pseudohalogens or alkyl halides to give gold(II) complexes containing a gold–gold bond.[24] However, when complex **1** is treated with an equimolar amount of $Cl_2IPh$ in dichloromethane a disproportionation reaction takes place, giving $[N(PPh_3)_2][AuCl_2]$ along with the gold(III) complex $[N(PPh_3)_2][Au\{\eta^2\text{-}S_2C{=}C(COMe)_2\}_2]$ **2**. The same behaviour has previously been observed for other dithiolato,[25] dialkyldithiocarbamato,[26] or trithiocarbonato[27] gold(I) complexes.

The isolated complexes **1** and **2** have been fully characterized by C, H, N, S analyses, IR spectroscopy and $^1H$ and $^{13}C$ NMR. The X-ray crystal structure of complex **2** (Fig. 1),‖ shows it to crystallize with two independent half-anions and one $[N(PPh_3)_2]$ cation in the asymmetric unit. Both anions show almost identical inversion-symmetric $[Au\{\eta^2\text{-}S_2C{=}C(COMe)_2\}_2]$ *E*,*Z*-conformations. The gold atoms are in distorted square-planar environments, the angles around gold differing from the ideal value of 90° because of the small bite of the dithiolate ligand [S(1)–Au(1)–S(2) 74.16(4), 74.46(4)°; S(1)–Au(1)–S(2′) 105.84(4), 105.54(4)°, respectively]. The Au(1), S(1), S(2), C(1) and C(2) atoms are coplanar (mean deviation 0.054, 0.044 Å), with both acetyl groups twisted out of this plane, one of them considerably (torsion angle 55, 48°), the other one slightly (torsion angle 9, 13°, respectively). The C(1)–C(4) bond distances [1.353(6), 1.365(4) Å] lie in the range expected for $C(sp^2){=}C(sp^2)$ double bonds (1.294–1.392)[28] and are similar to that found in the closely related ketene *S*,*S*-dithioacetal $(MeS)_2C{=}C\{C(O)Me\}_2$ (1.351 Å) which shows a twisted (torsion angle 14°) *E*,*E*-conformation.[29]

Apart from bands due to the cation, the solid-state IR spectrum of **1** shows two strong $\nu$(C=O) bands at 1698 and 1678 $cm^{-1}$ and a strong $\nu$(C=C) band at 1580 $cm^{-1}$, while the $\nu$(AuS) band(s) cannot be assigned unequivocally because of the presence of bands from the $[N(PPh_3)_2]$ cation in the 400–300 $cm^{-1}$ region. The position of the $\nu$(C=O) band suggest that conjugation plays at best a marginal role.[29] The IR spectrum of **2** shows two strong $\nu$(C=O) bands at 1664 and 1636 $cm^{-1}$ and a medium $\nu$(AuS) band at 370 $cm^{-1}$. The frequency of the $\nu$(C=C) band is expected to decrease because of conjugation with one of the acetyl groups and cannot be unequivocally assigned.

We thank DGICYT (PB92-0982C) and the Fonds der Chemischen Industrie for financial support. P. G.-H. is grateful to Ministerio de Educación y Cultura for a Grant.

## Footnotes and References

† Dedicated to Professor Pascual Royo on the occasion of his 60th birthday.

‡ E-mail: jvs@fcu.um.es
§ E-mail: p.jones@tu-bs.de
¶ WWW: http://www.scc.um.es/gi/gqo/

‖ *Crystal data* for complex **2**: $C_{48}H_{42}AuNO_4P_2S_4$, triclinic, space group $P\bar{1}$, $T$ = 143 K, $a$ = 10.729(3), $b$ = 11.853(3), $c$ = 18.076(4) Å, $\alpha$ = 83.13(2), $\beta$ = 81.62(2), $\gamma$ = 79.75(2)°, $U$ = 2227.6(10) $Å^3$, $Z$ = 2, $\lambda$(Mo-K$\alpha$) = 0.710 73 Å, $\mu$ = 3.61 $mm^{-1}$, $D_c$ = 1.616 Mg $m^{-3}$. Data collection: Yellow prism 0.55 × 0.40 × 0.30 mm, Stoe STADI-4 diffractometer, 9522 intensities of which 7867 independent, $2\theta_{max}$ 50°, absorption corrections based on $\psi$-scans with transmissions 0.776–0.933. *Structure solution and refinement*: heavy-atom method, refined anisotropically on $F^2$ (program SHELXL-93, G.M. Sheldrick, University of Göttingen). H atoms with riding model or as rigid methyl groups. In the C(=O)Me groups of the second anion, the slightly short C–C and long C=O bonds and the difficulty in locating methyl H may indicate some disorder. Final $wR(F^2)$ 0.0742, $R(F)$ 0.0296, 547 parameters, 464 restraints, $S$ = 1.09, max $\Delta\rho$ 1.4 e $Å^{-3}$. CCDC 182/591.

1 A. N. Papazian, *Gold Bull.*, 1982, **15**, 81.
2 A. Lorber and T. M. Simon, *Gold Bull.*, 1979, **12**, 149; K. C. Dash and H. Schmidbaur, *Metal Ions in Biological Systems*, ed. H. Sigel, Marcel Dekker, New York, 1982; P. J. Sadler, *Adv. Inorg. Chem.*, 1991, **36**, 1.
3 T. Okada, B. K. Patterson, S.-Q. Ye and M. E. Gurney, *Virology*, 1993, **192**, 631.
4 T. M. Simon, D. H. Kunishima, D. H. Vibert and A. Lorber, *Cancer Res.*, 1981, **41**, 94.
5 C. K. Mirabelli, R. K. Johnson, C. M. Sung, L. Faucette, K. Muirhead and S. T. Crooke, *Cancer Res.*, 1985, **45**, 32.
6 J. Vicente, M. T. Chicote, I. Saura-Llamas and M. C. Lagunas, *J. Chem. Soc. Chem. Commun.*, 1992, 915.
7 K. K. Pandey, *Coord. Chem. Rev.*, 1995, **140**, 37; V. Cadierno, M. P. Gamasa, J. Gimeno and E. Lastra, *J. Organomet. Chem.*, 1996, **510**, 207.
8 H. Otto and H. Werner, *Chem. Ber.*, 1987, **120**, 97.
9 D. Jentsch, P. G. Jones, C. Thöne and E. Schwarzmann, *J. Chem. Soc. Chem. Commun.*, 1989, 1495.
10 J. Vicente, M. T. Chicote, P. González-Herrero and P. G. Jones, *J. Chem. Soc. Chem. Commun.*, 1995, 745.
11 M. Bardají, M. C. Gimeno, P. G. Jones, A. Laguna, M. Laguna, F. Merchán and I. Romeo, *Organometallics*, 1997, **16**, 1083.
12 Z.-T. Huang and X. Shi, *Synthesis*, 1990, 162.
13 A. K. El-Shafei, A. M. M. El-Saghier and E. A. Ahmed, *Synthesis*, 1994, 152.
14 D. Villemin and A. B. Alloum, *Synthesis*, 1991, 301.
15 J. Sandström and I. Wennerbeck, *Acta Chem. Scand.*, 1970, **24**, 1191.
16 L.-B. Wang and Z.-T. Huang, *Synth. Commun.*, 1996, **26**, 459; Z.-T. Huang and X. Shi, *Chem. Ber.*, 1990, **123**, 541.
17 F. A. Abu-Shanab, M. H. Elnagdi, F. M. Ali and B. J. Wakefield, *J. Chem. Soc., Perkin Trans. 1*, 1994, 1449.
18 E. C. Taylor and P. W. Ronald, *Heterocycles*, 1977, **8**, 243.
19 K. Mohanalingam, M. Nethaji and P. K. Das, *J. Mol. Struct.*, 1996, **378**, 177.
20 J. Sandström and U. Sjöstrand, *Tetrahedron*, 1978, **34**, 3305.
21 D. Smith and P. J. Taylor, *J. Chem. Soc., Perkin Trans. 2*, 1979, 1376.
22 F. P. Colonna, G. DiStefano, J. Sandström and U. Sjöstrand, *J. Chem. Soc., Perkin Trans. 2*, 1978, 279.
23 W. U. Malik, R. Bembi and V. K. Bharddwaj, *J. Indian Chem. Soc.*, 1984, **65**, 379.
24 J. P. Fackler Jr., *Polyhedron*, 1997, **16**, 1.
25 M. N. I. Khan, S. Wang and J. P. Fackler Jr., *Inorg. Chem.*, 1989, **28**, 3579.
26 D. C. Calabro, B. A. Harrison, G. T. Palmer, M. K. Moguel, R. L. Rebbert and J. L. Burmeister, *Inorg. Chem.*, 1981, **20**, 4311.
27 J. Vicente, M. T. Chicote, P. González-Herrero and P. G. Jones, unpublished work.
28 F. H. Allen, O. Kennard, D. G. Watson, L. Brammer, A. G. Orpen and R. Taylor, *J. Chem. Soc., Perkin Trans. 2*, 1987, S1.
29 A. J. Jarvis and P. J. Taylor, *J. Chem. Soc., Perkin Trans. 2*, 1978, 972.

*Received in Cambridge, UK, 15th July 1997; 7/05052F*

# Selenoketenyl and selenoalkyne complexes *via* the reactions of ketenyl complexes with Woollins' reagent

**Ian Baxter, Anthony F. Hill,* John M. Malget, Andrew J. P. White and David J. Williams**

*Department of Chemistry, Imperial College of Science, Technology and Medicine, London, UK SW7 2AY*

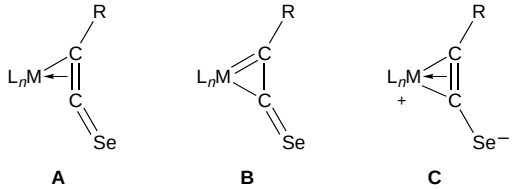
**The complexes [ML(η²-OCCR)(CO)(Tp)] [M = W, Mo; L = $PMe_2Ph$, $PPh_3$, $P(OMe)_3$; R = $C_6H_4Me$-4; Tp = hydrotris(pyrazol-1-yl)borate] react with 'Woollins' reagent' [$4(PPh)_5/5Se_8$] to provide the first examples of selenoketenyl complexes [ML(η²-SeCCR)(CO)(Tp)], alkylation of which provides selenoalkyne complexes; the crystal structures of [W(η²-SeCCR)(CO)($PMe_2Ph$)(Tp)] and [W(η²-MeSeCCR)(CO)($PPh_3$)(Tp)]I are also reported.**

The study of ligands featuring carbon–selenium multiple bonds is hampered by the shortage of suitable ligand precursors, with the majority of studies involving $CSe_2$ and CSSe as source molecules. Thioketenyl ligands have recently begun to attract attention[1–3] however no reports have appeared concerning the preparation of selenoketenyl complexes (Scheme 1). This report is concerned with (*i*) the development of synthetic routes to the first examples of selenoketenyl complexes; (*ii*) the structural characterisation of one such complex, [W(η²-SeCCR)(CO)($PMe_2Ph$)(Tp)] **2b** [hereafter R = $C_6H_4Me$-4, Tp = hydrotris(pyrazol-1-yl)borate]; (*iii*) alkylation of selenoketenyl ligands to provide rare examples of mononuclear selenoalkyne complexes; (*iv*) structural characterisation of one example in the salt [W(η²-MeSeC≡CR)(CO)($PPh_3$)(Tp)]I **4a**.

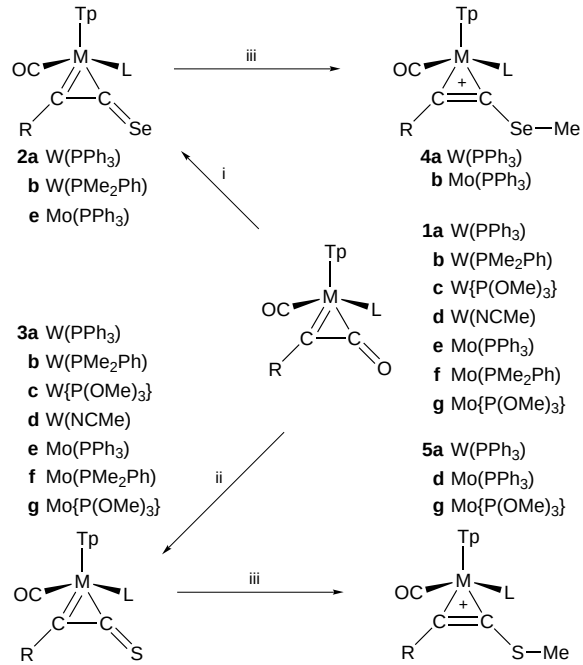
We have recently described two routes for the conversion of ketenyl complexes of tungsten to their sulfur congeners.[3] The first involves the initial conversion of a ketenyl ligand to a chloroalkyne and then treatment with sodium hydrosulfide. In our hands, this approach has so far failed in the case of sodium hydroselenide or lithium selenide, with intractible mixtures being obtained. The second approach involves the reaction of a ketenyl ligand with Lawesson's oxygen/sulfur transfer reagent and appeared attractive except that the selenium analogue has yet to be reported.[4,5] Woollins has prepared a range of organophosphorus selenides from the reaction of cyclopolyphosphines with selenium.[5] For brevity, we shall refer to as Woollins' reagent, the compound which is presumed to be 2,4-bis(phenyl)-1,3-diselena-2,4-diphosphetane-2,4-diselenide, obtained from $(PPh)_5$ and elemental selenium (P : Se ratio 1 : 2). Studies to date suggest a similar reactivity profile, at least in part, to that of Lawesson's reagent.[5] The ketenyl complex [W(η²-OCCR)(CO)($PPh_3$)(Tp)] **1a**[6] reacts cleanly with Woollins' reagent to provide [W(η²-SeCCR)(CO)($PPh_3$)(Tp)] **2a** in high yield as the only isolable species (Scheme 2). The formulation follows from spectroscopic data† which are comparable to those for the related thioketenyl complexes[3] and the complexes [ML(η²-SeCCR)(CO)(Tp)] [ML = $WPMe_2Ph$, $MoPPh_3$, $MoP(OMe)_3$] which may be obtained in a similar manner from Woollins' reagent and [ML(η²-OCCR)(CO)(Tp)] (Scheme 2). The series of complexes **1a**, **3a** and **2a** shows a steady increase in the IR frequency of the carbonyl-associated absorption [**1a**, 1883; **2a**, 1909; **3a**, 1919 $cm^{-1}$], suggesting that the π-acidity of chalcoketenyl ligands increases in the order O, S, Se.

One example, **2b**, of this new class of compound was characterised by X-ray crystallography (Fig. 1).‡ The overall structure is remarkably similar to that of [W(η²-OCCR)(CO)($PPh_3$)(Tp)].[6] The bonding of the selenoketenyl ligand is dihapto through C(1) and C(36), the C=C=Se grouping lying in the equatorial coordination plane which also contains the carbonyl ligand. The W–N distances are unremarkable and in the range 2.188(9)–2.251(8) Å, the shortest of these being that *trans* to the phosphine, whilst the N–W–N angles are similar [79.8(3)–82.2(3)°]. The binding of the selenoketenyl ligand is best described by three resonance forms **A**–**C** (Scheme 1). There is clearly multiple bonding between W and C(1) [2.003(11) Å], W and C(36) [2.078(10) Å] and C(1) and C(36) [1.328(13) Å]. Furthermore, whilst there is little appropriate crystallographic precedent,[7] the C(36)–Se(37) separation [1.834(11) Å] clearly indicates a degree of partial double bond character.

Consistent with their alternative formulation as chalcogenoxyalkyne complexes (**C**, Scheme 1), the new complexes **2** and the related thioketenyl complexes [ML(η²-SCCR)(CO)(Tp)][3] are readily alkylated at the chalcogen to provide complexes of selenolato and thiolato alkynes (Scheme 2). Thus the new complexes **4** and **5** were readily obtained from the reaction of




**Scheme 1** Valence bond descriptions for selenoketenyl ligands




**Scheme 2** *Reagents*: i, $4(PPh)_5/5Se_8$; ii, $(S_2PC_6H_4OMe\text{-}4)_2$; iii, MeI; M = Mo, W; R = $C_6H_4Me$-4; L = $PPh_3$, $P(OMe)_3$, $PMe_2Ph$, MeCN; Tp = hydrotris(pyrazol-1-yl)borate

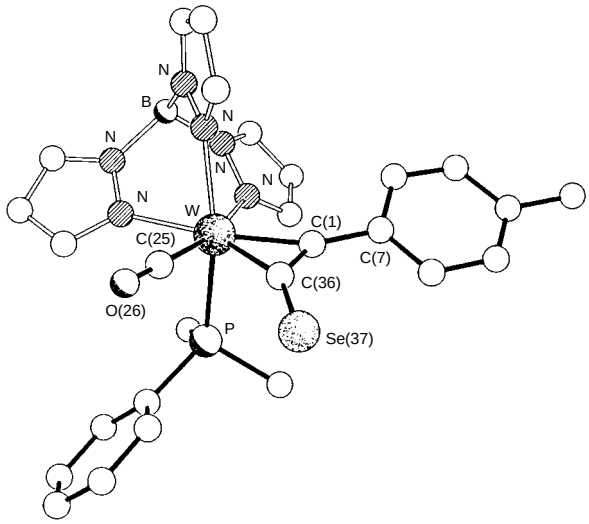



**Fig. 1** Molecular geometry of **2b** (hydrogen atoms omitted)

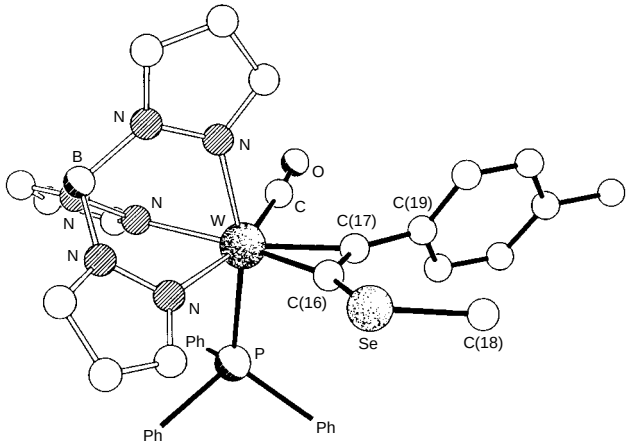



**Fig. 2** Molecular geometry of **4a** (phenyl groups, hydrogen atoms and iodide counter-anion omitted)

selected examples of **2** or **3** with iodomethane. The salts **4**† provide rare examples of mononuclear selenoalkyne complexes.[8] Notably, alkylation of **2** is considerably more rapid than for **3** and the ketenyl complexes **1** fail to react with alkyl halides.

The tungsten salt [W($\eta^2$-MeSeCCR)(CO)($PPh_3$)(Tp)]I **4a**, has been structurally characterised.‡ The molecular geometry of the cation (Fig. 2) is topologically similar to that of **2b** with the notable exception that the alkyne orientation now places the tolyl group *syn* to the carbonyl ligand *cf*. the *anti* arrangement of these groups in **2b**. Within the Tp scorpionate, the W–N bond *trans* to the carbonyl [2.172(13) Å] is somewhat shorter that the other two W–N distances [2.216(13), 2.218(12) Å]. The dimensions associated with the selenoalkyne coordination are somewhat similar to those of **2b**. Once again there is multiple bonding between W and C(17) [2.05(2) Å], and between W and C(16) [2.02(2) Å], however there is a notable loss of double bond character between C(16) and C(17) [1.39(2) Å] *cf*. **2b**. The C(16)–Se separation [1.81(2) Å] suggests that the partial double bond character observed in **2b** is retained upon alkylation, this being shorter than for the Se–C(18) separation [1.97(2) Å] which is typical for a Se–C($sp^3$) bond. The modest perturbation of these dimensions on alkylation lends further support to the significant contribution of resonance form **C** to the bonding description of **2b**.

The successful deployment of Woollins' reagent for the oxygen/selenium transfer conversion of coordinated organometallic ligands bodes well for the elaboration of further unsaturated organoselenium ligands, an avenue we are currently investigating. Ketenyl complexes are typically formed from the often reversible coupling of alkylidyne and carbonyl ligands. It remains to be seen if thioketenyl and selenoketenyl ligands may decouple to serve as precursors for chalcocarbonyl co-ligated alkylidyne complexes, $L_nM(\equiv CR)(CA)$ (A = S, Se).

We gratefully acknowledge the EPSRC (UK) for the award of a studentship (to J. M. M.) and the provision of a diffractometer. A. F. H. wishes to thank the Leverhulme Trust and the Royal Society for the award of a Senior Research Fellowship.

## Footnotes and References

* E-mail: a.hill@ic.ac.uk

† *Data for selected complexes* (satisfactory microanalytical data obtained for all complexes): **2b**: yield 90%. IR ($CH_2Cl_2$) 1906 $cm^{-1}$ [$\nu$(CO)]. NMR ($CDCl_3$, 25 °C). $^1$H: $\delta$ 1.35, 1.60 [d × 2, 6 H, ($PMe_2$), $^2J$(PH) 8.6 Hz], 2.30 (s, 3 H, CMe), 5.96, 6.17, 6.25 [app. t × 3, 3 H, H$^4$(pz), $^3J$(HH) 2 Hz], 6.76–7.91 [m, 15 H, $C_6H_4$, Ph and H$^{3,5}$(pz)]. $^{13}$C{$^1$H}: $\delta$ 237.6 [W*C*Se], 231.6 [WCO], 222.4 [W=CCSe], 146.6, 145.7, 142.4 [C$^3$(pz)], 136.4, 135.6, 135.5 [C$^5$(pz)], 130.0–128.0 (Ph and $C_6H_4$), 106.7, 106.2, 106.0 [C$^4$(pz)], 21.5 (C*Me*), 15.6, 14.1 [d × 2, ($PMe_2$), $^1J$(PC) 24 Hz]. $^{31}$P{$^1$H}: $\delta$ −5.1 [$^1J$(WP) 328.9 Hz]. FABMS: *m/z* (%) 757(14) $[M]^+$, 728(45) $[M - CO]^+$, 592(82) $[M - CO - PMe_2Ph]^+$. **4a**: Yield 90%. The complex exists in solution as two isomers related by alkyne rotation: major isomer: IR ($CH_2Cl_2$): 1949 $cm^{-1}$ [$\nu$(CO)]. NMR ($CDCl_3$, 25 °C). $^1$H: $\delta$ 1.96 (s, 3 H, C*Me*), 2.40 (s, 3 H, SeMe), 5.93–7.35 [m, 22 H, $C_6H_4$, $C_6H_5$ and H$^5$(pz)], 7.79, 8.04, 8.09 [H$^3$(pz), $^3J$(HH) 2 Hz]. $^{13}$C{$^1$H}: $\delta$ 232.2 [WCO, $^1J$(WC) 140 Hz], 220.6 (W=*C*R), 147.4–128.3 [$C_6H_4$, Ph and C$^{3,5}$(pz)], 107.9, 107.6, 107.4 [C$^4$(pz)], 21.6(C*Me*), 10.7 (Se*Me*). $^{31}$P{$^1$H}: $\delta$ 32.8 [$^1J$(WP) 309 Hz]. FABMS: *m/z* (%) 897(80) $[M]^+$, 852(6) $[M - CO]^+$.

‡ *Crystal data*: **2b**: $C_{27}H_{28}BN_6OPSeW{\cdot}CHCl_3$, $M$ = 876.51, orthorhombic, space group *Pbca*, $a$ = 14.691(3), $b$ = 15.940(4), $c$ = 28.162(7) Å, $U$ = 6595(3) Å$^3$, $Z$ = 8, $D_c$ = 1.766 g $cm^{-3}$, $\mu$(Mo-K$\alpha$) = 4.93 $mm^{-1}$, $F$(000) = 3408. A dark green needle of dimensions 0.53 × 0.22 × 0.10 mm was used. **4a**: $C_{38}H_{35}BIN_6OPSeW{\cdot}2CH_2Cl_2$, $M$ = 1193.06, triclinic, space group $P\bar{1}$, $a$ = 9.642(3), $b$ = 13.010(3), $c$ = 19.500(5) Å, $\alpha$ = 70.54(1), $\beta$ = 86.76(2), $\gamma$ = 86.67(2)°, $U$ = 2299(1) Å$^3$, $Z$ = 2, $D_c$ = 1.724 g $cm^{-3}$, $\mu$(Mo-K$\alpha$) = 4.28 $mm^{-1}$, $F$(000) = 1156. A blue block of dimensions 0.33 × 0.27 × 0.17 mm was used. For **2b** and **4a**, 5809 and 7980 independent reflections were measured, respectively, on a Siemens P4/PC diffractometer (graphite-monochromated Mo-K$\alpha$ radiation, 293(2) K) using $\omega$ scans. The structures were solved by direct methods and all the non-hydrogen atoms were refined anisotropically using full-matrix least squares based on $F^2$ and absorption-corrected data to give for **2b**, $R_1$ = 0.058, and $wR_2$ = 0.093 [3179 observed reflections, $|F_o| > 4\sigma(|F_o|)$, $2\theta \leqslant 50°$, 368 parameters] and for **4a** $R_1$ = 0.075, and $wR_2$ = 0.144 [4865 observed reflections, $|F_o| > 4\sigma(|F_o|)$, $2\theta \leqslant 50°$, 514 parameters]. CCDC 182/594.

1 A. Mayr and T.-Y. Lee, *Angew. Chem., Int. Ed. Engl.*, 1993, **32**, 1726.
2 T. Y. Lee and A. Mayr, *J. Am. Chem. Soc.*, 1994, **116**, 10 300.
3 A. F. Hill and J. M. Malget, *Chem. Commun.*, 1996, 1177.
4 The compounds [$Se_2PC_6H_2Bu^t_2(CH_2NR_2)$] have been reported: M. Yoshifuji, S. Sangu and K. Kamijo, *Chem. Ber.*, 1996, **129**, 1049. Compound $Ph_3P$=CPhP(=Se)$_2$ has also been described: G. Jochem, K. Karaghisoff, S. Plank, S. Dick and A. Schmidpeter, *Chem. Ber.*, 1995, **128**, 1207; G. Jochem, H. Noth and A. Schmidpeter, *Angew. Chem., Int. Ed. Engl.*, 1993, **32**, 1089.
5 J. C. Fitzmaurice, D. J. Williams, P. T. Wood and J. D. Woollins, *J. Chem. Soc., Chem. Commun.*, 1988, 741; P. T. Wood and J. D. Woollins, *J. Chem. Soc., Chem. Commun.*, 1988, 1190; P. T. Wood and J. D. Woollins, *Phosphorus Sulfur. Relat. Elements*, 1989, **41**, 51; M. J. Pilkington, A. M. Z. Slawin, D. J. Williams and J. D. Woollins, *Phosphorus Sulfur Relat. Elements*, 1992, **64**, 289; I. P. Parkin, M. J. Pilkington, A. M. Z. Slawin, D. J. Williams and J. D. Woollins, *Polyhedron*, 1990, **9**, 987; S. W. Hall, M. J. Pilkington, A. M. Z. Slawin, D. J. Williams and J. D. Woollins, *Polyhedron*, 1991, **10**, 261.
6 A. F. Hill, J. M. Malget, A. J. P. White and D. J. Williams, *Chem. Commun.*, 1996, 721.
7 [Rh($\eta^2$-SeCSe)Cl{$\kappa^3$-($PPh_2CH_2)_3$CMe}], exocyclic 1.711, metallacyclic 1.904 Å; C. Bianchini, C. Mealli, A. Meli and M. Sabat, *J. Chem. Soc., Chem. Commun.*, 1984, 1647; [Rh($\eta^2$-SeC=$CH_2$)($PPr^i_3$)($\eta$-$C_5H_5$)], 1.81 Å; J. Wolf, R. Zolk, U. Schubert and H. Werner, *J. Organomet. Chem.*, 1988, **340**, 161; [Se=C($C_6H_4OMe)_2$], 1.79 Å; K. Okuma, K. Kojima, I. Kaneko, Y. Tsujimoto, H. Ohta and Y. Yokomori, *J. Chem. Soc., Perkin Trans. 1*, 1994, 2151.
8 P. Neumann and K. Dehnicke, *Z. Naturforsch., Teil B*, 1991, **46**, 999.

*Received in Cambridge, UK, 16th July 1997; 7/05083F*

# Platinum catalysed 1,4-diboration of α,β-unsaturated ketones

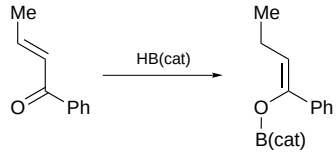
**Yvonne G. Lawson,[a] M. J. Gerald Lesley,[a] Todd B. Marder,*[b]† Nicholas C. Norman*[a] and Craig R. Rice[a]**

[a] *The University of Bristol, School of Chemistry, Cantock's Close, Bristol, UK BS8 1TS*
[b] *The University of Waterloo, Department of Chemistry, Waterloo, Ontario, Canada N2L 3G1*

**Diborane(4) compounds react with α,β-unsaturated ketones to give the 1,4-addition product in the presence of a platinum catalyst at 80 °C.**

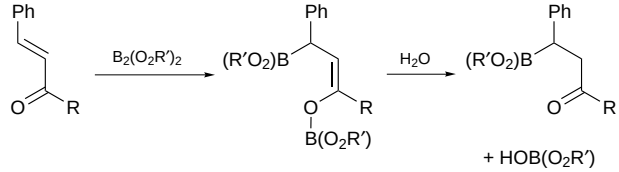
In contrast with the rhodium-catalysed hydroboration of alkenes, alkynes and α,β-unsaturated carbonyl compounds, which is now well established,[1] the related topic of metal-catalysed diboration reactions has only recently been studied in any detail. Thus the groups of Baker and Marder,[2] Miyaura[3] and Smith[4] have shown that alkenes can be diborated in the presence of rhodium,[2] gold[2] or platinum[3,4] catalysts affording 1,2-bis-(boronate) ester products, whilst platinum catalysed alkyne diboration yielding *cis*-1,2-bis(boronate) alkenes has been demonstrated by Miyaura and coworkers,[5a,b] Iverson and Smith[5c,d] and Norman and coworkers.[5e] Additional studies by Miyaura and coworkers[6] have also demonstrated 1,4-addition of a B–B bond to 1,3-dienes. In all cases, key steps are thought to involve oxidative addition of the B–B bond of a diborane(4) compound to the metal centre followed by coordination and insertion of the organic precursor and subsequent reductive elimination of the product.[7]

To date, however, the reaction of α,β-unsaturated carbonyl compounds with diborane(4) compounds has not been studied, although previous work has shown that HB(cat) (cat = 1,2-$O_2C_6H_4$) reacts with α,β-unsaturated carbonyl compounds in a 1,4 fashion[8] to give a synthetically useful[9] boron enolate as shown in Scheme 1. Here we report the reaction of α,β-unsaturated ketones with the diborane(4) compounds $B_2(pin)_2$ **1**[10] (pin = $OCMe_2CMe_2O$) and $B_2(cat)_2$ **2**.[11]




**Scheme 1**

Reaction of *trans*-4-phenylbut-3-en-2-one **3a** or *trans*-1,2-diphenylprop-2-en-1-one **3b** with 1 equiv. of **1** in the presence of 5 mol% of $[Pt(C_2H_4)(PPh_3)_2]$ at 80 °C gave, after 12 h, the 1,4-bis(boronate) ester products **4a**,**b** quantitatively as judged by $^1$H NMR spectroscopy (Scheme 2).‡ Furthermore, the $^1$H NMR spectra of **4a** and **4b** showed that each was present as only a single isomer which, in the case of **4a** and, by implication **4b**, is assumed to be the *Z*-isomer on the basis of a $^1$H NMR NOE signal enhancement (13.1%) between the vinylic and methyl protons; both hydroboration of α,β-unsaturated ketones[8] and diboration of dienes[5] also produce only the *Z*-isomer. Compounds **4a** and **4b** are both sensitive to hydrolysis and exposure to $H_2O$ affords the hydrolysis products **5a** and **5b** (Scheme 2).§




**3a** R = Me
**b** R = Ph

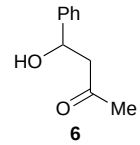
**4a** R = Me, $O_2R'$ = pin
**b** R = Ph, $O_2R'$ = pin
(**c** R = Me, $O_2R'$ = cat)

**5a** R = Me, $O_2R'$ = pin
**b** R = Ph, $O_2R'$ = pin
**c** R = Me, $O_2R'$ = cat

**Scheme 2**

In the corresponding reaction between **3a** and **2**, the 1,4-bis(boronate) ester **4c** analogous to **4a**,**b** was not observed but the hydrolysis product, **5c**, was identified by $^1$H NMR spectroscopy.¶ This observation indicates that the initial products formed from reactions involving **2** are more susceptible to hydrolysis than those involving **1** in keeping with observations made in the diboration of alkynes.[5e]

As further confirmation of the nature of the products formed in these reactions, compounds **5a** and **5c** were oxidised using $NaOH–H_2O_2$ to give the corresponding alcohol **6**‖ which was identified by the comparison of the spectra obtained with lit. values.[12]




**6**

Comparison of **4a**,**b** with the products formed from the hydroboration of similar α,β-unsaturated ketones shows that the regiochemistry is similar in both reactions, *i.e.* 1,4-addition occurs. However the reaction of diborane(4) compounds with α,β-unsaturated ketones results in the effective formation of a hydroxyl group in the β position (*i.e.* compound **6** in the case of **4a**), in contrast to hydroboration where no hydroxyl group is formed but in which the alkene function is effectively reduced.

We note finally that boron enolates such as **4a**,**c** are likely to be useful intermediates in organic synthesis providing starting materials in processes such as aldol condensations with aldehydes.[9] Reactions, of α,β-unsaturated ketones with chiral diborane(4) compounds will be reported elsewhere.

T. B. M. thanks NSERC of Canada and N. C. N. thanks the EPSRC, Laporte plc and The Royal Society for research support. T. B. M. and N. C. N. also thank NSERC and The Royal Society for supporting this collaboration *via* a series of Bilateral Exchange Awards. Johnson Matthey Ltd. are thanked for generous supplies of platinum salts.

## Footnotes and References

* E-mail: todd.marder@durham.ac.uk; n.c.norman@bristol.ac.uk
† Present address: The University of Durham, Department of Chemistry, Science Laboratories, South Road, Durham, UK DH1 3LE.

‡ *Synthesis* of **4a**: to a Schlenk tube charged with **1** (0.020 g, 0.079 mmol), $[Pt(C_2H_4)(PPh_3)_2]$ (5 mol%) and **3a** (0.013 g, 0.087 mmol), toluene (5 $cm^3$) was added and the reaction heated at 80 °C for 12 h. After this time the toluene was removed by vacuum affording a red oil containing **4a** as the major product (0.030 g, 90%) (the red colour is due to traces of decomposed catalyst). Compound **4b** was prepared similarly. *NMR data*: **4a**: $^1$H (300 MHz, $C_6D_6$) $\delta$ 7.6–7.1 (m, 5 H, Ph), 5.40 (dq, 1 H, C=CH, $^3J_{HH}$ 8.7, $^4J_{HH}$ 1.0 Hz), 4.06 [br d, 1 H, C*H*(B)Ph, $^3J_{HH}$ 8.7 Hz, coupling to Me not resolved

owing to broadening resulting from the adjacent boron], 2.05 (dd, 3 H, Me, $^4J_{HH}$ 1.0, $^5J_{HH}$ 1.0 Hz), 1.06 [s, 6 H, B(OC*Me*$_2$CMe$_2$O)], 1.04 [s, 6 H, B(OCMe$_2$C*Me*$_2$O)], 1.03 [s, 12 H, OB(OC*Me*$_2$C*Me*$_2$O)]; $^{13}$C{$^1$H} (75.4 MHz, $C_6D_6$) $\delta$ 146.5 (*ipso*-Ph), 143.6 [=*C*(Me)], 129.5, 129.1, 128.9 (Ph), 112.0 (=CH), 83.5, 83.0 [B(O*C*Me$_2$*C*Me$_2$O)], 25.3, 24.9, 24.7 [B(OC*Me*$_2$C-*Me*$_2$O)], 21.6 (Me), *C*H(B)Ph not observed; $^{11}$B{$^1$H} (96.3 MHz, $C_6D_6$) $\delta$ 30.8 (1B, CB), 20.0 (1B, OB). **4b**: $^1$H (300 MHz, $C_6D_6$) $\delta$ 7.3–7.0 (m, 10 H, Ph), 5.82 (d, 1 H, C=CH, $^3J_{HH}$ 8.7 Hz), 3.54 [br d, 1 H, C*H*(B)Ph, $^3J_{HH}$ 8.7 Hz], 1.16 [s, 6 H, B(OC*Me*$_2$CMe$_2$O)]; 1.14 [s, 6 H, B(OCMe$_2$C*Me*$_2$O)], 1.12 [s, 12 H, OB(OC*Me*$_2$CMe$_2$O)]; $^{13}$C{$^1$H} (75.4 MHz, $C_6D_6$) $\delta$ 146.9 [=*C*(Ph)], 141.9, 141.7 (*ipso*-Ph), 128.3, 128.2, 128.1, 128.0, 125.3, 124.4 (Ph), 112.8 (=CH), 83.5, 83.3 [B(O*C*Me$_2$*C*Me$_2$O)], 30.0 [br, *C*H(B)Ph], 24.7, 24.6, 23.0 [B(OC*Me*$_2$C*Me*$_2$O)]; $^{11}$B{$^1$H} (96.3 MHz, $C_6D_6$) $\delta$ 30.6 (1B, CB), 19.5 (1B, OB).

§ *Synthesis* of **5a**; Hydrolysis of **4a** was achieved by addition of $H_2O$ (0.5 cm$^3$) to a solution of **4a** (0.20 g, 0.5 mmol) in toluene (2 cm$^3$), removal of both the solvents by vacuum and extraction of the residue into hexane (3 $\times$ 1 cm$^3$) affording **5a** as a colourless oil (0.137 g, 100%). Compound **5b** was prepared similarly. *NMR data*: **5a**: $^1$H (400 MHz, $CDCl_3$) $\delta$ 7.25 (m, 5 H, Ph), 3.04 [dd, 1 H, C*H*(B)Ph/C*H*$_2$, $^3J_{HH}$ 11.0, $^3J_{HH}$ 18.3 Hz], 2.83 [dd, 1 H, C*H*(B)Ph/C*H*$_2$, $^3J_{HH}$ 5.1, $^3J_{HH}$ 18.3 Hz], 2.64 [dd, 1 H, C*H*(B)Ph/C*H*$_2$, $^3J_{HH}$ 5.1, $^3J_{HH}$ 11.0 Hz], 2.14 (s, 3 H, Me), 1.22 [s, 6 H, B(OC*Me*$_2$CMe$_2$O)], 1.16 [s, 6 H, B(OCMe$_2$C*Me*$_2$O)]; $^{13}$C{$^1$H} (75.4 MHz, $C_6D_6$) $\delta$ 206.6 (CO), 142.7 (*ipso*-Ph), 128.7, 128.6, 125.7 (Ph), 83.3 [B(O*C*Me$_2$*C*Me$_2$O)], 47.5 (*C*H$_2$), 28.9 (Me), 24.7 [B(OC*Me*$_2$CMe$_2$O)], 24.6 [B(OCMe$_2$C*Me*$_2$O)], *C*H(B)Ph not observed; $^{11}$B{$^1$H} (96.3 MHz, $C_6D_6$) $\delta$ 31.3. **5b**: $^1$H (300 MHz, $CDCl_3$) $\delta$ 8.00–7.00 (m, 10 H, Ph), 3.49 [dd, 1 H, C*H*(B)Ph/C*H*$_2$, $^3J_{HH}$ 10.8, $^3J_{HH}$ 18.3 Hz], 3.35 [dd, 1 H, C*H*(B)Ph/C*H*$_2$, $^3J_{HH}$ 5.1, $^3J_{HH}$ 18.3 Hz], 2.72 [dd, 1 H, C*H*(B)Ph/C*H*$_2$, $^3J_{HH}$ 5.1, $^3J_{HH}$ 10.8 Hz], 1.17 [s, 6 H, B(OC*Me*$_2$CMe$_2$O)], 1.10 [s, 6 H, B(OCMe$_2$C*Me*$_2$O)]; $^{13}$C{$^1$H} (75.4 MHz, $C_6D_6$) $\delta$ 199.7 (CO), 144.9, 142.0 (*ipso*-Ph), 132.9, 129.0, 128.5, 128.4, 128.0, 125.6 (Ph), 83.4 [B(O*C*Me$_2$*C*Me$_2$O)], 43.3 (CH$_2$), 24.6 [B(OC*Me*$_2$C-Me$_2$O)], 24.5 [B(OCMe$_2$C*Me*$_2$O)], *C*H(B)Ph not observed; $^{11}$B{$^1$H} (96.3 MHz, $CDCl_3$) $\delta$ 30.8.

¶ *NMR data* for **5c**: $^1$H (300 MHz, $C_6D_6$) $\delta$ 6.75 (m, 5 H, Ph), 6.45 [m, 4 H, B(1,2-O$_2$C$_6$H$_4$)], 2.64 [dd, 1 H, C*H*(B)Ph/C*H*$_2$, $^3J_{HH}$ 6.1, $^3J_{HH}$ 9.2 Hz], 2.48 [dd, 1 H, C*H*(B)Ph/C*H*$_2$, $^3J_{HH}$ 9.2, $^3J_{HH}$ 18.6 Hz], 2.24 [dd, 1 H, C*H*(B)Ph/C*H*$_2$, $^3J_{HH}$ 6.1, $^3J_{HH}$ 18.6 Hz], 1.61 (s, 3 H, Me); $^{13}$C{$^1$H} (75.4 MHz, $C_6D_6$) $\delta$ 210.0 (CO), 149.4 [C$^{1,2}$ of B(1,2-O$_2$C$_6$H$_4$)], 142.9 (*ipso*-Ph), 128.7, 128.6, 125.9 (Ph), 122.5 [C$^{4,5}$ of B(1,2-O$_2$C$_6$H$_4$)], 112.6 [C$^{3,6}$ of B(1,2-O$_2$C$_6$H$_4$)], 48.5 (CH$_2$), 28.1 (Me), *C*H(B)Ph not observed; $^{11}$B{$^1$H} (96.3 MHz, $C_6D_6$) $\delta$ 32.5.

‖ *Synthesis* of **6**: To a solution of **4a** (0.050 g, 0.18 mmol) in thf (1 cm$^3$), samples of EtOH (1 cm$^3$), NaOH(aq) (1 cm$^3$ of a 1 M solution) and $H_2O_2$ (30 vol%, 1 cm$^3$) (CAUTION: peroxides and organic solvents can be explosive) were added and the reaction mixture stirred at room temp. for 12 h. After this time the crude product was extracted into $Et_2O$ (2 $\times$ 5 cm$^3$), dried ($MgSO_4$) and evaporated to dryness affording **6** as an oily solid (0.024 g, 80%).


1 K. Burgess and M. J. Ohlmeyer, *Chem. Rev.*, 1991, **91**, 1179; I. Beletskaya and A. Pelter, *Tetrahedron*, 1997, **53**, 4957.
2 R. T. Baker, P. Nguyen, T. B. Marder and S. A. Westcott, *Angew. Chem., Int. Ed. Engl.*, 1995, **34**, 1336.
3 T. Ishiyama, M. Yamamoto and N. Miyaura, *Chem. Commun.*, 1997, 689.
4 C. N. Iverson and M. R. Smith, *Organometallics*, 1997, **16**, 2757.
5 (*a*) T. Ishiyama, N. Matsuda, N. Miyaura and A. Suzuki, *J. Am. Chem. Soc.*, 1993, **115**, 11 018; (*b*) F. Ozaura, A. Suzuki and N. Miyaura, *Organometallics*, 1996, **15**, 713; (*c*) C. N. Iverson and M. R. Smith, *J. Am. Chem. Soc.*, 1995, **117**, 4403; (*d*) C. N. Iverson and M. R. Smith, *Organometallics*, 1996, **15**, 5155; (*e*) M. J. G. Lesley, P. Nguyen, N. J. Taylor, T. B. Marder, A. J. Scott, W. Clegg and N. C. Norman, *Organometallics*, 1996, **15**, 5137.
6 T. Ishiyama, M. Yamamoto, and N. Miyaura, *Chem. Commun.*, 1996, 2073.
7 C. Dai, M. J. G. Lesley, T. B. Marder, N. C. Norman and C. R. Rice, *Main Group Chem. News*, 1997, in the press.
8 D. A. Evans and G. C. Fu, *J. Org. Chem.*, 1990, **55**, 5678.
9 Y. Matsumoto and T. Hayashi, *Synlett*, 1991, 349.
10 H. Nöth, *Z. Naturforsch., Teil B*, 1984, **39**, 1463.
11 F. J. Lawlor, N. C. Norman, N. L. Pickett, E. G. Robins, P. Nguyen, M. J. G. Lesley, T. B. Marder, J. A. Ashmore and J. C. Green, *Inorg. Chem.*, in the press.
12 A. Fauve and H. Veschambre, *J. Org. Chem.*, 1988, **53**, 5215.



*Received in Cambridge, UK, 6th August 1997; 7/05743A*

# Efficient synthesis of a molecular knot by copper(I)-induced formation of the precursor followed by ruthenium(II)-catalysed ring closing metathesis

**Christiane Dietrich-Buchecker, Gwénaël Rapenne and Jean-Pierre Sauvage***

*Laboratoire de Chimie Organo-Minérale, URA 422 CNRS, Université Louis Pasteur, Institut Le Bel, 4, rue Blaise Pascal, F-67070 Strasbourg, France*

**A double-stranded helix constructed around two copper(I) centres used as templates and bearing four terminal alkenes, is converted into a trefoil knot in 74% yield by ruthenium(II)-catalysed ring closing methathesis (RCM); the cyclic alkenes can be quantitatively reduced by catalytic hydrogenation to afford the copper(I)-complexed 82-membered knotted ring.**

In molecular biology, knots constructed on double-stranded DNA have been described more than twenty years ago.[1] Recently, the trefoil knot, but also more complex topologies, have been generated from single-stranded DNA.[2] Some proteins have also been shown to adopt knotted topologies.[3] The planned synthesis of chemical knots was first reported a few years ago,[4] but clearly the yield had to be increased both for the synthetic challenge that this improvement represented and for the interesting properties of this new family of compounds.[5] A more preparative procedure (30% yield) was recently described,[6] but we still looked for a more efficient and chemically milder method. The ring-closing metathesis approach (RCM)[7] which we now describe seems to be close to ideal: not only is the yield excellent considering the complexity of the reaction but the procedure takes place under very gentle conditions (without any acid or base, in $CH_2Cl_2$ at room temp.).

The strategy (Fig. 1) relies on (*i*) quantitative formation and high stability of the helical precursor composed of copper(I) bisphenanthroline units with 1,3-phenylene linkers between the phenanthroline nuclei,[5c,6] and (*ii*) the highly efficient RCM methodology developed by Grubbs and coworkers.[7]

Ligand **2** was obtained in 97% yield by reaction of **1** with 2-(2-chloroethoxy)ethanol in DMF at 80 °C, in the presence of $Cs_2CO_3$. It could be quantitatively converted to **3** by generating the dialcoholate with NaH and reacting it with an excess of allyl bromide in refluxing THF. The helical precursor $\mathbf{4}^{2+}$ was

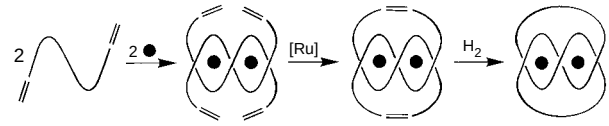



**Fig. 1** Synthetic strategy. Two coordinating fragments bearing terminal alkenes are gathered and interlaced around two copper(I) centres. RCM with ruthenium catalyst affords the knot.

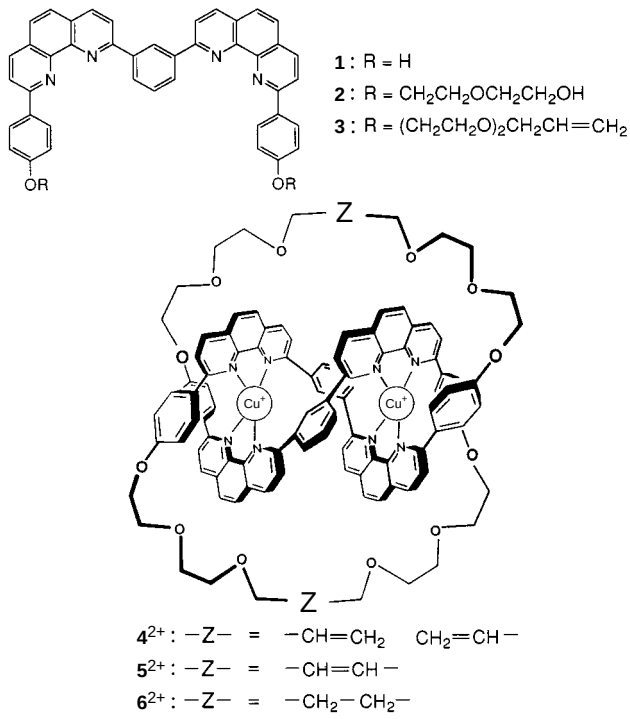



**Fig. 2** Chemical structure of the organic precursors and of the knots

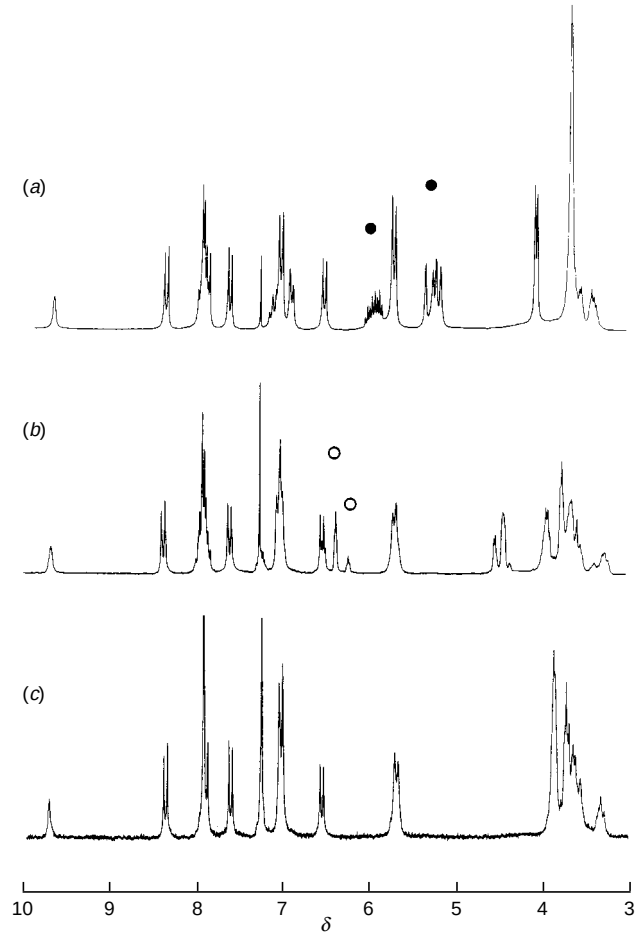



**Fig. 3** $^1$H NMR spectra of (*a*) the helical precursor $\mathbf{4}^{2+}$ with the signals corresponding to the four terminal alkenes (●), (*b*) the trefoil knot $\mathbf{5}^{2+}$ with the signals corresponding to the two alkenes incorporated in the molecule (○) and (*c*) the trefoil knot $\mathbf{6}^{2+}$ after catalytic reduction of the alkenes

formed quantitatively by the classical way: addition under argon of $[Cu(MeCN)_4]PF_6$ dissolved in MeCN onto a solution of the bis-chelate **3**. The metathesis was catalysed by $[RuCl_2\{P(C_6H_{11})_3\}_2(=CHPh)]$ (0.05 mol. equiv.) at a substrate concentration of 0.01 M in $CH_2Cl_2$ at room temp. The double coupling of the terminal alkenic groups afforded the trefoil knot $\mathbf{5}^{2+}$ in 74% yield after column chromatography (Fig. 2). The only other products were oligomers arising from intermolecular metathesis reactions.

The dicopper(I) trefoil knot $\mathbf{5}^{2+}$ is thus obtained in seven steps from commercially available 1,10-phenanthroline, with an overall yield of 35%.

The two cyclic alkenes remaining in $\mathbf{5}^{2+}$ appeared originally as a mixture of *cis* and *trans* alkenes in a 80 : 20 ratio, according to the $^1$H NMR spectrum. We thus obtained the *cis–cis*, *cis–trans* and *trans–trans* products [compare the broad signals in the spectrum in Fig. 3(*b*) to the narrow and well resolved ones of the spectrum in Fig. 3(*c*)]. The alkene functionalities could be easily and quantitatively reduced at room temp. by catalytic hydrogenation in EtOH–$CH_2Cl_2$ (1 : 1) with Pd/C (5 mol% Pd). Cyclisation and reduction could both be monitored by $^1$H NMR spectroscopy in the alkenic region, the signals corresponding to the cyclic alkenic groups in knot $\mathbf{5}^{2+}$ being sharply different from those of the terminal alkenic groups in the precursor $\mathbf{4}^{2+}$ (see Fig. 3). Moreover, the $^1$H NMR spectrum of the knot after reduction is clearly simplifed.

The knotted topology of $\mathbf{5}^{2+}$ could be unambiguously established by $^1$H NMR spectroscopy, the signals of the aromatic protons as well as those of the polyoxyethylenic chains in the 3–4 ppm region being highly characteristic.[8] Further evidence was obtained from FABMS which confirmed the absence of any starting material and displayed the expected mass: a peak at 1965.3 corresponding to $[\mathbf{5}(PF_6)]^+$ and a peak at 910.1 corresponding to $\mathbf{5}^{2+}$.

The here-described latest improvements now allow an easy access to trefoil knots and hence render the extensive study of their specific properties possible. It can also be envisaged that the two alkene functionalities of $\mathbf{5}^{2+}$, disposed in an antipodal fashion, can be utilized for further functionalization.

We thank the CNRS for financial support and the French Ministry of Research for a fellowship to G. R.

## Footnote and References

* E-mail: sauvage@chimie.u-strasbg.fr

1 L. F. Liu, R. E. Depew and J. C. Wang, *J. Mol. Biol.*, 1976, **106**, 439.
2 S. M. Du, B. D. Stollar and N. C. Seeman, *J. Am. Chem. Soc.*, 1995, **117**, 1194.
3 C. Liang and K. Mislow, *J. Am. Chem. Soc.*, 1995, **117**, 4201 and references therein.
4 C. O. Dietrich-Buchecker and J. P. Sauvage, *Angew. Chem., Int. Ed. Engl.*, 1989, **28**, 189; C. O. Dietrich-Buchecker, J. Guilhem, C. Pascard and J. P. Sauvage, *Angew. Chem., Int. Ed. Engl.*, 1990, **29**, 1154.
5 (*a*) C. O. Dietrich-Buchecker, J. P. Sauvage, J. P. Kintzinger, P. Maltese, C. Pascard and J. Guilhem, *New J. Chem.*, 1992, **16**, 931; (*b*) C. O. Dietrich-Buchecker, J. F. Nierengarten, J. P. Sauvage, N. Armaroli, V. Balzani and L. De Cola, *J. Am. Chem. Soc.*, 1993, **115**, 11 237; (*c*) M. Meyer, A. M. Albrecht-Gary, C. O. Dietrich-Buchecker and J. P. Sauvage, *J. Am. Chem. Soc.*, 1997, **119**, 4599; (*d*) C. O. Dietrich-Buchecker, J. P. Sauvage, N. Armaroli, P. Ceroni and V. Balzani, *Angew. Chem., Int. Ed. Engl.*, 1996, **35**, 1119.
6 C. O. Dietrich-Buchecker, J. P. Sauvage, A. De Cian and J. Fischer, *J. Chem. Soc., Chem. Commun.*, 1994, 2231.
7 G. C. Fu and R. H. Grubbs, *J. Am. Chem. Soc.*, 1992, **114**, 5426; A. Fürstner and N. Kindler, *Tetrahedron Lett.*, 1996, **37**, 7005; B. König and C. Horn, *Synlett*, 1996, 1013; B. Mohr, M. Weck, J. P. Sauvage and R. H. Grubbs, *Angew. Chem., Int. Ed. Engl.*, 1997, **36**, 1308.
8 R. F. Carina, C. O. Dietrich-Buchecker and J. P. Sauvage, *J. Am. Chem. Soc.*, 1996, **118**, 9110.

*Received in Basel, Switzerland, 10th July 1997; 7/04970F*

# Enantioselective syntheses of α-methylene butyrolactones *via* asymmetric aminocarbonylation of tungsten–prop-2-ynyl compounds

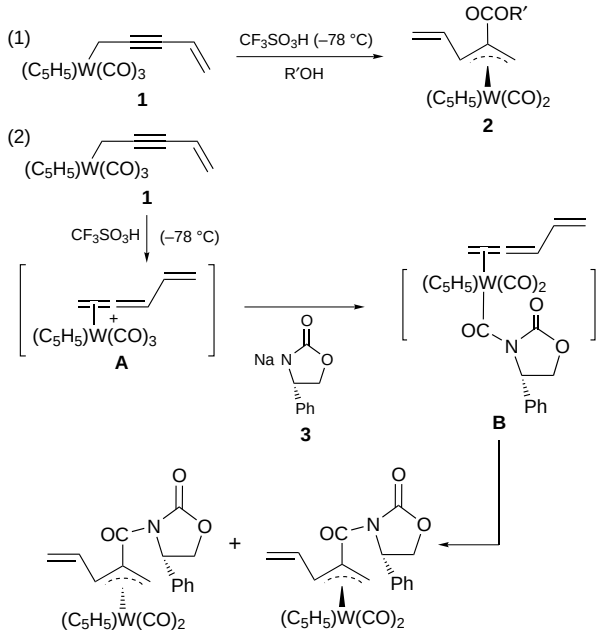
**Lin Hung Shiu,[a] Sue-Lein Wang,[a] Ming-Jung Wu[b] and Rai-Shung Liu*[a]**

[a] *Department of Chemistry, National Tsing Hua University, Hsinchu, 30043, Taiwan, ROC*
[b] *Department of Chemistry, Kaoshiung Institute of Medical College, Kaohsiung, Taiwan, ROC*

**A tungsten–η¹-vinylprop-2-ynyl compound undergoes enantioselective aminocarbonylation to afford an optically pure tungsten–π-γ-lactone; this π-allyl complex is useful for the efficient synthesis of optically pure α-methylene butyrolactone.**

In the last twenty years, utilization of stoichiometric transition-metal reagents in organic syntheses has undergone considerable progress.[1–3] The unique electronic properties of transition metals can direct and facilitate carbon–carbon bond formation of unusual types, providing easy access to useful organic substructures.[1–3] Nevertheless, most of these reactions[1–3] are carried out with racemic organometallic reagents although naturally occurring compounds often exist in optically pure forms. [M(η⁵-$C_5H_5$)(CO)$_2$(π-allyl)] (M = Mo, W) complexes have proved to be very useful in organic synthesis.[4,5] In this laboratory, we recently reported the use of complexes of this type for stereoselective syntheses of various oxygen heterocycles, 1,3-diols and 1,3,5-triols.[6] To further enhance the synthetic applications of these π-allyl complexes, we report herein an enantioselective aminocarbonylation of tungsten–vinylprop-2-ynyl complexes to afford an optically pure tungsten–π-γ-lactone that can be elaborated for asymmetric synthesis of α-methylene butyrolactones.

Although tungsten–prop-2-ynyl complexes are prone to alkoxycarbonylation[6b,c] to yield π-2-alkoxycarbonylallyl complexes **2** [Scheme 1, eqn. (1)], attempts to use chiral secondary alcohols such as (+)-menthol and (+)-neomenthol to induce enantioselective alkoxycarbonylation of **1** were unsuccessful.




**Scheme 1**

The resulting products **2** consisted of 1:1 diastereomeric mixtures that were inseparable by fractional crystallization and column chromatography. We found that (*S*)-4-phenyl-2,5-oxazolidinone[7] **3** was an effective chiral auxiliary for enantioselective aminocarbonylation of **1**. In a typical operation, $CF_3SO_3H$ acidification of **1** (*ca.* 1.50 g) in cold diethyl ether yielded a dark orange precipitate **A**, presumbly being containing η²-vinylallene cations.[8] After replacement of diethyl ether with THF, precipitate **A** was treated with the sodium oxazolidinonate **3** (1.2 equiv.) at −40 °C and 15-crown-5 (1.2 equiv.), followed by slowly warming the solution to 0 °C (*ca.* 12 h), yielding a mixture of **4a** {$[\alpha]_D$ −53.4 (*c* 0.5, $C_6H_6$)} and **4b** {$[\alpha]_D$ 282.1 (*c* 0.5, $C_6H_6$)} in 81% yield (**4a**/**4b** = 3.8). Further separation of these two diastereomers on a silica column gave **4a** and **4b** in 51 and 16% yields, respectively. In this aminocarbonylation, **3** initially attacks the coordinated carbonyl of **A** to yield tungsten–η¹-aminocarbonyl species **B** which subsequently undergoes insertion of the aminocarbonyl group into its central allene carbon, yielding the two isomers **4a**,**b**. The crystal structure of **4a** has been determined by an X-ray diffraction study† to clarify its absolute configuration; the ORTEP drawing is shown in Fig. 1.

As shown in Scheme 2, further treatment of **4a** with $CF_3SO_3H$ (1.1 equiv.) in cold ether (−40 °C) produced an orange precipitate **C**; subsequent hydrolysis of this salt with a saturated $Na_2CO_3$ solution yielded an optically active π-ε-lactonylallyl complex **5** {$[\alpha]_D$ 157.8 (*c* 0.5, $C_6H_6$)} in 80% yield. Fig. 2 shows the the crystal structure† of this optically active complex **5** which has an *anti*-configuration, *i.e.* the methyl group lies away from W(η⁵-$C_5H_5$)(CO)$_2$ fragment. The configuration of the tungsten–π-allyl fragment of **5** is retained relative to that of **2a**. To rationalize the stereochemical transformation of **4a** into **5**, we propose that η⁴-*s-trans*-diene **C** was first formed in the acidification of **4a** with $CF_3SO_3H$; subsequent attack of water at the η⁴-diene intermediate **C** occurs

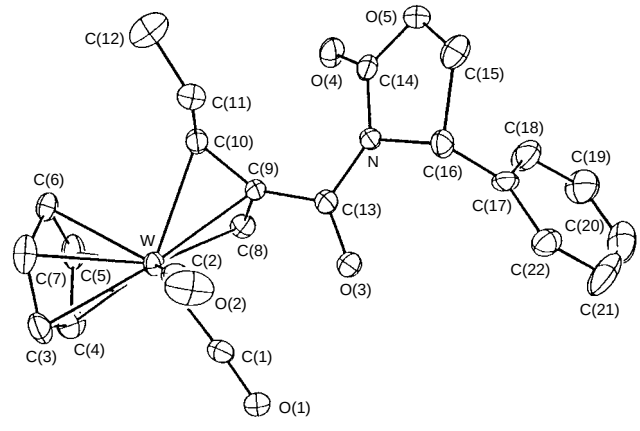
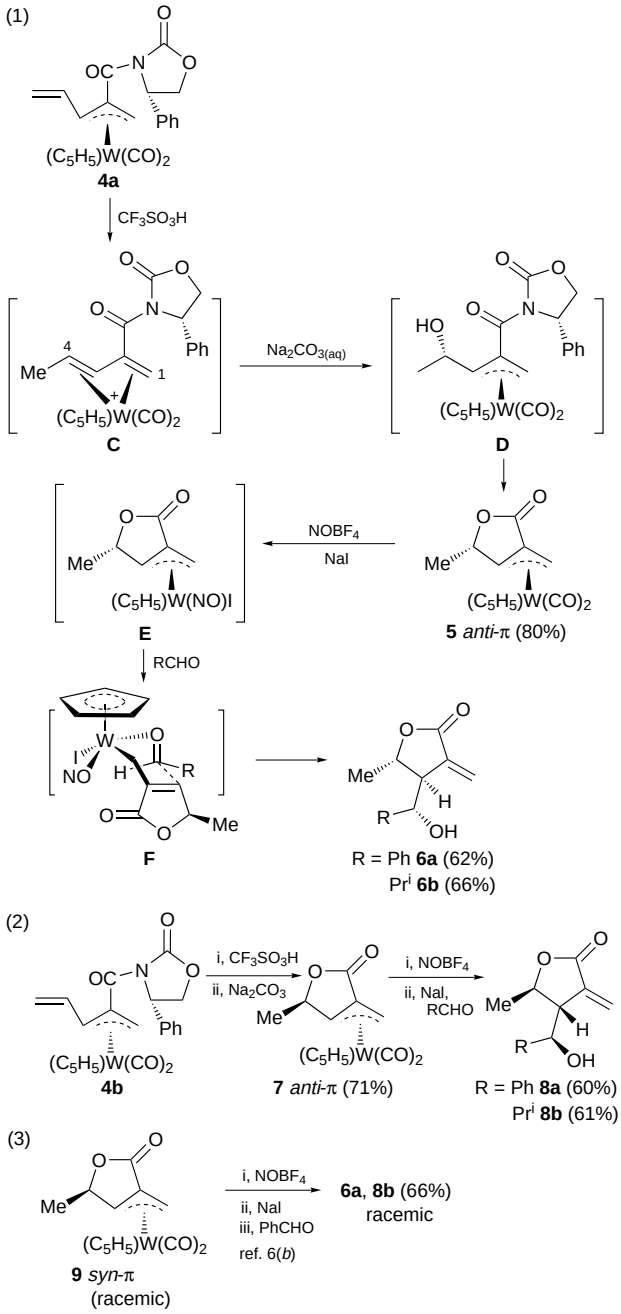



**Fig. 1** ORTEP drawing of the optically active tungsten–π-allyl complex **4a**. Pertinent bond lengths (Å): W–C(8) 2.252(7), W–C(9) 2.251(6), W–C(10) 2.321(6), C(8)–C(9) 1.427(9), C(9)–C(10) 1.411(8), C(10)–C(11) 1.459(9), C(11)–C(12) 1.320(10).




**Scheme 2**

regioselectively at the C(4)-carbon opposite W($\eta^5$-$C_5H_5$)$(CO)_2$ to yield an α-hydroxyallyl complex **D.** In aqueous $Na_2CO_3$ species **D** is prone to undergo base-catalyzed intramolecular lactonization, yielding the π-*anti*-allyl stereoisomer **5**.

To realize the synthetic utility of this asymmetric aminocarbonylation, compound **5** was sequentially treated with $NOBF_4$ (1.0 equiv.) and NaI (1.0 equiv.) in MeCN to generate the W($\eta^5$-$C_5H_5$)(NO)I derivative **E** that functions as an allyl anion;[9] this anion reacted *in situ* with RCHO (R = Ph, Pr$^i$) to afford optically active α-methylene butyrolactones **6a** {$[\alpha]_D$ −71.1 (*c* 0.5, $C_6H_6$)} and **6b** {$[\alpha]_D$ −90.2 (*c* = 0.5, $C_6H_6$)} in 62 and 66% yields, respectively. The ee values of **6a** and **6b** were 93 and 94% according to HPLC analysis (column: Chirasphere). Following the same procedure, the chiral π-allyl complex **4b** was converted to π-allyl–γ-lactone **7** {$[\alpha]_D$ −157.2 (*c* 0.5, $C_6H_6$)} in 71% yield. Sequential treatment of **7** with $NOBF_4$ and NaI, and then RCHO afforded α-methylene butyrolactones **8a** {$[\alpha]_D$ 70.3 (*c* = 0.5, $C_6H_6$)} and **8b** {$[\alpha]_D$ 90.4 (*c* 0.5, $C_6H_6$)} in 60 and 61% yields, respectively. HPLC analyses of **8a** and **8b** gave the ee values of 92 and 94%, respectively. Herein, a chair-like-transition state **F** is likely involved to control the stereochemistry of the products. We previously reported[6b] that the racemic form of **6a** (or **8a**) could also be produced from the π-*syn*-γ-lactone **9** following the same operation; the reaction mechanism was similarly elucidated to involve the transition state **F**.[6b] An interesting observation of this study is that two π-*anti* and -*syn*-stereoisomers **5** and **9** have the same transition states **F** for generation of α-methylene-γ-lactone **6a** (or **8a**).

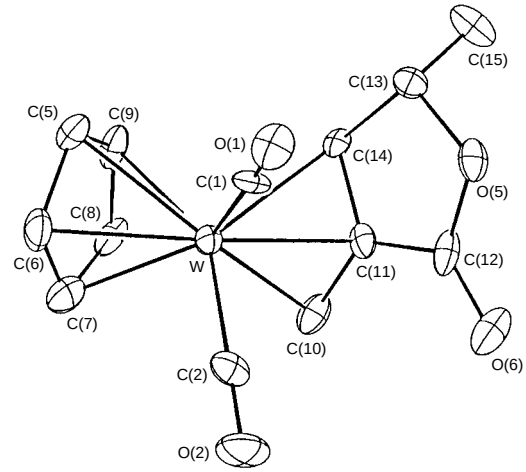



**Fig. 2** ORTEP drawing of the optically active tungsten–π-γ-lactone **5**. Pertinent band lengths (Å): W–C(10) 2.292(15), W–C(11) 2.241(14), W–C(14) 2.330(16), C(10)–C(11) 1.392(15), C(11)–C(14) 1.407(24), C(12)–O(6) 1.201(22).

## Footnotes and References

† *Crystal data*: **4a**: monoclinic, space group $P2_1$, $a$ = 8.9928(2), $b$ = 9.4679(2), $c$ = 12.0133(2) Å, $\beta$ = 93.881(3)°; $U$ = 1020.5(4) Å$^3$, $Z$ = 2. Final $R$ = 0.0170, $R_w$ = 0.0187 for 2381 reflections with $I > 3.0\sigma(I)$ out of 2531 unique reflections.

**5**: monoclinic, space group $P2_1$, $a$ = 8.8390(2), $b$ = 10.8836(3), $c$ = 13.6346(4) Å, $\beta$ = 101.23(2)°, $U$ = 1286.53(8) Å$^3$, $Z$ = 8. Each assymmetric unit contains two independent molecules. Final $R$ = 0.0360, $R_w$ = 0.0374 for 3191 reflections with $I > 3.0\sigma(I)$ out of 3902 unique reflections. CCDC 182/604.


1 *Advances in Metal–Organic Chemistry*, ed. L. S. Liebeskind, JAI Press Inc., Greenwich, CT, 1989–1996, vol. 1–5.
2 S. G. Davies, *Aldrichim. Acta*, 1990, 31.
3 L. S. Hegedus, *Transition Metals in the Synthesis of Complex Organic Molecules*, University Science Books, Mill Valley, CA, 1994, ch. 4, p. 103.
4 A. J. Pearson, *Synlett*, 1990, 10.
5 A. J. Pearson, in *Comprehensive Organometallic Chemistry*, ed. G Wilkinson, F. G. A. Stone and E. W. Abel, Pergamon, Oxford, 1995, vol. 12, p. 637.
6 (*a*) W.-J. Vong, S.-M. Peng, S.-H. Lin, W.-J. Lin and R.-S. Liu, *J. Am. Chem. Soc.* 1991, **113**, 573; (*b*) C.-C. Chen, J.-S. Fan, S.-J. Shieh, G.-H. Lee, S.-M. Peng, S.-L. Wang and R.-S. Liu, *J. Am. Chem. Soc.*, 1996, **118**, 9279.
7 D. A. Evans, F. Urpi, T. C. Somers, J. S. Clark and M. T. Bilodeau, *J. Am. Chem. Soc.*, 1990, **112**, 8215.
8 M.-H. Cheng, Y.-H. Ho, G.-H. Lee, S.-M. Peng, S.-Y. Chu and R.-S. Liu., *Organometallics*, 1994, **13**, 4082.
9 J. W. Faller and D. L. Linebarrier, *J. Am. Chem. Soc.*, 1989, **111,** 1939; J. W. Faller, J. A. John and M. R. Mazzier, *Tetrahedron Lett.*, 1989, **31**, 1769.


*Received in Cambridge, UK, 29th August, 1997; 7/06309A*

# Alternating ring-opening metathesis copolymerization of bicyclo[2.2.1]hept-2-ene and cyclopentene

**Basma Al Samak, Andrew G. Carvill, James G. Hamilton,* John J. Rooney and Jillian M. Thompson**

*School of Chemistry, The Queen's University of Belfast, Belfast, UK BT9 5AG*

**Almost alternating copolymers of bicyclo[2.2.1]hept-2-ene and cyclopentene have been formed by ring-opening metathesis polymerization using a $RuCl_3$–phenol catalyst system; this highly novel result is attributed to differential steric influences exerted by a hydrogen-bonded solvent cage which encloses the catalyst site.**

Copolymerization is an aspect of polymer chemistry that continues to attract widespread interest, not only because it affords the opportunity to prepare and study polymers with a wide variety of main chain architectures but also because of the mechanistic insights which may be gained from a detailed analysis of the microstructure of such materials.[1,2]

The primary microstructural variant in copolymers of a given comonomer composition is the distribution of the different monomer units in the chain and this variable depends to a large extent on the choice of monomer pairs. For example, in the field of coordination polymerization, monomers of similar polarity generally give rise to statistical copolymers, although block copolymers may be obtained by the sequential addition of a variety of monomers to living catalyst systems. Alternating distributions may be obtained either by copolymerization of monomers of dissimilar polarity; for example, the Ziegler–Natta copolymerization of CO[3] or styrene[4] with ethylene, or they may result from regiospecific ring-opening metathesis polymerization (ROMP)[5] or acyclic diene metathesis (ADMET)[6] homopolymerizations. Alternating copolymerization of olefinic monomers which have the same olefinic double bond polarity is extremely rare.[7–9]

We now report the alternating ring-opening metathesis copolymerization of cyclopentene and norbornene, two non-polar monomers, using a simple $RuCl_3$-based catalyst system.

Although readily available and remarkably tolerant of a wide range of monomer functionality, classical Ru-based ROMP initiators are rather sluggish, so a number of studies have been directed towards increasing the activity whilst retaining the robust properties of this class of catalyst.[10–12] The working catalytic species in metathesis polymerization is a metallacarbene[13] and a strategy we have employed is to increase the polarity of the Ru=C π-bond, and hence its activity, by providing harder acidic ligands at the Ru centre. A measure of success has been achieved using isolated complexes such as Ru(trifluoroacetate),[14] or $RuCl_3$ in the presence of acidic diol solvents, such as dimethyl tartrate,[15] and in these cases an enhanced catalyst activity, judged by the increased incorporation of the relatively unreactive cyclopentene in cyclopentene (CPE)–bicyclo[2,2,1]hept-2-ene (norbornene, NBE) copolymerizations, was noted. In continuation of these studies we have been examining the role of phenolic solvents both as reaction media and as potential ligands and we have found, not only a greatly enhanced catalyst activity, but remarkably, a highly alternating distribution of CPE and NBE units which is maintained throughout a range of yields (~2% to ~20%).† It is also significant that the final concentration of CPE in these copolymerizations, even at higher yields, exceeds its equilibrium monomer concentration.[7]

The alternating nature of these copolymers is unambiguously shown by the olefinic region of their rather simple $^{13}C$ NMR spectra, Fig. 1(*a*). Here the predominant signals at 128.2 and 135.13 ppm arise from isolated cyclopentene $M_2\mathbf{M}_1M_2$ (CPE = $M_1$) and norbornene $M_1\mathbf{M}_2M_1$ (NBE = $M_2$) units respectively,‡ the low intensity signals arising from homopolymer sequences, $M_1M_1M_1$ and $M_2M_2M_2$.[16] Fine structure is attributed to the effects of double bond isomerism and it is noteworthy that the *cis* double bond content (~30%) is higher than for less reactive Ru-based catalysts.[16]

The formation of such a copolymer requires that propagation occurs at a novel catalyst site and although its structure is at this stage a matter of some speculation we believe it to be based on

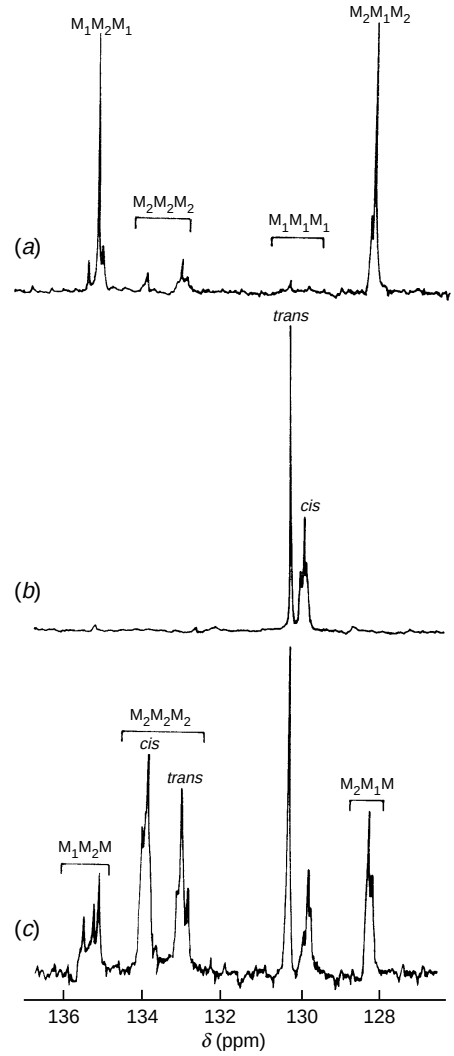



**Fig. 1** The olefinic regions of the 125 MHz $^{13}C$ NMR spectra (in $CDCl_3$ with $Me_4Si$ internal standard) of polymers prepared from NBE ($M_2$) and CPE ($M_1$) at a molar feed ratio of 1 : 8; (*a*) a highly alternating copolymer prepared using the $RuCl_3$–dry phenol catalyst, (*b*) a CPE homopolymer prepared using a $OsCl_3$–dry phenol catalyst and (*c*) a random copolymer prepared using the $OsCl_3$ catalyst in a 100 : 1 phenol–water solvent

$$\mathbf{P_C} + \text{CPE} \xrightarrow{k_{CC}} \mathbf{P_C} \qquad \mathbf{P_N} + \text{CPE} \xrightarrow{k_{NC}} \mathbf{P_C}$$

$$k_{CN} >> k_{CC} \qquad k_{NC} >> k_{NN}$$

$$\mathbf{P_C} + \text{NBE} \xrightarrow{k_{CN}} \mathbf{P_N} \qquad \mathbf{P_N} + \text{NBE} \xrightarrow{k_{NN}} \mathbf{P_N}$$

**Scheme 1**

a Ru-carbene complex bearing $\eta^1$-coordinated phenoxide ligands, formed *in situ* by the action of excess phenol on $RuCl_3$. Phenol (solvent) molecules are then associated with this complex through the medium of hydrogen bonding, in a manner analogous to that described recently for other Ru–phenoxy complexes,[17] forming, in effect, a cage around the catalyst site such that the differential steric effects of cyclopentylene and pentylene chain ends are greatly emphasised with respect to access of incoming monomer, NBE and CPE respectively.

The process is therefore governed primarily by the steric demands of the chain end coupled with the different steric and electronic properties of the approaching monomers and it is envisaged that propagation involves different forms of the metallacarbene, $\mathbf{P_N}$ and $\mathbf{P_C}$, (**N** = cyclopentylene, **C** = pentylene). Thus, with $\mathbf{P_N}$, the bulky norbornene is denied access to the site and the much less bulky cyclopentene has then the opportunity to react, leading to $\mathbf{P_C}$. The less sterically constrained $\mathbf{P_C}$ is now relatively accessible to both monomers but reacts preferentially with norbornene due to its electronically much more reactive double bond, and thus a $\mathbf{P_N}$ site is generated. This sequence of events may be described by the above kinetic scheme, Scheme 1, where the apparent reactivity ratios, $r_1 = k_{CC}/k_{CN}$, and $r_2 = k_{NN}/k_{NC}$, estimated from the spectra of the copolymers, are numerically very small, as demanded by an alternating mechanism.

We have accumulated several pieces of experimental evidence which support the existence of the proposed catalyst site and propagation mechanism. For example, the other noble metal-based metathesis catalysts, $IrCl_3$ and $OsCl_3$, behave in an analogous manner when used in phenolic solvents with the same monomer feed. $IrCl_3$, gives a somewhat less alternating product than $RuCl_3$ but significantly $OsCl_3$, Fig. 1(*b*), yields essentially a CPE homopolymer. This seemingly inconsistent result may however still be explained by the above mechanism if it is assumed that the hydrogen-bonded cage is now very tightly arranged around the Os-centred catalyst site, primarily as a consequence of the stronger ligand field exerted by the third row metal ion,[14] and that NBE is therefore denied access (Scheme 1, $k_{CN} = k_{NN} = 0$).

As expected, copolymers become less alternating as the solvent system is changed progressively from pure phenol to non-hydrogen bonded solvents such as chlorobenzene, but the essentially hydrogen-bonded nature of the cage is best illustrated by the effect of the addition of small quantities of water (1.0 wt% phenol) to the catalyst. Now with each metal a random copolymer is formed, illustrated here by reference to the $OsCl_3$, Fig. 1(*b*) and (*c*); we believe that random copolymer is formed as a result of propagation at a much less crowded site at which the hydrogen-bonding water has profoundly altered the nature of the solvent cage so that both monomers have now equal access. The high level of incorporation of CPE in these random copolymers however indicates that although water may have disrupted the solvent cage, a very active Mt(phenoxide) complex is still the propagating species.

Finally, we have noted that the *cis* double bond content of the polymer is essentially the same whether or not water is present in the system, and typically, in both $OsCl_3$ cases, Fig. 1(*b*) and (*c*), $M_1M_1$ units are 35% *cis*. We believe that this indicates that the solvent cage, which is not directly bonded to the metal, exerts a second order effect, merely helping to control monomer access but does not control the orientation of the intermediate metallacycle and hence the stereochemistry of the [2 + 2] cycloaddition step,[13] a first order effect. We have previously emphasised that these latter effects, *e.g.* a dramatic increase in the *cis* content of the polymer, may be caused by steric crowding due to various bulky spectator ligands directly bonded to the metal.[2] Examples are the addition of esters to $WCl_6$ and $MoCl_5$-based systems and various dienes and acetylenes to noble metal catalysts and can be used to modify catalyst systems and produce high *cis* content polymers.[2]

## Footnotes and References

* E-mail: j.g.hamilton@queens-belfast.ac.uk

† Catalyst systems were prepared by dissolving commercial samples of $RuCl_3{\cdot}xH_2O$, $OsCl_3$ or $IrCl_3{\cdot}3H_2O$ (8 mg) in phenol (2 ml) distilled from $P_2O_5$. A mixture of cyclopentene (1.7, 24 mmol) and norbornene (0.3, 3 mmol), both dried by distillation from $CaH_2$, was then added and the reaction mixture kept at room temperature overnight. Polymer was recovered by dissolving the gel in chloroform followed by precipitation in methanol and vacuum drying to yield typically 240 mg copolymer, $M_w$ 1.3 $\times$ $10^6$ (polystyrene standards). When other phenolic solvents such as *p*-chloro- and *p*-fluoro-phenol, as well as trifluoroethanol are used in the same manner, alternating copolymers are also produced.

‡ Taking into account variations due to *cis* and *trans* double bonds there are eight possible, closely positioned and partially overlapping, heterotriad resonances for the olefinic carbon atoms centred on $M_2$ units: $M_1t\mathbf{M_2}tM_1$, $M_1c\mathbf{M_2}tM_1$, $M_1t\mathbf{M_2}cM_1$, $M_1c\mathbf{M_2}cM_1$ and $M_2t\mathbf{M_2}tM_1$, $M_2c\mathbf{M_2}tM_1$, $M_2t\mathbf{M_2}cM_1$, $M_2c\mathbf{M_2}cM_1$. We have previously identified most of these[2] and are now confident that the three peaks labelled as $M_1M_2M_1$ in Fig. 1(*a*) are the first three of these with the central peak, $M_1tM_2tM_1$, the most abundant as expected from the higher *trans* content of the largely alternating copolymer. The corresponding resonances for the heterotriads centred around $M_1$ are less well resolved, but those labelled $M_2M_1M_2$ in Fig. 1(*a*) also agree with previous assignments as being $M_2tM_1M$ (major peak) and $M_2cM_1M$ (minor peak) (M is either $M_1$ or $M_2$).


1 D. A. Tirrell and J. Furukawa, in *Encyclopedia of Polymer Science and Engineering*, ed. J. I. Kroschwitz, 2nd edn., John Wiley and Sons, New York, 1986, vol. 4.
2 V. Amir-Ebrahimi, A. G. Carvill, J. G. Hamilton, J. J. Rooney and C. Tuffy, *J. Mol. Catal.*, 1997, **115**, 85.
3 M. Brookhart, F.-C. Rix and J. M. DeSimone, *J. Am. Chem. Soc.*, 1992, **114**, 5894.
4 C. Pellecchia, D. Pappalardo, M. D'Arco and A. Zambelli, *Macromolecules*, 1996, **29**, 1158.
5 Z. Wu and R. H. Grubbs, *Macromolecules*, 1995, **28**, 3502.
6 J. Konzelman and K. B. Wagener, *Macromolecules*, 1996, **29**, 7657.
7 K. F. Castner and N. Calderon, *J. Mol. Catal.*, 1982, **15**, 47.
8 J. G. Hamilton, K. J. Ivin, J. J. Rooney and L. C. Waring, *J. Chem. Soc., Chem. Commun.*, 1983, 159.
9 H. Cherdron, M.-J. Brekner and F. Osan, *Angew. Makromol. Chem.*, 1994, **223**, 121.
10 S. T. Nguyen, R. H. Grubbs and J. W. Ziller, *J. Am. Chem. Soc.*, 1993, **115**, 9858.
11 W. A. Herrmann, W. C. Schattenmann, O. Nuyken and S. C. Glander, *Angew. Chem., Int. Ed. Engl.*, 1996, **35**, 1087.
12 A. W. Stumpf, E. Saive, A. Demonceau and A. F. Noels, *J. Chem. Soc., Chem. Commun.*, 1995, 1127.
13 K. J. Ivin and J. C. Mol, *Olefin Metathesis and Metathesis Polymerization*, Academic Press, London, 1997.
14 J. G. Hamilton, K. J. Ivin, G. M. McCann and J. J. Rooney, *J. Chem. Soc., Chem. Commun.*, 1984, 1397.
15 B. Bell, J. G. Hamilton, E. E. Law and J. J. Rooney, *Macromol. Rapid Commun.*, 1994, **15**, 543.
16 K. J. Ivin, G. Lapienis and J. J. Rooney, *Makromol. Chem.*, 1982, **183**, 9.
17 K. Osakada, K. Ohshiro and A. Yamamoto, *Organometallics*, 1991, **10**, 404.


*Received in Liverpool, UK, 14th July 1997, 7/05046A*

# Heterogeneous electron transfer at the polarised water/1,2-dichloroethane interface studied by *in situ* UV–VIS spectroscopy and differential cyclic voltabsorptometry

**Zhifeng Ding, Pierre F. Brevet and Hubert H. Girault***

*Laboratoire d'Electrochimie, Département de Chimie, Ecole Polytechnique Fédérale de Lausanne, CH-1015 Lausanne, Switzerland*

**The heterogeneous electron transfer reaction between the redox couple ferricyanide–ferrocyanide in water and 7,7,8,8-tetracyanoquinodimethane (TCNQ) in 1,2-dichloroethane (DCE) is studied by combining conventional electrochemical measurements and UV–VIS absorption spectroscopy in total internal reflection (TIR) geometry.**

Heterogeneous electron transfer reactions are of biological interest, and polarised liquid/liquid interfaces represent a rather simple model system to study this type of reactions where reactants and products are located in their respective adjacent phases.[1–6] However, there is a paucity of reliable experimental data as electrochemical methods suffer from the difficulty of differentiating between currents originating from electron- and ion-transfer reactions occurring across the interface.[7–9] To circumvent the limitations of electrochemical studies, we have developed a novel spectroelectrochemical methodology.

Very few reports of spectroelectrochemical studies on electron transfer at liquid/liquid interfaces have been published.[10,11] *In situ* EPR has been used to study the product formation for the reduction of TCNQ and the oxidation of tetrathiofulvalene (TTF) by the ferro–ferricyanide redox couple at the water/DCE interface.[10] Time-resolved laser-induced fluorescence spectroscopy in TIR mode has been used to study photoinduced electron transfer between europium(III) in water and anthracene in DCE.[11] TIR fluorescence spectroscopy[12–14] and TIR UV–VIS spectroscopy[15] have recently been applied to the field of ion-transfer reactions across the water/DCE interface. The work outlined here shows that UV–VIS spectroscopy in TIR geometry can be used to detect interfacial changes of the products of electron-transfer processes at liquid/liquid interfaces.

The spectroscopic measurements involved the use of a 150 W xenon arc lamp (Applied Photophysics) which supplied white light within the UV–VIS spectral range. The output of the lamp was directed to the bottom face of the interface between water and DCE. The use of a 250 mm focal length lens and several aluminium mirrors then ensured that the light was focused on the interface in TIR mode and also allowed accurate adjustment of the light path to guarantee the optimum conditions for the spectroscopic measurements. An angle of approximately 75° was maintained in all of the experiments which allowed clear observation of the reflected beam at the opposite wall of the cell.[15] The spectroelectrochemical cell which held the solutions was a conventional four-electrode liquid–liquid electrochemistry cell modified to allow unhindered passage of the light beam. The reflected beam was either collected using a optical fibre of 400 μm in diameter attached to a spectrophotometer (Ocean Optics, Inc.) for *in situ* measurement of the whole spectrum, or collected using a water-filled optical waveguide of 1 cm in diameter attached to a high-voltage photomultiplier tube (PMT) *via* a monochromator (Applied Photophysics) equipped with a wavelength stepping motor for voltabsorptometry. The signal measured by either the fibre optic spectrophotometer or the PMT was then sampled and recorded directly on a microcomputer where further processing took place. The cell chosen for the simultaneous investigation of the electrochemistry and the absorptometry was cell 1,[5] where BTPPA represents bis(triphenylphosphoranylidene)ammonium, TPBCl represents tetrakis(4-chlorophenyl)borate. For the experiments conducted here the product of the electron-transfer reaction was $TCNQ^{\cdot-}$ in the DCE phase and was monitored spectroscopically. The potential difference imposed on the water/DCE interface and the whole data acquisition process were driven by LabView(Version 4, National Instruments). Using this set-up, the data acquisition program allowed the straightforward measurement of the whole absorption spectrum from the fibre optic spectrometer at frequencies up to 10 Hz or the signal intensity from the PMT, together with the applied interfacial potential and the corresponding electrochemical current at frequencies up to 20 kHz.

Cyclic voltammograms were recorded using a four-electrode potentiostat[16] which uses the positive feedback method for the compensation of potential drop due to solution resistance. All the potentials are absolute values obtained by comparison of the formal transfer potential of the tetramethylammonium cation: $\Delta_O^W\phi^0_{TMA^+}$, 0.160 V.

To obtain a whole spectrum, the raw data were processed in the following way. Since the data were in transmittance form which is effectively the final intensity incident at the fibre optic spectrometer, taking the negative logarithm of the ratio of signal data over the reference data at the beginning applied potential where there is no electron-transfer reaction gave the corresponding absorption spectrum directly. Fig. 1 shows the interfacial absorption spectra of the product *i.e.* $TCNQ^{\cdot-}$ in DCE following the application of a potential to the water/DCE interface, which drives the reduction of TCNQ in DCE by ferrocyanide in the aqueous phase. The acquisition frequency of a whole spectrum is 1 Hz. The electronic absorption spectrum of the $TCNQ^{\cdot-}$ following electroreduction of the parent TCNQ (the absorption maximum at 390 nm) by a platinum electrode in DCE exhibits clearly major absorption bands at 842, 744, 760,




cell 1

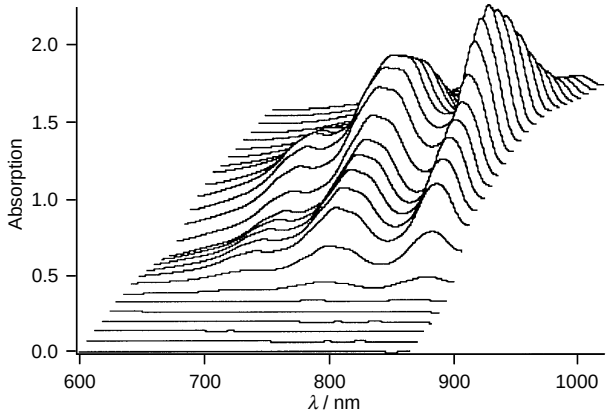



**Fig. 1** *In-situ* absorption spectra measured in TIR mode when the applied potential is scanned at 25 mV $s^{-1}$. From bottom to top, the applied potential $\Delta_O^W\phi$ varies from 0.187 to −0.26 V (forward scan) and from −0.26 to 0.187 V (backward scan) with a potential difference of *ca.* 40 mV between two spectra.

670 and 650 nm. This is similar to the spectrum reported for $TCNQ^{\cdot-}$ in acetonitrile.[17] The spectra shown in Fig. 1 can be attributed to the heterogeneous reduction of TCNQ to $TCNQ^{\cdot-}$ on forward sweep as the water phase becomes increasingly negative and the re-oxidation of the $TCNQ^{\cdot-}$ on the reverse sweep as the water becomes more positive relative to the DCE phase. TCNQ is totally water insoluble. The appearance and disappearance of the $TCNQ^{\cdot-}$ proves without any doubt that a heterogeneous electron-transfer process does take place at the water/DCE interface. The success of the experiment relies on the choice of the redox couple which must have distinct absorption spectra in the two oxidation states. The resolution of the experiment depends on the molar absorption coefficient of the product. A background spectrum was measured before and after addition of 0.6 mM TCNQ to the DCE phase and no absorption could be measured at any wavelength between 600 and 900 nm when the applied interfacial potential was held at a potential (0.258 V for example) far away from the formal electron transfer potential($\Delta_O^W\phi^0$ = −0.105 V).

The dependence of the absorbance waveform on scan rate has been established for the system in Fig. 2(*a*). By monitoring the absorbance of the $TCNQ^{\cdot-}$ species at 670 nm during a potential

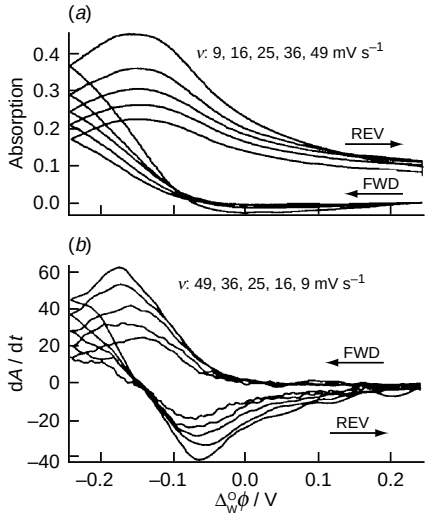



**Fig. 2** (*a*) Absorption data for cell 1 measured simultaneously during the voltammetry, and (*b*) corresponding differential cyclic voltabsorptograms. The monochromator was set to 670 nm and the scan rates (from top to bottom) are indicated.

sweep, an increase in absorbance until the zero current point and then a decrease in absorbance is observed at applied potentials corresponding to those of the electron-transfer voltammogram. Following the theory we have described elsewhere,[15] the shape is similar to that of an integrated voltammogram. The slower the scan rate, the larger the absorbance, because the absorption represents the amount of electron-transfer product which is formed during the electron-transfer reaction or the charge which has passed across the interface. Then differentiation of the absorbance data against time gave a voltammetric shape when plotted against applied potential. The results shown in Fig. 2(*b*) for several different scan rates corresponding to Fig. 2(*a*) are analogous to the measured electrochemical voltammograms with the observed peak height exhibiting a linear response as a function of the square root of scan rate. Because the concentration of ferrocyanide is very high in this case, the water phase acted analogously to a solid electrode and the electron-transfer rate was mainly controlled by the diffusion of TCNQ in DCE.

This study confirms the ability of *in situ* TIR UV–VIS spectroscopy to follow heterogeneous electron transfer at the liquid/liquid interface. The technique provides more information than conventional electrochemical techniques in mechanistic and kinetic studies. The kinetics of electron transfer for this system is currently under investigation based on spectroscopic approaches, such as chronoabsorptometry[15] and potential modulated reflectance spectroscopy.[18]

This work was supported by the European Community, Human Capital and Mobility scheme under Grant No. CHRx-CT92-0076, and Fonds National Suisse de la Recherche Scientifique. ZFD is also indebted to the Commission Fédérale pour les étudiants étrangers for financial support from 1994 to 1996.

## Footnote and References

* E-mail: hubert.girault@icp.dc.epfl.ch

1 H. H. Girault and D. J. Schiffrin, in *Electroanalytical Chemistry*, ed. A. J. Bard, Marcel Dekker, New York, 1989, vol. 15, p. 1.
2 Z. Samec, V. Marecek and J. Weber, *J. Electroanal. Chem.*, 1979, **103**, 11.
3 G. Geblewicz and D. J. Schiffrin, *J. Electroanal. Chem.*, 1988, **244**, 27.
4 V. J. Cunnane, D. J. Schiffrin, C. Beltran, G. Geblewicz and T. Solomon, *J. Electroanal. Chem.*, 1988, **247**, 203.
5 Y. Cheng and D. J. Schiffrin, *J. Electroanal. Chem.*, 1991, **314**, 153.
6 Y. F. Cheng and D. J. Schiffrin, *J. Chem. Soc., Faraday Trans.*, 1994, **90**, 2517.
7 J. Hanzlik, Z. Samec and J. Hovorka, *J. Electroanal. Chem.*, 1987, **216**, 303.
8 V. J. Cunnane, G. Geblewicz and D. J. Schiffrin, *Electrochim. Acta*, 1995, **40**, 3005.
9 K. Maeda, S. Kihara, M. Suzuki and M. Matsui, *J. Electroanal. Chem.*, 1991, **303**, 171.
10 R. A. W. Dryfe, R. D. Webster, B. A. Coles and R. G. Compton, *Chem. Commun.*, 1997, 779.
11 R. A. W. Dryfe, Z. F. Ding, R. G. Wellington, P. F. Brevet, A. M. Kuznetzov and H. H. Girault, *J. Phys. Chem. A*, 1997, **101**, 2519.
12 T. Kakiuchi, Y. Takasu and M. Senda, *Anal. Chem.*, 1992, **64**, 3096.
13 T. Kakiuchi and Y. Takasu, *Anal. Chem.*, 1994, **66**, 1853.
14 Z. F. Ding, R. G. Wellington, P. F. Brevet and H. H. Girault, *J. Phys. Chem.*, 1996, **100**, 10 658.
15 Z. F. Ding, R. G. Wellington, P.-F. Brevet and H. H. Girault, *J. Electroanal. Chem.*, 1997, **420**, 35.
16 Z. Samec, V. Marecek and J. Weber, *J. Electroanal. Chem.*, 1979, **100**, 841.
17 L. R. Melby, R. J. Harder, W. R. Hertler, W. Mahler, R. E. Benson and W. E. Mochel, *J. Am. Chem. Soc.*, 1962, **84**, 3374.
18 D. J. Fermin, Z. Ding, P.-F. Brevet and H. H. Girault, *J. Electroanal. Chem.* in press.

*Received in Exeter, UK, 18th July 1997; 7/05156E*

# Photo- and thermo-chromism of a ruthenium(II) complex and viologen-containing polymer film

**Masahiro Suzuki, Mutsumi Kimura, Kenji Hanabusa and Hirofusa Shirai***

*Department of Functional Polymer Science, Faculty of Textile Science and Technology, Shinshu University, Ueda, Nagano 386, Japan*

**A ruthenium(II) complex and a viologen-containing partially quaternized poly(1-vinylimidazole) film demonstrates both photochromism and thermochromism as a result of photosensitized and thermosensitized charge separations.**

1,1′-Dialkyl-4,4′-bipyridinium dications, so called viologens, are one of a group of electrochromic materials.[1,2] Electrochromism takes place in bipyridinium segments because the positive charge in radical cations formed by one electroreduction is delocalized. Electrochromic devices (ECDs) have been fabricated by electrostatic incorporation of such viologens into anionic polyelectrolyte films.[3–7] On the other hand, viologen radicals can be readily formed by photoinduced electron transfer from ruthenium(II) complexes to viologens in sacrificial systems.[8–12] The facts indicate that photochromism using photoinduced electron transfer is possible. Under an air atmosphere, however, the lifetime of viologen radicals is very short owing to reaction with $O_2$. Recently, we have reported that the viologen radical is efficiently formed by a photosensitized charge-separation reaction using a partially quaternized poly(1-vinylimidazole)-bound ruthenium(II) complex as a photosensitizer, alkylviologen and triethanolamine (TEOA) as a sacrificial donor.[13] In this work a ruthenium(II) complex and a viologen containing partially quaternized poly(1-vinylimidazole) is synthesized and the photo- and thermo-chromic properties of this polymer film are investigated.

Poly(1-vinylimidazole) and ruthenium(II) complex-containing poly(1-vinylimidazole) (RuPIm) were prepared as described elsewhere.[13,14] 1-(6-Bromohexyl)-1′-hexadecyl-4,4′-bipyridinium dibromide was prepared by refluxing of an acetonitrile solution of 1,6-dibromohexane and 4-(4′-pyridyl)-1-hexadecylpyridinium bromide[15] and identified by elemental analysis, $^1$H NMR and FTIR spectroscopy. Ruthenium(II) complex and viologen-containing partially quaternized poly(1-vinylimidazole) (RuVQPIm) was prepared by refluxing RUPIm and 1-(6-bromohexyl)-1′-hexadecyl-4,4′-bipyridinium dibromide in ethanol for 24 h under an argon atmosphere. After addition of *n*-hexadecyl bromide, the solution was further refluxed for 24 h. The RuVQPIm was purified by reprecipitation from methanol into acetone and identified by its UV–VIS absorption spectrum and $^1$H NMR spectroscopy (Fig. 1). The RuVQPIm film casting on a glass plate was *via* a methanol solution of RuVQPIm (5–10 mass%). The resulting film thickness was *ca.* 0.15 mm.

Upon light irradiation on an RuVQPIm film in air, the film changed from orange to blue, and reverted to orange on standing in the dark. Similarly, changes in film colour to blue with heating and to orange upon standing (cooling) were also observed. These colour change reactions were reversible† with the responses being more rapid for the irradiated relative to the thermal system. In both systems, the blue to orange response was slower. These results indicate that the colour change to blue is caused by formation of viologen radicals which are formed by electron transfer from the photoexcited ruthenium(II) complex residue to the viologen. Absorbances at 611 and *ca.* 400 nm, corresponding to absorption maxima of the viologen radical,[16] increased upon light irradiation or heating as shown in Fig. 2. The absorption spectrum of RuVQPIm showing an absorption maximum at 490 nm does not change even when viologen radicals are formed, indicating that the photo- and thermo-sensitized charge separation reactions take place in the film. In

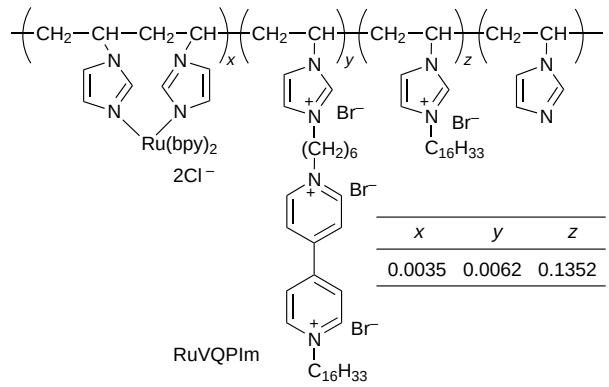



**Fig. 1** Chemical structure of RuVQPIm

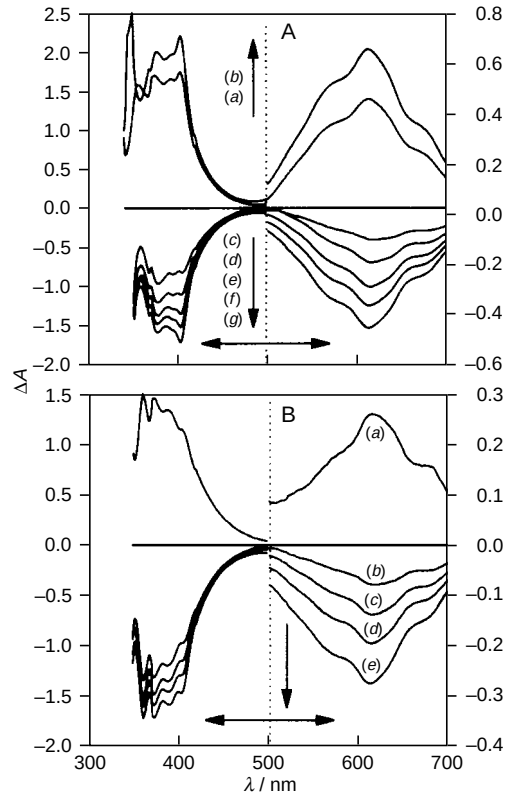



**Fig. 2** UV–VIS absorption spectral changes for photochromism (A) and thermochromism (B) of RuVQPIm film. (A): (*a*) light irradiation for 5 min, (*b*) 10 min, (*c*) standing in the dark for 5 min, (*d*) 10 min, (*e*) 20 min, (*f*) 30 min, (*g*) 50 min. (B): (*a*) heating at 120 °C for 2 min, (*b*) standing at room temp. for 10 min, (*c*) 20 min, (*d*) 30 min, (*e*) 50 min.

methanol solution, charge separation is observed in the presence of the sacrificial donor triethanolamine under an argon atmosphere, but not in the absence of triethanolamine in air.[13] In Fig. 2, the absorbance at *ca.* 350 nm, which is independent of viologen radical and RuVQPIm, increases with formation of viologen radicals. We have reported that the reaction product in intra-polymer electron-transfer between a cobalt(II) Schiff-base complex and quaternized imidazolium residue would be 3-ethylimidazoline(4−) having $\lambda_{max}$ at *ca.* 340 nm.[17] Considering this fact, 3-hexadecylimidazoline(4−) would also be formed in the charge separation reaction; the quaternized imidazolium residue acting as an electron donor.

On the other hand, the colour change to orange in air is caused by decrease in the viologen radical species concentration as shown in Fig. 2. It is likely that a reaction between 3-hexadecylimidazoline(4−) and viologen radical residues takes place. In addition, viologen radical reacts with dioxygen in air, although this is slow since the rate of colour change is little different from that in an argon atmosphere.‡ This is supported by the fact that the absorbance at *ca.* 350 nm corresponding to the 3-hexadecylimidazoline(4−) roughly disappears and little colour change was observed after 24 h under dioxygen.

The thermal blue to orange colour change is slow in comparison to the system under irradiation. Since the glass transition temperature of the RuVQPIm film is *ca.* 220 °C, a phase transition does not occur upon heating at 120 °C for 2 min. However, the DSC curve of the RuVQPIm film shows endothermic behavior at 120–150 °C, suggesting that a conformational change takes place in the film. The heating treatment brings about charge separation in addition to conformational change. Therefore, the reverse colour change after heating is caused by decrease in viologen radical concentration through electron transfer and a concomitant conformational change.

The present results reveal orange to blue photo- and thermochromism using a new polymer film. The blue colour arises from viologen radicals formed by charge separation in which the quaternized imidazolium residue acts as an electron donor in the film. A detailed investigation on the photo- and thermochromism is now in progress in our laboratory.

## Footnotes and References

* E-mail: smasa@giptc.shinshu-u.ac.jp

† The film is very stable for repeated experiments with light on and off as well as heating and cooling. Even after 30 repetitions, the spectroscopic properties of the film were unchanged.

‡ The decrease in viologen radical concentration after standing for 30 min in air was 1.2 times larger than that under Ar.

1 C. J. Schoat, J. J. Ponjee, H. T. van Dam, R. A. van Doaru and P. T. Bolwijn, *Appl. Phys. Lett.*, 1973, **23**, 64.
2 P. M. S. Monk, R. J. Mortimer and D. R. Rosseinsky, *Electrochromism: Fundamentals and Applications*, VCH, Weinheim, 1995.
3 J. M. Calvert, T. J. Manuccia and R. J. Nowak, *J. Electrochem. Soc.*, 1986, **133**, 951.
4 A. F. Sammells and N. U. Pujare, *J. Electrochem. Soc.*, 1986, **133**, 1270.
5 R. J. Mortimer, *J. Electrochem. Soc.*, 1991, **138**, 633.
6 R. J. Mortimer, *J. Electroanal. Chem.*, 1995, **397**, 79.
7 R. J. Mortimer and J. L. Dillingham, *J. Electrochem. Soc.*, 1997, **144**, 1549.
8 A. Juris, V. Balzani, F. Barigelletti, S. Campagna, P. Belser and A. von Zelewsky, *Coord. Chem. Rev.*, 1988, **84**, 85.
9 K. Kalyanasundaram, *Coord. Chem. Rev.*, 1982, **46**, 159.
10 E. Danielson, C. M. Elliott, J. W. Merkert and T. J. Meyer, *J. Am. Chem. Soc.*, 1987, **109**, 2519.
11 L. F. Cooly, S. L. Larson, C. M. Elliott and D. F. Kelley, *J. Phys. Chem.*, 1991, **95**, 10694.
12 J. R. Schoonover, G. F. Strouse, P. Chen, W. D. Bates and T. J. Meyer, *Inorg. Chem.*, 1993, **32**, 2618.
13 M. Suzuki, Y. Mori, M. Kimura, K. Hanabusa and H. Shirai, *J. Chem. Soc., Faraday Trans.*, 1996, **92**, 3599.
14 S. M. Geraty and J. G. Vos, *J. Chem. Soc., Dalton Trans.*, 1987, 3073.
15 T. Nishijima, T. Nagamura and T. Matsuo, *J. Polym. Sci., Polym. Lett.*, 1981, **19**, 65.
16 M. Wolszczak and Cz. Stradowski, *Radiat. Phys. Chem.*, 1989, **33**, 355.
17 M. Suzuki, S. Kobayashi, T. Koyama, K. Hanabusa, H. Shirai, F. L. Oliveira, S. Maruoka and Y. Kurimura, *J. Chem. Soc., Faraday Trans.*, 1995, **91**, 2877.

*Received in Cambridge, UK, 17th July 1997; 7/05107G*

# Preparation of new branched poly(triphenylamine)

**Susumu Tanaka,*[a] Tomoaki Iso[b] and Yasuo Doke[a]**

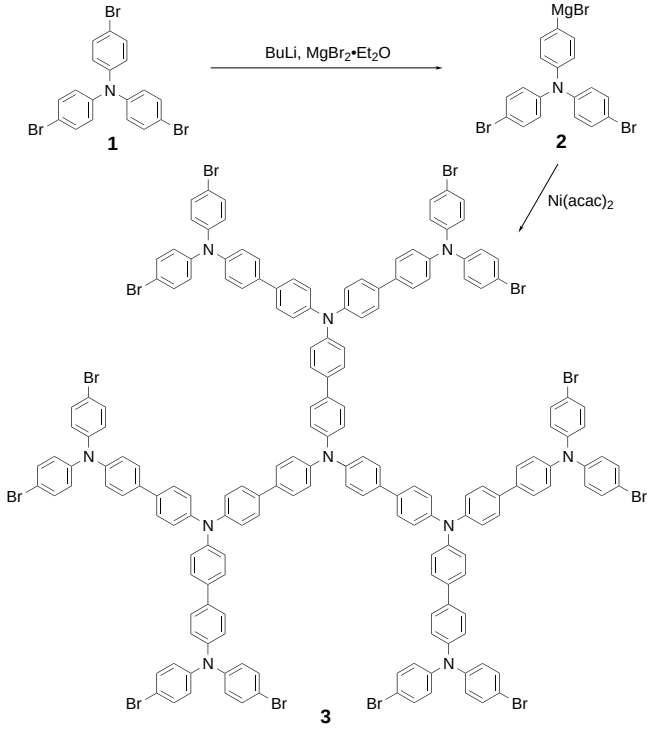
[a] *National Institute of Materials and Chemical Research, 1-1 Higashi, Tsukuba, Ibaraki 305 Japan*
[b] *Ibaraki Prefectural Industry and Technology Center, 189 Kanakubo, Yuhki, Ibaraki 307 Japan*

**New branched poly(triphenylamine) is conveniently prepared by the Grignard reaction of tris(4-bromophenyl)-amine.**

Oligomeric and polymeric materials based on triphenylamine have attracted much attention because of their stability and useful properties such as electrical conductivity and electroluminescence.[1–3] Typical conductive polymers have a linear conjugated system like polythiophene, polyphenylene and polypyrrole. Until now, only a few reports have appeared on three dimensionally conjugated polymers.[4–6]

We report here the first preparation of a branched conjugated polymer containing triphenylamine, *via* the coupling of *N*,*N*-bis(4-bromophenyl)-*N*-(4-bromomagnesiophenyl)amine **2**, by the Grignard reaction of tris(4-bromophenyl)amine **1** (Scheme 1).

Branched polymers can be prepared through two distinct synthetic approaches. One is a stepwise growth process,[7,8] in which a protection–deprotection step is required at every stage. Although this approach yields monodisperse polymers with well-defined structure, it usually requires extensive purification of the products at every protection–deprotection step of the growth process. Another approach is the one-step process[9,10] where an $AB_x$-type monomer undergoes self-condensation polymerization, as first discussed theoretically by Flory in 1952,[11] which results in a branched product. The advantage of this one-pot $AB_x$ approach lies in its simple preparation process. But this method involves the loss of control in molecular weight, accompanied by a broad molecular weight distribution.




**Scheme 1**

Polymer **3** was prepared by monolithiation with $Bu^nLi$ at −78 °C in THF, followed by reaction with magnesium bromide–diethyl ether, and coupling the resulting Grignard reagent with the catalytic amount of $Ni(acac)_2$. Grignard reagent **2** reacted as an $AB_2$-type monomer to give branched conjugated polymer **3** in a one-step process. Polymer **3** had an average molecular weight of $4.0 \times 10^3$ and was found to be soluble in organic solvents such as THF and $CHCl_3$, which implies that the branched polymer is processable.

A FTIR spectrum of monomer **1** showed three bands at 510, 817 and 1269 $cm^{-1}$, assignable to the C–Br stretching vibration; the C–H deformation vibration of 1,4-disubstituted benzene rings and the C–N stretching vibration of tertiary amines, respectively. Polymer **3** had all these bands, but the band at 510 $cm^{-1}$ was weak, due to the C–Br stretching vibration of the terminal benzene rings. These results indicate that a C–C bond was formed between the monomers at the carbon atoms coupled with bromine originally and a highly conjugated system was formed.

The UV–VIS spectra of monomer **1** had a band at 307 nm assignable to the conjugation between benzene units and nitrogen atoms. In polymer **3** a new π–π* transition band was clearly observed at 360 nm, possibly brought about by the conjugation between biphenylene units and nitrogen atoms.

The $^{13}C$ NMR spectrum of polymer **3** had three bands at 124.4, 127.5 and 129.3 ppm, which were assignable to biphenylene carbon resonances. Monomer **1** did not have these bands.

GPC was performed in THF at 40 °C using a TOSOH TSKgel $G3000H_{XL}$ column which was calibrated with polystyrene standards. Fig. 1 shows a fully reproducible GPC trace. The molecular weight of the lowest oligomeric peak was *ca*. 1000, indicating that the lower oligomers had been removed in the course of the work-up. The GPC trace had another interesting feature; the splittings of the low oligomeric peaks reflect the resolution of the repeating unit of polymer **3**, $C_{18}H_{12}NBr$. The results of GPC indicated that the degree of polymerization was *ca*. 12. Considering that the repeating unit of polymer **3** contains three benzene rings, this degree of polymerization signifies that the polymer contained *ca*. 36 benzene rings, which was sufficient to show electroactivity as described below. The degree of polymerization estimated from the bromine content of polymer **3** was *ca*. 10, which implies that the value obtained by GPC was likely to be an overestimate of the real molecular weight.

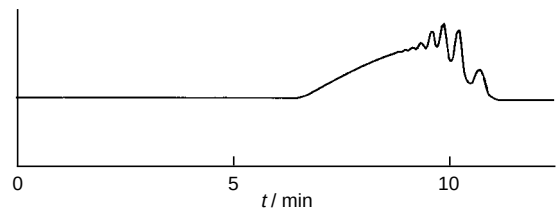



**Fig. 1** GPC of polymer **3** in THF

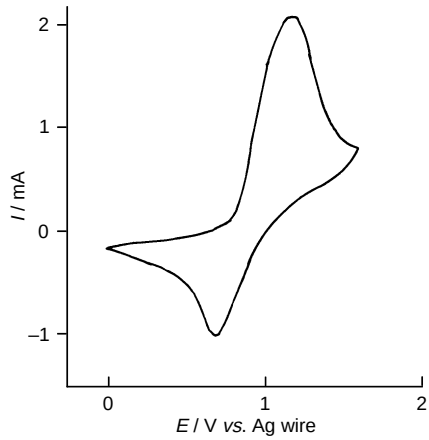



**Fig. 2** Cyclic voltammogram of polymer **3** in PC with 0.1 mol $l^{-1}$ $Bu_4NBF_4$; sweep rate, 100 mV $s^{-1}$

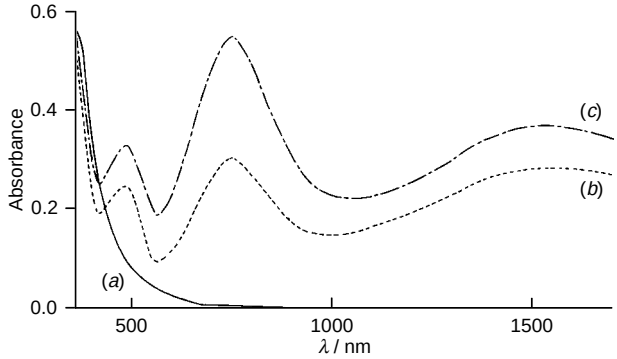



**Fig. 3** Spectral change during electrochemical $BF_4^-$ doping of polymer **3**. Applied voltage: (*a*) 0 , (*b*) 1.0 and (*c*) 1.2 V.

A cast film deposited on a platinum plate was used for cyclic voltammetry. The polymer showed a cathode-activity at applied voltages higher than 0 V; an anodic peak was observed at 1.20 V (Fig. 2). The film was dark blue above the oxidation potential and brown–yellow in the neutral state. The amount of charge, *Q*, exchanged during the redox cycle, was calculated from the integration of the absolute value of the current in Fig. 2 with respect to sweep time. The value of *Q* was found to be 0.20 electron per monomeric unit, which indicated that the polymer would be useful as a charge storage material.

Fig. 3 shows the change in the VIS–near IR spectra during electrochemical doping of polymer **3**. When the applied voltage was 0 V, the polymer film had only one band at 360 nm (3.44 eV) assigned to a π–π* transition. At 1.0 and 1.2 V, three new bands were observed around 500, 750 and 1500 nm (2.48, 1.65 and 0.83 eV). The first and last bands were considered to be assigned to the transition from the valence band to the higher and lower polaron bands,[12] respectively. The second band would be due to the transition from the lower to the higher polaron band. Electrochemically created charge carriers would be identified as polaron species in this case. The stability of the charge carriers would be brought about by the resonance effect of charged triphenylamine moiety.

Many conductive polymers are insoluble in organic solvents due to the rigid main chains but the introduction of a long alkyl or alkoxy group to the main chains is one way of enhancing solubility. However these groups do not contribute to an increase in π-conjugation length. A new branched conjugated polymer containing triphenylamine has been designed which has both a hyperbranched and conjugated backbone, and was found to be soluble in organic solvents without the addition of a long alkyl or alkoxy group. It showed a distinct anode-activity, indicating that it has a highly developed conjugated system.

## Footnote and References

* E-mail: sutanaka@ccmail.nimc.go.jp

1 Y. Kuwayama, H. Ogawa, H. Inada, N. Noma and Y. Shirota, *Adv. Mater.*, 1994, **6**, 677.
2 Y. Shirota, T. Kobata and N. Noma, *Chem. Lett.*, 1989, 1145.
3 H. Tanaka, S. Tokito, Y. Taga and A. Okada, *Chem. Commun.*, 1996, 2175.
4 L. Fomina and R. Salcedo, *Polymer*, 1996, **37**, 1723.
5 J. M. Tour, *Chem. Rev.*, 1996, **96**, 537.
6 R. Giesa, *J. Macromol. Sci. Rev. Macromol. Chem. Phys.*, 1996, **C36**, 631.
7 D. A. Tomalia, A. M. Naylor and W. A. Goodard, *Angew. Chem., Int. Ed. Engl.*, 1990, **29**, 138.
8 C. J. Hawker and J. M. J. Frechet, *J. Am. Chem. Soc.*, 1990, **112**, 7638.
9 Y. H. Kim and O. W. Webster, *J. Am. Chem. Soc.*, 1990, **112**, 4592.
10 T. M. Miller, T. X. Neenan, E. W. Kwock and S. M. Stein, *J. Am. Chem. Soc.*, 1993, **115**, 356.
11 P. J. Flory, *J. Am. Chem. Soc.*, 1952, **74**, 2718.
12 J. C. Scott, J. L. Bredas, K. Yakushi, P. Pfluger and G. B. Street, *Synth. Met.*, 1984, **9**, 165.

*Received in Cambridge, UK, 19th June 1997; 7/04299J*

# Syntheses of two kinds of dimeric hemicarcerand systems

**Juyoung Yoon and Donald J. Cram***

*Department of Chemistry and Biochemistry, University of California at Los Angeles, Los Angeles, CA 90095-1569, USA*

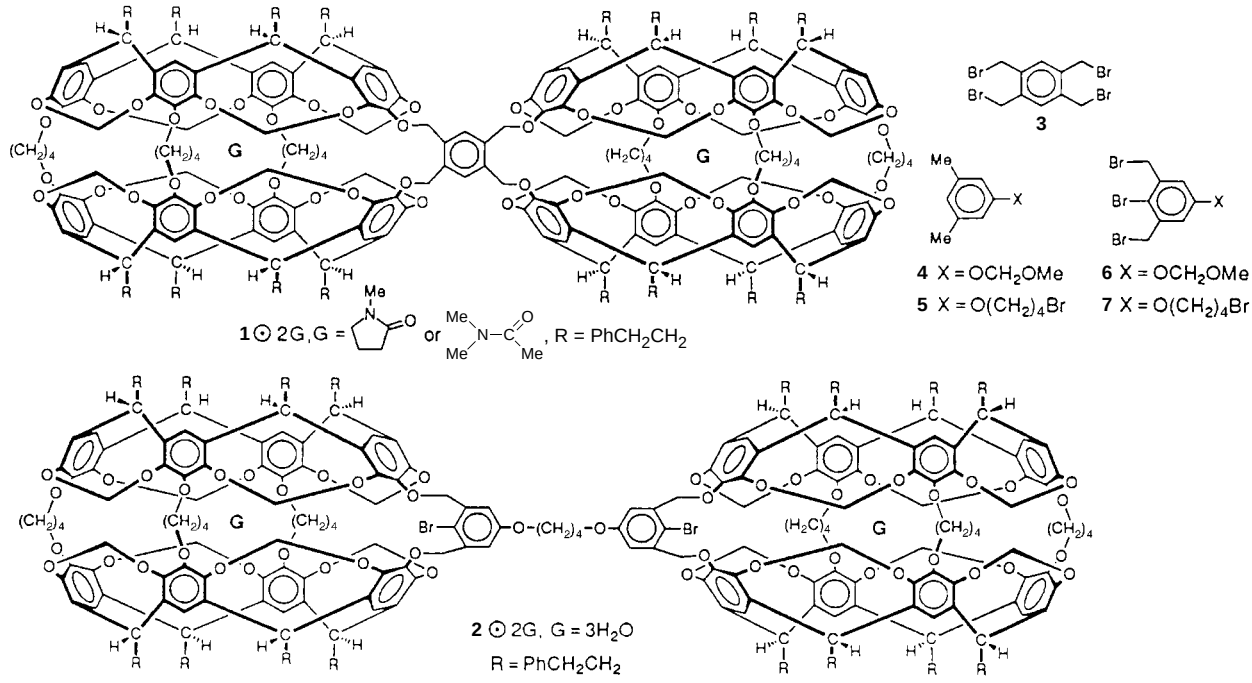
**The first dimeric hemicarcerand systems are reported, whose synthesis allows either identical or nonidentical cavities and their guests to be tethered at designed distances from one another.**

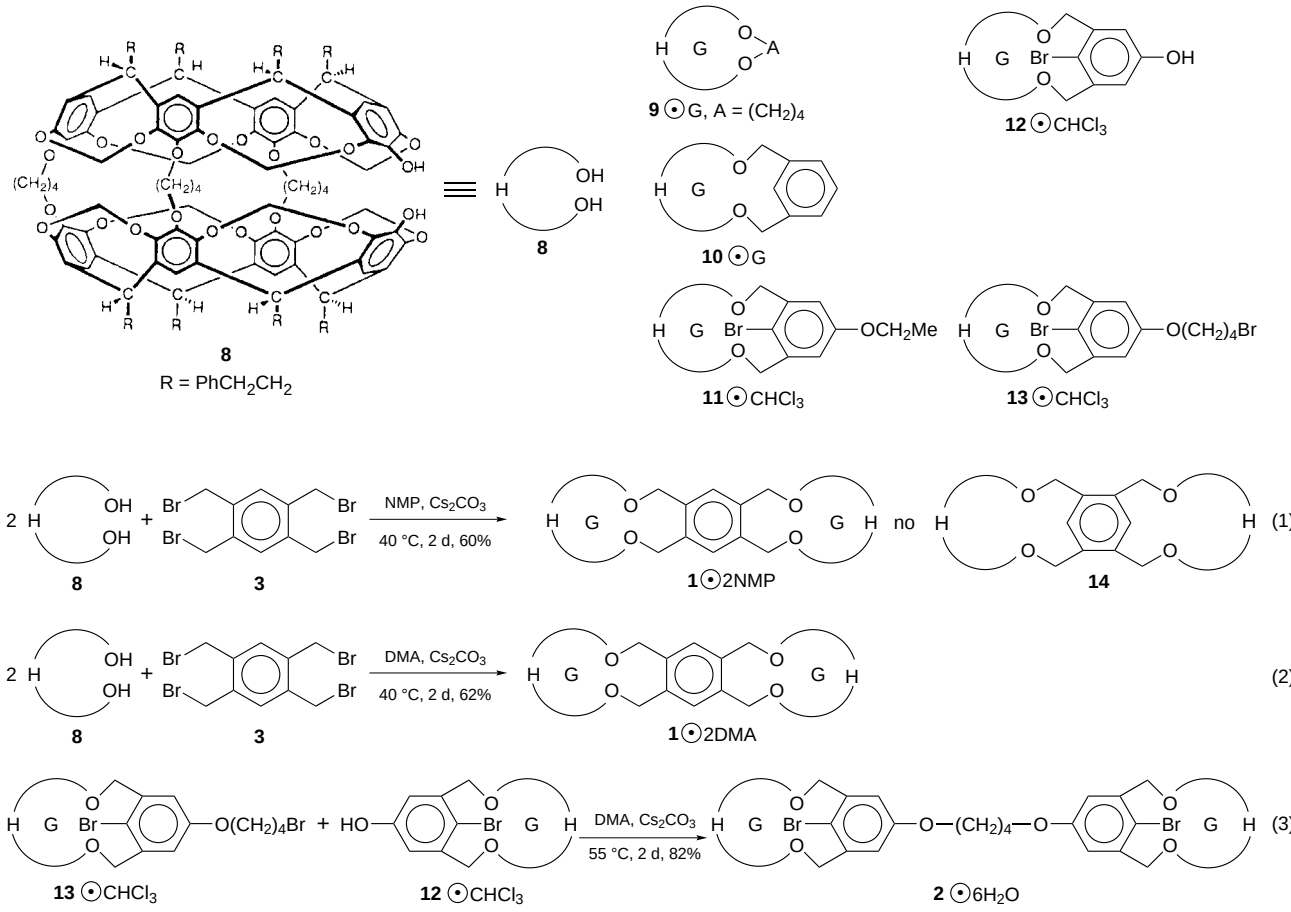
The objective of this research was to establish synthetic feasibility for the synthesis of hemicarcerands covalently attached to one another through groups of designable lengths and saturation, of which **1** and **2** are examples. We reported earlier that appropriate guests incarcerated in **9** underwent oxidation and reduction reactions in bulk solution containing a variety of reducing and oxidizing agents. Electron and water transfers through shells without physical contact between guest and reagent were demonstrated.[1] These results suggest the possibility of electron transfers occurring between two or more designable guests whose hosts of appropriate character are located at controllable distances from one another. We imagine the possibility of ultimately preparing robust polymer chains whose core of guests is conducting, whose proximate shells are electron-permeable, and whose R groups are insulating. Earlier papers report the easy synthesis of diol **8**,[2] and its convertibility to eight different hosts of general structure **9** that differ only in their A groups.[2–4] This family of hosts forms stable complexes with over 50 characterized guests representing a wide variety of structural types.[2–5]

The synthesis of **1**⊙2NMP† (NMP = *N*-methylpyrrolidinone) and of **1**⊙2DMA† (DMA = dimethylacetamide) was accomplished by the reaction of tetrabromide **3** with two moles of diol **8** under the conditions of eqns. (1) and (2), respectively.‡ Earlier, **8** had been shown to react with 1,3-$(BrCH_2)_2C_6H_4$ to give **10**⊙G, suggesting the possibility that a dimer might be formed in which each of the two shell closures involved *m*-xylyl rather than *o*-xylyl type reactions, as in **14**.[2] No evidence for formation of **14** was obtained. The rates of the product-determining steps involve formation of the second ether group which closes to form a 26-membered ring leading to **1** or to form a 27-membered ring to provide **14**. Apparently the former rate is faster than the latter.

The final step in the synthesis of **2**⊙6$H_2O$† is formulated in eqn. (3). The two hemicarceplexes, **12**⊙$CHCl_3$† and **13**⊙$CHCl_3$†, were prepared as follows. The hydroxy group of 3,5-$Me_2C_6H_3OH$ was protected by treating it with $BrCH_2OMe$–NaH–THF to give **4**† (95%), which was brominated with *N*-bromosuccinimide (NBS)–$CH_2Cl_2$–AIBN to give **6**† (40%). Shell closure of diol **8** with **6** in NMP–$Cs_2CO_3$ (40 °C, 2 d) gave **11**⊙$CHCl_3$† (NMP exchange with $CHCl_3$ solvent occurred during chromatography). Deprotection of the $ArOCH_2OMe$ group of **11**⊙$CHCl_3$ (THF–HCl, 35 °C, 4 h) gave **12**⊙$CHCl_3$.† Alternatively, 3,5-$Me_2C_6H_3OH$ was treated with excess $Br(CH_2)_4Br$–$K_2CO_3$–DMF (50 °C, 4 h) to provide **5** (60%) (characterized only by $^1H$ NMR), which was brominated with NBS–$CH_2Cl_2$–AIBN to give **7**† (40%). Shell closure of diol **8** with **7** in NMP–$Cs_2CO_3$ (30 °C, 2 d) resulted in **13**⊙$CHCl_3$† (72%), NMP again being exchanged for $CHCl_3$ as guest during chromatography. As indicated in eqn. (3), the DMA–$Cs_2CO_3$ catalyzed coupling of **13**⊙$CHCl_3$ and **12**⊙$CHCl_3$ gave **2**⊙6$H_2O$† (82%), the $CHCl_3$ guest of the starting materials being replaced by water during chromatography with $CH_2Cl_2$, drying and absorbing water from the atmosphere.‡

Corey–Pauling–Koltun model examinations of **1**, **2** and **14** provide the following estimates for the respective maximum and minimum distances the centres of the two cavities can be






from one another: **1**, 13–15; **2**, 13–26; **14**, 12.5–16 Å. For all three models, low-energy conformations appear to exist in which the outsides of the two shells contact one another. We believe it is more likely for electrons to pass from an appropriate guest in one shell of **1** to a second appropriate guest in the other shell of **1** than it is for electrons to pass between oxidizing or reducing agents and incarcerated guests dissolved in dilute solvent, an observed phenomenon.

## Footnotes and References

* E-mail: maverick@chem.ucla.edu

† These new compounds gave C and H elemental analyses within 0.30% of theory, $M^+$ *m/z* signals of 80–100% intensity (including guest) in their FAB-MS and $^1$H NMR spectra consistent with their structures.

‡ The procedures were patterned after those that are standard in the literature. All products were purified by chromatography (E. Merck silica gel 60, 70–230 mesh). The shell closures required reagent grade DMA or NMP, freshly distilled and stored over 3 Å molecular sieves (activated at 320 °C) and degassed just prior to use. The shell closures involved medium dilution and inert atmospheres, and were similar to those reported in refs. 2 and 5.

1 T. A. Robbins and D. J. Cram, *J. Am. Chem. Soc.*, 1993, **115**, 12 199.
2 J. Yoon, C. Sheu, K. N. Houk, C. B. Knobler and D. J. Cram, *J. Org. Chem.*, 1996, **61**, 9323.
3 J. Yoon C. B. Knobler, E. F. Maverick and D. J. Cram, *Chem. Commun.*, 1997, 1303.
4 J. Yoon and D. J. Cram, *Chem. Commun.*, 1997, 1505
5 T. A. Robbins, C. B. Knobler, D. R. Bellew and D. J. Cram, *J. Am. Chem. Soc.*, 1994, **116**, 111.

*Received in Columbia, MO, USA, 31st July 1997; 7/05537D*

# Dendritic solution viscosity behaviour in core terminated hyperbranched poly(amidoamine)s

**Lois J. Hobson and W. James Feast***

*I.R.C. in Polymer Science & Technology, University of Durham, Durham, UK DH1 3LE*

**A poly(amidoamine) hyperbranched $AB_2/B_6$ copolymer displays a viscosity/molecular weight profile similar to that shown by perfectly regular dendrimers.**

The physical properties of a polymer are heavily dependent upon its topology.[1–6] Dendrimers, prepared by stepwise iterative syntheses, represent a particularly interesting class of materials which are attracting considerable attention at present. A characterising feature of dendritic polymers is that past a critical point, their intrinsic viscosity decreases with increasing molecular weight.[7] It is often argued that the properties which distinguish dendrimers from other structures are associated only with those materials whose molecular weight is above this peak in the viscosity *versus* molecular weight curve.[8]

We have recently established a simple 'one-pot' route to the hyperbranched analogues of Tomalia's poly(amidoamine) dendrimers.[9,10] These polymers, prepared by the melt polymerisation of *N*-acryloyl-α,β-diaminoalkane hydrochlorides[11] $H_2C{=}CHCONH(CH_2)_nNH_3^+Cl^-$ ($n$ = 2–7), exhibit a degree of branching approaching one in the case where $n$ = 2. The observation of near perfect branching for this monomer is very unusual indeed; so far it is the only example we have found in more than twelve $AB_2$ polymer systems studied. Near perfect branching in $AB_n$ systems does not, of course, imply the formation of materials with dendritic topology. This is illustrated in Fig. 1, where structure (*b*) represents one possible topology in the spectrum between the linear structure (*a*) and the perfect dendritic wedge (*c*), all of which display a branching factor of one.

The peak in the log (molecular weight) *versus* log (intrinsic viscosity) relationship is widely believed to be a specific characteristic of dendritic materials and the possibility of regulating the molecular weight *versus* viscosity relationship within the limits defined by linear and true dendritic systems has technological attractions.

Here we report the preparation of a series of $AB_2/B_6$ copolymers, using the monomer *N*-acryloyl-1,2-diaminoethane hydrochloride ($n$ = 2) in conjunction with the $B_6$ core, tris(2-aminoethyl)amine. The polymerisations were carried out under dry nitrogen in the melt and it was readily shown by $^1$H NMR spectroscopy that the vinyl unit was rapidly and completely consumed in this system. For related monomers where $n > 2$ this did not occur and vinyl units remained after several hours reaction time. The high reactivity and high branching factor appears to be unique to the monomer where $n$ = 2. Since consumption of the monomer was complete, variation of the molar ratio of core terminating tris(2-aminoethyl)amine to $AB_2$ *N*-acryloyl-1,2-diaminoethane hydrochloride monomer allows regulation of product molecular weight. Unfortunately the water soluble polyelectrolytes produced in this work are not amenable to reliable molecular weight analysis by either GPC or MALDI–TOF MS, which prevents a direct check on their molecular weights and molecular weight distributions. However the knowledge that all the $AB_2$ wedges are terminated by cores and that all the monomers are consumed, taken with our earlier experience with less highly branched core-terminated polyesters,[12] gives some confidence in the calculated molecular weights used below. Our earlier work with $CHCl_3$ and THF soluble polyesters had established that the homo-$AB_2$ hyperbranched polyesters conformed to the Mark–Houwink relationship and that molecular weights calculated from $AB_2$ monomer to $B_n$ core molar ratios for the core terminated samples fell between the *M*n and *M*w values determined by GPC (see Fig. 2 in ref. 12), thus establishing a correlation between the molecular weight of the products and the $B_n$ core: $AB_2$ monomer molar ratio used in the polymerisation. Following this precedent, we have polymerised $AB_2/B_6$ mixtures with the molar ratios appropriate to the formation of successive generations of ideal dendrimers. Solution viscosity measurements on the resultant polyelectrolytes were carried out in 1% aqueous LiCl at 25 °C over a range of dilutions, using a Laude/Schott automated system. A plot of reduced viscosity against concentration allows extrapolation to zero concentration to give a value for intrinsic viscosity ($cm^3\ g^{-1}$).

The logs of the observed intrinsic viscosities were plotted against the logs of molecular weights calculated from the monomer to core terminator molar ratios and are shown in Fig. 2 in comparison with Tomalia's PAMAM dendrimer data.[13] We

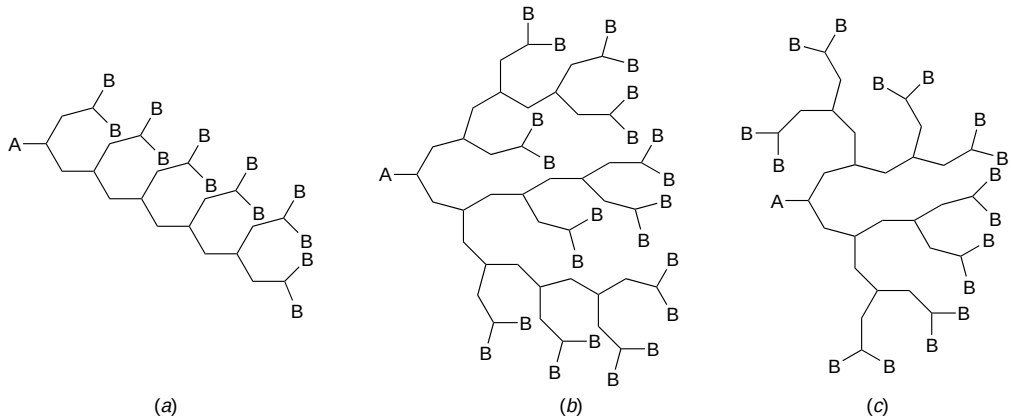



**Fig. 1** Possible structures of an $AB_2$ hyperbranched polymer with a branching factor of one

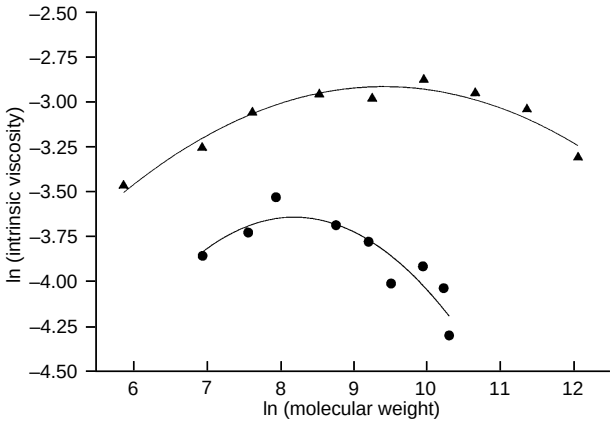



**Fig. 2** The molecular weight *vs.* intrinsic viscosity relationship for $AB_2/B_6$ copolymers: (●) $AB_2/B_6$ copolymers and (▲) Tomalia's PAMAM dendrimers (ref. 13)

do not expect that this simple 'one pot' synthesis will produce perfect monodisperse dendrimers; indeed, a distribution in both molecular weight and structure is to be expected. However it is clear that in the system examined the peak in the graph of log (intrinsic viscosity) *versus* calculated molecular weight is demonstrated and is consistent with the formation of polymeric materials with topologies giving rise to solution viscosity behaviour resembling that of dendrimers. These observations imply that at least some of the attractive materials properties of dendrimers may be obtained in materials synthesised by less laborious procedures than those reported to date.

We thank the EPSRC for support of this work through a ROPA grant.

## Footnote and References

* E-mail: w.j.feast@durham.ac.uk

1 D. A. Tomalia, A. N. Naylor and A. Goddard, *Angew. Chem., Int. Ed. Engl.*, 1990, 138.
2 E. M. M. de Brabander-van den berg, A. Nijenhuis, M. Mure, J. Keulen, R. Reintjens, F. Vandenbooren, B. Bosman, R. Denaat, T. Frijins, S. V. D. Wal, M. Castelijns, J. Put and E. W. Meijer, *Macromol. Symp.*, 1994, **77**, 51.
3 H. Ihre, A. Hult and E. Sonderlind, *J. Am. Chem. Soc.*, 1996, **118**, 6388.
4 B. I. Voit, *Acta Polym.*, 1995, **46**, 87.
5 Hawker, C. J. and J. M. J. Frechet, *J. Am. Chem. Soc.*, 1990, **112**, 7638.
6 J. M. J. Frechet and C. J. Hawker, *Comprehensive Polymer Science*, second supplement, volume, ed. S. L. Agarawal and S. Russo, Pergammon, Oxford, 1996, ch. 3.
7 T. H. Mourey, S. R. Turner, M. Rubinstein, J. M. J. Frechet, C. J. Hawker and K. L. Wooley, *Macromolecules*, 1992, **25**, 2401.
8 For example, E. W. Meijer, view expressed in lectures, *e.g.* E.U. SELOA Summer School, Siena, Italy, May 1997.
9 L. J. Hobson, A. M. Kenwright and W. J. Feast, *A.C.S. Polymeric Materials Science and Engineering, Las Vegas Meeting*, Sept. 1997, 77, 220.
10 L. J. Hobson, A. M. Kenwright and W. J. Feast, *Chem. Commun.*, 1997, 1877.
11 G. L. Stahl, R. Walter and C. W. Smith, *J. Org. Chem.*, 1978, **43**, 2285.
12 W. J. Feast and N. M. Stainton, *J. Mater. Chem.*, 1995, **5**, 405.
13 D. A. Tomalia, D. M. Hedstrand and L. R. Wilson, *Encyclopaedia of Polymer Science and Engineering*, 2nd edn., Wiley, New York, 1990, index vol., p. 46.

*Received in Liverpool, UK, 31st July 1997; 7/05572B*

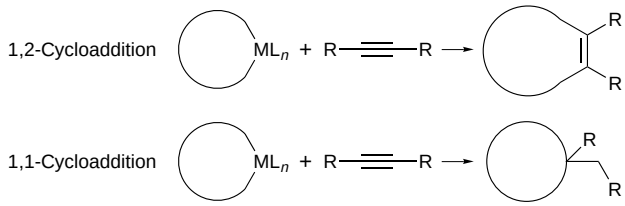
# 1,1-Cycloaddition of zirconacyclopentadienes to propynoates

**Tamotsu Takahashi,* Wen-Hua Sun, Chanjuan Xi and Martin Kotora**

*Catalysis Research Center and Graduate School of Pharmaceutical Sciences, Hokkaido University, Kita-ku, Sapporo 060, Japan*

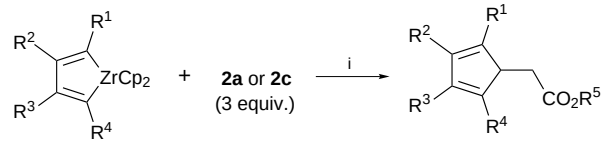
**Zinconacyclopentadienes react with propynoates in a 1,1-cycloaddition manner to give pentasubstituted cyclopentadiene derivatives in high yields.**

Metallacycles are convenient starting materials for the construction of carbocyclic compounds.[1] The formation of carbocycles can be accomplished by the addition reaction to (or insertion reaction of) unsaturated compounds such as alkenes, alkynes, CO and RNC. It is well documented that CO or its synthetic equivalents act as one-carbon units. For alkenes or alkynes, two types of addition reaction, *i.e.* 1,2-cycloaddition or 1,1-cycloaddition, are considered to be possible as shown in Scheme 1. There have been many examples of the 1,2-cycloaddition of metallacycles to alkynes, in which the alkynes behave as two-carbon units.[2] In contrast, 1,1-cycloaddition to alkynes or related reactions in which alkynes act as a one-carbon unit is very rare.[3,4] Here we report the 1,1-cycloaddition of zirconacyclopentadienes to propynoates to afford cyclopentadiene derivatives.




**Scheme 1**

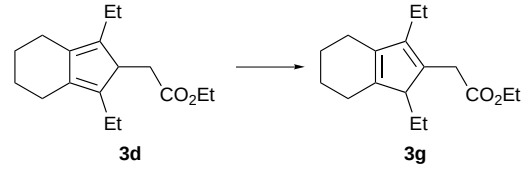
In a typical example, the reaction of tetraethylzirconacyclopentadiene **1b** with ethyl propynoate **2a** (3 equiv.) provided the cyclopentadiene **3b** in 97% (GC) yield (Scheme 2). The best results were obtained by stirring the reaction mixture first at −78 °C for 1 h followed by stirring at 0 °C for 1–3 h. Some further examples are presented in Scheme 2. In all cases yields of products were high. Monocyclic zirconacyclopentadienes afforded only the corresponding cyclopentadienes. In the case of bicyclic zirconacyclopentadiene **1d**, the desired product **3d** was easily isomerized to the more stable **3g** (Scheme 3) under the conditions used here. The reactions of




**1a** $R^1 = R^2 = R^3 = R^4 = Me$
**b** $R^1 = R^2 = R^3 = R^4 = Et$
**c** $R^1 = R^2 = R^3 = R^4 = Pr$
**d** $R^1 = R^4 = Et$, $R^2–R^3 = –(CH_2)_4–$

**3a** ($R^5$ = Et): 93% (73)
**b** ($R^5$ = Et): 97% (74)
**c** ($R^5$ = Et): 96% (78)
**d** ($R^5$ = Et): 93% (68)
**e** (from **1b**, $R^5$ = Me): 95% (78)
**f** (from **1c**, $R^5$ = Me): 93% (78)

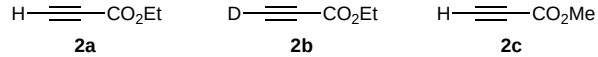
**Scheme 2** *Conditions*: i, −78 to 0 °C, 1–3 h; $H^+$. GC yields. Isolated yields are given in parentheses.




**3d** **3g**

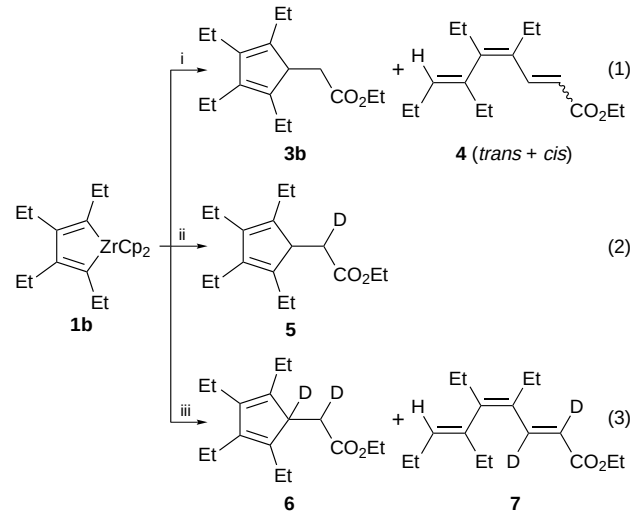
**Scheme 3**

zirconacyclopentadienes **1b**,**c** with methyl propynoate **2c** gave similar products **3e** and **3f**, respectively. Thus, the formation of cyclopentadiene derivatives proceeds under relatively mild conditions in high yields. Although its scope is limited only to zirconacyclopentadienes bearing alkyl substituents, and zirconacyclopentadienes bearing phenyl or trimethylsilyl substituents at the α-position did not react, clarification of the mechanism of 1,1-cycloaddition of **1** to **2** should be informative.



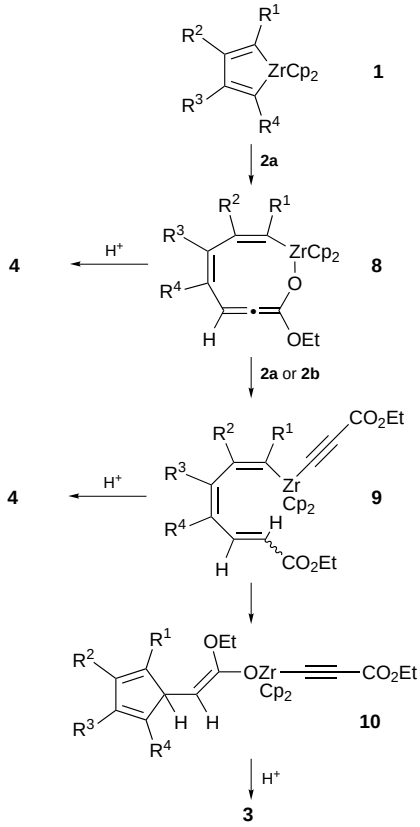

**2a** **2b** **2c**

To elucidate the reaction mechanism, the following experiments were conducted (Scheme 4). Firstly, the reaction was carried out at −78 °C. Interestingly, trienes **4** were obtained in 78% yield (*trans*-**4** 38% + *cis*-**4** 40%) as major products along with **3b** (18%), whereas at −40 °C the reaction gave a different ratio of the products: **3b** (49%), *trans*-**4** (29%) and *cis*-**4** (16%). Secondly, the reaction of the zirconacyclopentadiene **1b** with ethyl propynoate at −78 °C for 1 h and then 0 °C for 1 h afforded the monodeuterated cyclopentadiene **5** after deuterolysis with 3 M DCl. This result shows that the product of the reaction of **1b** with **2a** before hydrolysis contains only one Zr–C bond or one Zr-enolate moiety. One hydrogen atom must be transferred to the intermediate during the reaction. Obviously,




**1b** **3b** **4** (*trans* + *cis*) **5** **6** **7**

**Scheme 4** *Reagents and conditions*: i, **2a**, −78 °C, $H^+$; ii, **2a**, −78 to 0 °C, $D^+$; iii, **2b**, −78 to 0 °C, $H^+$



**Scheme 5** Proposed reaction mechanism of the cyclopentadiene formation

the only compound capable of acting as a possible hydrogen donor is the propynoate having a weakly acidic hydrogen atom bound to the sp carbon of the triple bond. This is consistent with the fact that 3-substituted propynoates, which do not have the acidic hydrogen, do not give the desired products. To clarify this point, the reaction of the zirconacyclopentadiene **1b** with ethyl [3-$^2$H]propynoate **2b**[5] was carried out. Hydrolysis of the reaction mixture with 3 M HCl afforded the dideuterated cyclopentadiene **6** in 61% yield and the *trans* triene **7** in 17% yield. This clearly indicates that Michael addition of one Zr–C bond of the zirconacyclopentadiene to propynoate is the first step. It is noteworthy that this is the first example of direct Michael addition of organozirconocene compounds. So far, the Michael addition was observed only after transmetallation of organozirconium compounds to Cu[2,6] or Ni[7] compounds. This demonstrated that a hydrogen (deuterium) atom is indeed transferred from the second propynoate (deuterated propynoate). It also explains why an excess of propynoate was necessary for this reaction and why 3-substituted propynoates did not give the desired products.

From these results, it is possible to propose the following reaction mechanism (Scheme 5). In the first step, the zirconacyclopentadiene **1** adds to the propynoate **2a** forming the nine-membered oxazirconacycle **8**. Hydrolysis of **8** gives the trienes **4**. Then, protonolysis **8** with the propynoate **2a** takes place forming the alkenylalkynyl zirconium compound **9**. Hydrolysis of **9** also affords trienes **4**. The intermediate **9** undergoes an intramolecular conjugate addition and forms **10** which, upon hydrolysis, affords **3**.

In conclusion, zirconacyclopentadienes unprecedentedly reacted with propynoates *via* inter- and intra-molecular Michael addition, resulting in a 1,1-cycloaddition to afford cyclopentadienes. This is in contrast to the reactions of late transition metal metallacyclopentadienes (*e.g.* Ir) which react with propynoates *via* vinylidene intermediates to yield stable organometallic compounds.[4,8]

## Footnote and References

* E-mail: tamotsu@cat.hokudai.ac.jp

1 (*a*) N. E. Schore, in *Comprehensive Organometallic Chemistry II*, ed. E. W. Abel, F. G. A. Stone and G. Wilkinson, Elsevier, Oxford, 1995, vol. 12; pp. 703–740; (*b*) D. B. Grothjahn, in *Comprehensive Organometallic Chemistry II*, ed. E. W. Abel, F. G. A. Stone and G. Wilkinson, Elsevier, Oxford, 1995, vol. 12, pp. 741–770; (*c*) E. Negishi, in *Comprehensive Organic Synthesis*, ed. B. M. Trost and I. Fleming, Pergamon, Oxford, 1991, vol. 5, pp. 1163–1184; (*d*) H.-W. Frühauf, *Chem. Rev.*, 1997, **97**, 523; (*e*) M. Lautens, W. Klute and W. Tam, *Chem. Rev.*, 1996, **96**, 49.

2 For example, for Zr see: T. Takahashi, M. Kotora and Z. Xi, *J. Chem. Soc., Chem. Commun.*, 1995, 361; for Ti: J. E. Hill, G. Balaich, P. E. Fanwick and I. P. Rothwell, *Organometallics*, 1993, **12**, 2911; for other metals see: K. P. C. Volhardt, *Angew. Chem., Int. Ed. Engl.*, 1984, **23**; see also refs. 1(*a*) and 1(*b*).

3 L. Miginiac, in *The Chemistry of Metal-Carbon Bond*, ed. F. R. Hartley and S. Patai, Wiley, New York, 1985, vol. 3, pp. 99–141.

4 J. M. O'Connor, K. Hiibner, R. Merwin, P. K. Gantzel, B. S. Fong, M. Adams and A. L. Rheingold, *J. Am. Chem. Soc.*, 1997, **119**, 3631 and references cited therein.

5 C. A. Townsend, A. M. Brown and T. T. Nguyen, *J. Am. Chem. Soc.*, 1983, **105**, 919.

6 M. Yoshifuji, M. J. Loots and J. Schwartz, *Tetrahedron Lett.*, 1977, 1303; B. H. Lipshutz and M. Segi, *Tetrahedron*, 1995, **51**, 4407.

7 M. J. Loots and J. Schwartz, *J. Am. Chem. Soc.*, 1977, **99**, 8045.

8 J. M. O'Connor, K. Hiibner, R. Merwin and L. Pu, *J. Am. Chem. Soc.*, 1995, **117**, 8861.

*Received in Cambridge, UK, 4th July 1997; 7/04740A*

# Pd–Cu–Exchanged montmorillonite K10 clay: an efficient and reusable heterogeneous catalyst for vinylation of aryl halides

**R. K. Ramchandani, B. S. Uphade, M. P. Vinod, R. D. Wakharkar, V. R. Choudhary and A. Sudalai***

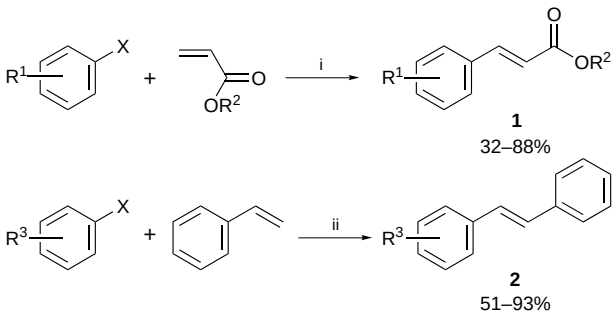
*National Chemical Laboratory, Pune 411 008, India*

**Palladium and copper exchanged montmorillonite K10 clay has been found to catalyse very efficiently the reaction between aryl halides (X = Br, I) and acrylates, and styrenes affording alkyl (*E*)-cinnamates and (*E*)-stilbenes respectively in high yields.**

The palladium-catalysed vinylation of aryl halides (X = Br, I) (Heck reaction) provides a very convenient and powerful method for forming carbon–carbon bonds at unsubstituted vinylic positions.[1] Major improvements in Heck-type reactions over the last decade have been brought about by the introduction of tetraalkylammonium salts, silver(I) or thallium(I) salts as promoting additives or by use of organotrifluoromethanesulfonates.[2] Two recent promising approaches involve reactions in aqueous (or water–organic solvent) media[3] and the use of vinyl iodonium salts.[4] For the Heck reaction, a $Pd^{II}$ salt or complex is employed which is reduced *in situ* to an active zero valent palladium species under homogeneous conditions. The $Pd^{II}$ species that is subsequently regenerated in the reaction[2] is very difficult to separate and reuse for the reaction directly without further processing. In view of the practical and industrial applications, improvements in catalyst efficiency and catalyst recycling are essential. To overcome these problems, heterogeneous catalysts such as polymer-supported palladium catalysts and Pd–$Ph_2$P–Si supported on clay have been reported for the arylation of alkenes.[5] However, these catalysts suffer from drawbacks such as (i) their preparation involves many steps and the use of expensive phosphorus and silicon compounds and (ii) deactivation of the catalyst on its reuse. We report here our preliminary results on the use of Pd and Cu exchanged montmorillonite K10 (Mont.K10) clay catalysts for the vinylation of aryl halides (X = Br, I) (Scheme 1).

Pd, Cu and Pd–Cu exchanged clay catalysts were prepared by exchanging the clay with dilute aqueous $PdCl_2$, $Cu(NO_3)_2$ or a mixture of two respectively. For example, Pd (0.29 wt%)–Cu (0.36 wt%)-exchanged Mont.K10 clay catalyst was prepared by treating Mont.K10 clay (25 g) with 600 ml aqueous $PdCl_2$ and $Cu(NO_3)_2$ under vigorous stirring at room temperature for 24 h, centrifuging and washing the Pd–Cu exchanged clay with distilled deionised water repeatedly until the discarded filtrate was free from $Cl^-$ and $NO_3^-$ ions, and drying the resulting mass at 110 °C for 12 h. The metal content of the catalysts was determined using an electron disperse X-ray microscope (EDX) (Kevex, US) connected to a JEOL (JSM-5200) scanning electron microscope (SEM). The surface area of Pd (0.29 wt%)–Cu (0.36 wt%)–Mont.10 and Cu (0.39 wt%)–Mont.K10 being 262.9 and 238.9 $m^2\ g^{-1}$ respectively (BET method). The XRD pattern and FT-IR spectra of these samples show that they are crystalline, however no significant differences were observed among their structures. Definite information about the nature of the metal species present in the catalyst could be obtained from cyclic voltammetry (CV). Fig. 1 shows the CV of Cu–Pd exchanged Mont.K10 clay at a scan rate of 50 mV $s^{-1}$. It clearly indicates two reversible peaks with $E_{1/2}$ (*vs.* saturated calomel electrode) at −0.119 and +0.117 V. We attribute, after comparing the potential values from literature,[6] the peak at +0.117 to a Pd/$Pd^{2+}$ process and the one at −0.119 V to a Cu/$Cu^{2+}$ process. Although two one-step electron processes (*i.e.* $Cu^{2+}/Cu^+$ and $Cu^+/Cu$) are possible, separate experiments with Cu and Pd exchanged Mont.K10 clay have shown that the CV behaviour corresponds to $Cu^{2+}/Cu$ and Pd/$Pd^{2+}$ redox processes. Hence the presence of Pd is mediating the Cu redox process (Fig. 2). This explains the high activity of the Pd–Cu exchanged catalyst compared to the Cu or Pd exchanged catalyst.

Results of the reaction of iodobenzene with acrylates, over different catalysts and over the best catalyst Pd (0.29 wt%)–Cu (0.36 wt%)-exchanged Mont.K10 clay catalyst are presented in Tables 1 and 2 respectively.† A comparison of the results in




**Scheme 1** *Reagents and conditions*: i, Pd–Cu–Mont.K10 (10% m/m), $K_2CO_3$, DMF, reflux, 2 h; ii, Pd–Cu–Mont.K10 (15% m/m), $K_2CO_3$, DMF, reflux, 2–3 h

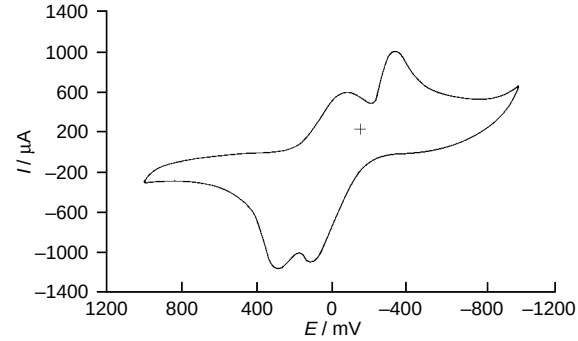



**Fig. 1** Cyclic voltammogram of Pd–Cu exchanged Mont.K10 clay at a scan rate of 50 mV $s^{-1}$

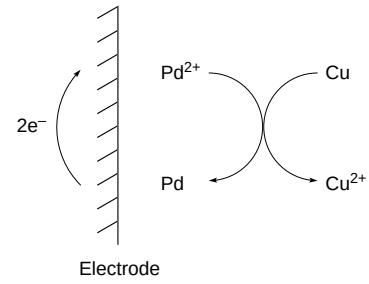



**Fig. 2** Pd mediates the redox behaviour of Cu

**Table 1** Results of Heck reaction between methyl acrylates and iodobenzene or *p*-methoxyiodobenzene over different catalysts[a]

| Entry | Catalyst | Yield (%) of methyl cinnamate **1** | |
|---|---|---|---|
| | | $R^1$ = H | $R^1$ = OMe |
| 1 | Cu (0.07 wt%)–Mont.K10 | 0 | 0 |
| 2 | Cu (0.39 wt%)–Mont.K10 | 30 | 51 |
| 3 | Pd (0.33 wt%)–Mont.K10 | 41 | 56 |
| 4 | Pd (0.29 wt%)–Cu (0.36 wt%)–Mont.K10 | 83 | 88 |
| 5 | Pd (1.73 wt%)–Cu (0.16 wt%)–Mont.K10 | 56 | 61 |
| 6 | Cu (0.32 wt%)–kaolin | 0 | 0 |

[a] *Reaction conditions*: iodobenzene (3 mmol), methyl acrylate (6 mmol), anhydr. $K_2CO_3$ (8 mmol), catalyst (10% m/m), DMF (5 ml), reflux, 2 h. [b] Isolated yield obtained after chromatographic purification.

Table 1 shows that among the catalysts, the Pd (0.29 wt%)–Cu (0.36 wt%)-exchanged Mont.K10 clay catalyst gives the best results for the Heck reaction. The higher activity of this catalyst seems to be due to a synergistic effect produced by the presence of Pd and Cu in close vicinity. The results also indicate that for this catalyst to be more active, enough copper must be present along with the palladium. It is remarkable that Cu (0.39 wt%)–Mont.K10 clay also catalyses the Heck reaction leading to the formation of (*E*)-cinnamate esters. The choice of solvent for the arylation reaction catalysed by the Pd (0.29 wt%)–Cu (0.36 wt%)–Mont.K10 clay catalyst is also critical as the reaction fails when carried out in MeCN under reflux. Among the different bases tried for this reaction, *viz.* $NaHCO_3$, K or Na acetate, $K_2CO_3$, $Et_3N$ and $Bu_3N$, $K_2CO_3$ gave the best results (*i.e.* high yields with 100% selectivity).

Table 2 lists the results for different types of aryl halides (X = Br, I) that have been vinylated with methyl or ethyl acrylate to afford the corresponding cinnamates in high yields using the Pd (0.29 wt%)–Cu (0.36 wt%)–Mont.K10 clay catalyst. In all the substrates examined, exclusive formation of the (*E*)-cinnamate was observed (GC, $^1$H and $^{13}$C NMR and mass spectroscopy). Table 3 shows the results of the reaction of various aryl halides (X = Cl, Br, I) with styrene producing (*E*)-stilbenes in high yields using Pd–Cu–Mont.K10 catalyst (15% m/m). A remarkable feature of these catalytic systems is that even less reactive substituted bromobenzenes react with styrene to give (*E*)-stilbenes in excellent yields. The reaction however did not proceed using aryl iodides with substituents such as nitro, amino, chloro *etc.* The reaction also failed when methyl vinyl ketone and cyclohexenone were used as alkenylating agents instead of acrylate. Mechanistically, it is proposed that aryl halides react with copper presumably to yield an organocopper species, which then transmetallates to $Pd^{II}$ followed by olefin insertion, β-hydride elimination and dissociation of palladium hydride species[2] (Scheme 2).

**Table 2** Results of the reaction of aryl halides with acrylates over Pd (0.29 wt%)–Cu (0.36 wt%)–Mont.K10 clay catalyst

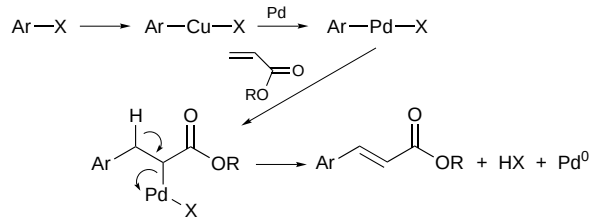
| Entry | Aryl halide | | Acrylate | Yield (%) of cinnamate **1**[a,b] |
|---|---|---|---|---|
| | $R^1$ | X | $R^2$ | |
| 1 | H | I | Me | 83 |
| 2 | H | Br | Me | 32 |
| 3 | 4-OMe | I | Me | 88 |
| 4 | 4-Me | I | Me | 76 |
| 5 | 2-OMe | I | Me | 69 |
| 6 | 2-Me | I | Me | 58 |
| 7 | 4-OMe | I | Et | 86 |

[a] Characterised by IR, $^1$H and $^{13}$C NMR and mass spectroscopy. [b] Isolated after chromatographic purification.

**Table 3** Results of the reaction of aryl halides with styrene over Pd (0.29 wt%)–Cu (0.36 wt%)–Mont.K10 clay as catalyst

| Entry | Aryl halide | | *t*/h | Yield (%) of stilbene[a,b] |
|---|---|---|---|---|
| | $R^3$ | X | | |
| 1 | H | I | 2 | 93 |
| 2 | H | Br | 2 | 51 |
| 3 | H | Cl | 12 | 0 |
| 4 | Cl | Br | 3 | 81 |
| 5 | Cl | I | 3 | 88 |
| 6 | OMe | I | 3 | 72 |

[a] Characterized by IR, $^1$H and $^{13}$C NMR and mass spectroscopy. [b] Isolated after chromatographic purification.




**Scheme 2**

The catalyst from the reaction mixture was recovered by simple filtration and was successfully reused three times without loosing its activity in the alkenylation of 4-methoxyiodobenzene with methyl acrylate.

In conclusion, the Pd (0.29 wt%)–Cu (0.36 wt%)–Mont.K10 clay catalyst has high activity for the Heck reaction in which aryl halides (X = Br, I) are reacted with acrylates and styrenes to form the corresponding (*E*)-cinnamates and (*E*)-stilbenes respectively in high yields. The high activity of the catalyst is attributed to a synergistic effect produced by the presence of Pd and Cu species in the catalyst.

The authors R. K. R. and B. S. U. thank CSIR, New Delhi, India for the award of Senior Research Fellowships.

## Footnotes and References

* E-mail: otech@ems.ncl.res.in

† In a typical reaction procedure, iodobenzene [580 mg, 2.8 mmol (1 : 1 styrene)], methyl acrylate (500 mg, 5.8 mmol), anhydr. $K_2CO_3$ (1 g, 7.2 mmol) and catalyst (58 mg, 10% by weight of PhI) in DMF (5 ml), were refluxed for 2 h. After completion of the reaction (TLC monitoring), the catalyst was separated by filtration and the reaction mixture was poured into water followed by its extraction with ethyl acetate to give the crude product which was subsequently purified by column chromatography to afford methyl (*E*)-cinnamate (380 mg, 83%), $\delta_C$ (50.3 MHz, $CDCl_3$) 51.6, 117.9, 127.9, 128.3, 128.9, 129.2, 130.3, 134.4, 144.8 and 167.3; *m/z* 162 ($M^+$, 65%), 161 (45), 131 (100), 117 (5), 103 (82) and 73 (91).

1 R. F. Heck, *Org. React.*, 1982, **27**, 345; R. F. Heck, *Palladium Reagents in Organic Synthesis*, Academic Press, London, 1985; L. S. Hegedus, in *Organometallics in Synthesis*, ed. M. Schlosser, Wiley, Chichester, 1994, p. 383.
2 A. de Meijere and F. E. Meyer, *Angew. Chem., Int. Ed. Engl.*, 1994, **33**, 2379.
3 J. P. Genet, E. Blart and M. Sarignac, *Synlett*, 1992, 715 and references cited therein.
4 R. M. Moriarty, W. R. Epa and A. K. Awasthi, *J. Am. Chem. Soc.*, 1991, **113**, 6315.
5 C. M. Anderson, K. Korabelas and A. Hallberg, *J. Org. Chem.*, 1985, **50**, 3891; B. M. Choudhary, R. M. Sarma and K. K. Rao, *Tetrahedron*, 1992, **48**, 719.
6 V. Bertocci and D. R. Turner, in *Encyclopedia of Electrochemistry of the Elements*, ed. A. J. Bard, Marcel Dekker, New York, 1974, vol. 2, p. 383 and vol. 6, p. 253.

*Received in Cambridge, UK, 11th August 1997; 7/05870E*

# Enantioselective bioelectrocatalyzed oxidation of glucose by glucose oxidase at chiral-monolayer-electrodes

**Guoliang Tao, Eugenii Katz and Itamar Willner***

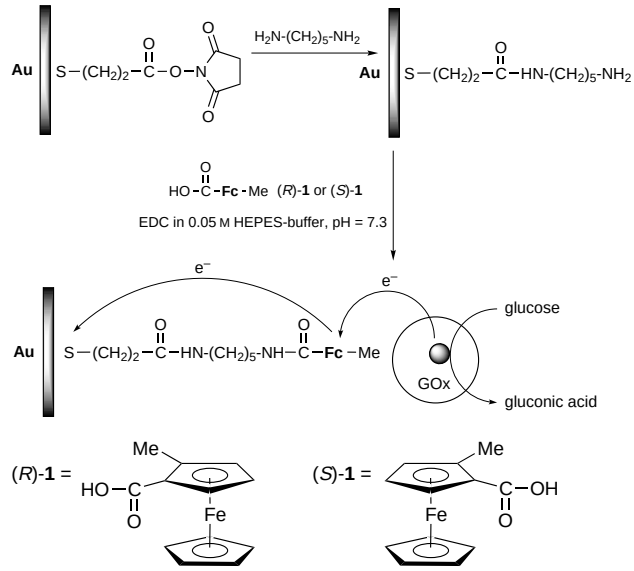
*Institute of Chemistry, The Hebrew University of Jerusalem, Jerusalem 91904, Israel*

**(*R*)- or (*S*)-2-Methylferrocenecarboxylic acid monolayers assembled onto Au-electrodes stimulate chiroselective bioelectrocatalysed oxidation of glucose in the presence of glucose oxidase**

Chiral discrimination in electron transfer or energy transfer processes in biological assemblies has been a subject of extensive research.[1,2] Chiroselectivity was observed in the association of optically-active transition metal complexes to DNA[3] and enantioselective electron transfer in the DNA microenvironment was reported.[4] Chiroselective electron transfer between transition metal complexes and redox proteins such as plastocyanine,[5] cytochrome c,[6] plant ferredoxin[7] and reconstituted $Zn^{II}$-myoglobin[8] was reported, although in low discrimination yields. Mediated electron transfer between low molecular-weight redox-relays and redox proteins has been studied in the general context of electrochemical biosensors.[9,10] In particular, ferrocenyl cation-mediated[11] oxidation of oxidoreductases was extensively explored, and the mediated electron transfer rates were controlled by the ferrocene substituent groups and the redox potentials of the relays. As the association rate of ligands to proteins is lower than diffusion-controlled (*k ca.* $10^7$–$10^8$ $M^{-1}$ $s^{-1}$) it is anticipated that chiral discrimination could play an important role in the affinity interactions of ligands and proteins. Indeed, we have reported the first example of enantioselective, diffusionally mediated, bioelectrocatalysed oxidation of glucose in the presence of chiral ferrocene mediators.[12] These results were later criticized by Alzari *et al.*,[13] though recent examples by Sadeghi and co-workers[14] nicely support the concept of chiroselective, diffusionally mediated, electron transfer within enzymes. Mediated bioelectrocatalytic transformations at redox-relay functionalized monolayer electrodes was recently exemplified.[15] Chiral monolayer-modified electrodes were developed for some electrochemical,[16] but not bioelectrochemical applications. Here we report on the assembly of chiral monolayers consisting of (+)-2-methylferrocene carboxylic acid, (*R*)-**1** and (−)-2-methylferrocenecarboxylic acid, (*S*)-**1**.[17] The resulting chiral monolayer interfaces stimulate the enantioselective mediated bioelectrocatalysed oxidation of glucose. Mechanistic analysis of the electron transfer process using a rotating disc electrode (RDE), reveals chiral discrimination in the affinity associative interactions between the chiral monolayer and the redox enzyme glucose oxidase (from *Aspergillus niger* type X-S, E.C. 1.1.2.4, Sigma).

The assembly of the amide-functionalized chiral ferrocene monolayers on Au-electrodes is shown in Scheme 1. The ferrocene monolayer-functionalized electrodes exhibit a reversible cyclic voltammogram, $E^\circ$ = 0.235 V *vs.* SCE, and the surface coverage of the two enantiomers is similar, $6 \times 10^{-11}$ mol $cm^{-2}$ (±2%). The electron transfer rates to the two chiral ferrocene relays was determined by Laviron's method[18] and were found to be identical, $k_{et}$ *ca.* 18.0 $s^{-1}$. Fig. 1 shows the cyclic voltammograms of the chiral ferrocene-functionalized electrodes, in the presence of glucose oxidase, GOx, in the electrolyte solution in the absence of glucose [curves (*a*) and (*b*)] and in the presence of added glucose, $5 \times 10^{-2}$ M [curves (*c*) and (*d*)]. In the presence of glucose electrocatalytic anodic currents are observed in the presence of the two redox-functionalized electrodes. The electrocatalytic anodic current in the presence of the (*S*)-**1**-functionalized monolayer is higher by *ca.* 90% as compared to the electrocatalytic current in the presence of the (*R*)-**1**-functionalized monolayer electrode. These results clearly demonstrate that chiroselective bioelectrocatalysed oxidation of glucose occurs at the functionalized electrodes.

To understand the origin of chiroselective mediated electron transfer at the chiral monolayer electrodes, the bioelectro-




**Scheme 1** Organization of the chiral ferrocene monolayer-modified Au-electrodes and their electrochemical interaction with reduced glucose oxidase, $GOx^{red}$

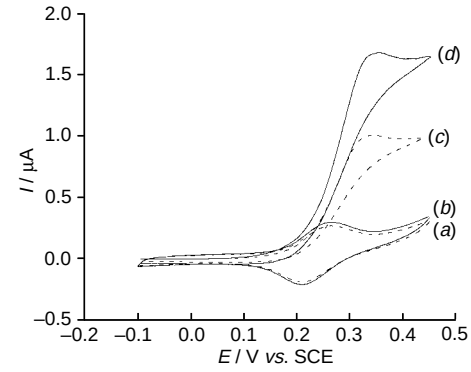



**Fig. 1** Cyclic voltammograms of the chiral ferrocene monolayer-modified Au-electrodes (0.5 mm diameter Au-wire, 0.2 $cm^2$ geometrical area, roughness coefficient, *ca.* 1.3); (*a*) and (*b*) (*S*)-**1** and (*R*)-**1** monolayer-modified electrodes, respectively, in the presence of $1 \times 10^{-5}$ M GOx and in the absence of glucose; (*c*) and (*d*) (*R*)-**1** and (*S*)-**1** monolayer-modified electrodes, respectively, in the presence of $1 \times 10^{-5}$ M GOx and 50 mM glucose. Background electrolyte, 0.1 M phosphate buffer, pH 7.0. Potential scan rate, 5 mV $s^{-1}$.

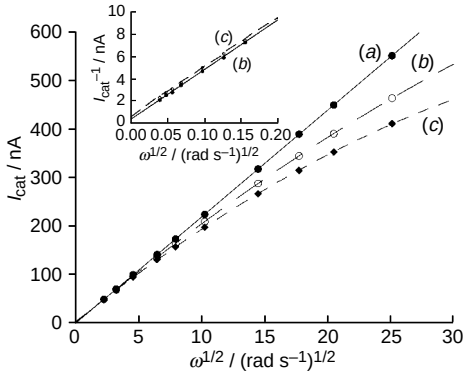



**Fig. 2** Currents generated at the chiral ferrocene monolayer-modified Au-electrodes (Au-disk, 0.16 cm² geometrical area, roughness coefficient, *ca.* 1.3) in the presence of $1 \times 10^{-5}$ M GOx and $5 \times 10^{-5}$ M glucose at applied potential +0.4 V *vs.* SCE. (*a*) Theoretical Levich plot, (*b*) **(*S*)-1** monolayer-modified electrode, (*c*) **(*R*)-1** monolayer-modified electrode. Background electrolyte, 0.1 M phosphate buffer, pH 7.0. Inset: Koutecky–Levich plots for the experimental results shown.

catalysed process was examined at a rotating disc electrode (RDE).[19] The two chiral ferrocenes, (*R*)-**1** and (*S*)-**1** were assembled on an Au-disc electrode as described in Scheme 1, and the resulting catalytic currents were monitored at a low glucose concentration, $5 \times 10^{-5}$ M, and under Ar in order to preserve the flavo enzyme redox centres in their reduced states, GOx$^{red}$. Fig. 2 (*b*) and (*c*) shows the experimental Levich plots for the electrocatalysed oxidation of GOx$^{red}$ by the (*S*)-**1** and (*R*)-**1** monolayers, respectively. For comparison, the theoretical Levich plot for the oxidation of GOx$^{red}$ by the ferrocene monolayer is shown in curve (*a*) (assuming the transfer of 2 electrons, $n = 2$; and the diffusion coefficient $D_{GOx} = 4 \times 10^{-7}$ cm² s$^{-1}$). The inset in Fig. 2 shows the related Koutecky–Levich plots for the electrocatalysed oxidation of GOx$^{red}$ by (*R*)-**1** and (*S*)-**1** monolayers, respectively. The slopes of the two plots are identical and correspond to the transfer of two-electrons (Fig. 2, inset). Thus, even though GOx consists of a dimer and the oxidation of each of the FAD sites in the subunits involves two electrons, the transfer of only two electrons is observed in the RDE experiments. This is rationalized by the fact that only one subunit is appropriately aligned in respect to the monolayer within the electron transfer event. It should be noted that in the RDE experiments, analysing the electron transfer rate between the chiral ferrocene monolayers and GOx, a *low* concentration of glucose was used under anaerobic conditions. The use of a low glucose concentration is essential to derive the electron transfer rate constant from reduced GOx, GOx$^{red}$, to oxidized ferrocene under conditions where the regeneration of GOx$^{red}$ by glucose is impossible (very slow) during monolayer and enzyme interaction time. From the intercepts of the respective Koutecky–Levich plots, the electrochemical electron transfer rates from the (*R*)-**1** and (*S*)-**1** monolayer were derived to be $0.51 \times 10^{-2}$ and $0.9 \times 10^{-2}$ cm s$^{-1}$, where the overall rate constants ($k_{overall} = k_{el}/\Gamma_{ferrocene}$, where $\Gamma_{ferrocene}$ is the surface coverage of the electron mediator) correspond to $0.85 \times 10^5$ and $1.5 \times 10^5$ M$^{-1}$ s$^{-1}$, respectively. The overall electron transfer rates for the oxidation of GOx by the two chiral monolayer-electrodes depend inversely on the concentration of GOx. This indicates that the electrocatalysed oxidation of GOx by the ferrocene monolayer proceeds via the formation of a complex between the monolayer and GOx$^{red}$, rather than by outer sphere electron transfer,[19] Scheme 2.

$$\left|-Fc^{+} + GOx^{red} \underset{k_{-1}}{\overset{k_{+1}}{\rightleftharpoons}}\right| -Fc^{+} \cdots GOx^{red} \xrightarrow{k_{+2}} \left|-Fc + GOx^{ox}\right.$$

**Scheme 2**

Following Scheme 2, the overall rate constant is given by eqn. (1), where $K_M$ is given by eqn. (2). We find that the electron transfer rates from the GOx$^{red}$ to the (*R*)-**1** and (*S*)-**1** monolayer differ substantially, $k_{+2}$(*R*)-**1** = 0.3 s$^{-1}$, $k_{+2}$(*S*)-**1** = 0.5 s$^{-1}$, while the $K_M$ values characterizing the chiral monolayer and GOx$^{red}$ are identical, $K_M = 1.2 \times 10^{-5}$ M.

$$k_{overall} = k_{+2}/(K_M + [GOx^{red}]) \quad (1)$$

$$K_M = (k_{-1} + k_{+2})/k_{+1} \quad (2)$$

We thus conclude that the affinities for the association of GOx$^{red}$ to the chiral ferrocenyl cation monolayer are similar. The electron transfer rates between the reduced flavin centre and the chiral ferrocenyl cations differ substantially. The diastereoisomeric nature of the complexes between GOx$^{red}$ and the chiral ferrocenyl cations could yield different electron transfer distances to the flavin sites, thereby stimulating the enantioselective bioelectrocatalysed oxidation of glucose.

This research was supported by the Bundesministerium für Bildung, Wissenschaft, Forschung und Technologie, BMBF, Germany, and a Consortium with Wacker Industries, München.

## Footnote and References

* E-mail: willnea@vms.huji.ac.il

1 L. Casella and A. Marchesini, *Biochemistry* 1994, **33**, 6377; R. A. Marushak, T. A. Shields and A. G. Lappin, in *Electron Transfer in Biology and the Solid State*, ed. M. K. Johnson, R. B. King, D. M. Kurtz, Jr., C. Kutal, M. L. Norton and R. A. Scott, ACS Advances in Chemistry 226, American Chemical Society, Washington, DC, 1990, p. 237.
2 A. Fersht, *Enzyme Structure and Function*, Freeman WH and Co., New York, 2nd edn., 1984, pp. 221–247.
3 A. M. Pyle, T. Morii and J. K. Barton, *J. Am. Chem. Soc.* 1990, **112**, 9432; N. J. Turro, J. K. Barton and D. A. Tomalia, *Acc. Chem. Res.* 1991, **24**, 332.
4 M. D. Purugganan, C. V. Kumar, N. J. Turro and J. K. Barton, *Science* 1988, **241**, 1970.
5 K. Bernauer and J.-J. Sauvain, *J. Chem. Soc., Chem. Commun.*, 1988, 353; J. R. Pladziewicz, M. A. Accola, P. Osvath and A. M. Sargeson, *Inorg. Chem.*, 1993, **32**, 2525.
6 S. Sakaki, J. Nishijima, H. Koga and K. Ohkubo, *Inorg. Chem.*, 1989, **28**, 4063; S. Sakaki, J. Nishijima and K. Ohkubo, *J. Chem. Soc., Dalton Trans.*, 1991, 1143; S. J. Meskers, M. Ubbink, G. W. Canters and H. P. J. M. Dekkers, *J. Phys. Chem.*, 1996, **100**, 17 957.
7 K. Bernauer, M. Monzione, P. Schürmann and V. Viette, *Helv. Chim. Acta*, 1990, **73**, 346; K. Bernauer, in *Electron-Transfer Reactions*, in *Metalloproteins, Metal Ions in Biological Systems*, 27, ed. H. Sigel and A. Sigel, Marcel Dekker, New York, 1991, p. 265.
8 K. Tsukahara, C. Kimura, J. Kaneko and T. Hara, *Chem. Lett.*, 1994, 2377.
9 P. N. Bartlett, P. Tebbutt and R. G. Whitaker, *Prog. React. Kinet.*, 1991, **16**, 55.
10 W. Schuhmann and H.-L. Schmidt, in *Advances in Biosensors*, ed. A. P. F. Turner, JAI, London, 1992, vol. 2, p. 79.
11 A. E. G. Cass, G. Davis, M. J. Green and H. A. O. Hill, *J. Electroanal. Chem.*, 1985, **190**, 117.
12 S. Marx-Tibbon, E. Katz and I. Willner, *J. Am. Chem. Soc.*, 1995, **117**, 9925.
13 P. Alzari, N. Anicet, C. Bourdillon, J. Moiroux and J.-M. Savéant, *J. Am. Chem. Soc.*, 1996, **118**, 6788.
14 S. J. Sadeghi, G. Gilardi, G. Nicolosi and A. E. G. Cass, *Chem. Commun.*, 1997, 517.
15 R. Blonder, E. Katz, Y. Cohen, N. Itzhak, A. Riklin and I. Willner, *Anal. Chem.*, 1996, **68**, 3151.
16 B. F. Watkins, J. R. Behling, E. Kariv and L. L. Miller, *J. Am. Chem. Soc.* 1975, **97**, 3549; B. E. Firth and L. L. Miller, *J. Am. Chem. Soc.*, 1976, **98**, 8272.
17 V. I. Sokolov, L. L. Troitskaya and O. A. Rentov, *J. Organomet. Chem.* 1979, **182**, 537.
18 E. Laviron, *J. Electroanal. Chem.*, 1979, **101**. 19.
19 V. J. Razumas, A. V. Gudavicius and J. J. Kulys, *J. Electroanal. Chem.*, 1986, **198**, 81.

*Received in Cambridge, UK, 4th June 1997; 7/03890I*

# First EPR characterisation of the structures and reactivities of α- and β-boryl radicals derived from boronic esters

**Andrew McCarroll,[a] John C. Walton,*[a]† Roger Nziengui[b] and Bertrand Carboni*[b]‡**

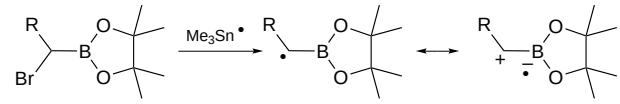
[a] *University of St Andrews, School of Chemistry, St Andrews, Fife KY16 9ST, UK*
[b] *Université de Rennes I, Avenue du Général Leclerc, 35042 Rennes CEDEX, France*

**The first EPR observations of carbon-centred radicals with α- and β-boronic ester substitutents indicated moderate thermodynamic stabilisation for the former whereas the latter had an inclination towards β-scission.**

Boronic acids and esters are convenient synthetic intermediates which have been widely applied in stereocontrolled reactions.[1] Recent research has shown that α-boryl radicals, generated by addition of carbon-centred radicals to alkenyl-[2] and alkynylboronic esters,[3] can take part in inter- and intra-molecular chain addition reactions. α-Boryl radicals have also been generated by iodine abstraction from α-iodoboronic esters[4] and high yields of useful homoallylboronic esters were obtained in allylation reactions. These developments led us to apply EPR spectroscopy to identify the radical intermediates and examine key reaction rates for several types of carbon-centred radicals possessing a boronic ester functionality. Little is known about the EPR spectra of boron-containing species in solution, apart from the impressive spectroscopic experiments of Roberts and co-workers with amine–boryl and other ligated-boryl radicals,[5] a report on the $Me_2BCH_2^{\bullet}$ radical in the solid state[6] and some aminoxyl species.[7]

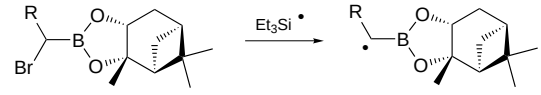
The α-bromoboronic esters **1a**,**b** were prepared according to the protocols developed by Matteson and co-workers from $B(OPr^i)_3$, $CH_2Br_2$ and $Bu^nLi$ for **1a**,[8] from pinacol *n*-hexyl boronate, $CH_2Br_2$ and $Pr^i_2NLi$ for **1b**.[9] EPR spectra, recorded during abstraction of the bromine atoms of these boronic esters by photochemically generated $Me_3Sn^{\bullet}$ radicals (or $Et_3Si^{\bullet}$ radicals) in *tert*-butylbenzene, cyclopropane or propane could be positively assigned to the corresponding α-boryl radicals **2a**,**b** (EPR parameters in Table 1). The hyperfine splittings (hfs) from the α-Hs are somewhat smaller than in analogous unsubstituted primary and secondary alkyl radicals [*e.g.* for $^{\bullet}CH_2CH(OEt)_2$ $a(H_\alpha)$ = 22.2 G][10] which suggests there is some electron delocalisation into the vacant boron p-orbital (**3**). This is also consistent with the comparatively large $^{11}B$ hfs.

If **3** makes a significant contribution to the ground state there should be an appreciable barrier to rotation about the $C_\alpha$–B bond. To try and detect this we examined the EPR spectra of radicals generated from the unsymmetrical boronic esters **4a**,**b** prepared by transesterification of **1a**,**b** with (+)-pinanediol.




**1** **2** **3**

**a** R = H, **b** R = n-$C_6H_{13}$




**4** **5**

**a** R = H, **b** R = n-$C_6H_{13}$

In the resulting radical **5a** the two α-Hs will be magnetically non-equivalent in the slow exchange limit. The spectrum of **5a** at 150 K [(Fig. 1(*a*)] shows hfs from $^{11}B$, the single δ-H of the pinane ring and two equivalent $H_\alpha$. Between 150 and 100 K selective line broadening occurred [Fig. 1(*b*)] due to restricted rotation about the $C_\alpha$–B bond with a coalescence temperature ($T_c$) of < 100 K. The $C_\alpha$–B torsion barrier ($E_t$) is therefore significantly greater than the analogous $C_\alpha$–$C_\beta$ barrier in alkyl radicals like $^{\bullet}CH_2CHR_2$ which show no exchange broadening.[11,12] Due to freezing of the propane solvent at lower temperatures, we were unable to determine the hfs of the non-equivalent $H_\alpha$. However, in analogous radicals $^{\bullet}CH_2$—X, (X = OH, OMe, $CHR_2$, SMe),[13–15] δ*a* is always in the range 0.5–1.5 G. Computer simulations[16] of the exchange broadened region (160–110 K) gave best fit with δ*a* = 0.6 G and led to log ($A_t$/s$^{-1}$) = 11.9, $E_t$ = 12.2 ± 3.0 kJ mol$^{-1}$. This established that alkyl radicals with α-boronic ester substituents possess a small but significant thermodynamic stabilisation and supports the contention that boron stabilises neighbouring radical centres.

Additional data on the stabilising influence of an α-boronic ester group was obtained *via* methyl boronic ester **6**. $Bu^tO$ radicals were known to displace alkyl radicals from trialkylboranes with comparative ease (homolytic substitution at boron)[17–19] and therefore a similar homolytic displacement of $Me^{\bullet}$ was expected from **6**. In fact, however, photolysis (150–160 K) of a solution of **6** and $Bu^tOOBu^t$ in cyclopropane

**Table 1** 9.4 GHz EPR spectral parameters of radicals derived from boronic esters[a]

| | | | Hfs/G | | | | | |
|---|---|---|---|---|---|---|---|---|
| Radical | R | *T*/K | H(α) | H(β) | H(β) | $^{11}B$ | $^{10}B$ | Other |
| **2a** | H[b] | 220[d] | 20.9 (2 H) | | | 12.3 | 4.1 | |
| **2b** | $C_6H_{13}$ | 220[d] | 20.0 | 23.5 | 23.5 | 12.0 | 4.0 | 0.5 (2 H) |
| **10a** | $Et_3SiCH_2$ | 195[d] | 18.3 | 23.8 | 9.1 | 10.8 | 3.6 | |
| **10b** | $Me_3SnCH_2$ | 235[d] | 16.7 | 16.7 | 11.8 | 10.1 | 3.4 | |
| **5a** | H | 145[c] | 21.1 (2 H) | | | 12.4 | 4.2 | 1.1 (1 H) |
| **5b** | $C_6H_{13}$ | 220[d] | 19.0 | 23.6 | 23.6 | 12.2 | 4.1 | |
| **12** | $Bu^n$ | 180[c] | 22.1 | 27.0 (2 H) | 22.1 (2 H) | 17.7 | 5.9 | |

[a] Hfs checked by computer simulations; 10 G = 1 mT. [b] *g*-Factor 2.0028; *g*-factors of all other radicals 2.003 ± 0.001. [c] In cyclopropane. [d] In $Bu^tPh$.

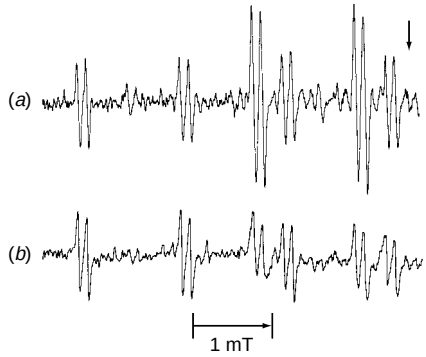
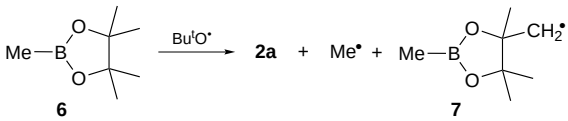


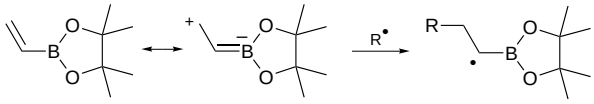

**Fig. 1** Low field halves of 9.4 GHz EPR spectra of radical **5a** in *n*-propane solution at (*a*) 150 and (*b*) 110 K. Arrow indicates spectrum centre.

gave a spectrum containing Me•, **2a** and a primary radical [*a*(2H) = 22.7 G] which we identify as **7**. Measurements of the relative concentrations of **2a** and $CH_3$• showed that abstraction of hydrogen adjacent to boron by $Bu^tO$• was about a factor of five more rapid than displacement of $CH_3$• from boron at 160 K.




**6** **7**

Addition to vinylborane **8** by a range of free radicals including $Bu^tO$•, Ph•, $CCl_3$•, $Ph_2N$• and BnS• was examined by EPR spectroscopy. However, only the radicals $Et_3Si$• and $Me_3Sn$• added efficiently enough, under EPR conditions (200–250 K), for adduct radicals **10a**,**b** to be detected (see Table

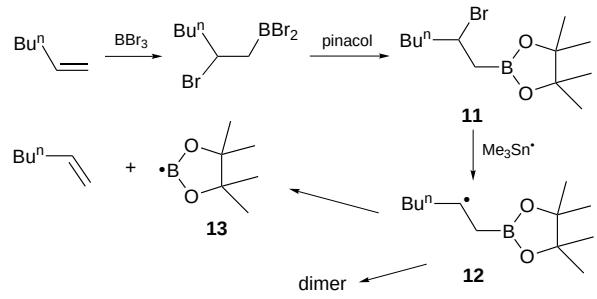



**8** **9** **10**

**a** R = $Et_3Si$, **b** R = $Me_3Sn$

1). These observations do not conflict with reports on the production of adducts from a variety of radicals at higher temperatures, where all rates of addition will be faster, but they do suggest that nucleophilic radicals add most efficiently. This conclusion is in good accord with the idea that structures such as **9** make an appreciable contribution to the ground state.[20]

The β-bromoboronic ester **11** was prepared in good yield by bromoboration of hex-1-ene followed by esterification with pinacol. Although this reaction was reported to give mixtures of products,[21] in our hands, and under different experimental conditions, addition proceeded in good yield.§ Bromine atom abstraction from ester **11** afforded a spectrum of the β-boryl radical **12** (see Table 1) in the temperature range 180–220 K. As expected, the hfs of the β-B-atom was larger than that of an α-B-atom, due to a hyperconjugative effect. At temperatures above *ca*. 220 K the spectrum of **12** unexpectedly disappeared leaving only noise. GC–MS analysis of the photolysate at 250 K showed hex-1-ene as the major product together with minor amounts of a dimer and other unidentified components. Product analysis of a photolysis at 180 K showed the dimer to be the main product with only minor amounts of hex-1-ene. A mechanism (Scheme 1) in which dimerisation of radical **12** gives way to β-scission producing hex-1-ene and radical **13** at higher temperatures is consistent with the known facts. Boron-centred radical **13** was EPR 'silent' probably because of extensive broadening. Attempts to spin trap **13** with 2-methyl-2-nitrosopropane and *tert*-butyl hyponitrite were unsuccessful. Radical **13** might become EPR visible when ligated with a suitable donor. However, when **12** was generated in the presence of excess pyridine, no signals due to [$C_5H_5N \rightarrow$ **13**]• were obtained.




**Scheme 1**

We thank the EPSRC for financial support (grant GR/L49185).

## Footnotes and References

† E-mail: jcw@st-and.ac.uk
‡ E-mail: bertrand.carboni@univ-rennes1.fr

§ To $BBr_3$ in hexane (5 cm³, 7 mmol) at −78 °C was added hex-1-ene (7 cm³ of a 1 M soln. in hexane, 7 mmol). The mixture was allowed to warm slowly to room temperature and then cooled to −10 °C. Pinacol in $Et_2O$ (5 cm³, 7 mmol) was then added. After stirring for 0.5 h, the reaction mixture was diluted with $Et_2O$ (20 cm³), washed with water, dried and concentrated. Purification by bulb-to-bulb distillation afforded **11** as a colourless oil. Yield 68%, bp 80-85 °C/0.1 Torr, $\delta_H$(200 MHz, $CDCl_3$) 0.91 (3H, t, *J* 7.1), 1.20–1.70 (4H, m), 1.25 (12 H, s), 1.63 (2 H, d, *J* 4.9), 4.25–4.38 (1H, m); $\delta_C$(50.3 MHz) 13.9 ($CH_3$), 22.0 ($CH_2$), 24.7 ($CH_3$), 29.9 ($CH_2$), 41.4 ($CH_2$), 54.7 (CH), 83.5 (C). The carbon α to boron was not found. HRMS; [M − Br•]⁺ found: 211.1868. Calc. for $C_{12}H_{24}{}^{11}BO_2$: 211.1869.

1 D. S. Matteson, in *Stereodirected Synthesis with Organoboranes*, Springer, Berlin, 1995; M. Vaultier and B. Carboni in *Comprehensive Organometallic Chemistry II*, ed. G. Wilkinson, F. G. A. Stone and E. V. Abel, Pergamon, Oxford, 1995, vol. 11, p. 191.
2 D. S. Matteson, *Organomet. Chem. Rev*., 1966, **1**, 1; W. G. Woods and I. S. Bengelsdorf, *J. Org. Chem*., 1966, **31**, 2769; R. H. Fish, *J. Organomet. Chem*., 1972, **42**, 345. N. Guennouni, C. Rassat-Deloge, B. Carboni and M. Vaultier, *Synlett*, 1992, 581.
3 D. S. Matteson and K. Peacock, *J. Am. Chem. Soc*., 1960, **82**, 5759; F. Lhermitte and B. Carboni, *Synlett*, 1996, 377.
4 R. A. Batey, B. Pedram, K. Yong and G. Baquer, *Tetrahedron Lett*., 1996, **37**, 6847; N. Guennouni, F. Lhermitte, S. Cochard and B. Carboni, *Tetrahedron*, 1995, **51**, 6999.
5 J. A. Baban, V. P. J. Marti and B. P. Roberts, *J. Chem. Soc., Perkin Trans 2*, 1985, 1723; H. S. Dang, V. Diart, B. P. Roberts and D. A. Tocher, *J. Chem. Soc., Perkin Trans. 2*, 1994, 1039.
6 A. R. Lyons and M. C. R. Symons, *J. Chem. Soc., Faraday Trans. 2*, 1972, **68**, 502.
7 M. Lucarini, G. F. Pedulli and L. Valgimigli, *J. Org. Chem*., 1996, **61**, 4309.
8 T. J. Michnick and D. S. Matteson, *Synlett*, 1991, 631.
9 D. S. Matteson, R. Soundararajan, O. C. Ho and W. Gatzweiler, *Organometallics*, 1996, **15**, 152.
10 A. J. Dobbs, B. C. Gilbert and R. O. C. Norman, *J. Chem. Soc., Perkin Trans. 2*, 1972, 786.
11 J. K. Kochi, *Adv. Free Radical Chem.*, 1975, **5**, 198.
12 K. U. Ingold, D. C. Nonhebel and J. C. Walton, *J. Phys. Chem.*, 1986, **90**, 2859.
13 I. Biddles, A. Hudson and J. T. Wiffen, *Tetrahedron*, 1972, **28**, 867.
14 P. J. Krusic, P. Meakin and J. P. Jesson, *J. Phys. Chem*., 1971, **75**, 3438.
15 J. C. Walton, *Magn. Reson. Chem.* 1987, **25**, 998.
16 J. Heinzer, *Quantum Chemistry Program Exchange*, No. 209, University of Indiana, Bloomington, IN, 1972.
17 A. G. Davies and B. P. Roberts, *J. Organometal. Chem*., 1969, **19**, P17.
18 A. G. Davies and B. P. Roberts, *J. Chem. Soc., Chem. Commun*., 1969, 699.
19 P. J. Krusic and J. K. Kochi, *J. Am. Chem. Soc.*, 1969, **91**, 3942.
20 D. S. Matteson, *Progress in Boron Chemistry*, ed. R. J. Brotherton and H. Steinberg, Pergamon, Oxford, 1970, vol. 3, p 117.
21 B. M. Mikhailov and M. E. Nikolaeva, *Izv. Akad. Nauk. SSSR, Ser. Khim*., 1963, 1368 (*Chem. Abstr*., **59**, 15296f).

*Received in Cambridge, UK, 6th June 1997, 7/03950F*

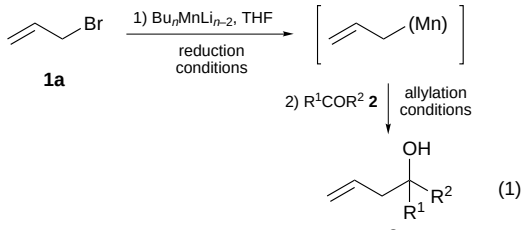
# A new type of allyl- and prop-2-ynyl-manganese species: generation and reactions with electrophiles

**Makoto Hojo, Hajime Harada, Hajime Ito and Akira Hosomi***

*Department of Chemistry, University of Tsukuba, Tsukuba, Ibaraki 305, Japan*

**Tetrabutylmanganese ate complex '$Bu_4MnLi_2$' reacts with allylic and prop-2-ynylic bromides to generate the corresponding allyl- and prop-2-ynyl-manganese species which further react with electrophiles such as aldehydes, ketones, epoxide and chlorosilanes to afford the corresponding allylated and prop-2-ynylated and/or allenylated products in high yields.**

Reactions of many kinds of allyl- and prop-2-ynyl-metals have been reported so far while new types of such reagents will attract much attention.[1] The creation of these new species may provide new methods for selective allylation and prop-2-ynylation. We report here reactions of a new type of allyl- and prop-2-ynyl-manganese reagent generated by the direct reduction of allyl and prop-2-ynyl bromides using manganese ate complex [eqn. (1)]. All of these reagents react with electrophiles efficiently.




Tributylmanganate '$Bu_3MnLi$' reacted with allyl bromide **1a** in THF at −78 °C, and upon addition of benzaldehyde **2a** to the mixture, the allylated product, 1-phenylbut-3-en-1-ol **3a** was obtained in 50% yield. Even if the amount of the manganate was increased to 1.5 equiv. the yield of the product **3a** was at most 66% [eqn. (1), $R^1$ = Ph, $R^2$ = H]. In sharp contrast to these facts, tetrabutylmanganate '$Bu_4MnLi_2$' showed high reactivity and the allylated product **3a** was produced in 80% yield using an equimolar amount of the reagent.† These results deserve comment. Considering this stepwise procedure, an allylmanganese reagent is possibly generated from allyl bromide by the action of the manganese ate complex as a reductant.[2] Hitherto, two methods for the generation of allylmanganese reagents, by transmetalation[3,4] and direct reduction of allyl halides with low valent manganese (Grignard-type procedure),[5] have been reported.[6]‡ The present reaction is clearly different from these reactions, in view of both the procedure and the reductant used. The substantial difference between the reducing ability of tributylmanganate and that of tetrabutylmanganate is also interesting. Tributylmanganate seems possibly to be in equilibrium between dibutylmanganese and tetrabutylmanganate. Our experiments showed that even reaction with tributylmanganate gave allylated product, but the yield of the product did not exceed 50% based on manganese. These results are likely due to the disproportionation of tributylmanganate, and the present reaction is the first example showing the peculiar reactivity of tetraalkylmanganate, although comparable relative reactivities of tetraalkylmanganates and trialkylmanganates have previously been reported.[7]§ Selected results for the allylation of carbonyl compounds are summarized in Table 1.¶ Aliphatic and aromatic aldehydes as well as ketones are allylated in high yield under mild conditions.

A characteristic feature of the reactivity of the allylmanganese reagent also emerged, as shown in eqns. (2)–(4). From chalcone **2e**, the 1,4-adduct **3e** was obtained as the major product. This is in marked contrast to previously reported reactions using low valent manganese, where only the 1,2-adduct was produced.[5,6]‖ This selectivity may possibly be due to the ate character of the allylmanganese reagent.[8] The allylation even took place with cyclohexene oxide,[9]** while with the keto ester **2g**, the keto moiety was allylated rather than the ester function.[6b]

Tetrabutylmanganate also reduced prop-2-ynylic bromides [eqn. (5)]. In this case, allenic and/or prop-2-ynylic products were produced depending on the bulkiness of the electrophiles and the substituent R on the prop-2-ynyl bromides (Table 2). From prop-2-ynyl bromide **1d** (R = H), only the prop-2-ynylic adduct **3o** was obtained in quantitative yield [eqn. (6)].††

As shown here, tetrabutylmanganate reacts with allyl and prop-2-ynyl bromides to generate allyl- and prop-2-ynyl-

**Table 1** Generation of an allylmanganese reagent from allyl bromide **1a** *via* reduction with manganese ate complexes and its reaction with carbonyl compounds **2**[a]

| Manganese ate complex (equiv.) | Reduction conditions | Carbonyl compound **2** $R^1$ | $R^2$ | | Allylation conditions | Product | Yield (%)[b] |
|---|---|---|---|---|---|---|---|
| '$Bu_3MnLi$' (1.0) | −78 °C, 1 h | Ph | H | **2a** | −78 °C to room temp., 4 h | **3a** | 50 |
| '$Bu_3MnLi$' (1.5) | −78 °C, 1 h | Ph | H | **2a** | −78 °C to room temp., 4 h | **3a** | 66 |
| '$Bu_4MnLi_2$' (1.0) | −98 °C, 1 h | Ph | H | **2a** | −78 °C, 0.5 h | **3a** | 80 |
| '$Bu_4MnLi_2$' (1.0) | −98 °C, 1 h | Pr | H | **2b** | −78 °C, 3 h | **3b** | 70 |
| '$Bu_4MnLi_2$' (1.0) | −98 °C, 1 h | Ph | Me | **2c** | −98 °C to room temp., 4 h | **3c** | 76 |
| '$Bu_4MnLi_2$' (1.0) | −98 °C, 1 h | -$(CH_2)_5$- | | **2d** | −78 °C, 3 h | **3d** | 84 |

[a] Conditions: allyl bromide **1a** (0.50 mmol) was added to a mixture of manganese ate complex (0.50 mmol) in THF at the temperature shown in the column 'reduction conditions', and the mixture stirred for 1 h. An electrophile was added to the flask, and the resultant mixture was further stirred under the conditions shown in the column 'allylation conditions'. After quenching with saturated $NH_4Cl$ and extraction with $Et_2O$ (30 ml × 3), an organic layer was washed with saturated EDTA and saturated $NaHCO_3$, and the organic layer was dried over $MgSO_4$. After evaporation of solvents, the crude mixture was subjected to chromatography to give the pure product. [b] Isolated yield.

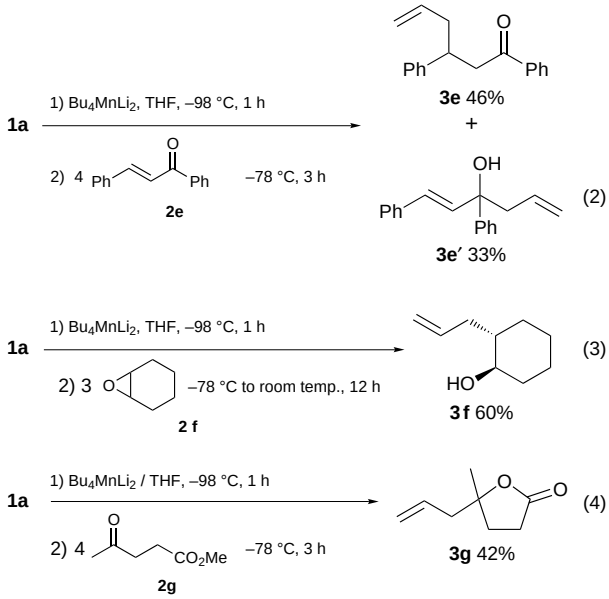


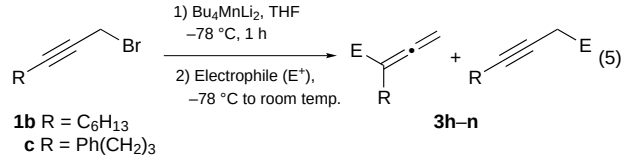

**Table 2** Generation and reaction of allenyl- and prop-2-ynyl-manganese species[a]

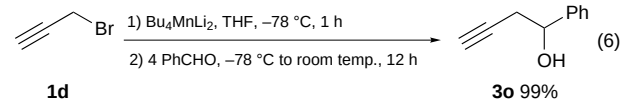
| Prop-2-ynyl bromide | Electrophile | Product | Yield (%)[b] (allenic : prop-2-ynylic) |
|---|---|---|---|
| **1b** | PhCHO **2a** | **3h** | 82 (100 : 0) |
| **1b** | EtCHO **2h** | **3i** | 75 (100 : 0) |
| **1b** | PhCOMe **2c** | **3j** | 74 (100 : 0) |
| **1b** | $Et_2CO$ **2i** | **3k** | 82 (67 : 33) |
| **1c** | $PhMe_2SiCl$ **2j** | **3l** | 80 (0 : 100) |
| **1c** | $Me_3SiCl$ **2k** | **3m** | 94 (1 : 99) |
| **1c** | $Me_2HSiCl$ **2l** | **3n** | 86 (61 : 39) |

[a] Conditions: prop-2-ynyl bromide (0.50 mmol) was added to a mixture of '$Bu_4MnLi_2$' (0.50 mmol) in THF at −78 °C, and the mixture was stirred for 1 h. An electrophile was added to the flask, at −78 °C and the temperature was allowed to rise to room temp. over > 4 h. After quenching was saturated $NH_4Cl$ and extraction with $Et_2O$ (30 ml × 3), the organic layer was washed with saturated EDTA and saturated $NaHCO_3$, and the organic layer was dried over $MgSO_4$. After evaporation of solvents, the crude mixture was subjected to chromatography to give the pure product. [b] Isolated yield.

manganese reagents where the manganate serves as a reducing agent, not as an alkylating agent. This is a new approach to allylic and prop-2-ynylic manganese reagents which react with aldehydes, ketones, oxirane and chlorosilanes to give the corresponding allylated and prop-2-ynylic and/or allenic products. Further study on the generation and reaction of these reagents is now under investigation.

This work was partly supported by Grants-in-Aid for Scientific Research and Grants-in-Aid for Scientific Research on Priority Areas from the Ministry of Education, Science, Sports and Culture, Japan and Pfizer Pharmaceuticals Inc. H. H. acknowledges support from the Research Fellowships of the Japan Society for the Promotion of Science for Young Scientists.




## Footnotes and References

* E-mail: hosomi@staff.chem.tsukuba.ac.jp

† The formulae '$Bu_3MnLi$' and '$Bu_4MnLi_2$' and the terms 'tributylmanganate' and 'tetrabutylmanganate' are used tentatively, since the precise structures of the species are not clear at present.

‡ Barbier-type allylations with metallic manganese were also reported (ref. 6).

§ It is known that the reactions of tetraalkylmanganates with acyl chlorides to produce ketones proceed at lower temperature, compared to the reactions of trialkylmanganates, while the yields in these reactions are equally good [ref. 7(*a*)].

¶ A solution of BuLi in hexane (1.6 M; 1.25 ml, 2.0 mmol) was added at −20 °C to a suspension of manganese(II) chloride in THF (63 mg, 0.50 mmol in 5 ml) and the mixture was stirred at −40 to −20 °C for 30 min. Allyl or prop-2-ynyl bromide (0.50 mmol) was added at −98 or −78 °C (at the specified temperature), and the mixture was stirred for 1 h. An electrophile (1.5–2.5 mmol) was added to the mixture, which was further stirred under the conditions shown. After quenching with saturated $NH_4Cl$ and extraction with $Et_2O$ (30 ml × 3), the organic layer was washed with saturated ethylenediaminetetraacetic acid (EDTA) and saturated $NaHCO_3$. The organic layer was dried over $MgSO_4$. After evaporation of solvents, the crude mixture was subjected to chromatography to give the pure product.

‖ The selective 1,4-addition to ethylidenemalonate, which is a good acceptor for the 1,4-addition [*cf.* refs. 3(*c*), 5, 6 and 8], using allylmanganese chloride was also reported [ref. 3(*c*)].

** It was reported that alkylmanganese chloride reacted with oxiranes in the presence of a copper chloride catalyst (ref. 9).

†† This is to the best of our knowledge, the first case of the generation and reaction of prop-2-ynylic manganese reagents.

1 Y. Yamamoto and N. Asao, *Chem. Rev.*, 1993, **93**, 2207.
2 M. Hojo, H. Harada, H. Ito and A. Hosomi, *J. Am. Chem. Soc.*, 1997, **119**, 5459.
3 (*a*) G. Cahiez, A. Alexakis and J. F. Normant, *Synth. Commun.*, 1979, **9**, 639; (*b*) G. Friour, G. Cahiez, A. Alexakis and J. F. Normant, *Bull. Soc. Chim. Fr.*, 1980, 515; (*c*) G. Cahiez and M. Alami, *Tetrahedron*, 1989, **45**, 4163.
4 K. Okada, K. Oshima and K. Utimoto, *J. Am. Chem. Soc.*, 1996, **118**, 6076.
5 T. Hiyama, M. Obayashi and A. Nakamura, *Organometallics*, 1982, **1**, 1249.
6 (*a*) T. Hiyama, M. Sawahata and M. Obayashi, *Chem. Lett.*, 1983, 1237; (*b*) G. Cahiez and P.-Y. Chavant, *Tetrahedron Lett.*, 1989, **30**, 7373.
7 (*a*) G. Cahiez and B. Laboue, *Tetrahedron Lett.*, 1992, **33**, 4439; (*b*) G. Cahiez, P.-Y. Chavant and E. Metais, *Tetrahedron Lett.*, 1992, **33**, 5245.
8 G. Cahiez and M. Alami, *Tetrahedron Lett.*, 1986, **27**, 569.
9 G. Cahiez and S. Marquais, *Synlett*, 1993, 45.

*Received in Cambridge, UK, 7th August 1997; 7/05771G*

# Stereochemistry of the methyl→methylene elimination in the enzyme-catalysed cyclization of geranyl diphosphate to (4*S*)-limonene

**Robert M. Coates,*[a] Charles S. Elmore,[a] Rodney B. Croteau,[b] David C. Williams,[b] Hiromi Morimoto[c] and Philip G. Williams[c]**

[a] *Department of Chemistry, University of Illinois, 600 S. Mathews Avenue, Urbana, IL 61801, USA*
[b] *Institute of Biological Chemistry, Washington State University, Pullman, WA 99164-6340, USA*
[c] *National Tritium Labelling Facility, E.O. Lawrence Berkeley National Laboratory, One Cyclotron Road, Berkeley, CA 94720, USA*

**The cyclization of (*R*)-[9-$^2H_1$,$^3H_1$]geranyl diphosphate catalysed by a recombinant form of (4*S*)-limonene synthase from spearmint leaf (*Mentha spicata*) is terminated predominantly by *re*-facial, *anti* proton elimination at the *cis* methyl group, producing (4*S*, 8*E*)-[8-$^2H_1$,$^3H_1$]limonene.**

(4*S*)-Limonene synthase from *Mentha* species catalyses the coupled isomerization–cyclization of geranyl diphosphate **1** (GPP) to (4*S*)-limonene **3** by way of the enzyme-bound intermediate, (3*S*)-linalyl diphosphate **2** (LPP) (Scheme 1).[1] (4*R*)-Limonene synthase in *Citrus* species is responsible for producing the enantiomeric component of peel oil.[2] (4*S*)-Limonene synthase has been purified from both peppermint (*M. piperita*) and spearmint (*M. spicata*) and characterized.[3]

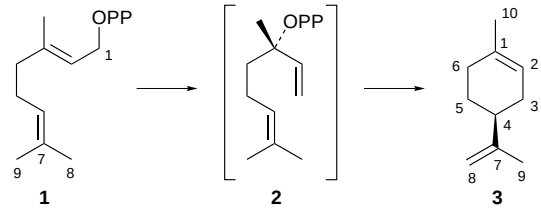
The mechanism of action and structural features of both (4*S*)- and (4*R*)-limonene synthases have been investigated using enzymes from *Mentha*, *Citrus* and other plant species.[4–6] The reaction leading to (4*S*)-limonene proceeds *via* stepwise, suprafacial isomerization of **1** to **2** followed by *anti*, *endo* $S_N'$ cyclization with overall retention of configuration at C(1)[4] and terminating proton transfer from the *cis* methyl group [C(9)].[4,5] Here we report evidence that establishes the stereochemistry of the final $CH_3 \rightarrow CH_2$ elimination.

A protein-based cloning strategy was employed to isolate a cDNA encoding (4*S*)-limonene synthase from a spearmint leaf cDNA library.[7] The 1800 nucleotide open-reading frame translates a 500 amino acid protein bearing a putative plastidial targeting peptide. The cDNA isolate was functionally expressed in *E. coli* to give catalytically active protein that affords (*S*)-limonene and its minor co-products [2% each of myrcene, (−)-α-pinene and (−)-β-pinene]. The recent development of a high level heterologous expression system[8] provided sufficient quantities of the crude recombinant protein for product analyses by $^3H$ NMR spectroscopy.

Substrate bearing a chiral methyl group of (*R*) configuration at the *cis* C(9) position (**5c**) was synthesized as outlined in Scheme 2. Z-Selective condensation of (*E*)-6-benzyloxy-4-methylhex-4-enal with ethyl 2-(diethoxyphosphoryl)propionate followed by $AlD_3$ reduction afforded dideuterio alcohol **4a**. Catalytic ruthenate oxidation and asymmetric reduction of the labile *Z*-aldehyde with (*S*)-Alpine-Borane[9] provided **4b**, the expected *R* configuration and enantiomeric purity (≥97%) of which were confirmed by $^1H$ NMR analysis of its (1′*S*)-camphanate derivative.[10]† Evidence that the methanesulfonate (MsO) of **4b** undergoes nucleophilic substitution with inversion was obtained by its conversion to the *S* enantiomer of **4b** (≥97% *S*) with $Bu_4NOAc$ in $Et_2O$ followed by $LiAlH_4$ cleavage and $^1H$ NMR analysis of the (1′*S*)-camphanate.

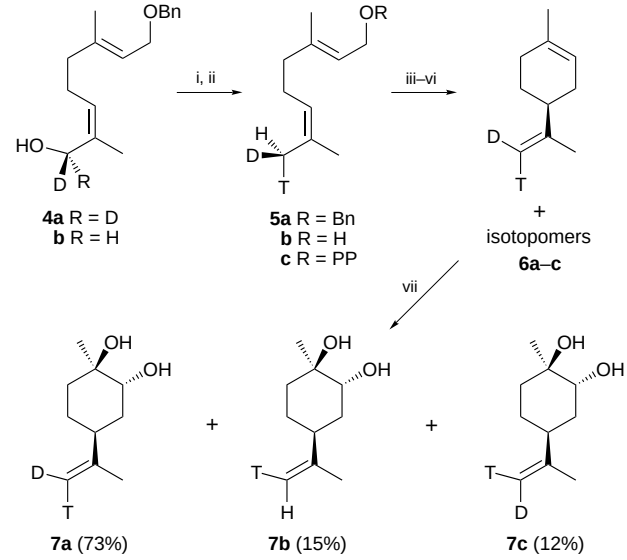
Reduction of **4b**–OMs with $LiBEt_3T$[11] (THF, 0 °C) was assumed to proceed with inversion, creating an *R* chiral methyl group in **5a** (1.0 Ci, *ca*. 6.7 Ci mmol$^{-1}$). Conversion to (*R*)-[9-$^2H_1$,$^3H_1$]GPP **5c** (23 mCi, 66%) was accomplished by literature procedures[12] adapted for radiochemical operations. The radiochemical purity of (*R*)-[9-$^2H_1$,$^3H_1$]geraniol **5b** (114 m Ci, 88%) was established by radio TLC, $^3H$ NMR spectroscopy and isotopic dilution analysis as the 3,5-dinitrobenzoate derivative.†

Incubation of **5c** with the crude recombinant (*S*)-limonene synthase[8]‡ afforded, after dilution with 1 mg of cold carrier and filtration over silica gel, [8-$^2H$,$^3H$]limonenes **6a**–**c**, (4.1 m Ci, 21%). Regioselective epoxidation followed by acid-catalysed hydrolysis and chromatographic purification gave [8-$^2H$,$^3H$]-menth-7-ene-1,2-diols **7a**–**7c** (1.0 m Ci, 24%), judged to be of high radiochemical purity by radio TLC and dilution analysis. Assignments of the isopropenyl vinyl proton signals at $\delta$ 4.81 and 4.77 in the 500 MHz $^1H$ NMR spectrum ($C_6D_6$) of unlabelled diol to $H_Z$ and $H_E$, respectively, were secured by




**1** **2** **3**

**Scheme 1**




**4a** R = D
**b** R = H

**5a** R = Bn
**b** R = H
**c** R = PP

**6a–c**

**7a** (73%) **7b** (15%) **7c** (12%)

**Scheme 2** *Reagents and conditions:* i, $Pr_4NRuO_4$, *N*-methylmorpholine *N*-oxide, MeCN; (*S*)-*B*-isopinocampheyl-9-borabicyclo[3.3.1]nonane, THF; ii, $MeSO_2Cl$, $NEt_3$, $Et_2O$, 0 °C; $LiBEt_3T$, THF, 0 °C; iii, Li, $NH_3$, THF; iv, $MeSO_2Cl$, $Et_4NCl$, 2,4,6-collidine, $CH_2Cl_2$, 0 °C; v, $(Bu_4N)_3HP_2O_7$, MeCN; vi, (*S*)-limonene synthase lyophilisate, 50 mM $MgCl_2$, Tris buffer, pH 7, 31 °C (see footnote ‡); vii, MCPBA, $NaHCO_3$, 0 °C; $HClO_4$, aq. THF

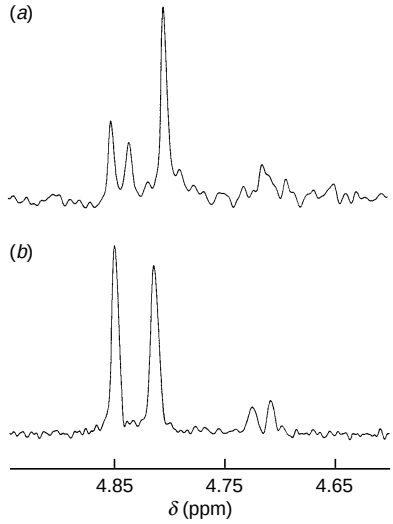



**Fig. 1** (*a*) Vinyl proton region of the 640 MHz $^3H\{^1H\}$ NMR spectrum of [8-$^3$H]menth-7-ene-1,2-diols (**7b**, **7c** and **7a**) in $C_6D_6$. (*b*) The same region of the 600 MHz $^1$H NMR spectrum of the unlabelled carrier diol for comparison. A slight impurity appears in the $^1$H NMR spectrum at $\delta$ 4.71 and 4.73.†

NOE measurements. The magnitude of the intramolecular primary kinetic isotope effect for the $CH_3 \rightarrow CH_2$ elimination ($k_H/k_D$ = 4.6 ± 0.5) was independently determined by GC–MS analysis of [8-$^2$H]limonene biosynthesized similarly using [9-$^2H_2$]-**1** as substrate.

The 640 MHz $^3$H NMR spectrum (Fig. 1) of [8-$^2$H,$^3$H]diols **7a**–**c** ($C_6D_6$) shows peaks at $\delta_T$ 4.849 (0.15 T), 4.833 (0.12 T), and 4.802 (0.73 T).† The most intense peak is assigned to the doubly labelled species **7a** generated by kinetically favored proton elimination. The signal at $\delta_T$ 4.849 is ascribed to the singly labelled species **7b** arising from deuteron elimination since its downfield position relative to **7a** ($\Delta\delta_T$ = +0.047) corresponds to the chemical shift difference between the vinyl protons ($\Delta\delta_H = \delta_{H_Z} - \delta_{H_E}$ = +0.037) plus a typical upfield deuterium isotope shift for **7a** of ($\Delta\delta_T$ = − 0.10).[13] The ratio of integrals (0.73/0.15 = 4.9) for the high and low field peaks is consistent with the primary deuterium isotope effect. The small centre peak is attributed to the minor doubly labelled form **7c** (isotope shift $\Delta\delta$ − 0.016 ppm from $\delta^{H_E}$ 4.849).

The results establish that the major doubly labelled product **6a** has arisen by proton elimination from the *R* chiral methyl group *anti* to the C(3)–C(4) bond formed in the cyclization step (Scheme 3). It is unclear whether the minor doubly labelled product **6c** is formed by competing *syn* elimination from **5c** or by *anti* elimination from a contaminant of the *S* chiral methyl enantiomer. The predominant *anti* $S_E'$ stereochemistry of this cyclization–elimination sequence is the same as that observed for the bridging cyclization–elimination in the formation of (+)- and (−)-α-pinene catalysed by pinene cyclases I and II from sage.[14] A plausible explanation for the *anti* elimination producing limonene is the preservation of a through-space bonding interaction between C(4) and C(7) of the presumed (*S*)-terpinyl ion intermediate required for cyclization to the pinenes.

The identity and radiochemical purity of all [$^3$H] compounds were verified by radio TLC analyses and comparisons with the unlabelled substance. All compounds were characterized by $^1$H and/or $^3$H NMR spectroscopy and other appropriate data.†

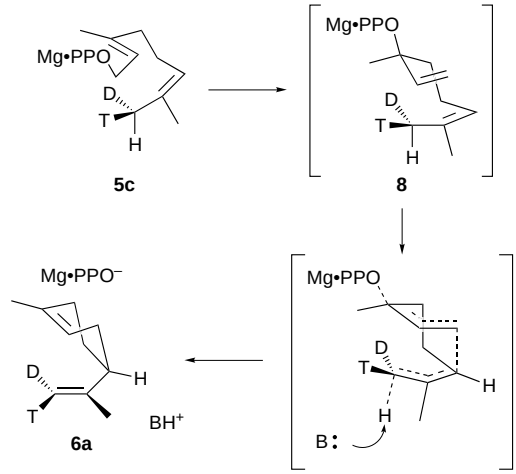
This research was supported by NIH grants GM 13956 (RMC), GM 31354 (RBC), and NCRR P41 RR01237(PGW).

## Footnotes and References

* E-mail: coates@aries.scs.uiuc.edu

† *Selected data* for the (1′*S*)-camphanate of **4b**: $^1$H NMR (400 MHz, $CDCl_3$): $\delta$ 4.69 (s, 1 H, C*H*DOR). For the (1′*S*)- camphanate of *ent*-**4b**: $^1$H NMR (400 MHz, $CDCl_3$): $\delta$ 4.72 (s, 1 H, CD*H*OR). For **5a**: $^3$H NMR (310 MHz, $C_6D_6$): $\delta$ 1.58 (d, *J* 15.6, CHDT). For **5b**: $^3H\{^1H\}$ NMR (310 MHz, $C_6D_6$): $\delta$ 1.51 (t, *J* 2.2, CHDT). For the 3,5-dinitrobenzoate of **5b** diluted with carrier: 236 μCi mmol$^{-1}$, mp 59–61 °C. For **5c**: radio TLC $R_f$ 0.5 (silica gel, 1 : 2 : 1 MeCN–Pr$^i$OH–50 mM aq. $NaHCO_3$). For unlabelled **7**: mp 69 °C. For **7a**–**c** $^3H\{^1H\}$ NMR, see Fig. 1. The $^1$H NMR spectrum was referenced to $C_6D_5H$ and the $^3$H NMR peak positions were computed using the average Larmor frequency ratio 1.066639739 (ref. 15).

‡ Preparative incubation procedure: **5c** (20 mCi; 3.6 μmol, 0.8 mM), $MgCl_2$ (50 mM), Tris buffer (pH 7), lyophilised enzyme (133 mg), 4.5 ml total volume with hexane overlay (1 ml), 31 °C, 12h.




**Scheme 3** mechanism for the enzyme-catalysed conversion of (*R*)-[9-$^2$H,$^3$H]GPP **5c** through *anti* $S_N'$ cyclization of (3*S*,9*R*)-[9-$^2$H,$^3$H]LPP **8** in the *endo* conformation showing cisoid, *anti* elimination to (4*S*,8*E*)-[8-$^2$H,$^3$H]limonene **6a**

1 R. Croteau, in *Progress in Flavor Precursor Studies: Analysis, Generation, Biotechnology*, ed. P. Schreier and P. Winterhalter, Allured Publishing Co., Wheaton, IL, 1993, p. 113.
2 O. Cori and M.C. Rojas, *Methods Enzymol*., 1985, **110**, 406.
3 W. R. Alonso, J. I. M. Rajaonarivony, J. Gershenzon and R. Croteau, *J. Biol. Chem*., 1992, **267**, 7582.
4 T. Suga, Y. Hiraga, M. Aihara and S. Izumi, *J. Chem. Soc., Chem. Commun*., 1992, 1556; Y. Hiraga, W. Shi, D. I. Ito, S. Ohta and T. Suga, *J. Chem. Soc., Chem. Commun*., 1993, 1370.
5 H.-J. Pyun, R. M. Coates, K. C. Wagschal, P. McGeady and R. Croteau, *J. Org. Chem*., 1993, **58**, 3998.
6 J. I. M. Rajaonarivony, J. Gershenzon and R. Croteau, *Arch. Biochem. Biophys*., 1992, **296**, 49; J. I. M. Rajaonarivony, J. Gershenzon, J. Miyazaki and R. Croteau, *Arch. Biochem. Biophys*., 1992, **299**, 77; R. Croteau, W. R. Alonso, A. E. Koepp, J. H. Sim and D. E. Cane, *Arch. Biochem. Biophys*., 1993, **307**, 397.
7 S. M. Colby, W. R. Alonso, E. J. Katahira, D. J. McGarvey and R. Croteau, *J. Biol. Chem*., 1993, **268**, 23016.
8 R. Croteau and D. C. Williams, unpublished work.
9 M. M. Midland, S. Greer, A. Tramontano and S. A. Zderic, *J. Am. Chem. Soc*., 1979, **101**, 2352.
10 H. Gerlach and B. Zagalak, *J. Chem. Soc., Chem. Commun*., 1973, 274; P. C. Prabhakaran, S. J. Gould, G. R. Orr, and J. K. Coward, *J. Am. Chem. Soc*., 1988, **110**, 5779 and references cited therein.
11 H. Andres, H. Morimoto and P. G. Williams, *J. Chem. Soc., Chem. Commun*., 1990, 627.
12 E. W. Collington and A. I. Meyers, *J. Org. Chem*., 1971, **36**, 3044; A. B. Woodside, Z. Huang, and C. D. Poulter, *Org. Synth*., 1993, Coll. Vol., **8**, 616.
13 F. A. L. Anet and M. Kopelevich, *J. Am. Chem. Soc*., 1989, **111**, 3429.
14 H.-J. Pyun, K. C. Wagschal, D.-i. Jung, R. M. Coates and R. Croteau, *Arch. Biochem. Biophys*., 1994, **308**, 488.
15 E. A. Evans, D. C. Warrell, J. A. Elvidge and J. R. Jones, *Handbook of Tritium NMR Spectroscopy and Applications*, Wiley, Chichester, 1985, p. 7.

*Received in Corvallis, OR, USA, 20th June 1997; 7/04370H*

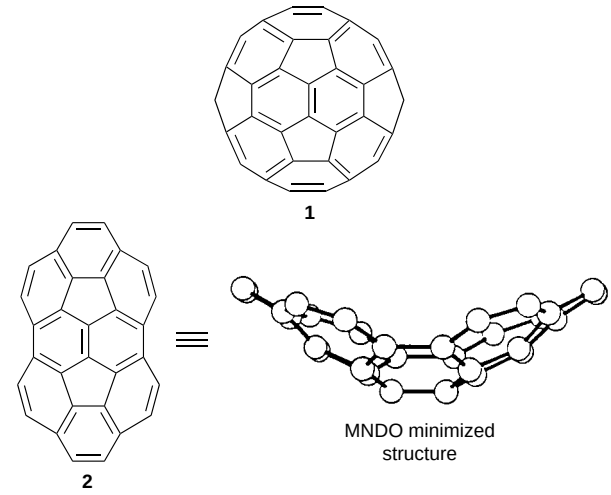
# Buckybowls: a simple, conceptually new synthesis of $C_{2v}$-semibuckminsterfullerene ($C_{30}H_{12}$, [5,5]-fulvalene circulene)

**Goverdhan Mehta* and Gautam Panda**

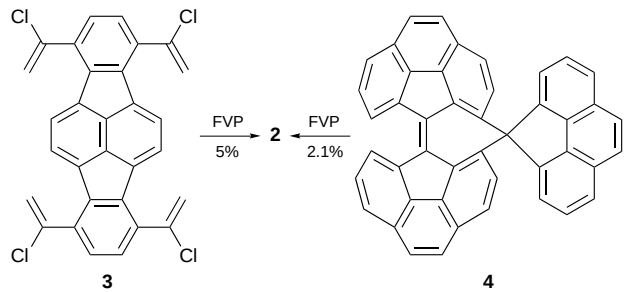
*Molecular design and synthesis laboratory of JNCASR, School of Chemistry, University of Hyderabad, Hyderabad 500 046, India*

**An extremely simple synthesis of decacyclic, $C_{30}H_{12}$ 'buckybowl' 2 from *m*-xylene, employing a strategy of wider applicability for the synthesis of diverse curved aromatic surfaces, is described.**

The onset of the fullerene era, following the discovery of buckminsterfullerene **1**, has generated a great deal of interest in the synthesis and chemistry of 'bowl-shaped' polycyclic aromatic hydrocarbons (PAHs), particularly those representing a dominant motif on the fullerene surface.[1] Such PAHs, with curved surfaces, can be expected to exhibit novel physicochemical characteristics and mimic some of the properties of fullerenes. Since buckybowls have never been encountered during the graphite vapourization processes, the only way to access them is through logically orchestrated synthetic methodologies. Efforts in this direction have been mounted in several laboratories during the past few years[1] and among the notable successes is the synthesis of $C_{2v}$-semibuckminsterfullerene **2**,[2] representing half the carbon content of **1** and endowed with substantial curvature (calculated bowl depth 2.7 Å).[2a]

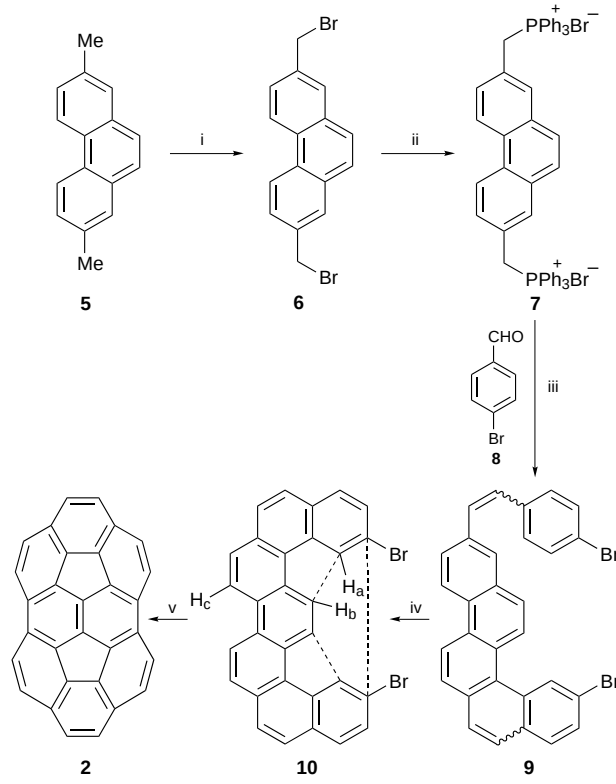



Rabideau *et al.*[2a] were the first to report the synthesis of **2** *via* flash vacuum pyrolysis (FVP) of **3**, following a variant of the Scott's seminal synthesis of corannulene (Scheme 1).[3] Very recently, in 1997, the groups of Scott and Zimmermann accomplished[2b] a synthesis of **2** *via* FVP of **4**, a compound obtained serendipitously from cyclopenta[*def*]phenanthrene. We now report a new synthesis of **2** which is conceptually different from the earlier efforts and notable for its simplicity and brevity.[4]




**Scheme 1**

Readily available 2,7-dimethylphenanthrene **5**[5] was transformed to the bis-ylide precursor **7** *via* the bis(2,7-bromomethyl)phenanthrene **6** (Scheme 2). Two-fold Wittig coupling between the ylide derived from **7** and *p*-bromobenzaldehyde **8** furnished **9** as a mixture of *E*- and *Z*-isomers. On irradiation, **9** underwent facile two-fold oxidative photocyclization with high regioselectivity to furnish the desired **10** as the only characterizable product. The symmetry of **10** and its structure followed from its characteristic $^1$H NMR spectrum [bay-region protons: $\delta$ 9.41 (s, $H_a$), 9.02 (s, $H_b$), 8.93 (d, $J$ 9 Hz, $H_c$)] and 15 line $^{13}$C NMR spectrum [$\delta$ 132.0, 131.4, 131.3, 130.6, 130.0(2C), 129.3, 128.1, 127.2(2C), 127.0(2C), 125.7, 122.7, 120.6]. We had planned to effect in tandem, three-fold cyclization in **10** (see dotted lines) as the pivotal step and for that purpose strategically positioned the two bromine atoms as promoters of such a process.[2b] To our great delight, we found that **10** on FVP furnished **2**, which was isolated from the pyrolysate through




**Scheme 2** *Reagents and conditions*: i, NBS, $CCl_4$, heat, 4 h, 80%; ii, $PPh_3$, benzene, room temp., 2–3 days, 79%; iii, $K_2CO_3$, THF, 18-crown-6, 10 h, 40%; iv, *hv* (450 W), Pyrex, benzene, 2 h, 60%; v, FVP, 1150 °C, 0.5 mm, $N_2$, 2–3%

extensive chromatography (alumina) and characterized through its mass spectrum [*m*/*z* 372 ($M^+$)] and diagnostic three line $^1$H NMR spectrum [$\delta$ 7.92 (d, *J* 9 Hz, 4 H), 7.55 (d, *J* 9 Hz, 4 H), 7.42 (s, 4 H)] which was found to be identical with the reported values.[2] Admittedly, the yield (2–3%) of **2** in the FVP step is low and as yet unoptimised, but it compares well with the earlier reports (2.1 and 5% in FVP).[2]

Our approach to **2** from dimethylphenanthrene **5** involves the following sequence: NBS bromination–Wittig olefination–photocyclization and pyrolysis. Interestingly, the phenanthrene precursor **5** itself is assembled from *m*-xylene through the same sequence involving NBS bromination–Wittig olefination–photocyclization.[5] Thus, in an overall sense, through an iterative three step sequence and a final pyrolysis step, *m*-xylene is elaborated into the decacyclic, $C_{30}H_{12}$, aromatic 'bowl' **2**. We believe that the simple strategy outlined here can be adapted towards the synthesis of several bowl-like non-planar PAHs. Efforts along these lines are currently underway.

We thank CSIR for the research support and a fellowship to G. P. We also appreciate the help of Mr Anirban Banerjee in performing some important preliminary experiments. We also thank Professor L. T. Scott and Dr S. Hagen, Boston College, USA, for sending the $^1$H NMR spectrum of [5,5]-circulene for comparison.

## Footnote and References

* E-mail: gmchem@uohyd.ernet.in

1 R. Faust, *Angew. Chem., Int. Ed. Engl.*, 1995, **34**, 1429; P. W. Rabideau and A. Sygula, *Acc. Chem. Res.*, 1996, **29**, 235; L. T. Scott, *Pure Appl. Chem.*, 1996, **68**, 291; G. Mehta and H. S. P. Rao, in *Advances in Strain in Organic Chemistry*, ed. B. Halton, JAI Press, London, 1997, vol. 6, pp. 139–187.

2 (*a*) P. W. Rabideau, A. H. Abdourazak, H. E. Folsom, Z. Marcinow, A. Sygula and R. Sygula, *J. Am. Chem. Soc.*, 1994, **116**, 7891; (*b*) S. Hagen, M. S. Bratcher, M. S. Erickson, G. Zimmermann and L. T. Scott, *Angew. Chem., Int. Ed. Engl.*, 1997, **36**, 406.

3 L. T. Scott, M. M. Hashemi, D. T. Meyer and H. B. Warren, *J. Am. Chem. Soc.*, 1991, **113**, 7082.

4 The synthetic strategy followed presently is generally along the lines pursued previously by us for the synthesis of other fullerene fragments, see G. Mehta, G. V. R. Sarma, M. A. Krishna Kumar, T. V. Vedavyasa and E. D. Jemmis, *J. Chem. Soc., Perkin Trans. 1*, 1995, 2529; G. Mehta, K. Venkateswara Rao and K. Ravikumar, *J. Chem. Soc., Perkin Trans. 1*, 1995, 1787; G. Mehta and K. Venkateswara Rao, *Synlett*, 1995, 317; G. Mehta and G. Panda, *Tetrahedron Lett.*, 1997, **12**, 2145; G. Mehta, G. Panda, S. R. Shah and A. C. Kunwar, *J. Chem. Soc., Perkin Trans. 1*, 1997, 2269.

5 F. B. Mallory and C. W. Mallory, *J. Am. Chem. Soc.*, 1972, **94**, 6041.

*Received in Cambridge, UK, 1st September 1997; 7/06336I*

# Synthesis of optically active allenes using tandem enzyme and palladium-catalysed reactions

**Pierre H. Dixneuf,[a] Thierry Guyot,[b] Mark D. Ness[b] and Stanley M. Roberts‡[b]**

[a] *UMR 6505 CNRS, Université de Rennes I, Laboratoire de Chimie de Coordination et Catalyse, Campus de Beaulieu, 35042 Rennes, France*

[b] *Department of Chemistry, University of Liverpool, Liverpool, UK L69 7ZD*

**The propargylic carbonates (*S*)-6 and (*R*)-9 are converted into the chiral allenes 10, 11, 13 and 14 (ee 82–85%) using organozinc reagents and tetrakis(triphenylphosphine)-palladium as catalyst.**

The importance of allenes is well-established and the variety of chemical reactions that they undergo is documented.[1] Recently, methods have been reported for the construction of allenes of the type $R^1CH{=}C{=}CHR^2$, in optically active form.[2]

In this paper, we report the enzymatic resolution of secondary[3] and the classical resolution of tertiary propargylic alcohols, their conversion into chiral allenes of the type $R^1R^2C{=}C{=}CR^3R^4$ *via* the corresponding carbonates[4] and their activation with palladium catalysts[5] in the presence of a zinc derivative.[6]

The optically active compounds required as starting materials for this study were obtained by a variety of methods. The alcohols **1** and **2** were prepared in high enantiomeric purity using enzymatic resolution methods (Table 1), while the alcohol (*R*)-**3** (99% ee) was obtained from the racemate by fractional crystallisation of the brucine salt from acetone.[7] Treatment of alcohol (*R*)-**3** with bromobenzene, piperidine and a catalytic amount of tetrakis(triphenylphosphine)palladium(0) in DMF at 80 °C furnished the alcohol (*S*)-**4** (86%).[8] Finally, the alcohol (*S*)-**5** (99% ee) was prepared by enzyme-catalysed acetylation of racemic material (Table 1),[9] while the alcohol (*R*)-**5** (92% ee) was prepared from 1-phenyl-3-(trimethylsilyl)prop-2-ynone by selective reduction using dipinanylborane,[10] followed by desilylation with potassium carbonate in methanol.

The alcohol (*S*)-**1** was converted quantitatively into the corresponding carbonate (*S*)-**6** using ethyl chloroformate in pyridine, in the presence of a catalytic amount of 4-*N*,*N*-dimethylaminopyridine (DMAP). Alcohols (*S*)-**2** and (*R*)-**5** afforded the carbonates (*S*)-**7** and (*R*)-**9** after similar treatment, while the alcohol (*S*)-**4** furnished the carbonate (*S*)-**8** (97%) on treatment with butyllithium for one hour followed by treatment with methyl chloroformate at low temperature.

The carbonate (*S*)-**6** was treated with phenylzinc bromide† and a catalytic amount of tetrakis(triphenylphosphine)palladium (TTPP) in THF to provide the (a*R*)-allene **10** in 84% yield and 83% ee (Scheme 1). This reaction is very similar to one

**Table 1** Resolution of alcohols **1**, **2** and **5** using *Pseudomonas amano* sp. AK and *Candida antarctica* lipases[a]

| Substrate | Enzyme | *t*/h | Alcohol Yield (%) (ee) (%) configuration | Ester Yield (%) (ee) (%) configuration |
|---|---|---|---|---|
| **1** | *P. amano* | 4 | 41 (93) *S* | 41 (97) *R* |
| **1** | *C. antarctica* | 2 | 39 (99) *S* | 42 (94) *R* |
| **2** | *P. amano* | 3 | 45 (86) *S* | 42 (99) *R* |
| **5** | *C. antarctica* | 3.5 | 46 (99) *S* | 50 (98) *R* |

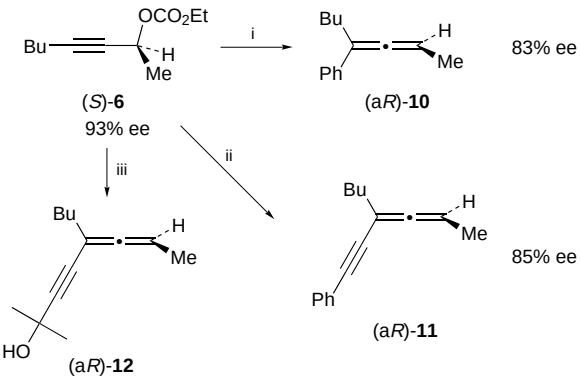
[a] The substrate, enzyme and vinyl acetate were reacted for the specified time in hexane.




**1** $R^1$ = Bu; $R^2$ = H; $R^3$ = Me; $R^4$ = Et **6**
**2** $R^1$ = Ph; $R^2$ = H; $R^3$ = Me; $R^4$ = Et **7**
**3** $R^1$ = H; $R^2$ = $Bu^t$; $R^3$ = Ph
**4** $R^1$ = $R^3$ = Ph; $R^2$ = $Bu^t$; $R^4$ = Me **8**
**5** $R^1$ = $R^2$ = H; $R^3$ = Ph; $R^4$ = Et **9**

performed by Vermeer *et al.*[6] The Dutch group reported a lower degree of stereocontrol, but these earlier studies were hampered by having a starting material of low optical purity (28% ee) and by having an uncertain amount of biphenyl in the product allene. Similarly, reaction of (*S*)-**6** with phenylacetylene in the presence of diisopropylamine, zinc chloride and catalytic amounts of copper(I) iodide and TTPP furnished the trisubstituted (a*R*)-allene **11** in 63% yield and 85% ee. The enantiomeric excesses of the products **10** and **11** were assessed by $^1$H NMR spectroscopy using a mixture of a silver salt and a chiral ytterbium salt (ratio 1 : 1) as recommended previously.[11] The enantiomeric purity of the starting material and products suggests a high degree of control in the transfer from point to axial chirality. While the enantiomeric excess of the (a*R*)-dienynol **12**, obtained from the carbonate (*S*)-**6** and 2-methylbut-3-yn-2-ol, could not be assessed by physical methods, a high degree of stereocontrol in the reaction could be anticipated.

The absolute configuration of the allenes **10**–**12** has not been established conclusively but is assumed on the basis of the established mechanism of the reaction (Fig. 1). The palladium(0) is expected to activate the chiral carbonate by nucleophilic attack antiperiplanar to the leaving group, forming the chiral allenylpalladium intermediate (A). A cross-coupling on the intermediate (A) affords the chiral allene (B), regenerating the palladium(0) catalyst.




**Scheme 1** *Reagents and conditions*: i, PhZnBr–Pd($PPh_3$)$_4$, THF–$Et_2O$, 84%; ii, CuI–$ZnCl_2$–$Pr^i_2NH$–Pd($PPh_3$)$_4$–THF–PhC≡CH, 63%; iii, CuI–$ZnCl_2$–$Pr^i_2NH$–Pd($PPh_3$)$_4$–THF–$Me_2C(OH)C{\equiv}CH$, 59%

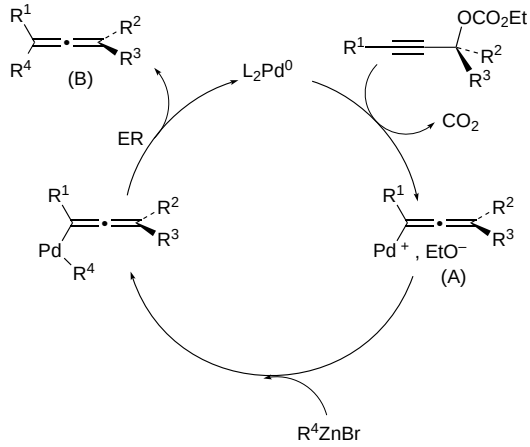
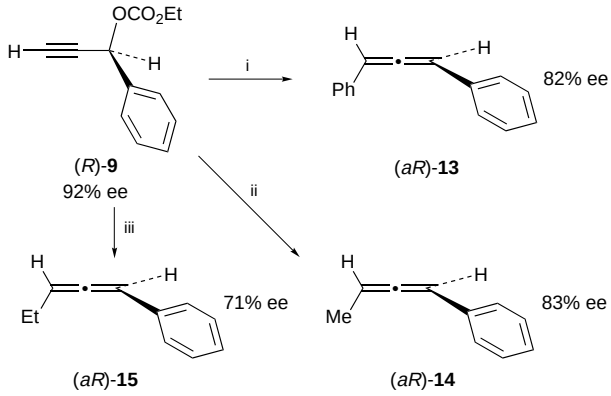


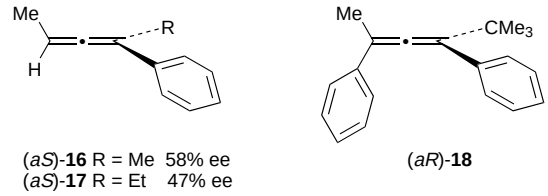

**Fig. 1** Mechanism




**Scheme 2** *Reagents and conditions*: i, $PhZnBr–Pd(PPh_3)_4–THF–Et_2O$, 65%; ii, $Me_2Zn–KBr–Pd(PPh_3)_4–THF$, 40%; iii, $EtZnBr–Pd(PPH_3)_4–THF–Et_2O$, 67%

In agreement with this proposal, the carbonate (*R*)-**9** (92% ee) reacts with phenylzinc bromide† in the presence of TTPP (Scheme 2) to furnish the (a*R*)-diphenylallene **13** (82% ee) {$[\alpha]_D^{22}$ −932 (*c* 1.0, $CHCl_3$); lit.[12] $[\alpha]_D$ +1137 ($CHCl_3$), for the (a*S*) enantiomer}. This carbonate (*R*)-**9** also reacts with dimethylzinc–potassium bromide or ethylzinc bromide in the presence of TTPP to give allenes **14** and **15** in 83 and 71% ee respectively (Scheme 2), as confirmed by $^1$H NMR spectroscopy (Yb/Ag salts).

Incorporation of a phenyl group at the alkyne terminus, such as in compound (*S*)-**7**, leads to a poorer transfer of chirality on reaction with dimethylzinc–TTPP or diethylzinc–TTPP as shown with the allenes **16** and **17** being formed in 58 and 47% ee respectively. Thus, while the carbonate (*R*)-**8** reacts smoothly with dimethylzinc and TTPP in the presence of potassium bromide to give the allene **18** in 78% yield, the optical rotation of the product, $[\alpha]_D$ −250 (*c* 0.96, $CHCl_3$), may reflect only a moderate enantiomeric excess. (The optical purity of this tetrasubstituted allene could not be established by $^1$H NMR spectroscopy using the silver–ytterbium chiral shift reagent.)




In summary, the preparation of highly substituted allenes of good to excellent optical purity can be accomplished by transformations involving secondary and tertiary propargylic carbonates.

We thank the CROUS de Rennes for support (to T. G.).

## Footnotes and References

‡ E-mail: sj11@liverpool.ac.uk

† Made *in situ* from bromobenzene, magnesium turnings and zinc chloride.

1 *Chemistry of the Allenes*, vol. 1–3, ed. S. R. Landor, Academic Press, New York, 1982; H. F. Schuster and G. M. Coppola, *Allenes in Organic Synthesis*, Wiley–Interscience, New York, 1984; C. Bruneau and P. H. Dixneuf, *Allenes and Cumulenes*, in *Comprehensive Organic Functional Group Transformations*, ed. A. R. Katritzky, O. Meth-Cohn and C. W. Rees, Pergamon, Oxford, 1995, vol. 1, ch. 20.

2 A. G. Myers and B. Zheng, *Tetrahedron Lett.*, 1996, **37**, 4841; *J. Am. Chem. Soc.*, 1996, **118**, 4492; J. Tsuji and T. Mandai, *Synthesis*, 1996, 1; see also J. Tsuji, *Palladium Reagents and Catalysts: Innovation in Chemical Synthesis*, Wiley, New York, 1995.

3 For earlier papers detailing resolutions of secondary propargyl alcohols–acetates, see C. Chan, P. B. Cox and S. M. Roberts, *J. Chem. Soc., Chem. Commun.*, 1988, 971; M. Shimizu, H. Kawanami and T. Fujisawa, *Chem. Lett.*, 1992, 107; K. Burgess and L. D. Jennings, *J. Am. Chem. Soc.*, 1991, **113**, 6129.

4 T. Mandai, T. Matsumoto, R. Kawada and J. Tsuji, *Tetrahedron Lett.*, 1993, **34**, 2161; T. Mandai, T. Nakata, H. Murayama, H. Yamaoki, M. Ogawa, M. Kawada and J. Tsuji, *Tetrahedron Lett.*, 1990, **31**, 7179.

5 C. Darcel, S. Bartsch, C. Bruneau and P. H. Dixneuf, *Synlett*, 1994, 457; *cf.* J. A. Marshall and M. A. Wolf, *J. Org. Chem.*, 1996, **61**, 3238.

6 C. J. Elsevier, P. M. Stehouwer, H. Westmijze and P. Vermeer, *J. Org. Chem.*, 1983, **48**, 1103.

7 F. Toda, K. Tanaka, H. Ueda and T. Oshima, *Isr. J. Chem.*, 1985, **25**, 338; *Tetrahedron Lett.*, 1981, **22**, 4664; tertiary propargyl alcohols are not readily resolved in high ee using enzyme-catalysed acylation procedures; see I. Brackenridge, R. McCague, S. M. Roberts and N. J. Turner, *J. Chem. Soc., Perkin Trans. 1*, 1993, 1093; D. O'Hagan and N. A. Zaidi, *Tetrahedron: Asymmetry*, 1994, **5**, 111.

8 M. Alami, F. Ferri and G. Linstrumelle, *Tetrahedron Lett.*, 1993, **34**, 6403.

9 *Cf.* B. I. Glanzer, K. Faber and H. Griengl, *Tetrahedron*, 1987, **43**, 5791.

10 H. C. Brown and G. G. Pai, *J. Org. Chem.*, 1982, **47**, 1606; P. Bartmettler and H. J. Hansen, *Helv. Chim. Acta.*, 1990, **73**, 1515.

11 A. Mannscheck, W. Munninger, T. Burgemeister, J. Gore and B. Cazes, *Tetrahedron*, 1986, **42**, 399.

12 R. Rossi and P. Diversi, *Synthesis*, 1973, 25.

*Received in Cambridge, UK, 23rd June 1997; 7/04374K*

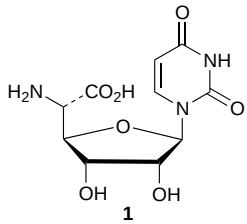
# Total synthesis of carbocyclic nikkomycin C

**Simon E. Ward,[a] Andrew B. Holmes[a]* and Ray McCague[b]**

[a] *University Chemical Laboratory, Lensfield Road, Cambridge, UK CB2 1EW*
[b] *Chiroscience Ltd, Cambridge Science Park, Milton Road, Cambridge, UK CB4 4WE*

**The carbocyclic analogue 11 of nikkomycin C 1 is prepared by a sequence involving allylic rearrangement of the imino ester adduct 3, palladium-mediated substitution of the allylic lactone 4c with uracil bis(trimethylsilyl)ether 6, and osmylation of the double bond.**

The imino Diels–Alder reaction is a versatile tool for the preparation of a variety of natural products.[1–4] As part of a programme to investigate the synthesis of amino acid derivatives, we were interested in elaboration of the azabicyclo-[2.2.1]heptene skeleton *via* acid catalysed rearrangement.[5] We have investigated the scope of these rearrangements, and the palladium catalysed allylic substitutions of the resulting lactones, to prepare cyclopentene amino acid derivatives. The methodology has been exemplified in the synthesis of a carbocyclic nikkomycin analogue.[6,7]



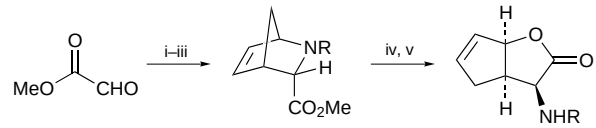

**1**

The nikkomycins and polyoxins are a family of nucleoside-type antibiotics which exhibit a broad spectrum of biological activity.[8–12] Carbocyclic nucleosides display comparable biological activity to the natural furanose materials, whilst maintaining an inherent stability towards β-glycosidase hydrolysis *in vivo*.[13–15] Our synthesis of a carbocyclic nikkomycin analogue **11** using bicyclic lactones illustrates a general approach to carbocyclic nucleosides.

The required lactone **4** was synthesised from the imino Diels–Alder adduct **3**. The stereochemistry of the amino acid side chain of nikkomycin necessitated use of the *endo* cycloadduct. The *endo* adducts are inherently more difficult to prepare than their *exo* diastereoisomers, since the imines required for the Diels–Alder reactions with unactivated dienes need to be activated by the presence of electron withdrawing groups on the nitrogen terminus. These electron withdrawing groups then appear to exert a greater requirement to adopt the *endo* conformation in the transition state and so give rise to the *exo* adducts. The solution to this problem is to use iminium salts as dienophiles[5] and to effect a resolution to produce enantiomerically pure material.

Cycloaddition of the iminium ion derived from methyl glyoxylate[16] to cyclopentadiene gave the azabicyclo-[2.2.1]heptene **3** (R = H) (Scheme 1). Derivatisation of the nitrogen with an electron withdrawing group [*e.g.* Ts, Bz, BnOCO (Z)] enables the acid-catalysed allylic rearrangement to occur. This is effected in good yield by treatment of the derived carboxylic acids with trifluoroacetic acid to give the lactones **4a**–**c**.

Treatment of the lactones with a variety of palladium(0) reagents effected efficient conversion into the π-allyl palladium complexes. Initial attempts to couple uracil as its sodium salt

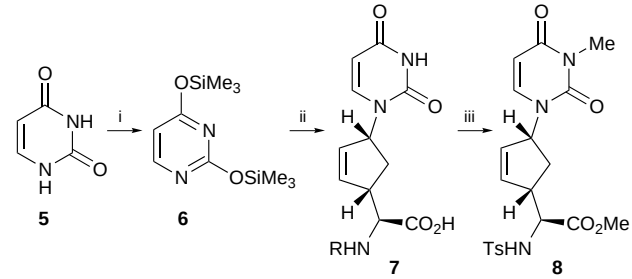



**2** **3** **4a** R = Ts **b** R = Bz **c** R = Z

**Scheme 1** i, $NH_4Cl$ (aq.); ii, cyclopentadiene; iii, *N*-derivatisation (see text) (70–82% overall); iv, LiOH, $H_2O$–THF; v, trifluoroacetic acid, $CH_2Cl_2$ (80–85% overall)

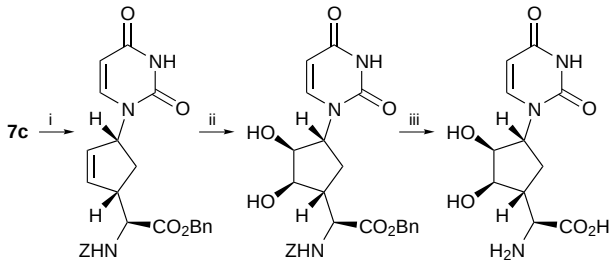
using a palladium-catalysed π-allyl substitution reaction proved fruitless.[17] More positive results were achieved using uracil bis(trimethylsilyl)ether† following the report of Benneche and co-workers for the preparation of a thymidine-substituted cyclopentene (Scheme 2).[18] Treatment of the *N*-tosyl lactone **4a** with tetrakis(triphenylphosphine)palladium(0) in the presence of DIPHOS at 25 °C in acetonitrile gave rise to a moderate yield (31%) of the required substitution product **7** (R = Ts). Somewhat unexpectedly, treatment of this product with (trimethylsilyl) diazomethane[21] gave the dimethylated derivative **8**, where the uracil nitrogen had also been methylated.[22] The uracil substitution reactions can be considerably improved by the use of chlorotrimethylsilane to promote formation of the π-allyl palladium intermediate.[7] It is thought that the function of the chlorotrimethylsilane is to trap the carboxylate species produced during formation of the π-allyl complex, and thus favour this in the equilibrium with the starting lactone. Repetition of the uracil substitution reaction under these conditions with the *N*-benzyloxycarbonyl derivative **4c** afforded the analogous cyclopentene **7c**. Benzylation of **7c** gave the ester **9** from which the protecting groups were later cleaved by hydrogenolysis (Scheme **3**). Dihydroxylation of the alkene **9** afforded an approximately 2 : 1 mixture of the diol **10** and its all-*cis* diastereoisomer. The poor selectivity of cyclopentene dihydroxylations can be rationalised on steric[23] or electronic[24] grounds.[7] Finally, hydrogenolysis of the benzyl protecting groups gave the required target molecule **11** in good yield.‡

In summary, this route has therefore demonstrated a rapid assembly of the nikkomycin skeleton and has further demonstrated the synthetic versatility of cycloadducts of imino Diels–Alder reactions.




**5** **6** **7** **8**

**Scheme 2** i, HMDS, $(NH_4)_2SO_4$, reflux, 3 h; ii, $Pd(PPh_3)_4$, DIPHOS, **4**, $Me_3SiCl$, MeCN, (20–55% overall); iii, $Me_3SiCHN_2$, MeOH, 91% (R = Ts)




**Scheme 3** i, BnBr, $NaHCO_3$, DMF, 90%; ii, $OsO_4$, NMO·$H_2O$, Bu$^t$OH, THF, 18 h, 52%; iii, $H_2$ Pd/C, EtOH, 2 h, 95%

We thank the EPSRC and the LINK Asymmetric Synthesis Initiative (Chiroscience Ltd and the Department of Trade and Industry) for financial support, the EPSRC Swansea Mass Spectrometry Service for mass spectrometry data, Dr V. K. Aggarwal for helpful advice and pre-prints of refs. 7*b*,*c* and Professor J. M. Williams and Dr B. Adger for their interest in this work.

## Footnotes and References

* E-mail: abh1@cus.cam.ac.uk

† Preparation of the bis(trimethylsilyl)uracil **6** using Vorbrüggen[19] or Cossy[20] methodology was, in our hands, difficult to reproduce consistently. Development of the Benneche protocol using refluxing hexamethyldisilazane with a catalytic quantity of ammonium sulfate gave reproducibly good results, provided the reflux time was prolonged to 3–4 h.

‡ All new compounds exhibited spectroscopic and combustion analysis (or high resolution mass spectrometry) properties in accordance with the assigned structures.

1 S. M. Weinreb, in *Comprehensive Organic Synthesis*, ed. B. M. Trost and I. Fleming, Pergamon Press, Oxford, 1991, vol. 5, ed. L. A. Paquette, p. 401.
2 S. M. Weinreb and P. M. Scola, *Chem. Rev.*, 1989, **89**, 1525.
3 A. B. Holmes, A. Kee, T. Ladduwahetty and D. F. Smith, *J. Chem. Soc., Chem. Commun.*, 1990, 1412.
4 D. L. Boger and S. M. Weinreb, *Hetero Diels–Alder Methodology in Organic Synthesis*, Academic Press Inc., London, 1987.
5 T. Kobayashi, K. Ono and H. Kato, *Bull. Chem. Soc. Jpn.*, 1992, **65**, 61.
6 H. Baumgartner, C. Marschner, R. Pucher, M. Singer and H. Griengl, *Tetrahedron Lett.*, 1992, **33**, 6443.
7 (*a*) V. K. Aggarwal, N. Monteiro, G. J. Tarver and S. D. Lindell, *J. Org. Chem.*, 1996, **61**, 1192; (*b*) V. K. Aggarwal, N. Monteiro, G. J. Tarver and R. McCague, *J. Org. Chem.*, 1997, **62**, 4665; (*c*) V. K. Aggarwal and N. Monteiro, *J. Chem. Soc., Perkin Trans. 1*, 1997, 2531.
8 H. Hagenmaier, A. Keckeisen, H. Zähner and W. A. König, *Liebigs Ann. Chem.*, 1979, 1494.
9 H. Hagenmaier, A. Keckeisen, W. Dehler, H. P. Fiedler, H. Zähner and W. A. König, *Liebigs Ann. Chem.*, 1981, 1018.
10 W. A. König, W. Hass, W. Dehler, H. P. Fiedler and H. Zähner, *Liebigs Ann. Chem.*, 1980, 622.
11 M. Uramoto, K. Kobinata, K. Isono, T. Higashijima, T. Miyazawa, E. E. Jenkins and J. A. McCloskey, *Tetrahedron*, 1982, **38**, 1599.
12 K. Kobinata, M. Uramoto, M. Nishii, H. Kusakabe, G. Nakamura and K. Isono, *Agric. Biol. Chem.*, 1980, **44**, 1709.
13 A. D. Borthwick and K. Biggadike, *Tetrahedron*, 1992, **48**, 571.
14 L. Agrofoglio, E. Suhas, A. Farese, R. Condom, S. R. Challand, R. A. Earl and R. Guedj, *Tetrahedron*, 1994, **50**, 10 611.
15 V. E. Marquez and M.-I. Lim, *Med. Res. Rev.*, 1986, **6**, 1 (*Chem. Abstr.*, 1986, **104**, 144 017z).
16 J. M. Hook, *Synth. Commun.*, 1984, **14**, 83.
17 F. Liotta, C. R. Unelius, J. Kozak and T. Norin, *Acta Chem. Scand.*, 1992, **46**, 686.
18 L. L. Gundersen, T. Benneche, F. Rise, A. Gogoll and K. Undheim, *Acta Chem. Scand.*, 1992, **46**, 761.
19 H. Vorbrüggen, K. Krolikiewicz and B. Bennau, *Chem. Ber.*, 1981, **114**, 1234.
20 J. Cossy and P. Pale, *Tetrahedron Lett.*, 1987, **28**, 6039.
21 T. Aoyama and T. Shioiri, *Chem. Pharm. Bull.*, 1981, **29**, 3249.
22 M. Jokic and V. J. Skaric, *J. Chem. Soc., Perkin Trans. 1*, 1990, 2225.
23 G. Poli, *Tetrahedron Lett.*, 1989, **30**, 7385.
24 N. Katagiri, Y. Ito, K. Kitano, A. Toyota and C. Kaneko, *Chem. Pharm. Bull.*, 1994, **42**, 2653.

*Received in Cambridge, UK, 11th August 1997; 7/05825J*

# Synthetic carbohydrate-based vaccines: synthesis of an L-*glycero*-D-*manno*-heptose antigen–T-epitope–lipopeptide conjugate

**Frank Reichel, Peter R. Ashton and Geert-Jan Boons***

*School of Chemistry, The University of Birmingham, Edgbaston, Birmingham, UK B15 2TT*

**A facile and highly efficient synthesis of a glycopeptidolipid containing a heptose sugar, a synthetic T-epitope and a synthetic immunoadjuvant is presented which represents an important step towards the development of a fully synthetic vaccine against *Neisseria meningitidis*.**

*Neisseria meningitidis* can cause a severe form of meningitis and bacteriamia and is the only bacterium that is capable of generating epidemics of meningitis.[1] Although it is more than a century since meningococcus was discovered, no vaccine has been developed that matches requirements such as safety, long-lasting immunity to all age groups and cross-protection against meningococcal serotypes and sub-serotypes.

Saccharides representing partial structures of the inner-core oligosaccharide of meningococcal lipopolysaccharides (LPS) have been synthesised.[2] These structures were equipped with an artificial spacer which enabled controlled conjugation to tetanus toxoid (TT). The conjugates were used to immunise mice and evoked an L-2 or L-3,7,9 specific immune response.[3] Thus, small synthetic saccharides derived from meningococcal LPS functioned as effective B-epitopes. Furthermore, tetanus toxoid acted as a carrier protein as well as a source of T-epitopes to give immunological memory.

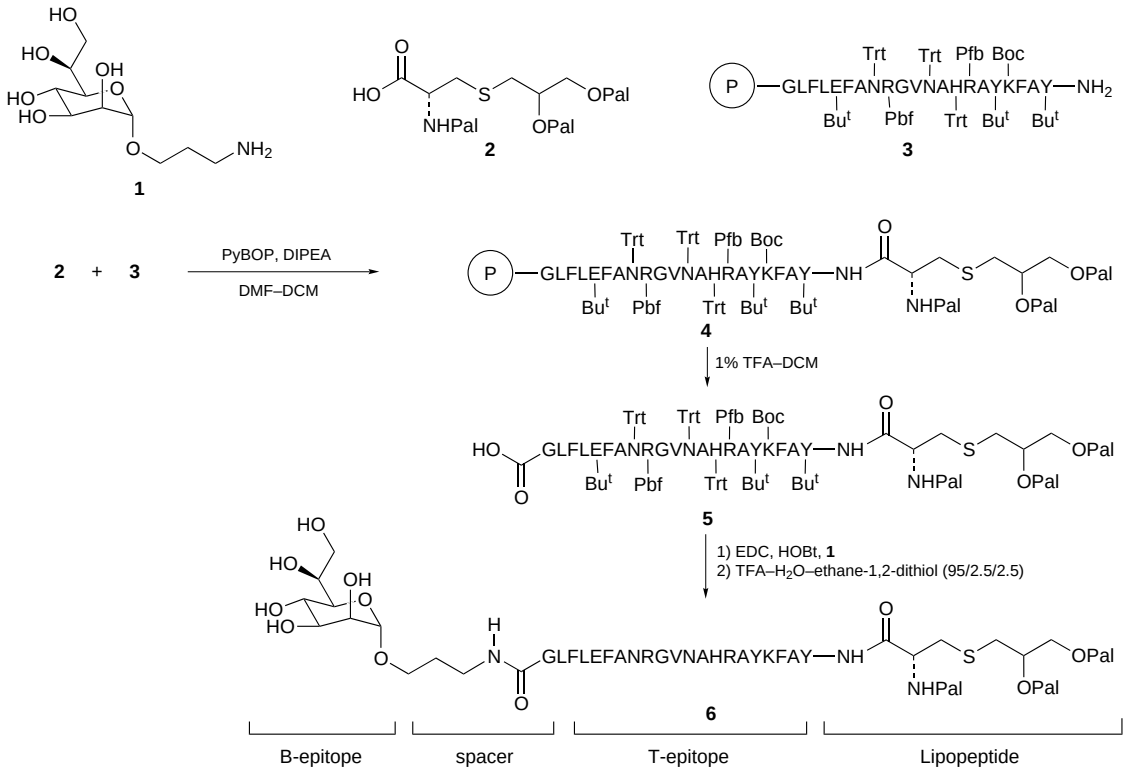
The use of TT as a carrier protein is problematic in several respects. For example, the antibody response to a haptan which is coupled to a carrier protein can be ineffective when vaccines have previously been immunised with the carrier protein.[4] Furthermore, heterologous memory T-cells (for example induced with TT conjugates) may not be reactivated during infection. Therefore, incorporation of homogeneous (*i.e.* meningococcal-derived) T-cell epitopes into a vaccine will be advantageous as the memory response will be more effective.[5] In addition, the advantages of the use of synthetic peptides derived from immunodominant T-cell epitopes compared to bacterial protein carriers are obvious: the immune response is directed selectively towards effective determinants, whereas sequences homologous to human self-protein can be excluded from the vaccine. The feasibility of the use of synthetic T-epitopes as vaccine components has recently been shown[6] by a conjugate composed of a *Heamophilus influenzae* capsular polysaccharide and functional T-helper cell peptide epitope, that elicited protective levels of antibodies in rabbits.

We report here a synthetic methodology that makes it possible to construct fully synthetic glycopeptidolipids that contain a carbohydrate-based B-epitope, a peptide T-epitope and a lipopeptide. Such a conjugate constitutes the minimal structural features required for an effective immunological response. We have synthesised a compound (**6**) that contains a L-*glycero*-D-*manno*-heptose sugar that will act as a B-epitope, the peptide sequence YAFKYARHANVGRNAFELFL that has been identified as a MHC class II restricted site for human T-cells and is derived from an outer-membrane protein of *N. meningitidis*[7] and the lipopetide *S*-[(*R*/*S*)-2,3-dipalmitoyloxypropyl]-*N*-palmitoyl-(*R*)-cysteine ($Pam_3Cys$). The lipopeptide $Pam_3Cys$ is a highly potent B-cell and macrophage activator derived from the immunologically active N-terminal sequence of the principal lipoprotein of *Escherichia coli*[8] and has been used in synthetic peptide-based vaccine and cancer vaccine development.[9] The lipid moiety will also serve as a membrane anchor in the lipid layer of cell membranes which will ensure efficient and long-term delivery of the antigen.

The synthesis of the complex target compound **6** requires a highly convergent strategy and the synthetic methods selected should be compatible with the requirements of carbohydrate, peptide and lipid chemistry. It was envisaged that the artificial spacer containing saccharide building block **1**, the lipopeptide **2** and solid supported peptide **3** would be suitable starting materials. As can be seen in Scheme 1, they will be coupled by well-established amide-bond forming reactions. Thus, the carboxylic acid of the glycolipid **2** will be coupled to the amino terminus of a peptide (**3**) that has been assembled on a solid support. Next, cleavage of the lipopeptide from the solid support followed by coupling of the released C-terminus to the amino containing spacer of saccharide **1** will afford a fully protected conjugate. An additional glycine residue has been incorporated at the C-terminus of the peptide to avoid epimerisation during the latter coupling step. The proposed assembly and deprotection requires only four synthetic steps and extensive purification procedures are avoided since most of the reactions have been performed on a solid support.

The preparation of the spacer containing saccharide unit **1** is rather straightforward and was performed as described previously.[2] Lipopeptide **2** was prepared from cysteine in five steps according to the procedure of Wiesmüller *et al.*[10] The peptide **3** was prepared by automated continuous flow solid-phase peptide synthesis on a commerically available HMPB–MBHA-resin using $N^{\alpha}$-fluorenylmethoxycarbonyl (Fmoc) amino acid derivatives, according to standard procedures.[11] The hyper acid sensitive linker allows the cleavage of the lipopeptide from the solid support without removal of the side-chain protecting groups. This feature is important since the unprotected side chains of aspartic acid, glutamic acid and lysine will interfere with the incorporation of the saccharide unit. The following side chain protecting groups were selected: Trt for Asn and His, Pbf for Arg, Boc for Lys and $Bu^t$ for Tyr and Glu. Deprotection can be performed under mild acid conditions without affecting the glycosidic linkages and palmitoyl ester moieties.

The N-terminus of the solid supported peptide **3** was linked to the carboxylic acid unit of the $Pam_3Cys$ **2** to give lipopeptide **4**. Model studies had established that the benzotriazol-1-yloxytris-(pyrrolidino)phosphonium hexafluorophosphate–$Pr^i_2EtN$ coupling reagents allowed highly efficient and fast coupling. Furthermore, this method required less of the rather precious $Pam_3Cys$ **3** compared to the use of a carbodiimide–1-hydroxybenzotriazole (HOBT) coupling system. Next, the conjugate was released from the solid support by treatment with 1% TFA in $CH_2Cl_2$ followed by immediate neutralisation with 10% pyridine–MeOH. The crude product was purified by size-exclusion column chromatography (Sephadex LH-20, $CH_2Cl_2$–MeOH 1 : 1, v/v) and 2D NMR and mass spectrometric analysis of the product obtained showed that the side-chain protecting groups had not been effected. Compound **5** was isolated in a yield of 75% based on a resin loading of 30 μmol. The revealed carboxylic acid at the C-terminus of the lipopeptide **5** was




**Scheme 1**

coupled with the amino-containing spacer moiety of the sugar unit **1** and in this case the coupling was best performed with EDC and HOBT in the presence of $Pr^{i}_{2}EtN$. Purification was accomplished by gel filtration and the fully protected conjugate was isolated in a yield of 91%. The molecular structure was confirmed by 1D and 2D NMR spectroscopy and mass spectrometry. FAB mass analysis of **5** showed a peak at *m*/*z* 5108 corresponding to $[M + Na]^+$. Scanning was also performed over a narrow mass range between 4800 and 5200. Peaks were present at *m*/*z* 5086 and 5108 corresponding to $[M + H]^+$ and $[M + Na]^+$, respectively. Further peaks at *m*/*z* 4843 and 4865 correspond to a fragment lacking one trityl protecting group and its sodium adduct, respectively. It is noteworthy that the hydroxy groups of the sugar moiety were unprotected and did not interfere with the coupling reaction. This feature is important because the most commonly used permanent protecting groups in carbohydrate chemistry are benzyl ethers or acetyl or benzoyl esters. Removal of these protecting groups would cause problems as base-catalysed deacylation of a product may result in the loss of the palmitoyl moieties. Furthermore, catalytic hydrogenation of benzyl ethers would be difficult because of poisoning of the palladium catalyst by the sulfur residues in the compound. Finally, the side chain protecting groups of the peptide were removed by treatment with TFA–water in the presence of ethane-1,2-dithiol as a scavenger. The obtained compound was purified by HPLC on a phenogel 5 μ 100 Å column (eluent: DMSO) and after freeze drying the structural integrity of **6** was confirmed by FAB mass spectrometry and 1D and 2D NMR spectroscopy. FAB mass analysis of **6** showed a peak at *m*/*z* 3586 corresponding to $[M + H]^+$.

In conclusion, we have developed a highly convergent strategy for the assembly of compounds that contain a carbohydrate B-epitope, a peptide T-epitope and a lipopeptide adjuvant. The use of these glycoconjugates as vaccines will have several advantages compared to conventional polysaccharide-protein conjugate vaccines. They are well-defined and can be purified to homogeneity and are chemically stable. The incorporation of homogeneous T-epitopes will enhance the immunological response.

Financial support for this project was provided by the Medical Research Council.

## Footnote and References

* E-mail: gjboons@chemistry.bham.ac.uk

1 D. A. A. Ala'Aldeen and K. A. C. Cartwright, *J. Infect.*, 1996, **33**, 153.
2 G. J. P. H. Boons, G. A. van der Marcel and J. H. van Boom, *Tetrahedron Lett.*, 1989, **30**, 229; G. J. P. H. Boons, M. Overhand, G. A. van der Marcel and J. H. van Boom, *Angew. Chem., Int. Ed. Engl.*, **28**, 1989, 1504; G. J. P. H. Boons, P. Hoogerhout, J. T. Poolman, G. A. van der Marel and J. H. van Boom, *Biomed. Chem. Lett.*, 1991, **1**, 303.
3 A. F. M. Verheul, G. J. P. H. Boons, G. A. van der Marcel, J. H. van Boom, H. J. Jennings, H. Snippe, J. Verhoef, P. Hoogerhout and J. T. Poolman, *Infect. Immun.*, 1991, **59**, 3566.
4 T. Barington, M. Skettrup, L. Jull and C. Heilmann, *Infect. Immun.*, 1993, **61**, 432.
5 L. M. Bradley, M. Croft and S. I. Swain, *Immunol. Today*, 1993, **14**, 197.
6 A. A. Kandil, N. Chan, M. Klein and P. Chong, *Glycoconjugate J.*, 1997, **14**, 13.
7 E. J. H. J. Wiertz, J. A. M. van Gaans-van den Brink, G. M. Th. Schreuder, A. A. M. Termijtelen, P. Hoogerhout and J. T. Poolman, *J. Immunol.*, 1991, **147**, 2012; E. J. H. J. Wiertz, J. A. M. van Gaans-van den Brink and H. Gausephol, *J. Exp. Med.*, 1992, 79.
8 P. Hoffmann, K. H. Weismüller, J. Metzger, G. Jung and W. G. Bessler, *Biol. Chem.*, 1989, **370**, 575; W. G. Bessler, M. Cox, A. Lex, B. Spur, K. Weismüller and G. Jung, *J. Immunol.*, 1985, **135**, 1900.
9 T. Toyakuni, B. Dean, S. Cai, D. Boivin, S. Hakomori and A. K. Singhal, *J. Am. Chem. Soc.*, 1994, **116**, 395; K. H. Wiesmüller, W. G. Bessler and G. Jung, *Int. J. Pept. Protein Res.*, 1992, **40**, 255; J. P. Defoort, B. Nardelli, W. Huang, D. D. Ho and J. P. Tam, *Proc. Natl. Acad. Sci. USA*, 1992, **89**, 3879.
10 K. H. Wiesmüller, W. G. Bessler and G. Jung, *Hoppe-Seyler's Z. Physiol. Chem.*, 1983, **364**, 593.
11 E. Atherton and R. C. Sheppard, *Solid phase synthesis: A practical approach*, IRL Press, Oxford University Press, Oxford, 1989.

*Received in Glasgow, UK, 12th June 1997; 7/04127F*

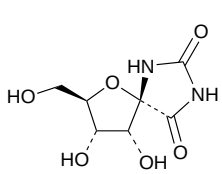
# A new class of anomeric spironucleosides

**Thanasis Gimisis,[a] Carlo Castellari[b] and Chryssostomos Chatgilialoglu*[a]**

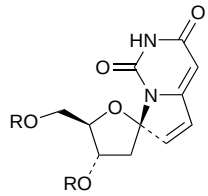
[a] *I.Co.C.E.A., Consiglio Nazionale delle Ricerche, Via P. Gobetti 101, I-40129 Bologna, Italy*
[b] *Dipartimento di Chimica 'G. Ciamician', Università di Bologna, Via Selmi 2, I-40126 Bologna, Italy*

**A 1,5-hydrogen migration of a conveniently situated alkoxyl radical affords spironucleosides which possess an unusual orthoamide structure at the anomeric position; X-ray crystallography establishes the configuration of the C-1′ position.**

Anomeric spironucleosides are useful modifications of natural nucleosides in that they contain the base unit in a fixed conformation around the *N*-glycosidic bond.[1] In recent years, they have gained in importance with the discovery of hydantocidin[2] **1**, a natural spironucleoside with herbicidal and plant growth regulatory activities, and generally, with the notion that important pharmaceutical leads can be found among modified nucleoside analogues.



**1**



**2**

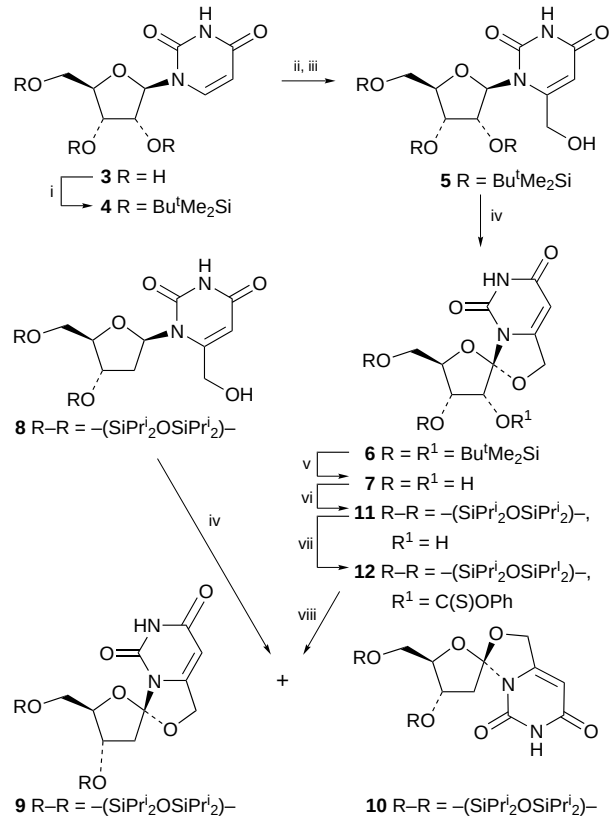
The first anomeric spironucleosides to be synthesized were derivatives of psiconucleosides.[3,4] All recent developments on the synthesis of anomeric spironucleosides are based on free-radical chemistry.[3b,5,6]

Modification of the anomeric position of nucleosides can also be attained *via* the intermediacy of C-1′ radicals.[7] We recently reported the first example of this kind of transformation for the preparation of compound **2**.[8] We report herein the synthesis of a new class of anomeric spironucleosides *via* a [1,5]-radical translocation of alkoxyl radicals to the anomeric position.

When the protected 6-hydroxymethylribouridine **5**, prepared from the corresponding protected uridine **4** by fine tuning of literature procedures,[9] was treated under the standard Suárez conditions[10] a major product was obtained in moderate (36%) yield after flash column chromatography (Scheme 1). The structure of the product could be assigned to compound **6** based on its $^1$H NMR spectrum, in which 2′-H appeared as a doublet and the 7-Hs appeared as a well resolved AB quartet. This, coupled with the lack of a 1′-H or 7-OH signal, corroborated the assignment of an orthoamide function to the product nucleoside, although the configuration of the anomeric centre remained ambiguous. Deprotection of the silyl groups provided the water soluble compound **7**. A single crystal of this material grown from MeOH–$H_2O$ with mp 172–173 °C was subjected to X-ray diffraction analysis in order to determine unambiguously the stereochemistry of the C-1′ position.

The independent part of the cell contains two formula units. An ORTEP diagram of **7** (molecule 1) is shown in Fig. 1. All atoms in molecule 1 were well defined, while atom O(5A) in molecule 2 exhibited a split image, as a consequence of two-fold rotational disorder around the C(4A)–C(5A) axis. An occupation factor for the latter was refined for O(5A) and the accompanying hydrogens, the final value being 0.57(1). The two independent molecules have strictly comparable parameters. In both molecules the stereogenic centre C(1A) is in the *R* configuration. The oxazolo[3,4-*c*]pyrimidine moiety is flat [maximum deviation from the average plane is 0.137(3) and 0.171(3) Å for atom O(7) in molecules 1 and 2, respectively]. The dihedral angle between the five membered ring and the fused pyrimidine moiety is 82.3(2) and 86.5(2)° for molecules 1 and 2, respectively.

When the Suárez conditions,[10] were applied to the 2′-deoxynucleoside analogue **8**, prepared from the corresponding protected 2-deoxyuridine,[9] two spironucleoside products were isolated in 71% combined yield and in a 1.1 : 1 ratio after flash column chromatography (Scheme 1). The structures of the products were assigned to compounds **9** and **10** based on their $^1$H NMR spectra, in which the two diastereotopic 2′-Hs appeared as well resolved doublets of doublets and the 7-Hs appeared as an AB quartet. The determined absolute configuration of the anomeric centre in the spiroribonucleoside **7** was linked with that of the 2′-deoxy analogues through a straightfor-




**Scheme 1** *Reagents and conditions*: i, Bu$^t$Me$_2$SiCl (5.0 equiv.) imidazole (7.0 equiv.), DMF, room temp., overnight, 98%; ii, LDA, THF, −70 °C, 3 h; $HCO_2Et$, −60 °C, 2 h; iii, $NaBH_4$, MeOH, room temp., 30 min, 68% based on consumption of **4**; iv, PhI(OAc)$_2$, $I_2$, cyclohexane, *hv*, 28 °C, 5 h, 36% for **6**, 71% for **9** and **10**; v, $Bu_4NF$ on $SiO_2$, THF, room temp., 2 h, 90%; vi, (Pr$^i_2$SiCl)$_2$O, pyridine, room temp., overnight, 61%; vii, PhOC(S)Cl, DMAP, $CH_2Cl_2$, 1 h, room temp., 84%; viii, (Me$_3$Si)$_2$SiH, AIBN, toluene, 80 °C, 6 h, 95%

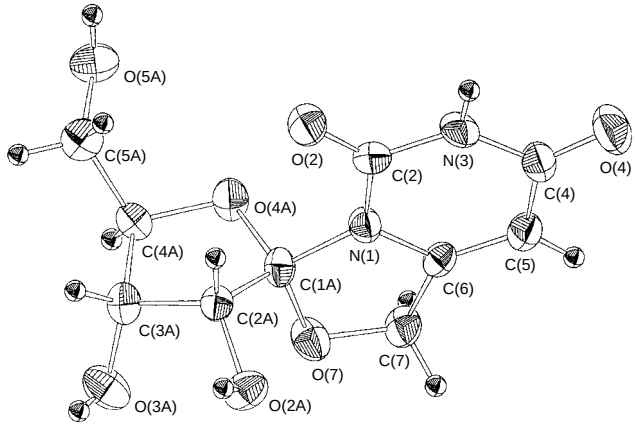
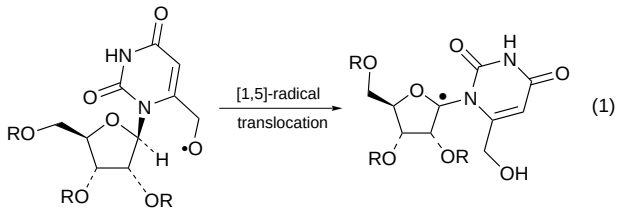



**Fig. 1** ORTEP drawing of one of the independent molecules of **7** (molecule 1) in the unit cell

ward, three-step chemical transformation, as outlined in Scheme 1. Standard regioselective protection of the 3′- and 5′-positions with the 1,1,3,3-tetraisopropyldisiloxane-1,3-diyl group to afford **11**, followed by transformation of the 2′-hydroxy group to give the thiocarbonate **12**,[11] and finally Barton–McCombie radical deoxygenation in the presence of $(Me_3Si)_3SiH$[12] produced the chromatographically less polar stereoisomeric 2′-deoxyspironucleoside **9**. These transformations, apart from establishing unequivocally the configuration of the C-1′ anomeric centre in **9** and **10**, also demonstrated the inherent stability of the orthoamide structure.

The mechanism for the formation of the spironucleoside involves generation, under the Suárez conditions, of the alkoxyl radical intermediate **13** which undergoes a [1,5]-radical translocation reaction[13] to yield the anomeric C-1′ radical intermediate **14** [eqn. (1)], which in turn produces the observed




**13** **14** (1)

orthoamide **6** after oxidation and cyclization. It is worth pointing out that the steric hindrance induced by the bulky 2′-substituent in the ribo series is likely responsible for the stereospecificity of the cyclization. The absence of the epimeric spironucleoside with *S* configuration in the reaction product can be attributed to the steric interaction between the carbonyl in the 2-position of the base and the bulky-2′ substituent as can be envisaged by inspection of the crystal structure in Fig. 1.

The spironucleosides reported herein correspond to the first spiro[tetrahydrofuran-2,3′-(1,5,6,7-tetrahydro-3*H*-[1,3]-oxazolo[3,4-*c*]pyrimidine)] nucleosides, possessing a remarkably stable orthoamide modification of the C-1′ anomeric position. Further work on the preparation and chemical transformations of this class of compounds is in progress.

We are grateful to the European Commission for a ‘Marie Curie’ post-doctoral fellowship to T. G.

## Footnote and References

* E-mail: chrys@area.bo.cnr.it

1 M. H. el Kouni, F. N. M. Naguib, R. P. Panzica, B. A. Otter, S.-H. Chu, G. Gosselin, C. K. Chu, R. F. Schinazi, Y. F. Shealy, N. Goudgaon, A. A. Ozerov, T. Ueda and M. H. Iltzch, *Biochem. Pharmacol.*, 1996, **51**, 1687.
2 M. Nakajima, K. Itoi, Y. Tamamatsu, T. Kinoshita, T. Okasaki, K. Kawakubo, M. Shindou, T. Honma, M. Tohjigamori and T. Haneishi, *J. Antibiot.*, 1991, **44**, 293.
3 (*a*) S. G. Zavgorodny, *Tetrahedron Lett.*, 1981, **22**, 3003; (*b*) for a recent approach to 6,1′-anhydro-6-hydroxypsicouridine, see M. S. P. Sarma, S. Megati, R. S. Klein and B. A. Otter, *Nucleosides Nucleotides*, 1995, **14**, 393.
4 H. Hrebabesky and J. Farkas, *Collect. Czech. Chem. Commun.*, 1974, **39**, 1098; A. Grouiller and J. Chattopadhyaya, *Acta Chem. Scand., Ser. B*, 1984, **338**, 367.
5 Y. Yoshimura, B. A. Otter, T. Ueda and A. Matsuda, *Chem. Pharm. Bull.*, 1992, **40**, 1761.
6 A. Kittaka, N. Yamada, H. Tanaka, K. T. Nakamura and T. Miyasaka, *Nucleosides Nucleotides*, 1996, **15**, 1447.
7 C. Chatgilialoglu and T. Gimisis, in *Free Radicals in Biology and Environment*, ed. F. Minisci, Kluwer, Dordrecht, 1997, pp. 281–292.
8 (*a*) T. Gimisis and C. Chatgilialoglu, *J. Org. Chem.*, 1996, **61**, 1908; (*b*) A. Kittaka, H. Tanaka, N. Yamada and T. Miyasaka, *Tetrahedron Lett.*, 1996, **37**, 2801.
9 M. P. Groziak, A. Koohang, W. C. Stevens and P. D. Robinson, *J. Org. Chem.*, 1993, **58**, 4054.
10 P. de Armas, C. G. Francisco and E. Suárez, *J. Am. Chem. Soc.*, 1993, **115**, 8865; R. L. Dorta, A. Martin, J. A. Salazar, E. Surárez and T. Prangé, *Tetrahedron Lett.*, 1996, **37**, 6021.
11 M. J. Robins and J. S. Wilson, *J. Am. Chem. Soc.*, 1981, **103**, 932.
12 C. Chatgilialoglu and C. Ferreri, *Res. Chem. Intermed.*, 1993, **19**, 755.
13 A. L. J. Beckwith and K. U. Ingold, in *Rearrangements in the Ground and Excited States Vol. 1*, ed. P. de Mayo, Academic, New York, 1980, pp. 161–310.

*Received in Glasgow, UK, 5th August 1997; 7/05742C*

# Reactions of 1,3,5-triazine with organolithium compounds yielding 1,4-dihydrotriazines or the ring-opened products, a 3-lithio-1,3,5,7-tetraazaheptatriene or -1,3,5-triazaheptatriene†

**Willem M. Boesveld, Peter B. Hitchcock and Michael F. Lappert***

*The Chemistry Laboratory, University of Sussex, Falmer, Brighton, UK BN1 9QJ*

**1,3,5-Triazine 1 reacts with the lithium alkyl LiR′ (R′ = $CHR_2$, $CH_2R$, Me, $Bu^n$ or Ph; R = $SiMe_3$) to give 1,4-adducts which on hydrolysis yield the first simple 1,4-dihydrotriazines; however, 1 with $LiNR_2$ or $LiCR_3(thf)_2$ gives the crystalline ring-opened 3-lithio-1,3,5,7-tetraazaheptatriene 5 or -1,3,5-triazaheptatriene 6 $[Li\{RNC(H)NC(H)NC(H)ER\}]_n$(μ-L) (E = N, *n* = 3 and L is absent 5, or E = CR, *n* = 2 and L = thf = tetrahydrofuran 6).**

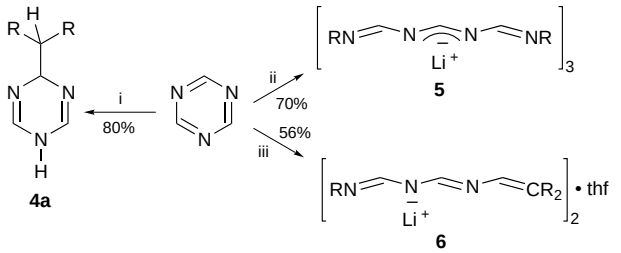
As part of our study of the reactions of nitriles free from α-hydrogen with organometallic reagents such as $LiCH(SiMe_3)_2$,[1] we now describe our initial findings with $(HCN)_3$, the 1,3,5-triazine **1**. The behaviour of **1** towards organometallic reagents is largely unexplored,[2] in contrast to its 2,4,6-triphenyl-derivative NC(Ph)NC(Ph)NC(Ph) **2**.[3] In rare cases **1** behaved as an HCN-synthon, but no intermediates were isolated.[4] For example, **1** with 2 $LiNR_2$ and subsequent treatment with RCl gave on sublimation the formamidine $RNC(H)NR_2$ (R = $SiMe_3$).[5]

We now report on the reactions of lithium hydrocarbyls or bis(trimethylsilyl)amide with **1**. Treatment of **1** in benzene with LiR′ (R′ = **a** $CHR_2$, **b** $CH_2R$, **c** Me, **d** $Bu^n$ or **e** Ph) at ambient temperature produced 1,4-adducts **1**·LiR′ **3a**–**e** which, because of their insolubility, were not adequately characterised, but presumably are analogues of 1-lithio-4-alkyltriphenyldihydrotriazines derived from **2**.[6] Hydrolysis of a diethyl ether slurry of each of the compounds **3a**–**e** with 1.1 equiv. of $H_2O$ and drying of the filtrate ($Na_2SO_4$) yielded the first 'simple' (*i.e.* monosubstituted) 1,4-dihydrotriazines, the colourless, crystalline **4a** (mp 104–106 °C) (or crystalline **4b** or the liquids **4c**–**e**), (Scheme 1, i). Such simple dihydrotriazines were hitherto believed merely to be transients[7] unlike the stable 1,4-dihydro adducts of **2** such as 1-*n*-butyl-2,4,6-triphenyl-1,4-dihydrotriazine.[3] Compound **4a**, possibly stabilised by the bulky $CH(SiMe_3)_2$-substituent (**4b** was markedly less robust), gave satisfactory microanalysis, $^1H$ and $^{13}C\{^1H\}$ NMR spectroscopic‡ and EI MS (parent molecular ion) data; the molecular structure of crystalline (boat-shaped) **4a** was also established by its X-ray structure (to be reported in the full paper). In $C_6D_5CD_3$ **4a** was in equilibrium with its 1,2-dihydro tautomer (*ca.* 50 : 1 at 295 K), a previously observed behaviour of substituted dihydrotriazines.[8]

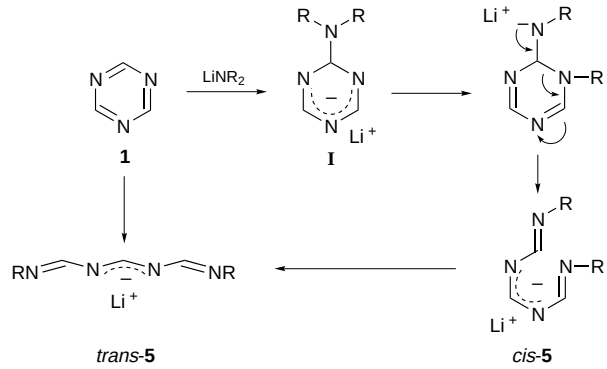
Reaction of **1** with $LiNR_2$ or $LiCR_3(thf)_2$ under similar conditions, however, took a different course: the triazine ring opened and, formally, an α → ω migration of an $Me_3Si$ group occurred; thus the 3-lithio-1,3,5,7-tetraazaheptatriene **5** or -1,3,5-triazaheptatriene **6** was obtained (Scheme 1, ii and iii). Compounds **5** and **6** were air- and moisture-sensitive both in the solid state and in solution and, in marked contrast to **3**, extremely soluble in hydrocarbons. Both have been characterised by microanalysis, $^1H$ and $^{13}C\{^1H\}$ NMR spectroscopy,‡ EI MS (parent molecular ion) and single-crystal X-ray analysis.

The pathway leading stereospecifically to the *trans*-product **5** or **6** is believed to implicate initially a 1,4-adduct analogous to **3**, followed successively by a 1,3-$Me_3Si$ shift from $NR_2$ or $CR_3$ and then its ring scission. This is illustrated for the system **1** + $LiNR_2$ → **5** in Scheme 2. Evidence for the Meisenheimer complex **I** (or its $CR_3$ analogue for **6**) is supported by NMR-scale experiments, which revealed intermediates having chemical shifts and coupling patterns resembling those of dihydrotriazine **4a**. Relevant precedents exist for anionic 1,3-$Me_3Si$ shifts from N → N[9] or C → N.[1] This migration might be stereoelectronically promoted, since for the case of **1** + $LiCHR_2$ the adduct **3a** was transformed into Li[RNC(H)NC(H)NC(H)CHR] **7** upon heating to 140 °C.

The X-ray molecular structure of crystalline **6** (Fig. 1) shows it to be dinuclear and lying on a crystallographic twofold rotation axis.§ The lithium atoms are bridged by a thf molecule, a rare phenomenon.[10] The atoms C(2), N(1), C(3), N(2), C(4) and N(3) are coplanar, largest deviation from least-squares plane is 0.048, and comparison of the bond lengths with known formamidinates[11,12] suggest that the NC(H)NC(H)N unit has some degree of delocalisation, while the values of 1.406 Å for N(1)–C(2) and 1.351 Å for C(2)–C(1) are unexceptional for a $N(sp^2)$–$C(sp^2)$ and $C(sp^2)$=$C(sp^2)$ bond, respectively.[13] The X-ray molecular structure of the crystalline, trinuclear compound **5** will be discussed in more detail in the full paper, but representative fragments of the molecular structures of **5** and **6**




**Scheme 1** *Reagents and conditions*: i, $LiCHR_2$, $Et_2O$, 4 h, −40 to *ca.* 20 °C, then 1.1 $H_2O$ and drying ($Na_2SO_4$); ii, $LiNR_2$, $C_6H_6$, 2 h, *ca.* 20 °C; iii, $LiCR_3(thf)_2$, $C_6H_6$, 2 d, *ca.* 20 °C




**Scheme 2** Proposed pathway for formation of **5**

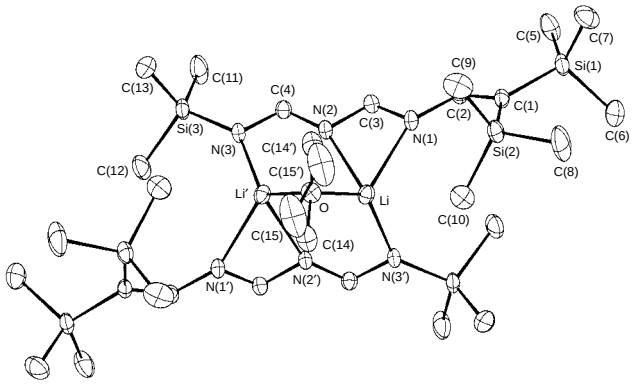
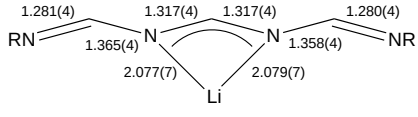
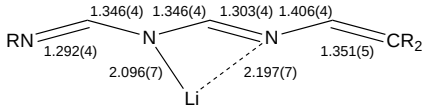



**Fig. 1** ORTEP representation of the molecular structure of **6**. Selected bond lengths (Å) and angles (°): Li–O 2.133(7), Li–N(1) 2.197(7), Li–N(2) 2.096(7), Li–N(3′) 2.058(7), C(1)–C(2) 1.351(5), C(2)–N(1) 1.406(4), N(1)–C(3) 1.303(4), C(3)–N(2) 1.346(4), N(2)–C(4) 1.346(4), C(4)–N(3) 1.292(4); N(2)–Li–N(1) 63.9(2), N(2)–Li–O 86.9(2), N(1)–Li–O 114.0(3), N(3′)–Li–O 129.4(3), N(3′)–Li–N(2) 125.4(3), N(3′)–Li–N(1) 115.3(3), Li′–O–Li 77.4(4), C(1)–C(2)–N(1) 124.6(4), N(1)–C(3)–N(2) 118.2(3), N(2)–C(4)–N(3) 120.5(3).




**5**




**6**

**Fig. 2** Bond lengths of selected fragments of the molecular structures of **5** and **6**

(Fig. 2) show that for **5**, unlike **6**, there is complete delocalisation of the central NC(H)N moiety with a bond length of *ca*. 1.32 Å.

On the basis of further exploratory experiments we consider that the results here reported have significant implications in that (*i*) compounds such as **4** upon hydrolysis in acidic or basic media are sources of aldehydes, (*ii*) compounds **5**–**7** are of interest as both sources of unusual tetra- or tri-azaheptatrienyl ligands and of nitrogen macrocycles.

We thank the European Community for a Human Capital and Mobility (category 20) grant for W. M. B. and EPSRC for other support.

## Footnotes and References

* E-mail: m.f.lappert@sussex.ac.uk

† No reprints available.

‡ *Selected NMR spectroscopic data* ($^1$H 300.13, $^{13}$C{$^1$H} 75.48, $^7$Li{$^1$H} 116.64 MHz, *ca*. 293 K, $C_6D_6$). **4a**: $^1$H: $\delta$ 6.23 (dd, $^3J$ 2.5, $^4J$ 2.3 Hz, 2 H, HCN), 5.01 [dt, $^3J$ 3.9 Hz, 1 H, NC(H)N], 4.74 (br s, 1 H, NH), 1.04 (d, 1 H, C*H*R$_2$), 0.38 (s, 18 H, 2 R). $^{13}$C{$^1$H}: $\delta$ 141 (HCN), 71 [NC(H)N], 25 (*C*R$_2$), 2 (2 R). **5**: $^1$H: $\delta$ 8.24 (s, 6 H), 7.85 (s, 3 H), 0.37 (s, 54 H, 6 NR). $^{13}$C{$^1$H}: $\delta$ 177.83, 170.48, 0.84. $^7$Li{$^1$H}: $\delta$ 5.18 (1 Li), 4.39 (2 Li) **6**: $^1$H: $\delta$ 8.20 (s, 2 H), 7.89 (br s, 2 H), 7.47 (s, 2 H), 3.59 (ddd, 4 H, thf), 1.41 (m, 4 H, thf), 0.36, (s, 18 H, *C*R), 0.34 (s, 18 H, *C*R), 0.17 (s, 18 H, NR). $^{13}$C{$^1$H}: $\delta$ 171.48, 169.95, 159.84, 121.7 (*C*R$_2$), 68.07, 25.65, 2.67, 1.18, 0.31. $^7$Li{$^1$H}: $\delta$ 3.85.

§ *Crystal data* for **5** and **6** [*T* 173 K: Enraf-Nonius CAD-4 diffractometer, $\lambda$(Mo-K$\alpha$) 0.710 73 Å, no crystal decay, direct methods, full-matrix least-squares refinement on $F^2$ (SHELXL-93) with non-hydrogen atoms anisotropic]. Hydrogens were included in riding mode with $U_{iso}$ = 1.2 $U_{eq}$ or 1.5 $U_{eq}$ for methyl groups. **5**: $C_{27}H_{63}Li_3N_{12}Si_6(C_5H_{12})_{\frac{1}{2}}$, $M$ = 781.3, monoclinic, space group $P2_1/n$ (non-standard no. 14), $a$ = 18.869(7), $b$ = 14.603(4), $c$ = 19.523(4) Å, $\beta$ = 112.10(2)°, $U$ = 4984(3) Å$^3$, $Z$ = 4, $D_c$ = 1.04 g cm$^{-3}$, $F$(000) = 1692, $\mu$(Mo-K$\alpha$) = 2.0 cm$^{-1}$, specimen 0.4 × 0.4 × 0.4 mm$^3$. 8753 unique reflections for 2 < $\theta$ < 25°, $R_1$ = 0.061 [for 5240 reflections with $I > 2\sigma(I)$], $wR_2$ = 0.132 (all data). **6**: $C_{30}H_{68}Li_2N_6OSi_6$, $M$ = 711.3, monoclinic, space group $P2/n$ (non-standard no. 13), $a$ = 13.022(3), $b$ = 8.134(4), $c$ = 22.607(6) Å, $\beta$ = 106.43(2)°, $U$ = 2296.8(14) Å$^3$, $Z$ = 2, $D_c$ = 1.03 g cm$^{-3}$, $F$(000) = 776, $\mu$(Mo-K$\alpha$) = 2.1 cm$^{-1}$, specimen 0.3 × 0.3 × 0.2 mm$^3$. 4041 unique reflections for 2 < $\theta$ < 25°, $R_1$ = 0.062 [for 2570 reflections with $I > 2\sigma(I)$], $wR_2$ = 0.162 (all data). CCDC 182/592.

1 M. F. Lappert and D.-S. Liu, *J. Organomet. Chem.*, 1995, **500**, 203.
2 Examples of 1,3,5-triazine in organic synthesis: C. Grundmann, *Angew. Chem., Int. Ed. Engl.*, 1963, **2**, 309; A. Kreutzberger, *Fortschr. Chem. Forsch.*, 1963, **4**, 273.
3 L. S. Cook, G. Prudhoe, N. D. Venayak and B. J. Wakefield, *J. Chem. Res.* (*S*), 1982, 113.
4 A. Kreutzberger, *Angew. Chem., Int. Ed. Engl.*, 1967, **6**, 940.
5 A. W. Cordes, C. D. Bryan, W. M. Davis, R. H. de Laat, S. H. Glarum, J. D. Goddard, R. C. Haddon, R. G. Hicks, D. K. Kennepohl, R. T. Oakley, S. R. Scott and N. P. C. Westwood, *J. Am. Chem. Soc.*, 1993, **115**, 7232.
6 D. R. Armstrong, K. W. Henderson, M. MacGregor, R. E. Mulvey, M. J. Ross, W. Clegg and P. A. O'Neil, *J. Organomet. Chem.*, 1995, **486**, 79.
7 A. L. Weis, *Adv. Heterocycl. Chem.*, 1985, **38**, 1; *cf*. p. 91.
8 K. Maeda, N. Kihara and N. Ishimura, *J. Chem. Soc., Perkin Trans. 2*, 1985, 887.
9 R. T. Boeré, R. T. Oakley and R. W. Reed, *J. Organomet. Chem.*, 1987, **331**, 161; M. Wedler, F. Knösel, M. Noltemeyer and F. T. Edelmann, *J. Organomet. Chem.*, 1990, **388**, 21.
10 Selected examples of μ-thf in lithium chemistry: G. Boche, C. Boie, F. Bosold, K. Harms and M. Marsch, *Angew. Chem., Int. Ed. Engl.*, 1994, **33**, 115; W. Clegg, L. Horsburgh, F. M. Mackenzie and R. E. Mulvey, *J. Chem. Soc., Chem. Commun.*, 1995, 2011.
11 J. Barker and M. Kilner, *Coord. Chem. Rev.*, 1994, **133**, 219.
12 Recent examples: F. A. Cotton, J. H. Matonic and C. A. Murillo, *Inorg. Chem.*, 1996, **35**, 498; F. A. Cotton, S. C. Haefner, J. H. Matonic, X. Wang and C. A. Murillo, *Polyhedron*, 1997, **16**, 541.
13 M. Burke-Laing and M. Laing, *Acta Crystallogr., Sect. B*, 1976, **32**, 3216.

*Received in Basel, Switzerland, 23rd April 1997; 7/02792C*

# Palladium-induced rearrangement of a $Fe_2Sn_2$ metal core leading to the first Fe–Pd–Sn cluster $[(OC)_3Fe(\mu\text{-}SnBu^n_2)(\mu\text{-}dppm)Pd(\mu\text{-}dppm)Fe(CO)_3]$†

**Pierre Braunstein,*[a] Chantal Charles,[a] Guido Kickelbick[b] and Ulrich Schubert[b]**

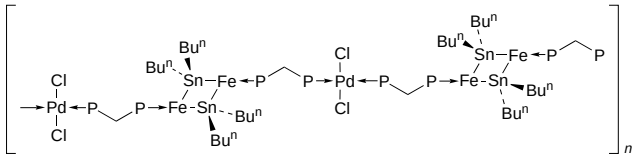
[a] *Laboratoire de Chimie de Coordination, URA 416 CNRS, Université Louis Pasteur, 4 rue Blaise Pascal, F-67070 Strasbourg Cedex, France*

[b] *Institut für Anorganische Chemie, Technische Universität Wien, Getreidemarkt 9/153, A-1060 Wien, Austria*

**A new tetranuclear FePdFeSn four-membered ring cluster, which could be viewed as a bent chain complex FePdFe bridged by a stannylene ligand, is obtained from a $Fe_2Sn_2$ precursor by $Ph_2PCH_2PPh_2$ (dppm)-assisted palladium incorporation; it provides the first example of a Sn–Fe–Pd linkage.**

Molecules which associate transition metals with group 14 elements currently enjoy increased attention because they provide opportunities for the formation of unusual structures and new bonds between transition metals and main-group elements, they are used as single-source precursors for new materials and display interesting catalytic properties.[1]

We have recently reported the synthesis of $[Fe(CO)_3(\eta^1\text{-dppm})(SnBu^n_2)]_2$ **1** (dppm = $Ph_2PCH_2PPh_2$) from $K[Fe(CO)_3\{Si(OMe)_3\}(\eta^1\text{-dppm})]$ and $[Sn(OAc)_2Bu^n_2]$ where a silicon/tin exchange reaction has taken place.[2] The silyl ligand may be considered as a protecting group for the unknown dianion $[Fe(CO)_3(\eta^1\text{-dppm})]^{2-}$.[3] Since the uncoordinated phosphorus lone pair in **1** can be used for further metal complexation,[2] we considered using a palladium educt with two labile ligands which could lead to an inorganic cyclic or a linear polymer.



Addition of 1 equiv. of $[PdCl_2(SEt_2)_2]$ to the solution of **1** in $CH_2Cl_2$ at −40 °C, gave after 2 h a dark-red solution which was filtered at −30 °C and yielded a bright-red powder which should be kept below −30 °C.‡ Its IR spectrum [$\nu$(CO) region] is similar to that found for **1**. However two main products, in approximately 1 : 1 ratio, were detected by $^{31}P\{^1H\}$ NMR and have very similar data. The former is characterized by two doublets at $\delta$ 58.0 and 35.3 with $^2J$(PP) 70.5 Hz and the latter by two other doublets at $\delta$ 56.7 and 34.7 with $^2J$(PP) 69.1 Hz. Further stirring of this red solution for 2 h at −30 °C did not result in any change and there was no evolution from one product to the other. However, if the reaction mixture is left standing in $CH_2Cl_2$ at room temp. for 2 d, $^{31}P\{^1H\}$ NMR monitoring shows the progressive formation of two new products and the disappearance of those described above. After one week, the solution became bright-green and contained only the two new products. Product **2** is characterized by a pair of doublets at $\delta$ 64.2 and 28.8 with $^2J$(PP) 107.2 Hz, and product **3** by a pair of triplets centered at $\delta$ 63.1 and 21.7 with $^2J$(PP) 99.8 Hz. Very dark single crystals of **2** were obtained by fractional crystallisation (slow diffusion of hexane into a concentrated solution in $CH_2Cl_2$) and their structure was determined by X-ray diffraction (Fig. 1).§

This rhombus-like molecule provides the first structure of a SnFePd ring. The Pd, two Fe and four P atoms are nearly coplanar and the four membered ring $PdFe_2Sn$ is folded by 9.97(9)° along the Fe–Fe axis. The sum of the angles around the Pd atom is exactly 360°, *i.e.* the coordination sphere around this atom is perfectly planar. The Fe(1)–Pd–Fe(2) angle is 93.51(8)° whereas the opposite Fe(1)–Sn–Fe(2) angle of 106.89(8)° reflects the nearly tetrahedral arrangement around the Sn atom. The coordination sphere around the Fe atoms is distorted octahedral.[1l,n,4] The Fe–Sn distances are 2.517(3) and 2.520(3) Å and are smaller than those found in **1** [2.6736(9) and 2.645(1) Å]. The Fe–Pd distances [2.763(3), 2.791(3) Å] are longer than those found in related dppm bridged complexes such as $[Fe(CO)_3\{\mu\text{-}Si(OMe)_2(OMe)\}(\mu\text{-dppm})PdCl]$ [2.582(1) Å] or $[Fe(CO)_3\{Si(OMe)_3\}(\mu\text{-dppm})Pd(\eta^3\text{-}C_3H_4Me\text{-}2)]$ [2.6994(7) Å] or $[Fe(CO)_3\{Si(OMe)_2(OMe)\}(\mu\text{-dppm})Pd(SnPh_3)]$ [2.6655(5) Å].[5] Neither the Pd–Sn (3.389(2) Å) nor the Fe(1)–Fe(2) distances [4.046(3) Å] indicate a metal–metal interaction across the ring.

During attempts to optimize the yield of **2**, we have reacted a solution of **1** with 1 equiv. of $[PdCl_2(SEt_2)_2]$ in refluxing

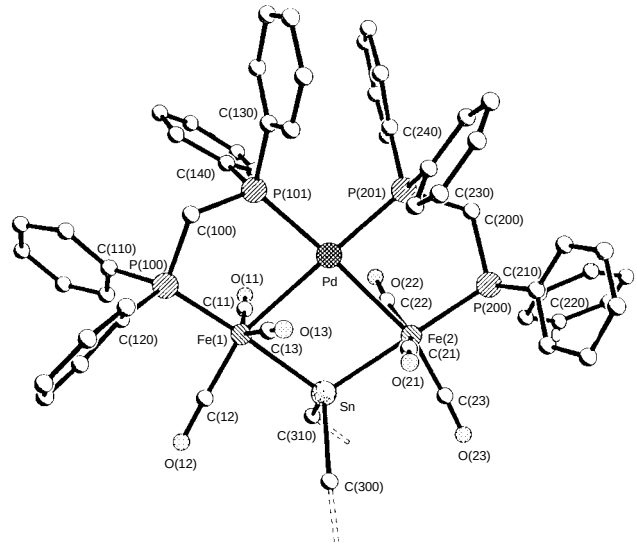
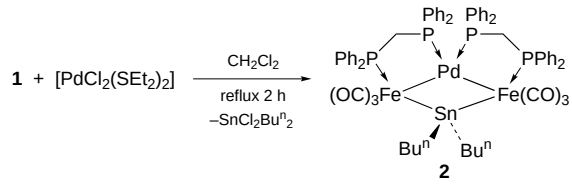


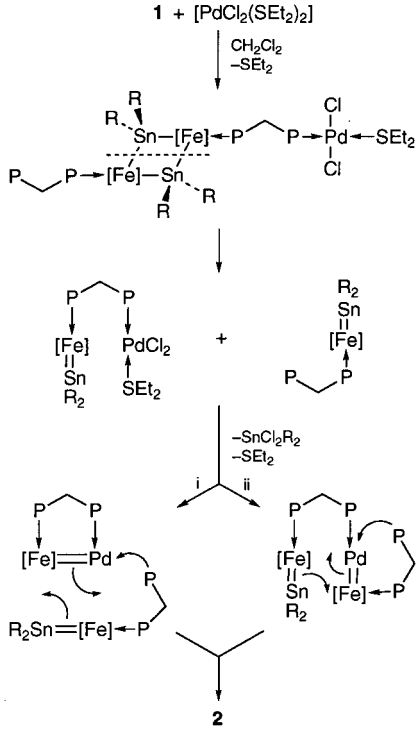

**Fig. 1** View of the structure of **2**. The dotted lines at C(300) and C(310) indicate the disorder of the butyl groups. Selected bond distances (Å) and angles (°): Pd–Fe(1) 2.763(3), Pd–Fe(2) 2.791(3), Sn–Fe(1) 2.520(3), Sn–Fe(2) 2.517(3), Pd–P(101) 2.347(4), Pd–P(201) 2.325(4), Sn–C(300) 2.421(12), Sn–C(310) 2.31(2), Fe(1)–C(11) 1.79(2), Fe(1)–C(12) 1.74(2), Fe(1)–C(13) 1.79(2), Fe(1)–P(100) 2.210(5), Fe(2)–C(21) 1.76(2), Fe(2)–C(22) 1.78(2), Fe(2)–C(23) 1.76(2), Fe(2)–P(200) 2.201(5); Fe(1)–Pd–Fe(2) 93.51(8), Fe(1)–Sn–Fe(2) 106.89(8), Sn–Fe(1)–Pd 79.69(7), Sn–Fe(2)–Pd 79.20(7), P(201)–Pd–P(101) 97.1(2), P(101)–Pd–Fe(1) 83.52(12), P(201)–Pd–Fe(2) 85.91(11), C(300)–Sn–C(310) 106.9(8), C(13)–Fe(1)–C(11) 147.6(8), C(21)–Fe(2)–C(22) 149.7(8).




**Scheme 1**

$CH_2Cl_2$ for 2 h. The solution became green and a dark-green powder of **2** was isolated in 51% yield (Scheme 1).

The first step of this unusual reaction is likely to be palladium coordination to a phosphorus lone pair of **1** (Scheme 2). The subsequent steps can only be speculative at this stage. Fragmentation of the $Fe_2Sn_2$ ring would occur and it is conceivable that replacement of one 'Fe=$SnR_2$' unit with an isolobal 'Fe=PdLL' moiety with elimination of $SnCl_2Bu^n_2$ would be followed by combination of this moiety with the remaining equivalent iron–stannylene.




**Scheme 2** Tentative pathways to the formation of **2**. Alternatives i and ii correspond to formal intra- or inter-molecular elimination of $SnCl_2R_2$. R = $Bu^n$; [Fe] = $Fe(CO)_3$.

During attempts to extend the formation of this complex to other metal centers we have found that reaction of **1** with $[PtCl_2(NCPh)_2]$ under similar conditions ($CH_2Cl_2$, 2 h, reflux) appears less selective but yields a product **4** similar to **2** on the basis of spectroscopic data.‡

We are grateful to the Ministère de l'Enseignement Supérieur et de la Recherche for a PhD Grant for C. C., the CNRS, the Ministère des Affaires Etrangères (Paris) (Amadeus 1996) and the Commission of the European Communities (contract ERBCHRXCT93 277) for financial support.

## Footnotes and References

* E-mail: braunst@chimie.u-strasbg.fr

† Dedicated to Professor Pascual Royo (Universidad de Alcala) on the occasion of his 60th birthday.

‡ All reactions were performed under purified nitrogen, using carefully dried solvents.

*Syntheses*: $[(OC)_3\overline{Fe(\mu\text{-}SnBu^n_2)(\mu\text{-}dppm)Pd}(\mu\text{-}dppm)Fe(CO)_3]$ **2**: to a solution of **1** in $CH_2Cl_2$ (0.258 g, 0.17 mmol) was added $[PdCl_2(SEt_2)_2]$ (0.061 g, 0.17 mmol). The solution was refluxed for 2 h, then filtered and concentrated. Yield: 51%. IR ($CH_2Cl_2$) $\nu$(C≡O) 1980m, 1949m, 1918vs $cm^{-1}$; (KBr) 1959m, 1925s, 1895vs, 1884vs $cm^{-1}$. NMR $^1H$ ($CD_2Cl_2$): $\delta$ 0.88 (t, 3 H, $CH_2CH_3$), 0.98 (t, 3 H, $CH_2CH_3$), 1.20–2.05 (m, 12 H, $CH_2$), 3.56 [t, 2 H, $PCH_2P$, $^2J$(PH) 9.48 Hz], 3.57 [t, 2 H, $PCH_2P$, $^2J$(PH) 9.56 Hz], 6.79–7.40 (m, 40 H, Ph). NMR $^{31}P\{^1H\}$ ($CD_2Cl_2$): $\delta$ 64.2 [d, P(Fe), $^2J$(PP) 107.2, $^2J(P^{117,119}Sn)$ 212.9 Hz], 28.8 [d, P(Pd), $^2J$(PP) 107.3 Hz].

$[(OC)_3\overline{Fe(\mu\text{-}SnBu^n_2)(\mu\text{-}dppm)Pt}(\mu\text{-}dppm)Fe(CO)_3]$ **4**: to a solution of **1** in $CH_2Cl_2$ (0.300 g, 0.20 mmol) was added $[PtCl_2(NCPh)_2]$ (0.095 g, 0.20 mmol). The solution was refluxed for 2 h, then filtered and concentrated. The brown powder was precipitated by addition of hexane. Yield: 55%. IR ($CH_2Cl_2$) $\nu$(C≡O) 1990w, 1955m, 1920s $cm^{-1}$. NMR $^{31}P\{^1H\}$ ($CD_2Cl_2$): $\delta$ 77.5 [d, P(Fe), $^2J$(PP) 49.3 Hz], 20.5 [d, P(Pd), $^2J$(PP) 49.3 Hz].

§ *Crystal data* for **2**. Dark red crystals (0.4 × 0.3 × 0.2 mm) were mounted on a Siemens SMART CCD area detector diffractometer. Mo-K$\alpha$ radiation ($\lambda$ = 0.710 73 Å, graphite monochromated). Monoclinic, space group $P2_1/n$, $a$ = 17.5349(7), $b$ = 18.6137(7), $c$ = 17.8860(7) Å, $\beta$ = 90.781(1)°, $U$ = 5837.3(4) $Å^3$, $Z$ = 4, $D_c$ = 1.797 g $cm^{-3}$. The cell dimensions were refined with all unique reflections. The data collection at 303(2) K covered a hemisphere of the reciprocal space, by a combination of three sets of exposures. Each set had a different $\phi$ angle for the crystal and each exposure took 20 s and covered 0.3° in $\omega$. The collected data range was $1.58 \leqslant \theta \leqslant 23.00°$ ($-25 \leqslant h \leqslant 24$, $-22 \leqslant k \leqslant 26$, $-16 \leqslant l \leqslant 25$) with a crystal-to-detector distance of 5.85 cm. 27 071 reflections were collected, and 8134 unique reflections ($R_{int}$ = 0.136) were obtained after correction of polarization and Lorentz effects ($\mu$ = 2.09 $mm^{-1}$). An empirical absorption correction with the program SADABS was carried out.[5] The structure was solved by direct methods (SHELXS86). Refinement was performed by the full-matrix least-squares method based on $F^2$ (SHELXL93). All non-hydrogen atoms were refined with anisotropic thermal parameters with exception of the $Bu^n$ carbon atoms. The hydrogen atoms were added in idealized positions and were refined with a riding model. We were not able to refine the two $Bu^n$ groups due to their strong disorder. Only the anchor C atoms were found and were refined isotropically. The positions C(2)–C(4) were totally smeared over the whole cone angle opened by the vector originating in the Sn atom. Various routines and ways of modelling the disorder of the Bu groups were attempted without success. There was neither convergence of the refinements nor an improvement of the $R$ factors. The missing $Bu^n$ groups cause the relatively high $R$ values [$R$ = 0.103, $R_w$ = 0.28 for 5265 reflections with $I \geqslant 2.0\,\sigma(I)$; $w = 1/[\sigma^2(F_o^2) + (0.1437\,P)^2 + 118.83\,P]$ [$P = (F_o^2 + 2\,F_c^2)/3$]. The largest residual electron density was 2.486 e $Å^{-3}$. CCDC 182/588.

1 (*a*) G. W. Parshall, *J. Am. Chem. Soc.*, 1966, **88**, 704; (*b*) R. Kummer and W. A. G. Graham, *Inorg. Chem.*, 1968, **7**, 1208; (*c*) J. A. Zubieta and J. J. Zuckerman, *Prog. Inorg. Chem.*, 1978, **24**, 251; (*d*) E. Colomer and R. J. P. Corriu, *Top. Curr. Chem.*, 1981, **96**, 79; (*e*) H. Natatsuji, J. Ushio and T. Yonezawa, *J. Organomet. Chem.*, 1983, **258**, C1; (*f*) W. Petz, *Chem. Rev.*, 1986, **86**, 1019; (*g*) J. K. Stille, *Angew. Chem., Int. Ed. Engl.*, 1986, **25**, 508; (*h*) M. S. Holt, W. L. Wilson and J. H. Nelson, *Chem. Rev.*, 1989, **89**, 11; (*i*) N. A. Compton, R. J. Errington and N. C. Norman, *Adv. Organomet. Chem.*, 1990, **31**, 91; (*j*) K. C. Molloy, *Adv. Organomet. Chem.*, 1991, **33**, 171; (*k*) P. Braunstein, M. Knorr, H. Piana and U. Schubert, *Organometallics*, 1991, **10**, 828; (*l*) P. Braunstein, M. Knorr, M. Strampfer, M. Lanfranchi and A. Tiripicchio, *Organometallic*, 1994, **13**, 3038; (*m*) P. Braunstein, X. Morise and J. Blin, *J. Chem. Soc., Chem. Commun.*, 1995, 1455; (*n*) P. Braunstein, C. Charles, A. Tiripicchio and F. Ugozzoli, *J. Chem. Soc., Dalton Trans.*, 1996, 4365; (*o*) P. Braunstein, V. Huch, C. Stern and M. Veith, *Chem. Commun.*, 1996, 2041; (*p*) M. Veith, A. Müller, L. Stahl, M. Nötzel, M. Jarczyk and V. Huch, *Inorg. Chem.*, 1996, **35**, 3848; (*q*) M. Veith, C. Mathur and V. Huch, *J. Chem. Soc., Dalton Trans.*, 1997, 995.

2 P. Braunstein, C. Charles, R. D. Adams and R. Layland, *J. Cluster Sci.*, 1996, **7**, 145.

3 U. Schubert, U. Kirchgäßner, J. Grönen and H. Piana, *Polyhedron*, 1989, **8**, 1589; P. Braunstein, M. Knorr, M. Strampfer, A. DeCian and J. Fischer, *J. Chem. Soc., Dalton Trans.*, 1994, 117.

4 P. Braunstein, M. Knorr, A. Tiripicchio and M. Tiripicchio-Camellini, *Angew. Chem., Int. Ed. Engl.*, 1989, **28**, 1361; M. Knorr, P. Braunstein, A. Tiripicchio and F. Ugozzoli, *Organometallics*, 1995, **14**, 4910.

5 SADABS, Program for empirical absorption correction for Siemens area detectors, G. M. Sheldrick, University of Göttingen, 1996.

*Received in Cambridge, UK, 14th July 1997; 7/05019D*

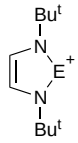
# Cyclic phosphenium and arsenium cations with 6π electrons and related systems

**Claire J. Carmalt, Viviana Lomeli, Brian G. McBurnett and Alan H. Cowley***

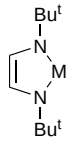
*Department of Chemistry and Biochemistry, The University of Texas at Austin, Austin, Texas 78712, USA*

**Cyclic phosphenium (1a) and arsenium (1b) cations are formed either by treatment of germylene 2b with $ECl_3$ (E = P, As) or *via* the metathetical reaction of LiN(Bu$^t$)C=CN(Bu$^t$)Li with $ECl_3$ and the structures of 1a and 1b are compared with those of pertinent saturated analogues.**

Cyclic phosphenium (**1a**) and arsenium (**1b**) cations are isoelectronic with the corresponding silylenes **2a**[1] and germylenes **2b**.[2] As such, they raise interesting questions concerning



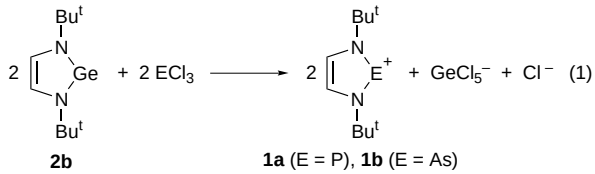
**1a** (E = P), **1b** (E = As)



**2a** (M = Si), **2b** (M = Ge)

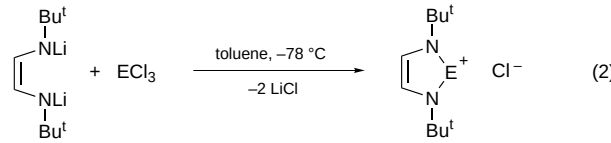
circumannular delocalisation since, in principle, **1a**,**b** and **2a**,**b** possess six π electrons. Given that the group 15 systems bear a formal positive charge at the phosphorus or arsenic centre, it might be expected that these species would exhibit more extensive delocalisation than their neutral group 14 counterparts. (For a similar argument for nitrenium ions *vis-à-vis* carbenes, see ref. 3). A cyclic phosphenium ion with the same skeleton as **1a** was structurally characterised several years ago;[4] however, this cation features a 2-chloro substituent thus potentially complicating interpretations of bonding. More recently, **1a** has been synthesised and identified spectroscopically.[5] We report the following new developments in this field: (*i*) a novel synthetic route to **1a** and **1b** based on the redox reactions of **2b** with $ECl_3$ (E = P, As); (*ii*) X-ray crystallographic data for **1a** and **1b** and (*iii*) syntheses and X-ray crystallographic data for pertinent saturated analogues of **1a** and **1b**.

The reaction of **2b** with $PCl_3$ or $AsCl_3$ takes place under mild conditions and affords moderate yields of the corresponding phosphenium or arsenium ions [eqn. (1)].† The reaction



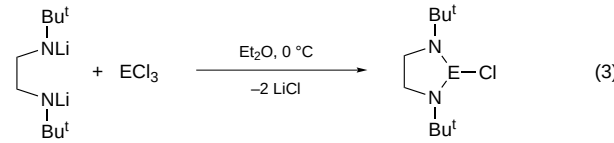
**2b** **1a** (E = P), **1b** (E = As)

mechanism has not been elucidated; however, it is clear that germanium is oxidised from the +2 to the +4 state and that **1a** and **1b** crystallise with equimolar quantities of $GeCl_5^-$ and $Cl^-$ anions. A noteworthy feature of **1b** is that it is monomeric in contrast to the previously reported cyclic arsenium cation, $MeNCH_2CH_2N(Me)As^+$, which is dimeric.[6,7] Since it was not obvious from the foregoing whether autoionisation of the E–Cl bonds of the products would occur, we sought a system free of chloride ion acceptors. It was found that the metathetical reactions summarised in eqn. (2) proceed in good yields.†



**1a** (E = P), **1b** (E = As)

Analogous metathetical reactions were employed for the synthesis of the related saturated systems [eqn. (3)].



**3a** (E = P), **3b** (E = As)

The structures of **1a**,**b** (Fig. 1) and **3a**,**b** (Fig. 2) have been determined by X-ray crystallography.‡ Autoionisation is observed in the case of **1a**. While shorter than the van der Waals radii, the P···Cl separation in **1a** [2.715(2) Å] is nevertheless considerably longer than those of typical covalent P–Cl bonds *e.g.* $PCl_3$ 2.043 Å, mes*NPCl 2.142(4) Å.[9] Anion–cation interactions which are less than the sum of the van der Waals radii are common for non-metals and certain phosphenium salts.[10] It has been observed previously that such anion–cation interactions have little or no effect on the structural features within the cation or anion.[11] Indeed, the structural features of **1a** derived from either the germanium exchange or metathetical route are identical within experimental error. Interestingly, the P–Cl distance in the corresponding C–C saturated analogue, **3a** [2.425(4) Å] is also longer than that of typical P–Cl bonds but shorter than that in **1a** thus implying that this compound is partway along the P–Cl heterolysis pathway. There is therefore an interesting parallel with carbene chemistry in the sense that the unsaturated imidazol-2-ylidenes (Arduengo type)[12] are more stable than the C–C saturated imidazol-2-ylidenes (Wanzlick type).[13] The case of the analogous arsenic system is not as clear because we have only been successful in isolating X-ray quality crystals of the mixed anion species, $[\mathbf{1b}]_2[GeCl_5]Cl$.

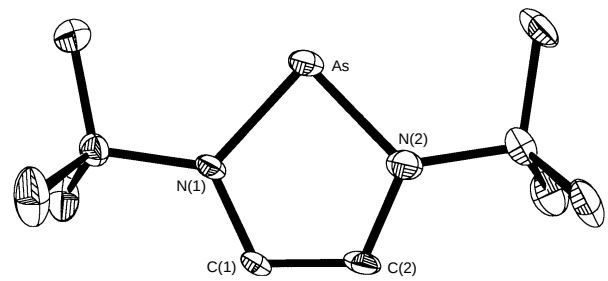



**Fig. 1** Molecular structure of **1b** showing the atom numbering scheme. Selected distances (Å) and angles (°) for **1b** (corresponding values for **1a** shown in parentheses): As–N(1) 1.810(9) [P–N(1) 1.650(4)], As–N(2) 1.812(9) [P–N(2) 1.651(4)], N(1)–C(1) 1.38(1) [1.370(6)], N(2)–C(2) 1.38(2) [1.383(6)], C(1)–C(2) 1.36(2) [1.330(6)], N(1)–As–N(2) 86.2(4) [N(1)–P–N(2) 90.4(2)].

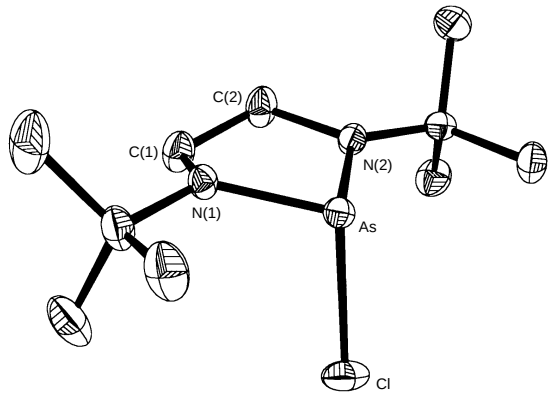
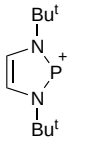
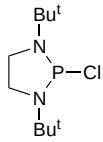
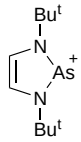
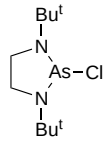



**Fig. 2** Molecular structure of **3b** showing the atom numbering scheme. Selected distances (Å) and angles (°) for **3b** (corresponding values for **3a** shown in parentheses): As–N(1) 1.773(6) [P–N(1) 1.629(9)], As–N(2) 1.789(6) [P–N(2) 1.645(9)], As–Cl 2.375(2) [P–Cl 1.425(4)], N(1)–C(1) 1.468(9) [1.41(1)], N(2)–C(2) 1.464(9) [1.43(1)], C(1)–C(2) 1.44(1) [1.43(1)], N(1)–As–N(2) 88.7(3) [N(1)–P–N(2) 90.6(5)], N(1)–As–Cl 103.7(2) [N(1)–P–Cl 103.1(4)], N(2)–As–Cl 101.8(2) [N(1)–P–Cl 101.9(3)].

However, it is interesting to note that the C–C saturated chloride, **3b**, also possesses an elongated As–Cl bond with a bond length of 2.375(2) Å, a feature which is also observed in the related compounds, MeNCH$_2$CH$_2$N(Me)AsCl [2.390(5) Å] and MeN(CH$_2$)$_3$N(Me)AsCl [2.357(2) Å].[8]

The metrical parameters for **1a**,**b** and the C–C saturated analogues **3a**,**b** (Table 1) are pertinent to the question of electron delocalisation in these systems. One of the first points to note is that the P–N bond distance in **1a** is longer than that in the acyclic phosphenium cation, [P(NPr$^i_2$)$_2$]$^+$ [av. 1.613(4) Å].[14] Moreover, the P–N and As–N bond lengths in **1a,b** are longer than those in the corresponding saturated derivatives **3a,b,** and the C–C bond lengths in **1a** and **1b** correspond to localised double bonds. The EN$_2$C$_2$ rings of **1a** and **1b** are planar within experimental error, as are the geometries at the nitrogen centres. However, it is interesting that the PN$_2$C$_2$ ring of **3a** is planar whilst the AsN$_2$C$_2$ ring of **3b** is not. Thus, in contrast to the view[5] that **1a** 'possesses aromatic 6π-stabilisation,' the foregoing metrical parameters indicate that the cyclic phosphenium and arsenium cations **1a** and **1b** possess relatively localised electronic structures.

**Table 1** Metrical parameters for compounds **1a**,**b** and **3a**,**b**

| |  **1a** |  **3a** |  **1b** |  **3b** |
|---|---|---|---|---|
| E–N(av.)/Å | 1.651(4) | 1.637(9) | 1.812(9) | 1.781(6) |
| N–CH(av.)/Å | 1.376(6) | 1.42(1) | 1.38(2) | 1.466(9) |
| C–C/Å | 1.330(6) | 1.43(1) | 1.36(2) | 1.44(1) |
| N–E–N/° | 90.4(2) | 90.6(5) | 86.2(4) | 88.7(3) |

## Footnotes and References

* E-mail: cowley@mail.utexas.edu

† *Experimental procedures*: the experimental procedures outlined below relate to the preparations of **1a** and **3a**; however, similar methods were employed for the preparations of **1b** and **3b**.

[**1a**]$_2$[GeCl$_5$]Cl: a solution of PCl$_3$ (0.433 g, 3.16 mmol) in thf (20 cm$^3$) was added dropwise to a stirred solution of **2b** (0.76 g, 3.16 mmol) in thf (30 cm$^3$) resulting in the formation of an orange coloured solution and precipitate. The reaction mixture was stirred overnight and then filtered through Celite resulting in a dark orange solution which was reduced *in vacuo* to a volume of approximately 20 cm$^3$. Cooling of this solution to −20 °C overnight afforded a 40% yield of orange, crystalline [**1b**]$_2$[GeCl$_5$]Cl.

[**1a**]Cl: a toluene solution (40 cm$^3$) of LiN(Bu$^t$)C=CN(Bu$^t$)Li (2.09 g, 11.47 mmol) was added dropwise to a solution of PCl$_3$ (1 cm$^3$, 11.47 mmol) in toluene (20 cm$^3$) at −78 °C. The reaction mixture was stirred overnight with slow warming to room temp. After filtering through Celite, the volume of the filtrate was reduced to 20 cm$^3$ and cooling of the solution to −20 °C afforded a 55% yield of orange crystalline [**1a**]Cl.

Further experimental details can be obtained as supplementary material upon request from the authors.

‡ *Crystal data*: [**1a**]$_2$[GeCl$_5$]Cl: $C_{20}H_{40}Cl_6GeN_4P_2$, $M$ = 683.79, monoclinic, space group $P2_1/c$, $a$ = 10.445(2), $b$ = 17.059(2), $c$ = 19.846(3) Å, $\beta$ = 93.35(2)°, $U$ = 3530(1) Å$^3$, $Z$ = 4, $D_c$ = 1.287 g cm$^{-3}$, $T$ = 298(2) K, $\mu$ = 1.428 mm$^{-1}$. $wR_2$ = 0.2347 (6187 independent reflections), $R$ = 0.0995 [$I > 2\sigma(I)$].

[**1b**]$_2$[GeCl$_5$]Cl: $C_{20}H_{40}As_2Cl_6GeN_4$, $M$ = 771.69, monoclinic, space group $P2_1/c$, $a$ = 10.567(4), $b$ = 16.954(5), $c$ = 19.675(7) Å, $\beta$ = 93.02(2)°, $U$ = 3520(2) Å$^3$, $Z$ = 4, $D_c$ = 1.456 g cm$^{-3}$, $T$ = 183(2) K, $\mu$ = 3.207 mm$^{-1}$. $wR_2$ = 0.2433 (4364 independent reflections), $R$ = 0.0765 [$I > 2\sigma(I)$].

[**1a**]Cl·0.5C$_7$H$_8$: $C_{13.5}H_{24}ClN_2P$, $M$ = 280.77, monoclinic, space group $C2/c$, $a$ = 20.535(4), $b$ = 11.356(4), $c$ = 13.939(4) Å, $\beta$ = 97.30(2)°, $U$ = 3224(2) Å$^3$, $Z$ = 8, $D_c$ = 1.157 g cm$^{-3}$, $T$ = 298(2) K, $\mu$ = 0.322 mm$^{-1}$. $wR_2$ = 0.2320 (2835 independent reflections), $R$ = 0.0686 [$I > 2\sigma(I)$].

**3a**: $C_{10}H_{22}ClN_2P$, $M$ = 236.72, orthorhombic, space group *Pbca*, $a$ = 11.978(2), $b$ = 11.439(3), $c$ = 19.533(3) Å, $U$ = 2676.4(8) Å$^3$, $Z$ = 8, $D_c$ = 1.175 g cm$^{-3}$, $T$ = 298(2) K, $\mu$ = 0.375 mm$^{-1}$. $wR_2$ = 0.1603 (2348 independent reflections), $R$ = 0.0883 [$I > 2\sigma(I)$].

**3b**: $C_{10}H_{22}AsClN_2$, $M$ = 280.67, orthorhombic, space group *Pbca*, $a$ = 12.140(1), $b$ = 11.405(1), $c$ = 19.907(3) Å, $U$ = 2756.3(6) Å$^3$, $Z$ = 8, $D_c$ = 1.353 g cm$^{-3}$, $T$ = 298(2) K, $\mu$ = 2.631 mm$^{-1}$. $wR_2$ = 0.1275 (2419 independent reflections), $R$ = 0.0529 [$I > 2\sigma(I)$]. CCDC 182/645.

1 M. Denk, R. Lennon, R. Hayashi, R. West, A. V. Belyakov, H. P. Verne, A. Haaland, M. Wagner and N. Metzler, *J. Am. Chem. Soc.*, 1994, **116**, 2691.
2 W. A. Herrmann, M. Denk, J. Behm, W. Scherer, F.-R. Klingan, H. Bock, M. Soluki and M. Wagner, *Angew. Chem., Int. Ed. Engl.*, 1992, **31**, 1485.
3 G. Boche, P. Andrews, K. Harms, M. Marsch, K. S. Rangappa, M. Schimeczek and C. Willeke, *J. Am. Chem. Soc.*, 1996, **118**, 4925.
4 A. M. Kibardin, I. A. Litvinov, V. A. Naumov, Yu. T. Struchkov, T. V. Gryaznova, Yu. B. Mikhailov and A. N. Pudovik, *Dokl. Akad. Nauk SSSR*, 1988, **298**, 369; Ya. M. Paushkin, Yu. M. Zhorov, A. L. Lapidus and E. G. Gorlov, *Dokl. Akac. Nauk SSSR*, 1988, **298**, 374.
5 M. K. Denk, S. Gupta and R. Ramachandran, *Tetrahedron Lett.*, 1996, **37**, 9025.
6 N. Burford, T. M. Parks, B. W. Royan, B. Borecka, T. S. Cameron, J. F. Richardson, E. J. Gabe and R. Haynes, *J. Am. Chem. Soc.*, 1992, **114**, 8147.
7 Interestingly however, the six-membered cyclic arsenium cation, MeN(CH$_2$)$_3$N(Me)As$^+$, is monomeric thus implying that the association between monomers is weak in the five-membered ring system.[8]
8 N. Burford, C. L. B. Macdonald, T. M. Parks, G. Wu, B. Borecka, W. Kwiatkowski and T. S. Cameron, *Can. J. Chem.*, 1996, **74**, 2209.
9 N. Burford, P. Losier, C. Macdonald, V. Kyrimis, P. K. Bakshi and T. S. Cameron, *Inorg. Chem.*, 1994, **33**, 1434 and references therein.
10 E. Niecke, M. Nieger and F. Reichert, *Angew. Chem., Int. Ed. Engl.*, 1988, **27**, 1715.
11 N. Burford, S. Mason, R. E. v H. Spence, J. M. Whalen, J. F. Richardson, and R. D. Rogers, *Organometallics*, 1992, **11**, 2241.
12 A. J. Arduengo, III, R. L. Harlow and M. Kline, *J. Am. Chem. Soc.*, 1991, **113**, 361; A. J. Arduengo, III, H. V. Rasika Dias, R. L. Harlow and M. Kline, *J. Am. Chem. Soc.*, 1992, **114**, 5530.
13 H.-W. Wanzlick and E. Schikora, *Angew. Chem.*, 1960, **72**, 494; H.-W. Wanzlick, *Angew. Chem.*, 1962, **74**, 129.
14 A. H. Cowley, M. C. Cushner and J. S. Szobota, *J. Am. Chem. Soc.*, 1978, **100**, 7784.

*Received in Bloomington, IN, USA; 8th July 1997; 7/04838F*

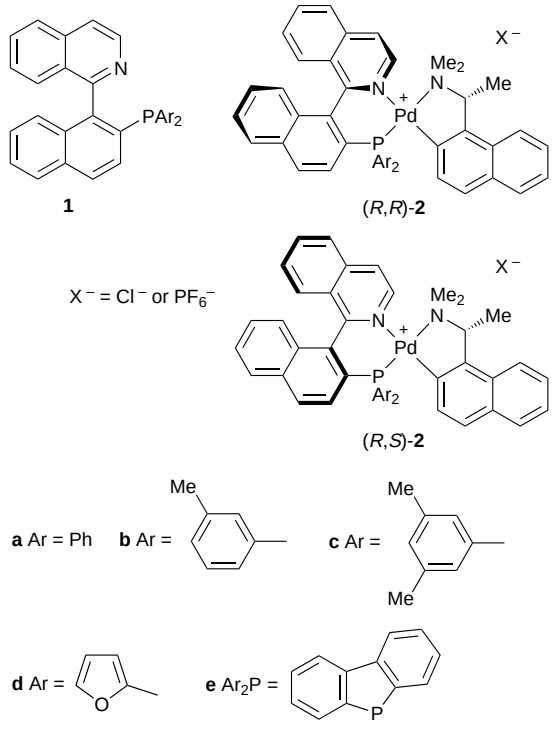
# Stereoselectivity in the mass-spectral fragmentation of palladium phosphinamine complexes

**Robin T. Aplin, Henri Doucet, Mark W. Hooper and John M. Brown***

*Dyson Perrins Laboratory, South Parks Rd., Oxford, UK OX1 3QY*

**The diastereoisomers of cyclopalladated 1-naphthyldimethylethylamine complexes of several phosphinoarylisoquinolines demonstrate distinct fragmentation in their electrospray MS, diagnostic of the ligand enantiomer.**

In previous work we have described the synthesis and resolution of a class of P–N chelating ligands based on 2-aza-1,1′-binaphthyl, the parent being **1a**.[1] These P–N chelates have proved useful for catalytic hydroboration and for allylic alkylation and considerable structure variation in the ligand is afforded by minor synthetic variations.[2] The chloropalladium complex derived (*R*)- or (*S*)-*N*,*N*-dimethyl-1-naphthylethylamine[3] proved to be uniquely effective for resolution of the racemic ligand, and this was rationalised in terms of an enforced conformational rigidity in the chelate ring of the complexed resolving agent.[4]




With a number of the resolution intermediates isolated in pure state as chloride or hexafluorophosphate salts, we were interested in making fuller spectroscopic comparisons. A difference became apparent on comparing electrospray MS of the diastereomeric pairs of the parent (*R*,*R*)-**2a** and (*R*,*S*)-**2a** at a standard cone voltage of 55 V. For the (*R*,*R*)-diastereomeric salt, the parent peak of the cation is evident, and a fragment $[LPdH]^+$ where the naphthylamine entity has been lost is also present with around twice the intensity of the parent peak. For the (*R*,*S*)-diastereomer, the same two peaks are observed but now the parent peak is about twice the intensity of the fragment peak. This pattern is repeated with related complexes at the same cone voltage, and under these conditions the spectrum is clean. More profound fragmentation to $[Ar_2PPd]^+$ occurs above 90 V.

In order to obtain more systematic information, three pairs of complexes of known configuration were subjected to electrospray MS over a range of cone voltages where both $[M^+]$ and $[M - 197]^+$ were evident, and the results are shown in Fig. 1. For **2a**, the parent compounds in the series, it can be seen that fragmentation is more pronounced for the (*R*,*R*)-enantiomer than for the (*R*,*S*)-enantiomer across the range of cone voltages [Fig. 1(*a*)]. The diastereomers of the phenanthridine analogue **3** behave quite similarly [Fig. 1(*b*)], although here the counter ion is $Cl^-$ for the (*R*,*R*)-isomer and $PF_6^-$ for the (*R*,*S*)-isomer.[5] For the phenylethylamine analogue **4** [Fig. 1(*c*)], where both complexes are $PF_6^-$ salts, it can be seen that the (*R*,*S*)-diastereomer fragments to a lesser degree than does the (*R*,*R*)-diastereomer.† However the difference is much smaller here; the ease of fragmentation is comparable for all the (*R*,*S*)-diastereomers in the series but the (*R*,*R*)-diastereomer of **3** is

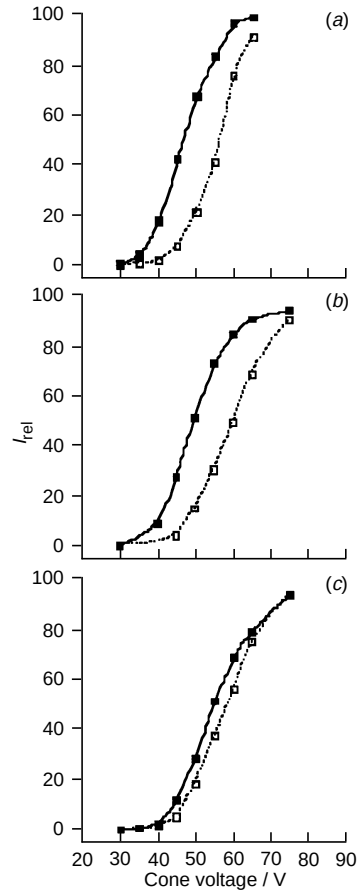
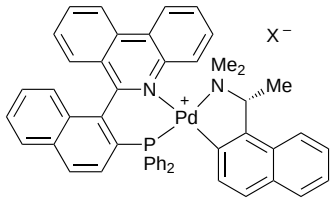
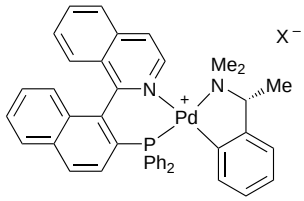



**Fig. 1** Relative signal intensity $I_{rel}$ *vs*. cone voltage for complexes **2a** (*a*), **3** (*b*) and **4** (*c*); intensity expressed as $(M - 197)^+/[M^+ + (M - 197)^+]$ for the $^{106}Pd$ isotopomer. The upper trace is the (*R*,*R*)-diastereomer (■) and the lower trace the (*R*,*S*)-diastereomer (□).




(*R*,*R*)- or (*R*,*S*)-**3**

$X^- = Cl^-$ or $PF_6^-$




(*R*,*R*)- or (*R*,*S*)-**4**

more stable to ESI cone voltage fragmentation than the other (*R*,*R*)-complexes.

A series of related ligands **1b–e** have been prepared in order to elucidate aryl substituent effects on asymmetric catalysis.[6] The resolution protocol was successful in separating enantiomers of each ligand, but the order of crystallisation was not predictable and in some cases the $PF_6^-$ salt was formed but in others the $Cl^-$ salt was isolated. Whilst it was possible to infer the absolute configuration in other cases by an accumulation of evidence (sign of optical rotation, sense of rhodium catalytic asymmetric hydroboration[7]) the furylphosphine **1d** proved anomalous. The (+)-isomer gave closely similar results in rhodium-catalysed asymmetric hydroboration to the (*R*)-(+)-isomer of **1a**, but the opposite hand of secondary alcohol was formed, indicating the (*S*)-(+) configuration for **1d**. This was confirmed by comparative CD spectra of (*S*)-(−)-**1a** and (−)-**1d** in $CHCl_3$ which are similar but mirror-related. It was observed that all the four pairs of diastereomeric complexes **2b–e** showed clear-cut behaviour in their electrospray mass spectra of 55 V; one of the pair was dominated by the parent $M^+$ and the other by the fragment $[M - 197]^+$. In each case it was the compound inferred to be the (*R*,*S*)-diastereomer which showed the strong parent peak and correspondingly the compound inferred to be the (*R*,*R*)-diastereomer which showed the strong fragment (Fig. 2). Hence the electrospray MS provides a simple and general method for defining the absolute configuration of the ligand. This is consistent with our earlier suggestions that the success of the palladium–naphthylamine resolving agent is due to enforced rigidity in the resolution complexes which specifically destabilises one diastereomer through unfavourable steric interactions.[4] Although these examples relate to P–N chelate ligands, some preliminary observations have been made which indicate that chiral diphosphines exhibit similar behaviour.[8]

The application of mass spectrometry to stereochemical problems is uncommon, although there are established cases where diastereomers can be identified from differences in their fragmentation patterns. For example, collision-induced dissociation is capable of defining ring-junction stereochemistry where that is the site of a retro-Diels–Alder reaction.[9] Electrospray MS in tandem with cone-voltage CID has been used to distinguish between $C_2$-epimeric pairs of ammine–nickel glycoside complexes.[10] The present case provides a simple method for direct assay of the configuration of a family of ligands useful in asymmetric catalysis, which may have more general applicability.

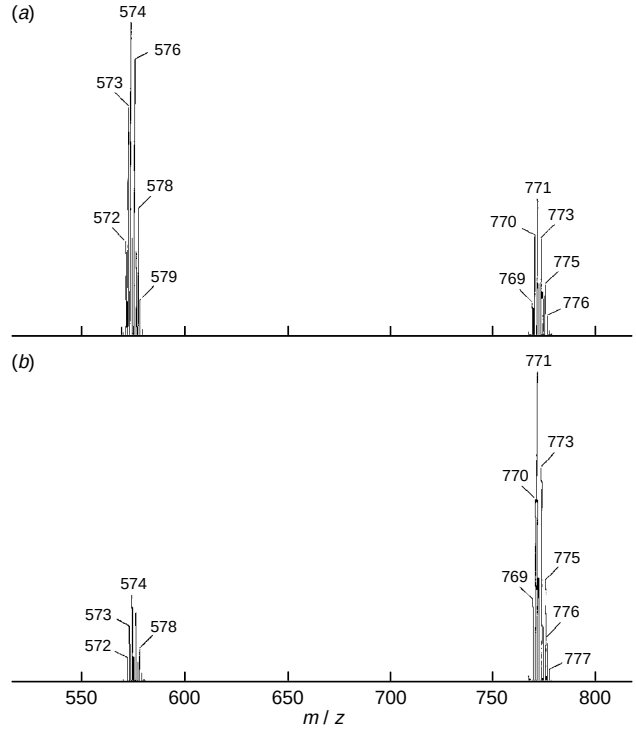



**Fig. 2** The electrospray mass spectra of (*a*) the (*R*,*R*) and (*b*) the (*R*,*S*) isomers of complex **2b** taken at a cone voltage of 55 V from a *ca.* 1% solution in MeCN–MeOH

We thank the EPSRC for support under the Catalysis Initiative to (H. D.) and for a Quota Studentship to (M. W. H.). Johnson-Matthey kindly provided a loan of Pd salts. Supporting CD spectra from the EPSRC Chiroptical Spectroscopy Service are gratefully acknowledged.

## Footnotes and References

* E-mail: john.brown@dpl.ox.ac.uk

† In this case the (*S*)-enantiomer of the resolving agent was used, but the chirality is reversed in the discussion for consistency.

1 N. W. Alcock, J. M. Brown and D. I. Hulmes, *Tetrahedron: Asymmetry*, 1993, **4**, 743.
2 T. D. W. Claridge, J. M. Long, J. M. Brown, D. Hibbs, M. B. Hursthouse and N. A. Cooley, *Tetrahedron*, 1997, **53**, 4035, and references therein.
3 D. G. Allen, G. M. McLaughlin, G. B. Robertson, W. L. Steffen, G. Salem and S. B. Wild, *Inorg. Chemistry*, 1982, **21**, 1007.
4 N. W. Alcock, D. I. Hulmes and J. M. Brown, *J. Chem. Soc., Chem. Commun.*, 1995, 395; *c.f.* ref. 1, figure 1.
5 J.-M. Valk, T. D. W. Claridge, J. M. Brown, D. Hibbs and M. B. Hursthouse, *Tetrahedron: Asymmetry*, 1995, **7**, 2597.
6 H. Doucet and J. M. Brown, *Tetrahedron: Asymmetry*, submitted.
7 J. M. Brown, D. I. Hulmes and T. P. Layzell, *J. Chem. Soc., Chem. Commun.*, 1993, 1673; E. Fernandez, M. W. Hooper, F. I. Knight and J. M. Brown, *Chem. Commun.*, 1997, 173.
8 J. M. Long, unpublished observations; similar effects have been observed with the corresponding complexes derived from heterocyclic analogues of BINAP, *cf.* U. Berens, J. M. Brown, J. Long and R. Selke, *Tetrahedron: Asymmetry*, 1996, **7**, 285.
9 A. Etinger and A. Mandelbaum, *Org. Mass Spectrom.*, 1992, **27**, 761; K. P. Madhusudanan, T. S. Dhami, A. Rani and S. N. Suryawanshi, *Rapid Commun. Mass Spectrom.*, 1993, **7**, 92.
10 G. Smith, S. F. Pedersen and J. A. Leary, *J. Org. Chem.*, 1997, **62**, 2152.

*Received in Cambridge, UK, 8th August 1997; 7/05803I*

# Synthesis and characterization of high-nuclearity osmium–rhodium mixed-metal carbonyl clusters; molecular and crystal structures of $[Os_{12}Rh_9(CO)_{44}(\mu_3\text{-}Cl)]\cdot 2CH_2Cl_2$ and $[Os_4Rh_3(\mu_3\text{-}H)(CO)_{14}(\mu_3\text{-}CO)(\eta^4\text{-}C_7H_8)_2]$

**Sarah Yeuk-Wah Hung and Wing-Tak Wong***

*Department of Chemistry, The University of Hong Kong, Pokfulam Road, Hong Kong, PR China*

**The anionic triosmium cluster $[N(PPh_3)_2][Os_3(\mu\text{-}H)(CO)_{11}]$ reacts with $[Rh(nbd)Cl)_2$ (nbd = norbornadiene) in the presence of $AgPF_6$ to give two new high-nuclearity osmium–rhodium clusters $[Os_{12}Rh_9(CO)_{44}(\mu_3\text{-}Cl)]$ 1 and $[Os_4Rh_3(\mu_3\text{-}H)(CO)_{14}(\mu_3\text{-}CO)(\eta^4\text{-}C_7H_8)_2]$ 2 in moderate yields.**

Mixed-metal clusters of osmium and rhodium are of interest as the rhodium tends to have a stable, coordinatively unsaturated 16 electron configuration,[1] while the osmium clusters display very rich chemistry and are kinetically stable. In addition, both osmium and rhodium metals have a well established background of catalytic applications.[2–6] One route to synthesize the mixed-metal osmium clusters is *via* nucleophilic addition of rhodium reagents to the coordinatively unsaturated cluster $[Os_3(\mu\text{-}H)_2(CO)_{10}]$ which has been extensively applied for the development of Os–Rh clusters.[7] An obvious alternative route into these systems is the interaction of the anion $[Os_3(\mu\text{-}H)(CO)_{11}]^-$ and cationic rhodium fragment but this has previously met limited success. However, this kind of ionic coupling strategy works well in many other mixed-metal systems.

Herein we report the reaction of a cationic mononuclear rhodium complex, $[Rh(nbd)]^+$,[8] (nbd = norbornadiene) with the anionic carbonyl cluster, $[Os_3(\mu\text{-}H)(CO)_{11}]^-$, which results in a novel class of high-nuclearity mixed-metal osmium–rhodium clusters. A mixture of $[Rh(nbd)Cl]_2$ and $AgPF_6$ (1 : 1) in thf was filtered and then treated with $[N(PPh_3)_2][Os_3(\mu\text{-}H)(CO)_{11}]$ under nitrogen at room temp.[9] An immediate change from red to brown was observed. Separation of the brown solution by TLC on silica [eluent: *n*-hexane–dichloromethane (1 : 4)] gave red $[Os_{12}Rh_9(CO)_{44}(\mu\text{-}Cl)]$ **1** (20%) and brown $[Os_4Rh_3(\mu_3\text{-}H)(CO)_{14}(\mu_3\text{-}CO)(\eta^4\text{-}C_7H_8)_2]$ **2** (10%) together with two uncharacterized products in low yield. Complexes **1** and **2** were fully characterized by spectroscopic techniques† and X-ray crystallography.‡

Single crystals of $\mathbf{1}\cdot 2CH_2Cl_2$ suitable for X-ray analysis were obtained by slow evaporation of a $CH_2Cl_2$–*n*-hexane solution. Its molecular structure, together with some important bond parameters, is depicted in Fig. 1. The structure of **1** [Fig. 1(*a*)] can be viewed as four '$Os_3(CO)_{11}$' units clipping onto the nanorhodium cluster metal core so that an asymmetric metal core results as illustrated in Fig. 1(*b*). The $Rh_9$ core geometry may be described as the fusion of an octahedron, Rh(1)Rh(2)Rh(3)Rh(4)Rh(5)Rh(6), with another virtual octahedron, Rh(4)Rh(5)Rh(6)Rh(7)Rh(8)Rh(9), in which there is no direct bonding between Rh(7) and Rh(9) or Rh(8) and Rh(9).

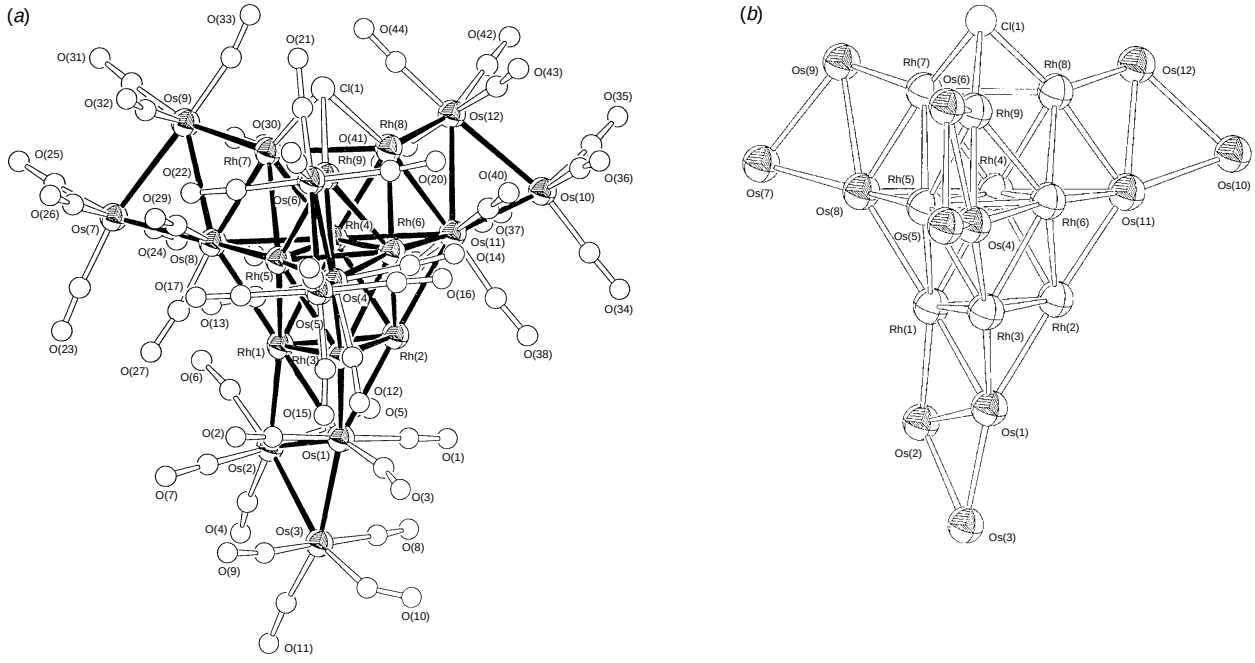



**Fig. 1** (*a*) Molecular structure of the cluster $[Os_{12}Rh_9(CO)_{44}(\mu_3\text{-}Cl)]$ **1** showing the atom numbering scheme. Selected bond lengths (Å) and angles (°): Os(1)–Os(2) 2.983(2), Os(1)–Os(3) 2.842(2), Os(2)–Os(3) 2.903(2), Os(4)–Os(5), 2.882(2) Os(4)–Os(6) 3.063(2), Os(5)–Os(6), 2.906(2) Os(7)–Os(8) 2.874(4), Os(7)–Os(9), 2.898(2) Os(8)–Os(9) 3.094(2), Os(10)–Os(11), 2.890(2) Os(10)–Os(12) 2.897(2), Os(11)–Os(12), 3.078(2) Os(1)–Rh(1) 2.806(3), Os(1)–Rh(2), 2.867(3) Os(1)–Rh(3) 2.766(3), Os(2)–Rh(1), 2.996(3) Rh(1)–Rh(2) 2.868(6), Rh(1)–Rh(3), 3.051(3) Rh(1)–Rh(5) 2.991(4), Rh(2)–Rh(3), 2.716(3) Rh(5)–Rh(7) 2.981(3), Rh(7)–Rh(8), 2.976(4) Rh(7)–Rh(9) 3.372(2), Rh(8)–Rh(9), 3.361(2) Os(1)–C(2) 2.867(3), Rh(7)–Cl(1), 2.533(7) Rh(8)–Cl(1) 2.586(7), Rh(9)–Cl(1), 2.558(6); Os(11)–Rh(4)–Rh(2) 59.65(7), Rh(7)–Cl(1)–Rh(8), 71.1(2) Rh(7)–Cl(1)–Rh(9) 83.0(2), Rh(8)–Cl(1)–Rh(9), 81.5(2). (*b*) The metal core geometry of **1**.

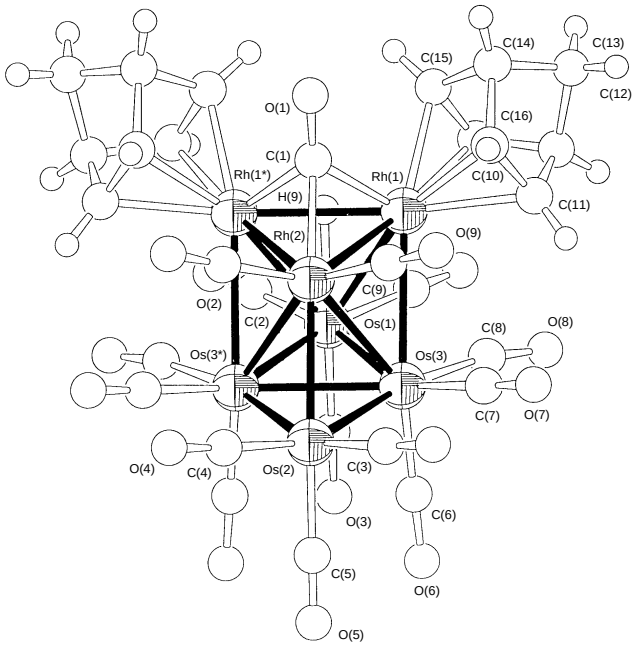



**Fig. 2** Molecular structure of the cluster $[Os_4Rh_3(\mu_3\text{-}H)(CO)_{14}(\mu_3\text{-}CO)(\eta^4\text{-}C_7H_8)_2]$ **2** showing the atom numbering scheme. Selected bond lengths (Å) and angles (°): Os(1)–Os(3) 2.839(1), Os(2)–Os(3) 2.800(1), Os(3)–Os(3*) 2.795(2), Os(1)–Rh(1) 3.003(2), Os(2)–Rh(2) 2.741(3), Os(3)–Rh(1) 2.915(2), Rh(1)–Rh(1*) 2.847(4), Rh(1)–Rh(2) 2.761(3), Rh(1)–C(1) 2.15(2), Rh(2)–C(1) 2.11(3), Rh(1)–C(10) 2.22(2), Rh(1)–C(11) 2.24(3), Rh(1)–C(15) 2.19(2), Rh(1)–C(16) 2.21(2), Os(1)–H(9) 2.03, Rh(1)–H(9) 1.85, O(1)–C(1) 1.19(3); Rh(1)–C(1)–Rh(1*) 83.1(9), Rh(1)–C(1)–Rh(1*) 83.0(9), Rh(1)–C(1)–Rh(2) 80.9(8), Os(1)–H(9)–Rh(1) 101.5, Rh(1)–H(9)–Rh(1*) 100.8.

In the $Rh_9$ core, one chloro-ligand caps onto three rhodium atoms, Rh(7), Rh(8) and Rh(9), and the rest of rhodium atoms, Rh(1), Rh(2), Rh(3), Rh(4), Rh(5) and Rh(6), have no ligand groups attached to them but are coordinated to metal atoms only. A salient structural feature of **1** is these relatively exposed Rh atoms which may facilitate the coordination of nucleophiles. All the carbonyl ligands are essentially terminally bonded to the osmium atoms except an incipient bridging CO interaction which is found between Os(4) and Rh(3), [Rh(3)···C(12) 2.44(3) Å]. However, in solution all carbonyls are terminally bonding as suggested by IR spectroscopic data. We do not detect any hydride in the variable-temperature $^1$H NMR studies [−50 to 25 °C]. Although satisfactorily elemental analysis was obtained, a satisfactory mass spectrum of **1** cannot be obtained by either EI, FAB or ESI techniques. If the triosmium units are each considered to have a formal 2− charge, $[Os_3(CO)_{11}]^{2-}$, each rhodium atom should be in an oxidation state of +1. Cluster **1** contains 50 metal–metal bonds and 268 cluster valence electrons (CVE) and hence does not obey the simple electron counting rules.[10–12] This is not entirely unexpected as it is common for rhodium to have a stable 16 electron configuration.

Brown crystals of **2** were grown from a $CH_2Cl_2$–*n*-hexane solution of the complex. A perspective drawing of cluster **2** with atomic numbering scheme is shown in Fig. 2 together with some selected bond parameters. Cluster **2** is much more symmetrical and consists of a crystallographic mirror plane that relates the two halves of the molecules. The metal framework contains a mixed-metal monocapped octahedron with four osmium atoms and three rhodium atoms. A $\mu_3$-bridging hydride capping the Os(1)–Rh(1)–Rh(1*) face is suggested by potential-energy calculations[13] and supported by $^1$H NMR spectroscopic measurements and difference Fourier synthesis based on log-angle data in the X-ray analysis. The metal core geometry of cluster **2** is similar to that of $[Os_7(CO)_{21}]$,[14] where both compounds have 98 CVE. This can be rationalised by the polyhedral skeletal electron pair theory[15] and the condensed polyhedral approach.[16] The mechanisms of formation of **1** and **2** have not been established. However, it seems reasonable to suggest that $[Rh(nbd)Cl]_2$ undergoes chloride dissociation upon reaction with silver(I) salts to give the active rhodium reagent, $[Rh(nbd)]^+$,[8] which reacts with the osmium cluster anion, $[Os_3(\mu\text{-}H)(CO)_{11}]^-$ *via* a complicated redox condensation, instead of a simple ionic coupling reaction. Cyclic voltammetric studies of $[N(PPh_3)_2][Os_3(\mu\text{-}H)(CO)_{11}]$ in thf at 25 °C showed an irreversible oxidation at +0.66 V *vs*. $Ag/AgNO_3$ while the preformed $[Rh(nbd)]^+$ cation showed an irreversible reduction at −0.02 V in thf *vs*. $Ag/AgNO_3$.[17] Further work on the mechanistic details and the chemical reactivities of these new high-nuclearity clusters is in progress.

We gratefully acknowledge financial support from the Hong Kong Research Grants Council and the University of Hong Kong. S. Y.-W. H. acknowledges the receipt of a postgraduate studentship, administrated by the University of Hong Kong.

## Footnotes and References

* E-mail: chemmail@hkucc.hku.hk

† *Spectroscopic data*: **1**: IR [$\nu$(CO), $CH_2Cl_2$] 2109m, 2099m, 2068vs, 2035vs, 2016m(sh), 2001m(sh). Elemental analysis: Anal. Calc. for $C_{44}ClO_{44}Os_{12}Rh_9$: C, 11.80. Found: 12.02%.

**2**: IR[$\nu$(CO), $CH_2Cl_2$] 2082m, 2068s, 2055vs, 2032m(sh), 2016vs, 1607m. Positive FAB mass spectrum: *m/z* 1674 (calc. 1674). $^1$H NMR ($CD_2Cl_2$): $\delta$ −19.47 (m, 1 H, metal hydride), 1.62 (m, 2 H, methylene), 4.33 (m, 2 H, methine), 4.96 (m, 4 H, alkene). Elemental analysis: Anal. Calc. for $C_{29}H_{17}O_{15}Os_4Rh_3$: C, 20.78, H, 1.01. Found: 20.99, 0.98%.

‡ *Crystal data*: $Os_{12}Rh_9C_{44}O_{44}Cl\cdot 2CH_2Cl_2$ **1**, $M$ = 4474.5 (4646.33 with solvents), triclinic, space group $P\bar{1}$ (no. 2), $a$ = 14.853(4), $b$ = 22.012(5), $c$ = 14.259(4) Å, $\alpha$ = 95.429(2)°, $\beta$ = 113.50(2)°, $\gamma$ = 71.06(2)°, $U$ = 4040(2) Å$^3$, $Z$ = 2, $D_c$ = 3.819 g cm$^{-3}$, $F$(000) = 4068.00, Mo-K$\alpha$ radiation ($\lambda$ = 0.710 73 Å), $\mu$(Mo-K$\alpha$) = 207.96 cm$^{-1}$, dimensions 0.12 × 0.14 × 0.16 mm. 11 035 observed diffractometer data [$I > 3.00\sigma(I)$]; $\psi$-scan absorption correction, structure solved by direct methods (SIR92) and Fourier techniques, refined by full-matrix least-squares analysis to $R$ = 0.047, $R'$ = 0.049, $w = 1/\sigma(F_o)$.

**2**: $C_{29}H_{17}O_{15}Os_4Rh_3$, $M$ = 1674.96, orthorhombic, space group *Pnma* (no. 62), $a$ = 17.425(3), $b$ = 17.828(4), $c$ = 10.963(3) Å, $U$ = 3405(1) Å$^3$, $Z$ = 4, $D_c$ = 3.266 g cm$^{-3}$, $F$(000) = 3000, Mo-K$\alpha$ radiation ($\lambda$ = 0.710 73 Å), $\mu$(Mo-K$\alpha$) = 163.37 cm$^{-1}$, dimensions 0.12 × 0.18 × 0.23 mm 4804 observed diffractometer data [$I > 3.00\sigma(I)$]; $\psi$-scan absorption correction, structure solved and refined as for **1** to $R$ = 0.038, $R'$ = 0.041. CCDC 182/607.

1 R. P. Hughes, in *Comprehensive Organometallic Chemistry*, ed. G. Wilkinson, F. G. A. Stone and E. Abel, Pergamon, Oxford, 1982, ch. 35.
2 R. L. Pruett, *Adv. Organomet. Chem.*, 1979, **17**, 1.
3 D. Forster, *Adv. Organomet. Chem.*, 1979, **17**, 255.
4 B. R. James, *Adv. Organomet. Chem.*, 1979, **17**, 319.
5 C. K. Rofer-DePoorter, *Chem. Rev.*, 1981, **81**, 447.
6 B. D. Dombek, *Adv. Catal.*, 1983, **32**, 325.
7 S. G. Shore, W. L. Hsu, M. R. Churchill and C. Bueno, *J. Am. Chem. Soc.*, 1983, **105**, 655.
8 R. R. Schrock and J. A. Osborn, *J. Am. Chem. Soc.*, 1971, 3089.
9 E. W. Abel, M. A. Bennett and G. Wilkinson, *J. Chem. Soc.*, 1959, 3178.
10 D. M. P. Mingos and A. S. May, in *The Chemistry of Metal Cluster Complexes*, ed. D. F. Shriver, H. D. Kaesz and R. D. Adams, VCH, New York, 1990, ch. 2.
11 C. Couture and D. H. Farrar, *J. Chem. Soc., Dalton Trans.*, 1987, 2251.
12 R. D. Adams and T. S. A. Hor, *Inorg. Chem.*, 1984, **23**, 4723.
13 A. G. Orpen, *J. Chem. Soc., Dalton Trans.*, 1980, 2509.
14 C. R. Eady, B. F. G. Johnson, J. Lewis, *J. Chem. Soc., Chem. Commun.*, 1977, 385.
15 D. M. P. Mingos, *Acc. Chem. Res.*, 1984, **17**, 311.
16 D. M. P. Mingos, *J. Chem. Soc., Chem. Commun.*, 1983, 706.
17 C. J. Cathey, B. F. G. Johnson and J. Lewis, P. R. Raithby and W. T. Wong, *J. Organomet. Chem.*, 1993, **450**, C12.

*Received in Cambridge, UK, 19th August 1997; 7/06080G*

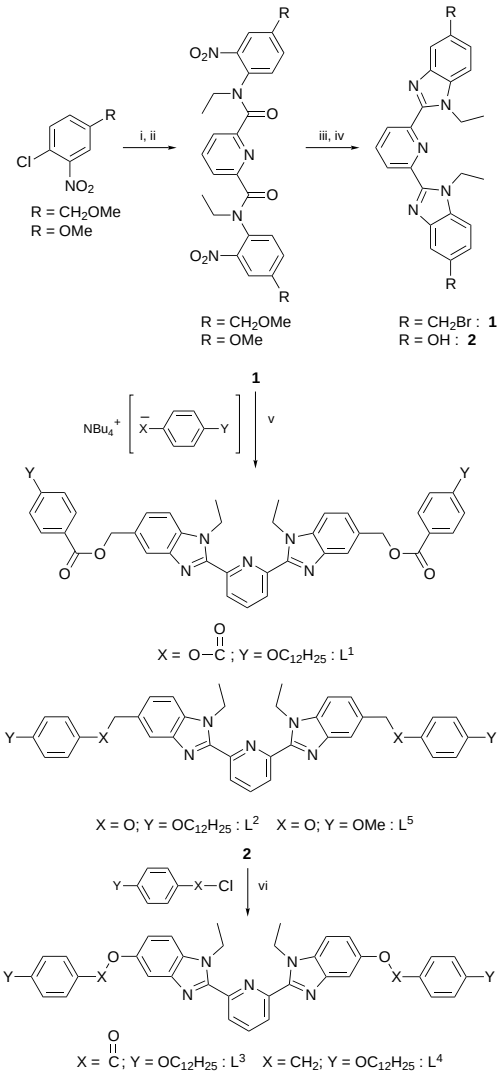
# Toward lanthanide-containing metallomesogens with tridentate ligands

**Homayoun Nozary,[a] Claude Piguet,*[a] Paul Tissot,[a] Gérald Bernardinelli,[b] Robert Deschenaux*[c] and Maria-Teresa Vilches[c]**

[a] *Department of Inorganic, Analytical and Applied Chemistry, University of Geneva, 30 quai E. Ansermet, CH-1211 Geneva 4, Switzerland*
[b] *Laboratory of X-ray Crystallography, University of Geneva, 24 quai E. Ansermet, CH-1211 Geneva 4, Switzerland*
[c] *Institute of Chemistry, University of Neuchâtel, Av. de Bellevaux 51, CH-2000 Neuchâtel, Switzerland*

**Tridentate aromatic receptors L¹–L⁴ containing the 2,6-bis-(benzimidazol-2-yl)pyridine chelating unit are designed to exhibit thermotropic calamitic liquid-crystalline phases; the mesomorphic behaviour is essentially retained in the complex [LuL²(NO₃)₃].**

We have recently launched into a research program aimed at developing lanthanide building blocks with tailored tridentate binding units.[1] It is now possible to finely control and tune the thermodynamic, structural, electronic and magnetic properties of the resulting mononuclear 1 : 1 and 1 : 3 complexes.[2–4] The incorporation of these building blocks into extended organized polynuclear architectures has been demonstrated,[4–6] but this approach is severely limited by the large amount of structural information required by segmental ligands for the selective recognition of 4f-block metal ions.[5,6] An alternative approach could take advantage of the molecular order associated with liquid-crystalline phases. Only a few lanthanide-containing metallomesogens have been prepared[7] and none with tridentate ligands, most likely as a consequence of their bent arrangement which results upon coordination.




**Scheme 1** *Reagents*: i, $EtNH_2$, EtOH; ii, pyridine-2,6-dicarbonyldichloride, $NEt_3$, $CH_2Cl_2$; iii, Fe, HCl–EtOH–$H_2O$; iv, $BBr_3$, $CH_2Cl_2$; v, $CH_2Cl_2$; vi, $NBu_4OH$, $CH_2Cl_2$

We report here on the design of semi-rigid tridentate receptors tailored for the preparation of calamitic lanthanide-containing liquid crystals. Substituted 2,6-bis(1′-ethylbenzimidazol-2′-yl)pyridine binding units (L¹–L⁴) have been selected for their peculiar electronic and structural properties which fit the $Ln^{III}$ stereochemical preferences, leading to stable complexes with predetermined properties.[3,8] Semi-rigid lipophilic substituents have been connected to the 5-positions of the benzimidazole rings in order (*i*) to extend the rigid core and the axial anisotropy, (*ii*) to improve intermolecular interactions and (*iii*) to limit the stability of the crystalline phase owing to flexible lipophilic chains. The spacers between the tridentate unit and the *para*-substituted phenyl side-arms are crucial since they must be flexible enough to allow the ligands to adopt suitable conformations in the free form (*trans–trans*)[5] and in the complexes (*cis–cis*), and rigid enough to ensure a rod-like shape compatible with the formation of calamitic mesophases. The synthons **1** and **2** are obtained in satisfying yields (28 and 38%, respectively) according to a multistep strategy based on the recently developed cyclisation of unsymmetrical benzimidazole rings from *N*-(2-nitroaryl)arenecarboxamide (Scheme 1).[9] Nucleophilic substitutions using **1** as electrophile give L¹, L² and L⁵. Deprotonation of **2** with $NBu_4OH$ followed by alkylation or acylation provides the ligands L³ and L⁴.

$^1H$ NMR nuclear Overhauser enhancement effects (NOE) in solution suggest that the tridentate units adopt the expected *trans–trans* conformation in all free ligands L¹–L⁵, which is confirmed in the solid state by the crystal structure of the non-mesogenic model compound L⁵ [N(4) is *trans* to N(3) and N(1) is *trans* to N(3), Fig. 1].† All C–C, C–N and C–O bonds are standard[10] and the $C_{ar}$–C–O–$C_{ar}$ atoms of the two spacers adopt all-*trans* conformations leading to an approximate rod-like shape of the receptor (Fig. 1). Reaction of L² with stoichiometric amounts of $Ln(NO_3)_3$ (Ln = La, Lu) in acetonitrile produces quantitatively the complexes $[LnL^2(NO_3)_3]\cdot nH_2O$ (Ln = La, *n* = 3; Ln = Lu, *n* = 1) where $Ln^{III}$ is nine-coordinated by the tridentate aromatic unit which adopts the *cis–cis* conformation (NOE effects observed between $H^{38}$–$H^{17}$) and three bidentate nitrate anions as similarly reported for the analogous complexes with unsubstituted 2,6-bis(1′-alkylbenzimidazol-2′-yl)pyridine ligands.[8,11]

The thermal and liquid-crystal properties were investigated by a combination of differential scanning calorimetry (DSC)

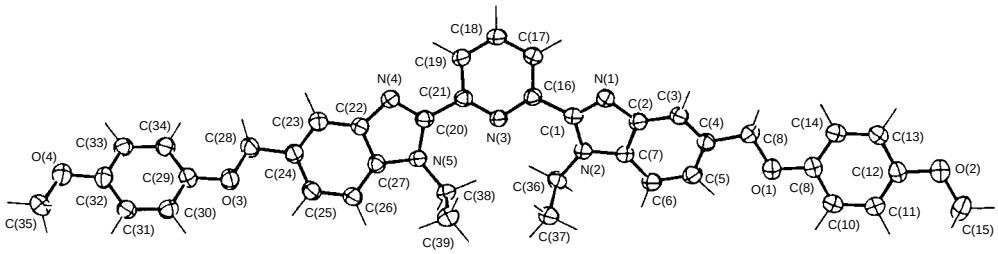



**Fig. 1** ORTEP[15] view of the ligand $L^5$ with ellipsoids represented at 50% probability level

**Table 1** Phase-transition temperatures and enthalpy and entropy changes for ligands $L^1$–$L^4$ and complex $[LuL^2(NO_3)_3]\cdot H_2O$

| Compound | Transition[a] | $T$/°C | $\Delta H$/kJ mol$^{-1}$ | $\Delta S$/J mol$^{-1}$ K$^{-1}$ |
|---|---|---|---|---|
| $L^1$ | K–I | 107 | 80 | 211 |
| $L^2$ | K–$S_A$ | 132 | 50 | 122 |
| | ($S_C$–$S_A$)[b] | 98 | —[c] | — |
| | $S_A$–I | 188 | 17 | 37 |
| $L^3$ | K–$S_C$ | 131 | 35 | 86 |
| | $S_C$–$S_A$ | 217 | —[c] | — |
| | $S_A$–N | 223 | —[d] | — |
| | N–I | 226 | 7[e] | 14[e] |
| $L^4$ | K–$S_A$ | 144 | 28 | 66 |
| | ($S_C$–$S_A$)[b] | 107[f] | — | — |
| | $S_A$–I | 193 | 18 | 39 |
| $[LuL^2(NO_3)_3]$ | K–$S_A$ | 133 | 72 | 176 |
| | ($S_C$–$S_A$)[b] | 98 | —[c] | — |
| | $S_A$–I | 188 | 23 | 50 |

[a] K = crystal, $S_C$ = smectic C phase, $S_A$ = smectic A phase, N = nematic phase, I = isotropic fluid; temperatures are given as the onset of the peak (Seiko DSC 220C differential scanning calorimeter, 5 °C min$^{-1}$, under $N_2$); the liquid crystalline phases were identified from their optical textures: $S_C$ = broken focal-conic fan and *schlieren* textures; $S_A$ = focal-conic fan texture and homeotropic zones; N = *schlieren* and marbled textures. [b] Monotropic transition. [c] Second-order transition determined by polarized optical microscopy. [d] Masked by isotropization. [e] Cumulated enthalpies and entropies. [f] Approximate value: the $S_C$ phase formed during the crystallization process.

and polarized optical microscopy (Table 1). The ligand $L^1$ (three-atom spacers) does not show mesogenic behaviour. However, the ligands $L^2$–$L^4$, which possess two-atom spacers, display interesting mesomorphism: they all present disordered smectic C and smectic A phases. An additional nematic phase is obtained for $L^3$. Interestingly, the mesomorphic behaviour of $L^2$ is essentially retained in the lanthanide complexes. In $[LaL^2(NO_3)_3]\cdot 3H_2O$, the melting process (130 °C) is associated with a fast decomposition which prevents an unambigous characterization of the mesophase(s), but the analogous complex $[LuL^2(NO_3)_3]\cdot H_2O$ melts at 133 °C to give a stable $S_A$ phase which isotropizes at 188 °C. Although the temperatures of the $K \rightarrow S_A$ and $S_A \rightarrow I$ transitions are similar for $L^2$ and its complex $[LuL^2(NO_3)_3]\cdot H_2O$, the enthalpy and entropy changes are significantly larger for the latter compound.

In conclusion, two-atom spacers as in $L^2$–$L^4$ are suitable for the incorporation of bent tridentate units into rod-like shape receptors exhibiting thermotropic calamitic behaviours. A fine tuning of the thermal properties results from the nature of the spacer, while metallic size effects are responsible for the larger stability of the Lu complex as previously reported for other lanthanide-containing metallomesogens.[7] The introduction of spectroscopically and magnetically active $Ln^{III}$ into smectic phases is currently under investigation.

We gratefully thank Mrs Hélène Lartigue, Dr J.-P. Rivera and C. Fouillet for their technical assistance. C. P. thanks the Werner Foundation for a fellowship. This work is supported through grants from the Swiss National Science Foundation.

## Footnotes and References

* E-mail: claude.piguet@chiam.unige.ch

† *Crystal data* for $L^5$: $C_{39}H_{37}N_5O_4$, $M$ = 639.8, triclinic, space group $P\bar{1}$, $a$ = 10.315(1), $b$ = 11.8767(7), $c$ = 14.170(1) Å, $\alpha$ = 105.076(5), $\beta$ = 108.972(6), $\gamma$ = 95.109(5)°, $U$ = 1556.2(2) Å$^3$ (by least-squares refinement of 24 reflections, 57 ⩽ 2$\theta$ ⩽ 76°), $Z$ = 2, $D_c$ = 1.37 g cm$^{-3}$, $F$(000) = 676. Yellow prisms. Crystal dimensions 0.15 × 0.20 × 0.37 mm, $\mu$(Cu-K$\alpha$) = 0.721 mm$^{-1}$. *Data Collection and Processing*: Stoe STADI4 diffractometer, $T$ = 200 K, $\omega$–2$\theta$ scan, scan width = 1.05 + 0.35 tan$\theta$, scan speed 0.06° s$^{-1}$, Cu-K$\alpha$ radiation ($\lambda$ = 1.5418 Å); 3741 reflections measured (3 ⩽ 2$\theta$ ⩽ 105°, −10 < $h$ < 10, −12 < $k$ < 11, 0 < $l$ < 14), 3561 unique reflections ($R_{int}$ for equivalent reflections = 0.017) of which 3091 were observable [$|F_o| > 4\sigma(F_o)$]. Two reference reflexions were measured every 45 min and showed no variation in intensity. *Structure analysis and refinement*: data were corrected for Lorentz, polarization and absorption effects[12] ($A^*_{min}$ = 1.102, $A^*_{max}$ = 1.186). The structure was solved by direct methods using MULTAN 87;[13] all other calculations used XTAL[14] system and ORTEP II[15] programs. Full-matrix least-squares refinements (on $F$) using weights of $w = 1/[\sigma^2(F_o) + 0.0001(F_o^2)]$ gave final values $R$ = 0.044, $R_w$ = 0.049, for 434 variables and 3091 contributing reflections. All non-H atoms were refined with anisotropic displacement parameters. H-atoms were placed in calculated positions and contributed to $F_c$ calculations. CCDC 182/599.

1 For reviews see: C. Piguet and J.-C. G. Bünzli, *Eur. J. Solid State Inorg. Chem.*, 1996, **33**, 165; C. Piguet, J.-C. G.Bünzli, G. Bernardinelli, G. Hopfgartner and A. F. Williams, *J. Alloys Compd.*, 1995, **225**, 324; C. Piguet, *Chimia*, 1996, **50**, 144.
2 S. Petoud, J.-C. G. Bünzli, F. Renaud and C. Piguet, *J. Alloys Compd.*, 1997, **249**, 14.
3 C. Piguet, A. F. Williams, G. Bernardinelli and J.-C. G. Bünzli, *Inorg. Chem.*, 1993, **32**, 4139; C. Piguet, J.-C. G. Bünzli, G. Bernardinelli, C. G. Bochet and P. Froidevaux, *J. Chem. Soc., Dalton Trans.*, 1995, 83.
4 C. Piguet, E. Rivara-Minten, G. Bernardinelli, J.-C. G. Bünzli and G. Hopfgartner, *J. Chem. Soc., Dalton Trans.*, 1997, 421.
5 C. Piguet, J.-C. G. Bünzli, G. Bernardinelli, G. Hopfgartner, S. Petoud and O. Schaad, *J. Am. Chem. Soc.*, 1996, **118**, 6681.
6 C. Piguet, J.-C. G. Bünzli, G. Bernardinelli, G. Hopfgartner and A. F. Williams, *J. Am. Chem. Soc.*, 1993, **115**, 8197.
7 Z. K. Wang, C. H. Huang and F. Q. Zhou, *Solid State Commun.*, 1995, **95**, 223; Y. Galymetdinov, A. M. Athanassopoulou, O. Kharitonova, E. A. Soto-Bustamante, I. K. Ovchinnikov and W. Hasse, *Chem. Mater.*, 1996, **8**, 922; I. Bikhantaev, Y. Galymetdinov, O. Kharitonova, I. K. Ovchinnikov, D. W. Bruce, D. A. Dunmur, D. Guilter and B. Heinrich, *Liq. Cryst.*, 1996, **20**, 489.
8 C. Piguet, A. F. Williams, G. Bernardinelli, E. Moret and J.-C. G. Bünzli, *Helv. Chim. Acta*, 1992, **75**, 1697.
9 C. Piguet, B. Bocquet and G. Hopfgartner, *Helv. Chim. Acta*, 1994, **77**, 931.
10 F. H. Allen, O. Kennard, D. G. Watson, L. Brammer, A. G. Orpen and R. Taylor, *J. Chem. Soc., Dalton Trans.*, 1987, S1.
11 S. Petoud, J.-C. G. Bünzli, K. J. Schenk and C. Piguet, *Inorg. Chem.*, 1997, **36**, 1345.
12 E. Blanc, D. Schwarzenbach and H. D. Flack, *J. Appl. Crystallogr.*, 1991, **24**, 1035.
13 P. Main, S. J. Fiske, S. E. Hull, L. Lessinger, D. Germain, J. P. Declercq and M. M. Woolfson, MULTAN 87; Universities of York, England, and Louvain-La-Neuve, Belgium, 1987.
14 *XTAL 3.2 User's Manual*, ed. S. R. Hall and J. M. Stewart, Universities of Western Australia and Maryland, 1992.
15 C. K. Johnson, ORTEP II, Report ORNL-5138, Oak Ridge National Laboratory, Oak Ridge, TN, 1976.

*Received in Cambridge, UK, 7th August 1997; 7/05776H*

# The first synthetic microporous yttrium silicate containing framework sodium ions

**João Rocha,* Paula Ferreira, Zhi Lin, Paula Brandaõ, Artur Ferreira and Júlio D. Pedrosa de Jesus**

*Department of Chemistry, University of Aveiro, 3810 Aveiro, Portugal*

**The synthesis and structural characterization of AV-1, the first synthetic microporous yttrium silicate containing stoichiometric amounts of framework sodium cations, are reported.**

Recently, much research has been carried out aimed at preparing inorganic microporous framework solids containing metal atoms in different coordination geometries. Two such families of materials are of considerable interest, microporous titanosilicates (known at ETS materials) and derivatives contain $Ti^{4+}$ usually in octahedral coordination,[1,2] while porous molybdophosphates display an amazing variety of crystal structures.[3] We have been interested in the synthesis of microporous framework silicates of several elements of the Periodic Table.[4,5] When attempting to prepare yttrium silicates we have obtained a synthetic analogue (named AV-1, Aveiro microporous solid no. 1) of the rare mineral montregianite (Mont St-Hilaire, Québec, Canada), $Na_4K_2Y_2Si_{16}O_{38}\cdot 10H_2O$, which possesses a most unusual structure.[6,7] In montregianite the sodium (and yttrium) cations are an integral part of the framework. In sharp contrast, in zeolites and zeolite-type materials the charge-balancing sodium cations usually reside within the channels and, thus, are not part of the framework.

AV-1 of composition (determined by bulk chemical analysis and TG) $Na_2KYSi_8O_{19}\cdot 5H_2O$, was prepared in Teflon-lined autoclaves under hydrothermal conditions. An alkaline solution was prepared by mixing 5.07 g sodium silicate solution (27% m/m $SiO_2$, 8% m/m $Na_2O$, Merck), 18.26 g $H_2O$, 0.20 g KOH (Carlo Erba), 0.29 g NaOH (Merck) and 0.22 g NaCl (Aldrich). $Y_2(SO_4)_3\cdot 8H_2O$ (Aldrich) (1.73 g) was added to this solution and stirred thoroughly. The gel with composition 0.53 $Na_2O$ : 0.078 $K_2O$ : 1.0 $SiO_2$ : 0.12 $Y_2O_3$ : 44 $H_2O$ was autoclaved for 6 d at 230 °C. The crystalline product was filtered, washed with distilled water and dried at ambient temperature, the final product being an off-white microcrystalline powder.

The crystal structure of montregianite consists of two different types of layers alternating along the [010] direction (Fig. 1): (*a*) a double silicate sheet, where the single silicate sheet is of the apophyllite type with four- and eight-membered rings, and (*b*) an open octahedral sheet composed of $[YO_6]$ and three distinct $[NaO_4(H_2O)_2]$ octahedra. The layers are parallel to the (010) plane. The K atoms are ten-coordinate and the six water molecules (not shown) are located within large channels formed by the planar eight-membered silicate rings.

The powder X-ray diffraction patterns of AV-1 and montregianite[6] (Fig. 2) are similar. The small differences observed are mainly due to the fact that extensive framework substitution of Y and Si by Ca, Mg, Ba and Al, respectively, occurs in the mineral.[6] The unit-cell parameters of AV-1 have been calculated assuming a monoclinic unit cell ($P2_1/n$, $Z = 2$)[7] and cell dimensions $a = 9.595$, $b = 23.956$, $c = 9.583$ Å, $\beta = 93.850°$.

The AV-1 $^{29}Si$ solid-state MAS NMR spectrum (Fig. 3) displays two groups of resonances in the ranges $\delta -96$ to $-102$ and $-105$ to $-108$. The spectrum can be deconvoluted into eight peaks with equal intensities, revealing the presence in AV-1 of eight non-equivalent Si sites. In accord with this observation, the crystal structure of montregianite calls for the

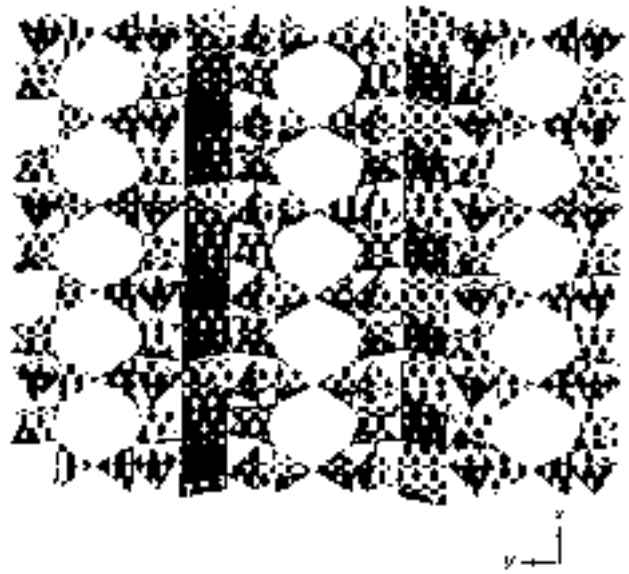


**Fig. 1** Polyhedral representation of the montregianite (and AV-1) structure viewed along [001] showing the alternating octahedral sheet and double silicate sheet along [010]

presence of eight unique Si sites with equal populations.[7] Two silicate tetrahedra [Si(1) and Si(4)], one each within the four-membered rings belonging to a single sheet, have upward-pointing apices [O(1)] which are shared with the apices of the two downward-pointing corresponding tetrahedra [Si(4) and Si(1), respectively] in the second silicate sheet.[7] Clearly, Si(1) and Si(4) are Si(4Si) environments (Si linked to four other Si *via* oxygen bridges) and the $^{29}Si$ MAS NMR resonances at $\delta -105.5$ and $-106.9$ are attributed to them. The assignment of the peaks at high frequency is more difficult. Si(6) is of the type Si(3Si, 1Y). Si(6)–O(12) is the shortest non-bridging bond length (1.562 Å) involving the most charge-deficient oxygen which is bonded to a Y atom.[7] Considering the well known correlation between the $^{29}Si$ chemical shifts and the SiO bond lengths in silicates,[8] we tentatively assign the peak at $\delta -100.8$

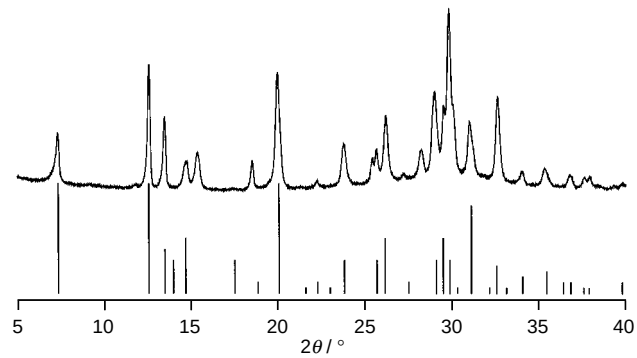



**Fig. 2** Powder XRD pattern of AV-1. For comparison, the solid lines depict the montregianite reflections.[6]

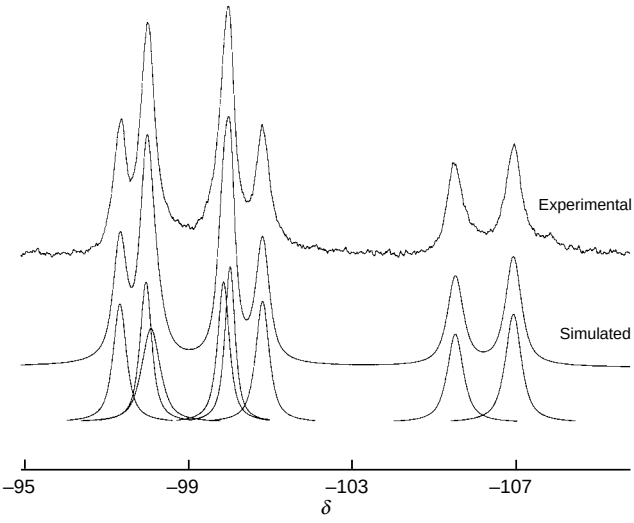



**Fig. 3** Experimental and simulated $^{29}$Si MAS NMR spectrum of AV-1 recorded at 79.5 MHz on a Bruker MSL 400P. Chemical shifts are quoted in ppm from $SiMe_4$.

to Si(6). The other five unique Si atoms are connected to three other silicons *via* bridging oxygens.[7] However, the fourth oxygen atom is non-bridging and is bonded to one Y and two Na atoms. [Si(2a) and Si(2b)] and [Si(5a) and Si(5b)] have very similar local environments and thus the resonances overlapping at $\delta$ *ca.* −98 and *ca.* −100 are probably associated with these sites. The resonance at $\delta$ −97.3 is assigned to the remaining Si(3) site.

The $^{23}$Na triple-quantum (3Q) MAS NMR spectrum[9] of AV-1 (not shown) displays two resonances with intensities close to 1 : 1. Although montregianite contains three non-equivalent Na sites the $[Na(2A)O_4(H_2O)_2]$ and $[Na(2B)O_4(H_2O)_2]$ octahedra (populations 0.47 and 0.45, respectively) are very similar in configuration and it is unlikely that they can be distinguished by solid-state $^{23}$Na NMR.[7] The $[Na(1)O_4(H_2O)_2]$ site (population 0.95) forms a weak seventh bond with O(5B) and is, thus, distorted. The 3Q peak S1 displays a relatively broad powder pattern and, hence, is ascribed to the distorted Na(1) site. S2 is assigned to sites Na(2A) and Na(2B). The single-quantum ('normal') spectrum (not shown) can be simulated assuming the presence of two resonances, ascribed to sites Na(1) and [Na(2A) and Na(2B)], with intensities of *ca.* 1 : 0.9 and the following parameters: isotropic chemical shifts: $\delta$ 1.8 and 9.0 (from 1 M aqueous NaCl); quadrupole coupling constants 1.92 and 1.24 MHz; asymmetry parameters 0.50 and 1.0, respectively.

The Raman spectrum of AV-1 (not shown) displays a main, strong and sharp, peak at 607 $cm^{-1}$ which we assign to relatively undistorted $[YO_6]$ octahedra. Indeed, in montregianite the $[YO_6]$ octahedron is fairly regular.[7]

The Fourier transform infrared spectra of AV-1 (not shown) and montregianite[6] are very similar. In particular, the medium intensity band at 1630 $cm^{-1}$, due to the H–O–H bending, confirms that water is present in the structure. Three O–H stretching bands are observed at 3610, 3510 and 3460 $cm^{-1}$.

Thermogravimetry (TG) and differential scanning calorimetry (DSC) data (not shown) provide further evidence that the structures of AV-1 and montregianite[6] are very similar. The dehydration of AV-1 is essentially complete at *ca.* 450–500 °C and the total mass loss is 11.4%. AV-1 materials calcined at 650 °C and rehydrated overnight at room temperature display TG and DSC curves similar to the parent solid. Three stages of dehydration occur, at *ca.* 20–80 °C (loss of disordered zeolitic water molecules adsorbed within the channels), 80–200 °C and 200–450 °C.

In conclusion, the novel synthetic microporous yttrium-silicate AV-1 and the rare mineral montregianite possess the same structure. These materials contain stoichiometric amounts of sodium cations which are an integral part of the framework and, thus, are fundamentally different from zeolites and other zeolite-type solids.

This work was supported by Junta Nacional de Investigação Científica e Tecnológica, PRAXIS XXI and FEDER.

## Footnote and References

* E-mail: rocha@dq.ua.pt

1 S. M. Kuznicki, *US Pat.*, 4 853 202, 1989.
2 M. W. Anderson, O. Terasaki, T. Ohsuna, A. Phillippou, S. P. Mackay, A. Ferreira, J. Rocha and S. Lidin, *Nature*, 1994, **367**, 347.
3 R. C. Haushalter and L. A. Mundi, *Chem. Mater.*, 1992, **4**, 31.
4 M. W. Anderson, A. Philippou, Z. Lin, A. Ferreira and J. Rocha, *Angew. Chem., Int. Ed. Engl.*, 1995, **34**, 1003.
5 J. Rocha, P. Brandão, Z. Lin, A. Ferreira and M. W. Anderson, *J. Phys. Chem.*, 1996, **100**, 14 978.
6 G. Y. Chao, *Can. Mineral.*, 1978, **16**, 561.
7 S. Ghose, P. K. S. Gupta and C. F. Campana, *Am. Mineral.*, 1987, **72**, 365.
8 G. Engelhardt and D. Michel, *High-Resolution Solid-State NMR of Silicates and Zeolites*, Wiley, New York, 1987.
9 A. Medek, J. S. Harwood and L. Frydman, *J. Am. Chem. Soc.*, 1995, **117**, 12 779.

*Received in Cambridge, UK, 1st August 1997; 7/05591I*

# Gemini surfactants, the effect of hydrophobic chain length and dissymmetry

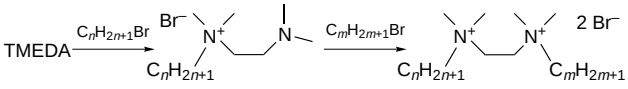
**Reiko Oda,*[a] Ivan Huc[b] and Sauveur J. Candau[a]**

[a] *Laboratoire d'Ultrasons et de Dynamique des Fluides Complexes, 3 rue de l'Université 67084 Strasbourg Cedex, France*
[b] *Laboratoire de Chimie Supramoléculaire, 4 rue Blaise Pascal 67070 Strasbourg Cedex, France*

**The synthesis of a new series of dimeric surfactants is reported; chain length and dissymmetry are shown to be critical factors for the richness of phases observed in water.**

In recent years, bis(quaternary ammonium) gemini surfactants have received increasing attention. Dimeric compounds with the structure $C_sH_{2s}$-α,ω-$(Me_2N^+C_mH_{2m+1}Br^-)_2$ which are referred to as *m*-*s*-*m*, show very low critical micellar concentrations (cmc) compared to the corresponding monomeric surfactants.[1] Some have been found to form giant worm-like micelles[2] at low concentration without any salt or hydrophobic counterions as was the case for the classically studied systems.[3,4] Zana and co-workers have reported detailed studies about the effect of the spacer chain length on the cmc of these surfactants as well as on the morphology of their aggregates.[5] Trimeric quaternary ammonium surfactants have also been prepared.[6] In this communication, we report on a new series of surfactants *n*-2-*m*, and on the effect of the dissymmetry of surfactant molecules on their self-assembled structures in aqueous solutions.

Their synthesis proceeds in two steps from *N*,*N*,*N*′,*N*′-tetramethylethylenediamine and two *n* and *m*-alkyl bromides. Thus, the diamine (0.1 mol) and the first alkyl bromide (0.8 equiv.) were heated in MeCN (250 ml) at 40 °C for 3 days. After evaporation and crystallisation from $Et_2O$, the corresponding pure alkyl dimethyl[1-(2-dimethylamino)ethyl] ammonium bromide was isolated in 70–80% yield. This compound (20 mmol) and the second alkyl bromide (4 equiv.) were refluxed in EtOAc (250 ml) for 2 days. After evaporation, the residue was recrystallised several times from $CHCl_3$–acetone yielding the *n*-2-*m* surfactant (50–60%).




When dissolved in water, the different surfactants assemble into various phases depending on their structure (Fig. 1). The symmetrical surfactants 14-2-14, 16-2-16, 18-2-18, as well as the almost-symmetrical surfactants 16-2-14 and 18-2-16 form turbid and rather viscous solutions which present a transition to isotropic and strongly viscoelastic phases upon heating. Rheometric studies (see below) allowed this latter phase to be characterised as entangled worm-like micelles. For the symmetrical surfactants, the solutions at room temperature are slightly birefringent. As shown in Fig. 2, DIC microscope observations reveal the presence of aggregated clusters of long and entangled tubule-like structures above 0.4, 0.2 and 0.1% for 14-2-14, 16-2-16 and 18-2-18 respectively. These tubules are quite stable and static, and their diameters do not exceed a micron. The phase observed with 16-2-14 at room temperature is somewhat different. It is also viscous, but shows much higher birefringence than those mentioned above. Microscopic observations show some indication of a lamellar phase. The phase observed with 18-2-16 also shows high birefringence, but the structure observed under the microscope was more reminiscent of a tubular phase. These structures as well as the nature of the transparent phase in-between are currently being investigated in detail by neutron scattering as well as with cryo-TEM.

The transition temperatures of these tubular/lamellar phases to worm-like micelles strongly depend on the overall length (*n* + *m*) as well as on the dissymmetry (*n* − *m*) of the surfactants (Fig. 1). The tubular/lamellar phases are more stable for longer chain lengths. In the symmetrical series, we observed a 15 °C drop in the transition temperature when both chains of a surfactant are shortened by two carbons, leading to transitions at 60, 45 and 30 °C for 18-2-18, 16-2-16 and 14-2-14 respectively.† Interestingly, the same 15 °C drop in transition temperature occurs when only one chain of a symmetrical surfactant is shortened by two carbons (*e.g.* from 18-2-18 to 18-2-16 or from 16-2-16 to 16-2-14). For example, 18-2-16 and 16-2-16, or 16-2-14 and 14-2-14 have almost identical transition temperatures. Thus, symmetry is a critical factor for the formation of the tubular/lamellar phases. In the range of *n* and *m* studied, these phases were never observed for $n - m > 2$ even for 18-2-14 which has the same overall chain length as 16-2-16.

Rheometric studies of the worm-like micellar phases obtained at high temperatures were performed, and we investigated the concentration dependence of the viscosity at low shear rate for various surfactants to determine the crossover concentration (overlap concentration) between dilute and semi-dilute regimes. Here, the crossover between these two regimes occurs when the micellar lengths become comparable to the screening length of electrostatic interactions. For salt-free worm-like micellar solutions, this happens approximately at the concentration at which the average distance between micelles equals the average length of micelles. As shown in Fig. 3, the overlap concentration of 16-2-16 is ten times lower than that of 14-2-14, which is itself ten times lower than that of 12-2-12. This can be

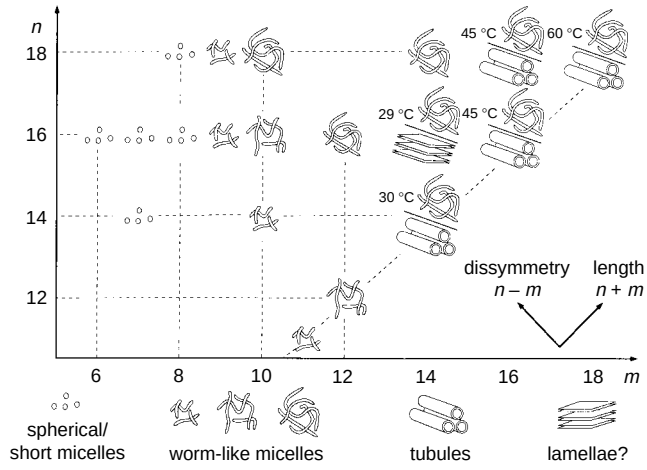



**Fig. 1** Phases observed in aqueous solutions of *n*-2-*m* surfactants as a function of *n* and *m*. The investigated concentrations were between 0.1 and 10% w/w (*ca.* 1.6–160 mM). Transition temperatures are indicated whenever a phase transition was observed upon heating. The worm-like micelles are divided into three categories according to their overlap concentrations: (*i*) lower than 0.5% w/w for the longer micelles; (*ii*) between 0.5 and 2%; (*iii*) between 2 and 10%.

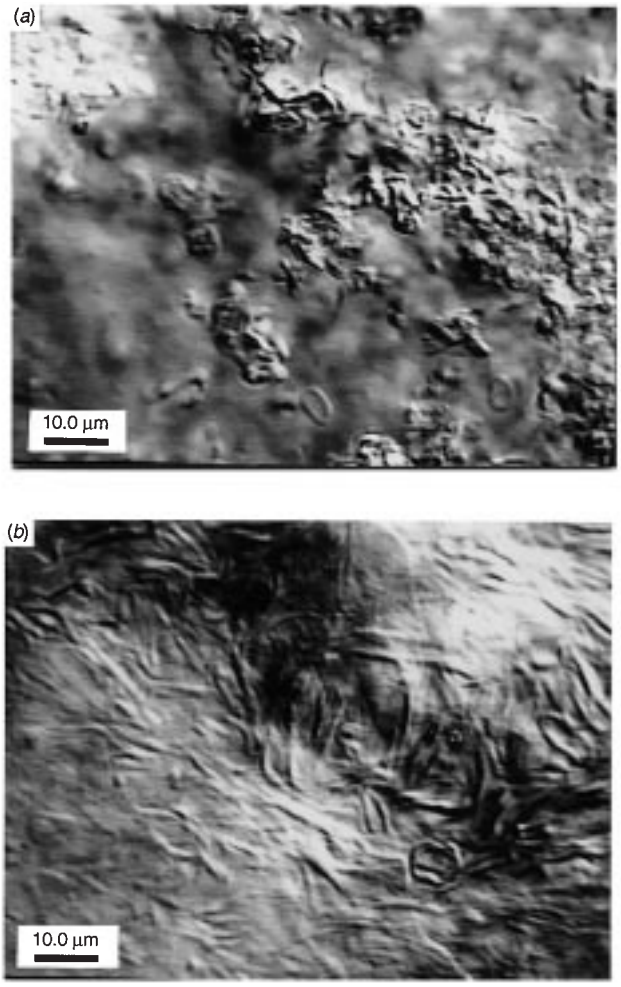



**Fig. 2** Tubule-like structures at room temperature in 1% solutions of (*a*) 16-2-16 and (*b*) 18-2-18. Observations were made with a video-enhanced differential interference contrast (DIC) Zeiss Axiovert 135 Microscope using a 100× objective (numerical aperture 1.3). The images were processed using a Hamamatsu CCD camera (C2400-77) and an Argus20 real time image processor.

understood geometrically as an increase of the spontaneous curvature for shorter hydrophobic chains.[7] A higher curvature reduces the cap-energy and favours the formation of shorter micelles.[8] It is striking that a 0.1% solution of 16-2-16 (1.6 mM) shows a viscosity of 0.15 Pa s at temperatures as high as 45 °C! In order to study the effect of the dissymmetry, we compared surfactants with the same $n + m$, but with different $n - m$: 12-2-12 *vs*. 14-2-10, 14-2-14 *vs*. 16-2-12 and 16-2-16 *vs*. 18-2-14. In all these cases, the symmetric surfactants showed higher viscosity and lower overlap concentrations. Thus, the dissymmetry also causes an increase of the spontaneous curvature. This effect is particularly pronounced when one chain is less than half the length of the other. The solutions are then fluid at all temperatures and at concentratons as high as 20%, indicating the presence of spherical or short micelles only. Rather than being true geminis, these surfactants feature a single hydrophobic chain linked to a very voluminous and polar head, which leads to a large spontaneous curvature.

The cmcs of the surfactants were measured by conductimetry. They show a monotonous decrease as the overall hydrophobic chain length is increased. The smallest measured cmc was that of 16-2-18, at 17 μM. The cmc of 18-2-18 was too low to be evaluated accurately with this technique. Surfactants with equal $n + m$ such as 12-2-12, 10-2-14 and 8-2-16, or 14-2-18 and 16-2-16 have similar cmcs. Unlike the other properties of the surfactant aggregates presented above, the cmc

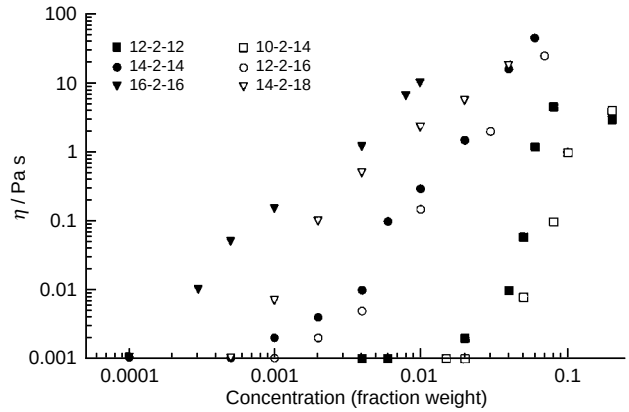



**Fig. 3** The low-shear viscosity ($\eta$) of 12-2-12, 14-2-14, 16-2-16, 14-2-10, 16-2-12 and 18-2-14 as a function of concentration at 45 °C. Measurements were performed with a Rheometrics Fluid Spectrometer RFS II.

does not depend on the symmetry but only on the overall hydrophobicity of the surfactant.

In conclusion, we have been able to correlate the morphology and the physical properties of the phases formed by new gemini surfactants with structural elements such as overall chain length and symmetry. Both decreasing the chain length and decreasing the symmetry result in larger spontaneous curvatures. This latter factor is particularly significant, allowing one to assess the arrangement of the surfactant hydrophobic chains in the various phases. Indeed, the increase in curvature for dissymmetric surfactants implies that in an aggregate, two diametrically opposed surfactant molecules cannot compensate their dissymmetry by overlapping their longer hydrophobic chains (see Graphical Abstract). The formation of pairs of surfactants spanning across a membrane in an arrangement comparable to that of bolamphiphiles is probably entropically disfavoured, and the thermal disorganisation of the hydrophobic chains proscribes such an overlap at the low concentrations studied. We are currently pursuing investigations to see whether interdigitation is possible in concentrated solutions of surfactants as was observed for hydrated dissymetrical phospholipids in the gel state.[9]

This work was supported by Rhône-Poulenc, and the Centre National de la Recherche Scientifique. We thank R. Zana for stimulating discussions. We are also grateful to G. Waton for the conductivity measurements.

## Footnotes and References

* E-mail: reiko@fresnel.u-strasbg.fr

† These transition temperatures are those of 1% solutions, they increase slightly with concentration. Typically, we observed a variation of about 2 °C between 0.1 and 2% solutions.

1 R. Zana, M. Benrraou and R. Rueff, *Langmuir*, 1991, **7**, 1072.
2 F. Kern, F. Lequeux, R. Zana and S. J. Candau, *Langmuir*, 1994, **10**, 1714.
3 S. J. Candau, E. Hirtsche, R. Zana and M. Adam, *J. Colloid Interface Sci.*, 1988, **122**, 430; F. A. L. Anet, *J. Am. Chem. Soc.*, 1986, **108**, 7102; H. Thurn, M. Löbl and H. Hoffmann, *J. Phys. Chem.*, 1985, **89**, 517.
4 M. E. Cates and S. J. Candau, *J. Phys.: Condens. Matter*, 1990, **2**, 6869.
5 M. Frindi, B. Michels, H. Levy and R. Zana, *Langmuir*, 1994, **10**, 1140; E. Alami, H. Levy, R. Zana and A. Skoulios, *Langmuir*, 1993, **9**, 940.
6 D. Danino, Y. Talmon, H. Levy, G. Beinert and R. Zana, *Science*, 1995, **269**, 1420.
7 P. G. De Gennes and C. Taupin, *J. Phys. Chem.*, 1982, **86**, 2294; D. J. Mitchell and B. W. Ninham, *J. Chem. Soc., Farad. Trans.*, 1981, **77**, 601.
8 F. C. MacKintosh, S. A. Safran and P. A. Pincus, *Europhys. Lett.*, 1990, **1**, 697.
9 T. J. McIntosh, S. A. Simon, J. C. Ellington and N. A. Porter, *Biochemistry*, 1984, **23**, 4038; H. N. Halladay, R. E. Stark, S. Ali and R. Bittman, *Biophys. J.*, 1990, **58**, 1449.

*Received in Liverpool, UK, 10th June 1997; 7/04069E*

# New hydrotalcite-like anionic clays containing $Zr^{4+}$ in the layers

**S. Velu,[a] Veda Ramaswamy,[a] A. Ramani,[b] Bhanu M. Chanda[b] and S. Sivasanker*[a]**

*[a] Catalysis Division, [b] Division of Organic Chemistry, Technology, National Chemical Laboratory, Pune 411 008, India*

**New hydrotalcite-like anionic clays containing $Zr^{4+}$ in the brucite-like layers are synthesised by a simple coprecipitation technique; these materials show very interesting properties as catalysts for liquid-phase hydroxylation of phenol with $H_2O_2$.**

Hydrotalcite (HT)-like anionic clays are a new family of interesting materials with applications as catalysts, catalyst supports, ion exchangers and composite materials.[1–3] The structure of these compounds can be visualised as being made of brucite [$Mg(OH)_2$]-like octahedral layers in which a part of $Mg^{2+}$ is isomorphously substituted by trivalent cations. The excess positive charge of the layer is compensated by hydrated anions, such as $CO_3^{2-}$, present in the interlayer. The materials are represented generally by the formula: $[M^{II}_{1-x},M^{III}_x,(OH)_2]^{x+}[(A^{n-})_{x/n}\cdot yH_2O]^{x-}$, where $M^{II}$ = $Cu^{2+}$, $Ni^{2+}$, $Co^{2+}$, $Zn^{2+}$, $Mn^{2+}$; $M^{III}$[4,5] = $Al^{3+}$, $Fe^{3+}$, $Cr^{3+}$, $Ga^{3+}$, $V^{3+}$, and more recently,[6] $Ru^{3+}$ and $Rh^{3+}$. A large number of HT-like compounds with a wide variety of cation pairs including a Co–$Ti^{IV}$ layered double hydroxide[7] have been reported in recent years. We now report the synthesis of a $Zr^{4+}$ containing HT-like material using a simple coprecipitation technique. The importance of Zr or Ti containing HT-like compounds stems from the fact that, similar to zeolites containing Zr (Zr-silicalites) or Ti (Ti-silicalites), they can be used as catalysts for liquid-phase hydroxylation/oxidation of various organic substrates.[8–11] In the present investigation, we report our preliminary studies on the synthesis of new Zr-containing anionic clays and their catalytic performance in the liquid-phase hydroxylation of phenol.

Zr-containing hydrotalcites with various Mg : Al : Zr atomic ratios were synthesized by a coprecipitation method at room temperature by reacting aqueous solutions containing a mixture of $Mg(NO_3)_2$, $Al(NO_3)_3$ and $ZrO(NO_3)_2$ and a mixture of NaOH and $Na_2CO_3$ at a constant pH (*ca.* 10). The resulting precipitate was filtered, washed with distilled water several times until the pH of the filtrate was 7 and then dried at 373 K overnight. The incorporation of Zr in the brucite-like layers was confirmed by powder X-ray diffraction (PXRD/Rigaku, D-MAX III VC model, with Ni-filtered Cu-K$\alpha$ radiation), UV–VIS diffuse reflectance spectroscopy (UV–VIS DRS; Shimadzu, UV–VIS Spectrophotometer 2101 PC model) and catalytic hydroxylation of phenol using hydrogen peroxide ($H_2O_2$) as the oxidant.

Fig. 1 shows the PXRD patterns of Mg : Al : Zr-HT with Mg : Al : Zr atomic ratio ranging from 3 : 1 : 0 to 3 : 0 : 1. A single phase corresponding to HT is obtained for all the samples although the crystallinity of the samples decreases with increasing Zr content (Table 1). A binary Zr containing HT without Al forms a poorly crystalline $ZrO_2$ phase [Fig. 1(*k*)] rather than a HT phase, indicating that the presence of Al favours the formation of a pure HT-like phase. The crystallographic parameters were evaluated employing least-squares refinement assuming a hexagonal crystal system for samples Zr0.0-HT–Zr0.6-HT whose PXRD peaks were intense and sharp enough for accurate determination. The increase in lattice parameters *a* and *c* with a concomitant increase in the unit cell volume *U* (Table 1) with increasing Zr content clearly demonstrates the effective incorporation of $Zr^{4+}$ in the HT framework. The increase in *a* can be attributed to the isomorphous substitution of $Al^{3+}$ (Shannon ionic radius 0.53 Å)[12] in the octahedral coordination by $Zr^{4+}$ (Shannon ionic radius 0.72 Å) in the HT matrix. The increase in *c* may be due to the weakening of the interaction between the brucite-like layer and the interlayer anions or due to the larger number of anions. Furthermore, since a part of the trivalent cation $Al^{3+}$ is being substituted by the tetravalent cation $Zr^{4+}$, the interlayer should accommodate more $CO_3^{2-}$ anions for charge compensation. This is supported by an increase in carbon content from 2.44% for Zr0.0-HT to 3.55% for Zr0.6-HT (Table 1). Hence, based on the chemical composition presented in Table 1, the Zr containing HT-like compounds with Mg/Al + Zr = 3 can be represented by the following general formula: $Mg_6Al_{2-x}Zr_x(OH)_{16}\cdot[(x + 2)/2]CO_3\cdot yH_2O$, where *x* can vary from 0 to at least 1.2.

Thermal calcination of these samples at 723 K results in the formation of an MgO phase whose *d*(200) value increases from 2.0934 Å for Zr0.0-HT to 2.1174 Å for Zr0.5-HT, indicating the dissolution of $Zr^{4+}$ in the MgO lattice. However, a poorly crystalline $ZrO_2$ phase, in addition to an MgO phase is noticed in the PXRD of the samples above Zr0.5-HT.

The dispersion of Zr in the HT framework was studied by UV–VIS DRS (Fig. 2). All these samples, including that

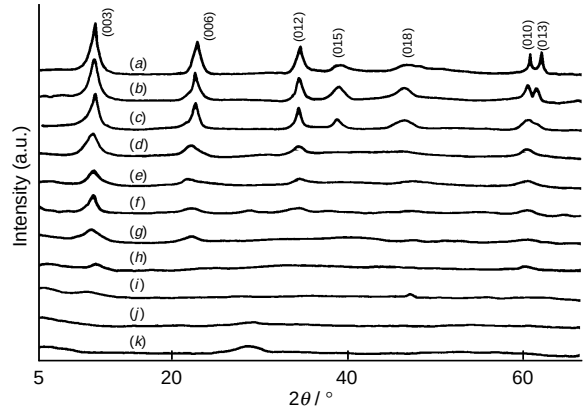



**Fig. 1** PXRD patterns of MgAlZr-HT: (*a*) Zr0.0-HT, (*b*) Zr0.1-HT, (*c*) Zr0.2-HT, (*d*) Zr0.3-HT, (*e*) Zr0.4-HT, (*f*) Zr0.5-HT, (*g*) Zr0.6-HT, (*h*) Zr0.7-HT, (*i*) Zr0.8-HT, (*j*) Zr0.9-HT, (*k*) Zr1.0-HT

**Table 1** Chemical compositions and lattice parameters of MgAlZr-HT

| Sample | Mg : Al : Zr atomic ratio[a] | Carbon content[b] (%) | Lattice parameters[c] | | |
|---|---|---|---|---|---|
| | | | *a*/Å | *c*/Å | *U*/Å$^3$ |
| Zr0.0-HT | 3 : 0.96 : 0.00 | 2.44 | 3.0584 | 23.1811 | 187.8 |
| Zr0.1-HT | 3 : 0.85 : 0.07 | — | 3.0643 | 23.4570 | 190.8 |
| Zr0.2-HT | 3 : 0.78 : 0.14 | 2.71 | 3.0688 | 23.5305 | 191.9 |
| Zr0.3-HT | 3 : 0.68 : 0.21 | 2.91 | 3.0687 | 23.7243 | 193.5 |
| Zr0.4-HT | 3 : 0.67 : 0.33 | 3.01 | 3.0732 | 23.7681 | 194.4 |
| Zr0.5-HT | 3 : 0.57 : 0.37 | — | 3.0773 | 23.9383 | 196.3 |
| Zr0.6-HT | 3 : 0.52 : 0.50 | 3.51 | 3.0780 | 24.1184 | 197.9 |

[a] Determined by X-ray fluorescence spectroscopy. [b] Determined by CHN microanalysis. [c] Refined using least square fitting method for hexagonal crystal system.

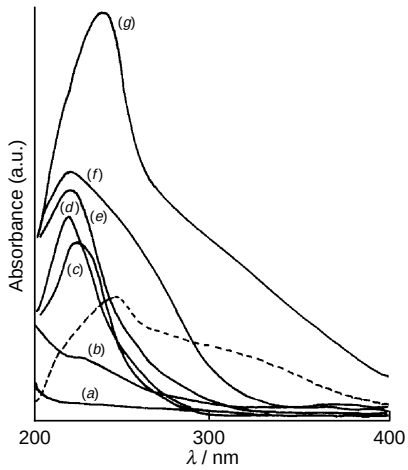



**Fig. 2** UV–VIS diffuse reflectance spectra of MgAlZr-HT: (*a*) Zr0.0-HT, (*b*) Zr0.1-HT, (*c*) Zr0.3-HT, (*d*) Zr0.3-CHT, (*e*) Zr0.5-HT, (*f*) Zr0.8-HT, (*g*) pure $ZrO_2$, (---) Zr0.0-HT + pure $ZrO_2$ (physical mixture)

calcined at 723 K [Fig. 2(*d*)], exhibited a single narrow band around 210 nm. This absorption band is attributed to charge transfer involving isolated $Zr^{IV}$ species.[9,10] Both pure $ZrO_2$ and a physical mixture of Zr0.0-HT and $ZrO_2$ exhibited bands around 240 and 320 nm. These results clearly demonstrate the absence of any $ZrO_2$ species within the sample and indicate that the $Zr^{4+}$ cations are well dispersed in the HT matrix, similar to that in Zr-silicates.[9–11]

Some of the Zr containing hydrotalcites have been tested as catalysts in the hydroxylation of phenol using $H_2O_2$ as the oxidant. Preliminary studies with $H_2O_2$/phenol ratios from 0.5 to 8 using solvents such as water, $CCl_4$ or MeOH did not show any catalytic activity. However, appreciable activity (up to around 10% conversion of phenol) was observed when light petroleum (bp 60–80 °C) was used as the solvent. Table 2 summarizes the results of hydroxylation of phenol over various Zr containing hydrotalcites. It is interesting to note from the Table that the turnover number (TON; moles of phenol converted per mole of Zr atom) increases four-fold (1.0 to 3.8) when $H_2O_2$ is added dropwise using a syringe pump. Similarly, a two-fold increase (1.0 to 1.9) in catalytic activity is noticed if the sample is calcined at 723 K for 5 h. In all these cases, catechol is obtained as a unique product (100% selectivity). Upon increasing the $H_2O_2$/phenol ratio, the TON also increases considerably, but the selectivity of catechol decreases at the expense of hydroquinone. The absence of catalytic activity in the case of pure MgAl-HT without Zr (Zr0.0-HT) or pure $ZrO_2$ clearly indicates that the Zr incorporated in the HT framework plays a pivotal role in catalytic activity. Surprisingly, under similar experimental conditions, the Zr-containing silicalite (ZrS-1) which showed appreciable conversion in aqueous medium,[8] is found to be inactive in the hydroxylation of phenol. Further work is in progress in order to investigate the above differences and also to compare the catalytic performance with new Ti-containing hydrotalcites.

**Table 2** Hydroxylation of phenol with $H_2O_2$ over MgAlZr-HT

| Catalyst | $H_2O_2$/phenol molar ratio | TON[a] | Product selectivity (mass%) | |
|---|---|---|---|---|
| | | | Catechol | Hydroquinone |
| Zr0.0-HT | 5.0 | — | — | — |
| Zr0.1-HT | 5.0 | 1.4 | 100 | — |
| Zr0.3-HT | 5.0 | 1.0 | 100 | — |
| Zr0.3-HT[b] | 5.0 | 3.8 | 100 | — |
| Zr0.3-CHT[c] | 5.0 | 1.9 | 100 | — |
| Zr0.3-HT | 7.0 | 29.1 | 73.8 | 26.2 |
| Zr0.3-HT | 10.0 | 40.5 | 65.1 | 34.9 |
| ZrS-1 | 5.0 | — | — | — |
| $ZrO_2$ | 5.0 | — | — | — |

[a] TON = Turnover number (mole of phenol converted per mole of Zr atom). [b] $H_2O_2$ was added dropwise using a syringe pump at a rate of 0.5 ml $h^{-1}$. [c] Sample calcined at 723 K for 5 h. *Reaction conditions*: solvent light petroleum (bp 60–80 °C) 30 ml; phenol, 1 g; catalyst, 100 mg; temperature 353 K; time 8 h.

Based on the above experimental evidence, we report that pure and crystalline Zr containing HT-like compounds can be easily synthesized by a simple coprecipitation method. The Zr atoms are highly dispersed in the HT matrix and the resulting Zr-HT-like compounds are active in the catalytic hydroxylation of phenol to catechol.

S. V. and A. R. thank CSIR, New Delhi, for research fellowships.

## Footnote and References

* E-mail: prs@ncl.ernet.in

1 F. Cavani, F. Trifiro and A. Vaccari, *Catal. Today*, 1991, **11**, 173.
2 J. M. L. Nieto, A. Dejoz and M. I. Vazquez, *Appl. Catal.*, 1995, **132**, 41.
3 S. Velu and C. S. Swamy, *Catal. Lett.*, 1996, **40**, 265.
4 M. Belloto, B. Rebours, O. Clause, J. Lynch, D. Bazin and E. Elkaim, *J. Phys. Chem.*, 1996, **100**, 8527.
5 F. M. Labajos, V. Rives, P. Malet, M. A. Centeno and M. A. Ulibarri, *Inorg. Chem.*, 1996, **35**, 1154.
6 F. Basile, L. Basini, G. Fornasari, M. Gazzano, F. Trifiro and A. Vaccari, *Chem. Commun.*, 1996, 2435.
7 A. de Roy, C. Forano, F. El Malki and J. P. Besse, in *Expanded clays and other microporous solids*, ed. M. L. Occelli and H. F. Robson, Van Nostrand Reinhold, New York, 1992, p. 108.
8 M. K. Dongare, P. Singh, P. Moghe and P. Ratnasamy, *Zeolites*, 1991, **11**, 690.
9 B. Rakshe, Veda Ramaswamy and A. V. Ramaswamy, *J. Catal.*, 1996, **163**, 501.
10 A. Tuel, S. Gontier and R. Teissier, *Chem. Commun.*, 1996, 651.
11 B. Rakshe, Veda Ramaswamy, R. Vetrivel, S. G. Hegde and A. V. Ramaswamy, *Catal. Lett.*, 1997, **45**, 41.
12 R. D. Shannon, *Acta Crystallogr., Sect., A*, 1976, **32**, 751.

*Received in Cambridge, UK, 4th July 1997; 7/04752E*

# Ti(μ : η¹,η¹-$OCMe_2CH_2PPh_2)_3$Rh has a cylindrically symmetric triple bond

**LeGrande M. Slaughter and Peter T. Wolczanski***

*Cornell University, Baker Laboratory, Department of Chemistry, Ithaca, New York, USA 14853*

**The cylindrical symmetry of Ti(μ : η¹,η¹-$OCMe_2CH_2PPh_2)_3$Rh permits maximum $Rh(d_\pi) \rightarrow Ti(d/p_\pi)$ overlap, resulting in a 2.2142(11) Å metal–metal triple bond.**

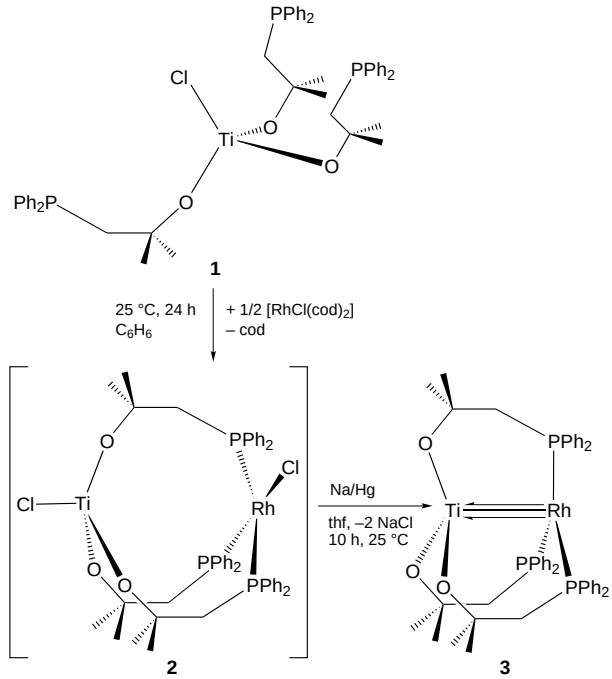
Aspects of heterogeneous materials exhibiting the strong metal–support interaction (SMSI)[1] have been modeled by homogeneous systems,[2–6] some containing M–M′ bonds of disparate metals.[5,6] Previously, we conducted an X-ray structural study of Cp*Zr(μ : η¹,η¹-$OCH_2PPh_2)_2RhMe_2$ (Cp* = η⁵-$C_5Me_5$) that revealed a short 2.444(1) Å ZrRh bond which was evaluated *via* extended Hückel molecular orbital (EHMO) calculations of an appropriately configured model, $Cp(HO)_2ZrRh(PH_3)_2Me_2$.[5] The metal–metal interaction, which is approximately 0.25 Å shorter than the sum of Zr (1.454 Å) and Rh (1.252 Å) covalent radii, was described in terms of a σ bond and a $Rh(d_\pi) \rightarrow Zr(d_\pi)$ bond. While the geometry of the alkoxyalkylphosphine bridges and the single critical π interaction resulted in a strong bond, at least by bond length criteria, the low symmetry of the complex prevented a second π interaction from being significant. As a consequence, we turned our attention to the synthesis of a cylindrically symmetric metal–metal bond in order to increase and perhaps maximize the strength of π interactions between group 4 and 9 metal centers.[5,7,8]

Treatment of $TiCl_4(thf)_2$ with 3 equiv. of $LiOCMe_2CH_2PPh_2$[4] in benzene at 25 °C for 3 h afforded $(Ph_2PCH_2CMe_2O)_3TiCl$ **1**† as a viscous, clear yellow oil in 80% yield. Although **1** was typically contaminated with *ca*. 5% $HOCMe_2CH_2PPh_2$, this was of sufficient purity to continue. Upon stirring a benzene solution of tris(alkoxyphosphine)-titanium chloride **1** and 0.5 equiv. of $[RhCl(cod)]_2$[9] for 24 h at 25 °C, a color change from yellow to deep red was noted, and an amorphous red solid was isolated from hexane. The major product displayed broad resonances in its $^1H$ and $^{31}P\{^1H\}$ NMR spectra at 23 °C in $C_6D_6$, the latter implying a 2 : 1 ratio of bound and free phosphines, while the $^{31}P\{^1H\}$ NMR spectrum at −8 °C exhibited broad, complex multiplets at $\delta$ 52.17 and 56.42 in a 2 : 1 ratio corresponding to bound phosphines. At −80 °C, we postulate the complex as ClTi(μ : η¹,η¹-$OCMe_2CH_2Ph_2P)_3RhCl$ (**2**, Scheme 1),† but suggest that dimerization to $[ClTi(OCMe_2CH_2Ph_2P)(\mu : \eta^1,\eta^1\text{-}OCMe_2CH_2Ph_2P)_2Rh]_2(\mu\text{-}Cl)_2$ is plausible at room temperature. Recrystallization and chromatographic purification efforts failed, and the chemical shifts attributed to impurities (*ca*. 20–25% integrated intensity) were consistent with the formation of various aggregates with bridging alkoxyalkylphosphines {*i.e.* $[TiCl(\mu : \eta^1,\eta^1\text{-}OCMe_2CH_2Ph_2P)_2ClRh(\mu : \eta^1,\eta^1\text{-}PPh_2CH_2CMe_2O)]_n$}.

Since **2** or any oligomeric variant could be a useful precursor to the desired heterobinuclear metal–metal bonded species, the red powder was reduced with 2 equiv. of Na/Hg in thf for 10 h at 25 °C. After separation from the salt and Hg, the resulting red–orange solid was dissolved in thf and chromatographed on basic alumina (activity I). The solid generated upon removal of thf was dissolved in toluene (60 °C) and crystallized at −78 °C to afford deep red Ti(μ : η¹,η¹-$OCMe_2CH_2Ph_2P)_3Rh$ **3**† as a $C_7H_8$ solvate in 24% overall yield. Reactivity studies implicated a robust titanium–rhodium bond: (*i*) no reaction with $H_2$ (10 equiv.) was observed upon heating in $C_6D_6$ at 140 °C for 2 weeks (sealed tube); (*ii*) reversible formation of a CO adduct, Ti(μ : η¹,η¹-$OCMe_2CH_2Ph_2P)_3RhCO$ **4**† was noted [ν(CO) 1956 $cm^{-1}$] and (*iii*) within 12 h, 2 equiv. of HCl converted **3** to precursor **2**, generating $H_2$ and a significant amount of impurities (*ca*. 50%) in the process.

An X-ray crystallograpic investigation of Ti(μ : η¹,η¹-$OCMe_2CH_2Ph_2P)_3Rh\cdot 0.5C_7H_8$, **3**·$0.5C_7H_8$, revealed a $C_3$ symmetry for the $O_3TiRhP_3$ core of **3** [dihedral angle $OTiRhP_{av}$ 15.8(20)°] that is broken when the external framework is included (Fig. 1). The OCCP bridge conformations adjust to maximize the number of favourable edge-to-face phenyl–phenyl interactions, thereby skewing the periphery.[10] A distorted trigonal monopyramidal geometry is evident for Rh, with Ti positioned apically and P–Rh–P angles of 113.22(5), 120.59(5) and 124.18(5)° describing an equatorial plane approximately perpendicular to the TiRh vector [Ti–Rh–P(1–3) 96.29(5), 89.72(5), 97.30(5)°]. The Ti center is roughly tetrahedral [O–Ti–O 107.7(2), 109.8(2), 112.4(2)°; $O–Ti–Rh_{av}$ 108.9(5)°] and the titanium–oxygen [$d(Ti–O)_{av}$ 1.830(3) Å] and rhodium–phosphine bond lengths [$d(Rh–P)_{av}$ 2.319(3) Å] are normal.

The titanium–rhodium bond distance of 2.2142(11) Å characterizes an extremely short heterobimetallic metal–metal bond. When compared to the sum of Ti (1.324 Å) and Rh covalent radii, the 0.362 Å reduction in bond length represents a large deviation (FSR = 0.860)[11] that supports formulation of a Ti≡Rh bond comprised of one $Ti(d/p_\sigma)–Rh(d/p_\sigma)$ and two $Rh(d_\pi) \rightarrow Ti(dTp_\pi)$ interactions. This appraisal is in accord with our EHMO investivations of Cp*Zr(μ : η¹,η¹-$OCH_2PPh_2)RhMe_2$,[5] and more recent Fenske–Hall calculations




**Scheme 1**

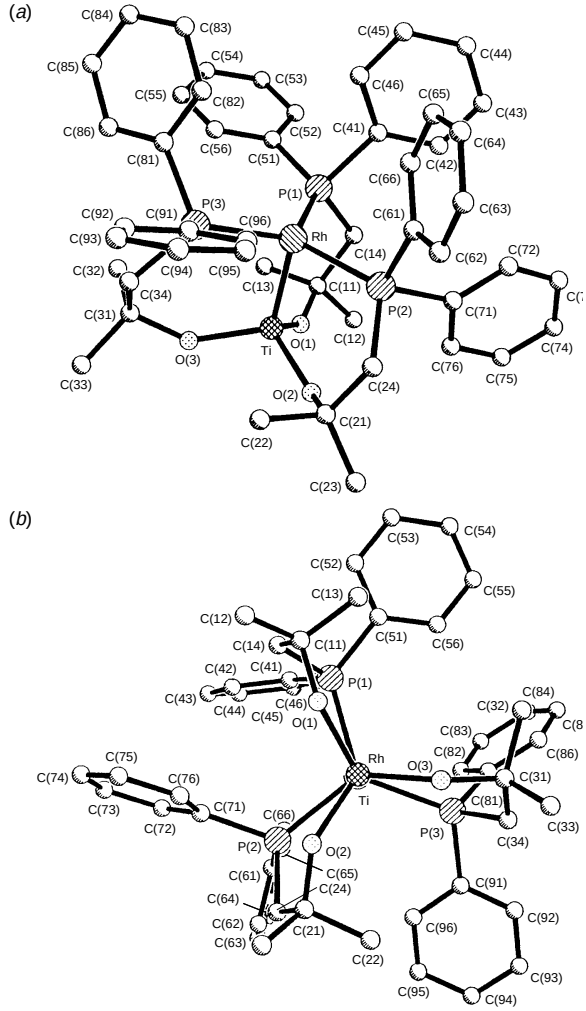



**Fig. 1** Side (*a*) and Ti–Rh parallel (*b*) views of Ti(μ : η¹,η¹-OC-$Me_2CH_2PPh_2)_3$Rh **3**. Selected (see text) interatomic distances (Å) and angles (°): Ti–Rh 2.2142(11), Ti–O(1) 1.833(4), Ti–O(2) 1.831(4), Ti–O(3) 1.827(4), Rh–P(1) 2.318(2), Rh–P(2) 2.316(2), Rh–P(3) 2.322(2); O(1)–Ti–Rh 109.5(1), O(2)–Ti–Rh 108.5(1), O(3)–Ti–Rh 108.9(1), Ti–O(1)–C(11) 143.8(3), Ti–O(2)–C(21) 137.9(4), Ti–O(3)–C(31) 144.1(3), O(1)–C(11)–$C_{av}$ 108.3(14), O(2)–C(21)–$C_{av}$ 109.0(25), O(3)–C(31)–$C_{av}$ 108.4(12), (O)C–C–$P_{av}$ 117.3(25), O(1)–Ti–Rh–P(1) 17.5(2), O(2)–Ti–Rh–P(2) 13.7(2), O(3)–Ti–Rh–P(3) 16.2(2).

on models of $\{MeC(CH_2NSiMe_3)_3\}MFe(CO)_2Cp$ (M = Ti, Sn) by Gade and coworkers.[7] While it is difficult to assess the influence of the alkoxyalkylphosphine bridges on *d*(Ti–Rh), none of the bond angles and distances are characteristically strained while imparting the desired cylindrical symmetry.

We thank the National Science Foundation and Cornell University for support of this research, and Emil B. Lobkovsky for experimental assistance in the X-ray crystallographic study.

## Footnotes and References

* E-mail: ptwz@cornell.edu

† *Selected analytical data*: **1** ($C_6D_6$), $\delta_H$ 1.46 (6 H, s, $CH_3$), 2.63 (2 H, d, $J_{PH}$ 3.2 Hz, $PCH_2$), 7.01–7.09 (6 H, m, Ph), 7.50 (4 H, td, *J* 7.5, 1.8 Hz, Ph); $\delta_C$ 32.08 (d, $J_{PH}$ 7.6 Hz, $CH_3$), 45.70 (d, $J_{PH}$ 16.8 Hz, $PCH_2$), 88.44 (d, $J_{PH}$ 18.3 Hz, OC), 129.04 (d, *J* 2.2 Hz, *m*-Ph), 129.12 (s, *p*-Ph), 133.75 (d, $J_{PH}$ 19.1 Hz, *o*-Ph), 140.44 (d, $J_{PH}$ 12.3 Hz, *ipso*-Ph); $\delta_P$ −24.19 (s). **2** (major, $C_6D_6$), $\delta_H$ 1.64 (12 H, br s, $CH_3$), 1.71 (6 H, br s, $CH_3$), 2.77 (4 H, br d, $J_{PH}$ 10 Hz, $PCH_2$), 3.07 (2 H, br d, $J_{PH}$ 2 Hz, $PCH_2$), 6.62–6.93 (12 H, m, Ph), 6.95–7.10 (6 H, m, Ph), 7.34–7.54 (8 H, m, Ph), 7.67–7.80 (4 H, m, Ph); $\delta_P$ −17.3 (1 P, br s, $\nu_{1/2}$ 450 Hz, free $Ph_2P$), 48 (2 P, br s, $\nu_{1/2}$ 1300 Hz, bound $Ph_2P$); (−80 °C, $C_7D_8$); $\delta_P$ 52.17 (2 P, br m, $J_{RhP}$ 200 Hz, bound $Ph_2P$), 56.42 (1 P, br m, $J_{RhP}$ 180 Hz, bound $Ph_2P$). **3** ($C_6D_6$), $\delta$1.40 (18 H, s, $CH_3$), 3.07 (6 H, br s, $PCH_2$), 6.94–6.97 (18 H, m, Ph), 7.26 (12 H, m, Ph); $\delta_C$ 34.83 (s, $CH_3$), 45.22 (dd, *J* 16.5, 8.8 Hz, $PCH_2$), 77.96 (dd, *J* 3.8, 3.0 Hz, OC), 128.32 (s, Ph), 128.51 (s, Ph), 133.17 (dd, *J* 10.7, 5.3, *o*-Ph), 141.76 (ddd, *J* 18.3, 11.1, 3.4, *ipso*-Ph); $\delta_P$ 24.13 (d, $J_{RhP}$ 208 Hz); UV–VIS (thf), 310 nm ($\varepsilon$ 12,100 $dm^3$ $mol^{-1}$ $cm^{-1}$); Anal. Calc. for $C_{48}H_{54}O_3P_3$-$TiRh{\cdot}0.5C_7H_8$. C, 63.85; H, 6.03. Found: C, 63.45; H, 5.98%. **4** ($C_6D_6$) $\delta_H$ 1.31 (18 H, s, $CH_3$), 3.53 (6 H, br s, $PCH_2$), 6.92–7.11 (18 H, m, Ph), 7.48–7.68 (12 H, m, Ph); $\delta_P$ 17.6 (d, $J_{RhP}$ 177 Hz).

‡ *Crystallograpic data*: $\mathbf{3}{\cdot}0.5C_7H_8$: monoclinic, space group $P2_1/c$, *a* = 13.899(2), *b* = 14.527(2), *c* = 24.016(3) Å, $\beta$ = 96.040(10)°, *U* = 4822.2(11) $Å^3$, *Z* = 4, *T* = 293(2) K, $\mu$ = 0.648 $mm^{-1}$, 6308 independent reflections, $R_1$ = 0.0783, $wR_2$ = 0.1297. CCDC 182/612.

1 *Strong Metal–Support Interactions*, ed. R. T. K. Baker, S. J. Tauster and J. A. Dumesic, ACS Symp. Ser. 298, American Chemical Society, Washington, DC, 1986; S. J. Tauster, *Acc. Chem. Res.*, 1987, **20**, 389.
2 G. S. Ferguson and P. T. Wolczanski, *Organometallics*, 1985, **4**, 1601.
3 S. M. Baxter, G. S. Ferguson and P. T. Wolczanski, *J. Am. Chem. Soc.*, 1988, **110**, 4231.
4 S. M. Baxter and P. T. Wolczanski, *Organometallics*, 1990, **9**, 2498.
5 G. S. Ferguson, P. T. Wolczanski, L. Párkányi and M. C. Zonnevylle, *Organometallics*, 1988, **7**, 1967.
6 W. J. Sartain and J. P. Selegue, *Organometallics*, 1989, **8**, 2153; W. J. Sartain and J. P. Selegue, *Organometallics*, 1989, **6**, 1812; W. J. Sartain and J. P. Selegue, *J. Am. Chem. Soc.*, 1985, **107**, 5818.
7 S. Friedrich, H. Memmler, L. H. Gade, W.-S. Li, I. J. Scowen, M. McPartlin and C. E. Housecroft, *Inorg. Chem.*, 1996, **35**, 2433; S. Friedrich, L. H. Gade, I. J. Scowen and M. McPartlin, *Organometallics*, 1995, **14**, 5344; S. Friedrich, L. H. Gade, I. J. Scowen and M. McPartlin, *Agnew. Chem., Int. Ed. Engl.*, 1996, **35**, 1338.
8 D. Selent, R. Beckhaus and J. Pickardt, *Organometallics*, 1993, **12**, 2857; G. Schmid, B. Stutte and R. Boese, *Chem. Ber.*, 1978, **111**, 1239.
9 G. Giordano and R. H. Crabtree, *Inorg. Synth.*, 1990, **28**, 88.
10 C. A. Hunter, *Chem. Soc. Rev.*, 1994, **23**, 101; C. A. Hunter and J. K. M. Sanders, *J. Am. Chem. Soc.*, 1990, **112**, 5525.
11 F. A. Cotton and R. A. Walton, *Multiple Bonds Between Metal Atoms*, Oxford University Press, New York, 2nd edn., 1993; L. Pauling, *The Nature of the Chemical Bond*, Cornell University Press, Ithaca, NY, 1960.

*Received in Bloomington, IN, USA, 9th July 1997; 7/04890D*

# A simple synthesis for donor-stabilized $Ga_2I_4$ and $Ga_3I_5$ species and the X-ray crystal structure of $Ga_3I_5{\cdot}3PEt_3$

**Andreas Schnepf, Clemens Doriat, Evelyn Möllhausen and Hansgeorg Schnöckel***

*Institut für Anorganische Chemie, Universität Karlsruhe, Engesserstraße, 76128 Karlsruhe, Germany*

**The reaction of 'GaI' synthesized by ultrasonic irradiation of gallium and diiodine in the presence of phosphanes leads to new gallium subhalides in which gallium–gallium bonds are involved.**

The molecular chemistry of the heavier low-valent group 13 elements has gained special interest during recent years.[1] One reason for this rapid development is the cryochemical preparation method in which the high-temperature molecules AlX and GaX (X = Cl, Br, I) are trapped in suitable cooled solvents.[2] By this method donor-stabilized $Al_4I_4$[2] and $Ga_8I_8$[3] compounds can be synthesized.

A much more convenient starting material for many low-valent gallium species is $Ga_2Cl_4$, which consists of $Ga^+GaCl_4^-$ ions in the solid[4] as well as in the molten state.[5] By addition of arenes a series of $Ga^+$–arene compounds with interesting Ga–π interactions has been prepared.[6] On the other hand geniune gallium(II) species with Ga–Ga bonds are formed by addition of special donor compounds. $Ga_2Cl_4{\cdot}2$dioxane[7] was the first prominent example which was followed by the analogous bromides and very recently by two examples of donor-stabilized $Ga_2I_4$ compounds.[3,8] Here we present a new route to low-valent donor-stabilized, gallium iodides, based on a method described by Green *et al.*, in which pale green 'GaI' is formed from a reaction of gallium with iodine in toluene under ultrasonic conditions at *ca.* 35 °C;[9] however, no definite species have, as yet, been isolated.

On treating 'GaI' in toluene with $PEt_3$ at −78 °C a yellow solution was obtained which exhibited $^{31}P$ NMR signals at $\delta$ −24 and −8 (doublet, triplet, coupling constants of 35 Hz) and a singlet at $\delta$ −20, which provides evidence for new molecular species.

The solid metallic residue was analyzed to be elemental gallium. This means that the soluble compound cannot be a pure GaI species since the amount of gallium and iodine was originally 1 : 1.

When the yellow solution was concentrated two new species could be isolated. The first was obtained as a white solid at −78 °C. The white powder can be recrystallized from toluene to provide colourless crystals. X-Ray analysis indicates the formation of $(GaI_2{\cdot}PEt_3)_2$ **1**, the third example of donor-stabilized $Ga_2I_4$, $Ga_2I_4{\cdot}2AsEt_3$ **2**[8] and $Ga_2I_4{\cdot}2NEt_3$ **3**[3] having been characterized very recently.

These iodides exhibit the expected structure with tetrahedrally coordinated gallium atoms and gallium–gallium bonds, Fig. 1.

The gallium–gallium distances are nearly identical for **1** [243.6(2) pm] and **2** [242.8(2) pm] but are shorter than in **3** [249.8(7) pm]. These changes in bond length may be explained with a decrease of donor strength in the series $NEt_3 \rightarrow PEt_3 \rightarrow AsEt_3$. This interpretation is based on an increase of the I–Ga–I bond angle in the same direction [**3**, 101.83(5)°, **1** 107.64(4)°; **2**, 109.0(1)°], which demonstrates that a weaker donor bond is in line with a more $sp^2$-like geometry at the Ga atom.[10]

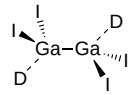



**Fig. 1** Schematic presentation of $GaI_2$ compounds (D = donor group)

However, steric interaction may also influence the Ga–Ga distance since $Ga_2I_4{\cdot}2PPh_3$ **4**, which has been synthesized by ultrasonic treatment of 'GaI' with $PPh_3$ exhibits a Ga–Ga distance of 244.4(2) pm.

The second compound isolated from the yellow solution is $Ga_3I_5{\cdot}3PEt_3$ **5** and its molecular structure is shown in Fig. 2. It is the first neutral compound containing a $Ga_3$ unit (similar to $B_3F_5$[11]).

In **5** a $Ga^I$ centre is the bridging entity for two $Ga^{II}$ units with Ga–Ga distances of 245.1(1) and 246.0(1) pm. As expected, the Ga–I distances in the terminal $GaI_2$ units [261.0(1) pm], are shorter than for the central GaI [262.7(1) pm], a fact which is in line with the larger size of $Ga^I$ relative to $Ga^{II}$. The same argument is valid for the corresponding Ga–P distances: 242.7(3) and 240.5(3) pm. More unexpected are the $^{31}P$ NMR shifts in comparison with that of uncoordinated $PEt_3$ ($\delta$ −19). The shifts of the $PEt_3$ groups at the $Ga^{II}$ centers are observed at $\delta$ −24 and of $PEt_3$ at the central $Ga^I$ unit at $\delta$ −8. Owing to the more positively polarized P atom coordinated to $Ga^I$ ($\delta$ −8) and to a more tetrahedral like geometry at phosphorus [sum of C–P–C bond angles is 310.3(13)° cf. 320.5(7)° for terminally coordinated $PEt_3$ ligands] a stronger donor bonding from $PEt_3$ to $Ga^I$ than to $Ga^{II}$ is concluded.

The overall reaction pathway may be described by Scheme 1. This scheme demonstrates the easy synthesis of donor-

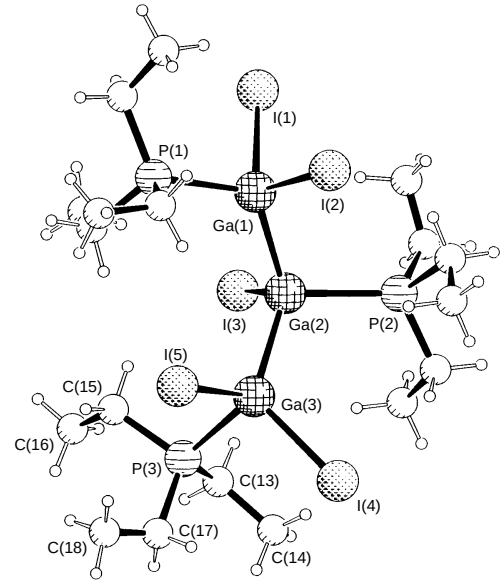
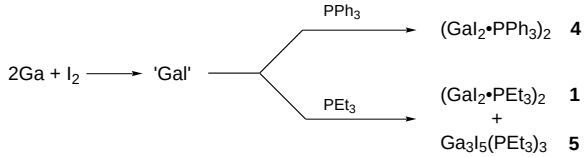



**Fig. 2** Perspective view of the molecular structure of $Ga_3I_5(PEt_3)_3$ **5**. Selected bond lengths (pm) and angles (°): Ga(1)–Ga(2) 245.1(1), Ga(2)–Ga(3) 246.0(1), Ga(1)–I(1) 260.1(1), Ga(2)–I(3) 262.7(1), Ga(3)–I(4) 260.8(1), Ga(1)–P(1) 240.4(3), Ga(2)–P(2) 242.7(3); Ga(1)–Ga(2)–Ga(3) 121.9(1), Ga(2)–Ga(1)–I(1) 117.76(5), Ga(2)–Ga(1)–I(2) 109.34(5), I(1)–Ga(1)–I(2) 107.23(5), P(1)–Ga(1)–Ga(2) 121.85(8), P(2)–Ga(2)–I(3) 98.76(8).




**Scheme 1** Overall reaction pathway

stabilized low-valent gallium iodides, although it does not explain the reaction pathway. However, the results presented here are a strong encouragement to apply this simple synthetic method, besides co-condensation techniques, in order to prepare uncoordinated gallium subhalides.

## Footnotes and References

* E-mail: hg@achpc9.chemie.uni-karlsruhe.de

† $(GaI_2{\cdot}PPh_3)_2$ **4**: colourless crystals, *ca*. 30% yield, $^{31}$P NMR: $\delta$ −18.23 (s). $(GaI_2{\cdot}PEt_3)_2$ **1**: colourless crystals, 22% yield, $^{31}$P NMR: $\delta$ −20.09 (s). $Ga_3I_5(PEt_3)_3$ **5**: yellow crystals, 33% yield, $^{31}$P NMR: $\delta$ −8.38 (t, *J* 35 Hz), −24.05 (d, *J* 35 Hz).

‡ *Crystal data*: STOE STADI IV diffractometer, Mo-K$\alpha$ radiation, $T$ = 200 K. All structures have been solved by direct methods and refined by full-matrix least squares on $F^2$. Programs used: SHELXL-93 and SHELXS.

$(GaI_2{\cdot}PEt_3)_2$ **1**: monoclinic, space group $P2_1/n$, $a$ = 10.034(2), $b$ = 11.857(2), $c$ = 10.763(2) Å, $\beta$ = 92.60(2)°, $U$ = 1279.2(4) Å$^3$, $Z$ = 4, $D_c$ = 2.293 g cm$^{-3}$, $\mu$ = 70.51 cm$^{-1}$, $F$(000) = 812. The structure analysis was based on 4311 reflections ($2\theta_{max}$ 49.98°), observed 2044 [$F > 4\sigma(F)$], 94 parameters. Absorption correction (min., max. transmission 0.47, 0.73). Final residuals: $R$ = 0.068, $R_w$ = 0.180.

$(GaI_2{\cdot}PPh_3)_2$ **4**: monoclinic, space group $C2/c$, $a$ = 14.271(3), $b$ = 15.964(3), $c$ = 17.310(3) Å, $\beta$ = 95.16(3)°, $U$ = 3927.7(14) Å$^3$, $Z$ = 8, $D_c$ = 1.981 g cm$^{-3}$, $\mu$ = 46.21 cm$^{-1}$, $F$(000) = 2200. The structure analysis was based on 4141 reflections ($2\theta_{max}$ 49.98°), observed 2187 [$F > 4\sigma(F)$], 199 parameters. Final residuals: $R$ = 0.038, $R_w$ = 0.081.

$Ga_3I_5(PEt_3)_3$ **5**: orthorhombic, space group $Pna2_1$, $a$ = 13.961(3), $b$ = 12.550(3), $c$ = 21.080(4) Å, $U$ = 3693.3(13) Å$^3$, $Z$ = 4, $D_c$ = 2.155 g cm$^{-3}$, $\mu$ = 64.89 cm$^{-1}$, $F$(000) = 2224. The structure analysis was based on 6255 reflections ($2\theta_{max}$ 55.02°), observed 3728 [$F > 4\sigma(F)$], 264 parameters. Absorption correction (min., max. transmission 0.0125, 0.0517). Final residuals: $R$ = 0.036, $R_w$ = 0.074. CCDC 182/610.

1 W. Uhl, *Angew. Chem., Int. Ed. Engl.*, 1993, **32**, 1386.
2 H. Schnöckel, D. Loos and C. Dohmeier, *Angew. Chem., Int. Ed. Engl.*, 1996, **35**, 129.
3 C. Doriat, M. Friesen, E. Baum, A. Ecker and H. Schnöckel, *Angew. Chem.*, in the press.
4 G. Garton and H. M. Powell, *J. Inorg. Nucl. Chem.*, 1957, **4**, 84.
5 J. W. Akitt, N. N. Greenwood and A. Storr, *J. Chem. Soc.*, 1965, 4410.
6 H. Schmidbaur, *Angew. Chem., Int. Ed. Engl.*, 1985, **24**, 893.
7 J. C. Beamish, R. W. H. Small and I. J. Worrall, *Inorg. Chem.*, 1979, **18**, 220.
8 B. Beagley, S. Godfrey, K. Kelly, S. Kungwankunakorn, C. McAuliffe and R. Pritchard, *Chem. Commun.*, 1996, 2179.
9 M. L. H. Green, P. Mountford, G. Smout and S. Speel, *Polyhedron*, 1990, **22**, 2763.
10 Extensive *ab initio* calculations (DFT, SCF, MP2) have been performed to obtain a better understanding of the bonding. However, these results are not presented here, since they did not allow a deeper understanding than the data provided by experiments described herein.
11 P. L. Timms, *J. Am. Chem. Soc.*, 1967, **89**, 1629.

*Received in Basel, Switzerland, 30th May 1997; 7/03776G*

# Synthesis of pure clinoptilolite without the use of seed crystals

**Craig D. Williams**

*School of Applied Sciences, University of Wolverhampton, Wulfruna Street, Wolverhampton, UK WV1 1SB*

**The present work re-examines the work of Chi and Sand together with that of Satokawa and Itabashi and reports the modifications required to obtain a pure clinoptilolite using conventional reagents, in the absence of seed crystals, at temperatures between 150 and 175 °C under autogeneous pressure.**

The natural zeolite clinoptilolite is widely distributed in nature, being the most abundant of natural zeolites.[1] However it has proved quite difficult to synthesise clinoptilolite under laboratory conditions. This has been ascribed to the rather narrow ranges of gel Si/Al and OH/Si ratios found to produced an acceptable final product. There have been three principal contributions to the synthesis of clinoptilolite in the laboratory. Hawkins *et al.*[2] produced Na,K-clinoptilolite, with the aid of seeds, at temperatures between 130 and 150 °C using volcanic glass as a reagent and high pressures, the final product was impure. Goto[3] produced Na,K-clinoptilolite from more standard chemical reactants at temperatures of 200 °C and autogeneous pressure, however the products were contaminated with mordenite. Chi and Sand[4] produced both Na,Na,K and K-clinoptilolite from standard laboratory reagents at temperatures between 120 and 200 °C and autogeneous pressure, using seed crystals. Recently Satokawa and Itabashi[5] reported the formation of Na,K-clinoptilolite, without the addition of seeds, using conventional chemical reagents.

The materials used in this work were as follows: Silica sources were fumed silica, 99.8 mass% [Cab-o-sil M5 (Carbot Corp; supplied by BDH)], colloidal silica, 40 mass% [Ludox AS40 and HS40 (Du Pont, supplied by Aldrich)]. Alumina sources were aluminium wire, 99.9 mass% (BDH), Versal 900 alumina, 72 mass% [pseudoboehmite (La Roche)], reagent-grade sodium and potassium hydroxide, 98+ mass% (Scientific & Chemical Supplies) and deionised water. The seed crystals (if used) were natural Anaconda 1010A clinoptilolite. Syntheses were carried out in 250 or 500 ml stainless steel autoclaves, stirred at 100 rpm at temperatures between 150 and 175 °C under autogeneous pressure. The reaction gels were prepared as follows; the alkali hydroxide was weighed out into a Teflon beaker and the required mass of aluminium wire or Versal 900 was added together with water (50 ml). This solution was stirred by hand and allowed to cool for 15 min. After this time the silica source was added, together with the outstanding water and the resultant gel was stirred electrically for 5 min until a fluid homogenised gel was obtained. If seed crystals were to be added they were added at this stage. The gel was then transferred to the autoclave and allowed to react for the required time. Both autoclaves were fitted with sampling devices to allow the degree of crystallization to be monitored. Once the gel had fully crystallized the products were recovered by filtration on a Buchner funnel and washed with water ($3 \times 50$ ml), they were then dried in air at 40 °C for 16 h. The synthesised samples were analysed by powder X-ray diffraction using a Philips PW1710 diffractometer utilizing Cu-K$\alpha$ radiation. The scan was run between $2\theta$ 3.5 and 50°, using a scan speed of 1° min$^{-1}$. The diffractometer is linked to a DEC 3100 MicroVAX using Sandman Search and Match routines to search the ICDD database. The purity of the natural and synthesised clinoptilolite was determined using Philips computerised quantitative software in conjunction with the ICDD database. Scanning electron microscopy (SEM) was performed on the samples using a Philips SEM 515 microscope.

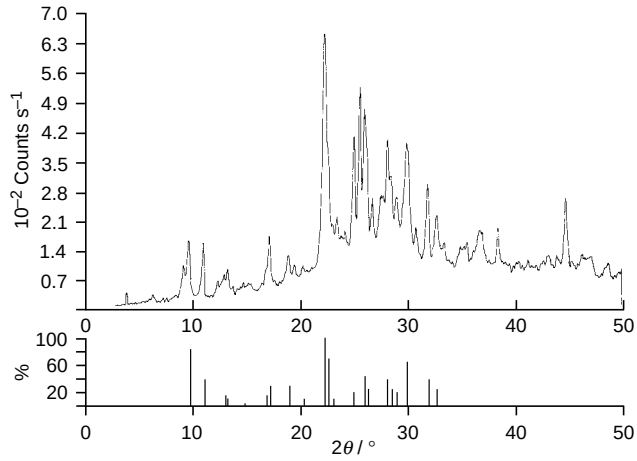



**Fig. 1** Powder X-ray diffractogram for pure clinoptilolite $(NaKCa)_6(SiAl)_{36}O_{72}\cdot 20H_2O$ (JCPDF 25–1349)

**Table 1** Reaction compositions and conditions used for clinopltilolite synthesis

| Attempt | Reaction gel compostion | Seeds (%) | *T*/°C | *t*/h | Silica source | Alumina source | Ref. |
|---|---|---|---|---|---|---|---|
| 1 | $2.1K_2O:0Na_2O:Al_2O_3:10SiO_2:105H_2O$ | 0 | 175 | 20 | Ludox HS40 | Versal 900 | 4[a] |
| 1a | $2.1K_2O:0Na_2O:Al_2O_3:10SiO_2:105H_2O$ | 0 | 175 | 20 | Ludox HS40 | Al wire | 4[a] |
| 2 | $2.1K_2O:0Na_2O:Al_2O_3:10SiO_2:105H_2O$ | 1 | 175 | 96 | Ludox HS40 | Versal 900 | 4[a] |
| 2a | $2.1K_2O:0Na_2O:Al_2O_3:10SiO_2:105H_2O$ | 1 | 175 | 96 | Ludox HS40 | Al wire | 4[a] |
| 3 | $2.1K_2O:0Na_2O:Al_2O_3:10SiO_2:105H_2O$ | 10 | 175 | 96 | Ludox HS40 | Versal 900 | 4[a] |
| 3a | $2.1K_2O:0Na_2O:Al_2O_3:10SiO_2:105H_2O$ | 10 | 175 | 96 | Ludox HS40 | Al wire | 4[a] |
| 4 | $0.72K_2O:0.27Na_2O:Al_2O_3:8.4SiO_2:210H_2O$ | 0 | 150 | 360 | Ludox HS40 | Versal 900 | 5[b] |
| 4a | $0.72K_2O:0.27Na_2O:Al_2O_3:8.4SiO_2:210H_2O$ | 0 | 150 | 360 | Ludox HS40 | Al wire | 5[b] |
| 5 | $0.72K_2O:0.27Na_2O:Al_2O_3:8.4SiO_2:210H_2O$ | 0 | 150 | 336 | Ludox AS40 | Versal 900 | 5[b] |
| 5a | $0.72K_2O:0.27Na_2O:Al_2O_3:8.4SiO_2:210H_2O$ | 0 | 150 | 336 | Ludox AS40 | Al wire | 5[b] |

[a] Run 211. [b] Example 1.

**Table 2** Phase compositions of the final products obtained

| Attempt | Phase composition mass%[a] | $t_b$/h |
|---|---|---|
| 1 | 100% Merlinoite | 20 |
| 1a | 90% Merlinoite–10% philipsite | 20 |
| 2 | 37% Merlinoite–63% potassium feldspar | 96 |
| 2a | 21% Merlinoite–60% potassium feldspar–19% quartz | 96 |
| 3 | 100% Sanidine | 96 |
| 3a | 91% Sanidine–9% quartz | 96 |
| 4 | 69% Clinoptilolite–31% potassium feldspar | 360 |
| 4a | 20% Clinoptilolite–75% potassium feldspar–5% quartz | 360 |
| 5 | 100% Clinoptilolite | 336 |
| 5a | 88% Clinoptilolite–12% mordenite | 336 |

[a] Derived by quantitative XRD analysis. [b] Reaction time.

The molar compositions used in this work and their original reference are detailed in Table 1. All experimental synthesis procedures were repeated three times to check for reproducibility. The powder X-ray diffractogram for the pure clinoptilolite sample is shown in Fig. 1. The mass% of the various phases formed are given in Table 2. Chemical analysis was carried out on the pure clinoptilolite sample using X-ray fluorescence analysis and thermal analysis, the results are shown in Table 3.

As can be seen, several attempts were made to repeat the work outlined by Chi and Sand, however, for each attempt the required phase, clinoptilolite, appeared elusive. It would appear that the substitution of Ludox AS40 for Ludox HS40 can lead to the successful synthesis of a pure clinoptilolite without the need to use seed crystals. It is well known that clinoptilolite has a high affinity for the ammonium ion and Ludox AS40 is stabilised by the ammonium ion, as opposed to Ludox HS40 which is sodium stabilised. It can also be seen that the fast dissolution characteristics of aluminium wire favour the formation of denser phases, with all reaction runs producing

**Table 3** Elemental compositions fo the pure clinoptilolite obtained

| Elemental oxide[a] | Conc. (%) |
|---|---|
| $SiO_2$ | 61.0 |
| $Al_2O_3$ | 11.8 |
| $K_2O$ | 8.13 |
| $Na_2O$ | 1.78 |
| $Fe_2O_3$ | 0.066 |
| $ZrO_2$ | 0.030 |
| $H_2O$ (LOI) | 17.3 |

[a] Determined by XRF and TG.

mixed final products. Therefore it would seem expedient to use an alumina source which dissolves into solution more slowly, such as the Versal 900 or similar hydrated aluminium oxides. Finally it can be concluded that it is difficult to synthesise clinoptilolite in the laboratory free from impurities and that pure clinoptilolite is transitory in nature. This observation may explain why so few reports of a successful pure clinoptilolite synthesis method can be found in the literature.

The author would like to thank Dr Mick Morris of British Gas for the gift of the 250 ml autoclave, Dr Alan Dyer for supplying the Anaconda 1010A natural clinoptilolite and La Roche for the Versal 900 alumina source.

## Footnote and References

* E-mail: cs1920@wlv.ac.uk

1 G. Gottardi and E. Galli, *Natural Zeolites*, Springer Verlag, Berlin, 1985, p. 256.
2 D. B. Hawkins, R. A. Sheppard and A. J. Gude, *Natural Zeolites: Occurrence, Properties and Use*, ed. L. B. Sand and F. A. Mumpton, Pergamon, Oxford, 1978, p. 337–343.
3 Y. Goto, *Am. Mineral.*, 1977, **62**, 330.
4 C.-H. Chi and L. B. Sand, *Nature*, 1983, **304**, 255.
5 S. Satakawa and K. Itabashi, *Eur. Pat. Appl.*, EP 0681 991 A1, 1995.

*Received in Cambridge, UK, 21st July, 1997; 7/05198K*

# Peroxo-bridged dinuclear cobalt(III) complexes containing *N*-glycoside ligands from tris(2-aminoethyl)amine and D-glucose and their reversible dioxygen binding properties

**Tomoaki Tanase,*[a] Tomoko Onaka,[a] Masako Nakagoshi,[a] Isamu Kinoshita,[b] Kozo Shibata,[b] Matsumi Doe,[b] Junko Fujii[b] and Shigenobu Yano*[a]**

*Department of Chemistry, Faculty of Science, Nara Women's University, Nara 630, Japan*
*Department of Chemistry, Faculty of Science, Osaka City University, Sumiyoshi-ku, Osaka 662 Japan*

**Peroxo-bridged dinuclear cobalt(III) complexes containing *N*-glycoside ligands from tris(2-aminoethyl)amine (tren) and D-glucose (D-Glc), $[\{Co[(D\text{-}Glc)_2tren]\}_2O_2]X_3\cdot 5H_2O$ (X = Cl 2, Br 3), and their reversible dioxygen binding properties are reported [$(D\text{-}Glc)_2$tren = bis(*N*-D-glucosyl-2-aminoethyl)(2-aminoethyl)amine].**

Interactions of carbohydrates with metal ions have become an important subject in bioinorganic chemistry, since many sugar-processing enzymes have been revealed to function with redox non-active metal ions such as $Mg^{2+}$, $Mn^{2+}$ and $Zn^{2+}$ in the active sites.[1] Elucidation of reactivity and behavior of sugars around redox active metal ions is also potentially important in relevance to ribonucleotide reductases which utilize non-haem diiron or coenzyme $B_{12}$ functional units.[2]

We have recently reported mononuclear cobalt(II) complexes ligated by a heptadentate *N*-glycoside formed from tris(2-aminoethyl)amine (tren) and mannose-type aldohexoses, $[Co\{(aldose)_3tren\}]X_2$ **1**, where $(aldose)_3$tren = tris(*N*-aldosyl-2-aminoethyl)amine, aldose = D-mannose (D-Man), L-rhamnose (L-Rha), and X = Cl, Br, $1/2SO_4$. Complex **1** showed a dynamic chiral inversion around the metal centre ($\Delta\leftrightarrow\Lambda$) induced by the interaction of sugars with the sulfate anion.[3] In general, mannose-type aldoses such as D-Man and L-Rha have 2,3-*cis* configuration and the sugar ring is axially oriented with respect to the chelate ring upon coordination through the 1,2-functional groups with the β-anomeric form being adopted.[4] The axial orientation of D-Man and L-Rha enables close sugar–sugar interactions around the metal centres.[5] The present study was carried out by utilizing D-glucose (D-Glc) as the sugar component, which has 2,3-*trans* configuration and was equatorially oriented on ligating through the 1,2-functional groups with the β-anomeric form being adopted.[4] We report herein novel μ-peroxo dicobalt(III) complexes supported by β-D-glucosyl polyamine ligands and their reversible dioxygen binding properties.

A methanolic solution of $Co^{II}X_2\cdot 6H_2O$ (X = Cl, Br) was treated in air with tris(*N*-D-glucosyl-2-aminoethyl)amine [$(D\text{-}Glc)_3$tren], which was prepared from D-glucose (D-Glc) and tris(2-aminoethyl)amine (tren) *in situ*. The resultant dark brown solution was chromatographed on a Sephadex LH-20 gel permeation column, eluted with methanol, and the brown band was collected. Slow evaporation of the solution yielded brown crystals formulated as $[\{Co[(D\text{-}Glc)_2tren]\}_2O_2]X_3\cdot 5H_2O$ (X = Cl **2**, Br **3**) in low yields, where $(D\text{-}Glc)_2$tren is bis(*N*-D-glucosyl-2-aminoethyl)(aminoethyl)amine.† Elemental analyses indicated that complexes **2** and **3** contained a *N*-glycoside ligand, $(D\text{-}Glc)_2$tren, formed by a loss of one D-glucose residue from $(D\text{-}Glc)_3$tren, per metal. The presence of a peroxo bridge between the two cobalt ions is demonstrated by the intense electronic absorption band around 400 nm (log $\varepsilon$ 3.46–3.58), corresponding to a peroxo–metal charge-transfer band, and the IR peak at 888 $cm^{-1}$ assignable to $\nu_{O-O}$. Two environmentally different D-glucose moieties were confirmed by the $^1H$ and $^{13}C$ NMR spectra of **3** in $D_2O$ assignments being carried out by combination of $^1H$–$^1H$ and $^{13}C$–$^1H$ COSY, HMBC, and HMQC NMR spectra. The *N*-glycosidic bond formation was unambiguously determined by the isotopic multiplets observed in the $^{13}C$ NMR spectrum in $D_2O$–$H_2O$ (1 : 1). Two resonances for the C(1) carbon atoms of D-glucose were observed as doublets owing to the isotope induced shifts of the neighboring N–H and N–D species.[6]†

ORTEP diagrams for the complex cation of **2** are illustrated in Fig. 1 and 2.‡ The complex cation consists of two $Co^{III}$ ions bridged by a peroxo unit [O(1)–O(2) 1.452(10) Å]. The cation has a pseudo-$C_2$ symmetry with respect to an axis passing through the middle of the O–O bond (Fig. 2). The metal–metal separation is 4.114(2) Å. Each cobalt ion is ligated by the *N*-glycoside, $(D\text{-}Glc)_2$tren, through the four nitrogen atoms and the C(2) oxygen atom of a sugar moiety together with the peroxide to give distorted *cis*-(O,O)-$[CoN_4O_2]$ octahedral geometry. The other D-glucose residue is anchored on the metal by only the *N*-glycosidic nitrogen atom; hydroxyl groups of the sugar lie away from the coordination sphere of the metal.[5] The $Co^{III}_2(\mu\text{-}O_2)$ core is supported by hydrogen bonds between the sugar moieties [O(112)···O(212) 2.42(1) Å, O(113)···O(213) 2.70(1) Å, O(122)···N(23) 2.95(1) Å, O(222)···N(13) 2.92(1)

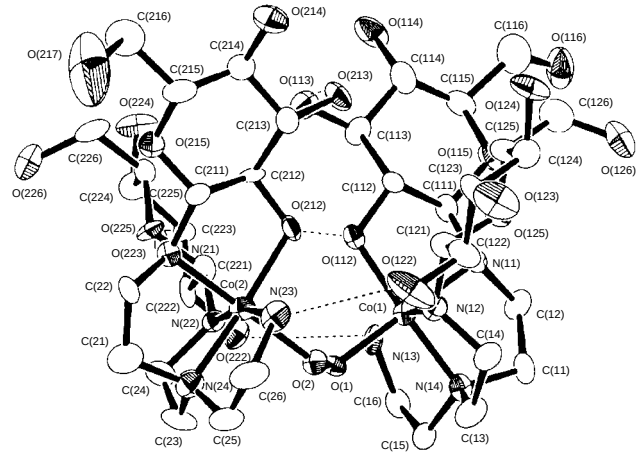



**Fig. 1** ORTEP diagram of the complex cation of **2**, $[\{Co[(D\text{-}Glc)_2tren]\}_2O_2]^{3+}$. Selected bond distances (Å) and angles (°); Co(1)–O(1) 1.895(7), Co(1)–O(112) 1.910(7), Co(1)–N(11) 1.963(9), Co(1)–N(12) 1.999(9), Co(1)–N(13) 1.977(8), Co(1)–N(14) 1.918(9), Co(2)–O(2) 1.916(7), Co(2)–O(212) 1.973(7), Co(2)–N(21) 1.954(9), Co(2)–N(22) 1.993(9), Co(2)–N(23) 1.98(1), Co(2)–N(24) 1.95(1), O(1)–O(2) 1.452(10); O(1)–Co(1)–O(112) 92.1(3), O(112)–Co(1)–N(11) 87.6(3), N(11)–Co(1)–N(14) 87.2(4), N(12)–Co(1)–N(14) 86.7(4), N(13)–Co(1)–N(14) 84.6(4), O(2)–Co(2)–O(212) 92.9(3), O(212)–Co(2)–N(21) 87.2(3), N(21)–Co(2)–N(24) 87.6(4), N(22)–Co(2)–N(24) 87.6(4), N(23)–Co(2)–N(24) 84.4(4), Co(1)–O(1)–O(2) 118.1(5), Co(2)–O(2)–O(1) 115.8(5),O(1)–Co(1)–N(11) 175.7(3), O(112)–Co(1)–N(14) 173.8(3), N(12)–Co(1)–N(13) 167.5(4), O(2)–Co(2)–N(21) 177.8(4), O(212)–Co(2)–N(24) 173.2(4), N(22)–Co(2)–N(23) 167.6(4).

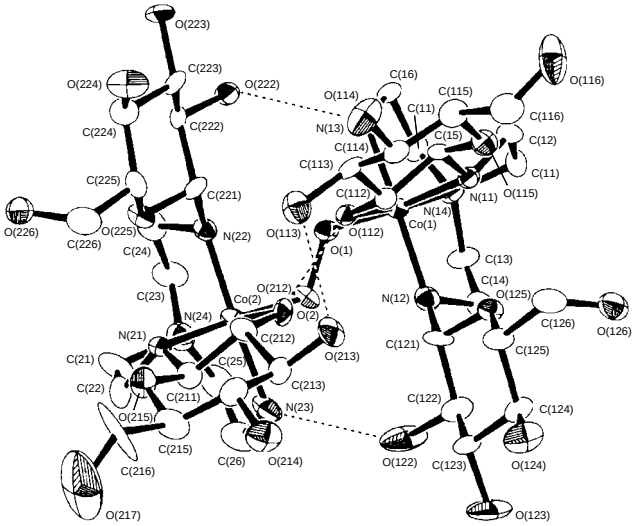



**Fig. 2** ORTEP plot of the complex cation of **2**, $[\{Co[(D\text{-}Glc)_2tren]\}_2O_2]^{3+}$, viewed along the pseudo-$C_2$ axis.

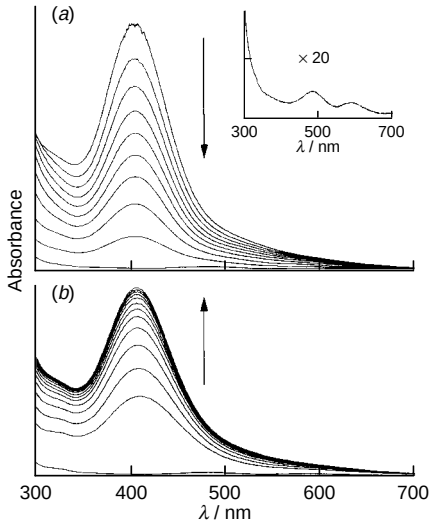



**Fig. 3** (*a*) An electronic absorption spectral change of **2** in $CH_3OH$ upon irradiation with a high-pressure mercury lamp at room temp. under a nitrogen atmosphere, monitored every 5 min. The final spectrum is expanded in the upper-right. (*b*) Absorption spectral changes measured in air every 5 min after the irradiation.

Å]. In particular, the short interatomic distance O(112)···O(212) suggests the presence of O$^-$···H–O type strong hydrogen bond, similar to that observed in the dinuclear nickel(II) complex bridged by a β-D-mannofuranoside residue.[7] This hydrogen-bonding system distorts the Co–O–O–Co torsional angle from planarity to 100.4(6)°, between 0–65° found in $Co^{III}_2(\mu\text{-}O_2)(\mu\text{-}X)$ double-bridged complexes (X = OH, NH) and 145–180° in $Co^{III}_2(\mu\text{-}O_2)$ single-bridged structures.[8]

The electronic absorption spectrum of **2** in methanol rapidly changed upon irradiation with a high-pressure mercury lamp at room temp. under a nitrogen atmosphere [Fig. 3(*a*)]. The absorption intensity around 400 nm, characteristic of a μ-peroxo dicobalt(III) complex, decreased and finally very weak absorptions around 480 and 590 nm were observed. This spectral change could correspond to deoxygenation of **2** leading to a cobalt(II) species and $O_2$, by analogy with the photolysis of $[(en)_2Co^{III}(\mu\text{-}OH)(\mu\text{-}O_2)Co^{III}(en)_2]^{3+}$ (en = 1,2-diaminoethane).[9]

When the resultant solution was exposed to air after irradiation, the absorption peak at 400 nm was immediately restored, and finally, almost 80% of complex **2** was recovered on the basis of its absorbance [Fig. 3(*b*)]. These spectral changes clearly indicated an almost reversible dioxygen binding through the μ-peroxo dimer **2**.§

The sugar units dramatically influence the redox property of the cobalt centre, which was demonstrated by the differential reactivity toward dioxygen molecule between the complex with mannose-type aldoses (D-Man, L-Rha) and that with D-glucose. Studies using other glucose-type aldoses are now in progress.

This work was partially supported by a Grant-in-Aid for Scientific Research from the Ministry of Education of Japan and Grants from Iwatani, Nippon Itagarasu, Mitsubishi-Yuka and Nagase Foundations, and the San-Ei Gen Foundation for Food Chemical Research.

## Footnotes and References

* E-mail: tanase@cc.nara-wu.ac.jp; yano@cc.nara-wu.ac.jp

† Synthetic procedures and analytical and spectral data for **2** and **3**, and the $^{13}C$ NMR spectra of **3** in $D_2O$ and in $D_2O$–$H_2O$ (1:1) are available as supplementary materials upon request to the authors.

‡ *Crystal data* for $\mathbf{2}\cdot 4H_2O\cdot CH_3OH$: orthorhombic, space group $P2_12_12_1$ (no. 19), $a$ = 19.384(8), $b$ = 23.468(5), $c$ = 13.195(5) Å, $U$ = 6002(2) Å$^3$, $Z$ = 4, $D_c$ = 1.440 g cm$^{-3}$, $T$ = −99 °C, $R$ = 0.078, $R_w$ = 0.085 [$w = 1/\sigma^2(F_o)$] for 4961 reflections with $I > 3\sigma(I)$. The structure was solved and refined with teXsan program package. CCDC 182/605.

§ Detailed photochemistry and kinetic parameters will be reported elsewhere.

1 R. W. Gracy and E. A. Noltmann, *J. Biol. Chem.*, 1968, **243**, 4109; R. W. Gracy and E. A. Noltmann, *J. Biol. Chem.*, 1968, **243**, 5410; R. L. Root, J. R. Durrwachter and C.-H. Wong, *J. Am. Chem. Soc.*, 1985, **107**, 2997; J. Jenkins, J. Janin, F. Rey, M. Chiadmi, H. Tilbeurgh, I. Lasters, M. D. Maeyer, D. V. Belle, S. J. Wodak, M. Lauwereys, P. Stanssens, N. T. Mrabet, J. Snauwaert, G. Matthyssens and A.-M. Lambeir, *Biochemistry*, 1992, **31**, 5449; M. Whitlow, A. J. Howard, B. C. Finzel, T. L. Poulos, E. Winborne and G. L. Gilliland, *Proteins*, 1991, **9**, 153; Y. Zhang, J.-Y. Liang, S. Huang, H. Ke and W. N. Lipscomb, *Biochemistry*, 1993, **32**, 17; Y. Xue, S. Huang, J.-Y. Liang, Y. Zhang and W. N. Lipscomb, *Proc. Natl. Acad. Sci. USA*, 1994, **91**, 12482; K. D. Hardman, R. C. Agarwal and M. Freiser, *J. Mol. Biol.*, 1982, **157**, 69.

2 S. J. Lippard and J. M. Berg, *Principles of Bioinorganic Chemistry*, University Science Book, CA, 1994, ch. 11.

3 T. Tanase, M. Nakagoshi, A. Teratani, M. Kato, Y. Yamamoto and S. Yano, *Inorg. Chem.*, 1994, **33**, 6; S. Yano, M. Nakagoshi, A. Teratani, M. Kato, T. Tanase, Y. Yamamoto, H. Uekusa and Y. Ohashi, *Mol. Cryst. Liq. Cryst.*, 1996, **276**, 253; S. Yano, M. Nakagoshi, A. Teratani, M. Kato, T. Onaka, M. Iida, T. Tanase, Y. Yamamoto, H. Uekusa and Y. Ohashi, *Inorg. Chem.*, in the press.

4 S. Yano, *Coord. Chem. Rev.*, 1988, **92**, 113, and references therein; S. Yano and M. Ohtsuka, *Metal Ions in Biological Systems*, ed. H. Sigel and A. Sigel, Marcel Dekker, New York, 1996, vol. 32, p. 27.

5 T. Tanase, M. Doi, R. Nouchi, M. Kato, Y. Sato, K. Ishida, K. Kobayashi, T. Sakurai, Y. Yamamoto and S. Yano, *Inorg. Chem.*, 1996, **35**, 4848.

6 K. Ishida, M. Yashiro, S. Yano, M. Hidai and S. Yoshikawa, *J. Am. Chem. Soc.*, 1988, **110**, 2015; K. Ishida, M. Yashiro, S. Yano, M. Hidai and S. Yoshikawa, *J. Chem. Soc., Dalton Trans.*, 1989, 1241.

7 T. Tanase, K. Kurihara, S. Yano, K. Kobayashi, T. Sakurai, S. Yoshikawa and M. Hidai, *Inorg. Chem.*, 1987, **26**, 3134.

8 C.-H. Yang and M. W. Grieb, *Inorg. Chem.*, 1973, **12**, 663; W. P. Schaefer and R. E. Marsh, *Acta Crystallogr.*, 1966, **21**, 735; W. P. Schaefer, *Inorg. Chem.*, 1968, **7**, 725; U. Thewalt, *Z. Anorg. Allg. Chem.*, 1972, **393**, 1; T. Shibahara and M. Mori, *Bull. Chem. Soc. Jpn.*, 1973, **46**, 2070; J. R. Fritch, G. G. Christoph and W. P. Schaefer, *Inorg. Chem.*, 1973, **12**, 2170; F. R. Fronczek, W. P. Schaefer and R. E. Marsh, *Acta Crystallogr., Sect. B*, 1974, **30**, 117; M. Zehnder, U. Thewalt and S. Fallab, *Helv. Chim. Acta*, 1976, **59**, 2290; U. Thewalt and G. Struckmeier, *Z. Anorg. Allg. Chem.*, 1976, **419**, 163; S. Fallab, M. Zehnder and U. Thewalt, *Helv. Chim. Acta*, 1980, **63**, 1491; F. Bigoli and M. A. Pellinghelli, *Cryst. Struct. Commun.*, 1981, **10**, 1445; T. Shibahara, M. Mori and S. Ooi, *Bull. Chem. Soc. Jpn.*, 1981, **54**, 433; U. Thewalt, *Z. Anorg. Allg. Chem.*, 1982, **485**, 122; G. G. Christoph, R. E. Marsh and W. P. Schaefer, *Inorg. Chem.*, 1969, **8**, 291; U. Thewalt and R. E. Marsh, *Inorg. Chem.*, 1972, **11**, 351; B. M. Gatehouse and L. Spiccia, *Aust. J. Chem.*, 1991, **44** 351.

9 M. Kikkawa, Y. Sasaki, S. Kawata, Y. Hatakeyama, F. B. Ueno and K. Saito, *Inorg. Chem.*, 1985, **24**, 4096.

*Received in Cambridge, UK, 12th August 1997; 7/05876D*

# Synthesis of *meso* substituted porphyrins in air without solvents or catalysts

**Charles M. Drain* and Xianchang Gong**

*Department of Chemistry, Hunter College of the City University of New York, 695 Park Avenue, New York, NY 10021, USA*

***meso*-Tetraarylporphyrins are synthesized from pyrrole and aryl aldehydes cleanly and efficiently in one step without solvents or catalysts by reactions at temperatures 10–15 °C above the boiling point of the starting aldehydes using air as oxidant.**

The remarkably diverse photo-, electro- and bio-chemical properties of the porphyrins continue to attract the attention of researchers even after well over a hundred years. In this century porphyrin research has gone from Hans Fischer's pioneering synthesis of hemin in the 1920s,[1] to their use as redox catalysts,[2] molecular electronic devices[3] and photodynamic therapy agents. In order to exploit their chemistry and fine tune their properties, a variety of synthetic methods have been developed for non-natural porphyrins, especially for the *meso* tetra-substituted porphyrins.[4–8] We have developed a simple way to synthesize many *meso* substituted porphyrins without solvents, catalysts or man-made oxidants, and the reaction is complete in minutes. This is the synthesis of porphyrins at high temperatures and/or in the gas phase.

Previous syntheses using pyrrole and aromatic aldehydes are typified by the Ruthemund sealed-tube anaerobic reaction in pyridine at 200 °C (*ca*. 5% yield),[4] the Adler–Longo reaction in propionic or acetic acid under aerobic conditions (10–30% yield),[5] the MacDonald coupling of dipyrroles (10–20% yield)[6] and most recently the Lindsey, anaerobic condensation to form the porphyrinogen followed by oxidation to the porphyrin (10–60% yield).[7] The rapid appearance of water and what is now known to be the porphyrinogen[8] in a pseudo zero-order reaction in the Adler–Longo method, the equilibrium conditions of the Lindsey method, and the stability of the porphyrin to high temperatures of the Rothemund method, led us to attempt porphyrin synthesis at high temperatures and in the gas phase.

Although solventless mixtures of the pyrrole and aldehyde rapidly heated to > 200 °C form the corresponding porphyrins,[9] better yields but similar side product distributions are observed by mixing the two reagents in the gas phase at the same temperature.† Whether the porphyrin is formed entirely in the gas phase is unknown at present, but a brown–purple vapour is observed within *ca*. 2 s of adding the pyrrole to gaseous aldehyde, and a blue–black tar begins to condense on the sides of the reaction vessel soon afterwards. In the rapid heating experiments, porphyrins condense at the top of the reaction vessel, which is below the reaction temperature, with the same purity as that found in the bottom containing the original solution.

High temperature gas phase conditions allow for the rapid aldehyde–pyrrole condensation, for the removal of water from the proximity of the intermediate and for an increase in the rate of oxidation by dioxygen. This latter reaction is proposed to be the rate limiting step in the Adler–Longo method.[5] Examination of yield and products *versus* time indicates that oxidation of the porphyrinogen, or its intermediates, occurs very rapidly, since we detect no porphyrinogen and no chlorin in the UV–VIS spectra (Fig. 1) even after reaction times of a few seconds. Anaerobic reaction conditions result in very low porphyrin yields and only traces of porphyrinogen, indicating the crucial role of dioxygen in trapping the porphyrin products. Studies show that the reaction temperature must be above the boiling point of benzaldehyde to result in yields of *meso*-tetraphenylporphyrin (TPP) greater than a few percent, but the yield levels off by 210 °C. That the rapid removal of water from the condensing porphyrin (intermediates) is one key to these reaction conditions is shown by the decreased yield (*ca*. 12%) when a 5 : 1 water : aldehyde mixture is used.[10] Consistent with the known chemistry of aryl aldehydes, benzaldehyde can serve as an oxidant, since greater than 20% yields are obtained in experiments where the ratio of benzaldehyde to pyrrole is 3 : 1 and the amount of dioxygen is limiting. Catalytic amounts ( < 5 mol%) of HCl or $NH_3$ block porphyrin formation almost entirely, but washing the reaction vessel with 1.0 M HCl or KOH and thorough drying has no effect. TFA diminishes the formation of TPP, but increases the yield of tetramesityl-porphyrin from trace amounts to about 7% for reasons still under investigation.

This method is general enough to make a wide variety of *meso* substituted porphyrins in yields ranging from 7 to 23% (not optimized) (Table 1). For those reactions using aldehydes that have boiling points greater than *ca*. 250 °C at 1 atm, where the pyrrole begins to decompose too rapidly, a thin film of the melted or liquid aldehyde is coated into the reaction vessel sides at *ca*. 220 °C before the pyrrole is injected. Thus a 15% yield of tetrakis(4′-*tert*-butylphenyl)porphyrin are obtained.

We are currently examining the complex balance between temperature, pressure and concentrations of all three reactants in order to maximize the yield and gain a deeper understanding of the reaction mechanism and thermodynamics. Porphyrin formation is believed to be driven by enthalpic changes[9] and the macrocycle is preferred over the polymer for entropic reasons ($\Delta H$ −212 kcal mol$^{-1}$, $\Delta G$ −166 kcal mol$^{-1}$, and $\Delta S$ −153 e.u.).[7–9] If this data is correct, then the favourable $\Delta G$ is dominated by the entropy term, and cooler temperatures should favour porphyrin formation. However, the porphyrin yield increases with temperature up to *ca*. 250 °C, thus under these conditions the high temperature gas phase formation of porphyrins represents a kinetically controlled reaction dominated by the reactivity of dioxygen—as the oxidation studies suggest. The glass walls of the vial do not directly participate in

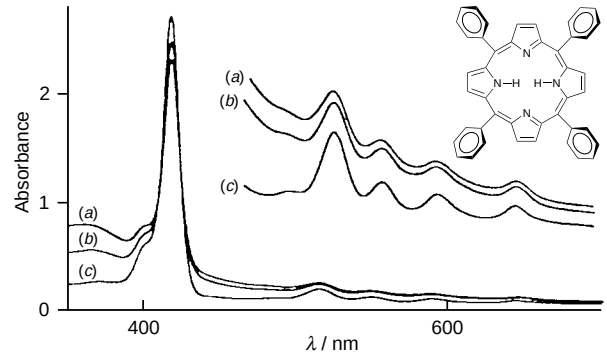
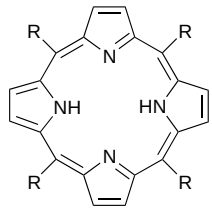



**Fig. 1** Unpurified $CHCl_3$ rinses from two gas phase reactions: (*a*) a 3 : 1 and (*b*) a 1 : 1 ratio of benzaldehyde to pyrrole are compared to (*c*) the UV–VIS absorption spectra of known pure $H_2$TTP from a large gas phase reaction, showing the purity of the soluble materials and the lack of dipyrromethanes and chlorins in the product mixture. The inset absorbance scale is ×10.

**Table 1** Isolated, unoptimized yields of porphyrin derivatives



| R | Yield (%)[a] |
|---|---|
| Ph | 23 |
| 4-$MeC_6H_4$ | 20 |
| 4-$Pr^iC_6H_4$ | 12 |
| 4-$Bu^tC_6H_4$ | 15 |
| 4-$ClC_6H_4$ | 10 |
| 4-$MeOC_6H_4$ | 20 |
| 4-$MeSC_6H_4$ | 10 |
| Mes[b] | 7 |
| $C_5H_{11}$ | 1–2 |
| 4-Pyridyl | 10[c] |

[a] ± 3%. [b] 5 mol% TFA added to reaction. [c] 25 mol% $Zn(Ac)_2$ added to reaction.

the reaction since control experiments, whereby glass wool is inserted into the reaction vial or the vial has been silanated, show similar yields and reactivities. We are further investigating the possibilities of surface catalysis.

Our results show that the commercially important *meso* arylporphyrins may be synthesized without catalysts or solvent, and using only dioxygen as an oxidant. The polymeric byproducts are insoluble, so washing the reaction vessel with minimal amounts of solvent followed by a short silica gel column results in pure porphyrin. Dioxygen is a key requirement for porphyrin synthesis under these conditions. While the unoptimized 7–23% isolated yields resulting from our high temperature gas phase method are typically not as good as the Lindsey method and on a par with the Adler–Longo and MacDonald methods, the great advantages of this method are its simplicity and minimal waste production. Purification is generally easier since there is virtually no chlorin formation and the tarry byproducts are less soluble than other byproducts from other procedures. We have been able to scale up this method for the synthesis of 0.1–0.3 g of several porphyrins using a glass tube wrapped with heating tape (or in a zone refining furnace) whereby the aldehyde is slowly injected at one end, and the pyrrole is slowly added at the other end, of a 1.5 × 60 cm tube closed with glass wool to allow sufficient dioxygen for the reaction. The product is removed with 100–200 ml $CHCl_3$ and a very short silica gel column yields pure material. Thus, this method is quite amenable for industrial-type reactors.

We thank D. Mauzerall for his consistently insightful ideas. Financial support from MBRS (GM08176-18) and Research Centers in Minority Institutions (RR-03037) grants to Hunter College are acknowledged, as is a Eugene Lang Faculty development award to C. M. D.

## Footnotes and References

* E-mail: cdrain@shiva.hunter.cuny.edu

† Synthesis of *meso*-tetraphenylporphyrin is used as an example. A 5 ml vial is closed by a cap fitted with a rubber septum, placed in a temperature controlled sand bath and heated to *ca*. 200 °C, at which time benzaldehyde (10 μl, 0.1 mM) is injected into the system. After a few minutes, when the aldehyde is in the gas phase, 1 equiv. of pyrrole is injected slowly into the vial. (Alternatively both reagents can be placed in the vial, stirred and placed in the sand bath, but the yields are 25–30% lower.) The vial is kept at *ca*. 200 °C for another 15 min. Rinsing the reaction vessel sparingly with $CH_2Cl_2$ or $CHCl_3$ removes most of the porphyrin in *ca*. 80% purity as measured by UV–VIS spectroscopy,[7] while the remaining insoluble material contains < 1% of the porphyrin yield. Isolated yields are listed in Table 1. All compounds had satisfactory $^1H$ NMR, UV–VIS and FAB mass spectra. **Caution**: the rapid formation of gases and the flash point of all compounds should be considered. Under these conditions there is some benzaldehyde decomposition, and little decomposition of the pyrrole.

‡ A plethora of methods result in spectroscopically detectable quantities of porphyrins, including gamma ray irradiation, supercritical fluids, very high pressures, DC plasmas and fluidized bed reactors (ref. 9).

1 For a remarkable book on porphyrin history, chemistry, and applications, see *The Chemical and Physical Behavior of Porphyrin Compounds and Related Structures*, ed. A. D. Adler, *Ann. N.Y. Acad. Sci.*, 1973, vol. 206.
2 For a review, T. Mlodnicka, *J. Mol. Catal.*, 1986, **36**, 205.
3 For example, C. M. Drain and J.-M. Lehn, *J. Chem. Soc., Chem. Commun.*, 1994, 2313; C. M. Drain, K. C. Russell and J.-M. Lehn, *Chem. Commun.*, 1996, 337; C. M. Drain and D. Mauzerall, *Biophys. J.*, 1992, **63**, 1556; C. M. Drain and D. Mauzerall, *Bioelectrochem. Bioenerg.*, 1990, **24**, 263.
4 P. Rothemund, *J. Am. Chem. Soc.*, 1939, **61**, 2912; P. Rothemund and A. R. Menotti, *J. Am. Chem. Soc.*, 1941, **63**, 267.
5 A. D. Adler, F. R. Longo and W. Shergalis, *J. Am. Chem. Soc.*, 1964, **86**, 3145; A. D. Adler, F. R. Longo, J. D. Finarelli, J. Goldmacher, J. Assour and L. Korasakoff, *J. Org. Chem.*, 1967, **32**, 476; R. A. W. Johnstone, M. L. P. G. Nunes, M. M. Pereira, A. M. Gonsalves and A. C. Serra, *Heterocycles*, 1996, **43**, 1423.
6 G. P. Arsenault, E. Bullock and S. F. MacDonald, *J. Am. Chem. Soc.*, 1960, **82**, 4384; L. T. Nguyen, M. O. Senge and K. M. Smith, *J. Org. Chem.*, 1996, **61**, 998.
7 J. S. Lindsey, I. C. Schreiman, H. C. Hsu, P. C. Kearney and A. M. Marguerattaz, *J. Org. Chem.*, 1987, **52**, 827; J. S. Lindsey, K. A. MacCrum, J. S. Tyhonas and Y.-Y. Chuang, *J. Org. Chem.*, 1994, **59**, 579 and references cited therein.
8 D. Mauzerall, in *The Porphyrins*, ed. D. Dolphin, Academic Press, New York, 1978, vol. 2.
9 P. George, p. 84 in ref. 1; trace amounts of porphyrin are formed at room temperature and pressure: G. W. Hodgson, *Ann. N.Y. Acad. Sci.*, 1972, **194**, 86.
10 These results suggest that the porphyrin condensation reactions in the presence of clays may be enhanced by the local removal of water or salt effects rather than by specific surface interactions. For example, T. Shinoda, Y. Izumi and M. Onaka, *J. Chem. Soc., Chem. Commun.*, 1995, 1801.

*Received in Columbia, MO, USA, 1st July 1997; 7/04600F*

# Multivalent neoglycoconjugates: solid-phase synthesis of N-linked α-sialodendrimers

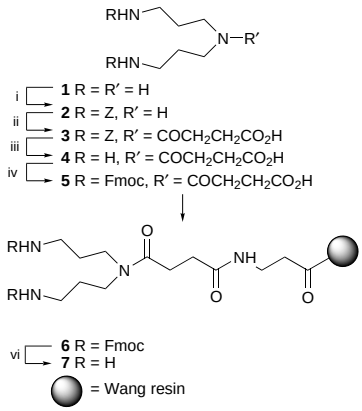
**Muriel Llinares and René Roy***

*Department of Chemistry, University of Ottawa, Ottawa, ON, K1N 6N5 Canada*

**A series of N-linked α-sialodendrimers with valencies of 2, 4 and 8 has been scaffolded on an *N*,*N*-bis(3-aminopropyl)succinamic acid core using Wang resin and 9-fluorenylmethoxycarbonyl and 2-(1*H*-benzotriazol-1-yl)-1,1,3,3-tetramethyluronium tetrafluoroborate solid-phase chemistry.**

Dendrimers are attractive monodispersed macromolecules with broad spectrum applications from physics to medicine.[1] The design of novel dendrimers represents an active research area and their syntheses are considered challenging owing to their size and highly branched structures. Traditionally, divergent[2] and convergent[3] strategies have been used to synthesize dendrimers. However, more recently a double exponential growth strategy[4] and a self-assembling method[5] have been developed. To date, the synthesis of most dendrimers has been carried out in solution, although Tam[6] has built hyperbranched L-lysine dendrimers on a solid-phase for multiple antigen peptide (MAP) presentation. Because of the critical role of carbohydrate-containing macromolecules in many cellular proceses, glycodendrimers have also become a growing research area.[7] There is increasing evidence that the multivalent effect displayed by these novel biopolymers may overcome the characteristic low-affinity binding interactions between carbohydrate ligands and proteins.[8,9]

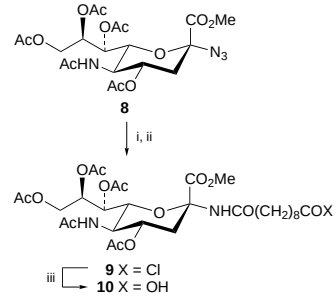
Potent L-lysine-based dendritic α-thiosialoside inhibitors of *Influenza* virus's hemagglutination to human erythrocytes have been previously described.[10] Similarly, different series of symmetrical dendrimers containing *N*-acetylneuraminic acid (NeuAc or sialic acid), representing one of the most widespread mammalian cell surface carbohydrate ligands,[11] have been successfully synthesized in solution.[12,13] Therefore, it was attractive to build a new series of sialodendrimers on a solid-phase. The present approach differs from previous S-linked sialosides[10,11] by the use of N-linked sialylated derivatives which are also expected to be sialidase resistant. Thus, the solid-phase synthesis of a new family of symmetrical N-linked sialodendrimers based on *N*,*N*-bis(3-aminopropyl)succinamic acid **4** core is described.



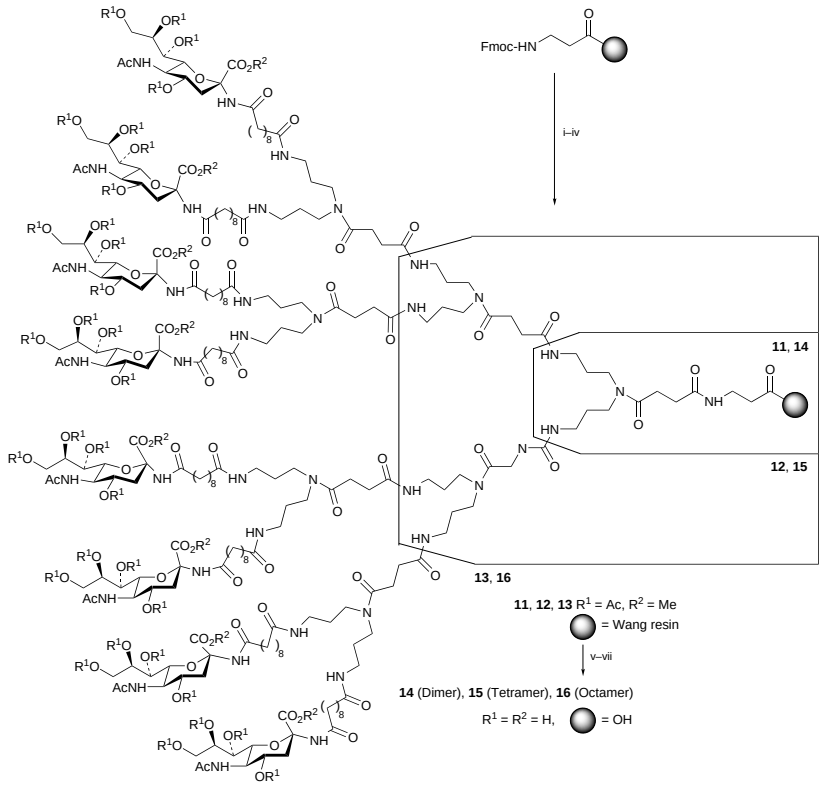

**Scheme 1** *Reagents and conditions*: i, $BnO_2CCN$, $CH_2Cl_2$, 2 h, 72%; ii, succinic anhydride, $Et_3N$, $CH_2Cl_2$, 1 h, 96%; iii, $H_2$, 10% Pd–C, MeOH, 2 h, quant.; iv, FmocCl, 10% $Na_2CO_3$–dioxane, 12 h, 72%; v, H-βAla-Wang resin, TBTU, $Pr^i_2EtN$, DMF, 30 min; vi, 20% piperidine–DMF (1 × 5 min, 1 × 15 min)

In order to provide a strategy which could be used with other carbohydrate ligands, a divergent approach was used to build these novel poly(amidoamine) dendrimers on a solid-phase. Suitably acid-functionalized carbohydrate derivatives could then be added onto polyamino dendrimers to afford glycodendrimes with even valencies. The dendritic core was prepared as follows (Scheme 1). The primary amine groups of *N*-(3-aminopropyl)propane-1,3-diamine **1** were regioselectively protected with benzyloxycarbonyl (Z) groups using benzyl cyanoformate in $CH_2Cl_2$[14] to give secondary amine **2** in 72% yield. Acylation of the residual amine with succinic anhydride (triethylamine, $CH_2Cl_2$, 96%) provided key building block **3** having a divalent structure with a bis-Z-protected monoacid core. In order to use the Fmoc strategy, the Z-protecting groups were removed by catalytic hydrogenation (10% Pd–C, MeOH) to give **4**, which was then treated with 9-fluorenylmethyl chloroformate (FmocCl, 10% $Na_2CO_3$–dioxane, 0 °C) to afford **5**† in 72% yield. The dendritic polyamine scaffolds were built on a β-alanine spacer attached to Wang resin [4-(hydroxymethyl)phenoxymethyl–*co*-poly(styrene–1% divinylbenzene), 0.58 mmol $g^{-1}$], using the Fmoc-strategy and performing the deprotection–coupling cycles as follow: (i) Fmoc deprotection by treatment with 20% piperidine in DMF (1 × 5 min, 1 × 15 min), (ii) coupling of Fmoc–protected acid **5** (2 equiv.) using 2-(1*H*-benzotriazol-1-yl)-1,1,3,3-tetramethyluronium tetrafluoroborate (TBTU) (2 equiv.) as activating agent and $Pr^i_2EtN$ (4 equiv.) in DMF during 30 min. Coupling completion was determined by a ninhydrin test for residual amino groups.[15] To characterize the dendrimers, 30 mg of resin from each sequential generation was Fmoc-deprotected and the dendrimers were released from the solid support following conventional acid treatment (95% aq. TFA, 2 h, 30–79% yield).

Glycodendrimer synthesis required sialic acid residues suitably functionalized at the anomeric position for coupling with amine-terminated dendrimers. The readily available α-sialic acid azide derivative **8**[16] was reduced by catalytic hydrogenation (10% Pd–C, MeOH) to provide α-sialic acid amine in quantitative yield (Scheme 2). To minimize anomerisation, the next acylation step was performed within 1 h. To




**Scheme 2** *Reagents and conditions*: i, $H_2$, 10% Pd–C, MeOH, 1 h, quant.; ii, $ClCO(CH_2)_8COCl$, $Pr^i_2EtN$, $CH_2Cl_2$, 3 h; iii, $H_2O$, 53% overall yield




**Scheme 3** *Reagents and conditions*: i, 20% piperidine–DMF (1 × 5 min, 1 × 15 min); ii, **5**, TBTU, $Pr^i_2EtN$, DMF, 30 min; iii, repeat cycle or 20% piperidine–DMF; iv, **10**, TBTU, $Pr^i_2EtN$, DMF, 0.5–8 h; v, 95% aq. TFA, 2 h; vi, 1 M NaOMe, MeOH, 2–8 h; vii, 0.05 M NaOH, 2–8 h

offer suitable carbohydrate accessibility, introduction of a spacer arm between the sialic acid residues and the dendrimer was carried out using excess $ClCO(CH_2)_8COCl$ ($CH_2Cl_2$, $Pr^i_2EtN$, 0 °C) to give unstable monoacid chloride **9** which was immediately hydrolysed to afford **10** in 53% overall yield. Attempts to isolate **9** for subsequent attachment to the resin were unsuccessful. α-Sialic acid derivative **10** was then ready to be coupled to the dendritic polyamine core on the solid-phase using the same TBTU coupling strategy described to scaffold the dendrimer generations. After coupling, peracetylated sialodendrimers with the valencies of 2, 4 and 8 (**11**, **12** and **13**) were released from the resin by treatment with 95% TFA. The sialodendrimers were then deprotected by sequential ester hydrolysis [(i) de-*O*-acetylation with 1 M NaOMe in MeOH, (ii) 0.005 M NaOH]. Purification of each independent generation by size exclusion chromatography over Biogel-P2 ($H_2O$ as eluent) provided pure deprotected glycodendrimers **14**, **15** and **16** in moderate yields (25–56%) (Scheme 3). The purity of each compound was readily established from the relative integration of key signals in the $^1H$ NMR spectrum. MALDI-TOF mass spectral data (negative mode) further confirmed the integrity of the dendrimers. Biological properties of these novel N-linked sialodendrimers will be reported in due course.

We thank Qing Quan Wu and Denis Carrière for providing α-sialic acid azide derivative **8**. We are also grateful to Drs P. Thibault and D. Krajcarski from NRC, Ottawa, for running the MALDI-TOF experiments on a Perspective Elite-STR instruments.

## Footnotes and References

* E-mail: rroy@science.uottawa.ca

† All compounds showed consistent NMR and mass spectral data. Because of dendrimers' repetitive structures, only selected data are reported. *Selected data* for **5**: $\delta_H$([$^2H_6$]acetone) 1.69 and 1.91 (2 m, 4 H, β-$CH_2$), 2.6 [m, 2 H, succinyl C*H*$_2$C(O)OH], 4.3 (dd, 4 H, Fmoc-$CH_2$s); $\delta_C$ 28.7 and 30.5 (β-C), 29.8 [succinyl *C*$H_2$C(O)OH]; FAB-MS (positive): calc. for $C_{40}H_{41}N_3O_7$: 675.7. Found: 676.3 (M + 1). For **10** (spacer identification from anomeric position to acid is a to h): $\delta_H$($CDCl_3$) 1.59 (m, 4 H, b-, g-$CH_2$s), 1.87 (s, 3 H, NAc), 2.07 (m, 1 H, H-3$^{ax}$), 2.74 (m, 1 H, H-3$^{eq}$), 3.74 (s, 3 H, $OCH_3$), 5.35 (dd, 1 H, $J_{6,7}$ 2.2, $J_{7,8}$ 6.1, H-7); $\delta_C$ 23.14 (NAc), 24.58 (g-C), 52.9 ($OCH_3$), 83.3 (C-2); FAB-MS (positive): calc. for $C_{30}H_{46}N_2O_{15}$: 674.7. Found: 675.4 (M + 1). For **14**: $\delta_H$($D_2O$) 1.62 (m, b-, g-$CH_2$s), 1.84 (m, 6 H, β-$CH_2$, H-3$^{ax}$), 2.08 (s, 6 H, NAc), 2.44 (m, 2 H, β-alanyl α-$CH_2$), 2.73 [m, 4 H, succinyl C*H*$_2$C(O)N, H-3$^{eq}$], 4.16 (d, 2 H, *J* 9.9, H-7); $\delta_C$ 21.5 (NAc), 24.5 (g-C), 26 and 27 (β-Cs), 36.2 (γ-Cs, β alanyl α-C and β-C), 72.4 (C-7), 84.4 (C-2); FAB-MS (positive): calc. for $C_{55}H_{94}N_8O_{24}$: 1250.64. Found: 1251.5 ($M^+$ + 1, 1%); MALDI-TOF (negative): Found: 1250.03 (M − 1)$^-$. For **15**: MALDI-TOF (negative): calc. for $C_{117}H_{200}N_{18}O_{48}$: 2625.37. Found: 2626 (M − 1)$^-$. For **16**: $\delta_H$ ($D_2O$) 1.86 (m, 28 H, β-$CH_2$s), 2.11 (s, 24 H, NAc), 4.18 (m, 8 H, H-7); $\delta_C$ 21.57 (NAc), 26.2 (β-Cs), 72.5 (C-7), 85.2 (C-2); MALDI-TOF (negative) calc. for $C_{241}H_{412}N_{38}O_{96}$: 5,374.85. Found: 5374 (M − 1)$^-$.

1 D. Astruc, *C. R. Acad. Sci. Paris*, 1996, **322**, 757.
2 D. A. Tomalia and H. D. Durst, *Top. Curr. Chem.*, 1993, **165**, 193.
3 C. J. Hawker and J. M. J. Fréchet, *J. Am. Chem. Soc.*, 1990, **112**, 7638.
4 T. Kawaguchi, K. L. Walter, C. L. Wilkins and J. S. Moore, *J. Am. Chem. Soc.*, 1995, **117**, 2159.
5 S. C. Zimmerman, F. W. Zeng, D. E. G. Reichert and S. V. Kolotuchin, *Science*, 1996, **271**, 1095.
6 J. P. Tam, *Proc. Natl. Acad. Sci. USA*, 1988, **85**, 5409.
7 R. Roy, *Polym. News*, 1996, **21**, 226; R. Roy, *Top. Curr. Chem.*, 1997, **187**, 241; K. Aoi, K. Itoh and M. Okada, *Macromolecules*, 1995, **28**, 5391, and references therein.
8 E. J. Toone, *Curr. Opin. Struct. Biol.*, 1994, **4**, 719.
9 R. Roy, *Curr. Opin. Struct. Biol.*, 1996, **6**, 692 and references cited therein.
10 R. Roy, D. Zanini, S. J. Meunier and A. Romanoska, *J. Chem. Soc., Chem. Commun.*, 1993, 1862.
11 J. C. Paulson, in *The Receptors*, ed. M. Conn, Academic Press, Orlando, 1985, vol. 2, p. 131.
12 D. Zanini and R. Roy, *J. Org. Chem.*, 1996, **61**, 7348.
13 D. Zanini and R. Roy, *J. Am. Chem. Soc.*, 1997, **119**, 2088.
14 S.-I. Murahashi, T. Naota and N. Nakajima, *Chem. Lett.*, 1987, 879.
15 E. Kaiser, R. L. Colescott, C. D. Bossinger and P. I. Cook, *Anal. Biochem.*, 1971, **34**, 595.
16 F. Tropper, F. O. Andersson, S. Braun and R. Roy, *Synthesis*, 1992, 618.

*Received in Corvallis, OR, USA, 27th May 1997; 7/03679E*

# Dendroids: a building block for the synthesis of polymodal dendritic structures

**Joanne V. Allen, David C. Horwell,* Julia A. H. Lainton, Jacqueline A. O'Neill and Giles S. Ratcliffe**

*Parke-Davis Neuroscience Research Centre, Cambridge University Forvie Site, Robinson Way, Cambridge, UK CB2 2QB*

**Differentially substituted 1,8-naphthalene and 1,2,3-trihydroxybenzene derivatives are synthesised and termed 'dendroids'; these may be differentially derivatised with mimetics of amino acid side chains.**

Dendritic polymers are synthetic polymers that are characterised by a non-linear array of monomeric species. They are self-organising moieties that have unique physico-chemical properties with respect to their linear counterparts and have a range of potentially novel industrial applications.[1–5]

The topographical features of starburst dendrimers have been compared with those found in globular proteins.[1] However, proteins display heterogeneous functional moieties on their surfaces, such as the constituent amino acid side-chains or the peptide backbone.

We describe here the synthesis of simple aromatic compounds with low molecular weight ( < 1000 Daltons) which can serve as a structural motif that is able to display *different* functional groups which correspond to the side-chains of amino acids. Such polymodal 'dendritic wedges'[2] we term 'dendroids' (**1**, Fig. 1). The dendroid motif is anticipated to facilitate *intramolecular* self-organisation (*cf. intermolecular* self-assembly associated with nanostructures[6,7]) by choice of suitable spacer groups B and C, which may non-covalently interact with each other by steric crowding, hydrophobic collapse and stereoelectronic attractive or repulsive effects. For example,

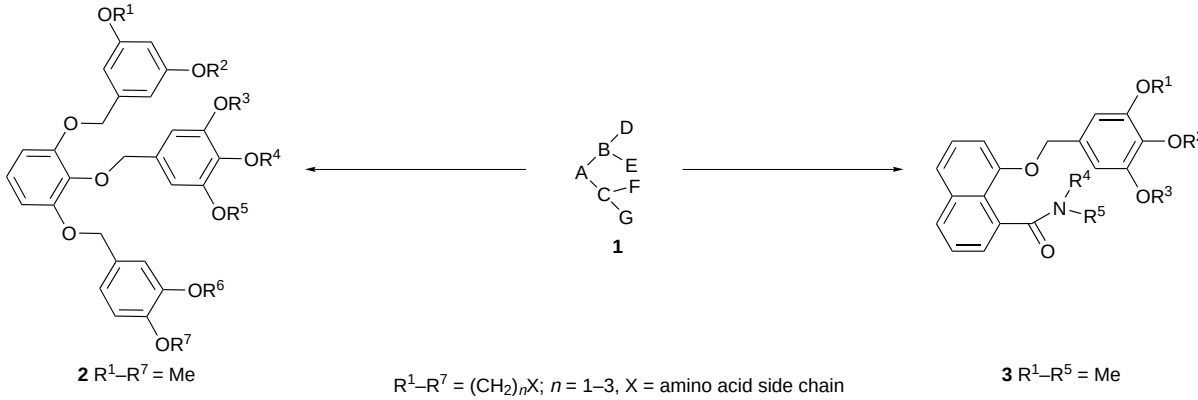
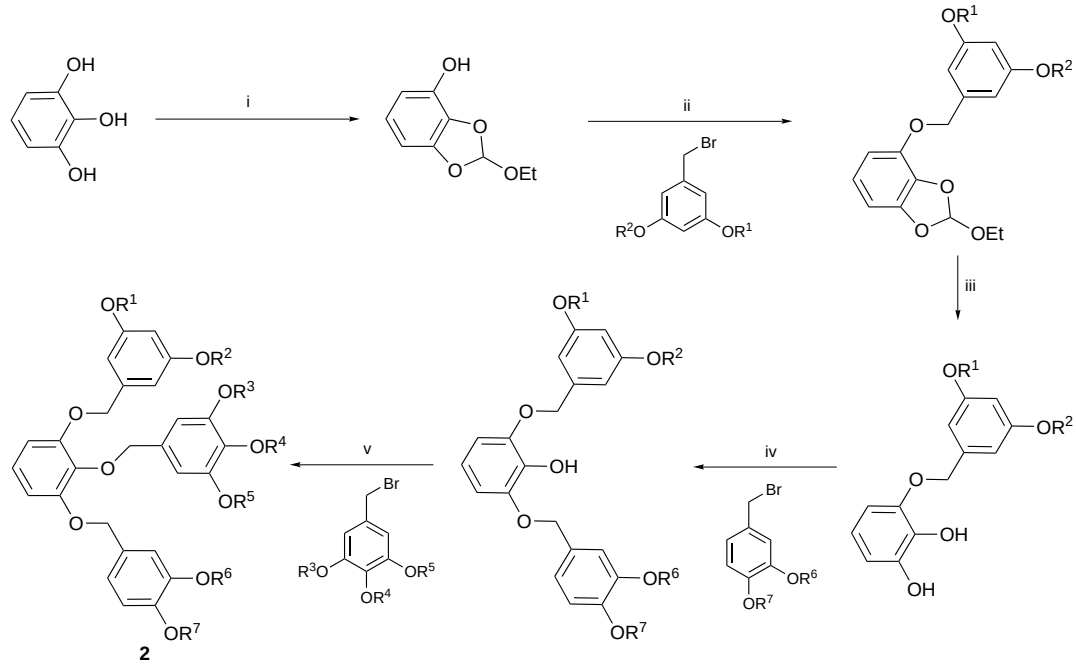
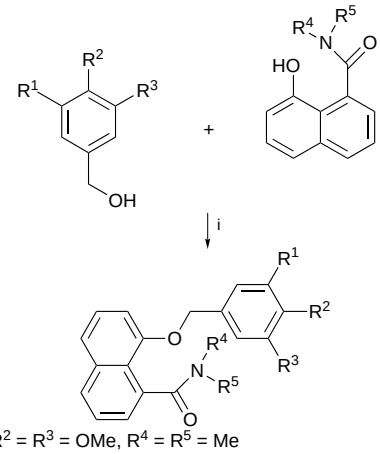



**Fig. 1** Dendroid motif **1** exemplified by 1,2,3-trialkoxybenzenes **2** and 1,8-disubstituted naphthalenes **3**




**Scheme 1** *Reagents and conditions*: i, $CH(OEt)_3$, Amberlyst-IR-120(plus), reflux, 28 h, 92%; ii, $K_2CO_3$, 18-crown-6, room temp., 18 h, 92%; iii, TsOH, room temp., 20 h, 90%; iv, $K_2CO_3$, 18-crown-6, room temp., 21 h, 32%; v, $K_2CO_3$, 18-crown-6, room temp., 21 h, 46%




**3a** $R^1 = R^2 = R^3 = OMe$, $R^4 = R^5 = Me$
**b** $R^1 = R^3 = H$, $R^2 = OBn$, $R^4 = R^5 = Me$
**c** $R^1 = R^3 = H$, $R^2 = OBn$, $R^4 = Pr^i$, $R^5 = (R,S)$CHMe-(indol-3-yl)
**d** $R^1 = R^3 = H$, $R^2 = OBn$, $R^4 = Bn$, $R^5 = CH_2C_6H_4OMe$-*p*
**e** $R^1 = R^3 = H$, $R^2 = OBn$, $R^4 = Bn$, $R^5 = CH_2CH_2$-(indol-3-yl)
**f** $R^1 = R^3 = H$, $R^2 = OBn$, $R^4 = CH_2C_6H_4OMe$-*p*, $R^5 = CH_2CH_2$-(indol-3-yl)
**g** $R^1 = R^3 = H$, $R^2 = OBn$, $R^4 = CH_2CH_2C_6H_4OMe$-*p*, $R^5 = CH_2$-(indol-3-yl)

**Scheme 2** *Reagents and conditions*: i, $PPh_3$ (1 equiv.), diisopropyl azodicarboxylate (1 equiv.), THF, 0 °C to room temp., 4 h

1,2,3-trisubstituted benzenes[8–11] and 1,8-disubstituted naphthalenes[12–15] have been shown to adopt non-planar arrangements by X-ray, NMR and chemical reactivity analysis. As one example, the dendroid motif **2**† may be synthesised from 1,2,3-trihydroxybenzene (Scheme 1). This type of molecule is able to achieve a non-planar structure by virtue of the electronic repulsion between the crowded 1,2,3-aryl ether oxygen atoms, so that the central 2-aryl ether oxygen substituent is forced out of plane with respect to the benzene ring.[8,9]

The 1,8-disubstituted naphthalene dendroids **3a**–**g** are prepared from 8-hydroxy-*N*,*N*-dimethylnaphthalenecarboxamide[12] (Scheme 2). Such 1,8-naphthalenes have been shown by X-ray analysis to exhibit a non-planar preference *via* a truly remarkable stereoelectronic attraction between the 8-naphthalene oxygen substituent atom and the 1-substituted carbonyl group of the amide moiety,[12] allowing the attached groups $R^1$–$R^5$ in **3** to be splayed into a polymodal surface. Examples of where this dendroid motif has been derivatised to give amino acid side-chains include the mimetics of phenylalanine **3b**, β-methyltryptophan **3c**, tyrosine (as its *O*-methyl ether) **3d** and tryptophan **3e**. The examples **3f** and **3g**† also mimic tryptophan and tyrosine side-chains bearing differing methylene spacer groups.

In these cases, the synthetic schemes allow *separate* functionalisation of the dendroid motif, which can be converted by further synthesis into separate amino acid side-chains. Hence the polymodality of part protein structures can be mimicked by use of the dendroid motif. The elaboration of the dendroid motif to give protein mimetics of the 'hot spots' of key amino acids in interleukin-Ira,[16] interleukin-8[17] and the conotoxin derivative SNX-III[18] is under investigation in our laboratory.

## Footnotes and References

* E-mail: david.horwell@camb.wl.com

† *Selected data* for **2**: $\delta_H$ ($CDCl_3$) 3.69 (s, 3 H, $OCH_3$), 3.75 (s, 6 H, 2 × $OCH_3$), 3.80 (s, 6 H, 2 × $OCH_3$), 3.85 (s, 3 H, $OCH_3$), 3.86 (s, 3 H, $OCH_3$), 5.02 (s, 2 H, $CH_2$), 5.04 (s, 2 H, $CH_2$), 5.06 (s, 2 H, $CH_2$), 6.40 (t, *J* 2.0, 1 H, ArH), 6.61 (d, *J* 2.0, 2 H, ArH), 6.65–6.68 (m, 4 H, ArH), 6.75 (d, *J* 8.4, 1 H, ArH), 6.92–6.97 (m, 2 H, ArH), 7.03 (d, *J* 1.6, 1 H, ArH). For **3g**: $\delta_H$ ($CDCl_3$) 2.45–2.50 (m, 1 H, C*H*H), 2.79–2.84 (m, 1 H, C*H*H), 3.00–3.18 (m, 1 H, C*H*H), 3.60 and 3.69 (2 × s, 3 H, OMe), 3.58–3.75 (m, 1 H, C*H*H), 4.40 (AB q, 1 H, C*H*H), 4.90 (AB qt, 1 H, C*H*H), 4.94–4.96 (m, 2 H), 5.01–5.02 (m, 1 H, ArH), 6.51–6.52 (m, 1 H, ArH), 6.67–6.68 (m, 1 H, ArH), 6.77–6.85 (m, 2 H, ArH), 6.85–7.00 (m, 7 H, ArH), 7.00–7.23 (m, 7 H, ArH), 7.23–7.37 (m, 7 H, ArH), 7.68–7.78 (m, 2 H, ArH), 8.88 (br s, 1 H, NH).

1 D. A. Tomalia, A. M. Naylor and W. A. Goddard, *Angew. Chem.*, 1990, **102**, 119; *Angew. Chem., Int. Ed. Engl.*, 1990, **29**, 138.
2 K. L. Wooley, C. J. Hawker and J. M. J. Fréchet, *J. Chem. Soc., Perkin Trans. 1*, 1991, **5**, 1059.
3 J. M. J. Fréchet, *Science*, 1994, **263**, 1710.
4 D. A. Tomalia and P. R. Dvornic, *Nature*, 1994, **372**, 617.
5 S. C. Zimmerman, F. Zeng, D. E. C. Reichert and S. V. Kolotuchin, *Science*, 1996, **271**, 1095.
6 G. M. Whitesides, J. P. Mathias and C. T. Seto, *Science*, 1990, **254**, 1312.
7 J. M. Lehn, *Pure Appl. Chem.*, 1994, **66**, 1961.
8 W. J. Gensler, C. M. Samour, S. Y. Wang and F. Johnson, *J. Am. Chem. Soc.*, 1960, **82**, 1714.
9 T. Banerjee and S. Chaudhuri, *Can. J. Chem.*, 1986, **64**, 876.
10 P. Sykes, *Guide Book to Mechanism in Organic Chemistry*, Longman Scientific and Technical, 6th edn., Wiley, New York, 1986, pp. 26–27, 173, 243.
11 P. G. Sammes and O. J. Weller, *Synthesis*, 1995, 1205.
12 W. B. Schweitzer, G. Procter, M. Kaftory and J. D. Dunitz, *Helv. Chim. Acta*, 1978, **61**, 2783.
13 P. Deslongchamps, *Stereoelectronic Effects in Organic Chemistry*, Pergamon Press, Oxford, 1983, ch. 4, pp. 106–108.
14 F. Cozzi, R. A. Ponzini, M. Cinquini and J. S. Siegel, *Angew. Chem.*, 1995, **107**, 1092; *Angew. Chem., Int. Ed. Engl.*, 1995, **34**, 1019.
15 J. A. Zoltewicz, N. M. Maier and W. M. F. Fabian, *Tetrahedron*, 1996, **52**, 8703.
16 R. J. Evans, J. Bray, J. D. Childs, G. P. A. Vigers, B. J. Brandhuber, J. J. Skalicky, R. C. Thompson and S. P. Eisenberg, *J. Biol. Chem.*, 1995, **270**, 11 477.
17 C. A. Hébert, R. V. Vitangcol and J. B. Baker, *J. Biol. Chem.*, 1991, **226**, 18 989.
18 L. Nadaski, D. Yamashiro, D. Chung, K. Tarczy-Hornock, P. Adriaenssens and J. Ramachandran, *Biochemistry*, 1995, **34**, 8076.

*Received in Glasgow, UK, 22nd July 1997; 7/05304E*

# Chiral–achiral ligand synergy: activation of a zirconium–BINOL Lewis acid complex by the addition of 4-*tert*-butylcalix[4]arene

**Sonia Casolari, Pier Giorgio Cozzi, Paolo Orioli, Emilio Tagliavini and Achillo Umani-Ronchi**

*Dipartimento di Chimica 'G. Ciamician', Università di Bologna, Via Selmi 2, 40126 Bologna, Italy*

**4-*tert*-Butylcalix[4]arene activates the enantioselective allylation of aldehydes catalyzed by a new zirconium–BINOL Lewis acid system allowing the use of less than 2% of the catalyst.**

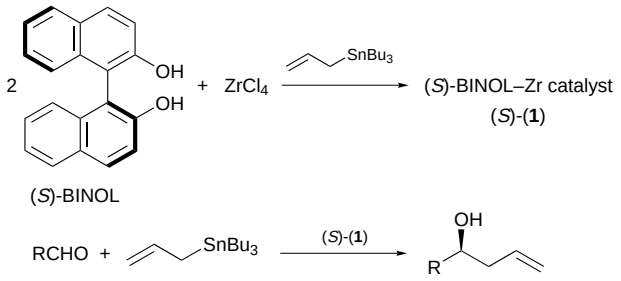
Enantioselective allylation reaction is becoming an important methodology in the total synthesis of complex chiral molecules. In order to enhance the broad applicability and the efficiency of this process for catalytic applications, a large number of groups have published different allylation methodologies which have been realized through the use of different metal–BINOL complexes.[1] The major drawback in all the reported methods is the high loading of the catalyst employed in the reaction (10–20%) which reduces the interest of this simple methodology.

Recently, an acceleration effect on the catalytic cycle of the allylation reaction was discovered whereby an additive, $R_2MSR$ (where M = Al, B), was introduced *in stoichiometric amount* into the reaction mixture.[2]

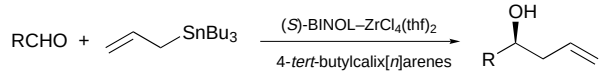
In searching for more active and efficient catalysts, we discovered that zirconium–BINOL Lewis acid **1** can be prepared by dissolving the $ZrCl_4$ in MeCN in the presence of BINOL, followed by the addition of allyltributyltin in $CH_2Cl_2$ (Scheme 1).[3]† After stirring the reaction mixture for 1–2 h at room temperature, the aldehyde was successively added at lower temperature (Scheme 1). The resulting data from this reaction are collected in Table 1. The drawback of this method is that two equivalents of BINOL (with respect to the zirconium) are needed to obtain high enantiomeric excesses (ees). Furthermore good reproducibility was difficult to obtain. We realized that another catalyst which could be prepared from commercially available $ZrCl_4(thf)_2$[4] could considerably enhance the applicability and the reproducibility of the procedure. Moreover, the higher solubility of $ZrCl_4(thf)_2$ in organic solvent, as compared to $ZrCl_4$, simplifies the procedure for the preparation of the catalyst. In fact, the catalyst can be simply prepared starting from BINOL and $ZrCl_4(thf)_2$ in $CH_2Cl_2$ or in $Et_2O$. As shown in Table 1 high ees were achieved by employing $Et_2O$ as the reaction solvent. Despite the high ees which we obtained, those reported for the same reactions promoted by $Zr(OiPr)_4$·$^i$PrOH–BINOL Lewis acid[5] were higher. Moreover, at least 10% mol of the zirconium catalyst was necessary to achieve good levels of ees.

Recently Mikami and Matsukawa reported that certain titanium–BINOL Lewis acids, capable of promoting the ene reaction, are activated by the addition of chiral phenols.[6] In particular, they showed that the presence of enantiopure BINOL enhances the reactivity of racemic titanium–BINOL catalysts and increases the ees of ene[6] and Diels–Alder reactions.[7]

We report here a spectacular activation of the zirconium–BINOL catalyst by adding achiral 4-*tert*-butylcalix[4]arene,[8] a phenol derivative, to the reaction mixture (Scheme 2). This new Lewis acid system is generated *in situ* by treating a mixture of BINOL, $ZrCl_4(thf)_2$ and 4-*tert*-butylcalix[4]arene with allyltributyltin.‡ The 4-*tert*-butylcalix[4]arene has low solubility in the reaction solvent ($Et_2O$) and the addition of allyltributyltin to




**Scheme 1**




**Scheme 2**

**Table 1** Enantioselective allylation of aldehydes promoted by (*S*)-**1**[a]

| Entry | Zr salt | Solvent | BINOL : Zr | RCHO | *T*/°C | Time/h | Yield (%)[d] | ee (%)[e] |
|---|---|---|---|---|---|---|---|---|
| 1 | $ZrCl_4$[b] | $CH_2Cl_2$ | 1 : 1 | PhCHO | 0 | 3 | 83 | 50 |
| 2 | $ZrCl_4$[b] | $CH_2Cl_2$ | 1 : 1 | PhCHO | −20 | 19 | 52 | 40 |
| 3 | $ZrCl_4$[b] | $CH_2Cl_2$ | 2 : 1 | PhCHO | −20 | 21 | 53 | 54 |
| 4 | $ZrCl_4$[b] | $CH_2Cl_2$ | 2 : 1 | PhCHO | −20 | 72 | 64 | 62 |
| 5 | $ZrCl_4$[b] | $Et_2O$ | 2 : 1 | PhCHO | −20 | 36 | 10 | 79 |
| 6 | $ZrCl_4(thf)_2$[c] | $CH_2Cl_2$ | 1 : 1 | *n*-$C_7H_{15}$CHO | 0 | 36 | 70 | 53 |
| 7 | $ZrCl_4(thf)_2$[c] | $CH_2Cl_2$ | 2 : 1 | *n*-$C_7H_{15}$CHO | −20 | 24 | 78 | 73 |
| 8 | $ZrCl_4(thf)_2$[c] | $Et_2O$ | 2 : 1 | *n*-$C_7H_{15}$CHO | −20 | 24 | 65 | 85 |
| 9 | $ZrCl_4(thf)_2$[c] | $Et_2O$ | 2 : 1 | PhCHO | −20 | 24 | 40 | 87 |

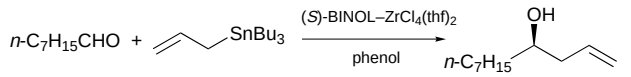
[a] All reactions were run by the employment of 10% catalyst based on Zr. Reactions performed with lower % of the catalyst gave lower yield and enantioselectivity. [b] The catalyst was prepared by dissolving $ZrCl_4$ (0.1 mmol) and BINOL in MeCN followed by the evaporation of the solvent. The solid residue was suspended in $CH_2Cl_2$ and allyltributyltin (2 mmol) was added. The resulting mixture was stirred for 1 h followed by the addition of the aldehyde (1 mmol). [c] The catalyst was prepared in $CH_2Cl_2$ or $Et_2O$ by stirring $ZrCl_4(thf)_2$ (0.1 mmol) and BINOL for 1 h followed by the addition of allyltributyltin (1.7 mmol) in the same solvent. The resulting yellow solution was stirred for another hour at room temp., then the mixture was cooled to the temperature reported in the Table and the aldehyde was added (1 mmol). [d] Isolated yield after chromatographic purification. [e] The ees were determined by GC analysis with a chiral Megadex-5 column.

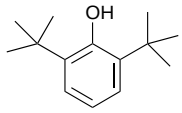
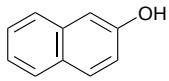
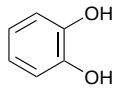
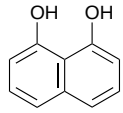
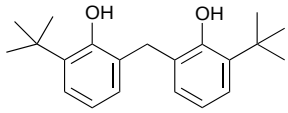
**Table 2** Enantioselective allylation with Zr–BINOL complex activated by 4-*tert*-butylcalix[*n*]arenes[a]

| Entry | $ZrCl_4(thf)_2$ (%)[b] | Calix[*n*]arene | % | RCHO | Time/h | Yield (%)[c] | ee (%)[d] |
|---|---|---|---|---|---|---|---|
| 1 | 10 | Calix[4]arene | 10 | *n*-$C_7H_{15}CHO$ | 60 | 68 | 93 |
| 2 | 5 | Calix[4]arene | 5 | *n*-$C_7H_{15}CHO$ | 60 | 65 | 96 |
| 3 | 2 | Calix[4]arene | 1 | *n*-$C_7H_{15}CHO$ | 60 | 40 | 92 |
| 4 | 2 | Calix[4]arene | 0.5 | *n*-$C_7H_{15}CHO$ | 60 | 57 | 95 |
| 5 | 10 | Calix[4]arene | 10 | *c*-$C_6H_{11}CHO$ | 72 | 52 | 90 |
| 6[e] | 6 | Calix[4]arene | 6 | PhCHO | 50 | 78 | 78 |
| 7 | 5 | Calix[4]arene | 5 | PhCHO | 72 | 85 | 85 |
| 8 | 10 | Calix[4]arene | 10 | PhCH=CHCHO | 90 | 38 | 77 |
| 9[f] | 4 | Calix[6]arene | 3 | PhCH=CHCHO | 50 | 43 | 62 |
| 10[f] | 4 | Calix[8]arene | 3 | PhCH=CHCHO | 50 | 30 | 70 |

[a] All reactions were carried out in $Et_2O$ at −20 °C. [b] For all reactions the molar ratio between $ZrCl_4(thf)_2$ and BINOL was 1 : 1. [c] Isolated yield after chromatographic purification. [d] The ees were determined by GC analysis with a chiral Megadex-5 column. [e] The reaction was performed at 0 °C. [f] The reaction was performed in $CH_2Cl_2$.

**Table 3** Enantioselective allylation promoted by BINOL–zirconium–phenol systems[a]




| Entry | Phenol | Yield (%)[b] | ee (%)[c] |
|---|---|---|---|
| 1 |  | 30 | 66 |
| 2 |  | 40 | 71 |
| 3 |  | 47 | 19 |
| 4 |  | 0 | — |
| 5 |  | 0 | — |

[a] All reactions were performed employing the following stoichiometric ratio: BINOL : $ZrCl_4(thf)_2$ : phenol : allyltributyltin : aldehyde; 0.1 : 0.1 : 0.1 : 1.6 : 1.0 at −20 °C for 48 h. [b] Isolated yield after chromatographic purification. [c] The ees were determined by GC analysis with a chiral Megadex-5 column.

the mixture solubilizes the complex with the appearance of a yellow colour only in the case of low catalyst loading (2–3%). In addition, the experimental procedure is simple, all the reagents are commercially available, and no particular drying procedure is required for the calixarene.

The remarkable aspect of this procedure is that, even without the use of molecular sieves, it is possible to obtain very high ees (up to 96% with linear aldehydes) using only 2% of the chiral promoter. Our results indicate that the amount of calixarene added to the mixture can be reduced (entries 3 and 4, Table 2). As shown in Table 2, the results are generally good with both aliphatic and aromatic aldehydes. Only in the case of cinnamaldehyde the yield and the ees are not satisfactory. Other calixarenes can be used with comparable results (entries 9 and 10, Table 2). It is noteworthy that this dramatic activation is obtained specifically with the calixarenes, whereas other phenols do not show the same activating effect (Table 3). Our system is interesting not only from the point of view of low catalyst loading giving high ees, but from the perspective that new frontiers can be opened in the field of metal–BINOL complexes in asymmetric catalytic applications.

Future work in our laboratory will address the general scope of Lewis acid catalyst activation and the characterization of the species responsible for the performance of the catalyst.

We thank MURST and CNR (Rome) for financial support. We wish to thank the University of Bologna for funds for selected research topics.

## Footnotes and References

* E-mail: Umani@ciamserv.ciam.unibo.it

† Preliminary spectroscopic investigations have shown that the catalyst formation probably occurs through the proton abstraction from an initial adduct between the $ZrCl_4$ and BINOL due to the allylating reagent, as previously described by Carreira and co-workers[3] for the $TiF_4$–BINOL system. Tributyltin chloride and propene are the products of the reaction.

‡ Typical experimental procedure: a suspension of (*S*)–BINOL (0.05 mmol), 4-*tert*-butylcalix[4]arene (0.05 mmol) and $ZrCl_4(thf)_2$ (0.05 mmol) was stirred for 1 h in $Et_2O$ (1.5 ml), then allyltributyltin (1.7 mmol) was added at room temperature. After stirring for 1 h and cooling to −20 °C, the aldehyde (1 mmol) was added. The mixture was stored in the freezer at −20 °C for 50–90 h, then diluted with $Et_2O$ and quenched with a saturated solution of $NaHCO_3$. The insoluble materials were filtered and the organic phase separated. The aqueous phase was extracted with $Et_2O$. The organic phases were collected, dried, evaporated under reduced pressure and purified by flash chromatography.

1 A. L. Costa, M. G. Piazza, E. Tagliavini, C. Trombini and A. Umani-Ronchi, *J. Am. Chem. Soc.*, 1993, **115**, 7001; G. E. Keck, K. H. Tabert and L. S. Geraci, *J. Am. Chem. Soc.*, 1993, **115**, 8467; G. E. Keck, D. Krishnamurthy and M. C. Grier, *J. Org. Chem.*, 1993, **58**, 6543; G. E. Keck, D. Krishnamurthy and X. Chen, *Tetrahedron Lett.*, 1993, **35**, 8323; S. Weigand and R. Brukner, *Chem. Eur. J.*, 1996, **2**, 1072; J. W. Faller, O. W. I. Sams and X. Liu, *J. Am. Chem. Soc.*, 1996, **118**, 1217; P. G. Cozzi, E. Tagliavini and A. Umani-Ronchi, *Gazz. Chim. It.*, in the press.

2 C.-M. Yu, H.-S. Choi, W.-H. Jung, H.-J. Kim and J. Shin, *Chem. Commun.*, 1997, 761. Although high enantiomeric excesses were obtained using only 2% of a titanium–BINOL Lewis acid complex, the additive is used in stoichiometric amount and is not commercially available.

3 D. R. Gauthier and E. M. Carreira, *Angew. Chem., Int. Ed. Engl.*, 1996, **35**, 2363; R. O. Duthaler and A. Hafner, *Angew. Chem., Int. Ed. Engl.*, 1997, **36**, 43.

4 L. E. Manzer, *Inorg. Synth.*, 1982, **21**, 136.

5 P. Bedeschi, S. Casolari, A. L. Costa, E. Tagliavini and A. Umani-Ronchi, *Tetrahedron Lett.*, 1995, **36**, 7897.

6 K. Mikami and S. Matsukawa, *Nature*, 1997, **385**, 613.

7 S. Matsukawa and K. Mikami, *Tetrahedron: Asymmetry*, 1997, **8**, 815.

8 V. Böhmer, *Angew. Chem., Int. Ed. Engl.*, 1995, **34**, 713.

*Received in Liverpool, UK, 14th July 1997; 7/05045C*

# A 24 mer peptide derived from RecA protein can discriminate a single-stranded DNA from a double-stranded DNA

**Naoki Sugimoto* and Shu-ichi Nakano**

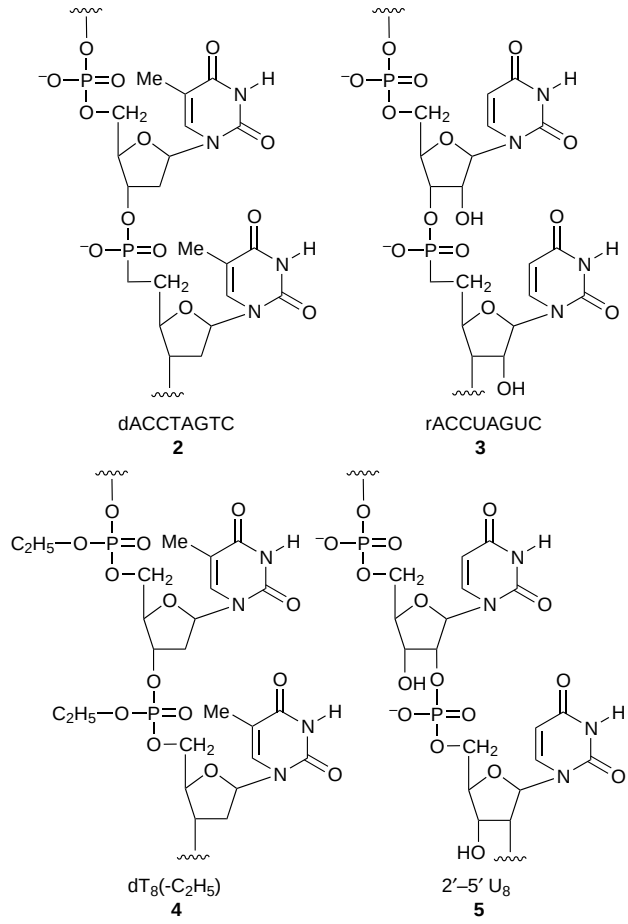
*Department of Chemistry, Faculty of Science, Konan University, 8-9-1 Okamoto, Higashinada-ku, Kobe 658, Japan*

**A novel 24 residue peptide, Ile-Arg-Met-Lys-Ile-Gly-Val-Met-Phe-Gly-Asn-Pro-Glu-Thr-Thr-Thr-Gly-Gly-Asn-Ala-Leu-Lys-Phe-Tyr, derived from RecA protein can discriminate a single-stranded DNA (ssDNA) from a double-stranded DNA (dsDNA) and a new developed support with this peptide recognizes ssDNA but not dsDNA.**

RecA protein plays an essential role for homologous DNA recombination and DNA repair in prokaryote.[1–3] The X-ray structure of 352 amino acids of *E. coli* RecA protein in the absence of DNA showed that two disordered loop domains, L1 (157–164) and L2 (195–209), composed of highly conserved amino acids project towards the polymer axis near DNA strands.[4] Based on several investigations of mutated RecA proteins, it was proposed that L1 and L2 are dsDNA and ssDNA binding domains, respectively. Helix G (210-218) lying next to loop L2 amino acids is a conserved domain including two Gly residues (211 and 212) which are absolutely invariant among bacterial RecA proteins, T4 UvsX, yeast Dmc 1 and mouse Rad 51 proteins.[5] Recently, it was reported that a 20 amino acid peptide (named FECO peptide) derived from *E. coli* RecA protein, which contains L2 and the conserved amino acids at both L2 termini including the invariant Gly residues (193–212), showed an enzymatic activity for the homologous recombination of DNA strands without any cofactors.[6] However, the FECO peptide which lacks the full helix G amino acids except both Gly residues, bound both ssDNA and dsDNA with similar affinity. Here, we have synthesized a 24 amino acid peptide including L2 and all helix G residues (195–218), Ile-Arg-Met-Lys-Ile-Gly-Val-Met-Phe-Gly-Asn-Pro-Glu-Thr-Thr-Thr-Gly-Gly-Asn-Ala-Leu-Lys-Phe-Tyr **1**, and investigated its recognition ability specific to ssDNA.[7]

Binding behaviors of the synthesized L2-G peptide **1** with four single-stranded octanucleotides, dACCTAGTC **2**, rACCUAGUC **3**, $dT_8(\text{-}C_2H_5)$ **4**, and 2′–5′ $U_8$ **5**, a double-stranded DNA (dsDNA) d(GTCAGGAATCTG)/d(CAGATTCCTGAC) **6**, and a hairpin-looped DNA $dCGTCA_8GACG$ **7** were investigated by surface plasmon resonance (SPR) analysis. Octamers **2** and **3** are unmodified ssDNA and ssRNA, respectively. Octamers **4** and **5** are unnatural strands; **4** has neutral charges on its backbone and **5** is linked by a phosphodiester bond between 2′ and 5′ positions. The DNA sequences of **6** and **7** were confirmed to form double-stranded and hairpin-looped structures, respectively, with an alternative secondary structure of two molecules of **7** forming an internal-looped one also being possible.

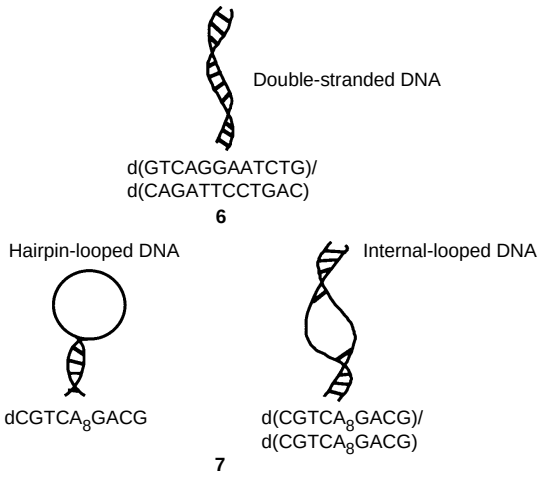
The L2-G peptide was immobilized on the SPR sensorchip,[8] and the octanucleotides were flowed across the sensorchip.† After the injection of 320 μM octanucleotides **2**–**5** to the flowcell, the response of the refractive index increased as the sample was flowed. Final intensities were approximately 1200, 400, 50 and 200 RU (resonance unit) for **2**, **3**, **4** and **5**, respectively, at 300 seconds after the injection. Although the refractive index for the ssDNA seems only three-fold greater than that for the ssRNA, the signal for **2** continued increasing even 300 seconds after the injection. Thus, affinity of **2** for the L2-G peptide is much greater than **3**. These results indicate **3** and **5** have much lower binding abilities to the peptide on the sensorchip than **2**, although these three nucleotides possess the same negative charges. Apparently, the neutral nucleotide of **4** could not bind to the L2-G peptide, suggesting the L2-G peptide recognizes nucleotides not only by their electronegativity but also by their backbone structure. A lower dissociation process for **2** was observed when the running buffer was flowed at 300 seconds after the injection, suggesting the interactions for the ssDNA with the L2-G peptide are not simple.




Ac-Ile-Arg-Met-Lys-Ile-Gly-Val-Met-Phe-Gly-Asn-Pro-Glu-Thr-Thr-Thr-Gly-Gly-Asn-Ala-Leu-Lys-Phe-Tyr-$NH_2$

L2 site — Helix G

**1**



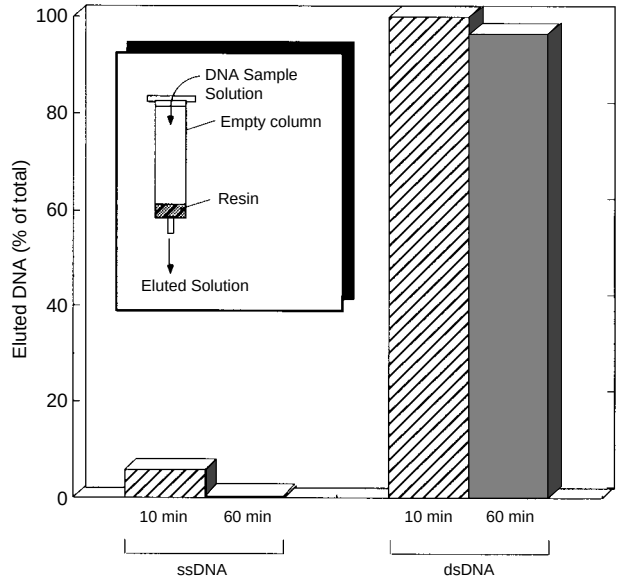




**Fig. 1** Binding properties of the control and L2-G columns to ssDNA of d(TAATACGACTCACTATAGGG) and dsDNA of d(TAATACGACTCACTATAGGG)/d(CCCTATAGTGAGTCGTATTA) at room temperature. Percentages of the eluted DNAs through these columns against the total DNA amount were calculated with absorbance differences at 260 nm of the eluted solutions through the control and the L2-G columns.

When **6** was flowed over the sensorchip with the L2-G peptide, only an increment of 100 RU was observed. Even if a high concentration of this dsDNA (up to 6 mM) was examined, the response was at most 200 RU. Thus, the L2-G peptide bound to ssDNA, but not to ssRNA, unnatural nucleotides or structured DNAs. This binding affinity was also supported by circular dichroism (CD) spectra (data not shown). On the other hand, as we expected, **7** had a smaller signal (450 RU) than **2**, because this DNA strand was designed to form a hairpin-looped structure easily. However, there was a relatively larger response of **7** than that of the ssRNA **3**. This result might be due to its ability to form not only a hairpin-looped structure but also an internal-looped structure of the self-complementary duplex which would be bound by the L2-G peptide.

Furthermore, we prepared an ssDNA affinity column by using the ssDNA recognizing peptide (L2-G peptide). The peptide was attached to a polystyrene supported PEG-PS resin (PerSeptive Biosystems). This resin was put in an empty column (L2-G column), then ssDNA, d(TAATACGACTCACTATAGGG), or dsDNA, d(TAATACGACTCACTATAGGG)/d(CCCTATAGTGAGTCGTATTA), was poured into the column.‡ In addition, a control resin without attached amino acid residues on the PEG-PS resin was prepared as a control column.

Absorbance at 260 nm of the elution buffers was compared. In the case of the ssDNA, no decrement of absorbance was observed for elution through the control column. However, through the L2-G column, much less absorbance ($Abs_{260}$ = 0.04) compared to that before pouring ($Abs_{260}$ = 0.73) was found. The percentages of the eluted DNA strand flowing through these resins against the total DNA amount are shown in Fig. 1. This indicates that most ssDNAs bound to the L2-G resin even after mixing for 10 min. When the dsDNA was poured into these columns, no significant difference of the measured absorbance was observed between the control column and the L2-G column. Thus, there is no specific interaction of the L2-G resin with the dsDNA. These results indicate that the L2-G resin is very useful as an ssDNA binding support.

In summary, the 24 amino acid peptide (L2 and helix G domains of RecA protein) discriminated ssDNA from ssRNA, unnatural nucleotides, and dsDNA. The helix G amino acids were required for the discrimination property of the L2-G peptide. A useful support recognizing DNA secondary structures was able to be developed with the L2-G peptide derived from the DNA binding protein.

We would like to thank Drs H. Mihara (Tokyo Institute of Technology), H. Aoyagi and T. Niidome (Nagasaki Univ.) for advice on the synthesis of the peptide, Dr H. Sawai (Gunma Univ.) for providing 2′–5′ linked $U_8$, and Dr Y. Hayakawa (Nagoya Univ.) for providing ethoxy-$dT_8$. We also acknowledge Dr P. C. Bevilacqua at Penn. State University for critical reading of the manuscript and helpful comments. This work was supported in part by Grants-in-Aid from the Ministry of Education, Science, Sports and Culture, Japan, and from the 'Research for the Future' Program of the Japan Society for the Promotion of Science.

## Footnotes and References

* E-mail : sugimoto@konan-u.ac.jp

† Nucleotide concentrations are expressed as base concentrations. All experiments were conducted in a buffer including 100 mM NaCl, 10 mM $Na_2HPO_4$ and 1 mM $Na_2EDTA$ (pH 7.0).

‡ 100 mg of the L2-G resin and the PEG-PS resin without attached amino acid residues was prepared. The quantity of the peptide bound to the resin was calculated to be 1.7 mmol if the synthesis was completed with 100% yield. The L2-G resin or the PEG-PS resin was put into a empty column (named L2-G column or control column, respectively). The single-stranded DNA of d(TAATACGACTCACTATAGGG) or double-stranded DNA of d(TAATACGACTCACTATAGGG)/d(CCCTATAGTGAGTCGTATTA) was dissolved in a buffer including 100 mM NaCl, 10 mM $Na_2HPO_4$ and 1 mM $Na_2EDTA$ (pH 7.0) to a concentration of 1.3 nmol. These DNA solutions were poured into the two columns and the percentages of the bound DNA on the resin were estimated from the absorbance at 260 nm of the eluted solution.

1 R. R. Meyer and P. Laine, *Microbiol. Rev.*, 1990, **54**, 342.
2 C. M. Radding, *J. Biol. Chem.*, 1991, **266**, 5355.
3 S. C. Kowalczykowski, *Annu. Rev. Biophys. Biophys. Chem.*, 1991, **20**, 539.
4 R. M. Story, I. T. Weber and T. A. Steitz, *Nature*, 1992, **355**, 318.
5 R. M. Story, D. K. Bishop, N. Kleckner and T. A. Steitz, *Science* 1993, **259**, 1892.
6 O. N. Voloshin, L. Wang and R. D. Camerini-Otero, *Science*, 1996, **272**, 868.
7 S. Nakano, M. Sasaki and N. Sugimoto, *Nucleic Acids Symp. Ser.*, 1995, **34**. 61.
8 N. Sugimoto and S. Nakano, *Nucleic Acids Symp. Ser.*, 1996, **35**, 303.

*Received in Cambridge, UK, 1st August 1997; 7/05575G*



Typeset and printed by Black Bear Press Limited, Cambridge, England

ChemComm
FEATURE ARTICLE

# New titanium imido chemistry

**Philip Mountford***

*Department of Chemistry, The University of Nottingham, Nottingham, UK NG7 2RD*

**A general entry point to new titanium imido chemistry is gained *via* the readily prepared synthons [Ti(NR)Cl$_2$(py)$_3$] (R = Bu$^t$ or aryl) and their homologues, from which straightforward metathesis reactions afford a wide range of derivatives. The structures, solution dynamics and reactivity of these new compounds are reviewed.**

## Introduction

Transition metal imido chemistry is one of the growth areas of inorganic research and has been reviewed up to the end of 1993.[1–4] The dianionic terminal imido ligand in complexes of the general formula [M(NR)$_n$(L)$_m$] [R = alkyl or aryl usually; (L)$_m$ = ancilliary ligand set] can act as a four-electron donor that is capable of forming a strong triple bond to the metal centre.† As such the M=NR linkage is valence isoelectronic with the terminal oxo group M=O, and the {NR}$^{2-}$ moiety is isolobal with {C$_5$R$_5$}$^-$.[5,6] The π-donor imido functional group gives rise to chemistry that is generally dominated by medium to high metal oxidation states; this contrasts with the familiar low to medium oxidation state chemistry that is characteristic of transition metal complexes supported by the neutral, π-acceptor carbonyl ligands.

While there has clearly been a strong curiosity-driven element to the development of transition metal imido chemistry, the importance of imido compounds and of their isolobal analogues in industrial processes, organic synthesis and catalysis is now very well recognised.[3,4,7] Generally speaking, by the end of the 1980s the chemistry of terminal imido compounds of Group 5–8 transition metals was firmly (although by no means comprehensively) established. By way of contrast, well defined derivatives for Groups 4 and 9 did not appear until about this time.[4] The primary objective of this article is to highlight the more recent advances in titanium imido chemistry. However, it will be helpful to begin by summarising some of the early developments in order to set the later work in context.

Structurally characterised terminal titanium imido complexes were only first described in 1990. These were the five-coordinate [Ti(NPh)(OC$_6$H$_3$Pr$^i_2$-2,6)$_2$(py′)$_2$] (py′ = 4-pyrrolidinopyridine) and six-coordinate [Ti{NP(S)Ph$_2$}Cl$_2$(py)$_3$], prepared by Rothwell and coworkers[8] and Roesky *et al.*[9] respectively [Fig. 1(*a*) and (*b*)]. In 1991 Wolczanski and coworkers described the preparation and chemistry of the highly reactive transient species [Ti(NSiBu$^t_3$)(NHSiBu$^t_3$)$_2$] [Fig. 1(*c*)] which can activate benzene C–H bonds.[10] Other reactive transient titanium imido species were also described around this time.[11] By 1993 a number of five- and six-coordinate complexes analogous to those shown in Fig. 1(*a*) and (*b*) had been reported,[4] but the range of titanium imido reaction chemistry appeared to be very polarised. In other words, it looked as though titanium imido compounds could either be isolated but were (apparently) unreactive, or could be generated *in situ* and were extremely reactive. In 1994 we started work in titanium imido chemistry by identifying a synthetic strategy that we hoped would allow us to extend significantly the range of ancilliary ligand environments for the Ti=NR functional group, and hence to find new reaction chemistry.[12] The remainder of this article describes this general entry to new titanium imido chemistry, an overview of the scope and range of new compounds that can be prepared, and some aspects of their structures, solution dynamics and reactivity.

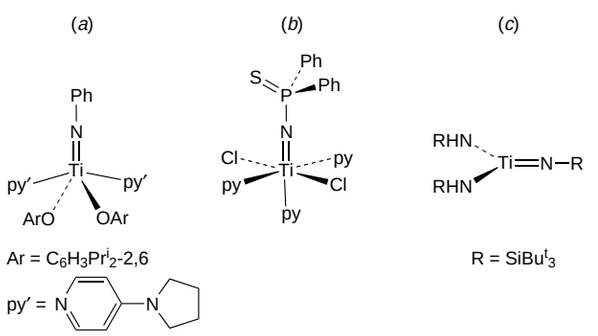



**Fig. 1** The first crystallographically characterised (*a*) five-[8] and (*b*) six-coordinate[9] titanium imido complexes, and (*c*) a highly reactive transient species[10]

## A convenient entry point to new titanium imido chemistry

### *Syntheses*

Being aware of the fairly facile reduction of Ti$^{IV}$ to Ti$^{III}$ in much of the element's chemistry, we decided to introduce the titanium imido group first, and any desired ancilliary ligands last. We have found that the compounds [Ti(NR)Cl$_2$(L)$_n$] (R = Bu$^t$ or aryl; L = py or NC$_5$H$_4$Bu$^t$-4; *n* = 2 or 3; see Fig. 2) are excellent synthons in this regard.[12,13] The success of these complexes as entry points to new titanium imido derivatives (*vide infra*) may partly be attributed to the π-donor imido ligand's ability to stabilise higher oxidation states. Hence almost none of the anion metathesis reactions described herein are complicated by reduction of the Ti$^{IV}$ centre.

The *tert*-butyl imido complexes [Ti(NBu$^t$)Cl$_2$(L)$_n$] (**1a** L = py, *n* = 3; **2a** L = py, *n* = 2; **3** L = NC$_5$H$_4$Bu$^t$-4, *n* = 2) are readily and efficiently obtained from TiCl$_4$, Bu$^t$NH$_2$ and the appropriate L (Fig. 2).‡ Compound **1a** in particular is available on a 35–40 g scale in near-quantitative yield.[12,13] Analogous aryl imido pyridine derivatives cannot be obtained directly from ArNH$_2$ and TiCl$_4$, but arylamine/*tert*-butyl imide exchange reactions of [Ti(NBu$^t$)Cl$_2$(py)$_3$] **1a** readily afford the desired [Ti(NAr)Cl$_2$(py)$_3$] (Ar = C$_6$H$_3$Me$_2$-2,6 **1**b; C$_6$H$_3$Pr$^i_2$-2,6 **1c**; C$_6$H$_5$ **1d**; C$_6$H$_4$Me-4 **1e**; C$_6$H$_4$NO$_2$-4 **1f**).[13,14] These were the first such exchange reactions for Group 4 imido compounds. The 2,6-disubstituted aryl derivatives **1b** and **1c** are by far the most stable and readily prepared; compounds **1a** and **1d**–**1f** have been crystallographically characterised. Five-coordinate bis(pyridine) derivatives [Ti(NAr)Cl$_2$(py)$_2$] (Ar = C$_6$H$_3$Me$_2$-2,6 **2b**; C$_6$H$_3$Pr$^i_2$-2,6 **2c**) are also easily obtained, reflecting the *trans*-labilising ability of the imido group.

The homologous series [Ti(NR)Cl$_2$(py)$_3$] (R = Bu$^t$ **1a**, Ph **1d**, C$_6$H$_4$Me-4 **1e** or C$_6$H$_4$NO$_2$-4 **1f**) provided the first opportunity to use crystallographic results to compare the general structural and *trans* influence [the average difference between the *cis*-Ti–N(py) and *trans*-Ti–N(py) bond lengths] of different imido ligands within a series of simple six-coordinate, d$^0$ complexes as a function of the imido N-substituent. The

absence of aryl ring 2,6-substituents in **1d–f** meant that steric effects were minimised as far as possible. Interestingly, despite the significantly different nitrogen substituents in **1a** and **1d–f**, there is no experimental difference in *trans* influence between them.[13,14]

### *Bi- and tri-dentate amine adducts*

Early transition metal, $d^0$ complexes with *cis*-dichloride ligands are potential precursors to alkene polymerisation catalysts.[15,16] As shown in Fig. 2, the bis- and tris-pyridine adducts **2a** and **1a** afford fourteen- and sixteen-electron, bi- and tri-dentate amine adducts $[Ti(NBu^t)Cl_2(tmeda)]$ (**4**; tmeda = tetramethylethylenediamine),[17] $[Ti(NBu^t)Cl_2(pmdeta)]$ (**5**; pmdeta = pentamethyldiethylenetriamine) and $[Ti(NBu^t)Cl_2(Me_3[9]aneN_3)]$ (**6**; $Me_3[9]aneN_3$ = 1,4,7-trimethyl-1,4,7-triazacyclononane) in good yields.[13,18] The crystallographically characterised compounds **5** and **6** are isolobal analogues of $[Ti(\eta^5\text{-}C_5H_5)_2Cl_2]$. The open-chain triamine adduct $[Ti(NBu^t)Cl_2(pmdeta)]$ **5** is highly labile in solution whereas the cyclic triamine analogue $[Ti(NBu^t)Cl_2(Me_3[9]aneN_3)]$ **6** is rigid on the NMR timescale and generally more easily handled. Compound **6** is the first structurally characterised, triazacyclonane-supported transition metal imido complex. Studies of the substitution chemistry and polymerisation activity of **4–6** and their heavier Group 4 and Group 5 analogues are currently in progress.

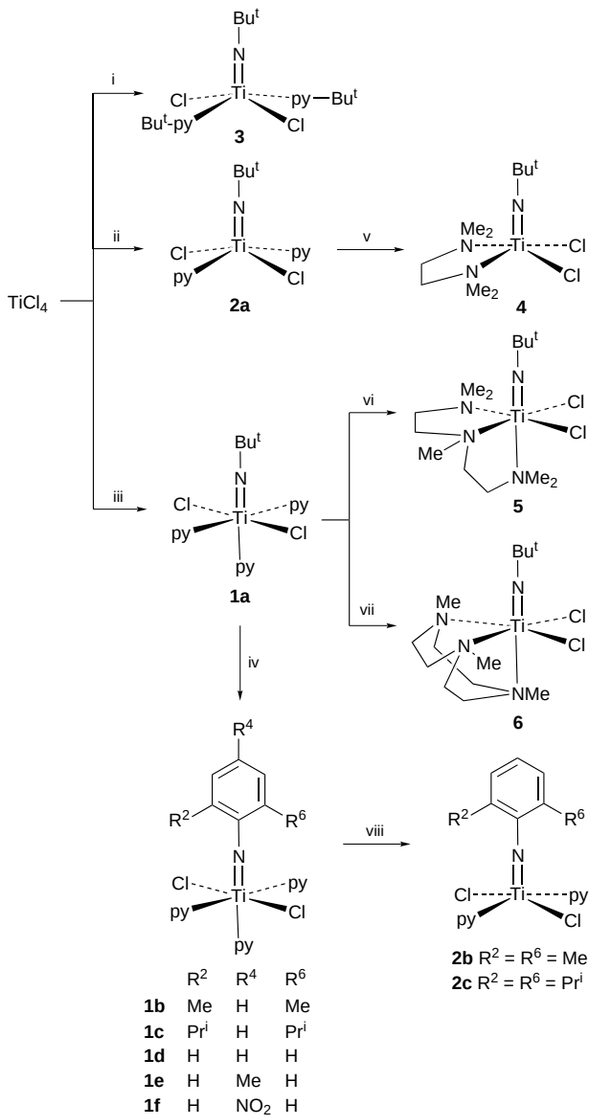



**Fig. 2** Versatile synthons for new titanium imido compounds and some pyridine substitution reactions.[13,18] *Reagents and conditions*: (i) $Bu^tNH_2$ (6 equiv.), py-$Bu^t$ (2.2 equiv.); (ii) $Bu^tNH_2$ (6.0 equiv.), py (2.3 equiv.); (iii) $Bu^tNH_2$ (6.3 equiv.), py (4.1 equiv.); (iv) aniline or substituted aniline; (v) tmeda; (vi) pmdeta; (vii) $Me_3[9]aneN_3$; (viii) 65 °C, dynamic vacuum. py-$Bu^t$ = $NC_5H_4Bu^t$-4.

## Cyclopentadienyl and indenyl derivatives

### *Half-sandwich compounds*

Straightforward metathesis reactions of $[Ti(NBu^t)Cl_2(NC_5H_4R\text{-}4)_n]$ (**1a**, **2a** or **3**) with sodium or lithium cyclopentadienides gives the range of half-sandwich derivatives $[Ti(\eta^5\text{-}C_5R'_5)(N\text{-}Bu^t)Cl(NC_5H_4R\text{-}4)]$ (**7–14**, Fig. 3).[12,19,20] Similarly, treatment of **3** with lithium trimethylindenide afforded the first Group 4 indenyl imido derivative $[Ti(\eta^5\text{-}C_9H_4Me_3)(NBu^t)Cl(NC_5H_4\text{-}Bu^t\text{-}4)]$ **15** for which a pentahapto coordination of the indenyl ligand was inferred from $^{13}C$ NMR data. Compound **15** is relatively labile and ring non-substituted indenyl analogues could not be isolated. The structurally characterised compound $[Ti(\eta^5\text{-}C_5Me_5)(NBu^t)Cl(py)]$ **12** was first obtained *via* dehydrohalogenation of $[Ti(\eta^5\text{-}C_5Me_5)(NHBu^t)Cl_2]$ in the presence of pyridine.[21] The ring non- or mono-substituted compounds **9** and **10** lose pyridine in solution or the solid state forming μ-imido bridged dimers. However, the ring penta-substituted homologues **12–14** are stable to pyridine loss under comparable conditions.

Bis(pyridine), half-sandwich titanium imides analogous to those of zirconium and hafnium[22] were not isolated, but variable temperature NMR measurements identified $C_s$-symmetric complexes $[Ti(\eta^5\text{-}C_5Me_4R)(NBu^t)Cl(py)_2]$ as intermediates in the free/coordinated pyridine exchange reactions of **7–14**; $^{13}C$ NMR lineshape and coalescence measurements for $[Ti(\eta^5\text{-}C_5Me_4C_4H_7)(NBu^t)Cl(py)]$ **14** yielded activation parameters for this process.

### *Sandwich compounds*

The Bergman group has developed an extensive reaction chemistry of zirconocene imido derivatives.[23,24] We were thus interested to find an entry point to analogous titanium imido systems.§

*Syntheses*: Fig. 3 shows that addition of two equivalents of sodium cyclopentadienide to $[Ti(NBu^t)Cl_2(py)_3]$ **1a** gave reasonable yields of $[Ti(\eta^5\text{-}C_5H_5)_2(NBu^t)(py)]$ **17**. Mixed ring analogues $[Ti(\eta^5\text{-}C_5H_5)(\eta^5\text{-}C_5Me_4R)(NBu^t)(py)]$ (R = Me **18** or Et **19**) were prepared from $Na[C_5H_5]$ and **12** or **13**. Attempts to prepare bis(pentamethylcyclopentadienyl)titanium imides from **12** and $Li[C_5Me_5]$ were unsuccessful and appeared to result in reduction to $Ti^{III}$.¶ The X-ray structure of **17** confirmed the pentahapto coordination of the cyclopentadienyl rings in the solid state and revealed a near-linear Ti=$NBu^t$ linkage. The sandwich titanium imido compounds are considerably more air- and moisture-sensitive than their half-sandwich analogues.

At first sight, the titanocene imido complexes **17–19** are twenty valence electron species. However, it appears that in these and related metallocene imido and oxo compounds[25,26] two of the 'excess' electrons are located in a ligand-based, non-bonding orbital having both $C_5H_5$ carbon and $NBu^t$ nitrogen character. Thus the actual Ti=$NBu^t$ bond order in compounds **17–19** is probably somewhere between two and three, with the titanium–cyclopentadienyl interactions presumably also somewhat weakened relative to 'normal' sixteen- and eighteen-electron titanocene derivatives. The Ti–$Cp_{cent}$ distances and $Cp_{cent}$–Ti–$Cp_{cent}$ angles ($Cp_{cent}$ = computed $C_5H_5$ centroid) for **17** are consistent with this hypothesis. Furthermore, reaction of lithium indenide with $[Ti(\eta^5\text{-}C_5H_5)(NBu^t)Cl(py)]$ **9** afforded the eighteen-electron, ring-slipped derivative $[Ti(\eta^5\text{-}C_5H_5)(\eta^3\text{-}C_9H_7)(NBu^t)(py)]$ **20**. Moreover, an equimolar mixture of $[Ti(NBu^t)Cl_2(py)_2]$ **2a** and $[Ti(\eta^5\text{-}C_5H_5)_2(NBu^t)(py)]$ **17** in $C_6D_6$ underwent a very facile, room temperature redistribution reaction in $C_6D_6$ to give **9** quantitatively, again indicative of $C_5H_5$ ligand labilisation in the bis(cyclopentadienyl) com-

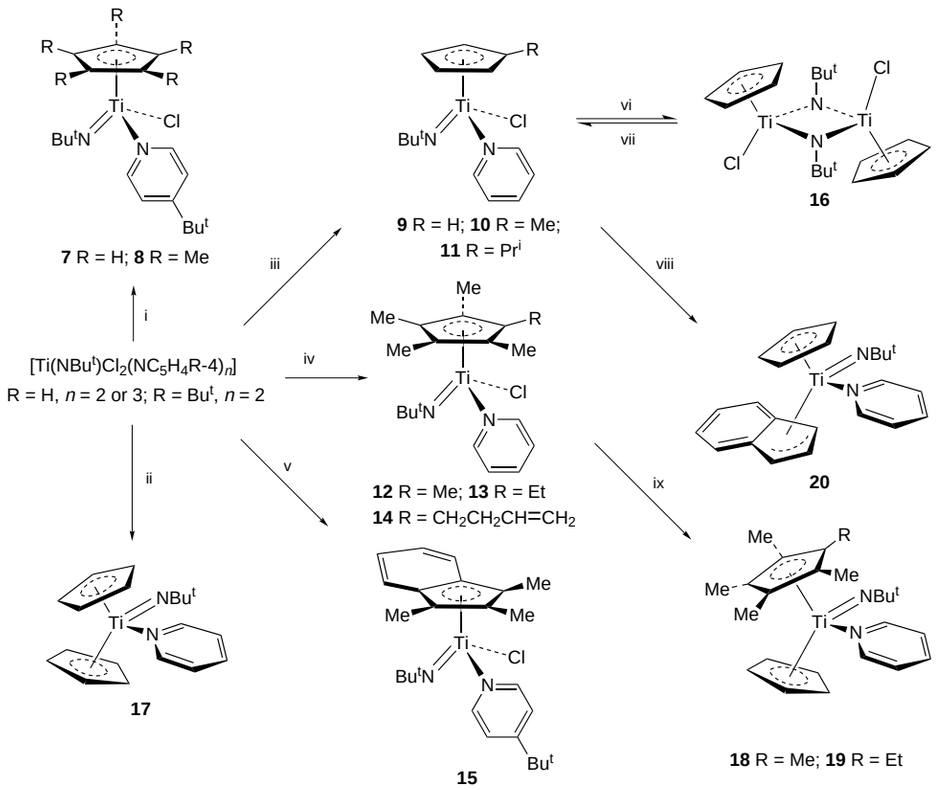



**Fig. 3** Sandwich and half-sandwich titanium imido derivatives.[20] *Reagents and conditions*: (i) for **7**: Na[$C_5H_5$], for **8**: Li[$C_5Me_5$]; (ii) Na[$C_5H_5$] (2 equiv.); (iii) for **9**: Na[$C_5H_5$], for **10**: Li[$C_5H_4Me$], for **11**: Li[$C_5H_4Pr^i$], (iv) for **12**: Li[$C_5Me_5$], for **13**: Li[$C_5Me_4Et$], for **14**: Li[$C_5Me_4C_4H_7$]; (v) Li[$C_9H_4Me_3$]; (vi) $1 \times 10^{-2}$ mbar, 85 °C; (vii) py (3 equiv.); (viii) Li[$C_9H_7$]; (ix) Na[$C_5H_5$].

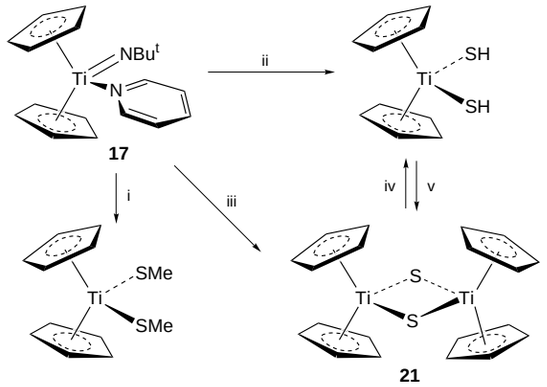



**Fig. 4** Reactions of [$Ti(\eta^5\text{-}C_5H_5)_2(NBu^t)(py)$] **17** with S–H bonds.[28] *Reagents*: (i) MeSH (excess); (ii) $H_2S$ (excess); (iii) $H_2S$ (1 equiv.); (iv) $H_2S$ (excess); (v) **17** (1 equiv.).

plexes. By way of comparison, the analogous $C_5H_5$ ring redistribution reaction between [$Ti(\eta^5\text{-}C_5H_5)_2Cl_2$] and $TiCl_4$ required elevated temperatures and longer reaction times.[27]

*Reactions with S–H bonds:* Tetraazamacrocycle-supported titanium *tert*-butyl imido derivatives (*vide infra*) undergo facile exchange of Ti=NBu$^t$ for terminal Ti=E (E = O, S, NAr or $NNPh_2$) groups on treatment with $H_2E$. We have investigated possible analogous routes to titanocene mono(sulfide) complexes (Fig. 4).[28] Not surprisingly, reaction of [$Ti(\eta^5\text{-}C_5H_5)_2(NBu^t)(py)$] **17** with an excess of MeSH affords the previously described [$Ti(\eta^5\text{-}C_5H_5)_2(SMe)_2$]. An intermediate species formulated as [$Ti(\eta^5\text{-}C_5H_5)_2(NHBu^t)(SMe)$] was observed by $^1$H NMR spectroscopy but was not isolated. With an excess of $H_2S$, **17** gives high yields of [$Ti(\eta^5\text{-}C_5H_5)_2(SH)_2$], but with one equivalent of $H_2S$ the new bis(μ-sulfide) [$Ti_2(\eta^5\text{-}C_5H_5)_4(\mu\text{-}S)_2$] **21** was obtained. Compound **21** may also be prepared by reaction of **17** with [$Ti(\eta^5\text{-}C_5H_5)_2(SH)_2$]. In neither of these reactions was evidence for a titanocene terminal sulfido derivative found.¶ The thermally labile compound **21** is a possible intermediate in the formation of [$Ti(\eta^5\text{-}C_5H_5)_2(SH)_2$] since treatment of **21** with an excess of $H_2S$ gave a quantitative yield of [$Ti(\eta^5\text{-}C_5H_5)_2(SH)_2$].

These reactions comprised the first reports of S–H bond 'activation' for Group 4 metal imido complexes. Furthermore, the complex [$Ti_2(\eta^5\text{-}C_5H_5)_4(\mu\text{-}S)_2$] **21** represents a kind of 'missing link' both in the titano- and zircono-cene bis(μ-chalcogenido) series [$M_2(\eta\text{-}C_5R_5)_4(\mu\text{-}E)_2$] (M = Ti or Zr; E = S or Se) and in the bis(titanocene) μ-(poly)sulfido series [$Ti_2(\eta\text{-}C_5H_4R)_4(\mu\text{-}S_x)_2$] ($x$ = 1, 2 or 3), which have been the subject of considerable research activity.

## Mono- and bi-nuclear derivatives with aryloxide ligands: fine control by *ortho*-substituents

As mentioned, five-coordinate aryloxide-supported derivatives were among the first terminal titanium imido compounds to be structurally characterised.[8,29] The transient imido complex [$Ti(NSiBu^t)(OSiBu^t)_2$] has been proposed as a reactive intermediate.[30] We were interested in extending these studies by exploring in detail the dependence of the structures, nuclearity and metal coordination number of aryloxide-supported titanium imides upon the steric demands of the ligand O- and N-substituents.[31]

The reaction products of [$Ti(NBu^t)Cl_2(py)_3$] **1a** with lithium aryloxides (Fig. 5) show the relationship between the product nuclearity and coordination number and the steric bulk of the aryloxide ligand *ortho*-substituents. The structure of [$Ti_2(\mu\text{-}NBu^t)_2(OC_6H_3Me_2\text{-}2,6)_4$] **22** was confirmed by X-ray crystallography and [$Ti(NBu^t)(OC_6H_3Bu^t_2\text{-}2,6)_2(py)$] **24** was established as a monomer by solution molecular mass determinations. The {$Ti(\mu\text{-}NBu^t)_2Ti$} core in compound **22** can be

cleaved by an excess of pyridine to form mononuclear $[Ti(NBu^t)(OC_6H_3Me_2\text{-}2,6)_2(py)_2]$ **25a**. Although the *tert*-butyl imido compound **25a** slowly dimerises to **22** over time, the aryl imido homologues $[Ti(NC_6H_3R_2\text{-}2,6)(OC_6H_3Me_2\text{-}2,6)_2(py)_2]$ [R = Me **25b** (X-ray structure) or $Pr^i$ **25c**] are stable.

We have analysed the bonding in $[Ti_2(\mu\text{-}NBu^t)_2(O\text{-}C_6H_3Me_2\text{-}2,6)_4]$ **22** using extended Hückel molecular orbital (EHMO) calculations and reached two important conclusions.[31] First, symmetry constraints mean that the Ti centres in **22** can only ever achieve a valence electron count of sixteen, even though the formal hybridisation of the imido N- and terminal aryloxide O-atoms suggests that metal electron counts of eighteen are apparently possible. Second, the deviation of the μ-imido $Bu^t$ substituents from coplanarity with the $Ti_2N_2$ unit in both **22** and related species such as $[Ti_2(\mu\text{-}NBu^t)_2(NMe_2)_4]$ can be attributed to a second-order Jahn–Teller distortion which arises because of competition between the terminal and bridging π-donor ligands for metal $d_\pi$-acceptor orbitals.

## Amidinate derivatives

In contrast to other areas of main group and transition metal chemistry, amidinate ligands[32,33] have been little used in metal imido systems.[34–38] We have recently reported new niobium imido (and oxo) benzamidinate derivatives,[39] and this work is complemented by the titanium imido amidinate chemistry summarised below.

The steric and solubility properties of amidinate ligands $R'C(NR)_2$ may be modified by changing the R′ and R groups. We have compared (Fig. 6) the reactions of lithium *N*,*N*′-bis(trimethysilyl)benzamidinate and lithium *N*,*N*′-bis(cyclohexyl)acetamidinate with $[Ti(NR)Cl_2(py)_3]$ (R = $Bu^t$ **1a**, $C_6H_3Me_2$-2,6 **1b** and $C_6H_3Pr^i_2$-2,6 **1c**).[40] Reaction of $Li[PhC(NSiMe_3)_2]$ with **1a**–**1c** afforded the corresponding mononuclear compounds $[Ti(NR)\{PhC(NSiMe_3)_2C\}l(py)_2]$ **26a**–**c** as confirmed by X-ray crystallography for **26b**. In contrast, reaction of $Li[MeC(NC_6H_{11})_2]$ with **1a** led to the structurally characterised binuclear derivative $[Ti_2(\mu\text{-}NBu^t)_2\{MeC(NC_6H_{11})_2\}_2Cl_2]$ **27** which contains no pyridine coligands. Attempts to prepare aryl imido analogues of **26** or **27** from $Li[MeC(NC_6H_{11})_2]$ and $[Ti(NC_6H_3Me_2\text{-}2,6)Cl_2(py)_3]$ **1b** were unsuccessful.

All three compounds **26a**–**c** form six-coordinate bis(pyridine) adducts in the solid state, but in solution they exist in temperature-dependent dynamic equilibrium with the fourteen valence electron, mono(pyridine) homologues **26a′**–**c′** (Fig. 6). Thermodynamic parameters (Table 1) associated with these equilibria have been determined by NMR spectroscopy and

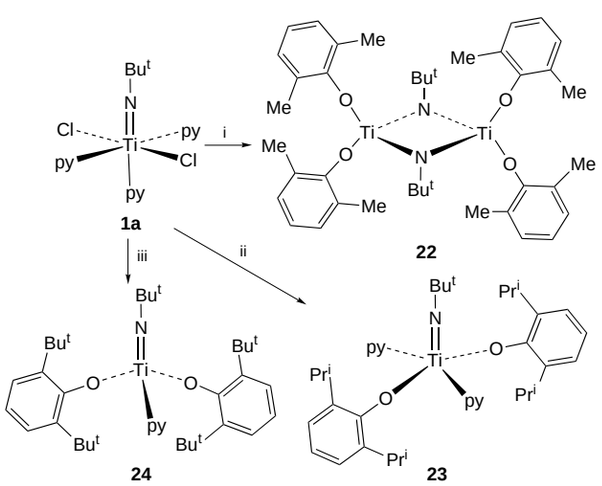



**Fig. 5** Reactions of $[Ti(NBu^t)Cl_2(py)_3]$ **1a** with $Li[OC_6H_3R_2\text{-}2,6]$: fine control by *ortho*-substituents.[31] *Reagents*: (i) $Li[OC_6H_3Me_2\text{-}2,6]$ (2 equiv.); (ii) $Li[OC_6H_3Pr^i_2\text{-}2,6]$ (2 equiv.); (iii) $Li[OC_6H_3Bu^t_2\text{-}2,6]$ (2 equiv.).

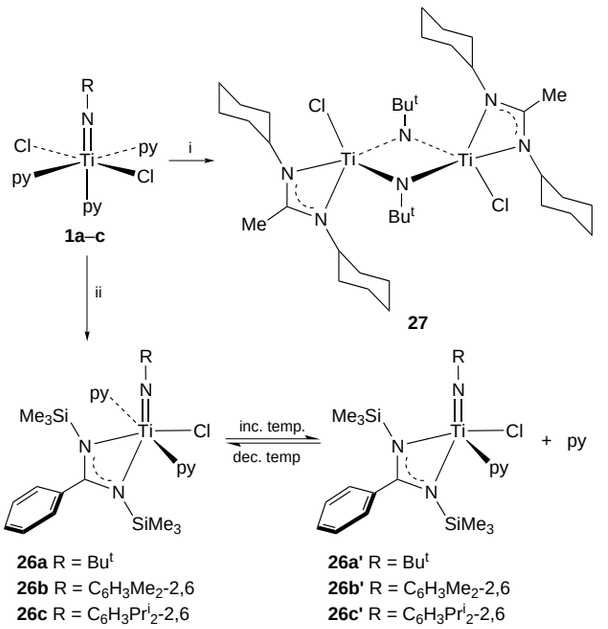



**Fig. 6** Mono- and bi-nuclear titanium imido complexes with amidinate ligands.[40] *Reagents*: (i) $Li[MeC(NC_6H_{11})_2]$; (ii) $Li[PhC(NSiMe_3)_2]$.

reveal the underlying effects of the different imido N-substituents. Activation parameters for the forward (*i.e.* **26a** or **26b** → **26a′** or **26b′** + py) and reverse (**26a′** or **26b′** + py → **26a** or **26b**) processes have also been measured. The differences between the derived $\Delta G^{\ddagger}_{258\,K}$ values for the forward and reverse steps compare very well with the equilibrium thermodynamic $\Delta G_{258\,K}$ values which show that all three equilibria are effectively thermochemically neutral. The large positive $\Delta S$ values are consistent with the dissociative equilibria as written and nearly compensate for the endothermic $\Delta H$ term at higher temperatures.

Very recent results for $[Ti(NBu^t)\{PhC(NSiMe_3)_2C\}l(py)_2]$ **26a** promise an extensive reaction chemistry for the amidinate-supported titanium imido compounds.[18] Straightforward metathesis reactions afford a range of organometallic and inorganic derivatives in good to excellent yields (Fig. 7). The half-sandwich compound **29** can also be prepared from $Li[PhC(NSiMe_3)_2]$ and $[Ti(\eta^5\text{-}C_5Me_5)(NBu^t)Cl(NC_5H_4Bu^t\text{-}4)]$ **8**.[18]

## Tris(pyrazolyl)hydroborate derivatives

Fig. 8 summarises the synthesis of sixteen valence electron tris(pyrazolyl)hydroborate derivatives $[Ti(L)(NBu^t)Cl(NC_5H_4Bu^t\text{-}4)]$ (L = $Tp^{Me2}$ **34**, $Tp^{Pri}$ **35** or $Tp^{Pri,Br}$ **36**) *via* reaction of $[Ti(NBu^t)Cl_2(NC_5H_4Bu^t\text{-}4)_2]$ **3** with one equivalent of $K[Tp^{Me2}]$, $K[Tp^{Pri}]$ or $K[Tp^{Pri,Br}]$ [$Tp^{Me2}$ = tris(3,5-dimethylpyrazolyl)hydroborate; $Tp^{Pri}$ = tris(3-isopropylpyrazolyl)hydroborate; $Tp^{Pri,Br}$ = tris(3-isopropyl-4-bromopyrazolyl)hydroborate] respectively.[41] Compounds **34**–**36** are the first Group 4 tris(pyrazolyl)hydroborate-supported imido complexes and are isolobal analogues of the half-sandwich

**Table 1** Thermodynamic parameters for the dissociative equilibria of $[Ti(NR)\{PhC(NSiMe_3)_2\}Cl(py)_2]$ [R = $Bu^t$ **26a**, $C_6H_3Me_2$-2,6 **26b** or $C_6H_3Pr^i_2$-2,6 **26c**][40]

| R | $\Delta H$/ kJ mol$^{-1}$ | $\Delta S$/ J mol$^{-1}$ K$^{-1}$ | $\Delta G_{258\,K}$/ kJ mol$^{-1}$ |
|---|---|---|---|
| $Bu^t$ **26a** | 38.7 ± 1.5 | 108 ± 5 | 10.8 ± 2.8 |
| $C_6H_3Me_2$-2,6 **26b** | 47.3 ± 1.9 | 142 ± 5 | 10.7 ± 3.2 |
| $C_6H_3Pr^i_2$-2,6 **26c** | 45.7 ± 2.0 | 172 ± 5 | 1.2 ± 3.3 |

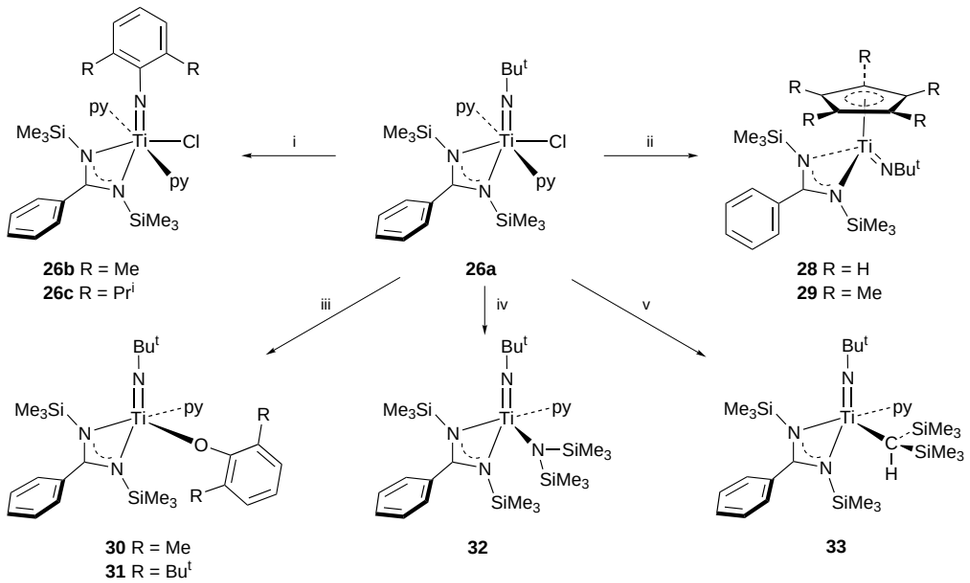
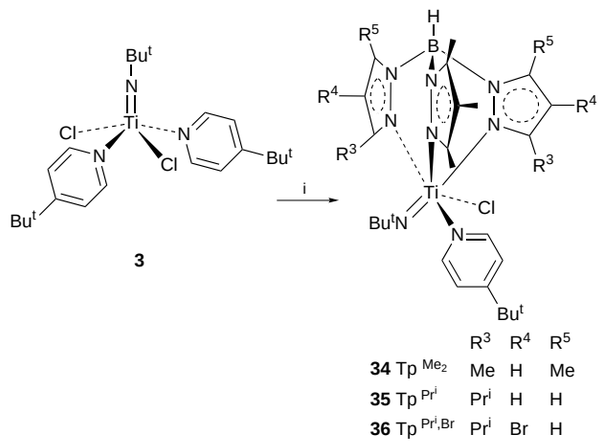


**Fig. 7** Substitution reactions of [Ti(NBu$^t$){PhC(NSiMe$_3$)$_2$}Cl(py)$_2$] **26a**.[18] *Reagents*: (i) $H_2NC_6H_3R_2$-2,6 where for **26b**: R = Me, for **26c**: R = Pr$^i$; (ii) for **28**: Na[$C_5H_5$], for **29**: Li[$C_5Me_5$]; (iii) Li[$OC_6H_3R_2$-2,6] where for **30**: R = Me, for **31**: R = Bu$^t$; (iv) Li[N(SiMe$_3$)$_2$]·Et$_2$O; (v) Li[CH(SiMe$_3$)$_2$].



| | $R^3$ | $R^4$ | $R^5$ |
|---|---|---|---|
| **34** Tp$^{Me_2}$ | Me | H | Me |
| **35** Tp$^{Pr^i}$ | Pr$^i$ | H | H |
| **36** Tp$^{Pr^i,Br}$ | Pr$^i$ | Br | H |

**Fig. 8** Titanium imido complexes with tris(pyrazolyl)hydroborate ligands.[41] *Reagents*: (i) for **34**: K[Tp$^{Me_2}$], for **35**: K[Tp$^{Pr^i}$], for **36**: K[Tp$^{Pr^i,Br}$].

complexes [Ti($\eta^5$-$C_5R'_5$)(NBu$^t$)Cl($NC_5H_4$R-4)] (**7**–**14**). Unlike the cyclopentadienyl compounds, however, the tris(pyrazolyl)hydroborate species are fluxional on the $^1$H and $^{13}$C NMR timescales, the spectra indicating restricted rotation about the Ti–($NC_5H_4$Bu$^t$-4) bond. Activation parameters were determined for **34** and the barrier to pyridine rotation obtained from coalescence measurements ($\Delta G^{\ddagger}_{267\,K}$ = 51.1 kJ mol$^{-1}$) compared very well with that calculated (51.4 kJ mol$^{-1}$) from the $\Delta S^{\ddagger}$ and $\Delta H^{\ddagger}$ values using lineshape analysis.

## Diamidoamine and diamidopyridine derivatives

The tetradentate, triamidoamine (tren) ligands [(RNCH$_2$CH$_2$)$_3$N]$^{3-}$ have been used with spectacular success for developing the metal–ligand multiple bond chemistry of groups 5–7.[42] We have started to explore the potential of tridentate diamidoamine[43] and diamidopyridine[44] ligands in Group 4 imido chemistry. While being related to the triamidoamines, the dianionic diamidoamine and diamidopyridine ligands have a dative nitrogen donor 'arm' which can in principle readily detach from the metal centre to open up reversibly a more reactive site. Furthermore, they require only two d electrons for metal–ligand bonding, thus enabling neutral imido derivatives for the Group 4 metals. Although our work in this area is at a very early stage, some important results have already been obtained (Fig. 9).[18,45]

Reaction of Li$_2$[Me$_3$SiN(CH$_2$CH$_2$NSiMe$_3$)$_2$] with [Ti(NBu$^t$)Cl$_2$(py)$_3$] **1a** gave the crystallographically characterised derivative [Ti(NBu$^t$){Me$_3$SiN(CH$_2$CH$_2$NSiMe$_3$)$_2$}py)] **37** in good yield. Similarly, addition of [Li$_2${MeC($C_5H_4$N-2)(CH$_2$NSiMe$_3$)$_2$}]$_2$ to **1a** in benzene gave [Ti(NBu$^t$){MeC($C_5H_4$N-2)(CH$_2$NSiMe$_3$)$_2$}(py)] **38** which has also been crystallographically characterised. Compounds **37** and **38** are the first fully characterised examples of terminal titanium imides supported by amido ligands, although the complex [Ti(NSiBu$^t_3$)(NHSiBu$^t_3$)$_2$] has been proposed as a reactive transient in C–H bond activation reactions.[10] Fig. 9 shows the product of the remarkable reaction between **38** and methyl isocyanide, namely [Ti{MeC($C_5H_4$N-2)(CH$_2$NSiMe$_3$)$_2$}{N(Me)N(Bu$^t$)-1,2-($C_4H_3N_2$Me-3)}] **39**, which has been structurally characterised. The Ti=NBu$^t$ linkage of **1a** has clearly undergone a C–N and C–C coupling reaction (with concomitant C–H bond migration) with three molecules of MeNC to form a coordinated 3-methyl-5,6-diamino-2,3-dihydropyrimidine derivative. The type of reaction giving rise to **39** is unprecendented in Group 4 imido chemistry. It is also highly selective with **39** being the only new species formed when the reaction was

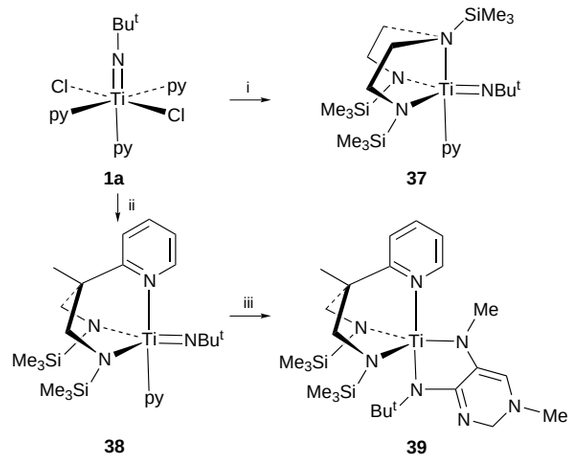


**Fig. 9** Titanium imido complexes with diamidoamine and diamidopyridine ligands.[18,45] *Reagents*: (i) Li$_2$[Me$_3$SiN(CH$_2$CH$_2$NSiMe$_3$)$_2$]; (ii) [Li$_2${MeC($C_5H_4$N-2)(CH$_2$NSiMe$_3$)$_2$}]$_2$; (iii) MeNC (3 equiv.).

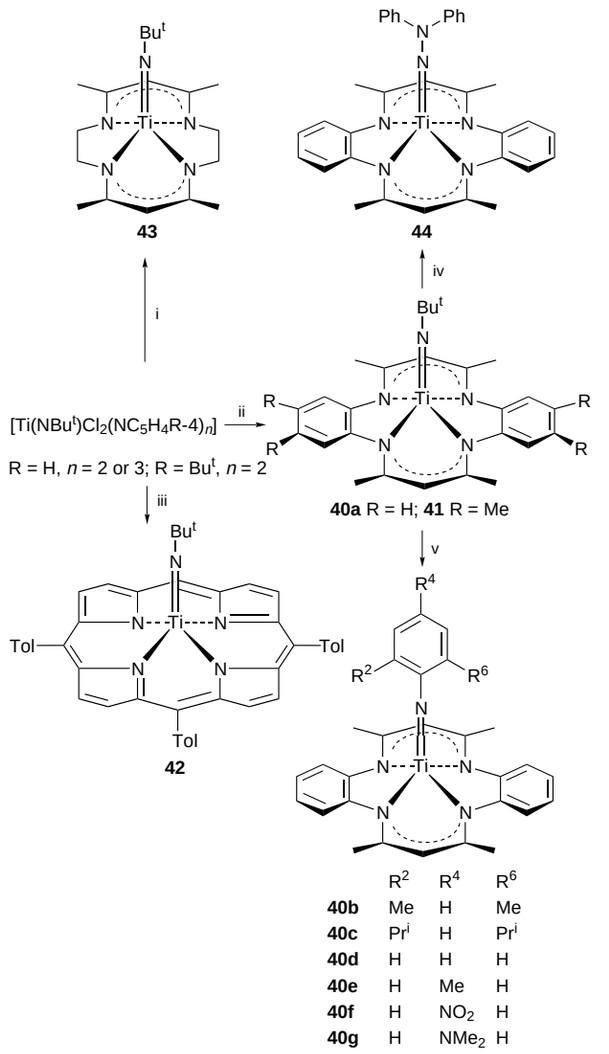



**Fig. 10** Titanium imido complexes with dibenzotetraaza[14]annulene and some other tetraazamacrocyclic ligands.[12,18,52] *Reagents*: (i) $Li_2[Me_4taen]$; (ii) for **40a**: $Li_2[Me_4taa]$, for **41**: $Li_2[Me_8taa]$; (iii) $Li_2[ttp]$; (iv) $Ph_2NNH_2$; (v) aniline or substituted aniline.

followed by $^1$H NMR spectroscopy. The Ti=NBu$^t$ functional group in **38** also reacts with a range of other unsaturated organic substrates and work is in progress to determine the scope of this chemistry.

## Tetraazamacrocycle-supported derivatives

### *Syntheses*

Prompted by reports that the Ti=O linkage in the tetraazamacrocycle-supported compound [Ti(O)($Me_4$taa)][46] ($H_2Me_4$taa = tetramethyldibenzotetraaza[14]annulene) is reactive towards a range of organic and inorganic substrates,[47] we prepared (Fig. 10) the titanium *tert*-butyl imido analogues [Ti(NBu$^t$)($Me_n$taa)] (*n* = 4 **40a** or 8 **41**; $H_2Me_8$taa = octamethyldibenzotetraaza[14]annulene) from [Ti(NBu$^t$)$Cl_2(L)_n$] and $Li_2[Me_n taa]$.[12,48] Compounds **40a** and **41** were the first reported macrocycle-supported Group 4 imido compounds. Woo and coworkers subsequently reported the synthesis of [Ti(NR)(ttp)] (R = Bu$^t$ **42**, Ph, $C_6H_4$Me-4 or $C_6H_{11}$; $H_2$ttp = tetratolylporphyrin) from [Ti(ttp)$Cl_2$].[49] We have shown that **42** can also be obtained in good yield by treating [Ti(NBu$^t$)$Cl_2(py)_3$] **1a** with $Li_2$[ttp].[18] In related studies (Fig. 10) we found that reactions of $Li_2[Me_4taen]$ ($H_2Me_4$taen = 5,7,12,14-tetramethyl-1,4,8,11-tetraazacyclotetradeca-4,6,11,13-tetraene) with **1a** gives [Ti(NBu$^t$)($Me_4$taen)] **43**. We have also recently prepared related $Me_4$taa-supported zirconium imido and amido complexes.[50,51]

Exchange reactions (Fig. 10) of [Ti(NBu$^t$)($Me_4$taa)] **40a** with a range of anilines or *N*,*N*-diphenylhydrazine afforded the homologues [Ti(NAr)($Me_4$taa)] (Ar = $C_6H_3Me_2$-2,6 **40b**, $C_6H_3Pr^i_2$-2,6 **40c**, Ph **40d**, $C_6H_4$Me-4 **40e**, $C_6H_4NO_2$-4 **40f** or $C_6H_4NMe_2$-4 **40g**) and [Ti($NNPh_2$)($Me_4$taa)] **44** respectively.[18,52] Although most of these reactions were quantitative by $^1$H NMR spectroscopy, they were noticeably slower than those of [Ti(NBu$^t$)$Cl_2(py)_3$] **1a** (Fig. 2). Indeed, the 2,6-diisopropylphenyl imido derivative **40c** was only obtained in trace quantities after long reaction times. The X-ray structures of **40b**[52] and **41**[12] have been determined. No bis(amide) intermediates were observed when the reactions of [Ti(NBu$^t$)($Me_4$taa)] **40a** with anilines were followed by $^1$H NMR spectroscopy and no evidence was found for equilibrium concentrations of [Ti($NHR)_2$($Me_4$taa)] in solutions containing [Ti(NR)($Me_4$taa)] and $H_2$NR (R = Bu$^t$ or $C_6H_3Me_2$-2,6). In contrast, the zirconium aryl imido homologue (which is obtained as a pyridine adduct) [Zr($NC_6H_3Pr^i_2$-2,6)(py)($Me_4$taa)] reacts immediately and irreversibly with $H_2NC_6H_3Pr^i_2$-2,6 to form the bis(anilide) [Zr($HNC_6H_3Pr^i_2$-2,6)$_2$($Me_4$taa)].[50] Interestingly, we note that [Ti(NBu$^t$)(ttp)] **43** does not undergo exchange reactions with anilines.[49] This underlines the importance of the choice of macrocyclic ligands.

### *Reactions of [Ti(NBu$^t$)($Me_4$taa)]* **40a** *with O–H and S–H bonds*

Treatment of **40a** with $H_2E$ (E = O or S) gave the previously described[46] [Ti(E)($Me_n$taa)] in quantitative yield (Fig. 11). Compound **40a** also undergoes protonolysis with aryl and alkyl alcohols and diols to form [Ti($OR)_2$($Me_4$taa)] (R = Me **45** or $OC_6H_3Me_2$-2,6 **46**; $(OR)_2 = O_2C_2Me_4$ **47** or $O_2C_6H_4$ **48**[46]), and with MeSH to form [Ti($SMe)_2$($Me_4$taa)] **49** by $^1$H NMR spectroscopy. Reaction of **49** with $H_2S$ forms [Ti(S)($Me_4$taa)] and MeSH. By analogy with the *tert*-butyl imide/aniline exchange processes (Fig. 10), when reactions of [Ti(NBu$^t$)($Me_4$taa)] **40a** with $HOC_6H_3Me_2$-2,6, MeSH or $H_2S$ were followed by $^1$H NMR spectroscopy, no six-coordinate intermediates [Ti(ER)(NHBu$^t$)($Me_4$taa)] (ER = $OC_6H_3Me_2$-2,6, SMe or SH) were observed. Furthermore, reaction of **40a** with one equivalent of $HOC_6H_3Me_2$-2,6 gave a *ca.* 50% yield of [Ti($OC_6H_3Me_2$-2,6)$_2$($Me_4$taa)] and unreacted **40a**.

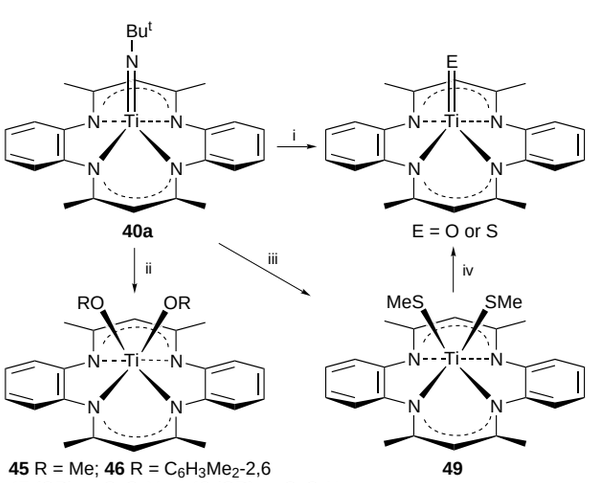



**Fig. 11** Reactions of [Ti(NBu$^t$)($Me_4$taa)] **40a** with O–H and S–H bonds.[12,18] *Reagents*: (i) $H_2E$ (E = O or S); (ii) ROH (2 equiv. of OH functional group); (iii) MeSH (2 equiv.); (iv) for [Ti(S)($Me_4$taa)]: $H_2S$ (excess).

### *Reactions of [Ti(NAr)(Me$_4$taa)] (Ar = Ph* **40d** *or Tol* **40e**) *with isocyanates, CO$_2$ and carbodiimides*

We have studied the cycloaddition and metathesis reactions of the compounds [Ti(NR)(Me$_4$taa)] **40** with a range of organic substrates.[18,50] Fig. 12 summarises some of the reactions of [Ti(NAr)(Me$_4$taa)] (Ar = Ph **40d** or Tol **40e**), along with some new, comparative reactions of [Ti(O)(Me$_4$taa)].

Reaction of **40d** or **40e** with isocyanates PhNCO or TolNCO gave the *N*,*N*′-bonded ureates [Ti{N(Ar)C(O)N(Ar)}(Me$_4$taa)] (Ar = Ph **50** or Tol **51**, respectively) in good yields.[50] The mixed N-aryl substituent ureate [Ti{N(Ph)C(O)N-(Tol)}(Me$_4$taa)] **52** was prepared similarly from **40e** and PhNCO. In related studies, [Zr(N-C$_6$H$_3$Pr$^i_2$-2,6)(py)(Me$_4$taa)] reacted with Bu$^t$NCO to give the crystallographically characterised *N*,*N*′-bound ureate [Zr{N(C$_6$H$_3$Pr$^i_2$-2,6)C(O)N(Bu$^t$)}-(Me$_4$taa)].[50] The titanium congener **52** exhibits novel reactivity such that treatment with an excess of PhNCO gave [Ti{N(Ph)-C(O)N(Ph)}(Me$_4$taa)] **50** with extrusion of TolNCO from the ureate ligand. $^1$H NMR crossover experiments eliminated [Ti(NPh)(Me$_4$taa)] **40d** as an intermediate, thus suggesting that the PhNCO–TolNCO exchange involves an unusual associative mechanism proceeding *via* a biuret-type species, [Ti{N(Ph)C(O)N(Ph)C(O)N(Tol)}(Me$_4$taa)]. The exchange reaction of **52** was the first example of the reversible insertion of an isocyanate into the metal–N bond of a ureate ligand.

Reaction of [Ti(NTol)(Me$_4$taa)] **40e** with di-*p*-tolylcarbodiimide gave [Ti{N(Tol)C(NTol)N(Tol)}(Me$_4$taa)] **53** which is a rare example of a triazatrimethylene methane metal complex.[53] Reaction of **40e** with $CO_2$ gave the *O*,*O*′-bonded carbamate species [Ti{OC(NTol)O}(Me$_4$taa)] **54**. Compound **54** is presumably a thermodynamic (as opposed to kinetic) product since the expected first-formed product would be the *N*,*O*-bonded linkage isomer [Ti{N(Tol)C(O)O}(Me$_4$taa)]. In comparative studies, we found that treatment of [Ti(O)(Me$_4$taa)] with TolNCO also formed **54** exclusively. This is again consistent with compound **54** being the thermodynamically favoured isomer. Thus rearrangements of the macrocycle-supported titanium-imido and -oxo cycloaddition products appears to be facile, as emphasised by the reaction of [Ti(O)(Me$_4$taa)] with di-*p*-tolylcarbodiimide (Fig. 12). This gave the *N*,*N*′-bound ureate **51** (also obtained from **40e** and TolNCO) rather than the *N*,*O*-bonded linkage isomer [Ti{OC(NTol)N(Tol)}(Me$_4$taa)] which would presumably form as a first intermediate in a Ti=O + TolN=C=NTol [2 + 2] cycloaddition reaction. Furthermore, even if the reactions in Fig. 12 proceed *via* nucleophilic attack of the imido N- or oxo O-atom at the central cumulene carbon E=C=E′ (*i.e.*, instead of going *via* direct cycloaddition), the formation of **54** from **40e**, and of **51** from [Ti(O)(Me$_4$taa)], still require rearrangement processes involving Ti–N and Ti–O bond cleavage respectively.

### Titanium imides with other dianionic ligands

Ongoing work in our group with other dianionic ligands has established further new classes of organometallic and coordination titanium imido compounds. As with the syntheses of the tetraazamacrocyle-supported derivatives [Ti(NBu$^t$)(Me$_4$taa)] **40a**, [Ti(NBu$^t$)(ttp)] **42** and [Ti(NBu$^t$)(Me$_4$taen)] **43**, straighforward reactions of disodium or dilithium salts Li$_2$[C$_8$H$_6$-(SiMe$_3$)$_2$], [Na$_2$(L)]$_2$ (LH$_2$ = 1,3-dimethyl ether *p*-*tert*-butylcalix[4]arene) or Na$_2$[Bu$^t_4$salen] [H$_2$Bu$^t_4$salen = tetrakis(*tert*-butyl)salen] with [Ti(NBu$^t$)Cl$_2$(py)$_3$] gave good yields of the corresponding new imido complexes [Ti(NBu$^t$){$\eta^8$-C$_8$H$_6$(SiMe$_3$)$_2$}] **55**, [Ti(NBu$^t$)(L)] **56** or [Ti(NBu$^t$)(Bu$^t_4$salen)] **57** repectively.[18,48,54] Studies of these and related systems are currently underway.

### Concluding remarks

Over the last three years we have shown that many new types of titanium and other Group 4 metal imido complex can be readily accessed through high-yielding, straightforward synthetic methods. A variety of both new and familiar reaction types have already been found for the new compounds. It is very likely that the next phase of Group 4 imido chemistry will focus much more on developing new reactions towards organic substrates and catalytic processes.


### Acknowledgements

I am indebted to my current and former graduate and postdoctoral coworkers for their contributions to the chemistry described in this article. I thank also my collaborators and colleagues in Nottingham and elsewhere for many valuable discussions, and the EPSRC, Leverhulme Trust, British Council, Nuffield Foundation, University of Nottingham, Royal Society and NATO for funding.

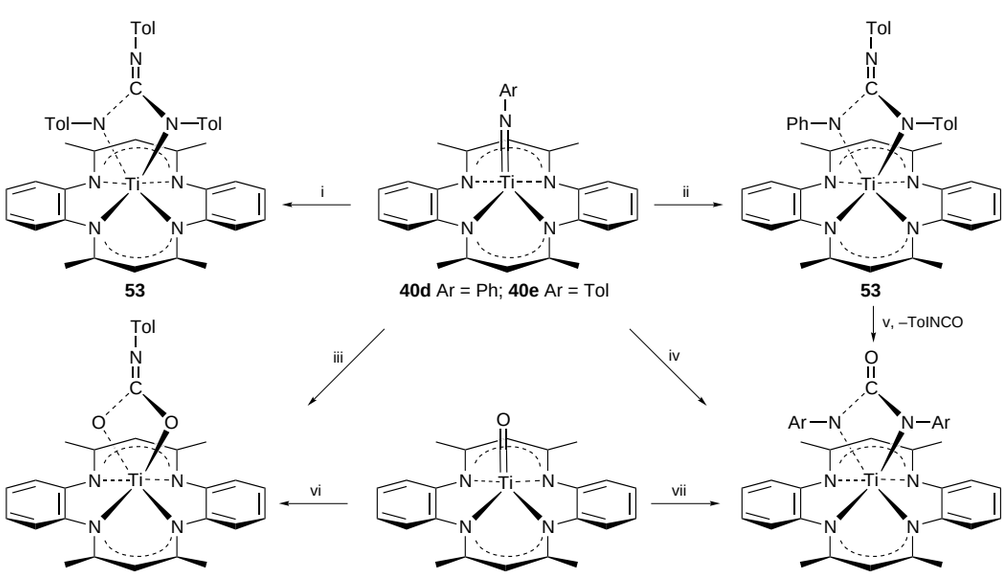




**Fig. 12** Selected reactions of [Ti(NAr)(Me$_4$taa)] and [Ti(O)(Me$_4$taa)] with cumulenes.[18,50] *Reagents*: (i) from **40e**: TolN=C=NTol; (ii) from **40e**: PhNCO; (iii) from **40e**: $CO_2$; (iv) from **40d**: PhNCO, from **40e**: TolNCO; (v) for **50**: PhNCO (5 equiv.); (vi) TolNCO; (vii) for **51**: TolN=C=NTol.

**Philip Mountford (b. 1962) gained a BSc (Hons) degree at Hatfield Polytechnic (1982–1986) and a DPhil degree at the University of Oxford (1986–1989) under the supervision of Professor M. L. H. Green. He remained at Oxford as a Junior Research Fellow at Wolfson College (1989–1992), Departmental Demonstrator at the Inorganic Chemistry Laboratory (1990–1992), and College Lecturer at Keble College (1990–1992). In 1992 he was appointed to a lectureship at the University of Nottingham. His research interests centre around studies of the synthesis, structure, bonding and reactivity of organometallic and coordination compounds and he is author or coauthor of over 75 publications in this area.**

## Footnotes and References

* E-mail: philip.mountford@nottingham.ac.uk
www: http://www.nottingham.ac.uk/~pczwww/Inorganic/PMount.html

† Although for ease of representation all metal–imido or –oxo linkages are drawn M=NR or M=O, the formal metal–ligand multiple bond order in the Group 4 imido compounds described herein is probably best thought of as three (pseudo-$\sigma^2\,\pi^4$; triple bond) rather than as two.[4] Formal bond orders for the imido linkage in the bis($\eta^5$-cyclopentadienyl)titanium imido and related compounds have been addressed.[4,20] General bond order assignments in a number of poly(imido) transition metal compounds have been proposed.[55]

‡ Throughout this review the suffixes **a**, **b** and **c** for homologous series of imido compounds $[Ti(NR)(L)_n]_m$ refer to those with R = $Bu^t$, $C_6H_3Me_2$-2,6 and $C_6H_3Pr^i_2$-2,6, respectively.

§ Vinylimido titanocene derivatives have been described but their reactions invariably involve [4 + 2] cycloadditions. Hence the reactivity of the non-conjugated Ti=NR functional group cannot be studied in these systems.[56]

¶ Although bis(pentamethylcyclopentadienyl) derivatives cannot be obtained *via* our route, Andersen and co-workers have recently found that reaction of $[Ti(\eta\text{-}C_5Me_5)_2(\eta^2\text{-}C_2H_4)]$ with $ArN_3$ or with $S_8$ and pyridine affords $[Ti(\eta\text{-}C_5Me_5)_2(NAr)]$[57] and $[Ti(\eta\text{-}C_5Me_5)_2(S)(py)]$ respectively.[58]

This ChemComm is also available in enhanced multi-media format *via* the World Wide Web: http://chemistry.rsc.org/rsc/ccenha.htm which contains more details of the bonding in the dibenzotetraaza[14]annulene systems

1 W. A. Nugent and B. L. Haymore, *Coord. Chem. Rev.*, 1980, **31**, 123.
2 M. H. Chisholm and I. P. Rothwell, in *Comprehensive Coordination Chemistry*, ed. G. Wilkinson, R. D. Gillard and J. A. McCleverty, Pergamon Press, Oxford, 1987, vol. 2, p. 162.
3 W. A. Nugent and J. M. Mayer *Metal–Ligand Multiple Bonds*, Wiley-Interscience, New York, 1988.
4 D. E. Wigley, *Prog. Inorg. Chem.*, 1994, **42**, 239.
5 D. N. Williams, J. P. Mitchell, A. D. Poole, U. Siemeling, W. Clegg, D. C. R. Hockless, P. A. O'Neil and V. C. Gibson, *J. Chem. Soc., Dalton Trans.*, 1992, 739.
6 D. S. Glueck, J. C. Green, R. I. Michelman and I. N. Wright, *Organometallics*, 1992, **11**, 4221.
7 R. R. Schrock, *Acc. Chem. Res.*, 1990, **23**, 158.
8 J. E. Hill, R. D. Profilet, P. E. Fanwick and I. P. Rothwell, *Angew. Chem., Int. Ed. Engl.*, 1990, **29**, 664.
9 H. W. Roesky, H. Voelker, M. Witt and M. Noltemeyer, *Angew. Chem., Int. Ed. Engl.*, 1990, **29**, 669.
10 C. C. Cummins, C. P. Schaller, G. D. Van Duyne, P. T. Wolczanski, A. W. E. Chan and R. Hoffmann, *J. Am. Chem. Soc.*, 1991, **113**, 2985.
11 P. L. McGrane, M. Jensen and T. Livinghouse, *J. Am. Chem. Soc.*, 1992, **114**, 5459.
12 S. C. Dunn, A. S. Batsanov and P. Mountford, *J. Chem. Soc., Chem. Commun.*, 1994, 2007.
13 A. J. Blake, P. E. Collier, S. C. Dunn, W.-S. Li, P. Mountford and O. V. Shishkin, *J. Chem. Soc., Dalton Trans.*, 1997, 1549.
14 P. E. Collier, S. C. Dunn, P. Mountford, O. V. Shishkin and D. Swallow, *J. Chem. Soc., Dalton Trans.*, 1995, 3743.
15 M. Bochmann, *J. Chem. Soc., Dalton Trans.*, 1996, 255.
16 H. H. Brintzinger, D. Fischer, R. Mülhaupt, B. Rieger and R. M. Waymouth, *Angew. Chem., Int. Ed. Engl.*, 1995, **34**, 1143.
17 T. S. Lewkebandra, P. H. Sheridan, M. J. Heeg, A. L. Rheingold and C. H. Winter, *Inorg. Chem.*, 1994, **33**, 5879.
18 Unpublished results from our group.
19 K. A. Butakoff, D. A. Lemenovskii, P. Mountford, L. G. Kuz'mina and A. V. Churakov, *Polyhedron*, 1996, **15**, 489.
20 S. C. Dunn, P. Mountford and D. A. Robson, *J. Chem. Soc., Dalton Trans.*, 1997, 293.
21 Y. Bai, M. Noltemeyer and H. W. Roesky, *Z. Naturforsch., Teil B*, 1991, **46**, 1357.
22 D. J. Arney, M. A. Bruck, S. R. Huber and D. E. Wigley, *Inorg. Chem.*, 1992, **31**, 3749.
23 S. Y. Lee and R. G. Bergman, *ACS Abstr.*, 1994, **208**, no. 64.
24 P. J. Walsh, F. J. Hollander and R. G. Bergman, *Organometallics*, 1993, **12**, 3705.
25 J. C. Green, M. L. H. Green, J. T. James, P. C. Konidaris, G. H. Maunder and P. Mountford, *J. Chem. Soc., Chem. Commun.*, 1992, 1361.
26 A. J. Bridgeman, L. Davis, S. J. Dixon, J. C. Green and I. N. Wright, *J. Chem. Soc., Dalton Trans.*, 1995, 1023.
27 R. D. Gorsich, *J. Am. Chem. Soc.*, 1958, **80**, 4744.
28 P. Mountford, *J. Organomet. Chem.*, 1997, **528**, 15.
29 C. H. Zambrano, R. D. Profilet, J. E. Hill, P. E. Fanwick and I. P. Rothwell, *Polyhedron*, 1993, **12**, 689.
30 J. L. Bennett and P. T. Wolczanski, *J. Am. Chem. Soc.*, 1994, **116**, 2179.
31 P. E. Collier, A. J. Blake and P. Mountford, *J. Chem. Soc., Dalton Trans.*, 1997, 2911.
32 J. Barker and M. Kilner, *Coord. Chem. Rev.*, 1994, **133**, 219.
33 F. T. Edelmann, *Coord. Chem. Rev.*, 1994, **137**, 403.
34 D. Y. Dawson and J. Arnold, *Organometallics*, 1997, **16**, 1111.
35 M. H. Ribeiro da Costa, M. T. Avilez and J. H. Teuben, unpublished results cited in ref. 33.
36 J. R. Hagadorn and J. Arnold, *Organometallics*, 1994, **13**, 4670.
37 F. A. Cotton and W. A. Wojtczak, *Polyhedron*, 1994, **13**, 1337.
38 J. R. Hagadorn and J. Arnold, *J. Am. Chem. Soc.*, 1996, **118**, 893.
39 P. J. Stewart, A. J. Blake and P. Mountford, *Inorg. Chem.*, 1997, **36**, 1982.
40 P. J. Stewart, A. J. Blake and P. Mountford, *Inorg. Chem.*, 1997, **36**, 3616.
41 S. C. Dunn, P. Mountford and O. V. Shishkin, *Inorg. Chem.*, 1996, **35**, 1006.
42 R. R. Schrock, *Acc. Chem. Res.*, 1997, **30**, 9.
43 H. C. S. Clark, F. G. N. Cloke, P. B. Hitchcock, J. B. Love and A. P. Wainwright, *J. Organomet. Chem.*, 1995, **501**, 333.
44 S. Friedrich, L. H. Gade, A. J. Edwards and M. McPartlin, *J. Chem. Soc., Dalton Trans.*, 1993, 2861.
45 A. J. Blake, P. E. Collier, L. H. Gade, P. Mountford, M. Schubart and I. J. Scowen, *Chem. Commun.*, 1997, 1555.
46 V. L. Goedken and J. A. Ladd, *J. Chem. Soc., Chem. Commun.*, 1982, 142.
47 C. E. Housemekerides, D. L. Ramage, C. M. Kretz, J. T. Shontz, R. S. Pilato, G. L. Geoffroy, A. L. Rheingold and B. S. Haggerty, *Inorg. Chem.*, 1992, **31**, 4453.
48 S. C. Dunn, PhD Thesis, University of Nottingham, 1996.
49 S. D. Gray, J. L. Thorman, L. M. Berreau and L. K. Woo, *Inorg. Chem.*, 1997, **36**, 278.
50 A. J. Blake, P. Mountford, G. I. Nikonov and D. Swallow, *Chem. Commun.*, 1996, 1835.
51 G. I. Nikonov, A. J. Blake and P. Mountford, *Inorg. Chem.*, 1997, **36**, 1107.
52 P. Mountford and D. Swallow, *J. Chem. Soc., Chem. Commun.*, 1995, 2357.
53 M. B. Dinger and W. Henderson, *Chem. Commun.*, 1996, 211.
54 S. R. Dubberley, A. J. Blake and P. Mountford, *Chem. Commun.*, 1997, 1603.
55 Z. Lin and M. B. Hall, *Coord. Chem. Rev.*, 1993, **123**, 149.
56 K. M. Doxsee, J. K. M. Mouser and J. B. Farahi, *Synlett*, 1992, 13.
57 R. A. Andersen and R. G. Bergman, personal communication.
58 Z. K. Sweeney, J. L. Polse, R. A. Andersen, R. G. Bergman and M. G. Kubinec, *J. Am. Chem. Soc.*, 1997, **119**, 4543.

*7/04194B*

# Gas phase molecular recognition of aromatic amino acid and aromatic carboxylic acid guests with a supramolecular [(η$^5$-pentamethylcyclopentadienyl)rhodium(2′-deoxyadenosine)]$_3^{3+}$ cyclic trimer host *via* non-covalent π–π interactions utilizing electrospray ionization mass spectroscopy†

**Ray Bakhtiar,[a] Hong Chen,[b]‡ Seiji Ogo[b]§ and Richard H. Fish*[b]**

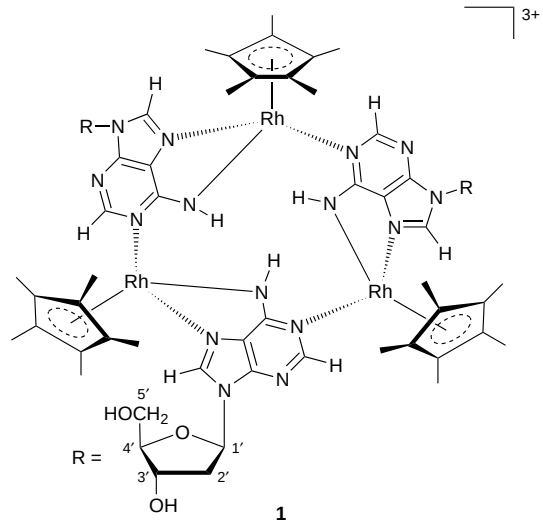
[a] *Department of Chemistry, Stevens Institute of Technology, Castle Point on The Hudson, Hoboken, NJ 07030, USA*
[b] *Lawrence Berkeley National Laboratory, University of California, Berkeley, California 94720, USA*

**A novel, gas phase, host–guest molecular recognition process, detected by electrospray ionization mass spectrometry, using guests that encompass aromatic amino acids and aromatic and aliphatic carboxylic acids with a supramolecular, bioorganometallic host, [Cp*Rh(2′-deoxyadenosine)]$_3$[OTf]$_3$ (Cp* = η$^5$-C$_5$Me$_5$), is found to occur predominately *via* non-covalent π–π interactions; non-covalent hydrophobic forces apparently being weak or non-existent.**

Molecular recognition is the cornerstone of many important biological processes; for example, drug and protein interactions with selective DNA sequences.[1–3] Recently, we reported on the molecular recognition of aromatic and aliphatic amino acids, as well as aromatic and aliphatic carboxylic acid guests with supramolecular, bioorganometallic (η$^5$-pentamethylcyclopentadienyl)rhodium (Cp*Rh)–nucleobase/nucleoside/nucleotide cyclic trimer hosts in aqueous solution at pH 7.2.[4] More importantly, in that study, the non-covalent hydrophobic interactions were found to be fully operational in aqueous solution by solvophobic forces that enhanced host–guest complexation, along with the equally important non-covalent π–π interactions.

It was intriguing to extend these above-mentioned aqueous molecular recognition studies to the gas phase, to compare and to better understand the role of water and its effect on the important π–π, hydrophobic, and hydrogen-bonding parameters, including steric, electronic, and conformational effects, that we found controls the host–guest process; to our knowledge, this is the first reported gas phase, host–guest molecular recognition study using a bioorganometallic host. Moreover, it has been clearly demonstrated that the soft electrospray ionization mass spectroscopy (ESIMS) technique was ideally suited for detecting such gas phase host–guest complexes in the absence of solvent.[5–11]

We started our gas phase molecular recognition ESIMS studies with a perusal of the various triangular, bowl-shaped Cp*Rh–nucleobase/nucleoside/nucleotide cyclic trimer molecular receptors we had studied in water, using L-tryptophan (L-Trp) as the guest in all cases.[4] To our surprise, we found that the best host in water, [Cp*Rh(2′-deoxyadenosine)]$_3$(OTf)$_3$ **1**, was also the best host in the gas phase. Thus, when we mixed equimolar amounts of host **1** with guest L-Trp in an aqueous 10 mM $NH_4OAc$ solution at pH 7.0, ions for **1** and the host–guest complex (**1**·L-Trp) were observed at *m/z* 488 (100%) and *m/z* 556 (35%), respectively (Fig. 1). As well, by further increasing the orifice potential from 45 to 80 V, we are able to follow the dissociation of the *m/z* 556 ion for the **1**·L-Trp host–guest complex in the gas phase. From these latter results, we had our first indication of favorable non-covalent π–π interactions in the gas phase between host **1** and L-Trp, as in aqueous solution [association constant, $K_a$ = 607 dm$^3$ mol$^{-1}$; free energy of complexation, $\Delta G^0$ = −3.8 kcal mol$^{-1}$ (1 cal = 4.184 J) in $H_2O$].[4]




We also conducted additional gas phase, ESIMS host–guest experiments with L-Phe and G1–G5 (see Guest structures) in the presence of host **1**. Table 1 contains the results, and what was very interesting, was the fact that G4, which had an association constant, $K_a$ = 760 dm$^3$ mol$^{-1}$, and a free energy of complexation, $\Delta G^0$ = −3.9 kcal mol$^{-1}$, with **1** in water, provided no detectable host–guest complex in the gas phase. Thus, initial indications clearly show that non-covalent hydrophobic interactions between G4 and **1** appear to be weak in the gas phase, and opposite to what occurred in water.[4,9,10]

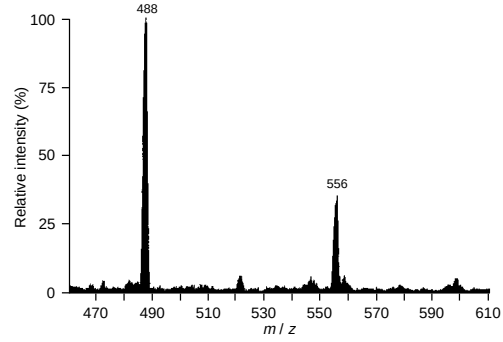
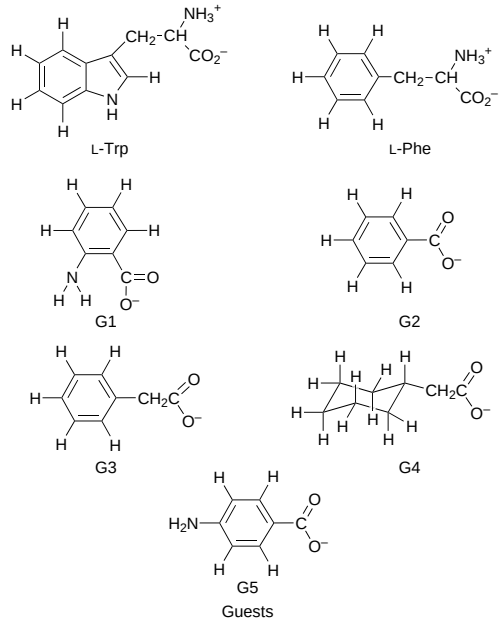



**Fig. 1** ESIMS of host **1** (*m/z* = 488) and host–guest, **1**·LTrp (*m/z* = 556) (experimental conditions, Table 1 footnotes)




Additionally, guest L-Phe, an aromatic amino acid that had a $K_a$ value of 456 dm$^3$ mol$^{-1}$ ($\Delta G^0$ = −2.8 kcal mol$^{-1}$) with **1** in aqueous solution, provided no corresponding detectable gas phase host–guest complex. Therefore, in water, L-Phe is in the prevalent zwitterion form at pH 7, and is more soluble in water and has a favorable Hansch partition coefficient, log $P_{octanol}$, in comparison to L-Trp; these factors appear to further demonstrate the solvophobic effect of water on the ability of L-Phe to form a strong host–guest complex in the aqueous phase.[4] Interestingly, in the gas phase, the water desolvated zwitterion form of L-Phe must inhibit host–guest complexation, apparently for reasons associated with its pronounced hydrophilicity.

In contrast, *o*-aminobenzoic acid ($K_a$ = 810 dm$^3$ mol$^{-1}$; $\Delta G^0$ = −4.0 kcal mol$^{-1}$, in $H_2O$ with **1**), G1, provides a detectable host–guest complex with **1** in the gas phase, since the free $NH_2$ group, in this instance, provides electron-donation to the aromatic ring thereby increasing π-electron density, and further facilitating non-covalent π–π interactions in the absence of solvent. Moreover, a positional isomer of G1, G5, which was found in the aqueous phase to sterically inhibit π–π interactions with host **1**, also did not provide a detectable host–guest complex in the gas phase, thus verifying a similar inhibition with the desolvated guest. Furthermore, aromatic carboxylic acids, G2 and G3, also readily provide detectable host–guest complexes in the gas phase with **1**, and again, dramatizes the dominance of the aromatic π electron effect in the gas phase molecular recognition process with the electron deficient host **1**.

**Table 1** Host–guest complexes in the gas phase with host **1**[a]

| Guest | Host ion, *m/z* (%) | Host–guest ion, *m/z* (%) |
|---|---|---|
| L-Trp | 488 (100) | 556 (35) |
| L-Phe | 488 (100) | ND[b] |
| G1 | 488 (100) | 534 (25) |
| G2 | 488 (100) | 528 (36) |
| G3 | 488 (100) | 533 (40) |
| G4 | 488 (100) | ND |
| G5 | 488 (100) | ND |

[a] An API III plus triple quadrapole spectrometer (PE-Sciex), equipped with an ion spray interface, was used for these ESIMS experiments. Host **1** and the guests in equimolar concentrations were dissolved in an 10 mM ammonium acetate solution at pH 7.0 and then delivered at 2.5 μl min$^{-1}$ to the ion-spray tip *via* a 50 μm id fused silica capillary. The ion-spray tip was held at a potential of 4.8 kV and compressed air (45 psi) was employed to assist liquid nebulization. Interface temperature (55 °C); orifice potential (45 V); positive ion detection mode; 5–10 scans summed for each host–guest experiment (±5–10%), which were performed three times. [b] Not detected.

The ESIMS literature with organic hosts and various guests has reported few comparisons of aqueous solution and gas phase molecular recognition chemistry.[5–11] However, the limited reported studies also demonstrate that the aqueous solvent is an important parameter especially for hydrophobic effects.[4,9,10] Thus, in the absence of water; *i.e.* under ESIMS conditions, this solvophobic force is missing, and therefore, non-covalent hydrophobic effects are greatly weakened in the gas phase, as is corroborated in this ESIMS study.

Future ESIMS molecular recognition studies will focus on the gas phase host–guest complexes of substituted aromatic carboxylic acid guests with **1** for a further understanding of steric and electronic effects involving non-covalent π–π interactions. As well, we will also focus on the molecular recognition of peptides containing terminal Trp or Phe groups with host **1**, and a comparison of the gas phase results with similar peptide–host **1** non-covalent π–π interactions in water, as analyzed by $^1$H NMR spectroscopy. In a preliminary experiment in both the gas phase (ESIMS) and in water ($^1$H NMR spectroscopy), it was found that the Trp–Met–Asp–Phe tetrapeptide with host **1** formed a host–guest complex in water that is detected in the gas phase; $^1$H NMR shows π–π interactions with the both terminal Trp or Phe groups.[12] Thus, complex **1** can be thought of as a simplified model DNA host which selectively binds peptides with terminal Trp or Phe groups *via* non-covalent π–π interactions in aqueous solution that are detected in the gas phase.

The studies at LBNL were generously supported by the Department of Energy under Contract No. DE AC03-76SF00098. R. B. wishes to acknowledge Merck Research Laboratories for the use of the ESIMS equipment and facilities.

## Footnotes and References

* E-mail: rhfish@lbl.gov
† Bioorganometallic chemistry: Part 9.
‡ Present address, Bio-Rad Laboratories, 2000 Alfred Nobel Dr Hercules, CA 94547, USA.
§ Present address, Department of Applied Molecular Science, Institute for Molecular Science, Okazaki National Research Institutes, Myodaiji, Okazaki 444, Japan.

1 J.-M. Lehn, *Angew. Chem., Int. Ed. Engl.*, 1988, **27**, 90 and references therein.
2 B. Alberts, D. Bray, J. Lewis, M. Raff, K. Roberts and J. D. Watson, *Molecular Biology of the Cell*, Garland Publishing, New York, 1989, pp. 481–612.
3 H.-J. Bohm and G. Klebe, *Angew. Chem., Int. Ed. Engl.*, 1996, **35**, 2589.
4 H. Chen, S. Ogo and R. H. Fish, *J. Am. Chem. Soc.*, 1996, **118**, 4993.
5 M. Vincenti, *J. Mass Spectrom.*, 1995, **30**, 925 and references therein.
6 M. Przybylski and M. O. Glocker, *Angew. Chem., Int. Ed. Engl.*, 1996, **35**, 807 and references therein.
7 E. Lamcharfi, S. Chuilon, A. Kerbal, G. Kunesch, F. Libot and H. Virelizier, *J. Mass Spectrom.*, 1996, **31**, 982.
8 M. Sawada, Y. Takai, T. Kaneda, R. Arakawa, M. Okamoto, H. Doe, T. Matsuo, K. Naemura, K. Hirose and Y. Tobe, *Chem. Commun.*, 1996, 1735.
9 Y.-T. Li, Y.-L. Hsieh, J. D. Henion, T. D. Ocian, G. A. Schiehser and B. Ganem, *J. Am. Chem. Soc.*, 1994, **116**, 7487.
10 Q. Wu, J. Gao, D. Joseph-McCarthy, G. B. Sigal, J. E. Bruce, G. M. Whitesides and R. D. Smith, *J. Am. Chem. Soc.*, 1997, **119**, 1157.
11 D. V. Dearden, C. Dejsupa, Y. Liang, J. S. Bradshaw and R. M. Izatt, *J. Am. Chem. Soc.*, 1997, **119**, 353.
12 S. Ogo, S. Nakamura, R. Bakhtiar, Y. Watanabe and R. H. Fish, unpublished work.

*Received in Columbia, MO, USA, 6th May, 1997; 7/03100I*

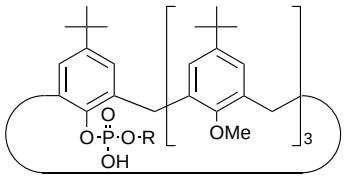
# Syntheses of phosphate diesters having *p-tert*-butylcalix[4]arene and alkyl group as ester moieties, and their selective lithium cation transport abilities through liquid membranes

**Sadatoshi Akabori,* Hideyuki Itabashi, Hisako Shimura and Masayuki Inoue**

*Department of Chemistry, Faculty of Science, Toho University, Funabashi-shi, Chiba 274, Japan*

**Phospate diesters, 2a, 2b and 2c, having *p-tert*-butylcalix-[4]arenes and alkyl groups as ester moieties exist as an equilibrium of cone and partial-cone conformations in solution and selectively transport $Li^+$; however, the conformations of the calix[4]arene moieties in the Li and Na complexes of 2a as the methyl ester and/or 2b as the ethyl ester in solution are cone only, although that of the K complex exists as a mixture of cone and partial-cone conformers.**

Calix[4]anene derivatives show highly selective complexing abilities, toward transition metal,[1–3] Na,[4–7] K[6–8] and Cs[9,10] cations. However, reports of selective complexing ability for the $Li^+$ are rare.[11] Also, the relationship between the complexing ability for metal cations and the conformation of calix[*n*]arene derivatives has been reported.[12] In previous papers, we reported that photoresponsive azocrown ethers,[13] benzocrown ethers,[13] dibenzocrown ethers[15,16] and crown ethers[17] having alkylphosphoric acid groups as side arms are useful as selective and efficient $Li^+$ carriers for liquid–liquid extraction and liquid membrane transport. In connection with these findings, we have synthesized phosphate diesters, **2a**, **2b** and **2c** having 25,26,27-trimethoxy-28-hydroxy-*p-tert*-butylcalix[4]arenes and alkyl groups (R = Me, Et, $Pr^n$) as ester moieties and studied the complexing abilities with alkali metal cations.




**2a** R = Me
**b** R = Et
**c** R = $Pr^n$

The host molecules **2a**, **2b** and **2c**, were prepared by the treatment of 25,26,27-trimethoxy-28-hydroxy-*p-tert*-butylcalix[4]arene **1**[18] with alkyldichlorophosphate followed by hydrolysis in 37, 22 and 35% yields, respectively.† The $^1$H NMR spectra of **2a** showed the signals of the methyl protons of the $Bu^t$ groups as singlets at $\delta$ 1.27, 1.30 and 1.33, the signals of the methylene protons as doublets at $\delta$ 3.20, 3.25, 4.32 and 4.65, the signals of the methoxy protons of the anisole moieties as singlets at $\delta$ 3.81 and 3.88 together with the other proton peaks. These results show the presence of the cone conformers of **2a**. In addition to these peaks, the $^1$H NMR spectra arising from the partial-cone of **2a** contained the signals of the methyl protons of the $Bu^t$ groups as singlets at $\delta$ 1.06, 1.33 and 1.41, the signals of the methylene groups as a doublet at 3.14 and 4.57 and a singlet at 3.73 (4 H), and the signals of the methoxy protons of the anisole moieties as singlets at 3.14 and 3.67 together with other proton peaks. The $^{31}$P NMR spectra‡ of **2a** showed two peaks at $\delta$ −5.77 and −6.29. From these data and other NMR measurements (COSY, DEPT, NOSY), **2a** in solution at 25 °C exists as an equilibrium between the cone and partial-cone conformations. As shown in Fig. 1, in order to convert the cone to partial-cone only the *p-tert*-butyl anisole moiety, which is *trans* to the phosphate ester substituted ring, needs to invert. The conformation of **2b** and **2c** were determined by similar methods. The spectral data showed that **2a**, **2b** and **2c** exist as a mixture of cone and partial-cone isomers (5 : 3) in $CD_3CN$–$CDCl_3$ (7 : 3) at 25 °C (2 : 3 ratio in $CDCl_3$). These results suggest that the equilibrium between the cone and partial-cone isomers in **2a**, **2b** and **2c** is sensitively affected by the solvent polarity; the cone % increases with solvent polarity. These findings are consistent with the result obtained for 25,26,27,28-tetramethoxy-*p-tert*-butylcalix[4]arene by Iwamoto *et al.*[12] In the cone conformation, four dipoles in **2** are forced to orient into the same direction whereas in the partial-cone conformation, one dipole is reversed.

The comparative complexing abilities of **2a**, **2b**, **2c** and **1** toward alkali metal cations ($Li^+$, $Na^+$ and $K^+$) were evaluated using solvent extraction and competitive liquid membrane transport experiments[13–17] and results are summarized in Table 1. The extraction abilities of **1** toward $Li^+$, $Na^+$ and $K^+$ are very low (9.3–11.7%) compared with those of **2a**, **2b** and **2c** and the selectivities for $Li^+/Na^+$, $Li^+/K^+$ and $Na^+/K^+$ are nearly of the same order (0.79–1.15). However, **2a**, **2b** and **2c** showed much higher cation extraction abilities (57–67%) toward alkali metal cations compared with those of **1**, although **2** did not show remarkable selectivities toward alkali metal cations. These results suggest that the alkylphosphoric acid moiety of **2** plays an important role in the complexation of **2** with alkali metal cations under our experimental conditions. Therefore, the selective extraction of **2** toward alkali metal cations could not observed. Next, in order to investigate the selectivity of the complexing abilities toward alkali metal cations in more detail, competitive liquid membrane transport experiments were carried out. In this experiment, practically no ion transport occurred in the absence of **2a**, **2b** or **2c**. The host molecule **1** also exhibited no transport abilities toward the alkali metal cations under these conditions, owing to its hydrophilic character. In contrast, drastic enhancement in the transport abilities was observed by introduction of an alkylphosphoric acid moiety into **1**. These results suggest that the transport ability order of **2a**, **2b** and **2c** toward alkali metal cations was $Li^+ > Na^+ > K^+$, although the alkali cations transport tendency of **2a**, **2b** and **2c** are very similar. $Li^+$ selectivity (4.55) over $K^+$ by **2b** was superior to those of **2a** and **2c**. However, **2a** showed higher selectivity of $Li^+$ over $Na^+$ compared with those of **2b** and **2c**.

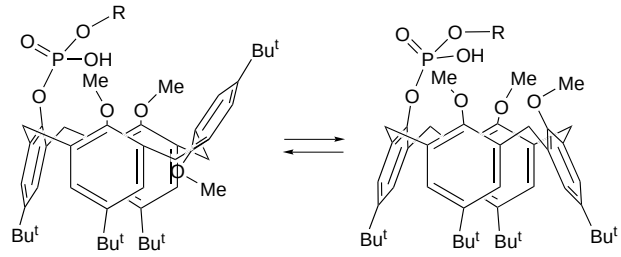



**Fig. 1** Equilibrium of **2** between cone and partial-cone conformers

**Table 1** Competitive extraction and competitive facilitated transport with **1, 2a, 2b** and **2c**

| | Extractability[a] (%) | | | Selectivity | | | Transported amount[b]/ $10^{-3}$ mol | | | Selectivity | | |
|---|---|---|---|---|---|---|---|---|---|---|---|---|
| Compound | $Li^+$ | $Na^+$ | $K^+$ | $Li^+/Na^+$ | $Li^+/K^+$ | $Na^+/K^+$ | $Li^+$ | $Na^+$ | $K^+$ | $Li^+/Na^+$ | $Li^+/K^+$ | $Na^+/K^+$ |
| **1** | 11 | 9 | 12 | 0.91 | 0.79 | 0.0 | 0.0 | 0.0 | 0.0 | — | — | — |
| **2a** | 60 | 57 | 65 | 1.05 | 0.93 | 0.89 | 4.33 | 2.90 | 1.80 | 1.49 | 2.41 | 1.61 |
| **2b** | 63 | 66 | 67 | 0.95 | 0.93 | 0.97 | 5.89 | 4.36 | 1.30 | 1.35 | 4.55 | 3.35 |
| **2c** | 55 | 57 | 62 | 0.97 | 0.89 | 0.92 | 3.41 | 2.62 | 1.41 | 1.30 | 2.42 | 1.30 |

[a] The extraction abilities of the host molecule with alkali metal cation was examined by the extraction method described previously.[13–17] [b] Conditions: [membrane phase] = $1.0 \times 10^{-3}$ M of the host molecule in $CH_2Cl_2$ (6.0 $cm^3$). [Source phase] = aqueous solution (3 $cm^3$) containing 1.0 M MOH (M = Li, Na, K); [receiving phase] = 1.0 M HCl (3 $cm^3$).

Furthermore, **2b** showed the highest selectivity for $Na^+/K^+$ (3.35) among the investigated host molecules. Therefore, the effects of the length of alkyl groups on transport abilities were negligibly small, however, the length of the alkyl groups affected the selectivity for $Li^+/Na^+$, $Li^+/K^+$ and $K^+/Na^+$.

In order to investigate the conformations of the host moiety in the complexes of **2** with alkali metal cations, the following experiments were carried out. A solution of **2** ($3.0 \times 10^{-6}$ mol) in $CD_2Cl_2$ (0.45 $cm^3$) was shaken 100 times with a $D_2O$ solution (0.45 $cm^3$) containing an alkali metal deuteroxide ($1.5 \times 10^{-5}$ mol) at 25 °C and then the $^1H$ and $^{31}P$ NMR spectra of the organic layer were measured. As shown in Fig. 2, the methoxy and methyl protons peaks of the methylphosphoric acid moieties in the Li and Na complexes of **2a** due to the cone conformer shifted down- and up-field by *ca*. 0.25–0.33 and 0.24–0.31 ppm, respectively, while all of the proton peaks due to the partial-cone conformer disappeared. Also, the $^{31}P$ NMR spectra of $Li^+$ and $Na^+$ complexes of **2a** showed only one peak at $\delta$ −5.87 and −6.22, respectively, despite the fact that for **2a** itself two peaks were observed. In contrast, the $^1H$ NMR spectra of the complex of **2a** with $K^+$ showed the presence of both cone and partial-cone conformers, although the methoxy protons of the anisole moiety due to the cone and partial-cone conformers were shifted down- and up-field by *ca*. 0.03 and 0.01 ppm, respectively; the $^{31}P$ NMR spectra also showed two peaks at $\delta$ −6.13 and −6.40. These results suggest that the host moieties in the complexes of **2a** and/or **2b** with $Li^+$ and $Na^+$ adopt only the cone conformation, although the host moiety of the $K^+$ complex exists as a mixture (1 : 2) of the cone and partial-cone conformers together with a very small amount of other conformers.

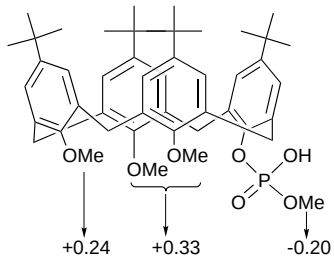



**Fig. 2** $^1H$ NMR chemical shift changes between **2a** and the $Li^+$ complex of **2a**. Positive and negative values mean down- and up-field shifts, respectively.

Furthermore, titration experiments in $CD_3CN$–$CDCl_3$ (7 : 3) were carried out by adding 0.25–3.0 equiv. of alkali metal thiocyanate to **2**. Remarkable chemical shift changes appeared in the $^1H$ and $^{31}P$ NMR spectra. The downfield shift of the methoxy protons in the cone conformer increases almost linearly with increase in $Li^+$ and/or $Na^+$ salt until addition of 1 equiv. relative to **2a**; further addition of alkali metal salt results in only a slight downfield shift change, which suggests the formation of a 1 : 1 complex of **2a** with $Li^+$ or $Na^+$. Also, all of the proton peaks in the $^1H$ NMR spectra due to the partial-cone conformer of **2a** disappeared, and the $^{31}P$ NMR spectra showed only one peak of the cone conformer when 1 equiv. of the thiocyanate was added. However, when KSCN was added to **2a** and/or **2b**, no chemical shift changes in the $^1H$ and $^{31}P$ NMR spectra were observed. This suggests that the host molecules **2a** and **2b** did not complex KSCN, although **2a** and **2b** complex with KOD.

In summary, we have shown that the phosphate diesters, **2a** and **2b**, containing calix[4]arene and alkyl groups as ester moieties selectively complexed $Li^+$ among the investigated alkali metal cations and the most moieties in the complexes of **2a** and/or **2b** with $Li^+$ and $Na^+$ cations adopt only a cone conformation, although the host moiety of the $K^+$ complex exists as a mixture (1 : 2) of cone and partial-cone conformations.

## Footnotes and References

* E-mail: akabori@ns2.toho-u.ac.jp

† Assignment of the $^1H$ NMR spectra and conformations of **2a**, **2b** and **2c** were carried out using $^1H$–$^1H$ COSY, $^{13}C$–$^1H$ COSY, DEPT and NOESY spectroscopy. Satisfactory elemental analyses were obtained for all new compounds.

‡ The chemical shifts of $^{31}P$ measured from external 85% $H_3PO_4$.

1 Reviews: M. Takeshita and S. Shinkai, *Bull. Chem. Soc. Jpn.*, 1995, **68**, 1088; C. D. Gutsche, *Calixarenes*, Monograph, The Royal Society of Chemistry, Cambridge, England, 1989.
2 K. Ohto, E. Murakami, K. Shiratsuchi, K. Inoue and M. Iwasaki, *Chem. Lett.*, 1996, 173.
3 J. F. Malone, D. J. Marrs, M. A. Mckervey, P. O'Hagan, N. Thompson, A. Walker, F. Armaud-Neu, O. Mauprivez, M.-J. Schwing-Weil, J.-F. Dozol, H. Rouquette and N. Simon, *J. Chem. Soc., Chem. Commun.*, 1995, 2151.
4 H. Yamamoto, K. Ueda, K. R. A. Samankumaru and S. Shinkai, *Chem. Lett.*, 1995, 497.
5 F. Ohsetsu and S. Shinkai, *J. Chem. Soc., Perkin Trans. 2*, 1995, 1103.
6 K. Iwamoto and S. Shinkai, *J. Org. Chem.*, 1992, **7**, 7066.
7 S.-K. Chang and I. Cho, *J. Chem. Soc., Perkin Trans. 1*, 1986, 212.
8 K. N. Koh, K. Araki, S. Shinkai, Z. Asfari and J. Vicens, *Tetrahedron Lett.*, 1995, **36**, 6095.
9 F. Inokuchi, Y. Miyahara, T. Inazu and S. Sinkai, *Angew. Chem., Int. Ed. Engl.*, 1995, **34**, 1364.
10 A. Casnati, A. Pochini, R. Ungaro, F. Ugozzoli, F. Armaud-Neu, S. Fanni, M.-J. Schwing, R. J. M. Egberink, F. de Jong and D. N. Reinhoudt, *J. Am. Chem. Soc.*, 1995, **117**, 2767.
11 A. Varnek and G. Wipff, *J. Phys. Chem.*, 1993, **97**, 10 840.
12 K. Iwamoto, A. Ikeda, K. Arai, T. Harada and S. Shinkai, *Tetrahedron Lett.*, 1993, **49**, 9937.
13 S. Akabori, Y. Miura, N. Yotsumoto, K. Uchida, M. Kitano and Y. Habata, *J. Chem. Soc., Perkin Trans. 1*, 1995, 2589.
14 Y. Habata, M. Ikeda and S. Akabori, *J. Chem. Soc., Perkin Trans. 1*, 1992, 2651.
15 Y. Habata and S. Akabori, *Tetrahedron Lett.*, 1992, **33**, 5815.
16 Y. Habata, M. Ikeda and S. Akabori, *Tetrahedron Lett.*, 1992, **33**, 3157.
17 H. Habata, H. Ugajin and S. Akabori, *J. Org. Chem.*, 1994, **59**, 676.
18 K. Arai, K. Iwamoto, S. Shinkai and T. Matsuda, *Bull. Chem. Soc. Jpn.*, 1990, **63**, 3480.

*Received in Cambridge, UK, 14th July 1997; 7/05000C*

# A simple construction of chiral fused benzoxocine ring ethers from D-glucose by regioselective 8-*endo*-aryl radical cyclisation

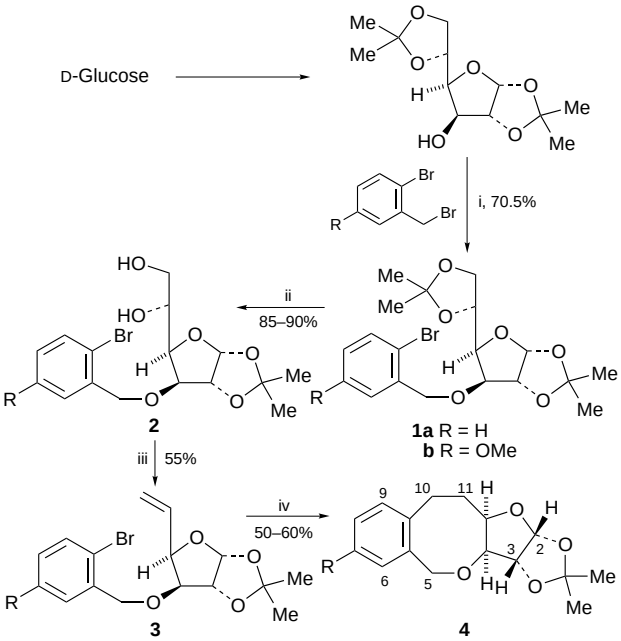
**Partha Chattopadhyay,*[a] Monika Mukherjee[b] and Soma Ghosh[b]**

[a] *Indian Institute of Chemical Biology, Calcutta-700 032, India*
[b] *Department of Solid State Physics, Indian Association for the Cultivation of Science, Jadavpur, Calcutta-700 032, India*

**A regioselective 8-*endo-trig* aryl radical cyclisation of the 5,6-deoxy-D-*xylo*-5-enofuranosides 3a and 3b with tri-*n*-butyltin hydride provides the chiral furo[3,2-*c*][2]benzoxocines 4a and 4b in good yields; the crystal structure of 4a is reported.**

The synthesis of condensed cyclic ethers incorporating medium size rings, a unique structural feature present in some highly bioactive marine natural products,[1] is a challenging problem. The development of new and general methodology for the synthesis of this class of compound,[2,3] especially in chiral form, has become an attractive area for investigation in recent years. The syntheses of chiral 5-, 6- and 7-membered cyclic ethers have been achieved from D-glucose by intramolecular nitrone cycloaddition reactions.[4] More recently, functionalised 9-membered chiral ethers have been prepared from D-glucose through oxy-Cope rearrangement.[5] We report herein a simple and convenient conversion of D-glucose to highly functionalised chiral condensed tricyclic benzoethers incorporating a *cis* 8-5 bicyclic system by regioselective 8-*endo-trig* aryl radical cyclisation.[6]

The transformation of the easily accessible 5,6-deoxy-*O*-isopropylidene-3-*O*-(*o*-bromobenzyl)-α-D-*xylo*-5-enofuranose **3a** and the corresponding 5′-methoxy derivative **3b** to the tricyclic furo[3,2-*c*][**2**]benzoxocines **4a** and **4b** is shown in Scheme 1. D-Glucose was converted to the 3-*O*-(*o*-bromobenzyl) ethers **1a**† and **1b** through *O*-benzylation of 1,2 : 5,6-diisopropylidene-α-*D*-glucofuranose with 50% aq. NaOH in a biphasic medium ($CH_2Cl_2$–$H_2O$) using $Bu_4NBr$ as phase transfer catalyst. Under mild acidic condition, the 5,6-*O*-isopropylidene group in **1a**,**b** was selectively deprotected to give **2a**,**b** which on treatment with $Ph_3P$, $I_2$ and imidazole in boiling toluene[7] gave the desired dideoxy furanose derivatives **3a** and **3b**. Radical cyclisation of each of the alkenes **3a** and **3b** in refluxing benzene (0.008 mol $dm^{-3}$) for 8–10 h with $Bu_3SnH$ (1.5 equiv.) and a catalytic amount of AIBN furnished the respective crystalline tricyclic ethers **4a** and **4b** in 50–60% yield as the only isolable products in each case after separation of the tin compounds[8] followed by chromatography on silica gel. The assigned structures of the products **4a** and **4b** resulting from 8-*endo-trig* aryl radical cyclisation were based upon spectroscopic data. Unequivocal confirmation of the structure of **4a** was obtained from an X-ray crystal structure‡ determination (Fig. 1).




**Scheme 1** *Reagents and conditions*: $Bu_4NBr$, 50% NaOH, $CH_2Cl_2$, 25 °C, 12 h; ii, 75% AcOH, 25 °C, 12 h; iii, $PPh_3$, $I_2$, imidazole, PhMe, reflux, 2 h; iv, $Bu_3SnH$, AIBN, benzene, 200 W lamp, reflux, 10 h

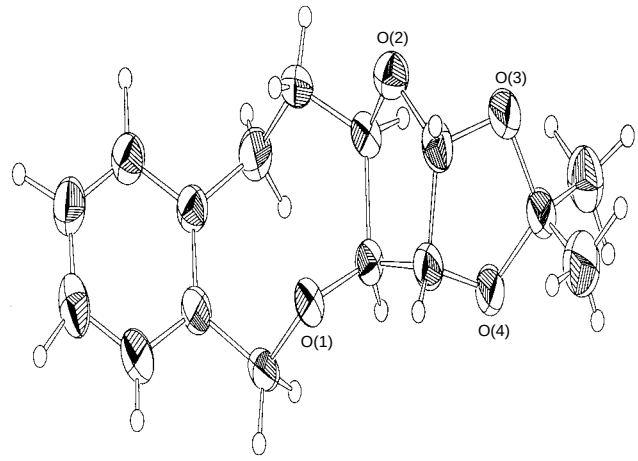



**Fig. 1** ORTEP diagram of **4a**

In conclusion, the present investigation clearly shows the potential of regioselective aryl radical cyclisation from carbohydrate derived substrates in the synthesis of chiral condensed cyclic ethers incorporating medium sized rings.

Grateful acknowledgement is due to Professor U. R. Ghatak, INSA Senior Scientist, for his kind interest and valuable suggestions. We also extend our thanks to the Regional Sophisticated Instruments Center, Bose Institute, Calcutta, India, for the use of its single crystal diffractometer facility.

## Footnotes and References

* E-mail: iichbio@giasclo1.vsnl.net.in

† Satisfactory elemental analyses and spectroscopic data were obtained for all new compounds. *Selected data* for **4a** mp 151–152 °C; $[\alpha]_D^{27}$ −20.6 (*c* 0.34, $CHCl_3$); $\delta_H(CDCl_3)$ 1.3 (s, 3 H), 1.46 (s, 3 H), 2.04–2.28 (m, 2 H), 2.44–2.68 (m, 1 H), 3.18–3.44 (m, 1 H), 4.04 (d, 1 H, *J* 4, H-3a), 4.28 (dt, 1 H, *J* 6 and 4, H-11a), 4.58 (d, 1 H, *J* 14), 4.62 (d, 1 H, *J* 4, H-3), 5.1 (d, *J* 14, 1 H), 5.90 (d, 1 H, *J* 4, H-2), 7.02–7.34 (m, 4 H, Ar-H); $\delta_C(CDCl_3)$ 26.2, 27.7, 28.6, 31.0, 75.0, 79.0, 84.5, 85.4, 104.0, 111.1, 126.1, 128.3, 128.8, 130.5, 135.7, 140.6; MS (EI) *m*/*z* 276 ($M^+$). For **4b**: mp 106–107 °C; $[\alpha]_D^{24}$ + 2.6 (*c* 0.23, $CHCl_3$); $\delta_H(CDCl_3)$ 1.31 (s, 3 H), 1.46 (s, 3 H),

2.09–2.21 (m, 2 H), 2.45–2.57 (m, 1 H), 3.17–3.31 (m, 1 H), 3.78 (s, 3 H, OMe), 4.02 (d, 1 H, *J* 4, H-3a), 4.22–4.29 (dt, 1 H, *J* 6 and 4, H-11a), 4.56 (d, 1 H, *J* 14), 4.62 (d, 1 H, *J* 4, H-3), 5.05 (d, *J* 14, 1 H), 5.89 (1 H, d, *J* 4, H-2), 6.64 (d, 1 H, *J* 2.5), 6.76–6.80 (1 H, dd, *J* 8 and 2.5), 7.08 (1 H, d, *J* 8); $\delta_C(CDCl_3)$ 26.2, 26.7, 27.8, 31.3, 55.2, 74.9, 78.9, 84.2, 85.4, 103.9, 111.2, 113.3, 114.4, 131.6, 134.6, 136.8, 157.8; MS (EI) *m*/z 360 ($M^+$).

‡ *Crystal data* for **4a**: $C_{16}H_{20}O_4$, $M$ = 276.33, orthorhombic, space group $P2_12_12_1$, $a$ = 8.6733(6), $b$ = 9.1234(6), $c$ = 17.9110(11) Å, $U$ = 1417.3(2) Å$^3$, $Z$ = 4, $D_c$ = 1.295 g cm$^{-3}$, $\mu$(Mo-K$\alpha$ radiation, $\lambda$ = 0.71073 Å) = 0.86 cm$^{-1}$, $2\theta_{max}$ = 50°. 1412 reflections were recorded on an Enraf-Nonius CAD-4 diffractometer at 293 K. The structure was solved by direct method (MULTAN88) and refined by the full-matrix least-squares technique (SHELXL93). The function minimised was $\Sigma w(F_0^2 - F_c^2)$ [$w = 1/\sigma^2(F_0^2) + (0.06P)^2$ where $P = (F_0^2 + 2F_c^2)/3$]. Anisotropic refinement of nonhydrogen atoms and isotropic refinement of hydrogen atoms, located from difference Fourier maps, converged at $R_1$ = 0.0415 ($wR_2$ = 0.0881) for 1069 reflections with, $I > 2\sigma(I)$. Goodness of fit = 1.146 maximum/minimum residual electron densities +0.204/−0.244 e Å$^{-3}$. CCDC 182/616.


1 Y.-Y. Lin, M. Risk, S. M. Roy, D. van Engen, J. Clardy, J. Golik, J. C. James and K. Nakanishi, *J. Am. Chem. Soc.*, 1981, **103**, 6773; M. Murata, M. Kumagai, J. S. Lee and T. Yasumoto, *Tetrahedron Lett.*, 1987, **28**, 5869; H. Nagai, K. Torigoe, M. Satake, M. Murata, T. Yasumoto and H. Hirota, *J. Am. Chem. Soc.*, 1992, **114**, 1102; M. Satake, M. Murata and T. Yasumoto, *Tetrahedron Lett.*, 1993, **34**, 1975; M. Satake, M. Murata and T. Yasumoto, *J. Am. Chem. Soc.*, 1993, **115**, 361; M. Murata, H. Naoki, T. Iwashita, S. Matsunaga. M. Sasaki, A. Yokoyama and T. Yasumoto, *J. Am. Chem. Soc.*, 1993, **115**, 2060; T. Yasumoto and M. Murata, *Chem. Rev.*, 1993, **93**, 1897.

2 For the synthesis of 8-membered condensed ether ring systems, see J.-i. Yamada, T. Asano, I. Katoda and Y. Yamamoto, *J. Org. Chem.*, 1990, **55**, 6066; E. Alvarez, M.-L. Candenas, R. Perez, J. L. Ravelo and J. D. Martin, *Chem. Rev.*, 1995, **95**, 1953; K. C. Nicolaou, *Angew. Chem., Int. Ed. Engl.*, 1996, **35**, 589 and references cited therein; E. Alvarez, M. Delgado, M. T. Diaz, L. Hanxing, R. Perez and J. D. Martin, *Tetrahedron Lett.*, 1996, **37**, 2865; J. S. Clark and J. G. Kettle, *Tetrahedron Lett.*, 1997, **38**, 123 and 127.

3 For the synthesis of 9-membered ether ring systems, see M. Inoue, M. Sasaki and K. Tachibana, *Tetrahedron Lett.*, 1997, **38**, 1611 and references cited therein.

4 A. Bhattacharjya, P. Chattopadhyay, A. T. McPhail and D. R. McPhail, *J. Chem. Soc., Chem. Commun.*, 1990, 1508; 1991, 136; P. M. Collins, M. S. Ashwood, H. Eder, S. H. B. Wright and D. J. Kennedy, *Tetrahedron Lett.*, 1990, **31**, 2055; S. Dutta, P. Chattopadhyay, R. Mukhopadhyay and A. Bhattacharjya, *Tetrahedron Lett.*, 1993, **34**, 3585; T. K. M. Shing, W.-C. Fung and C.-H. Wong, *J. Chem. Soc., Chem. Commun.*, 1994, 449; A. Bhattacharjee, A. Bhattacharjya and A. Patra, *Tetrahedron Lett.*, 1995, **35**, 4677.

5 A. V. R. L. Sudha and M. Nagarajan, *J. Chem. Soc., Chem. Commun.*, 1996, 1359 and references cited therein.

6 K. Ghosh, A. K. Ghosh and U. R. Ghatak, *J. Chem. Soc., Chem. Commun.*, 1994, 629.

7 P. J. Garegg and B. Samuelsson, *Synthesis*, 1979, 469.

8 G. Stork and N. H. Baine, *J. Am. Chem. Soc.*, 1982, **104**, 2321.



*Received in Cambridge, UK, 27th August 1997; 7/06249D*

# 5-*endo-trig* Cyclisations in heterocycle synthesis: enantiospecific synthesis of (+)-monomorine I

**Malcolm B. Berry,[a] Donald Craig,*[a] Philip S. Jones[b] and Gareth J. Rowlands[a]**

[a] *Department of Chemistry, Imperial College of Science, Technology and Medicine, London, UK SW7 2AY*
[b] *Roche Discovery Welwyn, Broadwater Road, Welwyn Garden City, Hertfordshire, UK AL7 3AY*

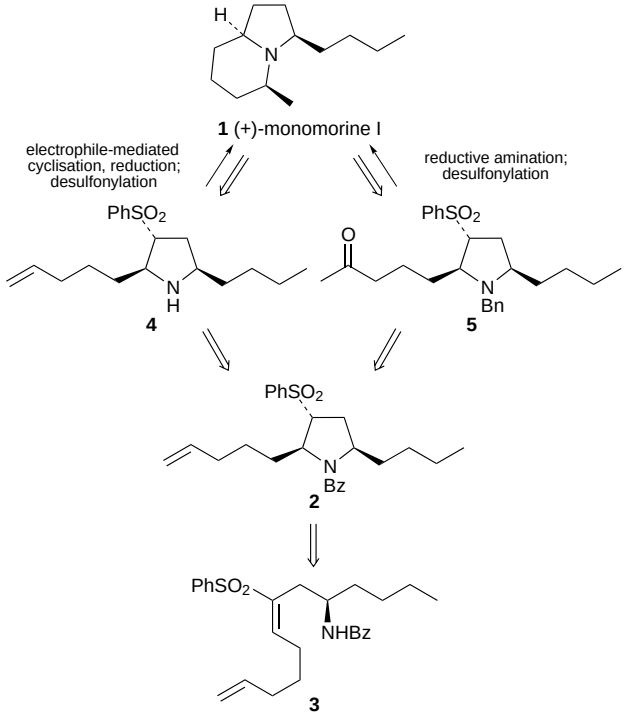
**The indolizidine alkaloid monomorine I is synthesised from D-norleucinol using 5-*endo-trig* cyclisation and intramolecular reductive amination as the key ring-forming steps.**

Pyrrolidines occur widely in nature as pheromones, venoms and toxins, and as structural motifs in more complex molecules such as pyrrolizidines and indolizidines.[1] As part of our programme investigating 5-*endo-trig* cyclisation reactions[2] for heterocycle construction[3] we have been looking at sulfone-mediated assembly of pyrrolidines, and have discovered that 2,5-disubstituted pyrrolidines may efficiently and stereoselectively be prepared from amino acid-derived precursors.[4] Here we report the application of this methodology to the total synthesis of the indolizidine alkaloid monomorine I **1**, the trail pheromone of the Pharaoh worker ant *Monomorium pharaonis*.[5,6]

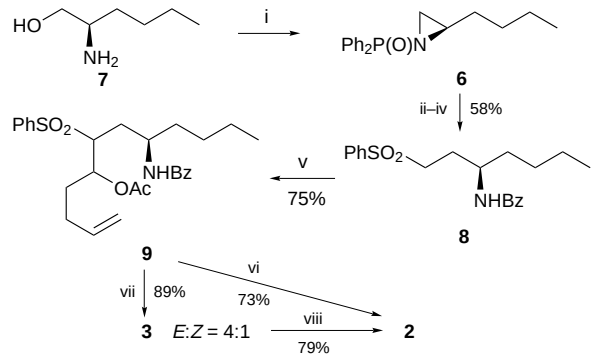
Our synthetic plan for **1** involved initial assembly of the pyrrolidine ring in **2** by 5-*endo-trig* cyclisation reaction of a substrate such as **3**. Closure of the remaining, six-membered cycle would be effected either by electrophile-induced addition of the pyrrolidine nitrogen atom to the distal double bond, as in **4**, or by intramolecular reductive amination of a derived side-chain ketone moiety, as in **5** (Scheme 1).

Retrosynthetic analysis of the cyclisation substrate **3** indicated *N*-protected aziridine **6** as the starting material. This was synthesised in two steps from commercially available D-norleucine;† reduction using the $NaBH_4$–iodine reagent system described by Meyers[7] gave D-norleucinol **7**, which was converted directly into **6** by treatment with diphenylphosphinic chloride and triethylamine in THF followed by excess sodium hydride according to the method of Sweeney (Scheme 2).[8] Addition of **6** to a THF–*N*,*N*,*N*′,*N*′-tetramethylethylenediamine solution of lithio(phenylsulfonyl)methane followed by proton quench gave the expected product of aziridine ring-opening at the less substituted carbon atom. This was dephosphinylated and reprotected as the benzamide **8** in good overall yield for the three steps from **6**.[9] Exposure of **8** to 2 equiv. of base followed by hex-5-enal, and *in situ* trapping of the intermediate alkoxides, gave ester **9**, mostly as one diastereoisomer.‡ Pyrrolidine formation was effected *in a single step* by treating a dilute THF solution of **9** with 2 equiv. of potassium *tert*-butoxide in the presence of *tert*-butyl alcohol, which effected one-pot elimination to give **3** followed by cyclisation. Pyrrolidine **2** formed in this way was a single, 2,5-*syn* diastereoisomer as evidenced by single-crystal X-ray diffraction analysis.§ Interestingly, treatment of **9** with 1 equiv. of base followed by *immediate* proton quench gave in 89% isolated yield a 4:1 *E*:*Z* mixture of geometric isomers of **3**, which could be converted into **2** in a separate operation by treatment with a further 1 equiv. of base. Compound **2** prepared in this way was identical in all respects to material made in the one-pot reaction.

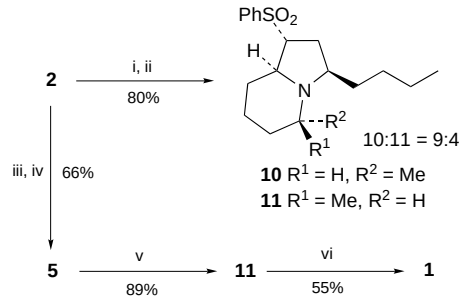
Initial attempts to complete the assembly of the indolizidine nucleus by closure of the six-membered ring involved mercury(II)-assisted cyclisation. Thus, debenzoylation of **2** using Super-Hydride®,[10] and treatment of the resulting free amine with $Hg(OAc)_2$ followed by *in situ* reduction with $NaBH_4$,[11] gave in 90% yield a 9 : 4 mixture of **10** and the desired




**Scheme 1**




**Scheme 2** *Reagents and conditions*: i, $Ph_2P(O)Cl$, (2.1 equiv.), $Et_3N$ (3 equiv.), THF (0.3 M), 0 °C→room temp., 12 h, then excess NaH, room temp., 1–2 weeks; ii, $PhSO_2Me$ (1 equiv.), BuLi (1 equiv.), 3 : 1 THF–$Me_2N(CH_2)_2NMe_2$ (0.4 M), −78 °C, add **6**, −78 °C→room temp., 12 h; iii, $BF_3{\cdot}OEt_2$ (10 equiv.), 1 : 1 $CH_2Cl_2$–MeOH (0.1 M), room temp., 12 h; iv, BzCl (1.2 equiv.), pyridine (1.1 equiv.), $CH_2Cl_2$ (0.2 M), room temp., 12 h, work-up with $Me_2N(CH_2)_3NH_2$; v, BuLi (2.1 equiv.), 3 : 1 THF–$Me_2N(CH_2)_2NMe_2$, −78 °C, add hex-5-enal (1.3 equiv.), −78 °C, 40 min, then add $Ac_2O$ (5 equiv.), −78 °C→room temp., 12 h; vi, $Bu^tOK$ (2.1 equiv. of a 1 M solution in THF), $Bu^tOH$ (10 equiv.) in THF (0.033 M), room temp., 12 h; vii, $Bu^tOK$ (1.05 equiv. of a 1 M solution in THF), $Bu^tOH$ (5 equiv.) in THF (0.1 M), room temp., < 1 min; viii, $Bu^tOK$ (1.05 equiv. of a 1 M solution in THF), $Bu^tOH$ (10 equiv.) in THF (0.033 M), room temp., 12 h




**Scheme 3** *Reagents and conditions*: i, $LiBHEt_3$ (2.2 equiv.), THF (0.23 M), room temp., 8 h; ii, $Hg(OAc)_2$ (1.05 equiv.), 1 : 1 THF–$H_2O$ (0.25 M), then $NaBH_4$–NaOH (0.75 equiv.); iii, DIBAL-H (4 equiv.), $CH_2Cl_2$ (0.1 M), −78 °C→room temp., 2 h; iv, $Hg(OAc)_2$ (1.05 equiv.), 3 : 1 THF–$H_2O$ (0.2 M), room temp., 1 h, then add to $PdCl_2$ (0.6 equiv.), $CuCl_2$ (3 equiv.), THF (0.2 M), room temp., 1.5 h; v, 10% Pd(C), cyclohexa-1,4-diene (15 equiv.), MeOH (0.1 M), reflux, 4 h; vi, $Na^+C_{10}H_8^-$ (3.5 equiv.), THF (0.05 M), room temp., 5 min

C-2 epimer **11**. The stereochemical assignment of **11**, and therefore that of **10** followed from the nuclear Overhauser enhancements of the signals corresponding to the α-hydrogen atoms at C-6 and C-9 observed on irradiation of the C-2 methyl group. In view of this adverse selectivity, the reductive amination route was pursued. Partial reduction of **2** to the *N*-benzyl analogue using DIBAL-H, and oxidation of the side-chain double bond in the product using a modified Wacker procedure[12] gave ketone **5**. This was subjected to catalytic transfer hydrogenation,[13] which effected sequential hydrogenolytic debenzylation and intramolecular reductive amination[14] to give exclusively **11**, which was identical in all respects to material prepared *via* the mercury-mediated cyclisation route. Finally, *brief* exposure¶ of **11** to sodium naphthalenide in THF followed by $NH_4Cl$ work-up gave (+)-monomorine I **1** (Scheme 3), which showed $^1H$ and $^{13}C$ NMR, IR and mass spectral and optical rotation characteristics in agreement with published values.[6]

In summary, the synthesis of (+)-monomorine I has been achieved in nine steps from aziridine **6**, which is available in two steps by known methods from D-norleucine. Both ring-forming steps are highly stereoselective, and our synthesis compares favourably with published approaches.[6] The complete selectivity of the pyrrolidine-forming reaction is particularly notable, and should be applicable to the synthesis of other pyrrolidine-containing alkaloids, and related pyrrolizidines and indolizidines.

We thank the SERC/EPSRC (CASE Studentships to M. B. B. and G. J. R ) and Roche Discovery Welwyn for financial support of this research.

## Footnotes and References

* E-mail: dcraig@ic.ac.uk

† All yields reported herein refer to isolated, pure materials which had $^1H$ and $^{13}C$ NMR, IR and high-resolution mass spectral characteristics in accord with the proposed structures.

‡ We have not been able to assign the configurations of the phenylsulfonyl- and acetoxy-substituted stereocentres.

§ We thank Professor David J. Williams and Dr Andrew J. P. White of this Department for this determination.

¶ Work-up after no more than 5 min was crucial to the success of this reaction. We thank Mr Simon Ward (University of Cambridge) for informing us of the importance of short reaction times in these transformations.

1 For reviews, see A. R. Pinder, *Nat. Prod. Rep.*, 1992, **9**, 17; J. P. Michael, *Nat. Prod. Rep.*, 1994, **11**, 17.
2 J. E. Baldwin, *J. Chem. Soc., Chem. Commun.*, 1976, 734.
3 D. Craig and A. M. Smith, *Tetrahedron Lett.*, 1992, **33**, 695; D. Craig, N. J. Ikin, N. Mathews and A. M. Smith, *Tetrahedron Lett.*, 1995, **36**, 7531. For other pyrrolidine-forming 5-*endo-trig* cyclisation reactions, see P. Knochel and J. F. Normant, *Tetrahedron Lett.*, 1985, **26**, 4455; A. Padwa and B. H. Norman, *J. Org. Chem.*, 1990, **55**, 4801.
4 M. B. Berry, Ph.D. thesis, University of London, 1993; G. J. Rowlands, Ph.D. thesis, University of London, 1996.
5 Isolation and characterisation: F. J. Ritter, I. E. M. Rotgans, E. Talman, P. E. J. Verwiel and F. Stein, *Experientia*, 1973, **29**, 530.
6 For a comprehensive collection of references to published syntheses of both racemic and enantiomerically pure monomorine I, see M. J. Munchhof and A. I. Meyers, *J. Am. Chem. Soc.*, 1995, **117**, 5399.
7 M. J. McKennon and A. I. Meyers, *J. Org. Chem.*, 1993, **58**, 3568.
8 H. M. I. Osborn, J. B. Sweeney and W. Howson, *Synlett*, 1994, 145.
9 We did not investigate reactions of lithio(phenylsulfonyl)methane with *N*-benzoylaziridines, in light of an account describing their non-chemoselective reaction with certain carbon nucleophiles: J. E. Baldwin, R. M. Adlington and N. G. Robinson, *J. Chem. Soc., Chem. Commun.*, 1987, 153.
10 H. C. Brown and S. C. Kim, *Synthesis*, 1977, 635.
11 J. J. Perie, J. P. Laval, J. Roussel and A. Lattes, *Tetrahedron*, 1972, **28**, 675.
12 G. T. Rodeheaver and D. T. Hunt, *J. Chem. Soc., Chem. Commun.*, 1971, 818.
13 A. M. Felix, E. P. Heimer, T. J. Lambros, C. Tzougraki and J. Meienhofer, *J. Org. Chem.*, 1978, **43**, 4194.
14 R. V. Stevens and A. W. M. Lee, *J. Chem. Soc., Chem. Commun.*, 1982, 102.

*Received in Liverpool, UK, 29th August 1997; 7/06333D*

# Self-assembling of bis-*ortho* chelated diaminobenzyl- (NC′N) and butyl-lithium units to give 2 : 2 mixed alkyllithium aggregates $(NC'N)Li_2Bu_2Li_2(NC'N)$ with a ladder structure

**Peter Wijkens,[a] Johann T. B. H. Jastrzebski,[a] Nora Veldman,[b] Anthony L. Spek[b] and Gerard van Koten*[b]**

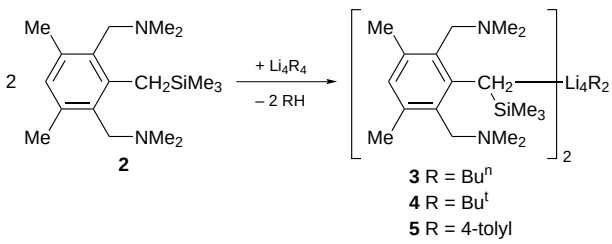
[a] *Debye Institute, Department of Metal-Mediated Synthesis, Utrecht University, Padualaan 8, 3584 CH Utrecht, The Netherlands*
[b] *Bijvoet Center for Biomolecular Research, Laboratory of Crystal and Structural Chemistry, Utrecht University, Padualaan 8, 3584 CH Utrecht, The Netherlands*

**The lithiation reaction of 1,3-bis(dimethylaminomethyl)-4,6-dimethyl-2-(trimethylsilylmethyl)benzene 2 with $Bu^nLi$ (2 equiv.) affords a unique aggregated species 3 of the parent lithiated compound and $Bu^nLi$ in a 2 : 2 ratio in which the bridging carbon atoms and the lithium atoms are arranged in an unprecedented ladder-type arrangement with exclusively bridging alkyl groups.**

Heteroatom-assisted lithiation of the bis(*ortho*-amino) substituted 2-methyl group in 1,3-bis(dimethylaminomethyl)-2,4,6-trimethylbenzene (NC′N–H)† with $Bu^nLi$ resulted in the formation of an unprecedented 2 : 2 mixed alkyllithium aggregate $(NC'N)_2Li_4Bu_2$ **1**.[1] The structure of **1** suggests considerable stability for the $[(NC'N)_2Li_4]^{2+}$ dication, which comprises a lithium tetrahedron of which two faces are capped by two NC′N terdentate monoanionic ligands, leaving two faces open for the binding of a C-monoanion *via* $\eta^3$-coordination (in **1**, two $\eta^3$-bonded Bu groups).

As a possible approach to overcome the formation of tetrahedral $Li_4$ aggregates like **1** we explored the effect an $\alpha$-$Me_3Si$ group would have on the aggregate formation. We now report that lithiation of 1,3-bis(dimethylaminomethyl)-4,6-dimethyl-2-(trimethylsilylmethyl)benzene **2** (NC′N–$SiMe_3$)[1] with $Bu^nLi$ likewise results in the formation of a 2 : 2 mixed alkyllithium aggregate having $(NC'N–SiMe_3)_2Li_4Bu_2$ stoichiometry, but with a novel structure comprising a ladder type frame-work with exclusively bridging alkyl groups.

The 1 : 2 molar reaction of **2** with $Bu^nLi$ in pentane afforded a pale yellow crystalline solid. According to its $^1H$ NMR spectrum this material appeared to be a mixed alkyl species **3** of $\alpha$-lithiated **2** and $Bu^nLi$ in a 1 : 1 molar ratio (Scheme 1), suggesting that **3** would have a similar 2 : 2 mixed alkyl aggregate structure as found earlier for **1**. Interestingly, the X-ray crystal structure determination‡ of **3** revealed that the 2 : 2 mixed aggregate was comprised of four lithium atoms and four carbon atoms, but now arranged in a unique ladder-type C–$Li_2$–C′$_2$–$Li_2$–C framework [see Fig. 1(*a*)]. It should be noted that X–Li–C–Li structural units have been reported before,[2–4] but **3** is the first heteroleptic organolithium aggregate containing a ladder framework consisting of only lithium and carbon atoms.§




**Scheme 1**

The 2 : 2 mixed alkyllithium aggregate **3** may be regarded as consisting of two (NC′N–$SiMe_3$)$Li_2$ cationic units linked together by two butyl anions. The two cationic units are symmetry-related by a crystallographic centre of symmetry. In the (NC′N–$SiMe_3$)$Li_2$ unit the benzylic carbon atom, C(7), is asymmetrically bonded to Li(1) [2.456(6) Å] and Li(2) [2.152(7) Å], while the two nitrogen atoms of the NC′N–$SiMe_3$ anion are each coordinating to one lithium atom, *i.e.* Li(1) [2.140(6) Å] and Li(2) [2.032(7) Å].

The two butyl anions connecting the two (NC′N–$SiMe_3$)$Li_2$ cationic units are each binding to three lithium atoms in an asymmetric manner: C(19) to Li(1) 2.386(9) Å, to Li(1a) 2.274(8) Å and to Li(2) 2.088(8) Å. As a consequence of different bonding modes of the NC′N–$SiMe_3$ and butyl bridging carbon atoms the coordination geometry of Li(1) is distorted tetrahedral and that of Li(2) more or less trigonal [see Fig. 1(*b*)]. This difference in coordination number and geometry is nicely

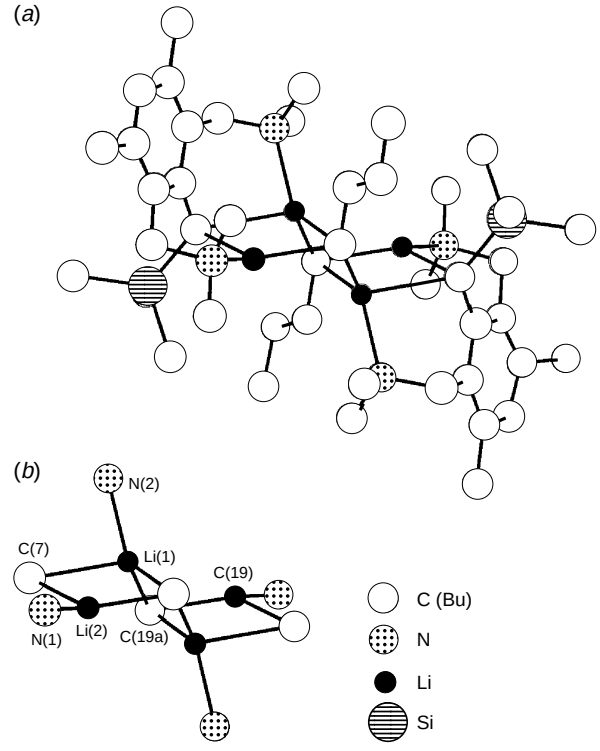



**Fig. 1** (*a*) Overall molecular geometry of **3**. (*b*) Schematic structure showing the ladder type structure with the arrangement of the lithium atoms, the multi-centre bonded carbon atoms and the coordinating nitrogen atoms. Important bond lengths (Å): Li(1)–C(7), 2.456(6); Li(1)–C(19), 2.386(9); Li(1)–C(19a), 2.274(8); Li(1)–N(2), 2.140(6); Li(2)–C(7), 2.152(7); Li(2)–C(19), 2.088(8); Li(2)–N(1), 2.032(7).

reflected in the shorter bonding interactions ($\Delta$Li–$C_{av}$, 0.23 Å; $\Delta$Li–N, 0.1 Å) around Li(2) as compared to Li(1).

Comparison of the closed tetrahedral–$Li_4$ **1** and the open ladder-$Li_4$ structure **3** leads to the following conclusions. α-Substitution leads to a change of the **4c**–**2e** $CLi_3$ bonding in **1** to **3c**–**2e** $CLi_2$ bonding in **3**. Although the charge at the α-C anion changes considerably on introduction of the α-$Me_3Si$ substituent it is most likely for steric reasons that instead of three (see **1**), only two lithium cations are bonded by the NC′N–$SiMe_3$ anion. This makes the NC′N–$SiMe_3$ anion unsuited to forming a well-defined dicationic species $[(NC'N–SiMe_3)_2Li_4]^{2+}$ similar to **1**, but stabilises $[(NC'N–SiMe_3)Li_2]^+$ monocationic building blocks instead.

The observed single resonance pattern in the $^{13}C$ NMR spectrum of **3** at room temperature comprises two $CH_2N$ resonances ($\delta$ 58.0 and 59.6), two ArMe resonances ($\delta$ 21.7 and 21.9) and four NMe resonances ($\delta$ 42.6, 43.1, 46.7 and 47.5). These observations indicate the lack of a symmetry plane, both in-plane and perpendicular to the plane of the aryl moiety of the benzylic ligand, and is, moreover, evidence that Li–N coordination is inert on the NMR timescale at this temperature. Also the $^1H$ NMR spectrum of **3** clearly illustrates the asymmetric fashion in which the benzylic ligand is bonded to two lithium atoms. Two AB patterns were observed for the two $NCH_2$ groups ($\delta$ 3.00 and 3.40, $^2J_{HH}$ 14 Hz, and $\delta$ 3.10 and 3.95, $^2J_{HH}$ 14 Hz). In the region between $\delta$ 1.60 and 2.10 several overlapping broad lines, attributed to the two $NMe_2$ and two ArMe groups were observed. $^1H$, $^{13}C$ and $^6Li$ NMR spectra recorded at lower temperatures (+10 down to −80 °C) did not provide further information, and only extensive line broadening was observed. At higher temperatures a fluxional process becomes operative on the NMR timescale, generating a symmetry plane perpendicular to the aryl moiety of the benzylic ligand. The observation of only one resonance pattern for the two $NMe_2$ groups (one singlet) and the $NCH_2$ (one AB pattern) indicates that a process involving Li–N dissociation/association becomes fast on the NMR timescale. However, the fact that the $CH_2$ protons are still diastereotopic is proof for the configurational stability of the stereogenic α-C atom which is bound to the lithium atoms.

During the lithiation of **2** a stereocentre at the benzylic position, having either (*R*) or (*S*) stereochemistry, is formed in equal amounts. The observation of only one resonance pattern in the $^1H$ and $^{13}C$ NMR spectra of **3** indicates that, most likely as a consequence of differences in thermodynamic stability of the possible aggregates, a diastereoselective aggregation to **3** [*i.e.* (*R,S*)] as found in the solid state has occurred.

That anionic organic groups other than primary alkyl anions are also capable of linking two cationic $(NC'N–SiMe_3)Li_2$ units to a ladder type arrangement may be concluded from the independent synthesis of the corresponding $Bu^t$ and 4-$MeC_6H_4$ aggregates **4** and **5**, respectively (see Scheme 1). The observed $^1H$ and $^{13}C$ NMR spectra of **4** and **5** are almost identical (with respect to the benzylic ligand) to that of **3**, suggesting a close structural resemblance. Obviously, the formation of these mixed hetero-aggregates from the homo-aggregates is driven by the difference in their thermodynamic stability. The observed selectivity of the self-assembling process in the present study is connected to the use of well-designed heteroatom-containing ligands such as NC′N in **1** and NC′N–$SiMe_3$ in **2**.

For synthetic purposes the present findings are relevant as ample evidence exists in the literature[5] that for the *in situ* preparation of various LiR species excess metallating reagent is often required.¶ When this is due to the formation of stable aggregates like **1** or **3**, subsequent reactions will be hampered as a consequence of the presence of trapped, but still reactive, Bu groups, *e.g.* with transition metals both MR as well as often unstable MBu may be formed. The use of $Bu^tLi$, for example, can sometimes solve this problem, most probably not because of the higher nucleophilicity of the $Bu^tLi$ anion but because of the lower stability of species such as **1** and **3** containing bridging $Bu^t$ instead of $Bu^n$ groups as compared with the respective parent alkyllithiums.

## Footnotes and References

* E-mail: vankoten@xray.chem.ruu.nl

† The NC′N abbreviation is used to distinguish this monoanionic benzylic ligand from the monoanionic NCN ligand $[C_6H_3(CH_2NMe_2)_2\text{-}2,6]^-$ we commonly use in our studies.

‡ *Crystal data* for **3**: $C_{44}H_{84}Li_4N_4Si_2$, triclinic, $P\bar{1}$, $a$ = 10.309(2), $b$ = 10.3220(13), $c$ = 12.890(3) Å, $\alpha$ = 103.85(2) $\beta$ = 101.19(2), $\gamma$ = 106.293(15)°, $V$ = 1227.0(4) Å$^3$, $D_{calc}$ = 1.019 g cm$^{-3}$, $\mu$(Mo-Kα) = 1.0 cm$^{-1}$, $Z$ = 1, 4333 unique reflections ($1.7 < \theta < 25.0°$), 3046 with $F_o > 4.0\ \sigma(F_o)$. Enraf-Nonius CAD4T/rotating anode diffractometer, graphite monochromated Mo-Kα radiation, $\lambda$ = 0.71073 Å, $T$ = −123 °C. Solution by direct methods (SHELXS86), refinement on $F^2$ with SHELXL-93 converged at $R_1$ ($wR_2$) = 0.066 (0.1779), $w = 1/[(\sigma^2(F_o) + (0.0736P)^2 + 1.0293P]$, $P = (F_o^2 + 2F_c^2)/3$, for 260 refined parameters (anisotropic temperature factors for the non-hydrogen atoms). Hydrogen atoms were included on calculated positions, riding on their carrier atoms. The structure contains some unresolved disorder as indicated by the anisotropic displacement parameter of C(19), the nature of which is unclear. CCDC 182/578.

§ One example of a homoleptic alkyllithium compound exhibiting a cyclic 'ladder' structure is $(c\text{-}HexLi)_6$ (ref. 6).

¶ In this respect it should be noted that we have proposed earlier, based on chemical evidence, that a mixed aryl-butyl aggregate $[2\text{-}Me_2NCH(Me)C_6H_4]_2Bu_2Li_4$ **6** is formed during the heteroatom assisted lithiation of $Me_2NCH(Me)C_6H_5$, irrespective the molar ratio of amine and BuLi used, *i.e.* excess amine is not reacting further with **6** (ref. 7). Furthermore $(C_6H_2Bu^t_3\text{-}2,4,6)_2Li_4Bu_2$, obtained as one of the products from the reaction of $C_6H_2BrBu^t_3$-2,4,6 with $Bu^nLi$, represents the first example of a well characterised mixed aryl-alkyllithium aggregate (ref. 8).

1 P. Wijkens, E. M. van Koten, M. D. Janssen, J. T. B. H. Jastrzebski, A. L. Spek and G. van Koten, *Angew. Chem., Int. Ed. Engl.*, 1995, **34**, 219.
2 M. A. Beswick and D. S. Wright, in *Comprehensive Organometallic Chemistry II*, ed. E. W. Abel, F. G. A. Stone, G. Wilkinson and C. E. Houscroft, Pergamon, Oxford, 1995, vol. 1, p. 1; F. Pauer and P. P. Power, in *Lithium Chemistry*, ed. A.-M. Sapse and P. v. R. Schleyer, Wiley, New York, 1995, p. 295.
3 K. Sorger, P. v. R. Schleyer and D. Stalke, *J. Chem. Soc., Chem. Commun.*, 1995, 2279.
4 K. Sorger, P. v. R. Schleyer, R. Fleischer and D. Stalke, *J. Am. Chem. Soc.*, 1996, **118**, 6924.
5 H. W. Gschwend and H. R. Rodriguez, *Org. React.*, 1976, **26**, 1.
6 R. Zerger, W. Rhine and G. Stucky, *J. Am. Chem. Soc.*, 1974, **96**, 6048.
7 G. van Koten and J. T. B. H. Jastrzebski, *Tetrahedron*, 1989, **45**, 569.
8 K. Ruhlandt-Senge, J. J. Ellison, R. J. Wehmschulte, F. Pauer and P. P. Power, *J. Am. Chem. Soc.*, 1993, **115**, 11353.

*Received in Liverpool, UK, 27th June 1997; 7/04548D*

# Efficient conversion of 9-Isopropenylphenanthrene to 4,6,6-trimethyl-6*H*-benz[*de*]anthracene in $FSO_3H$; 5,6-dihydro-4*H*-benzanthracen-4-ium ion and its charge delocalization mode

**Sandro Hollenstein and Kenneth K. Laali***

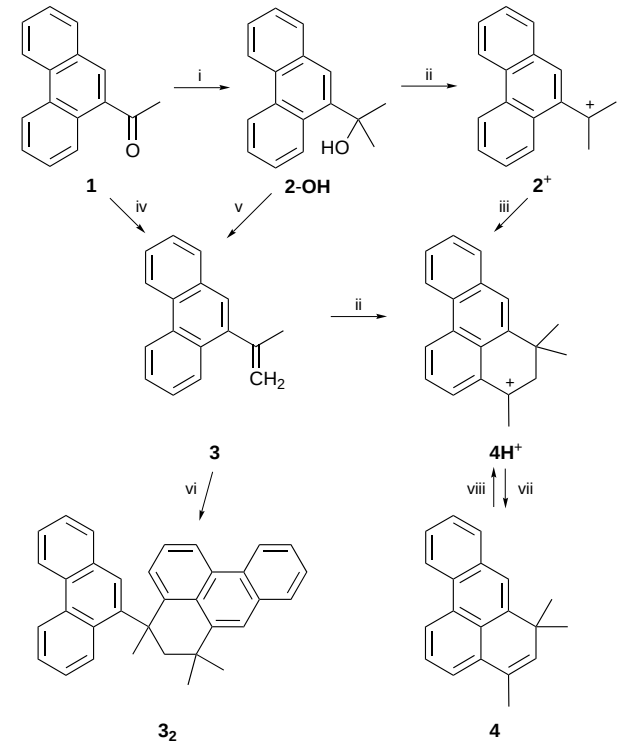
*Department of Chemistry, Kent State University, Kent, OH 44242, USA*

**Low temperature protonation of 9-isopropenylphenanthrene in $FSO_3H$–$SO_2ClF$ (or $FSO_3H$–$CH_2Cl_2$) leads to direct observation of 5,6-dihydrobenzanthracenium cation $4H^+$ from which the corresponding benz[*de*]anthracene is obtained in 92% yield upon quenching.**

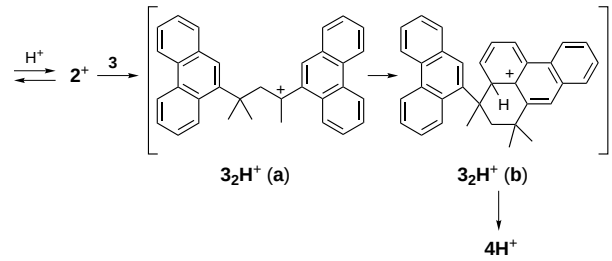
In the course of our work on charge delocalization mapping in arenium ions of polycyclic aromatic hydrocarbons (PAHs) and on various classes of PAH–$C^+R_2$ carbocations as models of epoxide ring opening,[1] we had prepared several regioisomeric phenanthrylpropane-2-carbenium ions including $\mathbf{2}^+$ which was stable up to room temperature. Attempted conversion of **2-OH** to the chloro derivative (**2-Cl**) led only to elimination to give the isopropenyl derivative **3**,[2] which was also independently synthesized by a Wittig type reaction[3] from **1** (Scheme 1).

Surprisingly, the expected quantitative conversion to $\mathbf{2}^+$ did not occur by low temperature protonation with $FSO_3H$–$SO_2ClF$; a mixture of the benzanthracene cation $\mathbf{4H}^+$ and 2-(9-phenanthryl)propane-2-carbenium ion $\mathbf{2}^+$ were formed, even if highly diluted PAH solutions were added to a large excess of the superacid. Raising the temperature led to increased formation of $\mathbf{4H}^+$ at the expense of $\mathbf{2}^+$ (NMR) and complete conversion to $\mathbf{4H}^+$ occurred at room temp. Quenching of the superacid solution furnished the benzanthracene **4** in 92% yield.†

The mechanistic scheme outlined in Scheme 2 is suggested, with intermediate formation of the dimer cation $\mathbf{3_2H}^+$**(a)** and the cycloalkylation product $\mathbf{3_2H}^+$**(b)**, converting rapidly to $\mathbf{4H}^+$. The proposed pathway requires the formation of a stoichiometric amount of phenanthrene. However, no protonated




**Scheme 1** *Reagents and conditions*: i, MeLi, $Et_2O$, 92%; iii, $FSO_3H$, $SO_2ClF$ or $CH_2Cl_2$, −78 °C–room temp.; iii, cat. phenanthrene; iv, $MePr(Ph)_3Br$, $NaNH_2$–THF, 94%; v, $SOCl_2$, $CH_2Cl_2$; vi, $TiCl_4$, $CH_2Cl_2$ (ref. 5); vii, NaOH–$H_2O$, 92%; viii, $FSO_3H$, $SO_2ClF$ or $CH_2Cl_2$




**Scheme 2**

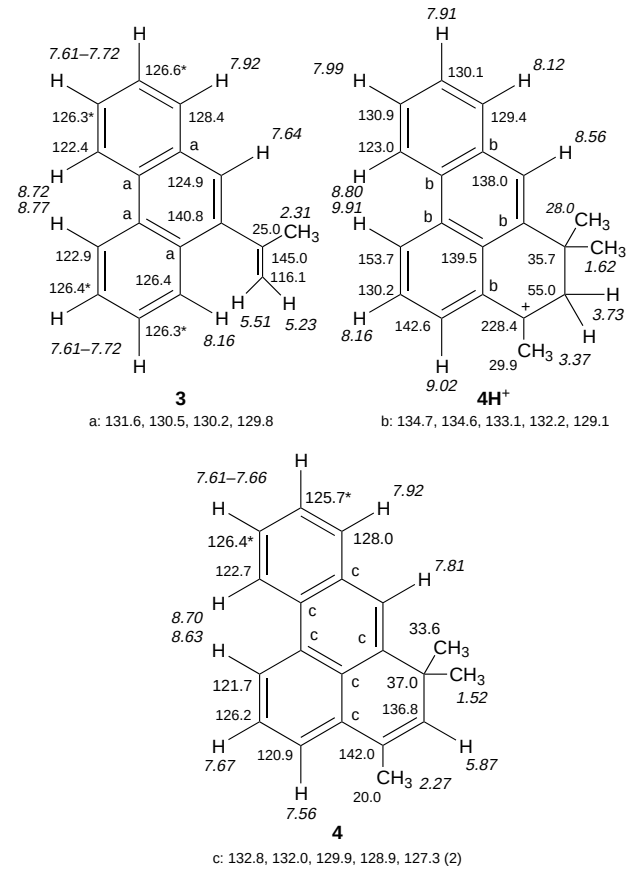



**Fig. 1** $^1H$ NMR (300 MHz, *italic*) and $^{13}C$ NMR (75 MHz) chemical shifts, referenced to internal $CHCl_3$ (7.26 ppm, 77.0 ppm, **3** and **4**) or $CH_2Cl_2$ (5.32 ppm, 53.8 ppm, $\mathbf{4H}^+$) *assignment may be interchangeable

phenanthrene was observed in the superacid solution and no phenanthrene could be isolated on work-up. This can be rationalized since in line with previous studies, the parent phenanthrenium ion is elusive;[4] furthermore control experiments confirm that once phenanthrene is reacted with $FSO_3H$, no intact phenanthrene can be isolated on work-up ($\rightarrow$polymer). An important question that remained was why $\mathbf{2}^+$ generated from the propan-2-ol would not undergo dimerization and cyclization. Addition of catalytic amounts of phenanthrene to a solution of $\mathbf{2}^+$ (generated *via* **2-OH**) gave $\mathbf{4H}^+$, demonstrating that either phenanthrene or its polymer induces *in situ* deprotonation forming **2** in equilibrium, which can then react with $\mathbf{3}^+$, cyclize and eliminate ($\rightarrow\mathbf{4H}^+$).

The $TiCl_4$-mediated dimerization of **3** to give an isolable dimer $\mathbf{3_2}$[5] and similar dimerization of other isopropenyl-PAHs[6*a–c*] have been reported where depending on the regioisomer, isopropenyl-PAHs would either undergo polymerization or dimerization. The observed facile dimerization, cyclization and cleavage in the superacid, offers synthetic potential for preparation of various benzophenalenes in simple one-pot reactions. Another noteworthy feature of this chemistry is facile access to 1-phenanthryl-substituted carbocations which are otherwise not available due to difficulties associated with synthesis of 1-substituted phenanthrene derivatives by electrophilic chemistry.

In the $^{13}C$ NMR, the $C^+$ centre in $\mathbf{4H}^+$ is at 228.4 ppm which is slightly shielded if compared to the $C^+$ of $\mathbf{2}^+$ (230.1 ppm),[1*c*] indicating a similar degree of charge delocalization into the phenanthrene moiety and therefore comparable $C^+$–C(*ipso*) double bond character (Fig. 1). Charge delocalization mapping in $\mathbf{4H}^+$ as deduced from $\Delta\delta^{13}C$ values shows arene $\pi$-participation primarily *via* a naphthalenium ion (AB ring of phenanthrene moiety) and is in qualitative agreement with the overall mode of charge delocalization deduced based on the AM1-calculated[7] carbon charges.[1]

We are grateful to the NCI of NIH (R15 CA63595-01A1) for financial support.

## Footnotes and References

* E-mail: klaali@kentvm.kent.edu

† *Experimental procedure for the synthesis of* **4**: 9-isopropenylphenanthrene (170 mg, 0.78 mmol) was dissolved in 5 ml of $CH_2Cl_2$ under argon and cooled to −78 °C. Fluorosulfonic acid (*ca.* 1 ml) was slowly added to the stirred solution; the colour suddenly turned deep red. After 5 min, the solution was warmed to room temp. (blue colour), stirred for additional 20 min, and poured into ice-cold aqueous 5% NaOH. Extraction with $CH_2Cl_2$ and column chromatography (hexane) gave 93 mg (92%) of a white solid (mp 80–81 °C; for NMR spectral data see Fig 1; *m/z* 258 ($M^+$).

‡ AM1 semi-empirical calculations[7] were carried out using the HYPERCHEM package (HYPERCUBE 1995).

1 (*a*) K. K. Laali, *Chem. Rev.*, 1996, **96**, 1873; (*b*) K. K. Laali and P. E. Hansen, *J. Org. Chem.*, 1997, **62**, 5804; (*c*) K. K. Laali and S. Hollenstein, unpublished work.
2 E. Bergmann and F. Bergmann, *J. Am. Chem. Soc.*, 1937, **59**, 1443; D. F. Church and G. J. Gleicher, *J. Org. Chem.*, 1976, **46**, 2327.
3 R. M. Pike, D. W. Mayo, S. S. Butcher, D. J. Butcher and J. Hinkle, *J. Chem. Educ.*, 1986, **63**, 917.
4 K. Laali and H. Cerfontain, *J. Org. Chem.*, 1983, **48**, 1092.
5 J. Coudane, M. Brigodiot and E. Marechal, *Polym. Bull.*, 1979, **1**, 475.
6 (*a*) C. Bunel, M. Brigodiot and E. Marechal, *J. Macromol. Sci. Chem.*, 1978, **A12**, 1283; (*b*) J. Coudane, M. Brigodiot and E. Marechal, *Polym. Bull.*, 1979, **1**, 465; (*c*) J. Coudane, M. Brigodiot and E. Marechal, *Polym. Bull.*, 1979, **1**, 469.
7 M. J. S. Dewar, E. G. Zoebisch, E. F. Healy and J. J. P. Stewart, *J. Am. Chem. Soc.*, 1985, **107**, 3902.

*Received in Corvallis, OR, USA, 2nd June 1997; 7/03840B*

# An extreme water exchange rate: the europium(II) aqua ion

**P. Caravan and André E. Merbach***

*Institut de Chimie Minérale et Analytique, Université de Lausanne-BCH, CH-1015 Lausanne, Switzerland*

**The rate of water exchange at the europium(II) aqua ion is measured by a combined variable-temperature $^{17}O$ NMR and EPR study; it is the fastest aqua exchange rate ever directly measured by magnetic resonance for a non Jahn–Teller ion, $3.5 \times 10^9$ s$^{-1}$ at 25 °C.**

Water exchange on an aqua ion is one of the most fundamental chemical processes. An established field, water exchange rates have been measured on many of the aqua ions across the Periodic Table and span 20 orders of magnitude.[1] To date, no solvent exchange rates have been reported for the divalent lanthanides. The most easily accessible divalent lanthanide is europium(II). This report describes water exchange on $Eu^{2+}_{(aq)}$ as a function of temperature determined by a combined $^{17}O$ NMR and EPR study. Apart from its intrinsic interest, and to develop an understanding of ligand substitution kinetics at $Eu^{II}$, this work sheds light on two other areas. Europium(II) is very similar in size to $Sr^{II}$ and exhibits a similar chemistry (excluding electron transfer).[2] Since water exchange on the heavier group 2 elements cannot be directly measured, $Eu^{II}$ may provide insight as a spectroscopic probe in the chemistry of $Ca^{II}$ and $Sr^{II}$.[3] Also, $Eu^{II}$ is isoelectronic with $Gd^{III}$; we, and others, have extensively studied the factors influencing water exchange on $Gd^{III}$ based contrast agents for magnetic resonance imaging (MRI).[4] Europium(II) being another $f^7$ ion allows us to further understand relaxation processes in $^8S$ ions.

The approach taken was the same as in our previous analyses† of $Gd^{III}$ water exchange kinetics.[5] The source of $Eu^{II}$ was the triflate salt, $Eu(O_3SCF_3)_2{\cdot}H_2O$.‡ From the measured relaxation rates and angular frequencies of $Eu^{2+}_{(aq)}$ solutions, $1/T_1$, $1/T_2$ and $\omega$, and of a dilute triflic acid reference solution, $1/T_{1A}$, $1/T_{2A}$ and $\omega_A$, the reduced relaxation rates and chemical shift $1/T_{1r}$, $1/T_{2r}$, and $\omega_r$ can be calculated, eqns. (1)–(3). Here,

$$\frac{1}{T_{1r}} = \frac{1}{P_m}\left[\frac{1}{T_1} - \frac{1}{T_{1A}}\right] = \frac{1}{T_{1m} + \tau_m} \tag{1}$$

$$\frac{1}{T_{2r}} = \frac{1}{P_m}\left[\frac{1}{T_2} - \frac{1}{T_{2A}}\right] = \frac{1}{\tau_m}\,\frac{T_{2m}^{-2} + \tau_m^{-1}T_{2m}^{-1} + \Delta\omega_m^2}{\left(\tau_m^{-1} + T_{2m}^{-1}\right)^2 + \Delta\omega_m^2} \tag{2}$$

$$\Delta\omega_r = \frac{1}{P_m}\left(\omega - \omega_A\right) = \frac{\Delta\omega_m}{\left(1 + \tau_m T_{2m}^{-1}\right)^2 + \tau_m^2\Delta\omega_m^2} \tag{3}$$

the subscript m refers to the relaxation rates of bound water and the chemical shift difference between bound and bulk water, $P_m$ is the mole fraction of bound water, and $\tau_m = k_{ex}^{-1}$ is the residency time of a bound water molecule. The chemical shift of bound water is given by eqn. (4), where $A/\hbar$ is the

$$\Delta\omega_m = \frac{g_L\mu_B S(S+1)B}{3k_BT}\,\frac{A}{\hbar} \tag{4}$$

hyperfine coupling constant and the other symbols are constants.§ The longitudinal relaxation rate is dominated by the dipole–dipole and quadrupolar mechanisms, eqn. (5).

$$\frac{1}{T_{1m}} = \left[\frac{2}{5}\left(\frac{\mu_0}{4\pi}\right)^2 \frac{\hbar^2\gamma_I^2\gamma_S^2}{r_{EuO}^6}\,S(S+1) + Q\right]\tau_R \tag{5}$$

The rotational correlation time is given by $\tau_R$ which has an exponential temperature dependence with an activation energy $E_R$, eqn. (6). The dipole–dipole mechanism is dependent on

$$\tau_R = \tau_R^{298}\exp\left[\frac{E_R}{R}\left(\frac{1}{T}\,\frac{1}{298.15}\right)\right] \tag{6}$$

the Eu–O bond length ($r^6_{EuO}$) which we have set to 2.65 Å.[6] The reduced transverse relaxation rate allows the determination of the rate constant by eqn. (7), where $1/\tau_{1S} = k_{ex} + 1/T_{1e}$.

$$\frac{1}{T_{2sc}} = \frac{(A/\hbar)^2}{3}\,S(S+1)\tau_{1S} \tag{7}$$

The transverse electronic relaxation rates have been determined by EPR linewidth measurements, denoted $\Delta_{Hpp}$. Eqns. (8) and (9) introduce three more parameters, $\Delta^2$, the trace of the square

$$\frac{1}{T_{2e}} = \frac{g_L\mu_B\pi\sqrt{3}}{h}\,\Delta H_{pp} = \Delta^2\tau_v\left[\frac{5.26}{1 + 0.372\omega_S^2\tau_v^2} + \frac{7.18}{1 + 1.24\omega_S\tau_v}\right] \tag{8}$$

$$\tau_v = \tau_v^{298}\exp\left\{\frac{E_V}{R}\left(\frac{1}{T} - \frac{1}{298.15}\right)\right\} \tag{9}$$

of the zero field splitting (ZFS) tensor $\tau_v$, the correlation time modulation of the ZFS, and $E_v$, the activation energy defining the temperature dependence of $\tau_v$. The longitudinal electronic relaxation rate can then be determined by the following relationship, eqn. (10). Finally, the temperature dependence

$$\frac{1}{T_{1e}} = \frac{1}{25}\,\Delta^2\tau_v\left\{4S(S+1) - 3\right\}\left(\frac{1}{1 + \omega_S^2\tau_v^2} + \frac{4}{1 + \omega_S^2\tau_v^2}\right) \tag{10}$$

of the exchange rate follows the Eyring equation (11). The

$$\frac{1}{\tau_m} = k_{ex} = \frac{k_BT}{h}\exp\left\{\frac{\Delta S^\ddagger}{R} - \frac{\Delta H^\ddagger}{RT}\right\} = \frac{k_{ex}^{298}T}{298.15}\exp\left\{\frac{\Delta H^\ddagger}{R}\left(\frac{1}{298.15} - \frac{1}{T}\right)\right\} \tag{11}$$

reduced relaxation rates, reduced chemical shifts, and electronic transverse relaxation rates were fitted simultaneously as a function of temperature using eqns. (1)–(11). The fitted parameters are given in Table 1, and the fitted data shown in Fig. 1.

**Table 1** Comparison of parameters for $Gd^{III}$[a] and $Eu^{II}$ water exchange

| Parameter | $[Eu(H_2O)_8]^{2+}$ | $[Gd(H_2O)_8]^{3+}$ |
|---|---|---|
| $10^{-9}\ k_{ex}^{298}/s^{-1}$ | 3.5 ± 0.4 | 0.80 ± 0.06 |
| $\Delta H^{\ddagger}$/kJ mol$^{-1}$ | 18.2 ± 2 | 15.3 ± 1 |
| $\Delta S^{\ddagger}$/J mol$^{-1}$ K$^{-1}$ | −0.2 ± 6 | −23.1 ± 4 |
| $10^{-6}\ (A/\hbar)$/rad s$^{-1}$ | −3.70 ± 0.07 | −5.3 ± 0.1 |
| $\tau_R^{298}$/ps | 12 ± 1 | 41 ± 2 |
| $E_R$/kJ mol$^{-1}$ | 18.2 ± 0.6 | 15.0 ± 1.3 |
| $\tau_v^{298}$/ps | 0.4 ± 0.1 | 7.3 ± 0.5 |
| $E_v$/kJ mol$^{-1}$ | 8.6 ± 0.8 | 18.4 ± 1.4 |
| $10^{-20}\ \Delta^2$/ s$^{-2}$ | 5.4 ± 1.4 | 1.19 ± 0.09 |

[a] Ref. 4.

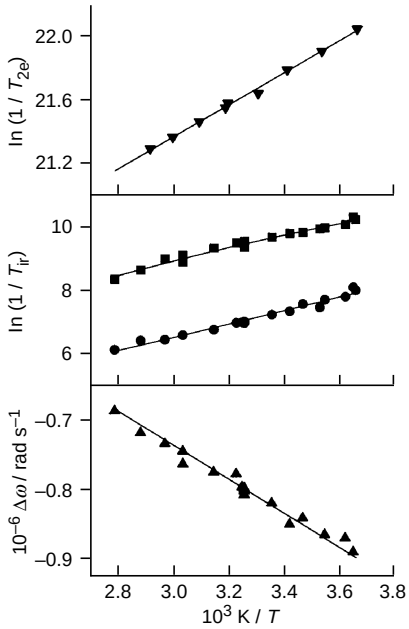



**Fig. 1** Temperature dependence of the reduced $^{17}O$ chemical shifts (bottom), reduced $^{17}O$ longitudinal (circles) and transverse (squares) relaxation rates (middle), and of the transverse electronic relaxation rates (top)

As expected, the larger, less highly charged $[Eu(OH_2)_8]^{2+}$ ion undergoes water exchange faster than $[Gd(OH_2)_8]^{3+}$. The hyperfine coupling constant is lower for $Eu^{II}$, again, as expected since $A/\hbar$ is determined by the degree of interaction between the electron spin of the metal and the $^{17}O$ nucleus; the larger, less charged ion should interact less strongly with the oxygen donor atom. The rotational correlation time is very short for the $Eu^{II}$ aqua ion. Although the precision associated with this number is very good, the actual error could be much larger since the measured $T_1$ of the sample was close to the $T_1$ of the reference (within 90%). Hence the rotational correlation time is based on the small difference between two large numbers, and $\tau_R$ should not be considered too meaningful. In contrast, the transverse relaxation rates provide a very good representation of the exchange rate. The value of $1/T_{2m}$ is dependent on contributions from electronic relaxation and chemical exchange. Since $Eu^{II}$ has a longer electronic lifetime than $Gd^{III}$ (shorter $\tau_v$, larger $\Delta^2$), the contribution of $1/T_{1e}$ to $1/T_{2m}$ is much less for the $Eu^{II}$ aqua ion (only about 10%). The differences between measured $T_2$ values for $Eu^{II}$ and reference are more than ten times greater than for the $T_1$ difference leading to increased accuracy.

The coordination number of the $Eu^{II}$ aqua ion is not known. This report assumes a coordination number of eight based on analogy with $Sr^{II}$.[7] A coordination number of nine would lead to a value 8–9 times lower for $k_{ex}^{298}$, which is within the experimental error.

This report describes the second fastest water exchange rate ever measured [behind $Cu^{2+}_{(aq)}$] and its represents the fastest rate of water exchange measured on a non-Jahn–Teller ion.[8] Currently, this work is being expanded to examine the effects of magnetic field strength on both the NMR and EPR data, the effect of pressure on the rate of water exchange, and a molecular dynamics study on $Eu^{II}$ solvation and water exchange.

Acknowledgement is made to NSERC of Canada for a postdoctoral fellowship (P. C.), the Swiss National Science Foundation for a research grant, and to Drs. L. Helm and E. Tóth for useful discussions.

## Footnotes and References

* E-mail: andre.merbach@icma.unil.ch

† The equations listed are those used in the analysis and, in some cases, are simplified versions of the equations found in ref. 5. The simplifications are based on assumptions justified in ref. 5.

‡ $Eu(O_3SCF_3)_2$ was prepared by distilling degassed triflic acid onto $EuCO_3$[9] and then removing the water and excess triflic acid under reduced pressure. This process was repeated twice more, followed by drying at 90 °C *in vacuo* overnight to give $Eu(O_3SCF_3)_2{\cdot}H_2O$. Anal. Calc. for $C_2H_2EuF_2O_7S_2$: C, 5.13; H, 0.43; S, 13.70; F, 24.35. Found: C, 5.37; H, 0.46; S, 13.54; F, 23.91%. Solutions were prepared under nitrogen in a glove box by dissolving $Eu(O_3SCF_3)_2$ in water degassed by a triple freeze–pump–thaw cycle. Solutions were enriched with $H_2{}^{17}O$ labelled water. Solutions ranged from 0.02 to 0.15 mol kg$^{-1}$ and enriched 3–6% in $H_2{}^{17}O$. Solution composition was checked by determination of total Eu content by titration with EDTA; the concentration agreed with that calculated from dissolution of solid $Eu(O_3SCF_3)_2$.

§ Constants: $g_L$ = isotropic Landé factor, here 2.0; $\mu_B$ = Bohr magneton; $B$ = magnetic field, 9.4 T; $k_B$ = Boltzmann constant; $\gamma_I$ = nuclear gyromagnetic ratio; $\gamma_S$ = electron gyromagnetic ratio; $Q = (3\pi^2/10)\ \{(2I + 3)/[I^2(2I - 1)]\}\ \chi^2\ (1 + \eta^2/3)$; $I$ = nuclear spin; $\chi$ = quadrupolar coupling constant; $\eta$ = an asymmetry parameter; $\omega_S = \gamma_S B$. Values of the parameters are given in ref. 5.

1 S. F. Lincoln and A. E. Merbach, *Adv. Inorg. Chem.*, 1995, **42**, 1; A. Cusanelli, U. Frey, D. T. Richens and A. E. Merbach, *J. Am. Chem. Soc.*, 1996, **118**, 5265.
2 N. N. Greenwood and A. Earnshaw, *The Chemistry of the Elements*, Pergamon, Oxford, 1984, p. 1448.
3 R. A. Dwek, R. E. Richards, K. G. Morallee, E. Nieboer, R. J. P. Williams and A. V. Xavier, *Eur. J. Biochem.*, 1971, **21**, 204.
4 D. H. Powell, O. M. Ni Dhubhghaill, D. Pubanz, L. Helm, Y. S. Lebedev, W. Schlaepfer and A. E. Merbach, *J. Am. Chem. Soc.*, 1996, **118**, 9333 and references therein.
5 K. Micseki, D. H. Powell, L. Helm, E. Brücher and A. E. Merbach, *Magn. Reson. Chem.*, 1993, **31**, 1011.
6 G. W. Nielson and R. D. Broadbent, *Chem. Phys. Lett.*, 1990, **167**, 429.
7 D. H. Powell, L. Helm and A. E. Merbach, *J. Chem. Phys.*, 1991, **95**, 9258.
8 The coordination number of $Sr^{II}$ is not well defined; however based on the available evidence it appears to be eight: D. T. Richens, *The Chemistry of Aqua Ions*, Wiley, Chichester, 1997, p. 138 and references therein.
9 R. A. Cooley and D. M. Yost, *Inorg. Synth.*, 1946, **2**, 69.

*Received in Basel, Switzerland, 14th August 1997; 7/05971J*

# [1,2,3]Triazolo[4,5-*d*][1,3,2]thiazaphospholes: a new fused NPS ring system from a cycloaddition–rearrangement sequence with Lawesson's reagent, a super dipolarophile

**Richard N. Butler,* Elaine C. McKenna and (in part) Denise C. Grogan**

*Chemistry Department, University College, Galway, Ireland*

**A new fused NPS ring system has been obtained from the reaction of substituted 1,2,3-triazolium-1-imide 1,3-dipoles with Lawesson's reagent**

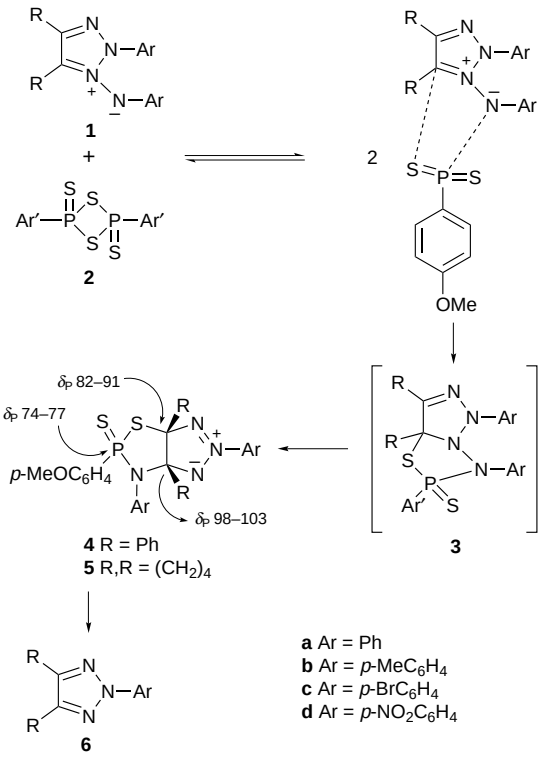
Recently there has been renewed interest in sulfur–nitrogen and sulfur–nitrogen–phosphorus containing ring systems.[1,2] The use of Lawesson's reagent as a possible P=S 1,3-dipolarophile has been established by Bertrand.[2] The cycloaddition–1,4-sigmatropic rearrangement sequences which we developed[3,4] for the triazolium imide 1,3-dipole system **1** opened the prospect of possible new fused nitrogen–phosphorus–sulfur ring systems such as **4** if these would be stable. Herein we describe routes to the new ring system **4** and the new tricyclic structure **5**, both of which proved to be reasonably stable in the solid state but unstable in solution, where they broke down rapidly to 1,2,3-triazoles **6** and uncharacterised N–P–S compounds. Kinetic studies on the rate of consumption of the dipole **1** by Lawesson's reagent showed it to be 2000 times faster than for acrylonitrile and twice as fast as the C=S dipolarophile of MeSC(S)CN, indicating that Lawesson's reagent is a super-dipolarophile comparable to thiones.[5–7]

Solutions of the dipoles **1** (*ca.* 0.4 mmol) in dry THF under an atmosphere of dry nitrogen were treated with Lawesson's reagent **2** (0.5 equiv.) and stirred at ambient temperature for *ca.* 1 h. The solvent was removed under reduced pressure and the flaky residue leached with cold $Et_2O$ until the ethereal extracts were colourless. Evaporation of the ethereal extracts gave the products **4** and **5** as low melting yellow–orange solids. A single product only was obtained in each case. Due to the instability of the fused ring system in solution low temperatures (−30 °C) and a carefully chosen number of scans were necessary to obtain good NMR spectra since the products **4** and **5** readily broke down to **6** in NMR solvents. The compounds were fully characterised by their $^1$H and $^{13}$C NMR spectra measured in $CDCl_3$, which showed all of the expected signals. Key signals were the two bridgehead carbon signals (see Table 1 and Scheme 1). We have previously established[4] that the N–C–N fused bridgehead $^{13}$C NMR signal for related systems without P occurs at $\delta$ 95–105 and the N–C–S bridgehead occurs at $\delta$ 80–95. These quaternary bridgehead signals were particularly weak and were made more difficult to detect because of the ongoing decomposition of the products. Small splittings (*ca.* 3–10 Hz) of the bridgehead carbon signals were observed due to the phosphorus. This is in agreement with the structures **4** and **5**, where P is not bonded directly to the bridgehead carbons. The *endo* or *exo* alignment of the substituents on the P atom has not been established. The $^{31}$P signal for **4** and **5** appeared at $\delta$ 74–77 (downfield from $H_3PO_4$) and the P-bonded *p*-methoxyphenyl group showed the expected $^{31}$P splittings although precise $J_{PC}$ values could not be measured in all cases due to signal spreading caused by the ongoing decomposition. Despite the fact that they could not be recrystallised and only cold washing procedures could be used for purification, the solid compounds **4** and **5** gave satisfactory CHN microanalyses. Energy dispersive X-ray analyses (EDAX) of the solid compounds using a scanning electron microscope confirmed the presence of sulfur and phosphorus in **4** and **5** in the expected atomic ratio of 2 : 1.

UV spectral measurements of the disappearance of the dipole **1a** (R = Ph) at 37 °C in acetone were carried out using pseudo-first-order conditions with 10–1000-fold excesses of dipolarophile giving $k_1$ values. Second-order rate constants $k_2$ were obtained from plots of these $k_1$ values against the dipolarophile concentration, giving the following $k_2$ values at 37 °C: dimethyl maleate = $0.108 \times 10^{-3}$; ethyl acrylate = $0.57 \times 10^{-3}$, acrylonitrile = $1.47 \times 10^{-3}$, dimethyl acetylene-

**Table 1** Substituted [1,2,3]triazolo[4,5-*d*][1,3,2]thiazaphospholes

| | | | Chemical shifts (ppm) | | |
|---|---|---|---|---|---|
| | Mp/°C | Yield (%) | P | NCN | NCS |
| **4a** | unstable oil | 83 | 74.0 | 100.2 | 91 |
| **4b** | 45–47 | 65 | 75.4 | 99.6 | 92 |
| **4c** | 48–49 | 84 | 75.3 | 100.2 | 91.4 |
| **4d** | 55–58 | 71 | 73.9 | 100.4 | 90 |
| **5a** | 42–43 | 64 | 75 | 100.4 | 90.3 |
| **5b** | 34–36 | 80 | 75.4 | 100.2 | 91.4 |
| **5c** | 35–36 | 90 | 75.3 | 100.5 | 92 |
| **5d** | 55–57 | 74 | 73.9 | 99.4 | 89.2 |




**Scheme 1**

dicarboxylate = 0.80, MeSC(S)CN = 1.65 and Lawesson's reagent = 2.2 l mol$^{-1}$ s$^{-1}$. Hence the P=S bond reacted with the dipole **1** at a rate which is faster than a C=S bond, and Lawesson's reagent is a superdipolarophile.[7]

We thank Dr W. Carroll of this Department for the EDAX spectral measurements.

## Footnote and References

* E-mail: r.debuitleir@ucg.ie

1 C. W. Rees, *J. Heterocyclic Chem.*, 1996, **33**, 1419.
2 N. Dubau-Assibat, A. Baceiredo and G. Bertrand, *J. Org. Chem.*, 1995, **60**, 3904.
3 For a review, see R. N. Butler and D. F. O'Shea, *Heterocycles*, 1994, **37**, 571.
4 R. N. Butler, A. M. Evans, A. M. Gillan, J. P. James, E. McNeela, D. Cunningham and P. McArdle, *J. Chem. Soc., Perkin Trans. 1*, 1990, 2537; R. N. Butler, A. M. Evans, E. McNeela, G. A. O'Halloran, P. D. O'Shea, D. Cunningham and P. McArdle, *J. Chem. Soc., Perkin Trans. 1*, 1990, 2527.
5 R. Sustmann, W. Sicking and R. Huisgen, *J. Am. Chem. Soc.*, 1995, **117**, 9679.
6 R. Huisgen, L. Fisera, H. Giera and R. Sustmann, *J. Am. Chem. Soc.*, 1995, **117**, 9671.
7 L. Fisera, R. Huisgen, I. Kalwinsch, E. Langhals, X. Li. G. Mloston, K. Polborn, J. Rapp, W. Sicking and R. Sustmann, *Pure Appl. Chem.*, 1996, **68**, 789.

*Received in Liverpool, UK, 28th August 1997; 7/06306G*

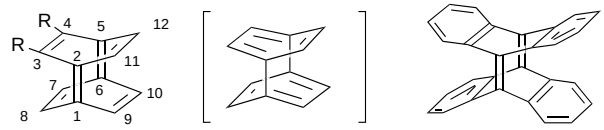
# Tricyclo[4.2.2.2$^{2,5}$]dodeca-1,3,5,7,9,11-hexaene: generation and chemical trapping of the 3,4-dicyano derivative

**Takashi Tsuji,* Masahiro Okuyama, Masakazu Ohkita, Toshiro Imai and Takanori Suzuki**

*Division of Chemistry, Graduate School of Science, Hokkaido University, Sapporo 060, Japan*

**The 3,4-dicyano derivative of hitherto unknown tricyclo-[4.2.2.2$^{2,5}$]dodeca-1,3,5,7,9,11-hexaene, in which six double bonds are uniquely arranged, is generated and chemically trapped with 1,2-dimethylenecyclopentane and *tert*-butyllithium.**

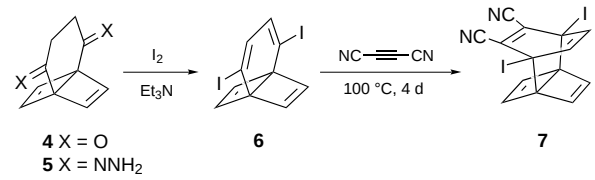
The title compound **1a** is a highly strained and symmetrical, fully unsaturated hydrocarbon[1] in which four double bonds are arranged longicyclically[2] and the residual two doubly bridgehead unsaturated bonds are disposed face-to-face in close



**1a** R = H
**b** R = CN

**2** **3**

proximity. It is also of interest that the species may be regarded as a π-bond-shift isomer of [0.0]paracyclophane **2** although, according to theoretical calculations, the latter appears neither to represent a local energy minimum on the potential energy surface nor to appreciably contribute to the molecule as a canonical form.† To the best of our knowledge, the tetrabenzo derivative **3**[3] is the only known compound closely related to **1a**. We envisaged that the title hexaene structure might be accessible *via* 1,4-elimination in **7** in which the cleaving bonds are ideally disposed antiperiplanar to each other.[4] Moreover, strain release by the concomitant cleavage of the highly strained central σ-bond is expected to facilitate the reaction. Here the generation of the 3,4-dicyano derivative **1b** from **7** and its chemical trapping is reported.

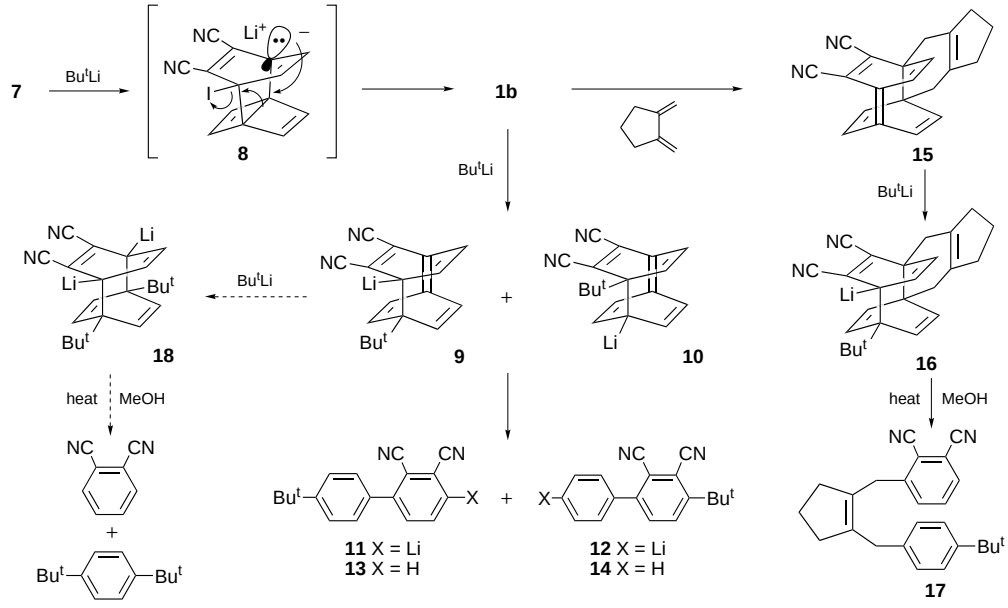


**4** X = O
**5** X = $NNH_2$

**6** **7**

**Scheme 1**

The preparation of **7** started with tricyclic diketone **4**,[5] from which diiodo[4.2.2]propellatetraene **6** was obtained *via* the bis(hydrazone) **5** using Barton's procedure (Scheme 1).[6] The [2 + 4] cycloaddition of dicyanoacetylene to **5** furnished **7** in 45% yield after 4 d at 100 °C.‡ Treatment of **7** with 3.3 equiv. of *tert*-butyllithium in the presence of 1,2-dimethylenecyclopentane (0.33 mol dm$^{-3}$) in THF at −78 °C followed by the addition of MeOH after 1 h provided **13** (40%), **14** (5%) and **17** (10%), along with several minor unidentified products. The formation of these products seems to be best explained by postulating the generation of **1b** *via* **8** as a short lived intermediate (Scheme 2), which undergoes [2 + 4] cycloaddition with 1,2-dimethylenecyclopentane[7] to give **15**, in competition with the regioselective addition of *tert*-butyllithium to give **9** and **10**. The addition of alkyllithium to strained carbon–carbon double bonds is well documented[1] and the observed regioselectivity is in accord with the expected electronic polarization of the double bond and/or the steric effect exerted by the cyano substituents. The resulting adducts **9** and **10** would suffer rapid ring-cleavage to give **11** and **12**, respectively, being facilitated by an enormous gain in energy, and end up as **13** and **14** after protonation by MeOH. According to semiempirical



**11** X = Li
**13** X = H

**12** X = Li
**14** X = H

**Scheme 2**

calculations (PM3),[8] the isomerization of the 1,2-dihydro derivative of **1a** to biphenyl is exothermic by 93 kcal mol$^{-1}$.§

Conspicuously absent in the product mixture were the substituted benzenes expected from the addition of another molecule of *tert*-butyllithium to **9** and **10** followed by ring fission, *e.g.* 1,4-di-*tert*-butylbenzene and phthalonitrile. Thus, the further addition of *tert*-butyllithium to **9** and **10** must be unimportant. The cycloadduct **15**, which is still highly strained but restrained from isomerizing to a biphenyl derivative by the side chain, would eventually be converted to **17** *via* the addition of *tert*-butyllithium,¶ followed by the fission in the benzene *p*,*p*-dimer moiety of the resultant adduct and protonation by MeOH under the reaction conditions or during the isolation.[9] When 1.1 equiv. of *tert*-butyllithium was used in an attempt to suppress its addition to **1b**, only one third of **7** was consumed and the residual two thirds were recovered intact. Apparently, the lithiation of **7** is rate-determining and the subsequent elimination of LiI from **8** and the addition of *tert*-butyllithium to the resulting **1b** must be much faster.‖ The reported isolation of highly strained alkenes whose alkenic carbons are more highly pyramidalized than the central carbons of **1a**,[10–12] however, suggests that the title hexaene may well become isolable if a generation method not requiring the use of strongly nucleophilic or electrophilic reagents is devised, or the skeleton is kinetically stabilized by the introduction of suitable substituents.

We thank the Ministry of Education, Science and Culture of Japan for a Grant-in-Aid for Scientific Research (No. 06453031).

## Footnotes and References

* E-mail: tsuji@science.hokudai.ac.jp

† The structure of **1a** optimized at the B3LYP/6-31G* level of theory is $D_{2h}$ symmetric; the interatomic distances C(1)–C(2), C(2)–C(3), C(3)–C(4) and C(1)–C(6) are 1.369, 1.515, 1.345 and 2.399 Å, respectively, and the angle between the bond C(1)–C(2) and the plane C(1)–C(8)–C(9) is 37.0°.

‡ *Selected data* for **6**; $\delta_H(CDCl_3)$ 5.86 (2 H, s), 6.38 (4 H, s); $\delta_C(CDCl_3)$ 65.20, 98.04, 129.88, 143.25; Calc. for $C_{10}H_6I_2$: 379.8559. Found: 379.8535. For **7**: $\delta_H(CDCl_3)$ 6.26 (2 H, s), 6.29 (2 H, s), 6.42 (2 H, s); $\delta_C(CDCl_3)$ 32.08, 66.00, 113.53, 136.08, 140.14, 140.64, 141.70; Calc. for $C_{14}H_6N_2I_2$: 455.8620. Found: 455.8616.

§ The formation of 10-methylbianthryl upon treatment of **3** with methyllithium has recently been reported. The addition of methyllithium in a transannular fashion, however, predominates in the reaction: R. Herges, H. Neumann and F. Hampel, *Angew. Chem., Int. Ed. Engl.*, 1994, **33**, 993.

¶ According to semiempirical calculations (AM1 and PM3) (ref. 8), the degree of pyramidalization around the central alkenic carbons of the 1,2-dihydro derivative of **1a** is slightly more pronounced than around those of **1a**.

‖ It seems that *tert*-butyllithium also rapidly reacts with *tert*-butyl iodide arising from the lithiation of **7**. Thus, 3 equiv. of *tert*-butyllithium at least are consumed in the reaction with **7**.

1 For reviews of strained bridgehead alkenes, see G. Szeimies, *Reactive Intermediates*, ed. R. A. Abramovitch, Plenum, New York, 1983, vol. 3, ch. 5; W. Luef and R. Keese, *Top. Stereochem.*, 1990, **20**, 231; P. W. Warner, *Chem. Rev.*, 1989, **89**, 1067; W. T. Borden, *Chem. Rev.*, 1989, **89**, 1095.

2 J. Goldstein and R. Hoffmann, *J. Am. Chem. Soc.*, 1971, **93**, 6193.

3 R. L. Viavattene, F. D. Greene, L. D. Cheung, R. Majeste and L. M. Trefonas, *J. Am. Chem. Soc.*, 1974, **96**, 4342.

4 P. Deslongchamps, *Stereoelectronic Effects in Organic Chemistry*, Pergamon, Oxford, 1983.

5 M. Okuyama and T. Tsuji, *Angew. Chem., Int. Ed. Engl.*, 1997, **36**, 1085.

6 D. H. R. Barton, R. E. O'Brien and S. Sternhell, *J. Chem. Soc.*, 1962, 470; D. H. R. Barton, G. Bashiardes and J.-L. Fourrey, *Tetrahedron Lett.*, 1983, **24**, 1605; D. H. R. Baton, M. Chen, J. C. Jászberényi and D. K. Taylor, *Org. Synth.*, 1996, **74**, 101.

7 H.-D. Scharf, H. Plum, J. Fleischhauer and W. Schleker, *Chem. Ber.*, 1979, **112**, 862; R. Sustmann, M. Böhm and J. Sauer, *Chem. Ber.*, 1979, **112**, 883.

8 *CS ChemOffice Ultra*, Ver. 4.0, CambridgeSoft, Cambridge, MA, 1997.

9 For the thermal isomerization of benzene *p*,*p*-dimer derivatives, see N. C. Yang, M. Chen and P. Chen, *J. Am. Chem. Soc.*, 1984, **106**, 7310; H. Gan, J. L. King and N. C. Yang, *Tetrahedron Lett.*, 1989, **30**, 1205.

10 J.-P. Melder, R. Pinkos, H. Fritz and H. Prinzbach, *Angew. Chem., Int. Ed. Engl.*, 1990, **29**, 95; R. Pinkos, J.-P. Melder, K. Weber, D. Hunkler and H. Prinzbach, *J. Am. Chem. Soc.*, 1993, **115**, 7173; H. Prinzbach and K. Weber, *Angew. Chem., Int. Ed. Engl.*, 1994, **33**, 2239.

11 A. Schuster and D. Kuck, *Angew. Chem., Int. Ed. Engl.*, 1991, **30**, 1699; R. Haag, B. Ohlhorst, M. Noltemeyer, R. Fleischer, D. Stalke, A. Schuster, D. Kuck and A. de Meijere, *J. Am. Chem. Soc.*, 1995, **117**, 10 474.

12 G. Dyker, J.Körning, P. G. Jones and P. Bubenitschek, *Angew. Chem., Int. Ed. Engl.*, 1995, **34**, 2502.

*Received in Cambridge, UK, 18th August 1997; 7/06047E*

# A three stranded β-sheet peptide in aqueous solution containing *N*-methyl amino acids to prevent aggregation

**Andrew J. Doig***

*Department of Biomolecular Sciences, UMIST, PO Box 88, Manchester, UK M60 1QD*

**A three stranded β-sheet peptide of *de novo* design with *N*-methyl amino acids to prevent aggregation folds upon heating.**

Peptides which fold in isolation provide a useful way to study protein secondary structure and stability. The α-helix has been studied in this way for a number of years since the discovery that *de novo* designed peptides of 15–20 amino acids in length, composed primarily of alanine, form isolated α-helices in water.[1] In contrast to the mature field of α-helical peptides, β-sheet peptides are much less well understood. A challenge is to synthesise a peptide which will fold into a β-sheet in aqueous solution without aggregation. Synthetic polypeptides that form β-sheets generally form large, insoluble structures comprising many polypeptide chains that are intractable for further study in aqueous solution. However, success has been achieved using both peptides containing natural amino acids[2–13] and with β-sheet formation promoted by non-peptide units.[14–20] Here a peptide designed to fold into a three-stranded β-meander is synthesised, and the fact that it folds into a β-sheet is demonstrated by circular dichroism (CD) spectroscopy.

The β-meander, sequence Ac-YGD(*N*-Me-A)A(*N*-Me-A)APGVVDDVVPGD(*N*-Me-A)AVA(*N*-Me-A)-$CONH_2$, was designed to fold into the structure shown in Fig. 1. Aggregation is avoided in two ways. Firstly, negatively charged Asp side chains are located on both faces of the sheet to introduce intermolecular charge repulsions. Secondly, both outer edges of the sheet have two *N*-methylated amino acids. The *N*-methyl bonds are unable to participate in intermolecular hydrogen bonding and hence the peptides will remain monomeric. These residues are also restricted in their backbone conformations to the β-sheet geometry, which further facilitates folding.[21] *N*-Methylation has previously been used to prevent dimerisation of Interleukin-8 by blocking intermolecular hydrogen bonding.[22] Ghadiri *et al*. have *N*-methylated peptide nanotubes on one side so that they form dimers tractable to NMR spectroscopy and X-ray crystallography.[23]

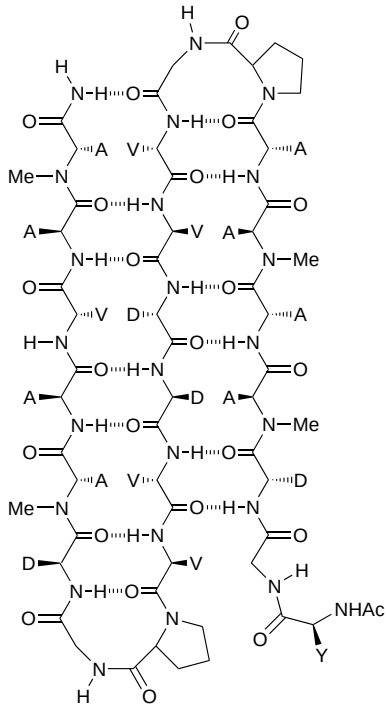



**Fig. 1** Design of the three stranded β-meander peptide

The other amino acids in the sheet were chosen as follows: Pro-Gly is the most commonly observed turn sequence in proteins,[24] while valine residues have a strong preference for β-sheets.[25,26] The formation of the N–Me to C=O bond is synthetically challenging.[27] This is generally made easier by forming *N*-Me-Ala to Ala bonds where possible. In particular, β-branched amino acids are avoided preceding *N*-methyl amino acids. The Gly-Tyr sequence is designed to give the peptide a UV absorbance unperturbed by secondary structure for accurate concentration determination.[28]

The syntheses of peptides containing *N*-methyl amino acids or those that form β-sheets are particularly difficult. The peptide designed here is therefore doubly challenging to synthesise. Peptides were synthesised by the solid phase method using Fmoc chemistry. Success was first achieved with Rink resin and Fmoc amino acids and the reagent TBTU [(benzotriazol-1-yloxy)tris(pyrrolidino)phosphonium hexafluorophosphate] in four-fold excess in the presence of $Pr^i_2EtN$, as judged by analytical fast protein liquid chromatography (FPLC) on the crude yield and confirmed by mass spectrometry. The yield was too low for further analysis so the powerful new reagents, HATU [*O*-(7-azabenzotriazol-1-yl)-1,1,3,3-tetramethyluronium hexafluorophosphate] and HOAt (1-hydroxy-7-azabenzotriazole)[29,30] were used with Fmoc-PAL-PEG-PS resin and double coupling cycles for the N–Me to C=O bonds. *N*-Termini were acetylated using pyridine and $Ac_2O$. Cleavage from the resin was achieved with TFA–anisole (19 : 1). After precipitation of the peptide–TFA mixtures into dry ice-coooled $Et_2O$, the peptides were purified by $C_{18}$ reverse-phase FPLC (Pharmacia) using a $H_2O$–MeCN gradient of 10–30% containing 0.1% TFA, followed by size-exclusion chromatography, giving a 10% yield (10 mg) of the target product.

The peptide is soluble in aqueous solution up to at least 2 mM concentration and appears to be monomeric by size exclusion chromatography and 1D NMR line shape analysis (data not shown). CD spectra were acquired at 18 μM concentration, pH 7, 5 mM phosphate buffer, 10 mM NaCl. Fig. 2 shows the CD spectra acquired at 293, 313 and 333 K. At 293 K the peptide is a mixture of random coil and β-sheet. Remarkably, it folds upon heating, giving a classic β-sheet spectrum at 333 K, with a minimum at 219 nm.[31] Hence, β-sheet formation is endothermic. The isodichroic point at 212 nm suggests that the sheet/coil transition is two-state.

It is proposed that *N*-methylation of NH groups on the outer edges of a β-sheet is a general solution to the problem of β-sheet aggregation. The peptide developed here may provide a suitable model system for investigating a range of aspects of β-sheet stability and folding.

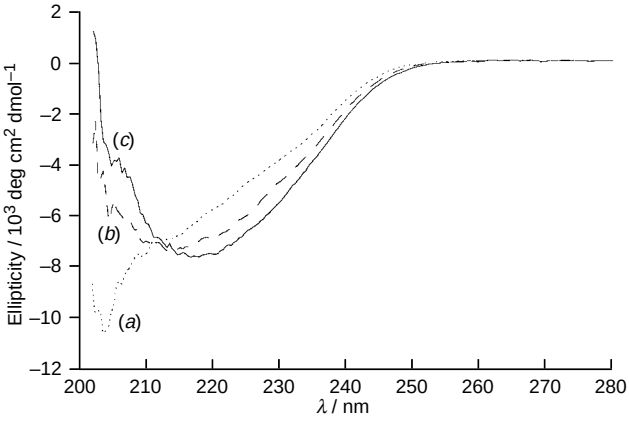



**Fig. 2** CD Spectra of the β-meander (pH 7, 5 mM phosphate, 10 mM NaCl) at (*a*) 20, (*b*) 40 and (*c*) 60 °C

This work was supported by grants from the BBSRC Seed Corn Initiative (36/SCI03358) and the Nuffield Foundation (SCI/180/94/9/G). We thank Ron Burke at the Department of Biomolecular Sciences, UMIST and Andy Felton at ABI for help with peptide synthesis, Derek Barratt at Zeneca Pharmaceuticals, Alderley Edge, for the use of the CD spectropolarimeter and Ian Fleet and Simon Gaskell at the Michael Barber Centre for Mass Spectrometry, UMIST for verification of peptide identity.

## Footnote and References

* E-mail: Andrew.Doig@umist.ac.uk

1 A. Chakrabartty and R. L. Baldwin, *Adv. Protein Chem.*, 1995, **46**, 141.
2 F. J. Blanco, M. A. Jimenez, J. Herranz, M. Rico, J. Santoro and J. L. Nieto, *J. Am. Chem. Soc.*, 1993, **115**, 5887.
3 F. J. Blanco, G. Rivas and L. Serrano, *Nat. Struct. Biol.*, 1994, **1**, 584.
4 M. S. Searle, D. H. Williams and L. C. Packman, *Nat. Struct. Biol.*, 1995, **2**, 999.
5 M. Ramírez-Alvarado, F. J. Blanco and L. Serrano, *Nat. Struct. Biol.*, 1996, **3**, 604.
6 M. S. Searle, R. Zerella, D. H. Williams and L. C. Packman, *Protein Eng.*, 1996, **9**, 559.
7 V. Sieber and G. R. Moe, *Biochemistry*, 1996, **35**, 181.
8 R. L. Fahrner, T. Dieckmann, S. S. L. Harwig, R. I. Lehrer, D. Eisenberg and J. Feigon, *Chem. Biol.*, 1996, **3**, 543.
9 E. DeAlba, F. J. Blanco, M. A. Jimenez, M. Rico and J. L. Nieto, *Eur. J. Biochem.*, 1995, **233**, 283.
10 E. DeAlba, M. A. Jimenez and M. Rico, *J. Am. Chem. Soc.*, 1997, **119**, 175.
11 T. S. Haque and S. H. Gellman, *J. Am. Chem. Soc.*, 1997, **119**, 2303.
12 E. DeAlba, M. A. Jimenez, M. Rico and J. L. Nieto, *Folding Des.*, 1996, **1**, 133.
13 A. J. Maynard and M. S. Searle, *Chem. Commun.*, 1997, 1297.
14 D. S. Kemp, B. R. Bowen and C. C. Muendel, *J. Org. Chem.*, 1990, **55**, 4650.
15 V. Brandmeier, W. H. B. Sauer and M. Fiegel, *Helv. Chim. Acta*, 1994, **77**, 70.
16 C. L. Nesloney and J. W. Kelly, *J. Am. Chem. Soc.*, 1996, **118**, 5836.
17 J. S. Nowick, E. M. Smith and M. Pairish, *Chem. Soc. Rev.*, 1996, **25**, 401.
18 J. S. Nowick, D. L. Holmes, G. Mackin, G. Noronhas, A. J. Shaka and E. Smith, *J. Am. Chem. Soc.*, 1996, **118**, 2764.
19 R. R. Gardner, G.-B. Liang and S. H. Gellman, *J. Am. Chem. Soc.*, 1995, **117**, 3280.
20 D. S. Kemp and Z. Q. Li, *Tetrahedron Lett.*, 1995, **36**, 4175.
21 P. Manavalan and F. A. Momany, *Biopolymers*, 1980, **19**, 1943.
22 K. Rajarathnam, B. D. Sykes, C. M. Kay, B. Dewald, T. Geiser, M. Baggiolini and I. Clark-Lewis, *Science*, 1994, **264**, 90.
23 M. R. Ghadiri, K. Kobayashi, J. R. Granja, R. K. Chadha and D. E. McRee, *Angew. Chem., Int. Ed. Engl.*, 1995, **34**, 93.
24 C. M. Wilmot and J. M. Thornton, *J. Mol. Biol.*, 1988, **203**, 221.
25 D. L. Minor, Jr. and P. S. Kim, *Nature*, 1994, **367**, 660.
26 C. K. Smoth, J. M. Withka and P. S. Kim, *Biochemistry*, 1994, **33**, 5510.
27 J. Coste, E. Frerot, P. Jouin and B. Castro, *Tetrahedron Lett.*, 1991, **32**, 1967.
28 A. Chakrabartty, T. Kortemme, S. Padmanabhan and R. L. Baldwin, *Biochemistry*, 1993, **32**, 5560.
29 L. A. Carpino, *J. Am. Chem. Soc.*, 1993, **115**, 4397.
30 L. A. Carpino, A. El-Faham, C. Minor and F. J. Alberico, *J. Chem. Soc., Chem. Commun.*, 1994, 201.
31 L. Tistra and W. L. Mattice, *Circular Dichroism and the Conformational Analysis of Biomolecules*, ed. G. D. Fasman, Plenum, New York, 1996, 261.

*Received in Glasgow, UK, 22nd August 1997; 7/06167F*

# Novel pyridyl-stabilised rigid-rod organometallic polymers and their monomeric precursors

**Christopher J. Adams, Stuart L. James and Paul R. Raithby***

*Department of Chemistry, University of Cambridge, Lensfield Road, Cambridge, UK CB2 1EW*

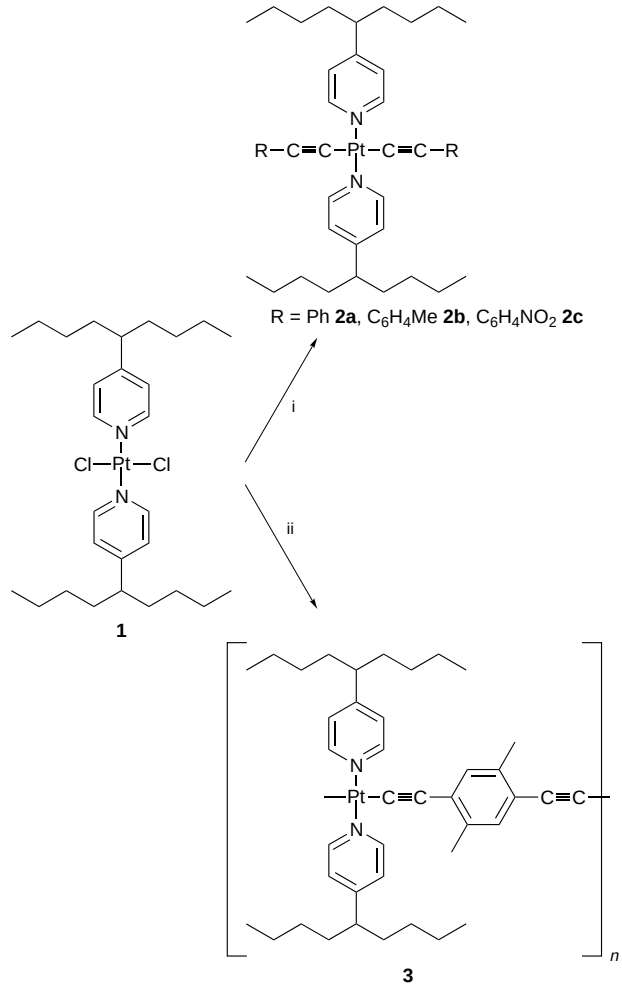
**Reaction of *trans*-[Pt(NC$_5$H$_4$CHBu$^n$$_2$)$_2$Cl$_2$] 1 with an excess of HC≡CR (R = Ph, C$_6$H$_4$Me, C$_6$H$_4$NO$_2$) affords the monomeric complex *trans*-[Pt(NC$_5$H$_4$CHBu$^n$$_2$)$_2$(C≡CR)$_2$] (R = Ph 2a, C$_6$H$_4$Me 2b, C$_6$H$_4$NO$_2$ 2c), the *trans* arrangement of the alkynyl ligands being confirmed from spectroscopic data and by an X-ray analysis of 2c; when 1 is treated with 1 equiv. of HC≡CC$_6$H$_2$(Me)$_2$C≡CH the polymer [Pt(NC$_5$H$_4$CHBu$^n$$_2$)$_2$C≡CC$_6$H$_2$Me$_2$C≡C]$_n$ is formed, which is soluble in a range of organic solvents.**

There is considerable current interest in σ-alkynyl transition-metal complexes and in the polymers formed from them because of their potential for use as non-linear optical, low-dimensional conducting, luminescent or liquid-crystalline materials.[1] Within this group the 'rigid-rod' *trans*-bis(σ-alkynyl) systems with the general formula [ML$_x$–C≡C–R–C≡C]$_n$ (M = Fe, Ru, Os, Ni, Pd, Pt; L = phosphine, arsine, *n* = 2,4; R = C$_6$H$_4$, C$_6$H$_2$Me$_2$, C$_6$H$_2$F$_2$, C$_4$H$_4$S, C$_{14}$H$_8$)[2] have been shown to exhibit a variety of novel electronic properties.[3] The ancillary ligands, L, in these metal-containing polymers are almost always phosphines, and this derives from the overwhelming proportion of monomeric platinum-group alkynyl precursor complexes which are stabilised by phosphines.[4] Imine donors are expected to impart different properties to both monomeric and polymeric systems, particularly with regard to their optical and redox behaviour.[5] We have, therefore, embarked on the development of platinum-group alkynyl chemistry with nitrogen donor ligands, and have recently reported the preparation of the *cis*-diimine stabilised complexes [(Me$_2$bipy)Pt(C≡CC$_6$H$_4$R-4)$_2$] (bipy = bipyridyl; R = H, Me, NO$_2$).[6] We now report the synthesis of the first diimine stabilised *trans*-bis(σ-alkynyl) platinum complex [Pt(NC$_5$H$_4$CHBu$^n$$_2$)$_2$(C≡CR)$_2$] (R = Ph **2a**, C$_6$H$_4$Me **2b**, C$_6$H$_4$NO$_2$ **2c**) and the formation of the novel polymer [Pt(NC$_5$H$_4$CHBu$^n$$_2$)$_2$C≡CC$_6$H$_2$Me$_2$C≡C]$_n$ **3**.

A frequent problem in the synthesis of σ-alkynyl complexes and the subsequent formation of the polymers is their insolubility in common organic solvents. In order to reduce this problem *trans*-[Pt(NC$_5$H$_4$CHBu$^n$$_2$)$_2$Cl$_2$] **1**, prepared by an adaption of the literature method,[7] was used as the starting material; the long hydrocarbon chains attached to the 4-position of the pyridine group greatly enhance the solubility. The reaction of **1** with 3 equiv. of HC≡CR (R = Ph, C$_6$H$_4$Me, C$_6$H$_4$NO$_2$), in the presence of catalytic amounts of CuI, in CH$_2$Cl$_2$ solution containing Pr$^i$$_2$NH, afforded [Pt(NC$_5$H$_4$CHBu$^n$$_2$)$_2$(C≡CR)$_2$] (R = Ph **2a**, C$_6$H$_4$Me **2b**, C$_6$H$_4$NO$_2$ **2c**) in high yield, after stirring for 1 h (Scheme 1). The products were isolated as crystalline solids after purification by column chromatography on alumina using CH$_2$Cl$_2$–hexane (1 : 1) as eluent. The products were characterised initially by IR, $^1$H and $^{13}$C NMR spectroscopy, and by mass spectrometry.† The single ν(C≡C) stretching frequency in the range 2102–2098 cm$^{-1}$ in the IR spectrum confirmed the presence of the σ-alkynyl ligands, consistent with the *trans* geometry.

In order to confirm the *trans* geometry of the products a single-crystal X-ray analysis of **2c** was undertaken. The molecular structure‡ is illustrated in Fig. 1 which includes selected bond parameters. The Pt atom sits on a crystallographic centre of symmetry, which imposes exact planarity at the metal centre, and requires the two alkynyl groups and the two substituted pyridine ligands to occupy mutually *trans* positions, respectively. The Pt–C(21)–C(22) alkynyl unit is essentially linear. The geometry is similar to that found in a number of *trans*-bis(phosphine) stabilised platinum bis(alkynyl) complexes,[8] and the Pt–C(21) distance lies within the range 1.98(1)–2.06(1) Å found in the other complexes.

The reaction of **1** with 1 equiv. of HC≡CC$_6$H$_2$Me$_2$C≡CH, under the same reaction conditions as described above, afforded, after purification, the polymer *trans*-[Pt(NC$_5$H$_4$CHBu$^n$$_2$)$_2$C≡CC$_6$H$_2$Me$_2$C≡C]$_n$ **3** as a brown solid in moderate yield (Scheme 1). The polymer was characterised by spectroscopic techniques,† and the presence of the σ-alkynyl confirmed by the presence of the ν(C≡C) stretching vibration in




**Scheme 1** i, 3 equiv. HC≡CR (R = Ph **2a**, C$_6$H$_4$Me **2b**, C$_6$H$_4$NO$_2$ **2c**), catalytic amount of CuI in Pr$^i$$_2$NH, CH$_2$Cl$_2$, stirred at room temp. for 1 h; ii, 1 equiv. HC≡CC$_6$H$_2$Me$_2$C≡CH, catalytic amount of CuI in Pr$^i$$_2$NH, CH$_2$Cl$_2$, stirred at room temp. for 1 h

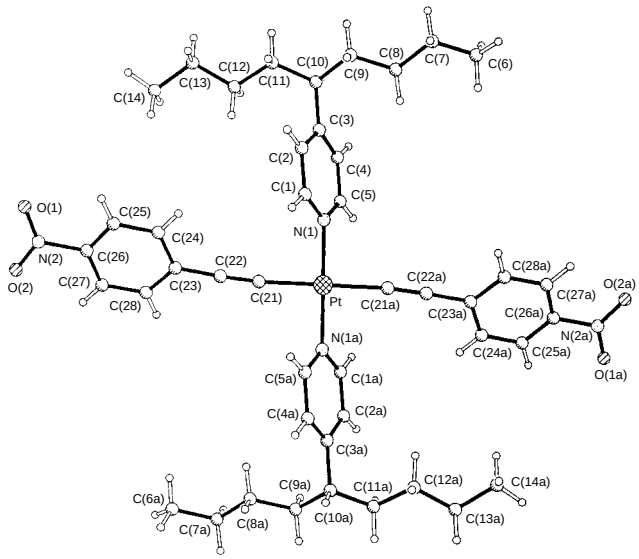



**Fig. 1** Molecular structure of **2c** showing the atom numbering scheme. Selected bond lengths (Å) and angles (°): Pt–N(1) 2.001(10), Pt–C(21) 2.02(2), C(21)–C(22) 1.21(2), C(22)–C(23) 1.42(2), C(26)–N(2) 1.49(2), N(2)–O(1) 1.22(2), N(2)–O(2) 1.22(2); N(1)–Pt–C(21) 88.2(4), N(1)–Pt–C(21A) 91.8(4), Pt–C(21)–C(22) 174.8(11), C(21)–C(22)–C(23) 174(2), O(1)–N(2)–C(26) 118.2(13), O(2)–N(2)–C(26) 116.1(14), O(1)–N(2)–O(2) 125.6(14).

the IR spectrum. As in other σ-alkynyl polymers[9] this $\nu$(C≡C) stretch does not show a significant shift from the position in the precursor complex. The $^{13}$C NMR spectrum confirmed the presence of both the arene spacer group and the substituted pyridine ligands, but in common with other 'rigid-rod' polymers chemical shifts corresponding to the σ-alkynyl carbons were not observed.[2,3]

Unlike many of the phosphine-stabilised 'rigid-rod' polymers **3** is soluble in a range of organic solvents. Therefore, it has been possible to run a series of electronic spectra to observe the shift in the absorption consistent with the greater delocalisation of electron density through the extended π-system along the polymer chain. In the free ligand, $HC{\equiv}CC_6H_2Me_2C{\equiv}CH$, two strong absorptions are observed at $\lambda_{max}$ = 263.8 nm ($\varepsilon$ = 1.9 × 10$^4$ dm$^3$ mol$^{-1}$ cm$^{-1}$) and $\lambda_{max}$ = 273.3 (2.31 × 10$^4$) in the UV region. For the precursor complex *trans*-[Pt(NC$_5$H$_4$CHBu$^n$$_2$)$_2$Cl$_2$] **1** one broad absorption is observed at $\lambda_{max}$ = 252.5 nm ($\varepsilon$ = 9.39 × 10$^3$ dm$^3$ mol$^{-1}$ cm$^{-1}$), while in the alkynyl-substituted monomer [Pt(NC$_5$H$_4$CHBu$^n$$_2$)$_2$-(C≡CPh)$_2$] **2a** the absorption is slightly shifted to $\lambda_{max}$ = 281.0 nm ($\varepsilon$ = 3.53 × 10$^4$ dm$^3$ mol$^{-1}$ cm$^{-1}$). In contrast, for the polymer there is a considerable shift in absorption to $\lambda_{max}$ = 342.2 nm ($\varepsilon$ = 2.92 × 10$^4$ dm$^3$ mol$^{-1}$ cm$^{-1}$), again a very broad band being observed. This shift in the position of the absorption is consistent with the greater delocalisation along the polymer chain. Similar shifts in the absorption spectra have been observed previously for related systems.[10]

We thank the EPSRC for support (to C. J. A. and S. L. J.), and Dr J. E. Davies for assistance with X-ray data collection.

## Footnotes and References

* E-mail: prr1@cam.ac.uk

† **2a**: IR $\nu$(C≡C)/cm$^{-1}$ ($CH_2Cl_2$) 2102; *m/z* 807.8 (M$^+$); $^1$H NMR ($CDCl_3$) $\delta$ 9.31 (d, 2 H, *J* 6.73 Hz), 7.23 (m, 5 H), 7.03 (d, 2 H, *J* 6.79 Hz), 2.50 (qnt, 1 H), 1.2 (m, 18 H); $^{13}$C NMR ($CDCl_3$) $\delta$ 158.05 (py), 155.44 (py), 131.67 (arene), 127.8 (arene), 125.46 (arene), 124.6 (py), 119.2 (C≡C), 100.13 (C≡C), 45.73 (nonyl), 35.64 (nonyl), 29.59 (nonyl), 22.67 (nonyl), 13.9 (nonyl). **2b**: IR $\nu$(C≡C)/cm$^{-1}$ ($CH_2Cl_2$) 2102; *m/z* 835.7 (M$^+$); $^1$H NMR ($CDCl_3$) $\delta$ 9.32 (d, 2 H, *J* 6.72 Hz), 7.22 (d, 2 H, *J* 8 Hz), 7.01 (d, 2 H, *J* 6.8 Hz), 6.98 (d, 2 H, *J* 8 Hz), 2.50 (qnt, 1 H), 2.27 (s, 3 H), 1.2 (m, 18 H); $^{13}$C NMR ($CDCl_3$) $\delta$ 157.92 (py), 155.5 (py), 135.14 (toluene), 131.5 (toluene), 128.6 (toluene), 124.8 (toluene), 124.5 (py), 118.2 (C≡C), 100.0 (C≡C), 45.7 (nonyl), 35.6 (nonyl), 29.5 (nonyl, 22.6 (nonyl), 21.3 (nonyl), 13.9 (nonyl). **2c**: IR $\nu$(C≡C)/cm$^{-1}$ ($CH_2Cl_2$) 2098; *m/z* 898.5 (M$^+$); $^1$H NMR ($CDCl_3$) $\delta$ 9.16 (d, 2 H, *J* 6.75 Hz), 7.36 (d, 2 H, *J* 5. Hz), 7.11 (d, 2 H, *J* 7 Hz), 3.05 (d, 2 H, *J* 5.Hz), 2.56 (qnt, 1 H), 1.25 (m, 18 H); $^{13}$C NMR ($CDCl_3$) $\delta$ 158.9 (py), 154.9 (py), 145.0 (arene), 132.0 (arene), 127.9 (arene), 124.9 (py), 123.4 (arene), 100.12 (C≡C), 82.3 (C≡C), 45.76 (nonyl), 35.6 (nonyl), 22.6 (nonyl), 13.9 (nonyl). **3**: IR $\nu$(C≡C)/cm$^{-1}$ ($CH_2Cl_2$) 2097; $^1$H NMR ($CDCl_3$) $\delta$ 9.29 (d, 2 H, *J* 6.98 Hz), 7.01 (s, 2 H), 6.98 (d, 2 H, *J* 6.8 Hz), 2.49 (qnt, 1 H), 2.16 (s, 6 H), 1.10 (m, 18 H); $^{13}$C NMR ($CDCl_3$) $\delta$ 157.6 (py), 155.43 (py), 135.97 (arene), 132.3 (arene), 124.51 (py), 124.3 (arene), 45.65 (nonyl), 35.64 (nonyl), 29.5 (nonyl), 22.61 (nonyl), 20.4 (arene), 13.88 (nonyl). Satisfactory microanalyses were obtained on all the complexes.

‡ *Crystal data* for **2c**: $C_{44}H_{54}N_4O_4Pt$, $M_r$ = 898.00, monoclinic, space group $P2_1/c$, $a$ = 7.693(2), $b$ = 22.908(5), $c$ = 11.738(2) Å, $\beta$ = 94.35(3)°, $U$ = 2062.6(8) Å$^3$, $Z$ = 2, $D_c$ = 1.446 g cm$^{-3}$, $\mu$ = 3.447 mm$^{-1}$ for Mo-K$\alpha$ radiation ($\lambda$ = 0.710 73 Å), $F$(000) = 912, $T$ = 153(2) K. 3471 Refelctions measured on a Rigaku AFC7R diffractometer, 2696 unique absorption corrected ($R_{int}$ = 0.082) used for structure solution (Patterson) and refinement (full-matrix least squares on $F^2$, anisotropic displacement parameters for non-H atoms, riding isotropic H-atoms); $R_1$ = 0.053 for 1670 reflections with $I > 2\sigma(I)$ and $wR_2$ = 0.172 for all data, goodness of fit = 1.079 for all $F^2$ values, 243 parameters; final difference map showed only ripples in the vicinity of the Pt atom. Programs: TeXsan, SHELXTL-PLUS and SHELXL 93. CCDC 182/614.

1 N. J. Long, *Angew. Chem., Int. Ed. Engl.*, 1995, **34**, 21; I. Manners, *Angew. Chem., Int. Ed. Engl.*, 1996, **35**, 1602; A. Harriman and R. Ziessel, *Chem. Commun.*, 1996, 1707.
2 S. J. Davies, B. F. G. Johnson, M. S. Khan and J. Lewis, *J. Chem. Soc., Chem. Commun.*, 1991, 187; B. F. G. Johnson, A. K. Kakkar, M. S. Khan and J. Lewis, *J. Organomet. Chem.*, 1991, **409**, C12; Z. Atherton, C. W. Faulkner, S. L. Ingham, A. K. Kakkar, M. S. Khan, J. Lewis, N. J. Long and P. R. Raithby, *J. Organomet. Chem.*, 1993, **462**, 265; M. S. Khan, A. K. Kakkar, S. L. Ingham, P. R. Raithby, J. Lewis, B. Spencer, F. Wittman and R. H. Friend, *J. Organomet. Chem.*, 1994, **472**, 247.
3 J. Lewis, M. S. Khan, A. K. Kakkar, B. F. G. Johnson, T. B. Marder, H. B. Fyfe, F. Wittmann and R. H. Friend, *J. Organomet. Chem.*, 1992, **425**, 165; M. S. Khan, A. K. Kakkar, N. J. Long, J. Lewis, P. R. Raithby, P. Nguyen, T. B. Marder, F. Wittmann and R. H. Friend, *J. Mater. Chem.*, 1994, **4**, 1227; A. E. Dray, F. Wittmann, R. H. Friend, A. M. Donald, M. S. Khan, J. Lewis and B. F. G. Johnson, *Synth. Met.*, 1991, **41**–**43**, 871; C. W. Faulkner, S. L. Ingham, M. S. Khan, J. Lewis, N. J. Long and P. R. Raithby, *J. Organomet. Chem.*, 1994, **482**, 139; A. Köhler, H. F. Wittmann, R. H. Friend, M. S. Khan and J. Lewis, *Synth. Met.*, 1994, **67**, 245; D. Beljonne, F. H. Wittmann, A. Köhler, S. Graham, M. Younus, J. Lewis, P. R. Raithby, M. S. Khan, R. H. Friend and J. L. Brédas, *J. Chem. Phys.*, 1996, **105**, 3868; D. Beljonne, M. C. B. Colbert, P. R. Raithby, R. H. Friend and J. L. Brédas, *Synth. Met.*, 1996, **81**, 179.
4 R. Nast, *Coord. Chem. Rev.*, 1982, **47**, 89; J. Manna, K. D. John and M. D. Hopkins, *Adv. Organomet. Chem.*, 1995, **38**, 79.
5 D. Collison, F. E. Mabbs, E. J. L. McInnes, K. J. Taylor, A. J. Welch and L. J. Yellowlees, *J. Chem. Soc., Dalton Trans.*, 1996, 329; E. J. L. McInnes, A. J. Welch and L. J. Yellowlees, *Chem. Commun.*, 1996, 2393.
6 S. L. James, J. Lewis, P. R. Raithby and M. Younus, *J. Organomet. Chem.*, in the press.
7 P.-C. Kong and F. D. Rochon, *Can. J. Chem.*, 1978, **56**, 441.
8 R. A. Mariezcurrena and S. E. Rasmussen, *Acta Chem. Scand.*, 1973, **27**, 2678; A. Sebald, C. Strader and B. Wrackmeyer, *J. Organomet. Chem.*, 1986, **311**, 233; J. P. Carpenter and C. M. Lukehart, *Inorg. Chim. Acta.*, 1991, **190**, 7; L. Manojlovic-Muir, A. N. Henderson, I. Treurnicht and R. J. Puddephatt, *Organometallics*, 1989, **8**, 2055.
9 A. J. Hodge, S. L. Ingham, A. K. Kakkar, M. S. Khan, J. Lewis, N. J. Long, D. G. Parker and P. R. Raithby, *J. Organomet. Chem.*, 1995, **488**, 205.
10 W. Blau, H. J. Byrne, D. J. Cardin and A. P. Davey, *J. Mater. Chem.*, 1991, **1** 245.

*Received in Basel, Switzerland, 9th September 1997; 7/06586H*

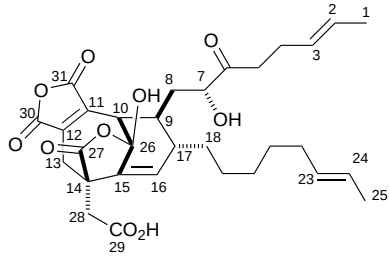
# Synthesis of the carbobicyclic substructure of CP-225,917 and CP-263,114

**Paulo W. M. Sgarbi and Derrick L. J. Clive***

*Chemistry Department, University of Alberta, Edmonton, Alberta, Canada T6G 2G2*

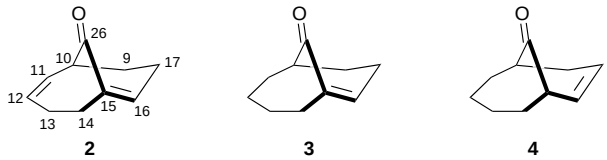
**The bridgehead alkenic ketones 22a and 22b, representing the carbobicyclic substructure of the squalene synthase and farnesyl transferase inhibitors CP-225,917 (1) and CP-263,114 (23), have been synthesized from the 7-norbornenone acetal 8, using an anionic oxy-Cope rearrangement of 21a and 21b in the key step; the synthesis serves as a test of a potential route to both natural products.**

The structurally complex anhydride **1** was isolated from the fermentation broth of an unidentified fungus, and described recently by chemists at Pfizer Central Research.[1,2] The substance is related to the nonadrides[3]—at least on the basis of its proposed[2] biosynthetic origin. It was given the designation CP-225,917, and was found[1] to inhibit squalene synthase[4] (from rat liver) and Ras farnesyl transferase[5] (from rat brain). Inhibition of these enzymes represents an opportunity for controlling serum cholesterol levels[6] as well as certain types of abnormal cell growth,[5] and so **1** may serve as a lead in the design of cholesterol-lowering and anticancer drugs.



**1**

CP-225,917 is the hemiacetal of a bicyclo[4.3.1]decadienone substructure **2**,† and one of its notable features is the bridgehead double bond. Although the related olefinic ketone **3** (which was obtained in admixture with the isomer **4**) has been prepared,[7] the method used to make that particular compound does not seem well-suited to the task of synthesizing the natural product. We report a model study[8,9] that establishes a route to **22a** and **22b** (see Scheme 2), both of which we take to represent the [4.3.1]-carbobicyclic substructure of CP-225,917.

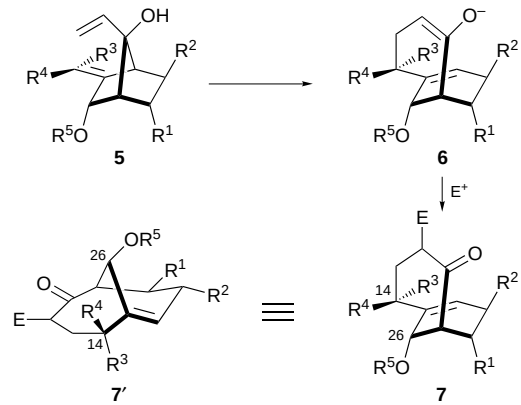


**2** **3** **4**

Our approach is based on the idea that anionic oxy-Cope rearrangement‡ of compounds such as **5** (Scheme 1) should lead to enolates **6**, which have a number of features that are appropriate for further elaboration in the desired manner (**6**→**7**/**7′**). In particular, the C(26) oxygen function of **7**/**7′** could provide the corresponding acetal unit of **1**, and the enolate **6** would offer several opportunities for constructing the anhydride, perhaps by initial capture with an electrophile, such as Mander's reagent.[11] The route summarized in Scheme 1 should also be able to accommodate introduction of two substituents at C(14) (see **7**/**7′**), which is a quaternary centre in the natural product.

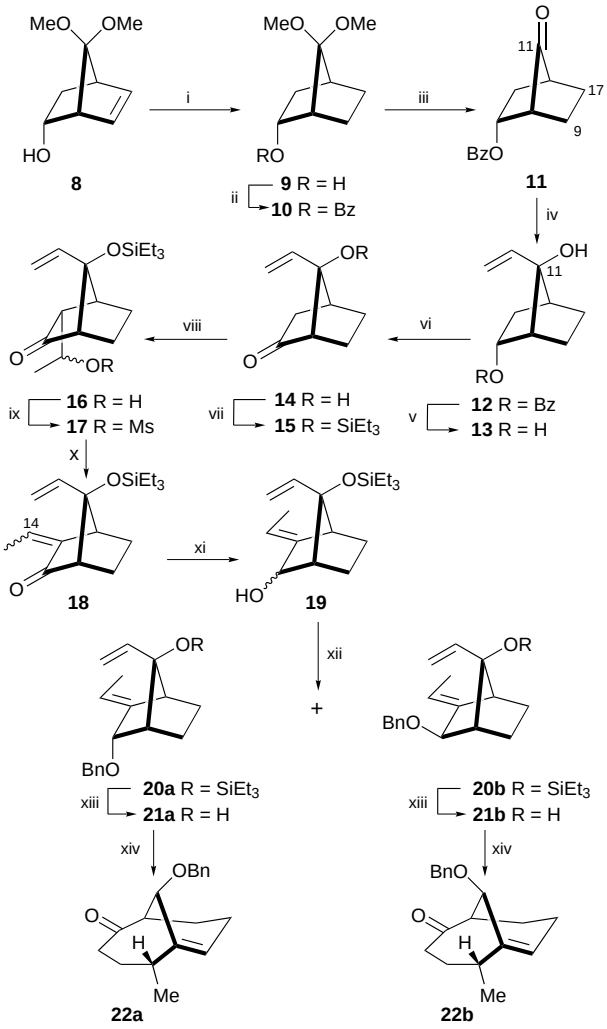
Our model study (Scheme 2) began with the readily available norbornene **8**.[12] The double bond was first saturated (**8**→**9**; Pd–C, $H_2$; 92%), and the resulting alcohol was then benzoylated (BzCl, pyridine; 98%) and treated with aqueous acetic acid to hydrolyse the acetal (**9**→**10**→**11**). When esterification was omitted, extensive decomposition occurred during attempts at deacetalization, presumably by a retroaldol process. Ketone **11** is quite sensitive, and so it was used without purification. While we had originally planned to introduce a vinyl group at C(11) (*cf.* **11**→**12**) by an intramolecular Barbier reaction, we wondered if adequate facial selectivity would be observed for a simple intermolecular process[13] and, in the event, treatment of crude **11** with vinylmagnesium bromide in $Et_2O$ gave a ≥5 : 1 mixture of tertiary alcohols, with the desired isomer **12** being the major product. In the present study, carbons C(9) and C(17) of **11** are unsubstituted; in a more advanced model those carbons would carry alkyl groups, and steric factors may improve the already satisfactory product ratio. Separation of the C(11) isomers could be performed chromatographically after hydrolysis of the benzoyl group (**12**→**13**; LiOH, 9 : 1 THF–water, 60 °C; 44% overall from **10**; 9% of C(11) isomer of **13**). Oxidation of the major diol (**13**) was initially problematic, until we tried the Dess–Martin reagent,[14] which smoothly converts **13** into keto alcohol **14** (93%).

The next task was to protect the tertiary hydroxy group (**14**→**15**) in order to avoid retroaldol fragmentation.[15] $Et_3$-SiOTf in the presence of 2,6-lutidine proved to be a satisfactory combination of reagents (84%); attempts to introduce *tert*-butyldimethylsilyl or *p*-methoxybenzyl groups were unsuccessful. The remainder of the hexa-1,5-diene subunit required for the anionic oxy-Cope rearrangement was assembled by a short sequence, beginning with aldol condensation (**15**→**16**; LDA, THF, −78 °C; excess of MeCHO; > 76%), so as to form the β-hydroxy ketones **16** as an isomer mixture. Without separation, these alcohols were converted into the corresponding mesylates **17** (MsCl, $Et_3N$, $CH_2Cl_2$, 0 °C) and, again without isomer separation, the mesylates were treated with DBU (THF, room temperature), affording the desired enones **18**, which were easily separable (*E*-isomer, 60% overall from **15**; *Z*-isomer, 11% overall from **15**).§ As a matter of convenience, only the major ketone was taken further. Reduction (**18**→**19**; $NaBH_4$,



**5** **6** **7′** **7**

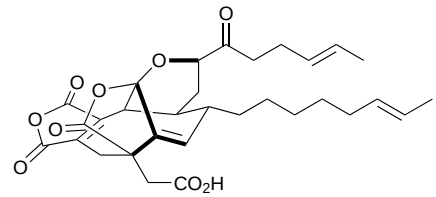
**Scheme 1**




**Scheme 2** *Reagents and conditions*: i, $H_2$, 10% Pd–C, MeOH, room temp., *ca*. 5 h, 92%; ii, BzCl, pyridine, room temp., 10 h, 98%; iii, 6 : 1 AcOH–$H_2O$, 150 °C, 40 min; iv, $H_2C$=CHMgBr, $Et_2O$, 0 °C, 40 min; v, LiOH·$H_2O$, 9 : 1 THF–$H_2O$, 80 °C, 12 h, 53% over 3 steps [44% for **13**, 9% for C(11) isomer of **13**]; vi, Dess–Martin periodinane, 33 : 1 $CH_2Cl_2$–DMSO, room temp., 12 h, 93%; vii, $Et_3SiOSO_2CF_3$, 2,6-lutidine, $CH_2Cl_2$, room temp., 1 h, 84%; viii, LDA, THF, −78 °C, 1 h, then MeCHO, −78 °C, 1 h; ix, $MeSO_2Cl$, $Et_3N$, $CH_2Cl_2$, 0 °C; x, DBU, THF, room temp., 1 h, 71% over 3 steps [60% isolated yield of (*E*)-alkene and 11% isolated yield of (*Z*)-alkene]; xi, $NaBH_4$, $CeCl_3$·$7H_2O$, MeOH, room temp., 1.5 h, 86% (*endo*-**19**, 42%; *exo*-**19**, 44%); xii, BnBr, NaH, THF, 70 °C, 24 h, 94% for **20a**, 70% for **20b**; xiii, $Bu_4NF$, THF, room temp., 2 min, 89% for **21a**, 89% for **21b**; xiv, $(Me_3Si)_2NK$, PhMe, 100 °C, 20 h, 95% for **22a**, 82% for **22b**

MeOH, $CeCl_3$·$7H_2O$; 86%) gave a 1 : 1 mixture of *endo*- (42% isolated yield) and *exo*-alcohols (44%), which were easily separated and individually protected by benzylation (*endo*-**19**→**20a**, 94%; *exo*-**19**→**20b**, 70%). At this point, desilylation of both **20a** and **20b** was accomplished under standard conditions ($Bu_4NF$, THF, room temperature; 89% for each compound) and finally, the resulting alcohols were subjected to anionic oxy-Cope rearrangement [$(Me_3Si)_2NK$, PhMe, 100 °C, *ca*. 20 h]. *endo*-Benzyl ether **21a** gave the bridgehead keto alkene **22a** (95%) and the *exo* isomer (**21b**) gave **22b** (82%), whose structures were confirmed by extensive $^1H$–$^1H$ COSY and ROESY NMR measurements. In neither case was the rate of oxy-Cope rearrangement noticeably increased by addition of 18-crown-6.

Formation of **22a** and **22b** (which is crystalline) serves as an initial test of the plan summarized in Scheme 1.




**23**

A closely related natural product (CP-263,114, **23**) was isolated along with CP-225,917, and found to have similar biological properties, although of a lower potency with respect to squalene synthase inhibition. The present work is, of course, equally relevant to the synthesis of the congener.

All new compounds, except **11**, one epimer of **16**, **17** and the C(11) epimer of **12**, were satisfactorily characterized by spectroscopic methods, including high resolution mass spectroscopic measurements.

Acknowledgment is made to the Natural Sciences and Engineering Research Council of Canada for financial support, and we thank Dr Yunxin Bo for advice. P. W. M. S. held a Graduate Scholarship from CNPq (Brazil).

## Footnotes and References

* E-mail: derrick.clive@ualberta.ca

† We use the non-systematic numbering given in ref. 2.

‡ For recent examples of the preparation of bicyclic systems by anionic oxy-Cope rearrangement, see ref. 10.

§ We have not yet explored the possibility of conjugate addition for introducing what will eventually be the second substituent at the quaternary centre [C(14)].

1 T. T. Dabrah, H. J. Harwood, L. H. Huang, N. D. Jankovich, T. Kaneko, J.-C. Li, S. Lindsey, P. M. Moshier, T. A. Subashi, M. Therrien and P. C. Watts, *J. Antibiot.*, 1997, **50**, 1.
2 T. T. Dabrah, T. Kaneko, W. Massefski, Jr. and E. B. Whipple, *J. Am. Chem. Soc.*, 1997, **119**, 1594.
3 *E.g.* J. E. Baldwin, D. H. R. Barton and J. K. Sutherland, *J. Chem. Soc.*, 1965, 1787 and earlier papers in the series; J. K. Sutherland, *Fortschr. Chem. Org. Naturst.*, 1967, **25**, 131.
4 N. S. Watson and P. A. Procopiou, *Prog. Med. Chem.*, 1996, **33**, 331.
5 S. B. Singh, J. M. Liesch, R. B. Lingham, M. A. Goetz and J. B. Gibbs, *J. Am. Chem. Soc.*, 1994, **116**, 11 606 and references cited therein.
6 J. D. Bergstrom, M. M. Kurtz, D. J. Rew, A. M. Amend, J. D. Karkas, R. G. Bostedor, V. S. Bansal, C. Dufresne, F. L. VanMiddlesworth, O. D. Hensens, J. M. Liesch, D. L. Zink, K. E. Wilson, J. Onishi, J. A. Milligan, G. Bills, L. Kaplan, M. Nallin Omstead, R. G. Jenkins, L. Huang, M. S. Meinz, L. Quinn, R. W. Burg, Y. L. Kong, S. Mochales, M. Mojena, I. Martin, F. Pelaez, M. T. Diez and A. W. Alberts, *Proc. Natl. Acad. Sci. USA*, 1993, **90**, 80; J. L. Goldstein and M. S. Brown, *Nature*, 1990, **343**, 425.
7 B. G. Cordiner, M. R. Vegar and R. J. Wells, *Tetrahedron Lett.*, 1970, 2285; *cf.* H. O. House and T. V. Lee, *J. Org. Chem.*, 1979, **44**, 2819.
8 *Cf.* K. C. Nicolaou, M. W. Härter, L. Boulton and B. Jandeleit, *Angew. Chem., Int. Ed. Engl.*, 1997, **36**, 1194.
9 *Cf.* H. M. L. Davies, R. Calvo and G. Ahmed, *Tetrahedron Lett.*, 1997, **38**, 1737.
10 S. F. Martin, J.-M. Assercq, R. E. Austin, A. P. Dantanarayana, J. R. Fishpaugh, C. Gluchowski, D. E. Guinn, M. Hartmann, T. Tanaka, R. Wagner and J. B. White, *Tetrahedron*, 1995, **51**, 3455; L. A. Paquette, *Chem. Soc. Rev.*, 1995, **24**, 9.
11 L. N. Mander and S. P. Sethi, *Tetrahedron Lett.*, 1983, **24**, 5425.
12 L. A. Paquette, K. S. Learn, J. L. Romine and H.-S. Lin, *J. Am. Chem. Soc.*, 1988, **110**, 879.
13 *Cf.* G. Mehta and F. Ahmad Khan, *J. Am. Chem. Soc.*, 1990, **112**, 6140; G. Mehta, F. Ahmad Khan, B. Ganguly and J. Chandrasekhar, *J. Chem. Soc., Perkin Trans. 2*, 1994, 2275.
14 R. E. Ireland and L. Liu, *J. Org. Chem.*, 1993, **58**, 2899.
15 *Cf.* L. A. Paquette and M.-A. Poupart, *J. Org. Chem.*, 1993, **58**, 4245.

*Received in Corvallis, OR, USA, 18th August 1997; 7/06075K*

# Copper(I) salt mediated 1,4-reduction of α,β-unsaturated ketones using hydrosilanes

**Atsunori Mori,* Akinori Fujita, Yasushi Nishihara and Tamejiro Hiyama**

*Research Laboratory of Resources Utilization, Tokyo Institute of Technology, Nagatsuta, Yokohama 226, Japan*

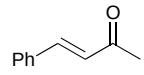
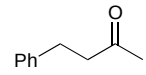
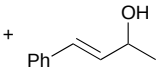
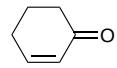
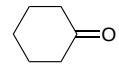
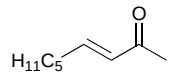
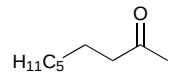
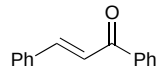
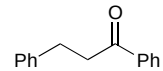
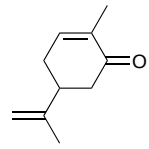
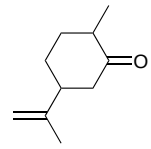
**Reduction of α,β-unsaturated ketones with $HSiPhMe_2$ in the presence of $CuF(PPh_3)_3{\cdot}2EtOH$ proceeds in a 1,4-selective manner to give the corresponding saturated ketones in excellent yields.**

Transfer of the organic groups of organosilanes to metallic species, *transmetalation*, has been our recent concern since a number of metal mediated synthetic reactions involve transmetalation as a key step.[1] The organometallic species thus formed may undergo further transformations, such as carbon–carbon or carbon–heteroatom bond formation, *via* reaction with several organic substrates.[2] We have disclosed that organosilicon compounds such as alkenyl-, aryl- and alkynyl-silanes induce homo-coupling reactions to yield the corresponding 1,3-dienes, biaryls and 1,3-diynes, respectively, in the presence of a copper(I) salt in a polar solvent.[3] The findings suggest that transmetalation of the organosilanes to copper occurs to give the organocopper species, the novel transmetalation being remarkable since an organic group on silicon is assumed to transfer onto copper without using an additional activator.[4,5] Our interest has accordingly turned to the transmetalation of hydrosilanes to copper to generate *copper hydride* species, with which reduction of a variety of organic molecules has been reported.[6] Although the combination of a copper salt and hydrosilane has rarely been studied when compared with reagents made from copper salts and the hydrides of metals such as aluminium and tin,[7] the desired reaction, we considered, would proceed with the proper choice of the counter ion and a ligand of copper. After screening several $Cu^I$ species, we found that the $CuF(PPh_3)_3$–$HSiPhMe_2$ system could effect 1,4-selective reduction of α,β-unsaturated ketones under mild conditions.

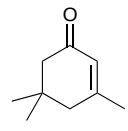
The reaction was studied using 1-phenylbut-1-en-3-one **1a** as substrate and HSiPhMe **2a** as the reducing agent in the presence of a copper(I) salt. The molar ratio of the substrate, hydrosilane and copper salt, as well as solvent, reaction temperature and reaction time were examined. We found that the use of 2 equiv. of **2a** and 1 equiv. of $CuF(PPh_3)_3{\cdot}2EtOH$[8] in *N*,*N*-dimethylacetamide (DMA) were the optimum conditions to yield 1-phenylbutan-2-one **3a** in a quantitative yield.† Results are summarized in Table 1. The yield decreased to 63% when 1 equiv. of **2a** was used. Using a catalytic amount of $CuF(PPh_3)_3{\cdot}2EtOH$, the reaction similarly proceeded with a slight decrease in yield, along with the formation of a small amount of unidentified product as well as a trace amount of 1,2-reduction product **4a**. Concerning the hydrosilane, **2a** and triethylsilane **2b** exhibited high 1,4-selectivities to give the corresponding ketone in excellent yields, but diphenylsilane **2c** considerably decreased the selectivity to give **3a** and **4a** in 49 and 36% yields, respectively, in contrast with the results on rhodium-catalysed hydrosilylation of α,β-unsaturated ketones.[9] No reaction occurred with $HSiPhCl_2$ **2d**.

Reactions using several other α,β-unsaturated ketones were carried out using similar optimized condition, as shown in Table 1. The reactions of **1a**–**e** proceeded in excellent yields with high 1,4-selectivity. However, sterically congested enones such as **1f**–**h** were recovered unchanged.‡ The results also contrast with those from the reactions catalysed by a rhodium complex,[9] which reduced enones **1f**–**h** smoothly in a highly 1,4-selective manner. In this sense, our systems appears to be highly chemoselective. Indeed, the reaction of a 1 : 1 mixture of **1a** and **1f** with **2a** in the presence of $CuF(PPh_3)_3{\cdot}2EtOH$ cleanly produced **3a** (99%), along with complete recovery of **1f** (97%) [eqn. (1)].

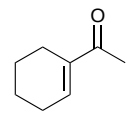
**Table 1** Copper(I) salt mediated reactions of α,β-unsaturated ketones with hydrosilanes in the presence of $CuF(PPh_3)_3{\cdot}2EtOH$[a]

| Substrate | Hydrosilane | Product (% yield) | |
|---|---|---|---|
|  | |  +  | |
| **1a** | **2a** $HSiPhMe_2$ | **3a** (>99) | — |
| **1a** | **2a** $HSiPhMe_2$ | **3a** (63)[b] | — |
| **1a** | **2a** $HSiPhMe_2$ | **3a** (69) | **4a** (trace)[c] |
| **1a** | **2b** $HSiEt_3$ | **3a** (95) | — |
| **1a** | **2c** $H_2SiPh_2$ | **3a** (49) | **4a** (36) |
| **1a** | **2d** $HSiPhCl_2$ | — | — |
|  | |  | |
| **1b** | **2a** $HSiPhMe_2$ | **3b** (91) | |
|  | |  | |
| **1c** | **2a** $HSiPhMe_2$ | **3c** (91) | |
|  | |  | |
| **1d** | **2a** $HSiPhMe_2$ | **3d** (98) | |
|  | |  | |
| **1e** | **2a** $HSiPhMe_2$[d] | **3e** (85)[e] | |

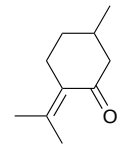
[a] Reactions were carried out using enone **1** (1.0 mmol), silane **2** (2.0 mmol) and $CuF(PPh_3)_3{\cdot}2EtOH$ **3** (1.0 mmol) unless otherwise specified. The yields are based on $^1H$ NMR analyses using $Cl_2C{=}CHCl$ as an internal standard. [b] One equiv. of **2a** was used. Accompanied by recovery of **1a** (21%). [c] $CuF(PPh_3)_3$ (5 mol%) was used. [d] 4 equiv. of **2a** was used. [e] Diastereoisomeric ratio was *ca.* 8 : 1.



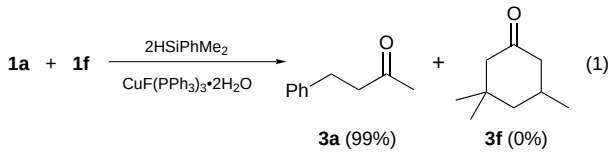
**1f**



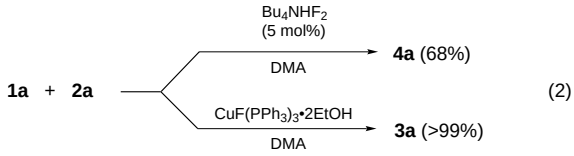
**1g**



**1h**




Although a mechanistic study of the transmetalation of organosilane to copper has yet to be undertaken, the activation of hydrosilanes by $CuF(PPh_3)_3{\cdot}2EtOH$ seems to be rather different from that by $Bu_4NF$ or the related reagents. The reaction of **1a** and **2a** in the presence of 5 mol% of $Bu_4NHF_2$[12] resulted in predominantly 1,2-reduced product **4a** in 68% yield. Thus, 1,4- and 1,2-selective reduction of α,β-unsaturated ketones with hydrosilanes are accessible by a suitable choice of copper(I) fluoride or $Bu_4NHF_2$ in a highly selective manner, respectively [eqn. (2)].




The authors thank Shin-Etsu Chemical Co. Ltd. for the generous donation of organosilicon reagents. This work was partially supported by a Grant-in-Aid for Scientific Research on Priority Areas (No. 09239102) from the Ministry of Education, Science, Sports and Culture, Japan.

## Footnotes and References

* E-mail: amori@res.titech.ac.jp

† *Typical experimental procedure*: $CuF(PPh_3)_3{\cdot}2EtOH$ (0.25 mmol) was dissolved in 2 ml of DMA to give a colourless clear solution, to which was added $HSiPhMe_2$ **2a** (0.5 mmol) at 0 °C to give a red homogeneous solution. The colour of the solution gradually changed to yellow after the addition of 1-phenylbut-1-en-3-one (**1a**, 0.25 mmol). The temperature of the reaction mixture was gradually raised to room temperature, and stirring was continued for 6 h to furnish **4a** in a quantitative yield after workup.

‡ The reaction of an α,β-unsaturated ester (methyl cinnamate) also resulted in no reaction. On the other hand, an α,β-unsaturated aldehyde (cinnamaldehyde) was found to effect 1,2-reduction, predominantly.

1 J. P. Collman, L. S. Hegedus, J. R. Norton and R. G. Finke, *Principles and Applications of Organotransition Metal Chemistry*, University Science Books, Mill Valley, CA, 1987.
2 E. W. Colvin, *Silicon Reagents in Organic Synthesis*, Academic Press, London, 1988.
3 K. Ikegashira, Y. Nishihara, K. Hirabayashi, A. Mori and T. Hiyama, *Chem. Commun.*, 1997, 1039; Y. Nishihara, K. Ikegashira, A. Mori and T. Hiyama, *Chem. Lett.*, in the press. See also: H. Ito, H.-o. Sensui, K. Arimoto, K. Miura and A. Hosomi, *Chem. Lett.*, 1997, 639; H. Ito, K. Arimoto, H.-o. Sensui and A. Hosomi, *Tetrahedron Lett.*, 1997, **38**, 3977; S.-K. Kang, T.-H. Kim and S.-J. Pyun, *J. Chem. Soc., Perkin Trans. 1*, 1997, 797.
4 The addition of a fluoride ion as an activator to form the pentacoordinate organosilicate is necessary for the palladium-catalysed cross-coupling of organosilanes: T. Hiyama and Y. Hatanaka, *Pure Appl. Chem.*, 1994, **66**, 1471 and references cited therein.
5 Another activation without fluoride ion is *in situ* generation of an activating species from allylic carbonates or diene monoxides as a substrate: H. Matsuhashi, S. Asai, K. Hirabayashi, Y. Hatanaka, A. Mori and T. Hiyama, *Bull. Chem. Soc. Jpn.*, 1997, **70**, 1943.
6 W. S. Mahoney, D. M. Brestensky and J. M. Stryker, *J. Am. Chem. Soc.*, 1988, **110**, 291 and references cited therein.
7 M. F. Semmelhack, R. D. Stauffer and A. Yamashita, *J. Org. Chem.*, 1977, **42**, 3180; D. Masure, P. Coutrot and J. F. Normant, *J. Organomet. Chem.*, 1982, **226**, C55; T. Tsuda, H. Satomi, T. Hayashi and T. Saegusa, *J. Org. Chem.*, 1987, **52**, 439; B. H. Lipshutz, C. S. Ung and S. Sengupta, *Synlett*, 1989, 64.
8 D. J. Gulliver, W. Levason and M. Webster, *Inorg. Chim. Acta*, 1981, **52**, 153.
9 I. Ojima and T. Kogure, *Organometallics*, 1982, **1**, 1390; G. Z. Zheng and T. H. Chan, *Organometallics*, 1995, **14**, 70.
10 A. Mori, A. Fujita, K. Ikegashira, Y. Nishihara and T. Hiyama, *Synlett*, 1997, 639. See also: M. Fujita and T. Hiyama, *J. Am. Chem. Soc.*, 1984, **106**, 4629.

*Received in Cambridge, UK, 18th August 1997; 7/06032G*

# Biomimetic methane generation and disulfide formation by catalysis with a nickel complex

**Masaru Tada* and Yoshihide Masuzawa**

*Department of Chemistry, Advanced Research Center for Science and Engineering and Materials Research Laboratory for Bioscience and Photonics, Waseda University, Shinjuku, Tokyo 169, Japan*

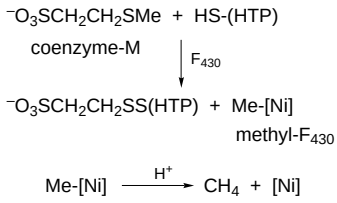
**The final metabolic process of *methanogen*, methane generation and simultaneous disulfide formation, is simulated by the reaction of thioanisole with a toluenethiyl radical in the presence of a nickel complex, which is generated by the photolysis of a toluenethiolato–nickel complex.**

Methanogens[1] are unique bacteria belonging to the Archae bacteria, which constitute the third domain of terrestrial life in addition to Eukaryotes and Prokaryotes.[2] A methanogen produces methane and water as metabolites to produce energy from hydrogen and carbon dioxide[3] [eqn. (1)]. The final step

$$4H_2 + CO_2 \xrightarrow{methanogen} CH_4 + 2H_2O \qquad (1)$$

$$\Delta G^0 = -131 \text{ kJ mol}^{-1}$$

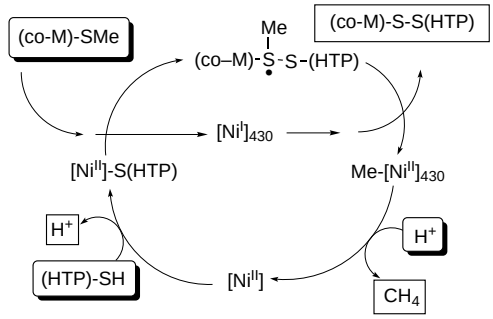
of this $C_1$-unit transformation is the generation of a mixed disulfide and methane (or methyl-$F_{430}$) from methyl-coenzyme M and 7-mercaptoheptanoylthreonine phosphate (HTP-SH) (Scheme 1).[3]




**Scheme 1**

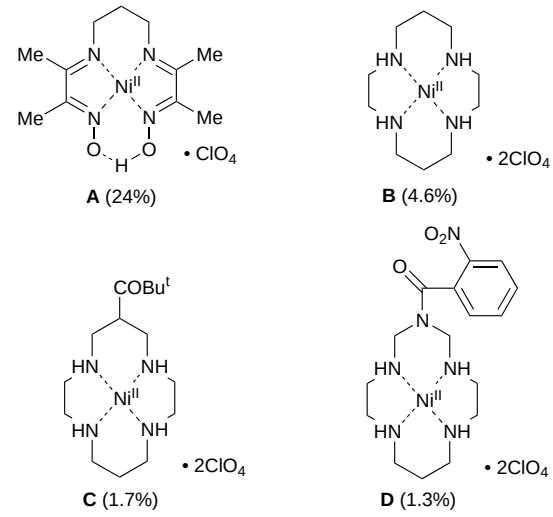
We have no analogy for this in organic or inorganic chemistry, and the main purpose of the present study is to establish a biomimetic reaction analogous to the biological methane production and gain insight into the biochemical reaction mechanism. Reported here is the first successful example of biomimetic production of methane and a mixed disulfide by catalysis with a nickel(II) complex, an $F_{430}$ model.[4] $F_{430}$ is a nickel complex having a modified corrin nucleus which is more flexible than the corrin nucleus in coenzyme $B_{12}$. This flexibility of $F_{430}$ is considered to enable variation in coordination number during the catalysis.

On starting the experimental study, we adopted the working hypothesis shown in Scheme 2, which was originally proposed by Jaun[5a] and Berkessel.[5b] Thus the formation of a thiolato–nickel complex [Ni]–S(HTP) and a sulfuranyl radical (co-M)S•Me– S(HTP)and a final methyl transfer from the sulfuranyl radical to the nickel complex ($F_{430}$) are the crucial features of this mechanism.



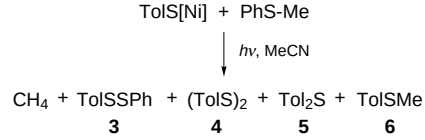

**Scheme 2**

Nickel(I) species have been reported to be active in an enzyme system;[6] therefore, we planned to produce the sulfuranyl radical and nickel(I) complex by the photolysis of the thiolato–nickel complex formed by the reaction of a nickel(II) complex and a thiolate ion. The colour of the MeCN solution of the nickel(II) complex **A** changed from orange to blue–violet on addition of the toluene-*p*-thiolate anion, which was prepared *in situ* from toluenethiol and NaH. A mixture of the toluene-*p*-thiolate ion ($1.5 \times 10^{-2}$ mol $l^{-1}$) and the nickel complex **A** ($5.0 \times 10^{-3}$ mol $l^{-1}$) was added to thioanisole ($1.5 \times 10^{-2}$ mol $l^{-1}$) in MeCN, and the mixture was irradiated at 350 nm under argon.†




Product analyses showed the formation of a mixed disulfide **3** in addition to ditolyl disulfide **4** and ditolyl sulfide **5** (Scheme 3). The time course of the formation of the mixed disulfide **3** and ditolyl disulfide **4** is shown in Fig. 1, which shows that the initial products **3** and **4** decompose on continuous irradiation. Reference irradiation showed the decomposition of these disulfides into the corresponding sulfides, and thus the initial products are the disulfides **3** and **4**.

Gas chromatography–mass spectral analysis (utilizing peaks at *m/z* 12 and 15 to avoid contamination by oxygen) of the top




**Scheme 3**

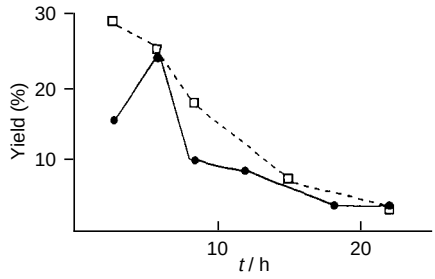
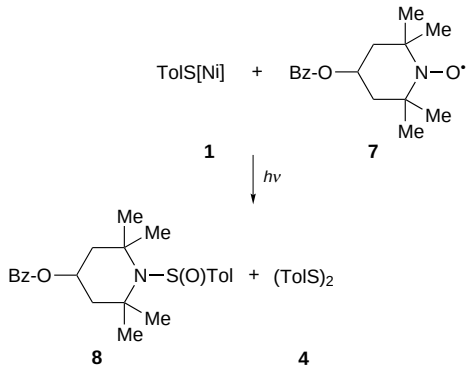



**Fig. 1** The time course of the formationn of disulfides (●) **3** and (□) **4**

gas of the reaction vessel showed the evident formation of methane, although the yield could not be determined due to the solubility of methane in MeCN. Irradiation of the same mixture containing an equivalent amount of compound **7** gave compound **8**‡ in 12% yield. The formation of **8** and ditolyl disulfide **4** shows the intervention of the toluenethiyl radical (Scheme 4).

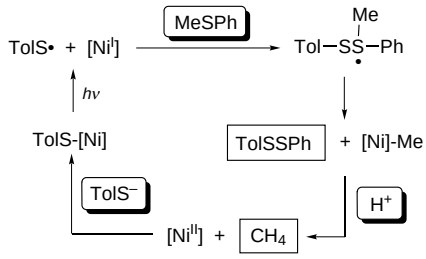



**Scheme 4**

Other nickel(II) complexes **B**–**D** showed some catalytic activity, although with less efficiency, and the yields of **3** after 6 h irradiation are shown in parentheses beneath their structures. Neutral complexes such as bis(dimethylglyoximato)nickel(II) and tetraphenylporphyrin–nickel(II) showed no activity.§ Formation of the mixed disulfide was not observed when either the nickel(II) complex or irradiation was absent. This reaction catalysed by the nickel(II) complex **A** is summarized by Scheme 5 and the net reaction is written as eqn. (2).

$$\mathrm{TolS^-} + \mathrm{MeSPh} + \mathrm{H^+} \rightarrow \mathrm{TolSSPh} + \mathrm{CH_4} \qquad (2)$$

There are two possible action modes of the nickel complex as shown in Fig. 2; (*a*) an $S_H2$ type substitution on the methyl group or (*b*) a ligand coupling on the hypervalent state sulfur.[7] We prefer mode (*a*) because the use of ω-phenylalkyl phenylsulfide instead of thioanisole yields no mixed sulfide and




**Scheme 5**

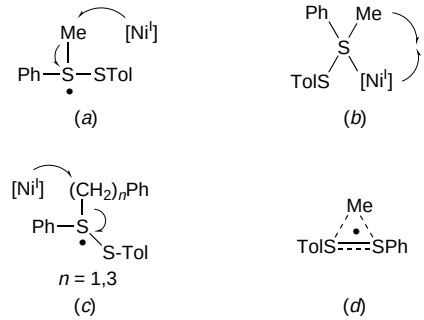



**Fig. 2** Possible reaction modes of the sulfuranyl radical

phenylalkane. Thus the transition state (*c*) of the nickel attack must be more hindered than the transition state (*a*) in which the least bulky methyl group is the reaction centre, and the present reaction seems to be under severe steric control. On the other hand, steric control is less important for mode (*b*) because the reaction centre is a sulfuranyl radical.

Finally, we detected a trace amount of methyl tolyl sulfide **6** from the present model reaction, and the methyl group on the sulfuranyl radical (*a*) seems to swing to some extent through a transition state (*d*). We are studying the effect of this methyl migration on the present intramolecular methyl transfer of biomimetic type.

We thank Waseda University and the Ministry of Education, Sports, and Culture of Japan for their financial support through the Annual Project Program (95A-252) and a 1997 Grant-in-aid (09640649) respectively.

## Footnotes and References

* E-mail: mtada@mn.waseda.ac.jp

† An MeCN solution (10 $cm^3$) of the reaction mixture was irradiated by a Rayonett Photoreactor equipped with 350 nm lamps for the specified periods. The products were identified by comparison with authentic material. The time course of the product yields was determined by gas chromatography using internal standards.

‡ We prefer the sulfinylamide structure **8** formed by the rearrangement of the direct radical coupling product because the base peak in the mass spectrum is seen at *m/z* 139, showing the existence of TolS(O), but only a weak peak corresponding to (TolS) was seen.

§ Addition of piperidine to those neutral complexes did not produce a major spectral change, but the UV absorption maxima of complex **A** (385.0 and 409.5 nm in EtOH) were replaced by maxima at 340.0, 454.5 and 578 (broad) nm or by a broad absorption band at *ca*. 560 nm upon addition of piperidine or toluenethiolate ion.

1 W. E. Balch, G. E. Fox, L. J. Woose and R. S. Wolfe, *Microbiol. Rev.*, 1979, **43**, 260; R. H. Crabtree, *Chem. Rev.*, 1995, **95**, 987.
2 C. R. Wooser and G. E. Fox, *Proc. Natl. Acad. Sci. USA*, 1977, **74**, 5088.
3 A. A. DiMarco, T. A. Bobik and R. S. Wolfe, *Annu. Rev. Biochem.*, 1990, **59**, 355; R. S. Wolfe, *Annu. Rev. Microbiol.*, 1991, **45**, 1; B. Jaun, *Metal ions in biological systems*, ed. H. Siegel and A. Siegel, Marcel Dekker, New York, 1993, vol. 29, ch. 9, p. 287.
4 R. P. Gunsalus and R. S. Wolfe, *FEMS Microbiol. Lett.*, 1978, **3**, 191; A. Pfaltz, D. A. Livingston, B. Jaun, D. Diekert, R. K. Thauer and A. Eschenmoser, *Helv. Chim. Acta*, 1985, **68**, 133.
5 (*a*) B. Jaun, *Helv.*, 1990, **73**, 2209; (*b*) A. Berkessel, *Bioorg. Chem.*, 1991, **19**, 101.
6 B. Jaun and A. Pfaltz, *J. Chem. Soc., Chem. Commun.*, 1988, 293; S. P. J. Albracht, D. Ankel-Fuchs, R. Bocher, J. Ellermann, J. Moll, J. W. Van Der Zwaan and R. K. Thauer, *Biochem. Biophys. Acta*, 1988, **955**, 86.
7 S. Oae, *Rev. Heteroatom Chem.*, Myu, Tokyo, 1988, vol. 1, p. 304; 1991, vol. 4, p. 195.

*Received in Cambridge, UK, 21st July 1997; 7/05187E*

# Highly stereoselective formation of *cis*-enediones from α-diazo carbonyl compounds catalysed by [RuCl(η$^5$-$C_5H_5$)($PPh_3$)$_2$]

**Walter Baratta, Alessandro Del Zotto and Pierluigi Rigo***

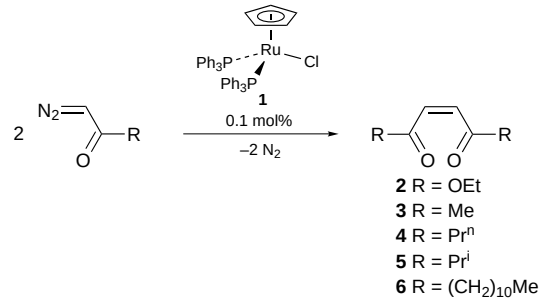
*Dipartimento di Scienze e Tecnologie Chimiche, Università di Udine, Via Cotonificio 108, I-33100 Udine, Italy*

**Stereoselective decomposition of the α-diazo carbonyl compounds $N_2CHCOR$ [R = Me, Pr$^n$, Pr$^i$, $(CH_2)_{10}CH_3$] catalysed by [RuCl(η$^5$-$C_5H_5$)($PPh_3$)$_2$] (0.1 mol%) in toluene at 65 °C affords quantitatively RCOCH=CHCOR carbene dimers, the *cis* isomers being formed in 95–97% yield; under the same experimental conditions $N_2CHCOEt$ gives diethyl maleate in a purity of greater than 99%, the highest value for a stereoselective carbene–carbene dimer formation reported to date.**

The metal-catalysed reactions of α-diazo carbonyl compounds have attracted a great deal of attention in recent years and have been used in an increasing number of syntheses, such as alkene cyclopropanation, carbene dimerisation and C–H insertion.[1] It is generally accepted that transition-metal complexes react with diazo compounds to generate transient metal–carbenes, although a few catalytically active species have been isolated.[2] Tuning of the electronic and steric properties of the catalyst has been proved to strongly affect the product distribution in reactions with diazo compounds, the control of both chemo- and stereo-selectivity still remaining an important goal.[3]

It has been reported that the metal-catalysed decomposition of diazo compounds occurs with loss of nitrogen to give alkenes, and both yield and *cis* : *trans* ratio vary according to the catalyst employed. We have now found that the readily available ruthenium(II) complex [RuCl(η$^5$-$C_5H_5$)($PPh_3$)$_2$] **1** catalyses the highly stereoselective formation of *cis*-enediones[4] from α-diazo carbonyl compounds. Thus, **1** in toluene at 65 °C converts ethyl diazoacetate (EDA) into diethyl maleate **2** quantitatively and in a purity of greater than 99%, diethyl fumarate being the only byproduct.† A comparison with other group 8 metal complexes shows that the metal–porphyrins [Ru(TMP)][1c] and [Os(TTP)]$_2$[5] induce formation of diethyl maleate in 94 and 96% purity, respectively, the highest values reported to date. Moreover, other complexes such as [$Rh_2(OAc)_4$], [$RuCl_2(PPh_3)_3$] and [$Ru_2Cl_4$(p-cymene)$_2$] also catalyse the conversion of EDA into alkenes, but with a considerably lower *cis* : *trans* ratio. Complex **1** has been previously used as a catalyst for the coupling of terminal alkynes with allyl alcohols,[6] but no investigations concerning its catalytic activity towards diazo compounds decomposition have been reported to date.

In order to explore the potential of **1** in the stereocontrolled carbene dimerisation reaction, other substrates have been tested (see Scheme 1). The conversion into alkene is always quantitative and the *cis* isomer is present in the reaction mixture in yields higher than 95%. Thus, when a toluene solution of $N_2CHCOR$ [R = Me, Pr$^n$, Pr$^i$, $(CH_2)_{10}CH_3$] is treated with 0.1 mol% of **1** under an inert atmosphere, dinitrogen evolution takes place rapidly (within 10 min) at 65 °C with quantitative formation of the product, as monitored by NMR spectroscopy. After removal of toluene, the *cis*-enediones **3**–**5** were distilled off *in vacuo* and isolated in 81–87% yield, while **6** was chromatographed on $SiO_2$ (84% isolated yield).† No cyclopropanation products, or other byproducts except *trans*-enediones were detected in the reaction mixtures by NMR and GC–mass spectrometry.

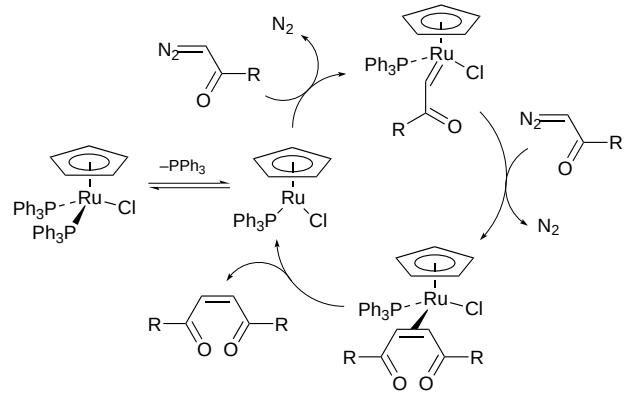



**Scheme 1** *Reaction conditions*: toluene, 65 °C, argon atmosphere

The catalytic carbene dimer formation has been extended to α,ω-bis(diazo carbonyl) compounds. For example, $N_2CHCO(CH_2)_4COCHN_2$ reacts in THF solution at 60 °C in the presence of **1** to give a mixture of cyclic *cis*-enediones, the *trans*-isomers being formed in less than 5% yield. The mononuclear *cis*-cyclooct-2-ene-1,4-dione[7] was distilled off from the reaction mixture and isolated in 19% yield. The solid residue, obtained in 60% yield, is a mixture of dicarbene dimer and trimer (in *ca.* 2 : 3 molar ratio), as inferred by $^1$H and $^{13}$C NMR and mass spectrometry.

Other ruthenium(II) cyclopentadienyl complexes obtained by substitution of one or both $PPh_3$ of **1**, such as [RuCl(η$^5$-$C_5H_5$)(CO)($PPh_3$)], [RuCl(η$^5$-$C_5H_5$)(CNBu$^t$)($PPh_3$)], [RuCl(η$^5$-$C_5H_5$){$P(OPh)_3$}$_2$] and [RuCl(η$^5$-$C_5H_5$)-($Ph_2PCH_2CH_2PPh_2$)], have been shown not to be catalytically active for the decomposition of EDA. In contrast, the indenyl complex [RuCl(η$^5$-$C_9H_7$)($PPh_3$)$_2$] **7** decomposes all the $N_2CHCOR$ compounds reported above, at a temperature (45 °C) lower than that necessary with **1**, but with similar high selectivity for the *cis*-enedione.

The decomposition of EDA catalysed by **1** has been examined in some detail and a plausible mechanism for the *cis*-enedione formation is depicted in Scheme 2. Since at room temperature no catalytic activity is shown by **1**, it is likely that the diazo compound decomposition takes place on the 16-electrons species [RuCl(η$^5$-$C_5H_5$)($PPh_3$)], which is formed upon




**Scheme 2** Proposed mechanism and catalytic cycle

$PPh_3$ dissociation induced by high temperature and concomitant reaction of the phosphine with EDA. In fact, it is known that EDA and $PPh_3$ give in an equilibrium reaction the phosphazine $EtOCOCHN_2{=}PPh_3$, and traces of this product were always found in our reaction mixtures. Furthermore, solutions containing equimolar amounts of EDA and $PPh_3$ and **1** as catalyst do not show dinitrogen evolution at 65 °C. At 90 °C only traces of diethyl maleate ( < 1%) are detected after 2 h reaction, the ylide $EtOCOCH{=}PPh_3$ being the major product present in solution.

As stated above, the indenyl complex **7** decomposes EDA at a lower temperature (45 °C) then **1** (65 °C), and this result is consistent with the kinetic studies of Gamasa *et al*.,[8] who found that complex **7** dissociates $PPh_3$ an order of magnitude faster than **1** to form [RuCl($\eta^5$-ligand)($PPh_3$)].

In the proposed catalytic cycle a neutral $Ru^{II}$ cyclopentadienyl carbene complex is involved, which is similar to [RuCl($\eta^5$-$C_5H_5$)($CPh_2$)($PPh_3$)], recently reported by Braun *et al*.[9] The high stereoselectivity observed for the nucleophilic attack of the α-diazo carbonyl compound on the coordinated carbene is probably related to the preferred orientation of the carbene moiety caused by the cyclopentadienyl ligand.[10] Furthermore, the steric constraint of the RuCl($\eta^5$-$C_5H_5$)($PPh_3$) fragment may favour the formation of the less sterically demanding *cis* alkene.[11]

The extension of this research towards the synthesis of unsymmetrical *cis*-enediones by using two different α-diazocarbonyl compounds is in progress. In particular, decomposition of a 1 : 1 mixture of EDA and $N_2CHCOMe$ yields **2**, **3** and *cis*-EtOCOCH=CHCOMe in *ca*. 1 : 1 : 3 molar ratio, respectively. The double coupling between carbene units derived from mono- and α,ω-bis-diazo carbonyl compounds is also under investigation and seems to give promising results.

This work was supported by the Italian Ministero dell'Università e della Ricerca Scientifica e Tecnologica (Rome). The authors thank Professor Giancarlo Verardo of the Dipartimento di Scienze e Tecnologie Chimiche, Università di Udine, for recording the mass spectra.

## Footnotes and References

* E-mail: inorg@dstc.uniud.it

† The typical procedure adopted for the synthesis of *cis*-enediones **2**–**6** is described here in detail for **3**. A solution of 1-diazopropan-2-one (700 mg, 8.33 mmol) in 5 ml of toluene was added dropwise to a solution of **1** (6 mg; 8 μmol) in 10 ml of toluene, at 65 °C under Ar atmosphere. The solvent was evaporated *in vacuo* and **3** was obtained as a pale yellow oily liquid by distillation at 55 °C and 1 mmHg (377 mg, 81%).

Compounds **2**–**6** gave satisfactory analytical and spectroscopic ($^1H$ and $^{13}C$ NMR and MS) data.

1 (*a*) M. P. Doyle, *Chem. Rev.*, 1986, **86**, 919; (*b*) H. Bock and H. P. Wolf, *J. Chem. Soc., Chem. Commun.*, 1990, 690; (*c*) J. P. Collman, E. Rose and G. D. Venburg, *J. Chem. Soc., Chem. Commun.*, 1993, 934; (*d*) W. J. Seitz, A. K. Saha and M. M. Hossain, *Organometallics*, 1993, **12**, 2604; (*e*) T. Ye and M. A. McKervey, *Chem. Rev.*, 1994, **94**, 1091; (*f*) A. Demonceau, C. A. Lemoine, A. F. Noels, I. T. Chizhevsky and P. V. Sorokìn, *Tetrahedron Lett.*, 1995, **36**, 8419; (*g*) M. P. Doyle, in *Comprehensive Organometallic Chemistry II*, ed. L. S. Hegedus, Pergamon Press, New York, 1995, vol. 12, ch. 5.1 and 5.2; (*h*) M. P. Doyle, A. V. Kalinin and D. G. Ene, *J. Am. Chem. Soc.*, 1996, **118**, 8837; (*i*) A. F. Noels and A. Demonceau, in *Applied Homogeneous Catalysis by Organometallic Complexes*, ed. B. Cornil and W. A. Herrmann, Verlag Chemie, Weinheim, Germany, 1996.

2 H. Nishiyama, Y. Itoh, H. Matsumoto, S.-B. Park and K. Itoh, *J. Am. Chem. Soc.*, 1994, **116**, 2223; P. Schwab, M. B. France, J. W. Ziller and R. H. Grubbs, *Angew. Chem., Int. Ed. Engl.*, 1995, **34**, 2039.

3 A. Padwa and D. J. Austin, *Angew. Chem., Int. Ed. Engl.*, 1994, **33**, 1797; M. P. Doyle, C. S. Peterson, Q.-L. Zhou and H. Nishiyama, *Chem. Commun.*, 1997, 211; M. P. Doyle and M. A. McKervey, *Chem. Commun.*, 1997, 983.

4 The synthesis of *cis*-enediones have been previously described through oxidative opening of furans: P. D. Williams and E. LeGoff, *Tetrahedron Lett.*, 1985, **26**, 1367; C. Domìnquez, A. G. Csáky and J. Plumet, *Tetrahedron Lett.*, 1990, **31**, 7669; B. M. Adger, C. Barrett, J. Brennan, M. A. McKervey and R. W. Murray, *J. Chem. Soc., Chem. Commun.*, 1991, 1553.

5 L. K. Woo and D. A. Smith, *Organometallics*, 1992, **11**, 2344.

6 B. M. Trost, G. Dyker and R. J. Kulawiec, *J. Am. Chem. Soc.*, 1990, **112**, 7809; B. M. Trost and R. J. Kulawiec, *J. Am. Chem. Soc.*, 1992, **114**, 5579; B. M. Trost and J. A. Flygare, *J. Am. Chem. Soc.*, 1992, **114**, 5476; B. M. Trost, R. J. Kulawiec and A. Hammes, *Tetrahedron Lett.*, 1993, **34**, 587; B. M. Trost and J. A. Flygare, *J. Org. Chem.*, 1994, **59**, 1078; B. M. Trost and J. A. Flygare, *Tetrahedron Lett.*, 1994, **35**, 4059.

7 Y. Kayama, M. Oda and Y. Kitahara, *Chem. Lett.*, 1974, 345.

8 M. P. Gamasa, J. Gimeno, C. Gonzalez-Bernardo, B. M. Martin-Vaca, D. Monti and M. Bassetti, *Organometallics*, 1996, **15**, 302.

9 T. Braun, O. Gevert and H. Werner, *J. Am. Chem. Soc.*, 1995, **117**, 7291.

10 B. E. R. Schilling, R. Hoffmann and J. W. Faller, *J. Am. Chem. Soc.*, 1979, **101**, 592; V. C. Gibson, *Angew. Chem., Int. Ed. Engl.*, 1994, **33**, 1565.

11 G. G. A. Balavoine, T. Boyer and C. Livage, *Organometallics*, 1992, **11**, 456.

*Received in Cambridge, UK, 4th September 1997; 7/06459D*

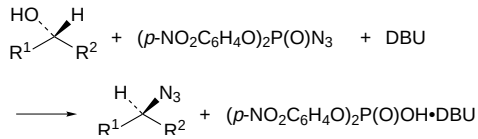
# Efficient method for the one-pot azidation of alcohols using bis(*p*-nitrophenyl) phosphorazidate

**Masanori Mizuno[a,b] and Takayuki Shioiri*[a]**

[a] *Faculty of Pharmaceutical Sciences, Nagoya City University, Tanabe-dori, Mizuho-ku, Nagoya 467, Japan*
[b] *Research and Development Department, Eisai Chemical Co. Ltd, Sunayama, Hasaki, Kashima-gun, Ibaraki 314-02, Japan*

**The direct stereoselective conversion of various alcohols and hexopyranoses into the corresponding alkyl azides and glycosyl azides, respectively, is efficiently accomplished by using bis(*p*-nitrophenyl) phosphorazidate and DBU.**

Azides have been used extensively in organic synthesis, especially for the introduction of primary amino groups and the construction of heterocyclic structures.[1] In most cases, aliphatic azides are prepared by nucleophilic substitution of the corresponding halides or sulfonates by the azide anion.[2] The only known methods for the direct conversion of alcohols into azides are the Mitsunobu reaction,[3] in which removal of the by-products is troublesome, and the diphenyl phosphorazidate (DPPA)–DBU method[4] which is effective only for activated alcohols. In the course of our investigation on the reactivity of some analogs of DPPA, we have discovered that bis(*p*-nitrophenyl) phosphorazidate (*p*-$NO_2$DPPA), prepared easily by nitration of DPPA,[5] in combination with DBU is quite useful and efficient for the direct conversion of alcohols into azides, as shown in Scheme 1.




**Scheme 1**

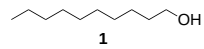
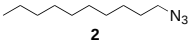
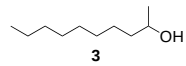
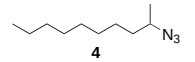
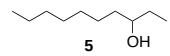
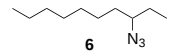
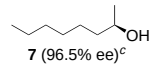
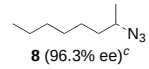
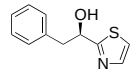
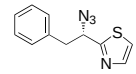
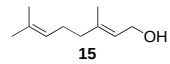
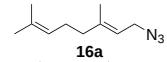
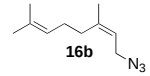
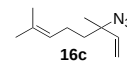
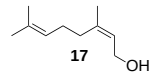
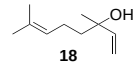
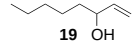
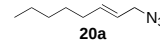
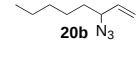
Treatment of decan-1-ol **1** or decan-2-ol **3** with *p*-$NO_2$DPPA (1.2 equiv.) and DBU (1.2 equiv.) in toluene (1 mol $l^{-1}$) smoothly afforded the corresponding azides **2** and **4** in good yield. Superior features of this method are that the reactions proceed with considerably faster rates than when DPPA–DBU is used (5 and 3% yields, respectively), and there are fewer byproducts to struggle with than in the Mitsunobu reaction. In the azidation of decan-2-ol **3**, DBU (81% yield) was much superior to triethylamine (28%), triethylamine with 0.1 part of DMAP (44%) and diisopropylethylamine (32%) under analogous reaction conditions. Toluene was the solvent of choice though THF and DMF can also be used.

Various azides prepared from alcohols according to this method are listed in Table 1. High stereoselectivity was observed in the reaction of optically active alcohols; for instance, (*R*)-(−)-octan-2-ol **7** and (*R*)-(+)-1-phenylethanol **9** afforded (*S*)-(+)-2-azidooctane **8** and (*S*)-(−)-1-phenylethyl azide **10**, respectively, in good yield with inversion of configuration without loss of stereochemical integrity. (*R*)-(+)-2-Phenyl-1-(thiazol-2-yl)ethanol **11** was also conveniently converted to the (*S*)-azide **12**, which was an intermediate for the synthesis of dolaphenine [(*S*)-(−)-2-phenyl-1-(thiazol-2-yl)ethylamine],[6] the C-terminal unit of dolastatin 10 having strong anticancer activity. Allylic alcohols gave a mixture of the isomeric azides (entries 8–11 and 13) due to rapid 1,3-rearrangement of the allylic azides.[7] However, the azidation of alicyclic alcohols such as cyclohexanol **31** and (−)-menthol **32** were unsuccessful under the same reaction conditions.

This method was extended to the preparation of glycosyl azides, key intermediates in the synthesis of glycosyl amino acids.[8] The results summarized in Table 2 demonstrate that this method selectively gives 1,2-*trans*-glycosyl azides. The stereochemical outcome of these direct azidations may be rationalized on grounds similar to those proposed by Sabesan and Neira[9] for the preparation of anomerically enriched glycosyl phosphates from hexopyranoses, *i.e.* probably the azidation occurs *via* initial formation of the thermodynamically stable 1,2-*cis*-glycosyl phosphate which subsequently undergoes the azide displacement with inversion of configuration.

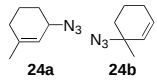
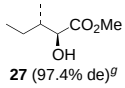
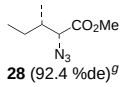
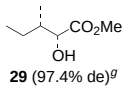
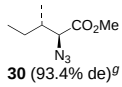
In summary, compared to other methods[2–4] that have been reported, this present method for the stereoselective synthesis of

**Table 1** Azidation of alcohols[a]

| Entry | Alcohol | Solvent | *t*/h | Azide | Yield (%) |
|---|---|---|---|---|---|
| 1 |  **1** | toluene | 16 |  **2** | 76 |
| 2[b] |  **3** | toluene | 6 |  **4** | 81 |
| 3[b] |  **5** | toluene | 6 |  **6** | 87 |
| 4[b] |  **7** (96.5% ee)[c] | toluene | 6 |  **8** (96.3% ee)[c] | 90 |
| 5 |  **9** (100% ee)[d] | THF | 1 |  **10** (100% ee)[d] | 94 |
| 6 |  **11** (95.9% ee)[e] | THF | 3 |  **12** (95.6% ee)[e] | 91 |
| 7 |  **13** (100% ee)[c] | THF | 2 |  **14** (81.3% ee)[f] | 82 |
| 8 |  **15** | toluene | 2 |  **16a**<br>  **16b**<br>  **16c** | 94 (9 : 5 : 2)[g] |
| 9 |  **17** | toluene | 0.5 | **16a** + **16b** + **16c** | 95 (3 : 4 : 1)[g] |
| 10 |  **18** | toluene | 2 | **16a** + **16b** + **16c** | 30 (7 : 10 : 3)[g]<br>Sm 61[h] |
| 11 |  **19** | toluene | 2 |  **20a**<br>  **20b** | 82 (1 : 1)[g] |

*continued*

**Table 1** *continued*

| Entry | Alcohol | Solvent | *t*/h | Azide | Yield (%) |
|---|---|---|---|---|---|
| 12 |  **21** | THF | 2 |  **22** | 74 |
| 13 |  **23** | THF | 1 |  **24a** **24b** | 77 (8 : 1)[g] |
| 14 |  **25** | THF | 2 |  **26** | 74 (*E* : *Z* 97 : 3)[g] |
| 15[b] |  **27** (97.4% de)[g] | toluene | 6 |  **28** (92.4 %de)[g] | 71 |
| 16[b] |  **29** (97.4% de)[g] | toluene | 6 |  **30** (93.4% de)[g] | 68 |
| 17[b] |  **31** | toluene | 24 | none | |
| 18[b] |  **32** | toluene | 24 | none | |

[a] The reaction was carried out at room temp. unless stated otherwise. The absolute configuration of the chiral products was assigned by comparison of the sign of specific rotation with the literature value. [b] At 50 °C. [c] Determined by GC analysis using a Chiraldex G-TA capillary column. [d] Determined by GC analysis using a Chiraldex B-PM capillary column. [e] Determined by HPLC analysis using a Chiralpak AS chiral column. [f] Determined by GC analysis using a Chiraldex B-DA capillary column. [g] Determined by $^1$H NMR analysis. [h] Sm = starting material.

azides has the advantages of simple procedure, mild reaction conditions and easy isolation of products.

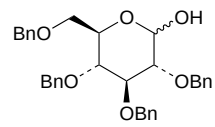
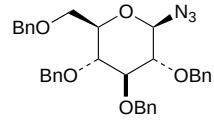
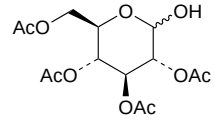
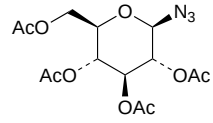
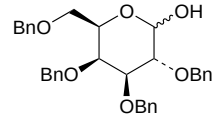
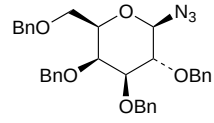
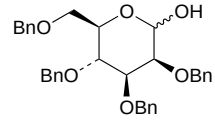
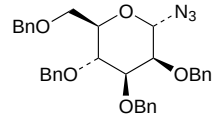
This paper is dedicated to Professor Yoshito Kishi on the occasion of his 60th birthday.

## Footnote and References

* E-mail: shioiri@phar.nagoya-cu.ac.jp

1 T. Sheradsky, in *The Chemistry of the Azido Group*, ed. S. Patai, Interscience, New York, 1971, p. 331.

**Table 2** Azidation of hexopyranoses[a]

| Entry | Hexopyranose | Azide | Yield (%)[b] |
|---|---|---|---|
| 1 |  **33** |  **34** | 76 Sm 18 |
| 2 |  **35** |  **36** | 34 Sm 56 |
| 3 |  **37** |  **38** | 85[c] α 9 |
| 4 |  **39** |  **40** | 75 β 13 |

[a] Reaction in DMF for 2 h at room temp. [b] Sm = starting material. [c] Determined by $^1$H NMR analysis.

2 (*a*) M. E. C. Biffin, J. Miller and D. B. Paul, in *The Chemistry of the Azido Group*, ed. S. Patai, Interscience, New York, 1971, p. 57; (*b*) S. G. Alvarez and M. T. Alvalez, *Synthesis*, 1997, 413.
3 (*a*) D. L. Hughes, *Org. Prep. Proced. Int.*, 1996, **28**, 127; (*b*) A. Saito, K. Saito, A. Tanaka and T. Oritani, *Tetrahedron Lett.*, 1997, **38**, 3955.
4 A. S. Thompson, G. R. Humphrey, A. H. DeMarco, D. J. Mathre and E. J. J. Grabowski, *J. Org. Chem.*, 1993, **58**, 5886.
5 T. Shioiri and S. Yamada, *Chem. Pharm. Bull.*, 1974, **22**, 855.
6 N. Irako, Y. Hamada and T. Shioiri, *Tetrahedron*, 1992, **48**, 7251.
7 A. Gagneux, S. Winstein and W. G. Young, *J. Am. Chem. Soc.*, 1960, **82**, 5956.
8 H. Kunz, *Angew. Chem., Int. Ed. Engl.*, 1987, **26**, 294.
9 S. Sabesan and S. Neira, *Carbohydr. Res.*, 1992, **233**, 169.

*Received in Cambridge, UK, 7th August 1997; 7/05768G*

# Facilitated transport of amino acids by fixed-site jumping

**Tracey A. Munro and Bradley D. Smith***

*Department of Chemistry and Biochemistry, University of Notre Dame, Notre Dame, IN 46556, USA*

**Amino acids are transported with high fluxes through plasticized cellulose triacetate membranes containing large amounts of quaternary tetraalkylammonium salts; similar results are obtained using analogous polymer-supported liquid membranes.**

The main aim in facilitated transport research is to develop selectively permeable, high-flux membranes with long-term durability. A major impediment to the industrial exploitation of this technology is the problem of membrane instability.[1] Recently, we discovered that plasticized cellulose triacetate (CTA) membranes containing large amounts of trioctylmethylammonium chloride (TOMAC) are selectively permeable to small, neutral carbohydrates.[2] The plastic films, which were originally designed as anion exchange membranes,[3] exhibit high saccharide fluxes and high membrane stabilities. Mechanistic studies produced evidence in favour of a fixed-site jumping mechanism, where the TOMAC acts as fixed 'stepping stones' and the sugar permeates through the membrane by jumping from one fixed-site to another.[2,4] These findings raise the possibility that facilitated transport through plasticized membranes by fixed-site jumping is a general way of improving membrane stability while still retaining high and selective permeability. As a consequence we have investigated the facilitated transport of other hydrophilic solutes through lipophilic CTA membranes. This report focuses on the neutral amino acids, phenylalanine, leucine and alanine.

Previous work has shown that liquid organic membranes incorporating TOMAC act as anion exchange membranes for amino acids at basic pH.[5,6] Under these conditions (relatively low concentration of TOMAC dissolved in the liquid membrane), transport occurs by membrane-diffusion of lipophilic ion-pairs of TOMA cation and amino acid anion.[7] At neutral pH very little of the amino acid is present in its anionic form, and transport enhancement is very weak.[8,9] We now report that amino acid transport can be greatly enhanced if the membrane contains enough TOMAC to induce fixed-site jumping.

Two related membranes were examined: plasticized CTA films and polymer-supported liquid membranes.† The plasticized films were prepared by evaporating a chloroform solution of CTA, 2-nitrophenyl octyl ether (2-NPOE) and TOMAC in a flat-bottomed glass petri dish.[3] The resulting plastic film (*ca.* 50 μm thick, depending on composition) was peeled off, trimmed and clamped into a cylindrical transport cell.† The supported liquid membranes were solutions of TOMAC dissolved in 2-NPOE that were absorbed by thin sheets of microporous polypropylene (Celgard 2500™, 25 μm thick). A selection of the transport fluxes observed with the plasticized CTA films is listed in Table 1. Even at neutral pH, the amino acid fluxes are very high, whereas the membranes are only weakly permeable to metal cations and hydrophilic organic cations such as dopamine.

**Table 1** Non-competitive transport through cellulose triacetate membranes at neutral pH

| Solute[a] | Flux/$10^{-8}$ mol m$^{-2}$ s$^{-1}$ TOMAC present[b] | TOMAC absent[c] |
|---|---|---|
| L-Phenylalanine | 1590 | 0.12 |
| L-Leucine | 520 | 0.12 |
| L-Alanine | 290 | 0.76 |
| Dopamine | 25 | 0.31 |
| NaCl[d] | 12 | 0.81 |

[a] Initially source contained 100 mM solute. Both aqueous phases contained 100 mM sodium phosphate, pH 7.3, $T$ = 298 K. [b] Membrane: 0.10 g CTA, 0.20 g 2-NPOE, 0.20 g TOMAC. [c] Membrane: 0.10 g CTA, 0.20 g 2-NPOE. [d] Source: 100 mM NaCl in deionised water; receiving: deionised water.

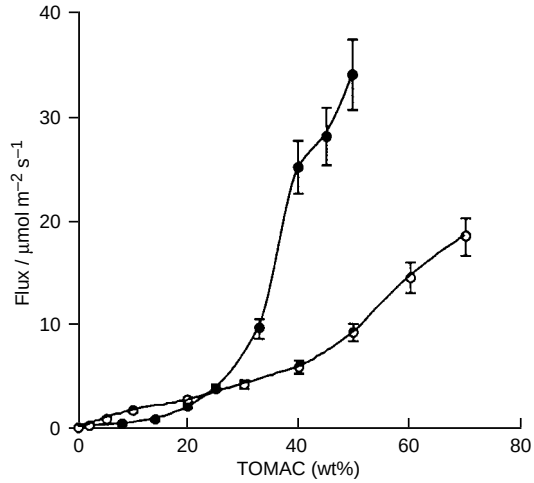



**Fig. 1** Initial phenylalanine flux *versus* wt% TOMAC in (●) plasticized membrane that also included CTA (0.1 g) and 2-NPOE (0.2 g) and (○) liquid membrane of 2-NPOE supported by a 25 μm thick sheet of Celgard 2500™. Both aqueous phases contained sodium phosphate (60 ml, 100 mM, pH 7.3), $T$ = 298 K. The source phase also contained phenylalanine (100 mM). To account for changes in flux due to changes in membrane thickness, the fluxes have been multiplied by the ratio (membrane thickness in presence of TOMAC)/(membrane thickness in absence of TOMAC).

Plots of phenylalanine flux *versus* wt% of TOMAC for both membranes with aqueous phases at neutral pH are shown in Fig. 1. The profiles do not exhibit the linear relationship that is typically found with transport systems that operate by carrier-diffusion.[4,12] Rather the profiles are non-linear, with the flux increasing dramatically at high TOMAC levels. This is indicative of a transport process that uses fixed-site jumping (Fig. 2).[4] In the case of the CTA films there is clear evidence of a percolation threshold at around 20% TOMAC. We postulate that below the threshold concentration, flux is negligible because the distance between the relatively immobile quaternary ammonium sites is too great ( > *ca.* 15 Å) to allow solute

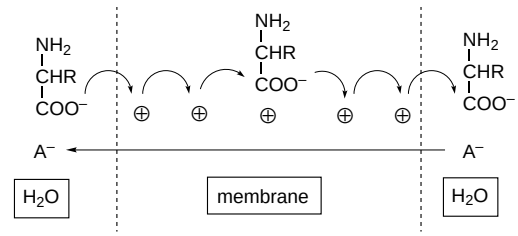



**Fig. 2** A transport process using fixed-site jumping

jumping and the high membrane viscosity greatly inhibits transport by carrier-diffusion. In the case of the supported liquid membrane, the flux *versus* percentage of TOMAC is first-order until about 40% TOMAC and then increases at a higher power. The difference in curve shape is attributed to a change in the relative contributions of the two transport pathways, *i.e.* carrier-diffusion at lower TOMAC concentrations and fixed-site jumping at higher TOMAC levels. The lower viscosity associated with a liquid membrane makes carrier-diffusion a more favourable pathway compared to a plasticized membrane, and the TOMAC concentration has to reach 40% before any flux enhancement due to fixed-site jumping is observed.

Amino acid flux through the CTA films is dependent on membrane thickness. Stacking multiple membranes together or preparing a single membrane of additional thickness lowers the flux in a linear fashion. Additional transport mechanism studies are ongoing, however, three pieces of evidence implicate an anion exchange process. (i) When the source phase but not the receiving phase contains sodium phosphate (100 mM, pH 7.3), phenylalanine flux is very low, but when the situation is reversed, (*i.e.* receiving phase contains sodium phosphate and the source phase does not) the flux is quite high. (ii) A plot of phenylalanine flux as a function of pH shows very low flux at pH $< 5.5$ (the isoelectric point for phenylalanine) and dramatically increasing flux after pH 5.5. At pH 10 the flux is five times higher than at pH 7.3. (iii) Changing the TOMA counter-anion from chloride to phosphate leads only to a 30% drop in initial flux, whereas changing the counter-anion to lipophilic bis(2-ethylhexyl)phosphate results in complete loss of phenylalanine permeability.

Previous work by others has shown that a crown–boronic acid mixture is a better transporter of phenylalanine through bulk, liquid membranes than TOMAC at neutral pH.[8] With CTA films containing high concentrations of transporting agent we find that TOMAC is superior. It appears that the crown–boronic acid mixture uses a carrier-diffusion process and, unlike TOMAC, does not switch to a fixed-site jumping mechanism at high membrane concentrations. A similar conclusion was recently reached by Lamb concerning metal cation transport mediated by crown carriers.[12] We have also examined the facilitated transport of dopamine through plasticized membranes using crown–boronic acid mixtures that are known to be effective dopamine carriers in supported liquid membranes.[13] Again there is no evidence for the onset of fixed-site jumping at high carrier concentrations. Thus, it remains to be seen if this remarkable transport effect, which we attribute to fixed-site jumping (*i.e.* the solute is rapidly relayed along a sequence of relatively immobile carriers), can be duplicated with transport agents other than quaternary alkylammonium salts.[4]

This research was supported by the National Science Foundation (USA) and the Herman Frasch Foundation of the American Chemical Society.

## Footnotes and References

* E-mail: smith.115@nd.edu

† The transport cell consisted of two identical, water-jacketed cylindrical halves (half-cell volumes 60 ml, membrane area 16 $cm^2$) that were stirred by turbines which in turn were driven by externally situated magnets (ref. 10). The side of the plastic film exposed to the air during the evaporation process was placed facing the source solution. Amino acid concentrations were determined by ninhydrin assay (ref. 11). Phenylalanine concentrations were also monitored spectrometrically at $\lambda = 262$ nm ($\varepsilon = 139$ l $mol^{-1}$ $cm^{-1}$) as were the dopamine levels ($\lambda = 279$ nm, $\varepsilon = 2675$ l $mol^{-1}$ $cm^{-1}$). Metal cation concentrations were determined by conductivity or inductively coupled plasma emission. All CTA films were prepared from CTA (0.10 g) and 2-NPOE (0.20 g). In the absence of TOMAC the films were 30 μm thick. Addition of TOMAC thickened the films up to 75 μm for a membrane containing 50 wt% TOMAC.

1 E. L. Cussler, in *Membrane Separation Systems. Recent Developments and Future Directions*, ed. R. W. Baker, E. L. Cussler, W. Eykamp, W. J. Koros, R. L. Riley and H. Strathmann, Noyes Data Corporation, Park Ridge, 1991, ch. 4; A. M. Neplenbroek, D. Bargeman, T. van den Boomgaard and H. Strathmann, *Sep. Sci. Technol.*, 1996, **31**, 2733.
2 J. A. Riggs and B. D. Smith, *J. Am. Chem. Soc.*, 1977, **119**, 2765.
3 T. Hayashita, M. Kumazawa and M. Yamamoto, *Chem. Lett.*, 1996, 37; T. Hayashita, in *Chemical Separations with Liquid Membranes*, ed. R. A. Bartsch and J. D. Way, *ACS Symp. Ser.*, Number 642, ACS, Washington, 1996, ch. 21; T. Hayashita, T. Fujimoto, Y. Morita and R. A. Bartsch, *Chem. Lett.*, 1994, 2385.
4 E. L. Cussler, A. Rutherford and A. Brown, *J. Membr. Sci.*, 1989, **43**, 149 and references cited therein; R. D. Noble, *J. Membr. Sci.*, 1992, **75**, 121; R. D. Noble, *J. Membr. Sci.*, 1991, **56**, 229.
5 A. M. Eyal and E. Bressler, *Biotechnol. Bioeng.*, 1993, **41**, 287.
6 J.-P.Behr and J.-M. Lehn, *J. Am. Chem. Soc.*, 1973, **95**, 6108; P. Deblay, M. Minier and H. Renon, *Biotechnol. Bioeng.*, 1990, **35**, 123; T. Hano, T. Ohtake, M. Matsumoto, D. Kitayama, F. Hori and F. Nakashio, *J. Chem. Eng. Jpn.*, 1991, **24**, 20.
7 E. V. Dehmlow and S. S. Dehmlow, *Phase Transfer Catalysis*, 2nd edn., Verlag Chemie, Weinheim, 1983, 17.
8 L. K. Mohler and A. W. Czarnik, *J. Am. Chem. Soc.*, 1993, **115**, 7037; M. T. Reetz, J. Huff, J. Rudolph, K. Töllner, A. Deege and R. Goddard, *J. Am. Chem. Soc.*, 1994, **116**, 11588.
9 Recent examples of amino acid transport at neutral pH: I. S. Antipin, I. I. Stoikov, E. M. Pinkhassik, N. A. Fitseva, I. Stibor and A. I. Konovalov, *Tetrahedron Lett.*, 1997, **38**, 5865; J. L. Sessler and A. Andrievsky, *Chem. Commun.*, 1996, 1119; H. Tsukube, S. Shinoda, J. Uenishi, M. Shiode and O.Yonemitsu, *Chem. Lett.*, 1996, 969; C. Seel, A. Galán and J. de Mendoza, *Top. Curr. Chem.*, 1995, **175**, 101.
10 W. van Straaten-Nijenhuis, F. de Jong and D. N. Reinhoudt, *Recl. Trav. Chim. Pays-Bas*, 1993, **112**, 317.
11 P. Scrimin, P. Tecilla and U. Tonellato, *Tetrahedron*, 1995, **51**, 217.
12 A. J. Schow, R. T. Peterson and J. D. Lamb, *J. Membr. Sci.*, 1996, **111**, 291.
13 M.-F. Paugam, J. T. Bien, B. D. Smith, L. A. J. Chrisstoffels, F. de Jong and D. N. Reinhoudt, *J. Am. Chem. Soc.*, 1996, **118**, 9820.

*Received in Columbia, MO, USA, 8th April 1997; 7/02390A*

# The first highly enantioselective catalytic hetero-Diels–Alder reaction of ketones

**Mogens Johannsen, Sulan Yao and Karl Anker Jørgensen***

*Center for Metal Catalyzed Reactions, Department of Chemistry, Aarhus University, DK-8000 Aarhus C, Denmark*

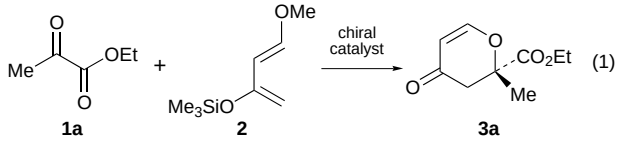
**The first highly enantioselective catalytic hetero-Diels–Alder reaction of various aliphatic and aromatic ketones with an activated conjugated diene catalysed by chiral copper(II) complexes with enantiomeric excesses up to 99% is presented.**

The hetero-Diels–Alder (HDA) reaction of carbonyl compounds with conjugated dienes is one of the cornerstone reactions in organic chemistry and has wide application for the synthesis of important compounds.[1] One of the most useful reactions in this field is the HDA reaction of aldehydes with activated conjugated dienes, such as Danishefsky's diene, leading to highly valuable oxygenated products.[2]

In recent years interest has been focused on the development of metal-catalysed enantio- and diastereo-selective HDA reactions of aldehydes with conjugated dienes.[3] Great progress has been made in the HDA reaction between activated conjugated dienes and simple unactivated aldehydes.[4] Recently, we have been involved in developing highly enantioselective HDA reactions of aldehydes, such as glyoxylates, with unactivated conjugated cyclic and acyclic dienes catalysed by bisoxazoline–copper(II) and –zinc(II) complexes[5] and BINOL-aluminium(III) complexes.[6]

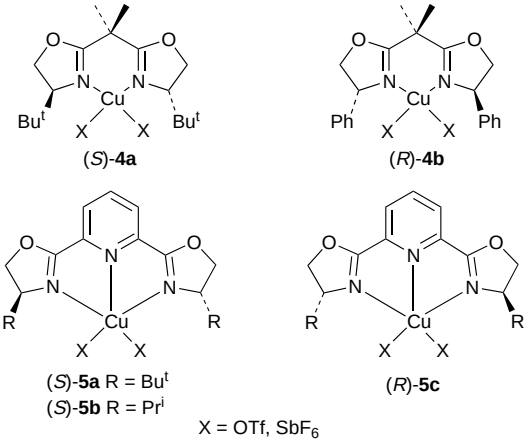
The challenge is to develop the metal-catalysed enantioselective HDA reaction of ketones with conjugated dienes, as this reaction will have wide potential in organic chemistry. Here we present the first highly enantioselective HDA reaction of both aliphatic and aromatic ketones with an activated conjugated diene using chiral catalysis.[7]

The reaction of ethyl pyruvate **1a** with *trans*-1-methoxy-3-(trimethylsilyloxy)buta-1,3-diene (Danishefsky's diene) **2** [eqn. (1)] has been studied in the presence of various bidentate

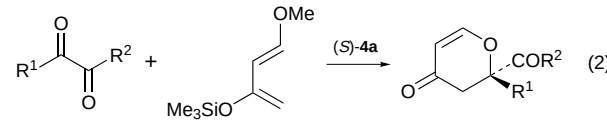



**1a** **2** **3a** (1)

bisoxazoline and tridentate bisoxazoline–pyridine ligands in combination with copper(II) salts [(*S*)-**4a**, (*R*)- **4b**, (*S*)-**5a**,**b** and (*R*)-**5c**, respectively] in order to investigate the catalytic properties of the different ligands on the HDA reaction. The reaction of **1a** with **2** in the presence of (*S*)-**4a**, (*R*)-**4b**, (*S*)-**5a**,**b** or (*R*)-**5c** (X = OTf) (10 mol%) as the catalyst in $CH_2Cl_2$ at room temperature gives the HDA product **3a** in various yields and enantiomeric excesses (ees) depending on the catalyst used. By application of (*S*)-**4a** as the catalyst, **3a** is isolated in 85% yield, with an ee of 92% (reaction time, 8 h), while (*R*)-**4b** gave the same yield of **3a**, but with an ee of only 26% (reaction time, 8 h). It should be noted that both catalysts give the same enantiomer of the HDA product **3a**.[5a,c] The catalysts (*S*)-**5a**,**b** and (*R*)-**5c** are less effective and much longer reaction times are required (*ca.* 100 h); with (*S*)-**5a**,**b**, the HDA product **3a** is isolated in 29 and 15% yield, and with an ee of 9 and 27%, respectively, while (*R*)-**5c** gave nearly the same yield (23%), but a slightly higher ee (55%).




It turned out the catalyst (*S*)-**4a** was the most promising chiral catalyst, both in terms of yield and ee of the HDA product formed. This catalyst was therefore applied for the reaction of different α-keto esters and an α-diketone **1a**–**d** with *trans*-1-methoxy-3-(trimethylsilyloxy)buta-1,3-diene **2** [eqn. (2)]




(2)

**1a** $R^1$ = Me, $R^2$ = OEt
**b** $R^1$ = Me, $R^2$ = OMe
**c** $R^1$ = Ph, $R^2$ = OEt
**d** $R^1$ = $R^2$ = Me

**2**

**3a** $R^1$ = Me, $R^2$ = OEt
**b** $R^1$ = Me, $R^2$ = OMe
**c** $R^1$ = Ph, $R^2$ = OEt
**d** $R^1$ = $R^2$ = Me

under various reaction conditions to extend the scope of the reaction.†

The results for the HDA reaction of the various ketones **1a**–**d** with *trans*-1-methoxy-3-(trimethylsilyloxy)buta-1,3-diene **2** catalysed by (*S*)-**4a** under various conditions are presented in Table 1.

**Table 1** Hetero-Diels–Alder reactions of the ketones **1a**–**d** with *trans*-1-methoxy-3-(trimethylsilyloxy)buta-1,3-diene **2** catalysed by (*S*)-**4a** [eqn. (2)] under various reaction conditions

| | | | | | | Diels–Alder product | |
|---|---|---|---|---|---|---|---|
| Entry | Ketone | (*S*)-**4a** X | *T*/°C | *t*/h | Solvent | Yield[a] (%) | Ee (%) |
| 1 | **1a** | OTf | room temp. | 8 | $CH_2Cl_2$ | **3a** 85 | 92[b] |
| 2 | **1a** | OTf | −40 | 30 | $CH_2Cl_2$ | **3a** 78 | 99[b] |
| 3 | **1a** | $SbF_6$ | room temp. | 24 | $CH_2Cl_2$ | **3a** 22 | 80[b] |
| 4 | **1a** | $SbF_6$ | −40 | 50 | $CH_2Cl_2$ | **3a** 37 | 89[b] |
| 5 | **1b** | OTf | room temp. | 23 | $CH_2Cl_2$ | **3b** 95 | 91[b] |
| 6 | **1c** | OTf | room temp. | 20 | THF | **3c** 77 | 77[c] |
| 7 | **1d** | OTf | −40 | 60 | THF | **3d** 90 | 94[b] |

[a] Isolated yield. [b] Ee determined by GC on a Chrompack Chirasil-DEX CB column. [c] Ee determined by HPLC on a Daicel Chiralpak AD column, eluent: hexane–$Pr^iOH$ (99 : 1).

Ethyl pyruvate **1a** reacts with *trans*-1-methoxy-3-(trimethylsilyloxy)buta-1,3-diene **2** in the presence of the catalyst (*S*)-**4a** having triflate as the anion at room temperature to give the HDA product in 85% yield with 92% ee (Table 1, entry 1). Performing the reaction at −40 °C leads to an improvement of the ee of **3a** to 99% without affecting the yield significantly (entry 2). Exchange of the anion from triflate to antimonate leads to a decrease in the yield of **3a** to only 22%, and also to a reduction of the ee (80%) (entry 3). Performing the reaction between **1a** and **2** in the presence (*S*)-**4a** (X = $SbF_5$) at −40 °C slightly increases the ee of the HDA product (entry 4). The ester substituent is of minor importance for the highly enantioselective HDA reaction as methyl pyruvate **1b** reacts with **2** in the presence of (*S*)-**4a** (X = OTf) as the catalyst to give **3b** in high yield (95%) and with high ee (91%) (entry 5). The reaction of the aromatic ketone **1c** with **2** in the presence of (*S*)-**4a** (X = OTf) also proceeds well, giving a 77% yield of the HDA product **3c** with an ee of 77%. The enantiomeric HDA reaction is not only restricted to α-keto esters such as **1a**–**c**; the α-diketo compound butane-2,3-dione **1d** also reacts with **2** in the presence of (*S*)-**4a** (X = OTf) as the catalyst to give **3d** in high yield (89%) and with very high ee (94%).

The potential of this new enantioselective HDA reaction for the various ketones is obvious from entries 2, 5–7 in Table 1. The HDA products are formed in high yields for both the aliphatic and aromatic ketones and, furthermore, the aliphatic ketones give up to 99% ee in these reactions, whereas 77% ee is found for the aromatic ketone. Work is in progress to develop this HDA reaction further and to understand the mechanistic aspects of the reaction.

Thanks are expressed to The Danish National Science Foundation for financial support.

## Footnotes and References

* E-mail: kaj@kemi.aau.dk

† *Typical procedure*: (*S*)-**4a** (X = OTf) was prepared by addition of $Cu(OTf)_2$ (36 mg, 0.1 mmol) to 2,2′-isopropylidenebis[(4*S*)-4-*tert*-butyl-2-oxazoline] (31 mg, 0.105 mmol) dissolved in dry $CH_2Cl_2$ (2 ml) under an inert atmosphere and stirred for 2 h. The catalyst was cooled to −40 °C, ethyl pyruvate **1a** (110 μl, 1 mmol) and *trans*-1-methoxy-3-(trimethylsilyloxy)buta-1,3-diene **2** (250 μl, 1.2 mmol) were added, and the solution stirred for 30 h at this temperature. Then TFA (0.1 ml) dissolved in $CH_2Cl_2$ (20 ml) was added at −40 °C and the solution stirred for 1 h at 0 °C. The solution was then neutralised with saturated $NaHCO_3$ and the solution was filtered through a plug of cotton. The organic phase was separated and the water phase was extracted twice with $CH_2Cl_2$. The combined organic phases were dried, filtered and the solvent evaporated. Purification of the crude product using flash chromatography (EtOAc–light petroleum, 1 : 4) gave **3a** in 78% yield and 99% ee (chiral GC); $[\alpha]_D^{25}$ + 149 (*c* 1.1, $CHCl_3$).

1 R. R. Schmidt, *Acc. Chem. Res.*, 1986, **19**, 250; D. L. Boger and S. M. Weinreb, *Hetero Diels–Alder Methodology in Organic Synthesis*, Academic Press, New York, 1987.
2 M. Bednarski, C. Maring and S. Danishefsky, *Tetrahedron Lett.*, 1983, 3451.
3 K. Narasaka, M. Inoue and N. Okada, *Chem. Lett.*, 1986, 1109; H. Waldmann, *Synthesis*, 1994, 535; K. Narasaka, *Synthesis*, 1991, 1; K. Maruoka and H. Yamamoto, in *Catalytic Asymmetric Synthesis*, ed. I. Ojima, VCH, Weinheim, 1993, p. 413; H. B. Kagan and O. Riant, *Chem. Rev.*, 1992, **92**, 1007.
4 G. E. Keck, X.-Y. Li and D. Krishnamurthy, *J. Org. Chem.*, 1995, **60**, 5998; K. Maruoka, T. Itoh, T. Shirasaka and H. Yamamoto, *J. Am. Chem. Soc.*, 1988, **110**, 310; T. Hanamoto, H. Furuno and J. Inanaga, *Synlett*, 1997, 79; Q. Gao, T. Maruyama, M. Mouri and H. Yamamoto, *J. Org. Chem.*, 1992, **57**, 1951; A. Togni, *Organometallics*, 1990, **9**, 3106; Y. Motoyama and K. Mikami, *J. Chem. Soc., Chem. Commun.*, 1994, 1563.
5 (*a*) M. Johannsen and K. A. Jørgensen, *J. Org. Chem.*, 1995, **60**, 5757; (*b*) M. Johannsen and K. A. Jørgensen, *Tetrahedron*, 1996, **52**, 7321; (*c*) S. Yao, M. Johannsen and K. A. Jørgensen, *J. Chem. Soc., Perkin Trans. 1*, 1997, 1234; (*d*) M. Johannsen and K. A. Jørgensen, *J. Chem. Soc., Perkin Trans. 2*, 1997, 1183.
6 A. Graven, M. Johannsen and K. A. Jørgensen, *Chem. Commun.*, 1996, 2373.
7 To the best of our knowledge this is the only other paper on enantioselective HDA reactions with ketones, albeit with modest ee: M. Quimpére and K. Jankowski, *J. Chem. Soc., Chem. Commun.*, 1987, 676. See also P. C. B. Page, P. H. Williams, E. W. Collington and H. Finch, *J. Chem. Soc., Chem. Commun.*, 1987, 756.

*Received in Cambridge, UK, 4th September 1997; 7/06463B*

# Effects of lanthanide complexes on the facial reactivity of 2-(2′,3′,4′,6′-tetra-*O*-acetyl-β-D-glucopyranosyloxy)benzaldehyde in hetero-Diels–Alder reactions and a model to account for such effects

**Richard P. C. Cousins,[a] Woan Chee Ding,[b] Robin G. Pritchard[b] and Richard J. Stoodley*[b]**

[a] *Medicinal Science, Glaxo Wellcome Medicines Research Centre, Stevenage, Hertfordshire, UK SG1 2NY*
[b] *Department of Chemistry, UMIST, PO Box 88, Manchester, UK M60 1QD*

**Changes in the facial reactivity of 2-(2′,3′,4′,6′-tetra-*O*-acetyl-β-D-glucopyranosyloxy)benzaldehyde towards (*E*)-1-methoxy-3-(*tert*-butyldimethylsiloxy)buta-1,3-diene in the presence of lanthanide(fod)$_3$ complexes can be correlated with the ionic radius of the lanthanide metal.**

Recently, we reported notable 1,5-asymmetric inductions in the reaction of the salicylaldehyde derivative **1** with Danishefsky's diene **2** in the presence of Lewis acids.[1] The use of $BF_3{\cdot}OEt_2$ and $SnCl_4$ (100 mol% of each) in THF led to *ca.* 27 : 3 : 63 : 7 mixtures of compounds **4**–**7**, which were transformed by the action of TFA into 90 : 10 mixtures of the dihydropyranones **6** and **7**. With $ZnCl_2$ (100 mol%) in THF and Eu(fod)$_3$ (5 mol%) in toluene, the cycloadducts **8** and **10** were produced in ratios of 86 : 14 and 25 : 75; the cycloadducts **8** and **10** were converted into the dihydropyranones **6** and **7** in the presence of TFA. Clearly, $BF_3{\cdot}OEt_2$ and $ZnCl_2$ in THF promoted attack mainly at the *si*-face of the aldehyde moiety of compound **1** whereas Eu(fod)$_3$ in toluene induced preferential *re*-face addition.

Here we describe efforts that have led to improvements in the practicality and stereoselectivity of the hetero-Diels–Alder reaction; we also propose a model to account for the variation in the facial reactivity of the salicylaldehyde derivative **1**.

Seeking initially to increase the stabilities of the cycloadducts† (compounds **8** and **10** were very prone to undergo desilylative eliminations to give the pyranones **6** and **7**), we investigated the reaction of the aldehyde **1** with the diene **3**[2]‡ under the afore-cited cycloaddition conditions. The use of $ZnCl_2$ in THF and Eu(fod)$_3$ in toluene afforded the cycloadducts **9** and **11** in ratios of 67 : 33 and 18 : 82. From the latter reaction, it was possible to isolate the cycloadduct **11**,§ mp 175–176 °C, $[\alpha]_D$ +53 (*c* 0.3, $CH_2Cl_2$), in 75% yield after crystallisation. In accord with its structure, the cycloadduct **11** was transformed into the dihydropyranone **7** (82% yield after crystallisation).

Expecting that a 'matched' chiral europium(III) complex would improve the diastereoselectivity, the use of (+)-Eu(hfc)$_3$, (−)-Eu(hfc)$_3$, (+)-Eu(tfc)$_3$ and (−)-Eu(tfc)$_3$ (5 mol% of each) as promoters was studied in toluene. Surprisingly, there was little difference in the effects of the enantiomeric catalysts and the selectivities were poor. Thus, the cycloadducts **9** and **11** were produced in ratios of 59 : 41 and 61 : 39 with (+)-Eu(hfc)$_3$ and (−)-Eu(hfc)$_3$, and in ratios of 45 : 55 and 47 : 53 with (+)-Eu(tfc)$_3$, and (−)-Eu(tfc)$_3$.

The importance of the metal in lanthanide(fod)$_3$ complexes in determining the facial reactivity of the aldehyde **1** towards the diene **3** is illustrated by the results shown in Table 1. In the first

**Table 1** Outcome of the reaction of aldehyde **1** and diene **3** in the presence of lanthanide(fod)$_3$ complexes[a]

| Catalyst | Lanthanide ionic radius/Å[b] | Ratio **9** : **11**[c] |
|---|---|---|
| La(fod)$_3$ | 1.06 | < 5 : 95 |
| Ce(fod)$_3$[d] | 1.03 | < 5 : 95 |
| Pr(fod)$_3$ | 1.01 | < 5 : 95 |
| Nd(fod)$_3$ | 0.99 | < 5 : 95 |
| Eu(fod)$_3$[e] | 0.95 | 18 : 82 |
| Gd(fod)$_3$ | 0.94 | 26 : 74 |
| Dy(fod)$_3$ | 0.91 | 55 : 45 |
| Ho(fod)$_3$ | 0.89 | 61 : 39 |
| Er(fod)$_3$ | 0.88 | 69 : 31 |
| Yb(fod)$_3$ | 0.86 | 66 : 34 |

[a] Typically, the reactions were conducted using aldehyde **1** (0.1 mmol), diene **3** (0.2 mmol) and the complex (*ca.* 4 mol%) in dry toluene (2 cm$^3$). [b] Ref. 3. [c] The ratio was determined by 300 MHz $^1$H NMR spectroscopic analysis of the crude product and/or the derived pyranones **6**/**7**. [d] The reaction involving Ce(fod)$_3$ was significantly slower than the others (requiring *ca.* 48 h for completion compared with *ca.* 5 h). [e] The use of different concentrations of Eu(fod)$_3$ (*ca.* 10 and *ca.* 0.5 mol%) did not affect the ratio of cycloadducts produced.

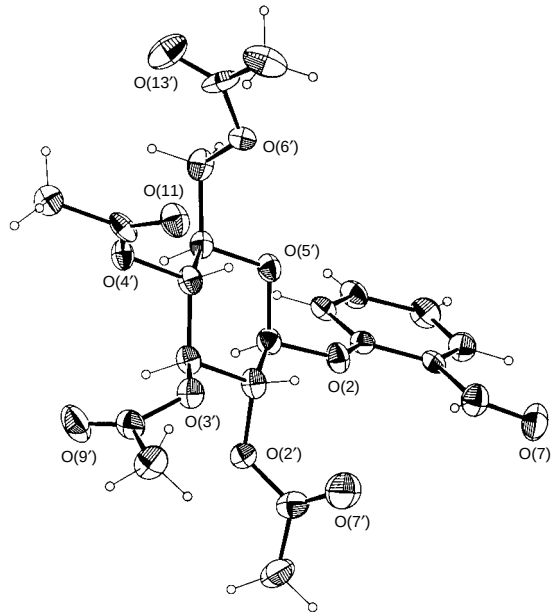



**Fig. 1** Molecular structure of compound **1**

four examples, essentially complete ( > 95 : 5) *re*-face selectivity of the aldehyde **1** was observed. In the remaining examples, there was (in the main) a gradual increase in *si*-face selectivity as the ionic radius of the lanthanide metal decreased. Significantly, from a synthetic standpoint, it was possible to isolate the cycloadduct **11** in 90% yield after crystallisation from the reaction of the salicylaldehyde **1** (11 mmol) and the diene **3** in the presence of $Pr(fod)_3$.

In the hope that its solid-state structure would reveal 'preorganisation' that might shed light on the stereoinductions, compound **1** was subjected to an X-ray crystallographic analysis. The molecular structure,¶ shown in Fig. 1 with its atomic labelling, indicates that the *re*-face of the aldehyde moiety is shielded by the 2′-*O*-acetyl group of the sugar.‖

Evidence that the solid-state conformation of compound **1** was maintained in solution ($C_6D_6$) was adduced from an NOED spectroscopic study. Thus, irradiation of the anomeric hydrogen atom (1′-H) caused an 8% enhancement of the aryl 3-hydrogen atom (3-H); similarly, irradiation of 3-H enhanced 1′-H by 6%.

From the afore-cited findings, we propose that compound **1** can be activated by Lewis acids in two ways. The formation of a monodentate complex of type **12**, in which the Lewis acid is coordinated to the aldehyde carbonyl O-atom *syn* to the aldehyde H-atom, is postulated to be the basis of the *si*-face reactivity; this pattern is predominant in aldol reactions induced by $BF_3{\cdot}OEt_2$ and $SnCl_4$ and in hetero-Diels–Alder reactions promoted by $ZnCl_2$ and the 'late' lanthanides. The generation of a chelated complex, *e.g.* of type **13** in which the Lewis acid is coordinated to the aldehyde carbonyl O-atom and the glycosidic O-atom, provides a possible explanation for the *re*-face selectivity; this behaviour is a feature of cycloaddition reactions initiated by the 'early' lanthanides. Presumably, because of the 'lanthanide contraction' (in which the radii of lanthanide cations decrease with increasing atomic number),[3] the 'late' lanthanides favour heptacoordination (and, therefore, the formation of monodentate complexes) whereas the 'early' lanthanides prefer octacoordination (and, as a consequence, are able to form chelated complexes).[4]

The results reported herein are of both mechanistic and synthetic note. Although the catalytic activity of lanthanide complexes in hetero-Diels–Alder reactions has been extensively investigated since Danishefsky's foundation studies,[5] the finding that the nature of the cation can have a significant impact upon the facial reactivity of a chiral aldehyde is novel.** The possibility that this effect is linked to the ionic radius of the lanthanide cation and its ability to form a monodentate *versus* a bidentate complex warrants further study. From a synthetic context, the technology permits the efficient assembly of compounds **7** and **11** in multi-gram quantities; earlier, only the dihydropyranone **6** was accessible in high yield.[1]

We thank the CVCP for an ORS award (to W. C. D.) and a referee for drawing our attention to ref. 8.

## Footnotes and References

* E-mail: richard.stoodley@umist.ac.uk

† Our interest in such cycloadducts stems from the expectation that their dihydropyran rings can be elaborated into glycopyranose-like structures; such products, which may be regarded as 'scaffolded' disaccharides, represent a novel and potentially interesting class of compounds.

‡ The diene **3** was prepared by a modification of the literature route (see ref. 2) in which (*E*)-4-methoxybut-3-en-2-one was treated with *tert*-butyldimethylsilyl triflate and triethylamine (see ref. 6).

§ New compounds displayed analytical and spectral properties that supported their assigned structures.

¶ *Crystal data* for **1**: $C_{21}H_{24}O_{11}$, $M$ = 452.4, monoclinic, space group $P2_1$ (no. 4), $a$ = 12.625(6), $b$ = 6.929(5), $c$ = 13.262(4) Å, $\beta$ = 97.89(3)°, $U$ = 1149(11) Å$^3$, $Z$ = 2, $D_c$ = 1.307 g cm$^{-3}$, $F(000)$ = 476, $\mu$(Mo-K$\alpha$) = 1.00 cm$^{-1}$, crystal size 0.40 × 0.15 × 0.15 mm. A total of 1947 reflections were measured, 1658 unique ($R_{int}$ = 0.084) after an empirical absorption correction (max., min. transmission = 1.00, 0.84), on a Rigaku AFC6S diffractometer using $\omega$–2$\theta$ scans ($\lambda$ = 0.71069 Å) at 20 °C. The structure was solved by direct methods and refined by full-matrix least-squares based on $F^2$, with all non-hydrogen atoms anisotropic and hydrogen atoms constrained in calculated positions. The final cycle converged to $R$ = 0.054 and $wR^2$ = 0.138 based on 679 observed reflections [$I > 2\sigma(I)$] and 293 variables ($R$ = 0.190, $wR^2$ = 0.210 for all data). CCDC 182/579.

‖ A related shielding effect was noted in the X-ray structure of 5-(2′,3′,4′,6′-tetra-*O*-acetyl-β-D-glucopyranosyloxy)-1,4-naphthoquinone and invoked to account for the high facial reactivity of the dienophile in Diels–Alder reactions (see ref. 7).

** The enantioselectivities of Diels–Alder reactions catalysed by complexes of lanthanide(OTf)$_3$ and (*R*)-binaphthol can be influenced by added achiral ligands and by the lanthanide metal (see ref. 8).

1 R. P. C. Cousins, A. D. M. Curtis, W. C. Ding and R. J. Stoodley, *Tetrahedron Lett.*, 1995, **36**, 8689.
2 R. E. Ireland, P. A. Aristoff and C. F. Hoyng, *J. Org. Chem.*, 1979, **44**, 4318.
3 F. A. Cotton, G. Wilkinson and P. L. Gaus, *Basic Inorganic Chemistry*, 3rd edn., Wiley, New York, 1995, p. 267 and 616.
4 S. Cotton, *Lanthanides and Actinides*, MacMillan, London, 1991, p. 58.
5 G. A. Molander, *Chem. Rev.*, 1992, **92**, 29.
6 H. Emde, D. Domsch, H. Feger, U. Frick, A. Götz, H. H. Hergott, K. Hofmann, W. Kober, K. Krägeloh, T. Oesterle, W. Steppan, W. West and G. Simchen, *Synthesis*, 1982, 1.
7 B. Beagley, A. D. M. Curtis, R. G. Pritchard and R. J. Stoodley, *J. Chem. Soc., Perkin Trans. 1*, 1992, 1981.
8 S. Kobayashi and H. Ishitani, *J. Am. Chem. Soc.*, 1994, **116**, 4083.

*Received in Liverpool, UK, 24th June 1997; 7/04463A*

# Asymmetric synthesis of protoberberine alkaloids *via* a tandem nucleophilic addition and intramolecular cyclisation of a chiral *o*-toluamide anion with 3,4-dihydroisoquinoline

**Ronald N. Warrener,* Ligong Liu and Richard A. Russell*†**

*Centre for Molecular Architecture, Central Queensland University, Rockhampton, Qld, Australia, 4702*

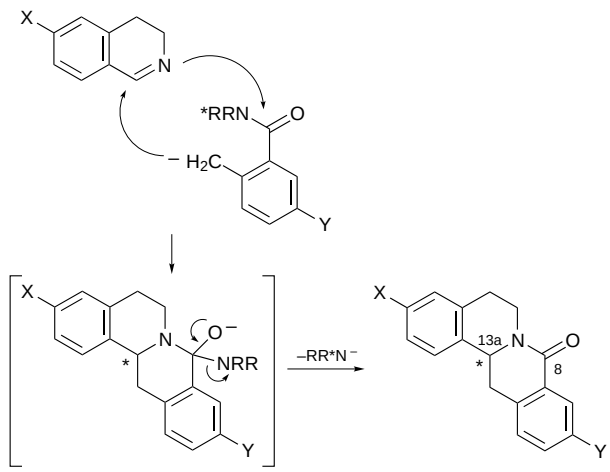
**The reaction of *o*-toluamide anions, derived from the (*S*)-(−)- and (*R*)-(+)-1-phenylethylamine, with 6,7-dimethoxy-3,4-dihydroisoquinoline gives (13a*S*)-(−)- and (13a*R*)-(+)-8-oxoprotoberberine, respectively, with enantiomeric excesses > 96%.**

The protoberberine alkaloids display a broad diversity of biological activities[1,2] and feature predominently as active components in many folkloric medicines especially in China and other Asian countries. A wide range of synthetic methods have been reported for the preparation of protoberberines and these have been the subject of several reviews.[2,3] In spite of this only a few methods deal with the enantioselective synthesis of protoberberines. Most asymmetric methods involve multi-step procedures, use of special reagents and occur in relatively low optical yields.[4,5] Recently, lateral metallation methodology has been developed for the synthesis of racemic heterocyclic compounds, including protoberberines, and shown to exhibit exceptional regiochemical control.[6] This feature, coupled with a direct approach to the products, offers efficient entry to the protoberberine skeleton and related structures.

In this communication we report the first successful application of lateral metallation to the efficient asymmetric synthesis of protoberberines *with* a chiral *o*-toluamide (Scheme 1).

The commercial availability of the two enantiomers of 1-phenylethylamine made this an attractive chiral auxiliary to incorporate into the *o*-toluamides. Our initial study, which involved the reaction the anion derived from the secondary *o*-toluamide **2a** (R = H) with the isoquinoline **1**, failed to afford any of the cyclised protoberberine **4** and only the ring-opened intermediate **3** could be detected. Whilst this intermediate could be cyclised by heating in refluxing toluene, the final product **4** exhibited very low enantiomeric purity (1.5% ee) (Table 1).

Since anions of tertiary amides, *e.g. N*,*N*-diethyl-*o*-toluamide, are known to condense with dihydroisoquinolines and



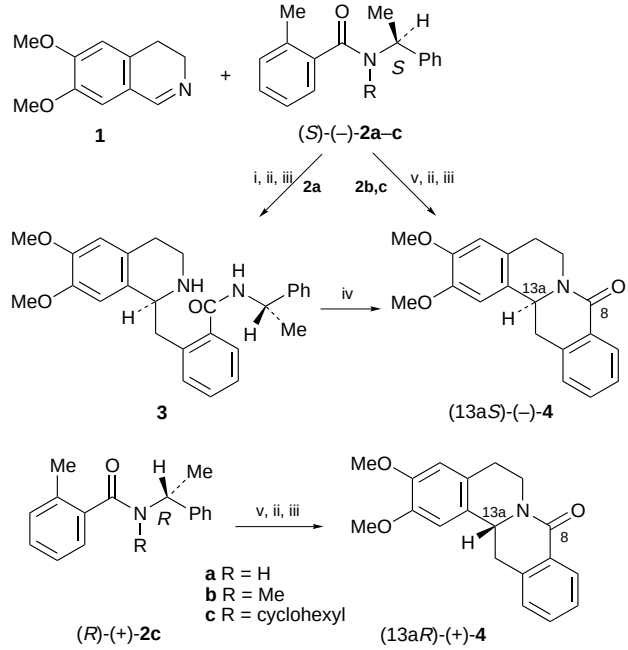

**Scheme 1** An approach to the asymmetric synthesis of protoberberines based upon lateral metallation

**Table 1** Chemical and optical yields of protoberberine **4** from reactions involving the toluamides **2a**–**c** with dihydrosioquinoline **3**

| | Yield (%)[a] | $[\alpha]_D^{20}$[b] | Ee (%)[c] |
|---|---|---|---|
| (*S*)-**2a** | 39 | −5.6 | 1.5 |
| (*S*)-**2b** | 14 | −19.9 | 5.2 |
| (*S*)-**2c** | 48 | −372.4 | 97 |
| (*R*)-**2c** | 51 | +366.6 | 96 |

[a] Chemical yields have not been optimised and refer to the sole product which was isolated by chromatography. [b] Rotations: *c* 0.359, $CHCl_3$. [c] Optical yields were calculated by comparison of the rotation with the reported data, *i.e.* rotations (in $CHCl_3$) of 10, 50, 67 and 73 corresponding to 3, 13, 18 and 19% ee.[5]

subsequently cyclise in the one pot,[7] we turned our attention to the chiral amide **2b**. Whilst reaction of **1** with **2b** afforded the 8-oxoprotoberberine in one step, there was only a slight improvement of the enantiomeric selectivity (5.2% ee) of the reaction. These rather disappointing results, we reasoned, were due to too great a conformational mobility of the chiral auxiliary and accordingly the more sterically demanding cyclohexyl group was introduced as a non-chiral substituent on the amide nitrogen atom, *i.e.* **2c**. The reaction of (*S*)-(−)-**2c** with the dihydroquinoline **1** gave as the product (*S*)-(−)-**4** (97% ee) in 48% chemical yield. Similarly pure (*R*)-(+)-**4** (96% ee) was prepared by replacement of the chiral auxiliary in the amide **2c** with (*R*)-(+)-1-phenylethylamine (Scheme 2), thereby provid-




**Scheme 2** *Reagents and conditions*: i, $Bu^nLi$ (2 equiv.), THF, 0 °C, 1 h; ii, **1**, THF, −78 to −30 °C, 1 h; iii, aq. $NH_4Cl$, −30 °C; iv, PhMe, 110 °C, 15 h; v, $Pr^i_2NLi$ (1 equiv.) THF, −78 °C, 25 min

ing the desired one-pot synthesis of the protoberberine ring system.

Although our research is at an early stage, it is clear that we have developed an efficient asymmetric synthesis for chiral 8-oxoprotoberberines based upon the regiospecific addition–cyclisation reaction of chiral *o*-toluamide anions with 3,4-dihydroisoquinolines. The extension of this methodology to other heterocyclic compounds and the understanding of the mechanism leading to chiral induction is an ongoing study in our laboratories.

The authors gratefully acknowledge the financial support of the Australian Research Council and The Central Queensland University. One of us (L. L.) also acknowledges the award of a postgraduate scholarship through the Centre for Molecular Architecture.

## Footnote and References

† E-mail: rarcat@deakin.edu.au

1 S. Simeon, J. L. Rios and A. Villar, *Plant Med. Phytother.*, 1989, **23**, 202.

2 D. A. Bhakuni and S. Jain, *The Alkaloids*, Academic Press, 1986, vol. 28, p. 95; M. Shamma and J. L. Moniot, *Isoquinoline Alkaloids Research 1972–1977*, Plenum Press, New York and London, 1978, p. 209; M. Shamma, *The Isoquinoline Alkaloids, Chemistry and Pharmacology*, Academic Press, New York and London, 1972, p. 268; Y. Kondo, *Heterocycles*, 1976, **4**, 197.

3 T. J. Kametani and K. Fukumoto, in *Isoquinolines*, ed. G. Grethe, Wiley-Interscience, New York, 1981, p. 139.

4 R. T. Dean and H. Rapoport, *J. Org. Chem.*, 1978, **43**, 4183; J. E. Johansen, B. D. Christie and H. Rapoport, *J. Org. Chem.*, 1981, **46**, 4914; Z. Czarnocki, D. B. MacLean and W. A. Szarek, *Bull. Soc. Chim. Belg.*, 1986, **95**, 749; Z. Czarnocki, *J. Chem. Res.* (*S*), 1992, 334; M. A. Matulenko and A. I. Meyers, *J. Org. Chem.*, 1996, **61**, 573; T. Kametani, N. Takagi, M. Toyota, T. Honda and K. Fukumoto, *J. Chem. Soc., Perkin Trans. 1*, 1981, 2830; *Heterocycles*, 1981, **16**, 591; T. Naito, Y. Tada and I. Ninomiya, *Heterocycles*, 1981, **16**, 1141; S. G. Pyne and B. Dikic, *J. Org. Chem.*, 1990, **55**, 1933; S. G. Pyne, *Tetrahedron Lett.*, 1987, **28**, 4737; K. Iwasa, Y. P. Gupta and M. Cushman, *Tetrahedron Lett.*, 1981, **22**, 2333; K. Iwasa and M. Cushman, *Heterocycles* 1981, **16**, 901; Y. Haraguchi, S. Kozima and R. Yamaguchi, *Tetrahedron: Asymmetry* 1996, **7**, 443.

5 T. Naito, K. Katsumi, Y. Tada and I. Ninomiya, *Heterocycles*, 1983, **20**, 779.

6 R. D. Clark and A. Jahangir, *Org. React.* (*N.Y.*), 1995, **47**, 1.

7 R. D. Clark and A. Jahangir, *J. Org. Chem.*, 1987, **52**, 5378.

*Received in Cambridge, UK, 15th August 1997; 7/06008D*

# One-step synthesis of tris(butylsulfanyl)sexithiophene from 3-butylsulfanyl-2,2′-bithiophene

**Francesca Goldoni, Dario Iarossi, Adele Mucci and Luisa Schenetti***

*Dipartimento di Chimica Università di Modena, Via Campi, 183, 41100 Modena, Italy*

**$FeCl_3$ converts, in high yield, 3-butylsulfanyl-2,2′-bithiophene into a tris(butylsulfanyl)sexithiophene, which shows interesting optical properties and forms a stable radical cation and dication.**

Oligothiophenes with defined structure are gaining increasing attention as a new class of organic π-electron systems. Among them, α-sexithiophene (α-6T) is a very promising material for field-effect transistors.[1] The optical and electrical properties as well as the processability of these materials can be modulated by adding substituents on the oligothiophene backbone. Recently, interesting methylsulfanylsexithiophenes with UV maximum absorption wavelengths near to, but lower than, those of sexithiophene have been reported.[2] Among alkylsulfanyl groups, butylsulfanyl shows interesting solubility and structural properties in poly(3-butylsulfanyl)thiophene[3] and in 4,4′-bis(butylsulfanyl)-2,2′-bithiophene.[4] To minimize the steric effect due to the bulky substituent we chose to build a sexithiophene from 3-butylsulfanylbithiophene.

Here, we report preliminary results on 3,3‴,3⁗-tris(butylsulfanyl)-2,2′ : 5′,2″ : 5″,2‴ : 5‴,2⁗ : 5⁗,2‴′-sexithiophene **1**, obtained by oxidative coupling of 3-butylsulfanyl-2,2′-bithiophene with $FeCl_3$ in $CHCl_3$–$MeNO_2$ (Scheme 1).† The product was identified by $^1H$ and $^{13}C$ NMR, mass and UV spectra. Mass analysis confirmed a molecular formula of $C_{36}H_{38}S_9$: *m/z* (70 eV) 762 (10%, $[M^+ + 4]$), 761 (15, $[M^+ + 3]$), 760 (41, $[M^+ + 2]$), 759 (43, $[M^+ + 1]$), 758 (100, $[M^+]$), 506 (18, $[M^+ - C_{12}H_{12}S_3]$).

$^1H$ NMR data enabled the regiochemistry of **1** to be determined. In the aromatic region of the $^1H$ NMR spectrum (Fig. 1), the presence of four doublets characterized by $^3J$(H-α,H-β) 5.2–5.3 Hz (H-4, H-5, H-4⁗ H-5⁗), six doublets characterized by $^3J$(H-β, H-β′) 3.7–3.9 Hz (H-3′, H-4′, H-3″, H-4″, H-3‴, H-4‴) and a singlet (H-4‴) demonstrates that the compound under investigation is actually a sexithiophene. Compound **1** proposed in Scheme 1 is the only structure compatible with the absence of monosubstituted terminal thiophenes. Three distinguishable triplets for $CH_2$(α) are found in the aliphatic region of the proton NMR spectrum, at δ 2.92, 2.88 and 2.87. Two further triplets, corresponding to the terminal methyls, are found at δ 0.92 (double intensity) and 0.90. Signals corresponding to $CH_2$(β) and $CH_2$(γ) are superimposed. Complete NMR characterization was achieved through $^1H$ and $^{13}C$ NMR inverse-detection techniques, HMQC[5] and HMBC.[6]

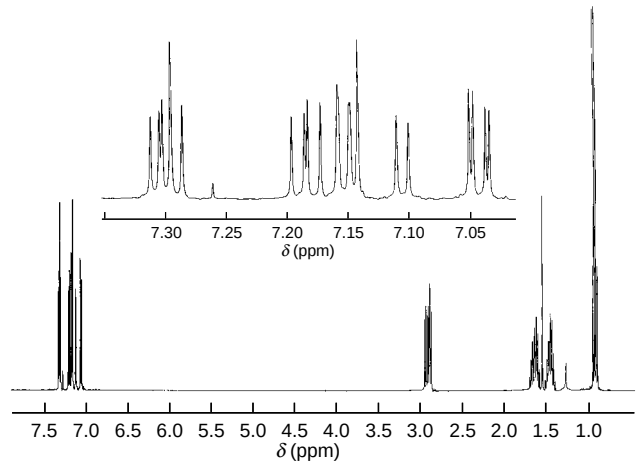
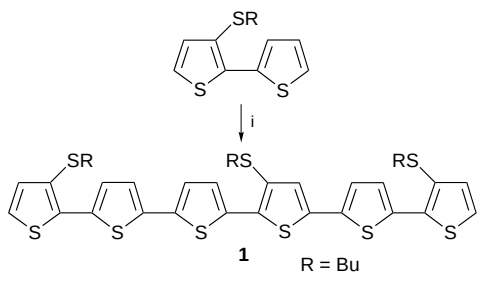



**Fig 1** $^1H$ NMR spectrum of sexithiophene **1**. The upper trace shows the expanded aromatic region.

The formation of the regioisomer **1**, out of the possible four that could in principle derive from the starting bithiophene, can be explained by considering the deactivation effect of the 3-methylsulfanyl group on the 5-position of thiophene or bithiophenes in oxidative coupling reactions with $FeCl_3$.[7] Another important result is the high reaction yield (70% of pure product) probably due to the stability of radical cation $\mathbf{1}^{+\cdot}$ in the reaction conditions. This stability was confirmed by a cyclic voltammetry investigation (Fig. 2) which showed the presence of two reversible oxidation peaks at 0.89 and 1.02 V (0.1 M $Bu_4NBF_4$–$CH_2Cl_2$, glassy carbon electrode, scan rate 100 mV $s^{-1}$, SCE) corresponding to the formation of the cation radical $\mathbf{1}^{+\cdot}$ and the dication $\mathbf{1}^{2+}$. Compound **1** shows $\lambda_{max}(CHCl_3)$ 449 nm, 17 nm higher than that reported for α-6T[8] and 19–43 nm higher than that reported for methylsulfanylsexithiophenes.[2] A further 19 nm bathochromic effect is observed in $CS_2$. In fact, $\lambda_{max}$ changes from 443 in MeOH, to 446 in MeCN, to 449 in $CHCl_3$ and to 468 nm in $CS_2$. The lowering of the optical gap with respect to α-6T and to methylsulfanylsexithiophenes is probably the consequence of a good balance between steric and




**Scheme 1** *Reagents and conditions*: i, $FeCl_3$, $CHCl_3$–$MeNO_2$ 1 : 1, room temp., 30 h

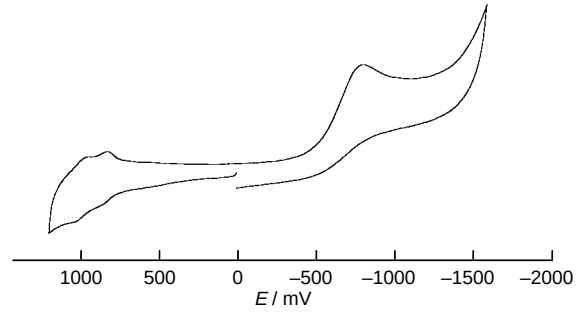



**Fig. 2** Cyclic voltammogram of sexithiophene **1**

electronic effects. The conjugational ability of the butylsulfanyl group acts on a π-conjugated system in which the steric hindrance, due to the bulky β-alkylsulfanyl groups, is diluted by the presence of unsubstituted rings. The regiochemistry of substitution should play a fundamental role in determining the optical characteristics of **1**. In fact, the lone pairs of the two sulfur atoms in the 3- and 3′′′′-positions can be delocalized onto the whole molecular skeleton. The sulfur lone pair could not exert the same conjugative effect if the outer butylsulfanyl groups were placed in the 4- and 4′′′′-positions. The 3′′′-butylsulfanyl group can only give rise to a less extended conjugation pattern (over four rings). In conclusion, through the accurate choice of the starting monomer we were able to synthesize a substituted sexithiophene with butylsulfanyl groups on the 3-, 3′′′- and 3′′′′-positions, having a $\lambda_{max}$ at a longer wavelength than that of α-6T and forming a stable radical cation and dication.

This work was supported by the Italian National Research Council (CNR). Thanks are due to the Centro Interdipartimentale Grandi Strumenti for the use of the Bruker AMX-400 WB spectrometer, and to Dr M. Borsari for electrochemical measurements.

## Footnotes and References

* E-mail: schene@unimo.it

† *Preparative details*: A solution of anhydrous $FeCl_3$ (10.4 g, 64 mmol) in dry nitromethane (240 ml) was added dropwise over a period of 2 h to a solution of 3-butylsulfanyl-2,2′-bithiophene (4.0 g, 15.7 mmol) in distilled $CHCl_3$ (240 ml) under a flow of dry nitrogen. The reaction mixture, stirred 30 h at room temperature, was evaporated and the residue was stirred with a solution of HCl acidified methanol (100 ml). The filtered dark product was washed with methanol (40 ml) and dissolved in $CHCl_3$ (150 ml). The chloroform solution was washed with a 3% hydrazine solution (100 ml) and then with water, and evaporated. The crude red oil was washed with pentane (400 ml). The pentane solution was evaporated and the product (3.7 g) chromatographed on silica gel (neutralized with a 2% solution of triethylamine) using light petroleum (bp 40–70 °C)–diethyl ether (90 : 10) as the eluent. The compound isolated (2.8 g, 70%) is a red oil identified as 3,3′′′,3′′′′-tris(butylsulfanyl)-2,2′ : 5′,2′′ : 5′′,2′′′ : 5′′′,2′′′′,: 5′′′′,2′′′′-sexithiophene **1**.

‡ *NMR data* for **1**: $\delta_H$ (400 MHz, $CDCl_3$, 27 °C, $Me_4Si$, *J*/Hz) 7.31 [d, $^3J$(H,H) 3.8, 1 H, H-4′′], 7.30 [d, $^3J$(H,H) 3.7, 1 H, H-3′], 7.29 [d, $^3J$(H,H) 3.9, 1 H, H-4′′′′], 7.19 [d, $^3J$(H,H) 5.3, 1 H, H-5′′′′] 7.18 [d, $^3J$(H,H) 5.3, 1 H, H-5], 7.15 [d, $^3J$(H,H) 3.8, 2 H, H-4′, H-3′′], 7.14 (s, 1 H, H-4′′′), 7.11 [d, $^3J$(H,H) 3.9, 1 H, H-3′′′′], 7.043 [d, $^3J$(H,H) 5.3, 1 H, H-4′′′′] 7.041 [d, $^3J$(H,H) 5.3, 1 H, H-4], 2.92 [t, 2 H, 3′′′-$CH_2$(α)], 2.88 [t, 2 H, 3′′′′-$CH_2$(α)], 2.87 [t, 2 H, 3-$CH_2$(α)], 1.64 [m, 6 H, $CH_2$(β)], 1.44 [m, 6 H, $CH_2$(γ)], 0.92 (t, 6 H, 3-$CH_3$, 3′′′′-$CH_3$), 0.90 (t, 3 H, 3′′′-$CH_3$); $\delta_C$ 137.61, 136.73, 137.36, 136.42, 135.50, 135.13, 134.67, 134.60, 134.39, 134.27, 132.23, 132.20, 128.76, 128.24, 128.02, 126.81, 126.77, 126.74, 123.72, 123.49, 123.48, 123.31, 123.13, 36.00, 35.89, 35.88, 31.66, 31.65, 21.86, 21.83, 13.58; $\lambda_{max}$/nm ($CHCl_3$) 449 (ε/dm$^3$ mol$^{-1}$ cm$^{-1}$ 75 000); *m/z* (70 eV) 762 (10%, [$M^+$ + 4]), 761 (15, [$M^+$ + 3]), 760 (41, [$M^+$ + 2]), 759 (43, [$M^+$ + 1]), 758 (100, [$M^+$]), 506 (18, [$M^+ - C_{12}H_{12}S_3$]).

1 G. Horowitz, F. Garnier, A. Yassar, R. Hajlaoui and F. Kouki, *Adv. Mater.*, 1996, **8**, 52; A. Dodabalapur, H. E. Katz, L. Torsi and R. C. Haddon, *Science*, 1995, **269**, 1560.
2 G. Barbarella, M. Zambianchi, R. Di Toro, M. Colonna, L. Antolini and A. Bongini, *Adv. Mater.*, 1996, **8**, 327.
3 F. Goldoni, D. Iarossi, A. Mucci, L. Schenetti and M. Zambianchi, *J. Mater. Chem.*, 1997, **7**, 593.
4 L. Antolini, U. Folli, F. Goldoni, D. Iarossi, A. Mucci and L. Schenetti, *Acta Polym.*, 1996, **47**, 265.
5 A. Bax, R. H. Griffey and B. L. Hawkins, *J. Magn. Reson.*, 1983, **55**, 301.
6 A. Bax and M. F. Summers, *J. Am. Chem. Soc.*, 1986, **108**, 2093.
7 G. Barbarella, M. Zambianchi, R. Di Toro, M. Colonna, Jr., D. Iarossi, F. Goldoni and A. Bongini, *J. Org. Chem.*, 1996, **61**, 8285.
8 C. Van Pham, A.Burkhardt, R. Shabana, D. D. Cunningham, H. B. Mark, Jr. and H. Zimmer, *Phosphorus, Sulfur, Silicon Relat. Elem.*, 1989, **46**, 153.

*Received in Cambridge, UK, 4th August 1997; 7/05613C*

# EPR study of the $H_2O_2$ interaction with $TiO_2$; evidence for a novel $S = 1$ surface radical pair

**Damien M. Murphy,*[a] Emyr W. Griffiths,[a] Christopher C. Rowlands,[a] Fred E. Hancock[b] and Elio Giamello[c]**

[a] *National EPSRC ENDOR Center, Department of Chemistry, University of Wales Cardiff, PO Box 912, Cardiff, UK CF1 3TB*
[b] *ICI Katalco, Research Technology and Engineering, PO Box 1, Billingham, Cleveland, UK TS23 1LB*
[c] *Dip. di Chimica Inorganica, Fisica e Materiali, Universita di Torino, Via P. Giuria 9, 10125 Torino, Italy*

**$H_2O_2$ reacts with rutile $TiO_2$ powder forming not only surface $O_2^-$ anions but also two newly identified surface $S = 1$ triplet radical anion pairs composed of two interacting $O^-\cdots O^-$ centers characterised by the EPR spin Hamiltonian parameters of $g_{iso} = 2.0104$ and $D = 13.7$ mT for triplet 1 and $g_{iso} = 2.0064$ and $D = 12.7$ mT for triplet 2.**

The role of free radical intermediates in the heterogeneous decomposition of organic substrates over metal oxides and zeolitic systems has been investigated for many years. In particular, the catalytic oxidation by $H_2O_2$ over $TiO_2$ or $V_2O_5$ has been studied in depth with a view to understanding the role of the active peroxo or peroxoacid species in the decomposition mechanism.[1] Despite the extensive literature available in this field, a well defined description of the basic phenomena occurring at the interface of the $H_2O_2$–oxide system is far from complete. Some of us have previously explored the reactivity of the $H_2O_2$–oxide system by EPR spectroscopy and a rich abundance of trapped radical species were identified.[2–5] It was found that for $H_2O_2$–MgO, a variety of oxygen based and protonated oxygen radicals including $O^-$, $O_2^-$ and $OH^\bullet$ were formed.[3] Here, we present preliminary results on the nature of the various radical centers, which are generated by interaction of $H_2O_2$ with rutile $TiO_2$. Evidence will be presented for the direct observation of a novel $S = 1$ triplet radical pair on the $TiO_2$ surface.

The $TiO_2$ powder (Rutile, ICI Tioxide) was stirred for 2 h at room temp. with an aqueous solution of $H_2O_2$ (27.5 mass%, Aldrich). The resulting slurry was then filtered and gently dried in air at 308–313 K for *ca.* 1 h. The EPR spectrum of the fresh sample (100 K) is shown in Fig. 1(*a*). This spectrum is clearly dominated by the presence of an intense orthorhombic signal with $g_1 = 2.0036$, $g_2 = 2.0095$, $g_3 = 2.0243$ and assigned to the superoxide $O_2^-$ anion. This anion is usually stabilised at a positive cationic site such that the electrostatic interaction splits the $2\pi^*$ antibonding orbitals by an amount ($\Delta$) depending on the local cationic crystal field. The magnitude of the $g_{zz}$ component ($g_3$ in this case) will give a measure of the cationic crystal field since $g_{zz} = g_e + 2\lambda/\Delta$ where $\lambda$ is the spin–orbit coupling constant of oxygen.[6] A $g_3$ value of 2.0263 clearly indicates that the $O_2^-$ anion is stabilised at a $Ti^{4+}$ cation in agreement with the $g$ values reported in the literature for $O_2^-$ adsorbed on $TiO_2$.[6]

Evacuation of the sample (30 min at 298 K, to $10^{-5}$ Torr) leads to the EPR spectrum shown in Fig. 1(*b*). Two very distinguishing features can be noted. First, the intensity of the $O_2^-$ signal has increased by a factor of about 40. This can be explained by the detection of predominantly surface $O_2^-$ anions with a much smaller abundance of bulk/subsurface superoxide. Only the bulk $O_2^-$ anions are visible in Fig. 1(*a*) since the surface $O_2^-$ anions undergo dipolar broadening with $O_2$ at low temperatures and so are not visible in the non-evacuated sample.

The second notable feature of Fig. 1(*b*) is the appearance of a new signal characterised by two low field and high field lines. The paramagnetic center(s) responsible for this signal are clearly stabilised on the rutile surface, since the signal is absent in the presence of $O_2$ due to the dipolar broadening. We propose that these new features correspond to the $\Delta M_s = 1$ transition of an $S = 1$ surface triplet arising from two interacting $S = 1/2$ species. This assignment is based on the following:

(*i*) the presence of a low field $\Delta M_s = 2$ transition at the expected magnetic field position of 165 mT [Fig. 1(*c*)];

(*ii*) it is not related in any way to the $O_2^-$ anions (*e.g.* as a superhyperfine interaction), since their respective saturation profiles are different and also the intensity of the new surface center varies slightly from one experiment to the next independent of the superoxide concentration.

Careful inspection of the new triplet signal reveals a 'splitting' of the two low field lines into an apparent doublet which is absent in the two high field lines. Assuming mutual orientation of the spin–spin and spin–nuclear axes with respect to the applied magnetic field, then simulation of the signal based on an $S = 1$ system with isotropic symmetry and $m_I = 1/2$ does not satisfactorily account for the line shape. In that case all $\Delta M_S = 1$ lines were split into doublets. The intensities of the

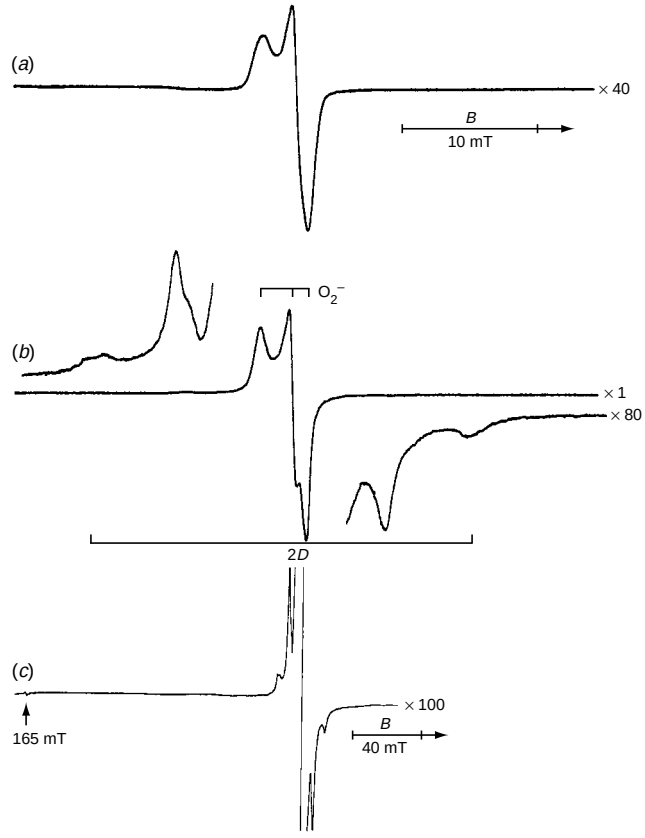



**Fig. 1** EPR spectrum (100 K) of rutile $TiO_2$ after contact with an aqueous solution of $H_2O_2$. (*a*) Sample prior to evacuation, (*b*) sample after evacuation at 298 K for 30 min, (*c*) sample as in (*b*) but recorded over wide scan range to show the half field feature at 165 mT.

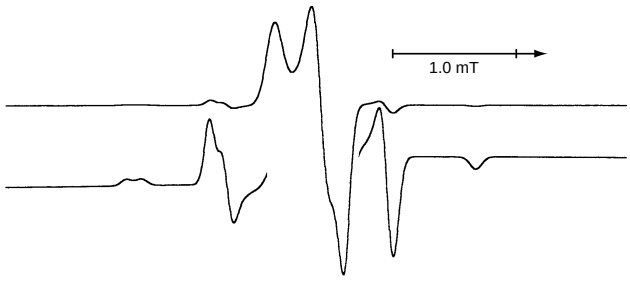



**Fig. 2** Computer simulation of Fig. 1(*b*) revealing the $O_2^-$ and the triplet $S = 1$ radical pair

apparent low field doublets also vary from one experiment to the next, suggesting the splitting arises from two separate signals rather than a hyperfine doublet. The best simulation obtained (Fig. 2) was based on two separate $S = 1$ centers having slightly different spin Hamiltonian parameters; *i.e.* triplet 1, $g_{iso} = 2.0104$ and $D = 13.7$ mT and triplet 2, $g_{iso} = 2.0064$ and $D = 12.7$ mT.

$D$ is the zero field splitting term and for randomly oriented triplets the separation between the $\Delta M_S = 1$ outer vertical lines is just $2D$ [Fig. 1(*b*)] so $D$ is easily extracted from the experimental spectrum.[7] The symmetry of the $g$ tensor, although reported as isotropic, may be slightly axial since small changes in the $g$ values did not produce drastic alterations to the simulation. Even though the individual $S = 1/2$ centers may have significantly lower symmetry (*e.g.* axial), in the coupled $S = 1$ state they appear to have a different symmetry, close to isotropic. Because the intensity of the $S = 1$ signal is so weak, precise analysis of the symmetry is not possible at present. Assuming $D$ is due entirely to a dipole–dipole interaction between two $S = 1/2$ species, then the distance $r$ separating the two species may be calculated using the equation $D = 3g^2\mu_B^2/2r^3 = -1.949 \times 10^{-4} g^2/r^3$ MHz.[8] This leads to a value of $r = 5.9$ and 6.0 Å riplet 1 and 2, respectively.

Based on the above EPR data, an assignment on the nature of the triplet center may be proposed. The absence of any hyperfine structure on the fine structure disfavours the possibility of any protonated $S = 1/2$ centers such as pairwise interacting $OH^\bullet$ or $H_2O^\bullet$ radicals. These radicals are involved in the homogeneous and heterogeneous decomposition of $H_2O_2$ and have been observed by EPR. $H_2O_2$ decomposition on MgO produces trapped $OH^\bullet$ radicals[3] and the pairwise trapping of $HO_2^\bullet$ radicals in aqueous glasses of $H_2O_2$ produce radical pairs with characteristic triplet state spectra.[9] Photoadsorption of $O_2$ on hydrated $TiO_2$ has also been reported to lead to the formation of surface trapped $HO_2^\bullet$ radicals but there was no observation of any $S = 1$ triplet centers.[10] However both $OH^\bullet$ and $HO_2^\bullet$ have appreciable hyperfine couplings of $a_{iso} \approx 2.7$ mT[3] and $a_{iso} \approx 1.1$ mT[11] respectively which should be visible in Fig. 1(*b*) where the line width of the $\Delta M_S = 1$ transition is only 0.9 mT. Furthermore ENDOR experiments failed to reveal the presence of any $^1H$ ENDOR lines. This would then indicate that the individual $S = 1/2$ species of the triplet pair do not contain a proton suggesting $O_2^-$ or $O^-$ as alternative candidates. A large number of oxide systems containing surface stabilised superoxide anions have been studied in the past. Despite the high concentrations of $O_2^-$ that may be formed, the pairing of two $O_2^-$ anions to produce a net $S = 1$ spin state has never been reported. Surface stabilised $O^-$ anions, with axial symmetry, have been reported on MgO but always as independent monomeric $S = 1/2$ centers.[12,13] However triplet state $O^-$ radical ion pairs have been observed in bulk monocrystals of alkaline earth oxides with $D$ terms ranging from 22.7 mT for MgO to 13.5 mT for SrO and spin–spin distances comparable to the lattice parameters of the oxides.[14] The observed $D$ terms in the present case (13.7 and 12.7 mT) are similar to those observed for other $O^-\cdots O^-$ radicals in oxides.

The formation of the triplet pair $O^-$ centers on the surface of rutile $TiO_2$ most likely occurs *via* the decomposition of the peroxide radical anion ($O_2^{2-} \rightarrow 2O^-$), the peroxide itself being formed directly or *via* the disproportionation of superoxide ($2O_2^- \rightarrow O_2 + O_2^{2-}$).[4] Indeed a similar mechanism has been proposed in the decomposition of surface $O_2^{2-}$ anions into active oxygen species, likely $2O^-$, over barium–lanthanum–oxygen mixed oxides, which have been postulated to be active in the oxidative coupling of methane.[15] We do not however speculate on any possible catalytic relevance of the $O^-\cdots O^-$ radical pair on $TiO_2$.

To summarise, a number of paramagnetic radicals have been observed following the heterogeneous decomposition of $H_2O_2$ over rutile $TiO_2$. Apart from the dominant presence of surface $O_2^-$ anions, a triplet state ($S = 1$) surface radical pair has been identified. This paramagnetic center arises from a pair of surface $O^-\cdots O^-$ anions in mutual interaction on rutile $TiO_2$ producing a net $S = 1$ triplet state. The observation of this surface centre is interesting since, despite the complex nature of the $H_2O_2$ interaction and the heterogeneous morphology of polycrystalline rutile $TiO_2$, the reproducibility of the results evidences the preferential stabilisation of $O^-$ anions at very specific surface sites consistently 5.9 or 6.0 Å apart. Similar surface triplet centers were not observed by us on anatase $TiO_2$ treated under similar conditions. This is to the best of our knowledge the first reported EPR spectrum of an $S = 1$ $O^-\cdots O^-$ radical anion pair stabilised on an oxide surface.

Funding of the National ENDOR center (by EPSRC) is gratefully acknowledged. E. W. G. would like to thank ICI Katalco and EPSRC for a CASE studentship.

## Footnote and References

* E-mail: sacdmm@cardiff.ac.uk

1 A. Sheldon and J. K. Kochi, *Metal Catalysed Oxidation of Organic Compounds*, Academic Press, New York, 1981.
2 A. Amorelli, C. J. Evans and C. C. Rowlands, *J. Chem. Soc., Faraday Trans. 1*, 1988, **84**, 1723.
3 E. Giamello, L. Calosso, B. Fubini and F. Geobaldo, *J. Phys. Chem.*, 1993, **97**, 5735.
4 E. Giamello, P. Rumori, F. Geobaldo, B. Fubini and M. C. Paganini, *Appl. Magn. Reson.*, 1996, **10**, 173.
5 B. D'Anna and E. Giamello, *Appl. Mag. Reson.*, 1996, **10**, 591.
6 M. Che and A. J. Tench, *Adv. Catal.*, 1983, **32**, 1.
7 E. Wasserman, L. C. Snyder and W. A. Yager, *J. Chem. Phys.*, 1964, **41**, 1763.
8 L. J. Beliner, *Spin Labelling; Theory and Applications*, Academic Press, New York, 1976, p. 149.
9 M. C. R. Symons, *Specialist Periodical Reports B, Electron Spin Resonance*, 1993, **13**, 215.
10 A. R. Gonzalez-Elipe, G. Munuera and J. Soria, *J. Chem. Soc., Faraday Trans. 1*, 1978, **75**, 748.
11 J. Bednarek and A. Plonka, *J. Chem. Soc., Faraday Trans. 1*, 1987, **83**, 3737.
12 N. B. Wong and J. H. Lunsford, *J. Chem. Phys.*, 1971, **55**, 3007.
13 M. Che and A. J. Tench, *Adv. Catal.*, 1982, **31**, 77.
14 J. Rubio O, H. T. Tohver, Y. Chen and M. M. Abraham, *Phys. Rev. B*, 1976, **14**, 5466 and references therein.
15 H. Yamashita, Y. Machida and A. Tomita, *Appl. Catal., A: General*, 1991, **79**, 203.

*Received in Exeter, UK, 11th August 1997; 7/05856J*

# CIT-5: a high-silica zeolite with 14-ring pores

**Paul Wagner,[a] Masahito Yoshikawa,[a]† Mark Lovallo,[b] Katsuyuki Tsuji,[a] Michael Taspatsis[b] and Mark E. Davis*[a]**

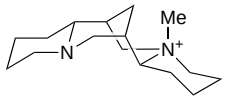
[a] *Division of Chemistry and Chemical Engineering, California Institute of Technology, Pasadena, CA 91125, USA*
[b] *Department of Chemical Engineering, University of Massachusetts, Amherst, MA 01003, USA*

**The synthesis and structure of a new zeolite, CIT-5 (California Institute of Technology Number Five), is described, which possesses one-dimensional pores comprised of 14 T-atoms (tetrahedrally coordinated silicon or aluminium atoms).**

Zeolites with pores comprised of larger than 12 T-atoms (extra-large pores) are much in demand[1–4] and have been so for many years.[4–7] The reason for this is the desire to perform catalysis/adsorption on molecules > 8 Å in size.

The first molecular sieve with extra-large pores was VPI-5 that is an aluminophosphate material with 18-ring pores.[8] Subsequently, other phosphate-based extra-large pore materials have been reported, *e.g.* cloverite.[2] All of the phosphate-based molecular sieves lack the desired properties of combined high acidity and thermal/hydrothermal stability and thus limit the practical potential. Recently, the first extra-large pore zeolite, UTD-1, was reported and shown to possess good acidity and thermal/hydrothermal stability.[9,10] Additionally, there have been numerous disclosures of ordered, aluminosilicate mesoporous materials with pore sizes of 20–100 Å.[11,12] Because the inorganic portions of the mesoporous materials are not crystalline, they lack the acidity and thermal/hydrothermal stability of high-silica zeolites.[13]

Here, we report a new extra-large pore zeolite denoted CIT-5. CIT-5 is synthesized under hydrothermal conditions. A reaction mixture of composition 0.2 ROH : 0.1 LiOH : 0.02 $Al_2O_3$ : 1 $SiO_2$ : 40 $H_2O$ is heated to 175 °C at autogenous pressure for *ca.* 12 d in order to produce CIT-5. In the absence of aluminium, pure-silica CIT-5 can be prepared in 5 d. The organic structure-directing agent (SDA), R, is *N*(16)-methylsparteinium **I** and is prepared as previously reported.[14] In the absence of lithium, **I** can form pure-silica or borosilicate SSZ-24.[13,14] Thus, the key to the successful preparation of CIT-5 is both the SDA **I** and the inclusion of lithium. Further synthetic details are forthcoming.[15]




**I**

Indexation[16] of the synchrotron powder X-ray diffraction (SPXRD) data from the pure-silica sample of CIT-5 revealed the presence of a small amount of an impurity phase together with the predominant CIT-5 phase. The CIT-5 material indexed in the orthorhombic crystal class with refined lattice constants $a$ = 13.694(2), $b$ = 5.0213(5), and $c$ = 25.4970(3) Å ($U$ = 1753.2 Å$^3$). The lattice constants for the impurity hexagonal phase were found to be $a$ = 13.63 and $c$ = 8.30 Å. The unit cell parameters and scanning electron micrographs helpd to identify the impurity phase as SSZ-24 (International Zeolite Association Code AFI).[17] Systematic absences for the orthorhombic CIT-5 phase indicate body-centering consistent with six possible space groups.

The starting model for Rietveld refinement of CIT-5 was obtained by an iterative process of model building, distance-least squares (DLS)[18] refinement of the atomic positions for the model, and comparison of the simulated powder X-ray pattern (CERIUS[19]) to the experimental pattern. The model with the closest match between the simulated X-ray powder pattern and the experimental XRD was found to have maximal topological symmetry of space group *Imma* (no. 74, standard setting) (consistent with the systematic absences).

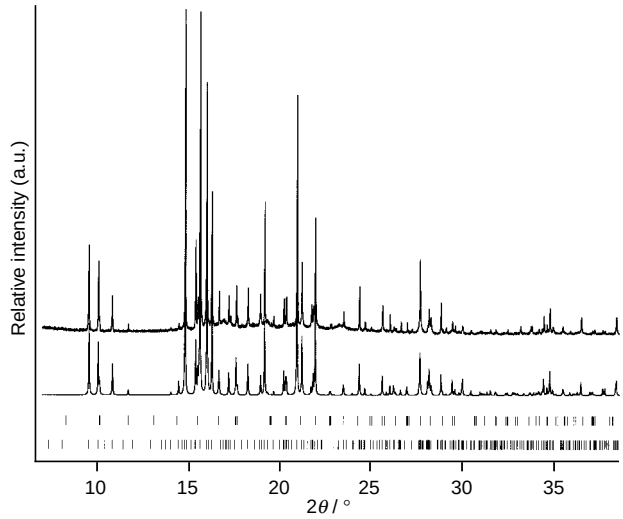



**Fig. 1** Experimental (top) and simulated (bottom) powder XRD data of CIT-5, $\lambda$ = 1.200 28(5) Å. The upper tick marks represents peak positions for the impurity phase, SSZ-24, while the bottom set of tick marks represents peak positions for CIT-5.

A two phase Rietveld refinement[20] was carried out using the structural parameters previously reported for the SSZ-24 impurity phase.[13] The background, scale factor and zero shift were refined, followed by refinement of the lattice parameters, peak shape function parameters and atomic positions for both

**Table 1** Crystallographic and refinement data

| | |
|---|---|
| Space group | *Imma* (no. 74) |
| $a$/Å | 13.6947(2) |
| $b$/Å | 5.0213(5) |
| $c$/Å | 25.4970(3) |
| $\lambda$/Å | 1.20028(5) |
| $T$/K | 298 |
| Profile range/° | 5–42.2 |
| Step scan increment/° | 0.005 |
| No observation | 7440 |
| No. structural parameters | 55 |
| No. profile parameters refined | 5 |
| No. background parameters | 20 |
| $R_{wp}$ (%) | 11.43 |
| $R_p$ (%) | 8.75 |
| $DW_d$[a] | 0.040 |
| Reduced $\chi^2$ | 6.898 |

[a] No serial correlation in fit at 90% confidence for 1.950 < $DW_d$ < 2.050.

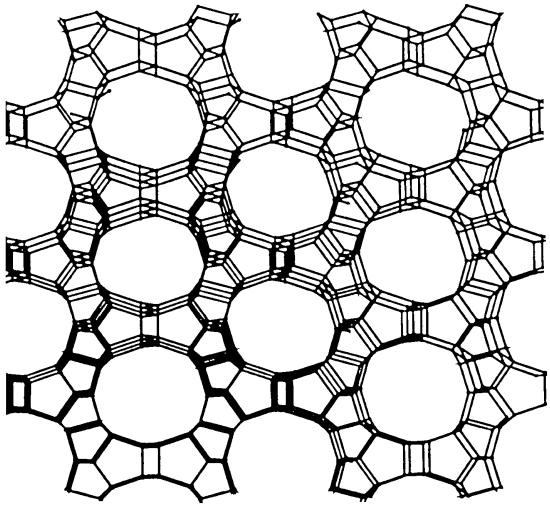


**Fig. 2** The [010] projection of CIT-5 showing the 14MR pores

CIT-5 and SSZ-24. Isotropic thermal parameters for the CIT-5 phase were also refined. The phase fraction refinement indicated *ca.* 4% SSZ-24 impurity. The low values of the residuals ($R_p$ = 8.7% and $R_{wp}$ = 11.4%) indicate close agreement between the calculated intensities from the refinement and the experimentally observed intensities (Fig. 1). Further details of the refinement results can be found in Table 1.

The structure of CIT-5 viewed down the *b*-axis is shown in Fig. 2 and is composed of one-dimensional, extra-large pores of nearly circular cross section (center of oxygen to center of oxygen distance 10.0 × 9.9 Å) circumscribed by 14-T-atom-membered rings (14MRs). The asymmetric unit contains 5 T-atoms and 8 oxygens resulting in a unit cell content of $[Si_{32}O_{64}]$, a framework density (FD) of 18.3 T-atoms/1000 Å$^3$, and a density of 1.821 g cm$^{-3}$. Table 2 contains the final atomic positional parameters and isotropic temperature factors obtained from the Rietveld refinement.

Comparison of the simulated, experimental and image processed experimental high resolution transmission electron micrographs (HRTEM) of CIT-5 viewed down the pores ([010] projection) are shown in Fig. 3, and confirm the topology of the structure. The primary building unit of CIT-5 is a zigzag ladder of four-membered rings (4MRs) with pendant five-membered rings (5MRs). These units are interconnected through single zigzag chains to form the body centered structure shown in Fig. 2. Electron diffraction patterns of CIT-5 show no signs of streaking indicating that the structure is not faulted or disordered.

Thermogravimetry showed an 11.2 mass% loss from **I** by 700 °C (in air). This amount of organic gives a pore volume of

**Table 2** Refined atomic positional parameters in space group *Imma* (No. 74) and isotropic thermal parameters (eds. in parentheses)

| Atom | *x* | *y* | *z* | $U_{iso}$/Å$^2$ |
|---|---|---|---|---|
| Si(1) | 0.1160(6) | 0.2500 | 0.0317(2) | 0.042(4) |
| Si(2) | 0.0000 | 0.7500 | 0.2788(6) | 0.082(6) |
| Si(3) | 0.2820(5) | 0.7500 | 0.1887(3) | 0.050(4) |
| Si(4) | 0.0000 | 0.2500 | 0.2177(4) | 0.020(4) |
| Si(5) | 0.1936(6) | 0.2500 | 0.1479(4) | 0.041(3) |
| O(6) | 0.0000 | 0.2500 | 0.0512(6) | 0.049(6) |
| O(7) | 0.0853(9) | 0.2500 | 0.1737(4) | 0.015(6) |
| O(8) | 0.0000 | 0.5776(31) | 0.2309(5) | 0.110(9) |
| O(9) | 0.1303(9) | 0.0000 | 0.0000 | 0.539(9) |
| O(10) | 0.1896(6) | 0.2500 | 0.0909(4) | 0.060(4) |
| O(11) | 0.2500 | 0.7500 | 0.2500 | 0.086(11) |
| O(12) | 0.0913(11) | 0.7500 | 0.3099(5) | 0.047(6) |
| O(13) | 0.2640(7) | 0.4474(22) | 0.1665(4) | 0.070(6) |

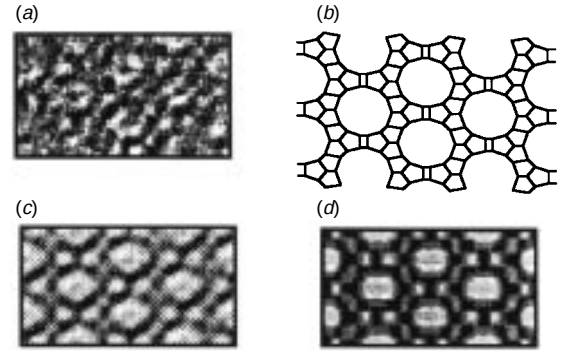



**Fig. 3** High-resolution transmission electron micrographs (HRTEM): (*a*) experimental, (*b*) [010] projection of CIT-5, (*c*) processed experimental image and simulated image (*d*). Samples for HRTEM were prepared by microtomy and images were recorded using a Phillips 430 electron microscope operating at 200 kV.

0.128 ml g$^{-1}$ and is consistent with the pore volume calculated from the structure (0.135 ml g$^{-1}$). While CIT-5 contains extra-large 14MR pores, temperature dependent powder XRD studies show that it has very high thermal and hydrothermal stability. The calcined material remains crystalline to over 900 °C, both under pure nitrogen atmosphere and under nitrogen atmosphere containing *ca.* 23 Torr $H_2O$.

Financial support for this work was provided by Chevron. We gratefully acknowledged R. Medrud and D. E. Cox for their assistance in collecting the synchrotron powder XRD data. The data were collected at the X7A beamline at the National Synchrotron Light Source at Brookhaven National Laboratory (Upton, NY), that is supported by the Department of Energy, Division of Material Science and Division of Chemical Sciences. P. W. thanks Air Products and Chemicals Inc. for financial support.

## Footnotes and References

* E-mail: mdavis@cheme.caltech.edu
† Current Address: Toray Industries Inc., Nagoya, 455, Japan.

1 M. E. Davis, *Chem. Ind. (London)*, 1992, **4**, 137.
2 M. Estermann, L. B. McCusker, Ch. Baerlocher, A. Merrouche and H. Kessler, *Nature*, 1991, **352**, 320.
3 M. E. Davis, *Nature*, 1991, **352**, 281.
4 M. E. Davis, *Nature*, 1989, **337**, 117.
5 R. M. Barrer and H. Villiger, *Z. Kristallogr.*, 1963, **128**, 352.
6 J. V. Smith and W. J. Dytrych, *Nature*, 1984, **309**, 607.
7 G. O. Brunner and W. M. Meier, *Nature*, 1989, **337**, 147.
8 M. E. Davis, C. Saldarriaga, C. Montes, J. Garces and C. Crowder, *Nature*, 1988, **331**, 698.
9 C. C. Freyhardt, M. Tsapatsis, R. F. Lobo, K. J. Balkus, Jr. and M. E. Davis, *Nature*, 1996, **381**, 295.
10 R. F. Lobo, M. Tsapatsis, C. C. Freyhardt, S. Khodabandeh, P. Wagner, C. Y. Chen, K. J. Balkus Jr., S. Zones and M. E. Davis, *J. Am. Chem. Soc.*, 1997, **119**, 8474.
11 C. T. Kresge, M. E. Leonowicz, W. J. Roth, J. C. Vartuli and J. S. Beck, *Nature*, 1992, **359**, 710.
12 P. T. Tanen and T. J. Pinnavaia, *Science*, 1995, **267**, 865.
13 R. F. Lobo and M. E. Davis, *Microporous Mater.*, 1994, **3**, 61.
14 Y. Nakagawa and S. Zones, *US Pat.*, 5 271 922, 1993.
15 M. Yoshikawa *et al.*, in preparation.
16 P. E. Werner, L. Erikson and M. Westdahl, *J. Appl. Crystallogr.*, 1985, **18**, 367.
17 W. M. Meier and D. H. Olson, *Atlas of Zeolite Structure Types*, Butterworth, 1987.
18 Ch. Baerlocher, A. Hepp and W. M. Meier, *DLS-76: A Fortran Program for the Simulation of Crystal Structures by Geometric Refinement*, Institute fur Kristallographie, ETH, Zurich, Switzerland, 1977.
19 CERIUS Version 3.2, Molecular Simulations, Cambridge, UK, 1993.
20 A. C. Larson and R. B. Von Dreele, *Los Alamos Laboratory Report*, 1987, No. LA-UR-86-748.

*Received in Cambridge, UK, 7th July 1997; 7/04774F*

# Electronic energy transfer between ruthenium(II) and osmium(II) polypyridyl luminophores in a hydrogen-bonded supramolecular assembly

**Nicola Armaroli,[a] Francesco Barigelletti,*[a] Giuseppe Calogero,[a] Lucia Flamigni,[a] Claire M. White[b] and Michael D. Ward*[b]**

[a] *Istituto FRAE–CNR, Via P. Gobetti 101, 40129 Bologna, Italy*
[b] *School of Chemistry, University of Bristol, Cantock's Close, Bristol, UK BS8 1TS*

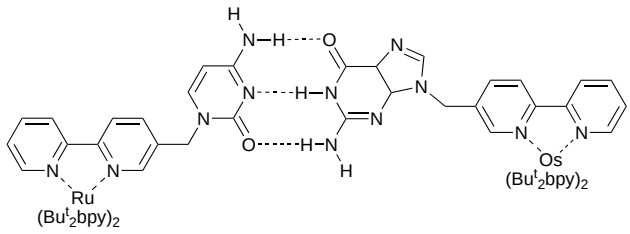
**Complexes Ru–C and Os–G are derivatives of $[Ru(bipy)_3]^{2+}$ and $[Os(bipy)_3]^{2+}$ bearing peripheral cytosine (C) or guanine (G) nucleobases respectively; in $CH_2Cl_2$ these undergo association ($K_A$ > 5000 dm$^{-3}$ mol$^{-1}$) by hydrogen bonding between the complementary C/G groups, and Ru → Os photoinduced energy-transfer occurs within Ru–C···G–Os associated pair.**

Many complexes are now known which display inter-component photoinduced energy transfer.[1–3] The study of such compounds is of fundamental interest both in relation to the mechanism of photosynthesis in nature,[2] and to recent efforts to prepare artificial molecular-scale electronic devices.[3] In virtually all cases the interacting components are covalently linked by a suitable bridging group, as this allows control of the inter-component separation, orientation, and the nature of the pathway between them through which the interaction can occur.

More recently supramolecular complexes have been prepared in which interacting components are associated by non-covalent interactions, in particular hydrogen bonding,[4] and photoinduced energy-transfer has been observed between metalloporphyrins and hydrogen-bonded organic fragments.[5] Although hydrogen bonding is widely used to promote self-assembly processes and to assist molecular recognition with organic compounds,[6] the association of metal complexes in the same way has received much less attention.[7,8]

Here we report on the association of ruthenium(II)– and osmium(II)–polypyridine units[3] driven by a triple hydrogen bond, and which results in photoinduced $Ru^{II} \rightarrow Os^{II}$ energy transfer across the hydrogen-bonded bridge. This was accomplished using metal complex components functionalised with the nucleotide bases cytosine (C) and guanine (G); the C/G pair gives Watson–Crick three-point hydrogen-bonding association with high constants (*ca.* $10^4$ dm$^3$ mol$^{-1}$) in low polarity solvents.[9]

The ligands bpy-C and bpy-G (Scheme 1) were prepared by alkylation of 5-bromomethyl-2,2′-bipyridine directly with cytosine at position $N^1$ to give bpy–C, or with 2-amino-6-chloropurine at position $N^9$ followed by acid hydrolysis to give bpy-G.[10]† Reaction of these with $[M(Bu^t_2bpy)_2Cl_2]$ [M = Ru, Os; $Bu^t_2bpy$ = 4,4′-di(*tert*-butyl)-2,2′-bipyridine][8] afforded $[Ru(Bu^t_2bpy)_2(bpy\text{-}C)][PF_6]_2$ (**Ru–C**) and $[Os(Bu^t_2bpy)_2(bpy\text{-}G)][PF_6]_2$ (**Os–G**).‡ The use of $Bu^t_2bpy$ ancillary ligands ensures good solubility in low-polarity solvents, to maximise association by hydrogen bonding. $[Os(Bu^t_2bpy)_2(bpy)][PF_6]$ (denoted **Os**) was also prepared.




**Scheme 1** Structure of the **Ru–C··Os–G** associate

The absorption properties in the visible region of **Ru–C** and **Os–G** dissolved in $CH_2Cl_2$ are as expected for ruthenium(II)– and osmium(II)–polypyridyl chromophores,[3] with band maxima occurring at 459 nm ($\varepsilon$ = 14 200 dm$^3$ mol$^{-1}$ cm$^{-1}$) and 484 (11 600), respectively, for population of the lowest-lying $^1$MLCT excited state. The luminescence band maxima of **Ru–C** and **Os–G** obtained in $CH_2Cl_2$ solvent are well separated with $\lambda_{max}$ = 626 and 744 nm, respectively. **Ru–C** is a much stronger emitter than **Os–G**, with $\Phi = 3.6 \times 10^{-2}$ ($\tau$ = 350 ns) and $2.9 \times 10^{-3}$ ($\tau$ = 44 ns), respectively.

We have demonstrated formation of a **Ru–C··G–Os** associate (where ··· signifies the triple cytosine/guanine hydrogen-bond; Scheme 1) by luminescence spectroscopy, comparing results obtained on 1 : 1 mixtures of **Ru–C** and **Os–G** in $CH_2Cl_2$ solution, before (*a*) and after (*b*) addition of drops of EtOH to break the hydrogen bonding between the components. The experiment was performed at three different concentrations: $[\mathbf{Ru–C}]_0 = [\mathbf{Os–G}]_0 = 1.0 \times 10^{-4}$ M, case (*i*); $2.2 \times 10^{-4}$ M, case (*ii*); and $4.5 \times 10^{-4}$ M, case (*iii*). Fig. 1 compares luminescence spectra recorded for case (*i*) (before and after additional of EtOH to break the hydrogen bonds), and those observed for a mixture of the reference couple **Ru–C** and **Os**. From Fig. 1 we see that EtOH addition causes an increase of the Ru-based luminescence intensity ($I_b/I_a$ = 1.4) for the **Ru–C**/**Os–G** pair, but has no effect on the Ru-based luminescence intensity for the **Ru–C**/**Os** pair. The absorption spectra of the mixtures are unaffected by the addition of EtOH. It follows that in the **Ru–C··G–Os** associate the Ru-based emission is

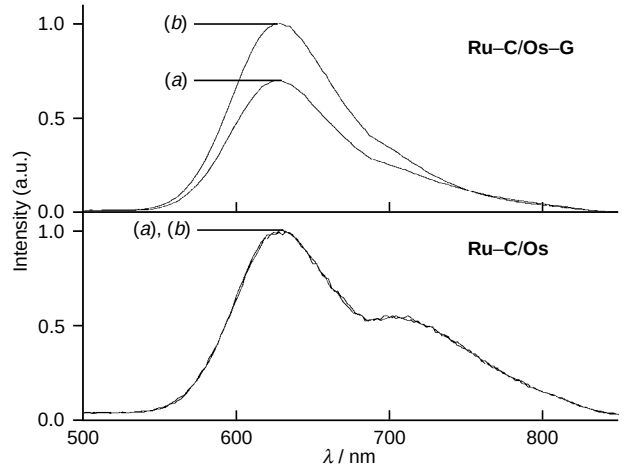



**Fig. 1** Upper: luminescence spectra of a $CH_2Cl_2$ solution of **Ru–C** and **Os–G** (both $1.0 \times 10^{-4}$ M), before (*a*) and after (*b*) EtOH addition. Lower: luminescence spectra of a $CH_2Cl_2$ solution of **Ru–C** ($3 \times 10^{-4}$ M) and **Os** ($7 \times 10^{-4}$ M), before (*a*) and after (*b*) EtOH addition. Excitation was at 458 nm.

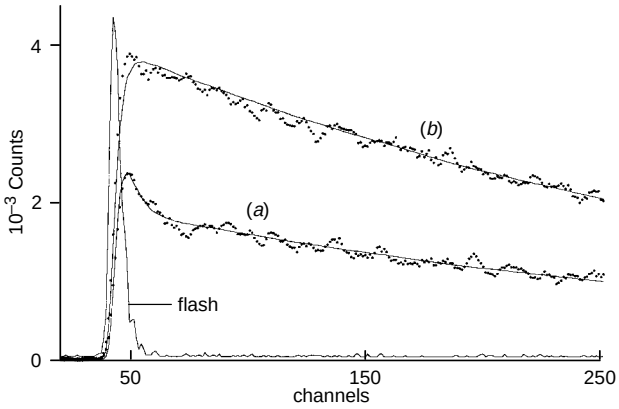



**Fig. 2** Decay of the luminescence intensity for a $CH_2Cl_2$ solution of **Ru**–**C** and **Os**–**G** (both $1.0 \times 10^{-4}$ M), before (*a*) and after (*b*) EtOH addition. Time axis was 1.03 ns/channel. Excitation was at 337 nm.

quenched, and this quenching is removed when the hydrogen bond is broken. In the latter case (**Ru**–**C**/**Os** pair) no hydrogen-bonding associate can be formed, so addition of EtOH had no effect on the emission properties of the mixture. For cases (*ii*) and (*iii*), the relative increases in luminescence intensity after addition of EtOH ($I_b/I_a$) were 1.6 and 4.0, respectively.

Fig. 2 shows the Ru-based time-resolved luminescence decay observed for case (*i*), as monitored at $\lambda_{em}$ = 626 nm. In neat $CH_2Cl_2$, case (*i*) (*a*), the decay follows a dual exponential law, $I(t) = B_1[\exp(-t/\tau_1)] + B_2[\exp(-t/\tau_2)]$, with $\tau_1$ = 10.5 ns, $\tau_2$ = 290 ns and $B_1/B_2$ = 0.7. EtOH addition, case (*i*) (*b*), results in a single exponential decay, $I(t) = B[\exp(-t/\tau)]$, with $\tau$ = 270 ns. Similar behaviour was shown for cases (*ii*) and (*iii*). From comparison of the luminescence intensity observed in $CH_2Cl_2$ before [cases (*a*)] and after [cases (*b*)] EtOH addition, and by entirely ascribing the residual Ru-based luminescence intensity of cases (*a*) to the unassociated **Ru**–**C** complex,§ it is possible to estimate an association constant $K_A > 5 \times 10^3$ dm$^3$ mol$^{-1}$ for formation of **Ru**–**C**··**G**–**Os**.¶

Use of time-resolved luminescence results allows estimates of the rate constants for both intermolecular and intra-associate quenching of the Ru-based luminescence of **Ru**–**C** by **Os**–**G**. Thus, for case (*i*), (*a*) intermolecular quenching controlled by diffusional processes results in $\tau_2$ = 290 ns as compared to $\tau$ = 400 ns for **Ru**–**C** alone in dilute solution.‖ The much more efficient quenching, resulting in $\tau_1$ = 10.5 ns, we ascribe to the process taking place within the **Ru**–**C**··**G**–**Os** associate because addition of EtOH [case (*i*), (*b*)], which is expected to cause disruption of the hydrogen bonds, results both in recovery of the Ru-based luminescence intensity at 626 nm (Fig. 1) and loss of the shorter-lived component of the luminescence decay (Fig. 2). Based on $k_{en} = 1/\tau_1 - 1/\tau$, the rate constant for this step is $k_{en} = 9.3 \times 10^7$ s$^{-1}$. For cases (*ii*) and (*iii*), $k_{en}$ was likewise found to be $9.5 \times 10^7$ s$^{-1}$ ± 10%. Attempts to obtain evidence for sensitization of the Os-based luminescence were unsuccessful because the Os-based luminescence ($\lambda_{max}$ = 744 nm) is hidden by the tail of the much stronger Ru-based luminescence (Fig. 1).

Energy transfer within the **Ru**–**C**··**G**–**Os** associate could in principle occur by the Förster (dipole–dipole)[11] or Dexter (exchange or through-bond)[12] mechanisms. Although the Förster mechanism is feasible at the shortest possible metal-to-metal separation,** estimated at *ca.* 13 Å from CPK models, the Dexter mechanism must be invoked for the greater metal–metal separations which are energetically favoured because of electrostatic repulsion. This implies a double electron exchange[13] *via* the hydrogen-bond interface, consistent with the recent finding that single electron transfer can be effectively mediated by H bonds.[14]

We thank the EPSRC (UK) for a Ph.D studentship (C. M. W.) and Johnson Matthey for the loan of ruthenium and osmium salts. We thank L. Ventura and M. Minghetti for technical support.

## Footnotes and References

* E-mail: mike.ward@bristol.ac.uk

† bpy-C: NaH (1 mmol) was added to a suspension of cytosine (111 mg, 1 mmol) and KI (30 mg, a catalytic amount) in dry, degassed *N*,*N*-dimethylformamide (dmf) and stirred for 0.5 h. A solution of 5-bromomethyl-2,2′-bipyridine (250 mg, 1 mmol) in dry dmf (2 cm$^3$) was added slowly to this mixture and the reaction was then stirred under $N_2$ at 50 °C overnight. Addition of water (100 cm$^3$) resulted in precipitation of clean bpy–C (175 mg, 62%).

bpy–G: a mixture of 1-amino-6-chloropurine (170 mg, 1 mmol), $K_2CO_3$ (276 mg, 2 mmol) and KI (30 mg, a catalytic amount) in dry $Me_2SO$ (10 cm$^3$) was stirred under $N_2$ for 10 min. A solution of 5-bromomethyl-2,2′-bipyridine (620 mg, 2.5 mmol) in dry $Me_2SO$ was then added slowly and the reaction was stirred under $N_2$ at room temp. for 3 h. Addition of water (50 cm$^3$) precipitated the intermediate 2-amino-6-chloro-9-{5-(2,2′-bipyridyl)methyl}purine (bpy–ACP) as an off-white solid (218 mg, 64%). bpy–ACP (215 mg, 0.6 mmol) was then heated to reflux in 0.1 M HCl (20 cm$^3$) for 4 h. After cooling and neutralisation (KOH), bpy-G precipitated as a white solid (156 mg, 77%). Satisfactory mass and $^1$H NMR spectroscopic data, and C, H, N, analyses, were obtained for both ligands and the intermediate bipy–ACP.

‡ The complexes were prepared in *ca.* 50% yield by reaction of $[M(Bu^t_2bpy)_2Cl_2]$ (M = Ru, Os, 1 mmol) with bpy-C or bpy-G as required (1 mmol) in ethylene glycol (10 cm$^3$) at 160 °C for 2 h followed by precipitation with aqueous $KPF_6$, followed by chromatography on alumina (Brockmann activity III) with $CH_2Cl_2$ containing 2–5% MeOH. ESMS of **Ru**–**C**: *m*/*z* 1062 $\{Ru(Bu^t_2bpy)_2(bpy–C)(PF_6)\}^+$, 459 $\{Ru(Bu^t_2bpy)_2(bpy–C)\}^{2+}$. ESMS of **Os**–**G**: *m*/*z* 1192 $\{Os(Bu^t_2bpy)_2(bpy–G)(PF_6)\}^+$, 523 $\{Os(Bu^t_2bpy)_2(bpy–G)\}^{2+}$. Satisfactory elemental analyses were also obtained.

§ For instance in case (*i*), $(B_1\tau_1)/(B_2\tau_2)$ = 0.014 (see text), so the contribution of the short-lived component to the steady state luminescence spectrum of Fig. 1 is < 2%.

¶ For instance, for case (*i*) and by using $[\mathbf{Ru}–\mathbf{C}]_0 = [\mathbf{Os}–\mathbf{G}]_0 = 1.0 \times 10^{-4}$ M and $[\mathbf{Ru}–\mathbf{C}]_0/[\mathbf{Ru}–\mathbf{C}]$ = 1.4 from Fig. 1, one may calculate [**Ru**–**C**··**G**–**Os**]; then $K_A$ = [**Ru**–**C**··**G**–**Os**]/([**Ru**–**C**][**Os**–**G**]) is evaluated.

‖ According to $\tau/\tau_2 = 1 + k_q\tau[\mathbf{Os}–\mathbf{G}]$, this is consistent with a second-order quenching constant $k_q = 9.5 \times 10^9$ dm$^3$ mol$^{-1}$ s$^{-1}$.

** According to the Förster treatment[11] the dipole–dipole rate constant for an intermetal separation of 13 Å is $k_F = 1.2 \times 10^8$ s$^{-1}$, to be compared with the experimental value $k_{en} = 9.3 \times 10^7$ s$^{-1}$, see text.

1 V. Balzani and F. Scandola, *Supramolecular Photochemistry*, Ellis Horwood, Chichester, 1991.
2 H. Kurreck and M. Huber, *Angew. Chem., Int. Ed. Engl.*, 1995, **34**, 849; M. R. Wasielewski, *Chem. Rev.*, 1992, **92**, 435.
3 V. Balzni, A. Juris, M. Venturi, S. Campagna and S. Serroni, *Chem. Rev.*, 1996, **96**, 759; A. Harriman and R. Ziessel, *Chem. Commun.*, 1996, 1707.
4 M. D. Ward, *Chem. Soc. Rev.*, 1997, in press.
5 J. L. Sessler, B. Wang and A. Harriman, *J. Am. Chem. Soc.*, 1995, **117**, 704; P. Tecilla, R. P. Dixon, G. Slobodkin, D. S. Alavi, D. H. Waldeck and A. D. Hamilton, *J. Am. Chem. Soc.*, 1990, **112**, 9408.
6 J.-M. Lehn, *Supramolecular Chemistry*, VCH, Weinheim, 1995; G. R. Desiraju, *Angew. Chem., Int. Ed. Engl.*, 1995, **34**, 2311; J. Bernstein, R. E. Davis, L. Shimoni and N.-L. Chang, *Angew. Chem., Int. Ed. Engl.*, 1995, **34**, 1555; S. Subramanian and M. J. Zaworotko, *Coord. Chem. Rev.*, 1994, **137**, 357.
7 A. D. Burrows, C. W. Chan, M. M. Chowdhry, J. E. McGrady and D. M. P. Mingos, *Chem. Soc. Rev.*, 1995, **24**, 329.
8 C. M. White, M. F. Gonzalez, D. A. Bardwell, L. H. Rees, J. C. Jeffery, M. D. Ward, N. Armaroli, G. Calogero and F. Barigelletti, *J. Chem. Soc., Dalton Trans.*, 1997, 727.
9 J. Pranata, S. G. Wiesschke and W. L. Jorgensen, *J. Am. Chem. Soc.*, 1991, **113**, 2810; J. L. Sessler, D. Magda and H. Furuta, *J. Org. Chem.*, 1992, **57**, 8181.
10 K. B. Mullah and W. G. Bentrude, *J. Org. Chem.*, 1991, **56**, 7218.
11 Th. Förster, *Discuss. Faraday Soc.*, 1959, **27**, 7.
12 D. L. Dexter, *J. Chem. Phys.*, 1953, **21**, 838.
13 G. L. Closs, M. D. Johnson, J. R. Miller and P. Piotrowiak, *J. Am. Chem. Soc.*, 1989, **111**, 3751.
14 P. J. F. De Rege, S. A. Williams and M. J. Therien, *Science*, 1995, **269**, 1409.

*Received in Basel, Switzerland, 14th August 1997; 7/05968J*

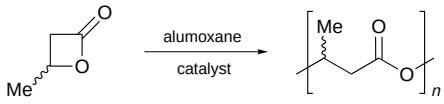
# The molecular structure of (*R*,*S*)-[$Al_6Bu^t_6(\mu_3\text{-}O)_4\{\mu_3\text{-}O_2CCH_2C(H)(Me)O\}_2$]: evidence for the latent Lewis acid catalyzed polymerization of (*R*,*S*)-β-butyrolactone

**C. Jeff Harlan,[a] Simon G. Bott,*[b] Bin Wu,[c] Robert W. Lenz*[c] and Andrew R. Barron*[a]**

[a] *Department of Chemistry, Rice University, Houston, Texas 77005, USA*
[b] *Department of Chemistry, University of Houston, Houston, Texas 77204, USA*
[c] *Department of Chemistry and Polymer Science and Engineering, University of Massachusetts, Amherst, MA 01003, USA*

**The reaction of $[Bu^tAl(\mu_3\text{-}O)]_6$ with 2 equiv. of (*R*,*S*)-β-butyrolactone resulted in the formation of the alumoxane, (*R*,*S*)-$[Al_6Bu^t_6(\mu_3\text{-}O)_4\{\mu_3\text{-}O_2CCH_2C(H)(Me)O\}_2]$, with a molecular structure consisting of two ring-opened lactone moieties inserted into, and bridging, the edge of the $Al_6O_6$ alumoxane. The role of this alumoxane in the latent Lewis acid catalyzed ring-opening polymerization of β-butyrolactone is discussed.**

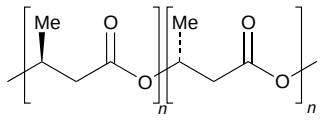
Alkylalumoxanes, $(RAlO)_n$, have been demonstrated to be catalysts for the ring opening polymerization of racemic β-butyrolactone, yielding a crystalline, high molecular mass polymer: poly-β-butyrolactone [eqn. (1)].[1]



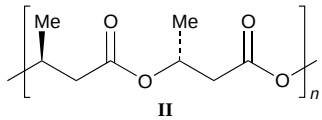

(1)

A range of alumoxane compounds have been investigated for this type of polymerization, including methylalumoxane (MAO), ethylalumoxane (EAO), and isobutylalumoxane (IBAO).[2] The activities of these alumoxane catalysts have been found to be highly dependent on the identity of the alkyl substituent, with the polymerization rates in the following order IBAO > EAO > MAO.

We have recently reported that the individual isolable *tert*-butylalumoxanes, $[Bu^tAl(\mu_3\text{-}O)]_n$ ($n$ = 6, 9), are also catalysts, as is a mixture of *tert*-butylalumoxanes (TBAO).[3] However, the stereoregular polymers prepared using MAO, EAO and IBAO are generally found to be isotactic in structure,[4] and it has been proposed that they consist of diads of isotactic sequences of approximately 5–10 repeating units of each configuration of (*R*)- and (*S*)-β-hydroxybutyrate unit sequences, **I**.[3] In contrast, the polymers formed using $[Bu^tAl(\mu_3\text{-}O)]_n$ were found to be predominantly syndiotactic in structure **II**.[3]



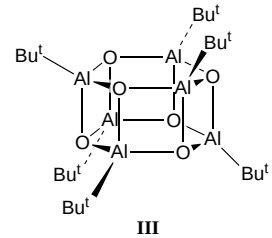

**I**




**II**

Irrespective of the details of the polymer microstructure obtained, it is clear that all alumoxane catalysts are able to convert a racemic mixture of (*R*,*S*)-β-butyrolactone into a stereoregular polymer by some type of stereospecific or steroselective propagation step; most likely one involving chain end control. The propagation process is generally agreed to occur by a coordination polymerization mechanism in which the monomer is insertion between the active site on the alumoxane and the growing, covalently bound, polymer chain. However, given the lack of understanding of the structure of alumoxanes in general it is not surprising that the initiation and propagation steps of polymerization are poorly understood.

We have previously demonstrated that the catalytic and co-catalytic activity of the isolable *tert*-butylalumoxanes, $[Bu^tAl(\mu_3\text{-}O)]_n$, is due to the opening of the $Al_nO_n$ cage, and we have postulated the term 'latent Lewis acidity' to describe this reactivity.[5] On the basis of these earlier results it is possible that the ring opening polymerization reaction of (*R*,*S*)-β-butyrolactone involves the alumoxane cage itself rather than the aluminium alkyl substituents. In that regard, our isolation of individual alkylalumoxanes[6,7] with proven catalytic activity has allowed us to investigate the initiation step in the ring opening polymerization of (*R*,*S*)-β-butyrolactone and we report herein the product formed from the reaction of hexameric alumoxane, $[Bu^tAl(\mu_3\text{-}O)]_6$ **III** with this monomer.




**III**

Addition of 2 equiv. of (*R*,*S*)-β-butyrolactone to a hexane solution of $[Bu^tAl(\mu_3\text{-}O)]_6$ at 25 °C, resulted in the formation of crystalline (*R*,*S*)-$[Al_6Bu^t_6(\mu_3\text{-}O)_4\{\mu_3\text{-}O_2CCH_2C(H)(Me)O\}_2]$ in *ca*. 30% yield. Use of only 1 equiv. of (*R*,*S*)-β-butyrolactone gave a lower yield of the same product. Although stable as a solid, (*R*,*S*)-$[Al_6Bu^t_6(\mu_3\text{-}O)_4\{\mu_3\text{-}O_2CCH_2C(H)(Me)O\}_2]$ decomposes in solution at room temp., producing unidentified products. However, X-ray quality crystals were obtained from the reaction mixture under suitable conditions. For example, reaction of $[Bu^tAl(\mu_3\text{-}O)]_6$ (650 mg) in hexane (25 $cm^3$) mixed with (*R*,*S*)-β-butyrolactone (0.18 $cm^3$) and allowed to stand, undisturbed, for 24 h.

The molecular structure of (*R*,*S*)-$[Al_6Bu^t_6(\mu_3\text{-}O)_4\{\mu_3\text{-}O_2CCH_2C(H)(Me)O\}_2]$, which resides on a crystallographic twofold axis, was determined by X-ray crystallography and is shown in Fig. 1.† The core structure consists of an $Al_6O_4$ ladder in a curved conformation, bridged by two $[O_2CCH_2C(H)(Me)O]^-$ ligands. The structure may be described as being derived from the opening of two adjacent edges of the hexagonal prismatic core of $[Bu^tAl(\mu_3\text{-}O)]_6$ and insertion of two

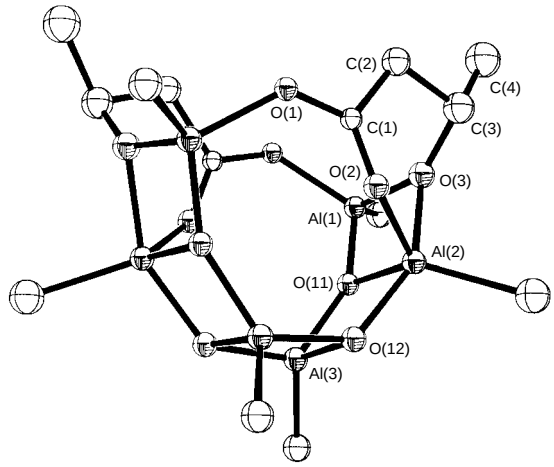



**Fig. 1** Molecular structure of (*R,S*)-[$Al_6Bu^t_6(\mu_3\text{-}O)_4\{\mu_3\text{-}O_2CCH_2C(H)(Me)O\}_2$]. Thermal ellipsoids are shown at the 30% level. All hydrogen atoms and *tert*-butyl methyl groups are omitted for clarity. Selected bond lengths (Å) and angles (°): Al(1)–O(1a) 1.82(1), Al(1)–O(3) 1.77(1), Al(1)–O(11) 1.71(1), Al(2)–O(2) 1.887(9), Al(2)–O(3) 1.99(1), Al(2)–O(11) 1.91(1); Al(2)–O(12) 1.807(9), Al(3)–O(11) 1.800(9), Al(3)–O(12) 1.84(1), Al(3)–O(12a) 1.79(1), C(1)–O(1) 1.29(1), C(1)–O(2) 1.23(1); O(1a)–Al(1)–O(3) 104.1(5), O(1a)–Al(1)–O(11) 108.6(5), O(3)–Al(1)–O(11) 85.9(5), O(2)–Al(2)–O(3) 85.4(4), O(2)–Al(2)–O(11) 118.2(4), O(2)–Al(2)–O(12) 89.1(4), O(3)–Al(2)–O(11) 75.0(4), O(3)–Al(2)–O(12) 152.1(5), O(11)–Al(2)–O(12) 83.7(4), O(11)–Al(3)–O(12) 85.7(4), O(11)–Al(3)–O(12a) 122.0(4), O(12)–Al(3)–O(12a) 86.7(4), Al(1a)–O(1)–C(1) 131.1(8), Al(2)–O(2)–C(1) 131.8(8), Al(1)–O(3)–Al(2) 96.8(5), Al(1)–O(3)–C(3) 138(1), Al(2)–O(3)–C(3) 119(1), Al(1)–O(11)–Al(2) 102.1(5), Al(1)–O(11)–Al(3) 155.1(5), Al(2)–O(11)–Al(3) 94.2(5), Al(2)–O(12)–Al(3) 96.2(5), O(1)–C(1)–O(2) 122(1).

molecules of β-hydroxybutyrate between the sides of the ladder. In this regard the cage opened core of (*R,S*)-[$Al_6Bu^t_6(\mu_3\text{-}O)_4\{\mu_3\text{-}O_2CCH_2C(H)(Me)O\}_2$] is unlike our previously characterized products from the latent Lewis acid reactions of [$Bu^tAl(\mu_3\text{-}O)]_6$ in which opposite edges are ordinarily opened.[5]

The geometries and bond distances around the Al and O atoms† are similar to those we have previously reported for other *tert*-butyl alumoxane compounds.[6,7] One unusual feature of the structure, however, is the presence of the two five-coordinate aluminium centers, Al(2) and Al(2a). As is common for five-coordinate aluminium, the geometry about Al(2) is that of a distorted trigonal bipyramid; O(3)–Al(2)–O(12) 152.1(5)°, and $\Sigma(X_{eq}\text{–Al–}X_{eq})$ = 359.3(6)°. The $[O_2CCH_2C(H)(Me)O]^-$ ligands, formed from the ring opening of the β-butyrolactone, each cap three of the aluminium atoms. The carboxylate moiety bridges atoms Al(1a) and Al(2), while the alkoxide terminus bridges atoms Al(1) and Al(2). The bond lengths and angles within the carboxylate unit are typical of such moieties[8] and are indicative of delocalization within the carboxylate group. The O–C–O angle [122(1)°] is similar to that in 'free' carboxylic acids. The carboxylate bite distance [Al(1a)···Al(2) 4.78 Å] is, however, significantly longer than previously observed for aluminium carboxylates (3.26–4.18 Å).[8] Unlike other types of bridging alkoxide compounds the Al(μ-OR)Al unit is asymmetrical, presumably due to the presence of both four- and five-coordinate aluminium centers and/or the ring strain within the cage.

Based on the structure described above, we can conclude that the ring-opening reaction of a β-butyrolactone by an alumoxane occurs by attack on the lactone's carbonyl group by the basic alumoxane oxo-ligands rather than by the alumoxane's alkyl substituents. This proposal is in line with our previous results which have shown that while the alkyl groups are relatively inert, the oxide ligands are basic, *e.g.*, they are readily protonated by even relatively weak acids.[9] Thus, it is clear from the structure of (*R,S*)-[$Al_6Bu^t_6(\mu_3\text{-}O)_4\{\mu_3\text{-}O_2CCH_2C(H)(Me)O\}_2$], and its activity as a polymerization catalyst, that the latent Lewis acid mechanism previously proposed for the ring opening of propylene oxide[10] is most likely involved in the initiation step in the polymerization of β-butyrolactone by *tert*-butylalumoxane. In addition, similar derivatives may be involved in the polymerization reactions of this monomer with other alkylalumoxanes.

Financial support of this work was provided by the Office of Naval Research (A. R. B.), and Robert A. Welch Foundation (S. G. B. and A. R. B.), and the Materials Research Laboratory of the University of Massachusetts funded by the National Science Foundation (R. W. L.).

## Footnotes and References

* E-mail: arb@ruf.rice.edu

† *Crystal data* for $C_{32}H_{66}Al_6O_{10}$, $M$ = 772.77, monoclinic, space group $C2/c$ (no. 15), $a$ = 25.819(2), $b$ = 10.5579(9), $c$ = 18.902(1) Å, $\beta$ = 118.030(7)°, $U$ = 4548.2(7) Å$^3$, $D_c$ = 1.128 g cm$^{-3}$, $Z$ = 4, $F(000)$ = 1664, Mo-Kα radiation, $\lambda$ = 0.710 73 Å, $\mu$ = 1.80 cm$^{-1}$. Enraf-Nonius CAD-4 automated diffractometer, 3033 reflections collected, $2 \leqslant 2\theta \leqslant 44°$, absorption (DIFABS) correction, 2967 unique reflections and 756 having with $F > 6\sigma(F)$. Structure solved by direct methods (SHELXS-86), and Fourier difference synthesis. Refinement by full-matrix least squares with all non-hydrogen atoms isotropic. Hydrogen atoms were placed in calculated positions [$d$(C–H) = 0.95 Å, $U$(H) = 1.2 $U_{eq}$ (attached carbon)], converged $R$ = 0.0567, $R_w$ = 0.0794. CCDC 182/624.

1 H. Tani, S. Yamashita and K. Teranishi, *Polym. J.*, 1972, **3**, 417; K. Teranishi, T. Araki and H. Tani, *Macromolecules*, 1972, **5**, 660; J. R. Shelton, J. B. Lando and D. E. Agostini, *J. Polym. Sci., Part B: Polym. Phys.*, 1971, **9**, 173; D. E. Agostini, J. B. Lando and J. R. Shelton, *J. Polym. Sci., Part A: Polym. Chem.*, 1971, **9**, 2775.
2 M. Benvenuti and R. W. Lenz, *J. Polym. Sci., Part A: Polym. Chem.*, 1991, **29**, 793; A. D. Pajerski and R. W. Lenz, *Makromol. Chem. Macromol. Symp.*, 1993, **73**, 7.
3 R. W. Lenz, J. Yang, B. Wu, C. J. Harlan and A. R. Barron, *Can. J. Microbiol.*, 1995, **41**, 274.
4 M. Yokouchi, Y. Chatani, H. Taddakoro, K. Teranichi and H. Tani, *Polymer*, 1973, **14**, 267.
5 C. J. Harlan, S. G. Bott and A. R. Barron, *J. Am. Chem. Soc.*, 1995, **117**, 6465; Y. Koide, S. G. Bott and A. R. Barron, *Organometallics*, 1996, **15**, 2213; Y. Koide, S. G. Bott and A. R. Barron, *Organometallics*, 1996, **15**, 5514.
6 M. R. Mason, J. M. Smith, S. G. Bott and A. R. Barron, *J. Am. Chem. Soc.*, 1993, **115**, 4971.
7 C. J. Harlan, M. R. Mason and A. R. Barron, *Organometallics*, 1994, **13**, 2957.
8 See, C. E. Bethley, C. L. Aitken, Y. Koide, C. J. Harlan, S. G. Bott and A. R. Barron, *Organometallics*, 1997, **16**, 329 and references therein.
9 C. C. Landry, C. J. Harlan, S. G. Bott and A. R. Barron, *Angew. Chem., Int. Ed. Engl.*, 1995, **34**, 1202.
10 B. Wu, C. J. Harlan, R. W. Lenz and A. R. Barron, *Macromolecules*, 1997, **30**, 316.

*Received in Columbia, MO, USA; 28th July 1997; 7/05437H*

# Post-synthesis grafting of Al onto MCM-41

**Robert Mokaya* and William Jones**

*Department of Chemistry, University of Cambridge, Lensfield Road, Cambridge UK CB2 1EW*

**Al-containing MCM-41 materials are prepared by grafting Al onto purely siliceous MCM-41; the resulting materials retain the hexagonal order and physical properties of the purely siliceous parent MCM-41 and exhibit higher Brønsted acid content compared to Al-MCM-41 prepared by direct hydrothermal synthesis.**

The recent synthesis of the M41S family of siliceous solids with sharply distributed pores of diameter in the mesoporous regime (20–100 Å) has greatly increased the range of heterogeneous catalysts.[1–3] Of particular interest is MCM-41 which possesses a hexagonally arranged array of uniform pores. Brønsted acid sites may be generated in MCM-41 by isomorphous substitution of Al for Si.[2,3] However, the direct synthesis of aluminium containing MCM-41 has proved to be challenging; the incorporation of even small amounts of aluminium in the MCM-41 framework causes a decrease in hexagonal ordering.[4,5] It has also been observed that when compared to zeolites, the concentration of Brønsted acid sites in such aluminosilicate MCM-41 is very low even at high aluminium concentrations.[2,3,6] It is therefore desirable to prepare aluminosilicate MCM-41 which exhibits both higher Brønsted acid content and long range order similar to that of the purely siliceous material. An alternative synthetic approach which may address both these challenges is the post synthesis grafting/incorporation of aluminium into MCM-41. This is possible due to the presence of a high density of silanol groups on the pore surface of MCM-41 to which guest species may be attached.[7–9] Here we report a grafting method which consists of reacting the silanol groups present in MCM-41 with discrete amounts of aluminium alkoxide in a non-aqueous environment, followed by calcination to anchor the Al.

The starting material, a purely siliceous MCM-41 (designated PSMCM), was prepared by adding tetramethylammonium hydroxide (TMAOH) and sodium hydroxide (NaOH) to an aqueous solution of hexadecyltrimethylammonium chloride (CTACl) of appropriate concentration with stirring for 10 min. Tetraethylorthosilicate (TEOS) was combined with the resulting solution at room temp. under stirring to give a gel of molar composition 0.25 TEOS : 0.06 NaOH : 0.03 TMAOH : 27.8 $H_2O$ : 0.06 CTACl which was left to react for 24 h at room temp. The solid product was obtained by filtration, washed with distilled water, dried in air at room temp. and finally calcined at 550 °C for 16 h. For alumination, 2.0 g of PSMCM was dispersed in 50 ml dry hexane, and added to 150 ml dry hexane containing the appropriate amount of aluminium isopropoxide, $Al(OPr^i)_3$, to give Si : Al ratio in the range 40–5 : 1. The resulting mixture was stirred for 10 min and allowed to react at room temp. for 24 h. The obtained powder was filtered, washed with dry hexane, dried at room temp. and calcined at 550 °C for 4 h. Four samples (designated Al-PSMCMX, where X is the Si : Al ratio) were prepared from PSMCM at Si/Al ratio 40, 20, 10 and 5.

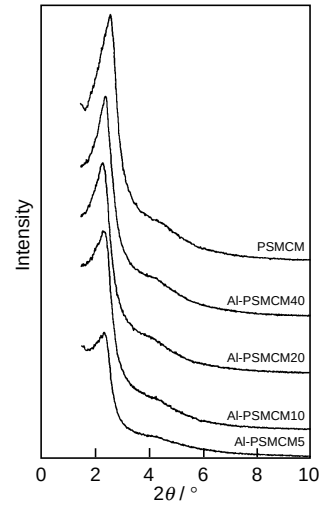



**Fig. 1** Powder XRD patterns of calcined purely siliceous sample (PSMCM) and Al-grafted (Al-PSMCM) samples

Fig. 1 shows that the powder X-ray diffraction patterns of the Al grafted materials are similar to that of the parent MCM-41 which is an indication that hexagonal order is maintained. TEM shows that, despite the gradual reduction in the intensity of the (100) peak, the hexagonal arrangement of the pores remains the same in all cases. Chemical analysis given in Table 1 shows that the Si/Al molar ratios of the Al-grafted samples are close to the expected bulk Si/Al ratios which is an indication of the potential of the present method in introducing discrete amounts of heteroatoms to purely siliceous MCM-41. $^{27}$Al MAS NMR spectra (of the calcined samples) shown in Fig. 2 indicate that all the samples contain tetrahedral (framework) and octahedral (non-framework) Al with resonances at $\delta$ 53.0 and 0, respectively. The amount of tetrahedral Al is always higher than the octahedral Al and generally increases with increasing Al content. For the dry samples, octahedral Al was always higher

**Table 1** Elemental composition, *d* spacing and textural properties and acidity of the study materials (CHA = cyclohexylamine)

| Sample | Si/Al | $d_{100}$/Å | Surface area/m$^2$ g$^{-1}$ | Pore volume/ cm$^3$ g$^{-1}$ | APD[a]/Å | $a_0$[b]/Å | Wall thickness/Å | Acidity/ mmol CHA g$^{-1}$ |
|---|---|---|---|---|---|---|---|---|
| PSMCM | | 33.8 | 1110 | 0.93 | 26.3 | 39.0 | 12.7 | |
| Al-PSMCM40 | 38.5 | 34.8 | 1000 | 0.82 | 26.8 | 40.2 | 13.4 | 0.16 |
| Al-PSMCM20 | 19.8 | 36.4 | 1004 | 0.81 | 26.7 | 42.0 | 15.3 | 0.29 |
| Al-PSMCM10 | 11.2 | 36.0 | 996 | 0.78 | 26.6 | 41.6 | 14.9 | 0.48 |
| Al-PSMCM5 | 6.1 | 35.7 | 980 | 0.77 | 26.5 | 41.2 | 14.7 | 0.51 |

[a] APD = Average pore diameter (determined using BJH analysis). [b] $a_0$ = Lattice parameter from XRD data using the formula $a_0 = 2d_{100}/\sqrt{3}$.

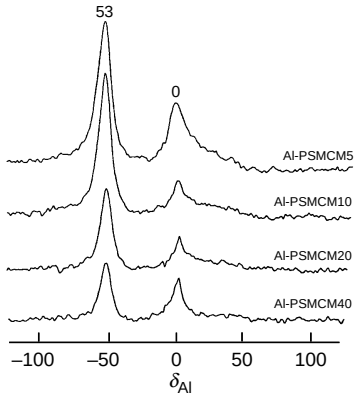



**Fig. 2** $^{27}$Al MAS NMR spectra of calcined Al-PSMCM samples. To ensure quantitative reliability all samples were hydrated and equilibrated with room air prior to measurement.

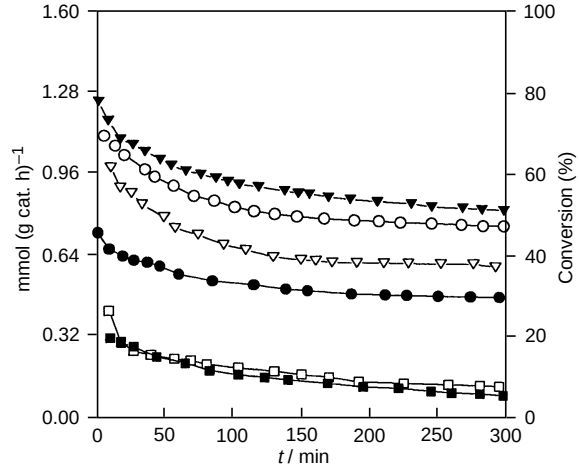



**Fig. 3** Cumene conversion over Al-PSMCM samples and reference materials compared at 300 °C and WHSV of 5.5. Al-PSMCM5 (▼), Al-PSMCM10 (○), Al-PSMCM20 (▽), Al-PSMCM40 (●), H$^+$-MCM41-20 (□), and SA10 (■)

than tetrahedral Al and therefore calcination serves to anchor some (octahedral) Al to the framework.

The *d* spacing of the Al-grafted materials was in all cases higher than that of the parent MCM-41 (see Table 1). This is consistent with the presence of tetrahedral Al in the framework. Table 1 also gives the textural properties obtained for the calcined Al-PSMCM materials. The surface area and average pore diameter (obtained by BJH analysis of the sorption data) of the Al-PSMCM materials are similar to that of the parent MCM-41 while the pore volume is lower probably due to the presence of non-framework Al in the pores. The pore wall thickness of the Al-grafted samples was in all cases higher than that of the parent purely siliceous MCM-41 sample in agreement with the incorporation of Al into the framework.

The acid content of the Al-PSMCM materials was obtained using thermally programmed desorption of cyclohexylamine.[3] Prior to analysis the base containing samples were heat treated at 250 °C for 2 h. This method principally determines the proton concentration which is of interest to catalysis. It is clear from the acidity values in Table 1 that the Al-grafting process generates acid sites and that the number of acid sites generated increases as the amount of framework aluminium increases. The acid content of Al-PSMCM10 and Al-PSMCM5 are very close in agreement with the $^{27}$Al MAS NMR which shows them to possess almost similar amounts of tetrahedral Al. We found that for similar bulk Si/Al ratios, the acidity of Al-PSMCM samples is higher than that of equivalent (protonic) aluminosilicate MCM-41 prepared using the conventional direct synthesis method (for example H$^+$-MCM-41-20 (see ref. 3 for sample details) had an acid content of 0.19 mmol g$^{-1}$ compared to 0.29 mmol g$^{-1}$ for Al-PSMCM20. We also prepared Al-grafted amorphous silica (designated SA10) at a Si/Al ratio of 10; the resulting material had an acid content of 0.22 mmol g$^{-1}$ compared to 0.48 for the equivalent (in terms of Al content) Al-PSMCM10 sample. Confirmation of the higher acid content of Al-grafted samples was provided by their activity in the cracking of cumene as shown in Fig. 3. The reaction, performed at 300 °C and a WHSV of 5.5 using a tubular stainless steel, continuous flow fixed-bed microreactor system with helium (25 ml min$^{-1}$) as carrier gas after activating the catalyst bed (100 mg; 30–60 mesh) for 1.5 h at 500 °C under helium (25 ml min$^{-1}$) proceeded almost exclusively *via* catalytic cracking to benzene and propene with only trace amounts of α-methylstyrene (product of dehydrogenation over Lewis acid sites) indicating that the active sites are of the Brønsted type.[10] The curves in Fig. 3 indicate that Al-PSMCM materials possess considerable catalytic activity, with the conversion of cumene increasing with increasing acid content and amount of framework aluminium. In particular we note that the activity of the Al-PSMCM materials is superior to that of equivalent MCM-41 prepared by direct synthesis (see comparison between H$^+$-MCM-41-20 and Al-PSMCM20). The Al-grafted amorphous silica (SA10), in line with the acid content, had a much lower activity compared to the equivalent Al-grafted MCM-41 (Al-PSMCM10). The purely siliceous material exhibited no catalytic activity.

We have demonstrated that Al-containing MCM-41 of good order can be prepared by post-synthesis grafting of Al by reacting purely siliceous MCM-41 with an Al–alkoxide in non-aqueous media. The Al is incorporated into the framework to generate materials with Brønsted acid sites whose content is higher than in equivalent Al-MCM-41 materials prepared *via* the conventional direct synthesis method. We attribute the higher acid content in the Al-grafted materials to the presence of Brønsted acid generating Al in accessible sites on the pore walls.

R. M. is grateful to the EPSRC for an Advanced Fellowship. The assistance of Laporte Absorbents in surface area measurements and Dr H. Y. He for NMR measurements is appreciated.

## Footnote and References

* E-mail: rm140@cus.cam.ac.uk

1 C. T. Kresge, M. E. Leonowicz, W. J. Roth, J. C. Vartuli and J. S. Beck, *Nature*, 1992, **359**, 710.
2 A. Corma, V. Fornés, M. T. Navarro and J. Pérez-Pariente, *J. Catal.*, 1994, **148**, 569.
3 R. Mokaya, W. Jones, Z. Luan, M. D. Alba and J. Klinowski, *Catal. Lett.*, 1996, **37**, 113.
4 C. Y. Chen, S. L. Burkett, H-X. Li and M. E. Davis, *Microporous Mater.*, 1993, **2**, 27.
5 Z. H. Luan, H. Y. He, W. Z. Zhou, C. F. Cheng and J. Klinowski, *J. Chem. Soc., Faraday Trans.*, 1995, **91**, 2955.
6 J. Weglarski, J. Datka, H. Y. He and J. Klinowski, *J. Chem. Soc., Faraday Trans.*, 1996, **92**, 5161.
7 T. Maschmeyer, F. Rey, G. Sankar and J. M. Thomas, *Nature*, 1995, **378**, 159.
8 R. Anwander and R. Roesky, *J. Chem. Soc., Dalton Trans.*, 1997, 137.
9 H. Hamdan, S. Endud, H-Y. He, M. N. M. Muhid and J. Klinowski, *J. Chem. Soc., Faraday Trans.*, 1996, **92**, 2311.
10 J. W. Ward, *J. Catal.*, 1967, **9**, 225; 1968, **11**, 251, 259.

*Received in Bath, UK, 15th July 1997; 7/05340A*

# Synthesis and characterization of intramolecular *N*-strapped porphyrins

**Yoshihiro Ishimaru,* Shigeki Sumida and Takeaki Iida**

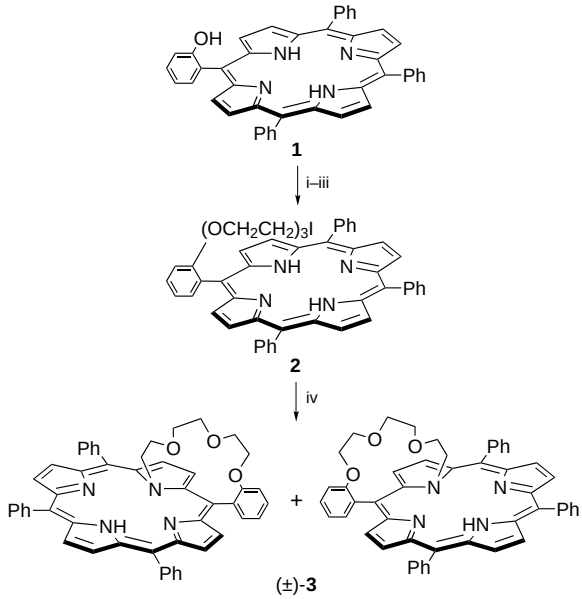
*Department of Functional Materials Science, Faculty of Engineering, Saitama University, 255 Shimo-ohkubo, Urawa 338, Japan*

**The first successful synthesis and characterization of intramolecular *N*-strapped porphyrins and the separation of a set of enantiomers are described.**

The functionalization of porphyrin macrocycles has become of interest in the field of supramolecular and biomimetic chemistry. Moreover, current investigations of porphyrin chemistry have led to the construction of new structural motifs using porphyrin rings.[1,2] *N*-Alkylporphyrins have been synthesized as biologically important compounds, after having been found to be formed by the reaction of alkenes with the cytochrome P-450 in the liver of mice. The aim of the present investigation was to synthesize the *N*-alkylporphyrins with new structural properties. Accordingly, we decided upon the preparation of intramolecular *N*-strapped porphyrins, that is, with one nitrogen atom alkylated by a tris(3-oxapropylene) bridge the other end of which was joined at the 2-position of a *meso* phenyl group.

The proposed intramolecular *N*-alkylation introduced three structural motifs into the porphyrin ring. (i) The generation of an asymmetric nitrogen atom. (ii) The steric distortion of the porphyrin ring. (iii) The construction of a half crown ether type bridge. To the best of our knowledge, despite the development of various methods for the alkylation of inner nitrogen atom(s),[3] no practical synthetic methods have yet been proposed for intramolecular *N*-alkylation. Accordingly, we propose here the synthetic method shown in Scheme 1.

Compound **1** was synthesized by condensation of pyrrole, benzaldehyde and 2-hydroxybenzaldehyde in a 4 : 3 : 1 molar ratio according to the method of Little *et al.*[4] The alkyl halide, 5-[2′-(9″-iodo-1″,4″,7″-trioxanonyl)phenyl]-10,15,20-triphenylporphyrin **2** was synthesized from **1** in 73% overall yield.




**Scheme 1** *Reagents and conditions*: i, NaOH, $I(CH_2CH_2O)_3THP$, dry DMSO, room temp., 12 h; ii, TsOH, MeOH–$CH_2Cl_2$, room temp., 12 h; iii, imidazole, $I_2$, $PPh_3$, benzene, room temp., 0.5 h; iv, $AgBF_4$, MeCN, reflux, 3 days

The detailed reaction conditions are shown in the caption to Scheme 1. The starting material **2** (0.3 mmol) and $AgBF_4$ (0.6 mmol) were stirred in refluxing dry MeCN (30 ml) for 3 days. After chromatographic purification, the desired product could be collected as a second purple band ($R_f$ 0.2, chloroform–methanol, 97 : 3) in 50% yield. Compound **3** has a UV–VIS spectrum that is fairly typical of *N*-alkylporphyrin free base derivatives.†

The reaction of **2** with $AgBF_4$ gave carbonium ion intermediates formed by the precipitation of AgI. The resulting intermediates were readily attacked by the intramolecular pyrrolic nitrogen atom *in situ* to give the proposed compound.

Fig. 1 shows $^1$H NMR spectrum of **3**. Extraordinarily up-field shifted signals at −4.08 and −4.31 ppm due to *N*-$CH_2$ protons and twelve multiplet signals due to the CH protons were evidence of the intramolecular conjugation of the tris(1-oxapropylene) bridge with asymmetric nitrogen atom. Signals at 8.78 (2 H), 8.67, 8.54, 8.47, 8.44, 7.61 and 7.52 ppm were assigned to the eight β-pyrrole protons on the basis of their peak intensity and coupling constants ($J$ 4.5 Hz). In particular, the signals at 7.61 and 7.52 ppm were strictly assigned to the *N*-alkylated β-pyrrole protons as explained by Kuila *et al.*[5] Signals at 7.66, 7.40 and 7.25 ppm were assigned to the *o*′-, *m*- and *m*′-protons of the 5-phenyl group, respectively, by 2D COSY measurement. This evidence suggested that the porphyrin ring was restrictively distorted by the introduction of an intramolecular strap.

As a result of the introduction of an intramolecular strap, two sets of enantiomers were expected to be formed at the different possible *N*-alkylation positions. Thus, a detailed two-dimensional NMR study (HMBC method) was performed to confirm which nitrogen atom is alkylated. The signal at 122.24 ppm† is correlated with the signals at 7.61 ppm due to the *N*-alkylated β-pyrrole proton and 7.66 ppm due to the *o*′-phenyl proton of the 5-phenyl group. Thus, we concluded that either the N(21) or N(22) atom of the pyrroles, which are adjacent to the 5-phenyl

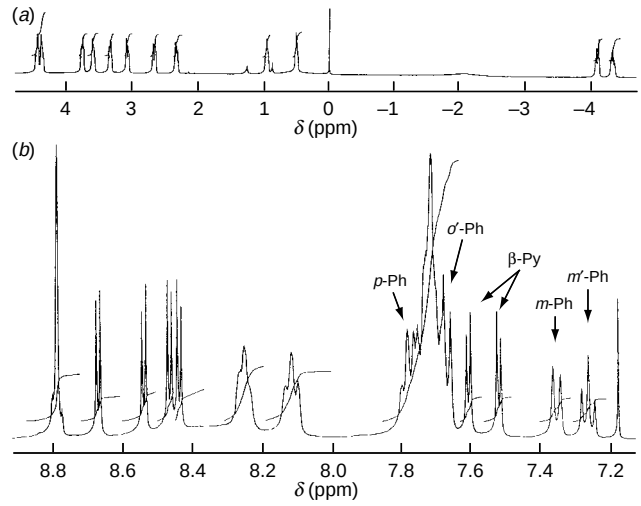



**Fig. 1** Portions of the $^1$H NMR spectrum of **3** in $CDCl_3$; (*a*) the tris(1-oxapropylene) region; (*b*) the aromatic region

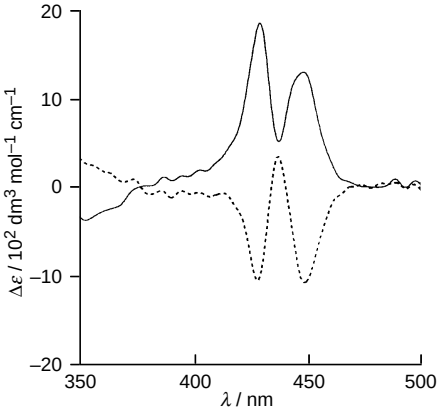



**Fig. 2** CD spectra of (+)-**3** (—) and (−)-**3** (- - -) in $CHCl_3$

group attached to the tris(1-oxapropylene) side chain, were alkylated. The length of the tris(1-oxapropylene) side chain is especially well-suited for connecting the 5-phenyl group and the nitrogen atom of the adjacent pyrrole rings.

It is considered that compound **3** is a set of enantiomers with an asymmetric nitrogen atom. Consequently, separation of racemic compound **3** was attempted using chiral HPLC (CHIRALCEL OD; Daisel Co. Lt. in Japan) eluted by *n*-hexane–propan-2-ol (7 : 3). Two fractions each of 100% ee were obtained.

The separated enantiomers, (+)-**3** and (−)-**3**, show mirror-image circular dichroism spectra and a split Cotton effect in the Soret region as shown in Fig. 2.

In summary, a new type of *N*-alkylporphyrin has been synthesized and characterized. The present work provides a unique technique for controlling the distortion of porphyrinoid macrocycles through intramolecular *N*-strapping. *N*-Alkylation studies with chains of different lengths is now under way.

We thank Dr J.-i. Setsune of Kobe university for useful discussions, Mr K. Fujikura of Varian Japan Limited for measurement of HMBC spectra and Mr T. Koyama for measurement of FAB mass spectra.

## Footnotes and References

* E-mail: ishimaru@apc.saitama-u.ac.jp

† *Selected data* for **3**: $\delta_H(CDCl_3)$ 8.78 (×2), 8.67, 8.54, 8.47, 8.44, 7.61, 7.52 (8 × d, 8 × 1 H, β-Py), 8.1–8.5 (3 × br, 3 × 2 H, *o*-Ph), 7.66 (d, 1 H, *o*′-Ph), 7.40 (d, 1 H, *m*-Ph), 7.25 (t, 1 H, *m*′-Ph), 7.7–7.8 (m, 10 H, *o*-, *p*-, *p*′-Ph), 4.36, 4.42 (2 × m, 2 × 1 H, 2″-$CH_2$), 3.73, 3.59 (2 × m, 2 × 1 H, 3″-$CH_2$), 3.31, 3.07 (2 × m, 2 × 1 H, 5″-$CH_2$), 2.67, 2.33 (2 × m, 2 × 1 H, 6″-$CH_2$), 0.96, 0.51 (2 × m, 2 × 1 H, 8″-$CH_2$), −4.08, −4.31 (2 × m, 2 × 1 H, 9″-$CH_2$), −2.11 (br, 1 H, NH); $\delta_C(CDCl_3)$ 126.11, 122.24, 119.54, 118.95 (*meso*-C). These signals were assigned to the four *meso* carbons on the basis of peak intensity and in comparison with the results of previous work (ref. 6). $\lambda_{max}(CHCl_3)$ (log $\varepsilon$) 675 (3.68), 574 (4.09), 533 (4.01), 434 (5.41), 421 (5.62); *m*/*z* (FAB) 744 ($M^+$, $C_{50}H_{40}N_4O_3$) (Calc. for $C_{50}H_{40}N_4O_3H_2O$: C, 78.72; H, 5.55; N, 7.34. Found: C, 78.42; H, 5.37; N, 7.26%).

1 For reviews, see J. L. Sessler, *Angew. Chem., Int. Ed. Engl.*, 1994, **33**, 1348; B. Franck and A. Nonn, *ibid.*, 1995, **34**, 1795; E. Vogel, *Pure Appl. Chem.*, 1996, **68**, 1355.

2 E. Vogel, M. Kocher, H. Schmickler and J. Lex, *Angew. Chem., Int. Ed. Engl.*, 1986, **25**, 257; J. L. Sessler and A. K. Burrell, *Top. Curr. Chem.*, 1991, **161**, 177; H. Furuta, T. Asano and T. Ogawa, *J. Am. Chem. Soc.*, 1994, **116**, 767; P. J. Chmielewski, L. Latos-Grazynski, K. Rachlewicz and T. Glowiak, *Angew. Chem., Int. Ed. Engl.*, 1994, **33**, 779; J. L. Sessler, *ibid.*, 1994, **33**, 1348; T. D. Lash, *ibid*., 1995, **34**, 2553; J. L. Sessler, S. W. Weghorn, Y. Hishaeda and V. Lynch, *Chem. Eur. J.*, 1995, **1**, 56; B. Franck and A. Nonn, *Angew. Chem., Int. Ed. Engl.*, 1995, **34**, 1795; T.. D. Lash and S. T. Chaney, *Chem. Eur. J.*, 1996, **2**, 944; T. D. Lash and M. J. Hayes, *Angew. Chem., Int. Ed. Engl.*, 1997, **36**, 840; K. K. Dailey, G. P. A. Yap, A. L. Rheingold and T. B. Rauchfuss, *ibid.*, 1996, **35**, 1833.

3 D. K. Lavallee, *The Chemistry and Biochemistry of N-Substituted Porphyrins*, VCH, Weinheim, 1987 and references cited therein; H. J. Callot, R. Cromer, A. Louati, B. Mets and B. J. Chevrier, *J. Am. Chem. Soc.*, 1987, **109**, 2946; A. L. Balch, C. R. Cornman, L. Latos-Grazynski and M. M. Olstead, *ibid.*, 1990, **112**, 7552; K. Konishi, Y. Takahata, T. Aida and S. Inoue, *ibid.*, 1993, **115**, 1169; J.-i. Setsune and H. Takeda, *Tetrahedron Lett.*, 1995, **36**, 5903.

4 R. G. Little, J. A. Anton, P. A. Loach and J. A. Ibers, *J. Heterocycl. Chem.*, 1975, **12**, 343.

5 D. Kuila, D. K. Lavallee, C. K. Schauer and O. P. Anderson, *J. Am. Chem. Soc.*, 1984, **106**, 448.

6 H. Scheer and J. J. Katz, in *Porphyrin and Metalloporphyrins*, ed. K. M. Smith, Elsevier, Amsterdam, 1975, p. 487; D. K. Lavallee, I. Morgenstern-Badarau, M. Lange and P. Gans, *Inorg. Chem.*, 1979, **18**, 1776.

*Received in Columbia, MO, USA, 28th July 1997; 7/05438F*

# Stereochemistry of the intramolecular carbolithiation of vinyl sulfides

**Reinhard W. Hoffmann,*[a] Ralf Koberstein,[a] Bruno Remacle[b] and Alain Krief[b]**

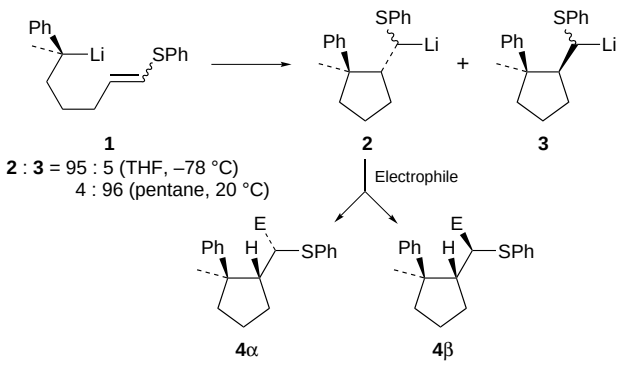
[a] *Fachbereich Chemie der Philipps-Universität Marburg, Hans-Meerwein-Strasse, 35032 Marburg, Germany*
[b] *Department of Chemistry, Facultés Universitaires Notre-Dame de la Paix, 61, rue de Bruxelles, 5000 Namur, Belgium*

**Intramolecular carbolithiation of vinyl sulfides to generate configurationally stable α-durylthioalkyllithium compounds at −105 °C in THF showed carbolithiation to be non-stereospecific regarding the newly formed lithium bearing stereocentre.**

The intramolecular carbolithiation of alkenes,[1] *i.e.* the addition of an organolithium entity across a C=C double bond is of interest, because it leads to carbo- and hetero-cycles with a stereochemically defined substitution pattern.[2] The detailed mechanism of the carbolithiation reaction is as yet not well-understood.

Cyclization of **1** in THF led to the *trans*-isomer **2** in high diastereoselectivity[3,4] (Scheme 1). Trapping of **2** by electrophiles generated two diastereoisomeric products **4α** and **4β**, the ratio of which depended on the electrophile used.[3] This demonstrates that the configurational stability of the α-phenylthioalkyllithium species **2** is too low to allow any conclusions regarding the initial configuration of the lithium-bearing stereocentre in **2**. Such information could, however, be obtained if a lithium-bearing stereocentre of higher configurational stability could be generated in the carbolithiation reaction. Previous studies[5] have indicated that α-durylthioalkyllithium compounds (duryl = 2,3,5,6-tetramethylphenyl) have a significantly higher barrier to enantioisomerization than α-phenylthioalkyllithium compounds. We therefore prepared the (*E*)- and (*Z*)-durylthio compounds **5**,† hoping to uncover further stereochemical details of the carbolithiation reaction of the derived benzyllithium compounds **6** (Scheme 2).

In order to preserve the initial configuration at the newly formed lithium-bearing stereocentre in **7** and **8**, we treated the seleno compound **5** with *tert*-butyllithium at −105 °C in THF. Quenching after 10 min with precooled $CD_3OD$ in a two compartment reaction vessel[6] showed that cyclization of **6** to **7** and **8** had occurred. The relative configuration of **9** at the ring carbon atoms corresponds to that of **4**, as supported by a crystal structure analysis of **9c**. The relative configuration of **9a** and **10a** at the exocyclic carbon atom is assigned by the similarity of their $^1$H NMR spectra to that of **4** (E = D). The ratio of the two diastereoisomeric deuterated compounds **9a** and **10a** was determined by $^2$H NMR spectroscopy.

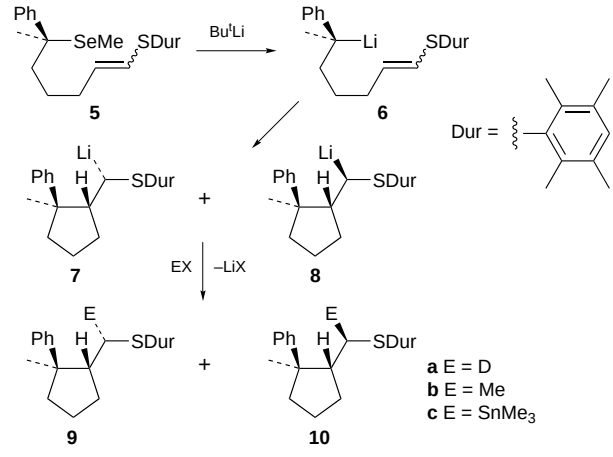



**Scheme 1**

Entries 1 and 2 of Table 1 show that carbolithiation occurred in an essentially stereospecific manner, when starting from a sample enriched in (*Z*)-**5**. Carbolithiation in the *E* series (entries 3 and 4) led to the α- and β-diastereoisomers **9a** and **10a** in a 4 : 6 ratio. The differences between the two series of experiments, and the fact that the time between carbolithiation and trapping had no influence on the diastereoisomer ratio of **9a** : **10a** indicates that the α-durylthioalkyllithium compounds **7** and **8** are configurationally stable under the reaction conditions. The diastereoisomer ratio is therefore kinetically controlled. Warming of the reaction mixture to −78 °C before quenching led to equilibration of **7** and **8**. Subsequent trapping then reflects the thermodynamic ratio of **7** and **8** (*cf.* entries 11–13 of Table 1). Moreover, dilution (entry 5) or trapping with methyl iodide to give **9b** and **10b** (entries 6 and 7) had no effect on the **9** : **10** ratio. For the carbolithiation reactions to occur at these low temperatures and with this stereochemistry, THF (a lithium-coordinating solvent) is essential. The reaction does also proceed in pentane at low temperatures, but only in the presence of at least one equivalent of THF.

The seemingly stereospecific cyclization of (*Z*)-**6** to **7** is in line with a concerted *syn*-addition of carbon and lithium to the double bond, but does not prove such a mechanism. The non-stereospecific cyclization of (*E*)-**6** suggests, however, a different scenario for the carbolithiation reaction in THF.

Carbolithiation reactions are greatly facilitated by all factors which help to detach the lithium from the carbon atom at the migration origin, *e.g.* an allyl-[7] or benzyl-lithium[3,4,8] entity at the migration origin, complexation assisted carbolithiation[9,10] and addition of lithium coordinating co-solvents.[10,11] This suggests that the carbon–lithium bond at the migration origin has to be broken first, in the extreme with the formation of a solvent separated ion pair **11**, a process favoured at lower temperatures.[12] C–C Bond formation, *i.e.* the cyclization, then proceeds in the carbanion part of the ion pair to give the ion pairs **12** and **13** (Scheme 3). The choreography of the cyclisation is probably such that $C_i$, S, $C_\alpha$ and the lone pair are initially antiperiplanar in **12** and **13**, in order to stabilize the transition state of the cyclization by delocalization of the negative charge

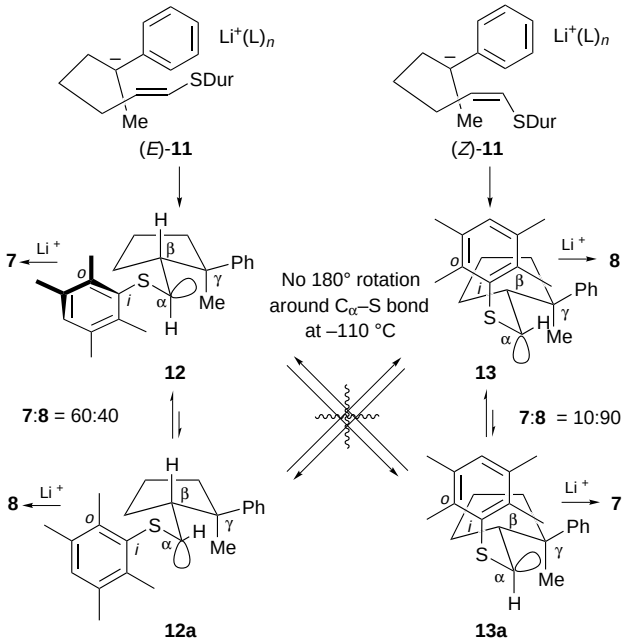



**Scheme 2**

**Table 1** Results of some carbolithiation experiments

| Entry[a] | *T*/°C[b] | Solvent | Substrate **5** *E* : *Z* | Electrophile | *t*/min[c] | Product Yield (%) | **9** : **10** |
|---|---|---|---|---|---|---|---|
| 1 | −105 | THF | 13 : 87 | $CD_3OD$ (neat) | 10 | | 88 : 12 |
| 2 | −105 | THF | 13 : 87 | $CD_3OD$ (neat) | 60 | | 88 : 12 |
| 3 | −107 | THF | 98 : 2 | $CD_3OD$ (neat) | 5.5 | | 41 : 59 |
| 4 | −104 | THF | 98 : 2 | $CD_3OD$ (neat) | 20 | 70 | 41 : 59 |
| 5[d] | −106 | THF | 98 : 2 | $CD_3OD$ (2.74 M in THF) | 15 + 30 | | 41 : 59 |
| 6 | −106 | THF | 13 : 87 | MeI (2.01 M in THF) | 30 | | 90 : 10 |
| 7 | −104 | THF | 98 : 2 | MeI (neat) | 20 | 70 | 43 : 57 |
| 8 | −107 | THF + HMPA (4 equiv.) | 15 : 85 | $CD_3OD$ (0.95 M in THF) | 15 | 67 | 86 : 14 |
| 9 | −104 | THF + HMPA (1 equiv.) | 98 : 2 | $CD_3OD$ (1.06 M in THF) | 20 | | 41 : 59 |
| 10[e] | −103 | Pentane + THF (1 equiv.) | 98 : 2 | $CD_3OD$ (1.06 M in THF) | 50 | 70 | 42 : 58 |
| 11 | −78 | THF | 13 : 87 | $CD_3OD$ (neat) | 90 | 62 | 94 : 6 |
| 12 | −78 | THF | 98 : 2 | $CD_3OD$ (neat) | 90 | | 94 : 6 |
| 13 | −78 | THF | 13 : 87 | MeI (2.01 M in THF) | 90 | 81 | 94 : 6 |

[a] Reactions were normally carried out with a 0.20 M solution of **5** in THF and with 1.2 equiv. of a 1.6 M solution of Bu$^t$Li in pentane. [b] All reactions were carried out with Bu$^t$Li and substrate solutions precooled to the given temperature. [c] Time between the start of the reaction and the addition of the electrophile ('15 + 30' means that the substrate was added over 15 min to the Bu$^t$Li solution and stirred for further 30 min before $CD_3OD$ was added). [d] Substrate concentration: 0.02 M, Bu$^t$Li concentration: 0.08 M. [e] Substrate concentration: 0.10 M.




**Scheme 3**

into the S–$C_i$ σ*-orbital. Next, a rotation about the $C_\alpha$–$C_\beta$ bond ensues to render the groups S–$C_\alpha$–$C_\beta$–$C_\gamma$ antiperiplanar, due to the quaternary nature of $C_\gamma$. Thus, the cyclization of (*E*)-**11** and (*Z*)-**11** leads to two distinct ion pairs **12** and **13**. Interconversion between the ion pairs **12** and **13** would require carbanion inversion and rotation about the $C_\alpha$–S bond, a process which should be slow at −110 °C,[5] but could be viable at −78 °C. The change in the stereochemistry of the carbolithiation reaction is then attributed to an inversion at the carbanion centre, which is calculated to have a rather low (< 2.5 kcal mol$^{-1}$) activation barrier.[13] This inversion to give **12a** and **13a** could therefore be competitive with or faster than the collapse of the ion pairs **12** and **13** to the configurationally stable organolithium compounds **7** and **8**. It should be noted, however, that the same stereoselectivity is observed in the absence or presence of HMPT and that further experiments may be needed to prove or to modify the interpretation given.

The carbolithiation of vinyl sulfides in THF was found to be non-stereospecific regarding formation of the new lithium-bearing stereocentre. This suggests that carbolithiation proceeds in a non-concerted fashion, in which collapse of an ion pair determines the configuration of the lithium-bearing centre at the migration terminus.

We are grateful to the Deutsche Forschungsgemeinschaft (SFB 260) and the Fonds der Chemischen Industrie for support of this study. We thank Professor H. J. Reich, Madison, Wisc., USA, for stimulating discussions and Dr N. Huser for carrying out preliminary studies.

## Footnotes and References

* E-mail: rwho@ps1515.chemie.uni-marburg.de

† The starting materials (*Z*)- and (*E*)-**5** were prepared using routes similar to the ones outlined in ref. 6.

1 W. F. Bailey and T. V. Ovaska, *Advances in Detailed Reaction Mechanisms*, ed. J. M. Coxon, JAI Press, Greenwich, CT, vol. 3, 1994, pp. 251–273. For more relevant studies, see I. Goldham and R. Hufton, *Tetrahedron Lett.*, 1995, **36**, 2157; *Tetrahedron*, 1996, **52**, 12 541; I. Goldham, R. Hufton and D. J. Snowden, *J. Am. Chem. Soc.*, 1996, **118**, 5322; M. P. Cooke and J.-J. Huang, *Synlett*, 1997, 535; W. F. Bailey, X. L. Jiang and C. E. McLeod, *J. Org. Chem.*, 1995, **60**, 7791; W. F. Bailey and E. R. Punzelan, *Tetrahedron Lett.*, 1996, **37**, 5435; W. F. Bailey and M. W. Carson, *Tetrahedron Lett.*, 1997, **38**, 1329.
2 L. R. Subramaniam, *Methoden der Organischen Chemie (Houben-Weyl*), ed. M. Hanack, Thieme, Stuttgart, vol. E19d, 1933, pp. 744–747.
3 A. Krief, B. Kenda and B. Remacle, *Tetrahedron*, 1996, **52**, 7435.
4 A. Krief and P. Barbeaux, *J. Chem. Soc., Chem. Commun.*, 1987, 1214; A. Krief, B. Kenda, C. Maertens and B. Remacle, *Tetrahedron*, 1996, **52**, 7465.
5 R. W. Hoffmann, R. K. Dress, T. Ruhland and A. Wenzel, *Chem. Ber.*, 1995, **128**, 861.
6 H. C. Stiasny and R. W. Hoffmann, *Chem. Eur. J.*, 1995, 619.
7 A. Krief, D. Derouane and W. Dumont, *Synlett.*, 1992, 907.
8 A. Krief and P. Barbeaux, *Tetrahedron Lett.*, 1991, **31**, 417.
9 G. W. Klumpp, *Recl. Trav. Chim. Pays-Bas*, 1986, **105**, 1; B. Mudryk and T. Cohen, *J. Org. Chem.*, 1991, **56**, 5761; R. F. Schmitz, F. J.-J. de Kanter, M. Schakel and G. W. Klumpp, *Tetrahedron*, 1994, **50**, 5933; F. Chen, B. Mudryk and T. Cohen, *Tetrahedron*, 1994, **50**, 12 793.
10 B. Mudryk and T. Cohen, *J. Am. Chem. Soc.*, 1993, **115**, 3855.
11 R. L. Funk, G. L. Bolton, K. M. Brummond, K. E. Ellestad and J. B. Stallman, *J. Am. Chem. Soc.*, 1993, **115**, 7023; W. F. Bailey, X.-L. Jiang and C. E. McLeod, *J. Org. Chem.*, 1995, **60**, 7791; W. F. Bailey and X.-L. Jiang, *J. Org. Chem.*, 1996, **61**, 2596.
12 J. Smid, *Ions and Ion Pairs in Organic Reactions*, ed. M. Szwarc, Wiley-Interscience, New York, vol. 1, ch. 3, 1972, pp. 106–110; G. Boche and F. Heidenhain, *J. Am. Chem. Soc.*, 1979, **101**, 738.
13 R. K. Dress, T. Rölle and R. W. Hoffmann, *Chem. Ber.*, 1995, **128**, 673.

*Received in Liverpool, UK, 7th August 1997; 7/05799G*

# Novel polycyclic polyprenoid sulfides in sediments

**Jacques Poinsot, Patrick Schneckenburger, Pierre Adam, Philippe Schaeffer, Jean Trendel and Pierre Albrecht*†**

*Institut de Chimie, URA 31 du CNRS, Université Louis Pasteur, 1 rue Blaise Pascal, 67000 Strasbourg, France*

**A series of polycyclic sulfides ($C_{15}$, $C_{20}$, $C_{25}$, $C_{30}$) deriving from regular isoprenoids has been characterized in sediments by mass spectrometry, synthesis of $C_{20}$ members, and NMR structural elucidation of two $C_{30}$ isomers isolated from a geological sample.**

The structure of numerous organo-sulfur compounds identified in sediments clearly indicates that incorporation of sulfur into biomolecules of decaying organisms takes place at the earliest stages of diagenesis.[1] Sulfurization most likely occurs by reaction of inorganic sulfur species (elemental S, $H_2S$, polysulfides) generated by bacterial processes with either organic components directly inherited from organisms or their functionalised derivatives. However, the precise mechanisms of these low-temperature sulfurization reactions still remain unclear and are at present the subject of many studies.[2] Structural determination of organo-sulfur components can give very useful information on their origin and their mode of formation. We report here the identification of a series ($C_{15}$, $C_{20}$, $C_{25}$, $C_{30}$) of novel polycyclic polyprenoid sulfides in immature sediments, the structures of which imply sulfur incorporation into partially cyclised regular isoprenoids.

Several organic extracts from sulfur-rich sediments were studied[3] and the aliphatic sulfide fraction was analysed by GC with a sulfur-specific FPD detector and by GC–MS. In all the samples selected, the *m/z* 169 mass fragmentogram shows the presence of two major isomeric compounds, the mass spectra of which exhibit a molecular ion at *m/z* 444 corresponding to an elemental composition of $C_{30}H_{52}S$ (verified by high resolution mass spectrometry) and a fragment triplet at *m/z* 156, 169 (base peak) and 185, all containing the sulfur atom as demonstrated by tandem mass spectrometry. In the peculiar case of an Italian Triassic marl, however, the *m/z* 169 mass fragmentogram highlighted four repetitive patterns of eight isomeric structures comprising two major, two minor and four extremely minor compounds more or less well resolved depending on the pattern considered. The molecular ions of each group,‡ respectively at *m/z* 240 ($C_{15}H_{28}S$), 308 ($C_{20}H_{36}S$), 376 ($C_{25}H_{44}S$) and 444 ($C_{30}H_{52}S$)—the two major $C_{30}$ skeletons being identical to that of the other samples—obviously point towards regular polyprenic structures differing by one isoprenic unit ($\Delta m/z$ = 68, respectively). Moreover, each compound displays the same fragment triplet as for the previous $C_{30}$ sulfides, thus suggesting the presence of a common sulfurized moiety. Small quantities of an almost pure major $C_{30}$ compound were obtained after argentation TLC fractionation of a particularly simple sulfide fraction where the two $C_{30}$ species were by far the major components. Desulfurization of the isolated product was achieved under drastic conditions with lithium–ethylamine and afforded a tetracyclic alkane, the mass spectrum of which shows a similar fragmentation pattern to that of scalarane, a tetracyclic sesterterpenoid which results from the cyclisation of a regular $C_{25}$ isoprenoid skeleton. Additional valuable information was obtained from the sulfone formed by treatment of the $C_{30}$ sulfide with OXONE®.[4] The lack of H–D exchange (BuLi, $CD_3SOCD_3$)[5] observed by MS showed the absence of any acidic proton α to the sulfur. These preliminary data indicated that all these closely related unknown compounds could result from sulfur incorporation into partially cyclised regular isoprenoids, leading to structure types **1**–**3** shown in Fig. 1.§

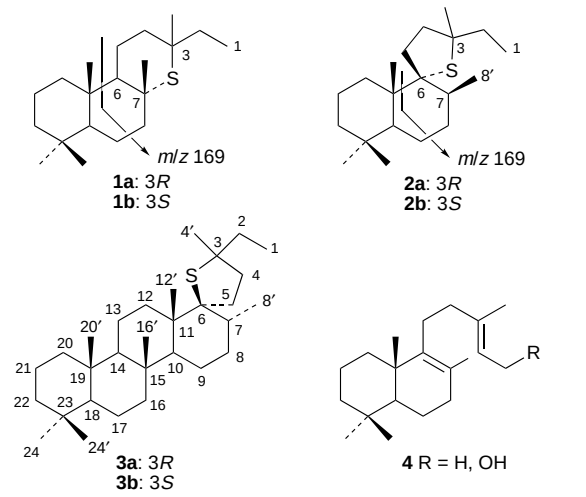
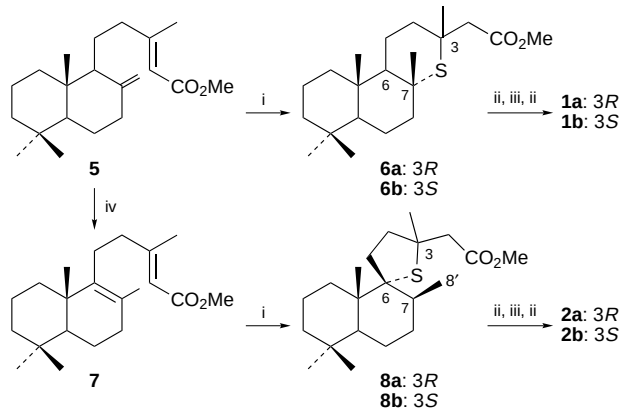



**Fig. 1** Postulated (**1**–**3**) and identified (**2** and **3**) structures of the geological sulfides and probable precursors **4** for **2**

Focusing first on the $C_{20}$ sulfide group of the Italian marl which comprises eight well-resolved isomers in the *m/z* 169 mass fragmentogram, we undertook the synthesis of reference compounds (Scheme 1), starting from methyl copalate here represented as its *ent*-isomer **5** for uniformity with other structures. Hence, sulfurization of **5**, achieved in DMF by means of $S_8$–NaSH in a 1 : 4 molar ratio ($HSSS^-$ major species),¶ gave exlusively a mixture of the two thiane epimers at position 3, **6a** and **6b**, which were fully characterised by 2D NMR after TLC separation. Complete reduction of the methoxycarbonyl function of **6a** and **6b** led to the corresponding thianes **1a** and **1b** whose mass spectra were markedly different from that of the sedimentary compounds, therefore allowing us to exclude this kind of structure for the naturally occurring components. Other suitable candidates were spiro-




**Scheme 1** Synthesis of the $C_{20}$ reference sulfides **1** and **2**: i, $S_8$–NaSH (1 : 4, mol/mol) in DMF under argon, 50 °C, 24 h (**6**, 90%) or 40 h (**8**, 10%); ii, $LiAlH_4$, THF; iii, $MeSO_2Cl$–$Et_3N$, $CH_2Cl_2$; iv, $HCO_2H$, $CH_2Cl_2$

**Table 1** $^1$H (500.1 MHz) and $^{13}$C (125.8 MHz) NMR data for the sulfide **3a** (Bruker ARX 500; in $C_6D_6$; $\delta$ in ppm relative to $SiMe_4$)

| C-atom | $\delta_C$ | $\delta_H$ | | C-atom | $\delta_C$ | $\delta_H$ | | C-atom | $\delta_C$ | $\delta_H$ | |
|---|---|---|---|---|---|---|---|---|---|---|---|
| 1 | 11.05 | 1.12 t | | 9 | 21.10 | 1.54 (eq) | 1.34 (ax) | 17 | 18.82 | 1.58 (eq) | 1.41 (ax) |
| 2 | 37.36 | 1.67 | 1.86 | 10 | 54.34 | 1.15 | | 18 | 56.69 | 0.86 | |
| 3 | 56.13 | | | 11 | 39.45 | | | 19 | 37.76 | | |
| 4 | 46.90 | 1.85 | 1.97 | 12 | 36.70 | 2.33 (eq) | 1.55 (ax) | 20 | 40.19 | 0.82 (ax) | 1.75 (eq) |
| 4′ | 27.82 | 1.46 s | | 12′ | 19.70 | 1.24 s | | 20′ | 16.68 | 0.92 s | |
| 5 | 28.96 | 1.85 | 2.02 | 13 | 17.85 | 1.66 (eq) | 1.44 (ax) | 21 | 19.06 | 1.49 (eq) | 1.72 (ax) |
| 6 | 76.27 | | | 14 | 61.72 | 0.77 | | 22 | 42.54 | 1.26 (ax) | 1.50 (eq) |
| 7 | 37.82 | 2.09 | | 15 | 38.35 | | | 23 | 33.45 | | |
| 8 | 32.81 | 1.17 (ax) | 1.71 (eq) | 16 | 42.54 | 0.91 (ax) | 1.79 (eq) | 24 | 33.55 | 1.02 s | |
| 8′ | 20.23 | 1.34 d | | 16′ | 17.43 | 0.90 s | | 24′ | 21.56 | 0.96 s | |

thiolanes **2**, which could account for the presence of eight isomers with regard to the possible configurations at C-3, C-6 and C-7. Two of them, **2a** and **2b**, were successfully obtained with the same reaction sequence as above, starting from the methyl copalate isomer **7**, the sulfurization of which specifically afforded, although in moderate yield, compounds **8a** and **8b** epimeric at C-3. Again, their structures were unambiguously determined by 2D NMR studies on the corresponding alcohols which were easily separated by HPLC. Based on comparison of mass spectra and GC retention times, thiolanes **2a** and **2b** were conclusively identified with two of the very minor sedimentary structures.

We finally isolated the two major ubiquitous $C_{30}$ sulfides **3a** and **3b** from the organic extract of a sedimentary rock (Toarcian, Paris basin, France) using a combination of liquid chromatographies. Their structures were established by NMR studies which led to the complete assignment of proton and carbon signals listed for **3a** in Table 1. For each compound, the basic carbon framework was deduced, with the help of the DEPT spectrum, from the HMBC spectrum correlation ($^{2,3}J_{CH}$ 7 Hz) network clearly showing that these structures indeed result from the cyclisation of a regular $C_{30}$ isoprenoid. Stereochemical information was obtained from the NOESY spectra which showed that **3a** and **3b** are epimeric at C-3 and bear the same *trans-transoid-trans* arrangement of the fused rings with axial ring-junction methyl groups on the same side of the mean plane of the molecule, a 6*S* configuration—*i.e.* the inverse of that of the synthetic references **2**—and a Me-8′ in the thermodynamically stable equatorial position.

In the light of these results, it was inferred that the eight structures belonging to a same molecular pattern are spirothiolanes isomeric at C-3, C-6 and C-7, the four extremely minor compounds being those which bear the 8′-methyl group at C-7 in the thermodynamically unfavourable axial position. Their formation most likely involves sulfur incorporation into partially cyclised regular isoprenoids, such as **4**, still possessing two double bonds in their skeleton. This implies that this process must operate at the earliest stages of diagenesis. Remarkably, apart from the case of the Italian marl, their distribution in all the geological samples investigated is almost exclusively restricted to the two $C_{30}$ members **3a** and **3b**, the other components, if any, being hardly detectable. This could reflect either a stereoselectivity in sulfur incorporation due to the mechanism itself—either linked or not to the existence of particular precursors—or that the 6*R* isomers formed initially are thermodynamically less stable and/or more susceptible to further geochemical transformations than their 6*S* epimers. Moreover, in most cases, the $C_{30}$ thiolanes overwhelmingly dominate the whole sulfide fraction, a fact which could indicate a major input of their biological precursors in sediments—although these $C_{30}$ tetracyclic terpenoids derived from regular isoprenoids are not known today in living organisms‖—or, more speculatively, that these sedimentary sulfides are directly inherited from producing oganisms.

We thank E. Mastio and P. Wehrung for their assistance in GC–MS analyses and R. Graff for recording NMR spectra.

## Footnotes and References

† E-mail: albrecht@chimie.u-strasbg.fr

‡ *MS data* (Finnigan MAT TSQ 700) EI (70 eV), *m/z* (rel. int.) for the first-eluting major sulfide of each group. $C_{15}H_{28}S$: 240 ($M^+$, 58%), 183 (3), 169 (100), 156 (22); $C_{20}H_{36}S$: 308 ($M^+$, 38%), 185 (3), 169 (100), 156 (22); $C_{25}H_{44}S$: 376 ($M^+$, 41%), 185 (18), 169 (100), 156 (38); $C_{30}H_{52}S$: 444 ($M^+$, 56%), 429 (8), 415 (3), 259 (12), 185 (38), 169 (100), 156 (40).

§ Since absolute configurations of the geological compounds are unknown, structures are arbitrarily drawn in the most usual way for terpenoid geochemical markers. All configurations subsequently discussed are relative to that represented on the drawings. Carbon numbering derives from that of the corresponding uncyclised regular isoprenols.

¶ Detailed mechanistic considerations concerning this sulfurization process will be included in an article on sulfur incorporation into unsaturated compounds (P. Schneckenburger, J. Poinsot, P. Adam and P. Albrecht, in preparation).

‖ Other polycyclic terpenoids derived from higher regular isoprenoids and of controversial or unknown origin have been identified in sediments: they are ubiquitous tricyclic hydrocarbons (D. Heissler, R. Ocampo, P. Albrecht, J.-J. Riehl and G. Ourisson, *J. Chem. Soc., Chem. Commun.*, 1984, 496) and optically-active highly cyclised hydrocarbons of more restricted distribution (P. Schaeffer, J. Poinsot, V. Hauke, P. Adam, P. Wehrung, J.-M. Trendel, P. Albrecht, D. Dessort and J. Connan, *Angew. Chem., Int. Ed. Engl.*, 1994, **33**, 1166; M. Li, C. L. Riediger, M. G. Fowler, L. R. Snowdon and T. A. Abrajano Jr., *Org. Geochem.*, 1996, **25**, 199).

1 J. Valisolalao, N. Perakis, B. Chappe and P. Albrecht, *Tetrahedron Lett.*, 1984, **25**, 1183; J. S. Sinninghe Damsté, W. I. C. Rijpstra, A. C. Kock-van Dalen, J. W. de Leeuw and P. A. Schenck, *Geochim. Cosmochim. Acta*, 1989, **53**, 1343; M. E. L. Kohnen, J. S. Sinninghe Damsté and J. W. de Leeuw, *Nature*, 1991, **349**, 775; P. Adam, J. C. Schmid, B. Mycke, C. Strazielle, J. Connan, A. Huc, A. Riva and P. Albrecht, *Geochim. Cosmochim. Acta*, 1993, **57**, 3395; M. E. L. Kohnen, J. S. Sinninghe Damsté, M. Baas, A. C. Kock-van Dalen and J. W. de Leeuw, *Geochim. Cosmochim. Acta*, 1993, **57**, 2515; P. Schaeffer, C. Reiss and P. Albrecht, *Org. Geochem.*, 1995, **23**, 567; for a review, see J. S. Sinninghe Damsté and J. W. de Leeuw, in *Advances in Organic Geochemistry*, 1989, ed. B. Durand and F. Béhar, Pergamon Press, Oxford, 1990, pp. 1077–1101.

2 W. De Graaf, J. S. Sinninghe Damsté and J. W. de Leeuw, *Geochim. Cosmochim. Acta*, 1992, **56**, 4321; S. Schouten, A. C. Van Driel, J. S. Sinninghe Damsté and J. W. de Leeuw, *Geochim. Cosmochim. Acta*, 1993, **57**, 5111; E. B. Krein and Z. Aizenshtat, *Org. Geochem.*, 1994, **21**, 1015; P. Adam, E. Philippe and P. Albrecht, *Geochim. Cosmochim. Acta*, in the press.

3 J. Poinsot, P. Schneckenburger, P. Adam, P. Schaeffer, J. Trendel, A. Riva and P. Albrecht, *Geochim. Cosmochim. Acta*, submitted.

4 B. M. Trost and D. P. Curran, *Tetrahedron Lett.*, 1981, **22**, 1287.

5 O. P. Strausz, E. M. Lown and J. D. Payzant, in *Geochemistry of Sulfur in Fossil Fuels*, ed. W. L. Orr and C. M. White, American Chemical Society, Washington, 1991, pp. 366–396.

*Received in Liverpool, UK, 2nd July 1997; 7/04649I*

# Preparation and characterization of titanocene silyl hydrides $[Cp_2Ti(\mu\text{-}HSiH_2)]_2$ and $[Cp_2Ti(\mu\text{-}HSiH_2)(\mu\text{-}H)TiCp_2]$

**Leijun Hao,[a] Anne-Marie Lebuis,[a] John F. Harrod*[a] and Edmond Samuel[b]**

[a] *Department of Chemistry, McGill University, Montreal, Canada H3A 2K6*
[b] *Laboratoire de Chimie Organométallique de l'ENSCP (URA 403 CNRS), 11 rue P. et M. Curie, 75005 Paris, France*

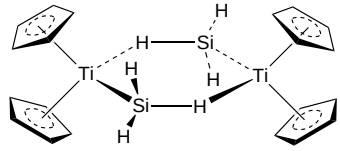
**The structure of a complex previously assigned as $[Cp_2Ti(\mu\text{-}SiH_2)]_2$ is shown to be $[Cp_2Ti(\mu\text{-}H\text{–}SiH_2)]_2$.**

Titanocene(IV) complexes containing a Ti–Si bond are extemely rare. To our knowledge, only three examples have been reported with convincing structural characterization.[1–3] We have previously reported the titanocene(III) hydrosilyl complexes $[Cp_2Ti(\mu\text{-}HSiHPh)]_2$ **1** and $[Cp_2Ti(\mu\text{-}HSiHPh)(\mu\text{-}H)TiCp_2]$ **2**, which are derived from intermediates in the polymerization of phenylsilane catalyzed by dimethyltitanocene (DMT).[4] The individual steps involved in the latter reaction are very complex and the mechanisms are still poorly understood.[5] Our experience in determining the structures of **1** and **2** sensitized us to the ease with which hydrogen atoms can be missed in the X-ray structures of such compounds. This in turn led us to consider the structure of $[Cp_2Ti(\mu\text{-}SiH_2)]_2$ **3**, reported two decades ago by Hencken and Weiss.[3]

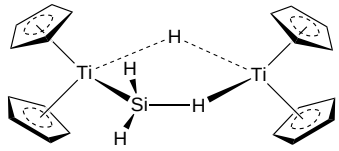
Our interest in this question was rekindled recently by the isolation of the complex $[Cp_2Ti(\mu\text{-}HSiH_2)]_2$ **4**, from the reaction of dimethyltitanocene (DMT) with trialkoxysilanes. In this reaction, the DMT catalyses the extremely rapid redistribution of $(RO)_3SiH$, according to eqn. (1).[6] The $SiH_4$ produced then reacts further to give the titanocene(III) silyl complex.

$$4\ (RO)_3SiH \rightarrow SiH_4 + 3\ (RO)_4Si \qquad (1)$$

The reaction of DMT with excess, chlorine-free,† $(MeO)_3SiH$ or $(EtO)_3SiH$ in dry hexane under argon gives **4** in good yield as air- and moisture-sensitive dark blue crystals.‡ Solutions of **4** in benzene, or toluene, under an argon atmosphere at room temperature are stable for several hours, decomposing slowly to a new compound $[Cp_2Ti(\mu\text{-}HSiH_2)(\mu\text{-}H)TiCp_2]$ **5**.§ This decompostition was evident from changes in the $^1H$ NMR spectrum of the solution and from a color change from greenish blue to dark yellowish green. Essentially the same result was obtained by the direct reaction of $SiH_4$ with $Cp_2TiMe_2$.




**4**




**5**

Complex **4** was readily characterized by comparison of its $^1H$ NMR spectrum to that of the known complex **1**.[4] At both room temperature and low temperature, the $^1H$ NMR spectrum of **4** in $[^2H_8]$toluene shows a single resonance at $\delta$ 4.58 for all four Cp rings, owing to a plane of symmetry containing the two titanium atoms, two silicon atoms and two hydrides in the six-membered ring, and a $C_2$ axis perpendicular to and through the center of the six-membered ring. The bridging hydride resonance appears as a triplet at $\delta$ −10.07, owing to coupling with the terminal $SiH_2$ protons. A doublet at $\delta$ 4.69 is assigned to the terminal $SiH_2$ protons. Similarly, **5** was characterized by comparison of its $^1H$ NMR spectrum to that of **2**.[4] At ambient temperature, **5** gives a broad single resonance at $\delta$ 5.50 due to the four Cp ligands. However, upon lowering the temperature to −20 °C the resonance splits into two equal intensity peaks, and a high-field hydride resonance appears at $\delta$ −13.22 assignable to the Si–H–Ti proton.[4] The coalescence temperature for the Cp resonances is at *ca.* 0 °C. A second high-field hydride was observed at $\delta$ −19.32 at −60 °C assignable to the Ti–H–Ti proton.[4] Integration of this spectrum indicates the formula $[Cp_2Ti(\mu\text{-}HSiH_2)(\mu\text{-}H)TiCp_2]$.

$^1H$ NMR measurements on the product prepared by reaction of $[Cp_2TiCl_2]$ with $SiH_3K$, carefully following the published procedure,[3] gave the same $^1H$ NMR specrum as **4**, indicating that the product of this reaction is not the $SiH_2$-bridged titanocene(IV) dimer **3**, originally proposed, but the titanocene(III) silyl dimer **4**. This result is consistent with the reported single crystal X-ray structure analysis.[3] The reported *R* value was high (*ca.* 9%) and disordering of the Si–H bridges would make detection of the third hydrogen unlikely.¶

We are continuing attempts to make higher quality crystals of **4** and **5** for X-ray diffraction to unequivocally assign their solid state structures. Further investigation of the chemistry of **4** and **5** is also under way.

We thank NSERC (Canada) and the Fonds FCAR de Quebec for financial support.

## Footnotes and References

* E-mail: harrod@omc.lan.mcgill.ca

† Most commercial samples of alkoxysilanes are adulterated with chlorosilanes to inhibit $SiH_4$ formation.

‡ $^1H$ NMR (200 MHz) data for **4** in $[^2H_8]$toluene: $\delta$ 4.69 [d, 4 H, $^2J$(HH) 5.4 Hz, $SiH_2$], 4.58 (s, 20 H, Cp), −10.07 [t, 2 H, $^2J$(HH) 5.4 Hz, SiHTi].

§ $^1H$ NMR (270 MHz) data for **5** in $[^2H_8]$toluene at 20 °C: $\delta$ 5.80 (br, 2 H, $SiH_2$), 5.50 (s, br, 20 H, Cp); at −20 °C, $\delta$ 5.65 (br, 1 H, SiH), 5.58 (s, br, 10 H, Cp), 5.41 (br, 1 H, SiH), 5.36 (s, br, 10 H, Cp), −13.22 (m, 1 H, SiHTi); at −60 °C, $\delta$ 5.64 (br, 1 H, SiH), 5.56 (s, br, 10 H, Cp), 5.38 (br, 1 H, SiH), 5.29 (s, 10 H, Cp) −13.3 (m, 1 H, SiHTi), −19.32 (m, 1 H, TiHTi).

¶ A problem with the reported structure is the extreme shortness of the Ti–Si bond (*ca.* 2.1 Å) compared to other values (ref. 2 and 4; *ca.* 2.5–2.7 Å) and the anomalously high temperature factor for the Si. Both of these problems disappear if it is assumed that the bridging group is OH, or O. The fact that the reported elemental analysis corresponds well to a product with an $SiH_2$ (or $SiH_3$) bridge, together with our NMR observations showing the presence of the $SIH_3$ bridged dimers in solution, suggests that the authors may have been unlucky in choosing a crystal of oxidized material.

1 L. Rösch, G. Altnau, J. Pickardt and N. Bruncks, *J. Organomet. Chem.*, 1980, **197**, 51.
2 V. A. Igonin, Yu. E. Ovchinnikov, V. V. Dement′ev, V. E. Shklover, T. M. Timofeeva, T. M. Frunze and Yu. T. Struchkov, *J. Organomet. Chem.*, 1989, **371**, 187.
3 G. Hencken and E. Weiss, *Chem. Ber.*, 1973, **106**, 1747.

4 C. T. Aitken, J. F. Harrod and E. Samuel, *J. Am. Chem. Soc.*, 1986, **108**, 4059.
5 B. Marciniec, in *Applied Homogeneous Catalysis with Organometallic Compounds*, ed. B. Cornils and W. A. Herrmann, VCH, New York, 1996, vol. 1, p. 487; E. Spaltenstein, P. Palma, K. A. Kreutzer, C. A. Willoughby, W. M. Davis and S. L. Buchwald, *J. Am. Chem. Soc.*, 1994, **116**, 10 308; H. G. Woo, J. F. Walzer and T. D. Tilley, *J. Am. Chem. Soc.*, 1992, **114**, 7047; J. Y. Corey, in *Advances in Silicon Chemistry*, ed. G. Larson, JAI Press, Greenwich, UK, 1995, vol. 1, p. 327; J. F. Harrod, T. Zeigler and V. Tschinke, *Organometallics*, 1990, **9**, 897; J. F. Harrod, in *Inorganic and Organometallic Polymers*, ACS Symp. Ser. 360, ed. M. Zeldin, K. J. Wynne and H. R. Allcock, American Chemical Society, Washington, DC, 1988; ch. 7; J. F. Harrod and S. S. Yun, *Organometallics*, 1987, **6**, 1381; C. T. Aitken, J. F. Harrod and E. J. Samuel, *Can. J. Chem.*, 1986, **64**, 1677; C. T. Aitken, J. F. Harrod and E. J. Samuel, *J. Organomet. Chem.*, 1985, **279**, C11.
6 S. Xin, C. Aitken, J. F. Harrod, Y. Mu and E. Samuel, *Can. J. Chem.*, 1990, **68**, 471.

*Received in Bloomington, IN, USA, 17th July 1997; 7/05102F*

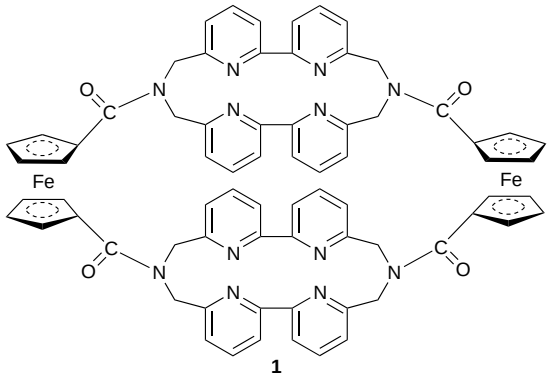
# Sodium springs another surprise

**C. Dennis Hall,* Thi-Kim-Uyen Truong, James H. R. Tucker† and Jonathan W. Steed**

*Department of Chemistry, King's College London, Strand, London, UK WC2R 2LS*

**The X-ray crystallographic structures of the novel redox-active cryptand 1 and its homobinuclear complex with sodium perchlorate are reported and discussed.**

The synthesis, structure, electrochemistry and complex formation of cryptands containing metallocene units have attracted considerable attention in recent years.[1] A common synthetic procedure to the compounds involves the condensation of 1,1′-ferrocene bis-acid chloride with diazamacrocycles which generally produces a mixture of monomeric and dimeric cryptands containing amide functions.[2] All the available solution NMR data and X-ray crystallographic data show that the amide functions are disposed *trans* to each other.[3–5] Complex formation with a range of mono-, di- and tri-valent cations then involves rotation of the amide carbonyl groups to *cis* orientations which allows their coordination to the guest cation usually in conjunction with other oxygen atoms of the polyether chains or heterocyclic units within the macrocyclic structure.[6,7] Recent work has involved the synthesis of analogous cryptands incorporating nitrogen ligands in the form of phenanthroline units which also have the carbonyl groups within the host cryptand disposed *trans* to each other.[8,9] These cryptands were designed with the objective of complexing lanthanide cations in order to create redox-active luminescent cryptates and the work reported here represents an extension of this concept to the synthesis of the dimeric cryptand **1** containing four 2,2′-bipyridyl units.




**1**

Cryptand **1**‡ was synthesised in the usual way from ferrocene bis-acid chloride and the appropriate diamine, prepared by a modification§ of the literature procedure.[10] No trace of the monomeric species was found but a trimeric amide was separated and characterised.¶ The $^{13}C$ NMR of **1** in $CDCl_3$ showed a total of 16 signals consisting of four ferrocene C–H carbons, one carbonyl carbon, two $CH_2N$ signals, six CH bipyridyl signals and three quaternary bipyridyl signals. The *ipso*-ferrocene carbons and one of the quaternary bipyridyl carbons were not observed but the spectrum is consistent with a structure in which the carbonyl groups on each ferrocene unit are either *cis* or *trans* to each other. The $^1H$ NMR data were also consistent with this conclusion. The definitive evidence, however, is provided by the X-ray crystal structure of the cryptand (Fig. 1).‖ It is immediately obvious that the carbonyl groups, located on the periphery of the cryptand, are mutually *trans* to each other with two of the bipyridyl units on the outside of the cryptand virtually orthogonal to the two corresponding bipyridyl units filling the cavity. Thus π–π stacking interactions are minimal and the crystal adopts a configuration which appears to minimise the dipole moment and maximise close packing.

Downfield shifts of most of the $^1H$ NMR signals of **1** were indicative of complex formation with $Na^+$ but at NMR concentrations (*ca.* $5 \times 10^{-2}$ M) complexes with other cations (*e.g.* $Ca^{2+}$ or $Eu^{3+}$) precipitated thus making it difficult to achieve a complete NMR analysis of the latter cryptates which is still in hand. The sodium complex was sufficiently soluble, however, to achieve a full analysis (by 2D NMR) and in summary, twice as many $^{13}C$ signals were observed in the complex as in the parent compound, a result which is entirely consistent with the crystal structure reported below. The binuclear sodium perchlorate complex of **1** crystallised from $CH_2Cl_2$–MeCN solution and the resultant single crystal was found to contain four molecules of solvent acetonitrile per molecule of the complex. Far more interestingly however, X-ray crystallography revealed the two sodium cations each bound in a centrosymmetrical structure by the four bipyridyl nitrogen atoms of one macrocyclic ring and one carbonyl oxygen of the other macrocyclic system in an approximate square pyramidal configuration (Fig. 2). Each uncomplexed amide function remained *trans* to its partner but was not involved in binding the cation. The sodium–nitrogen bond distances varied from 2.373(7) to 2.579(7) Å and the Na–O distance was unusually short at 2.191(6) Å. The N–Na–N bond angles in the square pyramid varied from 67.7(2) to 84.8(2)° and the O–Na–N bond angles from 105.2(2) to 136.0(2)°. The configuration achieved in the crystal enabled all the amide groups to remain planar and in the plane of the cyclopentadienyl rings in each case. This

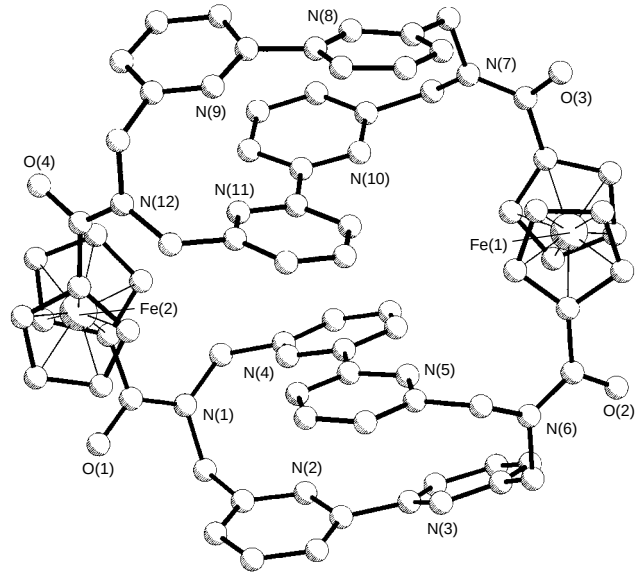



**Fig. 1** X-Ray crystallographic structure of ligand **1** showing all four amide carbonyl bonds *trans* relative to each other

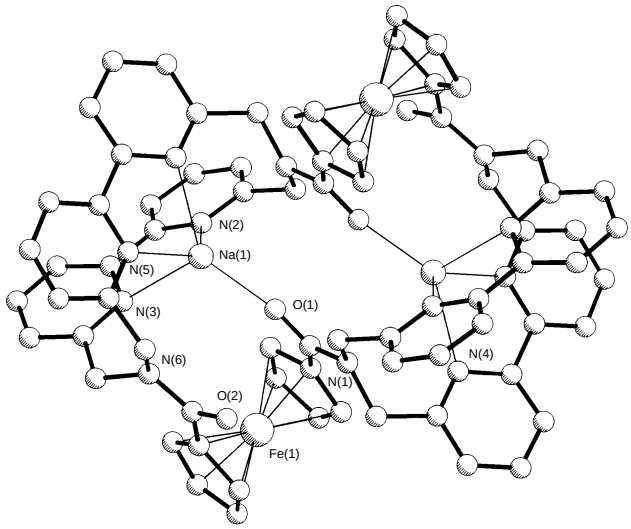



**Fig. 2** X-Ray crystallographic structure of the homo-binuclear complex of **1** with sodium perchlorate (counter-ions not included)

leaves a distance of 5.57 Å between the complexed sodium cations, a feature which should enable a suitable anion (*e.g* cyanate) or dianion (*e.g.* oxalate) to be accommodated within the cleft of the cryptate. This aspect of the complexation will be the subject of future work. The perchlorate counter ions are a considerable distance from the sodium cations with the nearest Na···Cl distance of $ClO_4$ at 7.88 Å and the nearest Na···O distance of $ClO_4$ at 6.66 Å. This confirms that the sodium cations are fully encapsulated by the cryptand which should therefore be effective as a redox-active phase transfer host. Finally, the highly unusual feature of sodium a 'hard' cation, complexed by four pyridyl nitrogens and an amide carbonyl oxygen in a five-coordinate square pyramidal configuration should be addressed. Preorganized rather than predisposed oligopyridine ligands are known to form helical complexes with sodium cations,[11,12] and macrocycles or cryptands containing phenanthroline[13] or bipyridyl[14] units are also known to complex sodium albeit in the latter case as a cryptatium species. There are very few examples, however, of sodium complexed by four nitrogen and one oxygen donor atoms and none in which the configuration of the complex is a square pyramid. Nelson and coworkers have characterised a mononuclear cryptate with a distorted trigonal bipyramidal configuration about the sodium composed of four nitrogen donors and a water molecule situated in an equatorial position.[15] The Na–N bond length varies from 2.520 to 2.636 Å and the Na–O distance is 2.241 Å significantly longer than that observed in the cryptate from **1**. It seems that sodium is indeed capable of more than one surprise.[11]

We thank King's College London for a Junior Research Studentship (to T.-K.-U. T.) and for financial support in purchasing X-ray equipment. Thanks are also due to Jane Hawkes and Jon Cobb (KCL/ULIRS) for NMR data and Dr K. Welham (School of Pharmacy/ULIRS) for mass spectra.

## Footnotes and References

* E-mail: c.d.hall@kcl.ac.uk
† Present address: Dept. of Chemistry, The University of Exeter, Stocker Road, Exeter, UK, EX4 4QD.
‡ All new compounds were characterised by accurate mass spectrometry and multinuclear NMR spectroscopy.
§ We are indebted to Dr. Anders Døssing (Copenhagen) for the generous gift of 6,6′-dimethyl-2,2′-bipyridine and a disclosure of their procedure to 6,6′-dibromomethyl derivatives.
¶ Details to be reported in the full paper.
‖ *Crystal data* for **1**. $C_{74}H_{60}Cl_4Fe_2N_{12}O_4$, $M$ = 1434.84, monoclinic, space group $P2_1/n$, $a$ = 14.450(1), $b$ = 28.621(1), $c$ = 16.181(1) Å, $\beta$ = 103.05(1), $U$ = 6517.51(6) Å$^3$, $Z$ = 4, $D_c$ = 1.462 Mg m$^{-3}$, $\mu$ = 0.67 mm$^{-1}$, $T$ = 293(2) K, 9856 unique reflections.

Refinement converged with $wR_2$ = 0.2278, which corresponds to a conventional $R$-factor of 0.081 for data with $I > 2\sigma(I)$.

*Crystal data* for the Na complex of **1**. $C_{72}H_{56}Fe_2N_{12}O_4{\cdot}2NaClO_4{\cdot}4CH_3CN$, $M$ = 1674.08, monoclinic, space group $P2_1/c$, $a$ = 9.3880(2), $b$ = 29.2720(8), $c$ = 13.2400(4) Å, $\beta$ = 97.895(1), $U$ = 3603.9(2) Å$^3$, $Z$ = 2, $D_c$ = 1.543 Mg m$^{-3}$, $\mu$ = 0.57 mm$^{-1}$, $T$ = 293(2) K, 3604 unique reflections.

*Experimental*: orange prismatic crystals (0.4 × 0.1 × 0.1 mm) were prepared by slow evaporation of an MeCN–$CH_2Cl_2$ solution of the compound (as the triflate salt) in the presence of excess $NBu_4ClO_4$ and mounted on a thin glass fibre using a fast setting epoxy resin. A total of 360 oscillation frames of 45 s exposure time with 0.5° rotation in $\phi$ were recorded using a Nonius Kappa CCD diffractometer, with a detector to crystal distance of 35 mm. The crystal was indexed from the first ten frames using the DENZO package[16] and positional data were refined along with diffractometer constants to give the final unit cell parameters. Integration and scaling of the whole data set resulted in a total of 3604 unique data which were corrected for Lorentz and polarisation effects and were used in subsequent refinement. The structure was solved using the direct methods option of SHELXS-86[17] and developed *via* alternating least squares cycles and difference Fourier synthesis (SHELXL-93).[18] All non-hydrogen atoms were modelled anisotropically except those of the two disordered molecules of acetonitrile and the oxygen atoms of the disordered perchlorate. Hydrogen atoms are assigned an isotropic thermal parameter 1.2 times that of the parent atom and allowed to ride. Hydrogen atoms were not included for the acetonitrile solvent molecules within the lattice as a consequence of their severely disordered nature. This disorder was eventually modelled in terms of a total of twelve different atom positions with refined occupancies ranging from 1.0 to 0.25. Even this model proved chemically unsatisfactory but since the solvent exhibits no significant interactions with the complex it was accepted as giving the best fit to the diffraction data. The disorder of the perchlorate anion was successfully modelled in terms of rotation about the Cl(1)–O(40) axis resulting in a total of nine different positions for the three oxygen atoms. Refinement converged with $wR_2$ = 0.2533, which corresponds to a conventional $R$-factor of 0.077 for data with $I > 2\sigma(I)$. CCDC 182/619.

1 P.D. Beer, *Adv. Inorg. Chem.*, 1992, **39**, 79; D. Dietrich, P. Viout and J.-M. Lehn, *Macrocyclic Chemistry*, VCH, Weinheim, 1993, ch. 3; J.-M. Lehn, *Supramolecular Chemistry*, VCH, Weinheim, 1995, ch. 8.
2 A. P. Bell, P. J. Hammond and C. D. Hall, *J. Chem. Soc., Perkin Trans. 1*, 1983, 707.
3 P. D. Beer, J. Elliot, P. J. Hammond, C. Dudman and C. D. Hall, *J. Organomet. Chem.*, 1984, **263**, C37.
4 P. D. Beer, C. D. Bush and J. A. Hamor, *J. Organomet. Chem.*, 1988, **339**, 133.
5 C. D. Hall, I. P. Danks, S. C. Nyburg, A. W. Parkins and N. W. Sharpe, *Organometallics*, 1990, **9,** 1602; C. D. Hall, A. W. Parkins, S. C. Nyburg and N. W. Sharpe, *J. Organomet. Chem.*, 1991, **407**, 107.
6 C. D. Hall, J. H. R. Tucker and N. W. Sharpe, *Organometallics*, 1991, **10**, 1727.
7 C. D. Hall, J. H. R. Tucker, A. Sheridan, S. Y. F. Chu and D. J. Williams, *J. Chem. Soc., Dalton Trans.*, 1992, 3133; C. D. Hall, J. H. R. Tucker, S. Y. F. Chu, A. W. Parkins and S. C. Nyburg, *J. Chem. Soc., Chem. Commun.*, 1993, 1505.
8 C. D. Hall and T.-K.-U Truong, *J. Organomet. Chem.*, 1996, **519**, 185.
9 C. D. Hall, T.-K.-U Truong and S. C. Nyburg, *J. Organomet Chem.*, 1997, in press.
10 J.-C. Rodriguez-Ubis, B. Alpha, D. Plancherel and J.-M. Lehn, *Helv. Chim. Acta*, 1984, **67**, 2264.
11 E. C. Constable, *Nature*, 1994, **367**, 415.
12 T. W. Bell and H. Jousselin, *Nature*, 1994, **367**, 441.
13 J. K. Judice, S. J. Keipert and D. J. Cram, *J. Chem. Soc., Chem. Commun.*, 1993, 1323.
14 L. Echegoyen, A. DeCian, J. Fischer and J.-M. Lehn, *Angew. Chem., Int. Ed. Engl.*, 1991, **30**, 838.
15 V. McKee, M. R. J. Dorrity, J. F. Malone, D. Marrs and J. Nelson, *J. Chem. Soc., Chem. Commun.*, 1992, 383.
16 Z. Otwinowski and W. Minor, *Methods Enzymol.*, 1996, **276**, ed. C. W. Carter and R. M. Sweet.
17 G. M. Sheldrick, *Acta Crystallogr., Sect. A.*, 1990, **46**, 467.
18 G. M. Sheldrick, SHELXL-93, University of Göttingen, 1993.

*Received in Cambridge, UK, 11th July 1997; 7/04975G*

# Novel ionogenic heterometal alkoxide derivatives

**Michael Veith,* Sanjay Mathur* and Volker Huch**

*Institute of Inorganic Chemistry, University of Saarland, D-66041 Saarbrücken, Germany*

**First examples of hydrocarbon soluble heterometal cation–anion systems containing metal alkoxide clusters as isolated ions, are reported.**

Although a few cationic alkoxides of yttrium against non-metallic counter ion $BPh_4^-$ have been reported,[1] the cation–anion systems based on different metals and discrete ions are unprecedented in heterometal alkoxide chemistry.[2] In view of the above, the title derivatives containing separated poly-metallic alkoxide ions, as solution and solid-state stable species, represent a new subset in alkoxide chemistry.

The equimolar interaction of $SnI_4$ with $KTi(OPr^i)_5$[2e] or $KTi_2(OPr^i)_9$[2c] in toluene–isopropyl alcohol, followed by removal of precipitated KI and leaving the deep orange solution at room temperature for a few hours, leads to crystallisation of the only isolable ionic complex $[\{Ti_3(OPr^i)_{11}\}^+][\{Sn_2I_6(OPr^i)_3\}^-]$ **1**, in both cases. **1** could be obtained in higher yield by the reaction of $SnI_4$, $KOPr^i$ and $Ti(OPr^i)_4$ in 2 : 2 : 3 molar ratio.†

The solid-state structure‡ of **1** consists of distinct $\{Ti_3(OPr^i)_{11}\}^+$ cations and $\{Sn_2I_6(OPr^i)_3\}^-$ anions (Fig. 1). The trinuclear cation, $Ti_3(OPr^i)_{11}^+$ is formed by three edge-sharing distorted octahedra, built about Ti(1), Ti(2) and Ti(3), which are also mutually confacial. The trimetallic $Ti_3$ core forms an equilateral triangle (non-bonding Ti···Ti distances = 3.082 Å) capped at both the faces by triply bridging $\mu_3$-$OPr^i$ ligands [O(8), O(9)], while the three doubly bridging $\mu$-$OPr^i$ ligands [O(6), O(7), O(12)] bridge the edges of the triangular frame. The cationic unit in **1** is a modification of the $M_3X_{11}$ structure type, well known among trimetallic alkoxides of the general formula $M_3(O)(OR)_{10}$.[3,4] Whereas one of the eleven ligands in $M_3O(OR)_{10}$ derivatives is dianionic ($O^{2-}$), the presence of only univalent anions in $Ti_3X_{11}$ unit produces a cationic species which acts as a stable entity due to the preferred six-coordination achieved by all the Ti atoms. The Ti–O bond lengths follow the trend $\mu_3$-$OPr^i$ (2.157 Å) > $\mu$-$OPr^i$ (2.044 Å) > terminal-$OPr^i$ (1.753 Å) and are in harmony with Ti–O bond lengths observed in molecular titanium isopropoxide derivatives.[2c,5] The anionic part in **1** is a bioctahedron formed by the two octahedral tin atoms [Sn(1), Sn(2)] sharing a face defined by the oxygen atoms of $\mu$-$OPr^i$ groups [O(1), O(2), O(3)]. It can be visualised as a modification of cluster anion $M_2(OPr^i)_9^-$ (M = Sn,[6] Ti,[2c] Zr,[2a] Hf,[2e]) observed as a versatile chelating metallo-ligand in a variety of hetero bi- and tri-metallic alkoxides. The Sn–I distances (av. 2.765 Å) are comparable with the Sn–I contacts observed in the crystal structures[7] of non-ionic compounds $[I_2Sn\{Ti(OPr^i)_5\}_2]$ (2.778 Å), $[I_2Sn\{Al(OPr^i)_4\}_2]$ (2.736 Å) and $[I_3Sn\{Zr(OPr^i)_5\text{-}(Pr^iOH)\}]$ (2.774 Å). It is noteworthy that bonding parameters of both the ions in **1** show no significant deviation when compared with analogous molecular compounds. The ambient-temperature $^1H$ NMR spectrum§ of **1** exhibits methyl resonances in the integrated ratio 6 : 3 : 3 : 2 which is consistent with the total number of alkoxide ligands observed in the solid-state structure; the methine protons are observed as several associated septets which overlap to give four multiplets in approximate intensity ratio 6 : 2 : 4 : 2. The solution $^{13}C$ NMR data corroborates the above observation. Although all the $OPr^i$ ligands in the solid-state structure of **1** are unique, the solid-state $^{13}C$ CP MAS NMR spectrum reveals only six signals of relative intensities 6 : 3 : 2 : 1 : 1 : 1, which possibly occur from an accidental overlapping of some of the alkoxy ligands [*e.g.* 6 terminal, 3 $\mu$- and 2 $\mu_3$-$OPr^i$ groups in $Ti_3(OPr^i)_{11}^+$], resonating at almost similar frequencies. The presence of a tin(IV)-based anionic species in the solution of **1** is evident in the significant lower frequency shift of the $^{119}Sn$ resonance ($\delta$ −1734.7) when compared with the $^{119}Sn$ NMR chemical shifts observed for neutral iodo-functionalised alkoxides $\{[I_2Sn\{Ti(OPr^i)_5\}_2]$, $\delta$ −1245.0; $[I_2Sn\{Al(OPr^i)_4\}_2]$, $\delta$ −1540.7$\}$ which also contain six-coordinate tin(IV) centers in an environment of terminal iodide and bridging isopropoxide ligands.[7] Various attempts to record a $^{119}Sn$ CP MAS NMR spectrum were thwarted by low signal to noise ratio which precluded an unambiguous assignment of anisotropic shifts.

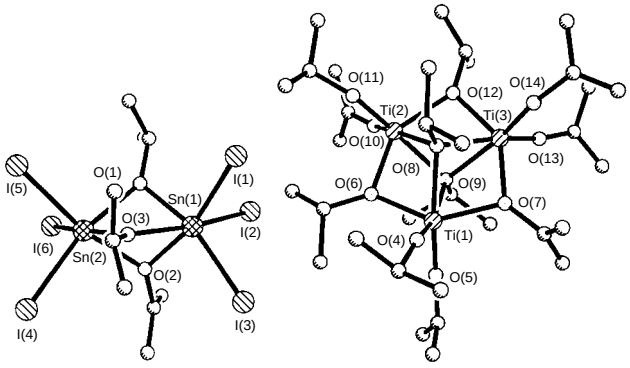



**Fig. 1** Crystal structure of **1**. Hydrogen atoms of isopropyl moieties are not drawn. Representative bond lengths (Å) and angles (°): Sn(1)–O(2) 2.104(8), Sn(1)–O(1) 2.108(9), Sn(1)–O(3) 2.164(8), Sn(2)–O(1) 2.119(8), Sn(2)–O(2) 2.140(9), Sn(2)–O(3) 2.103(8), Sn–I(1) 2.779(2), Sn–I(2) 2.776(2), Sn–I(3) 2.742(2); O(1)–Sn(1)–I(3) 164.8(2), O(2)–Sn(1)–I(2) 97.0(2), O(3)–Sn(1)–I(1) 97.8(2), I(2)–Sn(1)–I(3) 95.45(6), I(1)–Sn(1)–I(2) 93.39(5), I(1)–Sn(1)–O(1) 95.4(2), O(6)–Ti(1)–O(7) 140.7(3), O(5)–Ti(1)–O(9) 98.3(4), O(4)–Ti(1)–O(9) 162.3(3), O(4)–Ti(1)–O(5) 99.2(4), O(4)–Ti(1)–O(6) 100.6(4), O(4)–Ti(1)–O(8) 93.7(3).

The unique arrangement of large bi- and tri-metallic alkoxide clusters as distinct ions in **1**, inspired us to explore similar systems. Ionogenic heterometal alkoxide derivatives could be rationally constructed by abstracting halide ligand from the well defined heteroleptic heterometal alkoxides [eqn. (1)].

$$[ClSn\{M_2(OPr^i)_9\}]_2 + 2\ SnCl_2 \xrightarrow{\text{toluene}} 2\ [\{SnM_2(OPr^i)_9\}^+][SnCl_3^-] \quad (1)$$

M = Ti **2** M = Ti **4**
M = Zr **3** M = Zr **5**

The halide heterobimetallic precursors, **2** and **3** are obtained in nearly quantitative yields on treating anhydrous $SnCl_2$ with stoichiometric amount of alkali metal reagent $KM_2(OPr^i)_9$ (M = Ti, Zr[8]). Both **2** and **3** react [eqn. (1)] with 1 equiv. of $SnCl_2$ to afford **4** and **5**, respectively. In contrast to the fluxional behaviour of **3**, which could not be frozen to a static structure at even −70 °C, the room. temp. spectral data of **5** are structurally diagnostic. Both $^1H$ and $^{13}C$ NMR spectra show 4 : 2 : 1 : 2 pattern of resonances, characteristically observed for hetero-bimetallic alkoxides based on tetradentate interaction of the

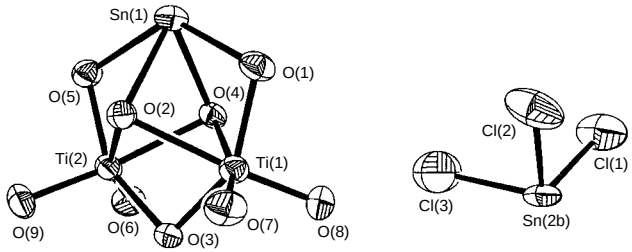



**Fig. 2** An ORTEP diagram of **4**. Displacement ellipsoids are drawn at 30% probability levels. $SnCl_3^-$ unit shows only one of the partially occupied tin sites. All oxygen atoms bear isopropyl groups which are not drawn from clarity. Pertinent bond lengths (Å) and angles (°): Sn(1)–O(1) 2.321(4), Sn(1)–O(2) 2.214(4), Sn(1)–O(4) 2.164(4), Sn(1)–O(5) 2.422(4), Ti(1)–O(3) 2.014(4), Ti(2)–O(3) 2.027(3), Ti(1)–O(8) 1.755(4); O(5)–Sn(1)–O(1) 131.58(12), Sn(1)–O(4)–Ti(1) 94.19(13), Ti(1)–O(1)–Sn(1) 97.7(2), Sn(1)–O(2)–Ti(1) 92.54(14), Ti(1)–O(3)–Ti(2) 102.7(2). Sn–Cl bond lengths and Cl–Sn–Cl angles in the $SnCl_3^-$ unit are in the range 2.329–2.488 Å and 93.1–99.4°, respectively.

bioctahedral $M_2(OPr^i)_9^-$ alkoxide sub-structure with a cationic fragment and possessing molecular $C_{2v}$ symmetry in solution.[2b,c] The $^{119}Sn$ NMR spectrum of **5** exhibits two resonances at $\delta$ −180.29 and −297.41 which according to the published data indicate the presence of two tin(II) species with coordination number at tin differing by one.[9] Ambient-temperature NMR data¶ of compound **4** shows a non-rigid behaviour, however, cooling a [$^2H_8$]toluene solution to −40 °C results in a static structure with spectral features essentially similar to that of **5**. The $^{119}Sn$ NMR chemical shifts ($\delta$ −147.2 and −281.3), similar to that observed for **5**, indicate a compositional similarity among the tin(II) species present in the solutions of both **4** and **5**.

The formulation of **4** and **5** suggested on the basis of spectroscopic and analytical data was established for **4**, by X-ray crystallography.‡ The crystal structure consists of discrete $\{SnTi_2(OPr^i)_9\}^+$ cation and $SnCl_3^-$ anion (Fig. 2). The heterobimetallic fragment based on the interaction of monoanionic $\{Ti_2(OPr^i)_9\}^-$ unit to $Sn^{2+}$, is of special interest as no $Sn^{II}Ti^{IV}$ mixed-metal species is formed in the reaction of neutral constituent alkoxides.[9b] Curiously, all the four alkoxide arms of $Ti_2(OPr^i)_9^-$ unit are used to cradle $Sn^{2+}$ in the $Sn\{Ti_2(OPr^i)_9\}^+$ unit, whereas only bidentate interaction of $\{M_2(OPr^i)_9\}^-$ moieties toward an $SnCl^+$ fragment is observed in $[ClSn\{M_2(OPr^i)_9\}]_2$ (M = Zr, Hf) derivatives.[8] The tin atom, in both cases, is present in a pseudotrigonal bipyramidal geometry. Whereas the lone pair of electrons occupies an equatorial position in the $SnTi_2(OPr^i)_9^+$ unit, the presence of a terminal halide ligand at tin in $[XSn\{M_2(OPr^i)_9\}]_2$ compounds[8] directs the lone pair of electrons to an axial position which inhibits the coordination of remaining isopropoxy ligands to tin(II).[6,8]

The 'bare' coordination hemisphere of tin(II) atom (no terminal ligands) makes the $Sn\{Ti_2(OPr^i)_9\}^+$ unit comparable, in a structural sense, with the molecular derivatives $K\{U_2(OBu^t)_9\}$[10] and $Na\{Th_2(OBu^t)_9\}$,[4] in which the alkali metals are devoid of any terminal ligands. Further, the Sn–$\mu_3$-OR (av. 2.189 Å) distances are significantly shorter than Sn–$\mu$-OR contacts which contrasts the usual trend ($\mu_3$-OR > $\mu$-OR > terminal OR) observed among $M'M_2$ heterobimetallic alkoxides containing a $M_2X_9^-$ unit. The repulsive forces between the Sn–O bonding electrons and the tin(II) electron lone pair along with the geometric constraints of the bioctahedral $Ti_2(OPr^i)_9^-$ unit result in a strained pseudotrigonal bipyramidal geometry at the tin center [O(2)–Sn(1)–O(4) 67.44(12)°, O(1)–Sn(1)–O(5) 131.58(12)°]. The ligand geometry about tin in $SnCl_3^-$ anion is trigonal pyramidal implying a stereochemically active lone pair; the tin atom, in the crystal structure, is disordered at two sites with partial site occupancy factors 0.66 : 0.34 [Sn(2A): Sn(2B)]. The Sn–Cl distances (av. 2.427 Å) fall in the range typically observed for $SnCl_3^-$ species.

This work was supported by the German Science Foundation (research programme SFB-277) and the Alexander von Humboldt Foundation, Germany.

## Footnotes and References

* E-mail: veith@rz.uni-sb.de

† Satisfactory elemental analyses were obtained for the new compounds **1** and **3**–**5**.

‡ *Crystallography* Both structures were solved by direct methods and refined on all $F^2$ data using the SHELX-97 suite of programs.[11]

*Crystal data*: **1**: $C_{56}H_{114}I_6O_{14}Sn_2Ti_3$, $M$ = 2152.98, orange bars, crystal size 0.60 × 0.45 × 0.50 mm, triclinic, space group $P\bar{1}$, $a$ = 15.867(3), $b$ = 15.970(3), $c$ = 16.684(3) Å, $\alpha$ = 80.60(3), $\beta$ = 79.56(3), $\gamma$ = 86.75(3)°, $U$ = 4100.2(13) Å$^3$, $Z$ = 2, $D_c$ = 1.732 g cm$^{-3}$, $T$ = 293(2) K, 26 338 reflections total, 12 179 unique ($R_{int}$ = 0.0756), 6474 observed [$I > 2\sigma(I)$], $R(wR_2)$ = 0.081(0.198).

**4**: $C_{27}H_{63}Cl_3O_9Sn_2Ti_2$, $M$ = 971.30, colourless cubes, crystal size 0.50 × 0.40 × 0.25 mm, triclinic, space group $P\bar{1}$, $a$ = 12.200(11), $b$ = 12.849(12), $c$ = 14.465(12) Å, $\alpha$ = 91.06(8), $\beta$ = 91.43(8), $\gamma$ = 107.95(7)°, $U$ = 2156(3) Å$^3$, $Z$ = 2, $D_c$ = 1.496 g cm$^{-3}$, $T$ = 293(2) K, 7249 reflections total, 5917 unique ($R_{int}$ = 0.0091), 5566 observed [$I > 2\sigma(I)$], $R(wR_2)$ = 0.0469(0.1308). CCDC 182/613.

§ *Spectral data*: **1**: $^1H$ NMR ($CDCl_3$, 20 °C, 200.13 MHz) $\delta$ 1.24 (d, 36 H), 1.31 (d, 18 H), 1.40 (d, 18 H), 1.63 (d, 12 H) ($CH_3$); 4.41 (m, 6 H), 4.58 (m, 2 H), 4.74 (m, 4 H), 5.02 (m, 2 H) (CH). $^{13}C$ NMR ($CDCl_3$, 20 °C, 50.3 MHz) $\delta$ 25.73, 25.93, 26.55, 29.86 ($CH_3$); 68.27, 69.57, 70.94, 74.15, 75.42 (CH). $^{13}C$ CP MAS NMR $\delta$ 24.89, 25.30, 25.65, 26.29, 27.04, 27.80 ($CH_3$); 71.63, 77.24, 77.98, 79.61, 84.15, 85.20 (CH). $^{119}Sn$ NMR ($C_6D_6$, 20 °C, 74.13 MHz) $\delta$ −1734.7.

**5**: $^1H$ NMR ($C_6D_6$, 20 °C, 200.13 MHz) $\delta$ 1.19 (d, 24 H), 1.29 (d, 12 H), 1.34 (d, 6 H), 1.42 (d, 12 H) ($CH_3$); 4.22, 4.29, 4.65 and 4.87 (spt, 9 H, CH). $^{13}C\{^1H\}$ NMR ($C_6D_6$, 20 °C, 50.3 MHz) $\delta$ 25.92, 25.99, 26.21, 26.74 ($CH_3$, intensity ratio = 4 : 2 : 1 : 2); 72.93, 73.45, 74.37, 74.89 (CH, intensity ratio = 2 : 1 : 4 : 2). $^{119}Sn\{^1H\}$ NMR ($C_6D_6$, 20 °C, 74.6 MHz): $\delta$ −180.3, −297.4.

¶ **4**: $^1H$ NMR ($CDCl_3$, 20 °C, 200.13 MHz) $\delta$ 1.25 (d, 54 H, $CH_3$), 4.61 (m, 9 H, CH). $^{13}C$ NMR ($CDCl_3$, 20 °C, 50.13 MHz) $\delta$ 26.21 ($CH_3$); 75.68 (CH). $^1H$ NMR ($CDCl_3$, −40 °C, 200.13 MHz) $\delta$ 1.34 (d, 24 H), 1.38 (d, 12 H), 1.41 (d, 6 H), 1.52 (d, 12 H) ($CH_3$); 4.53 (spt, 2 H), 4.65 (spt, 1 H), 4.82 (spt, 4 H), 4.99 (spt, 2 H). $^{13}C$ NMR ($CDCl_3$, −40 °C, 50.3 MHz) $\delta$ 24.74, 25.41, 25.87, 26.29 ($CH_3$, intensity ratio = 1 : 2 : 4 : 2); $\delta$ 72.49, 74.80, 76.06, 76.37, 76.69, 77.00, 77.33, 82.84 (CH, intensity ratio = 1 : 1 : 1 : 1 : 1 : 1 : 2). $^{119}Sn$ NMR ($CDCl_3$, 20 °C, 74.6 MHz) $\delta$ −147.2, −281.3.

1 W. J. Evans, J. M. Olofson and J. W. Ziller, *J. Am. Chem. Soc.*, 1990, **112**, 2308.
2 (*a*) M. Veith, *Chem. Rev.*, 1990, **90**, 3; (*b*) M. Veith, S. Mathur and V. Huch, *J. Am. Chem. Soc.*, 1996, **118**, 903; (*c*) M. Veith, S. Mathur and V. Huch, *Inorg. Chem.*, 1996, **35**, 7295; (*d*) M. Veith, S. Mathur, C. Mathur and V. Huch, *J. Chem. Soc., Dalton Trans.*, 1997, **12**, 2109; (*e*) M. Veith, S. Mathur and C. Mathur, *Polyhedron*, 1997, in press.
3 M. H. Chisholm, K. Folting, J. C. Huffman and C. C. Kirkpatrick, *J. Am. Chem. Soc.*, 1981, **103**, 5967.
4 D. L. Clark and J. G. Watkin, *Inorg. Chem.*, 1993, **32**, 1766.
5 M. Veith, S. Mathur and V. Huch, *Inorg. Chem.*, 1997, **36**, 2391.
6 M. Veith, S. Mathur and V. Huch, *J. Chem. Soc., Dalton Trans.*, 1996, **12**, 2485.
7 M. Veith and S. Mathur, manuscript in preparation.
8 M. Veith, C. Mathur, S. Mathur and V. Huch, *Organometallics*, 1997, **16**, 1292.
9 (*a*) S. Mathur, A. Singh and R. C. Mehrotra, *Polyhedron*, 1993, **12**, 1073; (*b*) D. J. Teff, J. C. Huffman and K. G. Caulton, *Inorg. Chem.*, 1996, **35**, 2981.
10 F. A. Cotton, D. O. Masler and W. Schwotzer, *Inorg. Chem.*, 1989, **23**, 4211.
11 G. M. Sheldrick, SHELX-97, University of Goettingen, Germany, 1997.

*Received in Basel, Switzerland, 24th July 1997; 7/05345B*

# Consistencies between experiments and quantum calculations of strained C–C single bond lengths

**Cheol Ho Choi and Miklos Kertesz***

*Department of Chemistry, Georgetown University, Washington, DC 20057-1227, USA*

**Modern electron correlated methods can accurately predict the unusually stretched C–C single bond lengths substantiating experimental structural information.**

Typical covalent bond lengths, such as 1.54 Å for C–C single bonds[1] have been one of the fundamental parameters in chemistry. At the same time, the possibility of unusually long C–C bond lengths has attracted much attention for its challenging nature raising the questions: is there an upper limit to the length of a stretched C–C single bond?

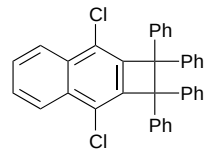
Recently, Toda *et al.*[2] have reported unusually long C–C bond lengths such as 1.720(4) Å in **1**, and 1.710(5) as well as 1.724(5) Å in **2**. They are considered the longest C–C single bonds accurately determined to date.[3] However, semiempirical methods have underestimated the length of the long bond in **1** by about 0.05 Å showing that special bonding effects exist that are not suitably covered by the current semiempirical parameters.[2]

In order to resolve these discrepancies between experiments and theories, full geometry optimizations[4] based on Hartree–Fock (HF) and density functional theory (DFT)[5] have been performed on **1**, as well as on other representative molecules (**3**, **4**, **5**) having strained long C–C bonds. Becke's 1988 (B)[6] and his three parameter hybrid (B3)[7] functionals incorporating exact exchange were used as gradient-corrected density functionals in combination with the Lee, Yang, and Parr (LYP)[8] correlation functional in the calculations.

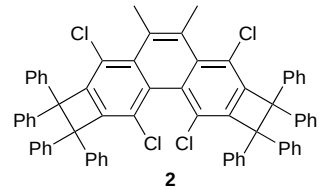
Hagler *et al.*[9] have shown that high-level quantum calculations, including HF and DFT in combination with available gas electron diffraction data, can assign a unique structure of **3** in which C–C bond length between the center methane carbon and that of a *tert*-butyl group is as long as 1.622(6) Å[10] (see Table 1). It can be seen that while HF slightly underestimates and BLYP overestimates the stretched bond length in **3**, our B3LYP/6-31G* calculation agrees perfectly with experiment.

The crystal structure of **4** has been refined by Choi and Marinkas[11] at room temperature and by Abboud *et al.*[12] at 198 K. They have shown that its two bridge bonds connecting the two anthracene components are 1.624[11] and 1.618(3)[12] Å, respectively. MNDO calculations[13] underestimate this long single bond by 0.04 Å. Again, while the B3LYP value is in perfect agreement with the experimental long C–C single bond length, HF underestimates and BLYP overestimates it. The same trend can also be found in the calculations for **5**. The C–C bond length, 1.77 Å for the two bridging bonds of **5** determined by Ehrenberg[14] has been disputed by several studies.[13,15] They have concluded that Ehrenberg had investigated a mixture of two photodimers[13] and found the bond lengths to be 1.663(4)[15*a*] and 1.648(3)[15*b*] in their X-ray diffraction studies. Our B3LYP/6-31G* calculation as well as the earlier two DFT calculations are in excellent agreement with Harata *et al.*'s experiment. However, BLYP/6-31G* calculation overestimates it by 0.035 Å.

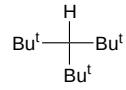
The overlong C–C bond length in **1** as calculated with B3LYP/6-31G* is in very good agreement with experiment showing excellent consistency between experiment and modern quantum calculations. The fact that HF systematically underestimates the stretched single C–C bond lengths indicates that



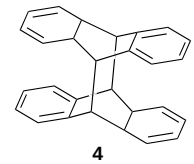

**1**



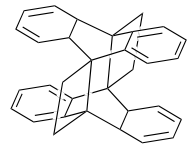

**2**




**3**



**4**



**5**

**Table 1** Experimental and theoretical long C–C bond lengths (Å)

| | | | | | |
|---|---|---|---|---|---|
| Tris(*tert*-butyl)methane **3** | | | | | |
| Exptl. | HF/6-13G*[b] | DFT/BLYP[b] | DFT/ACM[b] | B3LYP/6-31G*[c] | |
| 1.622(6)[a] | 1.616 | 1.639 | 1.609 | 1.621 | |
| Bis(9,10-dihydro-9,10-anthracenediyl) **4** | | | | | |
| Exptl. | MNDO[f] | HF/6-31G*[c] | BLYP/6-31G*[c] | B3LYP/6-31G*[c] | |
| 1.618(3)[d],1.624[e] | 1.585 | 1.605 | 1.645 | 1.623 | |
| Bis(anthracene-9,10-dimethylene) **5** | | | | | |
| Exptl. | HF/6-31G*[g] | DF/Local[g] | DF/Non-Local[g] | BLYP/6-31G*[c] | B3LYP/6-31G*[c] |
| 1.648(3)[g], 1.663(4)[h] | 1.635 | 1.661 | 1.673 | 1.698 | 1.667 |
| 1,1,2,2-Tetraphenylcyclobutaarenes: 3,8-dichloro-1,1,2,2-tetraphenylcyclobuta[b]naphthalene **1** | | | | | |
| Exptl. | MNDO[i] | HF/6-31G*[c] | BLYP/6-31G*[c] | B3LYP/6-31G*[c] | |
| 1.720(4) | 1.676 | 1.686 | 1.789 | 1.732 | |

[a] Ref. 10. [b] Ref. 9. [c] This work. [d] Ref. 12. [e] Ref. 11. [f] Ref. 13. [g] Ref. 15(*b*). [h] Ref. 15(*a*). [i] Ref. 12.

electron correlation effects in describing the lengthened bonds are essential. Since extreme bond lengthening is accompanied by large changes in electron correlation at the beginning of bond breaking, the underestimation of the bond length by HF is not surprising. Furthermore, our results show that incorporating the exact exchange term *via* Becke's three parameter methods (B3) is also very important to obtain accurate results in these kinds of chemical bonds.

In summary, on the basis of first principle calculations, the existence of the unusually long bond length of **1** has been further substantiated. The consistencies between experiments and modern quantum calculations have been demonstrated by comparing four representative molecules. It is clearly seen that electron correlation effects have to be included in the calculations to correctly describe lengthened bonds.[16]

We thank the National Science Foundation (CHE-9601976) for support and the National Center for Supercomputing Applications (NCSA, No. DMR-950029N) for the use of supercomputing facilities. An interdisciplinary grant from Georgetown University for support the Georgetown Molecular Modeling Center is also acknowledged.

## Footnote and References

* E-mail: kertesz@guvax.georgetown.edu

1 H.-B. Bürgi and J. D. Dunitz, *Structure Correlation*, VCH, Weinheim, 1994.
2 F. Toda, K. Tanaka, Z. Stein and I. Goldberg, *Acta Crystallogr., Sect. C*, 1996, **52**, 177.
3 G. Kaupp and J. Boy, *Angew. Chem., Int. Ed. Engl.*, 1997, **36**, 48.
4 Gaussian 94, Revision D.4, M. J. Frisch, G. W. Trucks, H. B. Schlegel, P. M. W. Gill, B. G. Johnson, M. A. Robb, J. R. Cheeseman, T. Keith, G. A. Petersson, J. A. Montgomery, K. Raghavachari, M. A. Al-Laham, V. G. Zakrzewski, J. V. Ortiz, J. B. Foresman, J. Cioslowski, B. B. Stefanov, A. Nanayakkara, M. Challacombe, C. Y. Peng, P. Y. Ayala, W. Chen, M. W. Wong, J. L. Andres, E. S. Replogle, R. Gomperts, R. L. Martin, D. J. Fox, J. S. Binkley, D. J. Defrees, J. Baker, J. P. Stewart, M. Head-Gordon, C. Gonzalez and J. A. Pople, Gaussian, Inc., Pittsburgh PA, 1995.
5 W. Kohn, L. J. Sham, *Phys. Rev. A*, 1965, **140**, 1133.
6 A. D. Becke, *Phys. Rev. A*, 1988, **38**, 3098.
7 A. D. Becke, *J. Chem. Phys.*, 1993, **98**, 1372.
8 C. Lee, W. Yang and R. G. Parr, *Phys. Rev. B*, 1988, **37**, 785.
9 A. T. Hagler, R. Sharon and M.-J. Hwang, *J. Am. Chem. Soc.*, 1996, **118**, 3759.
10 H. B. Bürgi and L. S. Bartell, *J. Am. Chem. Soc.*, 1972, **94**, 5239.
11 C. S. Choi and P. L. Marinkas, *Acta Crystallogr., Sect. B*, 1980, **36**, 2491.
12 K. A. Abboud, S. H. Simonsen and R. M. Roberts, *Acta Crystallogr., Sect. C*, 1990, **46**, 2494.
13 D. A. Dougherty, C. S. Choi, G. Kaupp, A. B. Buda, J.M. Rudzinski and E. Osawa, *J. Chem. Soc., Perkin Trans. 2*, 1986, 1063.
14 M. Ehrenberg, *Acta Crystallogr., Sect. C*, 1966, **20**, 183.
15 (*a*) J. Harada, K. Ogawa and S. Tomoda, *Chem. Lett.*, 1995, 751; (*b*) T. R. Battersby, P. Gantzel, K. K. Baldridge and J. S. Siegel, *Tetrahedron Lett.*, 1995, **36**, 845.
16 Fully optimized geometry is available upon request.

*Received in Columbia, MO, USA, 28th July 1997; 7/05439D*

# Novel low-valent zirconium porphyrin complexes: syntheses, characterization and X-ray crystal structures of ($\eta^5$-cyclopentadienyl)zirconium tetraphenylporphyrin and ($\eta^2$-diphenylacetylene)zirconium octaethylporphyrin

**Hee-Joon Kim, Sungkyung Jung, You-Moon Jeon, Dongmok Whang and Kimoon Kim***

*Department of Chemistry and Center for Biofunctional Molecules, Pohang University of Science and Technology, San 31 Hyojadong, Pohang 790-784, South Korea*

**Reactions of (por)$ZrCl_2$ [por = octaethylporphyrinato (oep) or tetraphenylporphyrinato (tpp) dianion] with TlCp and diphenylacetylene in the presence of Na/Hg or Mg produce novel low-valent zirconium porphyrin complexes (por)Zr($\eta^5$-Cp) 1 and (por)Zr($\eta^2$-PhC≡CPh) 2, respectively; spectroscopic and/or structural data for 1 and 2 are consistent with a formalism in which 1 is a resonance hybrid of a zirconium(III) metal-centered radical and a zirconium(IV) porphyrin radical anion while 2 is a zirconium(II) complex stabilized by a four-electron-donor alkyne ligand.**

Low-valent zirconium complexes have led to the development of novel routes to the functionalization of unsaturated organic molecules.[1] For example, zirconium(II) compounds have proved to be effective in converting a variety of enynes and diynes into the corresponding zirconabicycles in zirconocene chemistry.[2] We and others have been interested in development of zirconium porphyrin chemistry which has been, however, mainly focused on high-valent zirconium(IV) complexes.[3–5] In fact, there is no well characterized zirconium-(III) or -(II) porphyrin complex except for (oep)$ZrCH_2SiMe_3$.[3e] Extremely high sensitivity to air and moisture of such low-valent zirconium porphyrin complexes makes their synthesis and characterization challenging. Here we report the syntheses, characterization and X-ray crystal structures of the novel zirconium-(III) and -(II) porphyrin complexes (tpp)Zr($\eta^5$-Cp) **1** and (oep)Zr($\eta^2$-PhC≡CPh) **2**. The former is only the second example of formally zirconium(III) porphyrin complexes and the latter is the first zirconium(II) porphyrin complex.†

The cyclopentadienyl complex (tpp)Zr($\eta^5$-Cp) **1** was first obtained from the reaction of [(tpp)Zr(C≡CPh)$_3$][Li(thf)] **3**[6] and $Cp_2Ti(Me_3SiC{\equiv}CSiMe_3)$ **4** in toluene [eqn. (1)].[6]

$$\underset{\mathbf{3}}{[(tpp)Zr(C{\equiv}CPh)_3][Li(thf)]} + \underset{\mathbf{4}}{Cp_2Ti(Me_3SiC{\equiv}CSiMe_3)} \rightarrow \underset{\mathbf{1}}{(tpp)Zr(\eta^5\text{-}Cp)} + [Cp_2Ti(C{\equiv}CPh)]_2 + \textit{etc.} \quad (1)$$

Complex **1** can also be synthesized directly by reacting (tpp)$ZrCl_2$ with TlCp in the presence of Na/Hg [eqn. (2)].‡

$$(tpp)ZrCl_2 + TlCp + Na/Hg \rightarrow (tpp)Zr(Cp) \quad (2)$$

Complex **1** is paramagnetic as indicated by its broad $^1$H NMR peaks at $\delta$ 22.6, 11.0, 0.6 and −5.0. The mass spectrum of **1** shows a cluster of peaks centered at *m/z* 767.1 corresponding to the molecular mass of **1**. The structure of **1** was characterized by single crystal X-ray diffraction (Fig. 1).§ The zirconium ion is coordinated by the four nitrogen atoms of tpp and the $\eta^5$-Cp ligand in a sandwich fashion with the average Zr–N, and Zr–C bond distances being 2.177(10) and 2.49(2) Å, respectively. The four-nitrogen plane and the Cp plane are parallel (dihedral angle, 0.9°). The zirconium atom is 0.773(5) Å displaced out of the four nitrogen plane, and 2.206(6) Å away from the centroid of the Cp ligand. These values are almost the same as those found in (oep)Sc(Cp) (0.80 and 2.196 Å, respectively).[7]

The EPR spectrum of **1** in thf at 77 K is very similar to that of (oep)$ZrCH_2SiMe_3$;[3e] it shows a signal typical of a metal-centered radical, with $g_\perp$ = 2.004 and $g_\parallel$ = 1.991 but with no $^{14}$N hyperfine splitting. However, an isotropic signal with $g$ = 2.001, typical of an organic radical, is observed at room temperature. The electronic absorption spectrum of **1** recorded at room temperature exhibits a broad band centered at *ca*. 638 nm which is characteristic for a porphyrin anion radical. The electronic structure of **1** is therefore best described as a resonance hybrid of a zirconium(III) metal-centered radical and a zirconium(IV) porphyrin radical anion, as in the case of (oep)$ZrCH_2SiMe_3$.[3e]

The diphenylacetylene complex (oep)Zr($\eta^2$-PhC≡CPh) **2** was synthesized from the reduction of (oep)$ZrCl_2$ with equimolar amounts of magnesium in the presence of PhC≡CPh in thf at room temperature [eqn. (3)].‡

$$(oep)ZrCl_2 + PhC{\equiv}CPh + Mg \rightarrow (oep)Zr(\eta^2\text{-}PhC{\equiv}CPh) \quad (3)$$

Product **2** is diamagnetic exhibiting sharp $^1$H NMR signals. The $^1$H NMR spectrum of **2** is similar to that of the Ti analogue (oep)Ti($\eta^2$-PhC≡CPh).[8] The C≡C stretching frequency in **2** observed at 1697 cm$^{-1}$ is also similar to that of the Ti analogue (1701 cm$^{-1}$). The $\eta^2$-coordination of the alkyne ligand in **2** has been confirmed by X-ray crystallography (Fig. 2).§

The overall appearance of the molecular structure of **2** resembles that of (oep)Ti($\eta^2$-PhC≡CPh).[8] A crystallographic two-fold rotation axis passes through the Zr atom and the midpoint of the alkyne C–C bond. The geometry around the Zr atom is square pyramidal, with the four pyrrole nitrogens forming the basal plane and the alkyne triple bond at the apical position. All the metal to ligands distances, Zr–C [2.160(4) Å] and Zr–N [2.203(4), 2.205(4) Å] distances, are longer than the corresponding values for (oep)Ti($\eta^2$-PhC≡CPh) [Ti–C 2.016(5), 2.015(5) Å; Ti–N 2.083(8)–2.099(7) Å] apparently due to the larger ionic radius of Zr than that of Ti. The metal atom is displaced 0.90 Å out of the mean 24-atom porphyrin plane, which is larger than in the Ti analogue (0.54 Å). The alkyne C–C distance [1.333(8) Å] is comparable to that in the Ti complex [1.30(1) Å]. The bending of the alkyne ligand [C(19′)–C(19)-C(20) 133.4(3)°] is more severe than that (143°) in (oep)Ti($\eta^2$-PhC≡CPh).

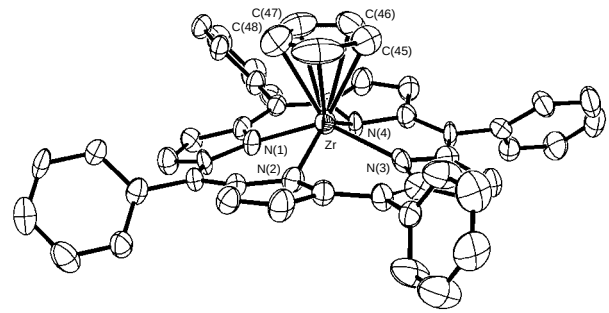



**Fig. 1** X-Ray crystal structure of (tpp)Zr($\eta^5$-Cp) **1**. Selected bond distances (Å): Zr–N(1) 2.183(10), Zr–N(2) 2.190(10), Zr–N(3) 2.169(10), Zr–N(4) 2.166(10), Zr–C(45) 2.47(2), Zr–C(46) 2.51(2), Zr–C(47) 2.50(1), Zr–C(48) 2.47(2), Zr–C(49) 2.50(1).

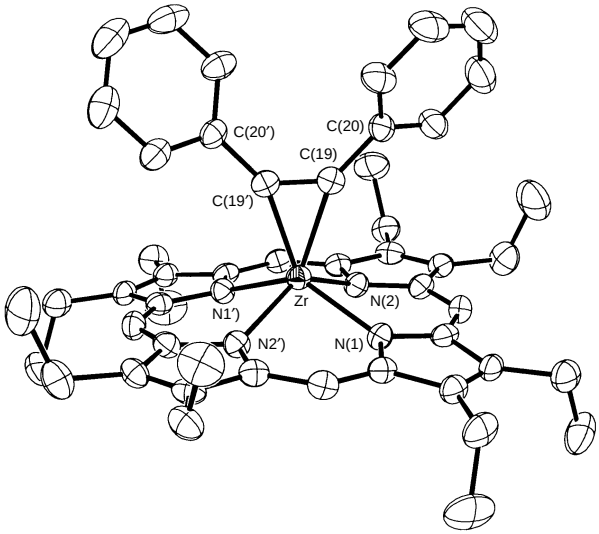



**Fig. 2** X-Ray crystal structure of (oep)Zr($\eta^2$-PhC≡CPh) **2**. Selected bond distances (Å) and angles (°) for **2**: Zr–C(19) 2.160(4), Zr–N(1) 2.203(4), Zr–N(2) 2.205(4), C(19)–C(19′) 1.333(8), C(19′)–C(19)–C(20) 133.4(3), N(1)–Zr-N(1′) 138.0(2), N(1)–Zr–N(2), 83.90(14).

Comparison of (oep)Zr($\eta^2$-PhC≡CPh) **2** with $Cp_2Zr(\eta^2$-PhC≡CPh)$(PMe_3)$[9] supports that the alkyne ligand in **2** behaves as a four-electron donor. According to the 18-electron rule the alkyne ligand is formally a two-electron donor in $Cp_2Zr(\eta^2$-PhC≡CPh)$(PMe_3)$. The longer Zr–C distances [2.20(4), 2.25(4) Å] in $Cp_2Zr(\eta^2$-PhC≡CPh)$(PMe_3)$ are in accord with this formalism. The $^{13}$C chemical shifts for the alkyne carbons in the two complexes are consistent with a two-electron-donor alkyne ($\delta$ 141.61, 156.42) in $Cp_2Zr(\eta^2$-PhC≡CPh)$(PMe_3)$ and a four-electron-donor alkyne ($\delta$ 218.4) in **2**.[10] Taking these into account, the alkyne complex **2** is best described as a zirconium(II) porphyrin complex stabilized by the $\eta^2$ four-electron $\pi$-donor ligand.

Preliminary reactivity studies of **2** also support the $Zr^{II}$ formalism. Stirring a [$^2H_8$]thf solution of **2** for several hours results in a change to brown. The $^1$H NMR spectrum of the resulting solution shows only sharp peaks corresponding to free diphenylacetylene with a broad background. This indicates that the diphenylacetylene ligand is displaced by thf to generate a paramagnetic zirconium porphyrin complex, which has not been fully characterized. When the solvent is removed by evaporation and the residue is taken up in $C_6D_6$ the original complex **2** is recovered as indicated by $^1$H NMR spectroscopy.

In summary, we have synthesized and characterized novel low-valent zirconium porphyrin complexes (tpp)Zr($\eta^5$-Cp) **1** and (oep)Zr($\eta^2$-PhC≡CPh) **2**. Spectroscopic and/or structural data for **1** and **2** are consistent with a formalism in which **1** is a resonance hybrid of a zirconium(III) metal-centered radical and a zirconium(IV) porphyrin radical anion while **2** is a zirconium(II) complex stabilized by a four-electron-donor alkyne ligand. Further studies on the reactivities of these novel complexes and their utilities in organic and organometallic syntheses are underway.

This work was supported by the Korea Research Foundation (Non Directed Research Fund, 1996) and in part by Center for Biofunctional Molecules.

## Footnotes and References

* E-mail: kkim@vision.postech.ac.kr

† Generation of a zirconium(II) porphyrin by photolysis of (tpp)$ZrMe_2$ has been clamed.[5b] However, neither its isolation nor characterization was reported to substantiate the claim.

‡ (tpp)Zr($\eta^5$-Cp) **1**: in a glove box a mixture of (tpp)$ZrCl_2$ (144 mg, 0.19 mmol), TlCp (75 mg, 0.28 mmol) and 6% Na/Hg (150 mg, 0.39 mmol) in thf (*ca*. 25 ml) was stirred for 1 d at room temp. After the solvent was removed *in vacuo*, the residue was taken up with diethyl ether. Insoluble salts were removed by filtration and the filtrate was concentrated to *ca*. 5 ml under reduced pressure. The violet crystalline product was filtered and dried *in vacuo* (110 mg, 77%). $^1$H NMR ($C_6D_6$): $\delta$ 22.6 (br s, 5 H, Cp), 11.0 (br s, 8 H, $H_\beta$), 0.6 (br s, 8 H, Ph), −5.0 (br s, 12 H, Ph). UV–VIS (toluene): $\lambda_{max}$ (log $\varepsilon$) 420 (4.76), 456 (4.10), 544 (3.10), 638 (3.43), 734 (2.91) nm. EPR (thf, 77 K): $g_\perp$ = 2.004, $g_\parallel$ = 1.991; (thf, 298 K) $g$ = 2.001. FABMS: *m/z* 767.1 ($M^+$). Despite numerous attempts with crystalline products no satisfactory elemental analysis has been obtained owing to extreme air sensitivity of the compound.

(oep)Zr($\eta^2$-PhC≡CPh) **2**. A mixture of (oep)$ZrCl_2$ (523 mg, 0.75 mmol), Mg powder (50 mesh, 19 mg, 0.78 mmol), and PhC≡CPh (135 mg, 0.76 mmol), in thf (*ca*. 50 ml) was stirred at room temp. in a glove box. The initially purplish red solution turned to dark green within 1 h. After 24 h, the solvent was removed *in vacuo*. The residue was extracted with toluene. The dark red extract solution was filtered and the filtrate was slowly concentrated to *ca*. 5 ml. Layering pentane (*ca*. 5 ml) over the solution yielded the microcrystalline product in 2 d, which was filtered, washed with pentane and dried *in vacuo* (329 mg, 54%). $^1$H NMR ($C_6D_6$): $\delta$ 10.42 (s, 4 H, *meso*-H), 6.34 (m, 6 H, *m*, *p*-Ph), 4.93 (d, 4H, *o*-Ph), 3.92 (m, 16 H, $CH_2CH_3$), 1.81 (t, 24 H, $CH_2CH_3$). $^{13}$C NMR ($C_6D_6$): $\delta$ 218.4 (C≡C), 147.6 (α-pyrrole), 144.2 (β-pyrrole), 132.1 (Ph), 126.9 (Ph), 126.0 (Ph), 125.1 (Ph), 101.5 (*meso*), 20.4 ($CH_2$), 18.6 ($CH_3$). IR (KBr): $\nu_{C\equiv C}$ 1697 $cm^{-1}$. UV–VIS (toluene): $\lambda_{max}$ (log $\varepsilon$) 408 (4.70), 458 (2.99), 534 (3.57), 570 (3.76) nm. Anal. Calc. for $C_{50}H_{54}N_4Zr$: C, 74.85; H, 6.80; N, 6.98. Found: C, 74.83; H, 6.39; N, 6.45%.

‡ *Crystal data*: for **1**: $C_{49}H_{33}N_4Zr\cdot C_6H_{14}$, $M$ = 855.19, triclinic, space group $P\bar{1}$, $a$ = 12.647(3), $b$ = 12.821(3), $c$ = 15.499(3) Å, $\alpha$ = 103.32(3), $\beta$ = 93.65(3), $\gamma$ = 118.97(3)°, $U$ = 2093.6(7) Å$^3$, $Z$ = 2, $\mu$(Mo-Kα) = 3.07 $cm^{-1}$, $T$ = 293 K, Enraf-Nonius CAD4 diffractometer, Mo-Kα (α = 0.710 73 Å), anisotropic refinement for all non-hydrogen atoms, final cycle of full-matrix least-squares refinement on $F^2$ with 3896 independent reflections and 493 variables (SHELXL-93), $R_1$ [$I > 2\sigma(I)$] = 0.0764, $wR_2$ (all data) = 0.1919, GOF = 1.18. For **2**: $C_{50}H_{54}N_4Zr$, $M$ = 802.19, monoclinic, space group $C2/c$ $a$ = 15.026(5), $b$ = 19.704(2), $c$ = 15.094(4) Å, $\beta$ = 106.97(1)°, $U$ = 4274(2) Å$^3$, $Z$ = 4, $\mu$(Mo-Kα) = 2.95 $cm^{-1}$, $T$ = 293 K, anisotropic refinement for all non-hydrogen atoms, final cycle of refinement on $F^2$ with 2298 independent reflections and 249 variables, $R_1$ [$I > 2\sigma(I)$] = 0.0462, $wR_2$ (all data) = 0.0974, GOF = 1.11.

1 R. D. Broene and S. L. Buchwald, *Science*, 1993, **261**, 1696; E. Negishi and T. Takahashi, *Acc. Chem. Res.*, 1994, **27**, 124; S. L. Buchwald and R. B. Nielsen, *Chem. Rev.*, 1988, **88**, 1047; P. Binger and S. Podubrin, in *Comprehensive Organometallic Chemistry II*, ed. M. F. Lappert, Elsevier, New York, 1995, vol 4, p. 439.
2 E. Negishi, S. J. Holmes, J. M. Tour, J. A. Miller, F. E. Cederbaum, D. R. Swanson and T. Takahashi, *J. Am. Chem. Soc.*, 1989, **111**, 3336; M. Jensen and T. Livinghouse, *J. Am. Chem. Soc.*, 1989, **111**, 4495; W. A. Nugent and D. F. Taber, *J. Am. Chem. Soc.*, 1989, **111**, 6435.
3 (*a*) H. Brand and J. Arnold, *J. Am. Chem. Soc.*, 1992, **114**, 2266; (*b*) J. Arnold, S. E. Johnson, C. B. Knobler and M. F. Hawthorne, *J. Am. Chem. Soc.*, 1992, **114**, 3996; (*c*) H. Brand and J. Arnold, *Organometallics*, 1993, **12**, 3655; (*d*) H. Brand, J. A. Capriotti and J. Arnold, *Organometallics*, 1994, **13**, 4469; (*e*) H. Brand and J. Arnold, *Angew. Chem., Int. Ed. Engl.*, 1994, **33**, 95.
4 H.-J. Kim, D. Whang, K. Kim and Y. Do, *Inorg. Chem.*, 1993, **32**, 360; H.-J. Kim, D. Whang, Y. Do and K. Kim, *Chem. Lett.*, 1993, 807; S. Ryu, D. Whang, H.-J. Kim, K. Kim, M. Yoshida, K. Hashimoto and K. Tatsumi, *Inorg. Chem.*, in press.
5 (*a*) K. Shibata, T. Aida and S. Inoue, *Tetrahedron Lett.*, 1992, **33**, 1077; (*b*) K. Shibata, T. Aida and S. Inoue, *Chem. Lett.*, 1992, 1173.
6 H.-J. Kim, S. Jung, D. Whang, Y.-M. Jeon and K. Kim, manuscript in preparation.
7 J. Arnold and C. G. Hoffman, *J. Am. Chem. Soc.*, 1990, **112**, 8620.
8 L. K. Woo, J. A. Hays, R. A. Jacobson and C. L. Day, *Organometallics*, 1991, **10**, 2102; L. K. Woo, J. A. Hays, V. G. Young, C. L. Day, C. Caron, F. D'Souza and K. M. Kadish, *Inorg. Chem.*, 1993, **32**, 4186.
9 T. Takahashi, D. R. Swanson and E. Negishi, *Chem. Lett.*, 1987, 623.
10 J. L. Templeton, *Adv. Organomet. Chem.*, 1989, **29**, 1.

*Received in Cambridge, UK, 21st July 1997; 7/05181F*

# Liquid phase oxidations using novel surface functionalised silica supported metal catalysts

**Janet Chisem (neé Bovey), Ian C. Chisem, John S. Rafelt, Duncan J. Macquarrie and James H. Clark***

*Department of Chemistry, University of York, Heslington, York, UK YO1 5DD*

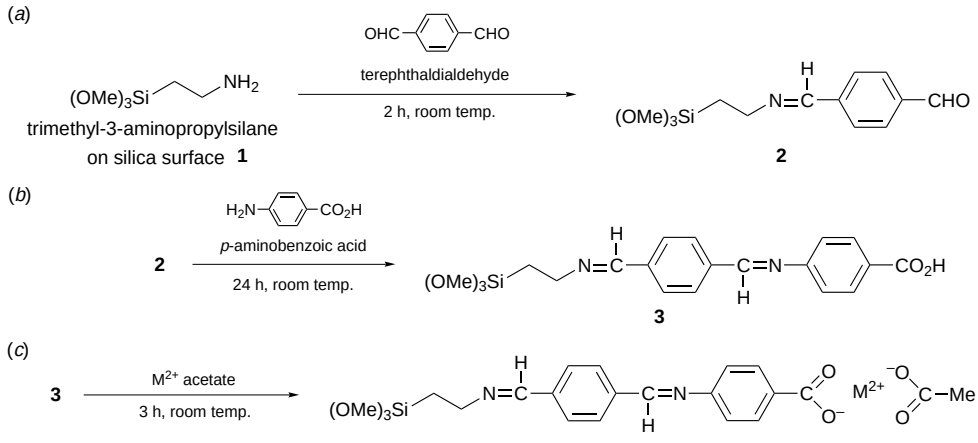
**Metal species supported on a surface functionalised silica gel are active heterogeneous catalysts for the liquid phase, room temperature epoxidation of cyclohexene and the aerobic oxidation of ethylbenzene.**

The oxidation of organic substrates leads to the production of many functionalised molecules which are of great commercial and synthetic importance. The oxidation of alkyl aromatic substrates is one such example, enabling the production of key groups such as ketones, aldehydes and esters. Epoxides are useful synthetic intermediates because they readily undergo ring-opening reactions to form bifunctional molecules. Alkene oxidation is a common method of epoxide synthesis. Use of a so-called sacrificial aldehyde as an oxygen transfer agent is a convenient and effective way of facilitating the epoxidation reaction.[1–5] However, in general, direct oxidation using organic oxygen donors such as peroxyacids and peroxides is the most important method of oxidation in industry.[6] The formation of by-products and decomposition of the desired product are often problems in these systems. The heterogenisation of reagents and catalysts and the use of molecular oxygen or air in place of homogenous oxidants is clearly desirable in economic and environmental terms.[6–7] However, air and oxygen are weak, non-selective oxidation reagents and suitable heterogeneous catalysts therefore need to be developed that work effectively in conjunction with these oxidants. Heterogeneous catalysts which have been used for liquid phase oxidations are often based on active species (notably transition metals, metal ions or metal complexes) adsorbed on supports (such as carbon, aluminas, silicas, zeolites, clays and ion exchange resins).[8] Chemically modified support materials offer great scope for the development of new catalysts.[5,9–11] Here we report on a new range of active oxidation catalysts based on chemically modified mesoporous silica with metal ions immobilised on a hydrophobic chain which, unusually, are capable of facilitating both alkene epoxidation and alkylaromatic oxidation reactions.

The preparation of the catalysts is illustrated in Scheme 1 and was carried out at room temperature. Silica with an average pore diameter of 100 Å (Kieselgel 100) was suspended in ethanol. Trimethyl-3-aminopropylsilane was added such that a ratio of 1.0 mmol silane (g silica)$^{-1}$ was obtained and the mixture was stirred for 24 h. The solid was then separated by filtration and washed thoroughly with diethyl ether to yield aminopropylsilica (AMPS). The AMPS was suspended in excess ethanol and terephthaldialdehyde added at a ratio of 1 mmol (g silica)$^{-1}$. The mixture was stirred for 2 h before being filtered and washed with diethyl ether. The resulting solid was then suspended in ethanol and *p*-aminobenzoic acid was added at a ratio of 1 mmol (g silica)$^{-1}$. The mixture was stirred for *ca.* 24 h. The solid was again separated by filtration and washed with diethyl ether. The product was resuspended in ethanol and the metal acetate (Cr, Mn, Co, Ni or Cu) was added at a ratio of 1.0 mmol metal (g silica)$^{-1}$ and the mixture stirred for 3 h. The excess solvent was removed using a rotary evaporator and the catalyst thoroughly washed with ethanol until the washings were colourless. Finally, the catalyst was dried under vacuum at *ca.* 95 °C for 16 h.

The epoxidation of cyclohexene to cyclohexene oxide was carried out as follows. A reaction flask under an $O_2$ atmosphere was charged with 17.5 mmol of cyclohexene, 60 mmol of isobutyraldehyde and 0.6 g of catalyst. Dichloromethane was used as the solvent and *tert*-butylbenzene as an internal standard. The reaction was run for 6 h at room temperature with constant stirring using a magnetic stirrer. The oxidation of ethylbenzene to acetophenone was carried out in a baffled flask with overhead stirring (1500 rpm). Air was used as the oxidant at a rate of 800 ml min$^{-1}$. 1.5 g of the Cr catalyst was added to 500 ml of neat substrate and the reactions carried out at reflux (130 °C) for 24 h. Water produced during the reaction was collected in twin Dean Stark traps. Both reactions were analysed by gas chromatography (GC) and the amount of product (mmol) thus determined.

The loading of metal on the catalysts was determined by atomic absorption spectroscopy (AAS). The solids were first dissolved in concentrated sulfuric acid and the resulting solution diluted with deionised water. Loadings were found to be in the




**Scheme 1** Diagrammatic representation of the functionalisation of the silica support (*a*,*b*) and the addition of the active metal species (*c*)

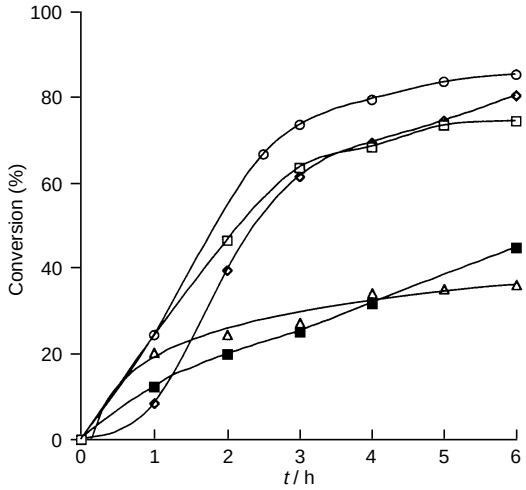



**Fig. 1** Percentage conversion of cyclohexene to cyclohexene oxide by various supported metals: Cr (□), Mn (△), Co (■), Ni (○) and Cu (◊)

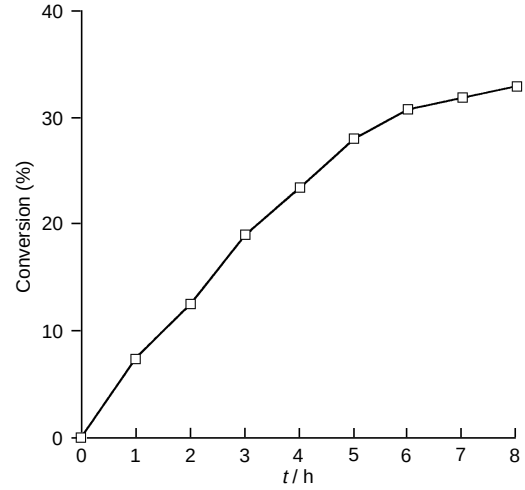



**Fig. 2** Percentage conversion of ethylbenzene to acetophenone by supported Cr catalyst

range 0.36–0.46 mmol $g^{-1}$, depending on the metal, which is typical of supported metal catalysts.[8] The loadings of metal are lower than the initial aminopropyl groups which may be due to incomplete metal binding during synthesis. Furthermore, the stoichiometry of the binding of the metal complexes has not yet been confirmed. Fourier-transform infrared spectroscopy revealed a band at 1684 $cm^{-1}$ which is indicative of the imine group, as shown in the proposed structure of the catalyst (see Scheme 1). Bands at 1584 and 1456 $cm^{-1}$ were attributed to the antisymmetric and symmetric stretching modes of the carboxylate group respectively. Preliminary leaching studies were carried out by performing AAS on the Ni catalyst following reaction. The loading of Ni was 0.36 mmol $g^{-1}$ for both the spent and fresh catalysts. This suggests that metal leaching is not occurring, which in turn is indicative of chemical bonding between the metal and the support of the catalyst.

In the cyclohexene epoxidations, all the catalysts showed excellent selectivity for the epoxide with only trace amounts (in total $< 1.0\%$) of by-products being detected by GC. Under homogeneous conditions, Murahashi *et al.*[1] obtained cyclohexenone as a by-product in the epoxidation of cyclohexene, in accordance with a peracid mechanism. Whilst we see only trace quantities of by-products in the heterogeneous reaction, we cannot rule out the possibility of cyclohexenone production. Fig. 1 shows the conversions (epoxide yields) achieved by each catalyst plotted *vs.* time. It should be noted that these activities have not been corrected for metal loadings but the range of loadings is narrow. It can be seen that the activity of the catalyst is dependent upon the identity of the supported cation, with high conversions being achieved for the Cr, Ni and Cu catalysts. The most active catalyst is the supported Ni variant which gives a conversion of 85% epoxide yield after 6 h. 80 and 74% epoxide yields are obtained with the Cu and Cr catalysts respectively. The fastest rates achieved are by the Ni and Cu catalysts and are 28 and 26.5% $h^{-1}$ respectively, over the first 3 h. These rates correspond to a frequency of 12 and 11 turnovers $h^{-1}$ per catalytic site (at an average loading of 0.41 mmol $g^{-1}$), respectively. Fig. 2 shows the conversion of ethylbenzene to acetophenone by the Cr catalyst *vs.* time. It can be seen that the catalyst showed excellent activity for the reaction, reaching 33% conversion after 8 h. A rate of *ca.* 5.5% $h^{-1}$ was reached over 5 h which is equivalent to $> 370$ turnovers $h^{-1}$ per catalytic site (assuming a loading of 0.41 mmol $g^{-1}$). After 5 h the rate decreased significantly which may be attributed to the inefficient removal of water from the system which leads to poisoning of the catalyst. The catalyst was highly selective to the ketone and no induction period was observed.

These new catalysts show remarkable and unusual versatility as they are capable of selectively catalysing reactions which proceed *via* very different mechanisms.[6] Further work is being directed at the use of other alkylaromatic and alkene substrates as well as Baeyer–Villiger systems. Catalyst re-use studies and the activities of other metal variants including Ti, V and Fe are also being investigated.

We thank the EPSRC for financial support, the RAEng/EPSRC for a Clean Technology Fellowship to J. H. C. and the Royal Society for a Research Fellowship to D. J. M.

## Footnote and References

* E-mail: jhc1@york.ac.uk

1 S.-I. Murahashi, Y. Oda, T. Naota and N. Komiya, *J. Chem. Soc., Chem. Commun.*, 1993, 139.
2 N. Mizuno, T. Hirose, M. Tateishi and M. Iwamoto, *Chem. Lett.*, 1993, 1839; N. Mizuno, M. Tateishi, T. Hirose and M. Iwamoto, *Chem. Lett.*, 1993, 1985.
3 E. Bouhlel, P. Laszlo, M. Levart. M.-T. Montaufier and G. P. Singh, *Tetrahedron Lett.*, 1993, **34**, 1123.
4 Z.-H. Ma, T.-J. Wang, Y.-Y. Yan, M.-Y. Huang and Y.-Y Jiang, *Angew. Makromol. Chem.*, 1996, **243**, 69.
5 A. J. Butterworth, J. H. Clark, P. H. Walton and S. J. Barlow, *Chem. Commun.*, 1996, 1859.
6 R. A. Sheldon and J. Dakka, *Catal. Today*, 1994, **19**, 215.
7 *Chemistry of Waste Minimisation*, ed. J. H. Clark, Chapman and Hall, London, 1995.
8 J. H. Clark, *Catalysis of Organic Reactions Using Supported Inorganic Reagents*, VCH, New York, 1994.
9 Y. Kurusu, *React. Polym.*, 1995, **25**, 63.
10 C. R. Dias, M. F. Portela, M. Galán-Fereres, M. A. Bañares, M. López Granados, M. A. Peña and J. L. G. Fierro, *Catal. Lett.*, 1997, **43**, 117.
11 Y. V. Subba Rao, D. E. De Vos, T. Bein and P. A. Jacobs, *Chem. Commun.*, 1997, 355.

*Received in Cambridge, UK, 8th September 1997; 7/06513B*

# Guest-responsive structural changes of porphyrinogen inclusion crystals: a long-range cooperative effect on guest inclusion

**Yoshio Furusho and Takuzo Aida***

*Department of Chemistry and Biotechnology, Graduate School of Engineering, The University of Tokyo, Hongo, Tokyo 113, Japan*

***meso*-Octaethylporphyrinogen inclusion crystals with lower alcohols undergo reversible guest-responsive structural changes, for which a long-range cooperative effect with a Hill coefficient of 40 is observed.**

Although porphyrinogen is a well known precursor of porphyrin, its chemistry has not been investigated until recently. Floriani *et al.* have extensively studied the chemistry of metal complexes of *meso*-octaalkylporphyrinogens,[1] and Sessler and co-workers have reported that free bases of porphyrinogens bind anions and neutral substrates in the solid state and in solution.[2] We have independently found that *meso*-octaethylporphyrinogen (hereafter OEP)[3] forms inclusion crystals with lower alcohols.[4] Herein we report guest-responsive structural changes of their inclusion crystals, and wish to highlight a long-range cooperative effect on the guest selection.

The crystalline inclusion compounds were obtained by recrystallization of OEP from alcoholic solutions, where the two host : guest mole ratios, 1 : 1 and 1 : 2, depending on the guest alcohol, were observed: 1 : 1 for MeOH, $HOCH_2OH$ [DHM] (from formalin–acetone), and $HOCH_2CH_2OH$ (EG) (from EG–acetone); 1 : 2 for EtOH, $Pr^nOH$ and $Pr^iOH$.† Crystallization of OEP from hexane gave crystals without guest molecules.

The crystal structures of some of the above inclusion compounds were successfully determined by X-ray crystallography (Fig. 1),‡ in which the porphyrinogen itself always adopts an $S_4$-saddle shape with the pyrrole units pointing up and down alternately. In the crystal of OEP without guest [Fig. 1(*a*)] the OEP molecules are stacked in an 'offset' geometry to fill cavities for guest inclusion, and form oblique columns, which are oriented in two directions perpendicular to each other. No intra- and inter-molecular hydrogen bonds were observed between OEP molecules in the crystal lattice. On the other hand, in the OEP·MeOH crystal [Fig. 1(*b*)], the OEP molecules are stacked along the crystallographic *b*-axis, and provide the cavity for MeOH. IR spectroscopy showed the presence of a hydrogen-bonding interaction between OEP and MeOH, for which the pyrrolic N–H serves as proton donor: A $\nu_{N-H}$ at 3440 $cm^{-1}$ for the OEP crystal without guest was observed at 3310 $cm^{-1}$ ($\Delta\nu_{N-H}$ −130 $cm^{-1}$) for the OEP·MeOH crystal. Interestingly, the oxygen atom of the guest MeOH is disordered along the *b*-axis,§ suggesting that it is hydrogen bonded with upper and lower OEP molecules. The packing mode of the OEP·EG crystal is very similar to that of the OEP·MeOH crystal, where the guest EG is not disordered due to simultaneous hydrogen bonding interaction with the upper and lower host molecules. The OEP·DHM crystal showed a virtually identical powder X-ray diffraction pattern to that of the OEP·MeOH crystal. On the other hand, in the OEP·2$Pr^iOH$ crystal [Fig. 1(*c*)], the OEP molecules are stacked tilting alternately to the left and right to give a cavity for two molecules of $Pr^iOH$, where each guest molecule is hydrogen bonded to the upper or lower OEP molecule. A similar packing mode was observed for the OEP·2EtOH crystal, although the crystal structure was not completely refined owing to its partial decomposition.

When finely pulverized OEP crystals without guest were exposed to an alcoholic vapor, the alcohol was included in the crystal. Likewise, the guest exchange of the inclusion crystals also took place reversibly. The guest inclusion or exchange under alcoholic vapors was usually complete within 48 h to furnish host : guest mole ratios identical to those for the clathrates grown from alcoholic solutions.¶ Of particular interest here is the fact that the OEP crystal exhibits guest-responsive structural changes of the lattice: from the powder X-ray diffraction pattern interconversions among the different crystals of OEP without guest, OEP·MeOH, OEP·2EtOH and

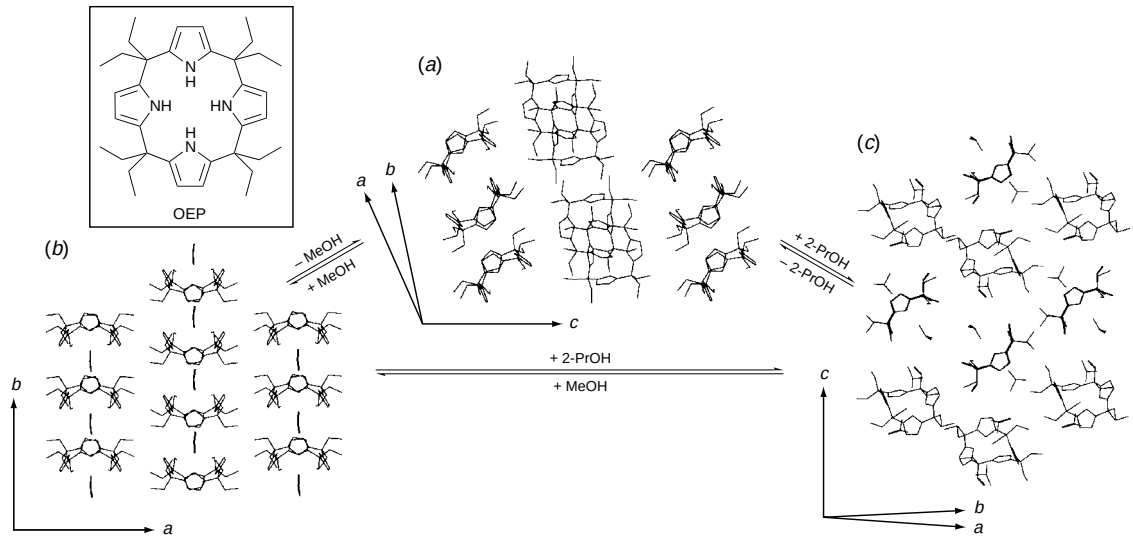



**Fig. 1** Crystal packing diagrams of OEP without guest (*a*), OEP·MeOH (*b*) and OEP·2$Pr^iOH$ (*c*)‡

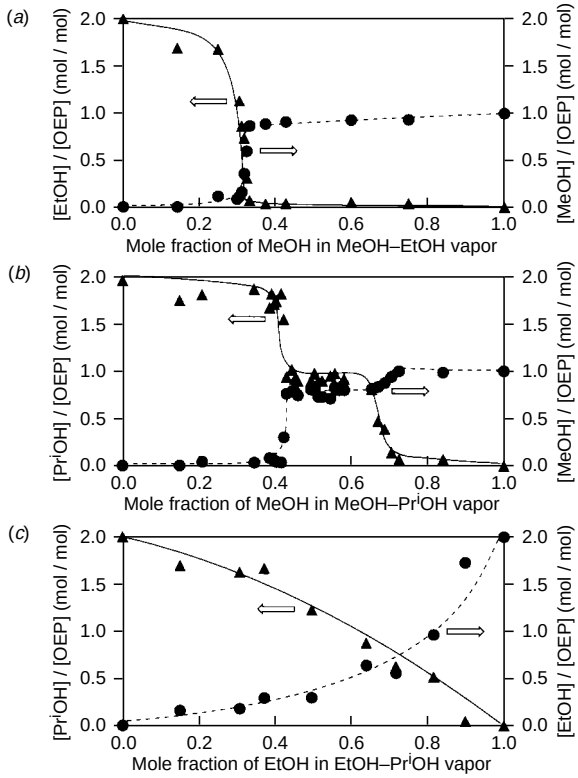



**Fig. 2** Relationships between mole ratios [guest]/[OEP] and vapor composition in competitive guest inclusion into OEP crystals without guest under mixed alcoholic vapors of MeOH–EtOH (*a*), MeOH–Pr$^{i}$OH (*b*) and EtOH–Pr$^{n}$OH (*c*) at 20 °C‖

OEP·2Pr$^{i}$OH took place without decomposition. Such a guest-responsive crystal-to-crystal transformation is rare, and has been reported for the inclusion crystals of cholic acid[5] and orthogonal aromatic triads.[6]

When powdery OEP crystals without guest were exposed to a mixed alcoholic vapor, a very clear cooperative (allosteric) effect, leading to a selective guest inclusion, was observed (Fig. 2).‖ In MeOH–EtOH vapor [Fig. 2(*a*)], MeOH was highly selectively incorporated into the host crystals over a wide range of vapor composition. However, at a mole fraction of MeOH below 30%, the selectivity was discretely reversed to EtOH. From Fig. 2(*a*), the Hill coefficient** was evaluated to be 40, which means that forty host molecules are cooperative for the guest inclusion.[7] The result was virtually identical to the above when started either from the inclusion crystals of OEP·MeOH or OEP·2EtOH. In MeOH–Pr$^{i}$OH vapor, the guest inclusion into the OEP crystals also showed a clear allosteric response [Fig. 2(*b*)]. However, an intermediate crystalline phase with [OEP]:[MeOH]:[Pr$^{i}$OH] of about 1:1:1 appeared, which is not a mixture of the OEP·MeOH and OEP·2Pr$^{i}$OH crystals, as judged from the powder X-ray diffraction pattern. In sharp contrast, in EtOH–Pr$^{i}$OH vapor, where the host:guest mole ratio was almost constant at 1:2 irrespective of the vapor composition, no allosteric response was observed for the guest inclusion [Fig. 2(*c*)].

From Fig. 2 together with the packing modes of the crystals (Fig. 1), the cooperative effect appears to operate when the guest inclusion or exchange requires a considerable structural change of the crystal lattice. For example, in the competition of MeOH and EtOH [Fig. 2(*a*)], the packing modes of the OEP·MeOH and OEP·2EtOH crystals are very different from each other, so that they may be unfavorable to coexist in a single crystal. As a consequence, either MeOH or EtOH is incorporated into the crystal depending on the vapor composition. Consistently, the exchange of $CH_3OH$ with $CD_3OD$ in the OEP crystal, which should require no structural change of the crystal lattice, took place extremely slowly ( < 10% in 48 h) compared with the exchange of MeOH with EtOH or Pr$^{i}$OH. Thus, the crystalline host of *meso*-octaethylporphyrinogen may be called an 'allosteric crystal'.

In conclusion, we have clearly demonstrated a long-range cooperative effect on the inclusion of lower alcohols into *meso*-octaethylporphyrinogen crystals. Although inclusion crystals have recently attracted particular attention as 'organic zeolites',[8] guest removal or exchange is very likely to result in decomposition of the crystal structure because of a low flexibility of the crystal packing. In contrast, the porphyrinogen inclusion crystal is a 'soft' organic zeolite, which is able to change its packing mode cooperatively depending on the guest molecule, leading to selective guest inclusion.

## Footnotes and References

* E-mail: aida@macho.t.u-tokyo.ac.jp

† Determined by $^{1}$H NMR, thermogravimetry and elemental analyses.

‡ *Crystal structure analysis* of OEP without guest, OEP·MeOH, OEP·EG and OEP·2Pr$^{i}$OH: Intensity data were collected on a Mac Science MXC18 diffractometer equipped with a graphite monochromator by using Cu-K$\alpha$ radiation ($\lambda$ = 1.541 78 Å) at room temperature with the $2\theta$–$\omega$ scan method. Structure solution and refinements were performed by using the SIR92 program package.

*Crystal data*: OEP ($C_{36}H_{52}N_4$, $M$ = 540): crystals from hexane, monoclinic, $C2/c$, $a$ = 19.038(2), $b$ = 16.655(3), $c$ = 22.937(3) Å, $\beta$ = 110.12(1)°, $U$ = 6829(2) Å$^3$, $Z$ = 8, $D_c$ = 1.05 g cm$^{-3}$, $F(000)$ = 2368, $R$ = 0.0560, $R_w$ = 0.0557. OEP·MeOH ($C_{37}H_{56}N_4O$, $M$ = 572): crystals from methanol, monoclinic, $C2/c$, $a$ = 23.129(6), $b$ = 6.894(2), $c$ = 23.045(6) Å, $\beta$ = 112.32(2)°, $U$ = 3399(2) Å$^3$, $Z$ = 4, $D_c$ = 1.12 g cm$^{-3}$, $F(000)$ = 1255, $R$ = 0.0804, $R_w$ = 0.0782. OEP·EG ($C_{38}H_{58}N_4O_2$, $M$ = 602): crystals from ethylene glycol, monoclinic, $C2/c$, $a$ = 27.52(1), $b$ = 16.510(5), $c$ = 20.462(6) Å, $\beta$ = 130.17(2)°, $U$ = 7105(4) Å$^3$, $Z$ = 8, $D_c$ = 1.13 g cm$^{-3}$, $F(000)$ = 2640, $R$ = 0.0717, $R_w$ = 0.0806. OEP·2Pr$^{i}$OH ($C_{42}H_{68}N_4O_2$, $M$ = 660): crystals from Pr$^{i}$OH, monoclinic, $P2_1/c$, $a$ = 17.239(4), $b$ = 11.513(2), $c$ = 20.793(5) Å, $\beta$ = 93.41(2)°, $U$ = 4119(2) Å$^3$, $Z$ = 4, $D_c$ = 1.07 g cm$^{-3}$, $F(000)$ = 1456, $R$ = 0.0775, $R_w$ = 0.0724. CCDC 182/622.

§ The disordered molecules are related by a twofold axis.

¶ In alcoholic solutions, the guest inclusion and exchange took place very rapidly and was complete within 1 h.

‖ Finely pulverized OEP crystals without guest were exposed for 48 h to a mixed alcoholic vapor at 20 °C in a 50 ml closed glass bottle, and the host:guests molar ratio was determined by $^{1}$H NMR in $CDCl_3$. The vapor composition was estimated from the vapor pressures at 20 °C (mmHg) for MeOH (91.8), EtOH (44.0) and Pr$^{i}$OH (32.4).

** The Hill coefficient ($n$) was calculated on the basis of the following equation: $\log [(x/(1-x)] = n \log P_{MeOH} - n \log P_{50}$, where $x$ is the molar ratio of OEP·MeOH to OEP·2EtOH; $P_{MeOH}$ and $P_{50}$ represent the partial pressure of MeOH and that of MeOH when a half of OEP molecules binds MeOH, respectively.

1 C. Floriani, *Chem. Commun.*, 1996, 1257 and references therein.
2 P. A. Gale, J. L. Sessler, V. Král and V. Lynch, *J. Am. Chem. Soc.*, 1996, **118**, 5140; W. E. Allen, P. A. Gale, C. T. Brown, V. M. Lynch and J. L. Sessler, *J. Am. Chem. Soc.*, 1996, **118**, 12 471; J. L. Sessler, A. Andrievsky, P. A. Gale and V. Lynch, *Angew. Chem., Int. Ed. Engl.*, 1996, **35**, 2782; P. A. Gale, J. L. Sessler, W. E. Allen, N. A. Tvermoes and V. Lynch, *Chem. Commun.*, 1997, 665.
3 D. Jacobi, C. Floriani, A. Chiesi-Villa and C. Rizzoli, *J. Am. Chem. Soc.*, 1993, **115**, 3595.
4 Y. Furusho, T. Aida and S. Inoue, *Abstr., 3D238 in the 67th Annual Meeting of the Chemical Society of Japan*, Tokyo, 1994.
5 M. Miyata, M. Shibakami, S. Chirachanchai, K. Takemoto, N. Kasai and K. Miki, *Nature*, 1990, **343**, 446; M. Shibakami, M. Tamura and A. Sekiya, *J. Am. Chem. Soc.*, 1995, **117**, 4499.
6 K. Kobayashi, K. Endo, Y. Aoyama and H. Masuda, *Tetrahedron Lett.*, 1993, **34**, 7929.
7 J. Rebek, Jr., T. Costello, L. Marshall, R. Wattley, R. C. Gadwood and K. Onan, *J. Am. Chem. Soc.*, 1985, **107**, 7481.
8 X. Wang, M. Simard and D. Wuest, *J. Am. Chem. Soc.*, 1994, **116**, 12119; *Molecular Inclusion and Molecular Recognition–Clathrate II*, ed. E. Weber, in *Top. Curr. Chem.*, Springer-Verlag, Berlin-Heidelberg, 1988, vol. 149.

*Received in Cambridge, UK, 9th July 1997; 7/04897A*

# The coupling of methylene and vinyl ligands at a ruthenium(II) centre

**Anthony F. Hill,* Chean T. Ho and James D. E. T. Wilton-Ely**

*Department of Chemistry, Imperial College of Science Technology and Medicine, South Kensington, London, UK SW7 2AY*

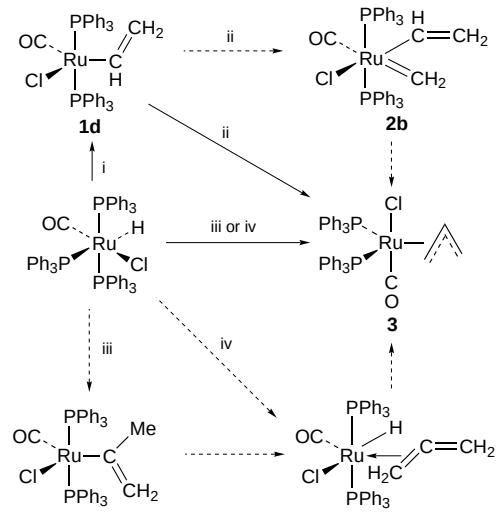
**The reaction of $[Ru(CH{=}CH_2)Cl(CO)(PPh_3)_2]$ with diazomethane provides the allyl complex $[Ru(\eta^3\text{-}CH_2CHCH_2)Cl(CO)(PPh_3)_2]$ which is also the product of the reactions of $[RuHCl(CO)(PPh_3)_3]$ with either allene or propyne and which reacts subsequently with $NaS_2CNMe_2$ to provide $[RuH(S_2CNMe_2)(CO)(PPh_3)_2]$ and allene.**

In a recent review,[1] Maitlis *et al*. drew attention to the potential significance of the coupling of vinyl and methylene groups in the Fischer–Tropsch synthesis. In particular the oxidation of $[Rh_2(\mu\text{-}CH_2)_2(CH{=}CH_2)_2(\eta\text{-}C_5Me_5)_2]$ by $AgBF_4$ in acetonitrile was shown to provide $[Rh(\eta^3\text{-}CH_2CHCH_2)(NCMe)(\eta\text{-}C_5Me_5)]BF_4$,[2] whilst diazomethane addition to the diruthenium complex $[Ru_2(\mu\text{-}CH{=}CH_2)(CO)_3(\eta\text{-}C_5H_5)_2]^+$ followed by deprotonation provides $[Ru_2(\mu\text{-}CHCH{=}CH_2)(\mu\text{-}CO)(CO)(\eta\text{-}C_5H_5)_2]$.[3] The operation of these couplings on bimetallic systems, whilst clearly significant in understanding Fischer–Tropsch processes, begs the question do they occur on monometallic systems? Werner and coworkers have reported that the reaction of $[RuCl(=CPh_2)(PPh_3)(\eta\text{-}C_5H_5)]$ with vinyl magnesium bromide provides the allyl complex $[Ru(\eta^3\text{-}CH_2CHCPh_2)(PPh_3)(\eta\text{-}C_5H_5)]$.[4] The complex $[Ru(CH{=}CH_2)(=CPh_2)(PPh_3)(\eta\text{-}C_5H_5)]$ is an attractive intermediate, however as the authors point out, the product is also consistent with direct nucleophilic attack at the carbene carbon. Such a process is typical of coordinatively saturated carbene complexes of divalent ruthenium.[5] Here, we report the unambiguous observation of the coupling of a vinyl and a methylene ligand on a ruthenium system. Furthermore, we show an unusual β-elimination process of the resulting $\eta^3$-allyl ligand which may be induced by dithiocarbamate coordination.

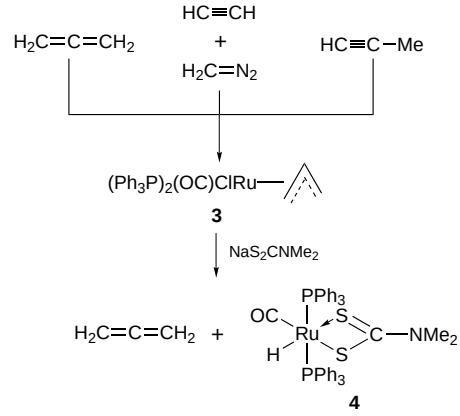
Roper and coworkers have shown that the coordinatively unsaturated complex $[Ru(Ph)Cl(CO)(PPh_3)_2]$ **1a** reacts with diazomethane to provide a remarkably stable methylene complex $[Ru(\eta^2\text{-}OCPh)Cl(=CH_2)(PPh_3)_2]$ **2a**, but that such a reaction has so far failed for the corresponding *trans* β-styryl analogue $[Ru(CH{=}CHPh)Cl(CO)(PPh_3)_2]$ **1b**.[6] An intriguing feature of the reactivity of **2a** is the apparent reluctance of the phenyl and methylene ligands to couple, despite the anticipated stability of the hypothetical product $[Ru(CH_2Ph)Cl(CO)(PPh_3)_2]$ **1c**. We find that the parent vinyl complex $[Ru(CH{=}CH_2)Cl(CO)(PPh_3)_2]$ **1d**[7] reacts readily with diazomethane in dichloromethane–diethyl ether to provide high yields of the $\eta^3$-allyl complex $[Ru(\eta^3\text{-}CH_2CHCH_2)Cl(CO)(PPh_3)_2]$ **3** (Scheme 1), the identity and stereochemistry of which follows unambiguously from spectroscopic data† and two unequivocal syntheses (*vide infra*). Whilst the reaction leading to **3** is unique, the class of compounds has precedent. Related examples, *e.g.* $[Ru(\eta^3\text{-}CH_2CHCH_2)Cl(CO)(PMe_2Ph)_2]$ have been obtained from the reaction of $[RuCl_2(CO)_2(PMe_2Ph)_2]$ with $Bu^n_3SnCH_2CH{=}CH_2$,[8]‡ whilst $[RuHCl(CO)(PPh_3)_3]$ hydroruthenates 1,3-dienes to provide substituted examples.[9] Although this result is surprising, the methylene complex $[Ru(CH{=}CH_2)Cl(=CH_2)(CO)(PPh_3)_2]$ **2b** is an obvious intermediate in the formation of **3**. It remains unclear to us why, in the case of **1a** methylene coordination is followed by (reversible) migration of a phenyl group to a carbonyl ligand, but in the case of **1d**, migration of the vinyl ligand occurs selectively and irreversibly to the introduced methylene ligand. Maitlis' studies of C–C bond forming processes for organorhodium species certainly point to a greater migratory aptitude for vinyl than phenyl ligands.[1] However, since the phenyl complex **2a** has been shown to be in equilibrium with $[Ru(Ph)Cl(=CH_2)(CO)(PPh_3)_2]$[6] the relative mobility of vinyl and phenyl ligands appears not to be the limiting factor here, but more likely one of product development control.

Complex **3** also results from two other approaches. Santos and coworkers have shown that in general, terminal alkynes RC≡CH (R = Ph, $Bu^t$, $Bu^n$) react with $[RuHCl(CO)(PPh_3)_3]$ to provide coordinatively unsaturated σ-vinyl complexes $[Ru(CH{=}CHR)Cl(CO)(PPh_3)_2]$.[10] We anticipated that a similar hydroruthenation of allene might provide **3** which indeed it does in high yield (Scheme 1). Somewhat surprisingly however, **3** is also the product of the reaction of $[RuHCl(CO)(PPh_3)_3]$ with propyne! This result can be explained by the formation of the usually less favoured α-substituted σ-vinyl complex $[Ru(C(Me){=}CH_2)Cl(CO)(PPh_3)_2]$, which can undergo β-Ru–H elimination to provide $[RuH(\eta^2\text{-}CH_2CCH_2)Cl(CO)(PPh_3)_2]$ followed by hydroruthenation to provide **3**.

The chemistry of $\eta^3$-allyl ligands is enriched by their ability to assume a monohapto coordination mode. We therefore attempted to induce monohapto coordination by replacing the chloride ligand in **3** with a potentially bidentate dithiocarbamate ligand. Surprisingly, the reaction of **3** with $Na[S_2CNMe_2]$ in dichloromethane–ethanol led to the formation of $[RuH(S_2CNMe_2)(CO)(PPh_3)_2]$ **4** with the organometallic ligand being lost from the coordination sphere. When the reaction was carried out in $CDCl_3$–MeOH (10 : 1), $^1H$ NMR integration confirmed allene as the organic product. The most reasonable course for this reaction would appear to be dissociation of chloride followed by the β-RuH elimination of allene to provide the coordinatively unsaturated, though presumably solvent-stabilised species '$[RuH(CO)(PPh_3)_2]^+$'. Although this type of elimination is unusual, we have observed[11] that treating




**Scheme 1** *Reagents and conditions*: i, HC≡CH ($CH_2Cl_2$, 25 °C); ii, $CH_2N_2$ ($Et_2O$, $CH_2Cl_2$, 25 °C); iii, $CH_3C{\equiv}CH$ (thf, 25 °C then heating); iv, $H_2C{=}C{=}CH_2$ (thf, 25 °C then heating)




**Scheme 2**

$[Ru(CH{=}CHCH_2PPh_3)Br(CO)(PPh_3)_2]^+$ with $Na[S_2CNMe_2]$ also leads to formation of **4**.

The above transformations taken together constitute the metal-mediated conversion of ethyne or propyne to allene (Scheme 2). The reactions are clearly not catalytic in nature, however they do add a further viewpoint to the complex picture of chain growth in Fischer–Tropsch processes, complimenting recent results obtained by Werner *et al*. for the coupling of vinyl ligands with vinylidenes on mononuclear rhodium centres.[12]

A. F. H. gratefully acknowledges the Leverhulme Trust and the Royal Society for the award of a Senior Research Fellowship. This work was supported by the EPSRC in the form of a studentship to J. D. E. T. W.-E.

## Footnotes and References

* E-mail: a.hill@ic.ac.uk

† *Selected data* for **3**: (*a*) complex **1d** (1.00 g) in dichloromethane (35 $cm^3$) was treated with an excess of diazomethane in diethyl ether and stirred for 15 min. Removal of solvent, chromatographic purification (silica gel, $CH_2Cl_2$ eluent) and crystallisation from $CH_2Cl_2$–EtOH provided **3**; yield 0.45 g (44%). (*b*) $[RuHCl(CO)(PPh_3)_3]$ (0.60 g) in allene-saturated thf was stirred for 1 h and then heated under reflux for 2 min. Addition of ethanol and slow concentration provided **3**; yield 0.39 g, (85%). $[RuHCl(CO)(PPh_3)_3]$ (0.50 g) in propyne-saturated thf was stirred for 1 h and then heated under reflux for 2 min. Addition of ethanol and slow concentration provided **3**; yield 0.32 g (84%). IR 1933 (Nujol), 1939 ($CH_2Cl_2$) [$\nu$(CO)] $cm^{-1}$. NMR (25 °C, $CDCl_3$). $^1$H: $\delta$ 2.57 [dd, 2 H, *J*(HH) 5.28, 12.54, $CH_2$], 2.97 [d, 2 H, *J*(HH) 7.26 Hz, $CH_2$], 5.03 [m (= tt), 1 H, ≡CH], 7.22–7.48 (m, 30 H, $C_6H_5$). $^{13}$C{$^1$H}: $\delta$ 202.2 [t, *J*(PC) 14 Hz], 134.4–127.9 ($C_6H_5$), 101.6 (≡CH), 62.1 [d, *J*(PC) 23.7 Hz, $CH_2$]. $^{31}$P {$^1$H}: $\delta$ 34.98. FABMS *m/z* (%): 730(3) $[M]^+$, 695 (51) $[M - Cl]^+$, 689 (73) $[M - C_3H_5]^+$, 653 (11) $[Ru(CO)(PPh_3)_2]^+$, 625 (17) $[Ru(PPh_3)_2]^+$. Anal. Found: C, 65.66; H, 4.75. $C_{40}H_{35}ClOP_2Ru$ requires C, 65.80; H, 4.83%.

‡ Notably **1a** rather than **3** is the product of the reaction of $[RuHCl(CO)(PPh_3)_3]$ with $Ph_3SnCH_2CH{=}CH_2$.

1 P. M. Maitlis, H. C. Long, R. Quyoum, M. L. Turner and Z.-Q. Wang, *Chem. Commun.*, 1996, 1.
2 J. M. Martinez, H. Adams, N. A. Bailey and P. M. Maitlis, *J. Chem. Soc., Chem. Commun.*, 1989, 286.
3 S. A. R. Knox, *J. Organomet. Chem.*, 1990, **400**, 255.
4 T. Braun, O. Gevert and H. Werner, *J. Am. Chem. Soc.*, 1995, **117**, 7291.
5 For a recent review of alkylidene and σ-vinyl complexes of ruthenium see: A. F. Hill, in *Comprehensive Organometallic Chemistry II*, ed. E. W. Abel, F. G. A. Stone and G. Wilkinson, Pergamon Press, Oxford, 1995, vol. 7.
6 D. S. Bohle, G. R. Clark, C. E. F. Rickard, W. R. Roper, W. E. B. Sheppard and L. J. Wright, *J. Chem. Soc., Chem. Commun.*, 1987, 563; D. S. Bohle, G. R. Clark, C. E. F. Rickard, W. R. Roper and L. J. Wright, *J. Organomet. Chem.*, 1989, **358**, 411.
7 J. C. Cannadine, A. F. Hill, A. J. P. White, D. J. Williams and J. D. E. T. Wilton-Ely, *Organometallics*, 1996, **15**, 5409.
8 C. F. J. Barnard, J. A. Daniels, P. R. Holland and R. J. Mawby, *J. Chem. Soc., Dalton Trans.*, 1980, 2418.
9 K. Hiraki, Y. Sasada and T.Kitamura, *Chem. Lett.*, 1980, 449; K. Hiraki, N. Ochi, Y. Sasada, H. Hayashida, Y. Fuchita and S. Yamanaka, *J. Chem. Soc., Dalton Trans.*, 1985, 873.
10 M. R. Torres, A. Vegas and A. Santos, *J. Organomet. Chem.*, 1986, **309**, 169; see also ref. 5.
11 N. W. Alcock, J. Cartwright, A. F. Hill, M. Marcellin and H. M. Rawles, *J. Chem. Soc., Chem. Commun.*, 1995, 369.
12 H. Werner, R. Wiedemann, P. Steinert and J. Wolf, *Chem. Eur. J.*, 1997, **3**, 127.

*Received in Cambridge, UK, 16th June 1997; 7/04157H; Revised manuscript 22nd August 1997; 7/06456J*

# Generation of stable and persistent carbocations from 4-vinylanisole within zeolites

**V. Jayathirtha Rao,[a] Nicolette Prevost,[a] V. Ramamurthy,*[a] Masanobu Kojima[b] and L. J. Johnston[c]**

[a] *Department of Chemistry, Tulane University, New Orleans, LA 70118, USA*
[b] *Department of Bioscience and Biotechnology, Faculty of Agriculture, Shinshu University, Matsumoto, Nagano 390, Japan*
[c] *Steacie Institute for Molecular Sciences, National Research Council of Canada, Ottawa, Ontario, Canada K1A OR6*

**Stable and ultrastable carbocations from 4-vinylanisole are spontaneously generated within zeolites; these reactive intermediates are stable for several weeks within the confined environments of zeolites.**

Spontaneous generation of long-lived organic cation radicals on the surfaces of zeolites has been known for over three decades.[1] However, only during the last few years has this phenomenon been widely recognized and the technique has been developed into a routine laboratory tool to generate stable cation radicals.[2,3] Simultaneous formation of carbocations may occasionally complicate the characterization of organic cation radicals within zeolites. This discrepancy prompted the present investigation. Our efforts to characterize stable reactive intermediates generated by inclusion of 4-vinylanisole within a number of zeolites are presented here. The behavior of 4-vinylanisole is typical of the many styrenes we have investigated. Persistent carbocations are formed more readily than cation radicals in all these cases.

Inclusion of 4-vinylanisole into activated Na ZSM-5 (Si/Al ≈ 15, the PQ Corporation-CBV 3010; Si/Al ≈ 25, Chemie Utikon) turned the zeolite blue–purple, as reported by Pollak *et al.*[4] The diffuse reflectance spectrum of the purple solid displayed in Fig. 1 consists of three maxima (*ca.* 280, 580 and *ca.* 640 nm). Of these the short-wavelength absorption is due to 4-vinylanisole. The appearance of an intense red–violet color and a visible absorption (*ca.* 580 nm) were general within a number of zeolites (Ca Y, H Y, Na omega-5, Na ZSM-11 and Na-beta). Of the zeolites examined, only Na X was totally inert. The appearance of a maximum at 640 nm was unique to ZSM zeolites. In no other zeolites was this peak recorded. The absorption spectrum of the 4-vinylanisole radical cation in solution consists of two maxima, one in the UV and the other in the visible region.[5] Close examination of the spectrum recorded for zeolite samples revealed that the absorption in the UV range (340–380 nm) in solution, was absent. To be sure that the zeolites do not influence the electronic transitions, the diffuse reflectance of the 4-vinylanisole radical cation included within Na Y was recorded by generating such a species by photoionization. The spectrum of such a generated 4-vinylanisole radical cation within Na Y was similar to that in solution. This indicated to us that no stable radical cation of 4-vinylanisole is generated under our conditions.

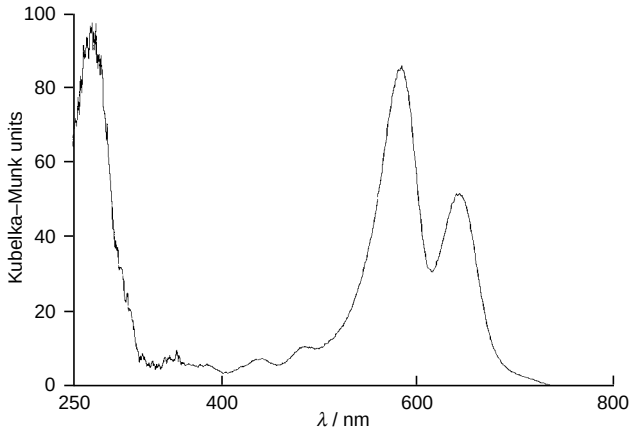



**Fig. 1** Diffuse reflectance spectrum of 4-vinylanisole upon inclusion in Na ZSM-5 (Si/Al ≈ 25)

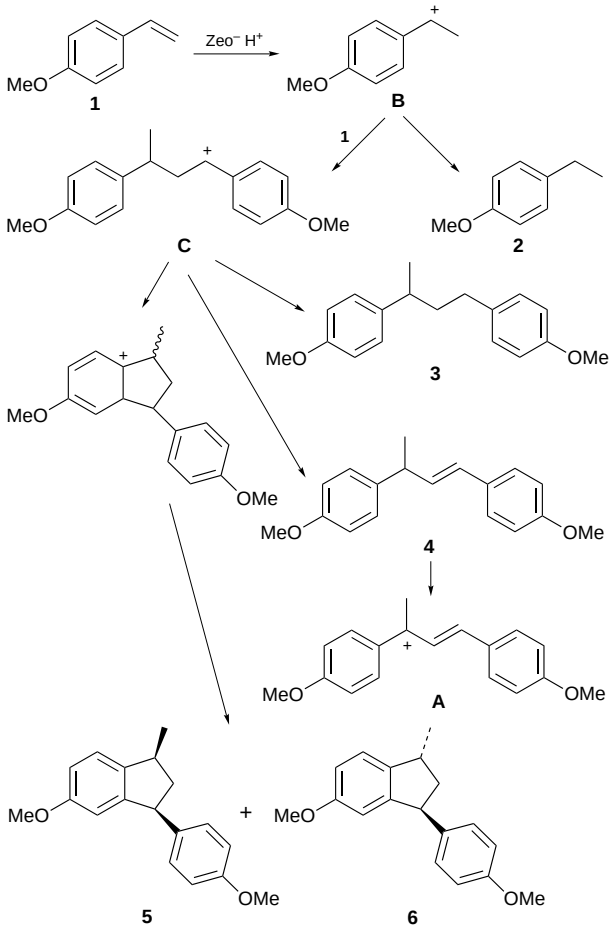
Extraction of the red–violet zeolite with either $CH_2Cl_2$ or tetrahydrofuran–$H_2O$ gave several products. The yields of products in various zeolites are summarized in Table 1. Since the total isolated yields of the products and the reactant after extraction amounted to *ca.* 90%, the species responsible for the red–violet color must be present only in small amounts within a zeolite. The formation of products **2**–**6** can be mechanistically rationalized on the basis of a primary step involving a proton transfer from the zeolite to 4-vinylanisole (Scheme 1). We believe that the acid sites, generated upon calcination, are directly involved in the formation of products **2**–**6**.[6]

Support for the involvement of the postulated reactive intermediates in Scheme 1 was obtained by recording the diffuse reflectance absorption spectrum of the colored zeolites. For example, activated Ca Y when dropped into a solution of 4-vinylanisole in hexane, developed a vibrant red–violet color. The diffuse reflectance spectrum of the solid zeolite sample presented in Fig. 2 consists of two broad absorption centered at 340 and 580 nm (note the absence of the transition at 640 nm). Of the two absorptions, the one at 580 nm was found to be permanent; the zeolite retained the red color and the absorption at 580 nm remained under all conditions including refluxing in HCl or NaOH solutions. The diffuse reflectance spectrum of the zeolite that has been extracted with a polar solvent did not show the absorption at 340 nm (Fig. 2). This leads us to suggest that an intermediate absorbing at 340 nm is responsible for the formation of products **2**–**6**. We attribute the absorption at *ca.* 340 nm to the carbocation(s) **B** and/or **C**. The absorption spectrum for the 4-methoxy phenylethyl cation has been reported in solution and that remarkably coincides with the

**Table 1** Product distribution (%) upon inclusion of vinylanisole within zeolites

| | Compound | | | | |
|---|---|---|---|---|---|
| Conditions[a,b] | **2** | **3** | **4** | **5 + 6** | Conversion |
| Ca, Y, oven, 500 °C | 22 | 36 | 37 | 6 | > 80% |
| Ca Y, vac. line, 400 °C | 10 | 78 | 6 | 6 | > 90% |
| H Y, oven 500 °C | 12 | — | 76 | 12 | > 90% |
| ZSM-5, oven, 500 °C | 4 | — | 5 | 65 | > 90% |
| Na Y, oven, 500 °C | 5 | — | 63 | 32 | < 20% |
| Na X, oven, 500 °C | — | — | — | — | — |

[a] Ca Y and H Y were prepared from Na Y obtained from Aldrich & Co; Na X was an Aldrich sample; Na Y received from Aldrich showed the most thermal reaction. Samples obtained from Zeolyst International (CBV-100) showed the least thermal reaction. [b] ZSM-5 samples were obtained from PQ Corporation and Chemie Utikon. Both samples showed similar behavior.




**Scheme 1** Mechanism of proton-transfer mediated reactions within zeolites

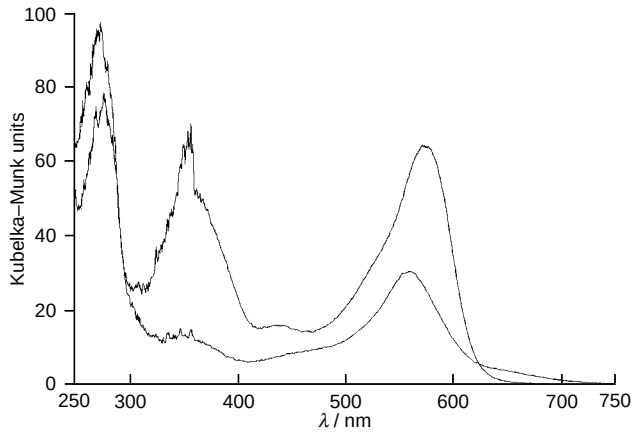
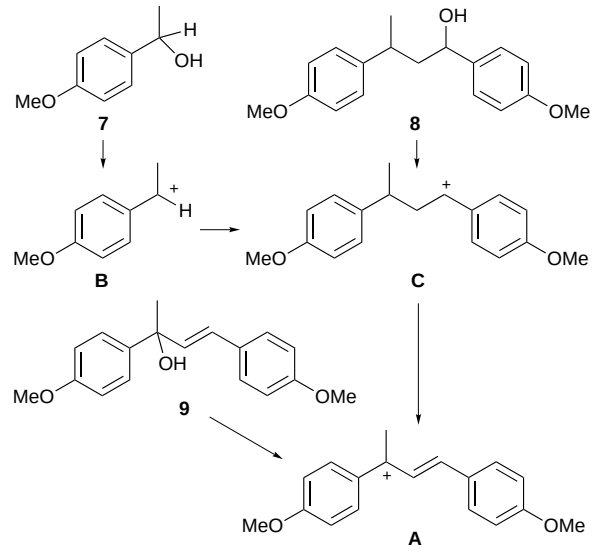



**Fig. 2** Diffuse reflectance spectrum of 4-vinylanisole upon inclusion into Ca Y. The spectrum with two maxima is before washing and that with one maximum is after washing.

absorption maximum observed in zeolite.[7] We propose that the absorption at *ca.* 580 nm is due to the persistent carbocation **A** shown in Scheme 1. This suggestion is consistent with the expected absorption for the 1,3-diphenyl propenyl cation.[8]

Support for the above assignment was obtained by generating the same carbocations from an independent source, from carbinols **7**, **8** and **9** (Scheme 2). Addition of activated Ca Y, H Y and Na ZSM-5 to hexane solutions of **7**, **8** and **9** resulted in an immediate development of a bright red–pink color. The diffuse reflectance spectrum, independent of the carbinol, possessed




**Scheme 2** Generation of carbocations from the corresponding carbinols

absorptions at 580 nm, identical to the one obtained when 4-vinylanisole was included into these zeolites. This suggested to us that independent of the source, within a zeolite, the cations **B** and **C** readily transform themselves into the persistent carbocation **A**.

It is clear from the above presentation that zeolites, when properly prepared, can generate and stabilize 'reactive' intermediates from neutral molecules. On the basis of the behavior of 1,2-diarylethylenes which yield stable cation radicals, we had expected the formation of cation radicals from these systems as well.[3] It is surprising to note that 1-arylethylenes yield persistent carbocations.[9] At this stage the origin of such a difference is not obvious.

The authors at Tulane University thank the Division of Chemical Sciences, Office of Basic Energy Sciences, Office of Energy Research, US Department of Energy for support of this program.

## Footnote and References

* E-mail: murthy@mailhost.tcs.tulane.edu

1 D. N. Stamires and J. Turkevich, *J. Am. Chem. Soc.*, 1964, **86**, 749.
2 P. S. Lakkaraju, D. Zhou and H. D. Roth, *Chem. Commun.*, 1996, 2605; E. A. Piocos, D. W. Werst and A. D. Trifunac, *J. Phys. Chem.*, 1996, **100**, 8408; C. J. Rhodes, *Colloids Surf. A: Physicochem. Eng. Asp.*, 1993, **72**, 111.
3 V. Ramamurthy, J. V. Caspar and D. R. Corbin, *J. Am. Chem. Soc.*, 1991, **113**, 594; J. V. Caspar, V. Ramamurthy and D. R. Corbin, *J. Am. Chem. Soc.*, 1991, **113**, 600.
4 S. S. Pollack, R. F. Sprecher and E. A. Frommell, *J. Mol. Catal.*, 1991, **66**, 195.
5 N. P. Schepp and L. J. Johnston, *J. Am. Chem. Soc.*, 1994, **116**, 6895; L. J. Johnston and N. P. Schepp, *J. Am. Chem. Soc.*, 1993, **115**, 6564; S. Tojo, S. Toki and S. Taklamuku, *J. Org. Chem.*, 1991, **56**, 6240; O. Brede, F. David and S. Steenken, *J. Chem. Soc., Perkin Trans. 2*, 1995, 23.
6 J. W. Ward, in *Zeolite Chemistry and Catalysis*, ed. J. A. Rabo, American Chemical Society, Washington, DC, 1976, p. 118.
7 R. A. McClelland, C. Chan, F. Cozens, A. Modro and S. Steenken, *Angew. Chem., Int. Ed. Engl.*, 1991, **30**, 1337.
8 J. Sondermann and H. Kuhn, *Chem. Ber.*, 1966, **99**, 2491; R. N. Young, B. Brocklehurst and P. Booth, *J. Am. Chem. Soc.*, 1994, **116**, 7885; H. Garcia, S. Garcia, J. P. Prieto and J. C. Scaiano, *J. Phys. Chem.*, 1996, **100**, 18 158.
9 Persistent carbocation formation from indene has been reported recently: K. Pitchumani and V. Ramamurthy, *Chem. Commun.*, 1996, 2763.

*Received in Columbia, MO, USA, 6th June 1997; 7/03946H*

# Synthesis and crystal structure of an unusual bimetallic mercury–dithiolene complex

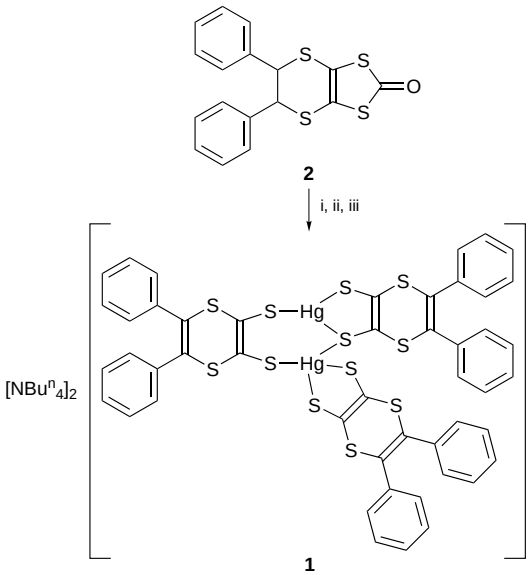
**Dong-Youn Noh,[a] Allan E. Underhill*[b] and Michael B. Hursthouse[c]**

[a] *Department of Chemistry, Seoul Womens University, Seoul 139-774, Korea*
[b] *Department of Chemistry, University of Wales, Bangor, Gwynedd, UK LL57 2UW*
[c] *Department of Chemistry, University of Wales, Cardiff, PO Box 912, UK CF1 3TB*

**A bimetallic mercury(II) dithiolene complex in which the ligand exhibits three different modes of coordination to the mercury atoms within the same molecular species is reported.**

Metal dithiolene complexes have been widely studied because of their potential in applications such as molecular conductors, ferromagnets, IR dyes, liquid crystals and catalysis.[1–3] As part of an extensive programme of research into these unusual compounds we have been studying the synthesis and properties of metal complexes of ligands derived from dmit (dmit = 1,3-dithiol-2-thione-4,5-dithiolate). During the course of these studies we have prepared a bimetallic mercury(II)–dithiolene complex **1**, which has a most unusual structure involving three differing modes of coordination by the same dithiolene ligand and contains a three-coordinate $Hg^{II}$. Here we report the synthesis and X-ray crystal structure of **1**.

The synthesis of the mercury–dithiolene complex **1** is outlined in Scheme 1. The 1,3-dithiole-2-one **2** was treated with KOH dissolved in MeOH under $N_2$ to open the five-membered ring.[5] To the solution were added separate solutions of $HgCl_2$ and TBABr in MeOH. The yellow precipitate was filtered off and washed with MeOH. The precipitate was recrystallised from acetone–ethyl acetate in a freezer to yield **1**† in 32% yield. Surprisingly, the precursor (or an intermediate thereof) has undergone oxidative dehydrogenation during this reaction to yield the fully conjugated system 1,4-dithiacyclohexadiene observed in **1**.




**Scheme 1** *Reagents and conditions*: i, KOH, MeOH, room temp.; ii, $HgCl_2$, MeOH then [$NBu^n_4$]Br, MeOH; iii, recrystallization from acetone–ethyl acetate, 32% yield

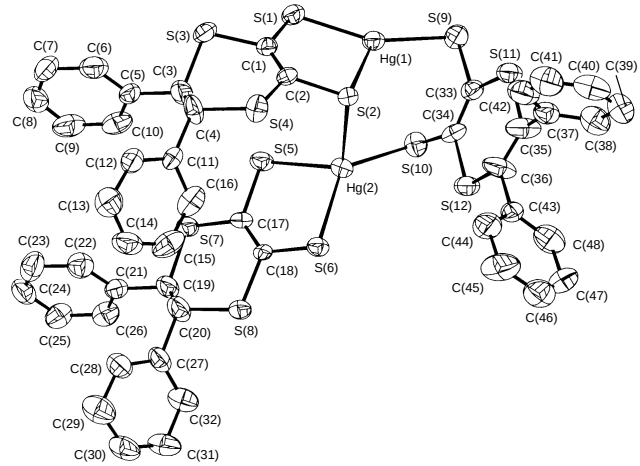



**Fig. 1** The single-crystal X-ray structure of [$NBu^n_4$][$Hg_2$(dithiolene)$_3$], with ellipsoids shown at 50% probability and [$NBu^n_4$]$^+$ ions omitted. For clarity only mercury and sulfur atoms are labelled, with all other atoms being carbon. Selected bond lengths (Å) and angles (°): Hg(1)–S(1) 2.367(3), Hg(1)–S(2) 2.609(2), Hg(1)–S(9) 2.348(3), Hg(2)–S(2) 2.748(2), Hg(2)–S(5) 2.502(2), Hg(2)–S(6) 2.484(2), Hg(2)–S(10) 2.481(3); S(1)–Hg(1)–S(2) 88.31(8), S(1)–Hg(1)–S(9) 155.40(8), S(2)–Hg(1)–S(9) 115.24(7), S(2)–Hg(2)–S(5) 108.31(8), S(2)–Hg(2)–S(6) 114.44(8), S(2)–Hg(2)–S(10) 95.26(9), S(5)–Hg(2)–S(6) 88.52(7), S(5)–Hg(2)–S(10) 120.97(8), S(6)–Hg(2)–S(10) 129.47(10).

The crystal structure of **1**‡ and selected interatomic parameters are presented in Fig. 1 and show two mercury atoms bridged and chelated by three dithiolene ligands, each of which have different binding modes. One ligand simply chelates a mercury ion, [Hg(2)], whilst another ligand acts as a normal $\mu_2$ bridge between Hg(1) and Hg(2) and the final ligand chelates Hg(1) and further bridges *via* one sulfur to Hg(2). As far as we are aware these variations in ligand behaviour (and indeed the resulting formations of oligomers) are unique in the area of dithiolate chemistry, but similar features are known in β-diketonate clusters.[6] The two mercury centres are in different coordination environments. Hg(1) is three coordinate with a very distorted trigonal planar geometry which is due to the ligand bonding constraints. Hg(2) however is four coordinate with very distorted tetrahedral geometry. These multiple forms of coordination have introduced considerable strain into the complex, as may be seen upon investigation of the Hg–S bond lengths. the conventionally coordinated ligand produces expected bond lengths [Hg(2)–S(5), Hg(2)–S(6)]. However around Hg(1) a longer bond is observed for the bridging sulfur [S(2)] and a shortening is seen for the chelating sulfur atoms [S(3), S(9)]. A lengthening is also observed for the Hg(2)–S(2) bridging sulfur, whilst the Hg(2)–S(10) bond has the expected length.

We thank the EPSRC and KOSEF for financial support.

## Footnotes and References

* E-mail: CH5013@bangor.ac.uk

† Selected analysis data for **1**, yellow crystal (from acetone–ethyl acetate), mp 180–181 °C. Elemental analysis: calc. C, 51.11; H, 5.47; N, 1.49; S, 20.42 for $C_{80}H_{102}Hg_2N_2S_{12}$; observed. C 51.04, H 5.89, N 1.11, S 21.34%. FTIR (KBr, $cm^{-1}$): 1479.9, 1451.4, 1378.0 (C=C), 765.8, 718.8, 694.6, (C–H phenyl) 513.5, 435.4, 408.8.

‡ *Crystal data*: $C_{80}H_{102}Hg_2N_2S_{12}$, $M_r$ = 1877.54, triclinic, space group $P\bar{1}$ (no. 2), $a$ = 12.144(2), $b$ = 12.219(2), $c$ = 29.588(8) Å, $\alpha$ = 96.82(4), $\beta$ = 91.326(9), $\gamma$ = 99.380(5)°, $U$ = 4297.3(14) Å, $Z$ = 2, $D_c$ = 1.451 g $cm^{-3}$, $F(000)$ = 1896, $\mu$(Mo-K$\alpha$) = 3.90 $cm^{-1}$. Data were collected at 293(2) K, for a crystal of dimensions 0.24 × 0.24 × 0.215 mm, on a FAST TV Area detector diffractometer following previously described procedures. 12291 data were recorded and merged to give 8421 unique ($R_{int}$ = 0.0669). The structure was solved *via* heavy-atom methods (SHELX),[8] to give two independent molecules in the asymmetric unit and then refined by full-matrix least squares on all $F_0^2$ data (SHELX-93).[9] An absorption correction was applied using DEFABS.[10] The final $R$, $R_w$ indices [$I > 2\sigma(I)$] were 0.0368, 0.0710 for 873 parameters (non-hydrogen atoms anisotropic hydrogen atoms in idealised positions, C–H = 0.96 Å, with $U_{iso}$ tied to $U_{eq}$ of the parent atoms). CCDC 182/620.

1 P. Cassoux, L. Valade, H. Kobayashi, R. A. Clark and A. E. Underhill, *Coord. Chem. Rev.*, 1991, **110**, 115.

2 C. S. Winter, S. N. Oliver, J. D. Rush, C. A. S. Hill and A. E. Underhill, *J. Mater. Chem.*, 1992, **2**, 443; T. Bjørnholm, T. Geisler, J. C. Petersen, D. R. Greve and N. C. Schiødt, *Non-linear Optics*, 1995, **10**, 129.

3 A. T. Coomber, D. Beljonne, R. H. Friend, J. L. Brédas, A. Charlton, N. Robertson, A. E. Underhill, M. Kurmoo and P. Day, *Nature*, 1996, **380**, 144.

4 A. E. Underhill, N. Robertson, J. Ziegenbalg, N. Le Narvor, J. D. Kilburn and K. Awaga, *Mol. Cryst. Liq. Cryst.*, 1996, **284**, 39.

5 D.-Y. Noh, H.-J. Lee, J. Hung and A. E. Underhill, *Tetrahedron Lett.*, 1996, **37**, 7603.

6 V-Cumaran Arunasalam, S. R. Drake, M. B. Hursthouse, K. M. A. Malik, S. A. S. Miller and D. M. P. Mingos, *J. Chem. Soc., Dalton Trans.*, 1996, **12**, 2435.

7 S. R. Drake, M. B. Hursthouse, K. M. A. Malik and S. A. S. Miller, *Inorg. Chem.*, 1993, **32**, 4653.

8 G. M. Sheldrick, *Acta Crystallogr., Sect. A*, 1990, **46**, 467.

9 G. M. Sheldrick, University of Göttingen, 1993, unpublished work.

10 N. P. C. Walker and D. Stuart, *Acta Crystallogr., Sect. A*, 1983, **39**, 158; adapted for FAST geometry by A. Karaulov, University of Wales, Cardiff, 1991.

*Received in Cambridge, UK, 4th September 1997; 7/06460H*

# Infrared spectroscopic evidence for an attractive intramolecular 1,5-CH···O interaction in 1-methoxy-2-(methylthio)ethane

**Hiroshi Yoshida, Takanori Harada, Keiichi Ohno and Hiroatsu Matsuura***

*Department of Chemistry, Faculty of Science, Hiroshima University, Kagamiyama, Higashi-Hiroshima 739-8526, Japan*

**An attractive intramolecular 1,5-CH··O interaction is evidenced in a conformer of 1-methoxy-2-(methylthio)ethane, in which the distance between a hydrogen atom of the SMe group and the oxygen atom is significantly shorter than the van der Waals separation.**

In 1992, we showed the importance of an intramolecular 1,5-CH··O interaction for determining the conformational stabilities of 1,2-dimethoxyethane (DME) in an argon matrix.[1] Since this work was reported, a considerable number of theoretical studies have been published, which dealt with the conformational properties of this molecule by paying special attention to this peculiar interaction.[2–6] These theoretical studies have shown the importance of this interaction in the conformational stabilisation of the DME molecule, in agreement with the experimental results by gas-phase electron diffraction[7] and matrix-isolation and gas-phase IR spectroscopy.[1,8] These experimental findings for the intramolecular 1,5-CH··O interaction were, however, not necessarily decisive because of the complexity involved in the analysis of the experimental data owing to the presence of many conformers. Here we report definitive detection by matrix-isolation IR spectroscopy of a conformer of 1-methoxy-2-(methylthio)-ethane (MMTE), $MeOCH_2CH_2SMe$, which is stabilised by an intramolecular 1,5-CH··O interaction. The characteristics of this intramolecular interaction should be similar in many respects to those of the well-recognised intermolecular CH··O interactions in organic crystals.[9]

The matrix-isolation IR spectra of MMTE were measured by depositing the premixed gases (Ar/MMTE = 2000) onto a caesium iodide plate kept at 11 K. Further experimental details are the same as described previously.[10] *Ab initio* molecular orbital calculations were performed using the GAUSSIAN 94 program[11] on all of the 14 possible conformers of MMTE by the second-order Møller–Plesset perturbation theory (MP2) using the 6-31G* basis set to evaluate the energies, optimized structures, partial charges, vibrational wavenumbers and IR intensities. The calculated wavenumbers were scaled by a uniform factor of 0.95 in the light of the previous systematic studies dealing with a large number of experimental wavenumbers.[12,13]

The IR spectrum of MMTE in an argon matrix at 11 K is shown in Fig. 1. The intensity behaviour of the bands with varying temperature has revealed that the spectrum consists of the bands arising from two conformers. To identify these conformers, the observed spectrum was critically compared with the *ab initio* calculated theoretical spectra of all the possible conformers. The observed bands coincide only with the bands of the TGG′ and TTG conformers.† The theoretical spectra of these conformers are shown in Fig. 1, in comparison with the observed spectrum. The existence of the TGG′ and TTG conformers in an argon matrix agrees with the calculated energies given in Table 1, corresponding as they do to the two lowest-energy conformers of MMTE.

It is noted that the TGG′ conformer, whose optimized structure is shown in Fig. 2, is highly stabilized in the isolated state. In this conformer, the distance (indicated by dots) between one of the hydrogen atoms of the SMe group and the oxygen atom is 0.244 nm, which is significantly shorter than the expected van der Waals separation of *ca*. 0.270 nm. It is obvious that an attractive intramolecular 1,5-CH··O interaction occurs between these non-bonded atoms and greatly stabilizes the TGG′ conformer. The H··O distance in MMTE is shorter than the corresponding distance in DME by 0.002 nm, indicating that the interaction in the former molecule is stronger than in the latter.

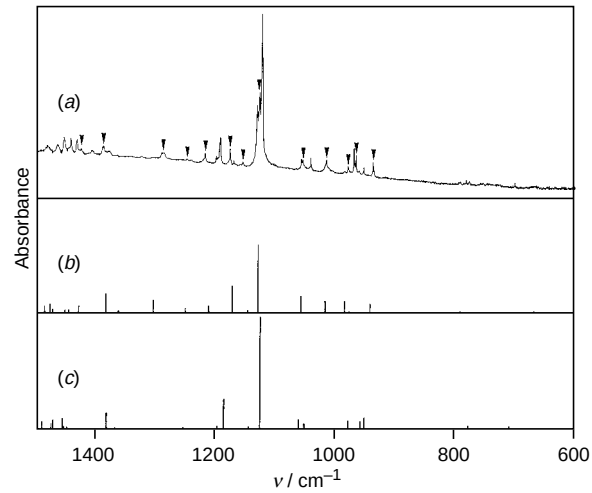



**Fig. 1** Observed and calculated IR spectra of MMTE: (*a*) observed matrix-isolation spectrum at 11 K, (*b*) calculated spectrum of the TGG′ conformer and (*c*) calculated spectrum of the TTG conformer. In the observed spectrum, the bands which are assigned exclusively to the TGG′ conformer are marked with an arrow.

The calculated partial charges of atoms are shown in Fig. 2. It is noteworthy that the methyl carbon atom bonded to the sulfur atom carries a large negative charge (−0.63 *e* units), which is comparable to the partial charge (−0.62 *e*) of the oxygen atom. The positive partial charge (+0.22 *e*) of the methyl hydrogen atom that interacts with the oxygen atom is larger than the partial charges (+0.18 and +0.19 *e*) of other hydrogen atoms

**Table 1** Energies of the 14 possible conformers of 1-methoxy-2-(methylthio)ethane (MMTE)

| Conformer[a] | Energy/ kJ mol$^{-1}$[b] | Conformer[a] | Energy/ kJ mol$^{-1}$[b] |
|---|---|---|---|
| TGG′[c] | 0.000 | GGG | 8.633 |
| TTG | 3.042 | GTG | 8.647 |
| TTT | 5.848 | GGT | 8.851 |
| GGG′[c] | 6.167 | GTT | 11.094 |
| TGT | 6.514 | G′GG[d] | 13.447 |
| G′TG | 7.662 | G′GT[d] | 14.745 |
| TGG | 7.688 | G′GG′[c,d] | —[e] |

[a] Conformation around the MeO–$CH_2$–$CH_2$–SMe bonds (T = *trans*, G = *gauche*). [b] Relative energies with respect to the energy of the TGG′ conformer, calculated at the MP2/6-31G* level. [c] 1,5-CH··O interaction is involved. [d] 1,5-CH··S interaction would be possible. [e] Transformed into the TGG′ conformer during structure optimization.

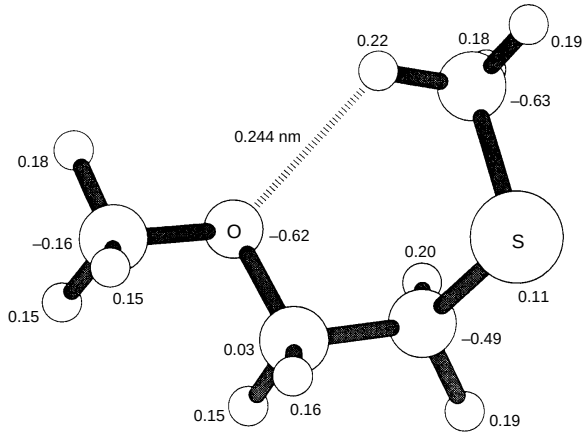



**Fig. 2** Optimized structure of the TGG′ conformer of MMTE. The intramolecular 1,5-CH··O interaction occurs between the methyl hydrogen atom and the oxygen atom as indicated by dots; the H··O distance is 0.244 nm and the C–H··O angle is 118.0°. The values shown are the partial charges of atoms in *e* units.

belonging to the same methyl group. These results indicate that the (S)C–H bond in the TGG′ conformer is like an alcoholic O–H bond in respect of partial charges and interacts attractively with the oxygen atom; this electrostatic interaction can therefore be described as $C^{\delta-}$–$H^{\delta+}\cdots O^{\delta-}$. In the MMTE molecule, an analogous intramolecular interaction may be anticipated to occur between one of the hydrogen atoms of the OMe group and the sulfur atom. The calculated energies (Table 1) indicate, however, that conformational stabilisation by this interaction is unlikely to occur.

The salient result in this work is that we have convincingly detected a conformer, TGG′, of MMTE which is highly stabilised by an intramolecular 1,5-CH··O interaction. Before the importance of this interaction was recognized, the conformers such as TGG′ of MMTE were thought to be unstable owing to apparent heavy steric repulsions between the relevant atoms which are in close proximity to each other. The comparison of the results for MMTE and DME indicates that the (S)CH··O interaction is stronger than the (O)CH··O interaction. The substituent atom, sulfur or oxygen, bonded to the C–H bond may change the strength of the 1,5-CH··O interaction.

## Footnotes and References

* E-mail: matsuura@sci.hiroshima-u.ac.jp

† T = *trans*, G = *gauche*. Conformation around the MeO–$CH_2$–$CH_2$–SMe bonds.

1 H. Yoshida, I. Kaneko, H. Matsuura, Y. Ogawa and M. Tasumi, *Chem. Phys. Lett.*, 1992, **196**, 601.
2 S. Tsuzuki, T. Uchimaru, K. Tanabe and T. Hirano, *J. Phys. Chem.*, 1993, **97**, 1346.
3 R. L. Jaffe, G. D. Smith and D. Y. Yoon, *J. Phys. Chem.*, 1993, **97**, 12745; G. D. Smith, R. L. Jaffe and D. Y. Yoon, *J. Phys. Chem.*, 1993, **97**, 12752; G. D. Smith, R. L. Jaffe and D. Y. Yoon, *J. Am. Chem. Soc.*, 1995, **117**, 530.
4 F. Müller-Plathe and W. F. van Gunsteren, *Macromolecules*, 1994, **27**, 6040; H. Liu, F. Müller-Plathe and W. F. van Gunsteren, *J. Chem. Phys.*, 1995, **102**, 1722.
5 O. Engkvist, P.-O. Åstrand and G. Karlström, *J. Phys. Chem.*, 1996, **100**, 6950.
6 D. J. Williams and K. B. Hall, *J. Phys. Chem.*, 1996, **100**, 8224.
7 E. E. Astrup, *Acta Chem. Scand., Ser. A*, 1979, **33**, 655.
8 H. Yoshida, T. Tanaka and H. Matsuura, *Chem. Lett.*, 1996, 637.
9 T. Steiner, *Chem. Commun.*, 1997, 727.
10 H. Yoshida, T. Harada, T. Murase, K. Ohno and H. Matsuura, *J. Phys. Chem. A*, 1997, **101**, 1731.
11 GAUSSIAN 94, Revision D.3, M. J. Frisch, G. W. Trucks, H. B. Schlegel, P. M. W. Gill, B. G. Johnson, M. A. Robb, J. R. Cheeseman, T. Keith, G. A. Petersson, J. A. Montgomery, K. Raghavachari, M. A. Al-Laham, V. G. Zakrzewski, J. V. Ortiz, J. B. Foresman, J. Cioslowski, B. B. Stefanov, A. Nanayakkara, M. Challacombe, C. Y. Peng, P. Y. Ayala, W. Chen, M. W. Wong, J. L. Andres, E. S. Replogle, R. Gomperts, R. L. Martin, D. J. Fox, J. S. Binkley, D. J. Defrees, J. Baker, J. P. Stewart, M. Head-Gordon, C. Gonzalez and J. A. Pople, Gaussian Inc., Pittsburgh PA, 1995.
12 A. P. Scott and L. Radom, *J. Phys. Chem.*, 1996, **100**, 16502.
13 H. Yoshida, T. Harada and H. Matsuura, *J. Mol. Struct.*, 1997, **413**/**414**, 217

*Received in Cambridge, UK, 18th August 1997; 7/06029G*

# Palladium-grafted mesoporous MCM-41 material as heterogeneous catalyst for Heck reactions

**Christian P. Mehnert and Jackie Y. Ying***

*Department of Chemical Engineering, Massachusetts Institute of Technology, Cambridge, MA 02139, USA*

**Palladium grafted mesoporous MCM-41 materials, prepared by vapor grafting, show remarkable activity in Heck carbon–carbon coupling reactions.**

Current research focuses on the synthesis and application of modified mesoporous MCM-41 materials[1,2] that have an active species attached to the framework *via* host–guest interactions, creating discrete and uniform catalyst sites on the inner walls of the porous systems. Herein we report the synthesis of palladium-grafted mesoporous materials, designated Pd-TMS11, and their application as heterogeneous catalysts in Heck reactions. Palladium catalyzed carbon–carbon bond formation, the Heck reaction,[3] represents one of the most versatile tools in modern synthetic chemistry and has great potential for industrial applications. Although recent advances in homogeneous[4] and heterogeneous[5] Heck catalysis have attracted considerable attention, the properties and activities of the existing catalysts have, as yet, limited industrial application. Here we report the synthesis of a highly active heterogeneous palladium catalyst, Pd-TMS11, that exhibits excellent activity towards activated and non-activated haloarene substrates.

Palladium-grafted mesoporous material (Pd-TMS11) is synthesized by vapor deposition of a volatile palladium complex onto the inside walls of the porous framework, followed by reduction. The success of grafting the inside of a porous material with a highly dispersed metal film is strongly dependent on the properties of the volatile complex and the reaction conditions.† To maintain the uniform structure, high surface area and accessibility of the molecular sieves, it is important to minimize the cluster growth inside and outside of the porous material. The concept of vapor grafting enables a uniform distribution of a volatile complex and ensures the discrete deposition of metal fragments throughout the porous structure of the material without cluster formation, giving metal-grafted molecular sieves.

The palladium grafting of the degassed silicate-based MCM-41 material‡ was carried out *via* sublimation of the volatile organometallic complex[6] [Pd($\eta$-$C_5H_5$)($\eta^3$-$C_3H_5$)] under vacuum through the porous material. After the palladium complex is deposited onto the inside walls of the pores, the material is reduced under a stream of hydrogen gas, giving an air-stable, black powder.

The prepared catalyst,§ Pd-TMS11, retains its hexagonally-packed porous structure as shown in X-ray diffraction (XRD) pattern. Although the diffraction patterns of Pd-TMS11 and the MCM-41 starting material are almost identical, the peak intensity for Pd-TMS11 is reduced owing to radiation diffusion caused by the grafted palladium metal. The XRD pattern of palladium metal has major diffraction peaks at $2\theta = 40.1°$ (111) and 46.7° (200), which are not found in the XRD pattern of Pd-TMS11, indicating that the palladium metal is highly dispersed in the latter. Further evidence is provided by transmission electron micrograph¶ (TEM) that shows the hexagonally packed porous structure of Pd-TMS11 (Fig. 1), with no noticeable palladium clusters. In addition, scanning transmission electron micrographs (STEM) and energy dispersive analysis by X-ray (EDAX) studies have been conducted on Pd-TMS11 particles, indicating that palladium is uniformly

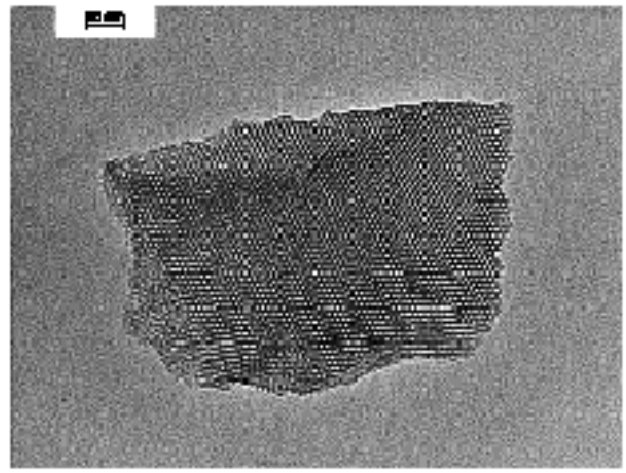
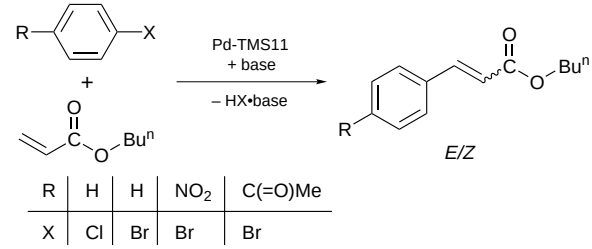


**Fig. 1** TEM of Pd-grafted mesoporous catalyst, Pd-TMS11, showing the hexagonal array of 26 Å pores

dispersed over the pore surface of the mesoporous support. Elemental analysis of Pd-TMS11 samples shows palladium metal contents of 10–30 mass%, depending on the amount of volatile complex [Pd($\eta$-$C_5H_5$)($\eta^3$-$C_3H_5$)] used in the vapor grafting process. The BET surface area of a typical sample of Pd-TMS11 with a palladium content of 19.1 mass% is 750 $m^2\ g^{-1}$. The BJH (Brunauer–Joyner–Halenda) pore size distribution of Pd-TMS11 illustrates a narrow peak centered at 26 Å for the pore diameter which is, as expected, slightly smaller than that determined for the MCM-41 starting material (27.4 Å) owing to the grafted palladium metal. The CO adsorption studies of Pd-TMS11 show metallic surface areas between 120 and 140 $m^2\ g^{-1}$ (Pd metal) with a metal dispersion of more than 30%. In comparison, commercially available Pd/$\gamma$-$Al_2O_3$ (Aldrich) shows a metallic surface area of only 60 $m^2\ g^{-1}$ (Pd metal) with a metal dispersion of 15%.

The Pd-TMS11 materials catalyze the Heck carbon–carbon coupling reaction of aryl halides (Scheme 1). The catalytic activity of these materials was investigated using activated and non-activated aryl halides and butyl acrylate as the vinylic substrate (Table 1). The yields for the activated aryl halides, with respect to reaction time and amount of catalyst, showed that the Pd-TMS11 catalysts have an excellent activity especially in view of other palladium-based heterogeneous systems.** Full conversion and a yield of 99% was obtained after




| R | H | H | $NO_2$ | C(=O)Me |
|---|---|---|---|---|
| X | Cl | Br | Br | Br |

**Scheme 1**

**Table 1** Heck alkenation[a] of aryl halides with *n*-butyl acrylate over Pd-TMS11 catalysts

| Aryl halide substrate[b] | Amount of catalyst (mol%) | *T*/°C | Time | % Conversion[c] % (Yield)[d] | *E* : *Z* | TON[e] |
|---|---|---|---|---|---|---|
| $C_6H_5Cl$ | 0.1 | 170 | 32 h | 16 (40) | 99 : 1 | 64 |
| $C_6H_5Br$ | 0.1 | 170 | 48 h | 67 (92) | 99 : 1 | 624 |
| 4-$BrC_6H_4NO_2$ | 0.1 | 120 | 90 min | 100 (99) | 99 : 1 | 1000 |
| 4-$BrC_6H_4C(O)CH_3$ | 0.1 | 120 | 25 min | 100 (99) | 99 : 1 | 1000 |
| 4-$BrC_6H_4C(O)CH_3$ | 0.02 | 120 | 60 min | 100 (99) | 99 : 1 | 5000 |

[a] All reactions are carried out in air. [b] 1.1 equiv. of base $NEt_3$ with respect to the aryl halide substrate is added to the reaction mixture. [c] Conversion of reactant is determined by gas chromatography. [d] Mol of coupling product (*E* + *Z*)/mol reactant converted. [e] TON = mol product/mol catalyst; recycled catalyst showed reduced activity.‖

only 1 h for the reaction of *n*-butyl acrylate and 4-bromoacetophenone using as little as 0.02 mol% catalyst. The Pd-TMS11 material therefore provides an extremely simple and efficient Heck catalyst that even rivals some of the best homogeneous catalysts.[7,††] A moderate conversion of non-activated aryl halides was observed, and a conversion of 67% for bromobenzene has been achieved (see Table 1).

The new catalyst system Pd-TMS11, prepared by vapor grafting, has successfully been used in carbon–carbon coupling reactions. Remarkable activity, easy accessibility and exceptional stability of the described material provides an excellent example for a new generation of heterogeneous Heck catalysts.

We thank Dr. T. J. Garrett-Reed and M. Frongillo (M.I.T. CMSE) for their assistance with transmission electron microscopy, and David Weaver for his assistance in conducting catalytic characterizations. The financial support of the David and Lucile Packard Foundation and the National Science Foundation (CTS-9257223) is gratefully acknowledged.

## Footnotes and References

* E-mail: jyying@mit.edu

† MCM-41 material was degassed at 60 °C under reduced pressure to prevent decomposition of the palladium complex due to air oxidation or hydrolysis *via* surface adsorbed water. To achieve a uniformly grafted Pd-TMS11 it is necessary that the surface of the MCM-41 be water-free and only consist of surface bound oxo and hydroxo groups.

‡ Modified synthesis of mesoporous MCM-41. Hexadecyltrimethylammonium bromide (15.9 g, 44.9 mmol) was dissolved in $H_2O$ (1.2 l) and treated with sodium silicate (14% NaOH/27% $SiO_2$) and 1 g (3.14 mmol) $Nb(OEt)_5$ in $H_2O$ (0.4 l) to give a white precipitate.‡‡ The pH value of the mixture was adjusted to pH = 11.5 using sulfuric acid (30%). The gel was aged at room temp. for 12 h before it was heated in pressure tubes to 100 °C for 7 d. The supernatant of the aged gel was decanted off and the resulting white residue washed with $H_2O$ (1 l) and EtOH (1 l). The isolated solid was dried in air at room temp. for 12 h before the material was calcined at 560 °C for 6 h giving MCM-41 with a hexagonally-packed cylindrical mesoporous structure.

§ Synthesis of palladium-grafted mesoporous material (Pd-TMS11). MCM-41 (0.5 g) [XRD (100) 39.9 Å, (110) 22.5 Å, (200) 19.6 Å, (210) 14.8 Å; BET surface area of 997 $m^2\ g^{-1}$, BJH adsorption pore size of 27.4 Å] was degassed at 600 °C under reduced pressure ($10^{-2}$ Torr) for 6 h. The resulting material was loaded into a short path frit and contained with glass wool under an inert gas atmosphere. A small round-bottom flask was filled with the red complex [Pd($\eta^3$-$C_3H_5$)($\eta$-$C_5H_5$)] (0.25 g, 1.2 mmol) and connected to a prepared frit that was further attached to a condensation bridge with a round-bottom flask. The apparatus was evacuated, and a constant pressure ($10^{-2}$ Torr) was maintained by cooling the empty round-bottom flask to −196 °C. The small round-bottom flask containing the volatile palladium complex and the loaded frit were heated to 120 °C (ramp 1 °C $min^{-1}$) using an oil bath. During the heating process, the white MCM-41 starting material turned black and the excess volatile organometallic complex was condensed into the cooled round-bottom flask. The resulting solid was reduced under a stream of hydrogen (50 ml $min^{-1}$) at 300 °C, giving a black powder designated Pd-TMS11 [XRD (100) 39.6 Å, (110) 22.4 Å, (200) 19.4 Å].

¶ An average of 50 particles per sample was investigated *via* TEM. No palladium clusters were observed on the as-synthesized Pd-TMS11 material, even at high magnification. TEM investigation of used Pd-TMS11 catalyst showed the formation of palladium clusters (*ca*. 50 Å diameter).

‖ Catalyst deactivation is noted in the form of palladium metal agglomeration, fracturing of the MCM-41 support material and coking of the catalyst surface. Pd-TMS11 recovered from the reaction of *n*-butyl acrylate and 1-bromo-4-nitrobenzene showed reduced activity in the second and third catalysis cycles under identical condition. The total lifetime of the catalyst is *ca*. 3000 TON for the latter reaction.

** Control experiments using commercially available $Pd/Al_2O_3$, $Pd/SiO_2$ and Pd/carbon (all containing *ca*. 10 mass% palladium) were conducted giving TONs which were 60% lower than those obtained for Pd-TMS11 with respect to activated aryl substrates. No activity was observed for non-activated aryl substrates in commercial supported catalysts.

†† Reaction between bromobenzene and *n*-butyl acrylate using homogeneous catalysts showed a TON of 96. In comparison, a TON of 624 was obtained for Pd-TMS11 at 170 °C in the same reaction. Unlike the existing homogeneous catalysts, our Pd-TMS11 is not air-sensitive and can be easily recovered by filtration after usage.

‡‡ The prepared MCM-41 had a niobium content of 1.5 mass% which contributed to the larger wall thickness of the material (18 Å). The dopant had no effect on the catalysis results.

1 C. T. Kresge, M. E. Leonowicz, W. J. Roth, J. C. Vartuli and J. S. Beck, *Nature*, 1992, **359**, 710; J. S. Beck, J. C. Vartuli, W. J. Roth, M. E. Leonowicz, C. T. Kresge, K. D. Schmitt, C. T-W. Chu, D. H. Olson, E. W. Sheppard, S. B. McCullen, J. B. Higgins and J. L. Schlenker, *J. Am. Chem. Soc.*, 1992, **114**, 10834.

2 T. M. Abdel-Fattah and T. J. Pinnavaia, *Chem. Commun.*, 1996, 665; T. Abe, Y. Tachibana, T. Uemastu and M. Iwamoto, *J. Chem. Soc., Chem. Commun.*, 1995, 1617; A. J. Butterworth, J. H. Clark, P. H. Walton and S. J. Barlow, *Chem. Commun.*, 1996, 1857; J. F. Diaz, K. J. Balkus, Jr., F. Bedioui, V. Kurshev and L. Kevan, *Chem. Mater.*, 1997, **9**, 61; C.-J. Liu, S. G. Li, W.-Q. Pang and C.-M. Che, *Chem. Commun.*, 1997, 65; T. Maschmeyer, F. Rey, G. Sankar and J. M. Thomas, *Nature*, 1995, **378**, 159; M. Morey, A. Davidson, H. Eckert and G. Stucky, *Chem. Mater.*, 1996, **8**, 486; Y. V. S. Rao, D. E. De Vos, T. Bein and P. A. Jacobs, *Chem. Commun.*, 1997, 355; P. Sutra and D. Brunel, *Chem. Commun.*, 1996, 2485; C.-G. Wu and T. Bein, *Chem. Mater.*, 1994, **6**, 1109; W. Zhang, J. Wang, P. T. Tanev and T. J. Pinnavaia, *Chem. Commun.*, 1996, 979.

3 Reviews: R. F. Heck, *Comprehensive Organic Synthesis*, ed. B. M. Trost and I. Fleming, Pergamon, Oxford, 1991, vol. 4, p. 833; A. de Meijer and F. E. Meyer, *Angew. Chem., Int. Ed. Engl.*, 1994, **33**, 2379; B. Cornils and W. A. Herrmann, *Applied Homogeneous Catalysis with Organometallic Compounds*, VCH, Weinheim, 1996, p. 712.

4 M. Beller, H. Fischer, W. A. Herrmann, K. Öfele and C. Broßmer, *Angew. Chem., Int. Ed. Engl.*, 1995, **34**, 1848; M. Beller, T. H. Riermeier, S. Haber, H.-J. Kleiner and W. A. Herrmann, *Chem. Ber.*, 1996, **129**, 1259; Y. Ben-David, M. Portnoy and D. Milstein, *Organometallics*, 1992, **11**, 1995; W. A. Herrmann, M. E. Elison, J. Fischer, C. Köcher and G. R. J. Artus, *Angew. Chem., Int. Ed. Engl.*, 1995, **34**, 2371.

5 M. T. Reetz and Gunther Lohmer, *Chem. Commun.*, 1996, 1921; R. L. Augustine and S. T. J. O'Leary, *Mol. Catal. A*, 1995, **95**, 277; M. Beller, H. Fischer, K. Kühlein, C.-P. Reisinger and W. A. Herrmann, *J. Organomet. Chem.*, 1996, **520**, 257.

6 B. J. Shaw, *J. Chem. Soc.*, 1960, 247.

7 W. A. Herrmann, C. Brossmer, K. Öfele, C.-P. Reisinger, T. Priermeier, M. Beller and H. Fischer, *Angew. Chem., Int. Ed. Engl.*, 1995, **34**, 1844.

*Received in Bloomington, IN, USA; 17th July 1997; 7/05104B*

# A solid state artificial muscle based on polypyrrole and a solid polymeric electrolyte working in air

**J. M. Sansiñena,[a] V. Olazábal,[a] T. F. Otero,[a] C. N. Polo da Fonseca[b] and Marco-A. De Paoli[b]**

[a] *Laboratorio de Electroquímica, Facultad de Química, Universidad del País Vasco, Apd 1072, 20080 San Sebastián, Spain*
[b] *Laboratório de Polimeros Condutores, Instituto de Química, Unicamp, C. Postal 6154, 13081-970 Campinas, SP, Brazil*

**A solid state artificial muscle based on polypyrrole(PPy) and poly(epichlorohydrin-co-ethylene oxide) [P(ECH-co-EO)]/$LiClO_4$ (solid polymeric electrolyte) is developed; an angular movement in air with rate, direction and electrical control similar to those obtained in a liquid electrolyte (aqueous solution of $LiClO_4$) is registered when an electrical current was applied.**

Conducting polymers like polypyrrole, polythiophene and polyaniline, can be electrochemically oxidized and reduced in a continuous and reversible way. Simultaneous changes in conductivity,[1] colour,[2] volume[3–5] and other parameters are observed. All these properties are linked to movement of ions and solvent inside and outside the conducting polymer. These movements are accompanied by conformational changes along the polymeric chains, driving the opening and closure of the polymeric entanglements. Artificial muscles based on reversible stress gradients linked to these reverse conformational changes have been developed in recent years.[6–14] All these prototypes are in the liquid configuration, usually a lithium salt dissolved in an aqueous solution.

In this work, we have investigated the construction of a new solid state artificial muscle, fully polymeric, based on two polypyrrole (PPy) film electrodes and a new polymeric electrolyte, poly(epichlorohydrin-co-ethylene oxide) [P(ECH-co-EO)]/$LiClO_4$.

Polypyrrole films were electrogenerated from 0.2 M pyrrole and 0.1 M $LiClO_4$ organic solutions (acetonitrile with a water content of 2%). Three AISI 304 stainless steel plates, having a surface area of 3.50 $cm^2$, were used as electrodes, one of them as the working electrode and the other two as counter electrodes. The electrogeneration was performed under an inert atmosphere of argon. Potential square waves were applied between −0.300 V (2 s) and 0.850 V (8 s) to control the morphology of the film and its adherence to the metal. A saturated calomel electrode (SCE) was used as reference electrode.

Polymer electrolytes were prepared from a tetrahydrofuran solution containing 2.5% (w/w) of [P(ECH-co-EO)] and $LiClO_4$. An elastomeric solid with high ionic conductivity is obtained after evaporation of the solvent (casting). Higher ionic conductivity was attained when the salt concentration, defined as $\eta$ = [O]/[$Li^+$], was fixed at $\eta$ = 6.[15]

The artificial muscle prototype was prepared by dripping the electrolyte solution on two polypyrrole films (mass = 3 mg, thickness = 6 μm) grown on two different stainless steel electrodes, followed by evaporation of the solvent under atmospheric pressure at room temperature. Two [steel ‖ PPy ‖ P(ECH-co-EO)/$LiClO_4$] systems were obtained. The evaporation of the THF gives increasingly viscous and adherent films. Once the polyelectrolyte was viscous and adherent enough, the two electrodes covered by the polyelectrolyte film (thickness = 3 μm) were put in contact and a [steel ‖ PPy ‖ P(ECH-co-EO)/$LiClO_4$ ‖ PPy ‖ steel] system was performed. After 30 min the polyelectrolyte is dry and the triple layer [PPy ‖ P(ECH-co-EO)/$LiClO_4$ ‖ PPy] was then peeled off the stainless steel plates. The two films of polypyrrole were held at the top with a metallic clamp to allow independent electrical contract to the PPy films. One polypyrrole film was connected as working electrode and the other as counter electrode short-circuited with the reference electrode contact of the potentiostat. The movement of the triple layer was studied at room temperature with a controlled humidity (60%).

The solid polymeric electrolyte provided the ionic contact between the two polypyrrole electrodes with a face to face

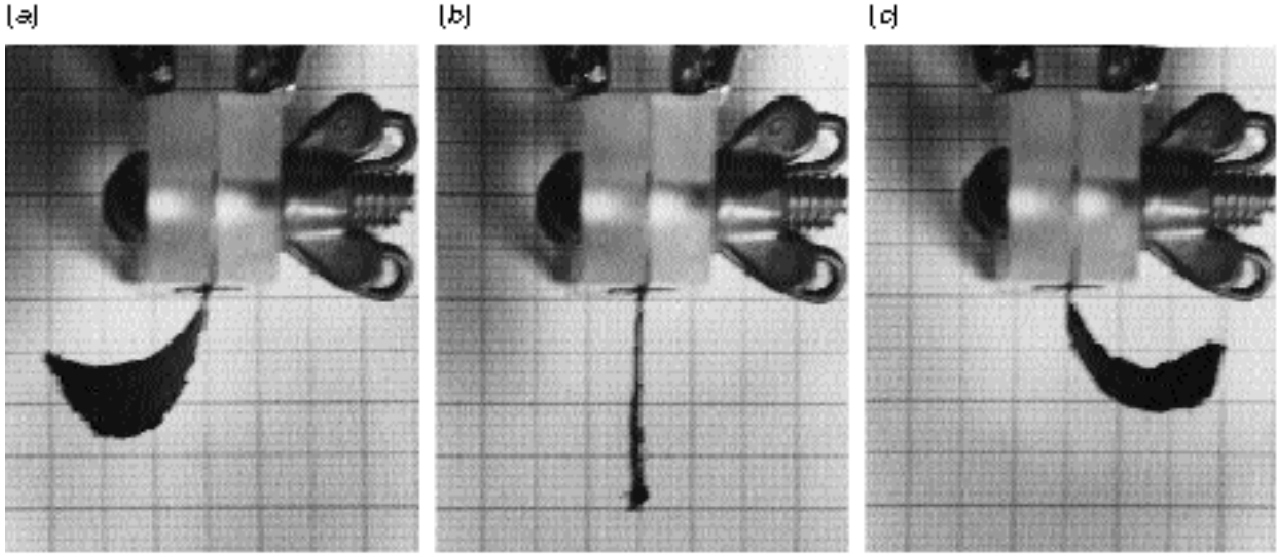



**Fig. 1** Movement of the solid artificial muscle during the application of an electric current: (*a*) position after 108 mC of reduction charge, (*b*) position at neutral electrical state and (*c*) position after 108 mC of oxidation charge

configuration. All experiments began from the vertical position as can be seen in Fig. 1(*b*) with the two PPy films in a semi-oxidised state (250 mV *vs.* SCE). The right face of the triple layer was the working electrode and the left side worked as a counter electrode.

The flow of a constant current through PPy films promotes an angular movement of the free end of the triple layer. An anodic current applied to the PPy film connected as working electrode produced an angular movement of the free end in the direction of the counter electrode, Fig. 1(*c*). A movement in the opposite direction was observed when a cathodic current was applied, Fig. 1(*a*). The triple layer bent in the direction of the working electrode. Under a constant current of 20 mA the free end of the artificial muscle delay 5.4 s to cross 90°.

The angular movement in air was similar to that obtained in a liquid medium.[10–12] The direction of the movement during the oxidation or reduction of the working electrode was the same to that obtained when a liquid electrolyte ($LiClO_4$ aqueous solution) was used. In this liquid electrolyte, $ClO_4^-$ anions enter into the PPy film during the oxidation process and the volume of PPy increases. These anions leave the film during reduction and the film volume decreases. In the solid configuration the flow of the current between both PPy films is supported by ionic movements inside the polymer electrolyte.

On the other hand, the electrical charge consumed during the movement of the solid state artificial muscle to cover 90° (36 mC per mg of PPy) was the same as that consumed when an aqueous $LiClO_4$, solution was used.

Taking into account that the covered angle depends directly on the volume change of the PPy film,[11,12] the PPy volume variation (covered angle) was the same for a similar electrical charge consumed when an aqueous $LiClO_4$ solution or a solid polymeric electrolyte (containing $LiClO_4$) was used.

The movement rate was also recorded. This parameter remained constant while the electrical current applied did not change. A linear relationship between movement rate and applied electrical current (similar to that showed in liquid configuration) was obtained [eqn. (1)].

$$\text{Movement rate rad s}^{-1} = 0.042\ I/\text{mass (mA mg}^{-1}) \quad (1)$$

Under these conditions both rate and direction of the angular movement are controlled by the intensity and direction of the current flow, respectively.

All the results obtained in this work show the feasibility of electrochemomechanical devices based on polypyrrole and a solid polyelectrolyte P(ECH-co-EO)/$LiClO_4$ film able to work in air. This fact starts a new development toward actuators and microrobotic applications.

The authors wish to express their gratitude to Gobierno Vasco, Iberdrola S.A., CNPq and FAPESP for their financial support. We also thank Oscar K. Kozima for the photographic work.

## Footnotes and References

* E-mail: qppfeott@sq.ehu.es

1 K. Naoi, M. M. Lien and W. H. Smyrl, *J. Electroanal. Chem.*, 1989, **272**, 273.
2 F. Garnier and G. Tourillon, *J. Electroanal. Chem.*, 1983, **148**, 299.
3 A. Robert Hillman, M. Swann and S. Bruckenstein, *J. Electroanal. Chem*., 1988, **92**, 356.
4 P. Marque and J. Roncali, *J. Phys. Chem.*, 1990, **94**, 8614.
5 R. H. Baughman and L. W. Shaklette, *Science and Applications of Conducting Polymers*, ed. W. R. Salanek, D. T. Clark and E. J. Samuelsen, IOP, Hilger: Bristol, UK, 1990.
6 T. F. Otero, E. Angulo, J. Rodriguez and C. Santamaría, *Eur. Pat.*, EP9200095, 1992.
7 T. F. Otero, J. Rodriguez and C. Santamaría, *Eur. Pat.*, EP9200095, 1992.
8 T. F. Otero, J. M. Sansiñena, V. Olazábal, M. Bengoechea, J. Rodríguez and C. Santamaría, *Polimeros Conductores—Conducting Polymers*, Video-Tape BI-1474-1995 distributed by the Institute of Science of the Education (ICE), Universidad del País Vasco, 1992 and 1995.
9 T. F. Otero and J. Rodríguez, *Intrinsically Conducting Polymers: An Emerging Technology*, ed. M. Aldissi, Kluwer, Dordrecht, Netherlands, 1993, 179.
10 T. F. Otero and J. M. Sansiñena, *Bioelectrochem. Bioenerg.*, 1995, **38**, 411.
11 T. F. Otero and J. M. Sansiñena, *Artificial Muscles: Influence of Electrolyte Concentration on Bilayer Movement, Third International Conference on Intelligent Materials and Third European Conference on Smart Structures and Materials*, Lyon, France, 1996, SPIE 2779, 365, ed. Pierre F. Gobin and Jacques Tatibouët, SPIE: Bellingham, WA.
12 T. F. Otero and J. M. Sansiñena, *Bioelectrochem. Bioenerg.*, 1977, **42**, 117.
13 E. Smela, O. Inganäs and Y. Lundström, *Science*, 1995, **268**, 1731.
14 T. Takashima, M. Kaneto and A. G. McDiarmid, *Synth. Met.*, 1995, **71**, 2265.
15 G. Goulart, N. H. T. Lemes, C. N. Polo da Fonseca and M-A. De Paoli, *Solid State Ionics*, 1997, **93**, 105.

*Received in Bath, UK, 16th July 1997; 7/05341J*

# Pore size regulation of $TiO_2$ by use of a complex of titanium tetraisopropoxide and stearic acid

**Satoshi Sato,* Satomi Oimatsu, Ryoji Takahashi, Toshiaki Sodesawa and Fumio Nozaki**

*Department of Applied Chemistry, Faculty of Engineering, Chiba University, Yayoi, Inage, Chiba 263, Japan*

**The pore size distribution of $TiO_2$ can be controlled by changing the molar ratio of stearic acid to titanium tetraisopropoxide.**

Materials with a controlled pore size, in addition to high specific surface areas, are attractive for use as catalysts and catalyst supports. Mesoporous amorphous silicas such as MCM-41[1] and FSM-16[2] have been recently synthesized, and have specific surface areas $> 1000$ m$^2$ g$^{-1}$ together with uniform mesopores. Interest in the synthesis of mesoporous materials are also focused on other oxides such as $Al_2O_3$, $WO_3$, and PbO.[3–7] Mesoporous aluminas with specific surface areas $> 500$ m$^2$ g$^{-1}$ have been prepared from aluminium alkoxide in the presence of a surfactant.[6,7] On the other hand, the pore size distribution of alumina can be regulated by a pH-swing process.[8] In the process, the particle size of aluminium hydroxide was controlled by altering the pH of the solution containing aluminium hydroxide gel. Here we demonstrate the control of pore size of titania by using stearic acid as a pore regulating reagent.

A measured amount of stearic acid ($C_{17}H_{35}CO_2H$, STA) was dissolved in propan-1-ol at 50 °C and titanium tetraisopropoxide [$Ti(OPr)_4$] dissolved in propan-1-ol at room temp. was added to the STA solution at room temp. The molar ratios of $Ti(OPr)_4$, STA, and propan-1-ol were $1:X:26$, where $X$ was varied from 0 to 2. After the mixed solution was stood at room temperature in an open container for at least 24 h, a white precipitate was formed. The solution was allowed to stand until no further precipitate was formed (up to 264 h). The precipitate was separated by decantation from the solution, and dried at 170 °C for 1 h. The dried sample was calcined at 400 °C for 4 h to obtain $TiO_2$. The pore size distribution of each $TiO_2$ sample was calculated from its $N_2$ adsorption isotherm at −196 °C according to a calcination method reported by Cranston and Inkray.[9]

Preliminarily, it was found that the addition of water to the starting solution decreased both the specific surface area and pore volume. Thus, we prepared samples without adding water to the solution. Since no STA was observed in the supernatant solution, almost all the added STA was included in the precipitate. When the samples were dried at 170 °C, the precipitates became yellow granules up to a molar ratio of STA/Ti ($X$) of 0.9, and melted above $X = 1.2$. Above $X = 0.2$, a white $TiO_2$ solid was obtained by calcining the dried sample at 400 °C, and the mass of the sample decreased. The mass decrease in the sample was nearly equal to the amount of added STA. For $X = 0.3$, the $TiO_2$ sample calcined at 400 °C had a specific surface area of 92 m$^2$ g$^{-1}$. For $X < 0.2$, however, carbon species remained in the samples calcined at 400 °C. The crystal structure, as confirmed by XRD, was anatase titania which at 500 °C, became a mixture of anatase and rutile (2.6 m$^2$ g$^{-1}$). At 600 °C, the crystal structure was completely converted to rutile and the specific surface area of the rutile titania was as low as 1 m$^2$ g$^{-1}$. Consequently, a calcination temperature of 400 °C was adopted.

The structural properties of the resulting $TiO_2$ altered with the amount of STA added in the starting solution (Figs. 1 and 2). At $X < 0.1$, specific surface areas of the samples were lower than 10 m$^2$ g$^{-1}$. A sample prepared without STA ($X = 0$) had a broad distribution of pore volume with a maximum at 5 nm, while the total volume was only 0.01 cm$^3$ g$^{-1}$. The specific surface area as well as the pore volume increased with increase in $X$ up to 1.2 (Fig. 1), and the pore size distribution could be regulated; the pore diameter was shifted from 5 to 15 nm in the STA/Ti ($X$) range between 0.3 and 1.2 (Fig. 2). At $X > 1.2$, no change was observed in the structural properties including the pore size distribution. In the calculation of the pore size distribution of $TiO_2$ samples, cumulative surface areas calculated from the pore volume and the pore diameter were consistent with the specific surface areas obtained by the BET method. Therefore, the pore size distribution of $TiO_2$ is controlled by changing the molar ratio of STA to $Ti(OPr)_4$ in the range $0.3 < X < 1.2$.

For different $X$ values, both the trend of the variation in structural properties and the behavior of the samples in the

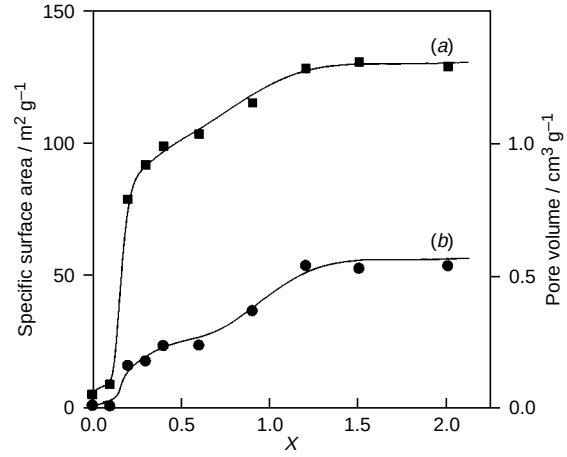



**Fig. 1** Structural properties of $TiO_2$ prepared with different amounts of stearic acid. The molar ratios of $Ti(OPr)_4$, stearic acid, and propan-1-ol were $1:X:26$; (*a*) specific surface area, (*b*) pore volume.

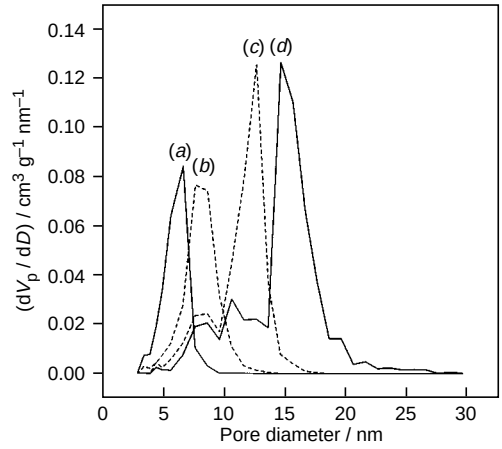



**Fig. 2** Pore size distribution of $TiO_2$ prepared from a $Ti(OPr)_4$–STA complex. The molar ratios of $Ti(OPr)_4$, stearic acid, and propan-1-ol were $1:X:26$; (*a*) $X = 0.3$, (*b*) 0.6, (*c*) 0.9, (*d*), 1.2.

preparation process were clearly altered at $X$ *ca*. 1. In the $Ti(OPr)_4$–$MeCO_2H$ system, two acetic acid molecules are known to coordinate with a titanium isopropoxide dimer to form a 2 : 2 complex.[10] In the $Ti(OPr)_4$–STA system, it is considered that the same type of complex is formed. In the IR spectrum of the precipitate dried at 170 °C, three characteristic absorption peaks were observed at 1450–1470, 1540–1560 and 1740 $cm^{-1}$. The broad peaks at 1450–1470 and 1540–1560 $cm^{-1}$ are assigned as stretching vibrations of a bidentate carboxylate ($CO_2^-$) ligand, and the sharp peak at 1740 $cm^{-1}$ as a stretching vibration of C=O in an ester bond of stearate. Because free STA was not detected in the sample dried at 170 °C, excess STA reacted with the solvent propan-1-ol to form *n*-propyl stearate.

For $X < 1.2$, the precipitates is a mixture of the $Ti(OPr)_4$–STA complex and titanium hydroxide contained residual alkoxide groups. For $X > 1.2$, the precipitate is a mixture of the $Ti(OPr)_4$–STA complex and *n*-propyl stearate. The results, for samples with $X > 1.2$, that the excess STA does not contribute to the formation of pore structure imply that the $TiO_2$ pores are formed upon decomposition of the $Ti(OPr)_4$–STA complex. In other words, an appropriate amount of STA acts as a template while excess of STA acts simply as a solvent. In conclusion, the pore size distribution of $TiO_2$ can be controlled by calcining the precipitate containing the $Ti(OPr)_4$–STA complex with different STA/Ti ratios.

## Footnote and References

* E-mail: satoshi@planet.tc.chiba-u.ac.jp

1 C. T. Kresge, M. E. Leonowicz, W. J. Roth, J. C. Vartuli and J. S. Beck, *Nature*, 1992, **359**, 710.
2 S. Inagaki, A. Koiwai, N. Suzuki, Y. Fukushima and K. Kuroda, *Bull. Chem. Soc. Jpn.*, 1996, **69**, 1449.
3 Q. Huo, D. I. Margolese, U. Ciesla, P. Feng, T. E. Gier, P. Sieger, R. Leon, P. M. Petroff, F. Schuth and G. D. Stucky, *Nature*, 1994, **368**, 317.
4 S. A. Bagshaw, E. Prouzet and T. J. Pinnavaia, *Science*, 1995, **269**, 1242.
5 U. Ciesla, D. Demuth, R. Leon, P. Petroff, G. Stucky, K. Unger and F. Schueth, *J. Chem. Soc., Chem. Commun.*, 1994, 1387.
6 F. Vaudry, S. Khodabandeh and M. E. Davis, *Chem. Mater.*, 1996, **8**, 1451.
7 S. A. Bagshaw and T. J. Pinnavaia, *Angew. Chem., Int. Ed. Engl.*, 1996, **35**, 1102.
8 T. Ono, Y. Ohguchi and O. Togari, *Preparation of Catalysts III, Third International Symposium on the Scientific Bases for the Preparation of Heterogeneous Catalysts*, Elsevier Science, Amsterdam, 1983, p. 631.
9 R. W. Cranston and F. A. Inkray, *Adv. Catal.*, 1954, **9**, 143.
10 C. J. Brinker and G. W. Scherer, *Sol–Gel Science, the Physics and Chemistry of Sol–Gel Processing*, Academic Press, New York, 1990, p. 55.

*Received in Cambridge, UK, 26th August 1997; 7/06197H*

# A novel aluminophosphate precursor that transforms to $AlPO_4$-5 molecular sieve at high temperature

**A. M. Prakash,[a] Martin Hartmann[b] and Larry Kevan*[a]**

[a] *Department of Chemistry, University of Houston, Houston, Texas 77204, USA*
[b] *Institute für Chemische Technologie, Universität Stuttgart, 70550 Stuttgart, Germany*

**A novel aluminophosphate microporous compound, denoted UHM-5, synthesized from an aqueous aluminophosphate gel at 150 °C in the presence of cyclohexylamine as the template, transforms upon calcination above 300 °C into $AlPO_4$-5 molecular sieve.**

Hydrothermal synthesis of microporous materials using organic structure directing templates normally leads to a crystalline solid (precursor) that possesses a three dimensional framework of $TO_4$ tetrahedra, where T is a tetrahedral atom, and the subsequent elimination of the template by calcination occurs without significant structural variation. Surprisingly, this is not the case for the precursor reported in this work. However, partial removal of the organic species from the precursor by calcination above 300 °C leads to the AFI type structure. A similar behavior has been reported recently in the structural transformation of JDF-20, an extra large pore molecular sieve with a 20-membered ring, to $AlPO_4$-5.[2] JDF-20 has been reported to be crystallized from a predominantly non-aqueous synthesis medium using triethylamine which is also a template for $AlPO_4$-5. Although both UHM-5 and JDF-20 exhibit similar transformation to $AlPO_4$-5, these materials differ significantly in their structural and compositional details. From various characterization results on UHM-5, we believe that this is a new member of the extra-large pore molecular sieve family.

Synthesis of UHM-5 was achieved from an aqueous aluminophosphate gel using cyclohexylamine (CHA) as the structure directing template. UHM-5 was prepared by a modification of a synthesis procedure which would otherwise yield $AlPO_4$-5 molecular sieve. Typically the molar composition of the gel was: 1 CHA : 1 $Al_2O_3$ : 1 $P_2O_5$ : 50 $H_2O$. In a typical synthesis procedure aluminium isopropoxide (Aldrich, 98+%) was slurried in deionized water. While stirring, orthophosphoric acid (Merck, 85%) diluted with water was added. After stirring for 10 min, cyclohexylamine (Aldrich, 99%) was added slowly. The mixture was then heated at 70 °C for 30 min using a water-bath. The final gel was crystallized at 150 °C for 74 h.

Fig. 1 shows the X-ray powder diffraction patterns of a sample in the as-synthesized form and after heating this sample in $O_2$ at 300 °C. The observed crystalline pattern for the as-synthesized material is novel. The very low $2\theta$ value ($d$ = 17.96 Å) of the most intense line in the XRD pattern is indicative of an extra-large pore molecular sieve. The weak line at $2\theta$ 7.57° is probably due to a very small amount of $AlPO_4$-5 which can probably crystallize along with UHM-5. After heating the sample at 300 °C, the structure changes to that of well crystallized $AlPO_4$-5 as also shown in Fig. 1. This structural transformation is brought about by the partial removal of the organic template. There is an extra line at $2\theta$ 21.80° in the XRD pattern which does not belong to $AlPO_4$-5. Note that a line at $2\theta$ 21.85° is also present in the XRD pattern of the as-synthesized sample. Thus, we believe that this extra line is possibly due to a small amount of a dense impurity phase present in the sample. By considering the first 15 lines after excluding the lines due to $AlPO_4$-5 ($2\theta$ 7.57°) and the impurity phase ($2\theta$ 21.85°) the powder pattern of UHM-5 has been indexed as a tetragonal unit cell with lattice parameters of $a$ = 18.15, $c$ = 20.59 Å and $U$ = 6786.3 Å$^3$.

To remove the organic template without effecting structural transformation, ion-exchange with $NH_4Cl$ was attempted. As in the case of thermal treatment, this procedure also leads to transformation of UHM-5 to $AlPO_4$-5 with significant loss in crystallinity. This suggests strong interaction between cyclohexylamine and the framework of UHM-5. The interaction between template and framework is further evidenced from thermal analysis results. Thermogravimetry (TG) and differential thermal analysis (DTA) of the material (Fig. 2) show two exothermic mass losses; a sharp loss at *ca*. 300 °C and a gradual loss between 300 to 500 °C due to the desorption and decomposition of the organic template. The total mass loss of 34 mass% observed on UHM-5 is significantly higher than the mass loss reported for any of the extra large pore molecular sieve materials and indicates the very high internal volume confined by the aluminophosphate framework. For example, both JDF-20 and VPI-5 show about 25% mass losses.[2,3] Interestingly, the material contains a very low amount of water as only < 1% of the total mass loss is accounted for by water desorption.

The product composition was estimated from electron microprobe analysis and TG results as 0.36 CHA $(Al_{0.5}P_{0.5})O_2 \cdot x\ H_2O$. The observed Al/P ratio of unity in UHM-5 is characteristic of three dimensional microporous solids with

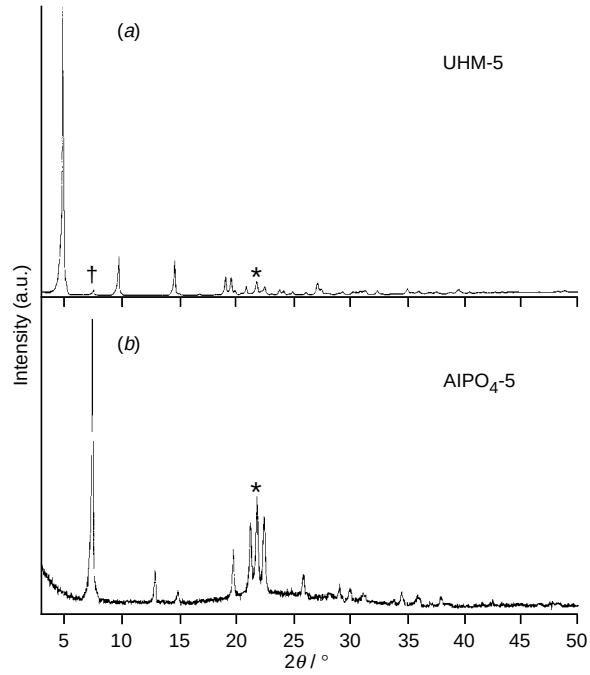



**Fig. 1** X-Ray powder diffraction patterns of (*a*) as-synthesized UHM-5 and (*b*) $AlPO_4$-5 obtained after calcination of UHM-5 at 300 °C in oxygen. In the as-synthesized sample the line marked with † is due to a small amount of $AlPO_4$-5 phase present. In both the as-synthesized and calcined samples, the lines marked by * are due to an impurity phase.

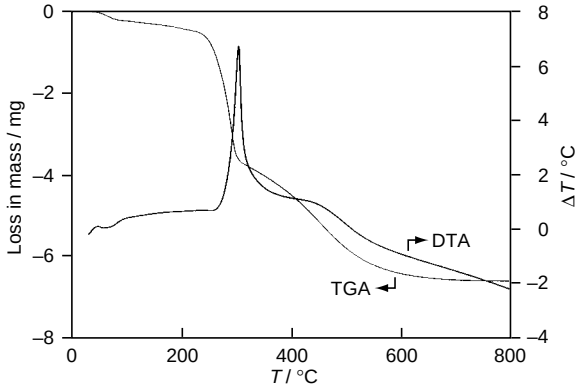



**Fig. 2** Thermogravimetry (TG) and differential thermal analysis (DTA) results on UHM-5. The data were recorded with a heating rate of 5 °C $min^{-1}$ in $O_2$ atmosphere. The initial mass of the sample was 17.418 mg.

alternate Al and P in the framework and is not observed in layered aluminophosphate materials. Previously synthesized layered aluminophosphates have a framework Al/P ratio of 0.75 and consist of vertices sharing $AlO_4$ and $PO_4$ tetrahedra with all of the vertices of the $AlO_4$ units being shared but only three-quarters of the $PO_4$ units being shared thus leaving formally a P=O group. It has been shown that these structure types can be related to two dimensional nets with the inclusion of a capping $PO_4^{3-}$ group.[4]

Fig. 3 shows the $^{27}Al$ and $^{31}P$ NMR spectra recorded on UHM-5 and after heating at 300 °C. The as-synthesized UHM-5 exhibits a single asymmetrical resonance in the $^{27}Al$ MAS NMR spectrum at $\delta$ 41.2 (reference: aqueous aluminium nitrate) characteristic of tetrahedral aluminium.[5] After the solid state transformation an additional peak is detected at $\delta$ 36.8. As-synthesized and calcined $AlPO_4$-5 is reported to exhibit a single resonance centered at $\delta$ *ca.* 35.[5] The fact that the line at $\delta$ 41.2 did not completely disappear during the transformation indicates that only a fraction of the Al sites undergo changes in environment during the transformation. The $^{31}P$ MAS NMR spectrum of as-synthesized UHM-5 exhibits a single sharp line at $\delta$ −4.6 and an additional broad line at $\delta$ −30 (reference 85% $H_3PO_4$). After the transformation, the line at $\delta$ −4.6 completely disappears while the line at $\delta$ −30 increases substantially. A $^{31}P$ line at $\delta$ −28.1 has been determined for $AlPO_4$-5.[6] Tetrahedral phosphorus in microporous materials generally exhibits resonances in the range $\delta$ −25 to −35 range characteristic of $P(OAl)_4$ environments.[5] The resonance at $\delta$ *ca.* −30 in UHM-5 is clearly due to tetrahedral phosphorus as found in several other microporous materials. The fraction of $AlPO_4$-5 present in the

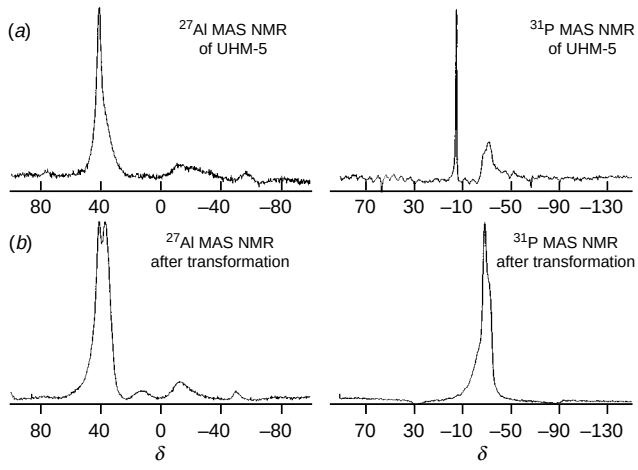



**Fig. 3** $^{27}Al$ and $^{31}P$ MAS NMR spectra recorded (*a*) for as-synthesized UHM-5 and (*b*) after heating UHM-5 at 300 °C in oxygen

original as-synthesized sample is very small. Thus, the relatively strong NMR signal at $\delta$ *ca.* −30 in an as-synthesized sample cannot be fully accounted for by an $AlPO_4$-5 phase, although a small contribution of this phase to the observed signal is obvious. In $AlPO_4$-based materials, the interaction of the framework phosphorus with extraframework species such as water or organic molecules can modify or shift the resonance signal considerably.[7] A wide range of chemical shifts spanning from $\delta$ 30 to −85 has been reported for five-coordinate phosphorus compounds.[8] A framework P/Al ratio of unity in UHM-5 implies an alternate arrangement of Al and P units in the framework. The observed resonance at $\delta$ −4.6 could be due to five-coordinate phosphorus of the form $P(OAl)_4(OH)$ formed by coordinating with four framework Al and an extraframework species such as a hydroxyl group. The presence of hydroxyl groups was observed in UHM-5 by FTIR measurements which show an intense sharp band at 3650 $cm^{-1}$ normally assigned to hydroxyl stretching vibrations.[9] The disappearance of the resonance at $\delta$ −4.6 after heating above 300 °C can be viewed as a consequence of phase transformation where the five-coordinated phosphorus transforms to tetrahedral to form $AlPO_4$-5 molecular sieve. Associated with each $P(OAl)_4(OH)$ unit one would expect a protonated template species. $AlPO_4$ units in which both Al and P are in tetrahedral coordination are neutral and do not require amine to balance any framework charge. From the observed chemical composition of UHM-5, it can be seen that for every ten P atoms there are about seven CHA species. This suggests that out of ten P atoms of the framework, roughly seven are in five-coordination and three in tetrahedral coordination consistent with the two $^{31}P$ NMR signals.

The observations made above suggest that the framework of UHM-5 probably consists of both $AlPO_4$ and $(AlPO_4)OH$ units. The framework structure of UHM-5 is stable in the presence of the organic species and transforms upon heating to the $AlPO_4$-5 structure. UHM-5 crystallizes in small 4–6 μm platelets bunched together to form large clusters of *ca.* 100 μm as revealed by scanning electron microscopy. Because of the small crystal size, single crystal analysis would be difficult. All the characterization results so far obtained on UHM-5 indicate an extra large pore material. Additional experiments are necessary for a better understanding of the transformation mechanism and work is in progress to determine the structure of UHM-5.

This work was supported by the Robert A. Welch Foundation and the National Science Foundation.

## Footnote and References

* E-mail: kevan@uh.edu

1 S. T. Wilson, B. M. Lok, C. A. Messina, T. R. Cannan and E. M. Flanigen, *J. Am. Chem. Soc.*, 1982, **104**, 1146.
2 Q. Huo, R. Xu, S. Li, Y. Xu, Z. Ma, Y. Yue and L. Li, in *Proceedings from the Ninth International Zeolite Conference*, ed. R. von Ballmoos, J. B. Higgins and M. J. M. Treacy, Butterworth-Heinemann, Boston, 1993, pp. 279–286.
3 M. E. Davis, C. Montes, P. E. Hathaway, J. P. Arhancet, D. L. Hasha and J. M. Garces, *J. Am. Chem. Soc.*, 1989, **111**, 3919.
4 P. A. Barrett and R. H. Jones, *J. Chem. Soc., Chem. Commun.*, 1995, 1979.
5 C. S. Blackwell and R. L. Patton, *J. Phys. Chem.*, 1984, **88**, 6137.
6 D. Müller, E. Jahn, B. Fahlke, G. Ladwig and U. Haubenreiser, *Zeolites*, 1985, **5**, 53.
7 M. Goepper, F. Guth, L. Delmotte, J. L. Guth and H. Kessler, in *Zeolites: Facts, Figures, Future*, ed. P. A. Jacobs and R. A. van Santen, Elsevier, Amsterdam, 1989, pp. 857–866 (*Stud. Surf. Sci. Catal.*, 1989, **49**, 857).
8 L. W. Dennis, V. J. Bartuska and G. E. Maciel, *J. Am. Chem. Soc.*, 1982, **104**, 230.
9 U. Lohse, E. Löffler, K. Kosche, J. Jänchen and B. Parlitz, *Zeolites*, 1993, **13**, 549.

*Received in Columbia, MO, USA, 10th July 1997; 7/04602B*

# Structure of a novel antimalarial gallium(III) complex with selective activity against chloroquine-resistant *Plasmodium falciparum*†

**Vijay Sharma,[a] Alicia Beatty,[b] Daniel E. Goldberg[c] and David Piwnica-Worms*[a]**

[a] *Laboratory of Molecular Radiopharmacology, Mallinckrodt Institute of Radiology and Department of Molecular Biology and Pharmacology, Washington University Medical School, St Louis, MO, USA*
[b] *Department of Chemistry, Kansas State University, Manhattan, KS, USA*
[c] *Howard Hughes Medical Institute, Departments of Medicine and Molecular Microbiology, Washington University Medical School, St Louis, MO, USA*

**The crystal structure of an amine phenol complex of gallium(III), [{1,12-bis(2-hydroxy-3-methoxybenzyl)-1,5,8,12-tetraazadodecane}gallium(III)] [Ga(madd)]$^+$, a potent new antimalarial which selectively targets chloroquine-resistant organisms is reported; the compound is shown to directly inhibit heme polymerization.**

Chloroquine, the mainstay of treatment and prophylaxis of malaria, disrupts polymerization of heme (ferriprotoporphyrin IX) released during catabolism of host hemoglobin within the causative organism, *Plasmodium falciparum*.[1–3] Given the importance attributed to iron metabolites in parasite toxicity, a variety of metal chelating agents such as deferoxamine and reversed siderophores have been explored as potential antimalarial chemotherapeutics.[4–6] We recently identified a class of Schiff-base and reduced amine phenol metal(III) complexes with $N_4O_2$ donor cores having potency as novel antimalarials.[7] We report herein the chemical characterization including crystal structure and direct demonstration of inhibition of heme polymerization by one distinctive complex, [{1,12-bis-(2-hydroxy-3-methoxybenzyl)-1,5,8,12-tetraazadodecane}gallium(III)] {[Ga(madd)]$^+$ **1**}. While the action of chloroquine is now circumvented by widely disseminated resistant organisms, **1** paradoxically possesses antimalarial activity only against chloroquine-resistant *P. falciparum* in whole cell assays. Thus, **1** may provide a lead for further development of analogous iron(III) antimalarials and, in addition, the crystal coordinates provide a structural template for exploration of the molecular determinants of chloroquine resistance in *P. falciparum*.

Large spectral linewidths and the accompanying poor resolution produced by high spin iron(III) pose difficulties for spectroscopic characterization of iron(III) complexes in solution through NMR studies. Thus, we have chosen diamagnetic gallium(III) as a template for iron(III), since both ions have the same charge and nearly identical six-coordinate ionic radii which typically result in similar coordination chemistry.[8] Furthermore, neither high spin $d^5$ iron(III) nor $d^{10}$ gallium(III) possess any crystal field stabilization energy and therefore often result in similar ligand exchange kinetics.[9] For analysis, the desired amine phenol ligand, $H_2$madd **2**, was obtained through *in situ* potassium tetrahydroborate reduction of the condensation product derived from appropriate stoichiometric amounts of bis(*N*,*N*′-aminopropyl)ethylenediamine and 3-methoxysalicylaldehyde.[10,11] [Ga(madd)]$^+$ **1** was obtained by dissolving **2** in methanol and treating with base and the hydrated salt of gallium(III) perchlorate.† The $^1$H NMR spectrum of **1** recorded in $(CD_3)_2SO$ demonstrated overlapping signals for the hydrocarbon backbone consistent with complex formation and a single set of signals for the aromatic protons consistent with chemically equivalent aromatic environments. The proton-decoupled $^{13}$C NMR spectrum recorded under similar conditions also revealed 12 resonances out of a possible 24 further indicating the maintenance of a high degree of symmetry around the ethylene moiety upon coordination of the metal to ligand **2**.

Definitive evidence that $Ga^{III}$ was coordinated simultaneously and symmetrically with the $N_4O_2$ donor core was provided by X-ray crystallography.‡ Crystals suitable for X-ray structure determination were grown through slow evaporation of methanol over a period of 2–3 d. An ORTEP drawing of **1** is shown in Fig. 1 along with selected bond angles and interatomic distances. The central $Ga^{III}$ is six-coordinate involving two phenolate oxygens and four amine nitrogens providing overall octahedral geometry. Furthermore, the structure reveals formation of four six-rings and one five-membered ring upon coordination of the metal. The smallest angle, N(2)–Ga–N(3), is attributable to restrictions by the five-membered chelate ring involving N(2), C(11), C(12), N(3) and Ga. The *trans* angles involving N(1)–Ga–N(3), N(2)–Ga–N(4) and O(1)–Ga–O(2) averaged 175.4°, whereas the *cis* angles involving O–Ga–N averaged 90.0°, providing minimally distorted octahedral

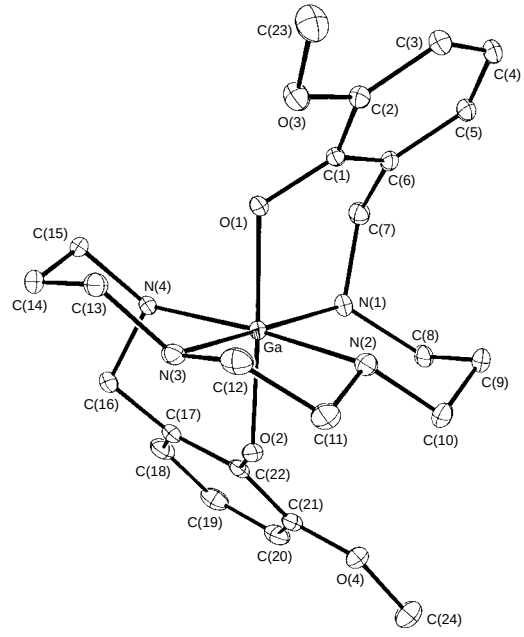



**Fig. 1** ORTEP drawing of the [Ga(madd)]$^+$ cation (**1**) in [Ga(madd)]$ClO_4$ showing the crystallographic numbering scheme. Atoms are represented by thermal ellipsoids corresponding to 20% probability. Selected bond angles (°) and interatomic distances (Å) for **1**: N(1)–Ga–N(2) 92.15(11), N(2)–Ga–N(3) 83.22(11), N(3)–Ga–N(4) 90.62(11), N(4)–Ga–N(1) 94.08(10), O(1)–Ga–O(2) 177.99(8), N(1)–Ga–N(3) 174.87(10), N(2)–Ga–N(4) 173.43(10), O(1)–Ga–N(1) 90.29(10), O(1)–Ga–N(4), 88.59(10), O(2)–Ga–N(2) 87.87(10), O(2)–Ga–N(3) 90.87(10), C(1)–O(1)–Ga 122.4(2), C(22)–O(2)–Ga 119.1(2); Ga–O(1) 1.911(2), Ga–O(2) 1.950(2), Ga–N(1) 2.130(3), Ga–N(2) 2.103(3), Ga–N(3) 2.109(3), Ga–N(4) 2.105(3), O(1)–C(1) 1.345(4), O(2)–C(22) 1.340(4).

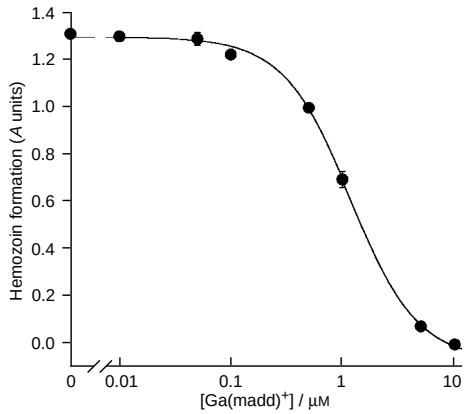



**Fig. 2** Inhibition of heme polymerization by $[Ga(madd)]^+$ **1**. Heme polymerization was assayed by the preformed hemozoin nucleation reaction[7] in the absence or presence of various concentrations of **1**. Data are shown as the mean ±SEM (when larger than symbol) of six determinations.

geometry around the central metallic core. Angles and distances of atoms directly participating in the coordination sphere of **1** are similar to those recently reported for the gallium(III) complexes of a 5-bromo substituted amine phenol[12] and an analogous substituted Schiff-base phenol.[13]

Chloroquine concentrates within the parasitic digestive vacuole[14] an acidic organelle wherein the host's hemoglobin is digested as a source of amino acids, releasing monomeric heme.[15] Toxic to parasites,[2,16,17] heme is polymerized by the organisms into a crystalline matrix known as hemozoin, a black insoluble pigment which constitutes heme units coordinated through iron–carboxylate linkages.[1] Chloroquine inhibits heme polymerization, resulting in accumulation of the toxic monomeric heme moiety.[2,3] Resistance appears to be mediated by an acquired ability of the parasite to reduce uptake[18] or pump chloroquine out of the digestive vacuole.[19,20] Because hemozoin formation is unique to the malaria organism, inhibition of heme polymerization has remained an attractive target for drug development, providing an agent can be designed to bypass the organism's chloroquine-evading mechanisms.

Among dozens of analogues, including the above 5-bromo complex[21] and several Schiff-base analogues,[7] **1** was found to be unique in possessing selective antimalarial activity against chloroquine-resistant Dd2 clones of *P. falciparum*. To further determine the potency of **1** to inhibit additional chloroquine-resistant lines of *P. falciparum*, growth of trophozoites in intra-erythrocyte culture was assayed by the hypoxanthine incorporation method.[7,22] Compared to a half-maximal inhibitory concentration ($IC_{50}$) value $>>20$ μM in the chloroquine-sensitive HB3 line, the $IC_{50}$ values for **1** were 0.5 and 0.6 μM in the chloroquine-resistant FCR-3 and Indo-1 lines, respectively, and further supported a general collateral selectivity of **1** for chloroquine-resistant *P. falciparum*.

However, the potency of **1** to directly inhibit heme polymerization *in vitro* was found to be similar to other agents in this class (Fig. 2). For example, to simulate the parasitic digestive vacuole environment,[16] heme was incubated along with preformed hemozoin nucleates under acidic conditions in the absence or presence of various concentrations of **1**.[2,7]§ Complex **1** was found to be a potent inhibitor of heme polymerization ($IC_{50}$ = 1.2 ± 0.08 μM; mean ±SEM; $n$ = 6), two- to three-fold more potent than chloroquine under identical conditions.[7] Thus, while **1** is not susceptible to the chloroquine resistance mechanism(s) in whole cell assays, it inhibits the same final molecular target as chloroquine *in vitro*. Careful evaluation of **1** revealed that the angles Ga–O(1)–C(1) and Ga–O(2)–C(22) which incorporate the aromatic rings averaged 120.8°, *ca*. 2.5° more acute than the reported 5-bromo complex, thereby suggesting that the unique targeting properties of **1** likely reside in the spatial orientation of the peripheral regions of the aromatic moieties, including the methoxy functionalities, rather than the central metal core.

The gallium(III) complex, $[Ga(madd)]^+$ **1**, is the first amine phenol metal(III) complex to show antimalarial activity selectively against chloroquine-resistant organisms. While important considerations regarding optimization of selectivity and bioavailability are under active investigation, **1** represents a significant step forward in the development of a novel antimalarial.

We thank George Gokel for critical review of the manscript, Ilya Gluzman and Anna Oksman for technical assistance. This work was funded in part by a grant from the US Department of Energy (ER61885) and by grants from the NIH (AI31615 and CA65735).

## Footnotes and References

* E-mail: piwnica-worms@mirlink.wustl.edu

† Details of synthesis and characterization of compounds **1** and **2**; structure determination, refinement methods and tables of X-ray crystallographic data for compound **1** (atomic coordinates, interatomic distances and angles, anisotropic and isotropic displacement parameters, and hydrogen coordinates) as well as the procedure for the heme polymerization inhibition assay are included as supporting material available upon request from the authors.

‡ Colorless crystals of $[Ga(madd)]ClO_4$ (formula, $C_{24}H_{36}ClGaN_4O_8$; $M$ = 613.74) belong to the monoclinic space group, $P2_1/n$, with $a$ = 10.8630(8), $b$ = 17.141(5), $c$ = 15.181(2) Å, $\beta$ = 107.711(7)°, $U$ = 2692.8(9) Å$^3$, $D_c$ = 1.514 g cm$^{-3}$, $Z$ = 4 and GOF = 1.165. Data were collected at 173 K using a Mo-Kα radiation source (0.710 73 Å) and the structure resolved and refined to $R_1$ [$I > 2\sigma(I)$] = 0.0409. CCDC 182/625.

§ Control experiments established that **1** was stable to acidic hydrolysis: $^1$H NMR spectra were superimposible before and after incubation in water for 72 h (37 °C, pH 4.5).

1 A. Slater, W. Swiggard, B. Orton, W. Flitter, D. Goldberg, A. Cerami and G. Henderson, *Proc. Natl. Acad. Sci. USA*, 1991, **88**, 325.
2 A. F. Slater and A. Cerami, *Nature* (*London*), 1992, **355**, 167.
3 D. J. J. Sullivan, I. Y. Gluzman, D. G. Russell and D. E. Goldberg, *Proc. Natl. Acad. Sci. USA*, 1996, **93**, 11 865.
4 S. Lytton, Z. Cabantchik, J. Libman and A. Shanzer, *Mol. Pharmacol.*, 1991, **40**, 584.
5 C. Hershko, E. Theanacho, D. Spira, H. Peter, P. Dobbin and R. Hider, *Blood*, 1991, **77**, 637.
6 C. Hershko, V. Gordeuk, P. Thuma, E. Theanacho, D. Spira, R. Hider, T. Peto and G. Brittenham, *J. Inorg. Biochem.*, 1992, **47**, 267.
7 D. E. Goldberg, V. Sharma, A. Oksman, I. Y. Gluzman, T. E. Wellems and D. Piwnica-Worms, *J. Biol. Chem.*, 1997, **272**, 6567.
8 R. D. Shannon, *Acta Crystallogr., Sect. A*, 1976, **32**, 751.
9 B. N. Figgis, *Introduction to Ligand Fields*, Wiley, New York, 1976, p. 74.
10 E. Wong, S. Liu, T. Lugger, F. E. Hahn and C. Orvig, *Inorg. Chem.*, 1995, **34**, 93.
11 V. Sharma, C. Crankshaw and D. Piwnica-Worms, *J. Med. Chem.*, 1996, **39**, 3483.
12 E. Wong, P. Caravan, S. Liu, S. J. Rettig and C. Orvig, *Inorg. Chem.*, 1996, **35**, 715.
13 B. W. Tsang, C. J. Mathias, P. E. Fanwick and M. A. Green, *J. Med. Chem.*, 1994, **37**, 4400.
14 D. J. Krogstad, I. Y. Gluzman, B. L. Herwaldt, P. H. Schlesinger and T. E. Wellems, *Biochem. Pharmacol.*, 1992, **43**, 57.
15 P. L. Olliaro and D. E. Goldberg, *Parasitol. Today*, 1995, **11**, 294.
16 A. Orjih, H. Banyal, R. Chevli and C. Fitch, *Science*, 1981, **214**, 667.
17 I. Gluzman, S. Francis, A. Oksman, C. Smith, K. Duffin and D. Goldberg, *J. Clin. Invest.*, 1994, **93**, 1602.
18 C. Sanchez, S. Wunsch and M. Lanzer, *J. Biol. Chem.*, 1997, **272**, 2652.
19 T. E. Wellems, L. J. Panton, I. Y. Gluzman, V. E. do Rosario, R. W. Gwadz, J. A. Walker and D. J. Krogstad, *Nature*, 1990, **345**, 253.
20 A. F. Cowman, S. Karcz, D. Galatis and J. G. Culvenor, *J. Cell Biol.*, 1991, **113**, 1033.
21 V. Sharma, D. E. Goldberg and D. Piwnica-Worms, unpublished work.
22 W. Trager and J. B. Jensen, *Science*, 1976, **193**, 673.

*Received in Columbia, MO, USA, 31st July 1997; 7/05563C*

# Generalised route to the preparation of mesoporous metallosilicates *via* post-synthetic metal implantation

**Ryong Ryoo,* Shinae Jun, Ji Man Kim and Mi Jeong Kim**

*Materials Chemistry Laboratory, Department of Chemistry and Center for Molecular Science, Korea Advanced Institute of Science and Technology, Taejon, 305-701, Korea*

**A post-synthesis route, through which various metal elements can be grafted onto siliceous frameworks using non-aqueous solutions of $AlCl_3$, $Al(NO_3)_3$, $SnCl_2$, $Zn(O_2CMe)_2$ $Mn(O_2CMe)_2$, *etc.*, is developed as a generalised means to obtain mesoporous metallosilicates molecular sieves with various structures such as MCM-41 (hexagonal), MCM-48 (cubic *Ia*3*d*), SBA-1 (cubic *Pm*3*n*), KIT-1 (disordered) and MSU-1 (disordered) with superior structural integrity, acidity and catalytic activity to those of materials having metals incorporated during synthesis.**

During the past five years, various kinds of mesoporous silica so-called MCM-41,[1,2] MCM-48,[1,2] SBA-1,[3] MSU-1,[4] KIT-1,[5,6] FSM-16,[7] *etc.* have been synthesized using surfactant micelles as the structure-directing agent. A large number of papers have reported the incorporation of aluminium and other metal elements within the siliceous frameworks of the mesoporous materials by adding metal precursors prior to hydrothermal synthesis reaction in order to improve ion exchange capacity, acidity and catalytic activity.[8] However, the method incorporating Al precursors into the surfactant–silicate gel requires specialised synthesis conditions depending on the respective structures of the materials being synthesised, incorporating metals, and silica sources. Besides, the synthesis method is often hindered by a severe decrease in the structural order as the metal content increases.

Here we report a generalised route through which various metal elements such as Al, Sn, Zn and Mn can be incorporated within various mesoporous materials such as MCM-41 (hexagonal), MCM-48 (cubic *Ia*3*d*), MSU-1 (disordered), SBA-1 (cubic *Pm*3*n*) and KIT-1 (disordered), after the synthesis of pure silica forms. We show that the resultant mesoporous aluminosilicates can have not only high ion exchange capacity due to tetrahedral Al, but also superior structural integrity, acidity and catalytic activity to those obtained by the mixed-gel approach.

The silica forms of MCM-41, MCM-48, MSU-1, SBA-1 and KIT-1 were obtained by hydrothermal synthesis following methods reported in the literature.[1–6] The as-synthesized materials except SBA-1 were washed with slurrying in EtOH–HCl at room temp.; less than 1 g of sample was washed with a mixture of 0.5 ml of 37% HCl and 20 ml of 95% EtOH. The sample was immediately dried in an oven at 393 K. The washing resulted in the removal of more than 95% of the surfactant, which was confirmed by IR absorption spectroscopy. The surfactant in SBA-1 was removed by calcination in $O_2$ flow at 823 K since the structure collapsed upon washing with EtOH–HCl. The mesoporous materials after the removal of surfactant, either by solvent extraction or calcination, were slurried in absolute EtOH solutions containing the anhydrous form of various metal compounds such as $AlCl_3$, $Al(NO_3)_3$, $SnCl_2$, $Zn(O_2CMe)_2$ and $Mn(O_2CMe)_2$, with magnetic stirring for 1 h at 298–333 K. The mesoporous materials were then washed with absolute EtOH, dried and calcined in air using a muffle furnace. The calcination temperature was increased to 823 K over 10 h and maintained there for 5 h.

The obtained materials were characterised by X-ray powder diffraction (XRD), BET surface area measurement, $^{27}Al$ MAS NMR, temperature programmed desorption (TPD) of $NH_3$, and $K^+$ ion exchange. XRD patterns and NMR spectra were obtained in the same manner reported in our recent papers.[9,10] Ammonia TPD and $K^+$ ion exchange capacity were measured following refs. 11 and 12, respectively.

All mesoporous metallosilicates obtained by the present metal-implantation route gave the same XRD patterns as those for their pure-silica analogues, as shown in Fig. 1. There were no significant changes in the XRD peak intensities and linewidths resulting from the implantation of Al, Sn, Zn and Mn throughout the investigated range of Si/Al $\geqslant$ 8, Si/Sn $\geqslant$ 20, Si/Zn $\geqslant$ 10 and Si/Mn $\geqslant$ 20. No additional XRD peaks appeared beyond the $2\theta$ region shown in Fig. 1, indicating that the implanted metal elements were well dispersed. The BET areas of the various samples ranged from 900 to 1200 $m^2\ g^{-1}$, and showed no more decreases than those attributable to increases in the sample mass due to the addition of the metal elements.

Recently, aluminosilicate forms of MCM-41 have been clarified to exhibit ion exchange capacity comparable to that for aluminosilicate zeolites whereas little ion exchange occurs with pure-silica MCM-41.[12] The ion exchange capacity can then be used as a means to probe the incorporation of metal elements with oxidation states less than +4. We have therefore measured the $K^+$-ion exchange capacity of our various metal-containing samples, and summarised results in Table 1. Note that the present Al-implanted samples showed a $K^+$-ion exchange capacity comparable to a result of 0.4 $K^+$/Al which was reported previously[12] with an AlMCM-41 (Si/Al = 39) sample prepared by the addition of sodium aluminate into the surfactant-silicate gel. The ion exchange capacity of the present Al-implanted samples depended more or less on structures and Si/Al ratios. The $K^+$/Al ratios decreased, in general, as the Si/Al ratios decreased. Sn-, Zn- and Mn-implanted samples also showed remarkable $K^+$ ion exchange capacity. It is thus evident that the

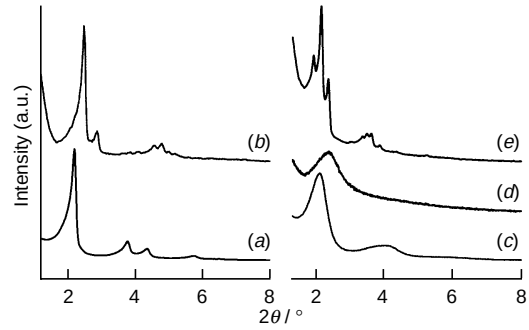



**Fig. 1** X-Ray diffraction patterns for various mesoporous molecular sieves obtained after calcination with metal implantation: (*a*) AlMCM-41 (Si/Al = 32), (*b*) AlMCM-48 (Si/Al = 8), (*c*) AlKIT-1 (Si/Al = 33), (*d*) AlMSU-1 (Si/Al = 53) and (*e*) AlSBA-1 (Si/Al = 11). The XRD patterns of the calcined samples with and without the metals were indistinguishable from each other.

**Table 1** Potassium ion exchange on mesoporous metallosilicates prepared by the metal-implantation method

| | Al implanted | | Sn implanted | Zn implanted | Mn implanted |
|---|---|---|---|---|---|
| Samples | Si/Al (K/Al[a]) | Si/Al (K/Al) | Si/Sn (K/Sn) | Si/Zn (K/Zn) | Si/Mn |
| KIT-1 | 47.7[b] (0.15) | 10.3[c] (0.07) | 71.7 (0.12) | 20.4 (0.09) | 68.5 |
| MCM-41 | 48.9[b] (0.20) | 8.3[c] (0.18) | 218 (0.39) | 21.1 (0.13) | 56.1 |
| MCM-48 | 37.1[b] (0.24) | 6.9[c] (0.10) | 56.7 (0.23) | 18.7 (0.26) | |
| SBA-1 | 56.3[b] (0.49) | 10.8[c] (0.27) | 79.2 (0.13) | 23.6 (0.29) | |
| MSU-1 | 53.4[b] (0.52) | 27.1[c] (0.33) | 230 (0.34) | | |

[a] Numbers in parentheses denote the atomic ratio between the ion exchanged $K^+$ and the implanted metal, determined by ICP emission spectroscopy. Metal leaching during ion exchange treatment occurred much less than $K^+$ exchange. Release of $H^+$ was also confirmed, indicating that the $K^+$ was exchanged with $H^+$. The pure-silica sample gave a K/Si ratio of 0.0004. [b] For Al incorporation, siliceous material was slurried in ethanol containing $AlCl_3$ at 298 K. [c] Slurry and filtration repeated three times using an excess of $AlCl_3$.

ion exchange capacity of the metal implanted samples arises from the incorporation of the metal elements within the silica framework, or at least in the form closely associated with it.

The incorporation of Al within the silica framework is consistent with a remarkable increase in the $^{27}$Al MAS NMR peak intensity for Al with tetrahedral coordination, upon calcination as shown in Fig. 2. The NMR spectrum before calcination shows a much lower peak intensity for the tetrahedral Al ($\delta$ 52) than that for octahedral aluminium ($\delta$ 0). The intensity order was reversed after calcination, throughout the range of Si/Al = 10 to infinity for the various mesoporous materials after calcination. This result indicates that a considerable proportion of the Al achieves tetrahedral coordination after calcination and probably becomes implanted within the silica framework.

Fig. 3 shows $NH_3$ TPD for the resulting Al-implanted samples. The other aluminosilicate samples also gave two TPD peaks which were centered around 430 and 830 K, respectively. The relative peak intensities and positions depended more or less on the structures and Si/Al ratios. The low temperature peak is similar to the TPD results reported previously for AlMCM-41. However, the high temperature peak was not reported previously.[9,13] The high temperature peak may be due to strong Lewis acidity of the extraframework Al species. The Al-

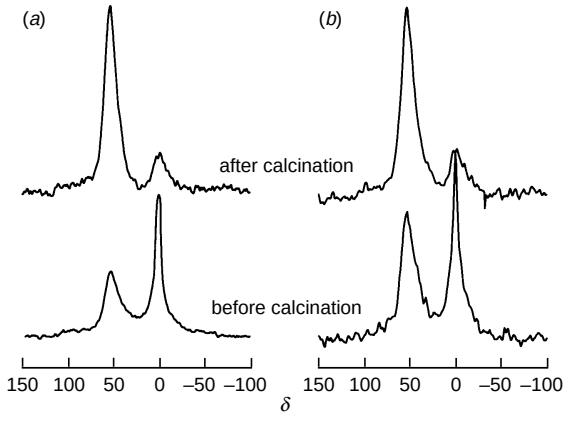



**Fig. 2** $^{27}$Al MAS NMR spectra for Al-implanted samples: (*a*) AlMCM-41 (Si/Al = 32) and (*b*) AlKIT-1 (Si/Al = 33). The NMR spectra show transition from octahedral to tetrahedral Al upon calcination.

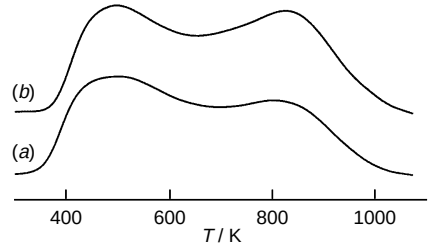



**Fig. 3** $NH_3$TPD spectra for Al-implanted samples: (*a*) AlKIT-1 (Si/Al = 33) and (*b*) AlMCM-41 (Si/Al = 32)

implanted samples exhibited 2–3 times higher catalytic activity for *n*-butane cracking under 0.5 kPa butane and 110 kPa He at 801 K. This can be due to the presence of a relatively large amount of Al on the framework surface of the implanted samples, while much A is imbedded within the pore wall of the samples which were synthesized with the addition of Al sources into the surfactant–silicate gel. Upon extrapolation to zero conversion, the turnover frequency for freshly calcined KIT-1 (Si/Al = 33) catalyst after Al implantation was 0.13 $s^{-1}$. This result is comparable to 0.30 $s^{-1}$, which was obtained for HZSM-5 (Si/Al = 25) based on the total number of Al sites under the same measurement conditions. Further details of the catalytic activity measurements will be reported in a full paper.

We have confirmed that it is important to use moisture-free EtOH or MeOH and anhydrous metal compounds since the presence of water inhibited metal implantation. It is believed that the metal species in the moisture-free solution was grafted onto silanol groups on the silica framework. The metal became probably incorporated within the siliceous framework *via* thermal activation during calcination. The resulting metallosilicate samples showed superior structural integrity, acidity and catalytic activity, compared to the materials obtained by the addition of a metal source into the surfactant-silicate gel. Thus, our metal implantation method can be useful for the preparation of various existing and new mesoporous metallosilicates.

The authors thank KOSEF for a grant supporting the present work.

## Footnote and References

* E-mail: rryoo@sorak.kaist.ac.kr

1 C. T. Kresge, M. E. Leonowicz, W. J. Roth, J. C. Vartuli and J. S. Beck, *Nature*, 1992, **359**, 710.
2 J. S. Beck, J. C. Vartuli, W. J. Roth, M. E. Leonowicz, C. T. Kresge, K. D. Schmitt, C. T-W. Chu, D. H. Olson, E. W. Sheppard, S. B. McCullen, J. B. Higgins and J. L. Schlenker, *J. Am. Chem. Soc*., 1992, **114**, 10834.
3 Q. Huo, R. Leon, P. M. Petroff and G. D. Stucky, *Science*, 1995, **268**, 1324.
4 S. A. Bagshaw, E. Prouzet and T. J. Pinnavaia, *Science*, 1995, **269,** 1242.
5 R. Ryoo, J. M. Kim, C. H. Ko and C. H. Shin, *J Phys. Chem*., 1996, **100**, 17 718.
6 R. Ryoo, J. M. Kim, J. Y. Lee and C. H. Shin, *Stud. Surf. Sci. Catal*., 1997, **105,** 45.
7 S. Inagaki, Y. Fukushima and K. Kuroda, *J. Chem. Soc., Chem. Commun*., 1993, 680.
8 A. Sayari, *Stud. Surf. Sci. Catal*., 1997, **102**, 1.
9 A. Corma, V. Fornés, M. T. Navarro and J. Pérez-Pariente, *J. Catal*., 1994, **148**, 569.
10 R. Ryoo and J. M. Kim, *J. Chem. Soc., Chem. Commun*., 1995, 711.
11 R. Ryoo, C. H. Ko and R. F. Howe, *Chem. Mater*., 1997, **9**, 1607.
12 J. M. Kim, J. H. Kwak, S. Jun and R. Ryoo, *J. Phys. Chem*., 1995, **99**, 16 742.
13 H. Kosslick, H. Landmesser and R. Fricke, *J. Chem. Soc., Faraday Trans*., 1997, **93**, 1849.

*Received in Cambridge, UK, 4th July 1997; 7/04745B*

# Heterobimetallic cycloheptatrienyl and cycloheptatrienylidene complexes

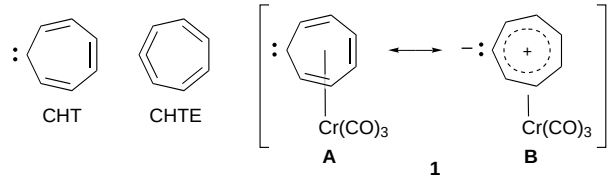
**Matthias Tamm,* Alexander Grzegorzewski, Irene Brüdgam and Hans Hartl**

*Institut für Anorganische und Analytische Chemie, Freie Universität Berlin, Fabeckstraße 34-36, D-14195 Berlin, Germany*

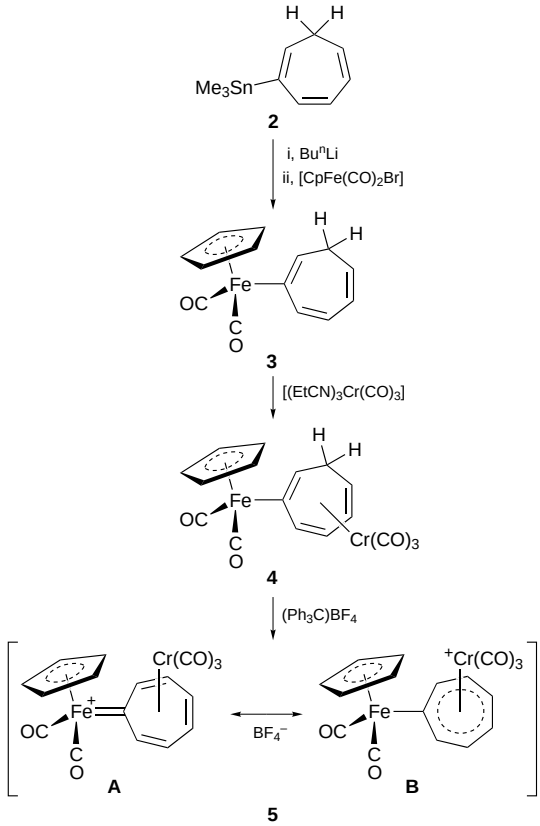
**The heterobimetallic μ-(η¹ : η⁶-1,3,5-cycloheptatrien-2-yl) complex 4 is obtained from 2-trimethylstannyl-1,3,5-cycloheptatriene 2 and [CpFe(CO)$_2$Br] followed by reaction with [(EtCN)$_3$Cr(CO)$_3$]; hydride abstraction results in the formation of the first heterobimetallic cycloheptatrienylidene (CHT) complex [CpFe(CO)$_2${μ-(η¹ : η⁷-CHT)}Cr(CO)$_3$]BF$_4$ 5; the crystal structure of 4 is reported.**

Cycloheptatrienylidene (CHT) and 1,2,4,6-cycloheptatetraene (CHTE) are well known isomers of the $C_7H_6$ potential-energy surface. Experimentally[1] and theoretically,[2] CHTE is the most stable species among the monocyclic $C_7H_6$ isomers. On the other hand, in transition metal complexes the ground state varies with the metal, and several η¹-CHT and η²-CHTE complexes have been reported by Jones and coworkers.[3]

In addition, these ligands offer the option to synthesize heterobimetallic complexes by coordination of the seven-membered ring to a second metal fragment.[4] Whereas the first heterobimetallic CHTE complex, [(PPh$_3$)$_2$Pt{μ-(η² : η⁶-CHTE)}Mo(CO)$_3$], has been reported only recently,[5] heterobimetallic CHT complexes have not yet been prepared. Attempts to generate and trap free [(η⁷-CHT)Cr(CO)$_3$] **1** were unsuccessful.[6] In the course of our work on ligands containing cycloheptatrienylium rings,[7] we have recently synthesized 2-trimethylstannyl-1,3,5-cycloheptatriene **2**,[7c] which can be used in a Stille coupling reaction. Here, we wish to report on the suitability of **2** for the preparation of heterobimetallic 1,3,5-cycloheptatrien-2-yl and cycloheptatrienylidene complexes.




Complex **3** was prepared by lithiation of **2** with Bu$^n$Li and reaction with [CpFe(CO)$_2$Br] in THF at low temperature (Scheme 1).†,[8] The $^1$H NMR spectrum clearly shows the exclusive formation of the 1,3,5-cycloheptatrien-2-yl derivative exhibiting a doublet of doublets for the allylic protons and five resonances for the vinylic protons in a 2 : 1 : 1 : 1 : 1 : 1 ratio. In order to avoid isomerization, **3** was treated with [(EtCN)$_3$Cr(CO)$_3$] at room temp., to form heterobimetallic **4** as stable red–orange crystals.† The $^1$H NMR spectrum exhibits five resonances due to the vinylic protons and two resonances due to the allylic *exo*- and *endo*-protons. As **4** is a racemic mixture of two enantiomers, two $^{13}$C NMR resonances are observed for the diastereotopic FeCO carbon atoms. The molecular structure of **4** is depicted in Fig. 1.‡ The 1,3,5-cycloheptatriene-2-yl ring is coordinated in a μ-(η¹ : η⁶)-fashion. The bond lengths and angles about the iron atom fall in the range observed for other alkenyl complexes,[9] and the Cr(CO)$_3$ coordination is similar to that reported for a manganese–chromium hydrosesquifulvalenyl complex.[7c]




**Scheme 1**

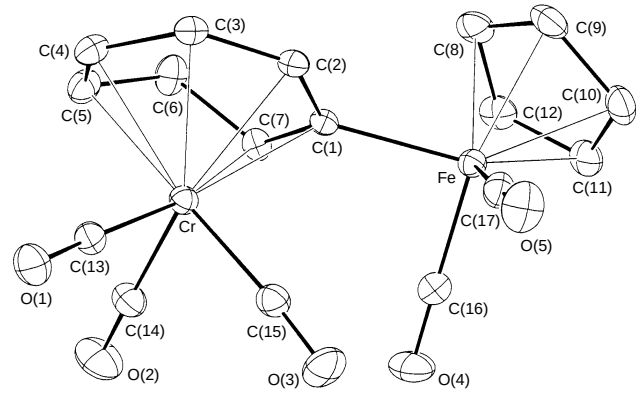



**Fig. 1** ORTEP drawing of **4**. Selected bond lengths (Å) and angles (°): Fe–C(1) 2.014(4), Fe–C(8) 2.139(6), Fe–C(9) 2.110(6), Fe–C(10) 2.117(4), Fe–C(11) 2.116(4), Fe–C(12) 2.125(5), Fe–C(16) 1.767(5), Fe–C(17) 1.761(5), Fe–C(17) 1.761(5), Cr–C(1) 2.272(3), Cr–C(2) 2.233(4), Cr–C(3) 2.220(5), Cr–C(4) 2.223(5), Cr–C(5) 2.386(6), Cr–C(7) 2.317(4), Cr–C(13) 1.847(4), Cr–C(14) 1.859(5), Cr–C(15) 1.848(5), O(1)–C(13) 1.151(5), O(2)–C(14) 1.138(7), O(3)–C(15) 1.139(7), O(4)–C(16) 1.132(6), O(5)–C(17) 1.140(7), C(1)–C(2) 1.446(5), C(1)–C(7) 1.397(7), C(2)–C(3) 1.406(5), C(3)–C(4) 1.449(7), C(4)–C(5) 1.385(7), C(5)–C(6) 1.514(5), C(6)–C(7) 1.516(7), C(8)–C(9) 1.434(9), C(8)–C(12) 1.434(7), C(9)–C(10) 1.458(8), C(10)–C(11) 1.415(8), C(11)–C(12) 1.425(8); C(1)–Fe–C(16) 90.8(2), C(1)–Fe–C(17) 94.3(2), C(16)–Fe–C(17) 95.7(2), Fe–C(1)–C(2) 119.3(3), Fe–C(1)–C(7) 118.2(2), Fe–C(16)–O(4) 178.5(4), Fe–C(17)–O(5) 176.2(4), Cr–C(13)–O(1) 177.4(4), Cr–C(14)–O(2) 178.5(3), Cr–C(15)–O(3) 175.7(4).

In **4** the 7-*exo*-hydrogen atom is easily accessible for hydride abstraction, and the carbene complex $[CpFe(CO)_2\mathbf{1}]BF_4$ **5** was formed quantitatively upon reaction with $(Ph_3C)BF_4$.† To the best of our knowledge, **5** represents the first heterobimetallic cycloheptatrienylidene complex. The carbene carbon resonance ($\delta$ 159.1) is observed at high field due to coordination of the $Cr(CO)_3$-unit to the μ-($\eta^1:\eta^7$-CHT) ligand. A direct relationship between the chemical shift of the cyclopentadienyl group and the degree of electron richness at the metal site has been suggested.[10] Consequently, the $^1$H cyclopentadienyl resonance of **5** is observed at substantially higher field ($\delta$ 5.14) than that of $[CpFe(CO)_2(\eta^1\text{-CHT})]PF_6$ ($\delta$ 5.50),[3a] thus indicating that $[(\eta^7\text{-CHT})Cr(CO)_3]$ **1** is a weaker π-acceptor than cycloheptatrienylidene and that the canonical form **B** contributes more strongly to the ground-state electronic structure of **5**.

Here, we have presented a new route for the preparation of isomerically pure mono- and bi-metallic cycloheptatrienyl complexes as suitable precursors for the synthesis of cycloheptatrienylidene complexes. In continuation of this program, we are currently studying the possibility to synthesize various bimetallic mono- and poly-carbene complexes by this method.

## Footnotes and References

* E-mail: tammm@chemie.fu-berlin.de

† *Spectroscopic data*: **3**: IR ($CH_2Cl_2$): $\bar{\nu}$ 2013, 1956 cm$^{-1}$ (CO). $^1$H NMR (400 MHz, $CDCl_3$): $\delta$ 6.70 (d, 1 H, 3-CH), 6.12 (dd, 1 H, 4-CH), 6.05 (dd, 1 H, 5-CH), 5.30 (td, 1 H, 6-CH), 5.14 (t, 1 H, 1-CH), 4.64 (s, 5 H, $C_5H_5$), 2.23 (dd, 2 H, 7-$CH_2$). $^{13}$C NMR (62.9 MHz, $CDCl_3$): $\delta$ 216.3 (Fe-CO), 146.2 (C-3), 133.0 (C-2), 126.7 (C-1), 124.8 (C-5), 122.8 (C-4), 120.7 (C-6), 85.8 ($C_5H_5$), 32.3 (C-7).

**4**: IR ($CH_2Cl_2$): $\bar{\nu}$ 2025, 1972, 1958, 1893, 1860 cm$^{-1}$ (CO). $^1$H NMR (400 MHz, $CDCl_3$): $\delta$ 6.08 (d, 1 H, 3-CH), 5.63 (dd, 1 H, 4-CH), 4.88 (s, 5 H, $C_5H_5$), 4.78 (dd, 1 H, 5-CH), 3.25 (dd, 1 H, 1-CH), 3.16 (m, 1 H, 6-CH), 2.90 (m, 1 H, 7-*endo*-CH), 1.46 (m, 1 H, 7-*exo*-CH). $^{13}$C NMR (62.9 MHz, $CD_3CN$): $\delta$ 235.1 (CrCO), 217.5, 216.7 (FeCO), 128.4 (C-2), 115.3, 100.7, 97.1 ($C_7$ ring: CH), 87.7 ($C_5H_5$), 64.6, 56.1 ($C_7$ ring: CH), 26.9 (C-7).

**5**: IR (MeCN): $\bar{\nu}$ 2052, 2025, 1999 cm$^{-1}$ (CO). $^1$H NMR (250 MHz, $CD_3CN$): $\delta$ 6.69 (d, 2 H, $C_7$ ring: CH), 6.35 (m, 2 H, $C_7$ ring: CH), 6.05 (m, 2 H, $C_7$ ring: CH), 5.14 (s, 5 H, $C_5H_5$). $^{13}$C NMR (62.9 MHz, $CD_3CN$): $\delta$ 225.2 (CrCO), 214.8 (FeCO), 159.1 (C-1), 119.0, 105.6, 104.0 ($C_7$ ring: CH), 89.0 ($C_5H_5$). UV–VIS (MeCN) $\lambda$/nm (log [$\varepsilon$/dm$^3$ mol$^{-1}$ cm$^{-1}$]) 322 (3.74), 348 (sh), 420 (sh).

‡ *Crystal data* for $C_{17}H_{12}CrFeO_5$ **4**: $M$ = 404.12, triclinic, space group $P\bar{1}$ (no. 2), $a$ = 7.859(2), $b$ = 9.320(2), $c$ = 12.403(4) Å, $\alpha$ = 99.94(4), $\beta$ = 102.55(4), $\gamma$ = 109.13(4)°, $U$ = 808.0(5) Å$^3$, $Z$ = 2, $D_c$ = 1.66 g cm$^{-3}$, Mo-K$\alpha$ radiation ($\lambda$ = 0.710 73 Å), $\mu$ = 16.44 cm$^{-1}$. 4652 unique data collected on a CAD-4 four-circle diffractometer at 20(3) °C in the range $4.8 < 2\theta < 60°$. Structure solution with direct methods, refined to $R$ = 0.053, $R_w$ = 0.066 for 3879 absorption corrected ($\psi$-scan) structure factors [$F_0 \geqslant 2\sigma(F_0)$] and 217 variables. CCDC 182/617.


1 For a review, see: R. P. Johnson, *Chem. Rev.*, 1989, **89**, 1111.
2 For recent reviews, see: S. Matzinger, T. Bally, E. V. Patterson and R. J. McMahon, *J. Am. Chem. Soc.*, 1996, **118**, 1535; M. W. Wong and C. Wentrup, *J. Org. Chem.*, 1996, **61**, 7022; P. R. Schreiner, W. L. Karney, P. von Ragué Schleyer, W. T. Borden, T. P. Hamilton and H. F. Schaefer III, *J. Org. Chem.*, 1996, **61**, 7030.
3 (*a*) N. T. Allison, Y. Kawada and W. M. Jones, *J. Am. Chem. Soc.*, 1978, **100**, 5224; (*b*) P. E. Riley, R. E. Davies, N. T. Allison and W. M. Jones, *J. Am. Chem. Soc.*, 1980, **102**, 2458; (*c*) F. J. Manganiello, M. D. Radcliffe and W. M. Jones, *J. Organomet. Chem.*, 1982, **228**, 273; (*d*) W. R. Winchester and W. M. Jones, *Organometallics*, 1985, **4**, 2228; (*e*) Z. Lu, W. M. Jones and W. R. Winchester, *Organometallics*, 1993, **12**, 1344; (*f*) Z. Lu, K. A. Abboud and W. M. Jones, *Organometallics*, 1993, **12**, 1471.
4 M. L. H. Green and D. K. P. Ng, *Chem. Rev.*, 1995, **95**, 439.
5 J. Klosin, X. Zheng and W. M. Jones, *Organometallics*, 1996, **15**, 3788.
6 R. W. Hoffmann, M. Lotze, M. Reiffen and K. Steinbach, *Liebigs Ann. Chem.*, 1981, 581.
7 (*a*) M. Tamm, A. Grzegorzewski and I. Brüdgam, *J. Organomet. Chem.*, 1996, **519**, 217; (*b*) M. Tamm, A. Grzegorzewski, T. Steiner, W. Werncke and T. Jentzsch, *Organometallics*, 1996, **15**, 4984; (*c*) M. Tamm, A. Grzegorzewski and T. Steiner, *Chem. Ber./Recueil*, 1997, **130**, 225; (*d*) M. Tamm, W. Werncke and T. Jentzsch, *Organometallics*, 1997, **16**, 1418.
8 Alternatively, **3** could also be isolated after $Pd^0$-catalyzed coupling between **2** and $[CpFe(CO)_2I]$, albeit in much lower yield. For palladium-catalyzed metal–carbon bond formation, see: P. Cianfriglia, V. Narducci, C. Lo Sterzo, E. Viola, G. Bocelli and T. A. Kodenkandath, *Organometallics*, 1996, **15**, 5220 and references therein.
9 See, for example: M. J. Heeg, *Acta Crystallogr., Sect. C*, 1988, **44**, 361; R. P. Hughes, R. T. Carl, S. J. Doig, R. C. Hemond, D. E. Samkoff, W. L. Smith, L. C. Stewart, R. E. Davis, K. D. Holland, P. Dickens and R. P. Kashyap, *Organometallics*, 1990, **9**, 2732, R. D. Adams and M. Huang, *Organometallics*, 1995, **14**, 2887.
10 E. S. Bolton, G. R. Knox and C. G. Robertson, *Chem. Commun.*, 1969, 664.


*Received in Cambridge, UK, 29th July 1997; 7/05502A*

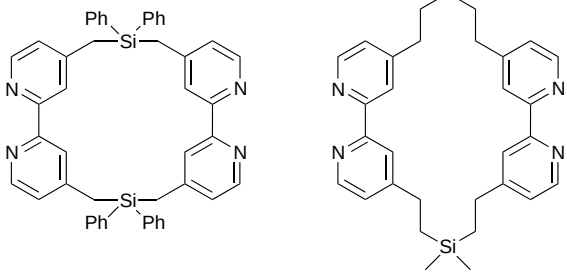
# Synthesis and structural analysis of a *exo*-ditopic macrocyclic ligand bearing 2,2′-bipyridine units interconnected by silane spacers and of its binuclear ruthenium complex

**Christian Kaes,[a] Mir Wais Hosseini,*[a] André De Cian[b] and Jean Fischer[b]**

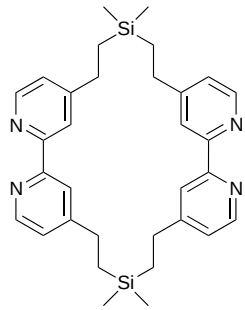
[a] *Université Louis Pasteur, Laboratoire de Chimie de Coordination Organique (UMR 7513 CNRS), F-67000 Strasbourg, France*
[b] *Université Louis Pasteur, Laboratoire de Cristallochimie et Chimie Structurale (UMR 7513 CNRS), F-67000 Strasbourg, France*

**The synthesis and structural analysis of a macrocyclic *exo*-ditopic ligand bearing two 2,2′-bipyridine units interconnected at the 4 and 4′ positions by two $-(CH_2)_2Si(CH_2)_2-$ spacers and of its acyclic analogue is achieved; for both compounds ruthenium homobinuclear complexes were prepared; for the complex obtained with the cyclic ligand, both diastereoisomers were separated and the structure of the *meso* form was elucidated by X-ray analysis.**

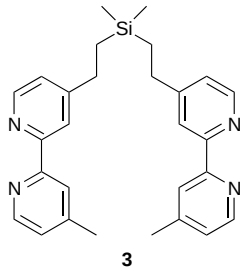
Whereas considerable effort has been invested in designing *endo*-di- and poly-topic ligands affording discrete *endo* complexes in which metal centres are located in close proximity, over the last few years much interest seems to be focused on *exo* ligands in which the coordination sites are outwardly oriented.[1] This increase in interest is related to the development of coordination polymers in which *exo*-ditopic ligands play the role of connectors between metallic centres. Although many examples of coordination polymers are available, most of the reported cases deal with bis-monodentate ligands.[2] Only few coordination polymers based on bridging of metallic centres by bis-tridentate ligands have been published so far.[3] Our approach to the formation of coordination polymers is based on the use of bis-bidentate ligands. 2,2′-Bipyridine derivatives are the most widely used chelates for metal binding.[4] We have previously reported *exo*-ditopic ligands based on two 2,2′-bipyridine units interconnected at the 4 and 4′ positions imposing the divergent orientation of the binding sites either by $(CH_2)_n$[5] or by $CH_2SiCH_2$ fragments (compound **1**).[6] In the latter case, probably owing to the presence of fragile benzylic positions, we were unable to prepare the ruthenium binuclear complexes.




**1**




**2**




**3**

In order to overcome this problem, ligand **2**, in which the two 2,2′-bipy chelates are interconnected at the 4 and 4′ positions by two $(CH_2)_2Si(CH_2)_2$ fragments was designed. Introduction of two silicon atoms within the macrocyclic framework has been previously reported for silacrown ether derivatives.[7] The silane moieties might be used either as connecting groups or as reactive centres allowing further structural modification. Prior to elaboration of coordination polymers using ligand **2**, a detailed structural analysis of discrete binuclear complexes based on such a ligand is needed. Here, we present the synthesis of both the free ligand **2** and its acyclic analogue **3** and of their homobinuclear ruthenium(II) complexes **2**-$Ru_2$ and **3**-$Ru_2$. For the **2**-$Ru_2$ complex, we also report a solid state structural analysis. The synthesis of ligand **2** was achieved by reacting the dilithium derivative of 4,4′-dimethyl-2,2′-bipyridine,[8] prepared by treating at 0 °C the latter with lithium diisopropyl amide (LDA) in dry THF, with bis(chloromethyl)dimethylsilane in dry THF at 25 °C (slow addition, 4–5 h and further stirring at room temp. overnight). To the blue–violet solution thus obtained a few drops of MeOH were added to quench the excess LDA before it was evaporated to dryness. In order to separate polymeric species, the residue was taken up in $CHCl_3$ and filtered. The solid was further washed with $CHCl_3$. The filtrate and washes were combined and evaporated to dryness affording a mixture of ten different products. Both compound **2** and **3** were obtained as a mixture after chromatography [$SiO_2$, $CH_2Cl_2$–MeOH (0–3%)]. Their separation (3% yield for compound **2**) appeared to be only feasible upon crystallisation from a hexane–$CH_2Cl_2$ mixture. However, compound **3** was also prepared in 50% yield by treating the monolithium derivative of 4,4′-dimethyl-2,2′-bipyridine with bis(chloromethyl)dimethylsilane in dry THF at 25 °C.

The X-ray analysis (Fig. 1) of the free ligand **2** revealed the following features:† (*i*) the two bipy units, both in *transoid* conformation, were almost parallel to each other leading thus to a cyclophane type situation (box dimension of 2.9 × 11.6 Å); (*ii*) the coordination geometry around both silicon atoms was tetrahedral with an average Si–C distance of 1.86 Å and C–Si–C angle of 109.5°; (*iii*) on each silane moiety, both methyl groups were pointing towards the exterior of the macrocycle.

The homobinuclear complexes $(\mathbf{2}\text{-}Ru_2)^{4+}4PF_6^-$ and $(\mathbf{3}\text{-}Ru_2)^{4+}4PF_6^-$ were obtained upon treatment under reflux of **2** or **3** with $Ru(bipy)_2Cl_2\cdot 2H_2O$ in degassed EtOH followed by addition of $NH_4PF_6$ which caused the precipitation of both

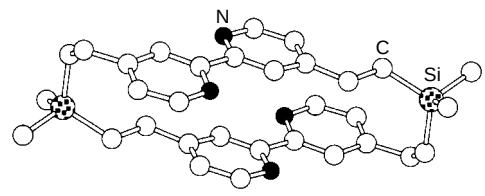
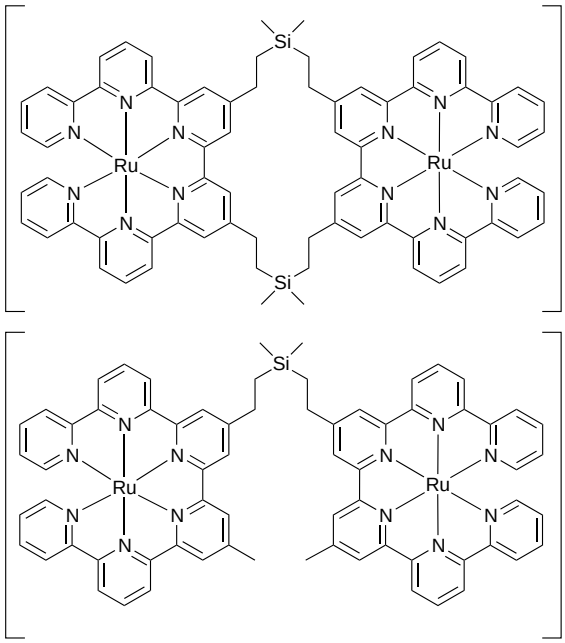



**Fig. 1** X-Ray crystal structure of ligand **2**; H atoms are not shown for clarity (for distances and angles see text)







stereoisomeric (Δ,Δ; Λ,Λ) and *meso* (Δ, Λ) complexes in a 1 : 1 mixture. The latter was further recrystallised from acetone–ether. For (**2**-$Ru_2$)$^{4+}$4$PF_6^-$, the 1 : 1 ratio of stereoisomers was deduced from the $^1$H NMR spectrum (300 MHz, $CD_3CN$, 25 °C) of the mixture which revealed that among the signals present, three singlets corresponding to MeSi fragments were the most differentiated. The diastereomeric separation of the mixture was achieved by crystallisation of the *meso* form by slow diffusion of benzene into a nitromethane solution. The assignment of singlets corresponding to MeSi groups was based on the $^1$H NMR study of both the pure *meso* form which showed two singlets at $\delta$ 0.02 and 0.1 and of the remaining mixture of enantiomers which revealed only one singlet at $\delta$ 0.06.

In the solid state (Fig. 2), the structure of the *meso* form of (**2**-$Ru_2$)$^{4+}$4$PF_6^-$ was studied by X-ray diffraction† which revealed the following features: (*i*) in addition to (**2**-$Ru_2$)$^{4+}$4$PF_6^-$ complex, six MeCN and two MeOH molecules are present in the solid state but without any interaction with the metallic centres; (*ii*) in marked contrast with the free ligand **2**, both bipy units in the complex adopt a *cisoid* conformation allowing, as expected, the chelation of $Ru^{II}$ cations; (*iii*) the cationic moiety of the complex possesses a centre of symmetry; (*iv*) the coordination geometry around Si atoms was tetrahedral with an average Si–C distance and C–Si–C angle of 1.86 Å and 109.4° respectively; (*v*) owing to the conformation of the $(CH_2)_2Si(CH_2)_2$ fragments (CCCSi, and CSiCC dihedral angles of 171.0 and −87.2 °, respectively), in marked contrast with the free ligand adopting a cyclophane type conformation, the two bipy units oppositly oriented are almost parallel but not coplanar; (*vi*) both Me groups of both silane moieties are, as in the case of the free ligand, outwardly oriented; (*vii*) for both $Ru^{II}$ centres, the coordination sphere is composed of six nitrogen atoms amongst which four are belonging to the two auxiliary bipy units and the remaining two are part of the macrocyclic ligand **2**. The coordination geometry around each $Ru^{II}$ was almost octahedral with an average Ru–N distance of 2.05 Å; (*viii*) the two $Ru^{II}$ centres were separated by 13.58 Å; (*ix*) quite interestingly and unexpectedly, among the four $PF_6^-$ anion present, two of them were localised below and above the mean plane of the macrocyclic core and pointing almost towards the centre of the macrocycle.

It is worth noting that a systematic Cambridge Database search revealed that only three homobinuclear ruthenium complexes bearing three bipyridine type ligands have been structurally characterised (KIKHOB,[9] ZADLAR,[5a] ZELCIC[1d]). Preparation of linear coordination polymers based on compound **2** is under current investigation.

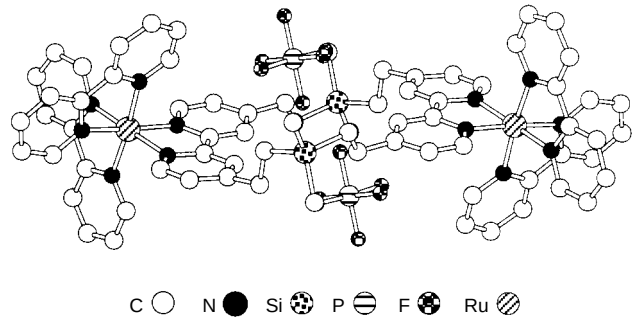



**Fig. 2** Crystal X-ray structure of the *meso* form of the ruthenium binuclear complex obtained with ligand **2**; solvent molecules as well as H atoms are not shown for clarity (for distances and angles see text)

We thank the CNRS and the Institut Universitaire de France (IUF) for financial support. C. K. thanks the Ministry of Education of Luxembourg for a scholarship.

## Footnotes and References

* E-mail: hosseini@chimie.u.strasb.fr

† *Crystallographic data*: **2** (slightly yellow crystals, 294 K): $C_{32}H_{40}N_4Si_2$, $M$ = 536.87, monoclinic, space group $P2_1/c$, $a$ = 9.408(2), $b$ = 12.506(2), $c$ = 12.651(3) Å, $\beta$ = 90.31(2)°, $U$ = 1488.5 Å$^3$, $Z$ = 2, $D_c$ = 1.20 g cm$^{-3}$, Mo-K$\alpha$ graphite-monochromated radiation ($\lambda$ = 0.7103 Å), 17.36 data with $I > 3\sigma(I)$, $R$ = 0.047, $R_w$ = 0.068.

(**2**-$Ru_2$)$^{4+}$4$PF_6^-$ (orange crystals, −173 K): $C_{72}H_{72}N_{12}Si_2Ru_2$·4$PF_6$·$CH_3CN$·2$CH_3OH$, $M$ = 2254.03, triclinic, space group $P\bar{1}$, $a$ = 12.1109(8), $b$ = 13.486(1), $c$ = 18.456(2) Å, $\alpha$ = 103.678(7), $\beta$ = 95.143(6), $\gamma$ = 111.723(7)°, $U$ = 2667(1) Å$^3$, $Z$ = 1, $D_c$ = 1.40 g cm$^{-3}$, Mo-K$\alpha$ graphite-monochromated radiation ($\lambda$ = 0.7103 Å), 7379 data with $I > 3\sigma(I)$, $R$ = 0.049, $R_w$ = 0.080. CCDC 182/634.

1 (*a*) O. Kocian, R. J. Mortimer and P. D. Beer, *Tetrahedron Lett.*, 1990, **31**, 5069; (*b*) X. Delaigue, J. McB. Harrowfield, M. W. Hosseini, A. De Cian, J. Fischer and N. Kyritsakas, *J. Chem. Soc., Chem. Commun.*, 1994, 1579; (*c*) X. Delaigue, M. W. Hosseini, A. De Cian, M. Kyritsakas and J. Fischer, *J. Chem. Soc., Chem. Commun.*, 1995, 609; (*d*) J. Bolger, A. Gourdon, E. Ishow and J.-P. Launay, *J. Chem. Soc., Chem. Commun.*, 1995, 1799; (*e*) B. Whittle, N. S. Everest, C. Howard and M. D. Ward, *Inorg. Chem.*, 1995, **34**, 2025; (*f*) P. D. Beer and F. Szemmes, *J. Chem. Soc., Chem. Commun.*, 1995, 2245; (*g*) G. Mislin, E. Graf and M. W. Hosseini, *Tetrahedron Lett.*, 1996, **37**, 4503; (*h*) A. Harriman and R. Ziessel, *Chem. Commun.*, 1996, 1707; (*i*) A. Rudi, D. Gut, F. Lellouche and M. Kol, *Chem. Commun.*, 1997, 17; (*j*) F. Barigelletti, L. Flamigni, J.-P. Collin and J.-P. Sauvage, *Chem. Commun.*, 1997, 333; (*k*) M. Schmittel and A. Ganz, *Chem. Commun.*, 1997, 999.

2 R. Robson, in *Comprehensive Supramolecular Chemistry*, ed. D. D. Macnicol, F. Toda and R. Bishop, Pergamon, New York, 1996, p. 733.

3 E. C. Constable and A. M. W. Cargill Thompson, *J. Chem. Soc., Dalton Trans.*, 1992, 3467; M. Ferigo, P. Bonhôte, W. Marty and H. Stoeckli-Evans, *J. Chem. Soc., Dalton Trans.*, 1994, 1549; E. C. Constable, A. J. Edwards, D. Phillips and P. R. Raithby, *Supramol. Chem.*, 1995, **5**, 93.

4 V. Balzani, A. Juris, M. Venturi, S. Campagna and S. Serroni, *Chem. Rev.*, 1996, **96**, 759.

5 (*a*) C. Kaes, M. W. Hosseini, R. Ruppert, A. De Cian and J. Fischer, *J. Chem. Soc., Chem. Commun.*, 1995, 1445; (*b*) C. Kaes, M. W. Hosseini, A. De Cian and J. Fischer, *Tetrahedron Lett.*, 1997, **38**, 3901; (*c*) C. Kaes, M. W. Hosseini, A. De Cian and J. Fischer, *Tetrahedron Lett.*, 1997, **38**, 4389.

6 C. Kaes, M. W. Hosseini, R. Rupert, A. De Cian and J. Fischer, *Tetrahedron Lett.*, 1994, **35**, 7233.

7 G. Oddon and M. W. Hosseini, *Tetrahedron Lett.*, 1993, **34**, 7413.

8 W. H. F. Sasse, *Org. Synth.*, 1966, **46**, 5.

9 R. Hage, J. G. Haasnoot, H. A. Nieuwenhuis, J. Reedijk, D. J. A. De Ridder and J. G. Vos, *J. Am. Chem. Soc.*, 1990, **112**, 9245.

*Received in Basel, Switzerland, 4th August 1997; 7/05664H*

# Self-assembly of a symmetric tetracopper box-grid with guest trapping in the solid state

**Paul N. W. Baxter,[a] Jean-Marie Lehn,*[a] Boris O. Kneisel[b] and Dieter Fenske[b]**

[a] *Laboratoire de Chimie Supramoléculaire, Institut Le Bel, Université Louis Pasteur, 4 rue Blaise Pascal, 67000, Strasbourg, France*

[b] *Institut Für Anorganische Chemie der Universität, Engesserstrasse, D-76128 Karlsruhe, Germany*

**Reaction of ligand 2 with Cu$^{I}$ ions leads to the self-assembly of the distorted [2 × 2] grid complex 1 of box-like shape, featuring a well defined cavity and trapping of guest molecules.**

The controlled generation of molecular entities that contain geometrically precisely defined arrangements of metal ions is of considerable current interest within the fields of supramolecular chemistry and materials science.[1] The presence of metal ions in such coordination arrays may result in the development of many varied physicochemical properties such as electrochemical, optical, magnetic, mechanical and catalytic activity for example.

Metal ion-directed self-assembly currently provides a very efficient method of access to coordination arrays of predetermined nuclearity and spatial composition[2] such as helicates,[3] pseudorotaxane racks,[4] grids,[5,6] rings[7] and cages.[8] The inorganic grids represent a particularly intriguing class of coordination arrays which may potentially function as components of systems such as molecular memory devices, in which information might be stored in the form of electron holes or occupancies at specific sites or areas within the architecture.

With ligands presenting a greater spatial separation between the metal ion binding sites than previously reported,[5,6] a cavity of controlled dimensions would be opened up within the grid structure. Such a cavity may exhibit selective guest inclusion, which if combined with redox activity of the grid itself, may result in a class of electrochemical guest sensors. Towards this goal, the linear ditopic tetradentate ligand **2** was constructed. A grid composed of four **2** ligands and four metal ions of tetrahedral coordination geometry should possess an internal box-shaped cavity lined by aromatic rings, of suitable dimensions for the inclusion of small molecules.

We herein report the structural characterisation and some physicochemical features of the self-assembled symmetric [2 × 2]G tetracopper grid (**1**) which is generated from **2**† and copper(I) ions; it is electrochemically active and exhibits guest inclusion in the solid state.

The tetracopper grid **1** forms in almost quantitative yield‡ in nitromethane solution upon admixture of a 1 : 1 stoichiometric ratio of the linear ligand **2** and $[Cu(MeCN)_4PF_6$. The structure of **1** both in solution and in the solid state has been established on the basis of $^1$H and $^{13}$C NMR, FAB and ES mass spectroscopy, microanalysis and X-ray crystallography.

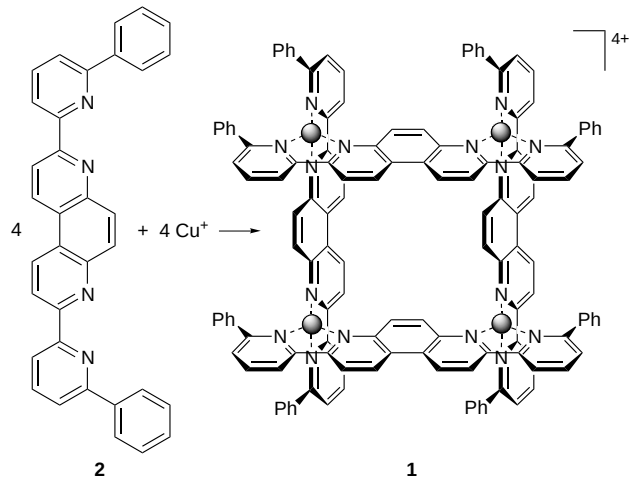
The $^1$H NMR spectrum‡ of the above reaction product in nitromethane solution consisted of a very simple pattern of peaks corresponding to ligand **2** in a single magnetic and chemical environment, and suggestive of the formation of a highly symmetrical species. The $^{13}$C spectrum also consisted of the expected fifteen peaks.

FAB and ES mass spectroscopy were found to be especially informative in identifying the above reaction product as **1**. The highest *m*/*z* peaks observed in the FAB mass spectrum, were assignable to the tetracopper grid **1** with succesive loss of $PF_6^-$ counter ions, *i.e.* 2635.2 $\{[Cu_4(\mathbf{2})_4](PF_6)_3\}^+$, 2490.2 $\{[Cu_4(\mathbf{2})_4](PF_6)_2\}^{\cdot+}$ and 2345.3 $\{[Cu_4(\mathbf{2})_4]PF_6\}^{\cdot\cdot+}$. Peaks at lower *m*/*z* ratios corresponded to mono- and di-nuclear species which arise through fragmentation/dissociation of **1**. The EMS peaks (recorded at $10^{-4}$ in $MeNO_2$) of the reaction product at *m*/*z* 1245.3, 781.9 and 550.3 were assignable to the species $\{[Cu_4(\mathbf{2})_4](PF_6)_2\}^{2+}$, $\{[Cu_4(\mathbf{2})_4]PF_6\}^{3+}$ and $[Cu_4(\mathbf{2})_4]^{4+}$, respectively. Upon dilution to $10^{-6}$ M, the peaks corresponding to counter ion loss from **1** decrease in intensity and peaks which arise from the dissociation of **1** increase in height showing that **1** undergoes dissociation at high dilution.

An X-ray crystal structural analysis finally provided unambiguous evidence that the identity of the above reaction product was that of **1**.§ The cation is indeed a tetranuclear distorted square grid composed of four copper(I) ions and four **2** ligands, with overall external dimensions (including van der Waals radii) of 22.5 × 15.4 × 12.5 Å (depth). The ligands are divided into two parallel pairs, one of which lies above and the other below the mean plane through the four copper ions. The grid is not a square but a rhombus (inner angles, *i.e.* angles between the mean planes of **2** of 74.5 and 105.5°) owing to deviation from perfect tetrahedral coordination geometry about each metal centre, with the ligands forming the sides and the copper(I) ions (7.7 Å apart) lying at the corners. The Cu–N bond lengths, 2.055–2.002 Å and N–Cu–N angles are unexceptional. The complex cation possesses an internal box-shaped void of area 4.2 × 3.8 Å and 12.5 Å depth.[9] Six guests, four benzenes and two nitromethane molecules are trapped in the grooves defined by the parallel pairs of the ligands, with a benzene lying in the mouth of the cavity on each side of the cation (Fig. 1).

Cyclic voltammetric measurements showed **1** to be electrochemically active, giving a single reversible oxidation wave at 0.44 V, and three closely spaced reversible reduction waves at −1.56, −1.65 and −1.79 V (*vs.* $Fc/Fc^+$).¶

The [2 × 2]G symmetric tetracopper grid **1** forms by the self-assembly of eight articles, four metal ions and four ligand components. It exhibits multiple guest inclusion in its box-




**Scheme 1** Self-assembly of the inorganic [2 × 2] box-grid **1**

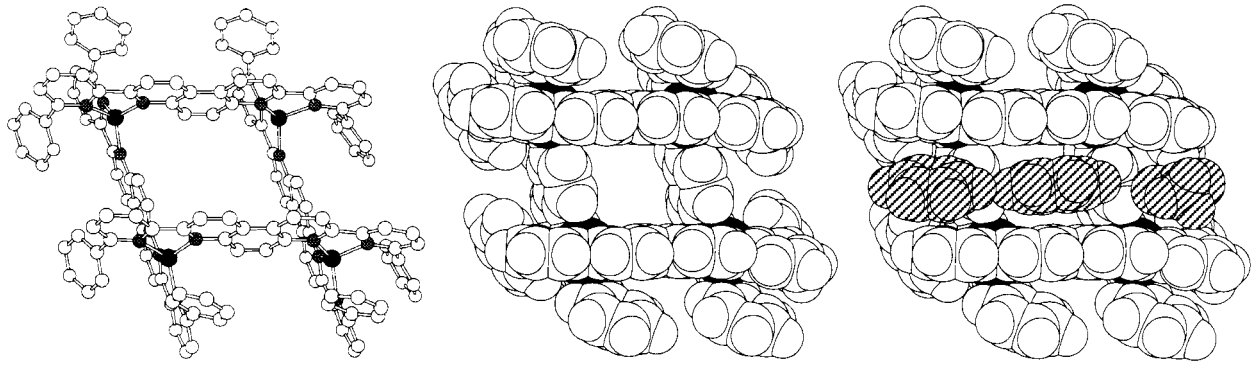


**Fig. 1** Crystal structure of the grid-type complex **1**; ball and stick representation (left); space-filling representation (centre); space-filling representation of **1** with guests in upper groove (right); guests in lower groove omitted for clarity

shaped cavity in the solid state. The presence of the phenyl rings on the ligands appears to be essential for its formation. If the phenyl rings of **2** are replaced by H or Me groups, then 1 : 1 mixtures with $[Cu(MeCN)_4]PF_6$ under identical conditions to the formation of **1** yield oligomeric mixtures and insoluble coordination polymers as the only products.

In addition to their possible use as components of molecular electronics devices, inorganic grids capable of trapping guest species may be of potential interest for chemical catalysis and selective guest sensing. They could therefore find various applications in materials science and nanotechnology.

We thank Annick Dupont-Gervais, Emmanuelle Leize and Alain Van Dorsselaer for the ES Mass spectroscopic and Marcel Mayor for the electrochemical measurements.

## Footnotes and References

* E-mail: lehu@chimie.u-strasbg.fr

† Ligand **2** was prepared from 2-trimethylstannyl,6-phenylpyridine and 3,8-dibromo-4,7-phenanthroline *via* a Stille coupling protocol.

‡ *Experimental*: to a mixture of 0.030 g ($6.17 \times 10^{-5}$ mol) of **2** and 0.023 g ($6.17 \times 10^{-5}$ mol) of $[Cu(MeCN)_4]PF_6$ under an atmosphere of argon was added 4 ml of $MeNO_2$ *via* syringe, and the dark-brown solution stirred at ambient temperature for 48 h. All solvent was then removed under vacuum and the remaining solid purified by gel permeation chromatography on a column of SX-1 biobeads using nitrobenzene as eluent. The product was collected in one fraction, reduced in volume to 3 ml under vacuum at 70 °C and precipitated by the addition of an excess of toluene. The solid was collected by filtration under vacuum, washed with toluene, recrystallised twice from $MeNO_2$–toluene and finally dried under vacuum at 90 °C/2 × $10^{-6}$ mmHg. The above work-up yielded 0.039 g (91%) of the product complex **1** $(PF_6)_4$ as a dark-brown microcrystalline solid. $^1$H NMR spectral assignments were made on the basis of $^1$H–$^1$H COSY and ROESY measurements.

**1** $(PF_6)_4$: $^1$H NMR ($CD_3NO_3$, 500 MHz, 25 °C), $\delta$ 9.39 [d, 8 H, H(**2**-1′,10), $J_{1'2'/10',9'}$ 8.9 Hz], 8.59 [d, 8 H, H (**2**-2′,9′), $J_{2'1'/9'10'}$ 9.0 Hz], 8.31 [d, 8 H, H (**2**- 3,3″), $J_{3,4/3'',4}$ 8.0 Hz], 8.10 [t, 16 H, H (**2**-4,4″), $J_{4,3/4,5;\ 4'',3''/4'',5''}$ 7.8 Hz], 7.70 [s, 8 H, H (**2**-5′,6″)], 7.63 [d, 8 H, H (**2**-5,5″), $J_{5,4/5'',4''}$ 7.5 Hz], 7.06 [d, 16 H, H (**2**-*ortho*), $J_{0,m}$ 7.3 Hz], 6.99 [t, 8 H, H (**2**-*para*), $J_{p,m}$ 7.4 Hz], 6.60 [t, 16 H, H[(**2**-*meta*), $J_{m,o/m,p}$ 7.5 Hz]. $^{13}$C NMR ($CD_3NO_3$, 75 MHz, 25 °C), δ 159.92, 154.72, 153.04, 145.75, 140.50, 140.15, 134.93, 133.39, 130.37, 128.72, 128.43, 127.60, 127.31, 123.23, 122.15. FABMS, *m*/z (rel. intensity %); 2635.2 (4.3) $\{[Cu_4(\mathbf{2})_4](PF_6)_3\}^+$, 2490.2 (2.1) $\{[Cu_4(\mathbf{2})_4](PF_6)_2\}^{\cdot+}$, 2345.3 (0.3) $\{[Cu_4(\mathbf{2})_4]PF_6\}^{\cdot+}$, 1245.1 (6.6) $\{[Cu_2(\mathbf{2})_2]PF_6^{-\cdot+}$, 1173.1 (2.3) $\{[Cu_4(\mathbf{2})_4]PF_6\}^{\cdot 2+}$, 1035.9 (7.6) $\{Cu(\mathbf{2}_2\}^+$, 549.5 (100) $\{Cu(\mathbf{2})\}^+$. ESMS ($10^{-4}$ M $MeNO_2$), *m*/z (rel. intensity %); 1245.3 (3.2) $\{[Cu_4(\mathbf{2})_4](PF_6)_2\}^{2+}$, 944.1 (19.0) $\{[Cu_4(\mathbf{2})_5]PF_6\}^{3+}$, 781.9 (59.7) $\{[Cu_4(\mathbf{2})_4]PF_6\}^{3+}$, 671.9 (39.6) $[Cu_4(\mathbf{2})_5]^{4+}$, 550.3 (100) $[Cu_4(\mathbf{2})_4]^{4+}$. UV–VIS ($CH_2Cl_2$), $\lambda$/nm ($\varepsilon$/dm$^3$ mol$^{-1}$ cm$^{-1}$); 593 (6391), 482 (14 164), 341 (118 331), 259 (83 672). Microanal. (Calc. for $C_{136}H_{88}Cu_4F_{24}N_{16}P_4$ C, 58.75; H, 3.19; N, 8.06. Found: C, 58.83; H, 3.41; N, 8.10%.

§ *Crystal data* for $\{[Cu_4(\mathbf{2})_4](PF_6)_4 \cdot 10C_6H_6 \cdot 4CH_3NO_2\}$: Brown blocks grown by benzene diffusion into nitromethane solution. Crystal size = 0.1 × 0.1 × 0.2 mm. STOE.IPDS diffractometer (−80 °C), graphite-monochromated Mo-K$\alpha$ radiation ($\lambda$ = 0.710 73 Å), monoclinic, space group *C*2/*c*, *a* = 24.782(5), *b* = 26.645(5), *c* = 29.101(6) Å, $\beta$ = 110.02(3)°, *U* = 18055(6) Å$^3$, *Z* = 8, $D_c$ = 1.400 Mg m$^{-3}$, $\mu$ = 0.590 mm$^{-1}$, *F*(000) = 7824, *M* = 1902.76, $2\theta_{max}$ = 52°. Primary structure solution by direct methods (SHELXS-92).[10] Anisotropic refinement for all non-hydrogen atoms (SHELXL-93).[11] The structure was refined against $F^2$ (full-matrix lest squares). The final weighting scheme was $w^{-1} = \sigma^2(F_o^2) + (0.0776P)^2 + 12.3113P$, with $P = (F_o^2 + 2F_c^2)/3$, $R_1$ = 0.0503 ($F > 4\sigma F$) and $wR_2$ = 0.1487 (all data), GOF on $F^2$ = *S* = 1.041, max. min. residual density: +0.458, −0.401 e Å$^{-3}$, ($R_1 = \Sigma \mid |F_o| - |F_c| \mid / \Sigma |F_o|$, $wR_2 = [\Sigma w(F_o^2 - F_c^2)^2 / \Sigma wF_o^4]^{1/2}$, GOF = $S = \{\Sigma[w(F_o^2 - F_c^2)^2]/(n - p)\}^{1/2}$, where *n* = no. of reflections and *p* = no. of parameters). CCDC 182/649.

¶ Electrochemical measurements were performed under argon in $CH_2Cl_2$ with 0.1 M $[NBu^n_4]ClO_4$ (oxidation) and $[NBU^n_4]PF_6$ (reduction) as the supporting electrolytes.

1 J.-M. Lehn, *Supramolecular Chemistry: Concepts and Perspectives*, VCH, Weinheim, 1995; D. Philp and J. F. Stoddart, *Angew. Chem.*, 1996, **108**, 1242; *Angew. Chem., Int. Ed. Engl.*, 1996, **35**, 1154.

2 (*a*) P. N. W. Baxter, in *Comprehensive Supramolecular Chemistry*, ed. J. L. Atwood, J. E. D. Davies, D. D. MacNicol, F. Vögtle and J.-M. Lehn. Pergamon, Oxford, 1996; vol. 9, ch. 5, pp. 165–211; (*b*) M. Fujita, *ibid.*, ch. 7, pp. 253–282.

3 E. C. Constable, in *Comprehensive Supramolecular Chemistry*, ed. J. L. Atwood, J. E. D. Davies, D. D. MacNicol, F. Vögtle and J.-M. Lehn. Pergamon, Oxford, 1996; vol. 9, ch. 6, pp. 213–252; K. T. Potts, M. Keshavarz-K, F. S. Tham, H. D. Abruña and C. Arana, *Inorg. Chem.*, 1993, **32**, 4436 and references therein.

4 H. Sleiman, P. N. W. Baxter, J.-M. Lehn and K. Rissanen, *J. Chem. Soc., Chem. Commun.*, 1995, 715.

5 M.-T. Youinou, N. Rahmouni, J. Fischer and J. A. Osborn, *Angew. Chem., Int. Ed. Engl.*, 1992, **31**, 733.

6 P. N. W. Baxter, J.-M. Lehn, J. Fischer and M.-T. Youinou, *Angew. Chem., Int. Ed. Engl.*, 1994, **33**, 2284.

7 B. Hasenknopf, J.-M. Lehn, B. O. Kneisel, G. Baum and D. Fenske, *Angew. Chem., Int. Ed. Engl.*, 1996, **35**, 1838; D. P. Funeriu, J.-M. Lehn, G. Baum and D. Fenske, *Chem. Eur. J.*, 1997, **3**, 99.

8 P. N. W. Baxter, J.-M. Lehn, A. De Cian and J. Fischer, *Angew. Chem., Int. Ed. Engl.*, 1993, **32**, 69; M. Fujita, S. Nagao and K. Ogura, *J. Am. Chem. Soc.*, 1995, **117**, 1649.

9 For other approaches to the generation of inorganic box-like structures, see: ref. 2(*b*); M. Fujita, *J. Synth. Org. Chem. Jpn.*, 1996, **54**, 953; H. Rauter, I. Mutikainen, M. Blomberg, C. J. L. Lock, P. Amo-Ochoa, E. Freisinger, L. Randaccio, E. Zangrando, E. Chiarparin and B. Lippert, *Angew. Chem., Int. Ed. Engl.*, 1997, **36**, 1296; P. J. Stang and B. Olenyuk, *Angew. Chem., Int. Ed. Engl.*, 1996, **35**, 732, and references therein; M. J. Hannon, C. L. Painting and W. Errington, *Chem. Commun.*, 1997, 307.

10 G. M. Sheldrick, *Acta Crystallogr., Sect. A*, 1990, **46**, 467.

11 G. M. Sheldrick, SHELXL-93, program for crystal structure refinement, University of Göttingen, 1993.

*Received in Cambridge, UK, 24th September 1997; 7/06919G*

# Synthesis of tetrasubstituted derivatives of $[Fe_3(CO)_{12}]$

**Xuetai Chen and Brian E. Mann**

*Department of Chemistry, The University of Sheffield, Sheffield, UK S3 7HF*

**The treatment of $[Fe_3(CO)_{10}L^1L^2]$ [$L^1$, $L^2$ = CO, $P(OMe)_3$, $P(OCH_2)_3CMe$] with $CNBu^t$ in the presence of $Me_3NO$ yields the tetrasubstituted derivatives, $[Fe_3(CO)_8(CNBu^t)_4]$, $[Fe_3(CO)_8(CNBu^t)_3\{P(OMe)_3\}]$, $[Fe_3(CO)_8(CNBu^t)_3\{P(OCH_2)_3CMe\}]$, $[Fe_3(CO)_8(CNBu^t)_2\{P(OCH_2)_3CMe\}_2]$, $[Fe_3(CO)_8(CNBu^t)_2\{P(OCH_2)_3CMe\}\{P(OMe)_3\}]$ and $[Fe_3(CO)_8(CNBu^t)_2\{P(OMe)_3\}_2]$; the compounds were characterised by analysis, mass spectrometry, IR, and (in part) $^1H$ and $^{31}P$ NMR spectroscopy.**

Highly substituted derivatives of $[Ru_3(CO)_{12}]$ and $[Os_3(CO)_{12}]$ are well known, with crystal structures having been determined for $[Os_3(CO)_8\{P(OMe)_3\}_2(\mu\text{-dppm})]$,[1] $[Os_3(CO)_8\{P(OMe)_3\}_2(PPh_3)_2]$,[1] $[Ru_3(\mu\text{-}CO)_2(CO)_6\{PPh(OMe)_2\}_4]$,[2] $[Ru_3(CO)_8[\{(MeO)_2P\}_2NEt]_2]$,[3] $[Ru_3(CO)_8\{AsMe_2C{=}C(AsMe_2)CF_2CF_2\}_2]$,[4] $[Ru_3(CO)_8\{P(OPh)_3\}_4]$,[5] $[Ru_3(CO)_8\{P(OMe)_3\}_4]$,[5] $[Ru_3(\mu\text{-}CO)_3(CO)_5\{P(OEt)_3\}_4]$,[5] and $[Ru_3(CO)_{10}(dpam)]$.[6] In addition, hexasubstituted derivatives are known *i.e.* $[Ru_3(CO)_6(dppm)_3]$[7,8] and $[Os_3(CO)_6\{P(OMe)_3\}_6]$.[9]

In contrast, substitution of carbonyls in $[Fe_3(CO)_{12}]$ is only known as far as the tris derivatives, with crystal structures having been determined for $[Fe_3(CO)_9(PMe_2Ph)_3]$,[10] $[Fe_3(CO)_9\{P(OMe)_3\}_3]$,[11] and $[Fe_3(CO)_9\{P(OPr^i)_3\}_3]$.[11] $[Fe_3(CO)_{12}]$ readily fragments on substitution to give mainly monomeric compounds.[12] Recently it has been shown that substitution of $[Fe_3(CO)_{12}]$ proceeds smoothly when $Me_3NO$ is used as the reagent.[13] We have been using this procedure to synthesise a range of derivatives of $[Fe_3(CO)_{12}]$. When $[Fe_3(CO)_{10}\{P(OMe)_3\}_2]$ is reacted with $CNBu^t$ in $CH_2Cl_2$ in the presence of $Me_3NO$, in addition to the expected product, $[Fe_3(CNBu^t)(CO)_9\{P(OMe)_3\}_2]$, a second green band due to $[Fe_3(CNBu^t)_2(CO)_8\{P(OMe)_3\}_2]$ was observed on the silica gel column. The production of this second derivative was optimised by using *ca*. 10 mol of $CNBu^t$ and *ca*. 20 mol of $Me_3NO$ per mol of $[Fe_3(CO)_{10}\{P(OMe)_3\}_2]$ in $CH_2Cl_2$ and allowing the reaction to procede for 2–3 d at room temp. under nitrogen. Subsequent chromatography on silica gel using $CH_2Cl_2$ as eluent yielded the product, $[Fe_3(CNBu^t)_2(CO)_8\{P(OMe)_3\}_2]$ in 5% yield. The compound was characterised by $^1H$ and $^{31}P$ NMR and IR spectroscopy, mass spectrometry and elemental analysis.[14] Attempts to grow suitable crystals for X-ray diffraction have failed.

The same procedure was used to synthesise $[Fe_3(CNBu^t)_2(CO)_8\{P(OCH_2)_3CMe\}_2]$, $[Fe_3(CNBu^t)_2(CO)_8\{P(OMe)_3\}\{P(OCH_2)_3CMe\}]$, $[Fe_3(CNBu^t)_3(CO)_8\{P(OMe)_3\}]$, $[Fe_3(CNBu^t)_3(CO)_8\{P(OCH_2)_3CMe\}]$ and $[Fe_3(CNBu^t)_4(CO)_8]$ except in that an alumina column was used for $[Fe_3(CNBu^t)_3\{P(OMe)_3\}]$ and $[Fe_3(CNBu^t)_4(CO)_8]$. Yields are low varying between 5 and 15%, with the highest yield being obtained for $[Fe_3(CNBu^t)_3(CO)_8\{P(OCH_2)_3CMe\}]$. The compounds decompose quite readily in solution and this prevented the observation of $^{13}C$ NMR spectra. All the compounds were characterized using elemental analysis, IR spectroscopy and mass spectrometry.† In solution they slowly decompose to give significant concentrations of the monomeric derivatives. This coupled with the exchange between stereoisomers made it difficult to obtain reliable NMR spectra.

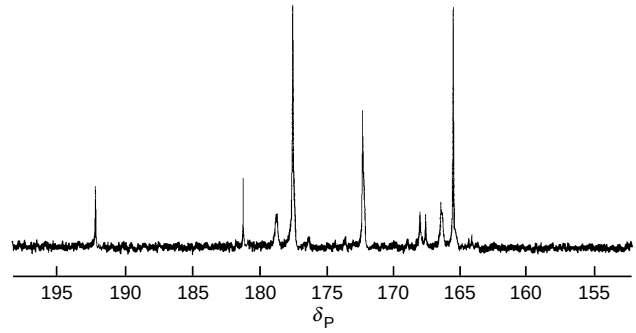
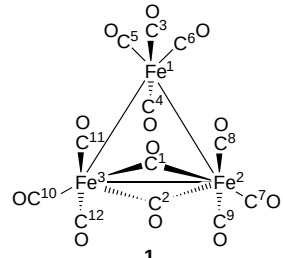


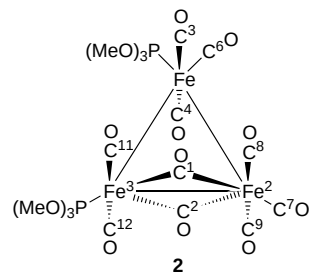

**Fig. 1** The 162 MHz $^{31}P$ NMR spectrum of $[Fe_3(CNBu^t)_2(CO)_8\{P(OMe)_3\}_2]$ in $[^2H_8]$toluene at 223 K. Note that the signals at $\delta$ 181 and 192 are impurities.

In general, the $^{31}P$ NMR spectra were the most informative. For example for $[Fe_3(CNBu^t)_2(CO)_8\{P(OMe)_3\}_2]$, which in solution exists as a mixture of at least four isomers, the $^{31}P$ NMR spectrum] in $[^2H_8]$toluene at room temp. is broad, but at 223 K has seven $^{31}P$ NMR signals at $\delta$ 165.7, 166.4 ($J$ 13 Hz), 167.7, 168.1, 172.3, 177.5 and 178.8 ($J$ 13 Hz) in significant intensities for $[Fe_3(CNBu^t)_2(CO)_8\{P(OMe)_3\}_2]$, Fig. 1. By using signal intensity and the coupling constant, these signals form three pairs and one singlet in the ratio 1.00 : 0.30 : 0.30 : 0.14, the pairs being $\delta$ 177.5 and 165.7, $\delta$ 178.8 and 166.4 and $\delta$ 168.1 and 167.7. It has been previously shown that $P(OMe)_3$ on the unbridged iron is at higher frequency than when on a bridged iron, and when the $P(OMe)_3$ ligands are in a linear arrangement, P–Fe–Fe–P, then a $J(^{31}P^{31}P)$ of *ca*. 6–25 Hz is observed.‡

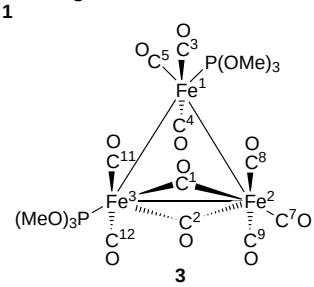
It is known that the concerted bridge-opening bridge-closing mechanism is far too rapid to stop even at −100 °C when phosphorus substitution is only in positions 6 and/or 10, numbering as in **1**.[15] The introduction of a $CNBu^t$ does slow the




**1**




**2**




**3**

rate of the concerted bridge-opening bridge-closing mechanism sufficiently to cause substantial broadening at −100 °C in $[Fe_3(CNBu^t)(CO)_{11}]$ or $[Fe_3(CNBu^t)(CO)_{10}\{P(OMe)_3\}]$.[16] It is also known that the $CNBu^t$ ligand has a preference for an axial site on the unbridged iron, $Fe^1$, in so far as the crystal structures of $[Fe_3(CNBu^t)(CO)_{11}]$,[17] $[Fe_3(CNBu^t)_2(CO)_{10}]$[18] and $[Fe_3(CNBu^t)(CO)_{10}\{P(OMe)_3\}]$[16] have an isonitrile in this position. In the case of $[Fe_3(CNBu^t)_2(CO)_{10}]$, the second $CNBu^t$ is also on the unbridged iron, $Fe^1$, but in the equatorial position.

The $^{31}P$ NMR signals at $\delta$ 177.5 and 165.7 do not show $J(^{31}P^{31}P)$ and arise from an isomer with a bent phosphorus ligand arrangement as in **2**. The $^{31}P$ NMR signal at $\delta$ 172.3 arises from the concerted bridge-opening bridge-closing mechanism averaging the $P(OMe)_3$ ligands. This is consistent with the phosphorus ligands being arranged as in **3** and one $CNBu^t$ ligand being substituted into the ligand set 3, 5, 4, 9, 8 and the other $CNBu^t$ ligand being substituted into the ligand set 1, 12, 11, 2, 7. The third most intense set of signals at $\delta$ 166.4 and 178.8, $J(^{31}P^{31}P)$ 13 Hz, arises from **3** with both $CNBu^t$ ligands in one ligand set, probably, 3, 5, 4, 9, 8.

There is less information available to assign the structures of the other compounds.

We wish to thank the University of Sheffield for financial support.

## Footnotes and References

* E-mail: b.mann@sheffield.ac.uk

† $[Fe_3(CNBu^t)_2(CO)_8\{P(OMe)_3\}_2]$. Anal. Calc. C, 35.76; H, 4.50; N, 3.48 for $C_{24}H_{36}Fe_3N_2O_{14}P_2$. Found: C, 35.71; H, 4.43; N, 3.33%. Mass spectrum: *m/z* 806 ($M^+$). IR ($CH_2Cl_2$): 2139m, 2014w, 1973s, 1956s, 1750w (br), 1753w $cm^{-1}$. $^1H$ NMR ($CD_3C_6D_5$): $\delta$ 1.20 (18 H), 3.33 (18 H). $[Fe_3(CNBu^t)_2(CO)_8\{P(OCH_2)_3CMe\}_2]$. Anal. Calc. C, 39.38; H, 4.25; N, 3.28 for $C_{28}H_{36}Fe_3N_2O_{14}P_2$. Found: C, 39.26; H, 4.21; N, 3.12%. Mass spectrum: *m/z* 854 ($M^+$). IR ($CH_2Cl_2$): 2145m, 2020w, 1981s, 1963s, 1762w (br) $cm^{-1}$. $[Fe_3(CNBu^t)_2(CO)_8\{P(OMe)_3\}\{P(OCH_2)_3CMe\}]$. Anal. Calc. C, 37.62; H, 4.37; N, 3.37 for $C_{26}H_{36}Fe_3N_2O_{14}P_2$. Found: C, 38.10; H, 4.45; N, 3.42%. Mass spectrum: *m/z* 830 ($M^+$). IR ($CH_2Cl_2$): 2142m, 2017w, 1976s, 1960s, 1751w (br) $cm^{-1}$. $^1H$ NMR ($CD_3C_6D_5$): $[Fe_3(CNBu^t)_2(CO)_8\{P(OMe)_3\}\{P(OCH_2)_3CMe\}]$ shows the integral of the overlapped signals at $\delta$ 3.3, which are due to methyl groups of $P(OMe)_3$ and methylene of $P(OCH_2)_3CMe$, and the overlapped signals around $\delta$ 1.20, which arise from the protons of $CNBu^t$ and methyl groups of $P(OCH_2)_3CMe$, is 15 : 21. $[Fe_3(CNBu^t)_3(CO)_8\{P(OMe)_3\}]$. Anal. Calc. C, 40.82; H, 4.74; N, 5.49 for $C_{26}H_{36}Fe_3N_3O_{11}P$. Found: C, 40.73; H, 4.88; N, 5.14%. Mass spectrum: *m/z* 765 ($M^+$). IR ($CH_2Cl_2$): 2162sh, 2132m, 2010w, 1971s, 1958s, $cm^{-1}$. $^1H$ NMR ($CD_3C_6D_5$): (room temp.), $\delta$ 1.20 (27 H), 3.48 (9 H). The $^{31}P$ NMR spectrum of $[Fe_3(CNBu^t)_3(CO)_8\{P(OMe)_3\}]$ in [$^2H_8$]toluene at 223 K shows there are at least seven signals at $\delta$ 164.1, 165.1, 165.9, 167.3, 169.0, 172.7 and 177.3 in the ratio 0.10 : 0.04 : 0.42 : 1.00 : 0.35 : 0.40 : 0.04, suggesting there are at least seven isomers in solution.

$[Fe_3(CNBu^t)_3(CO)_8\{P(OCH_2)_3CMe\}]$. Anal. Calc. C, 42.62; H, 4.60; N, 5.32 for $C_{28}H_{36}Fe_3N_3O_{11}P$. Found: C, 42.27; H, 4.56; N, 5.22%. Mass spectrum: *m/z* 789 ($M^+$). IR ($CH_2Cl_2$): 2162(sh), 2136m, 2013w, 1975s, 1960s, 1800w (br), 1758w, (br) $cm^{-1}$. $[Fe_3(CNBu^t)_4(CO)_8]$. Anal. Calc. C, 46.44; H, 5.01; N, 7.74 for $C_{28}H_{36}Fe_3N_4O_8$. Found: C, 46.23; H, 4.92; N, 7.56%. Mass spectrum: *m/z* 724 ($M^+$). IR ($CH_2Cl_2$): 2135m, 2067w, 1998w, 1969s, 1956s, 1800w, (br) 1759w, (br) $cm^{-1}$.

‡ The $^{31}P$ NMR spectrum of $[Fe_3(CO)_9\{P(OMe)_3\}_3]$ in $CD_2Cl_2$ at −92 °C shows coupling between the signals at $\delta$ 171.5 and 163.8 which have previously been assigned to the $P(OMe)_3$ ligands on $Fe^1$ and $Fe^3$ respectively, see ref. 14.

1 M. P. Brown, P. A. Dolby, M. M. Harding, A. J. Mathews and A. K. Smith, *J. Chem. Soc., Dalton Trans.*, 1993, 1671.
2 M. I. Bruce, J. G. Matisons, J. M. Patrick, A. H. White and A. C. Willis, *J. Chem. Soc., Dalton Trans.*, 1985, 1223.
3 J. S. Field, R. J. Haines and J. A. Jay, *J. Organomet. Chem.*, 1989, **377**, C35.
4 P. J. Roberts and J. Trotter, *J. Chem. Soc. A*, 1970, 3246.
5 M. I. Bruce, M. J. Liddell, O. bin Shawkataly, I. Bytheway, B. W. Skelton and A. H. White, *J. Organomet. Chem.*, 1989, **369**, 217.
6 S.-G. Teoh, H.-K. Fun and O. bin Shawkataly, *Z. Kristallogr.*, 1990, **190**, 287.
7 S. Cartwright, J. A. Clucas, R. H. Dawson, D. F. Foster, M. M. Harding and A. K. Smith, *J. Organomet. Chem.*, 1986, **302**, 403.
8 H. A. Mirza, J. J. Vittal and R. J. Puddephatt, *Inorg. Chem.*, 1993, **32**, 1327.
9 R. F. Alex, F. W. B. Einstein, R. H. Jones and R. K. Pomeroy, *Inorg. Chem.*, 1987, **26**, 3175.
10 G. Raper and W. S. McDonald, *J. Chem. Soc., A*, 1971, 3430.
11 H. Adams, X. Chen and B. E. Mann, *J. Chem. Soc., Dalton Trans.*, 1996, 2159.
12 A. F. Clifford and A. K. Mukherjee, *Inorg. Chim. Acta*, 1963, **2**, 151; B. F. G. Johnson, *Inorg. Chim. Acta*, 1986, **115**, L39; S. L. Yang, C. S. Li and C. H. Chang, *J. Chem. Soc., Chem. Commun.*, 1987, 1872; F.-H. Luo, S.-R. Yang, C.-S. Li, J.-P. Duan and C.-H. Cheng, *J. Chem. Soc., Dalton Trans.*, 1991, 2435.
13 J.-K. Shen, Y.-L. Shi, Y.-C. Gao, Q.-Z. Shi and F. Basolo, *J. Am. Chem. Soc.*, 1988, **110**, 2414; J.-K. Shen, Y.-C. Gao, Q.-Z. Shi and F. Basolo, *Inorg. Chim. Acta*, 1988, **27**, 4236.
14 H. Adams, N. A. Bailey, G. W. Bentley and B. E. Mann, *J. Chem. Soc., Dalton Trans.*, 1989, 1831; S. Aime, M. Botto, O. Gambino, R. Gobetto and D. Osella, *J. Chem. Soc., Dalton Trans.*, 1989, 1277.
15 H. Adams, N. A. Bailey, G. W. Bentley and B. E. Mann, *J. Chem. Soc., Dalton Trans.*, 1989, 1831; B. E. Mann, *J. Chem. Soc., Dalton Trans.*, 1997, 1457.
16 H. Adams, A. G. Carr, B. E. Mann and R. Melling, *Polyhedron*, 1995, **14**, 2771.
17 M. I. Bruce, T. W. Hambley and B. K. Nicholson, *J. Chem. Soc., Dalton Trans.* 1983, 2385.
18 J. B. Murray, B. K. Nicholson and A. J. Whitton, *J. Organomet. Chem.*, 1990, **385**, 91.

*Received in Cambridge, UK, 18th August 1997; 7/06054H*

# Approaching a cluster of aluminium(III) selenide: $[Al_4Se_5(H)_2(NMe_3)_4]$

**Peter D. Godfrey,[a] Colin L. Raston,*[a] Brian W. Skelton,[b] Vicki-Anne Tolhurst[a] and Allan H. White[b]**

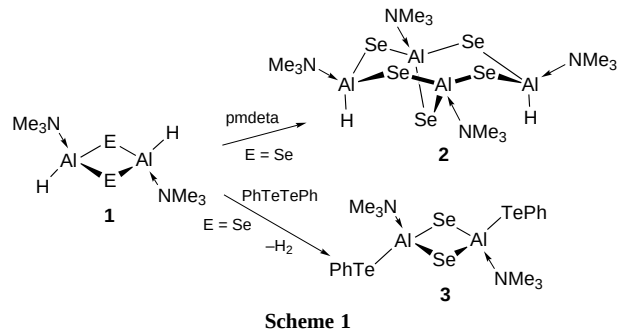
[a] *Department of Chemistry, Monash University, Clayton, Melbourne, Victoria 3168, Australia*
[b] *Department of Chemistry, University of Western Australia, Nedlands, WA 6907, Australia*

**The reaction of *trans*-[{$Me_3N(H)Al(\mu\text{-}Se)$}$_2$] with *N,N,N′,N″,N″*-pentamethyldiethylenetriamine (pmdeta) in toluene affords the tetranuclear, alane selenide cluster $[Al_4Se_5(H)_2(NMe_3)_4]$ (structurally authenticated and *ab initio* modelled), and with PhTeTePh yields a mixed chalcogenide *trans*-[{$Me_3N(PhTe)Al(\mu\text{-}Se)$}$_2$].**

We recently showed that elemental selenium or tellurium react under mild conditions with the trimethylamine adduct of alane, $[H_3AlNMe_3]$, in toluene affording the dimeric chalcogenidoalane, *trans*-[{$Me_3N(H)Al(\mu\text{-}E)$}$_2$] (E = Se, Te) **1**, Scheme 1, with the elimination of hydrogen.[1] This new class of compounds can be regarded as tertiary-amine-stabilised adducts of the simplest selenido- and tellurido-aluminium(III) species, *viz* [{$HAl(\mu\text{-}E)$}$_2$] (E = Se, Te) and should prove to have a rich chemistry. Instead of the adducts, base-free cubane structures are conceivable, [{$HAl(\mu_3\text{-}E)$}$_4$], noting that organometallic analogues have been prepared, [{$(\eta^5\text{-}C_5Me_5)Al(\mu_3\text{-}E)$}$_4$] (E = Se, Te)[2] and [{$Bu^tAl(\mu_3\text{-}S, Se or Te)$}$_4$.[3] For our system, such cubane type structures are computed to be less stable than the solvated dimers.

In developing the chemistry of the adducts we report reactions of *trans*-[{$Me_3N(H)Al(\mu\text{-}Se)$}$_2$] **1a** with (*i*) *N,N,N′,N″,N″*-pentamethyldiethylenetriamine (pmdeta) and (*ii*) PhTeTePh. Reaction (*i*) was an attempt to gain access to a stabilised Lewis-base-saturated monomeric H–Al=Se complex by chelation of the metal centre. This was deemed a synthetic target on theoretical grounds. Rather, an unprecedented tetranuclear cluster formed, $[Al_4Se_5(H)_2(NMe_3)_4]$ **2**, which approaches a stabilised cluster of aluminium(III) selenide. Reaction (*ii*) was successful in forming a mixed chalocogenide aluminium(III) species **3**, arising from metal hydride cleavage of the diorganoditelluride. This is related to the recently established facile cleavage of diorganoditellurides and diorganodiselenides by $[H_3AlNMe_3]$ affording $[(Me_3N)Al(ER)_3]$, (E = Se, Te, R = alkyl, aryl).[4]

Compounds **2** and **3** were prepared in toluene, Scheme 1.† While compound **2** is isolated in low yield, and crystallises over several weeks, its formation is reproducible. On mixing **1a** and pmdeta, a flocculant, insoluble, white precipitate was formed which is difficult to characterise: this product may be the ionic species $[\{(pmdeta)AlH_2\}^+]_2Se^{2-}$, and its formation would account for the change in Al : hydride : Se ratio from 1 : 1 : 1 in **1a** to 2 : 1 : 2.5 in **2**. It shows an IR band at 1789 $cm^{-1}$ *cf.* 1822 $cm^{-1}$ for $[(pmdeta)AlH_2]^+AlH_4^-$, a compound which has been structurally authenticated.[5] While the hydrides in **1** are resistant to further reaction with selenium or tellurium, reaction with a diorganoditelluride takes place, as demonstrated for **1a**, with elimination of hydrogen. Interestingly the integrity of the *trans*-isomer is maintained, whereas in the more complicated tetranuclear cluster this is lost with respect to the two residual hydrogens which are now in a *cis*-arrangement.




**Scheme 1**

Assignment of structure of the two compounds rests on X-ray diffraction studies.‡ Compound **2** crystallises as a toluene solvate with a single toluene and molecule of **2** as the asymmetric unit. The $Al_4Se_5$ metal core can be described as two six-membered rings, both in a boat conformation, sharing an $Al_2Se$ plane and the molecule approximates to $C_2$ symmetry, with *cis*-hydrido groups, Fig. 1. Indeed, departure from a higher potential $C_{2v}$ symmetry relates to puckering of the boat conformation of the two six-membered rings and angular distortion in $Al_3Se_4$ ring with angles subtended by Se(2,4) by two metal centres being more open at 98.6° (mean) relative to

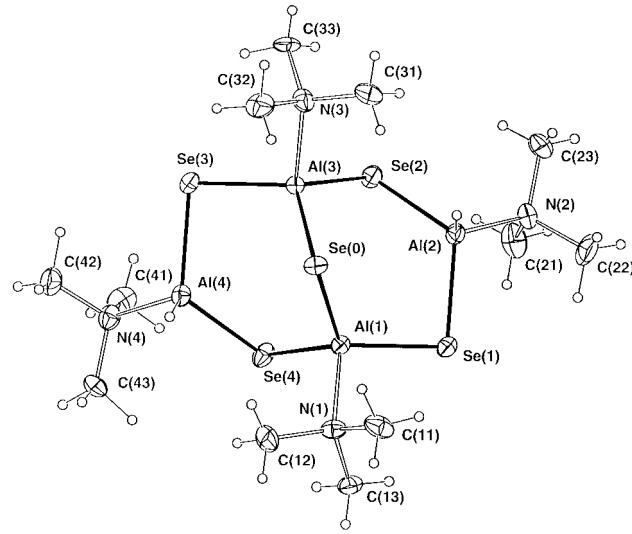



**Fig. 1** Projection of $[Al_4Se_5(H)_2(NMe_3)_4]$. **2** Selected distances (Å) and angles (°): Se(0)–Al(1,3) 2.361(4), 2.354(4), Se(1)–Al(1,2) 2.345(3), 2.358(4), Se(2)–Al(2,3) 2.356(4), 2.334(4), Se(3)–Al(3,4) 2.345(3), 2.360(5), Se(4)–Al(1,4) 2.332(4), 2.355(3), Al(1,2,3,4)–N(1,2,3,4) 2.05(1), 2.00(1), 2.05(1), 1.98(1); Al(1)–Se(0)–Al(3) 94.6(1), Al(1)–Se(1)–Al(2) 92.2(1), Al(2)–Se(2)–Al(3) 98.7(1), Al(3)–Se(3)–Al(4) 91.5(1), Al(1)–Se(4)–Al(4) 98.5(1), Se(0)–Al(1)–Se(1,4), N(1) 115.7(2), 113.2(1), 103.2(3), Se(1)–Al(1)–Se(4), N(1) 115.6(2), 102.2(3), Se(4)–Al(1)–N(1) 104.7(3), Se(1)–Al(2)–Se(2), N(2) 115.7(2), 101.8(4), Se(2)–Al(2)–N(2) 101.0(3), Se(0)–Al(3)–Se(2,3), N(3) 114.6(1), 114.5(2), 103.9(4), Se(2)–Al(3)–Se(3), N(3) 113.9(2), 104.7(3), Se(3)–Al(3)–N(3) 103.3(3), Se(3)–Al(4)–Se(4), N(4) 116.5(2), 104.2(4), Se(4)–Al(4)–N(4) 100.0(3). Computed values for the same molecule with $C_{2v}$ symmetry: Al(1)–N(1) 2.059, Al(2)–N(2) 2.086, Al(1)–Se(1,4) 2.431, Al(2)–Se(1,2) 2.445, Al(2)–H 1.600, Al(1)–Se(0) 2.437, Se(0)–Al(1)–N(1), Se(1,4) 103.49, 114.44, Se(1)–Al(1)–N(1), Se(4) 103.18, 115.78, N(1)–Al(1)–Se(4) 103.16, Se(1)–Al(2)–Se(2), N(2), H 119.33, 101.57, 115.27, Se(2)–Al(2)–N(2), H, 101.57, N(2)–Al(2)–H 98.90, Al(1)–Se(0)–Al(3) 99.75, Al(1)–Se(1)–Al(2) 111.99, Al(1)–Se(4)–Al(4) 111.99.

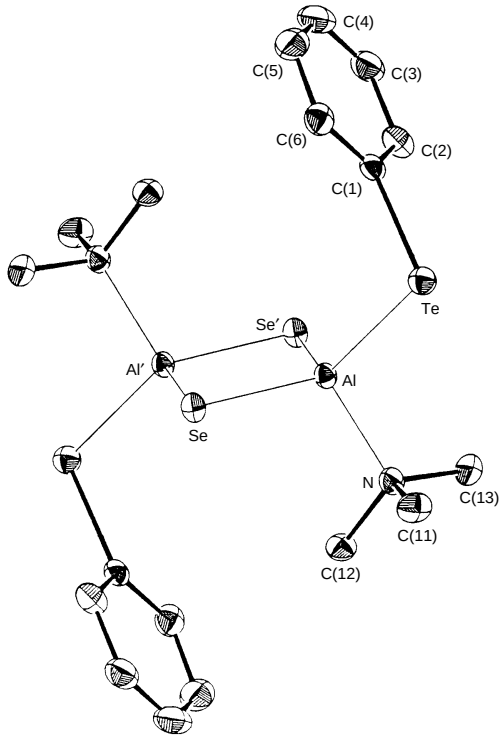



**Fig. 2** Projection of *trans*-[{$Me_3N$(PhTe)Al(μ-Se)}$_2$] **3**. Selected distances (Å) and angles (°): Te–Al, 2.610(2), Se–Al 2.359(2), Se–Al′ 2.347(2), Al–N 1.998(5); Al–Te–C(1), Al′ 94.6(1), 76.37(6), Te–Al–Se, N, Se′ 117.16(7), 102.1(1), 117.31(7), Se–Al–N, Se′ 107.2(2), 103.63(6), N–Al–Se′ 108.9(2)

those subtended by Se(1,3), 91.9° (mean). The corresponding angle at the unique selenium, Se(0), is intermediate at 94.6(1)°. All aluminium centres are four-coordinate. The bond distances around Al(1,3) which have the coordinated Lewis base $NMe_3$ are similar to those in [$(Me_3N)Al(SeEt)_3$], but the angles subtended by two seleniums are slightly more open at *ca*. 114.50, *cf*. 111.5(5), as are the Se–Al–N angles at *ca*. 113.4, *cf*. 87(1)°.[4] Similarly the bond distances around Al(2,4) are similar to those in *trans*-[{$Me_3N$(H)Al(μ-Se)}$_2$] (and **3**, see below) with the Se–Al–Se angles more open, at *ca*. 116.0°, *cf*. 103.10(7)°,[1] as expected for a larger ring system. Molecules of **3** are centrosymmetric, as the *trans*-isomer, Fig. 2. The $Al_2Se_2$ core is very similar to that in *trans*-[{$Me_3N$(H)Al(μ-Se)}$_2$].[1] The Te–Al distance at 2.610(2) Å is similar to that in [$(Me_3N)Al(TePh)_3$],[4] 2.589(2) Å.

An *ab initio* molecular-orbital calculation involving $C_{2v}$ structure optimisation at the RHF/LanL2DZ level was undertaken on **2** giving reasonable correlation of structural parameters with experimental values, except for the angular distortions associated with $C_2$ rather than $C_{2v}$ symmetry (Fig. 1).[6] Constraining the symmetry to $C_{2v}$ was necessary for computational convenience. In order to estimate the energy change on production *via* hydrogenation, a similar calculation was performed under $C_{2v}$ symmetry at the MP2/LanL2DZ level on the simpler analogous compound [$Al_4Se_5(H)_2(NH_3)_4$] and its hypothetical precursor [$Al_4Se_6(NH_3)_4$], the latter under $T_d$ symmetry as shown in Fig. 3. The MP2/LanL2DZ energies (in $E_h$) of the reactants [$Al_4Se_6(NH_3)_4$] (−287.918 974 1) and $H_2$ (−1.143 905 1) in combination with those of the products [$Al_4Se_5(H)_2(NH_3)_4$] (−279.906 603 9) and $H_2Se$ (−10.198 084 0) indicate that the formation of [$Al_4Se_5(H)_2(NH_3)_4$] *via* hydrogenation is exothermic by 654 kcal mol$^{-1}$ (1 cal = 4.184 J). Thus the analogous reverse reaction of converting **2** to [$Al_4Se_6(NMe_3)_4$] on treatment with $H_2Se$ is energetically unfavourable. However other sources of selenium, for example $Se(SiMe_3)_2$, may favour formation of [$Al_4Se_6(NMe_3)_4$], an area we are currently exploring.

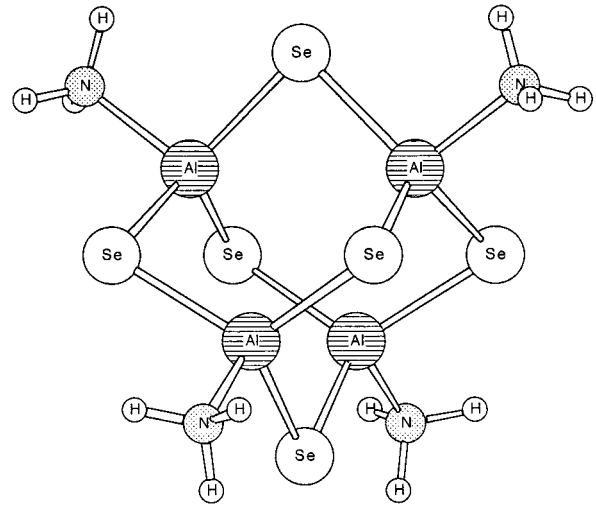



**Fig. 3** Computed structure of [$Al_4(\mu\text{-}Se)_6(Me_3N)_4$] with $T_d$ symmetry: Al–Se, N, 2.460, 2.059 Å; Se–Al–Se 116.16, Se–Al–N 101.46, Al–Se–Al 93.45°

We thank the Australian Research Council for support of this work.

## Footnotes and References

* E-mail: c.raston@sci.monash.edu.au

† *Synthesis*: **2**: pmdeta (0.28 ml, 1.34 mmol) was added to a stirred solution of *trans*-[{$Me_3N$(H)Al(μ-Se)}$_2$] (0.44 g, 1.32 mmol) in toluene at room temp. A white precipitate formed immediately and after 2 h the reaction mixture was filtered. Recrystallisation from toluene (*ca*. 40 ml) afforded colourless crystals (0.15 g, 20%). Mp (*in vacuo*); partial sublimation at 78–81 °C leaving a white powder which decomposes > 310 °C; IR $\nu_{Al-H}$ 1779 cm$^{-1}$ (s). NMR: $^1$H (300 MHz, $C_6D_6$, 25 °C) $\delta$ 2.10, 2.09 ($NCH_3$), $^{13}$C (75.5 MHz, $C_6D_6$, 25 °C) $\delta$ 47.6, 47.5 ($NCH_3$). Anal. Found C, 23.11; H, 5.06; N, 6.58. Calc. for $C_{12}H_{38}Al_4N_4Se_5{\cdot}0.5C_7H_8$: C, 23.65; H, 5.38; N, 7.12%.

**3**: PhTeTePh (0.65 g, 1.6 mmol) in toluene (10 ml) was added to *trans*-[{$Me_3N$(H)Al(μ-Se)}$_2$] (0.53 g, 1.6 mmol) in toluene (20 ml) at room temp. with gas evolution. After 17 h the resulting orange solution was filtered, and volatiles removed *in vacuo*. Recrystallisation from toluene (*ca*. 15 ml) afforded orange crystals (0.48 g, 41%). Mp 145–147 °C (*in vacuo*). NMR: $^1$H (200 MHz, $C_6D_6$, 25 °C) $\delta$ 8.17 (6 H, m, *o*-$C_6H_5$), 6.91 (4 H, m, *m*-, *p*-$C_6H_5$), 2.10 (18 H, s, $NCH_3$); $^{13}$C (50.3 MHz, $C_6D_6$, 25 °C) $\delta$ 141.0 (*o*-$C_6H_5$), 129.1, 126.6 (*m*-, *p*-$C_6H_5$), 107.6 (*ipso*-$C_6H_5$), 47.1 ($CH_3$). Anal. Found C, 29.31; H, 4.03; N, 3.79. Calc. for $C_{18}H_{28}N_2Al_2Se_2Te_2$: C, 29.24; H, 3.82; N, 3.79%.

‡ *Crystallographic data* (CAD4 diffractometer, crystals mounted in a capillaries): **2**·$C_6H_5Me$: $C_{19}H_{46}Al_4N_4Se_5$, $M$ = 833.3, orthorhombic, space group $Pna2_1$, $a$ = 12.294(2), $b$ = 27.769(5), $c$ = 10.285(5) Å, $U$ = 3511(2) Å$^3$, $D_c$ ($Z$ = 4) = 1.576 g cm$^{-3}$, $F$(000) = 1640, $\mu_{Mo}$ = 53.3 cm$^{-1}$, specimen: 0.21 × 0.50 × 1.10 mm, $A^*_{min,max}$ = 3.15, 12.08, $2\theta_{max}$ = 50°, final $R$, $R_w$ = 0.040, 0.038 (0.043, 0.041 other hand) $N_o$ = 1934 'observed' [($I > 3\sigma(I)$] reflections out of $N$ = 3270 unique.

**3**: $C_{18}H_{28}Al_2N_2Se_2Te_2$, $M$ = 739.5, monoclinic, space group $P2_1/n$, $a$ = 6.746(4), $b$ = 10.725(3), $c$ = 17.529(7) Å, $\beta$ = 90.57(4), $U$ = 1268.3(9) Å$^3$, $D_c$ ($Z$ = 2) = 1.936 g cm$^{-3}$, $F$(000) = 696, $\mu_{Mo}$ = 52.5 cm$^{-1}$, specimen: 0.35 × 0.20 × 0.22 mm, $A^*_{min,max}$ = 2.20, 3.59, $2\theta_{max}$ = 55°, final $R$, $R_w$ = 0.033, 0.042, $N_o$ = 2042 'observed' [($I > 3\sigma(I)$] reflections out of $N$ = 2915 unique. For both structures all H-atoms were included as invariants. CCDC 182/611.

1 M. G. Gardiner, C. L. Raston and V.-A. Tolhurst, *J. Chem. Soc., Chem. Commun.*, 1995, 2501.
2 S. Schultz, H. W. Roesky, H. J. Koch, G. Sheldrick, D. Stalke and A. Kuhn, *Angew. Chem., Int. Ed. Engl.*, 1993, **32**, 1729.
3 A. H. Cowley, R. A. Jones, P. R. Harris, D. A. Atwood, L. Contreras and C. J. Burek, *Angew. Chem., Int. Ed. Engl.*, 1991, **30**, 1143.
4 M. G. Gardiner, C. L. Raston and V.-A. Tolhurst, *J. Chem. Soc., Chem. Commun.*, 1995, 1457.
5 J. L. Atwood, K. D. Robinson, C. Jones and C. L. Raston, *J. Chem. Soc., Chem. Commun.*, 1991, 1697.
6 GAUSSIAN 94, Revision D.3, Gaussian, Inc., Pittsburgh, PA, 1995.

*Received in Columbia, MO, USA, 13th May, 1997; 7/03324I*

# First structural characterization of an eight-coordinate cobalt(II) complex containing five-membered chelate rings: evidence for d-orbital σ-stabilization energy favoring eight- over six-coordination at cobalt(II) ions

**Welf O. Koch, Jens T. Kaiser and Hans-Jörg Krüger***

*Institut für Anorganische und Angewandte Chemie der Universität Hamburg, Martin-Luther-King-Platz 6, D-20146 Hamburg, Germany*

**For the first time, an eight-coordinate cobalt(II) complex is presented where only five-membered chelate rings are formed with the coordinated ligand; evidence is put forward that in addition to reasons of the tetraazamacrocyclic nature of the ligand 2,11-diaza-[3.3](2,6)pyridinophane (L), eight-coordination at cobalt(II) ions is, to some extent, favored with respect to six-coordination by the presence of d-orbital σ-stabilization energy as calculated by angular overlap methods.**

Structurally established eight-coordination at a cobalt ion is very rare and, to our knowledge, has only been reported for $[Co(NO_3)_4]^{2-}$ ions where the oxygen donor atoms assume a dodecahedral arrangement.[1] The existence of eight-coordinate cobalt(II) ions has also been implied to exist, without any structural proof, in another cobalt complex containing the ligand 1,8-naphthyridine.[2] Here we introduce the first structural characterization of an eight-coordinate cobalt(II) complex in which the ligand forms only five-membered instead of four-membered chelate rings with the metal ion and, further, we present evidence that eight-coordination at cobalt(II) ions is favored, to some extent, by d-orbital σ-stabilization energy as calculated by angular overlap methods.[3]

In a recent publication[4] we demonstrated that eight-coordinate iron-(II) and -(III) complexes can be obtained with the tetraazamacrocyclic ligand 2,11-diaza-[3.3](2,6)pyridinophane (L). In these complexes the metal ion is positioned in a sandwich-like fashion between the two ligand moieties. We showed that a distorted dodecahedral coordination geometry is achieved because of the *syn* boat–boat conformation of the two coordinated macrocyclic ligands.

The lilac cobalt(II) complex $[CoL_2]^{2+}$ was prepared by the addition of 1 equiv. of cobalt(II) perchlorate to a methanolic solution containing 2 equiv. of the tetraazamacrocyclic ligand. Upon recrystallization from acetonitrile–diethyl ether, the complex was isolated either directly as the perchlorate salt $[CoL_2][ClO_4]_2$ **1** or, after a preceding metathesis with sodium tetraphenylborate, as the tetraphenylborate salt $[CoL_2][BPh_4]_2 \cdot Et_2O$ **2**. Analogous procedures render the violet nickel(II) complexes $[NiL_2][ClO_4]_2 \cdot MeCN$ **3** and $[NiL_2][BPh_4]_2$ **4**.

The structure determinations† of both cobalt complexes unambiguously establish eight-coordination at the cobalt(II) ions. The coordination geometry around the cobalt(II) ion in **2** (Fig. 1) is best described as a distorted dodecahedron. Thus, the two diazapyridinophane ligands form a torsional angle of approximately 70° and there are substantial differences in lengths ( > 0.1 Å) observed between the two crystallographically distinct $Co–N_{py}$ and the two $Co–N_{amine}$ bonds, respectively. In contrast, in **1** (structure not shown) the cobalt ion is located in a nearly perfect dodecahedral coordination environment (torsional angle of 90°), providing the complex with $D_{2d}$ overall symmetry. The average $Co–N_{py}$ and $Co–N_{amine}$ bond lengths in **1** (which are approximately the same as the average bond lengths in **2**) are 2.308 ± 0.002 and 2.389 ± 0.005 Å, respectively; the average $N_{py}–Co–N_{py}$ and $N_{amine}–Co–N_{amine}$ angles, defined by the Co–N bonds to the same ligand moiety, are determined to be 72.96 and 132.61°, respectively. The magnetic moment of the solid cobalt(II) complex **2**, 4.45 $\mu_B$, is considerably lower than that of an octahedral cobalt(II) complex[5] but similar to that of cobalt(II) complexes with a tetrahedral[5] or a dodecahedral coordination geometry[2,6] around the metal ion. Because the magnetic moment scarcely changes upon dissolving the complex in dimethyl sulfoxide (4.41 $\mu_B$) and because eight-coordinate cobalt complexes are obtained in the solid state irrespective of the counter anions used in the preparation, it is difficult to imagine that the coordination number eight at the cobalt ion is just the result of some solid state effect and that it prevails only in the solid state. Thus, this study demonstrates that coordination number eight can be readily achieved with the 'relatively small', late first row transition metal ion cobalt in the moderately low +2 oxidation state. In the two previously investigated cobalt complexes where eight-coordination is observed or assumed, the ligands have rather small chelate bites forming four-membered chelate rings, whereby the interaction of the two donor atoms of a

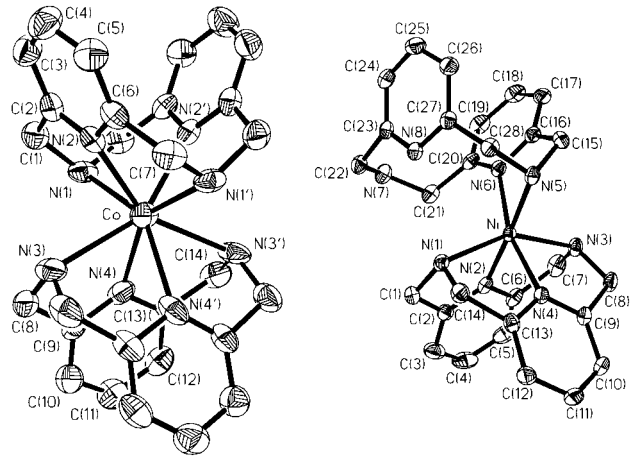



**Fig. 1** Perspective views of the complex cations $[CoL_2]^{2+}$ and $[NiL_2]^{2+}$ in **2** and **3**, respectively, showing thermal ellipsoids at 50% probability and the atom numbering scheme. The primed and unprimed atoms in **2** are related by a twofold rotation axis. Selected bond lengths (Å) and angles (°): **2**: Co–N(1) 2.316(2), Co–N(2) 2.229(2), Co–N(3) 2.438(3), Co–N(4) 2.366(3); N(1)–Co–N(2) 73.38(8), N(1)–Co–N(3) 86.26(10), N(1)–Co–N(4) 77.55(8), N(1)–Co–N(1′) 136.05(11), N(1)–Co–N(2′) 72.34(8), N(1)–Co–N(3′) 112.44(10), N(1)–Co–N(4′) 145.56(8), N(2)–Co–N(3) 78.28(8), N(2)–Co–N(4) 137.73(8), N(2)–Co–N(2′) 76.09(11), N(2)–Co–N(3′) 150.35(8), N(2)–Co–N(4′) 122.80(8), N(3)–Co–N(4) 69.75(9), N(3)–Co–N(3′) 129.97(11), N(3)–Co–N(4′) 70.00(9), N(4)–Co–N(4′) 71.08(11). **3**: Ni–N(1) 2.172(2), Ni–N(2) 2.021(3), Ni–N(3) 2.187(2), Ni–N(4) 2.029(2), Ni–N(5) 2.085(2), Ni–N(6) 2.138(2); N(1)–Ni–N(2) 79.45(9), N(1)–Ni–N(3) 150.43(9), N(1)–Ni–N(4) 78.46(9), N(1)–Ni–N(5) 97.55(9), N(1)–Ni–N(6) 116.19(9), N(2)–Ni–N(3) 79.07(10), N(2)–Ni–N(4) 84.34(10), N(2)–Ni–N(5) 176.68(10), N(2)–Ni–N(6) 102.38(10), N(3)–Ni–N(4) 79.42(9), N(3)–Ni–N(5) 104.24(10), N(3)–Ni–N(6) 88.19(9), N(4)–Ni–N(5) 96.50(10), N(4)–Ni–N(6) 164.60(9), N(5)–Ni–N(6) 77.60(9).

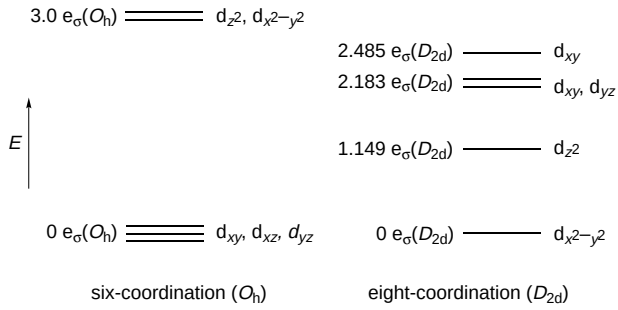



**Fig. 2** Energy diagrams for the d orbitals of a six-coordinate metal ion in an octahedral coordination geometry ($O_h$) and of an eight-coordinate metal ion in a dodecahedral coordination geometry ($D_{2d}$). The indicated energies of d orbitals are calculated by angular overlap methods[3] in units of $e_\sigma = \beta S_R^2$, assuming only σ-interactions between the metal ion and ligand donor atoms.

ligand with the metal ion is significantly favored by the spacial proximity of the donor atoms. In this study, for the first time, eight-coordination has been structurally established for a cobalt(II) ion where only five-membered chelate rings are present in the complex.

In contrast, the nickel(II) ion in **3**† is coordinated to all nitrogen donor atoms of one of the tetraazamacrocyclic ligands and to one each of the pyridine and amine nitrogen atoms of the second ligand (Fig. 1). Thus, the nickel ion assumes an octahedral coordination geometry which is also found in a preliminary structure determination of **4**.

Fig. 2 compares the energy levels obtained for an ideal octahedral and dodecahedral (using the angles within complex **1**) metal ion by angular overlap methods. With the assumption that π bonding can be neglected in these complexes, the dodecahedral site preference expressed as the difference in d-orbital σ-stabilization energies (calculated by angular overlap methods)[3] is: $8\ e_\sigma(D_{2d}) - 6\ e_\sigma(O_h)$ for high-spin $d^6$, $6.85\ e_\sigma(D_{2d}) - 6\ e_\sigma(O_h)$ for high-spin $d^7$ and $4.67\ e_\sigma(D_{2d}) - 6\ e_\sigma(O_h)$ for a $d^8$ metal ion. Considering that $|e_\sigma(D_{2d})|$ is smaller than $|e_\sigma(O_h)|$ owing to the larger M–N bond lengths in eight-coordinate complexes, eight- as well as six-coordination is possible for the cobalt(II) complex [depending on the relative magnitude of $e_\sigma(D_{2d})$ with respect to $e_\sigma(O_h)$], while only six-coordination is predicted to occur with nickel(II) ions according to angular overlap methods.‡ Clearly, eight coordination at the cobalt(II) as well as at the iron(II) ion[4] is favored by the distinct spacial properties of the tetraazamacrocyclic ligand L. However, in light of the finding that, in comparison with the cobalt(II) ion, the only slightly smaller nickel ion prefers octahedral over dodecahedral coordination geometry, evidence has been put forward that to some extent eight-coordination at iron(II) and cobalt(II) centres is stabilized with respect to six-coordination by electronic factors as illustrated by the d-orbital σ-stabilization energy calculated by angular overlap methods.

We are grateful to the Deutsche Forschungsgemeinschaft for financial support. We also thank Professor Dr O. Jarchow, Professor Dr U. Behrens and Dr J. Hanss for their assistance with the crystal structure determination of compound **1**.

## Footnotes and References

* E-mail: krueger@xray.chemie.uni-hamburg.de

† *Crystal data*: **1**: $C_{28}H_{32}Cl_2CoN_8O_8$, triclinic, space group $P\bar{1}$ (eightfold-primitive with the equivalent positions at *x*, *y*, *z*; 0.5 + *x*, *y*, 0.5 + *z*; 0.25 + *x*, 0.25 + *y*, 0.75 + *z*; 0.75 + *x*, 0.75 + *y*, 0.25 + *z*; 0.5 + *x*, 0.5 + *y*, 0.5 + *z*; *x*, 0.5 + *y*, *z*; 0.75 + *x*, 0.25 + *y*, 0.25 + *z*; 0.25 + *x*, 0.75 + *y*, 0.75 + *z*), $a$ = 23.162(5), $b$ = 23.162(5), $c$ = 11.380(4) Å, $\alpha$ = 90.00, $\beta$ = 90.00, $\gamma$ = 90.00, $U$ = 6105(3) Å$^3$, $Z$ = 8, $D_c$ = 1.607 g cm$^{-3}$; 8938 unique reflections [6055 reflections with $F_o > 4\sigma(F_o)$]; $T$ = 293 K; μ(Mo-Kα) = 8.03 cm$^{-1}$; 428 parameters; $R$ = 0.0508 [$F_o > 4\sigma(F_o)$]. The crystal is a non-merohedral twin composed of four components.

**2**: $C_{80}H_{82}B_2CoN_8O$, monoclinic, space group $C2/c$ (no. 15), $a$ = 22.772(11), $b$ = 15.050(2), $c$ = 21.595(15) Å, β = 115.70(3)°, $U$ = 6669(6) Å$^3$, $Z$ = 4, $D_c$ = 1.247 g cm$^{-3}$; 6847 unique reflections [4175 reflections with $F_o > 4\sigma(F_o)$]; $T$ = 153 K; μ(Mo-Kα) = 3.11 cm$^{-1}$; 428 parameters; $R$ = 0.0529 [$F_o > 4\sigma(F_o)$].

**3**: $C_{30}H_{35}Cl_2N_9NiO_8$, monoclinic, space group $P2_1/n$ (no. 14), $a$ = 11.216(3), $b$ = 15.995(5), $c$ = 17.981(5) Å, $\beta$ = 92.23(3)°, $U$ = 3223(2) Å$^3$, $Z$ = 4, $D_c$ = 1.606 g cm$^{-3}$; 7536 unique reflections [5665 reflections with $F_o > 4\sigma(F_o)$]; $T$ = 153 K; $\mu$(Mo-Kα) = 8.35 cm$^{-1}$; 464 parameters; $R$ = 0.0456 [$F_o > 4\sigma(F_o)$]. CCDC 182/627.

‡ The calculation of the ligand field stabilization energies for dodecahedral and octahedral high-spin metal ions with $d^6$, $d^7$ and $d^8$ electron configurations shows that eight-coordination geometry is favored for a $d^6$ metal ion, while six-coordination is preferred by $d^8$ metal ions. For a $d^7$ metal ion, the difference in ligand field stabilization energy between both geometries is small, but favors octahedral coordination geometry.

1 J. G. Bergman and F. A. Cotton, *Inorg. Chem.*, 1966, **5**, 1208.
2 R. L. Bodner and D. G. Hendricker, *Inorg. Chem.*, 1973, **12**, 33.
3 J. K. Burdett, *Adv. Inorg. Chem. Radiochem.*, 1978, **21**, 113.
4 W. O. Koch, A. Barbieri, M. Grodzicki, V. Schünemann, A. X. Trautwein and H.-J. Krüger, *Angew. Chem., Int. Ed. Engl.*, 1996, **35**, 422.
5 R. L. Carlin, *Magnetochemistry*, Springer Verlag Berlin, 1986, pp. 65.
6 F. A. Cotton and T. G. Dunne, *J. Am. Chem. Soc.*, 1962, **84**, 2013.

*Received in Basel, Switzerland, 4th August 1997; 7/05665F*

# Single-molecule magnets: isomeric $[Mn_{12}O_{12}(O_2CC_6H_4Me\text{-}4)_{16}(H_2O)_4]$ complexes exhibiting different rates of resonant magnetization tunnelling

**Sheila M. J. Aubin,[a] Ziming Sun,[a] Ilia A. Guzei,[b] Arnold L. Rheingold,*[b] George Christou*[c] and David N. Hendrickson*[a]**

[a] *Department of Chemistry and Biochemistry-0358, University of California at San Diego, La Jolla, CA 92093-0358, USA*
[b] *Department of Chemistry and Biochemistry, University of Delaware, Newark, DE 19716, USA*
[c] *Department of Chemistry, Indiana University, Bloomington, IN 47405-4001, USA*

**Two different isomeric forms of $[Mn_{12}O_{12}(O_2CC_6H_4Me\text{-}4)_{16}(H_2O)_4]$, differing in the positioning of $H_2O$ ligands, are structurally characterized and shown to have considerably different magnetization hysteresis loops.**

Single-molecule magnets have attracted considerable attention.[1–3] The presence of appreciable magnetic anisotropy in a big spin ground-state molecule leads to a potential-energy barrier for reversal of the direction of magnetization and an isolated molecule exhibits hysteresis in its magnetization *vs.* magnetic field response. The most thoroughly studied[4,5] single-molecule magnet $[Mn_{12}O_{12}(O_2CMe)_{16}(H_2O)_4]$ **1** has a magnetization that decays with a half-life of 2 months at 2.0 K after a magnetic field is removed. One of the most interesting aspects of complex **1** is that there are steps observed at regular intervals of magnetic field in the magnetization loop for oriented crystals. These steps have been attributed[6–8] to resonant magnetization tunnelling. We herein describe the preparation and X-ray structures of two new single-molecule magnets, $[Mn_{12}O_{12}(O_2CC_6H_4Me\text{-}4)_{16}(H_2O)_4]\cdot 3H_2O$ **2** and $[Mn_{12}O_{12}(O_2CC_6H_4Me\text{-}4)_{16}(H_2O)_4]\cdot HO_2CC_6H_4Me\text{-}4$ **3**, that differ in their space group and the positioning of their $H_2O$ ligands on the $Mn_{12}$ complexes.

The reaction of $Mn(ClO_4)_2$ (11 mmol) with $NBu^n{}_4[MnO_4]$ (4.3 mmol) and 4-methylbenzoic acid (140 mmol) in ethanol gives complexes **2** and **3**. When anhydrous ethanol is used complex **3** results, whereas a 20% $H_2O$–80% EtOH reaction medium yields the hydrate complex **2**. X-Ray quality crystals of **2** and **3** were grown from a $CH_2Cl_2$–hexanes mixture.

The structure† of complex **2** shows a $Mn_{12}$ complex with a $[Mn_{12}(\mu_3\text{-}O)_{12}]$ core, comprising a central $[Mn^{IV}{}_4O_4]^{8+}$ cubane held within a non-planar ring of eight $Mn^{III}$ ions by eight $\mu_3\text{-}O^{2-}$ ions. Peripheral ligation of complex **2** is provided by sixteen $\eta^2,\mu$-carboxylate groups and four $H_2O$ ligands. The eight $Mn^{III}$ ions fall into two groups of four $Mn^{III}$ ions. In group I each $Mn^{III}$ ion is bonded to a single $Mn^{IV}$ *via* two $\mu_3\text{-}O^{2-}$ bridges, while in group II each $Mn^{III}$ is bonded to two $Mn^{IV}$ ions *via* two $\mu_3\text{-}O^{2-}$ bridges. The four $H_2O$ ligands coordinate only to $Mn^{III}$ ions in group II. Complex **2** has two $H_2O$ ligands bonded to one $Mn^{III}$ ion and one $H_2O$ ligand on each of two other $Mn^{III}$ ions. The structure† of complex **3** shows that it is an isomer of the same $Mn_{12}$ complex. A drawing showing a superposition of the two $Mn_{12}$ complexes is shown in Fig. 1. It can be seen that the $Mn_{12}$ complexes in complexes **2** and **3** differ in the positioning of the four $H_2O$ ligands. Consequential rearrangements in the 4-methybenzoate ligands also occur.

Out-of-phase ac magnetic susceptibility ($\chi_M''$) signals are seen for both complexes **2** and **3**. Fig. 2 shows a plot for $\chi_M''$ *vs.* *T* for complex **3** (upper) and for hydrated complex **2** (lower) in the region 2–10 K, measured at frequencies of 50, 250 or 1000 Hz. Both samples of these two complexes exhibit two frequency-dependent $\chi_M''$ ac peaks, one in the region 2–4 K and the other in the region 4–7 K. However, complex **3** has predominantly a peak in the region 2–4 K, whereas hydrated complex **2** has predominantly a peak in the region 4–7 K. Several crystalline samples of $[Mn_{12}O_{12}(O_2CC_6H_4Me\text{-}4)_{16}(H_2O)_4\cdot xH_2O\cdot yHO_2CC_6H_4Me\text{-}4$ were prepared by varying the level of dryness of the EtOH reaction medium. As *x* and *y* varied, so did the intensity ratio of the two $\chi_M''$ peaks.

Fig. 3 shows magnetization hysteresis data obtained for oriented crystal samples of complexes **2** and **3**. A few small crystals of a given complex were suspended in eicosane at 40 °C, oriented in a 5.5 kG field and then the eicosane matrix was cooled to room temp. This gives a waxy cube with the crystals aligned with their easy axes of magnetization parallel. Steps are seen in the hysteresis loops for both complexes. The sample of complex **2** is first magnetically saturated in a +3.5 kG field. All of the complexes at 2.0 K will be in the $m_s = -10$ level of the $S = 10$ double-well potential. When the field is decreased to zero, each of the $m_s = -10, -9, -8, \cdots -1, 0$ levels on the right-hand side of the double well become equal in energy to the corresponding $m_s = 10, 9, 8, \cdots 1, 0$ level of the left-hand side. As the field is decreased from +3.5 kG to zero, there is the first step at zero field. The energy alignment leads to a resonant magnetization tunnelling. Individual molecules tunnel from one $m_s < 0$ level to an $m_s > 0$ level. If all molecules

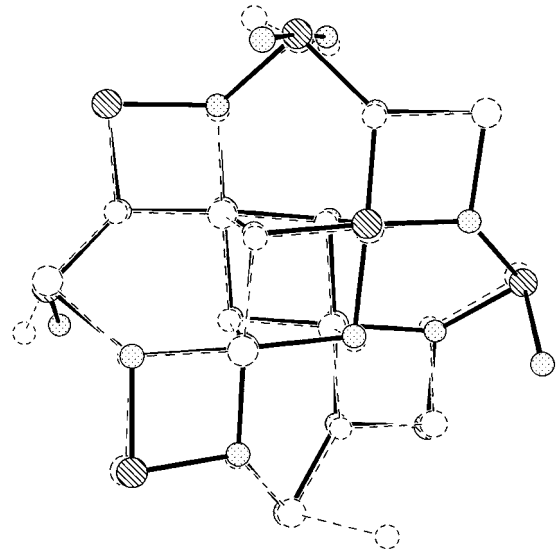


**Fig. 1** Drawing showing a superposition of the cores, without 4-methylbenzoate ligands, of the $[Mn_{12}O_{12}(O_2CC_6H_4Me\text{-}4)_{16}(H_2O)_4]$ molecules in complexes **2** (---) and **3** (—). The crosshatched and stippled spheres represent manganese and oxygen atoms, respectively, in the structure of **3**. The two isomers differ in the arrangements of four $H_2O$ ligands. Complex **2** has a 1,1,2 pattern of $H_2O$ ligand positions, where one $H_2O$ ligand is bonded to the Mn atom at the bottom of the drawing, one to the Mn atom at the left and two $H_2O$ ligands bonded to the 'top' Mn atom. Complex **3** has a 1,2,1 pattern of $H_2O$ ligands.

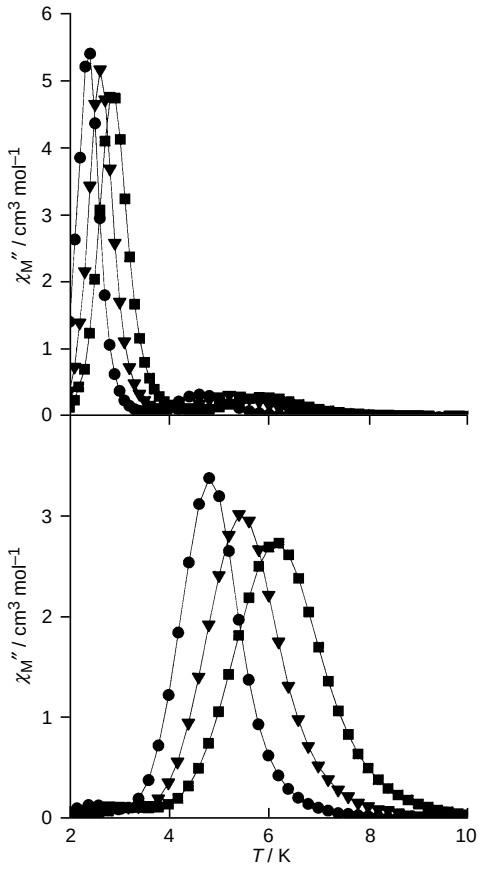



**Fig. 2** Plots of the out-of-phase ac magnetic susceptibility $\chi_M''$ *vs.* temperature for polycrystalline samples of the $Mn_{12}$ complexes **2** (lower) and **3** (upper). Data were collected with zero dc magnetic field and with an 1.0 G ac field oscillating at: (●) 50; (▼) 250 and (■) 1000 Hz.

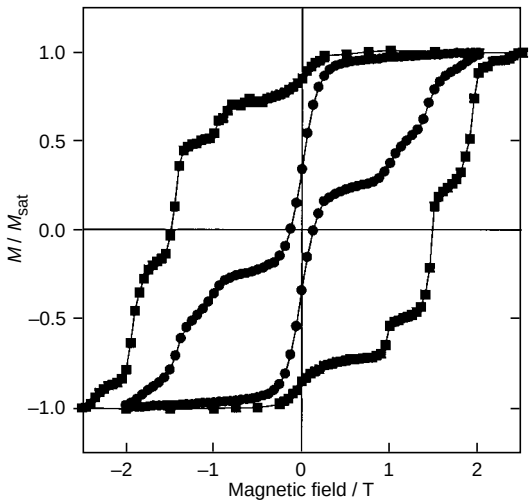



**Fig. 3** Magnetization hysteresis loops measured at 1.90 K for oriented crystals in eicosane matrix for complexes **2** (■) and **3** (●). The magnetization for each complex is plotted in units of the saturation magnetization $M_{sat}$ for that complex. The saturation magnetization values for complexes **2** and **3** are $1.20 \times 10^5$ and $1.05 \times 10^5$ cm$^3$ G mol$^{-1}$, respectively.

changed their direction of magnetization by thermal activation over the barrier, then the hysteresis loop would be a smooth function with no steps.

As can be seen in Fig. 3, it is of considerable interest to note there are appreciable differences in step heights between complexes **2** and **3**. The hysteresis loop of hydrated complex **2** is similar to that reported[6–8] for the acetate complex **1**. On the other hand, complex **3** shows a much steeper step at zero field than does complex **2**. Thus, complex **3** is exhibiting an appreciably faster rate of tunnelling of the magnetization than does complex **2**. This is the case in spite of the fact that complexes **2** and **3** have the same ligands and differ in their arrangements of four $H_2O$ ligands and space groups. The greater rate of tunnelling for complex **3** is consistent with the fact that this complex shows its $\chi_M''$ ac signal at a lower temperature than does hydrated complex **2**.

The origin of the faster rate of tunnelling for complex **3** than **2** is unclear. One possibility is that hydrated complex **2** has a $S = 10$ ground state as found for complex **1**, whereas complex **2** has a $S = 9$ ground state. The barrier height $\Delta$ in the double-well potential-energy diagram is equal to $\Delta = S^2|D|$, where $D$ gauges the axial zero-field splitting ($D\hat{S}_{z^2}$) in the ground state. The smaller thermal barrier ($\Delta$) for a $S = 9$ complex would also lead to larger tunnelling rates. A second possibility is that complexes **2** and **3** both have $S = 10$ ground states, but there are larger higher-order (quartic) zero-field interactions present for complex **3** and this leads to a faster tunnelling. Finally, the differences in rates between complexes **2** and **3** could be due to differences in rates of positioning a $Mn_{12}$ complex into the $m_s = -3$ level from which tunnelling occurs.

High-field EPR experiments are in progress to determine whether complexes **2** and **3** differ in their ground-state spins. Understanding the differences in hysteresis loops between complexes **2** and **3** should give insight into the unknown mechanism of magnetization tunnelling. This is essential if the potential application of single-molecule magnets to memory devices is to be realized.

This work was supported by the National Science Foundation. The W. A. Keck Foundation provided funds for the SQUID magnetometer used in the ac susceptibility experiments.

## Footnotes and References

* E-mail: dhendrickson@ucsd.edu

† *Crystal data*: $C_{128}H_{126}Mn_{12}O_{51}$ **2**: $M_w = 3139.46$, monoclinic, space group $I2/a$, $a = 29.2794(4)$, $b = 32.3271(4)$, $c = 29.8738(6)$ Å, $\beta = 99.2650(10)°$, $U = 27907.2(8)$ Å$^3$, $Z = 8$, $T = 223(2)$ K, $\mu$(Mo-K$\alpha$) = 11.31 cm$^{-1}$, $D_c = 1.488$ g cm$^{-3}$, $R(F) = 0.0880$ for 13 048 observed independent reflections ($4 \leqslant 2\theta < 56°$).

$C_{136}H_{128}H_{128}Mn_{12}O_{50}$ **3**: $M_w = 3221.66$, monoclinic, space group $C2/c$, $a = 40.4589(5)$, $b = 18.2288(2)$, $c = 26.5882(4)$ Å, $\beta = 125.8359(2)°$, $U = 15897.1(4)$ Å$^3$, $Z = 4$, $T = 193(2)$ K, $\mu$(Mo-K$\alpha$) = 7.94 cm$^{-1}$, $D_c = 1.346$ g cm$^{-3}$, $R(F) = 0.1021$ for 7155 observed independent reflections ($4 \leqslant 2\theta < 56°$).

For complex **2** three solvate $H_2O$ molecules were located. The 4-methylbenzoic acid solvate molecule of complex **3** is highly disordered. CCDC 182/636.

1 B. Schwarzschild, *Phys. Today*, January 1997, 17.
2 E. M. Chudnovsky, *Science*, 1996, **274**, 938.
3 S. M. J. Aubin, M. W. Wemple, D. M. Adams, H.-L. Tsai, G. Christou and D. N. Hendrickson, *J. Am. Chem. Soc.*, 1996, **118**, 7746.
4 R. Sessoli, D. Gatteschi, A. Caneschi and M. A. Novak, *Nature*, 1993, **365**, 141; D. Gatteschi, A. Caneschi, L. Pardi and R. Sessoli, *Science*, 1994, **265**, 1054.
5 R. Sessoli, H.-L. Tsai, A. R. Schake, S. Wang, J. B. Vincent, K. Folting, D. Gatteschi, G. Christou and D. N. Hendrickson, *J. Am. Chem. Soc.*, 1993, **115**, 1804.
6 J. R. Friedman, M. P. Sarachik, J. Tejada and R. Ziolo, *Phys. Rev. Lett.*, 1996, **76**, 3830.
7 L. Thomas, F. Lionti, R. Ballou, D. Gatteschi, R. Sessoli and B. Barbara, *Nature*, 1996, **383**, 145.
8 J. Tejada, R. F. Ziolo and X. X. Zhang, *Chem. Mater.*, 1996, **8**, 1784.

*Received in Bloomington, IN, USA; 21st August 1997; 7/06144G*

# Development of a site-selective copper-ion-exchanging method for HZSM-5 by vapourization of a hexafluoroacetylacetonato–copper complex

**Yasushige Kuroda,*[a] Kazunori Yagi,[a] Yuzo Yoshikawa,[a] Ryotaro Kumashiro[b] and Mahiko Nagao[b]**

[a] *Department of Chemistry, Faculty of Science, Okayama University, Tsushima, Okayama 700, Japan*
[b] *Research Laboratory for Surface Science, Faculty of Science, Okayama University, Tsushima, Okayama 700, Japan*

**The deposition of copper ion into a single type of ion-exchange site in HZSM-5-type zeolite is successful using bis(1,1,1,5,5,5-hexafluoroacetylacetonato)copper(II) as a volatile complex, and the sample thus prepared gives a single IR absorption band at 2158 $cm^{-1}$ upon adsorption of CO, differing from a sample prepared by aqueous ion-exchange, which gives two bands at 2158 and 2151 $cm^{-1}$.**

Many applications of zeolites rely on their unique surface properties that are largely determined by the concentration, distribution and nature of exchanged ions, such as protons, alkali metal and transition metal ions. Among many kinds of zeolites, the copper-ion-exchanged ZSM-5-type zeolite (Cu-ZSM-5) has become one of the most promising materials for the catalytic decomposition reaction of $NO_x$ to $N_2$ and $O_2$.[1,2] This material has also a specific adsorption property for $N_2$ at room temperature; and hence it can be used as a catalyst for $N_2$ separation, fixation and activation.[3,4] From the viewpoints of the development of more effective catalysts, it is useful and important to obtain information on the nature of the active sites on Cu-ZSM-5 for $NO_x$ decomposition and specific $N_2$ adsorption. Thus far we have investigated the state of copper ion exchanged in mordenite-type zeolites by using CO as a probe molecule and have found that there are at least two main types of sites in this substance, giving IR bands at 2160 and 2150 $cm^{-1}$ when CO is adsorbed on each site.[5] This situation is consistent with the results obtained independently by Zecchina and coworkers[6] and by Iwamoto and Hoshino for the Cu-ZSM-5 system.[7] A great deal of effort has so far been made to analyze these exchanging sites. However, the understanding of the role of each site for $NO_x$ decomposition reaction and $N_2$ fixation is still far from being complete.[8,9] The presence of a number of different ion-exchanged sites leads to complications in such studies. The most pertinent approach is to prepare site-selectively copper-ion-exchanged ZSM-5.

In the present work, we succeeded in site-selective copper-ion deposition in this zeolite and the results obtained shed light on the analysis of active sites for $NO_x$ decomposition and $N_2$ adsorption.

Bis(1,1,1,5,5,5-hexafluoroacetylacetonato)copper(II), [Cu(hfac)$_2$] (Aldrich), was used as a vapourizing source in chemical vapour deposition (CVD).[10] For the measurement of IR spectra, the HZSM-5 sample (supplied from Tosoh Co.) was pressed into a pellet (5 mg) of 10 mm diameter, and it was initially treated at 300 K for 2 h under a reduced pressure of 1 mPa in the *in situ* cell. The [Cu(hfac)$_2$] complex was then vapourized onto this pellet at room temperature. The sample thus prepared was evacuated at 873 K under a reduced pressure of 1 mPa and then treated with CO at 300 K. The ion-exchanging operation of HZSM-5 with copper ions was also carried out in an aqueous solution in the same manner as described in the literature.[3]

Fig. 1 shows the transmission FTIR spectra for the HZSM-5 sample evacuated at 873 K (*a*) and for the HZSM-5 sample with modified surface by deposition of [Cu(hfac)$_2$] followed by evacuation at 873 K (*b*). The spectrum in Fig. 1(*a*) shows intense bands at 3746 and at *ca*. 3613 $cm^{-1}$, which are due to hydroxyl groups of free silanol and of the Brönsted acid site,

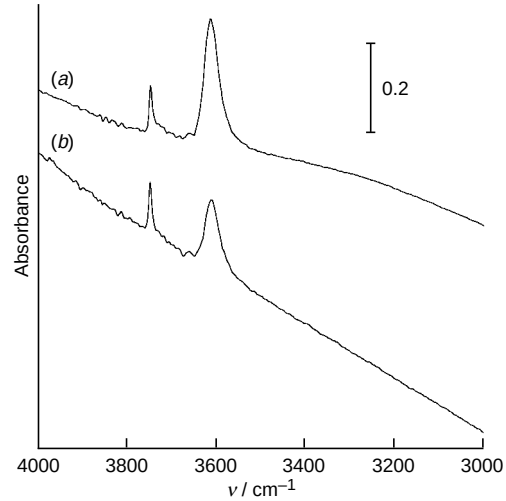



**Fig. 1** IR spectra of the HZSM-5 sample evacuated at 873 K (*a*) and for the surface-modified HZSM-5 sample with Cu(hfac)$_2$ and then subsequently evacuated at 873 K (*b*)

respectively. At first glance, the spectrum in Fig. 1(*b*) appears to be similar to the spectrum in Fig. 1(*a*). However, the relative intensity of the 3613 $cm^{-1}$ band to the 3746 $cm^{-1}$ band is lower for the surface-modified HZSM-5 sample, compared with that for the original HZSM-5 sample. These data suggest ion exchange of the proton on the Brönsted acid site with copper ion in the course of the evacuation process at higher temperatures.

Fig. 2 shows IR spectra for the sample prepared by deposition of [Cu(hfac)$_2$], as well as for a sample prepared by ion-exchange from aqueous solution. The spectra in Fig. 2(*b*) and (*d*) are those

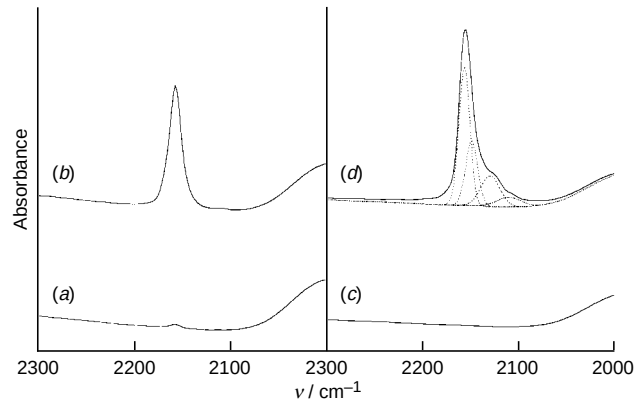



**Fig. 2** IR spectra for the Cu(hfac)$_2$-deposited HZSM-5 sample (*a*) and (*b*) and for the copper-ion-exchanged HZSM-5 sample (*c*) and (*d*). These samples were pretreated in the following manner: (*a*) and (*c*), evacuated at 873 K; (*b*) and (*d*), equilibrated with CO gas at 300 K under nearly zero pressure after evacuation at 873 K. The deconvolution (dotted line) curves for spectrum (*d*) are also depicted.

for samples equilibrated with CO under nearly zero pressure, *i.e.* the chemisorption region. The spectra for both samples evacuated at 873 K after CVD [Fig. 2(*a*)] or ion-exchange from aqueous solution [Fig. 2(*c*)] are also included for comparison. As can be seen from the Fig. 2(*a*) and (*c*), scarcely any band is discernible in the 873 K treated sample in the region shown. It is clearly seen that chemisorption of CO takes place on the sample prepared by the CVD method to give a single band at 2158 $cm^{-1}$ [Fig. 2(*b*)]. Chemisorption of CO also occurs for the sample prepared by ion-exchange from aqueous solution and the resultant CO species adsorbed give a broad IR band centred at *ca*. 2155 $cm^{-1}$ [Fig. 2(*d*)], which is slightly but obviously tailing to the lower wavenumber side. Based on the information accumulated so far,[11–14] it is generally agreed that an absorption band at *ca*. 2150 $cm^{-1}$ can be assigned to the C–O stretching mode of a CO species adsorbed on $Cu^{I}$; the copper complex was deposited on HZSM-5 by CVD and subsequent heat treatment reduced the $Cu^{II}$ to $Cu^{I}$. For the ion-exchanged sample, it is apparent that heat treatment *in vacuo* reduces $Cu^{II}$ to $Cu^{I}$, based on data described in previous papers.[3,5] A numerical deconvolution technique was applied to identify the bands in Fig. 2(*b*) and (*d*). For the CVD sample, only a single absorption band centred at 2158 $cm^{-1}$ is present, *i.e.* the copper ion-exchange occurred only at one type of site. For the sample prepared by ion-exchange from aqueous solution, the observed broad band at *ca*. 2155 $cm^{-1}$ is seen to be composed of two major components at 2158 and 2151 $cm^{-1}$. From the present experimental result, it is clear that for the sample prepared by ion-exchange from aqueous solution that both types of sites are occupied by copper ions. Recently, Zecchina and coworkers have reported, on the basis of EXAFS data, that two types of ion-exchanged sites exist on ZSM-5,[15] consistent with the above observations.

Taking the experimental data into consideration, it is also apparent that one of the two types of exchangeable sites in HZSM-5 is occupied selectively by copper ion in the sample prepared by CVD using $[Cu(hfac)_2]$, while in the sample prepared by ion-exchange from aqueous solution both types of sites are occupied by copper ion. This new ion-exchanging method (CVD) has potential to be utilized for the analysis of the active sites in the $NO_x$ decomposition reaction and also for the $N_2$ fixation reaction.

This work was supported by the Foundation from the Ministry of Education, Science, Sports and Culture of Japan (Nos. 08640750 and 09218242). We also thank Mr. T. Ozaki in the glassblowing workshop of Hiroshima University for technical assistance in making the *in situ* glass cell for IR measurements.

## Footnote and References

* E-mail: kuroda@cc.okayama-u.ac.jp

1 M. Iwamoto, S. Yokoo, K. Sakai and S. Kagawa, *J. Chem. Soc., Faraday Trans.*, 1981, **77**, 1629.
2 J. Valyon and W. K. Hall, *J. Phys. Chem.*, 1993, **97**, 1204.
3 Y. Kuroda, Y. Yoshikawa, S. Konno, H. Hamano, H. Maeda, R. Kumashiro and M. Nagao, *J. Phys. Chem.*, 1995, **99**, 10621.
4 G. Spoto, S. Bordiga, G. Ricchiardi, D. Scarano, A. Zecchina and F. Geobaldo, *J. Chem. Soc., Faraday Trans.*, 1995, **91**, 3285.
5 Y. Kuroda, H. Maeda, Y. Yoshikawa, R. Kumashiro and M. Nagao, *J. Phys. Chem. B*, 1997, **101**, 1312.
6 G. Spoto, A. Zecchina, S. Bordiga, G. Ricchiardi, G. Martra, G. Leofanti and G. Petrini, *Appl. Catal. B*, 1994, **3**, 151.
7 M. Iwamoto and Y. Hoshino, *Inorg. Chem.*, 1996, **35**, 6918.
8 M. Iwamoto, H. Yahiro, N. Mizuno, W.-X. Zhang, Y. Mine, H. Furukawa and S. Kagawa, *J. Phys. Chem.*, 1992, **96**, 9360.
9 M. Shelef, *Chem. Rev.*, 1995, **95**, 209.
10 J. Farkas, M. J. H. Smith and T. T. Kodas, *J. Phys. Chem.*, 1994, **98**, 6753.
11 J. Howard and J. M. Nicol, *Zeolites*, 1988, **8**, 142.
12 J. Sárkány, J. L. d'Itri and W. M. H. Sachtler, *Catal. Lett.*, 1992, **16**, 241.
13 V. Y. Borovkov and H. G. Karge, *J. Chem. Soc., Faraday Trans.*, 1995, **91**, 2035.
14 K. I. Hadjiivanov, M. M. Kantcheva and D. G. Klissurski, *J. Chem. Soc., Faraday Trans.*, 1996, **92**, 4595.
15 C. Lamberti, S. Bordiga, M. Salvalaggio, G. Spoto, A. Zecchina, F. Geobaldo, G. Vlaic and M. Bellatreccia, *J. Phys. Chem. B*, 1997, **101**, 344.

*Received in Cambridge, UK, 22nd August 1997; 7/06147A*

# Further demonstration of the higher reactivity of the vinyl hydrogen rather than the allyl hydrogen towards singlet oxygen

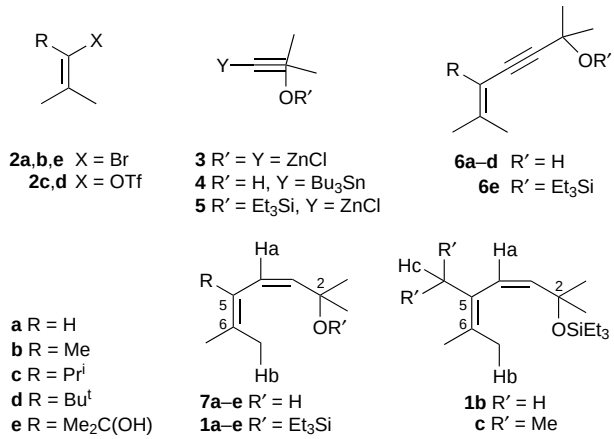
**Hajime Mori, Keiichi Ikoma and Shigeo Katsumura***

*School of Science, Kwansei Gakuin University, Uegahara 1-1-155, Nishinomiya 662, Japan*

**In a new linear twisted 1,3-diene, an anomalously high reactivity of the vinyl hydrogen rather than the allyl hydrogen towards singlet oxygen is observed.**

Previously, we reported the photosensitized oxygenation of significantly twisted *cis*-β-ionol derivatives, and found the vinyl hydrogen to be anomalously more reactive towards singlet oxygen than the allyl hydrogen in some significantly twisted compounds of *cis*-β-ionol derivatives. We proposed that this unusually high reactivity of the vinyl hydrogen in a significantly twisted 1,3-diene should be attributed to a large interaction between the σ* orbital of the vinyl hydrogen and the π orbital of another double bond.[1] Since only a few examples of significantly twisted 1,3-dienes are found in the literature,[2] although conjugated dienes are some of the most common systems in organic reactions as represented by pericyclic reactions, further investigation on the design, synthesis and photosensitized oxygenation of significantly twisted 1,3-dienes has been required. Here we report the photosensitized oxygenation of a newly designed linear twisted 1,3-diene, and describe a further demonstration of the unusually high reactivity of the vinyl hydrogen towards singlet oxygen.

The substrates **1a**–**e** were chosen for the photosensitized oxygenation because the substituent R on the olefin can be changed from hydrogen to methyl, isopropyl and *tert*-butyl, and when R is a bulky substituent the 1,3-diene structure would be twisted. Syntheses of these *cis*-1,3-diene derivatives were accomplished by palladium catalysed coupling of the appropriate vinyl halides or enol trifluoromethanesulfonates (triflates) with zinc or stannyl acetylides followed by partial hydrogenation and then protection of the tertiary hydroxy group. Thus, compounds **6a**,**b** were prepared from commercially available vinyl bromides **2a**,**b** by reaction with zinc acetylide **3** in the presence of tetrakis(triphenylphosphine)palladium (THF, 60 °C; **6a**, 80%; **6b**, 45% yield), respectively.[3] Compounds **6c**,**d** which have bulky substituents were synthesized by coupling of stannyl acetylide **4** with enol triflates **2c**,**d**,[4] which were prepared from the corresponding ketones[5] (LDA, *N*-phenyltrifluoromethanesulfonimide, THF), in the presence of the same palladium reagent (THF, room temp.; **6c**, 45%; **6d**, 52% yield).[6] Another enyne compound **6e** was also synthesized by coupling of vinyl bromide **2e**, prepared from methyl 3,3-dimethylacrylate ($Br_2$–$CH_2Cl_2$, DBU–THF, MeMgI–THF; 46% yield), with **5** under the same conditions as those of **2a**,**b** (**6e**, 84% yield). Partial reduction of the acetylene groups of **6a**–**e** to the corresponding *cis*-olefins by catalytic hydrogenation in hexane reflected the reactivity of their acetylene groups. Thus, **7a**,**b** were obtained with Lindlar catalyst in the presence of a catalytic amount of quinoline (**7a**, 47%; **7b**, 49% yield). In the absence of quinoline with Lindlar catalyst, **7c** was obtained (47% yield). Hydrogenation of **6d** with palladium on barium sulfate gave **7d** (60% yield) and of **6e** with palladium on charoal gave **1e** (MeOH, 90% yield). The *cis*-alcohols obtained were transformed into the corresponding triethylsilyl ethers **1a**–**d** in excellent yield ($Et_3SiCl$, DMAP, $Et_3N$, DMF).† The maximum absorption values in the electronic spectra of compounds **1b**–**e** were less than 210 nm, whereas that of **1a** was 238 nm. These data clearly show that **1b**–**e** are significantly twisted around the central single bond of the 1,3-diene. The most stable conformations of **1b**–**e** obtained by molecular mechanics calculations and molecular obrital calculations also support the significantly twisted structures.[1]§

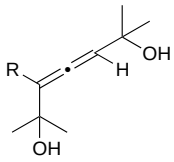



The photosensitized oxygenation of **1a**–**e** was carried out in $CH_2Cl_2$ (1.0–2.0 mmol scale) by irradiation using a halogen lamp under an oxygen atmosphere in the presence of a catalytic amount of tetraphenylporphine and 1 equiv. of triphenylphosphine at 0 °C. The products were isolated by column chromatography and all of them were characterized by $^1H$, $^{13}C$ NMR and IR spectroscopy, and by elemental analysis or high resolution mass spectra for some compounds. The ene reaction of Ha and Hb gave allene **8** and isopropenyl compound **9**, respectively. In the case of **1b**,**c**, the ene reaction of Hc gave compounds **10b**,**c**, which might produce allene **11** by further oxygenation. The results of the photosensitized oxygenation are shown in Table 1. For compounds **1d**,**e**, allenes **8d**,**e** (mp 76–77 °C) were produced in 75 and 74% yield along with isopropenyl compounds **9d**,**e** in 8 and 9% yield, respectively. In these cases, the abstracted vinyl hydrogen Ha and allyl hydrogen Hb are located at the opposite sides of the C5–C6 double bond, and the vinyl hydrogens Ha were much more reactive than the allyl hydrogens Hb toward singlet oxygen.[7]¶

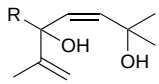
**Table 1** Ene reaction of acyclic twisted 1,3-dienes with singlet oxygen

| | Yield (%) | | | |
|---|---|---|---|---|
| Substrate | **8**[a] | **9**[a] | **10**[a,b] | **11**[a,b] |
| **1a** | 29[b] | 45[b] | — | — |
| **1b** | 32[b] | 12[b] | 42 | — |
| **1c** | 38[b] | 27[b] | 8 | 17 |
| **1d** | 75[b] | 8[b] | — | — |
| **1e** | 74[c] | 9[c] | — | — |

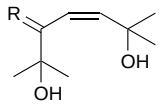
[a] Isolated yield. [b] The yields are over three steps; silylation of the corresponding alcohol followed by photosensitized oxygenation and then desilylation. [c] The yields are over two steps; photosensitized oxygenation and desilylation.



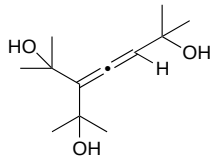

**8a–e**




**9a–e**




**10b** R = $CH_2$
**10c** R = $Me_2C$




**11** (≡**8e**)

These results are compatible with those of the cyclic system reported previously. On the other hand, compound **1a** produced allene **8a** in 29% and isopropenyl compound **9a** in 45% yield, respectively. Photosensitized oxygenation of **1b** gave allene **8b** and allyl alcohol **10b** in 32 and 42% yield, respectively, along with isopropenyl compound **9b** in 12% yield. Since both the abstracted vinyl hydrogen Ha and the allyl hydrogen Hc in **1b** are located at the same side of the C5–C6 double bond, and the ene reactions of the Ha and the Hc with singlet oxygen gave the allene **8b** and the allyl alcohol **10b**, respectively, the relative yields of **8b** and **10b** obviously reflect the relative reactivity of the vinyl hydrogen and the allyl hydrogen. It is worth noting that the vinyl hydrogen shows comparable reactivity to the allyl hydrogen. Next, in the photooxygenation of **1c**, allene **8c**, isopropenyl compound **9c**, diene **10c** and trihydroxyallene **11**, which is identical to **8e**, were obtained in 38, 27, 8 and 17% yield, respectively. In this case, compound **11** must be produced from **10c**, giving a 25% yield of allyl hydrogen Hc abstracted products. It is noteworthy that the vinyl hydrogen Ha of **1c** was more reactive than the isopropyl hydrogen Hc, and that the sterically hindered hydrogen Hc in **1c** reacted with singlet oxygen to a similar extent as the allyl hydrogen Hb.

Unfortunately, we did not observe a clear relationship between the bulkiness of the C5 substituent and the twisting of the two double bonds, and hence between the extent of twisting and the yield of the oxygenated products. However, the evidence suggests that twisting and/or the C5 substituent have an effect on the reactivity of 1,3-dienes, since the relative proportions of C6 and C5 hydroxy products in the significantly twisted **1b**–**e** were the opposite to that of the conjugated **1a**, thus the proportions of C6 and C5 hydroxy products in **1b**–**e** were 63–75 *vs*. 27–8, while for **1a** the proportion was 29 *vs*. 45.

The results obtained here seem to support our proposal on the activation of the vinyl hydrogen based on σ*–π orbital interaction between the vinyl C–H bond and another double bond in significantly twisted 1,3-dienes.[1]

This work was partly supported by Grant-in-Aid for Scientific Research on Priority Areas (No. 283, 'Innovative Synthetic Reactions') from Monbusho.

## Footnotes and References

* E-mail: z89019@kgupyr.kwansei.ac.jp

† The triethyl group on the silyl ethers is essential. See ref. 1.

§ The calculations were performed using software packages INSIGHT II 2.1.0 program, Biosym. Technol. Inc. San Diego, USA, with CFF91 forcefield and SPARTAN version 3.1 and 4.0 Wavefunction, Inc., Irvine, CA with STO-3G basis set.

¶ The regioselectivity of an ene reaction with singlet oxygen is discussed in ref. 7.

1 H. Mori, K. Ikoma, Y. Masui, S. Isoe, K. Kitaura and S. Katsumura, *Tetrahedron Lett.*, 1996, **37**, 7771.
2 D. Miller, M. Trammel, A. Kini and R. S. H. Liu, *Tetrahedron Lett.*, 1981, **22**, 409; G. Becher and A. Mannschreck, *Chem. Ber.*, 1983, **116**, 264; N. Sakai, J. Decatur and K. Nakanishi, *J. Am. Chem. Soc.*, 1996, **118**, 1559.
3 A. O. King, N. Okukado and E. Negishi, *J. Chem. Soc., Chem. Commun.*, 1977, 683.
4 J. E. McMurry and W. J. Scott, *Tetrahedron Lett.*, 1983, **24**, 979.
5 J. E. Dubois, M. Boussu and C. Lion, *Tetrahedron Lett.*, 1971, 829.
6 J. K. Stille and J. H. Simpson, *J. Am. Chem. Soc.*, 1987, **109**, 2138.
7 M. Orfanopoulos, M. Stratakis and Y. Elemes, *J. Am. Chem. Soc.*, 1990, **112**, 6417; W. Adam and J. Richer, *Tetrahedron Lett.*, 1993, **34**, 8423; M. Stratakis and M. Orfanopoulos, *Tetrahedron Lett.*, 1995, **36**, 4291.

*Received in Cambridge, UK, 13th August 1997; 7/05924H*

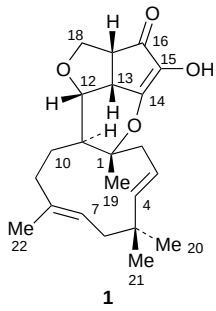
# Biosynthesis of Xenovulene A®: formation of a cyclopentenone *via* a unique ring expansion–ring contraction mechanism

**Mairi E. Raggatt,[a] Thomas J. Simpson*[a] and M. Inês Chicarelli-Robinson[b]**

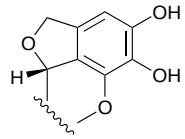
[a] *School of Chemistry, University of Bristol, Cantock's Close, Bristol, UK BS8 1TS*
[b] *Natural Products Chemistry Department, Xenova Discovery Ltd, 545 Ipswich Road, Slough, Berkshire, UK SL1 4EQ*

**Incorporation studies with $^{13}$C-labelled acetates and methionine in *Acremonium strictum* indicate that the cyclopentenone moiety in Xenovulene A® is formed *via* a unique pathway in which a C-methylated phenolic precursor undergoes ring expansion to a tropolone followed by two successive ring contractions resulting in incorporation of the C-methyl carbon into the five-membered ring.**

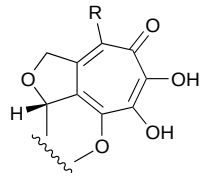
Xenovulene A® **1**, a novel inhibitor of benzodiazepine binding to the GABA-benzodiazepine receptor,[1] was isolated from cultures of *Acremonium strictum*.[2] The structure of **1** contains an unusual furocyclopentenone moiety fused to a humulene-derived 11-membered ring. A number of minor co-metabolites of **1** have been isolated[3] in which the cyclopentenone moiety is replaced by a trioxygenated benzene **2** or highly oxygenated tropolone rings, **3** and **4**. While fungal metabolites containing all of these types of rings are known, the presence of all three in a single family is unique.



**1**



**2**



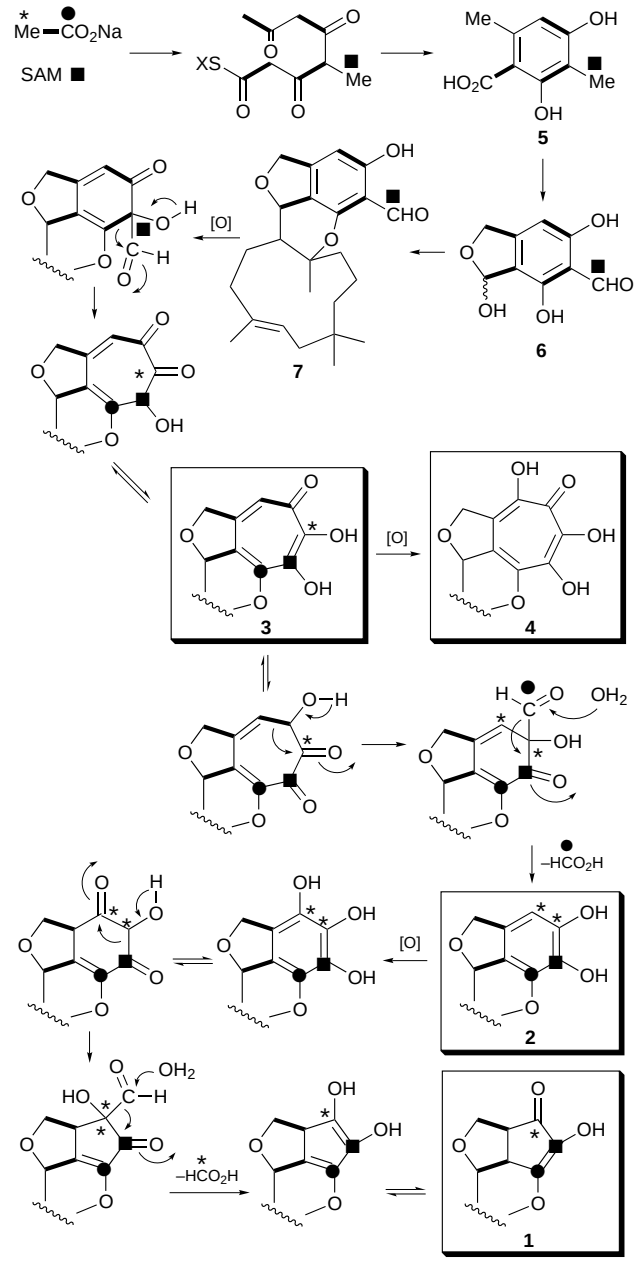
**3** R = H
**4** R = OH

Recently, two very similar fungal metabolites, pycnidione[4] and eupenifeldin[5] were isolated. These both contain a similar fusion of a tropolone to humulene. The higher plant metabolite, lucidene, also contains a humulene ring fused to an *o*-hydrobenzyl moiety.[6] The fungal tropolone, stipitatonic acid is derived from 3-methylorsellinic acid **5** with incorporation of the methionine-derived 3-methyl group into the polyketide-derived aromatic ring.[7] In addition, the fungal cyclopentenone metabolites, terrein[8] and cryptosporiopsonol[9] have been shown to be derived by ring contraction of the aromatic ring of dihydroisocoumarin intermediates. Thus a plausible pathway to the Xenovulene metabolites **1**–**4** appeared to be *via* the polyketide-derived 3-methylorsellinic acid **5** (Scheme 1) which would be converted by standard biosynthetic modifications to the lactol **6**. This would react with the 6,7 double bond of humulene, either *via* a carbocation mediated addition or cycloaddition of the readily derived quinomethane to give the key tetracyclic intermediate **7**.

Ring expansion of the phenolic ring in **7** followed by hydroxylation would give the tropolones **3** and **4**, whereas oxidative decarboxylation of **7** would give **2**, ring contraction and decarboxylation of which would lead to Xenovulene A® **1**.

We now report incorporation studies with $^{13}$C-labelled acetates and methionine which render this branched pathway untenable and indicate a linear relationship among the metabolites.

The results of incorporations† of [1-$^{13}$C]-, [2-$^{13}$C]- and [1,2-$^{13}C_2$]-acetates and [*methyl*-$^{13}$C]methionine into Xenovulene A® are summarised in Fig. 1. Surprisingly, no intact acetate unit was present in the cyclopentenone ring and C-15 was not



**Scheme 1**

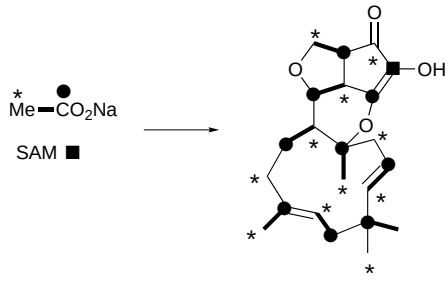



**Fig. 1**

derived from either the methyl or carboxy carbons of acetate. This was accounted for on feeding $^{13}$C-labelled methionine which gave an approximately 8% enrichment at C-15. To accommodate these results, the remarkable sequence outlined in Scheme 1 is proposed. Hydroxylation of **7** allows ring expansion *via* an α-ketol rearrangement to give **3** which, after further tautomeric adjustment, can ring contract and lose formic acid to form the trioxygenated benzenoid metabolite **2** with incorporation of the methionine-derived carbon into the aromatic ring. Further oxidation, α-ketol mediated ring contraction and loss of formate generates Xenovulene A® with the observed labelling pattern.

Work is in progress to obtain further information on the detailed mechanisms and the exact oxidation levels of the intermediates on the pathway. For example, analogous pathways in which the formyl group in **7** is at the hydroxymethyl or carboxy level can be proposed, but these necessitate more extensive reductive and oxidative adjustments to obtain the final structures. Overall, this represents a remarkable and unprecedented pathway in which a cyclopentenone is formed from a phenolic precursor *via* one ring expansion and two successive ring contractions.

## Footnotes and References

* E-mail: tom.simpson@bristol.ac.uk

† Precursors were fed to shake flask cultures of *A. strictum* at levels of 1.0 g $l^{-1}$ ([1-$^{13}$C]- and [2-$^{13}$C]-acetates) or 0.5 g $l^{-1}$ ([1,2-$^{13}C_2$]acetate and [*methyl*-$^{13}$C]methionine). Xenovulene A® (approximately 10 mg $l^{-1}$) was purified by flash chromatography followed by reversed phase HPLC. Incorporation of singly $^{13}$C-labelled acetates resulted in enrichments of 1–3 atom%. No significant differences in level of labelling were observed between the polyketide and terpenoid moieties. The minor metabolites **2**–**4** were not isolated.

1 P. Thomas, H. Sundaram, B. J. Krishek, P. Chazot, X. Xie, P. Bevan, S. J. Brocchini, C. J. Latham, P. Charlton, M. Moore, S. J. Lewis, D. M. Thorton, F. A. Stephenson and T. G. Smart, *J. Pharmacol. Exp. Ther.*, 1997, **282**, 513.
2 A. M. Ainsworth, M. I. Chicarelli-Robinson, B. R. Copp, U. Fauth, P. J. Hylands, J. A. Holloway, M. Latif, G. B. O'Beirne, N. Porter, D. V. Renno, M. Richards and N. Robinson, *J. Antibiot.*, 1995, **48**, 568.
3 Xenova Discovery Ltd., manuscript in preparation.
4 G. H. Harris, K. Hoogsteen, K. C. Silverman, S. L. Raghoobar, G. F. Bills, R. B. Lingham, J. L. Smith, H. W. Dougherty, C. Cascales and F. Pelaez, *Tetrahedron*, 1993, **49**, 2139.
5 F. Mayerl, Q. Gao, S. Huang, S. E. Klohr, J. A. Matson, D. R. Gustavson, D. M. Pirnik, R. L. Berry, C. Fairchild and W. C. Rose, *J. Antibiot.*, 1993, **46**, 1082.
6 H. Weenen, M. H. H. Nkunya, A. A. El-Fadl, S. Harkema and B. Zwanenburg, *J. Org. Chem.*, 1990, **55**, 5107.
7 A. I. Scott, H. Guildford and E. Lee, *J. Am. Chem. Soc.*, 1971, **93**, 3534.
8 R. A. Hill, R. H. Carter and J. Staunton, *J. Chem. Soc., Chem. Commun.*, 1975, 380.
9 J. S. E. Holker and K. Young, *J. Chem. Soc., Chem. Commun.*, 1975, 525.

*Received in Glasgow, UK, 8th July 1997; 7/04864E*

# Hydrogen-bonded porous solid derived from trimesic amide

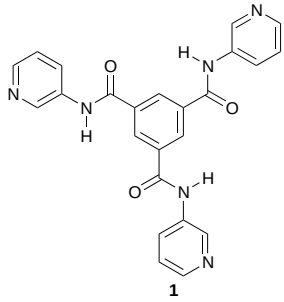
**Anja R. A. Palmans,[a] Jef A. J. M. Vekemans,*[a] Huub Kooijman,[b] Anton L. Spek[b]† and E. W. Meijer[a]**

[a] *Laboratory of Organic Chemistry, University of Technology, PO Box 513, 5600MB Eindhoven, The Netherlands*
[b] *Bijvoet Center for Biomolecular Research, Crystal and Structural Chemistry, University of Utrecht, Padualaan 8, 3584 CH Utrecht, The Netherlands*

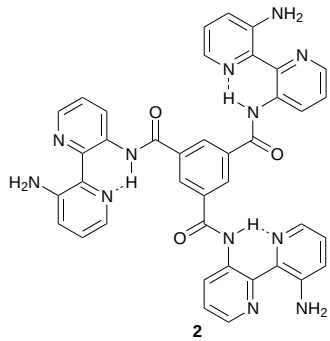
***N*,*N*′,*N*″-Tris(3-pyridyl)trimesic amide, 1, forms a unique *P*$\bar{3}$ symmetrical crystal containing pores with a mean diameter of 8.26 Å.**

Supramolecular assembly and crystal engineering are fruitful concepts to use in the design and development of structures with a desired shape. Recently these concepts evolved to be used in the construction of tubular superstructures[1] and porous solids.[2] Hydrogen bonding is one of the major tools which can be used to achieve the desired order.[3]

Here we report on the highly ordered infinite bilayer crystal structure of triamide **1**,‡ derived from trimesic acid (benzene-1,3,5-triacarboxylic acid) and 3-pyridylamine.§ In contrast to recently designed structures,[4] our result was entirely serendipitous. Structure **1** served just as a model for comparison with intramolecularly hydrogen-bonded structure **2**, a precursor for extended core discotic liquid crystals of enhanced thermal stability.[5]



**1**



**2**

The transparent, hexagon-shaped crystals of **1**, obtained upon crystallization from methanol, suggested hexagonal symmetry and prompted us to investigate a single crystal by X-ray diffraction. As indicated in Fig. 1 the asymmetric cell comprises only one third of a molecule while the unit cell is populated by two molecules.‡ Intermolecular hydrogen bonding between the pyridyl nitrogens and the amide NHs of adjacent molecules provides the basis for a macrocyclic organization in a rosette-like structure. A 30-membered macrocycle is formed with participation of six molecules and the 3-aminopyridyl units constitute the walls of a cavity with a mean diameter of 8.26 Å (Fig. 2).

The $C_3$-symmetry of the molecule then allows for the creation of an infinite two-dimensional honeycomb grid with repeating units at 13.87 Å in six directions and with a thickness of approximately 8.40 Å. According to Etter's[6] graph set analysis the nitrogen hydrogen bond donors and acceptors are involved in a $R_6^6(30)$ pattern. Closer inspection reveals the bilayer structure of an ensemble of molecules in one sheet (Fig. 3). The benzene units occupy alternating up and down positions. All the amide carbonyls point outwards, while the pyridyl units orientate their nitrogens inwards in the bilayer structure. This implies that although the crystal is achiral, the structure is a combination of trimesic units of *P*-helicity with units of *M*-helicity.

The infinite bilayer sheets themselves belong to a three dimensional super structure in which all the sheets are in fact repeating units placed exactly on top of each other. This results in the formation of a real porous structure with channels of

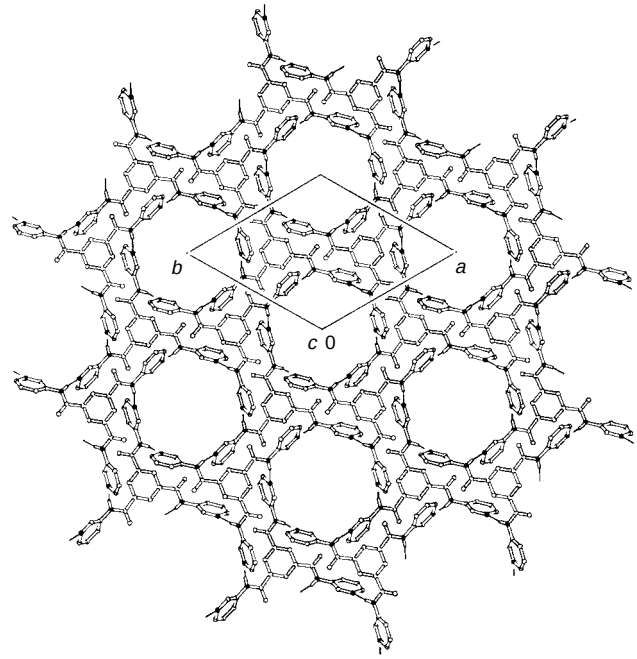



**Fig. 1** Infinite rosette structure of **1**

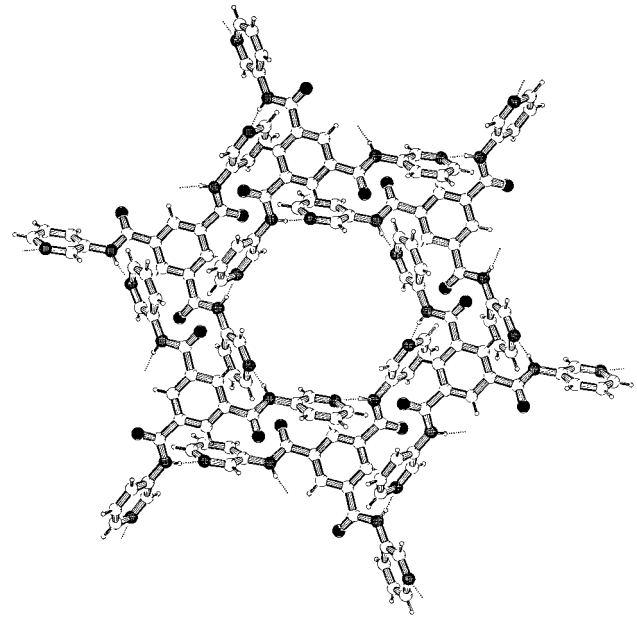


**Fig. 2** Cavity in **1** as a result of six-fold intermolecular hydrogen bonding

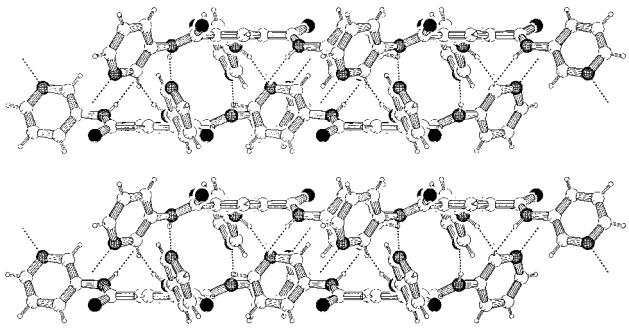


**Fig. 3** Superimposed bilayer structure of **1** creating channels

nanometer scale diameter and millimeter scale length. The formation of this 3D structure may rest simply on optimal packing. Alternatively it is rationalized by cooperative C–H··O interactions[7] (total length 3.39 Å) between each amide oxygen and a pyridyl C–H belonging to an adjacent bilayer.

Methanol is essential to guarantee the stability of the crystals, undoubtedly due to its role as a template and guest filling some of the void space in the interior of the channels, more specifically in the cavity surrounded by the six pyridyl units. The X-ray determination does not allow accurate localization of methanol in **1** but a molar ratio of 3 : 1 is estimated. According to the $^1$H NMR spectrum in [$^2H_6$]DMSO the molar content of methanol ranges from 1.5 to 3.0, depending on sample preparation. Elemental analysis of the crystals is irreproducible due to partial loss of methanol during analysis while analysis after removal of methanol at high temperature shows a deviation, presumably due to uptake of atmospheric (water) vapours. Upon heating between glass the crystals undergo, far below the melting point, a phase transition at 190 °C, suggesting loss of methanol. In air or in solvents like toluene the crystals become opaque and disintegrate. In pentane, by contrast, the crystals are stable.

To provide evidence for the accessibility of the channels for external molecules, a methanol–$CD_3OD$ exchange experiment was conducted¶ and the $^1$H NMR spectrum in [$^2H_6$]DMSO unambiguously demonstrates the complete disappearance of non-deuteriated methanol from the crystals. Analogous experiments have been conducted in other trimesic acid derivatives and in other tectonic molecules.[8] The calculated density of **1** without guests amounts to 1.0395 g cm$^{-3}$ and of **1**·**3** MeOH to 1.267 g cm$^{-3}$. This relatively low density contrasts with the higher density of many trimesic derivatives including the parent acid (1.449 g cm$^{-3}$).[9]

The presence of $C_3$-symmetry tends to induce void space in crystals, which Nature may compensate for by producing concatenated or interpenetrated structures or by incorporation of appropriate guest molecules. To our surprise, up to now no X-ray data are available on symmetrical secondary trimesic amides. In trimesic acid three-fold interpenetration of two-dimensional layers composed of three parallel molecules is observed,[9] unless guests like pyrene and ethanol are built in.[10] A pattern such as the one found in compound **1** is, to the best of our knowledge, unprecedented. It seems that in this particular molecule an acceptable compromise is found between void space, concatenation of molecules and inclusion of guests. The formation of a bilayer structure in compound **1** is reminiscent of the Piedfort units observed in other $C_3$-symmetric systems like 2,4,6-tris[4-(2-phenylpropan-2-yl)phenoxy]-1,3,5-triazine,[11] in which two π-stacked molecules are mutually rotating by 60° to resemble a spatially filled hexagonal system.

This work was supported in part by the Netherlands Foundation of Chemical Research (SON) with financial aid from the Netherlands Organization for Scientific Research (NWO). DSM Research is gratefully acknowledged for an unrestricted grant.

## Footnotes and References

* E-mail: tgtojv@chem.tue.nl
† Correspondence address for crystallographic data.

‡ *Crystal structure data* for **1**: $C_{24}H_{18}N_6O_3$, $M_r$ = 438.45, colourless, block-shaped crystal (0.3 × 0.5 × 0.5 mm), trigonal, space group $P\bar{3}$ (no. 147) with $a$ = 13.8762(10), $c$ = 8.4005(5) Å, $V$ = 1400.80(17) Å$^3$, $Z$ = 2, $D_c$ = 1.039 g cm$^{-3}$, $F$(000) = 456, $\mu$(Mo-Kα) = 0.7 cm$^{-1}$, 4819 reflections measured, 2135 independent, $R_{int}$ = 0.0288, 1.7° < $\theta$ < 27.5°, $\omega$ scan, $T$ = 150 K, Mo-Kα radiation, graphite monochromator, $\lambda$ = 0.71073 Å on an Enraf-Nonius CAD4 Turbo diffractometer on rotating mode. Data were corrected for Lp effects and for a linear instability of 1% of the reference reflections, but not for absorption. The structure was solved by automated direct methods (SHELXS96). Refinement on $F^2$ was carried out by full-matrix least-squares techniques (SHELXL96); no observance criterion was applied during refinement. Electron density in a disordered solvent area (the unit cell contains a channel parallel to the $c$-axis, through the origin, with a volume of 450 Å$^3$ and containing 111 electrons per $c$-translation period, suggesting the presence of approximately six molecules of methanol) was taken into account in the refinement *via* PLATON/SQUEEZE. Where relevant, data cited above are given without disordered solvent contribution. Positional parameters for hydrogen atoms were included in the refinement; initial values were obtained from a difference Fourier map. Refinement converged at a final $wR2$ value of 0.0973 $R1$ = 0.0376 [for 1727 reflections with $F_o > 4\,\sigma(F_o)$], $S$ = 1.071, for 118 parameters. A final difference Fourier showed no residual density outside −0.20 and 0.24 e Å$^{-3}$. CCDC 182/632.

§ *Synthesis* of **1**: Standard reaction of trimesic chloride (0.90 g, 3.39 mmol) with 3-pyridylamine (1.00 g, 10.6 mmol) in THF (20 ml) in the presence of triethylamine (1.6 ml, 1.13 g, 11.2 mmol) afforded a precipitate which after washing with water and diethyl ether and drying *in vacuo* gave **1** (1.18 g, 79%) as a white solid. Recrystallization from methanol (200 ml) afforded large, transparent hexagonal crystals, mp 287–289 °C; $\delta_H$([$^2H_6$]DMSO) 10.87 (s, NH), 9.01 (d, H-2′), 8.82 (s, H-2, 4, 6), 8.39 (dd, H-6′), 8.26 (ddd, H-4′), 7.47 (dd, H-5′), 4.15 (s, OH), 3.18 (s, $CH_3$); *m/z* (ES) (MeOH + $HCO_2H$) Calc. for $C_{24}H_{18}N_6O_3$ 438.142. Found: 439.1 (M + H)$^+$ and 219.9 (M + 2 H)$^{2+}$. Analysis (after exhaustive removal of methanol at 150 °C) Calc. C, 65.75; H, 4.14; N, 19.17. Found: C, 64.80; H, 4.17; N, 18.78%.

¶ Crystals of **1**·$(MeOH)_x$ were unloaded from exterior MeOH by repetitive immersion in pentane. Crystals were kept in $CD_3OD$ for four days. The crystals remained intact and were then filtered and washed with pentane. The $^1$H NMR spectrum in [$^2H_6$]DMSO indicated the complete replacement of MeOH by $CD_3OD$.

1 E. Weber, R. Pollex and M. Czugler, *J. Org. Chem.*, 1992, **57**, 4068; D. Venkataraman, S. Lee, J. Zhang and J. S. Moore, *Nature*, 1994, **371**, 591; M. R. Ghadiri, *Adv. Mater.*, 1995, **7**, 675.
2 G. B. Gardner, D. Venkataraman, J. S. Moore and S. Lee, *Nature*, 1995, **374**, 792; P. Brunet, M. Simard and J. D. Wuest, *J. Am. Chem. Soc.*, 1997, **119**, 2737.
3 V. A. Russell and M. D. Ward, *Chem. Mater.*, 1996, **8**, 1654; E. Fan, C. Vicent, S. J. Geib and A. D. Hamilton, *Chem. Mater.*, 1994, **6**, 1113.
4 N. Khazanovich, J. R. Granja, D. E. McCree, R. E. Milligan and M. R. Ghadiri, *J. Am. Chem. Soc.*, 1994, **116**, 6011; M. D. Ward, *Nature*, 1995, **374**, 764; R. E. Melendez, C. V. Krishnamohan Sharma, M. J. Zarawotko, C. Bauer and R. D. Rogers, *Angew. Chem., Int. Ed. Engl.*, 1996, **35**, 2213; M. Mascal, N. M. Hext, R. Warmuth, M. H. Moore and J. P. Turkenburg, *Angew. Chem., Int. Ed. Engl.*, 1996, **35**, 2204; R. Bishop, *Chem. Soc. Rev.*, 1996, 311.
5 A. R. A. Palmans, J. A. J. M. Vekemans, H. Fischer, R. A. Hikmet and E. W. Meijer, *Chem. Eur. J.*, 1997, **3**, 300.
6 M. C. Etter, *Acc. Chem. Res.*, 1990, **23**, 120.
7 Z. Berkovich-Yellin and L. Leiserowitz, *Acta Crystallogr., Sect. B*, 1984, **40**, 1596; G. R. Desiraju, *Acc. Chem. Res.*, 1996, **29**, 441.
8 (*a*) A. Mahdyarfar and K. D. M. Harris, *J. Chem. Soc., Chem. Commun.*, 1993, 51; (*b*) X. Wang, M. Simard and J. D. Wuest, *J. Am. Chem. Soc.*, 1994, **116**, 12119; (*c*) O. M. Yaghi, G. Li and H. Li, *Nature*, 1995, **378**, 704.
9 D. J. Duchamp and R. E. Marsh, *Acta Crystallogr., Sect. B*, 1969, **25**, 5.
10 S. V. Kolotuchin, E. E. Fenlon, S. R. Wilson, C. J. Loweth and S. C. Zimmerman, *Angew. Chem., Int. Ed. Engl.*, 1995, **34**, 2654.
11 A. S. Jessiman, D. D. MacNicol, P. R. Mallinson and I. Vallance, *J. Chem. Soc., Chem. Commun.*, 1990, 1619.

*Received in Bath, UK, 23rd July 1997; 7/05339H*

ChemComm
FEATURE ARTICLE

# Parlaying C–O chirality into C–C chirality: improving the cost/benefit ratio of carbohydrate templates

**J. Cristobal Lopez[a] and Bert Fraser-Reid*[b]**

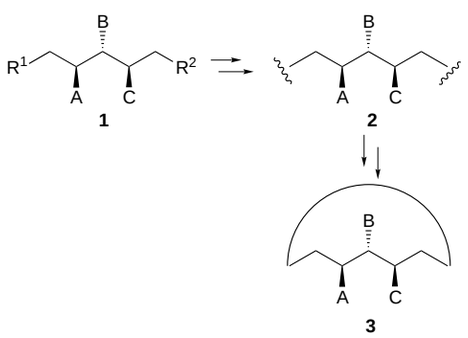
[a] *Instituto de Quimica Organica General (CSIC) Juan de la Cierva 3, 28006 Madrid, Spain*
[b] *Natural Products and Glycotechnology Research Institute Inc., 4118 Swarthmore Road, Durham NC, 27707 USA*

**Use of sugars as chirons for complex carbocyclic targets requires that C–O chirality be transmuted into C–C chirality. The cost/benefit ratio in such syntheses is one index of efficiency. For example, the process involving oxidation of a secondary alcohol followed by methylenation and hydrogenation gives, at best, a 1 : 1 ratio. The aim of lowering this ratio has been a feature of our synthetic studies, some of which are described in this article. Among other things, the studies show that the stereochemistry of pendant, off-template mixed acetals can direct the stereo- and regioselectivity choices (*e.g.* 5-*exo-trig versus* 6-*exo-trig*) in radical cyclization reactions.**

The term 'chirality transfer'[1] is generally used[2] in the context of the transformation profiled generically in Scheme 1, whereby a chiron[3] **1** is used to furnish a chiral fragment **2**, which is subsequently embedded in the target molecule **3**. The literature[4] is rich in examples of this basic strategy particularly with macrolide syntheses where the 'visual dialogue'[3] between the C–OH bonds of the starting sugar and the polyhydroxylic target is apt. In such examples chirality transfer refers to a prefabricated building block,[2] *e.g.* **2**, that is utilized convergently. However, the term may also refer to the process by which one type of asymmetry is transmuted into another, *e.g.* **4** → **5** or **5** → **6** (Scheme 2). The latter examples are abstracted from Stork's synthesis of prostaglandin $F_{2\alpha}$, notable for the fact that all of the sugar's C–OH bonds were utilized for some type of stereocontrol.[4] This study provided an excellent example of how to make optimum use of a sugar's many C–OH chiral centres.

Unfortunately this standard was not met in many syntheses that were to follow, as may be illustrated by the examples in Schemes 3 and 4, taken from the published work of one of the authors.[5,6]

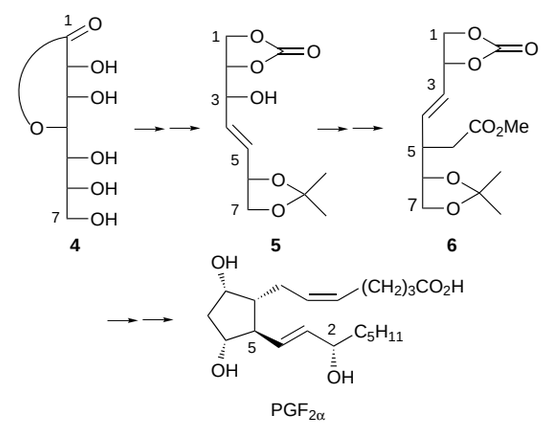
Thus in a synthesis of frontalin enantiomers (Scheme 3), ketone **8a** was used to give diastereoisomers **8b**, **c**, each of which was processed to furnish optically pure (*R*)- and (*S*)-**9**, which were then elaborated into (+)- and (−)-frontalin, respectively. In this exercise, the cost/benefit ratio is 4 : 1, based on the number of chiral centres lost and gained in going from the hexose to **9**.



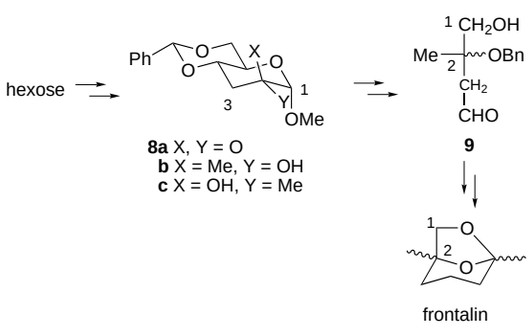

**Scheme 1**

This synthesis had merit in being enantiodivergent, as was also true for the chrysanthemic acid syntheses in Scheme 4; however, with the latter the cost/benefit ratio was improved to 2 : 1.

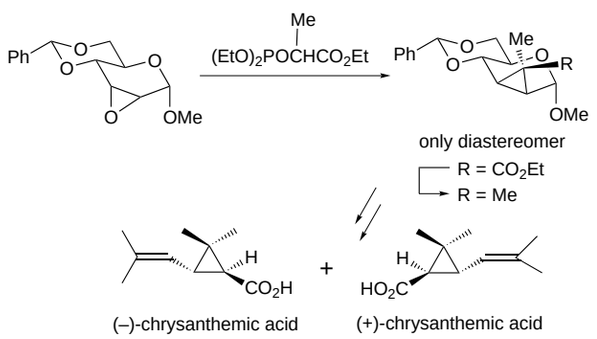
Ultimately, the case studies in Schemes 3 and 4 return to the challenge posed by Stork's prostaglandin synthesis (Scheme 2),



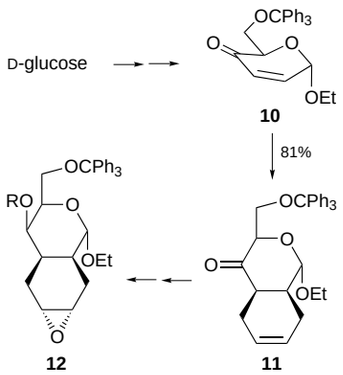

**Scheme 2**




**Scheme 3**




**Scheme 4**




**Scheme 5**

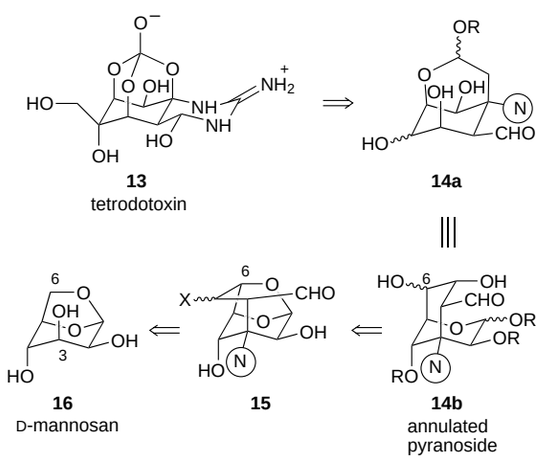
namely the problem of parlaying C–O into C–C stereochemistry.

*En route* to the well investigated α-enone **10**[7] (Scheme 5), three of the four chiral centres of D-glucose are 'destroyed', but because additions to **10** are facially selective, and the resulting adducts, *e.g.* **11**, are conformationally inflexible,[8] future transformations are highly diastereoselective.[9,10] As a result the cost/benefit ratio can sometimes be over compensated. In the case of **12**, for example, the ratio is 4 : 6 (ignoring the anomeric centre).

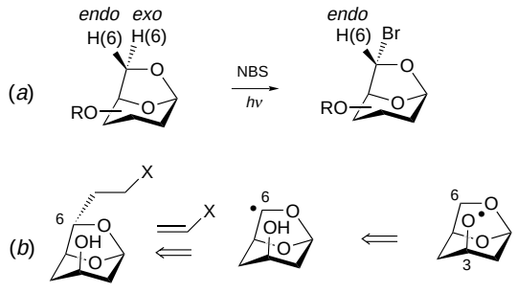
The indirect conversion of C–O into C–C chirality, as reported in Scheme 5, may be ascribed to the unique topographical features of enone **10**. However, with other substrates the prospect may not be as felicitous. In this article we give an account of some recent studies on the application of free radical methods for addressing the problem of C–O to C–C chirality transfer in connection with our program on converting carbohydrates into densely functionalized carbocycles.[11,12]

### C–O to C–C chirality transfer *via* serial 1,5-hydrogen transfer/intermolecular radical addition: the carbocyclic core of tetrodotoxin

Tetrodotoxin (TTX), **13**[13] occupies a unique place in natural products chemistry and efforts in our laboratory towards its synthesis employ the retrosynthetic plan summarized in Scheme 6.[14] The bicyclic entity **14a**, when displayed as in **14b**, emphasizes the relationship to an annulated pyranoside. Retron **15** indicates the need for a functionalized two-carbon bridge between C-3 and C-6 of an anhydropyranoside and further 'visual dialogue'[3] leads to commercially available D-mannosan **16** (1,6-anhydro-β-D-mannopyranose).




**Scheme 6**




**Scheme 7**

Retron **15** requires a functionalized branch at C-6. This requirement is facilitated by the unusual $^1C_4$ conformation of 1,6-anhydro sugars which enables remarkably reactions as exemplified by the elegant site-, regio- and stereo-selective bromination described by Ferrier and Furneaux[15] [Scheme 7(*a*)]. Thus hydrogen abstraction and subsequent bromination both take place from the less hindered *exo* face of the dioxabicyclo[3.2.1]octane system.

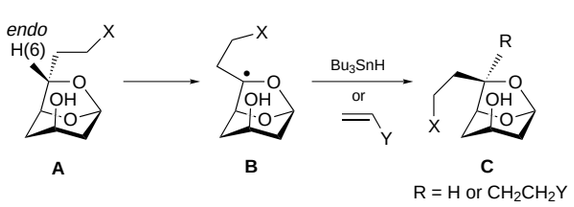
Could these facile stereodirecting capabilities of 1,6-anhydro sugars be of service to us? As expressed retrosynthetically in Scheme 7, we could conceivably employ the enthalpy driven C–O → C–OH 1,5-hydrogen transfer process, which is the basis of the original Barton reaction for functionalizing a remote angular methyl group.[16] Thus an axial C(3)–O radical should generate a carbon-centred radical at C(6), which should trap an external alkene from the less hindered *exo* face[17] [Scheme 7(*b*)].

However, in the context of the TTX plan in Scheme 6, retron **15** requires the C(6)-substituent to be *endo* oriented. This requirement could be met by taking advantage of a highly remarkable facet of our strategy, *viz*. (i) that it is *endo*-H(6) which is transferred, and (ii) that the process is amenable to iteration. Therefore an alkyl substituent, stereoselectively introduced at C(6) (**A**, Scheme 8) still presents an *endo* H(6) for transfer leading to the planar π-radical (**B**, Scheme 8).

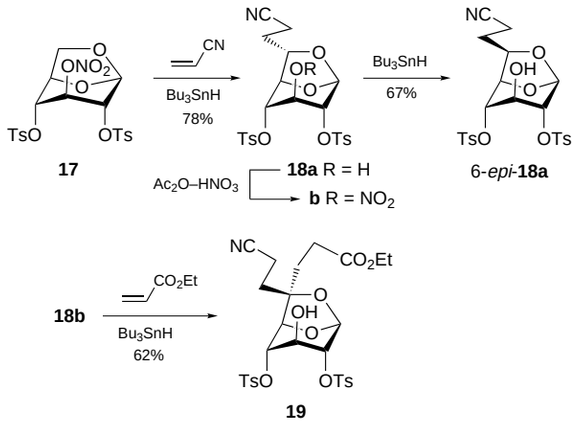
The latter radical could, in its turn, react from the *exo* face again with $Bu_3SnH$, *e.g.* **B** → **C** (R = H). Alternatively, we could take advantage of the nucleophilic character of the stabilized α-oxygenated radical[17] to foster reaction with electron-deficient alkenes. The method would then permit complete control in the creation of a secondary or tertiary branch at C-6, with either *R* or *S* orientation.

The design of this strategy was facilitated by studies in our laboratory which had shown that alkoxy radicals could be conveniently generated by reaction of nitrate esters with tri-*n*-butyltin hydride.[18] Accordingly, reaction of **17** with tri-*n*-butyltin hydride in the presence of acrylonitrile led to **18a**[19] (Scheme 9), and iteration of the process led to nitrate ester **18b** which on treatment with tri-*n*-butyltin hydride afforded 6-*epi*-**18a**.

On the other hand, a second branch at C-6 could be introduced stereoselectively by reaction of **18b** with tri-*n*-butyltin hydride in the presence of the appropriate radical trap, ethyl acrylate in the case of **19**.[19]




**Scheme 8**




**Scheme 9**

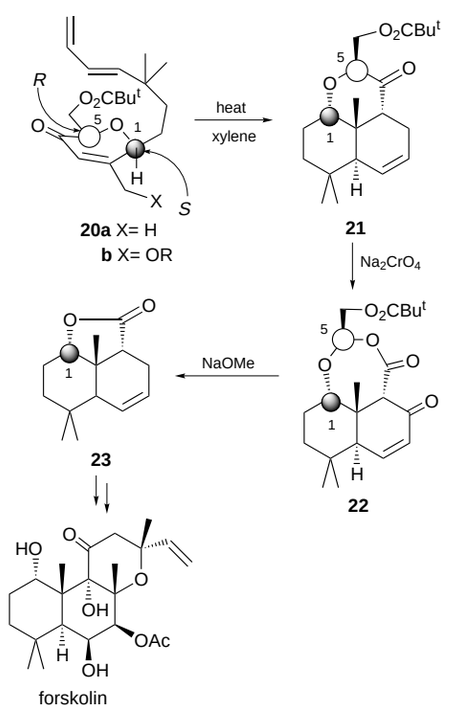
In this exercise the cost/benefit ratio is a highly rewarding 0 : 1 and it is noteworthy that the C(3)–OH is recovered unprotected after each operation.

### C–O to C–C chirality transfer *via* serial radical reactions on glycals: preliminary studies for the decalin portion of azadirachtin

Carbohydrate based Diels–Alder strategies are specially useful in the preparation of carbocyclic natural products, and it is in that context that α-enones were investigated in our laboratories.[11] Thus intermolecular Diels–Alder reactions (see Scheme 5) led to an early synthesis of actinobolin.[20]

We have also reported a relay synthesis of forskolin which features an intramolecular Diels–Alder (IMDA) reaction as the key step, wherein the trienic enoce **20a** was used to furnish the *trans*-decalin precursor **21**[21](Scheme 10). Further functionalization employed simultaneous Baeyer–Villiger and allylic oxidations leading to **22**. Treatment of this acetal lactone with mild base provided **23**, which had served as a forskolin precursor in the laboratories of Ziegler[22] and Rúveda.[23]

However, the potential of this strategy was undermined by the many steps leading to **20a** from D-glucose. In particular,




**Scheme 10**

introduction of the vinyl methyl residue proved to be especially demanding. This challenge, together with cognizance that the C(10) alkyl residue of clerodane terpenoids, such as azadirachtin, is frequently oxygenated, compelled us to consider appropriately functionalized synthons such as **20b**.

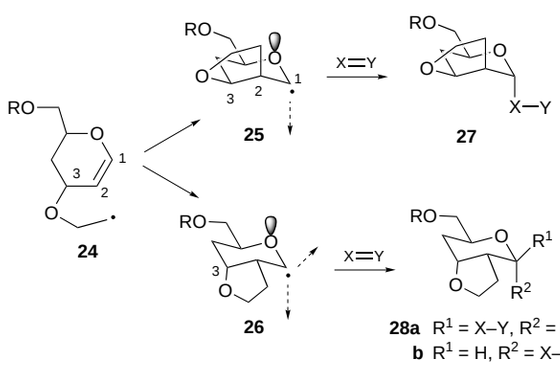
Our retrosynthetic analysis made use of the observation that, *en route* to decalin **23**, the chiral information at C(5) of enone **20a** was discarded (Scheme 10). The only essential chiral centre was therefore C(1). Thus either a D or an L sugar could be used as the starting material provided that the resulting stereogenic centre at C(1) would be *S*. This realization greatly simplified the synthetic planning because *S* chirality is found in β-D-*C*-glycosides as well as their α-L counterparts. The latter, in which the anomeric substituent is (normally) axially oriented, can be readily accessed through an anomeric radical.

Besides this conceptual viability it was also of help to note that the functionalization of C(6) of the sugars was also irrelevant. Therefore L-rhamnal (a 6-deoxy L-sugar) could be used as the starting material, thus adding economical viability to the synthetic approach (compare: L-rhamnose, 1 kg = £280; L-glucose, 1 kg = £16 400).

The need for a carbon branch at C(2) suggested that our recently developed strategy for serial radical reaction on glycals could be pressed into service (Scheme 11).[24] In this strategy, modelled after the Stork–Sher method,[25] serial radical reactions of C(3)-tethered glycals, *e.g.* **24**, leads to intermediate anomeric radicals *e.g.* **25** and **26**, which trap suitable reactants, *e.g.* X=Y, to afford *C*-glycosides *e.g.* **27** and **28**, respectively. We had also shown that the degree of stereocontrol depends on the interplay of 'shape selectivity'[25] (*vide infra*) and the radical anomeric effect.[26] When both are congruent, as in **25** → **27**, stereoselectivity is exquisite; however when both forces are in opposition, as in **26** → **28a,b**, lower preference in favour of 'shape selectivity' is observed.[24*a*]

Selected examples illustrating the scope and viability of this procedure are shown in Table 1.[24*b*] The sequence takes place with complete stereoselectivity at the anomeric carbon for the formation of α-*C*-glycosides (entries 1–5, 7–9). However, the protocol is less exclusive in the case of β-*C*-glycosides since anomeric mixtures are obtained (see entry 6), Notably the procedure allows for introduction of one- or two-carbon branches at C(2), according to precedents from Stork and coworkers,[25] Nishiyama *et al.*[27] and Tamao *et al.*[28]

Implementation of the protocol for the decalin moiety (Scheme 12), takes advantage of the O(3) bond of **31** for installing carbon branches at C(1) and C(2). The latter stereocentre is 'destroyed' in going from **40** → **41**, but this event is inconsequential because it is the surviving stereogenic centre at C(1) that dictates stereoselectivity on the IMDA process, wherein three new chiral centres are created in **42b**.[29,30] The overall cost/benefit ratio in terms of C–O to C–C chirality transfer is 2 : 2 for the radical process, and increases to 3 : 4 if the IMDA process is included.

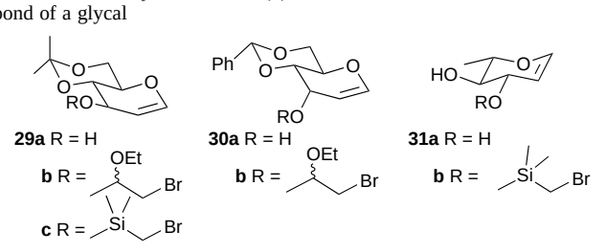


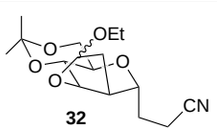
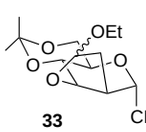
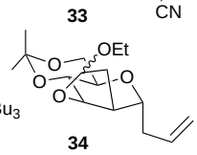
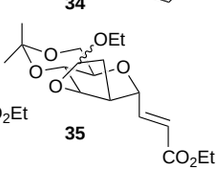
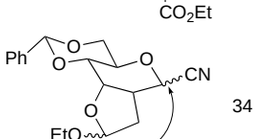
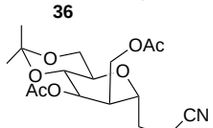
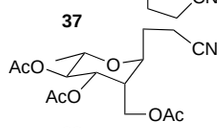
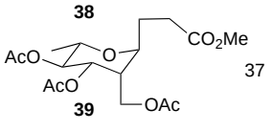

**Scheme 11**

## C–O to C–C chirality transfer *via* serial radical reactions on hex-2-enopyranosides: the cyclohexane fragment of reserpine

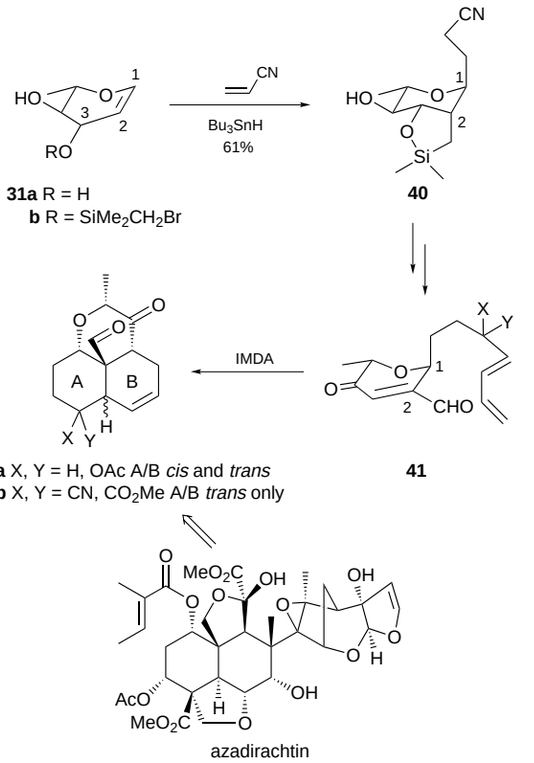
Reserpine, [Scheme 13(*a*)], a prominent member of the yohimbine family of indole alkaloids, possesses a pentacyclic skeleton which contains six chiral centres.[31] Woodward's landmark synthesis featured the richly functionalized E-ring intermediate **43** [Scheme 13(*b*)].[32] This densely functionalized cyclohexane which by itself accounts for five of the six chiral centres was especially appealing to us.

**Table 1** Radical cyclization of C(3) tethered radicals onto the $\Delta^{1,2}$ double bond of a glycal



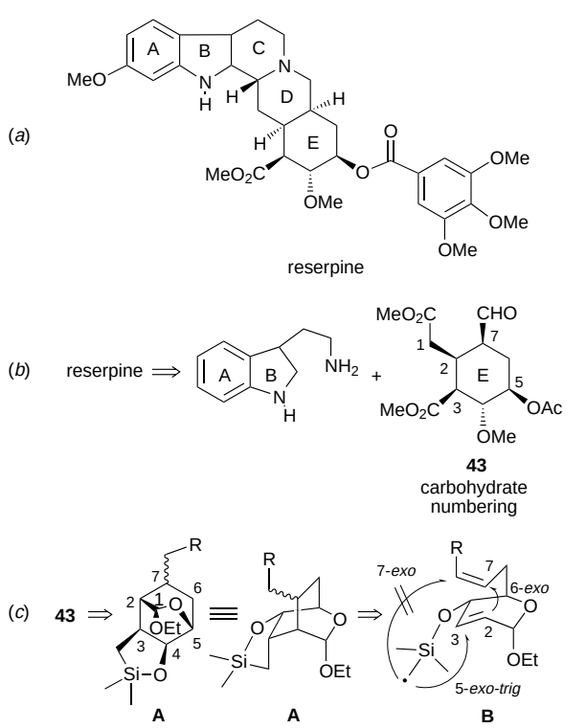

| Entry | Substrate | Reaction conditions[a] | Radical trap | Product | Yield (%) |
|---|---|---|---|---|---|
| 1 | **29b** | A | CN |  **32** | 75 |
| 2 | **29b** | B | CN | **32** | 78 |
| 3 | **29b** | B | C=N–Bu$^t$ |  **33** | 76 |
| 4 | **29b** | C | SnBu$_3$ |  **34** | 68 |
| 5 | **29b** | D | Bu$_3$Sn, CO$_2$Et |  **35** | 63 |
| 6 | **30b** | B | C=N–Bu$^t$ |  (5:1) β:α mixture **36** | 34 |
| 7 | **29c** | E | CN |  **37** | 61 |
| 8 | **31b** | E | CN |  **38** | 32 |
| 9 | **31b** | E | CO$_2$Me |  **39** | 37 |

[a] For reaction conditions see ref. 24(*b*).

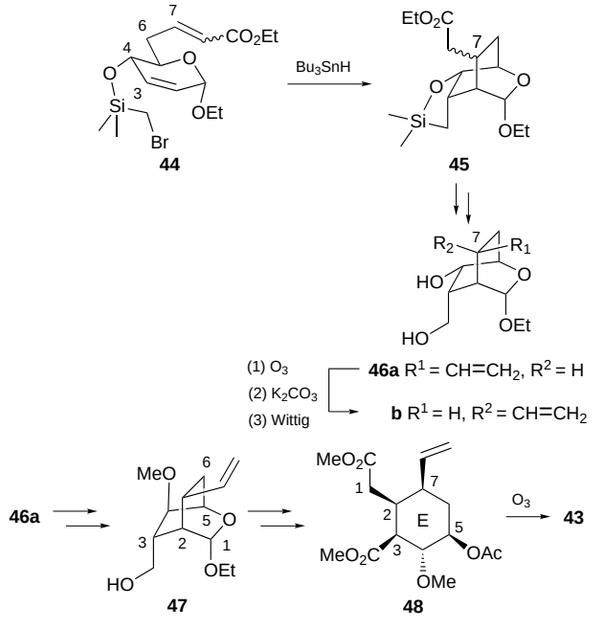



**Scheme 12**

Our strategy for this project was based on the correlation of a tricyclic cage **A**, with **43** [Scheme 13(*c*)].[33] Intermediate **A**, which already fulfills all functional and stereochemical requirements, could be accessed by serial radical cyclizations of a dienic pyranoside **B**. The latter contains two unsaturated sites, but the 5-*exo* mode should prevail over the 7-*exo* alternative, thereby presenting the resulting C(2) radical to C(7) for 6-*exo* cyclization. A C–O bond, this time at C(4), is once again key to




**Scheme 13**

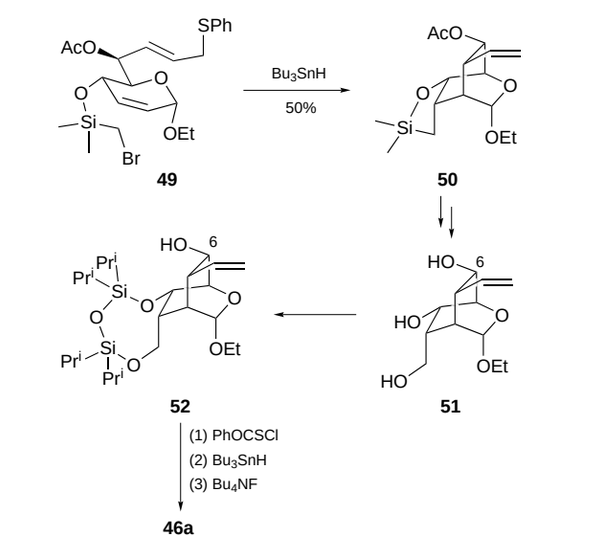


Scheme 14

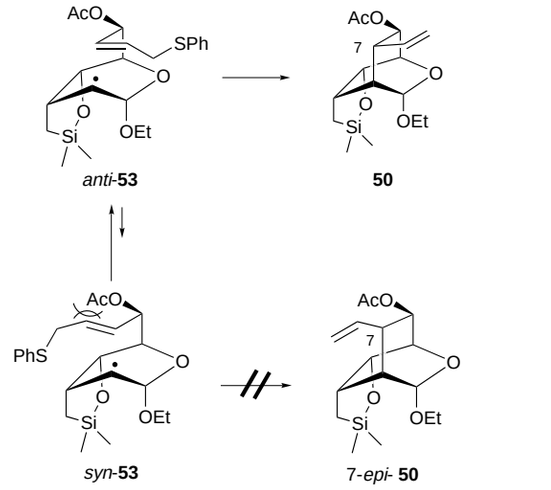
the plan, since it directs the stereochemical outcome in the formation of two [C(3), C(2)] of the three new stereogenic centres.

The strategy was first tested on pyranoside diene **44**[34] (Scheme 14), which furnished a mixture of caged compounds **45**. Oxidation of the silicon bridge in **45**, according to Tamao *et al.*,[28] gave a diol which was protected. Processing of the ethoxycarbonyl group into a vinyl moiety paved the way to epimers **46a,b**, which were readily separated. 'Unwanted' **46b** was transformed into **46a** (see Scheme 14), which could then be processed, *via* **47**, into **48**. Cyclohexane **48** is a masked precursor of Woodward's intermediate, in that the pendant vinyl residue at C(7) is retrosynthetically correlated with the aldehyde group of **43**.

Although the above mentioned strategy worked well, we were dissatisfied, because virtually no stereocontrol had been exerted over the C(7) vinyl residue. We therefore explored a parallel route in which a C–O bond at C(6) could be used to dictate the developing orientation at C(7).[35] Accordingly, radical cyclization of **49** (Scheme 15) led stereoselectively to **50** from which triol **51** was readily obtained. Selective protection



Scheme 15



Scheme 16

of the hydroxy groups paved the way for C(6) deoxygenation, furnishing **46a**.

The stereochemical model, based on the release of 1,3-allylic strain[36] (*e.g.* **53** → **50**, Scheme 16), therefore worked well and represents an additional mode of C–O to C–C chirality transfer.

The overall result, in terms of C–O to C–C chirality transfer, is 2 : 2 for the first synthetic route, and it increases to 2 : 3 if the oxygenated substituent at C(6) is incorporated.

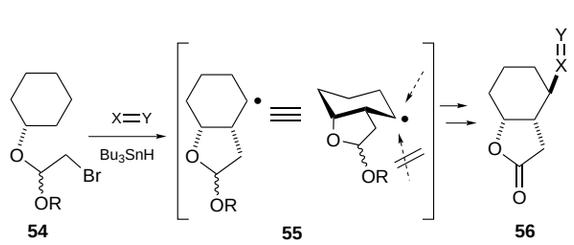
### C–O to C–C chirality transfer. Effects of the 'irrelevant' configuration at the anomeric centre of mixed haloacetals on the chemo- and stereo-selectivity of serial radical reactions.

Much of the chemistry utilized in the two preceding sections has relied on Stork's bicyclic radical **55**[25] (Scheme 17) which shows remarkable 'shape selectivity' in promoting reactions that occur *anti* to the fused five-membered ring. The latter, in turn, is formed by 5-*exo*-*trig* radical cyclization of haloacetals **54**. The configuration at the anomeric centre of these structures has always been considered as irrelevant,[25] a fact which is not surprising since the concept was developed in the context of the corresponding lactones **56**.

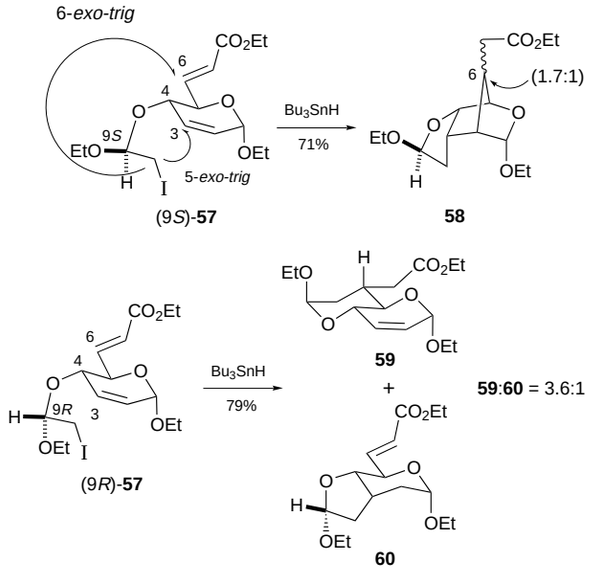
However, in the course of our exploratory studies,[37] we were intrigued by the suspicion that the configuration at the anomeric centre of the haloacetals was defining the stereoselectivity of the radical reaction. Accordingly, it was desirable to examine the reactions of diastereopure isomers.

The *R* and *S* haloacetals **57**[38] were chosen for this study because radical cyclization could take place at C(3) or at C(6). Interestingly, (9*S*)-**57** furnished exclusively tricyclic compounds **58** (Scheme 18), while (9*R*)-**57** gave rise to a mixture of regioisomeric bicyclic compounds **59** and **60**, with no evidence of a tricyclic product.

The opposite regioselectivity preferences observed for the epimers **57** may be rationalized by invoking intermediates, in which the ethoxy group enjoys an anomeric effect as in **A** and **C**, (Scheme 19). These gain precedence over those alternatives



Scheme 17



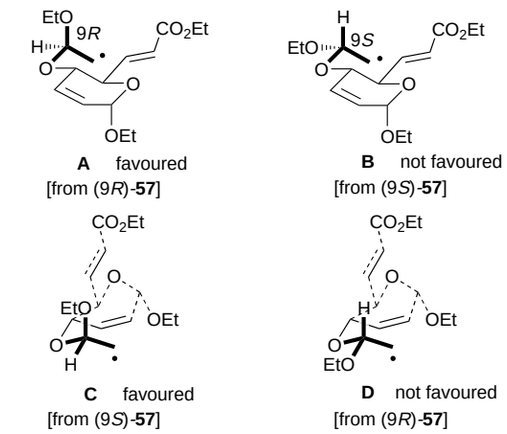

**Scheme 18**

where the ethoxy group occupies the more sterically advantageous pseudo-equatorial position, *e.g.* **B** and **C** (Scheme 19), as would be the case in the classical Beckwith–Schiesser model for 5-*exo-trig* ring closure of substituted hexenyl radicals.[39,40]

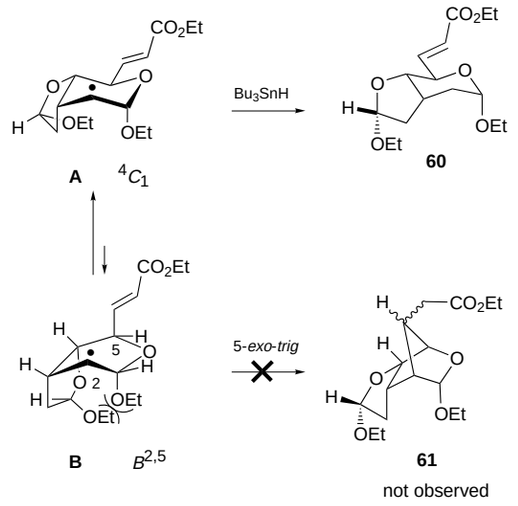
It is clear that in order for the second cyclization [C(2) to C(6)] to take place, the radical at C(2) must change conformation from a $^4C_1$ chair (**A**, Scheme 20), which enjoys an anomeric effect, to a $B^{2,5}$ boat (**B**, Scheme 20), which does not, and where all the substituents reside in pseudo-axial orientations. The fact that the double-cyclization product, **61**, is not obtained from (9*R*)-**57** [*cf.* (9*S*)-**57**, Scheme 18] may be associated with an additional destabilizing steric interaction between the two anomeric ethoxy groups in the required $B^{2,5}$ conformation as shown in Scheme 20.

In analysing the stereoelectronic factors depicted in Scheme 11, it was noted (see Table 1) that selectivity for the installation of an anomeric branch varied from complete (*i.e.* **25** → **27**) to selective (*ca.* 5–3 : 1) (*i.e.* **26** → **28a,b**).[24a] In light of the results in Schemes 18–20, it seemed wise to reexamine the reaction of **30b** (Scheme 21). In the presence of *tert*-butyl isocyanide,[24b] sequential cyclization–intermolecular radical trapping led to a *ca.* 5 : 1 mixture of epimeric cyanides **36a,b**, each one being itself a mixture of epimeric acetals.

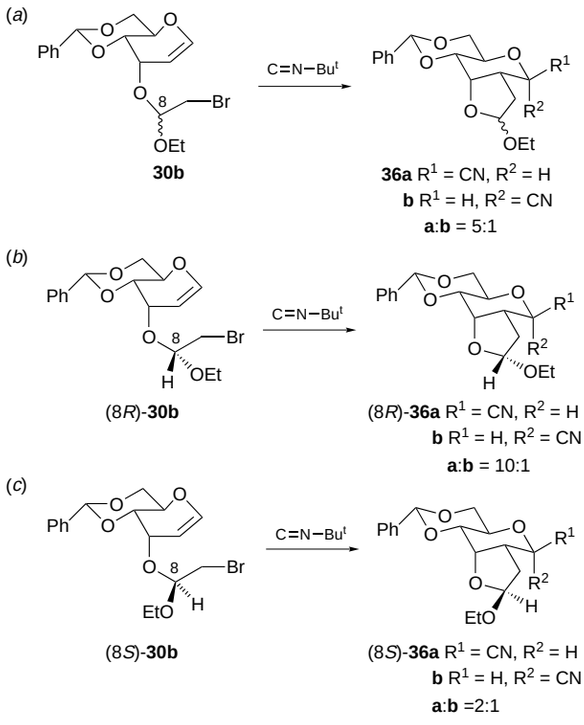
It was therefore justifiable to study each isomer. Remarkably, each showed distinctly different behaviour (Scheme 21), for which Stork's carbocyclic series (Scheme 18) did not provide a precedent.[25] Obviously the radical anomeric effect is responsible for the high percentage of α-*C*-glycoside (8*S*)-**36b** obtained on the cyclization of (8*S*)-**30b**. On the other hand, in the cyclization of (8*R*)-**30b**, the presence of an *endo*-oriented ethoxy substituent efficiently shields the α-face and overrides the radical anomeric effect (see **62**, Scheme 22).



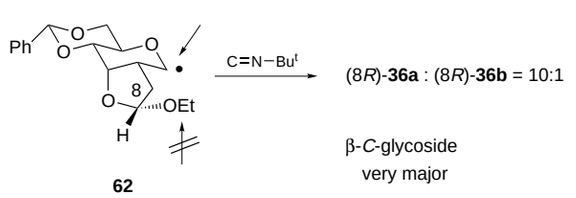

**Scheme 19**




**Scheme 20**




**Scheme 21**




**Scheme 22**

## Summary

We have presented a view on stereoselective radical transformations in which C–O bonds play a leading role on inducing C–C bond stereochemistry. One of the starting sugar's several C–O bonds has been used to induce C–C chirality for a variety of synthetic targets. Owing to their wealth of oxygen atoms, carbohydrates have been the substrates of choice for these transformations. However, from the last two examples it is clear that even 'imported' oxygen atoms can have a dramatic influence on newly formed C–C bonds.



## Acknowledgments

J. C. L is grateful to the Consejo Superior de Investigaciones Cientificas (C.S.I.C) and Consejeria de Educacion, Comunidad Autonoma de Madrid for financial support. These studies were made possible by grants from the National Science Foundation (CHE 892003 and 9311356) and National Institutes of Health (GM 51237).


---

**J. Cristobal López was born in Madrid Spain. He received his PhD degree with Dr S. Valverde from the Universidad Complutense (Madrid) in 1986. He was a postdoctoral associate at the Institut de Chimie des Substance Naturelles (Gif sur Yvette) with Dr Gabor Lukacs (1986–1987) and at the Chemistry Department of Duke University with Professor B. Fraser-Reid (1988–1990). He was subsequently Visiting Professor at Duke University (1992–1994). Since 1989 he has been Research Associate at the Instituto de Quimica Organica General (CSIC) in Madrid. His research interests involve several aspects of the chemical transformation of carbohydrates, including glycosylation, radical reactions and natural product synthesis.**

**Bert Fraser-Reid was born in Jamaica in 1934 and received his early education there. He attended universities in Canada (Queen's and Alberta), obtaining his PhD at the latter in 1964 (Lemieux). He spent 1964–1966 at Imperial College, London, as a post doctoral fellow (Barton). He has held faculty positions at Waterloo (1966–1980), Maryland (1980–1983) and Duke (1983–1996) and is currently President and Director of the Natural Products and Glycotechnology Research Institute, Inc., Research Triangle Park, NC. He is winner of the Merck, Sharp & Dohme Award (Canadian Institute of Chemistry, 1977), Hudson Award (American Chemical Society, 1991) and the Haworth Memorial Medal (UK, 1995). He is a Fellow of the American Academy of Arts and Sciences, and an Alexander von Humboldt Senior Scientist (Germany) awardee.**

---

## Footnotes and References


* E-mail: dglucose@aol.com



1 M. M. Joullie, P. C. Wang and J. E. Semple, *J. Am. Chem. Soc.*, 1980, **102**, 887.
2 We are grateful to Professor Joullie for bringing our attention to the recent suggestion that *retention* should replace *transfer* in this description. See *Asymmetric Synthesis* ed. R. A. Aitken and S. N. Kilanyi, Blackie Academic and Professional, Glasgow 1992, p. 31.
3 S. Hanessian, *Total Synthesis of Natural Products: The Chiron Approach*, Pergamon, New York, 1983.
4 G. Stork and S. Raucher, *J. Am. Chem. Soc.*, 1976, **98**, 1583; G. Stork, T. Takahashi, I. Kawamoto and T. Suzuki, *J. Am. Chem. Soc.*, 1978, **100**, 8272.
5 D. R. Hicks and B. Fraser-Reid, *J. Chem. Soc., Chem. Commun.*, 1976, 869.
6 B. J. Fitzsimmons and B. Fraser-Reid, *Tetrahedron* 1984, **40**, 1279; B. J. Fitzsimmons and B. Fraser-Reid, *J. Am. Chem. Soc.*, 1979, **101**, 6123.
7 B. Fraser-Reid, A. McLean and E. W. Usherwood, *J. Am. Chem. Soc.*, 1969, **91**, 5392.
8 B. Fraser-Reid, M. A. Rahman, D. R. Kelly and R. M. Srivastava, *J. Org. Chem.*, 1984, **49**, 1835.
9 J. S. Prasad, D. L. J. Clive and C. V. J. da Silva, *J. Org. Chem.*, 1986, **51**, 2717.
10 S. Chew and R. J. Ferrier, *J. Chem. Soc., Chem. Commun.*, 1984, 911.
11 B. Fraser-Reid and R. Tsang, *Strategies and Tactics in Organic Synthesis*, ed. T. Lindberg, Academic Press, New York, 1989, vol. 2, pp. 123–162.
12 Review: R. J. Ferrier and S. Middleton, *Chem. Rev.*, 1993, **93**, 2779.
13 H. S. Mosher and F. A. Furman, in *Seafood Toxins*, ed. E. P Ragelis, *ACS Symp. Ser.*, 262, American Chemical Society, Washington DC, 1986, pp. 333–344; Y. Kotaki and Y. Shimizu, *J. Am. Chem. Soc.*, 1993, **115**, 827.
14 R. A. Alonso, C. S. Burgey, B. V. Rao, G. D. Vite, R. Vollerthun, M. A. Zottola and B. Fraser-Reid, *J. Am. Chem. Soc.*, 1993, **115**, 6666.
15 R. J. Ferrier and R. H. Furneaux, *Aust. J. Chem.*, 1980, **33**, 1025.
16 D. H. R. Barton, J. M. Beaton, E. L. Geller and M. M. Pechet, *J. Am. Chem. Soc.*, 1960, **82**, 2640; D. H. R. Barton and J. M. Beaton, *J. Am. Chem. Soc.*, 1960, **82**, 2641; 1961, **83**, 4076.
17 H.-G. Korth, R. Sustmann, K. R. Gronninger, M. Leisung and B. Giese, *J. Org. Chem.*, 1988, **53**, 4364; B. Giese and W. Mehl, *Tetrahedron Lett.*, 1991, **32**, 4275.
18 G. D. Vite and B. Fraser-Reid, *Synth. Commun.*, 1988, **18**, 1339.
19 J. C. López, R. A. Alonso and B. Fraser-Reid, *J. Am. Chem. Soc.*, 1989, **111**, 6471.
20 M. A. Rahman and B. Fraser-Reid, *J. Am. Chem. Soc.*, 1985, **107**, 5576.
21 R. Tsang and B. Fraser-Reid, *J. Org. Chem.*, 1992, **57**, 1065.
22 F. E. Ziegler, B. H. Hayner and M. T. Saindane, *J. Am. Chem. Soc.*, 1987, **109**, 8115.
23 C. Somoza, J. Darias and E. A. Rúveda, *J. Org. Chem.*, 1989, **54**, 1593; M. I. Colombo, J. Zinczuk, J. A. Bacigaluppo, C. Somoza and E. A. Rúveda, *J. Org. Chem.*, 1990, **55**, 5631.
24 (*a*) J. C. López and B. Fraser-Reid, *J. Am. Chem. Soc.*, 1989, **111**, 3450; (*b*) J. C. López, A.M. Gómez and B. Fraser-Reid, *J. Org. Chem.*, 1995, **60**, 3871.
25 G. Stork, *Bull. Soc. Chim. Fr.*, 1990, **127**, 675; G. Stork and M. Sher, *J. Am. Chem. Soc.*, 1983, **105**, 6765.
26 B. Giese and J. Dupuis, *Tetrahedron Lett.*, 1984, **25**, 1349; S. D. Richnovsky, J. P. Powers and T. J. LePage, *J. Am. Chem. Soc.*, 1992, **114**, 8375.
27 H. Nishiyama, T. Kitajima, M. Matsumoto and K. Itoh, *J. Org. Chem.*, 1984, **49**, 2298.
28 K. Tamao, N. Ishida and M. Kumada, *J. Org. Chem.*, 1983, **48**, 2120.
29 J. C. López, A. M. Gómez and B. Fraser-Reid, *J. Chem. Soc., Chem. Commun.*, 1993, 762.
30 A. M. Gómez, J. C. López and B. Fraser-Reid, unpublished results.
31 E. W. Baxter and P. S. Mariano, *Alkaloids: Chemical and Biological Perspectives*, ed. S. W. Pelletier, Springer-Verlag, New York, 1992, vol. 8, pp. 197–319.
32 R. B. Woodward, F. E. Bader, H. Bickel, A. J. Frey and R. W. Kierstead, *Tetrahedron*, 1958, **2**, 1.
33 A. M. Gómez, J. C. López and B. Fraser-Reid, *J. Org. Chem.*, 1994, **59**, 4048.
34 A. M. Gómez, J. C. López and B. Fraser-Reid, *J. Chem. Soc., Perkin Trans 1*, 1994, 1689.
35 A. M. Gómez, J. C. López and B. Fraser-Reid, *J. Org. Chem.*, 1995, **60**, 3859.
36 T. V. RajanBabu, *Acc. Chem. Res.*, 1991, **24**, 139; J. C. López, A. M. Gómez and S. Valverde, *J. Chem. Soc., Chem. Commun.*, 1992, 613.
37 J. C. López, A. M. Gómez and B. Fraser-Reid, *Aust. J. Chem.*, 1995, **48**, 333; J. C. López, A. M. Gómez and B. Fraser-Reid, *J. Chem. Soc., Chem. Commun.*, 1994, 1533.
38 A. M. Gómez, J. C. López and B. Fraser-Reid, *Synlett*, 1993, 557.
39 A. L. J. Beckwith and C. H. Schiesser, *Tetrahedron Lett.*, 1985, **26**, 373; A. L. J. Beckwith and C. H. Schiesser, *Tetrahedron*, 1985, **41**, 3925.
40 D. C. Spellmeyer and K. N. Houk, *J. Org. Chem.*, 1987, **52**, 959.



*7/04040G*

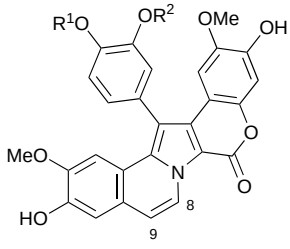
# Convergent total synthesis of lamellarin K†

**Martin Banwell,*‡ Bernard Flynn* and David Hockless**

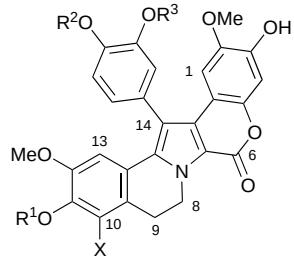
*Research School of Chemistry, Institute of Advanced Studies, The Australian National University, Canberra, ACT 0200, Australia*

**The azomethine ylide derived from dihydroisoquinolinium salt 24 undergoes an intramolecular [3 + 2] cycloaddition reaction to give pyrrole 25 which upon de-isopropylation affords the marine alkaloid lamellarin K 4.**

In 1985 Faulkner and his colleagues reported[1] the isolation of four members of a new class of marine natural product which they had obtained from a *Lamellaria* sp. of marine prosobranch mollusc collected in the waters off Palau. These compounds were called lamellarins A–D and through a combination of spectroscopic and X-ray crystallographic studies were shown to be highly oxygenated derivatives of 14-phenyl-6*H*-[1]benzopyrano[4′,3′ : 4,5]pyrrolo[2,1-*a*]isoquinolin-6-one or its 8,9-dihydro analogue. Thus, lamellarin D possesses structure **1** while congener C has structure **2**. Subsequently, Fenical[2] isolated further members of this type of compound (lamellarins E–H) from the Indian Ocean marine ascidian *Didemnum chartaceum*. More recently Bowden[3] reported obtaining lamellarins I–N from a Pacific ascidian *Didemnum* sp. collected off the north east coast of Australia, while Urban and Capon[4] have isolated lamellarin S from the same species.§ In 1997, Faulkner described[5] the isolation of nine new alkaloids of the lamellarin class, including the first examples of lamellarin sulfates, from an unidentified ascidian found in the Arabian Sea.



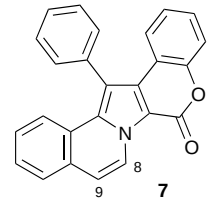
**1** $R^1$ = H, $R^2$ = Me
**6** $R^1$ = Me, $R^2$ = H



**2** X = OMe, $R^1$ = $R^3$ = Me, $R^2$= H
**3** X = OMe, $R^1$ = $R^2$ = $R^3$ = Me
**4** X = OH, $R^1$ = $R^3$ = Me, $R^2$ = H
**5** X = $R^1$ = $R^3$ = H, $R^2$ = Me

A number of the lamellarins exhibit highly interesting biological properties. For example, at concentrations of 19 μg $ml^{-1}$, compound **1** caused a 78% inhibition of cell division in a fertilised sea urchin assay while congener **2** caused 15% inhibition.[1] Lamellarins I **3**, K **4** and L **5** all showed comparable and significant cytotoxicity against P388 and A549 cell lines in culture ($IC_{50}$ ≈ 0.25 μg $ml^{-1}$ against each cell line).[3] Lamellarins K and L also exhibited moderate immunomodulatory activity (LcV : MLR 147 and 98, respectively).[3] In the NCl 60 cell-line panel, lamellarin N **6** showed some selectivity toward melanoma cell lines SK-MEL-5 ($LC_{50}$ 1.87 × $10^{-7}$ M) and UACC-62 ($LC_{50}$ 9.88 × $10^{-6}$ M).[5] Perhaps most significantly, very recent work at Pharma Mar S. A.[6] has raised the possibility that certain of the lamellarins, especially lamellarin K, may be highly effective in the treatment of multidrug resistant tumours.

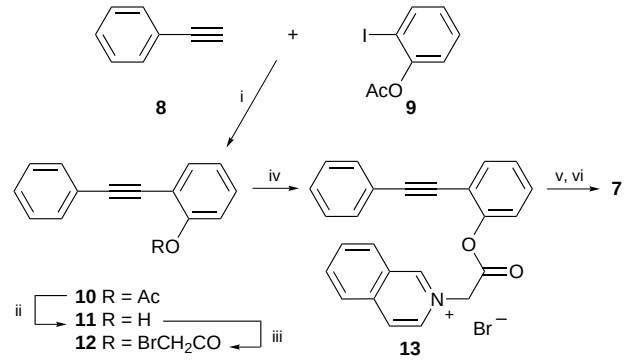
Despite the intriguing biological properties and the unprecedented structures of lamellarins A–N and S–X (the parent frameworks are unknown) only two studies directed towards the total synthesis of these marine natural products appear to have been reported to date.§ Thus, very recently Steglich[7] described a biomimetic synthesis of lamellarin G trimethyl ether, while Ishibashi *et al*.[8] have completed total syntheses of lamellarins D and H. These reports prompt us to disclose a quite different and highly convergent method for the synthesis of the title compound **4** and the parent ring-system **7**.



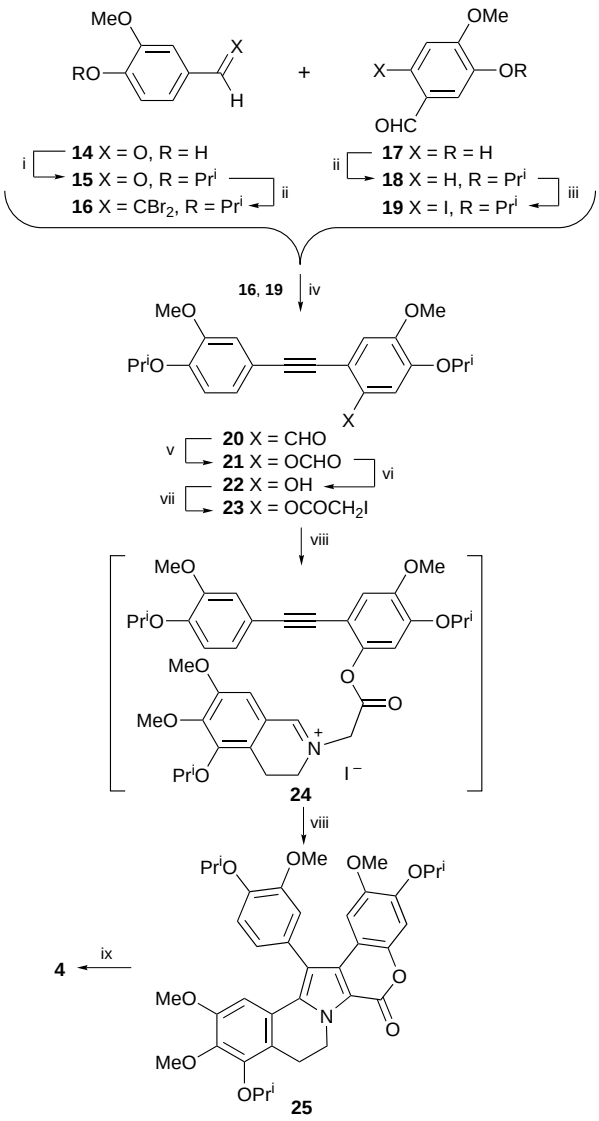
**7**

The pivotal step in our approach to the lamellarin ring systems involves construction of the central pyrrole moiety *via* an intramolecular [3 + 2] cycloaddition of an isoquinoline-based azomethine ylide to a suitably tethered tolan,[9] a hitherto unproven process. The reaction sequence leading to the parent framework (Scheme 1) starts with Sonogashira cross-coupling[10] of phenylacetylene **8** and *o*-iodophenyl acetate **9**[11] to give, after hydrolysis of the initial coupling product **10**[11] (99%), *o*-hydroxytolan **11**.[11] This last compound was subjected to dicyclohexylcarbodiimide (DCC)-promoted coupling with α-bromoacetic acid and the resulting ester **12** (91% from **10**) treated with isoquinoline to give the isoquinolinium salt **13**. Compound **13** was immediately reacted with $Et_3N$ so as to generate the associated azomethine ylide which underwent intramolecular cycloaddition to the tethered triple bond upon heating. The resulting mixture of dihydropyrrole-type products thereby obtained was subjected to oxidation with 2,3-dichloro-5,6-dicyano-1,4-benzoquinone (DDQ). In this manner, the target compound **7** (92% from **12**, mp 313–315 °C) was obtained and its structure established by single-crystal X-ray analysis.‖

The highly convergent nature of the reaction sequence outlined here would suggest that this approach could be readily



**Scheme 1** *Reagents and conditions*: i, $Pd(PPh_3)_4$ (1 mol%), CuI (2 mol%), $Et_3N$, 18 °C, 4 h; ii, $K_2CO_3$ (1.5 equiv.), MeOH, 18 °C, 0.25 h; iii, $BrCH_2COBr$ (1 equiv.), DMAP (5 mol%), DCC (1.05 equiv.), $CH_2Cl_2$, 18 °C, 3 h; iv, isoquinoline (1 equiv.), THF, 18 °C, 6 h; v, $Et_3N$ (1 equiv), THF, 66 °C, 4 h; vi, DDQ (1 equiv.), $CH_2Cl_2$, 18 °C, then silica gel chromatography




**Scheme 2** *Reagents and conditions*: i, Pr$^i$Br (1.2 equiv.), $K_2CO_3$ (3.5 equiv.), DMF, 18 °C, 19 h; ii, $CBr_4$ (2 equiv.), Zn (2 equiv.), $PPh_3$ (2 equiv.), 0 to 18 °C, 22 h, then 0 °C, **15**, 18 °C, 1 h; iii, $AgOCOCF_3$ (1.1 equiv.), $I_2$ (1.1 equiv.), $CHCl_3$, reflux, 7 h; iv, **16**, Bu$^n$Li (2.05 equiv.), THF, −78 °C, 0.83 h then $ZnCl_2$ (1.1 equiv.), −78 to 18 °C, 1 h then **19** (0.95 equiv.), $Pd(PPh_3)_4$ (*ca*. 2 mol%), 18 °C, 4 h; v, MCPBA (1.5 equiv.), $KHCO_3$ (3 equiv.), $CH_2Cl_2$, 18 °C, 1 h; vi, $NH_3$ in MeOH (sat.), 18 °C, 1 h; vii, $ICH_2CO_2H$ (1.05 equiv.), DCC (1.05 equiv.), DMAP (5 mol%), $CH_2Cl_2$, 18 °C, 3 h; viii, 3,4-dihydro-6,7-dimethoxy-5-isopropoxyisoquinoline (1.1 equiv.), $ClCH_2CH_2Cl$, 18 °C, 7 h, then Hünig's base (1.0 equiv.), 83 °C, 32 h; ix, $AlCl_3$ (3.6 equiv.), $CH_2Cl_2$, 18 °C, 2 h

adapted to the preparation of lamellarins A–N and S–X as well as many analogues thereof. Certainly, compounds in the 8,9-dihydroseries would seem to be readily accessible as evidenced by our synthesis of lamellarin K **4** (Scheme 2). Thus, the isopropyl ether **15**[12] (100%), prepared from vanillin **14** under standard conditions,[13] was subjected to a Corey–Fuchs *gem*-dibromomethylenation reaction[14] thereby affording styrene **16** (100%, mp 36–38 °C). This latter compound was treated with Bu$^n$Li and the lithium acetylide so formed was *trans*-metallated using zinc(II) chloride. Palladium-mediated cross-coupling of the resulting alkynylzinc chloride with aryl iodide **19** (mp 75–76 °C) (obtained in 93% yield by iodination of the isopropyl ether **18**[15] of isovanillin **17** using $AgOCOCF_3$–$I_2$) then gave tolan **20** (84%, mp 121–122 °C) which was subjected to a Baeyer–Villiger reaction using MCPBA as oxidant. The resulting formate ester **21** was readily hydrolysed to the corresponding phenol **22** (92% from **20**, mp 130–131 °C). DCC-mediated condensation of this last compound with α-iodoacetic acid then provided ester **23** (97%, mp 127–128 °C) which was reacted with 3,4-dihydro-6,7-dimethoxy-5-isopropoxyisoquinoline (readily available by standard methods) to give salt **24**. This last compound was not isolated but immediately treated with Hünig's base. The resulting mixture was heated at reflux in 1,2-dichloroethane and in this manner cycloaddition (followed by *in situ* aromatisation) took place to give lamellarin K triisopropyl ether **25** (81% from **23**, mp 244–245 °C). Treatment of this last compound with 3.6 mol equiv. of $AlCl_3$ in $CH_2Cl_2$ at 18 °C resulted in three-fold de-isopropylation and formation of the target compound **4** (96%, mp 230–232 °C) which was identical, by $^1$H and $^{13}$C NMR spectroscopy, with an authentic sample.

We thank the Institute of Advanced Studies for financial support including the provision of a post-doctoral Research Fellowship to B. L. F. Associate Professor B. Bowden (James Cook University of North Queensland) is thanked for providing spectral data on lamellarin K.

## Footnotes and References

† The work described herein is the subject of a patent application (AIPO Patent Office Provisional Application No. PO6565, May 2nd, 1997).

‡ E-mail: mgb@rsc.anu.edu.au

§ A series of structurally simpler lamellarins (O–R) have been isolated by Capon from a southern Australian marine sponge *Dendrilla cactos* (see work cited in ref. 4). Certain members of this simpler class of lamellarins have been the subject of synthetic studies (see M. G. Banwell, B. L. Flynn, E. Hamel and D. C. R. Hockless, *Chem. Commun.*, 1997, 207 and references cited therein) but the strategies used are quite different from those reported here.

‖ *Crystal data* for **7**: $C_{25}H_{15}NO_2$, $M$ = 361.40, $T$ = 296(1) K, orthorhombic, space group P*nma*, $a$ = 23.441(2), $b$ = 6.804(4), $c$ = 11.175(4) Å, $U$ = 1782(2) Å$^3$, $D_c$ ($Z$ = 4) = 1.347 g cm$^{-3}$, $F$(000) = 752, μ(MoKα) = 0.80 cm$^{-1}$, semi-empirical absorption correction; 2381 unique data ($2\theta_{max}$ = 55.0°), 661 with $I > 2\sigma(I)$; $R$ = 0.065, $wR$ = 0.049, GOF = 2.88. CCDC 182/606.

1 R. J. Andersen, D. J. Faulkner, H. Cun-heng, G. D. Van Duyne and J. Clardy, *J. Am. Chem. Soc.*, 1985, **107**, 5492.
2 N. Lindquist, W. Fenical, G. D. Van Duyne and J. Clardy, *J. Org. Chem.*, 1988, **53**, 4570.
3 A. R. Carroll, B. F. Bowden and J. C. Coll, *Aust. J. Chem.*, 1993, **46**, 489.
4 S. Urban and R. J. Capon, *Aust. J. Chem.*, 1996, **49**, 711.
5 M. Venkata Rami Reddy, D. J. Faulkner, Y. Venkateswarlu and M. Rama Rao, *Tetrahedron*, 1997, **53**, 3457.
6 A. R. Quesada, M. D. García Grávalos and J. L. Fernández Puentes, *Br. J. Cancer*, 1996, **74**, 677; J. L. Fernández Puentes, D. García Grávalos and A. Quesada, PCT Int. Appl., WO 9701336 (*Chem. Abstr.*, 1996, **126**, 166 474).
7 A. Heim, A. Terpin and W. Steglich, *Angew. Chem.*, 1997, **109**, 158; *Angew. Chem., Int. Ed. Engl.*, 1997, **36**, 155.
8 F. Ishibashi, Y. Miyazaki and M. Iwao, *Tetrahedron*, 1997, **53**, 5951.
9 For reviews on azomethine ylide chemistry see: R. Grigg, *Chem. Soc. Rev.*, 1987, **16**, 89; O. Tsuge and S.Kanemasa, *Adv. Heterocycl. Chem.*, 1989, **45**, 232; A. Padwa, in *Comprehensive Organic Synthesis, Vol. 4*, ed. B. M. Trost and I. Fleming, Pergamon, New York, 1991, pp. 1085–1089; P. A. Wade, in *Comprehensive Organic Synthesis, Vol. 4*, ed. B.M. Trost and I. Fleming, Pergamon, New York, 1991, pp. 1134–1141.
10 For a review see K. Sonogashira, in *Comprehensive Organic Synthesis, Vol. 3*, ed. B. M. Trost and I. Fleming, Pergamon, New York, 1991, pp. 521–549.
11 A. Arcadi, S. Cacchi, M. D. Rosario, G. Fabrizi and F.Marinelli, *J. Org. Chem.*, 1996, **61**, 9280.
12 M. F. Comber and M. V. Sargent, *J. Chem. Soc., Perkin Trans. 1*, 1991, 2783.
13 T. Sala and M. V. Sargent, *J. Chem. Soc., Perkin Trans. 1*, 1979, 2593.
14 E. J. Corey and P. L. Fuchs, *Tetrahedron Lett.*, 1972, 3769.
15 H. Ishii, I.-S. Chen and T. Ishikawa, *J. Chem. Soc., Perkin Trans. 1*, 1987, 671.

*Received in Cambridge, UK, 12th August 1997; 7/05874H*

# Bis[1,2,3,4,5,6,7,8-octahydro-1,4 : 5,8-di(ethano)anthryl]carbene. The first all-hydrocarbon triplet diphenylcarbene having a half-life over one second under normal conditions

**Hideo Tomioka,* Hidehiko Mizuno, Hidetaka Itakura and Katsuyuki Hirai**

*Chemistry Department for Materials, Faculty of Engineering, Mie University, Tsu, Mie 514 Japan*

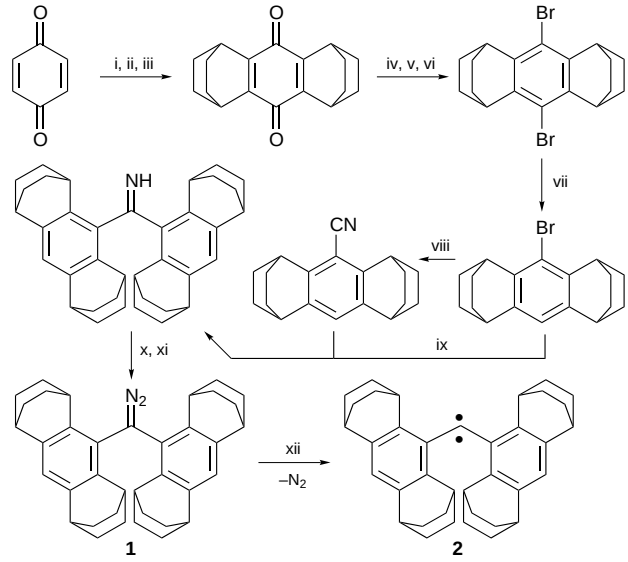
**Bicyclo[2.2.2]octyl groups are demonstrated to be very effective kinetic protectors for triplet carbenes.**

The stabilization of a triplet carbene[1] has emerged as a challenging target since the recent syntheses of stable singlet carbenes[2,3] upset the long-standing view that carbenes are not stable enough to be isolated in macroscopic scale at room temperature.[4] Steric protection is an ideal method for stabilizing the triplet since a protecting group when introduced near a carbene center not only blocks the carbene center from external reagents but also results in thermodynamic stabilization by increasing the carbene angle.[5–7] However, due to the voracious appetite of carbenes for electrons, which they can abstract even from very poor sources of electrons such as C–H bonds, this strategy encounters a limitation when alkyl groups are employed as protecting groups. For instance, dimesitylcarbene was shown to decay by undergoing dimerization and to have a half-life of 160 ms, some five orders of magnitude longer lived than triplet diphenylcarbene. However, when more methyl groups are introduced on the phenyl rings, the carbenic center is more effectively blocked from external reagents due to a buttressing effect, but it becomes more easily trapped by the *ortho* methyl groups, which are brought closer to the carbene center, to form benzocyclobutene: didurylcarbene ($t_{1/2}$ 410 ms) was twice as long-lived as dimesitylcarene, while decamethyldiphenylcarbene ($t_{1/2}$ 180 ms) decayed mainly unimolecularly by abstracting H from the *o*-methyl group and hence was shorter lived.[5a,d]

In this light, it is crucial to develop a protecting group which is sterically congesting but unreactive toward triplet carbenes. Bicycloalkyl groups are very attractive since bridgehead C–H bonds are less susceptible to hydrogen abstraction, although not entirely unsusceptible,[8] and thus the bridging chains will act as protectors. Thus, we generated diphenylcarbene protected by bicyclo[2.2.2]octyl groups and compared its reactivity with that of an open-chain 'counterpart', *i.e.* didurylcarbene (DDC).

The desired precursor diazomethane **1**† was prepared starting from a benzoquinone–cyclohexa-1,4-diene Diels–Alder reaction according to the reaction procedure as outlined in Scheme 1 and was obtained as a rather stable red solid with a mp of 183 °C (decomp.) after purification by gel permeation chromatography.

Irradiation of **1** in a 2-methyltetrahydrofuran (MTHF) glass at 77 K gave a fine structured EPR line shape characteristic of randomly oriented triplet molecules with a large *D* value attributable to a one-center nπ spin–spin interaction at the divalent carbon of diarylcarbene. The fine-structure constants were $|D|$ = 0.3951 cm$^{-1}$ and $|E|$ = 0.0106 cm$^{-1}$, showing unequivocally that the triplet signals are due to diphenylcarbene **2** generated from **1** as a result of $N_2$ elimination upon irradiation. The EPR signals were persistent at this low temperature but disappeared irreversibly when the matrix was thawed. Since the *E* value measures the difference of the magnetic dipole interaction along the *x* and *y* axes, it allows one to estimate the bond angle at the carbene center especially when weighted by *D*.[9] Comparison of the *E*/*D* value (0.0269) of **2** with that observed for DDC (*E*/*D* = 0.0279),[5c,d] an open chain 'counterpart' of **2**, indicates that carbenic center of **2** is slightly more sterically congested than that of DDC.




**Scheme 1** *Reagents and conditions*: i, cyclohexa-1,4-diene, 120 °C; ii, $H_2$–Pd/C; iii, $Br_2$; iv, $NH_2OH$; v, $SnCl_2$–$Br_2$; vi, $NaNO_2$–HBr and Cu, 20 °C; vii, Bu$^n$Li and $H_2O$; viii, CuCN; ix, Bu$^n$Li; x, $N_2O_4$; xi, $LiAlH_4$; xii, $h\nu$ ($\lambda$ > 300 nm)

Irradiation of **1** in MTHF glass at 77 K was then monitored by UV–VIS spectroscopy, which revealed the rapid appearance of new absorption bands at the expense of the original absorption due to **1**. As shown in Fig. 1, the new spectrum consists of two identifiable features, two intense UV bands with maxima at 318 and 333 nm and a weak and broad one with an apparent maximum around 483 nm. These features are usually present in the spectra of triplet diarylcarbenes in organic glasses at 77 K.[10] The glassy solution did not exhibit any changes for several hours when kept at 77 K. However, when it was allowed to warm to room temp. and then cooled to 77 K, the characteristic bands disappeared. On the basis of these observations, coupled with the EPR data, the absorption spectrum can be attributed to triplet carbene **2**.

Again essentially the same spectral features were noted in the case of DDC. However, in this case, as the matrix thawed and carbene absorption bands decreased, a new broad absorption at 375 nm appeared. This secondary intermediate was assigned to *o*-xylylene presumably formed by an intramolecular 1,4 H shift from an *o*-methyl group to the carbene center and leading to benzocyclobutene.[5a,d] The decay of the transient absorption of **2** was rather monotonous, no new band being detected even upon gradual warming, indicating that no intramolecular H abstraction occurs. This is in accord with the product analysis data.

Laser flash photolysis (LFP) of **1** in a degassed benzene solution at 20 °C with a 10 ns, 70–90 mJ, 308 nm pulse from a

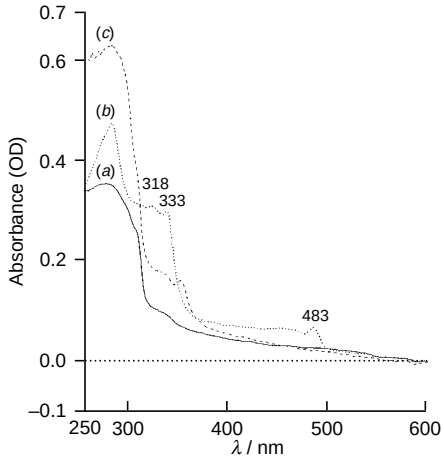



**Fig. 1** UV–VIS spectra obtained by irradiation of **1** in MTHF. (*a*) Spectrum of **1** in MTHF at 77 K. (*b*) Same sample after warming the matrix to room temperature and refreezing to 77 K. OD = optical density.

XeCl excimer laser produced a transient species showing a strong absorption around 320–330 nm and a weak absorption around 480 nm, which appeared coincident with the pulse (Fig. 2). On the basis of the low-temperature spectrum, we assign the transient product to triplet **2**. The inset in Fig. 2 shows the decay of **2**, which is found to be second order ($2k/\varepsilon l$ = 8.4 $s^{-1}$), suggesting that the carbene **2** decays mainly by undergoing dimerization. The approximate lifetime of **2** is estimated in the form of half-life, $t_{1/2}$, to be 1.5 ± 0.1 s.

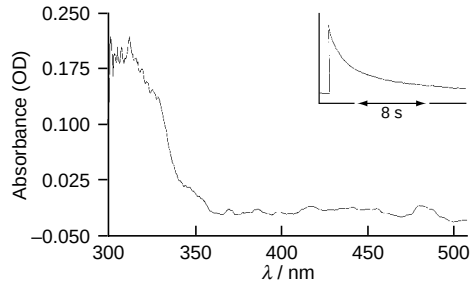



**Fig. 2** Absorption spectrum of the transient products formed during the irradiation of **1** in degassed benzene, recorded 50 μs after excitation. The inset shows the time course of the absorption at 480 nm (oscillogram traces).

The reactivities of **2** toward typical triplet quenchers, *i.e.* oxygen and cyclohexa-1,4-diene (CHD), were then investigated by using LFP. Thus, LFP of **1** on a degassed benzene solution in the presence of CHD generated a new signal attributable to the diarylmethyl radicals as the signals of **2** decayed, showing that triplet **2** abstracts H from the diene.[11] The rate constant ($k_{CHD}$) of H abstraction of **2** from CHD is determined from a plot of the apparent build-up rate constant of the radical *vs.* [CHD]. Similarly the rate constant ($k_{O_2}$) for the quenching of **2** by oxygen was determined from a plot of the observed pseudo-first-order growth rate of the carbonyl oxide[12] as a function of [$O_2$]. The data are summarized in Table 1 along with those obtained in the reaction of DDC.

**Table 1** Kinetic[a] and EPR data[b] for triplet diphenylcarbenes **1** and DDC

| Carbenes | $(2k/\varepsilon l)$/ $s^{-1}$ | $t_{1/2}$/s | $k_{CHD}$/ $M^{-1}$ $s^{-1}$ | $k_{O_2}$ $M^{-1}$ $s^{-1}$ | $D$/ $cm^{-1}$ | $E$/ $cm^{-1}$ |
|---|---|---|---|---|---|---|
| **2** | 8.4 | 1.5 | $3.6 \times 10^2$ | $2.3 \times 10^8$ | 0.3951 | 0.0106 |
| DDC | — | 0.41 | $3.4 \times 10$ | $7.1 \times 10^7$ | 0.3805 | 0.0106 |

[a] In benzene at 20 °C. [b] In MTHF at 77 K.

Thus, these observations clearly support our original idea that bicycloalkyl groups are not delivering hydrogens to triplet carbenic centers while they are acting as a fairly good kinetic protector for the carbene. In this way, the formation of a hydrocarbon triplet carbene having a half-life over a second under normal conditions, *i.e.* in degassed benzene solution at room temperature, was realized for the first time. It should be noted here that the reactivity of **2** toward typical triplet quenchers is somewhat higher than that of DDC, while the half-life of **2** in benzene is distinctly longer than that of DDC. Comparison of the optimized geometries between DDC and **2** obtained by the AM1/UHF method[13] reveals that there is slightly more space around carbene center in **2** compared to that in DDC, especially for a small particle such as hydrogen to attack, but that dimerization of the carbene center of **2** is obviously more severely retarded by the bulky rigid 'three-dimensional' bicyclic substituent compared to that of DDC which has more flexible methyl substituents.

The authors are grateful to the Ministry of Education, Science and Culture of Japan for support of this work.

## Footnotes and References

* E-mail: tomioka@chem.mie-u.ac.jp

† *Selected spectral data* for **1**: $\delta_H(CDCl_3)$ 1.13–1.38 (16 H, m), 1.55–1.75 (16 H, m), 2.93 (4 H, b s), 3.16 (4 H, br s), 6.89 (2 H, s); $\nu_{max}$(KBr)/$cm^{-1}$ 2032vs.


1 The first attempts to isolate triplet carbenes were made by Zimmerman and Paskovich: H. E. Zimmerman and D. H. Paskovich, *J. Am. Chem. Soc.*, 1984, **88**, 5251.

2 A. Igau, H. Grützmacher, A. Baceiredo and G. Bertrand, *J. Am. Chem. Soc.*, 1988, **110**, 6463; see also: M. Soleilhavoup, A. Baceiredo, O. Treutler, R. Ahlichs, M. Nieger and G. Bertrand, *ibid.*, 1992, **114**, 10 959 and references cited therein.

3 A. J. Arduengo, III, R. L. Harlow and M. Kline, *J. Am. Chem. Soc.*, 1991, **113**, 361; see also: A. J. Arduengo, III, J. R. Goerlich and W. J. Marshall, *ibid.*, 1995, **117**, 11 027 and references cited therein.

4 For discussion of the electronic structure for those stable singlet carbenes, see C. Heinemann, T. Müller, Y. Apeloig and H. Schwarz, *J. Am. Chem. Soc.*, 1996, **118**, 2039.

5 (*a*) H. Tomioka, H. Okada, T. Watanabe and K. Hirai, *Angew. Chem., Int. Ed. Engl.*, 1994, **33**, 873; (*b*) K. Hirai, K. Komatsu and H. Tomioka, *Chem. Lett.*, 1994, 503; (*c*) K. Furukawa, Y. Teki, T. Takui, K. Itoh, T. Watanabe, K. Hirai and H. Tomioka, *Mol. Cryst. Liq. Cryst.*, 1995, **271**, 183; (*d*) H. Tomioka, H. Okada, T. Watanabe, K. Banno, K. Komatsu and K. Hirai, *J. Am. Chem. Soc.*, 1997, **119**, 1582.

6 H. Tomioka, K. Hirai and C. Fujii, *Acta Chem. Scand.*, 1992, **46**, 680; H. Tomioka, K. Hirai and T. Nakayama, *J. Am. Chem. Soc.*, 1993, **115**, 1285.

7 H. Tomioka, T. Watanabe, K. Hirai, K. Furukawa, T. Takui and K. Itoh, *J. Am. Chem. Soc.*, 1995, **117**, 6376; H. Tomioka, M. Hattori, K. Hirai and S. Murata, *ibid.*, 1996, **118**, 8723.

8 V. R. Koch and G. J. Cleicher, *J. Am. Chem. Soc.*, 1971, **93**, 1657 and references cited therein.

9 For a recent review of EPR data of triplet arylcarbenes, see W. Sander, G. Bucher and S. Wievlacher, *Chem. Rev.*, 1993, **93**, 1583.

10 The optical absorption spectra of several aromatic carbenes in frozen media have been assigned: A. M. Trozzolo and E. Wasserman, in *Carbenes*, ed. R. A. Moss and M. Jones, Jr., Wiley, New York, 1975, vol. 2, pp. 185–206.

11 For review, see M. S. Platz and V. M. Maloney, in *Kinetics and Spectroscopy of Carbenes and Biradicals*, ed. M. S. Platz, Plenum, New York, 1990, pp. 239–352; J. E. Jackson and M. S. Platz, in *Advances in Carbene Chemistry*, ed. U. Brinker, JAI, Greenwich, CT, 1994, vol. 1, pp. 87–160.

12 It is well-documented that diarylcarbenes with triplet ground states are readily trapped by oxygen to generated the corresponding diary ketone oxides. For a review, see W. W. Sander, *Angew. Chem., Int. Ed. Engl.*, 1990, **29**, 344; see also J. C. Scaiano, W. G. McGimpsey and H. L. Casal, *J. Org. Chem.*, 1989, **54**, 1612.

13 J. J. P. Stewart, *J. Comput. Chem.*, 1989, **10**, 209, 221; MOPAC version 6.01 (JCPE No. P044) was used.


*Received in Cambridge, UK, 15th September 1997, 7/06663E*

# Construction of the tricyclo[5.3.1.0$^{1,5}$]undecane system by a tandem pinacol rearrangement–ene strategy: a formal synthesis of (±)-perhydrohistrionicotoxin

**Deukjoon Kim,* Sung Woo Hong and Cheol Won Park**

*College of Pharmacy, Seoul National University, San 56-1, Shinrim-Dong, Kwanak-Ku, Seoul 151-742, Korea*

**An advanced synthetic intermediate 4 for perhydrohistrionicotoxin 5 has been synthesized utilizing a novel tandem pinacol rearrangement–ene reaction as a key step.**

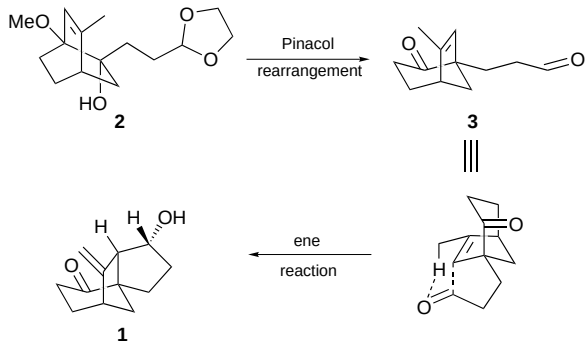
Construction of the tricyclo[5.3.1.0$^{1,5}$]undecane skeleton, which constitutes the carbon framework of natural products such as cedranes, has been a challenge to synthetic organic chemists and has led to the development of diverse and inspiring strategies.[1] We envisaged that highly functionalized tricyclo[5.3.1.0$^{1,5}$]undecane system **1** might be accessible by a novel tandem pinacol rearrangement–ene reaction on a Diels–Alder derived bicyclo[2.2.2]octene **2** *via* the intermediacy of bicyclo-[3.2.1]octene derivative **3** (Scheme 1).[2]

Reported herein is a stereoselective synthesis of an advanced intermediate **4**[3] for the synthesis of perhydrohistrionicotoxin **5**,[4] a hydrogenation product of a potent neurotoxin isolated from the Columbian frog *Dendrobates histrionicus*, which demonstrates the potential of our tandem pinacol rearrangement–ene protocol.

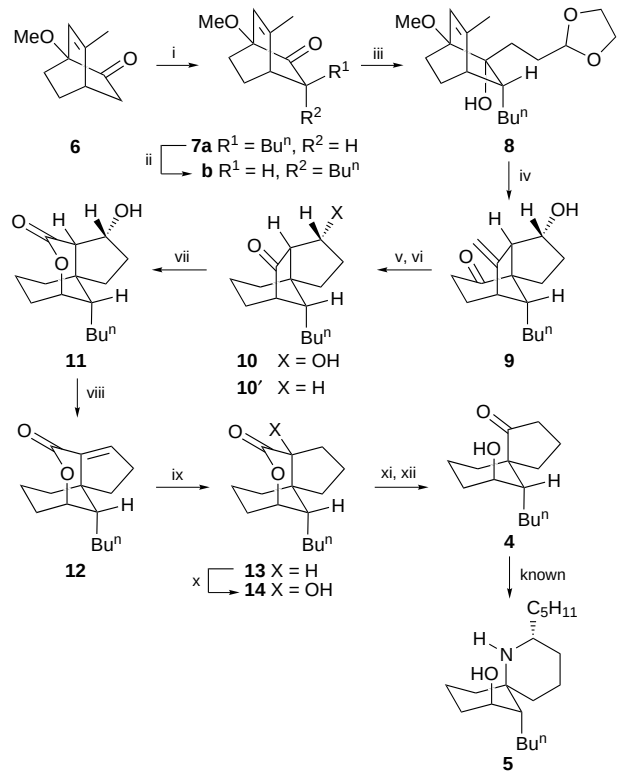
Alkylation of readily available ketone **6**[2a] by successive treatment with LDA and *n*-butyl iodide in THF containing HMPA produced a 75% yield of *exo* product **7a** (Scheme 2). Epimerization of *exo* isomer **7a** with methanolic NaOH produced a chromatographically separable 73 : 27 equilibrium mixture of *exo* and *endo* isomers **7a** and **7b** in a quantitative yield. Treatment of bicyclic ketone **7b**, secured in a large quantity by recycling of **7a**, with appropriate β-bromo ketal derived Grignard reagent under Barbier conditions[5] gave *endo* alcohol **8** in 92% yield stereospecifically. As we had planned, compound **8** underwent an efficient, novel, tandem pinacol rearrangement–ene reaction upon exposure to TsOH in refluxing acetone to afford tricyclic intermediate **9** and its epimeric alcohol in an 89 : 11 ratio (82% total yield).†

Next, we turned to the conversion of the key tricyclic intermediate **9** to our target compound **4** for a formal synthesis of perhydrohistrionicotoxin **5**. Removal of the keto function from **9** by Wolff–Kishner reduction,‡ followed by ozonolysis of the resulting alkene, produced hydroxy ketone **10** in 51% overall yield for the two steps. Regiospecific Baeyer–Villiger oxidation[6] of ketone **10** with MCPBA and subsequent elimination of the resulting β-hydroxy ester **11** gave α,β-unsaturated δ-lactone **12** (76% overall yield over two steps). Our originally projected synthetic plan for processing the key intermediate **4** by an ammonolysis–Hoffmann rearrangement protocol on **12** was thwarted by difficulties encountered in opening of the lactone. To circumvent these problems, catalytic hydrogenation of the alkene functionality in **12** and subsequent α-hydroxylation of the resulting lactone **13** *via* the method of Davis[7] yielded α-hydroxy lactone **14**. Finally, reductive opening of lactone **14** with $LiAlH_4$ to the corresponding diol, followed by oxidative cleavage with $NaIO_4$, delivered the desired keto alcohol **4** in 66% yield for the four steps from **12**.† $^1$H and $^{13}$C NMR spectral data of compound **4** were in good agreement with those of authentic samples kindly provided by Professors Ibuka and Smith.§

In summary, a formal synthesis of (±)-perhydrohistrionicotoxin **5** has been accomplished utilizing a novel tandem pinacol rearrangement–ene strategy and a regiospecific Baeyer–Villiger




**Scheme 1**




**Scheme 2** *Reagents and conditions*: i, $LN(SiMe_3)_2$, $Bu^nI$, HMPA, THF, −78 to −20 °C, 3 h, 75%; ii, NaOH, MeOH, room temp., 3.5 h (**7a** : **7b** = 73 : 27), 100%; iii, Mg, $Br(CH_2)_2Br$, 2-(2-bromoethyl)- 1,3-dioxolane, THF, room temp., 1.5 h, 92%; iv, TsOH, acetone, reflux, 11 h, (α : β = 89 : 11), 82%; v, $NH_2NH_2$, $HOCH_2C(=CH_2)CH_2OH$, KOH, $HO(CH_2)_2OH$, 110 to 190 °C, 8 h; vi, $O_3$, EtOAc, −78 °C, 4 h, then $Ph_3P$, EtOAc, room temp., overnight, 51%; vii, MCPBA, $NaHCO_3$, $CH_2Cl_2$, room temp., 1.5 h, 83%; viii, TsCl, DMAP, $Et_3N$ $CH_2Cl_2$, reflux, 3.5 h, 92%; ix, $H_2$, Pd–C, EtOH, room temp., 1.5 h, 97%; x, $KN(SiMe_3)_2$, *trans*-2-(phenylsulfonyl)-3-phenyloxaziridine, THF, −78 °C, 1.5 h; xi, LAH, THF, room temp., 2.5 h, 71% (2 steps); xii, $NaIO_4$, acetone–$H_2O$ (1 : 1), 1 h, 96%

reaction as key steps. Efforts are being made to apply this tandem pinacol–ene strategy to syntheses of other natural products.

We gratefully acknowledge financial support from KMOE (BSRI- 97-3420), KOSEF and OCRC. We also thank Mr Jong Sup Lee for his contributions in the early stages of the project.

## Footnotes and References

* E-mail: deukjoon@plaza.snu.ac.kr

† All new compounds exhibited satisfactory spectroscopic data. The ratio of isomers was determined by capillary GLC analysis and/or analysis of 500 MHz $^1$H NMR spectra. *Selected data* for **4**: $\delta_C$ ($CDCl_3$, 100 MHz) 14.0, 19.0, 20.2, 23.3, 29.1, 30.8, 31.9, 32.7, 35.0, 38.3, 47.7, 54.7, 73.3, 223.4.

‡ Addition of 2-methylenepropane-1,3-diol suppresses reduction of the double bond under these reaction conditions.

§ We thank Professors T. Ibuka (Kyoto University) and A. B. Smith, III (University of Pennsylvania) for copies of spectra of compound **4**.

1 Y. Chen and W. Lin, *Tetrahedron Lett.*, 1992, **33**, 1749 and references cited therein.

2 Pinacol rearrangement of a Diels–Alder derived bicyclo[2.2.2]octene **2** has previously been exploited in the synthesis of various natural products: (*a*) S. A. Monti, S. Chen, Y. Yang, S. Yuan and O. P. Bourgeois, *J. Org. Chem.*, 1978, **43**, 4062; (*b*) S. A. Monti and T. R. Dean, *J. Org. Chem.*, 1982, **47**, 2679 and references cited therein.

3 T. Ibuka, Y. Mitsui, K. Hayashi, H. Minakata and Y. Inubushi, *Tetrahedron Lett.*, 1981, **22**, 4425; E. R. Koft and A. B. Smith, III, *J. Org. Chem.*, 1984, **49**, 832.

4 E. J. Corey, J. F. Arnett and G. N. Widiger, *J. Am. Chem. Soc.*, 1975, **97**, 430 and references cited therein.

5 A. Greiner, *Tetrahedron Lett.*, 1989, **30**, 3547.

6 Baeyer–Villiger reaction of the deoxy ketone **10′**, prepared from **10** by elimination and catalytic hydrogenation, produced the desired lactone **13** and its regioisomeric lactone in a 5 : 1 ratio: T. Ho, in *Polarity Control for Synthesis*, Wiley, New York, 1991, p. 353.

7 F. A. Davis, L. C. Vishwaskarma, J. M. Billmers and J. Finn, *J. Org. Chem.*, 1984, **49**, 3241.

*Received in Cambridge, UK, 26th August 1997; 7/06193E*

# Enhancement of the photocyclization quantum yield of 2,2′-dimethyl-3,3′-(perfluorocyclopentene-1,2-diyl)bis(benzo[*b*]-thiophene-6-sulfonate) by inclusion in a cyclodextrin cavity

**Michinori Takeshita,* Chang Nam Choi† and Masahiro Irie***

*Department of Chemistry and Biochemistry, Graduate School of Engineering, Kyushu University, Hakozaki 6-10-1, Fukuoka, 812-81, Japan*

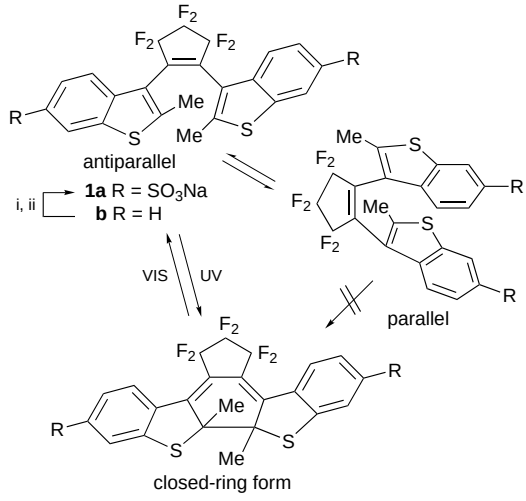
**The photocyclization quantum yield of 2,2′-dimethyl-3,3′-(perfluorocyclopentene-1,2-diyl)bis(benzo[*b*]thiophene-6-sulfonate) is found to increase in aqueous solution after the addition of β- and γ-cyclodextrin, in which a photoreactive antiparallel conformation of diarylethene is favourably included.**

Photochromic reaction of diarylethenes are based on reversible photocyclization of hexatriene structures, as shown in Scheme 1.[1] The opened ring form of diarylethene has two conformations, parallel and antiparallel. The photocyclization can proceed only from the antiparallel conformation, while the parallel conformation is photochemically inactive.[2] The conformational change between the antiparallel and parallel conformations in solution limits the maximum cyclization quantum yield to 0.5.[3] If one can increase the ratio of antiparallel : parallel conformation, the cyclization quantum yield is expected to increase accordingly.

It is well known that cyclodextrins (CDs) have cavities whose sizes are dependent on the number of glucopyranose units, and can include various types of organic compounds by hydrophobic interactions in aqueous media.[4] Here we have attempted to control the ratio of the two conformations in an aqueous solution by including the 3,3′-(perfluorocyclopentene-1,2-diyl)bis(benzo[*b*]thiophene-6-sulfonate) in the CD cavities.

2,2′-Dimethyl-3,3′-(perfluorocyclopentene-1,2-diyl)bis-(benzo(*b*]thiophene-6-sulfonate)‡ **1a** was prepared by treatment of 2,2′-dimethyl-3,3′-(perfluorocyclopentene-1,2-diyl)bis(benzo[*b*]thiophen)[5] **1b** with chlorosulfonic acid in $CHCl_3$ and subsequent hydrolysis with 1% aqueous NaOH (Scheme 1).

Fig. 1(*a*) shows the $^1$H NMR spectrum of the methyl groups of the open-ring form of **1a** in $D_2O$ ($3.0 \times 10^{-3}$ mol dm$^{-3}$, 20 °C, 200 MHz). The methyl signals of each conformation are




**Scheme 1** *Reagent and conditions*: i, $ClSO_3H$, $CHCl_3$, room temp.; ii, 1% NaOH, 78%

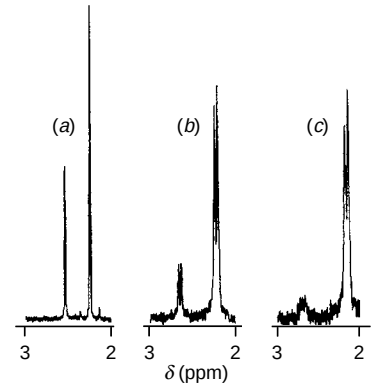



**Fig. 1** $^1$H NMR spectra of methyl protons in $D_2O$ ([**1**] = $3.0 \times 10^{-3}$ mol dm$^{-3}$); (*a*) **1a**, (*b*) **1a**–β-CD (1 : 5) and (*c*) **1a**–β-CD (1 : 10)

observed separately. This indicates that the conformational change takes place slowly relative to the NMR timescale ( < 56 Hz). The methyl protons at $\delta$ 2.27 (at higher magnetic field) are assigned to the antiparallel conformation.[2] Under the present conditions, the antiparallel conformation is favoured and the ratio of antiparallel : parallel was 64 : 36. This value shows that only 64% of **1a** is photoreactive. Upon addition of β- and γ-CD to this solution, the ratio of antiparallel : parallel conformations was increased, as shown in Fig. 2. When 10 equiv. of β-CD were added to the solution, the antiparallel conformation became dominant, as shown in Fig. 1(*c*). On the other hand, the addition of α-CD did not change the $^1$H NMR spectrum of **1a**. These results reveal that the cavity of β-CD is suitable for the antiparallel conformation of **1a**, whereas that of α-CD is too small to include **1a**. γ-CD is considered to have a small association constant with the diarylethene. The splitting of each

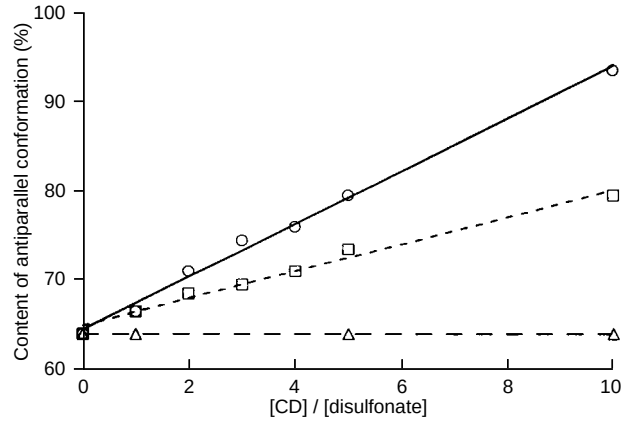



**Fig. 2** [CD]/[**1a**] *vs.* content of antiparallel conformation determined by $^1$H NMR spectroscopy ([**1a**] - $3.0 \times 10^{-3}$ mol dm$^{-3}$); (△) with α-CD, (○) with β-CD and (□) with γ-CD

**Table 1** Cyclization quantum yields of **1a** irradiated with 313 nm light in the presence of CD in aqueous solution[a]

| System | **1a** | **1a**–α-CD | **1a**–β-CD | **1a**–γ-CD |
|---|---|---|---|---|
| Quantum yield | 0.38 | 0.37 | 0.58 | 0.53 |

[a] [**1a**] = $4.0 \times 10^{-5}$ mol dm$^{-3}$; [CD] = $8.0 \times 10^{-3}$ mol dm$^{-3}$, 20 °C.

methyl proton of the both conformations of **1a** was observed in β-CD. The split suggests that the two methyl protons exist in different environments in the chiral CD cavity.

As described above, the diarylethene in the parallel conformation is not photoreactive. Therefore, the increase in the ratio of antiparallel : parallel conformations is expected to result in an increase in the cyclization quantum yield. Table 1 shows the cyclization quantum yields of **1a** irradiated with 313 nm light.[3,6]

As expected, the cyclization quantum yield of **1a** in the presence of a 200-fold excess of β-CD is *ca.* 1.5 times larger than that of **1a** in aqueous solution. NMR measurements indicated that almost all the diarylethene is in the antiparallel conformation in the presence of excess β-CD. The increase in the quantum yield is due to the increase in the proportion of molecules in the antiparallel conformation. On the other hand, no change was observed in either the $^1$H NMR spectrum or the quantum yield for cyclization of **1a** in the presence/absence of α-CD. The enhancement of quantum yield in the presence of β- and γ-CD is ascribed to the favourable antiparallel conformation of **1a** in the CD's cavities.

The authors are grateful to Professor S. Mataka and his coworkers at the Institute of Advanced Material Study, Kyushu University, for the measurement of mass spectra and elemental analyses. This work was partly supported by a Grant-in-Aid for Encouragement of Young Scientists (No. 09750956) from the Ministry of Education, Science and Culture, Japan.

## Footnotes and References

* E-mail: michi@cstf.kyushu-u.ac.jp
† Present address: Chonnam National University, Kwang-ju, Korea

‡ *Selected data* for **1a** (100% open form): $\delta_H$ (200 MHz, 20 °C, $D_2O$) 2.27 (3.84 H, s, ap), 2.55 (2.16 H, s, p), 7.58–7.96 (4 H, m, ap and p), 8.14 (0.72 H, s, p), 8.26 (1.28 H, s, ap) [although the spectrum shows parallel (p) and antiparallel (ap) conformers separately, these conformers exchange slowly relative to the NMR timescale]; Calc. for $C_{23}H_{12}F_6O_6S_4Na_2 \cdot H_2O$: C, 40.00; H, 2.04. Found: C, 39.56; H, 2.27%; $\lambda_{max}$/nm (ε) open-ring form: 233 (49 000), closed-ring form: 529 (9800); MS(FAB+) *m*/*z* 673 $[M + 1]^+$.

1 For a review, see M. Irie, *Photo-reactive Materials for Ultrahigh Density Optical Memory*, Elsevier, Amsterdam, 1994.
2 M. Irie, O. Miyatake, K. Uchida and T. Eriguchi, *J. Am. Chem. Soc.*, 1994, **116**, 9894.
3 M. Irie, K. Sakemura, M. Okinaka and K. Uchida, *J. Org. Chem.*, 1995, **60**, 8305.
4 For an example review, see F. Vögtle, *Supramolecular Chemistry*, Wiley, Chichester, 1991.
5 M. Hanazawa, R. Sumiya, Y. Horikawa and M. Irie, *J. Chem. Soc., Chem. Commun.*, 1992, 206.
6 Y. Yokoyama and Y. Kurita, *Yuki Gousei Kagaku Kyoukaishi*, 1991, **49**, 364 (*Chem. Abstr.*, 1991, **115**, 60 542F).

*Received in Cambridge, UK, 5th August 1997; 7/05677J*

# Synthesis of novel conformationally restricted L-glutamate analogues

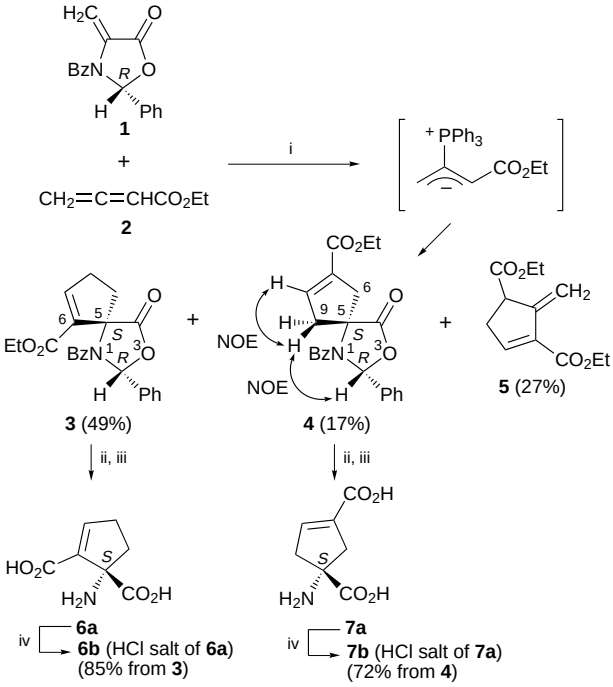
**Stephen G. Pyne,*[a] Karl Schafer,[a] Brian W. Skelton[b] and Allan H. White[b]**

[a] *Department of Chemistry, University of Wollongong, Wollongong, New South Wales, 2522, Australia*
[b] *Department of Chemistry, University of Western Australia, Nedlands, Western Australia, 6907, Australia*

**The novel, optically active and conformationally restricted L-glutamate analogues 6, 7 and 11 have been prepared *via* the $PPh_3$ catalysed cycloaddition of the allenes 2 and 9 with the chiral oxazolidinone 1.**

L-Glutamate is an excitatory neurotransmitter in the mammalian central nervous system (CNS). This amino acid activates both the metabotropic and the ionotropic group of glutamate receptors. The latter group includes the *N*-methyl-D-aspartic acid (NMDA), α-amino-3-hydroxy-5-methylisoxazole-4-propionate and kainate receptor subclasses. These receptors form ligand-gated ion channels and mediate excitatory neurotransmission. The former receptor group are coupled to G-proteins and activate or inhibit intracellular signals. Elevated glutamate concentrations can lead to excitoxicity which has been implicated in the pathogenesis of neurological disorders, including epilepsy and chronic neurodegenerative diseases.[1,2] Excitatory amino acid transporters (EAATs) in the CNS maintain extracellular glutamate concentrations below excitotoxic levels.[3] Selective agonists and antagonists for glutamate receptor subtypes[1] and selective blockers for EAATs are invaluable tools in understanding neuronal biochemistry. Furthermore, such compounds allow an understanding of the structural features of these receptor subtypes and the future design of new therapeutics for the treatment of neurodegenerative diseases.[1] One such compound is the conformationally restricted glutamate analogue, (1*S*,3*R*)-1-aminocyclopentane-1,3-dicarboxylic acid (ACPDA), which selectively activates metabotropic glutamate receptors and differentiates them from the ionotropic type.[4] Here we describe a novel synthesis of some dehydro derivatives of ACPDA *via* the cycloaddition reactions of the chiral oxazolidinone **1**[5] and allenic esters **2** and **9** and report some preliminary results on the pharmacological activities of these compounds.

Treatment of a benzene solution of the oxazolidinone **1** (1 equiv.) and ethyl buta-2,3-dienoate **2**[6] (5 equiv.) with $PPh_3$[7] (0.1 equiv.) at room temperature for 5 h gave, after purification by column chromatography, the major cycloadduct **3**† (49%), the minor cycloadduct **4**† (17%) and the dimer **5**[7a] (27%) (Scheme 1). The diastereoisomeric ratio of **3** and **4** was estimated to be 77 : 23 from $^1$H NMR analysis of the crude reaction mixture. The stereochemistry of **3** was revealed by a single crystal X-ray structural analysis, as shown in Fig. 1.‡ This analysis showed that the major cycloadduct had the 5*S* stereochemistry at the newly created stereogenic centre, consistent with the known tendency of **1** in [3 + 2] cycloaddition reactions to give products that arise from attack of the three-atom component *anti* to the C(2) phenyl substituent.[8] The minor cycloadduct **4** was a regioisomer of **3** and also had the 5*S* stereochemistry as shown by NOESY experiments which revealed cross-peaks between the signal for H-2 and that for one H-9 proton, as indicated in structure **4** (Scheme 1). Interestingly, the regiochemistry of the major cycloadduct **3** was different to that of the major cycloadduct formed from the reaction of ethyl acrylate or methyl methacrylate with **2**–$PPh_3$.[7a] The enantiomeric purity of **3** was determined to be 88% from $^1$H NMR analysis of its




**Scheme 1** *Reagents and conditions*: i, $PPh_3$ (10 mol%); ii, 6 M HCl, reflux, 16 h; iii, ion-exchange; iv, HCl

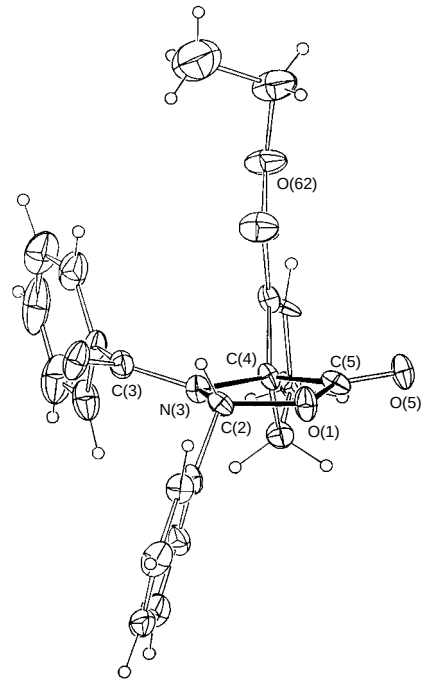
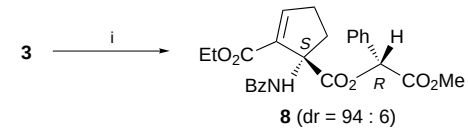



**Fig. 1** Projection of **3** through the heterocyclic ring plane (20% thermal ellipsoids are shown for C, N, O, H having arbitrary radii of 0.1 Å)



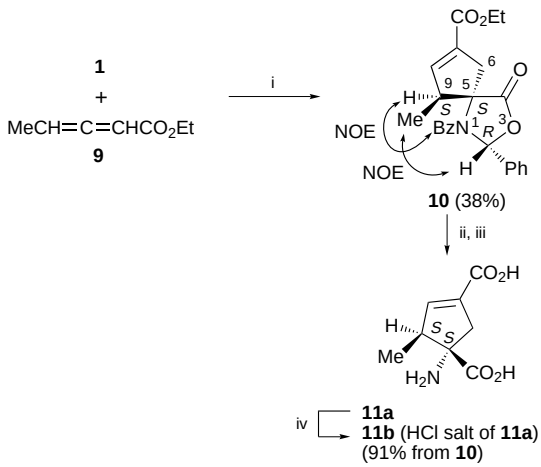

**Scheme 2** *Reagents and conditions*: i, (*R*)-methyl mandelate, $Et_3N$, $CH_2Cl_2$, 7 days, 63%

(*R*)-methyl mandelate derivative **8**, which was a 94 : 6 mixture of diastereoisomers [major: $\delta_H(CDCl_3)$ 5.99 (s), minor 5.98 (s)] (Scheme 2). Acid hydrolysis of **3** and **4** followed by purification *via* ion-exchange chromatography gave diastereoisomerically pure amino acids **6a** and **7a**, respectively, which were characterized as their respective hydrochloride salts, **6b**† and **7b**.† Amino acid **7a** has been reported recently, however this product was racemic and was obtained as a mixture of two isomers from which racemic **7a** could be obtained in 1.75% yield after selective crystallization.[9]

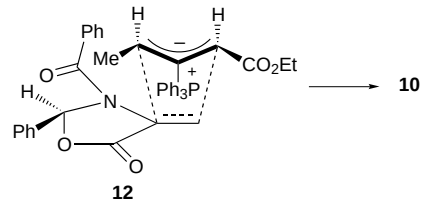
Treatment of a benzene solution of **1** and ethyl penta-2,3-dienoate **9**[6] (5 equiv.) with $PPh_3$ (0.1 equiv.) at room temperature for 5 h gave a single cycloadduct **10**† in 38% isolated yield after purification by column chromatography on silica gel. No other stereoisomer of **10** could be detected by $^1H$ NMR analysis of, or was isolated from, the crude reaction mixture. The 5*S*,9*S* stereochemistry of **10** was evident from NOESY experiments, which showed cross-peaks between H-2 and the C(9) methyl group and between H-9 and the *ortho* protons of the benzamido group, as shown in Scheme 3. Acid hydrolysis of **10** gave the amino acid **11a**, which was characterized as its hydrochloride salt **11b**.†

Thus the $PPh_3$ catalysed reactions of **2** and **9** with oxazolidinone **1** proceed in a different regiochemical sense. It is not clear if these reactions occur *via* a four step reaction sequence that involves initially a Michael addition reaction, then cyclization followed by proton transfer and then elimination of $PPh_3$,[7b] or *via* a three step mechanism *via* an initial 'concerted' 2,3-cycloaddition reaction.[7a] In the latter case, the transition state structure **12**, in which steric interactions between the substituents on the zwitterionic species formed between **9** and $PPh_3$ and the benzamido group on **1** are minimized, is consistent with the observed stereochemical outcome in **10** (Scheme 4). Attempts to obtain cycloadducts from the (2*S*)-*tert*-butyl analogue[5] of **1** and allene **2** gave only the dimer **5**.

In some preliminary studies, amino acids **6**, **7** and **11** showed no activity against NMDA-induced depolarizations in the rat neocortex at 500 μM concentrations.[10] Compound **11**, however, selectively blocks glutamate transport by EAAT2 expressed in




**Scheme 3** *Reagents and conditions*: i, $PPh_3$ (10 mol%); ii, 6 M HCl, reflux, 16 h; iii, ion-exchange; iv, HCl




**Scheme 4**

oocytes ($K_i$ = 62 μM) but is inactive on EAAT1.[11] Further biological studies are in progress and these will be reported in a future paper.

We thank the Australian Research Council for financial support and J. Ong and D. Kerr (University of Adelaide) and G. A. R. Johnston and R. J. Vandenberg (University of Sydney) for preliminary biological results on compounds **6**, **7** and **11**.

## Footnotes and References

* E-mail: s.pyne@uow.edu.au

† *Selected data* for **3**: colourless crystals, mp 144–146 °C, $[\alpha]_D^{21}$ +155 (*c* 0.60, $CHCl_3$); $\delta_H(CDCl_3)$ 1.35 (t, *J* 7.2, 3 H), 2.75–3.19 (m, 4 H, H-8α, H-8β, H-9α and H-9β), 4.28 (q, *J* 7.2, 2 H), 6.77 (br s, 1 H, H-2), 6.97 (br s, 1 H, H-7), 7.02 (d, *J* 6.9, 2 H), 7.25 (d, *J* 6.9, 2 H), 7.29–7.39 (m, 6 H). For **4**: white solid, mp 70–73 °C, $[\alpha]_D^{23}$ +202 (*c* 0.10, $CHCl_3$); $\delta_H(CDCl_3)$ 1.32 (t, *J* 7.2, 3 H), 3.20–3.26 (m, 1 H, H-9α), 3.32–3.39 (m, 2 H, H-6α and H-9β), 3.60–3.66 (m, 1 H, H-6β), 4.23 (q, *J* 7.2 , 2 H), 6.67 (br s, 1 H, H-2), 6.72 (br s, 1 H, H-8), 6.91 (d, *J* 7.5, 2 H), 7.12 (d, *J* 7.2, 2 H), 7.20–7.35 (m, 6 H). For **10**: pale yellow gum, $[\alpha]_D^{21}$ +90 (*c* 0.30, $CHCl_3$); $\delta_H(CDCl_3)$ 1.33 (t, *J* 7.2, 3 H), 1.38 (d, *J* 7.5, 3 H), 3.45–3.51 (m, 1 H, H-6α), 3.65–3.71 (m, 1 H, H-6β), 3.74–3.79 (m, 1 H, H-6β), 4.24 (q, *J* 7.2, 2 H), 6.57 (s, 1 H, H-2), 6.68 (br s, 1 H, H-8), 6.81, d, *J* 6.9, 2 H), 7.02 (d, *J* 6.9, 2 H), 7.1–7.33 (m, 6 H). For **6b**: white solid, mp > 250 °C, $[\alpha]_D^{22}$ +15 (*c* 0.20, 6 M HCl); $\delta_H(D_2O)$ 2.78–2.84 (app br d, *J* 16.2, 2 H, H-2α and H-5α), 3.22–3.27 (app br d, *J* 16.8, 2 H, H-2β and H-5β), 6.66 (br s, 1 H, H-4). For **7b**: white hygroscopic solid, mp > 250 °C, $[\alpha]_D^{22}$ +11 (*c* 0.40, 6 M HCl); $\delta_H(D_2O)$ 2.09–2.18 (m, 1 H, H-5α), 2.39–2.48 (m, 1 H, H-5β), 2.57–2.68 (m, 2 H, H-4α and H-4β), 6.82 (br s, 1 H, H-3). For **11b**: white hygroscopic solid, mp > 250, $[\alpha]_D^{22}$ +10 (*c* 0.10, 6 M HCl); $\delta_H(D_2O)$ 1.13 (d, *J* 7.5, 3 H), 3.30 (app t, *J* 1.8, 1 H, H-2α), 3.36 (app t, *J* 2.1, 1 H, H-2β), 3.55–3.65 (m, 1 H, H-5), 6.64 (s, 1 H, H-4).

‡ *Selected X-ray data* for **3**: $C_{23}H_{21}NO_5$, *M* = 391.4; orthorhombic, $P2_12_12_1$, *a* = 21.13(1), *b* = 11.22(1), *c* = 8.474(7) Å, *V* = 2009 Å$^3$, $D_c$ (*Z* = 4) = 1.29 g cm$^{-3}$, 795 'observed' [$I > 3\sigma(I)$] diffractometer reflections out of 2032 independent to $2\theta_{max}$ = 50° (monochromatic Mo-Kα radiation, λ = 0.7107 Å, no absorption correction) yielding conventional *R*, $R_w$ $|F|$ = 0.054, 0.046 (statistical weights). Anisotropic C, N, O thermal parameter refinement ($x$, $y$, $z$, $U_{iso})_H$ constrained at estimates *T* = 295 K. Chirality was assigned from the chemistry. CCDC 182/630.

1 T. Knöpfel, R. Kuhn and H. Allgeier, *J. Med. Chem.*, 1995, **38**, 1417.
2 S. Nakanishi, *Science*, 1992, **258**, 597.
3 R. J. Vandenberg, A. D. Mitrovic, M. Chebib, V. J.. Balcar and G. A. R. Johnston, *Mol. Pharmacol.*, 1997, **51**, 809.
4 D. Ma, J. Ma and L. Dai, *Tetrahedron: Asymmetry*, 1997, **8**, 825 and references cited therein.
5 S. G. Pyne, B. Dikic, P. Gordon, B. W. Skeleton and A. H. White, *Aust. J. Chem.*, 1993, **46**, 73.
6 R. W. Lang and H.-J. Hansen, *Org. Synth.*, 1984, **62**, 202.
7 (*a*) C. Zhang and X. Lu, *J. Org. Chem.*, 1995, **60**, 2906; (*b*) Z. Xu and X. Lu, *Tetrahedron Lett.*, 1997, **38**, 3461.
8 S. G. Pyne, J. Safaei-G and F. Koller, *Tetrahedron Lett.*, 1995, **36**, 2511; S. G. Pyne, J. Safaei-G, B. W. Skelton and A. H. White, *Aust. J. Chem.*, 1995, **48**, 1511.
9 R. D. Allan, R. K. Duke, T. W. Hambley, G. A. R. Johnston, K. N. Mewett, N. Quickert and H. W. Tran, *Aust. J. Chem.*, 1996, **49**, 785.
10 D. I. B. Kerr and J. Ong, personal communication.
11 G. A. R. Johnston and R. J. Vandenberg, personal communication.

*Received in Cambridge, UK, 22nd August 1997; 7/06148J*

# Cubic lanthanide sulfido clusters: $Ln_8S_6(SPh)_{12}(thf)_8$ (Ln = Pr, Nd, Gd)

**Jonathan H. Melman, Thomas J. Emge and John G. Brennan***

*Department of Chemistry, Rutgers, the State University of New Jersey, Piscataway, NJ 08854-8087, USA*

**Lanthanide thiolates react with elemental sulfur to give $Ln_8S_6(SPh)_{12}(thf)_8$ clusters in high yield.**

Lanthanide thiolates [$Ln(SPh)_3$; Ln = Pr, Nd, Gd] react with elemental sulfur to give crystalline octametallic $Ln_8S_6(SPh)_{12}(thf)_8$ clusters in high yield.

Inorganic clusters are important synthetic targets because their unique physical properties provide insight into the relationships between molecular and solid state properties. Lanthanide (Ln)[1] clusters are scarcer than main group[2] or transition metal clusters,[3] primarily because no general synthetic approach to such materials has as yet been identified. The recent explosion of interest in determining the properties of Ln thiolates (SR), selenolates (SeR), and tellurolates (TeR) has in effect created a wide variety of potential starting materials for cluster syntheses.[1a,4] Relative to more conventional O, N, or C based anions, these singly charged, electropositive chalcogenolate ligands should be considerably more susceptible to displacement from Ln coordination spheres. Here we present an extremely general approach to the synthesis of lanthanide sulfido cluster materials: $Ln(SPh)_3$ reacts with elemental sulfur to form thiolate capped lanthanide sulfide clusters in 40–60% isolated yields.

Addition of sulfur to a suspension of $Ln(SPh)_3$ in thf results in the formation of a homogeneous solution that can be saturated by layering with hexane to give crystals of $Ln_8S_6(SPh)_{12}(thf)_8$ (Ln = Pr, Nd, Gd) [eqn. (1)].†

$$8\ Ln(SPh)_3 + 6\ S \rightarrow Ln_8S_6(SPh)_{12}(thf)_8 + 6\ PhSSPh \quad (1)$$

The compounds were characterized by conventional methods and the Gd derivative (**1**) was also characterized by low temperature single crystal X-ray diffraction.‡ Unit cell data for the Pr and Nd compounds indicated that all three clusters are isostructural. The clusters (Fig. 1) contain a cube of $Ln^{III}$ ions, with the six faces of the cube all capped with $S^{2-}$, and the 12 edges of the cube all spanned by μ-SPh. The cubic structure appears to be particularly stable: thus far, $Ln_8S_6(SPh)_{12}(thf)_8$ clusters§ have crystallized in three distinct phases which differ in the amount of lattice thf present, and the related selenido cluster $Sm_8Se_6(SePh)_{12}$ can be isolated in low yield from the thermal decomposition of $Sm(SePh)_2$.[1c] The isolation of a neutral cluster compound is an additional benefit of $Ln(SR)_3$ starting materials: whereas in $Ln(SeR)_3$ chemistry SeR abstraction by excess $Hg(SeR)_2$ is a complicating side reaction,[1c,5] in related thiolate work Ln–S bonds have yet to be cleaved by the addition of excess $M(ER)_2$ (M = Zn, Cd, Hg),[6] and so more rational syntheses are possible.

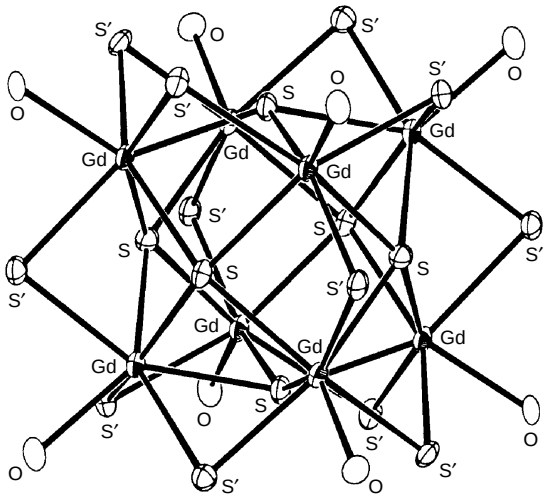



**Fig. 1** Molecular structure of $Gd_8S_6(SPh)_{12}(thf)_8$ **1**, with H and C atoms omitted for clarity. The unit cell contains two independent 'half' molecules that differ primarily in the orientation of the phenyl groups. The Gd–$S^{2-}$ bond lengths range from 2.746(4) to 2.835(4) Å and average 2.80 Å, while the Gd–S(Ph) (labeled S′) bond lengths range from 2.794(4) to 2.881(4) Å, and average 2.84 Å. Thermal ellipsoids are shown at the 50% probability level. The analogous Pr and Nd clusters are isostructural with the Gd cluster.

Thiolate displacement is clearly a general reaction that does not require a redox active metal. The reactivity can be understood in terms of 'hard', ionic metals preferentially binding harder, highly charged bases. The ability of $S^{2-}$ to bridge four metals must also contribute significantly to the stability of the final product. To date, only the middle of the Ln series (Pr–Tb) have yielded crystalline sulfido clusters from thf solution. The earlier (La, Ce) and later (Dy–Yb) lanthanides also react with elemental sulfur, as judged by the solubilization of $Ln(SPh)_3$, but these reactions precipitate microcrystalline materials from saturated thf solutions. Clusters of redox active Eu have also proven elusive. Solutions of europium(II) chalcogenoaltes in thf are colorless,[4f,g] and so the dark red solution color that results from the addition of S to a suspension of $Eu(SPh)_2$ in thf leads us to suggest that some form of $Eu^{III}$, with a visible S → Eu charge transfer absorption, is present in solution.

The facility with which lanthanide thiolates react with S–S bonds to form sulfido anions and PhSSPh at room temp. suggests the possibility that $Ln(SR)_3$ compounds may be valuable reagents for doping Ln into sulfide matrices.[7,8] Preliminary experiments indicate that reactions of $Ln(ER)_3$ (E = S, Se) with elemental Se procede similarly, and thus this is an extremely general synthetic route to lanthanide chalcogenide cluster compounds.

This work was supported by the National Science Foundation under Grant No. CHE-9628834.

## Footnotes and References

* E-mail: bren@rutchem.rutgers.edu

† *Cluster synthesis*: under nitrogen, Ln (2.42 mmol), PhSSPh (0.791 g, 3.62 mmol), and Hg (0.06 g, 0.3 mmol) were combined in thf (35 ml). The lightly colored solution was stirred for 1 d. Elemental sulfur was added (0.058 g, 1.8 mmol, 0.75 equiv. to Ln), and after 3 d the solution [yellow green (Gd), blue (Nd), blue green (Pr)] was filtered to remove a trace of black solid, and the filtrate was layered with hexane. Colorless (Gd), light blue (Nd), or light green (Pr) crystals of $Ln_8S_6(SPh)_{12}(thf)_8 \cdot 2.9thf$ were collected (0.44–0.57 g, yields range from 42 to 57% with longer saturation times giving larger yields). The compounds do not melt but begin turning yellow between 165 °C (Pr) and 175 °C (Gd). Upon isolation, the crystals lose thf and become amorphous within hours. Elemental analyses are consistent with the structure (less lattice thf) if the compound is analyzed immediately after isolation [*e.g.* Calc. for $Pr_8S_6(SPh)_{12}(thf)_8$: C, 38.9; H, 3.90. Found: C, 37.1; H, 3.80%], but the materials continue to lose coordinated thf upon standing

at room temp. The IR and NMR spectra are essentially identical for all three compounds. $^1$H NMR ([$^2H_8$]thf) revealed only peaks due to displaced thf at $\delta$ 1.754(t) and 3.604(m). IR (KBr, Nujol): 3151w, 2923s, 2854s, 2724w, 2672w, 2199w, 2036w, 1947w, 1874w, 1813w, 1571m, 1461s, 1377s, 1305w, 1262w, 1169m, 1154m, 1113w, 1075m, 1022m, 973w, 917w, 863w, 803w, 736m, 724m, 691m, 662w, 481m cm$^{-1}$. Unit cell data (−120 °C): Pr; triclinic space group $P\bar{1}$, $a$ = 17.661(5), $b$ = 18.297(5), $c$ = 20.490(5) Å, $\alpha$ = 102.84(2), $\beta$ = 94.56(2), $\gamma$ = 94.17(2)°, $U$ = 6407(3) Å$^3$. Nd; triclinic space group $P\bar{1}$, $a$ = 17.632(4), $b$ = 18.236(3), $c$ = 20.441(2) Å, $\alpha$ = 102.92(1), $\beta$ = 94.65(2), $\gamma$ = 94.21(2)°; $U$ = 6357(2)Å$^3$.

‡ Complex **1** crystallizes in the triclinic space group $P\bar{1}$, with $a$ = 17.513(4), $b$ = 18.136(4), $c$ = 20.382(4) Å, $\alpha$ = 102.94(2), $\beta$ = 94.39(2)°, $\gamma$ = 93.72(2)°, $U$ = 6268(3)Å$^3$, $Z$ = 2, $D_c$ = 1.878 g cm$^{-3}$, (Mo-K$\alpha$ radiation at −120 °C). Full-matrix least-squares refinement [8486 observations with $I > 2\sigma(I)$] gave $R(F)$ = 0.054, $wR(F^2)$ = 0.115. CCDC 182/621.

§ The terbium complex crystallizes in the monoclinic space group $C2/c$, with $a$ = 26.706(8), $b$ = 20.751(5), $c$ = 46.95(1)Å, $\beta$ = 90.21(2)°, $U$ = 26 020(11) Å$^3$. The Sm compound crystallizes from thf–dme in the tetragonal space group $I4/m$, with $a$ = 18.256(6), $c$ = 21.478(7) Å, and $U$ = 7158(4) Å$^3$.


1 (*a*) D. Cary, G. Ball and J. Arnold, *J. Am. Chem. Soc.*, 1995, **117**, 3492; (*b*) W. Evans, G. Rabe and J. Ziller, *Angew. Chem., Int. Ed. Engl.*, 1994, **33**, 2110; (*c*) D. Freedman, T. J. Emge and J. G. Brennan, *J. Am. Chem. Soc.*, 1997, **119**, 11 112.

2 C. B. Murray, D. J. Norris and M. G. Bawendi, *J. Am. Chem. Soc.*, 1993, **115**, 8706; N. Herron, J. Calabrese, W. E. Farneth and Y. Wang, *Science*, 1993, **259**, 1426; M. A. Marcus, W. Flood, M. Steigerwald, L. Brus and M. Bawendi, *J. Phys. Chem.*, 1991, **95**, 1572; A. N. Goldstein, C. M. Escher and A. P. Alivisatos, *Science*, 1992, **256**, 1425; B. Schreiner, K. Dehnicke and D. Fenske, *Z. Anorg. Allg. Chem.*, 1993, **619**, 1127; N. Herron, A. Duna and Y. Wang, *J. Chem. Soc., Dalton Trans.*, 1992, **15**, 2329.

3 See, for example: J. Brennan, T. Siegrist, S. Stuczynski and M. Steigerwald, *J. Am. Chem. Soc.*, 1992, **114**, 10334; L. F. Dahl, A. Johnson and S. Whoolery, *Inorg. Chem. Acta*, 1994, **227**, 269; D. Fenske and A. Fischer, *Angew. Chem.*, 1995, **34**, 307; P. Mathur and P. Sekar, *Chem. Commun.*, 1996, 727.

4 See, for example: (*a*) B. Cetinkaya, P. B. Hitchcock, M. F. Lappert and R. G. Smith, *J. Chem. Soc., Chem. Commun.*, 1992, 932; (*b*) A. R. Strzelecki, C. Likar, B. A. Hesel, T. Utz, M. C. Lin and P. A. Bianconi, *Inorg. Chem.*, 1994, **33**, 5188; (*c*) K. Tatsumi, T. Amemiya, H. Kawaguchi and K. Tani, *J. Chem. Soc., Chem. Commun.*, 1993, 773; J. Lee, M. Brewer, M. Berardini and J. Brennan, *Inorg. Chem.*, 1995, **34**, 3215; K. Mashima, Y. Nakayama, T. Shibahara, H. Fukumoto and A. Nakamura, *Inorg. Chem.*, 1996, **35**, 93; M. Berardini and J. Brennan, *Inorg. Chem.*, 1995, **34**, 6179; M. Berardini, T. Emge and J. Brennan, *J. Am. Chem. Soc.*, 1993, **115**, 8501.

5 M. Berardini, T. J. Emge and J. G. Brennan, *Inorg. Chem.*, 1995, **34**, 5327; J. Lee, T. J. Emge and J. G. Brennan, *Inorg. Chem.*, 1997, **36**, 5064.

6 M. Brewer, J. Lee and J. G. Brennan, *Inorg. Chem.*, 1995, **34**, 5919.

7 See for example: M. Pham-Thi, *J. Alloys Compd.*, 1995, **225**, 547; G. Harkonen, M. Leppanen, E. Soininen, R. Tornquist and J. Viljanen, *J. Alloys Compd.*, 1995, **225**, 552; G. Blasse, *J. Alloys Compd.*, 1995, **225**, 529; K. Karpinska, M. Godlewski, M. Leskela and L. Niinisto, *J. Alloys Compd.*, 1995, **225**, 544; C. R. Ronda, *J. Alloys Compd.*, 1995, **225**, 534.

8 See for example: P. K. Kumta and S. H. Risbud, *J. Mater. Sci.*, 1994, **29**, 1135; J. Nishii, S. Morimoto, R. Yokota and T. Yamagishi, *J. Non-Cryst. Solids*, 1987, **95/96**, 641; J. S. Sanghara, L. E. Busse and I. D. Aggarwall, *J. Appl. Phys.*, 1994, **75**, 4885; T. Katsugama and H. Matsumura, *J. Appl. Phys.*, 1994, **75**, 2743.


*Received in Cambridge, UK, 21st August 1997; 7/06129C*

# Novel lamella hydrated sodium zinc arsenate with 4-connected two-dimensional nets

**Xianhui Bu, Thurman E. Gier and Galen D. Stucky**

*Chemistry Department, University of California, Santa Barbara, California 93106, USA*

**Hydrothermal synthesis and crystal structure of a lamellar hydrated sodium zinc arsenate with an unusual sheet structure are reported.**

Metal phosphates and arsenates are of interest for their chemical and physical properties and resulting applications as catalysts, non-linear optical materials, ion-exchangers *etc.*[1] Since the 1980s, many phosphate based zeolite analogs and novel structures have been synthesized.[2] This has further expanded the possible applications of metal phosphate based materials. Divalent metal phosphates and arsenates have the same total charge (+2 and +5) as that of zeolite aluminosilicates (+3 and +4). This has generated a lot of interest in synthesizing zeolite structural analogs in the $T^{2+}/T^{5+}$ system (T refers to a tetrahedral atom).[3] A number of zeolite structural analogs have been synthesized, including $Na_6(H_2O)_8(ZnPO_4)_6$ (sodalite), $(Na, TMA)_{96}M_{96}P_{96}O_{192}$ (M = Be, Zn; zeolite X), $Li_4M_4P_4O_{16}\cdot 4H_2O$ (M = Be, Zn; zeolite Li-ABW) and $Li_{24}Be_{24}P_{24}O_{96}\cdot 4H_2O$ (zeolite RHO).[4] Very recently, a large family of cobalt phosphate based zeolite structural analogs have been reported.[5,6]

The framework of a zeolite structure has the general composition of $AB_2$, where A is a 4-connected atom (tetrahedral atoms such as Al, Si, Zn, Be, P, As . . .) and B is any 2-connected atom (usually oxygen) which is shared between two tetrahedral atoms. The topology of zeolite structures is usually viewed based on the connectivity of tetrahedral atoms. Such a tetrahedral atom connectivity can be regarded mathematically as 4-connected 3D nets, which are constructed from 3-connected 2D sheets.[7] Thus, both 4-connected 3D nets and 3-connected 2D sheets are common among known structures. To our knowledge, however, there is no reported example of a structure in which tetrahedral atoms form 4-connected 2D sheets. In known structures, when lamellar structures are formed from tetrahedral atoms, there are always interruptions involved and the resulting structures, even if polymeric, are not completely 4-connected.[8]

Here, we report an unprecedented occurrence of 4-connected 2D sheets in a new hydrated sodium zinc arsenate. Owing to the formation of 4-connected sheets, no pendant oxygen atoms, hydroxyl groups or water molecules are present on the anionic sheet. Such a novel sheet structure could lead to interesting properties such as the ion-exchange characteristics.

The title compound was synthesized under hydrothermal conditions typically used in the synthesis of zeolites. To a polypropylene bottle was added 9.36 g of $Na_2HAsO_4\cdot 7H_2O$ (30 mmol), 0.8 g of NaOH pellets (20 mmol) and 25 ml of water. To the clear solution was then added 12.0 ml of a 2 M solution of $Zn(NO_3)_2$ (24 mmol) and the resulting gel was shaken thoroughly to give a thick white slurry. The slurry settled rapidly (pH = 6.5) and after standing overnight at 50 °C was recovered by standard filtration and drying techniques. Small crystals (6.282 g) were obtained at 99.4% yield. Thermal analysis showed that the material had a mass loss of 13.2% up to 210 °C with no further loss to 500 °C (calc. 13.7% for $NaZnAsO_4\cdot 2H_2O$). The residue at 500 °C was identical to the hexagonal product from the calcination of $Na_6(ZnAsO_4)_6\cdot 6H_2O$ (sodalite structure).[9]

The pH and temperature are critical to the formation of this phase. At higher pH, the sodalite phase appears and at lower pH an unidentified material appears. Even at pH = 6.5, heating to 100 °C for any period of time converts the title compound to the latter unidentified phase.

The crystal structure was solved using data collected on a Siemens SMART CDD diffractometer.† A full sphere of intensity data were collected with $\omega$ scans (width of 0.30 and exposure time of 30 s per frame). Final full-matrix refinements were against $F^2$ with anisotropic thermal parameters for non-hydrogen atoms. Hydrogen atoms were not included.

The asymmetric unit is $NaZnAsO_4\cdot 2H_2O$ with two unique sodium cations located at inversion centers. Tetrahedral atoms (Zn and As) are connected by oxygen atoms to form an infinite sheet (Fig. 1). Like zeolite structures, there is a strict alternation of $ZnO_4$ and $AsO_4$ tetrahedra which explains the Zn/As ratio of unity. The unique feature of the title arsenate is that all corners of Zn and As tetrahedra are shared with adjacent tetrahedra. This is unprecedented for a lamellar structure constructed from tetrahedral centers. The resulting sheet can thus be described as a 4-connected 2D net.

Both two unique sodium cations are octahedrally coordinated. Each sodium cation is coordinated to two oxygen atoms in the anion sheet and four water molecules. Corner-sharing sodium octahedra form an infinite sheet similar in structure to anionic sheets formed by $ZnO_4$ and $AsO_4$ (Fig. 2). These cationic sheets are formed from sodium and water molecules and are connected to the anionic sheets through Na–O bondings. Note that the anionic sheet is far from planar. A side view of alternating anionic and cationic sheets is shown in Fig. 3.

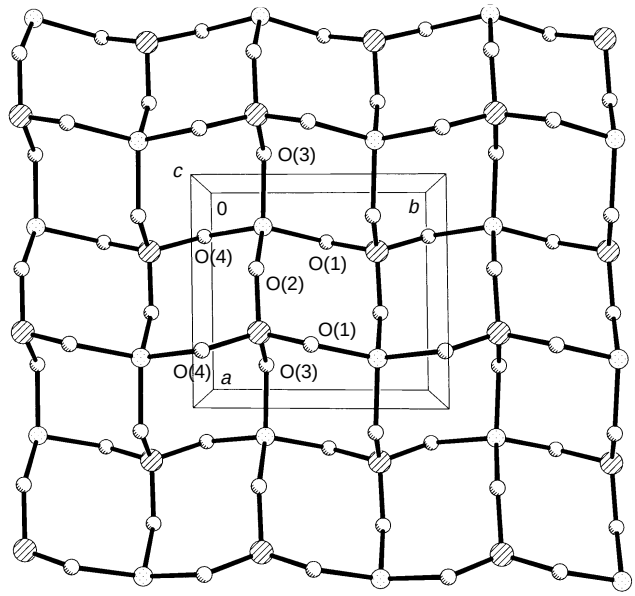



**Fig. 1** Projection down the *c*-axis showing the anionic sheet built from $ZnO_4$ and $AsO_4$ tetrahedra. There are four different 4-rings, all of which have a center of inversion.

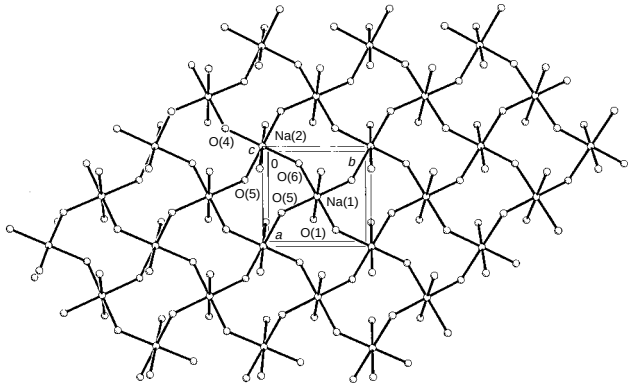



**Fig. 2** Projection down the *c*-axis showing the cationic sheet built from sodium octahedra. Two crystallographically unique sodium atoms are located at the unit cell origin and the face center which have inversion symmetry. Each ring contains four sodium cations and the center of each ring has inversion symmetry.

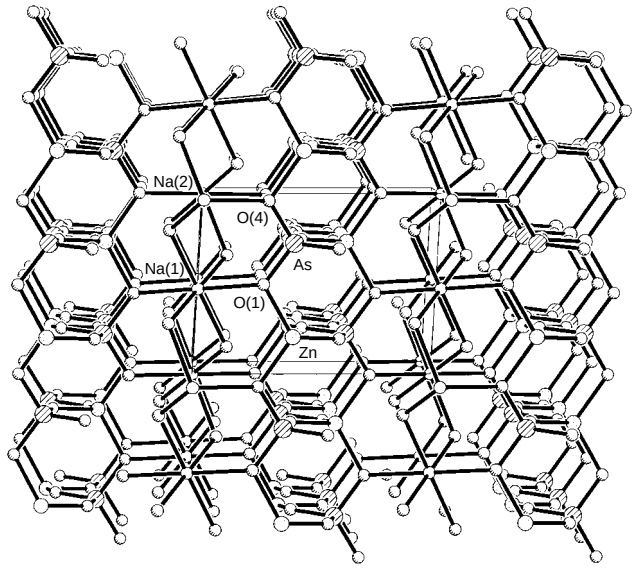



**Fig. 3** Side view (down the *a*-axis) of alternating anionic and cationic sheets

The circuit symbol, which enumerates the six distinct, smallest T-atom loop pathways[10] (including the central atom itself), can be written as ($4^4.6^2$) for all tetrahedral atoms. This type of tetrahedral atom configuration has never been previously known in either aluminosilicates or aluminophosphates. However, one chiral sodium zinc phosphate, $NaZnPO_4{\cdot}H_2O$, which has similar formula to the title compound, but monohydrated, has half of the zinc cations (a quarter of tetrahedral atom positions) in such a configuration.[11] Our arsenate represents an extreme case in which all tetrahedral atoms exist in the ($4^4.6^2$) configuration. The synthesis of the title compound suggests that there could be novel phases with framework topology intermediate between $NaZnPO_4{\cdot}H_2O$ and the title compound. This is an interesting possibility considering that $NaZnPO_4{\cdot}H_2O$ has a chiral symmetry and that chiral zeolites are very rare.[12]

Two other hydrated sodium zinc arsenates are known, both of which are tetrahedral framework structures. In $Na_6Zn_3(AsO_4)_4{\cdot}3H_2O$ which is a relatively dense phase, one corner of $AsO_4$ is terminated with a pendant As=O bond.[13] $Na_6(ZnAsO_4)_6{\cdot}8(H_2O)$ is a sodalite analog with a cage structure.[14] Compared to this sodalite structure, it is observed that the increased hydration transforms the structure from the 3D framework sodalite structure into a lamellar phase. We have synthesized and characterized phosphate analogs of these two hydrated sodium zinc arsenates,[4,15] but so far, the phosphate analog of the title compound has not been prepared.

It's of interest that both anionic and cationic sheets have the same grid pattern and that the two types of sheets strictly alternate. The interlayer interaction between two sheets is through Na–O bondings. It is clear that the translational periodicity in one type of sheet and the geometrical feature of the sheet structure can be imprinted onto the other type of sheet, which can in turn replicate the original sheet. The good match between the sodium sheet and the zinc arsenate sheet implies that it may be difficult for other tetrahedral atoms such as P, or other alkali metal cations to replace Zn, As or Na while maintaining the same type of structure. This may explain why the phosphate analog of the title compound has not been synthesized so far.

This research was supported in part by the National Science Foundation under Grant DMR 95-20971.

## Footnotes and References

* E-mail: bu@sbxray.ucsb.edu

† *Crystal data* for $NaZnAsO_4{\cdot}2H_2O$, $M$ = 263.31, space group $P\bar{1}$, $a$ = 5.6228(2), $b$ = 6.1039(3), $c$ = 7.9731 Å, $\alpha$ = 86.655(1), $\beta$ = 88.742(1), $\gamma$ = 89.174(1)°, $V$ = 273.09(2) Å$^3$, $Z$ = 2, $D_c$ = 3.202 g cm$^{-3}$, clear thin plate, crystal size 0.25 × 0.10 × 0.017 mm, Mo-K$\alpha$ radiation, $\lambda$ = 0.710 73 Å, $\mu$ = 10.541 mm$^{-1}$, $\theta_{max}$ = 56°, $R(F)$ = 0.0513, $wR(F^2)$ = 0.1210, GOF = 1.05 for 86 parameters and 1275 unique reflections with $I > 2.0\sigma(I)$. CCDC 182/623.

1 G. Le Flem, *Eur. J. Solid State Inorg. Chem.*, 1991, **28**, 3.
2 S. T. Wilson, B. M. Lok, C. A. Messina, T. R. Cannan and E. M. FLanigen, *J. Am. Chem. Soc.*, 1982, **104**, 1146.
3 X. Bu, P. Feng, T. E. Gier and G. D. Stucky, *Zeolites*, 1997, **19**, 200.
4 T. E. Gier and G. D. Stucky, *Nature*, 1991, **349**, 508.
5 P. Feng, X. Bu and G. D. Stucky, *Nature*, 1997, **388**, 735.
6 P. Feng, X. Bu, S. H. Tolbert and G. D. Stucky, *J. Am. Chem. Soc.*, 1997, **119**, 2497.
7 J. V. Smith, *Chem. Rev.*, 1988, **88**, 149.
8 J. R. D. DeBord, R. C. Haushalter and J. Zubieta, *J. Solid State Chem.*, **125**, 270.
9 T. M. Nenoff, W. T. A. Harrison, G. D. Stucky, J. M. Nicol and J. M. Newsam, *Zeolites*, 1993, **13**, 506.
10 J. V. Smith, *Am. Mineral.*, 1977, **62**, 703.
11 W. T. A. Harrison, T. E. Gier, G. D. Stucky, R. W. Broach and R. A. Bedard, *Chem. Mater.*, 1996, **8**, 145.
12 M. E. Davis and R. F. Lobo, *Chem. Mater.*, 1992, **4**, 756.
13 I. E. Grey, I. C. Madsen, D. J. Jones and P. W. Smith, *J. Solid State Chem.*, 1989, **82**, 52.
14 T. M. Nenoff, W. T. A. Harrison, T. E. Gier and G. D. Stucky, *J. Am. Chem. Soc.*, 1991, **113**, 378.
15 X.Bu, T. E. Gier, W. T. A. Harrison and G. D. Stucky, *Acta Crystallogr., Sect. C*, in press.

*Received in Columbia, MO, USA; 28th July 1997; 7/05442D*

# Thermochemical alkane dehydrogenation catalyzed in solution without the use of a hydrogen acceptor

**Wei-wei Xu,[a] Glen P. Rosini,[a] Mukta Gupta,[b] Craig M. Jensen,*[b] William C. Kaska,[c] Karsten Krogh-Jespersen[a] and Alan S. Goldman*[a]**

[a] *Department of Chemistry, Rutgers, The State University of New Jersey, New Brunswick, NJ 08903, USA*
[b] *Department of Chemistry, University of Hawaii, Honolulu, HI 96822, USA*
[c] *Department of Chemistry, University of California, Santa Barbara, CA 93106, USA*

**(PCP)$IrH_2$ [PCP = $\eta^3$-$C_6H_3(PBu^t_2)_2$-1,3] catalyzes the efficient (several hundred mol product/mol catalyst) dehydrogenation of alkanes under reflux to give the corresponding alkenes and dihydrogen.**

The development of effective systems for the functionalization of alkanes is one of the major goals in the field of homogeneous catalysis.[1] Conversion of alkanes to the corresponding alkenes is a particularly valuable functionalization reaction in view of the great versatility of alkenes as organic feedstock. Crabtree *et al.* first showed in 1979 that transition-metal phosphine complexes could effect stoichiometric dehydrogenation of alkanes;[2] this was later extended to catalytic dehydrogenation.[3,4] The high endothermicity of dehydrogenation was compensated for by either the use of a sacrificial hydrogen acceptor or by UV irradiation.[5]

Such systems were all plagued by ligand decomposition, however, and it was not until 1988 that the first 'high-turnover' ( > *ca.* 100 turnovers) dehydrogenation system was discovered: $Rh(PMe_3)_2(CO)Cl$ under UV irradiation.[6] This robust catalyst was later found to yield efficient thermochemical dehydrogenation through the use of sacrificial hydrogen acceptors and, surprisingly, added dihydrogen; unfortunately, the presence of $H_2$ atmosphere resulted in the hydrogenation of more than one mole sacrificial acceptor per mole dehydrogenated product.[7]

Most recently, the development of the first 'high-turnover' thermochemical catalysts not requiring $H_2$ atmosphere was reported: complexes of the 'pincer' ligand $\eta^3$-$C_6H_3(CH_2P$-$Bu^t_2)_2$-1,3 (PCP), including (PCP)$RhH_2$ or, more effectively, (PCP)$IrH_2$.[8]

The key to the effectiveness of the PCP-based catalysts appears to be their long-term stability at very high temperatures (*e.g.* 200 °C).[9] We considered that such temperatures are sufficiently high, in principle, to overcome the large positive enthalpy of dehydrogenation without the use of a sacrificial acceptor.†[10] This was indeed found to be the case and the remarkable stability of the catalyst is maintained under such conditions. Herein, we report the first example of efficient alkane dehydrogenation catalyzed homogeneously without the use of either light or a sacrificial hydrogen acceptor.

Refluxing a cyclooctane solution of (PCP)$RhH_2$ (10 mM) while passing a stream of argon above the condenser results in negligible rates of cyclooctene formation, ( < 2 mM after 24 h). As was found when sacrificial acceptors were used, the iridium analog is much more effective for 'acceptorless' dehydrogenation. Under similar conditions [2 mM (PCP)$IrH_2$], the initial rate of cyclooctene (COE) formation is 11 turnovers $h^{-1}$.‡

After 44 h, 104 turnovers are obtained; after 120 h, 190 turnovers are produced. These results may be compared with the most effective soluble 'acceptorless' dehydrogenation catalyst reported to date: $IrH_2(O_2CR)(PCy_3)_2$ (1.25 mM) was reported to yield 1.41 turnovers $h^{-1}$ COE, with a maximum of 28.5 turnovers obtained after 48 h.[11]

The high endothermicity of alkane dehydrogenation is obviously a key factor involved in the challenge of developing alkane dehydrogenation catalysts, particularly in developing an acceptorless dehydrogenation system. In this respect cyclooctane is anomalous, since its dehydrogenation enthalpy of 23.3 kcal $mol^{-1}$ contrasts with *ca.* 28–30 kcal $mol^{-1}$ required for the elimination of two secondary C–H bonds from more typical alkanes.[10] Extrapolation to typical alkanes, based on behavior observed with cyclooctane, is therefore, *a priori*, quite tenuous. We find, however, that the catalytic efficacy of (PCP)$IrH_2$ with other alkanes is at least comparable to that with cyclooctane and the higher reflux temperatures of less volatile solvents permit significantly greater rates. For example, in refluxing cyclodecane (201 °C), 170 and 360 turnovers cyclodecene are obtained after 4 and 24 h, respectively (*ca.* 3 : 1 *cis : trans*; 1.0 mM catalyst; see Fig. 1). This rapid dehydrogenation occurs in spite of the high dehydrogenation enthalpy of cyclodecane (30 and 33 kcal $mol^{-1}$ to form *cis*- and *trans*- cyclodecene, respectively).[10]

The decrease in the rate of alkene formation which invariably occurs with time is probably not due to inevitable decomposition of the catalyst but may be caused by build-up of alkene product. Accordingly, a fresh solution of catalyst in cyclooctane, to which had been added 10% COE, showed no increase in COE concentration upon reflux. The mechanism by which the alkene product inhibits the reaction remains to be determined.

Significant amounts of cyclooctane can also be dehydrogenated to give COE and molecular hydrogen in reactions carried out in a closed system under reduced pressure. In a typical experiment, a solution of cyclooctane (4.0 ml) and (PCP)$IrH_2$ (3 mg, 0.005 mmol) was sealed in a tube under 0.007 mbar of argon and fully immersed in a 200 °C oil bath. After 0.5 h, 10 turnovers of COE had been produced. The production of $H_2$ was confirmed by gas chromatographic analysis† of the vapor above

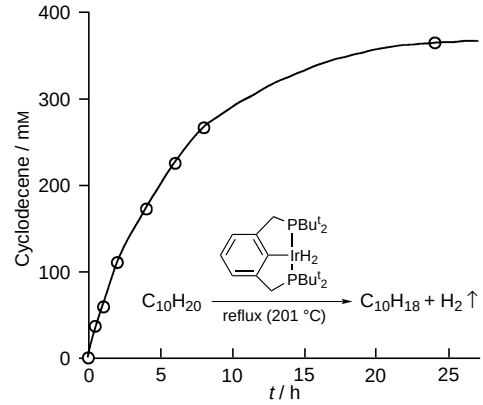



**Fig. 1** Cyclodecene formation (total, *ca.* 3 : 1 *cis*:*trans*) *vs.* time; (PCP)$IrH_2$ in refluxing cyclodecane (1.0 mM, 201 °C)

the reaction mixture. Increased levels of cyclooctane dehydrogenation were not observed in solutions which were heated for longer reaction times. However, additional dehydrogenation activity was achieved in solutions which had been heated to 200 °C for 0.5 h by removing the resulting $H_2$ by freeze–pump–thaw degassing. A total of 36 turnovers of COE were obtained in an experiment in which $H_2$ was removed four times through this procedure. These results demonstrate that under these conditions the catalysis is limited by equilibrium constraints rather than catalyst stability.

The PCP ligand clearly bears a close relationship (at least formally) to the ligand set in the putative catalytically active fragments $M(PR_3)_2Cl$ (M = Rh,[7] Ir[12]). In the case of the chloride complexes, rhodium has proven to be the more effective metal (for both transfer- and photo-dehydrogenation).[13] Thus the much greater efficacy of Ir *vs.* Rh in the case of the PCP complexes presents an issue which merits attention.

Although complexes $Rh(PR_3)_2ClH_2$ are classical dihydrides,[14] Milstein has reported the $T_1$ of $H_2Rh[\eta^3\text{-}HC(CH_2CH_2PBu^t_2)_2]$ to be 30–60 ms (−40 °C, 400 MHz)[15] strongly indicating the presence of a dihydrogen ligand. The closely related $(PCP)RhH_2$[16] is apparently also a dihydrogen complex: we find a $T_1$ value of 46 ms at 293 K (500 MHz)[17] and an H–D coupling constant of 33 Hz for (PCP)RhH(D).

We have previously reported that addition of $H_2$ to $Rh(PPr^i_3)_2Cl$ [to give $H_2Rh(PPr^i_3)_2Cl$] is highly exothermic ($\geqslant$ 33 kcal mol$^{-1}$).[18] The fact that $H_2$ addition to Rh(PCP) does not even cleave the H–H bond suggests that addition is much less favorable. Indeed, *ab initio* electronic structure calculations¶ yield remarkably different reaction energies for $H_2$ addition to the model fragments $Rh(PH_3)_2Cl$ and $Rh(PH_3)_2Ph$: −28.5 and −4.2 kcal mol$^{-1}$, respectively (producing dihydride and dihydrogen complexes, respectively, in accord with observation). In the case of Ir, the additions are much more exothermic though the difference between chloride and phenyl complexes is similar; respective values are $Ir(PH_3)_2Cl$: −54.1 kcal mol$^{-1}$ and $Ir(PH_3)_2Ph$: −23.0 kcal mol$^{-1}$.¶ These computational results strongly suggest a simple explanation for the very high catalytic activities of the $Rh(PR_3)_2Cl$ and Ir(PCP) fragments as compared with the 'converse' pair [*i.e.* Rh(PCP) and $Ir(PR_3)_2Cl$]. For Rh, the PCP complex adds $H_2$ too weakly. This implies not only that transfer of $H_2$ from alkane to rhodium is unfavorable, but it also suggests that C–H addition may be unfavorable, since $H_2$ normally adds much more favorably than C–H bonds. For Ir, $H_2$ addition to the chloride complex is highly exothermic; this may inhibit thermal loss of $H_2$ or even transfer of $H_2$ to a sacrificial acceptor. Thus, the similar affinities of the $Rh(PR_3)_2Cl$ and Ir(PCP) fragments for $H_2$ (*viz.*, −28.5 and −23.0 kcal mol$^{-1}$) may help explain their similarly high catalytic activities. In the case of the Rh complex, however, $H_2$ is needed to cleave the μ-Cl bridge and catalyst decomposition is observed at very high temperatures ($\gg$100 °C).[7] In the case of the Ir(PCP) unit, formation of analogous anion-bridged dimers is not possible and presumably the rigidity of the PCP ligand endows the complex with resistance to decomposition that is highly unusual for a transition-metal phosphine complex. Apparently, ligand stability and the appropriate (but unremarkable) energetics of oxidative addition to the Ir(PCP) fragment are the key factors resulting in the unprecedented ability to effect efficient alkane dehydrogenation without the use of light or a sacrificial acceptor.

This research was supported by the Division of Chemical Sciences, BES, OER, US Department of Energy and the US Department of Energy Hydrogen Program.

## Footnotes and References

* E-mail: goldman@rutchem.rutgers.edu; jensen@gold.chem.hawaii.edu

† For example, if $\Delta G^{\neq}$ = 30.0 kcal mol (1 cal = 4.184 J), at 200 °C the catalytic turnover rate would be 500 h$^{-1}$. Since the dehydrogenation enthalpy of typical alkanes is on the order of 28–30 kcal mol$^{-1}$,[10] reasonable rates could be obtained (in principle) even if the favorable reaction entropy does not make any contribution in the transition state. Of course, a significant concentration of alkene can only be obtained by allowing hydrogen to escape, thereby permitting entropy to predominate over enthalpy.

‡ Addition of liquid Hg to the solution has no measurable effect on the rate of COE formation, indicating that the catalyst is not colloidal iridium: D. R. Anton and R. H. Crabtree, *Organometallics*, 1983, **2**, 855.

§ Density functional theory calculations including geometry optimization employing the B3LYP hybrid functional; effective small-core potentials and double-zeta basis sets on Rh and Ir (LANL2DZ model); all-electron basis sets for main group atoms: D95(d) for C, P and Cl, 6-311G(p) for dihydrogen and hydrides, and 3-21G for other H atoms. To model the PCP structure, the phenyl groups in the $M(PR_3)_2Ph$ complexes were held coplanar with the Ir and P atoms.

¶ Similarly, methane C–H addition to $Ir(PH_3)_2Cl$ is reported to be 29 kcal mol$^{-1}$ more exothermic than addition to $Ir(PH_3)_2H$ (−41.6 and −12.8 kcal mol$^{-1}$, respectively): T. R. Cundari, *J. Am. Chem. Soc.*, 1994, **116**, 340.


1 For a recent review: B. A. Arndtsen, R. G. Bergman, T. A. Mobley and T. H. Peterson, *Acc. Chem. Res.*, 1995, **28**, 154.

2 R. H. Crabtree, J. M. Mihelcic and J. M. Quirk, *J. Am. Chem. Soc.*, 1979, **101**, 7738.

3 D. Baudry, M. Ephritikine, H. Felkin and R. Holmes-Smith, *J. Chem. Soc., Chem. Commun.*, 1983, 788.

4 M. J. Burk, R. H. Crabtree, C. P. Parnell and R. J. Uriarte, *Organometallics*, 1984, **3**, 816.

5 M. J. Burk, R. H. Crabtree and D. V. McGrath, *J. Chem. Soc., Chem. Commun.*, 1985, 1829.

6 (*a*) K. Nomura and Y. Saito, *J. Chem. Soc., Chem. Commun.*, 1988, 161; (*b*) T. Sakakura, T. Sodeyama, M. Tokunaga and M. Tanaka, *Chem. Lett.*, 1988, 263; (*c*) J. A. Maguire, W. T. Boese and A. S. Goldman, *J. Am. Chem. Soc.*, 1989, **111**, 7088.

7 (*a*) J. A. Maguire, A. Petrillo and A. S. Goldman, *J. Am. Chem. Soc.*, 1992, **114**, 9492; (*b*) K. Wang, M. E. Goldman, T. J. Emge and A. S. Goldman, *J. Organomet. Chem.*, 1996, **518**, 55.

8 (*a*) M. Gupta, C. Hagen, R. J. Flesher, W. C. Kaska and C. M. Jensen, *Chem. Commun.*, 1996, 2083; (*b*) M. Gupta, C. Hagen, W. C. Kaska, R. E. Cramer and C. M. Jensen, *J. Am. Chem. Soc.*, 1997, **119**, 840; (*c*) M. Gupta, W. C. Kaska and C. M. Jensen, *Chem. Commun.*, 1997, 461.

9 M. A. McLoughlin, R. J. Flesher, W. C. Kaska and H. A. Mayer, *Organometallics*, 1994, **13**, 3816.

10 NIST Standard Reference Database Number 69, 1996, http:// webbook.nist.gov/chemistry/

11 (*a*) T. Aoki and R. H. Crabtree, *Organometallics*, 1993, **12**, 294; (*b*) T. Fujii, Y. Higashino and Y. Saito, *J. Chem. Soc., Dalton. Trans.*, 1993, 517.

12 J. Belli and C. M. Jensen, *Organometallics*, 1993, **12**,294; T. Fujii, Y. Higashino and Y. Saito, *J. Chem. Soc., Dalton Trans.*, 1993, 517.

13 T. Sakakura, T. Sodeyama and M. Tanaka, *New J. Chem.*, 1989, **13**, 737.

14 R. L. Harlow, D. L. Thorn, R. T. Baker and N. L. Jones, *Inorg. Chem.*, 1992, **31**, 993.

15 A. Vigalok, Y. Ben-David and D. Milstein, *Organometallics*, 1996, **15**, 1839.

16 S. Nemeh, C. Jensen, E. Binamira-Soriage and W. C. Kaska, *Organometallics*, 1983, **2**, 1442.

17 This value (which is not minimized) is sufficiently low to permit characterization as a dihydrogen complex: D. G. Hamilton and R. H. Crabtree, *J. Am. Chem. Soc.*, 1988, **110**, 4126.

18 K. Wang, G. P. Rosini, S. P. Nolan and A. S. Goldman, *J. Am. Chem. Soc.*, 1995, **117**, 5082.


*Received in Bloomington, IN, USA; 17th July 1997; 7/05105K*

# Rôle for organic molecules in the oxidation of porous silicon

**James E. Bateman,[a] Robert D. Eagling,[a] Benjamin R. Horrocks,*[a] Andrew Houlton*[a] and David R. Worrall[b]**

[a] *Department of Chemistry, University of Newcastle-upon-Tyne, Newcastle-upon-Tyne, UK NE1 7RU*
[b] *Department of Chemistry, Loughborough University, Loughborough, Leicestershire, UK LE11 3TU*

**A simple rapid solution-based method for forming the oxide layer at porous silicon is described which uses amphiphilic molecules to wet the hydrophobic porous structure.**

Porous silicon (PS) has received much interest in recent years owing to its remarkable luminescent properties allied with the possible compatibility of the material with existing semiconductor processing techniques.[1] However, it is well known that as-prepared PS exhibits weak and unstable photoluminescence (PL) as a consequence of the slow oxidation of the hydrogen-terminated silicon surface in air.[2] As a result, numerous post-formation treatments of PS have been reported which aim to stabilize the PL through the formation of a passivating oxide layer.[3] Some of these treatments involve mild oxidation by immersion of the PS in organic solvents prior to thermal oxidation but little explanation has been given as to the mechanism of this initial oxidation.

Here we report on a simple, rapid chemical procedure for the formation of the oxide layer at porous silicon using a dilute aqueous solution of the surfactant, hexadecyltrimethylammonium bromide. These findings are discussed in terms of the influence of the wetting properties of porous silicon on the mechanism of oxide formation. The consequences of this have significant implications for the recent efforts towards the development of covalent modifications of porous silicon surfaces.[4,5]

Porous silicon was formed by galvanostatic anodisation of a p- doped Si(100) wafer in a 50 : 50 solution of 48% aqueous HF and ethanol in a Teflon cell, with a current density of 19 mA $cm^{-2}$ for 4 min. The PS was then rinsed in de-ionised water (Millipore, 18 MΩ) to remove ethanol, immersed in 48% aqueous HF to ensure removal of any remaining oxide and finally rinsed in de-ionised water (20 s) and dried in a $N_2$ stream. An FTIR spectrum indicated that samples so prepared were hydrogen-terminated with little, or no oxide, present. These samples were then immersed in 1 mM aqueous solution† of hexadecyltrimethylammonium bromide (CTAB) and comparisons were made with samples treated with de- ionised water. Oxidation of the PS in de-ionised water and CTAB solution was followed using FTIR spectroscopy and Fig. 1 shows the spectra for a CTAB-treated sample. In each case the spectra show loss of intensity of $Si–H_x$ modes ($Si–H_x$ stretching modes around 2100 $cm^{-1}$ and the $SiH_2$ scissors mode at 910 $cm^{-1}$ ) and an increase in intensity of bands due to Si–O (1135, 1075, 878 $cm^{-1}$) and $O_xSi–H$ (2250, 2220 $cm^{-1}$).[6] The CTAB-treated PS also showed some evidence for adsorption of surfactant with bands observed in the C–H stretch region.

Oxidation in de-ionised water was very slow, taking place over a few days, whereas the reaction in CTAB solution was extremely rapid accompanied by visible gas evolution, assumed to be hydrogen on the basis of the expected reactions (1) and (2).[7]

$$Si–H + H_2O \rightarrow Si–OH + H_2 \quad (1)$$

$$Si–OH + H_2O \rightarrow SiO_2 + 3/2\ H_2 \quad (2)$$

Figs. 2 and 3 show plots of the integrated intensity of the Si–O modes and Si–H stretch modes *vs.* log (immersion time/min), respectively, and give clear evidence for a correlation between loss of Si–H and gain of Si–O modes. In addition to the significantly increased rate in CTAB solution it is also evident that almost twice as much oxidation occurs compared to water. Moreover, the total surface area of the CTAB-treated sample was 13% less than the control, as evidenced by the integrated intensity of the $Si–H_x$ stretch modes prior to oxidation. This

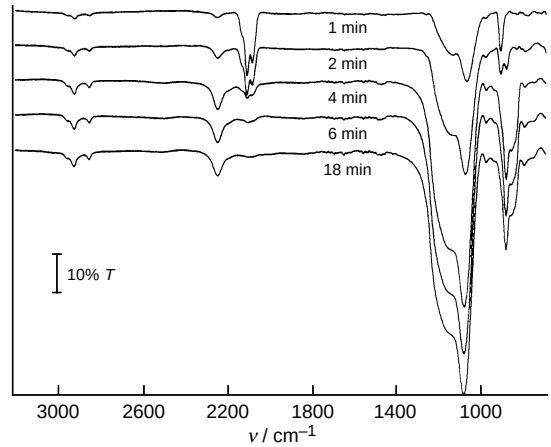



**Fig. 1** Transmission FTIR spectra for CTAB-treated porous silicon

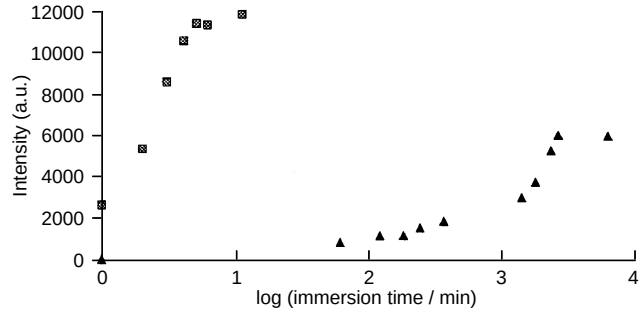



**Fig. 2** Plot of integrated intensity of the Si–O modes *vs.* log(immersion time/min) for water ( ▲ ) and CTAB-treated porous silicon (■)

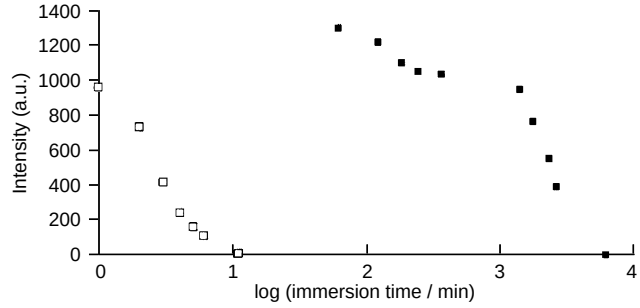



**Fig. 3** Plot of integrated intensity of the Si–H stretching mode *vs.* log(immersion time/min) for water (■) and CTAB-treated porous silicon (□)

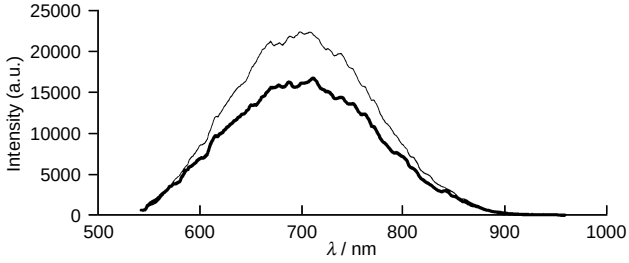



**Fig. 4** PL spectra of porous silicon before (—) and after treatment with CTAB (—)

shows that a greater percentage of the hydrogen-terminated surface is accessible to water molecules in the presence of CTAB.

PL spectra‡ of both as-prepared and CTAB-treated samples show a maximum at ~680 nm, typical of porous silicon (Fig. 4). Despite evidence from the IR spectra that no material is lost on CTAB-treatment, a small decrease in PL intensity is observed.§

The very significant enhancement of the oxidation by CTAB can be explained by considering the nature of the porous layer. Studies have shown that PS layers consist of silicon columns attached to the crystalline substrate with pore sizes in the nanometre range. The surface is highly hydrophobic with a large surface area (100–400 $m^2$ $cm^{-3}$).[1] The rapid oxidation observed in the CTAB-treated sample is explained as being due to a lowering of the surface tension ($\gamma$) of the liquid phase. Water can only oxidize the PS if it is in intimate contact with it. Immersion wetting of the PS is therefore a prerequisite to oxidation. Wetting will occur when:[8] $\gamma_{PS/air} > \gamma_{PS/H_2O} + \gamma_{H_2O/air}$.

Owing to the high surface tension of water ($\gamma_{H_2O/air}$ = 72.75 mN $m^{-1}$) and the hydrophobic nature of the PS surface, water does not spontaneously wet PS. The addition of CTAB lowers both $\gamma_{PS/H_2O}$ and $\gamma_{H_2O/air}$ thereby ensuring more complete wetting. Water molecules are therefore able to penetrate more effectively the porous structure leading to increased oxidation.

This finding has a considerable bearing on the post-preparation treatments and also for the more recent interest in the development of synthetic routes for the formation of molecular films at PS.[4,5] Specifically, the choice of solvent or reactant must take these effects into account. Most organic solvents have a significantly lower surface tension than water and may wet the PS surface more effectively on immersion.[9] Even nominally dry solvents will, if hygroscopic, absorb water from the surroundings thus enabling water, dissolved in the solvent, to penetrate, and oxidize, the PS.

Indeed, proof of this was demonstrated by immersion of PS in solvents under dry nitrogen using conventional Schlenk techniques to minimize contamination by water. Immersion in dry acetonitrile (distilled over $CaH_2$) for 30 min reveals considerable oxidation as observed by IR spectroscopy, equivalent to 4 h immersion in de-ionised water. Similar results were obtained with ethanol and ether, whereas no oxidation was observed with hexanes. The extent of oxidation is therefore clearly associated with the solvent's affinity for water.¶ These data reaffirm the acknowledged fact that under standard Schlenk line conditions adventitious water is present in sufficient quantity for oxidation to occur.[10]

These results suggest that the use of hygroscopic solvents in the chemical modification of PS is to be avoided if oxidation is undesirable. It is noteworthy that a recent report on the derivatization of PS using alcohols stresses the need for anhydrous conditions in the formation of alcohol-derived molecular films.[5]

In conclusion, the effect of organic molecules on the oxidation of hydrogen-terminated porous silicon is highly dependent on their hygroscopic nature and ability to lower the PS surface tension. This may be exploited for the rapid formation of an oxide layer. These findings are also relevant to chemists developing synthetic strategies for the covalent modification of PS.

A. H. and B. R. H. thank the Leverhulme Trust for a grant and Dr P. A. Christensen for access to instrumentation. The referees are thanked for useful comments.

## Footnotes and References

* E-mail: andrew.houlton@ncl.ac.uk

† This concentration is close to the critical micelle concentration of CTAB ($9.2 \times 10^{-4}$ M) ensuring a minimum in surface tension for the liquid phase at minimum CTAB concentration.[11]

‡ Photoluminescence spectra were recorded using an EG&G Princeton Applied Research Peltier cooled photodiode array system (150 ms exposure time, 0.7 nm spectral resolution). Excitation was at 488 nm using a Spectra-Physics model 2010 argon ion laser and measured at room temp. (20–21 °C).

§ A recent review[1] has emphasised that the effect of oxidative treatments on PS luminescence intensity and peak wavelength varies between laboratories. Reports of both intensity decreases and increases and red or blue shifts have been made. A decrease in PL intensity on oxidation may be explained as due to the production of a strained $SiO_2$ layer containing defects which act as nonradiative recombination centres.[12]

¶ Properties of solvents.[9]

| Solvent | $\gamma^a$/mN $m^{-1}$ | Solubility[b]/g (100 ml)$^{-1}$ |
|---|---|---|
| $H_2O$ | 72.75 | —[c] |
| MeCN | 29.1 | —[c] |
| EtOH | 22.3 | —[c] |
| $Et_2O$ | 17.0 | 1.3 |
| $C_6H_{14}$ | 18.4 | $1.1 \times 10^{-2}$ |

[a] At 20 °C. [b] Of water at 25 °C. [c] Completely soluble.

1 L. T. Canham, *Appl. Phys. Lett.*, 1990, **57**, 1046; for a review see, for example: M. J. Sailor, J. L. Heinrich and J. M. Lauerhaas, *Stud. Surf. Sci. Catal.*, 1996, **103**, 209.
2 L. T. Canham, M. R. Houlton, W. Y. Leong, C. Pickering and J. M. Keen, *J. Appl. Phys.*, 1991, **70**, 422.
3 V. Petrova-Koch, T. Muschik, A. Kux, B. K. Meyer, F. Koch and V. Lehman, *Appl. Phys. Lett.*, 1992, **61**, 943; G.-B. Li, L.-S. Liao, X.- B. Liu, X.-Y. Hou and X. Wang, *Appl. Phys. Lett.*, 1997, **70**, 1284; O. Belmont, C. Faivre, D. Bellet and Y. Brechet, *Thin Solid Films*, 1996, **276**, 219; X. Y. Hou, G. Shi, W. Wang, F. L. Zhang, P. H. Hao, D. M. Huang and X. Wang, *Appl. Phys. Lett.*, 1993, **62**, 2363; A. Nakajima, T. Itakura, S. Watanabe and N. Nakayama, *Appl. Phys. Lett.*, 1992, **61**, 46.
4 E. J. Lee, J. S. Ha and M. J. Sailor, *J. Am. Chem. Soc.*, 1995, **117**, 8295; E. J. Lee, T. W. Bitner, J. S. Ha, M. J. Shane and M. J. Sailor, *J. Am. Chem. Soc.*, 1996, **118**, 5375.
5 N. Y. Kim and P. E. Laibinis, *J. Am. Chem. Soc.*, 1997, **119**, 2297.
6 Y. Ogata, H. Niki, T. Sakka and M. Iwasaki, *J. Electrochem. Soc.*, 1995, **142**, 195.
7 T. Unagami, *Jpn. J. Appl. Phys.*, 1980, **19,** 231.
8 G. A. Somorjai, *Introduction to Surface Chemistry and Catalysis*, Wiley, New York, 1994.
9 I. M. Smallwood, *Handbook of Organic Solvent Properties*, Arnold, London, 1996.
10 M. J. Sailor and E. J. Lee, *Adv. Mater.*, 1997, **9**, 783.
11 J. H. Fendler, *Membrane Mimetic Chemistry*, Wiley, New York, 1982.
12 M. A. Tischier, R. T. Collins, J. H. Stathis and J. C. Tsang, *J. Electrochem. Soc.*, 1992, **60**, 639; K. H. Jung, S. Shih and D. L. Kwong, *J. Electrochem. Soc.*, 1993, **140**, 3046.

*Received in Cambridge, UK, 26th June 1997; Revised manuscript received 1st October 1997; 7/07107H*

# Porphyrins in aqueous amphiphilic polymers as peroxidase mimics

**Robert A. W. Johnstone,*[a] Anthony J. Simpson[b] and Paul A. Stocks[a]**

[a] *Department of Chemistry, University of Liverpool, Liverpool, UK L69 3BX*
[b] *Procter and Gamble Ltd., Newcastle Technical Centre, Newcastle, UK NE12 9TS*

**Water-insoluble porphyrins dissolve in aqueous solutions of amphiphilic polymers to give systems which mimic the action of peroxidase enzymes.**

Porphyrins hold an important position in oxidative mechanisms of metabolism, ranging from the oxygen-carrying capacity of haemoglobins to the oxidative reactions of cytochrome and peroxidase enzymes.[1] Mechanisms of reaction, in which an oxygen atom is transferred from a donor (*e.g.* $O_2$, $H_2O_2$, hydroperoxides, hypochlorites, iodates, iodosobenzene) to a substrate such as an alkene to form an epoxide or to an alkane or arene to form a hydroxy derivative, have been extensively examined, particularly for cytochrome P450 systems.[2] More recently, there has been considerable development of model cytochrome P450 enzyme systems as catalysts for oxidation.[3] Most research on peroxidases has been done with horse radish peroxidase[4] and sensitive tests have been developed to distinguish peroxidases from cytochromes P450.[5] However, relatively little research into peroxidase mimics has appeared and mostly has not distinguished between peroxidase and cytochrome P450 reaction mechanisms.[6] The present work describes a mimic for a peroxidase, which has intrinsic activity similar to that of horse radish peroxidase.

A variety of water-soluble iron or manganese porphyrins was prepared through sulfonation and metallation of 5,10,15,20-tetraarylporphyrins.[7] Other water-soluble metallo derivatives were prepared from 5,10,15,20-tetrakis(1-oxidopyridin-1-ium-4-yl)porphyrin[8] and from 5,10,15,20-tetrakis{4-[ω-hydroxypoly(ethoxy)ethoxy]phenyl}porphyrin.[8] As a quick test of the capacity of these water-soluble porphyrins for catalysing electron-transfer type oxidation with longevity of action, their ability to bleach a small range of red, orange and blue water-soluble dyes was examined, using $H_2O_2$ as the primary oxidant.[9] In all cases, 2–30% bleaching of the azo, anthraquinone and phthalocyanine dyes was observed but complete auto-oxidation and destruction of the porphyrin catalyst itself always occurred first and stopped the reaction. Indeed, with $H_2O_2$ alone and no added dye, the water-soluble manganese or iron 5,10,15,20-tetrakis(4-sulfophenyl)porphyrins were destroyed in 30 s and 2 min, respectively. Because cytochrome and peroxidase enzymes (albeit enveloped in a protein coat) can utilise $H_2O_2$ and porphyrin in an aqueous environment, it was decided to attempt to mimic the action of these proteins through use of synthetic porphyrins carried in amphiphilic water-soluble polymers. Two such examples of carriers used in the present work are poly(sodium styrene-4-sulfonate-*co*-2-vinylnaphthalene) (PSSS-VN) and poly(sodium styrene-4-sulfonate-*co*-2-vinylpyridine) (PSSS-VP).[10] It was found that porphyrins in PSSS-VN co-polymers formed systems that behaved like a typical peroxidase (horse radish peroxidase) and unlike P450 cytochromes.

Epoxidation of alkenes with $H_2O_2$ and P450 metalloporphyrin model catalysts is typically carried out under biphasic conditions.[11,12] Here, manganese(III) 5,10,15,20-tetraphenylporphyrin in aqueous PSSS-VN polymer with added imidazole effected the epoxidation of cyclooctene (48%), 1-methylcyclohexene (29%) and 2,3-dimethylbut-2-ene (7%) in $CH_2Cl_2$–aq. $H_2O_2$ but only very slowly and in the poor yields indicated. Significantly, the porphyrin survived these reactions with little auto-oxidation during 48 h. The percentage conversions are not only low but are in the reverse order of reactivity normally found for epoxidation of these alkenes with peroxy acids or cytochrome mimics, and indicate that the epoxidation was not the result of direct oxygen transfer from the metal centre of the porphyrin.

A number of substrates has been used to estimate peroxidase activity.[13] All of those tested in this work (phenols, amines, leuco dyes, ferrocyanide) gave positive responses with the PSSS-VN–porphyrin system, and were inactive in the presence of cyanide ion. Most of these substrates do not distinguish cytochrome P450 from peroxidase activity. The most definitive tests for peroxidase activity are generally considered to be colour reactions of guaiacol, mesidine and, particularly, the diammonium salt of 2,2′-azinobis(3-ethylbenzothiazoline-6-sulfonic acid) (ABTS).[5] The PSSS-VN–porphyrin system showed significant activity in all of the above tests[13] but only the last three[5] were examined in kinetic detail to distinguish peroxidase specifically from cytochrome P450 activity. The graphs in Fig. 1 compare the rates of oxidation of ABTS with hydrogen peroxide alone and also in the presence of authentic horse radish peroxidase or manganese(III) 5,10,15,20-tetraphenylporphyrin in aqueous PSSS-VN polymer. The results have been normalised for the amounts of porphyrin in the

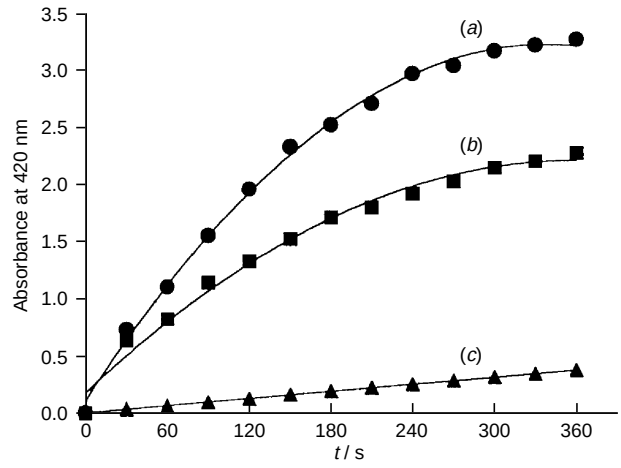



**Fig. 1** Graph showing the oxidation of ABTS by $H_2O_2$ in the presence of (*a*) horse radish peroxidase catalyst, (*b*) $Mn^{III}$ tetraphenylporphyrin–PSSS-VN polymer catalyst, and (*c*) no added catalyst. For (*a*), ABTS stock solution (0.2 ml) was mixed with $H_2O_2$ stock solution buffered to pH 8 (0.2 ml) and then horse radish peroxidase stock solution (2 ml) was added; the oxidation was monitored over a period of 6 min by the appearance and UV–VIS absorbance of a band at 405 nm due to the ABTS radical cation. After this time, the $H_2O_2$ had been used up. For (*b*), a similar solution was prepared and monitored but using a porphyrin–PSSS-VN stock solution in place of horse radish peroxidase. For (*c*), only $H_2O_2$ and ABTS solutions were mixed and monitored at 405 nm. For normalization purposes, the solutions were also monitored at 420 nm (porphyrin Soret band) so as to calculate the molar concentrations of porphyrin in the horse radish peroxidase and in the PSSS-VN system; the ABTS radical cation absorbance was divided by the molar concentration of porphyrin.

aqueous peroxidase and polymer solutions. Whilst horse radish peroxidase causes faster oxidation of ABTS, the biomimetic porphyrin–polymer system is 70% as fast; in the absence of either the authentic or artificial peroxidase, oxidation of ABTS with $H_2O_2$ is very slow. Similarly, the comparative effects of horse radish peroxidase and the PSS-VN–porphyrin system as catalysts in the $H_2O_2$ oxidation of guaiacol and mesidine showed that the authentic peroxidase and its mimic gave comparable rates of reaction and both exhibited a greatly increased rate compared with that for reaction with $H_2O_2$ alone. When the amphiphilic PSSS-VN polymer was replaced by the more hydrophilic PSSS-VP, the normally water-insoluble porphyrins dissolved as usual but the peroxidase-like activity was greatly reduced. It is notable that, in all these oxidations, the simple water-insoluble porphyrins such as manganese(III) 5,10,15,20-tetrakis(4-methoxyphenyl)porphyrin, when solubilised in water containing the amphiphilic polymer, were destroyed only very slowly as compared with the rapidity of auto-oxidation of similar water-soluble porphyrins in the absence of polymer. This stability suggests that the water-insoluble porphyrin molecules in the inner hydrophobic sphere of the PSSS-VN polymer must be isolated from each other so as to prevent mutual oxidation; the behaviour is characteristic of natural peroxidases.

The substrates to be oxidised (ABTS, guaiacol and mesidine) are soluble in water. For horse radish peroxidase, their approach to the metal centre in the porphyrin is prevented by the protein coat. For the PSSS-VN–porphyrin system it is probable that the porphyrin is not only held in the hydrophobic core of the PSSS-VN polymer in water but is isolated by intercalation between the many naphthalene residues in such a way that the oxidised metal centre is not open to approach by the substrate. Aggregation of polycyclic aromatic species through π–π interactions are well-known through UV effects[14] and it was found here that, in these PSSS-VN polymer–porphyrin systems, the Soret band near 420 nm is significantly broadened and reduced in height as compared with the free porphyrin.[8] Also, Mössbauer spectroscopy of the solid isolated by evaporation of water from a PSSS-VN polymer–iron porphyrin system revealed a small shift in the iron peak, suggesting electronic interaction of the porphyrin with surrounding groups.[8] Further, the substrates to be oxidised are water soluble and would not be expected to appear in the hydrophobic core of the polymer. Thus, for reaction to occur, an edge or edges of the porphyrin must be available for electron transfer reactions at the junction of the outer hydrophilic and inner hydrophobic surfaces of the polymer. If this is the case then the oxidation reactions catalysed by the PSSS-VN–porphyrin system would be closely similar to those typical of natural peroxidases and might be expected to have similar activity.

One difference between the natural enzymes and the PSSS-VN system lies in the absence of a formal apical ligand to the metal centre in the porphyrin in the latter. In horse radish peroxidase, this function is served by an imidazolyl nitrogen atom.[1b] In the PSSS-VN system at pH 8, the only apical ligand is likely to be $H_2O$ or $OH^-$. As catalytic activity in metalloporphyrins is influenced by the nature of such apical ligands, the activities of the horse radish peroxidase and the PSSS-VN–porphyrin mimic might not be expected to be identical. However, it has been demonstrated for oxidising systems with simple porphyrins as catalysts that the easily oxidised imidazole ligand can be profitably replaced by other ligands,[15a,b] including non-oxidisable inorganic varieties.[15a] It is encouraging that the rates of oxidation in the two systems are closely similar and that the porphyrin in the PSSS-VN polymer is not rapidly destroyed through auto-oxidation. In other work to be reported elsewhere, it is shown that a catalytic system, in which a porphyrin is covalently bonded between naphthalene residues in an analogue of PSSS-VN polymers, also behaves similarly and that even very simple sandwich molecules having a porphyrin covalently bonded between aromatic residues mimic the action of a peroxidase. It is concluded that porphyrins held in PSSS-VN amphiphilic polymers mimic peroxidase enzymic activity and do not behave like most other model porphyrin enzyme mimics, which resemble P450 cytochromes.

The authors thank the Eschenmoser Trust (UK) and Procter and Gamble (UK) for financial assistance (PAS).

## Footnote and References

* E-mail: rj05@liv.ac.uk

1 See for example (*a*) R. A. Sheldon and J. K. Kochi, *Metal-Catalysed Oxidations of Organic Compounds*, Academic Press, New York, 1981, pp. 216–268; (*b*) J. Frew and P. Jones, *Adv. Inorg. Bioinorg. Mechanisms*, 1984, **3**, 3175.
2 For examples, see T. McMurry and J. T. Groves, *Cytochrome P450, Structure, Mechanism and Biochemistry*, ed. P. Ortiz de Montellano, Plenum, London, 1986.
3 For some examples, see D. Mansuy, M. Fontecave and J.-F. Bartoli, *J. Chem. Soc., Chem. Commun.*, 1983, 253; K. Suslick and B. R. Cook, *J. Chem. Soc., Chem. Commun.*, 1987, 200; J. R. Lindsay-Smith and P. Sleath, *J. Chem. Soc., Perkin Trans 2*, 1983, 1991; A. M. d'A Rocha Gonsalves, R. A. W. Johnstone, M. M. Pereira, J. Shaw and A. J. F. N. Sobral, *Tetrahedron Lett.*, 1991, **32**, 1355.
4 S. Aibara, T. Kobayashi and Y. Morita, *J. Biochem.*, 1981, **90**, 489.
5 J. Putter and R. Becker, in *Methods of Enzymatic Analysis*, ed. H. U. Bergmeyer, VCH, Weinheim, 1985, vol. 3, p. 286.
6 G. Labat and B. Meunier, *J. Chem. Soc., Chem. Commun.*, 1990, 1414; N. Colclough and J. R. Lindsay-Smith, *J. Chem. Soc., Perkin Trans. 2*, 1994, 1139, and see ref. 1(*a*) therein.
7 R. A. W. Johnstone, M. L. P. G. Nunes, M. M. Pereira, A. M. d'A Rocha Gonsalves and A. C. Serra, *Heterocyclics*, 1996, **43**, 1423; A. M. d'A Rocha Gonsalves, R. A. W. Johnstone, M. M. Pereira, A. M. P. de SantAna, A. J. F. N. Sobral and P. A. Stocks, *Heterocycles*, 1996, **43**, 829.
8 P. A. Stocks, PhD Thesis, University of Liverpool, 1995.
9 R. A. W. Johnstone, P. A. Stocks, F. E. Hardy, J. G. L. Pluyter and A. J. Simpson, PCT Int. Appl. WO 9 525 267, 8th March, 1994; *Chem. Abstr.*, 1996, **46**, 599.
10 E. Sustar, M. Nowakowska and J. E. Guillet, *J. Photochem. Photobiol.*, 1990, **53**, 233.
11 For examples, see O. Almarsson and T. C. Bruice, *J. Am. Chem. Soc.*, 1995, **117**, 4533; P. Hoffmann, G. Labat, A. Robert and B. Meunier, *Tetrahedron Lett.*, 1990, **31**, 1991; S. Banfi, F. Montanari, S. Quici, S. V. Barkanova, O. L. Kaliya, V. N. Kopranenkov and E. A. Luk'yanets, *Tetrahedron Lett.*, 1995, **36**, 2317; T.-C. Zheng and D. E. Richardson, *Tetrahedron Lett.*, 1995, **36**, 837.
12 For some examples, see T. C. Bruice, *Aldrichim. Acta*, 1988, **21**, 87; A. M. d'A Rocha Gonsalves, R. A. W. Johnstone, M. M. Pereira, J. Shaw and A. J. F. N. Sobral, *Tetrahedron Lett.*, 1991, **32**, 1355.
13 For examples, see J. Putter and R. Becker, *Methods of Enzymatic Analysis*, ed. H. U. Bergmeyer, VCH, Weinheim, 1985, vol. 3, p. 286.
14 For references, see F. Ribo, J. Crustas, J. A. Farrera and M. Valero, *J. Chem. Soc., Chem. Commun.*, 1994, 681; R. F. Pasternack, L. Francesconi, D. Raff and E. Spiro, *Inorg. Chem.*, 1973, **12**, 2606.
15 (*a*) A. M. d'A Rocha Gonsalves, M. M. Pereira, R. A. W. Johnstone and J. Shaw, *J. Chem. Soc., Perkin Trans. 1*, 1991, 645; (*b*) A. Thellend, P. Battioni and D. Mansuy, *J. Chem. Soc., Chem. Commun.*, 1994, 23.

*Received in Cambridge, UK, 13th August 1997; 7/05934E*

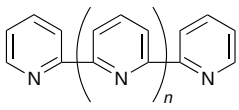
# New oligo-α-pyridylamino ligands and their metal complexes

**Ming-hwa Yang, Tzu-Wei Lin, Chin-Cheng Chou, Hsiao-Ching Lee, Hsiao-Chi Chang, Gene-Hsiang Lee, Man-kit Leung* and Shie-Ming Peng*†**

*Department of Chemistry, National Taiwan University, Taipei, Taiwan*

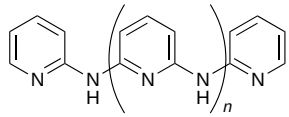
**Three novel oligo-α-pyridylamino ligands, tripyridyldiamine ($H_2$tpda), tetrapyridyltriamine ($H_3$teptra), pentapyridyltetramine ($H_4$peptea) are synthesized; the crystal structures of their metal complexes with the all-*anti* configuration of the chelating ligands are reported.**

Oligo-α-pyridines **I** exhibit an α-diimine functionality and chelating ability, they bind metal ions strongly and are used as building blocks for the self-assembly of metallosupramolecules.[1–3] We are interested in developing a new type of ligand which might bind oligonuclear metal ions chain; the oligo-α-pyridylamino ligands **II**.[4–6]



**I**

*n* = 0, bipyridine
*n* = 1, terpyridine
*n* = 2, quaterpyridine
*n* = 3, quinquepyridine
*n* = 4, sexipyridine

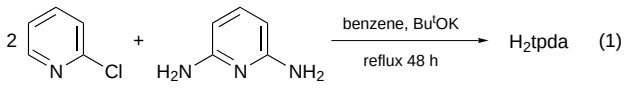


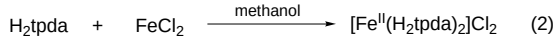
**II**

*n* = 0, dipyridylamine(Hdpa)
*n* = 1, tripyridyldiamine($H_2$tpda)
*n* = 2, tetrapyridyltriamine($H_3$teptra)
*n* = 3, pentapyridyltetramine($H_4$peptea)

Here, we report the synthesis of three novel oligo-α-pyridylamino ligands, tripyridyldiamine ($H_2$tpda), tetrapyridyltriamine ($H_3$teptra), and pentapyridyltetramine ($H_4$peptea). The crystal structure of their metal complexes with the all-*anti* conformation of the chelating ligands are presented.

The tripyridyldiamine ligand was synthesized by treating 2.2 equiv. of chloropyridine with 1 equiv. of 2,6-diaminopyridine under basic conditions [eqn. (1)]. The crude product was rinsed with water and recrystallized from propan-2-ol.[7] The iron complex of the ligand was synthesized by treating iron(II) chloride with 2 mol equiv. of $H_2$tpda in methanol [eqn. (2)]. The electronic spectrum (MeOH solution), shows maxima at 240 nm ($3.04 \times 10^4$ dm$^3$ mol$^{-1}$ cm$^{-1}$), 262 ($3.67 \times 10^4$), 278 ($3.81 \times 10^4$) and 334 ($3.72 \times 10^4$).




The molecular structure of $[Fe^{II}(H_2tpda)]^{2+}$ (Fig. 1)‡ reveals that the coordination geometry around $Fe^{II}$ is octahedral with two tridentate $H_2$tpda ligands arranged in a *mer*-configuration. The $H_2$tpda ligands coordinate to the iron(II) in an *anti–anti–anti–anti* conformation. The three pyridyl groups of the $H_2$tpda ligand are essentially planar and are twisted. The dihedral angle between each pair of neighboring pyridyl planes is 38°. The short Fe–N distances, ranging from 1.981(2) to 2.005(2) Å, are consistent with the low spin state of $Fe^{II}$.

The tetrapyridyltriamine ligand was synthesized by the palladium-catalyzed cross-coupling[8] of (6-bromo-2-pyridyl)(2′-pyridyl)amine and (6-amino-2-pyridyl)(2′-pyridyl)amine in the presence of catalyst [$Pd_2(dba)_3$, dppp, BuᵗOK, and 18-crown-6] in refluxing benzene [eqn. (3)]. The crude product was recrystallized from propan-2-ol. $H_3$teptra was characterized on the basis of $^1$H and $^{13}$C NMR spectroscopy, and mass spectrometry. $^1$H NMR in $(CD_3)_2SO$ clearly shows two singlets ($\delta$ 9.33, 9.07), four doublets ($\delta$ 8.19, 7.88, 7.72, 7.10) and three triplets ($\delta$ 7.62, 7.50, 6.84) which are consistent with the structural assignment.

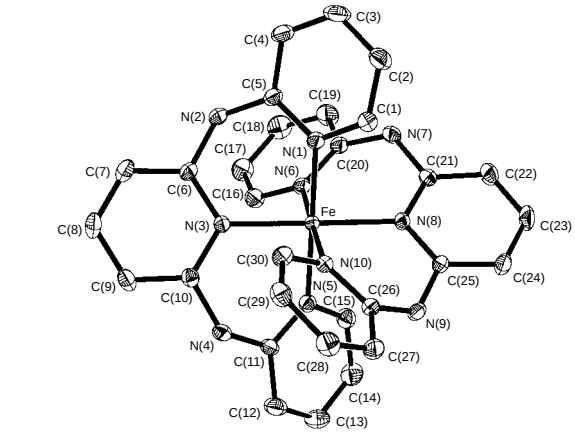
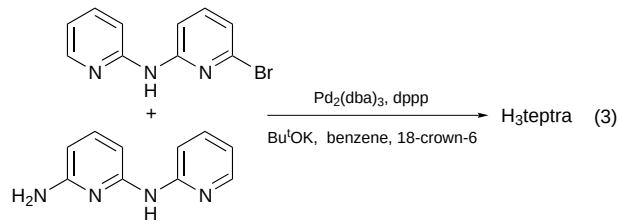
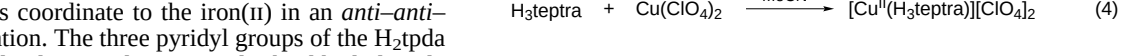



**Fig. 1** ORTEP view of $[Fe(H_2tpda)_2]^{2+}$. Selected bond lengths (Å) and angles (°): Fe–N 1.981(2)–2.005(2), av. 1.995; *cis*-N–Fe–N 88.68(9)–91.85(9), av. 90.0, N(1)–Fe–N(5) 179.2(1), N(3)–Fe–N(8), 179.2(1), N(6)–Fe–N(10), 178.6(1); dihedral angles between interpyridyl planes, Py(N1)–Py(N3), 40.8(1), Py(N3)–Py(N5), 34.4(1), Py(N6)–Py(N8), 40.2(1), Py(N8)–Py(N10), 37.6(1).

The $Cu^{II}$ complex of the ligand was synthesized by treating an equimolar amount of $Cu(ClO_4)_2$ and the $H_3$teptra in acetonitrile [eqn. (4)]. The electronic spectrum (MeCN solution), shows maxima at 239 nm ($2.70 \times 10^4$ dm$^3$ mol$^{-1}$ cm$^{-1}$), 270(sh) ($1.59 \times 10^4$), 328 ($3.77 \times 10^4$) and 368 ($9.71 \times 10^3$).




The molecular structure of $[Cu^{II}(H_3teptra)]^{2+}$ (Fig. 2)‡ reveals that the coordination geometry around $Cu^{II}$ is between planar and tetrahedral with the monohelical $H_3$teptra ligand having an all-*anti* comformation. The four pyridyl groups of the $H_3$teptra ligand are planar and the dihedral angle between each

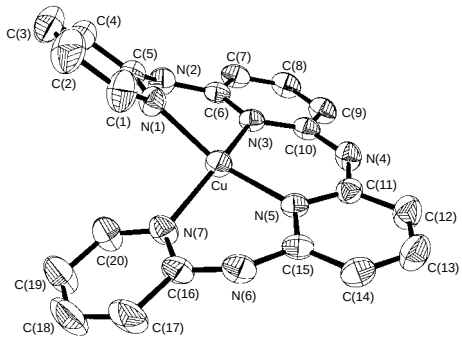
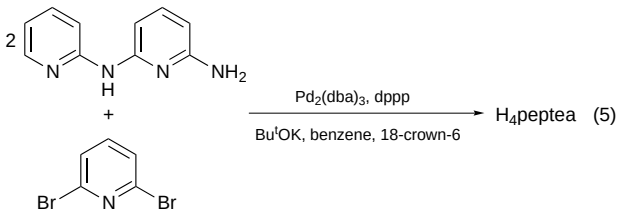


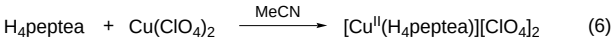

**Fig. 2** ORTEP view of $[Cu(H_3teptra)]^{2+}$. Selected bond lengths (Å) and angles (°): Cu–N 1.954(5)–1.982(5), av. 1.967; N(1)–Cu–N(3), 91.9(2), N(1)–Cu–N(5), 151.0(2), N(1)–Cu–N(7) 90.9(2), N(3)–Cu–N(5), 98.2(2) N(3)–Cu–N(7), 150.0(2), N(5)–Cu–N(7), 93.0(2); dihedral angles between interpyridyl planes, Py(N1)–Py(N3), 25.3(3), Py(N3)–Py(N5), 15.0(1), Py(N5)–Py(N7), 20.4(2).

pair of neighboring pyridyl planes is 25.3(3), 15.0(3), 20.4(3)°, respectively. The short Cu–N distances, ranging from 1.954(5) to 1.982(5) indicate a strong binding of the chelating ligand.

The synthesis of pentapyridyltetramine was similar to $H_3$teptra [eqn. (5)]. $H_4$peptea was characterized on the basis of its $^1$H and $^{13}$C NMR and mass spectrometry data. Although the $^1$H NMR spectrum of $H_4$peptea [in $(CD_3)_2SO$] only shows two singlets ($\delta$ 9.33, 9.06), five doublets ($\delta$ 8.19, 7.90, 7.28, 7.19, 7.08) and three triplets ($\delta$ 7.62, 7.50, 6.84), the intergrated area of the triplet at $\delta$ 7.50 is equivalent to that originating from three protons when compared to the area of the other triplet, indicating the existence of two independent triplets with an identical chemical shift at $\delta$ 7.50.

The $Cu^{II}$ complex of the ligand was synthesized by treating an equimolar solution of $Cu(ClO_4)_2$ and $H_4$peptea in acetonitrile and precipitated by adding diethyl ether [eqn. (6)]. The electronic spectrum (MeCN solution), shows maxima at 254 nm ($1.87 \times 10^4$ dm$^3$ mol$^{-1}$ cm$^{-1}$), 324 ($1.97 \times 10^4$), 344 ($1.65 \times 10^4$) and 378(sh) ($6.21 \times 10^3$).




The crystal structure of $[Cu^{II}(H_4peptea)]^{2+}$ (Fig. 3)‡ reveals that the coordination geometry around $Cu^{II}$ is trigonal bipyramidal with the monohelical $H_4$peptea ligand existing in an all-*anti* configuration. A crystallographic $C_2$ axis runs through the C(13)–N(5)–Cu chain. The three independent crystallographic pyridyl groups are planar and the dihedral angle between neighboring pyridine planes is *ca.* 21°.

In summary, the modified Buchwald's procedure[8] leads to the synthesis of new types of oligo-α-pyridylamino ligands. Their metal complexes were studied. The complexes demonstrate the chelating ability of the ligands. Attempts to isolate the metal complexes with different coordination modes of the ligands, *e.g.* the all-*syn* configuration of the ligands which bind metal ions in a chain are being undertaken.

We thank the National Science Council of the Republic of China for financial support.

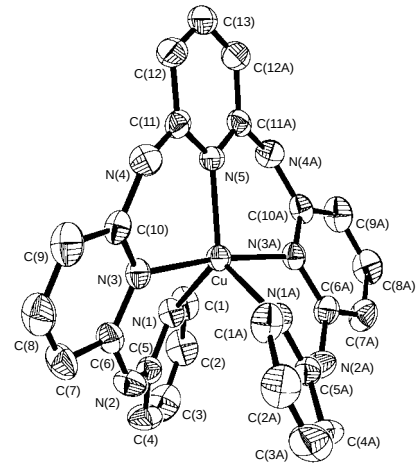



**Fig. 3** ORTEP view of $[Cu(H_4peptea)]^{2+}$. Selected bond length (Å) and angles (°): Cu–N(1) 2.102(5), Cu–N(3) 1.972(4), Cu–N(5) 2.017(6); N(1)–Cu–N(1A), 112.2(3), N(1)–Cu–N(3) 87.3(2), N(1)–Cu–N(3A), 88.4(2), N(1)–Cu–N(5), 123.9(1), N(3)–Cu–N(3A), 172.3(3), N(3)–Cu–N(5), 93.8(1); dihedral angles between interpyridyl planes, Py(N1)–Py(N3), 22.2(3), Py(N3)–Py(N5), 19.0(3).

## Footnotes and References

† E-mail: smpeng@chem35.ch.ntu.edu.tw

‡ *Crystal data*: for $[Fe(H_2tpda)_2]Cl_2 \cdot 2MeOH$: monoclinic, space group $P2_1/n$, $a$ = 15.0179(2), $b$ = 11.1499(2), $c$ = 20.2308(1) Å, $\beta$ = 98.864(1)°, $U$ = 3347.15(8) Å$^3$, $D_c$ = 1.424 g cm$^{-3}$, $Z$ = 4; $T_{min}$ = 0.236, $T_{max}$ = 0.296, 21 345 reflections were measured and 7613 unique reflections ($2\theta$ < 55°, $R_{int}$ = 0.046) were used in the refinement. Full-matrix least-squares refinement on $F^2$ (457 variables) converged to $R_F$ = 0.0506 $R_{wF^2}$ = 0.1026 for 5168 reflections with $I > 2\sigma(I)$.

$[Cu(H_3teptra)][ClO_4]_2 \cdot MeCN$: monoclinic, space group $P2_1/c$, $a$ = 12.0470(2), $b$ = 14.4324(1), $c$ = 15.4744(2) Å, $\beta$ = 92.883(1)°, $U$ = 2687.08(6) Å$^3$, $D_c$ = 1.629 g cm$^{-3}$, $Z$ = 4; $T_{min}$ = 0.2226, $T_{max}$ = 0.2830, 14 676 reflections were measured and 4721 unique reflections ($2\theta$ < 50°, $R_{int}$ = 0.0304) were used in the refinement. Full-matrix least-squares refinement on $F^2$ (354 variables) converged to $R_F$ = 0.0782 $R_{wF^2}$ = 0.2134 for 3877 reflections with $I > 2\sigma(I)$.

$[Cu(H_4peptea)][ClO_4]_2 \cdot 2H_2O$: monoclinic, space group $C2/c$, $a$ = 11.2720(4), $b$ = 36.0332(14), $c$ = 7.7793(2) Å, $\beta$ = 108.732(1)°, $U$ = 2998.6(2) Å$^3$, $D_c$ = 1.652 g cm$^{-3}$, $Z$ = 4; $T_{min}$ = 0.318, $T_{max}$ = 0.377), 8685 reflections were measured and 2652 unique reflections ($2\theta$ < 50°, $R_{int}$ = 0.056) were used in the refinement. Full-matrix least-squares refinement on $F^2$ (218 variables) converged to $R_F$ = 0.0723, $R_{wF^2}$ = 0.1843 for 1858 reflections with $I > 2\sigma(I)$. For all structures SMART diffractometer with graphite-monochromated Mo-Kα radiation ($\lambda$ = 0.710 73 Å), SADABS absorption correction. CCDC 182/638.

1 J.-M. Lehn, *Angew. Chem., Int. Ed. Engl*, 1988, **27**, 89; J.-M. Lehn, *Science*, 1993, **260**, 1762; J.-M. Lehn, *Supramolecular Chemistry*, VCH, Weinheim, 1995; G. S. Hanan, C. R. Arana, J.-M. Lehn and D. Fenske, *Angew. Chem., Int. Ed. Engl*., 1995, **34**, 1122.
2 E. C. Constable, *Chem. Commun.*, 1997, 1079; E. C. Constable, *Chem. Ind.*, 1994, 56; E. C. Constable, *Prog. Inorg. Chem.*, 1994, **42**, 67.
3 K. K. Ho, K. K. Cheung, S. M. Peng and C. M. Che, *J. Chem. Soc., Dalton Trans.*, 1996, 1411; K. K. Ho, S. M. Peng, K. Y. Wang and C. M. Che, *J. Chem. Soc., Dalton Trans.*, 1996, 1827; C. M. Che, Y. P. Wang, K. S. Yeung, K. Y. Wong and S. M. Peng, *J. Chem. Soc., Dalton Trans.*, 1992, 2675.
4 E. C. Yang, M. C. Cheng, M. S. Tsai and S. M. Peng, *J. Chem. Soc., Chem. Commun.*, 1994, 2377.
5 J. T. Sheu, C. C. Lin, I. Chao, C. C. Wang and S. M. Peng, *Chem. Commun.*, 1996, 315.
6 S. J. Shieh, C. C. Chou, G. H. Lee, C. C. Wang and S. M. Peng, *Angew. Chem., Int. Ed. Engl.*, 1997, **36**, 56.
7 The synthesis of this ligand was first reported in ref. 6. This procedure improved the yield to as much as 60%.
8 S. Wagaw and S. L. Buchwald, *J. Org. Chem.*, 1996, **61**, 7240.

*Received in Cambridge, UK, 3rd September 1997; 7/06439J*

# Mesoporous material containing framework tectosilicate by pore–wall recrystallization

**K. Richard Kloetstra, Herman van Bekkum and Jacobus C. Jansen**

*Laboratory of Organic Chemistry and Catalysis, Delft University of Technology, Julianalaan 136, 2628 BL Delft, The Netherlands*

**Partial recrystallization of the interporous aluminosilicate surface of MCM-41 and HMS by ion-exchanged tetrapropylammonium template results in a mesoporous material with surface-tectosilicate structures giving enhanced acidity and catalytic cracking activity.**

The development of the mesoporous molecular sieve MCM-41 by the workers of Mobil[1,2] has stimulated much research efforts in the field of acid[3,4] and base[5] catalysis. The strength of the acid sites of MCM-41 as well as of the related HMS material[6,7] is, however, rather weak compared to zeolites[8,9] owing to the amorphous character of the framework of both materials.[2,6–9] Here we report that upon increasing locally the crystallinity of the amorphous framework of MCM-41 and HMS, the acidity and catalytic activity improves substantially. The design of these catalysts is based on positioning tetrapropylammonium (TPA) cations at the interporous surface of MCM-41 and HMS which induces partial recrystallization of the pore wall *via* heterogeneous nucleation during thermal processing. Owing to short-range aluminosilicate–template interactions non-porous framework tectosilicate[10] is formed of the ZSM-5 precursor type.

Our approach to design a composite consisting of a mesoporous molecular sieve with interporous tectosilicate, denoted as porous nanocrystalline aluminosilicate (PNA) is based on the idea to recrystallize partially the amorphous framework of MCM-41 and HMS. By attachment of TPA cations, the template for ZSM-5,[11] onto the mesopore walls *via* an ion-exchange procedure a high dispersion of the TPA in the mesoporous material is achieved. This should result in a nucleation of ZSM-5 species and controlled conversion of MCM-41 and HMS. When the pre-positioning of TPA is omitted and a homogeneous aqueous mixture of TPAOH and MCM-41 is heated we observed that the MCM-41 is recrystallized overnight into aggregates of ZSM-5.[12] This process went even faster when purely siliceous MCM-41 was used, resulting in silicalite-1, which is however not useful in catalytic processes. Thus the need to pre-position TPA at the Al sites is a prerequisite to induce the recrystallization at the Al sites and suppress the diffusivity of TPA.

Considering partial recrystallization of MCM-41 and HMS, the ZSM-5 stoichiometry in the starting materials has to be optimized. It is well known that in as-synthesized ZSM-5 each TPA is surrounded by 24 tetrahedrally coordinated Si and/or Al atoms.[13] The Si/Al ratio (30) of the parent MCM-41 and HMS materials was chosen to be close to the above value. Here thirty one T-atoms (T = $SiO_4$ and/or $AlO_4^-$ tetrahedra) are neighbouring one TPA cation in TPA ion-exchanged MCM-41 (TPA-MCM-41). This ZSM-5 precursor-type situation is, according to Ostwald's rule of successive transformations,[10] expected to induce ZSM-5 crystallization Glycerol was selected as the solvent in the recrystallization, because it appeared to have unusual advantages in ZSM-5 synthesis. The high viscosity of glycerol will moderate zeolite growth and moreover glycerol can act as a stabilizing guest molecule.[14,15] It was proposed that various silicate structures are formed during aging due to the interaction of glycerol with silicate species.[15]

Calcined MCM-41 (1.0 g; Si/Al = 30; HNa-form)[5] was converted to TPA-MCM-41 by ion-exchange with a 50% excess of aqueous TPAOH ($2 \times 10^{-3}$ M solution) for 20 h, followed by washing and drying at 80 °C under vacuum. The Na/Al ratio decreased from 0.8 to 0.1 indicating a 90% substitution of $Na^+$ for TPA cations. TPA-MCM-41 with a tenfold excess mass of glycerol was loaded in a Teflon-lined autoclave and stirred for 2 h at room temp. and subsequently allowed to react at 120 °C statically for 24 h. Finally the material was collected by filtration, washed with demineralized water, dried at 100 °C and calcined at 500 °C for 5 h to remove the organics from the composite material (coded as PNA-1). Aluminosilicate HMS (Si/Al = 30; H-form)[16] was subjected to the same procedure resulting in the material PNA-2.

The substantial improvement of the catalytic activity, and thus the acidity, of the PNAs compared to the parent materials is demonstrated by the cracking of cumene (Table 1). The catalytic reactions were performed at 300 °C in a down-flow reactor (id = 7 mm) using 1 g of catalyst pellets (diameter 0.7–1.0 mm) and a $N_2$ flow of 25 ml $min^{-1}$ containing 14.4 μmol $min^{-1}$ of cumene. The parent MCM-41 and HMS materials in the $H^+$-form produce only benzene and propene with traces of α-methylstyrene. The enhanced cumene conversion over the PNAs is exclusively the result of a higher cracking activity.[17] The improved activity is therefore assigned to enhanced Brønsted acidity which is also reflected by the initial *n*-hexane cracking activity of the PNAs which is about four times higher than that of the MCM-41 and HMS materials. The PNAs showed no significant deactivation during 3 h on stream in the cumene reaction and showed similar activities after regeneration at high temperature indicating that the framework does not collapse and that the acid sites are still accessible. It may be mentioned that the cumene conversions over the four mesoporous aluminosilicates were not diffusion limited. This was, however, not the case for the cumene cracking over the microporous ZSM-5.

As shown in Fig. 1, the X-ray powder diffraction patterns of the parent MCM-41 and HMS materials and the corresponding PNAs do not differ significantly. The characteristic hexagonal features of MCM-41, which are reflected by the common $d_{100}$ diffraction peak and the 110, 200 and the much weaker 210 reflections in the 2θ range 4.0–7.0° are retained though with less

**Table 1** Conversion of cumene at 300 °C over PNAs and related parent materials

| Sample | Cumene conversion (%) at time on stream | |
|---|---|---|
| | 10 min | 3 h |
| MCM-41[a] | 14.7 | 13.6 |
| PNA-1 | 41.3 | 37.5 |
| HMS[a] | 24.8 | 26.8 |
| PNA-2 | 47.6 | 42.4 |
| ZSM-5[b] | 95.1 | 93.7 |

[a] MCM-41 and HMS in the $H^+$-form. [b] H-ZSM-5 with Si/Al = 78.

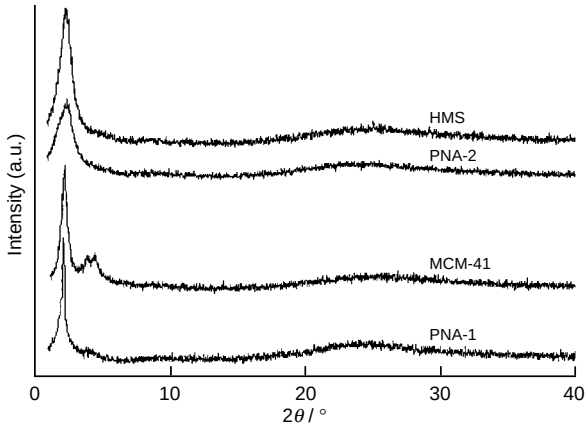



**Fig. 1** X-Ray powder diffraction patterns of the composite materials PNA-1 and PNA-2 together with the parent MCM-41 and HMS materials, respectively

intensity in PNA-1. The absence of high-order Bragg reflections in HMS, indicating small crystallite domains,[6,7] is also preserved in PNA-2. The intensity of the $d_{100}$ diffraction peak had decreased drastically when, instead of glycerol, water was used as the solvent. As indicated by the X-ray powder diffraction patterns the PNAs still possess mesoporous features and a large specific surface area measured by $N_2$ adsorption (1267 and 796 $m^2\ g^{-1}$ BET area and a pore size of 27 and 23 Å for HMS and PNA-2, respectively). TEM measurements showed that exclusively one solid phase was present.

FTIR spectroscopy reveals only for the PNA samples a distinct vibration at 550–560 $cm^{-1}$ (Fig. 2). Several researchers have assigned the 550 $cm^{-1}$ band to the asymmetric stretching mode of the five-membered ring present in ZSM-5 which should therefore be an indication of the presence of embryonal ZSM-5 structures.[18–22] The parent MCM-41 and HMS which have both an amorphous framework do not absorb at this wavenumber and therefore the 550 $cm^{-1}$ vibration is a good probe for detecting the degree of crystallinity of a siliceous MFI-type material even at this initial stage of ZSM-5 formation giving very small tectosilicate structures.[18,22]

Interestingly, $^{27}Al$ MAS NMR measurements show a transformation of strongly anisotropic Al into a quasi-isotropic tetrahedral environment going from HMS to PNA-2.

We conclude that thermally-treated TPA-MCM-41 and TPA-HMS recrystallize, assisted by glycerol, the amorphous aluminosilicate framework partly to such an extent that the framework Al environment is made more highly symmetric. Owing to the attachment of the TPA cations at the interporous framework in combination with the short TPA–aluminosilicate distance[23,24] the recrystallization process is forced to nucleate heterogeneously. The advantage of this process is the formation of embryonal ZSM-5 in a controlled way.

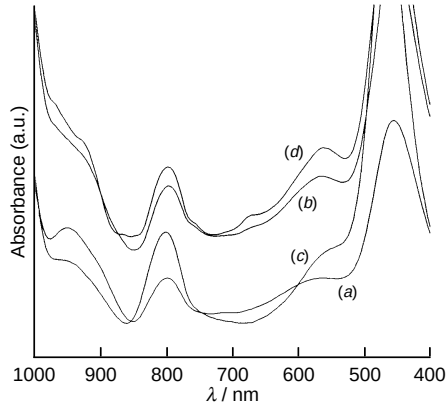



**Fig. 2** FTIR absorption spectra of MCM-41 (*a*), PNA-1 (*b*), HMS (*c*) and PNA-2 (*d*)

The importance of the TPA/T-atom ratio when partly recrystallizing MCM-41 and HMS materials is reflected by the production of only X-ray amorphous material when TPA/Al = 1 and Si/Al = 15 instead of 30. The higher amount of framework Al and therefore the increase of interattached TPA causes disturbance of the recrystallization of the framework. However, when the same mesoporous aluminosilicate is ion-exchanged at a TPA/Al ratio of 0.5 and subsequently thermally processed, the X-ray diffraction pattern was retained much better and an IR band at 550 $cm^{-1}$ was observed. The small size of the tectosilicate nanostructures makes detection of the 1220 $cm^{-1}$ band impossible.[22] Attempted preparation of PNA by interrupting the ZSM-5 crystallization using water as the medium appeared to be very difficult and not reproducible.[12]

In conclusion, the present approach to position the appropriate amount of template molecules inside a mesoporous aluminosilicate can lead to controlled partial reacrystallization and provide new interesting catalytic materials. Thus, upgrading of the catalytic properties of MCM-41 and related materials might lead to a more valuable component in commercial cracking catalysts used in oil refining of heavy feedstocks.[25]

We thank NIOK, the Dutch School of Catalysis, for financial support.

## Footnote and References

* E-mail: kloetstra@stm.tudelft.nl

1 C. T. Kresge, M. E. Leonowicz, W. J. Roth, J. C. Vartuli and J. S. Beck, *Nature*, 1992, **359**, 710.
2 J. S. Beck, J. C. Vartuli, W. J. Roth, M. E. Leonowicz, C. T. Kresge, K. D. Schmitt, C. T. W. Chu, D. H. Olson, E. W. Sheppard, S. B. McCullen, J. B. Higgins and J. L. Schlenker, *J. Am. Chem. Soc.*, 1992, **114**, 10 834.
3 K. R. Kloetstra and H. van Bekkum, *J. Chem. Res. (S)*, 1995, 26.
4 E. Armengol, M. L. Cano, A. Corma, H. Garcia and M. T. Navarro, *J. Chem. Soc., Chem. Commun.*, 1995, 519.
5 K. R. Kloetstra and H. van Bekkum, *J. Chem. Soc., Chem. Commun.*, 1995, 1005.
6 P. T. Tanev and T. J. Pinnavaia, *Science*, 1995, **267**, 865.
7 P. T. Tanev and T. J. Pinnavaia, *Chem. Mater.*, 1996, **8**, 2068.
8 A. Corma, V. Fornés, M. T. Navarro and J. Pérez-Pariente, *J. Catal.*, 1994, **148**, 569.
9 C.-Y. Chen, H.-X. Lin and M. E. Davis, *Microporous Mater.*, 1993, **2**, 17.
10 R. M. Barrer, *Hydrothermal chemistry of zeolites*, Academic Press, London, 1982.
11 E. G. Derouane, S. Detremmerie, Z. Gabelica and N. Blom, *Appl. Catal.*, 1981, **1**, 201.
12 K. R. Kloetstra, J. C. Jansen and H. van Bekkum, *Prepr. Am. Chem. Soc., Div. Pet. Chem.*, 1996, **41**, 412.
13 J. B. Nagy, Z. Gabelica and E. G. Derouane, *Zeolites*, 1983, **3**, 43.
14 R. M. Barrer, in *Zeolite Synthesis*, ed. M. L. Occelli and H. E. Robson, Am. Chem. Soc., Washington DC, 1989, pp. 11–27.
15 J. Dougherty, L. E. Iton and J. W. White, *Zeolites*, 1995, **15**, 640.
16 R. Mokaya and W. Jones, *Chem. Commun.*, 1996, 981.
17 R. Mokaya and W. Jones, *Chem. Commun.*, 1996, 983.
18 P. A. Jacobs, E. G. Derouane and J. Weitkamp, *J. Chem. Soc., Chem. Commun.*, 1981, 591.
19 K. F. M. G. J. Scholle, W. S. Veeman, P. Frenken and G. P. M. Velden, *Appl. Catal.*, 1985, **17**, 233.
20 G. Boxhoorn, O. Sudmeijer and P. H. G. van Kasteren, *J. Chem. Soc., Chem. Commun.*, 1983, 1416.
21 J. C. Jansen, F. J. van der Gaag and H. van Bekkum, *Zeolites*, 1984, **3**, 369.
22 B. J. Schoeman, *Stud. Surf. Sci. Catal.*, 1997, **105**, 647.
23 M. E. Davis, CHEMTECH., 1994, September, 22.
24 W. H. Dokter, T. P. M. Beelen and R. A. Van Santen, *Prepr. Am. Chem. Soc., Div. Pet. Chem.*, 1995, **40**, 235.
25 I. E. Maxwell and W. H. J. Stork, *Stud. Surf. Sci. Catal.*, 1991, **58**, 571.

*Received in Cambridge, UK, 5th August 1997; 7/05681H*

# Iron(III) oxamato-catalyzed epoxidation of alkenes by dioxygen and pivalaldehyde

**Rafael Ruiz,[a] Maria Triannidis,[a] Ally Aukauloo,[a] Yves Journaux,*[a] Isabel Fernández,[b] José R. Pedro,*[b] Beatriz Cervera,[c] Isabel Castro[c] and M. Carmen Muñoz[d]**

[a] *Laboratoire de Chimie Inorganique, URA 420, CNRS, Université de Paris-Sud, 91405 Orsay, France*
[b] *Departament de Química Orgànica, Facultat de Química, Universitat de València, 46100 Burjassot, València, Spain*
[c] *Departament de Química Inorgànica, Facultat de Química, Universitat de València, 46100 Burjassot, València, Spain*
[d] *Departamento de Física Aplicada, Universidad Politécnica de València, 46071 València, Spain*

**A new iron(III)–carbonato monomeric complex of *ortho*-phenylenebis(oxamato) (opba) 1 is synthesized, and spectroscopically and structurally characterized; it is a moderately efficient non-heme catalyst for the aerobic epoxidation of alkenes with co-oxidation of pivalaldehyde.**

There has been always a great interest in iron coordination chemistry owing to the relevant role that this transition metal ion plays in biology, particularly as the active metal center embedded in a large number of proteins involved in oxygen activation chemistry.[1] Now, this interest is directed towards mono- and di-nuclear non-heme iron proteins, owing to the surprisingly diverse functional properties exhibited by them.[2] Amido groups from asparagine or glutamine residues in the polypeptide backbone of some of these mononuclear iron proteins are frequently shown to coordinate to the iron metal center through their oxygen donor atom, like in lipid dioxygenase and isopenicillin *N*-synthase.[2a] Moreover, amido nitrogen coordination has been invoked in bleomycin, a natural iron-containing glycopeptide with antibiotic and antitumor properties of fundamental importance in medicine.[2a] That being so, it is evident that knowledge of the chemistry and reactivity properties of iron–amido complexes becomes particularly appropriate in order to understand the key steps of the enzymatic mechanism proposed for this class of non-heme iron proteins and antibiotics. Since the review of Sigel and Martin devoted to the coordinating properties of the amide bond with copper, nickel, cobalt and zinc metal ions,[3] a considerable effort has been made in the last fifteen years in order to detect iron ion interactions with the amide group.[4–6] Recently, we have initiated an investigation program to assess the possible use of bis-N-substituted oxamato ligands like *ortho*-phenylenebis-(oxamato) (opba) in the stabilization of unusual high oxidation state transition metal ions due to the high donor capacity of the deprotonated-amido group.[7] We report here on the synthesis and physical characterization,† and the crystal and molecular structure‡ of its corresponding oxamato iron(III) complex of formula $[NMe_4]_3[Fe(opba)(CO_3)]\cdot 5H_2O$ **1**, as well as its activity toward alkene epoxidation with dioxygen.

Complex **1** consists of mononuclear $[Fe(opba)(CO_3)]^{3-}$ complex anions (Fig. 1), tetramethylammonium cations and crystallization water molecules. The iron atom is bound to the two deprotonated amido nitrogens and two carboxylate oxygens of the opba ligand and to two oxygen atoms from the carbonate in a rhombically distorted octahedral coordination geometry. The carbonate chelating group is symmetrically bound to the metal (2.034, 2.045 Å for Fe–O) occupying two *cis* positions of the octahedron with a typical small bite angle [63.2° for O(7)–Fe–O(8)]. This imposes a non-planar conformation for the tetradentate opba ligand which is the only compatible with an octahedral environment at the metal ion. In fact, the opba ligand adopts a *cis*-β geometry with the N(1), N(2) and O(2) donor atoms occupying three meridional positions around iron. This situation contrasts to previous descriptions of mononuclear complexes with this ligand or its derivatives in which all four donor atoms form a plane (*trans* geometry).[7,8] The distortion from planarity of the opba ligand is accommodated by a disrotatory rotation of the C(3)–N(2) amide bond defined as the angle between the C(6)C(3)N(2) and C(3)N(2)C(4) mean planes [17 *cf.* 2° for the equivalent C(1)–N(1) amide bond], as previously observed in a related cobalt(III) diamido-*N*-dialkoxido complex.[9] This distortion is also reflected in the metal–ligand bond lengths, with a significant difference between the two Fe–O(carboxylate) bond distances of *ca.* 0.05 Å, the longer Fe–O(5) distance being *trans* to that of the carbonate ligand Fe–O(8) which is the longest bond of the octahedron. The Fe–N(amide) bond distances average 2.05 Å, a value very close to that observed in high-spin iron(III) complexes containing amido nitrogen bonds,[5] but significantly longer than those of the analogous intermediate[4b] or low-spin[6] iron(III)–amide bonds (1.93–1.96 Å).

In order to uncover the potential reactivity of this new iron(III) complex, we have examined its ability to catalyse the epoxidation of some representative disubstituted alkenes using dioxygen as oxidant in the presence of an aldehyde.[10] The

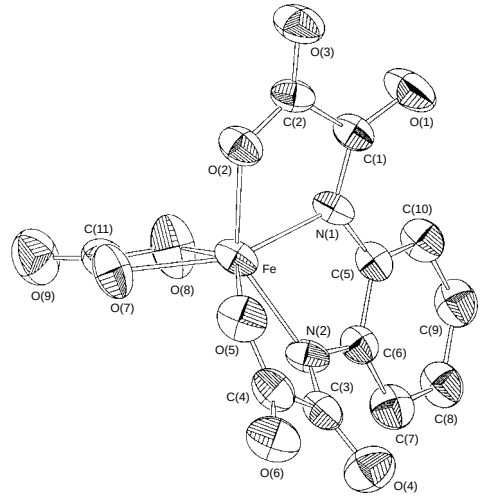



**Fig. 1** Perspective view of the anionic mononuclear unit of **1** with the atom numbering scheme (thermal ellipsoids are at the 30% probability level and hydrogen atoms have been omitted for clarity). Selected bond distances (Å) and angles (°) with standard deviations in parentheses: Fe–N(1) 2.048(5), Fe–N(2) 2.045(6), Fe–O(2) 1.986(4), Fe–O(5) 2.035(4), Fe–O(7) 2.034(5), Fe–O(8) 2.045(5); N(1)–Fe–N(2) 75.9(2), N(1)–Fe–O(2) 78.5(2), N(1)–Fe–O(5) 125.5(2), N(1)–Fe–O(7) 147.4(2), N(1)–Fe–O(8) 86.9(2), N(2)–Fe–O(2) 142.8(2), N(2)–Fe–O(5) 77.9(2), N(2)–Fe–O(7) 118.9(2), N(2)–Fe–O(8) 98.9(3), O(2)–Fe–O(5) 96.0(2), O(2)–Fe–O(7) 97.1(2), O(2)–Fe–O(8) 106.2(2), O(5)–Fe–O(7) 86.9(2), O(5)–Fe–O(8) 144.2(2), O(7)–Fe–O(8) 63.2(2).

**Table 1** Results for the epoxidation of alkenes by dioxygen and pivalaldehyde catalyzed by **1**[a]

| Entry | Alkene | *t*/h | Yield[b,c] (%) |
|---|---|---|---|
| 1 | *trans*-Stilbene | 3 | 95 |
| 2 | *cis*-Stilbene | 3[d] | 15 |
| 3 | Cyclohexene | 4 | 45 |
| 4 | 1,2-Dihydronaphthalene | 4 | 50 |
| 5 | 1,2-Dihydronaphthalene[e] | 4 | 80 |

[a] Reactions were carried out at room temperature by adding a fluorobenzene solution (0.2 ml) of the alkene (0.11 mmol) to a stirred mixture of the metal catalyst ($6.5 \times 10^{-3}$ mmol) and pivalaldehyde (0.33 mmol) in fluorobenzene (0.2 ml) under dioxygen atmosphere. The consumption of the alkene and the formation of the corresponding epoxide during the course of the reaction were monitored by TLC. The obtained epoxide and the unreacted alkene were separated by flash column chromatography on silica gel. [b] Yields refer to isolated and pure compounds (column chromatography on silica gel). All compounds exhibited spectral data consistent with their structures. [c] In the absence of catalyst some extension of epoxidation was observed. [d] With a reaction time of 24 h the final conversion was almost identical (*ca.* 20%). [e] In the presence of *N*-methylimidazole (0.11 mmol).

results are summarized in Table 1. Complex **1** catalyses the epoxidation of *trans*-stilbene by dioxygen plus pivalaldehyde in fluorobenzene solution with yields as high as 95% of the corresponding epoxide, *trans*-stilbene oxide, after 3 h (entry 1). By contrast, the percent conversion in the case of *cis*-stilbene is of only 15–20% even after a total reaction time of 24 h (entry 2), indicating that the catalytic epoxidation is greatly stereodependent. For both *cis*- and *trans*-stilbene, however, epoxides were the only oxidation products as confirmed by $^1$H NMR spectroscopy. As a matter of fact, no trace of the corresponding ketone or alcohol were detected for the epoxidation of cyclohexene which is typically regarded as a good substrate to check for competition of alkene epoxidation *vs*. allylic oxidation (entry 3). This observation suggests that typical free radical intermediates are not directly involved as potential epoxidizing agents. On the other hand, it is noteworthy that the amount of epoxide obtained with **1** increases in the presence of *N*-methylimidazole: for instance, almost a twofold yield enhancement was found for the epoxidation of 1,2-dihydronaphthalene, *i.e.* from 50 to 80% after 4 h (entries 4 and 5, respectively). Although it is premature to discuss the precise mechanism at the present stage, *N*-methylimidazole most likely acts as a monodentate donor ligand toward the iron(III) ion by replacement of the bidentate carbonate ligand, and thereby affording a vacant coordination site on the iron center for reaction with the potential oxidant. Furthermore, even if the exact role of the metal complex in the epoxidation of alkenes by dioxygen with co-oxidation of aldehydes is still unclear, recent studies by Valentine and coworkers[11] demonstrate that it coordinates to the acylperoxy radicals generated in the autoxidation of the aldehyde forming a metal-acylperoxo complex. That being so, iron(IV)–acylperoxo or iron(V)–oxo species derived by oxygen–oxygen bond cleavage of the acylperoxo group, seem to us the more probable candidates to play the role of active epoxidizing agents in our system. In this regard, it is interesting to note that Collins *et al*. have isolated stable iron(IV) complexes with amido-containing ligands which would be a model for the proposed catalytic entities in our oxidation system.[4a] Attempts to characterize these reactive intermediates species using other transition metal ions with more accessible high-valent oxidation states such as manganese are in progress in our laboratory.

This work was supported by the DGICYT, Ministerio de Educación y Ciencia (Spain) through projects PB94-0985 and PB94-1002. We acknowledge the financial support of the group Rhône-Poulenc. R. R. and B. C. thank the Ministerio de Educación y Ciencia (Spain) and the Conselleria de Educació i Ciència de la Generalitat Valenciana (Spain) for grants. We would also like to express our gratitude to Dr J. J. Girerd and Dr P. Mialane for fruitful discussions.

## Footnotes and References

* E-mail: jour@icmo.u-psud.fr

† *Syntheses and selected data* for **1**: A solution of the diethyl ester derivative of opba (1.54 g, 5 mmol) in methanol (100 ml) was charged with a 25% methanol solution of $NMe_4OH$ (10 cm$^3$, 25 mmol) and the resulting mixture was stirred at 60 °C for 15 min in order to facilitate the hydrolysis of the ethyl ester groups. A methanolic solution (50 ml) of iron(III) perchlorate hydrate (1.77 g, 5 mmol) was then added dropwise *via* a dropping funnel under stirring. The resulting intensely red coloured solution was filtered to eliminate the white precipitate of $NMe_4ClO_4$, and reduced to a final volume of 10 ml on a rotatory evaporator. The concentrated solution was treated successively with diethyl ether and acetone to give a very hygroscopic product (solid or oil) which was recuperated with acetonitrile (300 ml). The suspension obtained was gently heated for 5 h with vigorous stirring and then filtered to eliminate the remainder of the solid particles. Upon standing at room temperature, a first crop of a side product appeared which was also filtered and separated from the mother-liquor. Slow evaporation of the filtered solution in air afforded, after 2 weeks, red needles of **1** in small amounts which were picked by hand, dried on filter paper and stored under vacuum owing to its hygroscopic character. The crystals so obtained were suitable for X-ray diffraction. Satisfactory elemental analyses were obtained (C, H, N, Fe). $\nu_{max}$/cm$^{-1}$ (KBr) 1660s (sh), 1635vs (br) and 1571s (CO) (opba ligand and $CO_3^{2-}$) and 950s (NC) from $NMe_4^+$. UV–VIS (MeCN) $\lambda_{max}$/nm [ε dm$^3$ mol$^{-1}$ cm$^{-1}$)] 221 ($4.0 \times 10^4$), 257 ($4.2 \times 10^4$), 264 (sh), 308 ($3.0 \times 10^4$), 408 ($2.7 \times 10^3$). Magnetic moment (room temp.): 5.9 $\mu_B$. EPR spectrum (X-band, powder sample, liquid-$N_2$ temperature): a strong feature at $g_{eff} = 4.3$ which typically arises in a completely rhombic system ($E/D = 1/3$) for $D > 0.23$ cm$^{-1}$.

‡ *X-Ray crystal structure analysis*: Enraf-Nonius CAD-4 diffractometer, Mo-Kα radiation, λ = 0.710 69 Å, graphite monochromator, 293 K. Lorentz and polarization effects but not absorption correction (μ = 9.26 cm$^{-1}$). Data collection, solution and refinement: ω-θ, standard Patterson methods with subsequent full-matrix least-squares method refinement. SHELX86, SHELX93.[12] $C_{23}H_{50}FeN_5O_{14}$, monoclinic, space group $P2_1/a$, $a$ = 11.441(2), $b$ = 17.496(2), $c$ = 17.047(2) Å, β = 104.52(2)°, $U$ = 3303(1) Å$^3$, $Z$ = 4, $D_c$ = 1.36 g cm$^{-3}$, $1 \leqslant \theta \leqslant 25°$, crystal size 0.15 × 0.10 × 0.05 mm. 4456 unique reflections with 3362 assumed as observed with $I \geqslant 2\sigma(I)$. The hydrogen atoms were located from a difference synthesis and refined with an overall isotropic thermal parameter. Refinement on $F^2$ of 390 variables with anisotropic thermal parameters for all non-hydrogen atoms gave $R$ = 0.079 and $R_w$ = 0.108 with $S$ = 1.8 (observed data). CCDC 182/628.

1 *Active Oxygen in Biochemistry*, ed. J. S. Valentine, C. S. Foote, A. Greenberg and J. F. Liebman, Chapman and Hall, London, 1995.
2 (*a*) A. L. Nivorozhkin and J. J. Girerd, *Angew. Chem., Int. Ed. Engl.*, 1996, **35**, 609 and references therein; (*b*) L. Que, Jr. and Y. Dong, *Acc. Chem. Res.*, 1996, **29**, 190.
3 H. Sigel and R. B. Martin, *Chem. Rev.*, 1982, **82**, 385.
4 (*a*) T. J. Collins, K. L. Kostka, E. Münck and E. Uffelman, *J. Am. Chem. Soc.*, 1990, **112**, 5637; (*b*) K. L. Kostka, B. G. Fox, M. P. Hendrich, T. J. Collins, C. E. F. Rickard, L. J. Wright, E. Münck, *J. Am. Chem. Soc.*, 1993, **115**, 6746.
5 Y. Yang, F. Diederich and J. S. Valentine, *J. Am. Chem. Soc.*, 1991, **113**, 7195.
6 X. Tao, D. W. Stephan and P. K. Mascharak, *Inorg. Chem.*, 1987, **26**, 754.
7 R. Ruiz, C. Surville-Barland, A. Aukauloo, E. Anxolabehere-Mallart, Y. Journaux, J. Cano and M. C. Muñoz, *J. Chem. Soc., Dalton Trans.*, 1997, 745.
8 M. Tettouhi, L. Ouahab, A. Boukhari, O. Cador, C. Mathoniere and O. Kahn, *Inorg. Chem.*, 1996, **35**, 4932.
9 T. J. Collins and J. M. Workman, *Angew. Chem., Int. Ed. Engl.*, 1989, **28**, 912.
10 J. Estrada, I. Fernandez, J. R. Pedro, X. Ottenwaelder, R. Ruiz and Y. Journaux, *Tetrahedron Lett.*, 1997, **38**, 2377.
11 W. Nam, H. J. Kim, S. H. Kim, R. Y. N. Ho and J. S. Valentine, *Inorg. Chem.*, 1996, **35**, 1045 and references therein.
12 G. M. Sheldrick, SHELX. A Program for Crystal Structure Determination, University of Göttingen, DFR, 1986; G. M. Sheldrick, SHELXL93. Program for the Refinement of Crystal Structures, University of Göttingen, 1993.

*Received in Basel, Switzerland, 7th August 1997; 7/05787C*

# Application of TRISPHAT anion as NMR chiral shift reagent

**Jérôme Lacour,* Catherine Ginglinger, France Favarger and Sonya Torche-Haldimann**

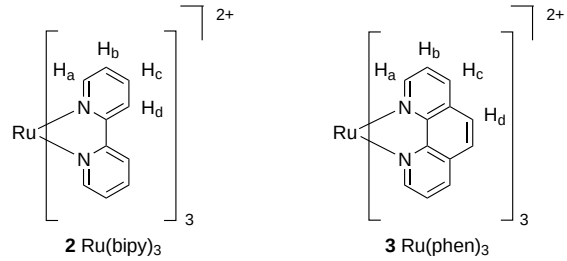
*Département de Chimie Organique, Université de Genève, quai Ernest Ansermet 30, CH-1211 Genève 4, Switzerland*

**TRISPHAT anion 1 is an efficient NMR chiral shift reagent for cationic tris(bisimine)ruthenium(II) complexes.**

Configurationally stable[1] tris(bisimine)ruthenium(II) complexes have been extensively studied in the fields of photochemistry, photophysics and as probes in DNA. Many applications require these compounds in an enantioenriched form and thus determination of their optical purity is a necessity.[2] Herein, we report the application of TRISPHAT anion **1** as a useful chiral NMR shift reagent[3] for two of these cationic complexes.

Recently, we have shown that chiral tris[tetrachlorobenzene-1,2-bis(olato)]phosphate anion **1** (or TRISPHAT) is configurationally stable in solution.[4] It was foreseen that **1** would be an interesting NMR chiral shift reagent† for chiral cationic compounds, and tris(bisimine) complexes of transition metals in particular. Addition of enantioenriched **1** to solutions of tris(bisimine)ruthenium(II) compounds would lead to the formation of diastereomeric ion pairs, which have, at least in principle, different chemical shifts. Furthermore, as cations and anion **1** possess the same $D_3$-symmetry, we thought that selective chiral discriminating interactions would likely occur, leading to a preferred association between the molecular propellers ($\Lambda^+ - \Lambda^-$ *vs.* $\Delta^+ - \Lambda^-$). As a result, enantiotopic protons, carbon atoms and other nuclei of the cationic complexes would be resolved. We decided to test this hypothesis with Ru(bipy)$_3$ **2** and Ru(phen)$_3$ **3** complexes using $Bu_3NH^+$–(*M*)-**1** salt [(+)-**1a**, 86% ee] as chiral shift reagent, which can be easily prepared as follows (Scheme 1). Addition of 0.5 equiv. of cinchonidine **4** to a solution of racemic tri-*n*-butylammonium salt [(±)-**1a**] in $CH_2Cl_2$ leads to the precipitation of a white solid **5** containing mainly cinchonidinium salts (72% de). Filtration and concentration of the mother liquor *in vacuo*, afford a white solid **6** containing the tri-*n*-butylammonium salt **1a** along with a minor amount of cinchonidinium salts. Recrystallisation of solid **6** in $CH_2Cl_2$–$CHCl_3$ affords, in the mother liquor, chemically and optically purified (+)-**1a** (86% ee).

Tris(bisimine)ruthenium(II) **2** and **3** were prepared as described by Broomhead and Young as dichloride salts (**2a**, **3a**).[5] Racemic Ru(phen)$_3$Cl$_2$ **3a** was resolved by recrystallization with (+)-antimonyl tartrate anion;[6] treatment of the tartrate or chloride salts with sodium perchlorate yielded the racemic or optically enriched [Ru(bipy)$_3$](ClO$_4$)$_2$·*x*H$_2$O (**2b**) and [Ru(phen)$_3$](ClO$_4$)$_2$·*x*H$_2$O (**3b**).‡




As foreseen, addition of 0.5–1.0 equiv. of (*M* or Λ)-TRISPHAT **1** to solutions of (±)-**2b** in $CD_2Cl_2$ (1–2 × $10^{-3}$ M), (±)-**3b** and (+)-**3b**[7] in 7–10% DMSO in $CD_2Cl_2$ (1–2 × $10^{-3}$ M)§ led to the resolution of the NMR spectra of the cations; we were able to distinguish between the two enantiomers and show that sample (+)-**3b** is optically pure. The resulting spectra at 400 MHz are shown in Figs. 1 and 2 and are compared to that of the same solutions in the absence of TRISPHAT. Upon addition of **1**, only the signals of one of the

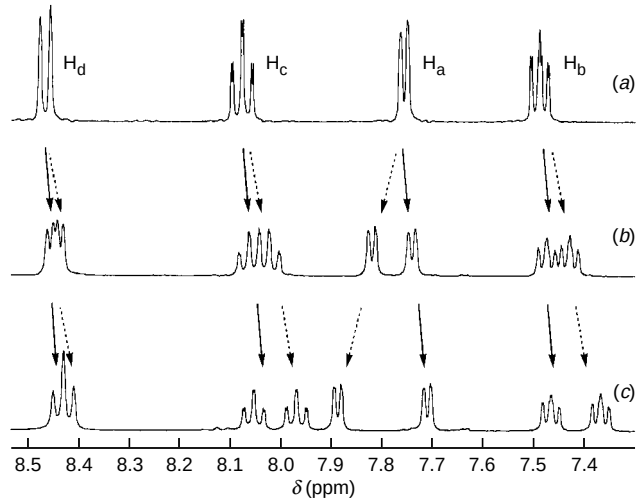
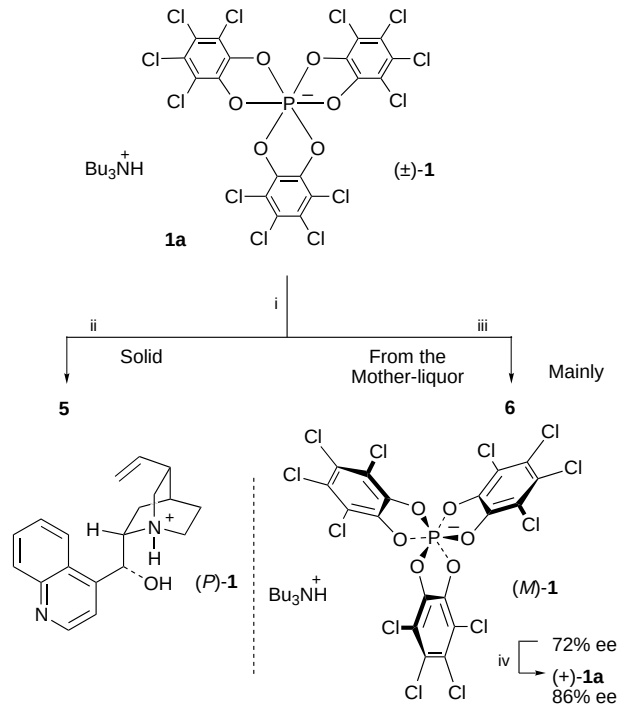



**Fig. 1** The $^1$H NMR spectra of racemic [Ru(bipy)$_3$(ClO$_4$)$_2$]·*x*H$_2$O **2** in the absence (*a*) and presence of (+)-**1a** [0.5 equiv. (*b*), 1.0 equiv. (*c*)]




**Scheme 1** *Reagents and conditions*: i, 0.5 equiv. of **4**, $CH_2Cl_2$, 20 °C, 6 h; ii, filtration, **5** (44%); iii, concentration of the mother liquor *in vacuo* (60 °C, $10^{-4}$ bar, 12 h), **6** (55%); iv, (+)-**1a** (86% ee) from the mother liquor after recrystallisation in $CH_2Cl_2$–$CHCl_3$

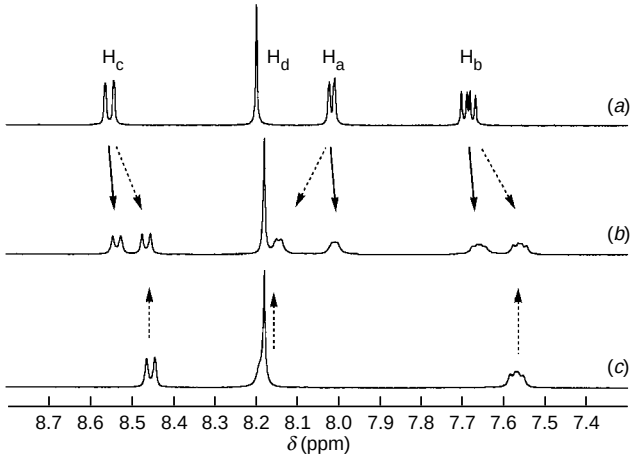



**Fig. 2** The $^1$H NMR spectra of $[Ru(phen)_3(ClO_4)_2]\cdot xH_2O$ **3** in the absence (*a*) and presence of 1.0 equiv. of (+)-**1a**: (±)-**3b** (*b*) and (+)-**3b** (*c*). Spectra (*a*), (*b*) and (*c*) were done in 10, 10 and 7% DMSO in $CD_2Cl_2$, respectively.

two enantiomers of **2** or **3** show strong shifts of its signals; observed chemical shifts ($\delta$), upfield or downfield shifts induced by the phosphate reagent ($\Delta\delta$), and the magnitude of the difference in chemical shifts of analogous protons of the two enantiomers of **2b** and **3b** upon addition of the shift reagent ($\Delta\Delta\delta$) are summarized in Tables 1 and 2 respectively.

As is shown in Tables 1 and 2, substantial differences between analogous $H_a$, $H_b$, $H_c$ protons of the enantiomers were found, while protons $H_d$ in **2**–**3b** remain essentially unchanged. Proton $H_a$, the closest from the $C_3$ axis, has the largest difference between the signals, and it is shifted downfield contrary to that of the others. We feel that the larger $\Delta\Delta\delta$ of $H_a$ and $H_b$ and smaller $\Delta\delta$ of $H_d$ are consistent with an ion-pairing model for anion induced shift, with cations and anions interacting most probably along their $C_3$ axes.

Finally, it is important to notice that the use of **1** as a NMR chiral shift reagent is not limited, in this case, by the presence of polar solvent such as DMSO or by non-coordinating ions.[2a,b]

In summary, by addition of chiral anion **1**, we have observed differences in the chemical shifts of enantiomers of cationic species. We have used this technique to confirm enantiomeric purity of a complex. We think that this technique will be quite general for chiral cationic species. The observation that only one enantiomer of the cation shows a strong shift upon addition of **1** is also important. Further studies are being conducted to determine if this effect is due to a preferred association of the two molecular propellers, the nature of the interaction and its effectiveness for chiral recognition processes.

**Table 1**

| Proton[a] | $\delta^b$ | | $\delta^c$ | | $\Delta\delta^c$ | $\Delta\Delta\delta^c$ |
|---|---|---|---|---|---|---|
| $H_a$ | 7.758 | 7.889 | 7.712 | 0.131 | −0.046 | 0.177 |
| $H_b$ | 7.490 | 7.370 | 7.467 | −0.120 | −0.023 | 0.097 |
| $H_c$ | 8.079 | 7.970 | 8.054 | −0.109 | −0.025 | 0.084 |
| $H_d$ | 8.467 | 8.420 | 8.440 | −0.047 | −0.027 | 0.020 |

[a] Chemical shifts for each enantiomer were assigned using a COESY experiment. [b] Without (+)-**1a**. [c] With 1.0 equiv. of (+)-**1a**.

**Table 2**

| | | $\delta^c$ | | $\Delta\delta^c$ | | |
|---|---|---|---|---|---|---|
| Proton[a] | $\delta^b$ | $\Lambda^d$ | $\Delta$ | $\Lambda^d$ | $\Delta$ | $\Delta\Delta\delta^c$ |
| $H_a$ | 8.015 | 8.144 | 8.009 | +0.129 | −0.006 | 0.135 |
| $H_b$ | 7.684 | 7.559 | 7.658 | −0.125 | −0.026 | 0.099 |
| $H_c$ | 8.554 | 8.464 | 8.536 | −0.090 | −0.018 | 0.072 |
| $H_d$ | 8.198 | 8.180 | 8.180 | −0.018 | −0.018 | 0.00 |

[a] Chemical shifts for each enantiomer of (±)-**3b** were assigned using a COESY experiment. [b] Without (+)-**1a**. [c] With 1.0 equiv. of (+)-**1a**. [d] Chemical shifts for $\Lambda$ enantiomer in (±)- and (+)-**3b**.

We are grateful for financial support of this work by the Swiss National Science Foundation. We thank Dr C. Piguet for a generous gift of **2a**, Mr A. Pinto, Mr J.-P. Saulnier, Mr W. Kloeti and Mrs E. Sandmeyer for NMR and mass spectroscopy measurements.

## Footnotes and References

* E-mail: Lacour@sc2a.unige.ch

† More particularly in $^1$H NMR spectra due to the lack of hydrogen atoms in **1**.

‡ The perchlorate salts were prepared to increase the solubility of the adducts in non-polar solvents.

§ Addition of DMSO (7–10%) is needed to insure the complete solubility of **3**. With 7% of DMSO in $CD_2Cl_2$, protons $H_a$(Δ-isomer) and $H_d$ are unfortunately isochronous.

1 F. P. Dwyer and E. C. Gyarfas, *J. Proc. R. Soc. NSW*, 1949, **83**, 174.
2 (*a*) J. K. Barton and J. S. Nowick, *J. Chem. Soc., Chem. Commun.*, 1984, 1650; (*b*) T. J. Rutherford, M. G. Quagliotto and F. R. Keene, *Inorg. Chem.*, 1995, **34**, 3857; (*c*) C. M. Shelton, K. E. Seaver, J. F. Wheeler and N. A. P. Kane-Maguire, *Inorg. Chem.*, 1997, **36**, 1532.
3 For a general article on NMR determination of enantiomeric purity, see D. Parker, *Chem. Rev.*, 1991, **91**, 1441.
4 J. Lacour, C. Ginglinger, C. Grivet and G. Bernardinelli, *Angew. Chem., Int. Ed. Engl.*, 1997, **36**, 608.
5 J. A. Broomhead and C. G. Young, *Inorg. Synth.*, 1990, **28**, 338.
6 F. P. Dwyer and E. C. Gyarfas, *J. Proc. R. Soc., NSW*, 1949, **83**, 170; R. D. Gillard and R. E. E. Hill, *J. Chem. Soc., Dalton Trans.*, 1974, 1217.
7 The absolute configuration of (+)-**3b** is (*M* or Λ): A. J. McCafferty, S. F. Mason and B. J. Norman, *J. Chem. Soc.* (*A*), 1969, 1428.

*Received in Cambridge, UK, 28th August 1997; 7/06916B*

# Synthesis and vesicle formation from novel pseudoglyceryl dimeric lipids. Evidence of formation of widely different membrane organizations with exceptional thermotropic properties

**Santanu Bhattacharya,*† Soma De and Shaji K. George**

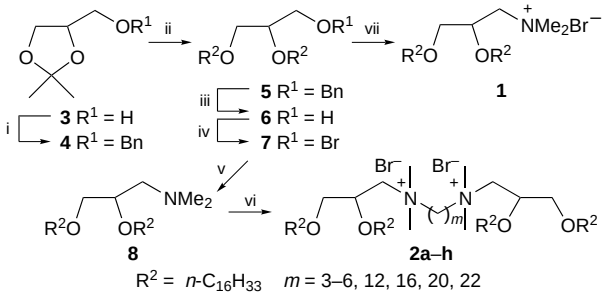
*Department of Organic Chemistry, Indian Institute of Science, Bangalore 560012, India*

**Eight new bis-cationic dimeric lipids 2a–h have been synthesized; TEM of their aqueous dispersions confirmed the vesicle formation and from the thermal, spectroscopic, DLS and XRD studies it has been revealed that they form three different kinds of membranous aggregate depending on the *m*-value.**

While the properties of vesicular membranes derived from a large number of 'monomeric' natural lipids[1] as well as their synthetic analogues[2] have been examined in great detail, there is no report in the literature that examines the properties of the membranes prepared from 'multimeric' lipids. This is despite the fact that several 'dimeric' and 'multimeric' lipid systems occur naturally and have important biological functions. Thus, cardiolipins (glycerol bridged dimeric phosphatidate lipids) constitute a class of complex phospholipids occurring mainly in the heart and skeletal muscles and show high metabolic activity.[3] Similarly, glycolipid A2 (composed of two phosphate headgroups and seven hydrophobic chains) serves as immunomodulator in mediating selective recognition of toxins, bacteria or viruses at the cell surfaces.[4]

Although dimeric (gemini) amphiphiles[5,6] that aggregate to form micelles are known, no analogous gemini form of lipids has been studied. Since cationic liposomes by themselves are receiving enormous current attention as effective non-viral gene transfection agents,[7] the resulting aggregates of dimeric lipids if cationic might be potentially useful. Along the lines of the above considerations, here we report the first synthesis of a family of bis-cationic, gemini lipids **2a**–**h** and their unusual membrane-forming properties on the basis of a combination of thermal, spectroscopic, dynamic light scattering (DLS), transmission electron microscopic (TEM) and reflection X-ray diffraction (XRD) methods supported by energy-minimization studies. To place the experimental data on these novel gemini membranes into appropriate perspective, we also include herein the related results from the vesicles of the corresponding 'monomeric' (control) lipid **1**.

Altogether eight new dimeric lipid systems **2a**–**h** were synthesized (Scheme 1). First the $CH_2OH$ group of the building block, 1,2-isopropylideneglycerol, **3** was protected in the form of a benzyl ether **4**. The isopropylidene group was then removed by treatment with HCl in aq. MeOH and the diol obtained upon preparative column chromatography over silica gel was alkylated with *n*-$C_{16}H_{33}Br$ (2.2 equiv.) to give **5** which upon hydrogenolysis afforded **6** in ~60% yield. Compound **6** was then converted to the corresponding bromide **7** by reaction with $PPh_3$–$CBr_4$; **7** was quaternized in the presence of $Me_3N$ in EtOH to give **1** in 80% yield. The bisquaternary systems **2a**–**h** were obtained from the corresponding dimethylamino derivative **8** upon refluxing with individual alkanediyl α,ω-dibromides in 60–75% yields.




**Scheme 1** *Reagents and conditions*: i, BnCl, KOH, $C_6H_6$, reflux, 87%; ii, aq. HCl–MeOH, reflux, 84%; *n*-$C_{16}H_{33}Br$, KOH, $C_6H_6$, reflux, 58%; iii, Pd–C/$H_2$, 60%; iv, $CBr_4$, $PPh_3$, $CH_2Cl_2$, 90%; v, $Me_2NH$–EtOH, heat, pressure tube, 95%; vi, $Br(CH_2)_mBr$, EtOH, reflux, 60–75% (exact yields depend on *m*); vii, $Me_3N$–EtOH, heat, pressure tube, 80%

Dispersion of lipids **1**, **2a**–**h** in water using probe or bath sonication afforded liposomes with a unimodal distribution of particle diameters as revealed by DLS (Table 1). Examination of DLS data on bath sonicated vesicles shows that vesicles from dimeric lipids were invariably larger. Within the vesicles among the dimeric lipid series, however, the hydrodynamic diameter variation as a function of *m*-value was very complex. The vesicular sizes were found to be the largest with lipids, **2**, of $m = 3$ and then decreased with increase in *m*-value up to $m = 12$ and then went up again with $m > 12$. Vesicle sizes were also found to strongly depend on the lipid concentration, thermal history and method of vesicle preparation. Thus while vortexing afforded mostly open lamellae and sonication gave small spherical, closed microstructures, reverse phase evaporation (REV) gave multilamellar vesicles (not shown).

**Table 1** The hydrodynamic diameters of vesicular aggregates, main phase-transition temperatures of vesicular **1**, **2a**–**h** and the unit-layer thicknesses of their corresponding self-supporting cast films

| Lipid (*m*-value) | DLS[a] size/nm | Main transition[b] (*T*/°C) | | Unit bilayer thickness/Å | |
|---|---|---|---|---|---|
| | | Microcal | Fluor. Pol. | Obs[c] | Calc.[d] |
| 0 | 15 | 45.2 | 45 | 45.9 | 49 |
| 3 | 93 | 57[e] | 57 | 45 | 49 |
| 4 | 52 | 48.3 | 48 | 45.9 | 49 |
| 5 | 29 | 44.2 | 43 | 45.9 | 49 |
| 6 | 29 | 43.9 | 43 | 44.2 | 49 |
| 12 | 30 | 46.5 | 45 | 31.3 | 49, 16.8,[f] 31[g] |
| 16 | 37 | 40.8 | 41 | 29.6 | 49, 21.9,[f] 31[g] |
| 20 | ND | 69.1 | 62 | 29.8 | 49, 27[f] |
| 22 | 52 | 66.3 | 53 | 30.8 | 49, 29[f] |

[a] Dynamic light scattering was examined with the vesicles prepared under identical conditions. All the vesicles ($1 \times 10^{-3}$ M) were prepared by bath sonication (Julabo USR3) for 10 min, at 70 °C and at 35 KHz. [b] Average deviation is ±0.5 °C for microcalorimetry; ±1.0 °C for fluorescence polarization method. [c] As obtained from reflection X-ray diffraction of cast films. [d] Lengths of two molecular layers of lipids as obtained from models. [e] Additional minor peaks at 66.1 and 71.6 °C were also observed. [f] Lengths of unit 'mono'layer-bilayer plans of lipids as obtained from models [g] Lengths of unit interdigitated and tilted bilayer plans of lipids as obtained from models.

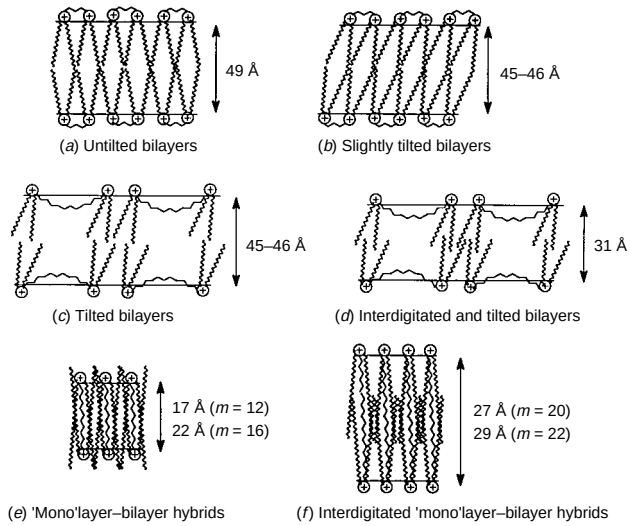



**Fig. 1** Schematic representation of possible bilayer forming motifs with gemini lipids as a function of *m*-value

The sonicated dispersions of different lipids (7 mM) were then converted to regular self-supporting films by casting on glass slides as described.[8] Reflection X-ray diffraction (Scintag XDS-2000) of these cast films gave the long spacings from individual lipid films as given in Table 1. Comparison of the corresponding molecular lengths of the gemini lipid units as determined from CPK models suggests the formation of slightly tilted bilayer arrangement [Fig. 1(*b*)] with **1** and with gemini lipids of *m*-values 3, 4, 5 and 6. But with **2e**, $m = 12$, the experimentally determined XRD data on the unit layer thicknesses cannot be explained by tilting alone suggesting the presence of additional interdigitations [Fig. 1(*d*)]. The alternative plan (*e*) is energetically unfavorable with the lipophilic chains protruding into the polar headgroup regions. To explain the reflection XRD data of **2g** and **2h**, we suggest a kind of monolayer–bilayer hybrid organization as shown in Fig. 1(*f*).

Independent examination of the thermotropic properties of the vesicles of **1** and **2a**–**h** by DSC, microcalorimetry and fluorescence methods showed that the changes in *m*-value in **2** profoundly influence their gel-to-liquid crystalline phase-transition temperatures (Table 1). Vortexing of 60 mM of either of **1** and **2a**–**h** in water afforded lameller gels which gave well-resolved, nearly reversible peaks as melting transitions ($T_m$) (Perkin Elmer DSC 7). Microcalorimetry (MC-2) of 1.0–2.5 mM sonicated vesicular specimens of either of the lipids reproduced the peaks due to $T_m$. Relative to **1**, there is a substantial increase in the gel-to-liquid crystalline transition temperature of the membranes derived from dimeric **2a**. In addition, unlike the membranes that are assembled from **1**, which show a sharp endothermic main transition at 45 °C, those made from **2a** exhibit a more complex melting pattern. For lipids with $m \geqslant 16$, the melting transition profiles appeared remarkably broadened (less cooperative), while for lipids with $m \leqslant 12$, the main transitions were quite sharp. Thus although the cooperativities of melting transitions with **2** ($m$ = 20–22) were severely reduced, alternative membrane organizational features allow broad but higher melting temperatures (see below). The latter could be a consequence of perturbation within the headgroup and/or direct interaction of the spacer chain with the hydrocarbon chain regions.

The fluorescence polarizations (*P*) due to the vesicle doped 1,6-diphenylhexa-1,3,5,-triene at various temperatures were then determined. The temperatures related to the break in *P vs. T* plot for the vesicles with $m$ = 0–16 were similar to the $T_m$ values obtained by calorimetric methods (Table 1). But the lipids with $m$ = 20 and 22 gave broader *P vs. T* variation, the mid-points of which were lower than the $T_m$ values obtained using microcalorimetry. Notably again the microviscosities (*ca.* 3.5–4.0 poise) of the vesicular aggregates of lipids with $m$ = 20–22 in their gel states were considerably lower than that of the lipids with lower *m*-values (*ca.* 10–11 poise) again suggesting gross differences in their suprastructural organizations.

Molecular mechanics calculation of the energy-minimized conformations of the dimeric lipids using DISCOVER (INSIGHT II) suggested that the packing in **2a** and **2b**, where $Me_2N^+$ headgroups are separated by three and four $CH_2$ units respectively, is much tighter than that in lipids with higher *m*-values. This should lead to a progressive decrease in $T_m$ as *m*-value increases from 3 to 10. As the *m*-value in lipid, **2**, reaches $\geqslant$12, this situation changes when the $(CH_2)_{12}$ connector in **2e** 'loops' into the vesicle interior to avoid 'undesirable' contacts with the bulk water. At $m$ = 16, the spacer chain should adopt an even more folded, wicket-like conformation further impairing the bilayer packing.‡ The greater extent of spacer chain looping into the membrane interior should disturb 'intra'-gemini lipid packing at $m$ = 16 even further [Fig. 1(*d*)]. This is consistent with the observation of lower $T_m$ value with vesicular **2f** than that with **2e**. As the *m*-value surpasses 16 in **2**, the suprastructural organizations in the membranes change again. This is because at $m \geqslant 20$, the length of spacer may now span as a 'monolayer' giving rise to 'mono'layer-bilayer hybrid type of suprastructures. Thus, strikingly, when *m*-value reaches $\geqslant$20, spacer chains probably hyperextend to produce (absolutely unrelated to the ones with lower *m*-values) 'monolayer' type organizations reminiscent of the assemblies seen in the bolaamphiphilic membranes [Fig. 1(*f*)].[9]

Since the freedom of motion of four independent hydrocarbon chains is critical to their properties at the membrane level, the present study clearly demonstrates that the interconnection of the 'monomeric' lipid by a polymethylene segment into a 'dimeric' lipid brings about ramifications far exceeding the seemingly trivial structural modification at the lipid level. These findings further emphasize the need for newer designs of synthetic lipid structures to expand the understanding of their behaviour upon membrane formation.

## Footnotes and References

* E-mail: sb@orgchem.iisc.ernet.in
† Also at the Chemical Biology Unit, Jawaharlal Nehru Centre for Advanced Scientific Research, Bangalore 560064, India.
‡ This is consistent with the observations of E. Alami, G. Beinert, P. Marie and R. Zana, *Langmuir*, 1993, **9**, 1465.

1 J. L. Slater and C.-H. Huang, in *The Structure of Biological Membranes*, ed. P. Yeagle, CRC Press, Baca Raton, FL, 1992, esp. pp. 175–210.
2 T. Kunitake, *Angew. Chem., Int. Ed. Engl.*, 1992, **31**, 709; H. Ringsdorf, B. Schlarb and J. Venzmer, *ibid.*, 1988, **27**, 113.
3 W. Hübner, H. H. Mantsch and M. Kates, *Biochim. Biophys. Acta*, 1991, **1066**, 166; S. M. Grunner and M. K. Jain, *ibid.*, 1985, **818**, 352.
4 O. Lockhoff, *Angew. Chem., Int. Ed. Engl.*, 1991, **30**, 1611.
5 F. M. Menger and C. A. Littau, *J. Am. Chem. Soc.*, 1991, **113**, 1451.
6 S. De, V. K. Aswal, P. S. Goyal and S. Bhattacharya, *J. Phys. Chem.*, 1996, **100**, 11 664; S. Bhattacharya and S. De, *J. Chem. Soc., Chem. Commun.*, 1995, 651.
7 S. Bhattacharya and S. S. Mandal, *Biochim. Biophys. Acta*, 1997, **1323**, 29; S. Bhattacharya and S. Haldar, *ibid.*, 1996, **1283**, 21; *Langmuir*, 1995, **11**, 4748; Y. Xu and F. C. Szoka, *Biochemistry*, 1996, **35**, 5616; M. S. Spector and J. M. Schnur, *Science*, 1997, **275**, 791; J. O. Rädler, I. Koltover, T. Salditt and C. R. Safinya, *ibid.*, 1997, **275**, 810.
8 S. Bhattacharya and S. De, *Chem. Commun.*, 1996, 1283; N. Kimizaka, T. Kawasaki and T. Kunitake, *J. Am. Chem. Soc.*, 1993, **115**, 4387.
9 J.-H. Fuhrhop and R. Bach, in *Advances in Supramolecular Chemistry*, ed. G. W. Gokel, JAI, Greenwich, CT, 1992, vol. 2, pp. 25–63.

*Received in Cambridge, UK, 16th June 1997; 7/04154C*

# First evidence of the formation of 5,8-endoperoxide from the oxidation of 1,4-disubstituted naphthalene by singlet oxygen

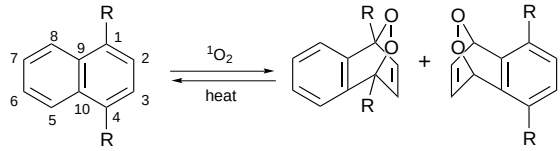
**Christel Pierlot and Jean-Marie Aubry***

*Equipe de Recherches sur les Radicaux Libres et l'Oxygène Singulet (URA CNRS 351) Faculté de Pharmacie, 3 rue du Professeur Laguesse BP 83 F59 006 Lille, France*

**Bulky water-soluble 1,4-disubstituted naphthalenes react with singlet oxygen giving the usual 1,4- and the unexpected 5,8-endoperoxides and showing that the regioselectivity of the [4 + 2] cycloaddition of singlet oxygen depends on the steric hindrance of the substrate.**

In contrast to anthracene and higher members of the acene series,[1] naphthalene does not react with singlet oxygen ($^1O_2$) to form the 1,4-endoperoxide.[2] However, the naphthalene 1,4-endoperoxide **2a** has been obtained indirectly in three steps from 1,6-imino[10]annulene.[3] When electron-donating substituents are introduced on the 1,4 positions of the naphthalene core, $^1O_2$ readily reacts leading regiospecifically to 1,4-endoperoxides.[4–6] 5,8-Endoperoxides have been solely observed when at least one additional methyl group was placed on the 6,7[7] or 8 positions[8,9] of the naphthalene core. In the course of our work on water-soluble carriers of $^1O_2$,[6,10] we have discovered that the photooxidation of the bulky non-ionic water-soluble 1,4-disubstituted naphthalene, *N*,*N*′,*N*″,*N*‴-tetrakis(2,3-dihydroxypropyl)2,2′-(naphthalene-1,4-diyldimethyl)bis(malonamide) **1b** (Scheme 1) leads to the simultaneous formation of the 1,4- and 5,8-endoperoxides (**2b** and **3b**). This example clearly shows that in addition to electronic effects, the steric hindrance of the substituents can modify the regioselectivity of the [4 + 2] cycloaddition of singlet oxygen on polycyclic aromatic hydrocarbons.

NMR and HPLC analysis of **1b**†‡ after dye-sensitized photooxygenation§ at −5 °C in $D_2O$–$CD_3OD$ (77 : 13) showed a 50% conversion in 2 h, and indicated that, beside the usual 1,4-endoperoxide **2b**, the unexpected 5,8-endoperoxide **3b** was also formed, with a time-independent ratio equal to 78 : 22 (Table 1). All spectra showed that the malonamide side chains remained unchanged during oxidation and the symmetry of each spectrum suggested that no other products of oxidation with lower symmetry, such as hydroperoxides, were formed.




**a** R = H
**b** R = $CH_2CH[CONHCH_2CH(OH)CH_2(OH)]_2$
**c** R = $CH_2CH_2CO_2Na$
**d** R = $CH_2CH(CO_2Na)_2$

**Scheme 1**

**Table 1** Product distribution after photooxidation of **1b**

| Solvent | *T*/°C | *t*/h | Conversion (%) | Regioselectivity **2b** : **3b** |
|---|---|---|---|---|
| $D_2O$–$CD_3OD$ (77 : 13) | −5 | 2 | 50 | 78 : 22 |
| $H_2O$–MeOH (77 : 13) | −5 | 2 | 3 | 100 : (< 1) |
| $D_2O$ | 25 | 1 | 26 | 69 : 31 |
| | 50 | 1 | 40 | (< 1) : 100 |
| $CD_3OD$ | 25 | 2 | 20 | 80 : 20 |

$^1$H and $^{13}$C NMR chemical shift assignments for **2b**¶ were in agreement with the spectral data of other 1,4-naphthalene endoperoxides such as **2c**.[10] The structure of the endoperoxide **3b**‖ was confirmed by comparison with **2b.** Thus, **3b** has four quaternary carbons in the aromatic region, in positions 1, 4, 9 and 10 (d, $J$ = 139.2 and 133.5 Hz) whereas **2b** has only two carbons of this type, C$^9$ and C$^{10}$ (d, $J$ = 142.2 Hz). Another telling difference was observed for the carbons supporting the peroxide bridge, which were the tertiary carbons C$^5$ and C$^8$ (d, $J$ = 75.7 Hz) for **3b** compared to the quaternary carbons C$^1$ and C$^4$ (d, $J$ = 83.4 Hz) for **2b**.

When the oxidation of **1b** was run over 2 h in $H_2O$–MeOH (77 : 13) instead of deuterated solvents, **2b** was formed with a 13 times lower yield (3% compared to 39%), and the concentration of **3b** became too small to be measurable. This lower yield was expected since the lifetime of $^1O_2$ is 15 times shorter in $H_2O$ than in $D_2O$. Chemical oxidation of **1b** by a chemical source of $^1O_2$ ($H_2O_2$–$MoO_4^{2-}$),[10] also led to the formation of **2b** and **3b**, confirming the involvement of singlet oxygen in the formation of both endoperoxides (Table 1).

Warming of the solutions of pure **2b** and **3b** obtained by semi-preparative HPLC indicated that both endoperoxides decompose giving the starting naphthalene **1b** and oxygen (Scheme 1) according to first order kinetics (Table 2). Comparison of the half-lives of decomposition ($t_{1/2}$) clearly showed the greater stability of **3b** since no significant decomposition occurred at 5 °C, and it was found to be ten times more stable than **2b** at 25 and 37 °C. On the contrary, **2b** was particularly thermolabile since its half-life at 37 °C ($t_{1/2}$ = 7 min) is three times shorter than that of other 1,4-endoperoxides such as **2c**. This phenomenon seems to be general, in fact we observed similar half-lives for other bulky 1,4-disubstituted endoperoxides such as **2d** ($t_{1/2}$ = 5 min at 37 °C). The poor stability of these 1,4-endoperoxides could result from the steric hindrance induced by the bulky substituents R in the 'butterfly' structure **2**, which would favour dissociation into the starting naphthalene derivative and oxygen.

$$\mathbf{1} + {}^1O_2 \xrightarrow{k_{r2}} \mathbf{2} \quad (1)$$

$$\mathbf{1} + {}^1O_2 \xrightarrow{k_{r3}} \mathbf{3} \quad (2)$$

**Table 2** Half-lives ($t_{1/2}$) of dissociation at 5, 25 and 37 °C for endoperoxides **2b**, **3b**, **2c** and **2d**, and rate constant ($k_r$) of their formation at −5 °C

| | $t_{1/2}$/min | | | $k_A/10^4$ M$^{-1}$ s$^{-1}$ |
|---|---|---|---|---|
| | 5 °C | 25 °C | 37 °C | ($D_2O$–$CD_3OD$ = 77 : 13) |
| **2b** | 540 | 30 | 7 | 3 |
| **3b** | stable | 300 | 70 | 1 |
| **2c** | stable | 113 | 23 | 142 |
| **2d** | 208 | 18 | 5 | 44 |

The rate constants, $k_{r2}$ [eqn. (1)] and $k_{r3}$ [eqn. (2)], for the chemical quenching of $^1O_2$ by **1b** were estimated by comparison with the well known $^1O_2$ acceptor **1c**[11] (Table 2). Thus, they were separately photooxidized in deuterated water at −5 °C under the same conditions. The kinetics of the disappearance of the starting materials indicated that **1b** ($k_{r2} + k_{r3} = 4 \times 10^4$ M$^{-1}$ s$^{-1}$) is about 13 times less reactive than **1c** ($k_r^{NDP} = 142 \times 10^4$ M$^{-1}$ s$^{-1}$). The constant regioselectivity observed at this temperature permits us to determine the contribution of each pathway: $k_{r2} = 3 \times 10^4$ M$^{-1}$ s$^{-1}$ and $k_{r3} = 1 \times 10^4$ M$^{-1}$ s$^{-1}$. The poor reactivity of **1b** towards $^1O_2$ could be explained by the electron-withdrawing effect of the amide function, which decreases the electronic density on the 1,4-positions of the naphthalene core, compared to the slight electron-donating effect of the sodium carboxylate functions of **1c**. However, since these groups are separated from the binding site by an ethylene linkage, it appears more likely that the difference of reactivity is mainly a consequence of the steric hindrance due to the side chains.[6]

To strengthen this hypothesis, we oxidized the tetra-(sodium carboxylate) **1d** which is more bulky than **1c**, but which exhibits a greater electronic density on the naphthalene ring due to the presence of four sodium carboxylate functions instead of two. Actually, the reactivity of **1d** towards $^1O_2$ is three times lower than that of **1c**. This result confirms the predominating contribution of steric hindrance over the electron-donating effects of the side chains of **1b** and **1d**.

It is noteworthy that the formation of the 5,8-endoperoxide **3b** is straightforward only when the oxidation of **1b** is carried out in deuterated water. Thus, in deuterated methanol, only 4% is obtained after 150 min at 25 °C (compared to 33% in deuterated water). This result seems astonishing if we refer to the lifetime of $^1O_2$, which is 3.5 times longer in $CD_3OD$ ($\tau_\Delta$ = 230 μs) than in $D_2O$ ($\tau_\Delta$ = 65 μs). In fact, contrary to a generally accepted principle, it was reported recently that the rate constants of singlet oxygen [4 + 2] cycloadditions ($k_r$) are strongly solvent-dependent. In particular, it was shown that highly structured solvents such as formamide and water considerably increase the reactivity of conjugated dienes and polycyclic aromatic derivatives.[2,12] Thus, the finding that **1b** exhibits a 15-fold higher rate constant in $D_2O$ than in $CH_3OD$ is just a further example of this accelerating effect.

Finally, it appears that the formation of the unusual 5,8-endoperoxide by reaction of $^1O_2$ with 1,4-disubstituted naphthalene is possible only when a number of stringent requirements are met: (i) substituents must be a little electron-donating to increase the electronic density of the whole naphthalene core; (ii) they must be very bulky to make difficult the approach of $^1O_2$ to the crowded ring and to impair the formation of the resulting butterfly structure; (iii) the peroxidation must be carried out in $D_2O$ in order to benefit from the rate-accelerating effect of water on the [4 + 2] cycloaddition of $^1O_2$ and from the enhancement of $^1O_2$ lifetime in deuterated solvents; (iv) a gentle warming of the reaction medium increases the ratio of 5,8- to 1,4-endoperoxides with oxidation time because of the greater thermolability of the 1,4-endoperoxide, which dissociates as it is forms whereas the 5,8-endoperoxide remains unchanged.

The authors are grateful to Dr A. Defoin for helpful discussions.

## Footnotes and References

* E-mail: jmaubry@phare.univ-lille2.fr

† High performance liquid chromatographic analyses (HPLC) were carried out with Waters pumps Model 600 with a reversed-phase column (Nova Pack RP 18, 25 cm) using 15 to 50% MeOH over 20 min at 0.7 ml/min and UV detection at 200 nm.

‡ *Synthesis* of **1b**: A solution of tetraethyl 2,2′-(naphthalene-1,4-diyldimethyl)bis(malonate) (ref. 11) (2 g, 4.2 mmol) and 3-aminopropane-1,2-diol (5.6 g, 73.3 mmol) in MeOH (30 ml) was stirred overnight under reflux. After evaporation of the solvent, acetone was added to the residue and the resulting suspension was filtered. The white precipitate was recristallised from MeOH (50%); mp = 195 °C; $\delta_H$ (300 MHz, $D_2O$) 8.10 (dd, $J_{5,6} = J_{5,7} = 3.15$, 2 H, H$^5$), 7.64 (dd, $J_{5,6} = J_{5,8} = 3.15$, 2 H, H$^6$), 7.26 (s, 2 H, H$^2$); $\delta_C$ (300 MHz, $D_2O$) 174.3 (s, CO), 136.0 and 134.4 (s, C$^1$, C$^9$), 129.9, 129.3 and 127.1 (s, C$^2$, C$^5$, C$^6$), 72.5 [d, CH(OH)], 65.9 [d, $CH_2$(OH)], 57.2 [$CH(C)_3$], 44.4 (d, $CH_2N$), 35.3 (s, Ar-$CH_2$); *m/z* 675 ($MNa^+$), 663 ($MH^+$).

§ *Photooxidation of* **1b** *into* **2b** *and* **3b**. A solution of **1b** (30 mg) and Methylene Blue ($1.6 \times 10^{-5}$ M in 1 ml of deuterated water was irradiated with a sodium lamp (150 W) under continuous bubbling of oxygen at constant temperature. During the reaction, some Methylene Blue was periodically added to compensate for its fading. HPLC analysis showed the ratio of each product.

‖ *Selected data* for $\delta_H$ (300 MHz, $D_2O$) 7.38 (m, 4 H, H$^5$, H$^6$), 6.87 (s, 2 H, H$^2$); $\delta_C$ (300 MHz, $D_2O$) 174.2 (CO), 142.2 (C$^9$), 140.5 (C$^2$), 130.3 (C$^6$), 123.6 (C$^5$), 83.4 (C$^1$), 72.5 [CH(OH)], 65.6 [$CH_2$(OH)], 51.1 [$CH(C)_3$], 44.3 ($CH_2N$), 31.9 ($CH_2C^1$).

** *Selected data* for **3b**: $\delta_H$ (300 MHz, $D_2O$) 7.15 (s, 2 H, H$^2$), 7.06 (dd, $J_{5,6} = J_{6,8} = 3.15$, 2 H, H$^6$), 6.10 (dd, $J_{4,5} = J_{5,7} = 3.15$, 2 H, H$^5$); $\delta_C$ (300 MHz, $D_2O$) 173.6 (CO), 139.2 (C$^9$), 138.1 (C$^6$), 133.5 (C$^1$), 131.5 (C$^2$), 75.7 (C$^5$), 72.5 [CH(OH)], 65.6 [$CH_2$(OH)], 58.0 [$CH(C)_3$], 44.3 ($CH_2N$), 33.2 ($CH_2C^1$).

1 J. Rigaudy, *Pure Appl. Chem.*, 1968, **16,** 169.
2 J. M. Aubry, B. Cazin, M. Rougee and R. V. Bensasson, *J. Am. Chem. Soc.*, 1995, **117**, 9159.
3 M. Schäffer-Ridder, U. Brocker and E. Vogel, *Angew. Chem., Int. Ed. Engl.*, 1976, **15**, 228.
4 H. H. Wassermann and D. L. Larsen, *J. Chem. Soc., Chem. Commum.*, 1972, 253.
5 H. H. Hart and A. Oku, *J. Chem. Soc., Chem. Commun.*, 1972, 254.
6 C. Pierlot, S. Hajjam, C. Barthélémy and J. M. Aubry, *J. Photochem. Photobiol. B.*, 1996, **36**, 31.
7 C. J. M. Van den Heuvel, H. Steinberg and T. J. de Boer, *Recl. Trav. Chim. Pays-Bas*, 1980, **99**, 109.
8 W. Adam, E. M. Peters, K. Peters, M. Prein and H. G. Von Schnering, *J. Am. Chem. Soc.*, 1995, **117**, 6686.
9 W. Adam and M. Prein, *Acc. Chem. Res.*, 1996, **9**, 1625.
10 J. M. Aubry, B. Cazin and F. Duprat, *J. Org. Chem.*, 1989, **54**, 726.
11 C. S. Marvel and B. D. Wilson, *J. Org. Chem.*, 1958, **23**, 1483.
12 B. Cazin, J. M. Aubry and J. M. Rigaudy, *J. Chem. Soc., Chem. Comm.*, 1986, 952.

*Received in Liverpool, UK, 4th August 1997; 7/05716D*

# Versatile intermediate for complete α/β stereocontrol in *O*-glycosidation reactions

**Giuseppe Capozzi,*† Francesca Mannocci, Stefano Menichetti, Cristina Nativi* and Serena Paoletti**

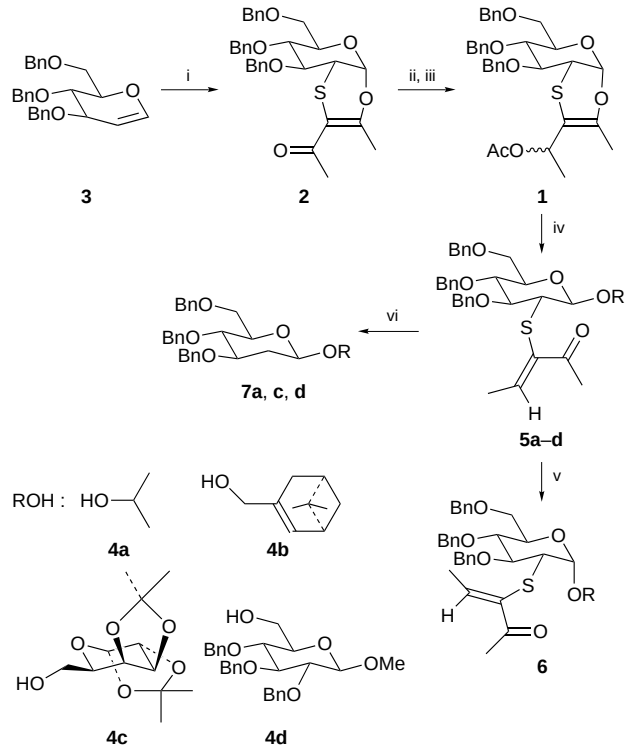
*Centro CNR 'Chimica e Struttura dei Composti Eterociclici', Dipartimento di Chimica Organica, Universita' di Firenze, via G. Capponi, 9 I-50121 Firenze, Italy*

**β-*O*-Glucosides 5, which can be completely converted to the α-anomers in the reaction medium, are obtained as single isomers by glycosidation of readily available donor 1 and are easily transformed into 2-deoxy-β-*O*-glucosides.**

Stereocontrol in *O*-glycosidation is a central matter in carbohydrate chemistry. A wide number of biologically important molecules originate from an aglycone and a saccharide by formation of a glycosidic linkage, moreover entire classes of polysaccharides are generated in nature by glycosidation of simpler carbohydrates.[1] A great effort has been devoted to optimise the glycosidation reaction as an indispensable transformation in organic chemistry. The crucial aspect has always been the achievement of a good level of stereocontrol on the formation of the glycosidic linkage, which usually leads to mixtures of α and β anomers. Efforts in this area have met with varying degrees of success.[2] While methods affording the α anomer with good selectivity are available, preparation of the pure β anomer is still a rare achievement. The problem is more serious for 2-deoxyglycosides, a class of derivatives of biological relevance, where the lack of assistance from proximal substituents and the low stability of precursors make the preparation of pure anomers, particularly the β anomer, a real challenge.[3] Our approach to the stereoselective synthesis of 2-deoxyglycosides was based on the exploitation of intermediates like **1**. We report here a synthetic protocol for *O*-glycosidation of tri-*O*-benzylglucal derivative **1** with complete stereocontrol of the glycosidic linkage, affording in a single reaction either α- or β-2-deoxyglucosides by simply controlling the experimental conditions. To the best of our knowledge, among the very few methods available, there is only one report of a selective preparation of β-2-deoxyglucosides that follows a similar approach.[4] The substantial improvement of the present protocol is the preparation of the β anomer as a pure isomer by using the readily available acetate **1** and the complete transformation of the β into the α anomer in the same reaction medium. The procedure is outlined in Scheme 1.

The oxathiine **1** is obtained from **2** which in turn is prepared in high yield as a single regioisomer by cycloaddition of tri-*O*-benzylglucal **3** with 2,4-dioxopentane-3-thione in a 95 : 5 α : β diastereomeric ratio.[5,6] Subsequent reduction of the carbonyl group to the alcohol and acetylation with acetic anhydride under standard conditions gave quantitatively the acetate **1**, which is further reacted without purification after removal under vacuum of pyridine and excess acetic anhydride. The glycosidic donor **1** is reacted in dry nitromethane at room temperature with the appropriate acceptor **4a**–**d** in the presence of a catalytic amount of methyl trifluoromethanesulfonate and quenching the reaction with pyridine.‡ Timing of quench is crucial for the success of β glycosidation. Quenching the reaction at the turning of the colour of the mixture from pale yellow to red affords the β glycosides **5** exclusively (reaction times and yields are given in Table 1). The stereochemistry of products is readily assigned by the chemical shift ($\delta$ 4.3–4.4) and coupling constants ($J_{1,2}$ 7.6–8.4 Hz) of the anomeric proton in the $^1$H NMR spectra.§ Chemically pure β-glycosides are obtained by flash column chromatography.

β-Glycosides **5** can be completely transformed into the α-anomers **6** by letting the product isomerise under the same reaction conditions; the isomerisation is presumably induced by acid catalysis. The aforementioned turning colour visually indicates the beginning of the isomerisation reaction, the time at which this occurs depends on the individual glycoside (from 0.5 h for **6a** to 1.5 h for **6d**¶). Thus, a single glycosidation reaction

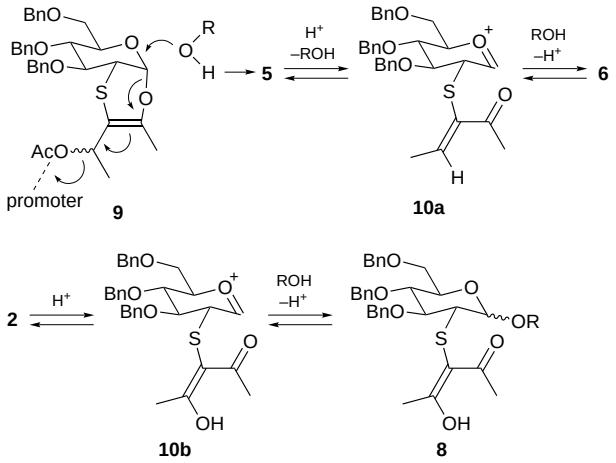



**Scheme 1** *Reagents and conditions*: i, see ref. 5; ii, $LiAlH_4$ (0.5 equiv.), THF, 0 °C to room temp., 30 min, 92%; iii, $Ac_2O$, pyridine, room temp., 96%; iv, ROH (2 equiv.), MeOTf (0.2 equiv.), $MeNO_2$, room temp., v, MeOTf (0.2 equiv.), $MeNO_2$, room temp., 1 h, quantitative yield; vi, Raney-Ni, wet THF, 0 °C to room temp.

**Table 1** Reaction times and yields of **5** and **7**

| Entry | Compound | *t*/min | Yield[a] (%) |
|---|---|---|---|
| 1 | **5a** | 5 | 82 |
| 2 | **5b** | 5 | 61 |
| 3 | **5c** | 35 | 40 |
| 4 | **5d** | 50 | 58 |
| 5 | **7a** | 45 | 72 |
| 6 | **7c** | 30 | 65 |
| 7 | **7d** | 30 | 68 |

[a] Isolated yield.




**Scheme 2**

provides both anomers in pure form by careful control of the reaction time. Glycosidation of the parent ketone **2** under acid catalysis is more sluggish than that of the acetate **1**, invariably providing mixtures of the α and β anomers **8** (Scheme 2). Since β-glycosidation of **1** is totally stereoselective we take this evidence as an indication of a different reaction pathway followed by **1** and **2**. In the former case, owing to the higher reactivity of the acetate, the developing positive charge induced on **1** by the catalyst might be trapped by the acceptor *before* ring-opening of the oxathiine, as shown in **9**, allowing for a β-stereospecific glycosidic linkage formation. Subsequent α–β equilibration might proceed through an oxonium intermediate **10a** analogous to that leading to product mixture in the glycosidation of the ketone **10b**.

Deprotection of the thiosubstituted glycosides **5a,c,d,** to the corresponding 2-deoxyglycosides **7a,c,d**‖ is readily achieved by desulfurisation with Raney-nickel[4,7] (Scheme 1). Reaction times and yield are reported in Table 1.

In conclusion these preliminary results clearly indicate that the aceate **1** is a readily available and effective new donor for the synthesis of 2-deoxy-β-*O*-glycosides and that the described procedure might represent a competitive protocol for an efficient α–β stereocontrol in the glycosidation reaction.

## Footnotes and References

† E-mail: capozzi@chimorg.unifi.it

‡ Running the reaction in the presence of molecular sieves causes an appreciable increase of reaction time (Table 1, entry 3: from 35 min to 2 h) without a significant increase in yield (entry 3: from 40 to 43%).

§ *Selected data* for **5d**: white solid, mp 98–100 °C; $[\alpha]_D$ −7 (*c* 0.3, $CHCl_3$); $\delta_H$(200 MHz, $CDCl_3$, *J*/Hz) 2.05 (d, 3 H, *J* 6.6), 2.27 (s, 3 H), 2.37 (s, 3 H), 3.30–3.75 (m, 14 H), 3.94–3.99 (m, 1 H), 4.33 (d, 1 H, *J* 7.6), 4.47 (d, 1 H, *J* 8.2), 4.45–4.97 (m, 12 H), 6.81 (q, 1 H, *J* 7.0), 7.10–7.41 (m, 30 H); $\delta_C$(50 MHz, $CDCl_3$) 16.7, 26.9, 52.1, 57.2, 68.2, 68.7, 73.5, 74.6, 74.7, 74.9, 75.6, 74.8, 75.1, 78.2, 78.6, 82.1, 83.3, 84.6, 104.3, 104.4, 127.5, 127.6, 127.8, 127.9, 128.0, 128.1, 128.2, 128.3, 128.4, 138.0, 138.1, 138.3, 138.5, 138.6, 138.9, 141.4, 196.7; $\nu_{max}$(neat)/cm$^{-1}$ 3032, 2874, 1676, 1602, 1452, 1068 (Calc. for $C_{60}H_{66}O_{11}S$: C, 72.40; H, 6.69; Found: C, 72.28; H, 6.88%).

¶ *Selected data* for **6d**: $\delta_H$(200 MHz, $CDCl_3$, *J*/Hz) 5.50 (d, 1 H, *J* 3.2), 7.14 (q, 1 H, *J* 7.0).

‖ *Selected data* for **7d**: white solid, mp 96–98 °C; $[\alpha]_D$ −60.2 (*c* 0.8, $CHCl_3$); $\delta_H$(200 MHz, $CDCl_3$, *J*/Hz) 1.64–1.75 (m, 1 H, H-$2_{ax}$), 2.22–2.30 (m, 1 H, H-$2_{eq}$), 3.37–3.73 (m, 13 H), 4.15–4.20 (m, 1 H), 4.30 (d, 1 H, *J* 7.8), 4.39 (m, 1 H), 4.37–4.97 (m, 12 H), 7.20–7.34 (m, 30 H); $\delta_C$(50 MHz, $CDCl_3$) 36.5, 57.0, 68.4, 69.2, 74.5, 74.7, 74.8, 74.9, 75.2, 75.6, 71.4, 73.4, 78.0, 78.1, 79.2, 82.2, 84.6, 100.4, 104.6, 127.5, 127.7, 127.8, 127.9, 128.0, 128.1, 128.3, 128.4, 138.1, 138.3, 138.4, 138.5 (Calc. for $C_{55}H_{60}O_{10}$. C, 74.96; H, 6.87. Found: C, 74.54; H, 6.92%).

1 *The Chemistry of Antitumor Antibiotics*, ed. W. A. Remers, Wiley, New York, 1978; *Lectins and Glycoconjugates in Oncology*, ed. H. J. Gabius and G. A. Nagel, Springer, New York, 1988.

2 R. R. Schmidt and W. Kinzy, *Carbohydr. Chem. Biochem.*, 1994, 21; S. J. Danishefsky and M. T. Bilodeau, *Angew. Chem., Int. Ed. Engl.*, 1996, **35**, 1380; J. R. Merritt, E. Naisang and B. Fraser-Reid, *J. Org. Chem.*, 1994, **59**, 4443; B. L. Lou, H. K. Huynh and S. Hanessian, in *Preparative Carbohydrate Chemistry*, ed. S. Hanessian, 1997, p. 413; A. Vasella, *Pure Appl. Chem.*, 1991, **63**, 507; S. David, A. Lubineau and J.-M. Vatele, *J. Chem. Soc., Chem. Commun.*, 1978, 535.

3 J. Thiem and W. Klaffke, *Top. Curr. Chem.*, 1990, **154**, 285; R. R. Schmidt, in *Comprehensive Organic Synthesis*, Pergamon, Oxford, 1991, **6**, 59; W. R. Roush and X.-F. Lin, *J. Am. Chem. Soc.*, 1995, **117**, 2236; G. Grewal, N. Kaila and R. W. Franck, *J. Org. Chem.*, 1992, **57**, 2084.

4 C. H. Marzabadi and R. W. Franck, *Chem. Commun.*, 1996, 2651.

5 G. Capozzi, A. Dios, R. W. Franck, A. Geer, C. Marzabadi, S. Menichetti, C. Nativi and M. Tamarez, *Angew. Chem., Int. Ed. Engl.*, 1996, **35**, 777.

6 G. Capozzi, R. W. Franck, M. Mattioli, S. Menichetti, C. Nativi and G. Valle, *J. Org. Chem.*, 1995, **60**, 6416.

7 G. Capozzi, C. Falciani, S. Menichetti, C. Nativi and R. W. Franck, *Tetrahedron Lett.*, 1995, 6755.

*Received in Liverpool, UK, 15th July 1997; 7/05338J*

# 1,4-Diselenine synthesis by Diels–Alder reaction of a novel exocyclic 1,2-diselone: X-ray crystal structure of (5,6-dimethoxycarbonyl-1,4-diselenine-2,3-dithiolate)Ni(dppe) [dppe = 1,2-$(Ph_2P)_2C_2H_4$]

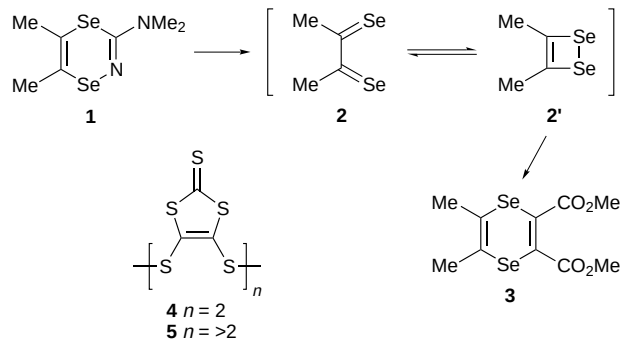
**Antony Chesney, Martin R. Bryce,* Andrei S. Batsanov and Judith A. K. Howard**

*Department of Chemistry, University of Durham, South Road, Durham, UK DH1 3LE*

**The salt $(NBu_4)_2[Zn(dsit)_2]$ 6 has been converted into the polymer $(C_3S_3Se_2)_n$ 7 which is a source of the reactive 1,2-diselone 8, trapping of which with dimethyl acetylenedicarboxylate affords the 1,4-diselenine derivative 9, which is subsequently transformed into the 1,4-diselenine-2,3-dithiolate species 11, characterised by the X-ray crystal structure of a nickel complex 12.**

The synthesis of unusual organoselenium heterocycles, especially *via* cycloaddition chemistry of reactive N=Se[1] and C=Se[2] bonds, has recently attracted considerable attention. For example, the low-yielding synthesis of 1,4-diselenine derivative **3** from the unstable 1,4,2-diselenazine **1** was presumed to occur *via* the transient 1,2-diselone intermediate **2**, or the 1,2-diselenete tautomer **2′** (Scheme 1).[2c] We now report an entirely different approach to an exocyclic 1,2-diselone intermediate and its efficient trapping reaction to yield the highly-functionalised bicyclic 1,4-diselenine system **9** which is subsequently transformed into the nickel complex **12**.

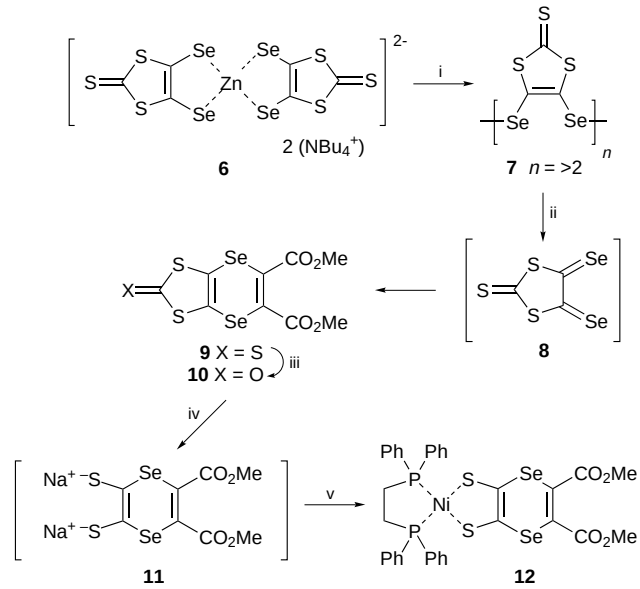
1,4-Dithiine synthesis by reactions of either the dimer **4**[3] or the polymer **5**[4] of the $C_3S_5$ unit[4b,5] has been reported. We chose to investigate the selenium-containing salt $(NBu_4)_2[Zn(dsit)_2]$ (dsit = 1,3-dithiole-2-thione-4,5-diselenolate) **6**[6] as a novel precursor for 1,2-diselones. Zinc salt **6** was easily prepared on a multi-gram scale, according to the literature procedure employing the more reactive red form of selenium.[6a] Oxidation of **6** with $I_2$ in EtOH–acetone at −50 °C afforded a highly insoluble, air-stable† compound $(C_3S_3Se_2)_n$, assumed to be polymer **7**, in excellent yield. Treatment of **7** with $PBu_3$ in $CH_2Cl_2$ at 20 °C in the presence of excess dimethyl acetylenedicarboxylate (DMAD) afforded the bicyclic 1,4-diselenine derivative **9** in 57% yield, presumably *via* the intermediacy of the highly-reactive 1,2-diselone **8** (or a $PBu_3$ complex of **8**) (Scheme 2). The use of $PBu_3$ to depolymerise **7** was more successful than the usual method employed for the sulfur analogue $(C_3S_5)_n$ **5**, which is heated in a solvent such as benzene, toluene, dioxane or chlorobenzene.[4] The use of these conditions with **7** led to poor yields of adduct **9**, which was contaminated with a variety of unidentified components. 1,2-Diselones are extremely rare species.[2c] Electron diffraction experiments[7] clearly revealed that a cyclic 1,2-diselenete structure (*cf*. structure **2′**) is favoured over the acyclic diselone structure $F_3CC(Se)–C(Se)–CCF_3$. However, this is less likely to be the situation for intermediate **8**, which is the first exocyclic 1,2-diselone: the diselenete tautomer of **8** would be a very strained bicyclic system.




**Scheme 1**

Conversion of the thione functionality in **9** into the oxo derivative **10** proceeded almost quantitatively on reaction with mercuric acetate in a mixture of $CHCl_3$ and AcOH. Opening of the 1,3-dithiole ring of **10** was achieved by reaction with MeONa in anhydrous MeOH: the disodium salt of 5,6-dimethoxycarbonyl-1,4-diselenine-2,3-dithiolate **11** thereby formed reacted *in situ* with $NiCl_2$(dppe) [dppe = 1,2-$(Ph_2P)_2C_2H_4$] to afford the dark green dithiolene complex (5,6-dimethoxycarbonyl-1,4-diselenine-2,3-dithiolate)Ni(dppe) **12**. Complexation of 1,4-dithiine-2,3-dithiolate units with nickel species has been previously reported both by Rauchfuss[3] and Bereman[8] but, to the best of our knowledge, this is the first time the 1,4-diselenine-2,3-dithiolate system has been prepared. X-Ray analysis of crystals of complex **12**, grown from MeCN, unambiguously proved the structure of the complex (Fig. 1).‡

In complex **12**, the nickel atom adopts a square planar coordination, distorted by a slight (6.5°) tetrahedral twist. The




**Scheme 2** *Reagents and conditions*: i, $I_2$ (2.1 equiv.), EtOH–acetone, −50 to 20 °C, 2 h; ii, $PBu_3$ (1 equiv.), DMAD (2 equiv.), $CH_2Cl_2$, 20 °C; iii, $Hg(OAc)_2$, $CHCl_3$–AcOH (3 : 1 v/v), 20 °C, 12 h; iv, NaOMe, MeOH, 30 min; v, $NiCl_2$ (dppe)

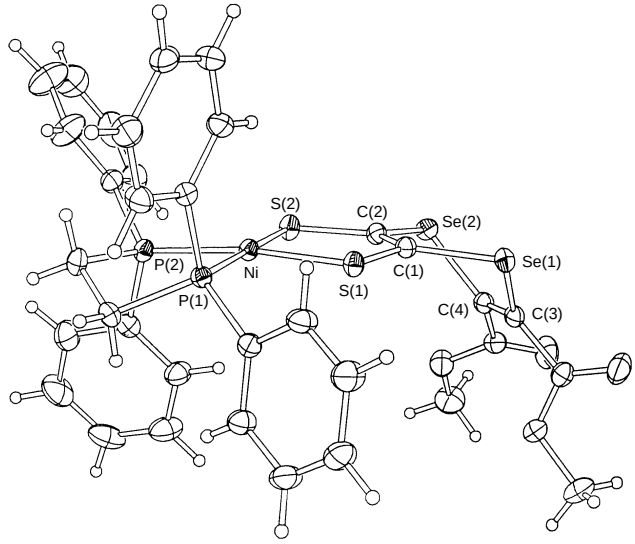



**Fig. 1** Molecular structure of **12**. Bond distances (Å): Ni–S(1) 2.168(1), Ni–S(2) 2.173(1), Ni–P(1) 2.175(1), Ni–P(2) 2.191(1), S(1)–C(1) 1.750(2), S(2)–C(2) 1.755(2), C(1)–Se(1) 1.917(2), C(2)–Se(2) 1.917(2), C(1)–C(2) 1.343(2), C(3)–Se(1) 1.918(2), C(4)–Se(2) 1.922(2), C(3)–C(4) 1.338(2).

Se(1)C(1)C(2)Se(2) moiety forms dihedral angles of 6.5° with the planar $NiS_2C_2$ ring and of 52.8° with the Se(1)C(3)C(4)Se(2) plane. The ester substituents at C(3) and C(4) are inclined to the latter plane by 48.5 and 55.3°, respectively.§ The folding of the diselenine ring in **12** is similar to that observed in [1,4]diselenino[2,3-*b*:5,6-*b′*]di[1]benzoselenole (54°) and 1,2,3,4,5,6,8,9,10,11,12,13-dodecahydrodicycloocta[1,4]diselenine[10] (49°), but larger than in nickel complexes with isoelectronic 2,3-dithiolato-1,4-dithiine ligands (28–43°).[3,11]

In summary, we have devised a short and expedient route to the 1,2-diselone **8** which has been converted to the 1,4-diselenine derivative **9** and hence the nickel complex **12**. This methodology affords a new and efficient approach to the synthesis of highly-functionalised derivatives of the rare 1,4-diselenine ring system. Further research into the Diels–Alder trapping of 1,2-diselone intermediate **8**, and the downstream organic and organometallic reactions of the products derived therefrom, will be reported in due course.

We are grateful to the EPSRC for funding this work and to the Leverhulme Trust for a scholarship (to A. S. B.) and the Royal Society for a Leverhulme Senior Research Fellowship (to J. A. K. H.).

## Footnotes and References

* E-mail: m.r.bryce@durham.ac.uk

† The analysis and reactivity of this material were unchanged by storage in a sealed container on the bench for at least three months.

‡ Satisfactory elemental analysis were obtained for **7**, **9**, **10** and **12**. *Selected data* for **9**: mp 215–217 °C; $\delta_H$ ($CDCl_3$) 3.86 (6 H, s); $\delta_C$ ($CDCl_3$) 53.72, 125.30, 136.15, 163.12 and 216.32; *m/z* (CI) 435 ($^{80}$Se, 25%), 58 (100); $\nu_{max}$ (KBr)/cm$^{-1}$ 1723, 1703, 1574, 1248 and 1049. For **12**: mp > 250 °C; $\delta_H$ ([$^2H_6$]DMSO) 3.56 (4 H, t, *J* 7.8), 3.66 (6 H, s), 7.55 (12 H, m) and 7.69 (8 H, m); $\nu_{max}$ (KBr)/cm$^{-1}$ 1721, 1566, 1434 and 1242.

§ *Crystal data* for **12**: $C_{34}H_{30}NiO_4P_2S_2Se_2{\cdot}C_2H_3N$, $M$ = 886.3, $T$ = 150 K, monoclinic, space group $C2/c$ (no. 15), $a$ = 41.722(2), $b$ = 9.199(1), $c$ = 19.599(1) Å, $\beta$ = 104.17(1)°, $V$ = 7293(1) Å$^3$, $Z$ = 8, $D_x$ = 1.61 g cm$^{-3}$, graphite-monochromated Mo-K$\alpha$ radiation, $\lambda$ = 0.71073 Å, $\mu$ = 27.7 cm$^{-1}$, crystal size 0.50 × 0.35 × 0.24 mm, 44429 reflections (10294 unique) with $\theta$ < 61.5° measured using a Siemens SMART CCD area detector; $R_{int}$ = 0.078 before, 0.047 after face-indexing (integration) absorption correction ($T_{min,max}$ = 0.310, 0.573), full-matrix least-squares refinement using SHELXTL software, on $F^2$ of all data to $wR$ = 0.067 (non-H atoms anisotropic, H isotropic; MeCN molecule disordered over two positions with occupancies of 78.3 and 21.7(5)%; total of 562 variables); for 9030 observed data with $I > 2\sigma(I)$, $R(F)$ = 0.026; residual $\Delta\rho_{min,max}$ = 0.51, −0.47 e Å$^{-3}$. CCDC 182/635.

1 M. R. Bryce and A. Chesney, *J. Chem. Soc., Chem. Commun.*, 1995, 195.
2 (*a*) H. Fischer, K. Treier, C. Troll and R. Stumpf, *J. Chem. Soc., Chem. Commun.*, 1995, 2461; (*b*) N. Takeda, N. Tokitoh and R. Okazaki, *Angew. Chem., Int. Ed. Engl.*, 1996, **35**, 660; (*c*) S. Yoshida, M. R. Bryce and A. Chesney, *Chem. Commun.*, 1996, 2375.
3 X. Yang, T. B. Rauchfuss and S. Wilson, *J. Chem. Soc., Chem. Commun.*, 1990, 34.
4 (*a*) O. Y. Neiland, Y. Y. Katsens and Y. N. Kreitsberga, *Z. Org. Chim.*, 1989, **25**, 592; (*b*) N. Svenstrup and J. Becher, *Synthesis*, 1995, 215.
5 G. Steimecke, H.-J. Sieler, R. Kirmse and E. Hoyer, *Phosphorus Sulfur*, 1979, **7**, 49.
6 (*a*) R. M. Olk, A. Röhr, B. Olk and E. Hoyer, *Z. Chem.*, 1988, **28**, 304; (*b*) H. Poleschner, R. Radeglia and J. Fuchs, *J. Organomet. Chem.*, 1992, **427**, 213; (*c*) J. Garín, J.Orduna, M. Savirón, M. R. Bryce, A. J. Moore and V. Morisson, *Tetrahedron*, 1996, **52**, 11063.
7 A. B. Borisenko, M. Broschag, I. Hargittai, T. M. Klapötke, D. Schröder, A. Schulz, H. Schwartz, I. C. Tornieporth-Oetting and P. S. White, *J. Chem. Soc., Dalton Trans.*, 1994, 2705.
8 J. H. Welch, R. D. Bereman, J. Bordner, W. Hatfield and J. H. Helms, *Inorg. Chem.*, 1985, **24**, 2905.
9 V. P. Litvinov, I. A. Dzhumaev, G. V. Gridunova, V. E. Shklover, Yu. T. Struchkov and B. M. Zolotarev, *Bull. Acad. Sci. USSR, Div. Chem. Sci.*, 1985, **34**, 782.
10 M. R. J. Dorrity, A. Lavery, J. F. Malone, C. P. Morley and R. R. Vaughan, *Heteroatom Chem.*, 1992, **3**, 87; F. R. Fronczek, H. E. Folsom and P. W. Rabideau, private communication to CCDC, 1995, ref. code PAPKUM01.
11 H. Kim, A. Kobayashi, Y. Sasaki, R. Kato, H. Kobayashi, T. Nakamura, T. Nogami and Y. Shirota, *Bull. Chem. Soc. Jpn.*, 1988, **61**, 2559.

*Received in Cambridge, UK, 12th September 1997; 7/06629E*

# First synthesis and properties of dendritic $Bi_n$-bismuthanes

**Hitomi Suzuki,* Haruto Kurata and Yoshihiro Matano**

*Department of Chemistry, Graduate School of Science, Kyoto University, Sakyo-ku, Kyoto 606-01, Japan*

**Directed tris-ortholithiation of tris[2-(diethylaminosulfonyl)phenyl]bismuthane 1 with *tert*-butyllithium followed by treatment with 3 equiv. of bis[2-(diethylaminosulfonyl)-phenyl]bismuth iodide 2a gives a symmetrically branched $Bi_4$-bismuthane 5a, which, on a similar treatment, is converted in a one-pot synthesis into a highly branched $Bi_{10}$-bismuthane 6a.**

Owing to excellent contrast density of bismuth toward X-rays of short wavelength, the synthesis of water-soluble non-ionic organobismuth compounds represents an interesting area of research in pursuit of iodine-free positive X-ray contrast agents. High bismuth content (m/m %) is a prerequisite for such a purpose and the incorporation of multiple bismuth atoms into a molecule is a straightforward approach to this. However, the literature to date contains no report of the synthesis of organobismuth compounds bearing more than two bismuth atoms in the molecule. Several tetraorganyldibismuthanes ($R_2BiBiR_2$) are known,[1] but they are quite sensitive to air and light and difficult to handle. During the course of our effort to synthesize polybismuth compounds, we came across a simple one-pot method for introducing three diarylbismuthyl units directly into the three aromatic rings of a triarylbismuthane and this methodology has now enabled us to gain easy access to highly branched aromatic polybismuth compounds. Herein we report the first synthesis of dendrimer-type aromatic polybismuth compounds bearing up to ten bismuth atoms in a single molecule,[2] utilizing the directed ortholithiation of triarylbismuthanes bearing a sulfonamide function at the *ortho* position of each aromatic ring.

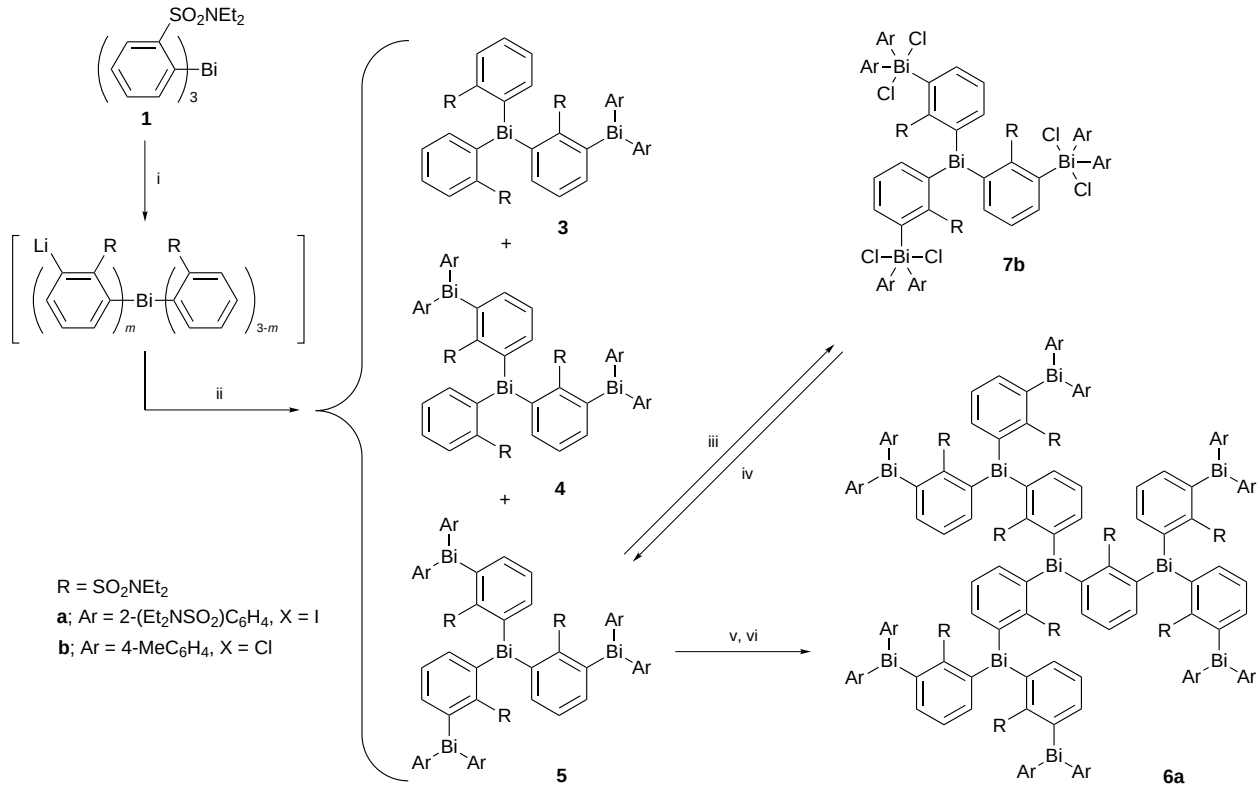
Since the sulfonamide group is a good directing group in the ortholithiation of arenes,[3] tris[2-(diethylaminosulfonyl)-phenyl]bismuthane[4] **1** was chosen as the starting material for water-soluble neutral polybismuth compounds. This bismuthane was synthesized by the ortholithiation of *N*,*N*-diethylbenzenesulfonamide with butyllithium followed by treatment with 1/3 $BiCl_3$ in THF at −78 °C. Compound **1** contains acidic protons *ortho* to the sulfonyl group on the three aromatic rings, so it can be further lithiated in the presence of an excess of an alkyllithium. When compound **1** was lithiated with 1.1 equiv. of *tert*-butyllithium in THF at −78 °C for 1 h and then treated with 1 equiv. of bis[2-(diethylaminosulfonyl)phenyl]-bismuth iodide[5] **2a**, $Bi_2$-bismuthane **3a** and $Bi_3$-bismuthane **4a** were obtained in 37 and 18% yields, respectively, together with 25% of recovered starting material **1**, where $Bi_n$-bismuthane represents a bismuthane bearing *n* bismuth atoms in one molecule (Table 1, entry 1). When 3.3 equiv. of *tert*-butyllithium was used under appropriate conditions, a symmetrically branched $Bi_4$-bismuthane **5a** was obtained as the main product. The yields of these bismuthanes varied considerably depending on the temperatures employed; compound **5a** was obtained in moderate and good isolated yield when the reaction mixture was warmed to −20 and 0 °C before iodide **2a** was added (entries 3 and 4, respectively), whereas $Bi_4$-bismuthane **5a** was not formed at all when bismuthane **1** was reacted with *tert*-butyllithium followed by iodide **2a** at −78 °C (entry 2). These results suggest that the tris-ortholithiation of compound **1** was the crucial step for the formation of a dendrimer-type $Bi_4$-bismuthane **5a** and that it did not proceed to completion at −78 °C. An isomeric linear $Bi_4$-bismuthane was not formed under the conditions employed. When bis(4-methylphenyl)bismuth chloride[4] **2b** was used in place of iodide **2a**, tolyl-substituted analogues **3b**, **4b** and **5b** were obtained in 2, 6 and 11% isolated yields, respectively (entry 5). Three of four bismuth atoms in $Bi_4$-bismuthane **5b** readily underwent oxidative chlorination with an excess of sulfuryl chloride in $CH_2Cl_2$ at room temp. to give a hexachloride **7b** in 55% yield, in which the central bismuth atom is intact, while the outer three bismuth atoms are oxidized to $Bi^V$ (Scheme 1). The reduction of hexachloride **7b** with saturated aqueous $Na_2S_2O_3$ smoothly regenerated the original $Bi_4$-bismuthane **5b** in 92% yield. All $Bi_n$-bismuthanes **3a,b**, **4a,b** and **5a,b** and hexachloride **7b** obtained were characterized by NMR and MALDI-TOF mass spectroscopies as well as by elemental analyses.

$Bi_4$-bismuthane **5a** bears acidic protons at the positions *ortho* to the sulfonamide group in the six outer aromatic rings. This structural advantage enabled us to extend the present methodology further, making access possible to a highly branched dendrimer-type $Bi_{10}$-bismuthane **6a**. Thus, treatment of $Bi_4$-bismuthane **5a** with 6.6 equiv. of *tert*-butyllithium in THF at 0 °C for 1 h followed by the addition of 6 equiv. of iodide **2a** at −78 °C afforded a crude $Bi_{10}$-bismuthane **6a** in *ca.* 20% yield, accompanied by small amounts of $Bi_8$- and $Bi_9$-congeners. The $Bi_{10}$-dendrimer **6a**, isolated by gel permeation chromatography and further purified by column chromatography on silica gel, is a white powder which begins to decompose above 180 °C without melting. It is readily soluble in dichloromethane and chloroform, but insoluble in methanol and ethanol. Its MALDI-TOF mass spectrum showed a $(M + Na)^+$ peak at *m/z* 6558.1 (calc; 6561.9). In its $^{13}C$ NMR spectrum, three distinct sets of $^{13}C$ absorptions were observed for non-equivalent ethyl groups at $\delta$ 41.8, 40.3 and 40.0 for methylene carbons and at $\delta$ 14.1, 13.0 and 12.7 for methyl carbons, respectively. Simple NMR peak patterns observed suggest a high molecular symmetry in accord with the dendritic structure of bismuthane **6a**. In the sense of atomic mass of a key element involved, the dendrimer **6a** represents the heaviest example of dendrimers so far reported. Attempts to elucidate the molecular geometry of compound **5a** by X-ray analysis have so far met with failure owing to the rapid efflorescence of the specimen crystals in air.

**Table 1** Reaction of lithiated bismuthane **1** with halides **2**

| | | Conditions for step i | | Yield (%)[a] | | | |
|---|---|---|---|---|---|---|---|
| Entry | Halide | $Bu^tLi$ (equiv.) | *T*/°C | **1** | **3** | **4** | **5** |
| 1 | **2a** | 1.1 | −78 | 25 | 37 | 18 | 0 |
| 2 | **2a** | 3.3 | −78 | 9 | 7 | 31 | 0 |
| 3 | **2a** | 3.3 | −78 to −20 | 4 | 9 | 11 | 13 |
| 4 | **2a** | 3.3 | −78 to 0 | 6 | 2 | 8 | 49 |
| 5 | **2b** | 3.3 | −78 to 0 | 2 | 2 | 6 | 11 |

[a] Based on total bismuth (**1** + **2**) employed.




**Scheme 1** *Reagents and conditions*: i, Bu$^t$Li, THF, −78 to *ca.* 0 °C, 1 h; ii, $Ar_2BiX$ **2**, −78 °C to room temp.; iii, $SO_2Cl_2$ (3.5 equiv.), $CH_2Cl_2$, room temp., 3 h, 55%; iv, $Na_2S_2O_3$ (aq), $CH_2Cl_2$, room temp., 1 h, 92%; v, Bu$^t$Li (6.6 equiv.), THF, −78 to 0 °C, 1 h; vi, $Ar_2BiI$ **2a** (6 equiv.), −78 °C to room temp.

## Footnotes and References

* E-mail: suzuki@kuchem.kyoto-u.ac.jp

† Selected data for **5a**: mp 162–164 °C (Found: C, 39.63; H, 4.61; N, 4.50. $C_{90}H_{123}Bi_4N_9O_{18}S_9$ requires C, 39.40; H, 4.52; N, 4.59%); $\delta_H$ (200 MHz, $CDCl_3$) 7.97 (6 H, d, *J* 7.6 Hz), 7.89 (3 H, d, *J* 7.3 Hz), 7.80 (3 H, d, *J* 7.3 Hz), 7.67 (6 H, d, *J* 7.6 Hz), 7.45 (6 H, t, *J* 7.6 Hz), 7.30 (6 H, t, *J* 7.6 Hz), 7.16 (3 H, t, *J* 7.3 Hz), 3.27 (36 H, q, *J* 6.6 Hz), 1.13 (54 H, t, *J* 6.6 Hz); MALDI-TOF, *m/z* 2766.2 ([M + Na]$^+$ requires 2766.5). For **5b**: mp 110–112 °C (Found: C, 43.03; H, 4.00; N, 2.03. $C_{72}H_{81}Bi_4N_3O_6S_3$ requires C, 42.88; H, 4.05; N, 2.08%); $\delta_H$ ($CDCl_3$) 8.11 (3 H, dd, *J* 7.3, 1.2 Hz), 7.85 (3 H, dd, *J* 7.3, 1.2 Hz), 7.58 (12 H, d, *J* 7.8 Hz), 7.3–7.1 (15 H, m), 3.22 (12 H, q, *J* 7.0 Hz), 2.30 (18 H, s), 1.01 (18 H, t, *J* 7.0 Hz); MALDI-TOF, *m/z* 2039.6 ([M + Na]$^+$ requires 2039.6). For **7b**: mp 156–157 °C (Found: C, 38.55; H, 3.62; N, 1.90. $C_{72}H_{81}Bi_4Cl_6N_3O_6S_3$ requires C, 38.79; H, 3.66; N, 1.88%); $\delta_H$ ($CDCl_3$) 8.5–8.3 (12 H, m), 7.87 (3 H, d, *J* 7.0 Hz), 7.79 (3 H, d, *J* 7.0 Hz), 7.63 (3 H, t, *J* 7.0 Hz), 7.5–7.3 (12 H, m), 3.34 (12 H, q, *J* 7.2 Hz), 2.42, 2.37 (18 H, two s), 1.02 (18 H, t, *J* 7.2 Hz); MALDI-TOF, *m/z* 2252.2 ([M + Na]$^+$ requires 2252.3). For **6a**: (Found: C, 38.72; H, 4.40; N, 4.62. $C_{210}H_{285}Bi_{10}N_{21}O_{42}S_{21}$ requires C, 38.57; H, 4.39; N, 4.50%); $\delta_H$ ($CDCl_3$) 8.0–7.8 (21 H, m), 7.8–7.7 (9 H, m), 7.7–7.6 (12 H, m), 7.5–7.2 (24 H, m), 7.2–7.1 (9 H, m), 3.26 (84 H, br q), 1.12 (126 H, br t); $\delta_C$ (200 MHz $CDCl_3$) 178.6, 175.5, 174.3, 147.1, 144.4, 140.8, 139.9, 138.3, 135.2, 129.3, 127.8, 41.8, 40.3, 40.0, 14.1, 13.0, 12.7.

‡ *General procedure*: To a solution of bismuthane **1** (0.42 g, 0.5 mmol) in THF (7 ml) was added *tert*-butyllithium (*n*-pentane solution; 1.9 M × 0.29 ml, 0.55 mmol) at −78 °C. After stirring for 1 h at this temperature, a THF solution (5 ml) of iodide **2a** (0.38 g, 0.5 mmol) was added. The reaction mixture was allowed gradually to warm to room temp. and quenched with brine. The aqueous phase was extracted twice with ethyl acetate, and the combined extracts were dried over $MgSO_4$, and evaporated under reduced pressure to leave a white solid, which was chromatographed on silica gel using hexane–ethyl acetate as the eluent to give bismuthane **1**, $Bi_2$-bismuthane **3a** and $Bi_3$-bismuthane **4a** in this elution order in 25, 37 and 18% isolated yields, respectively.

1 A. J. Ashe III, *Adv. Organomet. Chem.*, 1990, **30**, 77. Also see: H. Suzuki and Y. Matano, in *Chemistry of Arsenic, Antimony and Bismuth*, ed. N. C. Norman, Blackie Academic, Glasgow, 1997.
2 For a survey of dendrimers, see: J. M. J. Fréchet, C. J. Hawker, I. Gitsov and J. W. Leon, *J. Macromol. Sci., Pure Appl. Chem.*, 1996, **A33**, 1399; J. Issberner, R. Moors and F. Vögtle, *Angew. Chem., Int. Ed. Engl.*, 1994, **33**, 2413 and references therein.
3 A. I. Meyers and K. Lutomski, *J. Org. Chem.*, 1979, **44**, 4464; H. Watanabe, R. A. Schwarz, C. R. Hauser, J. Lewis and D. W. Slocum, *Can. J. Chem.*, 1969, **47,** 1543. For reviews of directed orthometalation, see: V. Snieckus, *Chem. Rev.*, 1990, **90,** 879; P. Beak and V. Snieckus, *Acc. Chem. Res.*, 1982, **15**, 306.
4 H. Suzuki, T. Murafuji and N. Azuma, *J. Chem. Soc., Perkin Trans. 1*, 1993, 1169.
5 H. Suzuki and T. Murafuji, *J. Chem. Soc., Chem. Commun.*, 1992, 1143.

*Received in Cambridge, UK, 1st September 1997; 7/06338E*

# Iron–carbene functionalities supported by a macrocyclic ligand: iron–carbon double bond stabilized by tetramethyldibenzotetraazaannulene

**Alain Klose,[a] Euro Solari,[a] Carlo Floriani,*[a] Nazzareno Re,[b] Angiola Chiesi-Villa[c] and Corrado Rizzoli[c]**

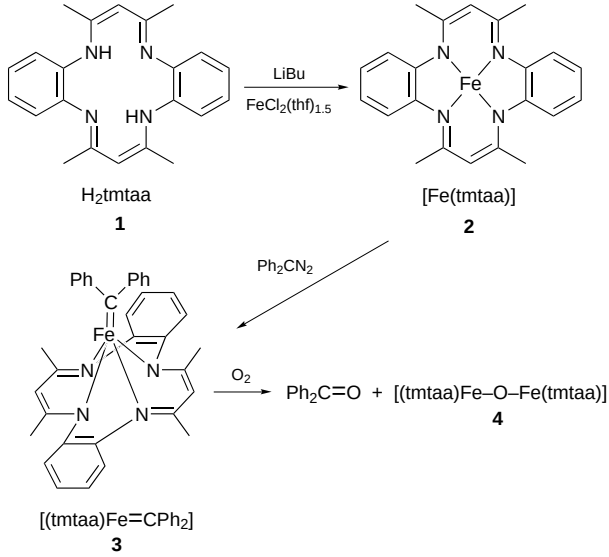
[a] *Institut de Chimie Minérale et Analytique, BCH, Université de Lausanne, CH-1015 Lausanne, Switzerland*
[b] *Dipartimento di Chimica, Università di Perugia, I-06100 Perugia, Italy*
[c] *Dipartimento di Chimica, Università di Parma, I-43100 Parma, Italy*

**We report an unprecedented entry to the chemistry of the iron–carbene functionality supported by an easily available macrocycle.**

The metal–carbene unit is a key functionality both in organometallic and organic chemistry.[1] It is usually bonded to conventional ancillary ligands, with a few remarkable exceptions in metal–porphyrin chemistry,[2–6] and particularly in the case of iron[2] and ruthenium.[2b,3,5] Despite of considerable effort in this field, owing to the relevance of metal–porphyrin carbene derivatives in chemistry and biology,[2,3] some facts are particularly surprising: (*i*) there is an absence of any modeling approach in macrocycle chemistry, *i.e.* the use of readily available macrocycles; (*ii*) the potential of the metal–carbene bonded to a macrocyclic structure is still to be explored; (*iii*) very few (three, at present) metal–porphyrin carbenes have been structurally characterized.[2a,6]

Here, we report a straightforward synthesis of iron–carbenes stabilized by the easily accessible tetramethyldibenzotetraazaannulene ligand ($H_2$tmtaa)[7] along with their structural characterization in solution and in the solid state. The availability of tetramethyldibenzotetraazaannulene encourages the use of [Fe(tmtaa)] for developing iron–carbene chemistry based on this and other macrocycles. The synthesis was performed by reacting **2**[8a] with the corresponding diazoalkane (Scheme 1).

The reaction of **2** with $Ph_2CN_2$ in THF at −30 °C, and then at room temperature, gave high yields of **3** as a green crystalline solid.† Complex **2** showed a very high thermal stability and resistance to hydrolysis. The reaction of **3** with dioxygen gave, almost quantitatively, benzophenone and the well known μ-oxo dimer **4**.[7a] The stability and the nature of the final compound




**Scheme 1**

derived from the reaction of **2** with diazoalkanes is strongly dependent on the substituents at the carbene carbon. In the case of $PhCHN_2$, the carbene derivative forms only at low temperature. It decomposes at room temperature leading to the starting material and *trans*-stilbene (81%) and *cis*-stilbene (19%), while in the presence of dioxygen it forms PhCHO and complex **4**. Owing to its diamagnetism, **3** has been readily characterized by $^1$H and $^{13}$C NMR spectroscopies and structural details have been revealed by X-ray analysis‡ (see Fig. 1). The coordination environment of iron is a distorted tetragonal pyramid, unlike iron–prophyrin[2a] or osmium–porphyrin[6b] examples, where the metal is always six-coordinate. The metal is displaced by 0.335(1) Å from the $N_4$ average plane. The Fe–C(23) vector is perpendicular to the $N_4$ core, the dihedral angle with the normal to the $N_4$ plane being 1.0(1)°. The carbene plane C(23)C(31)C(41) is almost parallel to the N(2)···N(4) vector, the torsion angles C(31)–C(23)–Fe–N(4) and C(41)–C(23)–Fe–N(2) being −15.5(3) and −15.2(3)°, respectively. The Fe–C(23) bond distance [1.794(3) Å] is particularly short compared to the only available iron–porphyrin [Fe=$CCl_2$ 1.83(3) Å][2a] or organometallic derivatives of iron, where it ranges from 1.978(3) to 1.85(3) Å.[9] The question whether the oxidation state of iron in **3** is +2 or +4 can be reasonably answered, in the absence of Mössbauer measurements, by considering the Fe distance from the $N_4$ plane. A correlation in tmtaa complexes has been established between the out of plane distance of the metal and its $d^n$ configuration.[7b] The value found in the present case [0.335(1) Å] is expected for low-spin $d^6$ five-coordinate iron(II), *e.g.* 0.29 Å in [Fe(tmtaa)(CO)].[8c] Much longer distances would be found for a $d^4$ configuration. The extended

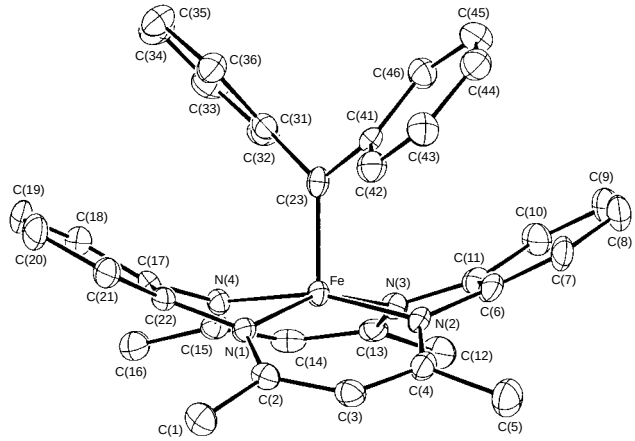



**Fig. 1** ORTEP drawing of complex **3** (50% probability ellipsoids. Selected interatomic distances (Å) and angles (°): Fe–N(1) 1.921(3), Fe–N(2) 1.926(2), Fe–N(3) 1.911(3), Fe–N(4) 1.920(2), Fe–C(23) 1.794(3), C(23)–C(31) 1.487(5), C(23)–C(41) 1.472(4); N(3)–Fe–N(4) 94.6(1), N(2)–Fe–N(4) 163.3(1), N(2)–Fe–N(3) 82.7(1), N(1)–Fe–N(4) 82.3(1), N(1)–Fe–N(3) 156.4(1), N(1)–Fe–N(2) 93.6(1), Fe–C(23)–C(41) 122.6(2), Fe–C(23)–C(31) 121.7(2), C(31)–C(23)–C(41) 115.7(3).

Hückel calculations further support the +2 oxidation state for iron in **3** and the use of carbene rather than alkylidene terminology for the present complexes. The tmtaa, which shows the usual saddle shape conformation,[7] has structural parameters quite close to those reported for the other iron complexes.[8]

We thank the 'Fonds National Suisse de la Recherche Scientifique' (Grant No. 20-46'590.96), Ciba Speciality Chemicals (Basel, Switzerland), and 'Fondation Herbette' (University of Lausanne, Switzerland) for financial support.

## Footnotes and References

* E-mail: carlo.floriani@icma.unil.ch

† *Preparation* of **3**: To a cooled (−30 °C) THF solution (140 ml) of [Fe(tmtaa)]·thf[8a] (1.79 g, 3.80 mmol) was added dropwise a THF solution (40 ml) of diphenyldiazomethane (0.78 g, 4.0 mmol). When warmed to room temperature the solution became red. Nitrogen gas was slowly given off. After stirring for 2 d, the green solution was concentrated *in vacuo* (20 ml) and then hexane (15 ml) added. A green crystalline solid was obtained (1.70 g, 75%). Crystals suitable for X-ray analysis were grown in toluene (Found: C, 74.53; H, 5.77; N, 9.91. $C_{35}H_{32}FeN_4$ requires C, 74.47; H, 5.71; N, 9.92%). $^1$H NMR (200 MHz, $C_6D_6$, 25 °C): $\delta$ 6.88–6.76 (m, 8 H), 6.35–6.33 (m, 10 H), 5.13 (s, 2 H), 2.12 (s, 12 H). $^{13}$C NMR (100.6 MHz, $C_6D_6$, 25 °C): $\delta$ 313.2 (C carbene), 166.6, 157.9, 149.3, 127.1, 124.8, 120.9, 120.5, 119.7, 107.3, 67.8, 25.8, 23.2.

‡ *Crystal data* for **3**: $C_{35}H_{32}FeN_4\cdot C_7H_8$, $M$ = 656.7, triclinic, space group $P\bar{1}$, $a$ = 11.670(3), $b$ = 13.593(4), $c$ = 11.234(3) Å, $\alpha$ = 106.72(2), $\beta$ = 96.21(2), $\gamma$ = 77.62(2)°, $U$ = 1665.0(8) Å$^3$, $Z$ = 2, $D_c$ = 1.310 g cm$^{-3}$, $F(000)$ = 692, Mo-K$\alpha$ radiation ($\lambda$ = 0.710 9 Å), $\mu$(Mo-K$\alpha$) = 4.87 cm$^{-1}$: crystal dimensions 0.08 × 0.72 × 0.85 mm. The structure was solved by the heavy atom method and anisotropically refined for all the non-H atoms. All the hydrogen atoms were located from difference Fourier maps and introduced as fixed contributors in the last stage of refinement ($U_{iso}$ = 0.05 Å$^2$). For 4428 unique observed reflections [$I > 2\sigma(I)$] collected at $T$ = 133 K on a Rigaku AFC6S diffractometer ($5 < 2\theta < 50°$) and corrected for absorption the final $R$ is 0.059 ($wR_2$ = 0.163 for the 5293 reflections having $I > 0$ used in the refinement). All calculations were carried out on a QUANSAN Personal Computer equipped with an INTEL PENTIUM processor. CCDC 182/644.

1 *Transition Metal Carbene Complexes*, VCH, Weinheim, 1983; W. D. Wulff, in *Advances in Metal–Organic Chemistry*, ed. L. S. Liebeskind, Jay, London, vol. 1, 1989, pp. 209; J. W. Herndon, S. U. Tumer, L. A. McMullen, J. J. Matasi and W. F. K. Schnatter, in *Advances in Metal–Organic Chemistry*, ed. L. S. Liebeskind, Jay, London, vol. 3, 1994, pp. 51–95; *Comprehensive Organometallic Chemistry*, ed. G. Wilkinson, F. G. A. Stone and E. W. Abel, Pergamon, Oxford, vol. 12, 1995, ch. 5.1–5.5.

2 (*a*) D. Mansuy, M. Lange, J. C. Chottard, J. F. Bartoli, B. Chevrier and R. Weiss, *Angew. Chem.*, 1978, **90**, 828; (*b*) P.J. Brothers and J. P. Collman, *Acc. Chem. Res.*, 1986, **19**, 209; (*c*) D. Mansuy, *Pure Appl. Chem.*, 1987, **59**, 759; (*d*) I. Artaud, N. Gregoire, J.-P. Battioni, D. Dupre and D. Mansuy, *J. Am. Chem. Soc.*, 1988, **110**, 8714; (*e*) I. Artaud, N. Gregoire, P. Leduc and D. Mansuy, *J. Am. Chem. Soc.*, 1990, **112**, 6899; (*f*) D. Mansuy and J. P. Mahy, in *Metalloporphyrins Catalyzed Oxidations*, ed. F. Montanari and L. Casella, Kluwer, Dordrecht, 1994, p. 175.

3 J. P. Collman, P. J. Brothers, L. McElwee-White, E. Rose and L. J. Wright, *J. Am. Chem. Soc.*, 1985, **107**, 4570; J. P. Collman, P. J. Brothers, L. McElwee-White and E. Rose, *J. Am. Chem. Soc.*, 1985, **107**, 6110.

4 H. Brand and J. Arnold, *Coord. Chem. Rev.*, 1995, **140**, 137; T. Aida and S. Inoue, *Acc. Chem. Res.*, 1996, **29**, 39.

5 J. P. Collman, L. S. Hegedus, J. R. Norton and R. G. Finke, *Principles and Applications of Organotransition Metal Chemistry*, University Science Books, Mill Valley, CA, 1987.

6 (*a*) T. Boschi, S. Licoccia, R. Paolesse and P. Tagliatesta, *Organometallics*, 1989, **8**, 330; (*b*) J.-P. Djukic, D. A. Smith, V. G. Young, Jr. and L. K. Woo, *Organometallics*, 1994, **13**, 3020.

7 Some leading references to the use of [tmtaa]$^{2-}$ as an ancillary ligand in the organometallic chemistry of the early transition metals are: (*a*) C. H. Jang, J. A. Ladd and V. L. Goedken, *J. Coord. Chem.*, 1988, **18**, 317; (*b*) S. De Angelis, E. Solari, E. Gallo, C. Floriani, A. Chiesi-Villa and C. Rizzoli, *Inorg. Chem.*, 1992, **31**, 2520; (*c*) L. Giannini, E. Solari, C. Floriani, A. Chiesi-Villa and C. Rizzoli, *Angew. Chem., Int. Ed. Engl.*, 1994, **33**, 2204; (*d*) L. Giannini, E. Solari, S. De Angelis, T. R. Ward, C. Floriani, A. Chiesi-Villa and C. Rizzoli, *J. Am. Chem. Soc.*, 1995, **117**, 5801; (*e*) D. G. Black, D. C. Swenson and R. F. Jordan, *Organometallics*, 1995, **14**, 3539; (*f*) H. Schumann, *Inorg. Chem.*, 1996, **35**, 1808; (*g*) G. I. Nikonov, A. J. Blake and P. Mountford, *Inorg. Chem.*, 1997, **36**, 1107.

8 (*a*) V. L. Goedken, J. J. Pluth, S. M. Peng and B. Bursten, *J. Am. Chem. Soc.*, 1976, **98**, 8014; (*b*) M. C. Weiss, B. Bursten, S. M. Peng and V. L. Goedken, *J. Am. Chem. Soc.*, 1976, **98**, 8021; (*c*) V. L. Goedken, S. M. Peng, J. A. Molin-Norris and Y. Park, *J. Am. Chem. Soc.*, 1976, **98**, 8391; (*d*) M. C. Weiss and V. L. Goedken, *Inorg. Chem.*, 1979, **18**, 819; (*e*) P. Berno, C. Floriani, A. Chiesi-Villa and C. Guastini, *J. Chem. Soc., Dalton Trans.*, 1988, 1409; (*f*) P. Berno, C. Floriani, A. Chiesi-Villa and C. Guastini, *J. Chem. Soc., Dalton Trans.*, 1989, 551.

9 P. E. Riley, R. E. Davis, N. T. Allison and W. M. Jones, *Inorg. Chem.*, 1982, **21**, 1321; D. Bauer, P. Härter and E. Herdtweck, *J. Chem. Soc., Chem. Commun.*, 1991, 829.

*Received in Basel, Switzerland, 4th July 1997; 7/04736C*

# X-Ray crystal structure of (tetraphenylimidodiphosphinato)silver(I): an unexpected tetranuclear complex with two modes of coordination of silver

**Henri Rudler,[a] Bernard Denise,[a] José Ribeiro Gregorio[a] and Jacqueline Vaissermann[b]**

*[a] Laboratoire de Synthèse Organique et Organométallique, URA 408, and [b] Laboratoire de Chimie des Métaux de Transition, URA 419, Université Pierre et Marie Curie, T44-45, 4 place Jussieu 75252 Paris Cedex 5, France*

**Potassium tetraphenylimidodiphosphinate reacts with silver nitrate to give, upon recrystallization from ethanol, an unexpected tetranuclear complex $[Ag\{N(OPPh_2)_2\}]_4\cdot 2EtOH$, the structure of which is established by X-ray crystallography; preliminary results concerning its use as a catalyst for the aerobic co-oxidation of alkenes and aldehydes are described.**

The tetraphenylimidodiphosphinate ligand (TPIP), the 'inorganic' equivalent of β-diketonate ligands, has proven to lead to interesting complexes especially in the field of lanthanide NMR shift reagents.[1–4] Thus, $Pr(TPIP)_3$, owing to its high stability with respect to hydrolysis even in the presence of acids (in contrast to β-diketonates), can be used as a shift reagent for carboxylic acids and induces important simplification in their $^1H$ NMR spectra. Moreover, $Pr(TPIP)_3$ reacts instantaneously with carboxylates to lead to dinuclear complexes: in the case of acids containing a chiral centre, these complexes can be used to control the optical purity of the starting acids. Along the same lines, the use of $Gd(TPIP)_3$ as a relaxation agent for carboxylic acids has recently been outlined.[5] A common feature of all the complexes so far described is the mode of coordination of the TPIP ligand to the metal: as for β-diketonates, TPIP acts as a bidentate ligand.[4]

A second interesting feature of this ligand is its high stability towards oxidants: its preparation from the related phosphine can be carried out in concentrated hydrogen peroxide without noticeable decomposition. This observation and our ongoing efforts to develop new catalysts for the efficient, possibly asymmetric, epoxidation of alkenes, prompted us to carry out the systematic synthesis of various lanthanide and transition metal complexes containing this and related ligands for that purpose.[6] Among the latter, we were interested in silver complexes containing such ligands. Indeed, silver-based catalysts are used in the epoxidation of ethene;[7] however, complexes containing this metal have, to the best of our knowledge, not been tested in the aerobic aldehyde alkene co-oxidation system (Mukayama reaction).[8,9]

Moreover, since silver chelates have also found interesting applications in NMR spectroscopy of alkenes,[10,11] we decided to attempt the preparation of Ag(TPIP).

Here, we describe the synthesis and the unexpected X-ray structure of the new complex Ag(TPIP) and to provide preliminary results concerning its use as an oxidation catalyst.

When aqueous solutions of silver nitrate (0.170 g, 1 mmol; 10 ml $H_2O$) and of KTPIP (0.46 g, 1 mmol; 10 ml $H_2O$) were mixed a precipitate formed. Filtration of the solid followed by recrystallization from $CH_2Cl_2$–EtOH gave colorless crystals 0.34 g, 65% yield) which were stable in the air and in solution, and were suitable for X-ray analysis.† According to the NMR spectrum of the crystals,‡ half an equivalent of EtOH solvent was present in the product and elemental analysis confirmed this observation.

The molecular structure of Ag(TPIP) is shown in Fig. 1. The molecule is built up of four Ag(TPIP) units which are arranged pairwise and which contains two solvent molecules per formula unit. These molecular pairs reside on a crystallographically imposed centre of symmetry. From a formal point of view, two $Ag^+$ cations adopt the preferred[12,13] linear coordination by combination with two TPIP ligands giving $Ag(TPIP)_2^-$, with N(1)–Ag(1)–N(2) 172.0(1)°, so leaving three pendent P=O groups, the remaining P=O group being linked *via* a hydrogen bond to ethanol. Two $Ag^+$ cations share six P=O ligands and thus hold together the two $Ag(TPIP)_2$ anions. Moreover, these two anions are also coupled by a pair of Ag···Ag contacts (3.210 Å). The coordination of the two silver atoms to the six suitably oriented P=O groups occurs in such a way as to lead to a central planar $Ag_2O_2$ ring with O(3)–Ag(2)–O(3′) 91.1(2)°, the two oxygen atoms being dissymmetrically bonded to silver with Ag(2)–O(3) 2.269(2) and Ag(2)–O(3′) 2.654(2) Å. The coordination around silver is thus distorted tetrahedral with the oxygen atoms of the P=O groups as closest neighbours, the shortest bond occurring between silver and a terminal oxygen atom is Ag(2)–O(1) 2.195 Å.

The P=O bond lengths are comparable or slightly shorter (especially the P=O group linked to ethanol by its oxygen atom) than those found *e.g.* in $Pr(TPIP)_3$. By contrast, the P–N bonds are in general longer than those observed in $Pr(TPIP)_3$ (1.620 *vs.* 1.590 Å) thus confirming their single bond character.[14]

Direct comparison of this structure with that of the corresponding unstable silver β-diketonates[15,16] could unfortunately not be established since the latter structures are so far unknown.

Although a number of mononuclear complexes in which the silver cation is surrounded by four oxygen (or sulfur) atoms giving distorted tetrahedral environment are known,[17,18] as well

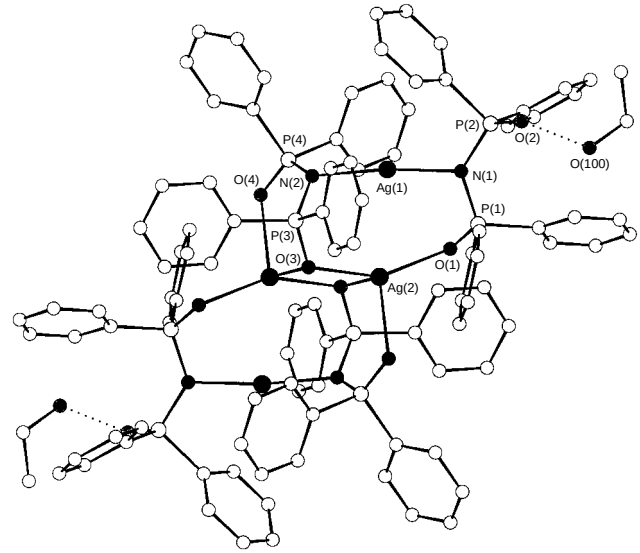



**Fig. 1** Molecular structure of $[Ag\{N(OPPh_2)_2\}]_4\cdot 2EtOH$ showing the atomic numbering scheme. Selected distances (Å) and angles (°): Ag(1)–N(1) 2.145(3), Ag(1)–N(2) 2.170(2), Ag(2)–O(1) 2.195(2), Ag(2)–O(3) 2.269(2), Ag(2)–O(3′) 2.654(2), Ag(2)–O(4′) 2.388(2); N(1)–Ag(1)–N(2) 172.0(2), O(3)–Ag(2)–O(3′) 90.84(8), P(1)–N(1)–P(2) 130.7(2), P(3)–N(2)–P(4) 124.6(2).

**Table 1** Epoxidation of various alkenes promoted by Ag(TPIP) in the presence of isobutyraldehyde and oxygen in dichloroethane

| Entry | Alkene (mmol) | *t*/h | Yield acid (%) | Yield epoxide (%) | Yield furan (%) | Yield pyran (%) |
|---|---|---|---|---|---|---|
| a | Cyclooctene (0.77) | 4 | 98 | 100 | | |
| b | Oct-1-ene (0.64) | 20 | 98 | 40 | | |
| c | Cholesteryl acetate (0.59) | 0.5 | 50 | 58[b] | | |
| | Cholesteryl acetate (0.59) | 2 | 80 | 100 | | |
| d | Linalool (0.57) | 3 | 70 | 26 | 30 | 4 |
| e | Linalool (0.57) | 21 | 99 | 5 | 85 | 10 |
| f | Linalool[c] (5.7) | 6 | 85 | 65 | 15 | |

[a] $P(O_2)$ = 1 atm, room temp.; aldehyde/alkene = 7; catalyst = 1 mol%. [b] α/β isomers: 32/68. [c] Linalool (1 ml), aldehyde (4 ml), catalyst (50 mg), dichloroethane (20 ml).

as an example of a trinuclear complex in which the silver atoms adopt both a linear and a tetrahedral coordination,[19] the central planar dinuclear structure with the two linear $Ag^-$ moieties found in the present complex is, to the best of our knowledge, unique.

Preliminary results of the catalytic properties of this complex in the oxidation of alkenes are promising. Many transition metals bearing various groups (usually β-diketonato ligands) are active in the aerobic co-oxidation of alkenes and aldehydes into epoxides and acids. However, one major problem is linked to the high rate of oxidation of the aldehyde to the acid: in such cases, the conversion of the alkenes into epoxides drops considerably, unless a large excess of aldehyde is used. We have now found that on the one hand that the lanthanide complexes (Pr, Eu, Dy) containing TPIP can be used for the epoxidation of alkenes: their activity are comparable to that of more classical complexes of Co and Mn.[6] On the other hand, as shown in Table 1, a series of alkenes gave, in the presence of Ag(TPIP), the corresponding epoxides (and their rearrangement products for linalool[20]) in yields and rates comparable to, or even higher than those observed for other metal TPIP complexes and also for the more classical metal β-diketonates (M = Mn, Co).[8,9,21,22] Although cyclooctene and cholesteryl acetate (entries a and c) are readily oxidized alkenes, the result achieved with Ag(TPIP) is striking since high rates and quantitative conversions into the epoxide are observed. However, and as for other catalysts, the results were rather sluggish for monosubstituted terminal alkenes (entry b). Finally, for linalool, the conditions could be varied in order to obtain either the epoxides or their rearrangement products[20] (entries d–f).

## Footnotes and References

† *X-Ray structure determination*: X-ray quality crystals were obtained by slow evaporation of $CH_2Cl_2$ from a solution of the silver complex in $CH_2Cl_2$–EtOH. Data were collected at room temperature on a Nonius CAD4 diffractometer. Empirical absorption correction using PSISCAN was applied. Anomalous dispersion terms and correction of secondary extinction were applied. The structure was solved by SHELXS[23] and refined by least-squares analysis using anisotropic thermal parameters for all non-hydrogen atoms. H atoms were located on a difference Fourier map, and their coordinates were refined as free atoms with an overall isotropic thermal parameter. 9260 reflections, with $F_o > 3\sigma(F_o)$ were used to solve and refine the structure to $R$ = 0.0338 and $R_w$ = 0.0324, 708 least-squares parameters. The programs used were CRYSTALS and CAMERON.[24,25]

*Crystal data*: $C_{100}H_{92}O_{10}N_4P_8Ag_4$, $M$ = 2189, triclinic, space group $P\bar{1}$, $a$ = 12.424(2), $b$ = 13.563(2), $c$ = 16.200(5) Å, α = 74.22(2), β = 69.06(2), γ = 71.24(2)°, $U$ = 2375(1) Å$^3$, $Z$ = 1, $D_c$ = 1.53 g cm$^{-3}$. CCDC 182/629.

‡ *Selected data*: $^1$H NMR ($C_6D_6$) δ 7.97 (m, 8 H), 6.97 (m, 12 H), 3.43 (q, 0.5 H, $OCH_2$), 1.02 (t, 0.75 H, $CH_3$). Analysis. Calc.: C, 54.87; H, 4.22; N, 2.42. Found: C, 54.24; H, 4.22; N, 2.56%.


1 I. Rodriguez, C. Alvarez, J. Gomez-Lara, R. Soriano-Garcia and R. A. Toscano, *Lanthanide–Actinide Res.*, 1986, **1**, 253.
2 C. Alvarez, N. Goasdoue, N. Platzer, I. Rodriguez and H. Rudler, *J. Chem. Soc., Chem. Commun.*, 1988, 1002.
3 C. Alvarez, L. Barkaoui, N. Goasdoue, J. C. Daran, N. Platzer, H. Rudler and J. Vaissermann, *J. Chem. Soc., Chem. Commun.*, 1989, 1507.
4 N. Platzer, H. Rudler, C. Alvarez, L. Barkaoui, B. Denise, N. Goasdoue, M. N. Rager, J. Vaissermann and J. C. Daran, *Bull. Chem. Soc. Fr.*, 1995, **132**, 95.
5 L. Barkaoui, M'hamed Charrouf, M. N. Rager, B. Denise, N. Platzer and H. Rudler, *Bull. Chem. Soc. Fr.*, 1997, **134**, 165.
6 H. Rudler, B. Denise and J. Ribeiro Gregorio, manuscript in preparation.
7 P. A. Kilty and W. M. H. Sachtler, *Catal. Rev.*, 1974, **10**, 1.
8 T. Yamada, T. Takai, O. Rhode and T. Mukaiyama, *Bull. Chem. Soc. Jpn.*, 1991, **64**, 2109.
9 T. Takai, E. Hata, T. Yamada and T. Mukaiyama, *Bull. Chem. Soc. Jpn.*, 1991, **64**, 2513.
10 D. F. Evans and J. N. Tucker, *J. Chem. Soc., Chem. Commun.*, 1975, 205.
11 T. J. Wenzel and R. E. Sievers, *J. Am. Chem. Soc.*, 1982, **104**, 382.
12 R. J. Lancashire, in *Comprehensive Coordination Chemistry*, ed. S. G. Wilkinson, vol. 5, p. 775.
13 D. R. Whitcomb and R. D. Rogers, *Polyhedron*, 1997, **16**, 863.
14 H. Nöth, *Z. Naturforsch., Teil B*, 1982, **37**, 1491.
15 J. V. Nef, *Liebigs Ann. Chem.*, 1893, **277**, 68.
16 R. West and R. Riley, *J. Inorg. Nucl. Chem.*, 1958, **5**, 295.
17 B. Lippert and D. Neugebauer, *Inorg. Chim. Acta*, 1980, **46**, 171.
18 K. B. Yatsimirsky, G. C. Talanova, E. A. Nazarova, M. I. Kabachnik, T. A. Mastryukova, I. M. Aladzheva, I. V. Leont'eva, M. Yu Antipin and Yu. T. Struchbov, *Koord. Khim.*, 1993, **19**, 469.
19 F. Guay and A. L. Beauchamp, *J. Am. Chem. Soc.*, 1979, **101**, 6260.
20 D. Felix, A. Melera, J. Seibl and E. sz. Kovats, *Helv. Chim. Acta*, 1963, **96**, 1513.
21 S. Bennett, S. M. Brown, G. Conole, M. Kessler, S. Rowling, E. Sinn and S. Woodward, *J. Chem. Soc., Dalton Trans.*, 1995, 367.
22 A. Atlamsani, E. Pedreza, C. Potvin, E. Dumprey, O. Mohammedi and J. M. Brégeault, *C.R. Acad. Sci. Paris*, 1993, **317**, 757.
23 G. M. Sheldrick, SHELXS-86, *Program for Crystal Structure Solution*, University of Göttingen, 1986.
24 D. J. Watkin, C. K. Prout, J. R. Carruthers and P. W. Betteridge, *Crystals Issue 10*, Chemical Crystallography Laboratory, University of Oxford, 1996.
25 D. J. Watkin, C. K. Prout and L. J. Pearce, CAMERON, Crystallography Laboratory, University of Oxford, 1996.


*Received in Cambridge, UK, 3rd September 1997; 7/06430F*

# A novel method for large-scale synthesis of AgI nanoparticles

**Sihai Chen, Takashi Ida and Keisaku Kimura***

*Department of Material Science, Faculty of Science, Himeji Institute of Technology, Harima Science Garden City, Kamigori, Hyogo 678-12, Japan*

**Thiol-derivatised I–VII nanoparticles of AgI (7–16 nm) are prepared in large quantities by the reaction of silver nitrate with potassium iodide containing 1-thioglycerol in aqueous solution.**

Solid electrolytes with high ionic conductivity have drawn much attention because of the possibility for applications in solid-state battery and chemical sensing systems. Recently, we have found that the ionic conductivity of polycrystalline pellet of AgI increased significantly when the particle size is decreased from the bulk to 140 nm.[1,2] Following this finding the synthesis of large amounts of small AgI nanoparticles is strongly desirable. Several wet chemical methods such as the use of gelatin[3] or polymer,[4–7] control release of iodide ions from $CH_2I_2$[8,9] have been studied. However these methods were all applied to very diluted solutions ($< 10^{-3}$ M), and thus AgI can not be separated as a solid powder in large quantities. Here, we report the synthesis of a large amount of AgI nanoparticles using 1-thioglycerol (TG) as the size controller. This is the first extension of the use of thiolates in the synthesis of II–VI nanoparticles[10] to I–VII nanoparticles.

In order to grow AgI clusters with simultaneous attachment of a thiol monolayer on the particle surface, silver ions are injected in the iodide solution containing thiols maintaining $[Ag^+] = [I^-] + [TG]$. The size of the particles can be controlled by the $[I^-]/[TG]$ ratio. For a typical preparation with a $[I^-]/[TG]$ ratio of 9.0, 20 ml of a 0.2 M $AgNO_3$ solution was rapidly added into a solution containing 18 ml 0.2 M KI and 2 ml 0.2 M TG under vigorous stirring. After 20 min of reaction, the resulting turbid yellow solution was sealed into cellulose tubing (Type 24/32, pore size 2.4 nm, Visking company) and dialysized against flowing water for 24 h in the dark. The pH of the solution changed from 2.13 to 7.16. After freeze drying, 0.92 g of yellow powder which corresponds to a yield of 98% was obtained. Fig. 1 shows the electron micrograph (recorded with Hitachi 8100 instrument at 200 kV) of the AgI particles sampling from a 200 times diluted initial solution. The particles were spherical with a mean diameter of 16 nm but characterized by a wide size distribution (standard deviation of 9.4 nm, calculated from the digitalized image with a NIH software package). The morphology of these particles is different from that prepared by simply mixing $AgNO_3$ and KI in dilute solutions[4,5] which often shows the shape of regular triangles with rounded corners or irregular polygons. This difference indicates that thiolates can effectively inhibit the anisotropic growth of the special crystal plane of AgI nuclei, leading to the formation of small particles even in concentrated solutions.

Fig. 2 shows a typical electron diffraction pattern of the sample in Fig. 1. The strong diffraction spots indicate that the samples are polycrystalline, this is also confirmed by HRTEM image in the insert of Fig. 1. The measured lattice spacings calibrated with a standard gold film were 3.969 (100), 3.737 (002), 3.483 (101), 2.723 (102), 2.296 (110), 1.954 (112), 1.326 (300) and 1.249 Å (302) of β-AgI (wurtzite structure). Also, the spacings at 3.737 (111), 2.296 (220), 1.949 (311), 1.673 (400), 1.480 (331) and 1.249 Å (511) can be attributed to γ-AgI (zinc blende structure). The existence of only these two types of diffraction rings indicates that the particles are composed of only β- and γ-AgI.

X-Ray diffraction spectra of the solid powder (recorded with a Rigaku RINT/Dmax-2000 diffractometer) confirmed the above assignment (Fig. 3). All diffraction peaks show broadening compared to that of the bulk sample. The average particle size was 15 nm estimated from the Scherrer's equation. Further simulation of the XRD pattern with a Rietveld method, utilizing a program RIETAN-94 developed by Izumi[11] revealed that the

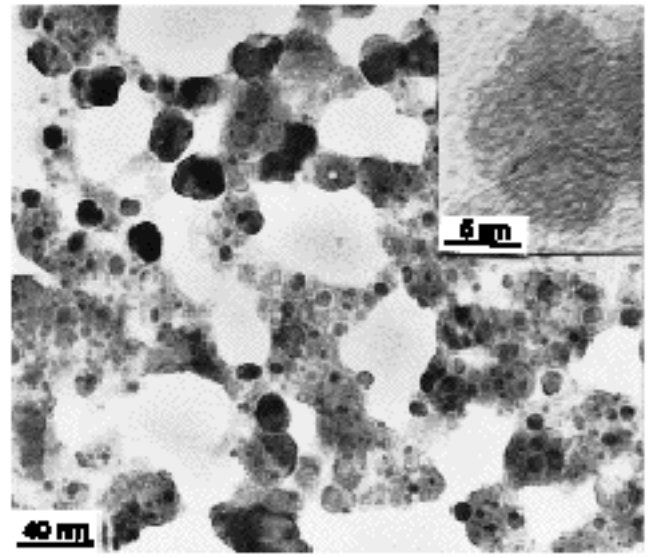



**Fig. 1** Transmission electron micrograph of AgI particles prepared with an initial $[I^-]/[TG]$ ratio of 9.0. The insert shows a high resolution TEM image of one particle.

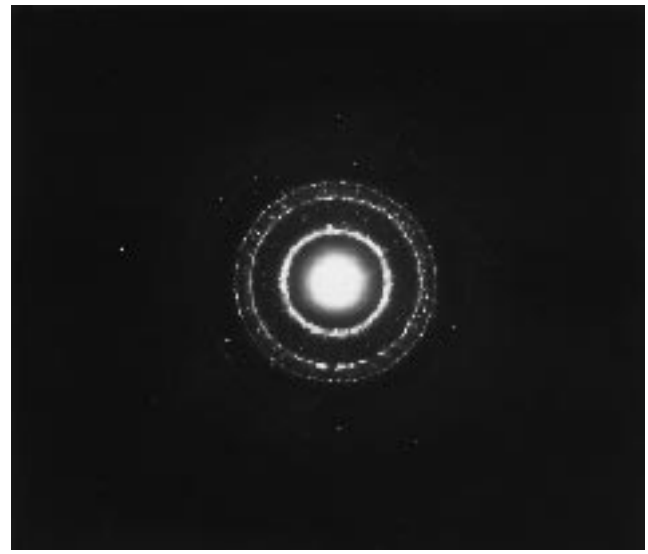


**Fig. 2** Electron diffraction pattern of the sample in Fig. 1

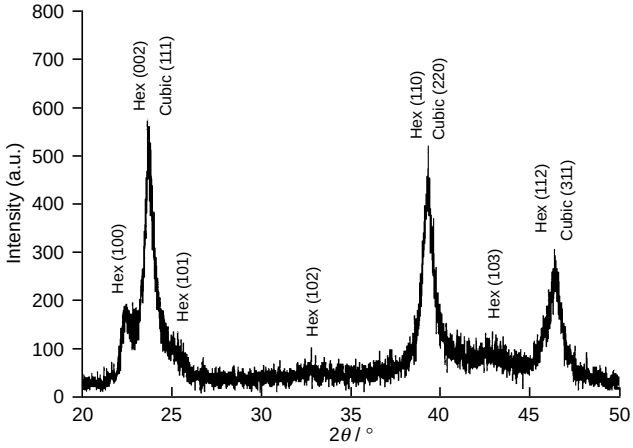



**Fig. 3** X-Ray diffraction pattern of the sample in Fig. 1

particles contain 36.5% of β- and 63.5% of γ-AgI. According to the theoretical dependence of X-ray diffraction peak intensity ratio, *R*, on the amounts of hexagonal and cubic AgI proposed by Berry (Fig. 1 in ref. 3, where *R* is the relative ratio of intensity of the center line of the diffraction triplet to the sum of intensities of the two outside lines, $[I(111)_{cubic} + I(002)_{hex}]/[I(100)_{hex} + I(101)_{hex}]$), a consistent result of 40.0% of β- and 60.0% of γ-AgI can be deduced.

The IR spectrum of the particles is similar with that of TG except for the absence of the S–H vibration peak at 2558 $cm^{-1}$. This phenomenon is also observed for other AgI particles prepared with lower $[I^-]/[TG]$ ratios, which contain more organics (up to 30.4%). Also, the resulting AgI solution is acidic (pH = 2.13). This shows that the following chemical reaction occurred (TG = R–SH):

$$R–SH + Ag^+ \text{ (surface)} \rightarrow R–SAg \text{ (surface)} + H^+ \qquad (1)$$

The thiolates are connected to the $Ag^+$ sites on the AgI particle surface *via* sulfur atoms, and act as the 'skin' of the AgI particles. Energy-dispersive X-ray microanalysis (Kevex system attached to Hitachi 8100) gave: Ag, 50.0; I, 45.2%. Thermogravimetry showed a 4.2% mass loss after heating the powder to 400 °C under a nitrogen atmosphere. If we assume that only the organics was lost after heat treatment (XRD confirmed that the residues were mainly AgI), about 88% of the organics were removed. After heating, the yellow powder turned black and bulk-like, with S still detected by EDX. This is reasonable owing to its strong interaction with silver ions. Upon decreasing the initial $[I^-]/[TG]$ ratio from 9.0 to 0.67, the size of the AgI particles decreased to *ca*. 7 nm as determined from XRD measurement, while the organic content increased to 30.4%.

We propose that this new method may find applications in large-scale synthesis of other I–VII nanoparticles such as AgBr or CuCl. Heat treatment may remove most of the organic layer. This suggests great potential in further increasing the electric conductivity of solid electrolytes by using nanometer sized AgI particles and futher work is under way.

This work was supported in part by Grant-in-Aids for Scientific Research on Basic Research (A: 09304068) and on Priority Areas (09215234), and a Grant-in-Aid for JSPS fellow from Ministry of Education, Science, Sports and Culture, Japan. One of us (S. C.) gratefully acknowledges a grant from the Japan Society for Promotion of Science for the postdoctoral fellowship.

## Footnote and References

* E-mail: kimura@sci.himeji-tech.ac.jp

1 T. Ida, H. Saeki, H. Hamada and K. Kimura, *Surf. Rev. Lett.*, 1996, **3**, 41.
2 T. Ida and K. Kimura, *Solid State Ionics*, in press.
3 C. R. Berry, *Phys. Rev.*, 1967, **161**, 848.
4 T. Tanaka, H. Saijo and T. Matsubara, *J. Photogr. Sci.*, 1979, **27**, 60.
5 H. Saijo, M. Iwasaki, T. Tanaka and T. Matsubara, *Photogr. Sci. Eng.*, 1982, **26**, 92.
6 M. I. Vucemilovic and O. I. Micic, *Radiat. Phys. Chem.*, 1988, **32**, 79.
7 A. Heiglein, M. Gutierrez, H. Weller, A. Fojtik and J. Jirkovsky, *Ber. Bunsen Ges. Phys. Chem.*, 1989, **93**, 593.
8 K. H. Schmidt, R. Patel and D. Meisel, *J. Am. Chem. Soc.*, 1988, **110**, 4882.
9 G. Hayes, K. H. Schmidt and D. Meisel, *J. Phys. Chem.*, 1989, **93**, 6100.
10 T. Vossmeyer, L. Katsikas, M. Giersig, I. G. Popovic, K. Diesner, A. Chemseddine and H. Weller, *J. Phys. Chem.*, 1994, **98**, 7665.
11 F. Izumi, H. Asano, H. Murata and N. Watanabe, *J. Appl. Crystallogr.*, 1987, **20**, 411.

*Received in Cambridge, UK, 28th July 1997; 7/05420C*

# Direct synthesis of gold nanodispersions in sol–gel derived silicate sols, gels and films

**S. Bharathi and O. Lev***

*Fredy and Nadine Herrmann School of Applied Sciences, The Hebrew University of Jerusalem, Jerusalem 91904, Israel*

**A simple method for the preparation of stable colloidal suspensions of gold nanoparticles in silicate sols, silicate based films and monoliths is presented; organically modified sol–gel monomers containing amine functional groups are used for the stabilisation of Au ions and the metal nanocrystalline sol.**

Several methods to produce metallic nanodispersions in aqueous and organic solvents have been recently reported.[1–4] In aqueous solutions colloids are stabilised by polymeric stabilisers [*e.g.* poly(vinyl pyrrolidine)][1] or buffer electrolytes such as *e.g.* citrate ions.[2] Long chain surfactants (*e.g.* quaternary ammonium compounds)[3] or specific ligands[4] are used to increase particle stability in organic solvents. In all these cases the removal of the stabilising agent causes immediate destabilisation of the sol. Encapsulation of metallic nanodispersions in sol–gel matrices is beset by additional complications. First, care should be taken to avoid aggregation or precipitation of the metal salts in the organic sol–gel precursors and additional means are required to prevent coalescence or precipitation of the metallic particles during sol–gel polymerisation. Two general schemes have been proposed for the encapsulation of metallic nanoparticles in sol–gel matrices. Silicate coated gold nanoparticles have been produced by preparing a gold sol by the citrate route and subsequent stabilisation by a 3-aminopropyltrimethoxysilane derived aminosilicate.[5] A second approach is based on sol–gel processing in inverse micelles.[6] Other methods to prepare highly dispersed metal particles in a porous support of silica or alumina were devised by hydrogen reduction or thermal decomposition of metal oxides or salts that were previously deposited on the support.[7] The method is simple to perform but gives a rather wide particle size distribution. Schubert and coworkers[8] developed a general methodology in which the metal ions are first attached to a silane monomer containing a chelating organofunctional group and then sol–gel polymerisation is initiated. The resulting gel is subsequently subjected to thermal oxidation giving a dispersion of metal oxide, which can then be reduced by treatment with hydrogen gas. Highly homogeneous monodispersions of nanocrystalline metals in sol–gel materials were produced by this method.

For practical reasons it is highly desirable that a single stabiliser should be employed for the stabilisation of the metal salt and the nanocrystalline sol. Additionally it is preferable that the sol will be stable for at least several weeks and that there should be no leaching of organic moieties or chelating agents from the supported catalysts. Sol–gel monomers containing amine functional chelating groups are very promising for this purpose. Alkylamines have been reported to form stable monolayers on bare gold substrates in the vapour phase[9] (although the stability of monolayers that were prepared from solvents was rather limited[10]). Furthermore, a recent report,[11] demonstrated that alkylamine can cap gold nanoparticles in a similar manner to that of thiols.[12]

Here, we use the precursors *N*-[3-(trimethoxysilyl)propyl]-ethylene diamine (EDAS) and aminopropyltrimethoxysilane (APS), which are capable of coordinating $AuCl_4^-$, stabilising the Au nanoparticles in the sol–gel solution, and becoming an integral and unleachable part of the supporting matrix after gelation. Gold colloid formation (*e.g.* by reduction with $NaBH_4$) can be initiated either before or after the polycondensation step. The preparation procedure involved the addition of the required amount of $HAuCl_4$ to EDAS or APS giving clear yellow solutions and subsequent sonication for 10 min. No phase separation or increased turbidity was noted, indicating a uniform dispersion of the gold salt in the silane precursor. The hydrolysis and condensation of the materials were then initiated by addition of a fixed quantity (3–5% by volume) of 0.1 M HCl and water (1–3% by volume) to the homogeneous solution. Formation of gold nanoparticles was achieved by subsequent dropwise addition of 0.4 M $NaBH_4$ solution (3–5% by volume) to the sol, causing an instantaneous purple coloration indicative of gold colloid formation.

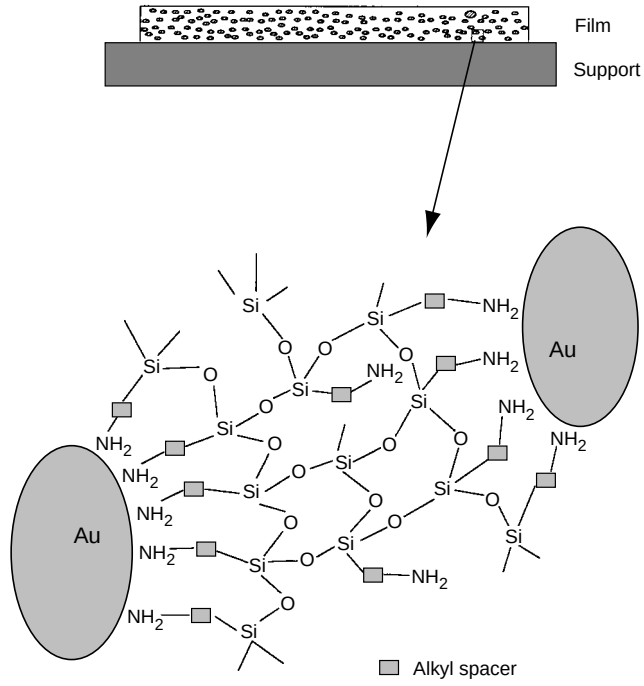
The general reaction can be represented by eqns. (1) and (2)

$$(MeO)_3Si–X–NH_2 + HAuCl_4^- \rightarrow (MeO)_3Si–X–NH_3^+AuCl_4^- \quad (1)$$

$$(MeO)_3Si–X–NH_3^+AuCl_4^- \xrightarrow{NaBH_4} (MeO)_3Si–X–NH_2Au_m \quad (2)$$

where X is an alkyl spacer. Thus, the tetrachloroaurate anions are bound to silane precursors, which assures good homogenisation, and after reduction of $AuCl_4^-$ the amine groups attach to and stabilize the metal nanoparticles. A schematic illustration of the gold nanoparticles in the aminosilicate network is shown in Scheme 1.

Absorbance spectra of typical sols are shown in Fig. 1. A surface plasmon peak at *ca*. 500–540 nm, characteristic of a




**Scheme 1** Schematic illustration of Au naoparticles in a silicate matrix

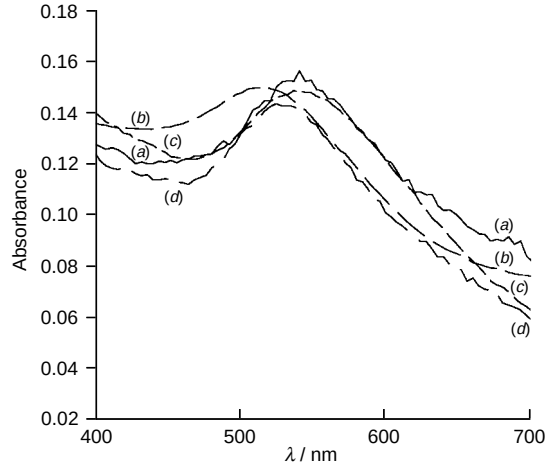



**Fig. 1** Visible spectra of different sols (*a*) EDAS : Au ratio 5 : 1 (*b*) EDAS : Au ratio 100 : 1, (*c*) the sol of (*a*) after a month and (*d*) thin film produced from sol (*a*)

gold sol, confirms the presence of Au nanoparticles. The surface plasmon absorbance of colloidal gold particles is affected by particle size as well as by the refractive index of the medium and thus it is impossible to determine the average particle size based on the optical characteristics alone.[13]

Gold sols were prepared with different EDAS : Au ratio, from < 1 : 1 to 100 : 1 in order to elucidate the sensitivity of particle size distribution to the gold loading. A stable gold sol was observed only for EDAS : Au ratio > 1. The absorbance spectra of the sols prepared using EDAS : Au = 5 : 1 and 100 : 1 are shown in Fig. 1(*a*) and (*b*). The absorbance maxima shifts from 540 to 514 nm as the Si : Au ratio is increased from 5 : 1 to 100 : 1. However, TEM investigations clearly showed that the particle size distribution was not affected by the Si : Au ratio, or by changing the aminosilane precursor. The small absorbance shift is probably caused by changes in the refractive index of the sol.[13] Fig. 1(*a*) and (*c*) show the absorbance spectra for a sol prepared with an Si : Au ratio of 5 : 1, taken 1 h after preparation and after a month. The time invariant spectra indicate good stability of the colloidal suspension. No visible aggregation of the particles took place over several months. Between the two silane precursors used, the EDAS–gold sols were stable for at least a few months as evidenced from the unchanged absorbance spectra. However gold sols prepared with APS were stable for only two weeks or so, after which slight deterioration of the sol homogeneity was observed. Attempts to prepare gold colloids using TEOS or methyltrimethoxysilane (MTMOS) without aminosilane precursors resulted in immediate aggregation of the gold particles during reduction with $NaBH_4$. This clearly establishes the role played by the aminosilanes in binding and dispersing the metal ions in addition to stabilising the Au nanoparticles.

The sol could be gelled to give monoliths of various shapes or films (1–10 μm thick) by dip or spin coating. A typical absorption spectrum of a thin silicate film containing a gold dispersion (prepared from a 5 : 1 EDAS : Au sol) is shown in Fig. 1(*d*). The resemblance of Fig. 1(*a*) and (*d*) indicates high stability of the dispersion which is maintained during sol–gel processing. Changes of sol–gel processing variables such as Si : HCl or Si : $H_2O$ ratio altered the rate of hydrolysis and gelation time but had no measurable influence on the particle size distribution of the resulting sol.

Transmission electron micrographs of the gold dispersed silica films were taken with a Philips electron microscope. A typical TEM image of gold nanoparticles prepared with EDAS : Au = 5 : 1 dispersed in a silicate network is shown in Fig. 2. It can be seen that the shape of the gold particles is mostly spherical with an average diameter of 5–6 nm. TEM images of particles obtained from the two aminosilane precursors were very similar. A few cylindrical (tubular) particles can also be seen which appear to be formed by coalescence of two or three particles.

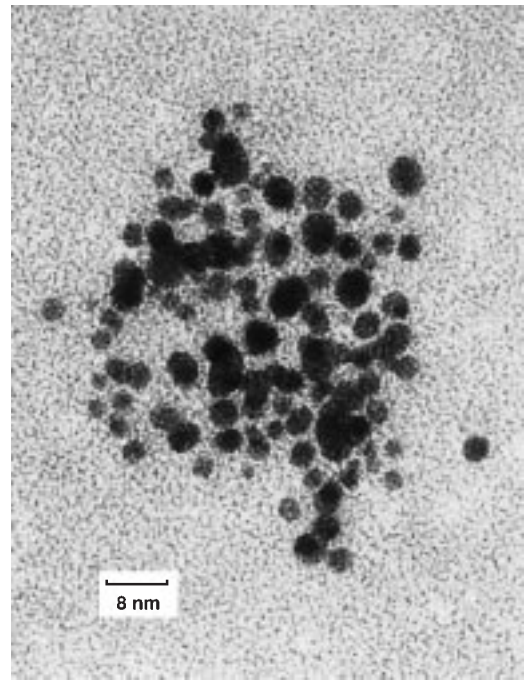



**Fig. 2** TEM image of Au nanoparticles with EDAS : Au ratio 5 : 1

In conclusion, it has been shown that Au nanoparticles can be stabilized in an organically modified silica sol, without the aid of any external stabilizing agent. Judicial selection of a suitable organo-functionalised sol–gel monomer can play a dual role of dispersing the metal salt precursors and stabilising the nanoparticles.

We thankfully acknowedge the financial help of MOS, Israel.

## Footnote and References

* E-mail: ovadia@vms.huji.ac.il

1 K. Megura, Y. Nakamura, Y. Hayashi, M. Torizuka and K. Esumi, *Bull. Chem. Soc. Jpn.*, 1988, 61, 347; N. Ishizuki, K. Torigoe, K. Esumi and K. Meguro, *Colloids Surf.*, 1991, **55**, 15.
2 G. Schmid, *Chem. Rev.*, 1992, **92**, 1709.
3 K. Torigoe and K. Esumi, *Langmuir*, 1992, **8**, 59.
4 G. Schmid and A. Lehnert, *Angew. Chem., Int. Ed. Engl.*, 1989, **28**, 780.
5 L. M. Liz-Marzan, M. Giersig and P. Mulvaney, *Langmuir*, 1996, **12**, 4329.
6 A. Martino, S. A. Yamanaka, J. S. Kawola and D. A. Loy, *Chem. Mater.*, 1997, **9**, 423.
7 T. Lopez, P. Bosch, M. Moran and R. Gomez, *J. Phys. Chem.*, 1993, **97**, 1671.
8 B. Breitscheidel, J. Zieder and U. Schubert, *Chem. Mater.*, 1991, **3**, 559; W. Morke, R. Lamber, U. Schubert and B. Brietscheidel, *Chem. Mater.*, 1994, **6**, 1659.
9 C. Xu, L. Sun, L. J. Kepley and R. M. Crooks, *Anal. Chem.*, 1993, **65**, 2102.
10 C. D. Bain, J. Evall and G. M. Whitesides, *J. Am. Chem. Soc.*, 1989, **111**, 7155.
11 D. V. Leff, L. Brandt and J. R. Heath, *Langmuir*, 1996, **12**, 4723.
12 M. Brust, M. Walker, D. Bethell, D. J. Schiffrin and R. Whyman, *J. Chem. Soc., Chem. Commun.*, 1994, 801.
13 P. Mulvaney and S. Underwood, *Langmuir*, 1994, **10**, 3427.

*Received in Cambridge, UK, 4th August 1997; 7/05609E*

# A short synthesis of conjugated unsaturated amides and esters *via* triphenylphosphine-catalysed isomerisation of acetylenic pentafluorophenyl esters†

**Uli Kazmaier**

*Organisch-Chemisches Institut der Universität, Im Neuenheimer Feld 270, 69120 Heidelberg, Germany*

**Isomerisation of acetylenic pentafluorophenyl esters in the presence of phosphines gives rise to activated dienoic acids, which can be coupled directly with amines and alcohols in a simple one-pot procedure.**

Highly unsaturated carboxylic and fatty acids are very common in different types of natural products.[1] Many of these sometimes very complex compounds show interesting biological activities and are applied as antibiotics.[2] Unsaturated esters are found as side-chains of sugars,[3] such as the antifungal active papulacandins,[4] or as parts of macrocyclic lactones.[5] Unsaturated amides find application as insecticides,[6] and modified peptides[7] and cyclopeptides[8] are highly interesting from a pharmaceutical point of view.

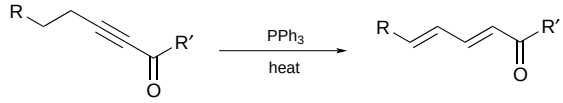
Apart from eliminations[9] and Knoevenagel condensations,[10] Wittig and Horner–Emmons[11] reactions are used frequently for the synthesis of conjugated unsaturated carboxylic acids. Besides these well established approaches, organometallic transformations, such as cross coupling reactions[12] or metal-catalysed isomerisations of acetylenes to dienes,[13] are also becoming more and more important.

Recently we described a new isomerisation of acetylenic carbonyl compounds in the presence of triphenylphosphine.[14] Similar results were obtained by Guo and Lu.[15] While acetylenic ketones can easily be isomerised in the presence of 5–10% of $PPh_3$ at 80–100 °C (Scheme 1), the corresponding less reactive esters react only in the presence of weak acids (*e.g.* acetic acid). If the reaction is applied to activated enynes or diynes, conjugated trienes or tetraenes can be obtained as well.[16]

The reaction probably starts with a nucleophilic addition of the phosphine on the activated triple bond, followed by a set of proton transfer steps. Perhaps these steps are accelerated by weak acids. This mechanism seams reasonable, because several of the possible intermediates could be trapped and used for further reactions, *e.g.* Michael additions.[17]

This procedure gives easy and cheap access to these interesting compounds, although problems may arise during the isomerisation process with acid- or thermo-labile compounds. Acetylenic amides only react, if at all, under even more drastic conditions,[14] which may not be 'survived' by sensitive amides, like peptides.

For an application of this process to natural product synthesis it would be desirable to work under mild conditions and/or to combine the isomerisation of an activated acetylene with a successive esterification (or amide formation), probably in a one-pot procedure. This approach can be realized by using the corresponding acetylenic pentafluorophenol esters. These relatively stable esters are used frequently in peptide syntheses, especially for the syntheses of strained cyclic peptides.[18] The isomerisation of these esters proceeds under much milder conditions (Table 1), because of the strong electron-withdrawing effect of the fluorine atoms and the resulting activation of the triple bond.




**Scheme 1**

Using 10 mol% of $PPh_3$ the isomerisation can be carried out at room temperature and under neutral conditions, which is important for the application of this procedure to sensitive substrates. Various acetylenic esters were investigated and, in general, the isomerisation was complete after stirring the reaction mixture overnight. The (*E*,*E*)-diene is formed almost exclusively (93–99%, as determined by NMR or GC analyses). If the esters tolerate higher temperatures, the amount of phosphine can be dramatically reduced, as shown with the last entries.‡ The higher temperatures are necessary for acceptable turnovers. From a synthetical point of view, it is convenient to carry out the isomerisation with 5% of phosphine at 50 °C, because under these conditions most reactions are complete after 4–5 h. The isomerisation only occurs in the presence of phosphines. No reaction was observed in the presence of tertiary amines, as determined by GC analysis, which is especially well-suited to monitoring the reaction progress. Obviously, the isomerisation proceeds directly from the acetylene to the conjugated diene. Allenic intermediates, as postulated in transition metal catalysed isomerisations,[13] could not be detected in any of the investigated examples.

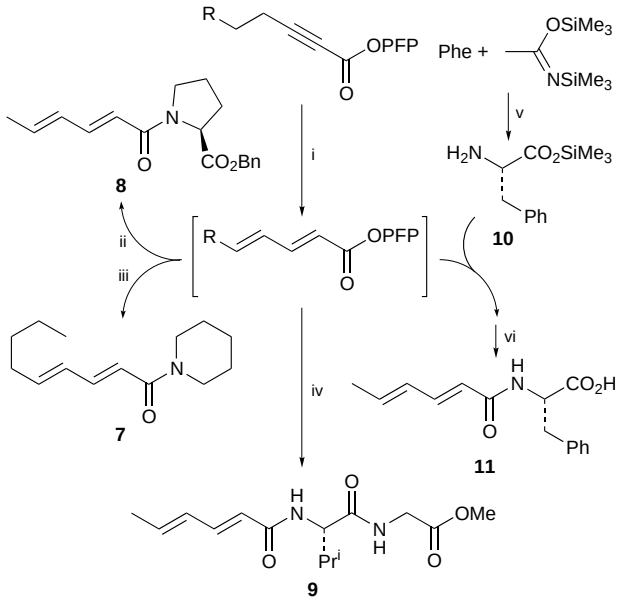
In general, the isomerisation proceeds in a very clean manner and without side reactions. Therefore the isomerised active esters can be coupled directly with nucleophiles in a one-pot procedure (Scheme 2).§ Thus conversion to the corresponding amides **7**, *e.g.* by reaction with amino acid esters **8** and peptides **9**, occurs at room temperature. To use this protocol in peptide syntheses, it would also be of interest to couple the dienoic acid to free amino acids, because the acylated amino acids obtained can be used directly for the next coupling step with further amino acids or peptides. This approach can be realized by heating the desired amino acid in toluene with bis(trimethylsilyl)acetamide (until the amino acid is completely dissolved) giving rise to the corresponding silyl ester **10**. The acylated amino acid **11** is obtained after acidic workup of the reaction mixture. The increased reactivity of the pentafluorophenol esters towards alkyl esters also allows their regioselective isomerisation and coupling, as illustrated with substrate **12** (Scheme 3).

**Table 1** $PPh_3$-catalysed isomerisations of **5**

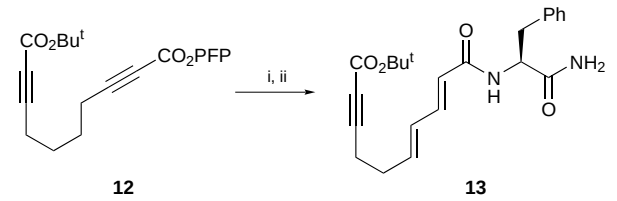
| $PPh_3$ (%) | *T*/°C | *t*/h | Conversion (%) |
|---|---|---|---|
| 10 | 25 | 2 | 43 |
| 10 | 25 | 14 | 67 |
| 10 | 25 | 14 | 97 |
| 5 | 50 | 4 | quant. |
| 1 | 50 | 4 | 46 |
| 0.1 | 100 | 40 | 59 |

The reaction is almost independent of the solvent used. Alcohols, especially sterically hindered ones, do not react under the conditions of amide formation, and they can be used as solvents for amines which are not soluble in less polar solvents. Nevertheless, esterification is possible under transesterification conditions, as described by Seebach *et al.*[19] (Scheme 4). In the presence of LiBr and 1,4-diazabicyclo[2.2.2]octane (DABCO) or DBU, acylated polyols (*e.g.* **14**) and steroids (*e.g.* **15**) can be obtained. The formation of the corresponding Weinreb amides[20] also needs higher temperatures (80 °C) in comparison to the reaction of other amines.

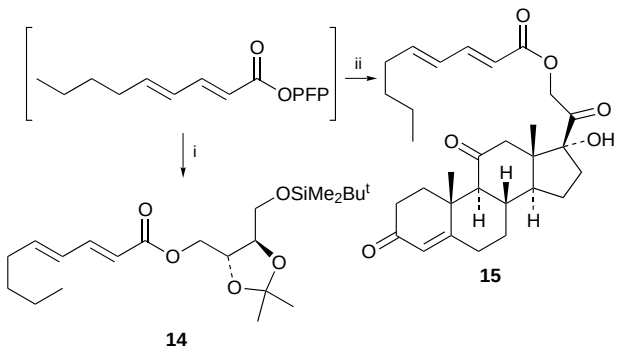
Professor Dr G. Helmchen is thanked for his generous support of this work. Financial support by the Deutsche Forschungsgemeinschaft and the Fonds der Chemischen Industrie is gratefully acknowledged.




**Scheme 2** *Reagents and conditions*: i, $PPh_3$, toluene, 50 °C, 5 h; ii, Pro-OBn, 74%; iii, piperidine, 81%; iv, Val-Gly-OMe, 75%; v, toluene, 110 °C, 4 h; vi, $H_3O^+$, 63%




**Scheme 3** *Reagents and conditions*: i, $PPh_3$ (5%), 50 °C, 5 h; ii, Phe-$NH_2$, room temp., 14 h, 66% over two steps




**Scheme 4** *Reagents and conditions*: i, Cortison, DBU, LiBr, DMF, toluene, 80 °C, 14 h, 64%; R*OH, DBU, LiBr, toluene–THF, 80 °C, 10 h

## Footnotes and References

* E-mail: ck1@ix.urz.uni-heidelberg.de

† Dedicated to Professor Huttner on the occasion of his 60th birthday.

‡ In these cases the reaction should be carried out under argon to avoid oxidation (deactivation) of the catalyst.

§ *General procedure* for the isomerisation/amide formation: 1 mmol each of alkynoic acid and pentafluorophenol were dissolved in 5 ml $CH_2Cl_2$ and, after addition of 0.1 mmol of DMAP, the solution was cooled to −20 °C. A solution of 1 mmol DCC in 1 ml $CH_2Cl_2$ was added and the mixture was allowed to warm to room temperature overnight. After filtration and evaporation of the solvent the residue was dissolved in 5 ml of toluene. After addition of 0.05 mmol of $PPh_3$ the solution was warmed to 50 °C for 5 h. After cooling to room temperature, 1–1.5 mmol of the corresponding amine were added and the mixture was stirred at room temperature overnight. The obtained crude product was purified by flash chromatography or crystallisation.

1 G. Habermehl and P. Hammann, *Naturstoffchemie*, Springer, Berlin, 1992.
2 U. Gräfe, *Biochemie der Antibiotika*, Spektrum, Heidelberg, 1992.
3 F. VanMiddlesworth, C. Dufrese, J. Smith and K. E. Wilson, *Tetrahedron*, 1991, **47**, 7563; Y. Doi, M. Ishibashi and J. Kobayashi, *Tetrahedron*, 1994, **50**, 8651; J. E. Hochlowski, D. N. Whittern, A. Buko, L. Alder and J. B. McAlpine, *J. Antibiot.*, 1995, **48**, 614.
4 P. Traxler, J. Gruner and J. A. L. Auden, *J. Antibiot.*, 1977, **30**, 289; A. G. M. Barrett, M. Pena and J. A. Willardsen, *J. Chem. Soc., Chem. Commun.*, 1995, 1145.
5 F. M. Arcamone, C. Bertazzoli, M. Ghione and T. G. Scotti, *Microbiol.*, 1959, **7**, 207.
6 F. Bohlmann and C. Zdero, *Chem. Ber.*, 1973, **106**, 1328.
7 A. Fredenhagen, S. Y. Tamura, P. T. M. Kenny, H. Komura, Y. Naya, K. Nakanishi, K. Nishiyama, M. Sugiura and H. Kita, *J. Am. Chem. Soc.*, 1987, **109**, 4409; J. Needham, M. T. Kelly, M. Ishige and R. J. Andersen, *J. Org. Chem.*, 1994, **59**, 2058.
8 R. Myokei, A. Sakurai, C. Chang, Y. Kodaira, N. Takahasi and S. Tamura, *Tetrahedron Lett.*, 1969, **9**, 695; M. Oka, Y.Nishiyama, S. Ohta, H. Kamei, M. Konishi, T. Miyaki, T. Oki and H. Kawaguchi, *J. Antibiot.*, 1988, **41**, 1331; H. Koshino, H. Osada, T. Yano, J. Uzawa and K. Isono, *Tetrahedron Lett.*, 1991, **32**, 7707.
9 K. Tanaka, M. Terauchi and A. Kaji, *Chem. Lett.*, 1981, 315, and references cited therein; T. Mandai, T. Moriyama, K. Tsujimoto, M. Kawada and J. Otera, *Tetrahedron Lett.*, 1986, **27**, 603.
10 J. Singh, K. L. Dhar and C. K. Atal, *Tetrahedron Lett.*, 1969, 4975.
11 D. Seebach, H. Chow, R. F. W. Jackson, K. Lawson, M. A. Sutter, S. Thaisrivongs and J. Zimmermann, *J. Am. Chem. Soc.*, 1985, **107**, 5292; U. Schmidt, A. Kleefeldt and R. Mangold, *J. Chem. Soc., Chem. Commun.*, 1992, 1687; R. W. Armstrong, *Tetrahedron Lett.*, 1994, **35**, 7743.
12 N. Lewis, P. W. McKeu and R. J. K. Taylor, *Synlett*, 1992, 898; F. Babudri, V. Fiandanese, F. Naso and A. Punzi, *Tetrahedron Lett.*, 1994, **35**, 2067; A. G. M. Barrett, M. Pena and J. A. Willardsen, *J. Chem. Soc., Chem. Commun.*, 1995, 1145.
13 B. M. Trost and T. Schmidt, *J. Am. Chem. Soc.*, 1988, **110**, 2301; D. Ma, Y. Lin, X. Lu and Y. Lu, *Tetrahedron Lett.*, 1988, **29**, 1045; D. Ma, Y. Lu and X. Lu, *J. Org. Chem.*, 1989, **54**, 1105.
14 B. M. Trost and U. Kazmaier, *J. Am. Chem. Soc.*, 1992, **114**, 7933.
15 C. Guo and X. Lu, *J. Chem. Soc., Chem. Commun.*, 1993, 394; C. Guo and X. Lu, *J. Chem. Soc., Perkin Trans. 1*, 1993, 1921.
16 S. D. Rychnovsky and J. Kim, *J. Org. Chem.*, 1994, **59**, 2659.
17 B. M. Trost and C. Li, *J. Am. Chem. Soc.*, 1994, **116**, 10 819; C. Zhang and X. Lu, *J. Org. Chem.*, 1995, **60**, 2906; C. Zhang and X. Lu, *Synlett*, 1995, 645; K. Liou and C. Cheng, *J. Chem. Soc., Chem. Commun.*, 1995, 1603.
18 U. Schmid, A. Lieberknecht, H. Griesser and J. Talbiersky, *J. Org. Chem.*, 1982, **47**, 3261.
19 D. Seebach, A. Thaler, D. Blaser and S. Y. Koo, *Helv. Chim. Acta*, 1991, **74**, 1102.
20 S. Nahm and S. M. Weinreb, *Tetrahedron Lett.*, 1991, **22**, 3815.

*Received in Liverpool, UK, 9th July 1997; 7/04927G*

# Solid-phase synthesis of tri-functionalised, α-substituted carbamoylmethyl-homocysteine compounds, their release from the resin and subsequent intramolecular cyclisation to give novel 1,3,3-trisubstituted succinimides

**J. Alan Girdwood and Richard E. Shute***

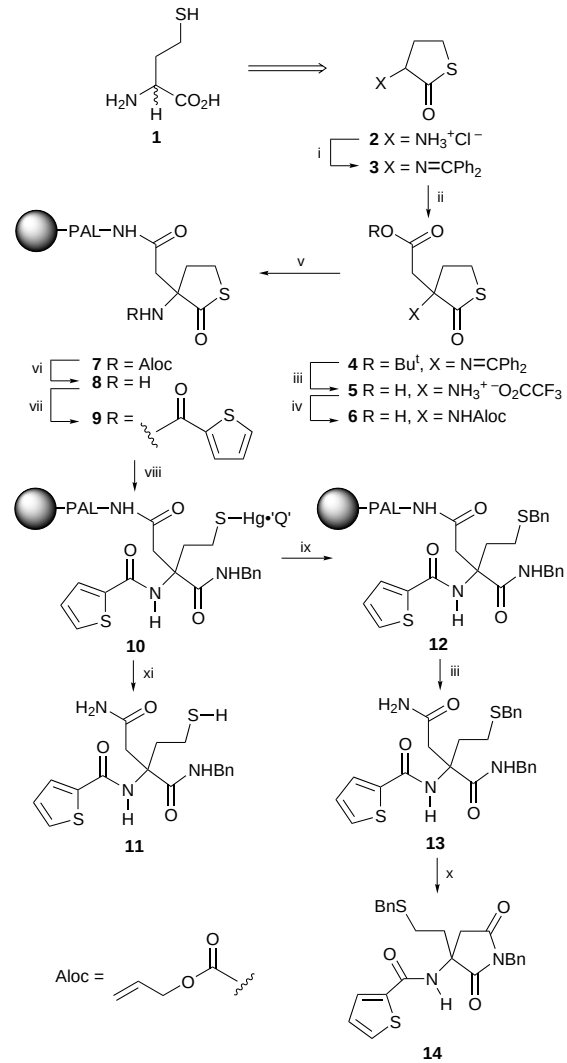
*ZENECA Pharmaceuticals, Mereside, Alderley Park, Macclesfield, Cheshire, UK SK10 4TG*

**Attachment of DL-homocysteine thiolactone to polystyrene resin *via* the PAL-linker and an α-carbamoylmethyl group, followed by amino, carboxy and thiol derivatisation, including a novel Hg-assisted thiolactone ring-opening, and acidolytic cleavage from the solid-phase yields novel 1,3,3-trisubstituted succinimides *via* intramolecular cyclisation.**

Recently, the pharmaceutical industry has undertaken far-reaching changes in order to foreshorten the timelines of drug discovery and development. Within the former of these two processes, the technology of combinatorial chemistry has assumed an ever-increasing importance.[1] Fundamental to the recent development of this technique has been the use of solid-phase organic chemistry (SPOC).[2] Here we report: (i) attachment of the amino acid homocysteine (hCys) **1** to a polystyrene-based solid-support *via* the PAL-linker[3] and an acetate-derived spacer group attached to the α-carbon of the amino acid; (ii) on-resin derivatisation of the orthogonal carboxy, amino and thiol functionalities; (iii) release of target compounds from the resin; and (iv) an unexpected intramolecular cyclisation of the target compounds leading to novel 1,3,3-trisubstituted succinimide compounds. Derivatisation of the amino functionality was achieved by means of a novel heavy metal-assisted ring-opening of the thiolactone. The chemistry described has been optimised to take place under mild conditions, to be high yielding, to use diverse substituents or building blocks which are readily available, and to yield compounds of high purity. It is thus eminently amenable to the generation of a compound library suitable for general biological screening purposes.

With the proviso that we wished to preserve the three hCys functionality handles for on-resin derivatisation, we envisaged connection of DL-hCys thiolactone **2**, a cheap and readily available precursor to hCys, to the resin *via* an acidolytic amide linker group attached to the α-carbon (Scheme 1). Off-resin reaction of **2** with benzophenone imine yielded the stable Schiff's base **3**.† Deprotonation of the α-position by KOBu$^t$ was followed by alkylation with $BrCH_2CO_2Bu^t$ to give **4** in good yield. Treatment of **4** with dilute acid gave the thiolactone amino acid **5** which could be readily $N^{\alpha}$-protected by treatment with allyl chloroformate (Aloc-Cl) under Schotten–Baumann conditions to give the crystalline, protected template **6**. Complete attachment of **6** to PAL-polystyrene resin[3] to give **7** was achieved by means of standard coupling reagents and a two-fold excess of **6**. $Pd^0$-catalysed Aloc-deprotection of **7** was achieved within 2 h at room temp. as indicated by cessation of $CO_2$ evolution, to give **8**. Coupling of the model carboxylic acid thiophene-2-carboxylic acid to **8** was achieved using an excess of symmetrical anhydride and yielded **9**.§

Attempts to ring-open the thiolactone of **9** to give amide and free thiol by treatment with $BnNH_2$ in *N*-methylpyrrolidone at elevated temperatures over many hours were unsuccessful. This was indicated by our failure, not only to observe the loss of the diagnostic thiolactone carbonyl absorption peak at *ca*. 1700 $cm^{-1}$ in the FT-IR spectrum of resin **9** (data gathered on a mull of **9** in $CHCl_3$), but also, on cleavage and analysis by HPLC and mass spectrometry, to see any compound other than that based on starting material. Addition of catalysts such as DMAP or NaCN also failed to effect the desired reaction. Finally, on-resin ring-opening was achieved by means of a novel Hg-assisted reaction in the presence of $BnNH_2$ to yield **10**.¶ The exact nature of the resultant resin-bound thiolate species, –S–Hg–'Q', remains unclear. Acidolytic cleavage of **10** using TFA (aq.) and




**Scheme 1** *Reagents and conditions*: i, $Ph_2C{=}NH$, $CH_2Cl_2$, room temp., 91%; ii, KOBu$^t$, THF, $BrCH_2CO_2Bu^t$, room temp., 89%; iii, TFA (aq.), 90%; iv, $CH_2{=}CHCH_2O_2CCl$, dioxane, $Na_2CO_3$ (aq.), room temp., 75%; v, PAL-resin, $Pr^iN{=}C{=}NPr^i$, 1-hydroxybenzotriazole, DMF, room temp. vi, $Pd(PPh_3)_4$, $Bu^n{}_3SnH$, AcOH, $CH_2Cl_2$, room temp. vii, thiophene-2-carboxylic anhydride, DMF, pyridine, room temp.; viii, $BnNH_2$, $Hg(O_2CCF_3)_2$, THF, room temp.; ix, BnBr, THF, room temp.; x, prolonged treatment with TFA–$H_2O$ 9 : 1, room temp. or 1% conc. HCl in MeOH, room temp., 90%; xi, TFA, $Et_3SiH$ 99 : 1

examination of the product by HPLC and mass spectrometry yielded material that contained 2–3 distinct chemical species, none of which was readily characterisable. On the other hand, when TFA–$Et_3SiH$ was used instead of TFA (aq.), the free thiol, **11**, as characterised by HPLC and mass spectrometry, was produced in high yield and purity. Elemental analysis of resin **10** showed Hg and F to be present as well as the other expected elements, suggesting that 'Q' comprised a $CF_3CO_2^-$ counterion derived from $Hg(O_2CCF_3)_2$. However, closer analysis of the elemental composition revealed a F : S ratio significantly less than 3 : 1. This further implied that 'Q' was not wholly $CF_3CO_2^-$ anion, but rather suggested a mixture of $CF_3CO_2^-$ and a putative crosslinked –S–Hg–S– form with two neighbouring on-resin hCys thiolates joined through a mercuric ion. Such a mixture of on-resin species might explain the observation of a mixture of products on cleavage of **10** under non-reducing conditions.

The final stage in the on-resin synthesis was achieved by direct treatment of **10** with excess BnBr to give **12**.**

Treatment of **12** with TFA (aq.) for 1 h gave **13,**‖ the conformationally flexible hCys product that was our initial target, in over 60% overall yield and with a purity greater than 90% by HPLC. Somewhat unexpectedly however, if the acid treatment time was increased, we observed in the reversed-phase HPLC a later running impurity, which, under prolonged TFA (aq.) treatment, became the predominant, and most stable chemical species. HPLC and mass spectrometry indicated that this material was derived from **13** by loss of $NH_3$. Furthermore, treatment of chromatographically purified **13** with HCl in MeOH (aq.) rapidly gave **14**‖ in greater than 90% yield. This material was identical to the later running impurity observed on prolonged treatment of **13** with TFA (aq.).

Compound **14** arises *via* an intramolecular cyclisation analogous to the peptidyl 'aspartimide' reaction, a rearrangement which can, in Asx-Gly/Ser containing peptides, lead to unnatural β-linked isoAsx-Gly/Ser sequences.[5] This cyclisation has a number of major consequences for the chemistry as originally conceived. Firstly, it removes the primary carboxamide functionality, that vestige of the compound's link to the solid support, by tying it back to the rest of the molecule in a succinimide ring. Secondly, and perhaps of greater significance in the context of this chemistry being of utility for the generation of compound libraries, the cyclisation does not cause any of the introduced diversity substituents to be lost. The final product **14** still retains all the functionality attached to hCys as was required in the original design, only now displayed around a different, more constrained scaffold.

Finally, it is of note that substituted succinimides have a long and rich history in medicinal chemistry particularly as bioisosteres of hydantoins,[6] and also that the hydantoin ring system itself was not only one of the very earliest heterocycles to be exploited in combinatorial chemistry,[7] but continues to be of interest for the generation of diverse compound libraries.[8] In a similar fashion, 1,3,3-trisubstituted succinimide-based compound libraries†† derived, as we have shown, either from α-carbamoylmethylhomocysteine, or potentially from other α-carbamoylmethyl-substituted amino acids, should also be of utility in drug discovery programmes. Our further studies on compounds of this general type[10] will be reported in due course.

The authors acknowledge the contributions of Peter Robins, Rachel Stead, Dearg Brown, Brian Main, David Hollinshead, Brian Wright, Kath Barber and Eddie Clayton to this work.

## Footnotes and References

* E-mail: richard.r.e.shute@alderley.zeneca.com

† For a recent reference to the solution-phase chemistry of amino acid Schiff's bases of this type see ref. 4(*a*). For a recent reference to on-resin, amino acid Schiff's base chemistry see ref. 4(*b*).

§ In order to confirm the integrity and follow the progress of any particular reaction, acidolytic cleavage of a few milligrams of resin was performed at various times throughout the course of all reactions by treatment with TFA in the presence of either $Et_3SiH$ or $H_2O$ and the products examined by HPLC and mass spectrometry. Also, all intermediate resins were analysed by quantitative elemental analysis for changes in heavy atom percentages as a means of estimating on-resin chemical yields.

¶ Further investigation of the scope of this reaction indicated that $Hg(O_2CCF_3)_2$ (2–3 equiv.) in the presence of excess amine was required for efficient and high yielding reaction, and also that only primary aliphatic amines were effective.

‖ *Selected physical data* for: **13**: $\delta_H([^2H_6]DMSO)$: 2.30 (m, 4 H), 2.96 (ABq, 2 H), 3.62 (s, 2 H), 4.30 (d, 2 H), 6.86 (br, 1 H), 7.23 (m, 12 H), 7.16 (m, 1 H), 7.27 (m, 1 H), 8.28 (s, 1 H), 8.49 (br, 1 H); $\nu_{max}(CHCl_3)/cm^{-1}$ 1667, 1638 (C=O). For **14**: $\delta_H([^2H_6]DMSO)$ 2.10 (m, 2 H), 2.42 (m, 2 H), 2.93 (ABq, 2 H), 3.72 (s, 2 H), 4.59 (ABq, 2 H), 7.16 (m, 1 H), 7.29 (m, 10 H), 7.78 (m, 1 H), 7.92 (m, 1 H), 8.80 (s, 1 H); $\nu_{max}(CHCl_3)/cm^{-1}$ 1777, 1708, 1619 (C=O).

** Extensive washing of the resin at this stage with solvents (THF, $CH_2Cl_2$, MeOH and $Et_2O$) and with dithiothreitol in THF gave material which, under stringent elemental analysis conditions, showed no evidence of any residual mercury (not greater than 1 ppm).

†† During the course of our development work on this chemistry we used the following nine diversity reagents: AcOH, thiophene-2-carboxylic acid, 2-naphthyloxyacetic acid (≡'A'–$CO_2H$); $BnNH_2$, isoamylamine, methoxyethylamine (≡'B'–$NH_2$); bromophenacyl bromide, 4-methoxybenzyl chloride and 4-nitrobenzyl bromide (≡'C'–$CH_2Br$), in the parallel synthesis of a $3 \times 3 \times 3$, 27-membered combinatorial library of discrete, single compounds. HPLC chromatography, with UV and evaporative light scattering detection (ref. 9), as well as mass spectrometry analyses of the 27 final products indicated that in all cases the correct succinimide products, which are analogues of **14**, were formed in greater than 50% overall yield and in greater than 70% purity. (Analytical data for these 27 succinimide compounds are available from the authors.)

1 M. A. Gallop, R. W. Barrett, W. J. Dower, S. P. A. Fodor and E. M. Gordon, *J. Med. Chem.*, 1994, **37**, 1233; E. M. Gordon, R. W. Barrett, W. J. Dower, S. P. A. Fodor and M. A. Gallop, *J. Med. Chem.*, 1994, **37**, 1385; N. K. Terrett, M. Gardner, D. W. Gordon, R. J. Kobylecki and J. Steele, *Tetrahedron*, 1995, **51**, 8135; G. Lowe, *Chem. Soc. Rev.*, 1995, **24**, 309; J. A. Ellman, *Acc. Chem. Res.*, 1996, **29**, 132; D. V. Patel and E. M. Gordon, *Drug Discovery Today*, 1996, **1**, 134.

2 For recent reviews, see: J. S. Fruchtel and G. Jung, *Angew. Chem., Int. Ed. Engl.*, 1996, **35**, 17; P. H. H. Hermkens, H. C. J. Ottenheijm and D. Rees, *Tetrahedron*, 1996, 5**2**, 4527; L. A. Thompson and J. A. Ellman, *Chem. Rev.*, 1996, **96**, 555; P. H. H. Hermkens, H. C. J. Ottenheijm and D. Rees, *Tetrahedron*, 1997, **53**, 5643.

3 F. Albericio, N. Kneib-Cordonier, S. Biancalana, L. Gera, R. I. Masada, D. Hudson and G. Barany, *J. Org. Chem.*, 1990, **55**, 3730.

4 (*a*) A. Lopez, M. Morenomanas, R. Pleixats, A. Roglans, J. Ezquerra and C. Pedregal, *Tetrahedron*, 1996, **52**, 8365; (*b*) M. J. O'Donnell, C. Zhou and W. L. Scott, *J. Am. Chem. Soc.*, 1996, **118**, 6070.

5 R. W. Roeske, in *The Peptides: Analysis Synthesis and Biology*, ed. E. Gross and J. Meienhofer, Academic Press, New York, 1981, vol. 3, pp. 102–136.

6 *Comprehensive Medicinal Chemistry*, ed. C. Hansch, P. G. Sammes and J. B. Taylor, Pergamon Press, Oxford, 1990, vol. 1, p. 55.

7 S. H. DeWitt, J. S. Kiely, C. J. Stankovic, M. C. Schroeder, D. M. Reynolds Cody and M. R. Pavia, *Proc. Natl. Acad. Sci. USA*, 1993, **90**, 6909.

8 B. A. Dressman, L. A. Spangle and S. W. Kaldor, *Tetrahedron Lett.*, 1996, **37**, 937; S. Hanessian and R.-Y. Yang, *Tetrahedron Lett.*, 1996, **37**, 5835.

9 M. Dreux, M. Lafosse and L. Morin-Allory, *LC GC Int.*, 1996, 148; C. Kibbey, *Mol. Diversity*, 1996, **1**, 247.

10 For recent references to similar 1,3,3-trisubstituted succinimides, see: W. L. Scott, C. Zhou, Z. Fang and M. J. O'Donnell, *Tetrahedron Lett.*, 1997, **38**, 3695; A. D. Abell and M. D. Oldham, *J. Org. Chem.*, 1997, **62**, 1509; D. Obrecht, C. Abrecht, M. Altorfer, U. Bohdal, A. Grieder, M. Kleber, P. Pfyffer and K. Mueller, *Helv. Chim. Acta*, 1996, **79**, 1315; M. L. Pedersen and D. B. Berkowitz, *J. Org. Chem.*, 1993, **58**, 6966; N. Sewald, J. Riede, P. Bissinger and K. Burger, *J. Chem. Soc., Perkin Trans. 1*, 1992, 267.

*Received in Glasgow, UK, 17th July 1997; 7/05757A*

# Inhibition of carboxypeptidase A by (*S*)-2-mercapto-3-phenylpropanoic acid

**Christopher M. Lanthier, Gregory R. MacKinnon and Gary I. Dmitrienko***

*Guelph-Waterloo Centre for Graduate Work in Chemistry, Waterloo Campus, Department of Chemistry, University of Waterloo, Waterloo, Ontario, Canada N2L 3G1*

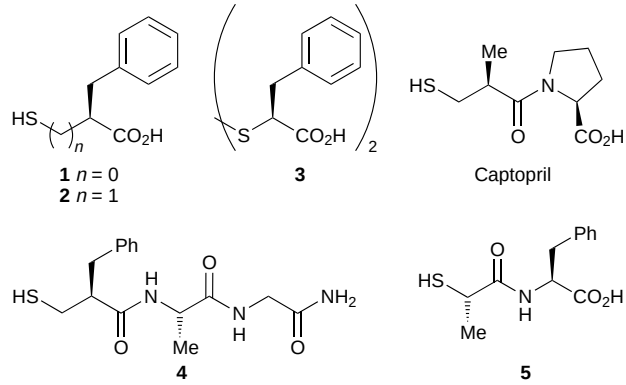
**(*S*)-2-Mercapto-3-phenylpropanoic acid is an effective competitive inhibitor of carboxypeptidase A, comparable in potency to (*S*)-3-mercapto-2-benzylpropanoic acid.**

Divalent metal ion-dependent proteolytic enzymes are involved in a wide variety of physiologically important processes and play a role in a number of disease states. It is widely recognized that selective inhibition of such enzymes is a viable strategy for therapeutic intervention. Notable successes have been reported in the development of very effective antihypertensive agents which function through inhibition of zinc-dependent angiotensin converting enzyme (ACE).[1] Intensive research efforts are underway aimed at developing related specific inhibitors for other zinc-dependent proteases such as neutral endopeptidase 24.11 and the matrix metalloproteases.[2,3] The ability to carry out rational design of inhibitors for such enzymes has been built upon detailed observations made in the development of specific inhibitors for the better characterized and understood zinc-dependent proteases such as carboxypeptidase A (CPA) and thermolysin.[4] Thus CPA has served as a valuable model system for the elucidation of guiding principles for the design of inhibition strategies for other less well understood but therapeutically important zinc-dependent proteases.

The now classical studies of the inhibition of CPA by benzylsuccinic acid[5] and by mercaptocarboxylic acid derivatives[6–8] played an important role in the definition of design criteria for the extremely successful commercial antihypertensive agents enaloprilat[9] and captopril.[10] The observation of the relative potencies of (±)-2-mercapto-3-phenylpropanoic acid **1** ($K_i$ = 1.2 μM)[7] and its homologue (*S*)-2-benzyl-3-mercaptopropanoic acid **2** ($K_i$ = 7.8 nM)[8] as competitive inhibitors of CPA has led to the conclusion that the insertion of a methylene group between the metal binding mercapto group and the α-carbon of an α-mercapto carboxylic acid derivative results in an optimal interaction between the active site and the mercapto, carboxylate and hydrophobic side chains of the inhibitor. The fact that inclusion of a similar methylene spacer between the mercapto group and the remainder of the structure of the ACE inhibitor captopril results in very high inhibitory potency ($K_i$ = 1.7 nM)[10] reinforced the belief that a spacing of approximately 4.1 Å between the sulfur atom and the carbonyl group carbon represents the ideal spatial relationship.

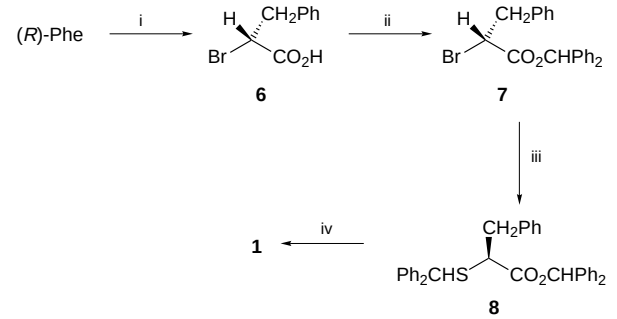
In the course of studies of the hydrolysis of thioesters by CPA we have prepared optically active 2-mercapto-3-phenylpropanoic acid **1** and have examined the kinetics of inhibition of CPA by this thiol. We report herein our observation that **1** is a much more effective inhibitor of the peptidase activity of CPA than previously believed, rivaling the potency of 3-mercapto-2-benzylpropanoic acid **2**, and point out the possible significance of this observation with respect to the rational design of specific zinc-binding inhibitors for metalloproteases.

The thiol **1** was synthesized *via* the route shown in Scheme 1. The known bromoacid **5**, prepared with retention of configuration by diazotization of (*R*)-phenylalanine in the presence of bromide, was converted to the benzhydryl ester **6** which was subjected to an $S_N2$ displacement with 1,1-diphenylmethanethiol as the nucleophile. Deprotection using trifluoroacetic acid–phenol yielded the free thioacid **1** (89% ee as measured by $^1$H NMR analysis of the Mosher's thioester[11] form of **1**.




Progress curves† for the CPA catalyzed hydrolysis of hippuryl-L-phenylalanine (HP)[12] in the presence of **1** were found to be biphasic with an initial low rate observed at short reaction times and a higher reaction rate at longer reaction times. That this phenomenon was associated with air oxidation of the thiol to the corresponding disulfide **3** was revealed by the fact that preincubation of solutions of **1** in air until no thiol could be detected using DTNB[13] assays prior to use in inhibition studies abolished the biphasic nature of the progress curves. The slopes of such progress curves were equal to those observed for the second phase of the biphasic curves observed in experiments employing solutions with equal concentrations of **1** which had not been preincubated in air. The inhibition by the disulfide **3**, which was isolated from such solutions and fully characterized, was found to be of the same order of magnitude as reported previously for the thiol **1** [$K_i$ = 3.6 ± 0.5 μM (competitive) for **3** *vs.* reported apparent $K_i$ of 1.2 μM (ref. 7) for racemic **1**].

Measurement of the true inhibitory potency of the thiol **1** required experimental conditions which inhibited the air oxidation process. This was eventually achieved by working with an argon atmosphere or, much more conveniently, by adding glutathione as an antioxidant. It was found that concentrations of glutathione as high as 0.1 mM could be tolerated without any observable influence on the rate of CPA




**Scheme 1** *Reagents and conditions*: i, NaBr, $NaNO_2$, $H_2SO_4$; ii, $Ph_2CN_2$, ether; iii, $Ph_2CHSH$, acetone; iv, $CF_3CO_2H$, $CH_2Cl_2$, PhOH

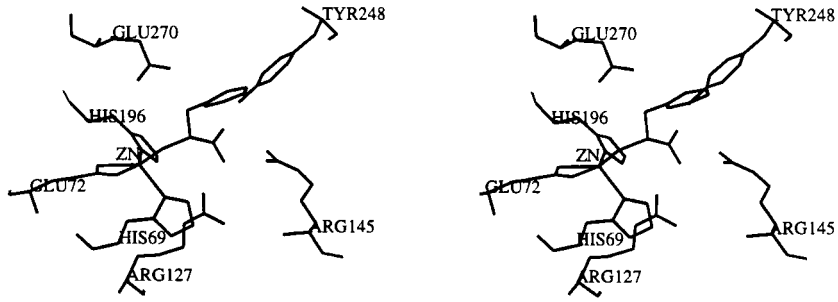



**Fig. 1** Stereoview of the predicted binding mode of **1** to the active site of CPA

catalyzed hydrolysis of HP. Inhibition of the CPA catalyzed hydrolysis of HP by **1** in the presence of glutathione was found to fit a competitive inhibition model as indicated in the Lineweaver–Burk plots.

Estimation of the potency of inhibition by **1** was complicated by the fact that the affinity of **1** for CPA was sufficiently high that inhibitor and enzyme depletion phenomena are significant and render invalid the normal assumptions associated with kinetic models of reversible inhibition. As a result, the graphical method of Dixon[14] which avoids such assumptions was employed to determine $K_i$ for inhibition of CPA catalyzed hydrolysis of HP to be 12.6 ± 1.0 nM. It thus appears likely that, in the earlier studies which concluded that the apparent $K_i$ for inhibition of peptidase activity by (±)-**1** was 1.2 μM (ref. 7), the inhibition observed resulted largely from the presence of the disulfide **3** rather than the thiol **1**.

The recognition that **1** ($K_i$ = 12.6 nM) is comparable in potency to **2** ($K_i$ = 7.8 nM)[8] raises interesting questions concerning the dimensions of the pharmacophore for selective zinc-binding inhibitors for $Zn^{2+}$-dependent proteases. It has been assumed previously that the apparent substantially higher inhibitory potency of **2** arose from the ability of the benzyl side chain of **2** to bind in the hydrophobic $S_{1'}$ pocket in the active site with the thiol sulfur atom interacting favorably with the $Zn^{2+}$ ion and the carboxylate group interacting with Arg-145. Docking of a model of **2** (not shown) in the active site of CPA‡ as defined by X-ray crystallographic coordinates suggests that such a hypothesis is reasonable and consistent with the active site interactions observed between the related thiol-type inhibitor **4** and the zinc-dependent endopeptidase thermolysin.[15] The apparent lower potency of the thiol inhibitor **1** has been assumed to result from an inability of the hydrophobic side chain, the thiol and the carboxylate group to simultaneously interact with the potential binding sites which are accessible to the same groups in the homologue **2**. A molecular modeling analysis of **1** docked in the active site of CPA confirms that the benzyl group in **1** has a diminished interaction with the hydrophobic pocket in the $S_{1'}$ subsite when the sulfhydryl sulfur atom is liganded to zinc and also reveals an interesting favorable interaction between the carboxylate of **1** and Arg-127 which might offset the loss of binding energy associated with the diminished hydrophobic interactions (Fig. 1). This model, although speculative, does suggest strategies for modification of the structure of 2-mercaptocarboxylic acid inhibitors to enhance inhibitor potency by increasing the interaction with the hydrophobic pocket which are now being pursued in this laboratory.

Although our observations clearly indicate the need for consideration of the stability of thiol type inhibitors in evaluation of inhibitory potency against zinc dependent proteases, it should be emphasized that some thiols are much better behaved than **1** and do not require the use of anaerobic conditions or radical scavengers in inhibition studies. For example the rates of air oxidation of the 3-mercaptocarboxylic acid **2** or the 2-mercaptocarboxamide **5**, which is a potent inhibitor of angiotensin converting enzyme,[16] are substantially lower than that observed for **1** such that no special precautions were found to be necessary in kinetic investigations with these compounds. Studies aimed at developing a mechanistic rationale for the susceptibility of 2-mercaptocarboxylates towards air oxidation are in progress.

## Footnotes and References

* E-mail: dmitrien@muskie.uwaterloo.ca

† CPA activity assays were conducted in 25 mM tris-HCl, 0.5 M NaCl, pH 7.5 containing 3.5% ethanol (v/v) at 25 °C using hippuryl-L-phenylalanine as substrate. Enzyme concentrations ranged from 113 to 126 nM, as determined using absorption at 280 nm ($\varepsilon_{280}$ = 6.42 × $10^4$ $M^{-1}$ $cm^{-1}$).[7]

‡ Molecular modeling studies were conducted using the software package SYBYL 6.2 (Tripos Associates Inc.) with crystal coordinates for carboxypeptidase A bound to [(−)-2-carboxy-3-phenylpropyl]methylsulfodiimine[17] (pdb1cps) obtained from the Brookhaven Protein Data Bank.

1 L. H. Opie, *Angiotensin Converting Enzyme Inhibitors*, Wiley-Liss, New York, 1992.
2 R. Bohacek, S. De Lombaert, C. McMartin, J. Priestle and M. Grütter, *J. Am. Chem. Soc.*, 1996, **118**, 8231; B. P. Roques, F. Noble, V. Daugé, M. C. Fournié-Zaluski and A. Beaumont, *Pharmacol. Rev.*, 1993, **45**, 87; E. Fillion and D. Gravel, *Bioorg. Med. Chem. Lett.*, 1996, **6**, 2097.
3 B. Lovejoy, A. Cleasby, A. M. Hassell, K. Longley, M. A. Luther, D. Weigl, G. McGeehan, A. B. McElroy, D. Drewry, M. H. Lambert and S. R. Jordan, *Science*, 1994, **263**, 375; M. F. Browner, W. W. Smith and A. L. Castelhano, *Biochemistry*, 1995, **34**, 6602; R. P. Beckett, A. H. Davidson, A. H. Drummond, P. Huxley and M. Whittaker, *Drug Discovery Today*, 1996, **1**, 16.
4 W. N. Lipscomb and N. Sträter, *Chem. Rev.*, 1996, **96**, 2375; B. W. Matthews, *Acc. Chem. Res.*, 1988, **21**, 333; H. Kim and W. N. Lipscomb, *Biochemistry*, 1991, **30**, 8171; D. W. Christianson and W. N. Lipscomb, *Acc. Chem. Res.*, 1989, **22**, 62–69; P. A. Bartlett and C. K. Marlowe, *Biochemistry*, 1983, **22**, 4618.
5 L. D. Byers and R. Wolfenden, *Biochemistry*, 1973, **12**, 2070; L. D. Byers and R. Wolfenden, *J. Biol. Chem.*, 1972, **247**, 606.
6 J. Suh, S. H. Lee and J. Y. Uh, *Bioorg. Med. Chem. Lett.*, 1995, **5**, 585.
7 B. Holmquist and B. L. Vallee, *Proc. Natl. Acad. Sci. USA*, 1979, **76**, 6216.
8 M. A. Ondetti, M. E. Condon, J. Reid, E. F. Sabo and H. S. Cheung, *Biochemistry*, 1979, **18**, 1427; D. H. Kim and Y. J. Kim, *Bioorg. Med. Chem. Lett.*, 1993, **3**, 2681.
9 A. A. Patchett, *Nature*, 1980, **288**, 280; R. Shiparo and J. F. Riordan, *Biochemistry*, 1984, **23**, 5225.
10 D. W. Cushman, H. S. Cheung, E. F. Sabo and M. A. Ondetti, *Biochemistry*, 1977, **16**, 5484.
11 J. A. Dale, D. L. Dull and H. S. Mosher, *J. Org. Chem.*, 1969, **34**, 2543.
12 J. E. Folk and E. W. Schirmer, *J. Biol. Chem.*, 1963, **238**, 3884.
13 P. W. Riddles, R. L. Blakely and B. Zerner, *Anal. Biochem.*, 1979, **94**, 75.
14 M. Dixon, *Biochem. J.*, 1972, **129**, 197.
15 A. F. Monzino and B. W. Matthews, *Biochemistry*, 1982, **21**, 3390.
16 C. M. Lanthier, PhD Thesis, University of Waterloo, 1996.
17 A. M. Cappalonga, R. S. Alexander and D. W. Christianson, *J. Biol. Chem.*, 1992, **267**, 19 192.

*Received in Corvallis, OR, USA, 4th August 1997; 7/05741E*

# Highly diastereoselective hetero-Diels–Alder reactions of alkenyldihydrooxazoles as an approach to novel pyrimidine derivatives

**Mark C. Elliott* and Elbertus Kruiswijk**

*Department of Chemistry, University of Wales Cardiff, PO Box 912, Cardiff, UK CF1 3TB*

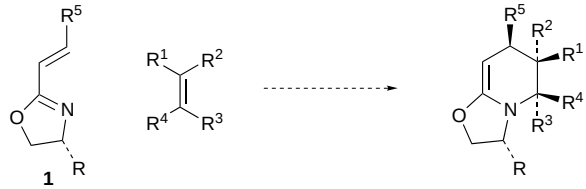
**Chiral 2-alkenyldihydrooxazoles react with two equivalents of aryl and arylsulfonyl isocyanates to give chiral non-racemic dihydropyrimidone derivatives in high yield and with complete diastereocontrol.**

Despite the proven synthetic utility of the all-carbon Diels–Alder reaction,[1] the aza analogue has been much less investigated.[2,3] It offers the opportunity to prepare a wide range of biologically interesting piperidines in a single step with control over three stereogenic centres. We considered the possibility that alkenyldihydrooxazoles **1** could act as aza-dienes,[4] and since these compounds are readily available in enantiopure form from amino alcohols, an asymmetric aza-Diels–Alder reaction as shown schematically in Scheme 1 is an attractive possibility. To the best of our knowledge there is only one example of the use of alkenyldihydrooxazoles as aza-dienes. However, the reported infrared stretching absorption of the product (1760 $cm^{-1}$) seems inconsistent with the assigned structure **2** (Scheme 2).[5] Since neither the yield nor reaction conditions were reported, we felt it would be useful to investigate the reactions of alkenyldihydrooxazoles with isocyanates as a prelude to a broader study.[6,7]

To this end, dihydrooxazoles **3**–**6** were prepared as shown in Scheme 3 from readily available (*R*)-2-aminobutan-1-ol.

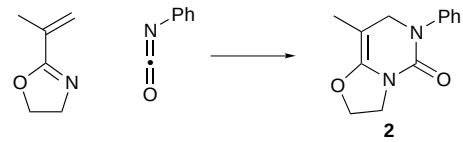
When **3** was heated in a sealed tube (150 °C, 1 h) with 2 equiv. of phenyl isocyanate, an essentially pure 2 : 1 adduct was obtained to which structure **8a** was assigned on the basis of spectroscopic data.†,‡ In fact, this reaction proceeds at room temp. (24 h), and at either temperature only a *single diastereoisomer was observed* (Scheme 4). Presumably this reaction proceeds *via* addition of a second molecule of phenyl isocyanate to compound **7**. The absence of any other products in the $^1H$ and $^{13}C$ NMR spectra of the crude reaction mixture conducted under a wide range of stoichiometries lead us to conclude that this process is faster than the hetero-Diels–Alder reaction. For a such a small chiral directing group this selectivity is particularly impressive.

The reactions of **3**–**5** with five different isocyanates gave similar results as shown in Table 1. In each case only a single



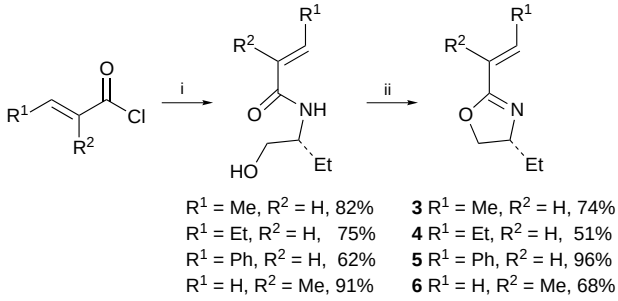
**1**

**Scheme 1**

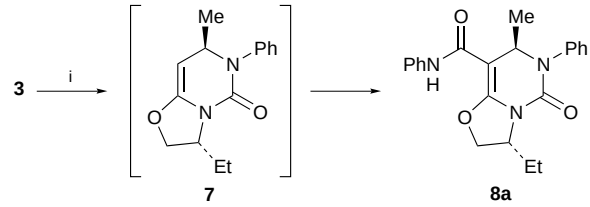


**2**

**Scheme 2**



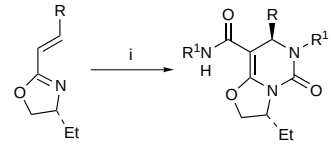

**Scheme 3** *Reagents and conditions*: i, (*R*)-2-aminobutan-1-ol, $Na_2CO_3$, $CH_2Cl_2$; ii, $MeSO_2Cl$, $Et_3N$, $CH_2Cl_2$



**7** **8a**

**Scheme 4** *Reagents and conditions*: i, 2 equiv. PhNCO, 150 °C for 1 h or 25 °C for 24 h

**Table 1** Reactions of **3**, **4** and **5** with selected isocyanates



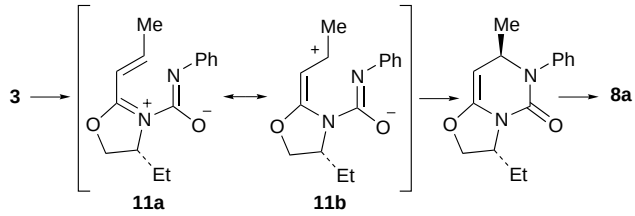
**3** R = Me
**4** R = Et
**5** R = Ph

**8** R = Me
**9** R = Et
**10** R = Ph

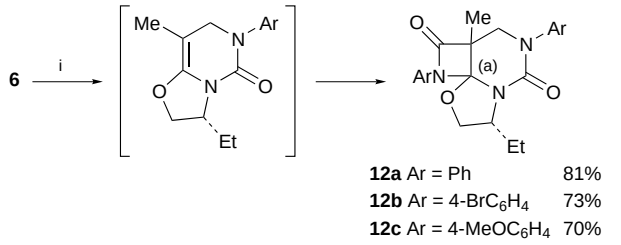
**a** $R^1$ = Ph
**b** $R^1$ = 4-$BrC_6H_4$
**c** $R^1$ = 4-$O_2NC_6H_4$
**d** $R^1$ = 4-$MeOC_6H_4$
**e** $R^1$ = 4-$MeC_6H_4SO_2$

| $R^1$ | $R^2$ | *t*/h | *T*/°C | Compound (yield %)[a] |
|---|---|---|---|---|
| Me | Ph | 48 | 25 | **8a** (58) |
| Me | 4-$BrC_6H_4$ | 24 | 25 | **8b** (61) |
| Me | 4-$O_2NC_6H_4$ | 21 | 25 | **8c** (82) |
| Me | 4-$MeOC_6H_4$ | 120 | 25 | **8d** (65) |
| Me | 4-$MeC_6H_4SO_2$ | 0.5 | 25 | **8e** (59) |
| Et | Ph | 1 | 150 | **9a** (53) |
| Et | 4-$BrC_6H_4$ | 1 | 150 | **9b** (61) |
| Et | 4-$O_2NC_6H_4$ | 1 | 150 | **9c** (71) |
| Et | 4-$MeOC_6H_4$ | — | — | **9d** (0)[b] |
| Et | 4-$MeC_6H_4SO_2$ | 0.5 | 25 | **9e** (90) |
| Ph | Ph | 1 | 150 | **10a** (76) |
| Ph | 4-$BrC_6H_4$ | 1 | 150 | **10b** (59) |
| Ph | 4-$O_2NC_6H_4$ | 1 | 150 | **10c** (74) |
| Ph | 4-$MeOC_6H_4$ | 1 | 150 | **10d** (10)[c] |
| Ph | 4-$MeC_6H_4SO_2$ | 0.5 | 25 | **10e** (94) |

[a] Yields refer to pure isolated compounds, and are not optimised. [b] The $^1H$ NMR spectrum of the crude reaction mixture shows a small amount of the desired product. No dihydrooxazole remains unreacted. [c] Not completely purified.




**Scheme 5**




**12a** Ar = Ph 81%
**12b** Ar = 4-$BrC_6H_4$ 73%
**12c** Ar = 4-$MeOC_6H_4$ 70%

**Scheme 6** *Reagents and conditions*: i, 2 equiv. ArNCO, 150 °C, 24 h

diastereoisomer was observed in the $^1$H and $^{13}$C NMR spectra of the crude reaction mixture. The stereochemistry of **8c** and **10e** were determined by single crystal X-ray diffraction. All other compounds are assumed, on the basis of similar spectroscopic data, to have the same stereochemistry.

There has been much debate about the concerted nature, or lack thereof, in both normal[8] and hetero[9] Diels–Alder reactions. Given the highly polarised nature of the reacting partners, the initial interaction may be best represented as initial acylation of the dihydrooxazole nitrogen as shown in Scheme 5.[10] However, the present results do not rule out a concerted (although probably asynchronous) aza-Diels–Alder reaction.

The subsequent addition of the isocyanate may proceed either by a direct [2πs + 2πa] cycloaddition followed by cleavage of the β-lactam or by a stepwise enamine acylation.[11] In fact, when **6** was subjected to similar reaction conditions (2 equiv. phenyl isocyanate, 150 °C, 24 h) compound **12a** was obtained§ as a 1.7 : 1 mixture of diastereoisomers (Scheme 6). Similar reactions were observed with 4-bromophenyl and 4-methoxyphenyl isocyanates. No product could be isolated from the reaction with 4-nitrophenyl isocyanate, presumably due to the ease of hydrolysis of the corresponding β-lactam.

The structures of compounds **12** were assigned by analogy with compounds **8**–**10**, and are supported by extensive NOE studies. Unfortunately we have been unable to assign the stereochemistry of the major isomer. Furthermore, the quaternary carbon (a) in Scheme 6 is significantly deshielded ($^{13}$C resonance in **12**, 152.6 ppm), which could be explained by the contribution of a zwitterionic resonance form **13** to the overall structure (Fig. 1). The existence of **12** as a full zwitterion seems unlikely on the grounds of polarity. Rigorous purification of **12a**–**c** proved difficult due to the lability of these compounds. Chromatography over neutral alumina gave essentially pure compounds, although traces of the diaryl urea, derived from the isocyanate, could not be completely removed. To the best of our knowledge this work represents the first synthesis of the azeto[3′,2′ : 5,6]pyrimido[6,1-*b*]oxazole ring system. We are unable to consolidate our data with that of Seeliger *et al.*[5]

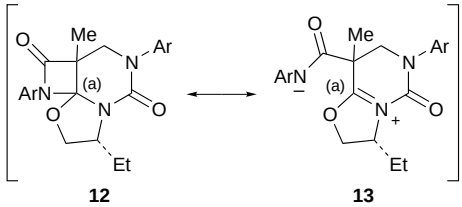



**Fig. 1**

This new variation on the Diels–Alder reaction has considerable potential in the provision of novel chiral nonracemic compounds. This is, as far as we are aware, only the second report of an asymmetric aza-Diels–Alder reaction of a chiral 1-azadiene.[3] Detailed experimental and computational studies are in progress to determine the mechanism and origin of stereoselectivity with a view to realising the potential of this reaction.

We thank the University of Wales, Cardiff for financial support of this research, Mrs A. Dams for microanalytical data and Mr R. Jenkins for mass spectrometric data. The X-ray crystallographic study of compounds **8c** and **10e** was carried out by Professor M. B. Hursthouse, Mr D. E. Hibbs and Mr D. S. Hughes of this department. Full details will be published elsewhere.

## Footnotes and References

* E-mail: elliottmc@cardiff.ac.uk

† All compounds exhibit satisfactory spectroscopic and analytical data.

‡ *Selected data* for **8a**: $\delta_H$(400 MHz; $CDCl_3$; *J*/Hz) 8.32 (1 H, s, N*H*), 7.47 (2 H, d, *J* 7.9, Ar-H), 7.33 (2 H, d, *J* 7.5, Ar-H), 7.28–7.20 (5 H, m, Ar-H), 7.00 (1 H, t, *J* 7.4, Ar-H), 4.89 (1 H, q, *J* 6.2, Me-C*H*), 4.60 (1 H, app. t, *J* 8.1, O-C*H*), 4.48 (1 H, dd, *J* 8.4 and 1.6, O-C*H*), 4.31 (1 H, m, *H*C-Et), 1.99–1.93 (1 H, m, one of C$H_2$), 1.90–1.83 (1 H, m, one of C$H_2$), 1.22 (3 H, d, *J* 6.2, C$H_3$), 0.87 (3 H, t, *J* 7.4, C$H_3$); $\delta_C$(100 MHz; $CDCl_3$) 162.6 (C=O), 152.1 (C=O), 150.4 (C=C), 140.3 (C), 139.0 (C), 129.6 (CH), 129.3 (CH), 128.3 (CH), 127.0 (CH), 123.9 (CH), 120.2 (CH), 83.8 (C=C), 74.1 (O-$CH_2$), 57.3 (CH), 56.2 (CH), 23.7 ($CH_2$), 21.2 ($CH_3$), 9.0 ($CH_3$); $\nu_{max}$($CHCl_3$)/cm$^{-1}$ 3424, 1686, 1649, 1595, 1535.

§ *Selected data* for **12a** (mixture of stereoisomers): $\delta_H$(400 MHz; $CDCl_3$; *J*/Hz) 7.7–6.9 (10 H, m, aromatic H), 4.40–4.20 (1 H, m) 4.14–4.04 (2 H, m), 3.95–3.85 (2 H, m), 1.58–1.46 (5 H, m, $CH_2$ and $CH_3$), 0.90 (3 H of major isomer, t, *J* 7.4, $CH_3$), 0.85 (3 H of minor isomer, t, *J* 7.5, $CH_3$); $\delta_C$(100 MHz; [$^2H_6$]DMSO) 170.1 (C=O), 165.2 (C=O), 165.2 (C=O), 152.6 (C), 152.6 (C), 142.9 (C), 142.7 (C), 137.7 (C), 137.6 (C), 129.8 (CH), 129.7 (CH), 129.6 (CH), 129.5 (CH), 128.7 (CH), 127.3 (CH), 127.1 (CH), 126.3 (CH), 126.0 (CH), 73.1 ($CH_2$), 72.9 ($CH_2$), 67.7 (CH), 67.7 (CH), 53.6 ($CH_2$), 53.1 ($CH_2$), 45.1 (C), 45.1 (C), 29.1 ($CH_2$), 28.6 ($CH_2$), 18.4 ($CH_3$), 18.0 ($CH_3$), 10.6 ($CH_3$), 10.2 ($CH_3$); $\nu_{max}$($CHCl_3$)/cm$^{-1}$ 3012, 2970, 1729, 1686 and 1498.

1 W. Carruthers, *Cycloaddition Reactions in Organic Synthesis*, Pergamon Press, Oxford, 1990.
2 Selected review articles: L. F. Tietze and G. Kettschau, *Top. Curr. Chem.*, 1997, **189**, 1; D. L. Boger and S. M. Weinreb, *Hetero Diels–Alder Methodology in Organic Synthesis*, Academic Press, New York, 1987.
3 Asymmetric hetero-Diels–Alder reactions of 1-azadienes: R. Beaudegnies and L. Ghosez, *Tetrahedron: Asymmetry*, 1994, **5**, 557; A. Waldner, *Tetrahedron Lett.*, 1989, **30**, 3061.
4 Langlois has investigated the use of alkenyloxazolines as *dienophiles* in asymmetric Diels–Alder cycloadditions: C. Kouklovsky, A. Poulihès and Y. Langlois, *J. Am. Chem. Soc.*, 1990, **112**, 6672; Y. Langlois and A. Poulihès, *Tetrahedron: Asymmetry*, 1991, **2**, 1223.
5 W. Seeliger, E. Aufderhaar, W. Diepers, R. Feinauer, R. Nehring, W. Thier and H. Hellmann, *Angew. Chem., Int. Ed. Engl.*, 1966, **5**, 875.
6 For a recent report of aza-Diels–Alder reactions of 1-azadienes with isocyanates, see T. Saito, H. Kimura, T. Chonan, T. Soda and T. Karakasa, *Chem. Commun.*, 1997, 1013.
7 For the use of achiral dihydrothiazoles as azadienes, see M. Sakamoto, K. Miyazawa, K. Kuwabara and Y. Tomimatsu, *Heterocycles*, 1979, **12**, 231.
8 B. R. Beno, K. N. Houk and D. A. Singleton, *J. Am. Chem. Soc.*, 1996, **118**, 9984; J. W. Storer, L. Raimondi and K. N. Houk, *J. Am. Chem. Soc.*, 1994, **116**, 9675.
9 M. A. McCarrick, Y.-D. Wu and K. N. Houk, *J. Org. Chem.*, 1993, **58**, 3330; L. F. Tietze, J. Fennen, H. Gießler, G. Schulz and E. Anders, *Liebigs Ann. Chem.*, 1995, 1681.
10 A recent computational study supports this mechanism: W. M. F. Fabian and G. Kollenz, *J. Phys. Org. Chem.*, 1994, **7**, 1.
11 J. March, *Advanced Organic Chemistry*, Wiley Interscience, New York, 4th edn., 1992, p. 978.

*Received in Liverpool, UK, 31st July 1997; 7/05571D*

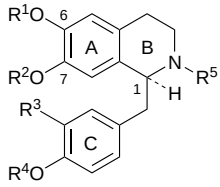
# (*S*)-Norreticuline is the precursor for the biosynthesis of *Erythrina* alkaloids

**Ulrich H. Maier and Meinhart H. Zenk***

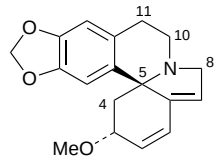
*Lehrstuhl für Pharmazeutische Biologie, Universität München, Karlstrasse 29, D-80333 München, Germany*

**In contrast to previous assumptions, the isoquinoline alkaloid (*S*)-norreticuline is the biosynthetic precursor to *Erythrina* alkaloids and, furthermore, this precursor is asymmetrically incorporated into these spirocyclic alkaloids.**

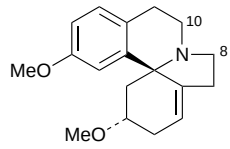
*Erythrina*-type alkaloids[1] suggest an unusual biosynthesis. Barton and co-workers[2,3] made the important observation that these spirocyclic alkaloids are formed by skeletal rearrangement from benzylisoquinoline alkaloids. Extensive application experiments of potential precursors to *Erythrina crista-galli* (Fabaceae) plants previously showed that (*S*)-norprotosinomenine **1** was the precursor for the *Erythrina* skeleton of erythraline **2**, although the incorporation was only in the range of 0.25%.[3–5] This finding was supported by the reported successful incorporation of labelled **1** into the *Erythrina* alkaloid cocculidine **3** (up to 0.66%) using plants of the taxonomically remote *Cocculus laurifolius* (Menispermaceae).[6,7] Norprotosinomenine **1** is a natural product and was isolated from *Erythrina variegata* (formerly *lithosperma*) fruits together with alkaloids possessing the *Erythrina*-type skeleton.[8]




**1** $R^1$ = H, $R^2$ = Me, $R^3$ = OH, $R^4$ = Me, $R^5$ = H
**4** $R^1$ = Me, $R^2$ = H, $R^3$ = H, $R^4$ = H, $R^5$ = H
**5a** $R^1$ = Me, $R^2$ = H, $R^3$ = OH, $R^4$ = Me, $R^5$ = H
**5b** $R^1$ = Me, $R^2$ = H, $R^3$ = OH, $R^4$ = Me, $R^5$ = Me
**6** $R^1$ = Me, $R^2$ = H, $R^3$ = OMe, $R^4$ = H, $R^5$ = H
**7** $R^1$ = H, $R^2$ = Me, $R^3$ = OMe, $R^4$ = H, $R^5$ = H
**8** $R^1$ = H, $R^2$ = H, $R^3$ = H, $R^4$ = H, $R^5$ = H




**2**




**3**

In the past, only 6-methoxy-7-hydroxytetrahydrobenzylisoquinoline alkaloids of the coclaurine **4** and reticuline **5b** type were recognized as biosynthetic precursors of a multitude of isoquinoline alkaloids occurring in plants such as aporphine-, benzophenanthridine-, bisbenzylisoquinoline-, morphinane-, pavine- and protoberberine-type alkaloids.[9] Norprotosinomenine **1** with a differing 6-hydroxy-7-methoxy substitution pattern is up to now the only biosynthetic exception to a phenol-coupled group of alkaloids and would require evolutionarily the development of a completely different and specific set of enzymes for the early steps of *Erythrina*-type alkaloid biosynthesis, since the enzymes of the coclaurine **4**–reticuline **5b** pathway are highly specific and do not accept alkaloidal substrates with the 6-hydroxy-7-methoxy pattern. This fact and the unusual carbon skeleton of the spirocyclic alkaloids prompted us to reinvestigate the structure of the precursors of *Erythrina* alkaloids.

Feeding experiments (cotton wick method)[3] with all four isomeric nortetrahydrobenzylisoquinoline alkaloids **1**, **5a**, **6** (nororientaline) and **7** (norisoorientaline), each tritium-labelled in the 6- or 7-methoxy group of ring A, were conducted using 4–5 month old plants, the same age as were used previously.[3] Erythraline **2**, the major alkaloid which is distributed in all parts of *E. crista-galli*, was isolated and found to be unlabelled ( < 0.0001%). Incubation of root, stem, leaf and flower tissue yielded the same result. Physiological transport experiments using $^3$H-labelled **4**–**7** showed that these potential precursor alkaloids were not transported at all in these plants. As a consequence, tissue slices (3–4 mm thick) were allowed to float on the aqueous tracer solution (0.5 μCi; 25 nmol) under constant shaking (150 strokes $min^{-1}$) for 24 h. Again, all vegetative tissue yielded no incorporation into erythraline **2**. However, fruit tissue showed considerable incorporation into erythraline **2** (11.8%) but only with (*S*)-norreticuline **5a** as precursor and not with **1**, **6**, **7**. All of the (*R*)-configurated potential precursors **1**, **5a**, **6**, **7** as well as their N-Me congeners were not incorporated. (*S*)-[6-O$C^3H_3$]Coclaurine **4**, however, was under these conditions incorporated to 11%. This clearly suggests that a coclaurine **4**–norreticuline **5a** pathway is operative in *Erythrina* alkaloid formation while the hitherto assumed norprotosinomenine **1** is not at all metabolized (confirmed by autoradiography of the fruit and other organ extracts). In spite of the high rate of incorporation of **4** and **5a** into the *Erythrina* alkaloids it could not be excluded that de- and re-methylation of potential precursors occurred under these feeding conditions as previously observed in other systems.[10]

To confirm specific incorporation and also to reinvestigate whether the later biosynthetic pathway to *e.g.* erythraline involves a symmetrical intermediate,[4,5] (*S*)-[1-$^{13}$C]-**1**,-**4**,-**5a**,-**6**,-**7** were synthesized by standard methods,[11] the correct position of the label was verified in each case by NMR analysis and the compounds applied at $10^{-4}$ M concentration to fruit slices (dry weight 18.2 g) as above. By isolation an average of 6 mg spectroscopically pure (UV, mass) erythraline **2** was obtained which was used for $^{13}$C NMR analysis of the enhanced signals (90.6 MHz, Bruker Aspect 3000) in $CDCl_3$. (*S*)-[1-$^{13}$C]Norprotosinomenine **1** yielded erythraline **2** that was unlabelled [Fig. 1(*a*)]. In contrast, (*S*)-[1-$^{13}$C]coclaurine **4** yielded **2** that was labelled at C-10 [Fig. 1(*b*), enrichment of 5.5% $^{13}$C, $^{13}$C atom excess calculated from mass spectral data]. (*S*)-[1-$^{13}$C]Norreticuline **5a** also labelled only C-10 of erythraline **2** [Fig. 1(*c*), enrichment of 9.3%]. If a symmetrical intermediate is occurring *en route* to the later steps to erythraline as postulated before,[4,5] $^{13}$C enrichment in the case of the **4** and **5a** feeding experiment would have occurred both at C-10 and C-8. Since at C-8 no enrichment is seen [Fig. 1(*b*), (*c*)], we have to conclude that *Erythrina* alkaloid biosynthesis does *not* involve a symmetrical intermediate of the diphenoquinone type. The previously observed labelling both of C-8 and C-10 of an *Erythrina*-type alkaloid after feeding [2-$^{14}$C]tyrosine[12] is easily explained. Norcoclaurine **8**, the precursor of coclaurine **4** and norreticuline **5a**, is formed from two different

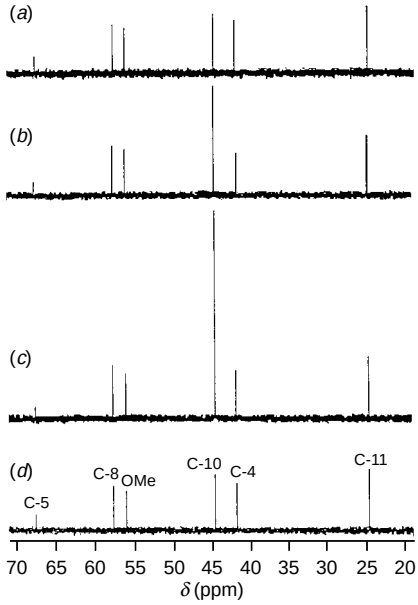
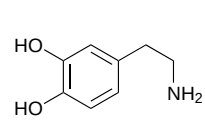


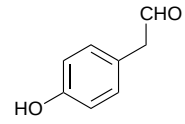

**Fig. 1** Proton-decoupled $^{13}C$ NMR partial spectrum of erythraline **2** (*a*) isolated after a feeding experiment with (*S*)-[1-$^{13}$C]norprotosinomenine **1**; (*b*) biosynthesized from (*S*)-[1-$^{13}$C]coclaurine **4**; (*c*) biosynthesized from (*S*)-[1-$^{13}$C]norreticuline **5a**; (*d*) unlabelled erythraline **2**

$C_6$–$C_2$ precursors analogous to all other 6,7-substituted isoquinoline alkaloids found in nature.[9,13,14] Tyrosine supplies both halves of the *Erythrina* alkaloids, while dopamine **9** is incorporated into the isoquinoline half of **4**, **5a**, **8** only. The benzyl part of these precursors is derived from 4-hydroxyphenylacetaldehyde **10** which in turn is also derived from tyrosine *via p*-hydroxyphenylpyruvate and subsequent decarboxylation to yield the aldehyde.[9] Thus the symmetrical labelling of an *Erythrina* alkaloid by [2-$^{14}$C]tyrosine in the reported experiment[12] is explained.

Finally, to probe the experiments reported on the incorporation of norprotosinomenine **1** into the *Erythrina*-type alkaloids in *Cocculus laurifolius*[6,7] we repeated these application experiments with the same plant. Again no incorporation of [1-$^{13}$C]-**1** into any of the *Cocculus* alkaloids was observed. **1** is, therefore, not a precursor to *Erythrina* alkaloids.




**9**




**10**

Future work on the biosynthesis of *Erythrina* alkaloids has to concentrate on the enzymes involved in (*S*)-norreticuline **5a** formation and on the later steps beyond precursor **5a** involving a non-symmetrical intermediate.

We thank Dr T. M. Kutchan for linguistic help in the preparation of this manuscript. This investigation was financially supported by SFB 369 of the Deutsche Forschungsgemeinschaft, Bonn, and by Fonds der Chemischen Industrie, Frankfurt/Main.

## Footnote and References

* E-mail: zenk@lrz.uni-muenchen.de

1 S. F. Dyke and S. N. Quessy, in *The Alkaloids*, ed. R. H. F. Manske. Academic Press, New York, 1981, vol. 18, p. 1.
2 D. H. R. Barton and T. Cohen, in *Festschrift Prof. Dr Arthur Stoll*, Birkhäuser, Basel, 1957, p. 117.
3 D. H. R. Barton, R. James, G. W. Kirby, D. W. Turner and D. A. Widdowson, *J. Chem. Soc*. (*C*), 1968, 1529.
4 D. H. R. Barton, R. B. Boar and D. A. Widdowson, *J. Chem. Soc.* (*C*), 1970, 1213.
5 D. H. R. Barton, C. J. Potter and D. A. Widdowson, *J. Chem. Soc*., *Perkin Trans. 1*, 1974, 346.
6 D. S. Bhakuni and A. N. Singh, *J. Chem. Soc., Perkin Trans. 1*, 1978, 618.
7 D. S. Bhakuni and S. Jain, *Tetrahedron*, 1980, **36**, 2153.
8 S. Ghosal, S. R. Majumdar and A. Chakraborti, *Austr. J. Chem.*, 1971, **24**, 2733.
9 M. H. Zenk, in *Organic Reactivity: Physical and Biological Aspects*, ed. B. T. Golding, R. J. Griffin and H. Maskill, RSC, London, 1995, p. 89.
10 B. Schneider and M. H. Zenk, *Phytochemistry*, 1993, **32**, 897.
11 R. Stadler and M. H. Zenk, *Liebigs Ann. Chem.*, 1990, 555.
12 E. Leete and A. Ahmad, *J. Am. Chem. Soc.*, 1966, **88**, 4722.
13 For review, see I. D. Spenser, in *Comprehensive Biochemistry*, ed. M. Florkin and E. H. Stotz, Elsevier, Amsterdam, 1968, ch. 20, p. 231.
14 R. Stadler, T. M. Kutchan and M. H. Zenk, *Phytochemistry*, 1989, **28**, 1083.

*Received in Glasgow, UK, 9th September 1997; 7/06595G*

# Homobimetallic vanadium $d^1$–$d^1$ complexes: structure and magnetism

**Robert Choukroun,*[a] Bruno Donnadieu,[a] Isabelle Malfant,[a] Simone Haubrich,[a] Richard Frantz,[b] Christian Guerin[b] and Bernard Henner[b]**

[a] *Equipe Précurseurs Moléculaires et Matériaux, Laboratoire de Chimie de Coordination du CNRS, 205 Route de Narbonne, 31077, Toulouse Cedex, France*

[b] *Laboratoire des Précurseurs Organométalliques des Matériaux, UMR CNRS 44, CC007, Université de Montpellier 2, Place E. Bastaillon, F-34095 Montpellier Cedex 5, France*

**From $Me_3SiC{\equiv}C–C{\equiv}CSiMe_3$ and $Ph_2PC{\equiv}C–C{\equiv}CPPh_2$ diynes and vanadocene $VCp_2$, homobimetallic vanadium $d^1$–$d^1$ complexes are synthesized and characterized by X-ray crystal structures of $(Cp_2V)_2$(1-2η:3-4η-RC=C–C=CR), (R = $SiMe_3$ 1 $PPh_2$ 2); magnetic moments of both complexes from 300 to 2 K indicate an antiferromagnetic *J* exchange coupling of −10.5 and −59.8 $cm^{-1}$ for 1 and 2, respectively.**

Many interesting reactions of the highly reactive $MCp_2$ species have been reported[1] and the zirconocene $ZrCp_2$ is of particular interest.[2] Numerous research has been devoted to the formation of organic synthetic products and more recently as a synthon in the reactivity of the alkynyl C≡C bond. This interest arises from the favourable electronic and structural features of C≡CR ligands *via* σ or σ–π networks. They can be modulated by varying either or both substituents and the metal centers.[3] In particular, vanadocene $VCp_2$ was studied with different classes of unsaturated molecules and different metallacyclopropene structures were identified.[4] Since the vanadocene unit easily binds alkyne derivatives, the reactivity of diynes $Me_3SiC{\equiv}C–C{\equiv}CSiMe_3$ and $Ph_2PC{\equiv}C–C{\equiv}CPPh_2$ was investigated.[5] One might expect that two identical species possessing one unpaired electron connected by diynes with various R end-groups could produce different structural and magnetic situations.[6]

Treatment of 2 equiv. of $VCp_2$ with 1 equiv. of $Me_3SiC{\equiv}C–C{\equiv}CSiMe_3$ or $Ph_2PC{\equiv}C–C{\equiv}CPPh_2$ in pentane, resulted in a brown solution from which, *via* the oxidative addition of $VCp_2$ on the alkyne bonds, $(Cp_2V)_2$(1-2η:3-4η-$Me_3SiC$=C–C=$CSiMe_3$) **1** and $(Cp_2V)_2$(1-2η:3-4η-$Ph_2PC$=C–C=$CPPh_2$) **2** were isolated as crystals in yields of *ca*. 50 and 40%, respectively. Formulation of **1** and **2** as homobimetallic vanadium complexes was confirmed by X-ray crystallography (Figs. 1 and 2).† The bond distances and angles associated with the vanadium acetylene interaction indicate that the acetylene molecule is symmetrically attached to the vanadium atom *via* two σ-type V–C bonds of 2.14 Å (av.) and 2.10 Å (av.) for **1** and **2**, respectively. This produces a metallacyclopropene structure for the central $VC_2$ moiety, with an acute C–V–C angle of 35° (av.). The acetylene coordination is reflected by the average 0.08 Å increase of the C≡C distance and by the geometrical alterations which accompany the acetylene upon coordination. The C–C–R bond angles (R = $SiMe_3$, $PPh_2$) are reduced from 180° in a free acetylene to 140° (av.) in the vanadocene adducts.[4] The distance of the C–C bond for **1** [C(2)–C(3) 1.39 Å] and **2** [C(2)–C(2) 1.40 Å] indicates the presence of a partial double bond. The essential aspects of the structures though are the dihedral angle between both $VC_2$ units in the molecules which are 110.8° for **1** and 165.61° for **2**, which leads to vanadium–vanadium distances of 4.886(5) and 5.384(2) Å in **1** and **2**, respectively. The different orientation of the $Cp_2VC_2$ unit in **1** and **2** may be due to the steric effects of the substituents $SiMe_3$ and $PPh_2$ on the diynes. Another difference in the structural aspects of **1** and **2** is the butadiene skeleton. This is deformed for **1** [C(4) is above the plane defined by C(1)–C(2)–

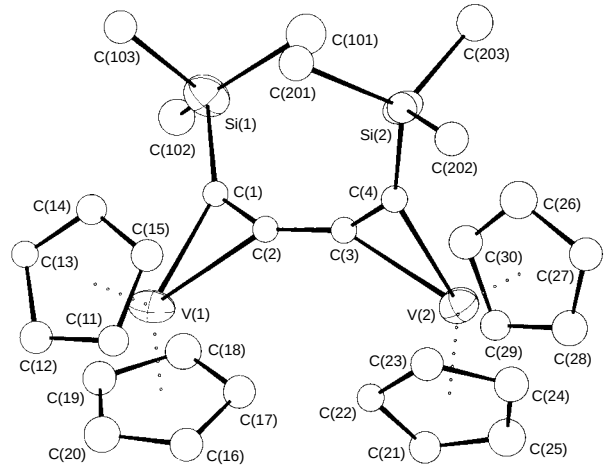



**Fig. 1** View of the molecular structure of **1** (bond lengths in Å, angles in °, hydrogen atoms omitted). V(1)–C(1) 2.14(2), V(1)–C(2) 2.15(2), V(2)–C(3) 2.16(2), V(2)–C(4) 2.13(2), C(1)–C(2) 1.25(3), C(2)–C(3) 1.39(2), C(3)–C(4) 1.28(3); C(1)–V(1)–C(2) 34.0(7), C(3)–V(2)–C(4) 34.7(8), Si(1)–C(1)–C(2) 139.8(20), Si(2)–C(4)–C(3) 140.2(20), C(1)–C(2)–C(3) 148.9(23), C(2)–C(3)–C(4) 149.1(23); V(1)···V(2) 4.886(5), V–Cp 1.977 (av.), Cp–V–Cp 138.4 (av.) [Cp are the centroids of the $C_5H_5$ rings C(11)–C(15), C(16)–C(20), C(21)–C(25), C(26)–C(30)].

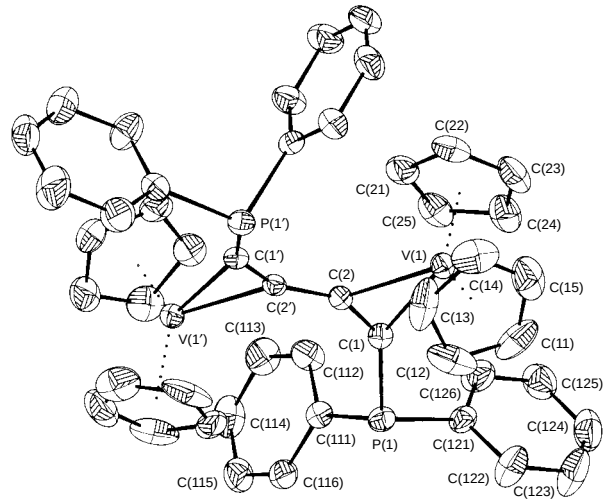



**Fig. 2** View of the molecular structure of **2** (bond lengths in Å, angles in °, hydrogen atoms omitted). V(1)–C(1) 2.092(5), V(1)–C(2) 2.116(4), C(1)–C(2) 1.283(6), C(2)–C(2′) 1.404(9); C(1)–V(1)–C(2) 35.5(2), P(1)–C(1)–C(2) 140.1(4), C(1)–C(2)–C(2′) 148.2 (6); V(1)···V(1′) 5.384(2), V(1)–Cp 1.968, V(1)–Cp′ 1.974, Cp–V(1)–Cp′ 137.57 [Cp, Cp′ are the centroids of the $C_5H_5$ rings C(1)–C(5), C(6)–C(10)].

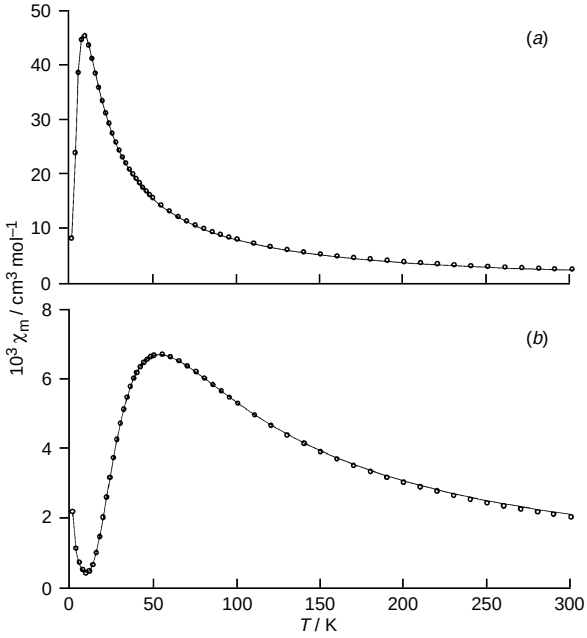
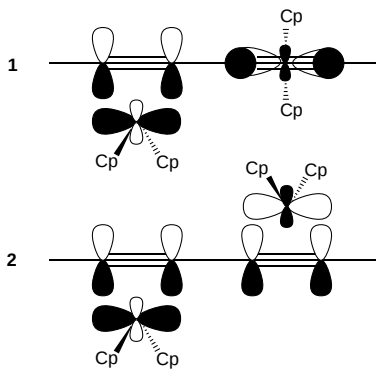



**Fig. 3** Temperature dependence of molar magnetic susceptibilities per vanadium (○) of (*a*) **1** and (*b*) **2** (the solid lines result from a least-squares theoretical fit)‡

C(3) by 0.63 Å] whereas all the carbon atoms are contained in a plane for **2**.

As a result of such situations, paramagnetic vanadium centers of $d^1$ electronic configuration could produce different magnetic behavior.[6,7] Variable-temperature magnetic susceptibility measurements have been carried out.‡ The effective magnetic moment $\mu_{eff}$ is 2.65 $\mu_B$ for **1** and 2.25 $\mu_B$ for **2** at 300 K. They decrease to reach 0.36 $\mu_B$ for **1** and 0.19 $\mu_B$ for **2** at 2 K. Fig. 3 show the plots of $\chi_m$, molar susceptibility per dimer, *vs.* temperature for **1** and **2**. The solid lines represent the good fit obtained to account for the observed dependence with an exchange interaction model. Fitting the data for **1** and **2** gives $J = -10.5$ and $-59.8$ cm$^{-1}$, respectively. The antiferromagnetic interaction for **2** is greater than that for **1** whereas the vanadium–vanadium distances show an opposite relation. In fact, the interaction is propagated by the carbon chain and a consideration of the bonding situation in the complex seems necessary. The orientation of the $Cp_2VC_2$ unit in the molecule suggests a favorable 'in-plane π type' geometry for complex **2**. This can be described as a linear combination of mainly p orbital character of the carbon of the diyne with the main contribution of the $d_{z^2}$ orbital of the HOMO in a $d^1$ type system.[4] This is disfavored in the complex **1** where the $Cp_2VC_2$ unit and their magnetic orbital contributions could be considered as orthogonal (Scheme 1).

In conclusion, our synthetic method is able to produce homobimetallic $d^1$ systems with organic substrates. Modification of the organic portion leads to different structure situations and varies the coupling propagated by extended bridges. We illustrate a strategy to potentially synthesize homobimetallic $d^1$ systems designed to produce differing metal–metal separations. The full extent of the interaction of metallocene $d^1$ $VCp_2$ with several unsaturated hydrocarbons is under investigation.




**Scheme 1**

S. H. is a recipient of the Erasmus program. We also thank A. Mari for helpful discussion.

## Footnotes and References

* E-mail: choukrou@lcctoul.lcc-toulouse.fr

† *Crystallographic data*: for **1**: $C_{30}H_{38}Si_2V_2$, $M$ = 557.70, triclinic, space group $P\bar{1}$, $a$ = 8.226(2), $b$ = 12.862(4), $c$ = 13.987(3) Å, $\alpha$ = 78.93(2), $\beta$ = 84.60(2), $\gamma$ = 82.05(2) °, $U$ = 1435.0 Å$^3$, $Z$ = 2, $D_c$ = 1.29 g cm$^{-3}$, $\mu$ = 7.28 cm$^{-1}$, $R(R_w)$ = 0.080(0.098), GOF = 1.5. For **2**: $C_{46}H_{40}P_2V_2$, $M$ = 780.34, orthorhombic, space group *Pbna*, $a$ = 12.940(2), $b$ = 16.757(2), $c$ = 17.638(2) Å, $U$ = 38.24.5 Å$^3$, $Z$ = 4, $D_c$ = 1.36 g cm$^{-3}$, $\mu$ = 5.87 cm$^{-1}$, $R(R_w)$ = 0.048(0.059), GOF = 0.85.

Data collection was performed at *ca.* 294 K on a IPDS STOE diffractometer using graphite monochromatized Mo-Kα radiation. The crystal of **1** is twinned and one of the two domains of the twin have been indexed; the integration was realized by using the program TWIN (STOE IPDS software), the overlapped reflections are automatically discarded by TWIN during the data reduction. The refinement of **1** was performed with the best data set containing once merging 60% of unique reflections. Computations were performed with the aid of CRYSTALS. The structure was solved by direct methods (SIR92[9]). All hydrogen atoms were found on difference Fourier maps but were introduced in the refinement as fixed contributors (C–H 0.96 Å) and recalculated after each cycle. For **2**, all non-hydrogen atoms were anisotropically refined; for **1**, only V and Si atoms were refined anisotropically owing to the low ratio of parameters to observations. CCDC 182/643.

‡ Magnetic susceptibilities were determined using a SQUID susceptometer within between 2 and 300 K. Using a Heisenberg Hamiltonian $H = -JS_AS_B$ with local spins $S_A = S_B = 1/2$, the magnetic interaction was estimated with a Bleaney–Bowers model for dimers[8] ($J$, $g$) including a percentage ($\rho$) of paramagnetic impurities. Parameters $J$, $g$ and $\rho$ were determined by least squares fitting. The average value of the $g$-factor was 2.12 for **1** and 1.95 for **2**. $\rho$ assumed as isolated $V^{IV}$ ions with the same molecular mass as the actual compounds **1** or **2**, so that the Curie constant $C$ was taken as $C = [N\beta^2/2k]g^2$, was found to be 0.018 for **1** and 0.006 for **2**.

1 In *Comprehensive Organometallic Chemistry II*, ed. E. W. Abel, F. G. A. Stone and G. Wilkinson, Pergamon, Fort Collins, 1995; M. Bochmann, vol. 4, ch. 4; P. Binger and S. Podubrin, vol. 4, ch. 7; R. D. Broene, vol. 12, ch. 3.7; S. L. Buchwald and R. D. Broene, vol. 12, ch. 7.4.

2 See, for example: K. Takagi, C. J. Rousset and E.-i. Negishi, *J. Am. Chem. Soc.*, 1991, **113**, 1440; H. Ito, Y. Ikeuchi, T. Taguchi, Y. Hanzawa and M. Shiro, *ibid.*, 1994, **116**, 5469; M. Takahashi, D. Y. Kondakov and N. Suzuki, *Organometallics*, 1993, **115**, 8485; N. Suzuki, D. Y. Kondakov and T. Takahashi, *J. Am. Chem. Soc.*, 1994, **13**, 3431; W. Ando, T. Ohtaki, T. Suzuki and T. Kabe, *ibid.*, 1991, **113**, 7782; S. L. Buchwald, B. T. Watson and J. C. Huffman, *ibid.*, 1986, **108**, 7411.

3 B. P. Warner, W. M. Davis and S. L. Buchwald, *J. Am. Chem. Soc.*, 1994, **116**, 5471; C. Lebefer, W. Baumann, A. Tillack, R. Kempe, H. Gorls and U. Rosenthal, *ibid.*, 1996, **15**, 3486; H. Lang, W. Frosch, I. Y. Wu, S. Blau and B. Nuber, *Inorg. Chem.*, 1996, **35**, 6266; V. Varga, J. Hiller, M. Polasek, U. Thewalt and K. Mach, *J. Organomet. Chem.*, 1996, **515**, 57; H. Lang, K. Köler and L. Zsolnai, *Chem. Commun.*, 1996, 2043.

4 G. Fachinetti, C. Floriani, A. Chiesi-Villa and C. Guastini, *Inorg. Chem.*, 1979, **18**, 2282; J. L. Petersen and L. Griffith, *ibid.*, 1980, **19**, 1852; K. Jonas, W. Rüsseler, C. Krüger and E. Raabe, *Angew. Chem., Int. Ed. Engl.*, 1986, **10**, 925.

5 R. J. P. Corriu, C. Guérin, B. J. L. Henner and A. Jolivet, *J. Organomet. Chem.*, 1997, **530**, 39.

6 L. C. Francesconi, D. R. Corbine, A. W. Clauss, D. N. Hendrickson and G. D. Stucky, *Inorg. Chem.*, 1981, **20**, 2059; L. S. Kramer, A. W. Clauss, L. C. Francesconi, D. R. Corbin, D. N. Hendrickson and G. D. Stucky, *ibid.*, 1981, **20**, 2070; E. Samuel, J. F. Harrod, D. Gourier, Y. Dromzee, F. Robert and Y. Jeannin, *ibid.*, 1992, **31**, 3252.

7 K. Yamamoto, K. Oyaizu and E. Tsuchida, *J. Am. Chem. Soc.*, 1996, **118**, 12665.

8 R. L. Carlin, *Magnetochemistry*, Springer-Verlag, Berlin, 1986.

*Received in Cambridge, UK, 24th June 1997; 7/04461E*

# Synthesis and structure of the first 2*H*-1,3,2-diazaphosphole complex

**Hendrik Wilkens, Jörg Jeske, Peter G. Jones and Rainer Streubel***

*Institut für Anorganische und Analytische Chemie der Technischen Universität Braunschweig, Postfach 3329, D-38023 Braunschweig, Germany*

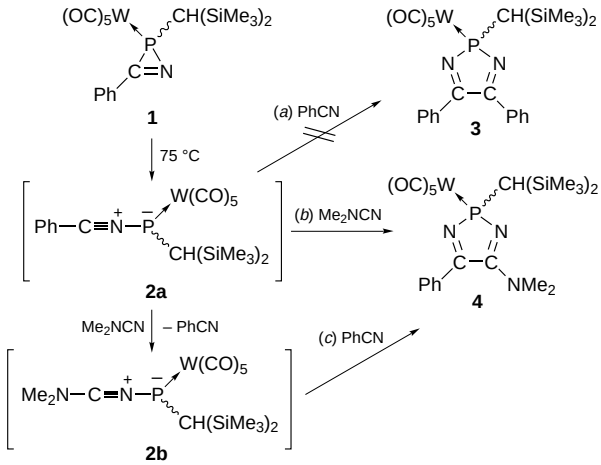
**Thermal decomposition of the 2*H*-azaphosphirene tungsten complex 1 in benzonitrile and in the presence of dimethylcyanamide yields the 2*H*-1,3,2-diazaphosphole tungsten complex 4, containing a novel five-membered heterocyclic ligand; the overall reaction may be described as a 1,3-dipolar cycloaddition of an *in situ* generated nitrilium phosphane ylide complex to benzonitrile.**

Nitrilium ylides, like nitrile oxides,[1] sulfides[2] and nitrileimines,[1,3] are versatile building blocks in heterocyclic chemistry. Very recently, we obtained the first evidence of a nitrilium phosphane ylide complex as a reactive intermediate in the thermolysis of 2*H*-azaphosphirene tungsten complexes in the presence of dimethylacetylenedicarboxylate (DMAD) in toluene.[4] The formation of the 2*H*-1,2-azaphosphole tungsten complexes, which were obtained as by-products, was explained as a 1,3-dipolar cycloaddition of a nitrilium phosphane ylide complex to the trapping reagent.[4]

We now report the first synthesis of a 2*H*-1,3,2-diazaphosphole tungsten complex **4**, which has been obtained in good yield by thermal decomposition of the 2*H*-azaphosphirene tungsten complex **1** in benzonitrile and in the presence of 2 equiv. of dimethylcyanamide. Under these reaction conditions the 1,3-dipolar cycloaddition is stereoselective and the exclusive formation of this regioisomer was observed.

This reaction is interpreted as a further example of a 1,3-dipolar cycloaddition of the transiently formed nitrilium phosphane ylide tungsten complex **2b** to benzonitrile (Scheme 1, pathway (*c*)]. Pathways (*a*) and (*b*) seem less plausible, especially, if taken into account that under these reaction conditions the formation of the diphenyl-substituted 2*H*-1,3,2-diazaphosphole tungsten complex **3** was not observed [pathway (*a*)].

The composition of 2*H*-1,3,2-diazaphosphole tungsten complex **4** is confirmed by elemental analysis and mass spectrometry;† the structural formulation is based on the characteristic




**Scheme 1** *Reagents and conditions*: 1 mmol **1** was treated with 2 mmol dimethylcyanamide in benzonitrile at 75 °C for 1.5 h. Work-up by column chromatography at low temperature afforded **4** in good yield (67%, mp 90 °C).

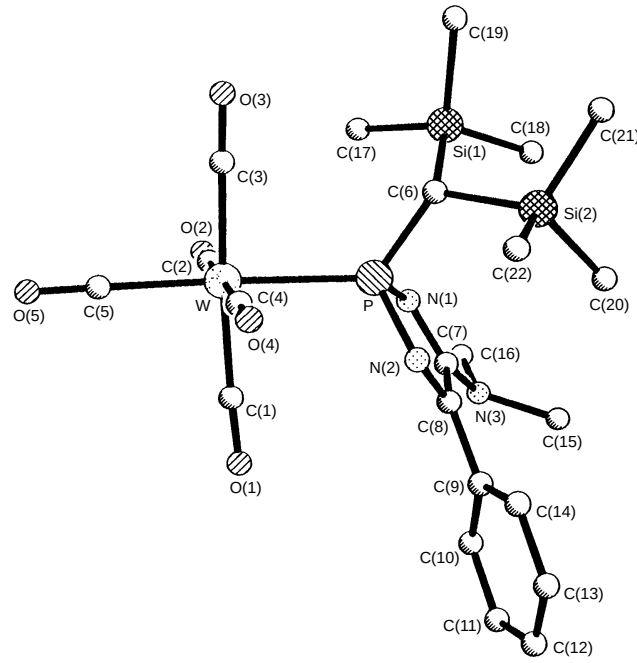



**Fig. 1** Molecular structure of complex **4** in the crystal. Radii are arbitrary. Selected bond lengths (Å) and angles (°): P–W 2.479(11), P–N(1) 1.705(3), P–N(2) 1.705(3), N(1)–C(7) 1.291(5), N(2)–C(8) 1.284(5), C(7)–C(8) 1.488(5); N(1)–P–N(2) 96.3(2), P–N(1)–C(7) 108.2(3), N(1)–C(7)–C(8) 114.0(3), N(2)–C(8)–C(7) 113.4(4), P–N(2)–C(8) 107.8(3).

NMR spectral data† in solution and was confirmed for the solid state by a X-ray crystal structure analysis.‡ In comparison to related 2*H*-1,2-azaphosphole tungsten complexes,[4] the 2*H*-1,3,2-diazaphosphole tungsten complex **4** displays a low-field shifted resonance signal of the phosphorus nucleus at $\delta$ 149.8 (*cf.* $\delta$ 102–105[4]) and a markedly increased phosphorus tungsten coupling constant of 257.1 Hz (*cf.* $^1J_{WP}$ 236–238 Hz[4]). The phosphorus–carbon coupling constants of the quaternary ring carbon atoms are 2–10 Hz, which are characteristically small for both five-membered heterocycles.

Remarkable features of the molecular structure of **4** and 2*H*-1,2-azaphosphole complexes[4] are the planar five-membered ring system and the localised double bonds; the latter being in contrast to the situation of aromatic heterocycles like 2*H*-1,2,3-diazaphospholes[5,6] and 2*H*-1,2,3-triazoles.[7] The coordination sphere of phosphorus is distorted tetrahedral and the phosphorus–tungsten bond length is 2.479(11) Å.

We are currently investigating the synthetic potential of nitrilium phosphane ylide complexes in 1,3-dipolar cycloaddition reactions.

This work was supported by the Fonds der Chemischen Industrie and by the Deutsche Forschungsgemeinschaft.

## Footnotes and References

* E-mail: streubel@mvs.anchem.nat.tu-bs.de

† Satisfactory elemental analysis was obtained for complex **4**. NMR data were recorded at room temp. in $CDCl_3$ solution at 50.3 MHz ($^{13}C$) and 81.0

($^{31}$P), using TMS and 85% $H_3PO_4$ as standard references; *J*/Hz. *Selected spectroscopic data* for **4**: $^{13}$C NMR, $\delta$ 162.4 (d, $\Sigma J_{PC}$ 9.4, P–N=C), 165.0 (d, $\Sigma J_{PC}$ 2.5, P–N=C); $^{31}$P NMR, $\delta$ 149.8 (5, $^1J_{WP}$ 257.1); MS (EI): $M^+$ at *m*/*z* 687.

‡ *Crystal data* for **4**: $C_{22}H_{30}N_3O_5PSi_2W$, $M$ = 687.49; triclinic, space group $P\bar{1}$: $a$ = 9.284(3), $b$ = 10.359(3), $c$ = 16.321(4) Å, $\alpha$ = 75.07(2), $\beta$ = 88.21(2), $\gamma$ = 67.67(2)°; $U$ = 1398.9(6) Å$^3$; $Z$ = 2, $D_c$ = 1.632 Mg m$^{-3}$, $T$ = 143 K, a crystal (0.7 × 0.7 × 0.6 mm) was mounted in inert oil. A total of 4946 absorption corrected intensities were measured to $2\theta$ = 50° using Mo-K$\alpha$ radiation on a STOE Stadi-4 diffractometer; 4915 were unique ($R_{int}$ = 0.0546) and used for all calculations (program SHELXL-93). The structure was solved by direct methods and refined anisotropically on $F^2$. The final $wR_2$ was 0.0686, with conventional $R(F)$ 0.0262 for 316 parameters and 151 restraints; max. $\Delta\rho$ 2.48 e Å$^{-3}$. CCDC 182/666.


1 P. Caramella and P. Grünanger, in *1,3 Dipolar Cycloaddition Chemistry*, ed. A. Padwa, Wiley, New York, 1984, ch. 3.
2 R. M. Paton, *Chem. Soc. Rev.*, 1989, **18**, 33.
3 G. Bertrand and C. Wentrup, *Angew. Chem., Int. Ed. Engl.*, 1994, **33**, 527.
4 R. Streubel, H. Wilkens, A. Ostrowski, C. Neumann, F. Ruthe and P. G. Jones, *Angew. Chem., Int. Ed. Engl.*, 1997, **36**, 1492.
5 J. H. Weinmaier, H. Tautz, A. Schmidpeter and S. Pohl, *J. Organomet. Chem.*, 1980, **185**, 53.
6 K. Karaghiosoff, W. S. Sheldrick and A. Schmidpeter, *Chem. Ber.*, 1986, **119**, 3213.
7 H. Dehne, in Houben-Weyl, *Meth. Org. Chem.*, Bd. E 8d, 1994, p. 305.



*Received in Basel, Switzerland, 18th June 1997; 7/04285J*

# Asymmetric total synthesis of antitumour antibiotic A83586C

**Karl J. Hale* and Jiaqiang Cai**

*Department of Chemistry, University College London, 20 Gordon Street, London, UK WC1H 0AJ*

**The first asymmetric total synthesis of antitumour antibiotic A83586C has been accomplished.**

A83586C **1** is a highly ornate hexadepsipeptide isolated from the fermentation broths of *Streptomyces karnatakensis* by Smitka *et al.*[1] It shows pronounced antimicrobial activity *in vitro* against Gram-positive strains of bacteria, and can combat the growth of a CCRF-CEM human T-cell leukaemia line ($IC_{50}$ = 0.0135 μg $ml^{-1}$). From a synthetic standpoint, A83586C **1** presents a formidable challenge owing to its ominous expanse of diverse functionality, which looks set to overwhelm most protecting group endgames conceived for its total synthesis. In light of this, we thought it prudent to dispense with protecting groups for the final stages, and some time ago, we synthesised the C(1)–C(47) sequence **2** *via* a chemoselective union between **3** and **4** (Scheme 1).[2] Unfortunately, difficulties later arose not only in the macrolactonisation of **2**, but also its *seco*-acid. This led us to consider new ways of completing this synthetic venture. One plan that looked particularly worthwhile featured a coupling between **6** and **3** to obtain **5** and a subsequent glycal hydration at C(30) to produce **1**. We now report the first total synthesis of A83586C based on this strategy.

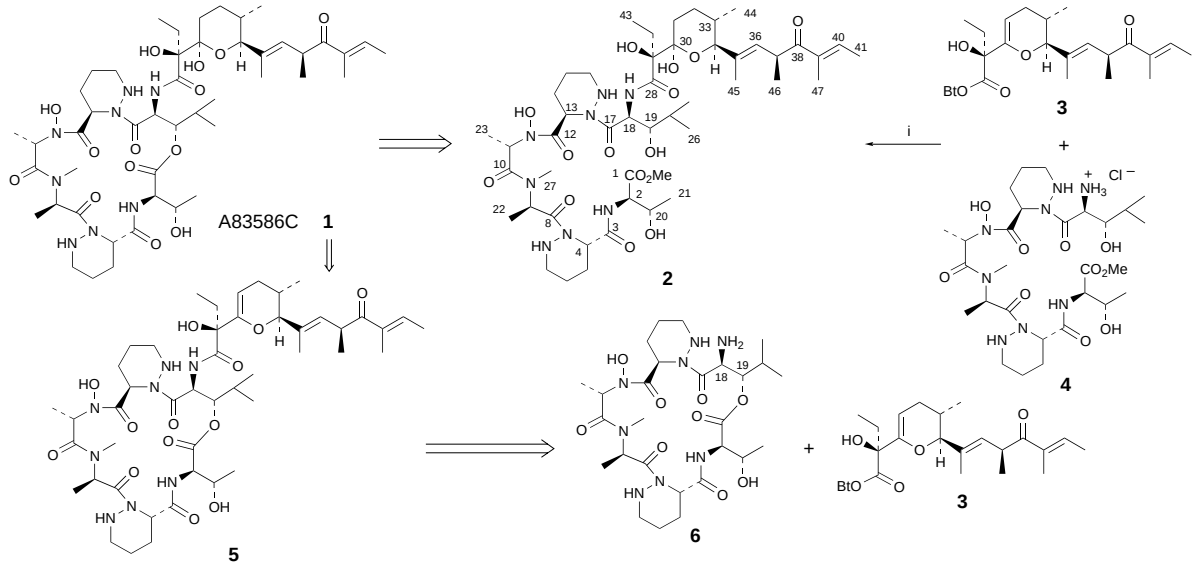
Initial attention focused on constructing **11** and **16** (Scheme 2). Tetrapeptide **11** was assembled in eight steps from known dipeptide **7**.[3] Our first manoeuvres replaced the $Ph_2CH$ ester[4] group in **7** with a Boc-NHNH group,[5] to prevent diketopiperazine formation occurring when the Fmoc group was removed with $Et_2NH$. Fortunately, this tactic worked very well, **8** being isolated uneventfully after Fmoc deprotection. Compound **8** coupled readily to acid **9**[3,6] in $CH_2Cl_2$ at 0 °C after sequential treatment with $Et_3N$ and bis(2-oxo-3-oxazolidinyl)phosphinic chloride (BOP-Cl);[7] **10** was obtained in 75% yield. The Boc group was cleaved from **10** with TFA, and the acyl hydrazine oxidised with *N*-bromosuccinimide (NBS) in aqueous THF.[8] Without further purification, the crude acid was esterified with $Ph_2CN_2$[4] and the Fmoc group excised to deliver **11**.

The synthesis of **16** was achieved from (2*S*,3*S*)-hydroxyleucine.[9] After Troc protection of the amino group,[6] a selective *O*-allylation was performed with $NaHCO_3$ and allyl bromide in DMF;[10] **13** was isolated in 92% yield. A range of coupling conditions were examined for establishing the O(19)–C(1) ester bond between **13** and **14**.[11] Success finally came using DCC and DMAP in $CH_2Cl_2$, but 5–10% epimerisation was always encountered at the α-carbon atom of the threonine unit. Notwithstanding this, **15** was usually prepared in 83–88% yield. The next two steps involved removal of the allyl ester group from **15** using palladium(0) catalysis,[12] and acid chloride formation with excess oxalyl chloride in benzene.

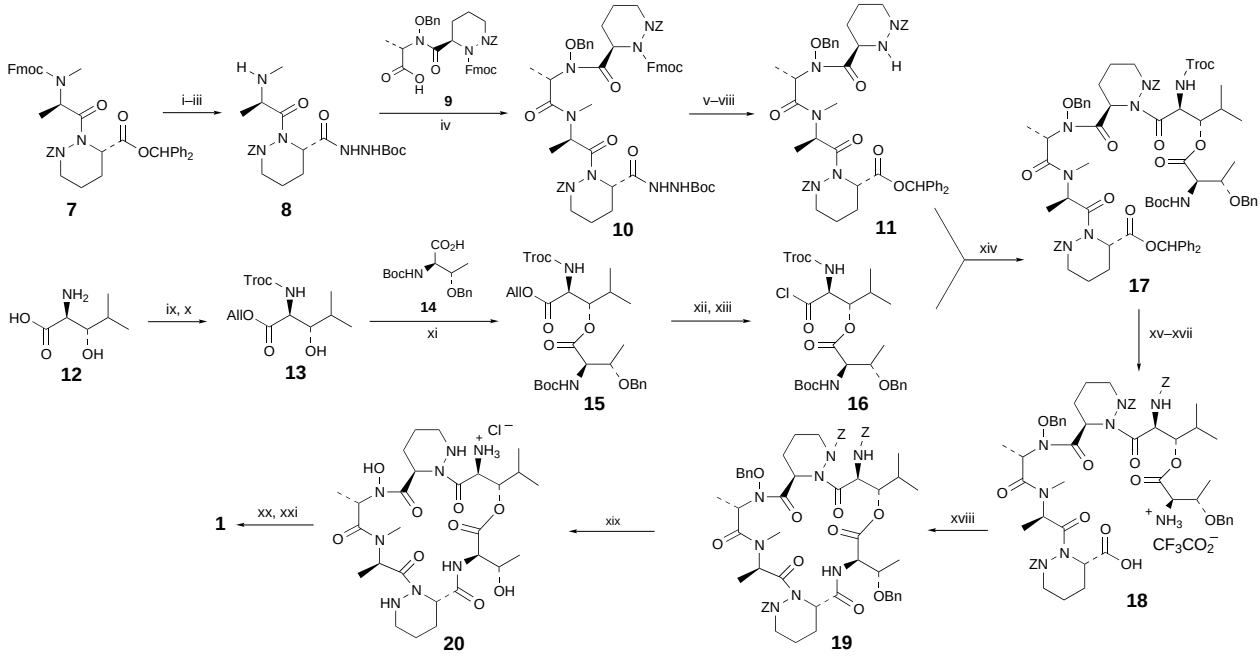
To our delight, [4 + 2]-fragment condensation between **11** and **16** was complete after 2 min when conducted in benzene at 60 °C in the presence of AgCN;[6] **17** was formed in yields of 73–86%.

Our next goal was to convert **17** into **18** and then macrolactamise at the (3*S*)-piperazic acid and D-threonine residues. The Troc group in **17** was substituted with a *Z* group by reacting **17** with excess zinc in acetic acid,[6] and acylating the crude amine with $BnO_2CCl$. TFA was then used to simultaneously deprotect the Boc and $Ph_2CH$ ester groups to give **18** in 78% overall yield for the three steps.

A significant number of peptide coupling reagents were evaluated for instigating the desired macrolactamisation of **18** to **19**, the majority of which performed poorly. Success was eventually attained with *O*-(7-azabenzotriazol-1-yl)-*N*,*N*,*N*′,*N*-tetramethyluronium hexafluorophosphate (HATU)[13] and *N*-ethylmorpholine (NEM) in $CH_2Cl_2$ under conditions of very




**Scheme 1** *Reagents and conditions*: i, $Et_3N$, $CH_2Cl_2$, −78 to 25 °C, $SiO_2$, 65%



**Scheme 2** *Reagents and conditions*: i, TFA–$CH_2Cl_2$ (10 : 1), PhOH (2 equiv.), 25 °C; ii, $BocNHNH_2$ (2 equiv.), DCC (2 equiv.), 1-hydroxybenzotriazole hydrate (HOBT) (2 equiv), THF (*ca.* 0.33 M), 0 to 25 °C, 93% (2 steps); iii, $Et_2NH$–MeCN (1 : 1) (*ca.* 0.55 M); iv, $CH_2Cl_2$ (*ca.* 0.15 M), add $Et_3N$ (2.3 equiv.) at −10 °C, stir 5 min, then add BOP-Cl (1.2 equiv.), warm to 0 °C, 4 h, 75% (2 steps); v, TFA–$CH_2Cl_2$ (1 : 1) (*ca.* 0.2 M), 0 °C; vi, NBS (2 equiv.), THF–$H_2O$ (1 : 1) (*ca.* 0.04 M), 0 to 25 °C; vii, $Ph_2CN_2$ (1.9 equiv.), $Me_2CO$ (*ca.* 0.16 M), 25 °C, 12 h, 68% (3 steps); viii, $Et_2NH$–MeCN (1 : 1) (*ca.* 0.24 M), 25 °C, 40 min; ix, Troc-Cl (1.05 equiv.), NaOH (2 equiv.), THF, $H_2O$, 25 °C, 90%; x, $NaHCO_3$ (4.3 equiv.), allyl bromide (6.2 equiv.), DMF (*ca.* 0.31 M), 25 °C, 92%; xi, DCC (1.2 equiv.), DMAP (1.25 equiv.), $CH_2Cl_2$ (*ca.* 0.322 M), 0 to 25 °C, 83–88%; xii, morpholine (6.5 equiv.), $(Ph_3P)_4Pd$ (5.9 mol%), THF (*ca.* 0.22 M), 0 to 25 °C, 59%; xiii, $(COCl)_2$ (20 equiv.), $C_6H_6$ (*ca.* 0.4 M), 25 °C, 2.5 h; xiv, AgCN (1.3 equiv.), $C_6H_6$ (*ca.* 0.12 M), 60 °C for 2 min, 73–86% (for viii, xiii, xiv); xv, Zn (70 equiv.), AcOH–$H_2O$ (10 : 1) (*ca.* 0.0685 M), 25 °C, 3 h; xvi, ZCl (3 equiv.), 10% aq. $NaHCO_3$, $CH_2Cl_2$, 25 °C, 2 h, 78% (2 steps); xvii, TFA–$CH_2Cl_2$ (2 : 1) (*ca.* 0.06 M), PhOH (2.2 equiv.), 0 °C, 1 h, 100%; xviii, HATU (10 equiv.), $CH_2Cl_2$ (500 ml), 0 °C, then slow addition of **18** (1.4 g) and NEM (13.5 equiv.) in $CH_2Cl_2$ (500 ml) over 3 h, then 0 °C, 2 h, then 25 °C, 30 h, 25%; xix, 10% Pd–C (= weight of **19** used), MeOH (*ca.* 0.01 M), HCl (1 equiv.), $H_2$ (1 atm.), 25 °C, 24 h; xx, **3** (1 equiv.), $CH_2Cl_2$ (*ca.* 0.03 M), −78 °C, add $Et_3N$ (9.3 equiv.), warm to 25 °C, stir 10 min, 31% (from **19**); xxi, $CDCl_3$ (wet), 72 h, 0 °C, 100%

high dilution. This produced **19** in a reproducible 25% yield after flash chromatography. Compound **19** was then deprotected by catalytic hydrogenolysis over palladium on carbon. We deliberately conducted this hydrogenation in methanolic HCl, so as to minimise the occurrence of O(19) to N(18) acyl rearrangement during this lengthy reaction. Without further purification, crude **20** was suspended in $CH_2Cl_2$ along with **3**.[2] After cooling to −78 °C, $Et_3N$ was added, and the reaction warmed to room temperature where it was stirred for 10 min. A rapid coupling ensued to deliver **5** in 31% yield after chromatographic purification. Upon standing in undried $CDCl_3$ (Aldrich) for 72 h, **5** readily hydrated to give A83586C in quantitative yield. The $^1H$ and $^{13}C$ NMR spectra of synthetic A83586C in $CDCl_3$ were identical in every respect with the spectra of authentic A83586C. In addition, synthetic A83586C also gave rise to an $(M + Na)^{+\cdot}$ ion at *m*/*z* 999.5360 in its high resolution FAB mass spectrum;† the calculated value for $C_{47}H_{76}N_8O_{14}Na$ is 999.5379.

We thank the EPSRC (Project Grant GR/J92590), Zeneca, Pfizer and Rhone-Poulenc Rorer for financial support. We thank Dr Tim Smitka of Eli Lilly for kindly supplying us with the original $^1H$ and $^{13}C$ NMR spectra of natural **1**. We are indebted to Dr Glyn Williams of Roche Products for obtaining the 500 MHz $^1H$ NMR spectrum of synthetic **1**, and to his colleague Dr B. K. Handa for urging us to try the HATU reagent. We thank the ULIRS MS Service for HRMS measurements.

† All new compounds reported in this synthetic route gave satisfactory 400 MHz $^1H$ and 100 MHz $^{13}C$ NMR and IR spectra, as well as HRMS and/or microanalyses within 0.4%.

## Footnotes and References

* E-mail: k.j.hale@ucl.ac.uk

1 T. A. Smitka, J. B. Deeter, A. H. Hunt, F. P. Mertz, R. M. Ellis, L. D. Boeck and R. C. Yao, *J. Antibiot.*, 1988, **41**, 726.
2 K. J. Hale, J. Cai and V. M. Delisser, *Tetrahedron Lett.*, 1996, **37**, 9345.
3 K. J. Hale, V. M. Delisser, L.-K. Yeh, S. A. Peak, S. Manaviazar and G. S. Bhatia, *Tetrahedron Lett.*, 1994, **35**, 7685.
4 G. C. Stelakatos, A. Paganou and L. Zervas, *J. Chem. Soc. C*, 1966, 1191.
5 R. A. Boissonnas, St. Guttmann and P.-A. Jaquenoud, *Helv. Chim. Acta*, 1960, **43**, 1349.
6 P. L. Durette, F. Baker, P. L. Barker, J. Boger, S. S. Bondy, M. L. Hammond, T. J. Lanza, A. A. Pessolano and C. G. Caldwell, *Tetrahedron Lett.*, 1990, **31**, 1273.
7 R. D. Tung and D. H. Rich, *J. Am. Chem. Soc.*, 1985, **107**, 4342.
8 H. T. Cheung and E. R. Blout, *J. Org. Chem.*, 1965, **30**, 315.
9 K. J. Hale, S. Manaviazar and V. M. Delisser, *Tetrahedron*, 1994, **50**, 9181.
10 V. Bocchi, G. Casnati, A. Dossena and R. Marchelli, *Synthesis*, 1979, 961.
11 Compound **14** was prepared by the same method described for its L-enantiomer by: Y. Nakamura, M. Hirai, K. Tamotus, Y. Yonezawa and C. Shin, *Bull. Chem. Soc. Jpn.*, 1995, **68**, 1369.
12 H. Kunz and H. Waldmann, *Angew. Chem., Int. Ed. Engl.*, 1984, **23**, 71.
13 L. A. Carpino, *J. Am. Chem. Soc.*, 1993, **115**, 4937.

*Received in Glasgow, UK, 26th August 1997; 7/06206K*

# Oxidation of tertiary diaryl alcohols catalyzed by a water-soluble metalloporphyrin: $C_{aliph}$–$C_{aliph}$ *versus* $C_{aliph}$–$C_{Ar}$ bond cleavage

**Karine Wietzerbin, Bernard Meunier*† and Jean Bernadou*‡**

*Laboratoire de Chimie de Coordination du CNRS, 205 route de Narbonne, 31077 Toulouse Cedex 4, France*

**In water and at room temperature, tertiary diaryl alcohols were easily cleaved by monopersulfate oxidation using a water-soluble metalloporphyrin catalyst to give mainly aryl methyl ketones and to a lower extent diaryl ketones, probably resulting from a β-fragmentation of the diarylethoxy radical $Ar_2MeC–O·$; a small amount of unexpected ester derivatives was also detected indicating at least one alternative pathway.**

As a part of our mechanistic studies on C–H bond oxidation catalyzed by water-soluble metalloporphyrins,[1–3] we wished to determine how the oxidation of some intermediate tertiary alcohols can give ketones through cleavage of a C–C bond. In addition, little is known about oxidative C–C bond cleavage by biomimetic catalysts, whereas this is a key step in the degradation of the lateral chain of cholesterol by cytochrome P-450.[4] Tertiary alcohols are usually resistant to oxidation and their oxidative conversion generally requires a sufficient intrinsic reactivity and the use of strong oxidants (*e.g.* concentrated $H_2O_2$ in sulfuric acid,[5] chromium(VI)[6] or cerium(IV)[7] reagents). We chose to develop this study on the two diarylmethyl alcohols 4-(1-hydroxy-1-phenylethyl)benzoic acid **1**§ and 1,1-diphenylethanol, using $KHSO_5$ as oxidant (hydrogen peroxide was also tested in similar conditions but proved to be inactive) and Mn-TMPyP¶ as catalyst. This water-soluble metalloporphyrin is well-known for its efficiency in epoxidation,[8] hydroxylation[2,3] or peroxidasic oxidation[9] reactions in aqueous media. The reaction products were identified by HPLC co-injection of authentic samples, and by NMR and GC–MS analyses of the product mixtures.

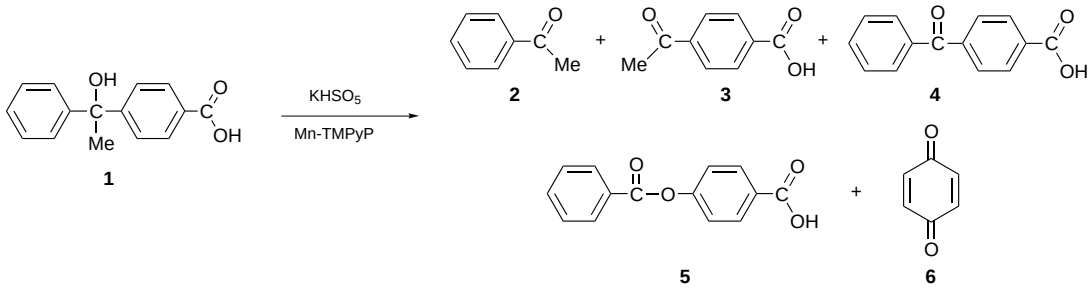
Among the compounds produced by the oxidation of **1**, two resulted from the loss of one of the two aromatic rings (**2**, **3**), two others from the loss of the methyl group (**4**, **5**) and the last one (**6**) was identified as benzoquinone (Scheme 1). Conversion and product yields are given in Table 1. More than 90% of the starting material was converted in 10 min at room temperature, with only 2% of catalyst (introduced in five consecutive additions). Such levels of conversion could not be obtained under similar conditions with cerium(IV) salts, which are well-known for their ability to oxidize some tertiary alcohols,[7] even in acetonitrile–water at reflux and/or raising the concentrations of substrate and oxidant by a factor of 100. The pool **2** + **3** + **4** + **5** represented about 50% yield (or 56% yield with respect to the starting material converted). Relative yields of ketones **2**, **3** and **4** show that cleavage of the $C_{aliph}$–$C_{Ar}$ bond (with release of a phenyl or a carboxyphenyl group) occurred more than 10 times faster than that of $C_{aliph}$–$C_{aliph}$ bond (with release of a methyl group). The relative scission of phenyl and 4-carboxyphenyl groups differed only by a factor of 2 (ratio **2**/**3** ≈ 2). Thus the relative rates of cleavage with formation of **2**, **3** and **4** were in the ratios 35 : 17.5 : 1.

These results are reminiscent of the oxidative cleavage of some tertiary alcohols by cerium(IV) salts in aqueous acetonitrile at reflux,[7] where *tert*-butyl, benzyl and allyl radicals were shown to be cleaved rapidly from the appropriate alcohol (the relative rates of formation of the *tert*-butyl : benzyl : allyl radicals were 20–63 : 4.4 : 1). In the present case, the formation of the ketones **2**–**4** suggests a mechanism involving the formation of a diarylethoxyl radical intermediate (Scheme 2) which is cleaved by β-fragmentation to give the three different ketones **2**, **3** and **4** and carboxyphenyl (route a), phenyl (route b) or methyl (route c) radicals. The diarylethoxyl radical could be formed from **1** in two steps by $e^-$ loss followed by $H^+$ abstraction, or directly by H· abstraction. Benzoquinone **6** might be an end-product deriving from one or both aryl radicals

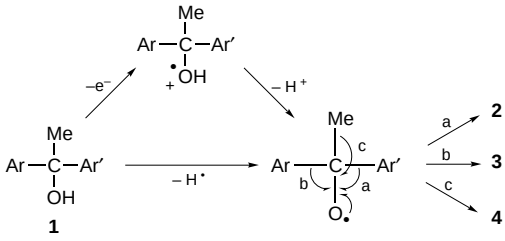
**Table 1** Yields of products obtained from oxidation of **1** catalyzed by Mn-TMPyP[a]

| Products | Yield (%)[b] | Selectivity (%)[c] |
|---|---|---|
| **2** | 27.9 ± 1.1 | 31.3 ± 0.7 |
| **3** | 14.0 ± 0.5 | 14.0 ± 0.4 |
| **4** | 0.8 ± 0.1 | 0.9 ± 0.1 |
| **5** | 7.7 ± 0.3 | 10.6 ± 0.3 |
| **6** | 9.2 ± 0.4 | 8.7 ± 0.2 |
| Conversion (%) | 90.5 ± 4.0 | |

[a] The reaction medium (1 ml of acetonitrile–water, 1 : 9) contained 66 mM phosphate buffer, pH 5 and 500 μM **1** (introduced as a 25 mM solution in acetonitrile) and 200 μM of *p*-diacetylbenzene as internal standard; [$KHSO_5$] was 10 mM, and [Mn-TMPyP] was 10 μM (introduced in five consecutive 2 nmol additions, every 2 min; the first addition initiated the reaction). The reaction was monitored by HPLC using a Nucleosil C18 10 μm column and 65 or 75% aqueous acetonitrile containing 0.1 M triethylammonium acetate as eluent (flow rate: 1 ml $min^{-1}$); the detection was performed at 240 nm and experimental errors were obtained from three independent experiments. [b] Yields were calculated after 10 min of reaction at room temperature. [c] Selectivity is defined as the ratio of product yield divided by substrate conversion.




**Scheme 1**



**Scheme 2** β-Fragmentation of a possible alkoxyl radical intermediate (Ar = phenyl and Ar′ = *p*-carboxyphenyl)

resulting from the β-scission (routes a, b), since we checked that phenol, benzoic acid and *p*-hydroxybenzoic acid, three putative evolution products of the released aryl radicals, could be quickly oxidized to **6** by the catalytic system. With this substrate, aryl (phenyl or carboxyphenyl) rather than methyl is lost, yielding acetophenone rather than benzophenone derivatives. This direction of cleavage differs from investigations on the decomposition of cumyloxyl radical[10,11] and from our recent results on oxidation of 4-(1-hydroxy-1-methylethyl)benzoic acid[3] where the loss of methyl is predominant. A plausible explanation of this special behaviour could be a combination of resonance stabilization of the resulting radicals (methyl less stable than aryl) and of the enhanced stability of acetophenone compared to acetone[10] or to benzophenone derivatives.

In the course of catalytic oxidation of **1**, the unexpected product **5** was detected. It was identified as benzoyloxybenzoic acid by MS and NMR analyses of a collected sample, and by comparison of its chromatographic behaviour with that of an authentic sample.§ Product **5** represented only about 8% yield when 10% acetonitrile was used in the reaction medium but this yield was increased up to 18% when the amount of acetonitrile was raised to 30%. At the same time, the yields of all other identified products were slightly lowered. Furthermore, the formation of **5** was dependent on oxygen concentration (yield of **5** was 1.5% under nitrogen and 7.5% under oxygen atmosphere, under experimental conditions slightly different from that of Table 1), while the formation of all the other products did not significantly depend on the atmospheric composition. It is also remarkable that the isomeric compound monophenyl terephthalate was not detected. A conceivable pathway to afford the ester **5** would be a Baeyer–Villiger oxidation of benzoylbenzoic acid (which is effectively produced in the reaction, product **4**) but this assumption can be discarded since, in a control experiment, we showed that benzoylbenzoic acid was stable under the catalytic oxidation conditions used. The results clearly demonstrate that pathway for formation of **5** is different from that of the other products **2**–**4** and **6** and, especially, that dioxygen probably plays a crucial role. The exact mechanism explaining the formation of this unexpected reaction product, which needs the cleavage of two C–C bonds, is presently unknown.

Similar experiments as with **1** were performed with 1,1-diphenylethanol. Here also, results show a high conversion of the substrate (more than 75%) and, while they are in qualitative agreement with the above data concerning the oxidation of **1** (oxidation products from 1,1-diphenylethanol were: acetophenone, benzophenone, *p*-benzoquinone and phenyl benzoate), the quantitative results differ significantly. Especially, the yield of phenyl benzoate was very low (about 1–2%), indicating that the carboxylic group present in **1** presumably plays a crucial role in orienting the reaction towards the ester **5**.

In summary, a highly efficient oxidative cleavage of a tertiary diaryl alcohol has been observed. Scission of the $C_{aliph}$–$C_{Ar}$ bond occurred preferentially compared to the $C_{aliph}$–$C_{Aliph}$ bond, yielding mainly acetophenone derivatives through a probable β-fragmentation mechanism. The presence of an ester derivative whose formation is oxygen dependent indicates that an alternative pathway is involved. An overall comprehensive mechanism of this oxidative cleavage reaction is presently under investigation using isotopic labelling experiments.

## Footnotes and References

† E-mail: bmeunier@lcc-toulouse.fr
‡ E-mail: bernadou@lcc-toulouse.fr
§ Compound **1** was synthesized from benzoylbenzoic acid **4** and methylmagnesium bromide according to ref. 13, and 4-benzoyloxybenzoic acid **5** was obtained by esterification of benzoyl chloride with 4-hydroxybenzoic acid.
¶ Mn-TMPyP denotes the pentaacetate of the diaqua-manganese(III) derivative of *meso*-tetrakis(1-methylpyridinium-4-yl)porphyrin, and was prepared according to ref. 12.

1 B. Meunier, *Chem. Rev.*, 1992, **92**, 1411.
2 M. Pitié, J. Bernadou and B. Meunier, *J. Am. Chem. Soc.*, 1995, **117**, 2935.
3 R. J. Balahura, A. Sorokin, J. Bernadou and B. Meunier, *Inorg. Chem.*, 1997, **36**, 3488.
4 P. R. Ortiz de Montellano, in *Cytochrome P-450: Structure, Mechanism and Biochemistry*, 2nd edn., ed. P. R. Ortiz de Montellano, Plenum, New York, 1995, p. 279.
5 M. Hudlicky, in *Oxidations in Organic Chemistry*, ACS Monograph 186, ed. M. Hudlicky, American Chemical Society, Washington, DC, 1990, p. 150.
6 T. G. Waddell, A. D. Carter and T. J. Miller, *J. Org. Chem.*, 1992, **57**, 381; J. J. Cawley and V. T. Spaziano, *Tetrahedron Lett.*, 1973, **47**, 4719.
7 W. S. Trahanovsky and D. B. Macaulay, *J. Org. Chem.*, 1973, **38**, 1497.
8 J. Bernadou, A. S. Fabiano, A. Robert and B. Meunier, *J. Am. Chem. Soc.*, 1994, **116**, 9375; J. T. Groves, J. Lee and S. S. Marla, *J. Am. Chem. Soc.*, 1997, **119**, 6269.
9 M. Vidal, M. Bonnafous, S. Defrance, P. Loiseau, J. Bernadou and B. Meunier, *Drug Metab. Dispos.*, 1993, **21**, 811; M. N. Carrier, P. Battioni and D. Mansuy, *Bull. Soc. Chim. Fr.*, 1993, **130**, 405; T. Ohe, T. Mashino and M. Hirobe, *Arch. Biochem. Biophys.*, 1994, **310**, 402.
10 C. Walling and A. Padwa, *J. Am. Chem. Soc.*, 1963, **85**, 1593.
11 E. Baciocchi, F. d'Acunzo, C. Galli and M. Ioele, *J. Chem. Soc., Chem. Commun.*, 1995, 429.
12 J. Bernadou, G. Pratviel, F. Bennis, M. Girardet and B. Meunier, *Biochemistry*, 1989, **28**, 7268.
13 M. M. J. Kubitscheck and W. A. Bonner, *J. Org. Chem.*, 1961, **26**, 2194.

*Received in Liverpool, UK, 5th August 1997; 7/05713J*

# Bifunctional catalytic membrane containing Brønsted acids and sites for enantioselective hydrogenation

**Diedrik Tas, Carla Thoelen, Ivo F. J. Vankelecom and Pierre A. Jacobs***

*Centre for Surface Chemistry and Catalysis, Faculty of Agricultural and Applied Biological Sciences, Katholieke Universiteit Leuven, Kardinaal Mercierlaan 92, 3001 Leuven, Belgium*

**The hydrogenation of methyl acetoacetate to give optically pure methyl 3-hydroxybutyrate is performed heterogeneously with high activity and enantioselectivity under mild reaction conditions due to the combination of Brønsted acid and Ru–binap sites in a polydimethylsiloxane membrane matrix.**

Binap based complexes are among the most versatile and selective catalysts used to produce chiral compounds.[1] Given their extremely high cost, immobilization of the catalyst is highly desirable to allow regeneration of the catalyst.

The first attempt at immobilization consisted of a triphasic approach in which the sulfonated form of the complex was dissolved in an ethylene glycol phase which adhered on one side to a support, with the other side in contact with an immiscible phase containing the substrate.[2] The system, however, is restricted in the choice of possible substrates and solvents. Recently, we reported a new, more versatile method to immobilize binap based complexes by simple occlusion in a polydimethylsiloxane (PDMS) membrane.[3]

The hydrogenation of β-keto esters, catalyzed by binap based complexes, is a very important class of enantioselective reaction. Unfortunately, it suffers from the need for high reaction temperatures ( > 60 °C) and high hydrogen pressures ( > 6 MPa).[4] In homogeneous reaction conditions, King *et al.* discovered that the addition of small amounts of strong inorganic acids allows the reaction to occur at 40 °C using reduced hydrogen pressures.[5] This, however, requires the separation of the acid from the products after reaction to keep the catalyst active and enantioselective.

In the present work, both a Ru–binap complex and toluene-*p*-sulfonic acid (PTSA) have been immobilized in a PDMS membrane *via* the same technique and used in the enantioselective hydrogenation of β-keto esters. This acidic chiral membrane shows substantially enhanced enantioselectivity and activity at room temperature, allowing catalyst separation and reuse after simple filtration.

Typically, binap–chloro(*p*-cymene)–ruthenium chloride was occluded in an elastomeric-type PDMS membrane together with PTSA. To do so, the PDMS membrane was synthesized in the presence of the binap complexes and the organic acid. A 20 vol% solution in chloroform of appropriate amounts of the prepolymer (RTV-615 A) and crosslinker (RTV-615 B) from General Electric was stirred in a 10 : 1 weight ratio together with an appropriate amount of PTSA (typically, 5 wt%) at room temp. for 1 h. The chiral complex (obtained from Aldrich) was then added (0.25 wt%), and the mixture was further stirred at room temp. for 1 h under a nitrogen atmosphere. After casting the mixture in a Petri dish, the solvent was allowed to evaporate for 18 h under nitrogen flux. The membrane was precured under vacuum at room temperature for 4 h, followed by curing under vacuum at 150 °C for 1 h. The catalyst membrane showed an average thickness of 0.2 mm, corresponding to a coverage of *ca.* 0.054 μmol $cm^{-2}$ for the Ru–binap complex. The complex and the acid are both wrapped in the elastomer network and retained by steric restrictions, in combination with van der Waals interactions between the occluded compounds and polymer chains.

Hydrogenation of methyl acetoacetate (MAA) (molar ratio MAA : Ru : solvent = 2500 : 1 : 25000) with the occluded Ru–binap complex was performed in a batch reactor at a pressure of 6 MPa at room temp. (RT), 40 or 60 °C.

An overview of the catalytic results obtained with the membrane occluded Ru–(*R*)-binap complex is given in Table 1. Entries 1–3 show that the Ru–binap PDMS membrane requires hydrogenation temperatures of at least 60 °C to exhibit reasonable activity and moderate enantioselectivity. Literature data show that the same is true for the homogeneous case.[4] Entries 4 and 5 show that strong organic acids like PTSA exert a comparable effect on catalyst activity as inorganic acids, allowing room temp. hydrogenation of methyl acetoacetate with high enantioselectivity. PTSA, added to the reaction mixture containing a Ru–binap membrane, activates the heterogeneous catalyst yielding good activity (entry 6). At the same time, a very significant increase in enantioselectivity from 61 to 93% is observed compared to the acid-free system at 60 °C (entry 3). However, this system still requires removal of PTSA from the reaction medium.

An acid/Ru–binap membrane, containing equal molar amounts of PTSA and Ru, shows a four-fold increase in activity at 40 °C while maintaining the high enantiomeric excess (entry 8) compared to the previous case (entry 6) in which PTSA was added to the reaction medium. The acid/Ru–binap membrane shows good activity and enantioselectivity at room temperature as well (entry 7). The ratio of PTSA to Ru–binap in the catalytic membrane was found to have a pronounced effect on the system's activity (Fig. 1). After an initial steep rise in activity resulting from an increase in concentration of the incorporated acid, an optimum activity is obtained at a molar ratio of $H^+$/Ru of about 10 (entry 9). The activity decrease at higher ratios is

**Table 1** Influence of PTSA addition to a Ru–binap PDMS membrane on the activity and enantioselectivity of the hydrogenation of methyl acetoacetate[a]

| Entry | Catalyst | PTSA | *T*/°C | TOF/$h^{-1}$[b] | Ee (%) |
|---|---|---|---|---|---|
| 1 | Ru–binap membrane | — | RT | — | — |
| 2 | Ru–binap membrane | — | 40 | — | — |
| 3 | Ru–binap membrane | — | 60 | 9.6 | 61 |
| 4 | Ru–binap homogeneous | 0.5[c] | RT | 8.2 | 97 |
| 5 | Ru–binap homogeneous | 0.5[c] | 40 | 59.2 | 96 |
| 6 | Ru–binap membrane | 0.5[c] | 40 | 1.8 | 93 |
| 7 | PTSA/Ru–binap membrane | 0.5[d] | RT | 3.7 | 79 |
| 8 | PTSA/Ru–binap membrane | 0.5[d] | 40 | 6.5 | 87 |
| 9 | PTSA/Ru–binap membrane | 2.0[d] | 40 | 41.6 | 92 |

[a] Reactions (4) and (5) (homogeneous), for reasons of solubility, were carried out in methanol, whereas the membrane reactions are carried out in ethylene glycol. [b] TOF = turnover frequency, calculated as turnover number per hour, is often referred to as turnover number (TON). [c] Amount of PTSA in the homogeneous reaction mixture (g per g Ru–binap). [d] Amount of PTSA incorporated in the PDMS membrane (g per g Ru–binap).

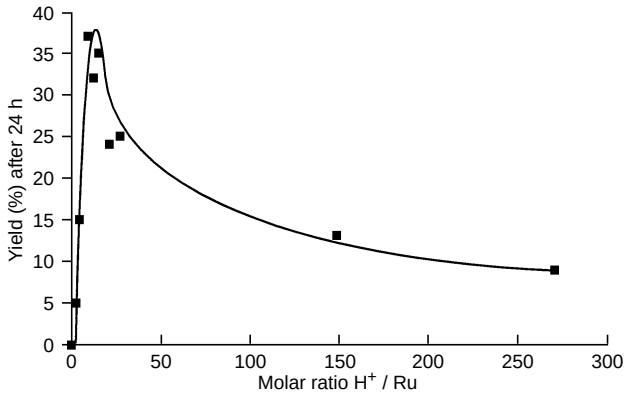



**Fig. 1** Influence of the amount of PTSA in PTSA/Ru–binap PDMS membranes, on the hydrogenation of methyl acetoacetate at 40 °C. The ee in all cases is 90 ± 3%.

probably due to a decreasing degree of crosslinking in the PDMS membrane when increasing amounts of acid are present. It seems that this results in moderate to severe leaching of the acid from the membrane, implying a decreasing concentration of incorporated acid and thus a drop in hydrogenation activity. Complex leaching is absent in all reported cases as measured by atomic absorbance spectrophotometry. The ruthenium content of the reaction mixture is lower than the detection limit of 0.16 ppm. Furthermore, after removing the membrane, the reaction mixture did not show any activity upon addition of fresh substrate. Up to the optimum point of activity, catalyst reuse after filtration is possible without loss of activity or enantioselectivity. These results clearly prove the heterogenity of the reported system.

In conclusion, a new highly active and enantioselective heterogeneous hydrogenation catalyst is presented, allowing room temp. hydrogenation of β-keto esters. The system consists of a Ru–binap complex, occluded in a PDMS membrane together with toluene-*p*-sulfonic acid activating the complex. The new catalyst has superior activity compared to its homogeneous equivalent. Moreover, reuse of the catalyst is possible after filtration.

This work was supported by the Belgian Federal Government in the frame of a IUAP-PAI grant on Supramolecular Catalysis. D. T. and C. T. thank the Flemish Fund of Scientific Research (FWO) for a grant as Aspirant Research Fellow. I. F. J. V. is indebted to the FWO for a fellowship as post doctoral research assistant.

## Footnote and References

* E-mail: pierre.jacobs@agr.kuleuven.ac.be

1 R. Noyori and H. Takaya, *Acc. Chem. Res.*, 1990, **23**, 345; S. Akutagawa, *Appl. Catal.*, 1995, **128**, 171.
2 K. T. Wan and M. E. Davis, *J. Catal.*, 1994, **148**, 1; *Nature*, 1994, **370**, 449; *J. Catal.*, 1995, **152**, 25.
3 I. F. J. Vankelecom, D. Tas, R. F. Parton, V. Van de Vyver and P. A. Jacobs, *Angew. Chem.*, 1996, **35**, 1346.
4 D. F. Taber and L. J. Silverberg, *Tetrahedron Lett.*, 1991, **32**, 4227; K. Mashima, K. Kusano, N. Sato, Y. Matsumura, K. Nozaki, H. Kumobayashi, N. Sayo, Y. Hori, T. Ishizaki, S. Akutagawa and H. Takaya, *J. Org. Chem.*, 1994, **59**, 3064.
5 S. A. King, A. S. Thompson, A. O. King and T. R. Verhoeven, *J. Org. Chem.*, 1992, **57**, 6689.

*Received in Cambridge, UK, 4th August, 1997; 7/05604D*

# Dibenzotetrathiafulvalenes inserted with cycloalkanes and their tricyclic valence isomers: reversible C–C bond making/breaking upon electron transfer

**Takanori Suzuki,*[a]† Masahide Kondo,[b] Tatsuo Nakamura,[b] Takanori Fukushima[b] and Tsutomu Miyashi*[b]‡**

[a] *Division of Chemistry, Graduate School of Science, Hokkaido University, Sapporo 060, Japan*
[b] *Department of Chemistry, Graudate School of Science, Tohoku University, Sendai 980-77, Japan*

**The title TTF derivatives and their tricyclic valence isomers afford the same bicyclic dications upon two-electron oxidation, and the resulting dications regenerate either one or the other of the two isomers selectively upon reduction.**

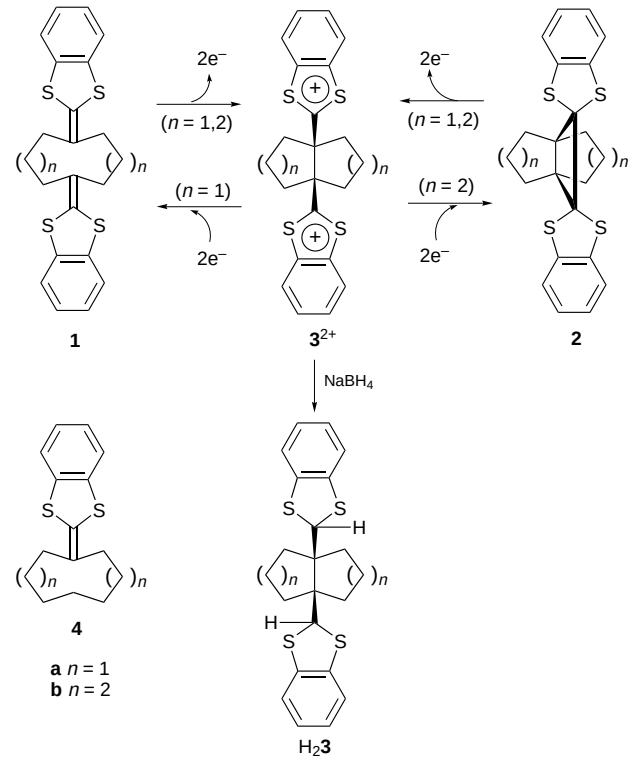
Recently much attention has been focused on molecules whose geometry and properties can be controlled by external signals.[1] From this point of view redox systems that undergo drastic structural changes upon electron transfer (ET) are interesting[2] and might be applicable to the construction of electrochemical switches or molecular devices based on their optical response and bistability. A series of tetraalkylhydrazines[3] was the first group of organic compounds reported to show such a 'dynamic redox' property. Various bicyclic diamines[4] and a variety of dithioethers[5] can also be classified as dynamic redox systems which are further advantageous in regard to the bistability gained by forming a transannular N–N or S–S bond upon ionization. ET-induced transannular C–C bond formation has been well studied in terms of homoconjugation,[6] yet little has been reported on carbocyclic ring systems other than 1,3-dimethylenecyclobutanes. We have designed and prepared the dibenzo-TTF derivatives **1** inserted with cyclooctane or cyclodecane, and their dynamic redox properties are reported herein along with those of their tricyclic valence isomers **2**. It is worth noting that the same bicyclic dications $\mathbf{3}^{2+}$ were formed upon two-electron oxidation of **1** and **2** by C–C bond formation in the former and breaking in the latter. Furthermore, the resulting dication $\mathbf{3}^{2+}$ regenerated either **1** or **2** selectively depending on their ring size upon reduction (Scheme 1).

The Wittig–Horner reactions of the corresponding diketones or ketones with 2-methoxyphosphinyl-1,3-benzodithiole[7] afforded **1**§ and monofunctionalized derivatives **4**,§ respectively. Their oxidation potentials ($E^{OX}$) measured by cyclic voltammetry in $CH_2Cl_2$ are summarized in Table 1. The donating ability of **1** is much stronger than that of **4**, and even stronger than the fully conjugated dibenzo-TTF, indicating the presence of considerable interaction between the two chromophores in the cyclooctane skeleton.[8]

Upon oxidation with iodine **1a** afforded the dication salt $\mathbf{3a}^{2+}(I_3^-)_2$ in 86% yield, the structure of which was deduced from the $^{13}C$ NMR spectrum in $Me_2SO$ [**1a** $\delta$ 22.98, 35.58, 121.47, 122.30, 125.46, 126.37, 135.69; $\mathbf{3a}^{2+}(I_3^-)_2$ $\delta$ 25.03, 37.61, 70.33, 116.95, 121.89, 125.53, 134.60]. Formation of a transannular C–C bond was confirmed by X-ray analyses¶ of the salt [1.63(3) Å] as well as its dihydro derivative $H_2$**3a** [1.584(6) Å] obtained by the reaction of $\mathbf{3a}^{2+}$ with $NaBH_4$ in quantitative yield. The two benzodithiolium moieties in $\mathbf{3a}^{2+}$ are arranged in a face-to-face manner in close proximity (Fig. 1), which causes the very large upfield shift of $\delta_C$ for C-2 of benzodithiolium ($\delta$ 116.95) in $\mathbf{3a}^{2+}$ from the normal value ($\delta$ 182.4). This salt regenerated **1a** in quantitative yield upon reduction with $SmI_2$, indicating that **1a** and $\mathbf{3a}^{2+}$ constitute a reversible redox pair undergoing facile C–C bond formation upon ionization and its breaking in the reverse cycle.

For cyclodecane **1b**, dication salt $\mathbf{3b}^{2+}(I_5^-)_2$ which has a *cis*-decalin structure was formed in quantitative yield by reaction with iodine.‖ Although this low solubility salt decomposed easily when dissolved in $Me_2SO$, its stereochemistry and the formation of a transannular bond were confirmed by the X-ray analysis¶ of $H_2$**3b** obtained by the reaction of this salt with $NaBH_4$ in 90% yield. In contrast to the dication $\mathbf{3a}^{2+}$, this salt did not regenerate the starting diolefin **1b** upon reduction with $SmI_2$. The reduction product obtained in 92% yield was proven to be the tricyclic isomer **2b** as determined by X-ray analysis.¶

In order to investigate the involvement of such tricyclic isomers in the whole redox cycle, **2a**§ and **2b**§ were prepared by




**Scheme 1**

**Table 1** Oxidation potentials[a] and synthetic yields of new donors **1**, **2** and **4** (reference compound)

| | **a** ($n$ = 1) | | **b** ($n$ = 2) | |
|---|---|---|---|---|
| Comp. | $E^{OX}$/V | Yield (%) | $E^{OX}$/V | Yield (%) |
| **1** | +0.55[b] | 37 | +0.69[c] | 13 |
| **2** | +1.03[b] | 71 | +0.95[c] | 98 |
| **4** | +1.03[d] | 91 | +1.13[d] | 61 |

[a] Anodic peak potentials ($E_{pa}$) *vs.* standard calomel electrode (SCE), 0.1 mol dm$^{-3}$ $Bu^n_4NBF_4$ in $CH_2Cl_2$, Pt electrode, scan rate 100 mV s$^{-1}$. Under the same conditions, $E_{pa}$ of dibenzo-TTF is +0.74 V and cathodic peak potential ($E_{pc}$) of 1,3-benzodithiolium is −0.13 V. [b] $E_{pc}$ = +0.36 V. [c] $E_{pc}$ = +0.14 V. [d] No cathodic peak was observed.

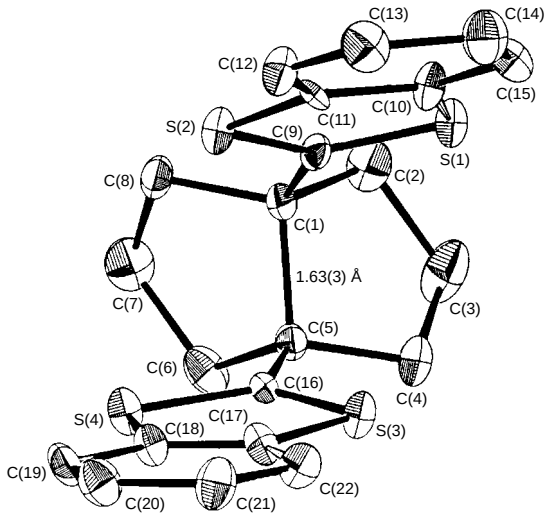



**Fig. 1** Molecular structure of the dication **3a**$^{2+}$ determined by X-ray analysis on its bis(triiodide) salt. The dihedral angle between 1,3-benzodithiolium moieties is 26°, and the torsion angle for C(9)–C(1)–C(5)–C(16) is 34°. Intramolecular contact between C(9)··C(16) is 2.80 Å.

the solid-state photoreaction of **1a** and *p*-$MeC_6H_4SO_3H$–catalyzed isomerization of **1b** in $CH_2Cl_2$, respectively, which are weaker electron donors than **1** (Table 1). Upon oxidation with iodine **2a** and **2b** afforded **3a**$^{2+}(I_3^-)_2$ and **3b**$^{2+}(I_5^-)_2$, in quantitative and 94% yield, respectively, thus making up the redox cycle shown in Scheme 1. These results indicate that **2b** and **3b**$^{2+}$ can be considered as a reversible dynamic redox pair, which is different from the previous case (**1a** and **3a**$^{2+}$) in the sense that the C–C bond breaking but not making occurs upon ionization. Although the reason of the divergent pathways for the dications **3a**$^{2+}$ and **3b**$^{2+}$ upon reduction is still unclear,** two different types of dynamic redox systems can be constructed by changing only the number of methylene units of the carbocyclic ring.††

This work was supported by the Ministry of Education, Science and Culture, Japan (No. 06640675 and 08640664).

## Footnotes and References

† E-mail: tak@science.hokudai.ac.jp
‡ E-mail: miyashi@org.chem.tohoku.ac.jp
§ All new compounds gave satisfactory analytical data.
¶ *Crystal data* for **2b**: $C_{24}H_{24}S_4$, *M* 440.70, triclinic $P\bar{1}$, *a* = 10.966(2), *b* = 13.137(2), *c* = 7.987(1) Å, α = 107.56(1), β = 109.07(1), γ = 79.49(1)°, *V* = 1032.4(6) Å$^3$, $D_c$ (*Z* = 2) = 1.418 g cm$^{-1}$, *R* = 0.065. For **3a**$^{2+}(I_3^-)_2$: $C_{22}H_{20}S_4I_6$, *M* 1174.07, monoclinic $P2_1$, *a* = 9.042(7), *b* = 19.016(7), *c* = 9.403(7) Å, β = 109.97(5)°, *V* = 1520(2) Å$^3$, $D_c$ (*Z* = 2) = 2.566 g cm$^{-1}$, *R* = 0.064. For $H_2$**3a**: $C_{22}H_{22}S_4$, *M* 414.64, monoclinic *C*2/*c* (molecule on the two-fold axis), *a* = 22.623(6), *b* = 7.402(1), *c* = 12.345(4) Å, β = 109.50(2)°, *V* = 1948.6(15) Å$^3$, $D_c$ (*Z* = 4) = 1.413 g cm$^{-1}$, *R* = 0.070. For $H_2$**3b**: $C_{24}H_{26}S_4$, *M* 442.69, orthorhombic *Pbca*, *a* = 12.493(1), *b* = 15.542(1), *c* = 21.381(2) Å, *V* = 4151.6(5) Å$^3$, $D_c$ (*Z* = 8) = 1.417 g cm$^{-1}$, *R* = 0.042. CCDC 182/642.
‖ Specific formation of the *cis*-decalin skeleton may result from kinetic control because the *trans*-isomer has nearly the same heat of formation as **3b**$^{2+}$. It seems that a much larger structural change has to take place to form the *trans*-isomer although no information is available on the conformation of the starting material **1b**. The authors are grateful to one of the referees for pointing out such a possibility.
** One possible explanation is postulating an interaction between the p-orbital of benzodithiolium and the transannular σ bond in **3a**$^{2+}$, thus adding the contribution from the σ* orbital to its LUMO. See ref. 9.
†† Unlike **1a** and **1b**, cyclohexane-1,4-diylidenebis[2-(1,3-benzodithiole)] ($E_{pa}$ = +0.96 V) does not form a transannular C–C bond upon oxidation with iodine. The product is the salt of 2-(4′-iodobicyclo[2.2.1]heptan-1′-yl)-1,3-benzodithiolium having a spiro(1,3-benzodithiole) unit at C-7′.

1 P. R. Ashton, R. Ballardini, V. Balzani, A. Credi, M. T. Gandolfi, S. Menzer, L. Pérez-García, L. Prodi, J. F. Stoddart, M. Venturi, A. J. P. White and D. J. Williams, *J. Am. Chem. Soc.*, 1995, **117**, 11 171; D. J. Cárdenas, A. Livoreil and J.-P. Sauvage, *J. Am. Chem. Soc.*, 1996, **118**, 11 980.
2 T. Suzuki, J. Nishida and T. Tsuji, *Angew. Chem., Int. Ed. Engl.*, 1997, **36**, 1329; T. Suzuki, H. Shiohara, M. Monobe, T. Sakimura, S. Tanaka, Y. Yamashita and T. Miyashi, *Angew. Chem., Int. Ed. Engl.*, 1992, **31**, 455.
3 S. F. Nelsen and C. R. Kessel, *J. Am. Chem. Soc.*, 1977, **99**, 2392; S. F. Nelsen, W. C. Hollinsed, C. R. Kessel and J. C. Calabrese, *J. Am. Chem. Soc.*, 1978, **100**, 7876; S. F. Nelsen, D. A. Trieber, J. J. Wolff, D. R. Powell and S. Roger-Crowley, *J. Am. Chem. Soc.*, 1997, **119**, 6873.
4 R. W. Alder, R. Gill and N. C. Goode, *J. Chem. Soc., Chem. Commun.*, 1976, 973; R. W. Alder and R. B. Sessions, *J. Am. Chem. Soc.*, 1979, **101**, 3651; R. W. Alder, A. G. Orpen and J. M. White, *J. Chem. Soc., Chem. Commun.*, 1985, 949; R. W. Alder, *Tetrahedron*, 1990, **46**, 683.
5 K.-D. Asmus, *Acc. Chem. Res.*, 1979, **12**, 436; W. K. Musker, *Acc. Chem. Res.*, 1980, **13**, 200; H. Fujihara, J.-J. Chiu and N. Furukawa, *J. Am. Chem. Soc.*, 1988, **110**, 1280.
6 M. Horner and S. Hünig, *J. Am. Chem. Soc.*, 1977, **99**, 6122; W. Freund and S. Hünig, *J. Org. Chem.*, 1987, **52**, 2154.
7 K. Akiba, K. Ishikawa and N. Inamoto, *Bull. Chem. Soc. Jpn.*, 1978, **51**, 2674.
8 R. Bishop, *Aust. J. Chem.*, 1984, **37**, 319.
9 A. Gleiter and W. Schäfer, *Acc. Chem. Res.*, 1990, **23**, 369.

*Received in Cambridge, UK 1st September 1997; 7/06342C*

# Regiospecific ring-opening reactions of aziridines bearing an α,β-unsaturated ester group with trifluoroacetic acid or methanesulfonic acid: application to the stereoselective synthesis of (*E*)-alkene dipeptide isosteres

**Hirokazu Tamamura,* Masaki Yamashita, Hiroyuki Muramatsu, Hiroaki Ohno, Toshiro Ibuka, Akira Otaka and Nobutaka Fujii**

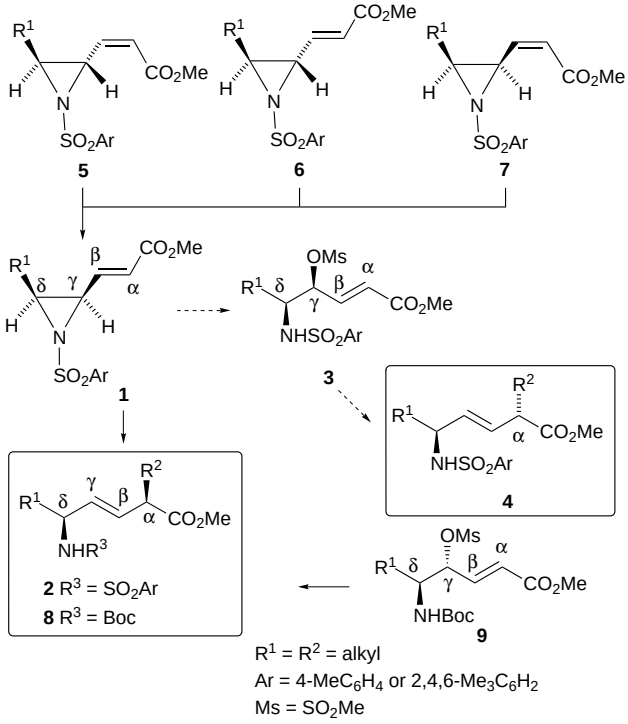
*Graduate School of Pharmaceutical Sciences, Kyoto University, Sakyo-ku, Kyoto 606-01, Japan*

**Reaction of *N*-(2,4,6-trimethylphenylsulfonyl)-γ,δ-*cis*- or -*trans*-γ,δ-epimino (*E*)-α,β-enoates with acids such as TFA or methanesulfonic acid (MSA) affords the stereo- and regioselective ring-opened products in high yields, and subsequent treatment of resulting δ-aminated γ-mesyloxy α,β-enoates with organocopper reagents yields diastereoisomerically pure (*E*)-alkene dipeptide isosteres.**

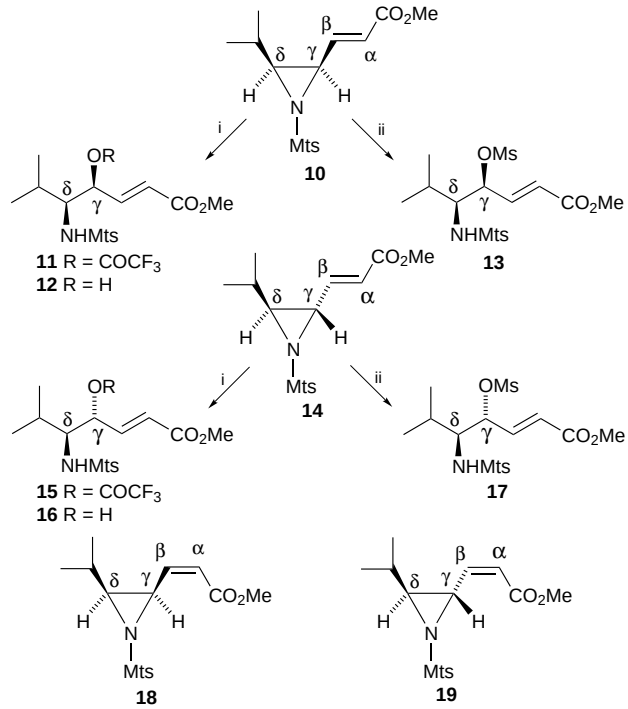
Among various dipeptide isosteres, use of (*E*)-alkene isosteres as backbone replacements of amide bonds in peptides has been well documented.[1] Recently we[2] and others[3] have reported that (*E*)-alkene isostere-containing peptides can exhibit potent biological activity. Because it has been reported that both the (*E*)-configuration and the stereochemistry at the α-position are important factors for biological activity, the stereocontrolled synthesis of both stereoisomers of types **2** and **4** from a single substrate of type **1** would be extremely valuable (Scheme 1). One advantage of such a strategy is that three other stereoisomeric enoates **5**, **6**, and **7** can be converted into the enoate **1** in synthetically acceptable yields merely by exposure to a palladium(0) catalyst (Scheme 1).[4] Previously we and others have developed two synthetic methods for the preparation of diastereomerically pure (*E*)-alkene dipeptide isosteres **2** and **8** by organocopper-mediated *anti*-$S_N2'$ reaction of β-aziridinyl α,β-enoate **1**[5] and δ-aminated γ-mesyloxy α,β-enoate **9**,[6] respectively.

Whereas ample precedent exists that various nucleophilic reagents,[7] including Lewis acids such as acetic acid,[8] TFA[9] and toluene-*p*-sulfonic acid in aqueous acetone,[10] attack simple *N*-unactivated or activated aziridines[11] at either of the two carbon atoms, yielding ring-opened products, the synthetically useful reactions involving γ,δ-epimino α,β-enoates of type **1** with TFA or methanesulfonic acid (MSA) have not previously been reported. Here we report the regio- and stereo-selective ring-opening reactions of aziridines and stereoselective synthesis of (*E*)-alkene dipeptide isosteres by treatment of the ring-opened products with organocopper reagents.

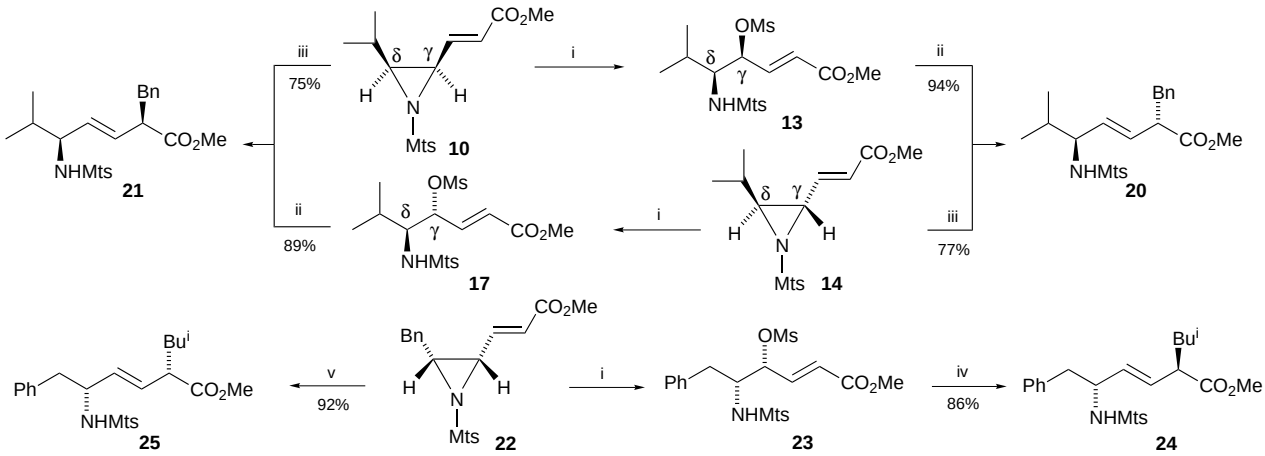
We initially examined ring-opening reactions using TFA. The required diastereoisomerically pure *N*-(2,4,6-trimethylphenylsulfonyl) (Mts)-protected aziridines bearing α,β-unsaturated esters were readily prepared according to reported methods.[4,5] Exposure of enoate **10** derived from L-valine to TFA at room temp. for 15 h afforded γ-trifluoroacetoxy α,β-enoate **11**, presumably *via* regioselective $S_N2$ ring-opening reaction at the γ-carbon position. Hydrolysis of **11** and silica gel flash chromatographic purification yielded the γ-hydroxy α,β-enoate **12** in 93% yield based on **10** (Scheme 2). In a similar manner, treatment of aziridine **10** with MSA (10 equiv.) in $CHCl_3$ at room temp. for 20 min gave exclusively γ-mesyloxy




**Scheme 1**



**Scheme 2** *Reagents*: i, TFA; ii, MSA



**Scheme 3** *Reagents*: i, MSA; ii, BnCu(CN)MgCl·$BF_3$; iii, BnCu(CN)MgCl·2LiCl; iv, Bu$^i$Cu(CN)MgCl·$BF_3$; v, Bu$^i$Cu(CN)MgCl·2LiCl

α,β-enoate **13** in essentially quantitative yield. It was found that the MSA-mediated ring-opening reaction proceeded much more faster than the reaction involving TFA. It is also noteworthy that, in both cases, ring-opened products generated by nucleophilic attack at the α- or δ-carbon positions could not be detected.

Regiochemical assignments for the trifluoroacetate **11** and the mesylate **13** were readily made by $^1$H NMR spectroscopy ($^1$H-$^1$H COSY). The γ,δ-*syn* stereochemistry of the *N*-protected amino alcohol **12** derived from **11** was confirmed by transformation of **12** into the original substrate **10** using the Mitsunobu conditions.[12] Since the mesylate **13** was prone to regenerate the original substrate **10** during silica gel flash chromatographic purification, the mesylate **13** could not be isolated.

Regioselective ring-opening of three other stereoisomeric enoates **14**, **18** and **19** with TFA or MSA was examined. Regioselective ring-opening was successfully carried out on the *trans*-(*E*)-isomer of the aziridine enoate **14** in a similar manner (the yield of **16** based on **14**: 78%). However, treatment of the *cis*-(*Z*)-enoate **18** and the *trans*-(*Z*)-enoate **19** with TFA or MSA gave complex product mixtures. This clearly demonstrates that a slight change in the structure of the substituents can significantly alter the reaction course. Since enoates **18** and **19** can be converted into the enoate **10** *via* Pd$^0$-catalysed reactions,[4] this ring-opening reaction has no significant problems associated with its practical use for the synthesis of (*E*)-alkene isosteres.

Next, treatment of the mesylate **13** with 4 equiv. of BnCu(CN)MgCl·$BF_3$ in THF at −78 °C for 30 min afforded the protected L,D-type (2*S*, 5*S*) dipeptide isostere Mts-L-Val-ψ[(*E*)-CH=CH]-D-Phe-OMe **20** in 94% yield based on **10** (diastereoselection > 99 : 1). This reaction occurred by an *anti*-$S_N2'$ reaction as shown in Scheme 3. In sharp contrast, an *anti*-$S_N2'$ reaction of the *cis*-(*E*)-enoate **10** with 4 equiv. of BnCu(CN)MgCl·2LiCl in THF at −78 °C for 30 min yielded the L,L-type (2*R*, 5*S*) isostere Mts-L-Val-ψ[(*E*)-CH=CH]-L-Phe-OMe **21** in 75% yield, as shown in Scheme 3. One important aspect of MSA-mediated ring-opening reactions is the inversion of configuration at the C-γ carbon *via* an $S_N2$ mechanism. Thus *cis*-(*E*)-enoates produce *syn*-(*E*)-mesylates, which are converted into L,D-type isosteres by organocopper reagents. On the other hand, *cis*-(*E*)-enoates themselves afford L,L-type isosteres with organocopper reagents. In a comparable study, the *trans*-(*E*)-enoate **14** was treated with MSA to yield the *anti*-(*E*)-mesylate **17**, which was converted with the organocopper reagent into the L,L-type isostere **21** in 89% yield based on **14**. In contrast, the organocopper-mediated reaction of the *trans*-(*E*)-enoate **14** afforded the L,D-type isostere **20** in 77% yield. As a result, two types of isosteres were stereoselectively synthesized from either *cis*- or *trans*-(*E*)-enoates. Likewise, the aziridine enoate **22** derived from D-phenylalanine produced the corresponding D,L-type isostere **24** and the D,D-type isostere **25** with the MSA–organocopper and the organocopper treatment, respectively.

In conclusion, regio- and stereo-selective ring-opening reactions of *N*-Mts-protected aziridines bearing an α,β-unsaturated ester by TFA or MSA have been found. These ring-opening reactions provide useful approaches for the stereoselective synthesis of both L,L-type (or D,D-type) and L,D-type (or D,L-type) (*E*)-alkene dipeptide isosteres from either γ,δ-*cis*- or -*trans*-γ,δ-epimino (*E*)-α,β-unsaturated esters. The authors are grateful to Dr Terrence R. Burke, Jr., NCI, NIH, for valuable discussions during the preparation of this manuscript.

## Footnote and References

* E-mail: tamamura@pharm.kyoto-u.ac.jp


1 J. S. Kaltenbronn, J. P. Hudspeth, E. A. Lunney, B. M. Michniewicz, E. D. Nicolaides, J. T. Repine, W. H. Roark, M. A. Steir, F. J. Tinney, P. K. W. Woo and A. D. Essenburg, *J. Med. Chem.*, 1990, **33**, 838; D. Tourwe, J. Couder, M. Ceusters, D. Meert, T. F. Burks, T. H. Kramer, P. Davis, R. Knapp, H. I. Yamamura, J. E. Leysen and G. van Binst, *Int. J. Peptide Protein Res.*, 1992, **39**, 131; for a review of syntheses of (*E*)-alkene dipeptide isosteres up to May 1992, see T. Ibuka, *J. Synth. Org. Chem. Jpn.*, 1992, **50**, 953.

2 M. Wada, R. Doi, R. Hosotani, T. Ibuka, H. Habashita, K. Nakai, N. Fujii and M. Imamura, *Pancreas*, 1995, **10**, 31.

3 T. E. Christos, A. Arvanitis, G. A. Cain, A. L. Johnson, R. S. Pottorf, S. W. Tam and W. K. Schmidt, *Bioorg. Med. Chem. Lett.*, 1993, **3**, 1035.

4 T. Ibuka, N. Mimura, H. Ohno, K. Nakai, M. Akaji, H. Habashita, H. Tamamura, Y. Miwa, T. Taga and N. Fujii, *J. Org. Chem.*, 1997, **62**, 2982.

5 P. Wipf and P. C. Fritch, *J. Org. Chem.*, 1994, **59**, 4875; N. Fujii, K. Nakai, H. Tamamura, A. Otaka, N. Mimura, Y. Miwa, T. Taga, Y. Yamamoto and T. Ibuka, *J. Chem. Soc., Perkin Trans. 1*, 1995, 1359.

6 T. Ibuka, H. Habashita, A. Otaka, N. Fujii, Y. Oguchi, T. Uyehara and Y. Yamamoto, *J. Org. Chem.*, 1991, **56**, 4370; M. J. Daly, R. A. Ward, D. F. Thompson and G. Procter, *Tetrahedron Lett.*, 1995, **36**, 7545.

7 D. Tanner and P. Somfai, *Tetrahedron Lett.*, 1987, **28**, 1211; J. Legters, J. G. H. Willems, L. Thijs and B. Zwanenburg, *Recl. Trav. Chim. Pays-Bas*, 1992, **111**, 59; C. M. Rayner, *Synlett*, 1997, 11.

8 A. Bongini, G. Cardillo, M. Orena, S. Sandri and C. Tomasini, *J. Chem. Soc., Perkin Trans. 1*, 1986, 1339; 1986, 1345.

9 D. A. Evans, M. M. Faul, M. T. Bilodeau, B. A. Anderson and D. M. Barnes, *J. Am. Chem. Soc.*, 1993, **115**, 5328; I. Coldham, A. J. Collis, R. J. Mould and R. E. Rathmell, *J. Chem. Soc., Perkin Trans. 1*, 1995, 2739; F. A. Davis and G. V. Reddy, *Tetrahedron Lett.*, 1996, **37**, 4349.

10 F. A. Davis and P. Zhou, *Tetrahedron Lett.*, 1994, **35**, 7525.

11 G. E. Ham, *J. Org. Chem.*, 1964, **29**, 3052.

12 O. Mitsunobu, *Synthesis*, 1981, 1.


*Received in Cambridge, UK, 18th August 1997; 7/06027K*

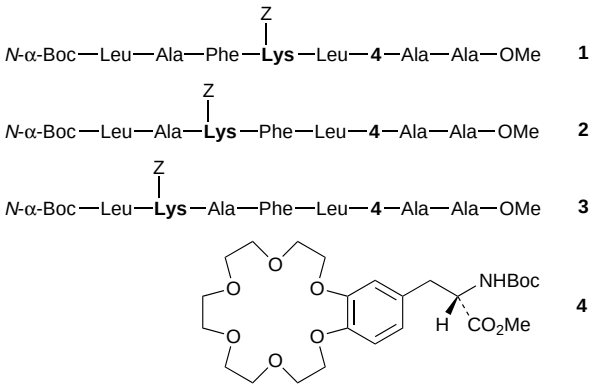
# Chiral recognition ability of peptide-based molecular receptors

**Normand Voyer*† and Brigitte Guérin**

*Département de chimie, Université de Sherbrooke, Sherbrooke, Québec, Canada J1K 2R1*

**Peptidic receptors bearing a crown ether side chain show enantioselective recognition of aromatic carboxylate and ammonium species and could be useful in chiral separation technology.**

The development of novel molecular systems that allow cost efficient separation of enantiomers is an active area of research.[1] In addition to the conventional fractional crystallization of diastereoisomeric salts, several new approaches are being investigated in this area: membrane separation, enzymatic resolution and chiral chromatography.[2] Herein we report that peptide-based molecular receptors could be used in enantiomer separation systems since they exhibit chiral recognition towards aromatic ammonium and carboxylate species by using distant aromatic–aromatic and electrostatic interactions.




The flexible crown ether modified peptides **1**–**3** were designed to complex aromatic ammonium and carboxylate species *via* an induced-fit mechanism, as depicted schematically in Fig. 1.[3] Receptors **1**–**3** were synthesized by a solid-phase strategy on a polystyrene-based oxime resin.[3] They showed both efficient complexation of phenylalkylamines and binding processes provoked conformational changes of the peptidic backbone, from a β-sheet to highly dissymetric β-turn structure. These observations lead us to investigate their chiral recognition ability towards synthetically useful compounds.

The chiral recognition ability of **1**–**3** was studied by a conventional enantioselective transport experiment through a $CHCl_3$ membrane.[4] Briefly, for the ammonium species, an aqueous source phase (0.08 M HCl) containing the substrate (0.24 mmol) and $LiPF_6$ (0.6 mmol) was separated from the receiving phase (0.01 M HCl) by a $CHCl_3$ phase containing the chiral receptors (8 mM). For the carboxylate species, KCl was used in the source phase (0.08 M LiOH) instead of $LiPF_6$ and pure water replaced the 0.01 M HCl solution in the receiving phase. The *R* and the *S* enantiomers of the $K^+$ salts of *N*-benzyloxycarbonylalanine (*N*-Z-Ala-O$^-$K$^+$) **5** and *N*-benzoylphenylalanine (*N*-Bz-Phe-O$^-$K$^+$) **6**, and α-methylbenzylammonium (MBA) **7** were used as substrates. Attempts to use α-methylnaphthylammonium as substrate failed due to its ability to cross the organic layer without receptors. The results are reported in Tables 1 and 2 as first order transport rates and enantiomeric discrimination constants.

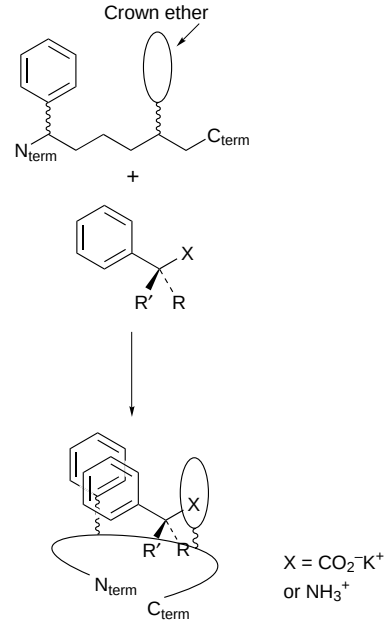



**Fig. 1** Working model for the chiral recognition ability of peptidic receptors **1**–**3** towards aromatic ammonium and carboxylate species. The binding of the guest by the cooperative action of the distant crown ether and benzyloxycarbonyl side chains induces conformational changes that lead to highly dissymetric complexes.

**Table 1** First order transport rates observed with peptidic receptors **1**–**3** and the crown ether **4** for the transport of substrates **5**–**7** across a $CHCl_3$ membrane[a]

| | | Rate/$10^5$ mol h$^{-1}$ | | | |
|---|---|---|---|---|---|
| | Substrates | **1** | **2** | **3** | **4** |
| **5** | (*S*)-Z-Ala-O$^-$K$^+$ | 6.16 | 4.73 | 1.40 | 10.3 |
| **5** | (*R*)-Z-Ala-O$^-$K$^+$ | 5.85 | 7.28 | 1.42 | 11.2 |
| **6** | (*S*)-Bz-Phe-O$^-$K$^+$ | 0.17 | 0.20 | 0.53 | 0.53 |
| **6** | (*R*)-Bz-Phe-O$^-$K$^+$ | 0.12 | 0.17 | 0.37 | 0.50 |
| **7** | (*R*)-(+)-MBA | 3.34 | 4.10 | 4.99 | 7.83 |
| **7** | (*S*)-(+)-MBA | 3.83 | 3.55 | 5.39 | 7.74 |

[a] Values reported are the average of three or more independent runs reproducible within ±5% performed at room temperature with a synchronized 6-position magnetic stirrer.

**Table 2** Enantiomeric discrimination constants (EDC = $k_S/k_R$) observed with peptidic receptors **1**–**3** and the crown ether **4** for the transport of substrates **5**–**7** across a $CHCl_3$ membrane

| | | EDC ($k_S/k_R$) | | | |
|---|---|---|---|---|---|
| | Substrate | **1** | **2** | **3** | **4** |
| **5** | (*S*/*R*)-Z-Ala-O$^-$K$^+$ | 1.05 | 0.65 | 0.99 | 0.92 |
| **6** | (*S*/*R*)-Bz-Phe-O$^-$K$^+$ | 1.42 | 1.18 | 1.43 | 1.06 |
| **7** | (*S*/*R*)-MBA | 1.15 | 0.89 | 1.08 | 0.99 |

One of the noteworthy features from the results is the enhanced enantioselectivity exhibited by the peptidic receptors as compared to their constituent crown ether amino acid **4** itself. This observation demonstrates the functional role of the peptidic frameworks in creating chiral clefts and the participation of aromatic–aromatic interactions in the complexation of the guests since the interplay of multiple binding sites is required for chiral recognition. Furthermore, no transport was observed in control experiments using the analogues of receptors **1**–**3** lacking the crown ring. Another point of importance is the different enantioselectivity demonstrated by peptidic receptor **2** compared to its positional analogues **1** and **3** in the cases of substrates **5** and **7**. Indeed, receptor **2** shows a preference for the *R* enantiomers whereas **1** and **3** transport the *S* enantiomers faster. It is worth considering a different complex structure between receptor **2** and the substrates. The peptidic receptors are known to exist in a β-sheet conformation in chlorinated solvents.[2] Under that conformation, the two binding side chains, the aromatic benzyloxycarbonyllysine and the crown ether, are on the same side of the peptidic framework for receptors **1** and **3**, but on opposite sides for their analogue **2** (Fig. 2). The different enantiomeric recognition ability of receptor **2** *versus* **1** and **3** is of importance since a subtle change in the spatial relationship of the binding elements (*i.e.* the relative position of the amino acids) allows the preparation of molecular systems selective for either enantiomer of a chiral compound of interest. The highest enantioselectivity was observed with receptors **1** and **3** and guest **5**, Bz-Phe-$O^-K^+$ [enantiomeric discrimination constant ($k_S/k_R$) = EDC = 1.42 and 1.43, respectively).

On the other hand, the three peptidic receptors transport the substrates at a slower rate than the monomeric crown analogue **4**. This could be due to the greater mobility and/or the faster decomplexation rate of the smaller and probably less stable crown complexes.

Even though several chiral receptors have been reported to achieve enantiomeric discrimination of carboxylate and ammonium compounds, the peptide-based molecular systems reported here have the advantages of being easily synthesized directly on polystyrene resin, the possibility of fine-tuning their enantioselectivity towards a desired enantiomer, and their suitability for optimization by combinatorial approach.[5] We are currently exploring the fundamental and practical aspects of peptidic receptors **1**–**3**.

The financial support of the NSERC of Canada, the Fonds FCAR du Québec, and the Université de Sherbrooke is gratefully acknowledged. B. G. thanks the NSERC of Canada for a postgraduate scholarship. The authors thank Dr Georges Dewynter (U. Montpellier-II, France) for critical reading of the manuscript.

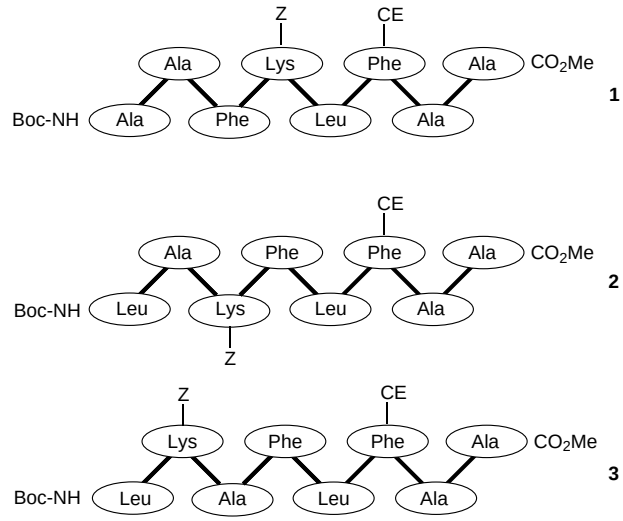



**Fig. 2** Schematic representations of peptidic receptors **1**–**3** under their β-sheet conformation (side view) that illustrate the orientation of the binding side chains (CE = crown ether; Z = benzyloxycarbonyl)

## Footnotes and References

* E-mail: normand.voyer@chm.ulaval.ca
† Address correspondence to: Professor Normand Voyer, Département de chimie, Université Laval, Québec, QC, Canada G1K 7P4.

1 S. C. Stinson, *Chem. Eng. News*, 1995, **73**, 44; 1993, **71**, 38; R. A. Sheldon, *Chirotechnology: Industrial Synthesis of Optically Active Compounds*, Marcel Dekker, New York, 1993.
2 For recent overviews on enantiomer separation techniques, see P. J. Pickering and C. R. Southern, *J. Chem. Technol. Biotechnol.*, 1997, **68**, 417; R. A. Sheldon, *J. Chem. Technol. Biotechnol.*, 1996, **67**, 1; *Chiral Separations by Liquid Chromatography*, *ACS Symp. Ser.*, ed. S. Ahuja, vol. 471, 1991; S. C. Stinson, *Chem. Eng. News*, 1992, **70**, 46.
3 N. Voyer and B. Guérin, *J. Chem. Soc., Chem. Commun.*, 1992, 1253.
4 For ammonium species: J.-P. Behr and J.-M. Lehn, *J. Am. Chem. Soc.*, 1973, **95**, 6108; M. Newcomb, R. C. Helgeson and D. J. Cram, *J. Am. Chem. Soc.*, 1974, **96**, 7367; for carboxylate species: H. Tsukube, *J. Chem. Soc., Perkin Trans. 1*, 1982, 2359; M. Zinic, L. Frkanec, V. Skaric, J. Trafton and G. W. Gokel, *J. Chem. Soc., Chem. Commun.*, 1990, 1726; *Supramol. Chem.*, 1992, **1**, 47.
5 For a recent report on a combinatorial approach towards chiral selectors, see G. Jung, H. Hofstetter, S. Feiertag, D. Stoll, O. Hofstetter, K.-H. Wiesmüller and V. Schurig, *Angew. Chem., Int. Ed. Engl.*, 1996, **35**, 2148.

*Received in Columbia, MO, USA, 20th June 1997; 7/04334A*

# Interaction between poly(ethylene glycol) and human serum albumin

**David L. Cocke,* Hai-Jun Wang and Jinjiang Chen**

*Jack M. Gill Chair of Applied Chemistry and Chemical Engineering, Lamar University, Beaumont, TX 77710, USA*

**The thermodynamic nature of the interaction between polyethylene glycol and human serum albumin has been determined by affinity capillary electrophoresis.**

Poly(ethylene glycol) (PEG) is of extreme interest in biomaterials chemistry because of its very unusual and unique lack of interaction with biological matter.[1] Surface bound PEG is known to reduce protein adsorption and has become a very high interest research area.[2] Major efforts are in progress to immobilize PEG and PEG-like molecules at surfaces by chemical grafting[3–7] and numerous coating and physical bonding schemes.[8–16] In addition, it has found extreme interest for use in one of the most challenging problems in biomaterials chemistry involving blood contact interactions with biomaterials. In this case, the clotting factor fibrinogen is not absorbed, the complement system is not activated, platelets are not bound and viral particles are not bound to PEG coated surfaces.[17] PEG's resistance to protein adsorption has been attributed to a steric stabilization effect, unique solution properties and its molecular conformation in aqueous solution.[1] However, the interaction that does occur between the protein and PEG is being used to stabilize proteins in solution and causes a decrease in thermal stability,[18] which have been attributed to steric exclusion[19] and binding to the nonpolar regions of the protein molecule,[20] respectively. It has been proposed that competition between steric expulsion forces and van der Waals attraction between the protein and PEG control the protein adsorption process. Although numerous theories and models have been proposed, there remains no consensus. Bergström *et al.*[2] found that very little fibrinogen adsorption occurs on surfaces treated with PEG in the molecular weight range from 1500 to 19 000 but that significant adsorption occurs if the molecular weights of the polymers fall below 1500 with 100% adsorption for 250 molecular weight PEG polymers. One explanation given is that the PEGs reject the protein because of an unfavourable entropy (negative entropy) change associated with compression of the configurationally random heavily hydrated PEG chains by the protein adsorption. There is, however, considerable ordering of water around the PEG chain since two or three waters are closely associated with each ethylene oxide unit.[21,22] Protein interaction would release some of this water of solvation and produce a positive entropy change. Their model discusses the need for the negative entropy of compression to be compensated by the latter and speculate that the enthalpy for water loss would be enthalpically unfavourable. In addition, the positive free energy change for this process would have to be overcome by other interactions for sorption to take place. It is clear that more information on the interaction between PEG and proteins is badly needed.

In recent experiments, we have used affinity capillary electrophoresis (ACE) to examine the interaction between PEG and human serum albumin (HSA) and have determined data that is extremely relevant to thermodynamic models that discuss entropic and enthaplic favorable and unfavorable scenarios. The ACE binding experiments were performed at 30 kV at 25, 40 and 60 °C using an open-tubular arrangement on a Hewlett-Packard Model G1600A system with HP$^3$D chemstation software. The PEG concentrations were 0, 0.500, 1.00, 2.50, 3.00, 4.00 and 7.00 mg ml$^{-1}$. The pH was maintained at 7.00 by a sodium phosphate buffer and the samples consisted of 30.0 μM human serum albumin. The neutral marker *N*,*N*-dimethylformamide served as a metric for the electroosmotic flow. The ACE method for measuring interaction energies and entropies of proteins and substrates involves measuring the change in electrophoretic mobility $\Delta\mu_{R,L}$ of the protein complex in the presence of various concentrations of ligand ([L]) such as PEG (23). Here $\Delta\mu_{R,L}$ is given by eqn. (1), where $\mu_R$ is the mobility

$$\Delta\mu_{R,L} = \mu_{R,L} - \mu_R \quad (1)$$

of the protein receptor and $\mu_{R,L}$ is the mobility of the protein–ligand complex. Form these values, Scatchard analyses can be performed using eqn. (2), where $\Delta\mu_{R,L,max}$ is the mobility of

$$\Delta\mu_{R,L}[L] = K_b\Delta\mu_{R,L,max} - K_b\Delta\mu_{R,L} \quad (2)$$

the protein receptor when it is saturated with ligand. Plotting $\Delta\mu_{R,L}[L]$ *vs.* $\Delta\mu_{R,L}$ gives a straight line with slope $-K_b$ and intercept of $K_b\Delta\mu_{R,L,max}$ and thus produces equilibrium constants. The typical Scatchard plot is shown in Fig. 1 for 25 °C. Measurements and similar treatments at 40 and 60 °C produce equilibrium constants that can be used in a second law treatment derived from the van't Hoff equation ($\ln K = -\Delta H/8.3145T + \Delta S/8.3145$) and plot a $\ln[K]$ *vs.* $T^{-1}$ produces the enthalpy and entropy changes associated with the interactions. The second law plot is shown in Fig. 2. Here the enthalpy change was determined from the slope to be $\Delta H$ = 18.1 kJ mol$^{-1}$ and from the intercept, the entropy change was determined to be $\Delta S$ = 166 J mol$^{-1}$ K$^{-1}$. At room temperature, the free energy is calculated to be −31.4 kJ mol$^{-1}$.

These results show that the enthalpy of interaction is endothermic and that the interaction is entropically driven. This supports the conjecture that protein interaction would release some of the water of 'hydration' and produce a positive entropy change. The negative but small value of the free energy shows that the overall interaction is favorable but is not chemisorption or chemical binding but rather a process driven by other events. This information should help in formualting models of interaction between PEG and proteins and points to the fact that thermodynamic models must consider the entire system, protein, solvent and PEG.

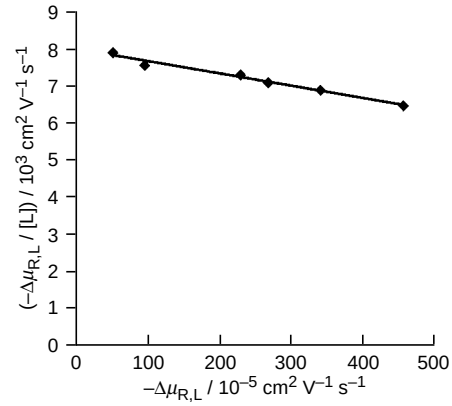



**Fig. 1** ACE-derived Scatchard plot for the interaction of the HSA with PEG at 25 °C

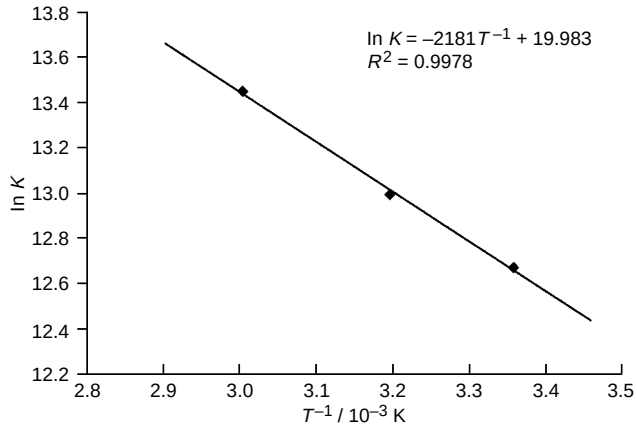



**Fig. 2** Second law plot of ln $K$ *vs.* $T$ with the equation for the line and the variance

The authors are grateful for the financial support of the Robert A. Welch Foundation (Houston, TX), the Texas Hazardous Waste Research Center (Gulf Coast Hazardous Substance Research Center) and the Texas Advanced Technology Program. We are particularly grateful to Dr Allan M. Ford for his insight concerning the importance of capillary electrophoresis and his support in obtaining the instrumentation. Special thanks go to Dr Jack M. Gill for his continuing support of the Gill Chair in Applied Chemistry and Chemical Engineering.

## Footnote and References

* E-mail: cockedl@hal.lamar.edu

1 *Poly(ethylene Glycol) Chemistry*, ed. J. M. Harris, Plenum Press, New York, 1992.
2 K. Bergström, E. Osterberg, K. Holmberg, A. S. Hoffman, T. P. Shuman, A. Kozlowski and J. M. Harris, in *Biomaterials in Solutions, as Interfaces and as Solids*, ed. S. L. Cooper, C. H. Bamford and T. Tsuruta, VSP Utrecht, The Netherlands, 1955, pp. 195–204.
3 E. Brinkman, A. Poot, L. van der Dose and A. Bantjes, *Biomaterials*, 1990, **11**, 200.
4 N. P. Desai and J. A. Hubbell, *J. Biomed. Mater. Res.*, 1991, **25**, 829.
5 Y. Mori, S. Nagaoka, H. Takiuchi, T. Takiuchi, N. Hoguchi, H. Tanzawa and Y. Noishiki, *Trans. Am. Soc. Artif. Intern. Organs*, 1982, **28**, 459.
6 S. Nagaoka and A. Nakao, *Biomaterials*, 1990, **11**, 119.
7 W. R. Gombotz, W. Guanghui and A. S. Hoffman, *J. Appl. Polym. Sci.*, 1989, **37**, 91.
8 J. H. Lee, J. Kopecek and J. D. Andrade, *J. Biomed. Mater. Res.*, 1989, **23**, 351.
9 C. Maechling-Strasser, P. Dejardin, J. C. Galin and A. Schmitt, *J. Biomed. Mater. Res.*, 1989, **23**, 1385.
10 E. W. Merrill, E. W. Salzman, S. Wan, N. Mahmud, L. Kushner, J. N. Lindon and F. Curme, *Trans. Am. Soc. Artif. Intern. Organs*, 1982, **28**, 482.
11 S. K. Hunter, D. E. Gregonis, D. L. Coleman, B. Hanover, R. L. Steohen and S. C. Jacobsen, *Trans. Am. Soc. Artif. Intern. Organs*, 1983, **29**, 250.
12 D. W. Granger, C. Nojiri, T. Okano and S. W. Kim, *J. Biomed. Mater. Res.*, 1989, **23**, 979.
13 N. P. Desai and J. A. Hubble, *Biomaterials*, 1991, **12**, 144.
14 N. P. Desai and J. A. Hubble, *Macromolecules*, 1992, **25**, 226.
15 K. Mukae, Y. H. Bae, T. Okano and S. W. Kim, *Polymer J.*, 1990, **22**, 250.
16 C. Sung, M. R. Sobarzo and E. W. Merrill, *Polymer*, 1990, **31**, 556.
17 E. W. Merrill, in *Biomaterials in Solutions, as Interfaces and as Solids*, ed. S. L. Cooper, C. H. Bamford and T. Tsuruta, VSP Utrecht, The Netherlands, 1995, pp. 919–929.
18 K. P. Antonsen, W. R. Gombotz and A. S. Hoffman, in *Biomaterials in Solutions, as Interfaces and as Solids*, ed. S. L. Cooper, C. H. Bamford and T. Tsuruta, VSP Utrecht, The Netherlands, 1995, pp. 943–953.
19 T. Arakawa, R. Bhat and S. N. Timasheff, *Biochemistry*, 1990, **25**, 1924.
20 R. Bhat and S. N. Timasheff, *Protein Sci.*, 1992, **1**, 1133.
21 K. P. Antonsen and A. S. Hoffman, in *Poly(ethylene Glycol) Chemistry*, ed. J. M. Harris, Plenum Press, New York, 1992, pp. 15–27.
22 N. B. Grahm, in *Poly(ethylene Glycol) Chemistry*, ed. J. M. Harris, Plenum Press, New York 1992, pp. 263–281.
23 J. P. Landers, *Handbook of Capillary Electrophoresis*, 2nd edn., CRC Press, Boca Raton, 1996.

*Received in Cambridge, UK, 18th August 1997; 7/06040H*



Typeset and printed by Black Bear Press Limited, Cambridge, England

ChemComm
FEATURE ARTICLE

# The renewed challenge of antibacterial chemotherapy†

**Daniela Niccolai, Luca Tarsi and Russell J. Thomas**

*GlaxoWellcome S.p.A, Medicines Research Centre, Via A. Fleming 4, Verona, 37100 Italy*

**We are currently witnessing a dramatic and alarming increase in the incidence of bacterial infections resistant to most common antibiotics. In this article, we examine briefly the background to this situation, and the mechanisms both of antibacterial action and bacterial resistance. Following this introduction is a discussion of the evolution of the various antibacterial classes and of the current approaches being adopted to keep at bay the threat of a return to a pre-antibiotic era.**

Undoubtedly one of the greatest discoveries of modern times was that of penicillin by Sir Alexander Fleming in the 1920s.[1] Prior to the clinical introduction of penicillin in the 1940s bacteria were responsible for many of the world's most lethal diseases such as pneumonia, plague, gas gangrene, wound sepsis and tuberculosis, which has killed more people than any other disease. As a result of the work of Fleming and contemporaries such as Howard Florey and Ernst Chain, few people today consider bacterial infections as being as life threatening as viral infections, heart disease or tumours.

However today, we are approaching a medical crisis which, according to some experts, could see us return to the 'dark age' of the pre-antibiotic era.

There are several reasons for this rapid reversal of fortune in man's battle against infection. The pressures of natural selection are favourable in bacteria due to their rapid rate of multiplication. Thus a colony treated with a particular antibiotic may contain a small number of organisms which have developed a random mutation which renders it less susceptible to the antibiotic. Should these bacteria survive the treatment, for example when the patient fails to complete the prescribed course, they can then multiply, causing an infection less susceptible to the antibiotic class previously used. A second factor is the over-prescription of antibiotics common throughout the world. Many people suffering from viral infections are given, as a matter of routine, antibacterial agents. Similarly, huge quantities of antibiotics are used indiscriminately in meat and dairy farming and crop spraying at doses below those necessary to eradicate bacteria. This is an ideal medium for the selection of resistant strains. Another reason is the increase in the number of immunocompromised patients such as those taking anticancer drugs, immunosuppressants following organ transplants and AIDS patients. These people need to take extended antibacterial regimens as prophylaxis against infection. Pharmaceutical companies also believed for many years that antibacterial agents were no longer a high priority and shifted their resources into other, less well-covered therapeutic areas. Thus, when resistance to the available antibiotics first started to become a problem, there were few novel agents ready to replace them.

However, in the last few years, most of the major pharmaceutical companies have committed themselves to large research programmes aimed at both improving the potency of existing classes and, more notably at discovering novel approaches to antibacterial therapy.

Some of the more common bacterial pathogens and their associated disease states are summarised in Table 1.

Various resistance mechanisms are present in a wide variety of bacteria (Table 2), in many cases because of the transfer of resistance genes between different organisms. Resistant bacteria colonising hospital wards, operating theatres, equipment and even healthcare workers are now a major problem. Only a few years after the introduction of penicillin, *Staphylococcus aureus* strains became resistant due to the production of β-lactamase enzymes which hydrolysed the antibiotic before it had a chance to act.[2] Scientists countered this problem by developing β-lactamase stable agents such as methicillin, but again the bacteria fought back by altering the cell-wall target for β-lactams, the penicillin binding proteins (PBPs), to give methicillin resistant *Staphylococcus aureus* (MRSA). For the life-threatening infections caused by MRSA, the only viable treatment is vancomycin. As will be discussed later, some *Enterobacter* strains, in addition to being unaffected by all other classes of antibiotics, are also resistant to vancomycin (VRE). It has also been shown to be possible to create vancomycin resistant *S. aureus* mutants in the laboratory.[3] If and when this occurs in a hospital man will find himself, for the first time in

**Table 1** Common bacterial pathogens and their associated disease states

| Class | Associated diseases |
|---|---|
| **Gram-positive** | |
| *Staphylococci* | abscesses |
| | endocarditis |
| | meningitis |
| | wound infections |
| *Streptococci* | pneumonia, ear, nose and throat infections |
| *Enterococci* | endocarditis |
| *Clostridium* spp. | gas gangrene |
| | tetanus |
| | colitis |
| *Bacillus* spp. | anthrax |
| | food poisoning |
| **Mycobacteria** | |
| *M. tuberculosis* | tuberculosis |
| *M. leprae* | leprosy |
| *M. avium-intracellulare* | disseminated mycobacterial disease in AIDS patients |
| **Gram-negative** | |
| *Escherichia coli* | food poisoning UTI[a] |
| *Enterobacter* spp. | UTI[a] |
| *Proteus* spp. | UTI[a] |
| *Pseudomonas aeruginosa* | burns infections, cystic fibrosis infections |
| | pneumonia |
| *Neisseria* spp. | meningitis |
| | gonorrhoea |
| *Klebsiella* spp. | pneumonia |
| | UTI[a] |
| *Salmonella* spp. | food poisoning |
| | typhoid fever |
| *Yersinia pestis* | plague |
| *Haemophilus* spp. | meningitis |
| | pneumonia |

[a] UTI = Urinary tract infection.

half a century, unable to treat one of the most problematic pathogens of the pre-antibiotic age.

The rest of this short review is dedicated to an analysis of the various classes of antibiotics currently in either clinical use or undergoing clinical trials and consideration of the problems they face, before taking a look at possible approaches towards the next generation of antibacterial agents which will hopefully arise from the rapid advances in both biology and chemistry we are currently witnessing.

A qualitative impression of the amount of research being carried out on the various antibiotic classes can be gained by examining the number of patents issued each year. A schematic representation of a study of this kind is given in Fig. 1.[4]

## Penicillins

The revolution brought about by Fleming's discovery was based on a very simple β-lactam molecule, penicillin, which acts by irreversibly acylating proteins vital for the construction of the bacterial cell wall. These penicillin binding proteins (PBPs) have no mammalian counterpart, making the β-lactams one of the most selective drug classes known. The evolution of the β-lactam antibiotics has led to the development of several distinct structural classes (Fig. 2). As can be seen, the amount of novel research being carried out on penicillins (penams) is now very limited, and will therefore not be discussed here.[5]

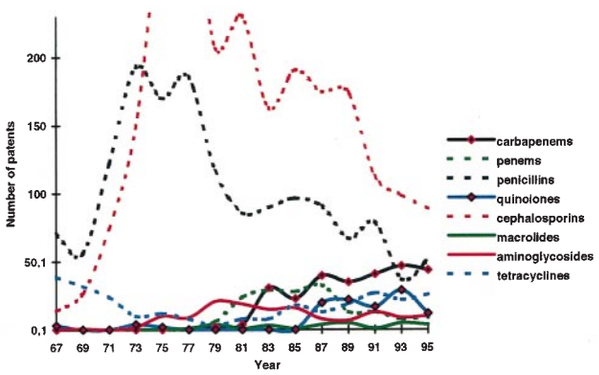



**Fig. 1** The changes in antibiotic research as shown by patent publications

## Cephalosporins

A similar overall picture is apparent also for the cephalosporins (cephems), with increasing structural complexity, heavy patent coverage and the development of resistant strains leading to a reduction in research effort on this class.[6]

What research is still being done on cephalosporins is aimed at trying to obtain activity against specific pathogens. As a way of improving activity against the notoriously impermeable pathogen *Pseudomonas aeruginosa*, some compounds have been made with the aim of exploiting the tonB-dependent iron uptake mechanism by incorporating a catechol or catechol-like group.[7,8] No catechol-bearing β-lactam has yet completed clinical trials but the approach is nevertheless an interesting one.

In an attempt to regain activity against MRSA some cephalosporins bearing bulky aromatic substituted chains on the six-membered ring have been made.[9,10]

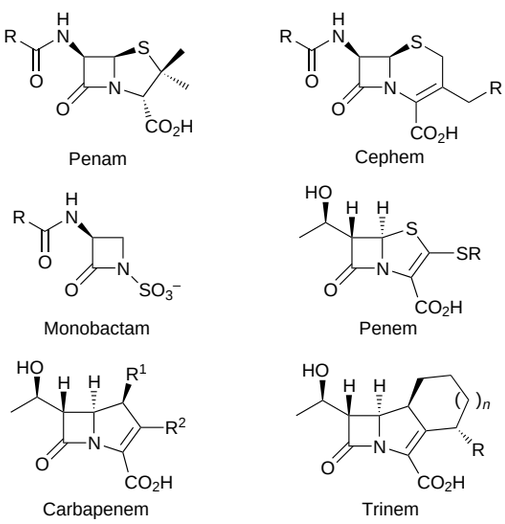


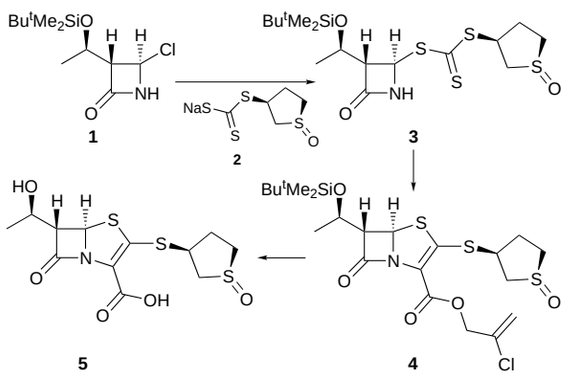

**Fig. 2** Structural classes of β-lactam antibiotics

**Table 2** Antimicrobial resistance by class

| Antimicrobial class | Mode of action | Baterial resistance mechanisms |
|---|---|---|
| β-Lactams | Cell wall biosynthesis inhibition | β-Lactamases<br>Altered PBP targets<br>Altered permeability |
| Glycopeptides | | |
| Fluoroquinolones | DNA gyrase A and topoisomerase IV inhibitors | Alteration of enzyme targets<br>Efflux pumps<br>Altered permeability |
| Aminoglycosides | Protein biosynthesis inhibitors | Enzymatic modification of antibiotic<br>Alteration of ribosome target |
| Chloramphenicol | | Enzymatic modification of antibiotic<br>Altered permeability |
| Macrolides | | Alteration of *23S* rRNA<br>Enzymatic modification of antibiotic |
| Streptogramins | | Alteration of ribosome target<br>Active efflux<br>Enzymatic modification of antibiotic |
| Tetracyclines | | Efflux pumps<br>Aleration of ribosome target<br>Altered permeability<br>Enzymatic modification of antibiotic |
| Sulfonamides<br>Trimethoprim | Folic acid biosynthesis inhibitors | Altered permeability |

## Penems

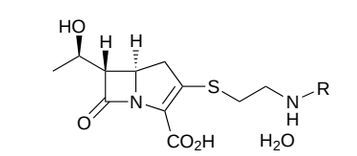
The penems are a purely synthetic class of β-lactam antibacterial agents.[11] It may be said, however, that considering the amount of extremely elegant research invested in the penem class, they have, from the clinical point of view, been decidedly disappointing. The main reasons for this are the difficulty of synthesis on a multi-tonne scale and the advent of the generally more potent carbapenem class. There is still however some interest in the penems, and there are currently a number of penems in clinical development including sulopenem **5** (Scheme 1). The key steps of the synthesis of compound **5** are the introduction of the thioxanthate substituent onto the transient azetinone generated from the 4-chloroazetidinone **1**. The resulting compound **3** is cyclised *via* an oxalimide route to the penem **4** which is then deprotected by standard methods to give sulopenem **5**.



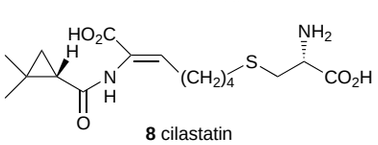
**Scheme 1**

## Carbapenems

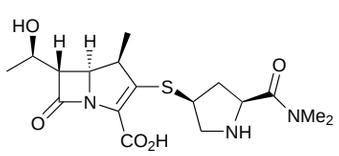
The first carbapenem, thienamicin **6**, was discovered as a natural product of *Streptomyces cattleya* in the late 1970s. Its formamidine derivative imipenem **7** was found to be much more chemically stable, and for a number of years has been an invaluable weapon against serious bacterial infection. Despite its chemical stability (due to the 6-hydroxyethyl side-chain it is also stable to all *conventional* β-lactamases), imipenem is rapidly inactivated in the kidney by mammalian dehydropeptidases (DHP) and is also nephrotoxic. This necessitates its co-administration with cilastatin **8**, which functions both as an inhibitor of DHP and reduces the renal accumulation of imipenem.[12]



**6** R = H
**7** R = CH=NH



**8** cilastatin



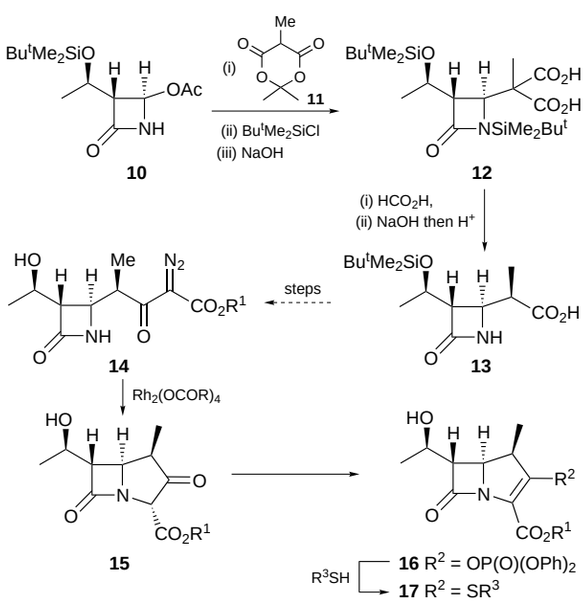
**9** meropenem

Meropenem **9** has, by the introduction of a 1β-methyl substituent, eliminated the necessity of co-administration with cilastatin.[13] This, along with the fact that it is possible to inject the compound as a single large bolus dose prior to surgery (whereas imipenem must be administered more gradually, both to reduce the risk of seizures and to overcome its lower solubility), is considered to be the main advantage of meropenem over imipenem as, in terms of clinical relevance, their antibacterial spectra are both impressive.

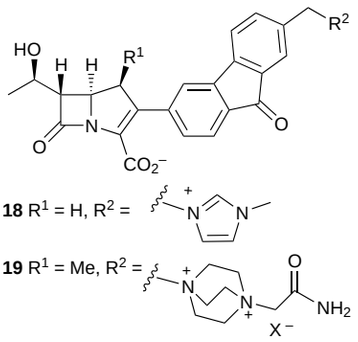
Although carbapenems have their origins as natural products, efficient, large-scale fermentation processes for key intermediates have yet to become commercially viable. Two key intermediates in the synthesis of 1β-methyl carbapenems are the 4-acetoxyazetidinone **10** and the propionic acid derivative **13**, in which all of the stereocentres in the final compounds are defined (Scheme 2).[14] While the need to explore novel syntheses of compound **10** (which is available commercially on a multi-tonne scale) is questionable, the control over the stereochemistry of the methyl group in **13** has led to many elegant approaches. One such route is shown in Scheme 2.[15] After alkylating the 4-acetoxyazetidinone **10** with the Meldrum's acid derivative **11**, *N*-silylation and saponification gave the diacid **12**, which was decarboxylated with catalytic formic acid to give the desired acid **13** in good yield and in a 94 : 6 ratio of β : α isomers. The transformation of acid **13** into a cyclised carbapenem system **17** is also outlined in Scheme 2.[16] Chain elongation to the diazo derivative **14** allowed an intramolecular rhodium octanoate-catalysed carbene insertion to the carbapenam keto ester **15** which was transformed into the enol phosphate **16**, an excellent substrate for a wide range of nucleophiles.

The current challenges in the discovery of novel carbapenems are largely based on broadening the spectrum even further, to include a wider range of problematic pathogens. As in the case of other β-lactams, carbapenems are largely ineffective against MRSA, as they have a low affinity for the PBP2' produced by these strains. The addition of a lipophilic group near the 'tail' of the molecule can increase affinity for PBP2', and workers at Merck have used this approach to synthesise anti-MRSA carbapenems such as L-695,256 **18** and its more soluble analogue L-742,728 **19**[17].

Resistance to carbapenems in *B. fragilis* and *P. aeruginosa* due to novel zinc-mediated metallo β-lactamases is starting to make an appearance, and will almost certainly increase in the coming years.[18] These enzymes are able to recognise the



**Scheme 2**

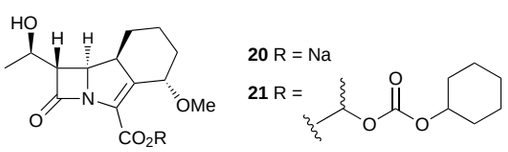



hydroxyethyl side-chain which protects carbapenems from more traditional serine β-lactamases and in order to have stable compounds in the future it will be necessary to either modify the hydroxyethyl side chain (while trying to maintain the affinity for the PBPs) or design a new generation of metallo β-lactamase inhibitors.

A third mechanism of resistance exploited by *P. aeruginosa* is to suppress the synthesis of the D2 porin in the outer membrane through which imipenem and amino acids pass. However, it has been shown that meropenem maintains activity against these resistant strains, indicating that it has an alternative method of reaching its target.[19]

## Trinems

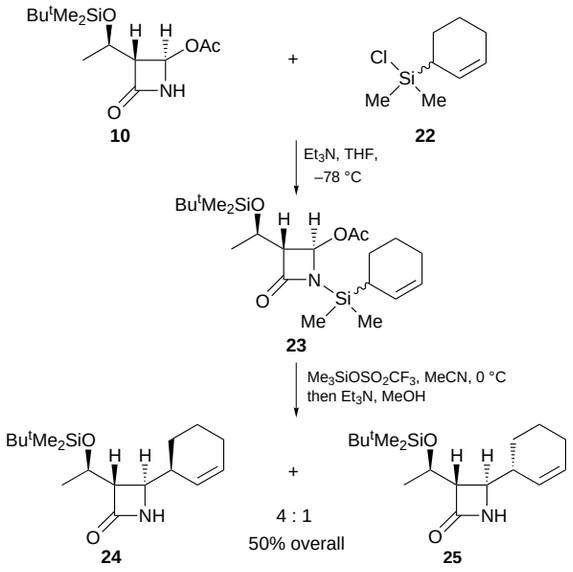
In the past few years there has been an increase in the exploration of novel β-lactam containing ring systems. Despite being structurally and synthetically interesting, many of the compounds generated in these programmes were unable, or unlikely, to exhibit significant antibacterial activity.[20] However, one both synthetically challenging and clinically relevant new class, the trinems, has emerged.[21]




Sanfetrinem **20**, the (4*S*)-methoxytrinem, and its orally bioavailable ester sanfetrinem cilexetil **21** are currently in Phase II clinical trials.[22] Its broad spectrum, which includes anaerobes and penicillin resistant *Streptococcus pneumoniae*, resistance to clinically relevant β-lactamases and stability to the renal dehydropeptidases which inactivate many penems and carbapenems, make it a promising agent for community acquired infections.

The challenge of the large-scale asymmetric synthesis of sanfetrinem has resulted in the recent publication of several quite different approaches. The original large-scale route to this compound, which was used successfully to produce the multikilogram quantity required for the Phase I study, suffered from a low overall yield and high number of steps.[21]

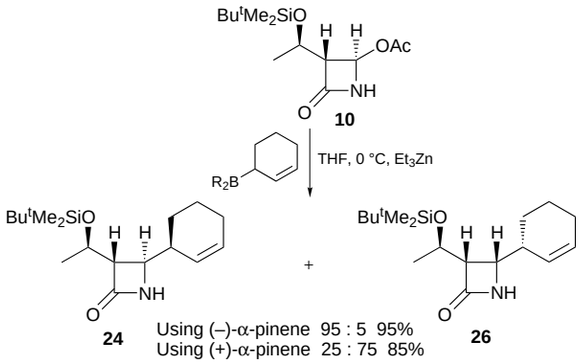
More recent approaches, however, have both reduced the number of steps and improved the overall yields to key intermediates. Two approaches to olefin **24** published recently involve an intramolecular Sakurai reaction with a cyclohexenylsilane[23] (Scheme 3), and dialkylcyclohexenylboranes[24] and appropriate Lewis acids (Scheme 4). An even more direct approach to sanfetrinem is *via* the direct condensation of (2*S*)-methoxycyclohexanone with the 4-acetoxazetidinone **10**. This has been achieved either *via* a Mukaiyama-like condensation (Scheme 5),[25] or more recently *via* zinc[26] or zirconium[27] enolates. A quite different approach to the key methoxy ketone **29** has also been published in a recent total synthesis of sanfetrinem.[28] With this method, the stereocontrol at the 6-position of the cyclohexanone ring is obtained by exploiting



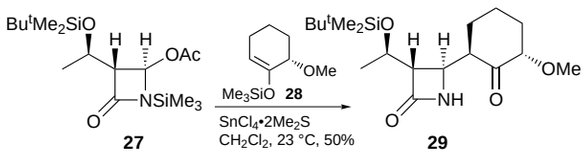

**Scheme 3**

the decarboxylation method originally applied to 1β–methyl carbapenems.[15] More recently still, a route to compound **29** using chelated tin(IV) enolates has been reported (Scheme 6).[29] In this method, optically active 2-methoxycyclohexanone is transformed into its stable tin(IV) chloride chelate **30**, which is then treated with a tertiary amine base, forming the corresponding enolate. This enolate then reacts with the 4-acetoxyazetidinone **10** and additional tin(IV) chloride to give the desired methoxy ketone **29**. This method, which was developed with the aid of low temperature NMR studies, has proved to give both high yields and stereocontrol and appears adaptable to a very large scale.

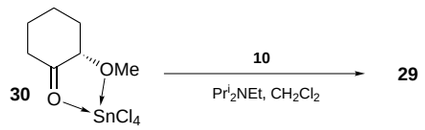
The promising biological activity obtained with sanfetrinem **20**, and the fact that this class presents a considerable synthetic




**Scheme 4**

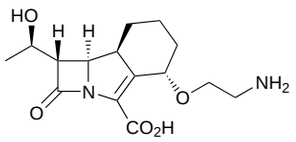



**Scheme 5**

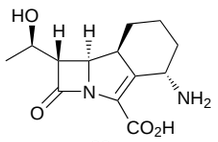



**Scheme 6**

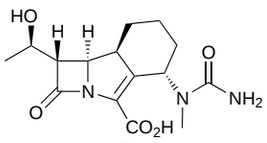
challenge, has encouraged research into other trinem molecules. Among the 4-alkoxy derivatives reported recently,[30] the 4-aminoalkoxy derivative **31** exhibited a promising biological



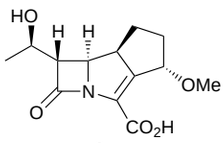
**31**



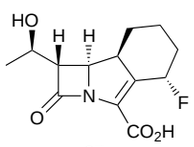
**32**



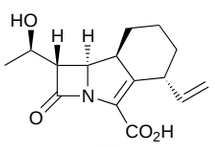
**33**



**34**



**35**



**36**

activity including *P. aeruginosa*. Other trinems reported recently include some 4-amino derivatives such as **32**,[31] 4-ureidotrinems including **33**,[32] the 5-membered ring analogue of sanfetrinem **34**,[33] stereo- and regio-isomers of sanfetrinem,[34] the highly unstable 4-fluorotrinem **35**[35] and a number of 4-alkenyl derivatives such as **36**.[36]

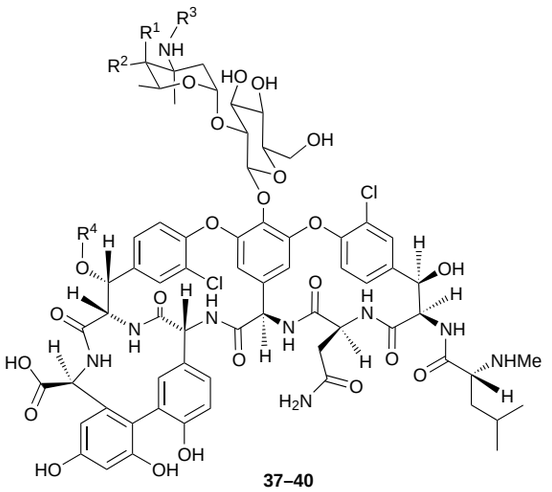
## Glycopeptides

The glycopeptides are a family of antibiotics isolated from a variety of species including actinoplanes and streptomyces.[37] Vancomycin **37** and teicoplanin **41** are the most well-known members of this class and are used widely in the clinic as the drugs of choice in treating resistant Gram-positive species such as (MRSA), coagulase-negative staphylococci and multi-resistant enterococci.

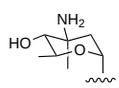
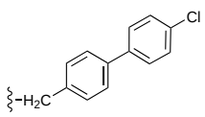
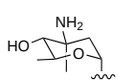
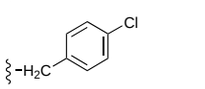
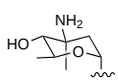
Five of the seven amino acids present are common to all glycopeptides, and their mode of action is to inhibit cell wall synthesis by interfering with a late stage in the assembly of the peptidoglycan. The conformation of the glycopeptides allows them to form a stable complex, by means of a hydrogen bond network, with the terminal dipeptide D-Ala-D-Ala of the peptidoglycan chain. This prevents both transglycosylation (chain elongation) and transpeptidation (cross-linking) with a consequent block of cell growth, subsequently leading to cell death. While the aglycone nucleus is responsible for the complexation of the D-Ala-D-Ala units, the sugar groups stabilise the complex (the modulation effect).

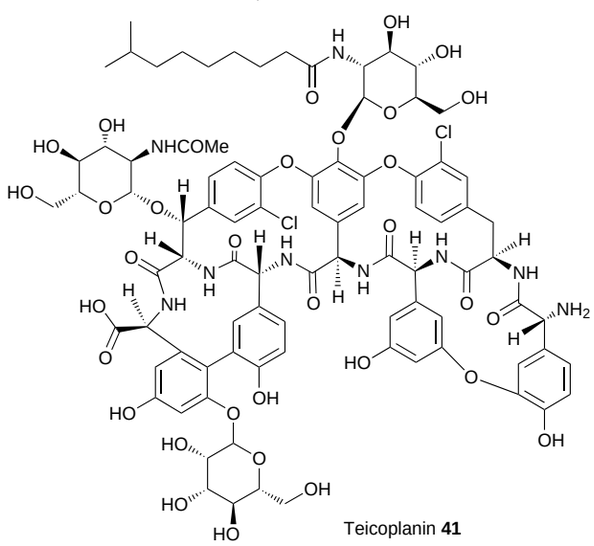
In recent years, a rapid increase in the incidence of infection and colonisation with vancomycin-resistant enterococci (VRE) has been reported from US hospitals, and the possibility of this resistance being transferred to *S. aureus* in the clinic is a cause for major concern. The mechanism of glycopeptide resistance in enterococci is well-understood and involves an alteration of the peptidoglycan precursor in which the terminal D-alanine is replaced with D-lactate, a change that reduces the ability of the antibiotic to bind to its target.[38]

In order to overcome these resistance problems, new semisynthetic glycopeptides have been synthesised. Based on the observation that the introduction of lipophilic chains onto the amino sugar vancosamine of vancomycin enhanced activity against resistant enterococci, several derivatives were prepared *via* reductive alkylation of LY264826 **38**[39] (a derivative of vancomycin). Among these, the *p*-chlorophenylbenzyl derivative LY333328 **39**[40] was identified as the most potent compound against vancomycin resistant enterococci and has undergone preclinical studies. Recent studies on the prototype



**37–40**

| | $R^1$ | $R^2$ | $R^3$ | $R^4$ |
|---|---|---|---|---|
| vancomycin **37** | OH | H | H | H |
| LY264826 **38** | H | OH | H |  |
| LY333328 **39** | H | OH |  |  |
| LY191145 **40** | H | OH |  |  |

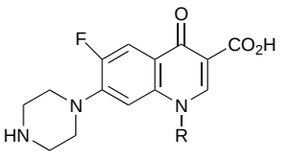


Teicoplanin **41**

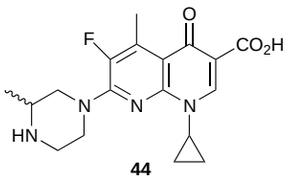
*p*-chlorobenzyl derivative LY191145 **40**[41] have shown it to still have a poor affinity for D-Ala-D-Lac residues. However, the ability of LY191145 **40** to inhibit peptidoglycan biosynthesis may be explained in part by strong dimerization, allowing it to bind to two D-Ala-D-Lac units at the cell surface. Moreover, the hydrophobic side chain confers the ability to bind to bacterial membranes, anchoring the agent at the membrane-associated target site.[38]

## Fluoroquinolones

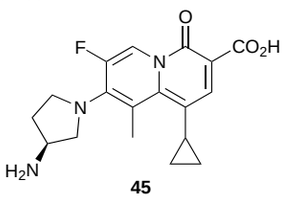
The introduction, in the 1980s of fluoroquinolones such as norfloxacin **42** and ciprofloxacin **43** provided clinicians with a valuable weapon against infections.[42] These compounds are orally active, have a broad-spectrum and favourable pharmacokinetic and safety profiles.



**42** R = Et
**43** R = cyclopropyl



**44**



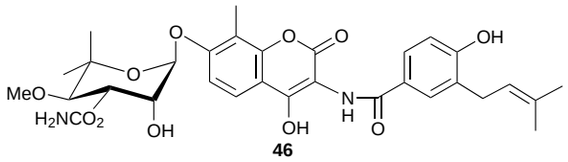
**45**

The primary mode of action of the quinolones is the inhibition of gyrase, a topoisomerase II responsible for the introduction of negative supercoils in bacterial DNA during its replication cycle.[43] Quinolones bind to the gyrase A subunit when it is complexed to the DNA, effectively blocking the supercoiling process. It has been shown that fluoroquinolones are also able to inhibit topoisomerase IV in several species including *S. pneumoniae*, *S. aureus* and *E. coli* and in some cases this may be the principal mode of antibacterial activity.[44]

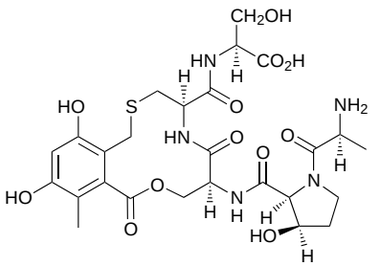
The main challenge of current quinolone research is to improve Gram-positive and anaerobe potency.[45] Two compounds currently addressing these issues are grepafloxacin **44** and the structurally interesting 2-pyridone ABT-719.1 **45**.[46]

## Cyclothialidines

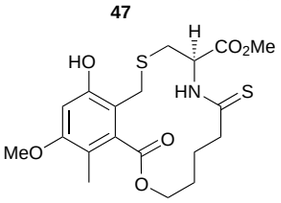
As mentioned previously, quinolones bind to the bacterial gyrase A subunit, thus blocking supercoiling. Gyrase is however a tetrameric protein comprised of two A and two B subunits. The B subunits have ATPase activity, necessary for the completion of the supercoiling cycle. When compared to the effort expended on quinolones, this target has, in the past, been largely overlooked. In the 1960s the coumarin antibiotics, such as novobiocin **46** were used clinically, although their toxicity and resistance development meant that they are now employed very rarely. Recently, however, scientists at both Hoffman-La Roche[47] and GlaxoWellcome discovered a new class of gyrase B inhibitors, the cyclothialidines. Despite having excellent activity against isolated gyrase B, cyclothialidine **47** has little or no activity against bacteria. More recently, scientists at Roche have been able to synthesise analogues, such as compound **48**, which act against a wide range of bacterial species. Several



**46**



**47**

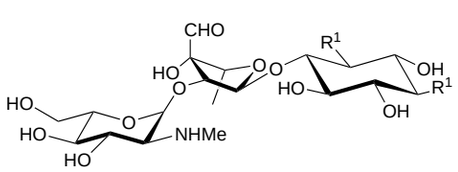


**48**

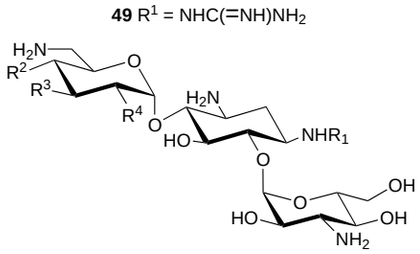
gyrase B protein subunit-inhibitor complexes have also been co-crystallised recently,[48] and it is hoped that the information gained from their X-ray crystal structures may aid the design and synthesis of novel gyrase B inhibitors.

## Aminoglycosides

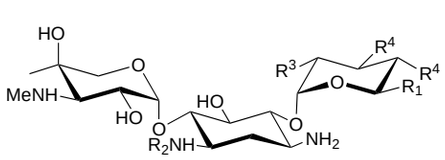
The first aminoglycoside discovered, streptomycin **49** was isolated from *Streptomyces griseus* in 1944. Since then, around ten compounds have found a clinical application, including the natural products gentamicin **50** and tobramycin **52**, and the semisynthetic derivatives amikacin **53**, netilmicin **55** and dibekacin **54**. The aminglycosides are an extremely useful class of antibiotics, especially against serious Gram-negative bacterial infections,[49] and are frequently used in a synergistic combination with β-lactams. The amino groups present in these molecules are essential for biological activity, but may also be the cause of the nephrotoxicity associated with this class. The binding of the aminoglycoside to the ribosome causes misreading of a protein which is then incorporated into membranes, causing the formation of abnormal membrane channels and



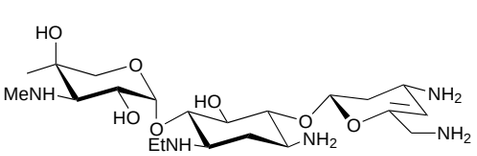
**49** $R^1$ = NHC(=NH)$NH_2$



**52** $R^1 = R^3$ = H, $R^2$ = OH, $R^4 = NH_2$
**53** $R^1$ = (*R*)-COCH(OH)$CH_2CH_2NH_2$, $R^2 = R^3 = R^4$ = OH
**54** $R^1 = R^2 = R^3$ = H, $R^4 = NH_2$



**50** $R^1$ = (*S*)-CH(Me)NHMe, $R^2$=$R^4$=H, $R^3$=$NH_2$
**51** $R^1$ = $CH_2NH_2$, $R^2$ = (*S*)-COCH(OH)$CH_2NH_2$, $R^3 = R^4$ = OH



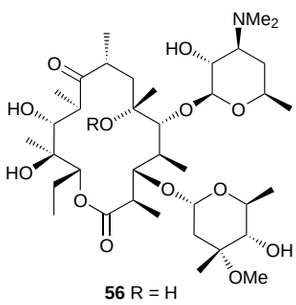
**55**

altered permeability into the bacterial cell. This provokes an autocatalytic increase in aminoglycoside uptake, leading to rapid cell death.

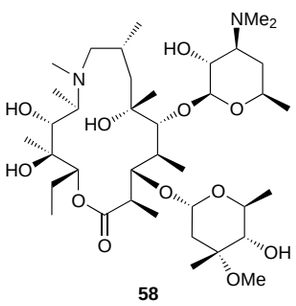
Resistance to aminoglycosides can come about *via* a number of mechanisms. The most significant is the chemical modification of the antibiotic by intracellular enzymes. Low-level resistance may also occur as a result of altered permeability across the cell wall or mutations of the ribosome target. Recently a novel aminoglycoside, isepamicin **51**, has been described as being less susceptible to enzymatic inactivation.[50]

### Macrolides and ketolides

The first macrolide, the 14-membered ring compound erythromycin A **56**, isolated from *Streptomyces erythraeus*, was introduced to clinical use in the early 1950s. Displaying similar activity to penicillins against Gram-positive bacteria, erythromycin A has the advantage of also being active against bacteria having altered outer structures such as *Mycoplasma pneumoniae* and those such as *Legionella* and *Chlamydia* which survive within the host's cells.[51]




**56** R = H




**58**

The macrolides act by inhibiting protein biosynthesis by blocking the peptidyl transferase centre of the *50S* subunit of the bacterial ribosome. Resistance to macrolides occurs either as a result of the enzymatic modification of the antibiotic or modification of targets (mutations of ribosomal proteins or rRNA genes).

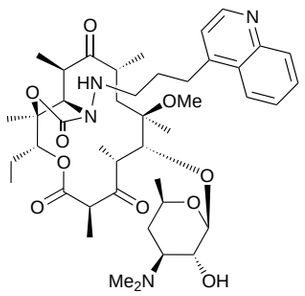
Further research led to the development of semisynthetic macrolides such as dirithromycin, roxithromycin, clarithromycin **57** and azithromycin **58**. These derivatives overcome some of the drawbacks of older agents: poor oral bioavailability as a result of acid instability, gastrointestinal disturbances, poor tissue concentration and short half-life. Azithromycin **58**, a 15-membered azalide antibiotic, is synthesised by a stereospecific Beckmann rearrangement of (9*E*)-erythromycin A oxime, followed by the reduction and reductive *N*-methylation under Eschweiler–Clarke conditions.[52]

Recent research on 14-membered macrolides has led to the discovery of a new distinct class of these macrocyclic lactones, characterized by a 3-keto function instead of the cladinose moiety (hence the name ketolide), well-known for its lability in even weakly acidic media. Currently, the most promising ketolides appear to be RU-66647,[53] RU-64004[54] **59** and TE-802[55] **60**.

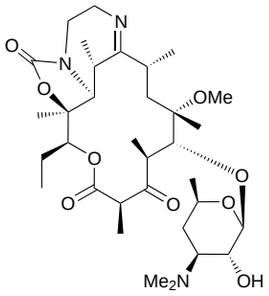
### Streptogramins

Macrolides have the same targets as the lincosamides and streptogramins, and these classes are frequently referred to as the MLS group. The streptogramins are a family of cyclic peptides produced by *Streptomyces* sp.[56] Each member of the class consists of at least two structurally different molecules, distinguished as being of either group A or group B agents. Group A molecules are polyunsaturated macrolactones, whereas group B compounds are cyclic hexadepsipeptides.

Quinupristin **61** and dalfopristin **62** are two injectable semisynthetic streptogramins currently in Phase III clinical trials. The compounds are used in synergistic combination

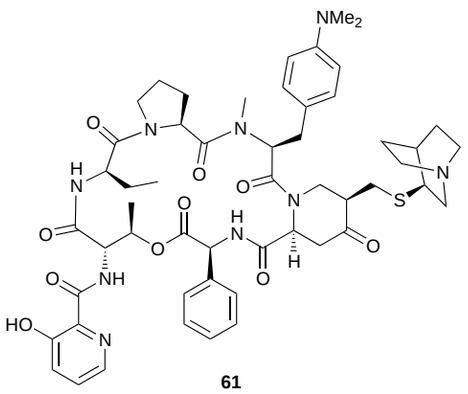



**59**

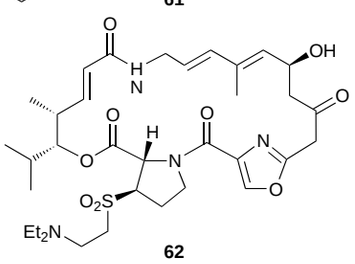



**60**

(RP59500, Synercid®) against Gram-positive bacteria, including multiresistant strains.




**61**




**62**

The synergy observed with the combination of quinopristin **61** and dalfopristin **62** can be explained in the remarkable way they bind to the peptidyl transferase domain of the *50S* ribosomal subunit. This synergy occurs because the attachment of a group A derivative such as dalfopristin **62** to the ribosome results in a conformational change, increasing the affinity for the group B compound quinopristin **61**. The resulting ternary complex is extremely stable and, unlike the bacteriostatic macrolides, streptogramins are bactericidal when used in combination.

More recent research into novel semisynthetic derivatives has allowed the discovery of an orally active streptogramin combination, RP106972, which is currently under investigation.[57]

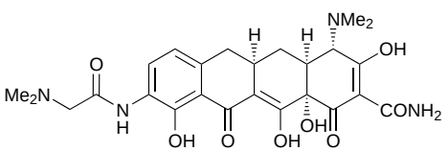
While resistance to single streptogramin components has been documented, it has been suggested that the quinupristin/dalfopristin combination should be less susceptible. However, according to a recent study reported at the 1996 Interscience Conference on Antimicrobial Agents and Chemotherapy (ICCAC) in New Orleans, resistance to the combination has already been seen in vancomycin resistant *Enterococcus faecium*.[58] Whether resistance to streptogramins will become a serious problem will only become apparent as their use in clinical situations becomes more widespread.

### Tetracyclines

Due to their broad spectrum, low toxicity, low incidence of side-effects and low cost, the tetracyclines were used intensively

both in clinical, agricultural and veterinary settings in the half century since their discovery.[59] The tetracyclines are bacteriostatic, and act by blocking the binding of aminoacyl-tRNA to the acceptor site on the *30S* ribosome.

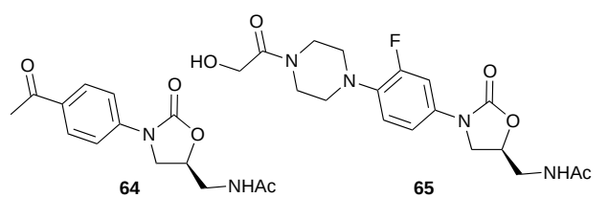
Recently, structurally modified tetracyclines have overcome the severe resistance problems affecting this class. The so-called glycylcyclines maintain potent activity against resistant strains containing ribosomial protection factors (*tetM* and *tetO*) or efflux (*tetA-E*, *-L* and *-K*) determinants.[60] The most promising member of the class is CL 331,928 (DMG-DMDOT) **63** and research into modified tetracyclines is now the subject of new research programmes in several laboratories.



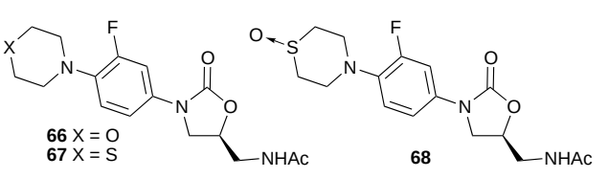
**63**

## Oxazolidinones

The last ten years have seen only one clinically significant novel class of antibiotics emerge from basic research, the oxazolidinones.[61] The pioneering work in this field was carried out at DuPont in the mid-1980s and culminated in the discovery of DUP 721 **64**. However, this molecule was found to exhibit



**64** **65**

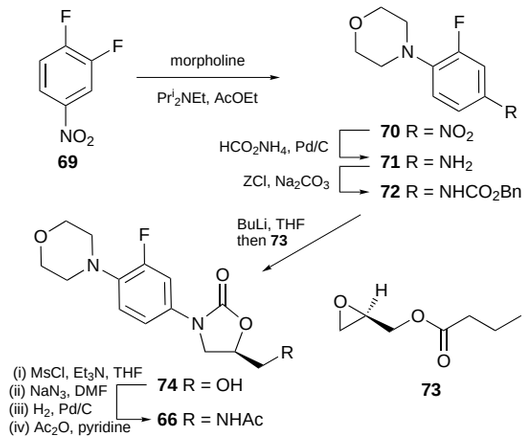


**66** X = O
**67** X = S **68**

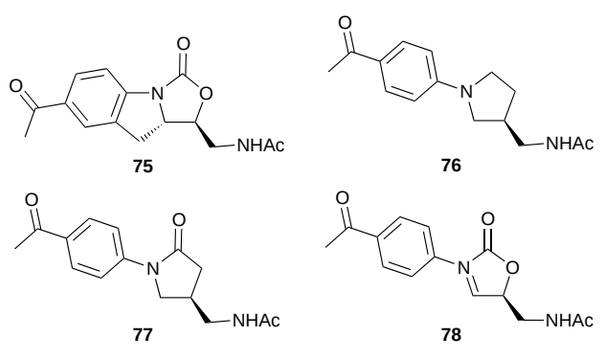
lethal toxicity in *in vivo* tests, and little further work was reported on this class until 1995, when Upjohn published a series of novel compounds. The toxicity problems encountered by DuPont and currently there are two oxazolidinones undergoing clinical trials, U-100592 **65** and U-100766 **66**.[62] Both compounds are active against Gram-positive bacteria, including resistant strains, and offer hope for the treatment of these extremely serious infections in the future. The oxazolidinones are believed to act by inhibiting an early step in bacterial protein synthesis. The versatile asymmetric synthesis of oxazolidinones, exemplified by U-100766 **66**, developed at Upjohn is shown in Scheme 7.

It has also been possible to extend the antibacterial spectrum of the class into mycobacterial species such as *M. tuberculosis* and *M. avium*, the latter being a life-threatening opportunistic infection of immunocompromised patients. Replacing the oxygen atom of the morpholine ring of U-100766 **66** with a sulfur atom gave the potent antimycobacterial oxazolidinone U100480 **67**. It is likely that the *in vivo* activity observed is due, at least in part, to its sulfoxide metabolite U-101603 **68**.

There have been other related but less well documented systems published in the last few years. While Upjohn has recently published *trans*-tricyclic systems such as **75**,[63] other groups have reported oxazolidinone ring-surrogate analogues. In one report, the inactive pyrrolidine **76** and pyrrolidinone **77** were contrasted with the active butenolide **78**.[64] This and related publications have prompted Brickner[62] to define a general structure–activity relationship, summarised in Fig. 3.



**Scheme 7**



**75** **76**

**77** **78**

## The resurgence of tuberculosis

One of the reasons for the interest being shown in the oxazolidinones is their activity against mycobacterial species such as *M. tuberculosis.* Prior to the discovery of the aminoglycoside streptomycin **49** in 1944, there were no effective treatments for tuberculosis (TB). This breakthrough was the start of a new age of chemotherapy for what had been a major killer throughout the world. With the introduction of streptomycin and even more effective therapies, the incidence of tuberculosis, especially in the more developed countries, went into sharp decline, to the point that the disease was no longer perceived to be a serious threat to most people. In recent years, however, this complacent attitude to TB has been seriously challenged. In the majority of the developing countries the number of cases is increasing, and more people died of TB in 1995 than in any other year in history. Even in the industrialised states there is a growing anxiety at the number of new cases being reported. Currently more than one third of the world's population carries *M. tuberculosis*, and in developing countries the disease accounts for over 25% of all preventable deaths.

There are several reasons for this alarming situation. Poverty, resulting in overcrowding and poor hygiene, is undoubtedly a

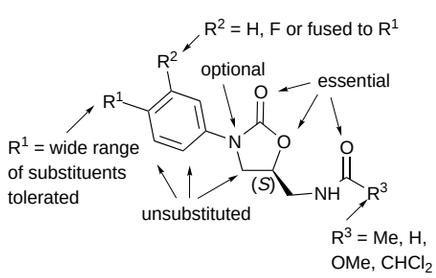
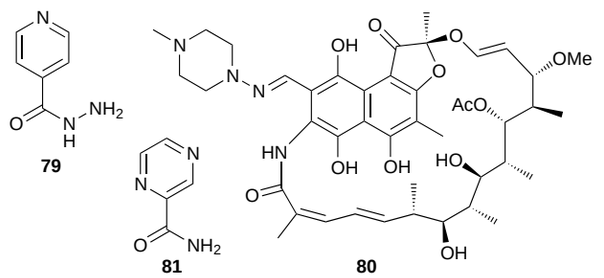


**Fig. 3** General structure–activity relationships

major factor in inner cities. The increase in the number of HIV seropositive people has also created a population less able to combat infection. In Asia, two-thirds of all TB cases are HIV-positive. A third reason is the increase in multidrug-resistant *M. tuberculosis* strains. A typical current therapeutic approach to TB may involve taking isoniazid **79**, rifampin **80** and pyrazinamide **81** for at least six months. As a result, non-



**79** **81** **80**

compliance, *i.e*. patients stopping therapy as soon as an improvement in the symptoms is felt, allows the remaining, more resistant bacteria to survive and spread.

Long-term benefits are unlikely to be gained by modifying existing antimycobacterial agents. The recent increase in research in this field will hopefully lead to the discovery of novel classes of compounds,[65] although the structures of these classes remain, as yet, unclear.

At present, studies are also being carried out to assess the efficacy of existing broad-spectrum antibacterials such as fluoroquinolones.[66] The possibility of using β-lactams in tuberculosis therapy has also been considered.[67] Although *M. tuberculosis* is naturally resistant to this class due to the production of intracellular β-lactamase, the use of elevated doses of newer, β-lactamase-stable agents such as carbapenems has been shown to work *in vitro*.

## Future approaches to antibacterial chemotherapy

The rapid emergence of multidrug resistant bacterial strains and the potential threat they pose to future generations means that the development of novel antibacterials is likely neither to be easy nor to offer a permanent solution to the problem.

Currently, there are two basic strategies for finding novel antibacterials. The first, which has been responsible for the discovery of most novel classes to date, is to screen natural product or corporate compound collections. This strategy provides a compound with demonstrable antibacterial activity, although it may take some time to discover the mode of action of the class, and working with a complex biological system such as a bacterial cell can make the generation of meaningful structure–activity relationships quite problematic, even before taking into account the inter-species diversity encountered.

The second strategy, which has become increasingly popular in recent years, is to identify the essential enzymes of the bacterial cell and to screen compounds as inhibitors of these systems. While this method allows a far greater control over the structure–activity relationship and in many cases facilitates the use of high-throughput screening technology, it involves taking at least one step back from the reality of bacterial infection in that it takes no account of how the compounds are able to permeate the bacterial cell to reach their target, or whether they are rapidly removed from the bacterial cell by efflux or enzymatic inactivation. At present, the number of targets is limited by our knowledge and understanding of gene and protein function. A significant improvement will be brought about by systematic elucidation of complete bacterial genomic sequences.[67] Genes and proteins found to be essential for bacterial cell survival are potential pharmaceutical targets.[68] Thus, using the current state-of-the-art technologies based around the high throughput screening of compound collections, high speed parallel synthesis and natural products will hopefully provide research groups with a number of novel lead classes for further optimisation. In some cases the further optimisation of the classes may be significantly helped by the availability of stuctural information on the target–inhibitor complexes provided by protein crystallography or high field protein NMR and mass spectroscopy.[69]

## Targeting bacterial virulence

An alternative approach currently being examined by several groups is that of modulating the virulence of bacteria.[70,71] For pathogenic bacteria to survive in the hostile environment of another organism they must first be able to attach themselves to host cells and then launch an assault whilst simultaneously debilitating the host immune system. To do this, bacteria produce products called virulence factors, which include attachment factors, toxins and lytic enzymes. Targeting these pathogenesis processes may give protection against a wide range of bacterial species, and result in an infection site-specific as opposed to microorganism specific therapy.

## Conclusions

Owing to the growing threat of infection due to multi-drug resistant bacteria we are already witnessing an increased effort not only aimed at finding more potent examples of existing agents but also, more encouragingly, a serious commitment to discover new classes of antibiotics. These new classes will hopefully evolve through the exploitation of the rapidly expanding number of known targets, the use of the latest techniques for combinatorial chemistry and high throughput screening, and by studying the processes used by the bacteria to establish infection.


## Acknowledgements

The authors thank Dr Daniele Donati, Dr Sergio Lociuro and Dr Tino Rossi for their support and suggestions, Dr Paul Wiedenau for proofreading and Dr Chiara Ghiron, both for discussions and help with the preparation of the manuscript.



**Daniela Niccolai was born in Sambuca Pistoiese in Italy in 1967, and received her Laurea in Industrial Chemistry from the University of Bologna in 1991. She studied for a further 18 months at the CNR institute in Bologna on antisense compounds, as antiviral and antitumour agents before joining GlaxoWellcome, Verona, where she has worked on both CNS and antibacterial projects in the Medicinal Chemistry Department.**

**Luca Tarsi was born in Cattolica in Italy in 1963, and received his Laurea in Chemistry, studying with Professor Diego Savoia in the University of Bologna. He joined Glaxo Wellcome, Verona, in 1993, where he has worked on antibacterial projects in the Medicinal Chemistry Department.**

**Russell J. Thomas was born in Swansea in 1966 and received his BSc from the University of Kent at Canterbury in 1987. Since completing his PhD at the University of Exeter with Professor Stanley M. Roberts he has worked in both the Medicinal Chemistry and Lead Discovery Departments of GlaxoWellcome, Verona. He is the co-author, with Chiara Ghiron, of *Exercises in Synthetic Organic Chemistry*, published in 1997 by Oxford University Press.**


## Footnote and References

† This ChemComm is also available in expanded format *via* the World Wide Web: http://chemistry.rsc.org/rsc/cccenha.htm


1 A. Fleming, *Br. J. Exp. Pathol.*, 1929, **10**, 226.
2 An excellent review of β-lactamases can be found in: D. M. Livermore, *Clin. Microbiol. Rev.*, 1995, **8**, 557.
3 K. Sieradzki and A. Tomasz, *FEMS Microbiol. Lett.*, 1996, **142**, 161.
4 The data used in Fig. 1 were generated using the SCIFINDER® programme, analysing the antibacterial patent publications for each antibiotic class by year. This approach is clearly approximative, but

gives an idea of the changing emphasis of research over the last three decades.
5 For a review on the use of penicillins, see D. Nathwani and M. J. Wood, *Drugs*, 1993, **45**, 866.
6 For a review of the evolution of the cephalosporins, and their classification by generation, see J. A. Garcia-Rodriguez, J. L. M. Bellido and J. E. G. Sanchez, *Int. J. Antimicrob. Agents*, 1995, **5**, 231.
7 M. E. Erwin and R. N. Jones, *36th Interscience Conference on Antimicrobial Agents and Chemotherapy*, 1996, Abstr. No. F145.
8 D. H. Klaubert, J. M. Essery and J. F. Barrett, *Expert Opin. Invest. Drugs*, 1994, **3**, 133.
9 H. Hanaki, H. Agaki, Y. Masaru, T. Otani, A. Hyodo and K. Hiramatsu, *Antimicrob. Agents Chemother*., 1995, **39**, 1120.
10 *36th Interscience Conference on Antimicrobial Agents and Chemotherapy*, 1996, Abstr. No. F138, 139, 140, 141 and 142.
11 For a comprehensive review on the most recent developments in penem research, see A. Bryskier, *Expert Opin. Invest. Drugs*, 1995, **4**, 705.
12 J. Birnbaum, F. M. Kahan, H. Kropp and J. S. MacDonald, *Am. J. Med.* 1985, **78**, 3.
13 J. L. Blumer, *Int. J. Antimicrob. Agents*, 1997, **8**, 73.
14 For an excellent review of approaches to the synthesis of key intermediates for 1β-methyl carbapenems, see A. H. Berks, *Tetrahedron*, 1996, **52**, 331.
15 W.-B. Choi, H. R. O. Churchill, J. E. Lynch, A. S. Thompson, G. R. Humphrey, R. P. Volante, P. J. Reider and I. Shinkai, *Tetrahedron Lett.*, 1994, **35**, 2275.
16 D. H. Shih, F. Baker, L. Cama and B. G. Christensen, *Heterocycles*, 1984, **21**, 29.
17 M. L. Greenlee, F. L. DiNinno and M. L. Hammond, WO 95-US1669
18 For a review on carbapenem-hydrolysing β-lactamases, see B. A. Rasmussen and K. Bush, *Antimicrob. Agents Chemother*., 1997, **41**, 223.
19 Y. Sumita, and M. Fikasawa, *Chemotherapy*, 1996, **42,** 47.
20 See, for example; B. Alcaide, C. Polanco and M. A. Sierra, *Tetrahedron Lett*., 1996, **37**, 6901; B. Alcaide, C. Polanco, E. Saez and M. A. Sierra, *J. Org. Chem*., 1996, **61**, 7125; B. Banik, G. V. Subbaraju, V. Gottumukkala, M. S. Manhas and A. K. Bose, *Tetrahedron Lett*., 1996, **37**, 1363; C. Niu, T. Pettersson and M. J. Miller, *J. Org. Chem*., 1996, **61**, 1014; S. Hanessian and G. B. Bhaskar, *Bioorg. Med. Chem. Lett*., 1994, **4**, 2285.
21 For an overview of research into trinems (formerly known as tribactams), see, S. Biondi, in *Recent Advances in the Chemistry of Anti-Infective Agents*, ed. P. H. Bentley and P. J. O'Hanlon, Royal Society of Chemistry, Cambridge, 1996, p. 86.
22 For recent reviews on the biological activity of sanfetrinem, see: J. Ngo and J. Castaner, *Drugs of the Future*, 1996, **21**, 1238; K. Singh, T. M. Coque and B. E. Murray, *Antimicrob. Agents Chemother*., 1996, **40**, 2142; R. Wise, J. M. Andrews and N. Brenwald, *ibid*, 1996, **40**, 1248; E. Di Modugno, I. Erbetti, L. Ferrari, G. L. Galassi, S. M. Hammond and L. Xerri, *ibid*, 1994, **38**, 2362.
23 C. Bismara, R. Di Fabio, D. Donati, T. Rossi and R. J. Thomas, *Tetrahedron Lett.*, 1995, **36**, 4283.
24 T. Rossi, S. Biondi, S. Contini, R. J. Thomas and C. Marchioro, *J. Am. Chem. Soc*., 1995, **117**, 9604.
25 C. Ghiron, E. Piga, T. Rossi, B. Tamburini and R. J. Thomas, *Tetrahedron Lett.*, 1996, **37**, 3891. For an analogous approach to various isomers of sanfetrinem using 3-unsubstituted 4-acetoxyazetidinone, see P. M. Jackson, S. M. Roberts, S. Davalli, D. Donati, C. Marchioro, A. Perboni, S. Provera and T. Rossi, *J. Chem. Soc., Perkin Trans. 1*, 1996, 2029.
26 G. Kennedy, T. Rossi and B. Tamburini, *Tetrahedron Lett.*, 1996, **37**, 7441.
27 S. Giacobbe and T. Rossi, *Tetrahedron: Asymmetry*, 1996, **7**, 3079.
28 S. Hanessian and M. J. Rozema, *J. Am. Chem. Soc*., 1996, **118**, 9884.
29 T. Rossi, C. Marchioro, A. Paio, R. J. Thomas and P. Zarantonello, *J. Org. Chem.*, 1997 **62**, 1653.
30 D. Andreotti, S. Biondi, R. Di Fabio, D. Donati, E. Piga and T. Rossi, *Bioorg. Med. Chem. Lett*., 1996, **6**, 2019; R. Di Fabio, D. Andreotti, S. Biondi, G. Gaviraghi and T. Rossi, *ibid*, 1996, **6**, 2025; R. Di Fabio, T. Rossi and R. J. Thomas, *Tetrahedron Lett.*, 1997, **38**, 3587.
31 M. E. Tranquillini, G. Araldi, D. Donati, G. Pentassuglia, A. Pezzoli and A. Ursini, *Bioorg. Med. Chem. Lett*., 1996, **6**, 1683.
32 S. Gehanne, E. Piga, D. Andreotti, S. Biondi and D. Pizzi, *Bioorg. Med. Chem. Lett.*, 1996, **6**, 2791.
33 S. Biondi, G. Gaviraghi and T. Rossi, *Bioorg. Med. Chem. Lett*., 1996, **6**, 525; R. Di Fabio, A. Feriani, G. Gaviraghi and T. Rossi, *ibid*, 1995, **5**, 1235.
34 D. Andreotti, T. Rossi, G. Gaviraghi, D. Donati, C. Marchioro, E. Di Modugno and A. Perboni, *Bioorg. Med. Chem. Lett*., 1996, **6**, 491; S. Hanessian, M. J. Rozema, G. B. Reddy and J. F. Braganza, *Bioorg. Med. Chem. Lett*., 1995, **6**, 2535.
35 A. Padova, S. M. Roberts, D. Donati, C. Marchioro and A. Perboni, *Tetrahedron*, 1996, **52**, 263; A. Padova, S. M. Roberts, D. Donati, C. Marchioro and A. Perboni, *J. Chem. Soc., Chem. Commun*., 1995, 661.
36 C. Ghiron, T. Rossi and R. J. Thomas, *Tetrahedron Lett.*, 1997, **38**, 3569.
37 For an excellent recent review on the structural modifications of glycopeptide antibiotics, see A. Malabarba, T. I. Nicas and R. C. Thompson, *Med. Res. Rev*., 1997, **17**, 69.
38 For an excellent review of the mechanism of glycopeptide binding to its target, see D. H. Williams, *Nat. Prod. Rep*., 1996, **13**, 469.
39 R. D. G. Cooper, N. J. Snyder, M. J. Zweifel, M. A. Staszak, S. C. Wilkie, T. I. Nicas, D. H. Mullen, T. F. Butler, M. J. Rodriguez, B. E. Huff and R. C. Thompson, *J. Antibiot*., 1996, **49**, 575.
40 T. I. Nicas, D. H. Mullen, J. E. Flokowitsch, D. A. Preston, N. J. Snyder, M. J. Zweifel, S. C. Wilkie, M. J. Rodriguez, R. C. Thompson and R. D. G. Cooper, *Antimicrob. Agents Chemother*., 1996, **40**, 2194.
41 N. E. Allen, D. L. LeTourneau and J. N. Hobbs, Jr., *Antimicrob. Agents Chemother*., 1997, **41**, 66.
42 T. D. Gootz and K. E. Brightly, *Med. Res. Rev*., 1996, **16**, 433.
43 For a review of gyrase as a drug target, see A. Maxwell, *Trends Microbiol*., 1997, **5**, 102.
44 X.-S. Pan and M. L. Fisher, *Antimicrob. Agents Chemother*., 1997, **41**, 471 and references cited therein.
45 E. J. C. Goldstein, *Clin. Infect. Dis*., 1996, **23**, S25.
46 L. S. Shen, S. K. Tanaka and D. T. W. Chu, *Curr. Pharm. Design*, 1997, **3**, 169.
47 E. Goetschi, C. J. Jenny, P. Reindl and F. Ricklin, *Helv. Chim. Acta*, 1996, **79**, 2219; J. Gewiz, E. Goetschi, P. Hebeisen, H. Link and T. Luebbers, EP675122, 1995.
48 F. T. F. Tsai, O. M. P. Singh, T. Skarzynski, A. J. Wonacott, S. Weston, A. Tucker, R. A. Pauptit, A. L. Breeze, J. P. Poyser, R. O'Brien, J. E. Ladbury and D. Wigley, *Proteins: Struct. Funct. Genet*., 1997, **28**, 41 and references cited therein.
49 G. Beaucaire, *J. Chemother*., 1995, **7** (suppl. 2), 111.
50 R. N. Jones, *J. Chemother*., 1995, **7**, (suppl. 2), 7.
51 For a review on macrolides, see A. Bryskier and C. Agouridas, *Antiinfect. Drugs Chemother*., 1996, **14**, 147.
52 G. Bright, *J. Antibiot.*, 1988, **41**, 1029; S. Dokic, G. Kobrehel, N. Lopotar, B. Kamenar, A. Nagl and D. Mrvos, *J. Chem. Res. (S)*, 1988, 152.
53 R. N. Jones and D. J. Biedenbach, *Diagn. Microbiol. Infect. Dis.*, 1997, **27**, 8.
54 T. Schulin, C. B. Wennerstein, R. C. Mollering, Jr. and G. M. Eliopoulos, *Antimicrob. Agents Chemother*., 1997, **41**, 1196.
55 Y. S. Or, K. Spina, M. Tufano, J. Plattner and D. Chu, Book of Abstracts, 212th ACS National Meeting, Orlando, 1996.
56 J.-C. Pechère, *Drugs*, 1996, **51** (suppl. 1), 13.
57 G. A. Pankuch, M. R. Jacobs and P. C. Applebaum, *Antimicrob. Agents Chemother.*, 1996, **40**, 2071.
58 C. A. Wood, H. D. Mandler, B. E. Fry-Arrighy, J. Smith-Davis, A. I. Hartstein and E. A. Blumberg, Poster LB13 presented at the *36th Interscience Conference on Antimicrobial Agents and Chemotherapy*, New Orleans, September, 1996.
59 D. Schnappinger and W. Hillen, *Arch. Microbiol*., 1996, **165**, 359.
60 F. T. Tally, G. A. Ellestad and R. T. Testa, *J. Antimicrob. Chemother*., 1995, **35**, 449.
61 For an excellent review on the oxazolidinones, see S. J. Brickner, *Curr. Pharm. Des*., 1996, **2**, 175.
62 S. J. Brickner, D. K. Hutchinson. M. R. Barbachyn, P. R. Manninen, D. A. Ulanowicz, S. A. Garmon, K. C. Grega, S. K. Hendges, D. S. Toops, C. W. Ford and G. E. Zurenko, *J. Med. Chem*., 1996, **39**, 673.
63 D. M. Gleave and S. J. Brickner, *J. Org. Chem*., 1996, **61**, 6470.
64 A. Denis and T. Villette, *Bioorg. Med. Chem. Lett*., 1994, **16**, 1925.
65 For a recent overview of the current status of tuberculosis research, see K. Duncan, *Expert Opin. Ther. Pat.*, 1997, **7**, 129.
66 C. Grassi and V. Peona, *Eur. Respir. J*., 1995, **8** (suppl. 20), 714s.
67 see I. Chopra, *Expert Opin. Invest. Drugs*, 1996, **5**, 241; E. J. Straus and S. Falkow, *Science*, 1997, **276**, 707.
68 I. Chopra, J. Hodgson, B. Metcalf and G. Poste, *J. Am. Med. Assoc*., 1996, **5**, 401.
69 For a review on the application of protein crystallography to drug design, see J. L. Martin, *Curr. Med. Chem*., 1996, **3**, 419.
70 For an excellent review on bacterial virulence as a therapeutic target, see R. M. Goldschmidt, M. J. Macielag, D. J. Hlasta and J. F. Barrett, *Curr. Pharm. Des.*, 1997, **3**, 125.
71 B. B. Finlay and P. Cossart, *Science*, 1997, **276**, 718.

*7/04497F*

# Total synthesis of 26-hydroxyepothilone B and related analogues

**K. C. Nicolaou,* Sacha Ninkovic, M. Ray V. Finlay, Francisco Sarabia and Tianhu Li**

*Department of Chemistry and The Skaggs Institute for Chemical Biology, The Scripps Research Institute, 10550 North Torrey Pines Road,, La Jolla, California 92037, USA and Department of Chemistry and Biochemistry, University of California, San Diego, 9500 Gilman Drive, La Jolla, California 92093, USA*

**A series of 26-substituted epothilones B (3, 22, 23a–n and 24a–h,j–l,o) have been constructed by total synthesis involving a selective Wittig olefination, an aldol reaction and a macrolactonization as key steps.**

The novel molecular structures and impressive antitumour properties of the epothilones[1] have captured the imagination of synthetic chemists, biologists[2,3] and clinicians. Isolated[1] from myxobacterium *Sorangium cellulosum*, these substances exhibit tubulin polymerization properties[2] similar to Taxol[4] and show potent cytotoxicity against Taxol-resistant tumour cells.[3] Research in this field has resulted in the total synthesis of the naturally occurring epothilones B **1**[5–7] and A **2**,[5,7–11] and a plethora of analogues.[5–17] Owing to the higher antitumour potency of the 12-methyl bearing epothilone B **2** as compared to epothilone A **1**, this substituent (the C26 methyl group) was considered a prime candidate for modification. An expedient entry into this series of compounds was sought. Here we report such a strategy which culminated in the total synthesis of 26-hydroxydesoxyepothilone B **3**, 26-hydroxyepothilone B **22** and a series of related analogues **23a**–**n** and **24a**–**h**,**j**–**l**,**o**.

The approach to the C26-modified epothilones B followed a similar path to that developed in these laboratories[5,7] for epothilone B **1**, and involved (i) stereoselective Wittig olefination, (ii) aldol condensation and (iii) macrolactonization (Fig. 1).

Protection of **4** (Scheme 1) as a trityl ($CPh_3$) ether furnished **5**† in 99%. Hydroboration of **5** led to **6** (94%), which was converted to **7** by the action of $PPh_3$, $I_2$ and imidazole (90%). Stereoselective alkylation of SAMP hydrazone **8**,[18] *via* its lithio derivative, with **7** led to **9**. The transformation of **9** to **10** proceeded under the influence of MMPP[7] (91%), and reduction of the latter with DIBAL-H provided aldehyde **11** (97%).

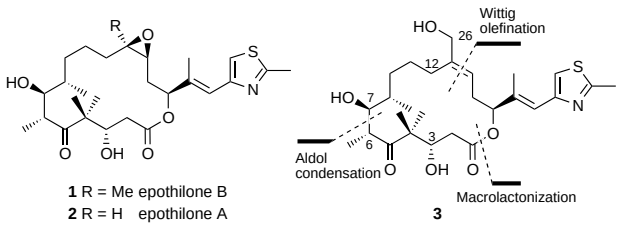
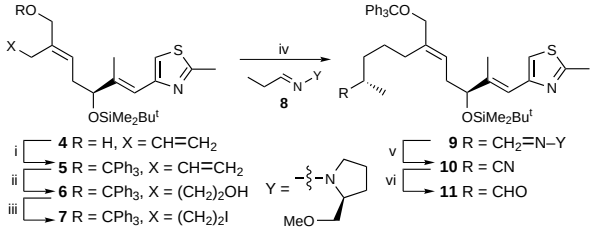



**Fig. 1** Structures of **1** and **2** and retrosynthetic analysis of **3**




**Scheme 1** *Reagents and conditions*: i, $Ph_3CCl$, DMAP, DMF, 70 °C, 1 h; ii, 9-borabicyclo[3.3.1]nonane, THF, 0 °C, 2 h, then aq. NaOH (3 M), then 30% $H_2O_2$; iii, $I_2$, imidazole, $PPh_3$, $Et_2O$–MeCN (3 : 1), 0 °C, 0.5 h; iv, **8**, LDA, THF, 0 °C, 14 h, then **7**, THF, −100 → −20 °C, 10 h; v, monoperoxyphthalic acid (Mg salt) (MMPP), MeOH–phosphate buffer (pH 7) (1 : 1), 0 °C, 1 h; vi, DIBAL-H, toluene, −78 °C, 1 h

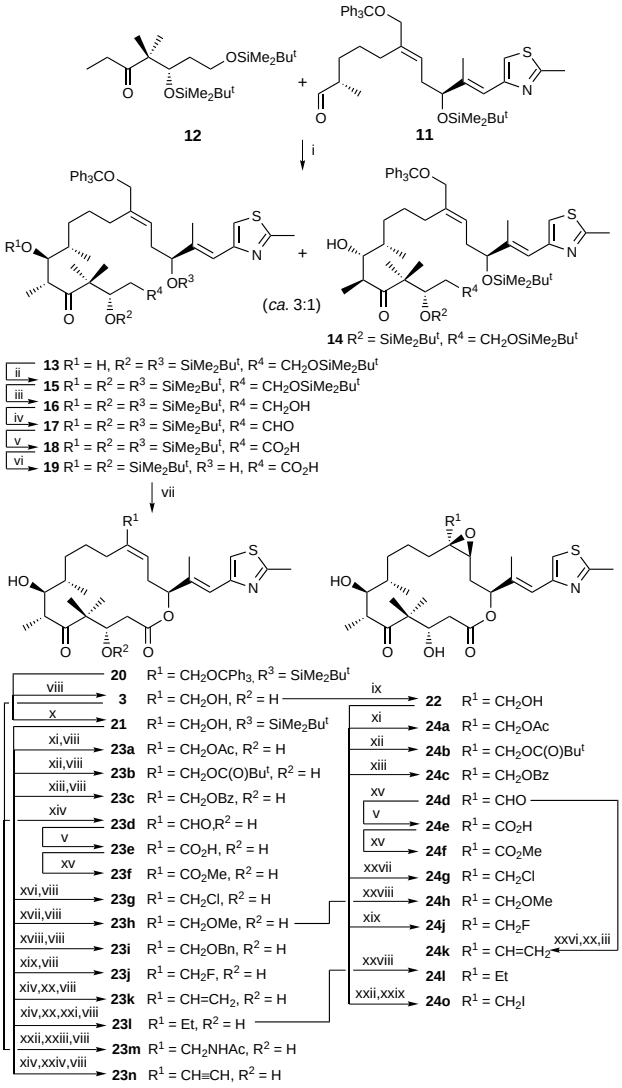
The coupling of the C1–C6 ketone fragment **12**[7,15] with **11** *via* a *syn*-selective aldol reaction (Scheme 2) furnished **13** along with its (6*S*,7*R*) diastereoisomer **14** (85% total yield, *ca.* 3 : 1). Chromatographic purification followed by silylation gave **15**. The use of buffered HF·pyridine in THF permitted selective desilylation of **15** giving **16** (74%), which was sequentially oxidized to **17**, and thence to carboxylic acid **18**. Selective desilylation at C15 was achieved by the use of $Bu_4NF$ in THF, providing **19** (89%). The latter compound was in turn subjected to the Yamaguchi macrolactonization forming **20** (75%). Exposure of **20** to HF·pyridine in THF promoted concomitant removal of both the silyl groups and the trityl moiety, leading to **3** (78%). Alternatively, treatment of **20** with camphorsulfonic acid in MeOH–$CH_2Cl_2$ resulted in the selective removal of the trityl group, giving **21** (70%). Sharpless asymmetric epoxidation of **3** then gave 26-hydroxyepothilone B **22** (76%).

The availability of **3**, **21** and **22** facilitated access to a number of 26-substituted epothilones. As indicated in Scheme 3, **21** was converted to **23a**–**c** by reaction with the corresponding acid anhydride or chloride under basic conditions followed by desilylation. $MnO_2$ oxidation of **3** proved highly efficient, providing α,β-unsaturated aldehyde **23d** (85%). Further oxidation of **23d** with $NaClO_2$ led to carboxylic acid **23e** (98%), which was converted to **23f** by treatment with $CH_2N_2$ (80%). Methylation and benzylation of **21** followed by desilylation afforded **23h** (58% overall) and **23i** (35% overall), respectively. Halogenation of **21** followed by desilylation led to chloride **23g** (73% overall) or fluoride **23j** (51% overall). Alternatively, treatment of **21** with $MnO_2$ and reaction of the resulting aldehyde with the anion derived from $Me_3SiCHN_2$ followed by

**Table 1** Biological activities of epothilone analogues

| Compound | Induction of tubulin assembly[a] (%) | $IC_{50}$/nM (relative resistance)[b] Parental 1A9 | Taxol-resistant PTX10 | Taxol-resistant PTX22 |
|---|---|---|---|---|
| **23g** | 88 | 90 | > 100 | > 100 |
| **23j** | 83 | 0.65 | 6 | 4 |
| **23k** | 95 | 8.7 | 30 | 14 |
| **23l** | 66 | 60 | > 100 | 93 |
| **24d** | 87 | 5 | 24 | 3.1 |
| **24g** | 69 | 0.25 | 0.50 | 0.55 |
| **24j** | 93 | 0.15 | 0.55 | 0.15 |
| **24k** | 94 | 0.63 | 4.7 | 0.95 |
| **24l** | 79 | 0.27 | 8.5 | 0.45 |
| **24o** | 41 | 25 | 55 | 20 |
| **Taxol** | 50 | 2 | 50 | 43 |
| Epothilone A | 72 | 2 | 19 | 4.2 |
| Epothilone B | 100 | 0.040 | 0.035 | 0.045 |

[a] Assays performed as in ref. 4. [b] Inhibition of human ovarian carcinoma cell growth. Assays performed as in ref. 7. Each $IC_{50}$ value shown is an average value obtained from three independent assays.



**Scheme 2** *Reagents and conditions*: i, LDA, THF, 0 °C, 15 min, then **12**, THF, −78 → −60 °C, 1 h, then **11**, THF, −78 °C; ii, $Bu^tMe_2SiOSO_2CF_3$, 2,6-lutidine, $CH_2Cl_2$, 0 °C, 2 h; iii, HF·pyridine, pyridine, THF, 0 → 25 °C, 4 h; iv, $(COCl)_2$, DMSO, $Et_3N$, $CH_2Cl_2$, −78 → 0 °C, 1.5 h; v, $NaClO_2$, $Me_2C$=CHMe, $NaH_2PO_4$, $Bu^tOH$–$H_2O$ (5 : 1), 25 °C, 2 h; vi, $Bu_4NF$, THF, 25 °C, 8 h; vii, 2,4,6-$Cl_3C_6H_2COCl$, $Et_3N$, THF, 0 °C, 1 h, then add to DMAP in toluene, 75 °C, 1 h; viii, 30% HF·pyridine (v/v), THF, 0 → 25 °C, 24 h; ix, (+)-diethyl L-tartrate, $Ti(OPr^i)_4$, $Bu^tOOH$, −30 °C, 2 h; x, camphorosulfonic acid, MeOH–$CH_2Cl_2$ (1 : 1), 0 → 25 °C, 3 h; xi, $Ac_2O$, DMAP, EtOAc, 0 °C, 0.5 h; xii, $Bu^tCOCl$, $Et_3N$, DMAP, $CH_2Cl_2$, 0 °C, 0.5 h; xiii, BzCl, $Et_3N$, DMAP, $CH_2Cl_2$, 0 °C, 0.5 h; xiv, $MnO_2$, $Et_2O$, 25 °C, 3 h; xv, $CH_2N_2$, $Et_2O$, 0 °C; xvi, $PPh_3$, $CCl_4$, 75 °C, 24 h; xvii, NaH, MeI, DMF, 0 °C, 1 h; xviii, NaH, BnBr, DMF, 0 → 25 °C, 1 h; xix, DAST, $CH_2Cl_2$, −78 → 25 °C, 1 h; xx, $Ph_3P^+CH_3Br^-$, $(Me_3Si)_2NLi$, THF, 0 °C; xxi, $H_2$, Lindlar catalyst, EtOAc, room temp., 15 min.; xxii, TsCl, $Et_3N$, DMAP, $CH_2Cl_2$, 0 °C, 1 h; xxiii, $NaN_3$, DMF, 25 °C, 10 h, then $PPh_3$, THF, 60 °C, 8 h, then $Ac_2O$, $CH_2Cl_2$, 10 min; xxiv, $Me_3SiCHN_2$, then $Bu^nLi$, THF, −78 → 0 °C, 1 h; xxv, TEMPO (0.008 M, $CH_2Cl_2$), NaOCl (0.035 M, 5% aq. $NaHCO_3$), aq. KBr (0.2 M), $CH_2Cl_2$, 0 °C, 0.5 h; xxvi, $Me_3SiCl$, $Et_3N$, $CH_2Cl_2$, 0 → 25 °C, 10 h; xxvii, $PPh_3$, MeCN–$CCl_4$ (1 : 3), 25 °C, 1 h; xxviii, methyl(trifluoromethyl)dioxirane, MeCN, 0 °C; xxix, NaI, acetone, 25 °C, 10 h

the usual desilylation conditions gave **23n** (68%). The aldehyde obtained from $MnO_2$ oxidation of **21** (90%) was also subjected to Wittig methylenation (85%) furnishing, after desilylation, alkene **23k** (85%). A similar sequence of reactions with this aldehyde (Wittig methylation and hydrogenation followed by desilylation) provided **23l**. Conversion of **3** to the corresponding tosylate, followed by displacement with $NaN_3$ in DMF and reduction with $PPh_3$, furnished the required primary amine. The latter was then exposed to $Ac_2O$ in $CH_2Cl_2$ providing the corresponding acetamide **23m** (39%, 4 steps). Similar chemistry was employed for the preparation of epothilones **24a–c, e–h** (Scheme 2). Compound **24d** was synthesized by selective oxidation of **22** with TEMPO–bleach (90%), and subsequent hydroxy protection, Wittig methylenation and deprotection allowed access to **24k** (49%, 3 steps). Iodide **24o** was prepared by selective tosylation of the primary hydroxy moiety of **22** and subsequent displacement with NaI (72%). Alternatively, treatment of **22** with DAST furnished fluoride **24j**. Reaction of **23h** and **23l** with methyl(trifluoromethyl)dioxirane provided, respectively, the epoxy methyl ether **24h** (20%) and the ethyl analogue **24l** (55%).

Table 1 shows the tubulin binding[5] and cytotoxicity properties of a selected number of the synthesized epothilones.

We thank Dr E. Hamel for a gift of purified tubulin and Dr P. Giannakakou for the cell lines. This work was supported by Novartis, the NIH, The Skaggs Institute for Chemical Biology, the CaP CURE Foundation, and the Fulbright Commission (M. R. V. F.).

## Footnotes and References

* E-mail: kcn@scripps.edu

† All new compounds exhibited satisfactory spectral and exact mass data.

1 G. Höfle, N. Bedorf, H. Steinmetz, D. Schomburg, K. Gerth and H. Reichenbach, *Angew. Chem., Int. Ed. Engl*., 1996, **35**, 1567.
2 D. M. Bollag, P. A. McQueney, J. Zhu, O. Hensens, L. Koupal, J. Liesch, M. Goetz, E. Lazarides and C. M. Woods, *Cancer Res.*, 1995, **55**, 2325.
3 R. J. Kowalski, P. Giannakakou and E. Hamel, *J. Biol. Chem.*, 1997, **272**, 2534.
4 S. B. Horwitz, J. Fant and P. B. Schiff, *Nature*, 1979, **277**, 665.
5 K. C. Nicolaou, N. Winssinger, J. A. Pastor, S. Ninkovic, F. Sarabia, Y. He, D. Vourloumis, Z. Yang, T. Li, P. Giannakakou and E. Hamel, *Nature*, 1997, **387**, 268.
6 D.-S. Su, D. Meng, P. Bertinato, A. Balog, E. J. Sorensen, S. J. Danishefsky, Y.-H. Zheng, T.-C. Chou, L. He and S. B. Horwitz, *Angew. Chem., Int. Ed. Engl*., **1997**, *36*, 757.
7 K. C. Nicolaou, S. Ninkovic, F. Sarabia, D. Vourloumis, Y. He, H. Vallberg, M. R. V. Finlay and Z. Yang, *J. Am. Chem. Soc*., 1997, **119**, 7974.
8 A. Balog, D. Meng, T. Kamenecka, P. Bertinato, D.-S. Su, E. J. Sorensen and S. J. Danishefsky, *Angew. Chem., Int. Ed. Engl.*, 1996, **35**, 2801; D. Meng, D.-S. Su, A. Balog, P. Bertinato, E. J. Sorensen, S. J. Danishefsky, Y.-H. Zheng, T.-C. Chou, L. He and S. B. Horwitz, *J. Am. Chem. Soc.*, 1997, **119**, 2733.
9 Z. Yang, Y. He, D. Vourloumis, H. Vallberg and K. C. Nicolaou, *Angew. Chem., Int. Ed. Engl*., 1997, **36**, 166; K. C. Nicolaou, F. Sarabia, S. Ninkovic and Z. Yang, *Angew. Chem., Int. Ed. Engl.*, 1997, **36**, 525.
10 D. Schinzer, A. Limberg, A. Bauer, O. M. Böhm, M. Cordes, *Angew. Chem., Int. Ed. Engl*., 1997, **36**, 523.
11 K. C. Nicolaou, Y. He, D. Vourloumis, H. Vallberg, F. Roschangar, F. Sarabia, S. Ninkovic, Z. Yang and J. I. Trujillo, *J. Am. Chem. Soc.*, 1997, **119**, 7960.
12 Isolation and structure elucidation: G. Höfle, personal communication.
13 K. C. Nicolaou, Y. He, F. Roschangar, N. P. King and D. Vourloumis, *Angew. Chem*., in the press.
14 K. C. Nicolaou, H. Vallberg, N. P. King, F. Roschangar, Y. He, D. Vourloumis and C. G. Nicolaou, *Chem. Eur. J*., in the press.
15 K. C. Nicolaou, F. Sarabia, M. R. V. Finlay, S. Ninkovic, N. P. King, D. Vourloumis and Y. He, *Chem. Eur. J*., in the press.
16 A. Balog, P. Bertinato, D.-S. Su, D. Meng, E. J. Sorensen, S. J. Danishefsky, Y-H. Zheng, T-C. Chou, L. He and S. B. Horwitz, *Tetrahedron Lett*., 1997, **38**, 4529.
17 K. C. Nicolaou, D. Vourloumis, T. Li, J. Pastor, N. Winssinger, Y. He, S. Ninkovic, F. Sarabia, H. Vallberg, F. Roschangar, N. P. King, M. R. V. Finlay, P. Giannakakou, P. Verdier-Pinard and E. Hamel, *Angew. Chem., Int. Ed. Engl*., 1997, **36**, 2097.
18 D. Enders, A. Plant, D. Backhaus and U. Reinhold, *Tetrahedron*, 1995, **51**, 10 699.

*Received in Corvallis, OR, USA, 11th August 1997; 7/05845D*

# Novel μ-methyl complexes of vanadium and their relevance to bimolecular deactivation of homogeneous imidovanadium polymerisation catalysts

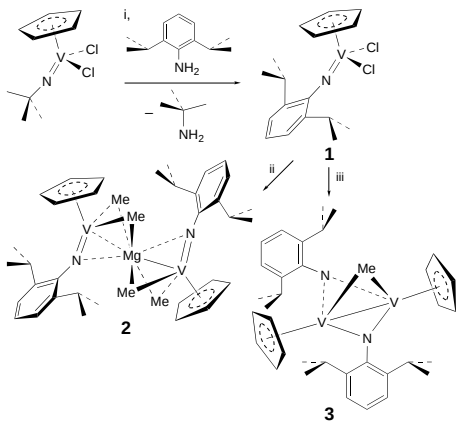
**Michael C. W. Chan,[a] Jacqueline M. Cole,[b] Vernon C. Gibson*[a] and Judith A. K. Howard[b]**

[a] *Department of Chemistry, Imperial College, South Kensington, London, UK SW7 2AY*
[b] *Department of Chemistry, University of Durham, South Road, Durham, UK DH1 3LE*

**Attempted dimethylation of [CpV(NC$_6$H$_3$Pr$^i_2$-2,6)]Cl$_2$ using Grignard reagents affords novel μ-methyl complexes arising by reductive dimerisation; the structure of one of these products, [CpV(NC$_6$H$_3$Pr$^i_2$-2,6)(μ-Me)$_2$]$_2$(μ-Mg) 2, reveals V–(μ-Me)–Mg, V–Mg, N–Mg and C–H···Mg interactions.**

There is presently much interest in the development of new-generation 'non-metallocene' catalysts for the polymerisation of α-alkenes. These include, for example, alkoxide,[1] thiolate,[2] amide,[3] imide,[4] tetradentate Schiff-base[5] and macrocyclic procatalysts.[6] In recent work we have been investigating the isolobal relationship between group 4 metallocenes and group 5 half-sandwich imido species[7] and have found that vanadium complexes of the type [CpV(NR)Cl$_2$] are particularly active amongst these group 5 metal pro-catalysts.[4a] Typically, they give high initial polymerisation activities but die over the course of a few minutes, a kinetic profile that is not uncommon in many homogeneous Ziegler-type polymerisation systems. In order to gain more insight into the deactivation process and to be able to control this behaviour, we set out to synthesise well defined cationic alkyl versions of these catalysts. Methyl derivatives were targeted since such species have proved to be suitable precursors in metallocene systems.[8] Here, we describe two highly unusual products arising from reactions of [CpV(NAr)Cl$_2$] (Ar = C$_6$H$_3$Me$_2$-2,6) **1** with methylmagnesium halides under differing conditions of solvent and Grignard reagent. The products are structurally exceptional and provide insight into the bimolecular deactivation process occurring in [CpV(NR)] polymerisation systems.†

The synthesis of the starting complex **1** has been described previously by Teuben and coworkers.[9] During the course of our studies, we have found that **1** and related imido complexes can also be prepared by an imido exchange route according to Scheme 1, a methodology that appears to be quite general.[10] Thus treatment of [CpV(NBu$^t$)Cl$_2$] with 2,6-diisopropylaniline in hot 1,2-dichloroethane affords [CpV(NAr)Cl$_2$] **1** in high yield.




**Scheme 1** *Reagents and conditions*: i, (CH$_2$Cl)$_2$, 75 °C, 10 d; ii, 2.5 MeMgBr, Et$_2$O, 12 h; iii, 3 MeMgCl in thf–Et$_2$O, 12 h

The paramagnetic magnesium-containing divanadium complex **2** was isolated from the reaction of **1** with excess MeMgBr in diethyl ether (Scheme 1). The molecular structure is shown in Fig. 1.‡ Complex **2** crystallises as a trimetallic V$_2$Mg cluster in the centrosymmetric space group $P2_1/c$, with the magnesium atom located at the centre of inversion. The structure consists of two methyl groups bridging between the vanadium atom of the [CpV(NAr)] fragment and the magnesium core. The V–Mg distance of 2.594(1) Å is similar to other proposed metal–Mg bonds[11,12] and therefore may be viewed as a direct V–Mg interaction. The N–Mg distance of 2.366(6) Å is within the range for a genuine bonding interaction,[13] although the V–N distance of 1.724(6) Å (1.60–1.68 Å in terminal imides,[14] 1.84–1.85 Å in bridging imides[3a,8,15]) and the V–N–C$_{ipso}$ angle of 160.6(5)° suggest that this interaction is weak and that the imido unit behaves more as a terminal ligand to the vanadium centre than a bridging group between V and Mg. The carbon atoms of the bridging methyl groups are located slightly closer to the vanadium [V–C$_{methyl}$ 2.200(7), 2.227(7) Å; Mg–C$_{methyl}$ 2.382(7), 2.408(7) Å] and the V–C$_{methyl}$ distances are longer than those reported for vanadium complexes with terminal alkyl groups (2.04–2.08 Å).[3,4,8,16] The two V–C$_{methyl}$–Mg angles are identical [68.4(2)°] and are typical for methyl groups bridging two metals.[11,16] The two highly distorted V–C–H angles (55, 77°) and the particularly short Mg–H separations (2.04, 2.35 Å) for H(18c) and H(19b) respectively,‡ indicate the presence of C–H···Mg agostic interactions [Fig. 1(*b*)]. The presence of the

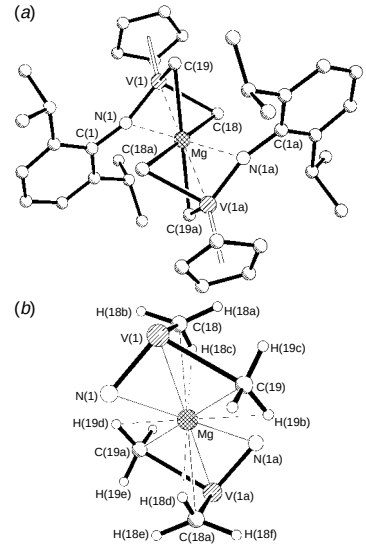



**Fig. 1** (*a*) The molecular structure of **2** with key atoms labelled. H atoms are omitted for clarity. Selected dimensions (Å and °): V(1)–N(1) 1.724(6), V(1)–C(18) 2.200(7), V(1)–C(19) 2.227(7), V(1)–Mg 2.594(1), Mg–N(1) 2.366(6), Mg–C(18) 2.408(7), Mg–C(19) 2.382(7); N(1)–V–C(18) 100.5, N(1)–V–C(19) 101.3(3), C(18)–V–V(19) 91.0(3), N(1)–V–Mg 62.7(2), C(18)–V–Mg 59.6(2), C(19)–V–Mg 58.6(2), V(1)–N(1)–C(1) 160.6(5), V(1)–C(18)–Mg 68.4(2), V(1)–C(19)–Mg 68.4(2); (*b*) view of the magnesium core showing the agostic C–H···Mg interactions.

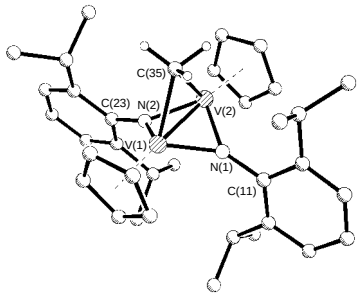



**Fig. 2** The molecular structure of **3** with key atoms labelled. H atoms are omitted for clarity. Selected dimensions (Å and °): V(1)–N(1) 1.867(3), V(1)–N(2) 1.882(3), V(2)–N(1) 1.896(3), V(2)–N(2) 1.894(3), V(1)–C(35) 2.215(4), V(2)–C(35) 2.310(4), V(1)–V(2) 2.324(1); V(1)–C(35)–V(2) 61.8(1), V(1)–N(1)–V(2) 76.3(1), V(1)–N(2)–V(2) 76.9(1), V(1)–N(1)–C(11) 143.8(2), V(2)–N(1)–C(11) 139.9(2), V(1)–N(2)–C(23) 142.4(2), V(2)–N(2)–C(23) 141.6(2).

magnesium core with its attendant weak ligand interactions (bonding distances 2.366–2.594 Å) appears to lend significant stability to this unusual product.

By contrast, in the presence of diethyl ether and tetrahydrofuran, **1** reacts with an excess of MeMgCl to afford the paramagnetic mono μ-methyl complex **3** (Scheme 1, Fig. 2). The crystal structure of **3**‡ consists of a single methyl and two arylimido groups bridging between two [CpV] units. The distances V(1)–C(35) [2.310(4) Å], V(2)–C(35) [2.215(4) Å] and the V(1)–C(35)–V(2) angle [61.8(1)°] are comparable with **2**. In this case, however, there are no close interactions of the bridging methyl C–H bonds with the adjacent metal centres. The V–N distances [av. 1.885(4) Å] are longer than for **2** owing to the decreased bond order resulting from the fact that the imido substituents are bridging. The V(1)–V(2) distance of 2.324(1) Å is within the range for a bonding interaction,[17] and the V–Cp(centroid) vectors are almost coaxial with the V–V bond. Finally, the bridging methyl and imides are arranged around the V–V axis such that C(35), N(1) and N(2) are approximately 120° to each other. We note that Teuben and coworkers have reported a related tolylimido complex, [CpV(μ-$NC_6H_4Me$-*p*)Me]$_2$, which contains bridging imido ligands and terminal methyl groups.[18]

Since dialkylation of a dihalide precursor is the prevalent route to a well defined cationic alkyl catalyst species, these observations provide an explanation for the rapid deactivation of [CpV(NR)] procatalysts and are likely to be of general relevance to other rapidly deactivating catalyst systems.

The EPSRC and the ILL are thanked for studentships to M. C. W. C. and J. M. C. respectively and BP Chemicals Ltd. is thanked for a CASE studnetship (to M. C. W. C.).

## Footnotes and References

* E-mail: v.gibson@ic.ac.uk

† Satisfactory elemental analyses have been obtained.

‡ *Crystal data*: **2**: $C_{19}H_{28}Mg_{0.5}NV$, $M_r$ = 333.52, orange-red irregular plate-shaped crystal (0.40 × 0.36 × 0.15 mm), monoclinic, space group, $P2_1/c$, $a$ = 10.220(2), $b$ = 9.909(2), $c$ = 18.658(3) Å, $\beta$ = 104.94(1)°, $U$ = 1825.6(6) Å$^3$, $Z$ = 4, $T$ = 150(2) K, $D_c$ = 1.213 g cm$^{-3}$, $F$(000) = 712, $\mu$ = 0.556 mm$^{-1}$. 2184 unique reflections ($2\theta$ < 45°) were measured on a Siemens P4 diffractometer with graphite monochromated Mo-Kα X-radiation ($\lambda$ = 0.710 73 Å); no absorption correction was made. Structure solved (by Patterson methods) and refined using SHELXL-93. 2179 reflections were used in the full-matrix least-squares refinement. Refinement of positional parameters for all non-H atoms and anisotropic thermal parameters for V (91 parameters) converged to $R_1[I > 2\sigma(I)]$ = 0.0602 and $wR_2[I > 2\sigma(I)]$ = 0.0912 [$w = 1/(\sigma^2F_0^2 + 0.0003P^2)$ where $P = (F_o^2 + 2F_c^2)/3$] with $S$ = 0.729. All bridging H atoms were found in the difference map but not refined. **3**: $C_{35}H_{47}N_2V_2{\cdot}0.5C_6H_{12}$, $M_r$ = 597.63, deep red diamond-shaped crystal (0.80 × 0.62 × 0.40 mm), monoclinic, space group, $P2_1/n$, $a$ = 9.924(2), $b$ = 21.653(4), $c$ = 16.235(3) Å, $\beta$ = 98.73°, $U$ = 3448(1) Å$^3$, $Z$ = 4, $T$ = 150(2) K, $D_c$ = 1.151 g cm$^{-3}$, $F$(000) = 1268, $\mu$ = 0.565 mm$^{-1}$. 4865 unique reflections ($2\theta$ < 46.5°) were measured on a Siemens SMART-CCD diffractometer with graphite monochromated Mo-Kα X-radiation ($\lambda$ = 0.710 73 Å); no absorption correction was made. Structure solved (by direct methods) and refined using SHELXL-93. 4857 reflections were used in the full-matrix least-squares refinement. Refinement of positional and anisotropic thermal parameters for all non-H atoms (364 parameters) converged to $R_1[I > 2\sigma(I)]$ = 0.0531 and $wR_2[I > 2\sigma(I)]$ = 0.1476 [$w = 1/(\sigma^2F_o^2 + 0.0650P^2 + 5.1588P)$] with $S$ = 1.208. Hexane solvent H atoms were not modelled. CCDC 182/609.

1 A. van den Linden, C. J. Schaverien, N. Meijboom, C. Ganter and A. G. Orpen, *J. Am. Chem. Soc.*, 1995, **117**, 3008.
2 T. Miyatake, K. Mizunuma and M. Kakugo, *Makromol. Chem. Macromol. Symp.*, 1993, **66**, 203.
3 For recent examples, see: (*a*) J. D. Scollard, D. H. McConville and S. J. Rettig, *Organometallics*, 1997, **16**, 1810; (*b*) F. G. N. Cloke, T. J. Geldbach, P. B. Hitchcock and J. B. Love, *J. Organomet. Chem.*, 1996, **506**, 343; (*c*) R. Baumann, W. M. Davis and R. R. Schrock, *J. Am. Chem. Soc.*, 1997, **119**, 3830; (*d*) S. Tinkler, R. J. Deeth, D. J. Duncalf and A. McCamley, *Chem. Commun.*, 1996, 2623; (*e*) F. Jäger, H. W. Roesky, H. Dorn, S. Shah, M. Noltemeyer and H.-G. Schmidt, *Chem. Ber.*, 1997, **130**, 399; (*f*) M. Oberthür, P. Arndt and R. Kempe, *Chem. Ber.*, 1996, **129**, 1087; (*g*) H. Mack and M. S. Eisen, *J. Organomet. Chem.*, 1996, **526**, 81 and references therein.
4 (*a*) M. P. Coles and V. C. Gibson, *Polym. Bull.*, 1994, **33**, 529; (*b*) M. P. Coles, C. I. Dalby, V. C. Gibson, W. Clegg and M. R. J. Elsegood, *J. Chem. Soc., Chem. Commun.*, 1995, 1709.
5 E. B. Tjaden, D. C. Swenson and R. F. Jordan, *Organometallics*, 1995, **14**, 371.
6 H. Brand, J. A. Capriotti and J. Arnold, *Organometallics*, 1994, **13**, 4469; R. Uhrhammer, D. G. Black, T. G. Gardner, J. D. Olsen and R. F. Jordan, *J. Am. Chem. Soc.*, 1993, **115**, 8493.
7 D. N. Williams, J. P. Mitchell, A. D. Poole, U. Siemeling, W. Clegg, D. C. R. Hockless, P. A. O'Neil and V. C. Gibson, *J. Chem. Soc., Dalton Trans.*, 1992, 739; J. K. Cockcroft, V. C. Gibson, J. A. K. Howard, A. D. Poole, U. Siemeling and C. Wilson, *J. Chem. Soc., Chem. Commun.*, 1992, 1668; U. Siemeling and V. C. Gibson, *J. Organomet. Chem.*, 1992, **426**, C25; P. W. Dyer, V. C. Gibson, J. A. K. Howard, B. Whittle and C. Wilson, *J. Chem. Soc., Chem. Commun.*, 1992, 1666.
8 See for example: R. F. Jordan, C. S. Bajgur, R. Willet and B. Scott, *J. Am. Chem. Soc.*, 1986, **108**, 7410; G. C. Hlatky, H. W. Turner and R. R. Eckman, *J. Am. Chem. Soc.*, 1989, **111**, 2728, J. A. Ewen and M. J. Elder, *Macromol. Chem., Macromol. Symp.*, 1993, **66**, 179; J. C. W. Chien, W. M. Tsai and M. D. Rausch, *J. Am. Chem. Soc.*, 1991, **113**, 8570; X. Yang, C. L. Stern and T. J. Marks, *J. Am. Chem. Soc.*, 1991, **113**, 3623; 1994, **116**, 10 015.
9 J.-K. F. Buijink, A. Meetsma, J. H. Teuben, H. Kooijman and A. L. Spek, *J. Organomet. Chem.*, 1995, **497**, 161.
10 For Ir: D. S. Glueck, J. Wu, F. J. Hollander and R. G. Bergman, *J. Am. Chem. Soc.*, 1991, **113**, 2041. For Os: R. I. Michelman, R. G. Bergman and R. A. Anderson, *Organometallics*, 1993, **12**, 2741. For Mo: P. W. Dyer, V. C. Gibson, E. L. Marshall, W. Clegg, M. J. Elsegood, A. Bell, *J. Chem. Soc., Chem. Commun.*, 1994, 2247; 2547. For Cr: M. P. Coles, C. I. Dalby, V. C. Gibson, W. Clegg and M. R. J. Elsegood, *Polyhedron*, 1995, **14**, 2455. For Ti: P. E. Collier, S. C. Dunn, P. Mountford, O. V. Shishkin and D. Swallow, *J. Chem. Soc., Dalton Trans.*, 1995, 3743.
11 Ni–Mg 2.615 Å: W. Kaschube, K. R. Pörschke, K. Angermund, C. Krüger and G. Wilke, *Chem. Ber.*, 1988, **121**, 1921.
12 Co–Mg 2.565, 2.480 Å: K. Jonas, G. Koepe and C. Krüger, *Angew. Chem., Int. Ed. Engl.*, 1986, **25**, 9; Mo–Mg 2.853, 2.737 Å: M. L. H. Green, G. A. Moser, I. Packer, F. Petit, R. A. Forder and K. Prout, *J. Chem. Soc., Chem. Commun.*, 1974, 839.
13 For example: H. Viebrock and E. Weiss, *J. Org. Chem.*, 1994, **464**, 121.
14 W. A. Nugent and J. M. Mayer, *Metal–Ligand Multiple Bonds*, Wiley Interscience, New York, 1988.
15 G. A. Solan, P. G. Cozzi, C. Floriani, A. Chiesi-Villa and C. Rizzoli, *Organometallics*, 1994, **13**, 2572.
16 S. K. Noh, S. C. Sendlinger, C. Janiak and K. H. Theopold, *J. Am. Chem. Soc.*, 1989, **111**, 9127; S. K. Noh, R. A. Heintz, S. C. Sendlinger, C. Janiak and K. H. Theopold, *Angew. Chem., Int. Ed. Engl.*, 1990, **29**, 775.
17 F. A. Cotton and M. J. Millar, *J. Am. Chem. Soc.*, 1977, **99**, 7886; H. Vahrenkamp, *Chem. Ber.*, 1978, **111**, 3472.
18 J.-F. K. Buijink, J. H. Teuben, H. Kooijman and A. L. Spek, *Organometallics*, 1994, **13**, 2922; J.-K. F. Buijink, A. Meetsma, J. H. Teuben, H. Kooijman and A. L. Spek, *J. Organomet. Chem.*, 1995, **497**, 161.

*Received in Basel, Switzerland, 22nd July 1997; 7/05256A*

# Synthesis of chiral half-sandwich rhodium oxazoline complexes and their use as asymmetric Diels–Alder catalysts

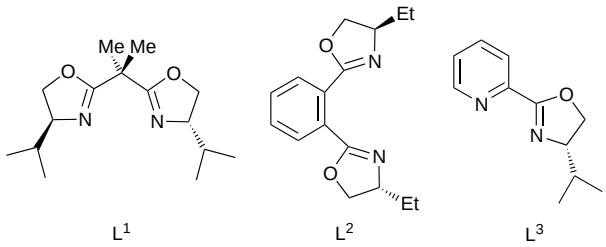
**Adam J. Davenport, David L. Davies,* John Fawcett, Shaun A. Garratt, Latesh Lad and David R. Russell**

*Department of Chemistry, University of Leicester, Leicester, UK LE1 7RH*

**The reaction of $[(\eta\text{-}C_5Me_5)RhCl_2]_2$ with bidentate oxazoline containing ligands provides the cations $[(\eta\text{-}C_5Me_5)RhClL]^+$ 1–3, of which {1, L = 2,2′-isopropylidenebis[4-isopropyl-2-oxazoline] and 3, L = 4-isopropyl-2-(2-pyridyl)-1,3-oxazoline} are structurally characterised by X-ray diffraction; treatment of these with $AgSbF_6$ gives dications which are enantioselective catalysts for the asymmetric Diels–Alder reaction between methacrolein and cyclopentadiene.**

Half-sandwich complexes have been extensively used in stoichiometric and catalytic asymmetric synthesis and have therefore attracted much study.[1] Such complexes can be chiral at the ligand and/or the metal. To date much transition metal catalysed asymmetric synthesis has utilised phosphines as chiral ligands, however recently, N-donor ligands have attracted more attention.[2] Oxazolines, in particular, have found extensive use in asymmetric catalysis.[3] For example, bis-oxazolinylpropanes (*cf*. $L^1$) provide high enantioselectivity in copper catalysed cyclopropanation, aziridination and Diels–Alder reactions[4] whilst pyridyloxazolines (*cf*. $L^3$) have been used in rhodium catalysed asymmetric hydrosilylation of ketones.[5] However, the use of oxazoline ligands with half-sandwich complexes is much less well studied, being limited to two reports of arene ruthenium complexes.[6,7]

The complexes $[(\eta\text{-}C_5Me_5)RhClL]X$ (X = $PF_6$, $SbF_6$) (**1**–**3**; $L^{1–3}$) were prepared in good yield by refluxing the appropriate




ligand with $[(\eta\text{-}C_5Me_5)RhCl_2]_2$ in methanol in the presence of NaX.† In the case of the $C_2$ symmetric ligands $L^1$ and $L^2$, coordination of the ligands is readily apparent in the $^1H$ NMR spectrum since the $C_2$ symmetry is lost and only one isomer is possible. For complex **3** containing the unsymmetrical ligand $L^3$ two diastereomers are possible, however complexation is highly diastereostereoselective, only one diastereomer being observed by $^1H$ NMR.

The X-ray structures of **1** and **3** were carried out and the structures of the cations with selected bond distances and angles are shown in Figs. 1 and 2 respectively.‡ In each case the rhodium has a pseudo-octahedral geometry with the $\eta\text{-}C_5Me_5$ occupying three *fac* coordination sites. In **1** the Rh–N(1) bond length 2.117(6) Å is slightly shorter than the Rh–N(2) length 2.157(6) Å; possibly the isopropyl on C(12) interacts with the $\eta\text{-}C_5Me_5$ inhibiting a closer approach of N(2). The N(1)–Rh–N(2) chelate bite angle is 84.0(2)°. In **3** the ligand is coordinated such that the isopropyl substituent is on the same side as the chloride rather than the $\eta\text{-}C_5Me_5$ presumably to miminise unfavourable steric interactions. The Rh–N(1) (ox) bond length 2.109(4) is shorter than that of Rh–N(2) (py) 2.142(4) Å, whilst the chelate bite angle N(1)–Rh–N(2) is 76.0(2)° as found for a related arene ruthenium complex with the same ligand.[6] The use of L-valine in the ligand preparation means that the configuration at the chiral carbon is *S* and the structure shows that the rhodium is also *S* [based on the priority

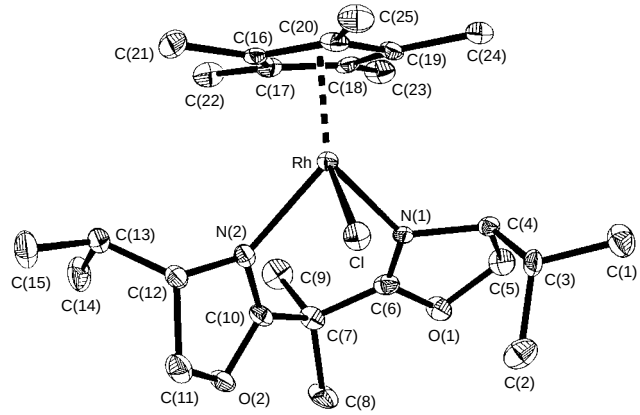



**Fig. 1** Molecular structure and atom numbering scheme for the cation of **1**. Selected bond distances (Å) and angles (°): Rh–N(1) 2.117(6), Rh–N(2) 2.157(6), Rh–Cl 2.406(2), N(2)–Ru–N(1) 84.0(2), N(1)–Rh–Cl 90.2(2), N(2)–Rh–Cl 82.1(2).

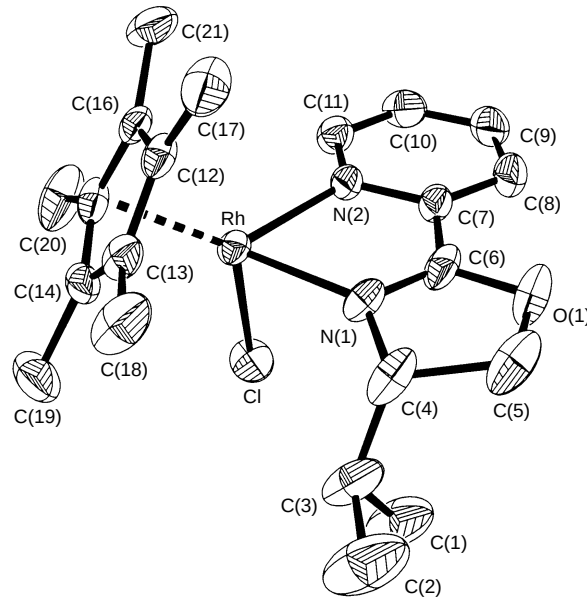
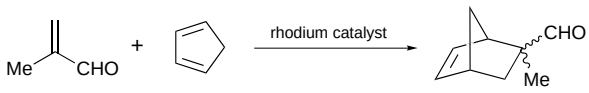



**Fig. 2** Molecular structure and atom numbering scheme for the cation of **3**. Selected bond distances (Å) and angles (°): Rh–N(1) 2.109(4), Rh–N(2) 2.142(4), Rh–Cl 2.407(1), N(2)–C(7) 1.345(6), C(7)–C(6) 1.456(8), C(6)–N(1) 1.260(6); N(2)–Rh–N(1) 76.0(2).

**Table 1** Enantioselective Diels–Alder reaction of methacrolein with cyclopentadiene in dichloromethane using catalysts prepared from $[(\eta\text{-}C_5Me_5)RhCl(L)]^+$




| Entry | Catalyst (mol%) | *T*/°C | *t*/h | Yield (%) | Isomer ratio (*exo*:*endo*) | Ee[a] (%) |
|---|---|---|---|---|---|---|
| 1 | **1**(5) | room temp. | 24 | 62 | 94:6 | 29 |
| 2 | **2**(5) | room temp. | 48 | 10 | 90:10 | 2 |
| 3 | **3**(1) | room temp. | 24 | 45 | 94:6 | 52 |
| 4 | **3**(2) | room temp. | 24 | 57 | 94:6 | 53 |
| 5 | **3**(2) | 0 | 72 | 81 | 95:5 | 68 |

[a] Enantiomeric excess of the major *exo* product.

arene > Cl > N (ox) > N (py)].[8] The observation of an NOE effect between the NCH and $\eta\text{-}C_5Me_5$ suggests that this geometry is retained in solution.

Asymmetric catalysis of Diels–Alder reactions mostly with Ti, Al, B or Ln complexes has been reported previously.[9] However, such catalysts are often extremely sensitive to water and may form dimers or oligomers in solution. As a result, characterisation of the actual catalytic species and understanding the mechanism of catalysis and selectivity are particularly difficult. Many of these drawbacks may be overcome with half-sandwich late transition metal Lewis acids. For example, cyclopentadienyl–rhodium[10] and –iron[11] complexes with chiral phosphorus ligands are catalysts for asymmetric Diels–Alder reactions and a related ruthenium complex is a catalyst for the hetero Diels–Alder reaction.[12]

The chloride in **1**–**3** is readily removed with $AgSbF_6$ to form dications. Solutions of these dications in $CH_2Cl_2$ have been tested as catalysts for the Diels–Alder reaction between methacrolein and cyclopentadiene and the results are shown in Table 1.§ The dication derived from **1** is a reasonable catalyst but gives only modest enantioselectivity (Entry 1) whilst that from **2** shows little or no activity and no enantioselectivity (Entry 2). However, the dication from **3** is a reasonable catalyst even at fairly low catalyst ratio (1 mol%) showing good *exo*:*endo* selectivity with moderate enantioselectivity (Entry 3). Increasing the catalyst ratio gives an increased yield but no increase in ee (Entry 4). However, carrying out the reaction at lower temperature leads to an increase in ee (Entry 5). The absolute configuration of the major *exo* product using **3** as catalyst is consistent with the isopropyl shielding the *Si* face of the coordinated methacrolein leading to attack of cyclopentadiene at the *Re* face as shown in Fig. 3. Coordination of the methacrolein with *Si* face exposed is disfavoured due to steric interactions of the alkene with the $\eta\text{-}C_5Me_5$. The reasons for the difference in catalytic activity of complexes **1**–**3** are not yet clear, though similar reactivity patterns are observed for related arene ruthenium complexes with the same ligands.[6,13]

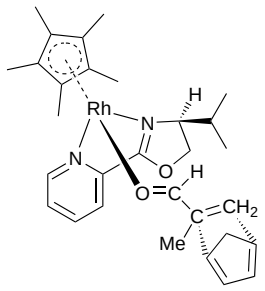



**Fig. 3** Model of the transition state

We thank the University of Leicester for a studentship (SAG) and Johnson Matthey for a loan of $RhCl_3$.

## Footnotes and References

* E-mail: did3@le.ac.uk

† *Selected spectroscopic data* for **2**: $^1$H NMR (250 MHz, $CDCl_3$, 20 °C, $SiMe_4$). $\delta$ 0.77 (t, 3 H, *J* 7 Hz, $CH_2$*Me*), 0.96 (t, 3 H, *J* 7 Hz, $CH_2$*Me*), 1.29 (s, 15 H, $C_5Me_5$), 1.60 (m, 2H, C*H*$_2$Me), 1.95 (m, 1 H, C*H*H′Me), 2.30 (m, 1 H, CHH′Me), 4.12 (tt, 1 H, *J* 5, 8.5 Hz, NCH), 4.6 (m, 5 H, 3 ×OCH + 2 × NCH), 7.84 (m, 2 H, aryl), 8.04 (m, 1 H, aryl), 8.16 (m, 1 H, aryl). Satisfactory elemental analysis (C, H, N) obtained for **1**–**3**.

‡ *Crystal data*: for **1**: $C_{25}H_{41}ClF_6N_2O_2RhSb$, $M$ = 775.71, orthorhombic, space group $P2_12_12_1$, $a$ = 13.335(2), $b$ = 13.496(2), $c$ = 17.740(3) Å, $U$ = 3192.7(9) Å$^3$, $Z$ = 4, $D_c$ = 1.614 g cm$^{-3}$, $\mu$ = 1.505 mm$^{-1}$, $F$(000) = 1552, graphite-monochromated Mo-K$\alpha$ radiation ($\lambda$ = 0.710 73 Å). Data collected on a Siemens P4 diffractometer at 190 K. 4829 reflections collected with 2.75 < $\theta$ < 26.99°, 4619 unique ($R_{int}$ = 0.0173). A $\psi$-scan absorption correction was applied. The structure was solved by Patterson methods and refined using full-matrix least squares on $F^2$ (SHELXL96).[14] Anisotropic displacement parameters used for all non-hydrogen atoms, hydrogens included in calculated positions (C–H 0.96 Å), with isotropic displacement parameters set to 1.2 $U_{eq}$(C). The $SbF_6^-$ anion was found to be disordered, this was modelled with each fluorine atom given equal site occupancy between two different sites. Final $R_1$ = 0.0743, $wR_2$ = 0.0784 (all data); Flack parameter, −0.06(3).

For **3**: $C_{21}H_{29}ClF_6N_2OPRh$, $M$ = 608.79, tetragonal, space group $P4_32_12$, $a$ = 12.844(5), $c$ = 30.542(13) Å, $U$ = 5038(3) Å$^3$, $Z$ = 8, $D_c$ = 1.605 g cm$^{-3}$, $\mu$ = 0.908 mm$^{-1}$, $F$(000) = 2464, graphite-monochromated Mo-K$\alpha$ radiation ($\lambda$ = 0.710 73 Å). Data collected as above. 7418 Reflections collected with 2.55 < $\theta$ < 27.09°, 5507 unique ($R_{int}$ = 0.0256). The structure was solved by Patterson methods and refined using full-matrix least squares on $F^2$ (SHELXL96).[14] One of the two anions (on special positions) exhibits positional disorder and the F atoms were each assigned fractional occupancy factors. All non-hydrogen atoms were refined anisotropically, hydrogen atoms were generated in their idealised positions (C–H 0.96 Å) and allowed to ride on their respective parent carbon atoms with isotropic displacement parameters set to 1.2 $U_{eq}$(C). Final $R_1$ = 0.0731, $wR_2$ = 0.0801 (all data); Flack parameter, −0.03(4). CCDC 182/648.

§ The catalysis was carried out as described in ref. 6.

1 H. Brunner, *Adv. Organomet. Chem.*, 1980, **18**, 151; S. G. Davies, *Pure Appl. Chem.*, 1988, **60**, 13; J. W. Faller, M. R. Mazzieri, J. T. Nguyen, J. Parr and M. Tokunaga, *Pure Appl. Chem.*, 1994, **66**, 1463; E. P. Kundig, A. Quattropani, M. Inage, A. Ripa, C. Dupré, A. F. J. Cunningham and B. Bourdin, *Pure Appl. Chem.*, 1996, **68**, 97; R. Noyori and S. Hashiguchi, *Acc. Chem. Res.*, 1997, **30**, 97.
2 A. Togni and L. M. Venanzi, *Angew. Chem., Int. Ed. Engl.*, 1994, **33**, 497.
3 A. Pfaltz, *Acc. Chem. Res.*, 1993, **26**, 339; A. Pfaltz, *Acta Chem. Scand.*, 1996, **50**, 189.
4 (*a*) D. A. Evans, K. A. Woerpel, M. M. Hinman and M. M. Faul, *J. Am. Chem. Soc.*, 1991, **113**, 726; (*b*) D. A. Evans, J. A. Murry, P. v. Matt, R. D. Norcross and S. J. Miller, *Angew. Chem., Int. Ed. Engl.*, 1995, **34**, 798.
5 H. Brunner and P. Brandl, *Tetrahedron Asymmetry*, 1991, **2**, 919.
6 D. L. Davies, J. Fawcett, S. A. Garratt and D. R. Russell, *Chem. Commun.*, 1997, 1351.
7 H. Asano, K. Katayama and H. Kurosawa, *Inorg. Chem.*, 1996, **35**, 5760.
8 T. E. Sloan, *Top. Stereochem.*, 1981, **12**, 1; K. Stanley and M. C. Baird, *J. Am. Chem. Soc.*, 1975, **97**, 6598.
9 H. B. Kagan and O. Riant, *Chem. Rev.*, 1992, **92**, 1007; K. Narasaka, *Synthesis*, 1991, 1.
10 D. Carmona, F. J. Lahoz, L. A. Oro, M. P. Lamata, F. Viguri and E. San Jose, *Organometallics*, 1996, **15**, 2961.
11 E. P. Kundig, B. Bourdin and G. Bernardinelli, *Angew. Chem., Int. Ed. Engl.*, 1994, **33**, 1856.
12 J. W. Faller and C. J. Smart, *Tetrahedron Lett.*, 1989, **30**, 1189
13 S. A. Garratt and D. L. Davies, unpublished work.
14 G. M. Sheldrick, in SHELXL 96, University of Göttingen, 1996.

*Received in Cambridge, UK, 28th August 1997; 7/06287C*

# Phosphinomethanide *versus* phosphinoenolate: thermodynamical preference for a three- instead of a five-membered chelate ring

**Gerhard Henig, Michael Schulz and Helmut Werner***

*Institut für Anorganische Chemie der Universität Würzburg, Am Hubland, D-97074 Würzburg, Germany*

**The phosphinoenolate complex 4, which is prepared stepwise from $[(mes)RuCl_2]_2$ 1 *via* the neutral and cationic compounds 2 and 3 as isolated intermediates, rearranges slowly in benzene to the thermodynamically more stable phosphinomethanide isomer 5; the presence of a three-membered RuCP ring in the latter is confirmed by X-ray crystallography.**

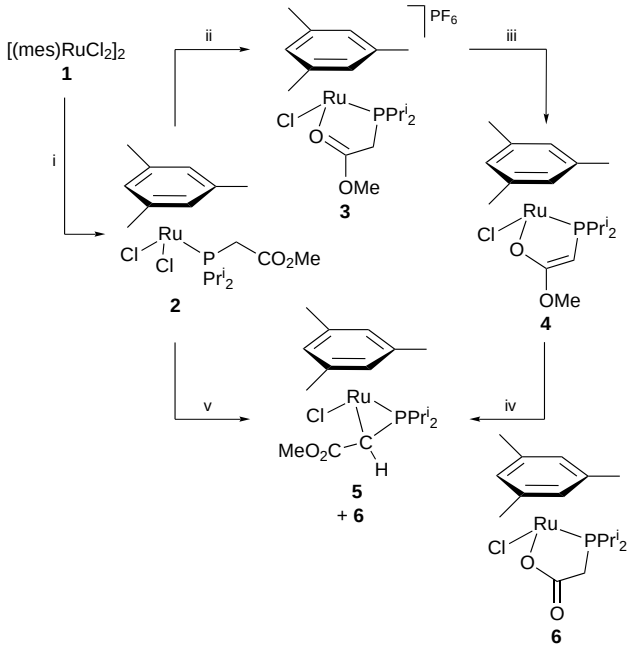
Following the development of the Shell Higher Olefin Process (SHOP),[1] the chemistry of phosphinoenolate metal complexes has become a focus of general interest.[2] While it has been shown by numerous examples that both β-phosphinoketones and β-phosphinoesters are easily converted to ligands of general composition $R_2PCH{=}C(R)O^-$ in the coordination sphere of transition metals,[3] we discovered more recently that from functional phosphines such as $Pr^i_2PCH_2CO_2R$ (R = Me, Et) phosphinomethanide units $Pr^i_2PCHCO_2R^-$ can also be generated.[4] However, it was not known which of the isomeric forms $Pr^i_2PCH{=}C(OR)O^-$ and $Pr^i_2PCHCO_2R^-$, the first forming a five-membered and the second a three-membered chelate ring, is more stable in a particular metal–ligand environment and whether the two types of ligands can be transformed into each other.

The half-sandwich-type complex **2**, which by analogy to previous work[5] was prepared from **1** and $Pr^i_2PCH_2CO_2Me$, reacts with an equimolar amount of $AgPF_6$ in $CH_2Cl_2$ to give the chelate compound **3** (Scheme 1) in almost quantitative yield.† The IR spectrum of the orange–red, nearly air-stable solid displays a C=O stretching frequency at 1618 $cm^{-1}$ (in $CH_2Cl_2$), which is lower by about 110 $cm^{-1}$ if compared with the frequency of $Pr^i_2PCH_2CO_2Me$.[6] This supports the assumption that the functional phosphine is coordinated *via* phosphorus and oxygen to the metal.

Treatment of the $PF_6^-$ salt **3** with $KOBu^t$ in THF led to a rapid change of colour from deep red to bright red and gave, after recrystallization from $CH_2Cl_2$–hexane (1 : 3), the phosphinoenolate complex **4** in 78% yield. The most characteristic features of the NMR spectroscopic data of **4** are the signal at $\delta$ 3.19 [*J*(PH) 3.7 Hz] for the vinylic proton and the two resonances at $\delta$ 180.5 ($CO_2$) and 44.5 (=CH) for the carbon atoms of the chelate ring, which display a strong P–C coupling of 28.6 and 70.6 Hz, respectively.

While phosphinoenolate complexes, such as those used for the oligomerization and polymerization of alkenes,[1,7] seem to be quite stable, compound **4** is thermally labile and slowly rearranges in benzene at room temp. to isomer **5**. After 3 d the reaction is complete. There is, to the best of our knowledge, no precedence for this type of isomerisation process which is probably driven by the conversion of the C=C double into a C–C single bond and the re-formation of the intact $CO_2Me$ unit. The IR spectrum of **5** (in KBr) displays a C=O stretch at 1661 $cm^{-1}$, the $^1H$ NMR spectrum a doublet at $\delta$ 2.71 [*J*(PH) 3.1 Hz] for the C*H*$CO_2Me$ proton and the $^{13}C$ NMR spectrum a singlet at $\delta$ 10.0 for the carbon atom of the RuPC three-membered ring.

The X-ray crystal structure analysis of **5** (Fig. 1) confirmed the structural proposal outlined in Scheme 1.‡ The ruthenium is coordinated by the mesitylene ring, one chloride and the P,C-




**Scheme 1** *Reagents and conditions*: i, $Pr^i_2PCH_2CO_2Me$, $CH_2Cl_2$, 25 °C, 3 h, 91%; ii, $AgPF_6$, $CH_2Cl_2$, 25 °C, 45 min, 90%; iii, $KOBu^t$, THF, 25 °C, 15 min, 78%; iv, $C_6H_6$, 25 °C, 3 d, 88%; v, $Al_2O_3$/NaH, THF, 25 °C, 45 min, 15% (for **5**) and 80% (for **6**)

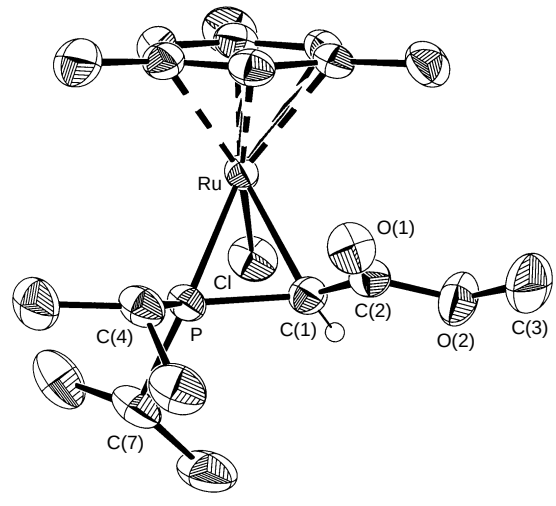



**Fig. 1** Molecular structure (ORTEP drawing) of **5**. Selected bond distances (Å) and angles (°): Ru–P 2.269(1), Ru–Cl 2.410(1), Ru–C(1) 2.201(2), P–C(1) 1.761(2), P–C(4) 1.832(2), P–C(7) 1.847(2), C(1)–C(2) 1.455(3), C(2)–O(1) 1.208(3), C(2)–O(2) 1.363(3); P–Ru–Cl 88.97(3), P–Ru–C(1) 46.37(6), C(1)–Ru–Cl 84.97(6), Ru–P–C(1) 64.77(7), Ru–C(1)–P 68.86(7), P–C(1)–C(2) 125.5(2), Ru–C(1)–C(2) 116.5(1), C(1)–C(2)–O(1) 128.6(2), C(1)–C(2)–O(2) 110.0(2), O(1)–C(2)–O(2) 121.3(2).

bonded phosphinomethanide ligand, the $CO_2Me$ substituent of which is pointing away from the Ru–Cl axis. The bond angles of the three-membered ring are comparable to those found in the osmium analogue of **5**[4] and in various [$L_nM\{\kappa^2$(P,C)-$Ph_2PCH_2\}$] complexes.[8] The distance P–C(1) is shorter by *ca*. 0.08 Å than the distances P–C(4) and P–C(7) indicating a substantial double-bond character of the phosphorus–carbon bond in the RuCP unit.

The phosphinomethanide and not the isomeric phosphinoenolate compound is also formed, although as the minor component, on treatment of **2** with $Al_2O_3$/NaH in THF (Scheme 1). The main product of this reaction is the phosphinocarboxylate complex **6**, which has been characterized by elemental analysis and spectroscopic techniques. Both the IR and $^1$H NMR data are similar to those of [(mes)RuCl{$\kappa^2$(P,O)-$Ph_2PCH_2C(O)O$}], obtained by acid hydrolysis of [(mes)-$RuCl_2(Ph_2PCH_2CO_2Bu^t)$] (mes = $C_6H_3Me_3$-1,3,5).[9] We note that in contrast to **2**, the related osmium compound [(mes)-$OsCl_2(Pr^i_2PCH_2CO_2Me)$] reacts with $Al_2O_3$/NaH in THF to give the corresponding phosphinomethanide complex [(mes)-OsCl{$\kappa^2$(P,O)-$Pr^i_2PCHCO_2Me$}] almost quantitatively.[4]

In conclusion, the present work has shown that, in connection with [(mes)RuCl] as a building block, a three-membered chelate ring of a phosphinomethanide complex is thermodynamically more stable than a five-membered ring of the phosphinoenolate metal isomer. At present, we are investigating whether an analogous isomerisation (as that of **4** to **5**) also occurs if the CH fragment of the $RuOC_2P$ five-membered ring is replaced, *e.g.* by a CC(O)NHR unit which is formed by insertion of an isocyanate into the C–H bond.[2a]

We gratefully acknowledge financial support from the Deutsche Forschungsgemeinschaft (SFB 347), the Fonds der Chemischen Industrie and Degussa AG.

## Footnotes and References

* E-mail: helmut.werner@mail.uni-wuerzberg.de

† All new compounds gave satisfactory elemental analyses. **2**: orange–red solid, mp 160 °C (decomp.). **3**: orange–red solid, mp 89 °C (decomp.), equiv. conductivity ($CH_3NO_2$) $\Lambda$ 68 cm² $\Omega^{-1}$ mol$^{-1}$. **4**: light red solid, mp 85 °C (decomp.). **5**: yellow crystals, mp 174 °C. **6**: pale yellow solid, mp 198 °C.

‡ *Crystal data* for **5**: crystals from hexane; $C_{18}H_{30}ClO_2PRu$, $M$ = 445.91; monoclinic, space group $P2_1/n$ (no. 14), $Z$ = 4, $a$ = 9.195(3), $b$ = 15.398(3), $c$ = 14.193(5) Å, $\beta$ = 94.69(2)°, $U$ = 2002.7(10) Å$^3$; $D_c$ = 1.479 g cm$^{-3}$; $T$ = 293(2) K; max $2\theta$ = 48°, graphite-monochromated Mo-K$\alpha$ radiation ($\lambda$ = 0.710 73 Å). 3117 unique data were obtained and 2776 of these with $I > 2\sigma(I)$ were used in the refinement; $R_1$ = 0.0178, $wR_2$ = 0.0522 [$I > 2\sigma(I)$]; $R_1$ = 0.0251, $wR_2$ = 0.0726 (all data); reflection/parameter ratio 14.15; residual electron density 0.245/−0.212. CCDC 182/637.

1 A.Behr, U. Freudenberg and W. Keim, *J. Mol. Catal.*, 1986, **35**, 17; U. Klabunde, T. H. Tulip, D. C. Roe and S. D. Ittel, *J. Organomet. Chem.*, 1987, **334**, 141; W. Keim, *J. Mol. Catal.*, 1989, **52**, 19; *Angew. Chem., Int. Ed. Engl.*, 1990, **29**, 235; *New. J. Chem.*, 1994, **18**, 93.

2 Reviews: P. Braunstein and D. Nobel, *Chem. Rev.*, 1989, **89**, 1927; A. Bader and E. Lindner, *Coord. Chem. Rev.*, 1991, **108**, 27.

3 Leading references: J. Andrieú, P. Braunstein and F. Naud, *J. Chem. Soc., Dalton Trans.*, 1996, 2903; P. Braunstein, Y. Chauvin, J. Nähring, A. De Cian, J. Fischer, A. Tiripicchio and F. Ugozzoli, *Organometallics*, 1996, **15**, 5551.

4 H. Werner, G. Henig, U. Wecker, N. Mahr, K. Peters and H. G. von Schnering, *Chem. Ber.*, 1995, **128**, 1175.

5 R. A. Zelonka and M. C. Baird, *J. Organomet. Chem.*, 1972, **44**, 383; M. A. Bennett and A. K. Smith, *J. Chem. Soc., Dalton Trans.*, 1974, 233; H. Werner and R. Werner, *Chem. Ber.*, 1982, **115**, 3766; H. Werner, H. Kletzin and K. Roder, *J. Organomet. Chem.*, 1988, **355**, 401.

6 W. Wolfsberger, W. Burkart, S. Bauer, A. Hampp, J. Wolf and H. Werner, *Z. Naturforsch., Teil B*, 1994, **49**, 1659.

7 D. Matt. M. Huhn, J. Fischer, A. De Cian, W. Kläui, I. Tkatchenko and M. C. Bonnet, *J. Chem. Soc., Dalton Trans.*, 1993, 1173; M. D. Fryzuk, X. Gao and S. J. Rettig, *Can. J. Chem.*, 1995, **73**, 1175.

8 E. Lindner, K. A. Starz, H.-J. Eberle and W. Hiller, *Chem. Ber.*, 1983, **116**, 1209; E. Lindner, E. U. Küster, W. Hiller and R. Fawzi, *Chem. Ber.*, 1984, **117**, 127.

9 B. Demerseman, C. Renoúard, R. Le Lagadec, M. Gonzalez, P. Chrochet and P. H. Dixneuf, *J. Organoment. Chem.*, 1994, **471**, 229.

*Received in Basel, Switzerland, 8th August 1997; 7/05821G*

# Chiral ruthenium complexes as catalysts in enantioselective Diels–Alder reactions. Crystal structure of the Lewis acid–dienophile adduct

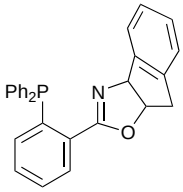
**Daniel Carmona,*[a] Carlos Cativiela,*[b] Sergio Elipe,[a] Fernando J. Lahoz,[a] M. Pilar Lamata,[c] M. Pilar López-Ram de Víu,[b] Luis A. Oro,[a] Cristina Vega[c] and Fernando Viguri[c]**

*[a] Departamento de Química Inorgánica and [b] Departamento de Química Orgánica, Facultad de Ciencias, Instituto de Ciencia de Materiales de Aragón, C.S.I.C.-Universidad de Zaragoza, 50009 Zaragoza, Spain*

*[c] Departamento de Química Inorgánica, Escuela Universitaria de Ingeniería Técnica Industrial, Instituto de Ciencia de Materiales de Aragón, C.S.I.C.-Universidad de Zaragoza, 50009 Zaragoza, Spain*

**On the basis of spectroscopic and structural studies a full catalytic cycle is proposed for the Diels–Alder reaction between methacrolein and cyclopentadiene when the new chiral aquo-complexes ($R_{Ru}$, $S_{Ru}$)-[($\eta^6$-*p*-cymene)Ru(PN)($H_2O$)][$SbF_6$]$_2$ {PN = (3a*S*, 8a*R*)-2-(2-diphenylphosphinophenyl)-3a,8a-dihydroindane[1,2-d]oxazole} are used as catalysts.**

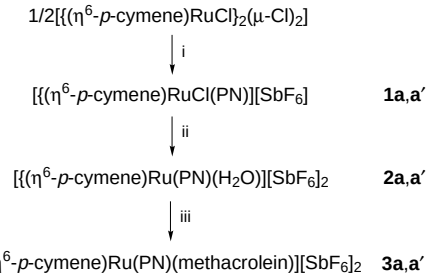
The Diels–Alder reaction is one of the most important reactions owing to its synthetic relevance and to its mechanistic implications.[1] For these reasons, considerable efforts have been devoted to the development of its enantioselective versions.[2] Among them the use of chiral transition-metal Lewis acids is one of the most recent and versatile variants.[3] It is commonly assumed that for activated alkenes, such as acroleins, the catalytic activity implies an $\eta^1$-coordination mode through the oxygen atom followed by subsequent attack of the diene.




**I**

However, studies supporting this assumption in transition metal catalyzed enantioselective Diels–Alder reactions are very scarce.[4] Following our studies on transition metal complexes with chiral metal centres,[5] we report here spectroscopic and crystallographic evidence that supports the aforementioned path for the Diels–Alder reaction between methacrolein and cyclopentadiene (HCp) catalyzed by the new aquo-complexes ($R_{Ru}$, $S_{Ru}$)-[($\eta^6$-*p*-cymene)Ru(PN)($H_2O$)][$SbF_6$]$_2$, including the X-ray crystal structure determination of the Lewis acid–dienophile adduct ($S_{Ru}$)-[($\eta^6$-*p*-cymene)Ru(PN)(methacrolein)][$SbF_6$]$_2$. The new enantiopure phosphinoxazoline ligand **I**, prepared from (1*S*,2*R*)-1-aminoindan-2-ol according to the Williams' procedure,[6] was used as a chiral auxiliary. The methacrolein complex was prepared following the sequence of reactions depicted in Scheme 1. Complexes **1** were prepared as a 70 : 30 mixture of epimers at ruthenium in essentially quantitative chemical yield. Enantiopure **1a** and **1a′** can be obtained by fractional crystallization from methanol and $CH_2Cl_2$–$Et_2O$, respectively.† NOE difference spectra support an *S* configuration at ruthenium[7] for **1a**.‡

The aquo-complexes **2** were obtained as a mixture of epimers at the metal.† The water molecule proceeds from the solvents. The epimeric composition is independent from the composition of the starting chloride compound **1**, but it depends on the solvent. $^1$H NMR spectra of aliquots of the same solid sample reveal 65 : 35 and 82 : 18 epimeric ratios in $(CD_3)_2CO$ and $CD_2Cl_2$, respectively. ROESY experiments indicated that the configuration at the metal for the major diastereomer is *S*.§




**Scheme 1** *Reagents*: i, PN, $NaSbF_6$, MeOH; ii, $AgSbF_6$, $CH_2Cl_2$–acetone (95 : 5, v/v); iii, methacrolein (excess)

At room temp., dichloromethane solutions of **2** catalyse rapidly the Diels–Alder reaction of methacrolein with HCp (91% conversion in 20 min), the system operating with low loading (5% mol), good *exo* : *endo* selectivity (92 : 8) and moderate enantioselectivity {46% in the *exo* adduct (1*R*,2*S*,4*R*)-2-methylbicyclo[2.2.1]hept-5-ene-2-carbaldehyde}.¶

In order to probe the mechanism of the Diels–Alder catalysis, **2** was combined separately with HCp and methacrolein (**2**: methacrolein or HCp, 1 : 20 molar ratio). While no interaction with HCp was detected by either $^1$H or $^{31}$P NMR, immediate adduct formation with methacrolein occurred to give **3** in 73% chemical yield as a 90 : 10 mixture of epimers at the metal† along with 27% of unreacted **2**. From the NMR solution single-crystals of complex **3** were obtained. An X-ray difraction study‖

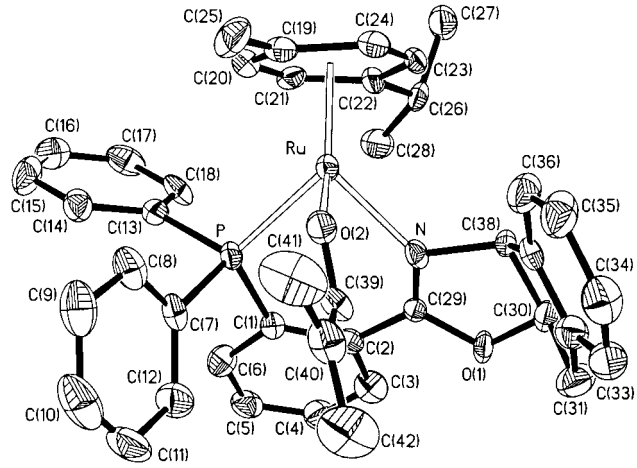
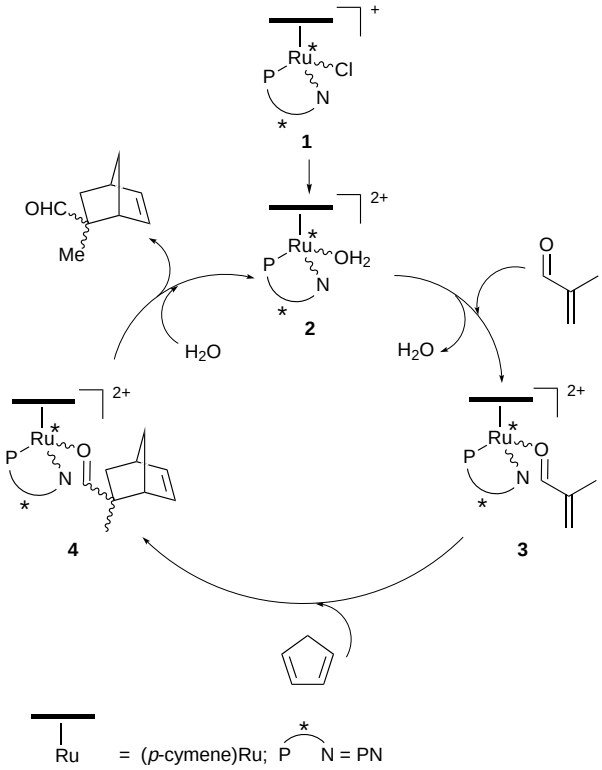



**Fig. 1** Molecular representation of ($S_{Ru}$)-**3**. Selected bond distances (Å) and angles (°): Ru–P 2.327(2), Ru—N 2.106(6), Ru–O(2) 2.110(5), O(2)–C(39) 1.219(8), C(39)–C(40) 1.448(11), C(40)–C(41) 1.475(13), C(40)–C(42) 1.329(13); P–Ru–N 89.0(2), P–Ru–O(2) 89.7(2), N–Ru–O(2) 85.7(2), Ru–O(2)–C(39) 131.2(5), O(2)–C(39)–C(40) 123.1(7), C(39)–C(40)–C(41) 118.3(8), C(39)–C(40)–C(42) 116.0(8), C(41)–C(40)–C(42) 125.7(8).




**Scheme 2**

showed an $\eta^1$-coordination mode through the oxygen atom for the methacrolein ligand which adopts an *S-trans* configuration. The methacrolein fragment maintains its planar structure upon coordination [O(2)–C(39)–C(40)–C(42) torsion angle −178.8(8)°], with the metal atom slightly out of this plane by 0.024(6) Å. The absolute configuration at the metal centre results to be *S*.[7] (Fig. 1).

Subsequent addition at 183 K of HCp to $CH_2Cl_2$ solutions of **3**, prepared as above, (**2** : methacrolein : HCp, 1 : 20 : 40 molar ratio) produced the appearance in the $^{31}P$ NMR spectrum of a new broad peak centred at $\delta$ 32.9 at the expense of the major epimer of **3**, the minor one and the aquo-complexes **2** retaining their relative intensities. At this temperature the Diels–Alder reaction was not observed and we assume that the new resonance would be due to one of several of the possible metal–complex diastereoisomers **4** in which the Diels–Alder adduct is still coordinated to the metal. On warming to 253 K the reaction starts and the sole species observed during the catalytic process are the aquo-complexes **2**. When the catalysis has been completed compounds **2** remain and, as expected, addition of methacrolein regenerates compounds **3** restarting the catalytic cycle.

In conclusion, the catalytic cycle depicted in Scheme 2 is proposed on the basis of spectroscopic data and of the X-ray molecular structure of the complex ($S_{Ru}$)-[($\eta^6$-*p*-cymene)Ru-(PN)(methacrolein)][$SbF_6$]$_2$. Further work in this area is in progress in order to optimise the catalytic conditions and to obtain information on the origin of the enantioselectivity.

## Footnotes and References

* E-mail: dcarmona@posta.unizer.es

† *Selected spectroscopic data*: for **1a**: $^{31}P\{^1H\}$ NMR [121.4 MHz, $(CD_3)_2CO$, 20 °C, $H_3PO_4$] $\delta$ 27.5 (s). $^1H$ NMR [300 MHz, $(CD_3)_2CO$, 20 °C, $SiMe_4$] $\delta$ 3.58, 3.78 (2 H, AB part of an ABX system, $J_{AB}$ 18.1, $J_{AX}$ 6.9, $J_{EX}$ 3.6 Hz, C$H_2$CHO); 5.95 (m, 2 H, CHO and CHN). For **1a′**: $^{31}P\{^1H\}$ NMR [121.4 MHz, $(CD_3)_2CO$, 20 °C, $H_3PO_4$] $\delta$ 37.3 (s). $^1H$ NMR [300 MHz, $(CD_3)_2CO$, 20 °C, $Me_4Si$] $\delta$ 3.52, 3.66 (2 H, AB part of an ABX system, $J_{AB}$ 18.1, $J_{AX}$ *ca.* 0, $J_{BX}$ 4.5 Hz, C$H_2$CHO); 5.75 (dd, 1 H, $J_{HH}$ 6.1, 4.5 Hz, CHO); 5.19 (d, 1 H, $J_{HH}$ 6.1 Hz, CHN). For **2a** (major diastereomer): $^{31}P\{^1H\}$ NMR (121.4 MHz, $CD_2Cl_2$, 20 °C, $H_3PO_4$) $\delta$ 36.1 (s). $^1H$ NMR (300 MHz, $CD_2Cl_2$, 20 °C, $SiMe_4$) $\delta$ 3.54, 3.68 (2 H, AB part of an ABX system, $J_{AB}$ 18.2, $J_{AX}$ 5.9, $J_{BX}$ *ca.* 0 Hz, C$H_2$CHO); 4.55 (br s, 2 H, $H_2O$); 5.90 (m, 2 H, CHO and CHN). For **2a′** (minor diastereomer): $^{31}P\{^1H\}$ NMR (121.4 MHz, $CD_2Cl_2$, 20 °C, $H_3PO_4$); $\delta$ 34.9 (s). $^1H$ NMR (300 MHz, $CD_2Cl_2$, 20 °C, $SiMe_4$) $\delta$ 4.26 (br s, 2 H, $H_2O$). For **3a** (major diastereomer): $^{31}P\{^1H\}$ NMR (121.4 MHz, $CD_2Cl_2$, −90 °C, $H_3PO_4$) $\delta$ 42.65 (s). For **3a′** (minor diastereomer): $^{31}P\{^1H\}$ NMR (121.4 MHz, $CD_2Cl_2$, −90 °C, $H_3PO_4$) $\delta$ 39.2 s.

‡ The X-ray crystal structure determination of **1a** confirm the assigned configuration: D. Carmona and F. J. Lahoz, unpublished work.

§ The priority orders for the chloride (**1**) and aquo-compounds (**2**) are *p*-cymene > Cl > P > N and *p*-cymene > P > O > N, respectively. Note that, comparing **1** to **2**, if the configuration at the metal is the same its descriptor changes and *vice versa*.

¶ *Catalytic Diels–Alder reaction*: a solution of the catalyst (0.025 mmol) in 2 ml of dry $CH_2Cl_2$ was prepared under argon. The dienophile (0.5 mmol in 2 ml of $CH_2Cl_2$) and freshly distilled cyclopentadiene (3 mmol in 2 ml of $CH_2Cl_2$) were added consecutively by syringe. The resulting solution was stirred until the dienophile was consumed (GC). Yields and *exo* : *endo* ratios were determined by GC analysis. The reaction mixture was concentrated and filtered through silica gel ($CH_2Cl_2$–hexane as eluent) before the determination of the enantiomeric purity. Ee values were determined by $^1H$ NMR spectroscopy in the presence of the chiral shift reagent Eu(hfc)$_3$. The configuration of the major adduct was assigned by comparing the sign of $[\alpha]_D$ with that in the literature.[9]

‖ *Crystal data* for ($S_{Ru}$)-**3**: $C_{42}H_{42}F_{12}NO_2PRuSB_2$, $M$ = 1196.32, orthorhombic, space group $P2_12_12_1$, $a$ = 11.3401(8), $b$ = 18.2209(12), $c$ = 20.7142(13) Å (by least-squares refinement of the setting angles for 92 reflections within $\theta$ = 12.5–19.5°), $U$ = 4280(1) Å$^3$, $Z$ = 4, $D_c$ = 1.857 g cm$^{-3}$, $T$ = 200.0(2)K, $\mu$ = 1.73 mm$^{-1}$, $F$(000) = 2344, orange irregular block (0.69 × 0.48 × 0.38 mm). Data were collected on a Siemens P4 diffractometer with graphite-monochromated Mo-K$\alpha$ radiation ($\lambda$ = 0.710 73 Å) within a 2$\theta$ range 4–50°. 8444 reflections collected, 7508 unique. Absorption correction applied according to $\psi$-scan method. The structure was solved by direct methods (SHELXS-86)[8] and refined by full-matrix least squares on $F^2$ using all unique data. Anisotropic displacement parameters used for all atoms except for the disordered $SbF_6^-$ groups. Hydrogens included in calculated (methyl groups) or found positions (all the remaining H atoms). Final $R_1$ = 0.0636; $wR_2$ = 0.0950 (SHELXL-93, all data) for 570 parameters. CCDC 182/640.

1 W. Carruthers, *Cycloaddition Reactions in Organic Synthesis*, Pergamon, New York, 1990, p. 1.
2 H. B. Kagan and O. Riant, *Chem. Rev.*, 1992, **92**, 1007.
3 S. Kobayashi and H. Ishitani, *J. Am. Chem. Soc.*, 1994, **116**, 4083; E. P. Kündig, B. Bourdin and G. Bernardinelli, *Angew. Chem., Int. Ed. Engl.*, 1994, **33**, 1856; D. A. Evans, J. A. Murry, P. von Matt, R. D. Norcross and S. J. Miller, *ibid.*, 1995, **34**, 798; J. Jaquith, J. Guan, S. Wang and S. Collins, *Organometallics*, 1995, **14**, 1079; S.-Y. Siah, P.-H. Leung and K. F. Mok, *J. Chem. Soc., Chem. Commun.*, 1995, 1747.
4 S. Shambayati, W. E. Crowe and S. L. Schreiber, *Angew. Chem., Int. Ed. Engl.*, 1990, **29**, 256; K. V. Gothelf, R. G. Hazell and K. A. Jorgensen, *J. Am. Chem. Soc.*, 1995, **117**, 4435.
5 D. Carmona, C. Cativiela, R. García-Correas, F. J. Lahoz, M. P. Lamata, J. A. López, M. P. López-Ram de Víu, L. A. Oro, E. San José and F. Viguri, *Chem. Commun.*, 1996, 1247 and references therein.
6 J. V. Allen, G. J. Dawson, C. G. Frost, J. M. J. Williams and S. J. Coote, *Tetrahedron*, 1994, **50**, 799.
7 K. Stanley and M. C. Baird, *J. Am. Chem. Soc.*, 1975, **97**, 6598; T. E. Sloan, *Top. Stereochem.*, 1981, **12**, 1.
8 G. M. Sheldrick, SHELXS-86, A program for Crystal Structure Solution, University of Göttingen, 1990; G. M. Sheldrick, SHELXL-93, A program for Crystal Structure Refinement, University of Göttingen, 1993.
9 K. Furuta, S. Shimizu, Y. Miwa and H. Yamamoto, *J. Org. Chem.*, 1989, **54**, 1481.

*Received in Cambridge, UK, 4th August 1997; 7/05605B*

# Asymmetric dihydroxylation with silica-anchored alkaloids

**Carsten Bolm,* Astrid Maischak and Arne Gerlach**

*Institut für Organische Chemie, RWTH Aachen, Professor-Pirlet-Strasse 1, D-52056 Aachen, Germany*

**Diols with excellent enantiomeric excesses are obtained from unfunctionalised alkenes in high yields by osmium-catalysed dihydroxylations using silica-bound pyrimidine and pyrazinopyridazine ligands.**

The Sharpless asymmetric dihydroxylation (AD) is an efficient catalytic method for the enantioselective oxidation of unfunctionalised alkenes.[1] Since its discovery in 1988[2] the catalyst system has been continuously optimised,[3] so that now almost any alkene can be transformed to the corresponding diol with high enantioselectivity. In order to ease the recovery of the ligands after the catalysis, the use of various polymer-supported cinchona alkaloids has been studied.[4–7] Most of the insoluble ligands are easily handled but suffer from disadvantages, such as longer reaction times and lower enantioselectivity. Recently, we[6] and others[7] introduced soluble polymer-supported alkaloids with MeO-PEG tethers which gave catalysts with similar reactivity and enantioselectivity as those reported for the original Sharpless system. Ligand recovery was easily accomplished by addition of ethereal solvents to the reaction mixture followed by filtration of the precipitated alkaloid. In our approach,[6] the MeO-PEG attachment was designed such that negative steric interactions between the polymer backbone and the alkaloid moiety were minimised. We now report on the anchoring of this type of specifically modified cinchona alkaloid on insoluble inorganic carriers based on silica. In contrast to organic polymers, this kind of heterogeneous support offers a variety of possible applications due to its mechanical and thermal stability.

The polysiloxane-anchored bis(9-*O*-dihydroquinidinyl)pyrazinopyridazine **1** and bis(9-*O*-dihydroquinidinyl)pyrimidine **2** were synthesised from the corresponding phenols ($R^1$, $R^2$ = H)[6] and commercial functionalised silica† using standard acylation or nucleophilic substitution reactions.

The catalysed asymmetric dihydroxylations of representative alkenes were performed under standard reaction conditions in $Bu^tOH$–$H_2O$ (1 : 1) using $K_3[Fe(CN)_6]$–$K_2CO_3$ as oxidant, 0.5–1 mol% of $K_2OsO_2(OH)_4$ and 2 mol% of immobilised ligand. Mechanical stirring was applied in order to avoid silica deterioration. The most significant results are summarised in Table 1.

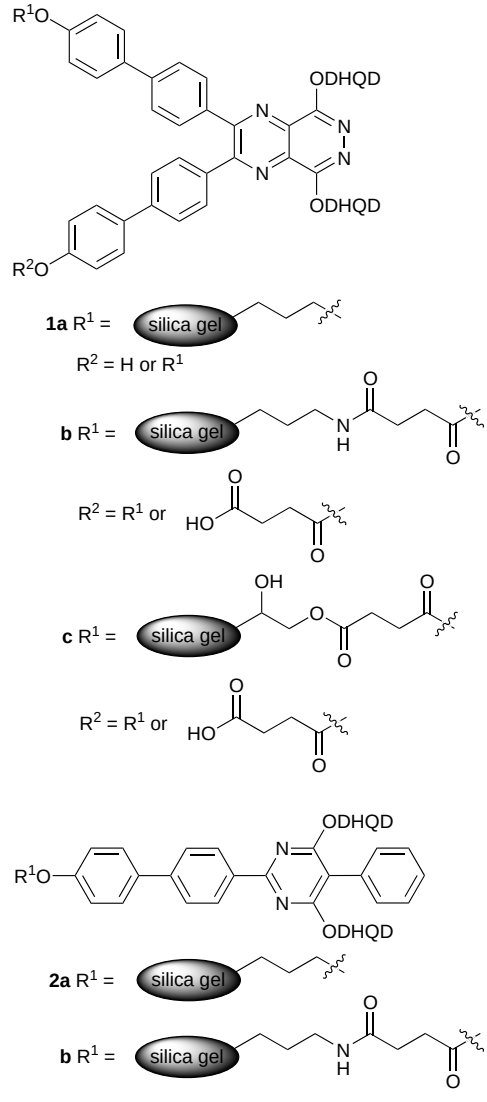
**Table 1** Enantioselectivities in the AD of various alkenes[a]

| Entry | Alkene | Ligand | Yield (%) | Ee (%)[b] | Configuration |
|---|---|---|---|---|---|
| 1 | *trans*-PhCH=CHPh | **1a** | 77 | 99 (99) | (*R*,*R*) |
| 2 | PhCH=$CH_2$ | **1a** | 93 | 98 (99) | (*R*) |
| 3 | PhCH=$CH_2$ | **1b** | 93 | 90 | (*R*) |
| 4 | PhCH=$CH_2$ | **1c** | 92 | 97 | (*R*) |
| 5 | $C_8H_{17}CH=CH_2$ | **2a** | 51 | 84 (89) | (*R*) |
| 6 | $C_8H_{17}CH=CH_2$ | **2b** | 53 | 61 | (*R*) |
| 7 | $Bu^tCH=CH_2$ | **2b** | 62 | 70 (92) | (*R*) |

[a] AD experiments as per typical protocol (see text). [b] Determined either by comparison of the specific rotation with the authentic samples or by HPLC using a chiral stationary phase [refs. 3(*a*), 4(*f*), 6]. The ee values of products which were obtained from catalyses with non-polymer supported DHQD ligands [ref. 3(*b*)] are given in parentheses.

In the AD of styrene and stilbene, exceedingly high enantioselectivities were achieved with heterogeneous silica-anchored ligands **1a** and **1c** having ether and ester linkers, respectively. A slightly lower asymmetric induction was observed when amido linked **1b** was applied (Table 1, entry 3). Presumably, residual amino groups on the silica surface or the amido linker itself have a negative influence, giving diols with reduced enantiomeric excess. Support of this hypothesis was gained in AD experiments performed with alkaloid-free amino functionalized silica gel. The rapid formation of racemic diol revealed the high catalytic activity of the support.

Under homogeneous conditions pyrimidine ligands are most suitable for the enantioselective dihydroxylation of aliphatic, terminal alkenes. Therefore, AD reactions of dec-1-ene were performed with silica-supported pyrimidines **2a** and **2b** (Table 1, entries 5 and 6). Catalyses with both ligands afforded the



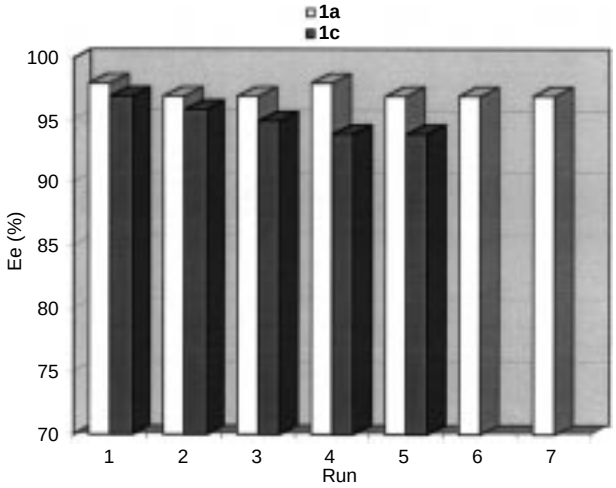



**Fig. 1** Enantioselectivities in consecutive AD reactions of styrene using silica-supported alkaloids **1a** and **1c**

corresponding diols in moderate yield with enantiomeric excesses of 84 and 61%, respectively. The former value compares well to the one obtained with the original homogeneous Sharpless system (89% ee).

In order to examine the stability of the catalyst and the possibility of ligand recovery, **1a** and **1c** were used in consecutive AD reactions of styrene. As shown in Fig. 1, silica-supported alkaloid **1a** was used seven times without significant loss of enantioselectivity. The enantiomeric excess of the diol stayed in the range of 97–98%, and the chemical yields were excellent. In contrast, in AD reactions with silica-attached **1c** the efficiency of the catalysis decreased with each run. Presumably, parts of the alkaloid were lost in each recycling process due to a minor ester hydrolysis under the basic reaction conditions. In order to ensure the presence of sufficient amounts of osmium in the reaction mixture, 0.5–1 mol% of $K_2OsO_2(OH)_4$ was added before each run in the experiments described above. Without this addition, a considerable decrease in activity was observed, indicating metal leaching during catalyst recovery. For example, in consecutive AD reactions of styrene in the presence of **1a** *without* the addition of osmium, the diol yield dropped from 93% in the first run to 50 and 34% yield in the second and third run, respectively. Even under these very unfavourable conditions, and despite the metal loss, the catalysis still benefits from the phenomenon of 'ligand acceleration'[8] and gives the products with high enantiomeric excess (run 1: 98% ee; run 2: 98% ee; run 3: 95% ee).

The results of this investigation can be summarised as follows. (i) The enantioselectivities in these heterogeneous AD reactions are excellent, and diols with up to 99% ee are formed. (ii) The new silica-bound alkaloids can be quantitatively recovered by simple filtration. (iii) Recycled ligands give catalysts which perform several times without loss of activity and enantioselectivity. (iv) Consecutive use of the immobilised ligands in AD reactions is possible but requires the addition of small quantities of osmium after each run. If no metal is added the enantioselectivity remains high but the catalyst activity is reduced.

This research was supported in part by grants from the BMBF and the Fonds der Chemischen Industrie.

## Footnotes and References

* E-mail: carsten.bolm@rwth-aachen.de

† The chloropropyl functionalised silica (2.5% chloride content) was obtained from Aldrich. Propylamino (0.19 mmol $g^{-1}$) and diol functionalised (0.35 mmol $g^{-1}$) polysiloxanes were purchased from Schuller. A double attachment of **1** onto the silica surface *via* the two phenolic hydroxy groups cannot be excluded.

1 H. C. Kolb, S. VanNieuwenhze and K. B. Sharpless, *Chem. Rev.*, 1994, **94**, 2483.
2 E. N. Jacobsen, I. Markó, W. S. Mungall, G. Schroeder and K. B. Sharpless, *J. Am. Chem. Soc.*, 1988, **110**, 1968.
3 (*a*) H. Becker and K. B. Sharpless, *Angew. Chem.*, 1996, **108**, 447; *Angew. Chem., Int. Ed. Engl.*, 1996, **35**, 448; (*b*) H. Becker, S. B. King, M. Taniguchi, K. P. M. Vanhessche and K. B. Sharpless, *J. Org. Chem.*, 1995, **60**, 3940; (*c*) K. B. Sharpless, W. Amberg, Y. L. Bennani, G. A. Crispino, J. Hartung, K.-S. Jeong, H.-L. Kwong, K. Morikawa, Z.-M. Wang, D. Xu and X.-L. Zhang, *J. Org. Chem.*, 1992, **57**, 2768; (*d*) E. J. Corey, A. Guzman-Perez and M. C. Noe, *J. Am. Chem. Soc.*, 1995, **117**, 10805.
4 (*a*) B. M. Kim and K. B. Sharpless, *Tetrahedron Lett.*, 1990, **31**, 3003; (*b*) D. Pini, A. Petri, A. Nardi, C. Rosini and P. Salvadori, *Tetrahedron Lett.*, 1991, **32**, 5175; (*c*) B. B. Lohray, E. Nandanan and V. Bhushan, *Tetrahedron Lett.*, 1994, **35**, 6559; (*d*) C. E. Song, E. J. Roth, S.-y. Lee and I. O. Kim, *Tetrahedron: Asymmetry*, 1995, **6**, 2687; (*e*) D. Pini, A. Petri and P. Salvadori, *Tetrahedron*, 1994, **50**, 11 321; (*f*) A. Petri, D. Pini, S. Rapaccini and P. Salvadori, *Chirality*, 1995, **7**, 580; (*g*) C. E. Song, J. W. Yang, H. J. Ha and S.-y. Lee, *Tetrahedron: Asymmetry*, 1996, **7**, 645; (*h*) P. Salvadori, D. Pini and A.Petri, *J. Am. Chem. Soc.*, 1997, **119**, 6929 and references cited therein.
5 For examples of other silica-supported alkaloids see: B. B. Lohray, E. Nandanan and V. Bhushan, *Tetrahedron: Asymmetry*, 1996, **7**, 2805; C. E. Song, J. W. Yang and H.-J. Ha, *Tetrahedron: Asymmetry*, 1997, **8**, 841.
6 C. Bolm and A. Gerlach, *Angew. Chem.*, 1997, **109**, 773; *Angew. Chem., Int. Ed. Engl.*, 1997, **36**, 773.
7 H. Han and K. D. Janda, *J. Am. Chem. Soc.*, 1996, **118**, 7632; H. Han and K. D. Janda, *Tetrahedron Lett.*, 1997, **38**, 1527; H. Han and K. D. Janda, *Angew. Chem.*, 1997, **109**, 1835; *Angew. Chem., Int. Ed. Engl.*, 1997, **36**, 1731.
8 D. J. Berrisford, C. Bolm and K. B. Sharpless, *Angew. Chem.*, 1995, **107**, 1159; *Angew. Chem., Int. Ed. Engl.*, 1995, **34**, 1050.

*Received in Cambridge, UK, 10th September 1997; 7/06605H*

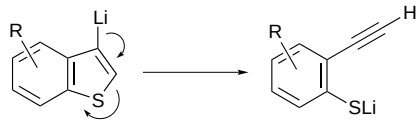
# Synthesis of polyfunctionalized thiophenes and enediynes *via* ring-opening reactions of 3-lithiated thieno[2,3-*b*](and [3,2-*b*])thiophenes, 3,4-dilithiated thieno[2,3-*b*]thiophenes and 3,6-dilithiated thieno[3,2-*b*]thiophenes

**Lance S. Fuller,[a] Brian Iddon MP*[b]† and Kevin A. Smith[b]**

[a] *Synthetic Chemicals Ltd., Four Ashes, Nr. Wolverhampton, UK WV10 7BP*
[b] *Chemical Sciences Division, Science Research Institute, University of Salford, Salford, UK M5 4WT*

**Solutions of the title lithiated thienothiophenes were synthesized from 2,5-disubstituted 3,4-dibromothieno[2,3-*b*]thiophenes or 3,6-dibromothieno[3,2-*b*]thiophenes *via* Br → Li exchange with 1.0 or 2.0 equiv. of BuLi (THF, −78 °C), respectively, and gave either polyfunctionalized thiophenes or polyfunctionalized enediynes (by a novel tandem ring-opening process in these cases) on being allowed to warm up to ambient temperature.**

Previously we have reported that ethereal ($Et_2O$ or THF) solutions of benzo[*b*]thiophen-3-yllithium[1–3] and its derivatives[2–4] (prepared from the corresponding 3-bromobenzo[*b*]-thiophene *via* Br → Li exchange with BuLi at −78 °C) undergo a ring-opening process, **1** → **2** (Scheme 1), as the solutions




**1** **2**

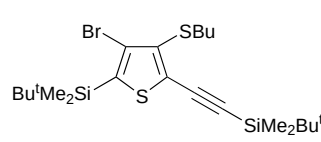
**Scheme 1**

are warmed up to give the lithium salt of an *o*-mercaptophenylacetylene, which can react further, *e.g.* by *S*-butylation with the bromobutane produced in the initial Br → Li exchange reaction or through metallation at the terminal alkyne position. Selenophen-3-yllithium[5–9] and 3-thienyllithium[2,6–12] behave similarly and yield enynes. We now report novel tandem ring-opening processes of 3,4-dilithiated thieno[2,3-*b*]thiophenes and 3,6-dilithiated thieno[3,2-*b*]thiophenes which afford novel enediynes. This work was prompted by intense current interest in enediynes as precursors to more complex molecular architectures.[13]

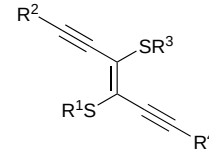
First we treated 2,3,5,6-tetrabromothieno[3,2-*b*]thiophene[14,15] successively with 2.0 equiv. of BuLi (THF, ambient temperature) and $Bu^tMe_2SiCl$, then the resulting solution of 3,6-dibromo-2,5-bis(*tert*-butyldimethylsilyl)thieno[3,2-*b*]thiophene[14] was cooled to −78 °C and a further 1.0 equiv. of BuLi was added. The resulting mixture was allowed to warm up slowly to ambient temperature, then it was quenched by addition of 20% aq. $NH_4Cl$. Following a standard work-up procedure (extraction of the crude product with $Et_2O$ and flash chromatography on silica with light petroleum as eluent) we obtained 3-bromo-2-*tert*-butyldimethylsilyl-5-*tert*-butyldimethylsilylethynyl-4-butylsulfanylthiophene **3** (70% yield) as a yellow oil.‡ Other 2,5-disubstituted 3,6-dilithiothieno[3,2-*b*]-thiophenes[14] can be prepared and converted similarly into polyfunctionalized thiophenes analogous to compound **3**.

When thiophene **3** was treated successively with 1.0 equiv. of BuLi (THF, 0 °C) and MeI, it gave the enediyne **4** (89% yield) as a yellow oil, thus demonstrating that each thiolate anion, as it is generated in this two-stage process, can be captured by a different alkylating reagent.

Both ring-opening processes can be carried out in tandem. Thus, we converted 2,3,5,6-tetrabromothieno[3,2-*b*]thiophene

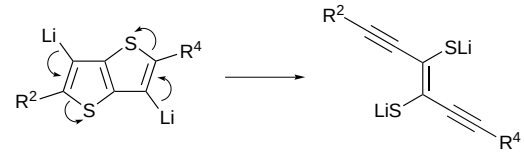



**3**




**4** $R^1$ = Me, $R^2$ = $R^4$ = $SiMe_2Bu^t$, $R^3$ = Bu
**5** $R^1$ = $R^3$ = Bu, $R^2$ = $R^4$ = $SiMe_2Bu^t$
**6** $R^1$ = $R^3$ = Bu, $R^2$ = $R^4$ = H

into 3,6-dibromo-2,5-bis(*tert*-butyldimethylsilyl)thieno[3,2-*b*]-thiophene[14] *in situ*, as described before, then added a further 2.0 equiv. of BuLi (THF, 0 °C) prior to allowing the reaction mixture to warm up slowly to ambient temperature which, after work-up in the standard way, gave the enediyne **5** (70% yield) as a yellow oil. The extremely unstable enediyne **6** (73.5% yield) was prepared by removal of the $Bu^tMe_2Si$ groups from compound **5** *via* treatment with $Bu_4NF$ in THF. Starting from 2,3,5,6-tetrabromothieno[3,2-*b*]thiophene we have prepared a number of other enediynes using this strategy. Essentially the thienothiophene ring is a template to which a variety of functional groups can be attached prior to the tandem ring-opening process **7** → **8** (Scheme 2), *e.g. via* Br → Li exchange

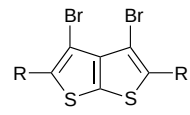



**7** **8**

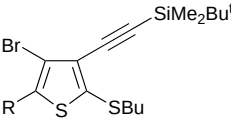
**Scheme 2**

techniques, by $Pd^0$-catalysed coupling reactions or through further modification of initial products such as by Wittig reactions of aldehydes.

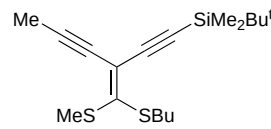
When 2,3,4,5-tetrabromothieno[2,3-*b*]thiophene[16] was treated successively with 3.4 equiv. of BuLi (THF, −65 °C) and 4.8 equiv. of $Me_3SiCl$, it gave 3,4-dibromo-2,5-bis(trimethylsilyl)thieno[2,3-*b*]thiophene **9** (51% yield) as a solid which decomposed when heated to 125 °C in a capillary tube. A similar attempt (2.6 equiv. BuLi, THF, but at 0 °C instead of




**9** R = $SiMe_3$
**10** R = $SiMe_2Bu^t$




**11** R = $SiMe_2Bu^t$
**12** R = H




**13**

−65 °C; 2.4 equiv. of $Bu^tMe_2SiCl$) to synthesize 3,6-dibromo-2,5-bis(*tert*-butyldimethylsilyl)thieno[2,3-*b*]thiophene **10** gave this compound (mp 112–114 °C) in only 23% yield together with 3-bromo-2-*tert*-butyldimethylsilyl-4-*tert*-butyldimethylsilylethynyl-5-butylsulfanylthiophene **11** (33%), a pale yellow solid with mp 35–37 °C, and 4-bromo-3-*tert*-butyldimethylsilylethynyl-2-butylsulfanylthiophene **12** (18%) as a pale yellow oil (formed by loss of the 2-$Bu^tMe_2Si$ group from compound **11**).

When treated successively with 2.0 equiv. of BuLi (THF, 0 °C) and an excess of MeI, the bromothiophene **11** was converted into 2-*tert*-butyldimethylsilylethynyl-1-butylsulfanyl-1-methylsulfanylpent-1-en-3-yne **13** (87% yield) as a yellow oil. In this reaction not only does the MeI capture the generated thiolate anion but it also displaces a $Bu^tMe_2Si$ group.

We thank the EPSRC (CASE award to K. A. S.) and Synthetic Chemicals Ltd. for financial support, Mrs Ruth Howard for recording mass spectra and Dr M. A. Stuckey for recording the 300 MHz $^1$H NMR spectra.

## Footnotes and References

* E-mail: iddonb@parliament.uk
† Present address: House of Commons, Westminster, London, UK SW1A 0AA.

‡ All new compounds (pure by TLC analysis) were characterised by recording their IR, $^1$H NMR and low- and high-resolution mass spectra. In most cases they were unstable in air at ambient temperature and we were unable to obtain satisfactory elemental microanalytical results (for C, H and N).

1 R. P. Dickinson and B. Iddon, *Tetrahedron Lett.*, 1970, 975; *Int. J. Sulfur Chem. C*, 1971, **6**, 59; *J. Chem. Soc. C*, 1971, 3447.
2 B. Iddon, *Heterocycles*, 1983, **20**, 1127.
3 R. M. Scrowston, *Adv. Heterocycl. Chem.*, 1981, **29**, 171.
4 R. P. Dickinson and B. Iddon, *J. Chem. Soc. C*, 1970, 2592; 1971, 182; 1971, 2504.
5 S. Gronowitz and T. Frejd, *Acta Chem. Scand.*, 1969, **23**, 2540.
6 S. Gronowitz, *Adv. Heterocycl. Chem.*, 1963, **1**, 1 (see p. 75).
7 S. Gronowitz and T. Frejd, *Chem. Heterocycl. Compds. (Engl. Transl.)*, 1978, **14**, 353.
8 S. Gronowitz, *Chem. Heterocycl. Compds. (Engl. Transl.)*, 1994, **30**, 1252.
9 T. Frejd, *Chem. Heterocycl. Compds.*, 1992, **44**, 257; *Thiophene and Its Derivatives*, ed. S. Gronowitz, Wiley-Interscience, New York, 1992, part 5, ch. II, p. 257 (in particular see p. 721).
10 P. Moses and S. Gronowitz, *Arkiv. Kemi*, 1962, **18**, 119.
11 S. Gronowitz, *Phosphorus, Sulfur, Silicon Relat. Elem.*, 1993, **74**, 113.
12 S. Gronowitz, A.-B. Hörnfeldt, E. Lukevics and O. Pudova, *Synthesis*, 1994, 40.
13 *e.g.* see *Modern Acetylene Chemistry*, ed. P. J. Stang and F. Diederich, VCH, Weinheim, 1995.
14 L. S. Fuller, B. Iddon and K. A. Smith, *J. Chem. Soc., Perkin Trans. 1*, 1997, in the press.
15 K. Yui, H. Ishida, Y. Aso, T. Otsubo, F. Ogura, A. Kawamoto and J. Tanaka, *Bull. Chem. Soc. Jpn.*, 1989, **62**, 1547.
16 T. Otsubo, Y. Kono, N. Hozo, H. Miyamoto, Y. Aso, F. Ogura, T. Tanaka and M. Sawada, *Bull. Chem. Soc. Jpn.*, 1993, **66**, 2033.

*Received in Cambridge, UK, 30th Septembert 1997; 7/07033K*

# Lewis acid mediated [3 + 2] cycloaddition of allylgermane: stereoselective synthesis of germyl substituted tetrahydrofurans

**Takahiko Akiyama* and Megumi Suzuki**

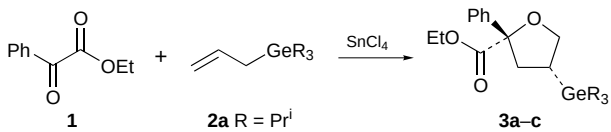
*Department of Chemistry, Faculty of Science, Gakushuin University, 1-5-1, Mejiro, Toshima, Tokyo 171, Japan*

**Tin(IV) chloride mediated [3 + 2] cycloaddition of allylgermanes to α-dicarbonyl compounds proceeds highly stereoselectively to give tetrahydrofurans in good yields.**

Cycloadditions are one of the most useful methods for the stereoselective construction of ring compounds. Numerous cycloadditions have been developed and have been effectively employed in the total synthesis of natural products.[1] Recently Lewis acid promoted [3 + 2] and [2 + 2] cycloadditions of allylsilane with α,β-unsaturated carbonyl compounds and ketones have been extensively studied.[2] For example, allylsilanes bearing bulky silyl substituents work as 1,3-dipole equivalents and both five-membered carbocycles[3] and heterocycles[4,5] have been constructed stereoselectively. Furthermore, allylsilanes have been found to act as 1,2-dipole equivalents depending on the reaction conditions to form four-membered carbocycles[6] and heterocycles stereoselectively.[7] We have recently reported that the Lewis acid promoted [3 + 2] cycloaddition of allylsilanes bearing sterically demanding silyl substituents to α-keto esters proceeded smoothly to afford tetrahydrofurans stereoselectively.[4] Furthermore the Lewis acid mediated cycloaddition of allylstannanes has been studied.[8] In striking contrast, the Lewis acid promoted cycloaddition of allylgermane has not been reported.[9] In connection with our interest in cycloaddition in allylsilane chemistry, we studied the cycloaddition of allylgermane. Reported here is the first [3 + 2] cycloaddition of allylgermane.

First, allyltriisopropylgermane **2a** was treated with an α-keto ester in the presence of a Lewis acid. After screening Lewis acids, we found that the use of tin(IV) chloride in toluene led to the formation of a cycloadduct **3a** as a single stereoisomer in 48% yield (Scheme 1).† Other conventional Lewis acids did not give the cycloadduct. Use of an allylgermane bearing a bulky germyl substituent is mandatory for the formation of the cycloadduct in good yield. Allylgermanes with less sterically demanding germyl substituents such as **2b** and **2c** decreased the yields of the tetrahydrofurans **3b** and **3c** to 17 and 7% yields respectively. In these cases, the normal allylation product was obtained predominantly.‡

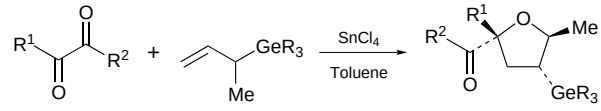
Furthermore, introduction of a methyl group at the α-germyl position improved the yield of the tetrahydrofurans significantly and the results are shown in Table 1. Treatment of **1** with allylgermane **4** and tin(IV) chloride in toluene at −78 °C for 40 min gave rise to the cycloadduct in 53% yield (entry 1). Ethyl pyruvate and an α-diketone also afforded the cycloadducts in good yields (entries 2 and 3). The reason why use of **4** inceased




**1** **2a** R = Pr$^i$, **b** R = Ph, **c** R = Et **3a–c**

**Scheme 1**

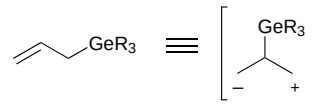
**Table 1** Results of the cycloaddition




**4** **5**

| Entry | R$^1$ | R$^2$ | Conditions | Product | Yield (%) |
|---|---|---|---|---|---|
| 1 | Ph | OEt | −78 °C, 40 min | **5a** | 53 |
| 2 | Me | OEt | −40 °C, 11 min | **5b** | 62 |
| 3 | Me | Me | −40 °C, 12 min | **5c** | 72 |

the yield of the adduct is accounted for as follows: the α-germyl methyl group stabilizes the β-germyl carbocation thus facilitating the germyl migration to produce cycloadducts in better yields than with **2b**.




The present cycloadditions exhibited excellent levels of diastereoselection, producing the tetrahydrofurans with diastereoisomeric excesses (des) reaching > 96% as determined by $^1$H and $^{13}$C NMR spectroscopy. The relative stereochemistry of **3a** and **5a** was unambiguously determined by a multiple NOE study. The stereochemistries of other tetrahydrofurans were estimated by analogy.

In conclusion, we have developed a novel method for the stereoselective formation of germyl substituted tetrahydrofurans by a tin(IV) chloride promoted [3 + 2] cycloaddition of allylgermane to α-keto esters. The utility of allylgermanes bearing sterically demanding germyl substituents as 1,3-dipole equivalents has been demonstrated for the first time.

## Footnotes and References

* E-mail: takahiko.akiyama@gakushuin.ac.jp

† Compound **3a** (R = Pr$^i$) was prepared as follows: in a two-necked round bottomed flask, a mixture of **1** (41.5 mg, 0.23 mmol) and **2a** (67.2 mg, 0.28 mmol) in dry toluene (3.2 ml) was stirred at −20 °C. To this mixture tin(IV) chloride (30 μl, 0.26 mmol) was added dropwise and the stirring was continued at the same temperature for 5 min. The reaction was quenched by the addition of 1 M aqueous HCl. The aqueous layer was extracted with ethyl acetate and the combined organic layers were washed with brine, dried over anhydrous $Na_2SO_4$ and concentrated to dryness. Purification of the crude mixture by preparative TLC ($SiO_2$, hexane–ethyl acetate, 7 : 1, v/v) gave **3a** (47.2 mg) in 48% yield.

*Selected data* for compound **3a**: $\delta_H$($CDCl_3$, *J*/Hz) 1.12 (d, *J* 7.3, 18 H), 1.21 (t, *J* 7.1, 3 H), 1.38 (septet, *J* 7.3, 3 H), 1.66 (dddd, *J* 7.7, 8.2, 12.3, 12.8, 1 H), 2.60 (dd, *J* 7.7, 12.8, 1 H), 2.67 (dd, *J* 12.8, 12.8, 1 H), 4.04 (dd, *J* 8.2, 12.3, 1 H), 4.17 (q, *J* 7.1, 2 H), 4.35 (dd, *J* 8.2, 8.2, 1 H) and 7.24–7.57 (m, 5 H); $\delta_C$($CDCl_3$) 14.06 ($CH_3$), 14.20 (CH × 3), 20.24 ($CH_3$ × 6), 23.39

(CH), 41.51 ($CH_2$), 61.43 ($CH_2$), 72.64 ($CH_2$), 86.41 (C), 125.56 (CH × 2), 127.44 (CH), 128.03 (CH × 2) and 141.80 (C).

‡ Compounds **2a–c** afforded the corresponding homoallyl alcohols in 36, 74 and 85% yield, respectively.


1 W. Carruthers, *Cycloaddition Reactions in Organic Synthesis*, Pergamon, Oxford, 1990; D. M. T. Chan, in *Transition Metal Mediated Cycloadditions*, ed. B. M. Trost and I. Fleming, Pergamon, Oxford, 1991, vol. 5, p. 271.

2 H.-J. Knölker, *J. Prakt. Chem.*, 1997, **339**, 304; J. S. Panek, in *Silicon Stabilization*, ed. B. M. Trost and I. Fleming, Pergamon, Oxford, 1991, vol. 1, p. 579; C. E. Masse and J. S. Panek, *Chem. Rev.*, 1995, **95**, 1293.

3 H.-J. Knölker, N. Foitzik, H. Goesmann, R. Graf, P. G. Jones and G. Wanzl, *Chem. Eur. J.*, 1997, **3**, 538; H.-J. Knölker and R. Graf, *Tetrahedron Lett.*, 1993, **34**, 4765; H.-J. Knölker and G. Wanzl, *Synlett*, 1995, 378; R. L. Danheiser, B. R. Dixon and R. W. Gleason, *J. Org. Chem.*, 1992, **57**, 6094; G. P. Brengel, C. Rithner and A. I. Meyers, *J. Org. Chem.*, 1994, **59**, 5144; G. P. Brengel and A. I. Meyers, *J. Org. Chem.*, 1996, **61**, 3230.

4 T. Akiyama, T. Yasusa, K. Ishikawa and S. Ozaki, *Tetrahedron Lett.*, 1994, **35**, 8401; T. Akiyama, K. Ishikawa and S. Ozaki, *Chem. Lett.*, 1994, 627.

5 J. S. Panek and M. Yang, *J. Am. Chem. Soc.*, 1991, **113**, 9868; J. S. Panek and R. T. Beresis, *J. Am. Chem. Soc.*, 1993, **115**, 7898.

6 H.-J. Knölker, G. Baum and R. Graf, *Angew. Chem., Int. Ed. Engl.*, 1994, **33**, 1612.

7 T. Uyehara, M. Yuuki, H. Masaki, M. Matsumoto, M. Ueno and T. Sato, *Chem. Lett.*, 1995, 789; T. Akiyama and M. Yamanaka, *Synlett*, 1996, 1095; T. Akiyama and M. Kirino, *Chem. Lett.*, 1995, 723.

8 J. W. Herndon, *J. Am. Chem. Soc.*, 1987, **109**, 3165; J. W. Herndon, C. Wu, J. J. Harp and K. A. Kreutzer, *Synlett*, 1991, 1.

9 For allylation with allylgermane, see: T. Akiyama and J. Iwai, *Tetrahedron Lett.*, 1997, **38**, 853.


*Received in Cambridge, UK, 5th September 1997; 7/06497G*

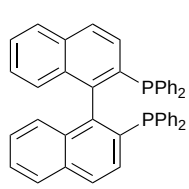
# Convenient and direct preparation of tertiary phosphines *via* nickel-catalysed cross-coupling

**David J. Ager, Michael B. East, Amihai Eisenstadt and Scott A. Laneman***

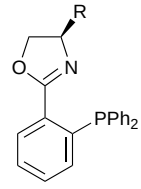
*NSC Technologies, A unit of Monsanto Company, 601 East Kensington Road, Mt. Prospect, Illinois 60056, USA*

**Nickel-catalysed cross-coupling of aryl sulfonates and aryl halides with chlorodiphenylphosphine and a reductant directly affords tertiary phosphines, which have application in a wide variety of asymmetric catalysis.**

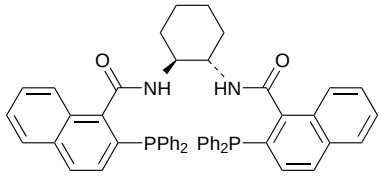
Tertiary phosphines are extremely useful ancillary ligands in homogeneous catalysis, especially as chiral ligands in asymmetric homogeneous catalysis as exemplified by **1**–**3**.[1–8] The preparations of tertiary phosphines can be divided into four major categories: Friedel–Crafts reactions,[9,10] the reaction of halophosphines with organometallic reagents[11,12] and the reaction of phosphides[13–15] or diarylphosphine compounds[16–18] in the presence of a transition metal catalyst with aryl halides or sulfonate esters. All of the methods have drawbacks ranging from limitations due to incompatabilities with other functional groups, the necessity for a separate step to reduce the phosphine oxide, to the use of pyrophoric reagents. We report here a convenient and direct route to tertiary phosphines by transition metal cross-coupling reaction that eliminates these problems.




**1**



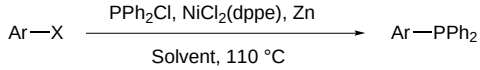

**2**




**3**

We have determined that tertiary phosphines can be prepared from aryl trifluoromethanesulfonates by nickel-catalysed cross-coupling with $Ph_2PCl$ in the presence of zinc in DMF at 110 °C (Scheme 1). $Ph_2PCl$ has the advantage that it is not pyrophoric, inexpensive and readily available for large scale usage. For example, 2-diphenylphosphinonaphthalene **5** is prepared from **4** *via* nickel-catalysed cross-coupling with $Ph_2PCl$ in 89% yield.† The zinc plays a dual role in the reaction. It reduces $Ni^{II}$ to $Ni^0$ as well as providing $Ph_2PZnCl$ for transmetallation.

This methodology appears to be quite general for the preparation of other tertiary phosphines (Table 1). The nickel-catalysed cross-coupling procedure successfully produces phosphines in good yields directly from aromatic sulfonates, aromatic halogens, benzylic bromides and vinyl bromides and iodides. Also, the cross-coupling can occur with aromatic



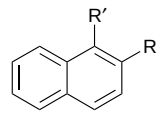

**Scheme 1**

**Table 1** Examples of nickel-catalysed cross couplings

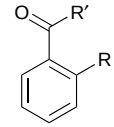
| Substrate | Product | Yield (%) |
|---|---|---|
| **4** | **5** | 89 |
| **6** | **5** | 78 |
| **7** | **8** | 95 |
| **9** | **10** | 84 |
| **11** | **10** | 46 |
| **12** | **13** | 67 |
| **14** | **15** | 46 |
| **16** | **17** | 90[a] |
| **18** | **19** | 80 |
| **20** | **21** | 45 |
| **22** | **1** | 52 |

[a] Isolated as the phosphine oxide by air oxidation during work up.

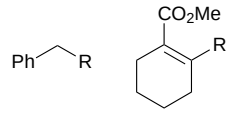
halides and sulfonates that contain *ortho*-substitution. Benzylic halides are extremely active substrates and reactions are completed in minutes. Surprisingly, the coupling reaction tolerates the presence of amides while carboxylic acid inhibit reaction.




**4** R = OTf, R′ = H
**5** R = $PPh_2$, R′ = H
**6** R = Br, R′ = H
**7** R = OTf, R′ = $CO_2Me$
**8** R = $PPh_2$, R′ = $CO_2Me$



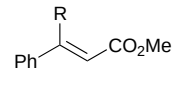

**9** R = OTf, R′ = OMe
**10** R = $PPh_2$, R′ = OMe
**11** R = Br, R′ = OMe
**12** R = OTf, R′ = NHBn
**13** R = $PPh_2$, R′ = NHBn
**14** R = Br, R′ = (*S*)-NHCHMePh
**15** R = $PPh_2$, R′ = (*S*)-NHCHMePh



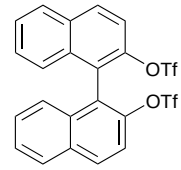

**16** R = Br
**17** R = $PPh_2$




**18** R = OTf
**19** R = $PPh_2$




**20** R = Br
**21** R = $PPh_2$




**22**
(Tf = $CF_3SO_2$)

Trifluoromethanesulfonate substrates give higher yields compared to the corresponding bromide substrate due to hydrodehalogenation side reaction. Double cross-coupling of the *S*-isomer of the bis(trifluoromethanesulfonate) **22** can be achieved to form *S*-BINAP **1** without any racemisation of the axial chirality.‡

This methodology is a convenient procedure to prepare a wide variety of tertiary phosphines. The use of a cheap phosphorus reagent coupled with the tolerance of the reaction to a wide variety of functional groups as well as direct access to phosphorus(III) products makes this a useful, versatile approach to phosphorus ligands.

## Footnotes and References

* E-mail: salane@monsanto.com

† *Typical reaction procedure*: to a solution of **4** (10.6 g, 40 mmol), $NiCl_2$(dppe) [dppe = ethylenebis(diphenylphosphine)] (0.315 g, 0.60 mmol) and $Ph_2PCl$ (8.85 g, 40 mmol) in anhydrous DMF (25 ml) was added Zn (4.10 g, 63 mmol) portionwise at 5–10 °C. The mixture was heated to 100–110 °C and monitored by GC. The reaction mixture was cooled to 80 °C, filtered and rinsed with a minimal amount of DMF. The combined filtrate was cooled to 5 °C and the product crystallised overnight. The solids were filtered, rinsed with MeOH and dried at room temp. under vacuum to give 11.21 g (89%) of **5** as an off-white solid. Satisfactory $^1H$ and $^{31}P$ NMR and mass spectral data were obtained on all the products.

‡ Optical purities of substrates and products were determined by optical rotation.


1 D. J. Ager and M. B. East, *Asymmetric Synthetic Methodology*, CRC Press, Boca Raton, FL, 1995.
2 P. von Matt and A. Pfaltz, *Angew. Chem., Int. Ed. Engl.*, 1993, **32**, 566.
3 P. von Matt, O. Loiseleur, G. Koch, A. Pfaltz, C. Lefeber, T. Feucht and G. Helmchen, *Tetrahedron: Asymmetry*, 1994, **5**, 573.
4 B. M. Trost and R. C. Bunt, *Angew. Chem., Int. Ed. Engl.*, 1996, **35**, 99.
5 S. Akutagawa, *Appl. Catal. A*, 1995, **128**, 171.
6 R. Noyori, *Science*, 1990, **248**, 1194.
7 R. Noyori and H. Takaya, *Acc. Chem. Res.*, 1990, **23**, 345.
8 H. Takaya, T. Ohta and R. Noyori, in *Asymmetric Hydrogenation*, ed. I. Ojima, New York, NY, 1993.
9 W. Ude, S. Besecke, A. Riemann and G. Schroeder, *Ger. Offen.*, 1986, DE 3425282 A1.
10 I.-Y. Wan, J. E. McGrath and T. Kashiwagi, *ACS Symp. Ser.*, 1995, **599**, 29.
11 E. P. Kyba, M. C. Kerby and S. P. Rines, *Organometallics*, 1986, **5**, 1189.
12 F. Langer, K. Puntener, R. Sturmer and P. Knochel, *Tetrahedron: Asymmetry*, 1997, **8**, 715.
13 S. J. Coote, G.J. Dawson, C. G. Frost and J. M. J. Williams, *Synlett*, 1993, 509.
14 M. D. Fryzuk and B. Bosnich, *J. Am. Chem. Soc.*, 1977, **99**, 6262.
15 M. D. Fryzuk and B. Bosnich, *J. Am. Chem. Soc.*, 1978, **100**, 5491.
16 D. Cai, J. F. Payack, D. R. Bender, D. L. Hughes, T. R. Verhoeven and P. J. Reider, *J. Org. Chem.*, 1994, **59**, 7180.
17 S. E. Tunney and J. K. Stille, *J. Org. Chem.*, 1987, **52**, 748.
18 S. R. Gilbertson and G. W. Starkey, *J. Org. Chem.*, 1996, **61**, 2922.


*Received in Corvallis, OR, USA, 16th July 1997; 7/05106I*

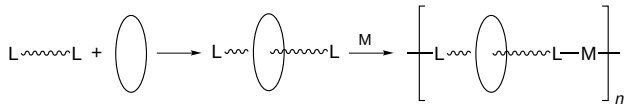
# Helical polyrotaxane: cucurbituril 'beads' threaded onto a helical one-dimensional coordination polymer

**Dongmok Whang, Jungseok Heo, Chang-Ahn Kim and Kimoon Kim***

*Department of Chemistry and Center for Biofunctional Molecules, Pohang University of Science and Technology (POSTECH) San 31 Hyojadong, Pohang 790-784, South Korea*

**Formation of a pseudorotaxane by threading a cucurbituril 'bead' with a *N*,*N*′-bis(3-pyridylmethyl)-1,4-diaminopentane 'string' followed by reaction of the pseudorotaxane with $AgNO_3$ yields a polyrotaxane, the X-ray crystal structure of which reveals the 'beads' threaded onto a helical one-dimensional coordination polymer.**

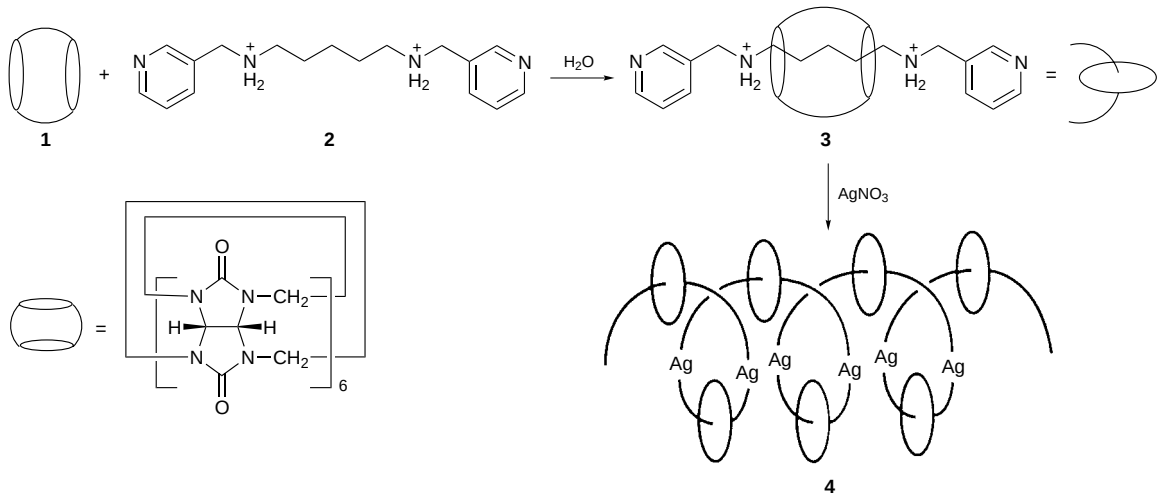
Polyrotaxanes[1] in which a number of cyclic molecular 'beads' are threaded onto a linear 'string' have received considerable attention in recent years due not only to their structures and properties but also to their potential applications as new materials.[1c] We have recently reported[2] a simple one-step approach to construct 1D and 2D polyrotaxane coordination polymers in the solid state. It involves formation of a pseudorotaxane first by threading a molecular 'bead' with a 'string' which has suitable functional groups at both ends and then formation of a polyrotaxane coordination polymer by allowing the end functional groups of the pseudorotaxane to coordinate to metal centers (Scheme 1). In this approach a




**Scheme 1**

judicious choice of metal ion is important to achieve the desired solid state structure. Under the same or similar conditions, for instance, $Mn^{2+}$, $Cu^{2+}$ and $Ag^{+}$ result in totally different structures; they are a simple rotaxane, a 1D polyrotaxane and a 2D polyrotaxane, respectively.[2] Counter-anions also play an important role in determining the solid state structure: for example, silver nitrate leads to a 2D polyrotaxane whereas silver tosylate yields a 1D polyrotaxane.[2b] A unique and interesting twist in this approach to construction of polyrotaxanes results from changing the 'string' from *N*,*N*′-bis(4-pyridylmethyl)-1,4-diaminobutane, used previously in this procedure,[2] to *N*,*N*′-bis(3-pyridylmethyl)-1,5-diaminopentane. Herein we report the first example of helical polyrotaxanes in which cyclic beads are threaded on helical one-dimensional coordination polymers.

The formation of the pseudorotaxane **3**, by threading cucurbituril **1**[3] with *N*,*N*′-bis(3-pyridylmethyl)-1,5-diaminopentane dihydronitrate **2**, followed by the reaction of **3** with $AgNO_3$ yielded **4** (Scheme 2).† The X-ray crystal structure‡ of **4** reveals a 1D polyrotaxane in which cucurbituril 'beads' are threaded on a 1D coordination polymer with a formula of $–[Ag–pyCH_2NH_2(CH_2)_5NH_2CH_2py–]_n^{3n+}$. The asymmetric unit consists of a Ag ion, a pseudorotaxane **3**, one of the pyridine units of which is coordinated to the silver ion, and three nitrate ions to balance the charge (Fig. 1). Most interestingly, the coordination polymer has a helical structure extended along the *b* axis with a pitch of 17.9 Å which is the same as the *b* axis length (Fig. 2). There are equal amounts of right- and left-handed helices in the crystal (it is a racemic mixture). In each helix, two 'supermolecules' of **3** and two silver ions constitute one turn. Each silver ion is coordinated by two 'supermolecule' **3** in a linear fashion: Ag–N(25) 2.133(8), Ag–N(28) 2.138(7) Å, N(25)–Ag–N(28) 177.9(3)°. A cucurbituril 'bead' is held tightly at the middle of each repeating unit by strong hydrogen bonds between the protonated amine nitrogen atoms of the 'string' **2** and the oxygen atoms of cucurbituril: N(26)···O(1) 2.914(10) Å, N(26)···O(2) 3.082(10) Å, N(26)···O(6) 2.893(10) Å, N(27)···O(8) 2.793(9) Å, N(27)···O(9) 2.754(9) Å, N(27)···O(10) 3.089(9) Å. It is interesting to note that N(26) is displaced from the six-oxygen plane of the portal by only 0.037(7) Å, but from the other amine nitrogen N(27) by 0.721(8) Å. Moreover, the 3-pyridyl unit attached to N(26) make a dihedral angle of 61° with the six-oxygen plane whereas that connected to N(27) is nearly parallel to the portal plane




**Scheme 2**

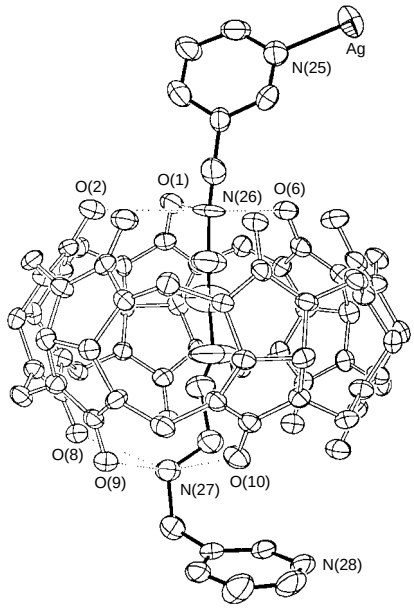



**Fig. 1** Asymmetric unit of the crystal structure of **4**. Counter-ions ($NO_3^-$) and water molecules in the lattice are omitted for clarity.

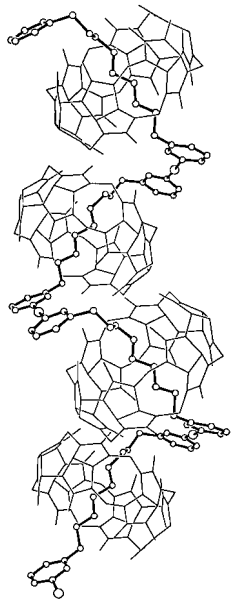


**Fig. 2** Structure of **4** showing cucurbituril 'beads' threaded onto a helical 1D coordination polymer

(angle 9°). The parallel conformation of the 3-pyridyl unit makes the polymer chain change its direction sharply, which eventually leads to a helical structure (Fig. 3).

In conclusion, we present here an unprecedented helical 1D polyrotaxane in which cyclic 'beads' are threaded onto a helical

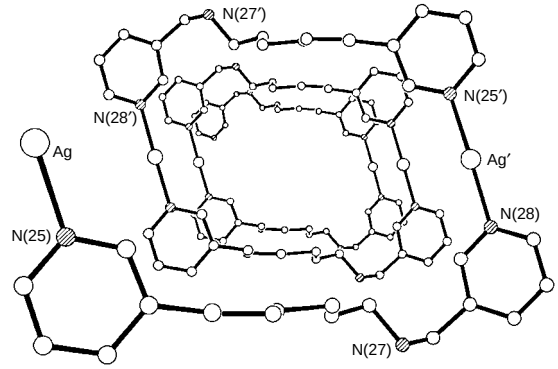



**Fig. 3** The helical 1D coordination polymer threading cucurbituril 'beads' (omitted) in **4**. The pitch of the helix is 17.9 Å. Bond distances (Å) and angle (°) around the silver ion: Ag–N(25) 2.133(8), Ag–N(28) 2.138(7), N(25)–Ag–N(28) 177.9(3).

coordination polymer. It still remains to be determined how one enantiomer, either right- or left-handed polyrotaxane helices can be enantioselectively constructed. Such chiral helical polyrotaxanes may have interesting applications.

We gratefully acknowledge the Korea Science and Engineering Foundation and POSTECH/BSRI (1997) for support of this work.

## Footnotes and References

* E-mail: kkim@vision.postech.ac.kr

† Cucurbituril (**1**) decahydrate (1.00 g, 0.85 mmol) and *N*,*N*′-bis(3-pyridylmethyl)-1,5-diminopentane dihydronitrate **2** (0.246 g, 0.60 mmol) were added to water (20 ml). After overnight stirring, undissolved cucurbituril was filtered. The $^1$H NMR spectrum of the filtrate (using $D_2O$) reveals the formation of a 1 : 1 complex (pseudorotaxane **3**) of **1** and **2**. A 0.2 M solution of $AgNO_3$ in methanol was layered over the filtrate in a diffusion tube to produce colorless X-ray quality crystals of **4** in one week (21%). Satisfactory elemental analysis was obtained.

‡ *Crystal data* for **4**: $AgC_{53}H_{86}N_{31}O_{33}$, $M$ = 1793.40, monoclinic, space group $P2_1/n$, $a$ = 16.680(4), $b$ = 17.889(2), $c$ = 24.335(4) Å, $\beta$ = 101.355(8)°, $U$ = 7119(2) Å$^3$, $Z$ = 4, $D_c$ = 1.673 g cm$^{-3}$, $\mu$(Mo-Kα) = 3.99 cm$^{-1}$, $T$ = 293 K; 7126 unique reflections measured; $R_1$ [$I > 2\sigma(I)$] = 0.063, $wR_2$ (all data) = 0.1693, GOF = 1.06. The intensity data were collected with an Enraf-Nonius CAD4 diffractometer using monochromated Mo-Kα radiation [$\lambda$(Kα) = 0.710 73 Å]. The structures were solved by direct methods (SHELXS-86) and refined by full-matrix least-squares methods (SHELXL-93). All non-hydrogen atoms were refined anisotropically. CCDC 182/674.

1 Recent review articles: (*a*) J. P. Sauvage, *Acc. Chem. Res.*, 1990, **23**, 319; (*b*) D. B. Amabilino and J. F. Stoddart, *Chem. Rev.*, 1995, **95**, 2725; (*c*) D. Philp and J. F. Stoddart, *Angew. Chem., Int. Ed. Engl.*, 1996, **35**, 1154; (*d*) H. Gibson, M. C. Bheda and P. T. Engen, *Prog. Polym. Sci.*, 1994, **19**, 843.

2 (*a*) D. Whang, Y.-M. Jeon, J. Heo and K. Kim, *J. Am. Chem. Soc.*, 1996, **118**, 11333; (*b*) D. Whang and K. Kim, *J. Am. Chem. Soc.*, 1997, **119**, 451.

3 Reviews on cucurbituril: W. L. Mock, *Top. Curr. Chem.*, 1995, **175**, 1; P. Cintas, *J. Incl. Phenom. Mol. Recognit. Chem.*, 1994, **17**, 205.

*Received in Cambridge, UK, 30th June 1997; 7/04574C*

# Isolation and comprehensive solid state characterization of $Cl_3Al–O–PCl_3$

**Neil Burford,*[a] Andrew D. Phillips,[a] Robert W. Schurko,[a] Roderick E. Wasylishen[a] and John F. Richardson[b]**

[a] *Department of Chemistry, Dalhousie University, Halifax, Nova Scotia, Canada B3H 4J3*
[b] *Department of Chemistry, University of Louisville, Louisville, Kentucky 40292, USA*

**The crystal structure of $Cl_3Al–O–PCl_3$ contains covalent molecular units with an essentially linear Al–O–P axis, and a similar solution structure is indicated by NMR spectroscopy.**

Binary mixtures of $AlCl_3$ and $OPCl_3$ have been under examination for nearly 150 years,[1] and the existence of various formulae has been envisaged. Conductivity measurements[2,3] and radiochlorine exchange studies[4] imply the formation of ionic systems of the type $[OPCl_2][AlCl_4]$[2,4] and $[Cl_2Al(OPCl_3)_2][AlCl_4]$.[3] The more complex salts $[Al(OPCl_3)_4][AlCl_4]_3$[5] and $[Al(OPCl_3)_6][AlCl_4]_3$[5,6] are postulated on the basis of Raman[5] and NMR[6] spectroscopic data. Most reports propose the covalent formulae, $Cl_3AlOPCl_3$,[7–16] $(Cl_3Al)_2OPCl_3$,[9,11] $Cl_3Al(OPCl_3)_2$,[9,13,17] or $(Cl_3Al)_2(OPCl_3)_3$,[7,15] on the basis of melting points,[17] thermal analysis,[16] vapour pressure measurements,[9,10] vibrational spectroscopy,[11,12,13] mass spectrometry,[14] NMR spectroscopy[5,7] or X-ray powder diffraction.[15] Nevertheless, definitive structural assignment for any of these is not yet available.

We now report the isolation and comprehensive solid state characterization of $Cl_3AlOPCl_3$, which can be crystallized from $CH_2Cl_2$ solution.† The melting point of the crystals (183–185 °C) corresponds to the well established dystectic for a 1 : 1 stoichiometry (186.5 °C,[17] 188 °C[8]). The crystal structure reveals $Cl_3AlOPCl_3$ as covalent molecular units without significant intermolecular interactions. As illustrated in Fig. 1, the plane defined by Cl(3), Al, O, P and Cl(1) lies on a crystallographic mirror plane so that the chlorine atoms adopt an eclipsed orientation. The Cl–Al and Cl–P bond lengths are typical of four-coordinate aluminium and phosphorus, respectively. Although the Al–O bond length is consistent with those in compounds containing $C_3AlO$ units,[18] it is significantly longer than observed for $Cl_3AlOPPh_3$ [1.733(4) Å].[19]

The similarity of the solution and solid state $^{31}P$ and $^{27}Al$ NMR chemical shifts implies retention of the covalent structure in solution. Although the Raman spectroscopic features (band intensities, assignments and interpretations) described in the literature are somewhat varied, the five most intense bands for the crystalline material correspond with five of the six strong bands reported for the 1 : 1 binary mixture (591, 452, 350, 210, 168, 118 $cm^{-1}$),[5] which has therefore previously been incorrectly assigned the ionic formula $[Al(OPCl_3)_4][AlCl_4]_3$.

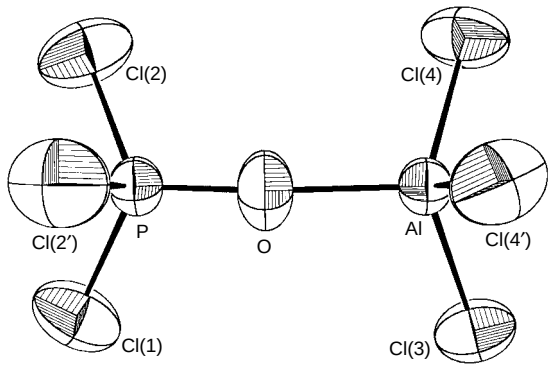



**Fig. 1** ORTEP view of $Cl_3AlOPCl_3$. Selected bond lengths (Å) and angles (°): Al–O 1.780(4), Al–Cl(3) 2.093(2), Al–Cl(4) 2.103(2), P–Cl(1) 1.929(2), P–Cl(2) 1.929(1), O–P 1.436(3); Al–O–P 176.0(4), O–Al–Cl(3) 106.9(2), O–Al–Cl(4) 106.18(9), Cl(3)–Al–Cl(4) 112.78(5), Cl(4)–Al–Cl(4′) 111.47(5), Cl(1)–P–Cl(2) 108.07(7), Cl(2)–P–Cl(2′) 107.71(8), O–P–Cl(1) 110.9(2), O–P–Cl(2) 111.0(1).

The most striking feature in the solid state structure of $Cl_3AlOPCl_3$ is the large Al–O–P angle [176.0(4)°], which is consistent with the near $C_{3v}$ symmetry assigned for a species in the melt on the basis of Raman spectra,[5] and with the structure assigned to $Br_3AlOPBr_3$ on the basis of single crystal NQR and NMR spectroscopy,[20] but is surprising when compared with the bent structure of $F_5AsOPCl_3$ [As–O–P 136.6(4)°].[21] While there are numerous examples of compounds containing a linear oxygen centre, most involve a transition metal.[22] Those between p block elements $\{(C_{10}H_8NO)_2Al–O–Al(NOC_{10}H_8)_2$,[23] $Ph_3Si–O–SiPh_3$,[24] $[(Me_2N)_3P–O–P(NMe_2)_3]^{2+}$,[25] $Ph(OMe)C–O–AlMe(BHT)_2$[26] and $X_3E–O–PPh_3$ ($X_3E$ = $Cl_3Al$, $Br_3Al$, $Cl_3Ga$)[19]$\}$ maybe imposed by substituent steric strain, but such interactions are insignificant in the title compound, as the intramolecular Cl(Al)···Cl(P) distances [Cl(1)···Cl(3) 4.645(2), Cl(2)···Cl(4) 4.428(2) Å] are substantially greater than the sum of the van der Waals' radii for chlorine (3.6 Å).[27] Moreover, the Al–P separation [3.213(2) Å] is greater than that between the silicon centres in the non-linear (Si–O–Si, 146°) isoelectronic molecule $Cl_3Si–O–SiCl_3$ (3.13 Å,[28] also the close contact limit for silicon centres).[29] $Cl_3AlOPCl_3$ is a useful and simple example of a non-VSEPR structure, although novelties or exceptions to the VSEPR model[30] were recognized at the outset (*e.g.* $H_3SiOSiH_3$[31] and $Cl_5RuORuCl_5$),[32] and internuclear repulsions may play a role in the determination of molecular geometry.[29]

$Cl_3AlOPCl_3$ is best viewed as one of an extensive series of phosphoryl coordination complexes which exhibit a range of angles (134–180°) at the dicoordinate oxygen centre,[22,33] although the widest angle previously reported for complexes of $OPCl_3$ is 164.1(4)°.[34] The O–P bond in $Cl_3AlOPCl_3$ is typical, in that it is essentially unchanged from that reported for the gas phase structure of the free ligand $OPCl_3$ [1.449(5) Å].[35] Therefore, we envisage the coordinative interaction to involve a purely non-bonding electron pair on oxygen, and invoke a similar model to that proposed for coordination complexes containing organo-carbonyl ligands, the M–O–C bond angle of which has a shallow energy minimum and is readily distorted by a number of factors.[36]

The observations and conclusions presented here have important structural implications for other $OPCl_3$ complexes, including the recently reported $Cl_3FeOPCl_3$.[37]

We thank the Natural Sciences and Engineering Research Council of Canada for funding, the Alexander von Humboldt Foundation for a fellowship (N. B.) and the Killam Trust for a scholarship (R. W. S.).

## Footnotes and References

* E-mail: burford@is.dal.ca

† Combination of $OPCl_3$ (1.95 g) and $AlCl_3$ (1.70 g) each in $CH_2Cl_2$ (25 ml) affects rapid solvation of $AlCl_3$. Slow evaporation of the solvent (20 min)

gives a white crystalline material which was washed with $CH_2Cl_2$, yield 83%; recrystallised from $CH_2Cl_2$, yield 25%; mp 183–185 °C; Anal. Calc. Cl, 74.20; P, 10.80. Found: Cl, 74.20; P, 10.70%. IR ($\nu$/cm$^{-1}$): 1233, 973, 642, 593, 521, 441, 347, 246. Raman (25 °C, cm$^{-1}$): 1225, 658, 636, 590, 559, 490, 435, 348, 310, 235, 209, 168, 136, 116, 84. NMR, solution ($CH_2Cl_2$): $^{31}$P, $\delta$ 35; $^{27}$Al, $\delta$ 93 ($\Delta\nu_{\frac{1}{2}}$, 270 Hz). CP MAS: $^{31}$P, $\delta$ 33; $^{27}$Al, $\delta$ 89.

*Crystal data*: $AlCl_6OP$, $M$ = 286.7, monoclinic, space group $P2_1/m$, $a$ = 6.341(2), $b$ = 10.087(3), $c$ = 8.122(2) Å, $\beta$ = 111.07(2)°, $U$ = 484.7 Å$^3$, $Z$ = 2, $D_c$ = 1.96 g cm$^{-3}$, $\mu$ = 19.7 cm$^{-1}$, $T$ = 22(1) °C, 806 observed reflections [$I > 3\sigma(I)$], $R$ = 0.038; $R_w$ = 0.037, GOF = 1.01. CCDC 182/658.


1 W. Casselmann, *Ann. Chem.*, 1852, **83**, 257; 1856, **98**, 213.
2 V. Gutmann and M. Z. Baaz, *Z. Anorg. Allg. Chem.*, 1959, **298**, 121.
3 V. Gutmann and M. Z. Baaz, *Monatsh. Chem.*, 1959, **90**, 729.
4 J. Lewis and D. B. Sowerby, *J. Chem. Soc.*, 1963, 1305.
5 F. Birkeneder, R. W. Berg and N. J. Bjerrum, *Acta Chem. Scand.*, 1993, **47**, 344.
6 R. G. Kidd and D. R. Truax, *Chem. Commun.*, 1969, 160.
7 S. Boghosian, G. Zissi and G. A. Voyiatzis, *Proc. Electrochem. Soc.*, 1994, 276.
8 A. S. Barabanova and B. A. Voitovich, *Russ. J. Inorg. Chem.*, 1964, **12**, 1455.
9 A. V. Suvorov and V. L. Shubaev, *Russ. J. Inorg. Chem.*, 1971, **16**, 166.
10 L. A. Nisel'son, T. D. Sokolova, Y. N. Lyzlov and S. I. Solov'ev, *Russ. J. Inorg. Chem.*, 1976, **21**, 1578.
11 S. Boghosian, D. A. Karydis and G. A. Voyiatzis, *Polyhedron*, 1993, **12**, 771.
12 H. Gerding, J. A. Koningstein and E. R. van der Worm, *Spectrochim. Acta*, 1960, **16**, 881.
13 E. W. Wartenberg and J. Goubeau, *Z. Anorg. Allg. Chem.*, 1964, **329**, 269.
14 V. L. Shubaev, A. V. Suvorov and G. A. Semenov, *Russ. J. Inorg. Chem.*, 1970, **15**, 479; A. V. Suvorov, *Koord. Khim.*, 1977, **3**, 1469.
15 B. A. Voitovich, A. S. Barabanova and G. N. Novitskaya, *Ukr. Khim. Z.*, 1967, **33**, 367.
16 I. L. Nadelyaeva, Yu. V. Kondrat'ev and A. V. Suvorov, *J. Gen. Chem. USSR*, 1974, **46**, 1413.
17 W. L. Groeneveld and A. P. Zurr, *Recl. Trav. Chim. Pays-Bas*, 1957, **76**, 1005; *J. Inorg. Nucl. Chem.*, 1958, **8**, 241.
18 See, for example, J. L. Atwood and M. J. Zaworotko, *J. Chem. Soc., Chem. Commun.*, 1983, 302.
19 N. Burford, B. W. Royan, R. E. v. H. Spence, T. S. Cameron, A. Linden and R. D. Rogers, *J. Chem. Soc., Dalton Trans.*, 1990, 1521.
20 T. Okuda, H. Ishihara, K. Yamada and H. Negita, *Bull. Chem. Soc. Jpn.*, 1978, **51**, 1273.
21 J. Petersen, E. Lork and R. Mews, *Chem. Commun.*, 1996, 1897.
22 N. Burford, *Coord. Chem. Rev.*, 1992, **112**, 1.
23 Y. Kushi and Q. Fernando, *J. Am. Chem. Soc.*, 1970, **92**, 91.
24 C. Glidewell and D. C. Liles, *J. Chem. Soc., Chem. Commun.*, 1977, 632.
25 A. Aaberg, T. Gramstad and S. Husebye, *Acta Chem. Scand.*, 1980, **34**, 717.
26 M. B. Power, S. G. Bott, D. L. Clark, J. L. Atwood and A. R. Barron, *Organometallics*, 1990, **9**, 3086.
27 R. Steudel, *Chemistry of the Non-Metals*, de Guyter, New York, 1977.
28 W. Airey, C. Glidewell, A. G. Robiette and G. M. Sheldrick, *J. Mol. Struct.*, 1971, **8**, 413.
29 C. Glidewell, *Inorg. Chim. Acta*, 1975, **12**, 219.
30 R. J. Gillespie and I. Hargittai, *The VSEPR Model of Molecular Geometry*, Allyn and Bacon, Boston, 1991; R. J. Gillespie, *Chem. Soc. Rev.*, 1992, 59.
31 R. C. Lord, D. W. Robinson and W. C. Schumb, *J. Am. Chem. Soc.*, 1956, **78**, 1327; A. Almenningen, O. Bastiansen, V. Ewing, K. Hedberg and M. Treatteberg, *Acta Chem. Scand.*, 1963, **17**, 7.
32 A. H. Mellor and N. C. Mathieson, *Acta Crystallogr.*, 1952, **5**, 185.
33 N. M. Karayannis, C. K. Mikulski and L. L. Pytlewski, *Inorg. Chim. Acta Rev.*, 1971, **5**, 69; M. W. G. de Bolster, *Top. Phosphorus Chem.*, 1983, **11**, 69.
34 G. Munninghoff, E. Hellner, M. El Essawi and K. Dehnicke, *Z. Kristallogr.*, 1978, **147**, 231.
35 T. Moritani, K. Kuchitsu and Y. Morino, *Inorg. Chem.*, 1971, **10**, 344.
36 T. J. LePage and K. B. Wiberg, *J. Am. Chem. Soc.*, 1988, **110**, 6642.
37 S. Boghosian, G. A. Voyiatzis and G. N. Papatheodorou, *J. Chem. Soc., Dalton Trans.*, 1996, 3405.


*Received in Bloomington, IN, USA, 7th August 1997; 7/05781D*

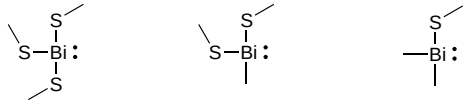
# Ammoniumthiolatobismuth halides: a new thiolate bonding environment for $Bi^{III}$ as an alternative to metathesis and chelation

**Glen G. Briand, Neil Burford* and T. Stanley Cameron**

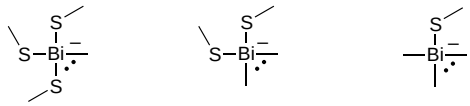
*Department of Chemistry, Dalhousie University, Halifax, Nova Scotia, Canada B3H 4J3*

**Synthesis, isolation and characterization of the first monothiolatobismuth complexes are contrary to the prominent thiophilicity, the tendency towards maximum metathesis and the extensive chelation chemistry of bismuth.**

The coordination chemistry of the heavier p block elements is diverse due primarily to the potential for both covalent and coordinative bonding, the access of coordination numbers up to nine, and facile ligand exchange in solution. Despite the rapid developments in the chemistry of bismuth resulting from demonstrated bioactivity[1] and the need for viable synthetic approaches to new materials,[2] systematic assessments of coordinative environments for bismuth still require the identification, characterization and classification of numerous structural possibilities. Thiobismuth derivatives are perhaps the most extensively studied series of bismuth compounds owing to their high thermal and reactive stability, and include complexes of thiolato,[3,4] dithiocarboxylato derivatives,[5] thione[6] and thioether[7] ligands. Numerous examples of multithiolato compounds (**1** and **2**) have been structurally characterized, but monothiolato complexes of type **3** have only been postulated on the basis of spectroscopic data.[8]



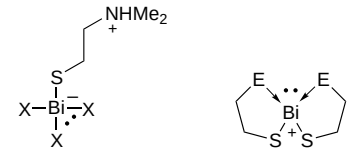
**1a** **2a** **3a**



**1b** **2b** **3b**

Here we describe the isolation and characterization† of ammoniumthiolatobismuth halides **4**, which are formed in high yield independent of stoichiometry in the reactions of $HSC_2H_4NMe_2HX$ with either $Bi(NO_3)_3$ or $BiX_3$ (X = Cl **a**, Br **b**). An X-ray crystallographic study of **4a** (Fig. 1) confirms the empirical formula and the pendant ammoniumethanethiolato moiety. The one-dimensional spirocyclic polymeric array, typical of bismuth halides,[4,9] is due to association of the bismuth centres by alternating chlorine and sulfur coordinative bridges, imposing a near octahedral, six-coordinate environment for bismuth. The two Bi–$Cl_{terminal}$ bonds [2.615(4), 2.636(3) Å] are predictably shorter than the Bi–$Cl_{bridging}$ bonds [2.776(4), 3.001(4) Å], and the Bi–S bond [2.669(3) Å] which is *trans* to the Bi–$Cl_{bridging}$ bonds is significantly shorter than that which is *trans* to the Bi–$Cl_{terminal}$ [2.927(3) Å] bond. These comparisons can be interpreted in terms of the bismuth centre engaging four covalent bonds (three to chlorine and one to sulfur) and two bridging coordinative bonds (one to chlorine and one to sulfur), which presumably dissociate on solvation to give the monomer in solution.

Although observation of a monothiolatobismuth environment of type **3b** in derivatives of **4** is contrary to the prominent thiophilicity of bismuth and the tendency towards maximum metathesis (which gives bonding environments **1** and **2**),[4,10–12] the quantitative halogenation of bismuth in the reaction of $Bi(NO_3)_3$ with $HSC_2H_4NMe_2HX$ implies that derivatives of **4** are thermodynamically favoured. In addition, formation of **4** contrasts the extensive chelation chemistry of bismuth, and specifically the reaction of aminoethanethiol (the conjugate base of $HSC_2H_4NH_3X$) with $Bi(NO_3)_3$ in acetic acid, which gives **5a** $(NO_3)\cdot H_2O$ as the result of a double metathesis.[12] We conclude that the thiophilicity of $Bi^{3+}$ is greater than that of $BiX_3$ (X = Cl, Br), and the higher basicity of the halide ligands restricts thiolation. Interestingly, $Bi(NO_3)_3$ and $BiX_3$ react with mercaptoethanol ($HSCH_2CH_2OH$) to give **5b** by virtue of bisthiolation,[10,11] implying that the higher protic basicity of the amine inhibits the chelation which is observed for the hydroxythiolate.



**4a** X = Cl
**b** X = Br

**5a** E = $NH_2$
**b** E = OH

Derivatives of **4**, as the first examples of bonding type **3b**, represent a fundamental missing link in the developing chemistry of bismuth, and their thermodynamically favoured formation bodes well for efficient and systematic assessment of a potentially extensive new direction, including anions of the type $[X_3BiSR]^-$, which we are currently examining.

We thank the Natural Sciences and Engineering Research Council of Canada for funding, the Atlantic Region Magnetic Resonance Centre and the Dalhousie Mass Spectrometry Centre for the use of instrumentation.

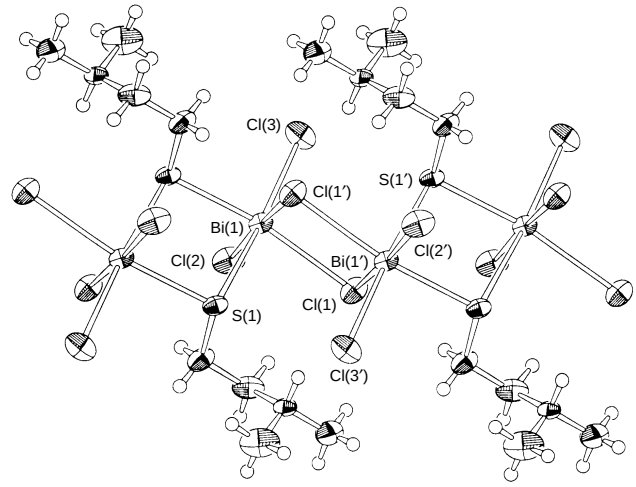



**Fig. 1** Crystallographic view of **4a**. Selected bond lengths (Å) and angles (°): Bi(1)–Cl(1′) 2.776(4), Bi(1)–Cl(2) 2.615(4), Bi(1)–Cl(3) 2.636(3), Bi(1)–Cl(1) 3.001(4), Bi(1)–S(1) 2.927(3), Bi(1)–S(1′) 2.669(3); Cl(1)–Bi(1)-Cl(1′) 85.31(10), Cl(1)–Bi(1)–Cl(2) 92.3(1), Cl(1)–Bi(1)–Cl(3) 100.2(1), Cl(1)–Bi(1)–S(1) 84.64(10), Cl(1)–Bi(1)–S(1′) 170.5(1).

## Footnotes and References

* E-mail: burford@is.dal.ca

† $BiX_3$ (6.6 mmol) in THF (50 ml) added to $HSC_2H_4NMe_2HX$ (13.3 mmol) in ethanol (125 ml), or $Bi(NO_3)_3{\cdot}5H_2O$ (5.0 mmol) with $HSC_2H_4NMe_2HX$ (15.0 mmol) in $H_2O$ (14 ml) and glacial acetic acid (6 ml), each give a yellow precipitate. **4a**: yield from $BiCl_3$, 97%. Anal. Calc.: C, 11.42; H, 2.62; N, 3.33%; Found: C, 11.98; H, 2.77; N, 3.42%; yield from $Bi(NO_3)_3{\cdot}5H_2O$, 67%. Anal. Found: C, 11.52; H, 2.64; N, 3.42%; 205 °C (decomp.); IR ($\nu$/cm$^{-1}$): 303w, 335m, 411w, 513w, 662w, 722m, 756w, 835w, 885w, 926s, 967w, 1011m, 1035w, 1048w, 1117w, 1149w, 1211w, 1226w, 1256w, 1305w, 1404w, 1429m. Raman (cm$^{-1}$): 107vs, 127vs, 172s, 220s (sh), 247vs, 334s, 412w, 446w, 514w, 663m, 757m, 885w, 927w, 967w, 1011w, 1037w, 1050w, 1213w, 1229w, 1258w, 1305w, 1365w, 1385m, 1431m, 1451m, 2896w (sh), 2939s (sh), 2955s, 2991m, 3020m, 3032m. $^1$H NMR [$(CD_3)_2SO$]; $\delta$ 2.77s, 3.30 (t, br), 4.98 (s, br), 9.02 (s, br). $^{13}$C NMR [$(CD_3)_2SO$], $\delta$ 23.2, 42.7, 60.8. Recrystallized (needle-like) from water by slow evaporation for 3–12 d, yield: 2.4%. Anal. Found: C, 11.57; H, 2.79; N, 3.32; consistent Raman and decomparison temperature. *Crystal data*: $C_4H_{11}BiCl_3NS$, $M$ = 420.54, monoclinic, space group $P2_1/c$, $a$ = 6.850(2), $b$ = 13.977(2), $c$ = 11.720(1) Å, $\beta$ = 106.14(1)°, $U$ = 1077.8(4) Å$^3$, $D_c$ = 2.591 g cm$^{-3}$, $Z$ = 4, $\lambda$(Mo-K$\alpha$) = 404.11 cm$^{-1}$, 1842 collected reflections, 1688 unique reflections, $2\theta_{max}$ = 120.2°, $R$ = 0.044, $R_w$ = 0.050 (Cu-K$\alpha$ radiation, $\lambda$ = 1.541 78 Å, $T$ = 23.0 °C). All measurements were made on a Rigaku AFC5R diffractometer with graphite monochromated Cu-K$\alpha$ radiation and a 12 kW rotating anode generator. The structure was solved by direct methods and refined by full-matrix least-squares techniques using 1417 reflections with $I > 3.00\sigma(I)$. The non-hydrogen atoms were refined anisotropically. A final difference-Fourier map yielded maximum and minimum peaks of 2.48 and −2.73 e Å$^{-3}$, respectively. CCDC 182/657.

**4b**: yield from $BiBr_3$, >95%. Anal. Calc.: C, 8.67; H, 2.00; N, 2.53; Found: C, 9.19; H, 2.07; N, 2.57%; yield from $Bi(NO_3)_3{\cdot}5H_2O$, 90%. Anal. Found: C, 8.94; H, 2.04; N, 2.62%; 195 °C (decomp.). IR ($\nu$/cm$^{-1}$) (Nujol): 513s, 588m, 658w, 721w, 752w (sh), 774s, 834m (br), 866m, 893w, 922m, 965w, 1007m, 1031w, 1045w, 1117w, 1145w, 1180m, 1226w (sh), 1256w (sh), 1321s, 1340m, 1425w (sh), 1513vs, 1570vs, 1623vs, 1639w (sh), 3402vs (br). Raman (cm$^{-1}$): 75vs, 101m, 119vs, 144m, 162vs, 210vs, 300w, 328s, 408w, 444w, 513m, 660m, 753m, 878m, 924w, 967w, 1008w, 1033m, 1045w (sh), 1117w, 1147w, 1212w, 1227w, 1257w, 1302w, 1359m, 1377m, 1394w, 1427m, 1451m, 1464w, 1475w (sh), 2841w (br), 2893w, 2932w (sh), 2947s, 2960s, 2983w, 3020m, 3074w (br). $^1$H NMR [$(CD_3)_2SO$], $\delta$ 2.78 (s), 3.30 (s, br), 5.04 (s, br), 8.99 (s, br). $^{13}$C NMR [$(CD_3)_2SO$], $\delta$ 24.2, 42.7, 60.9.


1 See, for example, G. F. Baxter, *Chem. Br.*, 1992, 445; *Pharm. J.*, 1989, 805; S. L. Gorbach, *Gastroenterology*, 1990, **99**, 863; R. Diemer, B. K. Keppler, U. Dittes, B. Nuber, V. Seifried and W. Opferkuch, *Chem., Ber.*, 1995, **128**, 335; U. Dittes, B. K. Keppler and B. Nuber, *Angew. Chem., Int. Ed. Engl.*, 1996, **35**, 67; S. P. Summers, K. A. Abboud, S. R. Farrah and G. J. Palenik, *Inorg. Chem.*, 1994, **33**, 88; P. J. Sadler, H. Sun and H. Li, *Chem. Eur. J.*, 1996, **2**, 701; P. J. Sadler and H. Sun, *J. Chem. Soc., Dalton Trans.*, 1995, 1395; H. Sun, H. Li and P. J. Sadler, *Chem. Ber.*, 1997, **130**, 669.

2 R. D. Rogers, A. H. Bond and S. Aguinaga, *J. Am. Chem. Soc.*, 1992, **114**, 2960; R. D. Rogers, A. H. Bond, S. Aguinaga and A. Reyes, *J. Am. Chem. Soc.*, 1992, **114**, 2967; M. A. Matchett, M. Y. Chiang and W. E. Buhro, *Inorg. Chem.*, 1990, **29**, 360.

3 See, for example: M. Dräger and B. M. Schmidt, *J. Organomet. Chem.*, 1985, **290**, 133; G. Hunter and T. J. R. Weakley, *J. Chem. Soc., Dalton Trans.*, 1983, 1067; G. E. Forster, M. J. Begley and D. B. Sowerby, *J. Chem. Soc., Dalton Trans.*, 1995, 383.

4 L. Agocs, N. Burford, T. S. Cameron, J. M. Curtis, J. F. Richardson, K. N. Robertson and G. B. Yhard, *J. Am. Chem. Soc.*, 1996, **118**, 3225.

5 See, for example: A. Müller, E. Krickemeyer, F. El-Katri, D. Rehder, A. Stammler, H. Bogge and F. Hellweg, *Z. Anorg. Allg. Chem.*, 1995, **621**, 1160; I. Haiduc, C. Silvestri and R. Cea- Olivares, *Polyhedron*, 1994, **13**, 547; M. J. Begley, D. B. Sowerby and I. Haiduc, *J. Chem. Soc., Dalton Trans.*, 1987, 145; M. R. Snow and E. R. T. Tiekink, *Aust. J. Chem.*, 1987, **40**, 743; C. L. Raston, E. L. Rowbottom and A. H. White, *J. Chem. Soc., Dalton Trans.*, 1981, 1352; 1366; 1369; 1372; 1379; 1383; C. L. Raston and A. H. White, *J. Chem. Soc., Dalton Trans.*, 1976, 791.

6 L. P. Battaglia, A. Bonamartini Corradi and G. Pelosi, *J. Cryst. Spectrosc. Res.*, 1992, **22**, 275; L. P. Battaglia and A. Bonamartini, Corradi, *J. Chem. Soc., Dalton Trans.*, 1983, 2425; W. Bensch, E. Blazso, E. Dubler and H. R. Oswald, *Acta Crystallogr., Sect. C*, 1987, **43**, 1699; G. R. Willey, J. R. Barras, M. D. Rudd and M. G. B. Drew, *J. Chem. Soc., Dalton Trans.*, 1994, 3025.

7 See, for example: W. Clegg, N. C. Norman and N. L. Pickett, *Polyhedron*, 1993, **12**, 1251; G. R. Willey, M. T. Lakin and N. W. Alcock, *J. Chem. Soc., Dalton Trans.*, 1992, 591; 1339.

8 T. Klapötke, *Polyhedron*, 1987, **6**, 1593.

9 See, for example: D. Mitzi, *Inorg. Chem.*, 1996, **35**, 7614.

10 L. Agocs, G. G. Briand, N. Burford, T. S. Cameron, W. Kwiatkowski and K. N. Robertson, *Inorg. Chem.*, 1997, **36**, 2855.

11 E. Asato, K. Kamamuta, Y. Akamine, T. Fukami, R. Nukada, M. Mikuriya, S. Deguchi and Y. Yokota, *Bull. Chem. Soc. Jpn.*, 1997, **70**, 639.

12 W. A. Herrmann, P. Kiprof, W. Scherer and L. Pajdla, *Chem. Ber.*, 1992, **125**, 2657.


*Received in Bloomington, IN, USA, 22nd July 1997; 7/05251K*

# Synthesis and redox properties of MCM-48 containing copper and zinc

**Martin Hartmann,* Sandrine Racouchot and Christian Bischof**

*Institute of Chemical Technology I, University of Stuttgart, D-70550 Stuttgart, Germany*

**MCM-48 materials, synthesized for the first time in the presence of copper and zinc salts, show remarkable redox properties in contrast to materials prepared by ion-exchange or impregnation.**

Since their rediscovery (as we learned recently[1] these materials were discovered more than 25 years ago) by researchers of the Mobil Oil Company in 1992[2,3] ordered mesoporous materials (denoted as M41S) have initiated intensive research resulting in an overwhelming number of publications. However, most studies have dealt with the hexagonal form, MCM-41.[4,5] MCM-48, the cubic member (space group $Ia\bar{3}d$) of the M41S family was investigated only in a limited number of studies.[6–9] The third member of the M41S family, MCM-50, is an unstable lamellar phase.[2,3]

The incorporation of transition metal ions into micro- or meso-porous molecular sieves is of considerable interest for catalytic applications. For MCM-48 to be useful with respect to catalytic applications, metal ions have to be incorporated into the amorphous walls. Attempts on the incorporation of Al, Mn, V, Ti and Cr have been reported so far.[11–14] Temperature programmed reduction (TPR) is a useful tool for collecting information on the redox properties of transition metal ions in zeolites and other porous supports.

The present work describes the first redox-type MCM-48 material containing copper and zinc introduced during the synthesis of the material. Temperature programmed reduction experiments of the calcined material show the availability of copper for redox reactions.

The MCM-48 materials were synthesized using cetyltrimethylammonium bromide (CTAB), tetraethylorthosilicate (TEOS) and NaOH. A gel with a molar composition of 0.61 CTAB : 1 $SiO_2$ : 0.25 $Na_2O$ : 61 $H_2O$ was prepared and different amounts of $Cu(MeCO_2)_2 \cdot H_2O$ and $ZnSO_4 \cdot 2H_2O$ were added. The resultant gel was loaded into autoclaves and heated to 373 K for 72 h. After synthesis the materials were recovered by filtration, washed with water and ethanol and finally calcined in flowing nitrogen up to 200 °C and in flowing air up to 540 °C for 18 h. For comparison, copper containing MCM-48 samples have been prepared by ion-exchange and impregnation, using standard procedures. The resulting materials were characterized by powder X-ray diffraction (XRD), atomic absorption spectroscopy, nitrogen adsorption and desorption (at 77 K) and temperature programmed reduction (TPR). The TPR measurements were performed in an Altamira AM1 instrument with a flow of 10 vol.% $H_2$ in Ar. A heating rate of 3 K $min^{-1}$ was chosen to enhance resolution and avoid 'hot spots'. Prior to the first reduction experiment, the samples were activated in a helium flow containing 10 vol.% $O_2$ up to a maximum temperature of 400 °C at a rate of 5 K $min^{-1}$.

The powder X-ray diffraction patterns of the calcined CuMCM-48, CuZnMCM-48 and ZnMCM-48 materials are presented in Fig. 1 and correspond well with those reported for pure siliceous MCM-48. XRD studies reveal that MCM-48 materials can be synthesized in the presence of copper and zinc salts. While the addition of copper acetate to the synthesis gel up a ratio $n_{Si}/n_{Cu} = 15$ has no influence on the quality of the XRD pattern, the ZnMCM-48 materials show XRD patterns with somewhat lower intensity. Assuming cubic symmetry, the unit cell size of the calcined materials was calculated to be 9.36 nm for CuMCM-48, 9.31 nm for CuZnMCM-48 and 8.45 nm for ZnMCM-48 (Table 1).

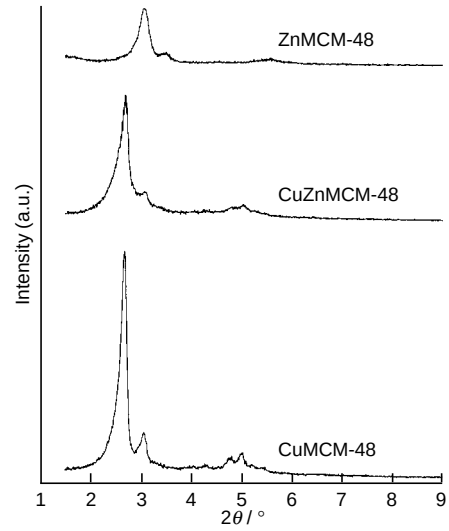



**Fig. 1** X-Ray diffraction pattern of as-synthesized CuMCM-48, CuZnMCM-48 and ZnMCM-48

The $N_2$ isotherms (Fig. 2) show no hysteresis in all samples under investigation. The surface area of the transition metal ion containing materials is reduced in comparison to the pure siliceous material. The surface areas and pore diameters were calculated from the nitrogen adsorption–desorption isotherms using BET and BJH analysis. The results of these calculations and the chemical analysis are collected in Table 1. The molar silicon/metal ratios of the starting gel were $n_{Si}/n_{Me} = 80$ leading to a reduced ratio in the calcined materials.

In agreement with the XRD powder pattern the nitrogen adsorption is largely reduced in ZnMCM-48 with $n_{Si}/n_{Zn} = 80$, while copper introduction does not affect the adsorption capacity. Similar findings were reported on AlMCM-41 materials,[15] showing that the mechanism of copper and zinc introduction might be significantly different. While co-precipitation of $Cu(OH)_2$ or complexation of $Cu^{2+}$ by the surfactant under the basic conditions of the synthesis prevent encapsulation of copper into the amorphous walls, Zn can be expected to be in the walls of MCM-48 as claimed in the Mobil patent.[16] The copper species can be removed by washing of the as-

**Table 1** Properties of the samples under investigation

| Sample | $n_{Si}/n_{(Cu+Zn)}$ | $n_{Cu}/n_{Zn}$ | $a_0$/nm | $A_{BET}$/ $m^2\ g^{-1}$ | $d_p$[a]/nm |
|---|---|---|---|---|---|
| MCM-48 | — | — | 8.33 | 1400 | 2.4 |
| CuMCM-48 | 35.8 | — | 9.36 | 1136 | 2.3 |
| CuZnMCM-48 | 48.5 | 1.4 | 9.31 | 1059 | 2.3 |
| ZnMCM-48 | 53.2 | — | 8.45 | 925 | 1.9 |

[a] The pore diameters were calculated from the desorption branch of the adsorption isotherm using the BJH model.

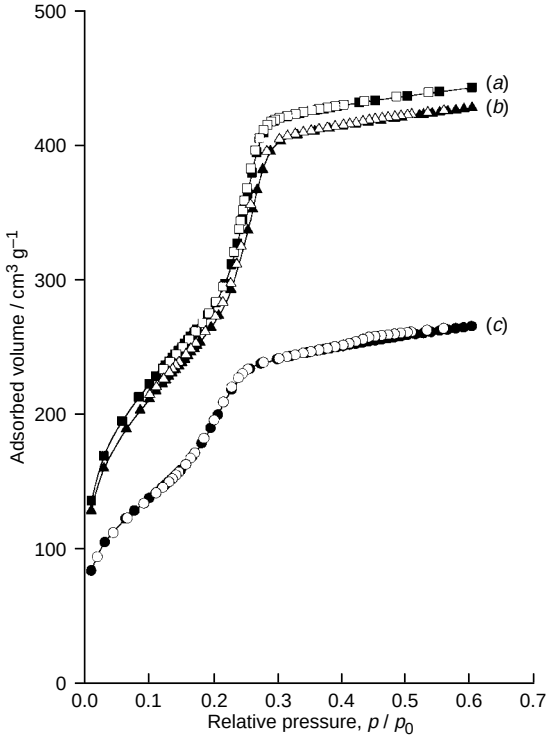



**Fig. 2** Nitrogen adsorption (closed symbols) and desorption (open symbols) at 77.3 K of (*a*) CuMCM-48, (*b*) CuZnMCM-48 and (*c*) ZnMCM-48

synthesized samples with 0.1 M HCl solution at 80 °C and are therefore most likely located within the channels. Complexation of copper by the surfactant has been established by EPR spectroscopy.[17]

The TPR profiles of CuMCM-48 and CuZnMCM-48 are displayed in Fig. 3. The sharp maximum of hydrogen consumption at 164 °C is accompanied by a shoulder at 184 °C (CuMCM-48). Temperatures in this range can be associated with the reduction of finely dispersed CuO to copper metal in the channels of MCM-48. The copper oxide is formed during calcination and/or sample pretreatment along with a color change from blue to brown. After the TPR experiment the sample exhibits a gray–red color, which is typical for copper metal clusters. The structural integrity of the sample has been checked by XRD and $N_2$ adsorption. The complete reduction of CuO dispersed on MCM-48 can be achieved at a substantial lower temperature than on $\gamma$-$Al_2O_3$ (210 °C)[18] or $SiO_2$ (350 °C).[19] Copper impregnated (Fig. 3) or ion-exchanged MCM-48

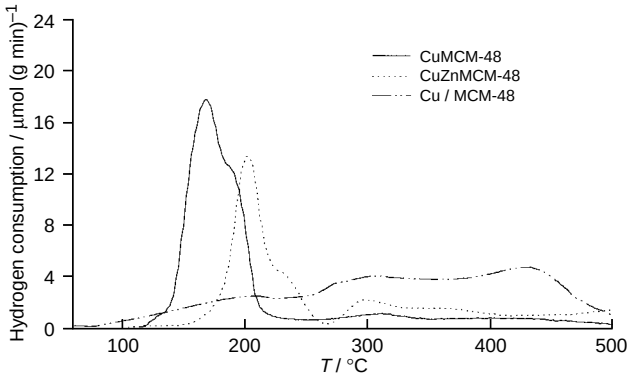



**Fig. 3** TPR profiles of CuMCM-48, CuZnMCM-48 and Cu/MCM-48

(not shown) do not exhibit a sharp signal in this temperature range. The reduction of CuO diluted with $SiO_2$ can be observed at 220 °C.

CuZnMCM-48 exhibits a somewhat different TPR profile. In comparison with the TPR profile of CuMCM-48 the reduction occurs at a significantly higher temperature (197 °C), but the halfwidth of the peak and the degree of reduction are remarkably reduced. The delay in copper reduction owing to the presence of zinc has been well observed in zeolites and CuO/ZnO catalysts.[20] The synergistic effect of zinc in reduction of copper is exploited for the commercial methanol catalyst (CuO/ZnO/$Al_2O_3$)[21] and has been shown for the first time to be effective in the M41S class of materials, with copper and zinc introduced *via* synthesis. The low reduction temperatures in the MCM-48 materials compared to silica might be associated with the size of the copper oxide particles. Smaller CuO particles are expected to be reduced at lower temperatures. This finding is further substantiated by an increase in reduction temperature with repeated redox cycles leading to agglomeration of smaller particles.[22]

Financial support by Deutsche Forschungsgemeinschaft (DFG) and Fonds der Chemischen Industrie is gratefully acknowledged. We are also grateful to Prof. J. Weitkamp for continuous support.

## Footnote and References

* E-mail: martin.hartmann@po.uni-stuttgart.de

1 F. Di Renzo, H. Cambon and R. Dutartre, *Microporous Mater.*, 1997, **10**, 283.
2 C. T. Kresge, M. E. Leonowicz, W. J. Roth, J. C. Vartuli and J. S. Beck, *Nature*, 1992, **359**, 710.
3 J. S. Beck, J. C. Vartuli, W. J. Roth, M. E. Leonowicz, C. T. Kresge, K. D. Schmidt, C. T.-W. Chu, D. H. Olson, E. W. Sheppard, S. B. McCullen, J. B. Higgins and J. L. Schlenker, *J. Am. Chem. Soc.*, 1992, **114**, 10 834.
4 F. Schüth, *Ber. Bunsen-Ges. Phys. Chem.*, 1995, **99**, 1306.
5 See, for example: X. S. Zhao, G. Q. Lu and G. J. Millar, *Ind. Eng. Chem. Res.*, 1995, **35**, 2075.
6 J. C. Vartuli, K. D. Schmidt, C. T. Kresge, W. J. Roth, M. E. Leonowicz, S. B. McCullen, S. D. Hellring, J. S. Beck, J. L. Schlenker, D. H. Olson and E. W. Sheppard, *Chem. Mater.*, 1994, **6**, 2317.
7 V. Alfredsson and M. W. Anderson, *Chem. Mater.*, 1996, **8**, 1141.
8 R. Schmidt, M. Stöcker, D. Akporiaye, E. H. Torstad and A. Olson, *Microporous Mater.*, 1995, **5**, 1.
9 A. A. Romero, M. D. Alba, W. Zhou and J. Klinowski, *J. Phys. Chem. B*, 1997, **101**, 5294.
10 R. Schmidt, H. Junggreen and M. Stöcker, *Chem. Commun.*, 1996, 875.
11 D. Zhao and D. Goldfarb, *J. Chem. Soc., Chem. Commun.*, 1995, 875.
12 M. Morey, A. Davidson, H. Eckert and G. Stucky, *Chem. Mater.*, 1996, **8**, 486.
13 W. Zhang and T. J. Pinnavaia, *Catal. Lett.*, 1996, **38**, 261.
14 M. Morey, A. Davidson and G. Stucky, *Microporous Mater.*, 1996, **6**, 99.
15 Z. Luan, C. F. Cheng, W. Zhou and J. Klinowski, *J. Phys. Chem.*, 1995, **99**, 1018.
16 C. T. Kresge, M. E. Leonowicz, W. J. Roth and J. C. Vartuli, *US Pat.*, 5 102 643, 1992.
17 A. Pöppl, P. Baglioni and L. Kevan, *J. Phys. Chem.*, 1995, **99**, 14 156.
18 W. P. Dow, Y. P. Wang and T. J. Huang, *J. Catal.*, 1996, **160**, 155.
19 K. P. Wendlandt, F. Vogt, W. Mörke and I. Achkar, in *Zeolite Chemistry and Catalysis*, ed. P. A. Jacobs, N. I. Jaeger, L. Kubelkova and B. Wichterlova, *Stud. Surf. Sci. Catal.*, 1990, **69**, 223.
20 J. M. Campos-Martin, A. Guerrero-Ruiz and J. L. G. Fierro, *Catal. Lett.*, 1996, **41**, 55.
21 K. C. Waugh, *Catal. Today*, 1992, **15**, 51.
22 M. Hartmann, S. Racouchot and C. Bischof, submitted.

*Received in Bath, UK, 8th September 1997; 7/06701A*

# Determination of localised corrosion mechanisms using a scanning vibrating reference electrode technique

**D. A. Worsley, H. N. McMurray and A. Belghazi**

*Department of Materials Engineering, University of Wales Swansea, Singleton Park, Swansea, UK SA2 8PP*

**A scanning electrochemical technique is used to show the influence of differential aeration on the kinetics and mechanism of corrosion reactions occurring at the exposed edge of galvanised sheet steels overcoated with organic layers of dissimilar thickness.**

Mass produced organic coated galvanised sheet steel is of increasing importance in the construction industry. Metallic corrosion at exposed cut edges is a potential failure mechanism[1] which must be assessed when evaluating the performance of new coating technologies. Conventional methods for evaluating cut edge performance are empirical and rely on the measurement of coating delamination rates under accelerated corrosion conditions. This is often time consuming and gives little mechanistic information. Various conventional electrochemical techniques, most notably electrical impedance spectroscopy,[2–4] have been used to study the corrosion of organic coated metals. However, none of these techniques possess the spatial resolution necessary to investigate properly the highly localised electrochemical reactions occurring at the cut edge, where dissimilar metal surfaces are closely approximated. The scanning vibrating reference electrode technique (SVRET) enables the quantitative mapping of localised ionic current fluxes by the measurement of potential gradients in solution, and has been successfully used to investigate both galvanic[5–10] and pitting[11,12] corrosion. Here we describe the use of SVRET to elucidate the kinetics and mechanism of cut edge corrosion in a model series of laboratory prepared organic coated galvanised steel samples.

SVRET measurements are carried out in aqueous electrolyte and employ a vibrating microtip electrode which is mechanically scanned at a small fixed distance from the corroding surface. It has been shown[5] that the ac voltage signal detected by the vibrating electrode is proportional to the potential gradient ($F$) parallel to the direction of vibration which is in turn proportional to the current density component in that direction. Thus for a point current source ($i$) in a medium of conductivity $\kappa$, the value of $F$ at any distance $x$, $y$ and $z$ from the source is given by:

$$F = \frac{iz}{2\pi\kappa(x^2 + y^2 + z^2)^{1.5}} \quad (1)$$

The apparatus used in this study comprised a 125 μm diameter platinum microdisc electrode vibrated normal to the scanned surface with a frequency of 140 Hz and amplitude of *ca*. 25 μm. The vibration frequency was set by a lock-in amplifier (EG & G model 5110) which also served to detect the SVRET signal. The vibrating electrode was positioned using a motorised, computer controlled, micromanipulator platform. All measurements were carried out in 0.86 M aqueous NaCl at 25 °C. The apparatus was calibrated using a known current density and was shown to exhibit an excellent linear response in the range 0.05–125 A m$^{-2}$ at the scan height of 125 μm.

Laboratory prepared model samples were prepared from 1 mm thick sheet steel (composition: Fe 99%), which had been hot-dip coated in a molten zinc bath containing *ca*. 0.2 mass% Al to produce a 20 μm coating of practically pure zinc (composition Zn 99.85%, Al 0.15%) with minimal formation of iron–zinc intermetallic phases.[13] The galvanised samples were pre-treated with chromic acid to aid polymer adhesion before being overcoated on both sides with a 5 μm thickness of a heat cured epoxy based polymer (Beckers PVC primer supplied by Beckers Paints Ltd). This was performed on a continuous coil coating line with the organic coating applied using rollers. A 140 μm laminate coating, consisting of PVC, was then applied to one or both sides of the sheet to produce asymmetrically and symmetrically coated samples. The coated samples were cut into 2 × 1 cm coupons and all but one cut edge masked using epoxy adhesive. The exposed cut edge was carefully polished flat using fine emery paper (down to 1200 grade). The polished coupons were immersed in a shallow electrolyte bath which was in contact with room air. The concentration of dissolved oxygen (in bulk solution) was therefore assumed to be approximately constant at 2 × 10$^{-5}$ mol dm$^{-3}$.[14] The exposed cut edge was positioned uppermost and horizontal, and scanned repeatedly with the vibrating probe moving in a plane 125 μm above the exposed metal surface. The results of this type of experiment are illustrated in Fig. 1(*a*)–(*c*) which show isocurrent contour maps of ionic current density in the plane of scan. Areas of positive current, associated with anodic activity at the metal surface, are shown as light and areas of negative current, associated with cathodic activity, are shown as dark. Free corrosion potentials of −0.65 and −1.05 V *vs*. SCE were measured in 0.86 M aqueous NaCl for mild steel and zinc respectively and it is therefore to be expected that zinc coating will cathodically protect steel at the cut edge. On this basis it is assumed that the predominant electrochemical reactions occurring under the experimental conditions are the anodic dissolution of zinc [eqn. (2)] and the cathodic reduction of oxygen at the steel surface [eqn. (3)].

$$Zn = Zn^{2+} + 2e \quad (2)$$

$$O_2 + 2H_2O + 4e = 4OH^- \quad (3)$$

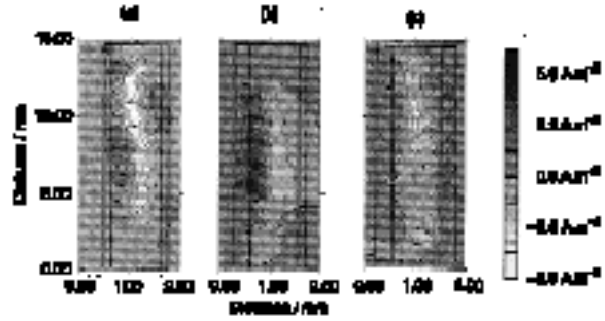


**Fig. 1** Isocurrent contour plots showing the anodic (light) and cathodic (dark) current density distributions over (*a*) a corroding cut edge with 5 μm epoxy primer both sides, (*b*) an identical sample with a 140 μm PVC coating applied to one side and (*c*) an identical sample with a 140 μm PVC coating applied to both sides. The sample position is shown together with schematic representations of the relative coating thicknesses applied to each side of the sample.

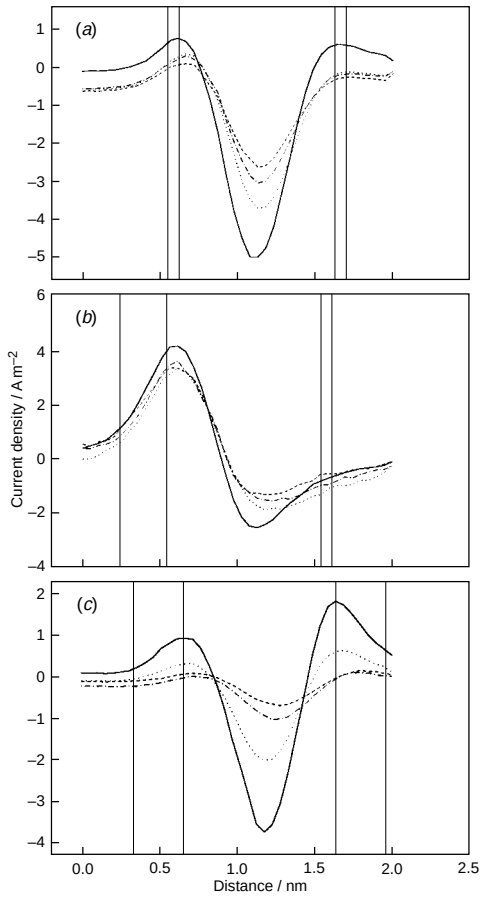



**Fig. 2** Normal component of current density distribution in plane of the scan across the thickness of the cut edge for successive scans over a 6 h period for (*a*) 5 μm epoxy primer both sides, (*b*) an identical sample with a 140 μm PVC coating applied to one side and (*c*) an identical sample with a 140 μm PVC coating applied to both sides after 0 h (—), 2 h (···), 4 h (–·–·–) and 6 h (---) immersion in 5% NaCl. The sample position is shown together with schematic representations of the relative coating thicknesses applied to each side of the sample.

Fig. 1 shows the differences in localised corrosion behaviour exhibited by cut edge samples prepared with symmetric and asymmetric thickness of organic coating. Symmetrically coated samples [Fig. 1(*a*) and (*c*)] show the anticipated symmetrical pattern of electrochemical activity with the cathodic steel surface bounded on either side by strips of anodic zinc. However, asymmetrically coated samples show a marked displacement of cathodic activity to the side where the organic coating is thinner, with a corresponding concentration of anodic activity on the more thickly overcoated zinc layer. This finding is perhaps more clearly illustrated in Fig. 2 in which current density data from individual, hourly repeated, area scans have been summed along the length of the cut edge so as to derive a series of current profiles representing the average current distribution across the thickness of the edge as a function of time. It may be seen from Fig. 2 that, in addition to any instantaneous differences in current distribution, current values decay markedly with time for symmetrical organic coatings, whereas for the asymmetric coating currents are substantially undiminished after 6 h.

The sharp difference in current distribution observed between the asymmetrically and symmetrically coated cut edge samples is probably due to the establishment of a differential aeration cell in the asymmetric case [illustrated in Fig. 1(*b*) and Fig. 2(*b*)]. Differential aeration arises for two reasons. Firstly, the thinner organic coating presents a smaller geometrical obstacle to oxygen diffusing or convecting through the electrolyte to the exposed metal surface. Secondly, the oxygen permeability of a coating will be inversely proportional to the coating thickness.[15] Higher steady state oxygen concentrations at the solution contacting zinc surface lying on the side of the thinner coating favour local cathodic activity through reaction (3).

In recent work[16] it has been shown that the cathodic reduction of oxygen, and hydrolytic processes catalysed by the $OH^-$ ions so produced, are key reactions in promoting the disbondment of organic polymer coatings. This implies that the extent of cathodic activity occurring immediately proximate to the polymer–metal interface will be the most significant factor determining rates of coating disbondment. The rapid decay of currents observed for the symmetrically coated samples may therefore be ascribed to blockage of the originally exposed metal surface by corrosion products with little or no fresh metal surface becoming available due to disbondment of the organic coating. Two basic chloride corrosion products [$6Zn(OH)_2{\cdot}ZnCl_2$ and $4Zn(OH)_2{\cdot}ZnCl_2$] have been identified for zinc corroding in NaCl solutions exceeding 0.1 M.[17] The much slower decay of currents observed for the asymmetrically coated samples may be ascribed to the continuous exposure of fresh metal surface through cathodic disbondment of the thinner organic coating as a result of intense cathodic activity immediately proximate to the zinc–polymer interface. Indeed, visible degradation of the thinner coating was observed in similar samples exposed to 5% NaCl for extended periods with *ca*. 500 μm delamination in 170 h.

The results obtained from the model system also indicate that differential aeration can be an important factor in the mechanism of cut edge corrosion in quiescent solutions of bulk electrolyte.

We thank British Steel Strip Products, Port Talbot and the EPSRC for funding this research under the Materials for Better Construction Initiative.

## Footnotes and References

* E-mail: d.a.worsley@swan.ac.uk

1 P. A. Ryan, R. P. Wolstenholme and D. M. Howell, *Durability of Cladding; A State of the Art Report*, Thomas Telford, London, 1994.
2 J. V. Standlish and H. Leidheiser, *Corrosion*, 1980, **36**, 390.
3 F. Mansfeld, M. W. Kenig and S. Tsai, *Corrosion*, 1982, **38**, 478.
4 J. C. Padget and P. J. Moreland, *J. Coatings Technol.*, 1983, 55.
5 H. S. Isaacs, *J. Electrochem. Soc.*, 1991, **138**, 723.
6 H. S. Isaacs, *Advances in localised corrosion*, ed. H. Isaacs, U. Bertocci, J. Kruger and S. Smialouzka, NACE, 1988, p. 221.
7 K. Komai, K. Minoshima and G. Kim, *JSME Int. J. Ser. I*, 1989, **32**, 282.
8 J. Hawkins, G. E. Thompson, G. C. Wood and H. S. Isaacs, *Abstracts of the American Chemical Society*, Washington DC, 1989, p. 65.
9 G. Pallos and G. Wallwork, *Corrosion*, 1982, **38**, 305.
10 M. J. Franklin, D. C. White and H. S. Isaacs, *Corrosion Sci.*, 1992, **33**, 251.
11 H. S. Isaacs, *Corrosion Sci.*, 1989, **28**, 547.
12 T. Shibata, T. Haruna and S. Fujimoto, *Corrosion Eng.*, 1990, **39**, 331.
13 I. Suzuki, in *Corrosion-Resistant Coatings Technology*, Marcel Dekker, New York, 1989, pp. 35–37.
14 A. Bonnel, F. Dabosi, C. Deslouis, M. Dupart, M. Kedam and B. Tribollet, *J. Electrochem. Soc.*, 1983, **130**, 753.
15 J. Crank and G. S. Park, in *Diffusion in Polymers*, Academic Press, London, 1968.
16 W. Furbeth and M. Stratmann, *Fresenius J. Anal. Chem.*, 1995, **353**, 337.
17 W. Feitknecht, *Chem. Ind.*, (Review article), 1959, 1102.

*Received in Cambridge, UK, 27th June 1997; 7/04530A*

# *Ab initio* structure determination of layered sodium titanium silicate containing edge-sharing titanate chains (AM-4) $Na_3(Na,H)Ti_2O_2[Si_2O_6]\cdot 2.2H_2O$

**M. S. Dadachov,[a] J. Rocha,[b] A. Ferreira,[b] Z. Lin[b] and M. W. Anderson*[c]**

[a] *Materials Division, Australian Nuclear Science and Technology Organisation, PMB 1 Menai NSW 2234, Australia*
[b] *Department of Chemistry, University of Aveiro, 3810 Aveiro, Portugal*
[c] *Department of Chemistry, UMIST, PO Box 88, Manchester, UK M60 1QD*

**The synthesis of a novel layered sodium titanosilicate, $Na_3(Na,H)Ti_2O_2[Si_2O_6]_2.H_2O$ (AM-4), and the solution of its crystal structure by *ab initio* methods are reported.**

Mixed framework minerals and synthetic compounds with structures built from common polyhedral units (octahedra and tetrahedra sharing all oxygens with at least two other neighbouring polyhedra) are of great interest, particularly with respect to host–guest chemistry, structural diversity, ion-exchange and adsorption properties, and shape selective catalysis. The large class of titanium silicates encompasses more than 70 minerals, mainly with mixed cation frameworks. During the last decade ynthetic inorganic and materials chemists have attempted to prepare titanium silicates by using high-temperature solid state ceramic and hydrothermal methods. Recently, we have reported the synthesis of analogues of minerals nenadkevichite,[1] umbite, narsarsukite[2] and penkvilksite.[3,4] We have also solved the structures of the important microporous material ETS-10,[5] as well as rhombohedrally distorted $Na_4[Ti_4O_4(SiO_4)_3]_6\cdot H_2O$.[6] Here, we wish to report the synthesis and structure determination of a novel titanium silicate layered compound, monoclinic $Na_3(Na,H)Ti_2O_2[Si_2O_6]_2\cdot 2H_2O$.

In a typical AM-4 synthesis, an alkaline solution was prepared by mixing 27.04 g sodium silicate solution (27% m/m $SiO_2$, 8% m/m $Na_2O$, Merck), 14.76 g NaOH (EKA Nobel) and 38.46 g $H_2O$. To this 40.30 g of $TiCl_3$ (15% m/m solution of $TiCl_3$ in 10% m/m HCl, Merck) were added and stirred thoroughly. The gel, with a composition 5.6 $Na_2O$ : 3.1 $SiO_2$ : 1 $TiO_2$ : 123 $H_2O$, was autoclaved at 230 °C under autogeneous pressure for 4 d. The Teflon-lined autoclaves were then quenched in cold water. The crystals, obtained in 80% yield, were filtered off, washed at room temp. with distilled water and dried overnight at 100 °C.

Thermogravimetry (TGA-50 Shimadzu analyzer) gives a total mass loss between 20 and 500 °C of *ca.* 7.4%. The crystal morphology and elemental analysis of crystals were studied on a JEOL JSM-6400 (SEM) and JEOL 2000FX (TEM). The sample studied has an Na : Ti : Si composition ratio of *ca.* 2 : 1 : 2. Diffraction data were collected with a Siemens D500 powder diffractometer using Co-K$\alpha$ X-radiation (1.799 Å). Intensity data for *h, k, l* were collected by the step counting method (step 0.01° and time 30 s) in the range 2$\theta$ 5–100°. X-Ray diffraction pattern autoindexing was performed with the PROSZKI package[7] from the well resolved first 40 lines with an absolute error of 0.02 (2$\theta$) on peak positions. A monoclinic cell swas indicated by the DICVOL[8] and POWDER[9] indexing programs with high figures of merit. Since different programs employing various indexing strategies yielded the same results, the unit cell parameters obtained were taken as correct and were refined with a non-peak weighting scheme by APPELMAN[10] which yielded $a$ = 5.19(3), $b$ = 8.59(5), $c$ = 29.35(5) Å and $\beta$ = 89.40(2)°. The space group $A2/a$ (no. 15) was unambiguously determined from systematic absences: $k + l = 2n$ ($hkl$) and $h + l = 2n$ ($h0l$). Peak intensities were altered by changing the method of sample preparation indicating the occurrence of preferred orientation effects. Scanning electron microscopic observations of crystal morphology showed that the crystalline material consists of 10–15 μm platelet single crystals likely to produce orientation effects. In order to reduce preferred orientation effects the side-loading technique was used. The program EXTRA[11] was used to extract structure factor amplitudes of 439 reflections occurring in the 2$\theta$ interval measured by the LeBail method.[12] At this stage, the following refined unit cell parameters were obtained: $a$ = 5.187, $b$ = 8.582, $c$ = 29.239 Å and $\beta$ = 89.49°.

In the absence of heavy atoms, the crystal structure was solved by direct methods using the program SIRPOW optimised for powder data.[13] Structure factors of 254 (excluding the first and several other high-angle overlappings) reflections were used. The solution of the crystal structure was performed in absence of reliable data on the chemical composition of the compound, its density and unit cell contents. This resulted in the

**Table 1** Atomic coordinates and isotropic thermal parameters for $Na_3(Na,H)Ti_2O_2[Si_2O_6]_2\cdot 2H_2O$

| Atom | Site | *x* | *y* | *z* | *B*/Å$^2$ |
|---|---|---|---|---|---|
| Ti | 8f | 0.580(3) | 0.4127(5) | 0.1686(4) | 0.5 |
| Na(1) | 8f | 0.113(5) | 0.193(2) | 0.1649(9) | 1.6 |
| Na(2) | 4e | 3/4 | 0.357(5) | 0 | 2.5 |
| Na(3) | 4e | 1/4 | 0.037(6) | 0 | 1.6 |
| Si(1) | 8f | 0.241(1) | 0.414(1) | 0.2705(6) | 0.6 |
| Si(2) | 8f | 0.597(5) | 0.108(1) | 0.0928(7) | 0.7 |
| O(1) | 8f | 0.538(7) | −0.031(8) | 0.2085(8) | 0.8 |
| O(2) | 8f | 0.723(9) | 0.260(2) | 0.2108(10) | 0.8 |
| O(3) | 8f | 0.516(5) | 0.254(3) | 0.1257(10) | 0.8 |
| O(4) | 8f | 0.547(6) | 0.117(4) | 0.0392(7) | 0.8 |
| O(5) | 8f | 0.922(4) | 0.393(2) | 0.1523(8) | 0.8 |
| O(6) | 8f | 0.878(6) | 0.029(5) | 0.1055(7) | 0.8 |
| O(7) | 8f | 0.280(6) | 0.460(4) | 0.2172(5) | 0.8 |
| Ow | 8f | 0.052(5) | 0.407(2) | 0.05223(11) | 2.5 |

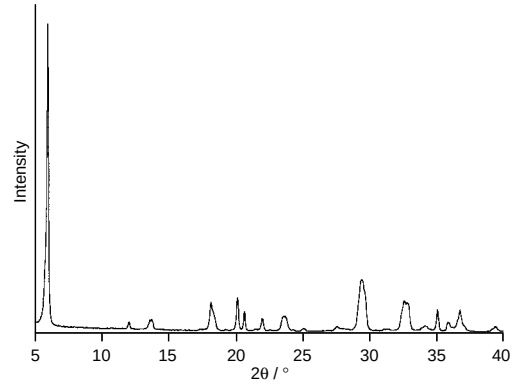



**Fig. 1** X-Ray diffraction pattern of AM-4 recorded with Cu-K$\alpha$ radiation (this was not the data used for structure refinement which was recorded with Co-K$\alpha$ radiation)

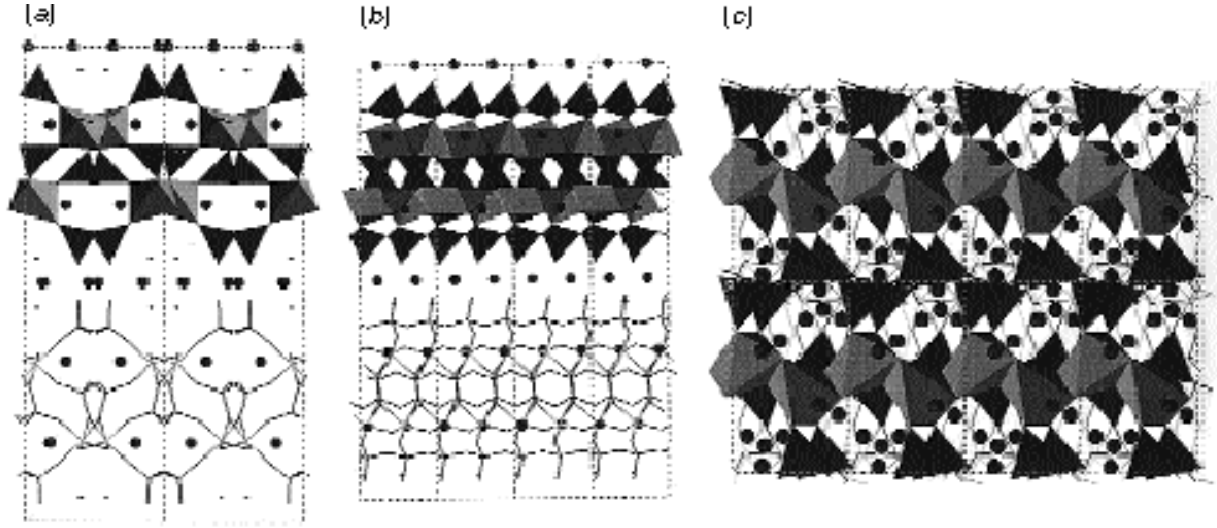



**Fig. 2** Structure of AM-4: (*a*) viewed down [100] showing the small cages containing sodium cations within the titanosilicate layers and further sodium cations between the layers; (*b*) viewed down [010]; (*c*) viewed down [001] showing chains of edge-sharing $TiO_6$ octahedra connected by chains of corner-sharing $SiO_4$ tetrahedra

need to vary the unit cell contents and the default settings of SIRPOW. Most atoms were located simultaneously, however, relabelling of atoms was necessary coupled with bond distance and bond angle changes. This procedure was alternated with least-squares refinement.

The coordinates of atoms obtained from direct methods were used in the Rietveld refinement of the structure by GSAS and are given in Table 1.[14] The final profile analysis refinement was carried out in the range $2\theta$ 13–70° and involved the following parameters: structural, 42 atomic coordinates, 14 isotropic temperature factors; profile, one scale factor, three halfwidth, three cell parameters, one peak asymmetry parameter; global parameters, one zero point, six coefficients of polynomial background. Because of instability of the peak shape coefficients several soft constraints to some of the bond distances were applied. The final results of the refinement fit correspond to a satisfactory model of the crystal structure, [$R(F^2$ = 4.5%] and profile factors ($R_p$ = 6.8%, $wR_p$ = 9.4%) indicators: space group *A*2/*a* (no. 15), *a* = 5.2012(8), *b* = 8.573(2), *c* = 29.300(6) Å, $\beta$ = 89.26(1)°, *U* = 1306.4(4) Å$^3$, *Z* = 4, $D_c$ = 2.74 g cm$^{-3}$, atoms in the asymmetric unit 14, relative mass of cell 2224.38. The experimental X-ray diffraction pattern for AM-4 is shown in Fig. 1.

The crystal structure of AM-4 is built from $TiO_6$ octahedra and $SiO_4$ tetrahedra which form layers perpendicular to [001]. Each layer consists of a five-tier sandwich of $Si_T : Ti_O : Si_T : Ti_O$-$Si_T$ (O = octahedral, T = tetrahedral) and this can be seen in Figs. 2(*a*) and (*b*). Between the layers are $Na^+$ cations and water molecules. Sodium cations also exist in small cages within the layers.

The major features of the structure are zigzag chains of edge-sharing $TiO_6$ octahedra running along [100] which are connected together by corner sharing pyroxene type $SiO_4$ tetrahedra, Fig. 2(*c*). Within the titanate chains the Ti···Ti cation repulsion is manifested in a shifting of the Ti by *ca.* 0.1 Å from the centre of the octahedron away from the shared edge. Consequently, Ti–O distances in the Ti octahedra vary widely, ranging from 1.841 Å in the oversaturated Ti–O(5) bond to 2.138 Å in the undersaturated Ti–O(7) bond. Such distortions from the average value of 1.969 Å have been observed in many so-called 'shared structures' and it produces a shortening of the shared edge O(5)···O(7) to 2.387 Å and an elongation of the opposite edge. Similar octahedral distortions take place in the structure of mineral vinogradovite.[15] The two one-dimensional and independent pyroxene-type [$Si_2O_6$] chains are also present in the structure of vinogradovite. The Si(1)–O(non-bridging) bonds are shorter than the Si(1)–O(bridging) bonds, and the O(2)–Si(1)–O(7) angle, with its two non-bridging oxygen atoms, is much larger (122.7°) than other angles.

In conclusion, we report the successful synthesis and structural determination of a novel layered titanosilicate, AM-4, which may have applications in heterogeneous catalysis, adsorption, molecular sieving and cation exchange. Work is in progress to determine whether such layered materials can be pillared in a similar manner to smectite clays.

## Footnotes and References

* E-mail: m.anderson@umist.ac.uk

† *Crystal data for AM-4*: $Na_3(Na,H)Ti_2O_2[Si_2O_6]_2 \cdot 2H_2O$, space group *A*2/*a*, *a* = 5.2012(8), *b* = 8.573(2), *c* = 29.300(6) Å, $\beta$ = 89.26(1)°, *U* = 1306.4(4) Å$^3$, *Z* = 4, $D_c$ = 2.74 g cm$^{-3}$, atoms in asymmetric unit 14, rel. mass of cell 2224.38, Co-K$\alpha$ radiation (1.799 Å). Intensity data for *h*,*k*,*l* were collected by the step counting method (step 0.01° and time 30 s) in the angular range $2\theta$ 5–100°.

1 J. Rocha, P. Brandão, Z. Lin, A. Kharlamov and M. W. Anderson, *Chem. Commun.*, 1996, 669.
2 M. Naderi and M. W. Anderson, *Zeolites*, 1996, **17**, 437.
3 Z. Lin, J. Rocha, P. Brandão, A. Ferreira, A. P. Esculcas, J. D. Pedrosa de Jesus, A. Philippou and M. W. Anderson, submitted.
4 M. S. Dadachov and A. Le Bail, *Eur J. Solid State Inorg. Chem.*, in press.
5 M. W. Anderson, O. Terasaki, T. Ohsuna, A. Philippou, S. P. Mackay, A. Ferrreira, J. Rocha and S. Lidin, *Nature*, 1994, **367**, 347; M. W. Anderson, O. Terasaki, T. Ohsuna, P. J. O'Malley, A. Philippou, S. P. MacKay, A. Ferreira, J. Rocha and S. Lidin, *Philos. Mag. B*, 1995, **71**, 813.
6 M. S. Dadachov and W. T. A. Harrison, *J Solid State Chem.*, submitted.
7 W. Lasocha and K. Lewinski, *Appl. Crystallogr.*, 1994, **27**, 437.
8 A. Boultif and D. Louer, *J. Appl. Crystallogr.*, 1991, **21**, 987.
9 S. Smith and R. L. Snyder, *J. Appl. Crystallogr.*, 1979, **12**, 60.
10 E. Appelman and H. T. Evans, Jr., US Geological Survey Computer Contribution 20, US National Technical Information Service Document PB2-16188.
11 A. Altomare, G. Cascarano, C. Giacovazzo, A. Guagliardi and A. G. G. Moliterni, *Appl. Crystallogr.*, 1995, **28**, 842.
12 A. Le Bail, H. Duroy and J. L. Fourquet, *Mater. Res. Bull.*, 1988, **23**, 447.
13 A. Altomare, G. Cascarano, C. Giacovazzo, A. Guagliardi, M. C. Burla, G. Polidori and M. Camalli, *Appl. Crystallogr.*, 1994, **27**, 435.
14 C. Larson and R. B. Von Dreele, GSAS User Guide, Los Alamos National Laboratory, NM.
15 K. Rastsvetaeva and V. I Andrianov, *Sov. Phys. Crystallogr.*, 1984, **29** 403.

*Received in Cambridge, UK, 23rd July 1997; Revised manuscript received 29th September 1997; 7/07106J*

# Catalytic and asymmetric aziridination of alkenes catalysed by a chiral manganese porphyrin complex

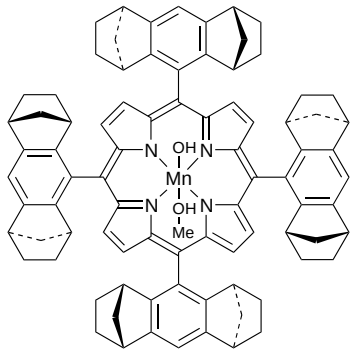
**Tat-Shing Lai,[a] Hoi-Lun Kwong,[b] Chi-Ming Che*[a] and Shie-Ming Peng[c]**

[a] *Department of Chemistry, The University of Hong Kong, Pokfulam Road, Hong Kong, PR China*
[b] *Department of Biology and Chemistry, City University of Hong Kong, Tat Chee Avenue, Kowloon Tong, Hong Kong, PR China*
[c] *Department of Chemistry, National Taiwan University, Taipei, Taiwan*

**A $D_4$-manganese(III) porphyrin is utilized to catalyze aziridination of styrene-type substrates with enantiomeric excess ranging from 43 to 68%; evidence for a $Mn^{IV}$ reactive intermediate in the catalysis was obtained from spectroscopic studies and organic product analysis.**

Metalloporphyrins have potential applications in asymmetric organic syntheses.[1] When compared to metal Schiff-base complexes, they can offer more robust catalysts[2] that can lead to high product turnover numbers and facilitate the detection and/or isolation of highly reactive intermediates in the catalyses.[3,4] Here, we report the evidence of a $Mn^{IV}$ reactive intermediate in a chiral manganese $D_4$-porphyrin-catalyzed nitrene transfer reaction. This reaction also features the first example of chiral porphyrin catalysts for asymmetric alkene aziridination with moderate enantioselectivities.

The chiral manganese(III)porphyrin catalyst Mn(P*)(MeOH)(OH) [$H_2$P* = 5,10,15,20-tetrakis(1,2,3,4,5,6,7,8-octahydro-1,4 : 5,8-dimethanoanthracen-9-yl)porphyrin] **1** used in this work was prepared by the method of Halterman and Jan.[5] Upon recrystallization of **1** from MeCN–MeOH–$CH_2Cl_2$ (1 : 10 : 2 v/v) red crystals of [Mn(P*)(MeOH)(OH)]·MeCN·MeOH·3$H_2O$ were obtained. Its structure was determined by X-ray crystal analysis† and a perspective view of the molecule is shown in Fig. 1.




**1**

With this bulky porphyrin ligand, a new manganese species which is capable of catalyzing nitrene transfer to alkenes is detected immediately after mixing stoichiometric amount of **1** and PhINTs in $CH_2Cl_2$ at room temp. This species has an apparent room temp. half-life of *ca.* 30 min in $CH_2Cl_2$ and is proposed to be a $Mn^{IV}$–PhINTs adduct (Scheme 1). The $Mn^{IV}$ formulation is based on the following reasons: its UV–VIS absorption spectrum (Fig. 2) with a Soret band at 433 nm, is similar to $Mn^{IV}$ porphyrin complexes reported previously;[6] its EPR spectrum shown in Fig. 3 is consistent with a high-spin octahedral $d^3$ ion.[6] It reacts rapidly with alkenes such as styrene to regenerate the starting complex **1** with the concomitant formation of aziridine in good yield and in moderate enantioselectivity ( > 70% yield and 50% ee for styrene) (Scheme 1). The UV–VIS spectral changes of its reaction with styrene are shown in Fig. 2. With excess styrene, the reaction follows pseudo-first-order kinetics (monitored at 480 nm) and the observed rate law is: rate = $k_2$[$Mn^{IV}$][styrene] with the second order rate constant being 2.0 × $10^{-3}$ $dm^3$ $mol^{-1}$ $s^{-1}$. Attempts were made to isolate this $Mn^{IV}$–PhINTs species in solid form by removal of the solvent at low temperature. A brown solid was obtained and its IR spectrum showed bands at 1340 and 1159 $cm^{-1}$ assigned to the tosyl moiety. However, this species slowly converted to

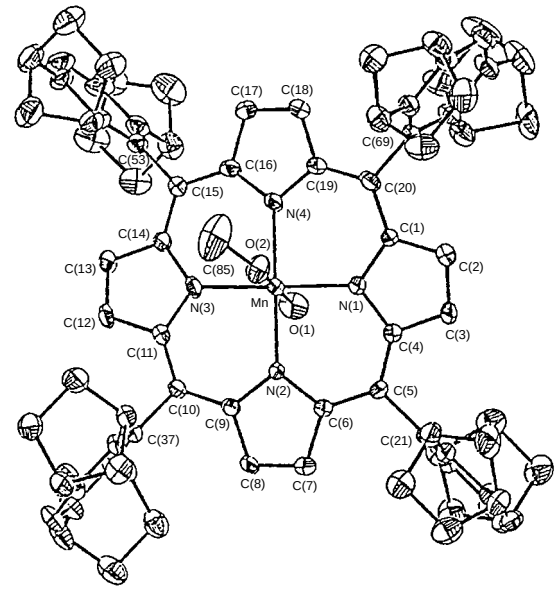
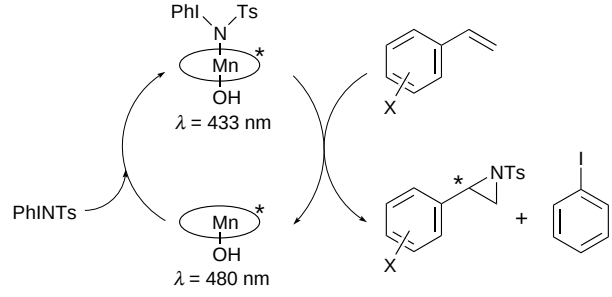



**Fig. 1** Perspective view of [Mn(P*)(MeOH)(OH)]. Selected bond lengths (Å) and angles (°): Mn–N(1) 2.004(7), Mn–N(2) 1.992(6), Mn–N(3) 2.019(7), Mn–N(4) 1.995(7), Mn–O(1) 2.268(7), Mn–O(2) 2.251(7); O(1)–Mn–O(2) 178.9(3), O(1)–Mn–N(1), 90.4(3), O(1)–Mn–N(2) 89.5(3), O(2)–Mn–N(1) 88.8(3), O(2)–Mn–N(2) 89.7(3), N(1)–Mn–N(2) 89.8(3), N(1)–Mn–N(4) 90.1(3)




**Scheme 1** Proposed catalytic cycle for enantioselective aziridination involving a $Mn^{IV}$–PhINTs adduct

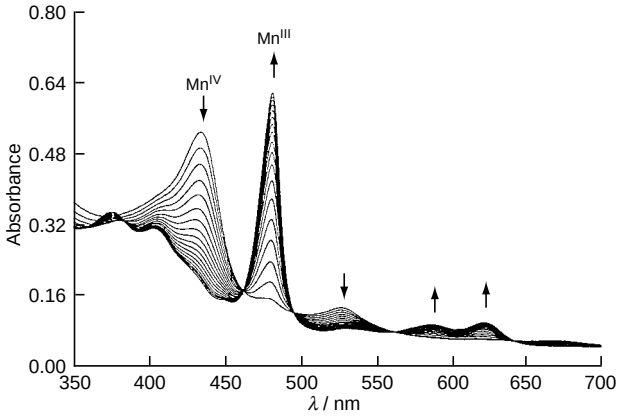



**Fig. 2** UV–VIS monitoring of the reaction between the $Mn^{IV}$–PhINTs adduct and styrene (0.48 mol $dm^{-3}$); scan interval, 1 min

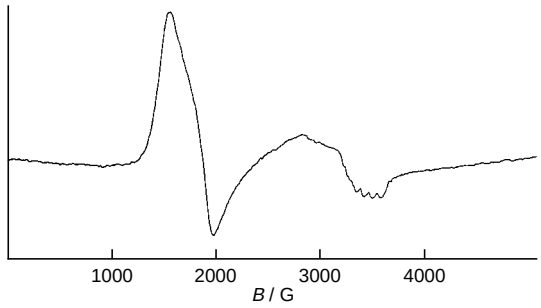


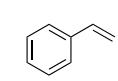
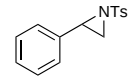
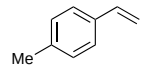
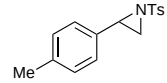
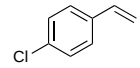
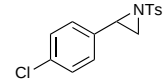
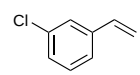
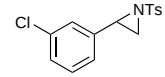
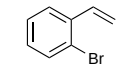
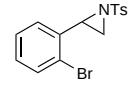
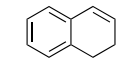
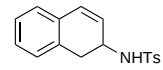
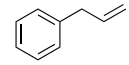
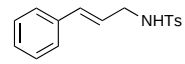

**Fig. 3** EPR spectrum of the reactive intermediate generated by mixing **1** and PhINTs in $CH_2Cl_2$ at room temp. and then cooled to 119 K

**1** and some unidentifiable substance in solution at room temperature.

The aziridination and amination of alkenes can be rendered catalytic and enantioselective by addition of PhINTs. The results are listed in Table 1. Enantioselectivity was moderate, ranging from 40 to 68% depending on both the position and the electronic demand of the substituents, with the best result obtained with *o*-bromostyrene. At a catalyst : PhINTs : alkene ratio of 1 : 200 : 4000, the chemical yields based on the amount of PhINTs used were moderate and note that the turnover numbers were good, usually around 100. With another portion of PhINTs added, the turnover number increased from 130 to *ca*. 292 in the case of styrene (Entries 2 and 3). At a catalyst : PhINTs : alkene ratio of 1 : 600 : 4000, a turnover number of 480 and aziridine at comparable ee were obtained (Entry 4). These turnover numbers are relatively high when compared with that of the reported chiral Mn–salen catalysts.[7] For alkenes that did not possess allylic hydrogen atom (Entries 1–11), aziridine was the only product. However, for alkenes that have allylic hydrogen (Entries 12 and 13), allylic amination became the major product with only minimal aziridination occurred. This result is intriguing since only a few methods for allylic amination are known.[8] From the yields and turnover numbers, the present findings feature one of the best results for catalytic allylic amination of alkenes. The absolute configuration of the aziridine obtained was *R*.

We acknowledge support from the Hong Kong Research Grants Council and The University of Hong Kong.

**Table 1** Catalytic asymmetric aziridination and amination of alkenes using PhINTs with complex **1** as the catalyst[a]

| Entry | Substrate | Product | Yield[b] (%) | % ee | Turnover |
|---|---|---|---|---|---|
| 1 |  |  | 71 | 49 | 130 |
| 2 | | | 73[d] | 55 | 142 |
| 3 | | | 72[e] | 51 | 292 |
| 4 | | | 60[f] | 43 | 480 |
| 5 |  |  | 66 | 44 | 132 |
| 6 |  |  | 43 | 45 | 86 |
| 7 | | | 47[d] | 51 | 94 |
| 8 |  |  | 49 | 49 | 98 |
| 9 | | | 53[d] | 52 | 106 |
| 10 |  |  | 44 | 62 | 88 |
| 11 | | | 56[d] | 68 | 112 |
| 12 |  |  | 73 | n.d.[g] | 146 |
| 13 |  |  | 76 | — | 152 |

[a] *Reaction conditions*: 0.50 mol% catalyst, 20-fold excess of substrate, 200 mg PhINTs and 2 ml $CH_2Cl_2$. [b] Isolated yield were based on the amount of PhINTs used. [c] Ee values are determined by HPLC analysis (Whelk-O1). [d] With 4-phenylpyridine *N*-oxide (5 mg) as additive. [e] Addition of another portion of 200 mg of PhINTs to the reaction after the first portion of PhINTs was consumed. [f] Catalyst : PhINTs : alkene = 1 : 600 : 4000. [g] Not determined.

## Footnotes and References

* E-mail: cmche@hkucc.hku.hk

† *Crystallographic data*: $C_{88}H_{94}MnN_5O_6$, $M$ = 1372.73, crystal size 0.30 × 0.50 × 0.60 mm, orthorhombic, space group $P2_12_12_1$, $a$ = 14.029(2), $b$ = 20.283(3), $c$ = 27.596(3) Å, $U$ = 7852.2(17) Å$^3$, $Z$ = 4, $D_c$ = 1.161 g cm$^{-3}$, $\mu$(Cu-K$\alpha$) = 17.83 cm$^{-1}$, $F$(000) = 2920, $2\theta_{max}$ = 140.0°, $\lambda$(Cu-K$\alpha$) = 1.5418 Å, scan type $\theta$–$2\theta$, $T$ = 298 K, no. of unique reflections = 8118, no. of observed reflections [$I > 2.0\sigma(I)$] = 4713, unit weights were used. No. of refined parameters = 902, refinement program NRCVAX, $R_f$ = 0.063, $R_w$ = 0.072, GOF = 1.87. The final Fourier difference map showed residual extrema in the range of 0.56 to −0.43 e Å$^{-3}$. CCDC 182/651.

1 (*a*) Y. Naruta, F. Tani, N. Ishihara and K. Maruyama, *J. Am. Chem. Soc.*, 1991, **113**, 6865; (*b*) J. P. Collman, L. J. Lee, C. J. Kellen-Yuen, X. Zhang, J. A. Ibers and J. I. Brauman, *J. Am. Chem. Soc.*, 1995, **117**, 692; (*c*) W. C. Lo, C. M. Che, K. F. Cheng and T. C. W. Mak, *Chem. Commun.*, 1997, 1205.
2 D. Dolphin, T. Traylor and L. Y. Xie, *Acc. Chem. Res.*, 1997, **30**, 251.
3 J. T. Groves and T. Takahashi, *J. Am. Chem. Soc.*, 1983, **105**, 2073; J. T. Groves and Y. Watanabe, *J. Am. Chem. Soc.*, 1988, **110**, 8443; W. H. Leung and C. M. Che, *J. Am. Chem. Soc.*, 1989, **111**, 8812; J. P. Collman, E. Rose and G. D. Venburg, *J. Chem. Soc., Chem. Commun.*, 1993, 935; S. M. Au, W. H. Fung, M.-C. Cheng, C. M. Che and S. M. Peng, *Chem. Commun.*, 1997, 1655.
4 R. Breslow and S. H. Gellman, *J. Chem. Soc., Chem. Commun.*, 1982, 1400; E. Svastit, J. H. Dawson, R. Breslow and S. H. Gellman, *J. Am. Chem. Soc.*, 1985, **107**, 6427; D. Mansuy, J.-P. Maby, A. Dureault, G. Bedi and P. Battioni, *J. Chem. Soc., Chem. Commun.*, 1984, 1161; J.-P. Mahy, G. Bedi, P. Battioni and D. Mansuy, *Tetrahedron Lett.*, 1988, **29**, 1927; J.-P. Mahy, G. Bedi, P. Battioni and D. Mansuy, *J. Chem. Soc., Perkin Trans. 2*, 1988, 1517.
5 R. L.Halterman and S.-T. Jan, *J. Org. Chem.*, 1991, **30**, 5253.
6 J. A. Smegal and C. L. Hill, *J. Am. Chem. Soc.*, 1983, **105**, 2920; J. A. Smegal, B. C. Schardt and C. L. Hill, *J. Am. Chem. Soc.*, 1983, **105**, 3510.
7 K. Noda, N. Hosoya, R. Irie, Y. Ito and T. Katsuki, *Synlett*, 1993, 469; H. Nishikori and T. Katsuki, *Tetrahedron Lett.*, 1996, **37**, 9245.
8 M. Johannsen and K. A. Jørgensen, *J. Org. Chem.*, 1994, **59**, 214; I. Nägeli, C. Baud, G. Bernardinelli, Y. Jacquier, M. Moran and P. Müller, *Helv. Chim. Acta*, 1997, **80**, 1087.

*Received in Cambridge, 2nd September 1997; 7/06395D*

# Absence of chiral discrimination in the interaction of tris(diphenylphenanthroline)ruthenium(II) with DNA

**Hye-Kyung Kim, Per Lincoln, Bengt Nordén and Eimer Tuite***

*Department of Physical Chemistry, Chalmers University of Technology, S-412 96 Göteborg, Sweden*

**Δ- and Λ-$[Ru(dpphen)_3]^{2+}$ (dpphen = 4,7-diphenyl-1,10-phenanthroline) bind non-intercalatively to B-form DNA and, unlike other octahedral metal complexes, show insignificant enantioselectivity in their interaction.**

Octahedral tris-diimine metal complexes possess two enantiomers having right (Δ)- and left (Λ)-handed propeller forms which might be intuitively anticipated to interact favourably with hosts having the same helical chirality, *e.g.* the right (B)- and left (Z)-handed forms of DNA, respectively. Indeed, most of these complexes have been found to interact to some degree stereoselectively with DNA.[1,2] The most dramatic reported example of such behaviour is that of $[Ru(dpphen)_3]^{2+}$, (dpphen = 4,7-diphenyl-1,10-phenanthroline) for which it has been claimed that the Δ-enantiomer interacts specifically with B-form DNA and the Λ-enantiomer specifically with Z-form DNA.[3–5] It was also suggested that this compound might bind to DNA by intercalation, perhaps with a single phenyl ring of one ligand threading through the helix to lie in the opposite grove.[6] However, the hydrophobicity and limited solubility of the salts of this complex which have been examined ($Cl^-$, $ClO_4^-$, $PF_6^-$) necessitated the addition of an organic solvent (10% $Me_2SO$ in the cited studies) which could potentially have perturbed the DNA structure and influenced the findings.

In order to study the interaction of $[Ru(dpphen)_3]^{2+}$ with DNA in purely aqueous medium, we have prepared the diacetate salt of the complex, which is more soluble than those previously examined.† The experiments have been carried out in acetate buffer which minimizes precipitation problems and allows spectroscopic measurements in aqueous solution.

Interaction with DNA is demonstrated by changes in the absorption spectrum of the complex when calf thymus (CT) DNA is present [Fig. 1]. The MLCT (metal-to-ligand charge transfer) band in the visible region experiences a red-shift, a change of band shape and hyperchromism, and the changes are of equal magnitude for both enantiomers. This contrasts with the behaviour of related metal complexes such as the externally binding $[Ru(bpy)_3]^{2+}$,[6] the non-intercalating $[Ru(phen)_3]^{2+}$,[7,8]

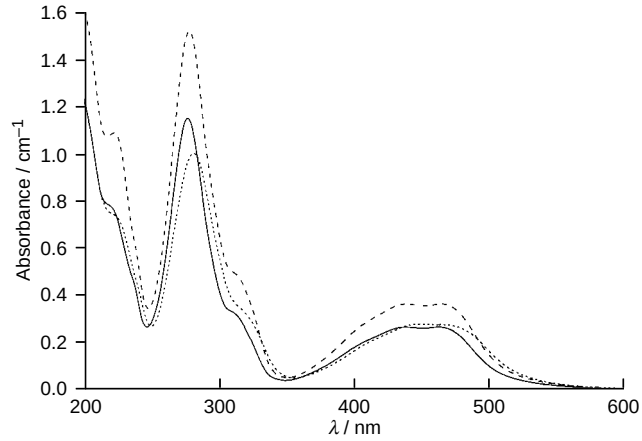
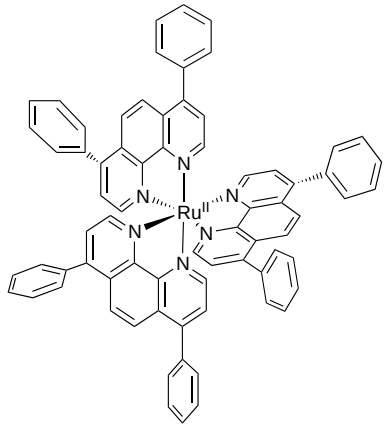
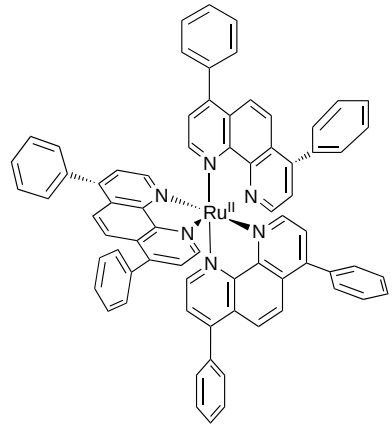



**Fig. 1** Absorption spectra of Δ-$[Ru(dpphen)_3]^{2+}$ (10 μM) in 5 mM sodium acetate buffer (pH 6.0) (—) and 50% ethanol (---) and, after subtraction of the DNA spectrum, in the presence of CT DNA (500 μM) (···). Identical changes were observed for Λ-$[Ru(dpphen)_3]^{2+}$.

and the intercalating $[Ru(phen)_2(dppz)]^{2+}$:[9] in these cases, the red-shifts in the MLCT band in the presence of DNA are accompanied by hypochromism. In order to further investigate the cause of the unusual spectral changes for $[Ru(dpphen)_3]^{2+}$, which are suggestive of a de-aggregation process, the effect of adding ethanol to an aqueous solution of the complex was examined.‡ In 50% ethanol [Fig. 1], *ca.* 33% hyperchromism, without substantial red-shifts or changes of band-shape, was observed over the entire spectrum for each enantiomer which likely results from de-aggregation of the hydrophobic metal complex, since addition of the same quantity of ethanol to a solution of the much less hydrophobic $[Ru(phen)_3]^{2+}$ (dichloride salt in the same buffer) has only a very slight hyperchromic effect (*ca.* 5%, data not shown). In the presence of DNA, it is likely that the observed spectral changes result from a combination of hyperchromism due to de-aggregation, and a




Λ-$[Ru(dpphen)_3]^{2+}$




Δ-$[Ru(dpphen)_3]^{2+}$

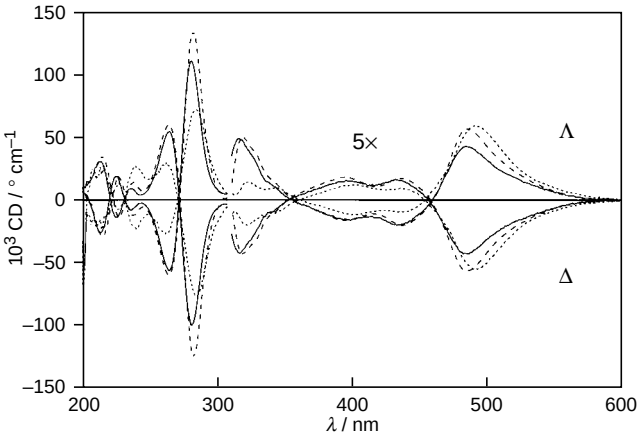



**Fig. 2** CD spectra of $[Ru(dpphen)_3]^{2+}$ enantiomers (10 μM) in 5 mM sodium acetate buffer (pH 6.0) (—) and 50% ethanol (---) and, after subtraction of the DNA spectrum, in the presence of CT DNA (500 μM) (···)

red-shift, altered band shape and hypochromism owing to the interaction with the nucleic acid (features which are quite marked in the UV region after subtraction of the DNA spectrum, assuming the latter is unaltered). The similarity of the absorption changes for Δ- and Λ-$[Ru(dpphen)_3]^{2+}$ indicates similar binding modes and affinities for both enantiomers.

In order to probe for enantioselectivity in the interaction of $[Ru(dpphen)_3]^{2+}$ with B-DNA, the circular dichroism (CD) of the complex was measured in the absence and presence of CT DNA. The Δ- and Λ-enantiomers have intrinsic CD spectra which are mirror images of each other. In the presence of DNA [Fig. 2], almost identical CD changes of equal magnitude but opposite sign were observed for the two enantiomers both in the VIS and, after subtraction of the DNA spectrum, in the UV. The CD changes due to addition of ethanol [Fig. 2] are not identical to the changes caused by DNA, so DNA binding does induce CD in addition to changes that accompany de-aggregation. Although changes of CD indicate interaction of the complex with DNA, it is not possible to interpret these changes in absolute structural terms. However, for other related metal complexes the interaction with DNA generally produces CD changes that are non-symmetric,[8,9] even for the external binder $[Ru(bpy)_3]^{2+}$. Hence, the CD spectroscopy indicates that both enantiomers interact in a similar manner with B-form DNA. This conclusion was supported by dialysis experiments of the racemate *vs*. CT DNA in which no enantioselectivity could be detected.

Linear dichroism (LD) spectroscopy has proven to be an excellent discriminator between different modes of binding of small molecules to DNA through comparison of the average orientation of the DNA bases with that of known transition moments in the molecule.[10] When $[Ru(dpphen)_3]^{2+}$ (25 μM) is added to a concentrated solution of CT DNA (500 μM), the linear dichroism observed for the metal complex in the visible region is extremely small (for Λ at *ca*. 420 nm, $LD^r$ = +0.023 normalized to perfect orientation), even by comparison with the non-intercalating $[Ru(bpy)_3]^{2+}$ complex (for Λ at *ca*. 420 nm, $LD^r$ = +0.261). This suggests that although $[Ru(dpphen)_3]^{2+}$ interacts with DNA, the orientation of the bound complex is very random which is not consistent with an intercalative geometry of the bound ligand. There is, however, a notable decrease of LD magnitude in the DNA band in the presence of $[Ru(dpphen)_3]^{2+}$ which indicates that the metal complex has a sufficiently intimate interaction with DNA to decrease its orientation.§ The DNA orientation in the presence of either Δ- or Λ-$[Ru(dpphen)_3]^{2+}$ is about 60% that of free DNA. This is a further indication of the similarity of binding of Δ- and Λ-$[Ru(dpphen)_3]^{2+}$ to B-DNA. Other metal complexes have also been found to influence DNA orientation[8,9,12] but unlike $[Ru(dpphen)_3]^{2+}$ the enantiomers usually have significantly different effects: for $[Ru(phen)_3]^{2+}$ which binds enantioselectively under similar conditions, the Δ-enantiomer causes a 50% reduction in orientation while the Λ-enantiomer affects orientation only slightly.[8]

Our conclusions are that $[Ru(dpphen)_3]^{2+}$ is an extremely hydrophobic molecule of low solubility that neither intercalates nor binds stereoselectively to B-form DNA.

This research was supported by the Carl Trygger and Wenner-Gren Foundations (E. T.), and the Swedish Natural Science Research Council (NFR) and the EU Biomed4 programme (B. N.). E. T. is grateful to the EU TMR programme for a postdoctoral fellowship.

## Footnotes and References

* E-mail: etuite@phc.chalmers.se

† Resolution of racemic $[Ru(dpphen)_3]^{2+}$ was accomplished by repetitive recrystallization of its arsenyl salt from ethanol–water [arsenyltartrate of L-(+)-tartaric acid gave the Δ-enantiomer and D-(−) gave Λ]. The complex was converted to its acetate salt by dissolution of the arsenyltartrate salt in hot acetic acid and subsequent precipitation with saturated aqueous sodium acetate. The enantiomeric purities were estimated to be > 95%.

‡ At concentrations < *ca*. 20 μM there was no precipitation of $[Ru(dpphen)_3]^{2+}$. Light-scattering experiments did not indicate the formation of large aggregates (detection limit *ca*. 40 nm) and no residual absorbance was observed above 600 nm which provided a qualitative indication of light scattering for concentrations above 50 μM.

§ The $LD^r$ of added methylene blue[11] at low binding ratio was used as an internal orientation reference.[9,12]

1 A. M. Pyle and J. K. Barton, in *Prog. Inorg. Chem.: Bioinorg. Chem.*, 1990, 413.
2 B. Nordén, P. Lincoln, B. Åkerman and E. Tuite, in *Probing of Nucleic Acids by Metal Ion Complexes of Small Molecules*, ed. A. Sigel and H. Sigel, New York, 1996, p. 177.
3 J. K. Barton, L. A. Basile, A. Danishefsky and A. Alexandrescu, *Proc. Natl. Acad. Sci. USA*, 1984, **81**, 1961.
4 C. V. Kumar, J. K. Barton and N. J. Turro, *J. Am. Chem. Soc.*, 1985, **107**, 5518.
5 A. E. Friedman, C. V. Kumar, N. J. Turro and J. K. Barton, *Nucleic Acids Res.*, 1991, **19**, 2595.
6 J. M. Kelly, A. B. Tossi, D. J. McConnell and C. OhUigin, *Nucleic Acids Res.*, 1985, **13**, 6017.
7 J. K. Barton, A. T. Danishefsky and J. M. Goldberg, *J. Am. Chem. Soc.*, 1984, **106**, 2172.
8 C. Hiort, B. Nordén and A. Rodger, *J. Am. Chem. Soc.*, 1990, **112**, 1971.
9 C. Hiort, P. Lincoln and B. Nordén, *J. Am. Chem. Soc.*, 1993, **115**, 3448.
10 B. Nordén, M. Kubista and T. Kurucsev, *Quart. Rev. Biophys.*, 1992, **25**, 51.
11 E. Tuite and B. Nordén, *J. Am. Chem. Soc.*, 1994, **116**, 7548.
12 P. Lincoln, A. Broo and B. Nordén, *J. Am. Chem. Soc.*, 1996, **118**, 2644.

*Received in Basel, Switzerland, 20th August 1997; 7/06122F*

# Solvent dependent anion selectivity exhibited by neutral ferrocenoyl receptors

**Paul D. Beer* and Matthew Shade**

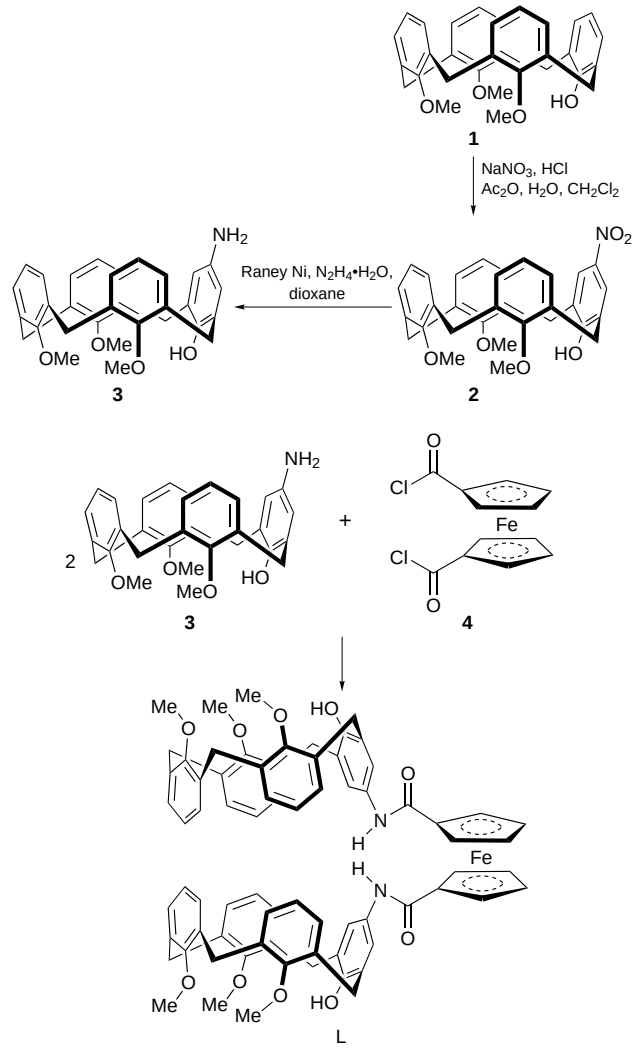
*Inorganic Chemistry Laboratory, University of Oxford, South Parks Road, Oxford, UK OX1 3QR*

**The nature of the solvent medium dramatically alters the anion recognition properties of a new bis(calix[4]arene) ferrocenoyl receptor L by influencing both the magnitude of stability constants and the anion binding selectivity trend the receptor displays.**

The recognition of anionic guest species of biochemical, medical and environmental importance by positively charged or neutral abiotic receptor molecules is an area of ever increasing research activity.[1] Although a wide range of solvents and solvent mixtures have been used in anion binding studies relatively little attention has been paid as to how the nature of the solvent affects the stability of anion–receptor complexes[2] and perhaps more importantly the anion selectivities of the receptors. We report here a preliminary investigation into the complexation of a number of anions in a range of solvents by a new neutral, amide functionalised ferrocenoyl bis(calix[4]arene) receptor[3] and demonstrate the novel finding that the solvent medium alone can dramatically influence the anion selectivity preference of a particular neutral amide containing receptor.

The trimethoxy lower-rim substituted calix[4]arene compound **1**[4] was treated with sodium nitrate and hydrochloric acid to produce the nitro derivative **2** in 80% yield. Using Raney nickel and hydrazine hydrate, **2** was reduced to the amine **3** and immediately condensed with 1,1′-bis(chlorocarbonyl) ferrocene **4**[5] to afford the new ferrocenoyl-bis(calix[4]arene) L as an orange solid in 82% yield (Scheme 1).

The anion coordination properties of L were investigated by $^1$H NMR anion titration experiments in $CD_2Cl_2$, $CD_3CN$ and $(CD_3)_2CO$ solutions with tetrabutylammonium chloride, benzoate and acetate salts. Significant downfield perturbations of the receptor's amide, cyclopentadienyl and upper-rim calix aromatic protons *ortho* to the amide groups were observed in all solvents suggesting anion binding is taking place at the bis(calix[4]arene)–ferrocenoyl upper-rim vicinity of the receptor. Stability constants were calculated from the resulting titration curves using EQNMR[6] and these values are presented in Table 1, and, for comparison purposes, Table 2 displays stability constant data for the non-calix[4]arene receptor **5**. It is immediately apparent from both Tables that the solvent exerts a very great effect on the complex equilibrium between the receptor and anionic guest with the magnitude of stability constant varying by over two orders of magnitude in some cases. A comparison of the data shows that there is no obvious relationship between complex stability and bulk solvent properties such as relative permittivity ($\varepsilon$) and dipole moment ($\mu$). It is noteworthy however, that there is a correlation between the stability constant values and the Gutmann acceptor number (AN) of the solvent,[7] which gives a quantitative measure of the solvent's hydrogen-bond donor ability. Both Tables show that as AN decreases, the stability constant values increase. A solvent with a greater AN acts as a more effective hydrogen-bond donor so solvates anions to a greater extent and competes with the receptor for binding of the anion. What is of real significance is the observation that the anion selectivity preferences of both receptors change as the solvent AN decreases. L exhibits the solvent dependent selectivity trends ($CD_2Cl_2$) $PhCO_2^-$ > $Cl^-$ > $MeCO_2^-$; ($CD_3CN$) $PhCO_2^-$ > $MeCO_2^-$ > $Cl^-$; [$(CD_3)_2CO$] $MeCO_2^-$ > $Cl^-$ > $PhCO_2^-$ while **5** shows ($CD_2Cl_2$) $PhCO_2^-$ ≈ $MeCO_2^-$ > $Cl^-$;

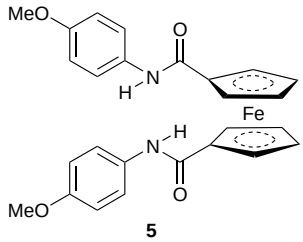



**Scheme 1**

**Table 1** Solvent effects on the stability constant values of the anion complexes of L

| | | | | $K^a$/dm$^3$ mol$^{-1}$ | | |
|---|---|---|---|---|---|---|
| | | | | Anion | | |
| Solvent | $\varepsilon$ | $\mu$ | AN | $Cl^-$ | $PhCO_2^-$ | $MeCO_2^-$ |
| $CD_2Cl_2$ | 8.9 | 1.5 | 20.4 | 40 | 117 | 26 |
| $CD_3CN$ | 36.0 | 3.96 | 18.9 | 70 | 360 | 120 |
| $(CD_3)_2CO$ | 20.7 | 2.86 | 12.5 | 5200 | 940 | 6000 |

[a] Estimated errors < 10%; $\varepsilon$ = relative permittivity, $\mu$ = dipole moment, AN = acceptor number of solvent.




**5**

**Table 2** Solvent effects on the stability constant values of the anion complexes of **5**[a]

| | | | | $K^b$/dm$^3$ mol$^{-1}$ | | |
|---|---|---|---|---|---|---|
| | | | | Anion | | |
| Solvent | $\varepsilon$ | $\mu$ | AN | $Cl^-$ | $PhCO_2^-$ | $MeCO_2^-$ |
| $CD_2Cl_2$ | 8.9 | 1.5 | 20.4 | 175 | 215 | 210 |
| $(CD_3)_2CO$ | 20.7 | 2.86 | 12.5 | 400 | 1500 | 3000 |

[a] Receptor **5** is insoluble in $CD_3CN$. [b] Estimated errors < 10%.

$[(CD_3)_2CO]$ $MeCO_2^-$ > $PhCO_2^-$ > $Cl^-$. These selectivity sequences may be rationalised in terms of relative anion solvation. As the hydrogen-bond donor ability of the solvent (AN) decreases the smaller, harder anions, acetate and chloride, become bound preferentially over the larger, charge diffuse benzoate. In the same manner that chloride and acetate are more heavily solvated in even very weakly protic solvents, in aprotic solvents they bind more strongly to the only protic source present, the ferrocene diamide receptor. As Tables 1 and 2 illustrate it can be concluded that the more heavily solvated anions are affected by changes in solvent to a greater extent than those which are less heavily solvated.

Interestingly with respect to receptor structure the introduction of the bis(calix[4]arene) cavity serves to amplify the solvent dependent anion stability constant values and selectivity effects. It can be seen from Tables 1 and 2 that the increases in stability constants (as AN decreases) for the bis(calix[4]arene) receptor are significantly larger than those for the non-calix[4]arene analogue **5**.

In conclusion the preliminary results presented here show that the nature of the solvent used in the study of anion binding by neutral hydrogen-bond donor receptors can determine both the magnitudes of stability constants and the anion binding selectivity. The selectivity of the receptors is best described in terms of the competition between the solvent and the receptor for the binding and solvation of the anions. The effect of the receptor's structure can be more clearly discerned when comparisons between stability constants and selectivities in different solvents are made and a suitable model compound is used.

We thank EPSRC for use of the mass spectrometry service at University College Swansea.

## Footnotes and References

* E-mail: paul.beer@icl.ox.ac.uk

1 B. Dietrich, *Pure Appl. Chem.*, 1993, **65**, 1457; P. D. Beer and D. K. Smith, *Prog. Inorg. Chem.*, 1997, **46**, 1.
2 T. R. Kelly and M. H. Kim, *J. Am. Chem. Soc.*, 1994, **116**, 7072.
3 For examples of calix[4]arene anion receptors, see: P. D. Beer, *Chem. Commun.*, 1996, 689 and references therein.
4 C. D. Gutsche, B. Dhawan, J. A. Levine, K. H. No and L. J. Bauer, *Tetrahedron*, 1983, **39**, 409.
5 H. J. Lorkowski, R. Pannier and A. Wende, *J. Prakt. Chem.*, 1967, **35**, 149.
6 M. J. Hynes, *J. Chem. Soc., Dalton Trans.*, 1993, 311.
7 U. Mayer, V. Gutmann and W. Gerger, *Monatsh. Chem.*, 1975, **106**, 1235; U. Mayer, *Coord. Chem. Rev.*, 1976, **21**, 159.

*Received in Cambridge, UK, 6th October 1997; 7/07181G*

# Ligand rotamers and redox isomerism: metallo-pseudo-prolines

**Marcus C. Durrant,[a] Shirley A. Fairhurst,[a] David L. Hughes,[a] Saad K. Ibrahim,[a] Mario Passos,[a,b] Arlete Queiros[b] and Christopher J. Pickett*[a]**

[a] *The Nitrogen Fixation Laboratory, John Innes Centre, Norwich Research Park, Colney, Norwich, UK NR4 7UH*
[b] *Departamento de Química, Escola de Ciências, Universidade do Mino, Campus de Gualtar, 4700 Braga, Portugal*

**A ligand rotation which orientates the oxygen atom of an amide group towards or away from a neighbouring metal centre provides rotamers A and B with *E*° potentials which differ by 150 mV; oxidation of the metal centre of B switches the system from a state in which there is a small difference in the relative populations of the rotamers to one in which the *cis*-amide conformation greatly predominates; this new metallocycle system can be viewed as a pseudo-proline with redox sensitive rotameric properties.**

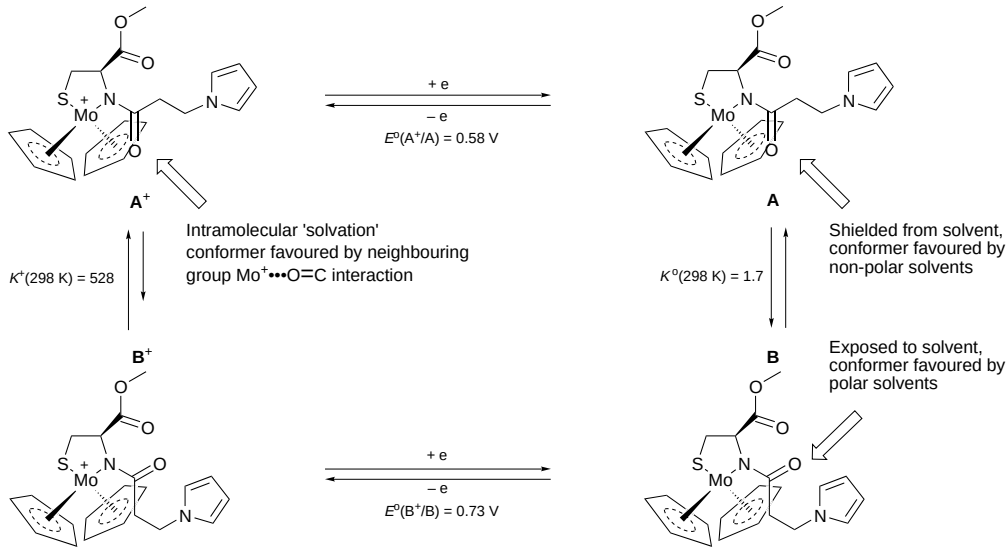
Redox-linked isomerism involving, for example, *cis–trans* rearrangement of ligands about a transition metal centre is a well established and much studied phenomenon, particularly for 17-/18-electron systems: well resolved redox processes for each isomer pair can sometimes be observed and the energetics and dynamics of interconversion of the geometric forms established.[1,2] Processes involving an essentially fixed geometric disposition of coordinating atoms about a transition metal centre and the isomerisation of a ligand rarely lead to discretely observable isomer redox processes[3] either because activation energy barriers are small and hence dynamics of isomer interconversion are fast, or because through-bond/through-space perturbations of the metal redox energetics in the two isomeric forms are weak or closely similar.

Herein we describe an exceptional system in which both the activation energy barrier for the interconversion of ligand states is sufficiently large, and electronic effects on the energetics of the redox chemistry sufficiently distinguished, to allow electrochemica observation of discrete redox isomers and their interconversion at and below ambient temperature, as set out in Scheme 1.

*N*-(3-Pyrrole-1-yl)propanoyl-L-cysteine methyl ester[4] ($H_2L$) reacts with $[Mo(\eta\text{-}C_5H_5)_2Cl_2]$ in EtOH–$NEt_3$ to give $[Mo(\eta\text{-}C_5H_5)_2L]$ which was isolated as an orange–brown crystalline material in 75% yield. $^1$H NMR [$CD_3CN$, $CD_2Cl_2$ or $(CD_3)_2NCDO$] spectroscopy of the product shows two distinct sets of resonances in each solvent, indicative of the presence of two isomeric forms of the complex. $^1$H NMR ($CD_2Cl_2$) exchange spectroscopy (EXSY) shows that the isomers interconvert. Cyclic voltammetry {MeCN, DMF or $CH_2Cl_2$–0.2 M $[NBu_4][BF_4]$; vitreous carbon} confirms the presence of two isomeric forms of $[Mo(\eta\text{-}C_5H_5)_2L]$ (**A** and **B**) each of which undergoes reversible one-electron oxidation at *E*° potentials separated by *ca.* 150 mV, Fig. 1. On the cyclic voltammetric timescale the isomer pairs **A**/**B** and $\mathbf{A}^+/\mathbf{B}^+$ are interrelated by dynamic square-scheme equilibria[2] (Scheme 1).

Cyclic voltammograms were recorded in the DMF electrolyte over a range of temperatures and scan rates and thermodynamic and kinetic parameters obtained by digital simulation of the current–potential data (Digisim 2.0).† The equilibrium constant, $K°(298\ K) = 1.7 \pm 0.1$ for the conversion of **A** to **B** estimated from the electrochemical analysis in the DMF electrolyte is concordant with that independently determined by integration of the cyclopentadienyl and methyl $^1$H NMR [$(CD_3)_2NCDO$] resonances.

X-Ray structural analysis of a crystalline sample of $[Mo(\eta\text{-}C_5H_5)_2L]$, from intensity measurements of poor quality, shows two independent molecules which are distinct conformers of the same rotamer.[5] In both molecules the Mo is chelated by cysteinyl S and amide N atoms which form part of a five-membered metallocycle ring, the amide carbonyl group is essentially co-planar with the metallocycle and its oxygen atom is deployed *trans* to the metal atom. The principal difference between the two molecules is the arrangement of the pendant $CH_2CH_2(NC_4H_4)$ group. In solution, $^1$H NMR [$CD_3CN$, $CD_2Cl_2$ or $(CD_3)_2NCDO$] data are consistent with free rotation




**Scheme 1**

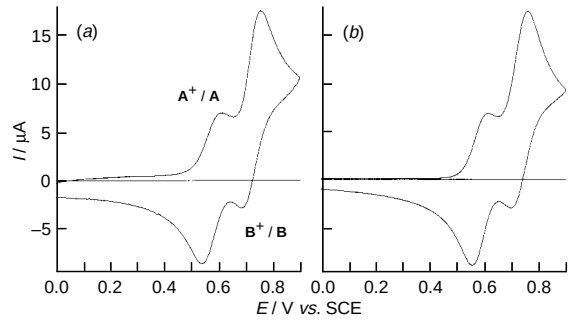



**Fig. 1** Experimental (*a*) and simulated (*b*) cyclic voltammograms for $[Mo(\eta\text{-}C_5H_5)_2L]$. Experimental data recorded in DMF–0.2 M $[NBu_4][BF_4]$ at a vitreous carbon working electrode of area 0.0707 $cm^2$; scan rate 100 mV $s^{-1}$, *T* 273 K; total concentration of $[Mo(\eta\text{-}C_5H_5)_2L]$ 2.3 mM.

about the C–C and C–N bonds in the $CH_2CH_2(NC_4H_4)$ group; evidently the difference in the solid state structures does not bear on the solution isomerism.

Molecular mechanics calculations[6] (ChemX, MM2) based on the two crystallographic structures also preclude the geometric arrangement of the pendant $CH_2CH_2(NC_4H_4)$ group as the origin of the solution isomerism. The activation energy calculated for the interconversion of the two crystallographic forms is $\Delta H^{\ddagger}_{calc.} < 5$ kcal $mol^{-1}$ (1 cal = 4.184 J) whereas the enthalpy of activation determined experimentally for the conversion of **A** to **B** in the DMF electrolyte is $\Delta H^{\ddagger}_{exp.} = 20.1$ kcal $mol^{-1}$. An activation energy barrier of this latter magnitude is more typically associated with processes involving restricted rotation about C–N amide bonds, *e.g.* DMF, 19.6 kcal $mol^{-1}$. MM2 calculations for the conversion of **A** to **B** through *cis–trans* amide bond isomerisation, as shown in Scheme 1, gives $\Delta H^{\ddagger}_{calc} = 24.7$ kcal $mol^{-1}$ which is in good agreement with the experimental data.

Further support for the *cis–trans* amide bond isomerisation process was obtained by nuclear Overhauser effect (NOE) difference spectroscopy. Irradiation of the β methylene protons of rotamer **A** in $CD_2Cl_2$ showed NOE enhancement of the γ-H resonance of the chiral centre but no enhancement of the cyclopentadienyl ring proton resonances, Fig. 2. Conversely, irradiation of the β methylene protons of rotamer **B** in $CD_3CN$ showed NOE enhancement of the cyclopentadienyl ring proton resonances but absence of NOE enhancement of the γ-H resonance, Fig. 2. This is consistent with the assignment of **A** and **B** as the *cis* and *trans*-amide isomers, respectively; the mean β-H–γ-H distances in the calculated structures are 2.3 and 4.5 Å for **A** and **B**, respectively.

The *cis–trans* amide bond isomerisation provides a rationale for other properties of the system. In the *cis* conformation the oxygen atom of the carbonyl is deployed towards the molybdenum atom (**A** calc. Mo···O distance, 3.23 Å) and through space interaction could contribute towards the stabilisation of the positive charge on the oxidised metal centre. The observation that *E*° (*cis*-rotamer $\mathbf{A}^+/\mathbf{A}$) is negative of *E*° (*trans*-rotamer $\mathbf{B}^+/\mathbf{B}$) is consistent with this (**B** calc. Mo···O distance, 4.3 Å). Stabilisation of $\mathbf{A}^+$ by what might be considered as intramolecular solvation by the amide oxygen explains why $\mathbf{A}^+$ is the thermodynamically favoured cation. The equilibrium constant for the conversion of $\mathbf{B}^+$ to $\mathbf{A}^+$ estimated from the electrochemical data is $K^+$ (298 K) ($CH_2Cl_2$) = 528, Scheme 1.

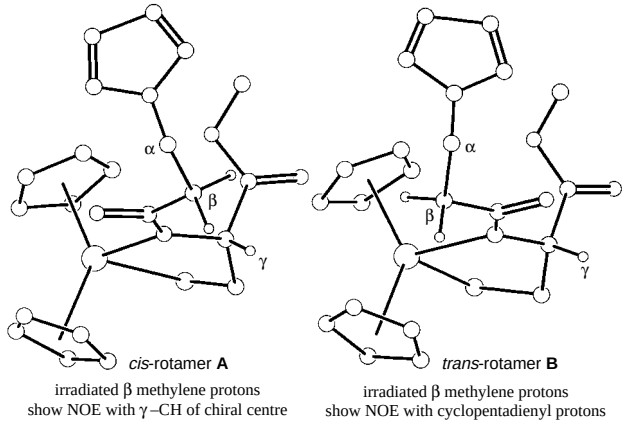



**Fig. 2**

The equilibrium between **A** and **B** is markedly solvent dependent: in polar solvents such as MeCN or DMF the *trans*-amide rotameter **B** is the more stable species, in the less polar solvent $CH_2Cl_2$ (or $CHCl_3$) the converse is true, for example, *K*° (298 K) ($CH_2Cl_2$) = 0.5 for the conversion of **A** to **B**. In the *trans* configuration, the amide oxgyen of **B** is exposed on the surface of the molecule whereas in the *cis* configuration of **A** it is shielded by the cyclopentadienyl rings. Thus polar interactions of the amide carbonyl group presumably stabilise **B** with respect to **A**. Consistent with this, IR spectroscopy in MeCN shows two distinct amide C=O bands with that for the major isomer **B** at a significantly lower energy (1562 $cm^{-1}$) than that for **A** (1582 $cm^{-1}$).

In conclusion, a ligand rotational isomerism which places the oxygen atom of an amide group close to or distant from a neighbouring metal centre can lead to redox isomers with substantially different *E*° potentials. In addition, it is evident that oxidation of the metal centre switches the system from a state in which there is a small difference in the relative thermodynamic stabilities of the isomers to one in which the *cis*-amide rotamer greatly predominates.

In a wider context, we note that the kinetics and energetics associated with *cis–trans* amide bond isomerism in prolines and in pseudo-prolines with ring heteroatoms is receiving considerable attention because of the importance of the rotamers in protein folding and recognition processes.[7] The metallocycle system described herein can be viewed as a pseudo-proline with redox-sensitive rotameric properties. Cyclopentadienyl ring substitution, N- or C-terminus modification, and/or changing the metal offer the prospect of refining the energetics and dynamics of the system. Notably, simply replacing the pyrrole group by a phenyl ring gives an analogous redox isomer system but with *K*° (298 K) (DMF) now close to unity.

We gratefully acknowledge the support of 'Comissao INVOTAN' for providing travel and subsistence funds for M. P. to work in the Nitrogen Fixation Laboratory and the BBSRC both for funding the research and for providing an equipment grant EQP05815.

## Footnotes and References

* E-mail: chris.pickett@bbsrc.ac.uk

† *Simulation parameters.* Digism 2.0 CV: heterogenous electron-transfer rate constants $k_s = 10^4$ cm $s^{-1}$ for all electron-transfer steps; electron-transfer coefficients $\alpha = 0.5$ for both rotamer couples; diffusion coefficients $D_{273\,K} = 2.0 \times 10^{-6}$ $cm^2$ $s^{-1}$ for all rotamers; uncompensated resistance $R_u = 500\ \Omega$; double layer capacitance $c_{dl} = 1$ μF; scan rate $\nu = 100$ mV $s^{-1}$ (simulation and experimental); electrode area = 0.0707 $cm^2$ (simulation and experimental); homogeneous rate-constants for decay of 17-electron cations, $k_{273\,K}$ ($\mathbf{A}^+$) = $3 \times 10^{-2}$ $s^{-1}$, $k_{273\,K}$ ($\mathbf{B}^+$) = $5 \times 10^{-2}$ $s^{-1}$; pre-equilibria enabled for all reactions; other values for *D* and *k* used for simulations at other temperatures.

1 F. L. Wimmer, M. R. Snow and A. M. Bond, *Inorg. Chem.*, 1974, **13**, 1617.
2 D. H. Evans, *Chem. Rev.*, 1990, **90**, 739.
3 T. Adachi, M. C. Durrant, D. L. Hughes, C. J. Pickett, R. L. Richards, J. Talarmin and T. Yoshida, *J. Chem. Soc., Chem. Commun.*, 1992, 1464.
4 C. J. Pickett and K. S. Ryder, *J. Chem. Soc., Dalton Trans.*, 1994, 2181.
5 D. L. Hughes, personal communication.
6 Chem-X, Chemical Design Ltd., Oxon., England, July 1996.
7 A. Yaron and F. Naider, *Crit. Rev. Biochem. Mol. Biol.*, 1993, **28**, 31.

*Received in Cambridge, UK, 12th September 1997; 7/06634A*

# Synthesis of the naturally occurring [3.3.3]propellane (±)-modhephene featuring a photocycloaddition–reductive fragmentation diquinane construction

**Curt A. Dvorak and Viresh H. Rawal†**

*Department of Chemistry, The University of Chicago, Chicago, IL 60637 and Department of Chemistry, The Ohio State University, Columbus, OH 43210, USA*

**Modhephene has been synthesized in 11 steps and 21% overall yield from cyclopentadiene, by a stereoselective route that features a photocycloaddition–fragmentation sequence for the construction of the diquinane core.**

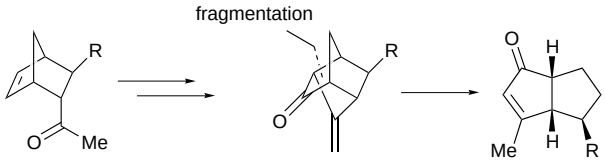
The fascinating realm of the polyquinane sesquiterpenes, recently reviewed,[1] has stimulated the development of new methodologies for the construction of fused five-membered rings. Previously we reported a route to di- and tri-quinanes that takes advantage of the connectivity gained when acylnorbornyl derivatives, obtained *via* the Diels–Alder reaction, are subjected to the Paterno–Büchi reaction (Scheme 1).[2] This expeditious assembly of a [3.3.0]bicyclic array is well suited for the synthesis of many members of the polyquinane class of natural products. We have completed concise, high-yielding syntheses of natural products having linear[2d] and angular triquinane[2b,e] frameworks using the photocycloaddition–fragmentation sequence. We report here a concise synthesis of naturally occurring propellane, modhephene **1**,[3] further extending the utility of our general strategy.

The propellane skeleton, the three contiguous quaternary centers, and the angular methyl group combine to make modhephene an attractive synthetic challenge, one taken on by several research groups.[4] We have examined two routes to modhephene, outlined retrosynthetically in Scheme 2. Appealing at first was a route that took advantage of enone **3**, a late-stage intermediate in our isocomene synthesis, wherein the methyl group stereochemistry was controlled through a Diels–Alder reaction.[2b,e] While it was possible to form the third ring by an alkylative cyclization of the terminal iodide derived from **3**,[5] the resulting enone **2** could not be converted to modhephene.[2h,l] An alternate route to the propellane framework of modhephene hinged on formation of the ring containing the angular methyl group, potentially by a radical cyclization.[6] The requisite diquinane precursor **6** was expected to be readily available through the photocycloaddition–reductive fragmentation sequence.

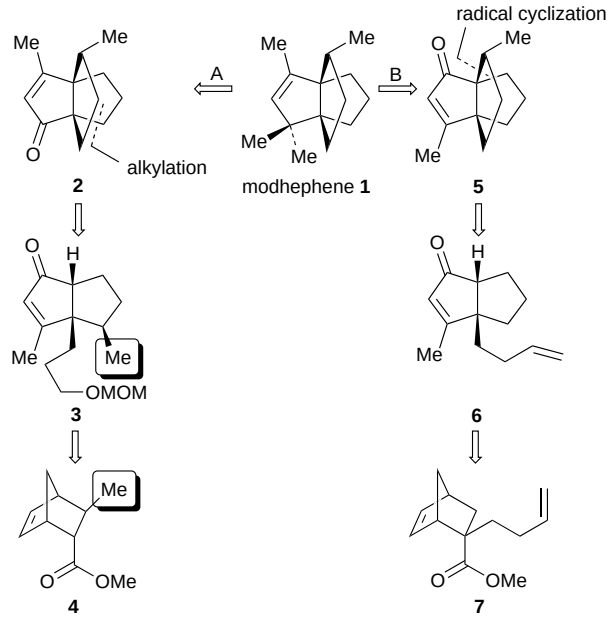
Diquinane **6** was prepared in high overall yield as described in Scheme 3. Norbornene **8**, obtained from cyclopentadiene and methyl acrylate ($H_2O$, room temp., 100%), was alkylated selectively on the *exo* face with 4-bromobut-1-ene using LDA in THF with 1,3-dimethyl-3,4,5,6-tetrahydropyrimidin-2(1*H*)-one (DMPU). The resulting ester **7** was converted into methyl ketone **9** by a one-pot modification of Corey's procedure,[7] affording the Paterno–Büchi precursor in 94% yield for the two steps. Irradiation of ketone **9** with Corex-filtered light provided oxetane **10** (89%), which possesses the connectivity required for a diquinane. Initially a three step sequence was used to convert oxetane **10** to a diquinane. Treatment of **10** with $Pr^i_2NMgI$ gave alcohol **11**, which on oxidation with pyridinium dichromate (PDC) gave keto alkene **12** in good overall yield. Reductive fragmentation of **12** afforded the expected diquinane, **6**, in 80% yield.

The hidden diquinane unit was also liberated by a novel, direct fragmentation of the strained oxetane precursor, which shortened the sequence by one step (Scheme 4). Treatment of oxetane **10** with LDBB (2.0 equiv.), the radical anion of 4,4′-di-*tert*-butylbiphenyl, in the presence of $Et_3Al$ (2.1 equiv.)[8] promoted the simultaneous scission of the oxetane C–O bond and the back-bond of the norbornane skeleton, affording diquinane moiety **13** in 86% yield.[9] The resulting allylic alcohol was then oxidized to enone **6** under standard conditions.

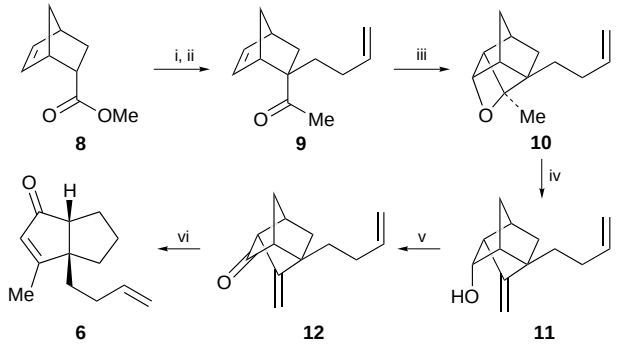
In preparation for closure of the final propellane ring, a suitable radical precursor was introduced α to the carbonyl group of **6** (Scheme 5). Selenation of the kinetic enolate of **6** afforded the desired phenyl selenide in 61% yield, provided inverse quenching conditions were employed. The bridgehead radical derived from **14** was expected to undergo 5-*exo*-*trig* cyclization onto the butenyl side-chain, concurrently setting the angular methyl group stereochemistry.[4m] Subjection of selenide **14** to standard radical conditions gave an excellent yield of the propellane (95%), albeit with a disappointing 2 : 1 ratio of inseparable diastereomers. This ratio was increased to a useful 6 : 1 level (69%) by carrying out the cyclization in toluene at −78 °C using $Et_3B$–air to initiate the radical chain.[10]



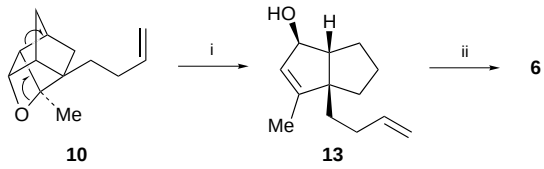

**Scheme 1**



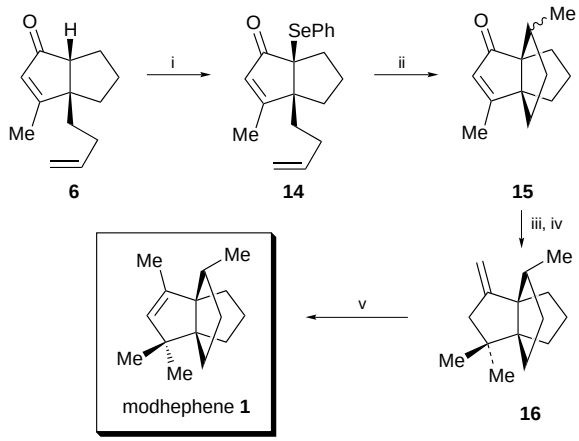

**Scheme 2**




**Scheme 3** *Reagents and conditions*: i, LDA, THF, DMPU, 4-bromobut-1-ene; ii, $MeS(O)CH_2Li$, THF; Zn, aq. NaOH, $PhCH_3$ (94% overall); iii, *hν*, PhH, corex filters (89%); iv, $Pr^i_2NMgI$ (2.6 equiv.) in THF (1.0 M), room temp., 1.5 days (87%); v, PDC (2.9 equiv.), DMF, room temp., 1 day (91%); vi, LDBB (3 equiv.) in THF (0.1 M), −78 °C (80%)




**Scheme 4** *Reagents and conditions:* i, LDBB, THF, $Et_3Al$, −78 °C, 4 h, warm to room temp., 12 h (86%); ii PDC, DMF, room temp., 16 h (91%)




**Scheme 5** *Reagents and conditions*: i, LDA, THF, −78 °C to room temp.; PhSeCl, −78 °C, inverse quench (61%); ii, $Bu_3SnH$, AIBN, PhH, reflux (2:1, 95%) (6:1 at −78 °C); iii, $Me_2CuLiCN$, THF, $Et_2O{\cdot}BF_3$; iv, $Ph_3P{=}CH_2$, THF (85% overall), MPLC separation; v, TsOH (cat.), $CH_2Cl_2$, 3 h (~100%)

The final two carbons were appended as previously described. Introduction of the geminal dimethyl unit to the hindered enone **15** requires a Lewis acid to assist the 1,4-addition of the higher order cuprate.[4b,l] Wittig olefination of the keto group with triphenylphosphonium methylide[4d] put in place the final carbon. The major diastereomer from the radical cyclization was separated at this stage by MPLC and then treated with a catalytic amount of TsOH, which isomerized the double bond to the endocyclic position, affording modhephene **1**. The minor diastereomer was similarly converted to epimodhephene.

The modhephene synthesis described here was accomplished in 11 steps from cyclopentadiene, with an overall yield of 21%, the highest to date. The synthesis illustrates the direct fragmentation of the cage-like oxetane **10** to diquinane **13** as well as the stereocontrolled formation of the propellane skeleton.

This work was supported financially by the National Institutes of Health (R01-GM-45624) and The University of Chicago. Pfizer and Merck are thanked for additional financial support in the form faculty awards to V. H. R.

## Footnote and References

† Present address: Department of Chemistry, The University of Chicago, 5735 S. Ellis Avenue, Chicago, IL 60637, USA.

1 G. Metha and A. Srikrishna, *Chem. Rev.*, 1997, **97**, 671.
2 (*a*) V. H. Rawal and C. Dufour, *J. Am. Chem. Soc.*, 1994, **116**, 2613; (*b*) V. H. Rawal, C. Dufour and A. Eschbach, *J. Chem. Soc., Chem. Commun.*, 1994, 1797; (*c*) V. H. Rawal, C. Dufour and S. Iwasa, *Tetrahedron Lett.*, 1995, **36**, 19; (*d*) V. H. Rawal, A. Fabre and S. Iwasa, *Tetrahedron Lett.*, 1995, **36**, 6851; (*e*) V. H. Rawal, A. Eschbach, C. Dufour and S. Iwasa, *Pure Appl. Chem.*, 1996, **37**, 675; (*f*) C. Dufour, S. Iwasa, A. Fabre and V. H. Rawal, *Tetrahedron Lett.*, 1996, **37**, 7867.
3 Isolation: L. H. Zalkow, R. N. Harris, III and D. Van Derveer, *J. Chem. Soc., Chem. Commun.*, 1978, 420; F. Bohlmann, C. Zdero, R. Bohlmann, R. M. King and H. Robinson, *Phytochemistry*, 1980, **19**, 579.
4 Syntheses: (*a*) M. Karpf and A. S. Dreiding, *Tetrahedron Lett.*, 1980, **21**, 4569; *Helv. Chim. Acta*, 1981, **64**, 1123; (*b*) A. B. Smith, III and P. J. Jerris, *J. Am. Chem. Soc.*, 1981, **103**, 194; *J. Org. Chem.*, 1982, **47**, 1845; (*c*) H. Schostarez and L. A. Paquette, *J. Am. Chem. Soc.*, 1981, **103**, 722; *Tetrahedron*, 1981, **37**, 4431; (*d*) W. Oppolzer and F. Marazza, *Helv. Chim. Acta*, 1981, **64**, 1575; W. Oppolzer and K. Battig, *Helv. Chim. Acta*, 1981, **64**, 2489; (*e*) P. A. Wender and G. B. Dreyer, *J. Am. Chem. Soc.*, 1982, **104**, 5805; (*f*) J. Wrobel, K. Takahashi, V. Honkan, G. Lannoye, J. M. Cook and S. H. Bertz, *J. Org. Chem.*, 1983, **48**, 139; (*g*) Y. Tobe, S. Yamashita, T. Yamashita, K. Kakiuchi and Y. Odaira, *J. Chem. Soc., Chem. Commun.*, 1984, 1259; (*h*) D. Wilkening and B. P. Mundy, *Tetrahedron Lett.*, 1984, **25**, 4619; B. P. Mundy, D. Wilkening and K. B. Lipkowitz, *J. Org. Chem.*, 1985, **50**, 5727; (*i*) G. Metha and D. Subrahmanyam, *J. Chem. Soc., Chem. Commun.*, 1985, 768; G. Metha and D. Subrahmanyam, *J. Chem. Soc., Perkin Trans. 1*, 1991, 395; (*j*) E. A. Marsh, S. K. Math and C. J. Flann, *Tetrahedron Lett.*, 1988, **29**, 2147; *Tetrahedron*, 1989, **45**, 4950; (*k*) L. Fitjer, A. Kanschik and M. Majewski, *Tetrahedron Lett.*, 1988, **29**, 5525; L. Fitjer, M. Majewski and A. Kanschik, *Tetrahedron Lett.*, 1988, **29**, 1263; (*l*) C. P. Jasperse and D. P. Curran, *J. Am. Chem. Soc.*, 1990, **112**, 5601; (*m*) C. Sha, T. Jean and D. Wang, *Tetrahedron Lett.*, 1990, **31**, 3745; (*n*) G. A. Kraus and J. Shi, *J. Org. Chem.*, 1990, **55**, 5423; *J. Org. Chem.*, 1991, **56**, 4147; (*o*) S. C. Suri, *Tetrahedron Lett.*, 1993, **34**, 8321; (*p*) T. Uyehara, T. Murayama, K. Sakai, M. Ueno and T. Sato, *Tetrahedron Lett.*, 1996, **37**, 7295; (*q*) H. Lee, D. Kim and S. Kim, *Chem. Commun.*, 1996, 1539.
5 The details of this alkylation will be reported in a full paper.
6 General reviews on radical chemistry: D. P. Curran, *Synthesis*, 1988, 417; 489; D. P. Curran, in *Comprehesnive Organic Synthesis*, ed. B. M. Trost and I. Fleming, Pergamon Press, Oxford, 1991; vol. 4, pp. 715–777; pp. 779–899; B. Giese, B. Kopping, T. Göbel, J. Dickhut, G. Thoma, K. J. Kulicke and F. Trach, *Org. React.*, 1996, **48**, 301.
7 E. J. Corey and M. Chaykovsky, *J. Am. Chem. Soc.*, 1965, **87**, 1345; J. S. Swenton, D. K. Anderson, D. K. Jackson and L. Narasimhan, *J. Org. Chem.*, 1981, **46**, 4825; K. Ishizumi, N. Ohashi and N. Tanno, *J. Org. Chem.*, 1987, **52**, 4477.
8 For an extensive investigation of the reductive fragmentation of simple oxetanes, see B. Mudryk and T. Cohen, *J. Org. Chem.*, 1989, **54**, 5657; *J. Org. Chem.*, 1991, **56**, 5760; For epoxide fragmentations, see: B. Mudryk and T. Cohen, *Org. Synth.*, 1993, **72**, 173 and references cited therein.
9 An extensive study has been carried out on the scope of this direct oxetane fragmentation, and the results have been submitted for publication.
10 K. Nozaki, K. Oshima and K. Utimoto, *J. Am. Chem. Soc.*, 1987, **109**, 2547; *Tetrahedron Lett.*, 1988, **29**, 6125; 6127.

*Received in Corvallis, OR, USA, 16th June 1997; 7/04260D*

# Conformational preferences of $R^1R^2C{=}O{\cdot}H_2BF$ complexes

**Mark D. Mackey and Jonathan M. Goodman***

*University Chemical Laboratory, Lensfield Road, Cambridge, UK CB2 1EW*

**Molecular orbital calculations have quantified both the C–H hydrogen bond and the anomeric effect in $R^1R^2C{=}O{\cdot}H_2BF$ complexes.**

It has recently been shown[1] that a hydrogen bond from a formyl C–H hydrogen to fluorine or oxygen is an important conformational restriction.[2] This is consistent with our calculations on $R^1R^2C{=}O{\cdot}H_2BF$ complexes, which prefer conformations with the fluoride eclipsing the carbonyl double bond (Fig. 1). We had suggested that this conformational preference may be due to a generalised anomeric effect,[3] which led to the interaction between fluorine and the adjacent group. The crystallographic results suggest that a formyl C–H to fluorine hydrogen bond is the controlling interaction. This can be used to explain the selectivity in many reactions. Here we report new *ab initio* calculations which allow us to investigate the relative importance of these two effects.

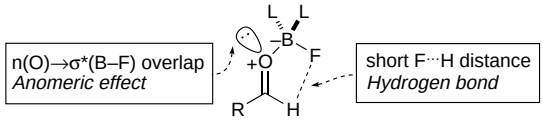



**Fig. 1** Carbonyl $H_2BF$ complexes: anomeric effect and hydrogen bond

The orientation of the coordinating Lewis acid will be affected by an anomeric effect (reinforced by a dipole–dipole interaction between the C=O and B–F bonds which we include in the anomeric effect for this analysis), a hydrogen bond and steric effects. It is not easy to separate these effects, because they will be combined in all molecules. The effect of changing from fluoride to chloride to bromide can be calculated. However, this may be expected to diminish both the anomeric effect (because the π–σ* energy match will be adversely effected) and also any H–halide interaction, because the orbital overlap will become less. This will not, therefore, help to distinguish these two effects.

We have already reported that the barrier for rotation around the O–B bond of formaldehyde complexed with $H_2BF$ (Fig. 2, structure 1) is 14 kJ mol$^{-1}$ at the MP2/6-31G*//3-21G level, using CADPAC.[4] We have now repeated this calculation at the MP2/6-31G**//MP2/6-31G** level and obtained a very similar figure (15 kJ mol$^{-1}$). In this complex, steric effects between the formyl hydrogen and the Lewis acid are likely to be small, so this should represent the sum of the anomeric effect and the hydrogen bond strength. In order to try and separate these effects, we performed calculations on the ketene complex **2** and the propynal complex **3**, reasoning that both these complexes should not have a hydrogen bond, but would show the anomeric effect. The results are summarised in Table 1.

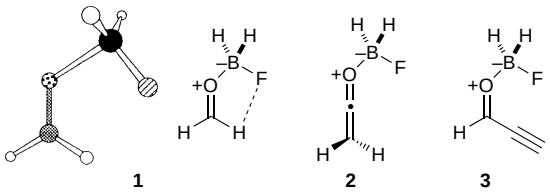



**Fig. 2** Complexes with and without hydrogen bonds

**Table 1** Results of calculations at the MP2/6-31G**//MP2/6-31G** level

| Molecule | Barrier to rotation about O–B kJ mol$^{-1}$ | H–F distance for lowest energy structure/Å | Strength of complexation/ kJ mol$^{-1}$ [a] | C=O–B–F torsion angle for lowest energy structure (°) |
|---|---|---|---|---|
| **1** | 15 | 2.20 | 48 | 0 |
| **2** | 1.4[b] | — | 15 | 0 |
| **3** | 6 | — | 34 | 0 |
| **4** | 13 | 2.04 | 54 | 60 |
| **5** | —[c] | 2.26, 2.34 | 50 | 14 |

[a] No correction for BSSE or zero-point energy was made. [b] MP2/6-31G**//3-21G level. [c] Not determined because of the size of the system.

The ketene complex **2** shows only weak association with the Lewis acid. The barrier to rotation is less than 2 kJ mol$^{-1}$, but the O–B bond is 2 Å long. We may take this as a minimum value for the magnitude of the anomeric effect, which is likely to be larger in molecules, such as **1**, for which the O–B bond is shorter.

The propynal complex **3** shows much stronger complexation. The barrier to rotation around the O–B bond is now 6 kJ mol$^{-1}$, which is a typical magnitude for an anomeric effect.[5] There is likely to be some steric repulsion between the triple bond and the fluorine, which suggests that this value may be slightly too low. However, if we accept the value of 6 kJ mol$^{-1}$ for the anomeric effect, we are left with 9 kJ mol$^{-1}$ to attribute to the hydrogen bonding interaction, for complex **1**. We may conclude, therefore, that both effects are important, but the hydrogen bonding interaction is probably larger.

Our calculations also suggested that there may be hydrogen bonding interactions to hydrogens further from the carbonyl group (Fig. 3). The barrier to rotation for the acetone complex **4** is 19 kJ mol$^{-1}$ (RHF/3-21G level). If we assume that the anomeric effect has a similar magnitude to the formaldehyde case, this gives a value of 13 kJ mol$^{-1}$ for the hydrogen bond. At a higher level of theory (MP2/6-31G**//MP2/6-31G**) the geometry of the global minimum structure changes. Instead of a C=O–B–F dihedral angle of about 0° (as found at the RHF/3-21G level and illustrated in Fig. 3), the preferred geometry has a dihedral angle of about 60°. The barrier to rotation falls to 14 kJ mol$^{-1}$. If, following Allinger,[6] we assume that the anomeric effect falls off as the square of the consine of the C=O–B–F angle, then the anomeric contribution at 60° rotation is about 1.5 kJ mol$^{-1}$. We may, therefore, suggest a strength of about 12

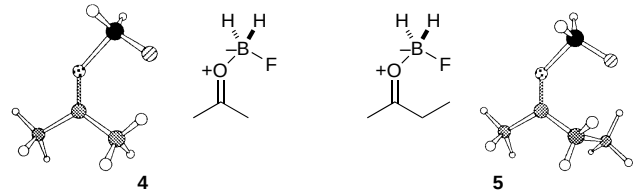



**Fig. 3** Acetone and butanone complexes (RHF/3-21G geometries)

kJ mol$^{-1}$ for the F–H hydrogen bond to the methyl group of acetone, which is similar to that estimated at the lower level of theory. This is stronger than the hydrogen bond for the formyl C–H, presumably because the geometry is better. The F–H distance in the formaldehyde complex is 2.20 Å, compared with 2.04 Å for the acetone complex. For comparison, the sum of the van der Waals radii for hydrogen and fluorine is 2.55 Å. The C–H–F angle is 100° for formaldehyde, and a more favourable 130° for acetone.

The structure of the (*Z*)-butanone complex **5**, in which the Lewis acid is complexed to the side of the ethyl group, appears to show hydrogen bonds both to the methylene adjacent to the carbonyl and also to the remote methyl group. Such an interaction is unusual, as the C–H bond is not activated by an adjacent group.[7] The geometries obtained at the low and high levels of theory are rather similar. If the energy is monitored as the O=C–C–C dihedral angle is rotated, there is a sudden change as the hydrogen bond to the methyl group breaks. This energy jump is about 4 kJ mol$^{-1}$ at the MP2/6-31G** level. The complexation energy is similar for complexation on the methyl side and the ethyl side of the ketone (there is a preference for complexation on the methyl side at the RHF/3-21G level, which diminishes at higher levels of theory), and so the energy of the interaction with the methylene hydrogen must be at about 8 kJ mol$^{-1}$, to balance the overall energy. In fact, the strength of the hydrogen bond is likely to be greater than this, because this figure does not take adverse steric effects into account.

A summary of the different effects controlling the preferred conformations of the Lewis acid complexes is given in Table 2. This should help with the further analysis of the many systems for which these effects are important.[8]

In conclusion, hydrogen bonds and anomeric effects are both important in determining the preferred conformations of carbonyl–Lewis acid complexes of this type. These calculations have allowed us to approximately quantify these effects, and this should be a useful guide in designing systems which take advantage of this interaction.

**Table 2** Quantification of anomeric and hydrogen bonding effects

| Parameter | | Energy/kJ mol$^{-1}$ |
|---|---|---|
| Anomeric effect: | (for eclipsing geometries) | 6 |
| Hydrogen bonds: | Formyl C–H | 9 |
| | α-Methyl C–H | 12 |
| | β-Methyl C–H | 4 |
| | α-Methylene C–H | 8 |

The Royal Society, the Cambridge Centre for Molecular Recognition and the EPSRC are thanked for support.

## Footnote and References

* E-mail: jmg11@cam.ac.uk

1 E. J. Corey, J. J. Rohde, A. Fischer and M. D. Azimioara, *Tetrahedron Lett.*, 1997, **38**, 33.
2 E. J. Corey and J. J. Rohde, *Tetrahedron Lett.*, 1997, **38**, 37; E. J. Corey, D. Barnes-Seeman and T. W. Lee, *Tetrahedron Lett.*, 1997, **38**, 1699; 1997, **38**, 4351.
3 J. M. Goodman, *Tetrahedron Lett.*, 1992, **33**, 7219.
4 Cambridge Analytical Derivatives Package, issue 5.0 and issue 6.0, N. C. Handy and R. Amos, Department of Chemistry, Cambridge University, UK.
5 P. P. Graczyk and M. Mikolajczyk, *Topics in Stereochemistry*, Wiley, New York, 1994, vol. 21, pp. 159–349.
6 U. Burkert and N. L. Allinger, *Molecular Mechanics*, ACS Monograph 177, Washington DC, 1982.
7 G. R. Desiraju, *Acc. Chem. Res.*, 1991, **24**, 290.
8 E. J. Corey and T. W. Lee, *Tetrahedron Lett.*, 1997, **38**, 5755; K. Ishihara, H. Kurihara and H. Yamamoto, *J. Am. Chem. Soc.*, 1996, **118**, 3049; K. Ishihara and H. Yamamoto, *J. Am. Chem. Soc.*, 1994, **116**, 1561; E. J. Corey, T.-P. Loh, T. D. Roper, M. D. Azimiora and M. C. Noe, *J. Am. Chem. Soc.*, 1992, **114**, 8290; K. Furuta, T. Maruyama and H. Yamamoto, *J. Am. Chem. Soc.*, 1991, **113**, 1041.

*Received in Cambridge, UK, 28th August 1997; 7/06288E*

# A new route for the synthesis of amphiphilic and water-soluble ligands: mono- and di-tertiary phosphines having an alkylene sulfate chain

**Henrik Gulyás, Péter Árva and József Bakos***

*Department of Organic Chemistry, University of Veszprém, H-8201 Veszprém, PO Box 158, Hungary*

**Cyclic sulfates react with $LiPPh_2$ to form a series of new amphiphilic or water-soluble ligands: monotertiary phosphines with one or two alkylene sulfate chains and ditertiary phosphines with one or two hydrophilic tails attached to bridgehead carbon atom; the application of zwitterionic $Rh^I$ complexes $(sulfatephos)_2Rh(cod)$ and (sulfatediphos)Rh(cod) in liquid biphasic catalysis has been demonstrated for the hydroformylation of styrene and oct-1-ene.**

Much effort has been directed toward the synthesis of new catalytic species, with some recent focus on water-soluble catalysts.[1] Transition metal complexes can easily be rendered water-soluble by incorporating polar substituents,[2] *e.g.* $SO_3Na$, $CO_2Na$, OH, $PMe_3^+$, $NMe_3^+$, $PO(ONa)_2$ and polyethers. We reasoned that a new route to amphiphilic or water-soluble phosphine ligands would be of particular interest because (i) a wide range of starting compounds (*e.g.* diol, triol, tetraol) is available, (ii) the synthesis is simple and (iii) it might be possible to access a series of amphiphilic or water-soluble phosphines. To the best of our knowledge, only a very few examples of ligands with amphiphilic properties have been reported,[3] and the 'sulfated' phosphines reported here are the first examples of this kind.

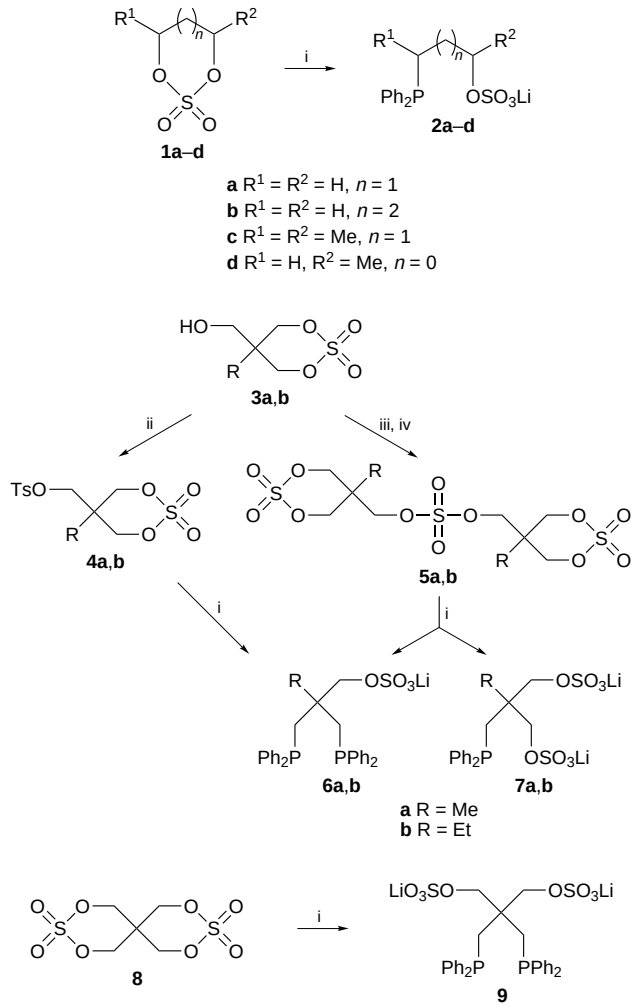
The mono- and bi-dentate phosphines were synthesized *via* the reaction of cyclic sulfates[4] with lithium diphenylphosphide. The water-solubility of these phosphines is provided by the sulfate group. Cyclic sulfates were obtained by a simple one-pot reaction from the corresponding diols, triols or tetraol following the procedure developed for 1,2-cyclic sulfates by Gao and Sharpless.[5] This involves the treatment of diols with $SOCl_2$ followed by ruthenium-catalysed oxidation.

The synthesis of the ligands is outlined in Scheme 1. A homologous series of monotertiary phosphines of the type $Ph_2PCH(R^1)(CH_2)_nCH(R^2)OSO_3Li$ ($n$ = 1,2, $R^1$ = $R^2$ = H; $n$ = 1, $R^1$ = $R^2$ = Me; $n$ = 0, $R^1$ = H, $R^2$ = Me) has been prepared. Nucleophilic attack occurred with complete inversion at the stereogenic centre of the electrophilic cyclic sulfate (**1c**) and with complete regioselectivity (**1d**).

The new ligands are monotertiary phosphine ligands (sulfatephos) with one (**2**) or two alkylene sulfate chains (**7**) or ditertiary phosphine ligands (sulfate-dppp) with one (**6**) or two hydrophilic tails (**9**) attached to the bridgehead carbon atom. A general procedure for the conversion of cyclic sulfates to amphiphilic or water-soluble phosphines was developed (Table 1). Our approach combines the introduction of the $PPh_2$ moiety and the formation of the charged β-, γ- or ω-sulfate functionality. Note that the anionic nature of the sulfate moiety, which is still a leaving group, renders it kinetically less reactive than the cyclic sulfate. Although β-substituted ethyl sulfates are subjected to hydrolyse slowly in water[6] or rapidly by using a catalytic amount of sulfuric acid,[5] the lithium salts of the sulfates in Table 1 proved to be stable in neutral or slightly basic aqueous solution. For example, when an aqueous solution of **9** was heated at 80 °C for 1 h, no appreciable decomposition or hydrolysis was detected.

The double 'sulfation' of triols (**5**) or the 'sulfation' of triols followed by tosylation (**4**) suggests a variety of useful transformations of these forgotten electrophiles. From a synthetic point of view, noteworthy applications of our methodology are those involving the mixed acyclic-bicyclic sulfate esters **5**; they lead to ditertiary phosphines **6** with very poor water-solubility and water-soluble monotertiary phosphines **7** in one reaction. In addition, **6** can also be obtained from **4**.

Compound **9** forms a complex when reacted in a 2 : 1 ratio with $[Rh(COD)Cl]_2$ in MeOH or EtOAc–$H_2O$. $^{31}P$ NMR spectroscopic data of this complex are characteristic of a cationic complex [$\delta$ 13.9 ($J_{RhP}$ 141 Hz) in $CD_3OD$ or in $D_2O$)] and do not significantly differ from those derived from dppp.[7] The MS FAB$^+$ spectrum displays a $[M + Li]^+$ peak at 855 and the MS FAB$^-$ spectrum displays a $M^-$ peak at 848. A zwitterionic structure for the complex $[Rh(COD)((Ph_2PCH_2)_2C(CH_2OSO_3Li)(CH_2OSO_3))]$ is suggested in which one of the $OSO_3^-$ groups of the ligand acts as the counterion for rhodium.




**Scheme 1** *Reagents*: i, $LiPPh_2$; ii, TsCl, pyridine; iii, $SOCl_2$; iv, $RuCl_3$, $NaIO_4$

**Table 1** Synthesis of cyclic sulfates, amphiphilic and water-soluble phosphines[a]

| Cyclic sulfate | | | Phosphine | | | Phosphine oxide[c] |
|---|---|---|---|---|---|---|
| | Yield[b] (%) | Mp/°C | | Yield[b] (%) | $\delta_P$ | $\delta_P$ |
| **1a** | 91 | 59–60 | **2a** | 84 | −16.1[d] | 43.8[d] |
| **1b** | 89 | 40–42 | **2b** | 81 | −15.9[e] | 44.2[d] |
| **1c** | 62 | 31 | **2c** | 86 | 1.1[e] | 48.1[d] |
| **1d** | 83 | oil | **2d** | 86 | −21.8[d] | 38.4[d] |
| **3a** | 77 | oil | | | | |
| **3b** | 83 | oil | | | | |
| **4b** | 50 | 74 | **6b** | 70 | −26.2[e] | 33.3[e] |
| **5a** | 36 | 152–4 | **6a** | 55 | −25.6[e] | 32.9[e] |
| | | | **7a** | 50 | −28.6[d] | 37.3[d] |
| **5b** | 41 | 95–98 | **6b** | 79 | −26.2[e] | 33.3[e] |
| | | | **7b** | 65 | −28.4[d] | 36.8[d] |
| **8** | 17 | 279 | **9** | 73 | −28.9[d] | 35.4[d] |

[a] Reactions were performed by the addition of sulfate to the solution of $LiPPh_2$ in THF at 0 to −5 °C. [b] Isolated but not optimized yields. [c] Phosphine oxide was obtained at room temperature by oxidation of the phospine with $H_2O_2$ in water or in a mixture of water and MeOH. [d] $^{31}P\{^1H\}$ NMR ($D_2O$). [e] $^{31}P\{^1H\}$ NMR ($CDCl_3$).

A preliminary investigation of the potential of **2c** and **9** in liquid biphasic catalysis has been carried out. Oct-1-ene is hydroformylated in a $H_2O$–PhMe or $H_2O$–oct-1-ene biphasic system in the presence of $[Rh(COD)Cl]_2$ associated with **2c** (35 bar of CO, 35 bar of $H_2$, 60 °C, 1 : 300 Rh to substrate ratio, 6 h, 100% conversion). In both cases, the reaction gives nonanal (54%), branched aldehydes (44%) [2-methyloctanal (38%) and 2-ethylheptanal (6%)] and isomerized octenes (2%). Most importantly, the catalytically active rhodiumcarbonyl–surfactant-phosphine complex is quantitatively recovered by simple extraction with water of the organic phase, which contains the product; the aqueous phase could be reused with a slight loss of catalytic activity. When styrene was hydroformylated in a $H_2O$–PhMe biphasic system, complete chemoselectivity for aldehydes and a high regioselectivity (up to 91%) for branched aldehydes were achieved in 3 h. Although the (1*R*,3*S*)-1-methyl-3-(diphenylphosphino)butyl lithium sulfate salt is chiral, no optical induction has been observed.

When the hydroformylation of styrene was performed with the highly water-soluble ligand **9**, complete chemoselectivity for aldehyde and an 81% regioselectivity for branched aldehydes was achieved. After reaction the organic phase was colourless, and the rhodium is located in the aqueous phase, which could be reused with a slight loss of catalytic activity. When the residue derived from the hydrocarbon layer was analysed by $^{31}P$ NMR spectroscopy, no appreciable amount of phosphorus was detected.

In conclusion we have introduced a new class of amphiphilic and water-soluble mono- and di-tertiary phosphines with considerable promise for the modification of liquid biphasic catalysis. The simplicity of the procedure and the rich achiral and chiral pool of diols, triols and tetraols should give synthetic chemists many ideas for the synthesis of achiral and even chiral water-soluble phosphines. With the homologous series of ligands, we are uniquely situated to vary the water-solubility imposed by the number of the sulfate groups and $PPh_2$ moieties without significantly varying the electronic nature of the metal centres in a corresponding series of complexes.

Financial support from the Hungarian National Science Foundation (OTKA-T016269) and the Ministry of Culture and Education (FKFP-0803/1997) is gratefully acknowledged. We are grateful to Mr Béla Édes for skillful assistance in the catalytic experiments.

## Footnote and References

* E-mail: bakos@almos.vein.hu

1 F. Joó and Á. Kathó, *J. Mol. Catal. A: Chem.*, 1997, **116**, 3; B. Cornils, W. A. Hermann and R. W. Eckl, *J. Mol. Catal. A: Chem.*, 1997, **116**, 27.
2 W. A. Hermann and C. W. Kohlpainter, *Angew. Chem., Int. Ed. Engl.*, 1993, **32**, 1524; D. Sinou, P. Kalck and F. Monteil, *Advances In Organometallic Chemistry*, Academic Press, 1992, vol. 34, p. 219; M. Barton and J. M. Atwood, *J. Coord. Chem.*, 1991, **24**, 43; M. J. Russel, *Platinum Metals Rev.*, 1988, **32**, 179.
3 B. Fell and G. Papandogianakis, *J. Mol. Catal.*, 1991, **66**, 143; H. Ding, B. E. Hanson, T. Bartik and B. Bartik, *Organometallics*, 1994, **13**, 3761; D. J. Bauer, J. Fischer, S. Kuchen, K. P. Langhans, O. Stelzer and N. Werferling, *Z. Naturforsch., Teil B*, 1994, **49**, 1511; T. Okano, N. Harada and J. Kiji, *Chem. Lett.*, 1994, **6**, 1057; H. Ding, B. E. Hanson and J. Bakos, *Angew. Chem., Int. Ed. Engl.*, 1995, **34**, 1645; E. Valls, J. Suades, B. Donadieu and R. Mathieu, *Chem. Commun.*, 1996, 771.
4 D. S. Breslow and H. Skolnik, *Multi-Sulfur and Sulfur and Oxigen Five- and Six-Membered Heterocycles, Part One*, Wiley-Interscience, New York, 1966, p. 17; G. W. Fischer and T. Zimmerman, in *Comprehensive Heterocyclic Chemistry*, ed. A. R. Katritzky and C. W. Rees, Pergamon, Oxford, 1984, vol. 6, p. 681, J. G. Tillet, *Phosphorus Sulfur*, 1987, **1**, 341.
5 Y. Gao and K. B. Sharpless, *J. Am. Chem. Soc.*, 1988, **110**, 7538.
6 D. A. Tomalia and J. Falk, *J. Heterocycl. Chem.*, 1972, **9**, 891.
7 D. A. Slack, J. Greveling and M. C. Baird, *Inorg. Chem.*, 1979, **18**, 3125.

*Received in Cambridge, UK, 10th September 1997; 7/06602C*

# 9-Alkylanthracene radical cations. An alternate route to apparent products of deprotonation

**J. M. Tanko* and Yonghui Wang**

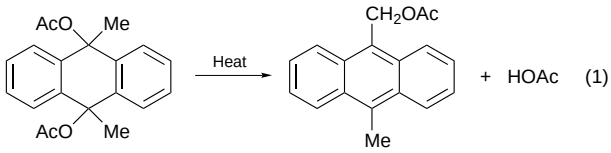
*Department of Chemistry, Virginia Polytechnic Institute and State University, Blacksburg, VA 24061-0212, USA*

**Side-chain oxidation products formed in the oxidation of 9-alkylanthracenes in MeOH–MeCN do not arise from radical cation deprotonation.**

The removal of an electron from a hydrocarbon dramatically increases its acidity. For example, the p$K_a$ of toluene drops from 41 to *ca.* −13 with the removal of a single electron. Consequently, there is a great deal of interest in the thermodynamic and kinetic acidity of radical cations.[1–4]

For an alkylaromatic radical cation, there are two competing pathways for reaction with a base (B:); side chain deprotonation (yielding a benzyl radical), and/or nucleophilic addition to the aromatic ring.[5–8] For alkylbenzenes, the side-chain deprotonation predominates. The effect of structure (of either the alkylbenzene or the base) on the rate of deprotonation has been extensively studied, and the deprotonation is believed to proceed *via* an early (reactant-like) transition state. Rate constants were successfully correlated to the Brønsted equation, with $\alpha \approx 0.25$–$0.30$.[4,9] The rate constant for deprotonation of $PhCH_3^{\bullet+}$ ($H_2O$ as base) is approximately $1.0 \times 10^7$ M$^{-1}$ s$^{-1}$.[6]

In the case of 9-alkylanthracenes, the situation is more complicated. Thermodynamically, these radical cations are quite acidic (9-methylanthracene is estimated to have a p$K_a$ of *ca.* −6.4),[2] however the literature is somewhat contradictory in terms of the extent to which these radical cations undergo deprotonation. In 1970, Parker reported that radical cations generated from 9-alkyl- and 9,10-dialkyl-anthracenes lead mainly to products derived from nucleophilic addition of solvent (water, alcohol, acetic acid, *etc*.) to the aromatic ring.[10] Moreover, when HOAc was the solvent and at elevated temperatures, the initially formed addition products were observed to eliminate HOAc and rearrange to yield a 'side-chain oxidation' product [eqn. (1)].[10] Similarly, Camaioni and

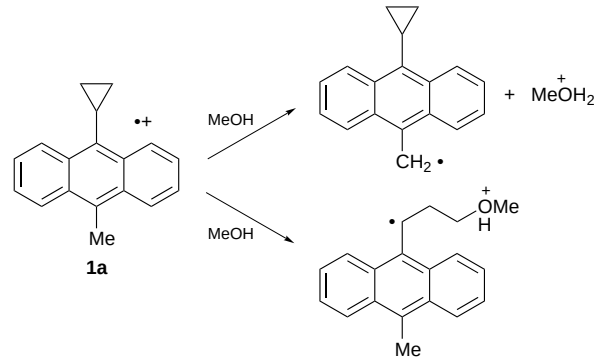



(1)

co-workers also found that a significant fraction of 'side-chain oxidation' products were derived from HOAc-addition products.[7,11] Others have generally ascribed the side-chain oxidation products as arising exclusively from deprotonation of a radical cation.[12,13]

We became interested in this problem as the result of a continuing study of the chemistry of radical cations derived from cyclopropylarenes.[14] Initially, using the radical cation generated from 9-cyclopropyl-10-methylanthracene **1a**, we had hoped to use the deprotonation reaction in an intramolecular competition to clock the rate of methanol-induced cyclopropane ring opening (Scheme 1).

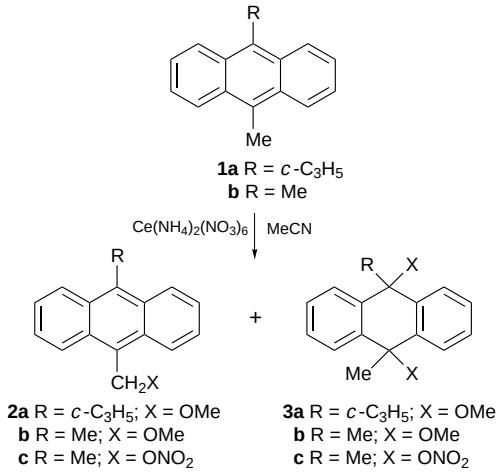
Treatment of **1a** with 1.9 equiv. of ceric ammonium nitrate in MeCN–MeOH at 45 °C led to side-chain oxidation product **2a** and ring-oxidation product **3a** (Scheme 2) in 37 and 57% yield, respectively. However, when the reaction was conducted at 0 °C, **3a** was formed in 91% yield, and no **2a** was detected (mass




**Scheme 1**

balances > 95%). This dramatic effect of temperature on the product ratio suggested that **2a** was *not* arising from the direct deprotonation of a radical cation.

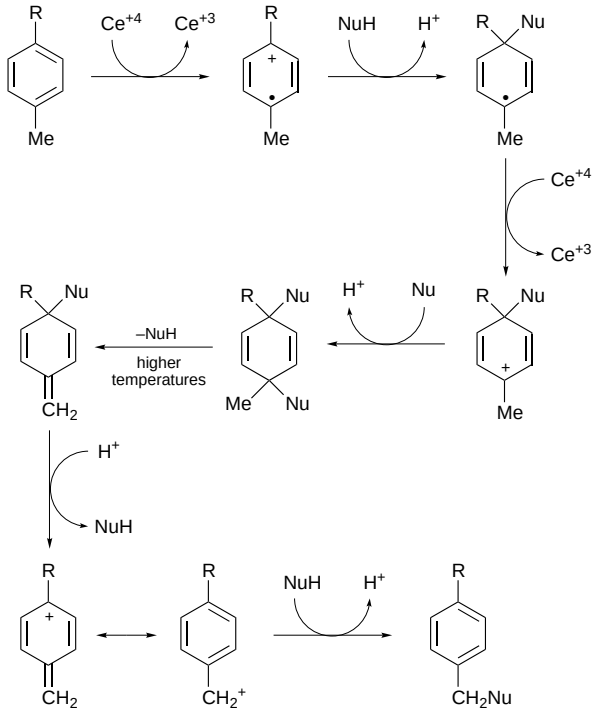
In order to test this hypothesis, 9,10-dimethylanthracene **1b** (Scheme 2) was treated with 1.9 equiv. of $Ce^{IV}$ under a variety of conditions (Table 1), and essentially the same results were obtained: at 0 °C, only ring-oxidation product **3b** was found; at 45 °C approximately equal amounts of **2b** and **3b** were formed. In order to determine whether **2b** was formed from **3b**, the following control experiment was run: **1b** was allowed to react




**Scheme 2**

**Table 1** Products arising from treatment of 9,10-dimethylanthracene with $Ce^{IV}$ under various conditions

| Reaction conditions | **2b** (%) | **3b** (%) |
|---|---|---|
| 0 °C; 30 min | 0.0 | 98.3 |
| 45 °C; 30 min | 40.8 | 53.0 |
| 0 °C; 30 min *then* 45 °C; 30 min | 0.0<br>43.0 | 94.3<br>49.0 |




**Scheme 3** Note: To conserve space, only the central ring of the 9,10-disubstituted anthracene is shown

with $Ce^{IV}$ at 0 °C for 30 min, and the reaction mixture was divided into two portions. The first portion was subject to work-up, and analyzed by $^1H$ NMR spectroscopy. The only product detected was **3b**. The second portion, which was warmed to 45 °C for 30 min and subsequently subject to the same work-up, was found to contain **2b** and **3b** in approximately the same ratio as when **1b** was reacted with $Ce^{IV}$ at 45 °C.

The conversion **3b** → **2b** is apparently favored by higher reaction temperatures, and requires the presence of a Lewis acid. (**3b** is stable at 50 °C indefinitely. However, in the presence of a small amount of $H^+$, **3b** is quantitatively converted into **2b** within 15 min.)

In the absence of MeOH, oxidation of **1b** at 0 °C, followed by work-up, leads exclusively to side-chain oxidation product **2c**. However, the failure to isolate **3c** is likely because of its instability. Indeed, when the reaction was conducted in $CD_3CN$ and analyzed by $^1H$ NMR *prior* to work-up, we found no resonances attributable to either **1b** or **2c**. We tentatively assign the observed resonances to **3c**. After work-up of the NMR sample, **2c** was the only observed product (85% yield). The presumed mechanism for these reactions is summarized in Scheme 3.

These results demonstrate that deprotonation (base = MeOH or $NO_3^-$) of 9-alkylanthracene radical cations is slow† relative to nucleophilic addition to the aromatic ring, and that little of the observed side-chain oxidation product can be attributed to deprotonation of the radical cation. The observed side-chain oxidation products actually arise from further reaction of the nucleophillic addition product. Conversion of this initially formed adduct to the side-chain oxidation product is facile in the presence of a Lewis acid and at higher reaction temperatures. Consequently, it is dangerous to draw mechanistic inferences pertaining to the deprotonation of 9-alkylanthracene radical cations based upon product analyses.‡

We gratefully acknowledge the National Science Foundation (CHE-9412814) for financial support

## Footnotes and References

* E-mail: jtanko@vt.edu

† The fact that deprotonation of radical cations is sluggish despite a potent thermodynamic driving force has been noted in the literature, see refs. 9 and 12.

‡ A reviewer has noted that our reaction conditions are non-aqueous, and that these observations may not apply to aqueous systems.

1 A. M. Nicholas and D. R. Arnold, *Can. J. Chem.*, 1982, **60**, 2165; A. M. Nicholas, R.J. Boyd and D. R. Arnold, *Can. J. Chem.*, 1982, **60**, 3011.
2 F. G. Bordwell and J. Cheng, *J. Am. Chem. Soc.*, 1989, **111**, 1792; X. Zhang and F. G. Bordwell, *J. Org. Chem.*, 1992, **57**, 4163; X. Zhang, F. G. Bordwell, J. E. Bares, J. Cheng and B. C. Petrie, *J. Org. Chem.*, 1993, **58**, 3051.
3 V. D. Parker, Y. Chao and B. Reitstöen, *J. Am. Chem. Soc.*, 1991, **113**, 2336.
4 E. Baciocchi, T. D. Giacco and F. Elisei, *J. Am. Chem. Soc.*, 1993, **115**, 12 290, and references therein.
5 V. D. Parker and L. Eberson, *Acta. Chem. Scand.*, 1970, **24**, 3542.
6 K. Sehested and J. Holcman, *J. Phys. Chem.*, 1978, **82**, 651.
7 L. A. Deardurff, M. S. Alnajjar and D. M. Camaioni, *J. Org. Chem.*, 1986, **51**, 3686.
8 E. Baciocchi, C. Rol and G. V. Sebastiani, *Gazz. Chim. Ital.*, 1982, **112**, 513.
9 C. J. Schlesener, C. Amatore and J. K. Kochi, *J. Am. Chem. Soc.*, 1984, **106**, 3567; C. J. Schlesener, C. Amatore and J. K. Kochi, *J. Am. Chem. Soc.*, 1984, **106**, 7472, and references therein.
10 V. D. Parker, *Acta Chem. Scand.*, 1970, **24**, 3455; V. D. Parker, *J. Chem. Soc., Chem. Commun.*, 1969, 873.
11 D. M. Camaioni, personal communication.
12 L. M. Tolbert and R. K. Khanna, *J. Am. Chem. Soc.*, 1987, **109**, 3477; L. M. Tolbert, R. K. Khanna, A. E. Popp, L. Gelbaum and L. A. Bottomley, *J. Am. Chem. Soc.*, 1990, **112**, 2373; P. Anzenbacker, T. Niwa, L. M. Tolbert, S. R. SIrimanne and F. P. Guengerich, *Biochemistry*, 1996, **35**, 2512.
13 Z. Li and L. M. Tolbert, *Gaodeng Xuexiao Huaxue Xuebao*, 1995, **16**, 380; Z. Li and L. M. Tolbert, *Acta Chimica Sinica*, 1995, **53**, 1204; Z. Li and L. M. Tolbert, *Youji Huaxue*, 1995, **15**, 303.
14 Y. Wang and J. M. Tanko, *J. Am. Chem. Soc.*, 1997, **119**, 8201.

*Received in Corvallis, OR, USA, 3rd July 1997; 7/04730D*

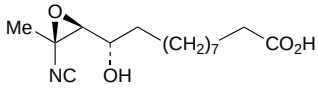
# On the synthesis of vinyl isonitriles

**Jack E. Baldwin, Deqi Chen and Andrew T. Russell**

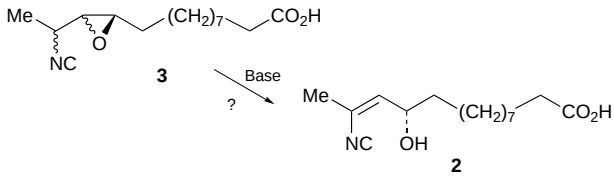
*The Dyson Perrins Laboratory, South Parks Road, Oxford, UK OX1 3QY*

**A reversal of the stereochemistry of base mediated isomerisation of some isonitrile epoxides to hydroxy-vinyl isonitriles on changing from lithium diisopropylamide to lithium bis(trimethylsilyl)amide is reported and applied to a synthesis of racemic desepoxyaerocyanidin.**

As part of our studies on the synthesis of the epoxy isonitrile antibiotic aerocyanidin **1**[1] we required access to vinyl isonitrile **2**.[2] We considered that base mediated isomerisation of an epoxide of general structure **3** could provide a stereocontrolled access to these systems (Scheme 1). During these studies we noted a pronounced dependence of the stereochemical outcome of the isomerisation on the choice of base.

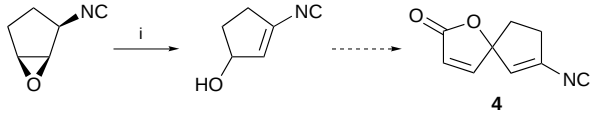



Aerocyanidin **1**

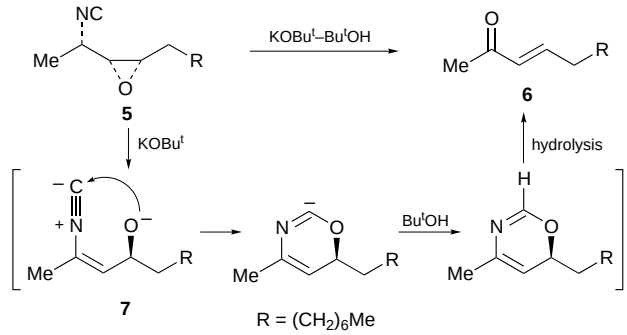



**Scheme 1**

Following our successful application of this approach to the synthesis of the spirocyclic isonitrile **4**, in which a proton *anti* to the epoxide was removed (Scheme 2),[3] we treated isonitrile epoxide **5** with Bu$^t$OK in Bu$^t$OH but obtained only the α,β-unsaturated ketone **6**. This presumably arises by rearrangement of the initially formed oxyanion **7** as proposed in Scheme 3. This result reflects observations made by Schöllkopf *et al.* regarding the stability of γ-hydroxy isonitriles in saturated acyclic systems.[4] They observed that under basic protic conditions cyclisation to the corresponding 5,6-dihydro-4*H*-1,3-oxazine occurs whereas under basic aprotic conditions the starting material was recovered. Thus we turned to the use of strong bases in an aprotic solvent system. In this context it has been shown that epoxides can be isomerised to allylic alcohols with lithium amide bases *via* a *syn*-elimination process and a cyclic six-membered transition state has been postulated to account for this.[5] Treatment of **8** with LDA in THF at −20 °C gave a 2 : 1 mixture of **9** : **10** with **9** presumably arising *via* a *syn*-β-elimination (Scheme 4).† In an attempt to optimise the selectivity of this process we exchanged the LDA for lithium bis(trimethylsilyl)amide and observed a reversal of stereoselectivity with a **9** : **10** ratio of 1 : 7. To take advantage of this enhanced selectivity we returned to diastereoisomer **5** and found



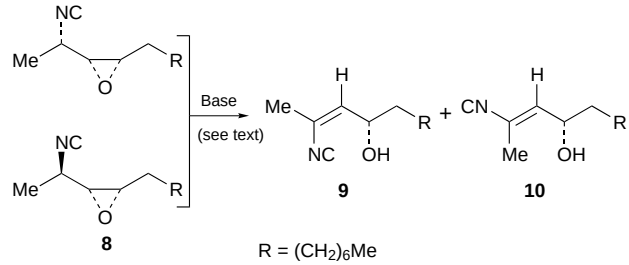

**Scheme 2** *Reagents and conditions*: i, KOBu$^t$, THF, −78 °C, 56%



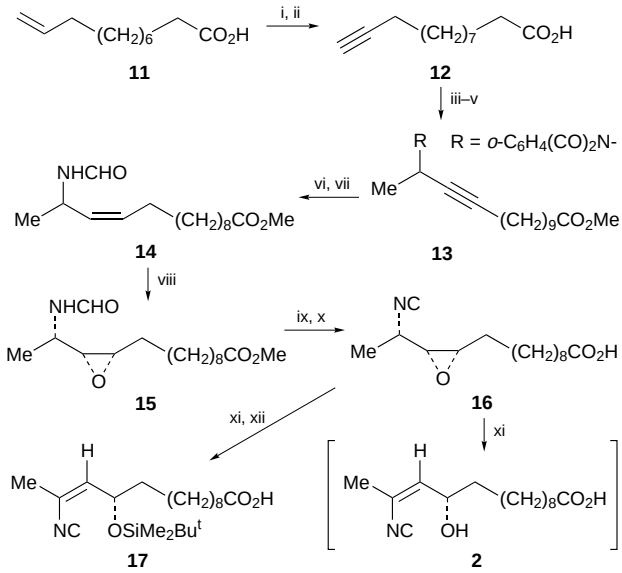

**Scheme 3**

it to rearrange with a 12 : 1 (**9** : **10**) selectivity and 96% yield. We speculated that this isomerisation proceeded through an *anti*-elimination *via* an open transition state and found that the relative rate of the *anti*-elimination could be increased by the addition of a small quantity of 12-crown-4 which resulted in an increase in selectivity for **9** to 20 : 1. Consistent with this is the observation that while LDA causes rearrangement of **5** with a 1 : 7 (**9** : **10**) ratio addition of 12-crown-4 depresses the ratio to 2 : 3.[6]

With this result in hand we undertook the synthesis of **2** (Scheme 5). Arndt–Eistert homologation of commercially available **11** afforded after bromination and elimination alkyne acid **12** in 66% overall yield. The dilithium anion of **12** was quenched with acetaldehyde and after conversion to the methyl ester introduction of the required amino group was effected under Mitsunobo conditions to give **13** (47% from **12**).[7] Hydrogenation over a Lindlar catalyst afforded the corresponding *Z*-alkene which, after deprotection of the phthalimide with methylamine, was smoothly formylated with acetic formic anhydride in 60% yield for the three steps. Taking advantage of the allylic strain in the *Z*-vinylformamide **14** we used MCPBA to affect a directed epoxidation to yield **15** as a single stereoisomer (79%).[8] Dehydration with trifluoromethanesulfonic anhydride[9] afforded the corresponding isonitrile epoxide (83%) which was saponified with $Ba(OH)_2$ (87%) to afford **16** for the key isomerisation reaction. Treatment of **16** with lithium bis(trimethylsilyl)amide at −15 °C in the presence of a small quantity 12-crown-4 afforded **2** which proved to be an unstable compound decomposing slowly to an α,β-unsaturated ketone corresponding to **6**. Therefore the lithium alkoxide of **2** was protected *in situ* as a *tert*-butyldimethylsilyl ether **17** (57%)




**Scheme 4**




**Scheme 5** *Reagents and conditions*: i, $(COCl)_2$, DMF, $CH_2Cl_2$; ii, (a) $CH_2N_2$, $Et_2O$, $Et_3N$ then $Ag_2O$, $Na_2S_2O_5$, dioxane, $H_2O$; (b) $Br_2$, $Et_2O$ then Na, liq. $NH_3$, 66% overall; iii, $Bu^nLi$, THF, −20 °C then MeCHO, THF, −5 °C, 58%; iv, $CH_2N_2$, $Et_2O$, 0 °C, 100%; v, phthalimide, $Ph_3P$, DEAD, THF, 16 h, 81%; vi, $H_2$, Lindlar's catalyst, quinoline, hexane, EtOAc, 24 h, 90%; vii, $MeNH_2$ (40% aq.) $CH_2Cl_2$, 16 h then AcOCHO, $CH_2Cl_2$, 67% (two steps); viii, MCPBA, $CH_2Cl_2$, 79%; ix, $Tf_2O$, $Pr^i_2NEt$, $CH_2Cl_2$, −78 °C, 83%; x, $Ba(OH)_2$, MeOH then citric acid, 87%; xi, LHMDS, THF, −15 °C; xii, TBSOTf, 57% (for two steps)

to permit full characterisation. The geometry of the double bond was supported by NOE spectroscopy, a 6% enhancement in the intensity of the vinylic proton resonance on irradiation of the vinyl methyl resonance being observed.

In summary we have noted a reversal of the stereochemistry of base mediated isomerisation of a series of isonitrile epoxides to allylic alcohols on switching from LDA to lithium bis-(trimethylsilyl)amide. Using this observation we have prepared racemic desepoxyaerocyanidin **2**.

## Footnotes and References

* E-mail: jack.baldwin@dpl.ox.ac.uk

† Given the established acidity of protons adjacent to isonitriles[10] we cannot preclude the possibility that the isomerisation goes, at least in part, *via* an $E_1cb$ mechanism. In circumstances where a substantial portion of the product derived from this mechanism the differences in stereochemical outcome between the diastereoisomers would require that ring opening of the epoxide is faster than bond rotation.

1 W. L. Parker, M. L. Rathnum, J. H. Johnson, J. S. Wells, P. A. Principe and R. B. Sykes, *J. Antibiot.*, 1988, **41**, 454.
2 J. E. Baldwin, R. M. Adlington, I. A. O'Neil, A. T. Russell and M.-L. Smith, *Chem. Commun.*, 1996, 41.
3 J. E. Baldwin, R. M. Adlington, J. Chondrogianni, M. S. Edenborough, J. W. Keeping and C. B. Ziegler, *J. Chem. Soc., Chem. Commun.*, 1985, 816.
4 U. Schöllkopf and R. Jentsch, *Angew. Chem., Int. Ed. Engl.*, 1973, **12**, 323.
5 J. K. Crandall and M. Apparu, in *Organic Reactions*, Wiley, New York, 1983, vol. 29, p. 345; R. P. Thummel and B. Rickborn, *J. Am. Chem. Soc.*, 1970, **92**, 2064.
6 K. M. Morgan and J. J. Gajewski, *J. Org. Chem.*, 1996, **61**, 820.
7 J. A. Marshall and A. W. Garofalo, *J. Org. Chem.*, 1993, **58**, 3675.
8 A. H. Hoveyda, D. A. Evans and G. C. Fu, *Chem. Rev.*, 1993, **93**, 1307; W. R. Roush, J. A. Straub and R. J. Brown, *J. Org. Chem.*, 1987, **52**, 5127.
9 J. E. Baldwin and I. A. O'Neil, *Synlett*, 1990, 603.
10 G. E. Niznik, W. H. Morrison and H. M. Walborsky, *J. Org. Chem.*, 1974, **39**, 600.

*Received in Cambridge, UK, 22nd September, 1997; 7/06830A*

# A new approach to peptide synthesis

**Christopher J. Moody,[a,b] Leigh Ferris,[b] David Haigh[c] and Elizabeth Swann[a]**

[a] *Department of Chemistry, University of Exeter, Stocker Road, Exeter, Devon, UK EX4 4QD*
[b] *Department of Chemistry, Loughborough University, Loughborough, Leicestershire, UK LE11 3TU*
[c] *Department of Medicinal Chemistry, SmithKline Beecham Pharmaceuticals, New Frontiers Science Park (North), Coldharbour Road, The Pinnacles, Harlow, Essex, UK CM19 5AD*

**A new approach to the synthesis of dipeptides is described based on the formation of the NHCHR[1]CONH–CHR[2]CO bond by carbenoid N–H insertion, rather than the formation of the peptide bond itself.**

Peptides and proteins play a central role in all living organisms, and hence the synthesis of such compounds has emerged as a subject in its own right.[1] In fact peptide synthesis is so highly developed that chemists rarely, if ever, consider any approach other than the formation of the amide bond (Fig. 1, disconnection 1). We now report a new approach to peptide synthesis which involves for formation of the CONH–CHRCO bond by a metal carbene N–H insertion reaction (Fig. 1, disconnection 2), and its application in the synthesis of dipeptides of dehydro amino acids, including the protected dehydro dipeptide component of the tunichrome Mm-2.

The N–H insertion reactions of metallocarbenoids, first described in 1952,[2] have found use in synthesis particularly in the construction of bicyclic β-lactams.[3] We have recently described the application of such N–H insertion reactions in the preparation of α-amino acids, α-aminophosphonates and phosphonoglycines,[4,5] and therefore were attracted by the possibility of using carbenoid N–H insertions in a synthesis of dipeptides which, unusually, does not rely on formation of the peptide bond itself. Two approaches starting from readily available *N*-protected amino acid amides **1** were considered (Scheme 1). Firstly, the use of diazo esters which would lead directly to dipeptides **2** [Scheme 1(*a*)]. There is one reported example of this approach which resulted in the synthesis of Z-Phe-α,α,α-trifluoroAla-OMe **2** (P = Z, $R^1$ = Bn, $R^2$ = $CF_3$, $R^3$ = Me) from methyl 2-diazo-3,3,3-trifluoropropionate,[6] and we have used both methyl 2-diazo-2-phenylacetate and methyl 2-diazo 3-oxobutanoate to give dipeptides **2** ($R^2$ = Ph and Ac respectively).[7,8] In the latter case the dipeptides **2** ($R^2$ = Ac) were cyclodehydrated to give oxazoles.[8,9] The second approach, which is reported herein, involves the rhodium(II)-catalysed reaction of diazophosphonoacetate to give phosphonates **3**, Wadsworth–Emmons reaction of which leads to the dehydro dipeptide **4** [Scheme 1(*b*)].

The key N–H insertion reaction was carried out by treating a mixture of the *N*-protected amino acid amide **5** and triethyl diazophosphonoacetate with a catalytic amount of rhodium(II) acetate in toluene, and resulted in the formation of the phosphonates **6** in good yield (Scheme 2, Table 1). The N–H insertion reaction was completely regioselective, in that no competing insertion into the carbamate N–H bond was

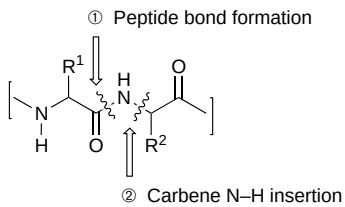
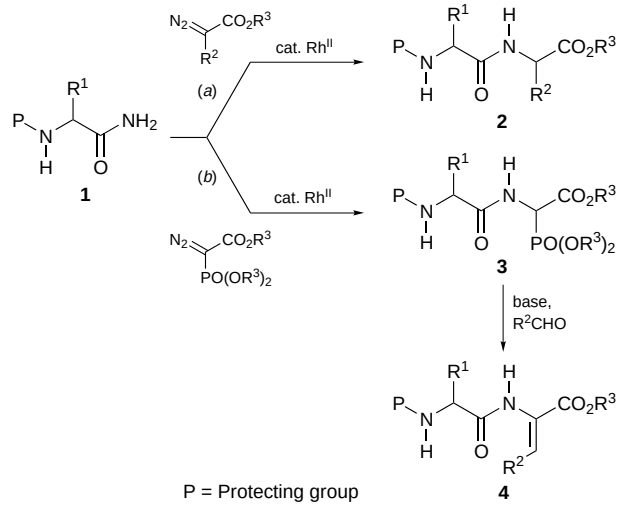
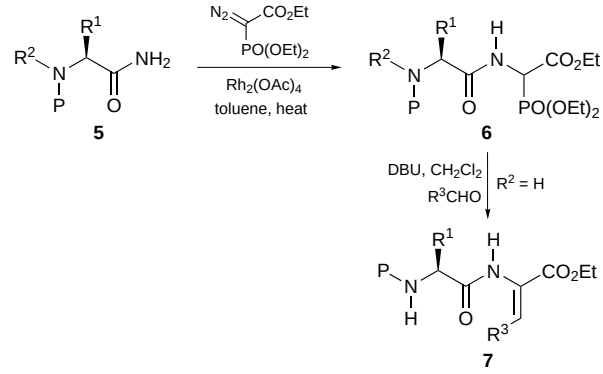



**Fig. 1**




**Scheme 1**

observed. Although related phosphonates have been prepared previously by synthesis of the corresponding α-aminophosphonate followed by peptide coupling,[10] the simplicity of this new method gives it some advantages. Wadsworth–Emmons reaction of the phosphonates **6** with a range of aldehydes using DBU as base[11] gave the corresponding dehydro dipeptides **7** in good yield (Scheme 2, Table 2). In each case a




**Scheme 2**

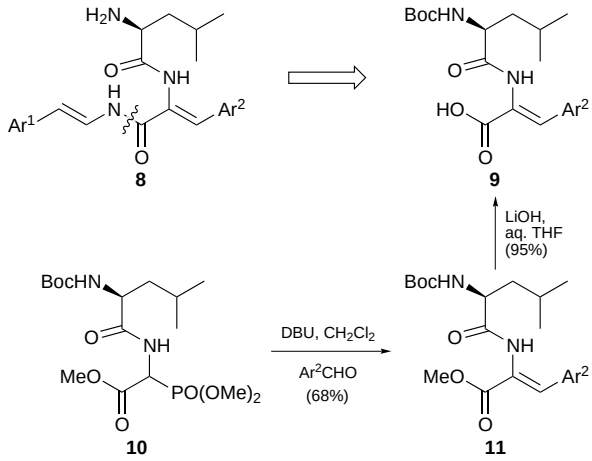
**Table 1** Formation of phosphonates **6** from amides **5**

| Amide | P | $R^1$ | $R^2$ | Phosphonate | Yield (%) |
|---|---|---|---|---|---|
| **5a** | Z | H | H | **6a** | 81 |
| **5b** | Boc | Me | H | **6b** | 88 |
| **5c** | Z | Me | H | **6c** | 80 |
| **5d** | Boc | $Pr^i$ | H | **6d** | 80 |
| **5e** | Boc | $Bu^i$ | H | **6e** | 82 |
| **5f** | Z | $-(CH_2)_3-$ | | **6f** | 80 |

**Table 2** Formation of dehydro dipeptides **7** from phosphonates **6**

| Phosphonate | P | $R^1$ | $R^3$ | Dehydro dipeptide | | Yield (%) |
|---|---|---|---|---|---|---|
| **6a** | Z | H | Ph | Z-Gly-ΔPhe-OEt | **7a** | 82 |
| **6b** | Boc | Me | Ph | Boc-Ala-ΔPhe-OEt | **7b** | 88 |
| **6e** | Boc | Bu$^i$ | Ph | Boc-Leu-ΔPhe-OEt | **7c** | 88 |
| **6e** | Boc | Bu$^i$ | Pr$^i$ | Boc-Leu-ΔLeu-OEt | **7d** | 82 |
| **6e** | Boc | Bu$^i$ | Ar$^a$ | Boc-Leu-ΔTrp-OEt | **7e** | 80 |

$^a$ Ar = *N*-Boc-indol-3-yl.




**Scheme 3**

single diastereoisomer was formed which on the basis of literature precedent was assigned the *Z*-configuration.

Finally, the new approach to dipeptides was applied to the synthesis of the dehydro dipeptide fragment of Mm-2 **8** ($Ar^1$ = $Ar^2$ = 3,4-dihydroxyphenyl), a blood pigment of the tunicate *Molgula manhattensis*.[12] Although this compound has been synthesised previously,[12] the projected disconnection (Scheme 3) to the protected dehydro dipeptide **9** ($Ar^2$ = 3,4-dibenzyloxyphenyl) differs from the published strategy. The phosphonate **10**, prepared from *N*-Boc-leucinamide and trimethyl phosphonoacetate in exactly the same way as its triethyl analogue **6e**, reacted readily with 3,4-dibenzyloxybenzaldehyde to give the required dipeptide **11** ($Ar^2$ = 3,4-dibenzyloxyphenyl) as a single *Z*-diasteromer. Hydrolysis of ester **11** gave the required acid **9** in 95% yield (Scheme 3).

In summary, we have shown that carbenoid N–H insertion reactions can be applied in a new approach to peptides which does not involve the formation of the peptide bond itself; such an approach may offer advantages in some cases.

We thank Loughborough University and SmithKline Beecham Pharmaceuticals for their support.

## Footnote and References

* E-mail: c.j.moody@exeter.ac.uk

1 For example, J. Jones, *The Chemical Synthesis of Peptides*, Clarendon, Oxford, 1991.
2 P. Yates, *J. Am. Chem. Soc.*, 1952, **74**, 5376.
3 For a compilation of references, see ref. 4.
4 E. Aller, R. T. Buck, M. J. Drysdale, L. Ferris, D. Haigh, C. J. Moody, N. D. Pearson and J. B. Sanghera, *J. Chem. Soc., Perkin Trans. 1*, 1996, 2879.
5 L. Ferris, D. Haigh and C. J. Moody, *J. Chem. Soc., Perkin Trans. 1*, 1996, 2885.
6 S. N. Osipov, N. Sewald, A. F. Kolomiets, A. V. Fokin and K. Burger, *Tetrahedron Lett.*, 1996, **37**, 615.
7 C. J. Moody and R. T. Buck, unpublished results.
8 M. C. Bagley, R. T. Buck, S. L. Hind, C. J. Moody and A. M. Z. Slawin, *Synlett*, 1996, 825.
9 C. J. Moody and M. C. Bagley, *Synlett*, 1996, 1171.
10 U. Schmidt and B. Riedl, *Synthesis*, 1993, 815.
11 U. Schmidt, H. Griesser, V. Leitenberger, A. Lieberknecht, R. Mangold, R. Meyer and B. Riedl, *Synthesis*, 1992, 487.
12 D. Kim, Y. Li, B. A. Horenstein and K. Nakanishi, *Tetrahedron Lett.*, 1990, **31**, 7119.

*Received in Cambridge, UK, 15th September 1997; 7/06658I*

# Molecular structure and magnetic properties of *N*,*N*-bis{4-methoxy-3,5-bis(*N*-*tert*-butyl-*N*-oxyamino)phenyl}aminoxyl. An approach to a stable and high-spin pentaradical

**Junpei Fujita,[a] Yoshihisa Matsuoka,[a] Kenji Matsuo,[a] Masakazu Tanaka,[a] Takeyuki Akita,[a] Noboru Koga*[a] and Hizu Iwamura*[b]**

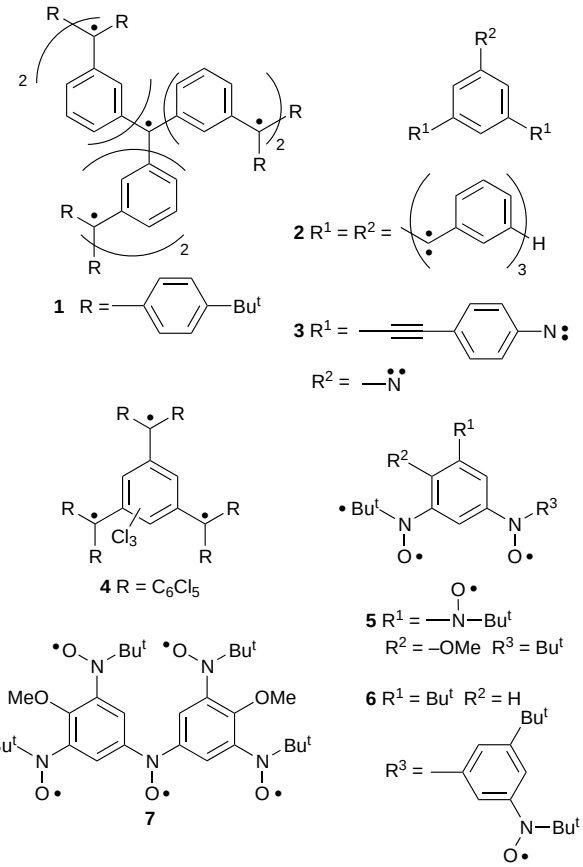
[a] *Faculty of Pharmaceutical Sciences, Kyushu University, Fukuoka 812-82, Japan*
[b] *Institute for Fundamental Research of Organic Chemistry, Kyushu University, Fukuoka 812-81, Japan*

**A stable pentaradical, *N*,*N*-bis{4-methoxy-3,5-bis(*N*-*tert*-butyl-*N*-oxyamino)phenyl)}aminoxyl, is prepared and its ground state determined to be a sextet ($S$ = 5/2) by SQUID magnetization measurements of the pentaradical diluted in poly(vinyl chloride) matrix.**

Poly(triarylmethyl) radical **1** ($S$ = 7/2),[1] nonacarbene **2** ($S$ = 9),[2] and trinitrene **3** ($S$ = 3)[3] are some of the highest-spin organic molecules rivalling high-spin $3d^5$ $Mn^{II}$, $Fe^{III}$ and $4f^7$ $Gd^{III}$ ions. However, these organic open-shell species are kinetically unstable and can be kept only in solid solution at cryogenic temperature under exclusion of air. Stable counterparts that can be bottled in the neat state under air are limited to perchlorinated triradical **4** ($S$ = 3/2).[4] Knowing that the methoxy group, while weakening the ferromagnetic coupling, increases the kinetic stability of **5**,[5] and that **6**[6] is a reasonably stable quartet, we designed pentakis(aminoxyl) radical **7** as a stable, high-spin, and high-spin-density pentaradical.

Pentaradical **7** was prepared in a manner similar to the procedure[6] for triradical **6** by using bis(hydroxyamino) derivatives protected with *tert*-butyldimethylsilyl groups in place of protected monohydroxylamines. A solution of 1-bromo-4-methoxy-3,5-bis[*N*-*tert*-butyl-*N*-(*tert*-butyldimethylsiloxy)-amino]benzene in THF was lithiated with *n*-butyllithium and coupled with 0.5 mol equiv. of pentyl nitrite to give monoradical **7a**† (7.7%) whose EPR spectrum ($\nu_0$ = 9.509 GHz) in benzene showed a hyperfine structure consisting of a triplet of quintets ($a_N$ = 10 G, $a_H$ = 1.85 G). Monoradical *N*,*N*-bis[4-methoxy-3,5-bis(*N*-*tert*-butyl{*N*-*tert*-butyldimethylsiloxy}-amino)phenyl]aminoxyl **7a** was deprotected in the presence of $NBu^n_4F$ followed by oxidation with silver oxide in ether and purification by column chromatography (silica gel/*n*-hexane–diethyl ether). Recrystallization from ether gave indefinitely stable pentaradical **7** as red needles.‡ It is somewhat unstable in dilute benzene and THF solution; a decrease of the EPR signal intensity by 5% was observed after 24 h under ambient conditions. Pentaradical **7** crystallizes in the monoclinic space group $P2_1/n$ (no. 14) with four molecules in the unit cell. An ORTEP drawing and stick model for the molecular and crystal structure of **7** are shown in Fig. 1(*a*) and (*b*), respectively.‡

The crystal was found to contain 0.5 of a molecule of diethyl ether per molecule of **7** and it is situated near the radical unit $S_{A1}$. The molecular structure of **7** has no symmetry axis and two sets of aminoxyl radicals $S_A$ and $S_B$ have *syn* and *anti*§ conformations, respectively, with respect to the benzene ring. The dihedral angles of the central *N*,*N*-diarylaminoxyl radical $S_C$ with the two aryl rings are 23.7 and 32.9° and those of $S_A$ and two $S_B$ with the benzene rings are relatively large [60–76°; Fig. 1(*a*)]. The average distances among the three aminoxyl radical moieties within a molecule are in the range 4.96–5.74 Å to construct a two-triangular five-spin system. As indicated in Fig. 1(*b*), there are two intermolecular short distances i and ii between the radical centers which should be responsible for the appearance of a strong intermolecular antiferromagnetic interaction at low temperature;[8] two molecules make a head-to-tail dimer structure with a separation of 3.35 Å and the resulting dimers align at a distance of 3.69 Å to form a chain structure along the *b* axis.




The X-band EPR spectrum of pentaradical **7** in toluene solution at room temp. showed one broad signal with $\Delta H_{PP}$ = 20 G at $g$ = 2.0064. In the corresponding spectrum ($\nu_0$ = 9.410 GHz) of **7** in frozen solution at 6.5 K, five signals (318.8, 327.2, 335.3, 343.4, and 351.8 mT) were observed in addition to the signal ($g$ = 4.019) due to a $\Delta m_S$ = 2 transition. The spectrum was simulated as a sextet with $S$ = 5/2 to afford $g$ = 2.0062 and zero-field splitting parameters $|D/hc|$ = 0.0039 and $|E/hc|$ = 0.0013 $cm^{-1}$.¶ As the temperature was increased from 12 to 100 K, the intensity of the signal at $g$ = 2 decreased in accordance with the Curie law, suggesting that the sextet was a ground state.

The magnetic susceptibility of a crystalline sample of pentaradical **7** was measured on a SQUID magnetometer/susceptometer in the temperature range 2–350 K at a constant field of 200 mT. The $\chi_{mol}T$ value at 350 K is 2.09 emu K $mol^{-1}$

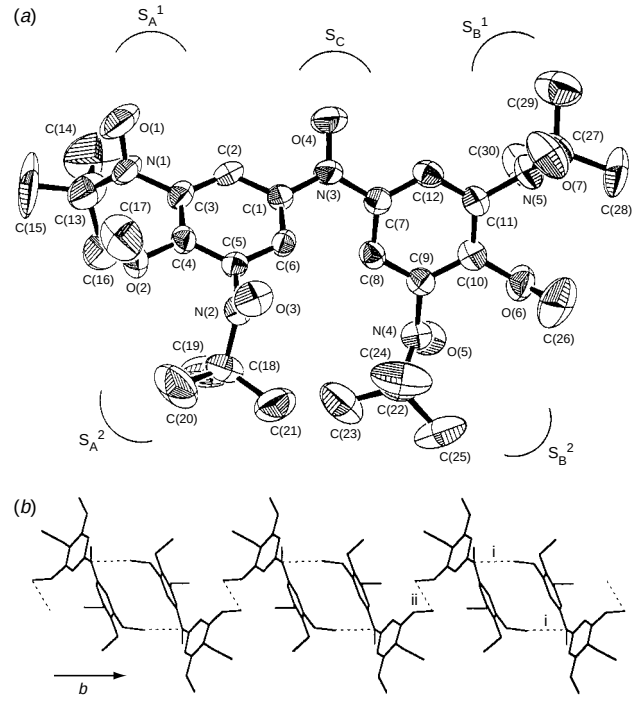



**Fig. 1** Molecular and crystal structure of pentaradical **7**: (*a*) ORTEP drawing with thermal ellipsoid plot at the 30% probability level. The diethyl ether molecule of crystallization is omitted for clarity; torsion angles between the benzene ring and the radical N–O bond are 75.8°, −62.9, −63.1 and 60.3° for $S_A^1$[O(1)N(1)C(3)C(2)], $S_A^2$[O(3)N(2)C(5)C(6)], $S_B^1$[O(7)N(5)C(11)C(12)] and $S_B^2$[O(5)N(4)C(9)C(10)], respectively. The average distances between the two nitrogens and two oxygens are 5.53, 5.56 and 4.96 Å for $r(S_{A1}S_{A2})$, $r(S_{A1}S_C)$ and $r(S_{A2}S_C)$ and 5.57, 5.74 and 5.04 Å for $r(S_{B1}S_{B2})$, $r(S_{B1}S_C)$ and $r(S_{B2}S_C)$, respectively, and (*b*) a stick model of crystal structure; Bu$^t$ groups are omitted for clarity. Broken lines indicate short contacts (Å) between the atoms of the radical centers; (i) 3.35 and (ii) 3.60.

which is slightly greater than 1.88 emu K mol$^{-1}$ calculated as a spin only value for five isolated radical centers. As the temperature was decreased from 350 K, $\chi_{mol}T$ values increased gradually and reached a maximum of 2.22 emu K mol$^{-1}$ at 120 K and then decreased sharply. The maximum value is considerably smaller than theoretical 4.38 emu K mol$^{-1}$ for $S$ = 5/2 and suggests that intermolecular antiferromagnetic interaction takes place predominantly below 120 K, as expected from the X-ray crystal structure of **7**.

In order to exclude the contribution of the intermolecular antiferromagnetic interaction at low temperature, a sample of **7** doped in poly(vinyl chloride) (PVC) matrix was prepared and employed for a SQUID measurement. The field dependence of a PVC film‖ containing 2% **7** was investigated at 2, 4, and 6 K and the $M/M_S$ *vs.* $H/T$ plot is shown in Fig. 2 together with a theoretical curve obtained on the basis of the Brillouin function** for $S$ = 5/2. The theoretical curve fitted the experimental data reasonably well indicating that the five aminoxyl radicals interact ferromagnetically to produce a sextet state.

In summary, stable pentaradical **7** was successfully prepared and its molecular structure was revealed by X-ray structure analysis. Its magnetic properties revealed that ferromagnetic interactions occur predominantly among the five spins within a molecule to produce a sextet ground state. However, the exchange coupling parameters ($J$) among them could not be estimated quantitatively from a $\chi_{mol}T$–$T$ plot since the intermolecular antiferromagnetic interaction among the pentaradical

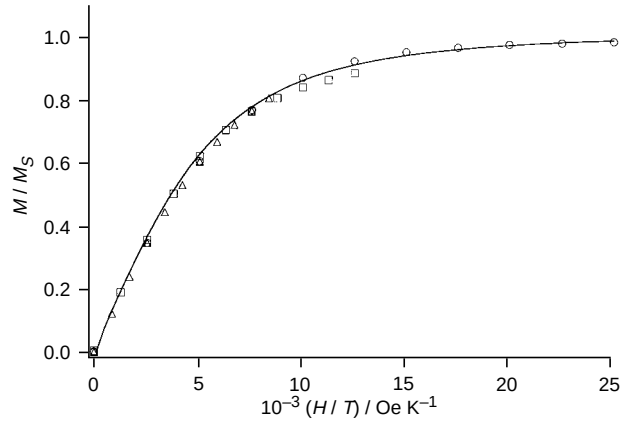



**Fig. 2** Field dependence of the magnetization at 2 (○), 4 (□), and 6 K (△) as expressed by $M/M_S$ *vs.* $H/T$ plots for pentaradical **7**. The solid curves are theoretical ones for $S$ = 5/2 as described in text.

molecules at low temperature caused by short intermolecular contacts between radical centers in the crystalline state was very strong.

## Footnotes and References

* E-mail: koga@yakukaws.phar.kyushu-u.ac.jp

† **7a**: mp (decomp.) 85–87 °C, FABMS (*m*-nitrobenzyl alcohol matrix) *m*/*z* 1049 ($M^+$ + 1), Anal. Calc. for $C_{54}H_{106}N_5O_7Si_4$: C, 61.71; H, 10.18; N, 6.67. Found: C, 62.08; H, 10.17; M, 6.37%.

‡ **7**: mp (decomp.) 139–141 °C, FABMS (*m*-nitrobenzyl alcohol matrix) *m*/*z* 592 ($M^+$ + 3), 591 ($M^+$ + 2), Anal. Calc. for $C_{30}H_{46}N_5O_7{\cdot}0.5C_4H_{10}O$: C, 61.41; H, 8.19; N, 11.18. Found: C, 61.42; H, 8.21; N, 11.19%. *Crystal data* for **7**: $C_{30}H_{46}N_5O_7{\cdot}0.5C_4H_{10}O$, $M$ = 625.78, monoclinic, space group $P2_1/n$ (no. 14), $a$ = 16.101(2), $b$ = 12.537(4), $c$ = 19.232(2) Å, $\beta$ = 113.687(8)°, $U$ = 3555(1) Å$^3$, $T$ = 296 K, $Z$ = 4, $D_c$ = 1.169 g cm$^{-3}$, $\mu$(Cu-Kα) = 6.83 cm$^{-1}$, 5729 total (5516 independent) reflections, $R$ = 0.072 and $R_{ws}$ = 0.071 for 404 reflections with $I > 3\sigma(I)$. Direct methods and refinement converged using the full-matrix least squares method of the TEXAN Ver. 1.6 program (Molecular Structure Corperation). CCDC 182/633.

§ The *anti* conformation is the first example in this series of methoxy substituted phenyl aminoxyl diradicals.[7]

¶ The simulation for the EPR fine structure was performed by using a program based on the second-order perturbation theory and provided by Professors K. Ito and K. Takui of Osaka City University.

‖ PVC films containing 1% of **7** were also prepared and similar $M/M_S$ *vs.* $H/T$ plots were obtained.

** $M = Ngj\mu_B B_J(x)$, where $B_J(x) = [(2J+1)/2J]\coth[(2J+1)/2J]x - 1/2J\coth(1/2J)x$ and $x = gJ\mu_B H/k_B T$.

1 A. Rajca and S. Utamapanya, *J. Am. Chem. Soc.*, 1993, **115**, 10 688; A. Rajca, *Chem. Rev.*, 1994, **94**, 871; A. Rajca, S. Rajca and S. R. Desai, *J. Am. Chem. Soc.*, 1995, **117**, 806.

2 N. Nakamura, K. Inoue and H. Iwamura, *Angew. Chem.*, 1993, **105**, 900; *Angew. Chem., Int. Ed. Engl.*, 1993, **32**, 872; K. Matsuda, N. Nakamura, K. Inoue, N. Koga and H. Iwamura, *Chem. Eur. J.*, 1996, **2**, 259.

3 S. Sasaki and H. Iwamura, *Chem. Lett.*, 1992, 1759.

4 J. Veciana, C. Rovira, N. Ventosa, M. I. Crespo and F. Palacio, *J. Am. Chem. Soc.*, 1993, **115**, 57.

5 F. Kanno, K. Inoue, N. Koga and H. Iwamura, *J. Phys. Chem.*, 1993, **97**, 13 267.

6 T. Ishida and H. Iwamura, *J. Am. Chem. Soc.*, 1991, **113**, 4238.

7 F. Kanno, K. Inoue, N. Koga and H. Iwamura, *J. Am. Chem. Soc.*, 1993, **115**, 847; J. Fujita, M. Tanaka, H. Suemune, N. Koga, K. Matsuda and H. Iwamura, *J. Am. Chem. Soc.*, 1996, **118**, 9347.

8 K. Yamaguchi, Y. Toyoda and T. Fueno, *Chem. Phys. Lett.*, 1989, **190**, 459; K. Yamaguchi, M. Okumura and M. Nakano, *Chem. Phys. Lett.*, 1989, **191**, 237.

*Received in Cambridge, UK, 16th June 1997; 7/04160H*

# Base-induced cyclization of 1-benzyloxy-2,2,4,4-tetramethylpentan-3-ones: intramolecular nucleophilic addition of an anion of a benzyl ether to the carbonyl moiety without the Wittig rearrangement or protophilic decomposition

**Masakatsu Matsumoto,* Nobuko Watanabe, Akio Ishikawa and Hiroyuki Murakami**

*Department of Materials Science, Kanagawa University, Tsuchiya, Hiratsuka, Kanagawa 259-12, Japan*

**Alkyl benzyl ethers bearing a carbonyl moiety in the alkyl chain (1) cyclize effectively, without the Wittig rearrangement or protophilic decomposition, to give hydroxytetrahydrofurans (*trans*-2) on treatment with Bu$^t$OK in DMSO at room temperature, whereas LDA–THF induces the cyclization of 1 to afford predominantly the stereoisomer *cis*-2.**

The α-carbanion of an alkyl benzyl ether is unstable and undergoes protophilic cleavage (elimination)[1,2] or Wittig rearrangement[3–5] even at low temperature (Scheme 1), so that little is known of its nucleophilic addition or substitution reactions, although extensive studies have been made on the rearrangement and the decomposition.[6] We report here that (i) the α-carbanion of an alkyl benzyl ether is able to add effectively to a carbonyl moiety in the alkyl chain *via* intramolecular nucleophilic addition without Wittig rearrangement or protophilic decomposition, and (ii) the addition is sterically controlled by the base–solvent system used.

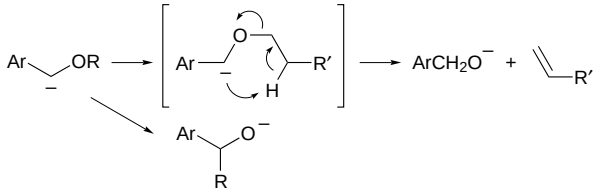
When benzyl ether **1a** (1.1 g, 4.0 mmol) was treated with Bu$^t$OK (8.0 mmol) in DMSO (12 ml) under $N_2$ at room temperature for 4 h, **1a** was exclusively transformed into tetrahydrofuran *trans*-**2a** (91%), which was isolated as a colourless oil in 88% yield after chromatographic purification ($SiO_2$) (Table 1, entry 1). The structure of *trans*-**2a** was determined by $^1$H NMR, NOESY, IR and mass spectral analysis.† A combination of base and solvent, *e.g.* Bu$^t$OK–THF or MeONa–DMSO, was ineffective for the cyclization of **1a**. On the other hand, after treatment of **1a** with LDA–THF at room temperature for 2 h, the cyclization took place smoothly to afford a stereoisomer *cis*-**2a** as colourless crystals (mp 83.0–83.5 °C) together with a small amount of *trans*-**2a** (*cis* : *trans* = 82 : 18) (94%) (entry 2). When the cyclization was carried out at 0 °C, the stereoselectivity was somewhat improved (*cis* : *trans* = 91 : 9) (entry 3). The reaction of **1a** with LDA–THF proceeded sluggishly at −78 °C. The other benzyl ethers **1b**–**d** also underwent base-induced cyclization to afford the corresponding tetrahydrofurans **2b**–**d** with similar stereoselectivities, as shown in Table 1. It is noteworthy that even benzyl ether **1c** bearing an electron-donating substituent at the *para*-position underwent cyclization in LDA–THF, even though Bu$^t$OK–DMSO was ineffective (entries 6 and 7).

The present results showed that (i) an alkyl benzyl ether is probably stable enough to undergo nucleophilic reaction without Wittig rearrangement or decomposition, so long as an electrophile such as a carbonyl moiety exists in a favourable situation, and (ii) the stereoselectivity of cyclization is tightly controlled by the base–solvent system used. The stereoselectivity can probably be rationalized as follows: for the Bu$^t$OK–DMSO system, a naked anion of **1** attacks the carbonyl *via* transition state **T-1**, in which interaction between the aryl and *tert*-butyl groups is minimized, thus giving the sterically less congested isomer *trans*-**2** (Scheme 2). On the other hand, in the

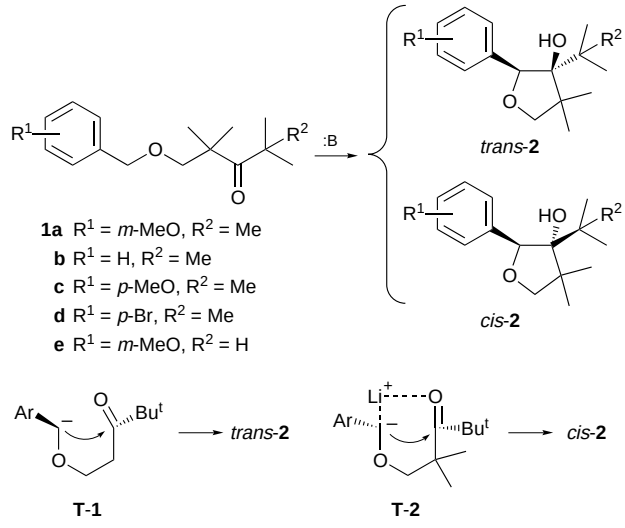
**Table 1** Base-induced cyclization of alkyl benzyl ethers **1**

| Entry | | System[a] | *t*/h[b] | Conversion (%)[c] | Ratio *trans* : *cis*[d] |
|---|---|---|---|---|---|
| 1 | **1a** | A | 4 | 91 | **2a** 100 : 0 |
| 2 | **1a** | B | 2 | 94 | **2a** 80 : 82 |
| 3 | **1a** | B | 2[e] | 95 | **2a** 9 : 91 |
| 4 | **1b** | A | 4 | 92 | **2b** 100 : 0 |
| 5 | **1b** | B | 2 | 99 | **2b** 9 : 91 |
| 6 | **1c** | A | 4 | 0 | — — |
| 7 | **1c** | B | 5[f] | 86 | **2c** 12 : 88 |
| 8 | **1d** | A | 4 | 99 | **2d** 100 : 0 |
| 9 | **1d** | B | 2 | 96 | **2d** 10 : 90 |
| 10 | **1e** | A | 4 | 72 | **2e** 93 : 7 |
| 11 | **1e** | B | 5[f] | 63[g] | **2e** 13 : 87 |

[a] A: **1** (4.0 mmol), Bu$^t$OK (8.0 mmol), DMSO (12 ml). B: **1** (4.0 mmol), LDA (8.0 mmol), THF (12 ml). [b] Carried out at room temp. unless stated otherwise. [c] No product other than **2** was observed, unless stated otherwide. [d] Determined *via* $^1$H NMR analysis of the crude product. [e] Reaction performed at 0 °C. [f] Reaction performed at −78 °C for 2 h and then at room temp. for 3 h. [g] *trans*-**2e** (5.5%), *cis*-**2e** (31%) and **1e** (37%) recovered after chromatography.



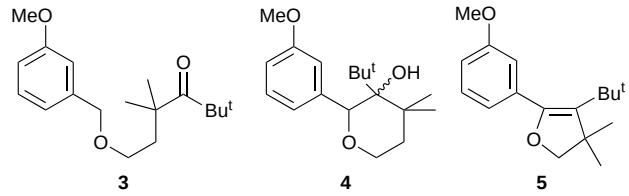

**Scheme 1**




**Scheme 2**

LDA–THF system a lithium ion might coordinate the carbonyl oxygen and the benzyl α-carbanion in transition state **T-2** to afford *cis*-**2** predominantly, even though the repulsive interaction between the aryl and *tert*-butyl moieties is thermodynamically unfavourable. This rationalization is consistent with the effect of temperature on the stereoselectivity in the cyclization of **1a** using LDA–THF. It is noteworthy that 18-crown-6 promoted the *trans*-selective cyclization of **1a** with Bu$^t$OK in THF to give *trans*-**2a** exclusively (room temp. for 4.5 h; 87%).

Since the substrate **1** lacks a β-hydrogen on the alkyl chain, it is not susceptible to protophilic decomposition to form a terminal alkene (Scheme 1), but it should undergo [1,2]-Wittig rearrangement. Thus, we examined the reaction of benzyl ether **3** as a representative ether bearing β-hydrogens on the alkyl chain. Treatment of **3** with LDA in THF (−78 °C to room




**3** **4** **5**

temp.) gave the expected cyclization product **4** in high yield,‡ while the use of Bu$^t$OK–DMSO induced almost no reaction. Thus, intramolecular nucleophilic addition of the α-carbanion of an alkyl benzyl ether to the carbonyl of the alkyl site takes place effectively even if it bears β-hydrogens. In addition, we should note that benzyl ether **1e** bearing an isobutyryl moiety also gave the corresponding cyclization product **2e** on treatment with a base even though **1e** possesses an acidic proton adjacent to the carbonyl moiety (entries 10 and 11).

Both isomeric hydroxytetrahydrofurans *trans*- and *cis*-**2a** were easily dehydrated to give dihydrofuran **5**, which is a key intermediate for the synthesis of a dioxetane used as a highly efficient chemiluminescent substrate[7]§ in high yield upon treatment with $SOCl_2$ and pyridine at room temperature. The other furans **2** obtained here were similarly dehydrated to give the corresponding dihydrofurans.

The present results show that the α-carbanion of an alkyl benzyl ether such as **1** or **3** undergoes nucleophilic addition to a carbonyl moiety existing in the same molecule without Wittig rearrangement or protophilic decomposition. Furthermore, the present cyclization should form a facile entry to sterically crowded cyclic enol ethers.

The authors gratefully acknowledge financial assistance in the form of a Grant-in-aid for Scientific Research from the Ministry of Education, Science, Sports and Culture of the Japanese Government.

## Footnotes and References

* E-mail: matsumo@info.kanagawa-u.ac.jp

† All products obtained here gave satisfactory NMR, IR and mass spectral data.

‡ A single isomer, with stereochemistry tentatively assigned as *cis*-**4** was isolated in 90% yield.

§ Previously, the dihydrofuran **5** had been synthesized by the McMurry reaction of 3-oxo-2,2,4,4-tetramethylpentyl 3-methoxybenzoate using $Ti^0$ (ref. 7). However, this method is expensive and not suitable for large-scale synthesis.

1 M. Maercker, *Angew. Chem., Int. Ed. Engl.*, 1987, **26**, 972.
2 M. Matsushita, Y. Nagaoka, H. Hioki, Y. Fukuyama and M. Kodama, *Chemistry Lett.*, 1996, 1039.
3 U. Schöllkopf, *Angew. Chem., Int. Ed. Engl.*, 1970, **9**, 763.
4 T. Nakai and K. Mikami, *Chem. Rev.*, 1986, **86**, 885.
5 J. A. Marshall, in *Comprehensive Organic Synthesis*, ed. G. Pattenden, Pergamon, Oxford, 1991, vol. 3, p. 975.
6 J.-F. Biellmann and J.-B. Ducep, *Org. React.*, 1982, **27**, 1.
7 M. Matsumoto, N. Watanabe, N. C. Kasuga, H. Hamada and K. Tadokoro, *Tetrahedron Lett.*, 1997, **38**, 2863.

*Received in Cambridge, UK, 19th September 1997; 7/06802F*

# Asymmetric synthesis of two diastereomeric P-chiral diphosphine ligands containing a pair of dissimilar asymmetric phosphorus donor atoms

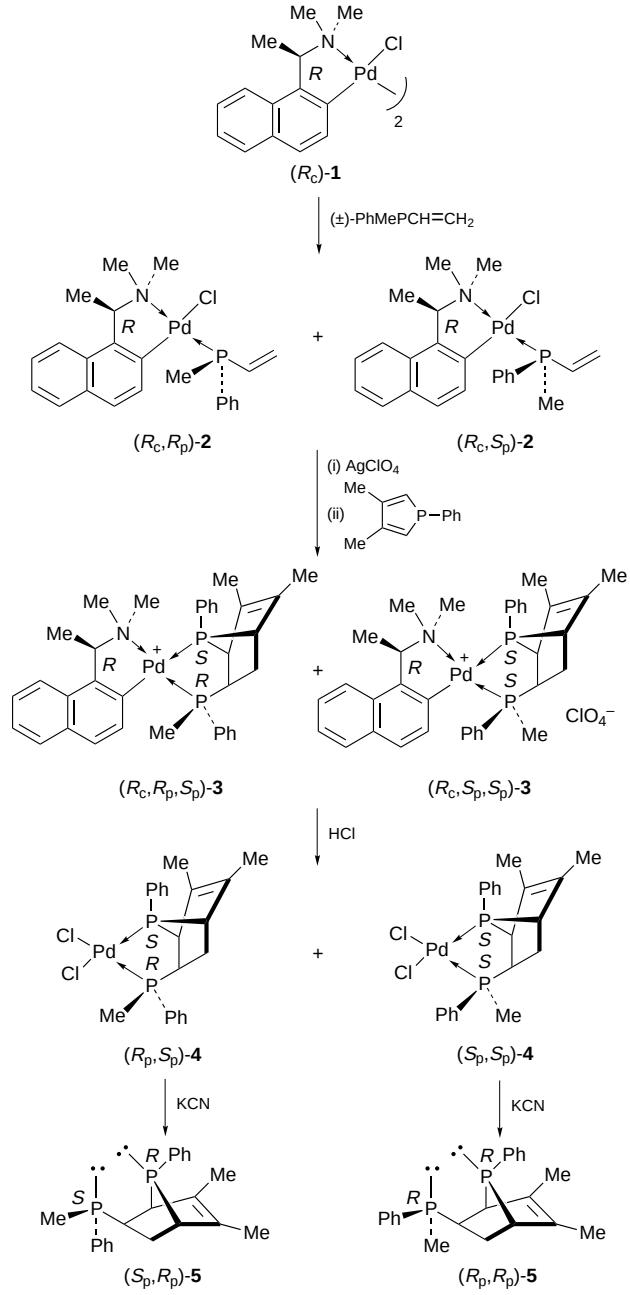
**Anming Liu, K. F. Mok and Pak-Hing Leung***

*Department of Chemistry, National University of Singapore, Kent Ridge 119260, Singapore*

**Two diastereoisomeric P-chiral diphosphine ligands, each containing a pair of dissimilar phosphorus donor atoms, have been prepared efficiently in their optically pure forms from a chiral organopalladium complex-promoted asymmetric Diels–Alder reaction between 1-phenyl-3,4-dimethylphosphole and methylphenylvinylphosphine.**

Enantiomerically pure P-chiral diphosphines are critically important as chiral auxiliaries in asymmetric catalysis.[1] To date, these chiral ligands are readily available from asymmetric synthesis[2] or from classic optical resolution.[1,3] However, no asymmetric synthesis of diphosphines containing a pair of dissimilar asymmetric phosphorus donor atoms have been reported hitherto. The sole example of optical resolution of a related ligand, 1-(methylphenylarsino)-2-(methylphenylphosphino)benzene, required the somewhat difficult separation of the (*R**,*R**) and (*R**,*S**) diastereoisomers prior to the individual resolution of the two racemic diastereoisomers.[3] We believe that the development of a more efficient asymmetric synthesis to all possible diastereoisomers of dissimilar P-chiral diphosphines may present a unique opportunity to probe in detail the subtle stereochemical interactions between diphosphine auxiliaries and the incoming reaction substrates in the important field of homogeneous asymmetric catalysis. We now delineate the first asymmetric synthesis of two diastereoisomeric P-chiral diphosphines without the prerequisite diastereoisomer separation which can be rather tedious.

As illustrated in Scheme 1, the racemic form of methylphenylvinylphosphine split the chlorine bridges in ($R_c$)-**1** regiospecifically[4] to give a pair of diastereoisomeric complexes ($R_c$,$R_p$)- and ($R_c$,$S_p$)-**2**. The neutral complexes could not be separated by fractional crystallization and were crystallized quantitatively as a 1 : 1 diastereoisomeric mixture from $CH_2Cl_2$–$Et_2O$. The 202 MHz $^{31}P$ NMR spectrum of the crystallized product in $CDCl_3$ exhibited two sharp singlets of equal intensity at $\delta$ 17.1 and 17.2. Treatment of this diastereoisomeric chloro complex mixture with silver perchlorate gave the corresponding perchlorato analogues.[5] These reactive intermediates were not isolated and were treated directly with stoichiometric quantities of 1-phenyl-3,4-dimethylphosphole in $CH_2Cl_2$ at room temperature for 4 h. Thus a 1 : 1 mixture of the diastereoisomeric complexes ($R_c$,$R_p$,$S_p$)-**3** and ($R_c$,$S_p$,$S_p$)-**3** was formed quantitively. The $^{31}P$ NMR spectrum of the crude reaction mixture in $CDCl_3$ exhibited only four doublets of identical coupling constants (41.9 Hz) and similar intensities. Two of these doublets were recorded at $\delta$ 116.2 and 116.7. These typical low-field $^{31}P$ NMR chemical shifts are consistent with the formation of two stereochemically distinct bridgehead phosphorus atoms with the *exo-syn* stereochemistry in the two diastereoisomers. The other two non-bridgehead phosphorus atoms exhibited doublet resonances at $\delta$ 38.4 and 44.2. The diastereoisomeric template complexes, however, could not be induced to crystallize. Treatment of the complex mixture with conc. HCl removed the naphthylamine auxiliary chemoselectively to give the dichloro complexes ($R_p$,$S_p$)-**4** and ($S_p$,$S_p$)-**4**. These diastereoisomeric complexes exhibited very different solubilities in organic solvents. Hence, upon crystallization from $CH_2Cl_2$–$Et_2O$, the less soluble ($S_p$,$S_p$) isomer was obtained as pale yellow prisms (90%), mp > 230 °C (decomp.), $[\alpha]_D$ +11.2 (*c* 0.5, $CH_2Cl_2$). The more soluble ($R_p$,$S_p$) isomer was subsequently obtained from $CHCl_3$–$Et_2O$ as beige prisms (70%), mp > 230 °C (decomp.), $[\alpha]_D$ +97.6 (*c* 0.5, $CH_2Cl_2$). The molecular structure and the absolute stereochemistry of both diastereoisomers were determined by X-ray structural analyses (Figs. 1 and 2).† The studies reveal that the absolute




**Scheme 1**

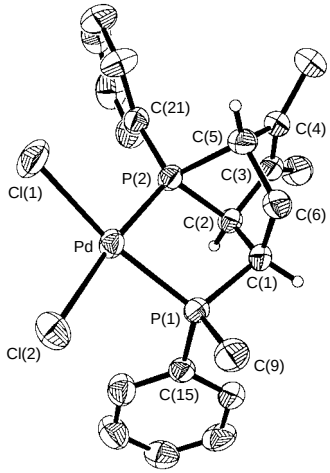



**Fig. 1** Molecular structure and absolute stereochemistry of ($R_p$,$S_p$)-**4**. Selected bond lengths (Å) and angles (°); Pd–P(1) 2.238(1), Pd–P(2) 2.219(1), Pd–Cl(1) 2.359(1), Pd–Cl(2) 2.365(1), P(1)–C(1) 1.836(3), P(1)–C(9) 1.815(3), P(1)–C(15) 1.809(3), P(2)–C(2) 1.847(3), P(2)–C(5) 1.850(3), P(2)–C(21) 1.804(3), C(1)–C(6) 1.570(4), C(3)–C(4) 1.341(5), P(1)–Pd–P(2) 83.0(1), P(1)–Pd–Cl(1) 170.4(1), P(1)–Pd–Cl(2) 90.1(1), P(2)–Pd–Cl(1) 91.6(1), P(2)–Pd–Cl(2) 172.8(1), Cl(1)–Pd–Cl(2) 95.5(1), C(2)–P(2)–C(5) 81.6(1).

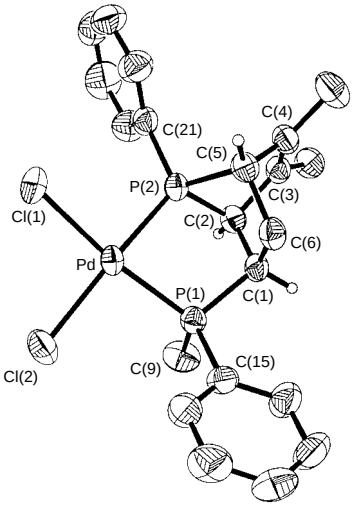



**Fig. 2** Molecular structure and absolute stereochemistry of ($S_p$,$S_p$)-**4**. Selected bond lengths (Å) and angles (°); Pd–P(1) 2.246(1), Pd–P(2) 2.223(1), Pd–Cl(1) 2.351(1), Pd–Cl(2) 2.380(1), P(1)–C(1) 1.825(3), P(1)–C(9) 1.801(3), P(1)–C(15) 1.806(3), P(2)–C(2) 1.833(3), P(2)–C(5) 1.837(3), P(2)–C(21) 1.801(3), C(1)–C(6) 1.561(4), C(3)–C(4) 1.325(4), P(1)–Pd–P(2) 82.8(1), P(1)–Pd–Cl(1) 172.7(1), P(1)–Pd–Cl(2) 93.0(1), P(2)–Pd–Cl(1) 90.4(1), P(2)–Pd–Cl(2) 170.4(1), Cl(1)–Pd–Cl(2) 94.1(1), C(2)–P(2)–C(5) 82.1(1).

configurations at P(2), C(1), C(2) and C(5) in both molecules are *S*, *R*, *S* and *S*, respectively, and the two isomers are diastereoisomeric at P(1) only.

Treatment of a $CH_2Cl_2$ solution of ($S_p$,$S_p$)-**4** with aqueous cyanide liberated the optically pure diphosphine ($R_p$,$R_p$)-**5** quantitatively as an air-sensitive oil with $[\alpha]_D$ −22.6 (*c* 0.5, $CH_2Cl_2$). The $^{31}$P NMR spectrum of the free diphosphine in $CDCl_3$ exhibited a pair of doublets at $\delta$ 91.2 and −22.6 ($J_{PP}$ 70.2 Hz). The low field $^{31}$P resonance indicates that the *exo–syn* stereochemistry is retained. It is noteworthy that the apparent inversion of configuration that takes place at both phosphorus stereogenic centres during the liberation reaction is merely a consequence of the Cahn–Ingold–Prelog (CIP) rules.[6] The optical purity of ($R_p$,$R_p$)-**5** was further confirmed by the quantitative repreparation of ($R_c$,$S_p$,$S_p$)-**3** from the liberated ligand and ($R_c$)-**1**: the 202 MHz $^{31}$P NMR spectrum of the crude product exhibited a pair of doublets at $\delta$ 116.7 and 38.4 only. Similarly, free diphosphine ($S_p$,$R_p$)-**5** was liberated from ($R_p$,$S_p$)-**4** as an air-sensitive oil with $[\alpha]_D$ +42.4 (*c* 0.5, $CH_2Cl_2$). The $^{31}$P NMR spectrum of ($S_p$,$R_p$)-**5** in $CDCl_3$ exhibited the two doublet resonances at $\delta$ 91.4 and −22.8 ($J_{PP}$ 66.6 Hz).

Finally, it should be noted that the enantiomeric forms of ($R_p$,$R_p$)- and ($S_p$,$R_p$)-**5** can be prepared similarly from methylphenylvinylphosphine and 1-phenyl-3,4-dimethylphosphole using ($S_c$)-**1** as the chiral reaction promoter. Investigations on the catalytic properties of transition metal complexes containing these optically active diastereoisomeric diphosphines are currently in progress.

We are grateful to the National University of Singapore for support of this research (Grant No. RP960675) and research scholarships to A. M. L.

## Footnotes and References

* E-mail: chmlph@nus.sg

† *Crystal data* for ($R_p$,$S_p$)-**4**: $[C_{21}H_{24}Cl_2P_2Pd]$, $M$ = 515.64, orthorombic, space group $P2_12_12_1$, $a$ = 8.949(1), $b$ = 10.300(1), $c$ = 23.606(2) Å, $V$ = 2175.9(4) Å$^3$, $Z$ = 4, $D_c$ = 1.574 g cm$^{-3}$, $\mu$(Mo-K$\alpha$) = 12.49 cm$^{-1}$, $F$(000) = 1040. A beige prism with dimensions 0.25 × 0.20 × 0.13 mm was used for diffraction studies. A total of 11 788 independent reflections were measured on a Siemens SMART CCD diffractometer with Mo-K$\alpha$ radiation (graphite monochromator) using $\omega$-scans. All the non-hydrogen atoms were refined anisotropically. In the full-matrix least-squares based on $F^2$ with absorption corrected data to give $R_1$ = 0.0214, $wR_2$ = 0.0533. The absolute stereochemistry was determined unambiguously by refining the Flack parameter [$x$ = 0.00(2)].

*Crystal data* for ($S_p$,$S_p$)-**4**: $[C_{21}H_{24}Cl_2P_2Pd]$, $M$ = 515.64, monoclinic, space group $P2_1$, $a$ = 11.090(2), $b$ = 8.875(1), $c$ = 12.060(3) Å, $\beta$ = 107.27(2), $V$ = 1095.2(4) Å$^3$, $Z$ = 2, $D_c$ = 1.564 g cm$^{-3}$, $\mu$(Mo-K$\alpha$) = 12.40 cm$^{-1}$, $F$(000) = 520. A pale yellow prism with dimensions 0.43 × 0.35 × 0.13 mm was used for diffraction studies. A total of 6418 independent reflections were measured on the above Siemens SMART CCD diffractometer using $\omega$-scans. All the non-hydrogen atoms were refined anisotropically. In the full-matrix least-squares based on $F^2$ with absorption corrected data to give $R_1$ = 0.0194, $wR_2$ = 0.0475. The absolute stereochemistry was determined unambiguously by refining the Flack parameter [$x$ = 0.001(1)]. CCDC 182/662.

1 B. Bosnich, *Asymmetric Catalysis*, Martinus, Dordrecht, 1986; R. Noyori, *Chem. Soc. Rev.*, 1989, **18**, 187; H. B. Kagan and M. Sasaki, in *The Chemistry of Organophosphorus Compounds*, ed. F. R. Hartley, Wiley, New York, 1990, vol. I, ch. 3; A. F. Noels, M. Graziani and A. J. Hubert, *Metal Promoted Selectivity in Organic Synthesis*, Kluwer, Dordrecht, 1991; K. M. Pietrusiewicz and M. Zablocka, *Chem. Rev.*, 1994, **94**, 1375.

2 E. J. Corey, Z. Chen and G. J. Tanoury, *J. Am. Chem. Soc.*, 1993, **115**, 11 000; P. H. Leung, S. K. Loh, K. F. Mok, A. J. P. White and D. J. Williams, *J. Chem. Soc., Dalton Trans.*, 1996, 4443; B. H. Aw, T. S. A. Hor, S. Selvaratnam, K. F. Mok, A. J. P. White, D. J. Williams, N. H. Rees, W. McFarlane and P. H. Leung, *Inorg. Chem.*, 1997, **36**, 2138.

3 G. Salem and S. B. Wild, *Inorg. Chem.*, 1983, **22**, 4049.

4 S. Y. M. Chooi, T. S. A. Hor, P. H. Leung and K. F. Mok, *Inorg. Chem.*, 1992, **31**, 1494.

5 S. K. Loh, K. F. Mok, P. H. Leung, A. J. P. White and D. J. Williams, *Tetrahedron: Asymmetry*, 1996, **7**, 45.

6 R. S. Cahn, C. K. Ingold and V. Prelog, *Angew. Chem., Int. Ed. Engl.*, 1966, **5**, 385.

*Received in Cambridge, UK, 29th September 1997; 7/06982K*

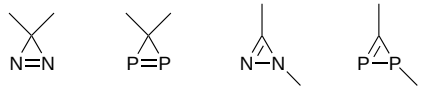
# New routes to free and coordinated 1*H*-diphosphirenes

**Didier Bourissou, Yves Canac, Maria Isabel Collado, Antoine Baceiredo and Guy Bertrand***

*Laboratoire de Chimie de Coordination du CNRS, 205 route de Narbonne, 31077 Toulouse Cédex 04, France*

**Diphosphirenium salt 1 reacts with $LiAlH_4$ leading to *P*-hydrophosphaalkene 2, which on treatment with a catalytic amount of $BF_3{\cdot}OEt_2$ affords 1*H*-diphosphirene 3, while with a stoichiometric amount of $W(CO)_5$(thf), complex 4 is obtained.**

Among the smallest dinitrogen- and diphosphorus-containing unsaturated heterocycles **A**–**D**, only the chemistry of 3*H*-diazirines **A** has been extensively explored.[1] So far, no 3*H*-diphosphirenes **B** have been observed,[2] and only one 1*H*-diazirine **C**[3] has been spectroscopically characterized. The only known free 1*H*-diphosphirene **D** was isolated as long ago as 1989 by Niecke *et al.*,[4a] although two complexes featuring heterocycle **D** as an $\eta^1$-ligand have been prepared more recently.[4b,c] The lack of simple synthetic methods for the preparation of heterocycles **D** has undoubtedly hampered the development of their chemistry. Indeed, all the known examples have been obtained by addition of free[4a] or coordinated phosphinidenes[4b,c] to phosphaalkynes. Here we report new synthetic routes to free and coordinated heterocycles **D** which are reminiscent of the Neber synthesis of 2*H*-azirines[5] and the Graham synthesis of 3-halogeno-3*H*-diazirines.[6]

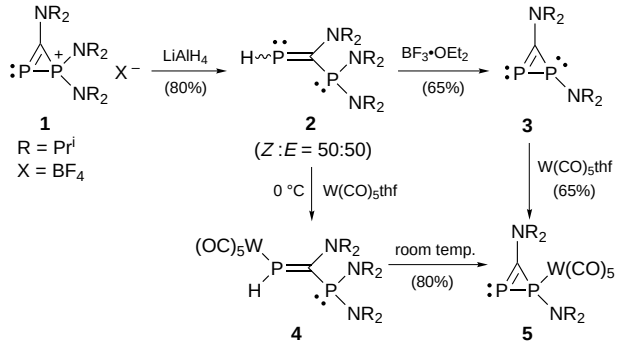



**A** **B** **C** **D**

We have already shown that ring opening reactions occur when the readily available diphosphirenium salt **1**[7a,b] is treated with nucleophiles.[7c,d] In a similar way, addition of one equivalent of lithium aluminium hydride to a thf solution of **1** afforded the corresponding *P*-hydrophosphaalkene **2** as a 50 : 50 mixture (according to NMR spectroscopy) of *Z* and *E* isomers in 80% total yield.†

The similarity between compound **2** and the Neber and especially the Graham amidine precursors is obvious. However, instead of using a base to induce the 1,3-elimination reaction, a thf solution of **2** was treated with a catalytic amount (5%) of $BF_3{\cdot}OEt_2$ at room temperature. After work up, the 1*H*-diphosphirene **3** was obtained as a light yellow oil in 65% yield. The spectroscopic data† for **3** compared well with those reported for the other known 1*H*-diphosphirene.[4a]

The corresponding coordinated 1*H*-diphosphirene **5** can be obtained by treatment of **3** with $W(CO)_5$(thf);[8] from **2**, the two step process gave access to complex **5** in 42% yield. Interestingly, addition of one equivalent of $W(CO)_5$(thf) to phosphaalkene **2** directly afforded **5** which was isolated after workup in 80% yield. Monitoring the reaction by $^{31}$P NMR spectroscopy at 0 °C showed the primary formation of complex **4** as a single isomer in an *E* configuration,[9] where the metal is $\eta^1$-bonded to the $\sigma^2$-phosphorus atom [$^{31}$P NMR: −71.0 (s, $^1J_{PH}$ 267.4, $^1J_{PW}$ 129.4 Hz, P–H), +66.5 (s, P–$NR_2$)]. The transformation of **4** into **5** involved both the elimination of diisopropylamine and the migration of the metal fragment. The former process is probably induced by a catalytic amount of $W(CO)_5$(thf) which acts as a Lewis acid. The metal shift is governed by the higher thermodynamic stability of **5** compared to the isomeric complex featuring the metal fragment at the $\sigma^2$-phosphorus atom.




**Scheme 1**

These new synthetic routes can be used on multi-gram scales readily allowing for the development of the chemistry of 1*H*-diphosphirenes, as shown by the recent preparation of a diphosphirenylium salt complex[8] and a diphosphirenyl radical dimer.[10]

## Footnotes and References

* E-mail: gbertran@lcctoul.lcc-toulose.fr

† Satisfactory elemental analyses for compounds **2** and **3** have been obtained.

*Selected spectroscopic data* for **2**, **3**, **4** and **5**: **2**, $\delta_P$($CDCl_3$, 32.438 MHz, *J*/Hz) +23.8 (d, $^2J_{PP}$ 39.8, $^1J_{PH}$ 137.6, $\sigma^2$-P–H), +53.7 (d, $^2J_{PP}$ 39.8, $\sigma^3$-P) and +34.3 (s, $^1J_{PH}$ 173.6, $\sigma^2$-P–H), +55.9 (s, $\sigma^3$-P); $\delta_C$($CDCl_3$, 62.896 MHz, *J*/Hz) 205.1 (dd, $^1J_{PC}$ 97.6 and 40.1, PCP) and 212.8 (dd, $^1J_{PC}$ 65.4 and 58.8, PCP); $\delta_C$($CDCl_3$, 200.132 MHz) 4.66 (dd, $^1J_{PH}$ 173.6, $^3J_{PH}$ 1.0, H–P) and 4.96 (dd, $^1J_{PH}$ 137.6, $^3J_{PH}$ 7.4, H–P). **3**, $\delta_P$($CDCl_3$, 32.438 MHz, *J*/Hz) −121.7 (d, $^1J_{PP}$ 121.3 P–$NPr^i_2$), −23.7 (d, $^1J_{PP}$ 121.3, $\sigma^2$-P); $\delta_C$($CDCl_3$, 100.614 MHz, *J*/Hz) 191.2 (dd, $J_{PC}$ 82.2 and 77.9, PCP), 58.4 (t, $J_{PC}$ 4.2, CNCH), 51.3 (s, CNCH), 43.4 (d, $^2J_{PC}$ 5.6, PNCH), 24.5 (d, $J_{PC}$ 5.2, $CH_3$), 24.2 (d, $J_{PC}$ 12.2, $CH_3$), 21.8 (s, $CH_3$), 21.6 (d, $J_{PC}$ 2.1, $CH_3$), 20.1 (d, $J_{PC}$ 2.7, $CH_3$), 19.1 (d, $J_{PC}$ 4.9, $CH_3$); $\delta_H$($CDCl_3$, 200.132 MHz, *J*/Hz) 4.19 (2 H, septet d, $^3J_{HH}$ 6.6, $^3J_{PH}$ 1.8, PNCH), 3.60 (2 H, septet, $^3J_{HH}$ 6.7, CNCH), 1.32 (6 H, d, $^3J_{HH}$ 6.7, $CH_3$), 1.15 (6 H, d, $^3J_{HH}$ 6.6, $CH_3$), 1.13 (6 H, d, $^3J_{HH}$ 6.7, $CH_3$), 0.95 (6 H, d, $^3J_{HH}$ 6.6, $CH_3$); CIMS ($NH_3$) *m/z* 275 (M + 1). **4**, $\delta_P$($C_7D_8$, 161.98 MHz, *J*/Hz) −71.0 (s, $^1J_{PH}$ 267.4, $^1J_{PW}$ 129.4, P–H), 66.5 (s, P–$NPr^i_2$); $\delta_C$($C_7D_8$, 100.614 MHz, *J*/Hz) 233.6 (dd, $^1J_{PC}$ 72.3 and 50.3, PCP), 203.3 (d, $^2J_{PC}$ 7.7, CO); $\delta_H$($C_7D_8$, 400.14 MHz, *J*/Hz δ 4.95 (d, $^1J_{PH}$ 267.4, H–P). **5**, $\delta_P$($C_6D_6$, 32.438 MHz, *J*/Hz) −123.0 (d, $^1J_{PP}$ 164.3, $^1J_{PW}$ 295.1, P–$NPr^i_2$), 15.0 (d, $^1J_{PP}$ 164.3, $\sigma^2$-P).

1 M. T. H. Liu, *Chem. Soc. Rev.*, 1982, **11**, 127; H. W. Heine, in *The Chemistry of Heterocyclic Compounds Small Ring Heterocycles, Part 2*, Wiley, New York, 1983, vol. 42, p. 588; *Chemistry of Diazirines*; ed. M. T. H. Liu, CRC Press, Boca Raton, FL, 1987, vols. I and II.

2 The transient formation of a 3*H*-diphosphirene has been postulated: E. Niecke, R. Streubel and M. Nieger, *Angew. Chem., Int. Ed. Engl.*, 1991, **30**, 90.

3 N. Dubau-Assibat, A. Baceiredo and G. Bertrand, *J. Am. Chem. Soc.*, 1996, **118**, 5216.

4 (*a*) E. Niecke, R. Streubel, M. Nieger and D. Stalke, *Angew. Chem., Int. Ed. Engl.*, 1989, **28**, 1673; (*b*) F. Mercier, L. Ricard, F. Mathey and M. Regitz, *J. Chem. Soc., Chem. Commun.*, 1991, 1305; (*c*) R. Streubel, L. Ernst, J. Jeske and P. G. Jones, *J. Chem. Soc., Chem. Commun.*, 1995, 2113.

5 V. Nair, *J. Org. Chem.*, 1968, **33**, 2121; H. G. Corkins, L. Storace and E. Osgood, *J. Org. Chem.*, 1980, **45**, 3146.
6 W. H. Graham, *J. Am. Chem. Soc.*, 1965, **87**, 4396; R. A. Moss, J. Wlostowska, W. Guo, M. Fedorynski, J. P. Springer and J. M. Hirshfield, *J. Org. Chem.*, 1981, **46**, 5048; X. Creary, *Acc. Chem. Res.*, 1992, **25**, 31.
7 (*a*) F. Castan, A. Baceiredo, J. Fischer, A. de Cian, G. Commenges and G. Bertrand, *J. Am. Chem. Soc.*, 1991, **113**, 8160; (*b*) M. Soleilhavoup, Y. Canac, A. M. Polozov, A. Baceiredo and G. Bertrand, *J. Am. Chem. Soc.*, 1994, **116**, 6149; (*c*) M. Soleilhavoup, A. Baceiredo, F. Dahan and G. Bertrand, *J. Chem. Soc., Chem. Commun.*, 1994, 337; (*d*) Y. Canac, M. Soleilhavoup, L. Ricard, A. Baceiredo and G. Bertrand, *Organometallics*, 1995, **14**, 3614.
8 D. Bourissou, Y. Canac, M. I. Collado, A. Baceiredo and G. Bertrand, *J. Am. Chem. Soc.*, 1997, **119**, 9923.
9 All the *P*-substituted-*C*-amino-*C*-phosphinophosphaalkenes we have obtained so far present the *E* configuration.
10 Y. Canac, A. Baceiredo, H. Gornitzka, W. W. Schoeller and Guy Bertrand, unpublished work.

*Received in Cambridge, UK, 15th September 1997; 7/06688K*

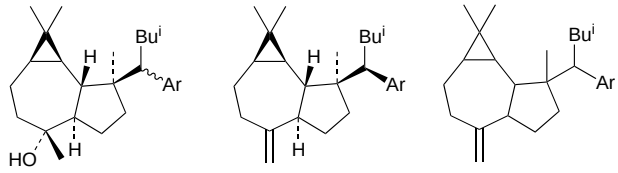
# First stereoselective total synthesis of macrocarpal C: structure elucidation of macrocarpal G

**Tetsuaki Tanaka,[a] Hidenori Mikamiyama,[a] Kimiya Maeda,[a] Toshimasa Ishida,[b] Yasuko In[b] and Chuzo Iwata*[a]**

[a] *Faculty of Pharmaceutical Sciences, Osaka University, 1-6 Yamadaoka, Suita, Osaka 565, Japan*
[b] *Osaka University of Pharmaceutical Sciences, 4-20-1 Nasahara, Takatsuki, Osaka 569-11, Japan*

**The first stereoselective total synthesis of macrocarpal C is achieved *via* a coupling reaction of a silyl dienol ether with a novel hexasubstituted benzene chromium tricarbonyl complex as an optically active benzyl cation equivalent, thereby clarifying the identity of macrocarpal C and G.**

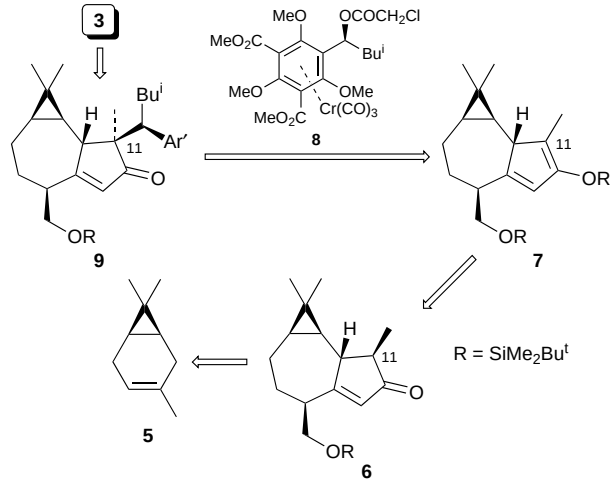
Macrocarpals[1,2] are structurally characterized by fusion of isopentylphloroglucinol dialdehyde to various sesquiterpene skeletons and are known to exhibit various interesting biological activities, such as antibacterial activity,[2a,c,e,g] inhibitory activity of HIV reverse transcriptase,[2b] aldose reductase[2d,e] and glucosyl transferase.[2e,g] Since the original isolation of macrocarpal A **1** from *Eucalyptus macrocarpa* in 1990,[2a] a number of macrocarpals have been isolated from *Eucalyptus* species.[2b–g] Complete structures have been elucidated for macrocarpals A (**1**), B (**2**) and C (**3**) using X-ray diffraction studies and spectral and chemical investigations, and the absolute stereochemistries of **1** and **3** have been determined by a modified Mosher's method.[2b] Macrocarpal G **4**,[2c] however, has been assigned the same planar structure as **3**,† and quite a few macrocarpals have not been designated relative stereochemistries. In this communication, we report the first and highly stereoselective total synthesis of macrocarpal C **3**, thereby clarifying its identity with respect to macrocarpal G **4**.




Macrocarpal A **1** (β-Ar) Macrocarpal C **3** Macrocarpal G **4**
Macrocarpal B **2** (α-Ar)

Ar = 2,4,6-trihydroxy-3,5-diformylphenyl

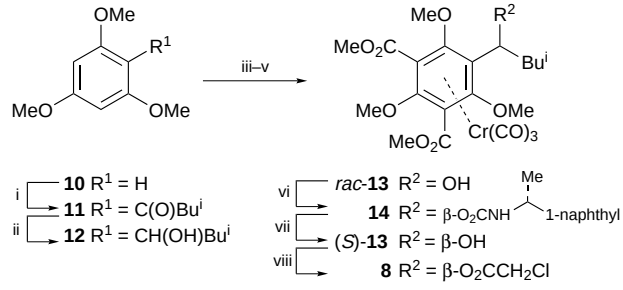
As illustrated in the retrosynthetic analysis of macrocarpal C **3** (Scheme 1), our synthetic approach began from the previously reported tricyclic enone **6**,[3] which we prepared from the commercially available and inexpensive (+)-3-carene **5**. The coupling reaction of the sesquiterpene moiety **6** with the isopentylphloroglucinol dialdehyde part is a crucial step requiring high stereoselectivity at both the benzylic and C11 positions. To this end, we planned the Lewis acid mediated coupling reaction of silyldienol ether **7** with a novel hexasubstituted benzene chromium tricarbonyl complex **8** as an optically active benzyl cation equivalent. Our previous studies suggested that an electrophile would be introduced stereoselectively at the C11 position from the less hindered β-side of **7**.[3] In connection with stereochemical control at the benzylic position, it is known that, with some nucleophiles, $S_N1$-type carbon–carbon bond formation *via* the $Cr(CO)_3$-stabilized carbonium ion proceeds with stereochemical retention at the benzylic position.[4] Hence, the desired coupling product **9**,



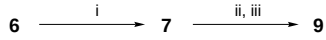

**Scheme 1**

which possesses the requisite functionalities and desired stereochemistry for the subsequent manipulations toward macrocarpal C **3**, would be obtained selectively after complexation.

Scheme 2 outlines the synthesis of the chiral chromium complex **8** starting from commercially available 1,3,5-trimethoxybenzene **10**. Friedel–Crafts acylation of **10** with isovaleryl chloride, followed by LAH reduction led to alcohol **12** *via* ketone **11**. After complexation of **12** with $Cr(CO)_6$, stepwise introduction of two methoxycarbonyl groups *via* direct nuclear lithiation[5] to the aromatic ring furnished diester *rac*-**13**. The resolution of this racemic benzyl alcohol was then examined. Diastereomeric carbamates derived from the CuCl assisted[6]




**Scheme 2** *Reagents and conditions*: i, isovaleryl chloride, $AlCl_3$, $CH_2Cl_2$, 0 °C, 81%; ii, LAH, $Et_2O$, 0 °C, 91%; iii, $Cr(CO)_6$, $Bu^n_2O$–1,4-dioxane–*n*-heptane (5 : 5 : 1), 120 °C, 43% (92% based on conversion); iv, $Bu^nLi$, TMEDA, THF, −78 °C, then $CO_2$, −78 °C, then $TMSCHN_2$, $C_6H_6$–MeOH (4 : 1); v, LDA, TMEDA, THF, −50 °C, then $CO_2$, −78 °C, then $TMSCHN_2$, $C_6H_6$–MeOH (4 : 1), 75% overall; vi, (*R*)-(−)-1-(1-naphthyl)ethyl isocyanate, CuCl, DMF, 99%, then separation; vii, $BF_3{\cdot}Et_2O$, wet MeCN, 0 °C, 81%; viii, $(ClCH_2CO)_2O$, pyridine, $CH_2Cl_2$, 0 °C, 92%

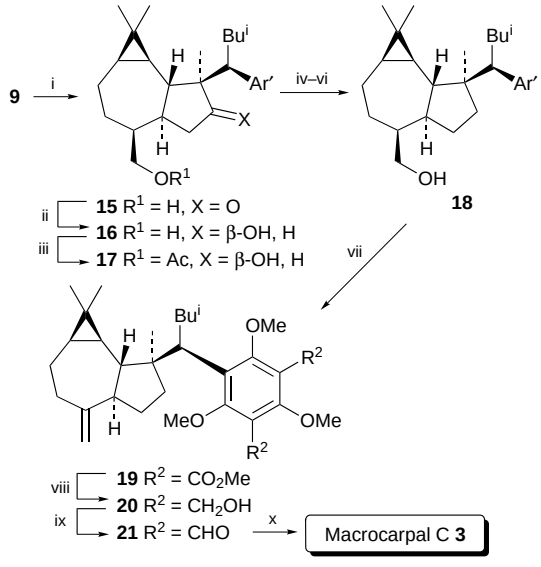



**Scheme 3** *Reagents and conditions*: i, Bu$^t$Me$_2$SiOTf, Et$_3$N, Et$_2$O–CH$_2$Cl$_2$ (1 : 1), 98%; ii, **8**, ZnCl$_2$, CH$_2$Cl$_2$; iii, CAN, MeOH, 0 °C, 61% from **8**

reaction of *rac*-**13** with (*R*)-(−)-1-(1-naphthyl)ethyl isocyanate[7] were separated by simple chromatography on silica gel. Hydrolysis of the polar carbamate **14** was achieved by treatment with $BF_3{\cdot}Et_2O$ in hydrous MeCN to provide the alcohol (*S*)-**13**, $[\alpha]_D^{26}$ −21.9 ( > 98% ee) without racemization.‡ Finally, (*S*)-**13** was converted to the chloroacetate **8**, which was expected to have the required reactivity.[8]

With the desired chiral complex **8** as an aromatic side-chain unit in hand, we subjected **8** to the coupling reaction (Scheme 3). For this purpose, the enone **6** was converted to the *tert*-butyldimethylsilyl dienol ether **7**. A 1.5-fold excess of this intermediate was then coupled with the chiral complex **8** in the presence of ZnCl$_2$[9] to afford **9** stereoselectively§ after decomplexation with ceric ammonium nitrate (CAN).

Since the stereoselective route to the promising precursor of macrocarpal C **9** had already been developed, we further pursued the total synthesis (Scheme 4). Catalytic hydrogenation of the enone **9** afforded desilylated ketone **15** with the desired stereochemistry.[3] NaBH$_4$ reduction of **15** followed by acetylation of the primary hydroxy group led to monoacetate **17**¶ *via* diol **16**. The application of modified Grieco's protocol[10] allowed dehydration of the C10 secondary hydroxy group of **17**. Deacetylation of the resulting product followed by catalytic hydrogenation afforded alcohol **18**, which was subjected to dehydration again, furnishing *exo*-olefin **19**. DIBAL-H reduction of diester **19** followed by oxidation afforded trimethyl macrocarpal C **21** *via* diol **20**. Finally, the cleavage of all three methyl ethers was fully achieved by our original method (10 equiv. of 4-MeC$_6$H$_4$SLi, 50 equiv. of HMPA, toluene, reflux)‖ to furnish macrocarpal C **3**, which was identical to a natural authentic sample ($^1$H and $^{13}$C NMR).** Moreover, the synthetic sample was found to be identical to natural macrocarpal G **4**.††




**Scheme 4** *Reagents and conditions*: i, $H_2$ (5 atm), 10% Pd–C, MeOH, 88%; ii, NaBH$_4$, MeOH, 96%; iii, Ac$_2$O, DMAP, CH$_2$Cl$_2$, 100%; iv, 2-NO$_2$C$_6$H$_4$SeCN, Bu$^n_3$P, THF, sealed tube, 75 °C, then 30% aq. $H_2O_2$ 0 °C; v, NaOMe, MeOH, 64% from **17**; vi, $H_2$ (5 atm), 10% Pd–C, MeOH, 100%; vii, 2-NO$_2$C$_6$H$_4$SeCN, Bu$^n_3$P, THF, 50 °C, then 30% aq. $H_2O_2$, 0 °C, 77%; viii, DIBAL-H, toluene, −78 °C, 100%; ix, Pr$^n_4$NRuO$_4$, 4-methylmorpholine *N*-oxide, molecular sieves 4 Å, MeCN, 87%; x, 4-MeC$_6$H$_4$SLi, HMPA, toluene, reflux, 58%

We thank Professor Mugio Nishizawa (Tokushima Bunri University) for provision of natural macrocarpal C **3** and copies of its spectra. We also thank Professor Seiichi Homma (Ochanomizu University) for copies of the spectra for natural macrocarpal G **4**. This research was supported in part by a Grant-in-Aid for Scientific Research from the Ministry of Education, Science, Sports and Culture of Japan (No. 08672425).

## Footnotes and References

* E-mail: iwata@phs.osaka-u.ac.jp

† The $^1$H and $^{13}$C NMR spectra of macrocarpals C **3** and G **4** were measured in different solvents, which made comparison difficult. In ref. 1, however, it has been considered that these were diastereomers due to the difference between their physicochemical properties.

‡ Enantiomeric purity was determined by $^1$H NMR analysis of Mosher ester derivatives.[11] Absolute stereochemistry was assigned by Mosher's method.[12]

§ A small amount (2%) of the benzylic epimer of **9** was obtained, but neither the C11 epimer nor the regioisomer was isolated.

¶ The structural assignment of **17** was confirmed by X-ray crystallographic analysis of its C10 carbonylimidazolide derivative **22**. *Crystal data* for **22**: $C_{39}H_{54}N_2O_{11}$, $M$ = 726.86, orthorhombic, space group $P2_12_12_1$, $a$ = 16.723(2), $b$ = 19.979(2), $c$ = 11.547(2) Å, $V$ = 3858.0(9) Å$^3$, $Z$ = 4, $D_c$ = 1.251 g cm$^{-3}$, $\mu$(Cu-K$\alpha$) = 7.13 cm$^{-1}$, $F$(000) = 1560, $T$ = 293 K. The structure was solved by direct methods and refined by full-matrix least-squares to $R$ = 0.052 and $R_w$ = 0.067 using 2185 reflections with $F_o > 3\sigma(F_o)$. CCDC 182/601.

‖ A preliminary study suggested that only bis-demethylation would occur by the use of sodium salt (4-MeC$_6$H$_4$SNa), as previously reported.[13]

** Synthetic **3** displayed $^1$H and $^{13}$C NMR spectra that were indistinguishable from those of the natural isolate and showed the following optical properties: $[\alpha]_D^{25}$ −22.1 (*c* 0.150, EtOH). A small rotation, $[\alpha]_D^{24}$ −3.0 (*c* 0.92, EtOH), was originally reported for **3** that had been isolated from *E. globulus*.[2b] This rotation, however, is believed to be erroneous due to contamination of the natural sample (M. Nishizawa, personal communication, April 15, 1997).

†† Synthetic **3** exhibited spectroscopic data ($^1$H, $^{13}$C, IR) identical to those for natural macrocarpal G **4**. The rotation for synthetic **3**, $[\alpha]_D^{25}$ −24.7 (*c* 0.135, MeOH), corresponded closely to the rotation reported for **4**, $[\alpha]_D$ −27.1 (*c* 0.59, MeOH).[2c]

1 For a review of bioactive acylphloroglucinol derivatives from *Eucalyptus* species, see: E. L. Ghisalberti, *Phytochemistry*, 1996, **41**, 7.
2 (*a*) M. Murata, Y. Yamakoshi, S. Homma, K. Aida, K. Hori and Y. Ohashi, *Agric. Biol. Chem.*, 1990, **54**, 3221; (*b*) M. Nishizawa, M. Emura, Y. Kan, H. Yamada, K. Ogawa and N. Hamanaka, *Tetrahedron Lett.*, 1992, **33**, 2983; (*c*) Y. Yamakoshi, M. Murata, A. Shimizu and S. Homma, *Biosci. Biotech. Biochem.*, 1992, **56**, 1570; (*d*) M. Murata, Y. Yamakoshi, S. Homma, K. Arai and Y. Nakamura, *Biosci. Biotech.Biochem.*, 1992, **56**, 2062; (*e*) K. Osawa, H. Yasuda, H. Morita, K. Takeya and H. Itokawa, *Phytochemistry*, 1995, **40**, 183; (*f*) I. P. Singh and H. Etoh, *Biosci. Biotech. Biochem.*, 1995, **59**, 2330; (*g*) K. Osawa, H. Yasuda, H. Morita, K. Takeya and H. Itokawa, *J. Nat. Prod.*, 1996, **59**, 823.
3 T. Tanaka, K. Maeda, H. Mikamiyama, Y. Funakoshi, K. Uenaka and C. Iwata, *Tetrahedron*, 1996, **52**, 4257.
4 M. Uemura, T. Kobayashi, K. Isobe, T. Minami and Y. Hayashi, *J. Org. Chem.*, 1986, **51**, 2859 S. G. Davies and T. J. Donohoe, *Synlett*, 1993, 323.
5 M. F. Semmelhack, J. Bisaha and M. Czarny, *J. Am. Chem. Soc.*, 1979, **101**, 768; H.-G. Schmalz, T. Volk, D. Bernicke and S. Huneck, *Tetrahedron*, 1997, **53**, 9219.
6 M. E. Duggan and J. S. Imagire, *Synthesis*, 1989, 131.
7 W. H. Pirkle and J. R. Hauske, *J. Org. Chem.*, 1977, **42**, 1839.
8 W. R. Roush and C. K. Wada, *Tetrahedron Lett.*, 1994, **35**, 7347.
9 M. T. Reetz and M. Sauerwald, *Tetrahedron Lett.*, 1983, **24**, 2837.
10 P. A. Grieco, S. Gilman and M. Nishizawa, *J. Org. Chem.*, 1976, **41**, 1485.
11 J. A. Dale, D. L. Dull and H. S. Mosher, *J. Org. Chem.*, 1969, **34**, 2543.
12 J. A. Dale and H. S. Mosher, *J. Am. Chem. Soc.*, 1973, **95**, 512.
13 C. Hansson and B. Wickberg, *Synthesis*, 1976, 191.

*Received in Cambridge, UK, 21st July 1997; 7/05231F*

# ≡CH··π *versus* ≡CH···Halogen interactions—the crystal structures of the 4-halogenoethynylbenzenes

**Hans-Christoph Weiss,[a] Roland Boese,*[a] Heather L. Smith[b] and Michael M. Haley[b]**

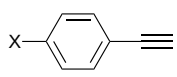
[a] *Institut für Anorganische Chemie, Universität Essen, Universitätsstrasse 3-5, D-45117 Essen, Germany*
[b] *Department of Chemistry, University of Oregon, Eugene, Oregon 97403, USA*

**The crystal structures of the 4-halogenoethynylbenzenes are quite similar and exhibit ≡CH···π interactions, whereas the structure of 4-fluoroethynylbenzene has very interesting and rare intermolecular ≡CH···F contacts.**

The X-ray crystal structures of 1,4-dihalogenobenzenes (α-form of 1,4-dichlorobenzene) are, for the most part, isomorphous;[1–6] notable exceptions are the structures of 1,4-diiodobenzene[7] and those which contain fluorine.[8] For mixed 1,4-dihalogenobenzenes a disorder was found such that the positions of the ring carbon atoms are almost fixed, but the sites of the halogens are crystallographically equivalent.[1,9] The packing motif typically found in 1,4-dihalogenobenzenes is a zigzag pattern of intermolecular X···X interactions.

Fluorine containing compounds, however, crystallize differently.[8] Fluorine often plays a special role in that it is expected not to exhibit intermolecular F···F contacts. We recently reported the crystal structures of a series of ethynylated benzenes in which ≡CH··π interactions predominated.[10] Combining both moieties (halogen and ethynyl group) in a single benzene derivative might lead to a deeper insight into the intermolecular interactions of the ethynyl group.

Accordingly we present the crystal structures of the 4-X-ethynylbenzenes (with X = F **4**, Cl **1**, Br **2** and I **3**).† The




**1** X = Cl
**2** X = Br
**3** X = I
**4** X = F

X-ray structures of compounds **1**, **2** and **3** are isomorphous. The cell dimensions are quite similar and remarkably also comparable to those of the 1,4-dihalogenobenzenes. The packing motif of **1** is easy to surmise: the molecules form a layer structure in the *bc* plane similar to that observed in the α-form of 1,4-dichlorobenzene,[2–4] in 1,4-dibromobenzene,[5] and also in 1,4-diethynylbenzene.[10,11] The molecules are tilted by 32.7° out of this plane (Fig. 1) and are held together by attractive ≡CH··π and Cl··Cl contacts, both of which dominate the packing. This geometry of T-shaped ≡CH··π hydrogen bridges is known from other alkynes,[12] as well as the zigzag pattern of the terminal chlorine atoms (*e.g.* in the α-form of 1,4-dichlorobenzene[2–4]). The ≡CH··π contacts to the center of the triple bond are quite short whereas the intermolecular Cl··Cl distances are relatively long (Table 1) but still have a significant attractive character.

Molecules **2** and **3** are disordered in the same manner as the mixed 1,4-dihalogenobenzenes: the center of inversion is in the center of the disordered ring system. This means that if the disorder is resolved 50% of the 1- and 4-positions of the benzene ring are occupied by the halogen atom and 50% by the ethynyl group (Fig. 2). Nevertheless, the packing motifs are the same as in **1** or in the 1,4-dihalogenobenzenes with the same zigzag pattern at the two ends of the molecules. For bromide **2**, two different positions of the ring system could be found and refined. The intermolecular interactions that determine the crystal packing are ≡CH··π and X···X. Hydrogen bridges between the ethynyl hydrogen atom to bromine or iodine might exist if statistical disorder is assumed; however, this is not very likely because the resulting ≡CH···X distances are much shorter than the sums of the van der Waals radii ($d_{H\cdots Br}$ = 243.9, $\Sigma_{vdW}$ = 299; $d_{H\cdots I}$ = 238.9, $\Sigma_{vdW}$ = 314 pm[13]). This indicates that the disorder is not statistical; instead there exists a disorder in which ordered domains or layers within the lattice are statistically distributed in the crystal.

**Table 1** Selected intermolecular geometric parameters of compounds **1–3**[a]

| Comp. | *d*(X–X)/pm | ∠(C–X···X)(°) | *d*(≡CH··M)/pm | ∠(≡CH··M)(°) |
|---|---|---|---|---|
| **1** | 379.0 | 92.5 | 357.9 | 171.9 |
| **2** | 386.7 | 96.1 | 266.9 | 173.6 |
| **3** | 394.9 | 97.0 | 255.7 | 174.9 |

[a] M represents the center of the triple bond, X the halogen atoms. The positions of the hydrogen atoms were normalized to a C–H distance of 108 pm.

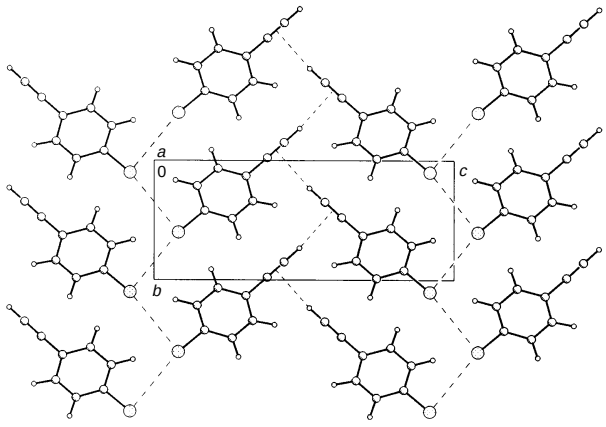



**Fig. 1** View along *a*-axis of the crystal structure of **1**

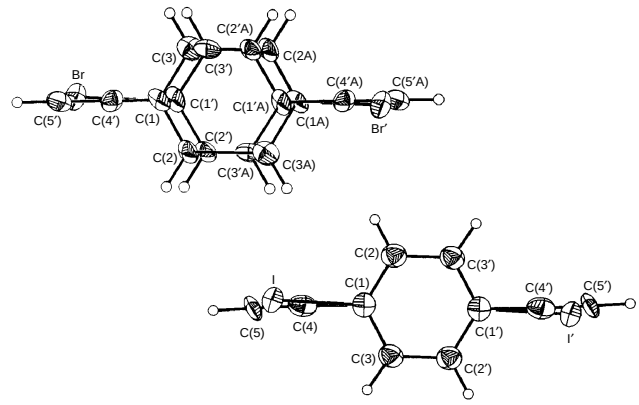



**Fig. 2** The type of disorder of **2** and **3**

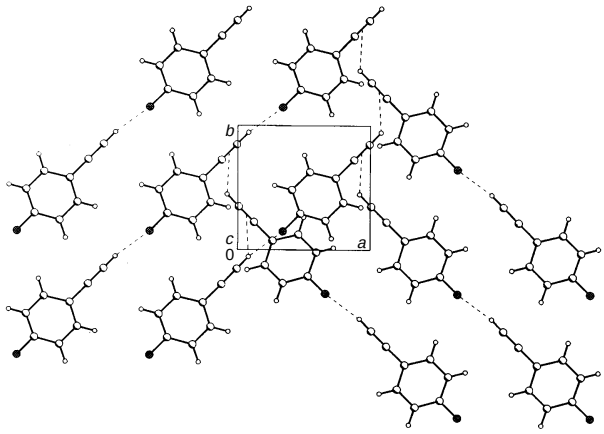



**Fig. 3** The two interactions which dominate the packing in the structure of **4**

In contrast to the other systems, the packing of fluoride **4** is totally different, as is shown in Fig. 3. Two attractive forces dominate the arrangement. In both cases the ethynyl hydrogen atoms serve as hydrogen bridge donors. One acceptor is the triple bond, but this contact does not possess an ideal geometry: The ≡CH··π distance is comparatively long (307.6 pm) and the angle ≡C–H··π is rather small (129.4°). The other attractive contact is much more interesting: a hydrogen bond to covalently bound organic fluorine is very much disputed.[14,15] The ≡CH··F distance in **4** is 226.4 pm and thus is significantly shorter than the sum of the van der Waals radii (254 pm[13]). The ≡CH··F angle of 140.4° supports the assumption that a ≡CH··F hydrogen bridge exists, at least if the carbon atom is sp-hybridized. This is also sustained by the fact, that the packing of **4** is totally different compared to 4-halogenoethynylbenzenes **1**–**3**. Therefore we must conclude that the predominant interactions in **4** consist of ≡CH··F hydrogen bridges.

We gratefully acknowledge the DFG, the Fonds der Chemischen Industrie and the NSF for financial support of this work.

## Footnotes and References

* E-mail: boese@structchem.uni-essen.de

† *Crystal data* for **1**: $C_8H_5Cl$ (Aldrich), no recrystallization necessary, space group $P2_1$, $a$ = 3.881(3), $b$ = 5.811(4), $c$ = 14.455(9) Å, $\beta$ = 95.02(5)°, $V$ = 324.7(4) Å$^3$, $Z$ = 2, $D_c$ = 1.40 g cm$^{-3}$, 1016 unique reflections $F_o > 4\sigma(F_o)$, 102 parameters, $2\theta_{max}$ = 60°, $R1$ = 0.039.

For **2**: $C_8H_5Br$,[16] crystals obtained by sublimation; space group $P2_1/c$, $a$ = 3.941(1), $b$ = 5.827(2), $c$ = 14.779(4) Å, $\beta$ = 94.57(2)°, $V$ = 338.3(2) Å$^3$, $Z$ = 2, $D_c$ = 1.78 g cm$^{-3}$, 1065 unique reflections $F_o > 4\sigma(F_o)$, 87 parameters, $2\theta_{max}$ = 80°, $R1$ = 0.062.

For **3**: $C_8H_5I$;[17] crystals obtained by sublimation; space group $P2_1/c$, $a$ = 4.046(1), $b$ = 5.888(2), $c$ = 15.322(5) Å, $\beta$ = 93.63(3)°, $V$ = 364.3(2) Å$^3$, $Z$ = 2, $D_c$ = 2.08 g cm$^{-3}$, 1255 unique reflections $F_o > 4\sigma(F_o)$, 64 parameters, $2\theta_{max}$ = 70°, $R1$ = 0.052.

For **4**: $C_8H_5F$ (Aldrich), no recrystallization necessary, space group $P2_1/c$, $a$ = 7.065(3), $b$ = 6.587(3), $c$ = 13.241(6) Å, $\beta$ = 99.65(3)°, $V$ = 607.5(4) Å$^3$, $Z$ = 4, $D_c$ = 1.31 g cm$^{-3}$, 1529 unique reflections $F_o > 4\sigma(F_o)$, 103 parameters, $2\theta_{max}$ = 60°, $R1$ = 0.055.

All measurements were performed on a Nicolet R3m/V X-ray four circle diffractometer at 125 K. Mo-Kα X-rays ($\lambda$ = 0.71073 Å), graphite monochromator and the program SHELXTL[18] refined on $F^2$, H-atom positions taken from difference fourier maps and refined free and isotropically. CCDC 182/650.

1 A. Koug, *Nature*, 1947, **160**, 570.
2 U. Croatto, S. Bezzi and E. Bua, *Acta Crystallogr.*, 1952, **5**, 825.
3 G. L. Wheeler and S. D. Colson, *J. Chem. Phys.*, 1976, **65**, 1227.
4 C. Panattoni, E. Frasson and S. Bezzi, *Gazz. Chim. Ital.*, 1963, **93**, 813.
5 A. Maiga, Nguygen-Ba-Chanh, Y. Haget and M. A. Cuevas-Diatre, *J. Appl. Crystallogr.*, 1984, **17**, 210.
6 D. Britton, *Acta Crystallogr., Sect. B*, 1976, **32**, 976.
7 A. Hinchliffe, R. W. Munn, R. G. Pritchard and C. J. Spicer, *J. Mol. Struct.*, 1985, **130**, 93.
8 R. Boese, H.-Chr. Weiss and M. Kirchner, unpublished results.
9 S. B. Hendricks, *Z. Kristallogr.*, 1933, **84**, 85.
10 H.-Chr. Weiss, D. Bläser, R. Boese, B. M. Doughan and M. M. Haley, *Chem. Commun.*, 1997, 1703.
11 N. A. Ahmed, A. I. Kitaigorodskij and M. I. Sirota, *Acta Crystallogr.*, 1972, **28**, 2875.
12 For example, see T. Steiner, *J. Chem. Soc., Chem. Commun.*, 1995, 95; P. E. Eaton, E. Galoppini and R. Gilardi, *J. Am. Chem. Soc.*, 1994, **116**, 7588; R. K. McMullan, Å. Kvick and P. Popelier, *Acta Crystallogr., Sect. B*, 1992, **48**, 726.
13 R. S. Rowland and R. Taylor, *J. Phys. Chem.*, 1996, **100**, 7384.
14 J. A. K. Howard, V. J. Hoy, D. O'Hagan and G. T. Smith, *Tetrahedron*, 1996, **38**, 12613.
15 J. D. Dunitz and R. Taylor, *Chem. Eur. J.*, 1997, **3**, 89.
16 R. P. Hsung, C. E. D. Chidsey and L. R. Sita, *Organometallics*, 1995, **14**, 4808.
17 1-Ethynyl-4-iodobenzene was prepared in two steps (84% yield) from the corresponding molecule where the terminal acetylene was protected as the trimethylsilyl derivative and the aryl iodide protected as a diethyltriazene using the procedures described in: J. Zhang, D. J. Pesak, J. L. Ludwick and J. S. Moore, *J. Am. Chem. Soc.*, 1994, **116**, 4227.
18 G. M. Sheldrick, SHELXTL, Program for Crystal Structure Solution and Refinement, University of Göttingen, 1993.

*Received in Cambridge, UK, 9th September 1997; 7/06564G*

# Macropolyhedral boron-containing cluster chemistry. Triple cluster fusion and the molecular structure of $[(PMe_3)_2IrB_{26}H_{24}Ir(CO)(PMe_3)_2]$. A 28-vertex metallaborane cluster with a polyboron core†

**Jonathan Bould,[a,b] John D. Kennedy,*[a] Lawrence Barton[b] and Nigam P. Rath[b]**

[a] *The School of Chemistry of the University of Leeds, Leeds, UK LS2 9JT*
[b] *The Department of Chemistry of the University of Missouri St. Louis, St. Louis, Missouri 63121, USA*

**$[(PMe_3)_2IrB_{26}H_{24}Ir(CO)(PMe_3)_2]$, from the thermolysis of $[(CO)(PMe_3)_2HIrB_8H_{12}]$ in molten $B_{10}H_{14}$, is a triple-cluster species that consists of *closo* twelve-vertex $\{IrB_{11}\}$ and *closo* ten-vertex $\{IrB_9\}$ units fused by (*a*) a common $\{IrB_2\}$ triangular face and (*b*) by an adjacent 'wedge' interboron linkage that also binds a *nido* nine-vertex $\{IrB_8\}$ subcluster; the resulting $\{Ir_2B_{26}\}$ cluster has a novel five-boron core.**

The extension of contiguous polyhedral boron-containing cluster chemistry beyond the constraints of single clusters of up to fourteen vertices is engendered by cluster fusion to generate so-called macropolyhedral species. Several compounds of up to about twenty vertices have been synthesized by the fusion of two clusters, but triple fusion to generate larger macropolyhedral assemblies has so far proved elusive. The *arachno* nine-vertex system appears to be particularly suitable for cluster-fusion chemistry, for example in the synthesis of $B_{18}H_{22}$ and its derivatives,[1] and in macropolyhedral platinaborane,[2] thiaborane,[3] and iridaborane formation.[4] These processes all appear to occur *via* reactive nine-vertex intermediates. We surmised that, if these intermediates are generated in the presence of suitable substrates of intermediate reactivity, then the possibility of mixed or multiple fusion to generate larger macropolyhedral assemblies arises. In this regard the *arachno*/*nido* $\{IrB_8\}$ system has interesting reactivity,[5] and we have recently reported preliminary results on the autofusion of the *arachno* nine-vertex compound $[(CO)(PMe_3)_2HIrB_8H_{12}]$ to give double-cluster $[(CO)(PMe_3)_2IrB_{16}H_{14}Ir(CO)(PMe_3)_2]$[4] and the mixed cluster fusion of molten *nido*-$B_{10}H_{14}$ with $[(CO)(PMe_3)_2HIrB_8H_{12}]$ to give double-cluster $[(PMe_3)_2(CO)IrB_{17}H_{20}]$ **1**.[6] We now report preliminary findings on the principle of multiple cluster fusion, as manifested in the isolation and characterization of a triple-cluster species of formulation $[(PMe_3)_2HIrB_{26}H_{24}(CO)(PMe_3)_2]$ **2** from the latter molten $B_{10}H_{14}$ system.

The sample of compound **2** was prepared by reaction of $[(CO)(PMe_3)_2HIrB_8H_{12}]$ (25 mg, 610 μmol) with $B_{10}H_{14}$ (134 mg; 1100 mmol; mp *ca*. 99 °C) under $N_2$ at 134 °C for 25 min. The excess of molten $B_{10}H_{14}$ was used to engender solubility of $[(CO)(PMe_3)_2HIrB_8H_{12}]$ and also to minimise the double-cluster autofusion[4] that would give $[(CO)(PMe_3)_2IrB_{16}H_{14}Ir(CO)(PMe_3)_2]$. The excess $B_{10}H_{14}$ was then removed by vacuum sublimation (bath *ca*. 80 °C). Extraction with $CH_2Cl_2$, filtration through silica gel, followed by repeated TLC (95 : 5 $CH_2Cl_2$–MeCN) on silica gel G revealed many coloured products, and ultimately gave an orange band [$R_F$ 0.7 using $CH_2Cl_2$–hexane (1 : 1)] as a predominant component. HPLC separation (silica, Lichrosorb Si60 7 μm; 260 × 16 mm column; rapid initial gradient 25% $CH_2Cl_2$ in hexane to 100% $CH_2Cl_2$, flow rate 4 ml $min^{-1}$) gave one impure major component of $R_T$ *ca*. 32 min, and several minor components, of which one has been identified as [7,7-$(PMe_3)_2$-7-(CO)-*syn*-7-$IrB_{17}H_{20}$] **1** ($R_T$ *ca*. 30 min).[6] Repeated fractional crystallisation of the principal component of the mixture with $R_T$ *ca*. 32 min gave a small sample ( < *ca*. 500 μg) of orange–yellow crystals of a $CH_2Cl_2$ solvate of $[(PMe_3)_2IrB_{26}H_{24}Ir(CO)(PMe_3)_2]$ **2** (Fig. 1). They were identified by single crystal X-ray diffraction analysis‡ and NMR spectroscopy.§ Although the very small quantities and complex nature of the compound have precluded chemical shift assignments by homonuclear $^1H$ or $^{11}B$ NMR COSY techniques, the NMR data on the bulk material are otherwise consistent with the structure of Fig. 1. Separation of the many reaction products is difficult; NMR spectroscopy suggests the presence of a number of other large iridaborane cluster compounds.

Structurally the compound is seen to be based on the conceptual fusion, with a common $\{IrB_2\}$ triangular face, of a *closo* twelve-vertex $\{IrB_{11}\}$ unit **IA** and a *closo* ten-vertex $\{IrB_9\}$ unit **IB**. The clusters are additionally linked by an interboron 'wedge' linkage that is also involved in multicentre bonding to the third subcluster, a *nido* nine-vertex $\{IrB_8\}$ unit **IC**. This latter linkage is reminiscent of the intercluster linkages in the simpler macropolyhedrals $B_{14}H_{22}$ and $B_{15}H_{23}$.[9] Mechanistically, *arachno* $[(CO)(PMe_3)_2HIrB_8H_{12}]$ will readily dehydrogenate to give *nido* $[(CO)(PMe_3)_2IrB_8H_{11}]$ under the

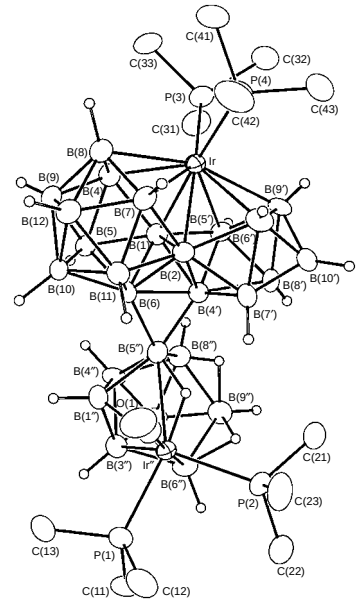
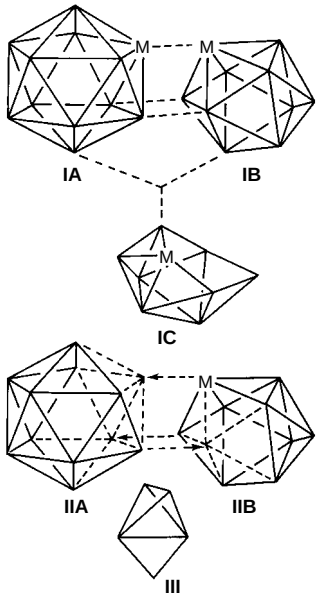



**Fig. 1** Representation of the crystallographically determined molecular structure of $[(PMe_3)_2IrB_{26}H_{24}Ir(CO)(PMe_3)_2]$ with non-hydrogen atoms as thermal ellipsoids of 50% probability, and with the methyl hydrogen atoms omitted for clarity. Selected interatomic distances (Å): to Ir: B(1) 2.149(8), B(2) 2.248(8), B(4) 2.296(9), B(7) 2.330(9), B(8) 2.329(9), B(5′) 2.416(8), B(6′) 2.273(10), B(9′) 2.351(9); to Ir″: B(1″) 2.161(8), B(3″) 2.263(9), B(5″) 2.533(8), B(6″) 2.287(9). Selected interboron distances: to B(6): B(1) 1.786(11), B(2) 1.874(12), B(5) 1.814(12), B(10) 1.776(11), B(11) 1.797(12), B(4′) 1.822(11), B(5″) 1.854(12); to B(7′): B(4′) 1.848(12), B(8′) 1.859(12), B(6′) 1.832(12), B(10′) 1.688(12), B(2) 1.803(12). Angles (°) between interatomic vectors at B(2) are in the ranges 53.4(4)–69.0(4), 98.9(4)–113.8(8), 121.4(5)–124.8(7) and 143.7(6)–155.4(7).




reaction conditions.[4,10] A *nido* {$IrB_8$} unit **IIB** will supply two vertices to the *nido* decaboranyl skeleton **IIA** to generate the {$IrB_{11}$} unit **IA**, with a reciprocal supply of one vertex to the *nido* unit **IIB** to generate the {$IrB_9$} unit **IB**. The fusion mechanism is thereby seen to be the successive addition of two *nido*-type {$IrB_8$} units **IC** and **IIB** to the *nido*-decaboranyl substrate **IIA**. Although a very minor product of a reaction system that yields several complex iridaboranes, a simple stoichiometry can be written as in eqn. (1).

$$2[(CO)(PMe_3)_2HIrB_8H_{12}] + B_{10}H_{14} \rightarrow [(PMe_3)_2IrB_{26}H_{24}Ir(CO)(PMe_3)_2] + CO + 8H_2 \quad (1)$$

Compound **2** has several noteworthy features. (*a*) It nicely demonstrates the principle of triple cluster fusion and (*b*) with 28 vertices it one of the biggest contiguous boron-cluster compounds yet synthesized. (*c*) There are two vertices, one boron and one iridium, that have the high cluster connectivity number eight. The iridium atom has the high overall coordination number ten. If multicentre bonding of boron is limited to participation in two- and three-centre bonding only, eight-connectivity represents the maximum for boron with its four valence orbitals. (*d*) The {$IrB_8$} subcluster still retains *nido* nine-vertex character, and is therefore in principle available for further cluster incorporation, either for increased condensation within the 28-vertex system, or for fusion with a further substrate to generate quadruple cluster character. (*e*) At the region of conjunction of the three subclusters there is a central five-boron unit **III** without *exo* substituents.

This last feature suggests new types of families of large borane-based species based on globular structures that have condensed inner borons-only cores surrounded by outer spheres based on boron hydride cluster features, as distinct from the rope-like structures envisaged by extension of classical two-borons-in-common macropolyhedral fusion modes.[11] The known species $B_{20}H_{16}$, with a four-boron core,[12] is a simpler example of this. At the other extreme, a boron ball surrounded by a boron–hydride skin could be envisaged. In principle a continuum of behaviour between the ropes and the globules is available. These globular-core configurations for large borane clusters contrast to (hypothetical) hollow fullerene-based boron structures upon which speculation has recently centred.[13] Metal cluster compounds can be regarded as domains of metal lattice with peripheral valencies occupied by ligands, and hydrocarbons can be regarded as based on fragments of diamond or graphite with peripheral valencies bound to hydrogen. In this context it may be noted that there is a tetrahedral {$B_4$} unit in β-rhombohedral boron itself,[14] at the point of fusion of three icosahedral units with a common vertex.

We thank the Johnson-Matthey Company for a loan of $IrCl_3 \cdot 3H_2O$, the National Science Foundation (USA) and the EPSRC (UK) for the financial support of this work, and the NSF for a grant to purchase the X-ray diffractometer used.

## Footnotes and References

* E-mail: johnk@chem.leeds.ac.uk

† A complete nomenclature would be: 3,3,2″,2″-tetrakis(trimethylphosphine)-3,2″-(dicarbonyl)-μ-6,4′-(*nido*-2″-iridanonaborane-5″-yl)-3(=2′)-irida-*closo*-decaborano-[1′,3′,2′ : 1,2,3][μ-4,6′]-*closo*-dodecaborane.

‡ *Crystallography*: All measurements were made at 193 K on a Siemens SMART CCD detector system with a sealed-tube X-ray source (50 kV × 40 mA) using Mo-Kα radiation ($\lambda$ = 0.710 73 Å). Data reduced using SAINT,[6] structure solution and refinement carried out using SHELXTL-PLUS (5.03)[7] by minimization of $\Sigma w(F_o^2 - F_c^2)^2$. All non-hydrogen atoms refined with anisotropic displacement parameters. All of the hydrogen atoms on the cage were located from Fourier difference maps and refined using a riding model. *Crystal data*: $C_{15}H_{62}B_{26}Cl_6Ir_2OP_4$, $M$ = 1260.69, monoclinic, space group $P2_1/n$, $a$ = 10.4293(1), $b$ = 24.1999(2), $c$ = 19.8959(2) Å, $\beta$ = 90.041(1)°, $U$ = 5021.49(8) Å$^3$, $Z$ = 4, $D_c$ = 1.668 Mg m$^{-3}$, $\mu$ = 5.761 mm$^{-1}$, $F(000)$ = 2424. $R_1$ = 0.0476 for 8198 observed reflections with $F > 4\sigma(F)$, $R_w(F^2)$ = 0.1212 for 11 478 reflections and $S$ = 1.142 for all data. CCDC 182/631.

§ Selected $^{11}$B and $^1$H NMR data, $CD_2Cl_2$ at 300 K, ordered as $\delta(^{11}B)$ (rel. $Et_2OBF_3$) [$\delta(^1H)$ of directly bound H(*exo*) in square brackets]: +38.0 [+6.84], +23.2 [+6.49], +19.0 [*conjuncto* site], +10.0 [+4.77], +8.8 [+3.84, doublet structure, splitting 28 Hz], *ca.* +5.4 [+4.53], *ca.* +5.4 [+1.76], *ca.* +5.4 [+1.21], *ca.* +3.4 [*ca.* + 2.80], *ca.* +3.4 [*ca.* +2.80], −1.5 [*conjuncto* site], −2.5 [+2.44], −3.5 [+1.79], *ca.* −7.0 [*conjuncto* site], *ca.* −7.2 [*ca.* +2.66], *ca.* −7.2 [*ca.* +2.66], −8.9 [+2.40], −12.0 [+3.04], −15.4 [*conjuncto* site], *ca.* −19.6 [+1.21], *ca.* −19.6 [+1.48], *ca.* −19.6 [+0.36] −23.6 [−0.43], − 28.0 [−1.21], −45.0 [−1.00], and −49.6 [*conjuncto* site]. Additional data are: $\delta(^1H)$ (bridge) at −17.78 [d, $^2J(^{31}P–^1H)$ 44 Hz], −2.40 and −1.82; and, at 213 K, $\delta(^{31}P)$ −33.0 and −56.0 [$^2J(^{31}P–^{31}P)$ *ca.* 15 Hz]; −38.0 and −39.7 [$^2J(^{31}P–^{31}P)$ *ca.* 4 Hz].

1 J. Bould, N. N. Greenwood and J. D. Kennedy, *Polyhedron*, 1983, **2**, 1401; D. F. Gaines, C. K.Nelson and G. A. Steehler, *J. Am. Chem. Soc.*, 1984, **84**, 7266; S. H. Lawrence, J. R. Wermer, S. K. Boocock, M. A. Banks, P. C. Keller and S. G. Shore, *Inorg. Chem.*, 1986, **25**, 367; G. B. Jacobsen, D. G. Meina, J. H. Morris, C. Thompson, S. J. Andrews, D. Reed, A. J. Welch and D. F. Gaines, *J. Chem. Soc., Dalton Trans.*, 1985, 1645; S. O. Kang and L. G. Sneddon, *Inorg. Chem.*, 1988, **27**, 587.

2 M. A. Beckett, J. E. Crook, N. N. Greenwood and J. D. Kennedy, *J. Chem. Soc., Dalton Trans.*, 1986, 1879; M. A. Beckett, N. N. Greenwood, J. D. Kennedy, P. A. Salter and M. Thornton-Pett, *J. Chem. Soc., Chem. Commun.*, 1986, 556.

3 T. Jelínek, J. D. Kennedy and B. Štíbr, *J. Chem. Soc., Chem. Commun.*, 1994, 1415; P. Kaur, J. Holub, N. P. Rath, J. Bould, L. Barton, B. Štíbr and J. D. Kennedy, *Chem. Commun.*, 1996, 273.

4 L. Barton, J. Bould, J. D. Kennedy and N. P. Rath, *J. Chem. Soc., Dalton Trans.*, 1996, 3145.

5 J. Bould, N. P. Rath and L. Barton, *Organometallics*, 1996, **15**, 4915.

6 J. Bould, W. Clegg, J. D. Kennedy, S. J. Teat and M. Thornton-Pett, *J. Chem. Soc., Dalton Trans.*, 1997, 2005.

7 SAINT, Program for reduction of X-ray data, Siemens Analytical X-ray Division, Madison, WI, 1995.

8 G. M. Sheldrick, Siemens Analytical X-ray Division, Madison, WI, 1995.

9 J. Rathke and R. Schaeffer, *Inorg. Chem.*, 1974, **13**, 3008.

10 J. Bould, J. E. Crook, N. N. Greenwood, J. D. Kennedy and W. S. McDonald, *J. Chem. Soc., Chem. Commun.*, 1992, 346; J. Bould, N. N. Greenwood and J. D. Kennedy, *J. Chem. Soc., Dalton Trans.*, 1984, 2477.

11 W. N. Lipscomb, *Inorg. Chem.*, 1980, **19**, 1415.

12 R. D. Dobrott, L. B. Friedman and W. N. Lipscomb, *J. Chem. Phys.*, 1964, **49**, 866.

13 W. N. Lipscomb and L. Massa, *Inorg. Chem.*, 1992, **31**, 2299; 1994, **33**, 5155.

14 See, for example (together with references therein): *GMELIN, Handbook of Inorganic Chemistry, Boron*, Supplement vol. 2: *Elemental Boron, Boron Carbides*, 1981, pp. 242.

*Received in Cambridge, UK, 23rd September 1997; 7/06905G*

# Formation of a novel tetranuclear iron(III) complex with a $\mu_4$-$PO_4$ bridge from 4-nitrophenyl phosphate

**Bao-Hui Ye,[a] Xiao-Yuan Li,*[a] Feng Xue[b] and Thoms C. W. Mak[b]**

[a] *Department of Chemistry, The Hong Kong University of Science and Technology, Clear Water Bay, Kowloon, Hong Kong, PR China*

[b] *Department of Chemistry, The Chinese University of Hong Kong, Shatin, New Territories, Hong Kong, PR China*

**A novel tetranuclear iron(III) complex, [{$Fe_2$(tren)$_2$($\mu$-O)}$_2$($\mu_4$-$PO_4$)][$ClO_4$]$_5$·2.5$H_2O$ 1 [tren = tris(2-aminoethyl)-amine], is synthesized; X-ray crystal structure analysis reveals that 1 contains a tetranuclear cation in which the iron atoms are linked by a $\mu_4$-$PO_4^{3-}$ bridge, which is a hydrolytic product from 4-nitrophenyl phosphate.**

The important and diversified roles of iron in biology have long been recognized and intensively studied. Non-heme iron proteins, besides iron–heme and iron–sulfur proteins, have attracted intensive attention in recent years.[1] This class of iron proteins contain either mono- or oxo-bridged binuclear or polynuclear iron cores, such as those found in hemerythrin, ribonucleotide reductase, purple acid phosphatase and ferritin.[1] Therefore, tremendous efforts have been devoted to the synthesis and characterization of binuclear and polynuclear iron model complexes to facilitate the understanding of structure and function of nonheme iron proteins. Hitherto, at least two tetranuclear iron(III) complexes were found to occur in nature.[2] Almost all of the synthetic tetranuclear iron(III) compounds can be envisaged as dimers of dimers, at least in terms of their molecular architecture.[3–9] These complexes can be further classified into three structure types: the first is termed 'butterfly' with a $[Fe_4(\mu_3\text{-}O)_2]^{8+}$ core[3] or $[Fe_4(\mu_3\text{-}OR)_2]^{10+}$ (R = H, Me) cores;[4,5] the second contains a distorted adamantane-like $[Fe_4(\mu\text{-}X)_2(\mu\text{-}OH)_2(\mu\text{-}O)_2]^{4+}$ (X = hydroxo, alkoxo or phenoxo) cores;[6] and the third can be viewed as consisting of two well separated $Fe_2(\mu\text{-}X)(\mu\text{-carboxylato})_n$ (X = O, OH, alkoxo; $n$ = 1, 2) cores,[7–9] which are linked through two non-interacting hydrocarbon tethers,[7] two oxo[8] or two alkoxy[9] bridges. Another interesting tetranuclear iron(III) system contains a 'metallocrown' core which consists of an $(Fe–N–O)_3$ ring capped by another iron(III).[10]

In our effort to synthesize model complexes for purple acid phosphatase which catalyzes the hydrolysis of certain phosphate esters under acidic conditions,[1] a novel tetranuclear iron(III) complex, [{$Fe_2$(tren)$_2$($\mu$-O)}$_2$($\mu_4$-$PO_4$)][$ClO_4$]$_5$·2.5$H_2O$ **1** was produced. The most interesting aspect of **1** is that the bridging $PO_4^{3-}$ group was a hydrolytic product of a phosphate monoester which was used as a precursor together with an iron(III) polyamine complex in our synthetic reaction. This suggests that the iron(III) polyamine actually expedites the hydrolytic cleavage of the ester bond in the phosphate monoester, a process likely involving a two- or poly-metal mechanism. To the best of our knowledge, this is the first example of a tetranuclear iron(III) complex in which the four iron(III) are linked with a $\mu_4$-$PO_4^{3-}$ bridge. Here we report the synthesis and structural characterization of the novel compound **1**.

When 4-nitrophenyl phosphate was treated with a methanol solution of $Fe^{III}$ and tren, a green solid was readily formed. The tetranuclear iron(III) complex **1** was isolated by filtration.† Its structure was determined by single crystal X-ray analysis.‡ Two other products were also obtained when the filtrate was evaporated in air. One is yellow and spectral analysis shows that it is 4-nitrophenol which is another hydrolytic product from 4-nitrophenyl phosphate. The second product is red and is insoluble in common organic solvents. Its IR and Raman spectra show that it may be a mononuclear iron(III) complex containing tren and 4-nitrophenyl phosphate ligands, but no $ClO_4^-$ anion.

The cation structure in complex **1** is shown in Fig. 1. Four iron centers, each chelated by a tetradentate tren ligand, are connected pairwise by two μ-oxo and further consolidated by a tetradentate phosphate. The complex can thus be viewed as consisting of two (tren)Fe–O–Fe(tren) units with a central tetradentate $PO_4^{3-}$ group bridging all four irons. The two 'dimers' are structurally similar but crystallographically independent. The Fe–O(oxo) distances and Fe–O–Fe angles fall in the normal range.[1a] However, the bond lengths of Fe(3)–O(6) [1.813(6) Å] and Fe(4)–O(6) [1.822(6) Å] are slightly longer than those of Fe(1)–O(5) [1.805(6) Å] and Fe(2)–O(5) [1.785(6) Å], the angle Fe(3)–O(6)–Fe(4) [129.4(3)°] is smaller than that of Fe(1)–O(5)–Fe(2) [134.2(3)°], and the distance of Fe(3)···Fe(4) (3.286 Å) is slightly shorter than that of Fe(1)···Fe(2) (3.307 Å). This can be elucidated by the formation of a hydrogen bond between the bridging O(6) and a neighboring water molecule [O(6)···O(1w) 2.743 Å]. The presence of this hydrogen bond confers a partial hydroxo character to O(6) and results in elongation of the Fe–O(6) bond

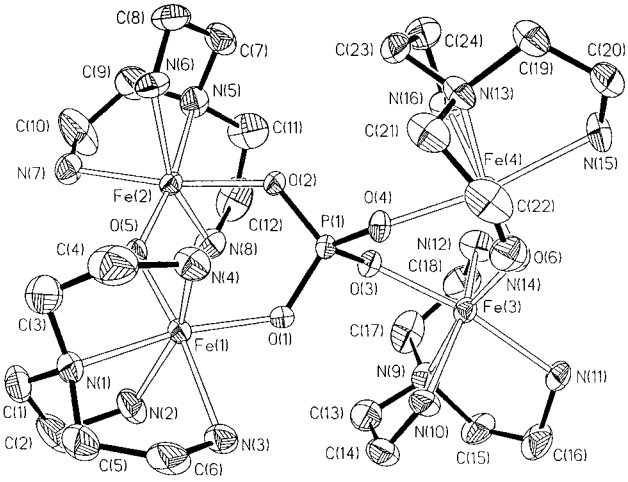



**Fig. 1** Structure of the tetranuclear iron cation in **1**. Selected interatomic distances (Å) and angles (°): Fe(1)···Fe(2) 3.307, Fe(3)···Fe(4) 3.286, Fe(1)···Fe(3) 5.768, Fe(1)···Fe(4) 5.942, Fe(2)···Fe(3) 6.014, Fe(2)···Fe(4) 6.013, Fe(1)–O(1) 1.955(6), Fe(1)–O(5) 1.805(6), Fe(1)–N(1) 2.204(8), Fe(1)–N(2) 2.180(9), Fe(1)–N(3) 2.223(8), Fe(1)–N(4) 2.195(8), Fe(2)–O(2) 2.008(6), Fe(2)–O(5) 1.785(6), Fe(2)–N(5) 2.237(8), Fe(2)–N(6) 2.163(8), Fe(2)–N(7) 2.177(8), Fe(2)–N(8) 2.216(8), Fe(3)–O(3) 2.005(6), Fe(3)–O(6) 1.813(6), Fe(3)–N(9) 2.225(8), Fe(3)–N(10) 2.185(8), Fe(3)–N(11) 2.196(8), Fe(3)–N(12) 2.182(9), Fe(4)–O(4) 1.984(6), Fe(4)–O(6) 1.822(6), Fe(4)–N(13) 2.231(8), Fe(4)–N(14) 2.172(8), Fe(4)–N(15) 2.197(8), Fe(4)–N(16) 2.186(8); Fe(1)–O(5)–Fe(2) 134.2(3), Fe(3)–O(6)–Fe(4) 129.4(3), Fe(1)–O(1)–P(1) 131.5(3), Fe(2)–O(2)–P(1) 129.9(4), Fe(3)–O(3)–P(1) 126.1(3), Fe(4)–O(4)–O(4) 130.7(3).

distances, narrowing of the Fe(3)–O(6)–Fe(4) angle, and shortening of the Fe(3)···Fe(4) distance. Furthermore, there is a small but significant structural *trans* influence exerted by the oxo-bridges on each of the four iron atoms in complex **1**. The four P–O lengths (av. 1.533 Å) and P–O–P angles (av. 109.8°) are almost equivalent within experimental error, indicating the trianionic charge of the $PO_4^{3-}$ is equally distributed over the four oxygen atoms of the phosphate. The phosphate can therefore be viewed as an ideal tetrahedron. All of the lattice water molecules are found to be involved in hydrogen bonds either to perchlorate [O(2w)···O(18) 2.841, O(2w)···O(21) 2.930, O(3w)···O(25) 2.426 Å] or toμ-oxo [O(6)···O(1w) 2.743 Å].

The UV–VIS spectrum of **1** in acetonitrile exhibits rich features in the 400–500 nm region similar to those of other tetranuclear iron(III) compounds.[7] It displays three strong absorption bands at *ca*. 213, 237 and 320 nm, which are readily assigned to the intraligand transitions. The weak band at *ca*. 693 nm is due to a ligand field transition. The IR spectrum of **1** shows two strong peaks at *ca*. 1145 and 978 $cm^{-1}$ which are characteristic of $PO_4^{3-}$ stretch vibrations. The peak at 778 $cm^{-1}$ can be assigned to the asymmetric Fe–O–Fe stretch vibration, comparable with that found in other oxo-bridged iron(III) compounds.[3b,6a,b,7a,b,8] The symmetric stretch vibration of the Fe–O–Fe unit is Raman active and was found at 464 $cm^{-1}$ in the Raman spectrum of **1**.

Although quite a few tetranuclear iron(III) complexes have been synthesized, almost all of them are bridged by carboxylate ligands. Hence **1** provides the first example of a tetranuclear iron(III) complex linked by a tetradentate phosphate. The most interesting observation in this reaction is that the phosphate monoester undergoes hydrolysis in the presence of the iron(III) polyamine complex, and the intermediate $PO_4^{3-}$ anion functions in the $\mu_4$-mode to generate tetranuclear iron complex **1**. This may involve either a two- or poly-metal mechanism in the hydrolysis reaction. Complex **1** also provides a good model for the hydrolysis of phosphate ester *in vivo* by purple acid phosphatase. Study of the detailed mechanism of the hydrolysis of phosphate mono-, di- and tri-esters by iron polyamine complexes is in progress.

This project is supported by the Hong Kong Research Grant Council and the Hong Kong University of Science and Technology.

## Footnotes and References

* E-mail: chxyli@usthk.ust.hk

† *Preparation of* **1**: to a red solution of methanol (10 ml) containing $Fe(ClO_4)_3 \cdot 9H_2O$ (0.492 g, 1 mmol) was added tren (0.15 g, 1.03 mmol) dissolved in methanol (10 ml) with stirring at room temp. After stirring for 20 min, to the brown solution was added $Na_2(O_2NC_6H_4OPO_3) \cdot 6H_2O$ (0.19 g, 0.51 mmol), the solution turned graminaceous in a few minutes, followed by precipitation of the complex as a green powder. The mixture was further stirred for 4 h and filtered. The green solid was dissolved in MeCN (5 ml) and filtered, and dark-green crystals were obtained by diffusing ethyl acetate into the acetonitrile solution. Anal. Found: C, 19.21; H, 5.40; N, 14.95. Calc. for $C_{24}H_{77}Cl_5Fe_4N_{16}O_{28.5}P$: C, 19.49; H, 5.21; N, 15.16%. UV–VIS spectrum (MeCN): $\lambda_{max}$ = 213 nm ($\varepsilon = 4.5 \times 10^4$ $dm^3$ $mol^{-1}$ $cm^{-1}$), 237 ($4.7 \times 10^4$), 320 ($3.4 \times 10^4$), 362 (sh), 415 (sh), 448 (712), 490 (540), 693 (br, 120). IR data ($\nu$/$cm^{-1}$, KBr pellet): 1145s ($\nu_{P-O}$), 1113–1088s ($\nu_{Cl-O}$ + $\nu_{P-O}$), 978s ($\nu_{P-O}$), 778m ($\nu_{Fe-O-Fe}$) 627s ($\nu_{Cl-O}$). Raman shift ($cm^{-1}$): 1026 ($\nu_{P-O}$), 941 ($\nu_{Cl-O}$), 627 ($\nu_{Cl-O}$), 464 ($\nu_{Fe-O-Fe}$).

‡ *Crystal data* for **1**: $C_{24}H_{77}Cl_5Fe_4N_{16}O_{28.5}P$, $M$ = 1477.64, monoclinic, space group $P2_1/c$ (no. 14), $a$ = 11.749(3), $b$ = 17.357(2), $c$ = 28.271(4) Å, $\beta$ = 97.41(1)°, $U$ = 5721.9(4) Å$^3$, $Z$ = 4, $D_c$ = 1.715 g $cm^{-3}$, $\mu$ = 1.351 $mm^{-1}$; 7873 independent reflections were collected, of which 7870 were used in the $F^2$ refinement; $R$ = 0.071 [5347 observed reflections with $I > 2\sigma(I)$]. The intensities were collected at 293 K on a Siemens P4 diffractometer using Mo-K$\alpha$ radiation ($\lambda$ = 0.710 73 Å). The crystal structure was solved by direct methods. Two of the five independent perchlorate groups exhibit two-fold orientational disorder. All non-hydrogen atoms were refined anisotropically by full-matrix least squares. Hydrogen atoms were placed in calculated positions with C–H 0.96 Å, assigned fixed isotropic thermal parameters and allowed to ride on their respective parent atoms. All computations were carried out on a PC-486 using the SHELXTL-PC program package. CCDC 182/659.

1 (*a*) S. J. Lippard, *Angew. Chem., Int. Ed. Engl.*, 1988, **27**, 344; (*b*) J. B. Vincent, G. L. Olivier-Lilley and B. A. Averill, *Chem. Rev.*, 1990, **90**, 1447; (*c*) A. K. Powell and S. L. Heath, *Comments Inorg. Chem.*, 1994, **15**, 255.
2 P. Susse, *Z. Kristallogr.*, 1968, **127**, 261; P. B. Moore, *Am. Mineral.*, 1972, **57**, 397.
3 (*a*) R. A. Stukan, V. I. Ponomarev, V. P. Nifontov, K. I. Turté and L. O. Atovmyan, *J. Struct. Chem.*, 1985, **26**, 197; (*b*) W. H. Armstrong, M. E. Roth and S. J. Lippard, *J. Am. Chem. Soc.*, 1987, **109**, 6318; (*c*) S. M. Gorun and S. J. Lippard, *Inorg. Chem.*, 1988, **27**, 149; (*d*) S. R. Boone, G. H. Purser, H.-R. Chang, M. D. Lowery, D. N. Hendrickson and C. G. Pierpont, *J. Am. Chem. Soc.*, 1989, **111**, 2292; (*e*) J. K. McCusker, J. B. Vincent, E. A. Schmitt, K. L. Mino, K. Shin, D. K. Coggin, P. M. Hagen, J. C. Huffman, G. Christou and D. N. Hendrickson, *J. Am. Chem. Soc.*, 1991, **113**, 3012; (*f*) P. Chaudhuri, M. Winter, P. Fleischhauer, W. Haase, U. Flörke and H.-J. Haupt, *Inorg. Chim. Acta*, 1993, **212**, 241; (*g*) K.-H. Lii and Y.-F. Huang, *Chem. Commun.*, 1997, 1311.
4 I.-P. Lorenz, W. Pohl and H. Nöth, *Angew. Chem., Int. Ed. Engl.*, 1997, **36**, 55; K.-H. Lii and Y.-F. Huang, *Chem. Commun.*, 1997, 839.
5 H. Li, Z. J. Zhong, W. Chen and X.-Z. You, *J. Chem. Soc., Dalton Trans.*, 1997, 463.
6 (*a*) B. P. Murch, F. C. Bradley, P. D. Boyle, V. Papaefthymiou and L. Que, Jr., *J. Am. Chem. Soc.*, 1987, **109**, 7993; (*b*) S. Drüeke, K. Wieghardt, B. Nuber, J. Weiss, E. L. Bominaar, A. Sawaryn, H. Winkler and A. X. Trautwein, *Inorg. Chem.*, 1989, **28**, 4477; (*c*) J. L. Sessler, J. W. Sibert, A. K. Burrell, V. Lynch, J. T. Markert and C. L. Wooten, *Inorg. Chem.*, 1993, **32**, 4277.
7 (*a*) H. Toftlund, K. S. Murray, P. R. Zwack, L. F. Taylor and O. P. Anderson, *J. Chem. Soc., Chem. Commun.*, 1986, 191; (*b*) J. L. Sessler, J. W. Sibert and V. Lynch, *Inorg. Chem.*, 1990, **29**, 4143; (*c*) J. L. Sessler, J. D. Hugdahl, V. Lynch and B. Davis, *Inorg. Chem.*, 1991, **30**, 334; (*d*) J. L. Sessler, J. W. Sibert, V. Lynch, J. T. Markert and C. T. Wooten, *Inorg. Chem.*, 1993, **32**, 621; (*e*) N. Arulsamy, J. Glerup and D. J. Hodgson, *Inorg. Chem.*, 1994, **33**, 3043.
8 Q. Chen, J. B. Lynch, P. Gomez-Romero, A. Ben-Hussein, G. B. Jameson, C. J. O'Connor and L. Que, Jr., *Inorg. Chem.*, 1988, **27**, 2673.
9 D. L. Jameson, C.-L. Xie, D. N. Hendrickson, J. A. Potenza and H. J. Schugar, *J. Am. Chem. Soc.*, 1987, **109**, 740.
10 M. S. Lah, M. L. Kirk, W. Hatfield and V. L. Pecoraro, *J. Chem. Soc., Chem. Commun.*, 1989, 1606.

*Received in Cambridge, UK, 12th August 1997; 7/05883G*

# Rigorous mathematical approaches to strategic bonds and synthetic analysis based on conceptually simple new complexity indices

**Steven H. Bertz*[a] and Toby J. Sommer[b]**

[a] *Complexity Study Center, 88 E. Main Street, Suite 220, Mendham, NJ 07945, USA*
[b] *Sphinx Pharmaceuticals, A Division of Eli Lilly and Company, Cambridge, MA 02139, USA*

**The enumeration of all possible subgraphs of the molecular graph is the basis for new complexity indices $N_S$ (number of kinds of subgraphs) and $N_T$ (total number of subgraphs) that are useful for synthetic analysis, *e.g.* the determination of topological strategic bonds.**

The first bonds to be broken in the retrosynthetic direction (*i.e.* the last formed in the synthetic direction) have been termed 'strategic bonds' by Corey *et al.*[1] Topological strategic bond identifies one selected on the basis of purely mathematical techniques,[2] and heuristic strategic bond on the basis of current methodology.[3] (Note that it is possible for a bond to be both.) The methods introduced here to calculate the topological strategic bonds are based on the enumeration of all possible subgraphs of a molecular graph $G$.[4] Topological approaches such as graph theory[5] are of interest, as they focus on the fundamental connectivity relationships inherent in a target structure. Setting these in place lies at the heart of synthetic strategy, as emphasized by Hendrickson.[6]

The number of kinds of subgraphs $N_S(G)$ and the total number of subgraphs $N_T(G)$ are new graph invariants,† which are useful indices of the complexity of $G$.[7,8] The relationship between graphs and subgraphs is analogous to that between structures and substructures, which chemists grasp intuitively. For simplicity, only connected skeletal ('hydrogen-suppressed'[5b]) graphs are considered. Then, the molecular graph of methane is a point, ethane is two points connected by a line (the path of length 1), and propane is the path of length 2.[9,10] The molecular graph of 2-methylpropane (2-Me-propane) has 3 'propane' subgraphs in addition to 3 'ethane' and 4 'methane' subgraphs. The graph itself is counted as a subgraph to preserve mathematical rigor.[5]‡ Consequently, $N_T$(2-Me-propane) = 11 and $N_S$(2-Me-propane) = 4.

It is easy to verify that the total number of subgraphs increases monotonically with chain length, branching and cyclization (homologous series), the major criteria of a complexity index.[11,12] Multiple bonds are included by considering multigraphs, *e.g.* ethyne has 1 'ethyne' {●≡●} and 3 'ethene' {●=●} subgraphs in addition to 3 'ethane' and 2 'methane.' Heteroatoms are included in a natural way by finding all possible (labelled) subgraphs of the corresponding labelled molecular graph: propan-2-ol has 1 'propan-2-ol' {(●–)$_2$●–○}, 2 'ethanol' {●–●–○}, 1 'propane' {●–●–●}, 1 'methanol' {●–○}, 2 'ethane' {●–●}, 1 'water' {○} and 3 'methane' {●} subgraphs. Thus, $N_T$(propan-2-ol) = 11, the same as '2-Me-propane' (above). However, 'propan-2-ol' has more kinds of subgraphs; thus, $N_S$(propan-2-ol) = 7, whereas $N_S$(2-Me-propane) = 4. For connectivity $N_T$ is a robust measure, and for the overall complexity $N_S$ is a simple and useful index. When applied to substructures, the latter is also useful in the measurement of molecular diversity.[13]

Fig. 1 illustrates the 1-bond (**2**–**5**), 2-bond (**6**–**15**) and selected 3-bond (**16**–**17**) disconnections for the fused 6-membered ring system **1**,§ which has long been a paramount synthetic problem. The ordered pair $N_S$, $N_T$ is given in parentheses for each structure. Based on $N_T(G)$, the order of increasing complexity in the 1-bond case is **5** < **4** < **3** < **2**, and in the 2-bond case it is **9**, **15** < **8** < **14** < **12** < **7** < **13** < **6** < **11** < **10**. Where the target is dissected into more than one piece, $N_T(G)$ is calculated for each and summed. Of all the possible 2-bond disconnections that break one bond in each ring, only the best one (**13**) is shown here, and it is not very effective.

In the 1-bond case the largest simplification involves breaking the fusion bond (**1**⇒**5**). This disconnection was eliminated from the heuristic bondset by LHASA rule 4: 'to avoid the formation of rings having greater than seven members during antithetic [retrosynthetic] bond cleavage, any bond common to a pair of bridged or fused primary rings whose envelope is eight-membered or larger cannot be considered strategic.'[1] Progress in eight-membered ring synthesis renders this rule archaic,[14] and also rule 1: 'because of the relative ease of formation of common-sized rings, a strategic bond must be in a four-, five-, six-, or seven-membered 'primary' ring.'[1]

If we restrict the problem to annulation of a 6-ring onto a pre-existing bond, then the greatest retrosynthetic simplification is **1**⇒**4**, which corresponds to the ring closure step of the Robinson Annulation. This is consistent with LHASA rule 2A: 'a strategic bond must be directly attached to another ring (*exo* to another ring). . .'.[1] This is one of the most important rules, and it has a purely topological basis. In contrast, the exception is completely heuristic, *viz*. rule 2B: 'due to the paucity of ring closure methods in which bonds are formed to pre-existing three-membered rings, strategic bonds may not be *exo* to rings of that size.'[1] Rule 2B may change with more research, rule 2A

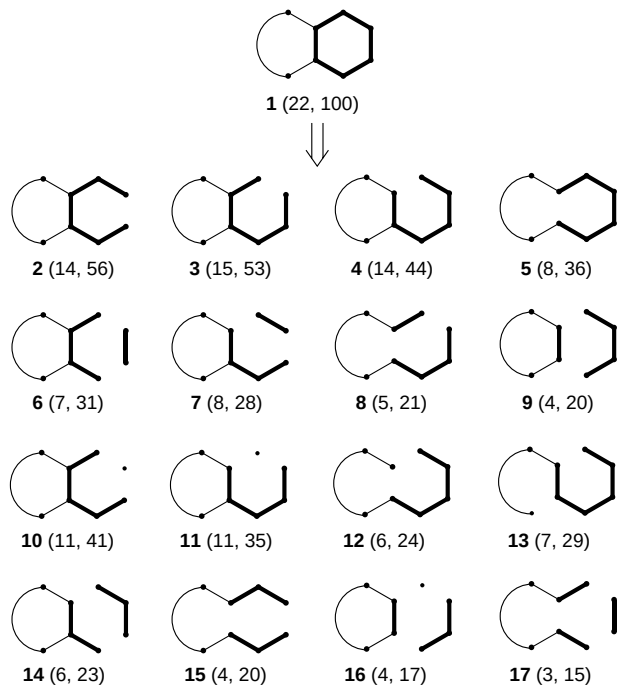



**Fig. 1** 1-bond (**2**–**5**), 2-bond (**6**–**15**), and selected 3-bond (**16**, **17**) disconnections of the fused six-membered ring system **1**; ($N_S$, $N_T$) is given below each structure

will not. Breaking the adjacent ('*exo*') bond minimizes the degrees of the points (valences of the atoms), which is also the basis for rule 3: '. . . strategic bonds should be in the ring (or rings) which exhibits the greatest degree of bridging.'[1]

Of the 2-bond 'Diels–Alder disconnections' resulting in daughters **6**–**9**, the one that affords two pieces of the same complexity (**1**⇒**9**)§ gives the greatest simplification, which is in harmony with the heuristic principle of convergence.[15] It is interesting to note that this 2-bond disconnection is also the overall disconnection for the Robinson Annulation. Furthermore, to minimize the total complexity of the synthetic route by maximizing the symmetry in the synthesis graph (reflexivity),[16] the two pieces should be identical if possible.

Particularly noteworthy is the impressive simplification provided by the 'bis-allyl disconnections' (*e.g.* **1**⇒**14**, **15**), which are comparable to the best Diels–Alder disconnections. This is clearly a reaction that would be worth developing.[17]¶ The 2-bond disconnections that produce an isolated 'methane' (*e.g.* **1**⇒**10**, **11**) are the least efficient of this class. (Synthetic equivalents include $CCl_2$, CN, CO, *etc*.) However, if the 1-carbon fragment is part of a process that forms other bonds as well, the overall result can be very efficient (next paragraph).

The most dramatic simplifications calculated here involve 3-bond disconnections. A particularly interesting 3-bond process is **1**⇒**16**. It corresponds to the Dötz–Wulff reaction, in which the 1-carbon (CO) and 3-carbon units derive from a metal–carbene complex and the 2-carbon unit comes from an alkyne.[18] Disconnection **1**⇒**17** is realized in the cobalt-mediated alkyne trimerization developed by Vollhardt and coworkers.[19] This reaction renders obsolete LHASA rule 5: 'Bonds within aromatic rings are not considered to have potential strategic character.'[1]

An example of the use of $N_S$ in synthetic analysis is provided by disconnections involving heteroatoms. The values of $N_S$ for pentan-1-ol, butyl methyl ether, and ethyl propyl ether are 11, 13, and 12, respectively. These molecules may be considered to be the daughters from the 1-bond disconnections of oxacyclohexane ($N_S$ = 18) at the C–O α-bond, the adjacent C–C β-bond, and the remote C–C γ-bond, respectively. These disconnections have $-\Delta N_S$(α-bond) = 7, $-\Delta N_S$(β-bond) = 5, and $-\Delta N_S$(γ-bond) = 6. ($\Delta N_S$ is the retrosynthetic change in complexity, daughter minus target; $-\Delta N_S$ is the change in complexity in the synthetic direction.) The greatest simplification involves breaking the C–O bond. This is consistent with the LHASA C-heterobond procedure: 'to the set of strategic bonds determined by application of rules 1–6 above is added the collection of bonds in the cyclic network between carbon and O, N and S. . .'.[1] Moreover, $N_S$ also identifies **1**⇒**5** as the most efficient 1-bond and **1**⇒**9**, **15** as the most efficient 2-bond disconnections.

The daughter structures are all subgraphs of the target *T*, as are all the second generation daughters obtained by considering the first generation to be new targets *T*′. Consequently, by generating all possible subgraphs of *T*, we also generate all possible retrosynthetic intermediates and thereby all possible direct synthetic routes. Actual intermediates are usually synthetic equivalents of these retrosynthetic ones and typically contain more atoms, making them more complex. The various routes can then be evaluated by using the principle of minimization of excess complexity[20] or the related principle of maximization of target-relevant complexity.[14]

While our new approach is conceptually simple, for large problems it is important to have a simpler index that parallels $N_T(G)$, and the number of pairs of adjacent bonds $\eta$ ('propane' subgraphs) does this well. Only one pair of structures (**12**, **14**) is ordered differently by $N_T(G)$ and $\eta$, which confirms the validity of our previous work on synthetic analysis.[2,8,11,20] (There are more degeneracies in the simpler index.) The number of spanning trees has also been proposed to be the 'complexity' of a planar graph,[21] but it is not useful for graphs without rings. A 'middle way' might be to count all paths[10] or walks.[22] Moreover, paths, walks or $N_T(G)$ include long-range 'interactions', which can be critically important, as emphasized by Lehn in his $MI_2$ approach to complexity.[23]

In conclusion, the total number of subgraphs $N_T(G)$ is a robust measure of connectivity ('topological complexity'), and the number of kinds of subgraphs $N_S(G)$ is a simple measure of the overall complexity of a molecular graph *G*. These new indices are useful for understanding strategic bond disconnections. Some of them correspond to powerful known reactions, while others suggest new reactions that would efficiently increase molecular complexity. The fact that we can derive certain of the 'heuristic' rules for strategic bonds mathematically establishes that they have a purely topological basis and suggests that topology may be the 'unseen hand' of synthesis. The other rules are revealed to be principally a function of the state of the art, for which our approach provides objective benchmarks.‖

We thank V. Shcherbukhin (Astra Hässle) and W. F. Wright (AT&T) for interesting discussions and useful references.

## Footnotes and References

* E-mail: sbertz@ispcorp.com

† Invariants are independent of isomorphism, *i.e.* how the graph is drawn.[5]

‡ By including the graph *G* as a subgraph of itself, $N_T(G)$ is given by simple formulas, *e.g.* $N_T(K_{1,n}) = 2^n + n$ for the star graphs and $N_T(P_{n-1}) = n(n + 1)/2$ for the *n*-alkanes.

§ Strictly speaking, the new 6-ring is annulated onto the middle bond of butane, as the arcs are not included in the subgraphs. Functionality need not be included at the strategic level; *cf*. the antepenultimate paragraph for tactical considerations.

¶ An intramolecular example has been reported;[17] however, it does not increase complexity significantly, as it is not a construction reaction.[6]

‖ A list of all the subgraphs of **1**–**17** is available upon request.*

1 E. J. Corey, W. J. Howe, H. W. Orf, D. A. Pensak and G. Petersson, *J. Am. Chem. Soc*., 1975, **97**, 6116.
2 S. H. Bertz and T. J. Sommer, in *Organic Synthesis: Theory and Applications*, ed. T. Hudlicky, JAI Press, New York, 1993, vol. 2, p. 67.
3 W.-D. Ihlenfeldt and J. Gasteiger, *Angew. Chem., Int. Ed. Engl*., 1995, **34**, 2613.
4 S. H. Bertz and W. C. Herndon, in *Artificial Intelligence Applications in Chemistry*, ed. T. H. Pierce and B. A. Hohne, ACS, Washington, D.C., 1986, p. 169.
5 (*a*) F. Harary, *Graph Theory*, Addison-Wesley, Reading, MA, 1969; (*b*) N. Trinajstić, *Chemical Graph Theory*, 2nd edn., CRC Press, Boca Raton, FL, 1992.
6 J. B. Hendrickson, *Angew. Chem., Int. Ed. Engl*., 1990, **29**, 1286.
7 S. H. Bertz, *J. Chem. Soc., Chem. Commun*., 1981, 818.
8 S. H. Bertz, *J. Am. Chem. Soc*., 1981, **103**, 3599.
9 M. Gordon and J. W. Kennedy, *J. Chem. Soc., Faraday Trans. 2*, 1973, **69**, 484.
10 M. Randić, *J. Chem. Inf. Comput. Sci*., 1996, **36**, 1092.
11 S. H. Bertz, in *Chemical Applications of Topology and Graph Theory*, ed. R. B. King, Elsevier, Amsterdam, 1983, p. 206.
12 S. H. Bertz, *Discrete Appl. Math*., 1988, **19**, 65.
13 C. Cheng, G. Maggiora, M. Lajiness and M. Johnson, *J. Chem. Inf. Comput. Sci*., 1996, **36**, 909.
14 P. A. Wender and B. L. Miller, ref. 2, p. 27.
15 L. Velluz, J. Valls and G. Nominé, *Angew. Chem., Int. Ed. Engl*., 1965, **4**, 181.
16 S. H. Bertz, *J. Chem. Soc., Chem. Commun*., 1984, 218.
17 W. W. Win, K. G. Grohmann and L. Todaro, *J. Org. Chem*., 1994, **59**, 2803.
18 K. H. Dötz, *Angew. Chem., Int. Ed. Engl*., 1975, **14**, 644; W. D. Wulff, in *Comprehensive Organometallic Chemistry*, Pergamon, Oxford, 1995, vol. 12, p. 469.
19 J. K. Cammack, S. Jalisatgi, A. J. Matzger, A. Negrón and K. P. C. Vollhardt, *J. Org. Chem*., 1996, **61**, 4798.
20 S. H. Bertz, *J. Am. Chem. Soc*., 1982, **104**, 5801.
21 E. C. Kirby, R. B. Mallion and P. Pollak, *Mol. Phys*., 1994, **83**, 599.
22 G. Rücker and C. Rücker, *J. Chem. Inf. Comput. Sci*., 1993, **33**, 683.
23 J.-M. Lehn, *Supramolecular Chemistry: Concepts and Perspectives*, VCH, Weinheim, 1995, p. 201.

*Received in Corvallis, OR, USA; 12th September 1997; 7/06192G*

# Synthesis and structural characterisation of tripodal titanium silsesquioxane complexes: a new class of highly active catalysts for liquid phase alkene epoxidation

**Mark Crocker,*[a] Ruud H. M. Herold[a] and A. Guy Orpen[b]**

[a] *Shell Research and Technology Centre Amsterdam, Postbus 38000, 1030 BN Amsterdam, The Netherlands*
[b] *School of Chemistry, University of Bristol, Cantock's Close, Bristol, UK BS8 1TS*

**Titanium silsesquioxane complexes [Ti(L)($R_7Si_7O_{12}$)], possessing tripodal geometry, represent models for heterogeneous titanosilicate catalysts; the new complexes are exceptionally active and selective catalysts for liquid phase alkene epoxidation reactions.**

The remarkable catalytic properties of titanosilicates such as titanium silicalite-1 (TS-1) have generated considerable scientific interest, particularly with regard to the nature of the active titanium species present. It is now generally accepted that a four-coordinate lattice titanium site is the catalytically active species in these materials.[1] Furthermore, recent studies point toward the involvement of titanium sites possessing tripodal geometry, representing so-called open lattice sites,[2,3] although the presence of closed lattice sites ('tetrapodal' sites) and bipodal sites has also been inferred (see Fig. 1).[1,2] With this in mind we have prepared soluble analogues of these different titanium species based on incompletely condensed silsesquioxane precursors and have studied the catalytic properties of the resulting complexes.[4] Recently we became aware of related studies aimed at modelling heterogeneous titanium-based epoxidation catalysts, which also employ silsesquioxane derivatives;[5,6] prompted by these reports we now describe our own findings.

Incompletely condensed silsesquioxanes have recently attracted interest as models for the silica surface.[7,8] Elegant work by Feher and coworkers has revealed that the molecular structure of **1** (see Scheme 1) shares many structural similarities with β-cristobalite (111) and β-tridymite (0001). Although the exact nature of the silica surface is a matter of great controversy, the occurrence of cristobalite- and tridymite-like surface structures has been frequently postulated on the basis of both experimental and theoretical studies. On this basis, we have prepared titanium complexes of **1** in which the silsesquioxane ligand functions as a model for the siliceous surface in a tripodal titanium site. Similarly, the monosilylated form of **1**, disilanol species **2** (Scheme 2) has been used to model the siliceous surface in bipodal and tetrapodal titanium sites.

Reaction of **1** with homoleptic titanium(IV) complexes $TiL_4$ (L = $CH_2Ph$, $NMe_2$, $OSiMe_3$, $OPr^i$) occurs with protonolysis, affording in each case a product with the empirical formula [TiL{(c-$C_6H_{11})_7Si_7O_{12}$}] (Scheme 1) on the basis of elemental analysis and solution $^1H$ NMR data. $^{29}Si$ NMR spectra of the products are particularly informative, the observation in each case of three resonances for the silsesquioxane Si atoms in a 3 : 1 : 3 ratio being consistent with the $C_{3v}$ symmetry expected

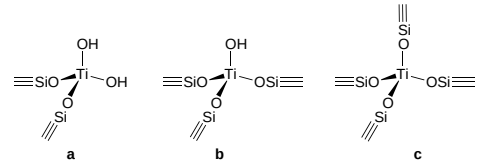
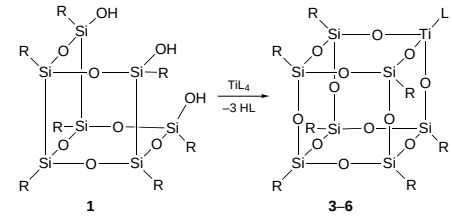


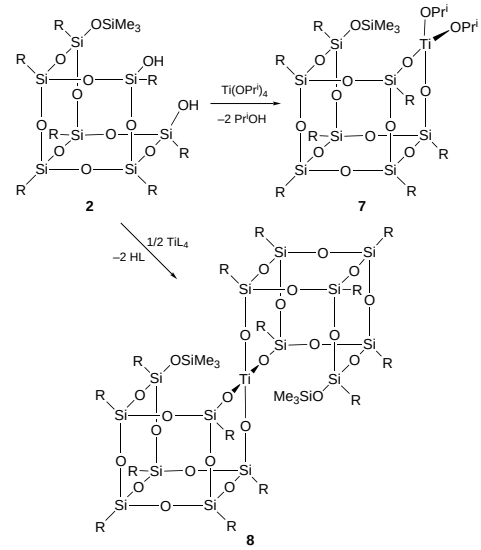

**Fig. 1** Possible framework titanium sites in titanosilicates: (*a*) bipodal site, (*b*) tripodal (open lattice) site, (*c*) tetrapodal (closed lattice) site




**Scheme 1** Synthesis of compounds **3**–**6**: L = $CH_2Ph$ **3**, $NMe_2$ **4**, $OSiMe_3$ **5**, $OPr^i$ **6**; R = cyclohexyl

for a tripodal TiL(silsesquioxane) species. In the case of **6**, $^{29}Si$ NMR data indicate the presence of a second species containing five distinct silicon environments (with relative ratios 2 : 2 : 1 : 1 : 1), corresponding to the dimer [Ti{(c-$C_8H_{11})_7Si_7O_{12}$}(μ-$OPr^i$)]$_2$ recently reported by Maschmeyer *et al.*[7] Freshly prepared solutions of **6** were found to contain exclusively the monomer, while at longer equilibration times a monomer : dimer ratio of *ca.* 5 : 2 was observed in $C_6D_6$.

The monomeric nature of **5** was confirmed by the results of a single crystal X-ray diffraction study (see Fig. 2). The crystal structure of **5** consists of isolated molecules separated by normal van der Waals contacts. Molecules of **5** lie in crystallographic special positions of $\bar{3}$ site symmetry and are consequently disordered; only one of the two centrosymmetrically related images of the disordered molecule is shown. The molecular structure of **5** consists of a pseudo-tetrahedral titanium(IV) centre coordinated by the tridentate silsesquioxane ligand and siloxy ($OSiMe_3$) ligand such that the complex has exact $C_3$ symmetry [disregarding the cyclohexyl substituent at Si(1′), the silicon opposite titanium]. As a consequence of the disorder the details of the apparent molecular geometry must be treated with scepticism. However, the gross geometry of **5** in the




**Scheme 2** Synthesis of **7** and **8** (L = $CH_2Ph$, R = cyclohexyl)

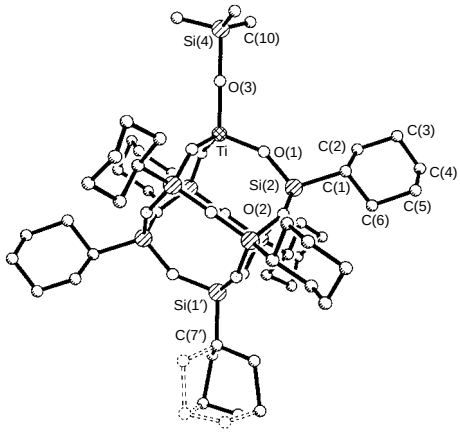



**Fig. 2** Molecular structure of **5** showing atom labelling scheme. All hydrogen atoms have been omitted for clarity. Only one of the two centrosymmetrically related images of the disordered molecule is shown. Selected distances (Å) and angles (°): Ti–O(1) 1.658(6), Ti–O(3) 1.84(2), Si(2)–O(1) 1.625(6), Si(2)–O(2) 1.641(6), O(3)–Si(4) 1.79(2); O(1′)–Ti–O(1) 107.4(2), O(1)–Ti–O(3) 111.4(2), O(1)–Si(2)–O(2) 108.0(3), Si(2)–O(1)–Ti 151.0(4), Si(4)–O(3)–Ti 180.0.

solid state is clearly established, and by inference so is the structure of the monomer form of the isopropoxy analogue **6**, which also crystallises in space group $R\bar{3}$ with similar cell dimensions to **5**, and has molecules lying at the same special positions as **5**. For **6** the disorder is less well resolved and refinement less satisfactory.

The reaction of disilanol **2** with [Ti(OPr$^i$)$_4$] was examined as a possible route to a model bipodal titanium site. Addition of a diethyl ether solution of **2** to the titanium complex resulted in a smooth reaction and the subsequent isolation of [Ti(OPr$^i$)$_2${(c-$C_6H_{11})_7Si_7O_{11}(OSiMe_3)$}] **7** as the sole product (Scheme 2). $^1$H NMR data are consistent with the presence of two inequivalent isopropoxy groups in **7**, while the observation of the five signals in the $^{29}$Si NMR spectrum corresponding to the silsesquioxane $Si_7O_{11}$ core indicates that, as for the free ligand, a plane of symmetry runs through the silsesquioxane ligand, with the alkoxide ligands lying in the plane.

The reaction of 2 equiv. of silsesquioxane **2** with [Ti(CH$_2$Ph)$_4$] was chosen as a convenient means of preparing a model for the closed lattice site. In aprotic solvents a rapid reaction occurs with the formation of a colourless solution, from which bis(silsesquioxane) complex **8** can be isolated in quantitative yield (Scheme 2).

$^1$H and $^{29}$Si NMR spectroscopy reveal the presence of only one type of –OSiMe$_3$ group in **8**, suggesting equivalence of the {(c-$C_6H_{11})_7Si_7O_{11}(OSiMe_3)$} ligands. The presence of molecular $C_2$ symmetry in **8** is confirmed by the results of X-ray crystallography.[9] Consistent with tetrahedral coordination of the Ti$^{IV}$ centre, seven resonances are observed in the $^{29}$Si NMR spectrum for the framework silsesquioxane Si atoms, indicating that the local mirror symmetry of the silsesquioxane ligands is not retained at titanium.

The epoxidation of oct-1-ene with Bu$^t$OOH (TBHP) was chosen as a convenient test of the epoxidation activity of complexes **3**–**8**. At the alkene/TBHP molar ratio of *ca.* 20 employed, pseudo-first order kinetics are observed corresponding to the rate equation:

$$\mathrm{d[epoxide]}/\mathrm{d}t = k_1[\mathrm{TBHP}]$$

(where $k_1 = k_2[\mathrm{Ti}] = k_3[\mathrm{Ti}][\mathrm{alkene}]$)

At high TBHP conversions (generally > 80%), some deviation from first order kinetics is observed, corresponding to a decrease in the reaction rate. This can be attributed to the fact that the reaction is autoretarded by the *tert*-butanol co-product, a phenomenon observed previously for epoxidation catalysts.[10]

The calculated second order rate constants for TBHP conversion ($k_2 = k_1/[\mathrm{Ti}]$) for complexes **3**–**8** are shown in Table 1. Most striking is the finding that the measured values of $k_2$ for the tripodal complexes **3**–**6** are *ca.* one order of magnitude greater than for **7** and **8**, while the former complexes also show superior selectivity. Complexes **3**–**6** are also considerably more active under these test conditions than titanosilicate catalysts such as Ti-MCM-41,[11] when compared on the basis of $k_2$ values. Our conclusion is that the (most) active site in these materials, as far as epoxidation catalysis is concerned, corresponds to the tripodal, open-lattice type of titanium site. The comparatively low epoxidation activity of Ti-MCM-41 can be ascribed to the fact that only a small fraction of the titanium sites in the material are exposed at the surface and possess the correct coordination environment.

**Table 1** Epoxidation of oct-1-ene with TBHP catalysed by titanium silsesquioxane complexes[a]

| Catalyst | $10^2\ k_2$/ dm$^3$ mol$^{-1}$ s$^{-1}$ | Selectivity to epoxide[b] (%) |
|---|---|---|
| **3** | 123 | 95 |
| **4** | 63 | 99 |
| **5** | 97 | 97 |
| **6** | 149 | 93 |
| **7** | 9.3 | 75 |
| **8** | 4.7 | 83 |
| Ti-MCM-41[c] | 2.6 | 94 |

[a] Conditions: $T$ = 80 °C, Ti = 0.2 mmol, TBHP = 30 mmol, oct-1-ene (75 g) as solvent. [b] Selectivity = (mol 1,2-epoxyoctane formed/mol TBHP consumed) × 100; selectivities were determined at 90% TBHP consumption. Data quoted are derived from at least two runs. [c] Ti content = 1.43 mass%.

## Footnotes and References

* E-mail: m.crocker@siop.shell.nl

† NMR data for selected compounds: **5**: $^1$H NMR (C$_6$D$_6$, 250.1 MHz): $\delta$ 2.13–0.97 (m, 77 H, c-C$_6$H$_{11}$), 0.21 (s, 9 H, SiMe$_3$). $^{29}$Si NMR (C$_6$D$_6$, 79.5 MHz): $\delta$ 2.76 (s, OSiMe$_3$), −65.80, −67.90, −68.85 (s, 3 : 1 : 3). **7**: $^1$H NMR (C$_6$D$_6$, 500.1 MHz); $\delta$ 4.62 [spt, 1 H, C*H*(CH$_3$)$_2$, *J* 6.1 Hz], 4.57 [spt, 1 H, C*H*(CH$_3$)$_2$, *J* 6.1 Hz], 2.17–1.05 (m, 77 H, *c*-C$_6$H$_{11}$), 1.32 (d, 6 H, CH$_3$, *J* 6.1 Hz), 1.30 (d, 6 H, CH$_3$, *J* 6.1 Hz), 0.47 [s, 9 H, Si(CH$_3$)$_3$]. $^{29}$Si NMR (C$_6$D$_6$, 99.4 MHz): $\delta$ 10.94 (s, OSiMe$_3$), −65.64, −66.37, −66.58, −67.49, −68.86 (s, 1 : 1 : 1 : 2 : 2). **8**: $^1$H NMR (C$_6$D$_6$, 250.1 MHz): $\delta$ 2.14–1.00 (m, 154 H, *c*-C$_6$H$_{11}$), 0.52 (s, 18 H, SiMe$_3$). $^{29}$Si NMR (C$_6$D$_6$, 79.5 MHz): $\delta$ 10.42 (s, SiMe$_3$), −66.35, −66.79, −66.92, −68.22, −69.26, −69.50, −69.72 (s, all × 1). All compounds analysed satisfactorily.

‡ *Crystal data* for **5**: C$_{45}$H$_{86}$O$_{13}$Si$_8$Ti, $M_r$ = 1107.8, rhombohedral, space group $R\bar{3}$ (no. 148), $a$ = 16.955(4), $c$ = 17.853(6) Å, $\alpha = \beta$ = 90, $\gamma$ = 120°, $U$ = 4445(2) Å$^3$, $Z$ = 3, $D_c$ = 1.24 g cm$^{-3}$, $\lambda$ = 0.710 73 Å, $\mu$(Mo-K$\alpha$) = 0.36 mm$^{-1}$, $F$(000) = 1782, $T$ = 200 K. The structure was solved by direct and Fourier methods: 1296 unique reflections collected; 113 parameters (11 restraints); $wR_2$ = 0.287, $R_1$ = 0.107 for the 775 data with $I > 2\sigma(I)$. CCDC 182/626.

1 G. Bellussi and M. S. Rigutto, *Stud. Surf. Sci. Catal.*, 1994, **85**, 177.
2 L. Le Noc, D. Trong On, S. Solomykina, B. Echchahed, F. Beland, C. Cartier dit Moulijn and L. Bonneviot, *Stud. Surf. Sci. Catal.*, 1996, **101**, 611.
3 T. Maschmeyer, F. Rey, G. Sankar and J. M. Thomas, *Nature*, 1995, **378**, 159.
4 M. Crocker and R. H. M. Herold, *Pat. Appl.*, PCT/EP96/05873.
5 H. C. L. Abbehuis, S. Krijnen and R. A. van Santen, *Chem. Commun.*, 1997, 331.
6 T. Maschmeyer, M. C. Klunduk, C. M. Martin, D. S. Shephard, J. M. Thomas and B. F. G. Johnson, *Chem. Commun.*, 1997, 1847.
7 F. J. Feher, D. A. Newman and J. F. Walzer, *J. Am. Chem. Soc.*, 1989, **111**, 1741.
8 F. J. Feher, S. H. Phillips and J. W. Ziller, *Chem. Commun.*, 1997, 829.
9 A. G. Orpen, unpublished work.
10 R. A. Sheldon and J. A. van Doorn, *J. Catal.*, 1973, **31**, 427.
11 A. Coma, M. T. Navarro and J. Perez-Pariente, *J. Chem. Soc., Chem. Commun.*, 1994, 147.

*Received in Basel, Switzerland, 10th July 1997; 7/04969B*